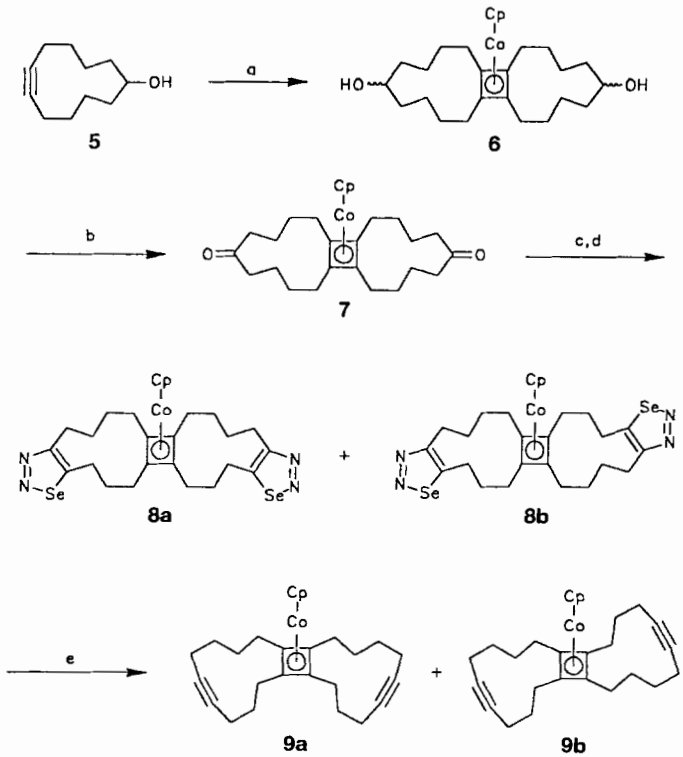
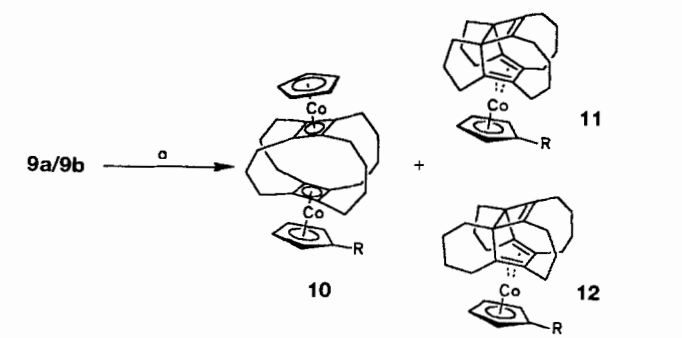


Scheme 2. a) [CpCo(cod)], decalin, 155 °C, 4 d; b) Oppenauer oxidation, acetone/toluene, $Al(OiPr)_3$, 20 h under reflux; c) semicarbazide · HOAc, ethanol, 30 min under reflux; d) SeO_2, HOAc, 40 °C, 4 h; e) *n*BuLi, THF, −40 °C.

Scheme 3 shows that heating the mixture of **9a**/**9b** with [CpCo(CO)$_2$] leads to three products in a 2:1:1 ratio and 75% yield: the superphane **10a** and the two fourfold bridged bicyclo[4.2.0]octa-2-4-7-triene complexes **11a** and **12a**.[10] X-ray studies on single crystals of **10a**[11] (Fig. 1) and **12a**[12] confirm the given structures.



Scheme 3. **10a**–**12a**, R = H; **10b**–**12b**, R = $SiMe_3$. a) R = H: [CpCo(CO)$_2$], cyclooctane, 5 h under reflux; R = $SiMe_3$: [$(Me_3SiC_5H_4)$Co(cod)], cyclooctane, 14 h under reflux.

The superphane **10a** is the first cyclobutadiene superphane containing different chain lengths in one molecule. Heating **9a**/**9b** with [$(Me_3SiC_5H_4)$Co(cod)] yielded, besides the anticipated "mixed" superphane **10b**, the bicyclo[4.2.0]octa-2,4,7-diene complexes **11b** and **12b** (Scheme 3). Thus, "labeling" of one Cp ring with the $SiMe_3$ group shows that during the formation of **11** and **12** the CpCo unit of **9a**/**9b** is removed. This observation was unexpected because CpCo-complexed cyclobutadienes are usually very inert towards the reaction with further triple

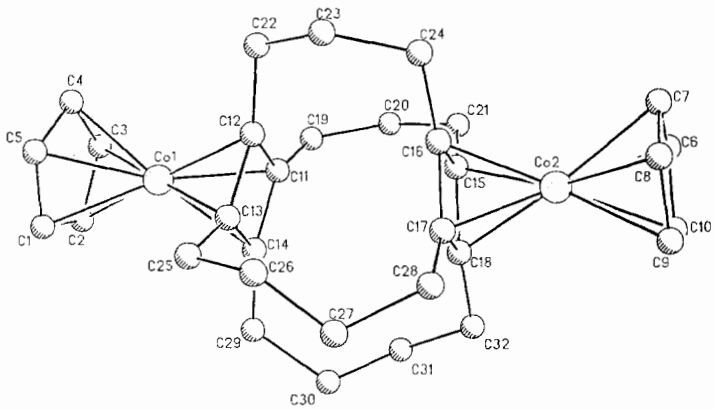
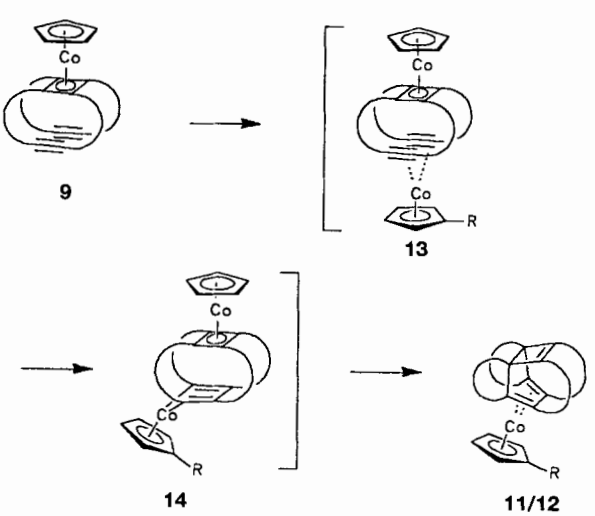


Fig. 1. Crystal structure of **10a** (H atoms omitted). Distances between the cyclobutadiene units [Å]: C11-C15 3.00, C12-C16 3.00, C13-C17 3.37, C14-C18 3.36. Other selected distances [Å] and angles [°]: Co1-C1 2.03(1), Co1-C11 1.97(1), C1-C2 1.36(2), C11-C12 1.44(1), C11-C14 1.45(1), C11-C12-C22 135.6(5), C12-C11-C19 133.8(5), C11-C14-C29 136.7(5), C14-C13-C25 134.8(5).

Table 1. NMR spectroscopic data of the most important compounds.

7: ^{1}H NMR (300 MHz, $CDCl_3$): δ = 4.55 (s, 5H), 2.47–2.60 (m, 4H), 2.28–2.42 (m, 4H), 1.97–2.18 (m, 8H), 1.39–1.78 (m, 16H); ^{13}C NMR (75.47 MHz, $CDCl_3$): δ = 214.2(s), 79.9 (d, Cp), 79.2(s), 40.9(t), 27.8(t), 24.7(t), 23.4(t).
9a + **9b**: ^{1}H NMR (300 MHz, $CDCl_3$): δ = 4.615 (s, 5H), 4.612 (s, 5H), 1.98–2.32 (m, 32H), 1.41–1.88 (m, 24H); ^{13}C NMR (75.47 MHz, C_6D_6): δ = 83.0(s), 81.0(s), 80.9(s), 79.9(s), 79.7(d, Cp), 79.3(s), 79.1(s), 29.3(t), 29.2(t), 29.0(t), 28.8(t), 25.2(t), 25.1(t), 25.0(t), 24.95(t), 24.9(t), 24.8(t), 19.7(t), 19.5(t), 17.8(t).
10a: ^{1}H NMR (200 MHz, $CDCl_3$): δ = 4.37 (s, 10H), 1.57–1.75 (m, 16H), 1.45–1.55 (m, 12H); ^{13}C NMR (75.47 MHz, C_6D_6): δ = 81.7(s), 81.0(d, Cp), 80.8(s), 29.5(t), 28.7(t), 28.6(t), 26.9(t).
11a + **12a**: ^{1}H NMR (300 MHz, $CDCl_3$): δ = 4.43 (s, 5H), 4.32 (s, 5H), 2.73–2.81 (m, 8H), 1.22–2.30 (m, 48H); ^{13}C NMR (75.47 MHz, C_6D_6): δ = 154.4(s), 154.0(s), 90.2(s), 87.5(s), 86.0(s), 83.3(d, Cp), 81.9(d, Cp), 66.8(s), 66.0(s), 38.0(t), 35.9(t), 35.5(t), 35.3(t), 31.0(t), 30.2(t), 29.2(t), 28.8(t), 28.5(t), 28.3(t), 26.7(t), 26.6(t), 26.3(t), 25.9(t), 25.8(t), 25.3(t), 25.2(t), 24.4(t).
16: ^{1}H NMR (300 MHz, $CDCl_3$): δ = 4.51 (s, 10H), 2.35–2.50 (m, 8H), 2.02–2.28 (m, 16H), 1.60–1.85 (m, 16H), 1.38–1.53 (m, 8H); ^{13}C NMR (75.47 MHz, $CDCl_3$): δ = 134.6(s), 79.6(d, Cp), 79.1(s), 32.7(t), 27.4(t), 26.9(t).
18: ^{1}H NMR (300 MHz, $CDCl_3$): δ = 4.45 (s, 10H), 2.10–2.48 (m, 24H), 1.22–1.78 (m, 40H); ^{13}C NMR (75.47 MHz, C_6D_6): δ = 133.7(s), 81.1(d, Cp), 80.5(s), 31.6(t), 28.3(t), 27.1(t), 25.9(t).

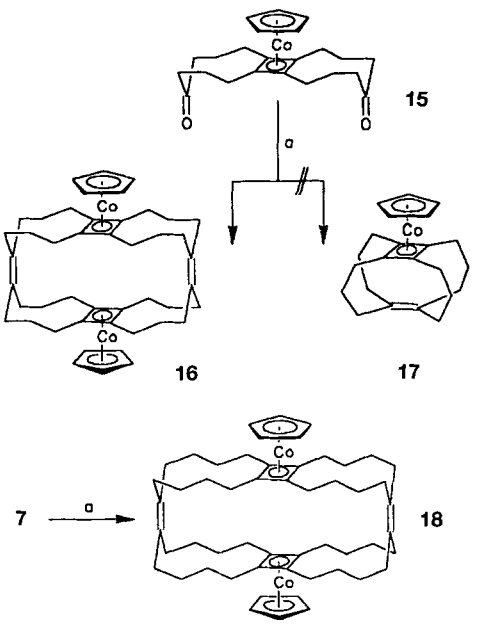
bonds.[4] To explain our results we suggest an intramolecular [4 + 2] cycloaddition between a reactive cobaltacyclopentadiene fragment[13] such as **14** and a CpCo-Co-complexed cyclo-



Scheme 4. Possible mechanism for the formation of complexes of bicyclo[4.2.0]-octa-2,4,7-trienes.

butadiene unit as indicated in Scheme 4. The isomers **11** and **12** are bridged C_8H_8 species like **2**–**4**.

Tricyclic diketones of type **7** are also useful for the synthesis of mixed superphanes of cyclobutadiene and ethylene. The McMurry reaction[14] with **7** and its congener (**15**) derived from 5-cyclononynol[15] leads to the respective products **16** in 3% and **18** in 1% yield. Anticipated derivatives of type **17** formed



Scheme 5. a) $TiCl_3$/Zn-Cu, 1,2-dimethoxyethane, high dilution, 80 °C, 3 d.

in an intramolecular reaction could not be found. Compounds **16** and **18** are a new type of superphane[16] that twice connects two different π-units with each other (Scheme 5).

Received: January 17, 1994 [Z 6622 IE]
German version: *Angew. Chem.* **1994**, *106*, 1350

[1] K. P. C. Vollhardt, *Acc. Chem. Res.* **1977**, *10*, 1; *Angew. Chem.* **1984**, *96*, 525; *Angew. Chem. Int. Ed. Engl.* **1984**, *23*, 539.
[2] H. Bönnemann, *Angew. Chem.* **1985**, *97*, 264; *Angew. Chem. Int. Ed. Engl.* **1985**, *24*, 248; H. Bönnemann, R. Goddard, J. Grub, R. Mynott, E. Raabe, S. Wendel, *Organometallics* **1989**, *8*, 1941.
[3] N. E. Schore, *Chem. Rev.* **1988**, *88*, 1081.
[4] Exceptions: R. Gleiter, D. Kratz, *Angew. Chem.* **1990**, *102*, 304; *Angew. Chem. Int. Ed. Engl.* **1990**, *29*, 276, and references therein.
[5] A. Efraty, *Chem. Rev.* **1977**, *77*, 691.
[6] R. Gleiter, *Angew. Chem.* **1992**, *104*, 29; *Angew. Chem. Int. Ed. Engl.* **1992**, *31*, 27, and references therein.
[7] R. Gleiter, V. Schehlmann, *Angew. Chem.* **1990**, *102*, 1450; *Angew. Chem. Int. Ed. Engl.* **1990**, *29*, 1426.
[8] R. Gleiter, H. Langer, W. Wittwer, unpublished results.
[9] I. Lalezari, A. Shafiee, M. Yalpani, *Tetrahedron Lett.* **1969**, 5105; *Angew. Chem.* **1970**, *82*, 484; *Angew. Chem. Int. Ed. Engl.* **1970**, *9*, 464; H. Petersen, H. Meier, *Chem. Ber.* **1980**, *113*, 2383.
[10] For unbridged $Fe(CO)_3$-stabilized bicyclo[4.2.0]octa-2,4,7-trienes see M. Cooke, J. A. K. Howard, C. R. Russ, F. Gordon, A. Stone, P. Woodward, *J. Orgmet. Chem.* **1974**, *78*, C43; W. Slegeir, R. Case, J. S. McKennis, R. Pettit, *J. Am. Chem. Soc.* **1974**, *96*, 287.
[11] X-ray structure analysis of **10a**: $C_{32}H_{38}Co_2$, $M_r = 2162.06$, monoclinic, space group C_{2h}^5, crystal size: $0.34 \times 0.45 \times 0.74$ mm, $a = 15.826(4)$, $b = 9.442(2)$, $c = 18.698(3)$ Å, $\beta = 111.05(2)°$, $V = 2607.6$ Å^3, $F(000) = 1136$, $Z = 4$, $\rho_{calcd} = 1.38$ g cm^{-3}, $\mu = 1.29$ mm^{-1}, $Mo_{K\alpha}$ radiation, $\lambda = 0.7107$ Å. Intensity data were collected on a SYNTEX R3 diffractometer. Of 4793 reflections collected, 3368 were within $I > 2.0\sigma(I)$ and 3034 within $I > 2.5\sigma(I)$. The structure was solved with Patterson-Fourier methods carried out with SHELXTL PLUS. $R = 0.054$, $R_w = 0.049$. Further details of the cristal structure investigation may be obtained from the Fachinformationszentrum Karlsruhe, Gesellschaft für wissenschaftliche-technische Information mbH, D-76344 Eggenstein-Leopoldshafen (FRG) on quoting the depository number CSD-58132, and the journal citation.
[12] R. Gleiter, H. Langer, B. Nuber, unpublished results.
[13] Y. Wakatsuki, O. Nomura, K. Kitana, K. Morokuma, H. Yamazaki, *J. Am. Chem. Soc.* **1983**, *105*, 1907.
[14] S. Tyrlik, I. Wolchowitz, *Bull. Soc. Chim. Fr.* **1973**, 2147; T. Mukaiyama, T. Sato, J. Hanna, *Chem. Lett.* **1973**, 1041; J. E. McMurry, M. P. Flemming, *J. Am. Chem. Soc.* **1974**, *96*, 4708; J. E. McMurry, *Chem. Rev.* **1989**, *89*, 1513.
[15] R. Gleiter, V. Schehlmann, *Tetrahedron Lett.* **1989**, *30*, 2893; V. Schehlmann, Dissertation, Universität Heidelberg, **1990**.
[16] R. Gleiter, D. Kratz, *Acc. Chem. Res.* **1993**, *26*, 311.

Micrometer-Scale Lateral Structuring of Organic Thiolate Layers through Self-Organization**

Claus Duschl,* Martha Liley, and Horst Vogel

Self-assembly techniques for the formation of ultrathin films based on sulfur-containing compounds show great potential for the modification of surfaces.[1,2] Films thus produced are remarkably free from defects and are highly stable and therefore very promising for technical applications. With these films, very precise control of chemical properties and thicknesses is possible, but it is difficult to control lateral properties, such as distribution of species in layers containing more than one component.[3–6] In contrast, Langmuir–Blodgett (LB) techniques produce ultrathin films in which a relatively high degree of lateral structuring is possible:[7–10] phase state and molecular density can be controlled, and two-dimensional domain structures in the plane of the film can be induced either by phase separation, or, in a mixed monolayer, by de-mixing. However, LB films are much less robust and generally exhibit a much higher defect density than layers prepared with self-assembly techniques. Using an amphiphilic disulfide, which can be spread as a Langmuir monolayer and which binds covalently to gold, it is possible to form ultrathin films which combine the advantages of these two techniques. The films produced are covalently attached to the surface, and therefore robust, and it is also possible to introduce two-dimensional structures with contrasting surface properties into the films. Unlike lithographic methods, this technique imposes no theoretical lower limit on the size of the lateral structures produced.

The generation of a laterally structured thiolate layer is depicted schematically in Figure 1 left. A mixture of palmitic acid and a lipid containing sulfur (thiolipid) is spread on the water/air interface of a Langmuir trough. On compression, the floating monolayer de-mixes and regularly distributed domains, containing predominantly fatty acid, are formed. Their size and shape depend on the self-organizing properties of the monolayer and its manipulation on the Langmuir trough. The film is transferred to a gold substrate where the thiolipids bind covalently to the gold surface. The physisorbed fatty acid is washed away to leave do-

[*] Dr. C. Duschl, Dr. H. Vogel
Institut de Chimie Physique II
Ecole Polytechnique Fédérale de Lausanne
CH-1015 Lausanne (Switzerland)
Telefax: Int. code + (21)693-4111
Dr. M. Liley
Institut de Microtechnique, Université de Neuchâtel
CH-2000 Neuchâtel (Switzerland)

[**] This work was supported by the Swiss National Science Foundation (SPP Biotechnology). We thank S. M. Zakeeruddin for the synthesis of the ω-mercaptoundecanoic acid.

mains of bare gold. A thiol monolayer is formed in these regions through a subsequent self-assembly step to give surface properties which contrast with those of the areas covered by the thiolipids. Here we present an example illustrating the potential of this new technique. Multilayers of ω-mercaptocarboxylic acid copper complex are formed according to the procedure of Evans et al.[11] (Fig. 1C left). This generates little "plateaux" on a molecular scale.

The structure formation is characterized by optical techniques. The lateral distribution of different phases of a monolayer floating on a water surface is studied by using fluorescence microscopy.[12–14] Small amounts of fluorophore-labeled lipids, which show different solubilities in different phases, are used to provide contrast between the phases. This technique allows optimization of the size and distribution of the patterns. Surface plasmon spectroscopy[15] and surface plasmon microscopy[16] are ideally suited for characterization of thin films on gold surfaces. They allow both the determination of the optical thickness of the films and the visualization of small variations in lateral optical thickness. Surface plasmon modes carry evanescent electromagnetic fields which probe the optical properties in the vicinity of a metal/dielectric interface. The sharp resonance which is observed in a reflected intensity vs. angle of incidence scan serves as a contrast mechanism for a surface plasmon microscope.

The fatty acid/thiolipid mixture is spread on the water surface from a chloroform solution. The thiolipid bis[8-(1,2-dipalmitoyl-*sn*-glycero-3-phosphoryl) 3,6-dioxaoctyl] disulfide)[17] consists of two phospholipid molecules, each attached to a hydrophilic spacer, and joined by a disulfide bond at the ends of the spacers. In addition to forming stable self-assembly monolayers on gold, the thiolipid also forms very stable Langmuir films at the air/water interface due to its amphiphilic nature. After the chloroform has evaporated, the film is compressed until a lateral pressure has been reached which lies a few $mN\,m^{-1}$ above the phase transition of the system. Figure 1A right is a fluorescence micrograph of such a mixed monolayer at the water/air interface. The film is a mixture of palmitic acid and thiolipid with, in addition, 1 mol% of the fluorescence probe *N*-(7-nitrobenz-2-oxa-1,3-diazol-4-yl)-1,2-dimyristoyl-*sn*-glycero-3-phosphoethanolamine (NBD-PE). The size and shape of the condensed domains in the monolayer are identical to those obtained in pure palmitic acid monolayers (results not shown), and the area occupied by the domains (at a given surface pressure) varies with the content of palmitic acid. We therefore conclude that the domains contain predominantly palmitic acid. The average size and number of domains per unit

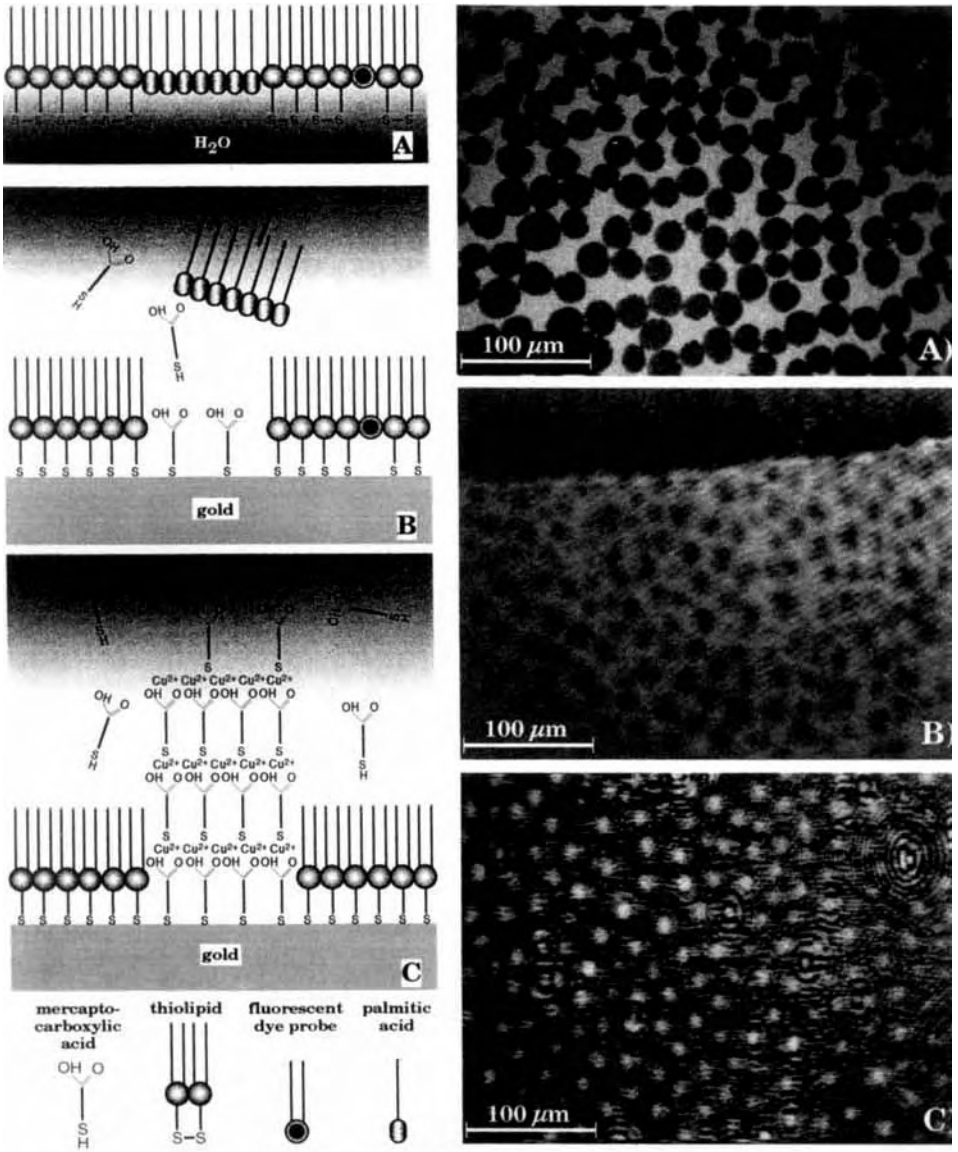


Fig. 1. Left: Generation of a laterally structured thiolate layer. Fig. 1A left shows a Langmuir film consisting of a mixture of palmitic acid and thiolipid at the water/air interface. In Fig. 1B left the Langmuir monolayer has been transferred to a gold surface by the LB technique [1]. After LB transfer the gold surface is washed in an appropriate solvent. The physisorbed palmitic acid domains are removed from the surface, while the thiolipid is not removed. Organic thiol molecules present in the solvent chemisorb to the newly exposed gold areas to form self-assembled monolayers. Fig. 1C left shows the formation of ω-mercaptocarboxylic acid copper complex multilayers on the carboxylic acid surface. Multilayers only form in those areas initially covered by the palmitic acid domains. Right: Experimental results which correspond to those steps presented in Fig. 1 left. A right: Fluorescence micrograph of a Langmuir monolayer consisting of palmitic acid and thiolipid (4:1 molar ratio) as well as 1 mol% NBD-PE. The fluorescence NBD-PE is sequeezed out of the condensed domains into the fluid phase, which therefore appears bright. B right: surface plasmon micrograph of a structured thiolipid film (3:1 palmitic acid/thiolipid ratio of the Langmuir layer) which has been transferred to a gold surface and then washed with ethanol and hexane. The horizontal line near the top of the picture is the limit of LB transfer: the dark area above this line is bare gold. Below, the surface has been covered with the LB film. The angle of incidence ($\theta = 31.95°$) of the laser beam has been tuned so that bare gold appears dark in the image, while adsorbed layers on the surface result in brighter areas. The dark domains in the lower part of the figure are bare gold. C right: Surface plasmon micrograph of a structured film (3:1 palmitic acid/thiolipid ratio of the transferred layer) on gold taken at $\theta = 32.45°$. After washing, multilayers of the copper complex of ω = mercaptoundecanoic acid were formed in the domains which appear bright due to their greater thickness.

 © VCH Verlagsgesellschaft mbH, D-69451 Weinheim, 1994 0570-0833/94/1212-1275 $ 10.00+.25/0

area are determined by the mixing ratio, the surface pressure, the subphase temperature, and the ionic strength. By manipulating these parameters the structures formed can be controlled to a high degree.

A freshly prepared (by vapor deposition), and thus hydrophilic, gold substrate is quickly dipped through the Langmuir film into the water, and then slowly drawn out (at a speed of 1 $\mu m\,s^{-1}$). As the substrate is drawn out through the film, the hydrophilic head groups of the monolayer come into contact with the gold surface and adsorb. After this LB transfer, the gold surface is washed in ethanol and hexane. This removes the physisorbed palmitic acid from the surface, while the thiolipid, which binds covalently to the gold, is not removed.[18]

Control experiments using surface plasmon resonance to measure LB layers consisting only of thiolipid show that a few percent of the thiolipid are removed when the same washing procedure is applied.[19] Examining the surface plasmon micrograph (Fig. 1B right) of a mixed monolayer, transferred by the LB technique to a gold substrate and then rinsed in organic solvents, confirms that during compression of the film on the water surface, de-mixing has taken place. Analyzing the local surface plasmon resonance by using the gray values of a sequence of micrographs taken at different angles,[20] shows that the dark domains in the lower part of Figure 1B right are bare gold patches. Their size and distribution correlate well with the domains of the floating monolayer. The stability of the structures has been checked in air, in water, and in ethanol. No change could be detected either in the lateral structure or in the thickness of the films over three days.

Next, the sample is immersed in an ethanolic solution of ω-mercaptoundecanoic acid, $HS(CH_2)_{10}COOH$, for 8 hours. Measurements of the local resonance minima clearly show the formation of a monolayer on those parts of the surface which are not covered by thiolipid. No increase in the thickness of the thiolipid-covered areas could be detected. To form a second thiol layer, we first immersed the sample in an aqueous solution of $Cu(ClO_4)_2$.[21] Monitoring of the angle of surface plasmon resonance in situ revealed a just detectable shift ($\approx 0.02^\circ$), caused by adsorption of copper ions to those parts of the surface where the carboxylic groups are exposed. Subsequent immersion in $HS(CH_2)_{10}COOH$ solution led to an increase in the thickness of 12–14 Å indicating formation of a second ω-mercaptocarboxylic acid monolayer[22] via a sulfur–copper complex. Alternate immersion in copper and ω-mercaptoundecanoic acid solutions results in multilayer formation in the domains only. We formed five layers, to give a surface where multilayers of ω-mercaptocarboxylic acid copper complex extend out of the surrounding thiolipid monolayer (Fig. 1C right). Analyzing the local angles of resonance, we find that the plateaux have a thickness of 50 Å (with refractive index $n = 1.45$) which is slightly less than that expected for five layers of mercaptoundecanoic acid.

This approach to the generation of selectively addressable structures is very general: in this paper we have described a chemical method for addressing the structures. Biochemical experiments using antibodies which selectively bind to antigens immobilized in the domains are in progress. The morphology of the structures can also be manipulated, for example, by using the procedure of Spratte et al.[23] to produce stripes. Experiments in our research group show the suitability of this technique for the structuring of thiolate layers. In principle, since the structures are formed by self-organization on the water surface, there is no lower limit on the size of the patterns that can be created. The method described here does not damage the delicate gold surface: a fact which is important for the application of such novel surface-sensitive methods as the use of evanescent light[24] or scanning probe[25] techniques. The exact nature of the structures on the gold surface (sharpness of domain boundaries, extent of de-mixing, etc.) is currently under investigation. Atomic force microscopy studies are already in progress, and Raman microscopy and imaging secondary ion mass spectrometry will also be applied.

Received: January 19, 1994 [Z 6630 IE]
German version: *Angew. Chem.* **1994**, *106*, 1361

[1] A. Ulman, *An Introduction to Ultrathin Organic Films: From Langmuir-Blodgett to Self-Assembly*, Academic Press, Boston, **1991**.
[2] G. M. Whitesides, J. P. Mathias, C. T. Seto, *Science* **1991**, *254*, 1312.
[3] N. L. Abbott, J. P. Folkers, G. M. Whitesides, *Science* **1992**, *257*, 1380.
[4] I. Rubinstein, S. Steinberg, Y. Tor, A. Shanzer, J. Sagiv, *Nature* **1988**, *332*, 4426.
[5] E. W. Wollman, C. D. Frisbie, M. S. Wrighton, *Langmuir* **1993**, *9*, 1517.
[6] A. Kumar, H. A. Biebuyck, N. L. Abbott, G. M. Whitesides, *J. Am. Chem. Soc.* **1993**, *114*, 9188.
[7] L. L. Evert, D. Leckband, J. N. Israelachvili, *Langmuir* **1994**, *10*, 303.
[8] H. Riegler, H. Möhwald in *Fluorescence Spectroscopy: New Methods and Applications* (Ed.: O. S. Wolfbeis), Springer, Berlin, **1993**, p. 111.
[9] C. M. Knobler, *Science* **1990**, *249*, 870.
[10] H. Möhwald, U. Höhne, P. Quint, *Polym. J. (Tokyo)* **1991**, *23*, 583.
[11] S. D. Evans, A. Ulman, K. E. Goppert-Berarducci, L. J. Gerenser, *J. Am. Chem. Soc.* **1991**, *113*, 5866.
[12] H. McConnell, L. K. Tamm, M. Weiss, *Proc. Natl. Acad. Sci. USA* **1983**, *81*, 3249.
[13] M. Lösche, E. Sackmann, H. Möhwald, *Ber. Bunsen Ges. Phys. Chem.* **1983**, *87*, 848.
[14] R. Peters, K. Beck, *Proc. Natl. Acad. Sci. USA* **1983**, *80*, 7183.
[15] H. Raether in *Physics of Thin Films, Vol. 9* (Eds.: G. Hass, M. H. Francombe, R. W. Hoffmann) Academic, New York, **1977**, p. 145.
[16] B. Rothenhäusler, W. Knoll, *Nature* **1988**, *332*, 615.
[17] H. Lang, C. Duschl, H. Vogel, *Langmuir* **1994**, *10*, 197.
[18] A slightly different procedure for the LB transfer involves first dipping the gold substrate into the water subphase of the film balance, and subsequently spreading and compressing the palmitic acid/thiolipid mixture on the water surface. The LB films produced by this procedure are not detectably different from the films produced as described in the text. However, the method described in the text exposes the fresh gold substrate to the laboratory atmosphere for a shorter time, thus minimizing contamination of the surface.
[19] No removal is observed on washing thiolipid films formed by self-assembly. This may indicate contamination of the gold surface in the laboratory atmosphere. Such surface contaminants are displaced by thiolates during the self-assembly process, but are probably not displaced during LB transfer of a film.
[20] W. Hickel, W. Knoll, *Appl. Phys. Lett.* **1990**, *67*, 3572.
[21] Multilayers of the copper complex of ω-mercaptoundecanoic acid were formed in the domains by using a modified procedure of Evans et al. [11], in which the $Cu(ClO_4)_2$ is dissolved in Millipore water, instead of ethanol. The sample was immersed for five min in the aqueous solution containing the copper ions. We obtained very similar results when we used cupric acetate monohydrate instead of cupric perchlorate. The thickness increase on immersion in the ω-mercaptoundecanoic acid solution was slightly greater after exposure to acetate ions. This is probably due to the increased deprotonation of the carboxylic acid in the more basic acetate solution.
[22] C. D. Bain, E. B. Troughton, Y.-T. Tao, J. Evall, G. M. Whitesides, R. G. Nuzzo, *J. Am. Chem. Soc.* **1989**, *111*, 321.
[23] K. Spratte, H. Riegler in *Organic Thin Films and Surfaces, Vol. 9* (Ed.: A. Ulman) Academic Press, Boston, **1993**, in press.
[24] W. Knoll, *MRS Bulletin* **1991**, *16*, 29.
[25] J. Frommer, *Angew. Chem.* **1992**, *104*, 1325; *Angew. Chem. Int. Ed. Engl.* **1992**, *31*, 1298.

 © VCH Verlagsgesellschaft mbH, D-69451 Weinheim, 1994 0570-0833/94/1212-1276 $ 10.00+.25/0

A New Method for the Synthesis of Heterometallic Complexes: Syntheses and Structures of $[(PhCH_2CH_2NLi)_3Sb(thf)]_2$ and $[Sb_3(cyN)_4(NMe_2)_2]Li$**

Andrew J. Edwards, Michael A. Paver, Paul R. Raithby, Moira-Ann Rennie, Christopher A. Russell, and Dominic S. Wright*

Recently we embarked on a reinvestigation of the use of $(NMe_2)_{3-x}ECl_x$ (E = As, Sb, Bi; $x = 0-2$) as metallating reagents in the syntheses of group 15 heteroatom complexes (containing N, P, O, S, etc.). None of the antimony complexes previously prepared in this manner had been characterized by single-crystal X-ray analysis or by NMR spectroscopy.[1, 2] It was with surprise that we observed Me_2NH, produced as a gaseous by-product in these reactions, as a stable ligand in the dimers $[(Me_2NH)Cl_2Sb(\mu\text{-}OEt)]_2$ and $[(Me_2NH)ClSb(\mu\text{-}t\text{BuN})]_2$ both in the solid state and in solution.[3] We report here our investigations on the metalation of primary amines by different metals ("mixed-metalation") as a method for the syntheses of heterometallic complexes containing amidoantimony anions. The heterometallic complexes **1** and **2** were synthesized by the metalation reactions of the neutral amidolithium complex $[PhCH_2CH_2N(H)Li]_n$ and of the antimony anion complex $Li[Sb(cyNH)_4]^-$, respectively, with $Sb(NMe_2)_3$ [Eq. (a) and (b), respectively]. Complex **1** has an $Sb_2N_6Li_6$ cage structure in the solid state and is the first structurally characterized example of an $[Sb(NR)_3]^{3-}$ trianion complex. In **2**, which is the first structurally characterized polynuclear amidoantimony anion complex, an Sb_3N_6Li "deck-chair" core is present.

$$\tfrac{3}{n}[PhCH_2CH_2N(H)Li]_n + Sb(NMe_2)_3 \xrightarrow{THF/C_6H_5CH_3} \underset{\mathbf{2}}{[(PhCH_2CH_2NLi)_3Sb(thf)]_2} + 3\,Me_2NH \quad (a)$$

$$2\,Sb(NMe_2)_3 + Li^+[Sb(cyNH)_4]^- \xrightarrow{THF/C_6H_5CH_3} \underset{\mathbf{2}}{[Sb_3(Ncy)_4(Me_2N)_2]Li} + 4\,Me_2NH \quad (b)$$

A low-temperature X-ray crystallographic study of **1**[4] shows it to be a fourteen-membered polyhedral cage $[(PhCH_2CH_2NLi)_3Sb(thf)]_2$ (Fig. 1). The structure can be regarded as being constructed from a hexameric amidolithium fragment, $(PhCH_2CH_2NLi)_6$,[5] bicapped at the open Li_3N_3 faces by two Sb atoms. Although $[\{^iPr_3Si)AsLi\}_3GetBu]_2$[6] and $[(RNLi)_3SiR']_2$ (R = Me_3Si, R' = Me, *t*Bu, Ph;[7] R = *t*Bu, R' = Ph;[8] R = Me, R' = *t*Bu[9]) have similar cores to **1**, none of these compounds are solvated by Lewis base donor molecules and all the Li atoms have identical environments. In the core of **1** four of the six Li centers are involved in agostic *ortho* C(-H)···Li interactions with the phenyl rings of adjacent $PhCH_2CH_2$ groups. These groups bend towards Li, straddling

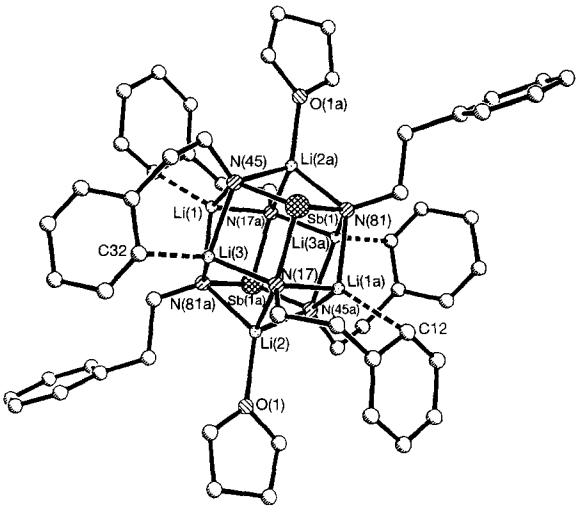


Fig. 1. Crystal structure of **1**. Selected bond lengths [Å] and bond angles [°]: Sb(1)-N(17) 2.070(3), Sb(1)-N(81) 2.059(3), Sb(1)-N(45) 2.059(3), Li(1a)-N(17) 2.035(7), Li(1a)-N(81) 2.116(8), Li(1a)-N(45a) 2.000(8), Li(2a)-N(81) 2.156(8), Li(2a)-N(45) 2.157(8), Li(2a)-N(17a) 2.137(8), Li(3)-N(17) 2.055(7), Li(3)-N(45) 2.093(7), Li(3)-N(81a) 1.988(7), Li(1a)···C(12) 2.505(8), Li(3)···C(32) 2.418(8), Li(2a)-O(1) 1.954(8); N-Sb-N 94.5 (mean).

the core N–Li bonds, and form loosely linked C_4NLi six-membered rings. These agostic C···Li distances (av. 2.472 Å) are of lengths intermediate between those observed in various organolithium compounds,[10] (e.g., the distance between tetramers in $(MeLi)_4$ 2.37 Å[11]) and those observed in certain amidolithium complexes (e.g., shortest *ortho* (C-H)···Li 2.70 Å in the trimeric amidolithium complex $[(PhCH_2)_2NLi]_3$[12]). For the remaining two Li centers of **1**, the agostic interactions are disrupted by the solvation of the metal centers by thf ligands. The result is that the pendant $PhCH_2CH_2$ groups lean away from the cage core and can no longer contact Li.

The geometry of the $Sb_2N_6Li_6$ core of **1** appears to be dictated both by the constraints imposed in accommodating the two capping Sb centers and by the inequivalent (agostic and THF) interactions of the Li^+ cations. In contrast to the largely symmetrical, pyramidal $[(PhCH_2CH_2N)_3Sb]^{3-}$ ions (av. N-Sb-N 94.5°, av. Sb–N 2.063 Å), the central Li_6N_6 fragment of **1** is highly distorted (Li–N range 1.998(7)–2.157(8) Å). The longest Li–N distances are made with the four-coordinate THF-solvated Li centers (av. 2.150 Å) and the shortest are made with the remaining coordinatively unsaturated Li centers (av. 2.050 Å).

A low-temperature X-ray crystal structure analysis of **2** shows it to have an Sb_3N_6Li ("deck-chair") core of two "back-to-back" distorted cubic fragments sharing a common face (Fig. 2).[4] Four μ-Ncy ligands link the central four-coordinate Sb center to the two terminal three-coordinate Sb atoms. Additionally, two of these μ-Ncy bridges and the NMe_2 groups attached to the terminal Sb atoms are coordinated to a Li^+ ion. Complex **2** can be regarded as an ion-pair of the trinuclear amidoantimony anion $[Me_2NSb(\mu\text{-}Ncy)_2Sb(\mu\text{-}Ncy)_2SbNMe_2]^-$ and Li^+.

Unsurprisingly, the geometry of the central Sb(2) atom, which is isoelectronic with (10 e^-) SF_4, is pseudo-square-based pyramidal. However, although the Sb(2)–N bond lengths are arranged almost symmetrically (two "short" (Sb(2)–N(11,41) av. 2.120 Å) and two "long" bonds (Sb(2)–N(21,31) av. 2.230 Å), there are large angular distortions about this center (N-Sb(2)-N range 73.8° to 150.3°). The two terminal three-coordinate Sb centers (Sb(1) and Sb(3)) are each bound to one NMe_2 and to two

[*] Dr. D. S. Wright, Dr. A. J. Edwards, M. A. Paver, Dr. P. R. Raithby, M.-A. Rennie, C. A. Russell
University Chemical Laboratory
Lensfield Road, Cambridge CB2 1EW (UK)
Telefax: Int. code +(223) 336-362

[**] We gratefully acknowledge the Science and Engineering Research Council (M. A. P., C. A. R., D. S. W., A. J. E.), the Associated Octel Co. Ltd., Ellesmere Port (UK), (M. A. P., D. S. W.) (Industrial Supervisors, Dr. S. L. Cook and Dr. D. Barr), the Royal Society (P. R. R., D. S. W.), the Nuffield Foundation (D. S. W.), and the Cambridge Crystallography Data Centre (M.-A. R.) for financial support. cy = cyclohexyl.

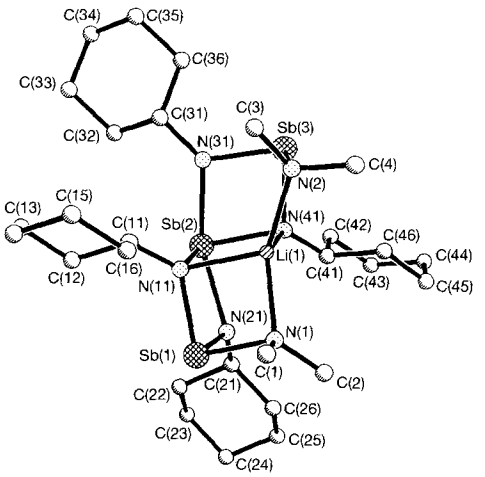


Fig. 2. The molecular structure of **2**. Hydrogen atoms have been omitted for clarity. Selected bond lengths [Å] and angles [°]: Sb(2)-N(11) 2.128, Sb(2)-N(41) 2.112, Sb(2)-N(31) 2.237, Sb(2)-N(21) 2.224, Sb(1)-N(21) 1.986, Sb(1)-N(11) 2.059, Sb(1)-N(1) 2.156, Sb(3)-N(31) 1.990, Sb(3)-N(41) 2.039, Sb(3)-N(2) 2.155, Li(1)-N(2) 2.074, Li(1)-N(1) 2.085, Li(1)-N(11) 2.128, Li(1)-N(41) 2.156; N(31)-Sb(2)-N(41) 73.8, N(31)-Sb(2)-N(11) 86.6, N(41)-Sb(2)-N(21) 84.1, N(41)-Sb(2)-N(11) 92.5, N(11)-Sb(2)-N(21) 74.6, N(31)-Sb(2)-N(21) 150.3, N(11)-Sb(1)-N(21) 81.4, N(11)-Sb(1)-N(1) 87.0, N(21)-Sb(1)-N(1) 96.0, N(31)-Sb(3)-N(2), 97.3, N(31)-Sb(3)-N(41) 80.9, N(2)-Sb(3)-N(41) 88.3, N(2)-Li(1)-N(11) 120.0, N(2)-Li(1)-N(41) 87.4, N(11)-Li(1)-N(41) 91.3, N(2)-Li(1)-N(1) 143.6, N(1)-Li(1)-N(11) 87.1, N(1)-Li(1)-N(41) 117.9.

μ-Ncy groups. These Sb centers both adopt similar, though not identical, distorted pyramidal geometries (N-Sb(1,3)-N range 80.9–97.3°). The Sb–(μ-Ncy) bond lengths at these Sb centers (av. 2.019 Å) are shorter than both the corresponding Sb(2)–(μ-Ncy) bonds (av. 2.175 Å) and the Sb–N bonds made with the terminal NMe_2 groups (av. 2.156 Å).

The Li^+ ion of **2** is captured by the pendant Me_2N groups (av. Li(1)–N(1,2) 2.080 Å) and by two of the Sb-attached μ-Ncy ligands (Li(1)–N(11,41) av. 2.142 Å). Although a four-coordinate geometry is typical for Li^+ ions,[5, 10] the coordination sphere of the Li center in **2** is exceptionally distorted (N-Li-N 87.1–143.6°). The angular distortions present within the core of **2** (particularly at Sb(2)) presumably partly arise from the strain induced by the coordination of this Li^+ ion to the anion of **2**. Although there are a variety of Sb[13–15] and other[16] p-block metal–amido cage complexes with structural features related to **2**, this complex is the first structurally characterized example of a compound containing a polynuclear amidoantimony anion.

Apart from the structural interest of **1** and **2**, this study highlights that $Sb(NMe_2)_3$ can be used as a metalating reagent for the synthesis of new anionic amidoheterometallic complexes. Both **1** and **2**, which are sources of $[Sb(NR)_3]^{3-}$ and $[Me_2N_2Sb_3(NR)_4]^-$ ions, respectively, are potential ligands for other main group and transition metals. We are currently preparing a range of such ligands and are investigating their coordination chemistry.

Experimental Procedure

1: A solution of 2-phenylethylamine (0.94 mL, 7.5 mmol) in THF (10 mL) was treated with *n*BuLi (4.69 mL, 7.5 mmol, 1.6 M in hexanes) at 0 °C. Heating the mixture to reflux and stirring (5 min) gave an intense red solution which was subsequently reduced to dryness under vacuum. Addition of toluene (20 mL) produced an orange solution. This was cooled to −78 °C and $Sb(NMe_2)_3$ (0.64 g, 2.5 mmol) was added. Gentle warming (60 °C) followed by stirring (1 h) gave a yellow solution and some decomposition. This solution was filtered through Celite and reduction of the filtrate under vacuum (ca. half volume) precipitated a yellow solid which was heated back into solution. Storage (5 °C, 24 h) gave yellow crystalline blocks of **1**. Isolation of **1** under vacuum resulted in loss of THF solvation. The crystal structure of the complex was obtained by mounting the crystals directly from solution so that THF solvation was maintained. The following data were obtained on the unsolvated powder after isolation; yield 0.25 g (20%, first batch); m.p. gradually darkens >90 °C to black solid, no melting below 300 °C; IR (Nujol), $\tilde{\nu}_{max}$ [cm^{-1}] = ca. 3070 (w, C-H (aryl)); ^1H NMR (C_6D_6, +25 °C, 250 MHz): δ = 7.2–7.0 (m, 5H, Ph), 2.70 (m, 2H, $-CH_2-$), 2.47 (m, 2H, $-CH_2-$); correct (C,H,N) analysis.

2: A solution of cyclohexylamine (0.99 g, 10 mmol) in THF (10 mL) was treated with *n*BuLi (6.25 mL, 10 mmol, 1.6 M in hexanes) at 0 °C. Addition of $SbCl_3$ (0.57 g, 2.5 mmol) followed by stirring at 30 °C (15 min) yielded a yellow solution. This was evaporated to dryness and the product separated from the LiCl by extraction from toluene (10 mL) and filtration. The yellow solution of $(cyNH)_4Sb^-Li^+$ in toluene (10 mL) was cooled to −78 °C and $(Me_2N)_3Sb$ added (1.27 g, 5 mmol). The reaction mixture was stirred at 60 °C (3 h) and subsequently at room temperature (16 h). During this time a faint yellow precipitate had developed and reduction of the mixture under vacuum yielded a mass of yellow solid which redissolved upon warming. Storage (10 °C, 24 h) produced yellow crystalline rods of **2**. First batch yield 0.67 g (32%), melting point 195–197 °C: ^1H NMR (25 °C, 250 MHz, [D_5]pyridine: δ = 3.34 (s, 12H, Me_2N), 0.5–2.5 (br.m, 44H, cyN); correct (C,H,N) analysis.

Received: December 2, 1993
Revised: March 9, 1994 [Z 6573/6628 IE]
German version: *Angew. Chem.* **1994**, *106*, 1334

[1] a) K. Moedritzer, *Inorg. Chem.* **1964**, *3*, 609; b) A. Kiennemann, G. Levy, F. Schué, C. Taniélian, *J. Organomet. Chem.* **1972**, *35*, 143.

[2] a) F. Ando, T. Hayashi, K. Ohashi, J. Koketsu, *J. Inorg. Nucl. Chem.* **1975**, *37*, 2011; b) W. Clegg, N. A. Compton, R. J. Errington, G. A. Fisher, M. E. Green, D. R. Hockless, N. C. Norman, *Inorg. Chem.* **1991**, *30*, 4680.

[3] a) A. J. Edwards, N. E. Leadbeater, M. A. Paver, P. R. Raithby, C. A. Russell, D. S. Wright, *J. Chem. Soc. Chem. Commun.*, submitted; b) A. J. Edwards, M. A. Paver, P. R. Raithby, M.-A. Rennie, C. A. Russell, D. S. Wright, *J. Chem. Soc. Dalton Trans.*, submitted.

[4] Crystal data for **1**: $C_{28}H_{35}Li_3N_3Sb$, M = 572.16, monoclinic, space group $P2_1/n$, a = 10.207(2), b = 11.361(2), c = 24.124(5) Å, β = 99.03(3)°, V = 2762.8(9) Å^3, Z = 4, ρ_{calcd} = 1.376 Mg m^{-3}, $F(000)$ = 1168, λ = 0.71073 Å, T = 153(2) K, $\mu(Mo_{K\alpha})$ = 1.022 mm^{-1}. Data were collected on a Siemens-Stoe AED diffractometer using an oil-coated rapidly cooled crystal (T. Kottke, D. Stalke, *J. Appl. Crystallogr.* **1993**, *26*, 615) of dimensions 0.39 × 0.32 × 0.25 mm by the θ/ω method ($7.00 \le 2\theta \le 45.00°$). Of a total of 3694 collected reflections, 3593 were unique. The structure was solved by direct methods (SHELXTL PLUS) and refined by full-matrix least-squares on F^2 (SHELXL-93; G. M. Sheldrick, Göttingen, **1993**) to $wR1$ = 0.0289 and $wR2$ = 0.1051 [$F > 4\sigma(F)$] and $wR1$ = 0.0353 and $wR2$ = 0.1281 (all data) [$R1 = \sum||F_o| - |F_c||/\sum|F_o|$, $R2 = \sqrt{\{\sum w(F_o^2 - F_c^2)^2/\sum wF_o^4\}}$, $w = 1/[\sigma^2(F_o^2) + (xP)^2 + yP]$, $P = (F_o^2 + 2F_c^2)/3$]. Largest peak and hole in the final difference map 0.843 and −0.936 e Å^{-3}. – Crystal data for **2**: $C_{28}H_{56}LiN_6Sb_3$, M = 848.98, triclinic, space group $P\bar{1}$, a = 9.624(2), b = 11.445(2), c = 17.006(3) Å, α = 105.11(3), β = 99.97(3), γ = 101.65(3)°, V = 1719.9(6) Å^3, Z = 2, ρ_{calcd} = 1.639 Mg m^{-3}, $F(000)$ = 844, λ = 0.71073 Å, T = 153(2) K, $\mu(Mo_{K\alpha})$ = 2.365 mm^{-1}. Data were collected on a Siemens-Stoe AED diffractometer using an oil-coated rapidly cooled crystal of dimensions 0.33 × 0.29 × 0.26 mm by the θ/ω method ($7.12 \le 2\theta \le 45.00°$). Of a total of 4686 collected reflections, 4505 were unique. The structure was solved by direct methods (SHELX TL PLUS) and refined by full-matrix least-squares on F^2 (SHELXL-93; G. M. Sheldrick, Göttingen, **1993**) to $wR1$ = 0.0197 and $wR2$ = 0.0702 [$F > 4\sigma(F)$] and $wR1$ = 0.0273 and $wR2$ = 0.1159 (all data) [$wR1 = \sum||F_o| - |F_c||/\sum|F_o|$, $wR2 = \sqrt{\{\sum w(F_o^2 - F_c^2)^2/\sum wF_o^4\}}$]. Largest peak and hole in the final difference map 1.088 and −1.405 e Å^{-3}. Further details of the crystal structure investigations are available on request from the Director of the Cambridge Crystallographic Data Centre, 12 Union Road, GB-Cambridge CB2 1EZ (UK), on quoting the full journal citation.

[5] a) R. E. Mulvey, *Chem. Soc. Rev.* **1991**, *20*, 167; b) K. Gregory, P. von R. Schleyer, R. Snaith, *Adv. Inorg. Chem.* **1991**, *37*, 47.

[6] L. Zsolnai, G. Huttner, M. Driess, *Angew. Chem.* **1993**, *105*, 1549–1551; *Angew. Chem. Int. Ed. Engl.* **1993**, *32*, 1439–1440.

[7] D. J. Brauer, H. Bürger, G. L. Liewald, J. Wilke, *J. Organomet. Chem.* **1985**, *287*, 305–320.

[8] D. J. Brauer, H. Bürger, G. L. Liewald, *J. Organomet. Chem.* **1986**, *308*, 119–130.

[9] M. Veith, A. Spaniol, J. Pöhlmann, F. Gross, V. Huch, *Chem. Ber.* **1993**, *126*, 2625–2635.

[10] W. Setzer, P. von R. Schleyer, *Adv. Organomet. Chem.* **1985**, *24*, 353.

[11] a) E. Weiss, E. A. C. Lucken, *J. Organomet. Chem.* **1964**, *2*, 197; b) E. Weiss, G. Hencken, *ibid.* **1970**, *21*, 265.

[12] a) D. R. Armstrong, R. E. Mulvey, G. T. Walker, D. Barr, R. Snaith, *J. Chem. Soc. Dalton Trans.* **1988**, 617; b) D. Barr, W. Clegg, R. E. Mulvey, R. Snaith, *J. Chem. Soc. Chem. Commun.* **1984**, 285.

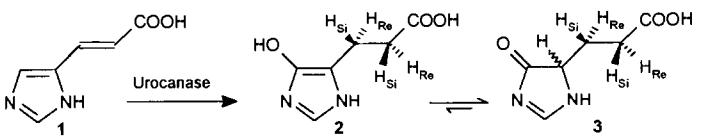
[13] O. J. Scherer, G. Wolmershäuser, H. Conrad, *Angew. Chem.* **1983**, *95*, 427–428; *Angew. Chem. Int. Ed. Engl.* **1983**, *22*, 404–405.
[14] W. Neubert, H. Pritkow, H. P. Latscha, *Angew. Chem.* **1988**, *100*, 298–299; *Angew. Chem. Int. Ed. Engl.* **1988**, *27*, 287–288.
[15] M. Björgvinsson, H. W. Roesky, F. Pauer, G. M. Sheldrick, *Chem. Ber.* **1992**, *125*, 767–769.
[16] M. Veith, *Chem. Rev.* **1990**, *90*, 3–16.

On the Mechanism of the Urocanase Reaction: Confirmation of the Structure of the NAD^+-Inhibitor Adduct by Direct ^{13}C-^{13}C Coupling**

Carsten Schubert, Ymin Zhao, Jung-Hyn Shin, and János Rétey*

Dedicated to Professor Joachim Knappe on the occasion of his 65th birthday

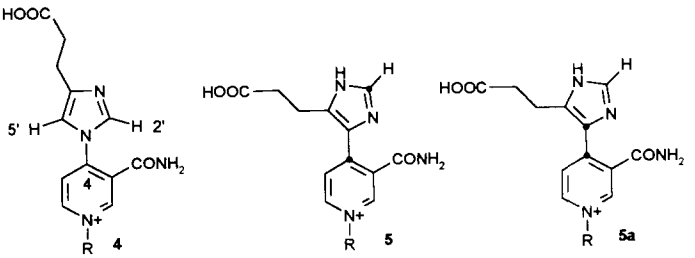
In oxidoreductases nicotinamide adenine nucleotide (NAD^+) functions as a redox reagent. In the urocanase reaction it plays a different and as yet unique role as electrophile (Scheme 1).



Scheme 1. Steric course of the urocanase reaction. The solvent protons are added to the *Re* positions of the side chains.

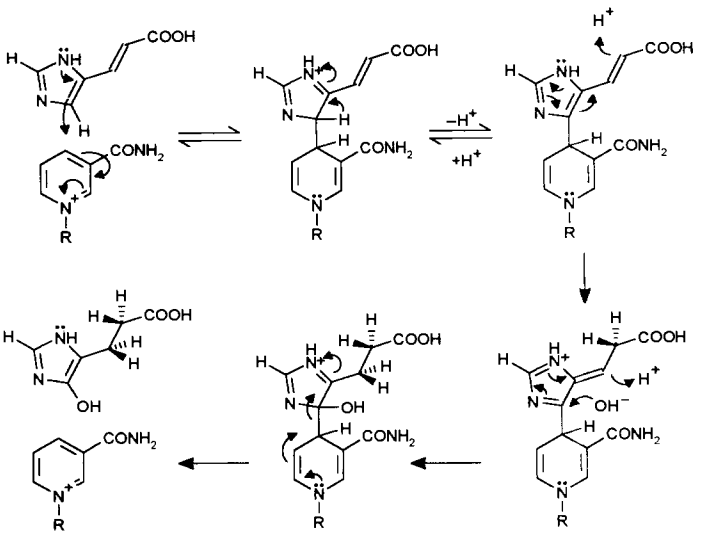
Urocanase (E.C. 4.2.1.49) occurs in most cells and catalyzes the second step in the degradation of histidine. In this process a water molecule is added to urocanic acid (**1**) in an unusual manner. In particular, the addition of an OH^- ion to the electron-rich imidazole nucleus seems to be chemically implausible. In overcoming this obstacle the tightly bound NAD^+ plays a crucial role. Using the competitive inhibitor imidazole propionic acid (**6**), an NAD^+-inhibitor adduct could be trapped by rearomatization of the dihydropyridine ring and then isolated. In the first postulated[1] structure **4**, the attachment of NAD^+ to the inhibitor was supposed to occur at the N1′ atom of the imidazole moiety (Scheme 2).

The assumption[1,2] that also urocanic acid forms the analogous covalent adduct in the initial step was supported convincingly by UV spectroscopy. This led to the proposal of a



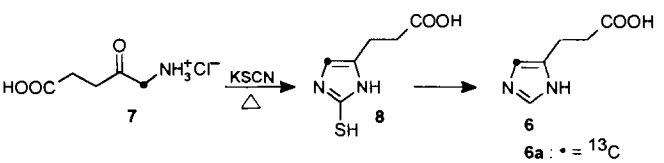
Scheme 2. Proposed structures for the NAD^+-imidazole propionate adduct (^{13}C-labeling indicated by filled circles). R = ADP-ribosyl.

reaction mechanism[3] which, however, did not solve the aforementioned chemical problem. Moreover, in the ^1H NMR spectrum of the adduct one of the signals for the imidazole protons was lacking. This was explained by a spontaneous exchange of the 2′-H atoms with solvent deuterium.[1] By specific ^{13}C-labeling of the 2′(imidazole) and 4 (nicotinamide) positions Klepp et al.[4] postulated structure **5** which was consistent with all experimental data and permitted the formulation of a plausible mechanism for the urocanase reaction (Scheme 3).



Scheme 3. Proposed mechanism for the urocanase reaction. R = ADP-ribosyl.

A definitive proof for structure **5** was provided by detection of direct ^{13}C-^{13}C coupling in the doubly ^{13}C-labeled adduct **5a**. Here we describe the synthesis of the [5′-^{13}C] imidazole propionic acid **6a** as well as the isolation and NMR spectroscopic characterization of the adduct **5a** enzymatically formed therefrom. The known 5-amino [5-^{13}C] levulinic acid · HCl **7** seemed to be a suitable precursor of **6a**. Starting from Cu^I [^{13}C]N (99% ^{13}C)[6] and methyl 3-chloroformylpropionate, **7** was prepared according to the method of Pfaltz et al.[5] The ring closure to



imidazole thiol **8** was accomplished by condensation of **7** with KSCN.[7] Subsequent oxidation with $Fe_2(SO_4)_3$[8] and ion-exchange chromatography (Dowex 50 W × 4, H^+-form) afforded

[*] Prof. Dr. J. Rétey, Dipl.-Chem. C. Schubert, Dr. Y. Zhao,[+] Prof. Dr. J.-H. Shin[++]
Lehrstuhl für Biochemie im Institut für Organische Chemie der Universität
Richard-Willstätter-Allee, D-76128 Karlsruhe (FRG)
Telefax: Int. code + (721)608-4823
[+] Current address: Xiao-qu-deng-tong 6, Dong-chen g-qu, 100850 Peking (PR China)
[++] Current address: Department of Chemistry, Seoul National University, Seoul 151–742 (Korea)

[**] This work was supported by the Deutsche Forschungsgemeinschaft and the Fonds der Chemischen Industrie. We thank Dr. M. Spraul, Bruker Analytische Meßtechnik GmbH, Rheinstetten/Karlsruhe for the 600 MHz H NMR spectrum, Dr. H. Röttele for the ^{13}C NMR spectrum of the adduct, Dr. M. Lenz for the urocanase overproducing *E. coli* strain, and Ms. J. Herman for her assistance in numerous enzyme isolations.

the desired product **6a** (Table 1). [4-^{13}C]Nicotinic acid (99% ^{13}C) was prepared by using the method of Oberfrank et al.[9] and biosynthetically incorporated into urocanase.[4] The cultivation of *Pseudomonas putida* nic II (a nicotinate auxotrophic mutant), the isolation of the labeled enzyme, and the enzymatic formation of the NAD$^+$-imidazole propionate adduct were carried out as described by Klepp et al.[4] 250 mg (2.03 μmol) ^{13}C-labeled urocanase and 48 mg (300 μmol) [5′-^{13}C]imidazole propionic acid · HCl were used.

Table 1. Spectroscopic data of compounds **5a** and **6a**. NMR spectra in D_2O, sodium 3-trimethylsilyl-[$^2H_4$]propionate as reference for ^{1}H, external dioxane as reference ($\delta = 68.0$) for ^{13}C NMR spectra. The water signal in the ^{1}H NMR spectra was suppressed by pre-saturation. A, I, and P refer to the corresponding positions in adenine, imidazole, and pyridinium rings, α and β for the positions in the propionic acid side chain.

5a: ^{1}H NMR (600 MHz; D_2O, pD = 9.0): $\delta = 8.88$ (d, ^3J(H2,^{13}C4) = 5.4 Hz, 1H, P2), 8.78 (t, ^3J(H6,^{13}C4) = 6.2 Hz, ^3J(H6,H5) = 6.8 Hz, 1H, P6), 8.33 (s, 1H, A8), 8.01 (s, 1H, A2), 7.93 (dd, ^3J(H5,^{13}C5′) = 6.7 Hz, ^3J(H5,H6) = 6.8 Hz, 1H, P5), 7.61 (d, ^3J(H2′,^{13}C5′ = 9.5 Hz, 1H, I2′); ^{1}H NMR (400 MHz; D_2O, pD = 9.0): $\delta = 3.05$ (dt, ^3J (β-H, α-H) = 7.0 Hz, ^3J(^{1}H,^{13}C) ≈ 2 Hz, 2H, β-H), 2.47 (t, ^3J(α-H, β-H) = 7.0 Hz, 2H, α-H); ^{13}C NMR (100 MHz; D_2O, pD = 8.0, ca. 320 μg): $\delta = 130.12$ (d, ^1J (^{13}C5′,^{13}C′4) ≈ 70 Hz, 1C, C5′), 151.12 (d, ^1J(^{13}C4, ^{13}C5′) = 70 Hz, 1C, C4).

6a: ^{1}H NMR (400 MHz; D_2O, pD = 4.6): $\delta = 2.60$ (t, ^3J(α-H, β-H) = 7.3 Hz, 2H, α-H), 2.96 (dtr, ^3J (β-H, α-H) = 7.3 Hz, ^3J (^{1}H,^{13}C) = 4.4 Hz, 2H, β-H), 7.20 (dd, ^1J(^{1}H,^{13}C) = 200.3 Hz, ^4J = 1.3 Hz, 1H, H5′), 8.55 (dd, ^3J = 5.4 Hz, ^4J = 1.4 Hz, 1H, H2′); ^{13}C NMR (100 MHz; D_2O, pD = 3.9): $\delta = 20.99$ (β-C), 34.80 (α-C), 116.44 (C5′), 133.85 (C2′), 133.69 (C4′), 179.25 (COOH); MS (70 eV): *m/z*: 141.14 [M^+].

In the ^{13}C NMR spectrum (Table 1) of the partially purified doubly labeled adduct **5a** (Fig. 1) two doublets at $\delta = 130.1$ and 155.1 with a coupling constant of 70 Hz are discernible, which

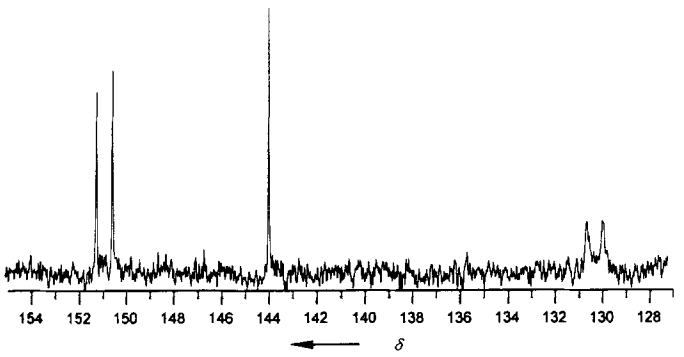


Fig. 1. Low-field portion of the ^{13}C NMR spectrum of the [4-^{13}C]NAD$^+$-[5′-^{13}C] imidazole propionate adduct **5a**.

is consistent with a direct ^{13}C-^{13}C coupling. The singlet at $\delta = 144.0$ arises from unreacted [4-^{13}C]NAD$^+$. In the low-field portion of the ^{1}H NMR spectrum of **5a** (Fig. 2; Table 1) most of the signals are identical with those of the adduct **5** formed from [4-^{13}C] NAD$^+$ and [2′-^{13}C] imidazole propionate.[4] One detects an additional coupling of $^3J = 6.7$ Hz in the 5-H signal ($\delta = 7.93$) of the nicotinamide ring (vicinal coupling with the 5′-^{13}C atom of the imidazole nucleus), and the 2′-H signal (doublet; $\delta = 7.61$) of the imidazole shows also a vicinal coupling constant of $^3J = 9.5$ Hz, instead of the direct one of $^1J = 212$ Hz in the spectrum of **5**.[4] An additional vicinal ^{1}H-^{13}C coupling is discernible also in the signal of the β-methylene

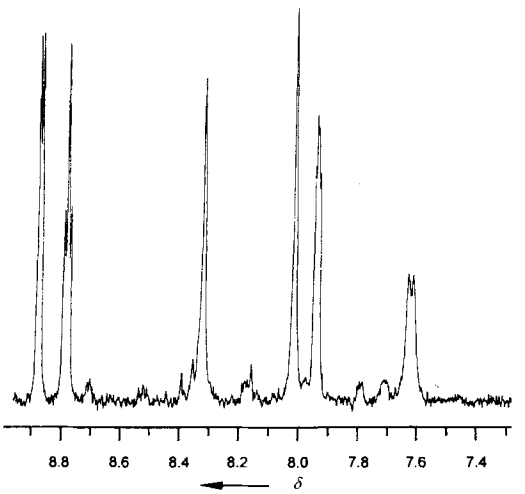


Fig. 2. Low-field portion of the ^{1}H NMR spectrum of the [4-^{13}C]NAD$^+$-[5′-^{13}C] imidazole propionate adduct **5a**.

group of the side chain of the imidazole propionic acid portion of the adduct **5a** (not shown).

All these findings support structure **5** proposed by Klepp et al. [4] for the isolated NAD$^+$-imidazole propionate adduct. In this light the mechanism of the urocanase reaction outlined in Scheme 3 seems to be even more likely.

Received: February 3, 1994 [Z 6665IE]
German version: *Angew. Chem.* **1994**, *106*, 1331

[1] L. H. Matherly, C. W. DeBrosse, A. T. Phillips, *Biochemistry* **1982**, *21*, 2789–2794.
[2] L. H. Matherly, K. A. Johnson, A. T. Phillips, *Biochemistry* **1982**, *21*, 2795–2798.
[3] R. M. Egan, L. H. Matherly, A. T. Phillips, *Biochemistry* **1981**, *20*, 132–137.
[4] J. Klepp, A. Fallert-Müller, K. Grimm, W. E. Hull, J. Rétey, *Eur. J. Biochem.* **1990**, *192*, 669–676.
[5] A. Pfaltz, S. Anwar, *Tetrahedron Lett.* **1984**, *25*, 2977–2980.
[6] H. J. Barber, *J. Chem. Soc.* **1943**, 79.
[7] R. W. Wynn, A. H. Corwin, *J. Org. Chem.* **1950**, *15*, 203–208.
[8] T. Furuta, M. Katayama, H. Shibasaki, Y. Kasuya, *J. Chem. Soc. Perkin Trans. 1* **1992**, 1643–1648.
[9] M. Oberfrank, W. E. Hull, J. Rétey, *Eur. J. Biochem.* **1984**, *140*, 157–161.

Cyclopropanes by Nucleophilic Attack of Mono- and Diaryl-Substituted (η^3-Allyl)palladium Complexes: Aryl Effect and Stereochemistry**

Andreas R. Otte, Andreas Wilde, and H. M. R. Hoffmann*

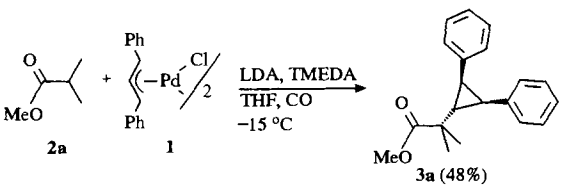
The reaction of (η^3-allyl)palladium complexes with stabilized carbon nucleophiles has matured into a major process for the formation of carbon–carbon bonds.[1] More recently the (η^3-1,3-diphenylallyl)palladium complex **1** has been investigated in

[*] Prof. Dr. H. M. R. Hoffmann, Dipl.-Chem. A. R. Otte, Dr. A. Wilde
Institut für Organische Chemie der Universität
Schneiderberg 1B, D-30167 Hannover (FRG)
Telefax: Int. code + (511)762-3011

[**] This work was supported by Deutsche Forschungsgemeinschaft and by Fonds der Chemischen Industrie (PhD fellowship for A. W.). We thank Erhard Barho for experimental contributions and Degussa AG for their generous gift of palladium salts.

great detail with respect to asymmetric allylic alkylation, and experimental conditions have been established for high asymmetric induction by using a wide variety of bidentate ligands (P/P, N/P, N/N, N/S).[2]

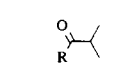
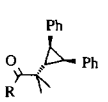
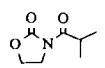
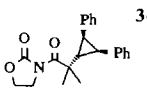
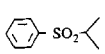
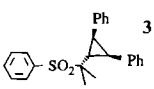
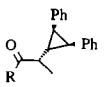
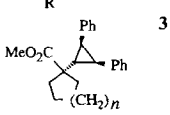
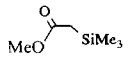
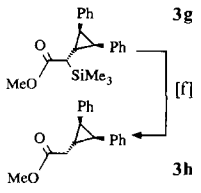
We now show that a slight change of nucleophile and ligand alters the product type decisively from that of allylic alkylation to (substituted) cyclopropane, by attack of the nucleophile at the *central* carbon of the allyl ligand. Thus, complex **1** reacted in the presence of the bidentate N/N ligand tmeda (N,N,N′,N′-tetramethylethylenediamine) with the lithium enolate of ester **2a** to give trisubstituted cyclopropane **3a** (Scheme 1). This cyclopropanation reaction is not limited to deprotonated esters, also deprotonated acid amides, modified Evans enolates (cf. **2c**), ketones, and sulfones afforded corresponding three-membered rings. Bulky tertiary carbanions were especially useful and reacted more satisfactorily than secondary carbanions (Table 1). The silylated nucleophile from methyl trimethylsilylacetate **2g** allows the indirect introduction of an unsubstituted acetic acid moiety after desilylation (**3g** → **3h**).



2a **1** **3a** (48%)

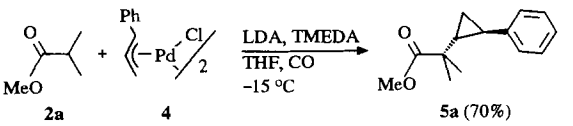
Scheme 1. LDA = Lithium diisopropylamide; analogous reactions see Table 1.

Table 1. *cis*-Diphenyl-substituted cyclopropanes **3** from the (η^3-1,3-diphenylallyl)palladium complex **1**.

Nucleophile [a]	No.	R (*n*)	Product [b]	No.	Yield [%] [c]
	**2b**:	NMe_2 $CHMe_2$ *p*-Me_2N-C_6H_4		**3b**	53 [e] 48 [d] 35 [e]
	**2c**	–		**3c**	73 [d]
	**2d**	–		**3d**	38 [d]
	**2e**	*p*-MeO-C_6H_4 C_6H_5		**3e**	35 [d] 25 [d]
	**2f**	(1) (2)		**3f**	34 [d] 48 [d]
	**2g**	–		**3g** **3h**	50 [d]

[a] Bases for deprotonation of the protonated nucleophile: lithium diisopropylamide (LDA)/TMEDA for esters, acid amides, and sulfones; potassium bis(trimethylsilyl)amide (KHMDS) for ketones, oxazolidinone derivatives, and methyl trimethylsilylacetate. [b] All products were fully characterized by spectroscopic methods (IR, ^1H and ^{13}C NMR spectroscopy, mass spectrometry, and high-resolution mass spectrometry). [c] Isolated yields. [d] Reaction temperature: −15 °C. [e] Reaction temperature: −35 °C. [f] F^- quant.

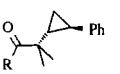
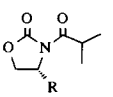
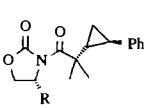
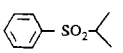
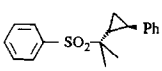
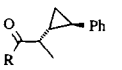
The monophenylated (η^3-1-phenylallyl)palladium complex **4** gave disubstituted cyclopropanes in good yields (Scheme 2, Table 2). However, attempts to transform simple alkyl-substituted (η^3-allyl)palladium complexes into cyclopropanes were not promising. For example, the (η^3-butenyl)palladium complex reacted with α-branched ester enolates, but not with other nucleophiles. Furthermore, introduction of a second methyl group as in the (η^3-1,3-dimethylallyl)palladium complex **6** provided no cyclopropanes at all, even when using experimental conditions optimum for converting the parent (η^3-allyl)palladium complex into cyclopropanes.[3]



2a **4** **5a** (70%)

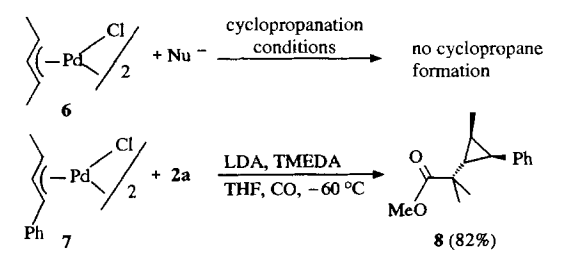
Scheme 2. Analogous reactions see Table 2.

Table 2. *trans*-1,2-Disubstituted cyclopropanes from the (η^3-1-phenylallyl)palladium complex **4**.

Nucleophile [a]	No.	R	Product [b]	No.	Yield [%] [c]
	**2b**	NMe_2 $CHMe_2$ *p*-MeO-C_6H_4		**5b**	64 [e] 67 [d] 57 [e]
	**2c**	H $CHMe_2$		**5c**	56 [d] 23 [d]
	**2d**			**5d**	50 [e]
	**2e**	*p*-Me_2N-C_6H_4 *p*-MeO-C_6H_4 Ph		**5e**	24 [d] (3:1) [f] 49 [d] (3:1) [f] 70 [d] (2:1) [f]

[a] Bases for deprotonation: see Table 1. [b] All products were fully characterized by spectroscopic methods. [c] Isolated yields. [d] Reaction temperature: −15 °C. [e] Reaction temperature: −60 °C. [f] Mixture of diastereomers (not separable by column chromatography).

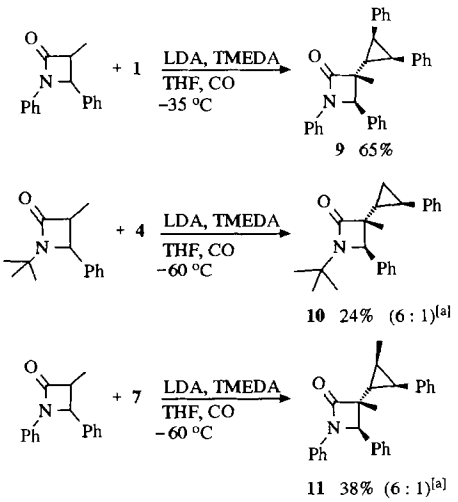
In contrast, introduction of a single phenyl group as in the (η^3-1-methyl-3-phenylallyl)palladium complex **7**, afforded cyclopropanation products in good yields (Scheme 3). Apparently, the phenyl substituent facilitates cyclopropanation (aryl effect) for reasons which are not completely clear at present.



6 **7** **8** (82%)

Scheme 3.

The cyclopropanation was also applied to β-lactams, which are of potential interest in medicinal chemistry. Again, preparation of the mixed 1-methyl-2-phenylcyclopropane derivative with complex **7** was feasible (Scheme 4). Regarding the stereochemis-



Scheme 4. [a] Mixture of diastereomers (not separable by column chromatography).

try, the phenyl groups, which are *W*-configurated in the η^3-allyl complex **1**, are *cis* to each other in the products and therefore, potentially repel each other. The incoming nucleophile is *trans* to the two phenyl groups. Similarly, the *W*-configurated η^3-allyl complex **7** furnishes cyclopropane derivatives **8** (Scheme 3) and **11** (Scheme 4), in which the methyl and phenyl groups are *cis* to each other. Thus, in all reactions studied the formation of substituted cyclopropane is clearly disrotatory (13 examples).[4]

In summary, nucleophilic cyclopropanation of (η^3-allyl)palladium complexes is facilitated by terminal phenyl groups relative to methyl groups in the allyl ligand (aryl effect). The cyclopropanes are built up stereoselectively, and a quarternary carbon center[5] exocyclic to the three-membered ring is installed with ease.

Experimental Procedure

Tetrahydrofuran was distilled over sodium/benzophenone under nitrogen. (η^3-Allyl)palladium complexes were prepared from allyl alcohols or allyl chlorides by the method of Bosnich et al. [2a].

General procedure for generating carbanions: To a solution of lithium diisopropylamide (LDA) (1.1 mmol) or potassium bis(trimethylsilyl)amide (KHMDS) (1.66 mL, 1.1 mmol, 15% in toluene) in dry THF (5 mL) under nitrogen was added the protonated nucleophile (1.1 mmol) at −78 °C. After the solution had been stirred for 10 min it was warmed up to 0 °C and 10 min later recooled to −78 °C. If LDA was used as a base, TMEDA (0.17 mL, 1.1 mmol) was added, and the resulting solution was stirred until required.

Cyclopropanation: The dimeric (η^3-allyl)palladium chloride complex (0.275 mmol) in dry THF (5 mL) was placed in an oven-dried flask under nitrogen. The solution was cooled to −78 °C and TMEDA (0.17 mL) was added. After warming the mixture to the temperature given in the Tables, the carbanion solution (see above) was added dropwise through a double-tipped needle. Attachment of a CO balloon caused the reaction mixture to turn black and palladium to precipitate. After stirring for 30 min and warming to room temperature, the solvent was evaporated in vacuo and diethyl ether (50 mL) was added. The mixture was filtered and the filtrate washed with water. The aqueous layer was re-extracted with diethyl ether and the combined organic layers were washed with brine (20 mL), dried with $MgSO_4$, and concentrated. The resulting oil was purified by flash chromatography (silica gel, cyclohexane/diethyl ether, 5:1) to give the product as a colorless oil or solid.

Spectroscopic data of **3a**: ^{1}H NMR ($CDCl_3$, 200 MHz): δ = 7.02 (m, 10H, H_{arom}), 3.72 (s, 3H, OCH_3), 2.45 (d, J = 6 Hz, 2H, PhC*H*), 2.09 (t, J = 6 Hz, 1H, cyclopropyl CH), 1.29 (s, 6H, $(CH_3)_2C$); ^{13}C NMR ($CDCl_3$, 50 MHz, APT(Attached Proton Test) technique: primary and tertiary carbons give negative (↓) signals, secondary and quarternary carbons give positive (↑) signals: δ = 177.78↑, 137.84↑, 128.96↓, 127.73↓, 125.73↓, 51.91↓, 41.71↑, 33.49↓, 27.41↓, 23.48↓.

Received: January 20, 1994 [Z 6635 IE]
German version: *Angew. Chem.* **1994**, *106*, 1352

[1] B. M. Trost, *Angew. Chem.* **1989**, *101*, 1199; *Angew. Chem. Int. Ed. Engl.* **1989**, *28*, 1173; B. M. Trost, T. R. Verhoeven in *Comprehensive Organometallic Chemistry, Vol. 8* (Eds.: G. Wilkinson, F. G. A. Stone, E. W. Abel), Pergamon, Oxford, **1982**, p. 799; S. A. Godleski in *Comprehensive Organic Synthesis, Vol. 4* (Ed.: B. M. Trost), Pergamon, Oxford, **1991**, p. 585; J. Tsuji, *Tetrahedron* **1986**, *42*, 4361.

[2] a) (P/P): P. B. Mackenzie, J. Whelan, B. Bosnich, *J. Am. Chem. Soc.* **1985**, *107*, 2046; M. Sawamura, H. Nagata, H. Sakamoto, Y. Ito, *ibid.* **1992**, *114*, 2586; B. M. Trost, *Organometallics* **1985**, *4*, 1143; T. Hayashi, A. Yamamoto, T. Hagihara, Y. Ito, *Tetrahedron Lett.* **1986**, *27*, 191; Y. Okada, T. Minami, Y. Sasaki, Y. Umezu, M. Yamaguchi, *ibid.* **1990**, *31*, 3905 (monodentate P ligands); M. Yamaguchi, T. Shima, T. Yamagishi, M. Hida, *ibid.* **1990**, *31*, 5049; Y. Okada, T. Minami, Y. Umezu, S. Nishikawa, R. Mori, Y. Nakayama, *Tetrahedron: Asymmetry* **1991**, *2*, 667; C. Breutel, H. Landert, A. Schnyder, F. Spindler, A. Tijani, A. Togni, *J. Am. Chem. Soc.*, **1994**, *116*, 4062; C. Breutel, A. Schnyder, A. Togni, *Chimia* **1993**, *47*, 283; b) (N/P), (N/N): P. von Matt, A. Pfaltz, *Angew. Chem.* **1993**, *105*, 614; *Angew. Chem. Int. Ed. Engl.* **1993**, *32*, 566; J. Sprinz, M. Kiefer, G. Helmchen, M. Reggelin, G. Huttner, O. Walter, L. Zsolnai, *Tetrahedron Lett.* **1994**, *35*, 1523; c) (N/N): A. Togni, *Tetrahedron: Asymmetry* **1991**, *2*, 683; V. Leutenegger, G. Umbricht, C. Fahrni, P. von Matt, A. Pfaltz, *Tetrahedron* **1992**, *48*, 2143; H. Kubota, M. Nakajima, K. Koga, *Tetrahedron Lett.* **1993**, *34*, 8135; d) (N/S): C. G. Frost, J. M. J. Williams, *ibid.* **1993**, *34*, 1785; G. J. Dawson, C. G. Frost, C. J. Martin, J. M. J. Williams, S. J. Coote, *ibid.* **1993**, *34*, 7793; e) Reviews: C. G. Frost, J. Howarth, J. M. J. Williams, *Tetrahedron: Asymmetry* **1992**, *3*, 1089; O. Reiser, *Angew. Chem.* **1993**, *105*, 576; *Angew. Chem. Int. Ed. Engl.* **1993**, *32*, 547; A. Pfaltz, *Acc. Chem. Res.* **1993**, *26*, 339.

[3] H. M. R. Hoffmann, A. R. Otte, A. Wilde, *Angew. Chem.* **1992**, *104*, 224; *Angew. Chem. Int. Ed. Engl.* **1992**, *31*, 234; A. Wilde, A. R. Otte, H. M. R. Hoffmann, *J. Chem. Soc. Chem. Commun.* **1993**, 615; C. Carfagna, R. Galarini, K. Linn, J. A. Lopez, C. Mealli, A. Musco, *Organometallics* **1993**, *12*, 3019; C. Carfagna, L. Mariani, A. Musco, G. Sallese, R. Santi, *J. Org. Chem.* **1991**, *56*, 3924; L. S. Hegedus, W. H. Darlington, C. E. Russel, *ibid.* **1980**, *45*, 5193.

[4] The stereochemistry was elucidated by differential NOE spectroscopy.

[5] Reviews: S. F. Martin, *Tetrahedron* **1980**, *36*, 419; K. Fuji, *Chem. Rev.* **1993**, *93*, 2037.

Copper(II)-Mediated Oxidative Coupling of Bis(dimethylaminomethyl)arylruthenium Complexes to give [(terpy)Ru^{III}(pincer-pincer)-Ru^{III}(terpy)](CuCl$_2$)$_4$**

Jean-Pascal Sutter, David M. Grove, Marc Beley, Jean-Paul Collin, Nora Veldman, Anthony L. Spek, Jean-Pierre Sauvage, and Gerard van Koten*

In the course of our studies on the catalytic, electro-, and photochemical properties of bis(dimethylaminomethyl)aryl metal complexes in which the aryl ligand is the monoanionic

[*] Prof. Dr. G. van Koten, Dr. J.-P. Sutter, Dr. D. M. Grove
Debye Institute, Department of Metal-Mediated Synthesis, Utrecht University
Padualaan 8, NL-3584 CH Utrecht (The Netherlands)
Telefax: Int. code + (30)52 3615
Dr. M. Beley, Dr. J.-P. Collin, Dr. J.-P. Sauvage
Laboratoire de Chimie Organo-Minérale, Université Louis Pasteur (France)
N. Veldman, Dr. A. L. Spek[+]
Bijvoet Center for Biomolecular Research,
Laboratory of Crystal and Structural Chemistry, Utrecht University
Padualaan 8, NL-3584 CH Utrecht, Utrecht (The Netherlands)
[+] Address queries related to the crystallographic study to this author.

[**] This work was supported in part (A. L. S. and N. V.) by the Netherlands Foundation of Chemical Research (SON) with financial aid from the Netherlands Organization for Scientific Research (NWO). This collaborative work is part of a COST-D4 approved programme. Ligand abbreviations: pincer = [2,6-(Me$_2$NCH$_2$)$_2$C$_6$H$_3$]$^-$, pincer-pincer = [2,6-(Me$_2$NCH$_2$)$_2$C$_6$H$_2$-C$_6$H$_2$-2,6-(CH$_2$NMe$_2$)$_2$]$^{2-}$, dpb-dpb = [2,6-(2-pyridyl)$_2$C$_6$H$_2$-C$_6$H$_2$-2,6-(2-pyridyl)$_2$]$^{2-}$, tterpy = 4′-(*p*-tolyl)-2,2′:6′,2″-terpyridine, terpy = 2,2′:6′,2″-terpyridine.

$[2,6\text{-}(Me_2NCH_2)_2\text{-}C_6H_3]^-$ (*trans*-pincer),[1] we synthesized a series of novel $16e^-$ and $18e^-$ complexes of Ru^{II} (Scheme 1).[2] We now report that **1**-Cl undergoes a selective C4–C4′ coupling mediated by $CuCl_2$ leading to the formation of a unique binuclear complex **2**-4$CuCl_2$, abbreviated as $[(terpy)Ru^{III}(pincer\text{-}pincer)Ru^{III}(terpy)](CuCl_2)_4$. Surprisingly $\mathbf{2}^{4+}$ is diamagnetic and

$[Ru^{II}Cl\{2,6\text{-}(Me_2NCH_2)C_6H_3\}PPh_3]$ 16e

$[Ru^{II}Cl\{2,6\text{-}(Me_2NCH_2)C_6H_3\}(nbd)]$ 18e

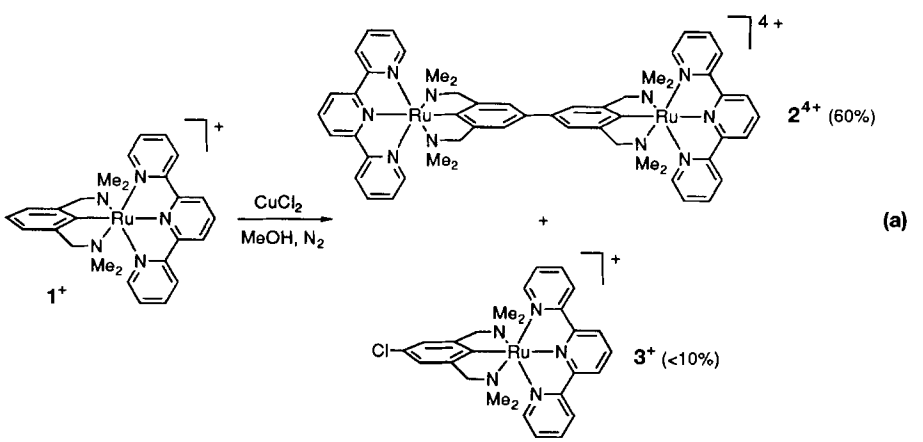
$[Ru^{II}\{2,6\text{-}(Me_2NCH_2)C_6H_3\}(terpy)]Cl$ 18e **1**-Cl

$[(terpy)Ru^{III}\{2,6\text{-}(Me_2NCH_2)C_6H_2\text{-}C_6H_2\text{-}2,6\text{-}(CH_2NMe_2)\}Ru^{III}(terpy)](CuCl_2)_4$ **2**-4$CuCl_2$

Scheme 1. Bis(dimethylaminomethyl)aryl Ru^{II} complexes. nbd = norbornadiene.

has as striking structural feature a perfectly planar 4,4′-biphenyldiyl bridge connecting the two Ru^{III} centers. Moreover, the mixed-valence complex $\mathbf{2}^{3+}$ displays strong electronic communication between the two metal centers.[3]

Complex **1**-Cl is an air-stable and water-soluble complex. Its reaction with three equivalents of $CuCl_2$ in dry and O_2-free MeOH, led to the green complex **2**-4$CuCl_2$ in good yield (60%) together with a minor deep red product (<10%), which was identified as **3**-PF_6 [Eq. (a)]. Complex **2**-4$CuCl_2$ is slightly soluble in CH_2Cl_2 but has a good solubility in polar solvents like MeCN, MeOH, or H_2O. Analytical data (^1H NMR, FAB-MS, and cyclic voltammetry (CV)) suggested that not only oxidation of the Ru^{II} center in **1** to Ru^{III} had occurred but also that $\mathbf{2}^{4+}$ is a diruthenium species formed by coupling of two units of $\mathbf{1}^+$.



The formation of **2**-4$CuCl_2$ by oxidation of **1**-Cl is unexpected in view of our early findings that oxidation of the arylnickel(II) complex $[Ni^{II}\{2,6\text{-}(Me_2NCH_2)_2C_6H_3\}X]$ (X = Cl, Br) with dihalogens or copper(II) halides results in quantitative formation of the trivalent arylnickel complex $[Ni^{III}\{2,6\text{-}(Me_2NCH_2)_2\text{-}C_6H_3\}X_2]$. Thus, in the latter reaction a clean one-electron oxidation of the nickel center occurs,[1] whereas the reaction of $\mathbf{1}^+$ with Cu^{II} leads to oxidation of both the ruthenium(II) center and the aryl ring. Formally the formation of $\mathbf{2}^{4+}$ can be seen as an oxidation of the C4–H bond. Obviously in the course of this process, besides C–C coupling, also competing ligand-transfer oxidation of the mononuclear ruthenium(III) intermediate with $CuCl_2$ takes place leading to formation of the 4-Cl derivative $\mathbf{3}^+$.

An X-ray structure determination[4] established that $\mathbf{2}^{4+}$ is indeed a binuclear complex containing a perfectly planar 4,4′-biphenyldiyl unit which connects the two octahedrally coordinated ruthenium centers through C1 and C1′, respectively. A PLUTON view is presented in Figure 1. Each ruthenium center

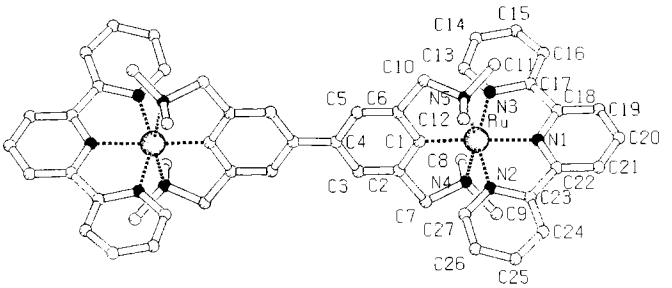


Fig. 1. PLUTON plot of the solid-state structure of **2**-4$CuCl_2$. The $CuCl_2^-$ ions, diethyl ether molecules (solvent of crystallization), and hydrogen atoms are omitted for clarity. Relevant bond lengths [Å], bond angles [°] and dihedral angles [°] are included in the text.

is coordinated by the three nitrogen atoms of a terpy and by three atoms of the *N,C,N′* bis-chelating pincer-pincer ligands. Both ruthenium atoms have a formal oxidation state of +3 leading to a cationic charge of +4 for the organometallic part, which is counterbalanced by the presence of four $CuCl_2^-$ ions in the unit cell.[4] The Ru···Ru intermetallic distance is 10.829(2) Å. A comparison of the various C–C bond lengths in the 4,4′-biphenyldiyl moiety of $\mathbf{2}^{4+}$ shows considerable differences amounting to 0.08 Å, (C2–C3, 1.361(12) vs. C3–C4, 1.441(15) Å), whereas the central C4–C4′ bond length has the value of a substantially shortened C–C single bond (1.436(12) Å). These data clearly show that at least in the solid state the π system of the 4,4′-biphenyldiyl bridging moiety in $\mathbf{2}^{4+}$ is completely conjugated between the two Ru^{III} metal centers. The extent of this conjugation is reflected in the electrochemical data (CV) of $\mathbf{2}^{4+}$ which have been compared with those of the mononuclear complexes $\mathbf{1}^+$ and $\mathbf{3}^+$ (Table 1). Cation $\mathbf{2}^{4+}$ can be reduced to the $Ru^{II}Ru^{III}$ mixed-valence complex, $\mathbf{2}^{3+}$, and subsequently to the $Ru^{II}Ru^{II}$ complex, $\mathbf{2}^{2+}$. Highly interesting is the large value of K_c (1250) (see Table 1) calculated from the electrochemical data

Table 1. Electrochemical data of complexes **1**–**4** in MeCN.

Complex [a]	$E_{1/2}$ [V] vs. SCE				K_c [b]
	III/II	III,III/III,II	III,II/II,II	II,I [c]	
$\mathbf{1}^+$	0.23	–		−1.63	
$\mathbf{2}^{2+}$	–	0.24	0.065	−1.66	1250
$\mathbf{3}^+$	0.27	–	–	–	–
$\mathbf{4}^{2+}$ [d]	–	0.505	0.34	−1.55	600

[a] The overall charge corresponds to the complexes with the ruthenium centers in the +2 formal oxidation state. [b] Comproportionation constant. [c] This situation most probably involves the reduced ligand (tterpy or terpy) and a divalent Ru center. [d] From ref. [6].

 © VCH Verlagsgesellschaft mbH, D-69451 Weinheim, 1994 0570-0833/94/1212-1283 $ 10.00+.25/0

which points to strongly coupled ruthenium centers. The $Ru^{II}Ru^{II}$ complex 2^{2+} could be independently synthesized from the reaction of 2^{4+} with hydrazine. The UV/VIS spectral values, λ_{max} and ε_{max}, for the mononuclear and binuclear Ru complexes are given in Table 2. The NIR spectrum of the mixed-valence $Ru^{II}Ru^{III}$ complex, 2^{3+}, obtained by in situ oxidation of the $Ru^{II}Ru^{II}$ complex with Br_2,[5] was recorded in MeCN from 900 to 2400 nm. It showed a broad, intense, intervalence charge

Table 2. UV/VIS data for the ruthenium complexes **1**–**4** in MeCN.

Complex	λ_{max} [nm] (ε[$10^4 M^{-1} cm^{-1}$])
1^+	632 (0.55), 593 (0.53), 523 (0.52), 392 (0.59), 324 (3.07), 280 (2.31), 238 (2.15)
1^{2+} [a]	574 (0.55), 331 (3.45), 269 (16.05)
2^{2+}	618 (1.58), 593 (1.67), 528 (1.81), 377 (3.72), 324 (7.30), 280 (5.95)
2^{4+}	657 (11.70), 306 (3.84), 275 (4.66), 201 (17.03)
4^{2+}	543 (3.06), 516 (3.06), 287 (11.29), 220 (6.75) [b]

[a] Obtained by in situ oxidation. [b] From ref. [6].

transfer (IVCT) band at 1875 nm ($\varepsilon = 33000\ M^{-1} cm^{-1}$) with a small overlapping band at 1650 nm (Fig. 2). As expected no NIR band was found for the $Ru^{II}Ru^{II}$ and $Ru^{III}Ru^{III}$ species.

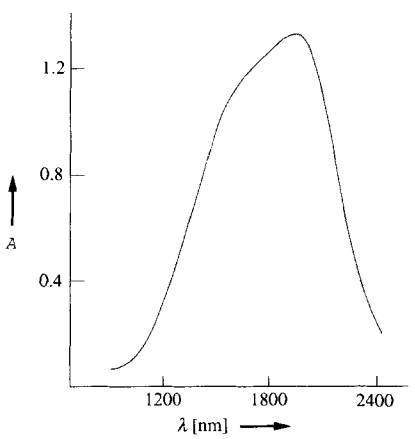
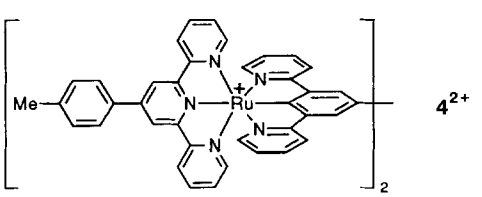
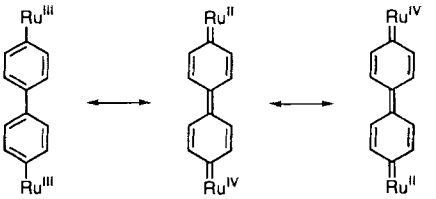


Fig. 2. NIR spectrum of complex 2^{3+} in the intervalence charge transfer region.

Recently, we reported a similar C–C coupling in the metalation reaction of the potentially terdentate N-C-N ligand 1,3-di(2-pyridyl)benzene (dpb-H) with $[Ru(tterpy)]^{3+}$ in the presence of oxygen and silver.[6] In the course of that reaction likewise not only a carbon–ruthenium but also a carbon–carbon bond was formed which led to 4^{2+}-$2PF_6$. The electrochemical and relevant spectroscopic data of 4^{n+} have been included in Tables 1 and 2. A comparison of these data and the structural features of 4^{n+} with those of 2^{p+} leads to the following results.



Binuclear 2^{3+} is among the strongest coupled diruthenium species ($K_c = 1250$, NIR band at 1875 nm, $\varepsilon = 33000\ M^{-1} cm^{-1}$) in spite of a large intermetallic distance ($Ru^{III} \cdots Ru^{III}$ separation of 10.829(2) Å; this distance is 11.009(2) Å in 4^{2+}). The dihedral angle between the phenyl rings in the 4,4′-biphenyldiyl moiety is practically 0° *in* 2^{4+} (vs. 22.2(7)° *in* 4^{2+}). The Ru^{III}-4,4′-biphenyldiyl-Ru^{III} central unit of 2^{4+} (Ru–C is 1.901(8) Å vs. 1.96(2) Å in 4^{2+}) can be envisaged as a diamagnetic formally Ru^{II}–Ru^{IV} conjugated polyene system (cf. ^1H NMR spectra and the double bond character of C4–C4′), as illustrated in Scheme 2. In 4^{2+}



Scheme 2. Limiting forms for the Ru^{III}-4,4′-biphenyldiyl-Ru^{III} system of 2^{4+}.

C4–C4′ is 1.51(1) Å with normal aromatic C–C distances in each ring. By changing the CH_2NMe_2 chelating groups of 2^{3+} for 2-pyridyl units as in 4^{3+}, the electronic communication between the metal centers is decreased ($K_c = 600$, NIR band at 1620 nm, $\varepsilon = 26000\ M^{-1} cm^{-1}$).

These results indicate that the amount of electron communication between the ruthenium centers may be modified by varying the electron-donating ability of the bridging ligand. The degree of twist between the two phenyl groups of the 4,4′-biphenyldiyl bridge should also be able to govern the extent of coupling. Further studies are directed to systems with larger and controllable torsion angles which would lead to tunable rates of electron transport through the molecule. Such systems may be useful building blocks for novel molecular switches.

Experimental Procedure

A suspension of complex **1**-Cl (0.20 g, 0.35 mmol) and $CuCl_2$ (0.13 g, 1.0 mmol) in MeOH (6 mL) was stirred at room temperature for 17 h to give a copper-colored solid and a deep red solution. The solvent was removed in vacuo and the residue dissolved in MeCN, to give a green solution which was subjected to chromatographic separation over a silica column with N_2 pressure. Elution with a solution of $MeCN/H_2O$/saturated KNO_3, (6/3/1 in volume) afforded a purple-blue band followed by a red one. The column was then eluted with a 5/5/1 mixture of the previous solvents to afford a major green band. The following workup was then applied to all three fractions: the solutions were concentrated to 1/3 in vacuo, an excess of NH_4PF_6 in solution in H_2O was added and the precipitate that formed was filtered off and washed with H_2O and Et_2O. The red fraction gave a deep red solid identified as complex **3**-PF_6 (0.04 g) and the green band gave a bronze-colored solid. The latter was dissolved in MeCN (2–3 mL), and the solution was added to CH_2Cl_2 (5 mL) and toluene (5–8 mL) to give the micro-crystalline red complex 2^{4+} (170 mg, 60%) with PF_6^- as counteranion.

Elemental analysis for **2**-$4PF_6$ + CH_2Cl_2 C 38.54, H 3.53, N 8.17 %; found C 38.88, H 3.76, N 7.98%. ^1H NMR (300 MHz, CD_3CN and some $N_2H_4 \cdot H_2O$, 25 °C TMS): $\delta(2^{2+})$ = 8.64 (d, ^3J(H,H) = 8.0, 4H), 8.49 (d, ^3J(H,H) = 7.8, 4H), 8.30 (d, ^3J(H,H) = 4.9, 4H), 7.98 (m, 6H), 7.68 (s, 4H), 7.50 (m, 4H), 3.75 (s, 8H; CH_2), 1.25 (s, 12H; NMe_2); δ(**3**-PF_6) = 8.60 (d, ^3J(H,H) = 8.0, 2H), 8.45, 8.19 (2m, 4H), 7.98 (t, ^3J(H,H) = 8.0, 1H), 7.91, 7.43 (2m, 4H), 7.24 (s, 2H), 3.60 (s, 4H; CH_2), 1.18 (s, 12H; NMe_2); FAB-MS (nitrobenzyl alcohol matrix): *m/z* (2^{2+}): 1195.0, (1195 for (**2**-PF_6)$^+$); *m/z* (3^{2+}): 705.0, (705.0 for (**3**-PF_6)$^+$).

Received: December 28, 1993 [Z 6589 IE]
German version: *Angew. Chem.* **1994**, *106*, 1359

[1] G. van Koten, *Pure Appl. Chem.* **1989**, *61*, 1681; *ibid* **1990**, *62*, 1155.
[2] J. P. Sutter, N. Veldman, W. J. J. Smeets, A. L. Spek, D. M. Grove, G. van Koten, unpublished results.
[3] Some representative references for Class II mixed-valence diruthenium complexes are: R. W. Callahan, F. R. Keene, T. J. Meyer, D. J. Salmon, *J. Am. Chem.*

Soc. **1977**, *99*, 1064–1073; C. A. Stein, N. A. Lewis, G. Seitz, *ibid.* **1982**, *104*, 2596–2599; D. E. Richardson, H. Taube, *ibid.* **1983**, *105*, 40–51; M.A.S. Aquino, F. L. Lee, E. J. Gabe, C. Bensimon, J. E. Greedan, R. J. Crutchley, *ibid.* **1992**, *114*, 5130–5140; D. E. Richardson, H. Taube, *Coord. Chem. Rev.* **1984**, *60*, 107–129; S. Woitellier, J. P. Launay, C. W. Spangler, *Inorg. Chem.* **1989**, *28*, 758–762; Y. Kim, C. M. Lieber; *ibid.* **1989**, *28*, 3990–3992; J. R. Reimers, N. S. Hush, *ibid.* **1990**, *29*, 3686–3697; J. P. Collin, P. Lainé, J. P. Launay, J. P. Sauvage, A. Sour, *J. Chem. Soc. Chem. Commun.* **1993**, 434–435.

[4] **2**-4$CuCl_2$ was crystallized without chromatographic purification, (see Experimental Procedure). Crystals suitable for the X-ray structure analysis were obtained from $MeOH/CH_2Cl_2$ layered with Et_2O. Crystal data for **2**-4$CuCl_2 \cdot 2Et_2O$. $M_r = 867.65$, dark crystal ($0.20 \times 0.20 \times 0.25$ mm), monoclinic, space group $P2_1/c$ with $a = 12.1907(19)$, $b = 18.115(3)$, $c = 18.9597(17)$ Å, $\beta = 125.01(1)°$, $V = 3429.3(10)$ Å^3, $Z = 2$, $\rho_{calcd} = 1.680$ g cm^{-3}, $F(000) = 1752$, $\mu(Mo_{K\alpha}) = 20.1$ cm^{-1}, 17010 reflections measured, 7877 independent ($1.7 < \theta < 27.5°$, $\omega/2\theta$ scan, $\Delta\omega = (1.28 + 0.35\tan\theta)°$), $T = 150$ K, $Mo_{K\alpha}$ radiation, graphite monochromator, $\lambda = 0.71073$ Å) on an Enraf-Nonius CAD4T rotating anode diffractometer. Data were corrected for Lorentz and polarization effects and for a linear decay of 3%. An empirical absorption correction was applied (DIFABS, correction range 0.819–1.277). The structure was solved by automated Patterson methods and subsequent difference Fourier techniques (DIRDIF-92). Refinement on F was carried out by full-matrix least squares techniques (SHELX76); final R value 0.0588, $wR = 0.0559$, $w = 1/[s^2(F) + 0.000114F^2]$, $S = 1.537$ for 399 parameters and 4379 reflections with $I > 2.5\sigma(I)$. Hydrogen atoms were included in the refinement on calculated positions (C–H = 0.98 Å) riding on their carrier atoms. All non-hydrogen atoms were refined with anisotropic thermal parameters; the hydrogen atoms were refined with two common isotropic thermal parameters. Weights were introduced in the final refinement cycles. A final difference Fourier showed no residual density outside -0.83 and 0.85 eÅ^{-3} (near Ru). Further details of the structure determination, including atomic coordinates, bond lengths and angles, thermal parameters, and a thermal motion ellipsoid plot are available on request from the Director of the Cambridge Crystallographic Data centre, 12 Union Road, Cambridge CB2 1EZ (UK) on quoting the full journal citation.

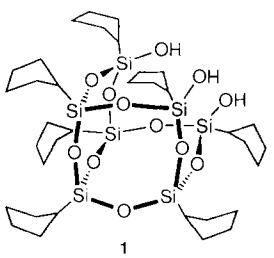
[5] Br_2 was gradually added to the solution while monitoring the NIR band. Its maximum intensity was reached at a Br_2 to Ru_2 ratio of 1:2 and it had disappeared completely at a 1:1 stoichiometry.

[6] M. Beley, J. P. Collin, R. Louis, B. Metz, J. P. Sauvage, *J. Am. Chem. Soc.* **1991**, *113*, 8521–8522; M. Beley, J. P. Collin, J. P. Sauvage, *Inorg. Chem.* **1993**, *21*, 4539–4543.

Molecular Siloxane Complexes of Rare Earth Metals—Model Systems for Silicate-Supported Catalysts?**

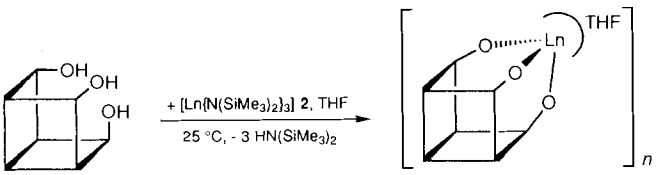
Wolfgang A. Herrmann,* Reiner Anwander, Veronique Dufaud, and Wolfgang Scherer

The preparation of realistic models of heterogeneous, SiO_2-supported transition metal catalysts eluded chemists for many years.[1] However, partially condensed oligosesquisiloxanes have lately proved to be reasonable model systems.[2] Since lanthanoid-doped zeolite catalysts are of considerable technical importance,[3] we have introduced oligosesquisiloxanes such as $[(c\text{-}C_5H_9)Si]_7O_9(OH)_3$ **1** as molecular models in the chemistry of the rare earth metals.[4]



1

We chose yttrium and neodymium as representatives of the lanthanoids. The metal complexes **3a**, **b** were obtained in quantitative yields according to the silylamide route given in Scheme 1. The course of the reaction was monitored by the



1

3a, Ln = Nd
3b, Ln = Y
$n = 1,2$

Scheme 1. Each corner of the formula representation corresponds to a cyclopentylsilicon group; oxygen atoms are found midway between the connected corners.

liberation of the silylamine (GC/MS analysis). **3a**, **b** are readily soluble in all organic solvents, even *n*-pentane, and were characterized by elemental analysis and IR spectroscopy (no ν(SiO–H) bands at ca. 3230 cm^{-1} typical of the starting material). Investigations by mass spectrometry (no signals < 300 °C) suggest dimeric structures in the solid state ($n = 2$) as found in the Al^{III} and Ti^{III} complexes.[2a, b] Whilst the ^1H, ^{13}C, and ^{29}Si NMR spectra could not be conclusively interpreted, the ^{89}Y NMR spectrum contains a single signal which indicates the presence of a well-defined compound and only one chemical environment of the Y atom. The shift of $\delta = 196.9$ is typical of lanthanoid siloxides (cf. $[Y(OSiMe_2tBu)_3(THF)_3]$, $\delta = 266.6$[5]). Attempts at recrystallization from common solvents such as THF, hexane, and benzene produced crystals that were amorphous by X-ray crystallography. However, with triphenylphosphane oxide as an auxiliary ligand, **3b** reacted to give the adduct **4** as single crystals.[6] Figure 1 shows the structure of the binuclear complex **4**.

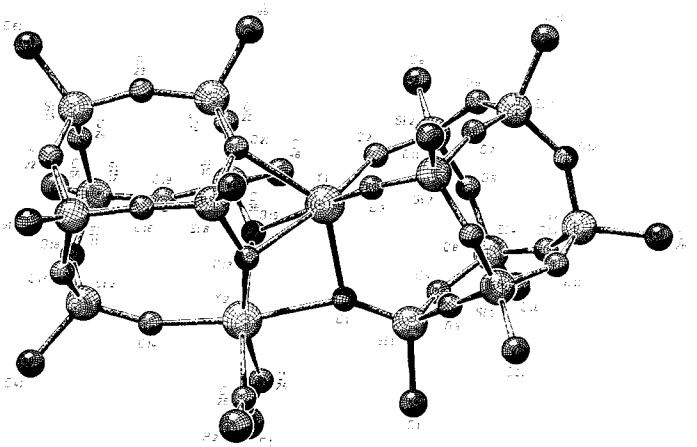


Fig. 1. Model of the molecular structure of **4** in the solid state (SHAKAL representation). To simplify the drawing, the cyclopentyl groups and the four solvent molecules are not completely represented. Selected bond lengths [Å] and angles [°]: Y1-O1 2.239(9), Y1-O2 2.119(7), Y1-O3 2.123(9), Y1-O13 2.422(7), Y1-O15 2.391(8), Y1-O21 2.509(9), Y2-O1 2.384(7), Y2-O13 2.25(1), Y2-O14 2.117(8), Y2-O15 2.255(8), Y2-O25 2.296(8), Y2-O26 2.26(1); Y1-O1-Y2 91.3(3); Y1-O13-Y2 90.0(4), Y1-O15-Y2 90.7(3), Y1-O21-Si8 92.9(4), Y1-O21-Si14 115.4(4), Si14-O21-Si8 141.1(5), Y2-O26-P1 157.0(6), Y2-O25-P2 153.3(6).

Both yttrium atoms have six-fold coordination. In contrast, the addition of the same phosphane oxide auxiliary ligand to the corresponding aluminum complex causes a *cleavage* of the dimer originally present.[2a]

[*] Prof. Dr. W. A. Herrmann, Dr. R. Anwander, Dr. V. Dufaud, W. Scherer
Anorganisch-chemisches Institut der Technischen Universität München
Lichtenbergstrasse 4, D-85747 Garching (FRG)
Telefax: Int. code + (89)3209-3473

[**] Lanthanoid Complexes, Part 7. This work was supported by Osram GmbH and the Alexander-von-Humboldt-Stiftung. We thank Dipl.-Chem. F.-R. Klingan for recording the NMR spectra. – Part 6: W. A. Herrmann, R. Anwander, W. Scherer, F. C. Munck, *J. Organomet. Chem.* **1993**, *462*, 163.

Furthermore, because of the considerable increase in the radius of the metal ion, as well as the increased oxophilicity of the metal compared to all other metal complexes containing this type of ligand, three bridging SiO units link the two metal centers (unsymmetrically). One of the yttrium atoms (Y1) achieves coordinative saturation by coordination to an oxygen atom in the ligand framework (O21; Fig. 2). This type of framework

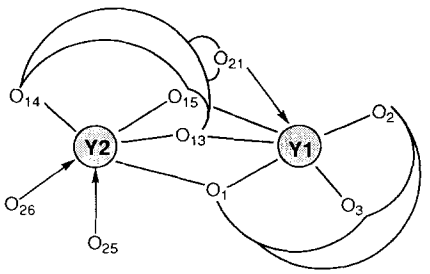


Fig. 2. Simplified representation of the coordination spheres of the yttrium atoms to emphasize the structural features of **4**. The *framework* oxygen atom O21 acts as a donor atom and completes the coordination sphere of Y1.

coordination is unknown for any of the known metal complexes of sesquisiloxanes, not even for any of the other lanthanoid siloxane complexes.[7] The distances from the yttrium center to the terminal [2.117(8)–2.123(9) Å] and bridging oxygen atoms [2.239(9)–2.422(7) Å] lie within the expected range.[7c] The Y–(O21) distance of 2.509(9) Å corresponds to a typical donor bond (cf. 2.374(20)–2.462(21) Å in $[Y(OSiR_3)_3(THF)_3]\cdot(THF)$, $R = C_6H_5$[7c]).

The Si-O-Si bridging oxygen atoms can act as Lewis bases in zeolite systems as well.[8] The binuclear complex units **4** are loosely packed in the solid state. Four crystallographically independent solvent molecules (toluene) are located in the resulting channels. The size of these solvent channels leads to a considerable disorder of the toluene molecules and explains the facile diffusion of the solvent out of the crystals even at low temperatures.

Organometallic compounds react preferentially with partially dehydroxylated silica surfaces, that is with $[Si(OH)_n]$ centers as opposed to [SiOSi] sites, towards which they usually behave indifferently.[4d] The yttrium complex **4** shows, for the first time, the coordination of [SiOSi] sites to an extremely oxophilic, electropositive metal center. This may permit interesting analogies with the structural chemistry of metal-doped zeolites. For example, in investigations of Ga-exchanged zeolites by IR spectroscopy altered lattice vibrations are observed,[3c, 9] which should correspond to a change in the catalytic properties. Furthermore, the attachment of neutral silicones of low molecular weight such as $(RSiO_{1.5})_4$ (R = *i*Pr, *t*Bu)[10] onto coordinatively unsaturated organolanthanoid compounds indicates the possibility of supporting a catalyst following the example in Scheme 1.

Experimental Procedure

In a glovebox (M. B. Braun) amides **2** and an equimolar quantity of **1** were weighed into a 100-mL round-bottomed flask. Roughly 40 mL of THF was added by condensation under high vacuum. The mixture was stirred for 1 h at 0 °C then allowed to warm to 25 °C. In the reaction of the yttrium amide a clear solution was obtained immediately, in the reaction of the neodymium amide only after 30 h. After ca. 40 h the solvent and the liberated amine were removed under vacuum (1 mbar). The colorless or light blue residue was dried for 3 h under vacuum (10^{-3} mbar). The residues are very soluble in *n*-pentane. Quantiative yields. **3a**: Starting from 0.58 g (0.92 mmol) **2a**, 0.81 g (0.93 mmol) **1**; light blue crystals; correct C,H,Si analysis (for two THF/Nd; no N); IR: $\tilde{\nu}$[cm^{-1}] = 1246 m, 1109 vs, 1088 (sh) vs, 1049 (sh) s, 998 s, 929 m, 875 w, 846 w, 525 m, 514 m. **3b**: Starting from 0.59 g (1.04 mmol) **2b**, 0.90 g (1.03 mmol) **1**; colorless crystals; m.p. 235 °C; correct C,H,N,Si analysis (for two THF/Y; no N); IR: $\tilde{\nu}$[cm^{-1}] = 1244 m, 1111 vs, 1087 vs, 1051 (sh) s, 1009 m, 954 m, 926 m, 914 m, 886 m, 841 (sh) w, 773 w, 519 m, 506 m, 483 m, 466 w. $^{13}C\{^1H\}$ NMR (400 MHz, C_7D_8, 25 °C): δ = 22.2–30.2 (complex pattern); ^{29}Si NMR (400 MHz, C_6D_6, 25 °C): δ = −65.64, −64.61, −62.74; ^{89}Y NMR (400 MHz, C_7D_8, 25 °C): δ = 196.9.

Received: November 25, 1993
Revised version: February 5, 1994 [Z 6512 IE]
German version: *Angew. Chem.* **1994**, *106*, 1338

[1] F. T. Edelmann, *Angew. Chem.* **1992**, *104*, 600; *Angew. Chem. Int. Ed. Engl.* **1992**, *32*, 586.

[2] a) F. J. Feher, T. A. Budzichowski, K. J. Weller, *J. Am. Chem. Soc.* **1989**, *111*, 7288; b) F. J. Feher, S. L. Gonzales, J. M. Ziller, *Inorg. Chem.* **1988**, *27*, 3440; c) F. J. Feher, J. F. Walzer, *ibid.* **1990**, *29*, 1604; d) T. A. Budzichowski, S. T. Chacon, M. H. Chisholm, F. J. Feher, W. Streib, *J. Am. Chem. Soc.* **1991**, *113*, 689; e) F. J. Feher, T. A. Budzichowski, J. W. Ziller, *Inorg. Chem.* **1992**, *31*, 5100; f) G. Calzaferri, *Nachr. Chem. Tech. Lab.* **1992**, *40*, 1106.

[3] a) M. Bruzzone in *Fundamental and Technological Aspects of Organo-f-Element Chemsitry* (Eds.: T. J. Marks, I. L. Fragalà), Reidel, Dordrecht, **1985**; b) W. Hölderich, M. Hesse, F. Näumann, *Angew. Chem.* **1988**, *100*, 232; *Angew. Chem. Int. Ed. Engl.* **1988**, *27*, 226; c) S. L. Suib, *Chem. Rev.* **1993**, *93*, 803; d) T. Baba, R. Koide, Y. Ono, *J. Chem. Soc. Chem. Commun.* **1991**, 691.

[4] Synthesis of oligosesquisiloxanes: a) J. F. Brown, Jr., L. H. Vogt, Jr., *J. Am. Chem. Soc.* **1965**, *87*, 4313; b) F. J. Feher, T. A. Budzichowski, R. L. Blanski, K. J. Weller, J. W. Ziller, *Organometallics* **1991**, *10*, 2526; c) F. J. Feher, D. A. Newman, J. F. Walzer, *J. Am. Chem. Soc.* **1989**, *111*, 1741; d) T. W. Hambley, T. Maschmeyer, A. F. Masters, *Appl. Organomet. Chem.* **1992**, *6*, 253; e) G. K. I. Magomedov, E. A. Chernyshev, L. V. Morozova, A. S. Frenkel, B. V. Molchanov, S. Y. Kochev, S. A. Sigachev, A. I. Sbrodov, E. V. Bulycheva, *Metalloorg. Khim.* **1992**, *5*, 151; *Organomet. Chem. USSR (English trans.)* **1992**, *5*, 81.

[5] P. S. Coan, L. G. Hubert-Pfalzgraf, K. G. Caulton, *Inorg. Chem.* **1992**, *31*, 1262.

[6] Growth, selection, and mounting of the crystals was carried out in a glove box with an integrated polarization microscope and capillary sealing apparatus. **4** crystallized from toluene at −35 °C in the triclinic space group $P\bar{1}$ with a = 1647.4(9), b = 2064.2(9), c = 2300.4(18) pm, α = 83.35(4), β = 71.83(4), γ = 89.50(3)°, T = −80 ± 3 °C, Z = 2, $V = 7379 \times 10^6$ pm^3, ρ = 1.289 $g\,cm^{-3}$, $F(000)$ = 3008, $Mo_{K\alpha}$ radiation, Enraf-Nonius CAD4 diffractometer, ω-scans, max. 50 s, 10634 measured reflections ($2° < \theta < 20°$), $h(-15/15)$, $k(0/20)$, $l(-21/21)$, 8625 independant reflections of which 6156 with $I > 3.0\,\sigma(I)$ were used for refinement; correction of intensity (30% decomposition), no correction for absorption ($\mu = 9.9\ cm^{-1}$), $R = \sum\|F_o| - |F_c\|)/\sum|F_o| = 0.079$; $R_w = [\sum w(|F_o| - |F_c|)^2/\sum w|F_o|^2]^{1/2} = 0.085$, residual electron density +0.80/−0.98 e_o $Å^{-3}$. Further details of the crystal structure investigation may be obtained from the Fachinformationszentrum Karlsruhe, D-76344 Eggenstein-Leopoldshafen (FRG), on quoting the depository number CSD-58155.

[7] a) P. S. Gradeff, K. Yunlu, A. Gleizes, J. Galy, *Polyhedron* **1989**, *8*, 1001; b) W. J. Evans, T. A. Ulibarri, J. W. Ziller, *Organometallics* **1991**, *10*, 134; c) M. J. McGeary, P. S. Coan, K. Folting, W. E. Streib, K. G. Caulton, *Inorg. Chem.* **1991**, *30*, 1723.

[8] F. Liebau, *Structural Chemistry of Silicates*, Springer, Berlin, **1985**.

[9] D. H. Dompas, W. J. Mortier, O. C. H. Kenter, M. J. G. Janssen, J. P. Verduijn, *J. Catal.* **1991**, *129*, 19.

[10] a) E. Wiberg, W. Simmler, *Z. Anorg. Allg. Chem.* **1955**, *282*, 330; b) R. Gewald, U. Scheim, K. Rühlmann, H. Goesman, D. Fenske, *J. Organomet. Chem.* **1993**, *450*, 73.

Olympiadane**

David B. Amabilino, Peter R. Ashton, Anatoli S. Reder, Neil Spencer, and J. Fraser Stoddart*

The appearance, toward the end of last year, of a remarkable paper in a special issue of the *New Journal of Chemistry*, edited by Sauvage, has drawn attention to the fact that, as long ago as 1960,

[*] Prof. J. F. Stoddart, Dr. D. B. Amabilino, P. R. Ashton, Dr. A. S. Reder, Dr. N. Spencer
School of Chemistry, University of Birmingham
Edgbaston, GB-Birmingham B15 2TT (UK)
Telefax: Int. code + (21)414-3531

[**] This work was supported in the UK by the Science and Engineering Research Council.

van Gulick[1] had likened the well-known symbol of the International Olympics (Fig. 1 top)[2] to a pentacatenane, for which he had gone as far as to suggest the trivial name olympiadane.

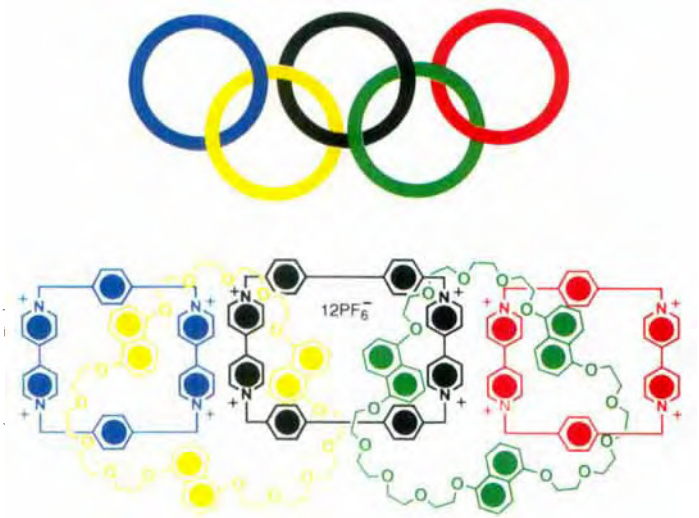
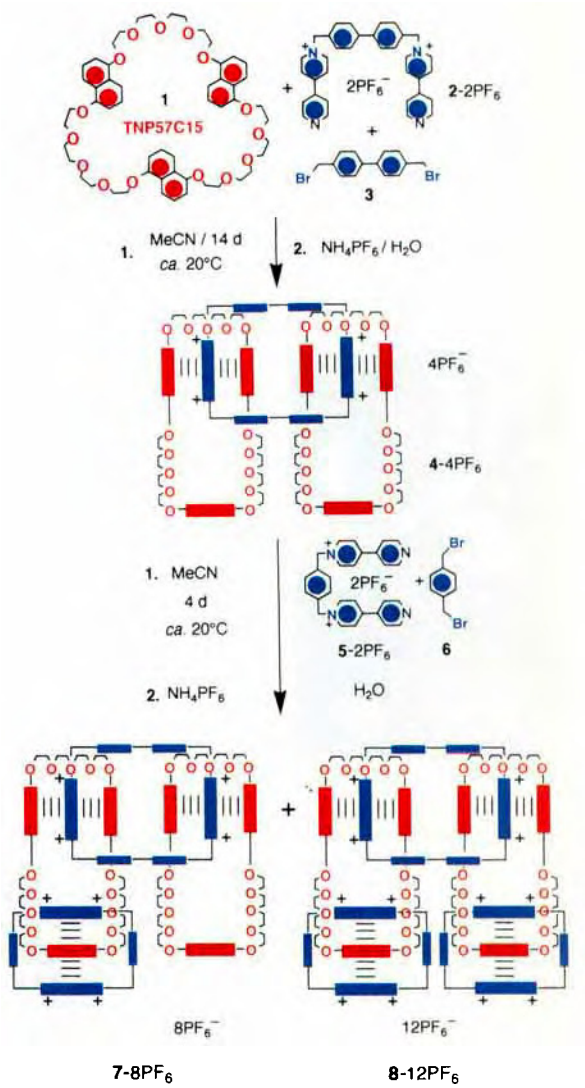


Fig. 1. The symbol of the International Olympics (top) and the structure of olympiadane (bottom).

Here, we describe the self-assembly (Scheme 1) and the characterization (Figs. 4–6) of the first molecular compound consisting of a *linear* array[3] of *five* interlocked rings. We propose to call this [5]catenane (Fig. 1 bottom) olympiadane.

Our first efforts[4] at making a [5]catenane culminated in a two-step self-assembly route (Fig. 2), which produced a [4]catenane and a whiff (< 0.5%) of a [5]catenane, which was only characterized by mass spectrometry. The reason for the reluctance of the [4]catenane to accept the addition of a fifth ring is enigmatic. Perhaps its templated formation is hindered by a negative intramolecular allosteric effect. Whatever the reason, it was clear that we needed to modify the recognition characteristics of the macrocyclic ether component. Since derivatives of 1,5-dihydroxynaphthalene are bound[5] within the receptor site of cyclobis(paraquat-*p*-phenylene) much more strongly than the analogous hydroquinone derivatives, we decided to replace the hydroquinone residues in the "failed" tris-*p*-phenylene[51]crown-15 with 1,5-dioxynaphthalene units. Here, we describe how this modification improves dramatically the templating features of the macrocyclic polyether component and enables the two-step self-assembly, *at ambient temperature and atmospheric pressure*, of a [5]catenane, which has been characterized conclusively by mass spectrometry (LSI-MS) and variable-temperature ^{1}H NMR (400 MHz) spectroscopy.

The trisnaphtho[57]crown-15 TNP57C15 **1** was prepared using a procedure[6] similar to that employed previously[4] in the preparation of tris-*p*-phenylene[51]crown-15. Reaction of **1** with two equivalents of 1,1′-[1,4-phenylenebis(methylene)]bis-4,4′-bipyridinium bis(hexafluorophosphate) (**5**-2 PF_6) and 1,4-bis(bromomethyl)benzene (**6**) in dimethylformamide (DMF) at ambient temperature and atmospheric pressure afforded[7] a [3]catenane as well as a [2]catenane, an outcome which boded well for the self-assembly of a [5]catenane under the same conditions. Next,



Scheme 1. The two-step template-directed synthesis of, firstly, the [3]catenane **4**-4 PF_6 from **1**, **2**-2 PF_6, and **3**, and secondly, the [4]catenane **7**-8 PF_6 and the [5]catenane **8**-12 PF_6 from **4**-4 PF_6, **5**-2 PF_6, and **6**. The chemical cartoons are defined as follows: *p*-phenylene rings: small blue rectangles; bipyridinium units: large blue rectangles; 1,5-dioxynaphthalene rings: red rectangles.

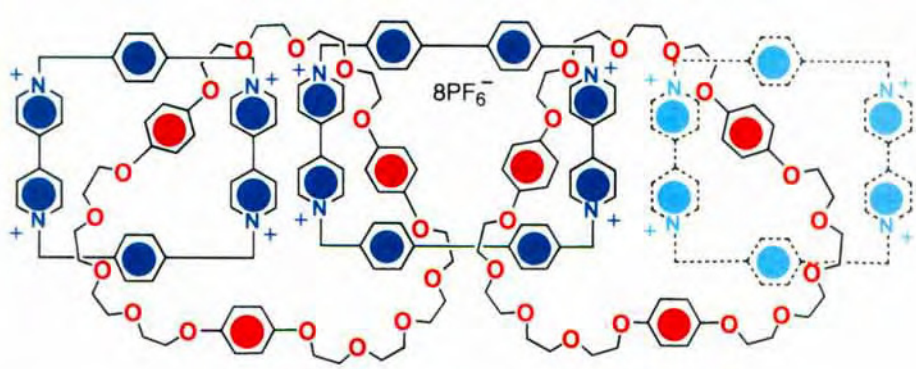


Fig. 2. The structure of the [4]catenane (solid-line drawing) comprising two tris-*p*-phenylene[51]crown-15 macrocycles, and the cyclophanes, cyclobis(paraquat-*p*-phenylene) and cyclobis(paraquat-4,4′-biphenylene). The [5]catenane (solid- plus dotted-line drawing) contains an additional cyclobis(paraquat-*p*-phenylene) macrocycle.

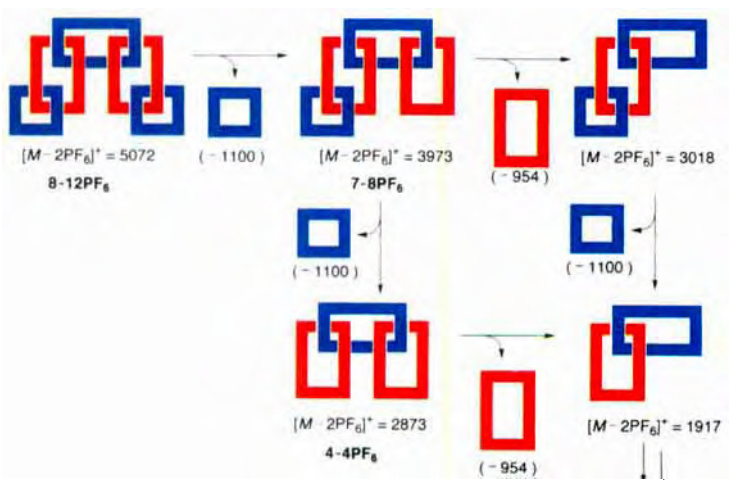
 © VCH Verlagsgesellschaft mbH, D-69451 Weinheim, 1994 0570-0833/94/1212-1287 $ 10.00+.25/0

treatment of **2**-2PF_6 with equimolar amounts of **3** in the presence of an excess of **1** afforded[8] the [3]catenane **4**-4PF_6 (Scheme 1), albeit in a rather low yield.[9] The [3]catenane was then treated with an excess of **5**-2PF_6 and **6** at ambient temperature and atmospheric pressure. After just four days, the reaction mixture was subjected to column chromatography on silica gel, yielding, after counterion exchange, the unchanged [3]catenane **4**-4PF_6 (45%), the intermediate [4]catenane **7**-8PF_6 (31%), and the [5]catenane **8**-12PF_6 (5%), all beautiful violet-colored compounds (Fig. 3).



Fig. 3. The violet bands of the [4]catenane **7**-8PF_6 and the [5]catenane **8**-12PF_6 after column chromatography of the reaction mixture with MeOH/2M NH_4Cl(aq)/$MeNO_2$ (7:2:1) on silica gel for 24 h. Note that the unchanged [3]catenane **4**-4PF_6 has already been eluted from the column and is contained in the two conical flasks.

The positive-ion FAB[10] and LSI mass spectra[11] of **4**-4PF_6, **7**-8PF_6, and **8**-12PF_6 show similar fragmentation patterns to those previously reported[4] for the analagous [3]-, [4]-, and [5]catenanes, self-assembled from the appropriate components with tris-*p*-phenylene[51]crown-15 as the template. In addition to the sequential loss of PF_6^- ions, there is also a stepwise loss (Scheme 2) of macrocycles from the parent catenanes. Figure 4



Scheme 2. Fragmentation sequence in the LSI mass spectrum of **8**-12PF_6. The large red rectangle represents the macrocyclic polyether **1**, the small blue rectangle, cyclobis(paraquat-*p*-phenylene) tetrakis(hexafluorophosphate), and the large blue rectangle, cyclobis-(paraquat-4,4′-biphenylene) tetrakis(hexafluorophosphate). The masses given correspond to the peaks observed in the mass spectrum of **8**-12PF_6.

shows the high-mass region of the positive-ion LSI mass spectrum of **8**-12PF_6. A comparison of the theoretical and observed isotopic distributions in the $[M - 2PF_6]^+$ ion of **8**-12PF_6 is shown in Figure 5. By the use of peak matching at high resolution, and

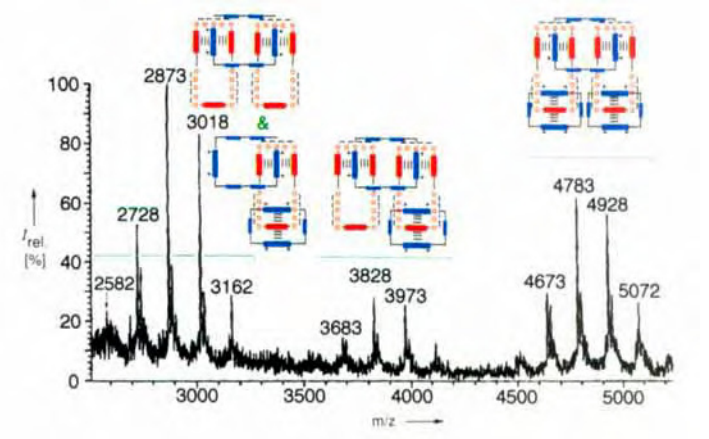


Fig. 4. The high-mass region of the positive-ion LSI mass spectrum of **8**-12PF_6, showing the sequential loss of hexafluorophosphate counterions, as well as the stepwise loss of the two smaller tetracationic cyclophanes and one of the macrocyclic polyethers.

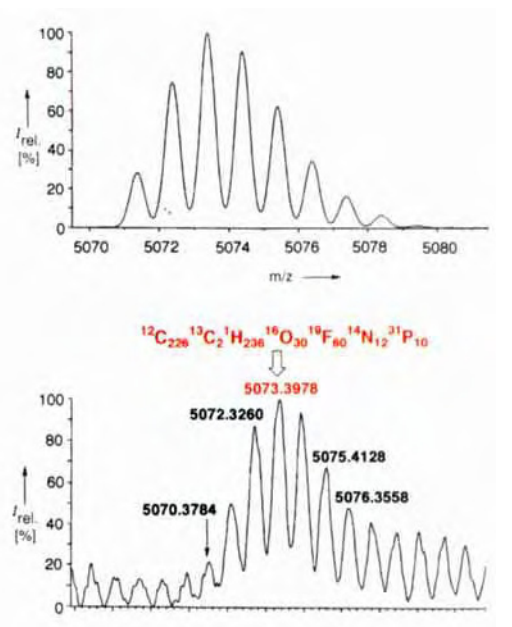


Fig. 5. A comparison of the theoretical isotopic distribution (top) for the $[M - 2PF_6]^+$ ion of the [5]catenane **8**-12PF_6 and its high-resolution LSI mass spectrum (bottom).

with CsI as a reference, the most abundant peak of this ion, which corresponds to $^{12}C_{226}{}^{13}C_2{}^{1}H_{236}{}^{16}O_{30}{}^{19}F_{60}{}^{14}N_{12}{}^{31}P_{10}$, was observed at *m/z* 5073.3978, a value that is within 5 ppm of the calculated mass.

The structure[12] of the [5]catenane **8**-12PF_6 was confirmed by variable-temperature ^1H NMR spectroscopy.[13] At ambient temperature, the 400 MHz ^1H NMR spectrum of **8**-12PF_6 recorded in CD_3CN shows well-resolved resonances at $\delta = 5.53$, 6.79, 7.72, 7.95, and 8.58 arising from the protons associated with the cyclobis(paraquat-4,4′-biphenylene) component, while all the other resonances are broadened by exchange processes. When the solution is warmed to 70 °C (Fig. 6), the four resonances for the nonequivalent protons in the two cyclobis(paraquat-*p*-phenylene) components become well resolved at $\delta =$ 5.68, 7.17, 7.94, and 8.58 as a result of relatively rapid movements and reorientations of the naphthalene rings in the macrocyclic polyether components out of and into the receptive cavities of these two smaller cyclophanes. Despite this observation, the reso-

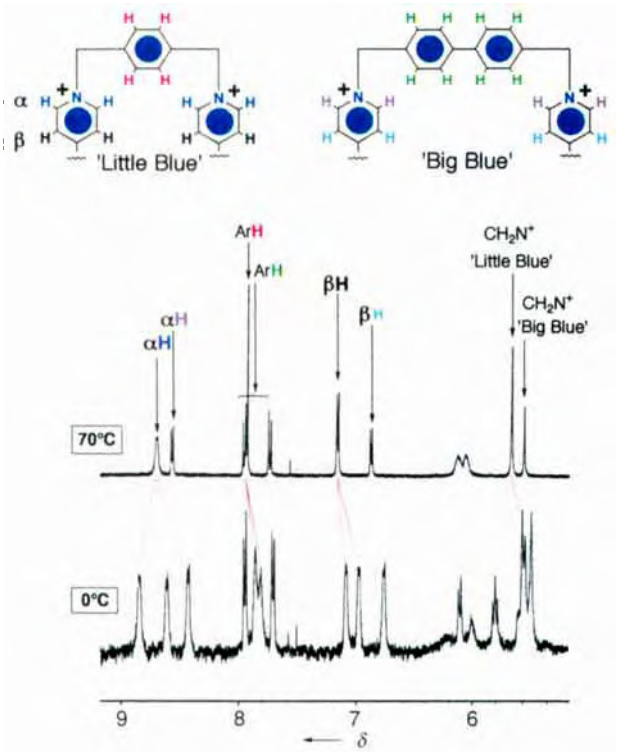


Fig. 6. The partial ^{1}H NMR spectra (400 MHz, CD_3CN) of the [5]catenane **8**-8 PF_6 recorded at 70 °C and 0 °C. The assignments of all the well-resolved signals at 0 °C have been confirmed by a two-dimensional homonuclear shift correlation experiment (COSY45). The spectrum obtained at 70 °C reflects the averaged D_{2h} symmetry of the molecule.

nances arising from the protons attached to the naphthalene rings remain broadened on account of the presumably larger limiting chemical shift differences associated with their resonances compared to those of the cyclophanes. Cooling the solution down to 0 °C results in a spectrum, wherein two sets of resonances are observed for each set of equivalent protons in the cyclobis(paraquat-*p*-phenylene) component. This doubling of the number of signals for the smaller cyclophanes is a result of the locally C_{2h}-symmetric 1,5-dioxynaphthalene units, which reside in their cavities and impose lower symmetries upon them. The "freezing" of the 1,5-dioxynaphthalene units inside the smaller cyclophanes is indicated by the emergence of resonances in the ^{1}H NMR spectrum at $\delta = 2.10$ (broad doublet for H-4/8), 5.82 (triplet for H-3/7), and 6.10 (doublet for H-2/6) arising from the naphthalene protons. The signals for the remaining two 1,5-dioxynaphthalene units in the polyether components remain broad, as these groups presumably oscillate between the interior and exterior of the larger tetracationic cyclophane. A $\Delta G_c^{\neq}$-value of 14.5 kcal mol^{-1} ($\pm$ 0.2 kcal mol^{-1}), corresponding to the reorganization of the smaller cyclophanes with respect to the included 1,5-dioxynaphthalene units, can be calculated[14] from the k_c-value of 369 s^{-1} at the coalescence temperature (T_c = + 37 °C) for the doublets centered on $\delta = 8.42$ and 8.84 (0 °C, $\Delta\nu$ = 166 Hz), which arise from the α-CH protons of the smaller cyclophane. A similar treatment of the coalescing doublets centered on $\delta = 6.97$ and 7.07 ($\Delta\nu = 41$ Hz) for the β-CH protons in the smaller cyclophanes affords a $\Delta G_c^{\neq}$-value of 14.7 kcal mol^{-1} ($\pm$0.2 kcal mol^{-1}) from a k_c of 92 s^{-1} at + 23 °C. This common free energy barrier of approximately 14.6 kcal mol^{-1} can be regarded as the one to be surmounted for the bound 1,5-dioxynaphthalene unit to be dislodged[15] from the centers of the smaller cyclophanes. The [3]catenane **4**-4 PF_6 and the [4]catenane **7**-8 PF_6 display similar multiple temperature dependencies in their ^{1}H NMR spectra.

The self-assembly[16] of olympiadane from eight components in two steps has been made possible as a result of programming sufficient molecular recognition into the constituent molecular components.[17] Reaching olympiadane—a structure some four nanometers in length when fully contracted—is symbolic in relation to developing the concept of self-assembly in chemical synthesis. When we can self-assemble a *high molecular weight, monodisperse* polymer, for example a polycatenane,[18] with *maximum efficiency*, *complete selectivity*, and *prescribed "information" content*, then the molecular self-assembly procedure will be a finely tuned and honed one. That is our ultimate goal.

Experimental Procedure

1: A solution of 1,5-bis[2-[2-[2-(1-naphthoxy-5-hydroxy)ethoxy]ethoxy]ethoxy]naphthalene (2.03 g, 2.55 mmol) in dry DMF (100 mL) was added to a stirred suspension of Cs_2CO_3 (19.39 g, 61.05 mmol) and CsOTs (1.98 g, 6.88 mmol) in dry DMF (200 mL) under nitrogen, and the temperature raised to 50 °C. After 1 h a solution of the tetraethyleneglycol bistosylate (1.39 g, 2.77 mmol) in dry DMF (100 mL) was then added during 1 h, and the temperature raised to 80 °C. Stirring and heating were continued for 4 d. The reaction mixture was then filtered, and the residue washed with DMF (100 mL) and EtOAc (100 mL). The solvent was removed under vacuum, and the residue was partitioned between CH_2Cl_2 (700 mL) and H_2O (250 mL). The CH_2Cl_2 phase was extracted once more with H_2O (250 mL), after which the organic solution was dried ($MgSO_4$) and concentrated under vacuum to afford a residue which was purified by column chromatography [SiO_2: CH_2Cl_2/EtOAc (9:1)] to yield **1** as a white solid (0.99 g, 40%, m.p. 81–83 °C); positive-ion FAB-MS: m/z = 954 for $[M]^+$; ^{1}H NMR ($CDCl_3$): $\delta = 3.64$–3.74 (m, 24H), 3.89 (t, J = 5 Hz, 12H), 4.17 (t, J = 5 Hz, 12H), 6.72 (d, J = 8.5 Hz, 6H), 7.28 (t, J = 8.5 Hz, 6H), 7.84 (d, J = 8.5 Hz, 6H); ^{13}C NMR ($CDCl_3$): δ = 68.0, 69.8, 70.8, 71.1, 105.7, 114.6, 125.1, 126.8, 154.4. When the same reaction procedure was repeated with 1,11-bis(1-naphthoxy-5-hydroxy)-3,6,9-trioxaundecane and 1,5-bis[2-[2-[2-(toluene-*p*-sulfonyl)-ethoxy]ethoxy]ethoxy]ethoxy]naphthalene as starting materials, a 35% yield of **1** was obtained.

4-4 PF_6: **2**-2 PF_6 (340 mg, 0.44 mmol), **3** (152 mg, 0.45 mmol), and **1** (1.023 g, 1.07 mmol) were combined as solids, and a dry mixture of MeCN (22 mL), DMF (1 mL), and CH_2Cl_2 (1 mL) was added. The suspension was allowed to stir at ambient temperature for 10 d, whereupon it was filtered, and the solvent was removed in vacuo yielding a purple solid. Column chromatography [SiO_2: MeOH/2 M NH_4Cl(aq)/$MeNO_2$ (7:2:1)], concentration in vacuo of the eluent containing the product, followed by solubilization of the residue in an H_2O/Me_2CO mixture, and precipitation by addition of aqueous NH_4PF_6 solution afforded **4**-4 PF_6 as a violet solid (83 mg, 6%, m.p. 109–111 °C) after filtration; positive-ion FAB-MS: m/z = 3016, 2871, 2062, 1917, and 1772 for $[M - PF_6]^+$, $[M - 2PF_6]^+$, $[M - 1 - PF_6]^+$, $[M - 1 - 2PF_6]^+$, and $[M - 1 - 3PF_6]^+$, respectively; ^{1}H NMR (CD_3CN): $\delta = 3.69$–3.74 (m, 48H), 3.75–3.81 (m, 24H), 3.82–3.88 (m, 24H), 5.51 (s, 8H), 6.21–6.42 (m, 24H), 6.50–6.64 (m, 20H), 7.65 (d, J_{AB} = 8 Hz, 8H), 7.88 (d, J_{AB} = 8 Hz, 8H), 8.42 (d, J = 7 Hz, 8H); ^{13}C NMR (CD_3COCD_3): δ = 65.6, 68.5, 70.5, 71.4, 71.5, 105.8, 114.2, 125.4, 125.9, 126.4, 128.7, 131.2, 134.5, 141.5, 144.7, 145.0, 154.0. See also ref. [9].

8-12 PF_6: **5**-2 PF_6 (58.4 mg, 0.083 mmol), **6** (24.2 mg, 0.092 mmol), and **4**-4 PF_6 (62.9 mg, 0.020 mmol) were dissolved in dry DMF (6 mL), and the solution was stirred for 2 d at room temperature and atmospheric pressure. Then, further quantities of **5**-2 PF_6 (60.2 mg, 0.085 mmol) and **6** (25.5 mg, 0.096 mmol) were added to the reaction mixture, which was stirred for an extra 2 d. The reaction was worked up as described above for **4**-8 PF_6, except that column chromatography was performed using a gradient elution [SiO_2: MeOH/2 M NH_4Cl(aq)/$MeNO_2$ (7:2:1) initially, increased slowly to 2 M NH_4Cl(aq)/DMF/MeOH/$MeNO_2$ (12:10:7:1)]. Counterions were exchanged by repeated precipitation from aqueous NH_4PF_6/Me_2CO mixtures, followed by thorough washing with water to remove all traces of ammonium salts. **4**-4 PF_6 was recovered from the column and was purified by crystallization from CH_2Cl_2/Et_2O (28.2 mg, 45%). Pure **7**-8 PF_6 was isolated as a violet solid (26.3 mg, 31%, m.p. > 250 °C); UV/VIS (MeCN, 25 °C): λ_{max} (charge transfer) = 531 nm, ε = 2190 mol^{-1} dm^3 cm^{-1}; LSI-MS: m/z = 4118, 3973, 3828, 3699, and 3554 for $[M - PF_6]^+$, $[M - 2PF_6]^+$, $[M - 3PF_6]^+$, $[M - 4PF_6]^+$, and $[M - 5PF_6]^+$, respectively; ^{1}H NMR (CD_3CN, 70 °C): $\delta = 3.60$–4.00 (m, 96H), 5.55 (s, 8H), 5.68 (s, 8H), 6.00–6.20 (br. m, 18H), 6.32 (d, J = 8 Hz, 6H), 6.47 (d, J = 8 Hz, 6H), 6.61 (t, J = 8 Hz, 6H), 6.70–6.85 (br. m, 8H), 7.16–7.20 (m, 8H), 7.70 (d, J_{AB} = 8 Hz, 8H), 7.92–7.99 (m, 16H), 8.45–8.55 (m, 8H), 8.68–8.76 (m, 8H). Pure **8**-12 PF_6 was isolated as a violet solid (5.1 mg, 5%, m.p. > 250 °C); UV/VIS (MeCN, 25 °C): λ_{max} (charge transfer) = 534 nm, ε = 2640 mol^{-1} dm^3 cm^{-1}; LSI-MS: m/z = 5072, 4928, 4783, and 4673 for $[M - 2PF_6]^+$, $[M - 3PF_6]^+$, $[M - 4PF_6]^+$, and $[M - 5PF_6]^+$, respectively; ^{1}H NMR (CD_3CN, 70 °C): $\delta = 3.60$–4.10 (m, 96H), 5.58 (s, 8H), 5.68 (s, 16H), 5.95–6.25 (br. m, 24H), 6.89 (d, J = 7 Hz, 8H), 7.17 (d, J = 7 Hz, 16H), 7.75 (d,

J_{AB} = 8 Hz, 8H), 7.94 (s, 16H), 7.97 (d, J_{AB} = 8 Hz, 8H), 8.73 (d, J = 7 Hz, 8H), 8.58 (d, J = 7 Hz, 16H). (The remaining 12H belong to one set of protons attached to the naphthalene rings. The resonances of these protons are broadened into the baseline by exchange processes.)

Received: January 18, 1994 [Z 6627 IE]
German version: *Angew. Chem.* **1994**, *106*, 1316

[1] The trivial name olympiadane has been proposed for the pentacatenane which resembles the symbol of the International Olympics. See N. van Gulick, *New J. Chem.* **1993**, *17*, 619 and the preface to this paper by D. M. Walba on p. 618. The special issue (Ed.: J.-P. Sauvage) of the *New Journal of Chemistry* published in October/November 1993 on "Topology in Molecular Chemistry" contains many excellent papers relating to catenanes.

[2] It has been pointed out (A. Nickon, E. F. Silversmith, *Organic Chemistry: The Name Game*, Pergamon, New York, **1987**, p. 160) that the coat of arms of the Ciba Foundation displays a [5]catenane with its rings portrayed slightly differently than the symbol of the International Olympics. It is noted that although "neither of these concatenated emblems has chemical significance"... "both symbols promote universal brotherhood among the five continents—the former in athletics and the latter in education and knowledge."

[3] A single macrocyclization afforded a series of catenanes containing three, four, five, six, and seven rings, in which one large ring was encircled by two, three, four, five and six small rings, respectively. The structure of these catenanes is different from the linear ones described in this communication. See C. O. Dietrich-Buchecker, J. Guilhem, A.-K. Khémiss, J.-P. Kintzinger, C. Pascard, J.-P. Sauvage, *Angew. Chem.* **1987**, *99*, 711; *Angew. Chem. Int. Ed. Engl.* **1987**, *26*, 661; J.-P. Sauvage, *Acc. Chem. Res.* **1990**, *23*, 319; F. Bitsch, C. O. Dietrich-Buchecker, A.-K. Khémiss, J.-P. Sauvage, A. Van Dorsselaer, *J. Am. Chem. Soc.* **1991**, *113*, 4023; C. Dietrich-Buchecker, J.-P. Sauvage, *Bull. Soc. Chim. Fr.* **1992**, *129*, 113. Most recently, three rings have been templated around a bicyclic core. See C. O. Dietrich-Buchecker, B. Frommberger, I. Lüer, J.-P. Sauvage, F. Vögtle, *Angew. Chem.* **1993**, *105*, 1526; *Angew. Chem. Int. Ed. Engl.* **1993**, *32*, 1434.

[4] D. B. Amabilino, P. R. Ashton, A. S. Reder, N. Spencer, J. F. Stoddart, *Angew. Chem.* **1994**, *106*, 450; *Angew. Chem. Int. Ed. Engl.* **1994**, *33*, 433.

[5] P. R. Ashton, M. Blower, D. Philp, N. Spencer, J. F. Stoddart, M. S. Tolley, R. Ballardini, M. Ciano, V. Balzani, M. T. Gandolfi, L. Prodi, C. H. McLean, *New J. Chem.* **1993**, *17*, 689.

[6] P. R. Ashton, C. L. Brown, E. J. T. Chrystal, K. P. Parry, M. Pietraszkiewicz, N. Spencer, J. F. Stoddart, *Angew. Chem.* **1991**, *103*, 1058; *Angew. Chem. Int. Ed. Engl.* **1991**, *30*, 1042.

[7] D. B. Amabilino, J. F. Stoddart, unpublished results.

[8] A minor product of this reaction was shown to be the [2]catenane comprising a cyclobis(paraquat-4,4'-biphenylene)cyclophane and *one* macrocycle **1**. The compound was isolated as a purple solid (2%, m.p. 159–161 °C); positive-ion FAB-MS: m/z = 2062, 1916, and 1770 for $[M - PF_6]^+$, $[M - 2PF_6]^+$, and $[M - 3PF_6]^+$, respectively; ^{1}H NMR (CD_3CN): δ = 3.72–3.76 (m, 24H), 3.81–3.86 (m, 12H), 3.97–4.02 (m, 12H), 5.69 (s, 8H), 6.43–6.53 (m, 12H), 6.78 (t, J = 8 Hz, 6H), 7.51 (d, J = 6.5 Hz, 8H), 7.56 (d, J_{AB} = 8 Hz, 8H), 7.64 (d, J_{AB} = 8 Hz, 8H), 8.75 (d, J = 6.5 Hz, 8H); ^{13}C NMR (CD_3CN): δ = 65.7, 68.7, 70.3, 71.2, 71.4, 106.4, 114.0, 126.5, 126.6, 126.7, 128.8, 130.7, 134.3, 141.6, 145.5, 147.4, 154.2.

[9] The low solubility of **1** in acetonitrile makes the self-assembly procedure leading to the [3]catenane difficult to perform in an efficient manner.

[10] FAB-MS (Fast Atom Bombardment Mass Spectrometry) for **4**-4PF_6 was carried out on a Kratos MS80RF mass spectrometer (accelerating voltage, 3 kV; resolution, 1000) coupled to a DS90 data system and off-line Sun Workstation for processing the raw data experiments. The atom gun was an adapted saddle-field source (Ion Tech Limited) operated at ca. 8 keV and a tube current of ca. 2 mA. Krypton was used to provide a primary beam of atoms, and the samples were dissolved in a small volume of 3-nitrobenzyl alcohol which had previously been coated onto a stainless steel probe tip. Spectra were recorded in the positive-ion mode at a scan speed of 30 s per decade.

[11] For samples **7**-8PF_6 and **8**-12PF_6 LSI-MS (Liquid Secondary Ion Mass Spectrometry) was carried out on a Kratos Concept 1H mass spectrometer (accelerating voltage, 8 kV; resolution, 1000) coupled to a Sun Sparc Station with Mach3 software. The samples were dissolved in acetone, and a small volume (1–2 μL) was added to the 3-nitrobenzyl alcohol matrix. Spectra were recorded in the positive-ion mode at a scan speed of 5 s per decade. We gratefully acknowledge the assistance of Kratos Analytical, and in particular Dr. M. Kimber, Dr. H. Wight, and Dr. J. Moncur, in the collection of the mass spectra for these compounds.

[12] Apart from the linear sequence of macrocycles, several different topological isomers could be formed in the reaction that self-assembles the [5]catenane **8**-12PF_6. In particular, we may consider the possibility that an isomeric [5]catenane is formed where two cyclobis(paraquat-*p*-phenylene) rings clip onto *one* and the same component **1**. Further, it is possible that the same clipping procedure could occur simultaneously on the other ring **1**, yielding both a [6]- and a [7]catenane. There is preliminary evidence that, under appropriate conditions, these products are indeed formed. Alternatively, a cyclic dimer of the tetracationic cyclophane may also form, threading through macrocycles **1** in the [3]catenane, so as to create a cyclic [4]catenane. All these and other possibilities can be discounted on the basis of the spectroscopic data obtained for **8**-12PF_6.

[13] The ^{1}H and ^{13}C NMR spectra were recorded on a Bruker AMX400 spectrometer operating at 400.13 MHz and at 100.63 MHz, respectively. All chemical shifts are referenced by means of the residual CHD_2COCHD_2 or CHD_2CN signals to Me_4Si.

[14] The values of k_c were obtained (I. O. Sutherland, *Annu. Rep. NMR Spectrosc.* **1971**, *4*, 71) from the limiting chemical shift differences for exchanging signals by using the approximate expression $k_c = \pi(\Delta\nu)/(2)^{1/2}$. Rate constants were employed, along with the observed coalescence temperatures of the doublets for the α-CH and β-CH protons (attached to the smaller tetracationic cyclophanes in **8**-12PF_6), to calculate the $\Delta G_c^{\ddagger}$-values at the coalescence temperatures using the Eyring equation.

[15] In a highly ordered [2]catenane, in which the crown ether component (DNP38C10) incorporates two 1,5-dioxynaphthalene units, two processes corresponding to movement of the cyclic polyether through cyclobis(paraquat-*p*-phenylene) were observed: one where the included naphthalene ring is displaced, reorients itself, and then enters the cavity once again ($\Delta G_c^{\ddagger}$ = 15.8 kcal mol^{-1}), and the other where the crown ether circumrotates through the cavity of the tetracationic cyclophane ($\Delta G_c^{\ddagger}$ = 17.2 kcal mol^{-1}). See P. R. Ashton, C. L. Brown, E. J. T. Chrystal, T. T. Goodnow, A. E. Kaifer, K. P. Parry, D. Philp, A. M. Z. Slawin, N. Spencer, J. F. Stoddart, D. J. Williams, *J. Chem. Soc. Chem. Commun.* **1991**, 634.

[16] J. F. Stoddart, *Host–Guest Molecular Interactions: From Chemistry to Biology (Ciba Found. Symp.* **1991**, *158*, 5–22); J. S. Lindsey, *New J. Chem.* **1991**, *15*, 153; G. M. Whitesides, J. P. Mathias, C. T. Seto, *Science* **1991**, *254*, 1312; J. Rebek, Jr. *Molecular Recognition: Chemical and Biochemical Problems II (Spec. Publ. R. Soc. Chem.* **1992**, *111*, 65–73).

[17] J.-M. Lehn, *Science* **1993**, *260*, 1762.

[18] D. B. Amabilino, J. F. Stoddart, *Pure Appl. Chem.* **1993**, *65*, 2351.

$[Cu_{96}P_{30}\{P(SiMe_3)_2\}_6(PEt_3)_{18}]$, a New Phosphorus-Bridged Copper Cluster**

Dieter Fenske* and Werner Holstein

Cluster complexes can be synthesized by treating halogeno(phosphane) transition metal complexes with silylated phosphanes.[1] For example, reactions of silylphosphanes R_2PSiMe_3 or $RP(SiMe_3)_2$ (R = organic group) with MCl and $M'Cl_2$ (M = Cu, Ag; M' = Zn, Cd) in the presence of phosphane ligands PR_3 result in a large number of cluster complexes that contain bridging phosphido and phosphinidene ligands.[2] Several examples are summarized in Scheme 1. The steric bulk of the organic groups at the bridging P atoms has a stabilizing effect on the framework of the cluster; however, this also prevents the formation of larger units.

$[Cu_4Cl(PPh_2)_3(PnPrPh_2)_3][Cu_4(PPh_2)_4(HPPh_2)_4]$
$[Cu_{18}(PPh)_4(PPh_2)_{10}(PHPh_2)_3][Cu_{13}Cl_6(PMe_2)_9]^{2-}$
$[Cu_5(PPh_2)_5(PR_3)_3]$(R = Ph,Me)$[Cu_{12}(PPh)_6(PR_2)_6]$(R = Ph, Tolyl)
$[Cu_{14}Cl_2(PPh)_6(PMe_3)_8][Cu_{14}Cl_2(PPH)_6(PEt_3)_6]$
$[Ag_4(PPh_2)_4(PMe_3)_4][Ag_6(PPh_2)_6(tBu_3)_2]$
$[M_4Cl_4(PPh_2)_4(PnPr_3)_2]$(M = Zn,Cd)

Scheme 1.

We have now investigated analogous reactions of CuCl in the presence of phosphanes PR_3 with $P(SiMe_3)_3$. If these reactions are carried out in THF, with the exception of PEt_3 which gave

[*] Prof. Dr. D. Fenske, Dipl.-Chem. W. Holstein
Institut für Anorganische Chemie der Universität
Engesserstrasse, Geb. Nr. 30.45, D-76128 Karlsruhe (FRG)
Telefax: Int. code + (721)661921

[**] This work was supported by the Deutsche Forschungsgemeinschaft (SFB 195) and the Fonds der Chemischen Industrie.

crystalline **1**,[3] no crystalline compounds could be isolated from the resulting black solutions. In the reaction (a) the components must be used in the ratio $CuCl:PEt_3:P(SiMe_3)_3$ 1:0.5:0.6, since otherwise also in this case no crystalline products can be isolated. Compound **1** forms black crystals which are sparingly soluble in organic solvents and which react with water under decomposition.

$$CuCl \xrightarrow[PEt_3]{P(SiMe_3)_3} \underset{\mathbf{1}}{[Cu_{96}P_{30}\{P(SiMe_3)_2\}_6(PEt_3)_{18}]} \qquad (a)$$

No signals appear in the ^{31}P NMR spectrum of the reaction mixture at room temperature which could be assigned to **1**; only the resonance signals of the starting materials are observed. Even at low temperatures only very broad ^{31}P NMR signals result from solutions of **1**. The IR spectrum likewise provides very little information. Therefore in order to determine the molecular structure an X-ray crystal structure analysis was carried out.[4]

A description of the structure is problematic, like those of the recently prepared Cu–Se[5] and Cu–Te clusters.[6] The reason for this is that no small cluster building blocks are recognizable from which the complete structure might be constructed. Remarkable is, however, that in **1** (without PEt_3 ligand) a Cu:P ratio of roughly 3:1 is present. Thus, it appears appropriate to discuss the structure of **1** in terms of its relationship to and similarities with that of Cu_3P.[7]

In the structure of Cu_3P a stacking order of Cu and P atoms is observed which could also be described as an arrangement of two differently composed layers. As a result the P^{3-} ions have the high coordination number eleven. In principle, this structure is based on a trigonal Cu_6 prism centered by P^{3-} ions; the faces of the prism are occupied by additional Cu^+ ions. The coordination numbers for the Cu^+ ions vary, namely 12 (8 Cu + 4 P; 9 Cu + 3 P) and 13 (9 Cu + 4 P).

A fragment of the Cu_3P structure occurs in **1** which has an unusual structure. The cluster core is sterically shielded by 18 PEt_3 ligands (P19–P27) and six μ_2-$P(SiMe_3)_2$ groups (P16–P18) (Fig. 1). Thus, the C atoms of the ethyl groups are strongly disordered.

The substituent-free P^{3-} ligands (P1–P15) show four forms of coordination: the P atoms at the cluster periphery act as μ_6 ligands (P5, P6, P8, and P13); P1, P3, P4, P7, P9–P12, and P15 function as μ_7 ligands. Similarly high coordination numbers as those observed in Cu_3P are only found for the four P atoms (P14, P14A, P2, P2A) in the center of the cluster, which are bound to nine and ten Cu atoms, respectively.

In **1** the Cu–P contacts differ in length: they are 216.5–255.6 to the substituent-free P atoms, 221.1–227.4 to the $P(SiMe_3)_2$ groups, and 217.9–224.0 pm to the PEt_3 groups. These values are significantly smaller than those of the Cu–P bonds in Cu_3P (236.7–257.5 pm); however, they can be compared to those of phosphane-substituted Cu clusters. If it assumed that P^{3-} and $P(SiMe_3)_2^-$ ligands occur, the Cu atoms in **1** attain the formal oxidation number 1 + (d^{10} configuration). The shortest distances between these Cu atoms are 240.3–279.8 pm; the corresponding values in Cu_3P are similar (262.8–277.5 pm). Ab initio calculations on smaller Cu complexes[8] show that bonding Cu–Cu interactions can be excluded if the Cu–Cu distances lie in this range. The reason for the relatively short Cu–Cu contacts in **1** could be dispersion interactions,[9] like those which occur in PR_3-stabilized Cu_2Se clusters.

The relationship of the structure of **1** to the Cu_3P type arises from the arrangement of the P^{3-} ions, which form an ABC order of layers. Nonbonding contacts between the P^{3-} ions are assigned to distances between 374 and 484 pm. The deviations from the average planes within these layers are ±38.2 pm (layer A, C) and ±61.8 pm (layer B). With the exception of P19, P21, and P25, the P atoms of the PEt_3 and $P(SiMe_3)_2$ ligands also lie within these layers. The layers show a network structure of corner-sharing rhombuses. The short and the long face-diagonals are each linked with one another in such a way that a section of a two-dimensional network results, which is indexed according to the Schläfli system as a 3^2434 net.[10] If these rhombuses are rotated by an angle of about 10° towards one another in the plane, hexagonal layers of P atoms are formed. Thus, the phosphorus framework in **1** can be considered as a distorted section of hexagonal packing.

The Cu atoms are inserted in different ways in this network. Fifty-two Cu atoms are inserted into the P layers, in which they are surrounded by two P atoms (Cu1–Cu4, Cu7, Cu10, Cu12, Cu14–Cu16, Cu18, Cu21, Cu24, Cu27, Cu30, Cu32, Cu35, Cu37, Cu40, Cu47, Cu48—this arrangement leads to slightly bent P-Cu-P angles of 152–168°) or by three P atoms (Cu5, Cu9, Cu19, Cu33, Cu44—this arrangement leads to a trigonal planar structure). Between the layers there are 44 Cu atoms, which are surrounded by P atoms either in a trigonal planar

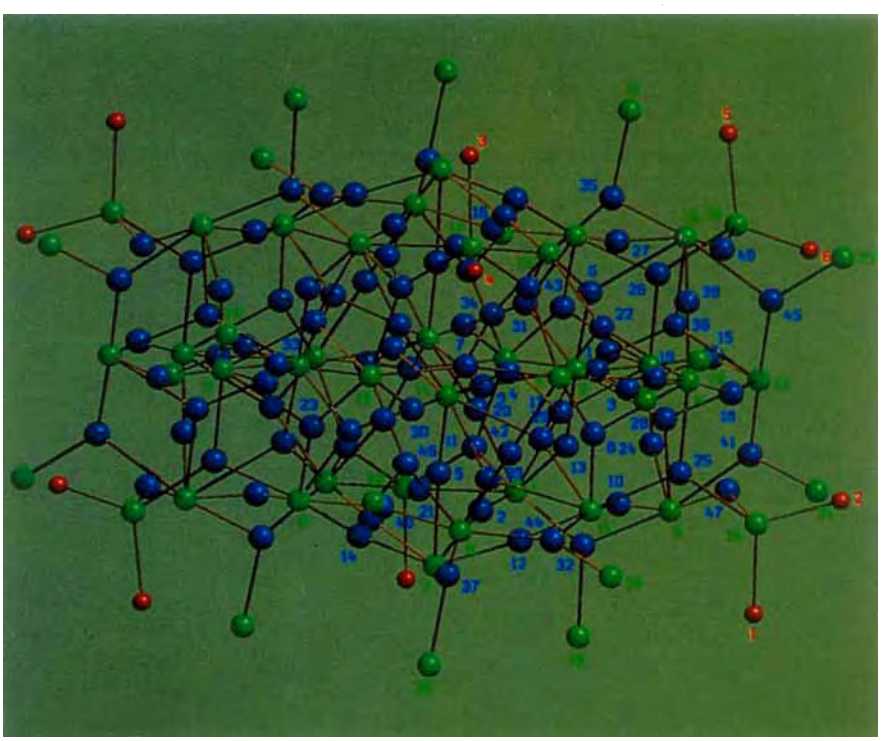


Fig. 1. Molecular structure of **1** in the crystal (without C atoms). For clarity no Cu–Cu contacts are drawn. The Cu atoms are blue, the P atoms green, and the Si atoms red. All atoms shown have been assigned color-coded numbers which correspond to the appropriate elements. In the figure only one set of symmetrically equivalent atoms is labeled (substituent-free P atoms: 1–15; $P(SiMe_3)_2$ groups: 16–18; PEt_3 ligands: 19–27).

 © VCH Verlagsgesellschaft mbH, D-69451 Weinheim, 1994 0570-0833/94/1212-1291 $ 10.00+.25/0

fashion (Cu17, Cu22, Cu23, Cu25, Cu26, Cu28, Cu36, Cu38, Cu41, Cu42, Cu45, Cu46) or in a distorted tetrahedral fashion (Cu6, Cu8, Cu11, Cu13, Cu20, Cu29, Cu31, Cu34, Cu39, Cu43).

Overall the structure of **1** can be considered as an intermediate in the formation of the Cu_3P structure. The course of events which take place during the growth of such a cluster cannot be described at present. NMR investigations show that CuCl–phosphane complexes are partly dissociated in solution and that an equilibrium exists between coordinated and free phosphane.[11] In contrast, the coordination of $P(SiMe_3)_3$ to Cu atoms is irreversible due to the elimination of $SiMe_3Cl$. The growth of the cluster is limited by the solubility of the units formed, since when cluster units become too insoluble they precipitate. The favorable position of the participating complex equilibria seems particularly important. If the stoichiometry of the reactants is changed and the PEt_3 contribution is increased, the formation of **1** can no longer be observed. From this point of view **1** is only an intermediate.

Attempts to use the reactive centers of **1** (the six μ_2-$P(SiMe_3)_2$ ligands) for the construction of larger units have been unsuccessful so far. The main reason is the poor solubility of **1**. Compound **1** decomposed on treatment with nonmetal halides such as PCl_3, $RPCl_2$, and R_2PCl; the cluster also did not react with additional CuCl.

Received: December 27, 1993 [Z6582IE]
German version: *Angew. Chem.* **1994**, *106*, 1311

[1] D. Fenske, J. Ohmer, J. Hachgenei, K. Merzweiler, *Angew. Chem.* **1988**, *100*, 1300; *Angew. Chem. Int. Ed. Engl.* **1988**, *27*, 1277.

[2] A. Eichhöfer, D. Fenske, W. Holstein, *Angew. Chem.* **1993**, *105*, 257; *Angew. Chem. Int. Ed. Engl.* **1993**, *32*, 242; A. Eichhöfer, J. Eisenmann, D. Fenske, F. Simon, *Z. Anorg. Allg. Chem.* **1993**, *619*, 1360.

[3] Preparation of **1**: $P(SiMe_3)_3$ (6.7 g) was added to a suspension of CuCl (5.3 g, 53.4 mmol) and PEt_3 (3.8 g, 32.1 mmol) in THF (50 mL). The reaction mixture turned black within a few minutes. After three hours reaction time the batch was left to stand. Black crystals of **1** formed within two weeks. (Yield 15%.)

[4] X-ray structure analysis: STOE IPDS, $Mo_{K\alpha}$, data collection and refinement: lattice constants: $a = 23.863(7)$, $b = 22.127(8)$, $c = 31.518(10)$ Å, $\beta = 98.75°$, $V = 16488 \times 10^6$ pm^3, space group: $P2_1/n$ (no. 14), $Z = 2$. $\mu(Mo_{K\alpha}) = 62.5$ cm^{-1}, $2\theta_{max} = 42°$; 51478 reflections, of which 29511 are independent. 12287 with $I > 4\sigma(I)$, 1109 parameters (Cu, P, Si1–Si4 anisotropically refined), $R_1 = 0.098$, two molecules THF per asymmetric unit could be localized. Further details of the crystal structure investigation may be obtained from the Fachinformationszentrum Karlsruhe, D-76344 Eggenstein-Leopoldshafen (FRG) on quoting the depository number CSD-58058.

[5] H. Krautscheid, D. Fenske, G. Baum, M. Semmelmann, *Angew. Chem.* **1993**, *105*, 1364; *Angew. Chem. Int. Ed. Engl.* **1993**, *32*, 1302; D. Fenske, H. Krautscheid, *ibid.* **1990**, *102*, 1513 and **1990**, *29*, 1453.

[6] D. Fenske, J. Steck, *Angew. Chem.* **1993**, *105*, 254; *Angew. Chem. Int. Ed. Engl.* **1993**, *32*, 238.

[7] O. Olofsson, *Acta Chem. Scand.* **1972**, *26*, 2777; M. Mansmann, *Z. Kristallogr. Kristallgeom. Kristallphys. Kristallchem.* **1966**, *122*, 399.

[8] C. Kölmel, R. Ahlrichs, *Z. Phys. Chem.* **1990**, *94*, 5536.

[9] S. Dehnen, A. Schäfer, D. Fenske, R. Ahlrichs, *Angew. Chem.* **1994**, *106*, 786; *Angew. Chem. Int. Ed. Engl.* **1994**, *33*, 746.

[10] W. B. Pearson, *The Crystal Chemistry and Physics of Metals and Alloys*, Wiley, New York, **1972**.

[11] G. Costa, E. Reisenhofer, L. Stefani, *J. Inorg. Nucl. Chem.* **1965**, *27*, 2581.

An Organic Molecule with a Rigid Cavity of Nanosize Dimensions

Peter Timmerman, Willem Verboom, Frank C. J. M. van Veggel, Willem P. van Hoorn, and David N. Reinhoudt*

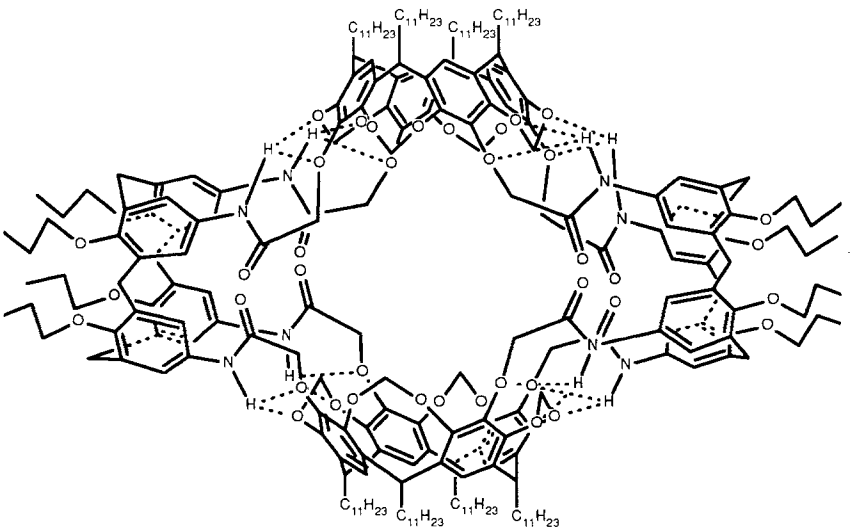
The rapidly expanding field of supramolecular chemistry[1–3] has revealed a number of useful building blocks for the synthesis of artificial receptor molecules, for example calixarenes,[4] cyclodextrins,[5] and resorcinol-based cavitands.[6] Nature constructs an almost infinite number of macromolecular receptors by the systematic combination of a limited number of building blocks. We are currently exploring an analogous approach for the synthesis of host molecules by the combination of simple rigid building blocks.[7] Recently, this method has resulted in the synthesis of several new receptor molecules with unique complexation properties.[8–11] These molecules possess small cavities suitable for the complexation of alkali metal cations, anions, or small organic molecules. The synthesis of receptor molecules with large cavities generally meets with the problem that such cavities collapse because of the inherent flexibility of large organic molecules. Recently, a few examples of receptor molecules with large, relatively open, rigid cavities were reported by Sanders et al.[12] in which rigid planar components (porphyrins and cholic acid derivatives) were linked by single covalent bonds.

In this paper we describe a new approach to receptor molecules with large cavities by the combination of building blocks which already possess a cavity, namely calix[4]arenes and resorcinol-based cavitands. The assembly of four such units in a cyclic array provides a convergent route for the synthesis of holand **1**,[13] an extremely rigid host molecule in which the cavities of the four components form a shielded hole of nanosize dimensions.

As part of our work on the synthesis of selectively functionalized resorcinol-based cavitands,[14] we studied the reaction between cavitand **2**[15] and upper rim 1,2-functionalized calix[4]arene **3**. Compound **3** was prepared in 72% overall yield by reduction of the corresponding 1,2-dinitro compound[16] and subsequent reaction with two equivalents of α-chloroacetyl chloride. When this reaction was performed in $CH_3CN/Cs_2CO_3/KI$ (ratio **2**/**3** 1:1), we isolated compound **4a** (20% yield), in which the calix[4]arene moiety is coupled in a 1,2 fashion, that is to two neighboring arene rings of **2** with the *endo* stereochemistry, together with 32% of the *exo* isomer **4b**.[17] In addition to these 1:1 adducts small amounts of the three possible isomeric 2:1 products **5a–c** were formed. Products in which the calix moiety is coupled in a 1,3 (distal) fashion to the cavitand could not be detected. When **2** was treated with two equivalents of **3** only the 2:1 addition products were isolated in an almost statistical ratio of *endo-endo* (**5a**, shown), *endo-exo* (**5b**), and *exo-exo* (**5c**) in a total yield of 64%.[18]

Apparently in this reaction there is a slight preference for the formation of the *exo* 1:1 product. The formation of the *endo* 1:1 product is favored by the introduction of functional groups at the calix[4]arene fragment that favorably interact with the cavitand moiety in the transition state. Reaction of a 1:1 mixture of **2** and calix[4]arene **6**,[19] in which two nitro groups have been introduced, exclusively gave the *endo* 1:1 isomer **7** together with small amounts of the 2:1 products **8a** (*endo-endo*) and **8b** (*endo-*

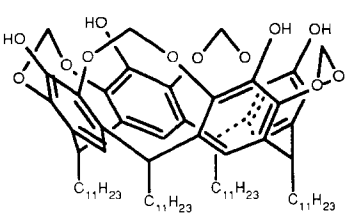
[*] Prof. Dr. Ir. D. N. Reinhoudt, Drs. P. Timmerman, Dr. W. Verboom, Dr. Ir. F. C. J. M. van Veggel, Ir. W. P. van Hoorn
Laboratory of Organic Chemistry, University of Twente
P.O. Box 217, NL-7500 AE Enschede (The Netherlands)
Telefax: Int. code + (31)53356024



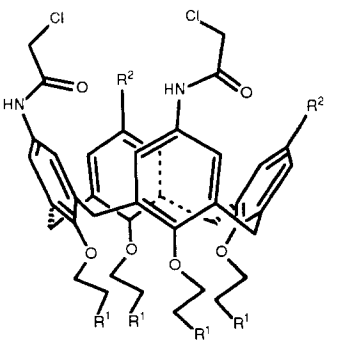
1

exo). Because of its instability **7** was isolated, after silylation of its free hydroxyl groups,[20] as **9** in 41% yield. The nitro groups in **9** could easily be reduced to amino groups by using Raney Ni/hydrazine.[16] The subsequent reaction with α-chloroacetyl chloride led to the bis(2-chloroacetamide) derivative **10** in quantitative yield. Compound **10** was dissolved in dimethylformamide (DMF; 5 mM) and desilylated with CsF at 80 °C; the solution was subsequently stirred for 48 hours in the presence of Cs_2CO_3 and KI to give two reaction products. The more polar product (isolated in 27% yield) is the calix[4]arene-based carcerand **11** with one molecule of DMF inside its interior. The presence of this permanent guest molecule is evident from both FAB mass spectrometry ($m/z = 2126$ (100%) $[M + DMF + Na^+]$) and ^1H NMR spectroscopy (two different singlets for the two methyl groups of DMF at $\delta = 0.66$ and -0.86.[21])

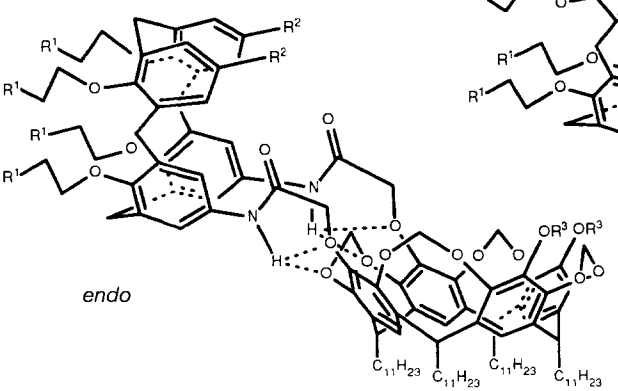
The second product (isolated in 26% yield) is the desired holand **1**. This compound could also be synthesized in 35% yield by dropwise addition of an equimolar solution of **12**[22] and **2** in DMF to a suspension of Cs_2CO_3 and KI in DMF. The FAB mass spectrum proves the formation of the 2:2 structure ($m/z = 4084$ (100%) $[M + Na^+]$) and the ^1H NMR spectrum (Fig. 1) reflects the high degree of symmetry expected for **1**. For its size, the molecule is extremely rigid: The calix[4]arene and cavitand moieties,



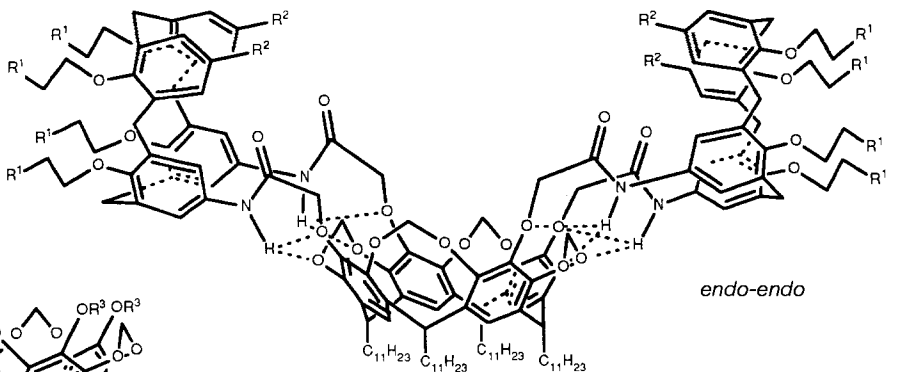
2



3: R^1=OCH_2CH_3, R^2=H
6: R^1=CH_3, R^2=NO_2



endo

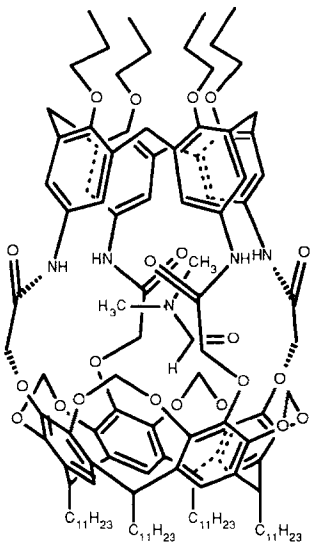


endo-endo

4: $R^1 = OCH_2CH_3$, $R^2 = R^3 = H$; **a**: *endo*, **b**: *exo*
7: $R^1 = CH_3$, $R^2 = NO_2$, $R^3 = H$; *endo*
9: $R^1 = CH_3$, $R^2 = NO_2$, $R^3 = Si(CH_3)_2C(CH_3)_3$; *endo*
10: $R^1 = CH_3$, $R^2 = NHC(O)CH_2Cl$, $R^3 = Si(CH_3)_2C(CH_3)_3$; *endo*

5: $R^1 = OCH_2CH_3$, $R^2 = H$
a: *endo-endo*, **b**: *endo-exo*, **c**: *exo-exo*
8: $R^1 = CH_3$, $R^2 = NO_2$
a: *endo-endo*, **b**: *endo-exo*
12: $R^1 = CH_3$, $R^2 = NHC(O)CH_2Cl$, *endo-endo*

 © VCH Verlagsgesellschaft mbH, D-69451 Weinheim, 1994 0570-0833/94/1212-1293 $ 10.00+.25/0



11

which are intrinsically rigid, are connected by two highly organized spacers. This becomes evident when the ^{1}H NMR spectra of compounds **3** and **5a** are compared with that of **1**. The signals of the aromatic protons *ortho* to the amide in **3** differ only by 0.08 ppm in chemical shift as a result of almost free rotation around the C(arene)–N bond. However, in **5a** the $\Delta\delta$ value is much greater because two of these calixarene moieties are coupled with the cavitand. The 0.85 ppm chemical shift difference is illustrative for the rigidity in the amide spacers of **5a**. In holand **1** the mobility of the calixarene fragments is further reduced to give a $\Delta\delta$ value of 1.0. The rigidity of the structure of **1** is even better exemplified when the chemical shift difference between the two methylene protons in the spacer in **3** and **5a** is compared with that in **1**. Whereas these protons in **3** give a singlet, this splits in **5a** to show an AB system with $\Delta\delta = 0.4$.

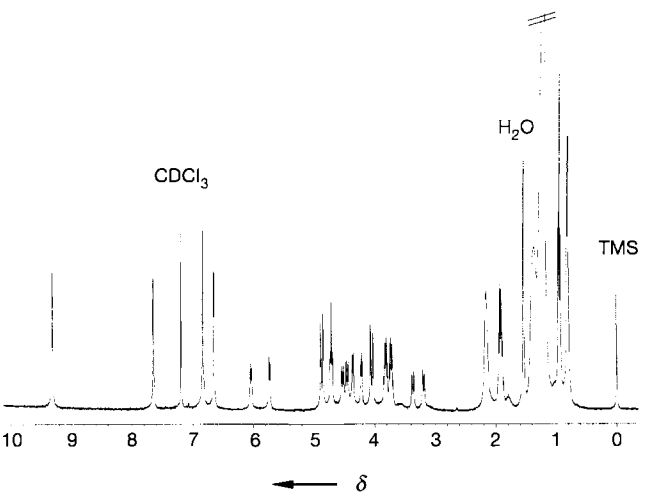


Fig. 1. ^{1}H NMR spectrum (400 MHz) of **1** in $CDCl_3$ at room temperature.

The motion of the calixarene fragments still present in **5a** mainly takes place by rotation around the O–CH_2 bond in the spacer. When this motion is finally frozen completely in **1** the $\Delta\delta$ value between the two AB doublets is 0.85. The above mentioned rigidity of **1** is partly a result of the three-center hydrogen bonds between the amide hydrogen atoms, the oxygen atoms in the spacer itself, and the oxygen atoms in the methylenedioxy bridges. These bonds are indicated in **1** with dashed lines.[23]

When compound **10** was used at a higher concentration (11 mM), the yields decreased from 27 (**11**) and 26% (**1**) to 12 (**11**) and 12% (**1**), respectively. Apparently, polymerization predominates at this concentration.

Holand **1** contains a cavity of nanosize dimensions. According to CPK models, the axes are about 1.5 and 2.0 nm long. The calculated internal volume is approximately 1.0 nm^3 (1000 $Å^3$). Figure 2 represents a picture of the energy-minimized structure

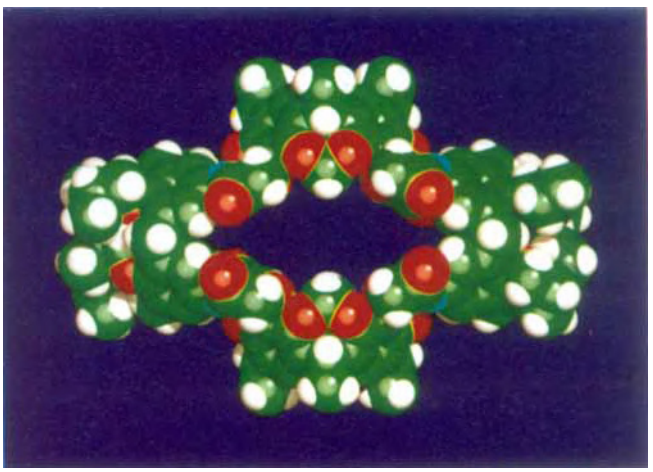


Fig. 2. Energy-minimized structure of holand **1** (undecyl chains have been replaced by methyl chains for simplicity).

of **1**. This minimized structure was subjected to a 50 ps dynamics simulation at 300 K in a $CHCl_3$ box with 46 Å edges. During this simulation four chloroform molecules entered the cavity and stayed there for the rest of the simulation without changing the shape of the cavity. This supports likewise the rigid structure of **1**. The organization of the amide spacers was clearly observed in this simulation. Although the hydrogen bonds were sometimes broken, they reformed after a short period of time. Rotation around the C(arene)–N bond was not observed.

Holand **1** is expected to have unique complexation properties. The size of the cavity permits complexation of host molecules which themselves are good complexing agents. Such complexation studies are currently under investigation.

Received: December 28, 1993 [Z 6587 IE]
German version: *Angew. Chem.* **1994**, *106*, 1313

[1] J. M. Lehn, *Angew. Chem.* **1990**, *102*, 1347–1362; *Angew. Chem. Int. Ed. Engl.* **1990**, *29*, 1304–1319.
[2] C. J. Pedersen in *Synthetic Multidentate Macrocyclic Compounds* (Eds.: R. M. Izatt, J. J. Christensen), Academic Press, New York, **1978**.
[3] a) D. J. Cram, K. N. Trueblood, *Top. Curr. Chem.* **1981**, *98*, 43–106; b) K. N. Trueblood, C. B. Knobler, E. F. Maverick, R. C. Helgeson, S. B. Brown, D. J. Cram, *J. Am. Chem. Soc.* **1981**, *103*, 5594–5596.
[4] a) C. D. Gutsche in *Calixarenes, Monographs in Supramolecular Chemistry, Vol. 1* (Ed.: J. F. Stoddart), The Royal Society of Chemistry, Cambridge, **1989**; b) *Calixarenes: a Versatile Class of Macrocyclic Compounds* (Eds.: J. Vicens, V. Böhmer), Kluwer, Dordrecht, **1991**.
[5] J. Szejtli in *Cyclodextrin Technology* (Ed.: J. Szejtli), Kluwer, Dordrecht, **1988**.
[6] a) D. J. Cram, S. Karbach, H.-E. Kim, C. B. Knobler, E. F. Maverick, J. L. Ericson, R. C. Helgeson, *J. Am. Chem. Soc.* **1988**, *110*, 2229–2237; b) J. A. Tucker, C. B. Knobler, K. N. Trueblood, D. J. Cram, *ibid.* **1989**, *111*, 3688–3699.
[7] L. C. Groenen, D. N. Reinhoudt in *Calix[4]arenes, Molecular Platforms for Supramolecular Structures*, in *Supramolecular Chemistry* (Eds.: V. Balzani, L. De Cola), Kluwer, Dordrecht, **1992**, p. 51.
[8] a) E. Ghidini, F. Ugozzoli, R. Ungaro, S. Harkema, A. A. El-Fadl, D. N. Reinhoudt, *J. Am. Chem. Soc.* **1990**, *112*, 6979–6985; b) E. J. R. Sudhölter, P. D. Van der Wal, M. Skowronska-Ptasinska, A. Van den Berg, P. Bergveld, D. N. Reinhoudt, *Recl. Trav. Chim. Pays-Bas* **1990**, *109*, 222–225; c) Z. Brzozka, B. H. M. Lammerink, D. N. Reinhoudt, E. Ghidini, R. Ungaro, *J. Chem. Soc. Perkin Trans. 2* **1993**, 1037–1040; d) W. F. Nijenhuis, E. G. Buitenhuis, F. De Jong, E. J. R. Sudhölter, D. N. Reinhoudt, *J. Am. Chem. Soc.* **1991**, *113*, 7963–7968.
[9] W. I. Iwema Bakker, M. Haas, C. Khoo-Beattie, R. Ostaszewski, S. M. Franken, H. J. den Hertog, Jr., W. Verboom, D. de Zeeuw, S. Harkema, D. N. Reinhoudt, *J. Am. Chem. Soc.* **1994**, *116*, 123–133.

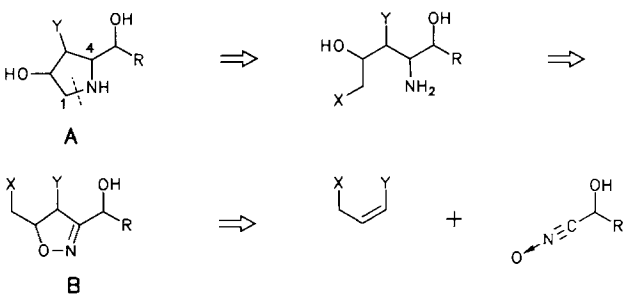
[10] W. F. van Straaten-Nijenhuis, A. R. van Doorn, A. M. Reichwein, F. de Jong, D. N. Reinhoudt, *J. Am. Chem. Soc.* **1991**, *113*, 3607–3608.
[11] D. M. Rudkevich, Z. Brzozka, M. Palys, H. Visser, W. Verboom, D. N. Reinhoudt, *Angew. Chem.* **1994**, *106*, 480–482; *Angew. Chem. Int. Ed. Engl.* **1994**, *33*, 467–468.
[12] a) S. Anderson, H. L. Anderson, J. K. M. Sanders, *Acc. Chem. Res.* **1993**, *26*, 469–475; b) L. G. Mackay, R. P. Bonar-Law, J. K. M. Sanders, *J. Chem. Soc. Perkin Trans. 1* **1993**, 1377–1378; c) R. P. Bonar-Law, L. G. Mackay, J. K. M. Sanders, *J. Chem. Soc. Chem. Commun.* **1993**, 456–458.
[13] A holand is defined as a ligand which contains a permanent hole (cavity).
[14] P. Timmerman, M. G. A. van Mook, W. Verboom, G. J. van Hummel, S. Harkema, D. N. Reinhoudt, *Tetrahedron Lett.* **1992**, *33*, 3377–3380.
[15] This compound was prepared as described in: J. C. Sherman, C. B. Knobler, D. J. Cram, *J. Am. Chem. Soc.* **1991**, *113*, 2194–2204.
[16] J.-D. van Loon, J. F. Heida, W. Verboom, D. N. Reinhoudt, *Recl. Trav. Chim. Pays-Bas* **1992**, *111*, 353–359.
[17] The configuration was determined by using NOE spectroscopy. In a compound very similar to **5c** in which the undecyl chains have been replaced by methyl chains, a short-distance contact was observed between the protons of the unsubstituted aromatic rings and the protons of the methyl groups, indicating that this compound adopts the *exo* configuration. The configurations of all the other compounds could be easily determined by comparing their ^{1}H NMR spectra with that of **5c**.
[18] Compounds **5a–c** have large hydrophobic surfaces and show selective complexation of several corticosteroids in $CDCl_3$ solutions. These results will be described elsewhere.
[19] P. Timmerman, W. Verboom, D. N. Reinhoudt, A. Arduini, S. Grandi, A. R. Sicuri, A. Pochini, R. Ungaro, *Synthesis*, **1994**, 185–189.
[20] The crude reaction mixture was first subjected to a silylation reaction with 20 equiv of *tert*-butyldimethylsilyl chloride, 20 equiv of NEt_3, and a catalytic amount of dimethylaminopyridine in CH_2Cl_2 for 24 h at room temperature, because of the instability of **7** on silica gel.
[21] This incarceration of solvent molecules has been frequently observed by Cram, see ref. [15] and also: a) D. J. Cram, S. Karbach, Y. H. Kim, L. Baczynskyj, K. Marti, R. M. Sampson, G. W. Kalleymeyn, *J. Am. Chem. Soc.* **1988**, *110*, 2554–2560; b) J. C. Sherman, D. J. Cram, *ibid.* **1989**, *111*, 4527–4528; c) J. A. Bryant, M. T. Blanda, M. Vincenti, D. J. Cram, *J. Chem. Soc. Chem. Commun.* **1990**, 1403–1405. The stability of **7** was determined by an exchange experiment in [D$_7$]DMF at 100 °C for 1 h. No exchange of DMF was observed at this temperature. Further work on these carcerands will be described elsewhere.
[22] Compound **12** was obtained from **8a** in quantitative yield in a similar way as **10** was prepared starting from **9**.
[23] Evidence for these hydrogen bonds was obtained from a quantitative NOE analysis performed with **5a** in which the distance between the aromatic protons *ortho* to the amide and the outer methylene proton was determined to be 2.5 Å and the distance between the amide protons and the outer methylene proton was determined to be 2.8 Å.

A New Synthesis of 1,3,4-Trideoxy-1,4-iminoglycitols of Varying Chain Length by (C_3 + C_n)-Coupling of Allyl Halides with Glyconitrile Oxides**

Rudolf Müller, Thomas Leibold, Michael Pätzel, and Volker Jäger*

Dedicated to Professor Heinz Günther Viehe on the occasion of his 65th birthday

Iminoglycitols such as **A** have attracted attention both as target compounds and as intermediates for polyhydroxylated N-bicycles. Some of the well-known representatives of this series that often act as powerful glycosidase inhibitors are pyrrolidine derivatives such as 1,4-dideoxy-1,4-imino-L-arabinitol (LAB)[2] and -D-lyxitol,[3–5] piperidines such as deoxynojirimycin (DNJ) and DNJ derivatives or analogues,[6] as well as indolizidine derivatives of the swainsonine[7] or castanospermine type.[8] The increasing interest in simple syntheses of specific compounds and derivatives with related unnatural structures stems from their potential for pharmaceutical application: inhibition of the corresponding enzymes is often accompanied by diverse physiological effects (anti-retroviral, -bacterial, -tumoral effects; reduction of the blood-sugar level). Topographical equivalence with the corresponding glycoside[3, 6, 9] or pyranosyl cation[4, 6] generally serves as a guideline to find active products of this type. The aim of our investigations is to provide access to unnatural analogues in the pyrrolidine series—by omission of OH groups, by placing them in different positions, or by inclusion of additional ones. Recently, two routes to *cis*-dihydroxypyrrolidines, based on a nitroaldol reaction and aminopentenediol cyclizations, have been presented.[5] Here we describe a third approach to 4-hydroxypyrrolidines (1,3,4-trideoxy-1,4-iminoglycitols) for which the highly selective, catalytic hydrogenation of 5-halomethyl-4,5-dihydro-1,2-oxazoles (**B**) has been developed as a new key step (Scheme 1). This route is exemplified in detail by the sequence leading to L-*ribo*-hexitol **5** and to the diastereomers **6**–**8** (Scheme 2).



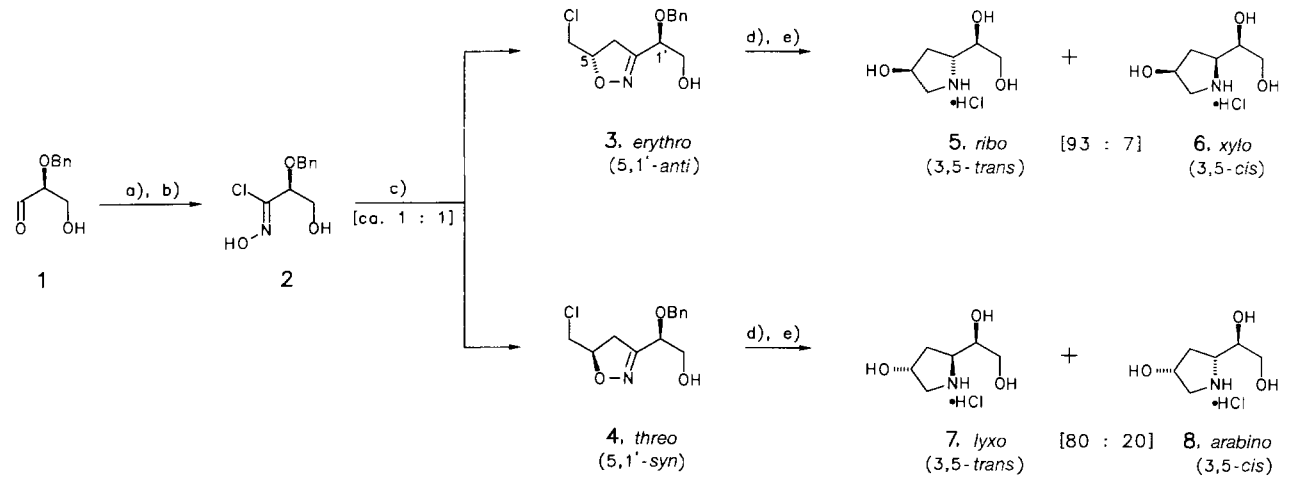
Scheme 1. Retrosynthesis of 1,4-iminoglycitols (hydroxypyrrolidines) **A** by the isoxazoline route. Y = H, R = $(CHOH)_xH$: this work; Y = OH, R = $(CHOH)_xH$: Refs. [10,19]. The hydroxypyrrolidines **A** are named as 1,4-iminoglycitols to facilitate the comparison with the structures and configurations of natural glycosidase substrates.

The glyceraldehyde **1**, available from diethyl L-(+)-tartrate,[13] was converted into the hydroxamic acid chloride **2** by oximation/chlorination.[12a] Cycloaddition of the nitrile oxide with allyl chloride according to Huisgen's in situ method[12b] gave, as expected,[14] the 5-chloromethyl-dihydro-1,2-oxazoles **3**/**4** as an approximately 1:1 mixture of diastereomers, each of which was isolated in 46% yield (in gram quantities) after chromatographic separation. Thus, an entry to two series of stereoisomers is provided (actually to four if the D-tartrate is also taken into account).

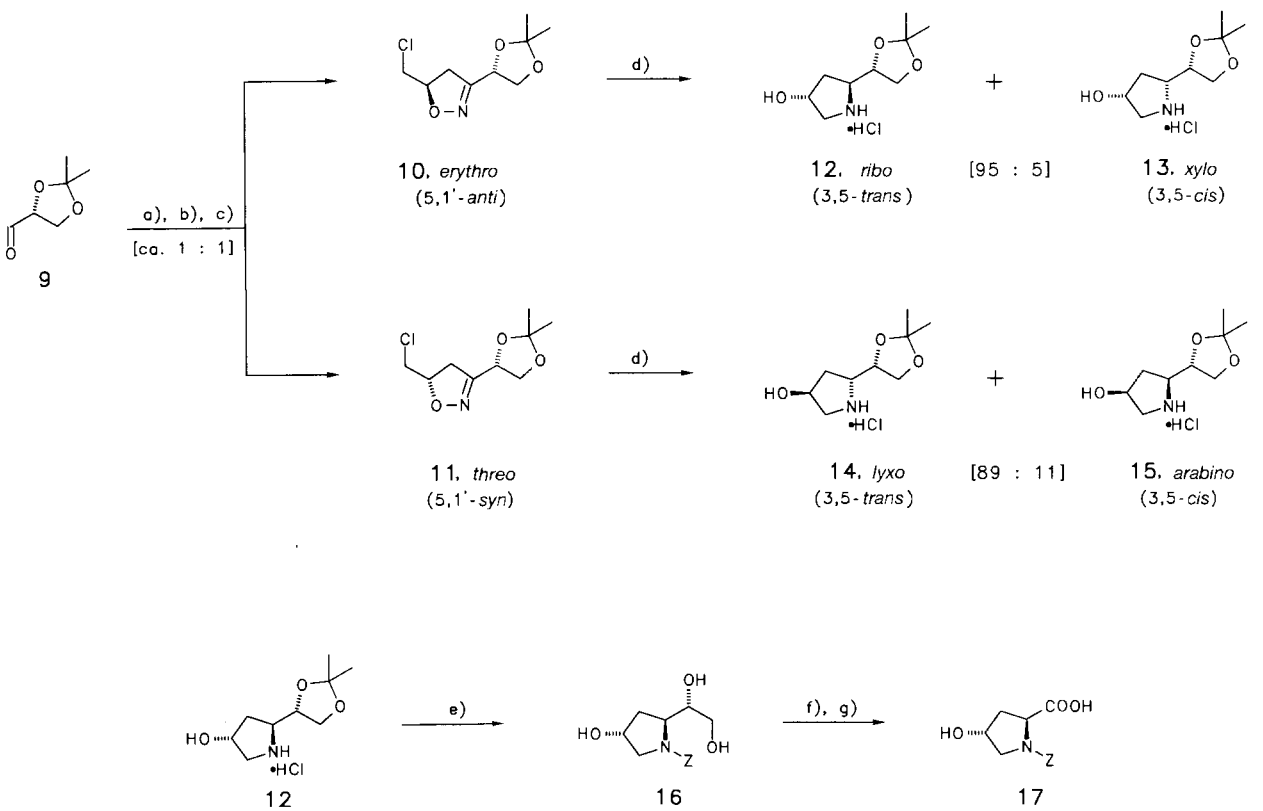
The catalytic hydrogenation of **3** and **4** in the presence of platinum on charcoal gave, in each case, the corresponding *trans*-hydroxypyrrolidine as major product. Thus, the 2-*O*-benzyl derivatives (L-*ribo*/L-*xylo*) were formed from **3** with a diastereomer ratio (*dr*) of 93:7, and the L-*lyxo*/L-*arabino*-isomers from **4** with *dr* = 80:20. The free iminoglycitols **5**/**6** and **7**/**8**, respectively, were obtained after removal of the O-protecting benzyl group with H_2/palladium on charcoal. The major isomer **5** was obtained pure in 73% yield from the mixture of **5**/**6** by crystallization (*dr* > 95:5 according to ^{1}H and ^{13}C NMR). The bromo compounds (from **2**/Et_3N and allyl bromide) corre-

[*] Prof. Dr. V. Jäger,[+] Dr. R. Müller, Dipl.-Chem. T. Leibold,[+] Dr. M. Pätzel
Institut für Organische Chemie der Universität
Am Hubland, D-97074 Würzburg (FRG)
[+] New address: Institut für Organische Chemie und
Isotopenforschung der Universität
Pfaffenwaldring 55, D-70569 Stuttgart (FRG)
Telefax: Int. code + (711)685-4321

[**] Syntheses with Isoxazolines, Part 22. This work was supported by the Deutsche Akademische Austauschdienst (postdoctoral fellowship for Dr. M. Pätzel), the Bundesministerium für Forschung und Technologie (AIDS-Forschungsförderung im Bundesgesundheitsamt), the Deutsche Forschungsgemeinschaft, the Fonds der Chemischen Industrie, and Bayer AG, Wuppertal; we thank Frau Sabine Ebeling for experimental assistance. Part 21: [1]



Scheme 2. Synthesis of 1,3,4-trideoxy-1,4-iminohexitols **5**–**8** of the L series from 2-*O*-benzyl-L-glyceraldehydes **1** [11,18]: a) $HONH_3Cl$, Na_2CO_3, H_2O, 25 °C, 20 h; 95% oxime as (83:17) *E*/*Z* mixture, $[\alpha]_D^{20} = -62.4$ ($c = 1.51$ in EtOH); b) *N*-chlorosuccinimide (NCS), *N*,*N*-dimethylformamide (DMF), HCl (cat.), 25 °C, 1 h (cf. ref. [12]); 96% **2**, colorless oil, $[\alpha]_D^{24} = -79.7$ ($c = 0.780$ in MeOH); c) 6 equiv $ClCH_2$-CH=CH_2, Et_3N, Et_2O, 25 °C, 3 d: diastereomer ratio (*dr*) of the crude product = 50:50; medium-pressure liquid chromatography (MPLC) LiChroprep Si60, 15–25 μm, *t*BuOMe: **3**, $[\alpha]_D^{24} = -7.4$ ($c = 0.85$ in CH_2Cl_2), and **4**, $[\alpha]_D^{24} = -193$ ($c = 0.645$ in CH_2Cl_2), each 46% of colorless, analytically pure oil; d) H_2, Pt/C, MeOH, 25 °C, 24 h; yield from **3** quant. with *dr* = 93:7 (^{13}C NMR), $[\alpha]_D^{22} = +29.4$ ($c = 0.715$ in MeOH); yield from **4**: 94% with *dr* = 80:20, $[\alpha]_D^{24} = +35.9$ ($c = 0.570$ in MeOH); e) H_2, Pd/C, MeOH/conc. HCl (10:1), 25 °C, 3 d; after crystallization from MeOH 73% 5 · HCl with *dr* > 97:3, m.p. 132–133 °C, $[\alpha]_D^{24} = +26.1$ ($c = 0.640$ in H_2O), and 93% **7**/**8** (hydrochloride) with *dr* = 80:20, light yellow oil, solidified at −20 °C (m.p. 109–110 °C).



Scheme 3. Synthesis of 1,3,4-trideoxy-1,4-iminohexitols of the D series from 1,2-*O*-isopropylidene-D-glyceraldehyde **9**, and correlation with *trans*-4-hydroxy-L-proline (Z derivative) [11, 18]. a) $HONH_3Cl$, K_2CO_3, H_2O, 0 → 25 °C, 2 h; after distillation (bath temp. 100–120 °C/0.1 Torr): 70% oxime, *E*/*Z* = 60:40 (^1H NMR), $[\alpha]_D^{20} = -74.6$ ($c = 1.60$ in $CHCl_3$); b) NCS, DMF, HCl (cat.), 25 °C, 18 h (cf. ref. [12]); 77%, colorless powder, m.p. 82–83 °C; c) 5 equiv $ClCH_2$-CH=CH_2, Et_3N, Et_2O, 3 d; crude product *dr* = 50:50. MPLC (cf. Scheme 2), eluent petroleum ether/EtOAc 4:1. **10**: 33%, $[\alpha]_D^{23} = -88.7$ ($c = 1.22$ in $CHCl_3$); **11**: 37% (3.64 g for 42.5 mmol batch), $[\alpha]_D^{23} = +85.1$ ($c = 1.02$ in $CHCl_3$); both colorless oils with b.p. 130 °C/0.04 Torr; d) H_2, Pd/C, MeOH, 25 °C, 18 h; **12**/**13** in 96% yield with *dr* = 95:5; **14**/**15** in 97% yield with *dr* = 89:11; e) ClCOOBn, Ag_2O, CH_2Cl_2/MeOH (20:1), 25 °C, 4 d, filtration/hydrolysis with silica gel; 73% of **16** as ca. (2:1)-rotamer mixture, $[\alpha]_D^{20} = -53.4$ ($c = 0.500$ in MeOH); f) $NaIO_4$, H_2O/MeOH 2:1, 25 °C, 45 min, then Br_2 (2 equiv)/MeOH, 25 °C, 1 h (according to ref. [16]); 79% of *Z*-L-4-hydroxyproline methyl ester as (55:45)-rotamer mixture, $[\alpha]_D^{21} = -50.1$ ($c = 0.340$ in MeOH); g) K_2CO_3, H_2O/EtOH 5:2, 25 °C, 7 d; MPLC (LiChroprep RP 18, 15–25 μm, CH_2Cl_2/MeOH 97:3); 66% of **17**, analytically pure (55:45)-rotamer mixture (based on NMR) and according to **12** probably about 95:5 *trans*/*cis*-mixture; $[\alpha]_D^{24} = -62.1$ ($c = 0.800$ in $CHCl_3$); ref. [17]: $[\alpha]_D^{20} = -72$ ($c = 1.00$ in $CHCl_3$) for Z-*trans*-4-hydroxyproline and $[\alpha]_D^{24} = +26.3$ ($c = 1.0$ in $CHCl_3$) for Z-*cis*-4-hydroxyproline.

sponding to **3**/**4** similarly gave the 2-*O*-benzyl derivatives of **5**/**6** and **7**/**8**, respectively, in the form of hydrobromides (*dr* = 91:9 and 73:27, respectively), but with somewhat lower stereoselectivity.[11, 15]

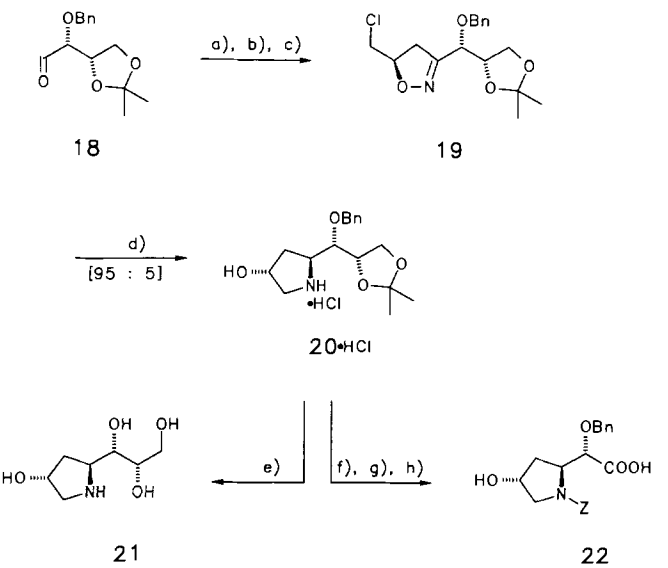
The route to compounds of the D series—in principle open by analogous elaboration of the enantiomeric D-tartrates—was started from 2,3-isopropylidene-D-glyceraldehyde (**9**), to simultaneously check if the structure of the side chain at the 3-position would somehow affect the course of the hydrogenation (Scheme 3). The *erythro*-dihydro-1,2-oxazole (**10**, 5,1′-*anti*) was hydrogenated with platinum on charcoal, again with high selectivitity (**12**/**13** with *dr* = 85:15; from **11**: **14**/**15** with *dr* = 73:27), although palladium on charcoal was shown to be more advantageous here: with Pd the product from the reduction/cyclization, the D-*ribo*-iminohexitol (**12**), was isolated in 96% yield; it contained only about 5% of the *xylo* isomer **13**. The D-*lyxo*/D-*arabino* products **14**/**15** were obtained in a 89:11 ratio from the *threo*-dihydro-1,2-oxazole (**11**, *syn*).[11] The configuration of **12** at C 2/C 4 (D-*ribo*) was established as follows: N-protection and hydrolysis to **16**, subsequent oxidative degradation with periodate/bromine in methanol according to Lichtenthaler et al.,[16] and finally hydrolysis of the methyl ester with base gave the known reference compound *N*-Z-4-hydroxyproline (**17**, Scheme 3).[17]

These cases—and others[19]—show that the stereochemical course of the hydrogenation of dihydro-1,2-oxazoles (isoxazolines) is determined by several factors. The configuration at C 1′ plays some role (cf. reduction of the pairs **3**/**4**, **10**/**11**),[20] as do the catalyst system and the structure of the side chains in the 3- and/or 5-position. Thus, with other adducts prepared from **9**, only insignificant induction (about 60:40) was observed for dihydro-1,2-oxazoles bearing $TosOCH_2$, MeOOC, or no substituent at the 5-position (see below). Nevertheless, with the appropriate combination of all of these factors this sequence should be suitable for the formation of higher trideoxyiminoglycitols from other glyconitrile oxides.

This expectation was confirmed by the outcome of the synthesis of imino-L-*talo*-heptitol **21**, a tetrol. For this synthesis we used the C_4 building block **18**, a threose derivative, also readily available[21] in both enantiomeric forms from tartrate or 2-*O*-benzylthreitol (Scheme 4).

The cycloadduct with allyl chloride (**19**) was obtained in 31% yield after chromatographic separation (in addition to 32% of the 5-epimer); hydrogenation with Pt catalyst gave the *trans*-hydroxypyrrolidine **20** as a single stereoisomer (>95:5 according to ^{13}C NMR) and further, after removal of the protecting groups, the iminoheptitol **21** (six steps, 16% overall yield from **18**). The configuration of **20** at C4 was established at the dihydro-1,2-oxazole stage, by degradation of the previously mentioned 5-epimer of **19** (hydrolysis, cleavage with periodate, and aldehyde reduction); in this manner the D-enantiomer of **4** (*threo*) was obtained. A similar degradation to the dihydroxyhomoproline derivative **22**[22] was carried out with **20** (Scheme 4).

The results described here show that the catalytic hydrogenation of isoxazolines (4,5-dihydro-1,2-oxazoles)[20] contains yet unrecognized possibilities for stereoselective reductions and thus supplements the well-investigated "predictable" $LiAlH_4$ reduction.[20, 23] The mechanism of this transformation is not yet apparent: the catalytic reduction of 5-halomethyl-isoxazolines, such as **3**, to the hydroxypyrrolidine **5** involves four steps (N–O and C=N reduction, rotation to a conformation suitable for cyclization, and intramolecular substitution at C1 by the N atom) moreover, the sequence might be structure-dependent (*dr* of 60:40 to 95:5). A point to be stressed is that all results on catalytic reductions of isoxazolines—whether leading to amino



Scheme 4. Synthesis of 1,3,4-trideoxy-1,4-imino-L-*talo*-hepitol **20** and dihydroxy-L-homoproline **21**. a), b), c) reactions as in Scheme 2. Oxime of **18**, 84%, $[\alpha]_D^{22} = +37.1$ (*c* = 0.675, MeOH), colorless, viscous, partially solidified oil (*E*/*Z* = 80:20); hydroxamic acid chloride 84%, $[\alpha]_D^{20} = +33.8$ (*c* = 0.685 in MeOH); **19**: (31%); m.p. 93–94 °C (from Et_2O/petroleum ether), $[\alpha]_D^{20} = 6.5$ (*c* = 0.535 in CH_2Cl_2); 5-epimer (32%): m.p. 36 °C, $[\alpha]_D^{20} = +152$ (*c* = 0.485 in CH_2Cl_2); d) H_2, Pt/C, MeOH, 25 °C, 25 h (reaction followed by H_2 consumption and by thin-layer chromatography; 95% **20** · HCl with *dr* = 95:5 (^{13}C NMR), m.p. (decomp.) 142–148 °C, $[\alpha]_D^{22} = -16.4$ (*c* = 0.510 in MeOH); e) 0.7 N HCl, 25 °C, 20 h, then Pd/C, MeOH/conc. HCl (15:1), 25 °C, 4 d; 79% of **21** · HCl, m.p. 154–155 °C (from MeOH), $[\alpha]_D^{19} = -16.1$ (*c* = 0.615 in H_2O), *dr* > 97:3 (NMR); fully analogous data for the D series (via 3-*O*-benzyldiacetone-D-glucose), ref. [19]; f) Z-Cl, Ag_2O, CH_2Cl_2, 25 °C, 3 d, filtration/hydrolysis with silica gel, eluent EtOAc/MeOH (85:15), 69% of *N*-Z,5-*O*-benzyltetrol as (75:25)-rotamer mixture, $[\alpha]_D^{19} = -81.8$, *c* = 0.183 in MeOH), m.p. 59–62 °C; g) $NaIO_4$, H_2O/MeOH (2:1), 25 °C, 75 min, then Br_2/CH_3OH [16] 2 h; 80% of methyl ester, $[\alpha]_D^{19} = -89.9$ (*c* = 0.300 in MeOH); h) K_2CO_3, H_2O/EtOH (5:2), 25 °C, 7 d; 81% of **22** as (55:45)-rotamer mixture (^1H NMR); colorless oil, $[\alpha]_D^{20} = -95.3$ (*c* = 0.395 in MeOH).

alcohols or to aldols—had led to the conclusion that N–O cleavage precedes the C=N hydrogenation.[15, 20a, 23]

The possibilities of combining other glyconitrile oxides with allyl chloride in a "building block fashion", according to $(C_3 + C_n)$, is currently being examined, the objectives being to provide "higher homologues", "other ring sizes", and "bicyclic structures". The new results presented here, namely, 1) the possibility of chromatographic separation of diastereomeric isoxazolines from chiral nitrile oxides on a preparative scale (gram quantities), 2) highly selective catalytic reduction of isoxazolines with specific combinations of side chains in 3- and 5-position, and 3) assignment of configuration of 5-epimeric isoxazolines based on consistent, markedly different specific optical rotations[24] should be essential assets to attain the above and related goals.

Received: December 6, 1993 [Z 6538 IE]
German version: *Angew. Chem.* **1994**, *106*, 1305

[1] W. Malisch, J. Zöller, M. Schwarz, V. Jäger, A. M. Arif, *Chem. Ber.*, in press.
[2] G. W. J. Fleet, P. W. Smith, *Tetrahedron* **1986**, *42*, 5685–5692.
[3] G. N. Austin, P. D. Baird, G. W. J. Fleet, J. M. Peach, P. W. Smith, D. J. Watkin, *Tetrahedron* **1987**, *43*, 3095–3108; G. W. J. Fleet, A. Karpas, R. A. Dwek, L. E. Fellows, A. S. Tyms, S. Petursson, S. K. Namgoong, N. G. Ramsden, P. W. Smith, J. C. Son, F. Wilson, D. R. Witty, G. S. Jacob, T. W. Rademacher, *FEBS Lett.* **1988**, *237*, 128–132; T. Ziegler, A. Straub, F. Effenberger, *Angew. Chem.* **1988**, *100*, 737–738; *Angew. Chem. Int. Ed. Engl.* **1988**, *27*, 716–717; C. H. Von der Osten, A. J. Sinskey, C. F. Barbas III, R. L. Pederson, Y.-F. Wang, C.-H. Wong, *J. Am. Chem. Soc.* **1989**, *111*, 3924–3927.
[4] D. A. Winkler, G. Holan, *J. Med. Chem.* **1989**, *32*, 2084–2089, and literature cited therein. We thank Dr. D. A. Winkler, CSIRO, Clayton, Victoria (Australia) for comments and suggestions concerning the compounds described in reference [5], and Drs. B. Junge and D. Häbich, Bayer AG, Wuppertal, for numerous discussions.

[5] V. Jäger, V. Wehner, *Angew. Chem.* **1990**, *102*, 1180–1182; *Angew. Chem. Int. Ed. Engl.* **1990**, *29*, 1169–1171; V. Jäger, W. Hümmer, *ibid.* **1990**, *102*, 1182–1183 and **1990**, *29*, 1171–1173.

[6] H. Paulsen, K. Todt, *Adv. Carbohydr. Chem.* **1968**, *23*, 116–232; G. Legler, E. Jülich, *Carbohydr. Res.* **1984**, *128*, 61–72; G. Legler, *Pure Appl. Chem.* **1987**, *59*, 1457–1464; *Adv. Carbohydr. Chem. Biochem.* **1990**, *48*, 318–384.

[7] D. R. P. Tulsiani, H. P. Broquist, L. F. James, O. Touster, *Arch. Biochem. Biophys.* **1984**, *232*, 76–85; U. Fuhrmann, E. Bause, H. Ploegh, *Biochim. Biophys. Acta* **1985**, *825*, 95–110; M. H. Ali, C. Hough, A. C. Richardson, *J. Chem. Soc. Chem. Commun.* **1984**, 447–448; S. A. Miller, A. R. Chamberlin, *J. Am. Chem. Soc.* **1990**, *112*, 8100–8112.

[8] A. M. Scofield, L. E. Fellows, R. J. Nash, G. W. J. Fleet, *Life Sci.* **1986**, *39*, 645–650; D. Taylor-Robinson, L. E. Fellows, *Lancet* **1987**, 1025–1028; R. C. Bernotas, B. Ganem, *Tetrahedron Lett.* **1984**, *25*, 165–168; K. Burgess, I. Henderson, *Tetrahedron* **1992**, *48*, 4045–4066.

[9] T. Kajimoto, K. K.-C. Liu, R. L. Pederson, Z. Zhong, Y. Ichikawa, J. A. Porco, Jr., C.-H. Wong, *J. Am. Chem. Soc.* **1991**, *113*, 6187–6196.

[10] V. Jäger, R. Müller, T. Leibold, G. Legler, unpublished; see also *Abstr. Pap. XVIth Int. Carbohydr. Symp. IUPAC*, Paris, July 5–10, 1992, IL-A9.

[11] Purity, structure, and configuration of the compounds mentioned are supported by satisfactory elemental analysis and by spectroscopic data.

[12] a) K.-C. Liu, B. R. Shelton, R. K. Howe, *J. Org. Chem.* **1980**, *45*, 3916–3918; b) R. Huisgen, *Naturwiss. Rundsch.* **1961**, *14*, 43–52; C. Grundmann, P. Grünanger, *The Nitrile Oxides*, Springer, Berlin, **1971**; K. B. G. Torssell, *Nitrile Oxides, Nitrones, and Nitronates in Organic Synthesis. Novel Strategies in Synthesis*, VCH, Weinheim, **1988**.

[13] V. Jäger, V. Wehner, *Angew. Chem.* **1989**, *101*, 512–513; *Angew. Chem. Int. Ed. Engl.* **1989**, *28*, 469–470.

[14] S. S. Ko, P. N. Confalone, *Tetrahedron* **1985**, *41*, 3511–3518; J. M. J. Tronchet, A. Jotterand, N. Le Hong, F. Perret, S. Thorndahl-Jaccord, J. Tronchet, J. M. Chalet, L. Faire, C. Hausser, C. Sebastian, *Helv. Chim. Acta* **1970**, 1484–1489; A. P. Kozikowski, S. Goldstein, *J. Org. Chem.* **1983**, *48*, 1139–1141; V. Jäger, P. Schohe, E. F. Paulus, *Tetrahedron Lett.* **1983**, *24*, 5501–5504.

[15] The catalytic hydrogenations of dihydro-1,2-oxazoles reported so far had consistently led to (40:60) *erythro*:*threo* mixtures; see, for example, synthesis of 4-hydroxyproline (racemic *erythro*:*threo* mixture 4:6): G. Drehfahl, H.-H. Hörfold, *Chem. Ber.* **1964**, *97*, 159–164; T. Kusumi, H. Kakisawa, S. Suzuki, K. Harada, C. Kashima, *Bull. Chem. Soc. Jpn.* **1978**, *51*, 1261–1262, as well as ref. [20a] (1979): *erythro*/*threo* 46:54.

[16] F. W. Lichtenthaler, P. Jarglis, K. Lorenz, *Synthesis* **1988**, 790–792.

[17] A. A. Patchett, B. Witkop, *J. Am. Chem. Soc.* **1957**, *79*, 185–192.

[18] Assignment of the stereochemical series of the cycloadducts is not possible by NMR spectroscopy, but can be made consistently and safely on the basis of numerous data (optical rotation, HPLC and MPLC retention factors) [19], cf. $[\alpha]_D$ values for **3**/**4**, **10**/**11**, **19**/5-epimer in the legends to the schemes. To check the enantiomeric purity and to ascertain whether a potential racemization/epimerization takes place at the nitrile oxide stage, correlations were undertaken by degradation of isoxazolines of all three series (from **1**, **9**, and **18**). The deviation in the optical rotation of enantiomers of isoxazoline-3-carboxylic acid derivatives produced by independent routes were of the order of $\leq 5\%$. Moreover, in a series of cycloadditions with optically active olefins only two diastereoisomers were observed in the crude products; a significant racemization/epimerization at the nitrile oxide stage would have led to the appearance of two additional diastereomers. For a summary of all correlations and degradation reactions see ref. [10,19].

[19] R. Müller, Dissertation, Universität Würzburg, **1992**; M. Pätzel, T. Leibold, V. Jäger, unpublished results 1991–1993.

[20] The asymmetric induction caused by the relative configurations at C5/C3', according to results obtained to date [19], appears to be additive, as recorded for "C4/C5 cases" of isoxazoline reductions with $LiAlH_4$: a) V. Jäger, Habilitationsschrift, Universität Gießen, **1979**; V. Jäger, V. Buß, W. Schwab, *Tetrahedron Lett.* **1978**, *19*, 3133–3136; *Liebigs Ann. Chem.* **1980**, 122–139; V. Jäger, J. Müller, R. Schohe, M. Frey, R. Ehrler, B. Häfele, D. Schröter, *Lect. Heterocycl. Chem.* **1985**, *8*, 79–98; V. Jäger, D. Schröter, *Synthesis* **1990**, 556–560, and references therein; b) see also the analogous match/mismatch concept: S. Masamune, W. Choy, J. S. Petersen, L. R. Sita, *Angew. Chem.* **1985**, *97*, 1–31; *Angew. Chem. Int. Ed. Engl.* **1985**, *24*, 1–30.

[21] E. Hungerbühler, D. Seebach, *Helv. Chim. Acta* **1981**, *64*, 687–702; S. Valverde, B. Herradon, M. Martin-Lomas, *Tetrahedron Lett.* **1985**, *26*, 3731–3734; cf. also B. Steuer, Diplomarbeit, Universität Würzburg, **1991**.

[22] The structure of an *N*-Val derivative of **22** has been proposed for the antibiotic TÜ 1718 B: A. Kern, G. Bovermann, G. Jung, M. Wanning, H. Zähner, *Liebigs Ann. Chem.* **1989**, 361–365; H.-T. Postels, W. A. König, *ibid.* **1992**, 1281–1287; revised structure: J. E. Baldwin, T. D. W. Claridge, K.-C. Goh, J. W. Keeping, C. J. Schofield, *Tetrahedron Lett.* **1993**, *34*, 5645–5648.

[23] V. Jäger, I. Müller, *Tetrahedron* **1985**, *41*, 3519–3528; V. Jäger, V. Buß, *Liebigs Ann. Chem.* **1980**, 101–121.

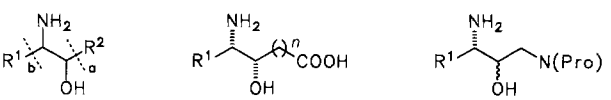
[24] Examples of 5-epimers of optically active 4,5-dihydro-1,2-oxazoles; optical rotations: **4**/**3**: −193°/−7.4; **10**/**11**: −88.7°/+85.1; **19**/5-epi-**19**: −6.5°/+151.8; (5*R*/5*S*)-3-[1-(*S*)-1,2-*O*-isopropylidene-1,2-(dihydroxyethyl)]-isoxazoline-5-carboxylic acid methyl ester: −165.0°/+145.8; the (5*R*) derivative, which shows the significantly smaller value of specific rotation, is given first in each case.

Simple and Versatile Synthesis of Optically Active 1,2-Amino Alcohols by Grignard Addition to *N*,*O*-Dibenzylglyceraldimine and -lactaldimine**

Thomas Franz, Matthias Hein, Ulrich Veith, Volker Jäger,* Eva-Maria Peters, Karl Peters, and Hans Georg von Schnering

Dedicated to Professor Ulrich Schmidt on the occasion of his 70th birthday

The 1,2-amino alcohol fragment **A** is found in many natural products and drugs, in particular as a central moiety of non-proteinogenic amino acids and amino polyols. Examples include statine,[1] norstatine,[2] and homostatine,[3] (see formula **B**), as well as related diamino alcohols **C**,[4a] which constitute



A **B** **C**

n = 0, 1, 2

R^1 = *i*Bu, CH_2Ph, $CH_2C_6H_{11}$

core units of peptide isosters that strongly inhibit a number of proteinases (aspartase, acetylcholine esterase, renin, pepsin, penicillopepsin, cathepsin D, HIV protease).[4b]

For the synthesis of compounds containing fragment **A**, mostly N-protected esters and aldehydes of the corresponding α-amino acids have been employed (path (a) indicated on formula **A**). This strategy imposes "natural" limitations on the choice of R^1. Until now these have rarely been overcome by devising "independent syntheses", that is, approaches not based on amino acids.

We now summarize the first part of our efforts to assemble disubstituted amino alcohols of type **A** by adding C-nucleophiles to the C=N bond of α-oxyaldehyde derivatives according to strategy (b) as outlined in **A**. Imine derivatives of 2-*O*-benzylglycerinealdehyde **1**, readily available in both enantiomeric forms,[5] were chosen as promising substrates that would allow for straightforward transformations at the other terminus. A survey of the literature up to 1990 on the addition of organometallic reagents to imines gave the following: 1) Additions to imines of enolizable aldehydes and ketones were found to be rather troublesome: "In general, these aldimines and ketimines are inert to alkyl Grignards and in their presence will

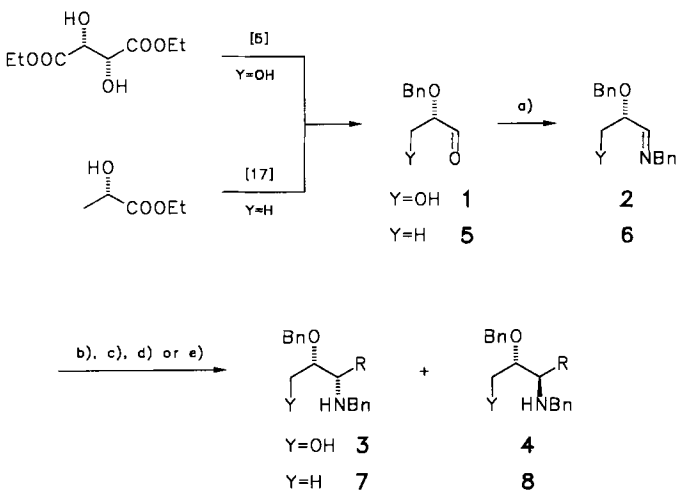
[*] Prof. Dr. V. Jäger,[+] Dr. T. Franz, Dipl.-Chem. M. Hein,[+] Dipl.-Chem. U. Veith[+]
Institut für Organische Chemie der Universität
Am Hubland, D-97074 Würzburg (FRG)
E.-M. Peters, Dr. K. Peters, Prof. Dr. H. G. von Schnering
Max-Planck-Institut für Festkörperforschung

[+] New address:
Institut für Organische Chemie und Isotopenforschung der Universität
Pfaffenwaldring 55, D-70569 Stuttgart (FRG)
Telefax: Int. code + (711)685-4321

[**] This work was supported by the Deutsche Forschungsgemeinschaft, the Fonds der Chemischen Industrie, the Bundesministerium für Forschung und Technologie (Aids-Forschungsförderung im Bundesgesundheitsamt) and Bayer AG. We thank Dr. Häbich for helpful discussions and Ms. Petra Schneider for experimental help. Results of these investigations were presented in Hamburg, Germany, at the Org.-Chem. Kolloquium, November 30th, 1990, and in Oxford, Great Britain, at the 13th International Symposium "Synthesis in Organic Chemistry", Perkin Division, RSC, July 20–22, 1993.

undergo complete enolization ... in refluxing THF."[6] 2) Except for a few cases of additions of Grignard,[7] organolithium,[7a, 8] and organocopper compounds[8, 9] to enolizable imines, primarily such reactions with the less basic allyl Grignard compounds[9] were known. In the course of our investigations, additions with organolithium,[10–12] organocopper,[12, 13] and organocerium compounds[11–13] as well as additions to several types of activated imines[11, 14] were reported.

After initial, unsatisfactory attempts to add *C*-nucleophiles stereoselectively,[15] a smooth and highly stereoselective reaction in what had appeared one of the less promising cases was observed: From the reaction of **2** with isobutylmagnesium bromide in ether, the amino diol **3**/**4** was isolated after 31 h at room temperature in 68% yield (Scheme 1), with an isomer ratio greater than 9:1. The major isomer was identified as **3d** and proved optically active.



Scheme 1. Synthesis of amino alcohols from N,O-dibenzylglyceraldimines and -lactaldimines. a) H_2NBn, neutral Al_2O_3, room temperature (RT), 1 h, quantitative; b) 4 RMgX, ether, 0 °C → RT, 12 h → 3 d, 41–92%; c) 4 RMgX, THF, 0 °C → RT, 3 d, incomplete conversion; d) 2.5 RLi, ether, −78 °C → RT, 79–83%, cf. reference [11]; e) 4 RMgX/4 $CeCl_3$, 0 °C → RT, 12 h, 62–70%, cf. reference [19].

Table 1 summarizes some of the results obtained in a more systematic study of this reaction.[16] At first questions about the possibility of varying the organo-Grignard moiety and about the origin of the unexpected high reactivity of the aldimine component had to be dealt with. Next, the possibilities for changing, improving, or reversing the diastereodifferentiation in the C–C bond-forming step were to be explored.

In general these additions were carried out at room temperature with four equivalents of the Grignard reagent; they proceeded at a moderate pace and gave satisfactory to good yields of isolated amino alcohols (41–92%) throughout, with rather varying diastereomer ratios—from approximately 1:1 to greater than 95:5 (runs 1–12). Apparently this increase in reactivity and the uniform course of the reaction is related to the presence of the alkoxymagnesium halide intermediate forming from **2**. The Grignard additions to the deoxy derivative, that is, the lactaldimine **6** (prepared analogously from **5**[17]), however, led to high yields of products under the same conditions (see runs 13–20 in Table 1). Hence, we attribute the successful outcome of all these cases to prior formation of a five-membered chelate with the 2-alkoxy group, due both to the inductive effect and the coordinative ability of OR,[18] and to the Lewis basicity of the

Table 1. Addition of organometallic compounds to *N*, 2-*O*-dibenzylglyceraldimine (**2**) and -lactaldimine (**6**).

Run	Starting material	RM	Product	Yield [%]	**3** (**7**): **4** (**8**) [a] *threo*/*erythro*
1	**2**	MeMgBr	**3a**/**4a**	78	63:37
2	**2**	*n*BuMgBr	**3b**/**4b**	73	73:27
3	**2**	*i*PrMgCl	**3c**/**4c**	81	80:20
4	**2**	*i*BuMgBr	**3d**/**4d**	92	88:12
5	**2**	3-MeBuMgBr	**3e**/**4e**	89	90:10
6	**2**	$CyCH_2MgBr$	**3f**/**4f**	58	>95: 5
7	**2**	*t*BuMgCl	**3b**/**4g**	86	56:44
8	**2**	AdMgBr	**3h**/**4h**	41	55:45
9	**2**	PhMgBr	**3i**/**4i**	61	76:24
10	**2**	vinylMgBr	**3j**/**4j**	91	83:17
11	**2**	allylMgBr	**3k**/**4k**	74	40:60
12	**2**	BnMgBr	**3l**/**4l**	87	40:60
13	**6**	MeMgBr	**7a**/**8a**	83	88:12
14	**6**	*n*BuMgBr	**7b**/**8b**	69	93: 7
15	**6**	*i*PrMgCl	**7c**/**8c**	86	91: 7
16	**6**	*i*BuMgBr	**7d**/**8d**	(74) [b]	>95: 5
17	**6**	$CyCH_2MgBr$	**7f**/**8f**	(83) [b]	>95: 5
18	**6**	PhMgBr	**7i**/**8i**	62	96: 4
19	**6**	allylMgBr	**7k**/**8k**	86	81:19
20	**6**	BnMgBr	**7l**/**8l**	89	>95: 5
21	**2**	*n*BuMgBr	**3b**/**4b**	(79) [b]	46:54
22	**2**	*i*BuMgBr	**3d**/**4d**	(93) [b]	47:53
23	**2**	MeLi	**3a**/**4a**	80	46:54
24	**2**	*n*BuLi	**3b**/**4b**	81	57:43
25	**2**	*t*BuLi	**3g**/**4g**	79	40:60
26	**2**	PhLi	**3i**/**4i**	83	44:56
27	**2**	MeMgCl/$CeCl_3$	**3a**/**4a**	69	9:91
28	**2**	*i*BuMgBr/$CeCl_3$	**3d**/**4d**	62	<5:95
29	**2**	BnMgCl/$CeCl_3$	**3l**/**4l**	70	76:24

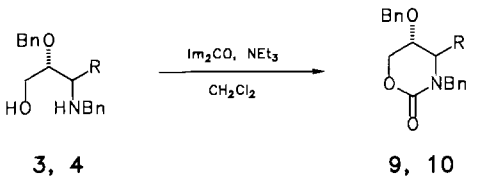
[a] Diastereomer ratio of the reaction mixture. Solvents: runs 21, 22, 27–29 in THF; others in diethyl ether. 3-MeBu = 3-methylbutyl; Cy = cyclohexyl, Ad = 1-adamantyl. [b] Crude yield, contaminated by imine **2** or **6**.

imine nitrogen atom. Further, the effect of R with respect to the 1,2-asymmetric induction is noteworthy: methyl, *tert*-butyl, adamantyl, allyl, and benzyl groups are taken up with rather low selectivity (runs 1, 7, 8, 11, 12), isopropyl and vinyl with satisfactory selectivity (approximately 4:1, runs 3, 10), and the β-branched groups, isobutyl and cyclohexylmethyl, with very good stereoselectivity (runs 4, 6). With lactaldimines, methyl and allyl groups show good inductions (run 13, 19), whereas benzyl (run 20) and other groups cause very high stereoselection. For the latter, the second diastereomer (run 16–18) could virtually not be detected by NMR analysis of the crude reaction mixtures.

The rate and stereoselectivity of the addition of RM to dibenzylglyceraldimine (**2**) was strongly dependent on the solvent and metal cation employed. Grignard additions to **2** in THF (instead of ether) proceeded much more slowly (in some cases the reaction was still incomplete after 76 h), with almost no induction (runs 21, 22). The corresponding reactions with organolithium compounds in ether again gave good yields but nearly no selectivity (runs 23–26).[11] Remarkably, on addition of $CeCl_3$[19] in THF the selectivity was reversed in favor of the adducts **4** with *erythro* (*anti*) configuration (R = alkyl, runs 27, 28). This observation was all the more surprising since related imines derived from threose had been reported to afford *xylo* (1,2-*syn*) isomers as the only products.[13] We therefore attribute the diastereomer ratios of **3**/**4** to the efficient formation of a cerium alkoxide coordinating to the N-atom, that is, the presence of a six-membered chelate with an $O^- \cdots Ce^{3+} \cdots N$ arrangement.

The amino diol products **3**/**4** were assigned the *threo* or *erythro* configuration based on analogies in ^1H and ^{13}C NMR spectro-

scopic data. The ^{13}C chemical shifts of the resonance signals from C1 to C4 showed characteristic and consistent differences even for OCH_2Ph/NCH_2Ph (of 12 data sets, only one deviation, for **3i/4i**, was observed). From run 6 the data of only one diastereomer were available; the assignment to the *threo* series was based on ^1H NMR coupling constants. Furthermore, the configuration of several adducts (run 1, 4, 5, 7, 12) was derived by analysis of ^1H NMR data of the tetrahydro-1,3-oxazin-2-ones **9**, **10** (prepared from the amino diols according to Scheme 2).[16]

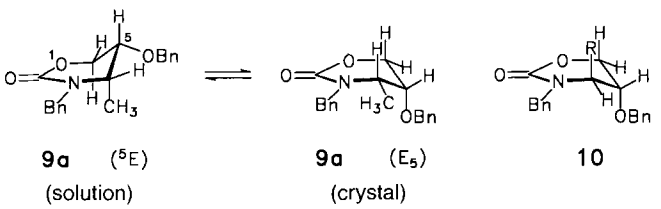


3, 4 **9, 10**

Scheme 2. Im = 1-imidazolyl.

From the ^1H NMR data of the N-protected oxazinones the coupling constants $J_{4,5} = 4.4-4.9$, $J_{4,6} = 0.8-1.0$, and $J_{5,6} = 4.4-4.9$ as well as 8.0–8.9 Hz for **9**, and $J_{4,5}$ and $J_{5,6} = 2.1-2.2$ for **10** were derived. These values agree well with results obtained from 3,4,5-substituted tetrahydrooxazinones[20] and show that **9** and **10** adopt sofalike conformations in $CDCl_3$ (Fig. 1, top). The *threo* configuration of the oxazinone **9a** was proven by crystal structure analysis (Fig. 1, bottom).[21] Notably the preferred conformation of **9a** in the crystalline state has the 4-methyl group in the equatorial position.[22]

The configurations of the lactaldimine adducts **7**, **8**[16] were deduced from comparison with data of known amino alcohols and oxazolidinones as well as from the consistent pattern of their ^{13}C NMR chemical shifts. The Grignard additions to glyceraldimine **2** and lactaldimine **6** proceed without discernible racemization; this was demonstrated by ^1H NMR experiments (addition of (*R*)-trifluoroanthrylethanol[23]) to the products of runs 4 and 5, and further by comparison of the optical rotation of an oxazolidinone derivative of **7l** with the value reported in the literature.[24]



9a (^5E) (solution) **9a** (E_5) (crystal) **10**

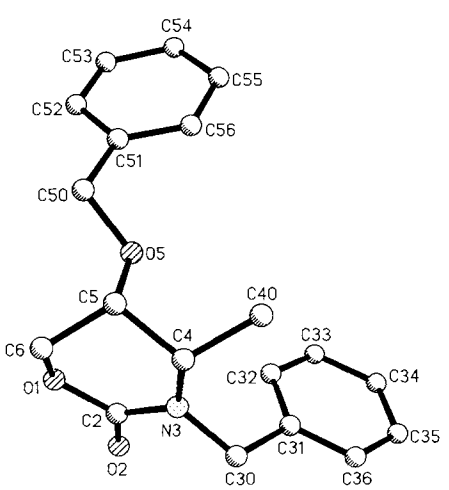


Fig. 1. Top: Conformations of **9a** and **10** (E_5). Bottom: Crystal structure of **9a**.

Received: December 6, 1993 [Z 6539 IE]
German version: *Angew. Chem.* **1994**, *106*, 1308

[1] U. Schmidt, B. Riedl, G. Haas, H. Griesser, A. Vetter, S. Weinbrenner, *Synthesis* **1993**, 216–220, and references therein.
[2] a) D. H. Rich, B. J. Moon, A. S. Boparai, *J. Org. Chem.* **1980**, *45*, 228–2290; b) K. Iizuka, T. Kamijo, T. Kubota, K. Akahane, H. Umeyama, Y. Kiso, *J. Med. Chem.* **1988**, *31*, 701–704; K. Iizuka, T. Kamijo, H. Harada, K. Akahane, T. Kubota, H. Umeyama, T. Ishida, Y. Kiso, *ibid.* **1990**, *33*, 2702–2714.
[3] H.-E. Radunz, V. Eiermann, G. Schneider, A. Riethmüller, *Tetrahedron* **1991**, *47*, 1887–1894.
[4] a) D. H. Rich, J. Green, M. V. Toth, G. R. Marshall, S. B. H. Kent, *J. Med. Chem.* **1990**, *33*, 1285–1288; D. H. Rich, C.-Q. Sun, J. V. N. Vara Prasad, A. Pathiasseril, M. V. Toth, G. R. Marshall, M. Clare, R. A. Mueller, K. Houseman, *ibid.* **1991**, *34*, 1222–1225; N. A. Roberts, J. A. Martin, D. Kinchingston, A. V. Broadhurst, J. C. Craig, I. B. Duncan, S. A. Galpin, B. K. Handa, J. Kay, A. Kröhn, R. W. Lambert, J. H. Merrett, J. S. Mills, K. E. B. Parkes, S. Redshaw, A. J. Ritchie, D. L. Taylor, G. J. Thomas, P. J. Machin, *Science* **1990**, *248*, 358–361; b) see review: D. Häbich, *HIV-Infektionen und AIDS (Chem. Unserer Zeit*, **1991**, *25*, 295–307).
[5] V. Jäger, V. Wehner, *Angew. Chem.* **1989**, *101*, 512–513; *Angew. Chem. Int. Ed. Engl.* **1989**, *28*, 469–470.
[6] R. A. Volkmann in *Comprehensive Organic Synthesis, Vol. 1* (Eds.: B. M. Trost, I. Fleming), Pergamon, Oxford, **1991**, p. 355–396.
[7] a) J. Yoshimura, Y. Ohgo, T. Sato, *J. Am. Chem. Soc.* **1964**, *86*, 3858–3862; Y. Ohgo, J. Yoshimura, T. Sato, *Bull. Soc. Chem. Jpn.* **1969**, *42*, 728–731; b) T. Fukumaru, T. Atsumi, T. Ogawa, M. Matsui, *Agric. Biol. Chem.* **1973**, *37*, 2617–2619; T. Atsumi, T. Fukumaru, T. Ogawa, A. Matsui, *ibid.* **1973**, *37*, 2621–2626; T. Atsumi, T. Fukumaru, M. Matsui, *ibid.* **1973**, *37*, 2627–2630; c) M. Carcano, F. Nicotra, L. Panza, G. Russo, *J. Chem. Soc. Chem. Commun.* **1989**, 297–298; see recent results of L. Lay, F. Nicotra, A. Paganini, C. Pangrazio, L. Panza, *Tetrahedron Lett.* **1993**, *34*, 4555–4558.
[8] M. Wada, Y. Sakurai, K.-y. Akiba, *Tetrahedron Lett.* **1984**, *84*, 1079–1082, 1083–1084; R. D. Clark, Jahangir, M. Souchet, J. R. Kern, *J. Chem. Soc. Chem. Commun.* **1989**, 930–931.
[9] Y. Yamamoto, T. Komatsu, K. Maruyama, *J. Am. Chem. Soc.* **1984**, *106*, 5031–5033; Y. Yamamoto, T. Komatsu, K. Maruyama, *J. Chem. Soc. Chem. Commun.* **1985**, 814–816; Y. Yamamoto, S. Nishii, K. Maruyama, T. Komatsu, W. Ito, *J. Am. Chem. Soc.* **1986**, *108*, 7778–7786.
[10] H.-W. Kleemann, H. Heitsch, R. Henning, W. Kramer, W. Kocher, U. Lerch, W. Linz, W.-U. Nickel, D. Ruppert, H. Urbach, R. Utz, A. Wagner, R. Weck, F. Wiegand, *J. Med. Chem.* **1992**, *35*, 559–567.
[11] M. T. Reetz, R. Jaeger, R. Drewlies, *Angew. Chem.* **1991**, *103*, 76–78; *Angew. Chem. Int. Ed. Engl.* **1991**, *30*, 103–106.
[12] Y. Ukaj, T. Watai, T. Sumi, T. Fujisawa, *Chem. Lett.* **1991**, 1555–1558.
[13] T. Matsumoto, Y. Kobayashi, Y. Takemoto, Y. Ito, T. Kamijo, H. Harada, S. Terashima, *Tetrahedron Lett.* **1990**, *31*, 4175–4176; Y. Kobayashi, K. Nakatani, Y. Ito, S. Terashima, *Chem. Lett.* **1990**, 1709–1710; Y. Kobayashi, T. Matsumoto, Y. Takemoto, K. Nakatani, Y. Ito, T. Kamijo, H. Harada, S. Terashima, *Chem. Pharm. Bull.* **1991**, *39*, 2550–2555.
[14] G. Cainelli, D. Giacomini, E. Mezzina, M. Panunzio, P. Zarantonello, *Tetrahedron Lett.* **1991**, *32*, 2967–2970; G. Cainelli, D. Giacomini, M. Panunzio, P. Zarantonello, *ibid.* **1992**, *33*, 7783–7786.
[15] Strecker reaction with *N*-benzylimine (**2**): 88% aminonitrile, low stereoselectivity (60:40); Grignard addition to the corresponding *N*-benzylnitrone: complete reaction, but a mixture of inseparable products; compare hetaryl-M additions to nitrones: A. Dondoni, F. Junquera, F. L. Merchan, P. Merino, T. Tejero, *Tetrahedron Lett.* **1992**, *33*, 4221–4224; A. Dondoni, S. Franco, F. L. Merchan, P. Merino, T. Tejero, *ibid.* **1993**, *34*, 5479–5482.
[16] Structure and configuration of the compounds prepared have been confirmed by spectroscopic data and correct elemental analyis.
[17] K. Mislow, R. E. O'Brien, H. Schaefer, *J. Am. Chem. Soc.* **1962**, *84*, 1940–1944; S. K. Massad, L. D. Hawkins, D. C. Baker, *J. Org. Chem.* **1983**, *48*, 5180–5182.
[18] For the influence of the α-benzyloxy group on the addition to ketones and for kinetic investigations concerning Cram's rule ("Cram chelate complex") see: E. L. Eliel, S. V. Frye, E. R. Hortelano, X. Chen, X. Bai, *Pure Appl. Chem.* **1991**, *63*, 1591–1598; X. Chen, E. R. Hortelano, E. L. Eliel, S. V. Frye, *J. Am. Chem. Soc.* **1990**, *112*, 6130–6131; *ibid.* **1992**, *114*, 1778–1784. We thank one of the referees for this comment.

[19] T. Imamoto, T. Kusumoto, Y. Tawarayama, Y. Sugiura, T. Mita, Y. Hatanaka, M. Yokoyama, *J. Org. Chem.* **1984**, *49*, 3904–3912; T. Imamoto, N. Takijama, K. Nakamura, T. Hatajima, Y. Kamija, *J. Am. Chem. Soc.* **1989**, *111*, 4392–4398; S. E. Denmark, T. Weber, D. W. Piotrowski, *ibid.* **1987**, *109*, 2224–2225.

[20] B. J. Kurtev, M. J. Lyapova, S. M. Mishev, O. G. Nakova, A. S. Orahovatz, I. G. Pojarlieff, *Org. Magn. Reson.* **1983**, *21*, 334–338; P. G. M. Wuts, Y.-W. Jung, *J. Org. Chem.* **1991**, *56*, 365–372; S. Akai, Y. Tsuzuki, S. Matsuda, S. Kitagaki, Y. Kita, *J. Chem. Soc. Perkin Trans. 1* **1992**, 2813–2820.

[21] Crystal structure data for **9a**: orthorhombic, space group $P2_12_12_1$, a = 1527.8(4), b = 1897.5(6), c = 574.7(1) pm; M = 311.38, V = 1666.0(8) × 106 pm^3, Z = 4, $\varrho_{ber.}$ = 1.241 gcm^{-3}, $Mo_{K\alpha}$ radiation, independent reflections: 2780, reflection with $F > 3\sigma(F)$: 1773. Refined by full-matrix, least squares analysis: R = 0.066, R_w=0.053 (SHELXTL PLUS). Further details of the crystal structure analysis are available on request from the Fachinformationszentrum Karlsruhe, D-76344 Eggenstein-Leopoldshafen, on quoting the depository number CSD-400480.

[22] The tetrahydrooxazinone ring of **9a** is nearly planar except in the vicinity of C5. O1 and C6 are approximately 10 pm on either side of the plane, while C5 is 65 pm out of the plane. The dihedral angle C6-O1-N3-C2 is 15.1°. The fold in the ring as determined by the (best) planes defined by O1, C2, N3, C4, C6 and C4, C5, C6 is 131°.

[23] W. H. Pirkle, D. L. Sikkenga, M. S. Pavlin, *J. Org. Chem.* **1977**, *42*, 384–387; W. H. Pirkle, *Top. Stereochem.* **1982**, *13*, 263–331. The enantiomers of the diastereomeric pairs **3d**/**4d** and **3e**/**4e** were prepared in an analogous way from L- and D-2-*O*-benzylglyceraldehyde. Groups of four signals could be discerned in the NMR spectrum of the racemic reaction mixture upon the addition of (*R*)-trifluoroanthrylethanol.

[24] **71** was transformed into *trans*-4-benzyl-5-methyloxazolidin-2-one: $[\alpha]_D^{21}$ = −70.7 (c = 0.920 in $CHCl_3$); literature value for the (4*S*, 5*S*) enantiomer: $[\alpha]_D$ = −71.8 (c = 0.9 in $CHCl_3$). S. Kano, Y. Yuasa, T. Yokomatsu, S. Shibuya, *Chem. Pharm. Bull.* **1989**, *37*, 2867–2869.

A stop-gap solution?



If the latest library copy of Angewandte spends more time off the shelf than on, stop the gap with a personal subscription.

Just call or fax

VCH

USA: Tel. 1-(800) 422-8824; Fax (305) 428-8201
UK: Tel. (0223) 321111, Fax (0223) 313221

Classics in Chemistry

Chemistry Imagined. Reflections on Science. By *R. Hoffmann* and *V. Torrence*. Smithsonian Institute Press, Washington, 1993. 168 pp., hardcover $ 23.95.—ISBN 1-50698-214-4

Among the treasures kept in the Herzog August Library in Wolfenbüttel are a number of "Malerbücher" (books of the painters), each of which is a two-author work in which an important artist of the day has illustrated a literary text of his own choosing.



Chemistry Imagined is a "Malerbuch" of chemistry, in which the text is by Roald Hoffmann and the illustrations are by Vivian Torrence, a well-known American artist. For Hoffmann this book is a continuation of his efforts, previously in the form of lectures, essays, and television programs, to help laypeople to understand those aspects of the sciences, and especially of chemistry, that relate to the arts and humanities.

Just as the words "imagined" and "reflections" in the title have various meanings, so also does the book itself. It is not a book to be read straight through, but rather one to enjoy looking at, to read a little and pause, to dream and speculate—about the elements as understood by the ancient Greeks and Chinese, or the Periodic Table, the Philosophers' Stone, phlogiston, or the relationship between theory and practice or between energy and form. A recurring theme throughout many of the chapters is the "fluxional" character of chemistry, which is the science of change and instability par excellence. They contain much that is of a very personal nature, for example thoughts based on childhood recollections, and are written in a style that is perhaps best described as bright and relaxed. No knowledge of chemistry is assumed, although the author is not immune from lapses into technical jargon and over-specialization.

Or could that perhaps have been intentional? In the same way as the chemist experiments with structures of all kinds, here the author plays with different literary forms—the essay, poetry, text arranged to form shapes (as in the chapter on the Periodic Table mentioned above), and even dialogue (in a chapter on "Possibilities and Pragmatism" that is surprisingly reminiscent of the radio dialogues of Arno Schmidt).

The pictures by Vivian Torrence are works of art in their own right, and yet at the same time serve to illustrate the text. The use of collage in these is very appropriate for a text dealing with such a creative science as chemistry. Most of them are packed with detail and invite one to make journeys of discovery, to smile at the Greek and Roman wrestlers in a chapter on force constants, or to follow the flows of liquids in the chapter on reaction steps and processes, which gives the reader a sort of "monochrome" introduction to the language of chemistry in the form of descriptions of experiments (although this will certainly be incomprehensible to lay readers). A very readable epilogue by Lea Rosson Delong serves to extend and add depth to one's own thoughts about the pictures. (In the copy sent to me for reviewing I marked the sentences that struck me as especially pertinent comments on the pictures, only to find at the end that I had highlighted practically everything.)

In his preface Carl Sagan writes that we need more books of this kind. That is probably true. Nevertheless, I have a sneaking feeling that books such as this which aim (once more) to reach a certain section of the reading public are no longer noticed by the people for whom they are intended. How many readers will find this book? Could it be as many as those who see the "Malerbücher" mentioned above? Probably far fewer. On one side "refinement, decline, sorrow" (G. Benn), on the other, much more numerous side, more and more pictures in more and more "channels" with ever less of the text which slows down the tempo. And between the two sides hardly any communication.

Henning Hopf
Institut für Organische Chemie
der Technischen Universität
Braunschweig (FRG)

Unraveling DNA. By *M. D. Frank-Kamenetskii*. VCH Verlagsgesellschaft, Weinheim/VCH Publishers, New York, 1993. 205 pp., hardcover DM 49.00, $ 25.95.—ISBN 3-527-89617-1/1-56081-617-1

The publication of a new English version of the Russian book "Samaya glavnaya molekula", which originally appeared in Moscow in the early 1980s, may seem surprising in view of the already enormous volume of literature on DNA throughout the world. However, *Unraveling DNA* is quite different from other books on the subject.

Only once before have I come across a book such as this about the information-carrying molecule that determines our lives. That was when I read, in the course of one evening and one night, Watson's book *The Double Helix*. Frank-Kamenetskii's *Unraveling DNA* too is unmistakably a very personal account of the history of DNA and its importance in our life processes, even though it comes 40 years after those events. It deals with the most fruitful period that has ever occurred in the interdisciplinary collaboration between physics, chemistry, and biology, describing the events in a way that is wide-ranging and at the same time profound, ensuring that the reader becomes captivated right from the first sentences of the preface and is held throughout by the fascination of the subject. The style is colorful and gripping, yet with consummate ease the author effectively brings together insights at very different levels, so that the descriptive quality of everyday

This section contains book reviews and a list of new books received by the editor. Book reviews are written by invitation from the editor. Suggestions for books to be reviewed and for book reviewers are welcome. Publishers should send brochures or (better) books to the Book Review Editor, Dr. Ralf Baumann, Redaktion Angewandte Chemie, Postfach 101161, D-69451 Weinheim, Federal Republic of Germany. The editor reserves the right of selecting which books will be reviewed. Uninvited books not chosen for review will not be returned.

language is constantly balanced by scientific precision, resulting in a vividness and clarity that is rarely found. By using a wealth of appropriate analogies even the most difficult process concepts are clearly explained, and the direct and forceful presentation broadens and liberates the reader's outlook. The result is a work into which the author and the translator have each put their whole soul.

As one expects, the book covers nearly all the ground that is nowadays common knowledge in the scientific world: the tedious "march across the plains" that began with Miescher and Altmann and continued through several decades; the tortuous pathways that were followed and eventually led, by an unexpected route, to the summit; the conquest of the summit by the four researchers whose discovery of the "sacred structure" and its inherent dynamics released a veritable flood of creativity; the "dogmas" concerning the flow of information between DNA, RNA, and proteins, and the partial revision of these that was so significant; the great efforts to discover the key to life in the DNA code; the role of the structures and long-range order of DNA molecules in the developing understanding of the static and dynamic behavior of genes, and the effects of natural and artificial stimuli in the complex information processing of DNA, RNA, and proteins; the new insights into evolution and the emergence of contradictions with genetics, a subject then experiencing an unprecedented surge of interest; the challenges and temptations of the technology of genetic engineering that began to emerge within the wider field of biotechnology—a technology that could be seen either as offering the realization of mankind's ancient dream of achieving a godlike omnipotence, or as perhaps the ultimate folly, already previously discovered by Oppenheimer in the case of physics, of "original sin", here in its truest sense; ultrastable cybernetic systems and the threatening disruption of their rhythms; DNA in the conflict between self/non-self recognition and discrimination, between new plagues on humanity and still unfulfilled needs, between the examples of the past and visions of the future.

So much of this we already know—and yet the "unwinding" and "decoding" DNA that Frank-Kamenetskii describes here contains much that is different. In what formerly seemed to be mainly an irregular mosaic of observations, previously unnoticed relationships are now becoming apparent. Whereas formerly the observer was content to look at mountains of statistical and ephemeral data, now he delights in the many new insights that are becoming clear for the first time in an exciting and action-packed film. In order to come closer to a scientific understanding of the processes of life, our approaches to the subject should preferably take account of the complexity involved. On the other hand, science is the science of human beings. Its endeavors in the many different skills are dependent on people, and thus it is subject to development and decay. Frank-Kamenetskii's praiseworthy attempt at a novel way of informing and inspiring the reader is based on a recognition of this dependence. It is an endeavor in which one must wish the author and publishers all success; it is also to be hoped that all kinds of readers and many areas of science will benefit from authors (and translators!) following this example.

"I am the original fragrance of the earth/ I am the life of all that lives/I am the original seed of all existences/All states of being are manifested by my energy/I am unborn and my transcendental form never deteriorates/Although I appear in so many configurations/You know not my true transcendental form"—Krishna's description of himself from the Bhagavad-gita, as applied by Ramaswamy H. Sarma to represent the informational component of life, would perhaps form a suitable epilogue to this book by Maxim D. Frank-Kamenetskii on the molecule of life and its "unraveling", again reflecting the preface's theme of the wonder of life, the "transfiguration of its molecule".

Siegfried Hoffmann
Institut für Biochemie
der Universität Halle-Wittenberg (FRG)

Electrode Kinetics for Chemists, Chemical Engineers, and Material Scientists. By *E. Gileadi*. VCH Verlagsgesellschaft, Weinheim/VCH Publishers, New York, 1993. 597 pp., hardcover DM 189.00.—ISBN 3-527-89561-2/1-56081-561-2

After a period of twenty years during which there was a shortage of good textbooks on electrochemistry, now in rapid succession several books have appeared dealing with general and special aspects of electrochemistry, and differing in their level of treatment and intended readership. This book by Gileadi, his second on this subject, is intended as an introduction to electrochemical kinetics, and sets out to familiarize students, and also scientists from related disiplines, with the classical methods of this field. Readers are assumed to have only a basic grounding in thermodynamics and chemical kinetics, and the amount of mathematics is kept to a minimum.

The book is in two parts. The first part contains, according to the author, the minimum basic knowledge that the reader needs to understand electrode processes. The second, more advanced, part treats some special topics in greater depth. Part 1 begins with two introductory chapters in which some basic concepts of electrochemical kinetics are explained from a phenomenological standpoint: current–voltage curves, material transport, and the capacitance of the double layer. The various potentials that can apply to a phase are then defined: the electrochemical and chemical potentials, internal and external potentials, and the conventional hydrogen scale. Next there are chapters on measurement principles and cell design, the relationship between chemical and electrochemical kinetics, and some simple measurement procedures. The core of this first part consists of the chapters on the kinetics of electrode processes, which deal with all the usual topics, such as overvoltage, the Butler–Volmer equation, the transfer coefficient, and simple and more complex reactions, and discuss these in relation to hydrogen and oxygen evolution. The author takes considerable time in discussing these aspects, describes practical examples, raises various relevant questions and answers them, and presents all this material clearly and skillfully. Nevertheless, one may not always agree with his views—for example, the answer to the question of whether the permeation factor depends on the potential must be yes, at least for simple electron transfer processes. Part 1 ends by discussing simple theories of the double layer and of electrocapillarity.

The more advanced part begins with a chapter on intermediates formed in electrode reactions including, interestingly, a discussion of underpotential deposition and the adsorption of halides. The latter topic is also included under the heading "underpotential deposition", although to thus broaden the meaning of this clumsy expression could well lead to confusion here. Next come two chapters on the electrosorption of neutral molecules; the prominence given here to the now obsolete "Gileadi combined adsorption isotherm" can be excused as a touch of vanity on the part of the author. Most of the space is then devoted to measurement techniques: current and voltage transients, cyclic voltammetry, electrochemical impedance spectroscopy, and microelectrodes. Here again it is pleasing to find that the treatment of these topics is lucid and practically-orientated. The only unsatisfac-

 © VCH Verlagsgesellschaft mbH, D-69451 Weinheim, 1994 0570-0833/94/1212-1304 $ 10.00+.25/0

tory chapter is that on impedance spectroscopy, which suffers from the author's self-imposed restriction to simple mathematics; the spectra given here cannot be understood without the relevant derivations. The book ends by discussing some examples of practical applications: batteries and fuel cells, corrosion, and electrodeposition. The review articles listed in the bibliography are mostly from the period 1970 to 1983, with only a few exceptions. That is also an indication of the state of knowledge covered by the book, which is not inappropriate for an introductory work such as this.

The book has evidently been produced in copy-ready form, and the author has made good use of modern desk-top publishing methods. The only aspects that I disliked were the inadequately small type size in the index and inaccurate positioning of the subscripts in some of the diagrams.

As can be seen from the list of contents, the subject matter is limited to classical electrochemistry, and therefore to the information obtainable from current–voltage curves. This restriction is appropriate for an introductory text, so the author should not be blamed for having omitted modern spectroscopic methods. Nevertheless, I would have liked to see the electrochemistry of semiconductors included, as it is undoubtedly within the classical domain. To summarize, however, this introduction to electrochemical kinetics is lucid and well written from a teaching standpoint, and the few shortcomings and omissions can willingly be forgiven.

Wolfgang Schmickler
Abteilung Elektrochemie
der Universität Ulm (FRG)

Dictionary of Trivial Names/Trivialnamen-Handbuch. Vols. 1–3. Edited by Fachinformationszentrum Chemie (FIZ Chemie), Berlin. VCH Verlagsgesellschaft, Weinheim, 1993. XIV, 2464 pp., hardcover DM 2100.00.—ISBN 3-527-29030-6

Having regard to the size of this reference work and what it claims to provide, it is at first glance very impressive and, despite the small print, easy to use. It lists 21812 compounds under eight data fields, which comes to a total of 174496 data field entries—a considerable amount of information which should be of interest to a large number of potential users. However, because of its price the number of actual purchasers will probably be much smaller than that. In any case, the high price makes it necessary to do a careful cost–benefit analysis, and that is what this review aims to provide.

The 14 pages of preliminaries in Volume 1 contain information about the contents, an introduction, and a more detailed explanation of the individual data fields and the indexes. This is followed by 1008 pages of text covering trivial names from A to H. Volume 2 (1196 pp.) covers trivial names from I to Z. Volume 3 contains an index of synonyms (60 pp.) and a reference index (200 pp.). Altogether 21812 compounds are listed, each page presenting ten compounds in miniature VDU-screen displays (5 cm × 9 cm). Each of these has fields containing the English and German trivial names, a sequential data-bank number, the structural formula with full stereochemistry, the molecular formula, the CAS Registry number, stereochemical information, and bibliographic information (a literature reference selected for maximum information about synthesis, structure, and activity). The print size of the text within the fields is uniform, about 1.5 mm, whereas the characters in the structural formulas are rarely more than 1.0 mm. Volumes 1 and 2 are each provided with a Fresnel lens that can be used as a bookmark and magnifier.

The work lists about 28000 entries (twice as many as in the German-language first edition published in the form of index cards), comprising trivial name of simple organic compound, names of natural products of known constitution, common abbreviations and acronyms for important compounds, and selected trade names of dyes, pharmaceuticals, and other industrial chemical products, together with an index of synonyms (in English), and a German–English index of names.

This reference work is intended as a resource that one can turn to for help when, for example, a compound is referred to in the literature by a trivial name with which one is unfamiliar, when one needs the correct structural formula of a compound for a publication or lecture and the trivial name is open to misunderstanding, or when one wishes to use an on-line data bank and needs search criteria such as synonyms or CAS Registry numbers. The *Dictionary of Trivial Names* is intended for use by everyone working in the areas of organic chemistry, biochemistry, or pharmaceutical chemistry, both in industry and in academic research.

After a thorough examination of this handbook (it would perhaps have been better to use the word "Handbook" instead of "Dictionary" in the English title, as on the back cover), a number of specific points occur to me:

1) Since the field containing the structural formula is of a constant size and each formula is always adjusted to fill the field so far as possible, the result is that small molecules are shown on a large scale and large molecules on a reduced scale. Consequently there is often a gross mismatch between the size of the characters and the length of the bond lines (an extreme example is acetaldehyde, where the CH_3 and CHO groups are linked by a bond 7.5 cm long!).

2) The editors have not followed the usual practice of distinguishing stereochemical descriptors from atomic symbols by means of italic type and/or brackets; also they are sometimes too far distant from the chiral center or too close to it, which can cause confusion (example: abienol).

3) The bibliographic information (which is not always in the form recommended in the *Chemical Abstracts System Source Index*) often seems very outdated (e.g., hystazarin: 1955), and sometimes cites exotic sources that are not easily accessible (e.g., hypotaurine: *Atti Accad. Naz. Lincei Cl. Sci. Fis. Mat. Nat. Rend.*). Occasionally publications in less common languages are cited (e.g., homostephanoline: *Yakugaku Zasshi*), or only a patent number is given (e.g., hetacillin: US 4321196). In such cases it would have been very useful to also include a reference to *Chemical Abstracts*.

4) In a few cases the CAS Registry number is not given, even though it is already known (e.g., inusoniolide: 129927-20-4).

5) In most cases the *Chemical Abstracts Index* name is also known, and could usefully have been included. Alongside the trivial name one would then have a name in accordance with nomenclature rules that would give the structure unambiguously and could be used for on-line searching.

6) Despite the size of the work there are, of course, some gaps here and there. Random checks showed, for example, that pseudilin and temaroten were both missing (the CAS Registry numbers of these compounds prove that they have been known for a long time). Surprisingly, some common acronyms such as AIBN, BBN, COT, and DABCO were also missing (showing that the claims made in the introduction regarding "Acronyms of Important Compounds" need to be qualified somewhat).

How serious these individual shortcomings are to be regarded is a question that potential purchasers or users must decide for themselves.

However, one must also ask at this point whether or not some works of comparable usefulness already exist. In principle the answer has to be yes—for ex-

 © VCH Verlagsgesellschaft mbH, D-69451 Weinheim, 1994 0570-0833/94/1212-1305 $ 10.00+.25/0

ample, there are the Chemical Abstracts publications *Registry Handbook—Common Names* and the *Index Guide*. The first of these contains, in its names section, over 1 300 000 names with their CAS Registry numbers and molecular formulas, and in its numbers section over 840 000 Registry numbers with more than 1 800 000 names (including the CA Index names that are so useful for on-line searching). This work is available at a cost of $ 1070.00 (1994 price) in microfiche or microfilm form. If one is unwilling to derive the structural formula from the CA Index name, it can easily be obtained by on-line retrieval or from the usual Chemical Abstracts printed volumes (as also can the bibliographic information). The *Index Guide* contains 2248 pages listing about 250 000 entries (mainly trivial names and acronyms with their CA Index names and CAS Registry numbers, and also structural formulas for "stereoparent" compounds), as well as numerous appendices that are also useful in dealing with questions of nomenclature; in printed form it costs $ 70.00 for a single issue, or $ 190.00 for three updated issues over a five-year period (1994 prices). The facilities for structural formulas and bibliographic information mentioned above for the *Registry Handbook—Common Names* are the same in this case.

A simple calculation gives "unit costs" of about DM 0.08 per name or DM 0.10 per compound in the case of the *Dictionary of Trivial Names*. Similar calculations for the *Registry Handbook—Common Names* and for the *Index Guide* give "unit costs" of less than DM 0.01 per name or per compound. Here again the potential purchaser or user must decide whether to pay more for fewer names and compounds *with* structural formulas and a literature reference (the latter subject to the reservations mentioned earlier), or to pay less for a greater number of names and compounds, usually *without* structural formulas and *without* literature references.

The decision in favor of one or the other publication will certainly depend on the detailed needs of the user. The reviewer hopes that the comments offered here will help in making the decision.

Udo Eberhardt
Chemische Berichte Editorial Office
Weinheim (FRG)

Scanning Electron Microscopy and X-Ray Analysis. By *R. E. Lee*. Ellis Horwood/PRT Prentice Hall, Englewood Cliffs, 1993. 464 pp., hardcover $ 60.00.—ISBN 0-13-813759-5

Scanning electron microscopy (SEM) has now become well established in many areas of chemistry, materials science, physics, biology, and medicine, in situations that demand high resolution imaging of materials and specimens or chemical analysis of microscopic regions. There is already plenty of literature, including some that is very recent, treating the methods of electron microscopy at a level suitable for specialists. However, this book has been written with a different objective, namely to explain, with a minimum of mathematics but with many well-chosen drawings, figures, and diagrams, the elementary physical and technical aspects of the scanning electron microscope. The author, who has many years of practical experience in this field, has certainly succeeded in this aim.

The first five of the twelve chapters are concerned with the construction of the scanning electron microscope, the generation of the electron beam, and the principles, functioning, and aberrations of magnetic lenses. The author describes applications-related aspects with detailed illustrations, for example, images of the surface of a cathode after overheating, and also discusses recent instrumental developments such as the use of field emission sources. The following chapters deal with the interaction of electrons with matter, different types of detectors, and in considerable detail with image formation and image processing. Scattering processes, contrast mechanisms, and many other aspects of importance to the user are explained in careful detail by text and figures. The chapters on vacuum pumping and pressure measurement and on specimen preparation are equally clear and detailed. The final chapter contains a thorough and detailed description of SEM X-ray microanalysis, explaining the principles of energy-dispersive and wavelength-dispersive spectroscopy, and the artefacts that can arise in qualitative and quantitative elemental analysis. The book ends with a useful appendix which includes data on the characteristic X-ray emissions of the elements, and also a short glossary of technical terms which is especially helpful.

I can thoroughly recommend this book for newcomers to SEM methods, as it covers all the important aspects and explains them in a simple, clear, and understandable way, but without being too superficial. Technical and scientific staff working in electron microscopy laboratories will also find the book very useful, and will obtain new insights from it. *Scanning Electron Microscopy and X-Ray Analysis* is certainly a very useful addition to the literature of the SEM laboratory, and I feel sure that it will come to be regarded as essential basic reading there. Lastly I recommend the book to the interested reader who simply wants to know something about how an electron microscope works and how it is used.

Werner Mader
Institut für Anorganische Chemie
der Universität Bonn (FRG)

 © VCH Verlagsgesellschaft mbH, D-69451 Weinheim, 1994 0570-0833/94/1212-1306 $ 10.00+.25/0

Fluorinated Isocyanides—More than Ligands with Unusual Properties

Dieter Lentz*

The substitution of hydrogen by fluorine in organic compounds usually results in drastic changes in their properties. For isocyanides, for which fluorinated examples have only recently become available in preparative quantities, this substitution leads to a significantly increased reactivity and a tendency to polymerize, which, on one hand, makes their handling more difficult. On the other hand, this high reactivity makes the fluorinated isocyanides useful building blocks for the synthesis of compounds like *N*-trimethylformamide. Energetically favorable π^* orbitals bestow excellent π-acceptor properties towards low-valent transition metal complexes, especially on the ligand trifluoromethyl isocyanide. The pronounced tendency of this ligand to bridge two metal atoms enables the formation of structural types that are not accessible with other π-acceptor ligands. Thus it was possible to prepare $[(Os_3(CO)_{11}(\mu_2\text{-}CNCF_3)_2]$ (a derivative of the hypothetical $[Os(CO)_{13}]$) which may be considered as a model for an associative mechanism of ligand substitution at carbonyl clusters. In contrast to the well-studied chemistry of trifluoromethyl isocyanide, that of the few other known fluorinated isocyanides is only now receiving attention. In particular the only recently synthesized trifluorovinyl isocyanide promises a rich chemistry as a result of its difunctionality.

1. Introduction

Isocyanides have been known for more than a hundred years. In 1867 Gautier[1] and Hofmann[2] recognized the nature of these compounds, which are isomeric to nitriles. Due to their repulsive odor and only limited synthetic accessibility, this class of compounds was long neglected. The synthesis of isocyanides from the corresponding formamides, developed by Ugi,[3] as well as the large number of subsequent studies of this class of compounds have demonstrated their great importance to organic synthesis.[3] The review by C. Grundmann gives a good survey of the current state of synthetic methods.[4]

Recently a number of novel isocyanides, some of which had been long sought after, have been prepared. Examples include CN–CN,[5] CN–NC,[6] NC–C≡C–NC, CN–C≡C–NC,[7] and HC≡C–NC.[8] The last species is not only of interest to chemists since it has been detected in interstellar space.[9]

The coordination chemistry of isocyanides has experienced a renaissance through the studies of Malatesta and Bonati.[10] Since then the interest in isocyanide complexes has not abated. The coordination chemistry of regular isocyanides has been summarized in several review articles.[11] The studies by Fehlhammer et al.[12] over the last few years on the coordination chemistry of functionalized isocyanides have led to remarkable compounds like $[(CO)_5Cr(CNCN)]$[13] or $[\mu_3\text{-}\{(CO)_5Cr(CN\text{–}C)\}\text{-}\{Co(CO)_3\}_3]$.[14] Multidentate isocyanides have been studied primarily with respect to their use as technetium complexes for radiological diagnostics.[15]

Fluorination of organic compounds usually leads to a drastic change in their properties,[16] particularly in the case of perfluorination. It is therefore somewhat surprising that the chemistry of fluorinated isocyanides has remained nearly unexplored for quite some time, even though the synthesis of trifluoromethyl isocyanide was first reported in 1967.[17]

2. The Synthesis of Fluorinated Isocyanides

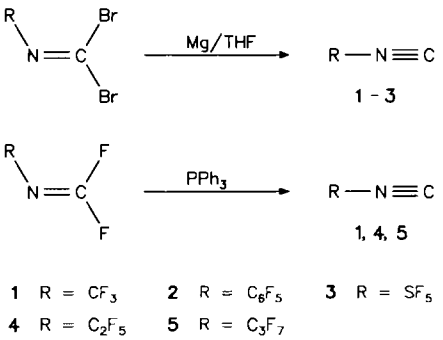
There are currently two main preparative methods for α-fluorinated and perfluorinated isocyanides, apart from the poorly reproducible syntheses for trifluoromethyl isocyanide (**1**)[17, 18] and pentafluorophenyl isocyanide (**2**)[19] described before the onset of our work that yield by-products that are difficult to remove. Simonneaux et al. recently discovered that isocyanides that are fluorine-substituted at the β position, like 2,2,2-trifluoroethyl and 2-fluoroethyl isocyanide, can be prepared by Ugi's synthetic method.[20]

2.1. Dehalogenation of Dihalomethanimines

The synthesis of **1**,[21] **2**,[22] and sulfurpentafluoride isocyanide (**3**)[23] is best performed by α-dehalogenation of the corresponding dibromomethanimines. Magnesium in THF has proven to be the best dehalogenation agent.[21–23] The reaction of $CF_3N{=}CBr_2$ with zinc in dimethylformamide leads directly to the isocyanide **1**;[24] it has not been possible to detect an organozinc inter-

[*] Priv.-Doz. Dr. D. Lentz
Institut für Anorganische und Analytische Chemie der Freien Universität
Fabeckstrasse 34-36, D-14195 Berlin (FRG)
Telefax: Int. code + (30)838-2424

 © VCH Verlagsgesellschaft mbH, D-69451 Weinheim, 1994 0570-0833/94/1313-1315 $ 10.00+.25/0



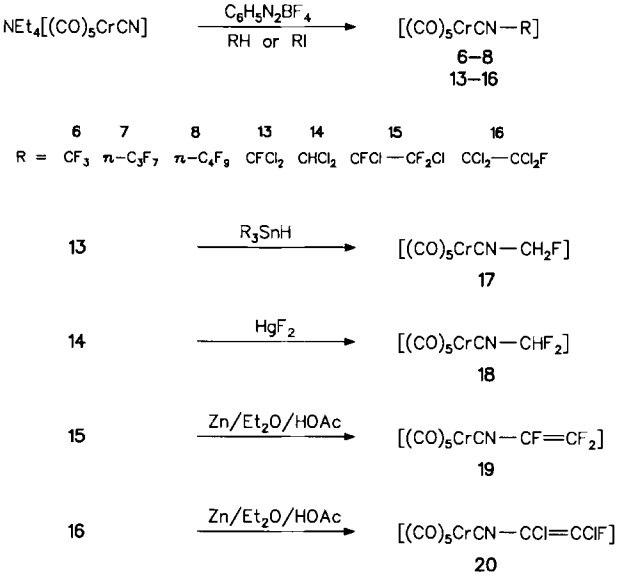
mediate. For **1** the yield is very high; for SF_5NC **3**, however, it is below 5%. The use of organolithium compounds does not improve the yields.[23] Recently Shreeve et al. reported an alternative synthesis for **1**, **4**, and **5**, utilizing the defluorination of difluoromethanimines with triphenylphosphane.[25]

2.2. Pyrolysis of Pentacarbonyl(isocyanide)chromium Complexes

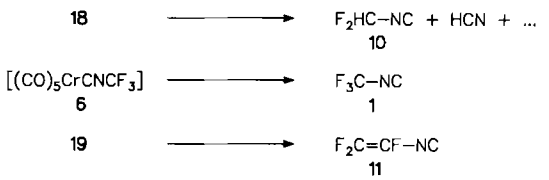
Fehlhammer et al. showed that pentacarbonyl(cyano)chromate can be alkylated by a radical pathway in the presence of diazonium salts.[26] The use of trifluoromethyl, heptafluoro-*n*-propyl, and nonafluoro-*n*-butyl iodide enabled the preparation of the corresponding isocyanide complexes $[(CO)_5Cr(CN-R)]$ (**6**–**8**) in low yields. A chlorine/fluorine exchange in pentacarbonyl(trichloromethyl isocyanide)chromium with $SbF_3/SbCl_5$ led at best to traces of the fluorinated isocyanide complex **6**.[27] The authors made no attempt to obtain the free isocyanides from these complexes.

There are no suitable organic precursors for the synthesis of the intermediate members of the series methyl, fluoromethyl (**9**), difluoromethyl isocyanide (**10**), and **1**, as well as for trifluorovinyl (**11**) and fluoroethynyl isocyanide (**12**). The formation of these isocyanides on the pentacarbonylchromium fragment proved to be advantageous.

Radical alkylation yields the corresponding starting compounds **13**–**16**, which can be modified by standard methods of organic synthesis. For instance, reduction of pentacarbonyl(dichlorofluoromethyl isocyanide)chromium (**13**) by tributyltin hydride leads to the fluoromethyl isocyanide complex **17**. Chlorine/fluorine exchange with mercuric fluoride yields the difluoromethyl isocyanide complex **18**.[28] Dechlorination of the dichlorotrifluoroethyl and tetrachlorofluoroethyl isocyanide complexes with zinc enables the preparation of the halogenated vinyl isocyanide complexes **19** and **20**,[29] which were supposed to serve as precursors for **11** and **12**.



Vacuum pyrolysis of these organometallic precursors, however, meets only with limited success. While the trifluoromethyl isocyanide complex **6** only yields the free isocyanide **1**,[30] the pyrolysis of **18** is accompanied by the release of significant amounts of HCN.[31] By using microwave spectroscopy, ethynyl isocyanide (**21**) was detected as an important, albeit trace impurity. This compound was subsequently directly prepared by pyrolysis of $[(CO)_5Cr(CN-CCl=CHCl)]$.[8] This method fails completely when applied to the fluoromethyl isocyanide complex **17**.[31]



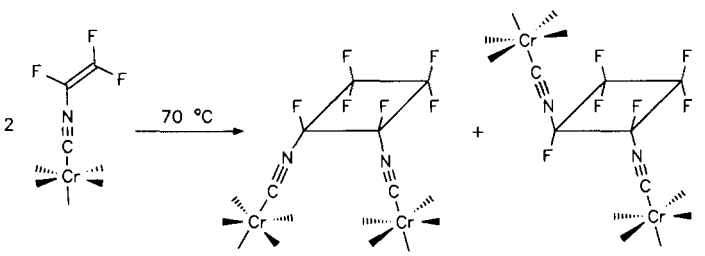
Much better results are obtained with the trifluorovinyl isocyanide complex **19**. Vacuum pyrolysis at 240 °C leads smoothly

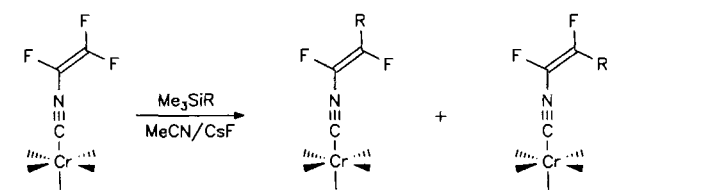


Dieter Lentz was born in Heidelberg in 1951. After finishing his Diplom in chemistry in 1977, he completed his studies in 1979 under the direction of Professor Konrad Seppelt with a Ph.D. thesis on pentafluoroorthoselenates and -tellurates of nonmetals. From 1980 to 1986, he worked on his habilitation at the Freie Universität Berlin, studying fluorinated isocyanides and bis(fluoromethylidyne)triiron clusters. Since 1986 he has been Privatdozent in the Institute for Inorganic and Analytical Chemistry at the Freie Universität Berlin. In 1991, he was a visiting professor in the Department of Chemistry, Clemson University, South Carolina.

to free **11**.[29] It has not yet been possible to detect **12** by microwave spectroscopy during the pyrolysis of **20** or **19** at high temperatures.[32] The action of electric discharges on **2** and H_5C_6NC does also not lead to **12** or **21**.[32] F–C≡C–C≡N can, however, be prepared from F_5C_6CN in this manner and characterized by mass spectrometry (MS), and photoelectron (PE), IR, and microwave spectroscopy.[33]

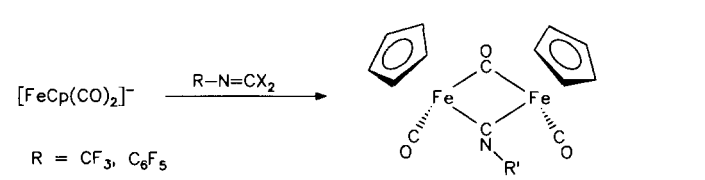
The trifluorovinyl isocyanide complex **19** proved to be an ideal starting material for other fluorinated isocyanides. As a fluorinated alkene, it can undergo [2 + 2]cycloaddition as well as nucleophilic substitution reactions. When **19** is heated under ambient pressure to 70 °C, one smoothly obtains an isomeric mixture of the *cis*- and *trans*-1,2,3,3,4,4-hexafluoro-1,2-diisocyanocyclobutane complexes **22a** and **22b**.[34] This reaction provides a convenient access to fluorinated cyclic diisocyanides. If the trifluoromethylation agent $F_3CSi(CH_3)_3$[35] or the pentafluorophenylating reagent $F_5C_6Si(CH_3)_3$[36] is treated with **19** in the presence of CsF a nucleophilic attack on the β-carbon atom yields an (*E*)/(*Z*) isomeric mixture of the perfluorinated alkenyl isocyanide complexes **23a** and **23b**, respectively.[37] The use of other nucleophilic reagents should make it possible to prepare numerous fluorinated vinyl isocyanides on the pentacarbonylchromium fragment.





23a R = CF_3 **23b** R = C_6F_5

Another pathway for the synthesis of fluorinated isocyanides on a complex fragment is the reaction between the highly nucleophilic anion $[FeCp(CO)_2]^-$ and the dihalomethanimines $CF_3–N=CBr_2$ and $C_6F_5–N=CCl_2$. The expected isocyanide complexes **24** and **25** are obtained in low yields. The main product of the reaction with $C_6F_5–N=CCl_2$, however, is the interesting isocyanide complex **26**, which is formed by a further nucleophilic attack on the fluorinated aromatic ring.[38]



24 R' = CF_3 **25** R' = C_6F_5
26 R' = 4–CpFe(CO)$_2$–C_6F_4

3. Physical Properties, Spectra, and Structures

The boiling point of **1**, −80 °C, is significantly lower than that of methyl isocyanide. This is due to the much smaller dipole moment of 1.153(20) D (determined by measuring the Stark effect in the microwave spectrum[39]) than the 3.8 D for methyl isocyanide.[40] The IR spectra of all fluorinated isocyanides synthesized up to now—except of SF_5NC—exhibit ν(NC) bands between 2100 and 2150 cm^{-1}. A complete analysis of the high-resolution spectrum of **1** is still in progress, but the following assignments of fundamental vibrations appear to be correct: $\nu_1(A_1)$ 2139, $\nu_2(A_1)$ 1209, $\nu_3(A_1)$ 840, $\nu_4(A_1)$ 552, $\nu_5(E)$ 1238, $\nu_6(E)$ 620, $\nu_7(E)$ 460, and $\nu_8(E)$ 145 cm^{-1}.[41]

The gas-phase structure of trifluoromethyl isocyanide (**1**) could be determined very accurately by a combination of microwave and electron diffraction data (Table 1).[39] During the course of this work, it was noted that the quadrupole coupling constants $\chi_{aa} = 1060(30)$, $\chi_{bb} = -530(30)$, and $\chi_{cc} = -530(30)$ kHz are unusually large for isocyanides.[39] The corresponding coupling constants for methyl isocyanides are only $\chi_{aa} = 489.4(4)$, $\chi_{bb} = -244.7(4)$, and $\chi_{cc} = -244.7(4)$ kHz.[42] In addition, it was possible to examine the rotational spectra of vibrationally excited $CF_3–NC$ more closely.[43] Dreizler et al. successfully obtained and analyzed the microwave spectra of difluoromethyl isocyanide[44] and pentafluorophenyl isocyanide.[45] They also determined the quadrupole coupling constants to be $\chi_{aa} = 599.0(10)$, $\chi_{bb} = -406.5(14)$, and $\chi_{cc} = -192.6(14)$ kHz for **10**, and $\chi_{aa} = 958.(113)$, $\chi_{bb} = -794.(60)$, and $\chi_{cc} = -165.(69)$ kHz for **2**.

It proved possible to perform low-temperature crystal structure analyses of pentafluorophenyl isocyanide (**2**)[46] and trifluorovinyl isocyanide (**11**).[47] Table 1 shows a comparison with the structural data of other isocyanides. It is noteworthy that the N≡C bond lengths in the solid state are shorter than those determined in the gas phase.

PE spectroscopic data for valence[53] as well as core[54] electrons are available only for **1** and methyl isocyanide. Noteworthy is the lowering of the $n_C(A_1)$ and the $\pi_{NC}(E)$ energy levels in trifluoromethyl isocyanide by 1.3 and 2.1 eV, respectively, rela-

Table 1. C–NC and CN≡C bond lengths in isocyanides [pm].

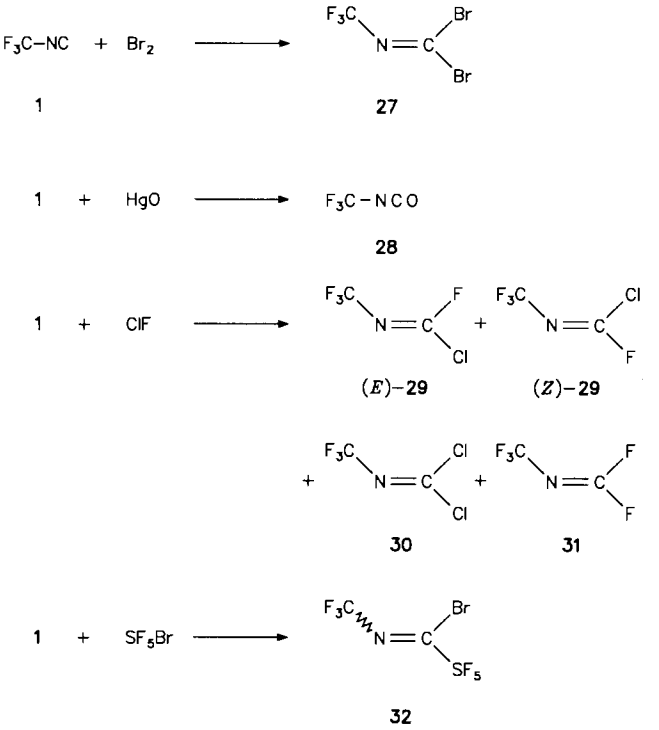
Isocyanide	r(C–NC)	r(CN≡C)	Phase	Ref.
$H_3C–NC$	142.8(2)	116.6(1)	gas.	[48]
$F_3C–NC$ **1**	140.7(3)	117.1(3)	gas.	[39]
H–NC		117.26(2)	gas.	[49]
$H_5C_6–NC$	141.0	114.2	gas.	[50]
$F_5C_6–NC$ **2**	138.0(2)	115.9(3)	solid	[46]
$F_2C=CF–NC$ **11**	137.2(1)	116.8(2)	solid	[47]
$H_2C=CH–NC$	137.9(6)	117.4(6)	gas.	[51]
NC–NC	131.60(26)	117.49(18)	gas.	[52]
HCC–NC	131.7(1)	117.5(1)	gas.	[8]

tive to methyl isocyanide. Assuming that an approximately equal $\pi-\pi^*$ splitting of the molecular orbitals occurs in both isocyanides, trifluoromethyl isocyanide possesses a LUMO that is lowered by about 2 eV. This explains the strong π-accepting behavior of trifluoromethyl isocyanide, which makes it an excellent ligand.

Ab initio calculations for the fluorinated methyl isocyanides **9**, **10**, and **1** indicate a distinct lowering of the LUMO energies with increasing degree of fluorination.[55] The lowest LUMO energy was calculated for **3**, which therefore should be a stronger π-acceptor than **1**.[55] Experimental evidence for this does not yet exist, as there are no known complexes of **3**.

With mass spectrometry on the negatively charged ions of CF_3NC and CF_3CN the dissociation energies of the C–C and C–N bonds were determined to be 4.4 ± 0.2 eV for CF_3CN and 3.9 ± 0.2 eV for CF_3NC, and the binding enthalpies ΔH_f^{298} to be 4.8 ± 0.3 eV for CF_3CN and 4.3 ± 0.3 eV for CF_3NC.[56]

The ^{19}F, ^{13}C, and ^{14}N NMR data for trifluoromethyl isocyanide show nothing unusual.[57] Due to the low electric field gradient at the nitrogen atom, an effect that is generally observed for isocyanides, the coupling between the ^{14}N and ^{19}F nuclei can be observed [$^2J_{^{19}F,\,^{14}N}=15.5$ Hz for CF_3NC[18, 57] **1**; $^2J_{^{19}F,\,^{14}N}=13$ Hz for CHF_2NC[31] **10**; $^2J_{^{19}F,\,^{14}N}=10$ Hz for C_2F_3NC[29] **11**].



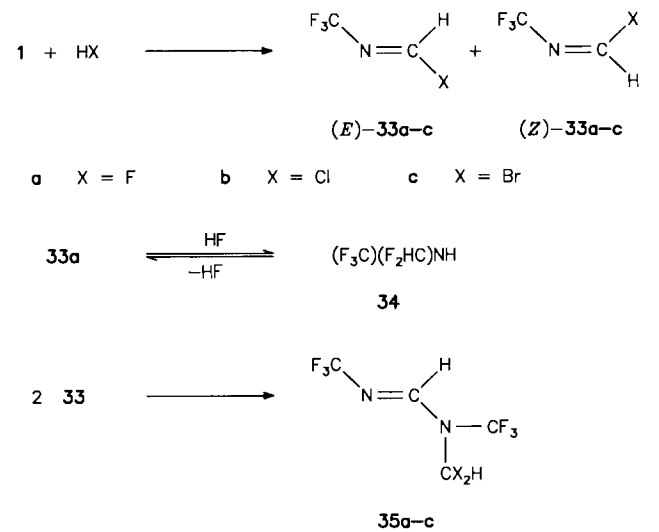
4. Fluorinated Isocyanides as Building Blocks for Synthesis

Fluorinated isocyanides are characterized by their increased reactivity relative to nonhalogenated isocyanides. This is especially evident in a very strong tendency towards polymerization. Trifluoromethyl isocyanide **1** decomposes even below its boiling point of $-80\,^\circ C$ to yield a polymer. According to Haszeldine et al. an α-polymer is formed.[18] Pentafluorophenyl isocyanide **2** decomposes rapidly above its melting point of $13\,^\circ C$;[22] trifluorovinyl isocyanide begins to decompose above $-40\,^\circ C$.[29]

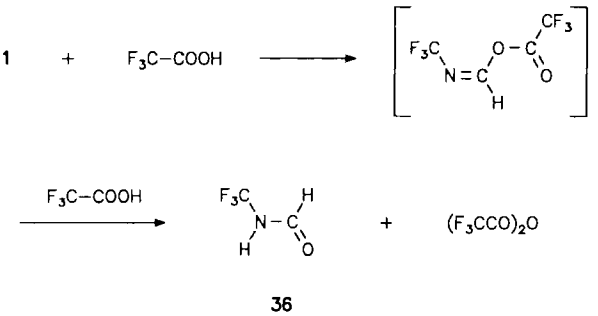
4.1. α-Additions

α-Additions have only been investigated for **1**. In a reversal of the formation of **1**, the α-addition of bromine to **1** yields dibromo-*N*-trifluoromethylmethanimine (**27**).[17] Mercuric oxide oxidizes the isocyanide to the isocyanate **28**.[18] The reaction of **1** with $(CF_3)_2NO$ leads to a mixture of CF_3-NCO, $(CF_3)_2N-O-N(CF_3)_2$, $CF_3-N=C[ON(CF_3)_2]_2$, and $CF_3-N=C[ON(CF_3)_2]-C[ON(CF_3)_2]=N-CF_3$.[58] With chlorine monofluoride, a mixture of the dihalomethanimines **29**–**31** is obtained, whereas the addition of SF_5Br leads to methanimine **32**.[59]

The addition of hydrogen halides is especially interesting, as it yields the *N*-trifluoromethylmethanimines **33**.[59] When performed with regular isocyanides, it is impossible to stop the reaction at this stage.[60] The methanimines **33** are present as mixtures of (*Z*) and (*E*) isomers; electron diffraction and NMR studies indicate that the (*E*) isomer predominates. The barriers for isomerization as well as the (*E*/*Z*) ratios depend on the substituents. Compound **33a** is capable of adding HF reversibly to give **34**.[59] Like $CF_3-N=CF_2$, the compounds **33** tend to dimerize, leading to the formation of the formamidines **35**.[59]



The reaction of **1** with trifluoroacetic acid enables the synthesis of *N*-trifluoromethylformamide **36**,[61] which cannot be prepared directly owing to the low stability of trifluoromethylamine.[62] The boiling point of **36** is lower than that of *N*-methylformamide. It is present as the formamide, and not in the form of the hydroxymethanimine. In contrast to *N*-methylformamide, for which 95% (*Z*) is present in the isomeric mixture, the (*E*) isomer is the thermodynamically more stable form for **36**. The isomers

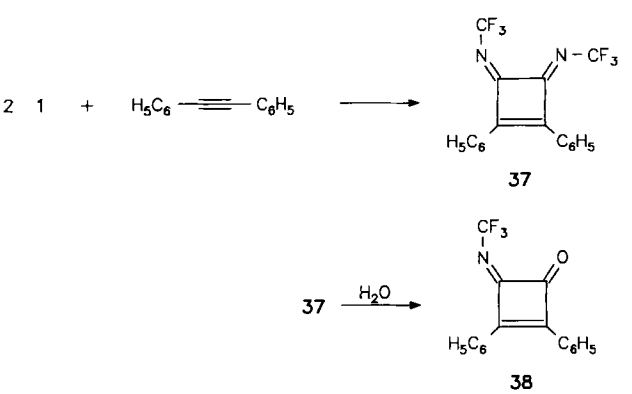


36

are interconverted by a hindered rotation, for which the free enthalpy of activation, determined by dynamic NMR methods, is 62 kJ mol^{-1}.[61]

4.2. Cycloadditions

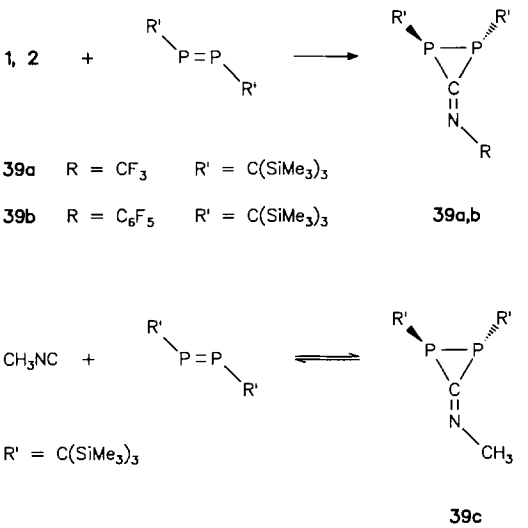
Reactions of alkynes with isocyanides lead to numerous products that depend on the substituents on both the isocyanide and the alkyne.[63] The simple [2 + 1]cycloaddition product, a cyclopropenimine,[64] is observed only in exceptional cases. The reactions generally require alkynes with either electron-donating or electron-withdrawing substituents.[63, 64] Isocyanide **1** reacts smoothly with diphenylacetylene in dilute solution to form colorless, crystalline 1,2-diphenyl-3,4-bis(trifluoromethylimino)-cyclobut-1-ene (**37**),[65] which has been completely characterized by its spectroscopic data and an X-ray crystal structure analysis. Partial hydrolysis of **37** leads to the formation of the pale yellow ketone derivative **38**. Similar reactions were also observed for 2-butyne and ethoxyacetylene.[66] Fluoroalkenes and hexafluorobutyne, however, do not react with trifluoromethyl isocyanide.[67]



37

38

So far, the cycloaddition of **1** and **2** (and other isocyanides) with diphosphenes is the most thoroughly investigated reaction. Depending on the substituents on the phosphorus atoms different products are obtained. The reactions of **1** and **2** with diphosphenes containing a tris(trimethylsilyl)methyl substituent are identical. The diphosphiranimines **39a** and **39b** are formed and have been characterized by their spectroscopic data[68] and by a crystal structure analysis of **39a** (Fig. 1).[69] These products



39a,b

39c

39a and **39b** form thermally extraordinarily stable crystals that are also not sensitive to air or hydrolysis. The analogous addition of methyl isocyanide leads to the diphosphiranimine **39c**, which undergoes a reverse cycloaddition reaction at room temperature to yield the diphosphene and methyl isocyanide.

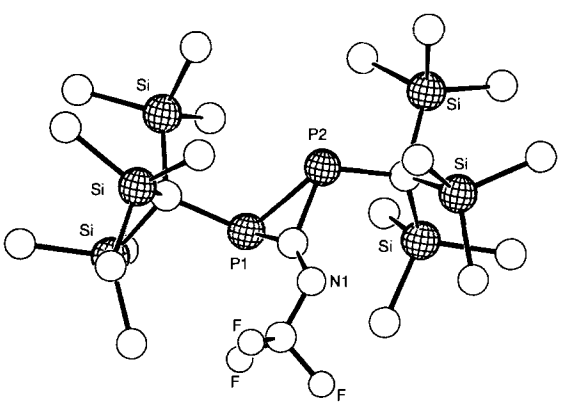
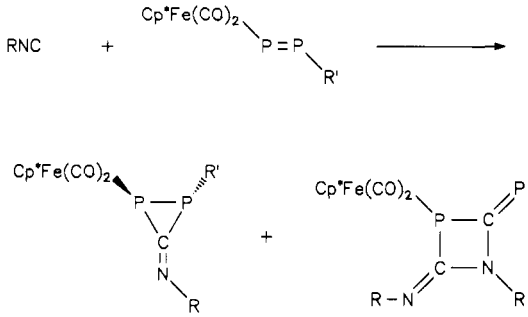


Fig. 1. Molecular structure of **39a** in the crystal.

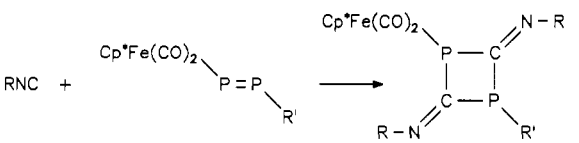
The metal-substituted diphosphenes Cp*Fe(CO)$_2$P=PR' (Cp* = C_5Me_5, R' = C[Si(CH$_2$)$_3$]$_3$) react to form the three-membered ring systems **40**.[70] In the case of the 2,4,6,-tri-*tert*-butylphenyl substituent, however, the reaction proceeds further to afford a product with the composition [Cp*Fe(CO)$_2$PPR'][RNC]$_2$ (**41**), which displays two sets of signals in the ^{31}P and ^{19}F NMR spectra. According to the spectroscopic data, **41** possesses a 1,3-azaphosphetane structure with an exocyclic P=C double bond. Regular isocyanides like *ortho*-tolyl isocyanide, however, lead to 2,4-diimino-1,3-diphosphetane derivatives, as demonstrated by a crystal structure analysis.[70]

If the diphosphene carries two 2,4,6,-tri-*tert*-butylphenyl substituents, the three-membered ring cannot be detected. Instead, the reaction with **1** leads, by an as yet unknown mechanism, to the five-membered ring system **42** with an exocyclic P=C double bond, whose structure was determined by a crystal structure analysis.[68]

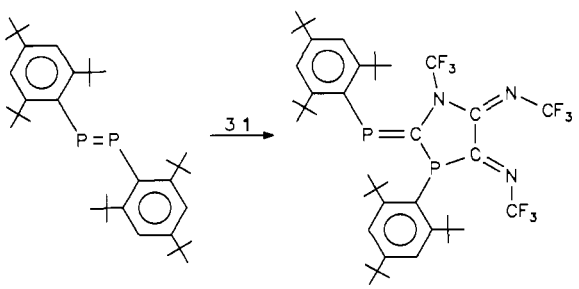


40 **41**

40a R = CF_3 R' = 2,4,6-tBu_3-C_6H_2
40b R = CF_3 R' = $C(SiMe_3)_3$
40c R = C_6F_5 R' = 2,4,6-tBu_3-C_6H_2
41 R = CF_3 R' = 2,4,6-tBu_3-C_6H_2

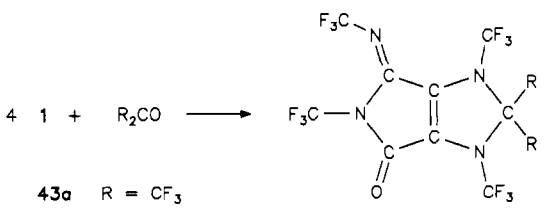


R = 2-CH_3-C_6H_4 R' = 2,4,6-tBu_3-C_6H_2



42

A similarly complicated course is taken by the reaction of hexafluoroacetone or 1,3-dichlorotetrafluoroacetone with **1**. The expected iminodioxolane is not formed,[71] but instead the hexahydropyrrolo-[3,4-d]imidazole **43** is found.[61, 72]



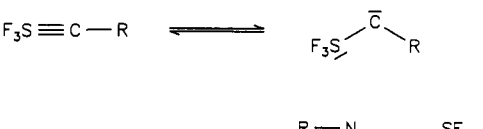
43a R = CF_3
43b R = CF_2Cl

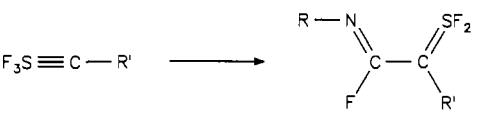
43

4.3. Reactions with Carbenoids

According to structural studies, the alkylidynesulfurtrifluoride compounds prepared by Seppelt et al. possess an energetically low-lying excited state with a C–S single bond and a carbene-like carbon atom in addition to the ground state with a C–S triple bond.[73] This readily explains the decomposition of these compounds to yield dimers with C–C double bonds.[73] Reactions of the P–C triple bond as well as of the carbene-like carbon atom can also be observed in the compound $(iPr_2N)_2PC-SiMe_3$, prepared by Bertrand et al.[74]

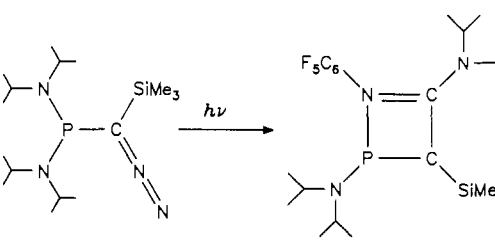
Recently the first successful reactions—apart from the trivial addition of hydrogen fluoride—of alkylidynesulfurtrifluorides (possessing a C≡S triple bond or a carbene-like carbon atom) with the fluorinated isocyanides **1** and **2** have been performed. The resulting alkylidenesulfurdifluoride **44** containing conjugated double bonds could stem from a ketenimine as well as from a three-membered ring species.[73] The compounds **44** can be





44a R = CF_3 R' = CF_3
44b R = C_6F_5 R' = CF_3
44c R = C_6F_5 R' = SF_5

44



45

three-membered ring species.[73] The compounds **44** can be present as several isomers. When the substituents are SF_5 and C_6F_5, only one isomer is observed. This enabled the first crystal structure analysis of an alkylidenesulfurdifluoride.[73]

The photochemical reaction of $(iPr_2N)_2P-C(N_2)-Si(CH_3)_3$ with C_6F_5NC (**2**) yields, by migration of the diisopropylamino group, the didehydroazaphosphetane derivative **45** (Fig. 2).[75]

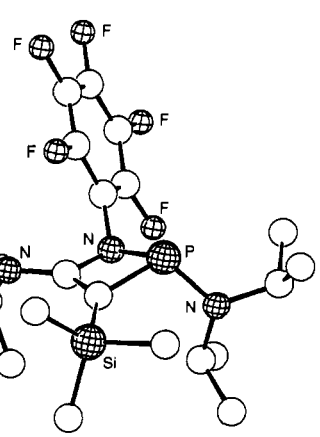
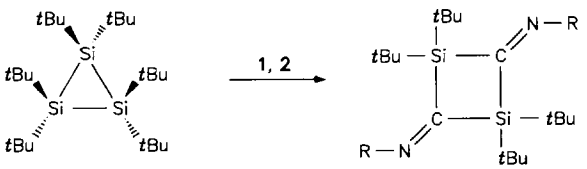


Fig. 2. Molecular structure of **45** in the crystal.

The expected primary product, a ketenimine, could again not be observed.

2,6-Dimethylphenyl isocyanide reacts with tetrakis(2,6-dimethylphenyl)disilene under the formation of a disilacyclopropanimine.[76] Although the photolysis of hexa-*tert*-butylcyclotrisilane yields a disilene, it appears that this compound does not react with isocyanides like **1** or **2**, but that the simultaneously formed silylene is the reactive species. Head-to-tail dimerization of the silaketenimine intermediates formed from the silylene leads to the observed 1,3-disilacyclobutane-2,4-diimines **46**.[77] The trifluoromethyl derivative **46a** was characterized by a crystal structure analysis.[77]

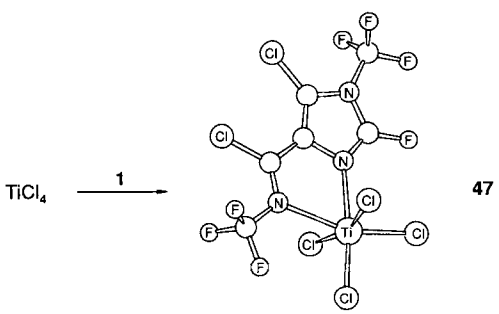


46

46a R = CF_3
46b R = C_6F_5

5. Fluorinated Isocyanides as Ligands in Coordination Complexes

According to results obtained from PE spectroscopy (see Section 3), trifluoromethyl isocyanide (**1**) should be a relatively weak Lewis acid; it should, however, possess rather good π-acceptor properties because of its energetically favorable π^* orbitals. Indeed, **1** does not form Lewis acid–base addition products with BF_3 or PF_5. The reaction with the stronger Lewis acid AsF_5 proceeds further, probably yielding $CF_3N{=}C(F)AsF_4$,[78] and even with titanium tetrachloride no simple trifluoromethyl isocyanide complex is formed. Instead, the linking of three CF_3NC units leads to an imidazole derivative that acts as a bidentate ligand in complex **47**.[79]

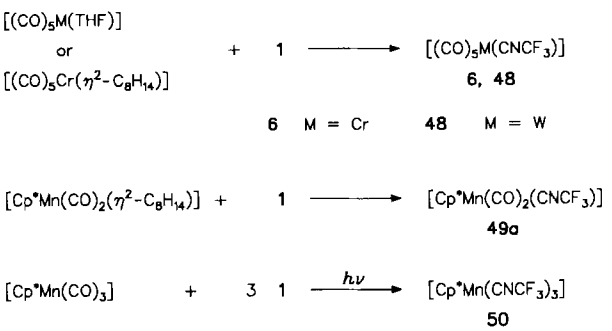


47

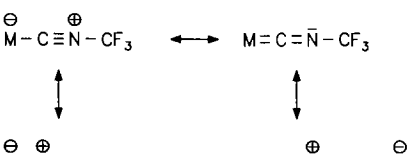
5.1. Mononuclear Trifluoromethyl Isocyanide Complexes and the Relative Ratio of the π-Acceptor and σ-Donor Strengths of the CF_3NC Ligands

Owing to the strong tendency of trifluoromethyl isocyanide **1** to polymerize, all syntheses must be performed at the lowest possible temperatures and at high dilution. In addition it is necessary to use reactive complex fragments, for example, those carrying readily substitutable ligands. It is frequently possible to perform ligand substitutions under photochemical conditions.

The synthesis of the first trifluoromethyl isocyanide complexes $[(CF_3NC)Cr(CO)_5]$ (**6**) and $[(CF_3NC)W(CO)_5]$ (**48**)[30] indicated



that the trifluoromethyl isocyanide ligand has a very similar, maybe even superior, ratio of π-acceptor to σ-donor strengths than CO. For instance, ^{13}C NMR spectra show the resonance of the *trans*-CO ligand at higher field than those of the *cis* ligands. This is the reverse of the effect that is observed for most other complexes containing the pentacarbonylchromium fragment—exceptions are thiocarbonyl and selenocarbonyl complexes.[80] Data from vibrational spectroscopy indicate the same trend. However, it is very difficult to analyze these data precisely, because the CO vibrations couple with those of the CN unit. Further proof is obtained from UV PE spectra of **6** and **48**. No splitting, but only a slight lowering of the "t_{2g}" level by 0.26 eV[81] relative to that of hexacarbonyl complexes is observed.[82] Results from X-ray PE spectra also confirm this trend.[54] The binding energies of the core electrons of all atoms in the trifluoromethyl isocyanide ligand in **6** and **48** are clearly lower than those found for free trifluoromethyl isocyanide. Especially notable is the decrease of the F-1s binding energy by more than 1 eV. In a valence bond description this can be explained by the participation of resonance structures with hyperconjugation. (Scheme 1).



Scheme 1.

A structural study of the chromium complex **6** in the gas phase, by electron diffraction,[83] indicates a significant bending at the isocyanide nitrogen atom to 142(4)° and a slight increase in the CN distance to 122.0(16) pm, relative to the free isocyanide.

Manganese halfsandwich complexes of the type $[Cp^*Mn(CO)_2L]$ (L = $CNCF_3$, CO, $CNCH_3$, CS) (**49a–d**),[84] $[Cp^*Mn(CO)(CNCF_3)L]$ (L = THF, η^2-C_8H_{14}, CH_3NC, C_6H_5NC, PF_3, $P(C_2H_5)_3$, $P(C_6H_5)_3$, CS) (**51**),[85] and $[\eta^6$-1,3,5-$C_6H_3(CH_3)_3]Cr(CO)(L)(CNCF_3)]$[86] (L = CO, $CNCH_3$) are much better suited for the comparison of π-acceptor and σ-donor strengths based

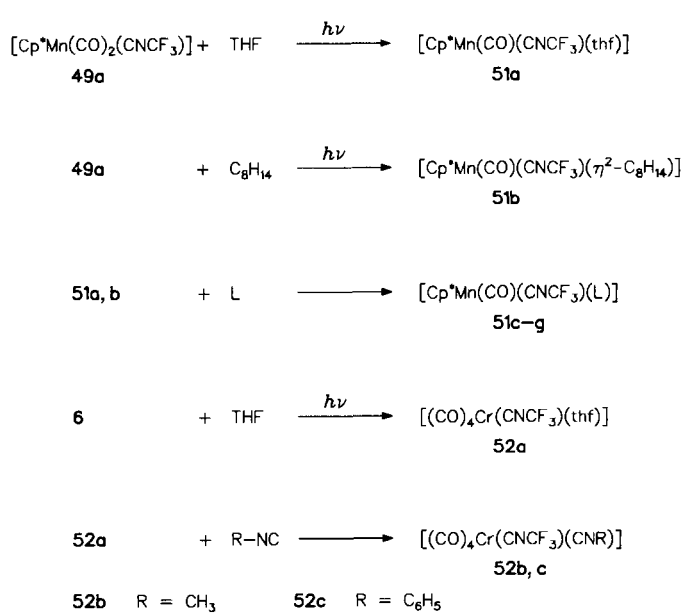
on vibrational spectroscopic data than the complexes **6** and **48**. The IR data of $[Cp^*Mn(CNCF_3)_3]$ (**50**) [ν(CN) = 1948, 1823 cm^{-1}] indicate unambiguously that the band between 1650 and 1850 cm^{-1} in the spectra of **49a** and **51** can be assigned to the CN valence vibration of the trifluoromethyl isocyanide ligands. In the case of the complexes **51** with donor ligands such as THF, this band is shifted to below 1700 cm^{-1}, which indicates a CN bond order in the isocyanide ligand of approximately 2. A comparison of the force constants of the CO valence vibrations of these complexes (Table 2), calculated according to the method

Table 2. Vibrational spectroscopic data of manganese halfsandwich complexes $[Cp^*Mn(CO)_2L]$ and $[Cp^*Mn(CO)(CNCF_3)L]$ (*n*-pentane solutions).

L =	CO	$CNCH_3$	CS
$[Cp^*Mn(CO)_2L]$			
$\tilde{\nu}$(CO) [cm^{-1}]	2010, 1918	1940, 1893	1996, 1945
$\tilde{\nu}$(CN) [cm^{-1}]		2105	
k(CO) [N cm^{-1}]	15.45	14.83	15.68
$[Cp^*Mn(CO)(CNCF_3)L]$			
$\tilde{\nu}$(CO) [cm^{-1}]	2007, 1945	1939	1988
$\tilde{\nu}$(CN) [cm^{-1}]	1810	1762, 2129	1831
k(CO) [N cm^{-1}]	15.77	15.1	15.9

of Cotton and Kraihanzel,[87] allows an estimate of the relative ratio of π-acceptor and σ-donor strengths of the trifluoromethyl isocyanide ligand relative to other ligands. This force constant is a measure of the CO bond order and, hence, of the contribution of the CO ligands to backbonding. If the force constant is large, the CO ligands do not contribute strongly to backbonding, and therefore the other ligands' contribution must be high. This is the case for the known strong π-acceptor ligands CS and PF_3 and apparently for the trifluoromethyl isocyanide ligand as well.

Further indications for the extraordinary properties of the trifluoromethyl isocyanide ligand stem from ligand substitution reactions on **49a** and **6**.[85, 88] Only the carbonyl ligands are substituted. This enables the synthesis of **52b**, which is formed preferentially as the *trans* isomer. This particular compound in



corporates all three ligands to be compared in one molecule. Its crystal structure analysis shows that there are significant differences among the $Cr-C_{ligand}$ distances. The bond to the trifluoromethyl isocyanide ligand is 20 pm shorter than that to the methyl isocyanide ligand, and also clearly shorter than the bonds to the carbonyl ligands. A further notable difference between the two isocyanide ligands is the distinct bending of the trifluoromethyl isocyanide ligand, relative to the nearly linear methyl isocyanide ligand.[85]

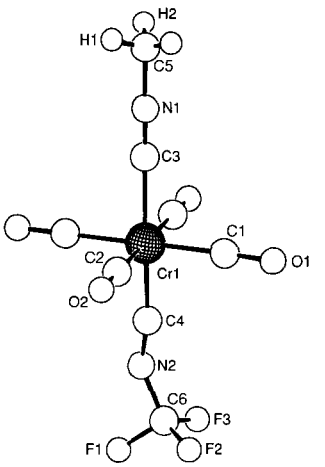
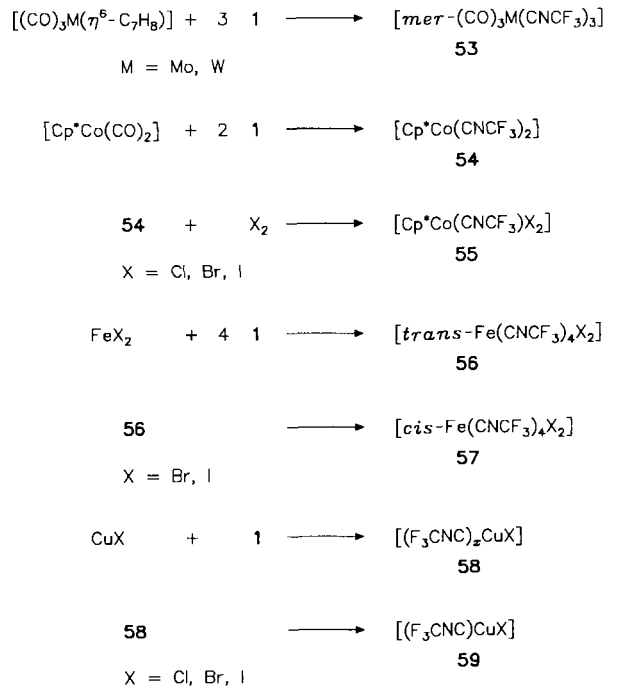


Fig. 3. Molecular structure of *trans*-**52b** in the crystal. Important distances [pm] and angles [°]: Cr1–C1 188.2(5), Cr1–C2 189.8(5), Cr1–C3 201.7(5), Cr1–C4 181.4(6), C3–N1 113.9(6), C4–N2 125.0(8), C3-N1-C5 179.7(3), C4-N1-C6 141.2(7).

According to NMR data, the molybdenum and tungsten complexes **53** are in the meridional form.[89] The exchange of carbonyl ligands in $[Cp^*Co(CO)_2]$ enables the synthesis of the halfsandwich complex **54**, which can be oxidized by halogens to give **55**.[90] The stability of these compounds decreases with increasing electronegativity of the halogen ligand. The low charge density on the metal center results in a distinct shift of the NC valence vibration to higher wavenumbers and a high-field shift of the ^{13}C resonance of the isocyanide carbon atom, in the order I < Br < Cl. According to its crystal structure, $[Cp^*Co(CNCF_3)I_2]$ crystallizes with one molecule of I_2 per complex to form chains of iodine molecules. These chains link the $[Cp^*Co(CNCF_3)]$ fragments;[91] however, the I_2 units are disordered.



The reaction of $FeBr_2$ or FeI_2 with **1** leads primarily to *trans*-**56**, which in dichloromethane slowly converts into the *cis*-isomer **57**.[92] The reaction of copper(I) halides with **1** in dichloromethane is especially interesting. In the presence of an excess of **1** the copper halide dissolves completely and forms **58**. These soluble species with an unknown number of isocyanide ligands, however, tend to liberate **1** to afford **59** in the form of small leaf-shaped crystals with a mother-of-pearl luster. These are insoluble in noncoordinating solvents, but dissolve in acetonitrile. The ^{19}F and ^{13}C NMR spectra confirm the presence of coordinated trifluoromethyl isocyanide.[93]

$[Ni(CO)_4]$ + 4 **1** ⟶ $[Ni(CNCF_3)_4]$ + 4 CO
60

$[Fe(CO)(\eta^4\text{-}C_4H_6)_2]$ + 5 **1** ⟶ $[Fe(CNCF_3)_5]$ + 2 C_4H_6 + CO
61

$[Cr(\eta^3\text{-}C_3H_5)_3]$ + 6 **1** ⟶ $[Cr(CNCF_3)_6]$ + . . .
62

Owing to the instability of **1**, the preparation of homoleptic trifluoromethyl isocyanide complexes is difficult. The most readily performed synthesis is that of the nickel complex **60** from tetracarbonylnickel.[94] The reaction with bis(η^4-butadiene)carbonyliron leads only to moderate yields of $[Fe(CF_3NC)_5]$ (**61**) and $[Fe_2(CF_3NC)_9]$ (**64**).[95] Like $[Fe(CO)_5]$[96] and $[Fe(CNR)_5]$ (R = Et, *i*Pr, *t*Bu)[97] **61**, which presumably possesses a trigonal-bipyramidal structure, is nonrigid on the NMR time scale. After many unsuccessful attempts the synthesis of the chromium complex **62** was achieved by the reaction of trisallylchromium and **1**.[98] The structural analysis shows the expected octahedral coordination by the trifluoromethyl isocyanide ligands. In this molecule, however, there are four crystallographically distinct isocyanide ligands, which differ in the degree of bending at the isocyanide nitrogen atom. Interestingly, an isocyanide ligand with a large C-N-C bond angle is *trans* to an isocyanide ligand with a small angle.

5.2. Multinuclear Trifluoromethyl Isocyanide Complexes

As is the case for the carbonyl ligand, the trifluoromethyl isocyanide ligand should be able to act not only as terminal ligand in mononuclear complexes, but also as bridging ligand in di- or multinuclear complexes and clusters. Due to its strong π-acceptor properties, the trifluoromethyl isocyanide ligand should have an especially high preference for the bridging position, since calculation by Howell et al. indicate that strongly π-accepting ligands favor the bridging position.[99] This was also confirmed for the thiocarbonyl ligand.[100]

5.2.1. Dinuclear Trifluoromethyl Isocyanide Complexes

Dinuclear trifluoromethyl isocyanide complexes have been prepared with nickel,[94] iron,[95] molybdenum,[101] ruthenium,[102] and tungsten.[103] Bis[η^5-cyclopentadienyl-μ-(trifluoromethyl isocyanide)nickel] (**63**) is formed, like the corresponding carbonyl complex, by the reaction of tetrakis(trifluoromethyl isocyanide)nickel (**60**) with bis(η-cyclopentadienyl)nickel. According to the spectroscopic data, the two isocyanide ligands bridge the nickel atoms.

60 + $[NiCp_2]$ ⟶ $[\{CpNi(\mu\text{-}CNCF_3)\}_2]$
63

61 ⟶ $[Fe_2(CNCF_3)_9]$
64

$[Cp(CO)_2M{\equiv}M(CO)_2Cp]$ + **1** ⟶ $Cp(CO)_2M(\mu\text{-}CNCF_3)M(CO)_2Cp$
65a, b, d

$[Cp(CO)_2M{\equiv}M(CO)_2Cp]$ + 2 **1** ⟶ $[\{Cp(CO)_2M(\mu\text{-}CNCF_3)\}_2]$
66a–d

66a–c ⟶ $Cp(CO)_2M(\mu\text{-}CNCF_3)_2M(CO)_2Cp$
67a–c

a M = Mo Cp = C_5H_5
b M = Mo Cp = C_5Me_5
c M = W Cp = C_5H_5
d M = W Cp = C_5Me_5

$[Fe_2(CNCF_3)_6(\mu_2\text{-}CNCF_3)_3]$ (**64**) is formed at room temperature by the decomposition of $[Fe(CNCF_3)_5]$ (**61**). According to spectroscopic data,[95] **64** has a structure that is analogous to $[Fe_2(CO)_9]$[104] and $[Fe_2(CNEt)_9]$.[105] On the NMR time scale there is no exchange of terminal and bridging ligands at room temperature. $[Ru_2(CO)_6(\mu_2\text{-}CNCF_3)_3]$ (**71**) is formed as a by-product during the reaction of $[Ru_3(CO)_{11}(CH_3CN)]$ or $[Ru_3(CO)_{10}(CH_3CN)_2]$ with **1**.[102] In contrast to the extremely unstable $[Ru_2(CO)_9]$[106] **71** is a very stable compound. According to its spectroscopic data, **71** has a structure that is analogous to $[Fe_2(CO)_9]$[104] and $[Ru_2(CN\text{-}iPr)_9]$.[107]

The tendency of the trifluoromethyl isocyanide ligand to occupy the bridging position is particularly apparent in the compounds $[CpM(CO)_2(\mu_2\text{-}CNCF_3)]_2$ (M = Mo, W; Cp = C_5H_5, C_5Me_5) (**66**).[101, 103] In the analogous carbonyl species[108] as well as in the substitution products with regular isocyanides,[109] only terminal ligands are found. The synthesis of these compounds proceeds by the addition of **1** to the metal–metal triple bond in $[Cp(CO)_2M{\equiv}M(CO)_2Cp]$.[101, 103]

Initially one molecule of **1** is added, forming the species **65**, which possesses a μ_2-η^2-bridging trifluoromethyl isocyanide ligand. According to the spectroscopic data, these complexes have a structure analogous to the corresponding phenyl isocyanide complex.[110] The reaction with an excess of **1** yields different products depending on the reaction conditions. At 0 °C, red $[CpM(CO)_2(\mu_2\text{-}CNCF_3)]_2$ (**66**) is formed, which transforms at

room temperature into the deep violet $[CpM(CO)_2(\mu\text{-}F_3C{-}N{=}C{=}C{=}N{-}CF_3)M(CO)_2Cp]$ (**67**). Both structures have been proven by a crystal structure analysis (Fig. 4).

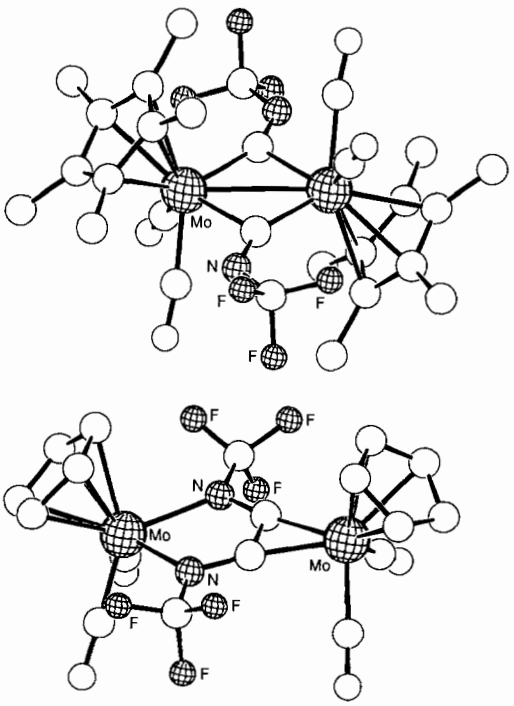


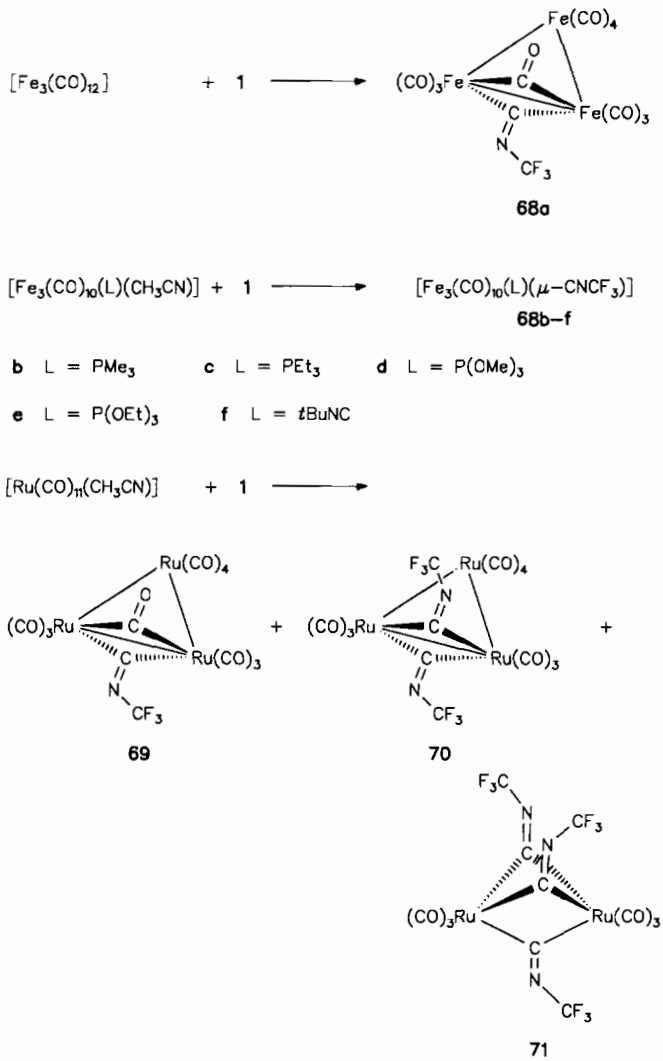
Fig. 4. Molecular structure of **66b** (top) and **67a** (bottom) in the crystal.

Even though **67** has (formally) an odd number of electrons at the metal centers, it is diamagnetic. It is still unclear how the dimerization can proceed so readily, forming a diazabutatriene ligand. In any case, the reaction is more straightforward than those of niobium(III) and tantalum(III) compounds with *tert*-butyl isocyanide, where dimeric isocyanide ligands occur as well.[111] The reductive coupling of coordinated isocyanide and carbonyl ligands has been the subject of extensive experimental as well as theoretical studies by the groups of Lippard,[112] Filippou,[113] and R. Hoffmann.[114]

5.2.2. Trinuclear Clusters Containing the Trifluoromethyl Isocyanide Ligand

The trinuclear carbonyl clusters of the iron triad $[M_3(CO)_{12}]$ (M = Fe, Ru, Os) have very interesting structural and dynamic properties. In the solid state $[Fe_3(CO)_{12}]$ contains two different types of iron atoms. Two of them have three terminal and two bridging ligands each, while one of them has only terminal ligands. Its symmetry is close to C_{2v}.[115] In contrast, the corresponding ruthenium[116] and osmium[117] compounds and their derivatives contain exclusively terminal ligands and hence display D_{3h} symmetry.

The synthesis of the trifluoromethyl isocyanide-substituted derivatives was performed by the replacement of a carbonyl or preferably a labile acetonitrile ligand. The crystal structure analyses of the isostructural compounds of iron (**68a**)[118] and ruthenium (**69**)[102] indicate that the trifluoromethyl isocyanide ligand



again occupies a bridging position. Thus the ruthenium species is forced into the $[Fe_3(CO)_{12}]$ structure. In contrast, regular isocyanides occupy terminal axial positions.[119]

Attempts to prepare the corresponding osmium compounds by substitution of the labile acetonitrile ligand in $[Os_3(CO)_{11}(CH_3CN)]$ lead to the isolation of $[Os_3(CO)_{11}(\mu_2\text{-}CNCF_3)_2]$ (**72**)

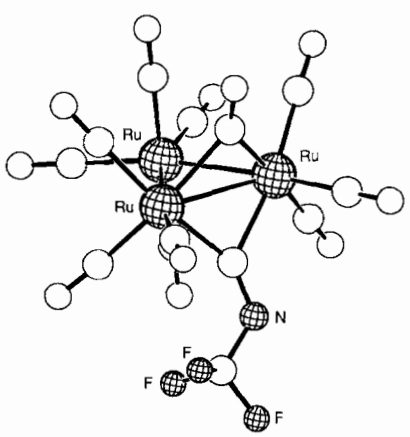
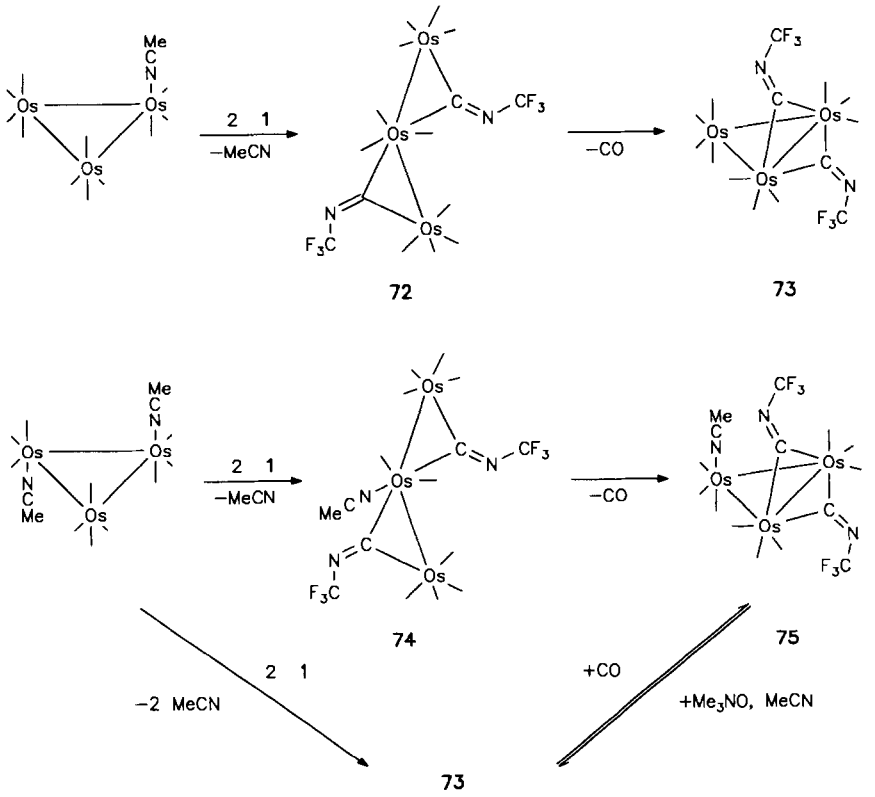


Fig. 5. Molecular structure of **69** in the crystal.



and its degradation product $[Os_3(CO)_{10}(\mu_2\text{-}CNCF_3)_2]$ (**73**).[120] Compound **72** is a derivative of the hypothetical compound $[Os_3(CO)_{13}]$ and hence a potential structural model for the products of ligand addition to $[M_3(CO)_{12}]$ clusters. Studies of these clusters with respect to ligand substitution and cluster fragmentation yielded a rate law that was interpreted as a combination of a dissociative and associative mechanism.[121] The isolation, structural analysis, and further reactivity of **72** as a metastable intermediate of such a reaction contributes to the understanding of the mechanism of these reactions, which are of fundamental interest in cluster chemistry.[122]

Cluster **72** is an "open" triosmium cluster, in which both $CNCF_3$ ligands bridge one metal–metal bond each. The two trifluoromethyl isocyanide ligands are structurally inequivalent (Fig. 6). One of them is located in the interior, the other one on the exterior of the open metal triangle. At low temperatures, this is also the case in solution. At −34 °C the ^{19}F NMR spectrum shows two singlets with an intensity ratio of 1:1. When the temperature is raised, however, the signals coalesce by a yet unknown mechanism; at room temperature only a broad signal at $\delta = -60.2$ is observed.

It is even more astonishing that the reaction of $[Os_3(CO)_{10}(CH_3CN)_2]$ and **1** also leads to the successful isolation and structural characterization of the "open" cluster **74**. This compound can react further, by loss of either the acetonitrile or a carbonyl ligand, to yield **73** or **75**.[123] The addition of a trifluoromethyl isocyanide ligand with breaking of the metal–metal bond therefore appears to compete successfully with the substitution of the second acetonitrile ligand. The structures of **74** and **75** are, with the exception of the presence of the acetonitrile ligand, very similar to those of the non-substituted compounds **72** and **73**. The two $CNCF_3$ ligands in **75** remain inequivalent in solution, while an increase in temperature leads to signal broadening for **74**.

Dodecacarbonyltriiron is nonrigid in solution; even at −150 °C all carbonyl ligands are equivalent on the NMR time scale.[124] Cotton and Troup explained this very low energy process ($\Delta G^{\ddagger} < 6\ kcal\,mol^{-1}$) with a "merry-go-round" mechanism requiring the simultaneous opening and reforming of carbonyl bridges. An alternative mechanism, proposed by B. F. G. Johnson, contains a rotation of the iron triangle around the C_2 axis, leading to a nonbridged D_3 structure.[125] A further rotation yields a structure with μ_3-carbonyl ligands. Recent EXAFS studies indicate that in frozen hexane solutions $[Fe_3(CO)_{12}]$ has most probably D_3 symmetry, while frozen solutions in the polar solvent dichloromethane contain unbridged as well as bridged structures.[126]

A number of different phosphane and phosphite derivatives have been synthesized in order to increase the activation barrier for the ligand exchange process; in no case, however, has it been possible to stop the

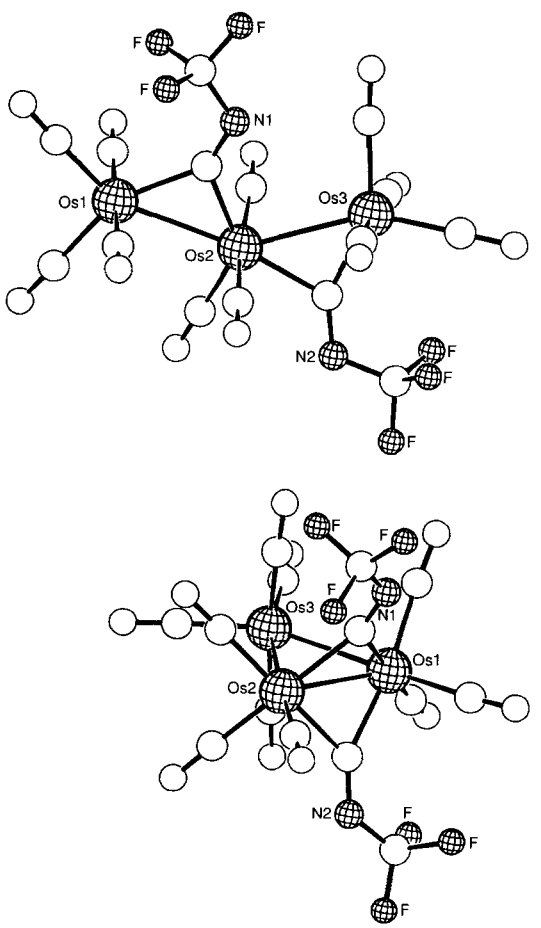
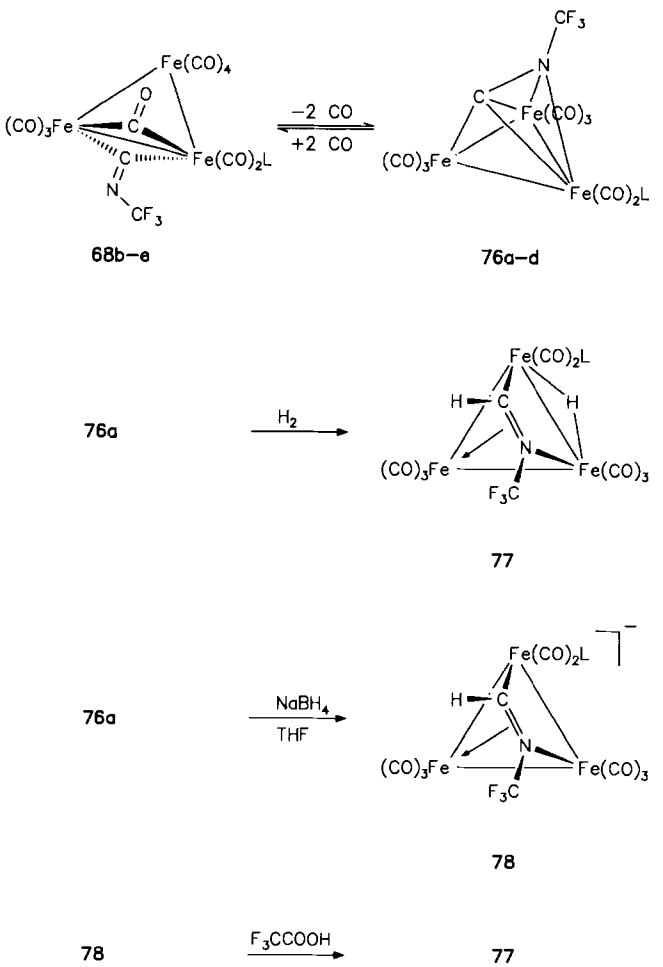


Fig. 6. Molecular structure of **72** (top) and **73** (bottom) in the crystal.

exchange process by decreasing the temperature.[127] Johnson et al. explained the spectra using the ligand polyhedron model,[127] while Mann et al. demonstrated that the ^{13}C NMR spectra of $[Fe_3(CO)_{11}(L)]$, $[Fe_3(CO)_{10}(L)_2]$, and $[Fe_3(CO)_9(L)_3]$ (L = a phosphane or phosphite ligand) can be explained by using the "merry-go-round" mechanism as well.[128] The bridged compound **68a**[129] was the first dodecacarbonyltriiron derivative for which it was possible to obtain a ^{13}C NMR spectrum, at $-110\,^{\circ}C$, that corresponds to the rigid solid-state structure. However, an unambiguous signal assignment was impossible. Only the introduction of additional phosphane or phosphite ligands in the compounds **68b–e** enabled the unambiguous signal assignment for the parent compound as well. When the temperature is increased, these compounds also undergo exchange of certain carbonyl ligands. Lentz and Marshall proposed a mechanism that is in accord with the experimental findings and leaves the trifluoromethyl isocyanide ligand in its preferred bridging position.[130] Mann later showed that our spectra can also be explained by a mechanism involving a concerted opening and reforming of bridges.[131] After a total of six intermediates with terminal $CNCF_3$ ligands, another isomer with a bridging trifluoromethyl isocyanide ligand is obtained. Recently Johnson et al. applied their ligand polyhedron model to these compounds and showed that an explanation of the experimental data is also possible using this model.[132]

In the course of the study of the compounds **68b–e** (L = PMe_3, PEt_3, $P(OMe)_3$, $P(OEt)_3$) it was noted that carbon monoxide is reversibly eliminated when the temperature is slightly raised, which leads to the clusters **76a–d**.[133] These compounds **76a–d** are the first examples for a η^2-(μ_3-C-μ_2-N)-bridging trifluoromethyl isocyanide ligand, which acts as a six-electron donor. The C=N bond is oriented perpendicular to an iron–iron bond. This coordination mode is also found in $[Fe_3(CO)_9(\mu_3\text{-}\eta^2\text{-CN-}t\text{Bu})]$.[119a] A η^2-(μ_3-C-μ_2-O)-bridging carbonyl ligand was first demonstrated in 1979 by W. A. Herrmann et al. in $Cp_3Nb_3(CO)_7$.[134] A similar coordination mode of CO with two or three metal centers is also assumed for the absorption of carbon monoxide on metal surfaces.[135] Metal clusters have been repeatedly proposed as highly simplified models for intermediates in reactions on the metal surface of heterogeneous catalysts.[136] As a result of these considerations, **76c** (L = $P(OMe)_3$) was allowed to react with molecular hydrogen. Even under mild conditions the hydrido-μ_3-η^2-N-(trifluoromethyl)formimidoyliron cluster **77** was formed nearly quantitatively[133] (see Section 5.3).



5.3. Reactions of Coordinated Trifluoromethyl Isocyanide

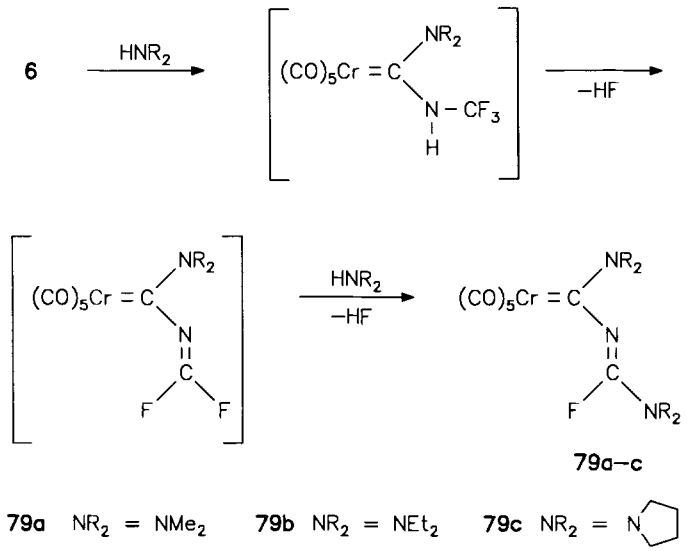
The coupling of two trifluoromethyl isocyanide ligands with the formation of a diazabutatriene ligand was discussed in Section 5.2.1.

Only five years after the designed synthesis of the first carbene complex by E. O. Fischer et al.,[137] Chatt et al. were able to demonstrate in 1969 that coordinated isocyanides are readily attacked by nucleophiles to afford carbene complexes.[138] Further reactions of isocyanide complexes have been discussed in several review articles.[11, 139] Fehlhammer et al. thoroughly examined the reaction of pentacarbonyl(trichloromethyl isocyanide)chromium with nucleophiles.[140]

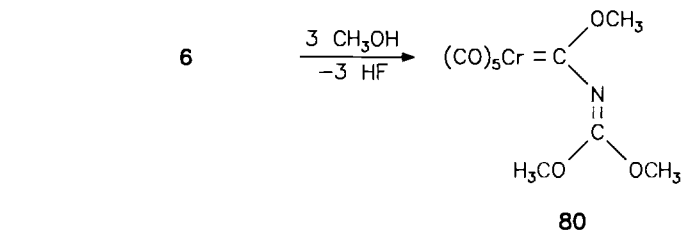
It is therefore not surprising that coordinated trifluoromethyl isocyanide also reacts readily with nucleophiles.[141] We have extensively studied these reactions on the pentacarbonylchromium complex **6**, and obtained the carbene complexes **79a–c** and **80**. It is noteworthy, however, that even such weak nucleophiles like methanol react without the addition of base and that in the course of the reaction the usually rather inert trifluoromethyl group is completely degraded. The hope of obtaining fluorinated heterocycles by the use of hydrazine derivatives was vain, because nucleophilic substitution replaced even the last fluorine substituent.[141]

An unexpected result was obtained from the reaction between nucleophiles and (pentamethylcyclopentadienyl)bis(trifluoromethyl isocyanide)cobalt **54**.[142] Only in the presence of water was it possible to obtain any crystalline products. According to the crystal structure analysis, the isolated cobaltacycle **81** contains a pentamethylcyclopentadienyl and an *N*-trifluoromethylformimidoyl ligand. The reaction scheme shows a plausible mechanism for the formation of this species. One of the two trifluoromethyl isocyanide ligands has become completely degraded by successive nucleophilic attacks by the amine and can be found integrated into the metallacycle. The second one has been transformed into the η^1-bound *N*-trifluoromethylformimidoyl ligand.

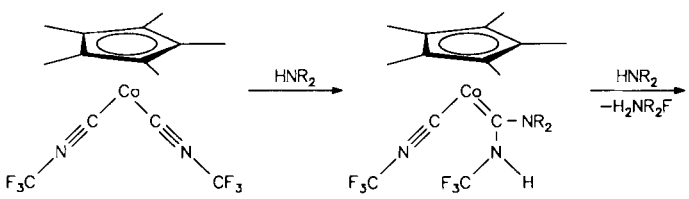
Another *N*-trifluoromethylformimidoyl ligand, in this case μ_3-η^2-bound, is obtained by the reaction of the trinuclear iron



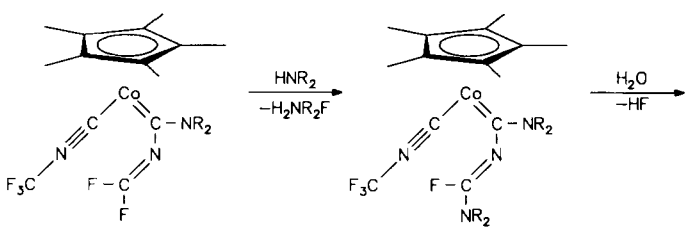
79a $NR_2 = NMe_2$ **79b** $NR_2 = NEt_2$ **79c** NR_2 = N

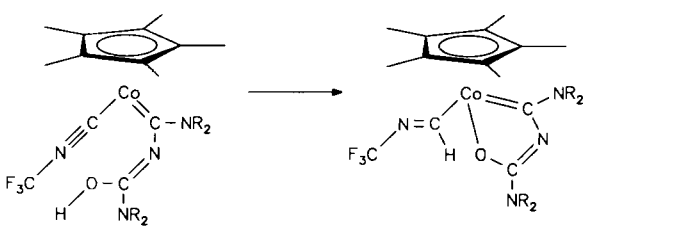


80



54

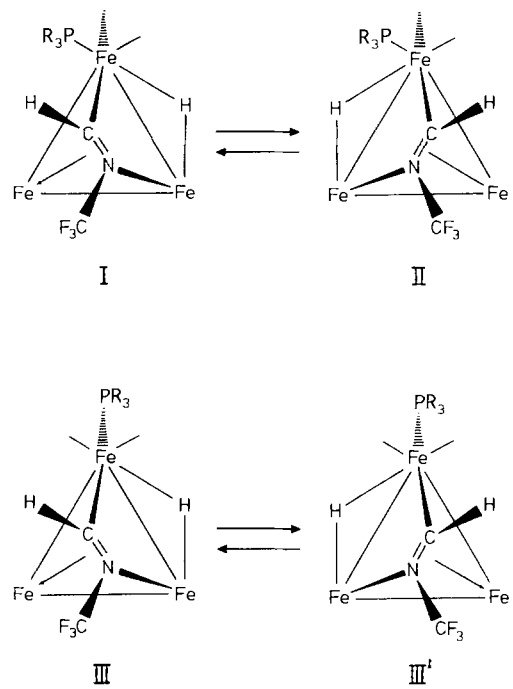




81a–c

81a $NR_2 = NMe_2$ **81b** $NR_2 = NEt_2$ **81c** NR_2 = N

cluster **76a** with hydrogen.[133] The iron cluster **77** that is formed contains, according to spectroscopic studies, an *N*-trifluoromethylformimidoyl as well as an μ_2-hydrido ligand. The μ_3-bridged **77** is present as a mixture of the isomers I–III, of which I and II, as well as III and III′ interconvert rapidly at room temperature (Scheme 2). The stepwise hydrogenation with sodium borohydride, followed by the protonation of the anionic cluster **76** by trifluoroacetic acid also leads to **77**, but in a different isomer ratio of I, II, and III.



Scheme 2. Structural isomers of compound **77** (only the framework of the cluster is shown).

5.4. Complexes of the Other Fluorinated Isocyanides

The coordination chemistry of fluorinated isocyanides other than CF_3NC is just beginning. The chromium complexes **7**, **8**, **13**,[26] **15**, **16**,[29] **17**, and **18**[28] are known for isocyanides with perfluoropropyl, perfluorobutyl, dichlorofluoromethyl, dichlorotrifluoroethyl, tetrachlorofluoroethyl, fluoromethyl, or difluoromethyl substituents. A crystal structure analysis is available for the difluoromethyl isocyanide complex **18** [Cr–CN 195.6(2), $Cr-CO_{trans}$ 190.0(2), $Cr-CO_{cis}$ 190.9-191.5(2) pm].[143] A slightly longer $metal-C_{isocyanide}$ bond and a slightly shorter bond to the *trans*-carbonyl ligand than to the *cis*-carbonyls are indications for the lower ratio of the π-acceptor and σ-donor strengths of the difluoromethyl isocyanide ligand. This had also been inferred from spectroscopic data. For 2-fluoroethyl and 2,2,2-trifluoroethyl isocyanide the complexes $[Ru(tpp)(CNCH_2CH_2F)_2]$, $[Ru(tpp)(CNCH_2CF_3)_2]$, and $[Fe(tpp)(CNCH_2CH_2F)_2]SO_3CF_3$ (tpp = *meso*-tetraphenylporphyrin) have been described.[20] The chromium complexes **19**, **20**,[29] and **23**[37] are known for the only recently prepared alkenyl isocyanides. The crystal structure analysis of **19** (Fig. 7) shows a somewhat longer $metal-C_{isocyanide}$ bond than $metal-C_{CO}$ bonds.[29]

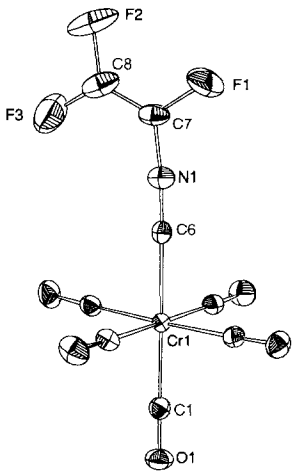


Fig. 7. Molecular structure of **19** in the crystal. Important distances [pm] and angles [°]: Cr1–C6 194.2(2), Cr1-C1 190.9(2), Cr1–CO_{cis} 190.2(2)-191.4(2), C6–N1 116.2(2), C7–N1 135.7(2), C7–C8 131.3(3), Cr1-C6-N1 177.8(1), C6-N1-C7 173.6(2), N1-C7-C8 123.8(2).

The reaction of **19** with pyrrolidine leads to a complete degradation of the complex, yielding $(C_4H_{10}N)_3[CrF_6]$.[144] Dimerization of **19** affords the first examples of complexes with 1,2,3,3,4,4-hexafluoro-1,2-diisocyanocyclobutane (**22a,b**).[34] The crystal structure of the *cis* isomer (Fig. 8) demonstrates that

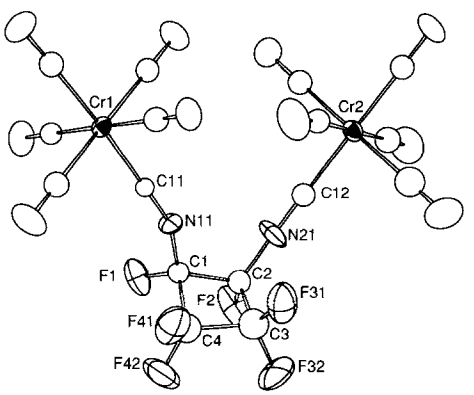
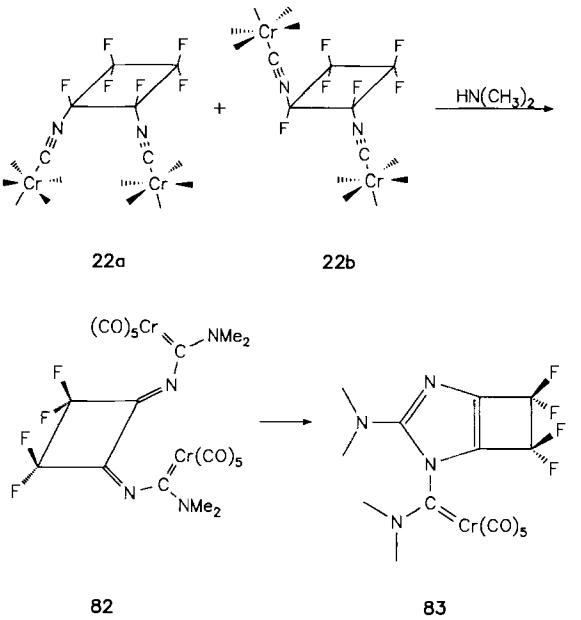


Fig. 8. Molecular structure of **22a** in the crystal.

it is clearly possible to accommodate two bulky substituents on the same side of the cyclobutane ring. Both chromium atoms have a nearly octahedral coordination environment; the various metal–$C_{carbonyl}$ bond lengths [188.1(7)–191.4(6) pm] are very similar and are not significantly different from the bond lengths to the isocyanide carbon atoms [Cr1–C11 190.3(6), Cr2–C21 190.0(6) pm]. In addition, the position of the intense carbonyl bands in the IR spectra indicate that these fluorinated diisocyanides are also excellent π-acceptors.

Correspondingly, **22a,b** react readily with nucleophiles like dimethylamine. Upon nucleophilic attack on both isocyanide carbon atoms and HF elimination, the primary product is the dicarbene complex **82**, which can be isolated in the form of deep blue crystals that are unstable at room temperature. The crystal structure analysis indicates that the lone pair on N1 is directed towards the p orbital of C26 (Fig. 9), which enables the facile cyclization to an imidazole ring with loss of a pentacarbonylchromium fragment, yielding the stable carbene complex **83**. If



this reaction could be generalized and the organometallic protecting group cleaved, it would represent a convenient synthesis for imidazole derivatives with an annelated fluorine-substituted four-membered ring.

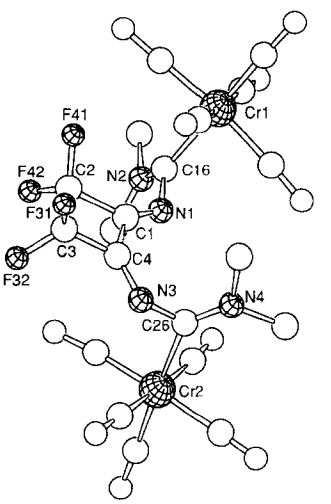


Fig. 9. Molecular structure of **82** in the crystal.

The fluorinated aryl isocyanide **2**, which is available in larger quantities, can be utilized for the direct synthesis of complexes. Previously, the manganese halfsandwich complex **84**,[22] as well as pentacarbonyl(pentafluorophenyl isocyanide)chromium **85**,

$$[Cp^*Mn(CO)_2(thf)] + 2 \longrightarrow [Cp^*Mn(CO)_2(CN{-}C_6F_5)]$$
84

$$[(CO)_5Cr(C_6H_{14})] + 2 \longrightarrow [(CO)_5Cr(CN{-}C_6F_5)]$$
85

$$[Ni(CO)_4] + 4\ 2 \longrightarrow [Ni(CN{-}C_6F_5)_4]$$
86

and the homoleptic nickel complex **86** had been prepared.[145] While there are only a few studies on pentafluorophenyl isocyanide complexes, they clearly indicate that **2** is by no means as good a π-acceptor ligand as **1**.

6. Outlook

Fluorinated isocyanides have proven to be a multifaceted class of compounds with a significant potential in synthesis. These compounds are excellent building blocks for two reasons: their unusual ligand properties, especially those of trifluoromethyl isocyanide, and their increased reactivity relative to regular isocyanides. The latter property, however, also increases the difficulty of handling. Unfortunately, some of these compounds, like the bifunctional trifluorovinyl isocyanide **11**, cannot be prepared by regular methods of organic synthesis and the pyrolysis of metal complexes only yields very small quantities. Early results indicate that **11**, in its "tamed" version (that is, stabilized on a pentacarbonylchromium moiety), is an excellent synthetic building block that enables the synthesis of further fluorinated isocyanides in the coordination sphere. For this and other reasons, further studies are necessary to explore the potential of fluorinated isocyanides in synthesis fully.

The research described in this article was made possible by my enthusiastic coworkers, to whom I wish to express my sincere gratitude. I wish to thank Prof. Dr. Konrad Seppelt for the constant support of my work. Numerous studies would not have been possible without the successful collaboration with the research groups of Prof. Dr. R. D. Adams, Dr. G. Bertrand, Prof. Dr. H. Bock, Prof. Dr. H. Bürger, Prof. Dr. P. Botschwina, Prof. Dr. H. Dreizler, Prof. Dr. J. Fuchs, Prof. Dr. H. Hartl, Prof. Dr. E. Illenberger, Prof. Dr. P. Luger, Prof. Dr. H. Oberhammer, Prof. Dr. K. Seppelt, Prof. Dr. J. S. Thrasher, Prof. Dr. L. Weber, Prof. Dr. M. Weidenbruch, and Prof. Dr. G. Wilke. My special gratitude belongs to Prof. Dr. D. D. DesMarteau (Clemson University, South Carolina), at whose institute I was allowed to work in 1991. This work was supported by the Deutsche Forschungsgemeinschaft, the Graduiertenkolleg "Synthese und Strukturuntersuchung niedermolekularer Verbindungen" der Freien und der Technischen Universität Berlin, and by the Fonds der Chemischen Industrie.

Received: July 15, 1993 [A 91E]
German version: *Angew. Chem.* **1994**, *106*, 1377
Translated by Dr. W. C. Wilisch, Ansbach (FRG)

[1] A. Gautier, *Justus Liebigs Ann. Chem.* **1867**, *142*, 289; *ibid.* **1868**, *146*, 124.
[2] A. W. Hofmann, *Justus Liebigs Ann. Chem.* **1867**, *144*, 114; *ibid.* **1868**, *146*, 107.
[3] I. Ugi, *Angew. Chem.* **1982**, *94*, 826; *Angew. Chem. Int. Ed. Engl.* **1982**, *21*, 810; *Isonitrile Chemistry* (Ed.: I. Ugi), Academic Press, New York, **1971**.
[4] C. Grundmann, *Methoden Org. Chem. (Houben-Weyl) 4th ed. 1952–1985, Bd. E5*, p. 611.
[5] T. van der Does, F. Bickelhaupt, *Angew. Chem.* **1988**, *100*, 998; *Angew. Chem. Int. Ed. Engl.* **1988**, *27*, 936 (described incorrectly as CN–NC); F. Stroh, M. Winnewisser, *Chem. Phys. Lett.* **1989**, *155*, 21; F. Stroh, M. Winnewisser, H. P. Reisenauer, G. Maier, S. J. Goede, F. Bickelhaupt, *ibid.* **1989**, *160*, 105.
[6] G. Maier, H. P. Reisenauer, J. Eckwert, C. Sierakowski, T. Stumpf, *Angew. Chem.* **1992**, *104*, 1287; *Angew. Chem. Int. Ed. Engl.* **1992**, *31*, 1218.
[7] A. M. Smith, G. Schallmoser, A. Thoma, V. E. Bondybey, *J. Chem. Phys.* **1993**, *98*, 1776.
[8] M. Krüger, H. Dreizler, D. Preugschat, D. Lentz, *Angew. Chem.* **1991**, *103*, 1674; *Angew. Chem. Int. Ed. Engl.* **1991**, *30*, 1644; L. Zanathy, H. Bock, D. Lentz, D. Preugschat, P. Botschwina, *J. Chem. Soc. Chem. Commun.* **1992**, 403; A. Guarnieri, R. Hinze, M. Krüger, H. Zerbe-Foese, D. Lentz, D. Preugschat, *J. Mol. Spectrosc.* **1992**, *156*, 39; H. Bürger, S. Sommer, D. Lentz, D. Preugschat, *ibid.* **1992**, *156*, 360.
[9] K. Kawaguchi, M. Ohishi, S.-I. Ishikawa, N. Kaifu, *Astrophys. J.* **1992**, *386*, L51.
[10] L. Malatesta, F. Bonati, *Isocyanide Complexes of Metals*, Wiley, London, **1969**.
[11] P. M. Treichel, *Adv. Organomet. Chem.* **1973**, *11*, 21; F. Bonati, G. Minghetti, *Inorg. Chim. Acta* **1974**, *9*, 95; Y. Yamamoto, *Coord. Chem. Rev.* **1980**, *32*, 193; E. Singleton, H. E. Oosthuizen, *Adv. Organomet. Chem.* **1983**, *22*, 209.
[12] W. P. Fehlhammer, *Nachr. Chem. Techn. Lab.* **1982**, *30*, 187; W. P. Fehlhammer, M. Fritz, *Chem. Rev.* **1993**, *93*, 1243.
[13] G. Christian, H. Stolzenberg, W. P. Fehlhammer, *J. Chem. Soc. Chem. Commun.* **1982**, 184.
[14] W. P. Fehlhammer, F. Degel, H. Stolzenberg, *Angew. Chem.* **1981**, *93*, 184; *Angew. Chem. Int. Ed. Engl.* **1981**, *20*, 214.
[15] F. E. Hahn, *Angew. Chem.* **1993**, *105*, 681; *Angew. Chem. Int. Ed. Engl.* **1993**, *32*, 650.
[16] B. Smart in *Chemistry of Functional Groups. Supplement D. The Chemistry of Halides, Pseudohalides and Azides* (Eds.: S. Patai, Z. Rapoport), Wiley, New York, **1983**, pp. 603–655; M. Hudlicky, *Chemistry of Organic Fluorine Compounds*, Ellis Horwood, Chichester, **1976**; R. D. Chambers, *Fluorine in Organic Chemistry*, Wiley-Interscience, New York, **1973**; *Synthesis of Fluoroorganic Compounds* (Eds.: I. L. Knunyants, G. G. Yacobson), Springer, New York, **1985**; *Fluorine-Containing Molecules: Structure, Reactivity, Synthesis, Application* (Eds.: J. F. Liebman, A. Greenberg, W. R. Dolbier, Jr.), VCH, New York, **1988**; *Synthetic Fluorine Chemistry* (Eds.: G. A. Olah, R. D. Chambers, G. K. S. Prakash), Wiley, New York, **1992**.
[17] S. P. Makarov, M. A. Englin, A. F. Videiko, T. V. Nikolaeva, *Zh. Obshch. Khim.* **1967**, *37*, 2781.
[18] R. E. Banks, R. N. Haszeldine, M. J. Stevenson, B. G. Willoughby, *J. Chem. Soc. C* **1969**, 2119; A. F. Gontar, N. A. Til'kunova, E. G. Bykhovskaya, I. L. Knunyants, *Izv. Akad. Nauk. SSR Ser. Khim.* **1977**, *10*, 2379.
[19] R. E. Banks, R. N. Haszeldine, B. G. Willoughby, *J. Chem. Soc. Perkin Trans.* **1975**, 2451.
[20] C. Gèze, N. Legrand, A. Bondon, G. Simonneaux, *Inorg. Chim. Acta* **1992**, *195*, 73.
[21] D. Lentz, *J. Fluorine Chem.* **1984**, *24*, 523.
[22] D. Lentz, K. Graske, D. Preugschat, *Chem. Ber.* **1988**, *121*, 1445.
[23] J. S. Thrasher, K. V. Madappat, *Angew. Chem.* **1989**, *101*, 1284; *Angew. Chem. Int. Ed. Engl.* **1989**, *28*, 1256.
[24] D. Lentz, D. D. DesMarteau, unpublished.
[25] B. Krumm, R. L. Kirchmeier, J. M. Shreeve, *ACS Eleventh Winter Fluorine Conference*, St. Petersburg, FL, **1993**.
[26] W. P. Fehlhammer, F. Degel, G. Beck, *Chem. Ber.* **1987**, *120*, 461.
[27] F. Degel, Dissertation, Universität Erlangen-Nürnberg, **1981**.
[28] D. Lentz, D. Preugschat, *J. Organomet. Chem.* **1992**, *436*, 185.
[29] D. Lentz, D. Preugschat, *J. Chem. Soc. Chem. Commun.* **1992**, 1523; D. Lentz, D. Preugschat, unpublished.
[30] D. Lentz, *Chem. Ber.* **1984**, *117*, 415.
[31] D. Lentz, D. Preugschat, unpublished.
[32] H. Dreizler, M. Krüger, D. Lentz, D. Preugschat, unpublished.
[33] G. Bieri, J.-P. Stadelmann, F. Thommen, J. Vogt, *Helv. Chim. Acta* **1978**, *61*, 357; K. Tanaka, T. Okabayashi, T. Tanaka, *J. Mol. Spectrosc.* **1988**, *132*, 467; M. Niedenhoff, K. M. T. Yamada, G. Winnewisser, K. Tanaka, T. Okabayashi, *J. Mol. Spectrosc.* **1991**, *145*, 290.
[34] D. Lentz, F. Nowack, D. Preugschat, M. Wasgindt, *Angew. Chem.* **1993**, *105*, 1547; *Angew. Chem. Int. Ed. Engl.* **1993**, *32*, 1456.
[35] G. K. S. Prakash in *Synthetic Fluorine Chemistry* (Eds.: G. A. Olah, R. D. Chambers, G. K. S. Prakash), Wiley, New York, **1992**; S. P. Kotun, J. D. O. Anderson, D. D. DesMarteau, *J. Org. Chem.* **1992**, *57*, 1124.
[36] N. R. Patel, R. L. Kirchmeier, *Inorg. Chem.* **1992**, *31*, 2537.
[37] D. Lentz, S. Kleinhenz, M. Holz, unpublished.
[38] G. Christian, D. Lentz, H. Hartl, W. P. Fehlhammer, *Chem. Ber.* **1992**, *125*, 1093.
[39] D. Christen, K. Ramme, B. Haas, H. Oberhammer, D. Lentz, *J. Chem. Phys.* **1984**, *80*, 4020.
[40] N. Ghosh, R. Trambarulo, W. Gordy, *J. Chem. Phys.* **1961**, *21*, 308.
[41] F. Heyder, Abschlußarbeit, BU-GH Wuppertal, **1983**; H. Bürger, BU-GH Wuppertal, personal communication.
[42] S. G. Kukolich, *J. Chem. Phys.* **1972**, *57*, 869.
[43] D. Christen, K.-J. Ramme, *Z. Naturforsch. A* **1984**, *39*, 865.
[44] M. Krüger, Dissertation, Universität Kiel, **1992**.
[45] M. Krüger, H. Dreizler, *Z. Naturforsch. A* **1992**, *47*, 865.
[46] D. Lentz, D. Preugschat, *Acta Crystallogr. Sect. C* **1993**, *49*, 52.
[47] J. Buschmann, S. Kleinhenz, D. Lentz, P. Luger, D. Preugschat, unpublished.
[48] L. Halonen, I. M. Mills, *J. Mol. Spectrosc.* **1978**, *73*, 494.
[49] E. F. Pearson, R. A. Cresswell, M. Winnewisser, G. Winnewisser, *Z. Naturforsch. A* **1976**, *31*, 1394.

[50] B. Bak, B. P. van Eijck, C. Kierkegaard, *J. Mol. Struct.* **1973**, *18*, 429.
[51] T.-A. Chang, M. D. Harmony, S. W. Staley, *J. Mol. Struct.* **1988**, *190*, 17.
[52] M. C. L. Gerry, F. Stroh, M. Winnewisser, *J. Mol. Spectrosc.* **1990**, *140*, 147.
[53] H. Bock, R. Dammel, D. Lentz, *Inorg. Chem.* **1984**, *23*, 1535.
[54] D. B. Beach, W. L. Jolly, D. Lentz, *Inorg. Chem.* **1985**, *24*, 1892.
[55] K. V. Madappat, J. S. Thrasher, unpublished; K. V. Maddapat, Dissertation, University of Alabama, **1993**.
[56] M. Heni, E. Illenberger, D. Lentz, *Int. J. Mass. Spectrom. Ion Phys.* **1986**, *71*, 199.
[57] D. Lentz, *J. Fluorine Chem.* **1988**, *39*, 305.
[58] R. E. Banks, R. N. Haszeldine, C. W. Stephens, *Tetrahedron Lett.* **1972**, 3699.
[59] D. Lentz, O. H. Oberhammer, *Inorg. Chem.* **1985**, *24*, 4665.
[60] J. N. Nef, *Justus Liebigs Ann. Chem.* **1892**, *270*, 267.
[61] D. Lentz, I. Brüdgam, H. Hartl, *Angew. Chem.* **1987**, *99*, 951; *Angew. Chem. Int. Ed. Engl.* **1987**, *26*, 921.
[62] G. Klöter, W. Lutz, K. Seppelt, W. Sundermeyer, *Angew. Chem.* **1977**, *89*, 754; *Angew. Chem. Int. Ed. Engl.* **1977**, *16*, 707; G. Klöter, K. Seppelt, *J. Am. Chem. Soc.* **1979**, *101*, 347.
[63] a) T. R. Oakes, H. G. David, F. J. Nagel, *J. Am. Chem. Soc.* **1969**, *91*, 4761; b) N. Obata, T. Takizawa, *Tetrahedron Lett.* **1969**, 3403; c) T. Takizawa, N. Obata, Y. Suzuki, T. Yanagida, *ibid.* **1969**, 3407; d) Y. Suziki, N. Obata, T. Takizawa, *ibid.* **1970**, 2667; e) H. J. Dillinger, G. Fengler, D. Schumann, E. Winterfeldt, *Tetrahedron* **1974**, *30*, 2553.
[64] A. Krebs, H. Kimling, *Angew. Chem.* **1971**, *83*, 401; *Angew. Chem. Int. Ed. Engl.* **1971**, *10*, 409.
[65] D. Lentz, *Z. Naturforsch. B* **1992**, *47*, 148.
[66] D. Lentz, unpublished.
[67] D. Lentz, D. D. DesMarteau, unpublished.
[68] D. Lentz, R. Marschall, *Z. Anorg. Allg. Chem.* **1992**, *617*, 53; D. Lentz, D. Preugschat, unpublished.
[69] D. Lentz, unpublished.
[70] S. Buchwald, D. Lentz, R. Marschall, D. Preugschat, O. Stamm, L. Weber, unpublished.
[71] W. J. Middleton, D. C. England, C. G. Krespan, *J. Org. Chem.* **1967**, *32*, 948.
[72] D. Lentz, D. D. DesMarteau, unpublished.
[73] J. Buschmann, R. Damerius, R. Gerhardt, D. Lentz, P. Luger, R. Marschall, D. Preugschat, K. Seppelt, A. Simon, *J. Am. Chem. Soc.* **1992**, *114*, 9465, and references therein
[74] A. Igau, H. Grützmacher, A. Baceiredo, G. Bertrand, *J. Am. Chem. Soc.* **1988**, *110*, 6463; A. Igau, A. Baceiredo, G. Tinquier, G. Bertrand, *Angew. Chem.* **1989**, *101*, 617; *Angew. Chem. Int. Ed. Engl.* **1989**, *28*, 621; G. R. Gillette, A. Baceiredo, G. Bertrand, *ibid.* **1990**, *102*, 1486 bzw. **1990**, *29*, 1429.
[75] G. Bertrand, D. Lentz, D. Preugschat, unpublished.
[76] H. B. Yokelson, A. J. Millevolte, K. J. Haller, R. West, *J. Chem. Soc. Chem. Commun.* **1987**, 1605.
[77] M. Weidenbruch, J. Hamann, H. Piel, D. Lentz, K. Peters, H. G. von Schnering, *J. Organomet. Chem.* **1992**, *426*, 35, and references therein
[78] D. Lentz, unpublished.
[79] D. Lentz, D. Dreissig, unpublished results. *cis*-$TiCl_4(CN\text{-}t\text{Bu})_2$ was obtained from $TiCl_4$ and *tert*-butyl isocyanide and characterized by X-ray crystallography. Compounds of the type $Cl_3Ti-C(Cl)=NR$, which had been described in earlier work, are probably isocyanide complexes as well. T. Carofiglio, C. Floriani, A. Chiesi-Villa, C. Guastini, *Inorg. Chem.* **1989**, *28*, 4417, and references therein.
[80] A. M. English, K. R. Plowman, I. M. Baibich, J. P. Hickey, I. S. Butler, G. Jaouen, P. Lemoux, *J. Organomet. Chem.* **1981**, *205*, 177.
[81] D. Lentz, H. Bock, R. Dammel, unpublished.
[82] D. W. Turner, C. Baker, A. D. Baker, C. R. Brandle, *Molecular Photoelectron Spectroscopy. A Handbook of He 584 Å Spectra*, Wiley-Interscience, London, **1970**.
[83] H. Oberhammer, D. Lentz, *Inorg. Chem.* **1985**, *24*, 1271.
[84] D. Lentz, J. Kroll, C. Langner, *Chem. Ber.* **1987**, *120*, 303.
[85] D. Lentz, R. Marschall, *Chem. Ber.* **1989**, *122*, 1223.
[86] D. Lentz, R. Marschall, *Z. Anorg. Allg. Chem.* **1991**, *593*, 181.
[87] F. A. Cotton, C. S. Kraihanzel, *J. Am. Chem. Soc.* **1962**, *84*, 4432.
[88] D. Lentz, B. Pötter, R. Marschall, I. Brüdgam, J. Fuchs, *Chem. Ber.* **1990**, *123*, 257.
[89] D. Lentz, *J. Organomet. Chem.* **1990**, *381*, 205.
[90] D. Lentz, B. Pötter, *J. Organomet. Chem.* **1987**, *336*, 393.
[91] D. Lentz, B. Pötter, I. Brüdgam, H. Hartl, unpublished.
[92] D. Lentz, unpublished.
[93] D. Lentz, R. Marschall, unpublished.
[94] D. Lentz, *Chem. Ber.* **1985**, *118*, 560.
[95] D. Lentz, *J. Organomet. Chem.* **1989**, *377*, 305.
[96] F. A. Cotton, A. Danti, J. S. Waugh, R. W. Fesseden, *J. Chem. Phys.* **1958**, *29*, 1427.
[97] J.-M. Basset, D. E. Berry, G. K. Barker, M. Green, J. A. K. Howard, F. G. A. Stone, *J. Chem. Soc. Dalton Trans.* **1979**, 1003.
[98] See [89].
[99] J. A. S. Howell, J.-Y. Saillard, A. Le Beuze, G. Jaouen, *J. Chem. Soc. Dalton Trans.* **1982**, 2533.
[100] P. V. Broadhurst, *Polyhedron* **1985**, *4*, 1801, and references therein; M. Herberhold, *Nachr. Chem. Tech. Lab.* **1981**, *29*, 365, and references therein.
[101] D. Lentz, J. Brüdgam, H. Hartl, *J. Organomet. Chem.* **1986**, *299*, C38.
[102] D. Lentz, R. Marschall, E. Hahn, *Chem. Ber.* **1991**, *124*, 777.
[103] D. Lentz, B. Lönnewitz, I. Brüdgam, H. Hartl, unpublished.
[104] F. A. Cotton, J. M. Troup, *J. Chem. Soc. Dalton Trans.* **1974**, 800.
[105] J.-M. Basset, M. Green, J. A. K. Howard, F. G. A. Stone, W. C. Wolsey, *J. Chem. Soc. Chem. Commun.* **1978**, 1000.
[106] J. R. Moss, W. A. G. Graham, *J. Chem. Soc. Dalton Trans.* **1977**, 95.
[107] J.-M. Basset, G. Barker, M. Green, J. A. K. Howard, F. G. A. Stone, W. C. Wolsey, *J. Chem. Soc. Dalton Trans.* **1981**, 219.
[108] R. D. Adams, R. M. Collins, F. A. Cotton, *Inorg. Chem.* **1974**, *13*, 1086.
[109] R. D. Adams, M. Brice, F. A. Cotton, *J. Am. Chem. Soc.* **1973**, *95*, 6594; N. J. Coville, *J. Organomet. Chem.* **1981**, *218*, 337.
[110] R. D. Adams, D. A. Katahira, L. W. Yang, *Organometallics* **1982**, *1*, 231.
[111] F. A. Cotton, S. A. Duraj, W. J. Roth, *J. Am. Chem. Soc.* **1984**, *106*, 6987.
[112] E. M. Carnahan, J. D. Protasiewicz, S. J. Lippard, *Acc. Chem. Res.* **1993**, *26*, 90; E. M. Carnahan, S. J. Lippard, *J. Am. Chem. Soc.* **1990**, *112*, 3230; R. N. Vrtis, C. P. Rao, S. Warner, S. J. Lippard, *ibid.* **1988**, *110*, 2669; R. N. Vrtis, C. P. Rao, S. G. Bott, S. J. Lippard, *ibid.* **1988**, *110*, 7564; P. A. Bianconi, R. N. Vrtis, C. P. Rao, I. D. Williams, M. P. Engeler, S. J. Lippard, *Organometallics* **1987**, *6*, 1968; P. A. Bianconi, S. Warner, S. J. Lippard, *ibid.* **1986**, *5*, 1716, and references therein.
[113] A. C. Filippou, W. Grünleitner, *J. Organomet. Chem.* **1990**, *393*, C10; *ibid.* **1990**, *398*, 99; *Z. Naturforsch. B* **1991**, *46*, 216; A. C. Filippou, W. Grünleitner, C. Völkl, P. Kiprof, *Angew. Chem.* **1991**, *103*, 1188; *Angew. Chem. Int. Ed. Engl.* **1991**, *30*, 1167.
[114] R. Hoffmann, C. N. Wilker, S. J. Lippard, J. L. Tempelton, D. C. Brower, *J. Am. Chem. Soc.* **1983**, *105*, 146.
[115] C. H. Wei, L. F. Dahl, *J. Am. Chem. Soc.* **1966**, *88*, 1821.
[116] R. Mason, A. I. Rae, *J. Chem. Soc. A* **1968**, 778; M. R. Churchill, F. J. Hollander, J. P. Hutchison, *Inorg. Chem.* **1977**, *16*, 2655.
[117] L. F. Dahl, E. R. Corey, *Inorg. Chem.* **1962**, *1*, 521.
[118] I. Brüdgam, H. Hartl, D. Lentz, *Z. Naturforsch. B* **1984**, *39*, 721.
[119] M. I. Bruce, T. W. Hambley, B. K. Nicholson, *J. Chem. Soc. Dalton Trans.* **1983**, 2385; M. I. Bruce, J. G. Matisons, R. C. Wallis, J. M. Patrick, B. W. Skelton, A. H. White, *ibid.* **1983**, 2365.
[120] R. D. Adams, Y. Chi, D. D. DesMarteau, D. Lentz, R. Marschall, *J. Am. Chem. Soc.* **1992**, *114*, 1909.
[121] N. M. J. Brodie, L. Chen, A. J. Poe, *Int. J. Chem. Kinet.* **1988**, *20*, 467; A. J. Poe, *Pure Appl. Chem.* **1988**, *60*, 1209; N. M. J. Brodie, A. J. Poe, *Inorg. Chem.* **1988**, *27*, 3156; A. J. Poe, M. V. Twigg, *J. Chem. Soc. Dalton Trans.* **1974**, 1860.
[122] D. Darensbourg in *The Chemistry of Metal Cluster Complexes* (Eds.: D. F. Shriver, H. Kaezs, R. D. Adams), VCH, Weinheim, **1990**; A. J. Poe in *Metal Clusters* (Ed.: M. Moskovits), Wiley-Interscience, New York, **1986**.
[123] R. D. Adams, Y. Chi, D. D. DesMarteau, D. Lentz, R. Marschall, A. Scherrmann, *J. Am. Chem. Soc.* **1992**, *114*, 10822.
[124] F. A. Cotton, J. M. Troup, *J. Am. Chem. Soc.* **1974**, *96*, 4155.
[125] B. F. G. Johnson, *J. Chem. Soc. Chem. Commun.* **1976**, 703; B. F. G. Johnson, A. Bolt, *J. Chem. Soc. Dalton Trans.* **1990**, 2437.
[126] N. Binstedt, J. Evans, G. N. Greaves, R. J. Price, *J. Chem. Soc. Chem. Commun.* **1987**, 1330.
[127] R. E. Benfield, P. D. Gavens, B. F. G. Johnson, M. J. Mays, S. Aime, L. Milone, D. Osella, *J. Chem. Soc. Dalton Trans.* **1981**, 1535; B. F. G. Johnson, A. Bott, *ibid.* **1990**, 2437.
[128] H. Adams, N. A. Bailey, G. W. Bentley, B. E. Mann, *J. Chem. Soc. Dalton Trans.* **1989**, 1831.
[129] D. Lentz, *Z. Naturforsch. B* **1987**, *42*, 839.
[130] D. Lentz, R. Marschall, *Organometallics* **1991**, *10*, 1487.
[131] B. E. Mann, *Organometallics* **1992**, *11*, 481.
[132] B. F. G. Johnson, E. Parisini, Y. V. Roberts, *Organometallics* **1993**, *12*, 233.
[133] D. Lentz, R. Marschall, *Chem. Ber.* **1991**, *124*, 497.
[134] W. A. Herrmann, M. L. Ziegler, K. Weidenhammer, H. Biersack, *Angew. Chem.* **1979**, *91*, 1026; *Angew. Chem. Int. Ed. Engl.* **1979**, *18*, 960; W. A. Herrmann, H. Biersack, M. L. Ziegler, K. Weidenhammer, R. Siegel, D. Rehder, *J. Am. Chem. Soc.* **1981**, *103*, 1692. A review on C- and O-coordinated carbonyl ligands can be found in C. P. Horwitz, D. F. Shriver, *Adv. Organomet. Chem.* **1984**, *23*, 219.
[135] E. L. Muetterties, *Angew. Chem.* **1978**, *90*, 577; *Angew. Chem. Int. Ed. Engl.* **1978**, *17*, 545; *The Nature of the Surface Chemical Bond* (Eds.: T. N. Rhodin, G. Ertl), North Holland, Amsterdam, **1979**; C. K. Rofer-DePoorter, *Chem. Rev.* **1981**, *81*, 447.
[136] P. Chini, *Inorg. Chim. Acta Rev.* **1968**, *2*, 31; B. F. G. Johnson, J. Lewis, *Pure Appl. Chem.* **1975**, *44*, 43; E. L. Muetterties, *Bull. Soc. Chim. Belg.* **1975**, *84*, 959; *Science* **1977**, *196*, 839; *Chem. Rev.* **1979**, *79*, 91; *Pure Appl. Chem.* **1982**, *54*, 83; R. Ugo, *Catal. Rev. Sci. Engl.* **1975**, *11*, 225; E. L. Muetterties, M. J. Krause, *Angew. Chem.* **1983**, *95*, 135; *Angew. Chem. Int. Ed. Engl.* **1983**, *22*, 135; G. Süss-Fink, *Nachr. Chem. Tech. Lab.* **1988**, *36*, 1110.

[137] a) E. O. Fischer, A. Maasböl, *Angew. Chem.* **1964**, *76*, 645; *Angew. Chem. Int. Ed. Engl.* **1964**, *3*, 580; b) review: K. H. Dötz, H. Fischer, P. Hofmann, F. R. Kreisl, U. Schubert, K. Weiss, *Transition Metal Carbene Complexes*, Verlag Chemie, Weinheim, **1983**. As early as 1915, Tchugajev et al. combined $[Pt(CNCH_3)_4]^{2+}$ and hydrazine; L. Tschugajeff, M. Skanawy-Grigorjewa, *J. Russ. Chem. Soc.* **1915**, *47*, 776; L. Tschugajeff, M. Skanawy-Grigorjewa, A. Posnjak, *Z. Anorg. Allg. Chem.* **1925**, *148*, 37. However, only in 1970 were these complexes recognized as cyclic carbene complexes; G. Rouschias, B. L. Shaw, *J. Chem. Soc. A.* **1971**, 2097; A. Burke, A. L. Balch, J. H. Enemark, *J. Am. Chem. Soc.* **1970**, *92*, 2555. The structure of Tchugajev's salt was determined in 1973 by X-ray crystallography; W. M. Butler, J. H. Enemark, J. Parks, A. L. Balch, *Inorg. Chem.* **1973**, *12*, 451.

[138] E. M. Badley, J. Chatt, R. L. Richards, G. A. Sim, *J. Chem. Soc. Chem. Commun.* **1969**, 1322.

[139] B. Crociani in *Reactions of Coordinated Ligands* (ed.: P. S. Braterman), Plenum, New York, **1986**.

[140] G. Beck, W. P. Fehlhammer, *Angew. Chem.* **1988**, *100*, 1391; *Angew. Chem. Int. Ed. Engl.* **1988**, *27*, 1344; W. P. Fehlhammer, G. Beck, *J. Organomet. Chem.* **1989**, *369*, 105; *Chem. Ber.* **1989**, *122*, 1907.

[141] D. Lentz, R. Marschall, *Chem. Ber.* **1990**, *123*, 751.

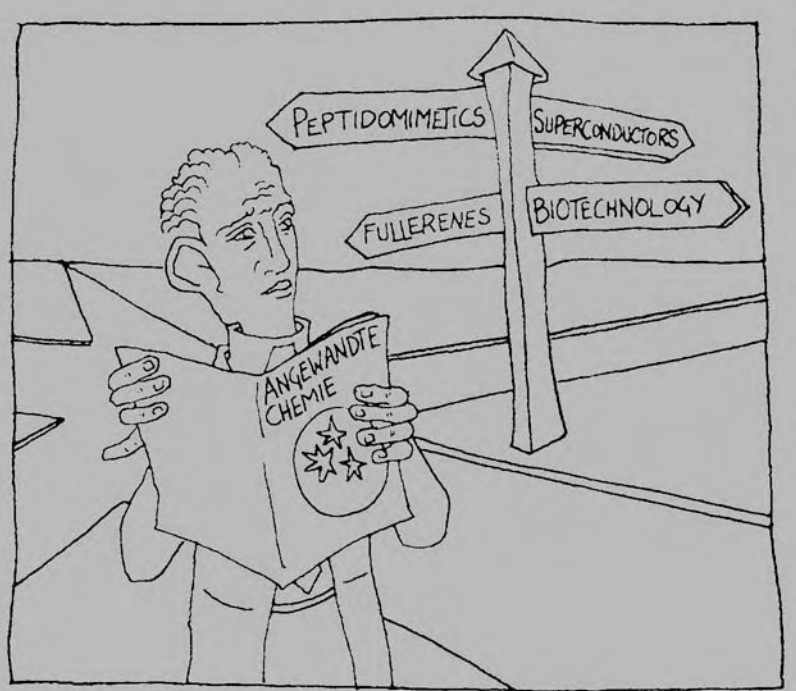
[142] D. Lentz, R. Marschall, *Chem. Ber.* **1990**, *123*, 467.

[143] D. Lentz, D. Preugschat, *Acta Crystallogr. Sect. C*, in press.

[144] D. Lentz, J. Fuchs, unpublished.

[145] D. Lentz, D. Preugschat, unpublished.

Chemistry at the crossroads



Pioneering scientists guide your way through newly charted territory with their topical reviews and discriminating highlights in **Angewandte Chemie.**

To start your own personal subscription, just fax.

An order form is provided on the last page for your convenience.

VCH

Gas-Phase Synthesis of Reactive Molecules Using Adsorbed Reagents

W. E. Billups* and Dianne J. McCord

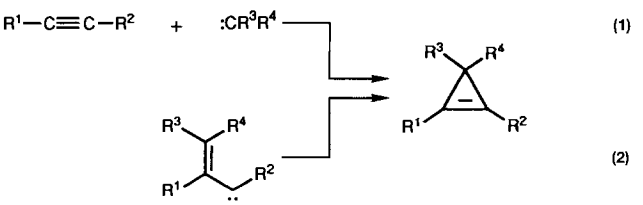
Base-induced elimination reactions have found wide application in the synthesis of strained alkenes. The method is often complicated by a competing process in which the incipient alkene is trapped by nucleophilic addition of the base. Recent studies have shown that the bimolecular side reactions can be avoided when bases such as potassium *tert*-butoxide are supported on an inert surface like silica gel and the reaction is carried out in vacuo. This vacuum gas-solid reaction (VGSR) procedure has the additional advantage that very unstable species may be isolated under conditions that allow detailed studies of their physical and chemical properties. The scope of this procedure has been extended to include the use of fluoride salts supported on glass helices to effect the elimination of β-halosilanes. The fluoride route to strained alkenes is particularly attractive since the reaction may be carried out at very moderate temperatures and the starting materials are readily available. This review describes the development of this vacuum gas-phase procedure and its application in the synthesis and characterization of small-ring alkenes and bicycloalkenes, including methylenecyclopropene, spiropentadiene, bicyclopropenyls, 1,2- and 1,3-bridged cyclopropenes, and other simple cyclopropenes.

1. Introduction

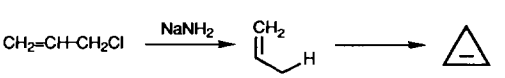
This review describes the development of a vacuum gas-phase procedure[1, 2] and its application in the synthesis and characterization of a wide variety of theoretically significant reactive intermediates which have, for the most part, not been accessible by known methodology. A common feature of these compounds is the incorporation of the cyclopropene ring. As the most highly strained cycloalkenes, the cyclopropenes have played a major role in the development of important concepts such as chemical reactivity and aromaticity.[3, 4] Their high strain energy often results in unexpected reactions such as facile [2+2] cycloaddition reactions and isomerization to species normally considered to be of high energy. The cyclopropenes thus represent one of the cornerstones of modern structural chemistry by virtue of their high energy content and the unusual properties that arise from their unique bonding. They continue to spark the imagination of organic chemists.

Historically, the syntheses of cyclopropenes fall into three general catagories:

1. The addition of carbenes[5, 6] to alkynes leads to the construction of the ring directly by either a concerted or stepwise process depending on the spin multiplicity of the carbene [Eq. (1)]. The ease with which halocarbenes can be generated has led to a plethora of halocyclopropenes.[7–17] This route is not limited to free carbenes, as carbenoids also add readily to alkynes yielding cyclopropenes.[18–30]



2. The formation of vinylcarbenes can be effected with relative ease from either 3*H*-pyrazoles or allylic diazo compounds. Subsequent ring closure of the vinylcarbene leads directly to the cyclopropene [Eq. (2)].[31–53] In a number of other cases, the vinyl carbene can be generated by the base-induced elimination of an appropriate allylic halide (Scheme 1).[54]

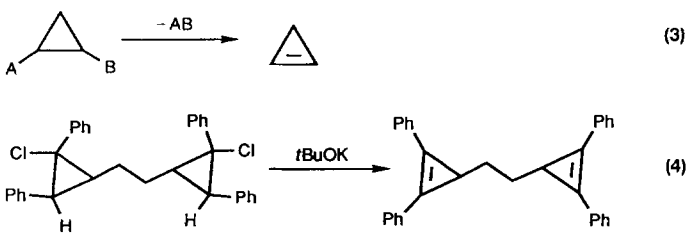


Scheme 1. Synthesis of cyclopropene.

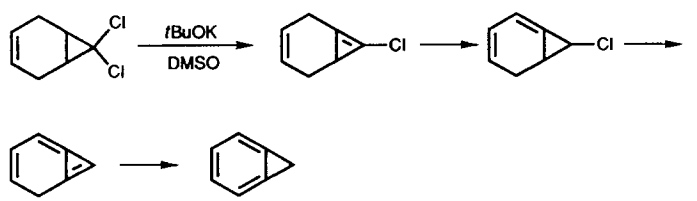
3. A final method is the 1,2-elimination of suitable precursors to yield a cyclopropene [Eq. (3)].[4] Indeed, the first authenticated synthesis of cyclopropene itself was reported in 1922 by Dem'yanov and Doyarenko, who found that trimethylcyclo-

[*] Prof. Dr. W. E. Billups, D. J. McCord
Department of Chemistry, Rice University
P.O. Box 1892, Houston, TX 77251 (USA)
Telefax: Int. code + (713)285-5155

propylammonium hydroxide undergoes a Hofmann elimination at 300 C on platinized clay.[55] Perhaps the most commonly employed procedure involves the dehydrohalogenation of a halocyclopropane with potassium *tert*-butoxide in either dimethyl sulfoxide (DMSO) or tetrahydrofuran (THF). A typical example is outlined in Equation 4.[56] In a number of in-



stances the cyclopropene has been observed to undergo a base-catalyzed prototropic rearrangement in which the endocyclic double bond isomerizes to an exocyclic position. This results usually in a thermodynamically more stable product, as illustrated by the formation of benzocyclopropene from 7,7-dichlorobicyclo[4.1.0]hept-3-ene and strong base (Scheme 2).[57, 58]



Scheme 2. Synthesis of benzocyclopropene.

The use of *tert*-butyllithium and other lithium reagents to effect the elimination of halogen from mono- and dihalocyclopropanes has also been reported.[59–63] The highly strained compounds **1**[62] and **2**[63] were synthesized by this procedure.

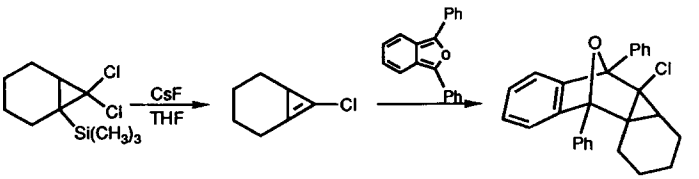


1



2

An important discovery by Chan and Massuda[64] demonstrated that halocyclopropenes can be prepared readily by the fluoride-induced elimination of β-dihalocyclopropylsilanes and trapped as illustrated in Scheme 3. The halocyclopropenes that result from these elimination reactions have become important building blocks in organic chemistry.[65, 66]



Scheme 3. Synthesis of a cyclopropene by fluoride ion mediated elimination of a β-halocyclopropylsilane and a subsequent trapping reaction.

Although these elimination reactions have found wide application in the synthesis of cyclopropenes, the method is often complicated by a competing process in which the incipient alkene is trapped by nucleophilic addition of the base that was used to induce the elimination.[67, 68] Several recent studies have shown that these bimolecular reactions can be avoided when the base is supported on an inert surface and the reaction is carried out in vacuo.[1, 2] This procedure, now commonly known as the vacuum gas–solid reaction (VGSR) technique, has the additional advantage that very unstable species may be isolated under conditions that permit detailed studies of their physical and chemical properties. Billups and Lin extended the scope of this procedure to include the use of fluoride salts supported on glass helices to effect the elimination of β-halosilanes.[2] This route to strained alkenes is particularly attractive, since the reaction can be carried out under very mild conditions and the starting materials are readily available.[69]

2. Experimental Techniques

2.1. The Gas-Phase Reactions

The apparatus used for these gas-phase reactions is illustrated in Figure 1. Dehydrohalogenation reactions can be carried out by using potassium *tert*-butoxide adsorbed onto inert surfaces such as Chromosorb W or silica gel. Dehydrochlorinations of



W. E. Billups is Professor of Chemistry at Rice University, Houston, Texas (USA), where he served as Chairman of the Department from 1985 until 1991. He received his bachelor's degree from Marshall University in 1961 and his Ph.D. from the Pennsylvania State University in 1970. He was employed as a research chemist by Union Carbide Corporation from 1961 until 1968. His research interests include the chemistry of small-ring systems, reactive intermediates, metal atom chemistry, and more recently fullerene chemistry.

chlorocyclopropanes have been carried out from 160 °C to 320 °C. The pressure is typically 10 mTorr (1.33 Pa). Dehydrobromination reactions have been carried out at ambient temperature. Ideally, products are collected in traps cooled by liquid nitrogen (labeled H in Fig. 1) for further studies on their chemical and physical properties. NMR spectra can be obtained by collecting the product in an NMR tube attached to the bottom of trap H with deuterated solvent that is introduced from the solvent trap G. This procedure allows compounds that are stable above −108 °C to be characterized readily using standard low-temperature techniques. In those cases where the intermediate is allowed to react with a trapping reagent, the material is introduced slowly from the solvent trap onto the walls of trap H as the product is collected.

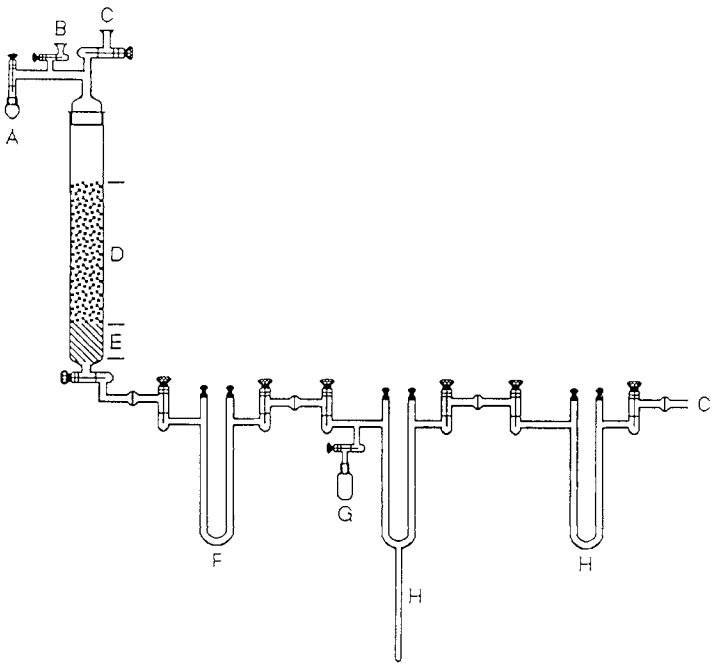


Fig. 1. Apparatus for gas-phase reactions. A) Flask containing starting material; B) connection to vacuum gauge; C) connection to vacuum pump (5–10 mTorr, 0.66–1.33 Pa); D) reagent adsorbed on support (*t*BuOK/Chromosorb W or nBu$_4$NF/glass helices); E) glass wool; f) cold trap (dry ice/acetone bath); G) flask containing NMR solvent or trapping reagent; H) cold trap (liquid nitrogen bath).

2.2. Matrix Isolation Spectroscopy

Although the gas-phase route described above allows very unstable molecules to be isolated and characterized by low-temperature NMR spectroscopy, in a number of instances we have used matrix isolation spectroscopy to identify reactive molecules. This usually involves low-temperature isolation of the reactive species followed by cocondensation with argon onto a matrix surface for characerization by FT-IR spectroscopy. Alternatively, the gas-phase reaction apparatus (actually a microversion) can be connected directly to the matrix apparatus so that the product is cocondensed with argon at 12 K directly onto the matrix surface. The infrared spectrum is recorded by reflection. A brief description of the state-of-the-art apparatus used in these studies follows.

The apparatus[70] shown in Figure 2A is interfaced to an FT-IR vacuum spectrometer. The multisurface copper block used in matrix isolation (labeled a in Fig. 2A) is shown in more detail in Figure 2B. This design permits independent matrix isolation studies with sixty rhodium-plated copper surfaces. In this way the contents of a cold trap can be fractionally distilled onto the various surfaces until the concentration of the desired species is optimized, and, when necessary, concentrations can be determined by direct measurement of the ratio of matrix gas to guest with an integral cooled quartz crystal microbalance.

The infrared spectrum of methylenecyclopropene, which is presented in Figure 3, was recorded using this technique (see Section 3.2). After the surface which contained the optimum concentration of methylenecyclopropene was identified, the ma-

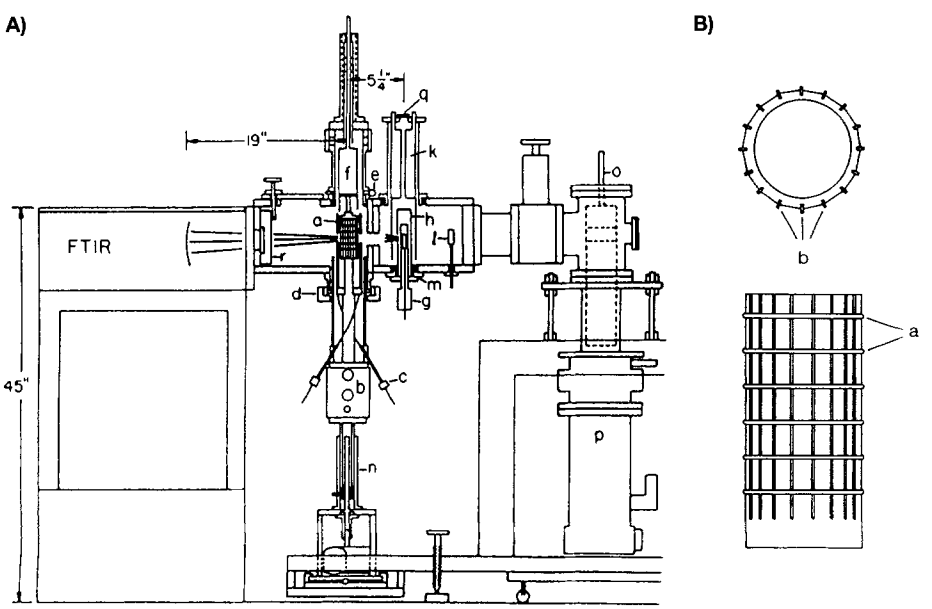


Fig. 2. A) Multisurface FTIR matrix isolation apparatus (side view). I. Matrix chamber. II. furnace chamber. a) multisurface matrix isolation copper block (can be adjusted vertically and rotated); b) helium refrigerator; c) shutter actuator; d) sliding O-ring seal for vertical positioning; e) worm gear for rotating the matrix block; f) dewar containing liquid nitrogen; g) high-temperature/water-cooled furnace assembly (can be adjusted vertically); h) water-cooled shield; k) liquid nitrogen cooled dewar and shield; l) water-cooled quartz crystal microbalance; m) rotation O-ring seal; n) electric screwjack for vertical positioning; o) dewar containing liquid nitrogen; p) diffusion pump; q) window for furnace temperature measurement; r) rotating window sets; one set of CsI is used for mid-IR, another set of polyethylene for far-IR. B) Multisurface matrix isolation copper block; view from above (top), side view (bottom). a) Viton 1/16"-thick O-rings; b) 1/32"-thick Teflon spacers.

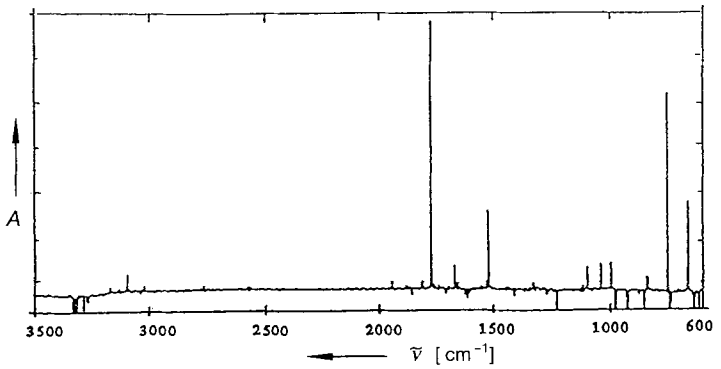


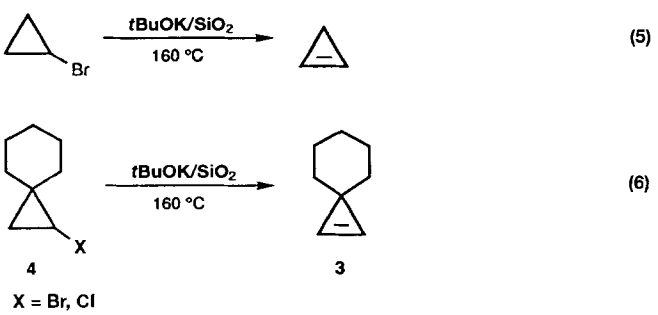
Fig. 3. FT-IR spectrum of methylenecyclopropene recorded after photolysis for five minutes in an argon matrix at 15 K.

trix was photolyzed. The absorption bands of the photolysis product, mainly vinylacetylene, point downward, whereas those of methylenecyclopropene point upwards.

3. Gas-Phase Dehydrohalogenation of Halocyclopropanes Using Potassium *tert*-Butoxide Supported on Chromosorb W

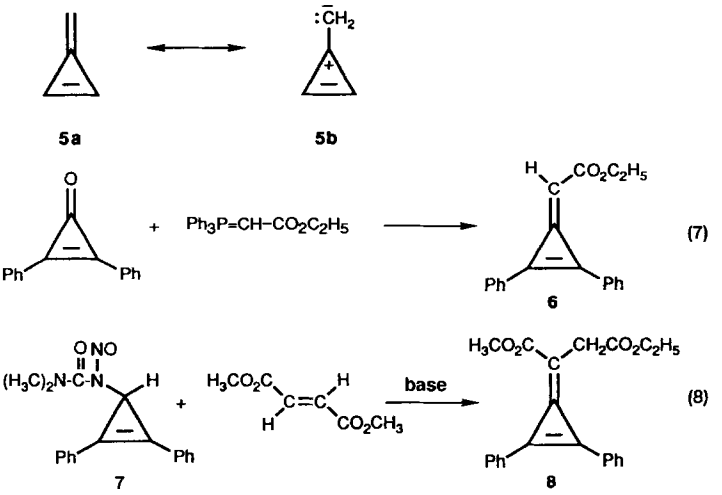
3.1. Simple Cyclopropenes

The use of adsorbed reagents to effect gas-phase elimination reactions was reported first by Denis et al. in 1980.[1a] They found that bromocyclopropane could be converted to cyclopropene in good yield by passing the bromide over solid potassium *tert*-butoxide supported on silica gel [Eq. (5)]. Spirocyclopropene **3** was synthesized from **4** under the same conditions [Eq. (6)].

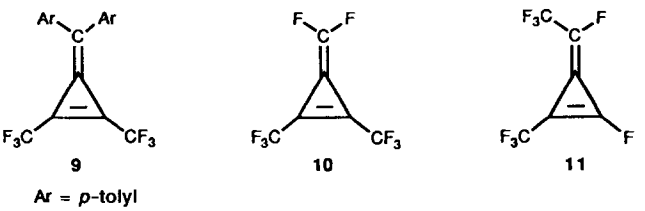


3.2. Methylenecyclopropene

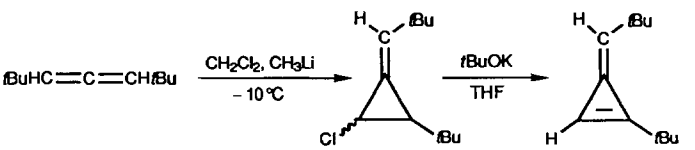
Our involvement in this field began with the synthesis of methylenecyclopropene (**5a**).[71-73] As a member of the C_4H_4 family of hydrocarbons, this, the simplest cross-conjugated cyclic hydrocarbon, has been of interest not only to theoreticians[74] but also to synthetic chemists.[75] Moderately stable derivatives of methylenecyclopropene were first reported in 1964 [Eqs. (7) and (8)]. Battiste[76] formed **6** by a Wittig reaction of diphenylcyclopropenone, and Jones and Denham[77] found that a base-induced reaction of the *N*-nitrosourea **7** with



dimethyl fumurate yielded **8**. These and other derivatives[78] owe their stability to the aromatic character obvious in the dipolar formula **5b**. Inductive effects caused by strong electron-withdrawing groups also lead to stable derivatives. For example, **9** is a perfectly stable compound with a dipole moment of 7.42 D.[79] Methylenecyclopropenes **10** and **11** most likely derive their stability from the same effect.[80,81]

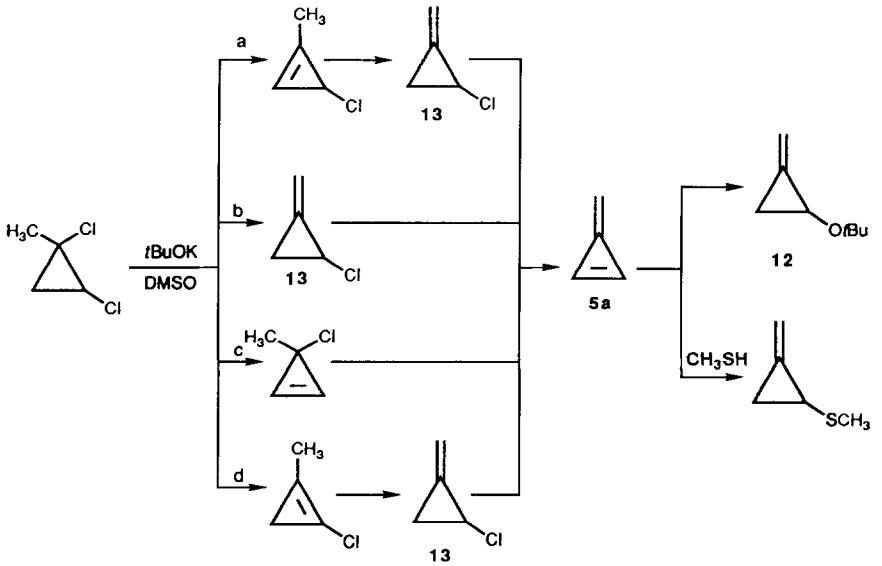


Moderately stable derivatives have also been synthesized in which the stability is derived from steric protection provided by bulky *tert*-butyl groups (Scheme 4).[82,83] The tetramethyl derivative, however, has only transient existence.[84]



Scheme 4. Synthesis of a sterically hindered methylenecyclopropene.

Despite the impressive array of derivatives, evidence for the parent hydrocarbon remained inconclusive prior to 1984.[71-73] Indirect evidence[75d] for methylenecyclopropene was provided by the isolation of **12** when 1,2-dichloro-1-methylcyclopropane was treated with potassium *tert*-butoxide in dimethylsulfoxide (Scheme 5). This observation can be rationalized by assuming the intermediacy of methylenecyclopropene (**5a**). Additional support for this assumption is found when an external nucleophile (MeS^-) is added to the reaction medium. Although the sulfide is not sufficiently basic to induce the elimination of HCl

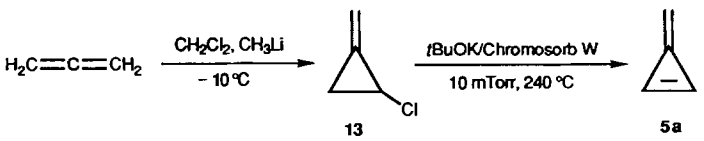


Scheme 5. Generation of methylenecyclopropene **5a** and subsequent reactions.

from the starting material, it is more nucleophilic than *tert*-butoxide and will add more readily to the cyclopropenyl double bond.

Factors that contribute to the instability of methylenecyclopropene include perhaps as much as 78 kcal mol^{-1} of strain energy, a high index of free valency at the exocyclic position resulting from the large contribution of the zwitterionic resonance structure, and the absence of steric protecting groups to inhibit bimolecular reactions. The gas-phase technique using a supported base to effect the dehydrohalogenation of a simple starting material would thus appear to provide the most direct approach to this elusive compound.

The precursor chosen for the gas-phase study, 1-chloro-2-methylenecyclopropane (**13**) appears in paths a, b, and d of Scheme 5 and would seem to be the starting material of choice for the synthesis of methylenecyclopropene. **13** can be synthesized from allene in a straightforward fashion. As expected, the elimination of HCl from **13** was accomplished readily by using the supported base.[71] The corresponding bromide[85] can be converted to **5a** at more modest temperatures.[72]

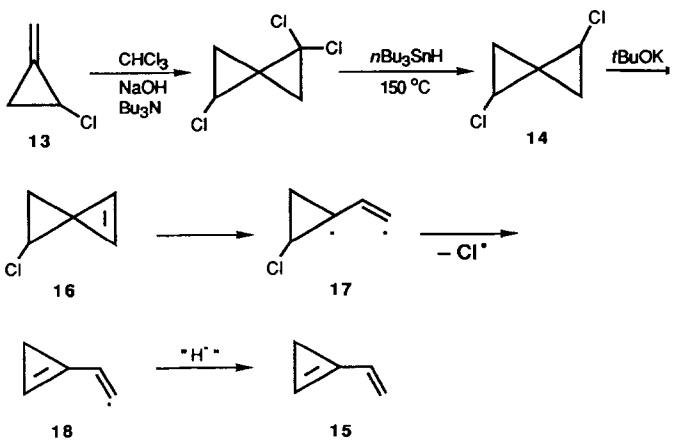


Photolysis of methylenecyclopropene in argon at 15 K through a quartz window using the matrix technique (see Section 2.2) gave mainly vinylacetylene. The two bands at 1770.3 and 1518.9 cm^{-1} arise from coupling between the stretching vibration of the *exo* double bond and that of ring deformation.[86] The NMR spectrum of methylenecyclopropene at $-98\,^{\circ}C$ in [D$_8$]THF displays two triplets ($J = 2.2$ Hz) at $\delta = 3.47$ (exocyclic protons) and 8.61 (ring protons). These chemical shifts emphasize the exceptional polarity of the π electron system.

With an abundant supply of methylenecyclopropene, other detailed spectroscopic measurements could be undertaken to answer some of the long-standing questions regarding the contribution of polar resonance structures to the ground state. Methylenecyclopropene has been thought of as pseudoaromatic,[74c, 87] nonaromatic,[88] and antiaromatic.[89] This issue has been largely resolved through the determination of the electric dipole moment and molecular structure by microwave spectroscopy.[90] Analysis of the experimental and calculated dipole moments, the calculated electron distribution, and the experimental and calculated molecular structures for methylenecyclopropene led to the conclusion that dipolar resonance structure **5b** constitutes about one-fifth of the ground state character of methylenecyclopropene, but it only contributes a π-delocalization energy comparable to that of 1,3-butadiene. These results infer that methylenecyclopropene is nonaromatic.

3.3. 1-Vinylcyclopropene

Elimination of HCl from dichlorospiropentane **14** provided an intriguing test for the gas-phase dehydrohalogenation, since the elimination of both equivalents of HCl would yield spiropentadiene (see Section 4.1.). When **14** was synthesized (Scheme 6) and introduced slowly into a column packed with



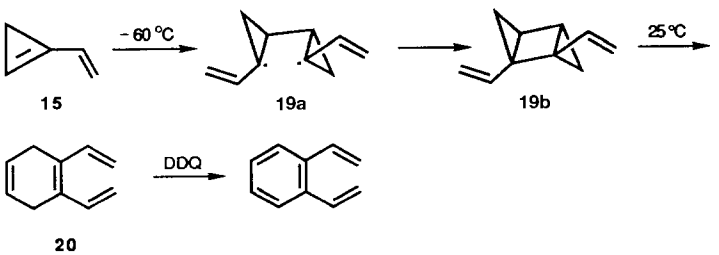
Scheme 6. Synthesis of dichlorospiropentane **14** and its transformation to vinylcyclopropene **15**.

potassium *tert*-butoxide supported on Chromosorb W at 320 °C and 5–10 mTorr (0.66–1.33 Pa), a major product, provisionally identified as 1-vinylcyclopropene **15** was isolated. Confirmation of this assignment was provided by comparison with an "authentic" sample prepared by subjecting 1-chloro-2-vinylcyclopropane to the same reaction conditions.[2]

A possible mechanism to explain the formation of 1-vinylcyclopropene is illustrated in Scheme 6. Elimination of HCl from

14 would yield spiropentene **16**. Cleavage of a C–C bond in **16** would give biradical **17**; this process would be facilitated by the high temperature required for the elimination. Subsequent scission of the C–Cl bond would afford radical **18**, which could then abstract a hydrogen atom from *tert*-butanol to give 1-vinylcyclopropene. The isolation of acetone along with **15** provides compelling evidence that *tert*-butanol serves as the hydrogen atom donor.

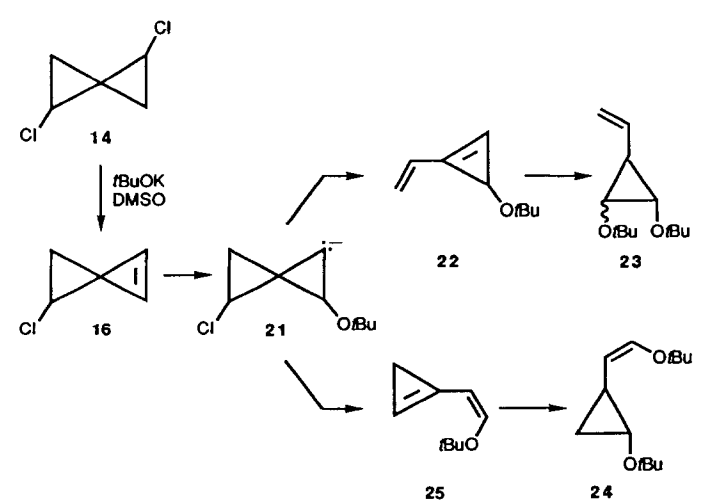
1-Vinylcyclopropene dimerizes readily at −60 °C via **19a** to give tricyclohexane **19b**, which rearranges slowly to **20**. *ortho*-Divinylbenzene was isolated when **20** was reacted with 2,3-dichloro-5,6-dicyano-1,4-benzoquinone (DDQ).



Scheme 7. Dimerization of vinylcyclopropene **15**.

Although the formation of a biradical would normally be an endothermic process, the facile dimerization of **15** can be understood from a thermodynamic standpoint. Benson's and O'Neal's additivity rules can be used to estimate the heats of formation of strain-free models of **15** and **20** as 26.2 and 65.6 kcal mol^{-1}, respectively.[91a] These values, along with the known strain energies[91b] of cyclopropene (55.2 kcal mol^{-1}) and cyclopropane (27.5 kcal mol^{-1}), can then be used to show that the dimerization to the biradical is exothermic by some 39 kcal mol^{-1}. The driving force for this dimerization is, of course, primarily the decrease in strain. The failure to observe products from ring opening of the cyclopropene to yield vinylcarbene intermediates is consistent with calculations which predict a high barrier for this process.[92]

Results from a study of the dehydrohalogenation of **14** in solution[67] stand in contrast to those from the gas-phase elimination and thus emphasize the advantages provided by the gas-phase method. Only products **23** and **24** resulting from nucleophilic addition reactions could be isolated from the solution-phase reaction. Experiments to elucidate the mechanism of formation of these products have not been carried out; however, the pathways illustrated in Scheme 8 are not unreasonable. Spiropentene **16** would be expected to undergo nucleophilic addition to yield anion **21**, which could collapse to **22**, followed by addition of *tert*-butoxide and protonation to yield **23**.[67] Alternatively, ring opening of the cyclopropyl anion with loss of chloride would yield **24** (via **25**). Formation of a single isomer of **24** (*cis* double bond) may result from a concerted ring opening of the anion.



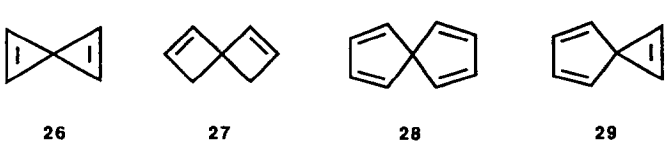
Scheme 8. Dehydrochlorination of **14** in solution.

4. Gas-Phase Elimination of β-Halocyclopropylsilanes Using Solid Fluoride Salts

Synthesis and characterization of methylenecyclopropene and vinylcyclopropene prompted investigation into the use of other supported reagents as a route to reactive intermediates. The fluoride route discovered by Chan and Massuda[64] (Scheme 3) seemed particularly attractive, since β-halocyclopropylsilanes are readily available and the reaction can be carried out at very mild temperatures. In the following section we describe some of our results in which solid fluoride salts were used to effect the gas-phase elimination of β-halocyclopropylsilanes.

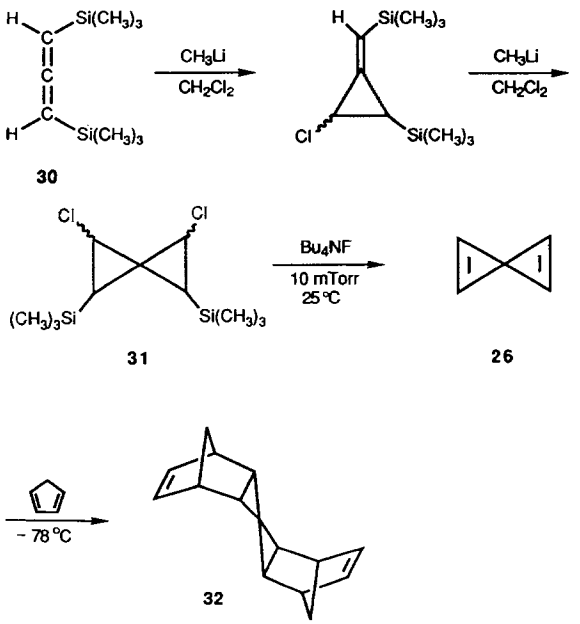
4.1. Spiropentadiene

Perhaps the greatest advertisement for the gas-phase fluoride route to highly energetic molecules is the synthesis of spiropentadiene **26** ("bowtiediene").[93] The spiro-connected cycloalkenes are of interest, since they can, in principle, exhibit interesting properties resulting from the two π systems being held in perpendicular planes by a common carbon atom. Such through-space interactions of nonconjugated π systems are commonly referred to as homoconjugation[94] or, in this case, spiroconjugation.[95, 96] Spectroscopic evidence would seem to support the presence of spiroconjugation in derivatives of **27**,[97] **28**,[98, 99] and **29**,[100] and calculations indicate that this may also apply for **26**.[94, 95] A range of values for the strain energy of spiropentadiene **26** from 110 to 145 kcal mol^{-1} has been calculated.[101–104]



The synthesis of **26** required the sterically hindered allene **30** as a point of departure. Although **30** had been synthesized previously by reaction of the anion of 1,3-bis(trimethylsilyl)propyne with sodium sulfate decahydrate,[105] a somewhat higher yield was obtained by treating the tosylhydrazone of

bis(trimethylsilyl)propynone with sodium cyanoborohydride in a two-phase system at pH 1.[106] Under these conditions none of the isomeric propyne could be detected by ^{1}H NMR spectroscopy. The allene could be converted in low yield to the desired precursor **31** by the sequential addition of chlorocarbene. Introduction of **31** into a column containing nBu$_4$NF on glass helices afforded **26** along with a complex mixture of products (Scheme 9).



Scheme 9. Synthesis of spiropentadiene **26**.

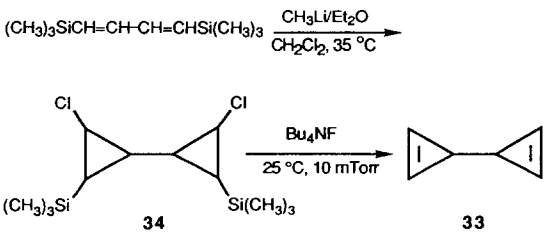
Although **26** exists only fleetingly, it was possible to detect a signal for the cyclopropenyl protons at $\delta = 7.62$ in the NMR spectrum ([D$_8$]THF, $-105\,^\circ$C). Upon warming, a sparingly soluble polymer is produced. Spiropentadiene **26** can be intercepted with cyclopentadiene to yield the Diels–Alder adduct **32**.

Experimental verification of the anticipated properties of **26** has not been reported; however, calculations[107] predict a standard heat of formation of 157.4 kcal mol^{-1}, which is more than twice the experimental heat of formation of 66.2 kcal mol^{-1} for cyclopropene,[108] and consistent with the high energy content expected for spiropentadiene.

4.2. Bicyclopropenyls

4.2.1. 2,2′-Bicyclopropenyl

(CH)$_6$ valence isomers of benzene have attracted the attention of chemists for well over a century.[109] Although Dewar benzene, benzvalene, and prismane have been known for a number of years, a fourth isomer, 2,2′-bicyclopropenyl **33**, was first prepared in 1989 (Scheme 10).[110] Starting material **34** was prepared by treating 1,4-bis(trimethylsilyl)buta-1,3-diene with an excess of chlorocarbene. Elimination of trimethylsilyl chloride from **34** by reaction with supported fluoride salts yielded **33**, which decomposes above approximately $-10\,^\circ$C.



Scheme 10. Synthesis of 2,2′-bicyclopropenyl (**33**).

Apart from historical interest, the possibility that the two double bonds might couple through the σ framework is intriguing from a theoretical perspective.[111–113] In order to confirm some of the properties of **33** anticipated earlier by theoreticians, high-quality crystals were prepared by Boese et al.[114] using a zone-melting procedure with focused infrared light, and the X-ray structure was determined at 103 K.[115, 116] As expected, the conformation of **33** in the solid state was found to be *anti* with C_i symmetry (Fig. 4). The most salient feature of **33** is the extremely short central bond (1.503(1) Å), which indicates significant sp^2 hybridization. This is also apparent from the C1′-C1-H1 angle of 113.7(6)° and the C1-C1′-(center C2, C3) angle of 124.7°.

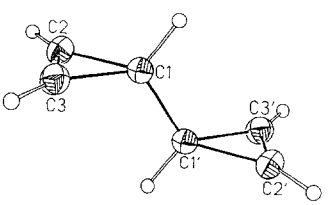


Fig. 4. Crystal structure of 2,2′-bicyclopropenyl.

The length of the double bond of **33** is comparable to that in cyclopropene, which was determined by microwave spectroscopy[117] to be 1.2939(4) Å; however, the single bonds in the ring (1.512(1) Å) are slightly longer than in cyclopropene (1.509(1) Å). This may be explained by the observation that, in general, bond lengths in the gas phase are found to be longer than in the solid state. Since a bond of similar length was found between the two rings of bicyclopropyl (X-ray structure, *anti* conformer[118] 1.4924(4) Å, gas electron diffraction[119] 1.508 Å), which was also shorter than the endocyclic bonds[119] (1.5052(3), vicinal; 1.5046(4), distal), we ascribe this effect to the higher σ character of this bond relative to a normal C–C bond.[120] In 3-vinylcyclopropene[121] (Section 4.5) the endocyclic double bond is even shorter (1.279(1) Å) than that in **33** and the conjugation in the exocyclic C–C bond shortens this distance to 1.476(1) Å.

In contrast to **33**, the hexa-*tert*-butyl derivative[122] was found to exist exclusively in the *gauche* conformation as a result of the severe steric interactions between the *tert*-butyl groups. This results in a lengthening of the central bond to 1.570(3) Å. The C–C bonds in the rings (1.550(2), 1.536(2) Å) are also longer, but the length of the double bond (1.294(2) Å) agrees well with that in **33**.

Electron density maps (Fig. 5) of **33** are particularly revealing with regard to the through-bond effect. In map A the expected circular pattern of the electron density in the plane of the σ bond is distorted to an elliptical shape owing to π-bonding contributions. Maps B and D show that the distortion is restricted to the plane of the bonds and not in all directions.

The photoelectron spectrum of **33** recorded by Gleiter et al.[114] exhibits three peaks of different heights well separated

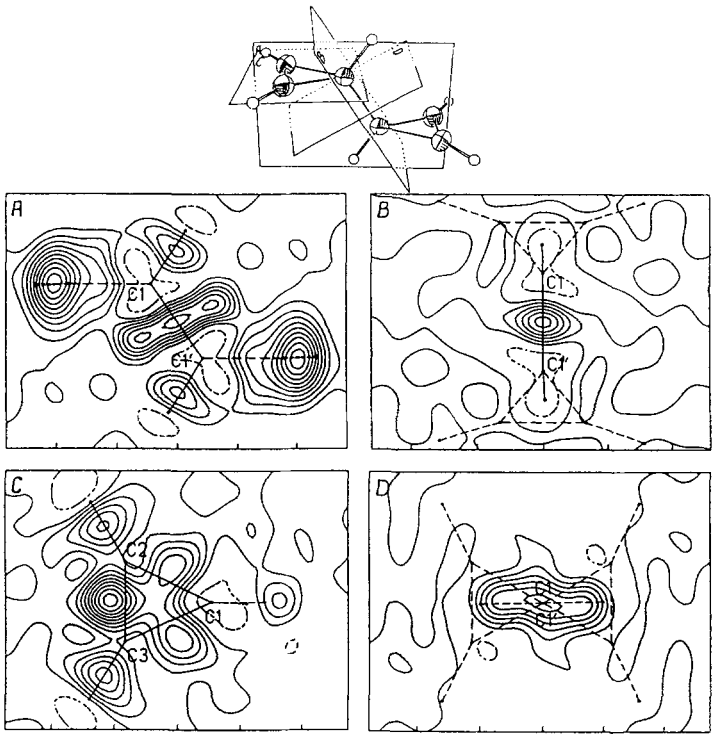
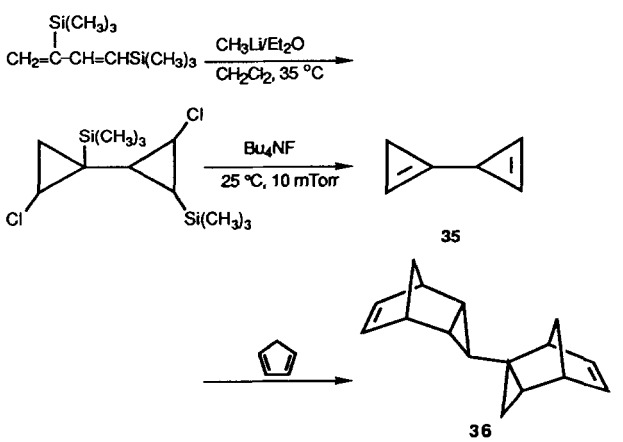


Fig. 5. X X electron density maps of 2,2'-bicyclopropenyl with a distance of 0.05 eÅ^{-1} (negative, dashed lines).

from a smaller fourth one. This result is rationalized in terms of a roughly 2:1 mixture of *anti* and *gauche* conformers in the gas phase.

4.2.2. 1,2'-Bicyclopropenyl

The synthesis of 1,2'-bicyclopropenyl **35** is illustrated in Scheme 11.[110] In view of the facile polymerization described earlier for **33**, it is perhaps not surprising that **35** was observed

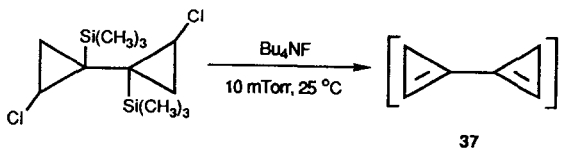


Scheme 11. Synthesis of 1,2'-bicyclopropenyl (**35**).

to polymerize above −30 °C. It was, however, possible to secure NMR spectral data at −50 °C and to trap the cyclopropene with cyclopentadiene to yield the Diels–Alder adduct **36**. Unfortunately, it was not possible to secure a single crystal, and X-ray structural data could not be obtained.

4.2.3. 1,1'-Bicyclopropenyl

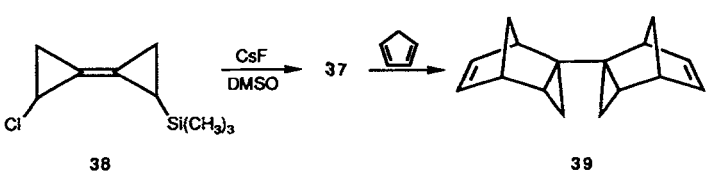
1,1'-Bicycloprop-1-enyl (**37**) is perhaps the most highly strained conjugated diene. Two sterically protected derivatives have been reported,[123] but no reports describing the synthesis of the parent compound have been published.[124] The elimination reaction presented in Equation 9 yielded a white polymeric



(9)

solid; however, in one instance a small amount of volatile material could be isolated which exhibited NMR signals at $\delta = 0.71$ and 7.36, consistent with what might be expected for the diene. Above −90 °C these signals began to diminish, and at room temperature rapid polymerization was observed. It was not possible to isolate a Diels–Alder adduct with cyclopentadiene.

An alternative precursor, compound **38**, was found to give the same polymeric material upon elimination in the gas phase;[125] however, when this precursor was allowed to react with cesium fluoride in dimethyl sulfoxide containing a large excess of cyclopentadiene, the cycloadduct **39** was formed as a mixture of diastereomers in 61 % yield. Since **38** can only yield **37** by means of a 1,4-elimination, the existence of **37** as a discrete species is indeed confirmed (Scheme 12). The use of **37** as a building block in synthesis remains to be exploited.



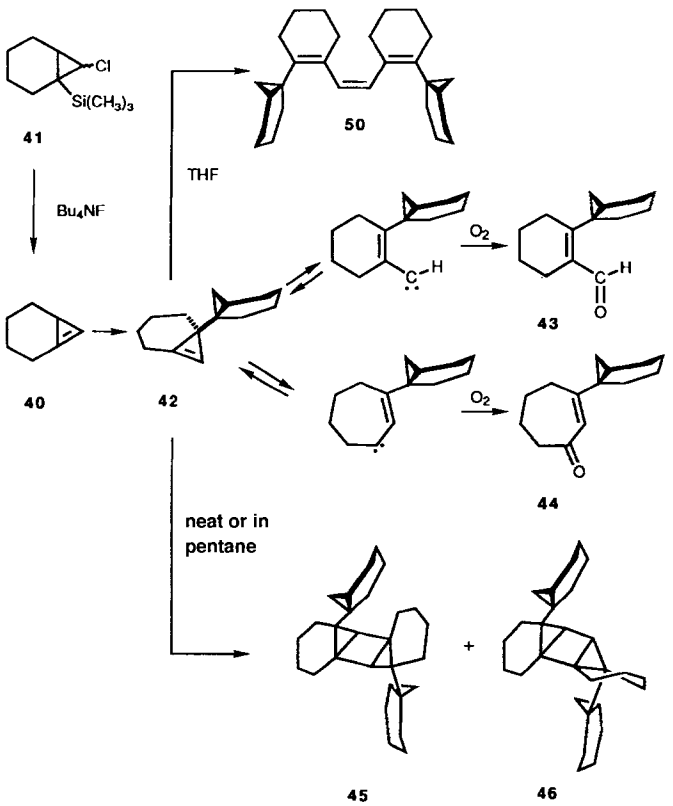
Scheme 12. Synthesis and trapping of 1,1'-bicyclopropenyl (**37**).

4.3. 1,3-Bridged Cyclopropenes

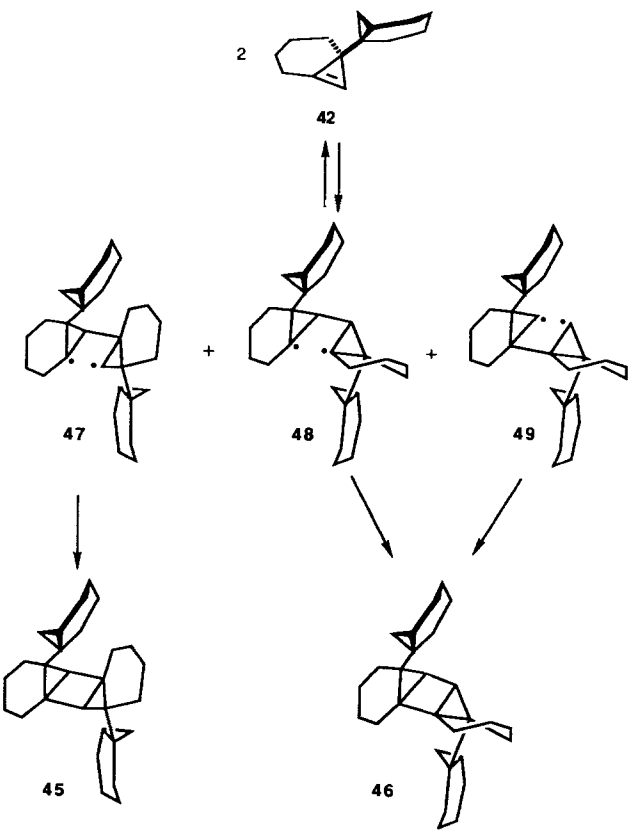
Although 1,3-bridged cyclopropenes can be isolated when the fused ring has more than seven carbon atoms, evidence for more highly strained systems has relied, for the most part, on trapping experiments.[126] The 1,3-bridged cyclopropene **40** was chosen for our work, since its properties had been the object of considerable speculation,[127] but no syntheses had been reported.

We found that **40** could be generated readily at room temperature by passing the precursor **41** over nBu$_4$NF deposited on glass helices.[128] The yield was nearly quantitative as shown by a trapping experiment with cyclopentadiene. The synthesis and chemistry of **40** is summarized in Scheme 13.

Dimerization of **40** by an ene reaction to yield **42** occurred readily below −90 °C. Cyclopropenes with a hydrogen atom at C3 often undergo ene reactions in which a hydrogen atom is transferred to the double bond of a second molecule with the simultaneous formation of a carbon–carbon bond.[129] The additional strain in **40** would probably account for this facile



Scheme 13. Synthesis and dimerization of **40** and other reactions.



Scheme 14. Dimerization of **42**.

dimerization. Steric interactions are presumably too severe to allow transfer of a hydrogen atom from a third molecule of **40** to yield a trimer.

Cyclopropene **42** is unexpectedly stable possibly due to steric protection provided by the bicycloheptyl pendant. The stabilization of reactive intermediates from bimolecular reactions by sterically hindered substituents is, of course, a strategy frequently used in the preparation of reactive molecules.[130, 131]

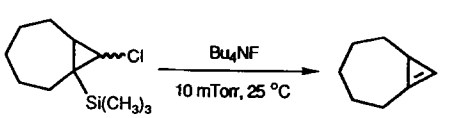
Exposure of **42** to dioxygen yields the oxidation products **43** and **44**. Although these unexpected products can be rationalized in terms of the carbenes[132] shown in the scheme, the direct reaction of the cyclopropene with molecular oxygen to yield the carbonyl derivatives is a viable alternative. Experiments to delineate these pathways have not been carried out.

When the ene dimer **42** was allowed to warm slowly to room temperature with rigorous exclusion of dioxygen, a white crystalline compound shown by mass spectroscopy to be a tetramer of **40** could be isolated. X-ray crystallographic studies established the structure of this compound as the tricyclohexane **45** with *trans,anti* configuration. A second tetramer identified by X-ray analysis as **46** was isolated when the dimer was diluted with pentane and allowed to stand at room temperature for several days. Isomers **45** and **46** are dimers of **42** that differ only in the configuration about the tricyclohexane framework.

A plausible rationalization for the formation of the tricyclohexanes is illustrated in Scheme 14.[133] Initial bond formation could occur to yield biradicals **47**, **48**, and **49**. Collapse of **47** with carbon–carbon bond formation would yield **45**. Formation of **46** would require either biradical **48** or **49** with subsequent formation of the four-membered ring. The factors controlling the regiochemistry of these dimerizations are obviously delicately balanced, since the biradicals have comparable stabilities.

A third tetramer **50** could be isolated to the complete exclusion of the tricyclohexanes when **42** was allowed to dimerize in tetrahydrofuran. The origin of this product has not been established.

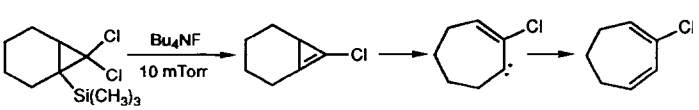
Other 1,3-bridged cyclopropenes, including the surprisingly stable hydrocarbon **51**, can also be synthesized readily [Eq. (16)].[129]



(10)

51

In contrast to **40**, the chloro derivative **52** trapped by Chan and Massuda[64] was observed to rearrange quantitatively in the gas phase to **53**, a product of thermal ring opening (Scheme 15).[128] The cyclopropene–vinylcarbene rearrangement depicted is an unusually facile process, as only **53** could be detected even at −90 °C.

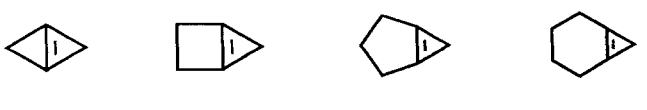


52 **53**

Scheme 15. Synthesis and rearrangement of **52** in the gas phase.

4.4. 1,2-Bridged Cyclopropenes

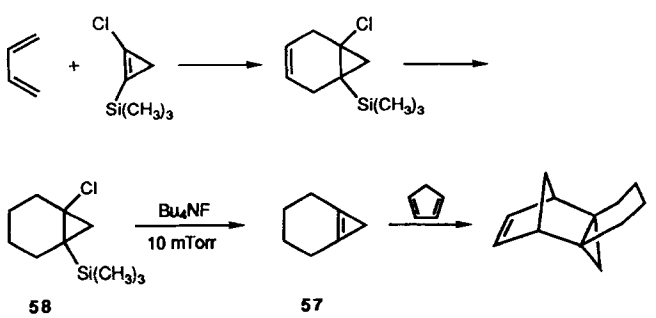
There has been much interest in the 1,2-bridged cyclopropenes, since calculations predict that pyramidalization will be important for those compounds in which the size of the bridging ring is small, as in **54**–**57**.[134] The predicted strain energies,



54 **55** **56** **57**

inversion barriers, bond properties, and atom properties indicate that bicyclopentene may be a transition state for the carbon scrambling of methylenecyclobutylidene and also indicate that bicyclobutene should have an unusual structure and charge density distribution.[135] Cyclopropenes **56** and **57** are expected to be fairly "normal" compounds exept for their high strain energies.

Compounds **56** and **57** have been synthesized in solution by dehalogenation of 1,5-dihalobicyclo[3.1.0]hexanes and 1,6-dihalobicyclo[4.1.0]heptanes, respectively.[61, 136] However, when the cyclopropenes were generated in the gas phase using either potassium atoms or solid methyllithium on glass helices, the products of thermal ring opening, methylenecyclopentene and methylenecyclohexene, were formed.[136] The less exothermic gas-phase route to **57** using solid fluoride salts was particularly attractive, since compound **58**, a viable precursor to **57**, can be synthesized readily by catalytic hydrogenation of the Diels–Alder adduct of 1-chloro-2-trimethylsilylcyclopropene[65] and 1,3-butadiene (Scheme 16).



58 **57**

Scheme 16. Synthesis and trapping of **57**.

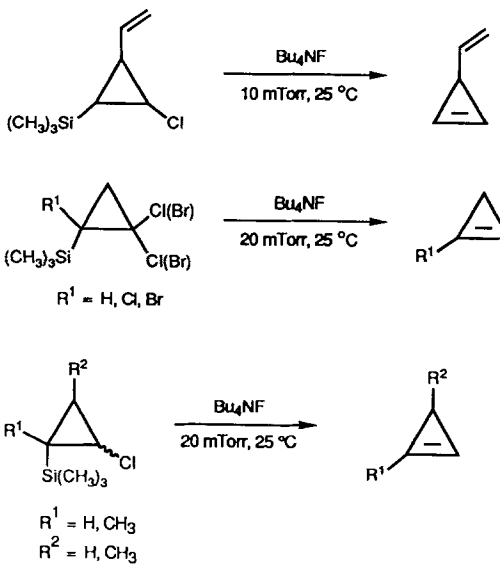
The discrete existence of **57** as a gas-phase entity could be demonstrated by subjecting **58** to the same reaction conditions used to synthesize **40** and trapping the short-lived intermediate with cyclopentadiene (Scheme 16).[2] It is interesting that this cyclopropene, in the absence of a trapping reagent, gives the ene dimer **42** described earlier for **40** as well as a new ene dimer identified as **42a**, a diastereomer of **42**. Attempts to record the spectral properties of **57** using both matrix isolation spectroscopy and low-temperature NMR spectroscopy have been unsuccessful.



42a

4.5. Other Simple Cyclopropenes

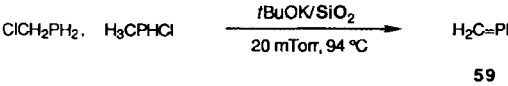
We have found the VGSR technique to be widely applicable to the synthesis of simple cyclopropenes which might be too unstable to isolate under ambient conditions.[127] 3-Vinylcyclopropene can be cited as an example [Eq. (11)]. It was possible to prepare this unstable compound and then secure a single crystal (m.p. 181 K) using the technique of Boese et al.[115, 116] so that high-quality structural data could be obtained.



Other simple cyclopropenes including cyclopropene itself could be synthesized [Eqs. (12) and (13)]. Although the halocyclopropenes [Eq. (12)] can be generated with equal ease in solution,[59, 60, 66, 137, 138] we find that it is sometimes advantageous to generate them in the absence of solvent.

4.6. Formation of Reactive Intermediates Containing Heteroatoms

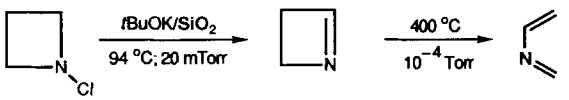
Phosphaethene (**59**), the unstable parent compound in the phosphaalkene series, can be generated very cleanly by vacuum dehydrochlorination of either chloromethylphosphane or 1-chloroethylphosphane over potassium *tert*-butoxide on silica gel [Eq. (14)].[139]



59

By connecting the vacuum apparatus directly to a photoelectron spectrometer, the photoelectron spectrum of **59** generated in situ could be recorded. The PE spectrum suggests a significant energetic separation between the $^2A''$ and $^2A'$ ionic states, implying that the double bond should exhibit an enhanced reactivity toward transition metals in competition with the lone pair on phosphorus.

Application of the VGSR technique to effect the elimination of HCl from *N*-chloroazetidine has also been reported.[140] The resulting 1-azetidine could be converted to the labile azadiene **60** by flash vacuum pyrolysis at 400 °C and 10^{-4} Torr (Scheme 17).



60

Scheme 17. Dehydrochlorination of *N*-chloroazetidine and pyrolysis of the resulting 1-azetidine.

No reports describing the chemistry of this potentially useful compound have appeared.

4.7. Summary and Outlook

Although applications of the VGSR technique have been limited to the few reagents described in this review, there is good reason to believe that numerous other reagents can be adsorbed onto inert surfaces and used in synthesis. For example, other more reactive forms of "naked fluoride" might prove to be useful.[141] Some preliminary results suggest that Peterson olefination might be carried out using the VGSR technique.

Finally, the technique described in this review benefits from the many other favorable attributes normally associated with heterogeneous reaction conditions. Most important perhaps is the accelerated rate under mild reaction conditions and the ability to isolate reactive species under conditions where their chemistry can be explored in detail.

We wish to thank our talented and motivated collaborators without whose contribution this article could not have been written. Thanks are also due to Professors Roland Boese (Essen) for X-ray structural data and Rolf Gleiter (Heidelberg) for the photoelectron spectrum of 2,2'-bicyclopropenyl. In acknowledging financial support for the work presented in this review, we extend our gratitude to the National Science Foundation (USA), the Robert A. Welch Foundation, the Petroleum Research Fund administered by the American Chemical Society, and the Humboldt Foundation who provided a Senior Scientist Award to W.E.B.

Received: September 21, 1992 [A 938 IE]
German version: *Angew. Chem.* **1994**, *106*, 1394

[1] a) J. M. Denis, R. Niamayoua, M. Vâta, A. Lablanche-Combier, *Tetrahedron Lett.* **1980**, *21*, 515; b) *Preparative Chemistry Using Supported Reagents* (Ed.: P. Laszlo), Academic Press, New York, **1987**; c) J. H. Clark, A. P. Kybett, D. J. Macquarrie, *Supported Reagents*, VCH, New York, **1992**.
[2] W. E. Billups, L.-J. Lin, *Tetrahedron* **1986**, *42*, 1575.
[3] J. F. Liebman, A. Greenberg, *Chem. Rev.* **1976**, *76*, 311.
[4] B. Halton, M. G. Banwell in *The Chemistry of the Cyclopropyl Group, Part 2* (Eds.: S. Patai, Z. Rappoport), Wiley, Chichester, **1987**, Chapter 21, p. 1223.
[5] F. L. Carter, V. L. Frampton, *Chem. Rev.* **1964**, *64*, 497.
[6] G. L. Closs, *Adv. Alicycl. Chem.* **1966**, *1*, 53.
[7] R. Breslow, R. Peterson, *J. Am. Chem. Soc.* **1960**, *82*, 4426.
[8] P. Weyerstahl in *The Chemistry of Halides, Pseudo-Halides and Azides, Suppl. D, Part 2* (Eds.: S. Patai, Z. Rappoport), Wiley, Chichester, **1983**, p. 1451.
[9] E. V. Dehmlow, *Tetrahedron Lett.* **1965**, 2317.
[10] K. Komatsu, M. Arai, K. Okamoto, *Tetrahedron Lett.* **1982**, *23*, 91.
[11] T. Niem, M. D. Rausch, *Org. Prep. Proced. Int.* **1976**, *8*, 271.
[12] O. Pelletier, K. Jankowski, *Can. J. Chem.* **1982**, *60*, 2383.
[13] R. A. Olofson, K. D. Lotts, G. N. Barber, *Tetrahedron Lett.* **1976**, 3779.
[14] G. N. Barber, R. A. Olofson, *Tetrahedron Lett.* **1976**, 3783.
[15] J. M. Birchall, K. Burger, R. N. Hazeldine, S. N. Nova, *J. Chem. Soc. Perkin Trans. 1* **1981**, 2080.
[16] P. B. Sargent, *J. Am. Chem. Soc.* **1969**, *91*, 3061.
[17] K. Komatsu, I. Tomioka, K. Okamoto, *Tetrahedron Lett.* **1980**, *21*, 947.
[18] M. Vincens, A. Dussauge, M. Vidal, *Tetrahedron* **1977**, *33*, 2937.
[19] M. Vidal, A. Dussauge, M. Vincens, *Tetrahedron Lett.* **1977**, 313.
[20] E. A. Shapiro, I. E. Dolgii, O. M. Nefedov, *Izv. Akad. Nauk SSSR Ser. Khim.* **1980**, 2096 [*Chem. Abstr.* **1981**, *94*, 83858]; *Tezisy Dokl. Vses. Konf. Khim. Atsetilena 5th 1975* **1975**, 68 [*Chem. Abstr.* **1978**, *88*, 190136].
[21] I. E. Dolgii, G. P. Okonnishnikova, O. M. Nefedov, *Izv. Akad. Nauk SSSR Ser. Khim.* **1979**, 822 [*Chem. Abstr.* **1979**, *91*, 38959].
[22] E. A. Shapiro, G. V. Lun'kova, A. O. Nefedov, I. E. Dolgii, O. M. Nefedov, *Izv. Akad. Nauk SSSR Ser. Khim.* **1981**, 2535 [*Chem. Abstr.* **1982**, *96*, 142932].
[23] G. Maier, M. Hoppe, H. P. Reisenauer, C. Krüger, *Angew. Chem.* **1982**, *94*, 445; *Angew. Chem. Int. Ed. Engl.* **1982**, *21*, 437.
[24] G. N. Suvorova, M. I. Komendantov, *Zh. Org. Khim.* **1982**, *18*, 1882 [*Chem. Abstr.* **1983**, *98*, 71511].
[25] V. E. Baikov, L. P. Danilkina, K. A. Oglobin, *Zh. Obshch. Khim.* **1981**, *51*, 2156 [*Chem. Abstr.* **1981**, *95*, 220097].
[26] E. Wenkert, K. J. Chou, R. P. Hatch, *Synth. Commun.* **1977**, *7*, 375.
[27] A. J. Hubert, A. F. Noels, A. J. Anciaux, P. Teyssié, *Synthesis* **1976**, 600.
[28] N. Petiniot, A. J. Anciaux, A. F. Noels, A. J. Hubert, P. Teyssié, *Tetrahedron Lett.* **1978**, 1239.
[29] I. N. Domnin, E. F. Zhuravleva, N. V. Pronina, *Zh. Org. Khim.* **1978**, *14*, 2323 [*Chem. Abstr.* **1979**, *90*, 137423].
[30] P. Dowd, P. Garner, R. Schappert, H. Irngartinger, A. Goldmann, *J. Chem. Soc. Chem. Commun.* **1981**, 455; *J. Org. Chem.* **1982**, *47*, 4240.
[31] C. Guiborel, R. Danion-Bougot, D. Danion, R. Carrie, *Tetrahedron Lett.* **1981**, *22*, 441.
[32] G. L. Closs, L. A. Closs, W. E. Boll, *J. Am. Chem. Soc.* **1973**, *85*, 3796.
[33] W. M. Jones, U. H. Brinker in *Pericyclic Reactions, Vol. 1* (Eds.: A. P. Marchand, R. E. Lehr), Academic Press, New York, **1977**, p. 126.
[34] T. T. Coburn, W. M. Jones, *J. Am. Chem. Soc.* **1974**, *96*, 5218.
[35] H. E. Zimmerman, M. C. Hovey, *J. Org. Chem.* **1979**, *44*, 2331.
[36] M. Franck-Neumann, C. Dietrich-Buchecker, *Tetrahedron Lett.* **1980**, *21*, 671; Eur. Pat. Appl. 7828 [*Chem. Abstr.* **1981**, *94*, 175329].
[37] W. Ando, Y. Hanyu, T. Takata, K. Ueno, *J. Am. Chem. Soc.* **1984**, *106*, 2216.
[38] G. L. Closs, W. A. Boll, *J. Am. Chem. Soc.* **1963**, *85*, 3904.
[39] G. L. Closs, H. Heyn, V. Dev, *J. Am. Chem. Soc.* **1968**, *90*, 173.
[40] H. Dürr, G. Klauck, K. Peters, H. G. von Schnering, *Angew. Chem.* **1983**, *95*, 321; *Angew. Chem. Int. Ed. Engl.* **1983**, *22*, 332; *Angew. Chem. Suppl.* **1983**, 347.
[41] J. E. Baldwin, K. A. Black, *J. Am. Chem. Soc.* **1984**, *106*, 1029.
[42] B. Coleman, M. Jones, *J. Organomet. Chem.* **1979**, *168*, 393.
[43] P. G. Gassman, J. J. Valcho, G. S. Proehl, *J. Am. Chem. Soc.* **1979**, *101*, 231.
[44] I. N. Domnin, E. F. Zhuravleva, V. L. Serebrov, R. R. Bekmukhametov, *Khim. Geterosikl. Soedin.* **1978**, 1091 [*Chem. Abstr.* **1979**, *90*, 6300].
[45] M. I. Komendantov, R. R. Bekmukhametov, *Tezisy Dokl. Vses. Konf. Khim. Atsetilena 5th 1975* **1975**, 374 [*Chem. Abstr.* **1978**, *88*, 190677].
[46] M. I. Komendantov, R. R. Bekmukhametov, I. N. Domnin, *Zh. Org. Khim.* **1978**, *14*, 759 [*Chem. Abstr.* **1978**, *89*, 23503].
[47] C. L. Leach, J. W. Wilson, *J. Org. Chem.* **1978**, *43*, 4880.
[48] M. W. Kett, R. P. Johnson, *Tetrahedron Lett.* **1983**, *24*, 2523.
[49] C. Dietrich-Buchecker, M. Franck-Neumann, *Tetrahedron* **1977**, *33*, 751.
[50] M. Franck-Neumann, M. Miesch, *Tetrahedron Lett.* **1982**, *23*, 1409; Eur. Pat. Appl. 25383 [*Chem. Abstr.* **1981**, *95*, 133192].
[51] M. Franck-Neumann, M. Miesch, *Tetrahedron Lett.* **1984**, *25*, 2909.
[52] M. Franck-Neumann, C. Dietrich-Buchecker, *Tetrahedron* **1978**, *34*, 2797.
[53] M. Franck-Neumann, J. J. Lohmann, *Tetrahedron Lett.* **1979**, 2397; *Angew. Chem.* **1977**, *89*, 332; *Angew. Chem. Int. Ed. Engl.* **1977**, *16*, 323.
[54] G. L. Closs, K. D. Krantz, *J. Org. Chem.* **1966**, *31*, 638.
[55] N. Y. Dem'yanov, M. N. Doyarenko, *Izv. Ross. Akad. Nauk* **1922**, *16*, 297 [*Chem. Abstr.* **1926**, *20*, 2988]; *Chem. Ber.* **1925**, *58*, 220; *Izv. Akad. Nauk SSSR Otd. Mat. Estestv. Nauk* **1929**, *7*, 653 [*Chem. Abstr.* **1930**, *24*, 1848].
[56] A. Padwa, M. J. Pulwer, *J. Chem. Soc. Chem. Commun.* **1982**, 783; A. Padwa, M. J. Pulwer, R. J. Rosenthal, *J. Org. Chem.* **1984**, *49*, 856.
[57] W. E. Billups, A. J. Blakeney, W. Y. Chow, *Org. Synth.* **1976**, *55*, 12.
[58] W. E. Billups, W. Y. Chow, *J. Am. Chem. Soc.* **1973**, *95*, 4099.
[59] M. S. Baird, W. Nethercott, *Tetrahedron Lett.* **1983**, *24*, 605.
[60] M. S. Baird, S. R. Buxton, J. S. Whitley, *Tetrahedron Lett.* **1984**, *25*, 1509.
[61] K. B. Wiberg, G. Bonneville, *Tetrahedron Lett.* **1982**, *23*, 5385.
[62] J. Harnisch, O. Baumgärtel, G. Szeimies, M. V. Meerssche, G. Germain, J.-P. Declercq, *J. Am. Chem. Soc.* **1979**, *101*, 3370.
[63] G. Szeimies, J. Harnisch, O. Baumgärtel, *J. Am. Chem. Soc.* **1977**, *99*, 5183.
[64] T. H. Chan, D. Massuda, *Tetrahedron Lett.* **1975**, 3383.
[65] W. E. Billups, L.-J. Lin, B. E. Arney, Jr., W. A. Rodin, E. W. Casserly, *Tetrahedron Lett.* **1984**, *25*, 3935.
[66] B. R. Dent, B. Halton, A. M. F. Smith, *Aust. J. Chem.* **1986**, *39*, 1621; B. R. Dent, Dissertation, Victoria University of Wellington, New Zealand, **1985**.
[67] T. C. Shields, P. D. Gardner, *J. Am. Chem. Soc.* **1967**, *89*, 5425.
[68] K. B. Wiberg, R. K. Barnes, J. Albin, *J. Am. Chem. Soc.* **1957**, *79*, 4994.

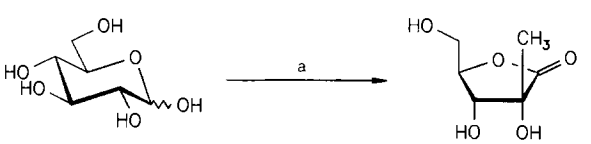
[69] L. A. Paquette, *Chem. Rev.* **1986**, *86*, 733.
[70] For a description of the apparatus see R. H. Hauge, L. Fredin, Z. H. Kafafi, J. L. Margrave, *Appl. Spectrosc.* **1986**, *40*, 588.
[71] W. E. Billups, L.-J. Lin, E. W. Casserly, *J. Am. Chem. Soc.* **1984**, *106*, 3698.
[72] S. W. Staley, T. D. Norden, *J. Am. Chem. Soc.* **1984**, *106*, 3699.
[73] G. Maier, M. Hoppe, K. Lanz, P. Reisenauer, *Tetrahedron Lett.* **1984**, *25*, 5645.
[74] a) M. J. S. Dewar, M. C. Kohn, *J. Am. Chem. Soc.* **1972**, *94*, 2699; b) J. Gayoso, A. Boucekkine, *J. Chim. Phys. Phys. Chim. Biol.* **1974**, *71*, 182; c) W. J. Hehre, J. A. Pople, *J. Am. Chem. Soc.* **1975**, *97*, 6941; d) R. P. Johnson, M. W. Schmidt, *ibid.* **1981**, *103*, 3244; e) H. Kollmar, F. Carrion, M. J. S. Dewar, R. C. Bingham, *ibid.* **1981**, *103*, 5292. f) G. Buemi, A. Raudino, F. Zuccarello, *THEOCHEM* **1981**, *1*, 285; g) H. M. Rosenstock, J. Dannacher, J. F. Liebman, *Radiat. Phys. Chem.* **1982**, *20*, 7.
[75] Review: a) T. Eicher, J. L. Weber, *Top. Curr. Chem.* **1975**, *57*, 1. For synthetic approaches to the parent hydrocarbon, see b) I. S. Krull, P. F. D'Angelo, D. R. Arnold, E. Hedaya, P. O. Schissel, *Tetrahedron Lett.* **1971**, 771; c) O. L. Chapman, *Pure Appl. Chem.* **1974**, *40*, 511; d) W. E. Billups, A. J. Blakeney, W. T. Chamberlain, *J. Org. Chem.* **1976**, *41*, 3771; e) W. E. Billups, A. J. Blakeney, N. A. Rao, J. D. Buynak, *Tetrahedron* **1981**, *37*, 3215; f) A. Weber, M. Neuenschwander, *Angew. Chem.* **1981**, *93*, 788; *Angew. Chem. Int. Ed. Engl.* **1981**, *20*, 774.
[76] M. A. Battiste, *J. Am. Chem. Soc.* **1964**, *86*, 942.
[77] W. M. Jones, J. M. Denham, *J. Am. Chem. Soc.* **1964**, *86*, 944.
[78] W. E. Billups, A. W. Moorehead in *The Chemistry of the Cyclopropyl Group, Part 2* (Eds.: S. Patai, Z. Rappoport), Wiley, Chichester, **1987**, Chapter 24, p. 1533.
[79] I. Agranat, M. R. Pick, *Tetrahedron Lett.* **1973**, 4079.
[80] G. Carnaggi, F. Gozzo, *J. Chem. Soc. C* **1970**, 178.
[81] P. Crabbé, R. Grezémkousky, L. Knox, *Bull. Soc. Chim. Fr.* **1968**, 789.
[82] W. E. Billups, A. J. Blakeney, *J. Am. Chem. Soc.* **1976**, *98*, 7817.
[83] W. E. Billups, L.-J. Lin, *Tetrahedron Lett.* **1983**, 1683.
[84] P. J. Stang, M. G. Mangum, *J. Am. Chem. Soc.* **1975**, *97*, 3854.
[85] B. Martel, J. M. Hiriat, *Synthesis* **1972**, 201.
[86] B. A. Hess, D. Michalska, L. J. Schaad, *J. Am. Chem. Soc.* **1985**, *107*, 1449.
[87] a) A. Sabljic, N. Trinajstic, *Croat. Chem. Acta* **1978**, *51*, 249; b) W. C. Herndon, *Pure Appl. Chem.* **1980**, *52*, 1459; c) K. Jug, *J. Org. Chem.* **1983**, *48*, 1344.
[88] a) B. A. Hess, Jr., L. J. Schaad, *J. Org. Chem.* **1972**, *37*, 4179; b) J. Aihara, *Bull. Chem. Soc. Jpn.* **1983**, *56*, 1935; c) P. H. M. Budzelaar, E. Kraka, D. Cremer, P. von R. Schleyer, *J. Am. Chem. Soc.* **1986**, *108*, 561.
[89] F. Fratev, D. Bonchev, V. Enchev, *Croat. Chem. Acta* **1981**, *53*, 545.
[90] T. D. Norden, S. W. Staley, W. H. Taylor, M. D. Harmony, *J. Am. Chem. Soc.* **1986**, *108*, 7912.
[91] a) "Kinetic Data on Gas Phase Unimolecular Reactions": S. W. Benson, H. E. O'Neal, *Natl. Stand. Ref. Data Ser. (US Natl. Bur. Stand)* **1970**, *21* (February); b) K. B. Wiberg, *Angew. Chem.* **1986**, *98*, 312; *Angew. Chem. Int. Ed. Engl.* **1986**, *25*, 312.
[92] J. A. Pincock, R. J. Boyd, *Can. J. Chem.* **1977**, *55*, 2482.
[93] W. E. Billups, M. M. Haley, *J. Am. Chem. Soc.* **1991**, *113*, 5084.
[94] Reviews: S. Winstein, *Spec. Publ. Chem. Soc.* **1967**, *21*, 5; P. M. Warner, *Topics in Nonbenzoid Aromatic Chemistry, Vol. 2*, Hirokawa, Tokyo, **1977**, p. 283; L. A. Paquette, *Angew. Chem.* **1978**, *90*, 114; *Angew. Chem. Int. Ed. Engl.* **1978**, *17*, 106.
[95] H. E. Simmons, T. Fukunaga, *J. Am. Chem. Soc.* **1967**, *89*, 5208; R. Hoffman, A. Imamura, G. D. Zeiss, *ibid.* **1967**, *89*, 5219.
[96] Review: H. Dürr, R. Gleiter, *Angew. Chem.* **1978**, *90*, 591; *Angew. Chem. Int. Ed. Engl.* **1978**, *17*, 559.
[97] L. A. Hulshof, H. Wynberg, *J. Am. Chem. Soc.* **1974**, *96*, 2191.
[98] M. F. Semmelhack, J. S. Foos, S. Katz, *J. Am. Chem. Soc.* **1972**, *94*, 8637.
[99] M. F. Semmelhack, J. S. Foos, S. Katz, *J. Am. Chem. Soc.* **1973**, *95*, 7325.
[100] H. Dürr, B. Ruge, H. Schmitz, *Angew. Chem.* **1973**, *85*, 616; *Angew. Chem. Int. Ed. Engl.* **1973**, *12*, 577.
[101] J. Kao, L. Radom, *J. Am. Chem. Soc.* **1978**, *100*, 760.
[102] Z. B. Maksic, K. Kovacevic, A. Mogus, *THEOCHEM* **1982**, *2*, 9.
[103] S. P. Zil'berg, A. I. Ioffe, O. M. Nefedov, *Izv. Akad. Nauk SSSR Ser. Khim.* **1983**, 261 [*Chem. Abstr.* **1993**, *98*, 159839a].
[104] M. J. S. Dewar, *The Molecular Orbital Theory of Organic Chemistry*, McGraw-Hill, New York, **1969**, p. 461.
[105] K. J. H. Kruithof, R. F. Schmitz, G. W. Klumpp, *Tetrahedron* **1983**, *39*, 3073.
[106] R. L. Danheiser, D. J. Carini, D. M. Fink, A. Basak, *Tetrahedron* **1983**, *39*, 935.
[107] I. Shavitt, D. W. Ewing, J. E. Del Bene, *J. Am. Chem. Soc.* **1991**, *113*, 9389.
[108] J. B. Pedley, R. D. Naylor, S. P. Kirby, *Thermochemical Data of Organic Compounds*, 2nd ed., Chapman and Hall, London, **1986**.
[109] J. H. Potgieter, *J. Chem. Educ.* **1991**, *68*, 280.
[110] W. E. Billups, M. M. Haley, *Angew. Chem.* **1989**, *101*, 1735; *Angew. Chem. Int. Ed. Engl.* **1989**, *28*, 1711.
[111] R. Gleiter, W. Schäfer, *Acc. Chem. Res.* **1990**, *23*, 369.
[112] R. Hoffmann, A. Imamura, W. Hehre, *J. Am. Chem. Soc.* **1968**, *90*, 1499; Reviews: R. Hoffman, *Acc. Chem. Res.* **1971**, *4*, 1; R. Gleiter, *Angew. Chem.* **1974**, *86*, 770; *Angew. Chem. Int. Ed. Engl.* **1974**, *13*, 696; M. N. Paddon-Row, *Acc. Chem. Res.* **1982**, *15*, 245; K. D. Jordan in *Modern Models of Bonding and Delocalization* (Eds.: J. F. Liebman, A. Greenberg), VCH, Weinheim, **1988**, p. 115; H. D. Martin, B. Mayer, *Angew. Chem.* **1983**, *95*, 281; *Angew. Chem. Int. Ed. Engl.* **1983**, *22*, 283.
[113] J. Spanget-Larsen, C. de Korswagen, M. Eckert-Maksic, R. Gleiter, *Helv. Chim. Acta* **1982**, *65*, 968; A. Greenberg, J. F. Liebman, *J. Am. Chem. Soc.* **1981**, *103*, 44.
[114] R. Boese, D. Bläser, R. Gleiter, K.-H. Pfeifer, W. E. Billups, M. M. Haley, *J. Am. Chem. Soc.* **1993**, *115*, 743.
[115] R. Boese, D. Bläser, N. Niederprüm, T. Miebach in *Organic Crystal Chemistry* (Eds.: J. Garbarczyk, D. W. Jones), Oxford University Press, Oxford, **1991**, p. 109.
[116] D. Brodalla, D. Mootz, R. Boese, W. Osswald, *J. Appl. Crystallogr.* **1985**, *18*, 316.
[117] W. M. Stigliani, V. W. Laurie, J. C. Li, *J. Chem. Phys.* **1975**, *63*, 1890.
[118] D. Nijvelt, Dissertation, Universität Groningen, **1985**.
[119] A. de Meijere, M. Traetteberg, *J. Mol. Struct.* **1987**, *161*, 97.
[120] Z. B. Maksic in *Theoretical Methods of Chemical Bonding, Part II* (Ed.: Z. B. Maksic), Springer, Berlin, **1990**, p. 137.
[121] R. Boese, unpublished.
[122] G. Maier, A. Schick, I. Bauer, R. Boese, M. Nussbaumer, *Chem. Ber.* **1992**, *125*, 2111.
[123] F. Grüger, G. Szeimies, *Tetrahedron Lett.* **1986**, *27*, 1563; P. J. Garratt, D. Payne, A. Tsotinis, *Pure Appl. Chem.* **1990**, *55*, 525.
[124] A. Greenberg, J. F. Liebman, *Strained Organic Molecules*, Academic Press, New York, **1978**, p. 104.
[125] M. M. Haley, Dissertation, Rice University, Houston, Texas, **1990**.
[126] For a review of this family of compounds see W. E. Billups, M. M. Haley, G.-A. Lee, *Chem. Rev.* **1989**, *89*, 1147.
[127] G. Köbrich, *Angew. Chem.* **1973**, *85*, 494; *Angew. Chem. Int. Ed. Engl.* **1973**, *12*, 464.
[128] W. E. Billups, G. A. Lee, B. E. Arney, Jr., K. H. Whitmire, *J. Am. Chem. Soc.* **1991**, *113*, 7980.
[129] R. Breslow, P. Dowd, *J. Am. Chem. Soc.* **1963**, *85*, 2729; Z. Yoshida, H. Miyahara, *Chem. Lett.* **1972**, 335.
[130] For some examples see R. L. Camp, F. D. Greene, *J. Am. Chem. Soc.* **1968**, *90*, 7349; J. K. Crandall, W. H. Machleder, *ibid.* **1968**, *90*, 7347.
[131] G. Maier, S. Pfriem, U. Schäfer, R. Matusch, *Angew. Chem.* **1978**, *90*, 552; *Angew. Chem. Int. Ed. Engl.* **1978**, *17*, 520.
[132] P. D. Bartlett, T. G. Traylor, *J. Am. Chem. Soc.* **1962**, *84*, 3408; W. Kirmse, *Carbene Chemistry*, Academic Press, New York, **1964**, p. 58; N. H. Werstiuk, H. L. Casal, J. C. Scaiano, *Can. J. Chem.* **1984**, *62*, 2391; M. Girard, D. J. Griller, *Phys. Chem.* **1986**, *90*, 6801; J. C. Scaiano, W. G. McGimpsey, H. L. Casal, *J. Org. Chem.* **1989**, *54*, 1612.
[133] 1,4-Diyls have been implicated to explain the products formed from the cycloaddition reactions of cyclopropenes. For an example see A. Padwa, G. D. Kennedy, G. R. Newkome, F. R. Fronczek, *J. Am. Chem. Soc.* **1983**, *105*, 137.
[134] H.-U. Wagner, G. Szeimies, J. Chandrasekhar, P. von R. Schleyer, J. A. Pople, J. S. Binkley, *J. Am. Chem. Soc.* **1978**, *100*, 1210; W. Hehre, J. A. Pople, *ibid.* **1975**, *97*, 6941.
[135] K. B. Wiberg, G. Bonneville, R. Dempsey, *Isr. J. Chem.* **1983**, *23*, 85.
[136] K. B. Wiberg, D. R. Artis, G. Bonneville, *J. Am. Chem. Soc.* **1991**, *113*, 7969.
[137] P. J. Garratt, A. Tsotinis, *J. Org. Chem.* **1990**, *55*, 84.
[138] M. S. Baird, H. H. Hussain, W. Nethercott, *J. Chem. Soc. Perkin Trans. 1* **1986**, 1845; M. S. Baird, *Functionalized Cyclopropenes as Synthetic Intermediates* (*Top. Curr. Chem.* **1988**, *4*).
[139] S. Lacombe, D. Gonbeau, J.-L. Cabioch, B. Pellerin, J. M. Denis, G. Pfister-Guillouzo, *J. Am. Chem. Soc.* **1988**, *110*, 6964.
[140] J. C. Guillemin, J. M. Denis, A. Lablache-Combier, *J. Am. Chem. Soc.* **1981**, *103*, 468.
[141] R. Schwesinger, R. Link, G. Thiele, H. Rotter, D. Honert, H.-H. Limbach, F. Männle, *Angew. Chem.* **1991**, *103*, 1376; *Angew. Chem. Int. Ed. Engl.* **1991**, *30*, 1372.

Ring Contractions in Carbohydrates

Hartmut Redlich*

The polyfunctional character of carbohydrates has always been a cause of the apparently unusual reactions that even an alert observer would not immediately consider as plausible. Thus, in the eyes of many chemists, "sugar chemistry" obtained a certain reputation that was not necessarily to its advantage. Certainly, those products, obtained occasionally from this group of compounds or their derivatives, that could be regarded as the result of a ring contraction have also contributed to this view.

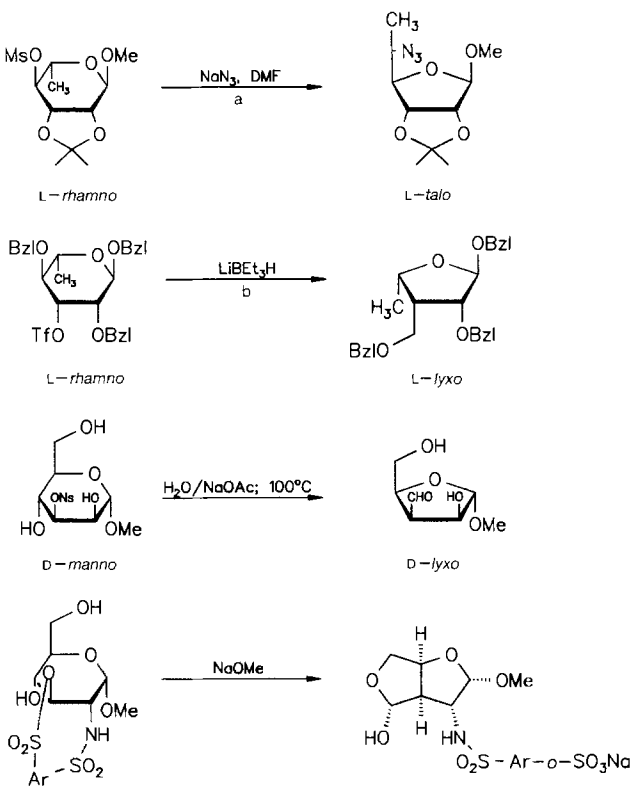
As early as 1838 (!) E. Peligot reported in his well-known publication[1] in which the name glucose was suggested for a certain hexose that sugars are converted into strong acids (acide tres énergique) with dilute calcium or barium hydroxide solution. Only a little later (according to the then prevalent understanding of time), in 1879, the same author reported on the base-induced conversion of glucose, fructose, or invert sugar into the crystalline product named by him as "α"-glucosaccharin.[2] Formation of this branched, ring-contracted lactone from the corresponding unbranched (cyclic?) starting compound can only be explained by exchange of position of O and C atoms (Scheme 1). More recently, this chiral, branched compound has attained importance as an extremely inexpensive starting material for the synthesis of chiral natural products from carbohydrates.[3]



D-glucose "α"-glucosaccharine

Scheme 1. Reaction conditions. a: 0.7 M $Ca(OH)_2$, room temperature, 1–2 months, about 10% yield. The systematic name for "α"-glucosaccharine is 2-C-methyl-D-*ribono*-1,4-lactone.

Initially the transformation of sugars in basic media into saccharinic, isosaccharinic, and metasaccharinic acids was traced to the activity of the carbonyl group in the unprotected sugar. Nevertheless it subsequently became clear that even complete protection of all the functional groups in a sugar was no guarantee against surprises—mostly of the unwanted variety. From the wealth of material compiled over the years only a selection of such reactions, which were initially planned as simple nucleophilic substitutions, is summarized below. It will be left to the reader to trace the devious path of the actual course of the reaction (Scheme 2; hint: the reaction always begins with an "internal" nucleophile).[4]

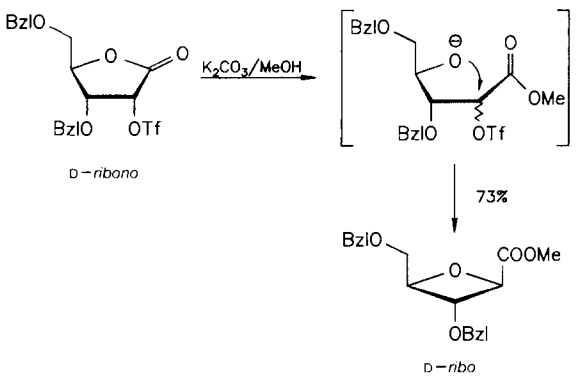


Scheme 2. a: Reflux. b: Dioxane. Ms = CH_3SO_2; Bzl = $C_6H_5CH_2$; Tf = CF_3SO_3; Ns = *p*-NO_2-C_6H_4-SO_2; Ar = arenediyl.

G. W. J. Fleet et al. used intramolecular substitution of carbohydrate lactones in the sense considered here as a deliberate element in the synthetic plan of a series of experiments. These compounds undergo facile ring contraction when a leaving group is situated in α-position to the lactone group, which thereby possesses electrophilic character. In the case of the four isomeric pentose-γ-lactones oxetanecarboxylic acid esters with various configurations were formed; the latter are suitable for the

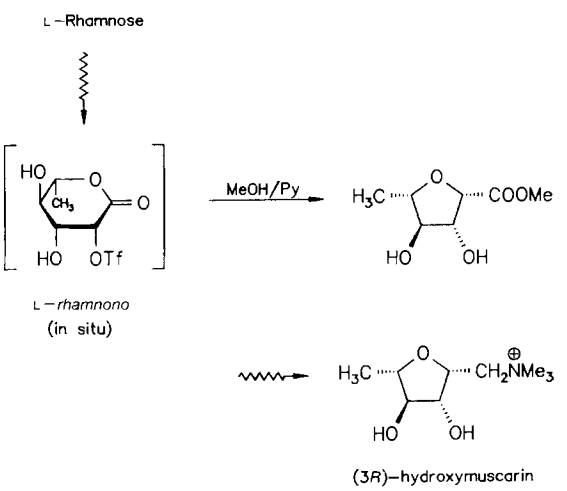
[*] Prof. Dr. H. Redlich
Organisch-chemisches Institut der Universität
Corrensstrasse 40, D-48149 Münster (FRG)
Telefax: Int. code + (531)391-5388

synthesis of nucleoside analogues.[5] Such oxetane nucleosides show biological activity against viruses. The stereochemical course of these substitutions (Scheme 3) suggests that an open-chain 4-hydroxy-2-*O*-trifluoromethanesulfonyl ester is formed initially. As a result of the low configurational stability of the leaving group in the position α to the ester group, the intramolecular substitution takes place with preferential formation of the oxetane with a *trans* configuration of the substituents at C2 and C3.



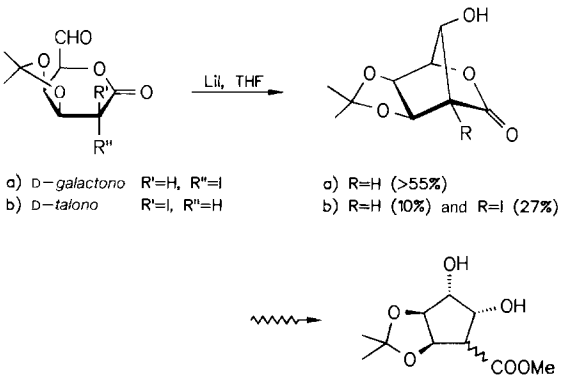
Scheme 3.

With the δ-lactones 2,5-disubstituted tetrahydrofurans are formed in the same fashion.[5] Fleet et al. were able to devise a very short synthesis of (3*R*)-hydroxy-(+)-muscarine and (+)-muscarine starting from L-rhamnose, without using protecting groups (Scheme 4).[5]



Scheme 4.

Without doubt the particular relationships at the α-position of the carbohydrate lactones play a central part in these reactions, which are facile for a very wide range of examples. The example given in Scheme 5, which formally shows the same exposition as that in the examples previously discussed (leaving group in the α-position to the lactone), demonstrates that quite unusual reactions are thereby also possible. If the α-position is offered an acceptor in the form of an aldehyde group at C6, this

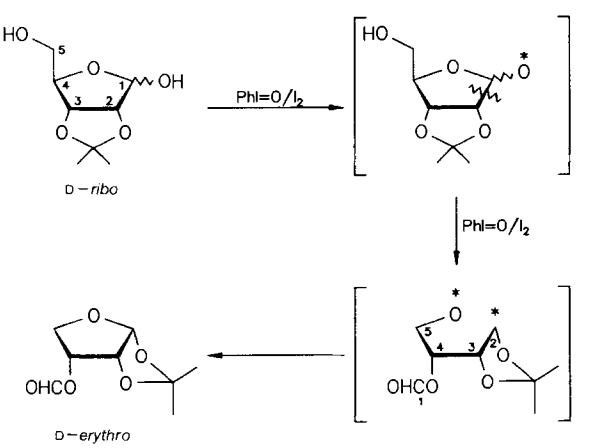


Scheme 5.

compound reacts in the sense of an intramolecular aldol addition on treatment with lithium iodide in THF at room temperature, to give a five-membered carbocyclic ring.[5] C2 acts here as a nucleophile; a reductive addition takes place for the *galactono*-configuration, whereas direct addition is found to a large extent for the *talono*-configuration. In the meantime this principle has been extended to the synthesis of six-membered rings.[5] The carbocycles obtained in this manner possess a high level of functionality and are thus suitable for numerous further syntheses.

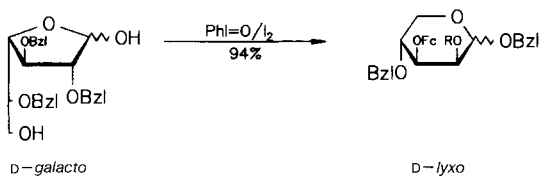
The advantage of carefully directed ring contraction with carbohydrates is obvious: from inexpensive starting materials one can obtain carbo- or heterocyclic compounds containing several functional groups in optically pure form, synthesis of which would otherwise be difficult.

This option has become particularly clear with two recent reports. Using the reagent iodosylbenzene/iodine E. Sua'rez et al.[6] have converted cyclic carbohydrate derivatives that are unblocked at the anomeric position and at a "suitable" distance therefrom (Scheme 6) into other cyclic derivatives that contain



Scheme 6.

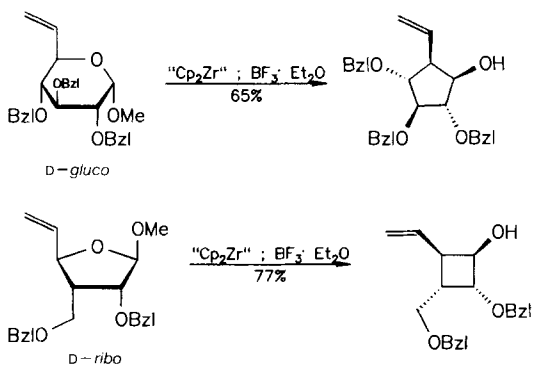
one less carbon atom and now blocked at the anomeric position. In this process, which takes place by a radical mechanism, the anomeric carbon atom is eliminated from the cyclic compound together with the oxygen atom. Recombination of the intermediate diradical leads to the formation of a new heterocycle. Depending on the starting compound, various ring sizes result



Scheme 7. Fc = CHO; R = $C_6H_5CH_2$.

from this process; as shown in Scheme 7, even ring expansions with excellent yields are possible.

Preparative advances in carbohydrate chemistry can frequently be regarded as a reflection of general developments in organic chemistry. While carbanionic and then radical processes were at the center of the development of new methods during the last two decades, the work of T. Taguchi et al.[7] heralds a new direction: reactions of carbohydrates catalyzed by transition metals. Thus, the action of $[Cp_2Zr(n\mathrm{Bu})_2]$ followed by $BF_3 \cdot OEt_2$ on carbohydrate derivatives containing a terminal double bond induces, according to the authors, quite unusual ring contractions (Scheme 8), which lead in a single synthetic step to highly functional carbocycles in very good yield and mostly with very high diastereoselectivity. Two examples from this work are the cyclopentane and cyclobutane shown in Scheme 8. Hitherto, products of this type could only be obtained by way of multistep reaction sequences.[8]

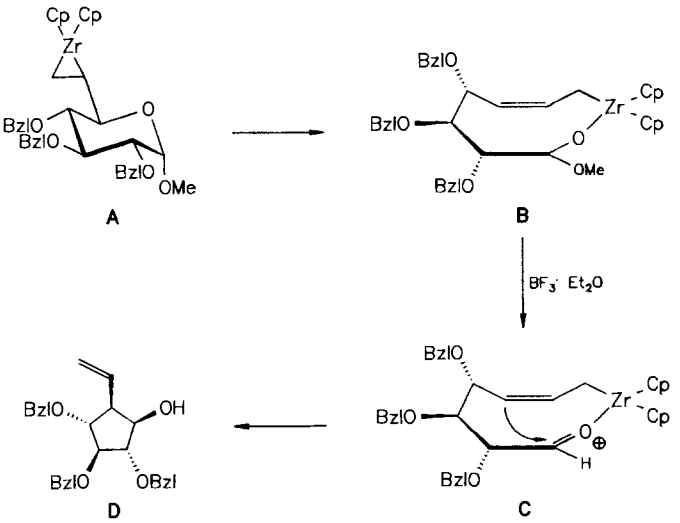


Scheme 8. $[Cp_2Zr(n\mathrm{Bu})_2]$ was used to generate the reactive Cp_2Zr unit.

The foundation for the initially surprising course of this process is the reaction, observed by the authors, of the zirconocene equivalent ("Cp_2Zr") with allyl ethers (Scheme 9), which apparently takes place smoothly even under such complicated circumstances as at protected carbohydrate derivatives (**A**, Scheme 10) and leads in that case to the nine-membered zirconacycle **B**. $BF_3 \cdot OEt_2$ promotes the decomposition of the hemiacetal-



Scheme 9.



Scheme 10.

zirconate to the oxonium ion **C**, which reacts intramolecularly to give the carbocycle **D**. The stereochemical course that is always observed (substituents on the new C–C bond *cis*, but *trans* to the other substituents adjacent to the side chain) is in very good agreement with this propposal.

One can only hope that such attractive synthetic successes will persuade other chemists (again) that carbohydrates are worthy objects for "their" chemistry.

German version: *Angew. Chem.* **1994**, *106*, 1407

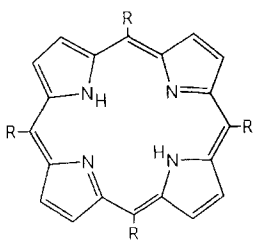
[1] E. Peligot, *C. R. Hebd. Seances Acad. Sci.* **1838**, *7*, 106–113.
[2] E. Peligot, *C. R. Hebd. Seances Acad. Sci.* **1879**, *89*, 918–922.
[3] R. E. Ireland, R. C. Anderson, R. Badoud, B. J. Fitzsimmons, G. J. Mc Garvey, S. Thaisrivongs, C. S. Wilcox, *J. Am. Chem. Soc.* **1983**, *105*, 1988–2006; M.-C. Trinh, J.-C. Florent, C. Monneret, *J. Chem. Soc. Chem. Commun.* **1987**, 615–616; K. Bock, J. M. Castilla, I. Lundt, C. Petersen, *Acta Chem. Scand.* **1987**, *41*, 13–17.
[4] J. Jary, P. Novák, Z. Ksandr, Z. Samek, *Chem. Int. (London)* **1967**, 1490–1491; V. Pozsgay, A. Neszmélyi, *Tetrahedron Lett.* **1980**, *21*, 211–212; P. W. Austin, J. G. Buchanan, R. M. Saunders, *J. Chem. Soc. C* **1967**, 372–377; K. Tatsuta, S. Miyashita, K. Akimoto, M. Kinoshita, *Bull. Chem. Soc. Jpn.* **1982**, *55*, 3254–3256.
[5] D. R. Witty, G. W. J. Fleet, K. Vogt, F. X. Wilson, Y. Wang, R. Storer, P. L. Myers, C. J. Wallis, *Tetrahedron Lett.* **1990**, *31*, 4787–4790; S. Choi, P. M. Myerscough, A. J. Fairbanks, B. M. Skead, C. J. F. Bichard, S. J. Mantell, C. Son, G. W. J. Fleet, J. Saunders, D. Brown, *J. Chem. Soc. Chem. Commun.* **1992**, 1605–1607; S. J. Mantell, P. S. Ford, D. J. Watkin, G. W. J. Fleet, D. Brown, *Tetrahedron Lett.* **1992**, *33*, 4503–4506; S. J. Mantell, G. W. J. Fleet, D. Brown, *J. Chem. Soc. Perkin Trans. 1* **1992**, 3023–3027; R. P. Elliot, G. W. J. Fleet, L. Pearce, C. Smith, D. J. Watkin, *Tetrahedron Lett.* **1991**, *32*, 6227–6230; B. M. Skead, G. W. J. Fleet, J. Saunders, R. B. Lamont, *ibid.* **1993**, *34*, 6115–6118.
[6] P. de Armas, C. G. Francisco, E. Suárez, *J. Am. Chem. Soc.* **1993**, *115*, 8865–8866.
[7] H. Ito, Y. Motoki, T. Taguchi, Y. Hanzawa, *J. Am. Chem. Soc.* **1993**, *115*, 8835–8836.
[8] R. J. Ferrier, *Chem. Rev.* **1993**, *93*, 2779–2831.

 © VCH Verlagsgesellschaft mbH, D-69451 Weinheim, 1994 0570-0833/94/1313-1347 $ 10.00+.25/0

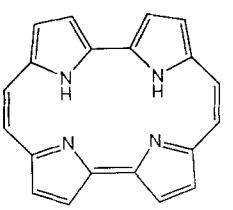
New Porphyrin Isomers

Jonathan L. Sessler*

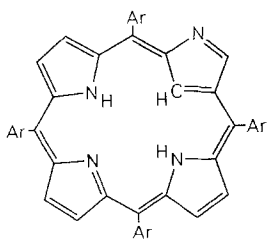
The porphyrins, derived from the parent $C_{20}H_{14}N_4$ system porphine (**1a**), are among the most widespread and important of all naturally occurring macrocycles. Not surprisingly, therefore, they have been both the subject of attention for synthetic chemists and a source of conceptual inspiration. Thus, in recent years reports have appeared not only of porphyrins, inspired by biological examples, that are capped, dimerized, or otherwise functionalized,[1] but also of abiotic, porphyrin-like systems whose frameworks are expanded,[2,3] fused,[4] or heteroatom substituted.[5–7] Interestingly, however, in spite of the increasing attention that is being given to chemistry of these latter analogues, relatively little work has been devoted to the generation of $C_{20}H_{14}N_4$ macrocyclic tetrapyrroles that are isomers of porphyrin per se. Indeed, with the obvious and important exception of Vogel's porphycene (**2**),[8] the seminal report of which was made in 1986, no nonnatural porphyrin isomers had been reported through the end of 1993. Now, two teams working on opposite sides of the globe have succeeded quite independently in preparing the α-to-β′-linked porphyrin isomers **3**.[9,10] Also, a conference abstract describing the synthesis of an alkyl-substituted derivative of the dimethine-containing isomer **4** has just



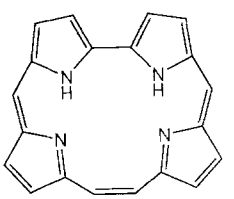
1a R = H
1b R = $C_6H_4CH_3$
1c R = C_6H_5



2



3a Ar = $C_6H_4CH_3$
3b Ar = C_6H_5

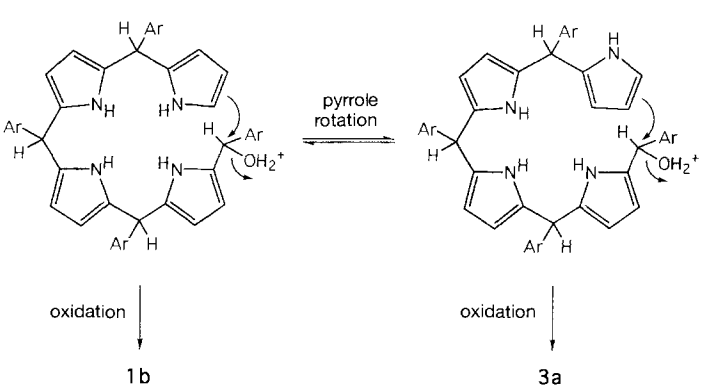


4

appeared.[11] Thus, in recent months the number of porphyrin isomers has suddenly doubled from two to four, while the lexicon of porphyrin-related trivial terms has expanded to include "mutant porphyrin", "N-confused prophyrin", and "corrphycene" used by the original authors to describe structures **3a**, **3b**, and **4**, respectively.[9–11]

The α-to-β′-linked porphyrin isomer **3**, which has appeared in two separate peer-reviewed publications, is the subject of this highlight. Here, the independent Polish and Japanese syntheses of the two α-to-β′-linked porphyrin derivatives **3a** and **3b** are worthy of special note. Taken together, the strategies serve not only to introduce a new type of porphyrin isomer but also to challenge the hitherto commonly held assumption that tetraarylporphyrins are the only useful porphyrinic products to result from classic[12,13] pyrrole + aryl aldehyde oxidative condensations. The Polish team led by Latos-Grażyńzki[9] found that the $BF_3 \cdot Et_2O$-catalyzed reaction of *p*-tolylaldehyde with excess pyrrole (1.75 molar equiv) at room temperature under nitrogen for one hour followed by oxidation with *p*-chloranil produces a 4:1 mixture of tetra-*p*-tolylporphyrin (**1b**) and **3a**; the overall yield of the latter compound is roughly 5%.[14] Interestingly, these workers report that when a 1:1 mixture of starting materials is first condensed and then oxidized under the same conditions, little or no α-to-β′-linked isomeric porphyrin (that is **3a**) is produced. By contrast, the Japanese team of Furuta et al. found that compound **3b** could be prepared, even from a 1:1 ratio of starting materials, provided that stoichiometric quantities of HBr are used to effect the acid-induced condensation.[10] However, as was true for their Polish competitors, these workers found that the product was only obtained in approximately 5–7% yields, being "contaminated" by about a 4 molar equivalent excess of the corresponding porphyrin **1c**.

Based on their findings Latos-Grażyńzki et al. have suggested that their mutant porphyrin **3a** is produced as the result of a final "twisted" porphyrinogen-forming macrocyclization (Scheme 1), while a more normal ring closure gives rise to the usual tetraarylporphyin **1b**.[9] Certainly, such a proposal is consistent with earlier suggestions[14,15] and also with the work of Furuta et al.[10] In this latter instance, however, the twisting needed to produce the β-linked "N-confused porphyrin" **3b**, or at least its porphyrinogen-like precursor, is possibly induced by a specific bromide anion template effect. If this proves true, the findings of Furuta et al.,[10] along with other earlier suggestions



Scheme 1. Ar = $C_6H_4CH_3$.

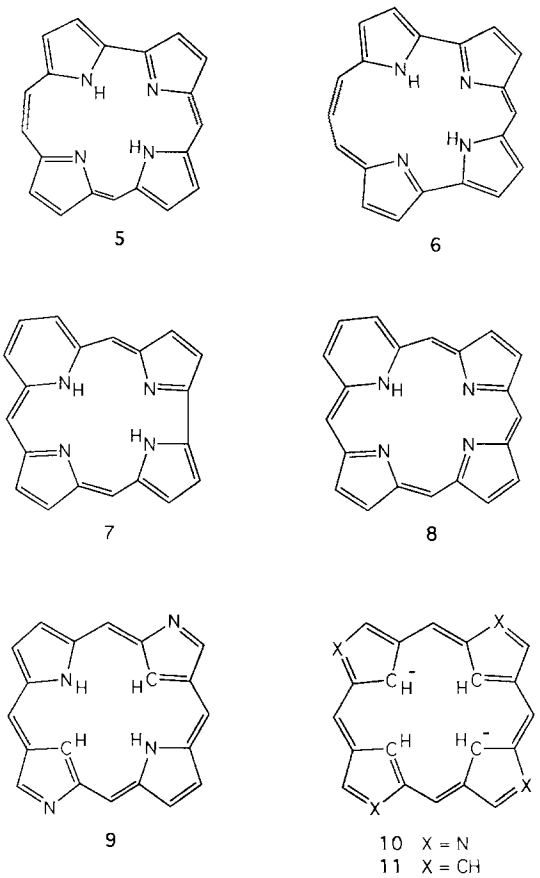
[*] Prof. J. L. Sessler
Department of Chemistry and Biochemistry, University of Texas
Austin, TX 78712 (USA)
Telefax: Int. code + (512)471-7550

in the literature,[16] might be of generalized significance: They would augur well for potential syntheses of other "unusual" porphyrin-like entities by anion-facilitated cyclization procedures.

Like porphine and porphycene, the new porphyrin isomers **3a** and **3b** can be considered as heteroatom-containing 18-π-electron annulenes. Not surprisingly, therefore, in solution both compounds display properties characteristic of [4*n* + 2] aromaticity. For instance, both **3a** and **3b** show porphyrin-like Soret and O-type absorption bands in their UV/Vis spectra.[9-10] Further, ^{1}H NMR spectra of these derivatives display signals for internal protons that are shifted to higher field as the result, presumably, of the porphyrin-like aromatic ring current. For instance, the unique internal β-protons of **3a** and **3b** resonate at approximately $\delta = -5.1$ vs. TMS, while the various external β-protons all resonate between $\delta = 8.5$ and 9.0.[9, 10] Thus, for this kind of porphyrin isomer, upfield shifts on the order of $\Delta\delta = 13.5-14$ are achieved as the result of the—figuratively speaking—isomer-inducing pyrrole ring flip.

The available structural information, although still limited, is also consistent with the formulation of **3a** and **3b** as aromatic compounds. For instance, the X-ray structure of the free-base form of **3b** reveals that this system, albeit not quite flat, deviates but slightly from planarity,[10] while that of the Ni^{II} complex of **3a**[9] reveals a structure that is essentially flat and thus, supports the notion that, at least in some instances, the new α-to-β′-linked porphyrin isomers **3** can assume the near-planar, porphyrin-like conformations expected of highly conjugated, aromatic systems. More importantly, it also serves to reveal that the nickel center is ligated at similar distances (about 1.96 Å) by four in-plane donor atoms, namely three porphyrin-like nitrogens and one anionic carbon. This, in turn, suggests an unusual labilization of the inner C–H bond in **3a** and lends credence to the suggestions[9, 10] that "mutant" or "N-confused" (depending on whether the Polish or Japanese nomenclature is preferred) α-to-β′-linked porphyrins could emerge as interesting ligands. They might, for instance, find application as alternatives to the more classic dianionic, tetraazaporphyrins in a range of metal-binding or bioinorganic modeling studies or serve as good systems with which to stabilize often labile metal-to-carbon coordination modes. Thus, it is possible that these new porphyrin analogues, like the porphycenes that preceded them,[8] will provide a portal into a new and rich subarea of porphyrin-related research.

Whether the above promise is realized remains, of course, to be seen. Nonetheless, the syntheses of **3** highlighted herein should provide a stimulus to all those that seek to prepare other new porphyrin isomers and analogues: They, in their own way, confirm that the already rich chemistry of porphyrins can bear still more fruit. Indeed, a wide range of porphine-type isomers of generalized formula $C_{20}H_{14}N_4$ can be conceived. These could include systems such as **5** and **6** that extend the porphycene concept,[17] those such as **7** that involve pyridine-for-pyrrole substitution, as well as ones such as **9** and **10** that represent intellectual extensions of the Latos-Grażyńzki and Furuta approach. While not all will prove to be useful, or even stable under normal laboratory conditions, these and other $C_{20}H_{14}N_4$ species stand, at the very least, as fascinating targets, tantalizing all those who might be challenged by exciting problems involving the organic synthesis of nonnatural products. In this context, the synthesis of **7** seems particularly challenging (and unlikely) given Breitmaier's recent unsuccessful efforts to obtain **8**,[6] while that of **10** and its long-dreamed-about all-carbon analogue **11**, both of



which require the presence of four carbon-bound hydrogens within the central macrocyclic space, seem particularly intriguing. It remains an open question when these or other enticing porphyrin congeners will actually be prepared.

German version: *Angew. Chem.* **1994**, *106*, 1410

[1] Brief review of functionalized, capped, and dimerized porphyrins: a) F. Vögtle, *Cyclophane Chemistry*, Wiley, Chichester, **1993**, Ch. 8, pp. 375–404. Some more recent examples of modified and oligomerized porphyrins: b) Y. Ramondenc, R. Schwenninger, T. Phan, K. Gruber, C. Kratky, B. Kräutler, *Angew. Chem.* **1994**, *106*, 934; *Angew. Chem. Int. Ed. Engl.* **1994**, *33*, 889; c) M. Veyrat, O. Maury, F. Faverjon, D. E. Over, R. Ramasseul, J.-C. Marchon, I. Turowska-Tyrk, W. R. Scheidt, *Angew. Chem.* **1994**, *106*, 200; *Angew. Chem. Int. Ed. Engl.* **1994**, *33*, 220; d) J. P. Collman, V. J. Lee, X. Zhang, J. A. Ibers, J. I. Brauman, *J. Am. Chem. Soc.* **1993**, *115*, 3834; e) A. Osuka, S. Nakajima, K. Maruyama, N. Mataga, T. Asahi, I. Yamazaki, Y. Nishimura, T. Ohno, K. Nozaki, *ibid.* **1993**, *115*, 4577; f) J.-C. Chambron, A. Harriman, V. Heitz, J.-P. Sauvage, *ibid.* **1993**, *115*, 7419; g) S. Prathapan, T. E. Johnson, J. S. Lindsey, *ibid.* **1993**, *115*, 7519; h) J. L. Sessler, V. L. Capuano, A. Harriman, *ibid.* **1993**, *115*, 4618; i) A. Helms, D. Heiler, G. McLendon, *ibid.* **1992**, *114*, 6227; j) S. Anderson, H. L. Anderson, J. J. K. M. Sanders, *Angew. Chem.* **1992**, *104*, 921; *Angew. Chem. Int. Ed. Engl.* **1992**, *31*, 907.

[2] Review of expanded porphyrins and related compounds: J. L. Sessler, A. K. Burrell, *Top. Curr. Chem.* **1991**, *161*, 177.

[3] New expanded porphyrins: a) T. W. Bell, P. J. Cragg, M. G. B. Drew, A. Firestone, A. D.-I. Kwok, J. Liu, R. T. Ludwig, A. T. Papoulis, *Pure Appl. Chem.* **1993**, *65*, 361; b) D. Dolphin, S. J. Rettig, H. Tang, T. Wijesekera, L. Y. Xie, *J. Am. Chem. Soc.* **1993**, *115*, 9301; c) F. H. Carre, R. J. P. Corriu, G. Bolin, J. J. E. Moreau, C. Vernhet, *Organometallics* **1993**, *12*, 2478; d) T. Wessel, B. Franck, M. Möller, U. Rodewald, M. Läge, *Angew. Chem.* **1993**, *105*, 1201;

Angew. Chem. Int. Ed. Engl. **1993**, *32*, 1148; e) J. L. Sessler, S. J. Weghorn, V. Lynch, M. Johnson, *ibid.* **1994**, *106*, (no. 14) and **1994**, *33*, (no. 14); see also refs. [7] and [8c].

[4] M. J. Crossley, P. L. Burn, *J. Chem. Soc. Chem. Commun.* **1991**, 1569.

[5] Examples of heteroatom-containing analogues of porphyrin: a) E. Vogel, W. Haas, B. Knipp, J. Lex, H. Schmickler, *Angew. Chem.* **1988**, *100*, 455; *Angew. Chem. Int. Ed. Engl.* **1988**, *27*, 406; b) E. Vogel, P. Röhrig, M. Sicken, B. Knipp, A. Hermann, M. Pohl, H. Schmickler, J. Lex, *ibid.* **1989**, *101*, 1683 and **1989**, *28*, 1651; c) E. Vogel, J. Dörr, A. Herrmann, J. Lex, H. Schmickler, P. Walgenbach, J. P. Gisselbrecht, M. Gross, *ibid.* **1993**, *105*, 1667 and **1993**, *32*, 1597.

[6] Novel porphyrin-like system in which a pyridine serves to replace a pyrrole: K. Berlin, E. Breitmaier, *Angew. Chem.* **1994**, *106*, 229; *Angew. Chem. Int. Ed. Engl.* **1994**, *33*, 219.

[7] New expanded porphyrins containing heteroatoms: a) M. R. Johnson, D. C. Miller, K. Bush, J. J. Becker, J. A. Ibers, *J. Org. Chem.* **1992**, *57*, 4414; b) D. C. Miller, M. R. Johnson, J. J. Becker, J. A. Ibers, *J. Heterocyclic Chem.* **1993**, *30*, 1485; c) Z. Hu, C. Scordilis-Kelley, M. P. Cava, *Tetrahedron Lett.* **1993**, *34*, 1879; d) G. Märkl, U. Striebl, *Angew. Chem.* **1993**, *105*, 1387; *Angew. Chem. Int. Ed. Engl.* **1993**, *32*, 1333; e) G. Märkl, H. Sauer, P. Kreitmeier, T. Burgemeister, F. Kastner, G. Adolin, H. Nöth, K. Polborn *ibid.* **1994**, *106*, 1211 and **1994**, *33*, 1151.

[8] a) E. Vogel, M. Köcher, H. Schmickler, J. Lex, *Angew. Chem.* **1986**, *98*, 262; *Angew. Chem. Int. Ed. Engl.* **1986**, *25*, 257; b) E. Vogel, *Pure Appl. Chem.* **1990**, *62*, 557; c) *ibid.* **1993**, *65*, 143; d) E. Vogel, P. Koch, X.-L. Hou, J. Lex, M. Lausmann, M. Kisters, M. A. Aukauloo, P. Richard, R. Guilard, *Angew. Chem.* **1993**, *105*, 1670; *Angew. Chem. Int. Ed. Engl.* **1993**, *32*, 1600, and references therein.

[9] P. J. Chmielewski, L. Latos-Grażyński, K. Rachlewicz, T. Glowiak, *Angew. Chem.* **1994**, *106*, 805; *Angew. Chem. Int. Ed. Engl.* **1994**, *33*, 779.

[10] H. Furuta, T. Asano, T. Ogawa, *J. Am. Chem. Soc.* **1994**, *116*, 767.

[11] J. L. Sessler, E. A. Brucker, S. J. Weghorn, E. Vogel, N. Jux, L. Neumann, *Abstracts of the 207th American Chemical Society National Meeting (Inorg. Abstract no. 295)*, San Diego, CA, USA, March 13–17, **1994**. In this abstract, the name "porphylene" was suggested for compounds of general formula **4**. However, given its more descriptive nature, the name "corrphycene" is now preferred. See also J. L. Sessler, E. A. Brucker, S. J. Weghorn, M. Kisters, M. Schäfer, E. Vogel, *Angew. Chem.* **1994**, *106*, and *Angew. Chem. Int. Ed. Engl.* **1994**, *33*, in press.

[12] a) P. Rothemund, *J. Am. Chem. Soc.* **1936**, *58*, 625; b) P. Rothemund, A. R. Menotti, *ibid.* **1941**, *63*, 267.

[13] a) A. D. Adler, F. R. Longo, W. Shergalis, *J. Am. Chem. Soc.* **1964**, *86*, 3145; b) A. D. Adler, F. R. Longo, J. D. Finarelli, J. Goldmacher, J. Assour, L. Korsakoff, *J. Org. Chem.* **1967**, *32*, 476.

[14] Biomimetic synthesis of porphyrinogen-like (i.e., nonaromatic), α-β'-linked pentapyrrole: K.-H. Schumacher, B. Franck, *Angew. Chem.* **1989**, *101*, 1292; *Angew. Chem. Int. Ed. Engl.* **1989**, *28*, 1243.

[15] B. Franck, *Angew. Chem.* **1982**, *92*, 327; *Angew. Chem. Int. Ed. Engl.* **1982**, *21*, 343.

[16] a) J. L. Sessler, T. D. Mody, V. Lynch, *J. Am. Chem. Soc.* **1993**, *115*, 3346; b) J. L. Sessler, T. Morishima, V. Lynch, *Angew. Chem.* **1991**, *103*, 1018; *Angew. Chem. Int. Ed. Engl.* **1991**, *30*, 977.

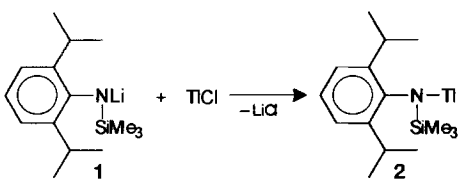
[17] For an interesting listing of putative porphycene-like porphyrin isomers: J. Waluk, J. Michl, *J. Org. Chem.* **1991**, *56*, 2729.

[2,6-*i*Pr$_2$C$_6$H$_3$(Me$_3$Si)NTl]$_4$—A Covalent Thallium(I)–Nitrogen Compound with Weak Arene–Thallium Interactions**

Said D. Waezsada, Thomas Belgardt, Mathias Noltemeyer, and Herbert W. Roesky*

Dedicated to Professor Wolfgang Lüttke on the occasion of his 75th birthday

Within the scope of our work on compounds of Group 13, which contain elements with low coordination numbers,[1–3] we achieved the first synthesis of a thallium(I) compound with the coordination number 2 a few years ago.[1] Obtaining a coordination number of 1 was the aim of subsequent investigations, to which end we have now tried coordination with the space-filling, nitrogen-containing 2,6-diisopropylphenyl-*N*-trimethylsilyl amine ligand.[4, 5] The lithium salt **1** reacts with TlCl in *n*-hexane to give the desired compound **2**.



1 2

The thallium compound **2** is a pale yellow solid, which is very sensitive to hydrolysis. A single-crystal X-ray structural analysis of **2** showed as the most important finding a tetrameric skeleton (**3**) in the solid state (Fig. 1). The aggregate contains, surprisingly, four arene–Tl interactions as well as four weak Tl–Tl contacts. The Tl atoms in **3** are each fixed approximately above the phenyl ring center of the neighboring molecule (mean distance 311 pm). The different substituents on the arene in **3** clearly hardly influence the η^6-coordination at the thallium center. Structural investigations on arene complexes of Group 13 have until now only been known for tetrahalometalates.[6] In [Mes$_6$Tl$_4$][GaBr$_4$]$_4$[7] (Mes = 1,3,5-Me$_3$H$_3$C$_6$) the corresponding arene–Tl distance is 294 pm and is thus noticeably shorter. These differences can easily be explained by the stronger donor–acceptor ability of the MesTl$^+$ unit relative to the tetrameric aggregate **3**. This leads to a strengthening of the arene–Tl bond. The Tl–Tl contacts (on average 406 pm) in **3** are clearly longer than those in the element (on average 340 pm[8]). The inter-

[2,6-*i*Pr$_2$C$_6$H$_3$(Me$_3$Si)NTl]$_4$ **3**

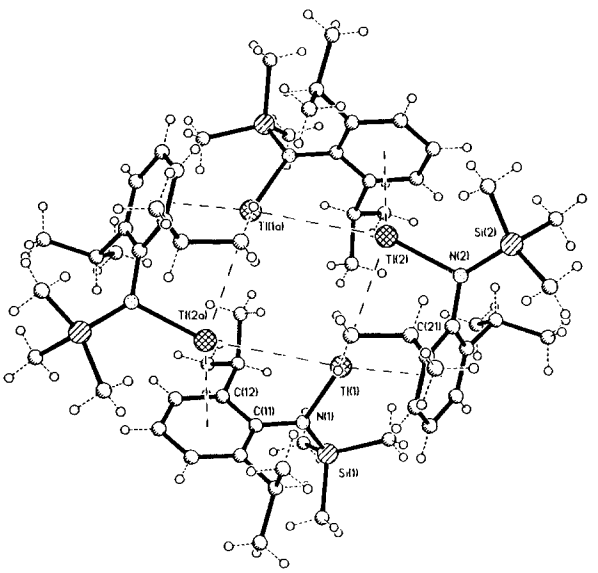


Fig. 1. Crystal structure of the tetramer **3**. Selected bond lengths [pm] and bond angles [°]: Tl(1)-N(1) 230.7(6), N(1)-Si(1) 170.1(7), N(1)-C(11) 140.5(11), Tl(2)-N(2) 230.5(6), N(2)-Si(2) 169.8(7); C(11)-N(1)-Si(1) 124.5(5), C(11)-N(1)-Tl(1) 109.4(5), Si(1)-N(1)-Tl(1) 126.1(3).

thallium bond in [AsPh$_4$]$_2$[Tl$_2$(Se$_2$C=C(CN)$_2$)$_2$] is, for comparison, 354.7(4) pm.[9]

The Tl–N bond lengths in **3** (on average 230 pm) lie between those of [Tl{N(SiMe$_3$)$_2$}$_3$] (on average 208.9 pm)[10] and those in (C$_9$H$_{21}$N$_2$SiTl)$_2$ (252.0(8)–273.7(8) pm).[11] To our knowledge no covalent arene complexes of Group 13 have yet been structurally described; the known compounds[6] are assembled ionogenically. Contrary to expectations H. Schumann et al. could not determine any thallium–arene interactions in [(Me$_4$C$_5$)Me$_2$Si(C$_6$H$_5$)Tl] in the solid state.[12] The arene–metal bond in lower homologues of Group 13 is plausibly interpreted as a HOMO–LUMO interaction.[6] This is not directly transferable to thallium complexes since the metal radius contracts strongly in this case, and the electrons are thus more strongly shielded (relativistic effects).[13] For the self-organization of **2** into the tetramer **3**, we assume weak donor–acceptor interactions; the metal–metal contacts can be considered as very weak.[14] Tetramer **3** is not stable in the gas phase and only the monomer **2** is found in the EI mass spectrum.

Experimental Procedure

A suspension of **1** (1.3 g, 5.1 mmol) in *n*-hexane (30 mL) was added dropwise to a slurry of TlCl (1.2 g, 5.1 mmol) in *n*-hexane (20 mL) at 0 °C. To allow the reaction to proceed to completion, the mixture was stirred for 12 h at room temperature. LiCl was subsequently separated by filtration, and the yellow solution was concentrated to 5 mL under vacuum. Compound **3** (1.8 g, 78%) precipitated as yellow crystals within 12 h. MS(EI): *m/z* 453 (M^+,7), 249 (M^+–Tl, 50), 73 (SiMe$_3$, 100%); ^{1}H NMR (C$_6$D$_6$, TMS): δ = 0.25 (s, 9H, SiMe$_3$), 1.20 (d, 6H, *i*Pr, J = 6.9 Hz), 1.33 (d, 6H, *i*Pr, J = 6.9 Hz), 3.77 (sept., 2H, *i*Pr, J = 7.0 Hz), 6.92 7.30 (m, 3H, arene).

Received: February 4, 1994 [Z6668IE]
German version: *Angew. Chem.* **1994**, *106*, 1413

[*] Prof. Dr. H. W. Roesky, Dipl.-Chem. S. D. Waezsada, Dipl.-Chem. T. Belgardt, Dr. M. Noltemeyer
Institut für Anorganische Chemie der Universität
Tammannstrasse 4, D-37077 Göttingen (FRG)
Telefax: Int. code + (551)39-3373

[**] This work was supported by the Deutsche Forschungsgemeinschaft and the Volkswagenstiftung.

[1] H. W. Roesky, M. Scholz, M. Noltemeyer, F. T. Edelmann, *Inorg. Chem.* **1989**, *28*, 3829.
[2] M. Scholz, M. Noltemeyer, H. W. Roesky, *Angew. Chem.* **1989**, *101*, 1419; *Angew. Chem. Int. Ed. Engl.* **1989**, *28*, 1383.
[3] S. Schulz, L. Häming, R. Herbst-Irmer, H. W. Roesky, G. M. Sheldrick, *Angew. Chem.* **1994**, *106*, 1052; *Angew. Chem. Int. Ed. Engl.* **1994**, *33*, 969.
[4] P. A. W. Porskamp, B. Zwanenburg, *Synthesis* **1981**, 368.
[5] Y.-W. Chao, P. A. Wexler, D. E. Wigley, *Inorg. Chem.* **1989**, *28*, 3868.
[6] H. Schmidbaur, *Angew. Chem.* **1985**, *97*, 893; *Angew. Chem. Int. Ed. Engl.* **1985**, *24*, 893.
[7] H. Schmidbaur, W. Bublak, J. Riede, G. Müller, *Angew. Chem.* **1985**, *97*, 402; *Angew. Chem. Int. Ed. Engl.* **1985**, *24*, 414.
[8] A. F. Wells, *Structural Inorganic Chemistry*, 5th ed., Clarendon, Oxford, **1984**.
[9] H.-U. Hummel, E. Fischer, T. Fischer, D. Gruß, A. Franke, W. Dietzsch, *Chem. Ber.* **1992**, *125*, 1565.
[10] R. Allmann, W. Henke, P. Krommes, J. Lorberth, *J. Organomet. Chem.* **1978**, *162*, 283.
[11] M. Veith, F. Goffing, V. Huch, *Chem. Ber.* **1988**, *121*, 943.
[12] H. Schumann, C. Janiak in *Unkonventionelle Wechselwirkungen in der Chemie metallischer Elemente* (Ed.: Deutsche Forschungsgemeinschaft), VCH, Weinheim, **1992**.
[13] K. S. Pitzer, *Acc. Chem. Res.* **1979**, *12*, 271.
[14] Crystal data for **3**: $C_{15}H_{26}NSiTi$, monoclinic, space group $C2/c$, $a = 2755.5(6)$, $b = 1052.8(2)$, $c = 2606.3(5)$ pm, $\beta = 111.11(3)°$, $V = 7.053(2)$ nm^3, $Z = 16$, $\rho_{calcd} = 1.706$ Mgm^{-3}, $F(000) = 3488$, $\lambda = 71.073$ pm, $(Mo_{K\alpha})$ $\mu = 9.214$ mm^{-1}. 4596 independent reflections were used for structure solution and refinement against F^2. $R1$ $[F > 4\sigma(F)] = 0.0382$, $wR2 = 0.1014$. Further details of the crystal structure investigation may be obtained from the Fachinformationszentrum Karlsruhe, D-76344 Eggenstein-Leopoldshafen (FRG) on quoting the depository number CSD-58165 and the journal citation.

Stable Silanetriols as Building Blocks for the Synthesis of Titanasilasesquioxanes—Model Compounds for Titanium-Doped Zeolites**

Norbert Winkhofer, Andreas Voigt, Hendrik Dorn, Herbert W. Roesky,* Alexander Steiner, Dietmar Stalke, and Armin Reller

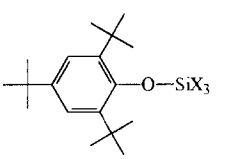
Dedicated to Professor F. Albert Cotton on the occasion of his 65th birthday

Titanium-doped zeolites catalyze the reaction of H_2O_2 with a variety of substrates such as arenes and alkenes.[1] The oxidative cleavage of hydrazones by TS1/H_2O_2 was also described recently,[2] and the oxidation of nonactivated hydrocarbons with this system is particularly impressive.[3, 4] The zeolites TS1 and TS2 are morphologically related to ZSM-5 (MEL) and ZSM-11 (MFI). In recent reports large-pore titanium zeolites have been described, which permit the oxidation of larger substrates.[5–7] The active centers were investigated by spectroscopic methods. In this way the structure of ETS-10 was recently determined by a combination of powder diffraction and solid-state NMR data.[8] All of the titanium zeolites studied display a characteristic IR band at 960 cm^{-1}.[9, 10]

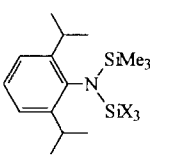
We have been interested for quite some time in the synthesis of defined metallasiloxanes as model compounds for catalytic metal systems on SiO_2 supports.[11, 12] In this context we are also directing efforts towards the preparation of three-dimensional structures starting from isolated silanetriols.

Syntheses of silasesquioxanes, in other words compounds with the composition $(RSiO_{3/2})_8$, have been reported.[13] For example, trisilanol *c*-Hex$_7$Si$_7$O$_9$(OH)$_3$ derived from cyclohexylsilasesquioxane can be prepared. The OH groups are bound to three silicon atoms and point in the direction of the unoccupied corner of this cubane-type structure. Feher et al. took advantage of this and prepared a series of monometalated polyhedral oligometallasilasesquioxanes (POMSS) by "corner-capping reactions" in which the polyhedral structure is completed or its unoccupied corners are capped.[14, 15]

Our goal was the simple synthesis of metallasilasesquioxanes with higher metal content. We started with monomeric silanetriols, which could be obtained by the controlled hydrolysis of trichlorosilanes **1a,b**. Several representatives of this class of compounds have been described; however, their chemistry is for the most part unexplored.[16, 17] The reaction of the kinetically stabilized silanetriols **2a,b** with titanium isopropoxides gives the target compounds in high yields.



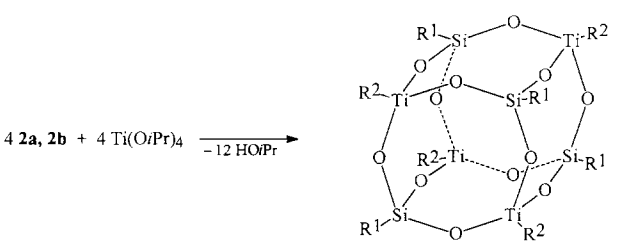
1a : X = Cl
2a : X = OH



1b : X = Cl
2b : X = OH

The main problem in syntheses with silanetriols is their tendency to undergo condensation reactions, particularly in the presence of acids. We have reported elsewhere on the condensation reaction of *t*BuSi(OH)$_3$ with Re_2O_7 to yield [(*t*BuSiO(OReO$_3$)]$_4$.[18]

Despite its bulky organic substituents, compound **2a** proved to be quite labile; it can be isolated in pure form, but in solution and in the presence of traces of acid **2a** undergoes condensation with cleavage of 2,4,6-tri(*tert*-butyl)phenol. Thus, deliberate reaction is possible only with halogen-free Ti(O*i*Pr)$_4$. Relative to **2a**, silanetriol **2b** is remarkably stable. It reacts smoothly with Ti(O*i*Pr)$_4$ and TiCl(O*i*Pr)$_3$ to give **3b**; condensation is not apparent in solutions of **2b** even after several hours. We attribute this behavior to the reduced electrophilicity of the OH-bound Si atom, owing to the neighboring donor atom. Products **3a** and



3a : R^1 = 2,4,6-*t*Bu$_3$C$_6$H$_2$O
3b : R^1 = 2,6-*i*Pr$_2$C$_6$H$_3$N(SiMe$_3$)
R^2 = O*i*Pr

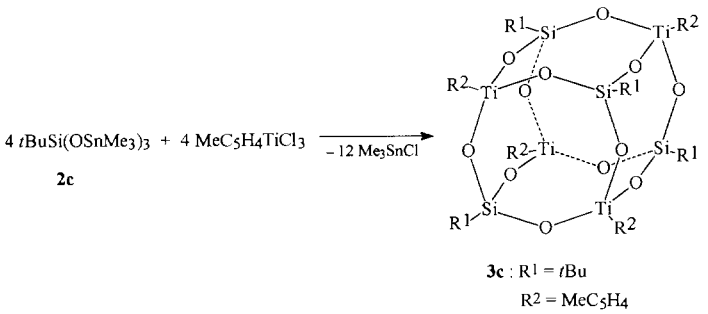
4 **2b** + 4 TiCl(O*i*Pr)$_3$ $\xrightarrow[-\ 4\ NEt_3\cdot HCl\ -\ 8\ HOiPr]{+\ 4\ NEt_3}$ **3b**

[*] Prof. Dr. H. W. Roesky, Dipl.-Chem. N. Winkhofer, Dipl.-Chem. A. Voigt, Dipl.-Chem. H. Dorn, Dipl.-Chem. A. Steiner, Priv.-Doz. Dr. D. Stalke
Institut für Anorganische Chemie der Universität
Tammannstrasse 4, D-37077 Göttingen (FRG)
Telefax: Int. code + (551) 39-3373
Prof. Dr. A. Reller
Institut für Anorganische und Angewandte Chemie
der Universität Hamburg

[**] This work was supported by Hoechst AG, the Deutsche Forschungsgemeinschaft, and the Fonds der Chemischen Industrie.

3b are metallasilasesquioxanes with completely hydrolyzable leaving groups.

In the reaction of silanetriol tBuSi(OH)$_3$ it proved advantageous to use SnMe$_3$ protecting groups (→ **2c**). In this way alkyl-



substituted silanetriols could be treated with titanium trihalides. The resulting product **3c** provided single crystals. An X-ray structure analysis[19] demonstrated that alternating silicon and titanium atoms form the corners of a cube with an average Si···Ti edge length of 332.1 pm (Fig. 1). The twelve Si···Ti edges are each bridged by an oxygen atom in an μ^2 fashion (average Si–O distance: 161.6 pm; average Ti–O distance: 179.4 pm). The average Si-O-Ti angle formed is 153.9°. The body diagonal of the Ti_4Si_4 cube is approximately 570 pm. The bond lengths and angles are within the range of the corresponding values for eight-membered siloxane rings.[23]

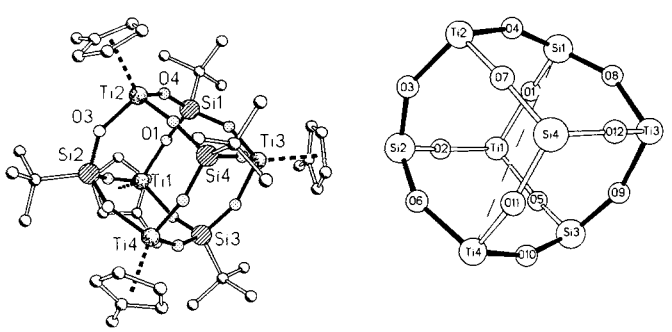


Fig. 1. Crystal structure of **3c**; left: with organic substituents, right: only the $Si_4O_{12}Ti_4$ framework is shown. Average distances [pm] and angles [°]: Ti-O 179.4, Si-O 161.6, Si···Si 458.1, Ti···Ti 480.6, Si···Ti 332.1; Si-O-Ti 153.9.

The IR spectra of **3a–c** show strong absorptions around $\tilde{\nu} \approx 960\ cm^{-1}$. A band in this region, whose assignment is not certain, is characteristic for the catalytically active forms of TS1, TS2, and TiZSM48. Huybrechts et al.[3] assign this band to the stretching vibration of the Ti=O group, whereas Corma et al.[6] attribute it to that of the SiO^- groups. Other authors interpret this band, the intensity of which depends on the titanium content of the zeolite, as the Si–O stretching vibration of the polarized $Si-O^{\delta-}-Ti^{\delta+}$ unit.[24] We believe that the data for the model compounds **3a–c** indicate that this band corresponds to the Si-O-Ti stretch, since Ti=O and $Si-O^-$ units do not exist in these compounds.

Our preparation of titanasilasesquioxanes is a facile synthetic route leading to a new class of compounds, the polytitanasilasesquioxanes, which are suitable model compounds for titanium-containing redox zeolites. We are currently studying the catalytic activity of these compounds. In addition the reactive substituents on the silicon and titanium atoms indicate that crosslinking to form zeolitic materials may be possible.

Experimental Procedure

1a: A suspension of 2,4,6-tBu$_3$C$_6$H$_2$OLi·Et$_2$O [25] (48.5 g, 0.14 mol) in toluene (ca. 130 mL) was added dropwise over 1 h to a solution of $SiCl_4$ (31.1 g, 0.18 mol) in toluene (ca. 450 mL). The reaction mixture was heated at reflux for 18 h, the precipitated LiCl removed by filtration over Celite, and the solvent removed under vacuum. The light brown solid was purified by fractional sublimation under vacuum (10^{-2} Torr, 90–95 °C). A small amount of 2,4,6-tri(*tert*-butyl)phenol sublimed first and was discarded. **1a** (40.8 g, 73%) was finally obtained as a white solid. M.p. 108 °C; ^{1}H NMR (250 MHz, C_6D_6, TMS): $\delta = 1.25$ (s, 9H, *p*-C(CH$_3$)$_3$), 1.49 (s, 18H, *o*-C(CH$_3$)$_3$), 7.46 (s, 2H, H$_{arene}$); ^{13}C NMR (63 MHz, $CDCl_3$, TMS): $\delta = 31.4$ (C(*C*H$_3$)$_3$), 31.5 (C(CH$_3$)$_3$), 34.7 (*C*(CH$_3$)$_3$), 35.3 (*C*(CH$_3$)$_3$), 123.4 (C$_{arene}$), 139.7 (C$_{arene}$), 145.4 (C$_{arene}$), 148.0 (C$_{arene}$); ^{29}Si NMR (80 MHz, C_6D_6, TMS): $\delta = -49.5$; IR (Nujol): $\tilde{\nu} = 1600$, 1422, 1224, 1122, 999, 881, 589, 460 cm^{-1}; MS (70 eV): *m/z* (%): 396 (11) [M^+], 247 (100) [$C_{17}H_{27}O^+$].

1b: A solution of (iPr$_2$C$_6$H$_3$)N(SiMe$_3$)Li [26] (60.1 g, 0.24 mol) in diethyl ether (200 mL) was added dropwise to a stirred solution of $SiCl_4$ (59.9 g, 0.35 mol) and diethyl ether (100 mL) at 0 °C. After 12 h of stirring at room temperature the precipitated LiCl was filtered off and washed with *n*-hexane (2 × 30 mL). The filtrate was concentrated to dryness under vacuum. Recrystallization from pentane furnished **1b** as a white solid. Yield: 84.6 (94%). M.p. 138 °C; ^{1}H NMR (400 MHz, $CDCl_3$, TMS): $\delta = 0.25$ (s, 9H, Si(CH$_3$)$_3$), 1.23 (d, $^3J_{HH} = 6.8$ Hz, 6H, CH(CH$_3$)(CH$_3$)), 1.26 (d, $^3J_{HH} = 6.8$ Hz, 6H, CH(CH$_3$)(CH$_3$)), 3.39 (sept, $^3J_{HH} = 6.8$ Hz, 2H, CH(CH$_3$)$_2$), 7.12 (m, 3H, H$_{arene}$); ^{29}Si NMR (49 MHz, $CDCl_3$, TMS): $\delta = -27.5$ ($SiCl_3$), 12.3 (Si(CH$_3$)$_3$); IR (Nujol): $\tilde{\nu} = 1255$, 1102, 980, 889, 871, 841, 609, 598 cm^{-1}; MS (70 eV): *m/z* (%): 383 (40) [M^+], 368(100) [M^+ – Me].

2a: A solution of **1a** (18.5 g, 46.7 mmol) in anhydrous diethyl ether (ca. 70 mL) was added dropwise within 1 h to a vigorously stirred emulsion of water (2.5 g, 0.14 mol) and aniline (13.1 g, 0.14 mol) in anhydrous diethyl ether (ca. 500 mL) in an ice bath. After 2 h the ice bath was removed, and the reaction mixture was stirred for 2 h at room temperature. The precipitated aniline hydrochloride was filtered off and the clear solution concentrated under vacuum. When the solution reached a volume of 50 mL, **2a** precipitated as a white solid, which was removed by filtration and washed with a small amount of pentane (15 mL) (12.3 g, 77%). M.p. 168 °C; ^{1}H NMR (250 MHz, [D$_6$]DMSO, TMS): $\delta = 1.23$ (s, 9H, *p*-C(CH$_3$)$_3$), 1.39 (s, 18H, *o*-C(CH$_3$)$_3$), 6.50 (s, 3H, OH), 7.14 (s, 2H, H$_{arene}$); ^{13}C NMR (63 MHz, [D$_6$]DMSO, TMS): $\delta = 31.2$ (C(*C*H$_3$)$_3$), 31.5 (C(*C*H$_3$)$_3$), 34.0 (*C*(CH$_3$)$_3$), 35.0 (*C*(CH$_3$)$_3$), 121.7 (C$_{arene}$), 139.5 (C$_{arene}$), 140.9 (C$_{arene}$), 150.0 (C$_{arene}$); ^{29}Si NMR (50 MHz, [D$_6$]DMSO, TMS): $\delta = -83.7$; IR (Nujol): $\tilde{\nu} = 3500$, 1602, 1246, 1125, 978, 907, 814 cm^{-1}; MS (70 eV): *m/z* (%): 340 (37) [M^+], 325 (100) [M^+ – Me].

2b: **1b** (61.9 g, 0.16 mol) was added dropwise over 3 h to a vigorously stirred emulsion of water (8.7 g, 0.49 mol) and aniline (45.1 g, 0.49 mol) in diethyl ether (1.3 L) at 0 °C. The solution was allowed to warm slowly to room temperature and then stirred a further 12 h. The solution was concentrated under vacuum to 1/3 of its volume. The precipitated aniline hydrochloride was filtered off and the remaining solvent removed under vacuum. The pale yellow crude product was washed with pentane (2 × 15 mL). The pure product (45.8 g, 88%) was a white solid. M.p. 131 °C; ^{1}H NMR (250 MHz, [D$_6$]DMSO, TMS): $\delta = 0.05$ (s, 9H, Si(CH$_3$)$_3$), 1.10 (d, $^3J_{HH} = 6.8$ Hz, 6H, CH(CH$_3$)(CH$_3$)), 1.15 (d, $^3J_{HH} = 6.8$ Hz, 6H, CH(CH$_3$)(CH$_3$)), 3.65 (sept, $^3J_{HH} = 6.8$ Hz, 2H, CH(CH$_3$)$_2$), 5.74 (s, 3H, OH), 6.92 (m, 3H, H$_{arene}$); ^{29}Si NMR (49 MHz, [D$_6$]DMSO, TMS): $\delta = -67.3$ (Si(OH)$_3$), 3.8 (Si(CH$_3$)$_3$); IR (Nujol): $\tilde{\nu} = 3344$, 1584, 1315, 1250, 1178, 987, 920, 836, 814 cm^{-1}; MS (70 eV): *m/z* (%): 327(54) [M^+], 312 (100) [M^+ – Me].

2c: A suspension of tBuSi(OH)$_3$ (3.3 g, 24.0 mmol) in *n*-hexane (40 mL) was treated with a solution of N(SnMe$_3$)$_3$ (12.2 g, 24.0 mmol) in *n*-hexane (20 mL), upon which the temperature of the reaction mixture increased. After 12 h of stirring at room temperature, the reaction mixture was heated at reflux for 1 h to ensure complete reaction. After the solvent was removed by distillation, the product was distilled (10^{-2} Torr, 95–100 °C). **2c** (13.6 g, 91%) was obtained as a colorless material which solidified in the receiving flask. ^{1}H NMR (250 MHz, C_6D_6, TMS): $\delta = 0.29$ (s, 27H, Sn(CH$_3$)$_3$), 1.18 (s, 9H, C(CH$_3$)$_3$); ^{29}Si NMR (49 MHz, C_6D_6, TMS): $\delta = -46.7$ (s); MS (70 eV): *m/z* (%): 567 (100) [M^+ – tBu].

3a: A solution of Ti(iOPr)$_4$ (1.36 g, 4.8 mol) in *n*-hexane (15 mL) was added dropwise over 30 min to a solution of **2a** (1.36 g, 4.0 mmol) in *n*-hexane/THF (30 mL/10 mL) at room temperature. The reaction mixture was stirred 12 h and then concentrated under vacuum, upon which a white solid precipitated. The crude product was filtered off, washed with *n*-hexane (5 mL), and then dried under vacuum to give **3a** (1.51 g, 85%) as a yellowish solid. M.p. 238 °C; ^{1}H NMR (250 MHz, $CDCl_3$, TMS): $\delta = 1.04$ (d, 6H, CH(CH$_3$)$_2$), 1.29 (s, 9H, *p*-C(CH$_3$)$_3$), 1.47 (s, 18H, *o*-C(CH$_3$)$_3$), 4.45 (sept, 1H, CH(CH$_3$)$_2$), 7.26 (s, 2H, H$_{arene}$); ^{13}C NMR (63 MHz, $CDCl_3$, TMS): $\delta = 25.5$ (CH(*C*H$_3$)$_2$), 31.4 (C(*C*H$_3$)$_3$), 31.7 (C(*C*H$_3$)$_3$), 34.5 (*C*(CH$_3$)$_3$), 35.2 (*C*(CH$_3$)$_3$), 82.1 (*C*H(CH$_3$)$_2$), 122.4 (C$_{arene}$), 139.7 (C$_{arene}$), 142.8 (C$_{arene}$), 148.8 (C$_{arene}$); ^{29}Si NMR (80 MHz, $CDCl_3$, TMS): $\delta = -116.4$; IR (Nujol): $\tilde{\nu} = 1430$, 1244, 1120, 1059, 973, 906, 645, 478 cm^{-1}; MS (70 eV): *m/z* (%): 1777(7) [M^+], 247(100) [$C_{17}H_{27}O^+$].

 © VCH Verlagsgesellschaft mbH, D-69451 Weinheim, 1994 0570-0833/94/1313-1353 $ 10.00+.25/0

3b: A solution of 1 N $TiCl(OiPr)_3$ in *n*-hexane (5.1 mL, 5.1 mmol) was added within 5 min to a suspension of **2b** (1.67 g, 5.1 mmol) and triethylamine (0.52 g, 5.1 mmol) in *n*-hexane/THF (30 mL/20 mL) at room temperature. The reaction mixture was stirred for 12 h and then heated to 60 °C for 3 h. The suspension was concentrated to dryness under vacuum and the residue taken up in pentane and filtered. The solution was stored at + 5 °C. After two weeks colorless, tetrahedral crystals (1.89 g, 86%) formed.

3b: A solution of $Ti(OiPr)_4$ (1.99 g, 7.0 mmol) in THF (15 mL) was added within 5 min to a stirred suspension of **2b** (2.29 g, 7.0 mmol) in THF (40 mL). The reaction mixture was stirred for 12 h and then heated to 60 °C for 3 h. Workup as in the other preparation of **3b** gave colorless, tetrahedral crystals (2.60 g, 86%). ^{1}H NMR (250 MHz, $CDCl_3$, TMS): $\delta = 0.02$ (s, 9H, $Si(CH_3)_3$), 0.95 (d, $^3J_{HH} = 6.1$ Hz, $CH(CH_3)_2$), 1.15 (d, $^3J_{HH} = 6.8$ Hz, 6H, $CH(CH_3)(CH_3)$), 1.24 (d, $^3J_{HH} = 6.8$ Hz, 6H, $CH(CH_3)(CH_3)$), 3.50 (sept, $^3J_{HH} = 6.8$ Hz, 2H, $CH(CH_3)_2$), 4.25 (sept, $^3J_{HH} = 6.1$ Hz, 1H, $CH(CH_3)_2$), 6.98 (s, 3H, H_{Aren}); ^{29}Si NMR (49 MHz, $CDCl_3$, TMS): $\delta = -96.5$ (Si-O), 6.3 ($Si(CH_3)_3$); IR (Nujol): $\tilde{\nu} = 1250$, 993, 968, 861, 842, 458 cm^{-1}; MS (70 eV): *m/z* (%): 1725 (100) [M^+].

3c: A solution of **2c** (1.90 g, 3.0 mmol) in 1,2-dimethoxyethane (DME) (8 mL) was added dropwise to a solution of $MeC_5H_4TiCl_3$ (0.70 g, 3.0 mmol) in DME (8 mL) at −60 °C. The reaction solution was allowed to warm slowly to room temperature and was then stirred for 2 d. A fine white precipitate was filtered from the turbid solution and washed with DME (2 mL). Yield 0.34 g (44%). ^{1}H NMR (250 MHz, C_6D_6, TMS): $\delta = 1.20$ (s, 9H, $C(CH_3)_3$), 2.23 (s, 3H, CH_3), 6.11 (m, 2H, C_5H_4), 6.25 (m, 2H, C_5H_4); ^{29}Si NMR (79 MHz, C_6D_6, TMS): $\delta = -68.6$ (s); IR (Nujol): $\tilde{\nu} = 1023$, 974, 799 cm^{-1}; MS (70 eV): *m/z* (%): 983 (100) [$M^+ - t$Bu].

Received: February 14, 1994 [Z 6691 IE]
German version: *Angew. Chem.* **1994**, *106*, 1414

[1] G. Perego, G. Ballussi, C. Corno, M. Tamarasso, F. Buonomo, A. Esposito in *Studies in Surface Science and Catalysis: New Developments in Zeolite Science and Technology* (Eds.: Y. Murakami, A. Iijima, J. W. Word), Elsevier, Amsterdam, **1986**.
[2] P. Kumar, V. R. Hegde, B. Pandey, T. Ravindranathan, *J. Chem. Soc. Chem. Commun.* **1993**, 1553.
[3] D. R. C. Huybrechts, L. De Bruycker, P. A. Jacobs, *Nature* **1990**, *345*, 240.
[4] T. Tatsumi, M. Nakamura, S. Negisbi, H. Tominaga, *J. Chem. Soc. Chem. Commun.* **1990**, 476.
[5] D. P. Serrano, H.-X. Li, M. E. Davis, *J. Chem. Soc. Chem. Commun.* **1992**, 745.
[6] M. A. Camblor, A. Corma, A. Martinez, J. Pérez-Pariente, *J. Chem. Soc. Chem. Commun.* **1992**, 589.
[7] T. Blasco, M. A. Camblor, A. Corma, J. Pérez-Pariente, *J. Am. Chem. Soc.* **1993**, *115*, 11 803.
[8] M. W. Anderson, O. Terasaki, T. Ohsuna, A. Philippou, S. P. MacKay, A. Ferreira, J. Rocha, S. Lidin, *Nature* **1994**, *367*, 347.
[9] M. A. Camblor, A. Corma, J. Pérez-Pariente, *J. Chem. Soc. Chem. Commun.* **1993**, 557.
[10] A. Zecchina, G. Spoto, S. Bordiga, A. Ferrero, G. Petrini, G. Leofanti, M. Padovan in *Zeolite Chemistry and Catalysis* (Ed.: P. A. Jacobs), Elsevier, Amsterdam, **1991**, p. 251.
[11] A. Haoudi-Mazzah, H.-G. Schmidt, M. Noltemeyer, H. W. Roesky, *Z. Naturforsch. B* **1991**, *46*, 587.
[12] H.-J. Gosink, H. W. Roesky, H.-G. Schmidt, M. Nolemeyer, E. Irmer, R. Herbst-Irmer, *Organometallics*, in press.
[13] J. F. Brown, L. H. Vogt, *J. Am. Chem. Soc.* **1965**, *87*, 4313.
[14] F. J. Feher, S. L. Gonzales, J. W. Ziller, *Inorg. Chem.* **1988**, *27*, 3440.
[15] F. J. Feher, K. J. Weller, *Organometallics* **1990**, *9*, 2638.
[16] S. S. Al-Juaid, N. H. Butturs, R. I. Damja, Y. Derouiche, C. Eaborn, P. B. Hitchcock, P. D. Lickiss, *J. Organomet. Chem.* **1989**, *371*, 287.
[17] H. Ishida, J. L. Koenig, K. C. Gardner, *J. Chem. Phys.* **1982**, *77*, 5748.
[18] N. Winkhofer, H. W. Roesky, M. Noltemeyer, W. T. Robinson, *Angew. Chem.* **1992**, *104*, 670; *Angew. Chem. Int. Ed. Engl.* **1992**, *31*, 599.
[19] Crystal data for **2c**: $[tBuSiO_3Ti(MeC_5H_4)]_4$, $M = 1040.87$, triclinic, space group $P\bar{1}$, $a = 1137.8(6)$, $b = 1145.7(6)$, $c = 2188.4(12)$ Å, $\alpha = 93.81(4)$, $\beta = 105.17(4)$, $\gamma = 110.23(3)°$, $V = 25.44(2)$ nm^3, $Z = 2$, $\rho_{calcd} = 1.359$ $Mg\,cm^{-3}$, $F(000) = 1088$, $\lambda = 71.073$ pm, $T = 0$ °C, $\mu(Mo_{K\alpha}) = 0.752$ mm^{-1}, crystal dimensions $0.3 \times 0.4 \times 0.6$ mm, $5° \le 2\theta \le 45°$; 7872 collected reflections, 6693 independent, of which 6686 were used for the refinement of 761 parameters with 2773 restraints; maximum residual electron density : 843 $e\,nm^{-3}$, $R1(F > 4\sigma(F)) = 0.078$ and $wR2 = 0.239$ (all data) with $R1 = \Sigma||F_o| - |F_c||/\Sigma|F_o|$ and $wR2 = (\Sigma(F_o^2 - F_c^2)^2/\Sigma w(F_o^2)^2)^{0.5}$. The data were collected on a Stoe-Huber integrated diffractometer. The intensity measurements were conducted on a cooled crystal in a drop of oil [20] with $2\theta/\omega$ scans. The structure was solved by direct methods (SHELX-90) [21] and refined versus F^2 by the least squares method [22]. The disordered MeC_5H_4 ligands were refined with distance and ADP restraints. Further details of the crystal structure investigation are available on request from the Director of the Cambridge Crystallographic Data Centre, 12 Union Road, GB-Cambridge CB2 1EZ (UK), on quoting the full journal citation.
[20] T. Kottke, D. Stalke, *J. Appl. Crystallogr.* **1993**, *26*, 615.
[21] G. M. Sheldrick, *Acta Crystallogr. Sect. A* **1990**, *46*, 467.
[22] G. M. Sheldrick, SHELXL-93, program for crystal structure refinement, Göttingen, **1993**.
[23] F-q. Liu, H.-G. Schmidt, M. Noltemeyer, C. Freire-Erdbrügger, G. M. Sheldrick, H. W. Roesky, *Z. Naturforsch. B* **1992**, *47*, 1085.
[24] M. R. Boccuti, K. M. Rao, A. Zecchina, G. Leofanti, G. Petrini in *Structure and Reactivity of Surfaces* (Eds.: C. Morterra, A. Zecchina, G. Costa), Elsevier, Amsterdam, **1989**, p. 133.
[25] B. Cetinkaya, I. Gümrükcü, M. F. Lappert, J. L. Atwood, R. Shakir, *J. Am. Chem. Soc.* **1980**, *102*, 2086.
[26] D. K. Kennepohl, S. Brooker, G. M. Sheldrick, H. W. Roesky, *Chem. Ber.* **1991**, *124*, 2223.

Trigonal-Bipyramidal Technetium and Rhenium Complexes with Tetradentate NS_3 Tripod Ligands**

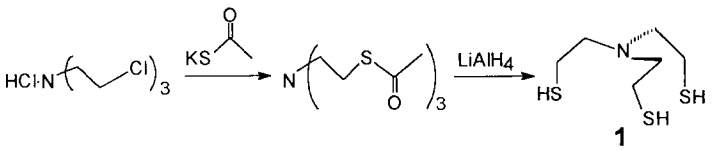
Hartmut Spies,* Matthias Glaser, Hans-Jürgen Pietzsch, F. Ekkehardt Hahn,* Oliver Kintzel, and Thomas Lügger

Our interest in coordination compounds of rhenium and technetium is based on the relevance of radionuclides of these metals for diagnosis and therapy in nuclear medicine. The gamma emitter ^{99m}Tc ($t_{1/2} = 6.02$ h, $E\gamma = 140.6$ keV) has already served for several years as the "work horse" in nuclear medicine for radiodiagnostic examinations. Coordination compounds of the β-emitter ^{186}Re are of current interest as cytotoxic radiotherapeuticals. In the concept of bifunctional pharmaceuticals, those technetium and rhenium complexes that are suitable for coupling to biologically relevant anchor groups lend themselves in particular to the design of new radiotracers. The previously known species suitable for coupling are almost without exception square-pyramidal oxo complexes of tetradentate ligands,[1-3] in which the properties, and thus the in vivo behavior, of a biomolecule is strongly influenced by the coupling to the polar M=O unit. In promising tracers, however, this influence should be kept as small as possible. It is to be expected that ligands which, in spite of extensive shielding of the metal,[4] still allow the coupling to a biomolecule, are particularly suitable. In this sense, complexes of tetradentate NS_3 tripod ligands present an interesting alternative to the oxo complexes. In the presence of a coligand, such ligands could lead to weakly polar, trigonal-bipyramidal complexes in which the metal atom is more strongly shielded than in the square-pyramidal oxo complexes. We report here on the syntheses, structures, and properties of trigonal-bipyramidal Re^{III} and Tc^{III} complexes which contain the tetradentate NS_3 tripod ligand 2,2′,2″-nitrilotris(ethanethiol) **1** and a triphenylphosphane or isocyanide ligand.

The ligand **1** was obtained by reaction of tris(2-chloroethyl)-amine with potassium thioacetate[6a] followed by reduction with $LiAlH_4$[6b] in accordance with Scheme 1.[5] A problem in the workup of the reaction mixture is posed by the presence of acidic and basic functions in the same molecule. The formation of ionic

[*] Dr. habil. H. Spies, Dipl.-Chem. M. Glaser, Dr. H.-J. Pietzsch
Forschungszentrum Rossendorf e. V.
Institut für Bioanorganische und Radiopharmazeutische Chemie
Postfach 510119, D-01314 Dresden (FRG)
Telefax: Int. code + (351)591-3232
Prof. Dr. F. E. Hahn, Dipl.-Chem. O. Kintzel, Dipl.-Chem. T. Lügger
Institut für Anorganische und Analytische Chemie der Freien Universität
Fabeckstrasse 34-36, D-14195 Berlin (FRG)
Telefax: Int. code + (30)838-2424

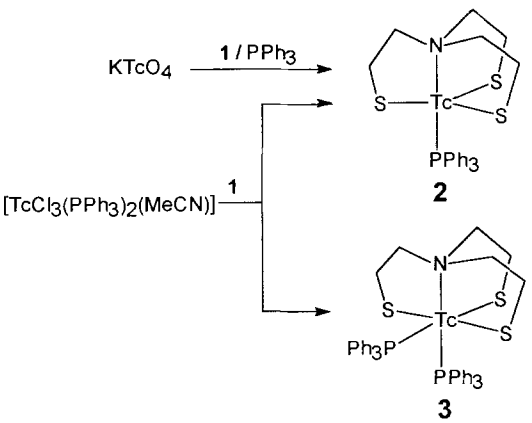
[**] This work was supported by the Deutsche Forschungsgemeinschaft, the Fonds der Chemischen Industrie, and by the BMFT through the Graduiertenkolleg "Synthese und Strukturaufklärung niedermolekularer Verbindungen".



Scheme 1. Synthesis of the ligand **1**.

reaction products (hydrochloride or thiolate) can be suppressed in a satisfactory manner by the introduction of CO_2 into the reaction mixture, which has previously been hydrolyzed with neutral, degassed water.

Technetium and rhenium complexes of the ligand **1** are possible in principle both by the in situ reduction of the metalates MO_4^-, as well as by ligand exchange on reactive M^{III} compounds (Schemes 2 and 3). In general, the ligand exchange reactions



Scheme 2. Synthesis of the technetium complexes **2** and **3**.

prove to be more advantageous as regards both the yield and the avoidance of side products.

The violet Tc^{III} complex **2** is formed in 62% yield by the action of a mixture of **1** and the pertechnate reducing agent triphenylphosphane[7] in an ethanol/water solution of pertechnate made acidic by acetic adic. The ligand exchange reaction of $[TcCl_3(PPh_3)_2(MeCN)]$[8] with **1** also leads to the complex **2** in good yield. In this reaction, a small amount of a blue complex **3** can be isolated as a side product, which is presumed to have the composition $[Tc(\mathbf{1})(PPh_3)_2]$[5] (Scheme 2).

The X-ray structure analysis on crystals of **2**[9] (Fig. 1) shows that a pentacoordinate trigonal-bipyramidal complex has indeed been formed. The tetradentate ligand **1** occupies three equatorial

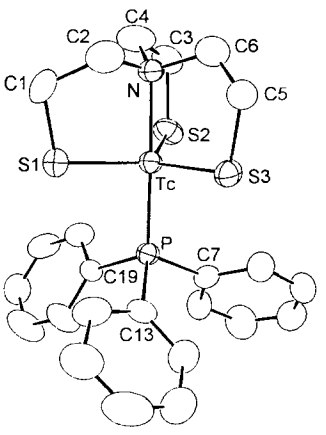
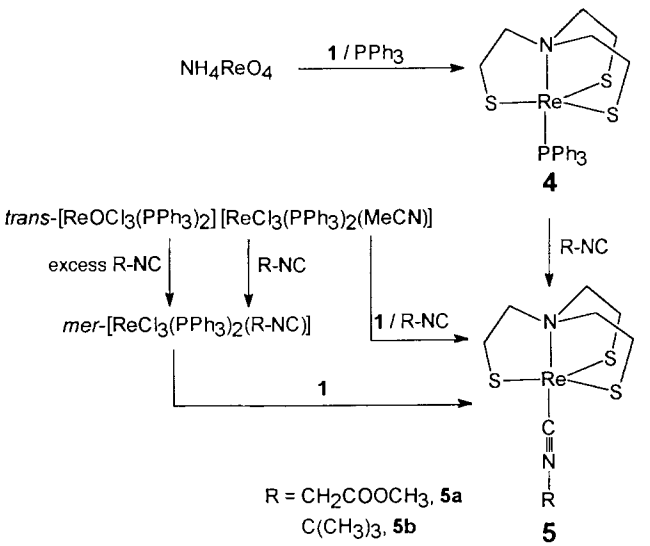


Fig. 1. Structure of the complex **2** in the crystal (ORTEP). Selected distances [Å] and angles [°]: Tc-S1 2.228(2), Tc-S2 2.224(2), Tc-S3 2.227(2), Tc-P 2.325(2), Tc-N 2.192(5); S1-Tc-S2 119.29(7), S1-Tc-S3 119.92(7), S1-Tc-P 93.83(6), S1-Tc-N 85.01(2), S2-Tc-S3 118.73(7), S2-Tc-P 95.61(7), S2-Tc-N 85.5(2), S3-Tc-P 94.92(6), S3-Tc-N 85.19(14), P-Tc-N 178.7(2) [9].

and one axial position, whereas the second axial position is occupied by a triphenylphosphane ligand. The tripodal topology of **1** obviously stabilizes the Tc^{III} ion and forces the formation of this coordination polyhedron. Only a very small number of trigonal-bipyramidal Tc^{III} complexes are known.[10] An example with the PS_3 tripod ligand 2,2′,2″-phosphanetriyltris(benzenethiol) was reported by de Vries et al.[10b] Bond lengths and angles in **2** lie within the expected range for Tc^{III} thiolates.[10b, 11] The small deviations of the angles on the technetium atom from the values for a trigonal bipyramid are remarkable.

The concept for the preparation of **2** can be applied to the synthesis of the analogous mixed-ligand rhenium(III) complex **4** (Scheme 3).[5] This can also be obtained by the reduction of per-



Scheme 3. Synthesis of the rhenium complexes **4** and **5**.

rhenate by triphenylphosphane in the presence of **1** in an ethanol/water solution made acidic by hydrochloric acid. Preliminary investigations show, moreover, that the rate of reaction is highly dependent on the type of the phosphane and is particularly high with alkylphenyl substituted phosphanes.[12] We found no indication for the formation of octahedral diphosphane complexes of the type $[Re(\mathbf{1})(PPh_3)_2]$.

Aside from perrhenate, Re^{III} compounds are also suitable starting reagents for the synthesis of trigonal-bipyramidal mixed-ligand Re^{III} complexes. In addition, these also provide a simple route to complexes in which the axial phosphane is replaced by an isocyanide ligand. Re^{III} complexes of the type *mer*-$[ReCl_3(PPh_3)_2(R{-}NC)]$ may be obtained by the exchange of acetonitrile in $[ReCl_3(PPh_3)_2(MeCN)]$ or by an excess of isocyanide in the combined reduction/substitution of $[Re^{V}OCl_3(PPh_3)_2]$.[12, 13] They react with **1** to give the complexes **5** (Scheme 3). Alternatively, **5** can also be obtained starting from $[ReCl_3(PPh_3)_2(MeCN)]$ in a "one pot" synthesis with an equimolar mixture of **1**/R−NC. In both cases an octahedral Re^{III} complex changes into a trigonal-bipyramidal complex on coordination of the ligand **1**, which confirms once again the preference for this coordination geometry in complexes of **1**. The most simple preparative method of obtaining **5** is, however, the direct exchange of the phosphane ligand in **4** for one equivalent of isocyanide in CH_2Cl_2.[5]

Compounds **4** and **5a** were characterized by X-ray structure analysis (Fig. 2).[9] Both complexes have trigonal-bipyramidal geometry. The molecular parameters of **4** are very similar to those of **2**. In the molecular structure of **5a**, the large deviation

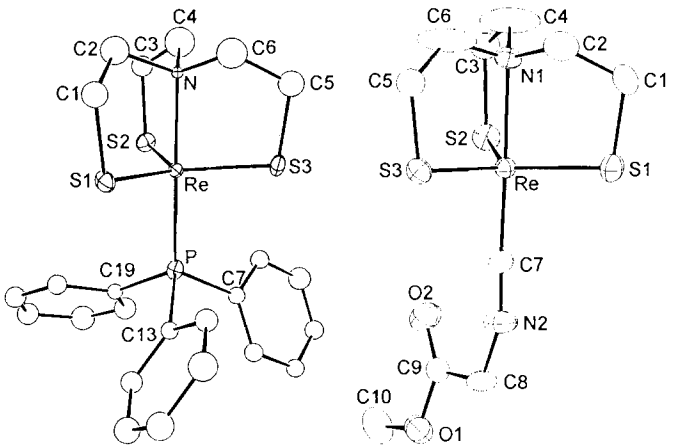


Fig. 2. Structure of the complexes **4** (left) and **5a** (right) in the crystal (ORTEP). Selected distances [Å] and angles [°] in **4**: Re-S1 2.243(6), Re-S2 2.222(6), Re-S3 2.240(6), Re-P 2.306(7), Re-N 2.18(2); S1-Re-S2 120.4(2), S1-Re-S3 119.3(2), S1-Re-P 93.6(2), S1-Re-N 85.2(5), S2-Re-S3 118.3(2), S2-Re-P 95.3(2), S2-Re-N 86.4(5), S3-Re-P 95.1(2), S3-Re-N 84.3(4), P-Re-N 178.2(5); in **5a**: Re-S1 2.231(2), Re-S2 2.235(2), Re-S3 2.238(2), Re-N1 2.231(7), Re-C7 1.905(9), C7-N2 1.200(12); S1-Re-S2 118.87(8), S1-Re-S3 119.31(8), S1-Re-N1 85.2(2), S1-Re-C7 96.1(2), S2-Re-S3 119.74(8), S2-Re-N1 85.3(2), S2-Re-C7 94.6(3), S3-Re-N1 85.2(2), S3-Re-C7 93.8(3), N1-Re-C7 178.7(3), Re-C7-N2 173.9(8), C7-N2-C8 150.8(9) [9].

of the C7–N2–C8 angle from the expected linearity [150.8(9)°] and the length of the C7–N2 bond [1.200(12) Å] (expected value approximately 1.150 Å) are particularly noticeable. These indicate, together with the very low wavenumber for the IR absorption of the NC stretching vibration (1940 cm^{-1}), a strengthened back bond to the isocyanide carbon atom from the rhenium atom, which, due to the coordination by sulfur, is very electron-rich. The great extent of the bending of an isocyanide due to coordination to an electron-rich transition metal has previously only rarely been observed in such clarity.[14]

With the complexes **2**, **4**, and **5**, we present a new type of neutral, trigonal-bipyramidal, mixed-ligand complex of Tc^{III} and Re^{III}. A similar coordination geometry is only to be found in the complex [Tc(PS_3)(*i*PrNC)] with the aromatic trithiol tripod PS_3.[10b] The complex **5a** is of special interest for further investigations. In principle, complexes of this type could be coupled to molecules with a specific biodistribution by the formation of an amide via the ester function, as has already been demonstrated for the $^{99m}Tc^{V}O$ complex of the tetradentate ligand 6-*p*-aminobenzyl-3,3,9,9-tetramethyl-4,8-diazaundecane-2,10-dionedioxime (PnAO).[3] The chelate unit in **5a** is less polar than in the square-pyramidal [TcO(PnAO)], however. For radiopharmaceutical preparations of complexes of the type **5a**—starting from MO_4^- reagents—the reaction conditions would have to be modified. We are currently investigating the possibility of coupling technetium and rhenium to biological anchor groups on the basis of the concept described above.

Received: January 13, 1994 [Z6616IE]
German version: *Angew. Chem.* **1994**, *106*, 1416

[1] S. Jurisson, D. Berning, W. Jia, D. Ma, *Chem. Rev.* **1993**, *93*, 1137–1156.
[2] J. Burgess, *Transition Met. Chem.* **1993**, *18*, 439–448.
[3] P. Koch, H. R. Mäcke, *Angew. Chem.* **1992**, *104*, 1492–1494; *Angew. Chem. Int. Ed. Engl.* **1992**, *31*, 1507–1509.
[4] a) F. E. Hahn, S. Rupprecht, K. H. Moock, *J. Chem. Soc. Chem. Commun.* **1991**, 224–225; b) F. E. Hahn, S. Rupprecht, *Chem. Ber.* **1991**, *124*, 481–486.
[5] Correct elemental analyses for **1**, **2**, **4**–**5**. Selected spectroscopic data for **1**: IR(KBr): ν[cm^{-1}] = 2543 (SH); $^{13}C\{^1H\}$ NMR (62.9 MHz, $CDCl_3$): δ = 57.01 (NCH_2), 22.81 (H_2CSH). – **2**: ^1H NMR (90 MHz, $CDCl_3$): δ = 7.35 (m, 15H; Ph-H), 2.97 (m, 12H; S-CH_2 and N-CH_2); UV/VIS($CHCl_3$): λ_{max}(lg ε) = 541 (2.7), 510 (sh), 347 (3.4), 290 (4.2) nm. **3**: Yield approx. 10%. The presumed composition results from the integrals in the ^1H NMR spectrum. **4**: Yield 57%, dark green needles from toluene; ^1H NMR (200 MHz, CD_2Cl_2): δ = 7.2 (m, 15H; Ph-H), 2.9 (m, 12H; S-CH_2 and N-CH_2); UV/VIS(CH_2Cl_2): λ_{max}(lg ε) = 598 (2.5), 461 (3.2), 334 (sh, 3.4), 306 (4.1), 247 (4.3) nm; MS (EI, 70 eV): m/z = 643 (M^+). – **5a**: yield 86%, brown rhombuses from CH_2Cl_2/Et_2O; IR(KBr): ν[cm^{-1}] = 1940 (NC); ^1H NMR (90 MHz, $CDCl_3$): δ = 5.46 (s, 2H; CH_2CO_2), 3.81 (s, 3H; OCH_3), 3.02 (m, 12H; S-CH_2 and N-CH_2); UV/VIS(CH_2Cl_2): λ_{max}(lg ε) = 570 (sh, 2.3), 437 (3.1), 355 (3.0), 314 (3.8), 251 (4.2) nm. – **5b**: yield 64%, olive-green platelets aus Ethanol; IR(KBr): ν[cm^{-1}] = 1976 (NC); ^1H NMR (90 MHz, $CDCl_3$): δ = 2.98 (m, 12H; S-CH_2 and N-CH_2), 1.54 (s, 9H; CH_3); UV/VIS(CH_2Cl_2): λ_{max}(lg ε) = 600 (sh, 2.4), 448 (3.1), 350 (3.1), 312 (4.0), 250 (4.2) nm.
[6] a) J. Y. Gauthier, F. Bourdon, R. N. Young, *Tetrahedron Lett.* **1986**, *27*, 15–18; b) P. A. Bobbio, *J. Org. Chem.* **1961**, *26*, 3023–3024.
[7] G. Bandoli, D. A. Clemente, U. Mazzi, E. Roncari, *J. Chem. Soc. Dalton Trans.* **1982**, 1381–1384.
[8] R. A. Pearlstein, W. M. Davis, A. G. Jones, A. Davison, *Inorg. Chem.* **1989**, *28*, 3332–3334.
[9] Structure analyses: red-violet crystals of **2** were obtained by evaporation of the solvent from a benzene/methanol solution. Crystals of **4** (crystallized from toluene) were very thin, air-sensitive platelets. The diffraction data for this compound were therefore measured at −100(5) °C. After measuring all symmetry-independent intensities in the 2θ range of 5.4–40°, crystal decomposition was observed and the data collection had to be interrupted. Only a relatively small data set was thus available. For this reason, only the Re, P, and S atoms were refined with anisotropicic thermal parameters in the least-squares procedure. While the quality of the diffraction data does not allow a detailed discussion of the bond lengths and angles in **4**, it is sufficient to allow an unequivocal determination of the geometry of the molecule. Compound **5a** can be crystallized from CH_2Cl_2/Et_2O. Structure parameters: **2** [**4**] {**5a**}: $C_{24}H_{27}NPS_3Tc$ [$C_{24}H_{27}NPReS_3$] {$C_{10}H_{17}N_2O_2ReS_3$}, monoclinic [monoclinic] {monoclinic}, space group $P2_1/c$ [$P2_1/n$] {$P2_1/c$}, a = 8.906(2) [10.855(3)] {7.827(4)}, b = 25.804(6) [16.707(4)] {13.866(3)}, c = 11.061(4) [15.441(5)] {13.627(6)} Å, β = 108.42(2) [92.62(2)] {93.19(7)}°, V = 2414(2) [2797(2)] {1476(2)} $Å^3$, Z = 4 [4] {4}, $\rho_{exp.}$ = 1.53 [1.53] {2.17}, $\rho_{ber.}$ = 1.527 [1.526] {2.157} $g\,cm^{-3}$, $Mo_{K\alpha}$ radiation (λ = 0.71073 Å), $\mu(Mo_{K\alpha})$ = 9.1 [46.8] {87.4} cm^{-1}, 4233 [2592] {2589} symmetry-independent data measured at 20(5) [−100(5)] {20(5)} °C in the 2θ range 2–50 [5.4–40] {2–50}. Structure solution with Patterson methods, refinement of the position parameters of all non-hydrogen atoms with anisotropicic thermal parameters (in **4** only Re, S, P anisotropicic). All hydrogen atoms on calculated positions [d(C–H) = 0.95 Å] with $B_{eq(H)} \approx 1.3\,B_{eq(C)}$. R = 3.73 [6.51] {4.10}, R_w = 4.56 [8.93] {6.09} for 2410 [1824] {2350} structure factors $F_o^2 \geq 3\sigma(F_o^2)$ and 271 [147] {163} variables, absorption correction for **4** and **5a**. Further details of the crystal structure investigation may be obtained from the Fachinformationszentrum Karlsruhe, D-76344 Eggenstein-Leopoldshafen (FRG) on quoting the depository number CSD-58128, the names of the authors, and the journal citation.
[10] a) H.-J. Pietzsch, H. Spies, S. Hoffmann, *Inorg. Chim. Acta* **1990**, *168*, 7–9; b) N. de Vries, J. Cook, A. G. Jones, A. Davison, *Inorg. Chem.* **1991**, *30*, 2662–2665.
[11] M. Melnik, J. E. van Lier, *Coord. Chem. Rev.* **1987**, *77*, 275–324.
[12] H. Spies, M. Glaser, F. E. Hahn, T. Lügger, unpublished.
[13] R. Richards, G. Rouschias, *J. Am. Chem. Soc.* **1976**, *98*, 5729–5731.
[14] J.-M. Bassett, D. E. Berry, G. K. Barker, M. Green, J. A. K. Howard, F. G. A. Stone, *J. Chem. Soc. Dalton Trans.* **1979**, 1003–1011.

Equilibrium between Isocyanide and Carbene Complexes in Coordination Compounds of 2,6-Dihydroxyphenyl Isocyanide**

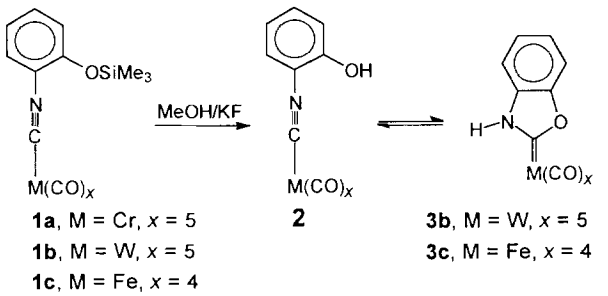
F. Ekkehardt Hahn,* Matthias Tamm, and Thomas Lügger

We reported recently on the reactions of $Fe(CO)_4$ and $M(CO)_5$ complexes (M = Cr, W) of 2-trimethylsiloxyphenyl isocyanide (**1**).[1] After hydrolysis of the Si–O bond, these react by intramolecular attack of the hydroxy group on the isocyanide carbon

[*] Prof. Dr. F. E. Hahn, Dr. M. Tamm, Dipl.-Chem. T. Lügger
Institut für Anorganische und Analytische Chemie der Freien Universität
Fabeckstrasse 34-36, D-14195 Berlin (FRG)
Telefax: Int. code + (30)838-2424

[**] This work was supported by the Deutsche Forschungsgemeinschaft and the Fonds der Chemischen Industrie. We thank the BASF Aktiengesellschaft for a doctoral grant (1991–1993) for M. T.

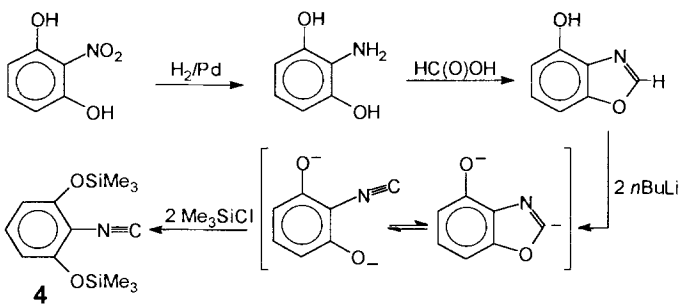
to form carbene complexes **3** (Scheme 1).[2, 3] The intermediately formed complex **2** could not be isolated. The driving force for the intramolecular reaction is the stability of the cyclic carbene ligand in **3**, which has a five-membered aromatic heterocycle.



Scheme 1. Reaction of coordinated 2-trimethylsiloxyphenyl isocyanide upon cleavage of the Si–O bond.

Normally, the intramolecular carbene formation from 2-hydroxyphenyl isocyanide is hindered when the latter is coordinated to a particularly electron-rich transition metal fragment. The nucleophilic attack of the oxygen atom on the isocyanide carbon atom is then made difficult, as this is deactivated by (d–p) π back bonding. In such cases, a mixture of isocyanide (**2**) and carbene (**3**) complexes is obtained.[4] The strength of the (d–p) π back bond, and consequently the position of the equilibrium between the complexes of types **2** and **3**, may be predicted from the force constant for the N≡C triple bond as calculated according to Cotton.[5]

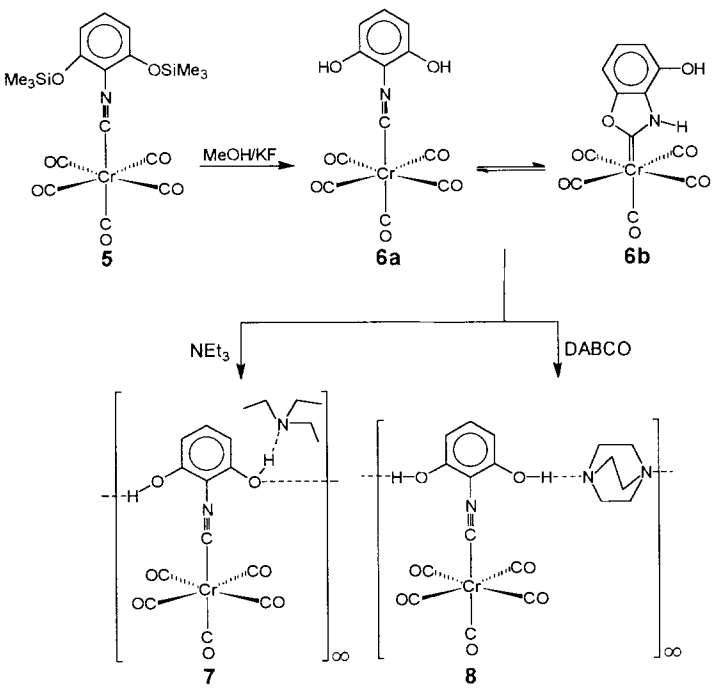
We have now investigated the behavior of the doubly trimethylsiloxy-substituted ligand 2,6-bis(trimethylsiloxy)phenyl isocyanide (**4**) coordinated to Cr(0), after hydrolysis of the Si–O bonds. In this case, a mixture is obtained in which the isocyanide (**6a**) and the carbene (**6b**) complexes are in equilibrium with one another (cf. Scheme 3). We report here on a new way of shifting the equilibrium completely to the side of either the isocyanide or the carbene, without altering the electronic properties of the metal center.



Scheme 2. Synthesis of the ligand **4**.

For the synthesis of the ligand **4** (Scheme 2),[6] the nitro group of commercially available nitroresorcinol is first reduced with Pd/H_2 and the resulting primary amine converted into 4-hydroxybenzoxazol according to Erlenmeyer et al.[7] After double deprotonation with two equivalents of *n*BuLi, this reacts regiospecifically with trimethylchlorosilane under *O*-silylation, as is known for benzoxazol.[1]

The reaction of **4** with $[Cr(CO)_5(thf)]$ leads to the isocyanide complex **5**.[8] This reacts after cleavage of the Si–O bonds to give a mixture containing the isocyanide complex **6a** and the carbene complex **6b**[9] (Scheme 3). The force constant for the N≡C stretching vibration in **6a** (1724 Nm^{-1}, calculated from the IR absorption measured in the mixture) indicates strong back bonding to the isocyanide carbon in **6a**, and explains the incomplete carbene formation. For comparison: Because of the weaker (d–p) π back bonding in **1c**, a force constant of 1791 Nm^{-1} was calculated,[2] and complete conversion into the carbene complex **3c** is observed on cleavage of the Si–O bond.[2] The mixture **6a/6b** can also be characterized quantitatively by ^1H NMR spectroscopy.[9] In the spectrum, resonances are found for the N*H* proton in **6b** at $\delta = 13.68$ and for the O*H* protons in **6a** and **6b** at $\delta = 9.57$. The amounts of the components in the mixture were determined from the integrals (59% **6a** and 41% **6b**).



Scheme 3. Reaction of a mixture of **6a/6b** with weak bases.

The reaction of isocyanide complexes with alcohols resulting in the formation of carbene complexes is normally catalyzed by bases.[10] In contrast to this, we found that by selection of specific bases, a stabilization of the coordinated 2,6-dihydroxyphenyl isocyanide is possible, even against the preferred intramolecular nucleophilic attack.

If two equivalents of triethylamine are added to a solution of the **6a/6b** mixture in dichloromethane, the expected shift in equilibrium to the carbene side is not observed. After removal of solvent, a colorless powder is obtained whose infrared spectrum shows exclusively absorptions for a pentacarbonyl(isocyanide)chromium complex (cf. **7**; $\nu(NC) = 2154\ cm^{-1}$).[11] The ^1H NMR spectrum of this complex contains signals which indicate the formation of a 1:2 adduct **6a**·$2NEt_3$. The reaction of the **6a/6b** mixture with one equivalent of the dibasic amine 1,4-diazabicyclo[2.2.2]octane (DABCO) proceeds similarly (exclusive formation of an isocyanide complex **6a**·DABCO; cf. **8**; $\nu(NC) = 2149\ cm^{-1}$).[11] The isocyanide complex **6a** is obviously stabilized by the addition of these amine bases to such an extent that the equilibrium **6a/6b** is shifted completely to the side of

 © VCH Verlagsgesellschaft mbH, D-69451 Weinheim, 1994 0570-0833/94/1313-1357 $ 10.00+.25/0

the pentacarbonyl(2,6-dihydroxyphenylisocyanide)chromium–amine adduct.

In order to understand the mechanism of the unusual stabilization of 2,6-dihydroxyphenyl isocyanide complexes by amine bases, X-ray structure analyses of the triethylamine and the DABCO adducts of **6a** were carried out.[1,2] These show that in both cases the isocyanide complex is stabilized by the formation of N···H hydrogen bridges to the hydroxy protons. In contrast to the structure in solution, crystals of the triethylamine adduct contain only one molecule of triethylamine per molecule **6a**, and consequently this complex can be formulated as **6a**·NEt_3 (**7**; Fig. 1, left).[1,3] Complex **7** crystallizes, polymerized through hydrogen bridges, as shown in Scheme 3. Crystals of the product of the reaction of **6a**/**6b** with DABCO consist of hydrogen-bridged polymers **6a**·DABCO (**8**, Scheme 3; Fig. 1, right).[1,3]

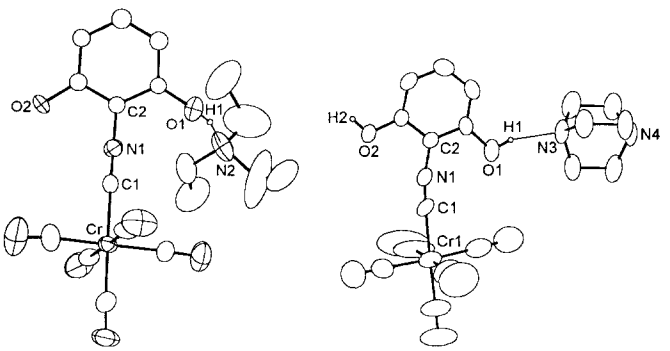


Fig. 1. Structures of the complexes **7** (left) and **8** (right) in the crystal (ORTEP). The asymmetric unit of **8** contains two almost identical molecules and one acetone molecule (not shown). Selected distances [Å] and angles [°] for **7**: Cr-C1 1.977(12), C1-N1 1.164(13), N1-C2 1.396(14), O1-H1 1.28(13), H1···N2 1.38(12), O1···N2 2.634(14), O1···O2* 2.525(11); Cr-C1-N1 177.7(10), C1-N1-C2 172.8(12), O1-H1···N2 164(8). The position of the H atom bonded to O2 could not be determined, symmetry code (*)x, 1/2−y, 1/2 + z; for **8**·0.5$(CH_3)_2CO$ (molecule 1, see [13] for further data): Cr1-C1 1.989(8), C1-N1 1.145(8), N1-C2 1.391(8), O1-H1 0.79(6), H1···N3 1.93(6), O1···N3 2.668(7), O2-H2 0.80(6), H2···N4* 1.87(6), O2···N4* 2.667(6); Cr1-C1-N1 176.3(6), C1-N1-C2 168.7(6), O1-H1···N3 154(7), O2-H2···N4* 170(6), symmetric code (*) x, 1/2 − y, 1/2 + z.

The use of weak bases (the pK_s values of phenol and the tertiary amines employed are of the same order of magnitude) obviously does not lead to deprotonation of the hydroxy groups and an increase in their nucleophilicity, but rather to the formation of hydrogen bridges and thus to the stabilization of the isocyanide complexes. A shift of the **6a**/**6b** equilibrium completely to the side of the isocyanide complexes stabilized by O–H···N hydrogen bonds is thereby achieved.

Attempts to shift the equilibrium to the carbene side must therefore be carried out with stronger bases which are capable of completely deprotonating the hydroxy groups. If a mixture of **6a**/**6b** is treated with two equivalents KO*t*Bu, and the dianion thus formed is then alkylated with two equivalents of methyl iodide, the *N*,*O*-dimethylated carbene complex **10** can be obtained in good yield (Fig. 2). The *N*-methylated complex **9** formed as intermediate can be obtained by the addition of only one equivalent of KO*t*Bu and MeI. After deprotonation, the phenolic oxygen atom of **6a** is sufficiently nucleophilic to allow the intramolecular cycloaddition to proceed to completion. The subsequent alkylation of the anion prevents the reverse reaction leading to the isocyanide complex, and a complete shift of the **6a**/**6b** equilibrium to the side of the mono- or dimethylated carbene complex is achieved.[2,3]

With the synthesis of the complexes **7**, **8**, and **10**, we present a procedure for the selective displacement of the **6a**/**6b** equilibrium between the isocyanide and carbene complexes by means of suitable bases. The complexes **7** and **8** are the first examples for which the normally preferred intramolecular carbene formation in coordinated 2-hydroxyphenyl isocyanides could be prevented.[2,3] This is the first time that such isocyanide complexes have been successfully stabilized without alteration of the electronic properties or the steric situation at the metal atom. Conversely, the carbene complexes **9** and **10** can be isolated when the $N-C_{carbene}$ atom in a mixture of **6a**/**6b** is alkylated by reaction with strong bases and MeI.

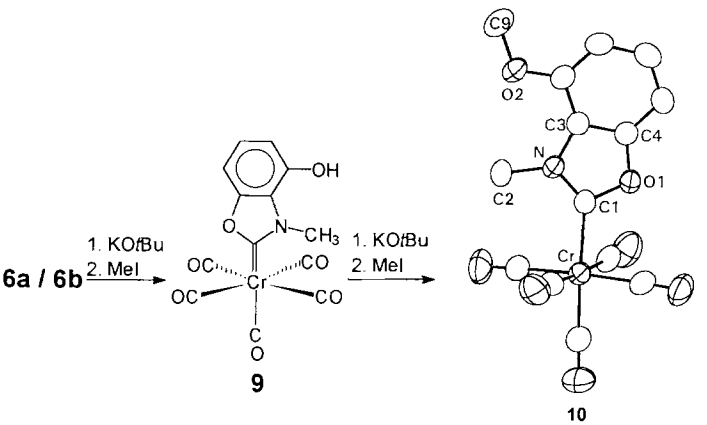


Fig. 2. Synthesis of the complexes **9** and **10** and the structure of **10** in crystals (ORTEP). Selected distances [Å] and angles [°]: Cr-C1 2.070(3), C1-O1 1.369(4), C1-N 1.343(4), O1-C4 1.379(4), N-C2 1.464(4), N-C3 1.399(4); Cr-C1-O1 118.6(2), Cr-C1-N 135.3(2), O1-C1-N 106.1(3), C1-N-C2 124.9(3), C1-N-C3 111.0(3), C2-N-C3 124.1(3) [13].

Received: January 28, 1994 [Z.6652IE]
German version: *Angew. Chem.* **1994**, *106*, 1419

[1] P. Jutzi, U. Gilge, *J. Organomet. Chem.* **1983**, *246*, 159–162.
[2] F. E. Hahn, M. Tamm, *J. Chem. Soc. Chem. Commun.* **1993**, 842–844.
[3] F. E. Hahn, M. Tamm, *J. Organomet. Chem.* **1993**, *456*, C11–C14.
[4] F. E. Hahn, M. Tamm, T. Lügger, unpublished.
[5] F. A. Cotton, C. S. Kraihanzel, *J. Am. Chem. Soc.* **1962**, *84*, 4432–4438.
[6] **4**: Correct elemental analysis. For the synthesis, 4-hydroxybenzoxazol [7] (10 g, 74 mmol) was dissolved in anhydrous THF (200 mL) at −78 °C. *n*BuLi (60 mL of a 2.5 M solution in hexane, 150 mmol) was added slowly by syringe. The monolithiated salt started to precipitate during the addition of the first half of the *n*BuLi. Further addition of *n*BuLi caused the precipitate to redissolve, however. After complete addition, stirring was continued for a further 3 h at −78 °C. Me_3SiCl (20 mL, 158 mmol) was subsequently added to the reaction mixture, and the clear brown solution was stirred for about 12 h at room temperature. All volatile components were then removed under vacuum. *n*-hexane (100 mL) was added, and the insoluble LiCl filtered off. The brown solution in *n*-hexane was concentrated by removing the solvent under reduced pressure; **4** was obtained as a colorless oil by distillation at 85 °C/0.06 mbar. Yield 18.73 g (91%). IR (KBr film): ν[cm^{-1}] = 2125 (NC); ^{1}H NMR (270 MHz, $CDCl_3$): δ = 7.09 (t, 1H; Ar-H), 6.52 (d, 2H; Ar-H), 0.32 (s, 18H, CH_3); $^{13}C\{^1H\}$ NMR (67.93 MHz, $CDCl_3$): δ = 170.3 (NC), 152.4 (Ar-C-O), 129.1 (*p*-Ar-C), 113.1 (*o*-Ar-C), 0.1 (Si-C), the signal Ar-*C*-NC was not observed.
[7] E. Sorkin, W. Roth, H. Erlenmeyer, *Helv. Chim. Acta* **1952**, *35*, 1736–1741.
[8] **5**: correct elemental analysis. Selected analytical data: green oil, yield 8.1 g (96%); IR (KBr-film): ν[cm^{-1}] = 2149 (s, NC), 2060 (s, CO), 1992 (sh, CO), 1945 (vs, br, CO); ^{1}H NMR (270 MHz, $CDCl_3$): δ = 7.06 (t, 1H; Ar-H), 6.50 (d, 2H; Ar-H), 0.32 (s, 18H; CH_3); $^{13}C\{^1H\}$ NMR (62.90 MHz, $CDCl_3$): δ = 217.1 (*trans*-CO), 214.8 (*cis*-CO), 174.0 (NC), 152.7 (Ar-C-O), 129.1 (*p*-Ar-C), 113.0 (*o*-Ar-C), 0.1 (Si-C), the signal Ar-*C*-NC signal was not observed; MS (70 eV): m/z 471 (M^+, 8.0%), 331 (M^+ − 5 CO, 100).
[9] Mixture **6a**/**6b**: For the preparation, **5** (8.1 g, 17 mmol) was dissolved in anhydrous methanol (50 mL). A small sample of KF (0.2 g) was added, and the mixture was stirred at room temperature for 2 d. All volatile components were removed under vacuum, and a colorless powder was obtained. After chromatographic purification (Al_2O_3, 4% H_2O, methanol:diethyl ether 1:1), a mixture of **6a**/**6b** (5.3 g, 95%) was obtained. Selected analytical data: IR (KBr): ν[cm^{-1}] = 3526 (m, NH **6b**), 3379 (m, OH **6a**,**b**), 2128 (s, NC **6a**), the bands for the CO absorptions could neither be resolved nor assigned; ^{1}H NMR

(250 MHz, [D$_6$]acetone): δ = 13.68 (s, br, 1H; NH **6a**), 9.57 (s, 3H; OH **6a**, **6b**), 7.25 (d, 2H; Ar-H **6b**), 7.10 (t, 1H; Ar-H **6a**), 6.89 (t, 1H; Ar-H **6b**), 6.56 (d, 2H; Ar-H **6a**); ^{13}C{^{1}H} NMR (62.90 MHz, [D$_3$COD]: δ = 230.0 (carbene-C), 222.7 (*trans*-CO **6b**), 218.8 (*trans*-CO **6a**), 218.2 (*cis*-CO **6b**), 216.0 (*cis*-CO **6a**), 175.6 (NC **6a**), 155.9, 130.7, 107.4, 106.9 (Ar-C **6a**), 156.0, 126.1, 114.4, 121.1, 111.6, 102.3 (Ar-C **6b**); MS (70 eV): *m/z* 327 (M^+ **6a**, **6b**, 17.0%), 187 (M^+ − 5CO, 100).

[10] a) K. H. Dötz, H. Fischer, P. Hofmann, F. R. Kreissl, U. Schubert, K. Weiss, *Transition Metal Carbene Complexes*, VCH, Weinheim, **1983**; b) B. Crociani in *Reactions of Coordinated Ligands, Vol. 1* (Ed.: P. S. Braterman), Plenum Press, New York, **1985**.

[11] Correct elemental analysis for **7**–**10**. **7**: ^{1}H NMR (250 MHz, [D$_6$]acetone, 1:2-triethylamine adduct): δ = 7.02 (m, 3H; Ar-H), 2.88 (quart, 12H; NCH_2), 1.15 (t, 18H; CH_2-CH_3), O-H-Resonance signal was not observed; IR (KBr, of the crystalline solid **7**): ν[cm^{-1}] = 3418 (m, O-H···N), 2154 (m, NC), 2062 (s, CO), 1988 (sh, CO), 1914 (vs br, CO). – **8**: ^{1}H NMR (250 MHz, [D$_6$]acetone): δ = 7.08 (m, 3H; Ar-H), 2.89 (s, 12H; NCH_2); IR (KBr): ν[cm^{-1}] = 3421 (m, O-H···N), 2149 (m, NC), 2061 (s, CO), 1990 (sh, CO), 1922 (vs br, CO). – **10**: ^{1}H NMR (250 MHz, $CDCl_3$): δ = 7.18 (t, 1H; Ar-H), 6.80 (d, 2H; Ar-H), 4.26 (s, 3H: NCH_3), 3.97 (s, 3H; OCH_3); ^{13}C{^{1}H} NMR (62.90 MHz, CD_2Cl_2): δ = 231.1 (carbene-C), 222.3 (*trans*-CO), 217.7 (*cis*-CO), 155.3, 147.2, 126.7, 122.6, 107.6, 104.2 (Ar-C), 57.0 (OCH_3), 37.4 (NCH_3); MS (70 eV): *m/z* 355 (M^+, 13.0%).

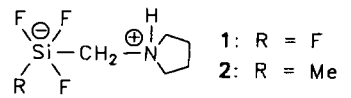
[12] The size and the scattering power of crystals of **7** were very small. For this reason, only a limited data set with $F_o^2 \geq 3\sigma(F_o^2)$ was available for the calculations. In order to keep the number of refinement parameters small, the six atoms of the aromatic ring were refined with isotropic thermal parameters. Crystals of **8** contained two almost identical molecules of **8** and one acetone molecule (the methyl groups of which were disordered) in the asymmetric unit. Structure parameters: **7** [**8**·0.5$(CH_3)_2CO$] {**10**}: $C_{18}H_{20}CrN_2O_7$ [$C_{19.5}H_{20}CrN_3O_{7.5}$] {$C_{14}H_9CrNO_7$}, monoclinic [orthorhombic] {monoclinic}, space group $P2_1/c$ [*Pbca*] {$P2_1/n$}, a = 12.713(8) [18.200(5)] {6.885(3)}, b = 15.328(8) [21.691(6)] {13.969(4)}, c = 11.950(6) [23.700(4)] {15.772(3)} Å, β = 117.92(4) [90.0] {97.83(2)}°, V = 2058(4) [9356(7)] {1502.8(14)} Å^3, Z = 4 [16] {4}, $\rho_{exp.}$ = 1.37 [1.32] {1.58}, $\rho_{calcd.}$ = 1.383 [1.330] {1.570} g cm^{-3}, $Mo_{K\alpha}$ radiation (λ = 0.71073 Å), $\mu(Mo_{K\alpha})$ = 5.8 [5.2] {7.8} cm^{-1}, 2688 [5821] {2641} symmetry-independent data measured at −100(5) [20(5)] {20(5)} °C in the 2θ range 2–45 [2–45] {2–50}°. Structure solution with Patterson methods, refinement of the position parameters of all non-hydrogen atoms with anisotropicic thermal parameters (ring atoms in **7** isotropic). C–H atomic positions calculated [d(C–H) = 0.95 Å] with $B_{eq(H)} = 1.3\,B_{eq(C)}$; no hydrogen atoms were calculated for acetone in **8**·0.5$(CH_3)_2CO$; H 1 in **7** and all O–H in **8**·0.5$(CH_3)_2CO$ were found and refined with constant B_{eq} = 4.0 Å^2. R = 4.90 [6.95] {3.76}, R_w = 6.14 [9.06] {4.85} for 901 [3551] {1764} structure factors $F_o^2 \geq 3\sigma(F_o^2)$ [absorption correction for **7** and **8**·0.5$(CH_3)_2CO$] and 226 [559] {208} variables.

[13] Further details of the crystal structure investigation may be obtained from the Fachinformationszentrum Karlsruhe, D-76344 Eggenstein-Leopoldshafen (FRG) on quoting the depository numcaled CSD-58127 and the journal citation.

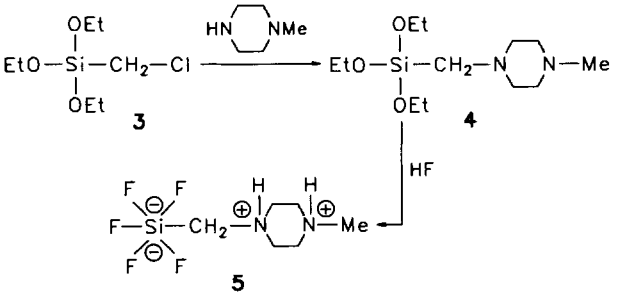
Hexacoordinate Silicon in a Compound with an F_5SiC Unit**

Reinhold Tacke* and Mathias Mühleisen

Anions with penta- and hexacoordinate silicon such as $[RSiF_4]^-$, $[RSiF_5]^{2-}$, and $[R_2SiF_4]^{2-}$ (R = organic substituent) have been known for about thirty years.[1] More recently salts containing the anions $[R_2SiF_3]^-$ [2] and $[R_3SiF_2]^-$ [2c, 3] have also been reported. Whereas the aforementioned λ^6Si-organofluorosilicates have not been structurally characterized, the structural chemistry of λ^5Si-organofluorosilicates has been investigated in great detail in the past few years.[4] We have recently extended these studies with investigations on zwitterionic (molecular) λ^5Si-organofluorosilicates[5] (examples: zwitterions **1**[5a] and **2**[5d]). We report here on the synthesis and structural characterization of **5**·H_2O, the first zwitterionic λ^6Si-organofluorosilicate. The zwitterion **5** is the first molecular compound of hexacoordinate silicon with an F_5SiC unit and contains a hexacoordinate (formally twofold negatively charged) Si atom and two tetracoordinate (formally single positively charged) N atoms. The crystal structure analysis of **5**·H_2O is the first solid-state structural characterization of an λ^6Si species with an F_5SiC unit.



The λ^6Si-silicate **5** was prepared by the reaction of (chloromethyl)triethoxysilane (**3**)[6] with 1-methylpiperazine to yield silane **4**, which was treated with hydrofluoric acid; the product was isolated as monohydrate **5**·H_2O.



Compound **5**·H_2O crystallizes in the space group $P\bar{1}$ with one pair each of crystallographically independent zwitterions and water molecules in the asymmetric unit.[7] The crystal structure is dominated by intermolecular N–H···F and O–H···F hydrogen bonds. All of the donor functions are involved in the three-dimensional hydrogen-bonding network, which has a marked surplus of acceptor functions (donor/acceptor ratio 8:34). The structures of the two independent zwitterions (Fig. 1) are very similar. The Si–C distances [194.6(1) and 194.3(2) pm] are distinctly greater than those in the zwitterionic λ^5Si-organofluoro-

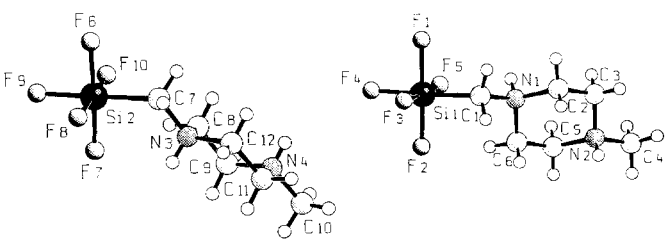


Fig. 1. Structures of the crystallographically independent zwitterions in the crystal of **5**·H_2O. Selected distances [pm] and angles [°] (standard deviations in parentheses): Si1-F1 174.0(1), Si1-F2 168.5(1), Si1-F3 171.6(1), Si1-F4 169.0(1), Si1-F5 170.8(1), Si1-C1 194.6(1); F1-Si1-F2 177.59(5), F1-Si1-F3 89.27(5), F1-Si1-F4 87.73(5), F1-Si1-F5 87.47(5), F1-Si1-C1 89.54(5), F2-Si1-F3 91.40(5), F2-Si1-F4 89.97(5), F2-Si1-F5 91.81(5), F2-Si1-C1 92.79(5), F3-Si1-F4 88.31(5), F3-Si1-F5 176.56(5), F3-Si1-C1 89.02(5), F4-Si1-F5 90.45(5), F4-Si1-C1 176.21(5), F5-Si1-C1 92.06(5). – Si2-F6 171.7(1), Si2-F7 168.8(1), Si2-F8 172.9(1), Si2-F9 169.2(1), Si2-F10 170.5(1), Si2-C7 194.3(2); F6-Si2-F7 177.87(5), F6-Si2-F8 89.24(5), F6-Si2-F9 88.13(5), F6-Si2-F10 89.69(5), F6-Si2-C7 89.33(5), F7-Si2-F8 89.59(5), F7-Si2-F9 90.04(5), F7-Si2-F10 91.38(5), F7-Si2-C7 92.47(5), F8-Si2-F9 87.82(5), F8-Si2-F10 176.57(5), F8-Si2-C7 91.03(5), F9-Si2-F10 88.89(5), F9-Si2-C7 177.23(6), F10-Si2-C7 92.21(5).

[*] Prof. Dr. R. Tacke, Dipl.-Chem. M. Mühleisen
Institut für Anorganische Chemie der Universität
Engesserstrasse, Geb. 30.45, D-76128 Karlsruhe (FRG)
Telefax: Int. code + (721)608-4290

[**] This work was supported by the Deutsche Forschungsgemeinschaft and the Fonds der Chemischen Industrie. We thank Priv.-Doz. Dr. A. Sebald, Bayerisches Geoinstitut/Universität Bayreuth, for the measurement of the ^{29}Si CP/MAS NMR spectrum.

silicates investigated previously.[5] In contrast, the Si–F distances [168.5(1)–174.0(1) pm] are comparable in length to the axial Si–F bonds in the latter compounds.[5] Similar distances were also determined for the $[SiF_6]^{2-}$ ion (typically in the region of 168–170 pm).[4a] The bond angles in $\mathbf{5}\cdot H_2O$ deviate only slightly from the ideal values of 180° [maximum deviation 3.8 and 3.4°] and 90° [maximum deviation 2.8 and 2.5°], and thus the coordination polyhedra around the two Si atoms may be described as only slightly distorted octahedra. The relevant structural parameters are listed in the legend to Figure 1.

NMR spectroscopic investigations[8] have shown that **5** is also present as a zwitterion in solution (D_2O, [D_6]DMSO). The presence of the quaternary ammonium centers can be inferred indirectly from the chemical shifts of the ring protons in D_2O and [D_6]DMSO and from the detection of the NH protons in [D_6]DMSO. The hexacoordination at silicon is demonstrated indirectly by the ^{19}F NMR spectrum of **5** in D_2O (two signals with an intensity ratio of 4:1); in contrast, the spectrum of **5** in [D_6]DMSO shows only a relatively broad ^{19}F resonance signal, which could indicate dynamic molecular processes. ^{29}Si NMR spectra of **5** in D_2O and [D_6]DMSO could not be obtained (^{29}Si CP/MAS NMR: $\delta = -177.2$).

Experimental Procedure

4: A solution of **3** [6] (16.9 g, 79.4 mmol), 1-methylpiperazine (7.95 g, 79.4 mmol), and triethylamine (12.1 g, 120 mmol) in toluene (200 mL) was stirred under reflux for 24 h and then at room temperature for 48 h. Solvent and unreacted triethylamine were removed under reduced pressure, and the residue was treated with *n*-pentane (300 mL). The precipitate was filtered off, and the filtrate was concentrated under reduced pressure and then fractionally distilled using a Vigreux column to provide a colorless, clear liquid; yield 17.9 g (82%), b.p. 90 °C/0.2 Torr; correct C,H,N analysis; ^1H NMR ([D_6]DMSO): $\delta = 1.13$ (t, $^3J(H,H) = 7.0$ Hz, 9H; CCH_3), 1.87 (s, 2H; $SiCH_2$), 2.10 (s, 3H; NCH_3), 2.10–2.40 (m, 8H; ring H), 3.76 (q, $^3J(H,H) = 7.0$ Hz, 6H; CH_2O); ^{13}C NMR ([D_6]DMSO): $\delta = 18.5$ (CCH_3), 44.0 ($SiCH_2$), 46.1 (NCH_3), 55.4, 56.2, 58.2 (CH_2O, ring C); EI-MS: *m/z* (%): 276 (21) [M^+], 261 (5) [$M^+ - CH_3$], 247 (14) [$M^+ - C_2H_5O$], 206 (100).

$\mathbf{5}\cdot H_2O$: Hydrofluoric acid (1.5 M, 12.1 mL, 18.2 mmol HF) was added dropwise at 0 °C over 1 h to a stirred solution of **4** (1.00 g, 3.62 mmol) in water (20 mL). The resulting clear solution was stirred for 2 h at 0 °C and then treated with ethanol (100 mL), which caused a solid to precipitate. After the solid was removed by filtration, the filtrate was concentrated to ca. 10 mL under reduced pressure. Ethanol (100 mL) was added and the precipitated solid filtered off. The combined precipitates were washed with ethanol (3 × 10 mL) and then recrystallized from water at room temperature (crystallization by slow evaporation of the solvent). The crystals obtained were dried in a stream of nitrogen (room temperature): yield 685 mg (74%) colorless crystals, M.p. 202–204 °C (decomp); correct C,H,N,F analysis; ^{29}Si CP/MAS NMR (59.6 MHz, $\nu_{rot} = 3740$ Hz, contact time 4 ms, time between pulses 3 s, 1958 accumulated spectra): $\delta = -177.2$ ($\nu_{1/2} = 675$ Hz); ^1H NMR (D_2O): $\delta = 2.25$ (s, 2H; $SiCH_2$), 3.00 (s, 3H; CH_3), 3.25–4.05 (m, 8H; ring H); ^1H NMR ([D_6]DMSO): $\delta = 2.15$–2.30 (m, 5H; CH_3, $SiCH_2$), 2.75–3.00 (m, 4H; ring H), 3.25–3.35 (m, 6H; ring H, H_2O), 8.4 (br. s, 2H; NH); ^{13}C NMR (D_2O): $\delta = 46.0$ (CH_3), 53.9, 54.9 (ring C), 60.5 (m, unresolved C,F couplings; $SiCH_2$); ^{13}C NMR ([D_6]DMSO): $\delta = 45.2$ (CH_3), 51.7, 54.4 (ring C), $SiCH_2$ not detected; ^{19}F NMR (D_2O): $\delta = -113.7$ (s, 4F), -123.5 (s, 1F); ^{19}F NMR ([D_6]DMSO): $\delta = -112.1$ (br. s, $\nu_{1/2} = 63$ Hz); FD-MS (DMSO, 11 kV): *m/z* (%): 236 (9) [$(M - 2H)^+$], 198 (100) [$(M - 2HF)^+$].

Received: January 14, 1994 [Z6617IE]
German version: *Angew. Chem.* **1994**, *106*, 1431

[1] Review: R. Müller, *Organomet. Chem. Rev.* **1966**, *1*, 359–377.
[2] a) D. Schomburg, R. Krebs, *Inorg. Chem.* **1984**, *23*, 1378–1381; b) R. Damrauer, S. E. Danahey, *Organometallics* **1986**, *5*, 1490–1494; c) J. J. Harland, J. S. Payne, R. O. Day, R. R. Holmes, *Inorg. Chem.* **1987**, *26*, 760–765; d) S. E. Johnson, J. S. Payne, R. O. Day, J. M. Holmes, R. R. Holmes, *ibid.* **1989**, *28*, 3190–3198; e) S. E. Johnson, J. A. Deiters, R. O. Day, R. R. Holmes, *J. Am. Chem. Soc.* **1989**, *111*, 3250–3258; f) R. O. Day, C. Sreelatha, J. A. Deiters, S. E. Johnson, J. M. Holmes, L. Howe, R. R. Holmes, *Organometallics* **1991**, *10*, 1758–1766; g) K. Tamao, T. Hayashi, Y. Ito, *ibid.* **1992**, *11*, 182–191.
[3] D. A. Dixon, W. B. Farnham, W. Heilemann, R. Mews, M. Noltemeyer, *Heteroatom Chem.* **1993**, *4*, 287–295.
[4] Reviews: a) S. N. Tandura, M. G. Voronkov, N. V. Alekseev, *Top. Curr. Chem.* **1986**, *131*, 99–189; b) W. S. Sheldrick in *The Chemistry of Organic Silicon Compounds, Part 1* (Eds.: S. Patai, Z. Rappoport), John Wiley, Chichester, **1989**, pp. 227–303; c) R. R. Holmes, *Chem. Rev.* **1990**, *90*, 17–31; d) C. Chuit, R. J. P. Corriu, C. Reye, J. C. Young, *ibid.* **1993**, *93*, 1371–1448.
[5] a) R. Tacke, J. Becht, G. Mattern, W. F. Kuhs, *Chem. Ber.* **1992**, *125*, 2015–2018; b) R. Tacke, A. Lopez-Mras, J. Becht, W. S. Sheldrick, *Z. Anorg. Allg. Chem.* **1993**, *619*, 1012–1016; c) R. Tacke, J. Becht, A. Lopez-Mras, J. Sperlich, *J. Organomet. Chem.* **1993**, *446*, 1–8; d) R. Tacke, J. Becht, A. Lopez-Mras, W. S. Sheldrick, A. Sebald, *Inorg. Chem.* **1993**, *32*, 2761–2766; e) for analogous zwitterionic Si–O compounds see R. Tacke, M. Mühleisen, P. G. Jones, *Angew. Chem.* **1994**, *106*, 1250–1252; *Angew. Chem. Int. Ed. Engl.* **1994**, *33*, 1186–1188, and references therein.
[6] Synthesis of **3**: J. E. Noll, J. L. Speier, B. F. Daubert, *J. Am. Chem. Soc.* **1951**, *73*, 3867–3871.
[7] Crystal data for $\mathbf{5}\cdot H_2O$: $C_6H_{17}F_5N_2OSi$, triclinic, $P\bar{1}$, $a = 743.8(1)$, $b = 1207.1(2)$, $c = 1240.7(2)$ pm, $\alpha = 74.25(1)$, $\beta = 82.28(1)$, $\gamma = 74.61°$, $V = 1.0313(3)$ nm^3, $Z = 4$, $T = -70$ °C. A colorless prism (0.80 × 0.55 × 0.21 mm) was mounted in paraffin oil (type DAB 8, USP XX, Merck). A STADI-4 Stoe diffractometer ($Mo_{K\alpha}$ irradiation, $2\theta_{max} = 56°$) was used to measure 5346 intensities, of which 4965 were independent ($R_{int} = 0.022$). After an empirical absorption correction, the structure was solved by direct methods and refined on F^2 (program SHELXL-93, G. M. Sheldrick, Universität Göttingen). The final $R_w(F^2)$ value was 0.101, the conventional $R(F)$ value was 0.036 (for 407 parameters). Further details of the crystal structure investigation may be obtained from the Fachinformationszentrum Karlsruhe, D-76344 Eggenstein-Leopoldshafen (FRG) on quoting the depository number CSD-58125.
[8] Measurement conditions: 250.1 (^1H), 62.9 (^{13}C), and 235.4 MHz (^{19}F); ca. 22 °C; [D_5]DMSO ($\delta = 2.49$) and (CH_3)$_3$Si(CH_2)$_3$$SO_3$Na ($\delta = 0$) as internal ^1H NMR standards in [D_6]DMSO and D_2O, respectively; [D_6]DMSO ($\delta = 39.90$) and (CH_3)$_3$Si(CH_2)$_3$$SO_3$Na ($\delta = 0$) as internal ^{13}C NMR standards in [D_6]DMSO and D_2O, respectively; $CFCl_3$ ($\delta = 0$) as internal ^{19}F NMR standard in [D_6]DMSO and as external ^{19}F NMR standard in D_2O.

Iterative Divergent/Convergent Approach to Linear Conjugated Oligomers by Successive Doubling of the Molecular Length: A Rapid Route to a 128Å-Long Potential Molecular Wire**

Jeffry S. Schumm, Darren L. Pearson, and James M. Tour*

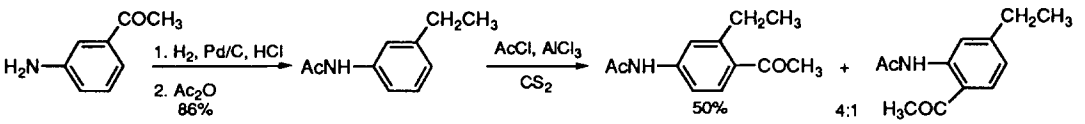
The ultimate computational system would consist of logic devices that are ultra dense, ultra fast, and molecular-sized.[1] Even though state-of-the-art nanopatterning techniques allow lithographic probe assemblies to be engineered down to the 100 Å gap regime,[2] the possibility of electronic conduction based upon single or small packets of molecules has not been addressed, and the feasibility of molecular electronics remains theoretically controversial.[1, 3] In an attempt to assess the possibility of molecular wire[4] conduction by spanning the 100 Å probe gaps with small packets of molecules, we describe here the synthesis of phenylalkyne oligomers that remain in a near-linear conformation owing to the 1,4-substitution of the phenylene units and the linearity of the alkyne moiety. This arrangement should minimize undesired conformational changes during adhesion and testing in the nanofabricated probes. Our approach to such a molecular framework involves a rapid iterative method that doubles molecular length with each iteration.[5] We obtained an air- and light-stable, linear conjugated oligomer that is 128 Å long which could also serve as a useful model for understanding

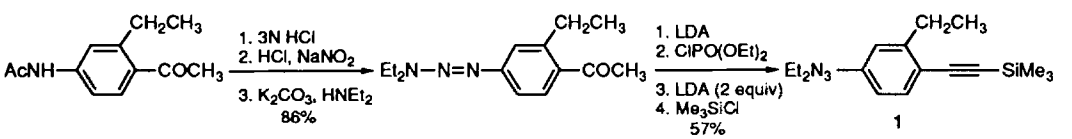
[*] Prof. J. M. Tour, J. S. Schumm, D. L. Pearson
Department of Chemistry and Biochemistry
University of South Carolina
Columbia, SC 29208 (USA)
Telefax: Int. code + (803)777-9521

[**] This research was supported by the Office of Naval Research and the Advanced Research Projects Agency. We also thank Molecular Design Ltd. for the use of their synthetic data base and Farchan Laboratories for a gift of trimethylsilylacetylene that was used in early model studies.

bulk properties of the polymeric material.[4i, j, 6] Moreover, since the the ends of this product should be easily functionalized, the ends may serve as "molecular alligator clips" for making surface contacts to metal probes for molecular electronics studies.[7]

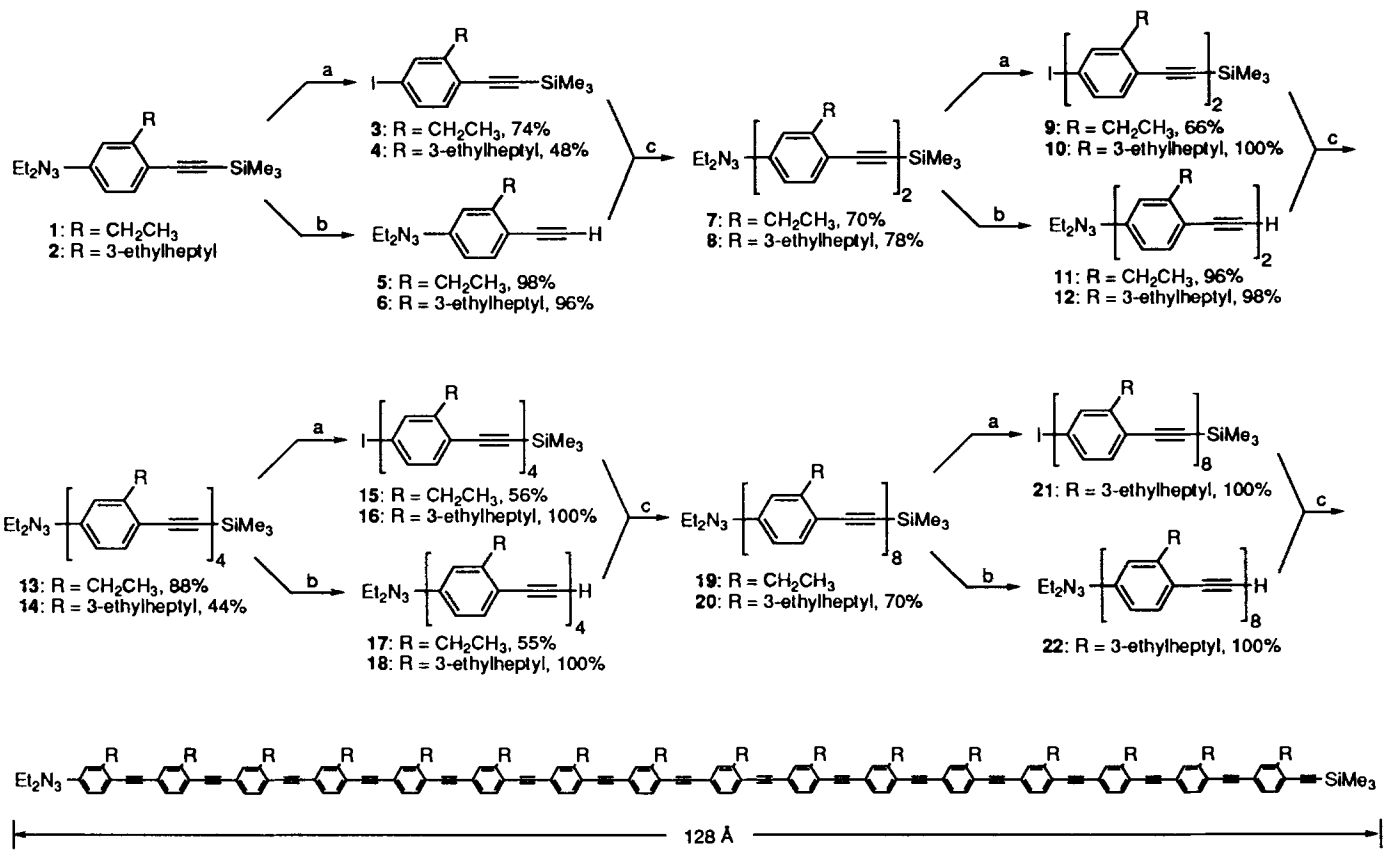
The synthesis of the ethyl-substituted monomer **1** is shown in Equations (1) and (2) (LDA = lithium diisopropylamide).[8]



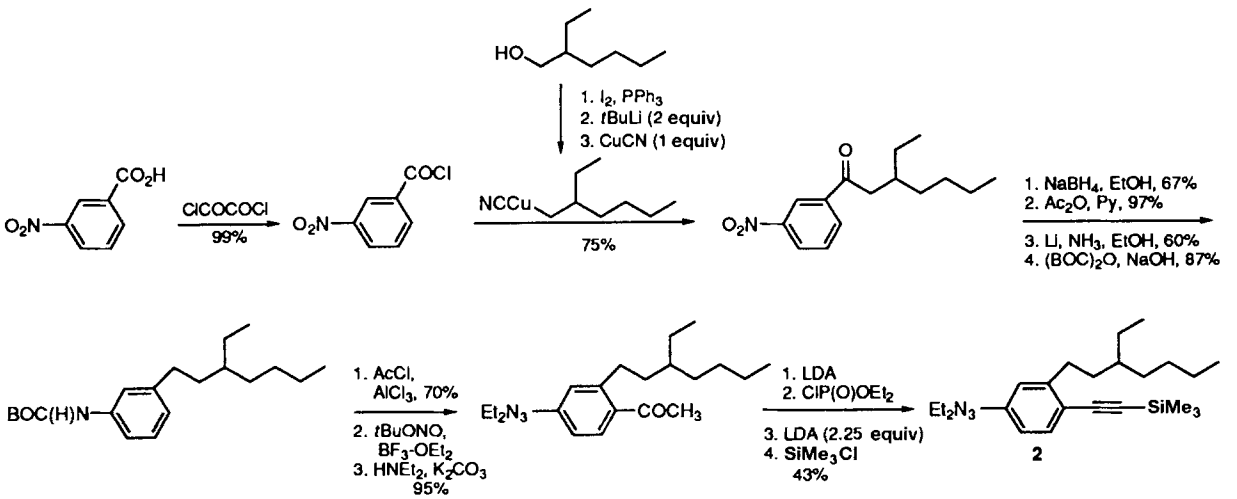


The iterative divergent/convergent approach to doubling the length of the molecule is shown in Scheme 1. Just three different reactions are needed at each stage to double the molecular length.[5c, d, 9] We initially conducted the synthesis starting from the monomer **1**, assuming that ethyl groups would provide sufficient solubility to permit formation of a 16-mer long enough to bridge the lithographically derived probe gaps. Unfortunately, the octamer **19** was nearly insoluble. Therefore, we were only able to obtain a UV/VIS spectrum and a mass spectrum (direct ionization) (Table 1).

In an effort to insure the solubility of the linear rigid-rod oligomer through to the 16-mer, we prepared the monomer **2** as shown in Scheme 2. We tried numerous methods to concomitantly reduce both the ketone and the nitro moieties; however, all methods failed, including the Pd-C/H_2/HCl reduction used in the synthesis of **1** [Eqs. (1) and (2)]. Therefore the multistep reaction sequence shown in Scheme 2 had to be utilized which also required a *tert*-butylnitrite-promoted[10] formation of the intermediate diazonium species. In addition to possessing a longer alkyl chain than **1**, **2** also has a stereogenic center. Successive dimerization thus affords numerous diastereomers that will retard crystallization and thereby increase solubility. Indeed, we were delighted to discover that both the octamer **20** and the



Scheme 1. The iterative divergent/convergent synthetic approach to the linear oligomers. a) MeI as solvent, 120 °C, in a screw-cap tube; b) K_2CO_3, MeOH, 23 °C or nBu_4NF, THF, 23 °C; c) $[Pd(dba)_2]$ (dba = dibenzylacetone) (5 mol%), CuI (10 mol%), PPh_3 (20 mol%), iPr_2NH/THF (1:5), 23 °C.



Scheme 2. Synthesis of the 3-ethylheptyl-substituted monomer **2**. Py = pyridine.

16-mer **23** (Scheme 1) were quite soluble and could be adequately characterized by spectroscopy. While **1**, **2**, **7**, **8**, **13**, **14**, and **19** were characterized by electron impact (EI) MS, in order to obtain MS data on **20** and **23**, it was necessary to use matrix-assisted laser desorption/ionization (MALDI) MS (Table 1). **23** is 128 Å long according to force field calculations (MMX) with extended Hückel and multiconformational parameters.

Table 1. Selected data for compounds **13**, **14**, **19**, **20**, and **23**.

13: IR (KBr): $\tilde{\nu}$[cm^{-1}] = 2965, 2872, 2151, 1590, 1503, 1401, 1246, 841; ^{1}H NMR (300 MHz, $CDCl_3$): δ = 7.46 (d, J = 7.9 Hz, 1H), 7.45 (d, J = 8.0 Hz, 1H), 7.45 (d, J = 8.2 Hz, 1H), 7.40 (d, J = 7.8 Hz, 1H), 7.39 (br. m, 2H), 7.35 (d, J = 1.3 Hz, 1H), 7.32 (dd, J = 7.9, 1.7 Hz, 1H), 7.32 (dd, J = 7.9, 1.7 Hz, 1H), 7.29 (d, J = 1.9, 1H), 7.27 (dd, J = 8.2, 1.6 Hz, 1H), 7.23 (dd, J = 8.2, 2.1 Hz, 1H), 3.76 (q, J = 7.2 Hz, 4H), 2.885 (q, J = 7.5 Hz, 2H), 2.884 (q, J = 8.2 Hz, 2H), 2.87 (q, J = 7.5 Hz, 2H), 2.79 (q, J = 7.6 Hz, 2H), 1.32 (t, J = 7.6 Hz, 6H), 1.31 (t, J = 7.6 Hz, 3H), 1.26 (t, J = 7.6 Hz, 3H), 0.25 (s, 9H); ^{13}C NMR (75 MHz, $CDCl_3$): δ = 151.75, 147.50, 147.22, 146.69, 146.62, 133.29, 132.75, 132.54, 132.50, 131.33, 131.26, 131.21, 129.18, 129.06, 129.03, 124.45, 123.85, 123.79, 122.78, 122.68, 122.16, 120.72, 118.88, 117.96, 103.82, 100.29, 94.99, 94.80, 93.08, 90.93, 89.98, 89.73, 28.33, 28.05, 28.03, 27.99, 15.21, 15.05, 15.01, 14.80, 0.33; Low-Resolution (LRMS) calcd for $C_{47}H_{51}N_3Si$: 685; found: 685.

14: IR (neat): $\tilde{\nu}$[cm^{-1}] = 2956, 2151, 1595, 1464, 1402, 1236, 1103; ^{1}H NMR (300 MHz, $CDCl_3$): δ = 7.48–7.27 (m, 12H), 3.76 (q, J = 7.1 Hz, 4H), 2.98–2.70 (m, 8H), 1.82–1.63 (m, 4H), 1.59–1.05 (m, 46H), 1.05–0.78 (m, 24H), 0.27 (s, 9H); LRMS calcd for $C_{75}H_{107}N_3Si$: 1077.8; found: 1077.9; UV/VIS (CH_2Cl_2): λ_{max} = 372 nm, UV 10% edge value = 421 nm; M_n = 1335, M_w = 1388, M_w/M_n = 1.06.

19: MS statistical isotopic range calculated for $C_{87}H_{83}N_3Si$: 1198 (95%), 1199 (100%), 1200 (55%); found: 1098.6 [M^+ – Et_2N_3, 100 amu]; UV/VIS (CH_2Cl_2): λ_{max} = 364 nm, UV 10% edge value = 500 nm.

20: IR (neat): $\tilde{\nu}$[cm^{-1}] = 2952, 2198, 2147, 1464, 827; ^{1}H NMR (300 MHz, $CDCl_3$): δ = 7.48–7.27 (m, 24H), 3.77 (q, J = 7.1 Hz, 4H), 2.98–2.63 (m, 16H), 1.84–1.58 (m, 8H), 1.58–1.10 (m, 86H), 1.10–0.78 (m, 48H), 0.27 (s, 9H); UV/VIS (CH_2Cl_2): λ_{max} = 376 nm; UV 10% edge value = 422 nm; M_n = 2800, M_w = 2960, M_w/M_n = 1.05; MALDI-MS (sinapinic acid matrix, positive ion mode) average molecular weight calculated for $C_{143}H_{195}N_3Si$: 1984; found for M + 1 m/z = 1791 ± 9(peak maximum, large error due to broad signal), [M^+ – $SiMe_3$ (73 amu), – N_3Et_2 (100 amu), – C≡C (24 amu), typical products of phenylalkyne cleavage [11]].

23: IR (neat): $\tilde{\nu}$[cm^{-1}] = 2956, 2927, 2360, 2340, 1506, 1458; ^{1}H NMR (300 MHz, $CDCl_3$): δ = 7.47–7.24 (m, 48H), 3.77 (q, J = 7.1 Hz, 4H), 2.95–2.65 (m, 32H), 1.82–1.58 (m, 16H), 1.58–1.10 (m, 166H), 1.10–0.70 (m, 96H), 0.26 (s, 9H); UV/VIS (CH_2Cl_2): λ_{max} = 376 nm, UV 10% edge value = 422 nm; M_n = 6649, M_w = 7114, M_w/M_n = 1.07; MALDI-MS (sinapinic acid matrix, positive ion mode) average molecular weight calculated for $C_{279}H_{371}N_3Si$: 3795; found for M + 1 m/z = 3486 ± 14 (peak maximum, large error due to broad signal), [M^+ – $SiMe_3$ (73 amu), N_3Et_2 (100 amu), – C≡C (24 amu), typical products of phenylalkyne cleavage, – C_8H_{17} fragment at 113 amu typical fragment from cleavage of a benzyl group [11]].

The optical spectra are interesting in that a saturation of the systems appears to have occurred by the octamer stage, such that doubling the length of the conjugated π-electron system causes no change in the position of the absorbance maximum (Figs. 1, 2). We also noticed that the extention of the π-electron system with the triazene substituent shifts the absorbance maxima bathochromically.

The results of the size exclusion chromatography (SEC) are shown in Figure 3 and compared with the actual molecular weights (MW) of the oligomers. SEC is not a direct measure of

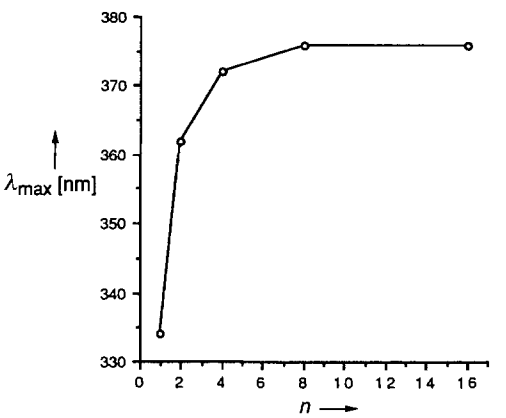


Fig. 1. UV absorbance maxima (CH_2Cl_2) of **2**, **8**, **14**, **20**, and **23** (monomer through 16-mer, respectively).

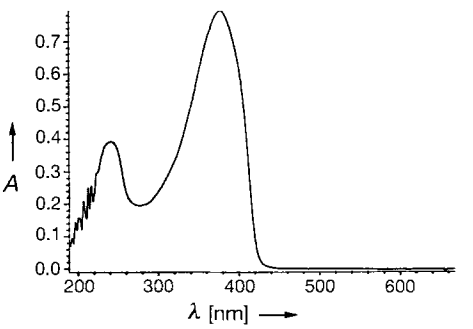


Fig. 2. UV/VIS spectrum of the 16-mer **23**. A = absorption (arbitrary units).

MW but a measure of the hydrodynamic volume. Thus, by SEC using randomly coiled polystyrene standards, the number average molecular weights (M_n) of rigid-rod polymers are usually greatly overestimated relative the actual molecular weights. Accordingly, the SEC-determined M_n values of the octamer **20** (M_n = 2800, actual MW = 1981) and the 16-mer **23** (M_n = 6650, actual MW = 3789) are much greater than the actual MWs. These results further confirm the formation of the 16-mer **23**. Also, as predicted, the monomer **2**, dimer **8**, and tetramer **14** have M_n values that are reasonably close to the actual MWs (slope $\approx$1.0 in Fig. 3) because they are in the low MW region, in which the polystyrene standards are not coiled. In all cases, the SEC-determined values of M_w/M_n are 1.04–1.07. Thus Figure 3 can serve as a useful calibration chart for very rigid linear oligomers as they compare to polystyrene standards by SEC.

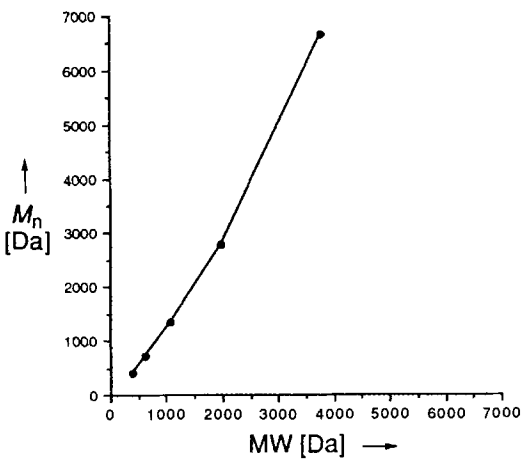


Fig. 3. M_n values determined by SEC (THF, polystyrene) versus the actual molecular weights MW of **2**, **8**, **14**, **20**, and **23**, (monomer through 16-mer, respectively).

Thus we have prepared rigid linear conjugated oligomers by an iterative divergent/convergent approach in which the monomeric unit is doubled. These oligomers may be well-suited as molecular wires in nanopatterned assemblies.

Received: November 22, 1993
Revised version: January 6, 1994 [Z 6507 IE]
German version: *Angew. Chem.* **1994**, *106*, 1445

[1] a) *Molecular Electronics: Science and Technology* (Ed.: A. Aviram), Conf. Proc. 262, American Institute of Physics, New York, **1992**; b) J. S. Miller, *Adv. Mater.* **1990**, *2*, 378; c) D. H. Waldeck, D. N. Beratan, *Science* **1993**, *261*, 576; d) J. Guay, A. Diaz, R. Wu, J. M. Tour, *J. Am. Chem. Soc.* **1993**, *115*, 1869.

[2] a) M. A. Reed (Yale University), personal communication, **1993**; b) *Nanostructures and Mesoscopic systems*, (Eds.: W. P. Kirk, M. A. Reed), Academic Press, San Diego, **1992**.

[3] a) J. S. Miller, *Adv. Mater.* **1990**, *2*, 495, 601.

[4] For some foundational work in the area of potential molecular wires, see: a) P. W. Kenny, L. L. Miller, *J. Chem. Soc. Chem. Commun.* **1988**, 85; b) S.-i. Kugimiya, T. Lazrak, M. Blanchard-Desce, J.-M. Lehn, *ibid.* **1991**, 1179; c) M. J. Crossley, P. L. Burn, *ibid.* **1991**, 1569; d) S. Zecevic, B. Simic-Glavaski, E. Yeager, *J. Electroanal. Chem. Interfacial Electrochem.* **1985**, *196*, 339; e) T. Yoshimura, S. Tatsuura, W. Sotoyama, A. Matsuura, T. Hayano, *Appl. Phys. Lett.* **1992**, *60*, 268; f) J. L. Sessler, V. L. Capuano, A. Harriman, *J. Am. Chem. Soc.* **1993**, *115*, 4618; g) H. Tachibana, R. Azumi, T. Nakamura, M. Matsumoto, Y. Kawabata, *Chem. Lett.* **1992**, 173; h) M. P. O'Neil, M. P. Niemczyk, W. A. Svec, D. Gosztola, G. L. Gaines III, M. R. Wasielewski, *Science* **1992**, *257*, 63; i) F. Wudl, S. P. Bitler, *J. Am. Chem. Soc.* **1986**, *108*, 4685; j) F.-L. Lu, F. Wudl, M. Nowak, A. J. Heeger, *ibid.* **1986**, *108*, 8311.

[5] An iterative synthetic method for doubling monomeric units was first described by Whiting et al. and then later used by Moore et al. to prepare oligo(1,3-phenylacetylene)s. a) E. Igner, O. I. Paynter, D. J. Simmonds, M. C. Whiting, *J. Chem. Soc. Perkin Trans. 1* **1987**, 2447; b) I. Bidd, D. J. Kelly, P. M. Ottley, O. I. Paynter, D. J. Simmonds, M. C. Whiting, *ibid.* **1983**, 1369; c) J. Zhang, J. S. Moore, Z. Xu, R. A. Aguirre, *J. Am. Chem. Soc.* **1992**, *114*, 2273; d) Z. Xu, J. S. Moore, *Angew. Chem.* **1993**, *32*, 1394; *Angew. Chem. Int. Ed. Engl.* **1993**, *32*, 1354; for related oligomers and polymers, see: e) R. H. Grubbs, D. Kratz, *Chem. Ber.* **1993**, *126*, 149; f) U. Scherf, K. Müllen, *Synthesis* **1992**, 23.

[6] a) J. Guay, A. Diaz, R. Wu, J. M. Tour, L. H. Dao, *Chem. Mater.* **1992**, *4*, 254; b) J. M. Tour, R. Wu, *Macromolecules* **1992**, *25*, 1901; c) J. Guay, P. Kasai, A. Diaz, R. Wu, J. M. Tour, L. H. Dao, *Chem. Mater.* **1992**, *4*, 1097; d) *Handbook of Conducting Polymers* (Eds.: T. A. Skotheim), Dekker, New York, **1986**.

[7] a) N. L. Abbott, J. P. Folkers, G. M. Whitesides, *Science* **1992**, *257*, 1380; b) D. H. Charych, M. D. Bednarski, *MRS Bull.* **1992**, *17*(11), 61.

[8] For the conversion of a methyl ketone to an alkyne, see: E. Negishi, A. O. King, J. M. Tour, *Org. Synth.* **1985**, *64*, 44.

[9] Iodination: a) J. S. Moore, E. J. Weinstein, Z. Wu, *Tetrahedron Lett.* **1991**, *32*, 2465; cross coupling: b) K. Sonogashira, Y. Tohda, N. Hagihara, *Tetradedron Lett.* **1975**, 4467; c) R. D. Stephens, C. E. Castro, *J. Org. Chem.* **1963**, *28*, 3313; d) J. Suffert, R. Ziessel, *Tetrahedron Lett.* **1991**, *32*, 757.

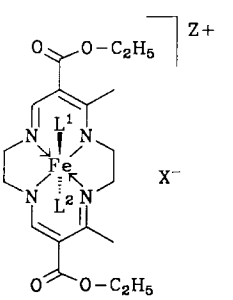
[10] M. P. Doyle, W. J. Bryker, *J. Org. Chem.* **1979**, *44*, 1572.

[11] F. W. McLafferty, F. Turecek, *Interpretation of Mass Spectra*, 4th ed., University Science Press, Mill Valley, CA, USA, **1993**.

Change of Orientation of Axial Imidazole Ligands in a Cytochrome b Model Complex in Response to a Change in the Oxidation State of the Metal Center**

Frank Wiesemann, Ralf Wonnemann, Bernt Krebs,* Heike Keutel, and Ernst-G. Jäger*

Iron complexes with anionic, tetraazamacrocyclic, Schiff base ligands exhibit a close relationship to iron porphyrins if the higher σ and π basicity of these ligands[1, 2] is attenuated by the electron-withdrawing effects of free carbonyl substituents in the *meso* position (COOEt in **1**, COMe in the more hydrophilic acetyl derivatives[3a]). For instance, in analogy to heme proteins of the metmyoglobin type, the iron(III) complex **1b** forms stable adducts in solution with a multitude of axial ligands, which can be exchanged through dynamic equilibria: amines, amino acids and N-heterocycles, phosphanes and phosphites, nitriles and isonitriles, hydroxide, halides, pseudohalides, as well as other



1

	Z	X	L^1	L^2
1a	0	—	HIm	HIm
1b	1	PF_6	HIm	HIm
1c	1	I	—	—

[*] Prof. Dr. B. Krebs, F. Wiesemann, R. Wonnemann[+]
Institut für Anorganische Chemie der Universität
Wilhelm-Klemm-Strasse 8, D-48149 Münster (FRG)
Telefax: Int. code + (251)838366
Prof. Dr. E.-G. Jäger, H. Keutel
Institut für Anorganische Chemie der Universität
August-Bebel-Strasse 2, D-07743 Jena (FRG)
Telefax: Int. code + (3641)635538

[+] Crystal structure analysis.

[**] This work was supported by the Deutsche Forschungsgemeinschaft and the Fonds der Chemischen Industrie. H. K. acknowledges a stipend from the Fonds der Chemischen Industrie.

anions, such as nitrite, sulfite, thiosulfate, complex cyanides, and ethynyl derivatives.[3b] In this respect, **1b** resembles the heme-containing iron proteins more closely than do free heme or most synthetic iron porphyrins.[4]

Cytochromes of the b group occupy a key position in the vectorial charge transfer during photosynthesis and in the respiratory chain.[5, 6] They contain hemes with low-spin iron centers and two axial imidazole (HIm) ligands. It is assumed that different orientations of the axial ligands with respect to the equatorial Fe–N bonds of the porphyrin are of importance for the function of the cytochromes.[6–13] These orientations depend on the valence state of the central atom. In low-spin iron(III) porphyrins one often finds a coplanar orientation in which both ligand planes lie above an equatorial N-Fe-N axis (Fig. 1, type a)).[7, 8] This orientation should be thermodynamically favored due to π interactions between the half-filled metal t_{2g} orbital and π orbitals of the imidazole ring.[8, 9] When the axial ligands are sterically encumbered or when they are not π donors, the mutually perpendicular (Fig. 1, type b) or coplanar (Fig. 1, type c) orientations dominate in which the ligand planes lie between the equatorial donor atoms.[10] These are also observed in the iron(II) complexes.[11] According to NMR data, the rotational barrier is low as long as there are no additional interactions.[12] The mutually perpendicular orientation in which each ligand plane lies above one N-Fe-N axis (Fig. 1, type d) has been postulated for certain cytochromes of the b group based on ESR data.[7] This orientation could be enforced by hydrogen bonds between the imidazole and carbonyl groups of the protein. Until now, this orientation may have been experimentally achieved but only in disordered crystals of a model porphyrin with different imidazole ligands.[13]

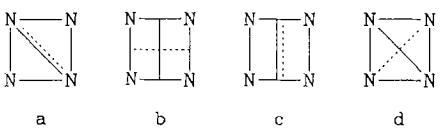


Fig. 1. Idealized orientations of the axial imidazole ligands in cytochrome b model complexes relative to the equatorial Fe–N bonds in the iron porphyrin complex [7-13].

We were able to obtain, crystallize, and structurally characterize the iron complexes **1a** and **1b** as low-spin bis(imidazole) adducts with iron in the oxidation states II and III, respectively. In iron(III) derivative **1b** the orientation of the imidazole rings is close to type d in Figure 1; this is the first occurrence of this orientation in a pure compound. The comparison of the two structures demonstrates impressively to what extent a change in oxidation state of the central atom, with no change in the first coordination sphere, can influence the orientation of the planes of axial ligands (coplanar in **1a**, nearly perpendicular in **1b**), the position of peripheral substituents (the carbonyl groups in **1a** are oriented in opposite directions, in **1b** in the same direction), the intermolecular interactions (four H bonds to four neighboring molecules in **1a**, and to two in **1b**), and the thus induced long-range order (three-dimensional network for **1a**, parallel, one-dimensional molecular strands for **1b**). Figures 2 and 3 show the crystal structures for both compounds; Figure 4 shows stereoprojections of the packing in the respective crystals.

The iron(II) complex **1a** crystallizes in the space group $P2_1/n$ with the iron atom at the inversion center. The ethoxy chains of the ester groups (O(2), C(7), C(8)) and the methyl group on the ring (C(4)) are disordered (1:1). The ^{1}H NMR spectra of the free ligands demonstrate that the methyl groups (C(4a), C(4b)) are *cis*.[14] The iron(III) derivative **1b** crystallizes in the space group $C2/c$; the atoms Fe(1), P(1), F(2), and F(4) are located on the two-fold axis. The anions in **1b** show no anomalies.

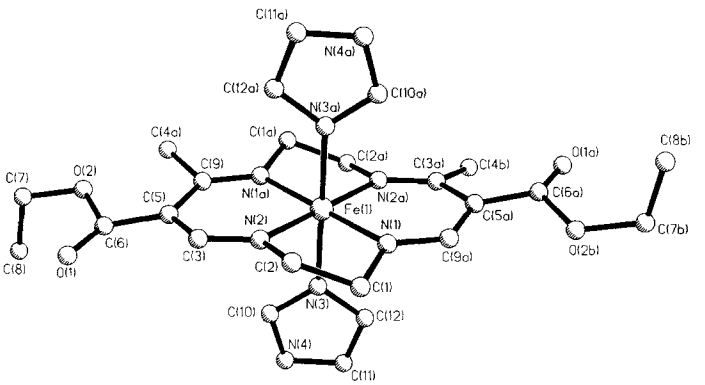


Fig. 2. Crystal structure of **1a**. Selected bond lengths [Å] and angles [°]: Fe(1)-N(1) 1.916(3), Fe(1)-N(2) 1.914(3), Fe(1)-N(3) 2.006(4), N(1)-C(1) 1.453(5), N(2)-C(2) 1.474(5), C(1)-C(2) 1.514(6), N(2)-C(3) 1.291(6), C(3)-C(5) 1.422(6), C(5)-C(9) 1.440(6), C(9)-N(1a) 1.300(5), C(5)-C(6) 1.421(6), C(6)-O(1) 1.202(7), C(6)-O(2) 1.465(10), C(10)-N(4) 1.345(6), N(4)-C(11) 1.353(6), C(11)-C(12) 1.362(6); N(1)-Fe(1)-N(2) 87.6(2), N(1)-Fe(1)-N(2a) 92.4(2), N(2)-Fe(1)-N(3) 91.14(15), N(1)-Fe(1)-N(3) 89.54(15), N(3)-Fe(1)-N(3a) 180.0; torsion angles [°]: C(1a)-C(2a)-N(2a)-Fe(1) 31.2, Fe(1)-N(1)-C(2) −30.9, N(1)-Fe(1)-N(3a)-C(10a) 43.2, N(2)-Fe(1)-N(3)-C(10) 49.2, C(5)-Fe(1)-N(3)-C(12) −179.5, C(10)-N(3)-N(3a)-C(10a) −180.0, C(3)-C(5)-C(6)-O(1) −1.7.

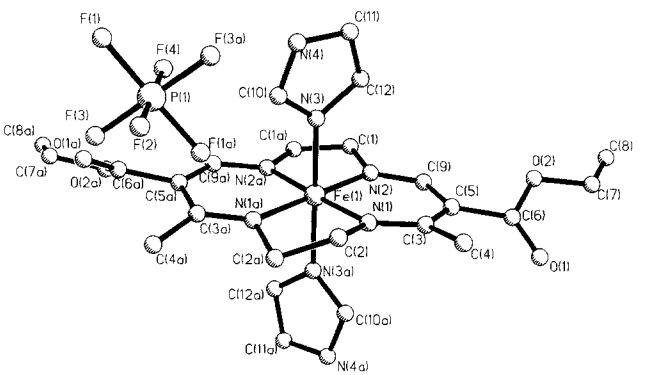


Fig. 3. Crystal structure of **1b**. Selected bond lengths [Å] and angles [°]: Fe(1)-N(1) 1.913(4), Fe(1)-N(2) 1.883(3), Fe(1)-N(3) 2.004(4), N(2)-C(1) 1.456(6), N(1)-C(2) 1.468(5), C(1)-C(1a) 1.431(10), C(2)-C(2a) 1.530(9), N(1)-C(3) 1.327(5), C(3)-C(5) 1.431(6), C(5)-C(9) 1.396(6), C(9)-N(2), 1.319(5), C(5)-C(6) 1.481(6), C(6)-O(1) 1.194(6), C(6)-O(2) 1.332(6), C(10)-N(4) 1.332(6), N(4)-C(11) 1.353(6), C(11)-C(12) 1.362(6); N(1)-Fe(1)-N(1a) 87.6(2), N(1)-Fe(1)-N(2) 93.84(15), N(2)-Fe(1)-N(3) 91.36(15), N(1)-Fe(1)-N(3) 87.93(15), N(3)-Fe(1)-N(3a) 177.2(2); torsion angles [°]: C(1)-C(1a)-N(2a)-Fe(1) −9.4, Fe(1)-N(1)-C(2)-C(2a) 31.0, N(1)-Fe(1)-N(3a)-C(10a) −9.7, N(2a)-Fe(1)-N(3)-C(10) 84.1, C(5)-Fe(1)-N(3)-C(12) 27.3; C(10)-N(3)-N(3a)-C(10a) −105.3, C(3)-C(5)-C(6)-O(1) 32.7.

In both cases, the central atom has octahedral coordination. The equatorial Fe–N distances (1.88–1.92 Å) are somewhat shorter than those in porphyrins (1.97–2.00 Å) and are also nearly independent of the oxidation state. In both complexes, the axial Fe–N distances (2.00 Å) are in the range characteristic for low-spin iron(II) porphyrins and somewhat longer than those found in most low-spin iron(III) porphyrins (1.97 Å).[8, 11] The bond angles around the iron atom reflect the lower symmetry of the equatorial ligand (alternating five- and six-membered rings) compared to that in porphyrins. In both cases the central atom lies exactly in the $[N_4]$ plane. The six-membered chelate rings are bent by only about 5–6° along the N–N axes.

The five-membered chelate rings in **1a** exhibit the normal half-chair conformation; the ethylene bridges are both rotated in the same direction 40° out of the central [N_4] plane. The bond angle and the C–C distance (1.51 Å) are typical for sp^3-hybridized carbon atoms. In contrast, in **1b** only the ethylene bridge on the side of the methyl substituents shows the normal torsion angle (− 40°). The opposite five-membered chelate ring is nearly planar; the nearly ideal eclipsed conformation of the methyl groups and the C–C distance of 1.43 Å indicate partial double bonds in the ethylene bridge. This could stem from interactions with the π system of the six-membered chelate rings and possibly from interactions with the partially occupied t_{2g}^5 orbital of the central atom.

Apart from this altered ring conformation, the following differences between the iron(II) and the iron(III) complex are especially noteworthy:

1. The planes of both imidazole rings in **1a** are exactly coplanar and point directly to the *meso* position of the six-membered rings (cf. Fig. 1, type c). In **1b**, they are rotated by 64° with respect to each other and are nearly aligned along the equatorial N-Fe-N axes (Fig. 1, type d).

2. The ester groups in **1a** are each rotated by 13° out of the central [N_4] plane, and the two carbonyl functionalities point in opposite directions. In **1b**, the orientation of the ester groups is characteristic for such chelate complexes, namely the carbonyl moiety points in the direction of the neighboring methyl group on the chelate ring.[12, 15] The rotation out of the central [N_4] plane (32° in both cases) is larger than that found in **1a**.

3. The crystal structures of both compounds are characterized by intermolecular hydrogen bonds between the NH groups of the axial imidazoles and the peripheral carbonyl groups on the macrocycle (Fig. 4). In **1a**, each molecule is linked by four single H bonds (N···O distance of 2.72 Å) to a total of four neighboring molecules, which results in a three-dimensional network. In **1b**, each complex cation forms two H bonds to each of two neighbors (N···O distance of 2.88 Å). This one-dimensional linkage leads to an arrangement of paired chains which are surrounded—without any covalent interactions—by the hexafluorophosphate counterions.

Without prior knowledge of the energies involved, it is impossible to say whether rearrangements on the molecular level lead to the different intermolecular networks, or whether differences in the crystal packing forces, which could be caused by the incorporation of the anions in **1b**, force the structural adjustment of the H bonds and the molecular units. Some arguments support the proposition that the change in orbital occupancy at the central atom from t_{2g}^6 to t_{2g}^5 affects primarily the immediate environment, that is, the conformation of the chelate rings and the orientation of the imidazole units.[16] On the other hand, there are examples among similar macrocyclic chelate complexes in which crystal packing forces and details of the molecular structure are determined by the water molecules that link peripheral ester groups of neighboring chelate molecules in a one-dimensional fashion through hydrogen bonds.[17]

In any case, the simple model system presented here is an instructive example for the far-reaching structural consequences of a valence change of the central atom. The conformation of chelate rings, the orientation of the π-electron systems of axial ligands or peripheral substituents, the formation of hydrogen bonds and the resulting order of larger molecular aggregates are all affected solely by this valence change. It is possible that the rearrangements that are linked to the charge change also influence the direction of the charge transfer—as long as all these events happen within the same time frame.

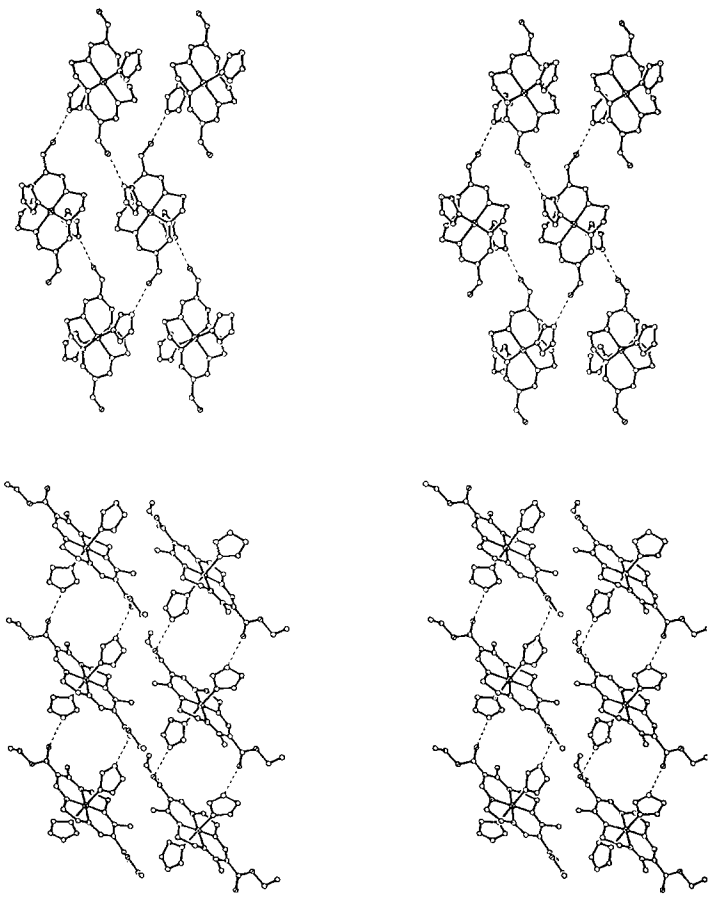


Fig. 4. Stereoprojections of the arrangements of **1a** (top) and **1b** (bottom) in their respective crystal lattices. For clarity the disordered methyl and ethyl groups in **1a** and the PF_6^- anions in **1b** have been omitted.

For iron(III) porphyrins, a conformation of axial imidazole ligands corresponding to Figure 1 type d has been predicted to lead to an ESR spectrum with a "strong g_{max}" > 3.[13] For samples of **1b** both in the form of a crystalline powder and in a methanol glass we have found normal rhombic ESR spectra with $g = 1.98, 2.09, 2.15$. It follows that the splitting in energy of the d_{xz} and d_{yz} orbitals is not determined by the relative position of the molecular planes of axial ligands, but more likely by the low symmetry of the equatorial ligand.

Experimental Procedure

Compound **1a** was prepared according to the general procedure outlined in ref. [18]. In order to avoid the formation of oligomeric products, a larger excess of imidazole was added: Under exclusion of air, iron(II) acetate [19] (3.48 g, 0.02 mol), 6,13-bis(ethoxycarbonyl)-5, 14-dimethyl-1, 4, 8, 11-tetraazatetradeca-4, 6, 12, 14-tetraene (7.31 g, 0.02 mol), and imidazole (10 g, 0.15 mol) in 120 mL of methanol were heated to reflux for 15 min. Upon cooling, dark red crystals of the diadduct **1a** formed, which were washed with a small amount of cold methanol. Insufficient exclusion of air leads to a color change to deep green. Yield: 9.2 g (83%), diamagnetic. $FeC_{24}H_{34}N_8O_4$, 554.4 g mol^{-1}, satisfactory elemental analyses for Fe, C, H, N.

1b: Iodide **1c** [3b] (0.3 g, 0.55 mmol) and imidazole (2 g, 30 mmol) were dissolved in 20 mL of methanol. A filtered solution (G4 sintered glass frit) of NH_4PF_6 (5 g, 30 mmol) in 20 mL of methanol was added. The resulting mixture was heated to reflux for 15 min. Slow cooling led to the separation of dark green crystals, which were washed with a small amount of very cold methanol and dried in air. Yield: 0.22 g (57%), $\mu_{eff} = 1.78\ \mu_B$. $FeC_{24}H_{34}N_8O_4PF_6$, 699.4 g mol^{-1}, satisfactory elemental analyses for Fe, C, H, N. ESR spectra: ERS-300 spectrometer (former Zentralwerkstatt für wissenschaftlichen Gerätebau, Berlin Adlershof); X band; $p = 0.2$ mW; 1,1-diphenyl-2-picrylhydrazyl (DPPH) as external standard. Compound **1b** was measured as a solid at 150 K, compound **1c** in a methanol glass (10^{-3} mol L^{-1}) at 77 K in the presence of 1 mol L^{-1} of imidazole.

Crystal structure analyses: Crystal data for **1a** ($C_{24}H_{34}N_8O_4Fe$): monoclinic, $P2_1/n$, $a = 11.973(3)$, $b = 7.473(1)$, $c = 14.604(4)$ Å, $\beta = 95.27(2)°$, $Z = 2$, $V = 1301.2$ Å^3, measurement temperature 150 K, $Mo_{K\alpha}$ radiation ($\lambda = 0.71073$ Å), 2848 independent reflections, 2046 with $I > 1.96\sigma(I)$, $R = 0.065$, $wR^2 = 0.1689$, structure solution by direct methods, refinement by full matrix least squares method on F^2 (SHELXL 93). Crystal data for **1b** ($C_{24}H_{34}N_8O_4PF_6Fe$): monoclinic, $C2/c$, $a = 17.430(13)$, $b = 17.746(9)$, $c = 10.164(7)$ Å, $\beta = 110.95(5)°$, $Z = 4$, $V = 2936.02$ Å^3, measurement temperature 290 K, $Mo_{K\alpha}$ radiation ($\lambda = 0.71073$ Å), 2316 independent reflections, 1419 with $I > 1.96\sigma(I)$, $R = 0.0479$, $wR^2 = 0.1406$, structure solution by direct methods, refinement by full matrix least squares method on F^2 (SHELXL 93). Further details of the crystal structure investigation may be obtained from the Fachinformationszentrum Karlsruhe, D-76344 Eggenstein-Leopoldshafen (FRG) on quoting the depository numbers CSD-400554 (**1a**) and CSD-400556 (**1b**).

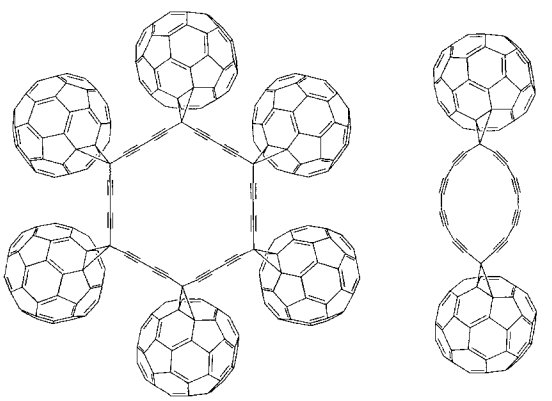
Received: January 14, 1994 [Z 6618 IE]
German version: *Angew. Chem.* **1994**, *106*, 1424

[1] Y. Nishida, K. Hayashida, N. Oishi, S. Kida, *Inorg. Chim. Acta* **1980**, *38*, 213–219; Y. Nishida, S. Kida, *Coord. Chem. Rev.* **1979**, *27*, 275–298.
[2] N. W. Alcock, W.-K. Lin, A. Jircinato, I. D. Mokren, P. W. R. Corfield, G. Johnson, G. Novotnak, C. Cairns, D. H. Busch, *Inorg. Chem.* **1987**, *26*, 440–452; H. Okawa, D. H. Busch, *ibid.* **1979**, *18*, 1555–1558.
[3] a) E.-G. Jäger, B. Schweder, S. Radzuweit, *Z. Chem.* **1988**, *28*, 152–153; E.-G. Jäger, J. Liehr, E. Morich, A. Dix, *Proc. Conf. Coord. Chem. 12th Smolenice/Bratislava*, **1989**, 123–128; E.-G. Jäger, *Z. Chem.* **1985**, *25*, 446–447; b) E.-G. Jäger, H. Hähnel, F. Klein, A. Schmidt, *J. Prakt. Chem.* **1991**, *333*, 423–430; E.-G. Jäger, H. Hähnel, *J. Inorg. Biochem.* **1991**, *43*, 305.
[4] An attractive feature of **1a**, apart from its solubility in water and its low tendency for association, is primarily the possibility of studying axial coordination by ligands [3] that usually lead to redox reactions with protein-free iron(III) porphyrins, e.g., cyanide or hydroxylamine; cf. D. W. Feng, M. D. Ryan, *Inorg. Chem.* **1987**, *26*, 2480–2483.
[5] T. Yamanaka in *Metalloproteins, Vol. 8* (Eds.: S. Otsuka, T. Yamanaka), Elsevier, Amsterdam, **1988**, p. 134–139; W. Cramer, J. Whitmarsh, P. Horton, *Porphyrins 1978–1979* **1979**, *7*, 71–106; F. S. Mathews, E. W. Czerwinski, P. Argos, *ibid.* **1979**, *7*, 107–147.
[6] J. D. Satterlee, *Met. Ions Biol. Syst.* **1987**, *21*, 121–185.
[7] F. A. Walker, B. H. Huynh, W. R. Scheidt, S. R. Osvath, *J. Am. Chem. Soc.* **1986**, *108*, 5288–5297; W. R. Scheidt, D. M. Chipman, *ibid.* **1986**, *108*, 1163–1167; M. K. Safo, G. P. Gupta, C. T. Watson, U. Simonis, F. A. Walker, W. R. Scheidt, *ibid.* **1992**, *114*, 7066–7075.
[8] W. R. Scheidt, Y. J. Lee, *Struct. Bonding (Berlin)* **1987**, *64*, 1–70.
[9] R. Quinn, J. S. Valentine, M. P. Byrn, C. E. Strouse, *J. Am. Chem. Soc.* **1987**, *109*, 3301–3308; S. M. Soltis, C. E. Strouse, *ibid.* **1988**, *110*, 2824–2829.
[10] F. A. Walker, U. Simonis, *J. Am. Chem. Soc.* **1991**, *113*, 8652–8657; M. K. Safo, G. P. Gupta, F. A. Walker, W. R. Scheidt, *ibid.* **1991**, *113*, 5497–5510.
[11] M. K. Safo, W. R. Scheidt, G. P. Gupta, *Inorg. Chem.* **1990**, *29*, 626–633.
[12] F. A. Walker, U. Simonis, H. Zhang, J. M. Walker, T. Ruscitti, C. Kipp, M. A. Amputch, B. V. Castillo, S. H. Cody, D. L. Wilson, R. E. Graul, G. J. Yong, K. Tobin, J. T. West, B. A. Barichievich, *New J. Chem.* **1992**, *16*, 609–620.
[13] K. Hatano, M. K. Safo, F. A. Walker, W. R. Scheidt, *Inorg. Chem.* **1991**, *30*, 1643–1650.
[14] E.-G. Jäger, B. Kirchhof, E. Schmidt, B. Remde, A. Kipke, R. Müller, *Z. Anorg. Allg. Chem.* **1982**, *485*, 141–172.
[15] H. Görls, G. Reck, E.-G. Jäger, K. Müller, D. Seidel, *Cryst. Res. Technol.* **1990**, *25*, 1277–1286; G. Reck, G. Bannier, B. Heyn, E.-G. Jäger, *ibid.* **1984**, *19*, 1603–1606; H. Elias, D. Hess, H. Paulus, E.-G. Jäger, F. Gräfe, *Z. Anorg. Allg. Chem.* **1990**, *589*, 101–114.
[16] The imidazole ligands could stabilize their orientations in **1b** by π-donor bonds, provided that the $d_{xz, yz}$ orbitals are higher in energy than the d_{xy} orbital and only slightly split in energy. This, however, should be evident in the ESR spectrum [7]. The bond lengths within the imidazole rings in **1b** are 1% shorter than those in **1a** (1.340(6) vs. 1.353(6) Å). While this change is not significant for the individual bonds, it is noteworthy and in agreement with π interactions in **1b** that this shift occurs in the same direction for all bonds. In the iron(II) complex **1a** no stabilization by π-donor bonds is possible, and the sterically most favorable orientation, in the direction of the six-membered chelate rings, is adopted.
[17] E.-G. Jäger, H. Keutel, M. Rudolph, B. Krebs, F. Wiesemann, *Chem. Ber.*, submitted.
[18] E.-G. Jäger, E. Stein, F. Gräfe, W. Schade, *Z. Anorg. Allg. Chem.* **1985**, *526*, 15–28; E.-G. Jäger, *Z. Chem.* **1968**, *8*, 470.
[19] H.-D. Hardt, W. Möller, *Z. Anorg. Allg. Chem.* **1961**, *313*, 57.

Fullerene–Acetylene Hybrids: On the Way to Synthetic Molecular Carbon Allotropes**

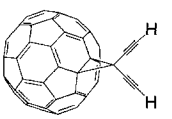
Harry L. Anderson, Rüdiger Faust, Yves Rubin, and François Diederich*

Our interest in carbon-rich materials[1] has prompted us to explore routes to molecular carbon allotropes based on both fullerenes and acetylenes. Among the attractive targets are the cyclic polyynes **1** and **2** in which peripheral C_{60} spheres stabilize a central acetylenic core through steric shielding and interact with this core through the cyclopropane rings. Related macrocyclic polyynes have been reported,[1, 2] but "end-capping" with methanofullerenes would avoid the incorporation of heteroatoms and yield new types of carbon allotropes.



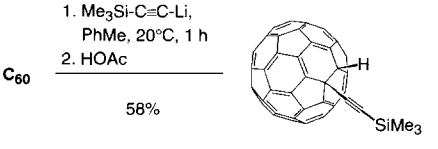
1 **2**

A common precursor for compounds **1** and **2** is diethynylmethanofullerene **3**[3] from which the desired acetylenic carbocycles could be assembled by oxidative coupling. In light of the radical-trapping properties of C_{60},[4] the viability of such a reaction for coupling fullerene derivatives was questionable.



3

Here we describe the first steps towards the construction of **1** and **2**, namely two synthetic entries to symmetrically and unsymmetrically substituted diethynylmethanofullerenes, as well as the previously unknown hydroethynylation of C_{60} leading to **4** (Scheme 1).[5] The formation of bis(butadiynyl)methanofullerene **5** (Scheme 3) and the dumbbell-shaped



4

Scheme 1. Synthesis of the hydroethynylated fullerene **4**.

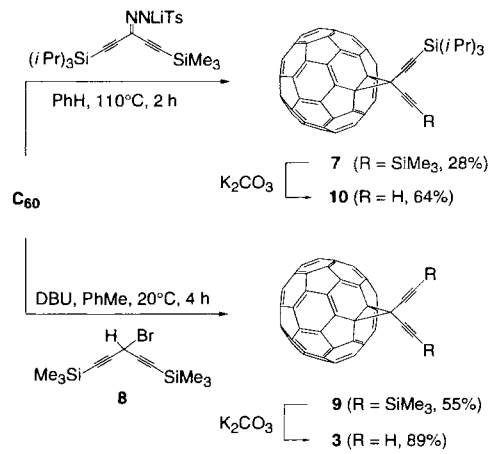
[*] Prof. Dr. F. Diederich, Dr. H. L. Anderson, Dr. R. Faust
Laboratorium für Organische Chemie, ETH Zentrum
Universitätstrasse 16, CH-8092 Zürich (Switzerland)
Telefax: Int. code + (1)261-3524
Prof. Dr. Y. Rubin
Department of Chemistry and Biochemistry
University of California at Los Angeles

[**] This work was supported by the Schweizerische Nationalfonds zur Förderung der wissenschaftlichen Forschung. H. L. A. thanks the Science and Engineering Research Council (UK) for a postdoctoral research fellowship.

derivative **6** (Scheme 4) under Hay coupling conditions demonstrates the feasibility of the proposed route to the new allotropes **1** and **2**.

Nucleophilic addition to C_{60} is among the most common reaction types in fullerene chemistry.[5, 6] Surprisingly, the use of acetylide nucleophiles has not previously been reported. Initial attempts to react C_{60} with chloromagnesium acetylide failed, and no reaction was observed in toluene at room temperature, even with a large excess of the nucleophile. Lithium trimethylsilylacetylide, on the other hand, reacted with the fullerene under these conditions to produce **4** upon quenching with acetic acid (Scheme 1). This reaction proceeded much slower than the addition of aromatic or aliphatic organolithium and Grignard reagents.[5] The structure of **4** is evident from its spectral data (Table 1); the characteristic ^{1}H NMR resonance at $\delta = 6.92$ corresponds to the fullerene proton. The addition proceeds in a 1,2 fashion across the junction of two six-membered rings, as judged by the 32 distinct fullerene resonances in the ^{13}C NMR spectrum of **4**. The signals of the newly formed sp^3 carbon centers appear at $\delta = 61.8$ (C_{sp^3}–H) and $\delta = 55.1$ (C_{sp^3}–C_{sp}). Evidently, the successful synthesis of **4** suggests a new entry into mixed fullerene–acetylene molecular scaffolding.[1b, 7]

Rubin et al.[3] recently prepared symmetrically protected bis(trimethylsilylethynyl)methanofullerene[60] by reacting C_{60} with carbenes derived from the tosylhydrazone of 1,5-bis(trimethylsilyl)-1,4-pentadiyn-3-one.[8] We applied this methodology to obtain the unsymmetrically protected species **7** in 28% yield (Scheme 2). We also explored an ionic route to diethynylmethanofullerenes inspired by Bingel's recent report[9] that fullerenes can be cyclopropanated by α-halocarbonyl compounds in the presence of base. We found that bromopentadiyne **8**[10] reacts with C_{60} to form bis(trimethylsilylethynyl)methanofullerene **9** in 55% yield (Scheme 2) in the presence of 1,8-diazabicyclo[5.4.0]undec-7-ene (DBU). Since the pK_a of **8** is probably less than 21 (in EtOH),[11] it should be acidic enough to be deprotonated by DBU (pK_a = 24.3 in MeCN).[12] Alternatively DBU could react as a nucleophile and displace bromide from **8** to give a more acidic salt,[13] which would be deprotonated to form an ylid, which could attack C_{60}.



Scheme 2. Syntheses of diethynylmethanofullerenes. Ts = *p*-tosyl.

Table 1. Selected physical data of **4**–**7** and **10** [a].

4: FT-IR: $\tilde{\nu}$ = 2951 (w), 2155 (w), 839 (s), 526 (s) cm^{-1}. ^{1}H NMR (CS_2): δ = 6.92 (s, 1 H), 0.37 (s, 9 H). ^{13}C NMR (CS_2): δ = 150.98, 150.77, 147.22, 146.96, 146.30, 146.06, 146.04, 145.88, 145.87, 145.43, 145.36, 145.31, 145.17, 145.08, 145.01, 144.34, 144.17, 142.81, 142.29, 142.25, 141.75, 141.72, 141.70, 141.51, 141.36, 141.31, 140.04, 140.02, 135.73, 134.74, 107.33, 88.15, 61.82, 55.10, −0.04. UV/VIS: λ_{max} [nm] = 256 (ε 104000), 306 (31200), 327 (32500), 404 (4270), 431 (3240), 701 (260). FAB-MS: *m/z* 818.9 (M^+), 719.8 (C_{60}). Satisfactory C,H analysis for $C_{65}H_{10}Si$.

5: FT-IR: $\tilde{\nu}$ = 2953 (m), 2894 (w), 2222 (w), 2105 (m), 1248 (s), 844 (s), 526 (s) cm^{-1}. ^{1}H NMR (CS_2): δ = 0.24 (s). ^{13}C NMR (CS_2): δ = 145.10, 145.08, 145.03, 144.84, 144.74, 144.70, 144.40, 143.82, 143.70, 142.71, 142.68, 142.53, 142.04, 141.76, 140.89, 138.84, 89.32, 87.57, 74.41, 70.88, 68.62, 27.23, −0.65. UV/VIS: λ_{max} [nm] = 256 (ε 127000), 329 (40700), 435 (2190), 487 (1580), 687 (170). FAB-MS: *m/z* 976.1 (M^+), 720.0 (C_{60}). Satisfactory C,H analysis for $C_{75}H_{18}Si_2$.

6: FT-IR: $\tilde{\nu}$ = 2933 (s), 2856 (s), 2167 (w), 1456 (m), 1422 (m), 878 (m), 678 (m), 522 (s) cm^{-1}. ^{1}H NMR (CS_2/C_6D_6): δ = 1.14 (s). ^{13}C NMR (CS_2/C_6D_6): δ = 145.92, 145.76, 145.73, 145.71, 145.70 (2×), 145.68, 145.67, 145.39, 145.30, 145.24, 145.01, 144.97, 144.95, 144.90, 144.30, 144.28, 143.32, 143.31, 143.28, 143.27, 143.19, 143.08, 142.76, 142.39, 142.34, 141.53, 141.39, 139.55, 139.35, 97.20, 88.90, 75.31, 73.95, 69.72, 28.61, 19.18, 11.98. UV/VIS: λ_{max} [nm] = 256 (ε 110000), 330 (37200), 434 (2300), 481 (1600), 687 (200). MALDI-TOF-MS (2,5-dihydroxybenzoic acid matrix): *m/z* 1877.6 (M^-), 722.03 (C_{60}).

7: FT-IR: $\tilde{\nu}$ = 2929 (s), 2856 (s), 2167 (w), 1461 (m), 1422 (m), 1248 (m), 843 (m), 525 (s) cm^{-1}. ^{1}H NMR ($CDCl_3$): δ = 1.19 (s, 21 H), 0.33 (s, 9 H). ^{13}C NMR ($CDCl_3$): δ = 146.41, 146.24, 145.74, 145.67, 145.38, 145.37, 145.36, 145.05, 144.85, 144.81, 144.75, 144.70, 144.02, 144.01, 142.99, 142.96, 142.95, 142.93, 142.88, 142.86, 142.36, 142.23, 142.10, 142.09, 141.05, 141.02, 139.24, 139.00, 98.18, 97.25, 90.69, 87.32, 75.58, 32.24, 18.60, 11.34, 0.00. UV/VIS: λ_{max} [nm] = 258 (ε 107000), 329 (35500), 436 (2200), 488 (1500), 687 (100). FAB-MS: *m/z* 1011.0 (M^+), 720.0 (C_{60}).

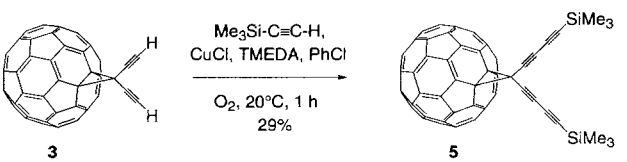
10: FT-IR: $\tilde{\nu}$ = 3289 (m), 2922 (s), 2856 (s), 2167 (w), 2119 (w), 1456 (m), 1422 (m), 672 (m), 522 (s) cm^{-1}. ^{1}H NMR ($CDCl_3$): δ = 2.88 (s, 1 H), 1.20 (s, 21 H). ^{13}C NMR (CS_2/C_6D_6): δ = 146.21, 146.12, 145.78, 145.65 (several overlapping peaks), 145.30, 145.19, 145.15, 144.97, 144.89, 144.28, 144.26, 143.28 (several overlapping peaks), 143.18, 142.61, 142.41, 142.36, 142.34, 141.38, 141.36, 139.42, 98.21, 87.61, 76.47, 74.94, 73.35, 29.51, 18.95, 11.66. UV/VIS: λ_{max} [nm] = 258 (ε 148000), 328 (45700), 406 (4700), 434 (3200), 493 (2200), 688 (890). FAB-MS: *m/z* 939.0 (M^+), 719.8 (C_{60}).

[a] ^{1}H and ^{13}C NMR spectra were measured at 500 MHz and 125.8 MHz, respectively; IR and UV/VIS spectra were recorded in KBr and CH_2Cl_2, respectively.

The silyl groups in **7** and **9** greatly enhance the solubility of these fullerene derivatives in common organic solvents (THF, hexane, aromatic hydrocarbons), which facilitates their spectroscopic characterization (Table 1). Both cyclopropanations occur at the 6,6 ring junction leading to structures with closed transannular bonds.[14] In the ^{13}C NMR spectra all 16 C_{sp^3} fullerene resonances expected for **9** (C_{2v} symmetry) are well resolved between δ = 147 and δ = 139, while only 28 out of the 31 C_{sp^3} resonances are clearly discernible for **7** with C_s symmetry. Diagnostic for both compounds are the resonances of the methano bridge C atoms at δ = 32.24 (**7**) and δ = 27.91 (**9**), along with their respective bridgehead carbon signals at δ = 75.98 (**7**) and δ = 76.04 (**9**).

Protodesilylation of **7** and **9** is rapidly effected by K_2CO_3 in MeOH/THF to generate regioselectively deprotected **10** and the parent hydrocarbon **3**.[3] The NMR signals of the acetylenic protons appear at δ = 2.87 (**3**) and δ = 2.88 (**10**, Table 1).

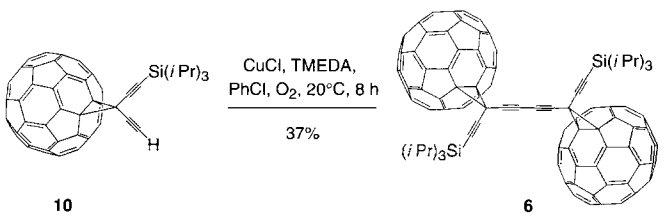
In order to probe the potential of diethynylmethanofullerenes as building blocks for molecular carbon allotropes, **10** and **3** were subjected to Hay coupling conditions (Schemes 3 and 4). Initial attempts at homocoupling of **3** did not yield tractable products, which prompted us to try heterocoupling to trimethylsilylacetylene under conditions previously developed for the preparation



Scheme 3. Synthesis of dibutadiynylmethanofullerene **5**. TMEDA = *N,N,N',N'*-tetramethylethylenediamine.

of butadiynyl porphyrins.[15] In situ preparation of the Hay catalyst [CuCl·TMEDA, O_2] in chlorobenzene in the presence of **3** and a large excess of trimethylsilylacetylene indeed furnished bis(butadiynyl)methanofullerene **5**, which was readily isolated by column chromatography (SiO_2, cyclohexane). The butadiynyl substructure of **5** is easily identified in its ^{13}C NMR spectrum by the four resonances observed in the typical range for acetylenic carbon atoms (δ = 89.32, 87.57, 70.88, and 68.62; Table 1). A total of 17 distinct fullerene carbon signals (16 between δ = 146 and 138, one at δ = 74.41) indicates no change of symmetry on passing from **3** to **5**, which demonstrates that the methanofullerene moiety remains intact in the course of the coupling reaction.

Similarly, monoprotected diethynylmethanofullerene **10** could be homocoupled to the butadiynyl-linked "dimeric" methanofullerene **6** in 37% yield (Scheme 4). In contrast to previously



10 **6**

Scheme 4. Synthesis of the dumbbell-shaped fullerene derivative **6**.

reported dumbbell-shaped molecules containing two fullerene moieties,[16] the black shiny crystals of **6** are reasonably soluble in cyclohexane, toluene, and CS_2, and complete spectroscopic characterization was possible (Table 1, Fig. 1). Matrix-assisted

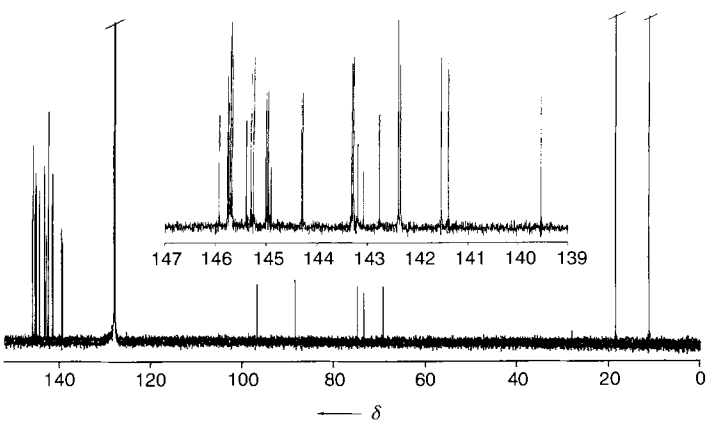


Fig. 1. ^{13}C NMR spectrum of **6** in CS_2/C_6D_6. The inset shows an expansion of the aromatic region of the fullerene signals.

laser-desorption time-of-flight (MALDI-TOF) mass spectrometry in the negative-ion mode with 2,5-dihydroxybenzoic acid as the matrix confirmed the "dimeric" nature of **6** with a signal at m/z 1877.6 ($C_{148}H_{42}Si_2$; calculated 1876.1 g mol^{-1}). In the ^{13}C NMR spectrum (Fig. 1) 31 fullerene resonances are distinguishable (30 in the aromatic region, one at δ = 73.95). The signals of the four acetylenic carbon atoms appear at δ = 97.20, 88.90, 75.31, and 69.72, while the methano bridge C atoms resonate at δ = 28.61. The electronic absorption spectrum is remarkably similar in shape and intensity to those of other methanofullerenes,[14] which indicates little electronic interaction between the two fullerene units. The electrochemistry of this material is currently under investigation, and we are working on transforming **5** and **6** into new molecular carbon allotropes.

Experimental Procedure

4: A solution of C_{60} (500 mg, 0.695 mmol) in toluene (600 mL) was treated with lithium trimethylsilylacetylide (10 mL of 0.2 M solution in THF, 2.0 mmol) under N_2. The purple solution slowly discolored, and a black precipitate formed. After 1 h thin-layer chromatography (TLC) showed that most of the C_{60} had been consumed, so the reaction was quenched with acetic acid (0.5 mL). The product was isolated by column chromatography (SiO_2/cyclohexane), and recrystallization from CS_2/Et_2O yielded 324 mg (58%) of black crystals.

9: DBU (300 μL, 2.01 mmol) was added under N_2 to a solution of C_{60} (500 mg, 0.694 mmol) and **8** (400 mg, 1.39 mmol) in toluene (550 mL). After 4 h the product was isolated by column chromatography (SiO_2/cyclohexane). The product was recrystallized from cyclohexane to yield 305 mg (47% or 55% based on recovered starting material) of large black cubic crystals.

10: To a solution of **7** (126 mg, 0.125 mmol) in THF (50 mL) was added MeOH (25 mL) and K_2CO_3 (50 mg, 0.362 mmol). After 20 min at room temperature the reaction was complete by TLC. The suspension was partitioned between toluene (100 mL) and H_2O (100 mL), and the organic phase was washed with H_2O (3 × 20 mL) and dried over $MgSO_4$. Filtration and removal of solvent left a red solid that was loaded on a short column of silica and eluted with hexane. Evaporation of solvent furnished a black material that was recrystallized from CS_2/Et_2O to yield 75 mg (64%) of bronze flakes.

6: A suspension of **10** (70 mg, 0.075 mmol) and CuCl (600 mg, 6.0 mmol) in chlorobenzene (100 mL) was stirred vigorously with TMEDA (0.85 mL, 5.5 mmol) under dry air for 8 h. The product was isolated by column chromatography (SiO_2/cyclohexane), and recrystallization from CS_2/Et_2O furnished 26 mg (37%) of black, shiny plates.

Received: March 7, 1994 [Z67351E]
German version: *Angew. Chem.* **1994**, *106*, 1427

[1] a) F. Diederich, Y. Rubin, *Angew. Chem.* **1992**, *104*, 1123–1146; *Angew. Chem. Int. Ed. Engl.* **1992**, *31*, 1101–1123; b) F. Diederich, *Nature (London)*, **1994**, *369*, 199–207.
[2] A. de Meijere, S. Kozkushkov, C. Puls, T. Haumann, R. Boese, M. J. Cooney, L. Scott, *Angew. Chem.* **1994**, *106*, 934–936; *Angew. Chem. Int. Ed. Engl.* **1994**, *33*, 869–871.
[3] Y.-Z. An, Y. Rubin, C. Schaller, S. W. McElvany, *J. Org. Chem.*, **1994**, *59*, 2927–2929.
[4] P. J. Krusic, E. Wasserman, P. N. Keizer, J. R. Morton, K. F. Preston, *Science (Washington)* **1991**, *254*, 1183–1185; P. J. Krusic, E. Wasserman, B. A. Parkinson, B. Malone, P. N. Keizer, J. R. Morton, K. F. Preston, *J. Am. Chem. Soc.* **1991**, *113*, 6274–6275; C. McEwen, R. McKay, B. Larsen, *ibid.* **1992**, *114*, 4412–4414; J. R. Morton, K. F. Preston, P. J. Krusic, S. A. Hill, E. Wasserman, *ibid.* **1992**, *114*, 5454–5455; M. A. Cremonini, L. Lunazzi, G. Placucci, *J. Org. Chem.* **1993**, *58*, 4735–4738.
[5] A. Hirsch, A. Soi, H. R. Karfunkel, *Angew. Chem.* **1992**, *104*, 808–810; *Angew. Chem. Int. Ed. Engl.* **1992**, *31*, 766–768.
[6] R. Taylor, D. R. M. Walton, *Nature (London)* **1993**, *363*, 685–693; A. Hirsch, *Angw. Chem.* **1993**, *105*, 1189–1192; *Angew. Chem. Int. Ed. Engl.* **1993**, *32*, 1138–1141; K.-D. Kampe, N. Egger, M. Vogel, *ibid.* **1993**, *105*, 1203–1205 and **1993**, *32*, 1174–1176; A. Hirsch, *Chem. Unserer Zeit* **1994**, *28*, 79–87.
[7] R. H. Baughman, D. S. Galvão, C. Cui, Y. Wang, D. Tománek, *Chem. Phys. Lett.* **1993**, *204*, 8–14.
[8] H. Hauptmann, *Tetrahedron* **1976**, *32*, 1293–1297.
[9] C. Bingel, *Chem. Ber.* **1993**, *126*, 1957–1959.
[10] H. Hauptmann, *Tetrahedron Lett.* **1974**, 3587–3588.
[11] The pK_a for the methylene protons of nonhalogenated 1,4-pentadiynes has been estimated to be less than 21 (in EtOH); I. M. Mathai, H. Taniguchi, S. I. Miller, *J. Am. Chem. Soc.* **1967**, *89*, 115–120.
[12] R. Schwesinger, H. Schlemper, *Angew. Chem.* **1987**, *99*, 1212–1214; *Angew. Chem. Int. Ed. Engl.* **1987**, *26*, 1167–1169.
[13] Y. Hori, Y. Nago, K. Tanaka, *Chem. Express* **1986**, *1*, 491–494 [*Chem. Abstr.* **1987**, *106*, 196380y].
[14] L. Isaacs, A. Wehrsig, F. Diederich, *Helv. Chim. Acta* **1993**, *76*, 1231–1250; L. Isaacs, F. Diederich, *ibid.* **1993**, *76*, 2454–2464.
[15] H. L. Anderson, *Inorg. Chem.* **1994**, *33*, 972–981.
[16] T. Suzuki, Q. Li, K. C. Khemani, F. Wudl, Ö. Almarsson, *J. Am. Chem. Soc.* **1992**, *114*, 7300–7301; P. Belik, A. Gügel, J. Spickermann, K. Müllen, *Angew. Chem.* **1993**, *105*, 95–97; *Angew. Chem. Int. Ed. Engl.* **1993**, *32*, 78–80.

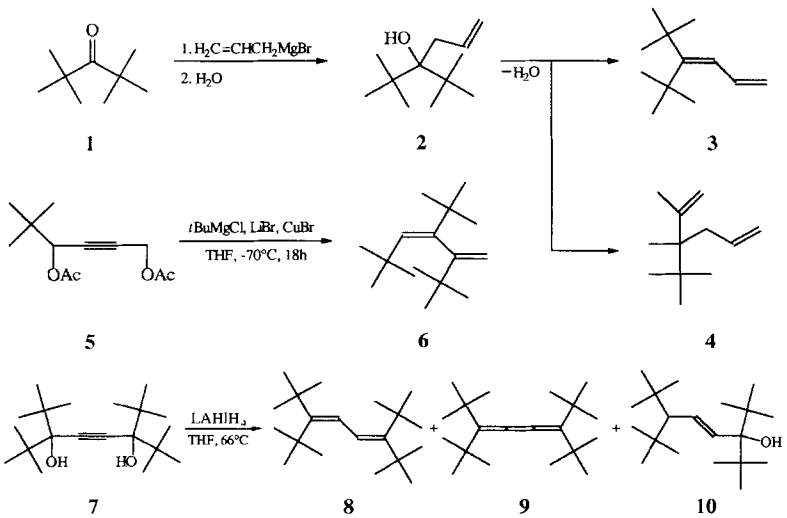
1,1-Di-, 1,2,3-Tri-, and 1,1,4,4-Tetra-*tert*-butyl-1,3-butadiene**

Henning Hopf,* Ralf Hänel, Peter G. Jones, and Peter Bubenitschek

Dedicated to Professor Virgil Boekelheide on the occasion of his 75th birthday

Highly substituted dienes exist predominantly in nonplanar, and in the extreme case orthogonal, conformations, which in turn result in chemical behavior distinctly different from that of planar 1,3-dienes.[1] Prerequisites for a systematic study of the relationship between orthogonality and reactivity of di- and polyenes are methods of synthesis that are not only efficient, but also offer sufficient scope for application. Now, after we presented a procedure for the convenient preparation of highly alkylated 1,3-dienes that have *tert*-butyl groups at C2 and C3 in 1991, we describe new routes to terminal *tert*-butylated butadienes.

5,5-Dimethyl-4-*tert*-butyl-1,3-hexadiene (**3**) is accessible by the reaction of di-*tert*-butylketone (**1**) with allylmagnesium bromide and dehydration of the resulting alcohol **2**. Depending on the reaction conditions, varying amounts of the Wagner–Meerwein product **4** are formed in this elimination: whereas this 1,5-hexadiene derivative arises exclusively with *para*-toluenesulfonic acid/benzene, the proportion when using thionyl chloride/pyridine is only about 70%, and a virtual reversal of the product ratio (89% **3**, 11% **4**, GC analysis) is achieved if **2** is initially converted into its *p*-nitrobenzoate, and this ester is finally decomposed thermally (100 → 160 °C); **3** is obtainable in gram quantities in this manner.



For the synthesis of (*Z*)-4-*tert*-butyl-2,2,6,6-tetramethyl-5-methylene-3-heptene (**6**) the previously employed "*tert*-butylcuprate" method with diacetate **5** as starting material proved advantageous (yield 63%). 3,6-Di-*tert*-butyl-2,2,7,7-tetramethyl-3,5-octadiene (**8**) was finally obtained by reduction of the diol **7** with $LiAlH_4$. All experiments afforded **8** as a mixture with the [3]cumulene **9** and the allyl alcohol **10** (typical composition of the reaction mixture after a reduction period of 33 days: 3% **7**, 16% **10**, 67% **8** + **9**, 13% unidentified product; GC analysis).

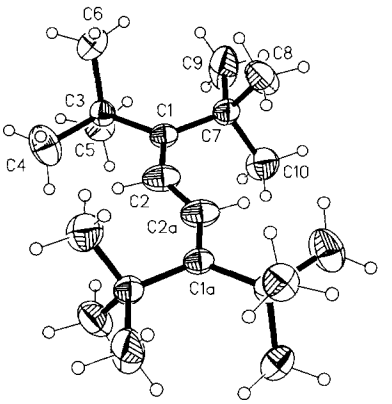


Fig. 1. The molecular structure of **8** in the crystal (ellipsoids represent 50% probability).

Although the complete chromatographic separation/purification of these compounds has not yet been successful, crystals that were suitable for an X-ray crystal analysis[3] could be picked out manually. As Figure 1 shows, **8** has crystallographic inversion symmetry. The bond lengths C1–C2 (134.6(3) pm) and C2–C2a (135.3(4) pm) differ only marginally. The torsion angle C3-C1-C2-C2a (−179.3(4)°) and C1-C2-C2a-C1a (180°) confirm the planarity of the molecular skeleton. The angle C1-C2-C2a is widened to 142.2(3)°,[4] which apparently in this sterically strained system is easier to tolerate than loss of planarity.

To gain a first impression of the reactivity of the new dienes, whose structures can deduced without ambiguity from the spectroscopic data (Table 1), we treated **6** with bromine in trichloro-

Table 1. Spectroscopic data of **3**, **6**, and **8** [a].

3: ^{1}H NMR ($CDCl_3$): δ = 1.23, 1.36 (2 × s, each 9H, *t*Bu), 5.03–5.09 (m, 2H, 1-H), 6.02 (d, J = 11.2 Hz, 1H, 3-H), 6.93–7.03 (m, J = 11.2 Hz, 1H, 2-H); ^{13}C NMR ($CDCl_3$): δ = 156.8 (s, C-4), 136.4, 124.4 (2 × d, C-2, C-3), 115.9 (t, C-1), 38.7, 37.7 (2 × s, C-5, C-7), 33.7, 31.8 (2 × q, CH_3); UV (CH_3CN): λ_{max} (ε) = 242 nm (8620); IR (film): $\tilde{\nu}$ = 3087 cm^{-1} (= CH_2), 1620 (C = C), 901(> C = CH_2); MS (70 eV): *m/z* (%) = 166 (12, M^+), 109 (100), 57 (92); elemental analysis for $C_{12}H_{22}$ (166.31): calc. C 86.67, H 13.33; found C 86.58, H 13.31

6: ^{1}H NMR ($CDCl_3$): δ = 1.04, 1.08, 1.18 (3 × s, each 9H, *t*Bu), 4.76 (d, J = 1.8 Hz, 1H, 8-H), 5.15 (d, J = 1.9 Hz, 1H, 8-H), 5.32 (s, 1H, 3-H); ^{13}C NMR ($CDCl_3$): δ = 156.3, 146.2 (2 × s, C-4, C-5), 135.2 (d, C-3), 114.3 (t, C-8), 36.2, 35.0, 33.4 (3 × s, C-2, C-6, C-9), 32.5, 31.6 (q, CH_3); UV (CH_3CN): λ_{max} (ε) = 195 nm (13600); IR (film): $\tilde{\nu}$ = 3078 cm^{-1} (= CH_2), 901 (> C = CH_2); elemental analysis for $C_{16}H_{30}$ (222.41): calc. C 86.40, H 13.60; found C 86.38, H 13.66

8: (mixture with **9**): ^{1}H NMR ($CDCl_3$): δ = 1.23, 1.33 (2 × s, each 18 H, *t*Bu), 6.42 (s, 2H, 4-H, 5-H); ^{13}C NMR ($CDCl_3$): δ = 151.2 (s, C-3, C-6), 123.0 (d, C-4, C-5), 39.1, 37.2 (2 × s, C-2, C-7, C-9, C-11), 32.74, 32.0 (q, CH_3); GC/MS (40 eV): *m/z* (%) = 278 (2, M^+), 165 (34), 109 (24), 57 (100)

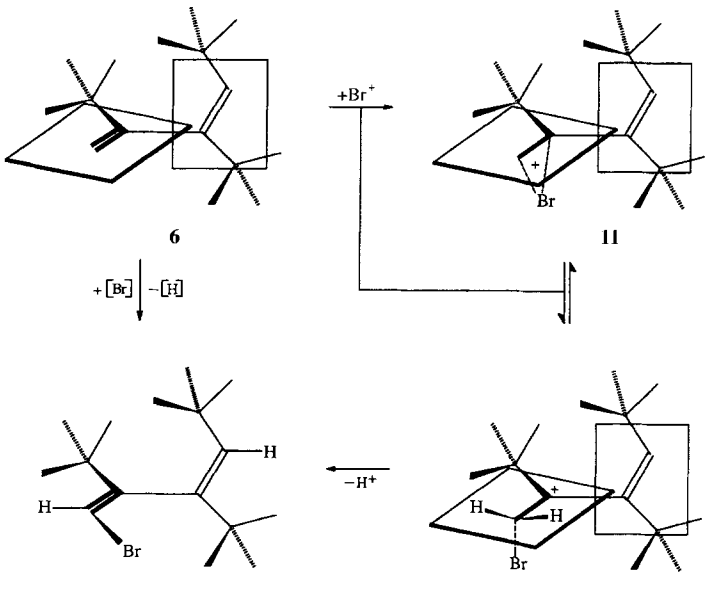
12: ^{1}H NMR ($CDCl_3$): δ = 1.05, 1.18, 1.22 (3 × s, each 9H, *t*Bu), 5.39 (s, 1H, 4-H), 6.28 (s, 1H, 1-H); ^{13}C NMR ($CDCl_3$): δ = 154.1, 140.0 (s, C-4, C-5), 137.9 (d, C-8), 106.8 (d, C-3), 37.5, 36.1, 33.9 (3 × s, C-2, C-6, C-9), 32.2, 31.2, 29.9 (3 × q, CH_3); UV (CH_3CN): λ_{max} (ε) = 194 nm (14400); IR (Film): $\tilde{\nu}$ = 3078 cm^{-1} (= CH_2), 647 (C–Br); GC/MS (40 eV): *m/z* (%) = 302/300 (2, M^+), 246/244(2), 165(7), 109(7), 57(100); elemental analysis for $C_{16}H_{29}Br$ (301.31): calc. C 63.78, H 9.70; found C 63.69, H 9.55.

[a] The NMR spectra were recorded at 400 MHz(^{1}H) and 100.6 MHz (^{13}C).

[*] Prof. Dr. H. Hopf, Dipl.-Chem. R. Hänel, Dipl.-Chem. P. Bubenitschek
Institut für Organische Chemie der Technischen Universität
Hagenring 30, D-38106 Braunschweig (FRG)
Telefax: Int. code + (531)-391-5388
Prof. Dr. P. G. Jones
Institut für Anorganische und Analytische Chemie
der Technischen Universität Braunschweig

[**] Sterically Hindered Double-Bond Systems, Part 6. We thank the Deutsche Forschungsgemeinschaft and the Fonds der Chemischen Industrie for the support of our research. Part 5: H. Hopf, M. Traetteberg, R. Hänel, *Chem. Ber.* in press.

methane at 0–5 °C. Instead of the expected 1,2- and/or 1,4-adducts, the monobromide **12** in which the butadiene part has been *retained* was isolated exclusively (yield 60%).



To explain this observation we postulate an initial Br attack at the sterically less hindered side of the less substituted double bond of **6**. Whether this forms a bromonium ion (**11**) or an "open carbenium ion" (**13**, orthogonal allyl cation) is unknown. At any rate this intermediate cannot be captured by the usual back-side attack because of extreme steric shielding. It can, however, be stabilized by deprotonation to form **12**. The *trans* arrangement of bromine and *tert*-butyl substituents in **12** is concluded from NOE difference measurements (Table 1). Thus **6** favors substitution (by addition/elimination) over addition, and thus behaves *regeneratively, like a classical arene*.

Received: February 4, 1993 [Z 6669 1E]
German version: *Angew. Chem.* **1994**, *106*, 1444

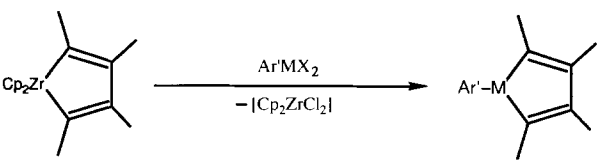
[1] H. Hopf, M. Traetteberg, H. Lipka, *Angew. Chem.* **1994**, *106*, 232–233; *Angew. Chem. Int. Ed. Engl.* **1994**, *33*, 204–205.
[2] H. Hopf, H. Lipka, *Chem. Ber.* **1991**, *124*, 2075–2084.
[3] Crystal data for **8**: $C_{20}H_{38}$. $P\bar{1}$, $a = 609.8(2)$, $b = 820.3(3)$, $c = 1028.0(3)$ Å, $\alpha = 75.73(2)$, $\beta = 85.71(2)$, $\gamma = 71.47(2)°$, $V = 0.4725(3)$ Å^3, $Z = 1$, $T = -100$ °C. A colorless prism 0.7 × 0.45 × 0.12 mm was mounted in inert oil (type RS3000, Fa. Riedel de Haën). On a Siemens R3 diffractometer, 2736 intensities ($Mo_{K\alpha}$ radiation, $\lambda = 71.073$ pm, $2\theta_{max} = 55°$) were measured, of which 2151 were independent ($R_{int} = 0.017$). The structure was solved with direct methods and refined anisotropically on F^2 (program SHELXL-93, G. M. Sheldrick, University of Göttingen). The final $wR(F^2)$ value was 0.186, with a conventional $R(F)$ of 0.061, for 97 parameters. Further details of the crystal structure investigation may be obtained from the Fachinformationszentrum Karlsruhe, Gesellschaft für wissenschaftlich-technische Information mbH, D-76344 Eggenstein-Leopoldshafen (FRG) on quoting the depository number CSD-400686 and the journal citation.
[4] A reviewer pointed out that the wide angle C1-C2-C2a could be a result of disorder in view of the "large displacement parameters" of the atom C2. Such effects are always possible in principle and cannot be completely ruled out here. With a U_{eq} value of only 0.046 Å^2 for C2, however, we see no reason to expect a particularly large error and also no chance to resolve any disorder.

Synthesis and Ligative Behavior of a Gallacyclopentadiene**

Alan H. Cowley,* François P. Gabbaï, and Andreas Decken

Boracyclopentadienes (boroles) have been known for several years[1] and continue to attract attention, for example, as ligands.[2] However, surprisingly little information is available regarding the heavier group 13 metallacyclopentadienes. In fact, structurally authenticated examples of such compounds are confined to one aluminacyclopentadiene, which was isolated as an Et_2O adduct and as a Ni(cod) complex (cod = 1,5-cyclopentadiene).[3] We report here the synthesis and X-ray crystal structure of the first neutral gallacyclopentadiene[4] and the corresponding $(\eta\text{-}C_5H_5)Co$ complex.

Since 1-phenyl-2,3,4,5-tetramethylboracyclopentadiene dimerizes,[5] it was clear that the isolation of the desired gallium analogue demanded the use of a bulkier aryl group. Accordingly, the zirconacyclopentadiene **1**[6] was treated with $Ar'GaCl_2$ (Ar' = 2,4,6-tBu$_3$C$_6$H$_2$)[7] in C_6H_6 solution. The reaction, which takes place over a 48 h period at 25 °C, affords a 73% yield of gallacyclopentadiene **2**.



1

2, M = Ga
3, M = In

Ar' = 2,4,6-tBu$_3$C$_6$H$_2$; X = Cl, Br

The proposed formula for **2** is consistent with elemental analysis data and with the observations that a) the base peak in the CI mass spectrum corresponds to M^+, b) no peaks are detectable at higher m/z values (Table 1), and c) ^{1}H and ^{13}C NMR spectra exhibit the anticipated resonances in the appropriate intensity ratios (Table 1).

An X-ray structure analysis of **2**[8] showed that the asymmetric unit contained two independent molecules. However, the metrical parameters for molecules I (Fig. 1) and II are very similar and neither molecule exhibits unusually short intermolecular interactions. The five-membered gallacyclopentadiene ring is planar, the maximum deviation from the least-squares plane being 0.013 Å for C(21). The Ar'Ga group is bonded to the tetramethylbutadiene moiety in a symmetrical fashion such that the endocyclic bond angle is about 45° smaller than the exocyclic angles. The Ga–C(aryl) bond is slightly shorter than the other two Ga–C bonds; however, all three distances fall in the range for single bonds. The double bonds within the gallacyclopentadiene ring are localized as indicated by the fact that the C(20)–C(21) distance is considerably larger than the other two C–C distances. A further interesting feature of the structure of **2** relates to the near orthogonality of the Ar' and gallacyclopentadiene rings (dihedral angles = 83.6 and 84.4° in molecules I and

[*] Prof. A. H. Cowley, F. P. Gabbaï, Dr. A. Decken
Department of Chemistry and Biochemistry
The University of Texas at Austin
Austin, TX 78712 (USA)
Telefax: Int. code + (512)471-6822

[**] This work was supported by the National Science Foundation and the Robert A. Welch Foundation.

Table 1. Important physical data for **2**–**4**.

2: ^{1}H NMR (300.15 MHz, C_6D_6, 295 K, TMS ext.): $\delta = 1.34$ (s, 9 H, *p*-*t*Bu), 1.39 (s, 18 H, *o*-*t*Bu), 1.95 (s, 6 H, 2,5-Me_2), 2.09 (s, 6 H, 3,4-Me_2), 7.51 (s, 2 H, H-aryl); $^{13}C\{^1H\}$ NMR (75.47 MHz, C_6D_6, 295 K, TMS ext.): $\delta = 14.71$, 16.98 (CMe), 31.58 (s, *p*-$(CH_3)_3C$), 32.26 (s, *o*-$(CH_3)_3C$), 34.99 (s, *p*-$(CH_3)_3C$), 37.67 (s, *o*-$(CH_3)_3C$), 120.49 (s, *m*-C(aryl)), 133.19 (s, 3,4-C_2), 133.92 (s, *ipso*-C(aryl)), 149.71 (s, 2,5-C_2), 150.17 (s, *p*-C(aryl)), 157.25 (s, *o*-C(aryl)). MS(CI, CH_4): *m/z* 423 ($M^+ + H$, 100%); HRMS(CI, CH_4): calcd for $C_{26}H_{42}{}^{69}Ga$ 423.2542, found 423.2529.

3: ^{1}H NMR (300.15 MHz, C_6D_6, 295 K, TMS ext.): $\delta = 1.34$ (s, 18 H, *p*-*t*Bu)), 1.39 (s, 9 H, *o*-*t*Bu), 2.06 (s, 6 H, 2,5-Me_2), 2.27 (s, 6 H, 3,4-Me_2), 7.54 (s, 2 H, H-aryl); $^{13}C\{^1H\}$ NMR (75.47 MHz, C_6D_6, 295 K, TMS ext.): $\delta = 15.51$, 20.14 (CMe), 31.78 (s, *o*-$(CH_3)_3C$), 32.61 (s, *p*-$(CH_3)_3C$), 35.10 (s, *o*-$(CH_3)_3C$), 37.04 (s, *p*-$(CH_3)_3C$), 120.46 (s, *m*-C(aryl)), 137.00 (s, 3,4-C_2), 149.66 (s, 2,5-C_2), 149.86 (s, *p*-C(aryl)), 157.08 (s, *o*-C(aryl)), C-*ipso* not detected. MS(CI, CH_4) *m/z* 469 ($M^+ + H$, 100%). HRMS(CI, CH_4): calcd for $C_{26}H_{42}In$ 469.2325, found 469.2338.

4: ^{1}H NMR (300.15 MHz, C_6D_6, 295 K, TMS ext.): $\delta = 1.32$ (s, 9 H, *p*-*t*Bu), 1.39 (s, 18 H, *o*-*t*Bu), 2.11 (s, 12 H, CMe), 4.34 (s, 5 H, C_5H_5), 7.58 (s, 2 H, H-aryl); $^{13}C\{^1H\}$ NMR (75.47 MHz, C_6D_6, 295 K, TMS ext.): $\delta = 13.62$, 20.10 (s, $C(CH_3)$), 31.66 (s, *p*-$(CH_3)_3C$), 33.23 (s, *o*-$(CH_3)_3C$), 35.14 (s, *p*-$(CH_3)_3C$), 37.41 (s, *o*-$(CH_3)_3C$), 81.58 (s, C_5H_5), 83.85, 96.48 (s, $C(CH_3)$), 119.65 (s, *m*-C(aryl)), 135.69 (s, *p*-C(aryl)), 149.48 (s, *o*-C(aryl)), C-*ipso* not detected. MS(CI, CH_4): *m/z* 526 (M^+, 100%), 423 ($M^+ -$ CpCo + H, 15%), 301($M^+ -$ Ar', 3%). HRMS(CI, CH_4): calcd for $C_{31}H_{46}Co^{69}Ga$ 546.2187, found 546.2196.

II, respectively). Such an arrangement, which minimizes the steric interactions between the *o*-*t*Bu and 2,5-methyl groups, undoubtedly contributes to the stability of the base-free gallacyclopentadiene **2**.

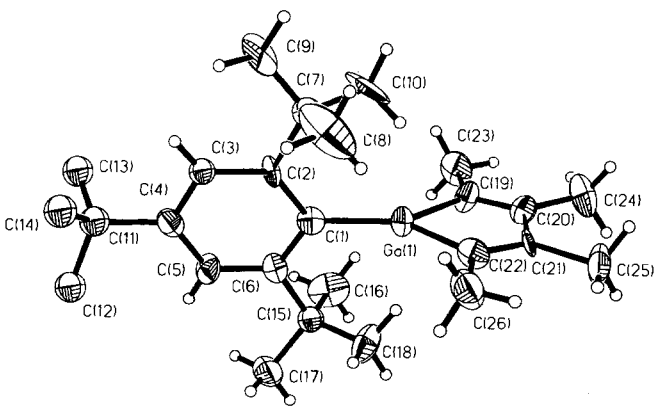
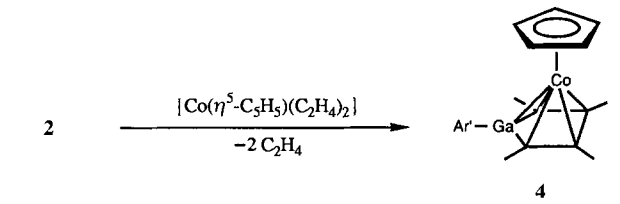


Fig. 1. View of **2** showing the atom labeling scheme. There are two independent molecules in the asymmetric unit; molecule I is shown here. The *p*-*t*Bu groups are disordered. Important bond lengths [Å] and angles [°]: Ga(1)-C(1) 1.888(21), Ga(1)-C(19) 1.953(22), Ga(1)-C(22) 1.937(26), C(19)-C(20) 1.313(37), C(20)-C(21) 1.542(37), C(21)-C(22) 1.312(37), C(1)-Ga(1)-C(19) 134.5(10), C(1)-Ga(1)-C(22) 135.4(10), C(19)-Ga(1)-C(22) 90.1(11), Ga(1)-C(19)-C(20) 108.0(18), C(19)-C(20)-C(21) 116.1(22), C(20)-C(21)-C(22) 118.9(22), Ga(1)-C(22)-C(21) 106.9(19).

The reaction of **1** with $Ar'InBr_2$[7a] proceeds analogously to that with $Ar'GaCl_2$ and affords the first neutral indacyclopentadiene **3**. It has not yet been possible to grow single crystals of **3** suitable for X-ray analysis. However, the mass spectral and NMR data for **3** (Table 1) are remarkably similar to those for **2**, hence an analogous structure can be proposed.

The ligative behavior of **2** is of potential interest in regard to the development of single-source precursors for the deposition of intermetallic phases such as β-CoGa.[9] Thus **2** reacts with $[Co(\eta^5\text{-}C_5H_5)(C_2H_4)_2]$ to afford the cyclopentadienylcobalt(I) complex **4**.



The proposed formula for **4** is in accord with elemental analysis data and the observation of the molecular ion together with satellites of the correct isotopic abundances in the CI mass spectrum (Table 1). Support was provided by the ^{1}H and $^{13}C\{^1H\}$ spectra which exhibit all the expected resonances in the appropriate relative intensities. An X-ray structure analysis of **4** (Fig. 2)[8] revealed that attachment of the $(\eta^5\text{-}C_5H_5)$Co moiety

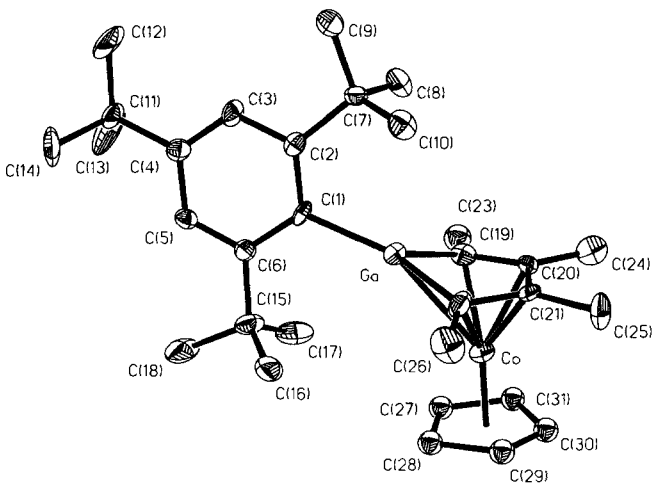


Fig. 2. View of **4** showing the atom labeling scheme. Important bond lengths [Å] and angles [°]: Ga-C(1) 1.988(12), Ga-C(19) 1.921(12), Ga-C(22) 1.918(15), C(19)-C(20) 1.414(22), C(20)-C(21) 1.459(19), C(21)-C(22) 1.434(19), Co-Ga 2.706(2), Co-C(19) 2.089(13), Co-C(20) 1.986(24), Co-C(21) 1.981(13), Co-C(22) 2.109(13), C(1)-Ga-C(19) 133.7(6), C(1)-Ga-C(22) 140.2(5), C(19)-Ga-C(22) 85.9(6), Ga-C(19)-C(20) 110.6(10), C(19)-C(20)-C(21) 113.6(11), C(20)-C(21)-C(22) 114.4(12), Ga-C(22)-C(21) 109.6(10). The dihedral angle between the C(19)-Ga-C(22) and Ga-C(1)-C(2)-C(3)-C(4)-C(5)-C(6) planes = 85.6 .

to the gallacyclopentadiene ring resulted in the following: a) the gallacyclopentadiene ring changes from a planar to an envelope conformation with an angle of 21.8° between the C(19)-Ga-C(22) and C(19)-C(20)-C(21)-C(22) planes such that the Ga atom resides 0.52 Å above the latter plane; b) within experimental error, all three C–C bond lengths in the gallacyclopentadiene ring became essentially equal; c) the Ga–C(aryl) bond length increases by about 0.1 Å. Although observation a) implies η^4 attachment of the $(\eta^5\text{-}C_5H_5)$Co moiety to the gallacyclopentadiene ring, it is interesting to note that the Co–Ga distance in **4** (2.706(2) Å) is considerably shorter than the sum of van der Waals radii and only slightly longer than the range of 2.38 to 2.58 Å that has been reported for the few compounds that feature this linkage.[10] From the standpoint of the number of skeletal bonding electrons, **4** can be viewed as a *nido* cluster provided the Ar'Ga moiety is included in the framework.

Experimental Procedure

2: Solid $Ar'GaCl_2$ (1.40 g, 3.63 mmol) and $[(C_5H_5)_2Zr(C_4Me_4)]$ (1.20 g, 3.63 mmol) were mixed in a 100 mL Schlenk flask, then dissolved in benzene (30 mL). The reaction mixture was stirred for 48 h at 25 °C following which the benzene was

removed under reduced pressure. Extraction of the resulting residue with pentane (15 mL), followed by solvent removal, afforded a 73% yield of white microcrystalline **2** (m.p. 103 °C). X-ray quality crystals were grown from a concentrated pentane solution.

4: A mixture of $[(C_5H_5)Co(C_2H_4)_2]$ (0.12 g, 0.69 mmol) and **2** (0.29 g, 0.69 mmol) in benzene (5 mL) was stirred for 15 h following which the benzene was removed under reduced pressure. Extraction of the residue with pentane, followed by cooling of the resulting solution to −20 °C resulted in two successive crops of crystals of **4** (m.p. 201 °C) in a combined yield of 40%.

Received: February 12, 1994 [Z 6687 IE]
German version: *Angew. Chem.* **1994**, *106*, 1429

[1] See, for example, J. J. Eisch, N. K. Hota, S. Kozima, *J. Am. Chem. Soc.* **1969**, *91*, 4575; J. J. Eisch, J. E. Galle, S. Kozima, *ibid.* **1986**, *108*, 379; J. J. Eisch, J. E. Galle, *J. Organomet. Chem.* **1977**, *127*, C 9; L. Killian, B. Wrackmeyer, *ibid.* **1978**, *148*, 137; W. Schacht, D. Kaufmann, *Angew. Chem.* **1987**, *99*, 682; *Angew. Chem. Int. Ed. Engl.* **1987**, *26*, 665.

[2] See, for example, G. E. Herberich, J. Hengesbach, U. Kölle, G. Huttner, A. Frank, *Angew. Chem.* **1976**, *88*, 450; *Angew. Chem. Int. Ed. Engl.* **1976**, *15*, 433; G. E. Herberich, J. Hengesbach, U. Kölle, W. Oschmann, *ibid.* **1977**, *89*, 63 and **1977**, *16*, 42; G. E. Herberich, T. Carlstensen, D. P. J. Köffer, N. Klaff, R. Boese, I. Hyla-Krypsin, R. Gleiter, M. Stephan, H. Meth, U. Zenneck, *Organometallics* **1994**, *13*, 619, and references therein.

[3] H. Hoberg, R. Krause-Göing, *J. Organomet. Chem.* **1977**, *127*, C 29; C. Krüger, J. C. Sekutowski, H. Hoberg, R. Krause-Göing, *ibid.* **1977**, *141*, 141.

[4] For the reaction of **1** with $GaCl_3$, see P. J. Fagan, W. A. Nugent, *J. Am. Chem. Soc.* **1988**, *110*, 2310.

[5] P. J. Fagan, E. G. Burns, J. C. Calabrese, *J. Am. Chem. Soc.* **1988**, *110*, 2979.

[6] E. Negishi, F. E. Lederbaum., T. Tamotsu, *Tetrahedron Lett.* **1986**, *27*, 2829.

[7] a) S. Schulz, S. Pusch, E. Pohl, S. Dielkus, R. Herbst-Irmer, A. Meller, H. W. Roesky, *Inorg. Chem.* **1993**, *32*, 3343; b) M. A. Petrie, P. P. Power, H. V. Rasika Dias, K. Ruhlandt-Senge, K. M. Waggoner, R. J. Wehmschulte, *Organometallics* **1993**, *12*, 1086.

[8] Crystal structure data for **2** ($C_{26}H_{61}Ga$): monoclinic, space group $P2_1/c$, $Z = 8$, $a = 21.540(4)$, $b = 9.860(1)$, $c = 24.832(3)$ Å, $\beta = 105.85(2)°$, $V = 5073(2)$ Å^3, $\rho_{calcd} = 1.108$ g cm^{-3}, $Mo_{K\alpha}$, $\lambda = 0.71073$ Å, $\mu = 10.9$ cm^{-1}. 6618 unique data were collected at 298 K on an Enraf Nonius CAD 4 diffractometer (2θ-θ scan technique, $4.0 < 2\theta < 45.0°$). Of these, 1668 had $I > 6\sigma(I)$ and were used for structure solution (direct methods) and refinement, $R = 0.0654$. The *p*-*t*Bu groups are disordered (C(12), C(13), and C(14) in molecule I and C(42), C(43), and C(44) in molecule II). Crystal structure data for **4** ($C_{31}H_{46}CoGa$): orthorhombic, space group $P2_12_12_1$, $Z = 4$, $a = 9.848(2)$, $b = 16.423(4)$, $c = 17.569(4)$ Å, $V = 2841(1)$ Å^3, $\rho_{calcd} = 1.279$ g cm^{-3}, $Mo_{K\alpha}$, $\lambda = 0.71073$ Å, $\mu = 15.5$ cm^{-1}. 2989 unique data were collected at 298 K on an Enraf Nonius CAD 4 diffractometer (2θ-θ scan technique, $4.0 < 2\theta < 50.0°$). Of these, 1703 had $I > 4\sigma(I)$ and were used for structure solution (direct methods) and refinement, $R = 0.0569$. Further details of the crystal structure investigations may be obtained from the Fachinformationszentrum Karlsruhe, D-76344 Eggenstein-Leopoldschafen (FRG), on quoting the depository number CSD-58142.

[9] Y. J. Chen, H. D. Kaesz, Y. K. Kim, H. J. Müller, Z. Xue, *Appl. Phys. Lett.* **1989**, *55*, 2760; R. A. Fischer, W. Scherer, M. Kleine, *Angew. Chem.* **1993**, *105*, 778; *Angew. Chem. Int. Ed. Engl.* **1993**, *32*, 748.

[10] N. A. Compton, R. J. Errington, N. C. Norman, *Adv. Organomet. Chem.* **1990**, *31*, 91; *Gmelin Handbook of Inorganic Chemistry. Organogallium Compounds*, Part 1, Springer, Berlin, **1987**.

$[Be(dad)_2]$: Synthesis and Structure of a Diazabutadieneberyllium Complex**

Karl-Heinz Thiele,* Volker Lorenz, Gerhard Thiele, Peter Zönnchen, and Joachim Scholz

Diazadiene complexes of electron-poor transition elements[1, 2] are most often prepared from metal halides and diazabutadienes in the presence of alkali metals or magnesium and are a well-investigated class of compounds. In contrast, little information is available about diazadiene complexes of elements of the second main group.[3–5] We report here on the synthesis of a diazadieneberyllium complex and its structure in the solid state and in solution.

On treatment of beryllium chloride with the diazadiene **1** and sodium according to Equation (a), crystals with a metallic luster of composition $[Be(dad)_2]$ (**2**) can be isolated.

$$\underset{\mathbf{1}}{BeCl_2 + 2\ dad} + 2\ Na \xrightarrow{\text{toluene}} \underset{\mathbf{2}}{[Be(dad)_2]} + 2\ NaCl \qquad (a)$$

In crystalline form **2** is astoundingly stable to oxygen and moisture. In finely powdered form or in solution an immediate reaction takes place, recognizable by the color change from black-green to yellow. In hydrocarbons **2** is only slightly soluble; these solutions are, however, strongly colored. The EI mass spectrum contains an intense molecular ion peak [*m*/*z* (%) 786 (75)] and the characteristic fragmentation pattern of a diazadiene. The volatility under conditions of the mass spectrometric experiment indicates that **2** is monomeric. The structure determined by X-ray diffraction is shown in Figure 1.[6]

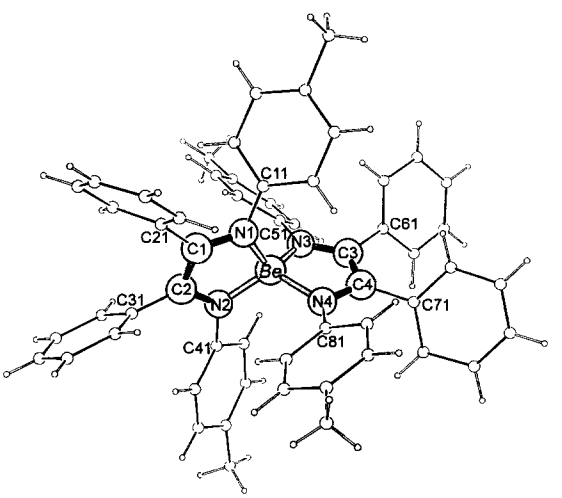


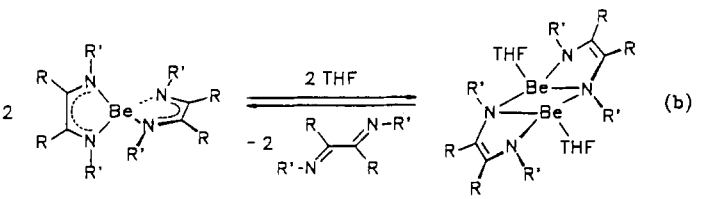
Fig. 1. Crystal structure of **2**. Selected bond lengths [pm] and angles [°]: Be-N1 170(2), Be-N2 169(2), Be-N3 168(2), Be-N4 173(2), N1-C1 132(1), N2-C2 137(1), N3-C3 134(1), N4-C4 135(1), C1-C2 141(1), C3-C4 140(1), N1-C11 141(1), C1-C21 151(1), C2-C31 148(1), N2-C41 143(1), N3-C51 143(1), C3-C61 148(1), C4-C71 150(1), N4-C81 141(1); N1-Be-N2 94.3(8), N3-Be-N4 94.4(8), N1-Be-N3 115.6(10), N1-Be-N4 113.4(10), N2-Be-N3 123.1(11), N2-Be-N4 117.6(10), Be-N1-C1 108.5(8), Be-N2-C2 109.4(9), Be-N3-C3 109.9(9), Be-N4-C4 106.7(8), N1-C1-C2 116.0(10), C1-C2-N2 111.4(10), N3-C3-C4 113.3(10), C3-C4-N4 115.2(10).

According to the crystal structure two *cis*-configured dad ligands surround the Be atom; the ligating N atoms occupy the vertices of a distorted tetrahedron. The Be–N distances lie between 167 and 174 pm and are thereby longer than those in beryllium amides, which are, for example, 157.3 pm in $[\{Be(NMe_2)_2\}_3]$ and 156.2 pm in $[Be\{N(SiMe_3)_2\}_2]$.[7, 8] The heterodiene frameworks N1–C1–C2–N2 and N3–C3–C4–N4 together with the Be atom form two planes that are almost orthogonal to each other. Thus, a spiranoid system is present. The C=N and C–C bond lengths in the free ligand are 127.0 and 152.7 pm, respectively.[9] Relative to these lengths, the N–C bonds in **2** are distinctly

[*] Prof. Dr. K.-H. Thiele, Dipl.-Chem. V. Lorenz, Dr. J. Scholz
Institut für Anorganische Chemie der Universität Halle
Geusaer Strasse, D-06217 Merseburg (FRG)
Telefax: Int. code + (3461)-46-2370
Prof. Dr. G. Thiele, Dipl-Chem. P. Zönnchen
Institut für Anorganische und Analytische Chemie
der Universität Freiburg (FRG)

[**] This work was supported by the Fonds der Chemischen Industrie. dad = 1,4-bis(4-methylphenyl)-2,3-diphenyl-1,4-diaza-1,3-butadiene.

lengthened and the C–C bonds shortened, from which a charge delocalization in the ligand may be concluded. The EPR spectrum of the crystalline compound displays an intense signal without fine structure ($g = 2.004$), which suggests that **2** is paramagnetic. The spectrum does not change on dissolving the compound in nonpolar solvents ($g = 2.006$). Since in the EPR spectrum of **2** no half field signal is observed, the dad ligands are independent radical anions each with spin $S = 1/2$, and the Be atom is in the oxidation state II. Analogous ions also exist in diazadiene complexes of aluminum and gallium. In these compounds only one diazadiene ligand is present as radical ion; the other can be formulated as an enediamide ion.[10, 11] Comparable with **2** are diazadienelanthanide complexes of the type $[Ln(NR{=}CH{-}CH{=}NR)_3]$ containing exclusively radical anions on the metal atom. Because the solubility of **2** is too small and its nature is paramagnetic, no interpretable ^{1}H NMR spectrum could be obtained in [D$_8$]toluene. Surprisingly, however, sharp signals are observed in the spectrum recorded in [D$_8$]THF. Under the influence of the donor, **2** is converted into the diamagnetic compound **3** accord-



R = C$_6$H$_5$, R' = C$_6$H$_4$-4-CH$_3$

ing to Equation (b): an intramolecular disproportionation takes place in which one of the radical anions transfers its electron to the other ligand at the Be atom to form a free dad ligand and an enediamide ion. Possibly a beryllium enediamide intermediate is formed first and stabilizes by dimerizing with the formation of enediamide bridging ligands to yield **3**. In the ^{1}H NMR spectrum this reaction can be monitored by the appearance of a singlet for the methyl protons of the free ligand **1** at $\delta = 2.16$ and two singlets for the methyl groups of the nonequivalent *p*-tolyl groups of the enediamide ions at $\delta = 2.24$ and 2.26. Analogously the ^{13}C NMR spectrum of **1**, recorded in [D$_8$]THF, displays the CH$_3$ signal of **1** at $\delta = 20.93$ and two singlets at $\delta = 23.19$ and 14.34 for the CH$_3$ groups of the enediamide ligands of **3**. Similar structures with enediamide bridging ligands were discussed for Mg complexes on the basis of NMR data, and were proven for the Mn complex $[\{Mn(NPh{-}CPh{=}CPh{-}NPh)\cdot THF\}_2]$ by X-ray structure analysis.[4] Dimeric structures and indications of equilibria in solution are also prevalent in the conversions of dialkylberyllium compounds with other chelating ligands like *N*,*N*,*N*′,*N*′-tetramethylethylenediamine, 2,2′-bipyridyl, and dimethoxyethane.[13]

Experimental Procedure

2: Anhydrous $BeCl_2$ (0.77 g, 9.66 mmol) were added to a solution of **1** (7.5 g, 19.3 mmol) in toluene (200 mL) at 20 °C. The mixture was stirred for 24 h, after which sodium (0.44 g, 19.3 mmol) was added, and the mixture again stirred for 3 days, during which time the color changes from the initial orange-yellow to deep red and finally dark brown. After the solvent was removed under vacuum, the residue was extracted in a continuous extractor with hot toluene. Compound **2** separates as a black-green, microcrystalline substance. Yield 3.5 g (46%). Repeated recrystallization from hot toluene produces crystals suitable for X-ray structure analysis. Correct elemental analysis (C, H, N); EI-MS (70 eV): *m*/*z* (%): 786 (75) [M^+], 388 (45) [dad$^+$], 194 (100) [Me-4-C$_6$H$_4$N=CPh$^+$].

3: ^{1}H NMR (300 MHz, [D$_8$]THF, 25 °C): $\delta = 7.85$–6.40 (m, C$_6$H$_5$, C$_6$*H*$_4$-4-Me), 2.26, 2.24 (s, C$_6$H$_4$-4-*Me*); ^{13}C NMR (75 MHz [D$_8$]THF, 25 °C): $\delta = 150$–120 (C$_6$H$_5$, C$_6$H$_4$-4-Me), 23.2, 14.3 (C$_6$H$_4$-4-*Me*).

1: ^{1}H NMR (200 MHz, [D$_8$]THF, 25 °C): $\delta = 2.16$ (s, 6H, C$_6$H$_4$-4-*Me*), 6.82 (d, 4H, $^3J_{(H,H)} = 8$ Hz, C$_6$*H*$_4$-4-Me), 6.44 (d, 4H, $^3J_{(H,H)} = 8$ Hz, C$_6$*H*$_4$-4-Me), 7.82 (m, 4H, C$_6$H$_5$), 7.32 (m, 4H, C$_6$H$_5$).

Received: December 27, 1993 [Z6578IE]
German version: *Angew. Chem.* **1994**, *106*, 1461

[1] J. Scholz, M. Dlikan, D. Ströhl, A. Dietrich, H. Schumann, K.-H. Thiele, *Chem. Ber.* **1990**, *123*, 2279–2285.
[2] J. Scholz, A. Dietrich, H. Schumann, K.-H. Thiele, *Chem. Ber.* **1991**, *124*, 1035–1039.
[3] a) P. Clopath, A. von Zelewsky, *J. Chem. Soc. Chem. Commun.* **1971**, 47–48; b) P. Clopath, A. von Zelewsky, *Helv. Chim. Acta* **1972**, 52–67.
[4] D. Walter, U. Ritter, R. Kempe, J. Sieler, B. Undeutsch, *Chem. Ber.* **1992**, *125*, 1529–1536.
[5] M. Rieckhoff, U. Pieper, D. Stalke, F. T. Edelmann, *Angew. Chem.* **1993**, *105*, 1102–1104; *Angew. Chem. Int. Ed. Engl.* **1993**, *32*, 1079–1081.
[6] X-ray crystal structure analysis for **2** ($BeN_4C_{56}H_{48}$): $M = 786.03$, black-green, dense crystal $0.8 \times 0.5 \times 0.5$ mm, mounted in a quarz tube under nitrogen with two-component adhesive, data collection temperature 20 °C, monoclinic, space group $P2_1/c$ (no. 14), $a = 1284.0(5)$, $b = 1530.8(4)$, $c = 2353.9(4)$ pm, $\beta = 101.54°$, $V = 4530.1$ Å^3, $Z = 4$, $\rho_{calcd} = 1.152$ g cm^{-3}, $2\theta_{max} = 50°$, $Mo_{K\alpha}$ radiation, $\lambda = 71.069$ pm, $\omega/2\theta$ scan, $\mu = 0.070$ mm^{-1}, $F(000) = 1664.0$, 8660 reflections in the range $2\theta = 2$–$50°$, reflections with $\theta > 18°$ consistently with $I < 2\sigma(I)$, 3111 independent reflections with $I > 2\sigma(I)$, 194 parameters, residual electron density + 0.41/−0.31 eÅ^{-3}, $R = 0.086$, $R_w = 0.083$, Enraf-Nonius CAD4 diffractometer; solution and refinement with SHELXTL-PC. The H atoms were positioned geometrically (riding model) and the phenyl groups were refined as rigid groups. Further details of the crystal structure investigation may be obtained from the Fachinformationszentrum Karlsruhe, Gesellschaft für wissenschaftlich-technische Information mbH, D-76344 Eggenstein-Leopoldshafen (FRG) on quoting the depository number CSD-58187 and the journal citation.
[7] J. L. Atwood, G. D. Stucky, *J. Am. Chem. Soc.* **1969**, *91*, 4426–4430.
[8] A. H. Clark, A. Haaland, *Acta Chem. Scand.* **1970**, *24*, 3025–3030.
[9] J. Wunderle, J. Scholz, R. Fröhlich, *Z. Kristallogr.* **1993**, *208*, 277–279.
[10] F. G. N. Cloke, G. R. Hanson, M. J. Henderson, P. B. Hitchcock, C. L. Raston, *J. Chem. Soc. Chem. Commun.* **1989**, 1002–1003.
[11] F. G. N. Cloke, Ch. I. Dalby, P. J. Daff, J. C. Green, *J. Chem. Soc. Dalton Trans.* **1991**, 181–184.
[12] a) F. G. N. Cloke, H. C. de Lemos, A. A. Sameh, *J. Chem. Soc. Chem. Commun.* **1986**, 1344–1345; b) F. G. N. Cloke, *Chem. Soc. Rev.* **1993**, 17–24.
[13] G. E. Coates, S. I. E. Green, *J. Chem. Soc. A* **1962**, 3340–3348.

Bis(tetramethylbutynediol)nickel(0), the First Pure Monoalkyne Complex of Nickel and Its Chemistry**

Dirk Walther,* Andreas Schmidt, Thomas Klettke, Wolfgang Imhof, and Helmar Görls

"Pure" alkyne complexes of nickel, which exclusively contain monoalkynes as ligands can be considered an attractive goal in organometallic synthesis as numerous catalytic transformations of alkynes on nickel(0) centers are known. The simplest stable compound should be of the type $[Ni^0(alkyne)_2]$; however, such complexes have not previously been isolated[1] even though stable platinum(0) complexes of this type exist.[2]

[*] Prof. Dr. D. Walther, Dipl.-Chem. A. Schmidt, T. Klettke
Institut für Anorganische und Analytische Chemie der Universität
August-Bebel-Strasse 2, D-07743 Jena (FRG)
Telefax: Int. code + (3641)6-35538
Dr. W. Imhof, Dr. H. Görls
Max-Planck-Gruppe CO_2-Chemie, Jena

[**] This work was supported by the Deutsche Forschungsgemeinschaft (SFB 247, Heidelberg), the Max-Planck-Gesellschaft (Arbeitsgruppe CO_2-Chemie) and the Fonds der Chemischen Industrie.

 © VCH Verlagsgesellschaft mbH, D-69451 Weinheim, 1994 0570-0833/94/1313-1373 $ 10.00+.25/0

We report here on the synthesis of bis(tetramethylbutynediol)nickel(0) (**1**) the first stable alkyne–nickel complex, which contains solely monoalkynes as ligands and which is formed surprisingly easily by treating $[Ni(cod)_2]$ (cod: cycloocta-1,5-diene) with alkyne [Eq. (a)] in boiling THF (reaction time 6 h). Compound **1** can be obtained from THF/hexane as lemon yellow crystals.

$$[Ni(cod)_2] + 2\ HO{-}C(CH_3)_2{-}C{\equiv}C{-}C(CH_3)_2{-}OH \longrightarrow [Ni\{(HO{-}C(CH_3)_2{-}C{\equiv}C)_2\}] \quad (a)$$

1

According to the results of the crystal structure analysis[3] (Fig. 1) the nickel(0) center is surrounded by four C atoms of the alkyne groups in a distorted tetrahedral fashion. Ni–C and C≡C bond lengths as well as the C≡C–C bond angles lie within the expected range. No agostic interactions are observed for the H atoms of the CH_3 groups and the nickel center; hence, compound **1** truly is an alkyne–nickel(0) complex.

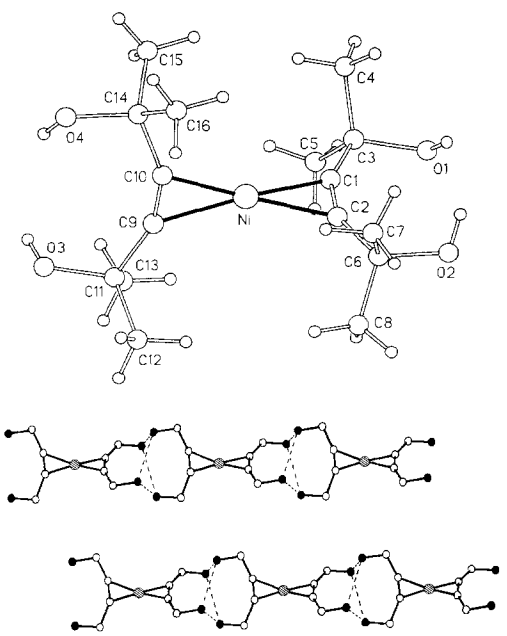


Fig. 1. Structure of molecules **1** and their packing in the crystal (the methyl groups were omitted for clarity). ●: O, ⊗: Ni, ○: C, ---: H bonds. Selected bond lengths [Å] and angles [°]: Ni-C1 1.90(1), Ni-C2 1.851(9), Ni-C9 1.905(7), Ni-C10 1.82(1), C1-C2 1.278(7), C9-C10 1.21(1), O1-O3A 2.74, O1-O4A 2.76, O2-O3A 2.72, O2-O4A 2.81; C1-Ni-C2 39.8(2), C9-Ni-C10 37.7(3), C2-C1-Ni 68.1(8), Ni-C2-C1 72.1(7), C10-C9-Ni 67.3(7), Ni-C10-C9 75.0(8), C2-C1-C3 156(1), C1-C2-C6 154(1), C10-C9-C11 158(1), C9-C10-C14 152(1).

In the solid state the molecules are connected by four intermolecular hydrogen bonds between neighboring, coordinated butynediols. The resulting polymer-like chain structure consists of C_4 tetrahedra that surround the coordinated nickel(0) and O_4 tetrahedra; the two types of tetrahedra are separated by CMe_2 "spacer" groups. (Fig. 1, bottom).

As expected, two signals (for CH_3 and OH) are observed in the ^1H NMR spectrum ($[D_8]$THF) of **1**. In addition to the signals for the $C(CH_3)_2$ groups, the ^{13}C NMR spectrum exhibits one signal for the coordinated alkyne carbon atoms at $\delta = 206$. This strong deshielding of the alkyne carbon atoms in **1** indicates– in conjunction with the short average Ni–C distance of 1.86 Å—that the alkyne ligand acts as a four-electron donor.[9] In contrast, the alkyne has to be considered a two-electron ligand in compounds of type $[NiL_2(butynediol)]$, where the solid-state structure is also influenced by hydrogen bonding.[4]

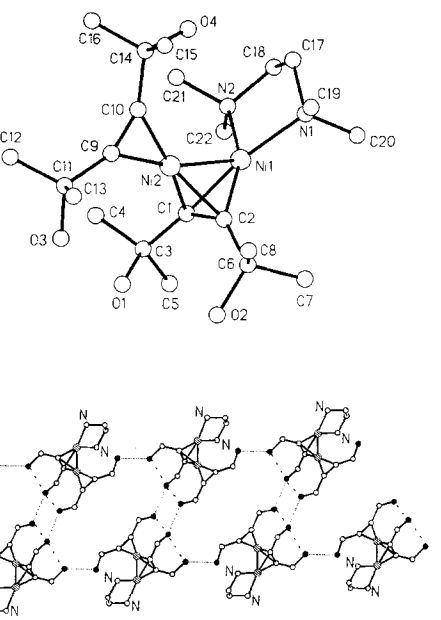
Compound **1** shows a rich chemistry, which will be illustrated by three examples: Addition of *N,N,N',N'*-tetramethylethylenediamine (tmeda) to **1** results in displacement of one alkyne ligand and formation of an intermediate, which, however, is not isolated but instead reacts further with **1** [Eq. (b)] to yield the

$$\mathbf{1} + \text{tmeda} \longrightarrow [Ni(\text{tmeda})\{\mu\text{-}(HOC(CH_3)_2C{\equiv}C)_2\}] \xrightarrow{\mathbf{1}} [(\text{tmeda})Ni\{\mu\text{-}(HOC(CH_3)_2C{\equiv}C)_2\}Ni\{(HOC(CH_3)_2C{\equiv}C)_2\}] \quad (b)$$

2

deep red, binuclear complex **2**. Binuclear nickel(0) complexes stabilized by phosphane-containing bridging and terminal alkyne ligands are already known for ethyne.[5]

The crystal structure analysis of **2** showed that the molecules are connected by four intermolecular hydrogen bonds to give a double-stranded structure (Fig. 2).[3] Furthermore, there are two intramolecular hydrogen bonds between bridging alkynes and between bridging and terminal alkynes. In contrast to **1**, the two OH groups of the terminal alkyne are far appart.



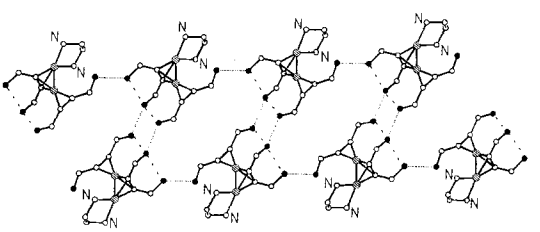


Fig. 2. Structure of molecules **2** and their packing in the crystal (cf. Fig. 1). Selected bond lengths [Å] and angles [°]: Ni1-Ni2 2.449(1), Ni1-C1 1.879(2), Ni1-C2 1.907(2), Ni2-C1 1.968(3), Ni2-C2 1.938(3), C1-C2 1.344(3), Ni1-N1 2.024(2), Ni1-N2 2.035(2), Ni2-C9 1.847(2), Ni2-C10 1.876(3), C9-C10 1.268(3), O1-O2 2.727, O1-O3 2.900, O1-O3A 2.735, O3-O1A 2.735, O2-O4B 2.726, O4-O2C 2.726; Ni1-C1-Ni2 79.04(9), Ni1-C2-Ni2 79.1(1), Ni1-Ni2-C1 48.86(7), Ni1-Ni2-C2 49.86(7), Ni1-C2-C1 68.1(1), Ni2-C1-C2 68.7(1), Ni2-Ni1-C1 52.10(7), Ni2-Ni1-C2 51.01(8), C1-Ni1-C2 41.59(9), Ni2-C2-C1 71.1(1), C1-Ni2-C2 40.24(9), Ni1-C1-C2 70.3(1), N1-Ni1-N2 87.25(9), C3-C1-C2 136.9(2), C6-C2-C1 138.4(2), C11-C9-C10 152.1(2), C14-C10-C9 149.6(2).

As the catalytic cyclotetramerization of alkynes probably proceeds via binuclear nickel species,[6] **2** can be regarded as a model compound for the initial steps of this reaction. Its structure makes it plausible that OH groups—fixed in distinct positions by hydrogen bonds—can influence the selectivity of C–C bond formations (cf. Ref. [7]).

 © VCH Verlagsgesellschaft mbH, D-69451 Weinheim, 1994 0570-0833/94/1313-1374 $ 10.00+.25/0

Substitution of an alkyne in **1** by a ligand without functional groups yields compound **3** [Eq. (c)] in which the OH groups

$$\mathbf{1} + \text{cod} \rightarrow [\text{Ni(cod)}\{(\text{HOC(CH}_3)_2\text{C}\equiv)_2\}] \quad \text{(c)}$$

3

form both intra- and intermolecular hydrogen bonds to neighboring complex molecules. This leads to a third "connecting" principle in the crystal, which results in a polymeric chain with helical structure for the coordinated alkynols (Fig. 3).[3]

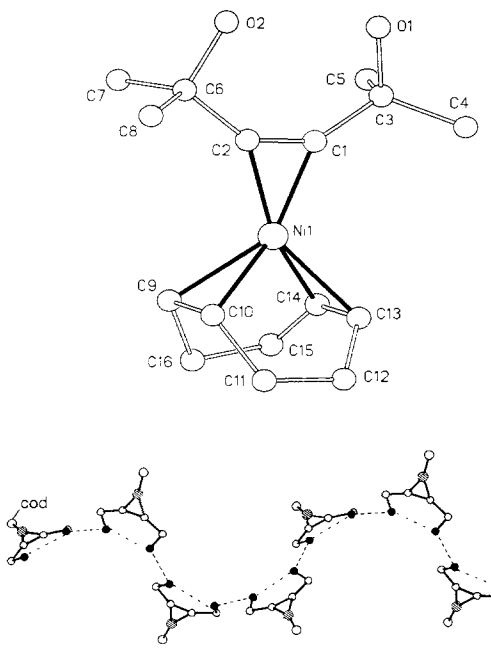


Fig. 3. Structure of molecules **3** and their packing in the crystal (cf. Fig. 1, in the bottom figure the cod ligand is represented by its center of gravity. O3 and O4 represent the hydroxyl groups of the second symmetry-independent molecule of **3**). Selected bond lengths [Å] and angles [°]: Ni1-C1 1.868(6), Ni1-C2 1.854(6), Ni1-C9 2.079(9), Ni1-C10 2.064(8), Ni1-C13 2.080(8), Ni1-C14 2.055(8), C1-C2 1.251(9), O1-O2 2.75, O1-O4A 2.74, O2-O3B 2.79; C1-Ni1-C2 39.3(3), C9-Ni1-C10 37.4(3), C10-Ni1-C13 84.6(4), C13-Ni1-C14 38.3(4), C14-Ni1-C9 86.8(5), C3-C1-C2 144.5(6), C6-C2-C1 142.8(6).

Rupture of the polymeric structure can be achieved by compounds that can interact with the OH groups of the alkynes but do not possess element–H bonds suitable for hydrogen bonding. For example, compound **4**, formed by treating **1** with Ph_3P in acetonitrile [Eq. (d)], has a dimeric structure in the crystal.

$$\mathbf{1} + \text{PPh}_3 \rightarrow [\text{Ni(PPh}_3)_2\{(\text{HOC(CH}_3)_2\text{C}\equiv)_2\}] \quad \text{(d)}$$

4

Acetonitrile is disordered in the crystal and binds to one OH group of the alkynediol. An intermolecular hydrogen bond between neighboring monomers and two intramolecular hydrogen bonds complete the binuclear structure (Fig. 4).[3]

The special significance of the OH groups becomes apparent when comparing the formation reactions of **1**–**3** with the reaction of the dimethoxy derivative of tetramethylbutynediol with $[Ni(cod)_2]$. When using this alkyne under the reaction conditions which otherwise cleanly yield **1**, thermal decomposition to elemental nickel is observed. Therefore, attempts to synthesize a binuclear complex analogous to **2** yielded only decomposition products.

This strengthens the notion that peripheral influences (here hydrogen bonds) do not only play a role in the formation and

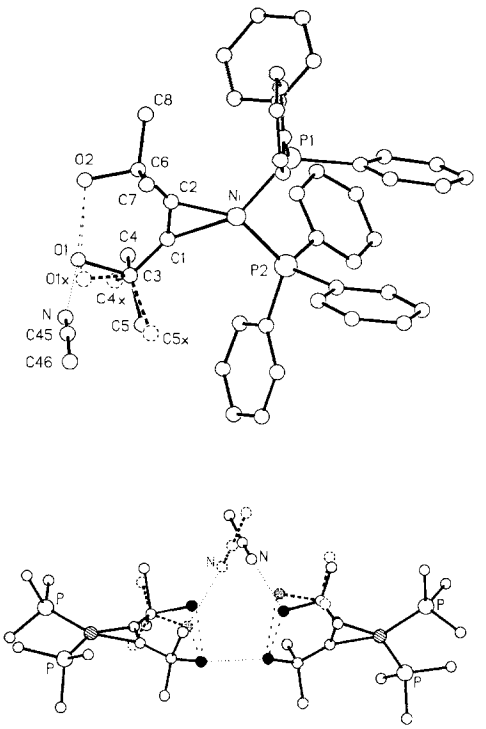


Fig. 4. Structure of molecules **4** and their packing in the crystal (for clarity the phenyl groups are represented in the figure by the ipso carbon atoms). Selected bond lengths [Å] and angles [°]: Ni-P1 2.1892(8), Ni-P2 2.1895(8), Ni-C1 1.88, Ni-C2 1.914(2), C1-C2 1.260(4), O1-O2 2.640, O1-N 2.911, O1X-O2 2.805, O2-O2A 2.828; P1-Ni-P2 101.86(3), C1-Ni-C2 38.7(1), C3-C1-C2 142.2(3), C6-C2-C1 139.9(2).

thermal stability of the solid-state structures but are also of significance in solution.

Experimental Procedure

All reactions were carried out under an inert argon atmosphere.

1: 10 mmol $[Ni(cod)_2]$ and 20 mmol tetramethylbutynediol were refluxed in 30 mL THF for 6 h. After removal of THF and cod by vacuum destillation followed by addition of ether, the reaction product was collected on a filter and washed with hexane. Yield: approximately 60%, lemon yellow powder; single crystals were obtained from THF/hexane. IR (Nujol) $\tilde{\nu} = 1889\ cm^{-1}$ (C≡C), 3271 cm^{-1} (OH). ^1H NMR ([D$_8$]THF): $\delta = 1.36$ (s, CH_3), 2.08 (s, OH). ^{13}C NMR ([D$_8$]THF): $\delta = 32.1$ (CH_3), 69.9 (CMe_2OH), 206.3 (C≡C) [8].

2: To a solution of **1**, prepared in situ by treating 2.8 mmol $[Ni(cod)_2]$ with 5.6 mmol alkyne, was added 10 mmol tmeda, and the mixture was stirred for 2 h. The solution was reduced in volume, and after layering with hexane, red crystals of **2** were obtained. IR (Nujol) $\tilde{\nu} = 1573\ cm^{-1}$ (C≡C), 1842 cm^{-1} (C≡C), 3266 cm^{-1} (OH). ^1H NMR ([D$_8$]THF): $\delta = 1.30$–1.60 (m, CH_3), 2.13–2.29 (m, CH_2), 2.50 (s, N–CH_3), 2.78 (s, N–CH_3), 3.44 (s, OH), 3.83 (s, OH), 4.20 (s, OH). ^{13}C NMR ([D$_8$]THF): $\delta = 32.7$ (CH_3), 33.5 (CH_3), 46.1 (CH_2), 49.3 (N–CH_3), 50.6 (N–CH_3), 58.9 (CMe_2OH), 59.5 (CMe_2OH), 117.9 (C≡) [8].

3: Compound **3** is prepared as described above for **1** from equimolar amounts of $[Ni(cod)_2]$ and alkyne. Orange powder; single crystals were obtained from THF/hexane. IR (Nujol) $\tilde{\nu} = 1807\ cm^{-1}$ (C≡C), 3247 cm^{-1} (OH). ^1H NMR ([D$_8$]THF): $\delta = 1.28$ (s, CH_3), 2.0–2.4 (m, CH_2), 4.24 (s, OH), 5.39 (s, CH=). ^{13}C NMR ([D$_8$]THF): $\delta = 30.8$ (CH_3), 32.0 (CH_2), 70.0 (CMe_2OH), 94.7 (CH=), 137.1 (C≡C) [8].

4: Compound **4** was prepared from $[Ni(Ph_3P)_2(tetramethylbutynediol)]$ [4c] in hot acetonitrile. IR (Nujol) $\tilde{\nu} = 1770\ cm^{-1}$ (C≡C), 2215 cm^{-1} (C≡N), 3286 cm^{-1} (OH) [8].

Received: February 1, 1994
Revised: March 11, 1994 [Z.6661IE]
German version: *Angew. Chem.* **1994**, *106*, 1421

[1] a) E. L. Muetterties, W. R. Pretzer, M. G. Thomas, B. F. Beier, D. L. Thorn, V. W. Day, A. B. Anderson, *J. Am. Chem. Soc.* **1978**, *100*, 2090–2096; b) G. A. Ozin, D. F. McIntosh, W. J. Power, R. P. Messmer, *Inorg. Chem.* **1981**, *20*, 1782–1792; c) A Ni(0) chelate containing macrocyclic trisalkyne ligand has been reported: J. D. Ferrara, C. Tessier-Youngs, W. J. Youngs, *J. Am. Chem. Soc.* **1985**, *107*, 6719–6721.

[2] F. D. Rochon, T. Theophanides, *Can. J. Chem.* **1972**, *50*, 1325–1327; b) R. J. Dubey, *Acta. Crystallogr. Sect. B* **1975**, *31*, 1860–1864; c) N. M. Boag, M. Green, D. M. Grove, J. A. K. Howard, J. L. Spencer, F. G. A. Stone, *J. Chem. Soc. Dalton Trans.* **1980**, 2170–2190.

[3] Crystal data: $Mo_{K\alpha}$, $\lambda = 0.71069$ Å, ω-2θ-scan, structure solution: direct methods (SHELXS-86), refinement on |F| (SHELXL-93), hydrogen atoms were calculated in idealized positions unless otherwise noted. **1**: $0.2 \times 0.2 \times 0.1$ mm, monoclinic, Cc, $a = 15.524(3)$, $b = 8.520(2)$, $c = 15.588(3)$ Å, $\beta = 108.64(3)^\circ$, $V = 1953.6(7)$ Å^3, $Z = 4$, $\rho_{calcd} = 1.166$ g cm^{-3}, $T = 293$ K, $\mu = 1.011$ mm^{-1}, 4262 measured reflections (triclinic), 2578 symmetry-independent reflections, of which 2014 were observed ($I > 2\sigma(I)$), 206 parameters refined, $R_1 = 0.0477$, $wR_2 = 0.1020$, residual electron density 0.234 e Å^{-3}. **2**: $0.6 \times 0.4 \times 0.3$ mm, triclinic, $P\bar{1}$, $a = 9.418(4)$, $b = 9.601(5)$, $c = 15.508(6)$ Å, $\alpha = 103.54(3)^\circ$, $\beta = 93.39(4)^\circ$, $\gamma = 102.77(5)^\circ$, $V = 1320(1)$ Å^3, $Z = 2$, $\rho_{calcd} = 1.303$ g cm^{-3}, $T = 193$ K, $\mu = 1.463$ mm^{-1}, 4807 measured reflections, 4616 symmetry-independent reflections of which 4199 were observed ($I > 2\sigma(I)$), 292 parameters refined, $R_1 = 0.0299$, $wR_2 = 0.0751$, residual electron density 0.591 e Å^{-3}. **3**: $0.4 \times 0.3 \times 0.1$ mm, monoclinic, $P2_1/c$, $a = 9.450(2)$, $b = 23.159(5)$, $c = 15.522(3)$ Å, $\beta = 102.77(3)^\circ$, $V = 3313(1)$ Å^3, $Z = 8$, $\rho_{calcd} = 1.239$ g cm^{-3}, $T = 293$ K, $\mu = 1.176$ mm^{-1}, 5419 measured reflections, 5208 symmetry-independent reflections of which 3710 were observed ($I > 2\sigma(I)$), 408 parameters refined, $R_1 = 0.0765$, $wR_2 = 0.1505$, residual electron density 0.481 e Å^{-3}. The unit cell contains two independent molecules of **3** per asymmetric unit. The olefinic hydrogen atoms of the cod ligand were determined by difference Fourier analysis and refined without parametric constraints. Because of poor crystal quality and disorder problems with the cod ligands, their C atoms could only partially be refined isotropically. **4**: $0.4 \xi 0.38 \xi 0.36$ mm, monoclinic, $C2/c$, $a = 19.809(4)$, $b = 12.564(3)$, $c = 32.788(7)$ Å, $\beta = 102.95(3)^\circ$, $V = 7953(3)$ Å^3, $Z = 8$, $\rho_{calcd} = 1.246$ g cm^{-3}, $T = 293$ K, $\mu = 0.605$ mm^{-1}, 9207 measured reflections, 9046 symmetry-independent reflections, of which 7012 were observed ($I > 2\sigma(I)$), 449 parameters refined, $R_1 = 0.0469$, $wR_2 = 0.1170$, residual electron density 0.46 e Å^{-3}. Further details of the crystal structure investigation may be obtained from the Fachinformationszentrum Karlsruhe, D-76344 Eggenstein-Leopoldshafen (FRG), on quoting the depository number CSD-58133.

[4] a) R. Diercks, J. Kopf, H. tom Dieck, *Acta Crystallogr. Sect. C* **1984**, *40*, 363–365; our own analyses of the structure data show the presence of dimers, which are—as in **1**—connected by four hydrogen bonds; b) H. Görls, B. Schulz, U. Rosenthal, W. Schulz, *Cryst. Res. Technol.* **1988**, *23*, 25–33; c) U. Rosenthal, H. Görls, *J. Organomet. Chem.* **1988**, *348*, 135–138.

[5] K.-R. Pörschke, *J. Am. Chem. Soc.* **1989**, *111*, 5691–5699.

[6] G. Wilke, *Pure Appl. Chem.* **1978**, *60*, 677–690.

[7] H. tom Dieck, A. M. Lauer, L. Stamp, R. Diercks, *J. Mol. Catal.* **1986**, *35*, 317–325; b) D. Walther, D. Braun, W. Schulz, U. Rosenthal, *Z. Anorg. Allg. Chem.* **1989**, *577*, 270–282.

[8] Correct elemental analyses (C, H, Ni).

[9] J. Templeton, *Adv. Organomet. Chem.* **1989**, *29*, 1.

Magnetic Properties of Aromatic Transition States: The Diels–Alder Reactions**

Rainer Herges,* Haijun Jiao, and Paul von Ragué Schleyer

Dedicated to Professor Werner Kutzelnigg on the occasion of his 60th birthday

Evans et al. first recognized the analogy between the π electrons of benzene and the six electrons in the cyclic transition state of the Diels–Alder reaction of butadiene and ethylene.[1] Generalized through the Woodward–Hoffmann rules[2] and the Hückel–Möbius method[3, 4] to many pericyclic reactions, it has often been suggested that thermal pericyclic reactions take place preferentially through aromatic transition states.[5] Although the parent Diels–Alder reaction between butadiene and ethylene is taken as the prototype of pericyclic processes,[6] the energy of concert is relatively small.[7]

We now apply magnetic properties as criteria[8–10, 11b] to investigate the nature of concerted transition states for the first time specifically for the Diels–Alder reactions of ethylene both with butadiene and cyclopentadiene. While the magnetic properties of transition states cannot be measured, both chemical shifts and magnetic susceptibilities can be computed conveniently. The accuracy of the IGLO[11a] results for ground states suggest that they may be applied to analyze the nature of transition structures as well. Moreover, we examine the changes of chemical shifts and magnetic susceptibilities along the reaction path for the reaction of ethylene with butadiene. These results are presented in Figures 1 and 2.

The geometries of the individual points on the reaction coordinate were optimized at the ab initio RHF/3-21G level[12] within the C_s point group, and were employed for IGLO calculations with a Huzinaga DZ basis set.[13] During the reaction (read Figures from right to left), eight of the ten olefinic protons of

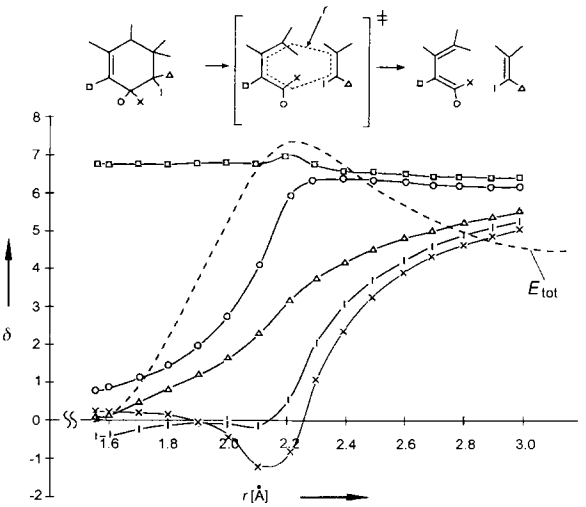


Fig. 1. Calculated ^{1}H chemical shifts in the retro-Diels–Alder reaction of cyclohexene as a function of the of reaction coordinate r. The total energy curve E_{tot} (reaction profile) is depicted with a broken line [8a].

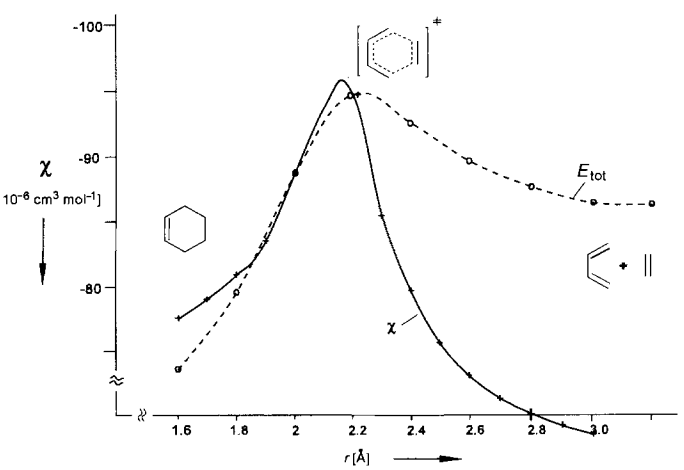


Fig. 2. Calculated diamagnetic susceptibility χ and total energy E_{tot} of the reaction in Fig. 1 as a function of the reaction coordinate r.

[*] Priv.-Doz. Dr. R. Herges, Dipl.-Chem. H. Jiao, Prof. Dr. P. v. R. Schleyer
Computer-Chemie-Centrum
Institut für Organische Chemie der Universität Erlangen-Nürnberg
Henkestrasse 42, D-91054 Erlangen (FRG)
Telefax: Int. code + (9131)85-9132

[**] This work was supported by the Deutsche Forschungsgemeinschaft and the Fonds der Chemischen Industrie. The authors thank Prof. W. Kutzelnigg for suggesting that magnetic susceptibility might be used to characterize aromatic transition states. Dr. U. Fleischer also provided helpful comments. H. J. is grateful for a fellowship of the Shanxi Normal University.

butadiene and ethylene gradually become aliphatic protons in cyclohexene. Similar to the ^{13}C chemical shifts,[14] the proton chemical shifts should decrease continuously (i.e. from $\delta \approx 5-7$ to $\delta \approx 1-2$). However, this is not the case. Electronic effects due to delocalization are not negligible. The delocalization of the six electrons in the transition state results in ring current shielding and deshielding effects similar to those in aromatic compounds. Most pronounced is the shielding of the "inner" protons of the butadiene moiety. The maximum upfield deviation from a hypothetical monotonous[15] function on the reaction path ($\Delta\delta \approx -3.5$) coincides with the transition state structure ($r = 2.1$ Å; see Fig. 1). Deshielding effects also are apparent. The chemical shifts of the "outer" protons of butadiene deviate from a monotonous sigmoidal relationship by $\Delta\delta \approx +2.8$ in the transition structure.

Besides ^1H chemical shifts, exaltation A of the magnetic susceptibility χ is a magnetic property uniquely associated with systems with cyclic delocalization of electrons.[16, 18] χ is more negative for aromatic compounds than for nonaromatic analogues, thus, for instance, the values for χ of benzene and fulvene are -54.8×10^{-6} and -43.0×10^{-6} cm^3 mol^{-1}, respectively.[16c] Similarly, we now find χ to be more negative in the aromatic transition states of pericyclic reactions, for example TS1 and TS2 (see Fig. 3), than in the starting materials or products (see also Fig. 4). In Figure 2 the magnetic susceptibility χ and the energy of the system ethylene + butadiene are plotted as a function of the reaction coordinate.[17] The maximum of the χ curve, which indicates an aromatic transition state, almost coincides with the energy maximum.

While Figures 1 and 2 illustrate the trends, calculations of the stationary points at higher levels of theory give a quantitative estimate of the effects (geometry optimizations and frequency calculations: MP2(fu)/6-31G*, single-point energies: MP4SDTQ/6-31G*//MP2(fu)/6-31G*; ^1H chemical shift calculations: IGLO/II//MP2(fu)/6-31G*). The stationary point geometries on the reaction path of the Diels–Alder reaction of ethylene and butadiene are shown in Figure 3a and those of the Diels–Alder reaction of ethylene and cyclopentadiene in Figure 3b. The energies of the seven structures are listed in Table 1. Note that the calculated and experimental activation entropies and energies agree remarkably well.

The optimized geometries (Fig. 3) were used to perform IGLO calculations (basis set II) of the ^1H chemical shifts and magnetic suceptibilities (Fig. 4).

For starting materials and products the calculated and experimental ^1H chemical shifts are in good agreement. Because transition states of symmetry allowed pericyclic reactions are described

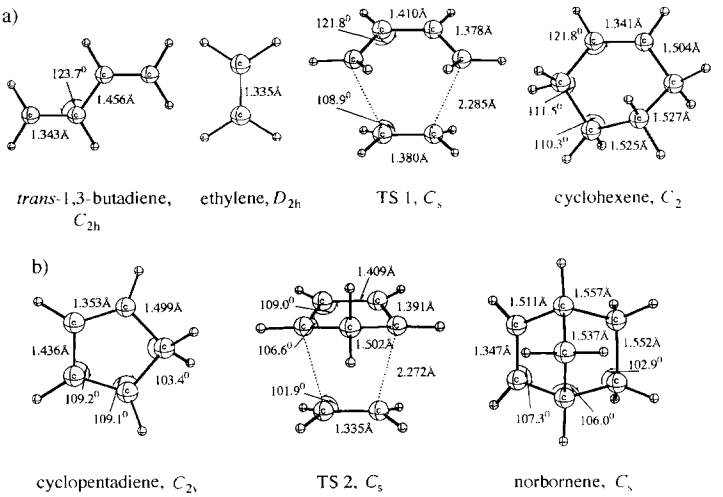


Fig. 3. Calculated geometries of the stationary points on the reaction path of the Diels–Alder reaction of a) butadiene with ethylene (MP2(fu)/6-31G*) and b) cyclopentadiene with ethylene (MP2(fu)/6-31G*).

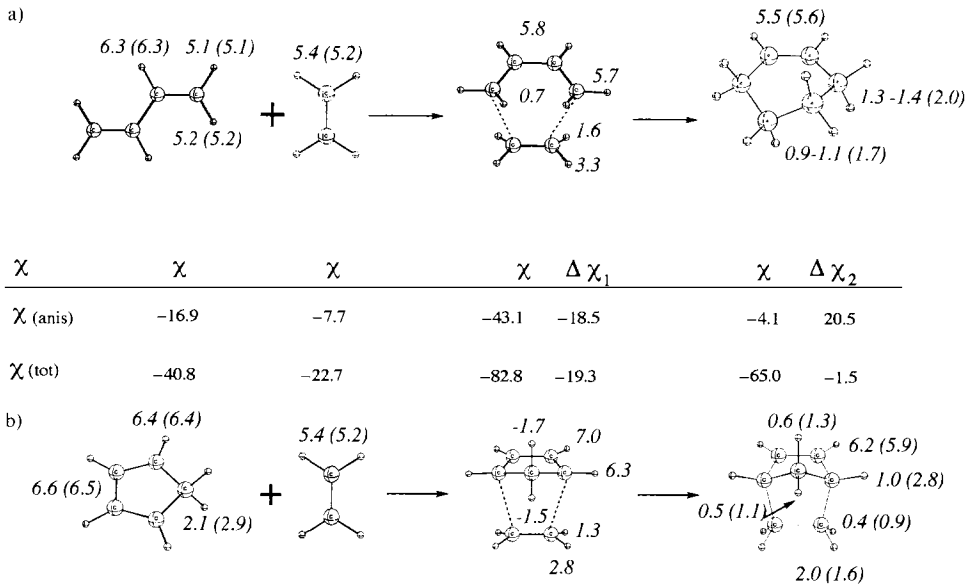
reasonably by single determinant wavefunctions,[6] an adequate treatment of the magnetic properties on the Hartree–Fock level can be expected for the transition structures as well. The general trends along the reaction path (Figs. 1 and 2) are confirmed by the stationary point computations at a considerably higher level of theory (Fig. 4). In general, upfield shifts in the shielding range of the ring current in the transition state are more pronounced than downfield shifts of the signals of the protons in the periphery. Note the large upfield shift of the two methylene protons located above the cyclic delocalized transition state system of the Diels–Alder reaction of cyclopentadiene and ethylene (Fig. 4b, $\delta = -1.5, -1.7$), indicating a strong shielding effect of the ring current.

The calculated magnetic susceptibilities χ(tot) for both transition states are 17.7×10^{-6} and 19.3×10^{-6} cm^3 mol^{-1}, respectively, more negative than those for the starting materials. (The differences from the values for the products are -14.5×10^{-6} and -17.8×10^{-6} cm^3 mol^{-1}, respectively). These values may be compared with the magnetic susceptibility exaltation[18] -13.4×10^{-6} computed for benzene at the same level. The magnetic susceptibility anisotropies, χ(anis), as is characteristic of aromatic compounds,[19] are more negative in the transition states by 18.5×10^{-6} and 20.9×10^{-6} cm^3 mol^{-1} than in the starting materials. Both, χ(tot) and χ(anis) indicate the

Table 1. Calculated total energies [Hartree], entropies (S/ΔS [cal mol^{-1} K^{-1}, 300 K]), number of imaginary frequencies (NIMAG), zero point vibrational energies (ZPE), activation energies (E_a), and reaction energies (ΔH_r^0 [kcal mol^{-1}] for structures in Fig. 3) compared with experimental values. PG = point group.

Compounds	PG	MP2(fu)/6-31G*					MP4SDTQ(fc)/6-31G*//MP2(fu)/6-31G*		exp. [6]
		E (NIMAG)	ZPE [a]	S	ΔS	E_a (ΔH_r^0) [b]	E	E_a (ΔH_r^0) [c]	E_a (ΔH_r^0)
1,3-butadiene	C_{2h}	−155.44171 (0)	49.4	66.3	..	..	−155.48359	..	..
ethylene	D_{2h}	−78.29429 (0)	29.7	52.4	–	–	−78.31980	..	..
TS 1	C_s	−233.70790 (1)	81.3	77.9	−40.8	18.5	−233.76812	22.4	23.6
cyclohexene	C_2	−233.82506 (0)	85.6	72.2	−46.5	(−54.8)	−233.88084	(−47.5)	(−42.5)
cyclopentadiene	C_{2v}	−193.44967 (0)	3.6	65.5	–	–	−193.49328	–	..
ethylene	D_{2h}	−78.29429 (0)	29.7	52.4	–	–	−78.31980	–	–
TS 2	C_2	−271.72596 (1)	85.6	77.0	−40.8	12.4	−271.78599	17.5	17.5
norbornene	C_s	−271.80388 (0)	89.4	72.7	−45.0	(−33.4)	−271.86460	(−29.0)	(−25.0)

[a] MP2(fu)/6-31G* values scaled with 0.93 [12a]. [b] MP2(fu)/6-31G* + ZPE (MP2(fu)/6-31G* + 300 K). [c] MP4SDTQ/6-31G*//MP2(fu)/6-31G* + ZPE (MP2(fu)/6-31G* 300 K).



	χ	χ	χ	$\Delta\chi_1$	χ	$\Delta\chi_2$
χ (anis)	−16.9	−7.7	−43.1	−18.5	−4.1	20.5
χ (tot)	−40.8	−22.7	−82.8	−19.3	−65.0	−1.5

	χ	χ	χ	$\Delta\chi_1$	χ	$\Delta\chi_2$
χ (anis)	−31.0	−7.7	−59.6	−20.9	−12.9	25.8
χ (tot)	−51.0	−22.7	−91.4	−17.7	−76.9	−3.2

Fig. 4. IGLO calculated magnetic susceptibilities χ [10^{-6} cm^3 mol^{-1}] (diamagnetic, paramagnetic, and nonlocal contributions), relative magnetic susceptibilities (relative to the sum of the χ values of the starting materials) $\Delta\chi_1$ and $\Delta\chi_2$ as well as the ^{1}H chemical shifts for the stationary points of the Diels–Alder reaction of a) 1,3-butadiene and ethylene (IGLO//MP2(fu)/6-31G*) and b) cyclopentadiene and ethylene (IGLO//MP2(fu)/6-31G*). The measured values of the chemical shifts are given in parentheses.

pronounced aromatic character of the transition structures TS1 and TS2.

Application of the term "aromatic" to pericyclic transition states is justified. This concept is useful in predicting the stereochemistry and mechanism of these reactions.[2–4] Criteria for aromaticity, such as bond length equalization, cyclic delocalization of electrons, and stabilization relative to open chain analogues also hold for pericyclic transition states.[5, 6] The magnetic properties are also criteria in this concept. The abnormal chemical shifts as well as the magnetic susceptibility and the anisotropy enhancement now provide an additional basis for the aromaticity concept of pericyclic transition states.[20]

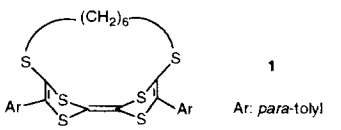
Received: November 26, 1993
Revised version: March 30, 1994 [Z 6515 IE]
German version: *Angew. Chem.* **1994**, *106*, 1441

[1] M. G. Evans, E. Warhurst, *Trans. Faraday Soc.* **1938**, *34*, 614; M. G. Evans, *ibid.* **1939**, *35*, 824; M. G. Evans, M. Polanyi, *ibid.* **1938**, *34*, 11.
[2] R. B. Woodward, R. Hoffmann, *Angew. Chem.* **1969**, *81*, 797; *Angew. Chem. Int. Ed. Engl.* **1969**, *8*, 781.
[3] H. E. Zimmerman, *Acc. Chem. Res.* **1971**, *4*, 272.
[4] M. J. S. Dewar, *Angew. Chem.* **1971**, *83*, 859; *Angew. Chem. Int. Ed. Engl.* **1971**, *10*, 761.
[5] For reviews see: P. J. Garratt, *Aromaticity*, Wiley, New York, **1986**, p. 285ff; V. I. Minkin, M. N. Glukhovtsev, B. Y. Simkin, *Aromaticity and Antiaromaticity* Wiley, New York, **1994**, p. 63ff.
[6] For a review see: K. N. Houk, Y. Li, J. D. Evanseck, *Angew. Chem.* **1992**, *104*, 711; *Angew. Chem. Int. Ed. Engl.* **1992**, *31*, 682, and references therein.
[7] The energy difference (energy of concert) between the activation energy of the concerted reaction of butadiene and ethene and the relative energy estimated for an alternative diradical intermediate has been given as 2 kcal mol^{-1} [6] and 5.7 kcal mol^{-1}: (W. von E. Doering, W. R. Roth, R. Breuckmann, L. Figge, H.-W. Lenartz, W.-D. Fessner, H. Prinzbach, *Chem. Ber.* **1988**, *121*, 1 and references therein). The cyclopentadiene + ethylene energy of concert was estimated to be larger, 13.7 kcal mol^{-1} in the same work.
[8] a) The results summarized in Figure 1 were attained in 1989. b) D. Cremer et al. used magnetic criteria to investigate the homoaromaticity of the barbaralyl cation, the 1,4-bishomotropylium cation and the homotropenylium cation: D. Cremer, P. Svensson, E. Kraka, Z. Konkoli, P. Ahlberg, *J. Am. Chem. Soc.* **1993**, *115*, 7445; D. Cremer, P. Svensson, E. Kraka, Z. Konkoli, P. Ahlberg, *ibid.* **1993**, *115*, 7457; D. Cremer, F. Reichel, E. Kraka, *ibid.* **1991**, *113*, 9459.
[9] H. Jiao, P. von R. Schleyer, *Angew. Chem.* **1993**, *105*, 1833; *Angew. Chem. Int. Ed. Engl.* **1993**, *32*, 1763.
[10] H. Jiao, P. von R. Schleyer, *J. Chem. Soc. Perkin Trans. 2*, **1994**, 407.
[11] a) IGLO (*I*ndividual *G*auge for *L*ocalized *O*rbitals), for a review see: W. Kutzelnigg, U. Fleischer, M. Schindler, *NMR Basic Princ. Prog.* **1990**, *23*, 165; b) for a recent study on magnetic properties and aromaticity see: W. Kutzelnigg, U. Fleischer, P. Lazzeretti, V. Mühlenkamp, *J. Am. Chem. Soc.*, submitted.
[12] a) W. J. Hehre, L. Radom, P. von R. Schleyer, J. A. Pople, *Ab initio Molecular Orbital Theory*, Wiley, New York, **1986**. b) The calculations were performed with the GAUSSIAN88 package of programs: M. J. Frisch, M. Head-Gordon, H. B. Schlegel, K. Raghavachari, J. S. Binkley, C. Gonzalez, D. J. Defrees, D. J. Fox, R. A. Whiteside, R. Seeger, C. F. Malius, J. Baker, L. R. Kahn, J. J. P. Stewart, E. M. Fluder, S. Topiol, J. A. Pople, Gaussian Inc., Pittsburgh, PA, **1988**.
[13] a) The calculations were performed with M. Schindler's CONVEX version of the IGLO program, version June 1988, see: M. Schindler, W. Kutzelnigg, *J. Chem. Phys.* **1982**, *76*, 1919; b) S. Huzinaga, *Approximate Atomic Wave Functions*, University of Alberta, Edmonton, Alberta, **1971**.
[14] The ^{13}C chemical shifts do not exhibit ring current effects in the transition state. The ^{13}C chemical shift functions of the carbon atoms in butadiene and ethylene changing hybridization from sp^2 to sp^3 exhibit a sigmoidal shape like the central Δ-Δ-curve in Figure 1.
[15] A sigmoidal function similar to the carbon chemical shift curve [14] was assumed.
[16] a) For a review see: H. J. Dauben, Jr., J. D. Wilson, J. L. Laity, *Nonbenzoid Aromaticity, Vol II*, (Ed.: J. P. Snyder), Academic Press, New York 1971, and references therein; b) *J. Am. Chem. Soc.* **1968**, *90*, 811; c) *ibid.* **1969**, *91*, 1991.
[17] The length of the forming π bonds between ethylene and butadiene was decreased in steps of 0.05 Å from 3.0 to 1.6 Å and the remaining geometry parameters were optimized on each point within the C_s point group.
[18] The magnetic susceptibility exaltation Λ, is defined as the difference between the measured bulk susceptibility and the susceptibility predicted on the basis of an increment system ($\Lambda = \chi_M - \chi_M$) [16].
[19] The magnetic susceptibility anisotropy is defined as the difference between the magnetic susceptibility value along the axis perpendicular to the ring and the average value along the in-plane axes. R. C. Benson, W. H. Flygare, *J. Am. Chem. Soc.* **1970**, *92*, 7523. Since the delocalized system in the transition state of the Diels–Alder reaction is not planar, the plane of the sp^2 carbon atoms of butadiene and cyclopentadiene were used as the reference plane. The susceptibility anisotropy was determined as the difference between the magnetic susceptibility value along the axis perpendicular to the reference plane and the average value along the in-plane axes.
[20] In nonpericyclic transition states, ring current effects are not to be expected. According to our calculations on the automeric reaction of CH_3F with F^- (3-21G opt, IGLO, DZ), χ even increases slightly along the reaction coordinate ($\Delta\chi = +25 \times 10^{-6}$ cm^3 mol^{-1}).

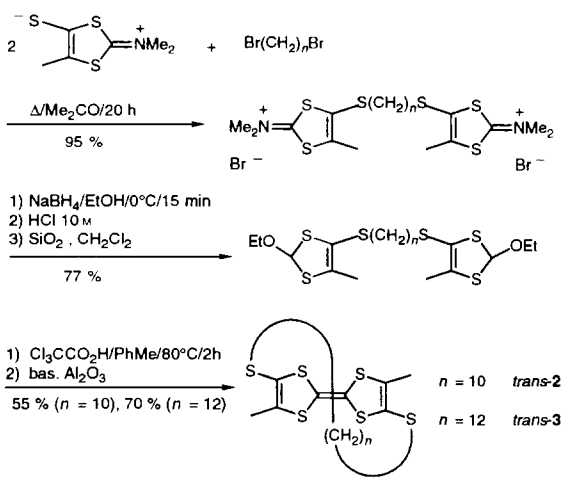
trans-cis Isomerization upon One-Electron Oxidation of [12]- and [14]Tetrathiafulvalenophanes

Kamal Boubekeur, Christine Lenoir, Patrick Batail,* Roger Carlier, André Tallec,* Marie-Pierre Le Paillard, Dominique Lorcy, and Albert Robert*

The effect of electron-transfer processes on the conformation of molecules[1] is a continuing central theme in many fields of molecular chemistry with implications on the structure of molecular assemblies, their electronic and chemical sensing properties, and the associated switching processes.[2] Here, we report on a remarkable conformational interconversion upon oxidation within a series of constrained cagelike molecules which function as reversible redox systems.[3] In addition, we present a correlation between the switching rate in solution, as determined by cyclic voltammetry, and the molecular cage constraints observed in the solid state. The general strategy for synthesizing such tetrathiafulvalenophanes was described recently.[4] It was found[5] that the $-S(CH_2)_6S-$ bridge is much too short to preserve the planarity of the central tetrathiafulvalene (TTF) core; thus **1**[4, 5] is *cis*-substituted. Because of the severe bending at the "dithiolene S···S hinges" (by 47° and 34°) compounds of this type only oxidize irreversibly.[6] The synthesis of **2**[7] and **3**[8] was designed (Scheme 1) in order to remove the inner redox unit constraints. In addition, the substitution of methyl for *para*-tolyl was favored in order to achieve a molecular shape better suited for compact intermolecular binding.



1 Ar: *para*-tolyl



Scheme 1. Syntheses of **2** and **3**.

Although the central TTF unit in the neutral cage with the $-S(CH_2)_{10}S-$ bridge, *trans*-**2**, is not planar, it is significantly less folded (23°) than **1**, and the bridge is now long enough to enable the *trans* configuration[9] (Fig. 1a). The analysis of the molecular structure of the oxidized donor cage in its cation radical salt $(cis\text{-}\mathbf{2}^{\bullet+})_2[Re_6S_6Cl_8]^{2-}$,[10] reveals that the neutral cage constraints have been removed since the central TTF core in *cis*-$\mathbf{2}^{\bullet+}$ is planar (Fig. 1b). Another salient effect is the evidence (Fig. 1) for a *cis* configuration of the oxidized cage molecule. In the neutral *trans* cage, *trans*-**3**,[11] the $-S(CH_2)_{12}S-$ bridge is now found to be long enough to bridge the planar, nonoxidized TTF unit (Fig. 1c). Likewise, one observes that the cage molecule switches from *trans* to *cis* upon oxidation, as revealed by the crystal structure of its cation radical salt, $(cis\text{-}\mathbf{3})_2^{\bullet+}[Re_6S_5Cl_9]^-$[12] (Fig. 1d). The *cis* configuration of $\mathbf{2}^{\bullet+}$ and $\mathbf{3}^{\bullet+}$, with the alkyl chains pointing away from the central TTF cores (Figs. 1b and 1d, respectively), allow for these TTF cores to be strongly dimerized in the crystal structures of $(cis\text{-}\mathbf{2}^{\bullet+})_2[Re_6S_6Cl_8]^{2-}$ and $(cis\text{-}\mathbf{3})_2^{\bullet+}[Re_6S_5Cl_9]^-$ (Fig. 2). Thus, uniform chains of non-interacting dimers develop across close-packed associations of the outer $-S(CH_2)_nS-$ bridges within the inorganic cluster anion framework (Fig. 2).

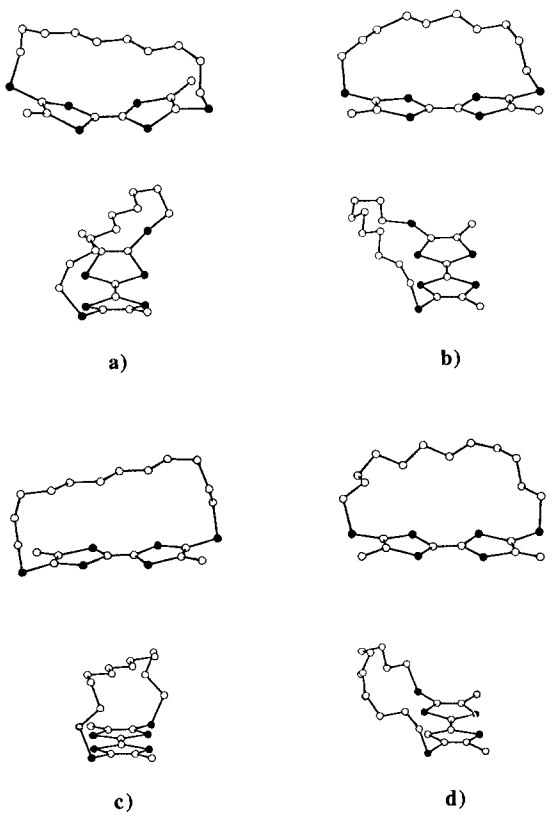


Fig. 1. Crystal structures of the tetrathiafulvalenophanes; views of the molecules parallel (bottom) and perpendicular (top) to the central C–C double bond. a) *trans*-**2**; b) *cis*-**2** in $(cis\text{-}\mathbf{2}^{\bullet+})_2[Re_6S_6Cl_8]^{2-}\cdot 2CH_3CN$; c) *trans*-**3**; d) *cis*-**3** in $(cis\text{-}\mathbf{3})_2^{\bullet+}[Re_6S_5Cl_9]^-$.

The cyclic voltammetry data shows that the coupled, heterogeneous electron transfer and isomerization reactions proceed according to an EC mechanism (EC = electron transfer with subsequent chemical reaction).[13] Thus, as exemplified in the case of **2** in Figure 3a, the first anodic scan reveals two one-elec-

[*] Dr. P. Batail, Dr. K. Boubekeur, C. Lenoir
Laboratoire de Physique des Solides
Unité Associée au CNRS No 2, Université de Paris-Sud
F-91405 Orsay (France)
Telefax: Int. code + (1)69416086
Prof. Dr. A. Tallec, R. Carlier
Laboratoire d'Electrochimie Organique
Unité Associée au CNRS No 439, Université de Rennes I
F-35042 Rennes (France)
Telefax: Int. code + 99281660
Prof. Dr. A. Robert, Dr. M.-P. Le Paillard, Dr. D. Lorcy
Groupe de Recherche de Physicochimie Structurale
Unité Associée au CNRS No 704, Université de Rennes I
F-35042 Rennes (France)
Telefax: Int. code + 99286738

 © VCH Verlagsgesellschaft mbH, D-69451 Weinheim, 1994 0570-0833/94/1313-1379 $ 10.00+.25/0

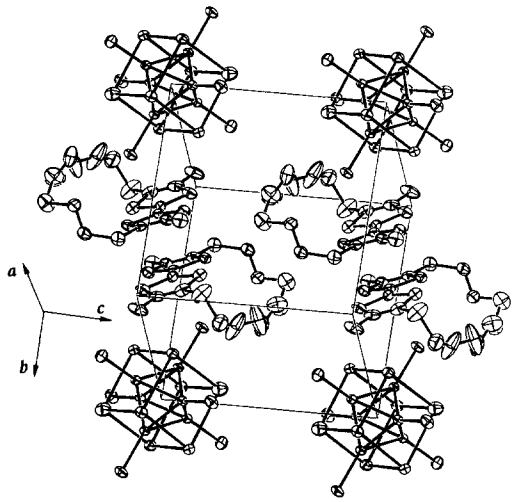


Fig. 2. ORTEP view of the unit cell packing in $(cis\text{-}\mathbf{2}^{\bullet+})_2[Re_6S_6Cl_8]^{2-} \cdot 2CH_3CN$. The solvent molecules as well as four cluster anion molecules have been omitted for clarity. The ellipsoïds are at the 40% probability level. A similar solid-state structure is observed in $(cis\text{-}\mathbf{3})_2^{+}[Re_6S_5Cl_9]^{-}$.

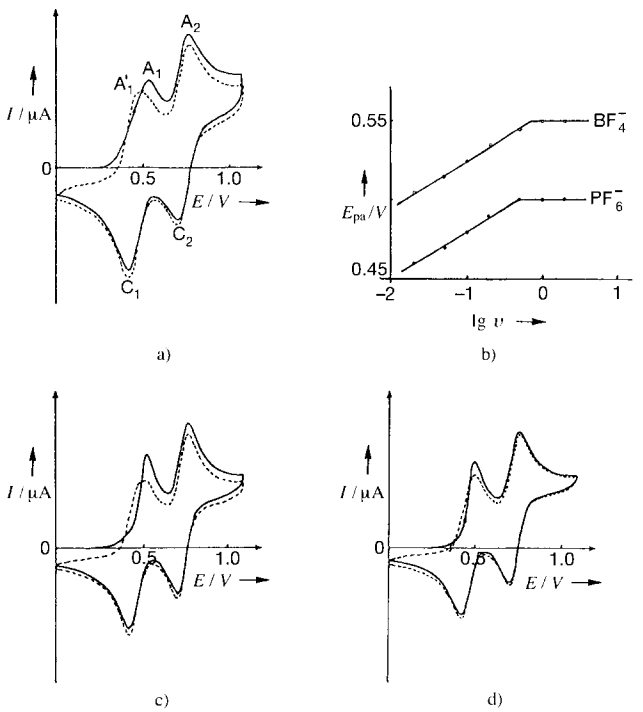
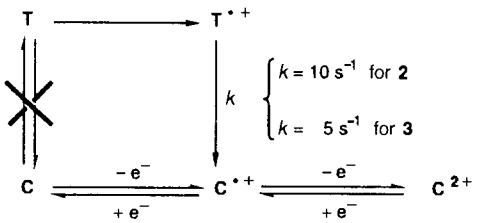


Fig. 3. Cyclic voltammograms of *trans*-**2** (10^{-3} M) in a solution of Bu_4NX (1 M; $X = BF_4^-$ or PF_6^-) in CH_2Cl_2. The cyclic voltammograms are recorded with a 1 mm^2 PT30 Tacussel electrode; potentials vs. standard calomel electrode (SCE). a) Scan speed 1 Vs^{-1}; b) variation with the scan speed v of the peak potential A_1 for *trans*-**2**; c) scan speed 100 mVs^{-1}; d) scan speed 20 mVs^{-1}.

tron waves A_1 and A_2, associated on the reverse scan with the cathodic waves C_1 and C_2, respectively. The peak potentials A_2, C_1 and C_2 are independent of the scan speed and the coupled peaks A_2/C_2 correspond to a reversible system ($\Delta E_p = 0.06$ V). Note that for slow scan speeds v ($v < 0.5$ Vs^{-1}), the peak potential for A_1 is shifted towards positive potentials as v increases, with shifts of 0.03 V per decade of v that is, $E_p(A_1) = 0.510(0.555) + 0.03 \lg v$ for PF_6^- (BF_4^-), respectively. For $v > 1$ Vs^{-1}, $Ep(A_1)$ is independent of the scan speed (Fig. 3b).

The shape of A_1 appears different when the second scan occurs at low speed (Fig. 3c, d), while a novel peak (A_1') involved in a reversible system with C_1 is observed for higher scan speeds (Fig. 3a). The same variation in the voltammogram shape is observed when the potential is reversed at 0.6 V. These are characteristic features of an EC mechanism.[13] Thus, the electrochemical oxidation of the *trans* molecule is followed (Scheme 2) by the chemical isomerization reaction (rate constant k). For the threshold scan speed v_i, the first oxidation peak potential becomes independent of v (Fig. 3b). Thus, for **2**, $k/v_i = 20.8$ at 25 °C,[13] which yields $v_i = 0.50$ Vs^{-1} and $k = 10.4$ s^{-1} with PF_6^- and $v_i = 0.6$ Vs^{-1} and $k = 12.5$ s^{-1} with BF_4^-. Therefore, the rate of isomerization appears to be essentially independent of the nature of the anion.



Scheme 2.

The features of the cyclic voltammograms shown in Figure 3 are consistent with the previously mentioned kinetic data. Thus, for high scan speeds (Fig. 3a), on the first scan, the neutral *trans* cage (T) is oxidized first and it is the neutral *cis* cage (C) which gets oxidized on the second scan (see Scheme 2). Note that the broadening of the second scan oxidation wave results from the concomitant oxidation of a small amount of the neutral *trans* cage T which by then had diffused to the electrode. Since larger amounts of T diffuse at lower scan speeds, the second scan oxidation peak in this case is much broader (Fig. 3c). At low scan speed ($v = 0.02$ Vs^{-1}, Fig. 3d), no broadening of the first oxidation peak occurs at the second scan. Indeed, at such low scan speed, there is essentially coalescence of the first oxidation peaks for T and C.

Finally, the standard oxidation potentials E^0 (Table 1) for the series of processes summarized in Scheme 2 have been determined from the cyclic voltammograms obtained for scan speeds higher than 1 Vs^{-1}. Interestingly the difference in E^0 between the $T^{\bullet+}/T$ and $C^{\bullet+}/C$ processes amounts to about 0.065 V (6 $kJ\,mol^{-1}$), regardless of the anion. Note that $E^0_{C^{2+}/C^{\bullet+}}$ is also independent of the anion (for **2**). Conversely, one observes (Table 1) that the first electron transfer from either T or C is always easier (by 1 $kJ\,mol^{-1}$) in the presence of PF_6^-, a more nucleophilic anion.

A similar study for *trans*-**3** has so far only been carried out in the presence of PF_6^-. The qualitative features of the cyclic voltammograms are identical to those of *trans*-**2**. The oxidation potentials of *trans*-**3** and *cis*-**3** being now closer (0.025 V), the quantitative analysis is more difficult than in the case of **2**. It is conclud-

Table 1. Standard oxidation potentials E^0 [V] for **2**/**3** (vs. SCE) in 1 M solutions of Bu_4NX in dichloromethane ($X = PF_6^-$, BF_4^-).

Potential	Anion	
	PF_6^-	BF_4^-
E^0 ($T^{\bullet+}/T$)	0.47/0.48	0.52/0.48
E^0 ($C^{\bullet+}/C$)	0.40/0.45	0.46/0.46
E^0 (C^{2+}/C)	0.75/0.83	0.74/0.73

 © VCH Verlagsgesellschaft mbH, D-69451 Weinheim, 1994 0570-0833/94/1313-1380 $ 10.00+.25/0

ed, however, that the isomerization rate for *trans*-**3** is half that for *trans*-**2** (Scheme 2). This observation nicely supplements the former structural analysis (Fig. 1) which also suggests that *trans*-**2**, (Fig. 1a) being significantly more strained than *trans*-**3** (Fig. 1c), would, given the opportunity, undergo a faster conformational change. Therefore, the present combination of structural and kinetic studies demonstrates that one driving force for the isomerization of such redox cage molecules is to achieve the less constrained planar configuration for their $TTF^{\bullet+}$ cores, that is, the *cis* configuration, even for the longer bridge. The first event of the EC mechanism now involves the creation of the oxidized *trans* cages $T^{\bullet+}$; one expects therefore that the subsequent lengthening of the inner TTF central double bond will result in an increase of the steric constraints within the cages in their *trans* configuration. Thus, the electron transfer also increases the tension within the *trans* cages, while at the same time weakening the central double bond. These combined events appear quite effective at driving the *trans* to *cis* isomerization even in the case of the somewhat less constrained *trans* cage **3**. Indeed, while the aliphatic fragment of the $-S(CH_2)_{12}S-$ bridge is properly locked in within the crystal structure of *trans*-**3** (Fig. 1c), it is found highly disordered within the structure of $(cis\text{-}\mathbf{3})_2^{\bullet+}[Re_6S_5Cl_9]^-$,[12] which indicates that the cage in the *cis* configuration is unconstrained and fairly flexible (Fig. 1d).

Future reports on this unique system will focus on the design and properties of molecular solid-state assemblies based on such redox-active nonplanar molecules whose molecular shape switches upon electron transfer.

Received: February 19, 1994 [Z 6700 IE]
German version: *Angew. Chem.* **1994**, *106*, 1448

[1] W. Huber, K. Müllen, *Acc. Chem. Res.* **1986**, *19*, 300–306.

[2] M. Jorgensen, K. Lerstrup, P. Frederiksen, T. Bjørnholm, P. Sommer-Larsen, K. Schaumburg, K. Bechgaard, *J. Org. Chem.* **1993**, *58*, 2785, and references therein.

[3] Only few cagelike π-donor molecules exhibiting reversible redox processes have been described so far: a) A. Renault, D. Talham, J. Canceill, P. Batail, A. Collet, J. Lajzerowicz, *Angew. Chem.* **1989**, *101*, 1251; *Angew. Chem. Int. Ed. Engl.* **1989**, *28*, 1249; b) M. Adam, V. Enkelmann, H.-J. Räder, J. Rörich, K. Müllen, *ibid.* **1992**, *104*, 331 and **1992**, *31*, 309; c) M. Adam, K. Müllen, *Adv. Mater.* **1994**, *6*, 439.

[4] F. Bertho-Thoraval, A. Robert, A. Souizi, K. Boubekeur, P. Batail, *J. Chem. Soc. Chem. Commun.* **1991**, 843.

[5] K. Boubekeur, P. Batail, F. Bertho-Thoraval, A. Robert, *Acta Crystallogr. Sect. C* **1991**, *47*, 1109.

[6] As observed recently for other cage donor molecules with strongly bent redox unit: a) T. Jorgensen, J. Becher, T. K. Hansen, K. Christiansen, P. Roepstorff, S. Larsen, A. Nygaard, *Adv. Mater.* **1991**, *3*, 486; b) R. Gasiorowski, T. Jorgensen, J. Møller, T. K. Hansen, M. Pietraszkiewicz, J. Becher, *ibid.* **1992**, *4*, 568.

[7] *trans*-**2**: M.p. 158–159 °C, correct elemental analysis (C, H, S). ^1H NMR (CD_2Cl_2, 300 MHz): $\delta = 3.07$ (dtt, 2H, S-CH_a), 2.52 (dt, 2H, S-CH_b), 2.17 (s, 6H, Me), 1.66 (m, 4H), 1.33 (m, 8H), 1.02 (m, 4H); MS: *m/z*: 434.037 (calcd 434.0358).

[8] *trans*-**3**: M.p. 115–116 °C, correct elemental analysis (C, H, S). ^1H NMR ($CDCl_3$, 80 MHz): $\delta = 2.62$ (m, 4H), 2.05 (s, 6H, Me), 1.20 (m, 20H); MS: *m/z*: 462.066 (calcd 462.067).

[9] Crystal structure for *trans*-**2**: $C_{18}H_{26}S_8$, $M = 434.79$, yellow flat crystals, monoclinic space group $P2/n$, $a = 11.874(2)$, $b = 7.745(2)$, $c = 12.996(2)$ Å, $\beta = 116.99(2)°$, $V = 1065.0$ Å^3, $Z = 2$, $\varrho_{calcd} = 1.36$ g cm^{-3}; $Mo_{K\alpha}$ radiation; absorption corrections by Ψ-scan; 1902 independent reflections with ω-2θ scans were measured up to $\theta = 25°$ at 293 K on an Enraf-Nonius CAD4 diffractometer. The structure was solved by direct methods. The full-matrix least-squares refinements of 109 parameters from 1519 reflections with $I > 3\,\sigma(I)$ converged at $R = 0.035$ and $R_w = 0.056$ [12].

[10] Shiny, black paralellepiped single crystals of $(cis\text{-}\mathbf{2}^{\bullet+})_2[Re_6S_6Cl_8]^{2-} \cdot 2CH_3CN$ were harvested after five days of anodic oxidation under constant low current (1.5 μAmp) at a platinum wire electrode of *trans*-**2** (0.025 mmol) in a 7/1 acetonitrile/dichloromethane solution of $(Bu_4N)_2(Re_6S_6Cl_8)$ (0.022 mmol). The latter was prepared according to published procedures [14]. Crystal structure for $(cis\text{-}\mathbf{2}^{\bullet+})_2[Re_6S_6Cl_8]^{2-} \cdot 2CH_3CN$: $C_{40}H_{58}Cl_8N_2Re_6S_{20}$, $M = 2.072.44$, triclinic, space group $P\bar{1}$, $a = 12.010(6)$, $b = 13.795(7)$, $c = 10.692(1)$ Å, $\alpha = 95.99(2)$, $\beta = 102.58(2)$, $\gamma = 75.61(5)°$, $V = 1672.7$ Å^3, $Z = 1$, $\varrho_{calcd} = 2.06$ g cm^{-3}; $Mo_{K\alpha}$ radiation; absorption corrections by Ψ-scan; 7598 independent reflections with ω-2 θ scans were measured up to $\theta = 28°$ at 293 K on an Enraf-Nonius CAD4 diffractometer. The structure was solved by the Patterson method. The full-matrix least-squares refinements of 334 parameters from 4244 reflections with $I > 3\,\sigma(I)$ converged at $R = 0.034$ and $R_w = 0.043$. The cation radical cores of the *cis* cage molecules form strong, discrete fully oxidized diamagnetic dimers in the crystal in agreement with the absence of an ESR signal.

[11] Crystal structure for *trans*-**3**: $C_{20}H_{30}S_6$, $M = 462.85$, yellow flat crystals, triclinic, space group $P\bar{1}$, $a = 9.633(2)$, $b = 10.308(2)$, $c = 13.350(2)$ Å, $\alpha = 110.16(1)$, $\beta = 98.04(1)$, $\gamma = 105.74(2)°$, $V = 1157.1$ Å^3, $Z = 2$, $\varrho_{calcd} = 1.33$ g cm^{-3}, $Mo_{K\alpha}$ radiation; absorption corrections by Ψ-scan; 4503 independent reflections with ω-2θ scans were measured up to $\theta = 26°$ at 293 K on an Enraf-Nonius CAD4 diffractometer. The structure was solved by direct methods. The full-matrix least squares refinements of 235 parameters from 2956 reflections with $I > 3\,\sigma(I)$ converged at $R = 0.029$ and $R_w = 0.034$.

[12] Brittle, black paralellepiped single crystals of $(cis\text{-}\mathbf{3})_2^{\bullet+}[Re_6S_5Cl_9]^-$ were harvested after five days of anodic oxidation under constant low current (1.5 μAmp) at a platinum wire electrode of *trans*-**3** (0.021 mmol) in a 7/1 acetonitrile/dichloromethane solution of $(Bu_4N)_2[Re_6S_5Cl_9]$ (0.026 mmol). The latter was prepared according to published procedures [14]. Crystal structure for $(cis\text{-}\mathbf{3})_2^{\bullet+}[Re_6S_5Cl_9]^-$: $C_{40}H_{60}Cl_9Re_6S_{17}$, $M = 2.522.25$, triclinic, space group $P\bar{1}$, $a = 12.086(6)$, $b = 13.939(8)$, $c = 11.306(2)$ Å, $\alpha = 90.69(3)$, $\beta = 103.67(3)$, $\gamma = 75.53(5)°$, $V = 1790$ Å^3, $Z = 1$, $\varrho_{calcd} = 2.34$ g cm^{-3}, $Mo_{K\alpha}$ radiation; absorption corrections by Ψ-scan; 8278 independent reflections with ω-2θ scans were measured up to $\theta = 28°$ at 293 K on an Enraf-Nonius CAD4 diffractometer. The structure was solved by the Patterson method. Note that, not only was the thermal motion for all atoms of the *cis*-**3** cation found to be significantly larger than for the other three structures but also the located carbon atoms of the $-S(CH_2)_{12}S-$ fragment, which are consistently found all on one side of the molecule only, exhibited considerable instability when treated as independent atoms in the refinement procedure, leading to unrealistic geometries. Therefore the final refinement stages were conducted imposing restraints on bond lengths and angles for this fragment using the program XTAL3.2 [15]. Thus, the full-matrix least-squares refinements of 253 parameters from 3950 reflections with $I > 3\,\sigma(I)$ converged at $R = 0.115$ and $R_w = 0.161$. Further details of the crystal structure investigations may be obtained from the Fachinformationszentrum Karlsruhe, D-76344 Eggenstein-Leopoldshafen (FRG) on quoting the depository number CSD-58143. A single, quasi-isotropic ESR line (temperature independent linewidth of 4.3 Gauss with g values extremes of 2.0065 and 2.010) is observed on a single crystal of $(cis\text{-}\mathbf{3})_2^{\bullet+}[Re_6S_5Cl_9]^-$. The spin susceptibility shows a Curie-type behavior in agreement with the presence of discrete, noninteracting mixed-valence dimers in the structure.

[13] C. P. Andrieux, J.-M. Savánt in *Electrochemical Reactions in Investigations of Rates and Mechanisms of Reactions, Techniques of Chemistry, Vol. VI/4E, Part 2* (Ed.: C. F. Bernasconi), Wiley, New York, **1986**, pp. 305–390.

[14] J.-C. Gabriel, K. Boubekeur, P. Batail, *Inorg. Chem.* **1993**, *32*, 2894.

[15] S. R. Hall, H. D. Flack, J. M. Stewart, *XTAL 3.2 Reference Manual*, Universities of Western Australia, Geneva and Maryland, **1992**.

Desulfurization of Benzo[*b*]thiophene by S/Ru Exchange: Formation and Structure of the Cluster $[Ru_3(CO)_8(C_8H_6)]$**

Alejandro J. Arce,* Ysaura De Sanctis, Arquímedes Karam, and Antony J. Deeming*

The organometallic chemistry of thiophenes has been developed extensively during the past few years.[1–3] The cleavage of C–S bonds in thiophenes is required for metals to abstract

[*] Dr. A. J. Arce, Y. De Sanctis, A. Karam
Centro de Química, Instituto Venezolano de Investigaciones Científicas (IVIC)
Apartado 21827, Caracas 1020-A (Venezuela)
Telefax: Int. code + (2)501-1350
Prof. A. J. Deeming
Department of Chemistry, University College London
20 Gordon Street, GB-London WC1H OAJ (UK)
Telefax: Int. code + (71)380-7463

[**] This work was supported by the Science and Engineering Research Council (SERC), by the Consejo Nacional de Investigaciones Científicas y Tecnológicas (CONICIT) (Venezuela), and the University of London Central Research Fund.

sulfur from the heterocycle, and the homogeneous desulfurization of thiophenes with transition-metal compounds has provided models for the catalytic heterogeneous dehydrosulfurization of thiophenic components of crude oil.

The cluster $[Fe_3(CO)_{12}]$ reacts with thiophene with loss of the sulfur atom to give the ferrole compound $[Fe_2(\mu\text{-}C_4H_4)(CO)_6]$,[4] while $[Fe_2(\mu\text{-}C_4H_3MeS)(CO)_6]$ as well as the sulfur-free species $[Fe_2(\mu\text{-}C_4H_3Me)(CO)_6]$ are formed from 2-methylthiophene.[5, 6] Similarly the reaction of $[Ru_3(CO)_{12}]$ with thiophene[7] gives the sulfur-free species $[Ru_2(\mu\text{-}C_4H_4)(CO)_6]$ derived by C–S bond cleavage as in the iron case, but in addition the tetranuclear cluster $[Ru_4(\mu_3\text{-}S)(\mu\text{-}C_4H_4)(CO)_{11}]$, which contains separate S and C_4H_4 ligands within the same molecule. Better yields were obtained from 2-methylthiophene, and in this case, products of both C–S and C–H bond cleavage were obtained: $[Ru_3(\mu\text{-}H)(\mu\text{-}C_4H_2MeS)(CO)_{10}]$ (*exo* and *endo* isomers) and $[Ru_4(\mu_3\text{-}S)(\mu\text{-}C_4H_3Me)(CO)_{11}]$. With osmium, C–H rather than C–S bonds are cleaved exclusively, and $[Os_3(CO)_{12}]$ or $[Os_3(CO)_{10}(MeCN)_2]$ react with thiophene to give the thienyl isomers $[Os_3(\mu\text{-}H)(\mu\text{-}C_4H_3S)(CO)_{10}]$ (*exo* and *endo* isomers in rapid equilibrium), which decarbonylate to the "thiophyne" cluster $[Os_3(\mu\text{-}H)_2(\mu_3\text{-}C_4H_2S)(CO)_9]$.[8–11]

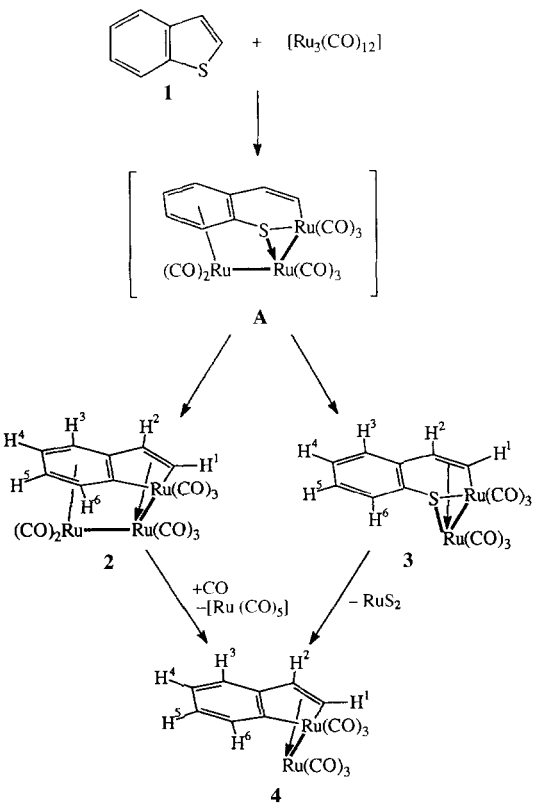
Benzo[*b*]thiophene **1** and dibenzothiophene more closely correspond to the major sulfur components in fossil fuels than thiophene, and these compounds are difficult to activate.[12] The first example of metal-assisted opening and hydrogenation of **1** was described by Rauchfuss et al.,[6] who treated **1** with $[Fe_3(CO)_{12}]$ to obtain the benzothiaferrole $[Fe_2(C_8H_6S)(CO)_6]$, which was hydrogenated to give ethylbenzene together with some 2-ethylbenzenethiol, bis(2-ethylphenyl) sulfide, and bis(2-ethylphenyl) disulfide. Also oxidative addition of the C–S bond of **1** with $[(C_5Me_5)Rh(PMe_3)(Ph)H]$ was reported.[13] Recently oxidative addition of **1** to iridium(I) gave an iridium(III) complex that could be selectively hydrogenated to give the 2-ethylbenzenethiolate ligand at iridium(III).[14] We now report the synthesis of the clusters $[Ru_3(C_8H_6)(CO)_8]$ (**2**), $[Ru_2(C_8H_6S)(CO)_6]$ (**3**), and $[Ru_2(C_8H_6)(CO)_6]$ (**4**), obtained from the reaction of $[Ru_3(CO)_{12}]$ with **1** under relatively mild conditions.

The reaction of $[Ru_3(CO)_{12}]$ with **1** under reflux in THF gave, compounds **2**, **3**, and **4** in 28, 17, and 10% yield, respectively, after TLC work-up (Scheme 1). The clusters were characterized by ^1H NMR and IR spectroscopy, and the X-ray structure of **2** was determined.[15]

Compounds **2** and **4** are formed by C–S bond cleavage and extrusion of the sulfur atom. Compound **3** is closely related to that obtained by Rauchfuss from the reaction of benzo[*b*]thiophene and $[Fe_3(CO)_{12}]$;[6] their ^1H NMR spectra correspond. The dinuclear compound **3** was isolated and heated in cyclohexane for 20 min to afford an insoluble black by-product, which suggests the formation of RuS_2, and the sulfur-free compound **4**, since the spectroscopic data of **4** resemble those of the product obtained from the debromination of 1,4-dibromocyclooctatetraene with $[Ru_3(CO)_{12}]$ in hydrocarbon solvent (the metallaindene complex $[Ru_2(C_8H_6)(CO)_6]$), the most likely structure is that shown in Scheme 1. The X-ray structure of the osmium analogue was reported.[16]

Although **4** was obtained in low yield (10%), this can be increased considerably if the reaction is carried out under carbon monoxide. ^1H NMR ($CDCl_3$ solution) and IR monitoring (showing the presence of $Ru(CO)_5$) confirmed that **2** can be converted quantitatively into **4** at room temperature under 1 atm of CO over a period of 24 h (Fig. 1).

Under our reaction conditions, no decacarbonyl or nonacarbonyl clusters such as the *exo* and *endo* isomers $[Ru_3(\mu\text{-}H)(\mu\text{-}C_8H_5S)(CO)_{10}]$ or their expected decarbonylation products



Scheme 1. Synthesis of **2**, **3**, and **4**.

$[Ru_3(\mu\text{-}H)_2(\mu\text{-}C_8H_4S)(CO)_9]$ were obtained on treating **1** with $[Ru_3(CO)_{12}]$. Probably compound **A** containing a ring-opened benzo[*b*]thiophene ligand bonded to an opened Ru_3 triangle is formed in the early stages of the reaction (Scheme 1) and con-

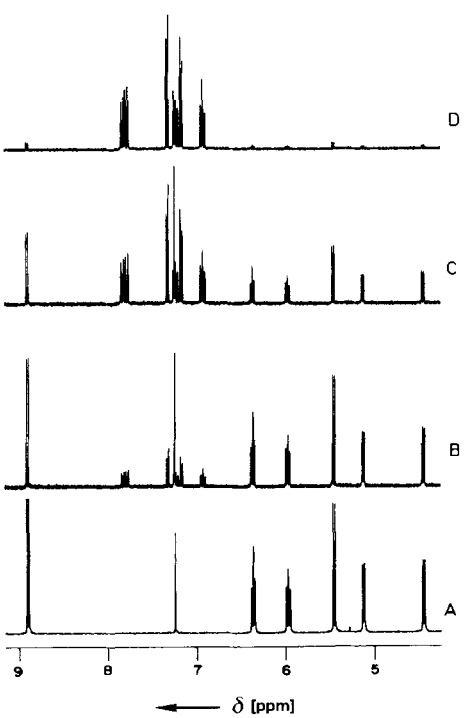


Fig. 1. Monitoring of the conversion **2** → **4** ($CDCl_3$, CO 1 atm) by ^1H NMR spectroscopy. A: Initial spectrum; B: after 70 min; C: after 5 h; and D: after 24 h, showing the clean, almost quantitative, conversion to compound **4**.

verts readily to the dinuclear ring-opened compound **3**, or is desulfurized to afford cluster **4**. A single-crystal X-ray structure for **2** (see Fig. 2) was needed to establish the mode of bonding. The desulfurized ligand is bonded to three metal atoms as an 10-electron donor to give a 50-electron cluster with only two Ru–Ru bonds.

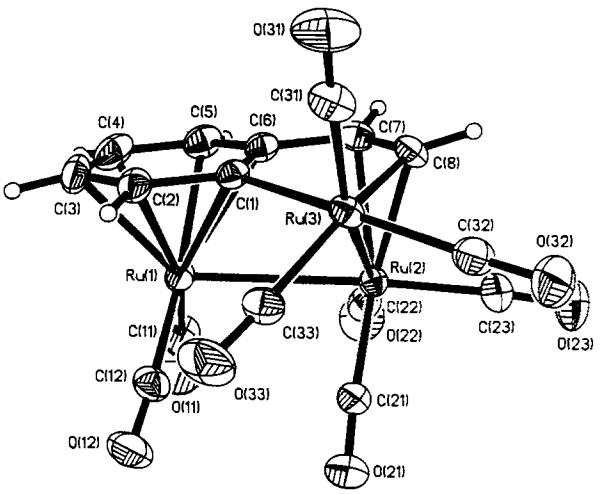


Fig. 2. Molecular structure of **2**: selected bond lengths [Å] and angles [°]: Ru(1)–Ru(2), 2.946(2); Ru(2)–Ru(3), 2.781(2); Ru(2)–C(7), 2.257(5); Ru(2)–C(8), 2.237; Ru(1)–C(1), 2.322(5); Ru(1) C(4), 2.294(6); Ru(3)–C(1), 2.088(6); Ru(3)–C(8), 2.058(6); C(1)–C(2), 1.413(8); C(2) C(3), 1.430(9); C(3)–C(4), 1.40(1); C(4)–C(5), 1.41(1); C(5)–C(6), 1.424(8); C(6)–C(7), 1.458(8); C(7)–C(8), 1.400(9); C(1)–C(6), 1.454(8); Ru(1)···Ru(3), 3.815(2); Ru(2)···C(1), 2.934(6); Ru(2)···C(6), 2.657(6); Ru(1)-Ru(2)-Ru(3), 83.5(1); Ru(1)-C(1)-Ru(3), 119.6(2); Ru(3)-C(1)-C(6), 113.9(4); Ru(1)-C(1)-C(6), 72.9(3); Ru(3)-C(8)-C(7), 116.8(4); Ru(3)-C(8)-C(7), 72.7(3); C(2)-Ru(1)-C(5), 76.0(2); C(3)-Ru(1)-C(6), 75.6(2); Ru(1)-C(6)-C(7), 128.3(3); Ru(2)-C(7)-C(6), 88.6(3).

$[Ru_3(C_8H_6)(CO)_8]$ (**2**) is the first example of a fully characterized trinuclear Ru complex containing a 1-ruthenaindene system. The nine atoms of the bicyclic metallaindene system are substantially coplanar; the $C_8H_6Ru(CO)_3$ unit can thus be regarded as an 8-electron-donor ligand π-complexed to the $Ru_2(CO)_5$ group.

Experimental Procedure

$[Ru_3(CO)_{12}]$ (0.200 g) and **1** (0.200 g) were heated at reflux in tetrahydrofuran (50 cm^3) for 24 h under N_2. The orange-brown solution was evaporated to dryness under reduced pressure, and the residue separated by TLC on silica with n-hexane as eluent into three bands, which yielded **2** (yellow, 28%), **3** (yellow-orange, 17%), and **4** (yellow, 10%). A solution of **2** (0.020 g) in $CDCl_3$ (0.5 cm^3) under CO (1 atm) showed complete conversion to compound **4** in 24 h at room temperature (monitored by ^1H NMR spectroscopy). Crystals of compound **2** for structure determination were obtained from cyclohexane. **2**: IR (cyclohexane): $\tilde{\nu}$(CO) [cm^{-1}] = 2077 s, 2045 vs, 2017 vs, 2003 s, 1980 m, 1963 m; ^1H NMR ($CDCl_3$, 300 MHz, 296 K, J in Hz): δ = 8.89 (d, H^1), 5.45 (d, H^2), 4.44 (dd, H^3), 5.96 (ddd, H^4), 6.36 (ddd, H^5), 5.11 (dd, H^6) [$J(H^1H^2)$ = 6.3, $J(H^3H^4)$ = 6.7, $J(H^3H^5)$ = 1.1, $J(H^4H^5)$ = 6.0, $J(H^4H^6)$ = 1.3, $J(H^5H^6)$ 5.8]. **3**: IR (cyclohexane): $\tilde{\nu}$(CO) [cm^{-1}] = 2088 m, 2061 s, 2021 s, 2014 vs, 2000 m. ^1H NMR (CD_3COCD_3, 300 MHz, 296 K, J in Hz): δ = 9.04 (d, H^1), 6.08 (dd, H^2), 7.18 (dddd, H^3), 6.91 (ddd, H^4), 7.05 (ddd, H^5), 7.22 (dd, br, H^6) [$J(H^1H^2)$ = 10.0, $J(H^2H^3)$ = 0.6, $J(H^3H^4)$ = 7.6, $J(H^3H^5)$ = 1.2, $J(H^3H^5)$ = 0.5, $J(H^4H^5)$ = 7.5, $J(H^4H^6)$ = 1.4, $J(H^5H^6)$ = 7.5]. $[Fe_2(C_8H_6S)(CO)_6]$ [6]: IR (cyclohexane): $\tilde{\nu}$(CO) [cm^{-1}] = 2077 m, 2044 vs, 2005 s, 1993 w. ^1H NMR (CD_3COCD_3, 300 MHz, 296 K, J in Hz): δ = 9.04 (d, H^1), 5.67 (d, H^2), 7.06 (dd, H^3), 6.81 (ddd, H^4), 6.99 (ddd, H^5), 7.12 (dd, H^6) [$J(H^1H^2)$: 9.1, $J(H^3H^4)$ = 7.6, $J(H^3H^5)$ = 1.2, $J(H^4H^5)$ = 7.5, $J(H^4H^6)$ = 1.2, $J(H^5H^6)$ = 7.5]. **4**: IR (cyclohexane): $\tilde{\nu}$(CO) [cm^{-1}] = 2082 m, 2051 vs, 2010 vs, 1992 m, 1984 s. ^1H NMR (CD_3COCD_3, 300 MHz, 296 K, J in Hz): δ = 7.53 (d, H^1), 7.45 (d, H^2), 8.04 (ddd, H^3), 7.35 (ddd, H^4), 7.05 (ddd, H^5), 7.89 (d, br, H^6) [$J(H^1H^2)$ = 6.5, $J(H^3H^4)$ = 8.5, $J(H^3H^5)$ = 1.1, $J(H^3H^6)$ = 1.0, $J(H^4H^5)$ = 6.7, $J(H^4H^6)$ = 1.2, $J(H^5H^6)$ = 8.3].

Received: January 28, 1994 [Z 6653 IE]
German version: *Angew. Chem.* **1994**, *106*, 1459

[1] R. J. Angelici, *Acc. Chem. Res.* **1988**, *21*, 387
[2] T. B. Rauchfuss, *Prog. Inorg. Chem.* **1991**, *39*, 259.
[3] T. Frejd in *Heterocyclic Compounds*, *Vol 44* (Ed.: S. Gronowitz), Wiley, New York, **1992**, Part 5, pp. 257–754.
[4] H. D. Kaesz, R. B. King, T. A. Manuel, L. D. Nichols, F. G. A. Stone, *J. Am. Chem. Soc.* **1960**, *82*, 4750.
[5] P. Hüberer, E. Weiss, *J. Organomet. Chem.* **1977**, *129*, 105.
[6] A. E. Ogilvy, M. Draganjac, T. B. Rauchfuss, F. R. Wilson, *Organometallics* **1988**, *7*, 1171.
[7] A. J. Arce, P. Arrojo, A. J. Deeming, Y. De Sanctis, *J. Chem. Soc. Dalton Trans.* **1992**, 2423.
[8] A. J. Arce, A. J. Deeming, Y. De Sanctis, R. Machado, J. Manzur, C. Rivas, *J. Chem. Soc. Chem. Commun.* **1990**, 1568.
[9] A. J. Arce, J. Manzur, M. Márquez, Y. De Sanctis, A. J. Deeming, *J. Organomet. Chem.* **1991**, *412*, 177.
[10] A. J. Deeming, A. J. Arce, Y. De Sanctis, M. W. Day, K. I. Hardcastle, *Organometallics* **1989**, *8*, 1408.
[11] M. W. Day, K. I. Hardcastle, A. J. Deeming, A. J. Arce, Y. De Sanctis, *Organometallics* **1990**, *9*, 6.
[12] R. Bartsch, C. Tanelian, *J. Catal.* **1974**, *35*, 353; D. R. Kilanowski, B. C. Gates, *ibid.* **1980**, *62*, 70.
[13] W. D. Jones, L. Dong, *J. Am. Chem. Soc.* **1991**, *113*, 559.
[14] C. Bianchini, A. Meli, M. Peruzzini, F. Vizza, P. Frediani, V. Herrera, R. A. Sánchez-Delgado, *J. Am. Chem. Soc.* **1993**, *115*, 7505.
[15] Crystal structure of **2**: $C_{16}H_6O_8Ru_3$, M = 629.43, monoclinic, space group $P2_1/n$, a = 9.447(4), b = 16.426(8), c = 11.857(8) Å, β = 102.81(5)°, V = 1794(2) $Å^3$, Z = 4, λ = 0.71073 Å, $\mu(Mo_{K\alpha})$ = 24.9 cm^{-1}, $F(000)$ = 1192. Solution with direct methods (SHELXTL-PLUS), 4101 unique absorption-corrected data between $5 \le 2\theta \le 55°$ and with $I_o \le 1.5\ \sigma(I_o)$ used, 244 parameters (all non-H atoms anisotropic), final R = 0.0418 and R_w = 0.00469, with $R_w = [\sum w(|F_o| - |Fc|)^2/\sum w|F_o|^2]^{1/2}$ and $w = 1/[\sigma^2(F_o) + 0.00122F_o^2]$. H atoms in calculated positions (C–H 0.96 Å, U_{iso} = 0.08 $Å^3$). Further details of the crystal structure investigation are available on request from the Director of the Cambridge Crystallographic Data Centre, 12 Union Road, GB-Cambridge, CB21EZ (UK) on quoting the full journal citation.
[16] P. J. Harris, J. A. K. Howard, S. A. R. Knox, R. P. Phillips, F. G. A. Stone, P. Woodward, *J. Chem. Soc. Dalton Trans.* **1976**, 377.

Samarium Iodide Induced Intramolecular C-Glycoside Formation: Efficient Radical Formation in the Absence of an Additive

Daniel Mazéas, Troels Skrydstrup,* Olivier Doumeix, and Jean-Marie Beau*

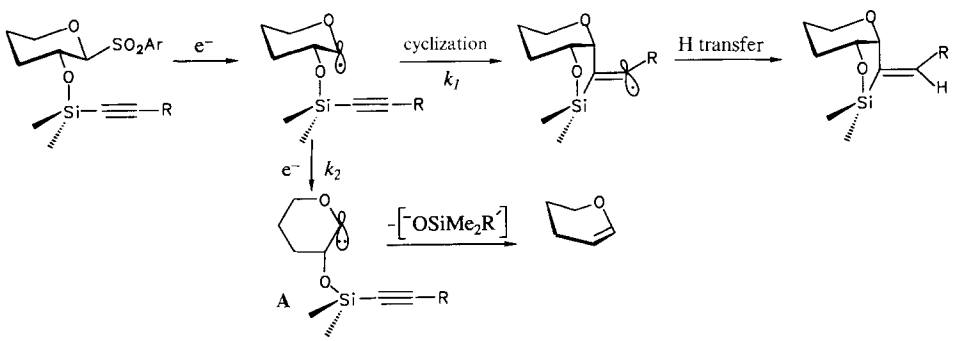
Of the numerous existing methods for C-glycoside construction,[1] the intramolecular free radical cyclization employing the temporary silicon connection reported by Stork et al. lends itself as the most attractive.[2] The reaction conditions are mild and complete stereochemical control at the anomeric center may be achieved by the judicious choice of the linking hydroxy group (i.e. the oxygen of the substrate which carries the silicon tether). Only a few examples of this reaction are known, however, and in each case the tin hydride based procedure coupled with phenylselenoglycosides has been applied for radical generation at the anomeric center.[2–4]

In the last few years samarium(II) iodide has not only emerged as a unique alternative for carrying out reductive radical cyclization reactions of unsaturated haloalkanes, but has shown greater versatility as well.[5, 6] However, for efficient single-electron transfer with concomitant radical formation, the reducing potential of SmI_2 has to be augmented by the addition of a cosolvent such as hexamethylphoshoramide (HMPA).[7] Reductive desulfonyl-

[*] Dr. T. Skrydstrup, Prof. Dr. J.-M. Beau, D. Mazéas, O. Doumeix
Université d'Orléans, Laboratoire de Biochimie Structurale
URA 499, BP 6759, F-45067 Orléans Cédex 2 (France)
Telefax: Int. code + 38417281

ation of phenylsulfones, which involves a transient radical species, has likewise been observed with the SmI_2/HMPA system.[8, 9] Again, in the absence of HMPA, the phenylsulfones are devoid of any reactivity, though a notable exception has been provided by Trost et al.[10] for geminal bis-sulfones. We now report an application of the SmI_2-promoted radical cyclizations that uses glycosyl aryl sulfones in connection with the above-mentioned silicon-tethered appraoch as an alternative to C-glycoside construction. The particular highlight of this procedure lies in the fact that by fine tuning the aryl sulfone moiety, SmI_2 alone is sufficient for effective radical formation at the anomeric center, thus avoiding the use of the additive HMPA. In addition, we report the first stereoselective synthesis of a C-disaccharide by employing the 5-*exo* cyclization mode.

The essential features of this strategy are illustrated in Scheme 1. One-electron transfer to the π^* (SO_2Ar) orbital of the



Scheme 1. The actual conformation of the α-orientated anionic species **A** of this kind is presently unknown which explains the Haworth representation of this intermediate. If an alkenylsilyl group is used instead of an alkynyl silyl group, a one-electron reduction and protonation occurs in the final step of the reaction.

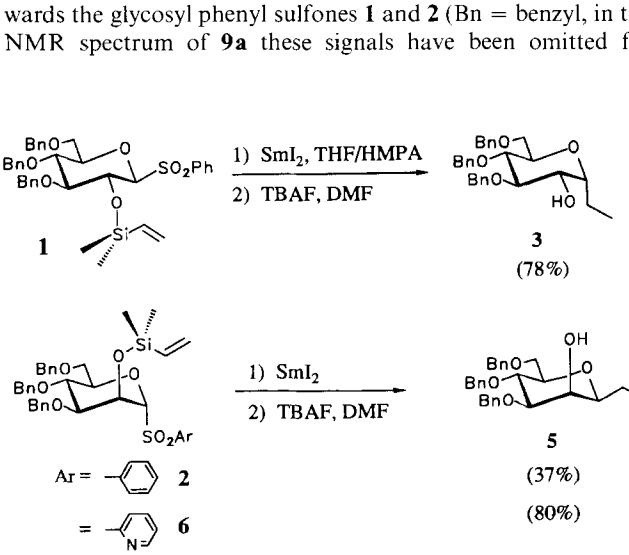
sulfonylglycoside from SmI_2 leads to fragmentation and generation of the radical at the anomeric position. At this stage, for efficient C-glycoside formation, 5-*exo* ring closure onto the silicon-tethered alkyne or alkene group (k_1) must precede the second electron transfer step (k_2). The newly formed radical center could then either abstract hydrogen from THF (C=C) or undergo one-electron reduction (C–C). Inefficient cyclization, on the other hand, would be measured by formation of the α-anion **A**, which would probably lead to the corresponding glucal by β elimination.

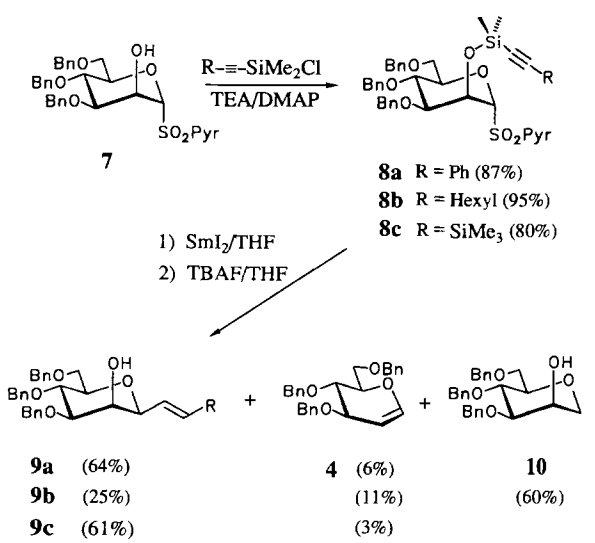
To examine this approach, our efforts were first directed towards the glycosyl phenyl sulfones **1** and **2** (Bn = benzyl, in the NMR spectrum of **9a** these signals have been omitted for clarity), each prepared from their corresponding C2-alcohols[9] and commercially available dimethylvinylsilyl chloride. Treatment of a 0.01 M THF solution of phenyl sulfone **1** and SmI_2 (5 equiv) with HMPA (11 equiv) at 20 °C led to rapid consumption of the starting material. Desilylation with four equivalents of tetrabutylammonium fluoride (TBAF) in dimethylformamide (DMF) (4 h, 60 °C)[11] gave the α-C-ethylglucoside **3** in good overall yield (78%) with no sign of 3,4,6-tri-*O*-benzyl glucal (**4**). In contrast, under identical conditions mannoside **2** led to a low yield of the β-C-mannoside **5** (37%) with essentially glucal **4** as the only other compound detected. Hence a slow cyclization rate (k_1) in the case of **2** appears as the major concern and may be attributed to the preference for an α configuration by the radical.[12]

One way of increasing the cyclization efficiency would be to extend the lifetime of the radical by simply slowing down the rate of the second electron transfer or, in other words, reducing the redox potential of SmI_2. Omission of HMPA would allow this, although at the expense of the first electron transfer into the $\pi^*(SO_2Ar)$ orbital. Therefore decreasing the LUMO energy level of the aryl sulfone group would be desirable and could be accomplished, for example, by including nitrogen in the arene ring.[13, 14]

Screening a variety of nitrogen-containing arenes revealed that mannosyl 2-pyridyl sulfones[15] proved to be the most convenient to prepare and, more importantly, were instantaneously reduced in the presence of SmI_2 without an additive.[16] Hence slow addition of two equivalents of SmI_2 (ca. 30 min) to a well-degassed 0.01 M THF solution of **6** at 20 °C provided the β-C-glycoside **5** in 80% overall yield after desilylation. No glucal was detected. An added advantage of this procedure is that completion of the reaction is easily monitored from the persistent blue color of excess SmI_2.

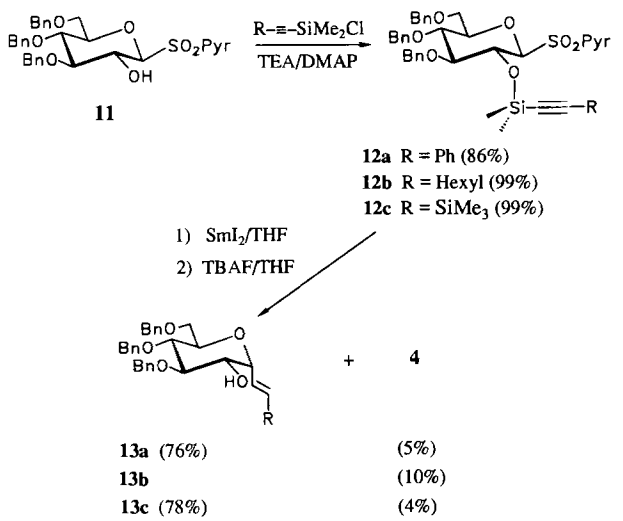
A series of acetylenic silyl-tethered derivatives **8a–c** were tested to expand the scope of this reaction. Each was prepared in good yields by adding dichlorodimethylsilane (3.0 equiv) to the pre-





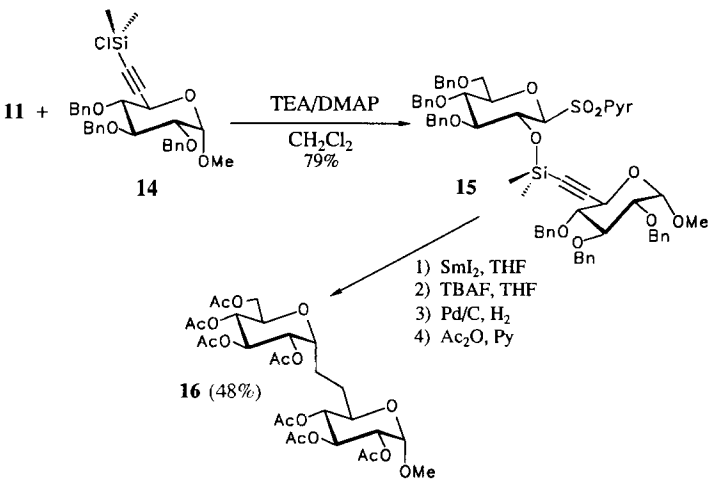
formed lithiated alkynes in THF at −78 °C (warming to 20 °C, 2 h) followed by evaporation of the excess Me_2SiCl_2, and silylation of alcohol **7** (0.2 equiv) in the presence of triethylamine (TEA) and dimethylaminopyridine (DMAP) in CH_2Cl_2.[17] Two-step reductive radical cyclization and desilylation (2 equiv. TBAF, THF, 0 °C) afforded the vinylic-β-C-glycosides **9a–c** under similar conditions as for the reactions of **6**. With the activated alkynes **8a** and **8c**, reasonable yields were obtained (*E*:*Z* ratio, ≈10:1) comparable to the one previously reported for **9a** using the tin hydride procedure.[2] On the other hand, **8b** gave a poor yield, clearly reflecting the lowered rate for the 5-*exo*-dig cyclization with respect to the 5-*exo*-trig mode of **6**. In all three cases, glucal **4** was also recovered albeit in low yields. Interestingly, the reduction product **10** was likewise isolated which, in the case of **8b**, corresponded to a remarkable 60% yield. This 1-deoxy sugar could have originated from protonation of a possible stable samarium mannoside species. The implications of this result are under further investigation.

Our attention was then directed towards the silylated glucose derivatives **12a–c**, each prepared in excellent yields from alcohol **11**. In contrast to **8**, rapid addition of SmI_2 (5–8 equiv) to a 0.007 M solution of glucosyl sulfones **12** in THF and subsequent desilylation afforded the best yields of the α-C-glycosides **13a–c**. As expected, the yields were generally higher than those of **9** and excellent *trans*-selectivities (*E*:*Z* ratio, >50:1) were also exhibited. A complex mixture of products was obtained with **12b**, nevertheless, exhaustive hydrogenation (H_2, Pd/C) and acetylation (Ac_2O, pyr) gave the tetra-*O*-acetyl-α-C-octylglucoside (Ac instead of Bn and CH_2CH_2 instead of CH=CH in **13b**) in a 53% overall yield with the major by-product again representing a 1-deoxy sugar.



Finally, a fast and efficient stereoselective synthesis of methyl-α-C-isomaltoside was performed by using the above strategem. Coupling of the two subunits **11** and **14** proceeded well providing intermediate **15** in 79% yield based on sulfone **11**. Cyclization in the presence of SmI_2 and further transformation furnished the methyl C-isomaltoside as its crystalline peracetate **16**[18] in a good 48% overall yield (four steps).[19]

In summary, samarium iodide promoted radical cyclizations provide a good alternative to the corresponding tin hydride method for intramolecular C-glycoside formation, with the added advantage of avoiding the sometimes tedious process of removing tin-containing by-products. Extension of this procedure to the preparation of C-glycoside analogues of biologically important O-glycosides is currently underway in our laboratory.



Experimental Procedure

C-Mannoside formation (**9a**): A 0.1 M solution of SmI_2 in THF (3.4 mL, 0.34 mmol) was added over a period of 30 min by syringe to a well-degassed solution of **8a** (59.5 mg, 0.081 mmol) in THF (8 mL) at 20 °C. Saturated aqueous NH_4Cl was added and the mixture was extracted twice with CH_2Cl_2. The combined organic phases were washed twice with water, dried (Na_2SO_4), and evaporated to dryness. The residue was redissolved in THF (3 mL), cooled to 0 °C, and 1.0 M TBAF in THF (165 μL, 0.165 mmol) was added. After stirring for 30 min, water and CH_2Cl_2 were added, and the organic phase was washed twice with water, dried (Na_2SO_4), and evaporated to dryness. Flash chromatography (heptane:EtOAc, 9:1) gave **9a** as a colorless syrup (28 mg, 64% yield, *E*/*Z* = 10:1). The *E*/*Z* mixture could be separated by column chromatography. *E* isomer: ^{1}H NMR ($CDCl_3$, 300 MHz): δ = 2.40 (br. s, 1H, OH), 3.54 (ddd, 1H, *J* = 9.6, 4.5, 2.3 Hz, H-5), 3.70 (dd, 1H, *J* = 9.1, 3.2 Hz, H-3), 3.77 (dd, 1H, *J* = 10.8, 4.5 Hz, H-6a), 3.81 (dd, 1H, *J* = 10.8, 2.3 Hz, H-6b), 3.89 (dd, 1H, *J* = 9.6, 9.1 Hz, H-4), 4.09 (d, 1H, *J* = 3.2 Hz, H-2), 4.10 (br. d, 1H, *J* = 6.2 Hz, H-1), 6.40 (dd, 1H, *J* = 16.1, 6.2 Hz, *H*C=CPh), 6.74 (br. d, 1H, *J* = 16.1 Hz, C=C*H*Ph), 7.21–7.46 (m, 20H, 4 Ph); *Z* isomer: δ = 6.13 (dd, 1H, *J* = 11.6, 8.8 Hz, *H*C=CPh), 6.77 (d, 1H, *J* = 11.6 Hz, C=C*H*Ph).

C-Glucoside formation (**13c**): A 0.1 M solution of SmI_2 in THF (13 mL, 1.3 mmol) was added quickly to a stirred solution of **12c** (122 mg, 0.167 mmol) in THF (24 mL). After stirring for 10 min, the reaction mixture was worked up and desilylated as for **9a**. Flash chromatography (heptane:EtOAc, 8:1) gave 69.5 mg of **13c** as a colorless syrup (78% yield, *E*/*Z* > 50:1): *E* isomer: ^{1}H NMR ($CDCl_3$, 300 MHz): δ = 0.13 (s, 9H, $SiMe_3$), 2.68 (d, 1H, *J* = 5.8 Hz, OH), 3.65–3.72 (m, 2H, H-3,4), 3.74 (dd, 1H, *J* = 10.4, 4.0 Hz, H-6a), 3.82 (ddd, 1H, *J* = 7.5, 5.8, 4.6 Hz, H-2), 3.83 (dd, 1H, *J* = 10.4, 5.2 Hz, H-6b), 4.04 (ddd, 1H, *J* = 9.2, 5.2, 4.0 Hz, H-5), 4.47 (ddd, 1H, *J* = 4.6, 4.1, 1.7 Hz, H-1), 4.55 (d, 1H, *J* = 12.1 Hz, C*H*Ph), 4.59 (d, 1H, *J* = 11.2 Hz, C*H*Ph), 4.64 (d, 1H, *J* = 12.1 Hz, C*H*Ph), 4.68 (d, 1H, *J* = 11.6 Hz, C*H*Ph), 4.71 (d, 1H, *J* = 11.2 Hz, C*H*Ph), 4.79 (d, 1H, *J* = 11.6 Hz, C*H*Ph), 6.11 (dd, 1H, *J* = 19.2, 1.8 Hz, C=C*H*$SiMe_3$), 6.24 (1H, dd, *J* = 19.2, 4.1 Hz, C*H*=C$SiMe_3$), 7.22–7.40 (m, 15H, 2 Ph). The *Z* isomer was not detected.

Received: February 11, 1994 [Z 6686 IE]
German version: *Angew. Chem.* **1994**, *106*, 1457

[1] For two recent reviews see: M. H. D. Postema, *Tetrahedron* **1992**, *48*, 8545–8599; J. Herscovici, K. Antonakis in *Studies in Natural Products Chemistry*, *Vol. 10* (Ed.: Atta-ur-Rahman), Elsevier, Amsterdam, **1992**, pp. 337–403.

[2] G. Stork, H. S. Suh, G. Kim, *J. Am. Chem. Soc.* **1991**, *113*, 7054–7056.

[3] An application of this approach using a 9-endo cyclization mode for the expedient construction of two C-disaccharides has just been described, although with the large ring size used, α-C-glycosides are predominantly obtained due to the anomeric effect: Y. C. Xin, J.-M. Mallet, P. Sinaÿ, *J. Chem. Soc. Chem. Commun.* **1993**, 864–865; B. Vauzeilles, D. Cravo, J.-M. Mallet, P. Sinäy, *Synlett* **1993**, 522–524.

[4] For examples of the construction of C-glycosides by intermolecular or nonsilicon-tethered intramolecular reactions of anomeric radicals see ref. [1].

[5] H. B. Kagan, J. L. Namy, P. Girard, *Tetrahedron* **1981**, *37*, 175–180; G. A. Molander, L. S. Harring, *J. Org. Chem.* **1990**, *55*, 6171–6176; J. Inanaga, O. Ujikawa, M. Yamaguchi, *Tetrahedron Lett.* **1991**, *32*, 1737–1740; S. M. Barrett, D. Larouche, *Synlett* **1991**, 805–806; M. J. Totleben, D. P. Curran, P. Wipf, *J. Org. Chem.* **1992**, *57*, 1740–1744.

[6] For two recent reviews on the application and mechanistic aspects of SmI_2 reactions see: G. A. Molander, *Chem. Rev.* **1992**, *92*, 29–68; D. P. Curran, T. L. Fevig, C. P. Jasperse, M. J. Totleben, *Synlett* **1992**, 943–961.
[7] E. Hasegawa, D. P. Curran, *Tetrahedron Lett.* **1993**, *34*, 1717–1720; E. Hasegawa, D. P. Curran, *J. Org. Chem.* **1993**, *58*, 5008–5010; G. A. Molander, J. A. McKie, *ibid.* **1992**, *57*, 3132–3139; J. Inanaga, M. Ishikawa, M. Yamaguchi, *Chem. Lett.* **1987**, 1485–1486.
[8] H. Künzer, M. Stahnke, G. Sauer, R. Wiechert, *Tetrahedron Lett.* **1991**, *32*, 1949–1952; P. de Pouilly, A. Chénedé, J.-M. Mallet, P. Sinaÿ, *ibid.* **1992**, *33*, 8065–8068.
[9] P. de Pouilly, A. Chénedé, J.-M. Mallet, P. Sinaÿ, *Bull. Soc. Chim. Fr.* **1993**, *130*, 256–265.
[10] B. M. Trost, J. B. Neilsen, K. Hoogsteen, *J. Am. Chem. Soc.* **1992**, *114*, 5432–5434.
[11] G. Stork, T. Y. Chan, G. A. Breault, *J. Am. Chem. Soc.* **1992**, *114*, 7578–7579.
[12] B. Giese, J. Dupuis, *Tetrahedron Lett.* **1984**, *25*, 1349–1352; T. Cohen, M. Bhupathy, *Acc. Chem. Res.* **1989**, *22*, 152–161, and references therein; B. Giese, J. Dupuis, K. Gröninger, T. Hasskerl, M. Nix, T. Witzel in *Substituent Effects in Radical Chemistry* (Eds.: M. G. Viehe, Z. Jarousek, R. Merenyi), Reidel, Dordrecht, **1986**, pp. 283–296; G. Giese, *Angew. Chem.* **1989**, *101*, 993–1004, *Angew. Chem. Int. Ed. Engl.* **1989**, *28*, 969–980; S. D. Rychnovsky, J. P. Powers, T. J. LePage, *J. Am. Chem. Soc.* **1992**, *114*, 8375–8384.
[13] J. Delaunay, G. Mabon, M. Chaquiq el Badre, A. Orliac, J. Simonet, *Tetrahedron Lett.* **1992**, *33*, 2149–2150.
[14] The essentials of this approach have been applied by A. Kende, J. S. Mendoga, *Tetrahedron Lett.* **1990**, *31*, 7105–7108, for the reductive elimination of β-hydroxy imidazolyl sulfones with only SmI_2. The corresponding phenyl sulfones were unreactive under identical conditions.
[15] For other applications of 2-pyridyl sulfones see: J. B. Baudin, G. Hareau, S. A. Julia, O. Ruel, *Bull. Soc. Chim. Fr.* **1993**, *130*, 336–357, and references therein.
[16] The 2-pyridylsulfonyl glycosides were easily prepared as previously described for the phenyl sulfones (see ref. [9]). Attempts to prepare the corresponding imidazolyl sulfones were problematic and interestingly, the free C2 hydroxyl group failed to be silylated.
[17] The procedure reported by Stork and Keitz led to low or no yields of silylated products (G. Stork, P. Keitz, *Tetrahedron Lett.* **1989**, *30*, 6981–6984). In the case of a nonvolatile alkyne, the excess could easily be recovered by desilylation of the major by-product, the dialkynyldimethylsilane. Attempts to prepare an alternative and more efficient silylation method is underway in our laboratory.
[18] **16**: Colorless crystals; m.p. 151–152 °C; $[\alpha]_D^{22} = 124$ ($c = 0.51$ in $CHCl_3$); ^1H NMR ($CDCl_3$, 300 MHz): $\delta = 1.42$–1.66 (m, 3H), 2.00 (m, 1H), 2.01, 2.03, 2.04, 2.05, 2.07, 2.09 (6 s (ratio of intensities 1:1:2:1:1:1, 21H, $COCH_3$), 3.40 (s, 3H, CH_3O), 3.78 (m, 1H, H-5), 3.80 (ddd, 1H, $J = 9.2$, 5.3, 2.6 Hz, H-5'), 4.02 (dd, 1H, $J = 12.3$, 2.6 Hz, H-6a'), 4.15 (ddd, 1H, $J = 12.2$, 6.0, 3.5 Hz, H-1'), 4.24 (dd, 1H, $J = 12.3$, 5.3 Hz, H-6b'), 4.84 (dd, 1H, $J = 10.2$, 3.7 Hz, H-2), 4.85 (dd, 1H, $J = 9.8$, 9.8 Hz, H-4), 4.91 (d, 1H, $J = 3.7$ Hz, H-1), 4.97 (dd, 1H, $J = 9.2$, 9.2 Hz, H-4'), 5.07 (dd, 1H, $J = 9.9$, 6.0 Hz, H-2'), 5.32 (dd, 1H, $J = 9.9$, 9.2 Hz, H-3'), 5.44 (dd, 1H, $J = 10.2$, 9.8 Hz, H-3).
[19] For previous C-isomaltoside syntheses see: P. G. Goekjian, T.-C. Wu, H.-Y. Kang, Y. Kishi, *J. Org. Chem.* **1991**, *56*, 6422–6434; O. R. Martin, F. Xie, R. Kakarla, R. Benhamza, *Synlett* **1993**, 165–167.

New Materials for Liquid Crystal Displays: Structure–Property Relationship of 2-Fluoropyridines**

Volker Reiffenrath* and Matthias Bremer

The development of improved liquid crystal displays (LCDs) for devices[1] for the automotive industry, lap-top computers, or television sets, for example, is a challenging interdisciplinary goal for the 1990s. Liquid crystals used in devices are anisotropic materials that exhibit two different dielectric constants parallel ($\varepsilon_\parallel$) and perpendicular ($\varepsilon_\perp$) to the long molecular axis. This is a prerequisite for the observation of electro-optical effects. Most LCDs produced today are based on the twisted nematic cell (TNC).[2] This requires liquid crystals with positive values of the dielectric anisotropies ($\Delta\varepsilon = \varepsilon_\parallel - \varepsilon_\perp$), which can be realized by the introduction of polar terminal substituents into the rodlike mesogenic molecules.

In contrast, for applications based on electrically controlled birefringence (ECB)[3] or positive-contrast guest–host (GH,[4] a technique in which a small amount of a dye is added) there is continuing interest in liquid crystalline materials with strongly negative $\Delta\varepsilon$, implying large values of $\varepsilon_\perp$. A negative value of $\Delta\varepsilon$ can be achieved by the introduction of lateral polar substituents. This often also leads to the formation of tilted smectic-C (S_C)[5] phases, which are essential for ferroelectric liquid crystal (FLC)[6] applications. The ideal substituent should be strongly polar, form an angle of 90° with the long molecular axis, and, for optimum switching speeds, should not increase viscosity. Our solution to this problem is based on 2-fluoropyridine as a new building block for liquid crystals.[7]



The fluoropyridines offer two possible 3,6-substitution patterns (**A** and **B**), which lead to different physical properties of the liquid crystals. Starting from two commercially available materials, we synthesized a host of new compounds based on the 2-fluoropyridine moiety (Schemes 1 and 2). Key steps are *ortho*-metallation,[8] carbon–carbon bond formation by palladium-catalyzed boronic acid coupling,[9] and displacement of aromatic sulfonyl groups by Grignard reagents.[10]

The iodopyridine, which appears as an intermediate in Scheme 2, is easily accessible by electrophilic iodination.[11] Interestingly, the use of 2-chloropyridine enables halogen-free 3-alkoxypyridines to be synthesized: The chlorine atom only serves as a directing group for metalation and is removed by hydrogenation in the final step.

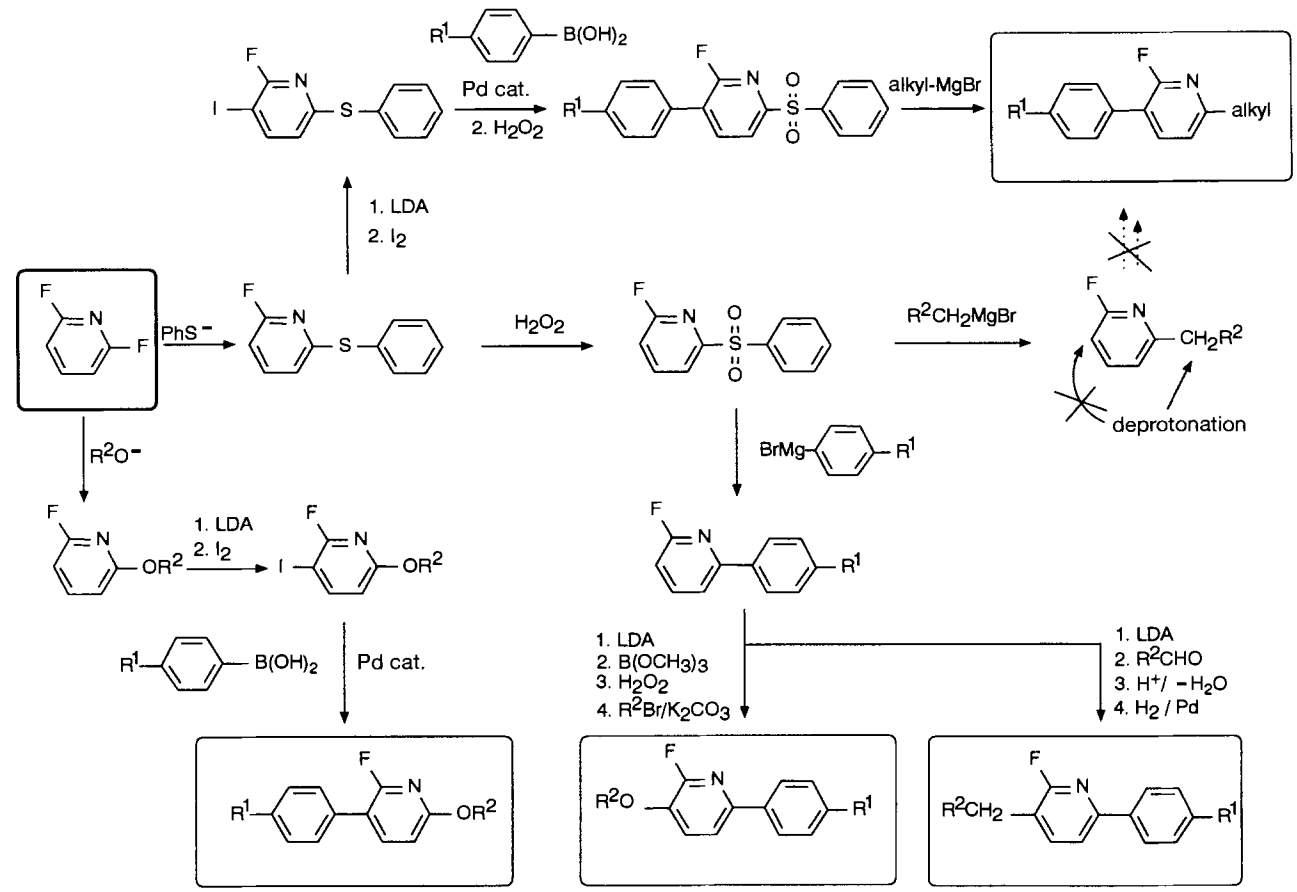
Because of the polar substituents, the molecular dipole moment of **1** exhibits strong components along the molecular axis and perpendicular to it. Therefore, large values for both $\varepsilon_\perp$ and $\varepsilon_\parallel$ and a small positive $\Delta\varepsilon$ are found.[12] Replacement of the terminal fluorine by an ethoxy group in **2** reduces both dielectric constants, and not only, as expected, $\varepsilon_\parallel$. "Flipping" the pyridine ring (**2** → **3**, Table 1) results in a dramatic increase of $\varepsilon_\perp$ and thus in a strongly negative $\Delta\varepsilon$.

As this intriguing effect was not observed for the corresponding alkyl-substitued pyridines **4** and **5**, the oxygen atoms in **2** and **3** must play a significant role. To understand this surprising behavior better we carried out semiempirical model calculations (AM1).[13] 2-Fluoro-6-methoxy- and 2-fluoro-3-methoxypyridine were used to model the polar head groups of compounds **2** and **3**. The C-O-C-N dihedral angle θ was varied stepwise from 0° to 180°, but kept fixed while all other geometric parameters were fully optimized in the energy minimization. The calculations show that rotation from the *syn* into the *anti* structure enhances the molecular dipole moment of both pyridines especially in the y direction (Fig. 1).

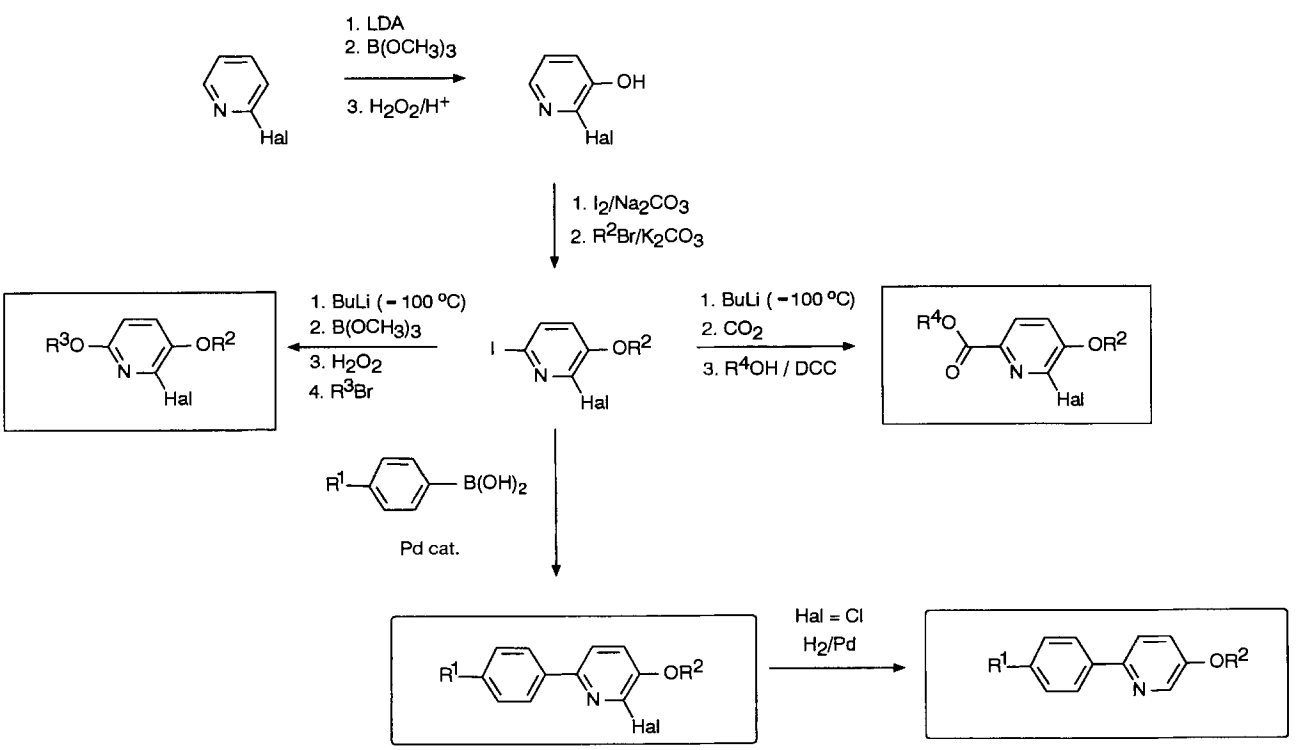
Figures 2 and 3 give the overall dipole moments and the rotational barriers as a function of the dihedral angle θ. Although the calculated dipole moments for the *syn* and *anti* conformers

[*] V. Reiffenrath, Dr. M. Bremer
E. Merck
Liquid Crystal Research
Frankfurter Strasse 250, D-64271 Darmstadt (FRG)
Telefax: Int. code + (6151) 72-2593

[**] We thank Dr. U. Finkenzeller for the determination of the physical parameters of the new liquid crystals.



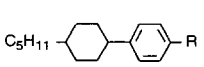
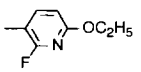
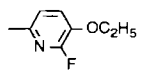
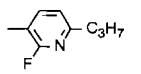
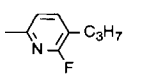
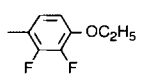
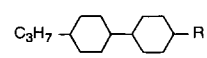
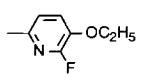
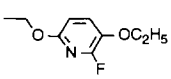
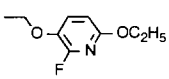
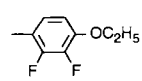
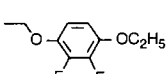
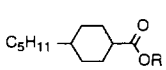
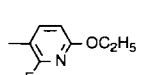
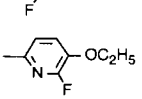
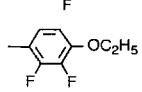
Scheme 1. Synthesis of liquid crystals starting from 2,6-difluoropyridine. For the specific compounds, see Table 1.

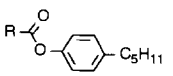
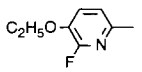
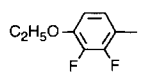
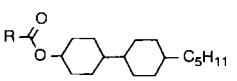
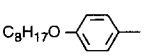
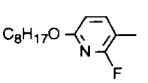
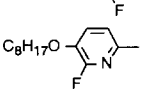
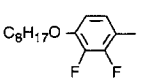
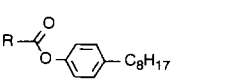
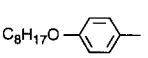
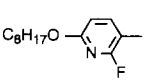
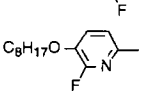
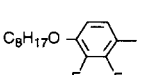


Scheme 2. Synthesis of liquid crystals starting from 2-halopyridine (halogen is F or Cl). For the specific compounds see Table 1.

 © *VCH Verlagsgesellschaft mbH, D-69451 Weinheim, 1994* *0570-0833/94/1313-1387 $ 10.00+.25/0*

Table 1. The influence of the substitution pattern of pyridine and the type of substituent on dielectric properties and on the mesophase behavior of fluoropyridines and corresponding 2,3-difluorobenzenes.

Compound	$\varepsilon_\parallel$	$\varepsilon_\perp$	$\Delta\varepsilon$	Mesophases [°C]
				
1, R = 	10.6	8.3	2.3	K 58 N 107 I
2, R = 	3.3	3.8	−0.5	K 72 N 147 I
3, R = 	4.1	9.4	−5.3	K 112 S_A (105) N 190 I
4, R = 	3.9	6.5	−2.6	K 64 S_A (63) N 122 I
5, R = 	3.4	6.5	−3.1	K 60 S_X 91 S_A 124 N 150 I
6, R = 	3.9	8.0	−4.1	K 74 S_A 86 N 171 I
				
7, R = 			−6.1	K 81 S_B 98 N 179 I
8, R = 			−2.7	K 90 N 108 I
9, R = 			−2.1	K 71 N 129 I
10, R = 			−4.4	K 76 S_B 79 N 186 I
11, R = 			−6.0	K 62 N 154 I
				
12, R = 			−1.1	K 62 N (28) I
13, R = 			−5.3	K 58 N (23) I
14, R = 			−4.6	K 51 N 63 I

Compound	$\varepsilon_\parallel$	$\varepsilon_\perp$	$\Delta\varepsilon$	Mesophases [°C]
				
15, R = 			−5.0	K 88 I
16, R = 			−3.5	K 61 N (51) I
				
17, R = 				K 80 S_A 140 N 182 I
18, R = 				K 81 S_A 109 N 149 I
19, R = 				K 117 S_C 130 S_A 145 N 156 I
20, R = 				K 90 S_C 98 N 170 I
				
21, R = 				K 54 S_A 64 N 66 I
22, R = 				K 29 N (20) I
23, R = 				K 75 S_C (73) I
24, R = 				K 37 S_C 49 N 57 I

of the two pyridines are qualitatively similar, the relative energies are reversed. Thus, 2-fluoro-6-methoxypyridine probably exists mainly in the *syn* conformation with a small dipole moment (Fig. 2), whereas 2-fluoro-3-methoxypyridine is dominated by the more stable *anti* structure (Fig. 3) and therefore should exhibit a much larger dipole moment, especially perpendicular to the long molecular axis (Fig. 1). Since the dielectric anisotropy of

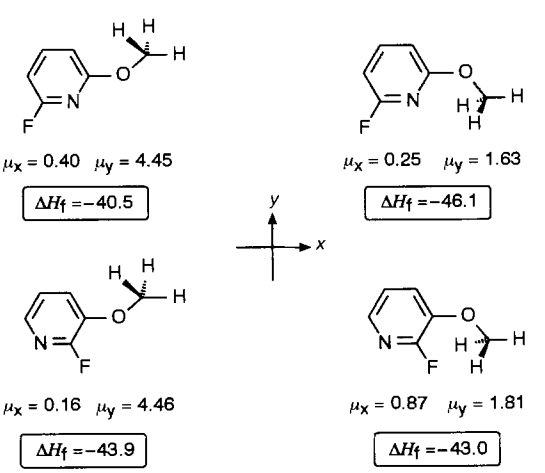


Fig. 1. Heats of formation calculated with AM1 [kcal mol^{-1}] and dipole moments [Debye] for conformers of methoxyfluoropyridines.

 © VCH Verlagsgesellschaft mbH, D-69451 Weinheim, 1994 0570-0833/94/1313-1388 $ 10.00+.25/0

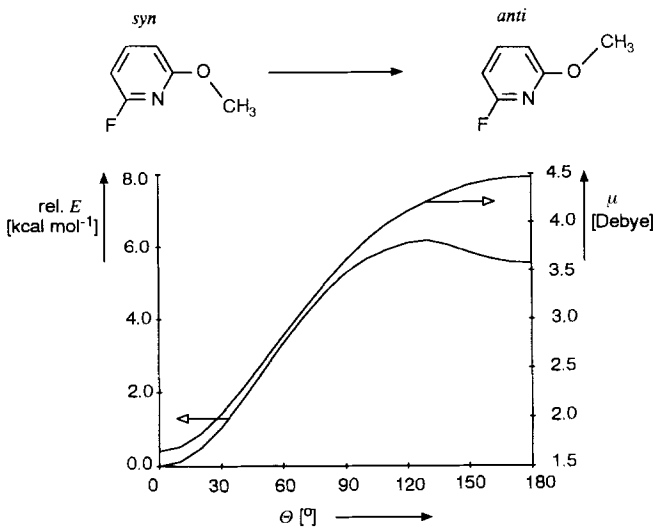


Fig. 2. The energy profile of the rotation about the pyridine-oxygen bond and total dipole moments in 2-fluoro-6-methoxypyridine.

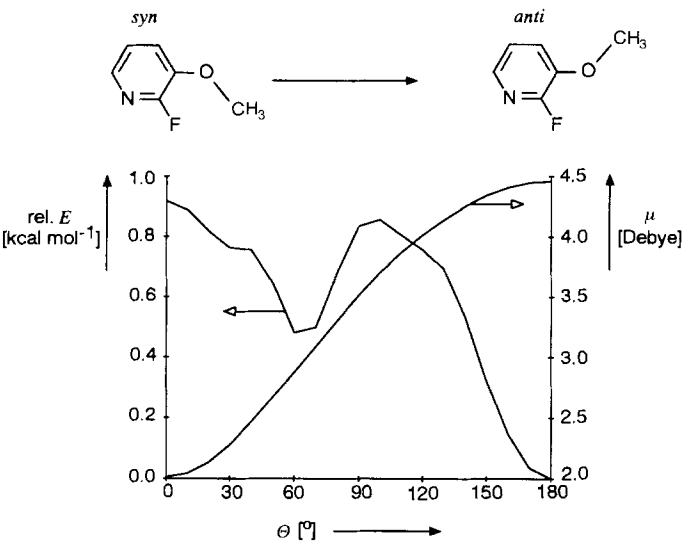


Fig. 3. The energy profile of the rotation about the pyridine-oxygen bond and total dipole moments in 2-fluoro-3-methoxypyridine.

a liquid crystal is directly related to the molecular dipole moment,[14] a simple explanation for this initially surprising result can be given.

While the introduction of a second alkoxy group (**10** → **11**, Table 1) into the difluorobenzenes[15] leads to an increase of $\Delta\varepsilon$ due to rotational preferences, the opposite behavior is found for the pyridines **7** and **8**. Now, flipping the pyridine ring (**8** → **9**) has, as expected, almost no effect on the dielectric anisotropy. The somewhat larger negative values of $\Delta\varepsilon$ found for **8** and **9** relative to **2** can also be rationalized by model calculations: The two-dimensional torsional energy surface of 2-fluoro-3,6-dimethoxypyridine was calculated, and the Boltzmann-weighted dipole moments[16] were computed for the gas phase at 298 K. The calculations yield an overall dipole moment of 2.1 Debye with a parallel contribution μ_x of only 0.1 Debye and a perpendicular dipole of 2.1 Debye (compare the values given in Fig. 1).

The examples **12**–**16** (Table 1) show the influence of incorporation of a carbonyl group. Depending on the substitution pattern of the pyridine ring, either a decrease or an increase of the dielectric anisotropy is observed.

Not only the dielectric properties can easily be tuned by the substitution pattern of the pyridine moiety, but also the mesophase behavior of long-chain liquid crystals. As indicated above, the introduction of lateral polar substituents in many cases favors the formation of S_C phases.[5, 15] In accord with earlier results for 2,3-difluorophenylene derivatives **20** and **24** (Table 1),[15] replacement of the phenyl rings by the fluoropyridine moiety in **17** and **21**[17] induces a S_C phase in **19** and **23**, respectively. Interestingly, this is not the case for the less polar compounds **18** and **22**. It appears that the substitution pattern leading to the more polar molecule favors the formation of the S_C phase.

We have shown that energetically preferred rotamers of alkoxy-substituted fluoropyridines strongly influence the dielectric properties of liquid crystals. We have synthesized new materials that offer broad S_C phases as well as distinctly negative dielectric anisotropy to improve the performance of modern liquid crystal displays with high information content.

Received: February 9, 1994 [Z 6682 IE]
German version: *Angew. Chem.* **1994**, *106*, 1435

[1] Reviews: B. S. Scheuble, *Kontakte (Darmstadt)* **1989** (1), 34; B. Bahadur, *Mol. Cryst. Liq. Cryst.* **1984**, *109*, 3; M. Schadt, *Displays* **1992**, *13*, 11.
[2] M. Schadt, W. Helfrich, *Appl. Phys. Lett.* **1971**, *18*, 127.
[3] M. Schiekel, K. Fahrenschon, *Appl. Phys. Lett.* **1971**, *19*, 391; G. Labrunie, J. Robert, *J. Appl. Phys.* **1973**, *44*, 4869; S. Matsumoto, M. Kawamoto, K. Mizunoya, *ibid.* **1976**, *47*, 3842.
[4] G. H. Heilmeier, L. A. Zanoni, *Appl. Phys. Lett.* **1968**, *13*, 91; G. H. Heilmeier, J. A. Castellano, L. A. Zanoni, *Mol. Cryst. Liq. Cryst.* **1969**, *8*, 293; D. L. White, G. N. Taylor, *J. Appl. Phys.* **1974**, *45*, 4718.
[5] W. L. McMillan, *Phys. Rev. A* **1973**, *8*, 1921; G. W. Gray, J. W. Goodby, *Smectic Liquid Crystals*, Leonard Hill, Glasgow, London, **1984**.
[6] U. Finkenzeller, A. E. Pausch, E. Poetsch, J. Suermann, *Kontakte (Darmstadt)* **1993** (2), 3; C. Escher, R. Wingen, *Adv. Mater.* **1992**, *4*, 189.
[7] V. Reiffenrath, E. Poetsch, V. Meyer, H. J. Plach (E. Merck), WO-B 91/04249 [*Chem. Abstr.* **1991**, *115*, P218994]; D. Coates, S. Greenfield, I. C. Sage, R. Clemitson, H. J. Plach, V. Reiffenrath (E. Merck), WO-B 91/04248 [*Chem. Abstr.* **1991**, *115*, P171066]; V. Reiffenrath, T. Geelhaar (E. Merck), WO-B 92/09576 [*Chem. Abstr.* **1992**, *117*, P191691].
[8] P. D. Leeson, J. C. Emmett, *J. Chem. Soc. Perkin Trans. 1* **1988**, 3085.
[9] M. Miyaura, T. Yanagi, A. Suzuki, *Synth. Commun.* **1981**, *11*, 513; T. Watanabe, M. Miyaura, A. Suzuki, *Synlett* **1992**, 207.
[10] N. Furukawa, M. Tsuruoka, H. Fujihara, *Heterocycles* **1986**, *24*, 3337.
[11] V. Koch, S. Schnatterer, *Synthesis* **1990**, 497.
[12] For the determination of electro-optical parameters, see U. Finkenzeller, *Kontakte (Darmstadt)* **1988** (2), 7; U. Finkenzeller, T. Geelhaar, G. Weber, L. Pohl, *Liq. Cryst.* **1989**, *5*, 313.
[13] M. J. S. Dewar, E. G. Zoebisch, E. F. Healy, J. J. P. Stewart, *J. Am. Chem. Soc.* **1985**, *107*, 3902; MOPAC 6.0 (QCPE 455) was used.
[14] W. Maier, G. Meier, *Z. Naturforsch. A* **1961**, *16*, 262.
[15] V. Reiffenrath, J. Krause, H. J. Plach, G. Weber, *Liq. Cryst.* **1989**, *5*, 159.
[16] M. Bremer, K. Tarumi, *Adv. Mater.* **1993**, *5*, 842.
[17] M. E. Neubert, M. R. Jirousek, C. A. Hanlon, *Mol. Cryst. Liq. Cryst.* **1986**, *133*, 233.

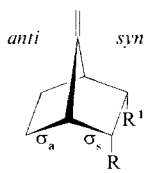
 © VCH Verlagsgesellschaft mbH, D-69451 Weinheim, 1994 0570-0833/94/1313-1389 $ 10.00+.25/0

Electrostatic vs. Orbital Control of Facial Selectivities in π Systems: Experimental and Theoretical Study of Electrophilic Additions to 7-Isopropylidenenorbornanes**

Goverdhan Mehta,* Faiz Ahmed Khan, Shridhar R. Gadre*, Rajendra N. Shirsat, Bishwajit Ganguly, and Jayaraman Chandrasekhar*

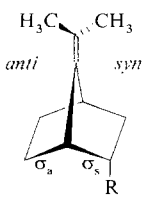
Dedicated to Professor C. N. R. Rao on the occasion of his 60th birthday

Evaluation of the relative importance of electrostatic and orbital effects in determining facial selectivities of π systems (π-facial selectivity) in nucleophilic and electrophilic additions to trigonal carbon centers is currently a topic of intense debate.[1–3] We have recently reported[2] the addition of electrophiles such as BH_3, peracid, and $Hg(OAc)_2$ to some *endo*-substituted 7-methylenenorbornanes, for example **1a**, with sterically indistinguishable π faces and reconciled the observed *syn*-face selectivity in terms of the Cieplak model,[4] according to which the electrophiles should approach **1a** from the face opposite to the more electron-rich σ_a bond. However, on the basis of PM3 calculations on 7-methylenenorbornyl derivatives **1a**, **1c**, and related systems, it has been proposed[3] that the initial approach of a charged reagent would be along the *anti* side, governed by electrostatics, and the subsequent nucleophilic attack (for example, by water) would lead to the observed product stereochemistry.



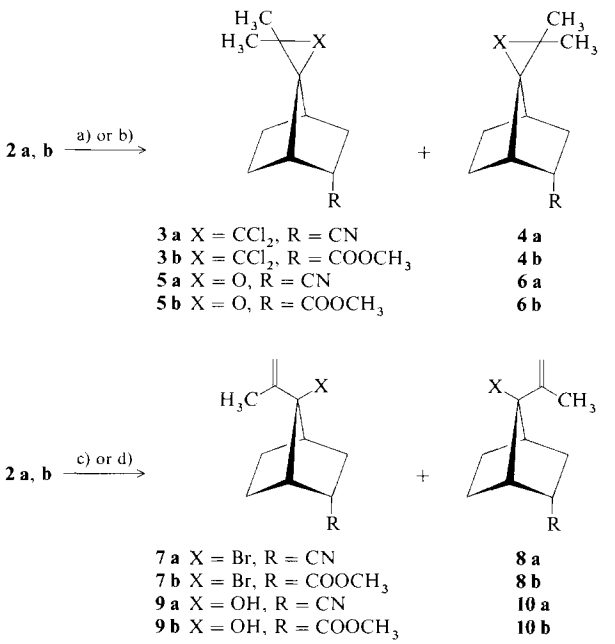
1a R = R¹ = $COOCH_3$
1b R = F, R¹ = H
1c R = R¹ = F
1d R = CN, R¹ = H
1e R = R¹ = CN

Studies on CCl_2 and halonium ion additions to these systems were suggested for providing further insights. We now report experimental facial selectivities for the addition of such electrophiles to 7-isopropylidenenorbornane derivatives (**2**) and provide interpretations on the basis of ab initio molecular electrostatic potentials (MEP) and electron densities, as well as semiempirical transition state energetics. The use of the isopropylidene unit offers significant advantages. From an experimental point of view, the double bond becomes more reactive, which enables the study of carbene additions.[5] Further, unlike in **1**, the site of electrophilic attack is likely to be at C7 and not at C8, a factor which is crucial for interpretation of the experimental results. Finally, the mechanistic details of electrophilic attack in **2** are unambiguous and the steric neutrality on the two π faces is maintained.



2a R = CN
2b R = $COOCH_3$

7-Isopropylidenenorbornanes **2** smoothly undergo dichlorocarbene and singlet oxygen addition, epoxidation, and reaction with the bromine(I) cation. The reaction conditions, yields, and products obtained are shown in Scheme 1, and the π-face selectivities are summarized in Table 1. Structures of diastereomers were determined on the basis of ^1H and ^{13}C NMR data, but more specifically through the greater deshielding of the C_2 *exo*-proton in the *syn*-addition products (**3**, **5**, **7**, **9**) relative to that of the *anti*-products (**4**, **6**, **8**, **10**).[2, 6, 7]



3a X = CCl_2, R = CN — **4a**
3b X = CCl_2, R = $COOCH_3$ — **4b**
5a X = O, R = CN — **6a**
5b X = O, R = $COOCH_3$ — **6b**

7a X = Br, R = CN — **8a**
7b X = Br, R = $COOCH_3$ — **8b**
9a X = OH, R = CN — **10a**
9b X = OH, R = $COOCH_3$ — **10b**

Scheme 1. Electrophilic additions to **2**. a) $Cl_3CCOO^-Na^+$, dimethoxyethane (DME)/tetrachloroethylene, Δ, 80–93%; b) *m*-chloroperbenzoic acid (*m*-CPBA), Na_2CO_3, CH_2Cl_2, 0–5 °C, 90–95%; c) *N*-bromosuccinimide, 10% aqueous DME, 95%; d) $^1O_2$, *hv*, methylene blue, CH_2Cl_2, then $NaBH_4$, MeOH, 75–81%.

Table 1. Experimental ratios of *syn*- and *anti*-addition products of **2** with $:CCl_2$, *m*-CPBA, Br^+, and $^1O_2$ [a].

Compound	$:CCl_2$		*m*-CPBA		Br^+		$^1O_2$	
	syn	*anti*	*syn*	*anti*	*syn*	*anti*	*syn*	*anti*
2a	78	22	77	23	72	28	78	22
	3a	**4a**	**5a**	**6a**	**7a** [b]	**8a** [b]	**9a**	**10a**
2b	60	40	62	38	59	41	61	39
	3b	**4b**	**5b**	**6b**	**7b** [b]	**8b** [b, c]	**9b**	**10b**

[a] Product ratios (±5%) are based on ^1H NMR spectra. [b] Exhibits marked propensity for allylic rearrangement. [c] Could not be obtained pure but its presence was inferred from high-field NMR data.

The results confirm that even a single electron-withdrawing substituent in the *endo* position is capable of inducing *syn*-facial electrophilic addition, thus reinforcing our earlier observations.[2] There is also no ambiguity about the initial direction of attack of Br^+. Since the nucleophilic attack on the bromonium ion is followed by an elimination to give the olefins **7** and **8**, the loca-

[*] Prof. G. Mehta, F. A. Khan
School of Chemistry, University of Hyderabad
Hyderabad 500134 (India)
Telefax: Int. code + (40)253145
Prof. S. R. Gadre, R. N. Shirsat
Department of Chemistry, University of Poona
Pune 411007 (India)
Prof. J. Chandrasekhar, B. Ganguly
Department of Organic Chemistry, Indian Institute of Science
Bangalore 560012 (India)

[**] Computational and financial assistance from the Centre for Development of Advanced Computing (C-DAC), Pune, is gratefully acknowledged. FAK, RNS, BG thank the Council for Scientific and Industrial Research (CSIR/UGC) for research fellowships. We also thank G. Gunasekaran for experimental assistence.

tion of the bromine atom in these products directly reveals the direction of the initial electrophilic attack. Based on the observed product ratios, the charged electrophile Br^+ as well as neutral CCl_2 prefer to approach the *syn* face of **2a** and **2b**.

To delineate the nature of the electronic control of the observed selectivities, we carried out a topographical analysis of the molecular electrostatic potentials of **1a**, **b** and **2a**, **b** at the ab initio level with the 6-31G basis set, using the parallel SCF program INDMOL.[8] In particular, we focused on the MEP minima whose depth generally correlates with electron density. For both series of compounds, the MEPs about the two π faces are unsymmetrical; the (3, +3) critical point on the *anti* face consistently has a more negative value (Table 2). A similar asymmetry computed for **1c** at the PM3 level has been identified as the principal factor determining facial selectivity for the approach of charged electrophiles.[3] However, as the MEP values at the critical points are significantly less negative than those obtained for typical C=C bonds,[9] electrostatic influences are probably not of primary importance in determining the facial selectivities in these compounds.

Table 2. MEP at (3, +3) minimum and electron density at bond critical point (all values in Hartree) [a].

Cmpd. [b]	MEP at critical point		Density at bond critical point	
	syn	*anti*	σ_s	σ_a
1a	−0.0208	−0.0269	0.2096	0.2174
1b	−0.0270	−0.0307	0.2121	0.2165
1c	−0.0129	−0.0202	0.2130	0.2166
1d	−0.0193	−0.0234	0.2112	0.2169
1e	−0.0012	−0.0083	0.2116	0.2172
2a	−0.0174	−0.0222	0.2114	0.2172
2b	−0.0278	−0.0305	0.2109	0.2171

[a] At a critical point of a scalar field f, $\nabla f = 0$. The critical points are classified in terms of the eigenvalues of the Hessian operator. The MEP and bond critical points are (3, +3) and (3, −1) types in the scalar fields. For details of MEP and density topography see Ref. [10]. [b] MNDO optimized geometries. The olefinic units are essentially planar in all the derivatives.

To confirm the potential role of orbital interactions in determining the facial selectivities in these substrates, the unsymmetrical donor abilities of the σ_s and σ_a bonds (see structures **1** and **2**) were characterized in terms of the electron densities at the corresponding bond critical points (Table 2). In all systems with electron-withdrawing groups, the σ_a bond consistently has a greater density. Operation of Cieplak-type orbital interactions[4] would then lead to the observed *syn*-facial selectivity.

Semiempirical MO calculations on the bromonium ion intermediates resulting from **2**, as well as carbene addition transition states, lead to several additional insights (Table 3). Optimization of the bromonium ion intermediates at the PM3 level[11] leads to classical structures, and cyclic forms are not minima.

Table 3. Calculated heats of formation in kcal mol^{-1} of classical intermediates formed by Br^+ additions and transition states for $:CCl_2$ additions to **2**.

Cmpd.	Site of electrophilic attack	Br^+ [a]		$:CCl_2$ [b]	
		syn	*anti*	*syn*	*anti*
2a	C-7	228.64	229.41	91.53	92.37
	C-8	236.29	236.55	93.17	93.21
2b	C-7	109.05	109.26	−23.11	−22.52
	C-8	115.64	115.76	−21.66	−21.65

[a] PM3 method. [b] AM1 method.

The calculations confirm that Br^+ prefers to attack the C7 center, rather than C8 (by 6–7 kcal mol^{-1}), as a less strained tertiary carbocation is formed in the former. The computed *syn*–*anti* energy differences are small. Nevertheless, for both **2a** and **2b**, the ion formed by addition to the *syn* face is consistently more stable, in agreement with the observed facial selectivities. Interestingly, the preference is larger for the ions formed by attack at C7 and not C8, particularly for **2a** [ΔE (*anti*–*syn*) = 0.8 and 0.3 kcal mol^{-1}, respectively)]. Greater unfavorable electrostatic interactions are anticipated between the Br^+ ion at C7 and *syn* face of **2a**. These are evidently overcome by effective orbital stabilization involving the Br-C-7σ* MO and the relatively electron-rich antiperiplanar σ_a bond.

Transition state energies determined with the AM1 procedure[11] for CCl_2 addition to **2** are also consistent with the observed stereoselectivities.[12] Since the least motion pathway for the addition of a carbene to an olefin is a forbidden pathway,[13] the transition structure is highly unsymmetrical. In effect, the carbene forms a bond to one of the olefinic carbon atoms with a C-C-C angle of about 90°. The chlorine atoms are tilted towards the other carbon, which has a planar coordination characteristic of a carbocation. These features have significant consequences for the facial selectivities of **2**. In view of the unsymmetrical nature of the olefins, two sets of first order saddle points, characterized by a closer approach of the carbene to C7 or C8, are obtained for the *syn*- as well as *anti*-facial additions. Interestingly, the energetically favored transition states correspond to CCl_2 attack at C7. As a result, the newly formed C–C bond is more responsive to the unsymmetrical orbital effects from σ_a and σ_s orbitals. Further, as the chlorine atoms are tilted upwards in the corresponding transition states, any contribution from electrostatic interactions from the norbornyl unit are precluded. Overall, a clear preference for *syn*-facial attack results. For the transition states for attack at C8, there is negligible facial selectivity. Orbital effects and electrostatic interactions seem to cancel.[14]

In summary, we have demonstrated a consistent, remote substituent control of the facial selectivities in electrophilic additions to *endo*-substituted 7-isopropylidenenorbornanes. With ab initio and semiempirical MO calculations, it has been clearly shown that the observed preferences are primarily due to orbital effects.

Received: December 17, 1993 [Z 6565 IE]
German version: *Angew. Chem.* **1994**, *106*, 1433

[1] Recent references: A. S. Cieplak, B. D. Tait, C. R. Johnson, *J. Am. Chem. Soc.* **1989**, *111*, 4635; J. M. Coxon, D. Q. McDonald, *Tetrahedron* **1992**, *48*, 3353; M. N. Paddon-Row, Y.-D. Wu, K. N. Houk, *J. Am. Chem. Soc.* **1992**, *114*, 10638; A. S. Cieplak, K. B. Wiberg, *ibid.* **1992**, *114*, 9226; R. L. Halterman, M. A. McEroy, *ibid.* **1992**, *114*, 980; G. Mehta, F. A. Khan, B. Ganguly, J. Chandrasekhar, *J. Chem. Soc. Chem. Commun.* **1992**, 1711; B. Ganguly, J. Chandrasekhar, F. A. Khan, G. Mehta, *J. Org. Chem.* **1993**, *58*, 1734. Y.-D. Wu, Y. Li, J. Na, K. N. Houk, *ibid.* **1993**, *58*, 4625. G. Mehta, G. Gunasekaran, S. R. Gadre, R. N. Shirsat, B. Ganguly, J. Chandrasekhar, *ibid.* **1994**, in press.
[2] G. Mehta, F. A. Khan, *J. Chem. Soc. Chem. Commun.* **1991**, 18.
[3] H. B. Broughton, S. M. Green, H. S. Rzepa. *J. Chem. Soc. Chem. Commun.* **1992**, 998.
[4] A. S. Cieplak, *J. Am. Chem. Soc.* **1981**, *103*, 4540.
[5] We have found **1a** and **1d** to be inert towards dichlorocarbene under usual conditions.
[6] G. Mehta, F. A. Khan, *J. Am. Chem. Soc.* **1990**, *112*, 6140.
[7] All new compounds reported here were characterized by spectral (IR, ^{1}H and ^{13}C NMR) data and elemental analysis.
[8] R. N. Shirsat, A. C. Limaye, S. R. Gadre, *J. Comp. Chem.* **1993**, *14*, 445.
[9] The MEP minimum for ethylene at the 6-31G level is −0.0383 Hartree.
[10] R. N. Shirsat, S. V. Bapat, S. R. Gadre, *Chem. Phys. Letters* **1992**, *200*, 373; R. F. W. Bader, *Atoms in Molecules, a Quantum Theory*, Clarendon, Oxford, **1990**, and references therein.
[11] J. J. P. Stewart, *J. Comput. Aided Mol. Design* **1990**, *4*, 1. Minimization of gradient norm for intermediates and transition states was carried out without

any symmetry constraints. Stationary points were characterized rigorously by computing vibrational frequencies. Minima have no modes with an imaginary frequency, while transition structures have one and only one vibration with an imaginary frequency.

[12] Optimized structural data for prototypical transition states for CCl_2 addition to ethylene are quite similar at AM1 and ab initio (3–21G) levels [13b]. We have also found that AM1 transition state energetics correctly reproduce the observed facial selectivities in CCl_2 additions to 8-methylenetricyclo-[3.2.1.$0^{2,4}$]octanes reported by R. W. Hoffmann, N. Hauel, B. Landmann, *Chem. Ber.* **1983**, *116*, 389.

[13] a) R. Hoffmann, *J. Am. Chem. Soc.* **1968**, *90*, 1475. b) Ab initio calculations on model systems confirm the qualitative predictions: 3-21G: K. N. Houk, N. G. Rondan, J. Mareda, *Tetrahedron* **1985**, *41*, 1563. MP2/6-31G*: J. F. Blake, S. G. Wierschke, W. L. Jorgensen, *J. Am. Chem. Soc.* **1989**, *111*, 1919.

[14] Ab initio calculations (3-21G) on the AM1 transition structures for CCl_2 addition to **2a** support the general conclusions. Total energies [Hartree] for *syn*- and *anti*-facial addition structures: −1429.12927 and −1429.12620 for C7 approach; −1429.12650 and −1429.12433 for C-8 approach, respectively. Thus, the former structures are energetically favored. Further, *syn*-face attack is preferred to a greater extent in the transition structures corresponding to C7 approach (1.9 vs 1.4 kcal mol^{-1} for C8 approach).

Asymmetric Michael Additions to Chiral α,β-Unsaturated Alkoxycarbene Chromium Complexes**

José Barluenga,* Javier M. Montserrat, Josefa Flórez, Santiago García-Granda, and Eduardo Martín

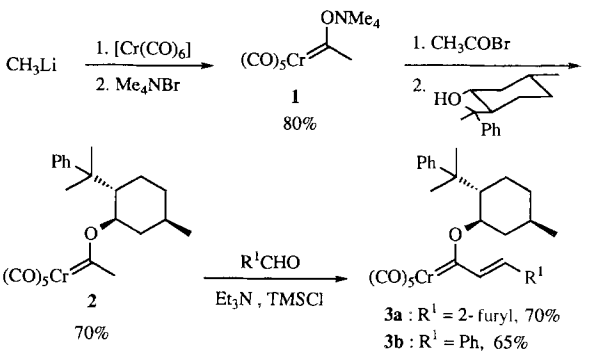
The Michael reaction is one of the fundamental processes for carbon–carbon bond formation; and significant advances in asymmetric 1,4-conjugate addition reactions, involving chirally modified substrates or a chiral reaction medium, have been achieved.[1] α,β-Unsaturated Fischer carbene complexes, which are increasingly playing an important role in organic synthesis,[2] behave as reactive Michael acceptors. Since the pioneering work by Casey et al. on additions[3] of carbon nucleophiles, several other nucleophiles have been 1,4-added to heteroatom-stabilized alkenyl-[4] and alkynylcarbene[5] complexes with good regioselectivities and diastereoselectivities;[6] but thus far no examples of enantioselective Michael additions to α,β-unsaturated Fischer carbene complexes are known. The asymmetric Michael reactions of chiral prolinol-derived aminocarbene complex anions to cyclic enones have been recently described.[7] We report herein on highly diastereoselective conjugate additions of β-oxygen-functionalized organolithium compounds, alkyllithium reagents, and lithium enolates to chirally modified α,β-unsaturated alkoxycarbenechromium complexes that are readily available in optically pure form.

In a previous report[8] we described the diastereoselective one-pot synthesis of strained tricyclic ethers by reaction of properly substituted β-oxygen-functionalized organolithium compounds with Fischer vinylcarbene complexes. In order to prepare these unusual tricyclic structures as enantiomerically pure compounds

[*] Prof. Dr. J. Barluenga, J. M. Montserrat, Dr. J. Flórez
Instituto Universitario de Química Organometálica *Enrique Moles*
Universidad de Oviedo
Julián Claveria, 8, E-33071 Oviedo (Spain)
Telefax: Int. code + (348) 510 3446
Dr. S. García-Granda,[+] E. Martín[+]
Departamento de Química Física y Analítica
Facultad de Química, Universidad de Oviedo (Spain)

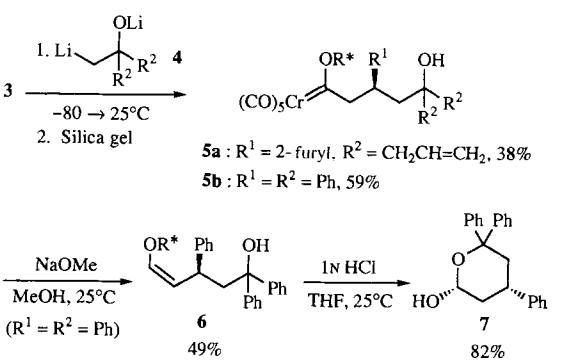
[+] X-ray crystal structure analyses.

[**] This work was supported by Dirección General de Investigación Científica y Técnica (DGICYT) (Grant PB89-0538). J. M. M. thanks the Ministerio de Educación y Ciencia de España for a doctoral fellowship.



Scheme 1. Synthesis of chiral carbene complexes **3**. TMS = $SiMe_3$.

we synthesized the (−)-8-phenylmenthol-derived vinylcarbenes **3**[9] (Scheme 1). The synthesis of these chiral carbene complexes was achieved starting from the tetramethylammonium complex **1**[10] by alkylation[11] and condensation.[12] The reaction of the organolithium reagent **4**[13] ($R^2 = CH_2{=}CHCH_2$) with the vinylcarbene complex **3a** (R^1 = 2-furyl) led to the acyclic 1,4-addition product **5a** (Scheme 2) with good diastereoselectivity (95% *de*; Table 1, entry 1); but the expected[8] intramolecular



Scheme 2. Asymmetric Michael additions of β-oxygen-substituted organolithium compounds. R*OH = (−)-8-phenylmenthol.

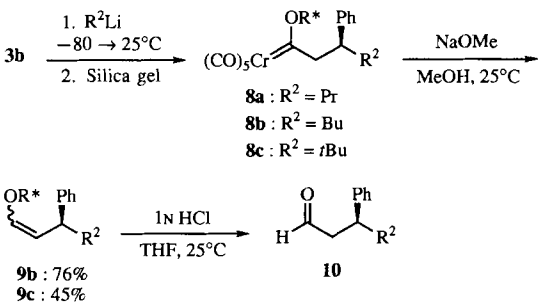
Table 1. Asymmetric Michael additions of organolithium compounds to optically active carbene complexes **3**.

Entry	R^1	R^2	R^3	Product [a]	Yield [%] [b]	*ee* [%]	*de* [c] [%]	$[\alpha]_D$ [d]	Config. [e]
1	2-furyl	allyl	–	**5a**	38	–	95	–	*S*
2	Ph	Ph	–	**7**	82 [f]	87 [g]	–	−137	*S*
3	Ph	Pr	–	**8a**	65	–	95		*S*
4	Ph	Bu	–	**10b**	82 [h]	90 [i]	–	−2.3	*S*
5	Ph	*t*Bu	–	**10c**	88 [h]	80 [i]	–	−9.7	*R*
6	Ph	Me	H	**12a**	55	–	93	–	*S*
7	Ph	Ph	H	**12b**	67	–	97	–	*S*
8	Ph	$(CH_2)_4$		**12c**	69	–	89	–	*R*

[a] Michael adduct used in each case to determine the enantiomeric excess. [b] Yield of isolated product after flash chromatography based on the corresponding carbene complexes **3**. [c] Determined by ^{1}H NMR spectroscopy (300 MHz) and further confirmed by HPLC analysis (Nucleosil 120-10, hexane:THF, 15–36:1). [d] Optical rotations were recorded in CH_2Cl_2 at 20–25 °C, c = 0.25–0.35 g 100 mL^{-1}. [e] Absolute configuration of the new stereogenic center formed in the addition step. Determined by X-ray analyses of compounds **8a** and **12a** (entries 3, 6) and proposed by analogy in all the other adducts assuming the same stereochemical model. [f] Based on enol ether **6**. [g] Determined by HPLC (Chiralcell OD-H, hexane:2-propanol, 3:1) of compound **7** in comparison with the corresponding racemic mixture. [h] Based on the corresponding enol ether **9b**, **9c**. [i] Determined by HPLC (Chiralcell OD-H, hexane:THF, 6–12:1) of 2,4-dinitrophenylhydrazone derivatives of the corresponding aldehydes **10** in comparison with the corresponding racemic products.

alkoxide exchange and cyclopropanation reactions were not observed, probably due to the bulkiness of the 8-phenylmenthyl group. While this approach has so far not led to tricyclic ring systems,[14] the high asymmetric induction observed in the reaction prompted us to study the addition of other organolithium compounds and these results represent the first examples of asymmetric conjugate additions to Fischer vinylcarbene complexes.

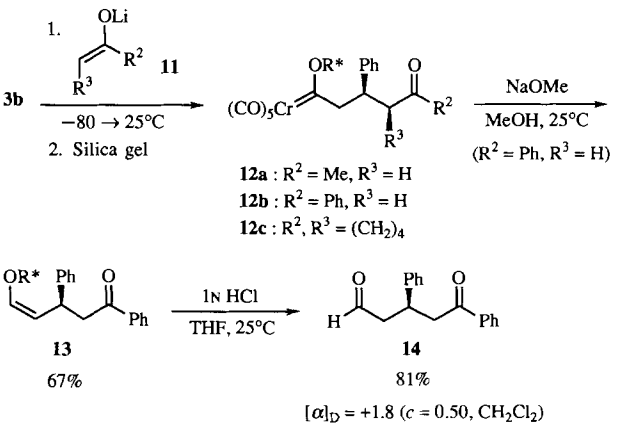
Scheme 2 shows the Michael reaction of another β-oxygen-functionalized organolithium **4** (R^2 = Ph) with carbene complex **3b** (R^1 = Ph) which gave, after purification by silica gel chromatography, adduct **5b**. Removal of the pentacarbonylchromium fragment by basic treatment with sodium methoxide[15] in methanol, afforded the less stable (*Z*)-enol ether[3c] **6** (*J* = 6 Hz, vinyl protons). The (−)-8-phenylmenthyl chiral auxiliary was removed and recovered (80%, after column chromatography) by acid hydrolysis (1 N, HCl) of **6** which led to the cyclic hemiacetal **7** as a single product (Table 1, entry 2), indicating high asymmetric induction in the conjugate addition and also in the intramolecular cyclization reaction. The relative configuration of the newly formed stereogenic carbon centers of **7** was established by analysis of the coupling constants for the methine protons and by a difference NOE experiment. Under the same reaction conditions, the addition of alkyllithium reagents to α,β-unsaturated carbene complex **3b** led diastereoselectively to the Michael adducts **8**. Removal of the transition metal moiety and the chiral auxiliary as previously described gave rise to the optically active β-substituted aldehydes **10** with high enantiomeric excesses (Scheme 3, Table 1, entries 3–5). Both vinyl ethers **9** were



Scheme 3. Asymmetric Michael additions of alkyllithium compounds. Yields of **9b** and **9c** are based on **3b**; both vinyl ethers are a mixture *Z*:*E*, 6:1.

isolated as a 6:1 mixture of diastereoisomers (*Z*:*E* ratio determined from the ^{1}H NMR spectrum; J_{cis} = 6.9 Hz, J_{trans} = 12.1 Hz, vinyl protons). The lithium enolates **11**, generated from the corresponding ketones by treatment with lithium diisopropylamide (LDA) at −78 °C in tetrahydrofuran,[16] may also be added as donors to the optically active acceptor **3b**, yielding the 1,4-adducts **12** in uniformly high diastereomeric excesses (Table 1, entries 6–8). The Michael addition of the lithium enolate of cyclohexanone to Fischer vinylcarbene complexes takes place with *syn* diastereoselectivity;[6] thus, this stereochemistry was assumed for compound **12c**. Metal and chiral auxiliary-free products are easily accessible in high enantiomeric purity as indicated in Scheme 4 with the transformation of **12b** into the 1,5-dicarbonyl compound **14**.[17]

The absolute configuration of the newly formed stereogenic center at the β position of the carbene complex was determined by the single-crystal X-ray structure analysis of compounds **8a**[18] (Fig. 1) and **12a**.[19] In all other products it was assigned by analogy.



Scheme 4. Asymmetric Michael additions of lithium enolates of ketones.

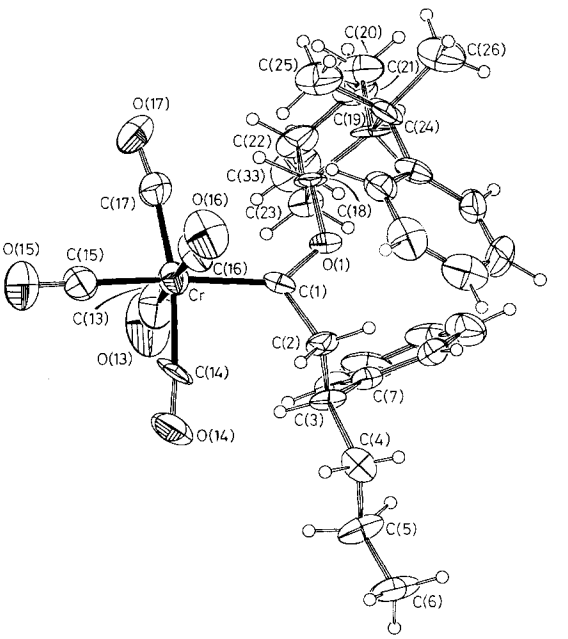


Fig. 1. Crystal structure of **8a**. Selected bond lengths [Å] and bond angles [°]: Cr(1)-C(1) 2.056(7), O(1)-C(1) 1.288(6), C(1)-C(2) 1.528(8), C(2)-C(3) 1.528(8), C(3)-C(7) 1.476(9), C(3)-C(4) 1.563(11); C(15)-Cr(1)-C(1) 172.8(4), C(1)-O(1)-C(18) 125.2(5), O(1)-C(1)-C(2) 103.4(5).

The asymmetric induction that has been observed in all these reactions can be explained in terms of the model shown in Figure 2. In this drawing of the most stable conformation the appropriately positioned phenyl group shields selectively the front face of the double bond by π,π-orbital overlap[20] forcing the nucleophile to attack preferentially on the opposite side.[21] This model is similar to the "π-stacking" one previously proposed by W. Oppolzer et al.[22] for cuprate additions to enoates and the one depicted by E. Nakamura et al.[6] to explain the diastereoselective *syn* Michael addition of enolates to Fischer vinylcarbene complexes.

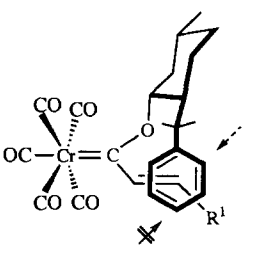


Fig. 2. Model proposed to explain the asymmetric induction of the Michael additions discussed here.

The net transformations described here are the synthetic equivalent of Michael additions of alkyllithium compounds and ke-

tone enolates to α,β-unsaturated aldehydes. The present carbene route offers an attractive alternative to this otherwise generally difficult reaction.[1a, d, 23]

Experimental Procedure

10b: To a cooled (−80 °C) solution of **3b** (1.44 g, 2.68 mmol) in THF (30 mL) was added a 2.5 M solution of BuLi in hexane (1.15 mL, 2.8 mmol) under nitrogen and the mixture was stirred at −80 °C for 1 h and between −80 °C and room temperature for 0.5 h. After removal of the solvents in vacuo a solution of NaOMe (ca. 0.5 M) in MeOH (20 mL) was added and the mixture was stirred at room temperature for 3 h. MeOH was removed and the residue was purified by column chromatography (silica gel, hexane: Et_2O, 4:1) to give 0.83 g (76%) of **9b**. To a solution of **9b** (0.75 g, 1.86 mmol) in THF (30 mL) was added 1 M HCl (3 mL) and the mixture stirred at room temperature for 10 h. The solvent was removed in vacuo and the residue was purified by column chromatography (silica gel, hexane: Et_2O, 10:1) to give 0.29 g (82%) of **10b**.

Received: January 31, 1994 [Z 6658 IE]
German version: *Angew. Chem.* **1994**, 106, 1451

[1] Recent reviews: a) H. G. Schmalz in *Comprehensive Organic Synthesis, Vol. 4* (Eds.: B. M. Trost, I. Fleming), Pergamon, New York, **1991**, p. 199; b) P. Perlmutter, *Conjugate Addition Reactions in Organic Synthesis*, Pergamon, Oxford, **1992**; for recent examples, see: c) K. Rück, H. Kunz, *Synthesis* **1993**, 1018; d) M. Yamaguchi, T. Shiraishi, M. Hirama, *Angew. Chem.* **1993**, *105*, 1243; *Angew. Chem. Int. Ed. Engl.* **1993**, *32*, 1176; e) E. J. Corey, I. N. Houpis, *Tetrahedron Lett.* **1993**, *34*, 2421; f) A. Tatsukawa, M. Dan, M. Ohbatake, K. Kawatake, T. Fukata, E. Wada, S. Kanemasa, S. Kakei, *J. Org. Chem.* **1993**, *58*, 4221; g) S. Hanessian, A. Gomtsyan, A. Payne, Y. Hervé, S. Beaudoin, *ibid.* **1993**, *58*, 5032.

[2] W. D. Wulff in *Comprehensive Organic Synthesis, Vol. 5* (Eds.: B. M. Trost, I. Fleming), Pergamon, New York, **1991**, p. 1065.

[3] a) C. P. Casey, W. R. Brunsvold, *J. Organomet. Chem.* **1974**, *77*, 345; b) *ibid.* **1975**, *102*, 175; c) *Inorg. Chem.* **1977**, *16*, 391.

[4] a) D. W. Macomber, M. H. Hung, A. G. Verma, R. D. Rogers, *Organometallics* **1988**, *7*, 2072; b) D. W. Macomber, P. Madhukar, R. D. Rogers, *ibid.* **1991**, *10*, 2121; c) S. Aoki, T. Fujimura, E. Nakamura, *J. Am. Chem. Soc.* **1992**, *114*, 2985; conjugate addition of alkyl radicals (formal Michael reactions); d) C. A. Merlic, D. Xu, *ibid.* **1991**, *113*, 9855; e) C. A. Merlic, D. Xu, M. C. Nguyen, V. Truong, *Tetrahedron Lett.* **1993**, *34*, 227.

[5] Carbon nucleophiles: a) S. L. B. Wang, W. D. Wulff, *J. Am. Chem. Soc.* **1990**, *112*, 4550; b) H. Fischer, T. Meisner, J. Hofmann, *Chem. Ber.* **1990**, *123*, 1799. Nitrogen nucleophiles: c) F. Stein, M. Duetsch, R. Lackmann, M. Noltemeyer, A. de Meijere, *Angew. Chem.* **1991**, *103*, 1669; *Angew. Chem. Int. Ed. Engl.* **1991**, *30*, 1658; d) M. Duetsch, F. Stein, R. Lackmann, E. Pohl, R. Herbst-Irmer, A. de Meijere, *Chem. Ber.* **1992**, *125*, 2051; e) R. Pipoh, R. van Eldik, *Organometallics* **1993**, *12*, 2668. Oxygen nucleophiles: f) F. Camps, A. Llebaria, J. M. Moretó, S. Ricart, J. M. Viñas, J. Ros, R. Yáñez, *J. Organomet. Chem.* **1991**, *401*, C17; g) R. Aumann, *Chem. Ber.* **1992**, *125*, 2773.

[6] E. Nakamura, K. Tanaka, T. Fujimura, S. Aoki, P. G. Williard, *J. Am. Chem. Soc.* **1993**, *115*, 9015.

[7] B. A. Anderson, W. D. Wulff, A. Rahm, *J. Am. Chem. Soc.* **1993**, *115*, 4602.

[8] J. Barluenga, J. M. Montserrat, J. Flórez, *J. Chem. Soc. Chem. Commun.* **1993**, 1068.

[9] First reported as chiral auxiliary: E. J. Corey, H. E. Ensley, *J. Am. Chem. Soc.* **1975**, *97*, 6908.

[10] E. O. Fischer, A. Maasböl, *Chem. Ber.* **1967**, *100*, 2445.

[11] a) E. O. Fischer, T. Selmayr, F. R. Kreissl, *Chem. Ber.* **1977**, *110*, 2947; b) M. F. Semmelhack, J. J. Bozell, *Tetrahedron Lett.* **1982**, *23*, 2931; c) B. C. Söderberg, L. S. Hegedus, M. A. Sierra, *J. Am. Chem. Soc.* **1990**, *112*, 4364.

[12] R. Aumann, H. Heinen, *Chem. Ber.* **1987**, *120*, 537.

[13] J. Barluenga, J. Flórez, M. Yus, *J. Chem. Soc. Perkin Trans. 1* **1983**, 3019.

[14] Other approaches to the tricyclic compounds are currently being investigated in our laboratory.

[15] This transformation is more frequently carried out with pyridine: E. O. Fischer, D. Plabst, *Chem. Ber.* **1974**, *107*, 3326. We first used sodium methoxide with the aim of inducing the intramolecular alkoxide exchange reaction of compound **5b**: C. A. Merlic, D. Xu, B. G. Gladstone, *J. Org. Chem.* **1993**, *58*, 538.

[16] H. O. House, M. Gall, H. D. Olmstead, *J. Org. Chem.* **1971**, *36*, 2361.

[17] All new compounds were characterized spectroscopically (^1H, ^{13}C NMR, IR) and by mass spectrometry.

[18] Crystal data for **8a**: $C_{33}H_{38}CrO_6$, $M_r = 582.63$, orthorhombic, space group $P2_12_12_1$, $a = 10.875(3)$, $b = 14.134(4)$, $c = 20.91(1)$ Å, $V = 3214.(2)$ Å^3, $Z = 4$, $\rho_{calcd} = 1.20$ g cm^{-3}, $F(000) = 1232$, $\lambda(Mo_{K\alpha}) = 0.71073$ Å, $\mu = 3.8$ cm^{-1}, $T = 293$ K. Yellow crystal (0.20 × 0.10 × 0.10 mm) obtained from a hexane solution at −30 °C. Enraf-Nonius CAD4 diffractometer. ω-2θ scan technique. Of 6609 reflections measured ($0 < \theta < 25°$), 5637 used in refinement. The structure was solved by Patterson methods with the program SHELXS86 [24] and expanded by DIRDIF [25]. An absorption correction was applied by using DIFABS [26]. Full-matrix least-squares refinement on $|F|^2$ was made with SHELXL93 [27]. All non-hydrogen atoms were anisotropically refined. Most hydrogen atoms were located by difference Fourier synthesis. Final conventional $R = 0.048$ (for 1550 $F_o > 4\sigma(F_o)$) and $wR2 = 0.131$ (for all reflections (5637)) $w = 1.0/[\sigma^2(F_o^2) + (0.0625P)^2]$ where $P = (\mathrm{Max}(F_o^2, 0) + 2F_c^2)/3$. The absolute configuration was checked with the BIJVOET Program [28] and gave $B = 0.46(7)$ for the 100 strongest Friedel pairs. (Flack χ parameter [29] 0.0076(402)). Total number of parameters 394. Residual electron density less than 0.18 eÅ^{-3}. The plot in Figure 1 was made by EUCLID package [30]. Further details of the crystal structure determination are available on request from the Director of the Cambridge Crystallographic Data Centre, 12 Union Road, GB-Cambridge CB2 1EZ (UK), on quoting the full journal citation.

[19] A complete description of the X-ray structure analysis and absolute configuration determination for **12a** has been deposited at the Cambridge Crystallographic Data Centre.

[20] Evidence for π,π-attractive interactions: a) E. J. Corey, Y. Matsumura, *Tetrahedron Lett.* **1991**, *32*, 6289; b) E. J. Corey, T. P. Loh, *J. Am. Chem. Soc.* **1991**, *113*, 8966; c) J. M. Hawkins, S. Loren, *ibid.* **1991**, *113*, 7794, and references therein.

[21] A *cisoid* conformation, less stable due to more steric interactions, and which would lead to the same sense of asymmetric induction cannot be ruled out at this time.

[22] a) W. Oppolzer, H. J. Löher, *Helv. Chim. Acta* **1981**, *64*, 2808; b) J. d'Angelo, J. Maddaluno, *J. Am. Chem. Soc.* **1986**, *108*, 8112.

[23] G. V. Kryshtal, V. V. Kulganek, V. F. Kucherov, L. A. Yanovskaya, *Synthesis* **1979**, 107.

[24] G. M. Sheldrick in *Crystallographic Computing 3*, SHELXS86, (Eds.: G. M. Sheldrick, C. Kruger, R. Goddard), Clarendon, Oxford, **1985**, pp. 175–189.

[25] P. T. Beurskens, G. Admiraal, G. Beurskens, W. P. Bosman, S. Garcia-Granda, R. O. Gould, J. M. M. Smits, C. Smykalla, *The DIRDIF program system. Technical Report of the Crystallography Laboratory*, University of Nijmegen, The Netherlands, **1992**.

[26] N. Walker, D. Stuart, *Acta Crystallogr. Sect. A*, **1983**, *39*, 158.

[27] G. M. Sheldrick in *Crystallographic Computing 6*, SHELXL93 (Eds. H. D. Flack, P. Parkanyi, K. Simon), Clarendon, Oxford, **1993**.

[28] G. Beurskens, J. H. Noordik, P. T. Beurskens, *Cryst. Struct. Commun.* **1980**, *9*, 23.

[29] H. D. Flack, *Acta Crystallogr. Sect. A*, **1983**, *39*, 876.

[30] A. L. Spek in *Computational Crystallography. The EUCLID Package* (Ed.: D. Sayre), Clarendon, Oxford, **1982**, p. 528.

New Cyclic Derivatives of 3′-Amino-3′-deoxyadenosine-5′-diphosphate, -triphosphate, and -methylenebis(phosphonate)**

Michael Morr* and Victor Wray

Dedicated to Professor Fritz Wagner on the occasion of his 65th birthday

Whereas a number of chemical syntheses of 3′-amino-3′-deoxyadenosine (3′-AdA) (**1**) have been described,[1] we have been engaged for a long time in its preparation by fermentation of *Helminthosporium* sp. 215.[2] Compound **1**, the basic component of the antibiotic nucleoside puromycin,[3] has also been modified by us in many ways. Thus **1** was phosphorylated to 3′-AdA-5′-monophosphate (**9**), which in turn was cyclized with dicyclohexylcarbodiimide (DCC) or water-soluble carbodiimide (1-ethyl-3-(3-dimethylaminopropyl)carbodiimide hydrochloride, EDC) to yield the cAMP-analogue 3′-AdA-3′,5′-cyclophosphate (**12**) (3′-NH-cAMP).[4, 5] This was used for inhibition studies with cAMP-dependent protein kinase.[6] A further derivative of **1**, 3′-AdA-5′-triphosphate (**7**) (3′-NH_2-ATP), proved to be of bio-

[*] Dr. M. Morr, Dr. V. Wray
GBF – Gesellschaft für Biotechnologische Forschung mbH
Mascheroder Weg 1, D-38124 Braunschweig (FRG)
Telefax: Int. code + (531)6181-302

[**] We are grateful to Mrs. D. Döring, Technical University of Braunschweig, for recording the FAB mass spectra.

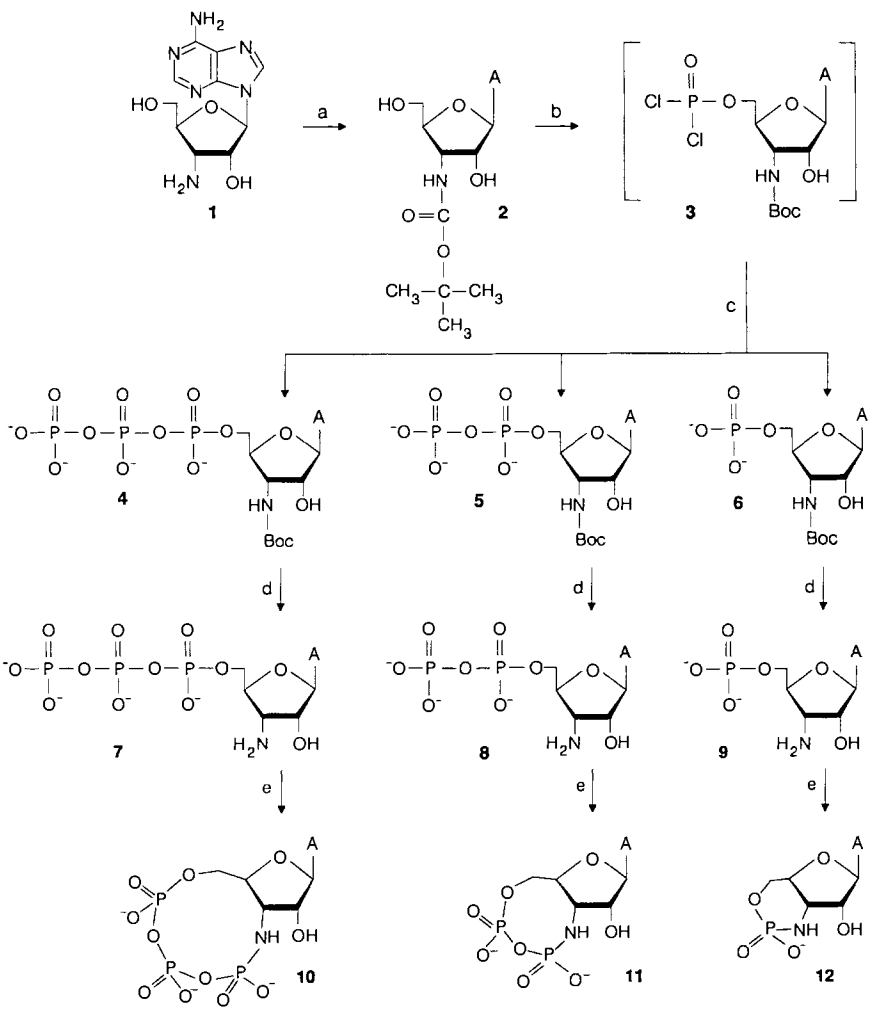
chemical interest. It was first prepared enzymatically by Marutzky[7] from **9** with myokinase and pyruvate kinase and served as an ATP-analogue in substrate binding studies with leucyl-tRNA-synthetase.[8] Van Boom et al. prepared **7** by phosphorylation of the 5′-OH group according to the triester method and by activation of protected **9** with morpholine and subsequent reaction with diphosphoric acid.[9] Apart from its use in the study of protein biosynthesis, **7** was shown to be an effective inhibitor of the DNA-dependent RNA polymerase from Ehrlich ascites tumor cells[10] and *E. coli*.[11–13]

Phosphorylation of **1** according to Yoshikawa[14] with $POCl_3$ in triethylphosphate furnishes different products depending on the reaction conditions. Thus, phosphorylation in suspension gives almost exclusively 3′-amino-5′-chloro-3′,5′-dideoxyadenosine[15] accompanied by a small amount of **9**. When **1** is dissolved in hot triethylphosphate and then phosphorylated with $POCl_3$, one obtains 3′-AdA-5′-phosphorodichloridate (not isolated) which is converted exclusively to **12** by alkaline hydrolysis.

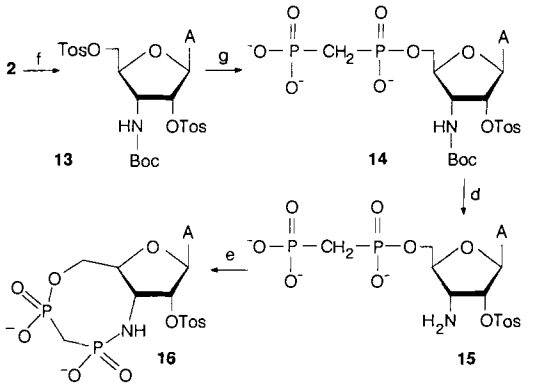
A repetition of the synthesis of **12** from impure **9** (containing some 3′-AdA-5′-diphosphate (**8**) and the triphospate (**7**) by the cyclization method with water-soluble carbodiimide led to the surprising observation that **7** and **8** also underwent complete cyclization to yield **10** and **11**, respectively. For subsequent studies on a larger scale, **7** and **8** were prepared according to Yoshikawa[14] and Ludwig.[16] The *tert*-butoxycarbonyl (Boc) protecting group is introduced into **1** with di-*tert*-butyldicarbonate[17] in *N*,*N*-dimethylformamide (DMF) to give 3′-*N*-Boc-3′-deoxyadenosine (**2**).[18] Phosphorylation with $POCl_3$ in triethylphosphate yields the intermediate **3** (not isolated), which is converted with bis(tri-*n*-butylammonium) diphosphate[16] in good yield to 3′-*N*-Boc-ATP (**4**), and small amounts of 3′-*N*-Boc-ADP (**5**) and 3′-*N*-Boc-AMP (**6**). By ion-exchange chromatography on DEAE-sephadex [HCO_3^- form, H_2O/triethylammonium hydrogencarbonate buffer (pH 7.5) gradient], removal of the *N*-Boc protective group with trifluoroacetic acid (TFA) and repeated chromatography, **7**, **8**, and **9** are obtained (Scheme 1).

Cyclization of **7** and **8** proceeds in very good yields with EDC (5- to 10-fold excess, nucleotide concentration 1–2 mg mL^{-1}) at pH 7.0–7.5 to 3′-AdA-3′,5′-cyclodiphosphate (**11**) and 3′-AdA-3′,5′-cyclotriphosphate (**10**), respectively. Purification is achieved by ion-exchange chromatography on DEAE-sephadex (see above). Compound **11** is the first derivative of the naturally occurring adenosine-3′,5′-cyclodiphosphate (cADP)[19] which has been isolated from the red alga *Porphyra perforata* and synthesized by cyclization of adenosine-3′,5′-diphosphate with DCC.[20, 21] cADP inhibits the cAMP-dependent protein kinase and bovine phosphodiesterase;[21] in the presence of N^6,2′-*O*-dibutyryl-3′,5′-cAMP it inhibits the spontaneous germinal vesicle breakdown (GVBD) of cultured mouse oocytes.[22] No naturally occurring cyclic ATP derivatives have been found so far; **10** is the first derivative of cATP. Straight chain γ derivatives of ATP with different amines were prepared by Knorre et al. by reaction with DCC.[23] Orgel et al. investigated the reactions of AMP, ADP, ATP, and ATeP (adenosine-5′-tetraphosphate) with water-soluble carbodiimide without observing any intramolecular cyclization.[24]

After tosylation of the 3′- and 5′-positions of **2** with tosyl chloride in pyridine/4-dimethylaminopyridine (DMAP) to **13**, a further interesting derivative, **14**, of **1** was obtained by selective nucleophilic substitution of the 5′-*O*-tosyl group with tris-(tetra-*n*-butylammonium) methylenebis(diphosphonate).[25] Removal of the 3′-*N*-Boc protective group with TFA and cyclization of **15** with EDC at pH 7.0–7.5 followed by the usual purification on DEAE-sephadex furnishes good yields of 3′-amido-3′-deoxy-2′-*O*-tosyladenosine-3′,5′-cyclomethylenebis(phosphonate) (**16**) (Scheme 2). The new cyclic derivatives are very stable with respect to hydrolysis of the P–N bond. Whereas **12** is already cleaved to **9** at pH 5 because of the large ring strain, compounds **10**, **11**, and **16** are completely stable at pH 3 since ring strain is less important here. At pH 2, the half-life times of P–N bond cleavage are about 30 h, 18 h, and 4 h for **10**, **11**, and **16**, respectively.



Scheme 1. a) $(Boc)_2O$, DMF, 92%; b) $POCl_3$, $OP(OEt)_3$, 90%; c) $(Bu_3NH)_2H_2P_2O_7$/Bu_3N/DMF, 0 °C, 5 min, 1 M $(Et_3NH)HCO_3$ buffer (pH 7.5), column chromatography: DEAE-sephadex (HCO_3^-), H_2O/$(Et_3NH)HCO_3$ buffer gradient, **4** 65%, **5** 20%, **6** 12%; d) TFA, 5 min, room temperature, column chromatography as under b), **7** 85%, **8** 70%, **9** 92%; e) EDC, pH 7–7.5, column chromatography as under b), **10** 88%, **11** 90%.



Scheme 2. cADP analogues with NH and CH_2 in the ring system: f) TsCl, DMAP, pyridine, 75%; g) $(Bu_4N^+)_3HOP(O)(O^-)CH_2P(O)(O^-)_2$, CH_3CN, 68%, d) see Scheme 1, **15** 85%; e) see Scheme 1, **16** 88%.

The structures of **7**, **8**, **10**, **11**, **15**, and **16** were confirmed from their FAB mass spectra[26] and from their ^1H, ^{13}C, and ^{31}P NMR data (Tables 1 and 2). The assignments of these NMR data followed from a straightforward comparison with detailed literature data for **9** and its 3′,5′-cyclophosphate **12**.[5] Two ^{31}P NMR signals were observed for **8**, **11**, **15**, and **16**, and three for **7** and **10**. Ring formation in **10**, **11**, and **16** was confirmed by the observation of ^{31}P spin coupling to H3′ and to C2′, C3′, C4′, and C5′. Two-dimensional $^1H,^1H$-COSY and a ^1H-detected heteronuclear multiple-quantum coherence $^{13}C,^1H$ correlation allowed unambiguous assignments of the signals in **16**. The presence of the methylene group bound directly to both phosphorus atoms in **15** and **16** was indicated by the two large $J(^{31}P,^{13}C)$ values observed for this carbon nucleus.

Table 1. ^1H NMR data of **7**, **8**, **10**, **11**, **15**, and **16** in D_2O.

Cmpd.	Chemical shifts [a] H-2/H-8	H-1′	H-2′	H-3′	H-4′	H-5′A	H-5′B
7	8.41/8.15	6.14	4.89	4.31	4.60	4.49	4.34
	s s	d	dd	dd	ddd	ddd	ddd
8	8.52/8.22	6.12	4.75	4.61	4.37	4.26	4.19
	s s	d	dd	dd	m	ddd	ddd
10	8.45/8.20	6.14	4.41	4.18	4.22	4.56	4.35
	s s	s	d	ddd	bd	bdd	bdd
11	8.28/8.22	6.09	4.54	4.02	4.22	4.39	4.22
	s s	s	d	ddd	m	m	m
15 [c]	8.34/8.16	6.11	5.54	4.13	4.37	4.29	4.29
	s s	d	dd	dd	m	m	m
16 [c]	8.26/8.19	5.82	5.43	4.42	4.20	4.37	4.28
	s s	d	dd	ddd	ddd	ddd	ddd

	Coupling constants [Hz] 1′-2′	2′-3′	3′-4′	4′-5′A	4′-5′B	5′A-5′B	P-5′A	P-5′B	P-3′
7	3.1	6.0	7.5	~2.3	~2.3	12.0	7.0	4.0	–
8	5.3	5.2	4.2	3	3	11.5	6	4	–
10	<2	3.2	~10	small	small	12.0	11	3.5	10
11	<2	5.1	9.0	[b]	[b]	[b]	[b]	[b]	12
15 [c]	6.3	7.2	5.3	[b]	[b]	[b]	[b]	[b]	–
16 [c]	3.9	7.5	9.8	4.1	6.3	11.7	11.8	11.7	11.7

[a] δ values relative to 3-(trimethylsilyl)-1-propanesulfonic acid-sodium salt (DSS); signal multiplicities are shown below the shifts. [b] These couplings were not determined as the spectrum was second order and broad. [c] Phosphorus-bound methyl groups: **15**: $\delta = 2.27$, J(P,H) 19.7 Hz; **16**: $\delta = 2.32$ (P(A)), 2.24 (P(B)), J(A,B) −15.6, J(A,P5) 20.3, J(A,P3) 20.3, J(A,P5) 18.0, J(B,P3) 18.9 Hz. Tosyl group: **15**: $\delta = 7.56$ ["d", H2″/6″, $J(2'',3'') + J(2'',5'')$ 8.2], 7.07 ["d", H3″/5″], 2.34 [s, CH_3-4″]; **16**: $\delta = 7.67$ ["d", H2″/6″, $J(2'',3'') + J(2'',5'')$ 8.2], 7.09 ["d", H3″/5″], 2.22 [s, CH_3-4″].

Table 2. ^{13}C and ^{31}P NMR data of **7**, **8**, **10**, **11**, **15**, and **16** in D_2O.

Cmpd.	^{13}C Shifts [a] C-2	C-4	C-5	C-6	C-8	C-1′	C-2′	C-3′	C-4′	C-5′
7	155.22	151.02	121.11	157.75	142.48	91.77	76.01	53.83	83.00	67.36
8	155.22	150.80	121.00	157.68	142.25	91.75	75.86	53.85	82.56	66.71
10	155.22	150.76	121.41	158.03	142.36	91.82	77.90	54.66	83.79	65.52
11	155.22	150.54	121.02	157.80	141.83	91.82	77.61 [b]	58.97	81.61 [b]	68.32
15 [c]	155.22	150.39	120.90	157.91	142.59	87.38	83.70	54.37	86.65	66.35
16 [c]	155.22	150.24	120.27	157.89	142.15	88.01	84.07	57.03	81.91	65.71

	^{31}P Shifts [d] α	β	γ	Coupling constants [Hz] P-2′	P-3′	P-4′	P-5′	α-β	β-γ
7	−8.98	−19.45	−4.23	–	–	9.5	5.7	19.5	20.1
8	−9.90	−6.37		–	–	8.8	[e]	20.3	
10	−10.73	−22.96	−3.50	3.2	1.6	8.0, 8.0	5.2	22.4	22.4
11	−10.78	−3.89		8.6 [b]	1.5	[b, e]	5.9	23.8	
15	18.8 [f]	13.5		–	–	7.4	5.2	9.1	
16	20.9 [f]	15.3		5.7	3.5	3.2	4.7	9.4	

[a] δ values; for consistency the chemical shift of C2 was used as a secondary reference (relative to DSS in D_2O at pH 7.5). [b] Signal assignments are interchangeable. [c] Additional signals were found at: **15**: $\delta = 30.40$ [PCH_2P, J(P,C) 124.8, 122.1 Hz] and of the tosyl group at $\delta = 150.39$ (s, C,1″), 132.79 (s, C,4″), 132.30, 129.63 (d × 2, C2″/6″, C3″/5″) and 23.50 (q, C7″); **16**: $\delta = 32.32$ [PCH_2P, J(P,C) 126.8, 112.7 Hz] and of the tosyl group at $\delta = 149.09$ (s, C1″), 132.98 (s, C4″), 132.36, 129.87 (d × 2, C2″/6″, C3″/5″) and 23.09 (q, C7″). [d] Standard H_3PO_4 external. [e] Signals broadened but coupling(s) not resolved. [f] The low-field signal belongs to the moiety bound to C5′ of ribose (P5 in Table 1).

In the near future, we intend to investigate to what extent the new cyclic derivatives can be transported through cell membranes by the aid of carriers such as 1,4-diazabicyclo[2.2.2]octane (DABCO).

Received: January 12, 1994 [Z 6604 IE]
German version: *Angew. Chem.* **1994**, *106*, 1439

[1] [1] M. C. Samano, M. J. Robins, *Tetrahedron Lett.* **1989**, *30*, 2329.
[2] N. N. Gerber, H. A. Lechevalier, *J. Org. Chem.* **1962**, *27*, 1731.
[3] J. N. Porter, R. I. Hewitt, C. W. Hesseltine, G. Krupka, J. A. Lowery, W. S. Wallace, N. Bohonos, J. H. Williams, *Antibiot. Chemotherapy* **1952**, *2*, 409.
[4] M. Morr, M.-R. Kula, G. Roesler, B. Jastorff, *Angew. Chem.* **1974**, *86*, 308; *Angew. Chem. Int. Ed. Engl.* **1974**, *13*, 280.
[5] M. Morr, M.-R. Kula, L. Ernst, *Tetrahedron* **1975**, *31*, 1619.
[6] N. Panitz, E. Rieke, M. Morr, K. G. Wagner, *Eur. J. Biochem.* **1975**, *55*, 415.
[7] R. Marutzky, Dissertation Technische Universität Braunschweig, **1975**.
[8] R. Marutzky, J. Flossdorf, M.-R. Kula, *Nucleic Acids Res.* **1976**, *3*, 2067.
[9] G. M. Visser, C. Schattenkerk, J. H. van Boom, *Recl. Trav. Chim. Pays-Bas* **1984**, *103*, 165.
[10] J. T. Trauman, H. Klenow, *Mol. Pharmacol.* **1968**, *4*, 77.
[11] V. W. Armstrong, F. Eckstein, *Eur. J. Biochem.* **1976**, *79*, 33.
[12] V. W. Armstrong, F. Eckstein, *Biochemistry* **1979**, *18*, 5117.
[13] T. Kutatemadze, R. Beabealashvili, A. Azhayev, A. Krayevsky, *FEBS Lett.* **1983**, *153*, 420.
[14] K. Kusashio, M. Yoshikawa, *Bull. Chem. Soc. Jpn.* **1968**, *41*, 142.
[15] M. Morr, M.-R. Kula, *Tetrahedron Lett.* **1974**, 23.
[16] J. Ludwig, *Acta Biochim. Biophys. Acad. Sci. Hung.* **1981**, *16*, 131.
[17] L. Moroder, A. Hallett, E. Wünsch, O. Keller, G. Wersin, *Hoppe-Seyler's Z. Physiol. Chem.* **1976**, *357*, 1651.
[18] M. Morr, L. Ernst, *Chem. Ber.* **1978**, *111*, 2152.
[19] J. C. Su, W. Z. Hassid, *Biochemistry* **1962**, *1*, 474.
[20] D. Lipkin, W. H. Cook, *Biochim. Biophys. Acta* **1963**, *68*, 136.
[21] H. N. Wood, D. G. Lynn, *Differentiation* **1981**, *18*, 51.
[22] E. Sato, S. S. Koide, *Endocr. Res.* **1987**, *13*, 399.
[23] D. G. Knorre, V. A. Kurbatov, V. V. Samukov, *FEBS Lett.* **1976**, *70*, 105.
[24] K. E. Ng, L. E. Orgel, *Nucleic Acids Res.* **1987**, *15*, 3573.
[25] V. J. Davisson, D. R. Davis, V. M. Dixit, C. D. Poulter, *J. Org. Chem.* **1987**, *52*, 1794.
[26] FAB-MS (glycerol): **10**: $C_{10}H_{15}N_6O_{11}P_3$, calcd 488 (free acid), found 487 $[M-H]^-$, 489 $[M+H]^+$; **11**: $C_{10}H_{14}N_6O_8P_2$, calcd 408 (free acid), found 407 $[M-H]^-$; **15**: $C_{18}H_{24}N_6O_{10}P_2S$, calcd 578 (free acid), found 577 $[M-H]^-$ 579 $[M+H]^+$; **16**: $C_{18}H_{22}N_6O_9P_2S$, calcd 560 (free acid), found 559 $[M-H]^-$, 581 $[M+Na-2H]^-$.

The Spin Density Distribution in the Tetracyanoethylene Radical Anion, $[TCNE]^{\bullet -}$, by Single-Crystal Polarized Neutron Diffraction**

Andrey Zheludev, André Grand, Eric Ressouche, Jacques Schweizer,* Brian G. Morin, Arthur J. Epstein,* David A. Dixon,* and Joel S. Miller*

Several classes of molecule/organic-based magnetic solids based upon the tetracyanoethylene radical anion, $[TCNE]^{\bullet -}$, have been reported.[1] These include $[Fe(C_5Me_5)_2]^{\bullet +}[TCNE]^{\bullet -}$, with a critical temperature T_c of 4.8 K,[1] $[V(TCNE)_x]\cdot y(CH_2Cl_2)$ ($T_c \approx 400$ K),[1, 2] and $[MnTPP]^{\bullet +}[TCNE]^{\bullet -}$ (TPP = *meso*-tetraphenylporphyrinato) ($T_c = 18$ K).[1, 3] In the former class of magnetic materials the $[TCNE]^{\bullet -}$ is an isolated ion approximately parallel to the plane of the C_5Me_5 rings of adjacent $[M(C_5Me_5)_2]^{\bullet +}$ radical cations. In contrast, the $[TCNE]^{\bullet -}$ radical anions coordinate directly to metal ions in a bridging *trans*-μ_2 arrangement for the latter classes of materials. In all cases the odd number of electrons in $[TCNE]^{\bullet -}$ is crucial to the magnetic properties of the material. To understand the spin coupling mechanism that leads to the cooperative magnetic behavior of these classes of materials it is important to understand the spin distribution in the $[TCNE]^{\bullet -}$ radical anion. Herein, we report the spin distribution within $[TCNE]^{\bullet -}$ as determined from the single-crystal polarized neutron diffraction of $Bu_4N^+[TCNE]^{\bullet -}$.

The spin density in a radical of a known structure can be determined from neutron scattering by aligning the spins by means of an external magnetic field at low temperature and measuring the magnetic neutron scattering amplitudes (magnetic structure factors) at the Bragg scattering positions. The use of polarized neutrons increases the sensitivity of the method, since the nuclear scattering enhances the magnetic signal.[4] The crystal structure of $Bu_4N^+[TCNE]^{\bullet -}$ was determined by both X-ray[5a] and unpolarized neutron diffraction.[5b] The planar $[TCNE]^{\bullet -}$ radical anions are isolated both from the cations and from each other in the crystal.

The magnetic structure factors F_M are the Fourier components of the magnetization (spin) density. Reconstruction of the spatial spin density from the experimental magnetic structure factors is an Inverse Fourier (IF) problem, which is solved within the limitations of the accuracy and completeness of the polarized neutron diffraction data.[6] Because the data are noisy, the sampling of data points in reciprocal space is somewhat arbitrary, and the spatial resolution of the diffraction experiment is limited, several approaches for solving the IF problem were utilized.

Model-independent IF methods not involving any a priori knowledge of the spin density distribution were used to determine the spin density. The most straightforward method requires calculation of the IF sum over the Bragg reflections for which the F_M values were determined. This widely used approach is not suitable for incomplete and noisy data. Furthermore, since not all of the Fourier components are known, there are many three-dimensional spin density distributions (maps) which fit the data.

The recently developed maximum of entropy (MaxEnt) technique[7-10] selects the most probable spin density distribution—the one which maximizes the Boltzmann entropy—and gives much better results than conventional Fourier inversion. Figure 1 represents the MaxEnt reconstructed spin density projected onto the $[TCNE]^{\bullet -}$ molecular plane. The MaxEnt reconstruction reveals three key features: 1) The unpaired electron resides only on the $[TCNE]^{\bullet -}$ radical anion. 2) Most of the spin is localized on the central sp^2-carbon atoms, with smaller, but significant, spin densities at the nitrogen atoms, and even smaller and *negative* spin densities on the sp-carbon atoms. 3) The spin density on the sp^2-carbon atoms is not centered on these atoms, but it is bent away from the midpoint of the central C–C bond.

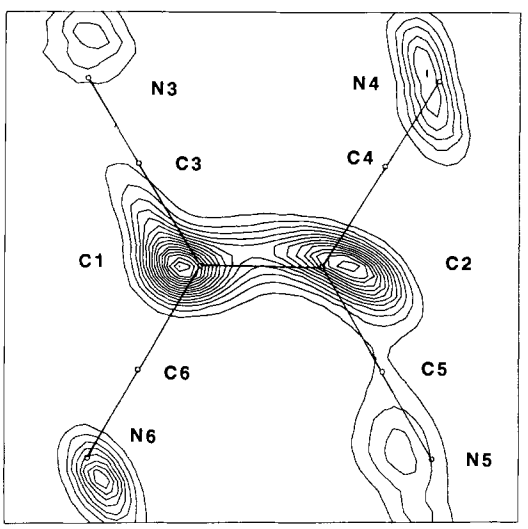


Fig. 1. Projection of the MaxEnt reconstructed spin density of $[TCNE]^{\bullet -}$ onto the molecular plane (xy).

Alternatively, the IF problem can be solved by using a parametrized model of the spatial spin density distribution and refining the parameters to fit the experimental structure factors. A good model should be flexible enough to describe the actual density with as few parameters as possible. A simple, frequently used model is based on individual atomic magnetic wavefunctions.[4] In this framework a LCAO-type wavefunction is constructed at each atomic site from standard Slater-type atomic orbitals.[11]

The simplest model for $[TCNE]^{\bullet -}$ uses the $|p_z\rangle$ orbitals (where z is the axis perpendicular to plane of the ion) for the C and N atoms. The atomic spin populations and radial exponents were refined by using a modification of the least-squares program MOLLY.[12] The results, however, are not very satisfactory as the residual estimated standard deviation (χ^2) is large (i.e. 1.8). The refined spin populations on each chemically equivalent sp^2-C are different [i.e. 0.185(7) and 0.256(7) μ_B].

The spin density on the sp^2-carbon atoms cannot be properly described by only using axially symmetrical $|p_z\rangle$ orbitals, since the unpaired electron resides in an antibonding π^* orbital which

[*] Dr. J. Schweizer, Dr. A. Zheludev, Dr. E. Ressouche
DRF/SPSMS/CENG, 85X, 38041 Grenoble (France)
Prof. A. J. Epstein, B. G. Morin
Department of Physics, The Ohio State University
Columbus, OH 43210-1106 (USA)
Dr. D. A. Dixon, Prof. J. S. Miller,[+]
DuPont Science & Engineering Laboratories
Experimental Station, E328, Wilmington, DE 19880-0328 (USA)
Dr. A. Grand
DRF/SESAM CENG, 85X, 38041 Grenoble (France)
[+] Current address: Department of Chemistry, University of Utah
Salt Lake City, UT 84112 (USA)
Telefax: Int. code + (801)581-8433

[**] Contribution No. 6619. The authors gratefully acknowledge the support of the Department of Energy, Division of Materials Sciences (Grant Nos. DE-FG03-93ER45504 and DE-FG02-86BR45271) has given to enable these studies and the single-crystal X-ray analysis provided by Carlos Vazquez, William J. Marshall, and Joseph C. Calabrese (DuPont).

is bent away from the center of the central C–C bond. Hence, a model permitting more freedom of the spin density shape is required. More flexibility can be obtained by directly modeling the spin density rather than the magnetic wavefunction. This can be accomplished by expanding the spin density around the nuclei in a multipolar series.[13] In this model the spin density is treated as a sum of real spherical harmonic functions centered at each atomic site.

After several trial refinements the hybrid model with only a minimal basis set of orbitals perpendicular to the molecular plane (i.e., the $|2p_z\rangle$ orbitals for the nitrogen and sp-carbon atoms) and a multipolar expansion of the spin density, was chosen. This multipolar expansion was truncated at orbital index = 3 (i.e., only mono-, di-, quadru-, and octapoles were included). To minimize the number of adjustable parameters, maximum advantage was taken of molecular symmetry. Only those functions which are even with respect to z and y were utilized (with the x axis parallel to the C–C double bond). Furthermore, the spin densities on the sp^2-carbon atoms were constrained to be symmetric with respect to the plane perpendicular to the central C–C bond and passing through its midpoint. The final refinement was improved ($\chi^2 = 1.4$) with refined spins on each sp^2-carbon atom of 0.255(3) μ_B (Table 1). The projection of the spin density along the z axis onto the approximate molecular plane is presented in Figure 2.

Table 1. Characteristic parameters of the spin densities calculated and refined atomic spin populations of $[TCNE]^{\bullet -}$ in μ_B and comparison with the results from NLDFT calculations [a].

	Wavefunction refinement	Multipolar expansion of the spin density	NLDFT TZVP [b]
Number of variables	13	17	
N_{obs}/N_{var} [c]	16.23	12.41	
χ^2 [d]	1.8	1.4	
C1 (sp^2)	0.185(7)	0.255(3)	0.30
C2 (sp^2)	0.256(7)	0.255(3)	0.29
C3 (sp)	−0.013(6)	−0.040(6)	−0.04
C4 (sp)	−0.012(7)	−0.030(6)	−0.05
C5 (sp)	−0.035(7)	−0.025(6)	−0.04
C6 (sp)	−0.018(7)	−0.057(7)	−0.05
N3	0.096(7)	0.095(6)	0.14
N4	0.097(7)	0.094(6)	0.16
N5	0.113(7)	0.096(6)	0.14
N6	0.120(8)	0.118(6)	0.15
total spin	0.789(22)	0.761(17)	1.00

[a] Negative values correspond to an excess of electrons with β spin. [b] A triple-zeta valence potential based on the structure determined from neutron diffraction was used for the NLDFT calculations. [c] N = number of parameters/number of observed flipping ratios. [d] Experimental estimated standard deviation.

To ascertain if the spin density on the other atoms of $[TCNE]^{\bullet -}$ has the $|2p_z\rangle$ shape, preliminary refinements in which the contributions from these atoms were reduced to spherical ones were made ($\chi^2 = 1.8$). Hence, the $|2p_z\rangle$ orbital model better fits the observed densities.

The model with only the sp^2 carbon atoms symmetrized provides the best fit[14] to the experimental data. The greatest spin contribution (66%) is from the sp^2-carbon atoms. The contribution from the nitrogen atoms is also significant (52%), while the total spin contribution from the sp-carbon atoms is small (−20%) and *negative*. The multipole expansion shows that the spin density is not centered over the nuclei at the sp^2-carbon atoms, but is bent away from the midpoint of the central C–C bond consistent with the results of the MaxEnt analysis shown in Figure 1.

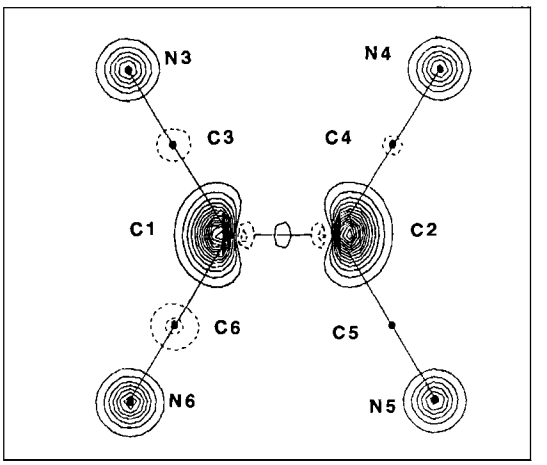


Fig. 2. Projection of the spin density reconstructed by model refinement of $[TCNE]^{\bullet -}$ onto the molecular plane.

The averaged experimental spin populations of the sp^2-carbon, sp-carbon, and nitrogen atoms are 33, −5, and 13%, respectively, of the total spin. The relative magnitudes of the spins per atom are in good agreement with previous estimates based on ESR spectroscopic data and molecular orbital models.[15] The signs and magnitudes of the spin populations are also consistent with the results of ab initio calculations.[16] Molecular orbital-based methods exaggerate the negative spin on the sp-carbon atoms and the spin populations on the nitrogen atoms, while calculations based on density functional theory (DFT) correctly predict the magnitudes of the spin populations. The calculated geometry at the self-consistent nonlocal DFT (NLDFT) level agrees well with the structure determined by neutron diffraction (Table 1). The central C–C distance is calculated to be 0.019 Å longer than the experimental value, but it is within two estimated standard deviations (esds). The C–CN distance is only 0.005 Å too long and the CN distance is 0.009 Å too long. The NC-C-CN angle is calculated to be smaller than the experimental value by 1.6°, and the calculated value for the C-C-N bond angle is slightly more linear than the average experimental value. The spin density on the sp^2-carbon atoms are bent away from the midpoint of this C–C bond. This is in agreement with the antibonding character of the SOMO and confirmed that the magnetic molecular orbital of the $[TCNE]^{\bullet -}$ radical is the π^* orbital.

Polarized neutron diffraction is presently the most powerful tool for determining the absolute spin density of a radical. In contrast to resonance techniques, it can be used to determine the shape of the spin density as well as the total spin populations. The results show that the excess α-spin on the $[TCNE]^{\bullet -}$ is not completely localized on the sp^2-carbon atoms, but is distributed across the radical since it has significant contributions from the nitrogen atoms. This is important since it demonstrates that both ionic $[TCNE]^{\bullet -}$ (as observed for $[Fe(C_5Me_5)_2][TCNE]$) and covalently bonded (as observed for [MnTPP][TCNE] and $[V(TCNE)_x]\cdot y(CH_2Cl_2)$) have the possibility for strong magnetic interactions with neighboring spin sites consistent with the bulk magnetic behavior observed for these materials. The combination of sophisticated experimental and theoretical techniques provide the basis for a better understanding of molecule-based magnetism.

Received: December 15, 1993 [Z6561IE]
German version: *Angew. Chem.* **1994**, *106*, 1454

[1] J. S. Miller, A. J. Epstein, *Angew. Chem.* **1994**, *106*, 399; *Angew. Chem. Int. Ed. Engl.* **1994**, *33*, 385, and references therein; J. S. Miller, A. J. Epstein, W. M. Reiff, *Chem. Rev.* **1988**, *88*, 201.

[2] J. M. Manriquez, G. T. Yee, R. S. McLean, A. J. Epstein, J. S. Miller, *Science* **1991**, *252*, 1415.

[3] J. S. Miller, J. C. Calabrese, R. S. McLean, A. J. Epstein, *Adv. Mater.* **1992** *4*, 498.

[4] B. Gillon, J. Schweizer, *Study of Chemical Bonding in Molecules: The interest of Polarized Neutron Diffraction*, (Ed.: J. Maruani) (*Molecules in Physics, Chemistry and Biology, Vol. II*, Kluwer, Dordrecht, **1989**, p. 111).

[5] a) X-ray analysis: A $0.40 \times 0.38 \times 0.45$ mm crystal of $[Bu_4N][TCNE]$ (M_r = 370.96) was grown from Et_2O/MeCN and belongs to the monoclinic space group $P2_1/n$ (no. 14); $a = 14.651(3)$, $b = 8.446(1)$, $c = 19.669(5)$ Å, $\beta = 106.21(1)^\circ$, $V = 2337.1$ Å^3, $Z = 4$, $\rho_{calcd} = 1.053$ g cm^{-3}, $\mu_{Mo} = 0.60$ cm^{-1} at $-70\,^\circ$C. Using an Enraf-Nonius CAD4 diffractometer, 4040 reflections were measured with graphite-monochromated $Mo_{K\alpha}$ radiation. With 244 variables, the structure was refined by using 1560 data for which $I > 3\sigma(I)$ to convergence of $R = 0.049$ and $R_w = 0.046$. b) Neutron diffraction (10 K): $a = 14.550(36)$, $b = 8.263(13)$, $c = 19.686(48)$ Å, $\beta = 106.14(15)^\circ$.

[6] Two series of polarized neutron measurements were performed on the DN2 diffractometer at the Siloe reactor (CEA, Grenoble). A $7.4 \times 3.6 \times 1.7$ mm crystal grown by slow diffusion of diethyl ether into an acetonitrile solution of the salt was mounted in a cryomagnet and cooled down to 1.8 K in an applied field of 4.65 T. In the first experiment, the crystal was mounted with the b axis parallel to the magnetic field. In the second experiment, the crystal was rotated to align the $[10\bar{1}]$ axis collinear to the magnetic field. With both orientations, 211 independent data were collected up to $\sin(\theta/\lambda) = 0.36$, with the incident wavelength $\lambda = 1.205$ Å for the neutrons. There is one significant restriction in the measurements. The construction of the lifting-counter and the split-coil cryomagnet permits access only to a "slice" in reciprocal space for each mounting of the sample. For example, in the first series of experiments only the $(h0l)$, $(h1l)$, and $(h2l)$ Bragg reflections could be measured. Thus, the resolution in the vertical direction is poor. Nevertheless, the data are sufficient for the reconstruction of a projection onto the ac plane which is essentially the $[TCNE]^{\cdot -}$ molecular plane. The problem is only partly solved by mounting the crystal in the second orientation since on projection along the $[10\bar{1}]$ axis two symmetrically equivalent $[TCNE]^{\cdot -}$ units overlap. Thus, the second series of experiments does not reveal much information of the spin density distribution perpendicular to the molecular plane.

[7] R. J. Papoular, B. Gillon, *Neutron Scattering Data Analysis* (Ed.: M. W. Johnson), *Inst. Phys. Conf. Ser.* **1990**, *107*, 101.

[8] R. J. Papoular, B. Gillon, *Europhys. Lett.* **1990** *13*, 429.

[9] R. J. Papoular, E. Ressouche, J. Schweizer, A. Zheludev, *Fundam. Theor. Phys.* **1993** *53*, 311.

[10] The MaxEnt technique strictly applies to positive densities, but the method can be modified to treat sign alternating densities by considering the α- and β-spin densities as being independent.

[11] Note that in this model the wavefunction is squared at each site and then their squares summed. This is formally incorrect as a linear combination of the atomic wavefunctions should be formed prior to squaring of the resulting wavefunction. As we allow for negative spin populations, this introduces a cross-term and significantly more complex equations. Considering the available data, the additional computational effort is not justified.

[12] N. K. Hansen, P. Coppins, *Acta Crystallogr. Sect. A* **1978**, *34*, 909.

[13] P. J. Brown, A. Capiomont, B. Gillon, J. Schweizer, *J. Magn. Magn. Mater.* **1979**, *14*, 286.

[14] Other calculations (i.e., enforced D_{2h} symmetry on the spin density distribution, but not on the structure and a multipolar expansion for $[TCNE]^{\cdot -}$ in D_{2h} symmetry) to determine if the fit could be improved were undertaken. The results are not substantially changed from those of the model given with only the sp^2-carbon atoms being symmetrized.

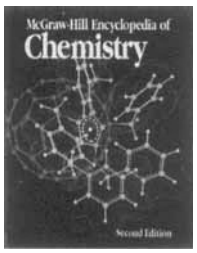
[15] M. L. Kaplan, R. C. Haddon, F. B. Bramwell, F. Wudl, J. H. Marshall, D. O. Cowan, S. Gronowitz, *J. Phys. Chem.* **1980**, *84*, 427. D. A. Dixon, J. S. Miller, *J. Am. Chem. Soc.* **1987**, *109*, 3656.

[16] A. Zheludev, A. Grand, E. Ressouche, J. Schweizer, B. G. Morin, A. J. Epstein, D. A. Dixon, J. S. Miller, *J. Am. Chem. Soc.* **1994**, in press.

To Help You Help Yourself

McGraw-Hill Encyclopedia of Chemistry. 2nd edition. Edited by *S. P. Parker*. McGraw-Hill, New York, 1993. 1236 pp., hardcover $ 95.50.—ISBN 0-07-045455-8

This alternate selection of the Library of Science is one of five new editions of McGraw-Hill technical encyclopedias, the others dealing with astronomy, engineering, environmental science and engineering, and physics. Much of the material has been taken from the 20-volume 7th edition of the *McGraw-Hill Encyclopedia of Science and Technology* (1992) (see G. B. Kauffman, *Angew. Chem.* **1993**, *105*, 1154; *Angew. Chem. Int. Ed. Engl.* **1993**, *32*, 1217), with additional articles prepared especially for the volume. Written to be accessible to nonspecialists, the hundreds of signed articles, replete with bibliographies for further reading, are the contributions of 407 distinguished authorities from around the world, including several Nobel laureates. In addition to comprehensive coverage of analytical, inorganic, organic, and physical chemistry, the book also deals with the related disciplines of biochemistry, physics, molecular biology, and materials science.



Each article begins with a definition and presents a concise but complete explanation of the topic. The material has been extensively revised, cross-referenced, and updated to reflect the latest developments such as fullerenes, light-scattering photometry, reactive intermediates, and ultrafast molecular processes (although cold fusion and superconductivity are neglected). The book is well-designed with an outstanding visual layout (wide margins, easy-to-read type, and bold headings), and the text is amplified and supplemented with hundreds of structural formulas, equations, graphs, tables, drawings, and photographs to clarify the presentation. A 36-page index (4 columns per page) facilitates the retrieval of information. Although most articles are authoritative and accurate, the entry on cobalt incorrectly states that the ammines of cobalt were discovered in 1894 by Werner, and the entry on coordination complexes does not employ the 1990 IUPAC inorganic nomenclature for formulas and names.

This attractive, moderately priced, user-friendly encyclopedia will be invaluable to chemists, chemical educators, students, librarians, science writers, and anyone seeking basic, clear, up-to-date information about the central science.

George B. Kauffman
California State University
Fresno, CA (USA)

This section contains book reviews and a list of new books received by the editor. Book reviews are written by invitation from the editor. Suggestions for books to be reviewed and for book reviewers are welcome. Publishers should send brochures or (better) books to Dr. Ralf Baumann, Redaktion Angewandte Chemie, Postfach 101161, D-69451 Weinheim, Federal Republic of Germany. The editor reserves the right of selecting which books will be reviewed. Uninvited books not chosen for review will not be returned.

Two Books on Capillary Electrophoresis

Capillary Electrophoresis of Small Molecules and Ions. By *P. Jandik* and *G. Bonn*. VCH Verlagsgesellschaft, Weinheim/VCH Publishers, New York, 1993. 298 pp., hardcover DM 108.00/$ 65.00.—ISBN 3-527-89533-7/1-56081-533-7

As the title indicates, this book concentrates on one particular area of application of capillary electrophoresis (CE), namely the analysis of small molecules and ions. The more familiar fields of application of CE, such as the analysis of biomolecules (DNA, proteins, polysaccharides, etc.), are treated only marginally. Of the nearly 300 pages, 210 are devoted to the principles of CE and the instrumental aspects and 70 to applications.

The book begins with a short introduction outlining the history of the development of the method. The second chapter, "Fundamentals of Capillary Electrophoresis" (about 60 pp.), explains the most important variables in the CE method and gives a simple and easily understandable account of the theory illustrated by many clear diagrams. The separation techniques are only outlined briefly here, so that one gets no more than an indication of the complexity. Micellar electrokinetic chromatography is only described very briefly, even though it is the most commonly used method for the separation of small molecules and ions. There is a very lucid account of band broadening effects caused by Joule heating and electrodispersion. In Chapter 3, "Instrumentation for Capillary Electrophoresis", the authors give a comprehensive description of the various components of a CE system. They also devote about a hundred pages to commonly encountered problem areas in CE, such as detection methods, the improvement of sensitivity, sample injection techniques, and reproducibility. The section on the handling of capillary columns is very useful, especially for beginners in CE. Coupling techniques are also described, and altogether this is a very useful review of modern CE technology. The last two chapters of this excellent book describe many practical examples under the titles "Selected Applications of Counterelectroosmotic Capillary Electrophoresis" and "Application Examples of Coelectroosmotic Capillary Electrophoresis". The concepts "coelectroosmotic" and "counterelectroosmotic" introduced here are a useful aid to understanding the migration processes occurring in the capillary column. These chapters explain a large variety of separation procedures, and describe not only direct detection methods but also the indirect UV detection method and methods based on the derivatization of samples.

One of the authors previously worked for a manufacturer of CE instruments, and has consequently been able to include many specialized illustrations in this book, which are a particular feature of the detailed description of indirect UV detection.

Despite some minor weaknesses this book can be strongly recommended for newcomers to CE. Readers experienced in

 © VCH Verlagsgesellschaft mbH, D-69451 Weinheim, 1994 0570-0833/94/1313-1401 $ 10.00+.25/0

the field should also find something of interest here, since this excellent survey of CE techniques reflects the current state of the art.

Practical Capillary Electrophoresis. By *R. Weinberger*. Academic Press, New York, 1993. 312 pp., hardcover $ 53.00.—ISBN 0-12-742355-9

This book of about 300 pages provides a more broadly based survey of the commonly used separation mechanisms in capillary electrophoresis than does the one reviewed above. It covers the instrumental and theoretical aspects, and also applications, which are in this case integrated into the descriptions of the various separation techniques. Rather than going into great detail, the author has set out to give the reader a general overview of the range of potential applications of CE. The basic chemistry underlying the separation procedures is described, and possible sources of error are discussed.

The twelve chapters cover the various separation techniques, such as capillary zone electrophoresis (CZE), capillary gel electrophoresis (CGE), capillary isoelectric focussing (CIEF), micellar electrokinetic chromatography (MEKC), and capillary electrochromatography (CEC), as well as sample injection, detection, and basic principles. One chapter summarizes all the separation techniques discussed, so as to help readers who wish to develop their own particular methods. Further help is available from the many clearly set out tables, which enable one to quickly review the possibilities. References to the original publications are provided so that one can go into specific points in greater depth if necessary. Another chapter includes a discussion of likely future developments in CE. Because of its textbook style this volume can be thoroughly recommended for beginners in the field. Those already experienced in the use of CE are unlikely to find much in the book that is new to them.

Thomas Schmitt, Heinz Engelhardt
Fachrichtung Angewandte Physikalische Chemie
der Universität des Saarlandes
Saarbrücken (FRG)

Analysis with Supercritical Fluids: Extraction and Chromatography. Edited by *B. Wenclawiak*. Springer, Berlin, 1992. XIV, 213 pp., hardcover DM 148.00—ISBN 3-540-554203/0-387-55420-3

There is currently a great interest in the use of supercritical fluids in chromatography, either as a mobile phase (supercritical fluid chromatography, SFC) or as a solvent (supercritical fluid extraction, SFE). Ten years ago, with the introduction of "capillary" (more precisely, open-tubular) column SFC, it was commonly predicted that it would replace many of the applications of gas chromatography (GC) and high-performance liquid chromatography (HPLC). Although this did not occur, SFC has now established itself as a viable variant of chromatography. On the other hand, SFE, the younger brother of SFC in analytical chemistry (though long familiar as an industrial process) rapidly established itself as a very important sample preparation technique.

In the case of a rapidly growing field, it is very important to have at intervals good, up-to-date compilations from which one can learn about the newest developments and their relationship to the fundamentals of the technique. Obviously, this was the purpose of this multi-authored book.

The book consists of eleven chapters. After a brief (8 pp.) "Introduction for Novices" on SFC and SFE by the editor, G. M. Schneider discusses in detail the physicochemical principles of supercritical fluid separation processes (23 pp.). This is followed by a chapter on the basic principles of analytical SFE by J. W. King and J. E. France (29 pp.). In the following chapters S. B. Hawthorne deals with the combination of SFE and GC (13 pp.), E. Klesper and F. P. Schmitz with gradients in SFC (26 pp.), and T. Greibrokk with sample introduction techniques in SFC (16 pp.). (I do not like the restriction to "injection techniques" implied by the title of the latter chapter). The next chapter by C. F. Poole and his associates discusses in detail the stationary phases used in packed-column SFC (18 pp.). This is followed by a chapter by M. Schleimer and V. Schurig on enantiomer separation by capillary SFC (17 pp.). The next two chapters deal with the combinations of SFC with mass spectrometry (J. D. Pinkston, 27 pp.) and FT-IR (L. T. Taylor and E. M. Calvey, 12 pp.). In the last chapter M. L. Lee and his associates discuss supersonic jet spectroscopy (SJS) with supercritical fluids (13 pp.). At the end of the book some basic references on SFE/SFC are given, followed by a three-page appendix listing "recommended literature" from 1992.

In my opinion the book has two major shortcomings. The first is that three chapters which should have been included are missing. (a) A chapter should have described the system of a supercritical fluid chromatograph, including pumps and detectors (FID and UV), the selection of analytical conditions including the mobile phase, and the instrumentation of SFE. (b) The book has a chapter devoted to the packed columns used in SFC. However, it is almost inconceivable that it does not also have a chapter on the *open-tubular* columns used in SFC. After all, as correctly pointed out by the editor in the preface, modern SFC could not exist without them. This can actually be seen from the illustrations in the book: practically every chromatogram (except those included in the packed-column chapter) was obtained on open-tubular columns (which are not discussed). How could the most important component of a modern SFC system be neglected? (c) The book deals with SFC and SFE, and includes discussions on the combination of a number of techniques ("hyphenated systems") such as SFE-GC, SFC-MS, SFC-FT/IR or SFC-SJS. However, the most obvious combination is missing, namely the coupling of SFE with SFC.

The second shortcoming concerns the up-to-dateness of the discussions. The editor's preface is dated August 1992 and in it he mentions that the articles were "collected over a period of one year", which would mean that the individual contributions should cover the field up to the first part of 1991. However, this is not the case. The chapter by Schleimer and Schurig is an exception, but in the ten other chapters one can find no references from 1991–1992 and only a very few from 1990; out of a total of 453 references only 14 (3.1%!) are from 1990. By contrast, in the chapter by Schleimer and Schurig 51.1% of the references (24 out of 47) are from 1990–1992. This is not a coincidence: it clearly indicates that all the other chapters were written in the period 1989–1990. Evidently the editor was aware of this discrepancy and added a supplement containing "recommended literature" from 1992, consisting of 53 citations. This is laudable, but it still omits results reported in 1990 and 1991.

I have a few minor criticisms. For example, I disagree with the use of the term "capillary columns" instead of "open-tubular columns"; after all, the small-diameter packed columns may also be described as "capillaries". In the figure

 © VCH Verlagsgesellschaft mbH, D-69451 Weinheim, 1994 0570-0833/94/1313-1402 $ 10.00+.25/0

captions, columns should be identified more precisely, and one should avoid trade names: stationary phases *must* be specified by their chemical composition and not by the particular manufacturer's fantasy name. Also the format of the references given in the book does not conform to the *Chemical Abstracts* usage.

These shortcomings, especially the missing chapters, restrict the book's general usefulness, particularly because its general title implies that it provides a unified discussion of analytical SFC and SFE. However, within this limitation the book presents a wealth of useful information. The chapters are well written and represent good summaries of the topics treated. Thus, everyone who is interested in SFC and SFE will find something valuable in it.

Leslie S. Ettre
Department of Chemical Engineering
Yale University, New Haven, CT (USA)

Chemical Vapor Deposition. Principles and Applications. Edited by *M. L. Hitchman* and *K. F. Jensen*. Academic Press, London, 1993. 677 pp., hardcover £ 75.00.—ISBN 0-12-349670-5

Chemical vapor deposition (CVD), as a method for preparing thin solid films, has undergone intensive development during the last twenty years, and is now of major importance in a wide variety of technological applications, for example in microelectronics, optoelectronics, energy technology, and the reduction of friction and wear. There has long been a need for a book treating the many different aspects of this method, which is of fundamental importance in surface coating technology. The book reviewed here fills this gap admirably, and has been written to meet the needs of readers from a variety of disciplines. The editors have brought together thirteen recognized experts in their individual fields to prepare ten chapters that deal with different aspects of this complex subject, and can be read independently of each other.

Chapter 1 outlines the historical development of the method and its main characteristics. The accompanying bibliography provides an introduction to the extensive literature on CVD, and is remarkably comprehensive. Chapter 2, "Fundamentals of Chemical Vapor Deposition", explains the interdependence between chemical kinetics, reaction mechanism, and the fluid dynamics of the reaction system in relation to the growth of the deposited film. Current ideas regarding the mathematical modeling of CVD processes are discussed, together with likely future developments. Chapter 3 contains a highly informative review of modern diagnostic methods for CVD processes, including techniques such as flow imaging, spatially resolved temperature measurements, and analysis of the composition of the gas phase. This is followed in Chapter 4 by a very useful and comprehensive discussion of low-pressure CVD, illustrated by the outstanding example of polycrystalline silicon. Potential applications to other systems such as dielectrics and to metals such as tungsten, aluminum, and copper for VLSI (very large scale integration) metal deposition are also discussed. Chapter 5 is concerned with silicon epitaxy, describing not only conventional methods but also new trends, for example the development of new semiconductor components such as Si:Ge heterobipolar transistors with a band-gap chosen to suit the application. Chapter 6 is the longest in the book, and addresses the problems of the gas phase epitaxy of III/V materials prepared from organometallic molecules. The treatment is a concise but updated sequel to recent monographs on this topic (M. Razeghi, *The MOCVD Challenge*, Hilger, London, **1989**; G. B. Stringfellow, *Organometallic Vapor-Phase Epitaxy*, Academic Press, London, **1989**). The next two chapters are concerned with variants of the CVD method that are not (purely) thermal in nature, plasma-CVD and photo-CVD. The aspects covered, each in an appropriate degree of detail, are the physico-chemical fundamentals, experimental techniques, reactor design, and modeling, with up-to-date examples of particular applications (dielectrics, metals, semiconductors, diamond) which provide good illustrations of the advantages of the methods (e.g., low process temperatures, selective deposition). Whereas most of the book is concerned with the physico-chemical processes involved in film deposition, Chapter 9 gives an interesting insight into electronic and optical characterization methods that are directly related to the electrical properties of electronic devices produced by CVD (e.g., optical reflection and transmission measurements, vibrational spectroscopy, electron spin resonance spectroscopy, determination of current–voltage characteristics, photoconductivity measurements, and capacitance spectroscopy). These methods are especially applicable to amorphous α-Si:H and α-Si_xN_{1-x} films prepared by plasma-CVD. The main emphasis here is on the problems of characterizing defect structures. To conclude the book, Chapter 10 deals with applications of CVD to the reduction of friction and wear, and with the special structural problems posed by thick CVD films, such as roughness and adhesion.

Starting from well-established CVD processes and applications, the book gives a very good account of the current state of knowledge, and also discusses the most recent development trends. The many literature references, extending up to about 1991, are arranged according to the individual chapters, thus affording a very good basis for further reading on special topics. The subject index too is excellent. The structure of the book results in a certain amount of overlapping on several of the topics. For example, ideas concerning the modeling of CVD processes are perhaps repeated more often than necessary. Altogether, however, the book is carefully written and nicely produced. It can be recommended not only for everyone working in the field of chemical vapor deposition, but also unreservedly for interested readers from other related disciplines and newcomers to the subject.

Roland A. Fischer
Anorganisch-chemisches Institut
der Technischen Universität München
Garching (FRG)

Solid State Chemistry. Synthesis, Structure, and Properties of Selected Oxides and Sulfides. By *A. Wold* and *K. Dwight*. Chapman and Hall, New York, 1993. 245 pp., hardcover $ 19.95.—ISBN 0-412-03621-5

How is it possible to compress the subject matter of a textbook designed for a one-semester course on solid state chemistry into less than 250 pages, even though these are closely printed? That is the feat that has been attempted by the authors of this book. It consists of a very superficial general part covering the structure, characterization, and properties of solids, followed by a highly subjective selection of topics which is strongly biased towards the special research interests of the two authors. In the course of this, some important aspects of the mental toolkit needed for solid state chemistry are abbreviated almost beyond recognition (e.g., spectroscopic methods are given one page, X-ray diffraction three pages), or are omitted completely (e.g., the sphere packing principle, lattice energy, defect chemistry). As is already indicated by the book's subtitle, the second part is concerned with a special class of solid compounds, namely some selected transition metal oxides and sul-

 © VCH Verlagsgesellschaft mbH, D-69451 Weinheim, 1994 0570-0833/94/1313-1403 $ 10.00+.25/0

fides. The authors justify this very personal choice of subject matter close to their own research interests by claiming that only in this way is it possible to include experimental results that are highly reproducible. The examples discussed in the book cannot represent more than a very tiny segment of the large and fascinating subject of solid state chemistry. In principle the inclusion of a chapter on preparative methods before the specialized part of the book is a good feature, but even here some important aspects are cut down to an unacceptable extent (flux methods are given seven lines, chemical transport one page, and high-pressure syntheses half a page). Without any introduction to the structural aspects or their geometrical basis, the following chapter goes straight into a description of the monoxides of transition metals. The first structural diagram in the book shows the crystal structure of CuO. Following the trend set by the general part of the book, where a lengthy chapter is devoted to the electronic properties of semiconductors, the book places particular emphasis throughout on transition metal oxide semiconductors. Even here, however, much space is wasted by reproducing numerous conductivity curves for the compounds concerned, sometimes filling the whole page and conveying little information. There is, of course, a mention at the end of the oxides chapter of the modern ceramic cuprate superconductors. The final chapter is devoted to transition metal sulfides. As in the oxides chapter, there are many large, and not particularly well drawn, crystal structure diagrams showing the basic structural types. The electronic properties of the compounds under discussion are explained by means of energy band schemes, usually greatly simplified. As in other textbooks on solid state chemistry, there are exercise problems at the end of each chapter (with answers at the end of the book), and also lists of original publications, some of which are quite extensive. Here, instead of listing, for example, over 150 references to original papers on ternary and higher transition metal oxides, it would have been much more useful to give a limited selection of relevant review articles and textbooks.

To summarize, one cannot really recommend this book to a large readership as an accompaniment to lecture courses. The main criticisms are that the choice of topics is very subjective and unrepresentative, that important concepts and facts are sometimes treated very superficially, and that the diagrams and the text layout are rather unattractive. The book will not succeed in awakening an enthusiasm for the fascinating subject of solid state chemistry in readers approaching it for the first time (including students).

Wolfgang Schnick
Laboratorium für Anorganische Chemie
der Universität Bayreuth (FRG)

Sulphones in Organic Synthesis. (Tetrahedron Organic Chemistry Series, Vol. 10.) By *N. S. Simpkins*. Pergamon, Oxford, 1993. 381 pp., paperback £ 30.00, hardcover £ 55.00.—ISBN 0-08-040284-4 (paperback), 0-08-040283-6 (hardcover)

The use of sulfones in organic synthesis has become much more important during the last twenty years. Their synthetic potential now rivals that of the carbonyl group in versatility. This monograph by N. S. Simpkins focuses attention on the synthetic aspects of SO_2 compounds, which have the important advantage of being easily obtainable. The book consists of nine chapters, and the literature coverage extends in general up to the end of 1990, including also some important original publications up to the end of 1991. A brief introduction to the chemistry of sulfones (4 pp.) is followed by a chapter of 94 pages on the preparation of sulfones (e.g., alkylaryl, dialkyl, vinyl and other unsaturated and functionalized sulfones), each class being treated in accordance with its relative importance. The next chapter (82 pp.) deals comprehensively with sulfonyl carbanions, describing their formation, structures, stereochemistry, and wide variety of reactions. This is followed by chapters on addition reactions of unsaturated sulfones (25 pp.), rearrangements of sulfones (19 pp.), the cycloaddition chemistry of unsaturated sulfones (26 pp.), and the formation of CC double bonds by sulfone elimination (35 pp.). The book ends with chapters on the chemistry of cyclic sulfones (43 pp.) and desulfonation reactions (38 pp.).

The author's method of classifying the now very broad subject of sulfones and their chemistry according to compound type and reaction type has turned out successfully. He has included not only well-established routine syntheses using sulfones but also others that are less well known and have only recently been developed; all of these are described in detail. In the discussion of the palladium-catalyzed synthesis of allylsulfones (Ch. 2) the author has omitted to mention the work of Y. Tamaru et al. (*J. Chem. Soc. Chem. Commun.* **1978**, 367) and of U. M. Dzemilev et al. (*Zh. Org. Khim.* **1978**, *14*, 2223; see also *J. Organomet. Chem.* **1993**, *455*, 1–27). In his introduction the author explains that the book's main purpose is to emphasize and illustrate the growing importance of sulfones in organic synthesis; this aim has certainly been achieved. In particular the many clearly set out reaction schemes make it easy for the reader to understand the reactions described and the related factual information.

The monograph gives a good account of the current state of knowledge regarding sulfones in organic synthesis, and forms an important addition to the relevant review articles in "Houben–Weyl" and "Patai". It is essential to all departmental libraries involved in any way with organic synthesis.

Eberhard Wenschuh
Fachbereich Chemie
der Humboldt-Universität
Berlin (FRG)

 © VCH Verlagsgesellschaft mbH, D-69451 Weinheim, 1994 0570-0833/94/1313-1404 $ 10.00+.25/0

Peptidyl-Prolyl *cis/trans* Isomerases and Their Effectors

Gunter Fischer*

Dedicated to Professor Alfred Schellenberger on the occasion of his 65th birthday

Changes in the conformation of the units within the peptide chain are the elementary processes in the folding of a protein into its native three-dimensional structure. Even a few years ago protein folding in vivo was considered to be an autonomous process not requiring the help of enzymes or auxiliary substances. Recently an increasing number of proteins that assist in the folding process have been found; these include enzymes that catalyze conformational interconversions. The *cis/trans* isomerization of the peptide bond N-terminal to a proline residue is catalyzed by peptidyl-prolyl *cis/trans* isomerases (PPIases). Two families of these ubiquitous and phylogenetically highly conserved enzymes are known, the cyclophilins and FK506-binding proteins. Their catalytic activity is extremely high —the rate constants for the bimolecular reactions they catalyze approach the diffusion-controlled limit for enzyme–substrate reactions. These enzymes increase the rate of isomerization in oligopeptides as well as in intermediates in protein folding. It is not yet known which structural units in the cell serve as substrates and exactly which reactions are catalyzed. However, these isomerases have been shown to interact with the heat shock proteins of the nonactivated steroid receptors and with the gag polyprotein of the AIDS HIV-1 virus. The immunosuppressive agents cyclosporin A and FK506 are highly effective inhibitors for PPIases. Surprisingly these compounds affect the signal cascade of T cells but not through enzyme inhibition; the inhibitor–enzyme complexes themselves are the active agents. These complexes exhibit properties not displayed by the individual components and thus are able to affect other cellular components. The current model of the suppression of the antigen- and mitogen-stimulated clonal expansion of T cells is presented here.

1. Introduction

There are a number of reactions in the cell for which increasing the rate or controlling the selectivity seems unnecessary or even wasteful, since they are rapid and seemingly specific without enzymatic catalysis. The production of an enzyme would be wasteful. Such autonomous processes within the cell generally include those in which biological substances undergo conformational interconversions. Biochemists are especially interested in conformational interconversions in proteins, since proteins are the central regulatory elements in living systems.

This view was confirmed by the results of many denaturing/renaturing experiments on proteins. It was shown that starting from denatured protein, in which residual elements of the original secondary structure of the polypeptide chain are not detectable, small single-domain globular proteins often refold rapidly to yield the conformation of the native protein under renaturing conditions. No external agents have to be added to enhance or speed up the process. These results indicate that there is not much evolutionary pressure for organisms to develop enzymes capable of recognizing proteins as substrates and speeding up the rate of conformational interconversions within proteins.

One specific intracellularly relevant conformational interconversion, namely the *cis/trans* isomerization of the N-terminal amide bond of the amino acid proline, requires a relatively long time. This apparent paradox was explained in 1984 when we discovered and isolated a peptidyl-prolyl *cis/trans* isomerase (PPIase) which was the first enzyme found to catalyze a conformational interconversion at a formally single bond.[1] New enzymes naturally become targets in screening studies of the culture filtrates of microorganisms for effectors and are particulary interesting in drug development.[2] However, in the case of the PPIases things developed a little differently. Long after the clinical use of the immunosuppressive cyclosporin A (CsA), a cyclic undecapeptide, and following the identification of a cytosolic receptor protein for CsA by Handschumacher et al.,[3] N. Takahashi et al.[4] and we[5] were able to demonstrate the PPIase activity of this receptor and the inhibitory effect of CsA on enzyme catalysis. Based on these results, studies on the immunosuppressive peptidomacrolide FK506 were carried out; isolation of the receptor and enzymological experiments were conducted simultaneously, and a PPIase, which proved to be insensitive to CsA, was detected and shown to be inhibited by FK506.[6]

[*] Prof. Dr. G. Fischer
Max-Planck-Gesellschaft, Arbeitsgruppe Enzymologie der Peptidbindung
Weinbergweg 16a, D-06120 Halle (FRG)
Telefax: Int. code + (345)647126

 © VCH Verlagsgesellschaft mbH, D-69451 Weinheim, 1994 0570-0833/94/1414-1415 $ 10.00+.25/0

Totally unexpected was the finding from American research groups that the suppressive effect of these drugs on the clonal expansion of T cells is not simply due to the direct inhibition of PPIase activity. According to current knowledge, the protein presents ligands with changed conformation in the drug–protein complex to another cellular component, the Ca^{2+}/calmodulin-dependent protein phosphatase, calcineurin, whose dephosphorylating activity is in turn inhibited (see Section 9).[7–9]

Therefore in this review we discuss not only the properties and mechanism of reactions catalyzed by PPIases, but also the biological effects of the complexes of these enzymes with immunosuppressives.

2. Proline—A Molecular Switch

In the restructuring of polypeptide chains, slow partial reactions taking up to hours are often found when proline forms part of the chain.[10, 59] Such folding processes are not only observed in the test tube in artificial denaturation/renaturation reactions, but are seen in vivo in ribosomal protein synthesis and maturation, in the transport of polypeptides through membranes, in the disposal of malfunctioning proteins, in ligand binding, and in the oligomerization of proteins.[11] In many processes the observed ratio of the *cis* and *trans* isomers transiently does not correspond to the thermodynamic equilibrium but reflects the immediate surroundings of the polypeptide.

To illustrate the folding problem a section of a polypeptide chain is shown in Figure 1. Rotation about the formally single bonds in the peptide backbone and in the side chains is responsible for the flexibility of the chain. These rotations determine most of the dynamic processes in proteins, including folding. As uncoupled elementary processes they are generally fast (relaxation times $\ll 1$ s), with the exception of changes in ω; however, owing to interactions and neighboring group effects the observed time scales in polypeptides range from 10^{-11} to 10^{3} s. Especially slow conformational changes arise from the well-known delocalization of electrons in the amide bond and are even more pronounced if additional steric constraints are imposed by the proline ring (Fig. 2.). In contrast to C(O)NH bonds, the two lowest energy arrangements of the prolyl peptide bond, *cis* ($\omega \approx 0^{\circ}$) and *trans* ($\omega \approx 180^{\circ}$), are of comparable thermodynamic stability. In principle polypeptides with n proline residues can form 2^n isomers as partners for recognition processes and as reaction partners at the molecular level in the cell. Proteins have the strong tendency to form three-dimensional structures. Since the *cis* and *trans* isomers in these structures are no longer equal in energy, the less preferred isomer is not likely to exist in the folded chain.

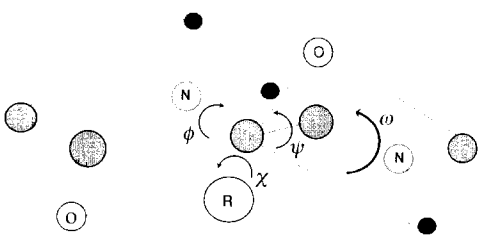


Fig. 1. Labeling of the torsion angles in a polypeptide chain.

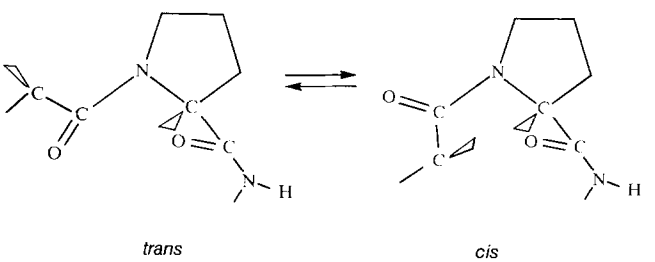


Fig. 2. The *cis/trans* isomerization of a peptide bond N-terminal to proline.

Obviously *cis/trans* isomerization leads to periodic changes in the positions of neighboring chain segments, because the propagation direction of the polypeptide backbone is different in each isomer. In this respect *cis/trans* isomerization at the peptide bond N-terminal to proline resembles a molecular switch with the following characteristics:

1. There are two switch positions; other positions are unstable.
2. The energy needed to operate the switch is high on the energy scale for biological recognition processes.
3. Operation of the switch leads to an amplification of an effect at the place where the signal arrives. In the case of the proline switch this amplification manifests itself chiefly in the form of a mechanical movement, which may be the movement of a segment of the protein backbone.



Gunter Fischer, born in 1943 in Altenburg, Thuringia (FRG), was trained as a chemical technician (1959–1962) before he completed his chemistry studies at the University of Halle in 1967. In 1971 he completed his first dissertation on research with A. Schellenberger on the reactivity of α-keto acids; in 1978 he finished his second dissertation on the reactivity of amide groups. After some time at the Forschungszentrum Biotechnologie/Berlin, he accepted positions in 1988 as "Dozent" of biochemistry at the University of Halle and in 1990 as a guest professor at the University of Würzburg. Since 1992 he has been the director of the research group "Enzymology of the Peptide Bond" of the Max Planck Society in Halle, and in 1993 he accepted a chair for molecular biochemistry at the University of Halle. His research focuses on the structure and activity of protein folding enzymes and the effect of imino acids on peptide conformation.

4. Isomerization catalysts such as the PPIases act as variable components for reducing the switch resistance, and in the presence of many switches they assure extra selectivity. The switching resistance (the rotation barriers) is controlled by varying the enzyme concentration, and the selection of switching elements by means of enzyme specificity.

An example of a photoactivated switching process is the biologically very important *cis/trans* isomerization of the C=C bonds in retinal and retinal proteins.[12]

3. Peptidyl-Prolyl *cis/trans* Isomerases and Other Immunophilic Proteins

When present even in catalytic amounts PPIases are able to increase the rate of isomerization of the prolyl-peptide bond (see Fig. 2.) in a suitable peptide substrate. In examinations of any mammalian cell material the activities of a number of PPIases, which differ in their molecular weight distribution and isoelectric behavior, are apparent (Figs. 3 and 4.). This supports the idea that a whole range of such enzymes could exist.

In enzyme nomenclature PPIases are classified under the *cis/trans* isomerases (EC number 5.2.1.8). In the literature they are often referred to as "rotamases"[13] or "rotomases"[14] based on the term "rotamerization" for the process of conformational change. At the present time two families of proteins with PPIase activity are known: the cyclophilins (Cyp) and the FK506-binding proteins (FKBP) (synonyms FK506-binding PPIases, macrophilins). Which specific enzymatic function characterizes the two groups of enzymes?

The enzyme-catalyzed isomerization at proline is reversible, and thus the *cis* and *trans* conformers must coexist. If irreversible reactions are coupled to the *cis/trans* equilibrium, then the catalyzed partial reactions *cis* → *trans* and *trans* → *cis* can be analyzed separately. For all three cases solid experimental data supporting in vitro PPIase catalysis are available. But which of these is primarily catalyzed by these enzymes in vivo can only be

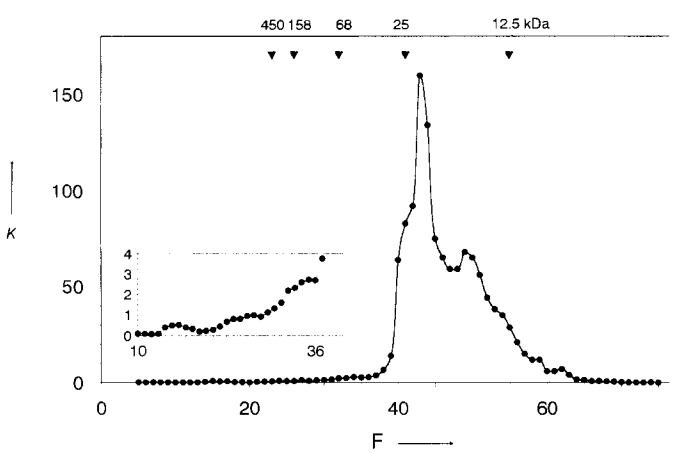


Fig. 3. Separation of the PPIase activity from pig kidney cytosol according to molecular weight [kDa]. The activity was determined with Suc-Ala-Phe-Pro-Phe-4-nitroanilide by measuring the catalytic factor K in each fraction F: $K = (k_c - k_u)/k_u$, where k_u is the first-order rate constant of the uncatalyzed isomerization and k_c is the first-order rate constant of the catalyzed isomerization. (FPLC separation on a Bio-GPC-Diol column (330 × 10 mm)). The insert shows the plot for fractions 10 to 36 on a larger scale.

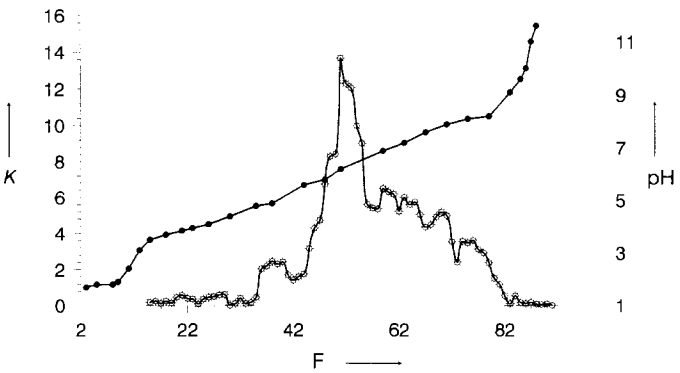


Fig. 4. Separation of PPIase activity (☼) from pig kidney cytosol according to the isoelectric behavior of the enzymes in a pH gradient (●); the activity determination as described for Fig. 3. Separation on a continuous free-flow electrophoresis system (Octopus, Dr. Weber Co., Ismaning (FRG)) at 5 °C in 0.2% Servalyt (pH 3–10), 0.1% dextran (M = 1 kDa).

the subject of speculation at present. If human Cyp18cy (for details on the nomenclature of the PPIase families see ref. [15]), is offered Suc-Ala-Ala-Pro-Phe-4-nitroanilide as substrate and the PPIase concentration is kept very low during the *cis* → *trans* isomerization, then normal Michaelis–Menten kinetics are observed for the conformational isomerism, without curves with sigmoid character at low substrate concentrations $[S]_0$ or other effects in plots of v versus $[S]_0$ (v corresponds to the reaction rate). The increase in reaction rate for the *cis* → *trans* isomerization in oligopeptide substrates (when $[S]_0 \ll K_m$) is linearly dependent on the enzyme concentration.[11, 16, 17]

Of course under the standard reaction conditions for activity tests (enzyme concentration $[E]_0 \ll [S]_0$) PPIases do not change the *cis/trans* ratio of the substrate. However, the isomer distribution after the substrates[18, 19] (and inhibitors)[20, 21] are bound to PPIase does not correspond to that of the free ligands in the solid state or in solution. Sometimes either the *trans* isomer or the *cis* isomer binds better to the enzyme. When the substrate and PPIase are present in stoichiometric amounts or when there is an excess of PPIase, the isomer equilibrium of proline-containing polypeptides can be completely changed. This is important in studies of cellular processes involving PPIases since high intracellular enzyme levels have been found. For example, in the cytosol of human erythrocytes the concentration of cyclophilins is at least 4 μM[22] and thus can easily exceed the concentration of a potential intracellular substrate.

For catalytic activity PPIases must also be able to recognize a specific proline residue forming part of a linear polypeptide chain and bind to it. The ability to bind substrate can be increased through a combination of secondary interactions at specific subsites. Under these circumstances PPIases could act as binding proteins with a specific proline recognition function. Indeed, the eight-stranded, antiparallel β-barrel structure of human Cyp18cy resembles that of typical binding and transport proteins for small hydrophobic molecules such as bilin-binding protein, retinol-binding protein, and streptavidin, although the binding sites of these proteins for their ligands have different structures.[23, 24]

According to our current knowledge, PPIases are not able to substantially increase the rate of isomerization for open-chain *N*-alkylpeptide bonds in oligopeptides. This implies that in the

catalysis of protein folding it is the proline moiety that is important and not a special property of the peptide bond itself.[25]

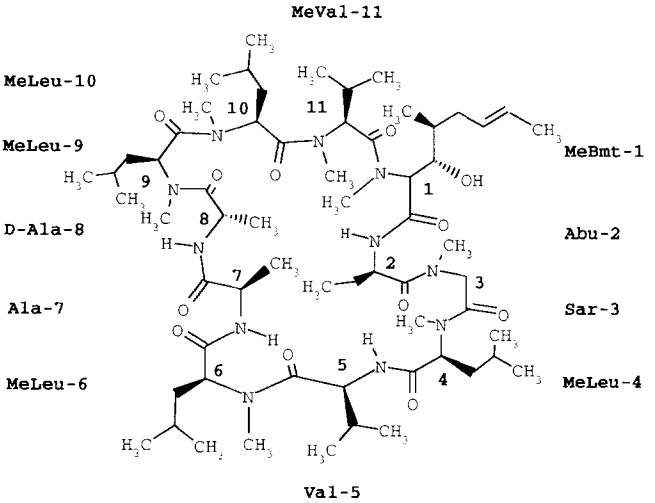
The amino acid sequences of cyclophilins and FKBPs have little in common,[26] not even in that part of the peptide chain probably important for enzyme activity; the structural homology of the putative active sites is also not very great.[27] The two groups of enzymes can be easily distinguished by their differing inhibition by cyclosporin A and peptide macrolides. Thus only CsA and its derivatives inhibit cyclophilins, while FKBPs are inactivated by specific peptide macrolides. Cross-inhibition has not been observed.

Within the two families the amino acid sequences are highly conserved throughout living systems. Within the isoforms of cyclophilins and FKBPs of a particular cell type a central region apparently important for enzyme activity is complemented by C-terminal and N-terminal extensions of differing lengths. Such sequence conservation in the course of evolution is indicative of a central role for the corresponding protein function within the cell.

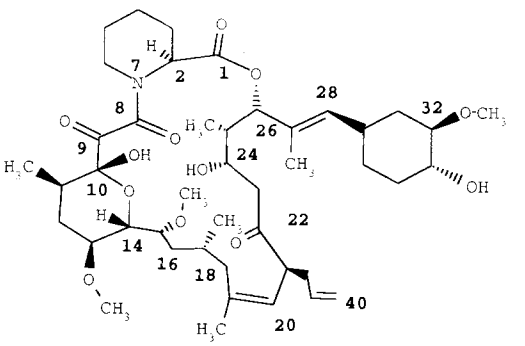
For a number of PPIase genes the position on the human genome is already known: human Cyp23sec is on chromosome 15,[28] Cyp150mem on chromosome 3,[29] FKBP12cy on chromosome 20, and FKBP13cy on chromosome 11.[30] In a human gene bank derived from leukocyte DNA, a single functional Cyp18cy gene and fifteen pseudogenes were found to be present.[31]

S. L. Schreiber et al. introduced the term "immunophilins"[32] for the families of PPIases in order to point out the role of PPIases as receptor proteins in the mammalian immune system. This term refers to the formation of drug–protein complexes with the immunosuppressive drugs cyclosporin A, rapamycin, and FK506 (Fig. 5.). Cyclosporin A, rapamycin, and FK506 (synonym: tacrolimus) are natural products derived from microorganisms, which have a specific effect on the immune system[33, 34] and also affect other systems and tissues.[35] In antigen-stimulated T lympocytes the immunosuppressive drugs block signal transduction in the Ca^{2+}-dependent pathways leading to clonal expansion of the cells. One of the main factors in the repression of the T-cell response after triggering of the receptor–CD3 complex by an antigen or mitogen is assumed to be the inhibition of gene expression of a number of important lymphokine genes. This could include the genes for a variety of interleukins (IL-2, IL-3, IL-4), factors such as GM-CSF (granulocyte macrophage colony stimulating factor), tumour necrosis factor α (TNFα), and γ interferon, as well as the oncogene c-myc.[36] Regulation seems to take place at the level of translocation of components of the hitherto not very well biochemically characterized transcription factors (AP-3, NF-AT, NF-κB) from the cytosol to the nucleus.[37]

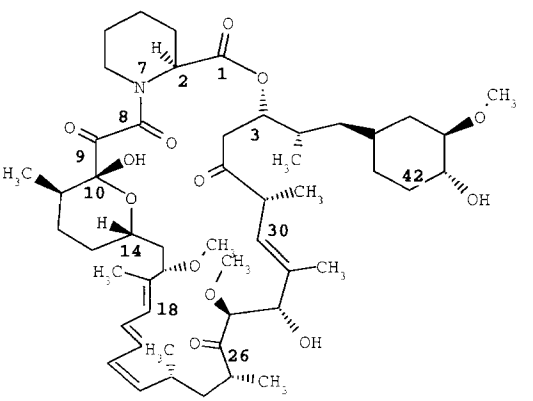
There are many more immunophilic proteins than just those with proven PPIase activity.[38, 39] Amongst others, the immunosuppressive CsA derivatives [D-Lys(ε-dansyl)^8]-CsA and [D-Dab(Boc)^8]-CsA with dissociation constants $K_d = 60 \pm 33$ nM and 570 ± 380 nM, respectively, bind as strongly to G-actin from Jurkat cells as to the PPIases from the same cell homogenate.[40] In addition, SSA1, a cytosolic yeast protein and analogue of the heat shock protein hsp70 which is structurally related to actin, can bind [D-Lys(ε-dansyl)^8]-CsA with a dissociation constant of



Cyclosporin A



FK506



Rapamycin

Fig. 5. Immunosuppressive inhibitors of the peptidyl-prolyl *cis*/*trans* isomerases. In cyclosporin A MeBMt is (4*R*)-4[(*E*)-2-butenyl]-4-*N*-dimethyl-L-threonine and Abu is L-α-butyric acid. Substitution of FK506 at C21 (ethyl group instead of allyl) yields the immunosuppressive ascomycin.

53 nM.[40] In situ affinity photolabeling of fibroblasts, hepatocytes, and lymphoid cell lines with [^{3}H]*N*-(diazotrifluoroethyl)benzyl-D-Lys^8-cyclosporin leads to a variety of specifically labeled proteins which can be detected and separated using SDS (sodium dodecylsulfate) polyacrylamide gel electrophoresis. The molecular weight of these proteins is in the range of about 20–200 kDa, and they can be assigned only in part to the known PPIases.[39, 41] Among the identifiable material is a membrane

protein of the Na^+/D-glucose cotransporter of the kidney with a molecular weight of 75 kDa.[42]

In fact the specific binding of interleukin-8 (IL-8) to CsA (K_d = 850 nM) is in some sense immunochemically similar to that with PPIases, since there is cross reactivity with an antiserum against human recombinant IL-8 with a cytosolic PPIase. However, interleukin-8 shows no PPIase activity in a standard test.[43] Interestingly, a cytosolic, 50 kDa immunophilic protein from Jurkat and spleen cells which has not been well characterized has a high affinity for both CsA (K_d = 39 nM) and FK506 (K_d = 2 mM) without showing any PPIase activity. Both rapamycin and CsA can be displaced from the binding site by [^{3}H]-dihydro-FK506.[44]

Investigation at the molecular level is still needed to understand the binding of cyclosporin derivatives to the membrane-bound P glycoprotein (170 kDa),[45] which is responsible for a special type of multidrug resistance in malignant cells. Like these cyclosporins, FK506 and the PPIase inhibitor rapamycin also prevent the P glycoprotein from pumping cytotoxic substances out of the cell by binding to it with high affinity.[46]

Thus immunophilic proteins are a much larger group than just the PPIases. On the other hand, amongst the PPIases are proteins with relatively little affinity for cyclosporin A (Table 1) and FK506 (Table 2) and which therefore cannot be classified as immunophilic.

Table 1. Properties of some cyclophilins. K_d = dissociation constant, K_i = inhibition constant.

Cyclophilin	N-Terminus [a]	PPIase activ. [b]	Inhibition by CsA [nM]	Ref.
human18cy	^{1}M(rec.); ^{2}V(nat.)	22	1.6 (K_i)	[97, 106, 107]
(porcine) bovine18cy	^{2}VNPTV; N-Block	13.4	2.6 (K_i); 20 (IC_{50})	[5, 51, 108]
rat18cy		+	sensitive	[109]
*L. esc.*18cy		+	sensitive	[75]
*P. vulgaris*18cy		+	sensitive	[110]
*C. albicans*18cy		+	sensitive	[80]
*S. cerevis*17cy		19	40 (IC_{50}); 4.1 (K_i)	[111, 112]
*N. crassa*24mito	^{45}SKVFFD	+	200 (K_d)	[113]
*D. melanog*26mem		[c]	probable	[88]
human41cy	N-Block	+	300 (IC_{50})	[90]
human24sec	^{32}ADEKK	+	sensitive	[92]
human23sec	^{26}DEKKK	+	84 (IC_{50})	[93]
mouse22sec		+	400 (K_d)	[95]
human22mito		8.0	8 (K_i)	[97]
mouse23sec		+	sensitive	[8]
*S. cerevis*20mito	^{21}GKKVF	9.2	9.3 (K_i)	[99]
*S. cerevis*23sec	^{21}SDVGE	+	101 (IC_{50})	[111, 114]
*S. chryso*18	^{4}KVYFD	+	25 (IC_{50})	[103]
*E. coli*18cy		67.4	25000–50000 (IC_{50})	[115]
*E. coli*21peri	^{25}AKGDP	57.1	25000–50000 (IC_{50})	[115]

[a] Sequenced N-terminal ends of isolated, mature proteins (one-letter code for amino acids). [b] The quotient k_{cat}/K_m [$\mu M^{-1} s^{-1}$] is a measure of PPIase activity. Suc-Ala-Ala-Pro-Phe-4-nitroanilide was used as substrate. Determination at 10 °C. [c] Not determined.

Table 2. Properties of some FK506-binding peptidyl-prolyl *cis/trans* isomerases (FKBP).

FKBP	N-Terminus [a]	PPIase activ. [b]	Inhibition by FK506 and Rap [nM] [c]	Ref.
human12cy	^{2}GVQVE	2.2, 0.64	1.7 (FK), 0.2 (Rap), K_i	[162, 190, 191]
bovine12cy	^{2}GVQVE	0.66	0.25 (Rap), K_i	[51, 168]
*S. cerevis*12cy	N-Block	82	0.9 (FK), 0.5 (Rap), K_d	[168, 180]
human16mem	^{22}TGT(A)EG	1.5	55 (FK), K_i	[192]
human25	N-Block	0.8 [d]	160 (FK), 0.9 (Rap), K_i [d]	[177]
human52	^{2}TAEE	0.39 [e]	10 (FK), 8 (Rap), K_i	[178, 193]
dog52	XAEEM	[f]	[f]	[194]
*S. cerevis*14	^{18}GSLSD	54	8.3 (FK), 0.7 (Rap), K_i	[180]
*S. chryso*13	^{2}SIEKP	+	≈40 (FK), ≈10 (Rap), IC_{50}	[181]
*N. crassa*13		+	≈20 (FK), IC_{50}	[182]
*N. meningitidis*12		+	sensitive FK	[183]
*C. trachomatis*27		+	sensitive FK and Rap	[195]
*L. pneumophila*25	^{21}ATDAT	1.2	210	[185, 218]

[a] Sequenced N-terminal ends of isolated, mature proteins. [b] k_{cat}/K_m [$\mu M^{-1} s^{-1}$]; Suc-Ala-Leu-Pro-Phe-4-nitroanilide as substrate; T = 10 °C. [c] FK506 = FK, rapamycin = Rap. [d] Bovine enzyme. [e] Determination at 15 °C. [f] Not determined.

4. Measuring Enzyme Activity

Table 3 lists the methods of measuring PPIase activity known up to the present. They are often based on the production of pure *cis* or *trans* isomers or at least an isomeric distribution different from that expected based on the reaction conditions alone. This allows investigation of the kinetics of the reestablishment of equilibrium and thus the rate of the *cis/trans* isomerization. When dynamic NMR spectrometry is employed, the activity for the compounds in the unperturbed *cis/trans* equilibrium is measured. The *cis* and *trans* forms of linear proline-containing oligopeptides can sometimes be separated by low-temperature HPLC,[47] but the lifetime of the isolated pure conformers is

Table 3. Methods for measuring the catalytic activity of peptidyl-prolyl *cis/trans* isomerases.

Method	Detection	Reaction direction	Substrate type	Application in homogenates	Ref.
Isomer specific proteolysis	UV/VIS; fluorescence	*cis* → *trans*	oligopeptides	yes	[1, 4, 51, 60]
NMR spectroscopy	saturation transfer line broadening	*trans* ⇄ *cis*	oligopeptides, short proteins	no	[55–57, 61]
Solvent jump	fluorescence; UV/VIS	*trans* → *cis* *cis* → *trans*	oligopeptides	yes	[52, 53]
Folding/refolding	fluorescence	*trans* → *cis*; *cis* → *trans*	proteins	no	[16, 62, 63]
	UV/VIS	*trans* → *cis*; *cis* → *trans*	proteins	no	[62, 64]
	circular dichroism	*trans* → *cis*; *cis* → *trans*	proteins	no	[65]
	proteolysis	*trans* → *cis*; *cis* → *trans*	proteins	no	[65, 136]
	enzymatic activity	*trans* → *cis*; *cis* → *trans*	proteins	yes	[66–68]

typically too short for kinetics experiments. Therefore it is better to hydrolyze the peptide bond with a isomer-specific protease and use the coupled irreversible bond cleavage to temporarily disturb the conformational equilibrium. This reaction allows the kinetics (and thermodynamics) of the conformational equilibrium to be analyzed, because many proteases are $>10^4$ times more specific for the all-*trans* conformer of a substrate (this number refers to the value of k_{cat}/K_m; k_{cat} is the turnover rate and K_m is the Michaelis constant). Isomer-specific proteolysis is also observed when the isomerizable bond is far away from the bond cleaved in the protease reaction (Fig. 6.).[48–50]

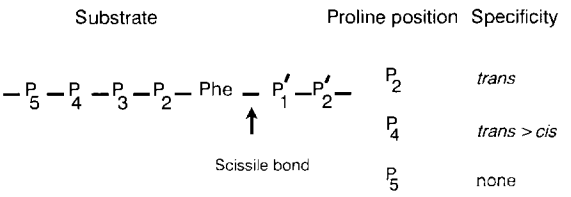


Fig. 6. Schematic representation of the *cis/trans* conformation specificity of α-chymotrypsin for proline-containing substrates with this amino acid in different positions within the peptide chain; based on the specificity constant k_{cat}/K_m. The positions of the other bonds of the protease substrate relative to the reactive bond between P_1 and P_1' are labeled according to the nomenclature of Berger and Schechter [264].

Figure 7 shows that when $[E]_0 k_{cat}^{S*} \gg k_{-1} K_m^S$, the rate of enzyme-catalyzed product formation v for a common reaction product starting from conformers in equilibrium can approach a limit when the equilibrium is affected by a very active isomer-specific protease. At higher enzyme concentrations $[E]_0$ and when an unreactive isomer S is present, the rate of product formation v is independent of the protease concentration. In this case it depends only on the rate of conversion of the unreactive conformer (k_1; for peptide bond isomers *cis* → *trans*), which can be easily followed by using a chromogenic protease substrate.

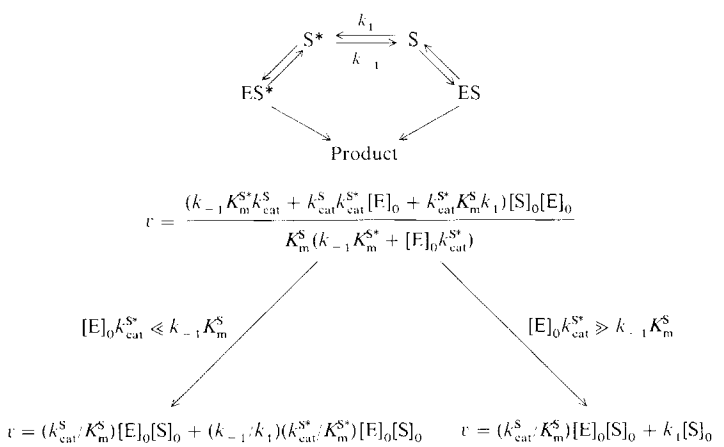


Fig. 7. The rate of formation v of a common product formed in an enzyme-catalyzed reaction from a substrate present in different conformations under steady-state conditions ($[S^* + S]_0 \ll K_m^{S*}, K_m^S$).

The resulting reaction is first order, and the increase of the reaction rate of the isomerization *cis* → *trans* upon addition of PPIase can be seen in the plot in Figure 8. If the substrate concentration is adjusted so that $[S]_0 \ll K_m$ is valid for the PPIase reaction, then the first-order rate constant k_b [s^{-1}] of the catalyzed reaction (k_u [s^{-1}] is the constant for the uncatalyzed reaction) directly gives the rate constant for the bimolecular PPIase-catalyzed reaction (k_{cat}/K_m [$M^{-1}s^{-1}$] = $(k_b - k_u)/[E]_0$). The isomer-specific proteolysis method can be varied in line with the molecular structure of the substrate and the protease sensitivity of the PPIase. It can be used to assay PPIase activity even in crudely prepared biological materials. The limit of detection for human recombinant Cyp18cy is an enzyme concentration of about 0.02 nM in the measuring solution.

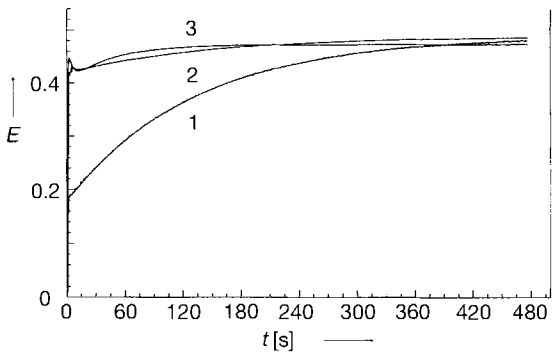


Fig. 8. Reaction course for the cleavage of Suc-Ala-Phe-Pro-Phe-4-nitroanilide by the isomer-specific protease subtilisin type VIII (0.15 mg mL^{-1} in 0.035 M hepes buffer, pH 7.8 at 13 °C); activity detected at 390 nm. 1) Uncatalyzed *cis* → *trans* isomerization started with the peptide dissolved in 0.2 M LiCl/trifluoroethanol; 2) uncatalyzed *cis* → *trans* isomerization started with the peptide dissolved in dimethyl sulfoxide; 3) as in curve 2, but with 5 nM Cyp18cy. The spikes at the beginning are mixing artifacts.

Since the amplitude of the isomerization reaction is limited owing to the low *cis* isomer level, (about 5–30% of the total concentration, depending on the peptide structure), obtaining an adequate signal/noise ratio is problematic; at high substrate concentrations solubility problems may arise. D. Rich et al.[51] were able to show that in a solution of the standard substrate Suc-Ala-Ala-Pro-Phe-4-nitroanilide in LiCl/trifluoroethanol (0.235–0.47 M) more than 50% *cis* isomer can be obtained, which makes the activity determination much easier (Fig. 8.).

If such a solvent jump is used for peptides whose fluorescence is quenched intramolecularly, for example the fluorogenic substrate 2-aminobenzoyl-Gly-Ala-Pro-Phe(4-NO_2)-Xaa-NH_2, then it is possible to measure the rate of isomerization without adding a protease enzyme.[52] After such a jump, conversion from the *cis* to the *trans* conformation leads to an increase in fluorescence. With the substrate Ala-Ala-Pro-Tyr(3-NO_2)-AlaNH_2 basically the same procedure can be used to measure the catalytic activity of PPIase in reversible equilibrium, although in this case a drop in absorbance at 428 nm in the UV/VIS spectrum is monitored.[53] The signal measured results from the differing pK_a values of the 3-nitrotyrosyl residue in the two conformational states of the peptide.[54]

One-dimensional NMR spectrometry can be used to determine the relaxation rates of the conformers in the presence of catalytic amounts of enyzme based on saturation transfer[17, 55, 56] or line broadening.[57, 58] The interconversion rate of the conformers of most *cis* and *trans* prolyl-peptide bonds is slow on the NMR timescale. Therefore separate signals are observed for nuclei near the isomerization center for both molecular forms. In the

presence of PPIase concentrations of >1 μM, the standard substrate Suc-Ala-Ala-Pro-Phe-4-nitroanilide displays coalesced NMR signals owing to a large increase in the interconversion rate. The catalyzed chemical exchange was also demonstrated in a NOESY experiment on human calcitonin$^{1-32}$ by the appearence of extra cross peaks in the presence of Cyp18cy (Fig. 9.).[58]

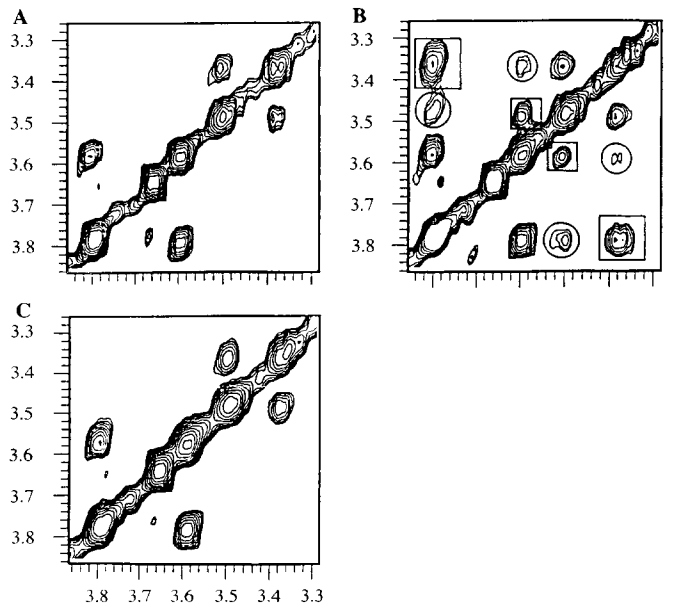


Fig. 9. The proline region (δ-ring signals) of the ^{1}H NMR NOESY spectrum of human calcitonin$^{1-32}$. **A**: in phosphate buffer, pH 6.8; **B**: as in **A** but in the presence of 25 μM Cyp18cy; **C**: as in **B** but with inhibition of the Cyp18cy activity by an excess of CsA. The extra cross peaks (in boxes) in **B** are due to rapid *cis/trans* exchange at the Phe-^{23}Pro in the presence of PPIase. The NOESY cross peaks between the δ ring protons in *cis* and *trans* ^{23}Pro resulting from the catalytic action of PPIase are circled [58]. The axes are labeled with the chemical shifts (δ).

When the kinetics of protein refolding and unfolding is examined,[10, 59] it is possible to find slower folding phases which often have their origins in the *trans* → *cis* isomerization of one or more prolyl-peptide bonds. Tyrosine and tryptophan residues in the neighborhood of the proline can act as probes for following the course of the isomerization, since changes in polarity during the folding process lead to changes in their fluoresence or absorbance. RNase T1 has proved to be a particularly suitable substrate for both families of PPIases having two *cis* bonds (namely Tyr$-^{39}$Pro and Ser$-^{55}$Pro) in the native state. Under conditions where both kinetic processes can be observed separately both were catalyzed by PPIases.[25] The low concentrations (<1 M) of urea and guanidinium hydrochloride in the refolding solution were tolerated by the cytosolic PPIase without substantial loss of activity.

5. Cyclophilins

For many of the 35 known protein sequences showing homology to the cyclophilin familiy of the PPIases (Scheme 1) isolation as proteins, characterization, and confirmation of their enzyme activity has been possible. A list of cyclophilins and their characteristic properties is given in Scheme 1.

Besides their tightly conserved central region comprising 130 amino acids, eukaryotic cyclophilins all have a high affinity for cyclosporin A ($K_i \ll 1$ μM) and many of its derivatives. Prokaryotic enzymes generally have a lower affinity,[104, 105, 115] though this may not always be the case.[103, 116]

The amino acids that are completely conserved in the sequence are distributed over the central region and most are coded for in the fourth exon.[166] The polypeptide chain of Cyp18 is relatively short, which implies that these amino acids are involved at the active site and have something to do with the activation of the catalytic process. For human Cyp18cy the three-dimensional structure has been determined down to a resolution of 1.63 Å by NMR spectrometry and X-ray crystallography.[18, 23, 24] The resulting structure shows that the conserved amino acids are located along a cleft along a β-sheet region (Fig. 10.). The conserved region is shown to be quite extended and is in fact larger than the hypothetical substrate binding site for short-chain oligopeptides. Amongst the presently known six isoforms of the human cyclophilins, Cyp18cy has a particularly broad distribution and is considered to be the receptor protein responsible for the immunosuppressive effect of CsA.

Amongst the sequence regions responsible for the localization of proteins in the cell, Cyp19cy has the terminal CXXL known as a signal for post-translational digeranylation. This sequence motif is mostly found in small G proteins and allows the regulated anchoring of the protein in the membrane.[117] Experimental results clearly demonstrating post-translational modification of cyclophilins are lacking at the present time. The cell adhesion signal motif RGD is present in a number of secretory cyclophilins in the core region of the sequence. However, the location of this sequence in the three-dimensional structure of the molecule is unknown, and no specific biological function has been assigned to it in the relevant cyclophilins.

Highly purified mammalian Cyp18cy enzymes are thermally and chemically stable (the enzymes retain full activity for months at 4 °C in buffer solution), but due to their highly hydrophobic nature, exposure to a plastic surface is enough to cause denaturation.[118] Cytosolic enzymes of the Cyp18cy type are widely distibuted in tissues and cell types of mammals and are found in high concentrations; however, the quantitative results seem to depend to a large extent on the method used for the determination. In mammals Cyp18cy is not restricted to lymphocytes—a fact which may help explain the side effects associated with CsA therapy.[119]

Kidney tubules and endothelial cells contain about 10 μg of Cyp18cy per mg of total protein, while T cells contain slightly less (3.1–7.0 μg mg^{-1}).[120, 121] In body tissues the concentration is about 1–3 μg mg^{-1}; skin and the deepest and most neuron-rich regions of the brain[122] have the highest levels.[121] There are large variations in localization and concentration within individuals,[123] and in other investigations lymph nodes and spleen were found to have the highest Cyp18cy levels.[118] A finding that tumor cells may have elevated levels[124] has not been confirmed by subsequent work.[121] Cyp18cy was detected by electron microscopy and confocal fluoresence microscopy not only in the cytosol but also in the nuclear membrane and in the outer regions of the Golgi apparatus. A cell-specific increase in Cyp18cy concentration, which was dramatic for liver and kidney, was found after treatment with CsA.[118, 125]

Scheme 1. For an explanation see p. 1423.

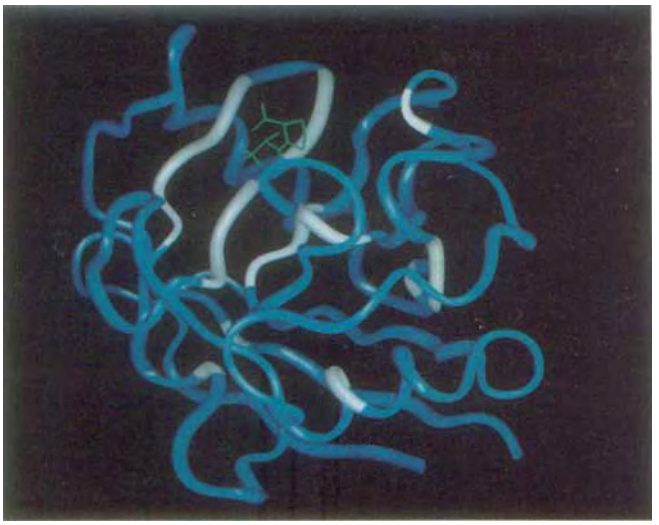


Fig. 10. A three-dimensional model of human recombinant Cyp18cy in the presence of the dipeptide Ala-Pro (shown in green) based on the results of X-ray diffraction studies [19]. Areas of highly conserved amino acids in the cyclophilin family are shown in white.

An unexpected high level of relatedness between human Cyp41cy and Cyp18cy in maize (67.3% identity) and the ubiquitous presence in tissues (brain > (liver, kidney, thymus, spleen) > lungs) is indicative of a special cellular function for this PPIase in mammals.[90, 108] This hypothesis is confirmed by the fact that this enzyme forms part of the oligomeric nonactivated estrogen receptor.[91] The long C-terminal extention on the PPIase homologous core region of Cyp41cy shows homology with the C-terminal of FKBP59, the PPIase component of the nonactivated progesterone receptor. Other components of the steroid receptors, the heat shock proteins hsp90 and hsp70, are also molecules specialized in mediating correct protein folding; their effect at the molecular level on the receptor function remains unknown.

This restriction also applies to Cyp158mem located on the outer membrane of $CD3^-$,$CD16^+$ granulocytes (natural killer cells), which plays a role in the recognition of tumor cells and in the cytotoxicity of killer cells. The amino acid sequence and the results of experiments with antibodies raised against sequence-derived peptides support the view that the N-terminal PPIase part of the molecule is extracelluarly anchored on the transmembrane segments and thus can take part directly in intercellular contact.[98]

It seems likely that *Drosophila* Cyp26mem, the tissue-specific ninaA protein from the compound eyes of fruit flies, plays a role in the catalysis of the synthesis, folding, and transport of the photosensitive Rh1-Rh6 rhodopsin and/or maintaining its stability. Cyp26mem is an integral membrane protein with a Cyp18cy-homologous sequence in the core region, which is located in the lumen of the endoplasmic reticulum (ER).[78, 88] If the Cyp26mem gene is deactivated, then abnormal opsin, the precursor of rhodopsin, accumulates in the ER to such an extent that it causes uncontrolled proliferation of the ER.[126] Random mutagenesis of fruit flies leads to point mutations in Cyp26mem, which lead to fruit fly phenotypes with defective rhodopsin production. Subsequent analysis showed that the amino acids affected are located in the postulated active site of the homologous Cy18cy, whose three-dimensional structure has been determined.[127]

There is also a group of cyclophilins that are secretory proteins and have the corresponding signal sequences added to the amino acid sequence (Scheme 1 and Table 2). Although it lacks an N-terminal signal sequence, Cyp18cy like IL-1 can be secreted through the cell membrane when certain stimuli are applied to the cell.[128] Secretory cyclophilins may contain the ER retention signal VEKPFAIKE at the C-terminus in addition to a signal sequence.[96] The transport of these cyclophilins out of the cell and their de novo synthesis is stimulated by growth factors.[129] This sequence motif data is consistent with the experimental finding that high PPIase activity levels are found in the lumen of the endoplasmic reticulum.[130] Of possibly biological significance is the observed colocalization of these proteins with typical ER proteins, such as the Ca^{2+}-binding protein calreticulin.[96] The hypothesis of C. M. Deber et al.[131] that the *cis/trans* isomerization of prolyl bonds plays a role in dynamic processes in membrane channels finds support in the fact that transport proteins that can be blocked by cyclosporin A have been observed, for example, in the inner mitochondrial membrane.[132] In studies of inhibitors analogous to CsA the inhibition constant K_i for the inactivation of the rat homologue of Cyp22mito was found to be proportional to the IC_{50} values for the blocking of the Ca^{2+} transport through these membrane pores.[133] In studies with CsA-resistant mutants of *Neurospora crassa* with a genetic defect for a functional Cyp24mito, M. Tropschug et al. were able to demonstrate for the first time that the inhibition of the PPIase activity itself is not responsible for the biological effect of CsA but rather that the CsA–Cyp complex must be cytotoxic.[87]

Deletion of the genes for Cyp20mito, Cyp17cy, and Cyp23sec even in the form of a triple mutant in the yeast *Saccharomyces cerevisiae* does not affect the viability of the cells.[99] However, when cells are exposed to stress conditions, the effect of the Cyp deletion becomes clear. Cyp20mito is essential for the growth of the yeast on L-lactate at 37 °C, and the Cyp20mito mutant is temperature sensitive.[100] In plant cells a Northern blotting

◀ Scheme 1. Amino acid sequences for cyclophilins known at the genetic level. The numbers above the sequences refer to the amino acids in human Cyp18cy. The letters in bold represent the highly conserved residues. Human Cyp18cy (human cyclophilin A, human cyclophilin 1) [69]; bovine (pig) Cyp18cy (bovine (pig) cyclophilin A) [4,5,70]; rat Cyp18cy (rat cyclophilin A) [71], (the sequence of hamster Cyp18cy to identical to 97.6%) [72]; mouse Cyp18cy (mouse cyclophilin A) [73]; chicken Cyp (partial sequence) [74]; *L. esculentum* Cyp18cy (tomato) [75]; *B. napus* Cyp18 (rape) [75]; *Z. mays* Cyp18 (maize) [75]; *P. vulgaris* Cyp18cy (bean) [76]; *A. thaliana* Cyp18 [77]; *D. melanogaster* Cyp18cy (fruit fly) [78]; *D. discoideum* Cyp18 (slime mold) [79]; *C. albicans* Cyp18cy (yeast) [80]; *S. pombe* Cyp18 (yeast) [81]; *S. cerevisae* Cyp17cy (yeast cyclophilin A) (yeast) [82,83]; *E. granulosus* Cyp17 (tapeworm) [84]; *S. japonicum* Cyp20 [85]; *N. crassa* Cyp24mito [86,87]; *D. melanogaster* Cyp26mem (ninaA) (fruit fly) [88,89]; chicken Cyp22sec (S cyclophilin) [74]; human Cyp41cy (Cyp-40, ERB cyclophilin) [90,91]; human Cyp24sec (secreted cyclophilin-like protein SCLP) [92]; human Cyp23sec (human cyclophilin B, cyclophilin-2)[93]; rat Cyp26sec (CyLP; rat cyclophilin B) [94] (the sequence in ref. [94] probably contains a mistake in the reading frame which was corrected in ref. [95]; the corrected sequence is shown here. It is possible that a further base insertion leads to a stop codon at amino acid ^{208}Glu) [96]; human Cyp22mito (human cyclophilin-3) [97]; human Cyp158mem (NK-TR protein) [98]; mouse Cyp22sec (mouse cyclophilin-2) [95]; mouse Cyp23sec (mouse cyclophilin C) [8]; *S. cerevisiae* Cyp20mito (yeast cyclophilin-3) (yeast) [99,100]; *S. cervisiae* Cyp23sec (yeast cyclophilin B) [101]; *S. cerevisiae* Cyp36 (Scc3) [102]; *S. chrysomallus* Cyp18 [103]; *Synechococcus sp.* Cyp15, [A. Kaplan, PIR CSYC42]; *E. coli* Cyp18cy (*E. coli* b) [104]; *E. coli* Cyp21peri (*E. coli* a) [104,105]; an open reading frame in *Salmonella typhimurium* (gene bank M32355) is almost indentical to *E. coli* Cyp21peri.

analysis demonstrated an increase in Cyp18cy mRNA in response to stress conditions.[76] The more than twofold increase in transcription of the Cyp18cy gene of *Saccharomyces cervisiae*, which was observed in response to heat shock, shows certain parallels to a typical stress 70 gene SSA1. The corresponding Cyp promoter proved to be heat inducible. Disabling the genes for Cyp17cy and Cyp23sec drastically reduces the ability of the yeast cells to survive heat shock.[134]

5.1. Catalytic Properties

Up until the present time, enzyme kinetic parameters have been determined almost exclusively for reactions of Cyp18cy (see Table 1). With regard to the enzyme–substrate interaction, the rate constants k_{cat}/K_m (*cis* → *trans*) for the bimolecular reaction approach the diffusion limit of 2×10^8 M^{-1}s^{-1} in the best cases.[135] A reliable method for determining the number of active sites by titration is not yet available; however, it is possible to use the increased intensity of the tryptophan fluorescence to follow the titration with the competitive inhibitor CsA. For human Cyp18cy the following kinetic constants were determined with the standard substrate Suc-Ala-Ala-Pro-Phe-4-nitroanilide: $K_m = 0.87$ mM (*cis*), $k_{cat} = 12\,700$ s^{-1} (*cis*) (0 °C).[51] These data show that the cytosolic cyclophilins at least are highly evolved enzymes with respect to their catalytic function. Because of the high k_{cat} values, these enzymes increase the rate of the reaction substantially, $k_{cat}/k_u \approx 10^6$, over that of the already fast uncatalyzed isomerization.

Information on the specificity of Cyp18cy for secondary binding sites (the nomenclature of the secondary binding sites is analogous to that of proteases;[264] isomerizable bond between positions P_1 and P'_1) is at present only available in some detail for the amino acids Xaa and Yaa in Suc-Ala-Xaa-Pro-Yaa-4-nitroanilide. In comparisons of the best and worst peptide substrates having uncharged and charged side chains Xaa, the values for the ratio k_{cat}/K_m differ by less than 20-fold.[97, 115, 162, 163] The differences for Yaa tend to be somewhat less, and for variations at at position P_1 the values of k_{cat} show a greater range of variation than those of k_{cat}/K_m.[266] The succinyl residue in the standard substrate can be replaced with a glutaryl residue without changing k_{cat}/K_m or even removed completely with minimal effect on the rate constants. The P_2 position also has an effect on specificity.[97]

At present three-dimensional structures have been determined only for substrate–Cyp18cy complexes.[18, 19, 23] For both the dipeptide Ala-Pro and a tetrapeptide substrate, whose *cis*/*trans* isomerization is readily catalyzed, only the *cis* isomer (angle at the peptide $\omega = -3°$) was observed as preferred bound conformation. The conformation of Cyp18cy on binding of the dipeptide does not change significantly compared to that of free Cyp18cy. However, since Ala-Pro is not a substrate but only a weak inhibitor, complex formation with longer peptide chains could lead to more significant changes in the enzyme structure. Our kinetic studies indicate that Cyp18cy binds the substrate calcitonin$^{1-32}$ with regiospecificity. The isomerization of the central Phe-^{23}Pro bond is strongly catalyzed; in contrast, the isomerization of the terminal Ala-^{32}ProNH_2 bond is not catalyzed at all.[58]

A number of slow processes in protein folding reactions can be catalyzed by cyclophilins,[62, 64–66] and thus have been identified without doubt as *cis*/*trans* isomerizations. During the refolding of a protein, the PPIases definitely act as true catalysts, and unlike molecular chaperones they do not depend on the presence of stoichiometric amounts of the helper protein or low molecular weight additives.[137] In the special case of recombinant carbonic anhydrase under certain refolding conditions the effect of porcine Cyp18cy was to increase the rate of refolding as well as the refolding yield.[138] The effect on yield seems to be independent of the enzymatic catalysis, and thus an additional chaperone function might be assigned to the enzyme. However, significant increases in refolding yield were also observed when stoichiometric amounts of foreign protein were added to the refolding solution (a nonspecific protective effect of added protein).[265] The catalytic effects of PPIases on refolding rates can always be blocked by inhibiting the PPIase with CsA. In contrast, cyclosporin H which is of similiar hydrophobicity but is noninhibitory did not affect the catalysis of the refolding processes.

Like the catalysis of *cis*/*trans* isomerizations by PPIases, which are linked in the assay to an isomer-specific proteolysis (see Section 4), the *cis* → *trans* or *trans* → *cis* isomerization in the PPIase-catalyzed refolding of proteins is linked to an irreversible reaction, namely the quasi-irreversible formation of a stable three-dimensional protein structure under renaturing conditions. It has already been demonstrated experimentally that during protein folding catalysis in both isomerization directions takes place.[62, 139] The catalytic efficiency of cyclophilins with macromolecular substrates under conditions where $[S] \ll K_m$ is at least ten times less than with short-chain substrates. This is certainly caused in part by the extended diffusion times with large molecules.

Kinetic analysis of PPIase-catalyzed protein refolding beyond the qualitative finding that the rate of reaction increases is very complicated because of the existence of many poorly defined substrate states. In the most thoroughly investigated refolding process, that of unfolded RNase T1,[25] the *trans* Ser-^{55}Pro unit is accessible to the catalyst while the *trans* Tyr-^{39}Pro bond is not because of steric shielding. The resulting formation of intermediate structures that already possess the *cis* Ser-^{55}Pro unit of the native structure is not a property of the fully unfolded chain, but rather it is reached in the early stages of refolding. The early formation of native structure elements may be the reason why Cyp18cy cannot catalyze certain partial reactions in protein refolding involving *cis*/*trans* isomerizations.[67] When cytosolic cyclophilins from a variety of organisms are used in the refolding of this model protein, parallels can be drawn between catalytic activity of all these enyzmes with a tetrapeptide substrate and the two slow, catalyzable processes in the formation of the native structure of RNase T1.[16] With the exception of *E. coli* Cyp18cy, which catalyzes the very slow *cis* Tyr-^{39}Pro isomerization relatively well, there are five other, not very phylogenetically related cyclophilins, which recognize the secondary binding sites of the RNase T1 polypeptide chain equally well and have similar substrate steric requirements. This finding can be taken as evidence of evolutionary conservation of protein-folding catalysis.

When attempting to develop models of de novo protein formation in the the cell it must be borne in mind that the oxidative refolding of reduced RNase T1 (the molecule contains two disulfide

bridges in the native state) is synergetically accelerated by the presence of protein disulfide isomerase and *E. coli* Cyp18cy.[140] Although protein unfolding catalyzed by PPIases is supported by the concept of microscopic reversibility, it is not so easy to demonstrate experimentally. This was achieved by Mücke and Schmid with reduced and *S*-carboxymethylated RNase T1 which can be unfolded simply by employing a concentration jump from 0.2 to 3 M NaCl. The surprisingly simple kinetics of the unfolding process showed a nonlinear catalytic increase in rate of reaction which was dependent on the concentration of *E. coli* Cyp18cy.[63]

The catalysis of isomer interconversion in native proteins, which is very interesting from a physiological point of view, did has not received much attention. However, 50 μM Cyp18cy (porcine) was found to have no effect on the rate of *cis/trans* isomerization of the Gly-^{43}Pro bond in native calbindin D_{9k}.[61]

At present quantitative data for protein folding catalyzed in vivo are lacking. Among the positive qualitative findings are the CsA-linked slowing down of the formation of the three-dimensional structure of transferrin in the endoplasmic reticulum,[141] the increased protein yield in coexpression experiments,[142] and the effect of gene deletions.[143] In addition a single kinetic value is known, namely the 1.4-fold reduction caused by CsA for the rate of triple helix formation in procollagen from fibroblasts.[144] Here, too, the inhibition of PPIase activity through CsA was used as an investigative tool. However, the relatively small kinetic effect led to considerable changes in the reaction product, because the increased time scale of protein folding due to the inhibition meant that a higher degree of posttranslational modification was possible in the triple helix.

5.2. Inhibition

All cyclophilins bind CsA with binding constants ranging from nM to several μM (Table 1). Their enyzme activity seems to be competitively inhibited by CsA; however, this result has been verified only for human Cyp18cy, which binds very tightly to the inhibitor. The CsA–Cyp18cy binding constants reported in the literature show a wide range (by a factor of greater than 100). This can be explained by the dependence of the association constants on the protein concentration, which has its origins in the oligomerization of free Cyp18cy or in the formation of a decamer complex[145] which has already been observed in the solid state.

The specificity of the binding and inhibition is demonstrated by the mininal affinity of cyclophilins for D-^{11}MeVal-cyclosporin (CsH). Further structures that act as reversible cyclophilin inhibitors at a comparable level of effectiveness are not known at present. A variety of proline-containing oligopeptides that appeared to be potential competitive inhibitors proved not very effective at inhibiting the test reaction with Suc-Ala-Ala-Pro-Phe-4-nitroanilide when both components were kept at less than 1 mM.[146]

Interesting from a pharmacological point of view is the finding of D. Rich et al. that the binding of CsA to Cyp18cy is a relatively slow, pseudo-first-order reaction under the reaction conditions and can be divided up into at least two or three kinetically relevant processes. In addition, the binding parameters depend on the type of solvent cyclosporin A was dissolved in prior to the start of the inhibition reaction.[51, 147, 148] The time dependence of the inhibition constants (with an apparent half-life of 29 s for the middle phase) is reflected by the different values: $K_i = 61$ nM shortly after addition of CsA to Cyp18cy, $K_i = 2.5$ nM after 30 min (Fig. 11.). The reaction with the mature form of

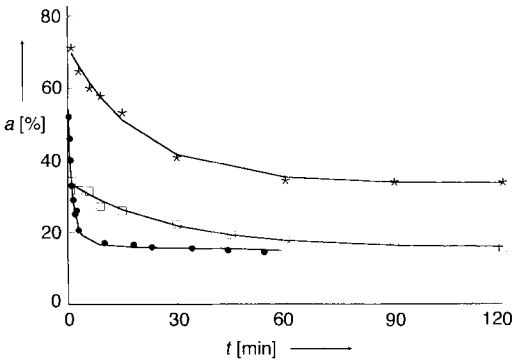


Fig. 11. Time dependence of the residual activity a [%] of the reaction of CsA (●) with Cyp18cy as well as FK506 (*) and rapamycin (□) with FKBP12cy at 10 °C and 15 °C (rapamycin). CsA (10 nM in reaction mixture) and Cyp18cy (1.5 nM); FK506 (25 nM in reaction mixture); rapamycin (34 nM in reaction mixture), FKBP12 40 nM each. All stock solutions of the effectors are in $EtOH/H_2O$ (50/50 vol%) [263].

Cyp22mito (rat) also exhibits phases with different reaction rates. In this case the half-life is significantly longer and indicative of an enzyme-dependent conformational change during the formation of stronger CsA–CsA complexes. The origin of the "memory" of CsA for nature of the solvent stems mainly from the conformational heterogeneity of CsA in solution.[149] The form of CsA active in inhibition with a *trans* conformation at ^{9}MeLeu-^{10}MeLeu[21, 150] is present in low concentrations in many solvents (e.g. tetrahydrofuran); in others CsA is almost exclusively present in the active form (tetrahydrofuran/LiCl[151]). Thus this concentration determines the K_i value at the start of the reaction which is usually calculated from the total amount of CsA. However, CsA does not seem to be a suicide inhibitor since according to current knowledge Cyp18cy cannot catalyze the *cis* → *trans* conversion in CsA. Many CsA derivatives only reach a final equilibrium after several hours when the ligands are optimally adapted to their host protein. When dimethyl sulfoxide is used as a solvent the approach to equilibrium is slowed even further. Even under these unfavorable conditions for structure–activity relationships a very nearly linear dependence for the binding of 96 CsA derivatives to bovine Cyp18cy versus the ability to suppress T-cell proliferation was found.[152] However, two derivatives ("off-diagonal analogues")[153] showed great deviations from this correlation which leads to doubt that the inhibition of the Cyp18cy activity alone leads directly to immunosuppression. ^{6}MeAla-CsA strongly inhibits the catalysis ($K_i = 9$ nM),[154] and although its structure is very similar to that of CsA, this derivative showed only 1% of the immunosuppressive effect of CsA.[155] In contrast, ^{1}MeBm$_2$t-cyclosporin binds weakly ($K_i = 2240$ nM; bovine Cyp18cy)[153] but still shows 12% of the immunosuppressive effect of CsA on the activiation of the IL-2 transcription factor NF-AT.[154, 156]

Macromolecular CsA derivatives prepared from aminodextran (molecular weight ca. 70 kDa) or serum albumin by covalent

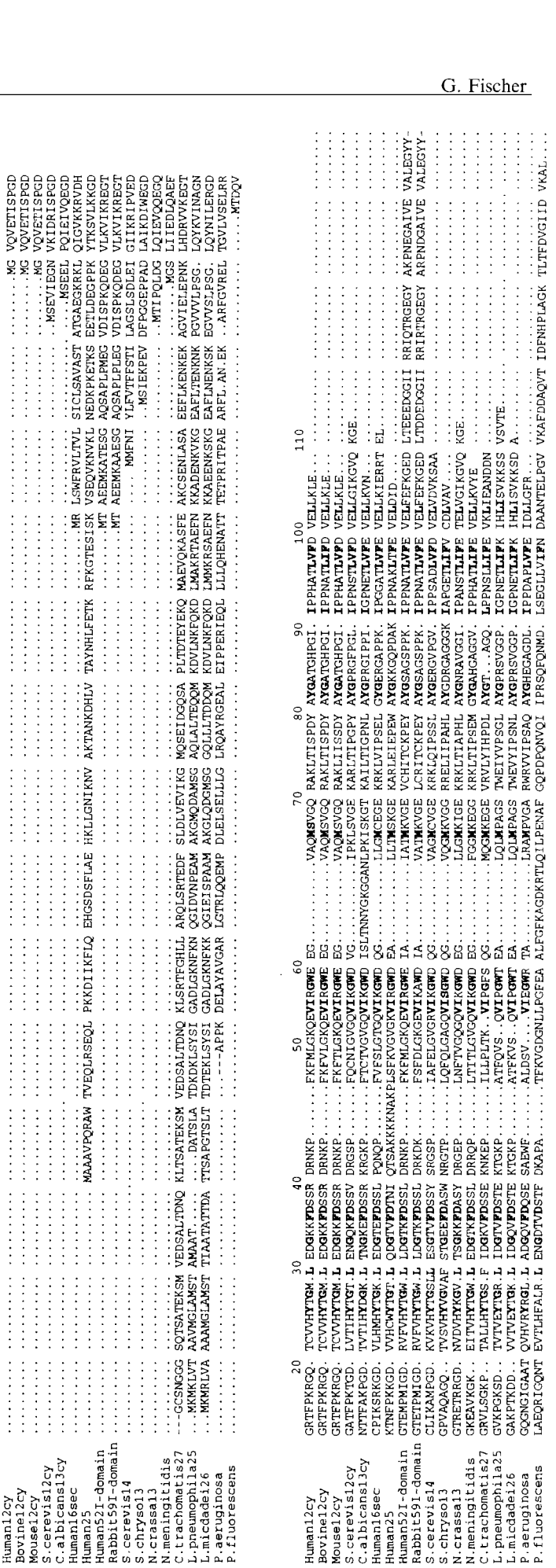
linkage of CsA with the side chain of the (4*R*)-4-[*trans*-butenyl]4,*N*-dimethyl-L-threonine residue inhibit Cyp18cy only ten times less effectively than CsA itself. The IL-2 release from EL-4 lymphocytes can be inhibited by this CsA derivative with an IC_{50} value of 60 nM (about 4% of the CsA activity under the same conditions). Even the coupling of aminodextran-CsA to agarose beads does not prevent the immunosuppressive effect, as long as contact to the cell surface is ensured.[157] This implies the existence of a(n) (additional?) receptor for CsA on the surface of T cells. However, one property of ^{6}MeAla-CsA does not fit the present model for the action of CsA (see Section 9)—this derivative does not act as a CsA antagonist in the (phorbol ester/ionomycin)-activated T-cell proliferation test.[153]

The three-dimensional structure of human CsA–Cyp18cy was determined by X-ray crystallography[145] and NMR spectrometry.[158] The structure of Cyp18cy was shown to be hardly affected by complex formation, whereas the three-dimensional structure of CsA in the complex is dramatically different from that in unpolar, nonaqueous solution[160] or in the solid state;[161] for example, intramolecular hydrogen bonds of CsA are not found in the complex. The CsA residues 1–3 and 9–11 (see Fig. 5) are involved in the contact to the cyclophilin surface, which binds the ligands in a hydrophobic pocket formed from the side chains of the amino acids ^{121}Trp, ^{60}Phe, ^{57}Ile, ^{122}Leu, ^{113}Phe, ^{126}His, ^{101}Ala, ^{103}Ala, and ^{73}Thr. As was already known from the increase in the fluorescence intensity on complex formation and from mutagenesis experiments,[163, 164] ^{121}Trp is a determinant for the especially strong binding of CsA to the cyclophilin.

The binding region consists of four antiparallel β-pleated sheets and is identical with the pocket for the substrate acetyl-Ala-Ala-Pro-Phe-amidomethylcoumarin.[23] However, compared to this peptide CsA binds to cyclophilins in the opposite propagation direction of the peptide chain.[150]

6. FK506-Binding Proteins

Cytosolic FKBPs (synonym: macrophilins), which are made up of less than 110 amino acids and have molecular weights of about 12 kDa, are amongst the smallest known enzymes. A common feature of these enzymes apart from sequence homology is their inhibition by FK506 and rapamycin (Table 2). There is no evidence of oligomerization of the enzyme at catalytic concentrations. FKBP12cy from mammalian tissues function as receptors for the immunosuppressive effect of peptidomacrolides, and it was receptor studies with these compounds that revealed the enzyme nature of the FK506-binding proteins.[6] At present 18 sequences with homology are known (Scheme 2) which were for



Scheme 2. Amino acid sequences for FK506-binding peptidyl-prolyl *cis/trans* isomerases known at the genetic level. The numbers above the sequences refer to the FKBP12cy (human) sequence. Human FKBP12cy [32,166,167]; bovine FKBP12cy [168]; mouse FKBP12cy [169]; *S. cerevisiae* FKBP12cy (RPB or RBP1 protein) [26,170,171]; *C. albicans* FKBP13 [172]; human FKBP16 (FKBP-13) [173]; human FKBP25 [174–176] (bovine FKBP25 is 97% homologous [177]); human FKBP52cy (p56, hsp56) [178]; rabbit FKBP52 (hsp binding immunophilin, HBI; p59 [179]; *S. cerevisiae* FKBP14 [180]; *S. chrysomallus* FKBP [181]; *N. crassa* FKBP13 [182]; *N. meningitidis* FKBP [183]; *C. trachomatis* FKBP27 (Mip-like protein) [184]; *L. pneumophila* FKBP25mem (Mip protein) [185,186]; *L. micdadei* FKBP26 (Mip protein) [187]; *P. aeruginosa* FKBP25 [188]; *P. fluorescens* FKBP [189].

the most part identified using the standard test for PPIases. In addition, there are FKBPs which have not been sequenced yet but whose inclusion in this family has been demonstrated by cross-reactivity with anti-FKBP12cy antibodies and FK506 sensitivity.[110, 165]

A high-resolution three-dimensional structure was determined for human FKBP12;[20, 219, 221] however, no structure is yet available for the enzyme–substrate complex. The structure of FKBP12cy with a bound FK506 molecule is shown in Figure 12. The highly conserved amino acids in the FKBP sequences (Scheme 2) are distributed all over the protein molecule.

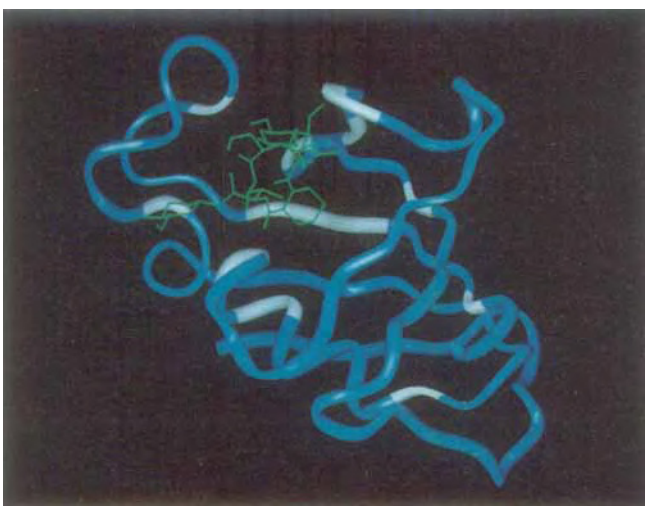


Fig. 12. Three-dimensional model of the FK506–FKBP12 complex [20]. FK506 is shown in green; amino acids that are highly conserved in FKBP sequences are shown in white.

The kinetic constants of recombinant FKBPs do not differ significantly from those of PPIases from natural sources,[180, 196] although a post-translational phosphorylation in vitro has been reported (the FKBP12 chain contains a consensus sequence for protein kinase C: ^{35}KKFDS*SRD).[197] The clustering of conserved residues is less pronounced than in the cyclophilins; however, these residues are also found in the cleft forming the binding site of FK506 (Fig. 12).

The stability of human FKBP12 is impressive ($T_m \approx 68$ °C) and increases further when complexed with peptidomacrolides.[198] In contrast to cyclophilins, after denaturation and unfolding with urea ($c_m \approx 4.3$ M) FKBP12 refolds to the native form and regains full enzyme activity.[199]

Like cyclophilins, FKBP12cy are widely distributed in human tissues, and especially high levels are found in certain regions of the brain.[200] The concentration of FKBP12cy in the cytosol of lymphocyte cells is extraordinarily high for an enzyme ($c \approx 20$ μM).[197, 201] The subcellular distribution pattern is not constant but depends on the functional state of the cell; FKBP12cy tends to be localized in regions near the cell nucleus, as is the case with Cyp18cy.[202] A further unexpected similarity between Cyp18cy and FKBP12cy is their chemotactic effect on neutrophils, an effect that is detectable down to nanomolar concentrations with FKBP12cy.[203] CsA and FK506 block the chemotactic activity of the corresponding binding partners, while the PPIase inhibitors ^{6}MeAla-CsA and rapamycin do not. This shows that the site of attack is actually the Ca^{2+}-dependent signal transduction. The observation that FKBP12cy possesses a hepatocyte growth stimulating activity at a dose of 1 μg per kg of tissue during liver perfusion fits in well with this extracellular activity.[204] The inhibition of the chemotactic effect of PPIases has been put forward as an alternative to the IL-2 model to explain the immunosuppressive effect of CsA and FK506.[205]

The yeast analogue of FKBP12cy is coded for by a nonessential gene, whose elimination, or simply the exchange of Tyr^{89}Asp in the enzyme,[206] blocks the fungicidal effect of rapamycin.[168, 170, 207] In the wild-type yeast rapamycin blocks growth by fixing the cells irreversibly in the G1 phase of the cell cycle. FK506 is an anatogonist of rapamycin. The rapamycin–FKBP12cy complex probably inhibits a phosphatidylinositol-3-kinase.[171, 208]

As is also the case for the second FKBP protein found in *Saccharomyces cerevisiae* (FKBP14mem), the activity of the yeast PPIases is greater than the FKBPs from other sources by almost 100-fold (Table 2). The signal sequence of FKBP14mem leads to the localization of this enzyme mainly in the microsomal fractions.[180] The deletion of the gene in this case as well does not lead to the generation of a phenotype under normal conditions. However, the level of nonglycosylated, unfolded precursor proteins in the endoplasmic reticulum is increased by a tunicamycin treatment, and the expression of FKBP14mem is also increased.[209]

The related human FKBP16sec is the major FKBP in mast cells,[210] and in the form of a FKBP16 homologue it is the major FKBP of leaf cells of plants.[110] However, in Jurkat cells it makes up only about 2% of the amount of FKBP12cy.[173] FKBP25 is especially interesting because it contains a localization signal for the cell nucleus and shows DNA binding properties through a helix-turn-helix motif.[174, 177, 211]

A further similarity with the biochemistry of the cyclophilins is the fact that both protein families have been demonstrated to form part of the steroid receptors. An integral component of the heterooligomeric, nonactiviated glucocorticoid receptor (ca. 300 kDa) is a heat shock protein (52 kDa) with two regions homologous to FKBPs.[194] The N-terminal domain has 49% homology with human FKBP12cy. There is an additional FKBP-related domain with a somewhat vague functional significance, and further similarity to a calmodulin-binding consensus sequence can be recognized.[212] FKBP52, which is probably dimeric in the native state, is directly connected to the cytoskeleton and binds to affinity columns for FK506.[193] It is PPIase active and inhibited by peptidomacrolides.[213] After initial unsuccessful attempts, an effect of FK506 on the functioning of the receptor was found—an increase in the rate of transcription of specific genes. Conditions of reduced steroid induction have to be used so that the effect can be monitored.[214]

The C-terminal region of FKBP52 is 34% identical with the same 140 amino acid region in Cyp41cy, the PPIase component of the nonactivated estrogen receptor.[90, 91]

Pathogenic bacteria seem to be predestined to express membrane-bound FKBPs on their surfaces (see Scheme 2).[215] For example *Legionella pneumophila*, the pathogen causing Legionnaires' disease, is an intracellular phagocytic parasite of lung macrophages and monocytes.[216] The mip protein

(FKBP25mem) is thought to be the pathogenicity factor on the surface of *Legionella* (about a 100-fold reduction in virulence is observed in FKBP25mem-negative mutants).[217] The N-terminal extension to the FKBP homologous core of the mature protein is predicted to have a high helix content, which could contribute to the anchoring of the protein to the membrane. The PPIase activity can be inhibited with FK506,[185] and the enzyme is probably present as a dimer.[218] However, the exact sites of interaction for FKBPs on the molecular level during pathogenesis remain unclear.[215]

6.1. Catalytic Properties

The catalytically active concentrations of FKBPs have been determined up until now by titration with FK506 or rapamycin by following the decrease in the intensity of the protein fluorescence[219] or approximated by blocking the enzyme activity with stoichiometric amounts of inhibitors. In contrast to cyclophilins FKBPs exhibit a high level of subsite specificity for the amino acid at position P_1 on the substrate chain.[162, 180, 185, 190] Especially high values of k_{cat}/K_m are observed with amino acids in this position having hydrophobic side chains, whereas glycine and charged amino acids lead to peptides that are hardly utilized by the enyzmes at all. Indeed, there is a linear relationship between k_{cat}/K_m (human FKBP12cy) and the hydrophobic capacity factor R' of the amino acid side chain.[146] Such a specificity distribution makes sense biologically only if the cell has different enzymes available with differing specificity for secondary binding sites, as is the case of proteases. However, this does not seem to be the case with FKBPs, since all enzymes examined so far show a similar catalytic pattern (Fig. 13). With the optimum substrate

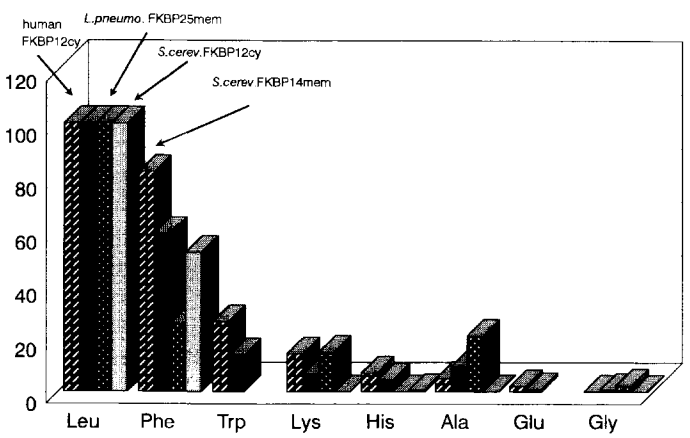


Fig. 13. Relative substrate specificity k_{cat}/K_m [%] is plotted on the y axis for a variety of FKBPs for substrates of the type Suc-Ala-Xaa-Pro-Phe-4-nitroanilide with Xaa = Leu (100%) [162,180,185].

Suc-Ala-Leu-Pro-Phe-4-nitroanilide for FKBP12cy, the k_{cat}/K_m value is about ten times less than with Cyp18cy. This is mostly due to the k_{cat} term [597 s^{-1}] and not the K_m constant.[220]

Although FKBPs are less effective than cyclophilins, they can also catalyze protein folding;[182] at present not much data is available.

6.2. Inhibition

Rapamycin and FK506 bind strictly stoichiometrically (1:1 with human FKBP12cy) and sometimes very strongly to FKBPs; in doing so they reversibly inhibit PPIase activity (Table 2). The rate of inhibition is time-dependent for both of the inhibitors, and thus the course of the reaction is comparable with the formation of the CsA–Cyp complex formation (see Fig. 11). The origin of this slow first-order process is probably the supply of *trans* isomer of the inhibitor by the uncatalyzed isomerization after the consumption of the equilibrium level of the *trans* isomer. Although the immunosuppressive effect of rapamycin differs from that of FK506 so much that a separate receptor seems likely, no specific rapamycin-binding protein has yet been found in Jurkat cells.[222] With rapamycin, too, inhibition of PPIase activity and rapamycin-specific immunosuppression can be separated from each other.[223]

In an FK506 dimer (FK1012), in which two units of FK506 are linked by a bis(carbamoyl)-4-xylylenediamine bridge at the C40 atom of FK506, both halves possess a high affinity for FKBP (K_i^1 = 0.06 nM; (K_i^2 = 0.76 nM). Thus chimeric proteins consisting of an FKBP part and an effector part can form dimers in situ and start a oligomerization-dependent signal cascade. Addition of FK506 monomers can be used to turn the signal cascade off.[224]

The enthalpy of formation for these complexes and other thermodynamic data suggest that hydrophobic interactions play a dominant role in complex formation.[225] This finds additional support in the structure of the FK506–FKBP complex, since all of the amino acid residues near the binding center possess hydrophobic side chains (Fig. 14).

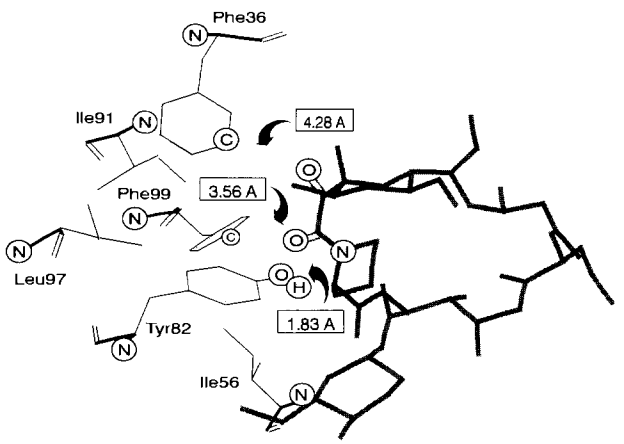


Fig. 14. All amino acids that have an atom located within 5.5 Å of the peptide carbonyl group of FK506 (section of the molecule represented with a thick gray line) in the FK506–FKBP12 complex [20]. The nitrogen atoms are marked in the backbone of the polypeptide chain (thick black lines). Distances are given for a number of atoms that are especially close together. The distances refer to the atoms connected by thin lines.

Similar to the situation with the cyclophilins, a linear relationship exists for FK506 derivatives between the parameter for the binding to FKBP12 ($\lg IC_{50}$) and the blocking of IL-2 release from stimulated Jurkat cells. Off-diagonal compounds include rapamycin and 506BD in particular (Fig. 15), a synthetic compound which first showed the discrepancy between inhibition of

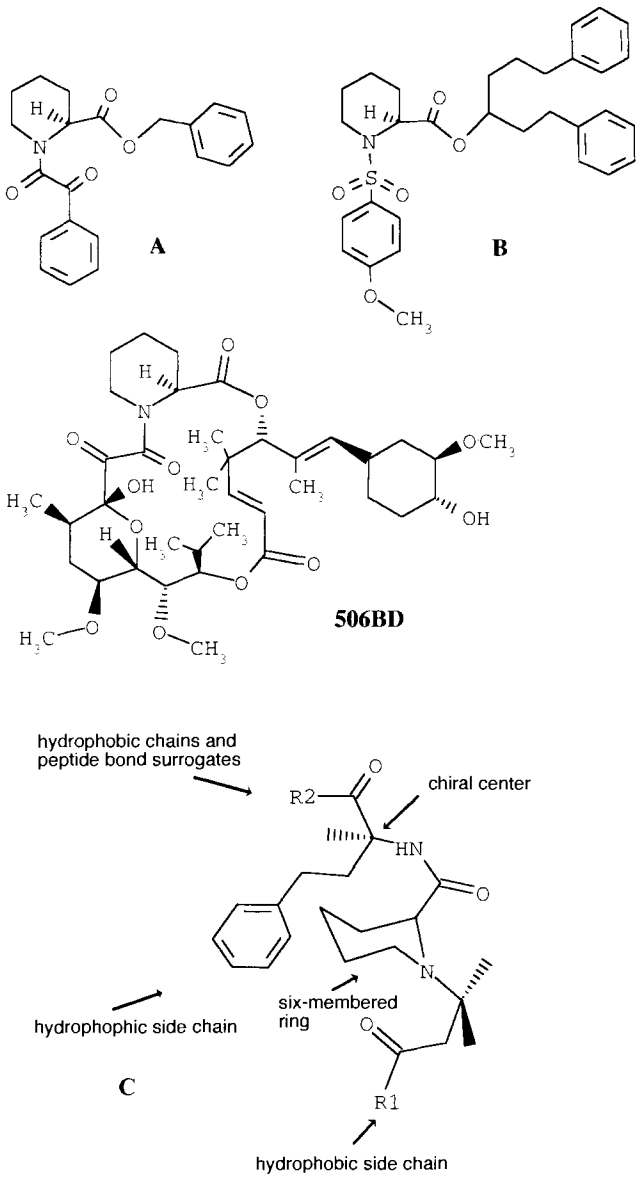


Fig. 15. Structures of a number of synthetic inhibitors of FKBP12cy.

PPIase activity and the effect on T cells.[226] Both compounds have a high affinity to PPIases and inhibit their activity while not affecting IL-2 production.[227] These off-diagonal derivatives act as sensitive probes for investigations into the calcineurin model of immunosuppression.

The α-dicarbonyl unit in FK506 and rapamycin deviates considerably from s-*trans* planarity. The α-carbonyl group is also situated perpendicular to the plane of the amide group in the enzyme–FK506 complex (see Fig. 12.).[20, 228] However, this is not a consequence of the macrocyclic structure, since local strain forces the α-carbonyl group out of the dicarbonyl plane even in simple pyruvdialkylamides.[229]

Complex formation leads to a change in conformation of the amide bond of FK506; the *cis* conformation is found in the solid state, a mixture of isomers is present in aqueous solution, and after binding to FKB12cy it acquires the *trans* conformation. The conformation of free rapamycin is the same as that found in the complex, which could explain the greater complex formation constant compared to that of the rapamycin–FKBP complex. In contrast to rapamycin, FK506 is not chemically stable, as was demonstrated in a solution of ethanol/water; it tautomerizes slowly at the hemiketal C10 atom with racemization and formation of a keto structure at C10.[230] Both macrolides are considered to be transition state analogues for the PPIase-catalyzed conversions, since the spatial arrangement of the α-carbonyl group relative to the peptide bond in the ground state corresponds to that in the transition state of the isomerization.[13] FK506 becomes less inhibitory after replacement of the OH group at position C10 with a peptide bond.[231] This implies that FK506 is probably not a transition state analogue for a natural substrate containing a Leu-Pro dipeptide unit.

The conformational homology of FK506 to α-ketoacid amides explains why new inhibitors were first based on this structural unit. Compound **4** in Figure 15, a phenylglyoxylic acid derivative, has a much simpler structure than FK506 but a K_i value of 1.5 μM and is thus is a fairly good inhibitor.[232] Compound **B** which has a sulfonamide group has improved inhibitory activity (K_i = 5 μM),[233] while structure **C** proposed by Hauske et al.[234] has the extrapolated structural elements for an optimum FKBP inhibitor based on the information extracted from the data of 56 structures.

7. Intracellular Binding Proteins for PPIases

Proteins that are specifically associated with PPIases in intact cells or in cell homogenates can give clues about the biological function of the enzymes and natural substrates. Owing to the high K_m values of human Cyp18cy and FKBP12 for oligopeptides and the projected low affinities of PPIases for protein substrates, it is not likely that complexes of PPIases with cellular substrates will accumulate. Therefore it is questionable whether the lifetimes of PPIase complexes with good polypeptide substrates are long enough to be detected by analytical methods. However, PPIase binding partners can be detected in stable heterooligomeric complexes.

The binding of immobilized proteins of the heat shock family hsp90 to human Cyp18cy depends on the Mg^{2+}/ATP concentration; however, binding does not require the hydrolysis of ATP and cannot be blocked by addition of CsA. Consequently, an affinity column with Cyp18cy as ligand binds the heat shock proteins hsp70 and hsp90.[235] A 77 kDa glycoprotein from AC-6 bone marrow cells was retained by a column with the immobilized PPIase-active fusion protein consisting of glutathione-S-transferase and Cyp23sec (mouse). The fusion protein was bound to glutathione agarose as carrier. Interestingly, the targeted glycoprotein was found to have a cysteine-rich sequence region typical for cell surface molecules.[8, 236]

An unexpected finding is that the proline-free peptide CGY-DVSTAQKIIAKL can integrate specifically with yeast Cyp17cy. This was demonstrated in cross-linking studies with bis(sulfosuccinimidyl)suberate. The cross-linking can be blocked by CsA and is not observed with the reverse sequence.[237]

An elegant molecular biological method[238] can detect protein–protein interactions in a yeast system by means of the transcription of a reporter gene in vivo. In the search for potential binding partners of the gag polyprotein of the HIV-1 virus

in a protein bank coded by human cDNA, the only specific binding partners for $Pr55^{gag}$ were Cyp18cy and Cyp23sec.[239] Gag proteins from related viruses do not bind or in the case of the simian virus SIV-1 only bind Cyp23sec. The formation of the $Pr55^{gag}$–Cyp complex occurs also in vitro with isolated proteins and was also observed with the p24 fragment of $Pr55^{gag}$. The associations can be disrupted by the addition of CsA. However, it is still unclear what relevance these results have to the pathogenesis after infection with HIV-1. The addition of CsA has been shown to block HIV-1 replication and especially the formation of syncytes with multiple nuclei from T cells.[240]

Fewer binding proteins for the FKBPs have been found thus far. FKBP12cy binds strongly and very specifically to the ryanodin receptor and can be copurified with it. The rynodin receptor is the 565kDa Ca^{2+} channel of skeletal muscle. It seems likely that FKBP12cy is located on the cytoplasmic side of the sarcoplasmic reticulum.[241]

8. Mechanisms of PPIase-Catalyzed Reactions

The rate of the uncatalyzed *cis/trans* isomerization of the prolyl-peptide bond depends relatively little on the nature of the adjacent amino acids but on the state of folding of the polypeptide chain.[25] Both a rate increase and a decrease are found for the isomerization of polypeptide chains compared to that found in oligopeptides. A specific intramolecular catalysis of the isomerization of the proline bond resulting from the arginine side chains in dihydrofolate reductase has been proposed;[242] however, it is very difficult to separate such a group-specific effect from structure-dependent effects.

Acid catalysis has not been detected except at extreme pH values, and the action of OH^- ions as nucleophiles in the isomerization reaction has been inferred only indirectly.[243] *cis/trans* Conformational interconversions are more rapid in nonaqueous solvents (the rate constant is increased by up to 100-fold) because the ground state of the isomers is destabilized and thus the electronic delocalization in the amide bond is reduced.[244]

We described the plausible reaction mechanisms for the enzyme-catalyzed *cis/trans* isomerization early on[245] and present a modified version in Figure 16. A number of these reaction paths imply that an intermediate with a covalently bound substrate is formed in the course of the catalysis. In any case the crucial elementary step is a reduction in the double bond character of the C–N bond. So far investigations on PPIases do not provide evidence to support the two postulated mechanisms involving cleavage of a C–H bond. The enzyme-bound nucleophile $E-X^-$ and the electrophile $E-X^+$ could also represent enzyme-bound water molecules, and in fact a role for water in the mechanism of the catalyzed isomerization is currently under consideration.

The interpretation of the kinetic data for PPIase-catalyzed reactions is made more difficult by the presence of multiple enzyme forms[146] with differing catalytic properties. The pH dependence of the reaction of Cyp18cy with tetrapeptide substrates, whose catalytic effect (k_{cat}/K_m) decreases at low pH, can

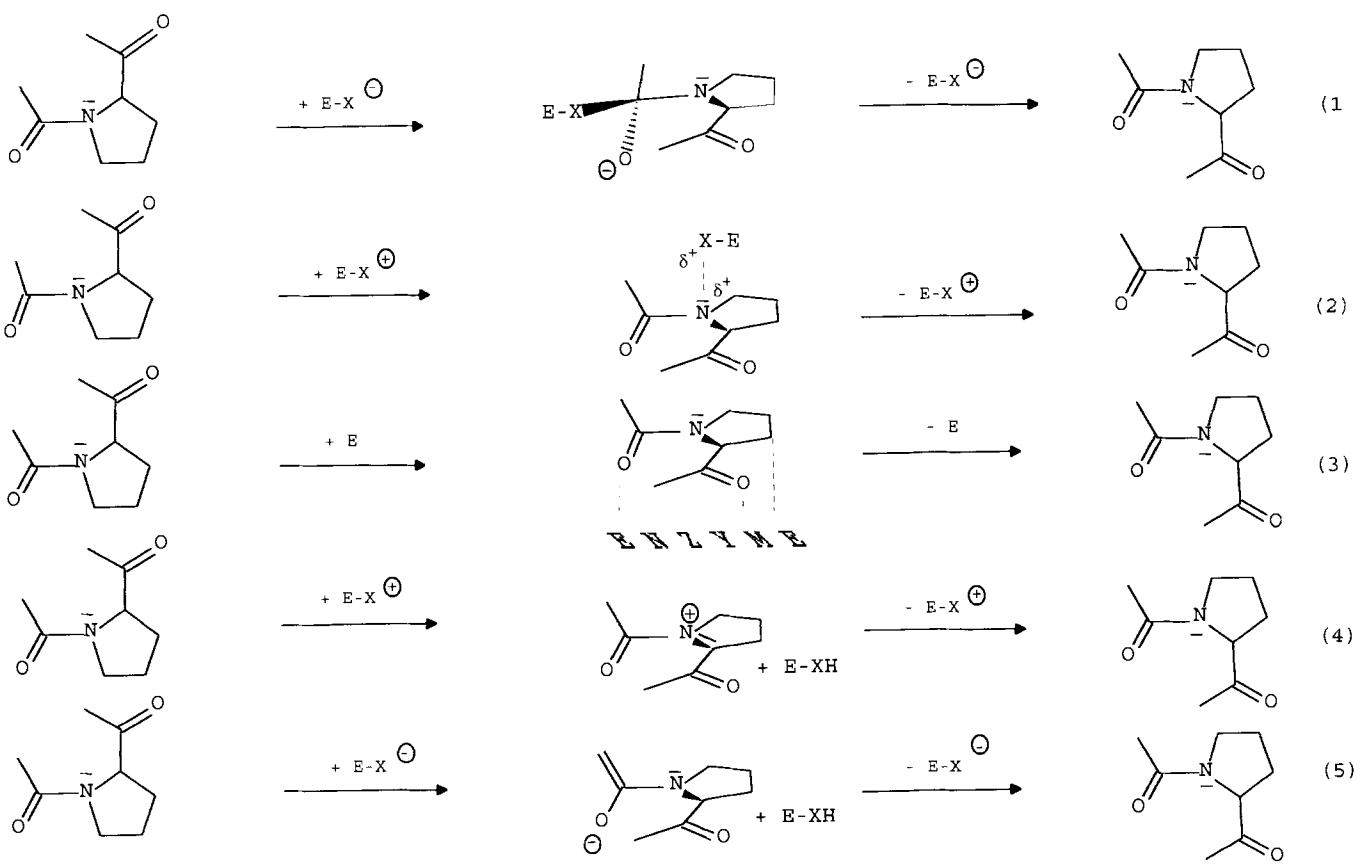


Fig. 16. Hypothetical reaction mechanisms for the PPIase-catalyzed *cis/trans* isomerization of the prolyl-peptide bond. E–X corresponds to an enzyme-bound reactive group. In every mechanism the lone pair is pushed towards the nitrogen atom; in other words, the electrons are not delocalized in the amide bond

be described by the transfer of a proton with a pK_a of 5.9[266] (literature value 4.92[246]). Together with the low enthalpy of activation, $\Delta H^{\neq} = 0.3-3$ kcal mol^{-1},[146, 246, 247] this parameter implies an unusual mechanism of catalysis.

At first glance secondary kinetic isotope effects greater than 1.0 for Xaa-Pro substrates with a $C_\alpha(D)H$ unit in the Xaa residue (found in both enzyme families), solvent deuterium isotope effects $(k_{cat}/K_m)_{H_2O}/(k_{cat}/K_m)_{D_2O} \approx 1$, and the fact that k_{cat}/K_m is largely independent of pH (for pH values above 7) seem to imply a very simple mechanism, possibly with a noncovalent transition state (Eq. (3) in Fig. 16). In this mechanism the strong binding of the transition state to the enzyme, reflected by an angle $\omega \approx 90°$ at the prolyl-peptide bond, must then be responsible for lowering the free enthalpy of activation $\Delta G^{\neq}$ (conformational twist mechanism).[146] The transfer of the substrates from the aqueous medium into the hydrophobic enzyme area could simultaneously lead to the reduced electron delocalization in the ground state and the contribution to the catalytic effect discussed previously.

As ^{126}His is near the isomerization center in the complex (Ala-Pro)–Cyp18cy, it is a good candidate for a catalytically active side chain (Fig. 17). A backbone segment (^{102}Asn to

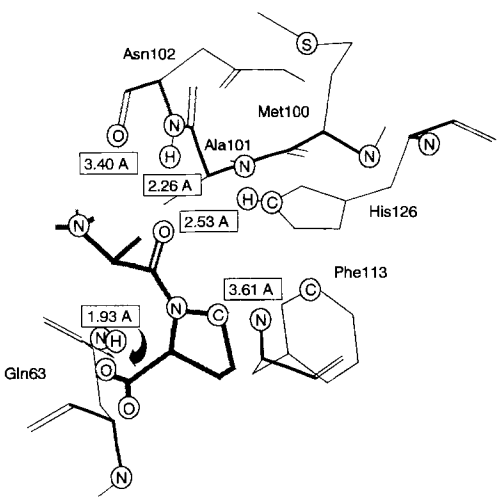


Fig. 17. All amino acid residues of the cytosolic cyclophilin [19] that have an atom located within 5.5 Å of the oxygen atom of the peptide carbonyl group of the bound dipeptide Ala-Pro (thick gray line). For the hidden amide group of the side chain of ^{63}Gln the H···O distance given is indicative of a strong hydrogen bond. For further information see Fig. 14.

^{100}Met) of the protein is almost parallel to the peptidyl residue Xaa in the Xaa-Pro unit but oriented opposite to the chain polarity. The carbonyl group adjacent to the Ala-Pro unit forms a hydrogen bond to the backbone NH group of ^{102}Asn; in the FK506–FKBP complex this function is performed by the ^{82}Tyr–OH group (see Fig. 14). In this complex no other functional amino acid side chains are in near the isomerization center. The effect of the hydrogen bond between the side chain of ^{63}Gln and the carboxyl group of Ala-Pro, which does not occur in polypeptide substrate, could differentiate structurally between this inhibitory dipeptide complex and the substrate–Cyp18 complex. In the tetrapeptide complex ^{55}Arg is also at a suitable position for hydrogen bonding.[118]

Site-specific mutagenesis was used to rule out the nucleophilic role of SH groups in the mechanism of catalysis in Cyp18cy.[248] This was inferred from inhibitor data and the identification of a cysteine residue protected from SH modification in the CsA–Cyp complex.[5] ^{115}Cys is near the active center but too far away from the peptidyl carbonyl unit of the substrate for nucleophilic attack. Furthermore, the binding of CsA and enzymatic activity can be separated from another by mutation experiments; for example, a more than 100-fold decrease in the ability of the W121A mutant enzyme to bind CsA is accompanied by only a 11.4-fold reduction in catalytic activity. Even the practically inactive enzymes H126Q, F60A, and R55A can still bind CsA; quantitative data is not available.[164]

Based on the qualitative results of the in vivo performance of Cyp26mem from *Drosophila melanogaster*,[127] mutations at Gly130Asp, Gly108Asp, Gly64Asp, Gly65Asp, and Asn35Lys (the numbering is based on that of human Cyp18cy) lead to enzymes with diminished activity.

Compared to cyclophilins, much more quantitative data is available for FKBP enzymes with point mutations. The exchange of the single cysteine residue (Cys22Ala), the successive exchange of all five serine residues, and exchange of two of the total of seven threonine residues (Thr75Ala, Thr96Ala) eliminated potential nucleophiles and hydrogen bond donors. None of the resulting enzymes showed significant reductions in activity or in affinity for FK506 or rapamycin.[220]

However, as observed for the cyclophilins, mutant enzymes in this protein family must exist whose enzyme activity can be separated from FK506 binding. For example, the Phe36Tyr mutation in FKBP12cy[213] does not affect the affinity for the inhibitor, but the enzyme activity is drastically reduced. In the case of Asp37Val exchange in the same enzyme, both processes are almost totally uncoupled, and this time a relatively great loss of affinity for FK506 is also observed.[249] This tendency is also seen to almost the same extent in *Legionella pneumophila* FKBP25mem upon the substitution of Asp37Leu (numbering based on human FKBP12cy), an amino acid that is highly conserved within the FKBP family.[218] Amongst those amino acids near the active center (see Fig. 17) that were tested in *Legionella pneumophila* FKBPmem, are ^{36}Phe and ^{99}Phe in addition to ^{82}Tyr. ^{87}His seems to play no role in catalysis.[249]

9. Immunosuppressor–PPIase Complexes and the Calcineurin Model

The loss of PPIase activity when the receptors Cyp18cy and FKBP12cy bind CsA and FK506, respectively, is not enough on its own to explain the blocking of T-cell activation by these compounds. The second highly effective immunosuppressive peptidomacrolide, rapamycin, is an even better inhibitor of FKBP12cy than of FK506, but its biological activity has a completely different molecular basis. Instead of blocking the transcription of key genes early in the signal transduction cascade, as was found for inhibition with CsA and FK506, rapamycin affects constitutive cell division by blocking the $G_1 \rightarrow S$ phase.[191, 250, 251] It appears that a rapamycin–FKBP complex blocks the rise in activity of p70S6 kinase which normally occurs when the IL-2

receptor or CD28 is stimulated.[252-253] This effect is not restricted to T cells.[254]

In addition, a series of CsA and FK506 derivatives (the off-diagonal analogues referred to previously) specifically inhibit PPIase activity with their excellent affinity but show a different effect or no effect at all in the in vitro IL-2 transcription models and T-cell activation tests.[153, 226] That these compounds, FK506, and CsA all have a common receptor binding site can be demonstrated by the antagonistic effect of the biologically inactive derivatives in transcription tests. These results along with those of deletion experiments carried out on the genes for Cyp12cy and FKBP12cy in yeast and *Neurospora crassa* make it clear that the specific binding of the immunosuppressive compounds to these receptors is a necessary step in blocking the T-cell response, but it is not in itself enough to cause the effect. Thus it seems that the components responsible for the immunosuppressive effect are in fact the ligand–PPIase complexes themselves. They possess properties not found in the free ligand or protein alone.

By using affinity chromatography with carrier-bound FK506–FKBP or CsA–Cyp, S. L. Schreiber et al. and Weissman et al. were able to demonstrate that calcineurin/calmodulin is the common binding protein for these complexes.[7, 8] However, rapamycin–FKBP12cy did not bind these proteins. This heteromeric protein phosphatase (consisting of calcineurin A, calcineurin B, calmodulin, Ca^{2+}) is inhibited in its hydrolysis activity towards protein phosphates (but not towards 4-nitrophenylphosphate) by CsA–Cyp18cy and FK506–FKBP with a K_i value of 35 nM. In a quantitative test of transcription activity of the IL-2 specific transcription factor NF-AT_p, a number of off-diagonal analogues of FK506 and CsA showed the expected correlation between K_i value for calcineurin and the IC_{50} value in the transcription model.[154] The cellular target molecule for the phosphatase activity of calcineurin was found to be the roughly 120 kDa, cytosolic, phosphorylated component of the multimeric transcription factor NF-AT.[255] NF-AT_p is present in the cell nucleus in the unphosphorylated form. A lack of calcineurin activity is thought to prevent translocation of NF-AT_p, such that the active transcription complex at the IL-2 promoter (which consists proteins of the Jun and Fos families and the DNA-binding NF-AT) cannot be turned on owing to the lack of the cytosolic component (Fig. 18).[256] This strong calcineurin inhibition is a special property of the cytosolic FKBP12 and Cyp18cy complexes. In comparison, the binding of FK506 to mature FKBP16mem leads to 200-fold reduction in inhibition for the phosphatase.[192]

It still remains to be explained at the molecular level why the PPIase–effector complexes inhibit calcineurin and not the free constituents of the complex. Structure–activity analyses for a large number of FK506 derivatives that all bind FKBP12cy but have different effects on IL-2 release indicate that very subtle effects are responsible. Based on these data and the three-dimensional structures of the complexes, an approximate effector region for the active substances has been postulated, which is responsible for the contact to calcineurin. In the case of CsA this is amino acids 5–8, and for FK506 the carbon chain C17–C32.

Thus in contrast to ascomycin (for structure see legend for Fig. 5), C18-hydroxyascomycin is inactive in the IL-2 test but a strong antagonist of FK506 and rapamycin effects.[257] As expected it does not affect calcineurin activity. The structures of

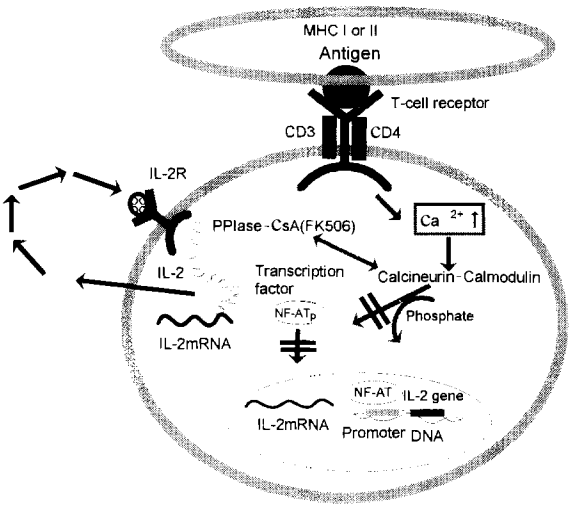


Fig. 18. Hypothetical mechanism for the suppression of antigen- or mitogen-stimulated clonal T-cell expansion by CsA or FK506. Inhibition of calcineurin activity by the CsA(FK506)–PPIase complex leads to the interruption of the signal transduction after T-cell stimulation. The IL-2 receptor triggers an independent signal pathway. MHC = major histocompatibility complex.

the two complexes with FKBP12 were determined.[258] A comparison reveals that the structural differences between biologically active and inactive complexes (F506–(human FKBPcy12) and ascomycin–(human FKBP12cy), respectively) are so minimal that the addition of the single OH group of hydroxyascomycin must affect the oligomeric calcineurin complex (which has a net molecular weight of 100 kDa).[213] If the C18-hydroxyascomycin–(yeast FKBP12cy) complex is used in an inhibition test for calcineurin, the phosphatase activity is blocked almost as effectively as with FK506–(human FKBP12cy). Surprisingly, the three-dimensional crystal structure of this complex shows the same peptidomacrolide conformation as in the inactive human complex. Thus whether a substance–protein complex is inactive or active is decided by the nonconserved amino acids in the sequences of each FKBP. Such subtle relationships are also seen in complexes of CsA derivatives with Cyp18cy and Cyp23sec.[156, 260]

The effects of CsA–PPIase complexes (and the FKBP–PPIase complexes) probably extend further than to just T cell and relatively slow transcription regulation. Stimulation of the IgE receptor results in the fast release of histamine ($t_{1/2} \approx 10$ min!) and can be blocked by FK506 and CsA. This fast release of histamine from mast cells was also found to be linked to inhibitor–PPIase complexes.[261] In the guard cells of higher plants the influx of K^+ ions is regulated by the intracellular level of Ca^{2+} which serves as a secondary messenger. The K^+ channel is blocked by high levels of Ca^{2+}, and this blocking effect can be eliminated by the addition of CsA–Cyp18cy or FK506–FKBP12cy. Deblocking can be achieved by addition of CsA alone but not with FK506 alone. The reason for this is that the major component of cells' own FKBPs (a FKBP16 homologue) gives an inhibitor complex that is inactive towards calcineurin.[110]

It should also be mentioned that a second proline-specific enzyme, dipeptidyl peptidase IV as CD26, specifically influences the antigen-induced signal transduction in T cells. The blocking of proteolytic activity by inhibition,[262] as demonstrated by CsA and FK506, leads to reduction of IL-2 secretion.

10. Outlook

Since the discovery of the first peptidyl-prolyl *cis/trans* isomerase the number of sequenced enzymes has increased dramatically. Many of these PPIases play a role in an as yet unexplained way in cellular regulation systems and may play a role in cell–cell interactions. In order to understand the course of events on a molecular level, the in vivo effectors or substrates must be identified and the effect of *cis/trans* isomerization on the properties of a polypeptide chain must be investigated. Naturally we expect that the number of known PPIase sequences will increase further, and perhaps new activity tests will identify new PPIase families. In addition, these proteins offer enzymologists the chance to study the mechanistic background of the simplest chemical "reaction", the rotation of a single bond. The PPIases are the first enzymes known that are specialized for the catalysis of conformational changes. They are probably specific for proline-containing polypeptides. It is interesting to speculate whether further conformases with completely different target molecules exist in cells.

I would like to thank my previous and current co-workers, those who conducted the first investigations after the discovery of these enzymes, Dr. Holger Bang and Dr. Carla Mech,† and those who joined our group later, Dr. habil. Gerhard Küllertz, Dr. Jens Rahfeld, and Dr. Mike Schutkowski. They have all worked enthusiastically on our contribution to the research discussed here. Without the flood of ideas and the work of the Ph. D. and M. Sc. students it would not have been possible to carry out the experiments presented here. The collaboration with the groups of Franz X. Schmid (Bayreuth), Jörg Hacker (Würzburg), Klaus Kühn (Martinsried), Kurt Lang (Penzberg), and Sture Forsen (Lund) enabled us to acquire the techniques and methods necessary for investigating the enzymes. I would like to thank Prof. Hengming Ke for the coordinates of the cyclophilin and cyclophilin–(Ala-Pro) structures which were used in creating Figures 10 and 17. The financial support of the Max-Planck-Gesellschaft, the Deutsche Forschungsgemeinschaft, the Volkswagenstiftung, the Boehringer-Ingelheim-Stiftung, and the Fonds der Chemischen Industrie is gratefully acknowledged.

Received: September 6, 1993 [A 221E]
German version: *Angew. Chem.* **1994**, *106*, 1479
Translated by: Dr. M. Griffiths, Edingen (FRG)

[1] G. Fischer, H. Bang, C. Mech, *Biomed. Biochim. Acta* **1984**, *43*, 1101.
[2] H. Umezawa, T. Aoyagi, H. Morishima, M. Matsuzaki, M. Hamada, T. Takeguchi, *J. Antibiot.* **1970**, *23*, 259; H. Tomoda, S. Omura, *ibid.* **1990**, *43*, 1207.
[3] R. E. Handschumacher, M. W. Harding, J. Rice, R. J. Drugge, D. W. Speicher, *Science* **1984**, *226*, 544.
[4] N. Takahashi, T. Hayano, M. Suzuki, *Nature* **1989**, *337*, 473.
[5] G. Fischer, B. Wittmann-Liebold, K. Lang, T. Kiefhaber, F. X. Schmid, *Nature* **1989**, *337*, 476.
[6] J. J. Siekierka, S. H. Hung, M. Poe, C. S. Lin, N. H. Sigal, *Nature* **1989**, *341*, 755; M. W. Harding, A. Galat, D. E. Uehling, S. L. Schreiber, *ibid.* **1989**, *341*, 758.
[7] J. Friedman, I. Weissman, *Cell* **1991**, *66*, 799.
[8] J. Liu, J. D. Farmer, Jr., W. S. Lane, J. Friedman, I. Weissman, S. L. Schreiber, *Cell* **1991**, *66*, 807.
[9] M. K. Rosen, S. L. Schreiber, *Angew. Chem.* **1992**, *104*, 413; *Angew. Chem. Int. Ed. Engl.* **1992**, *31*, 384.
[10] J. F. Brandts, H. R. Halvorson, M. Brennan, *Biochemistry* **1975**, *14*, 4953; B. T. Nall, *Comments Mol. Cell. Biophys.* **1985**, *3*, 123; F. X. Schmid, *Methods Enzymol.* **1986**, *131*, 70; P. S. Kim, R. L. Baldwin, *Annu. Rev. Biochem.* **1982**, *51*, 459; M. Levitt, *J. Mol. Biol.* **1981**, *145*, 251; J. Engel, D. J. Prockop, *Annu. Rev. Biophys. Biophys. Chem.* **1991**, *20*, 137.
[11] D. B. Wetlaufer, *Biopolymers* **1985**, *24*, 251; R. Jaenicke, *Prog. Biophys. Mol. Biol.* **1987**, *49*, 117; R. Jaenicke, *Angew. Chem.* **1984**, *96*, 385; *Angew. Chem. Int. Ed. Engl.* **1984**, *23*, 395; M. J. Gething, J. Sambrook, *Nature* **1992**, *355*, 33; P. Bruckner, E. F. Eikenberry, D. J. Prockop, *Eur. J. Biochem.* **1981**, *118*, 607.
[12] D. Oesterhelt, J. Tittor, E. Bamberg, *J. Bioenerg. Biomembr.* **1992**, *24*, 181.
[13] M. K. Rosen, R. F. Standaert, A. Galat, M. Nakatsuka, S. L. Schreiber, *Science* **1990**, *248*, 863.
[14] M. J. Bossard, P. L. Koser, M. Brandt, D. J. Bergsma, M. A. Levy, *Biochem. Biophys. Res. Commun.* **1991**, *176*, 1142.
[15] Because increasing numbers of isoenzymes in the PPIase family have been discovered, some of the abbreviations for the enzymes have become inexact and confusing. For the unequivocal naming of cyclophilins and FKBPs we assume the following abbreviations: Cyp and FKBP stand for the two respective families of PPIases. The abbreviations Cyp and FKBP are followed by the molecular weight (kDa) of the amino acid sequence of the complete preprotein obtained from the nucleotide sequence. When the location is known, then the abbreviations cy (cytosolic), mit (mitochondrial), sec (secretory), mem (membrane bound) follow the molecular weight. The organism from which the protein comes is noted in front of or after the enzyme abbreivation, if needed. The cross references to several of the other abbreviations in the literature are given in the footnotes to Scheme 1 (Cyp) and Scheme 2 (FKBP).
[16] E. R. Schönbrunner, S. Mayer, M. Tropschug, G. Fischer, N. Takahashi, F. X. Schmid, *J. Biol. Chem.* **1991**, *266*, 3630.
[17] R. E. London, D. G. Davis, R. J. Vavrek, J. M. Stewart, R. E. Handschumacher, *Biochemistry* **1990**, *29*, 10298.
[18] J. Kallen, M. D. Walkinshaw, *FEBS Lett.* **1992**, *300*, 286.
[19] H. Ke, D. Mayrose, W. Cao, *Proc. Natl. Acad. Sci. USA* **1993**, *90*, 3324.
[20] G. D. Van Duyne, R. F. Standaert, P. A. Karplus, S. L. Schreiber, J. Clardy, *Science* **1991**, *252*, 839.
[21] C. Weber, G. Wider, B. von Freyberg, R. Traber, W. Braun, H. Widmer, K. Wüthrich, *Biochemistry* **1991**, *30*, 6563.
[22] H. Akagi, A. Reynolds, M. Hjelm, *J. Int. Med. Res.* **1991**, *19*, 1.
[23] J. Kallen, C. Spitzfaden, M. G. Zurini, G. Wider, H. Widmer, K. Wüthrich, M. D. Walkinshaw, *Nature* **1991**, *353*, 276.
[24] H. M. Ke, *J. Mol. Biol.* **1992**, *228*, 539.
[25] F. X. Schmid, L. Mayr, M. Mücke, R. Schönbrunner, *Adv. Protein Chem.* **1993**, *44*, 25.
[26] G. Wiederrecht, L. Brizuela, K. Elliston, N. H. Sigal, J. J. Siekierka, *Proc. Natl. Acad. Sci. USA* **1991**, *88*, 1029.
[27] A. I. Denesyuk, M. Vihinen, J. Lundell, V. P. Zav'yalov, T. Korpela, *Biochem. Biophys. Res. Commun.* **1993**, *192*, 912.
[28] L. B. Peddada, J. D. McPherson, R. Law, J. J. Wasmuth, P. Youderian, R. J. Deans, *Cytogenet. Cell Genet.* **1992**, *60*, 219.
[29] H. A. Young, N. A. Jenkins, N. G. Copeland, S. Simek, M. I. Lerman, B. Zbar, G. Glenn, J. R. Ortaldo, S. K. Anderson, *Genomics* **1993**, *16*, 548.
[30] A. G. Difella, A. Hawkins, R. J. Craig, S. L. Schreiber, C. A. Griffin, *Biochem. Biophys. Res. Commun.* **1992**, *189*, 819.
[31] B. Haendler, E. Hofer, *Eur. J. Biochem.* **1990**, *190*, 477.
[32] R. F. Standaert, A. Galat, G. L. Verdine, S. L. Schreiber, *Nature* **1990**, *346*, 671.
[33] N. H. Sigal, F. J. Dumont, *Annu. Rev. Immunol.* **1992**, *10*, 519.
[34] J. Y. Chang, S. N. Sehgal, C. C. Bansbach, *Trends Pharmacol. Sci.* **1991**, *12*, 218.
[35] C. Yousry, J. Kanitakis, *Pathol. Biol.* **1991**, *39*, 293.
[36] P. A. Nelson, A. Kawamura, Y. Akselband, D. A. Peattie, R. A. Aldape, M. W. Harding, *Transplant. Proc.* **1991**, *23*, 2867; S. C. Wang, A. Zeevi, M. L. Jordan, R. L. Simmons, D. J. Tweardy, *ibid.* **1991**, *23*, 2920; M. J. Tocci, D. A. Matkovich, K. A. Collier, P. Kwok, F. Dumont, S. Lin, S. Degudicibus, J. J. Siekierka, J. Chin, N. I. Hutchinson, *J. Immunol.* **1989**, *143*, 718.
[37] E. A. Emmel, C. L. Verweij, D. B. Durand, K. M. Higgins, E. Lacy, G. R. Crabtree, *Science* **1989**, *246*, 1617; P. S. Mattila, K. S. Ullman, S. Fiering, E. A. Emmel, M. McCutcheon, G. R. Crabtree, L. A. Herzenberg, *EMBO J.* **1990**, *9*, 4425.
[38] P. M. Colombani, A. Robb, A. D. Hess, *Science* **1985**, *228*, 337; P. S. Bernstein, W. C. Law, R. R. Rando, *J. Biol. Chem.* **1987**, *262*, 16848; E. W. Palaszynski, J. G. Donnelly, S. J. Soldin, *Clin. Biochem.* **1991**, *24*, 63.
[39] K. Ziegler, M. Frimmer, *Biochim. Biophys. Acta* **1986**, *855*, 147.
[40] M. L. Moss, R. E. Palmer, P. Kuzmic, B. E. Dunlap, W. Henzel, J. L. Kofron, W. S. Mellon, C. A. Royer, D. H. Rich, *J. Biol. Chem.* **1992**, *267*, 22054.
[41] B. M. J. Foxwell, G. Woerly, H. Husi, A. Mackie, V. F. J. Quesniaux, P. C. Hiestand, R. M. Wenger, B. Ryffel, *Biochim. Biophys. Acta* **1992**, *1138*, 115; B. Ryffel, G. Woerly, V. F. J. Quesniaux, H. Husi, B. M. J. Foxwell, *Biochem. Pharmacol.* **1992**, *43*, 953.
[42] K. Ziegler, M. Frimmer, G. Fritzsch, H. Koepsell, *J. Biol. Chem.* **1990**, *265*, 3270.
[43] H. Bang, K. Brune, C. Nager, U. Feige, *Experientia* **1993**, *49*, 533.
[44] J. G. Donnelly, R. L. Russell, E. W. Palaszynski, K. R. Copeland, R. W. Yatscoff, M. M. Chan, S. J. Soldin, *Clin. Biochem.* **1991**, *24*, 71; J. G. Donnelly, Y. J. Chen, R. W. Yatscoff, K. R. Copeland, E. W. Palaszynski, S. J. Soldin, *Clin. Chem.* **1993**, *39*, 122.

[45] B. M. Foxwell, A. Mackie, V. Ling, B. Ryffel, *Mol. Pharmacol.* **1989**, *36*, 543; T. Saeki, K. Ueda, Y. Tanigawara, R. Hori, T. Komano, *J. Biol. Chem.* **1993**, *268*, 6077.

[46] N. Takeguchi, K. Ichimura, M. Koike, W. Matsui, T. Kashiwagura, K. Kawahara, *Transplantation* **1993**, *55*, 646; R. J. Arceci, K. Stieglitz, B. E. Bierer, *Blood* **1992**, *80*, 1528.

[47] W. R. Melander, C. Horvath, *J. Chromatogr.* **1982**, *234*, 269; J. C. Gesquiere, E. Diesis, M. T. Cung, A. Tatar, *ibid.* **1989**, *478*, 121; E. Watson, W. C. Kenney, *ibid.* **1992**, *606*, 165.

[48] L. N. Lin, J. F. Brandts, *Biochemistry* **1979**, *18*, 43, 5037; *ibid.* **1983**, *22*, 4480; *ibid.* **1985**, *24*, 6533.

[49] G. Fischer, H. Bang, E. Berger, A. Schellenberger, *Biochim. Biophys. Acta* **1984**, *791*, 87.

[50] G. Fischer, J. Heins, A. Barth, *Biochim. Biophys. Acta* **1983**, *742*, 452.

[51] J. L. Kofron, P. Kuzmic, V. Kishore, E. Colon Bonilla, D. H. Rich, *Biochemistry* **1991**, *30*, 6127.

[52] C. Garciaecheverria, J. L. Kofron, P. Kuzmic, V. Kishore, D. H. Rich, *J. Am. Chem. Soc.* **1992**, *114*, 2758.

[53] C. Garciaecheverria, J. L. Kofron, P. Kuzmic, D. H. Rich, *Biochem. Biophys. Res. Commun.* **1993**, *191*, 70.

[54] J. R. Garel, O. Siffert, *Biochem. Biophys. Res. Commun.* **1979**, *89*, 591.

[55] V. L. Hsu, R. E. Handschumacher, I. M. Armitage, *J. Am. Chem. Soc.* **1990**, *112*, 6745.

[56] R. M. Justice, Jr., A. D. Kline, J. P. Sluka, W. D. Roeder, G. H. Rodgers, N. Roehm, J. S. Mynderse, *Biochem. Biophys. Res. Commun.* **1990**, *171*, 445.

[57] D. Hübner, T. Drakenberg, S. Forsen, G. Fischer, *FEBS Lett.* **1991**, *284*, 79.

[58] D. Kern, T. Drakenberg, M. Wikstrom, S. Forsen, H. Bang, G. Fischer, *FEBS Lett.* **1993**, *323*, 198.

[59] F. X. Schmid in *Protein Folding* (Ed.: T. E. Creighton), Freeman, New York, **1992**, p. 197.

[60] L. N. Lin, J. F. Brandts, *Biochemistry* **1987**, *26*, 3537.

[61] J. Kordel, T. Drakenberg, S. Forsen, E. Thulin, *FEBS Lett.* **1990**, *263*, 27.

[62] K. Lang, F. X. Schmid, G. Fischer, *Nature* **1987**, *329*, 268.

[63] M. Mücke, F. X. Schmid, *Biochemistry* **1992**, *31*, 7848.

[64] K. Lang, F. X. Schmid, *Nature* **1988**, *331*, 453.

[65] H. P. Bächinger, *J. Biol. Chem.* **1987**, *262*, 17144.

[66] C. Fransson, P. O. Freskgard, H. Herbertsson, A. Johansson, P. Jonasson, L. G. Martensson, M. Svensson, B. H. Jonsson, U. Carlsson, *FEBS Lett.* **1992**, *296*, 90.

[67] L. N. Lin, H. Hasumi, J. F. Brandts, *Biochim. Biophys. Acta* **1988**, *956*, 256.

[68] T. Kiefhaber, R. Quaas, U. Hahn, F. X. Schmid, *Biochemistry* **1990**, *29*, 3053.

[69] B. Haendler, R. Hofer-Warbinek, E. Hofer, *EMBO J.* **1987**, *6*, 947.

[70] M. W. Harding, R. E. Handschumacher, D. W. Speicher, *J. Biol. Chem.* **1986**, *261*, 8547.

[71] P. E. Danielson, S. Forss Petter, M. A. Brow, L. Calavetta, J. Douglass, R. J. Milner, J. G. Sutcliffe, *DNA* **1988**, *7*, 261.

[72] D. J. Bergsma, D. Sylvester, *Nucleic Acids Res.* **1990**, *18*, 200.

[73] K. W. Hasel, J. G. Sutcliffe, *Nucleic Acids Res.* **1990**, *18*, 4019.

[74] P. Caroni, A. Rothenfluh, E. McGlynn, C. Schneider, *J. Biol. Chem.* **1991**, *266*, 10739.

[75] C. S. Gasser, D. A. Gunning, K. A. Budelier, S. M. Brown, *Proc. Natl. Acad. Sci. USA* **1990**, *87*, 9519.

[76] J. Marivet, P. Frendo, G. Burkard, *Plant Sci. Limerick Irel.* **1992**, *84*, 171.

[77] D. Bartling, A. Heese, E. W. Weiler, *Plant Mol. Biol.* **1992**, *19*, 529.

[78] M. A. Stamnes, B. H. Shieh, L. Chuman, G. L. Harris, C. S. Zuker, *Cell* **1991**, *65*, 219.

[79] K. Barisic, S. Mollner, A. A. Noegel, G. Gerisch, J. E. Segall, *Dev. Genet. N.Y.* **1991**, *12*, 50.

[80] P. L. Koser, G. P. Livi, M. A. Levy, M. Rosenberg, D. J. Bergsma, *Gene* **1990**, *96*, 189.

[81] R. de Martin, L. Philipson, *Nucleic Acids Res.* **1990**, *18*, 4917.

[82] K. Dietmeier, M. Tropschug, *Nucleic Acids Res.* **1990**, *18*, 373.

[83] B. Haendler, R. Keller, P. C. Hiestand, H. P. Kocher, G. Wegmann, N. R. Movva, *Gene* **1989**, *83*, 39.

[84] M. W. Lightowlers, A. Haralambous, M. D. Rickard, *Mol. Biochem. Parsitol.* **1989**, *36*, 287.

[85] V. P. Argaet, G. F. Mitchell, *J. Parasitol.* **1992**, *78*, 660.

[86] M. Tropschug, *Nucleic Acids Res.* **1990**, *18*, 190.

[87] M. Tropschug, I. B. Barthelmess, W. Neupert, *Nature* **1989**, *342*, 953.

[88] B. H. Shieh, M. A. Stamnes, S. Seavello, G. L. Harris, C. S. Zuker, *Nature* **1989**, *338*, 67.

[89] S. Schneuwly, R. D. Shortridge, D. C. Larrivee, T. Ono, M. Ozaki, W. L. Pak, *Proc. Natl. Acad. Sci. USA* **1989**, *86*, 5390.

[90] L. J. Kieffer, T. W. Seng, W. Li, D. G. Osterman, R. E. Handschumacher, R. M. Bayney, *J. Biol. Chem.* **1993**, *268*, 12303.

[91] T. Ratajczak, A. Carrello, P. J. Mark, B. J. Warner, R. J. Simpson, R. L. Moritz, A. K. House, *J. Biol. Chem.* **1993**, *268*, 13187.

[92] G. Spik, B. Haendler, O. Delmas, C. Mariller, M. Chamoux, P. Maes, A. Tartar, J. Montreuil, K. Stedman, H. P. Kocher, R. Kellert, P. C. Hiestand, N. R. Movva, *J. Biol. Chem.* **1991**, *266*, 10735.

[93] E. R. Price, L. D. Zydowsky, M. J. Jin, C. H. Baker, F. D. McKeon, C. T. Walsh, *Proc. Natl. Acad. Sci. USA* **1991**, *88*, 1903.

[94] N. Iwai, T. Inagami, *Kidney Int.* **1990**, *37*, 1460.

[95] K. W. Hasel, J. R. Glass, M. Godbout, J. G. Sutcliffe, *Mol. Cell. Biol.* **1991**, *11*, 3484.

[96] S. Arber, K. H. Krause, P. Caroni, *J. Cell Biol.* **1992**, *116*, 113.

[97] D. J. Bergsma, C. Eder, M. Gross, H. Kersten, D. Sylvester, E. Appelbaum, D. Cusimano, G. P. Livi, M. M. McLaughlin, K. Kasyan, T. G. Porter, C. Silverman, D. Dunnington, A. Hand, W. P. Pritchett, M. J. Bossard, M. Brandt, M. A. Levy, *J. Biol. Chem.* **1991**, *266*, 23204.

[98] S. K. Anderson, S. Gallinger, J. Roder, J. Frey, H. A. Young, J. R. Ortaldo, *Proc. Natl. Acad. Sci. USA* **1993**, *90*, 542.

[99] M. M. McLaughlin, M. J. Bossard, P. L. Koser, R. Cafferkey, R. A. Morris, L. M. Miles, J. Strickler, D. J. Bergsma, M. A. Levy, G. P. Livi, *Gene* **1992**, *111*, 85.

[100] E. S. Davis, A. Becker, J. Heitman, M. N. Hall, M. B. Brennan, *Proc. Natl. Acad. Sci. USA* **1992**, *89*, 11169.

[101] P. L. Koser, D. Sylvester, G. P. Livi, D. J. Bergsma, *Nucleic Acids Res.* **1990**, *18*, 1643.

[102] L. Franco, A. Jimenez, J. Demolder, F. Molemans, W. Fiers, R. Contreras, *Yeast* **1991**, *7*, 971.

[103] A. Pahl, M. Uhlein, H. Bang, W. Schlumbohm, U. Keller, *Mol. Microbiol.* **1992**, *6*, 3551.

[104] T. Hayano, N. Takahashi, S. Kato, N. Maki, M. Suzuki, *Biochemistry* **1991**, *30*, 3041.

[105] J. Liu, C. T. Walsh, *Proc. Natl. Acad. Sci. USA* **1990**, *87*, 4028.

[106] M. A. Levy, M. Brandt, G. P. Livi, D. J. Bergsma, *Transplant. Proc.* **1991**, *23*, 319.

[107] T. F. Holzman, D. A. Egan, R. Edalji, R. L. Simmer, R. Helfrich, A. Taylor, N. S. Burres, *J. Biol. Chem.* **1991**, *266*, 2474.

[108] L. J. Kieffer, T. Thalhammer, R. E. Handschumacher, *J. Biol. Chem.* **1992**, *267*, 5503.

[109] T. Thalhammer, L. J. Kieffer, T. Jiang, R. E. Handschumacher, *Eur. J. Biochem.* **1992**, *206*, 31.

[110] S. Luan, W. W. Li, F. Rusnak, S. M. Assmann, S. L. Schreiber, *Proc. Natl. Acad. Sci. USA* **1993**, *90*, 2202.

[111] L. D. Zydowsky, S. I. Ho, C. H. Baker, K. McIntyre, C. T. Walsh, *Protein Sci.* **1992**, *1*, 961.

[112] H. Hasumi, T. Nishikawa, *Biochim. Biophys. Acta* **1993**, *1161*, 161.

[113] M. Tropschug, D. W. Nicholson, F. U. Hartl, H. Kohler, N. Pfanner, E. Wachter, W. Neupert, *J. Biol. Chem.* **1988**, *263*, 14433.

[114] I. Tanida, M. Yanagida, N. Maki, S. Yagi, F. Namiyama, T. Kobayashi, T. Hayano, N. Takahashi, M. Suzuki, *Transplant. Proc.* **1991**, *23*, 2856.

[115] L. A. Compton, J. M. Davis, J. R. Macdonald, H. P. Bächinger, *Eur. J. Biochem.* **1992**, *206*, 927.

[116] M. Herrler, H. Bang, K. Brune, G. Fischer, M. A. Marahiel, *FEBS Lett.* **1992**, *309*, 231.

[117] P. J. Casey, *J. Lipid Res.* **1992**, *33*, 1731.

[118] M. L. McDonald, T. Ardito, W. H. Marks, M. Kashgarian, M. I. Lorber, *Transplantation* **1992**, *53*, 460.

[119] M. J. Mihatsch, G. Thiel, B. Ryffel, *Toxicol. Lett.* **1989**, *46*, 125; J. B. Kopp, P. E. Klotman, *J. Am. Soc. Nephrol.* **1990**, *1*, 162.

[120] B. Ryffel, B. M. Foxwell, A. Gee, B. Greiner, G. Woerly, M. J. Mihatsch, *Transplantation* **1988**, *46 (2 Supplemental Volumes)*, 90S.

[121] B. Ryffel, G. Woerly, B. Greiner, B. Haendler, M. J. Mihatsch, B. M. Foxwell, *Immunology* **1991**, *72*, 399.

[122] R. P. Lad, M. A. Smith, D. C. Hilt, *Mol. Brain Res.* **1991**, *9*, 239.

[123] W. H. Marks, M. W. Harding, R. Handschumacher, C. Marks, M. I. Lorber, *Transplantation* **1991**, *52*, 340.

[124] A. J. Koletsky, M. W. Harding, R. E. Handschumacher, *J. Immunol.* **1986**, *137*, 1054.

[125] A. H. Sarris, M. W. Harding, T. R. Jiang, D. Aftab, R. E. Handschumacher, *Transplantation* **1992**, *54*, 904.

[126] N. J. Colley, E. K. Baker, M. A. Stamnes, C. S. Zuker, *Cell* **1991**, *67*, 255.

[127] B. Ondek, R. W. Hardy, E. K. Baker, M. A. Stamnes, B. H. Shieh, C. S. Zuker, *J. Biol. Chem.* **1992**, *267*, 16460.

[128] B. Sherry, N. Yarlett, A. Strupp, A. Cerami, *Proc. Natl. Acad. Sci. USA* **1992**, *89*, 3511.

[129] T. R. Davis, L. Tabatabai, K. Bruns, R. T. Hamilton, M. Nilsen-Hamilton, *Biochim. Biophys. Acta* **1991**, *1095*, 145.

[130] S. Bose, R. B. Freedman, *Biochem. Soc. Trans.* **1992**, *20*, 256S.

[131] C. J. Brandl, C. M. Deber, *Proc. Natl. Acad. Sci. USA* **1986**, *83*, 917; K. A. Williams, C. M. Deber, *Biochemistry* **1991**, *30*, 8919.

[132] O. McGuinness, N. Yafei, A. Costi, M. Crompton, *Eur. J. Biochem.* **1990**, *194*, 671; E. J. Griffiths, A. P. Halestrap, *Biochem. J.* **1991**, *274*, 611.

[133] M. Schweizer, J. Schlegel, D. Baumgartner, C. Richter, *Biochem. Pharmacol.* **1993**, *45*, 641.

[134] K. Sykes, M. J. Gething, J. Sambrook, *Proc. Natl. Acad. Sci. USA* **1993**, *90*, 5853.

[135] A. Fersht, *Enzyme Structure and Mechanism*, Freeman, New York, **1985**, p. 152.

[136] J. M. Davis, B. A. Boswell, H. P. Bächinger, *J. Biol. Chem.* **1989**, *264*, 8956.
[137] G. Fischer, F. X. Schmid, *Biochemistry* **1990**, *29*, 2205.
[138] P. O. Freskgard, N. Bergenhem, B. H. Jonsson, M. Svensson, U. Carlsson, *Science* **1992**, *258*, 466.
[139] S. E. Jackson, A. R. Fersht, *Biochemistry* **1991**, *30*, 10436.
[140] E. R. Schönbrunner, F. X. Schmid, *Proc. Natl. Acad. Sci. USA* **1992**, *89*, 4510.
[141] H. F. Lodish, N. Kong, *J. Biol. Chem.* **1991**, *266*, 14835.
[142] A. Knappik, C. Krebber, A. Plückthun, *Biotechnology* **1993**, *11*, 77.
[143] M. A. Stamnes, S. L. Rutherford, C. S. Zuker, *Trends Cell Biol.* **1992**, *2*, 272.
[144] B. Steinmann, P. Bruckner, A. Superti-Furga, *J. Biol. Chem.* **1991**, *266*, 1299.
[145] G. Pflugl, J. Kallen, T. Schirmer, J. N. Jansonius, M. G. M. Zurini, M. D. Walkinshaw, *Nature* **1993**, *361*, 91.
[146] R. K. Harrison, R. L. Stein, *J. Am. Chem. Soc.* **1992**, *114*, 3464.
[147] J. L. Kofron, P. Kuzmic, V. Kishore, G. Gemmecker, S. W. Fesik, D. H. Rich, *J. Am. Chem. Soc.* **1992**, *114*, 2670.
[148] P. Kuzmic, M. L. Moss, J. L. Kofron, D. H. Rich, *Anal. Biochem.* **1992**, *205*, 65.
[149] H. Kessler, M. Gehrke, J. Lautz, M. Kock, D. Seebach, A. Thaler, *Biochem. Pharmacol.* **1990**, *40*, 169; J. Lautz, H. Kessler, W. F. van Gunsteren, H. P. Weber, R. M. Wenger, *Biopolymers* **1990**, *29*, 1669.
[150] S. W. Fesik, R. T. Gampe, Jr., T. F. Holzman, D. A. Egan, R. Edalji, J. R. Luly, R. Simmer, R. Helfrich, V. Kishore, D. H. Rich, *Science* **1990**, *250*, 1406; S. W. Fesik, P. Neri, R. Meadows, E. T. Olejniczak, G. Gemmecker, *J. Am. Chem. Soc.* **1992**, *114*, 3165; O. Vix, B. Rees, J. C. Thierry, D. Altschuh, *Proteins Struct. Funct. Genet.* **1993**, *15*, 339.
[151] M. Kock, H. Kessler, D. Seebach, A. Thaler, *J. Am. Chem. Soc.* **1992**, *114*, 2676.
[152] V. F. Quesniaux, M. H. Schreier, R. M. Wenger, P. C. Hiestand, M. W. Harding, M. H. Van Regenmortel, *Transplantation* **1988**, *46 (2 Supplemental Volumes)*, 23S.
[153] N. H. Sigal, F. Dumont, P. Durette, J. J. Siekierka, L. Peterson, D. H. Rich, B. E. Dunlap, M. J. Staruch, M. R. Melino, S. L. Koprak, D. Williams, B. Witzel, J. M. Pisano, *J. Exp. Med.* **1991**, *173*, 619.
[154] J. Liu, M. W. Albers, T. J. Wandless, S. Luan, D. G. Alberg, P. J. Belshaw, P. Cohen, C. Mackintosh, C. B. Klee, S. L. Schreiber, *Biochemistry* **1992**, *31*, 3896.
[155] P. L. Durette, J. Boger, F. Dumont, R. Firestone, R. A. Frankshun, S. L. Koprak, C. S. Lin, M. R. Melino, A. A. Pessolano, J. Pisano, J. A. Schmidt, N. H. Sigal, M. J. Staruch, B. E. Witzel, *Transplant. Proc.* **1988**, *20*, 51.
[156] P. A. Nelson, Y. Akselband, A. Kawamura, M. Su, R. D. Tung, D. H. Rich, V. Kishore, S. L. Rosborough, M. T. Decenzo, D. J. Livingston, M. W. Harding, *J. Immunol.* **1993**, *150*, 2139.
[157] N. A. Cacalano, B. C. Chen, W. L. Cleveland, B. F. Erlanger, *Proc. Natl. Acad. Sci. USA* **1992**, *89*, 4353.
[158] Y. Theriault, T. M. Logan, R. Meadows, L. P. Yu, E. T. Olejniczak, T. F. Holzman, R. L. Simmer, S. W. Fesik, *Nature* **1993**, *361*, 88.
[159] H. M. Ke, L. D. Zydowsky, J. Liu, C. T. Walsh, *Proc. Natl. Acad. Sci. USA* **1991**, *88*, 9483.
[160] H. Kessler, M. Kock, T. Wein, M. Gehrke, *Helv. Chim. Acta* **1990**, *73*, 1818.
[161] H.-R. Loosli, H. Kessler, H. Oschkinat, H. P. Weber, T. J. Petcher, A. Widmer, *Helv. Chim. Acta* **1985**, *68*, 682.
[162] R. K. Harrison, R. L. Stein, *Biochemistry* **1990**, *29*, 3813.
[163] J. Liu, C. M. Chen, C. T. Walsh, *Biochemistry* **1991**, *30*, 2306.
[164] L. D. Zydowsky, F. A. Etzkorn, H. Y. Chang, S. B. Ferguson, L. A. Stolz, S. I. Ho, C. T. Walsh, *Protein Sci.* **1992**, *1*, 1092.
[165] C. Lee, K. Hoffmann, R. Zocher, *Biochem. Biophys. Res. Commun.* **1992**, *182*, 1282.
[166] N. Maki, F. Sekiguchi, J. Nishimaki, K. Miwa, T. Hayano, N. Takahashi, M. Suzuki, *Proc. Natl. Acad. Sci. USA* **1990**, *87*, 5440.
[167] A. G. DiLella, R. J. Craig, *Biochemistry* **1991**, *30*, 8512.
[168] J. J. Siekierka, G. Wiederrecht, H. Greulich, D. Boulton, S. H. Hung, J. Cryan, P. J. Hodges, N. H. Sigal, *J. Biol. Chem.* **1990**, *265*, 21011.
[169] P. A. Nelson, J. A. Lippke, M. A. Murcko, S. L. Rosborough, D. A. Peattie, *Gene* **1991**, *109*, 255.
[170] Y. Koltin, L. Faucette, D. J. Bergsma, M. A. Levy, R. Cafferkey, P. L. Koser, R. K. Johnson, G. P. Livi, *Mol. Cell. Biol.* **1991**, *11*, 1718.
[171] J. Heitman, N. R. Movva, M. N. Hall, *Science* **1991**, *253*, 905.
[172] A. Ferrara, R. Cafferkey, G. P. Livi, *Gene* **1992**, *113*, 125.
[173] Y. J. Jin, M. W. Albers, W. S. Lane, B. E. Bierer, S. L. Schreiber, S. J. Burakoff, *Proc. Natl. Acad. Sci. USA* **1991**, *88*, 6677.
[174] Y. J. Jin, S. J. Burakoff, B. E. Bierer, *J. Biol. Chem.* **1992**, *267*, 10942.
[175] G. Wiederrecht, M. M. Martin, N. H. Sigal, J. J. Siekierka, *Biochem. Biophys. Res. Commun.* **1992**, *185*, 298.
[176] D. T. Hung, S. L. Schreiber, *Biochem. Biophys. Res. Commun.* **1992**, *184*, 733.
[177] A. Galat, W. S. Lane, R. F. Standaert, S. L. Schreiber, *Biochemistry* **1992**, *31*, 2427.
[178] D. A. Peattie, M. W. Harding, M. A. Fleming, M. T. Decenzo, J. A. Lippke, D. J. Livingston, M. Benasutti, *Proc. Natl. Acad. Sci. USA* **1992**, *89*, 10974.
[179] M. C. Lebeau, N. Massol, J. Herrick, L. E. Faber, J. M. Renoir, C. Radanyi, E. E. Baulieu, *J. Biol. Chem.* **1992**, *267*, 4281.
[180] J. B. Nielsen, F. Foor, J. J. Siekierka, M. J. Hsu, N. Ramadan, N. Morin, A. Shafiee, A. M. Dahl, L. Brizuela, G. Chrebet, K. A. Bostian, S. A. Parent, *Proc. Natl. Acad. Sci. USA* **1992**, *89*, 7471.
[181] A. Pahl, U. Keller, *J. Bacteriol.* **1992**, *174*, 5888.
[182] M. Tropschug, E. Wachter, S. Mayer, E. R. Schönbrunner, F. X. Schmid, *Nature* **1990**, *346*, 674.
[183] B. A. Shampson, E. C. Gotschlich, *Proc. Natl. Acad. Sci. USA* **1992**, *89*, 1164.
[184] A. G. Lundemose, D. A. Rouch, S. Birkelund, G. Christiansen, J. H. Pearce, *Mol. Microbiol.* **1992**, *6*, 2539.
[185] G. Fischer, H. Bang, B. Ludwig, K. Mann, J. Hacker, *Mol. Microbiol.* **1992**, *6*, 1375.
[186] N. C. Engleberg, C. Carter, D. R. Weber, N. P. Cianciotto, B. I. Eisenstein, *Infect. Immun.* **1989**, *57*, 1263.
[187] J. M. Bangsborg, N. P. Cianciotto, P. Hindersson, *Infect. Immun.* **1991**, *59*, 3836.
[188] J. Kato, L. Chu, K. Kitano, J. D. DeVault, K. Kimbara, A. M. Chakrabarty, T. K. Misra, *Gene* **1989**, *84*, 31.
[189] L. Isaki, R. Beers, H. C. Wu, *J. Bacteriol.* **1990**, *172*, 6512.
[190] M. W. Albers, C. T. Walsh, S. L. Schreiber, *J. Org. Chem.* **1990**, *55*, 4984.
[191] B. E. Bierer, P. S. Mattila, R. F. Standaert, L. A. Herzenberg, S. J. Burakoff, G. Crabtree, S. L. Schreiber, *Proc. Natl. Acad. Sci. USA* **1990**, *87*, 9231.
[192] M. K. Rosen, D. Yang, P. K. Martin, S. L. Schreiber, *J. Am. Chem. Soc.* **1993**, *115*, 821.
[193] P. K. K. Tai, M. W. Albers, H. Chang, L. E. Faber, S. L. Schreiber, *Science* **1992**, *256*, 1315.
[194] A. W. Yem, A. G. Tomasselli, R. L. Heinrikson, H. Zurcher Neely, V. A. Ruff, R. A. Johnson, M. R. Deibel, Jr., *J. Biol. Chem.* **1992**, *267*, 2868.
[195] A. G. Lundemose, J. E. Kay, J. H. Pearce, *Mol. Microbiol.* **1993**, *7*, 777.
[196] R. Edalji, T. J. Pilotmatias, S. D. Pratt, D. A. Egan, J. M. Severin, E. G. Gubbins, A. M. Petros, S. W. Fesik, N. S. Burres, T. F. Holzman, *J. Protein Chem.* **1992**, *11*, 213.
[197] J. J. Siekierka, G. Wiederrecht, J. Cryan, S. H. Y. Hung, M. Comisky, N. H. Sigal, *Transplant. Proc.* **1991**, *23*, 2720.
[198] D. Marquisomer, G. Sanyal, D. B. Volkin, A. I. Marcy, H. K. Chan, J. A. Ryan, C. R. Middaugh, *Biochem. Biophys. Res. Commun.* **1991**, *179*, 741.
[199] D. A. Egan, T. M. Logan, H. Liang, E. Matayoshi, S. W. Fesik, T. F. Holzman, *Biochemistry* **1993**, *32*, 1920.
[200] J. P. Steiner, T. M. Dawson, M. Fotuhi, C. E. Glatt, A. M. Snowman, N. Cohen, S. H. Snyder, *Nature* **1992**, *358*, 584; M. Asami, T. Kuno, H. Mukai, C. Tanaka, *Biochem. Biophys. Res. Commun.* **1993**, *192*, 1388.
[201] N. H. Sigal, J. J. Siekierka, F. J. Dumont, *Biochem. Pharmacol.* **1990**, *40*, 2201.
[202] M. Kobayashi, K. Ohtsuka, K. Tamura, K. Ohara, S. Fujihira, Y. Hirano, C. Kusunoki, M. Hayashi, S. Satoh, N. Katayama, T. Tsutsumi, K. Nakamura, M. Niwa, M. Kohsaka, *Transplant. Proc.* **1993**, *25*, 655.
[203] Q. Xu, M. C. Leiva, S. A. Fischkoff, R. E. Handschumacher, C. R. Lyttle, *J. Biol. Chem.* **1992**, *267*, 11968; M. C. Leiva, C. R. Lyttle, *Biochem. Biophys. Res. Commun.* **1992**, *186*, 1178.
[204] T. E. Starzl, S. L. Schreiber, M. W. Albers, K. A. Porter, C. S. Foglieni, A. Francavilla, *Transplantation* **1991**, *52*, 751.
[205] B. F. Erlanger, *Immunol. Today* **1993**, *14*, 369.
[206] P. L. Koser, W. K. Eng, M. J. Bossard, M. M. McLaughlin, R. Cafferkey, G. M. Sathe, L. Faucette, M. A. Levy, R. K. Johnson, D. J. Bergsma, G. P. Livi, *Gene* **1993**, *129*, 159.
[207] J. Heitman, N. R. Movva, P. C. Hiestand, M. N. Hall, *Proc. Natl. Acad. Sci. USA* **1991**, *88*, 1948.
[208] J. Kunz, R. Henriquez, U. Schneider, M. Deuterreinhard, N. R. Movva, M. N. Hall, *Cell* **1993**, *73*, 585.
[209] J. A. Partaledis, V. Berlin, *Proc. Natl. Acad. Sci. USA* **1993**, *90*, 5450.
[210] T. Hultsch, M. W. Albers, S. L. Schreiber, R. J. Hohman, *Proc. Natl. Acad. Sci. USA* **1991**, *88*, 6229.
[211] S. Riviere, A. Menez, A. Galat, *FEBS Lett.* **1993**, *315*, 247.
[212] I. Callebaut, J. M. Renoir, M. C. Lebeau, N. Massol, A. Burny, E. E. Baulieu, J. P. Mornon, *Proc. Natl. Acad. Sci. USA* **1992**, *89*, 6270; N. Massol, M. C. Lebeau, J. M. Renoir, L. E. Faber, E. E. Baulieu, *Biochem. Biophys. Res. Commun.* **1992**, *187*, 1330.
[213] G. Wiederrecht, S. Hung, H. K. Chan, A. Marcy, M. Martin, J. Calaycay, D. Boulton, N. Sigal, R. L. Kincaid, J. J. Siekierka, *J. Biol. Chem.* **1992**, *267*, 21753; V. A. Ruff, A. W. Yem, P. L. Munns, L. D. Adams, I. M. Reardon, M. R. Deibel, K. L. Leach, *ibid.* **1992**, *267*, 21285.
[214] Y. M. Ning, E. R. Sanchez, *J. Biol. Chem.* **1993**, *268*, 6073.
[215] J. Hacker, G. Fischer, *Mol. Microbiol.* **1993**, *10*, 445.
[216] R. Marre, J. Hacker, *BioEngineering* **1992**, *1*, 60.
[217] N. P. Cianciotto, B. I. Eisenstein, C. H. Mody, G. B. Toews, N. C. Engleberg, *Infect. Immun.* **1989**, *57*, 1255.
[218] B. Ludwig, J. Rahfeld, B. Schmidt, E. Wintermeyer, G. Fischer, J. Hacker, *FEMS Lett.*, **1994**, *118*, 23.
[219] J. M. Moore, D. A. Peattie, M. J. Fitzgibbon, J. A. Thomson, *Nature* **1991**, *351*, 248.
[220] S. T. Park, R. A. Aldape, O. Futer, M. T. DeCenzo, D. J. Livingston, *J. Biol. Chem.* **1992**, *267*, 3316.

[221] S. W. Michnick, M. K. Rosen, T. J. Wandless, M. Karplus, S. L. Schreiber, *Science* **1991**, *252*, 836.
[222] J. G. Donnelly, S. J. Soldin, *Transplant. Proc.* **1991**, *23*, 2886.
[223] T. D. Ocain, D. Longhi, R. J. Steffan, R. G. Caccese, S. N. Sehgal, *Biochem. Biophys. Res. Commun.* **1993**, *192*, 1340.
[224] D. M. Spencer, T. J. Wandless, S. L. Schreiber, G. R. Crabtree, *Science* **1993**, *262*, 1019.
[225] P. R. Connelly, J. A. Thomson, *Proc. Natl. Acad. Sci. USA* **1992**, *89*, 4781.
[226] B. E. Bierer, P. K. Somers, T. J. Wandless, S. J. Burakoff, S. L. Schreiber, *Science* **1990**, *250*, 556.
[227] R. V. Bundick, D. K. Donald, R. P. Eady, R. Hutchinson, R. W. Keogh, J. A. Schmidt, E. Wells, *Transplantation* **1992**, *53*, 1150.
[228] G. D. van Duyne, R. F. Standaert, P. A. Karplus, S. L. Schreiber, J. Clardy, *J. Mol. Biol.* **1993**, *229*, 105.
[229] G. Fischer, G. Oehme, A. Schellenberger, *Tetrahedron* **1971**, *27*, 5683.
[230] Y. Namiki, N. Kihara, S. Koda, K. Hane, T. Yasuda, *J. Antibiot.* **1993**, *46*, 1149.
[231] D. K. Donald, M. E. Cooper, M. Furber, E. Wells, R. Hutchinson, F. M. Black, *Tetrahedron Lett.* **1991**, *32*, 1375.
[232] D. M. Armistead, J. S. Boger, J. O. Saunders, R. D. Tung, WO-B 92/00278 (U.S. patent).
[233] J. P. Duffy, WO-B 92/21313 (U.S. patent).
[234] J. R. Hauske, P. Dorff, S. Julin, J. Dibrino, R. Spencer, R. Williams, *J. Med. Chem.* **1992**, *35*, 4284.
[235] K. Nadeau, A. Das, C. T. Walsh, *J. Biol. Chem.* **1993**, *268*, 1479.
[236] J. Friedman, M. Trahey, I. Weissman, *Proc. Natl. Acad. Sci. USA* **1993**, *90*, 6815.
[237] J. A. McNew, K. Sykes, J. M. Goodman, *Mol. Biol. Cell* **1993**, *4*, 223.
[238] S. Fields, O. Song, *Nature* **1992**, *340*, 245.
[239] J. Luban, K. L. Bossolt, E. K. Franke, G. V. Kalpana, S. P. Goff, *Cell* **1993**, *73*, 1067.
[240] M. A. Wainberg, A. Dascal, N. Blain, L. Fitz Gibbon, F. Boulerice, K. Numazaki, M. Tremblay, *Blood* **1988**, *72*, 1904; A. Karpas, M. Lowdell, S. K. Jacobson, F. Hill, *Proc. Natl. Acad. Sci. USA* **1992**, *89*, 8351.
[241] J. H. Collins, *Biochem. Biophys. Res. Commun.* **1991**, *178*, 1288; T. Jayaraman, A. M. Brillantes, A. P. Timerman, S. Fleischer, H. Erdjumbentbromage, P. Tempst, A. R. Marks, *J. Biol. Chem.* **1992**, *267*, 9474; A. P. Timerman, E. Ogubumni, E. Freund, G. Wiederrecht, A. R. Marks, S. Fleischer, *ibid.* **1993**, *268*, 22992.
[242] F. L. Texter, D. B. Spencer, R. Rosenstein, C. R. Matthews, *Biochemistry* **1992**, *31*, 5687.
[243] J. T. Gerig, *Biopolymers* **1971**, *10*, 2435.
[244] A. Radzicka, S. A. Acheson, R. Wolfenden, *Bioorg. Chem.* **1992**, *20*, 382; E. S. Eberhardt, S. N. Loh, A. P. Hinck, R. T. Raines, *J. Am. Chem. Soc.* **1992**, *114*, 5437.
[245] G. Fischer, E. Berger, H. Bang, *FEBS Lett.* **1989**, *250*, 267.
[246] R. K. Harrison, R. L. Stein, *Biochemistry* **1990**, *29*, 1684.
[247] G. Fischer, *Nova Acta Leopold.* **1989**, *61*, 35.
[248] J. Liu, M. W. Albers, C. M. Chen, S. L. Schreiber, C. T. Walsh, *Proc. Natl. Acad. Sci. USA* **1990**, *87*, 2304.
[249] R. A. Aldape, O. Futer, M. T. Decenzo, B. P. Jarrett, M. A. Murcko, D. J. Livingston, *J. Biol. Chem.* **1992**, *267*, 16029.
[250] R. E. Morris, *Immunol. Today* **1991**, *12*, 137.
[251] J. Chung, C. J. Kuo, G. R. Crabtree, J. Blenis, *Cell* **1992**, *69*, 1227.
[252] C. J. Kuo, J. K. Chung, D. F. Fiorentino, W. M. Flanagan, J. Blenis, G. R. Crabtree, *Nature* **1992**, *358*, 70.
[253] D. J. Price, J. R. Grove, V. Calvo, J. Avruch, B. E. Bierer, *Science* **1992**, *257*, 973.
[254] S. M. Hatfield, J. S. Mynderse, N. W. Roehm, *J. Pharmacol. Exp. Ther.* **1992**, *261*, 970.
[255] P. G. McCaffrey, C. Luo, T. K. Kerppola, J. Jain, T. Badalian, A. M. Ho, E. Burgeon, W. S. Lane, J. N. Lambert, T. Curran, G. L. Verdine, A. Rao, P. G. Hogan, *Science* **1993**, *262*, 750.
[256] P. G. McCaffrey, B. A. Perrino, T. R. Soderling, A. Rao, *J. Biol. Chem.* **1993**, *268*, 3747; J. Jain, P. G. McCaffrey, V. E. Valge-Archer, A. Rao, *Nature* **1992**, *356*, 801.
[257] F. J. Dumont, M. J. Staruch, S. L. Koprak, J. J. Siekierka, C. S. Lin, R. Harrison, T. Sewell, V. M. Kindt, T. R. Beattie, M. Wyvratt, N. H. Sigal, *J. Exp. Med.* **1992**, *176*, 751.
[258] R. P. Meadows, D. G. Nettesheim, R. X. Xu, E. T. Olejniczak, A. M. Petros, T. F. Holzman, J. Severin, E. Gubbins, H. Smith, S. W. Fesik, *Biochemistry* **1993**, *32*, 754; J. W. Becker, J. Rotonda, B. M. McKeever, H. K. Chan, A. I. Marcy, G. Wiederrecht, J. D. Hermes, J. P. Springer, *J. Biol. Chem.* **1993**, *268*, 11335.
[259] J. Rotonda, J. J. Burbaum, H. K. Chan, A. I. Marcy, J. W. Becker, *J. Biol. Chem.* **1993**, *268*, 7607.
[260] S. K. Swanson, T. Born, L. D. Zydowsky, H. Cho, H. Y. Chang, C. T. Walsh, F. Rusnak, *Proc. Natl. Acad. Sci. USA* **1992**, *89*, 3741; S. Elrouby, Y. Shi, G. H. Reem, *Clin. Exp. Immunol.* **1992**, *89*, 136; V. L. Hsu, I. M. Armitage, *Biochemistry* **1992**, *31*, 12778; M. K. Rosen, P. J. Belshaw, D. G. Alberg, S. L. Schreiber, *Bioorg. Med. Chem. Lett.* **1992**, *2*, 747.
[261] R. E. Kaye, D. A. Fruman, B. E. Bierer, M. W. Albers, L. D. Zydowsky, S. I. Ho, Y. J. Jin, M. C. Castells, S. L. Schreiber, C. T. Walsh, S. J. Burakoff, K. F. Austen, H. R. Katz, *Proc. Natl. Acad. Sci. USA* **1992**, *89*, 8542.
[262] G. R. Flentke, E. Munoz, B. T. Huber, A. G. Plaut, C. A. Kettner, W. W. Bachovchin, *Proc. Natl. Acad. Sci. USA* **1991**, *88*, 1556; T. Kubota, G. R. Flentke, W. W. Bachovchin, B. D. Stollar, *Clin. Exp. Immunol.* **1992**, *89*, 192.
[263] T. Zarndt, B. Janowski, K. Lang, G. Fischer, unpublished.
[264] I. Schechter, A. Berger, *Biochem. Biophys. Res. Commun.* **1967**, *27*, 157.
[265] H. Lilie, K. Lang, R. Rudolph, J. Buchner, *Protein Sci.* **1993**, *2*, 1490.
[266] S. Wöllner, G. Fischer, unpublished.

Conformational Requirements for Sweet-Tasting Peptides and Peptidomimetics

Toshimasa Yamazaki, Ettore Benedetti, Darin Kent, and Murray Goodman*

The molecular basis of taste has been extensively studied over many years. The research carried out in our laboratories is focused on the elucidation of detailed structure–taste relationships of peptides and peptidomimetics using an "integrated" approach employing synthesis, analysis of NMR spectra, computer simulations, and X-ray crystallography. Various peptidomimetic residues have been incorporated to introduce predictable structural constraints into taste ligands. These constraints eliminate some of the molecular flexibility and allow us to develop structure–activity relationships. We describe here the topochemical requirements of the sweet and bitter taste receptor(s) and develop detailed structure–taste relationships with considerable predictive power for peptides and related molecules.

1. Introduction

The transduction of taste is believed to be initiated by receptor proteins located on the surface of the taste cell. In terms of structural biochemistry, the taste ligand and the receptor protein form a host–guest complex which produces a sense of taste. The structures of taste receptors have not been identified, but it is clear that the taste ligand must assume specific three-dimensional structures, so-called bioactive conformations, when interacting with the taste receptor. The bioactive conformation must be one of the accessible conformations of the isolated ligand. We contend that interactions of receptors with ligands cannot convert inaccessible structures to allowed conformations.

A wide variety of unrelated compounds are known to elicit a sweet taste. An early attempt to generalize common structural features (glucophores) among sweet molecules was made by Shallenberger and Acree,[1] who proposed the existence of a hydrogen bond donor (AH) and a hydrogen bond acceptor (B) in sweet molecules (AH/B model). Based on results obtained from a systematic study of unrelated sweet molecules such as sugars, saccharin, chloroform, unsaturated alcohols, and 2-amino-1-propoxy-4-nitrobenzene, the distances between these two groups have been determined to be within a range of 2.5 to 4.0 Å.[1] The AH and B groups form a bioactive complex through two intermolecular hydrogen bonds between the taste ligand and the sweet receptor. Studies on a series of potently sweet 2-amino-4-nitrobenzene derivatives led Deutsch and Hansch[2] to suggest that a hydrophobic binding area is also necessary for a compound to taste sweet. Kier et al.[3] extended the theory of Deutsch and Hansch and estimated the distances between the hydrophobic site (X) and the AH and B groups to be approximately 3.5 Å for AH–X and 5.5 Å for B–X (AH/B/X model). In Figure 1, several types of sweet molecules are shown with labeled AH/B/X groups and calculated intergroup distances. Based on preferred conformations of various amino acids calculated by using the extended Hückel theory, it was

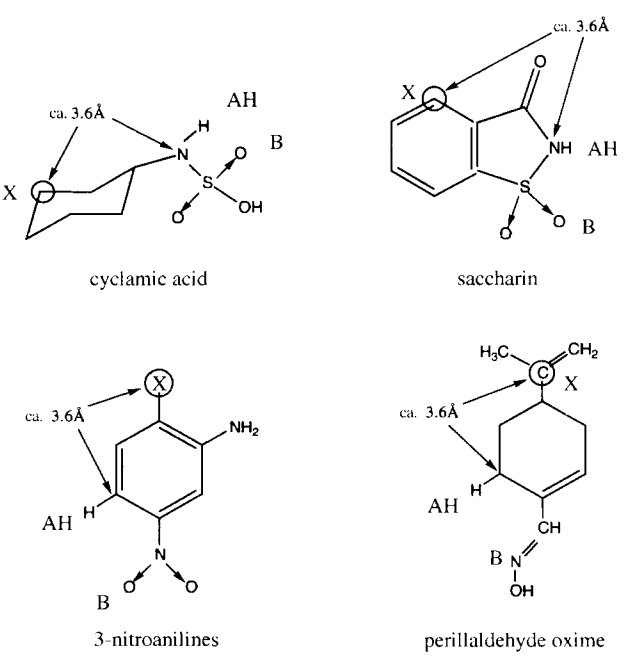


Fig. 1. Representatives of four classes of sweet molecules; the AH, B, and X groups are labeled and the AH–X distances are given.

[*] Prof. Dr. M. Goodman, D. Kent
Department of Chemistry
University of California, San Diego
La Jolla, CA 92093-0343 (USA)
Telefax: Int. code + (619)534-0202
Dr. T. Yamazaki
Bone Research Branch, National Institute of Dental Research
National Institutes of Health, Bethesda, MD (USA)
Prof. Dr. E. Benedetti
University of Naples (Italy)

concluded that the aromatic groups of D-phenylalanine, D-tyrosine, and D-tryptophan were ideal candidates for the hydrophobic X group and that side chains smaller than the isobutyl group of leucine did not fulfill the spatial requirements of the X glucophore. The AH/B system in amino acids is adequately represented by the charged amino and carboxylate groups. Similarly, third binding sites have been identified in sugars by Shallenberger and Lindly[4] and in dipeptide esters by van der Heijden et al.,[5] but the concepts of third binding sites are not identical to those proposed by Kier.

Since the initial discovery of the potent sweet taste of L-aspartyl-L-phenylalanine methyl ester (aspartame, L-Asp-L-Phe-OMe, **1**: approximately 200 times sweeter than sucrose) by Mazur et al.,[6] extensive structure–activity studies of peptide-based taste molecules have been carried out. Dipeptides containing two chiral amino acids can have four possible stereoisomers, which generally taste different. In the case of the aspartyl-phenylalanine methyl ester stereoisomers, only the L-L isomer is sweet, while all the other isomers are bitter.[6] The L-aspartic acid residue of **1** is necessary for a sweet taste and can be replaced by aminomalonic acid (Ama), which is a shorter homologue of aspartic acid.[7, 8] A higher homologue L-Glu-L-Phe-OMe is bitter.[6] As in the case of Asp-Phe-OMe, the absolute configuration of the Ama residue of Ama-L-Phe-OMe is also critical for sweet taste. It was originally proposed that (*S*)-Ama-L-Phe-OMe (**6**) would be sweet as its configuration is analogous to that of **1**;[7] however, we recently established that (*R*)-Ama-L-Phe-OMe (**5**) is 800 times sweeter than sucrose, while (*S*)-Ama-L-Phe-OMe (**6**) is tasteless.[8] We have determined these configurational assignments by X-ray analysis of the two isomers. The taste properties observed for the four diastereomers of Asp-Phe-OMe and for the two diastereomers of Ama-L-Phe-OMe demonstrate that distinct spatial requirements at the α-carbon atom of the N-terminal residues, namely, an L configuration for the Asp residue and an (*R*) configuration for the Ama residue, must be fulfilled for the molecule to elicit a sweet taste. In these analogues, the protonated amino and carboxylate groups of the N-terminal residue represent the AH and B groups of the Shallenberger and Acree glucophore hypothesis. The benzyl side chain of phenylalanine functions as the hydrophobic moiety X.

Although the N-terminal residue of L-Asp-L-Phe-OMe (**1**) and (*R*)-Ama-L-Phe-OMe (**5**) must be conserved, the C-terminal L-phenylalanine methyl ester can be replaced by a variety of other amino acid derivatives and related structures without a decrease in sweetness. The amino acid derivative must have a hydrophobic X group comparable in size to the benzyl side chain in the correct orientation. As suggested by Mazur[9] and Ariyoshi,[10] the C-terminal residue of sweet dipeptide derivatives has two hydrophobic groups of differing size. These groups are composed of the amino acid side chain and the ester or amide group. In the L configuration, the C-terminal amino acid side chain is required to be larger than the ester or amide group; the relationship is reversed in the D configuration.

Ariyoshi[10] explained the sweet taste of aspartyl dipeptides on the basis of Fischer projections. The Ariyoshi model is quite convenient for the prediction of taste properties of peptidelike molecules. The "sweet formula" (Fig. 2a) is consistent with those of the sweet L-aspartyl dipeptide derivatives reported in the literature, while the "non-sweet formula" (Fig. 2b) is consistent with the L-aspartyl dipeptides devoid of sweet taste.

The application of Fischer projections to the study of three-dimensional peptide taste ligands is limited because of the two-



Murray Goodman was born in New York, NY in 1928 and received his Ph.D. in chemistry from the University of California, Berkeley in 1953. He then carried out postdoctoral research at the Massachusetts Institute of Technology and at Cambridge University, England. In 1956 he joined the faculty of the Polytechnic Institute of Brooklyn as an Assistant Professor and was appointed Full Professor in 1964. Three years later he became Director of the Polymer Research Institute at the Polytechnic. In 1970 he accepted a position as Professor of Chemistry at the University of California, San Diego, where he served as Chairman of the Chemistry Department from 1976 to 1981. He has received many honors and awards, including the Scoffone Medal of the University of Padua, a Humboldt Professorship, and the Max Bergmann Medal. He is Editor of the journal Biopolymers and has published more than 350 original research papers in the area of biopolymers and their model structures. His research focuses on the use of computer-aided design of bioactive molecules, synthesis of peptides and peptidomimetics, and spectroscopic characterization of novel biomolecular systems.

Ettore Benedetti was born in Naples, Italy in 1940 and completed his Ph.D. research in chemical crystallography in 1965 under the direction of Professor Alfonso M. Liquori. During three years of postdoctoral research with Professor Murray Goodman at the Polytechnic Institute of Brooklyn he began his studies on the structure and conformation of peptides and polypeptides. He joined the Science Faculty of the University of Naples, where he was appointed Full Professor of General Chemistry and Director of the Institute of Chemistry in 1975. He is a member of the Advisory Board of Biopolymers and on the Editorial Board of the International Journal of Peptide and Protein Research. His research interests lie in peptide chemistry: the structure–activity relationships of numerous peptide systems have been the object of his investigations, which have been carried out with a variety of experimental and theoretical techniques, for the understanding of the mechanism of action of biologically relevant systems.

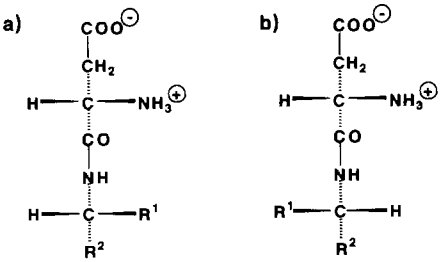


Fig. 2. Fischer projections of a) a sweet and b) a nonsweet aspartyl-based peptide. R^1 is a *small* hydrophobic substituent and R^2 is a *large* hydrophobic substituent.

dimensional nature of the model. The Ariyoshi model does not explain the sweet taste of L-Asp-(*S*)-gAla-TMCP (**12**) (see Table 1) which appears to fit the "non-sweet formula". This result indicates that the molecular basis of taste must be defined by the three-dimensional structure of the molecule, that is, the relative spatial arrangements of the three glucophores AH, B, and X. From the conformational analysis of a series of aspartyl-based dipeptides incorporating stereoisomeric peptides and peptidomimetics as the second residue, we have developed a three-dimensional model, the "L model", describing the conformational requirements for sweet and bitter tastes.[11]

In this paper, we describe how the L model for sweet taste has been developed through conformational studies of peptide-based taste ligands using X-ray crystallography, NMR spectroscopy, and computer simulations. The compounds examined are peptide-based taste ligands such as aspartame (**1**) and peptide-based analogues incorporating stereoisomeric changes in residues and peptidomimetics (Table 1). The X-ray crystal structures of all these analogues have been elucidated.[8, 11, 12] Compounds **5** and **6** contain an aminomalonyl residue at the first position, all others have the L-aspartyl residue of the parent dipeptide **1**. In all aspartame analogues studied the AH and B groups are represented by the protonated amino and the side-chain carboxylate groups of the N-terminal residue [L-Asp,(*R*)-Ama, or (*S*)-Ama] of the molecule. The first eight analogues **1**–**8** (Type A) contain the hydrophobic element X in the side chain of the second residue. In the remaining five analogues **9**–**13** (Type B), the X group is the C-terminal amide or ester group. The L-aspartyl derivatives shown in Table 1 are dipeptide derivatives in the cases of **1**, its hydrochloride salt **2**, and analogues **9** and **10**. The remaining compounds in Table 1 incorporate various peptidomimetics as the second residue such as α-methylphenylalanine in **3** and **4**, cyclohexylglycine in **7** and **8**, a retro-inverso peptide of alanine in **11** and **12**, and α-aminocyclopropanecarboxylic acid in **13**. The structures of the peptide-based taste ligands in Table 1 are illustrated in Figure 3. Our model requires that the N-terminal residue be conformationally fixed when the molecule binds to the taste receptor. The relative orientation of the X group to the fixed AH/B groups is determined by the conformation of the second residue. Each peptidomimetic residue used in this study displays unique conformational preferences. Therefore, it is possible to identify specific topochemical arrays that produce a sweet or bitter taste.

2. X-Ray Structure Analysis

The following sections describe the X-ray crystallography studies on the peptide-based taste ligands listed in Table 1. In Table 2, results of the crystallographic analyses relevant to the scope of this paper are presented. All crystal structures deter-

Table 2. Relevant results of the crystallographic analyses of dipeptide taste ligands **1**–**13**.

Cmpd.	Crystal system, space group [a]	No. of molecules in unit cell	No. of water molecules in unit cell	Conventional R-factor	Standard deviations of bond lengths and angles	Refs.
1	tetragonal, $P4_1$	1	1	0.045	0.006 Å, 0.6°	[12a]
2	orthorhombic, $P2_12_12_1$	1	8	0.033	0.002 Å, 0.1°	[12b]
3	orthorhombic, $P2_12_12_1$	1	8	0.038	[b]	[12c]
4	orthorhombic, $P2_12_12_1$	1	4	0.038	0.005 Å, 0.1°	[12d]
5	triclinic, $P1$	4	4	0.073	0.010 Å, 3°	[8]
6	monoclinic, $P2_1$	1	0	0.053	0.004 Å, 0.7°	[8]
7	monoclinic, $P2_1$	1	4	0.108	0.020 Å, 1.5°	[11g]
8	monoclinic, $P2_1$	1	2	0.062	0.010 Å, 0.5°	[11g]
9	triclinic, $P1$	4	10	0.079	0.015 Å, 0.9°	[11d]
10	monoclinic, $P2_1$	1	4	0.086	0.010 Å, 1.3°	[12e]
11, **12**	monoclinic, $P2_1$	4(2, 2)	6	0.090	0.015 Å, 0.6°	[11b]
13	orthorhombic, $P2_12_12_1$	1	4	0.056	0.002 Å, 0.3°	[12f]

[a] Crystal dimensions are listed in the references listed. [b] Value not provided by authors.

Table 1. Taste properties of peptide-based taste ligands.

	Compound [a]	Shorthand Form	Taste [b]
Type A			
1	L-aspartyl-L-phenylalanine methyl ester	L-Asp-L-Phe-OMe	sweet
2	L-aspartyl-L-phenylalanine methyl ester hydrochloride	HCl-L-Asp-L-Phe-OMe	sweet
3	L-aspartyl-(α-methyl)-L-phenylalanine methyl ester	L-Asp-L-(α-Me)Phe-OMe	sweet
4	L-aspartyl-(α-methyl)-D-phenylalanine methyl ester	L-Asp-D-(α-Me)Phe-OMe	bitter
5	(*R*)-aminomalonyl-L-phenylalanine methyl ester	(*R*)-Ama-L-Phe-OMe	sweet
6	(*S*)-aminomalonyl-L-phenylalanine ethyl ester	(*S*)-Ama-L-Phe-OEt	tasteless
7	L-aspartyl-(*S*)-cyclohexylglycine methyl ester	L-Asp-(*S*)-Chg-OMe	sweet
8	L-aspartyl-(*R*)-cyclohexylglycine methyl ester	L-Asp-(*R*)-Chg-OMe	bitter
Type B			
9	L-aspartyl-D-alanine *N*-(2,2,4,4-tetramethylthietanyl)amide	L-Asp-D-Ala-TAN	sweet
10	L-aspartyl-D-alanine 2,2,5,5-tetramethylcyclopentyl ester	L-Asp-D-Ala-OTMCP	sweet
11	*N*-L-aspartyl-*N'*-(2,2,5,5-tetramethylcyclopentanecarbonyl)-(*R*)-1,1-ethanediyldiamine	L-Asp-(*R*)-gAla-TMCP	sweet
12	*N*-L-aspartyl-*N'*-(2,2,5,5-tetramethylcyclopentanecarbonyl)-(*S*)-1,1-ethanediyldiamine	L-Asp-(*S*)-gAla-TMCP	sweet
13	L-aspartyl-α-aminocyclopropanecarboxylic acid *n*-propyl ester	L-Asp-Ac^{3}c-O*n*Pr	sweet

[a] Molecular formulas are shown in Fig. 3; for definitions of Types A and B see text. [b] The taste was determined by a three-member panel by a qualitative "sip and spit" taste assessment of a dilute solution of the molecule in water without any pH adjustment.

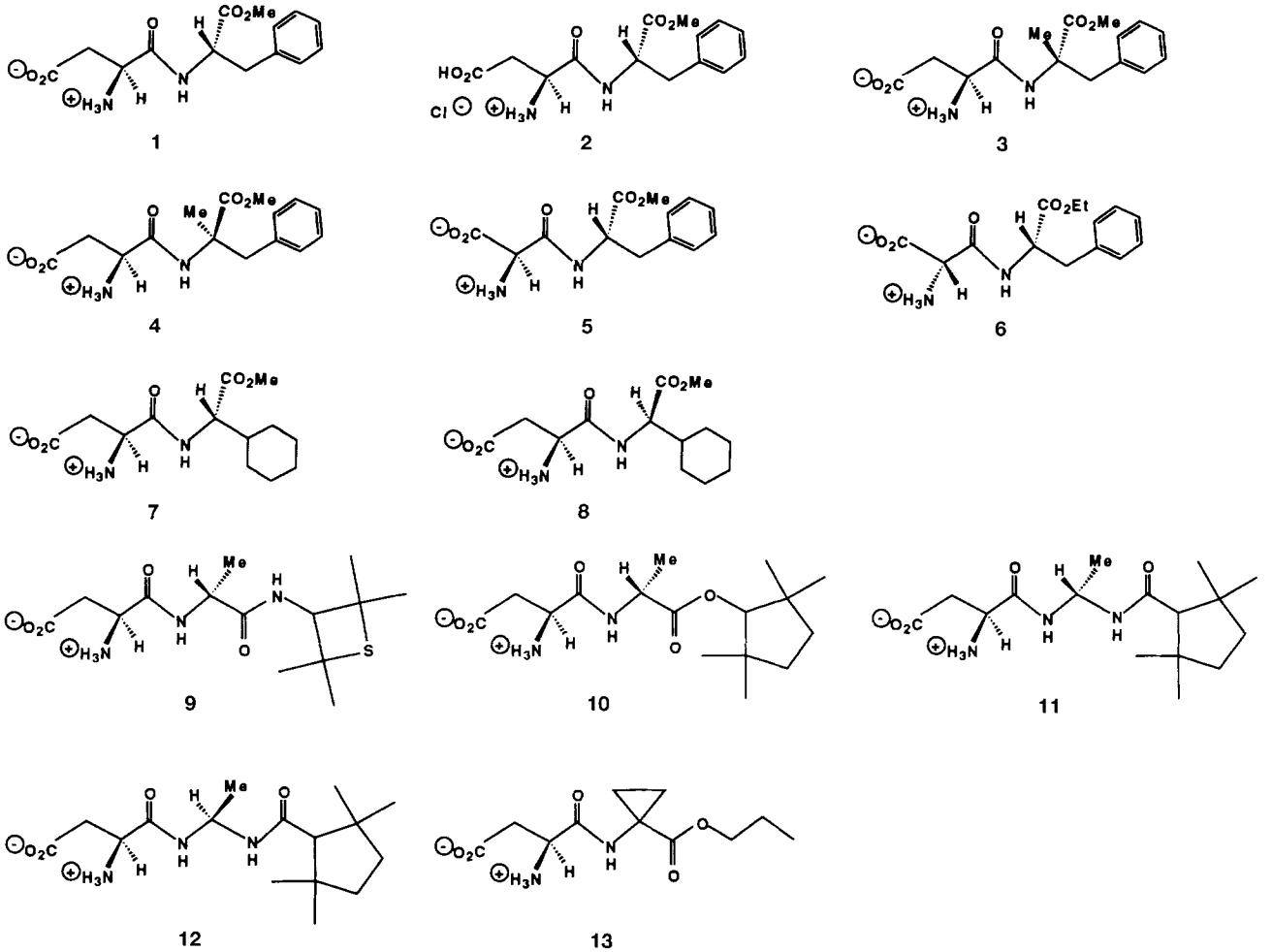


Fig. 3. Structures of peptide-based taste ligands presented in Table 1.

mined by diffraction techniques have been refined to a degree of accuracy ranging from very good to reasonable, with R-factor values between 0.033 and 0.103. The estimated standard deviations of bond lengths and bond angles are in the ranges of 0.002–0.02 Å and 0.1–1.4°, respectively; that of torsion angles is not greater than 5°. The crystals of all the compounds except **6** contain one or more molecules of water in the unit cell. In the crystals of **5** and **9**, four independent molecules with slightly different conformations constitute the asymmetric unit. The X-ray diffraction studies of the retro-inverso taste ligands **11** and **12** were carried out on a crystal composed of these two diastereomeric molecules. The torsion angles describing the backbone and side-chain conformations of all the peptide-based taste ligands studied are listed in Table 3.

Table 3. Torsion angles [°] of the dipeptide taste ligands **1**–**13** in the crystalline state [a].

[b]	ψ^1	ω^1	χ^1_1	$\chi^1_{2,1}$	$\chi^1_{2,2}$	ϕ^2	ψ^2	ω^2	χ^2_1
1	149.0	−178.5	−71.7	−173.4	4.0	−156.8	−173.6	179.1	61.7
2	165.5	170.9	−155.9	175.1	−4.8	−153.6	166.8	176.9	58.9
3	152.4	164.0	−63.9	−100.2	79.1	−42.3	−48.3	178.2	171.8
4	151.0	167.7	−68.9	177.2	−1.7	49.0	47.9	−177.3	173.2
5a	170.9	179.8	−159.4		–	−93.8	130.0	−176.8	−176.6
5b	174.3	−179.3	−161.4	–	–	−82.5	131.4	175.2	−172.5
5c	175.2	178.9	−164.1	–	–	−97.4	113.1	−179.2	−177.2
5d	168.4	−176.9	−159.9	–	–	−84.1	140.4	177.2	−175.0
6	−177.2	−175.3	162.0	–	–	−97.0	135.3	173.6	179.2
7	144.9	172.9	−66.9	151.0	−31.4	−118.2	63.4	−172.5	−48.9
8	167.1	176.5	−77.9	173.6	−6.3	88.1	−131.8	178.2	69.0
9a	158.5	170.5	−63.6	−175.5	5.9	126.0	−158.4	−172.1	–
9b	144.1	170.0	−66.8	−172.0	8.1	66.6	−151.9	175.4	–
9c	153.3	167.0	−64.0	−165.1	15.1	70.2	−151.1	171.2	–
9d	167.4	−174.2	−63.7	−168.4	8.7	74.1	−158.1	171.2	–
10	158.1	171.0	−61.8	−161.4	22.4	64.3	−140.9	176.2	–
11	172.0	−175.4	−82.6	−168.9	−1.3	104.4	−97.3	166.8	–
12	166.2	177.5	−75.4	177.8	−1.9	−99.7	104.8	−169.4	–
13	147.7	−179.9	−70.4	159.1	−21.9	−78.4	−0.6	179.1	103.7

[a] Torsion angles were measured according to IUPAC convention. [b] For **5** and **9** the independent molecules in the unit cell are denoted by **a**–**d**.

2.1. Conformations and Packing of Peptide-Based Taste Ligands in the Solid State

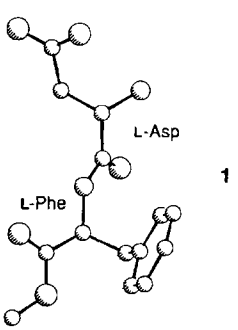
Dipeptide esters with an unprotected N-terminal residue can be considered rather flexible molecules. However, in their crystal structures only two areas of the (ϕ, ψ) map seem to be more densely populated with conformations characterized by (ϕ, ψ) values of (−160°, 180°) and (−70°, 170°).[13] The conformation of a molecule in the crystalline state is greatly affected by packing forces. Among the most important are electrostatic interactions between charged groups, hydrogen bonds, and van der

Waals and hydrophobic interactions, such as the stacking of aromatic groups, and alkyl–phenyl and alkyl–alkyl interactions. Molecules in the crystalline state assume conformations that maximize molecular packing. In general, the most efficient packing is achieved when molecules adopt extended or semi-extended conformations.

The crystal structures of aspartame and the related analogues are no exception to this trend, even though they show a more pronounced variety of conformations owing to the presence of more or less hindered peptidomimetics. In the crystalline state, all of the peptide-based taste ligands, except for aspartame hydrochloride (**2**), exist as zwitterions; the N-terminal amino group is positively charged, and the side-chain carboxylate of the N-terminal residue is negatively charged. Evidence of the zwitterionic structures is seen in the C–O bond lengths, which are intermediate between those of a single and a double bond, and in the fact that the NH_3^+ cation acts as a hydrogen bond donor to three acceptor groups. In these structures the charged groups of the zwitterion are close together allowing for better electrostatic interactions and intra- and intermolecular hydrogen bond formation. For this reason the AH/B unit is referred to as the zwitterionic ring. The conformation of the aspartyl residue is highly conserved. On the average, the torsion angles ψ^1, ω^1, χ_1^1, and $\chi_{2,1}^1$ assume values of +156, +175, −69, and −173° (or +7° for $\chi_{2,2}^1$), respectively. The conformation about the Asp C^α–C^β bond (χ_1^1) is *gauche*$^-$ (g^-). The carboxylate group of the aspartyl side chain is nearly coplanar with the C^α–C^β bond; the $\chi_{2,1}^1$ and $\chi_{2,2}^1$ dihedral angles are close to 180 and 0°, respectively. The conformations of the Ama residue in compounds **5** and **6** are very similar to those of the aspartyl-containing molecules.

The conformation of the second residue varies greatly, depending upon the configuration and the conformational constraints of the molecules. Aspartame (**1**) itself is the only compound that adopts a structure in which the second residue has an almost fully extended backbone conformation ($\phi^2 = -156.8°$ and $\psi^2 = -173.6°$) (Fig. 4).[20] The value of +61.7° (*gauche*$^-$: g^+) observed for the Phe side chain torsion angle χ_1^2 is allowed when the peptide backbone is in the extended conformation.

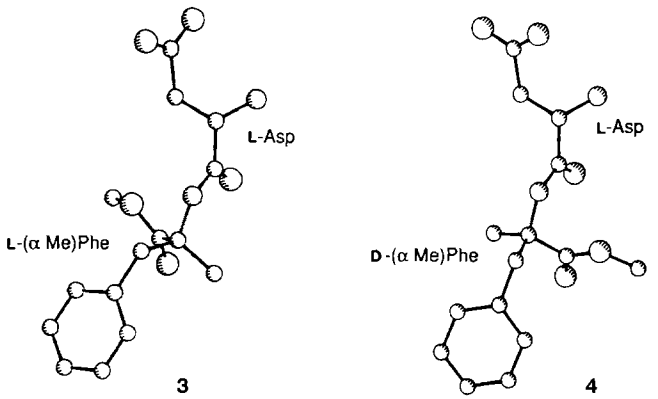
The torsion angles observed for aspartame hydrochloride (**2**)[12b] in the crystalline state are similar to those observed for aspartame itself with the exception of the χ_1^1 angle of the aspartyl residue. In aspartame hydrochloride χ_1^1 assumes a value of −155.9° (*trans* conformation, t); in other words, the side-chain carboxyl group is rotated away from the positively charged N-terminal NH_3^+ group. Electrostatic interactions between the N-terminal charged group and the chloride ions are mediated by the cocrystallized water molecules.



1

Fig. 4. Molecular structure of **1** in the crystalline state. The structure is drawn in a projection perpendicular to the plane defined by the atoms C^β, N, and C(O) of the Asp residue.

The X-ray structures of the diastereomeric aspartame analogues **3** (sweet)[12c] and **4** (bitter)[12d] are shown in Figure 5. In contrast to **1** in which the second residue has an extended backbone conformation, the α-methylphenylalanine residue assumes a right-handed helical conformation in **3** with $\phi^2 = -42.3°$ and $\psi^2 = -48.3°$, and a left-handed helical conformation in **4** with $\phi^2 = 49.0°$ and $\psi^2 = 47.9°$. Folded helical structures, in other words, 3_{10}- and α-helices, are highly preferred in peptides containing α,α-dialkylamino acid residues.[14] In both diastereomers, the (α-Me)Phe side chain assumes the *trans* conformation about the C^α-C^β bond defined by an angle $\chi_1^2 = 171.8°$ for the sweet L-L isomer and 173.2° for the bitter L-D isomer. The crystal structure of both diastereomers is essentially the same and determined primarily by molecular packing forces. In fact, the relative orientation of the zwitterionic ring of the aspartyl moiety and the benzyl side chain, which are major groups for hydrophilic and hydrophobic interactions, respectively, is exactly the same in both structures.

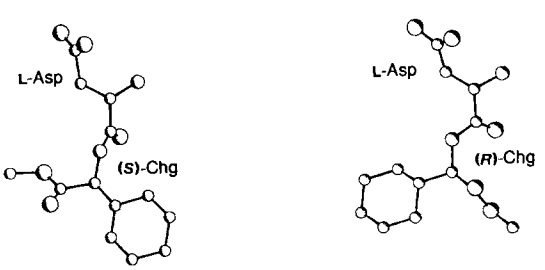


3 **4**

Fig. 5. Molecular structures of the diastereomeric taste ligands **3** and **4**.

In the crystalline state, both the sweet (*R*)-aminomalonyl compound **5** and its tasteless (*S*) analogue **6** adopt similar molecular structures in which the L-Phe residues assume semi-extended backbone conformations and the $\chi_1^2 = t$ side-chain conformation.[8] In these structures, the zwitterionic ring of the N-terminal residue and the benzyl side chain of the second residue are 180° apart from one another in a planar linear array as in sweet **3** and bitter **4**.

The X-ray crystal structures[11g] of the two diastereomeric molecules **7** (sweet) and **8** (bitter) are shown in Figure 6. Both compounds are highly hydrophilic at the N-terminus and have nearly identical conformations at that residue. Conversely, the C-terminal portions of the two molecules, which are hydrophobic, assume conformations in which the cyclohexyl moieties

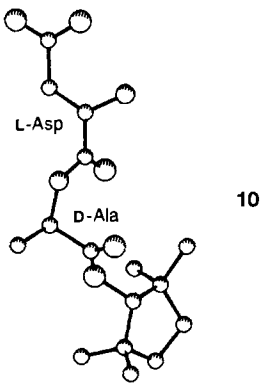


7 **8**

Fig. 6. X-ray crystal structures of the diastereomers **7** and **8**; projection perpendicular to the plane defined by the atoms C^β, N, and C(O) of the Asp residue.

point in opposite directions relative to the zwitterionic ring of the aspartyl residue.

The molecular structure of the sweet-tasting L-aspartyl-D-alanine derivative **10**[12e] is shown in Figure 7. The D-alanyl residue adopts a semiextended backbone conformation characterized by the torsion angles $\phi^2 = 64.3°$ and $\psi^2 = -140.9°$, which are appropriate for a residue with a D configuration. The zwitterionic ring of the aspartyl moiety and the C-terminal 2,2,5,5-tetramethylcyclopentyl ester group are arranged in an almost planar parallel array.



10

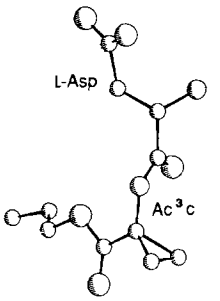
Fig. 7. An X-ray crystal structure of dipeptide ester **10**; projection perpendicular to the plane defined by the atoms C^{β}, N, and C(O) of the Asp residue.

The sweet-tasting L-aspartyl-D-alanine derivative **9** crystallizes with four molecules in the asymmetric unit.[11d] The conformation of the L-aspartyl residues in the four independent molecules is highly conserved with no torsional variance of more than 25°. The N-terminal aspartyl residues are zwitterionic in all four molecules. The backbone torsion angle of the D-Ala residue (ϕ^2) shows the greatest variability; that in one molecule (126.0°) differs from that in the other three (70.3° on the average) by approximately 60°. The C(O)-N-C^1-H torsion angle of the C-terminal TAN group in the former molecule (−36.0°) is approximately 60° away from the values observed in the latter three molecules (+24.0° on the average). However, the overall structure of the four independent molecules is essentially the same as that of the sweet-tasting **10**.

In the crystalline state the two retro-inverso diastereomers **11** and **12**, both intensely sweet, show ϕ^2 and ψ^2 values centered at −100 and +100° for the (*S*)-gAla residue and values equal and opposite for the (*R*)-gAla residue.[11b] Their conformations are influenced by the presence of two geminal NH groups, which are involved in the formation of intermolecular hydrogen bonds. The relative orientations of the zwitterionic ring of the aspartyl moiety and the largest hydrophobic group of the molecule (i.e. the C-terminal TMCP group) in the L-(*R*) and L-(*S*) isomers are similar to those of the sweet **7** and the bitter **8**, respectively (Fig. 6). This observation demonstrates clearly that X-ray crystal structures cannot provide clear, concise information on the structure–taste relationships of these flexible peptide-based taste ligands; both isomers are intensely sweet although they adopt equal but opposite conformations at the C-terminus.

In compound **13**[12f] (Fig. 8) the aspartyl moiety has the same conformation as that observed in all previously described compounds except aspartame hydrochloride. The Ac^3c residue contains an acute twist of the peptide backbone characterized by the ϕ^2 and ψ^2 angles of −78.4 and −0.6°, respectively. These values are in the "bridge" region of the Ramachandran map.

The molecular packing schemes for all of the peptide-based taste ligands investigated are quite similar, while the molecular structures in the crystalline state are substantially different. As examples, the packings of compound **9** and those of the diastereomeric aminomalonyl-containing compounds **5** and **6** are shown in Figures 9 and 10, respectively. Because of the presence of the positively charged NH_3^+ group and the negatively charged COO^- group of the side chain of the N-terminal residue, electrostatic interactions are the most important factors holding the molecules together in the solid state. The electrostatic interactions maximize the number of hydrogen bonds and donor groups involved in hydrogen bonding. The oppositely charged groups cluster with one another and with solvent molecules (mostly water), giving rise to complicated patterns of intermolecular hydrogen bonds. In all structures, the resulting hydrophilic core is surrounded by a hydrophobic surface which is formed by the stacking and packing of the hydrophobic side chains of the second residue or the C-terminal protecting groups. The peptide-based taste ligands assume conformations in the crystalline state that maximize this type of molecular packing. In all structures, with the exception of the aspartame hydrochloride salt (**2**), the N-terminal aspartyl or aminomalonyl residues assume the same zwitterionic form. In addition,



13

Fig. 8. An X-ray crystal structure of **13**; projection perpendicular to the plane defined by the atoms C^{β}, N, and C(O) of the Asp residue.

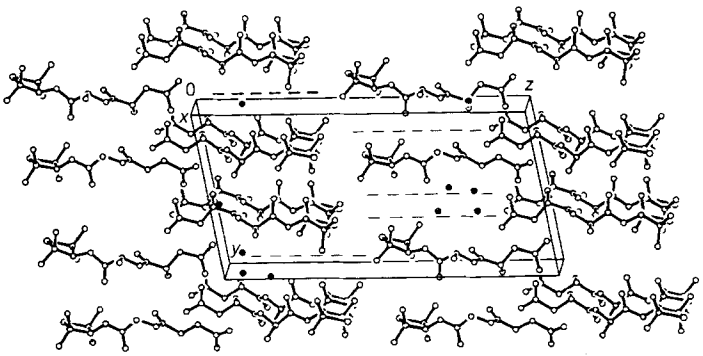


Fig. 9. Molecular packing of **9** in the crystal including water molecules in the unit cell. To clearly show the positions of the water molecules, several molecules of **9** are represented only by dashed lines.

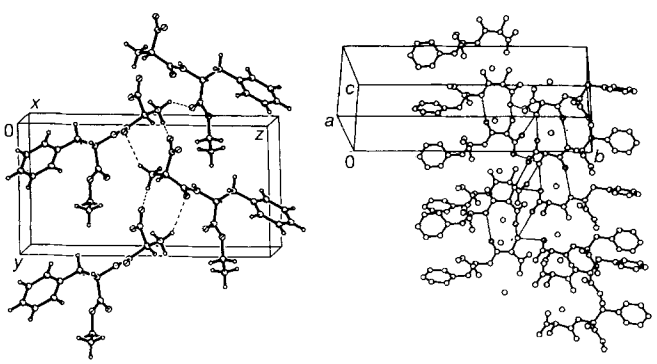


Fig. 10. Molecular packings for **6** (left) and **5** (right) in the crystal. Hydrogen bonds between the hydrophilic moieties are represented by dashed lines. The circles on the right-hand side that are not involved in any bonds correspond to the O atoms of water molecules.

the average ϕ^2 angle in the C-terminal residues assumes values of approximately $+85$ or $-85°$ depending upon the configuration. The other two torsion angles, ψ^2 and χ_1^2, describe the conformation of the second residue and exhibit great variation. In conclusion, the conformations assumed by each molecule in the crystalline state are mainly determined by packing forces.

2.2. Relationship between the Taste and the Crystal Structure of Peptide-Based Taste Ligands

All of the sweet, bitter, and tasteless ligands described here are zwitterionic at the N-terminus, except for aspartame hydrochloride (**2**). The topology of the zwitterionic portion is such that the protonated α-amino and the side-chain carboxylate groups of the N-terminal residue can act as the AH/B functionalities necessary to elicit the sweet taste.

The orientation of the hydrophobic X group with respect to the AH/B groups is substantially different from one analogue to the next. The sweet analogues **7** (Fig. 6) and **11** adopt L-shaped conformations, in which the zwitterionic ring of the L-aspartyl moiety containing the AH/B groups forms the stem of the L in the direction of the y axis, and the X group projects out along the base of the L in the direction of the $+x$ axis. The sweet analogues **12** and **13** (Fig. 8) adopt reversed L-shaped conformations, in which the X group projects along the $-x$ axis. The bitter analogue **8** also adopts a reversed L shape (Fig. 6). In the X-ray structures of the sweet analogues **3** (Fig. 5), **5**, **9**, and **10** (Fig. 7), the X group projects out along the $-y$ axis, resulting in extended structures in which the AH/B groups and the X group are planar and form an angle of roughly 180°. These extended structures are very similar to those observed for the bitter molecule **4** (Fig. 5) and the tasteless molecule **6**. In the X-ray structure of aspartame (**1**), the hydrophobic benzyl side chain (X) projects into the $+z$ dimension (Fig. 4).

The analyses of these crystal structures clearly indicate that the solid-state conformations alone give no information on the relationship between the taste properties and the structures of these peptide-based taste ligands.

3. NMR Spectroscopy and Computer Simulations

Since the X-ray crystal structures of the taste ligands of the aspartame family fail to provide a consistent relationship between taste and molecular structure, we must search for further accessible conformations of the molecules. For this purpose, preferred conformations in solution were estimated by NMR spectroscopy and computer simulations.[8, 11, 12] Packing forces are nonexistent in solution; the molecules are solvated and exist as equilibrium mixtures of various preferred conformers.

The preferred conformations of taste ligands **1**–**13** in solution were estimated from nuclear Overhauser effects (NOE) and ^1H–^1H vicinal coupling constants.[15] The results are summarized in Table 4. In all of the L-aspartyl-based analogues, the L-aspartyl residue shows the same conformational preferences independent of the structure and configuration of the second residue. The conformations of the L-aspartyl residue are defined by the ψ^1 angle (60–180°) and the preference of the side chain for the g^- conformation ($\chi_1^1 = -60°$). These conformations are preserved not only in the sweet molecules but also in the bitter molecules **4** and **8**. The ψ^1 angle of the (*R*)-Ama residue of the sweet-tasting molecule **5** is also restricted to the same range (60–180°) as the L-Asp residue, while that of the (*S*)-Ama residue of the tasteless molecule **6** is restricted to opposite values (-180 to $-60°$).

The preferred conformations of the second residues are divided into several categories depending upon molecular type. Among the molecules **1**–**8** belonging to Type A, which contain the hydrophobic glucophore X in the side chain of the second residue, the sweet-tasting molecules **1**, **3**, **5**, and **7** prefer negative values of -180 to $-60°$ for the ϕ^2 angle of the second residue. Conversely, the bitter molecules **4** and **8** prefer positive values for ϕ^2; for the D-(α-Me)Phe residue in **4**, ϕ^2 is 60–180°, and for the (*R*)-Chg residue in **8**, ϕ^2 is 98 and 142°. Although the N-terminal residues are different in **1**, **5**, and **6**, their L-Phe side chains display the same conformational preferences. The preferred conformer of the L-Phe side chain χ_1^2 was found to be g^- (43–48%); the t and g^+ conformers comprise 14–19% and 37–39%, respectively. The preferred conformations in solution are

Table 4. Conformations of taste ligands **1**–**13** determined by ^1H NMR spectroscopy.

Residue	Bond								
		Type A:	**1**	**3**	**4**	**5**	**6**	**7**	**8**
Asp/Ama	ψ^1: C^α-C(O)		60 to 180°	60 to 180°	60 to 180°	60 to 180°	−180 to −60°	60 to 180°	60 to 180°
	χ_1^1: C^α-C^β	g^- (ca. −60°)	55%	56%	55%	–	–	50%	49%
		t (ca. 180°)	21%	22%	23%	–	–	27%	26%
		g^+ (ca. 60°)	24%	22%	22%	–	–	23%	25%
Residue 2	ϕ^2: N-C^α		−180 to −60°	−180 to −60°	60 to 180°	−180 to −60°	−180 to −60°	−142, −98°	98, 142°
	χ_1^2: C^α-C^β	g^- (ca. −60°)	48%			44%	43%	[a]	[a]
		t (ca. 180°)	14%			19%	18%	17% [a]	[a]
		g^+ (ca. 60°)	38%			37%	39%	[a]	16% [a]
		Type B:	**9**	**10**	**11**	**12**	**13**		
Asp	ψ^1: C^α-C(O)		60 to 180°	60 to 180°	60 to 180°	60 to 180°	60 to 180°		
	χ_1^1: C^α-C^β	g^- (ca. −60°)	59%	60%	60%	58%	62%		
		t (ca. 180°)	19%	18%	18%	20%	16%		
		g^+ (ca. 60°)	22%	22%	22%	22%	22%		
Residue 2	ϕ^2: N-C^α		60 to 180°	60 to 180°			0° ± 90°		
	ψ^2: C^α-C(O)								
C-Terminus	τ^3		0° ± 60° [b]	0° ± 60° [c]	0° ± 60° [d]	0° ± 60° [d]			

[a] Since cyclohexylglycine has one β-proton, the rotational isomeric state analysis of the ^1H-^1H vicinal coupling constant $J(\alpha,\beta)$ provides only a fraction of the conformer in which the α- and β-protons orient *trans* to each other. [b] τ^3 is the C(O)-N-C^1-H angle of the C-terminal 2,2,4,4-tetramethylthietanylamide group. [c] τ^3 is the C(O)-O-C^1-H angle of the C-terminal 2,2,2,5-tetramethylcyclopentyl ester group. [d] τ^3 is the N-C(O)-C^1-H angle of the C-terminal 2,2,5,5-tetramethylcyclopentanecarbonyl group.

clearly different from the conformations of the L-Phe side chain of aspartame (**1**) ($\chi_1^2 = +61.7°$), **5** ($\chi_1^2 = -175.3 \pm 5.0°$), and **6** ($\chi_1^2 = 179.2°$) in the crystalline state.

Among the dipeptide taste molecules belonging to Type B, which contain the hydrophobic element X in the C-terminal amide or ester group, the D-Ala residue of compound **9** prefers positive values (60–180°) for ϕ^2 and a broad range of values for ψ^2. Similarly, the D-Ala residue of compound **10** prefers positive values of 60–180° for ϕ^2. The Ac^3c residue of compound **13** assumes a ϕ^2 angle of $0 \pm 90°$. In compounds **11** and **12**, which have retro-inverso gAla residues with (*R*) and (*S*) configurations, respectively, no clear conformational preferences were identified for the second residues from the ^{1}H NMR studies alone.

The accessible (or preferred) conformations of any given molecule are strongly influenced by van der Waals interactions. These steric interactions can be estimated by using any one of the many existing force fields such as CHARMm[16] and DISCOVER.[17] The conformational analyses carried out on the peptide-based taste ligands allow the identification of virtually all minimum-energy conformations. These conformations represent preferred structures within the accessible conformational space of the molecule.

An extensive search for minimum-energy conformations was carried out in a stepwise fashion, starting with small model compounds such as *N*-methylamide derivatives of the N-terminal residues [L-Asp-NHMe, (*R*)-Ama-NHMe, and (*S*)-Ama-NHMe] and *N*-acetyl derivatives of the C-terminal residues [Ac-L-Phe-OMe, Ac-L-Phe-OEt, L- and D-Ac-(α-Me)Phe-OMe, (*R*)- and (*S*)-Ac-Chg-OMe, Ac-D-Ala-TAN, Ac-D-Ala-OTMCP, (*R*) and (*S*)-Ac-gAla-TMCP, and Ac^3c-O*n*Pr] and working toward the structures of the peptide-based taste ligands. This treatment is based on the assumption that interresidue interactions are trivial for the determination of preferred conformations of the taste ligands. This assumption is supported by the ^{1}H NMR data which indicate that the N-terminal L-aspartyl residue shows the same conformational preferences independent of the structure and configuration of the second residue and that the conformation of the second residue is independent of the structure and configuration of the N-terminal residue.

The NMR studies revealed that the L-Asp side chain assumes three conformational states with a preference for the g^- state over the t and g^+ states (see Table 4). However, the AH/B-containing aspartyl moiety could be conformationally fixed when the molecules bind to the taste receptors. We, as well as other groups, have assumed that the g^- structure for the L-aspartyl residue is the bioactive conformation based on the following:

1) The distances between the AH (protonated α-amino) and B (β-carboxylate) groups required for sweet taste sensation (2.5–4.0 Å) are achieved only when the aspartyl side chain assumes either the g^- or g^+ state.

2) All of the peptide analogues studied prefer the g^- state about the aspartyl side chain in solution as revealed by the NMR studies, in other words, 50–60% for g^- and 20–25% for g^+.

3) All of the peptide analogues examined, with the exception of the aspartame hydrochloride salt (**2**), adopt the g^- state in the crystalline state.

Thus, in the following sections only the conformers with a g^- state for the aspartyl side chain are included. As a result, topological differences in molecular structures for each analogue are derived from differences in the conformations of the second residue.

3.1. Preferred Conformations of Type A Taste Ligands

Sixteen minimum-energy conformations consistent with the ^{1}H NMR parameters obtained in solution were calculated for L-Asp-L-Phe-OMe (**1**). The results indicate that the L-Phe residue has great flexibility, since the L-Asp residue adopts the same structure with (ψ^1, ω^1, χ_1^1, $\chi_{2,1}^1$) ≈ (175°, 180°, −56°, −170°) on the average in these conformations. The lowest energy conformation is very similar to the X-ray crystal structure.[12a]

The relative spatial arrangements of the three glucophores of **1**, the protonated N-terminal amino group (AH), the carboxylate group (B) of the Asp residue, and the aromatic group (X) of the Phe residue, are defined by a set of six angles: ψ^1, ω^1, χ_1^1, and $\chi_{2,1}^1$ of L-Asp, and ϕ_2 and χ_1^2 of L-Phe. Since the first four angles of the Asp residue are essentially the same for all minimum-energy conformations, the remaining two angles, ϕ^2 and χ_1^2, define the spatial arrays of the glucophores. According to the observed combinations of these two angles, six preferred topochemical arrays of the AH, B, and X glucophores are obtained for the sweet-tasting L-Asp-L-Phe-OMe (**1**) (Fig. 11). The

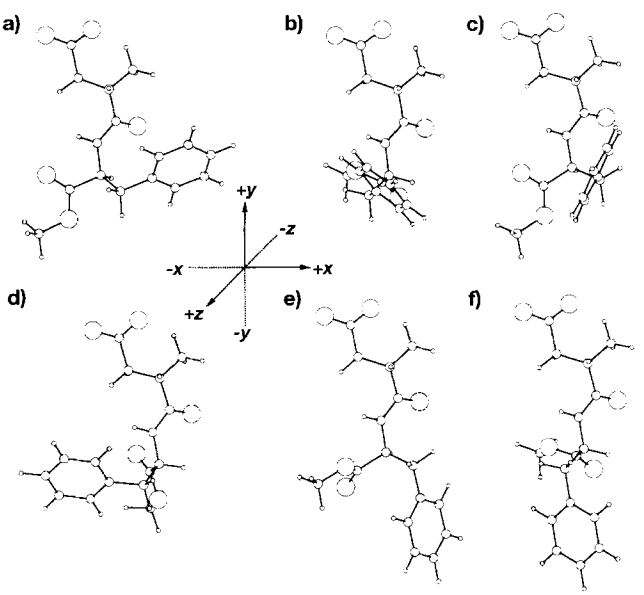


Fig. 11. Preferred conformations of aspartame (**1**). In all the conformations, the L-aspartyl moiety containing the AH and B glucophores assumes essentially the same zwitterionic structure which projects along the $+y$ axis. The hydrophobic phenylalanine side chain projects along the $+x$ axis in a), along the $+z$ axis in b) and c), along the $-x$ axis in d), and along the $-y$ axis in e) and f).

calculated ϕ^2 angle is restricted to two regions: between −165 and −140°, and between −90 and −60°. For the χ_1^2 angle, three values were calculated: ca. 180° (t), ca. −60° (g^-), and ca. +60° (g^+). The conformation shown in Figure 11a, in which the ϕ^2

and χ_1^2 angles assume values of -148 and $-61°$ (g^-), respectively, assumes an L-shaped structure; the AH- and B-containing zwitterionic ring of the aspartyl moiety forms the stem of the L along the $+y$ axis, and the hydrophobic X group projects along the base of the L along the $+x$ axis. The structure with the X group projecting into the $+z$ dimension shown in Figure 11b exhibits ϕ^2 and χ_1^2 angles of -67 and $-60°$ (g^-), respectively. A similar topochemical array is observed in Figure 11c, in which the Phe residue adopts the angles $\phi^2 = -163°$ and $\chi_1^2 = +58°$ (g^+). The structure shown in Figure 11d with $\phi^2 = -73°$ and $\chi_1^2 = +59°$ (g^+) is defined by a reversed L-shaped structure, in which the X group projects along the $-x$ axis. In Figures 11e and 11f, the X group projects along the $-y$ axis, which results in extended structures with the AH/B groups and the X group in a planar array. These extended structures require the side chain χ_1^2 angle to be roughly 180° (t) but are less dependent upon the ϕ^2 angle.

The minimum-energy conformations calculated for the sweet-tasting L-Asp-L-(α-Me)Phe-OMe (**3**) are very similar to those of **1**. Therefore, the preferred topochemical arrays of the AH, B, and X glucophores of both compounds are equivalent. These results indicate that substitution of an α-methyl group for the α-proton of the L-Phe residue does not affect the preferred conformations of the L-aspartyl dipeptide molecules.

The bitter L-Asp-D-(α-Me)Phe-OMe (**4**) adopts essentially the same structures for the L-Asp moiety as its diastereomer **3** and aspartame (**1**), both of which are sweet. The ϕ^2 angle calculated for the D-(α-Me)Phe residue of **4** has values between 157 and 187°, and between 58 and 78°. These ranges of angles are opposite to those calculated for the L-(α-Me)Phe residue of the sweet-tasting **3**. Consequently, the preferred topochemical arrays of the AH, B, and X glucophores of the bitter dipeptide **4** are different from those of the sweet analogues **1** and **3**. No L-shaped structures are accessible to **4**; instead, this bitter analogue assumes structures with a large $-z$ component, in which the hydrophobic benzyl side chain (X) projects into the $-z$ dimension and the D-(α-Me)Phe residue adopts the angles $\phi^2 = 160°$ and $\chi_1^2 = 71°$ (g^+). This kind of structure was not observed for the sweet analogues **1** and **3**.

The three-dimensional structures of the glucophores of sweet-tasting **5** are topochemically equivalent to those of **1**. In contrast, the preferred topochemical arrays of the AH, B, and X glucophores of the tasteless analogue **6** are different from those of the sweet analogues **1**, **3**, and **5**, and the bitter analogue **4**. Neither L-shaped structures nor structures with a large $-z$ component are accessible to **5**. When the zwitterion formed by the protonated amino group (AH) and carboxylate group (B) of the (*S*)-Ama residue is placed along the $+y$ axis, the hydrophobic Phe side chain mostly projects into the space defined by the $-x$, $-y$, and $+z$ axes.

In contrast to analogues **1**–**6**, which show large flexibilities in the second residue, the Chg residue in analogues **7** and **8** displays unique and restricted conformational preferences. Conformations are found in which the cyclohexyl side chain has substituents either in *axial* or in *equatorial* positions; the axial form is calculated to be at least 7 kcal mol^{-1} higher in energy than the equatorial.[11g] Therefore, only the conformers in which the substituent is *equatorial* will be considered. In both diastereomers **7** and **8**, the conformation about the N–C^α bond (ϕ^2) of the Chg residue is the primary determinant of the relative spatial arrangements of the AH, B, and X glucophores. Since the cyclohexane ring is directly attached to the α-carbon of the second residue, a rotation of the cyclohexyl side chain about the C^α–C^β bond (χ_1^2) causes minimal change in the relative position of the X group. In each diastereomer, the calculated ϕ^2 angles are restricted to two regions: from -145 to $-131°$ and from -97 to $-77°$ for the sweet-tasting **7** and from 77 to 102° and roughly 140° for the bitter-tasting **8**. These values agree with the experimental values estimated from the ^{1}H NMR studies (Table 4). In **7** the hydrophobic cyclohexyl side chain (X) orients along the $+x$ axis (forming an L-shaped structure) when the (*S*)-Chg residue adopts the ϕ^2 angle in the range of -145 to $-131°$ (Fig. 12a). With ϕ^2 in the range of -97 to $-77°$, the

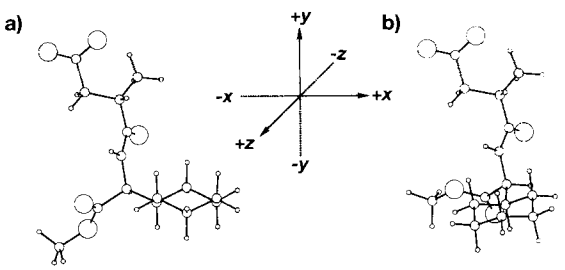


Fig. 12. Preferred conformations of **7**. In both, the L-aspartyl moiety containing the AH and B glucophores assumes essentially the same zwitterionic structure which projects along the $+y$ axis. The hydrophobic cyclohexyl side chain projects along the $+x$ axis in a) and along the $+z$ axis in b).

cyclohexyl side chain projects into the $+z$ dimension (in front of the stem of the L structure, Fig. 12b). In contrast, the cyclohexyl side chain of **8** orients along the $-x$ axis (reversed L shape, Fig. 13a) with $\phi^2 = 77$–$102°$ for the (*R*)-Chg residue, and in the $-z$ axis (behind the stem of the L, Fig. 13b) when the angle ϕ^2 is about 140°. In the latter structures the molecule possesses a large $-z$ component.

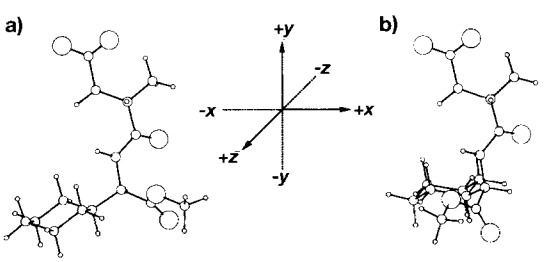


Fig. 13. Preferred conformations of **8**. In both, the L-aspartyl moiety containing the AH and B glucophores assumes essentially the same zwitterionic structure which projects along the $+y$ axis. The hydrophobic cyclohexyl side chain projects along the $-x$ axis in a) and along the $-z$ axis in b).

3.2. Preferred Conformations of Type B Taste Ligands

Fourteen minimum-energy conformations were calculated for the diastereomeric pair **11** and **12**, in which the L-Asp side chain is in the g^- state. These fourteen structures are subdivided into seven families according to the (ϕ^2, ψ^2) conformation of the gAla residue. Each family contains two minimum-energy con-

formations with different values of the torsion angle τ^3 of the C-terminal TMCP group which is defined as N-C(O)-C^1-H; one structure has $\tau^3 \approx +20°$ and the other has $\tau^3 \approx -20°$. The results of computer simulations lead to two interesting and important conclusions regarding the conformational features of these retro-inverso molecules:

1) None of the minimum-energy conformations has (ϕ^2, ψ^2) $\approx$ ($+100°$, $-100°$) or (ϕ^2, ψ^2) $\approx$ ($-100°$, $+100°$) in the gAla residue, although these values are observed in the X-ray crystal structures[11b] of **11** and **12**, respectively. There is no similarity observed between the calculated and X-ray structures. These results indicate that the X-ray crystal structures of the retro-inverso analogues **11** and **12** represent accessible conformations in solution but are not minimum-energy structures. The two geminal NH groups of the gAla residue are involved in intermolecular hydrogen bonds in the X-ray structure.

2) The gAla residue adopts both negative and positive ϕ^2 angles without preference, which is in agreement with the results of the ^{1}H NMR studies. These ϕ^2 values indicate that there are no clear conformational preferences for this residue. In this respect, the retro-inverso analogues are distinguished from the other dipeptides which show clear conformational preferences for the second residue.

Since the L-aspartyl residue assumes the same conformation in both analogues, the (ϕ^2, ψ^2) conformation of the second residue (gAla) determines the relative spatial orientation of the C-terminal hydrophobic TMCP group (X) and the AH/B glucophores in the aspartyl moiety. A rotation about the C(O)–C^1 bond (τ^3) causes little relative change in the position of the X group. Minimum-energy structures of the sweet-tasting **11** are shown in Figure 14. The molecule assumes extended structures when the (*R*)-gAla residue adopts conformations with (ϕ^2, ψ^2) = (163°, −165°), (ϕ^2, ψ^2) = (63°, −165°), and (ϕ^2, ψ^2) = (−52°, 161°), as shown in Figures 14a, 14b, and 14c, respectively. In the structure shown in Figure 14d, the (*R*)-gAla residue adopts a conformation with (ϕ^2, ψ^2) = (165°, −66°) which causes the hydrophobic TMCP group (X) to project into the $+z$ dimension. In the structure shown in Figure 14e, in which the (*R*)-gAla residue adopts a conformation with (ϕ^2, ψ^2) = (161°, 51°), the X group points into the space between the $+z$ axis and the $-x$ axis. The molecule forms a reversed L shape with the X group projecting along the $-x$ axis when the (*R*)-gAla residue adopts a conformation with (ϕ^2, ψ^2) = (−57°, −66°), as shown in Figure 14f. In the conformation with (ϕ^2, ψ^2) = (64°, 57°) the retro-inverso molecule is arranged in an L shape with the X group projecting along the $+x$ axis (Fig. 14g).

As shown in Figure 15, the sweet-tasting **12** assumes topochemical structures similar to those of its diastereomer **11**. Extended structures are observed when the (*S*)-gAla residue is in conformations with (ϕ^2,ψ^2) = (−164°, 163°), (ϕ^2, ψ^2) = (−67°, 164°), and (ϕ^2, ψ^2) = (52°, −160°), as shown in Figures 15a, 15b, and 15c, respectively. In the structure shown in Figure 15d, the (*S*)-gAla residue adopts a conformation with

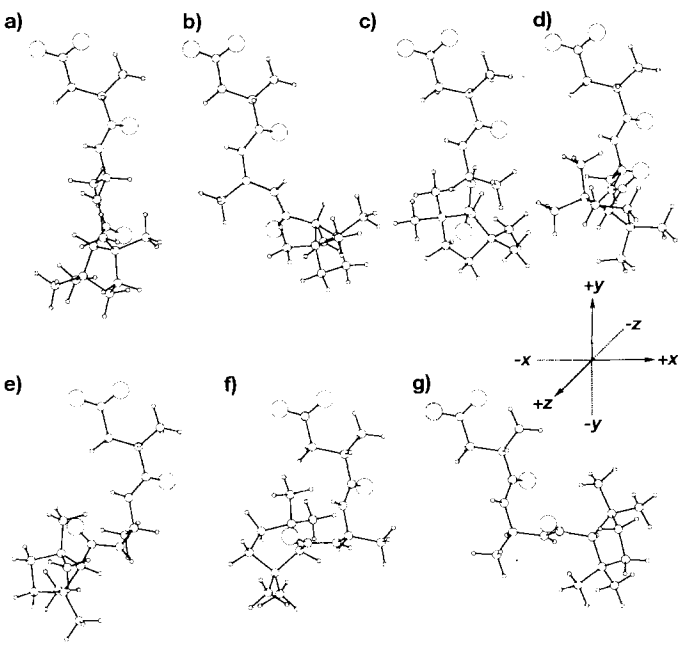


Fig. 14. Preferred conformations of **11**. In all the conformations, the L-Asp moiety containing the AH and B glucophores assumes essentially the same zwitterionic structure, which projects along the $+y$ axis. The C-terminal TMCP group, which serves as the hydrophobic X glucophore, projects into the $-y$ dimension in structures a), b), and c), into the $+z$ dimension in structure d), and into the space between the $+z$ axis and the $-x$ axis in structure e). Structure f) has a reversed L shape with the TMCP group projecting along the $-x$ axis; structure g) has an L shape with the same group projecting along the $+x$ axis.

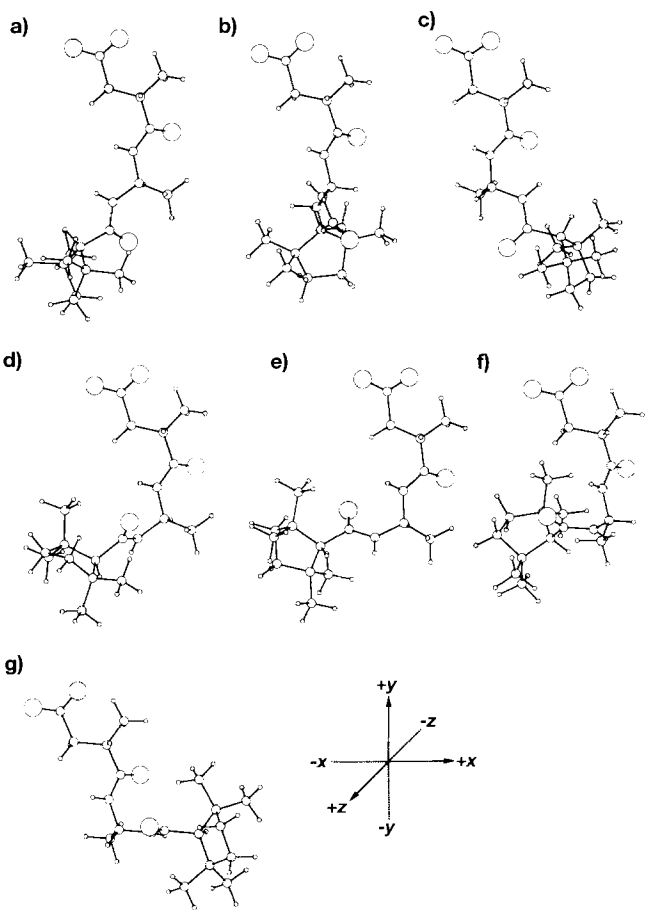


Fig. 15. Preferred conformations of **12**. In all the conformations, the L-Asp moiety containing the AH and B glucophores assumes essentially the same zwitterionic structure, which projects along the $+y$ axis. The C-terminal TMCP group, which serves as the hydrophobic X glucophore, projects into the $-y$ dimension in structures a), b), and c), and into the space between the $+z$ axis and the $-x$ axis in structure d). Structures e) and f) have reversed L shapes with the TMCP group projecting along the $-x$ axis; structure g) has an L shape with the same group projecting along the $+x$ axis.

$(\phi^2, \psi^2) = (-159°, -54°)$, which causes the X group to point into the space between the $+z$ axis and the $-x$ axis. In the reversed L-shaped structures shown in Figures 15e and 15f, the (*S*)-gAla residue is in conformations with $(\phi^2, \psi^2) = (-164°, 62°)$ and $(\phi^2, \psi^2) = (-66°, -57°)$, respectively. The L-shaped structure shown Figure 15g requires $(\phi^2, \psi^2) = (55°, 65°)$.

Similar topochemical arrays of the AH, B, and X glucophores were observed for the sweet D-Ala-containing analogues **9** and **10**, although the D-Ala residue of these molecules adopts only positive ϕ^2 values (60–180°).

The α-aminocyclopropanecarboxylic acid (Ac^3c) residue displays quite unique (ϕ, ψ) conformational preferences. For ϕ, only two narrow regions are equally accessible for Ac^3c: one with $\phi = 70 \pm 30°$ and the other with $\phi = -70 \pm 30°$. On the other hand, accessible regions for ψ of Ac^3c are relatively broad. Two energy minima are observed for each allowed ϕ value: $\psi \approx 55$ and 180° for $\phi \approx +70°$, and $\psi \approx -55$ and 180° for $\phi \approx -70°$. Because of the structural constraints of the Ac^3c residue, four families of minimum-energy conformations were calculated for the sweet L-Asp-Ac^3c-O*n*Pr (**13**). In all of the families, the aspartyl moiety assumes essentially the same structure $((\psi^1, \omega^1, \chi^1_1, \chi^1_{2,1}) \approx (175°, 180°, -56°, -170°))$. Four similar families have been reported by Taylor et al.,[18] but their ψ^2 values are different from ours because they have assumed a two-fold potential about the C^α–C(O) bond of the Ac^3c residue with minima at 0 and 180°. Each family consists of minimum-energy conformations that are different from one another in terms of the conformation of the C-terminal *n*-propyl ester group. The conformation of the *n*-propyl ester group is less critical to the relative spatial arrangements of the AH, B, and X glucophores than the (ϕ^2, ψ^2) conformation of the Ac^3c residue.

Figure 16 shows accessible conformations for the sweet-tasting **13**. In the Ac^3c conformation with $(\phi^2, \psi^2) = (70°, 57°)$ the dipeptide molecule is arranged in an L shape (Fig. 16a) with the hydrophobic *n*-propyl ester (X) projecting along the $+x$ axis. Conversely, in the conformation with $(\phi^2, \psi^2) = (-70°, -57°)$ a reversed L-shaped structure (Fig. 16c) is observed with the X group projecting along the $-x$ axis. In Figures 16b and 16d, the L-Asp-Ac^3c-O*n*Pr molecule assumes extended structures with $(\phi^2, \psi^2) = (73°, -177°)$ and $(\phi^2, \psi^2) = (-74°, 177°)$, respectively.

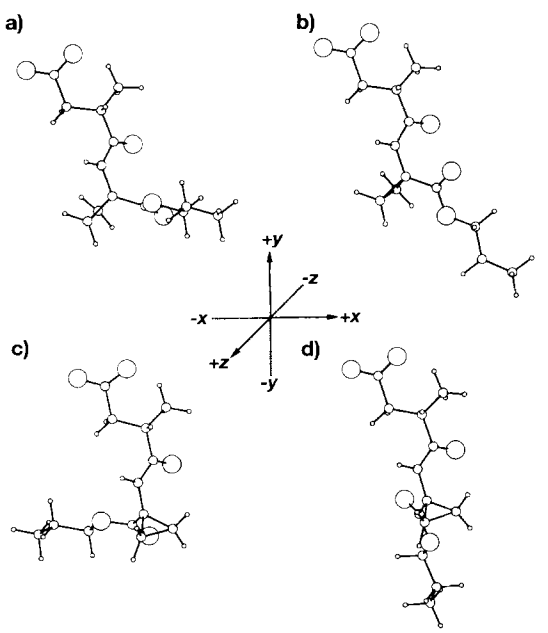


Fig. 16. Preferred conformations of **13**. In all the conformations, the L-Asp moiety containing the AH and B glucophores assumes essentially the same zwitterionic structure which projects along the $+y$ axis. The molecule assumes a) an L shape with the hydrophobic *n*-propyl ester group projecting along the $+x$ axis and c) a reversed L shape with the same group projecting along the $-x$ axis. The *n*-propyl ester group projects into the $-y$ dimension in structures b) and d).

4. A Three-Dimensional Model for Taste

The topochemical arrays of the AH (hydrogen bond donor), B (hydrogen bond acceptor), and X (hydrophobic element) glucophores accessible in the peptide-based taste ligands investigated are divided into five classes:

I: an L-shaped structure with the AH- and B-containing zwitterionic ring of the N-terminus (L-Asp, (*R*)-Ama, or (*S*)-Ama) forming the stem of the L in the y axis and the hydrophobic X group projecting along the base of the L in the $+x$ axis;

II: a reversed L-shaped structure with the X group projecting along the $-x$ axis;

III: an extended structure in which the AH/B moiety of the zwitterionic ring and the X group form an angle of nearly 180° in a planar linear array, and the X group projects into the $-y$ dimension;

IV: a structure with the X group projecting into the $+z$ dimension;

V: a structure with significant extension of the X group into the $-z$ dimension.

All of the sweet-tasting analogues with the exception of **7** and **13** adopt common topochemical arrays of the AH, B, and X glucophores (classes I–IV) as shown in Table 5. The topochemical array in which the X group projects into the $-z$ dimension (class V) is accessible to none of the sweet-tasting analogues including **7** and **13**. Therefore, this topochemical array is excluded as a candidate for the bioactive conformation necessary for sweet taste.

Table 5. Topochemical arrays of AH, B, and X glucophores in **1**–**13**.

Compound		Taste	Topochemical arrays [a]				
			I	II	III	IV	V
Type A							
1	L-Asp-L-Phe-OMe	sweet	yes	yes	yes	yes	no
3	L-Asp-L-(α-Me)Phe-OMe	sweet	yes	yes	yes	yes	no
4	L-Asp-D-(α-Me)Phe-OMe	bitter	no	yes	yes	yes	yes
5	(*R*)-Ama-L-Phe-OMe	sweet	yes	yes	yes	yes	no
6	(*S*)-Ama-L-Phe-OEt	tasteless	no	yes	yes	yes	no
7	L-Asp-(*S*)-Chg-OMe	sweet	yes	no	no	yes	no
8	L-Asp-(*R*)-Chg-OMe	bitter	no	yes	no	no	yes
Type B							
9	L-Asp-D-Ala-TAN	sweet	yes	yes	yes	yes	no
10	L-Asp-D-Ala-OTMCP	sweet	yes	yes	yes	yes	no
11	L-Asp-(*R*)-gAla-TMCP	sweet	yes	yes	yes	yes	no
12	L-Asp-(*S*)-gAla-TMCP	sweet	yes	yes	yes	yes	no
13	L-Asp-Ac^3c-O*n*Pr	sweet	yes	yes	yes	no	no

[a] For a definition of the topochemical arrays see text.

Among the sweet-tasting analogues, **7** is particularly informative with regard to the orientation of the X group relative to the

AH and B groups. Since the conformationally constrained cyclohexyl group is bonded directly to the α-carbon of the second residue in this analogue, the hydrophobic X group sweeps out an arc nearly coplanar with the xz plane. Thus, no extended structures (class III) in which the X group projects out along the $-y$ axis are accessible to this analogue. Dipeptide **7** can only assume two types of topochemical arrays, class I and class IV. The sweet-tasting **13** is also informative. This analogue adopts the L-shaped (class I), the reversed L-shaped (class II), and the extended (class III) structures. However, no structures in which the hydrophobic *n*-propyl ester (X) projects into either the $+z$ dimension (class IV) or the $-z$ dimension (class V) are accessible to this analogue because of the constrained Ac^3c residue. Only the L-shaped structure (class I) is common to both of the sweet analogues **7** and **13**. As is evident in Table 5, the L-shaped structure is the only topochemical array of the AH, B, and X glucophores that is accessible to all sweet-tasting analogues. From these results, we conclude that the L-shaped structure is necessary for sweet taste. Our conclusion is further strengthened by the fact that no L-shaped structures (class I) are accessible to either the tasteless analogue **6** or the bitter analogues **4** and **8** (Table 5). The L-shaped structures of aspartame (**1**) (Type A with the Phe side chain as the hydrophobic X group) and **9** (Type B with the C-terminal TAN group as the X group) are shown in Figure 17.

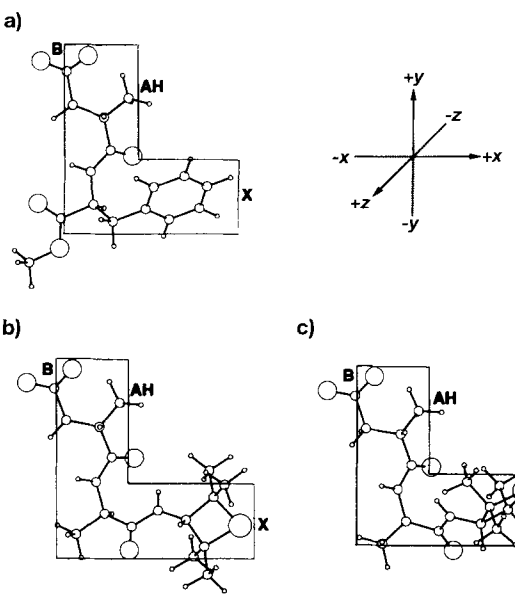


Fig. 17. The L-shaped structures of a) **1** and b), c) **9**, which produce a sweet taste. In all the structures, the AH- and B-containing zwitterionic ring of the L-Asp moiety forms the stem of the L in the $+y$ axis, and the hydrophobic X group projects out along the base of the L in the $+x$ axis. The zwitterionic ring is coplanar with the plane of the L.

Structural requirements for the bitter taste produced by peptide-based molecules can be deduced by comparing accessible topochemical arrays of the bitter molecules **4** and **8** with those of the sweet and tasteless analogues. Dipeptide **4** can assume four topochemical arrays: structures of classes II, III, IV, and V. In contrast, only two topochemical arrays, structures of classes II and V, are accessible to **8** because of the constrained cyclohexylglycine residue. Thus, the class II and class V structures are common to the bitter analogues **4** and **8**. In the class V structures, the molecules possess large $-z$ components. Although the reversed L-shaped array (class II) is also accessible to most of the sweet and tasteless analogues, the class V topochemical array is unique to the bitter analogues **4** and **8** (Table 5). We postulate that this topochemical array with a large $-z$ component, which results from the projection of the X group behind the stem of the L into the $-z$ dimension, produces a bitter taste. The class V topochemical structures of **4** and **8** are shown in Figure 18.

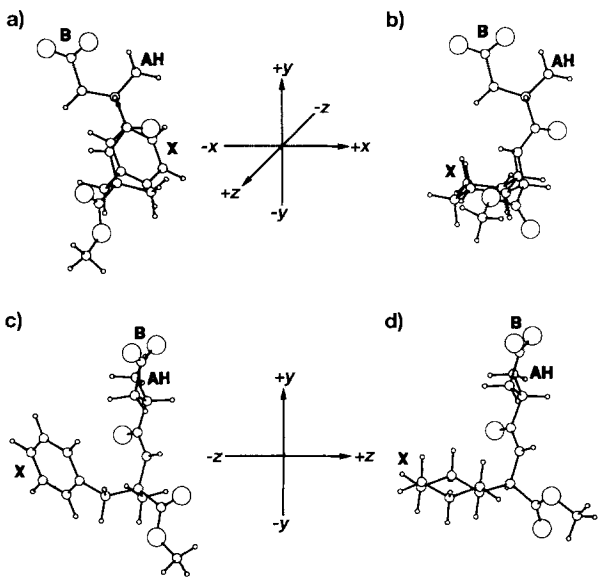


Fig. 18. The topochemical structures which produce the bitter taste of a) **4** and b) **8**. In these structures, the hydrophobic X glucophore projects into the $-z$ dimension, in other words, behind the stem of the L (see Fig. 14). Thus, these structures possess large $-z$ components which are clearly seen in the projections along the yz axes of the structures of **4** (c) and **8** (d).

The Type A dipeptide molecule **6** assumes topochemical arrays of classes II, III, and IV, but neither the class I L-shaped structures necessary for sweet taste nor the class V structures required for bitter taste are accessible. Thus, this molecule is tasteless. Although we have not discussed tasteless molecules belonging to Type B in this review, several such compounds such as D-aspartyl-D-alanine(2,2,4,4-tetramethylthietanyl)-amide,[11d] a stereoisomer of **9**, have been reported. Conformational studies by NMR spectroscopy and computer simulations reveal that this compound can assume structures of classes II, III, and IV but not of classes I or V.

The relationship between the topochemical arrays of the AH, B, and X glucophores and tastes developed here for peptide-based taste ligands is illustrated in Figure 19.

In all five classes of topochemical arrays of the AH, B, and X glucophores presented in Table 5, the N-terminal residue adopts essentially the same structure: $(\psi^1, \omega^1, \chi_1^1, \chi_{2,1}^2) \approx (175^\circ, 180^\circ, -56^\circ, -170^\circ)$ for L-Asp and $(\psi^1\ \omega^1, \chi_{1,1}^1) \approx (175^\circ, 180^\circ, -170^\circ)$ for (*R*)-Ama. In all compounds, the protonated amino (AH) and the side-chain carboxylate (B) groups are arranged in the correct geometry for them to act as the AH/B functionalities. The differences in overall structure and in taste arise from the

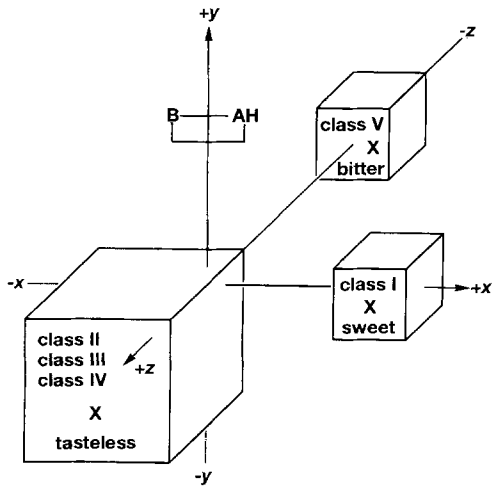


Fig. 19. A schematic illustration of the relationship between topochemical arrays of the AH, B, and X glucophores and tastes. The α-carbon atom of the second residue of the taste ligands is located at the origin of the *xyz* coordinate system, i.e. at (0, 0, 0).

conformation of the second residue. The ϕ^2 and χ_1^2 angles are critical for the overall structures and taste properties of Type A analogues. For Type B analogues, the ϕ^2 and ψ^2 angles are critical for their tastes. These angles determine the relative orientation of the hydrophobic X function with respect to the AH/B functions. In Type A analogues, the L-shaped structure necessary for sweet taste requires the torsion angles $\phi^2 = -150^\circ \pm 30^\circ$ and $\chi_1^2 \approx -60^\circ$ (g^-) in the second residue; in Type B analogues $\phi^2 = 70^\circ \pm 30^\circ$ and $\psi^2 = 0^\circ \pm 60^\circ$ are required.

The class V structures, which possess a large $-z$ component and produce a bitter taste, also require specific torsion angles for the second residue: $\phi^2 = +150^\circ \pm 30^\circ$ and $\chi_1^2 \approx +60^\circ$ (g^+) for Type A and $\phi^2 = -70^\circ \pm 30^\circ$ and $\psi^2 = +60^\circ \pm 30^\circ$ for Type B. The ϕ^2 and ψ^2 angle requirements for Type B analogues were estimated from conformational studies of the bitter Type B compounds L-asparty-L-alanine-2,2,4,4-(tetramethylthietanyl)amide[11d] and L-aspartyl-L-alanine-(2,2,5,5-tetramethylcyclopentyl)amide[19] by NMR spectroscopy and computer simulations. The former compound is a stereoisomer of the sweet-tasting L-Asp-(*S*)-gAla-TAN (**9**), and the latter is the parent compound of the sweet-tasting L-Asp-(*S*)-gAla-TMCP (**12**).

As mentioned in Section 1, the absolute configuration of the second residue is a critical factor in determining the taste properties of dipeptide taste ligands. For Type A taste ligands, an L-amino acid residue at position 2 is necessary for sweet taste, while incorporation of a D-amino acid at the same position produces bitter taste. For Type B analogues, a D-amino acid at position 2 is necessary for sweet taste, while incorporation of an L-amino acid at the same position results in a bitter or tasteless molecule. The configurational requirements of the second residue that must be fulfilled for a molecule to elicit a sweet taste can be explained with the ϕ^2 requirements of the L-shaped structures. The conformation with $\phi^2 = 70 \pm 30^\circ$ is required for the L-shaped structures of dipeptide taste ligands belonging to Type B. For L-amino acids, this structure is energetically less stable than the conformation with negative values of ϕ^2. The L-shaped structures of dipeptide analogues belonging to Type A require the angle ϕ^2 to assume a value of $-150 \pm 30^\circ$. Such a structure is not accessible to D-amino acids.

In order to generalize the angle requirements of dipeptides with sweet and bitter tastes, we introduce the dihedral angle θ_ϕ^2 defined by C(O)-N-C^α-R_2 [C(O)-N-C^α-X (hydrophobic glucophore) in Fig. 2a]. The θ_ϕ^2 angle can be related to the torsion angle ϕ^2 as $\theta_\phi^2 = \phi^2 - 120^\circ$ for taste ligands of Type A which have an L- or (*S*) configuration at position 2, $\theta_\phi^2 = \phi^2 + 120^\circ$ for analogues of Type A which have a D- or (*R*) configuration at position 2, and $\theta_\phi^2 = \phi^2$ for Type B dipeptide analogues. Therefore, the L shape needed for sweet taste requires $\theta_\phi^2 = 90 \pm 30^\circ$ for Type A and $\theta_\phi^2 = 70 \pm 30^\circ$ for Type B. These two θ_ϕ^2 angle ranges are very close to each other. In contrast, the class V structure which produces a bitter taste requires $\theta_\phi^2 = -90 \pm 30$ for Type A and $\theta_\phi^2 = -70 \pm 30^\circ$ for Type B. These results indicate that the positive θ_ϕ^2 value of $80 \pm 40^\circ$ is required for sweet taste, while the negative θ_ϕ^2 value of $-80 \pm 40^\circ$ is required for bitter taste.

5. Comparison of the L Model with Other Molecular Models for Sweet Taste

In addition to our L model, several other molecular models for sweet taste have been reported in the literature. In the following sections, comparison of the L model with other molecular models is addressed.

5.1. Comparison with the Temussi Model

Temussi et al.[22] analyzed the preferred conformations of aspartame (**1**) by using ^{1}H NMR spectroscopy and potential energy calculations. As a bioactive conformation of aspartame, they proposed an extended structure in which the AH/B-containing zwitterionic ring of the L-Asp moiety and the hydrophobic benzyl side chain (X) of the L-Phe residue form a planar parallel array with an angle of nearly 180° (Class III in this review). This structure resulting from the $\chi_1 = g^-$ (ca. -60°) and t (ca. 180°) states for the L-Asp and L-Phe side chains, respectively, was originally reported to be the most stable in solution. After Siemion and Picur[21] argued against the $\chi_1 = t$ preference of the L-Phe side chain, Temussi et al.[20] reported that the most stable form of aspartame in solution is a structure with both the L-Asp and L-Phe side chains in the $\chi_1 = g^-$ state. This revision was based on the assignments of the two β-protons of the L-Phe residue by the ^{1}H NMR studies of aspartame containing a stereospecifically β-monodeuterated phenylalanine, (2*S*, 3*S*)-[3-^{2}H]-Phe. However, they insisted that the bioactive conformation of aspartame remained the extended structure as originally reported.

Temussi's structural model differs from our L model in the side-chain χ_1 angle of the second residue (L-Phe of aspartame). This residue assumes the t (ca. 180°) state in Temussi's model and the g^- (ca. -60°) state in our model. Since the L-Phe residue of aspartame adopts both χ_1 states in solution with a preference of g^- over t, it is clear that the aspartame molecule adopts both extended and L-shaped structures (Fig. 11 and Table 5). Thus it

is impossible to discriminate between the two models on the basis of aspartame alone. However, our studies reveal that the L-shaped structure is the only topochemical structure accessible to all of the sweet analogues and that no L-shaped structures are accessible to the bitter and tasteless analogues (Table 5). In addition, extended structures which fit the Temussi model are not accessible to the sweet molecule **7**, and the bitter molecule **4** and the tasteless molecule **6** can also assume extended structures. These results provide evidence in favor of the L model over the extended structure model.

5.2. Comparison with the van der Heijden Model

It has been demonstrated that the sweetness potencies of a wide variety of L-aspartyl-based dipeptide derivatives are dependent on the length and size of the C-terminal amide or ester groups and the side-chain substituent of the second residue.[23] Based on these findings, van der Heijden et al.[24] criticized Temussi's model[22] and postulated an alternative structure as a bioactive conformation of aspartame, in which both the L-Asp and L-Phe side chains assume the $\chi_1 = g^-$ (ca. $-60°$) state. Molecular models and the STERIMOL approach were used to calculate the distances AH – B, AH – X, and B – X as 3.0, 4.5, and 7.3 Å, respectively. Van der Heijden et al. argued that their model correlates better with taste properties of a series of dipeptide taste ligands than Temussi's model. In terms of the side-chain conformations of the L-Asp and L-Phe residues, the van der Heijden model is in agreement with our L model. In addition, the AH–B, AH–X, and B–X distances calculated for our L-shaped structures of aspartame are 2.9, 5.2 and 7.5 Å, respectively, values which are close to those of the van der Heijden model. This suggests that the backbone conformations of the two proposed models are similar, although the torsion angles describing the backbone conformation have not been reported for the van der Heijden model.

5.3. Comparison with the Görbitz Model

As a bioactive conformation of aspartame, Görbitz[12b] has proposed a rather compact structure, with distances of 2.9 Å for AH–B, 3.7 Å for AH–X, and 5.2 Å for B–X. This structure correlates well with the Kier triangular model[3] developed for sweet-tasting amino acids. However, it should be mentioned that the AH–X and B–X distances required for sweet taste must be reevaluated, because dipeptide taste ligands are much sweeter than the amino acids used for development of the Kier triangular model. The Görbitz bioactive structure is described by the angles $\psi^1 = 82.0°$, $\omega^1 = -172.0°$, $\chi_1^1 = +60.0°$ (g^+), and $\chi_{2,1}^1 = -65.0°$ for the L-Asp residue, and $\phi^2 = -128.0°$, $\psi^2 = 166.8°$, $\chi_1^2 = -60.0°$ (g^-), and $\chi_{2,1}^2 = -85.0°$ for the L-Phe residue. As for the conformation of the L-Phe residue, the ϕ^2 and χ_1^2 angle values of Görbitz's structure agree with the angles of $\phi^2 = -150° \pm 30°$ and $\chi_1^2 \approx -60°$ (g^-) required in our L model. On the other hand, the conformations of the L-Asp residue are different in the two models. The major difference arises from the side chain χ_1^1 conformation. Görbitz's compact structure assumes the g^+ (ca. $+60°$) state about the L-Asp side chain, while our L model assumes the g^- (ca. $-60°$) state. Both states provide similar distances between the AH and B glucophores in the aspartyl moiety, in accordance with the AH–B distances found in many nonpeptide sweet-tasting molecules (2.5–4.0 Å). Because all of the aspartyl-based dipeptide analogues prefer the g^- state (50–60%) over the g^+ state (20–25%) about the aspartyl side chain in solution, as revealed by the NMR studies, we have assumed the $\chi_1^1 = g^-$ state for the L-Asp residue as a bioactive conformation. All aspartyl-based analogues studied, with the exception of the aspartame hydrochloride salt (**2**), adopt the g^- state in the solid state. It is not possible on the basis of the present data to choose between the $\chi_1^1 = g^+$ and g^- states for the active form of the L-aspartyl side chain. One method of answering this question is by examining a stereoisomer of the N-terminal L-aspartyl residue of taste ligands in the aspartame family.

5.4. Comparison with the Tinti–Nofre Model

Tinti, Nofre, et al.[25] demonstrated that the COO^- and NO_2 (or CN) groups, previously considered as B sites in the Shallenberger–Acree hypothesis,[1] participate by specific and distinct interactions with the taste receptors to elicit a sweet taste. They postulated that the NO_2 or CN group comprises a D site, in other words, a fourth binding site in addition to the AH, B, and X glucophores.[26] The significance of this fourth binding site was demonstrated with a highly potent, sweet *N*-(4-cyanophenylcarbamoyl)-L-aspartyl-L-phenylalanine methyl ester (14000 times sweeter than sucrose), which is a hybrid compound of the two sweeteners 4-cyanophenylcarbamoyl-β-alanine (450 times sweeter than sucrose)[27] and aspartame (**1**) (200 times sweeter than sucrose).[6] This hybrid contains the AH, B, X, and D glucophores within a single structure. On the basis of these findings, Tinti and Nofre[28] have proposed an eight recognition site model, with four high-affinity sites designated as AH (hydrogen bond donor), B (anionic group such as COO^-), G (hydrophobic group, equal to X in the AH/B/X model), and D (hydrogen bond acceptor), and with four secondary sites designated as Y, E_1, E_2 (hydrogen bond acceptors), and XH (hydrogen bond donor). The relative distances between these sites and their Cartesian coordinates have been outlined. However, the authors do not describe how they estimated these distances and coordinates. According to Tinti and Nofre, the simultaneous interaction of a taste ligand with all of these receptor recognition sites is not required to generate a sweet response. A lower number of interaction sites is often sufficient to initiate a sweet taste. The sweetness potency of a compound depends both on the number of active sites involved in the ligand–receptor interaction and on the effectiveness of each individual interaction.

The taste ligands discussed here (Table 1) contain six of the eight sites postulated by Tinti and Nofre,[28] namely, AH (NH_3^+), B (COO^-), G (hydrophobic group either in the side chain of the second residue or in the C-terminal amide or ester group), Y (C=O of the amide bond between residues 1 and 2), XH (NH of the amide bond between residues 1 and 2), and either E_1 (C=O of the second residue in Type A analogues) or E_2 (C=O of the second residue in Type B analogues). Of the

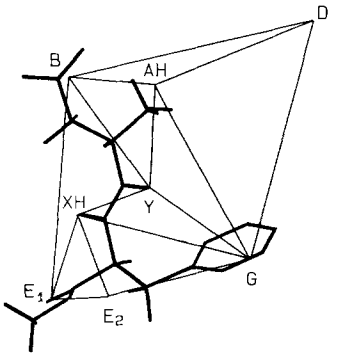


Fig. 20. Superposition of the Tinti–Nofre model (thin lines) with our L model (thick lines) for the bioactive structure of aspartame **1**. For a definition of the recognition sites in the Tinte–Nofre model see the text.

four high-affinity sites, the peptide derivatives lack the D site. Figure 20 shows a comparison of the Tinti–Nofre model with our proposed bioactive L-shaped structure of aspartame. The agreement between the two models is quite good as far as the relative positions of the AH, B, G, Y, XH, and E_1 sites are concerned.

6. Conclusion

We have presented the results of comprehensive structure–activity studies on a series of peptide derivatives of the aspartame family. The compounds fall into two classes. The first (Type A) are dipeptide derivatives containing the hydrophobic group X in the side chain of the C-terminal residue; the second (Type B) contain the hydrophobic group X as either an amide or ester functionality at the C-terminus. In both families, it is not possible to relate the crystal structure directly to the taste properties of the molecules. The solid-state conformation is determined primarily by packing forces. Therefore, it is not possible to assign bioactive conformations on this basis alone.

Examination of the molecules in solution using NMR spectroscopy and computer modeling has led us to propose a general structural model for the sweet and bitter tastes of these molecules. For sweet molecules an L shape is required, in which the zwitterionic ring of the N-terminal residue forms the stem of the L and the hydrophobic group X forms the base of the L. The two groups are coplanar. For bitter molecules, the orientation of the zwitterionic ring is identical, but the hydrophobic group X exhibits a large -*z* coordinate. All other topochemical arrays lead to tasteless molecules. The work presented in this review clearly demonstrated that all of the sweet molecules have accessible coplanar L-shaped structures; those molecules that are not sweet cannot assume these L-shaped structures.

Our model also incorporates many features of other molecular models for sweet taste described in the literature. However, as a result of the correlation and comparison of molecular structures, our model overcomes the limitations of other published structural studies. We are currently examining other peptidomimetic and non-peptide molecules to further refine and to test the the general predictive ability of our model.

The authors gratefully acknowledge the financial support of the National Institutes of Health (DE05476).

Received: April 6, 1993
Revised version: October 4, 1993 [A 939 IE]
German version: *Angew. Chem.* **1994**, *106*, 1502

[1] R. S. Shallenberger, T. E. Acree, *Nature* **1967**, *216*, 480–482.
[2] E. W. Deutsch, C. Hansch, *Nature* **1966**, *211*, 75.
[3] a) L. B. Kier, *J. Pharm. Sci.* **1972**, *61*, 1394–1397; b) H. D. Holtje, L. B. Kier, *ibid.* **1974**, *63*, 1722–1725.
[4] R. S. Schallenberger, M. G. Lindley, *Food Chem.* **1977**, *2*, 145–153.
[5] A. van der Heijden, L. B. D. Brussel, H. G. Peer, *Chem. Senses Flavour* **1979**, *4*, 141–152.
[6] R. H. Mazur, J. M. Schlatter, A. H. Goldkamp, *J. Am. Chem. Soc.* **1969**, *91*, 2684–2694.
[7] a) M. T. Briggs, J. S. Morley GB-B 1299265 **1972**; b) M. Fujino, M. Wakimatsu, K. Tanaka, H. Aoki, N. Nakajima, *Naturwissenschaften* **1973**, *60*, 351.
[8] T. Ando, M. Ota, T. Kashiwagi, N. Nagashima, Y. Ariyoshi, R. K. Chadha, T. Yamazaki, M. Goodman, *J. Am. Chem. Soc.* **1993**, *115*, 397–402.
[9] R. H. Mazur in *Symposium: Sweeteners* (Ed.: G. E. Inglett), Avi Publc. Westport, CT USA, **1974**, p. 159.
[10] Y. Ariyoshi, *Agric. Biol. Chem.* **1976**, *40*, 983–992.
[11] a) M. Goodman, J. Coddington, D. F. Mierke, W. D. Fuller, *J. Am. Chem. Soc.* **1987**, *109*, 4712–4714; b) E. Benedetti, B. D. Blasio, V. Pavone, C. Pedone, W. D. Fuller, D. F. Mierke, M. Goodman, *ibid.* **1990**, *112*, 8909–8912; c) M. Goodman, D. F. Mierke, D. W. Fuller in *Peptide Chemistry 1987* (Eds.: T. Shiba, S. Sakakibara), Peptide Research Foundation, Japan, **1988**, pp. 699–704; d) R. D. Feinstein, A. Polinski, A. J. Douglas, M. G. F. Beijer, R. K. Chadha, E. Benedetti, M. Goodman, *J. Am. Chem. Soc.* **1991**, *113*, 3467–3473; e) T. Yamazaki, Y.-F. Zhu, A. Pröbstl, R. K. Chadha, M. Goodman, *J. Org. Chem.* **1991**, *56*, 6644–6656; f) Y.-F. Zhu, T. Yamazaki, J. W. Tsang, S. Lok, M. Goodman, *ibid.* **1992**, *57*, 1074–1081; g) M. Goodman, T. Yamazaki, Y.-F. Zhu, E. Benedetti, R. K. Chadha, *J. Am. Chem. Soc.* **1993**, *115*, 428–432; h) T. Yamazaki, Y.-F. Zhu, E. Benedetti, M. Goodman in *Peptide Chemistry 1992* (*Proc. 2nd Jpn. Symp. Peptide Chem.* (Ed.: N. Yanaihara), Escom, Leiden, **1992**, pp. 343–346).
[12] a) M. Hatada, J. Jancarik, B. Graves, S. Kim, *J. Am. Chem. Soc.* **1985**, *107*, 4279–4282; b) C. H. Görbitz, *Acta Chem. Scand. Ser. B* **1987**, *41*, 87–92; c) S. Polinelli, Q. B. Broxterman, H. E. Schoemaker, W. H. J. Boesten, M. Crisma, G. Valle, C. Toniolo, J. Kamphuis, *Bioorg. Med. Chem. Lett.* **1992**, *2*, 453–456. d) The details of conformational studies of **4** by X-ray crystallography, NMR spectroscopy, and computer simulations will be reported elsewhere. e) The details of conformational studies of **10** by X-ray crystallography, NMR spectroscopy, and computer simulations will be reported elsewhere. f) C. Mapelli, M. G. Newton, C. E. Ringold, C. H. Stammer, *Int. J. Pept. Protein Res.* **1987**, *30*, 498–510.
[13] E. Benedetti, *Chem. Biochem. Amino Acids Pept. Proteins* **1982**, *6*, 105–184.
[14] a) C. Toniolo, E. Benedetti, *ISI Atlas Sci. Biochem.* **1988**, *1*, 225–230; b) A. Santini, V. Barone, A. Bavaso, E. Benedetti, B. Di Blasio, F. Fraternali, F. Lelj, V. Padone, C. Pedone, M. Crisma, G. M. Bonora, C. Toniolo, *Int. J. Biol. Macromol.* **1988**, *10*, 292–299; c) V. Padone, E. Benedetti, V. Barone, B. Di Blasio, F. Lelj, C. Pedone, A. Santini, M. Crisma, G. M. Bonora, C. Toniolo, *Macromolecules* **1988**, *21*, 2064–2070.
[15] a) A. Bax, D. G. J. Davis, *J. Am. Chem. Soc.* **1985**, *107*, 2820–2821; b) A. A. Bothner-By, R. L. Stephens, J. Lee, C. D. Warren, R. W. Jeanloz, *ibid.* **1984**, *106*, 811–813; c) A. Bax, D. G. J. Davis, *J. Magn. Reson.* **1985**, *65*, 355–360; d) G. Bodenhausen, R. L. Vold, R. R. Vold, *ibid.* **1980**, *37*, 93–106.
[16] a) B. R. Brooks, R. E. Bruccoleri, B. D. Olafson, D. J. States, S. Swaminathan, M. Karplus, *J. Comput. Chem.* **1983**, *4*, 187–217; b) L. Nilsson, M. Karplus, *ibid.* **1986**, *7*, 591–616.
[17] A. T. Hagler, *Peptides NY* **1985**, *7*, 214–296.
[18] E. W. Taylor, S. Wilson, C. H. Stammer in *Sweeteners: Discovery, Molecular Design, and Chemoreception* (Eds.: D. E. Walters, F. T. Orthoefer, G. E. Dubois), American Chemical Society, Washington, DC, **1991**, pp. 162–175.
[19] W. D. Fuller, M. Goodman, M. S. Verlander, *J. Am. Chem. Soc.* **1985**, *107*, 5821–5822.
[20] M. A. Castiglione Morelli, F. Lelj, F. Naider, M. Tallon, T. Tancredi, P. A. Temussi, *J. Med. Chem.* **1990**, *33*, 514–520.
[21] I. Z. Siemion, B. Picur, *Pol. J. Chem.* **1984**, *58*, 475.
[22] a) F. Lelj, T. Tancredi, P. A. Temussi, C. Toniolo, *J. Am. Chem. Soc.* **1976**, *98*, 6669–6675; b) P. A. Temussi, F. Lelj, T. Tancredi, *J. Med. Chem.* **1978**, *21*, 1154–1158; c) P. A. Temussi, F. Lelj, T. Tancredi, M. A. Castiglione Morelli, A. Pastore, *Int. J. Quantum Chem.* **1984**, *26*, 889–906.
[23] a) R. H. Mazur, J. A. Reuter, K. A. Swiatek, J. M. Schlatter, *J. Med. Chem.* **1973**, *16*, 1284–1287; b) L. B. P. Brussel, H. G. Peer, A. van der Heijden, Z. *Lebensm. Unters. Forsch.* **1975**, *159*, 337–343; c) G.-Z. Zeng, J.-T. Chen, H.-Z. He, Z.-Q. Wang, J.-S. Yan, *J. Agric. Food Chem.* **1991**, *39*, 782–785.
[24] a) A. van der Heijden, L. B. P. Brussel, H. G. Peer, *Food Chem.* **1978**, *3*, 207–211; b) see ref. [5].
[25] a) J.-M. Tinti, D. Durozard, C. Nofre, *Naturwissenschaften* **1980**, *67*, 193; b) J.-M. Tinti, C. Nofre, D. Durozard, *ibid.* **1981**, *68*, 143.
[26] J.-M. Tinti, C. Nofre, A. M. Peytavi, *Z. Lebensm. Unters. Forsch.* **1982**, *175*, 266.
[27] C. Nofre, J.-M. Tinti, EP-B 0 107 597, **1983**.
[28] J.-M. Tinti, C. Nofre in *Sweeteners: Discovery, Molecular Design, and Chemoreception* (Eds.: D. E. Walters, F. T. Orthoefer, G. E. Dubois), American Chemical Society, Washington, DC, **1991**, pp. 206–213.

Reactions in Supercritical Carbon Dioxide

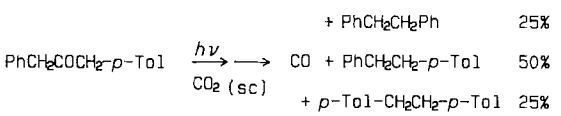
Gerd Kaupp*

The increasing global stress on the environment due to atmospheric pollutants from anthropogenic sources, in addition to those stemming from natural emissions, necessitates certain restrictions, for example on the use of organic solvents. For instance, lacquering is more and more frequently performed in a solvent-free fashion, and a great deal of effort is being made to avoid organic solvents in chemical syntheses, through the use of crystal photolyses,[1] gas/solid reactions,[2] and solid/solid reactions.[3] An additional environmentally friendly approach is the use of supercritical carbon dioxide $CO_{2(sc)}$ as solvent for chemical syntheses. It is nontoxic, cheap, and nonflammable. It has already proven useful in some large-scale extraction processes in the food industry (e.g., decaffeination of coffee or extraction of hops).[4] In these processes, pressure or density changes lead to solubility variations which can also be exploited for chemical reactions in $CO_{2(sc)}$.

The favorable ecological properties of CO_2, especially when it is used in a closed loop system, are counterbalanced by the effort and expense associated with the use of high-pressure installations. High-pressure operations are more readily realized in large-scale production processes than in university or research laboratories. These suffer not only from an increasing lack of funding, but also from the continually changing safety directions and lack of clearly assigned responsibilities. This has deterred academic researchers from undertaking and teaching high-pressure experiments. This misdirected development must be halted because of the detrimental effects on the environment. Many syntheses that cannot be performed as solid-state reactions rely on the use of inert solvents of medium polarity, which are frequently delicate. Therefore $CO_{2(sc)}$, with the critical temperature, pressure, and density values of $T_c = 31.06\,^{\circ}C$, $p_c = 73.83$ bar, $D_c = 0.467\,g\,mL^{-1}$, ought to be utilized.[5] In terms of polarity, $CO_{2(sc)}$ [Dimroth-Reichardt $E_T(30)$ value of 32[6]] is roughly comparable to carbon tetrachloride. However, differences remain when the Kamlet–Taft π^* solvatochromicity parameter ($\pi^* = -0.2$) [7] is taken into account. Thus, $CO_{2(sc)}$ could be used as a replacement for commonly used organic solvents. Until now, however, it appears that most experiments have been primarily governed by academic curiosity.

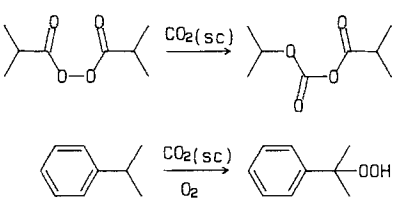
Diels–Alder reactions have shown no discontinuities in reaction rates when liquid CO_2 is replaced by $CO_{2(sc)}$, as long as the density is kept constant.[8] The reaction rates were roughly equal to those in solvents at normal pressures.[9, 10]

Laser flash photolysis studies of benzophenone with H donors in $CO_{2(sc)}$ have shown that the local substrate clusters, which are considered crucial for the reactivity, exchange rapidly (in picoseconds) with the supercritical medium.[11] The photochemical α-cleavage of asymmetric benzyl ketones also indicated that there is no cage effect for radical recombinations in $CO_{2(sc)}$.[12] The products are formed in a statistical ratio (see Scheme 1).



Scheme 1. Tol = tolyl.

The carboxy inversion of diacyl peroxides has been interpreted as being an ionic reaction. In $CO_{2(sc)}$ it proceeds with a 17% yield (40 °C, $d = 0.93\,g\,mL^{-1}$), but slower than in CCl_4 or $CHCl_3$ (Scheme 2).[7] Radical chain reactions like the well-known oxidation of cumene to cumene hydroperoxide also led to lower yields in $CO_{2(sc)}$ (110 °C, 200–414 bar), probably because it was not possible to prevent chain termination reactions due to the metal container (Scheme 2).[13]

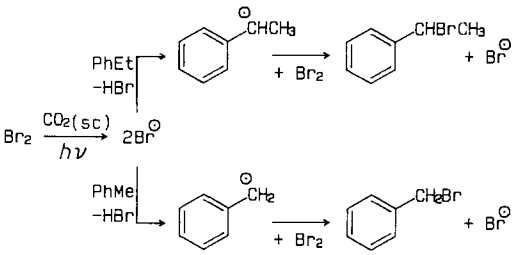


Scheme 2.

Recently, however, a number of studies were published which demonstrated that radical brominations[14] and polymerizations,[15] hydroxyformylations,[16] CO_2 hydrogenations,[17] catalytic additions/cycloadditions on CO_2,[18, 19] and enzymatic reactions[20, 21] in $CO_{2(sc)}$ can proceed providing better (or roughly equal[19]) results than the corresponding reactions in conventional solvents.

[*] Prof. Dr. G. Kaupp
FB-9 Organische Chemie I der Universität
Postfach 2503, D-26111 Oldenburg (FRG)
Telefax: Int. code + (441)798-3409

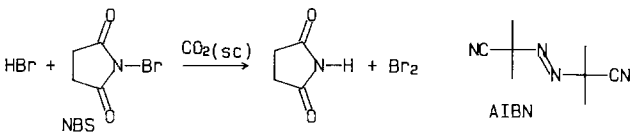
The bromination of toluene with bromine in $CO_{2(sc)}$, photochemically initiated through a sapphire window, led to benzyl bromide (74%) and 4-bromotoluene (11%). Ethylbenzene afforded 1-bromo-1-phenylethane in 95% yield (Scheme 3).[14] In



Scheme 3.

order to demonstrate that uncomplexed bromine atoms act as chain propagators, toluene and ethylbenzene were photobrominated in a competition study at pressures of 75 to 423 bar and at 40 °C. Over the entire pressure range, the reactivity of the benzylic secondary C–H bond in ethylbenzene was found to be about 30 times greater than that of the corresponding primary C–H bond in toluene. The analogous value for the reactivity in CCl_4 at 40 °C is 36. The bromine atoms in $CO_{2(sc)}$ are therefore particularly free. It would be important to determine quantum yields (chain lengths) at various pressures to learn more about mechanistic aspects and other details of the reaction.

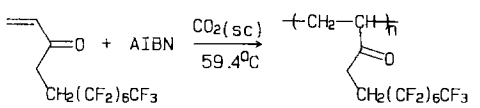
The same study[14] also dealt with the heterogeneous *N*-bromosuccinimide (NBS) bromination (Ziegler bromination; Scheme 4) of toluene in $CO_{2(sc)}$. The reaction (40 °C, 170 bar,



Scheme 4.

4 h) was initiated photochemically with azobis(isobutyronitrile) (AIBN). In CCl_4, this reaction proceeds without succinimidyl radicals, with the same selectivity as the direct bromination. The yield is quantitative on the 4 mmol scale; no 4-bromotoluene is observed.

Homogeneous fluoroalkene polymerizations (and copolymerizations) also proceed in $CO_{2(sc)}$ after AIBN initiation.[15] In this case it is advantageous that highly fluorinated polymers ($> 250000\ g\,mol^{-1}$) and copolymers are very soluble (up to 25%) in $CO_{2(sc)}$ at high pressures. This means that no chlorofluorocarbons must be employed as solvents. The homopolymer ($270000\ g\,mol^{-1}$) shown in Scheme 5 can be obtained from

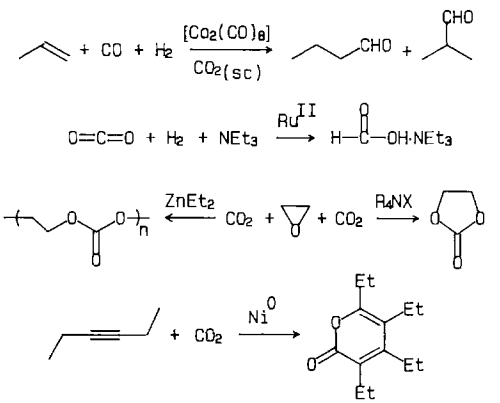


FOA

Scheme 5.

FOA in $CO_{2(sc)}$ (59.4 °C, 207 bar, 48 h, no Trommsdorff effect[15]) in 65% yield. The product can be precipitated from the homogeneous solution by pressure release. It would be useful, however, to develop a workup procedure that does not offset the use of $CO_{2(sc)}$ by the necessity to dissolve the raw product in 1,1,2-trifluorotrichloroethane. Statistical copolymers of FOA are also surprisingly soluble in $CO_{2(sc)}$. The kinetic parameters of the thermal AIBN decomposition in $CO_{2(sc)}$ have been determined accurately, and 1,1-difluoroethylene was telomerized correspondingly.[13] The basis for applications has been established.

$CO_{2(sc)}$ is an inert solvent for radical reactions. This is also true for cobalt-catalyzed hydroformylations of propene and other alkenes to the corresponding aldehydes.[16] These reactions profit from the good miscibility in $CO_{2(sc)}$ (Scheme 6). The

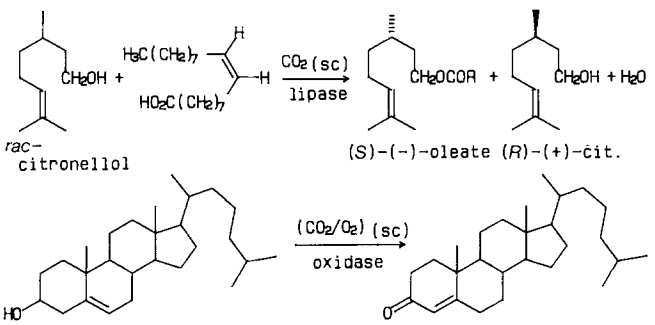


Scheme 6.

reaction mixture is less viscous, which leads to sharp ^{59}Co NMR signals (quadrupole nucleus), which in turn allows the identification of the catalytically active species by high-pressure NMR spectroscopy. The hydrogenation of double bonds is not a competing reaction in this instance. There are Ru^{II} catalysts, however, which hydrogenate the C_1 building block CO_2 homogeneously to formic acid as long as this reaction is coupled to salt formation. The reaction in $CO_{2(sc)}$ (50 °C, 86 bar H_2, 207 bar CO_2, dissolved NEt_3) proceeds with the highest rate of the numerous variants of this reaction, namely 1400 mole of formic acid per mole of catalyst per hour. This turnover frequency (TOF) is reduced to $1.3\ h^{-1}$ for the same composition when liquid CO_2 (at 15 °C) is employed. All other high-pressure variants of this reaction in liquid solvents yield much lower TOF values.[17] This behavior indicates the favorable effect of the high solubility of H_2 in $CO_{2(sc)}$ as well as the high mass transport rate. The well-known and well-studied copolymerizations of CO_2 and oxiranes and their cycloadditions to cyclic carbonates such as ethylene carbonate (Scheme 6) have also been successfully performed in supercritical mixtures.[18] It turned out, however, that the industrial production of ethylene carbonate (similar to propylene carbonate) in a liquid (product) phase (190–200 °C, total pressure 80 bar) is more economical for capacities of 4000 t per year and installation when it is run nearly stoichiometrically.[22] In the cases of substituted or polycyclic oxiranes, solvents are usually added and 1 to 40 bar of CO_2 are

introduced, depending on the catalyst employed.[18] Homologous cyclic ethers (oxetanes, tetrahydrofurans, etc.) are also expected to undergo cycloaddition to CO_2 and should be tried in $CO_{2(sc)}$. A [2 + 2 + 2]cycloaddition of two moles of 3-hexyne to one mole of CO_2 in the presence of the catalyst $[\{Ni(cod)_2\}Ph_2P(CH_2)_4PPh_2]$ and of benzene (25 °C, 50 bar, 20 h at 120 °C), led to tetraethylpyranone (57%) (Scheme 6).[23] A preliminary attempt to improve this yield by using the same catalyst in $CO_{2(sc)}$ failed (102 °C, 93 g of CO_2 in 200 mL, 69 h, 35%).[19] It appears, however, that attempts to improve this yield are still in progress in spite of a number of experiments that have reproduced it.[19]

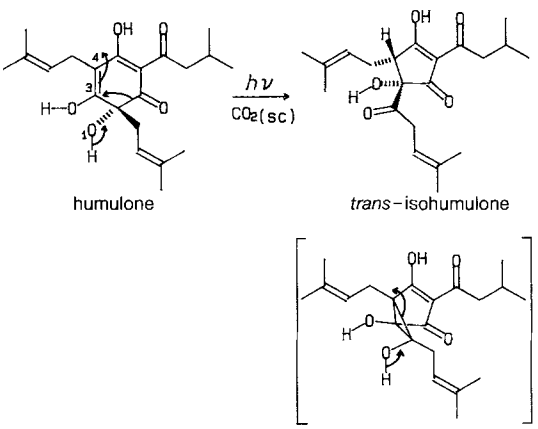
Enzyme-catalyzed esterifications (immobilized lipase MY) of *rac*-citronellol with oleic acid in $CO_{2(sc)}$ close to the critical point led stereoselectively to 1.2–5.8% of citronellol oleate (Scheme 7).[20] Only at the critical temperature (31 °C, 84 bar)



Scheme 7.

does the (*S*)-(−)-citronellol oleate form with 99% optical purity. Even small temperature increases (4–9 °C) led to a drastic reduction of the optical purity; pressure increases (up to 190 bar) had the same effect. This result was explained by the formation of clusters near the critical point, where pressure and temperature changes have particularly strong effects. No esterification took place in water-saturated cyclohexane. Good yields (75% at a residence time of only 13 s) were reported for the enzymatic oxidation (immobilized cholesterol oxidase from *G. chrysocreas*) of cholesterol in supercritical CO_2/O_2 (9:1) (Scheme 7).[21] Co-solvents, like *tert*-butyl alcohol, that increase the solubility and, to an even larger extent, those that assist aggregate formation, increase the rate of the reaction (fourfold in this case). Further examples for biocatalyses in $CO_{2(sc)}$ are summarized in reference [24].

Apparently, unnoticed by the recent studies, the photolysis of hops extracts in $CO_{2(sc)}$ has been developed into an established industrial process.[25] The $CO_{2(sc)}$ extract contains the so-called α-acids (vinylogous carboxylic acids), for instance humulone, which are primary bittering agents with limited stability. These are isomerized into α-isoacids, such as *trans*-isohumulone (Scheme 8), stable and more soluble bittering agents, which give beer its characteristic taste. The conventional brewing method achieved this transformation in low yields by boiling the hops in the wort. It is more efficient to add the ingredients stemming from hops to the cold finished beer. This, however, requires the isomerization of the air-sensitive α-acids to be performed photochemically in the $CO_{2(sc)}$ extract before the addition to the beer.



Scheme 8.

The quantum yield ϕ is 0.03. The mechanism of this [1,2,3,4] rearrangement[26] is unknown. Formally, the reaction can be considered an H migration from the OH group to the end of a four-membered chain with a concomitant acyl group migration from position 2 to 3 within that chain. According to the current canon of photochemistry, an oxa-di-π-methane rearrangement with subsequent [1,3]-H-migration and ring opening was formulated.[25] It is said that this procedure affords special protection to the flavors of the hops ingredients.

The current state of knowledge indicates the versatility of $CO_{2(sc)}$ as a reaction medium and gives reason to be optimistic that in the future more reactions will be carried out in the ecologically sound $CO_{2(sc)}$ (closed loop systems) rather than in organic solvents. The theoretical and mechanistic basics have essentially been established and a great deal of practical knowledge has been acquired from the widespread extraction processes utilizing $CO_{2(sc)}$. Therefore nothing should stand in the way of further industrial applications. For teaching purposes, it can only be hoped that textbooks on experimental techniques will soon include material about "unusual reaction media".

German version: *Angew. Chem.* **1994**, *106*, 1519

[1] V. Ramamurthy, *Tetrahedron* **1986**, *42*, 5753; G. Kaupp, *Adv. Photochem.* **1994**, *19*, in press; G. Kaupp in *Handbook of Organic Photochemistry and Photobiology* (Ed.: W. Horspool), CRC, Cleveland, OH, **1994**, in press.

[2] G. Kaupp, D. Matthies, *Chem. Ber.* **1986**, *119*, 2387; *Mol. Cryst. Liq. Cryst.* **1988**, *161*, 119; G. Kaupp, D. Lübben, O. Sauerland, *Phosphorus Sulfur Silicon Relat. Elem.* **1990**, *53*, 109; G. Kaupp, *Mol. Cryst. Liq. Cryst.* **1992**, *211*, 1; G. Kaupp, J. Schmeyers, *Angew. Chem.* **1993**, *105*, 1656; *Angew. Chem. Int. Ed. Engl.* **1993**, *32*, 1587, and references therein.

[3] F. Toda, K. Kiyoshige, M. Yagi, *Angew. Chem.* **1989**, *101*, 329; *Angew. Chem. Int. Ed. Engl.* **1989**, *28*, 320; Review: F. Toda in *Reactivity in Molecular Crystals* (Ed.: Y. Ohashi), VCH/Kodansha Weinheim/Tokyo, **1993**, p. 177.

[4] R. Eggers, *Angew. Chem.* **1978**, *90*, 799; *Angew. Chem. Int. Ed. Engl.* **1978**, *17*, 751; K. Zosel, *ibid.* **1978**, *90*, 748 and **1978**, *17*, 702; P. Hubert, O. G. Vitzthum, *ibid.* **1978**, *90*, 756 and **1978**, *17*, 710; E. Stahl, W. Schilz, E. Schütz, E. Willing, *ibid.* **1978**, *90*, 778 and **1978**, *17*, 731; K. Zosel (Studiengesellschaft Kohle), US-A 4260639, **1981**; A. B. Caragay, *Perfum. Flavor.* **1981**, *6*, 43; H. Brogle, *Chem. Ind. (London)* **1982**, 385; R. Vollbrecht, *ibid.* **1982**, 397; liquid: D. S. Gardner, *ibid.* **1982**, 402.

[5] According to its phase diagram, CO_2 can only be liquefied by compression between the triple point at −57 °C/5.2 bar and the critical point. Above T_c *and* p_c, CO_2 is in the supercritical state.

[6] Y. Ikushima, N. Saito, M. Arai, *J. Phys. Chem.* **1992**, *96*, 2293; Y. Ikushima, N. Saito, M. Arai, K. Arai, *Bull. Chem. Soc. Jpn.* **1991**, *64*, 2224; J. A. Hyatt, *J. Org. Chem.* **1984**, *49*, 5097.

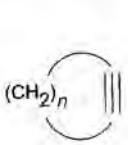
[7] M. E. Sigman, J. T. Barbas, J. E. Leffler, *J. Org. Chem.* **1987**, *52*, 1754.

[8] For example, reaction of 1.5 g cyclopentadiene with 0.5 g *p*-benzoquinone in 20 g CO_2: 25–40 °C, 60–240 bar, $k^1 = 0.597 \times 10^{-3}$ to $1.147 \times 10^{-3}\ s^{-1}$.
[9] N. S. Isaacs, N. Keating, *J. Chem. Soc. Chem. Commun.* **1992**, 876.
[10] M. E. Paulaitis, G. C. Alexander, *Pure Appl. Chem.* **1987**, *59*, 61.
[11] C. D. Roberts, J. E. Chateauneuf, J. F. Brennecke, *J. Am. Chem. Soc.* **1992**, *114*, 8455.
[12] K. E. O'Shea, J. R. Combes, M. A. Fox, K. P. Johnston, *Photochem. Photobiol.* **1991**, *54*, 571; C. B. Roberts, J. Zhang, J. F. Brennecke, J. E. Chateauneuf, *J. Phys. Chem.* **1993**, *97*, 5618; for high-resolution reference spectra see G. Kaupp, E. Teufel, H. Hopf, *Angew. Chem.* **1979**, *91*, 232; *Angew. Chem. Int. Ed. Engl.* **1979**, *18*, 215.
[13] G. J. Suppes, R. N. Occhiogrosso, M. A. McHugh, *Ind. Eng. Chem. Res.* **1989**, *28*, 1152.
[14] J. M. Tanko, J. F. Blackert, *Science* **1994**, *263*, 203.
[15] J. R. Combes, Z. Guan, J. M. DeSimone, *Macromolecules* **1994**, *27*, 865; Z. Guan, J. R. Combes, Y. Z. Menceloglu, J. M. DeSimone, *ibid.* **1993**, *26*, 2663; J. M. DeSimone, Z. Guan, C. S. Elsbernd, *Science* **1992**, *257*, 945.
[16] J. W. Rathke, R. J. Klingler, T. R. Krause, *Organometallics* **1991**, *10*, 1350.
[17] P. G. Jessop, T. Ikariya, R. Noyori, *Nature* **1994**, *368*, 231.
[18] U. Petersen, *Methoden Org. Chem. (Houben Weyl) 4th. ed. 1952*, Chap. E4, **1983**, p. 95.
[19] M. T. Reetz, W. Könen, T. Strack, *Chimia* **1993**, *47*, 493.
[20] Y. Ikushima, N. Saito, T. Yokoyama, K. Hatakeda, S. Ito, M. Arai, H. M. Blanch, *Chem. Lett.* **1993**, 109.
[21] T. W. Randolph, D. S. Clark, H. W. Blanch, J. M. Prausnitz, *Science* **1988**, *239*, 387.
[22] G. Hechler, *Chem. Ing. Tech.* **1971**, *43*, 903.
[23] Y. Inoue, Y. Itoh, H. Kazama, H. Hashimoto, *Bull. Chem. Soc. Jpn* **1980**, *53*, 3329.
[24] O. Aaltonen, M. Rantakylä, *CHEMTECH* **1991**, 240.
[25] J. C. Andre, A. Said, M. L. Viriot (Centre National de la Recherche Scientifique), FR-A1 2590589, **1987**; *J. Photochem. Photobiol. A* **1988**, *42*, 383; M. L. Viriot, J. C. Andre, M. Niclause, D. Bazard, R. Flayeux, M. Moll, *J. Inst. Brew.* **1980**, *86*, 21; *J. Am. Soc. Brew. Chem.* **1980**, *38*, 61; J. C. Andre, M. L. Viriot, J. Villermaux, *Pure Appl. Chem.* **1986**, *58*, 907.
[26] G. Kaupp, *Top. Curr. Chem.* **1988**, *146*, 57.

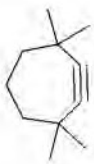
Triple Bonds in Small Rings: Testing the Limits of Chemical Bonds

Wolfram Sander*

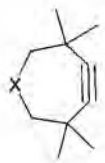
Since the pioneering work of Wittig et al.[1] on strained cycloalkynes, molecules with triple bonds deviating significantly from linearity have fascinated chemists. Cyclooctyne (**1**) is the last carbocyclic parent compound that is stable under "normal" conditions. The deviation from linearity in this compound, 21.5°,[2] is reflected in its increased reactivity. Cycloheptyne (**2**), bent by 30–35°, has a half-life of only one hour at −76 °C. To stabilize smaller cycloalkynes either substituents that suppress dimerization must be introduced α to the triple bond, or heteroatoms X (Si, S) with long C–X or X–X bonds must be incorporated in the ring to reduce ring strain. In the 1970s Krebs et al. used this approach to synthesize a series of derivatives of cycloheptyne (**2**) and characterize them chemically and by spectroscopy.[2] Tetramethylcycloheptyne **2a** can be isolated at room temperature, and thiacycloheptyne **2b** and silacycloheptyne **2c** are even more stable.



1 $n = 6$
2 $n = 5$
3 $n = 4$
4 $n = 3$
5 $n = 2$
6 $n = 1$



2a

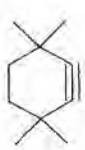


2b X = S
2c X = Si

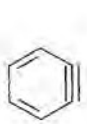
Carbocyclic derivatives of cyclohexyne (**3**) are considerably more reactive than **2** and are thus isolable only at low temperatures by matrix techniques. Wentrup et al.[3] reported on the matrix isolation of the parent compound, cyclohexyne (**3**), which could be characterized only by a pair of IR bands at 2105 and 2090 cm^{-1}. The tremendous reactivity of **3** was evident in studies of tetramethylcyclohexyne **3a**,[4] which dimerizes already at temperatures below 77 K. The first step in the dimerization is the abstraction of a hydrogen atom from one of the methyl groups, which is indicative of the strong diradical character of **3a**. Thus α-methyl groups do not suffice to effectively stabilize cyclohexyne. **3a** undergoes photochemical carbonylation to yield the corresponding cyclopropenone;[4] in contrast, cycloalkynes with larger rings can be prepared by irradiation of cyclopropenones.[5]

The derivative of cyclohexyne that has been investigated most thoroughly is *o*-didehydrobenzene (**3b**). Chapman et al.[6] reported on the matrix isolation of **3b** in the 1970s. The question of the position of the C≡C stretching vibration, which should give information on the strength of the triple bond, was disputed for some time and first determined in 1992 by Radziszewski et al.[7]

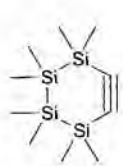
Recently Ando et al.[8] isolated the first six-membered cyclic alkyne at room temperature. Tetrasilacyclohexyne **3c** has an impressive half-life of 8 h in decane at 174 °C! This cycloalkyne is stabilized both by steric shielding and the long C–Si and Si–Si bonds.



3a



3b



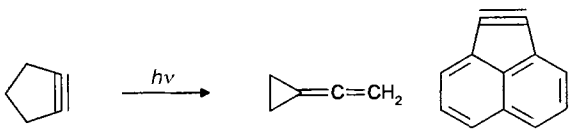
3c

To date the single derivative of cyclopentyne characterized unequivocally by spectroscopy is acenaphthyne **4a**, which was

[*] Prof. Dr. W. Sander
Lehrstuhl für Organische Chemie II der Universität
D-44780 Bochum (FRG)
Telefax: Int. code + (234) 709-4353

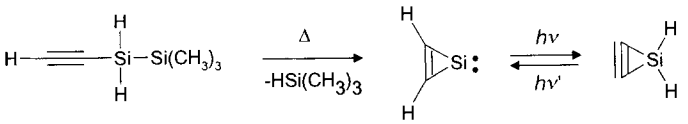
 © VCH Verlagsgesellschaft mbH, D-69451 Weinheim, 1994 0570-0833/94/1414-1455 $ 10.00+.25/0

obtained by Chapman et al.[9] in several steps by irradiation of a matrix-isolated diazoketone. Cyclopentyne (**4**) could not be prepared by this route, since this cycloalkyne is photolabile and rearranges to ethenylidenecyclopropane by a photochemical [1,3] shift.



4 **4a**

ameter of 1 mm was used; and the products were trapped directly on a cold spectroscopic window. The reaction of disilane **7** under these conditions allowed easy access to the C_2H_2Si potential energy surface. In agreement with the calculations of Schaefer et al.[13] the thermolysis yielded 1-silacyclopropenylidene (**8**)



7 **8** **6a**

Only calculations are available for cyclobutyne (**5**) and cyclopropyne (**6**), as spectroscopic proof is lacking. Extensive ab initio calculations by Schaefer III et al.[10] predict an activation barrier of 25 kcal mol^{-1} for the rearrangement of **5** into butatriene. This indicates that cyclobutyne (**5**) should be isolable in a matrix; however, suitable precursors have not yet been available for testing these predictions. Based on the typical scaling of calculated harmonic frequencies, a medium-intensity IR absorption of the triple bond is expected at 1800–1850 cm^{-1}. In contrast to **5**, the structure of cyclopropyne (**6**) does not correspond to a minimum on the potential energy surface but to the transition state for the degenerate rearrangement of propadienylidene.[10]

Considering all this, the successful synthesis and characterization of a three-membered ring compound with a C≡C bond by G. Maier, H. P. Reisenauer, and H. Pacl[11] is even more remarkable. The key here was the application of a new technique in gas-phase pyrolysis, which has considerable advantages over standard flash vacuum pyrolysis (FVP). This new method, first described by Chen et al.,[12] serves to decrease the typical contact times in flash pyrolysis from 1–100 ms to roughly 10 μs. Conditions in a conventional pyrolysis reactor include pressures of $\approx 10^{-3}$ mbar, temperatures from 400 to 1000 °C, and heating zones several cm in length; with the new experimental set-up pressures of roughly one bar, temperatures of up to 1700 °C, and very short heating zones only a few mm in length with pyrolysis tube nozzles having small cross-sections are employed. The precursor is mixed with a large excess of helium, and the gas mixture is cooled to 40 K by adiabatic expansion (jet-cooled) immediately after leaving the pyrolysis zone. The molecular beam is pulsed through a magnetic valve to maintain the high vacuum on the side of the expanding gas flow. In this experiment the sample is subjected to a temperature gradient of over 1600 K within 50 μs. In conventional flash pyrolysis the mean free path exceeds the dimensions of the reactor, and energy is thus transferred by collisions with the walls. Undesired reactions frequently occur with the result that very reactive molecules such as diradicals and carbenes do not "survive" these conditions and "stick" to the walls of the reactor. In the method described by Chen et al. energy is transferred by collisions with the inert gas and is thus much gentler.

Maier et al.[11] combined this method with the matrix isolation technique. Helium was replaced with argon; instead of a pyrolysis oven a heated corundum capillary with an inner di-

as the most stable C_2H_2Si isomer. Photolysis with monochromatic light led selectively to a series of C_2H_2Si isomers such as ethynylsilylene and vinylidenesilylene, which previously had been studied only theoretically and each of which are the first examples of their respective classes of compounds. A further C_2H_2Si isomer formed reversibly from **8** was assigned the structure of 3-silacyclopropyne (**6a**). The calculations by Schaefer et al.[13] predict that this structure, like cyclopropyne, does not correspond to a minimum on the potential energy surface but rather to a transition state. However, in comparison to cyclopropyne and relative to the open-chain reference compounds, silacyclopropyne was judged to be stabilized by the silicon atom by roughly 30 kcal mol^{-1}. Only when correlation interactions are considered (MP2/6-31G(d,p)) is a minimum found, and the calculated IR absorptions now agree quite well with the experimental.[11]

The research group of G. Maier has succeeded in characterizing the first cyclopropyne, a molecule previously not considered to exist. Is this compound a cycloalkyne or a diradical? How large is the singlet–triplet gap, and how does the tremendous ring strain affect the reactivity? Answers to these questions are eagerly awaited.

German version: *Angew. Chem.* **1994**, *106*, 1522

[1] a) G. Wittig, J. Weinlich, E. R. Wilson, *Chem. Ber.* **1965**, *98*, 458; b) G. Wittig, J. Heyn, *Justus Liebigs Ann. Chem.* **1969**, *726*, 57–68.
[2] A. Krebs, J. Wilke, *Top. Curr. Chem.* **1983**, *109*, 189.
[3] C. Wentrup, R. Blanch, H. Briehl, G. Gross, *J. Am. Chem. Soc.* **1988**, *110*, 1874–1880.
[4] W. Sander, O. L. Chapman, *Angew. Chem.* **1988**, *100*, 402–403; *Angew. Chem. Int. Ed. Engl.* **1988**, *27*, 398–399.
[5] A. Krebs, W. Cholcha, M. Müller, T. Eicher, H. Pielartzik, H. Scnöckel, *Tetrahedron Lett.* **1984**, *25*, 5027–5030.
[6] O. L. Chapman, K. Mattes, C. M. McIntosh, J. Pacansky, G. V. Calder, G. Orr, *J. Am. Chem. Soc.* **1973**, *95*, 6134–6135.
[7] J. G. Radziszewski, B. A. J. Hess, R. Zahradnik, *J. Am. Chem. Soc.* **1992**, *114*, 52–57.
[8] a) W. Ando, F. Hojo, S. Sekigawa, N. Nakayama, T. Shimizu, *Organometallics*, **1992**, *11*, 1009–1011; b) F. Hojo, S. Sekigawa, N. Nakayama, T. Shimizu, W. Ando, *Organometallics* **1993**, *12*, 803–810.
[9] O. L. Chapman, J. Gano, P. R. West, M. Regitz, G. Maas, *J. Am. Chem. Soc.* **1981**, *103*, 7033–7036.
[10] H. A. Carlson, G. E. Quelch, H. F. Schaefer III, *J. Am. Chem. Soc.* **1992**, *114*, 5344–5348.
[11] G. Maier, H. P. Reisenauer, H. Pacl, *Angew. Chem.* **1994**, 106, 1347–1349; *Angew. Chem. Int. Ed. Engl.* **1994**, *33*, 1248–1250.
[12] J. A. Blush, H. Clauberg, D. W. Kohn, D. W. Kohn, D. W. Minsek, X. Zhang, P. Chen, *Acc. Chem. Res.* **1992**, *25*, 385–392.
[13] G. Frenking, R. B. Remington, H. F. Schaefer III, *J. Am. Chem. Soc.* **1986**, *108*, 2169–2173.

Enantioselective Reactions in a Static Magnetic Field—A False Alarm!

On August 20, 1993, we received a communication from E. Breitmaier, Bonn, in which he, together with his coauthors, G. Zadel, C. Eisenbraun, and G.-J. Wolff, reported on "Absolute Asymmetric Syntheses in a Static Magnetic Field". In view of the potential importance of the disclosed results, the communication was immediately sent to three referees. Referee A recommended acceptance with minor alterations ("The results must be regarded as being of great importance to this field. They should be published in Angewandte Chemie with minor alterations."). Referee B requested major changes, and referee C recommended rejection. On September 22, the correspondence author was then informed that the manuscript would have to be revised before a decision could be made (the referees' reports were enclosed with the letter).

On September 29, we received a revised manuscript with the modified title "Enantioselective Reactions in a Static Magnetic Field". In the accompanying letter, the author commented on the two critical reports; in particular, the points not taken into consideration in the revised version were addressed. The new manuscript and the accompanying letter were presented to referees B and C, whereupon referee B then agreed to publication. He wrote, "The importance of these disclosures is such that they must now be made available to our professional colleagues in order to allow an international debate to take place." Referee C remained unconvinced. "This work is inherently flawed and is not suitable for publication." Both responses—each just under a page long—were sent to the correspondence author on October 11, together with a request that he examine the points raised. On October 13, he replied that the editorial office should not rush their decision on whether to publish, since "the results and potential applications have already been documented in a patent application." The correspondence author was then informed by telephone that the manuscript would be printed in the "most concise form possible."

Not long afterwards, in a letter dated October 24, the correspondence author asked for a delay in publication: "Next week our laboratory will be receiving a cryomagnet (4–5 tesla) on loan. We would like to repeat some of the experiments described in the communication before we send you the final version of the manuscript. Also, in view of the heavy criticism raised by one of the referees, we would once again like to carefully check the reproducibility of our results. The experiments will be completed by the beginning of December." The final version of the manuscript was received on December 8. The accompanying letter stated: "As explained previously, we have, once again, reproduced the most important experiments in response to the heavy criticism; in these experiments, a cryomagnet, which is at present charged to 2.1 tesla, was used. We have included 1-phenylpropanol as an additional example; *N*-methylamphetamine has been omitted as a precaution, since this compound is a highly active designer drug and a very desirable target. I hope that this version meets with your approval." The manuscript was then edited and published.[1]

The publication met with an enthusiastic response,[2] but even at an early stage misgivings were voiced. One such occasion was the discussion organized at short notice during this year's Bürgenstock "Stereochemistry Conference" in Switzerland,[3] where the coauthor G. Zadel presented the results.

The whole affair culminated at the beginning of June with two contributions to the Correspondence section describing many failed attempts at reproducing the results.[4, 5] These were sent to E. Breitmaier with a request that he respond to them by June 17. On June 21, E. Breitmaier broke the news to us that the coauthor G. Zadel had, after reinvestigation of his working procedure by other co-workers of the group,[6] confessed to having manipulated the reaction solutions prior to the experiments and that all results reported in the publication[1] must therefore be regarded as invalid.[6]

The most critical of the three referees was right, and I regret not having taken his advice. This publication certainly generated much excitement, and many groups worldwide invested time and money as a result, a situation which could have been avoided.[7] But, all too often, the established "peer review" system is accused of stifling unconventional publications which might introduce a paradigm change.[8] Had they been correct, the results described in the publication would have been of such great importance, regardless of how they might have been explained, that preventing publication would have been untenable.

Peter Gölitz

[1] G. Zadel, C. Eisenbraun, G.-J. Wolff, E. Breitmaier, *Angew. Chem.* **1994**, *106*, 460–463; *Angew. Chem. Int. Ed. Engl.* **1994**, *33*, 454-456.

[2] See, for example D. Bradley, *Science* **1994**, *264*, 906.

[3] W. Leitner, *Nachr. Chem. Tech. Lab.* **1994**, *42*, 714.

[4] B. L. Feringa, R. M. Kellogg, R. Hulst, C. Zondervan, W. H. Kruizinga, *Angew. Chem.* **1994**, *106*, 1526–1527; *Angew. Chem. Int. Ed. Engl.* **1994**, *33*, 1458–1459.

[5] G. Kaupp, T. Marquardt, *Angew. Chem.* **1994**, *106*, 1527–1529; *Angew. Chem. Int. Ed. Engl.* **1994**, *33*, 1459–1461.

[6] E. Breitmaier, *Angew. Chem.* **1994**, *106*, 1529; *Angew. Chem. Int. Ed. Engl.* **1994**, *33*, 1461.

[7] In order to minimize the damage, as far as this was still possible, E. Breitmaier's statement was immediately published in issue 12 of the English and issue 13 of the German edition of *Angewandte Chemie*; the weekly journals *Science* and *Chem. Eng. News* were also informed. Furthermore, all groups which, to our knowledge, were working on the verification of the results were notified by fax. The correspondence author informed all groups in contact with him who were attempting to reproduce the results.

[8] H.-D. Daniel, *Guardians of Science. Fairness and Reliability of Peer Review*, VCH, Weinheim, **1993**, pp. 3–7.

 © VCH Verlagsgesellschaft mbH, D-69451 Weinheim, 1994 0570-0833/94/1414-1457 $ 10.00+.25/0

Attempts to Carry Out Enantioselective Reactions in a Static Magnetic Field

Ben L. Feringa,* Richard M. Kellogg,* Ron Hulst, Charon Zondervan, Wim H. Kruizinga

In a recent article in this journal Zadel, Eisenbraun, Wolff, and Breitmaier reported enantioselective reactions in a static magnetic field.[1] The results were dramatic: prochiral aldehydes were treated with aliphatic Grignard reagents to produce (chiral) alcohols with enantiomeric excesses (*ee*) of 57–98%, and reductions of some aryl alkyl ketones with lithium aluminum hydride (LAH) proceeded with 11–68% *ee*.

These results have produced excitement in the chemical community. At an informal meeting during the recent Bürgenstock Stereochemical Conference in Switzerland Dr. Zadel reported on these remarkable experiments to a large group of highly interested stereochemists. The interest stems first from the fact that these results seem to contradict straightforward theory from which one concludes that static magnetic fields are not chiral.[2] Previous claims of enantioselective syntheses in magnetic fields have been shown to be spurious; a recent example not cited in reference [1] involves the electrochemical reduction of α-keto acids in magnetic fields.[3, 4] Circumventing these theoretical barriers might be possible; we mention, for example, the concept of "true" and "false" chirality as introduced by Barron.[5] Another possibility is that a small stereochemical bias might be amplified by a large nonlinear effect[6] or asymmetric autocatalysis.[7]

From the practical side these claims of enantioselective reactions could have profound implications for the manner in which asymmetric synthesis is carried out in academic and industrial laboratories. In an extreme scenario the painstakingly developed methods relying on chiral auxiliaries and optically active catalysts could be supplanted by simply conducting reactions in large magnets.

Independent confirmation of these important experiments is clearly of great importance to the chemical community.

We have repeated the Breitmaier experiments in our own laboratories with magnets having flux densities of 0.3 and 1.2 Tesla. In addition our colleague Prof. Bert Meijer in Eindhoven has also carried out these experiments in magnets available to him and has obtained results fully analogous to ours as described below. We have also contacted Prof. Breitmaier and have carried out experiments in his laboratories in Bonn with the same magnets used in his original work. Glassware and chemicals were brought from our laboratories, and the enantiomeric excesses were determined in Groningen.

We take this opportunity to express our sincere appreciation to Prof. Breitmaier and his co-workers for their hospitality, as well as openness and cooperativity in helping us to reproduce these experiments. The results of our experiments are summarized in Tables 1 and 2.

Table 1. Reduction of acetophenone [a] by addition to LAH.

Run	B_o [T]	LAH [mg]	Solvent	Aceto-phenone [a]	t [d] [min]	Con-version [%]	Isolated yield [%]
1 [b]	0.3	90	2 mL THF/ 2 mL C_6H_6	200 mg in 200 μL C_6H_6	30	100	86
2 [b]	0.3	80	2 mL THF/ 2 mL C_6H_6	204 mg in 1 mL C_6H_6	60	100	91
3 [b]	0.3	122	2 mL THF/ 2 mL C_6H_6	300 mg in 3 mL C_6H_6	60	100	86
4 [b]	0.3	80	2 mL THF/ 4 mL C_6H_6	206 mg in 200 μL C_6H_6	75	100	82
5–8 [b]	0.3	Runs 1–4 repeated in C_6H_6; comparable conversions					
9–12 [b]	0.3	Runs 1–4 repeated with twice the concentrations; yields ca. 70–75%					
13–15 [b]	0.3	Runs 1, 3, and 4 repeated in 1.5 mL THF and 0.5 mL C_6H_6; comparable conversions					
16–18 [b]	0.3	Runs 1, 3, and 4 repeated in 0.5 mL THF and 1.5 mL C_6H_6; comparable conversions					
19 [b]	0.3	Run 1 repeated in THF; comparable conversion					
20 [b]	0.3	130	1 mL THF	359 mg in 2.5 mL C_6H_6 [a]	40	100	> 75
21 [b]	0.3	25	0.6 mL THF/ 1.3 mL C_6H_6	90 mg in 2 mL C_6H_6 [a]	45	100	95
22 [c]	0.3	80	2 mL THF/ 4 mL C_6H_6	289 mg [a] in 6 mL C_6H_6	60	90	69
23–26 [b]	1.2	Runs 1–4 repeated; comparable conversions					
27–43 [b]	1.2	Runs 5–21 repeated; comparable conversions					
44 [c]	2.3	80	2 mL THF/ 4 mL C_6H_6	228 mg [a] in 6 mL C_6H_6	60	90	69

[a] Acetonaphthone was used in runs 20–22, propionaphthone in run 44. [b] Experiments conducted in Groningen. [c] Experiments conducted in Bonn in the Breitmaier laboratory. [d] Addition time.

All experiments were performed using Schlenck techniques except for the experiments conducted in Bonn, which were carried out without special precautions. Solvents were dried over Na/K. The solutions were added through a Teflon tube attached to a stainless steel needle that was kept 2–3 mm above the surface of the solution. Alternatively, the Teflon tube without an attached stainless steel needle was kept 2–3 mm above the surface of the solution. The experiments were performed at room temperature.

[*] Prof. Dr. B. L. Feringa, Prof. Dr. R. M. Kellogg, Dr. R. Hulst, Drs. C. Zondervan, W. H. Kruizinga
Department of Organic and Molecular Inorganic Chemistry
University of Groningen
Nijenborgh 4, NL-Groningen 9747 AG (The Netherlands)
Telefax: Int. code +(50)634296

 © VCH Verlagsgesellschaft mbH, D-69451 Weinheim, 1994 0570-0833/94/1414-1458 $ 10.00+.25/0

Table 2. Reaction of benzaldehyde with CH_3MgI in a magnetic field flux of 0.3 T.

Run	CH_3MgI	Benzaldehyde	Addition time [min]	Conversion [%]	Isolated yield [%]
1 [a]	1.4 mmol in 1 mL Et_2O	100 µL in 0.2 mL C_6H_6/ 1 mL Et_2O	60	100	80
2	Run 1 repeated; addition over 90 min; comparable conversion				
3 [b]	2.7 mmol in 3 mL Et_2O	300 µL in 0.2 mL C_6H_6/ 1 mL Et_2O	90	100	80

[a] The solution of benzaldehyde was added to the Grignard reagent. [b] The Grignard reagent was added to the solution of benzaldehyde.

Two magnets were used in Groningen: a 0.3 T permanent horseshoe magnet with a homogeneous magnetic field between the poles, dimensions: 4 cm (diameter) × 3 cm (separation); and an electromagnet (Bruker B-E 20 C 8) adjusted to 1.2 T with a homogeneous field between the poles, dimensions: diameter 7.8 cm (diameter) × 3 cm (separation). The field strengths were checked with a Gaussian meter. The magnets used in Bonn were like those described in reference [1]; the Bruker magnet was adjusted to 2.3 T. The field strengths were not checked.

The reaction mixtures were quenched with an excess of water and extracted with ether. Conversions were determined by ^1H NMR spectroscopy (300 MHz, recorded in $CDCl_3$) or gas chromatography (GC). Optical rotations were measured in methanol or toluene, and the enantiomeric excesses were determined by GC using a chiral column (WCOT fused silica, CP-cyclodextrine-β-2,3,6-M-19, 0.25 mm × 50 m, 7501 Chrompack). Baseline separations were obtained in all cases. The experimental error in the *ee* determination is estimated to be 1%. In no case did we observe a distribution of enantiomers that deviated within experimental error from a 50:50 ratio.

At this time on the basis of the experiments that have been carried out, we must conclude that we have been unsuccessful in reproducing the Breitmaier results. At the request of the editor of *Angewandte Chemie* we make these initial results available.

Received: June 3, 1994 [C 20005]

[1] G. Zadel, C. Eisenbraun, G.-J. Wolff, E. Breitmaier, *Angew. Chem.* **1994**, *106*, 460; *Angew. Chem. Int. Ed. Engl.*, **1994**, *33*, 454.
[2] a) C. A. Mead, A. Moscowitz, H. Wynberg, F. Meuwese, *Tetrahedron Lett.* **1977**, 1063; b) W. Rhodes, R. C. Dougherty, *J. Am. Chem. Soc.* **1978**, *100*, 6247.
[3] F. Takahashi, K. Tomii, H. Takahashi, *Electrochim. Acta*, **1986**, *31*, 127.
[4] W. A. Bonner, *Origins Life and Evol. Biosphere* **1990**, *20*, 1.
[5] L. D. Barron, *J. Am. Chem. Soc.* **1986**, *108*, 5539.
[6] H. Wynberg, B. L. Feringa, *Tetrahedron* **1976**, *32*, 2831.
[7] A. H. Alberts, H. Wynberg, *J. Am. Chem. Soc.* **1989**, *111*, 7265.

Absolute Asymmetric Synthesis Solely under the Influence of a Static Homogeneous Magnetic Field?

Gerd Kaupp* and Thorsten Marquardt

Absolute asymmetric synthesis is of utmost importance for the origin of chirality on earth. The physical and chemical foundations for the generation of chirality in the absence of chiral auxiliaries are well known.[1] Therefore it was surprising to read of the claim in a publication by Breitmaier et al.[2] that solely the application of a static homogeneous magnetic field (with a strength of 0.2–2.1 T) induces efficient (*Re*)/(*Si*) differentiation in homogeneous solutions of aromatic aldehydes and ketones when they are reduced or added to Grignard reagents (Scheme 1). It was mentioned that the alcoholates formed precipitate in gelatinous form. The *ee* values of the isolated alcohols were claimed to be very high (up to 98%) and easily reproducible.[2] (*R*) and (*S*) products were reported to form at random but always with the same *ee* value.[2]

$$ArCRO + LiAlH_4 \longrightarrow ArCHR(OH) \longleftarrow RMgX + ArCHO$$

Scheme 1.

[*] Prof. Dr. G. Kaupp, T. Marquardt
FB9 · Organische Chemie I der Universität
Postfach 2503, D-26111 Oldenburg (FRG)
Telefax: Int. + (441)798-3409

However, contrary to scientific practice, no explanation or comment was given regarding the basic question that inevitably arises: how can a homogeneous magnetic field alone create face differentiation in violation of basic principles? These circumstances should have halted publication of the paper but of course not its rapid dissemination through secondary bibliographical literature[3] after publication. Scrutiny of the case is, however, also required owing to possible implications in research funding policies. Supporting agencies and their referees should not judge the important field of absolute asymmetric synthesis as being unnecessarily complicated.

A *theoretical analysis* reveals severe self-contradictions in the work of Breitmaier et al.[2] A static magnetic field in its homogeneous range is clearly directional but not chiral. Therefore it cannot create chirality in the form of *ee* values in reactions of achiral molecules in the absence of further directional fields. It does not help to invoke the Faraday effect, which is well known from magnetooptic rotational dispersion, or magnetic circular dichroism. Only the superposition of additional directional fields could give rise to chiral field action.[4]

Breitmaier et al. reported[2] that the same reaction in the same magnetic field gives (*R*) and (*S*) products randomly though with the same *ee* values. For symmetry reasons one would have to

 © VCH Verlagsgesellschaft mbH, D-69451 Weinheim, 1994 0570-0833/94/1414-1459 $ 10.00+.25/0

conclude that the direction of the unknown chirality-donating additional fields in relation to the magnetic field is reset at random prior to every new run. Such a proposal cannot be considered seriously. Therefore, any analysis of the results of Breitmaier et al.[2] would have to be based on a chemical explanation.

The formation of gelatinous precipitates after the dropwise addition of the reagents into homogeneous solutions is mentioned very briefly in the publication. If we try to devise a model for the action of the magnetic field on the chemical reaction based on this observation, we will again fail due to symmetry reasons. Contrary to self-seeding in the crystallization of achiral molecules that organize in chiral space groups, an event that may yield only one kind of enantiomorphous crystals if the process is highly effective,[1, 5] there is no similar mechanism for the selective precipitation of chiral alcoholates from a homogeneous solution even under the influence of a homogeneous magnetic field. Thus, the products that might eventually precipitate in microcrystalline form must first be generated chemically. That means, any face differentiation would have to occur prior to the precipitation.

At constant field direction (note the relation to possible additional fields) the authors report that either (*Re*) or (*Si*) reactions predominate at random[2] (that is to say from the beginning until the end of the run) and that the reagents are added dropwise to the homogeneous solution. Therefore the gravitational field cannot be invoked. Since the magnetic field is achiral, there cannot be (*Re*)/(*Si*) differentiation at this stage, and the (local) transgression of the solubility product for the (*R*) alcoholate occurs at the same time as that for the (*S*) alcoholate. Enantiomeric (*R*) and (*S*) crystallites will precipitate side by side if the system does not favor amorphous phases or racemic mixed crystals instead. In the former case it would be conceivable that the directional magnetic field might select between the enantiomorphous species of crystals if it is assumed that these crystals may in some way enantioselectively catalyze the primary reaction while the reagent is added to the solution. However, even this model of magnetic activation of chiral catalysts is not applicable here, because it is reported that either the (*R*) or the (*S*) products predominate at random.

Furthermore according to Breitmeier et al. seeding (only in the magnetic field) with the (*R*) product results in the formation of the (*R*) product with a high *ee*-value, and seeding with the (*S*) product has the opposite effect.[2] For symmetry reasons similar inconsistencies would also emerge with other explanations. Therefore, it must be concluded that the experiments of Breitmaier et al.[2] can be reproduced only if further unspecified requirements are fulfilled.

Accordingly, our *attempts at verification* failed. We requested more detailed reaction conditions from the correspondence author, who provided some "tips"[6] which were more detailed than the experimental description in reference [2]. We followed these guidelines as closely as possible, even though we could not always understand their purpose (the end of the needle used in the addition should be centered within the field about 0.5 cm above the solution of substrate or reagent; addition should be very slow; one should not stir but pass a very slow stream of nitrogen through the solution or move the flask occasionally; diethyl ether or tetrahydrofuran (THF) may be used instead of diisoamyl ether; the aldehyde may be added to the solution of RMgX in ether/benzene, which is centered in the magnetic field; the choice of magnet was not critical in Bonn: a permanent magnet 0.35 T, 7 cm, an electromagnet 0.2–1.4 T, 7 cm, and a cryomagnet 2.1 T, 15 cm, were all successful in Bonn). We still obtained products with *ee* values of zero.

In our experiments we used the homogeneous magnetic field of a 90 MHz Perkin-Elmer R 32 NMR spectrometer without the probe inserts. As we had set out to prove or disprove expressly the claim that contrary to elementary principles[4] an achiral magnetic field solely might create the *ee* values,[2] we applied our magnetic field as efficiently as possible and used a vessel for the reported scale of the reaction that filled the homogeneous field space as completely as possible. This deviation from the conditions at Bonn (50 mL three-necked flask centered in the homogeneous range) should enforce any magnetic field action whatsoever, but not decrease it.

We never detected any optical rotation for the reaction products [pure enantiomer: $[\alpha]_D = \pm 46.3^\circ$ ($c = 1$, toluene)] in the reactions of acetophenone with $LiAlH_4$ and of benzaldehyde with CH_3MgI when the carefully worked-up raw material was analyzed polarimetrically (detection limit of the Polarotronic Universal of Schmidt and Hensch: $\alpha = \pm 0.01^\circ$; $d = 20$ cm). We conducted eight different runs with numerous variations according to reference [2] and later on taking into account the "tips" we received.[6]

Our *reaction flask* consisted of a glass cylinder which was flattened at its closed end (width 5.0 cm, o.d. 1.00 ± 0.01 cm, i.d. 0.60 ± 0.01 cm, filling height initially 2.0 cm, after addition of the reactants 4.0 cm; addition time ≥ 2 h; pole distance 1.4 cm; pole diameter 7.5 cm; distance between addition needle and surface of the reaction mixture 6–8 cm and 0.5–1.5 cm). The flask was fixed as close to the center of the magnetic field as possible with an external clamp and flushed with argon prior to the experiment. A strong or weak or no stream of argon was passed through the solution (in the latter case the vessel was shaken every 15 min).

The size of the runs was as described in reference [2]. CH_3MgI was prepared in THF or in diethyl ether, and in the latter case the solution was diluted with benzene (1:1 by volume). The chemical yields were quantitative in the reductions with $LiAlH_4$ and 85–95% in the Grignard reactions. Every reaction was terminated while still in the magnetic field by addition of water, and NH_4Cl was used for neutralization. The diethyl ether extracts were concentrated to dryness under vacuum, diluted with toluene up to a volume of 10 mL, and analyzed polarimetrically.

In view of the complete failure to reproduce either type of claimed absolute asymmetric syntheses in a homogeneous magnetic field, we did not repeat the other examples reported by Breitmaier et al.[2] outside Bonn for reasons of cost. There is no reason to expect to obtain *ee* values different from zero in those cases either.

In *conclusion* we maintain that in the experiments that provided the spectra in Figure 1 in reference [2] particular conditions must have prevailed which were neither mentioned in the publication[2] nor in the private communication.[6] Absolute asymmetric syntheses under the influence of physical fields continue to require that the field be chiral.[4] A homogeneous field alone is not chiral, and it cannot effect (*Re*)/(*Si*) differentiation. This

fact must be stated here plainly in view of the apparent sensation created[3] by the paper of Breitmaier et al.[2]

Received: June 12, 1994
German version: *Angew. Chem.* **1994**, *106* 1527

[1] References in G. Kaupp, M. Haak, *Angew. Chem.* **1993**, *105*, 727; *Angew. Chem. Int. Ed. Engl.* **1993**, *32*, 694, and L. Caswell, M. Garcia-Garibay, J. R. Scheffer, J. Trotter, *J. Chem. Educ.* **1993**, *70*, 785.

[2] G. Zadel, C. Eisenbraun, G.-J. Wolff, E. Breitmaier, *Angew. Chem.* **1994**, *106*, 460; *Angew. Chem. Int. Ed. Engl.* **1994**, *33*, 454.
[3] *Chem. Eng. News* **1994**, *72* (9), 36.
[4] R. C. Dougherty, *J. Am. Chem. Soc.* **1980**, *102*, 380; E. Edwards, K. Cooper, R. C. Dougherty, *ibid.* **1980**, *102*, 381, and references therein.
[5] J. M. McBride, R. L. Carter, *Angew. Chem.* **1991**, *103*, 298; *Angew. Chem. Int. Ed. Engl.* **1991**, *30*, 293.
[6] E. Breitmaier, personal communication, May 12, 1994.

No Enantioselective Reactions in a Static Magnetic Field

Based on part of the PhD thesis by G. Zadel (completed 1993) and parallel investigations by Catja Eisenbraun the communication "Enantioselective Reactions in a Static Magnetic Field" appeared under my auspices together with G. Zadel, C. Eisenbraun, and G. J. Wolff in this journal (*Angew. Chem.* **1994**, *106*, 460; *Angew. Chem. Int. Ed. Engl.* **1994**, *33*, 454). Several independent research groups have informed me since that the experiments reported (1,2-addition of Grignard compounds to aldehydes; reduction of prochiral ketones with lithium aluminum hydride), contrary to the results published by us gave no enantiomeric excesses. In light of this I instructed three experienced co-workers from my research group (F. Keller, K. Berlin, and T. Marx) to repeat the most important experiments [reduction of 2-acetylnaphthalene with lithium aluminum hydride to (*R*)- or (*S*)-1-(2-naphthyl)ethanol; 1,2-addition of methylmagnesium iodide to benzaldehyde to give (*R*)- or (*S*)-1-phenylethanol] completely independently from the chief experimentalist (G. Zadel). These co-workers carried out several experiments in Bonn and Karlsruhe, some in my presence but all in the absence of G. Zadel, and could detect no measureable enantiomeric excesses (NMR with $[Eu(hfc)_3]$, GC with β-cyclodextrin, polarimetry). In one case, we were able to prove quite clearly (GC-MS, polarimetry) that the starting solution prepared by G. Zadel for the reduction of propiophenone with lithium aluminum hydride also contained considerable amounts of (+)-1-phenylpropanol in addition to propiophenone. G. Zadel admitted this deception and two other manipulations in front of witnesses. Therefore we must assume that the data in the publication as well as "successful" attempts at reproducing the results by other co-workers in my research group and guest scientists in the presence of G. Zadel came about because of consistent and particularly cleverly disguised manipulations. I therefore wish to disassociate myself and the coauthors C. Eisenbraun and G. J. Wolff from all the experimental results in this publication.

E. Breitmaier
Institut für Organische Chemie und Biochemie der Universität
Gerhard-Domagk-Strasse 1, D-53121 Bonn (FRG)
Received: June 21, 1994

 © *VCH Verlagsgesellschaft mbH, D-69451 Weinheim, 1994* *0570-0833/94/1414-1461 $ 10.00+.25/0*

Bond-Stretch Isomers and Spin-State Isomers: A Comment on the Article "Bond-Stretch Isomers: Fact not Fiction"[1]

Gerard Parkin* and Roald Hoffmann

Molecules which differ only in the length of one or several bonds have been termed bond-stretch isomers. The first reports of this phenomenon, both theoretical[2] and experimental,[3] date back to the early 1970s, while the first comprehensive article was published in 1988 by Jean, Lledos, Burdett, and Hoffmann.[4] The 1988 article summarized the phenomenon and provided a theoretical rationalization, and thereby stimulated considerable interest in the subject.

However, in 1991 it was discovered that the original example of bond-stretch isomerism in transition metal complexes was an artifact due to crystallographic disorder[5, 6] Thus, it was demonstrated that the green "isomer" of *cis-mer*-$[MoOCl_2(PMe_2Ph)_3]$ was in fact a solid solution of blue *cis-mer*-$[MoOCl_2(PMe_2Ph)_3]$ and yellow *mer*-$[MoCl_3(PMe_2Ph)_3]$, and that the crystallographic disorder between an oxygen atom and a chlorine atom was manifested by an *apparent* increase in the Mo=O bond length. Indeed, it is presently recognized that impurities may commonly serve to modify apparent bond lengths.[7] There is therefore no longer a well-characterized example of bond-stretch isomerism for which it can be stated with certainty that the observed bond-length changes are not an artifact. Nevertheless, it is still possible that one day the phenomenon of bond-stretch isomerism will be experimentally verified.

It was, therefore, of great interest to read an article in this journal titled "Bond-Stretch Isomers: Fact not Fiction".[1] By its title, the article implies that examples of bond-stretch isomers have been discovered. However, the content of the article is not related to the concept of bond-stretch isomerism in the spirit in which it was originally discussed,[4] but rather is concerned with the well-established, valuable, and interesting phenomenon of *spin-state* isomerism, in which changes in bond length are associated with changes in spin-state.

Three review articles on bond-stretch isomerism[7–9] have indeed discussed the phenomenon of spin-state isomerism, and also related effects such as "deformational isomerism".[10, 11] However, bond-stretch isomerism was a concept that was introduced for isomers of the same spin-state, on the same potential energy curve, for which there was no obvious explanation. It may have been a failing of the original papers not to have excluded spin-state isomerism from the definition, but a reading of those papers and a general sense of the community make it clear that the interest of the bond-stretch isomerism phenomenon resides in those cases where the isomers belong to the same spin state. As interesting as they are, there is no special intrigue associated with the observed changes in bond lengths for spin-state isomers.

[*] Prof. Dr. G. Parkin
Department of Chemistry, Columbia University
New York, NY 10027 (USA)
Prof. R. Hoffmann
Department of Chemistry
Cornell University
Ithaca, NY 14853 (USA)

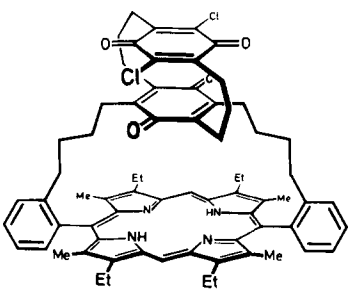
[1] P. Gütlich, H. A. Goodwin, D. N. Hendrickson, *Angew. Chem.* **1994**, *106*, 441–443; *Angew. Chem. Int. Ed. Engl.* **1994**, *33*, 425–427.
[2] a) W.-D. Stohrer, R. Hoffmann, *J. Am. Chem. Soc.* **1972**, *94*, 779–786; b) W.-D. Stohrer, R. Hoffmann, *ibid.* **1972**, *94*, 1661–1668.
[3] The term "distortional isomerism", rather than "bond-stretch isomerism", was originally used to describe the phenomenon in the following papers: a) J. Chatt, L. Manojlovic-Muir, K. W. Muir, *J. Chem. Soc. D* **1971**, 655–656; b) L. Manojlovic-Muir, K. W. Muir, *J. Chem. Soc. Dalton Trans.* **1972**, 686–690; c) L. Manojlovic-Muir, *J. Chem. Soc. D* **1971**, 147; d) L. Manojlovic-Muir, *J. Chem. Soc. A* **1971**, 2796–2800.
[4] Y. Jean, A. Lledos, J. K. Burdett, R. Hoffmann, *J. Am. Chem. Soc.* **1988**, *110*, 4506–4516.
[5] a) K. Yoon, G. Parkin, A. L. Rheingold, *J. Am. Chem. Soc.* **1991**, *113*, 1437–1438; b) *ibid.* **1992**, *114*, 2210–2218; c) G. Parkin, *Acc. Chem. Res.* **1992**, *25*, 455–460.
[6] P. J. Desrochers, K. W. Nebesny, M. J. LaBarre, S. E. Lincoln, T. M. Loehr, J. H. Enemark, *J. Am. Chem. Soc.* **1991**, *113*, 9193–9200.
[7] G. Parkin, *Chem. Rev.* **1993**, *93*, 887–911.
[8] J. M. Mayer, *Angew. Chem.* **1992**, *104*, 293–295; *Angew. Chem. Int. Ed. Engl.* **1992**, *31*, 286–287.
[9] V. C. Gibson, M. McPartlin, *J. Chem. Soc. Dalton Trans.* **1992**, 947–956.
[10] U. Kölle, J. Kossakowski, N. Klaff, L. Wesemann, U. Englert, G. E. Heberich, *Angew. Chem.* **1991**, *103*, 732–733; *Angew. Chem. Int. Ed. Engl.* **1991**, *30*, 690–691.
[11] J. K. Burdett, *Chemtracts: Inorg. Chem.* **1992**, *4*, 112–115.

 © VCH Verlagsgesellschaft mbH, D-69451 Weinheim, 1994 0570-0833/94/1414-1462 $ 10.00+.25/0

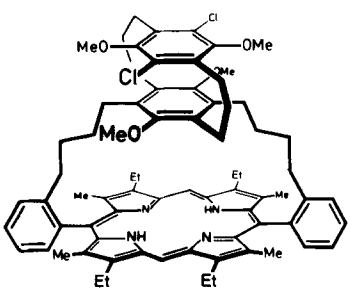
Synthesis and Properties of a Vertically Stacked Porphyrin-Quinone(1)-Quinone(2) Cyclophane**

Heinz A. Staab,* Moana Tercel, Rüdiger Fischer, and Claus Krieger

In multiple electron transfers, such as those assumed to occur in the primary process of biological photosynthesis, the question arises as to which structural factors favor a consecutive, stepwise electron transfer and which an integrated process relying on electronic coupling. Until now, the hypotheses (e.g. "superexchange") offering a theoretical explanation for the second of these mechanisms have frequently been developed in a rather ad hoc fashion. Further experimental investigations into the effect of structure, distance, and spatial orientation of the electron systems involved in these processes are required. In this context, a series of model compounds based on porphyrin-quinone(1)-quinone(2) cyclophane **1** have proved to be interesting because their steric and electronic structures can be defined unambiguously and varied systematically. In the vertically stacked P-Q(1)-Q(2) sequence, the weak acceptor Q(1), whose electron affinity is comparable to that of duroquinone, is adjacent to the porphyrin. The structure of the cyclophane dictates that the substantially stronger electron acceptor dichlorobenzoquinone Q(2) is fixed at such a distance from P that direct P···Q(2) interactions are negligible. In the classical case of a discrete, stepwise process, the slowest and thus rate-determining step in **1** is expected to be the photoinduced electron transfer from P* to Q(1). However, time-resolved fluorescence measurements[1] show that electron transfer in **1** does not occur at a rate comparable to that in the sterically and electronically analogous P–Q(1) system in the series of single-bridged quinone–porphyrin cyclophanes;[2] electron transfer is in fact approximately a thousand times faster (solvents *n*-hexane, toluene): for **1** the fluorescence lifetime of 2–3 ps, independent of solvent polarity, is of the same order of magnitude as the value recorded for the single-bridged porphyrin–dichloroquinone cyclophane P–Q(2).[2] The dramatic effect on the rate of photoinduced electron transfer produced by the higher electron affinity of Q(2) in P-Q(1)-Q(2), despite the remoteness of Q(2) from P, can be rationalized if we assume that the central Q(1) π-electron system mediates a sufficiently effective electronic coupling between P and Q(2). As an alternative explanation it might also be considered that the strong transannular interactions in the benzoquinone cyclophane moiety of **1**, Q(1)–Q(2), result in the formation of a coherent acceptor unit with an electron affinity greater than that of the isolated Q(1) acceptor.[1] Evidence for one or other of these mechanisms can be obtained from analogues of **1** in which the factors mentioned above can be influenced separately. On the one hand, spacers in porphyrin–quinone cyclophane analogues of **1** can be used to vary the P···Q distance systematically while leaving the vertical arrangement unchanged;[3] on the other hand, Q(1)···Q(2) interactions can be altered selectively by moving from the [3.3]paracyclophane system present in **1** to higher [n.n]paracyclophanes



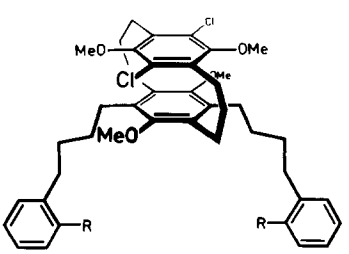
1



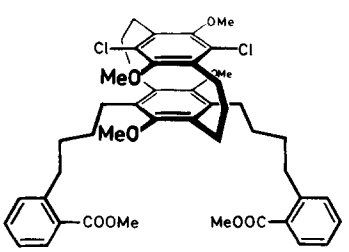
2

or by synthesizing the corresponding pseudogeminal isomers (see below). This approach has been used for investigating charge-transfer interactions in analogous paracyclophane quinhydrones.[4]

The synthesis of **1** described below establishes a general strategy for the preparation of a series of analogues of **1**, in which there is a graduated variation in the P···Q(1) and Q(1)···Q(2) interactions. In tackling this synthesis, we were able to draw on our experience from the syntheses of [n.n]paracyclophanes[4] and porphyrin–quinone cyclophanes.[5] The porphyrin–[3.3]-paracyclophane triad **2**, which already contains the complete carbon skeleton of **1** as well as the oxygen functionalities in the [3.3]paracyclophane moiety, was chosen as a suitable precursor to **1**. It was hoped that transformation of **2** into **1** could be achieved by cleavage of the methoxy groups followed by oxidation. By analogy with the synthesis of single-bridged porphyrin cyclophanes,[5] dicarboxylic ester **3** was expected to be a key intermediate in the preparation of **2**. Dialdehyde **5**, which is required for the porphyrin synthesis, should be accessible from **3** via **4** by standard procedures of reduction and partial oxidation. The only feasible route to the fully substituted carbocyclic [3.3]paracyclophane system in **3** involved the vapor-phase pyrolysis[6] of disulfones obtained from appropriately substituted dithia[4.4]paracyclophanes. A crucial question here concerned



3: R = COOMe; **4**: R = CH_2OH; **5**: R = CHO



6

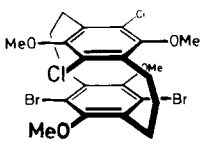
[*] Prof. Dr. H. A. Staab, Dr. M. Tercel, Dr. R. Fischer, C. Krieger
Abteilung Organische Chemie
Max-Planck-Institut für medizinische Forschung
Jahnstrasse 29, D-69120 Heidelberg (FRG)
Telefax: Int. code + (6221)486-219

[**] Photoinduced Electron Transfers in Porphyrin–Quinone Cyclophanes, Part 11. – Part 10: H. A. Staab, C. Krieger, C. Anders, A. Rückemann, *Chem. Ber.* **1994**, *127*, 231–236.

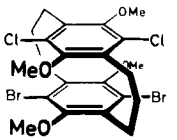
 © VCH Verlagsgesellschaft mbH, D-69451 Weinheim, 1994 0570-0833/94/1414-1463 $ 10.00+.25/0

the order in which the [3.3]paracyclophane unit and the long side chains attached to the "lower" ring in **3** should be assembled.

An attempt was first made to start the synthesis from dithia[4.4]paracyclophanes in which the required ring substituents, including the complete side chains of **3**, were already present. Unfortunately, the corresponding disulfones had such low volatilities that thermal decomposition predominated in the vapor-phase pyrolysis. The pseudogeminal [3.3]paracyclophane **6** was the only product that could be isolated in yields (ca. 3%) too poor to allow further transformations.[7] An attempt was then made to introduce the side chain after the [3.3]paracyclophane unit in **3** had been assembled. Coupling of 1,4-dibromo-2,5-bis(bromomethyl)-3,6-dimethoxybenzene[8] and 1,4-dichloro-2,5-bis(mercaptoethyl)-3,6-dimethoxybenzene[7] yielded the appropriately substituted dithia[4.4]paracyclophanes (methanol/THF, cesium carbonate, dilution technique; 52% yield). Oxidation to the disulfones followed by vapor-phase pyrolysis (535 °C, 10^{-5} Torr) gave, after chromatographic separation, the two isomeric 5,8-dibromo-14,17-dichloro-6,9,15,18-tetramethoxy[3.3]paracyclophanes **7** (26% yield) and **8** (29% yield).[9] It



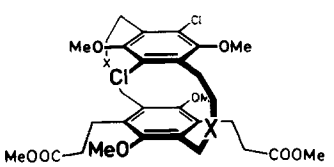
7



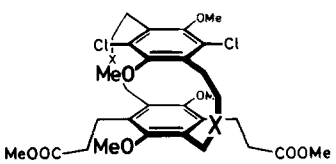
8

was hoped that a palladium-catalyzed Heck vinylation[10] at the bromo-substituted position would then allow introduction of the side chains (in this type of reaction, bromo substituents are known to react selectively in the presence of chloro substituents). It turned out, however, that **7** and **8** were totally inert, even though the conditions employed were identical to those used in the Heck reaction of 1,4-dibromo-2,5-dimethoxy-3,6-dimethylbenzene with methyl acrylate, in which yields of 80–90% were achieved.[5] Clearly, steric interactions with the [3.3]paracyclophane unit hindered the reaction. Attempts at increasing reactivity in the Heck reaction by using the iodo derivatives of **7**/**8** failed because of the poor, nonreproducible yields obtained in the cyclization and pyrolysis reactions.

As a compromise between these two unsuccessful synthetic strategies, a new concept for the synthesis of **3** via a central [3.3]paracyclophane unit with shorter side chains was developed. The side chain would have to be short enough to allow successful pyrolysis of the disulfones, but at the same time long enough to circumvent steric interactions with the fully substituted paracyclophane system. With a judicious choice of terminal functionality, the subsequent chain extension to give **3** could then be achieved in a short and promising reaction sequence. Dithia[4.4]paracyclophanes **9** and **10**, each bearing two C_3 side chains in the form of methoxycarbonylethyl groups, were chosen as starting materials for the synthesis of disulfones **11** and **12**, respectively.

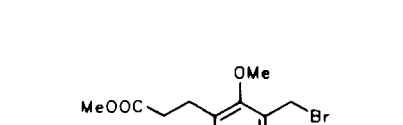


9: X = S
11: X = SO_2

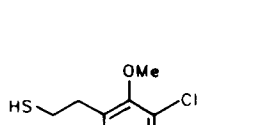


10: X = S
12: X = SO_2

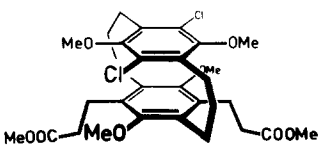
Cyclization of 1,4-bis(bromomethyl)-2,5-bis(2-methoxycarbonylethyl)-3,6-dimethoxybenzene (**13**) and 1,4-dichloro-2,5-(2-mercaptoethyl)-3,6-dimethoxybenzene (**14**)[11] (KOH, methanol/THF, dilution technique; 46% yield) gave the isomers **9** and **10** (1.2:1, according to ^{1}H NMR). The disulfone isomers **11** and **12** were obtained by oxidation with *m*-chloroperbenzoic acid (dichloromethane, 90 h at 20 °C; 85% yield).[12] Vapor-phase pyrolysis of the mixture of disulfone isomers **11**/**12** (535 °C, 10^{-5}–10^{-6} Torr) gave a mixture of carbocyclic [3.3]paracyclophanes in 45% yield. The isomers were separated by chromatography (silica gel, hexane/diethyl ether, 4:1) and recrystallized from methanol. The elemental analyses and spectroscopic data (^{1}H NMR, MS) for isomer A (22% yield, m.p. 191–192 °C) and isomer B (22% yield, m.p. 196–197 °C) were consistent with the expected structures. Assignment of the isomers to the pseudoortho and pseudogeminal series was only possible by X-ray structure analysis; it was thus established that A has the pseudoortho structure **15** and B the pseudogeminal structure **16**.[13]



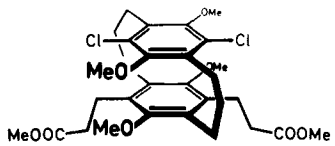
13



14



15



16

The molecular structures of both isomers show practically eclipsed orientations of the nearly planar six-membered rings, with an interplanar distance of 334 pm. The C_3 side chains on the "lower" six-membered ring lie in a plane perpendicular to that of the ring and point, as expected, away from the "upper" ring of the [3.3]paracyclophane. Figure 1 shows the molecular structure of **15** in a top view onto the plane of the ring (top) and in a side view (bottom). It may be assumed that the spatial arrangement in the [3.3]paracyclophane moiety of **1** largely corresponds to that shown for **15**. Starting the synthesis from **15** guarantees, above all, that the benzoquinone units in **1** will be in a pseudoortho relationship. An analogous synthetic sequence starting from **16** would then yield the pseudogeminal isomer. This compound is of interest because of the expected differences in Q(1)···Q(2) interactions as compared to **1**.

In the first step towards the synthesis of **3**, **15** was either converted directly into the corresponding aldehyde[9] (m.p. 216–220 °C, from cyclohexane) by reaction with diisobutylaluminum hydride (toluene, −78 °C; 62% yield), or else it was first reduced to the bis(3-hydroxypropyl) derivative[9] (lithium aluminum hydride, THF, 20 °C; 96% yield; m.p. 249–252 °C, from methanol) and then oxidized to the aldehyde with pyridinium

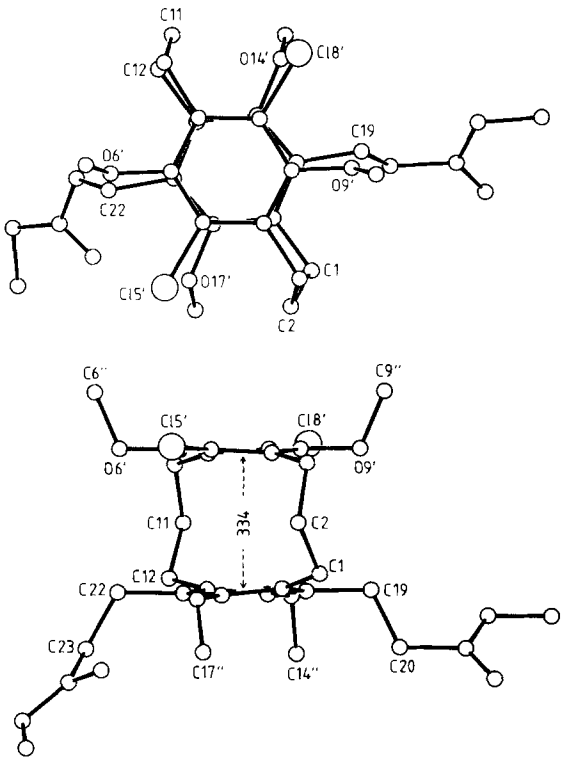
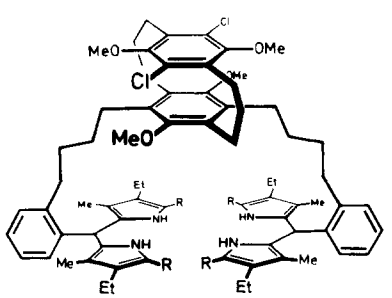


Fig. 1. Crystal structure of **15**. Top: top view onto the plane of the six-membered ring; bottom: side view.

chlorochromate (dichloromethane, celite/magnesium sulfate; 70% yield). The Wittig reaction of the dialdehyde with (2-methoxycarbonylbenzyl)triphenylphosphonium bromide[14] (sodium methanolate, THF; 85% yield, mixture of *cis* and *trans* isomers) followed by hydrogenation (Pd/C, ethyl acetate/methanol, 1 h, 20 °C) led to formation of **3**[9] (ca. 95% yield, m.p. 139–140 °C, from methanol/chloroform, 4:1).

The dicarboxylic ester **3** was reduced to the corresponding bis(2-hydroxymethylphenyl) compound **4**[9] (m.p. 109–110.5 °C) with lithium aluminum hydride (THF, 20 °C; nearly quantitative yield). Partial oxidation with pyridinium chlorochromate (dichloromethane, celite/magnesium sulfate; 92% yield) gave dialdehyde **5**[9] (m.p. 135–137 °C). In an analogous procedure to that described for the synthesis of single-bridged tetraethyltetramethylporphyrins,[5] **5** was condensed with 2-benzyloxycarbonyl-3-ethyl-4-methylpyrrole[15] to give the corresponding bis(dipyrrylmethyl) compound **17**[9] (conc. hydrochloric acid, ethanol, 4 h at reflux; 98% yield). Cleavage of the benzyl groups by hydrogenolysis (Pd/C, THF) yielded the tetracarboxylic acid **18**. Finally, the [3.3]paracyclophane-bridged porphyrin **2**[9] (crimson microcrystals; m.p. > 330 °C) was obtained from **18** by cyclization with triethyl orthoformate in dichloromethane/trichloroacetic acid followed by dehydrogenation with 2,3-dichloro-5,6-dicyano-1,4-benzoquinone (DDQ).

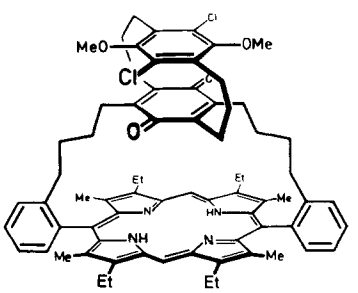


17: R = COOBz
18: R = COOH

The unusually poor yield of 2% obtained in the porphyrin synthesis may be ascribed to the steric hindrance presented by the two methoxy groups in the "lower" paracyclophane ring. The methoxy groups in both six-membered rings of the paracyclophane system are twisted out of the plane of the ring, so as to avoid steric interactions with other ring substituents; they are forced into a conformation—also observed in the molecular structures of **15** and **16** (Fig. 1)—in which the methoxy groups in the "upper" ring point upwards and those in the "lower" ring downwards. The latter hinder the formation of the porphyrin ring in **2**.

The ^{1}H NMR spectrum of **2** also provides evidence for the existence of such steric interactions: whereas in all the precursors of **2** both sets of [3.3]paracyclophane methoxy protons have very similar δ values (e.g. **3**: 3.46, 3.51; **5**: 3.45, 3.51; **17**: 3.42, 3.49), in the ^{1}H NMR spectrum of **2**, only one of the singlets, corresponding to two of the four methoxy groups, appears in this region [δ = 3.28 (s, 6H)]. The protons belonging to the other two methoxy groups absorb at δ = 1.12 (s, 6H) (all values given for $CDCl_3$, 500 MHz). This large upfield shift indicates that the methoxy protons in the central ring of **2** are positioned in very close proximity to the porphyrin system and thus experience an anisotropic shielding effect.[16]

Attempts to obtain **1** by demethylation of **2** with boron tribromide (dichloromethane, 70 min, 20 °C) and subsequent dehydrogenation with DDQ did not lead to formation of the expected product. Instead, a compound was obtained in which only one of the six-membered rings of the paracyclophane unit had been converted into a quinone. Surprisingly, it was found that the more sterically shielded methoxy groups of the middle ring had been demethylated, thus forming compound **19**[9] [^{1}H NMR: δ(MeO) = 3.38 (s, 6H), no methoxy signals at $\delta \approx 1.1$; $CDCl_3$, 500 MHz]. In order to find suitable reaction conditions for ether cleavage in **2**, preliminary experiments were performed with several demethylating agents on a model compound synthesized for this purpose.[17] Demethylation of **2** was finally achieved with boron triiodide (dichloromethane, 49 h under argon at 20 °C with exclusion of light). Subsequent oxidation with DDQ gave the target compound **1** (48% yield; purple-colored needles from hexane/benzene, 5:1; m.p. > 330 °C). Elemental analysis and spectroscopic data confirmed the proposed structure for **1**. Investigations into photoinduced electron transfers in **1** and **19** were recently described in a joint publication with Michel-Beyerle, Heitele, et al.;[1] some of the results obtained are summarized in the introduction to this communication.



19

Received: March 23, 1994 [Z 6790 1E]
German version: *Angew. Chem.* **1994**, *106*, 1531

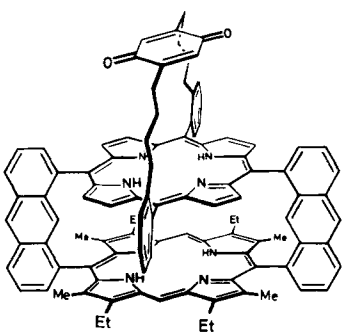
[1] F. Pöllinger, H. Heitele, M. E. Michel-Beyerle, M. Tercel, H. A. Staab, *Chem. Phys. Lett.* **1993**, *209*, 251–257.
[2] See H. Heitele, F. Pöllinger, K. Kremer, M. E. Michel-Beyerle, M. Futscher, G. Voit, J. Weiser, H. A. Staab, *Chem. Phys. Lett.* **1992**, *188*, 270–278; H. A. Staab, G. Voit, J. Weiser, M. Futscher, *Chem. Ber.* **1992**, *125*, 2303–2310.
[3] H. A. Staab, A. Feurer, R. Hauck, A. S. Kumar, C. Krieger, unpublished.

[4] H. A. Staab, C. P. Herz, C. Krieger, M. Rentea, *Chem. Ber.* **1983**, *116*, 3813–3830; H. A. Staab, B. Starker, C. Krieger, *ibid.* **1983**, *116*, 3831–3845, and references therein.
[5] H. A. Staab, J. Weiser, M. Futscher, G. Voit, A. Rückemann, C. Anders, *Chem. Ber.* **1992**, *125*, 2285–2301; H. A. Staab, T. Carell, A. Döhling, *ibid.* **1994**, *127*, 223–229; H. A. Staab, C. Krieger, C. Anders, A. Rückemann, *ibid.* **1994**, *127*, 231–236, and references therein.
[6] H. A. Staab, M. Haenel, *Chem. Ber.* **1973**, *106*, 2190–2202; M. W. Haenel, A. Flatow, V. Taglieber, H. A. Staab, *Tetrahedron Lett.* **1977**, 1733–1736; H. A. Staab, A. Döhling, C. Krieger, *Liebigs Ann. Chem.* **1981**, 1052–1064.
[7] R. Fischer, *Dissertation*, Universität Heidelberg, **1989**; also contains information on the synthesis of the [2.2]paracyclophane analogues of **2** and their precursors.
[8] H. A. Staab, W. Rebafka, *Chem. Ber.* **1977**, *110*, 3333–3350.
[9] The proposed structures were confirmed by elemental analysis and spectroscopic data (^{1}H NMR, MS).
[10] R. F. Heck, *Org. React.* **1982**, *27*, 345.
[11] The syntheses of cyclization components **13** and **14**, which were achieved via a total of 13 novel precursors, will be described in detail in a later publication.
[12] The isomers in the mixtures **9**/**10** and **11**/**12** were not separated, because isomerization was observed in the subsequent disulfone pyrolysis.
[13] X-ray structure analyses: Enraf-Nonius CAD4 diffractometer ($Mo_{K\alpha}$ radiation, graphite monochromator, ω/θ-scan); **15**: $C_{30}H_{38}Cl_2O_8$, $M_r = 597.54$; colorless prisms, $0.20 \times 0.20 \times 0.35$ mm; monoclinic, space group $P2_1/n$ (no. 14); $a = 1494.2(2)$, $b = 942.4(3)$, $c = 2102.6(3)$ pm, $\beta = 98.45(1)°$; $V = 2929(2) \times 10^6$ pm^3, $Z = 4$, $\rho_{calcd} = 1.356$ g cm^{-3}; a total of 5751 reflections were recorded up to $\sin\theta/\lambda = 6.2$ nm^{-1}, 3544 of which with $I \geq 3.0\sigma(I)$; the structure was solved by direct methods (SIR); $R = 0.065$. – **16**: $C_{30}H_{38}Cl_2O_8$, $M_r = 597.54$; pale yellow platelets, $0.25 \times 0.25 \times 0.10$ mm; triclinic, space group $P\bar{1}$ (no. 2); $a = 860.5(1)$, $b = 1036.7(1)$, $c = 1736.6(1)$ pm, $\alpha = 106.23(2)$, $\beta = 90.98(2)$, $\gamma = 93.64(2)°$; $V = 1483.3(6) \times 10^6$ pm^3, $Z = 2$. $\rho_{calcd} = 1.337$ g cm^{-3}; a total of 5813 reflections were recorded up to $\sin\theta/\lambda = 6.2$ nm^{-1}, 4499 of which with $I \geq 3.0\sigma(I)$; the structure was solved by direct methods (SIR); $R = 0.049$. Further details of the crystal structure investigations may be obtained from the Fachinformationszentrum Karlsruhe, D-76344 Eggenstein-Leopoldshafen (FRG) on quoting the depository number CSD-58193, the names of the authors, and the journal citation.
[14] H. A. Staab, J. Weiser, E. Baumann, *Chem. Ber.* **1992**, *125*, 2275–2283.
[15] See D. H. R. Barton, S. Z. Zard, *J. Chem. Soc. Chem. Commun.* **1985**, 1098–1100.
[16] This effect was also observed in the [2.2]paracyclophane analogue with the same substitution pattern as in **2** [$\delta = 1.19$ (s, 6H), 3.24 (s, 6H); CDCl3, 500 MHz]: R. Fischer, M. Tercel, H. A. Staab, unpublished.
[17] M. Tercel, H. A. Staab, unpublished.

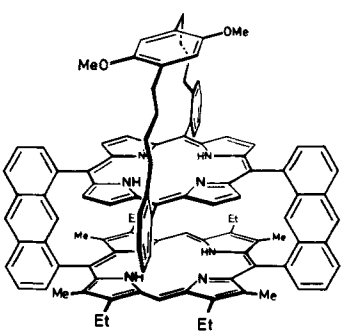
Synthesis and Properties of a Vertically Stacked Porphyrin(1)-Porphyrin(2)-Quinone Cyclophane**

Heinz A. Staab* and Thomas Carell

Photoinduced electron transfers over several successive porphyrin and quinone units have found increasing interest in the context of the primary process in biological photosynthesis. The mechanisms of these "multistep" electron-transfer reactions are not yet well understood. Further examination of model compounds is necessary in which the structure, distance, and orientation of the π systems involved are defined and can be varied systematically. Complementary to numerous studies conducted by other research groups concentrating primarily on porphyrin–quinone systems with lateral arrangements, we synthesized cyclophane-type structures, in which the double bridging of the vertically stacked porphyrin and quinone units leads to a relatively rigid structure.[1] In these systems the effect of single parameters—the electron affinity of the quinones, the donor strength of the porphyrins, and the distance and orientation of the porphyrin and quinone components—can be examined while the other parameters are held constant.[2] This "cyclophane concept" has been extended to multistep electron-transfer systems, as the porphyrin-quinone(1)-quinone(2) cyclophane described in the preceding communication[3] demonstrates. We report here on the vertically stacked porphyrin(1)-porphyrin(2)-quinone cyclophane **1**. The two different porphyrin units in **1** are aligned parallel to each other and separated by roughly 500 pm; the porphyrin that is the weaker donor is flanked by the quinone, which functions as an electron acceptor. The geometric relationships and electronic interactions in the "upper" portion of the triad correspond to those in 5,10,15,20-tetraarylporphyrins with one quinone bridge.[4]

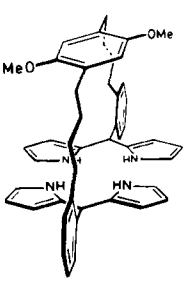


1

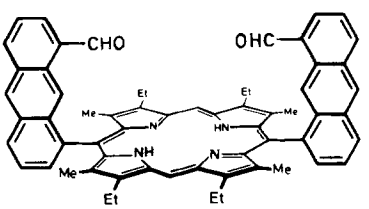


2

In analogy to previous syntheses of porphyrin–quinone cyclophanes[1, 3, 4] non-quinoid **2** was the targeted precursor of **1**, since it contains the complete carbon framework of **1** and should provide **1** upon cleavage of the methoxy groups and subsequent oxidation. For the construction of **2** we considered the condensation of 1,4-bis{4-[2-(bis-2-pyrrolylmethyl)phenyl]butyl}-2,5-dimethoxybenzene (**3**) with *syn*-5,15-bis(1-formyl-8-anthryl)-2,8,12,18-tetraethyl-3,7,13,17-tetramethylporphyrin (**4**). Since we had already prepared **3** in related work,[4] the main problems to be worked out in the synthesis of **2** were the synthesis of **4** and its cyclization with **3**.



3



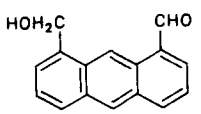
4

Anthracene 1,8-dicarboxylic acid[5] was converted via its dimethyl ester into 1,8-bis(hydroxymethyl)anthracene,[6] which was treated with triphenylmethyl chloride (1 equiv, pyridine, 15 h, 50 °C) to give 1-hydroxymethyl-8-triphenylmethoxymethylanthracene (32% yield)[7] in addition to 1,8-bis(triphenylmethoxymethyl)anthracene (20% yield).[7] Oxidation of the

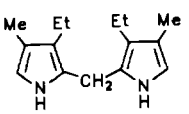
[*] Prof. Dr. H. A. Staab, Dr. T. Carell
Abteilung Organische Chemie
Max-Planck-Institut für medizinische Forschung
Jahnstrasse 29, D-69120 Heidelberg (FRG)
Telefax: Int. code + (6221)486-219

[**] Photoinduced Electron Transfer in Porphyrin–Quinone Cyclophanes, Part 12. – Part 11: ref. [3].

free hydroxymethyl group of the former (dimethylsulfoxide (DMSO), dichloromethane, oxalyl dichloride, −70 °C; yield 90%) led to 1-formyl-8-triphenylmethoxymethylanthracene (m.p. 215 °C),[7] and subsequent hydrolysis (acetic acid, 100 °C; yield 65%) furnished 1-formyl-8-hydroxymethylanthracene (**5**, m.p. 132 °C).[7] In a procedure better suited for large-scale preparation, **5** was obtained from 1,8-bis(hydroxymethyl)-anthracene by means of its partial acetylation to 1-acetoxymethyl-8-hydroxymethylanthracene (1 equiv acetyl chloride, sodium hydride, dioxane; m.p. 118–120 °C)[7] in 33% yield (18% yield of 1,8-bis(acetoxymethyl)anthracene as well). Oxidation of the free hydroxymethyl group (conditions as above; 90% yield) to give 1-acetoxymethyl-8-formylanthracene (m.p. 110 °C)[7] and cleavage of the acetyl group (ammonia/methanol, 12 h, 20 °C; yield 75%) led to **5**. The second component for the construction of the "lower" porphyrin unit of **2**, bis(3-ethyl-4-methyl-2-pyrrolyl)methane (**6**), was obtained from the corresponding α-ethoxycarbonyl compound by basic hydrolysis and decarboxylation.[8]

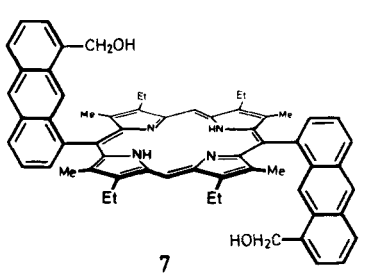


5

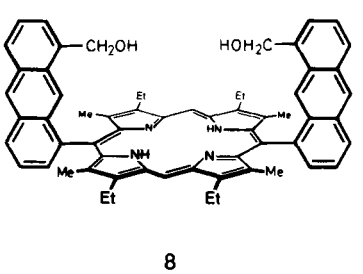


6

The cyclization of **5** and **6** was conducted in methanol under argon with *p*-toluenesulfonic acid as catalyst.[9] The porphyrin-containing precipitate was oxidized with chloranil (THF, 20 min, exclusion of light). Standard workup yielded a violet product, which was separated by chromatography (silica gel, toluene/ethyl acetate, 10:1) into product fractions A and B. Further purification of both fractions by medium-pressure chromatography and recrystallization from dichloromethane/methanol furnished two products in analytically pure form (A: 29%, B: 26% yield). The ^{1}H NMR spectra (500 MHz, [D$_6$]DMSO) and ^{13}C NMR spectra (90.6 MHz, CD_2Cl_2, ^{1}H broad band decoupled; assignment by ^{13}C–^{1}H COSY), as well as the mass spectra and other spectroscopic data for the two products, were very similar and corresponded to those of the anticipated *syn* and *anti* atropisomers **7**[7] and **8**.[7] In similar

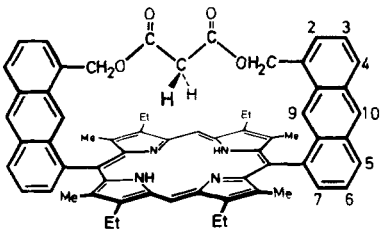


7



8

cases different R_f values have been used to differentiate between the isomers;[10] this was the case here as well (A: 0.37, B: 0.08; silica gel, toluene/ethyl acetate, 4:1). Unequivocal assignment of the isomers was possible by making use of the different spatial arrangement of the hydroxymethyl groups: only with B did reaction with malonyl dichloride (*N*-methylmorpholine, dichloromethane, 30 min, −78 °C) lead to an intramolecular malonate bridge, indicating that B must be the *syn* compound **8**. The compound obtained was unambiguously assigned structure **9** based on its analytical data (^{1}H and ^{13}C NMR, Liquid Secondary Ionization (LSI) MS, high-resolution MS). A noteworthy feature of **9** is the extremely high-field signal for the central methylene protons of the malonate unit at $\delta = -2.54$ (360 MHz, $CDCl_3$), which is explained by the position of these protons above and within the ring current of the porphyrin system. In an attempt to increase the overall yield of **8**, compound **7** was heated at reflux in ethylene glycol (200 °C). Some thermal *anti–syn* isomerization of **7** was indeed observed, but thermal decomposition dominated under these conditions.



9

Oxidation of the two hydroxymethyl groups in **8** to the formyl groups in **4** in the presence of the porphyrin unit was not possible under typical conditions for mild oxidation (e.g. pyridinium chlorochromate, dichloromethane; DMSO, oxalyl dichloride, dichloromethane; silver carbonate/silica gel, toluene). The transformation succeeded, however, with the molybdenum-picolinato-*N*-oxido-peroxo complex[10] (1,2-dichloroethane, 24 h at 50 °C under argon; 60% yield) and with the "hypervalent iodine" reagent ("periodinane"[11]) prepared from iodobenzoic acid, potassium bromate, and acetic anhydride in dichloromethane (5 °C, monitored by thin-layer chromatography; 82% yield). Following chromatography (silica gel, toluene/ethyl acetate, 4:1) and recrystallization from dichloromethane/methanol, compound **4** was obtained as violet crystals (m.p. > 300 °C). The spectroscopic data (^{1}H NMR, MS including high resolution of the molecular ion peak at *m/z* 886) confirmed the proposed structure.

The second porphyrin system in **2** was constructed by condensation of **3** and **4** in propionic acid (30 min at 20 °C, 30 min at 90 °C, 1 h at 140 °C).[12] Oligomers and polymers were removed by successive column chromatography (silica gel, toluene/ethyl acetate, 15:1), medium-pressure chromatography (silica gel 60, toluene/ethyl acetate, 100:1), and high-pressure chromatography (silica gel, toluene); each time only the first fraction was subjected to further purification. Due to this procedure after precipitation from dichloromethane/methanol/water (10:10:1) **2** was obtained in a yield of only 2%.

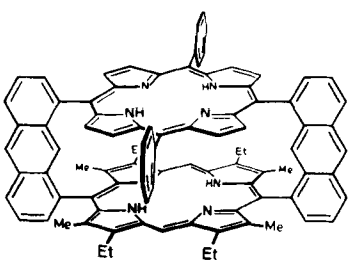
In the ^{1}H NMR spectrum (500 MHz, CD_2Cl_2) of **2** two NH signals (each s, 2H) are observed at $\delta = -4.58$ and -4.18, which correspond to the two differently substituted porphyrin systems. The extreme upfield shift compared to analogous signals of related porphyrins demonstrates that both pairs of NH protons are also affected by the ring current effect of the neighboring porphyrin ring. The other ^{1}H NMR signals could be assigned in almost complete accord with the structure of **2** with the help of COSY experiments and comparisons with other spectra. In the mass spectrum (LSI-MS positive ion mode) the expected cluster near the molecular ion peak at *m/z* 1534 is evident; high resolution of the M^+ and the MH^+ peaks confirms the molecular formula of **2** ($C_{108}H_{94}N_8O_2$).

The last steps in the synthesis of **1** were the demethylation of the dimethoxybenzene unit (boron trifluoride, dichloromethane) and the oxidation of the resulting hydroquinone with DDQ in analogy to the syntheses of simple quinone-bridged porphyrins.[1, 2] After medium-pressure chromatography (silica gel, toluene/ethyl acetate, 100:1) and precipitation from dichloro-

methane/methanol/water (10:10:1), **1** was obtained in 70% yield based on **2**. The purity and structure of **1** were confirmed by analytical high-pressure chromatography (Nucleosil, toluene/*n*-hexane, flow rate = 1 mL min^{-1}, t_R = 3.68 min) and by the ^{1}H NMR and mass spectra. The ^{1}H NMR spectrum (500 MHz, CD_2Cl_2, assignment with COSY and NOE experiments) corresponds to the ^{1}H NMR spectrum of the precursor **2** with the exception of signals reflecting the changes in the "upper" ring. In the mass spectrum (LSI-MS positive ion mode) the expected peak cluster occurs at the base peak *m/z* 1507, which arises from the $[M + 3H]^+$ ion. High resolution of the M^+ and $[M + 2H]^+$ signals confirms the molecular formula $C_{106}H_{88}N_8O_2$.

The absorption spectra of **1** and **2** are almost superimposable in the long-wavelength region dominated by the porphyrin chromophores. This implies that it makes no difference whether the porphyrin is bridged by a quinoid or a non-quinoid unit, which is in agreement with the results from related single-bridged systems.[2] In contrast to the porphyrin–quinone cyclophanes previously studied,[1–4] in **1** and **2** two different porphyrin chromophores are linked in a cyclophane-like fashion; the unit in the middle is a tetraarylporphyrin, that underneath is an octaalkyldiarylporphyrin. The absorptions of **1** and **2** in the regions of the Soret band and the Q bands show that the spectra are not simply superpositions of the absorptions of the two porphyrin chromophores. In particular the Soret bands of **1** and **2** are shifted to shorter wavelengths in comparison to those of the isolated porphyrins with the same substitution patterns; they also do not occur as separate absorptions that can be assigned to the individual porphyrin chromophores. This is apparently the result of electronic interactions between the two porphyrin units in **1** and **2**.

In studies of the fluorescence of **1** solvent-dependent quenching was observed. The "relative quantum yield" of the fluorescence of **1** based on that of the non-quinoid triad **2** is almost independent of the wavelength of the excitation and was determined to be 42% in *n*-hexane, 7% in toluene, and 2.5% in dichloromethane; these findings are in qualitative agreement with preliminary measurements of the fluorescence lifetimes.[13] Here, too, the participation of the porphyrin(1)–porphyrin(2) unit is unclear (e.g. with regard to the electron transfer versus energy transfer). Further insight should be provided by investigations on the porphyrin(1)–porphyrin(2) cyclophane **10**, which was prepared in this context and will be described elsewhere.[14] In compound **10**, which lacks only the quinone bridge of triad **1**, the interaction of the two porphyrin units should correspond to that in **1**.



10

Received: March 23, 1994 [Z 6791 IE]
German version: *Angew. Chem.* **1994**, *106*, 1534

[1] J. Weiser, H. A. Staab, *Angew. Chem.* **1984**, *96*, 602–603, *Angew. Chem. Int. Ed. Engl.* **1984**, *23*, 623–625; C. Krieger, J. Weiser, H. A. Staab, *Tetrahedron Lett.* **1985**, *26*, 6055–6058; H. A. Staab, J. Weiser, E. Baumann, *Chem. Ber.* **1992**, *125*, 2275–2284; H. A. Staab, J. Weiser, M. Futscher, G. Voit, A. Rückemann, C. Anders, *ibid.* **1992**, *125*, 2285–2301.
[2] H. A. Staab, G. Voit, J. Weiser, M. Futscher, *Chem. Ber.* **1992**, *125*, 2303–2310; H. A. Staab, C. Krieger, C. Anders, A. Rückemann, *ibid.* **1994**, *127*, 231–236, and references therein.
[3] H. A. Staab, M. Tercel, R. Fischer, C. Krieger, *Angew. Chem.* **1994**, *106*, 1531; *Angew. Chem. Int. Ed. Engl.* **1994**, *33*, Nr. 14; F. Pöllinger, H. Heitele, M. E. Michel-Beyerle, M. Tercel, H. A. Staab, *Chem. Phys. Lett.* **1993**, *209*, 251–257.
[4] H. A. Staab, T. Carell, A. Döhling, *Chem. Ber.* **1994**, *127*, 223–229.
[5] Prepared from 1,8-dichloroanthraquinone via 1,8-dicyanoanthraquinone and anthraquinone-1,8-dicarboxylic acid in analogy to the reaction described by M. E. Rogers, B. A. Averill, *J. Org. Chem.* **1986**, 51, 3308–3314.
[6] S. Akiyama, S. Misumi, M. Nakagawa, *Bull. Chem. Soc. Jpn.* **1960**, *33*, 1293–1298; **1962**, *35*, 1829–1836.
[7] Elemental analyses and spectroscopic data confirm the assumed structure.
[8] R. Young, C. K. Chang, *J. Am. Chem. Soc.* **1985**, *107*, 898–909; see also J. L. Sessler, J. Hughdahl, M. R. Johnson, *J. Org. Chem.* **1986**, *51*, 2838–2840.
[9] Based on the porphyrin syntheses of M. J. Gunter and L. N. Mander (*J. Org. Chem.* **1981**, *46*, 4792–4795).
[10] O. Bortolini, S. Campestrini, F. Di Furia, G. Modena, G. Valle, *J. Org. Chem.* **1987**, *52*, 5467–5469; S. Campestrini, F. Di Furia, G. Modena, O. Bortolini, *ibid.* **1990**, *55*, 3658–3660.
[11] D. B. Dess, J. C. Martin, *J. Org. Chem.* **1983**, *48*, 4155–4156.
[12] Based on A. D. Adler, F. R. Longo, J. D. Finarelli, J. Goldmacher, J. Assour, L. Korsakoff, *J. Org. Chem.* **1967**, *32*, 476.
[13] F. Pöllinger, H. Heitele, M. Michel-Beyerle, unpublished.
[14] T. Carell, H. A. Staab, unpublished; T. Carell, Dissertation, Universität Heidelberg, **1993**.

A Highly Convergent Synthesis of the Lewis^y Blood Group Determinant in Conjugatable Form**

Victor Behar* and Samuel J. Danishefsky*

Dedicated to Professor R. U. Lemieux

The role of carbohydrates as signaling molecules in the context of biological processes has only recently been appreciated.[1, 2] Carbohydrate molecules, carrying detailed structural information, tend to exist as glycoconjugates (cf. glycoproteins and glycolipids) rather than as free entities. Given the complexities often associated with isolating the conjugates in homogeneous form, the opportunities for synthesis are apparent.[3, 4]

The carbohydrate domains of the blood group substances, contained in both glycoproteins and glycolipids, are widely distributed. The early focus on these systems centered on their role in determining blood group specificities.[5] Intriguingly, ensembles related to the blood group substances in conjugated form are encountered as markers for the onset of various tumors.[6] Carbohydrate-based tumor antigenic factors may find applications at the diagnostic level, as resources in drug delivery, or, ideally, in immunotherapy.[7]

Major advances in glycoconjugate synthesis will require the attainment of high degrees of convergence, good stereocontrol,

[*] Prof. S. J. Danishefsky,[+] V. Behar
Department of Chemistry, Havemeyer Hall
Columbia University
New York, NY 10027 (USA)
Telefax: Int. code + (212)854-7142
[+] Alternative address:
Memorial Sloan-Kettering Cancer Center
1275 York Avenue, New York, NY 10021 (USA)
Telefax: Int. code + (212)772-8691

[**] This research was supported by the National Institutes of Health (grand nos. HL 25848 and AI 16943). A Pfizer Predoctoral Fellowship to V. B. is gratefully acknowledged.

and relief from the burdens associated with the manipulation of blocking groups. Another requirement is that of delivering the carbohydrate determinant with appropriate provision for conjugation to carrier proteins or lipids.[8] In this communication we show how the use of glycals both as glycosyl donors and as glycosyl acceptors can be exploited to accomplish such ends. We do so in the context of a straightforward synthesis of the Le^y (type 2) system.[9]

The Le^y hapten was first isolated from a blood group glycoprotein in 1966 by Kabat, Lloyd et al.[10a] Subsequently, Potapov[10b] discovered an antibody to this carbohydrate antigen. Interest in the Le^y antigen stems from the existence of a number of glycoproteins and glycolipids which contain this substructure and are associated with human colonic adenocarcinoma[11] as well as human liver adenocarcinoma.[12] Both Le^y and Le^x antigenic structures are of general interest due to the preponderance of highly fucosylated polylactosamine glycolipids that are found to accumulate in other human carcinomas.[7f, 13] Our synthesis provides for the determinant to be insulated from the conjugation device by a carbohydrate spacer module which can, in principle, be broadly varied (Fig. 1). Through appropriate insulation, the likelihood that the protein or lipid carrier might distort the recognition property of the determinant is thus minimized.

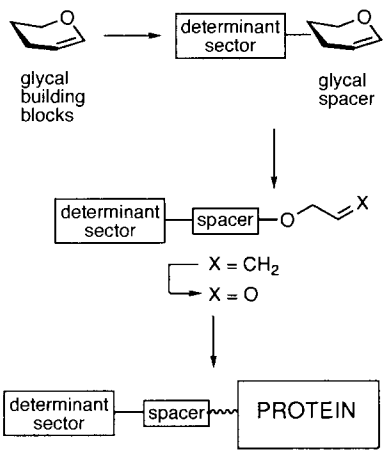
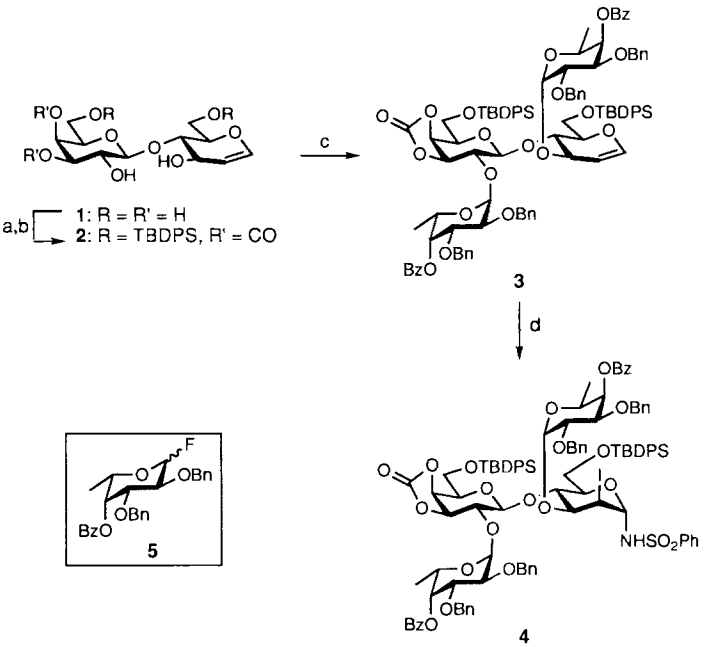


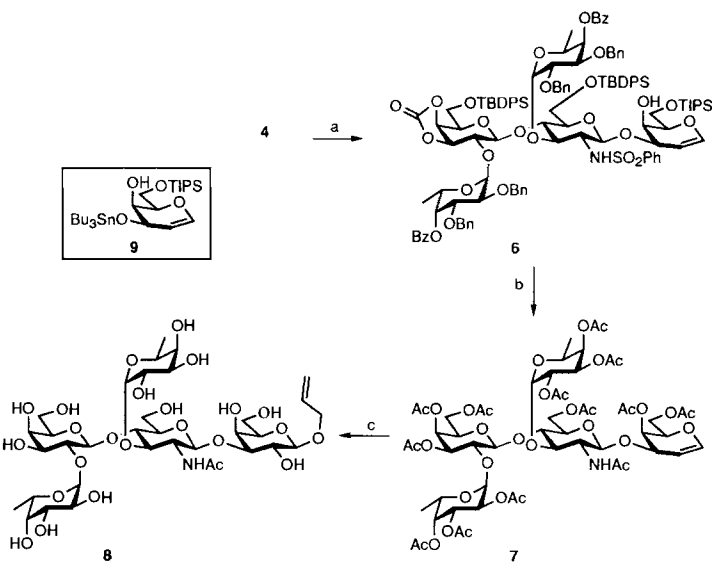
Fig. 1. Glycal assembly leading to neoglycoproteins.

Construction of the Le^y determinant commenced with lactal (**1**)[14] (Scheme 1). Capping both primary hydroxyl groups as their *tert*-butyldiphenylsilyl (TBDPS) ethers under standard conditions was followed by simple engagement of the 3′ and 4′ hydroxyl functions as a cyclic carbonate **2**. The stereospecific introduction of two α-linked fucose residues gave the tetrasaccharide glycal **3** in 51% yield in a single step. The donor used was the known fluorosugar **5**[15] following a modification of the original Mukaiyama conditions (see Experimental Procedure).[16] Glycal **3** corresponds to the Le^y hapten, lacking the N-acetyl function in the glucose residue. We next sought to introduce this group as well as a galactose spacer module.

Methodology which we developed previously[17] proved to be appropriate toward these goals. Glycal **3** was treated with iodonium dicollidine perchlorate ($I(coll)_2ClO_4$) and benzenesulfonamide to afford the iodosulfonamide **4**. Azaglycosylation with the 3-stannyl ether of galactal (**9**)[18] in the presence of silver tetrafluoroborate gave the pentasaccharide glycal **6** in 75% yield (Scheme 2; see also Experimental Procedure). Having **6** in hand, one can iterate the azaglycosylation sequence or activate the glycal as its epoxide and continue with further glycosylations. In terms of convergence, conciseness, and simplicity, we believe that this method offers advantages over earlier worthy efforts directed toward Le^y.



Scheme 1. a) TBDPSCl, imidazole/DMF, 84%; b) carbonyldiimidazole, cat. imidazole, THF, 65%; c) **5**, di-*tert*-butylpyridine, $AgClO_4$, $SnCl_2$, ether, 51%; d) $PhSO_2NH_2$, $I(coll)_2ClO_4$, 94%.



Scheme 2. a) **9**, $AgBF_4$, 4 Å molecular sieves, THF, 75%; b) i: tetrabutylammonium fluoride (TBAF), THF; ii: Na/NH_3; iii: Ac_2O, pyridine, 52%; c) i: 3,3-dimethyldioxirane; allyl alcohol, $ZnCl_2$, 72%; ii: NaOMe, MeOH, quant.

Anxious to demonstrate the ability to fashion a conjugatable form of Le^y hapten, we chose to concentrate on the formation of the allyl glycoside. The feasibility of converting the sulfonamido group into the target acetamide was demonstrated. Glycal **6** was deprotected in two steps as shown. Peracetylation afforded acetamido glycal **7**. Activation of the glycal as its epoxide with dimethyldioxirane,[19] followed by epoxide opening with allyl alcohol in the presence of zinc chloride, gave the

desired peracetylated β-allyl pentasaccharide which was deacetylated by the action of methoxide to provide the target Le^y hapten as its β-allyl glycoside **8**.[20] The aldehyde, derived by ozonolysis of **8**, was conjugated to BSA by the method of Bernstein and Hall.[8a] Approximately 15 carbohydrate pentamers were introduced, presumably at lysine residues.

In summary, the work demonstrates the versatility of glycals both as donors and as acceptors, takes advantage of 1,2 glycal epoxides and their presumed N-sulfonylaziridine counterparts, and opens the way for analogous syntheses of this kind. The biological properties of such systems linked to carrier proteins will be investigated and described in due course.

Experimental Procedure

3: To lactal carbonate **2** (2.00 g, 2.47 mmol) was added fucosyl fluoride **5** (4.44 g, 9.86 mmol). The mixture was azeotroped five times with benzene and placed under high vacuum for two hours. Under an argon atmosphere di-*tert*-butyl pyridine (2.77 mL, 12.33 mmol) and dry ether (16 mL) were added. 2.0 g of freshly activated 4 Å molecular sieves were added and the mixture stirred for one hour at room temperature. In an argon glove bag, $SnCl_2$ (2.34 g, 12.33 mmol) and $AgClO_4$ (2.56 g, 12.33 mmol) were added. The flask was equipped with a reflux condenser and the reaction heated to reflux for 72 h. The reaction was quenched with saturated bicarbonate (5 mL) and filtered through a pad of celite. The filtrate was diluted with ethyl acetate (50 mL) and washed twice with saturated bicarbonate, twice with saturated copper sulfate, and twice with saturated brine. The organic phase was dried over $MgSO_4$ and concentrated. Flash chromatography in 20% ethyl acetate/hexanes afforded 2.10 g (51%) of a white foam **3**: $[\alpha]_D = -78.9$ ($c = 0.555$, $CHCl_3$); IR (thin film): $\tilde{\nu}$ = 3040, 3000, 2905, 2860, 2830, 1820, 1800, 1710, 1635, 1585, 1570, 1480, 1460, 1440, 1415, 1370, 1350, 1300, 1260, 1205, 1145, 1100, 950, 735, 695 cm^{-1}; ^1H NMR (400 MHz, $CDCl_3$): δ = 8.09 (d, J = 8.12 Hz, 2H), 8.00 (d, J = 8.26 Hz, 2H) 7.66 (m, 4H), 7.59 (d, J = 6.74 Hz, 4H), 7.56 (t, J = 7.27 Hz, 1H), 7.30–7.50 (m, 22H) 7.16–7.26 (m, 10H) 7.09 (m, 2H), 6.99 (t, J = 7.59 Hz, 2H) 6.89 (t, J = 7.97 Hz, 1H), 6.43 (d, J = 6.08 Hz, 1H), 5.46 (bs, 1H), 5.38 (bs, 1H), 5.35 (d, J = 3.42 Hz, 1H), 4.89 (d, J = 11.35 Hz, 1H), 4.75–4.80 (m, 4H), 4.72 (d, J = 5.88 Hz, 2H), 4.69 (d, J = 4.27 Hz, 2H), 4.36–4.55 (m, 5H), 4.28 (q, J = 6.51 Hz, 1H), 4.17 (bd, J = 5.46 Hz, 1H), 3.90–4.00 (m, 6H), 3.85 (d, J = 2.99 Hz, 1H), 3.82 (d, J = 2.89 Hz, 1H), 3.56–3.78 (m, 4H), 1.07 (m, 24H); HR-MS (FAB): calcd for $C_{99}H_{106}O_{20}Si_2Na$ 1694.6740; found 1694.6787.

6: Iodosulfonamide **4** (230 mg, 0.12 mmol) was azeotroped five times with dry benzene and placed under high vacuum for two hours. A solution of tin ether **9** (15 equiv) (generated by azeotropic removal of water overnight with a Dean–Stark trap equipped with freshly activated 4 Å molecular sieves from 6-TIPS-galactal (561 mg, 1.80 mmol) and bis(tributyltin) oxide (673 µL, 1.32 mmol) in benzene (80 mL)) in THF (2.4 mL). To this solution stirring under an argon atmosphere was added 200 mg of freshly activated 4 Å powdered molecular sieves. After the mixture had been stirred for one hour at room temperature it was cooled to −78 °C and a solution of silver tetrafluoroborate (187 mg, 0.96 mmol) in THF (2.4 mL) was added by cannula. The mixture was allowed to warm to room temperature over 15 hours, during which time it had turned bright yellow, and the reaction was quenched by the addition of saturated bicarbonate (2 mL). The reaction mixture was filtered through a pad of celite into a separating funnel. The celite pad was washed thoroughly with ethyl acetate. The organic phase was washed twice with saturated bicarbonate and twice with saturated brine. The organic phase was dried over $MgSO_4$. Concentration and chromatography in 25% ethyl acetate/hexanes gave 193 mg (75%) as a white foam **6**: $[\alpha]_D$ −126.4 (c = 0.505, $CHCl_3$); IR (thin film): $\tilde{\nu}$ = 3500, 3040, 3000, 2905, 2840, 1820, 1800, 1705, 1635, 1590, 1440, 1410, 1255, 1195, 1100, 1080, 1035, 815, 730, 695 cm^{-1}; ^1H NMR (400 MHz, $CDCl_3$): δ = 8.09 (app t, 4H), 7.08–7.65 (m, 46H), 6.90 (t, J = 7.65 Hz, 3H), 6.76 (d, J = 6.91 Hz, 2H), 6.12 (d, J = 6.59 Hz, 1H), 5.50 (bs, 1H), 5.45 (bs, 1H), 5.28 (app t, 2H), 3.03–4.91 (m, 36H), 1.09 (m, 45H); LR-MS (FAB): calcd for $C_{120}H_{141}NO_{26}SSi_3Na$ 2153; found 2153.

Received: March 9, 1994 [Z 6744 IE]
German version: *Angew. Chem.* **1994**, *106*, 1536

[1] a) M. L. Phillips, E. Nudelman, F. C. A. Gaeta, M. Perez, A. K. Singhal, S. Hakomori, J. C. Paulson, *Science* **1990**, *250*, 1130; b) M. J. Polley, M. L. Phillips, E. Wagner, E. Nudelman, A. K. Singhal, S. Hakomori, J. C. Paulson, *Proc. Natl. Acad. Sci. USA* **1991**, *88*, 6224.

[2] a) Y. Hirabayashi, A. Hyogo, T. Nakao, K. Tsuchiya, Y. Suzuki, M. Matsumoto, K. Kon, S. Ando, *J. Biol. Chem.* **1990**, *265*, 8144; b) U. Spohr, R. U. Lemieux *Carbohyr. Res.* **1988**, *174*, 211, and references therein.

[3] For recent reviews of glycosylation see: a) K. Toshima, K. Tatsuta, *Chem. Rev.* **1993**, *93*, 1503; b) H. Paulsen, *Angew. Chem.* **1982**, *94*, 184; *Angew. Chem. Int. Ed. Engl.* **1982**, *21*, 155; c) R. R. Schmidt, *ibid.* **1986**, *98*, 213 and **1986**, *25*, 212; d) R. R. Schmidt, *Comprehensive Organic Synthesis, Vol 6*, Pergamon Press, Oxford, **1991**, Chapter 1 (2); e) R. R. Schmidt, *Carbohydrates, Synthetic Methods and Applications in Medicinal Chemistry, Part 1*, VCH, Weinheim, **1992**, Chapter 4.

[4] For pioneering work on the use of glycals as glycosyl donors in glycoside synthesis see a) R. U. Lemieux, *Can. J. Chem.* **1964**, *42*, 1417; b) R. U. Lemieux, B. Faser-Reid, *ibid.* **1965**, *43*, 1460; c) R. U. Lemieux, A. R. Morgan, *ibid.* **1965**, *43*, 2190; d) J. Thiem, P. Ossowski, *J. Carbohydr. Chem.* **1984**, *3*, 287; e) J. Thiem, A. Prahst, T. Wendt, *Liebigs Ann. Chem.* **1986**, 1044; f) J. Thiem in *Trends in Synthetic Carbohydrate Chemistry* (Eds.: D. Horton, L. D. Hawkins, G. L. McGarvvey), American Chemical Society, Washington D.C. **1989**, Chapter 8 (*ACS Symp. Ser.* **1989**, 386).

[5] R. R. Race, R. Sanger, *Blood Groups in Man*, 6th ed. Blackwell, Oxford, **1975**.

[6] a) K. O. Lloyd, *Am. J. Clinical Path.* **1987**, *87*, 129; b) *Cancer Biol.* **1991**, *2*, 421.

[7] a) T. Toyokuni, B. Dean, S. Cai, D. Boivin, S. Hakomori, A. K. Singhal, *J. Am. Chem. Soc.* **1994**, *116*, 395; b) G. Dranoff, E. Jaffee, A. Lazenby, P. Golumbek, H. Levitsky, K. Brose, V. Jackson, H. Hamada, D. Paardoll, R. Mulligan, *Proc. Natl. Acad. Sci. USA* **1993**, *90*, 3539; c) M.-H. Tao, R. Levy, *Nature* **1993**, *362*, 755.

[8] a) M. A. Bernstein, L. D. Hall, *Carbohydr. Res.* **1980**, *78*, C1; b) R. U. Lemieux, *Chem. Soc. Rev.* **1978**, *7*, 423; c) R. U. Lemieux, D. R. Bundle, D. A. Baker, *J. Am. Chem. Soc.* **1975**, *97*, 4076 and references therein.

[9] For previous syntheses see: a) J. C. Jacquinet, P. Sinay, *J. Org. Chem.* **1977**, *42*, 720; b) S. Nilsson, H. Lohn, T. Norberg, *Glycoconjugate J.* **1989**, *6*, 21; c) R. R. Schmidt, A. Topfer, *Tetrahedron Lett.* **1991**, *32*, 3353; d) W. Kinzy, A. Low, *Carbohydr. Res.* **1993**, *245*, 193.

[10] a) K. O. Lloyd, E. A. Kabat, E. J. Layug, F. Gruezo, *Biochem.* **1966**, *5*, 1489; b) M. I. Potapov, *Probl. Hematol. Blood Transfus.* (USSR) **1970**, *15*, 45.

[11] T. Kaizu, S. B. Levery, E. Nudelman, R. E. Stenkamp, S. Hakomori, *J. Biol. Chem.* **1986**, *261*, 11254.

[12] S. B. Levery, E. Nudelman, N. H. Anderson, S. Hakomori, *Carbohydr. Res.* **1986**, *151*, 311.

[13] a) S. Hakomori, E. Nudelman, S. B. Levery, R. Kannagi, *J. Biol. Chem.* **1984**, *259*, 4672; b) Y. Fukushi, S. Hakomori, E. Nudelman, N. Cochran, *ibid.* **1984**, *259*, 4681; c) Y. Fukushi, E. Nudelman, S. B. Levery, S. Hakomori, H. Rauvala, *ibid.* **1984**, *259*, 10511.

[14] W. N. Haworth, E. L. Hirst, M. M. T. Plant, R. J. W. Reynolds, *J. Chem. Soc.* **1930**, 2644.

[15] S. J. Danishefsky, J. Gervay, J. M. Peterson, F. E. McDonald, K. Koseki, T. Oriyama, D. A. Griffith, C.-H. Wong, D. P. Dumas, *J. Am. Chem. Soc.* **1992**, *114*, 8329.

[16] T. Mukaiyama, Y. Murai, S. Shoda, *Chem. Lett.* **1981**, 431.

[17] D. A. Griffith, S. J. Danishefsky, *J. Am. Chem. Soc.* **1990**, *112*, 5811.

[18] S. J. Danishefsky, K. Koseki, D. A. Griffith, J. Gervay, J. M. Peterson, F. E. McDonald, T. Oriyama, *J. Am. Chem. Soc.* **1992**, *114*, 8331.

[19] R. L. Halcomb, S. J. Danishefsky, *J. Am. Chem. Soc.* **1989**, *111*, 6661.

[20] **8**: $[\alpha]_D$ −72.7 (c = 0.1, MeOH); IR (thin film): $\tilde{\nu}$ = 3350, 2940, 2900, 2830, 1650, 1550, 1365, 1300, 1155, 1070, 1030 cm^{-1}; ^1H NMR (400 MHz, CD_3OD): δ = 5.95 (m, 1H), 5.32 (d, J = 17.25 Hz, 1H), 5.14–5.19 (m, 2H), 5.04 (d, J = 3.83 Hz, 1H), 5.02 (d, J = 3.50 Hz, 1H), 4.68 (d, J = 8.15 Hz, 2H), 4.51 (d, J = 5.70 Hz, 1H), 3.40–4.38 (m, 27H), 1.96 (s, 3H), 1.23 (m, 6H); FAB-HR-MS ($C_{35}H_{56}NO_{24}Na$): calcd 900.3325; found 900.3310.

An Interactive Strategy for the Assembly of Complex, Branched Oligosaccharide Domains on a Solid Support: A Concise Synthesis of the Lewis^b Domain in Bioconjugatable Form**

John T. Randolph* and Samuel J. Danishefsky*

In the previous communication, we described an application of the glycal assembly method to the construction of the Lewis^y

[*] Prof. S. J. Danishefsky, J. T. Randolph
Department of Chemistry, Havemeyer Hall
Columbia University, New York, NY 10027
Telefax: Int. code + (212)854-7142

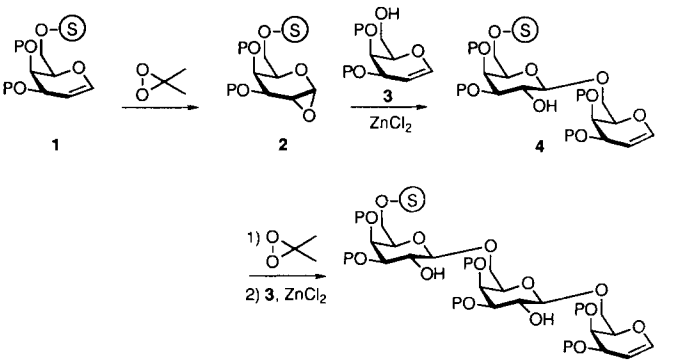
[+] Alternative address:
Memorial Sloan-Kettering Cancer Center
1275 York Avenue, New York, NY 10021
Telefax: Int. code + (212)772-8691

[**] This research was supported by National Institutes of Health (NIH, grant no. AI 16943). An NIH National Research Service Award Postdoctoral Fellowship to J. T. R. is gratefully acknowledged.

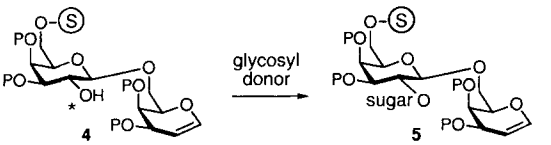
determinant.[1] In this report, we describe the construction of the Lewis^b determinant.[2] As before, our synthesis results in equipping the reducing end of the antigen with a suitable device for subsequent attachment to carrier protein. An intervening spacer element (lactose) is incorporated to insulate the recognition domain from the bioconjugation module.

The Le^b blood group determinant is of particular current interest. Thus, Borén et al. have recently identified the Le^b blood group antigen as a mediator for the binding of *Helicobacter pylori* to human gastric epithelium.[3] In addition, it was found that a Le^b hexasaccharide as well as a soluble neoglycopeptide conjugate of the Le^b antigenic determinant were highly effective agents for inhibiting bacterial binding. This finding is, in principle, of considerable interest. Thus, clinical studies have identified *H. pylori* as a causative agent in gastric and duodenal ulcers.[4] Considerable evidence exists to suggest that antimicrobial treatments are an effective means of dealing with *H. pylori* infection.[5] Since bacterial attachment is a prerequisite to infection,[6] soluble Le^b receptor analogues may emerge as therapeutic candidates which could well serve as alternatives to broad-spectrum antibiotics.

The assembly of the Le^b (type 1) domain was, from our perspective, a more difficult undertaking than was the Le^y (type 2) target, wherein lactal was used as a very convenient starting material. In the case of a type 1 determinant, lactal is obviously not a useful starting material. It seemed appropriate to use the synthesis of the Le^b system as an opportunity to explore significant extensions to our recently disclosed polymer-based oligosaccharide construction method.[7] The essence of that strategy is summarized in Scheme 1. Polymer-bound glycal **1** is activated for glycosyl donation by direct formation of a 1,2-anhydro derivative **2**. Reaction of **2** with acceptor glycal **3** furnishes **4**. Reiteration is achieved by direct epoxidation and reaction with the next acceptor **3**. The self-policing nature of the method, and the major simplification arising from "one time" purification at the end of the synthesis, have been described.[7, 8]



Scheme 1. A strategy for the solid-phase synthesis of oligosaccharides using the glycal assembly method. Ⓢ = solid support, P = protecting group.

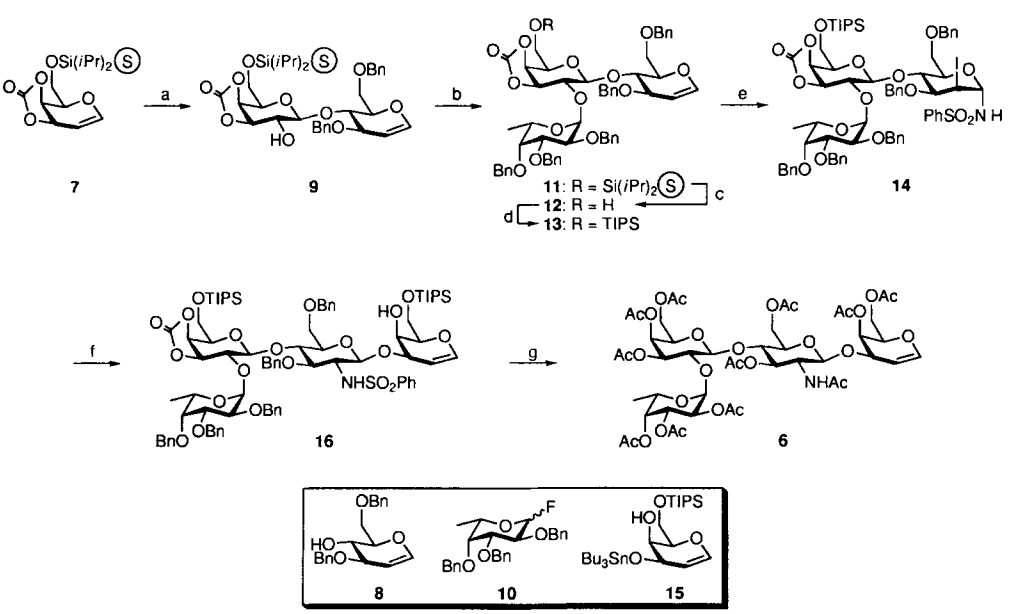


Scheme 2. Application of the solid-support method to the assembly of branching patterns of complex carbohydrates. Ⓢ = solid support, P = protecting group.

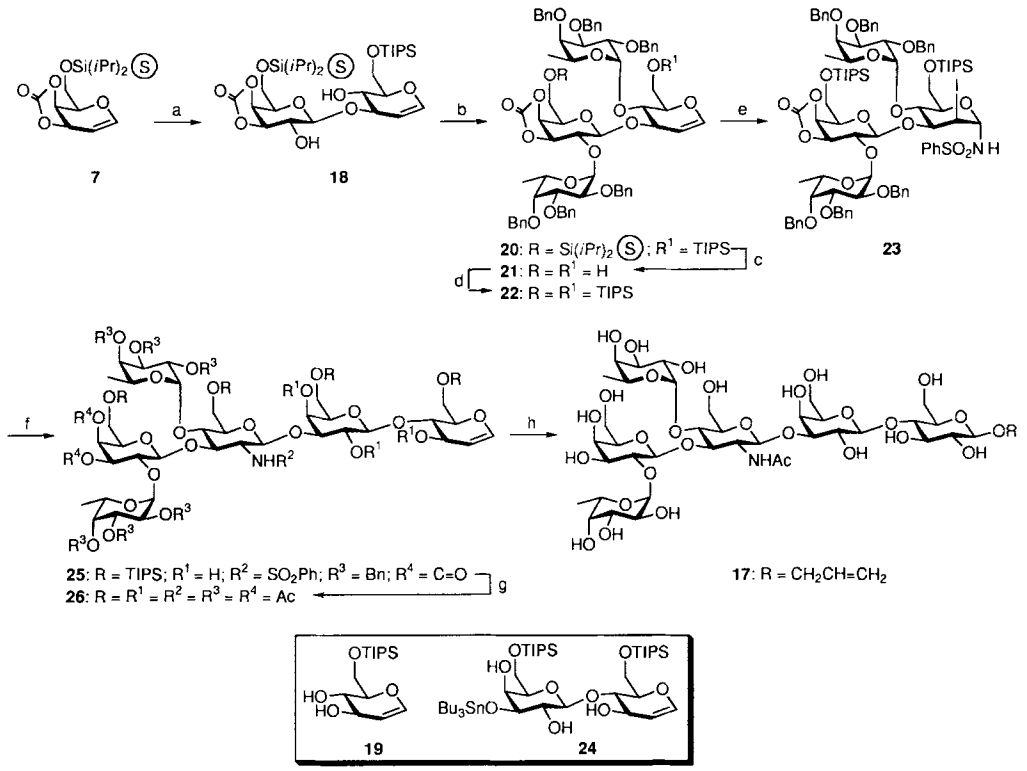
In the work reported herein, we explore an important additional dimension of the polymer-bound method. Here we take cognizance that each glycosylation event generates a unique C_2 hydroxyl (marked with an asterisk in Scheme 2). In principle, (and in fact, vida infra) this hydroxyl group can function as a glycosyl acceptor upon reaction with a solution-based donor. The glycal linkage of **5**, still housed on the support, can be further elongated. In this way, branching at C_2 is accomplished while minimizing the requirement for protecting group machinations.[9]

In principle, this branching can be implemented at any pyranose site in a growing chain. For such an application, it would be necessary to cap all previously generated hydroxyl groups generated on the "polymer side" (nonreducing end) of the growing domain. In short, the nexus of the proposal is that the polymer-bound oligosaccharide can serve as donor or as acceptor wherever appropriate.

The tetrasaccharide glycal **6**, bearing H-type 2 blood group specificity, was our initial goal (Scheme 3). Polymer-supported galactal **7**[10] was allowed to react with a solution of 3,3-dimethyldioxirane[11] to provide the corresponding 1,2-anhydrosugar glycosyl donor, which was treated with a solution of glucal derivative **8** in the presence of $ZnCl_2$ to provide **9**.[12] This polymer-bound disaccharide acted as a glycosyl acceptor upon treatment with a solution of fucosyl fluoride **10**[13] in the presence of $Sn(OTf)_2$. Polymer-bound **11** was thus generated. Retrieval of the trisaccharide glycal from the support was accom-



Scheme 3. Synthesis of a tetrasaccharide having H-type 2 blood group specificity. a) i: 3,3-dimethyldioxirane, CH_2Cl_2; ii: **8**, $ZnCl_2$, THF; b) **10**, $Sn(OTf)_2$, di-*tert*-butylpyridine, THF; c) TBAF, AcOH, THF; d) TIPSCl, imidazole, DMF; e) $I(coll)_2ClO_4$, $PhSO_2NH_2$, CH_2Cl_2; f) **15**, $AgBF_4$, 4 Å molecular sieves, THF; g) i: TBAF, AcOH, THF; ii: Na/NH_3; iii: Ac_2O, pyridine. Ⓢ = solid support.



Scheme 4. Synthesis of a Le^b hexasaccharide in bioconjugatable form. a) i: 3,3-dimethyldioxirane, CH_2Cl_2; ii: **19**, $ZnCl_2$, THF; b) **10**, $Sn(OTf)_2$, di-*tert*-butylpyridine, THF; c) TBAF, AcOH, THF; d) TIPSCl, imidazole, DMF; e) $I(coll)_2ClO_4$, $PhSO_2NH_2$, CH_2Cl_2; f) **24**, $AgBF_4$, 4 Å molecular sieves, THF; g) i: TBAF, AcOH, THF; ii: Na/NH_3; iii: Ac_2O, pyridine; h) i: 3,3-dimethyldioxirane, CH_2Cl_2; ii: allyl alcohol, $ZnCl_2$; iii: NaOMe, MeOH. S = solid support.

plished by using tetrabutylammonium fluoride (TBAF) to afford **12** in 50% overall yield from **7**.[14]

We next demostrated how the trisaccharide, retrieved from the polymer, could be further elaborated. Toward this end, compound **12** was converted to silyl ether **13** by reaction with triisopropylsilyl chloride (TIPSCl). The latter was converted to the iodosulfonamide derivative **14** by the action of $I(coll)_2ClO_4$ in the presence of $PhSO_2NH_2$.[15] Reaction of **14** with the galactal stannyl ether derivative **15** in the presence of $AgBF_4$ gave **16** in 77% yield.[16] Tetrasaccharide glycal **16** was deprotected and then peracetylated to afford **6** (62% overall yield for three steps).

Having accomplished the synthesis of the full H-type determinant by sequential polymer- and solution-based maneuvers, we could direct our attention to the synthesis of the more complex Le^b hexasaccharide **17** (Scheme 4). Polymer-bound galactal **7** was converted to **18** upon epoxidation with 3,3-dimethyldioxirane followed by reaction with glucal derivative **19**. This disaccharide diol was then bisfucosylated by using fucosyl donor **10** in the presence to $Sn(OTf)_2$ to afford **20**. Retrieval from the support with TBAF provided **21**, which was obtained in 40% overall yield from **7**. Compound **21** reacted with TIPSCl to give **22**.

Iodosulfonamide **23**, obtained from **22** using $I(coll)_2ClO_4$ and $PhSO_2NH_2$, reacted with lactal derivative **24** in the presence of $AgBF_4$ to provide the hexasaccharide glycal **25** in 55% yield.[16] Deprotection of **25** was accomplished in two stages (TBAF to remove the silyl ethers, followed by Na/NH_3 reduction to remove the aromatic protecting groups). The crude product was peracetylated to give **26** in a 51% overall yield. Compound **26** was converted, via the 1,2-anhydrosugar derivative, to allyl glycoside **17**, which was readily activated by ozonolysis to the aldehyde ($R = CH_2CHO$). Coupling to the protein human serum albumin (HSA) by the method of Bernstein and Hall was accomplished.[17] Approximately 33 carbohydrate hexamer units were incorporated, presumably at lysine residue sites.

In summary, we have extended our solid-support glycal assembly method for complex carbohydrate domain synthesis to include the branching patterns needed for critical systems in biorecognition processes. Specifically, the determinant for the binding of *H. pylori* to human gastirc epithelium has been stereospecifically fashioned, with simplicity, in a way which provides significant relief from some of the complexities of protecting group manipulations. The biological properties of our new glycoprotein construct will be reported in due course.

There is every reason to believe that the solid-phase methodology to date is only a first generation version of what is possible.[18, 19] Important new variations of the technique and new applications will be described shortly.

Experimental Procedure

6: ^1H NMR (400 MHz, $CDCl_3$): $\delta = 6.39$ (d, 1H, $J = 6.2$ Hz, H_1 galactal), 5.65 (d, 1H, $J = 8.9$ Hz, NHAc), 5.35 (d, 1H, $J = 3.8$ Hz), 5.33 (m, 1H), 5.29 (d, 1H, $J = 2.6$ Hz), 5.27 (d, 1H, $J = 3.1$ Hz), 5.17-5.09 (m, 2H), 4.97-4.90 (m, 2H), 4.81 (dd, 1H, $J = 3$ Hz, $J = 6.1$ Hz, H_2 galactal), 4.75 (d, 1H, $J = 8.0$ Hz), 4.52 (m, 1H), 4.48 (dd, 1H, $J = 12.0$ Hz, $J = 1.6$ Hz, 1H), 4.44-4.06 (m, 8H), 3.88-3.77 (m, 4H), 3.61 (m, 1H), 2.18-1.97 (m, 33H, $COCH_3$), 1.18 (d, 3H, $J = 6.5$ Hz, CH_3 fucose); ^{13}C NMR ($CDCl_3$): $\delta = 170.80$, 170.77, 170.72, 170.67, 170.62, 170.34, 170.21, 170.09, 170.01, 169.99, 169.65, 144.92 (C_1 galactal), 100.22, 98.83, 98.58, 95.55, 74.48, 73.38, 73.13, 73.06, 71.48, 71.01, 70.68, 67.97, 67.42, 67.18, 67.05, 65.94, 64.83, 62.35, 62.22, 60.88, 60.37, 54.21, 23.23, 22.15, 20.85, 20.82, 20.79, 20.76, 20.65, 20.61, 20.57, 15.51 (C_6 fucose); IR (thin film): $\tilde{\nu} = 3368.7$ (NH), 2965.6, 2934.6, 1746.5 (C=O), 1537.5, 1435.9, 1371.3, 1228.5, 1065.0, 1046.0 cm^{-1}; $[\alpha]_D^{23} = -51.1$ ($c = 1.8$, CH_2Cl_2); HRMS (FAB) ($C_{46}H_{63}NNaO_{28}$): calcd: 1100.3434, found 1100.3436.

21: Polymer-bound galactal **7** (loading = 0.75 mmol glycal g^{-1}), which had been placed in a round-bottom flask equipped with a fritted outlet, was suspended in CH_2Cl_2 under N_2, cooled to 0 °C, and then treated with a solution of 3,3-dimethyldioxirane. The mixture was stirred (teflon-coated magnetic stir bar) for 40 min at 0 °C, after which time the soluble material was removed by filtration through the fritted outlet (N_2 pressure). The polymer-bound 1,2-anhydrosugar was evacuated (ca. 0.1 Torr) for several hours in order to dry the material for the next step. This material was once again placed under N_2 before being treated with **19** (ca. 10 molar equivalents as a 0.5 M solution in THF). The suspension was cooled to 0 °C, and treated with $ZnCl_2$ (ca. 2 molar equivalents as a 1.0 M solution in THF). The reaction mixture was allowed to warm slowly to room temperature (over ca. 2 h), and then stirred for an additional 3-4 h. Soluble material was removed by filtration, and polymer **18** was washed several times with THF and then dried in vacuo. Solid $Sn(OTf)_2$ (ca. 4 molar equivalents) was added to compound **18** in a glove bag, and the mixture was placed under N_2 and cooled to 0 °C before being treated with **10** (ca. 5 molar equivalents as a 0.2 M solution in THF) and di-*tert*-butylpyridine (ca. 8 molar equivalents). The suspension was allowed to warm to room temperature and

stirred 8–10 h. The mixture was rinsed with anhydrous THF (2 times), 1,4-dioxane (2 times), again with THF, and then dried in vacuo. Compound **20** (100 mg) was suspended in THF, treated with a 1:3 mixture of AcOH and TBAF (ca. 0.2 M in TBAF, ca. 10 molar equivalents), and the mixture was stirred for 18 h at 40 °C. The polymer was rinsed with THF (3 times), and the combined rinsings were concentrated and purified by column chromatography on silica gel (1:1 EtOAc:hexanes). Compound **21** (18 mg) was obtained as a colorless solid (40% overall yield from 7): ^{1}H NMR (400 MHz, $CDCl_3$): δ = 7.40–7.25 (m, 30H, Ar*H*), 6.18 (d, 1H, J = 6.0 Hz, H_1 glucal), 5.26 (d, 1H, J = 3.5 Hz, H_1 fucose), 5.09 (d, 1H, J = 3.7 Hz, H_1 fucose), 4.96 (dd, J = 10.8 Hz, 2H, PhCH_2), (4.90–4.56 (m, 13H), 4.43 (m, 1H), 4.15–4.06 (m, 4H), 3.97 (dt, 1H, J = 8.3 Hz, J = 2.4 Hz), 3.87–3.65 (m, 10H), 3.64 (d, J = 1.7 Hz, 1H), 3.57 (d, J = 1.7 Hz, 1H), 2.69 (br, 1H, OH), 2.52 (br, 1H, OH), 1.11 (d, 3H, J = 7.0 Hz, CH_3 fucose), 1.09 (d, 3H, J = 7.0 Hz, CH_3 fucose); ^{13}C NMR ($CDCl_3$): δ = 153.37 (C=O), 145.75 (C_1 glucal), 138.60, 138.52, 138.19, 137.61, 128.55, 128.52, 128.44, 128.24, 128.16, 128.07, 127.62, 127.56, 127.45, 98.71, 98.38, 97.65, 97.34, 79.26, 78.87, 78.67, 78.01, 77.79, 77.65, 76.37, 76.10, 74.92, 74.40, 74.16, 73.95, 72.86, 72.64, 72.53, 67.43, 67.29, 61.31, 60.90, 16.65 (C_6 fucose), 16.53 (C_6 fucose); IR (thin film): $\tilde{\nu}$ = 3467.0 (OH), 3029.6, 2923.6, 1807.2 (C=O), 1647.3, 1496.0, 1453.5, 1358.1, 1240.2, 1095.6, 1049.2, 738.5, 697.2; $[\alpha]_D^{23}$ = −82.5 (c = 0.4, CH_2Cl_2); HRMS (FAB): ($C_{67}H_{74}NaO_{18}$): calcd. 1189.4772, found 1189.4757.

25: To a mixture of **23** (60 mg, 34 μmol) and powdered 4 Å molecular sieves (200 mg) under N_2 was added, by canula, a solution of **24** (0.21 mmol) in anhydrous THF (1.5 mL). The stirred suspension was cooled to −78 °C before being treated with a solution of $AgBF_4$ (0.21 mmol) in anhydrous THF (0.25 mL). The mixture was stirred and allowed to slowly warm to room temperature overnight. The suspension, which had developed a bright yellow color, was heated, with stirring, at 45 °C for an additional 36 h, until the TLC (2:5 EtOAc:hexanes) showed no trace of **23**. The mixture was treated with saturated aqueous NH_4Cl (5 mL) and then extracted with EtOAc (3 × 10 mL), and the organic phase was dried over $MgSO_4$. The crude product was purified by silica gel chromatography (1:3 EtOAc:hexanes) to give **25** as a colorless oil (42 mg, 55%): ^{1}H NMR (400 MHz, [D_6]acetone): δ = 8.17 (d, 2H, J = 7.3 Hz, $PhSO_2$), 7.50–7.20 (m, 33H, Ar*H*), 6.52 (d, 1H, J = 10.5 Hz, N*H*), 6.30 (dd, J = 6.0 Hz, J = 1.5 Hz, 1H, H_1 glucal), 5.35–5.32 (m, 2H), 5.25 (d, 1H, J = 7.9 Hz), 5.15 (m, 2H), 4.99–4.92 (m, 3H), 4.86–4.52 (m, 14H), 4.45 (dd, 1H, J = 7.91 Hz, J = 2.4 Hz), 4.32–4.23 (m, 3H), 4.22 (m, 1H), 4.17 (d, 1H, J = 10.1 Hz), 4.08–3.84 (m, 18H), 3.79–3.73 (m, 2H), 3.66 (m, 1H), 3.55 (t, 1H, J = 6 Hz), 3.50 (dd, J = 9.7 Hz, J = 2.8 Hz, 1H), 1.33 (d, 3H, J = 6.5 Hz, CH_3 fucose), 1.31 (d, 3H, J = 6.4 Hz, CH_3 fucose), 1.20–0.98 (m, 84H, 3 × Si(*i*Pr)$_3$); ^{13}C NMR ([D_6]acetone): δ = 145.66 (C=O), 132.72, 131.48, 131.45, 131.28, 131.16, 130.77, 130.48, 121.31, 120.11, 119.86, 119.78, 119.25, 95.63, 94.70, 91.37, 89.64, 89.31, 86.52, 73.38, 72.24, 71.00, 70.71, 70.37, 69.80, 69.59, 69.06, 68.23, 67.92, 67.38, 67.10, 66.49, 65.67, 65.33, 64.60, 64.34, 64.03, 63.45, 63.30, 59.46, 58.83, 58.37, 54.45, 53.32, 49.86, 19.67 (C_6 fucose), 18.42 (C_6 fucose), 9.55, 9.48, 9.45, 9.31, 9.23, 3.82, 3.70, 3.64; IR (thin film): $\tilde{\nu}$ = 3491.9 (OH), 3030.1, 2941.2, 2865.5, 1835.8, 1819.5, 1649.8, 1496.2, 1462.3, 1349.9, 1245.5, 1155.2, 1095.1, 1049.4, 882.2, 734.8, 692.0 cm^{-1}; $[\alpha]_D^{23}$ = −33.8 (c = 2.0, CH_2Cl_2); HRMS (FAB): ($^{12}C_{120}{}^{13}CH_{179}NNaO_{29}SSi_4$): calcd 2278.1292, found 2278.1296.

17: ^{1}H NMR (400 MHz, CD_3OD): δ = 6.00 (m, 1H, CH_2CH=CH_2), 5.37 (dd, 1H, J = 1.6 Hz, J = 7.3 Hz, CH_2CH=CH_2), 5.20 (dd, 1H, J = 1.6 Hz, J = 9.5 Hz, CH_2CH=CH_2), 5.18 (d, 1H, J = 3.9 Hz, H_1 fucose), 5.10 (d, 1H, J = 3.8 Hz, H_1 fucose), 4.64 (d, 1H, J = 6.9 Hz), 4.45 (d, 1H, J = 7.4 Hz), 4.43–4.23 (m, 2H), 4.27 (dd, 1H, J = 9.3 Hz, J = 10.6 Hz), 4.23–4.11 (m, 2H), 4.02–3.29 (m, 31H), 2.06 (s, 3H, NAc), 1.31 (d, 3H, J = 6.6 Hz, CH_3 fucose), 1.29 (d, 3H, J = 6.6 Hz, CH_3 fucose); ^{13}C NMR (CD_3OD): δ = 173.20 (C<=>O), 135.73 (CH_2CH=CH_2), 117.51 (CH_2CH=CH_2), 105.13, 103.30, 102.49, 101.62, 99.63, 96.86, 80.79, 80.67, 78.44, 76.67, 76.49, 75.89, 74.80, 74.59, 73.94, 73.61, 73.40, 71.55, 71.38, 71.16, 70.96, 70.42, 70.26, 70.14, 67.77, 67.30, 67.21, 62.79, 62.34, 61.99, 55.54, 22.97 (NAc), 16.65 (2 C's, C_6 fucose); IR (thin film): $\tilde{\nu}$ = 3376.6 (OH), 2924.2, 1652.5 (C=O), 1383.1, 1032.4 cm^{-1}; $[\alpha]_D^{23}$ = −12.8 (c = 0.25, MeOH); HRMS (FAB): ($C_{41}H_{69}NNaO_{29}$): calcd 1062.3853, found 1062.3837.

Received: March 9, 1994 [Z 6745 IE]
German version: *Angew. Chem.* **1994**, *106*, 1538

[1] V. Behar, S. J. Danishefsky, *Angew. Chem.* **1994**, *106*, 1536; *Angew. Chem. Int. Ed. Engl.* **1994**, *33*, 1468.

[2] For alternative methods for synthesizing Le^b oligosaccharides, see: a) S. S. Rana, J. J. Barlow, K. L. Matta, *Carbohydr. Res.* **1981**, *96*, 231; b) U. Spohr, R. U. Lemieux, *Carbohydr. Res.* **1988**, *174*, 211.

[3] T. Boren, P. Falk, K. A. Roth, G. Larson, S. Normark, *Science*, **1993**, *262*, 1892.

[4] J. Alper, *Science* **1993**, *260*, 159.

[5] a) D. Y. Graham, G. M. Lew, P. D. Klein, D. G. Evans, D. J. Evans, Z. A. Saeed, H. M. Malaty, *Ann. Intern. Med.* **1992**, *116*, 705; b) E. Hentschel, G. Brandstatter, B. Dragosics, A. M. Hirschl, H. Nemeg, K. Schutze, M. Taufer, H. Wurzer, *N. Engl. J. Med.* **1993**, *328*, 308.

[6] N. Sharon in *The Lectins: Properties, Functions and Applications in Biology and Medicine* (Eds.: I. E. Liener, N. Sharon, I. J. Goldstein), Academic, New York, **1986**, pp. 494–525.

[7] a) S. J. Danishefsky, K. F. McClure, J. T. Randolph, R. B. Ruggeri, *Science* **1993**, *260*, 1307. For additional references on the use of polymer supports for oligosaccharide synthesis, see: b) G. H. Veeneman, S. Notermans, R. M. J. Liskamp, G. A. van der Marel, J. H. van Boom, *Tetrahedron Lett.* **1987**, *28*, 6695; c) A. Malik, H. Bauer, J. Tschakert, W. Voelter, *Chem.-Ztg.* **1990**, *114*, 371; d) J. M. J. Frechet in *Polymer-Supported Reactions in Organic Synthesis* (Eds.: P. Hodge, D. C. Sherrington), Wiley, Chichester, UK, **1980**, Chapter 8.

[8] Recently, van Boom et al. (C. M. Timmers, G. A. van der Marel, J. H. van Boom, *Recl. Trav. Chim. Pays-Bas*, **1993**, *112*, 609) found that glycosylation of a particular acceptor with the α epoxide derived from 3,4,6-tri-*O*-benzyl-D-glucal gave only a 4:1 ratio of β:α linked disaccharides. The minor product was previously missed [12] because of its close chromatographic correspondence to the unreacted glycosyl acceptor. With a more complicated acceptor, van Boom confirmed strict β-glycoside preference. Subsequent to our earliest publication, it has been found that the epoxide derived from 3,4,6-tri-*O*-benzyl-D-glucal is the most problematic of the glycosyl donors, which we have occasionally employed, leading to modest amounts of α-glycoside. The implication that the finding of minor amounts of α-glycoside in a particular solution-based experiment invalidates the solid-phase method, which uses completely different resident protecting groups, is, as will be shown, premature.

[9] For an application of this strategy in the synthesis of a complex saponin, see: J. T. Randolph, S. J. Danishefsky, *J. Am. Chem. Soc.* **1993**, *115*, 8473.

[10] The polymer support used in this study was polystyrene crosslinked with 1% divinylbenzene, which was functionalized by using published procedures: T.-H. Chan, W.-Q. Huang, *J. Chem. Soc. Chem. Commun.* **1985**, 909; M. J. Farrall, J. M. J. Fréchet, *J. Org. Chem.* **1976**, *41*, 3877.

[11] R. W. Murray, R. Jeyaraman, *J. Org. Chem.* **1985**, *50*, 2847.

[12] R. L. Halcomb, S. J. Danishefsky, *J. Am. Chem. Soc.* **1989**, *111*, 6661.

[13] K. C. Nicolaou, C. W. Hummel, Y. Iwabuchi, *J. Am. Chem. Soc.* **1992**, *114*, 3126.

[14] We moved our operations to the solution phase because, at this writing, we can not yet implement the azaglycosylation protocols with complex acceptors in the solid phase mode. Work on this goal is in progress.

[15] D. A. Griffith, S. J. Danishefsky, *J. Am. Chem. Soc.* **1990**, *112*, 5811.

[16] S. J. Danishefsky, K. Koseki, D. A. Griffith, J. Gervay, J. M. Peterson, F. E. McDonald, T. Oriyama, *J. Am. Chem. Soc.* **1992**, *114*, 8331.

[17] M. A. Bernstein, L. D. Hall, *Carbohydr. Res.* **1980**, *78*, C1.

[18] Cf. A. Giannis, *Angew. Chem.* **1994**, *106*, 188; *Angew. Chem. Int. Ed. Engl.* **1994**, *33*, 178.

[19] A recent report by Wong et al. describes a major accomplishment in the field in which chemo-enzymatic methods are used to assemble a glycopeptide on a solid support: M. Schuster, P. Wang, J. C. Paulson, C.-H. Wong, *J. Am. Chem. Soc.* **1994**, *116*, 1135.

The First Mononuclear Nitrosyl(oxo)molybdenum Complex: Side-On Bonded and μ_3-Bridging NO Ligands in $[\{MoL(NO)(O)(OH)\}_2]NaPF_6 \cdot H_2O$**

Jochen Böhmer, Gabriele Haselhorst, Karl Wieghardt,* and Bernhard Nuber

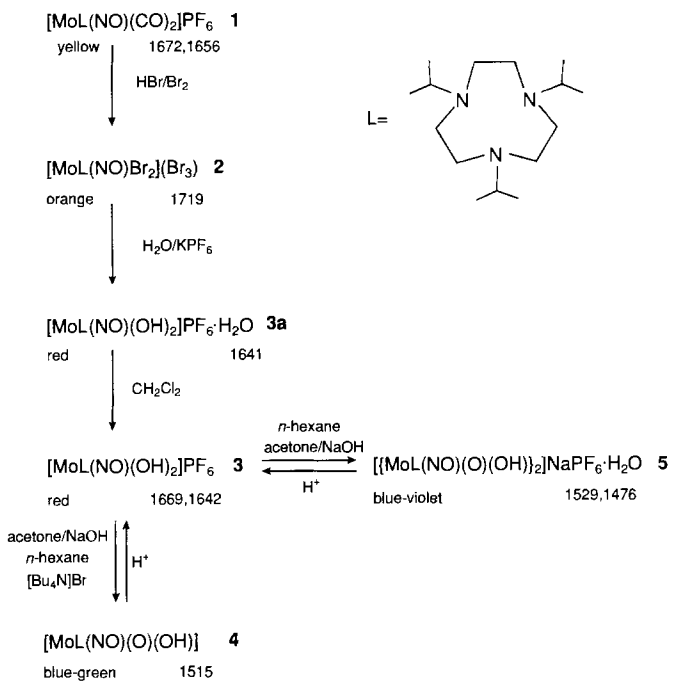
The combination of a strong π donor and a π acceptor ligand in a transition metal complex leads to an interesting situation in terms of electron density, because a strong ($p_\pi \rightarrow d_\pi$)-donor bond requires an electron-deficient metal center, whereas stable ($d_\pi \rightarrow p_\pi$)-backbonding requires an electron-rich metal center. An example of a strong π acceptor is the nitrosyl ligand, and the terminal oxo group is a good π donor. Mononuclear nitrosyloxo complexes are as yet unknown,[1] but two μ-oxo-bridged nitrosylmolybdenum complexes[2, 3] of the $\{Mo-NO\}^4$ type[4] have been structurally characterized. In both cases, the $Mo-O_{oxo}$ dis-

[*] Prof. Dr. K. Wieghardt, J. Böhmer, G. Haselhorst
Lehrstuhl für Anorganische Chemie I der Universität
D-44780 Bochum (FRG)
Telefax: Int. code + (234)7094-378
Dr. B. Nuber
Anorganisch-Chemisches Institut der Universität
Heidelberg (FRG)

[**] This work was supported by the Fonds der Chemischen Industrie.

tances are short (about 1.89 Å) and indicate multiple bond character. McCleverty et al.[5] have also shown that the Mo-O_{oxo} bonds of octahedral alkoxonitrosylmolybdenum(II) complexes have ($p_\pi \rightarrow d_\pi$) double-bond character. They explained this finding by the 18-electron configuration yielded by the formation of an oxygen–metal ($p_\pi \rightarrow d_\pi$) double bond.

We have now tried to synthesize nitrosylmolybdenum complexes of the $\{Mo-NO\}^4$ type containing a terminal oxo ligand based on the following considerations: although the $\{Mo-NO\}^4$ unit is sufficiently electron-rich to stabilize a linear Mo–NO group, it leads in octahedral complexes containing five purely σ ligands only to relatively electron-deficient 16-electron species. The formation of a ($p_\pi \rightarrow d_\pi$) oxygen–metal bond should therefore give a complex having a stable 18-electron configuration. Our intention was to suppress potential μ-oxo-bridging, by using the sterically demanding cyclic triamine 1,4,7-triisopropyl-1,4,7-triazacyclononane (L).[6] Scheme 1 shows the synthetic



Scheme 1. Preparation of **1**–**5**. The numbers indicate the ν(NO) stretching frequencies in cm^{-1} (KBr pellets).

route to the first mononuclear nitrosyloxomolybdenum complex. Nitrosylation of $[MoL(CO)_3]$[6] with $NaNO_2$ and HCl in methanol, followed by addition of KPF_6, gave yellow, air-stable crystals of salt **1**, which contains an 18-electron complex cation of the $\{Mo-NO\}^6$ type. Oxidation of **1** with bromine in 48% HBr yielded salt **2** (the 16-electron complex cation is of type $\{Mo-NO\}^4$). The bromide ions in the cation of **2** are relatively substitution-labile and can be exchanged for two OH^- groups in a boiling H_2O/tetrahydrofuran mixture (3:1). This exchange produced salt **3**, which could also be isolated in crystalline form as the monohydrate **3a**. Interestingly, a solution of **3** in acetone, which is initially red, changes its color to blue-green upon addition of NaOH. When such a solution was salted out with [nBu$_4$N]Br and overlaid with n-hexane, slow diffusion of the two layers gave blue-green crystals of the neutral complex **4**. When no $[Bu_4N]Br$ was added, blue-violet single crystals of **5** crystallized. Aqueous solutions of **4** and **5** slowly revert to red **3**; this conversion takes place rapidly when protons are added. The pK_a

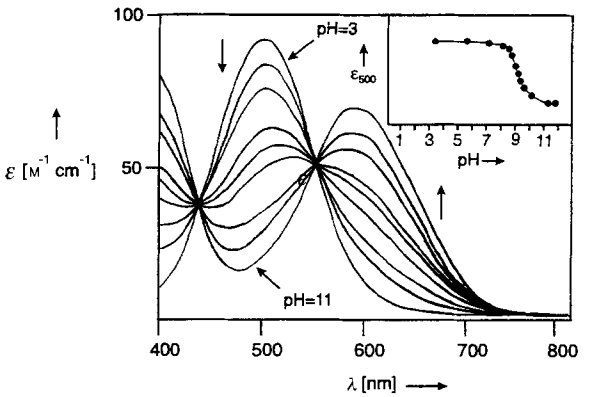


Fig. 1. Electronic spectrum of an aqueous solution of **3** as a function of pH (3–12). The insert shows the molar absorption coefficient at 500 nm as a function of pH.

of the acid/base equilibrium (a) was determined by spectrophotometry (Fig. 1) and, separately, by titration to be 9.0(1) at 20 °C in H_2O.

$$3 \rightleftharpoons 4 + H^+ \qquad \text{(a)}$$

The X-ray structure analyses[7] of **3** and **4** (Figs. 2 and 3 and Table 1) confirm the mononuclear structures. The MoL(NO)

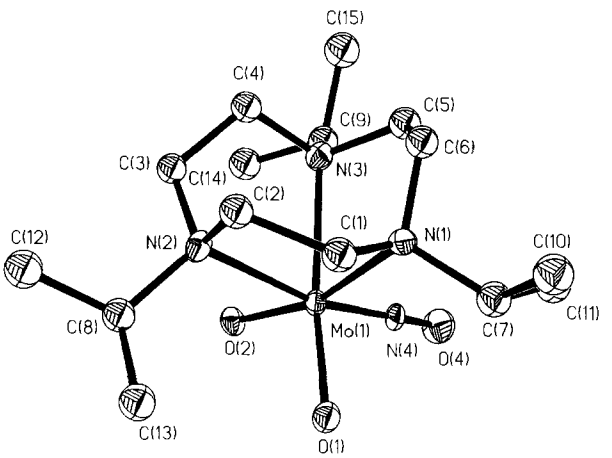


Fig. 2. Structure of the monocation in crystals of **3**.

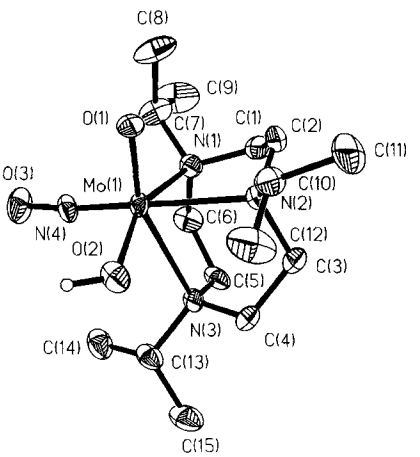


Fig. 3. Structure of the nitrosyloxo complex in crystals of **4**.

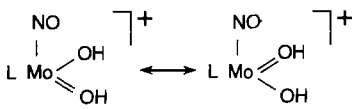
 © VCH Verlagsgesellschaft mbH, D-69451 Weinheim, 1994 0570-0833/94/1414-1474 $ 10.00+.25/0

Table 1. Selected bond lengths [Å] and angles [°] of the *fac*-[N_3Mo(NO)XY] skeleton in **3**–**5**.

	3	**4**	**5** [f]	
Mo-NO	1.748(4)	1.761(8)	1.748(4)	1.747(4)
N-O	1.195(6)	1.215(11)	1.241(5)	1.265(6)
Mo-X	1.903(4)	1.775(5) [c]	1.781(3) [c]	1.754(4) [c]
Mo-Y	1.919(4)	1.983(7) [d]	1.940(4) [d]	1.943(4) [d]
Mo-N_{trans} [a]	2.349(4)	2.424(8)	2.444(4)	2.448(4)
Mo-N_{cis} [b]	2.298(4)	2.460(7) [e]	2.452(4) [e]	2.475(4) [e]
	2.348(4)	2.310(7)	2.444(4)	2.332(4)
Mo-N-O	177.0(4)	175.0(8)	171.1(4)	173.8(4)
X-Mo-Y	103.0(2)	103.6(3)	103.5(2)	103.2(2)

[a] Mo–N distance *trans* to the Mo–NO unit. [b] Mo–N distances *cis* to the Mo–NO unit. [c] Mo=O distance. [d] Mo–$O_{hydroxy}$ distance; [e] Mo–N distance *trans* to Mo=O unit; [f] the data in the first column refer to the neutral complex [MoL(NO)(O)(OH)] with side-on coordination of the NO ligands to one Na^+ ion, and those in the second column to the complex with O coordination of the NO ligand to two Na^+ ions (Fig. 4).

fragment is present in both complexes; the Mo–NO unit is nearly linear and the M–NO distance of 1.75 Å is short and invariant; it corresponds to that of an Mo–N multiple bond displaying efficient ($d\pi \rightarrow p\pi$) backbonding. The differences in the N–O bond lengths are not significant within the relatively large experimental error. This is an astounding result in the light of the large variation in stretching frequency from 1719 cm^{-1} in **2** to 1476 cm^{-1} in **5**. The Mo–O bonds of the two *cis* hydroxo ligands in **3** are approximately 1.90 Å long and thus somewhat shorter than a Mo–O single bond, whose length is typically 1.98–2.10 Å. If the double bond is resonance-stabilized, the cation in **3** attains an 18-electron configuration (Scheme 2). The large O-Mo-O bond angle of 103.0(2)° also lends support to this interpretation.



Scheme 2.

Deprotonation of the cation in **3** yields the mononuclear nitrosyloxomolybdenum complex **4**, the structure of which is shown in Figure 3. The very short Mo–O_{oxo} distance of 1.775(7) Å is an indication of the ($p_\pi \rightarrow d_\pi$) double-bond character of the Mo=O group, whereas the Mo–$O_{hydroxo}$ bond of 1.983(7) Å must be interpreted as a single bond, since it is significantly longer than in **3**. In the IR spectrum of **4**, the ν(Mo=O) stretching band is at 813 cm^{-1}. The ν(OH) stretching band can also be detected unambiguously as a sharp band at 3648 cm^{-1}. Neither the oxo nor the hydroxo group is involved in the intermolecular O–H···O interactions in the crystal packing of **4**.

The crystal structure of **5** (Fig. 4) is notable. The unit cell contains two crystallographically independent neutral [MoL(NO)(O)(OH)] complexes that are coordinated to the Na^+ ions to give a tetranuclear structural unit and form the centrosymmetric dication $[\{MoL(NO)(O)(OH)\}_4Na_2(H_2O)_2]^{2+}$ in the crystal assembly. These units are linked to one another through an intermolecular O(4)···H–O(1a)–H hydrogen bond (not shown in Fig. 4); the charge is balanced by isolated PF_6 anions.

Interestingly the nitrosyl groups of the two crystallographically independent neutral complexes of the cluster are coordinated to the Na^+ ions in different ways. The NO groups of Mo(1) forms a side-on bond, since the N(4)–Na(1) and Na(1)–O(2) distances of 2.775(4) and 2.782(4) Å are almost identical. The shortest calculated distance of the Na^+ ion from the π electron density of this NO^+ ligand is 2.71 Å. In contrast, the NO group of Mo(2) is attached to two Na^+ ions through the bridging O(6)

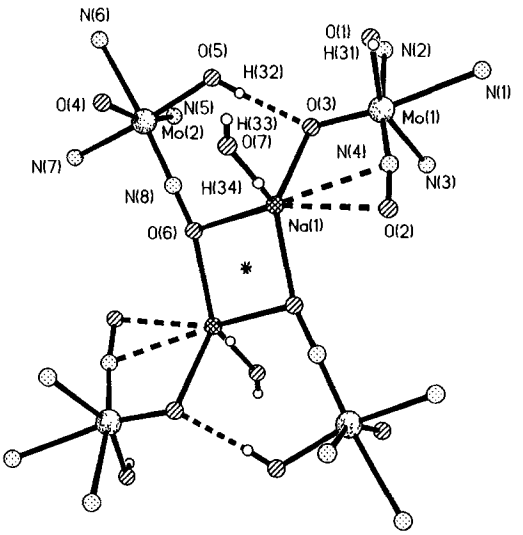
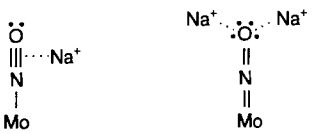


Fig. 4. Schematic structure of a $[\{MoL(NO)(O)(OH)\}_4Na_2(H_2O)_2]^{2+}$ cluster in crystals of **5**. The neutral [MoL(NO)(O)(OH)] unit corresponds largely to that in **4**. For clarity, the carbon atoms and the hydrogen atoms attached to this unit are not shown; * is a crystallographic center of symmetry. Selected distances [Å] (see also Table 1): Na(1)-N(4) 2.775(4), Na(1)-O(2) 2.782(4), Na(1)-O(3) 2.435(4), Na(1)-O(6a) 2.543(4), Na(1)-O(7) 2.366(4); Na(1)-O(6) 2.386(4); Na(1)···Na(1a) 3.791(3); O(3)···O(5) 2.748(6), O(4)···O(1a) 2.715(6).

(μ_3-(NO)-1-κN:2,3-$\kappa^2 O$). In an idealized form, the bonding of the two new structural motifs can be represented by the resonance structures shown in Scheme 3. The Na···O and Na···N interactions are likely to be predominantly of an ionic nature.



Scheme 3.

The Na^+ ion completes its coordination sphere by binding to the oxo group O(3) at Mo(1) and by binding to a water molecule; the overall structure is a strongly distorted NO_5Na octahedron. Within the cluster, the OH group at Mo(2) forms an intramolecular hydrogen bond to the oxo group O(3) at Mo(1). It is instructive to compare the IR spectroscopic properties of the neutral [MoL(NO)(O)(OH)] complexes in **4** and **5** with their structural properties, because the ν(NO) stretching frequency is a sensitive guage of different electron density distributions. In

Table 2. Selected physical data of **1**–**5**. ^1H NMR: 400 MHz; IR: KBr pellet

1: ^1H NMR (CD_3CN): $\delta = 1.21$ (d, 6H, -CH_3), 1.31 (d, 6H, -CH_3), 1.33 (d, 6H, CH_3), 2.79-3.13 (m, 12H, -CH_2-), 3.19 (sep, 1H, -$HC(CH_3)_2$), 3.48 (sep, 2H, -$HC(CH_3)_2$). IR: ν_{as}(CO) 2016; ν_s(CO) 1927,1913; ν(NO) 1672, 1656 cm^{-1}. UV/VIS (CH_3CN): λ_{max} (ε·L mol^{-1} cm^{-1}) 265 (3850), 395 nm (170).

2: IR: ν(NO) 1719 cm^{-1}; $[MoL(NO)Br_2]BF_6$: IR: ν(NO) 1724, 1708 cm^{-1}. UV/VIS (CH_3CN): λ_{max} (ε, L mol^{-1} cm^{-1}) 306 (2950), 438 nm (4590).

3: ^1H NMR (CD_3CN): $\delta = 1.05$ (d, 6H, -CH_3), 1.07 (d, 6H, -CH_3), 1.19 (d, 6H, -CH_3), 2.56–3.03 (m, 12H, -CH_2), 3.40 (sep, 2H, -$HC(CH_3)_2$), 3.55 (sep. 1H, -$HC(CH_3)_2$), 12.25 (s, 2H, OH); $^{13}C\{^1H\}$ NMR (100,6 MHz, CD_3CN): $\delta = 62.7$, 57.0, 52.6, 50.6, 49.8, 29.7, 19.2, 16.8. IR: ν(OH) 3564, 3546, ν(NO) 1669, 1642 cm^{-1}. UV/VIS (CH_3CN): λ_{max} (ε, L mol^{-1} cm^{-1}) 265 (7200), 495 nm (90).

4: ^1H NMR ($NaOCD_3/CD_3OD$): $\delta = 0.92$ (d, 6H, -CH_3), 0.97 (d, 6H, -CH_3), 1.04 (d, 6H, -CH_3), 2.32–2.73 (m, 12H, -CH_2-), 3.33 (sep, 2H, -$HC(CH_3)_2$), 3.76 (sep, 1H, $HC(CH_3)_2$); $^{13}C\{^1H\}$ NMR (100,6 MHz, $NaOCD_3/CD_3OD$): $\delta = 62.8$, 61.5, 57.9, 52,0, 51.1, 19.7, 18.2, 18.1. IR: ν(OH) 3648, ν(NO) 1515, ν(M=O) 813 cm^{-1}. UV/VIS (H_2O, pH 11.5): λ_{max} (ε, L mol^{-1} cm^{-1}) 230 (6500), 330 nm (480), 400(sh), 590 nm (75).

5: IR: ν(NO) 1529, 1476, ν(H_2O) 3401, 3247 cm^{-1}.

 © VCH Verlagsgesellschaft mbH, D-69451 Weinheim, 1994 0570-0833/94/1414-1475 $ 10.00+.25/0

the crystals of **4**, in which the neutral complexes are not linked to one another by hydrogen bonds or even Na^+ ions, the observed ν(NO) frequency is observed at 1515 cm^{-1}. It thus appears at a much lower energy than in **2** (1719 cm^{-1}) or in **3** (1669, 1642 cm^{-1}). This effect must be attributed to the different strengths of the ($p_\pi \rightarrow d_\pi$) donor bonds in the complexes: the two Br^- ligands in **2** are weaker π-donor ligands than the two HO^- ligands in **3**, whereas the terminal oxo group in **4** is a very strong π donor. The occupation of the π*(NO) orbitals increases in the order $Br^- < HO^- < O^{2-}$, which is related to a weakening of the N–O bond.

As described above, in the crystals of **5** the NO ligands are coordinated to the Na^+ ions in two ways. The IR spectrum therefore shows two ν(NO) vibrations of relatively low intensity, one at 1529 cm^{-1} and the other at the very low frequency of 1476 cm^{-1}(!). The corresponding oxo ligands are also coordinated in different ways: because of the coordination of O(3) to Na(1) and its participation in an intramolecular O-H···O bond, the Mo(1)–O(3) distance is 1.781(3) Å and thus significantly longer than the Mo(2)–O(4) distance of 1.754(3) Å where O(4) only participates in a weak intermolecular O-H···O bond. The oxo group Mo(1)=O(3) in **5** is therefore a comparatively weaker π donor, which is why the higher energy NO stretching frequency of 1529 cm^{-1} should be assigned to this neutral complex. The N–O bond in the complex containing the Mo(2)=O(4) group (stronger π donor) is weakened to a greater extent. This effect may even be intensified by coordination of the NO ligands to *two* Na^+ ions through the oxygen atom O(6). The low-energy ν(NO) stretching frequency of 1476 cm^{-1} is therefore assigned to the neutral complex containing the (μ_3-(NO)-1-κN:2,3-$\kappa^2 O$) bridge. Although this interpretation is supported by the two different N–O bond lengths of 1.241(5) and 1.265(6) Å, the difference is just within experimental error (3 σ).

Complexes **2**, **3**, **4**, and **5** are isoelectronic $\{Mo-NO\}^4$ compounds. The electron density on the molybdenum center is formally increased by the strong π donor O^{2-} in **4** and **5** but can again be lowered by occupation of the π*(NO) orbitals to give a nitrosyl ligand of typical NO^- character. This synergistic bonding model is shown in Figure 5: the d_{xz} orbital localized on the central atom is occupied by two electrons in the $\{Mo-NO\}^4$ complexes as is the p orbital on the O^{2-} ligand, whereas the π* orbital on the NO ligand is initially unoccupied, which implies that π electron density is transferred from the O^{2-} ligand to the Mo center and from there to the π*(NO) orbital.

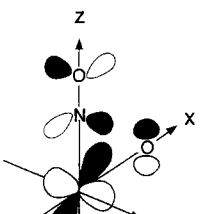


Fig. 5. Model of the π-bonding in the Mo(NO)(O) unit in **4** and **5**.

Experimental Procedure

1: 36% HCl (10 mL) was slowly added to a stirred mixture of [MoL(CO)$_3$] (1.0 g, 2.3 mmol) and $NaNO_2$ (0.30 g, 4.3 mmol) in methanol (100 mL) to give a clear yellow solution accompanied by foaming. After removal of the solvent, the yellow residue was dissolved in H_2O (200 mL), the resulting solution filtered, and a solution of KPF_6 (0.30 g) in H_2O (100 mL) added to the filtrate. A yellow precipitate formed. Yield: 1.20 g (90%).

2: Bromine (1.0 mL) was added to a solution of **1** (1.0 g, 1.7 mmol) in 48% HBr (30 mL), which was then stirred for 10 min. The orange, microcrystalline product obtained was filtered off and washed with ether. Yield: 1.0 g (75%). The analogous PF_6^- salt was obtained from **2** after addition of $NaPF_6$.

3, **3a**: A solution of **2** (1.0 g, 1.3 mmol) in H_2O (30 mL) and tetrahydrofuran (10 mL) was heated at reflux for 5 h. KPF_6 (1.0 g) was added to the filtered solution. Slow evaporation of the solvent gave red crystals of the monohydrate **3a**. Yield: 0.60 g (85%). The anhydrous compound **3** was obtained by recrystallization of **3a** from CH_2Cl_2.

4: Solid NaOH (0.05 g) was added to a solution of **3** (0.10 g, 0.17 mmol) in acetone (1.0 mL), followed by stirring. After the color had changed from red to blue-green, $[Bu_4N]Br$ (0.05 g) was added, and the solution was overlaid with *n*-hexane (1 mL). Slow diffusion of the two layers produced crystals of **4**. Yield: about 0.03 g.

5: When synthesis of **4** was carried out without the addition of $[Bu_4N]Br$, violet crystals of **5** precipitated. Yield: about 0.03 g.

All compounds gave correct elemental analyses (C,H,N).

Received: January 27, 1994
Revised version: February 19, 1994 [Z 6647 IE]
German version: *Angew. Chem.* **1994**, *106*, 1556

[1] G. B. Richter-Addo, P. Legzdins, *Metal Nitrosyls*, Oxford University Press, New York, **1992**.

[2] H. Adams, N. A. Bailey, G. Denti, J. A. McCleverty, J. M. A. Smith, A. Wlodarczyk, *J. Chem. Soc. Dalton Trans.* **1983**, 2287.

[3] D. Sellmann, B. Seubert, F. Knoch, M. Moll, *Z. Anorg. Allg. Chem.* **1991**, *600*, 95.

[4] J. H. Enemark, R. D. Feltham, *Coord. Chem. Rev.* **1974**, *13*, 339. According to this reference, the electron configuration of a nitrosyl complex is given in the $\{M-NO\}^n$ notation, where *n* is the number of electrons in metal d orbitals plus the number of electrons in the π*(NO) orbital, or, in more simple terms, the usual number of d electrons of the L_yM fragment if the NO is formally considered to be bonded as NO^+. Jones, J. A. McCleverty, *J. Chem. Soc. Dalton Trans.* **1990**, 3577.

[6] G. Haselhorst, S. Stoetzel, A. Strassburger, W. Walz, K. Wieghardt, B. Nuber, *J. Chem. Soc. Dalton Trans.* **1993**, 83.

[7] **3**: $C_{15}H_{35}N_4O_3MoPF_6$, crystals from CH_2Cl_2; monoclinic, space group $P2_1/c$, $a = 12.283(5)$, $b = 8.237(3)$, $c = 22.20(1)$ Å, $\beta = 91.15(4)°$, $Z = 4$; $\rho_{calcd} = 1.66\ g\,cm^{-3}$; $\mu_{Mo} = 0.73\ mm^{-1}$; 4869 observed reflections ($I \geq 2.5\,\sigma(I)$); empirical absorptions correction, Ψ scans; $2\theta_{max} = 60°$; $R = 0.059$; $R_w = 0.054$; max. residual electron density 0.48 $e^-\,Å^{-3}$; PF_6^- is disordered. C*H* in calculated positions, O*H* not located on last difference Fourier map. **4**: $C_{15}H_{34}N_4O_3Mo$, crystals from acetone, monoclinic, space group Cc, $a = 13.624(3)$, $b = 16.831(4)$, $c = 8.594(1)$ Å, $\beta = 107.1(1)°$, $Z = 4$, $\rho_{calcd} = 1.46\ g\,cm^{-3}$, $\mu_{Mo} = 0.716\ mm^{-1}$; 1404 observed reflections ($I \geq 2.0\,\sigma(I)$); no absorption correction; $2\theta_{max} = 50°$; $R = 0.040$; $R_w = 0.034$; max. residual electron density 0.62 $e^-\,Å^{-3}$, C*H* in calculated positions, O*H* position obtained from difference Fourier synthesis. The polarity was tested by carrying out refinement calculations in both enantiomeric configurations. The configuration giving smaller R values was assumed to be the correct one. **5**: $C_{30}H_{70}F_6Mo_2N_8NaO_7P$; crystals from acetone monoclinic, space group $P2_1/c$ (No 14), $a = 9.809(2)$, $b = 28.728(7)$, $c = 15.144(4)$ Å, $\beta = 95.34(2)°$, $Z = 4$, $\rho_{calcd} = 1.62\ g\,cm^{-3}$, $\mu_{Mo} = 0.716\ mm^{-1}$; 5505 observed reflections ($I \geq 2.0\,\sigma(I)$); no absorption correction, $2\theta_{max} = 50°$; $R = 0.045$; $R_w = 0.042$; max. residual electron density of 2.07 $e^-\,Å^{-3}$ in the vicinity of the slightly disordered PF_6^- anions; C*H* in calculated positions, O*H* positions obtained from difference Fourier synthesis. The attempts to model (split atom model) the disorder of the PF_6^- anions were unsuccessful; the intensities of the reflections were measured on a Syntex R3 (**3**) or on a Siemens P4 (**4**, **5**) diffractometer at room temperature using $Mo_{K\alpha}$ radiation ($\lambda = 0.71073$ Å). The structures were solved by Patterson syntheses (**3**) or direct methods (**4**, **5**) and refined for all independently observed reflections using *F* (heavy atoms calculated with anisotropic and H atoms with isotropic temperature factors); $R_w = \{\Sigma w(|F_o| - |F_c|)^2/|F_o|^2\}^{1/2}$. Program used: SHELTXL-PLUS (PC version; G. M. Sheldrick, Universität Göttingen). Further details of the crystal structure investigations are available on request from the Fachinformationszentrum Karlsruhe, D-76344 Eggenstein-Leopoldshafen (FRG), on quoting the depository number CSD-58173.

On the Helicity of Oligomeric Formaldehyde

Christian R. Noe,* Christian Miculka, and Jan W. Bats

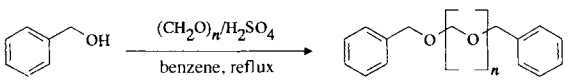
Since the formulation of the term "stereoelectronic factor" by E. J. Corey a multitude of work has been carried out illustrating the existence and the significance of this effect.[1] Nevertheless,

[*] Prof. C. R. Noe, Dr. C. Miculka
Christian Doppler Laboratorium
Institut für Pharmazeutische Chemie der Universität
Marie-Curie-Strasse 9, D-60439 Frankfurt/Main (FRG)
Telefax : Int. code + (69) 5800-9352
Dr. J. W. Bats
Institut für Organische Chemie der Universität Frankfurt

this concept still meets with skepticism.[2] The main reason for this is that most of the investigations are carried out on polar, multifunctional carbohydrates, in which the relatively weak stereoelectronic effects can often be hidden by other factors. In addition, certain cases of the stereoelectronic effect, such as the anomeric or *gauche* effect, are frequently interpreted as isolated phenomena of individual bonds, and the stereoelectronic properties of the molecule as a whole are neglected. The purpose of investigations into stereoelectronic effects should be to indicate the possibilities and limitations of the interpretation based on considerations of the relevant frontier orbital interactions such as $n-\sigma^*$, $\pi-\sigma^*$, $n-\pi^*$, $\sigma-\sigma^*$, and $\sigma-\pi^*$, which are offered by the very visual valence bond model.

Poly(oxymethylene) can be considered an almost ideal example of a compound with a stereoelectronically determined conformation, because in this simple molecule each bond can be fixed stereoelectronically. The helical conformation of polymeric formaldehyde has been known for a long time[3] and clearly differentiates this compound from polyethylene, which lacks special stabilization and prefers the expected achiral *anti* conformation on steric grounds. Previously, we interpreted the *gauche* configuration of oligomeric formaldehyde determined by X-ray data[4] as an indication of the stereoelectronic effect: we noticed a diastereoselective 1,10 induction between inducing and prochiral centers, which were separated by a tetra(oxymethylene) chain. The direction and extent of the observed induction in the reaction was attributed to the helical stabilization of the chain by stereochemical effects. An X-ray structure analysis of oligo- or poly(oxymethylene)s providing structural details such as bond lengths, bond angles, and torsion angles has not yet been reported.

The melting point of the dimethyl-substituted pentamer of formaldehyde is 18.3 °C.[5] We attempted, therefore, to obtain higher melting formaldehyde oligomers by simply heating paraformaldehyde and benzyl alcohol under acid catalysis. We chose benzyl alcohol since the phenyl group, as well as the oxygen atom, is a "stereoelectronically active", planar (pl) ligand[6] on account of its σ^* orbital. This reaction provided a mixture of chromatographically separable products **1**–**5**.[7]



$n = 1 - 5$

1 - 5

Crystals of the pentamer **5** suitable for X-ray analysis could be obtained by low-temperature crystallization from chloroform/hexane.[8] The unit cell contains two independent molecules, which have a C_2 axis passing through the central carbon atom (Fig. 1). All the torsion angles in the chain are between $-62°$ and $-68°$ and indicate the expected *gauche* configuration, which results in helicity. Since both helices have the same handedness and thus the same absolute configuration, it can be assumed that **5** crystallizes in two enantiomorphic crystal forms.

Consideration of the molecules in the unit cell indicates that they are not identical but rather conformational isomers differentiated by the orientation of the benzyl groups. In molecule **A** the continuous (−)-*gauche* conformation of the chain is continued up to C_{Ar} of the phenyl group; the aryl ligand thus assumes the expected position of a pl ligand following the critera of the b(ulky), pl(anar), H rule (Fig. 2).[6] In molecule **B** C_{Ar} of the phenyl group lies almost antiperiplanar to the first carbon atom

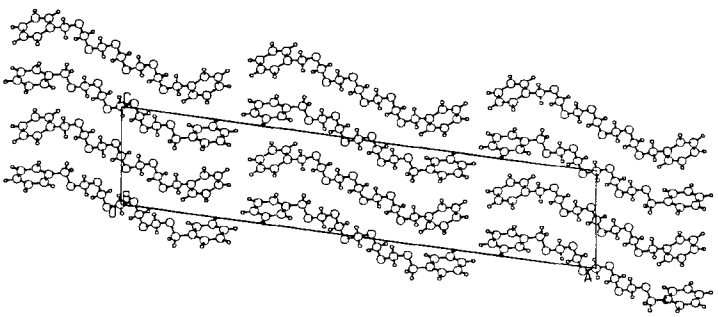


Fig. 1. Crystal structure of **5**; helical conformers with the same absolute configuration within the unit cell are shown.

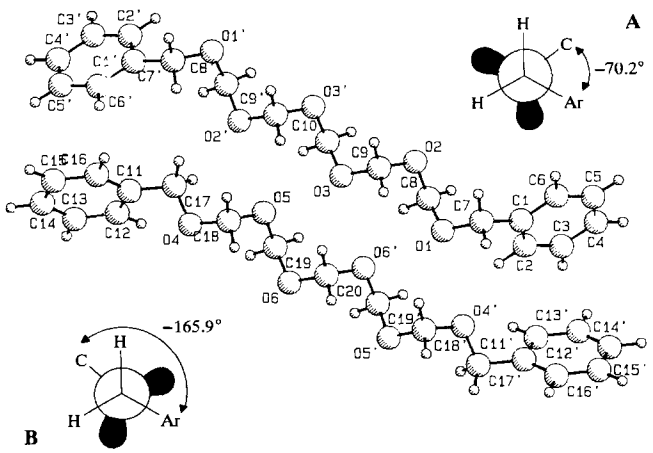


Fig. 2. The two conformational isomers of **5**. In molecule **A** a nonbonding electron pair of the first oxygen atom lies synperiplanar to the antibonding orbital of the aromatic unit (pl ligand).

in the chain, thus assuming the preferred position of a b ligand according to the b, pl, H classification.

The definition of "stereoelectronically determined" bond lengths and angles is provided best by an oligomeric oxymethylene structure. Uniform $n-\sigma^*$ interactions between all atoms along the chain occur without disturbance from other structural elements. The concomitant regular shortening of bonds should in turn be apparent in an X-ray structural analysis. In this respect the results are remarkable: there is not a continuous, symmetrical reduction in bond lengths such that the bonds are close to the same length. Rather a systematic pattern of bonding is seen along the chain (Table 1). In the middle of the chain two shortened bonds (bond lengths ca. 139 pm) alternate with two normal bonds (bond lengths ca. 142 pm). Each oxygen atom has one shortened bond and one of normal length. Partic-

Table 1. Observed bond lengths in the chain of **5** in pm (in each case the second half of the molecule is ignored).

Molecule **A**		Molecule **B**		**A** − **B**
C1-C7	149.7(5)	C11-C17	**147.2(4)** [a]	+2.5
C7-O1	**140.3(4)**	C17-O4	143.9(4)	−3.6
O1-C8	**139.5(4)**	O4-C18	**137.8(4)**	+1.7
C8-O2	142.0(4)	C18-O5	**139.8(4)**	+2.2
O2-C9	**138.6(4)**	O5-C19	141.6(4)	−3.0
C9-O3	**139.3(4)**	C19-O6	142.0(4)	−2.7
O3-C10	142.0(4)	O6-C20	**139.1(4)**	+2.9

[a] Values are given in boldface to emphasize the pairs of similar bond lengths.

 © VCH Verlagsgesellschaft mbH, D-69451 Weinheim, 1994 0570-0833/94/1414-1477 $ 10.00+.25/0

ularly amazing is that the molecules **A** and **B** in the unit cell are, to our knowledge, isomers of a type not previously known. For each bond in the chain the difference in the bond lengths in the two isomers is at least 1.7 pm (in the middle of the chain on average 2.8 pm).

In the benzyl groups of conformer **B** the $C_{Ar}-CH_2$ bond is shortened. This effect is made plausible by the almost orthogonal position of the aromatic unit to the C—O bond and the concomitant $\pi-\sigma^*$ interactions. As is indicated by the bond angle at the benzylic carbon atom (Fig. 3), this should be substantially weaker than the $n-\sigma^*$ interactions in molecule **A**. It is probable that the pattern of bond lengths in the oxymethylene chain in **A** is influenced by the ends of the molecule.

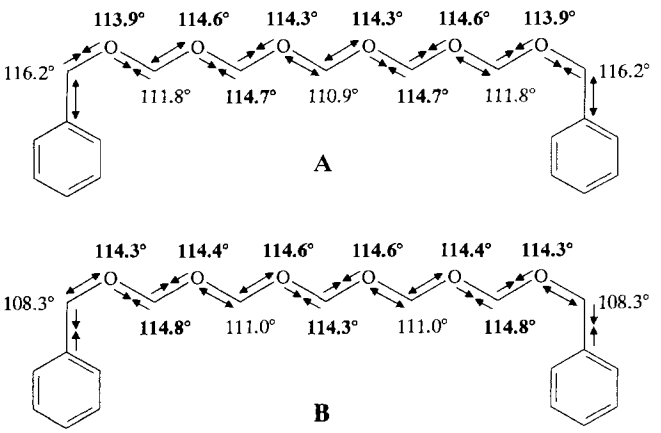


Fig. 3. Patterns of bond lengths and angles in the pentameric formaldehyde derivative **5**.

In connection with stereoelectronic effects the discussion often circles round the question of whether the geometry at the oxygen atom is better described by canonical orbitals or, on practical grounds, by the preferred, graphic model of sp^3 hybridization.[1a] Actually the observed angles lie consistently in a range between 120° (trigonal planar) and 109.5° (sp^3 tetrahedral angle). The oxymethylene structure offers the opportunity to define a standard value for a "stereoelectronically determined" bond angle at oxygen of 114.4° (Fig. 3).

While the bond angles at oxygen in both molecules **A** and **B** indicate almost no variation, the carbon atoms in the chain have an alternating pattern of bond angles, which should be eliminated by the stereoelectronic contribution to their bonding which imparts an increased double bond character (which would be characterized in turn by an increase in the bonding angle towards sp^2). Thus, the O-C-O angle at each carbon atom between two shortened bonds corresponds very closely to the angles at the oxygen atoms (average value 114.7°); the other bond angles are closer to the value at an sp^3 atom (average value 111.3°).

Table 2. Observed torsion angles in the chain of **5** in degrees (in each case the second half of the molecule is ignored).

Molecule **A**		Molecule **B**	
C6-C1-C7-O1	152.9(0.3)	O4-C17-C11-C16	100.4(0.4)
C1-C7-O1-C8	−70.2(0.3)	C18-O4-C17-C11	−165.9(0.3)
C7-O1-C8-O2	−68.4(0.3)	O5-C18-O4-C17	−67.1(0.4)
O1-C8-O2-C9	−66.5(0.3)	C19-O5-C18-O4	−68.5(0.3)
C8-O2-C9-O3	−65.7(0.3)	O6-C19-O5-C18	−64.9(0.3)
O2-C9-O3-C10	−65.2(0.3)	C20-O6-C19-O5	−62.1(0.4)
C9-O3-C10-O3'	−68.1(0.3)	O6'-C20-O6-C19	−66.4(0.3)

The torsion angles in the middle of the chain (Table 2) indicate the deviation from the ideal staggered *gauche* configuration because of the stereoelectronic effect, which leads to a slight twisting of the poly(oxymethylene) helix (Fig. 4).

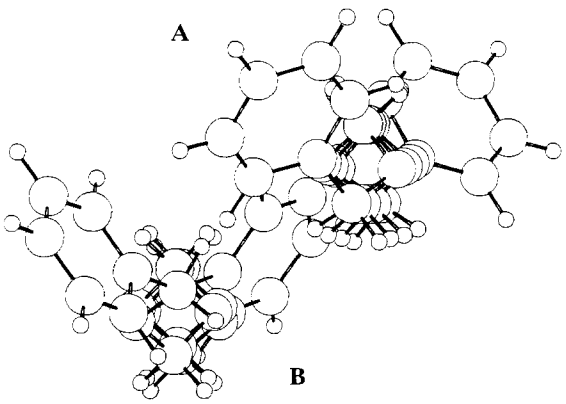


Fig. 4. Comparison of the secondary helices of molecules **A** and **B**. The smaller variation in torsion angles in molecule **A** lead to a more regular secondary helix.

In connection with the *exo* anomeric effect, the Φ torsion angle allows us to define a standard value of 66.3° (cf. that derived from the X-ray analysis of a glycolnitrile acetal[6] of 72.6°).

We are currently studying the structure of oligo- and poly(oxymethylene) helices and the asymmetric induction in their formation.

Received: December 6, 1993 [Z6540IE]
German version: *Angew. Chem.* **1994**, *106*, 1559

[1] a) A. J. Kirby, *The Anomeric Effect and Related Stereoelectronic Effects at Oxygen*, Springer, Berlin, **1983**; b) P. Deslongchamps, *Stereoelectronic Effects in Organic Chemistry (Org. Chem. Ser. Vol. 1)*, Pergamon, Oxford, **1983**.
[2] T.-C. Wu, P. G. Goekjian, Y. Kishi, *J. Org. Chem.* **1987**, *52*, 4819–4823.
[3] a) J. Hengstenberg, *Ann. Phys. (Leipzig)* **1927**, *84*, 245–278; b) E. Sauter, *Z. Phys. Chem. Abt. B* **1932**, *18*, 417–435; c) M. L. Huggins, *J. Chem. Phys.* **1945**, *13*, 37–42; d) C. F. Hammer, T. A. Koch, J. F. Whitney, *J. Appl. Polym. Sci.* **1959**, *1*, 169–178; e) G. Carazzolo, *Gazz. Chim. Ital.* **1962**, *92*, 1345–1361; f) G. Carazzolo, G. Putti, *Chim. Ind. (Milan)* **1963**, *45*, 771–776; g) G. Carazzolo, M. Mammi, *J. Polym. Sci. Part A Gen. Pap.* **1963**, *1*, 965–983; h) T. Uchida, H. Takokoro, *J. Polym. Sci. Polym. Phys. Ed.* **1967**, *5*, 63–81.
[4] C. R. Noe, M. Knollmüller, P. Ettmayer, *Angew. Chem.* **1988**, *100*, 1431–1433; *Angew. Chem. Int. Ed. Engl.* **1988**, *27*, 1379–1381.
[5] R. H. Boyd, *J. Polym. Sci.* **1961**, *50*, 133–141.
[6] C. R. Noe, M. Knollmüller, G. Göstl, B. Oberhauser, H. Völlenkle, *Angew. Chem.* **1987**, *99*, 467–469; *Angew. Chem. Int. Ed. Engl.* **1987**, *26*, 442–444.
[7] Experimental procedure: To a suspension of paraformaldehyde (12 g, 0.40 mol) in benzene (60 mL) was added benzyl alcohol (4.32 g, 0.04 mol) and sulfuric acid (0.5 mL), and the mixture was heated at reflux for 2 h. The reaction mixture was cooled and treated with solid sodium hydrogen carbonate (2 g), stirred for 30 min, and filtered. The residue was washed with ether and the filtrate concentrated to dryness. The crude mixture of oligomers (5.8 g) was separated by column chromatography (600 g fine silica gel, petroleum ether/ether, 15:1) to give 1.60 g of **1**, 0.90 g of **2**, 0.60 g of **3**, 0.20 g of **4**, and 0.10 g of **5**. For analytical details see C. Miculka, Dissertation, Technische Universität, Vienna, **1993**.
[8] Enraf-Nonius CAD4 diffractometer; room temperature, $Cu_{K\alpha}$ radiation, $a = 4076(1)$, $b = 545.4(2)$, $c = 841.6(3)$ pm, $\beta = 97.86(3)°$, $V = 1853(2) \times 10^6$ pm^3; space group $C2$, $Z = 4$; $\mu(Cu_{K\alpha}) = 7.3$ cm^{-1}, $2\theta_{max} = 120°$; 2594 reflections, of which 1496 were independent with $I > 0$; 227 parameters (C, O anisotropically refined; position of the H atoms calculated); $R = 0.039$; $R_w = 0.030$. Further details of the crystal structure investigation can be obtained fron the Fachinformationszentrum Karlsruhe, D-76344 Eggenstein-Leopoldshafen (FRG), on quoting the deposition number CSD-57971.

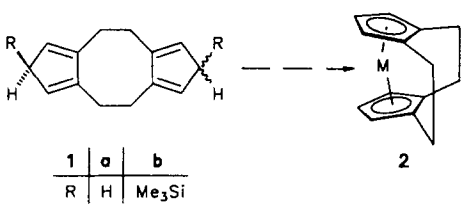
Synthesis and Structure of the First [2₂]Metallocenophanes**

Klaus Hafner,* Carsten Mink, and Hans Jörg Lindner

Dedicated to Professor Virgil Boekelheide on the occasion of his 75th birthday

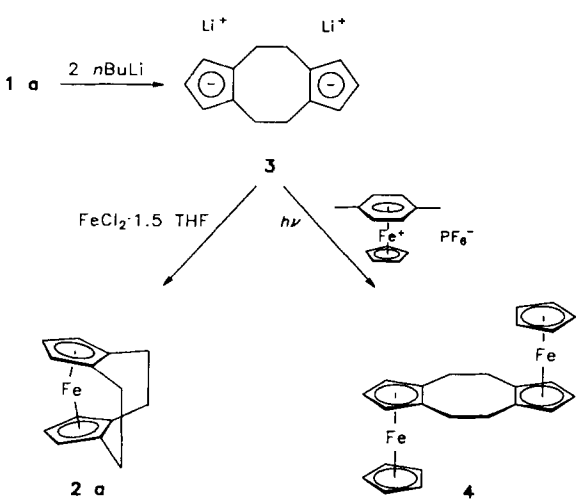
Bent metallocenes with a nonplanar arrangement of the ring ligands proved to be components of efficient catalysts for the stereoselective polymerization of alkenes.[1] Rigid metallocene derivatives of the fourth subgroup having a short bridge and consequently exposed metal center were found to be particularly well suited.[2] Numerous metallocenophanes have been prepared with one or more bridges of various lengths, but surprisingly [2](1,1')[2](2,2')-metallocenophanes **2** are not known,[3] even though the considerable conformational rigidity of the ligand system and the large dihedral angle between the planes of the rings indicates that they could serve as components of homogeneous catalysts.

In the course of investigations on dicyclopenta[*a*,*e*]cyclooctene, a 14π electron system with cyclic delocalization,[4] we discovered a simple route to tricyclo[9.3.0.0^{4,8}]tetradeca-4,7,11,14-tetraene (**1**),[5] which proved to be a suitable starting material for metallocenophanes of type **2**. We report here on the



synthesis and structure of ferrocenophane **2a** and zirconocenophane dichloride **2b**, the first [2₂]metallocenophanes.

The dilithium compound **3** was prepared by double deprotonation of **1a** with *n*BuLi in THF at 25 °C. The ^{1}H, ^{13}C, and ^{6}Li



NMR spectra of **3** indicate that it exists as a contact ion pair at −60 °C.[5] The reaction of **3** with (η^6-*p*-xylene)(η^5-cyclopentadienyl)iron hexafluorophosphate[6] at 25 °C by irradiation with a halogen lamp (300 W, Osram Concentra) provided the *trans*-[2₂](1,2)-ferrocenophane (**4**)[7] (18% yield, yellow crystals, decomp > 230 °C), which was previously synthesized by Schlögl et al.[8] from substituted ferrocenes in multistep procedures. Compound **3** reacted with $FeCl_2 \cdot 1.5\,THF$ in THF at 25 °C to afford [2](1,1')[2](2,2')-ferrocenophane **2a** as deep red plates (decomp > 210 °C)[9] in 41% yield.[10] The complex is stable at −50 °C under inert gas but rapidly decomposes at room temperature, particularly in solution.

The X-ray structure analysis of **2a**[11] (Fig. 1) indicates considerable torsion of the two decks. The dihedral angle between

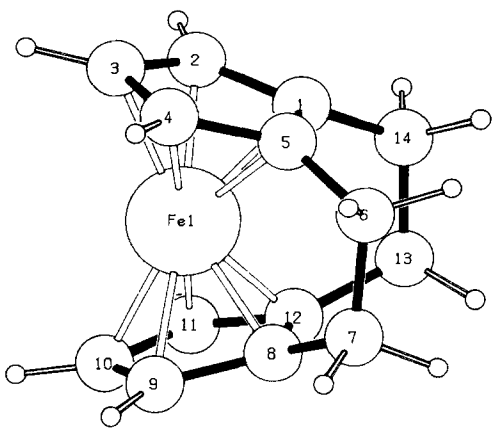
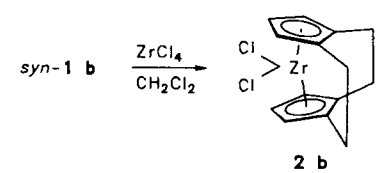


Fig. 1. Crystal structure of **2a** [11]. Selected distances [Å] and angles [°]: C1-C2 143.1(12), C5-C6 149.5(9), C6-C7 150.1(10); C5-C6-C7 113.7(5), C4-C5-C6 128.3(7).

the planes of the two rings is 28.8°, considerably larger than in the known ferrocenophanes.[3] The two small dihedral angles in the bridges (8.2(10) and 6.9(10)°) indicate that the five-membered rings are almost perfectly eclipsed. The average C–C bond length in the cyclopentadienyl ligands (141 pm) corresponds to that of other ferrocenophanes, whereas the average Fe–C distance in **2a** (201 pm) is much shorter.

In contrast to [2]ferrocenophane, which is more Lewis basic than ferrocene,[12] treatment of **2a** with trifluoroacetic acid in dichloromethane at −60 °C did not provide a well-defined protonation product but rather brown-black products insoluble in standard solvents.

In analogy to the synthesis of zirconocene dichloride[13] the reaction of *syn*-6,13-bis(trimethylsilyl)tricyclo[9.3.0.0^{4,8}]-tetradeca-4,7,11,14-tetraene (**1b**) with zirconium tetrachloride in dichloromethane at 25 °C furnished [2](1,1')[2](2,2')-zirconocenophane dichloride (**2b**) in 61% yield as colorless needles (decomp > 270 °C). Compound **2b** can be obtained in analytically pure form by sublimation at 230 °C/10^{-2} mbar.[14]



An X-ray structure analysis of **2b**[11] (Fig. 2) shows that the average Zr–C distance (249 pm) is considerably longer than that in the known [2]zirconocenophane dichlorides.[15] The dihedral angle between the planes of the rings (62.9°) in **2b** is the

[*] Prof. Dr. K. Hafner, Dr. C. Mink, Prof. Dr. H. J. Lindner
Institut für Organische Chemie der Technischen Hochschule
Petersenstrasse 22, D-64287 Darmstadt (FRG)
Telefax: Int. code + (6151) 163574

[**] This work was supported by the Fonds der Chemischen Industrie and by Degussa AG, Frankfurt/Main.

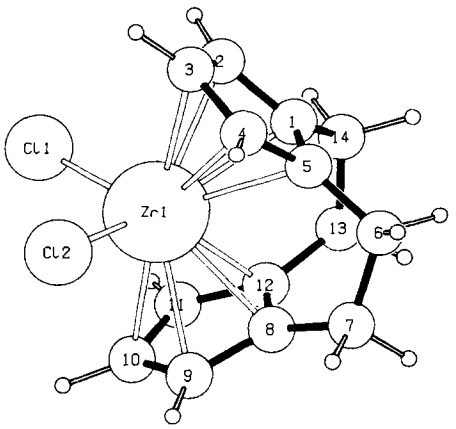


Fig. 2. Crystal structure of **2b** [11]. Selected distances [Å] and angles [°]: C1-C2 140.0(7), C5-C6 150.6(7), C6-C7 149.0(8), Zr-Cl 244.2(1); C5-C6-C7 114.1(4), C4-C5-C6 127.7(5), Cl-Zr-Cl 97.95(5).

largest observed in these compounds. As in **2a** the dihedral angles in the bridges of **2b** (18.6(7) and 20.7(8)°) indicate an approximately eclipsed configuration of the five-membered rings.

Owing to the molecular structure of the new rigid zirconocenophane **2b**, catalytic activity for the stereoselective polymerization of alkenes can be anticipated for this compound or substituted chiral derivatives. Moreover, application of complexes of type **2b** appears promising for C–C bond-forming reactions with metallocene derivatives from the fourth subgroup, which are currently of interest,[16] as well as for the synthesis of novel metallacycles.[16, 17]

Received: April 12, 1994 [Z6839IE]
German version: *Angew. Chem.* **1994**, *106*, 1566

[1] W. Kaminsky, A. Ahlers, N. Möller-Lindenhof, *Angew. Chem.* **1989**, *101*, 1304–1306; *Angew. Chem. Int. Ed. Engl.* **1989**, *28*, 1216–1218; J. Okuda, *Nachr. Chem. Tech. Lab.* **1993**, *41*, 8–14, and references therein; R. Mülhaupt, *ibid.* **1993**, *41*, 1341–1351; G. Erker, M. Aulbach, D. Wingbermühle, C. Krüger, S. Werner, *Chem. Ber.* **1993**, *126*, 755–761.

[2] W. Röll, H. H. Brintzinger, B. Rieger, R. Zolk, *Angew. Chem.* **1990**, *102*, 339–341; *Angew. Chem. Int. Ed. Engl.* **1990**, *29*, 279–280; W. Spaleck, M. Antberg, J. Rohrmann, A. Winter, B. Bachmann, P. Kiprof, J. Behm, W. A. Herrmann, *ibid.* **1992**, *104*, 1373–1376 and **1992**, *31*, 1347–1350, and references therein.

[3] U. T. Müller-Westerhoff, *Angew. Chem.* **1986**, *98*, 700–716; *Angew. Chem. Int. Ed. Engl.* **1986**, *25*, 702–717; M. Hisatome, *Rev. Heteroat. Chem.* **1992**, *6*, 142–176.

[4] K. Hafner, G. F. Thiele, C. Mink, *Angew. Chem.* **1988**, *100*, 1213–1215; *Angew. Chem. Int. Ed. Engl.* **1988**, *27*, 1191–1192.

[5] C. Mink, K. Hafner, *Tetrahedron Lett.* **1994**, *35*, 4087–4090.

[6] T. P. Gill, K. R. Mann, *J. Organomet. Chem.* **1981**, *216*, 65–71.

[7] C. Mink, Dissertation, Technische Hochschule Darmstadt, **1994**. The physical properties of **4** are identical to those described in ref. [8].

[8] M. Benedikt, K. Schlögl, *Monatsh. Chem.* **1978**, *109*, 805–822; K. Schlögl, W. Weissensteiner, *Synthesis* **1982**, 50–53; H. Paulus, K. Schlögl, W. Weissensteiner, *Monatsh. Chem.* **1983**, *114*, 799–808.

[9] MS (70 eV): *m/z* (%): 238 (100) (M^+), 93 (23) ($C_7H_9^+$), 56 (14) (Fe^+); UV (*n*-hexane) λ_{max} (lg ε) = 223 (4.36), 250 (3.85 (sh), 330 (2.31) (sh), 455 (2.61) (sh), 496 nm (2.70); ^{1}H NMR (300 MHz, C_6D_6): δ = 2.98 (s, 4H, $2CH_2$ (outer)), 3.20 (s, 4H, $2CH_2$ (inner)), 3.65 (s, 2H, 4,4′-H), 4.51 (s, 4H, 3,3′-H, 5,5′-H); ^{13}C NMR (75.47 MHz, $CDCl_3$): δ = 33.17 (CH_2), 64.39 (C-4, C-4′), 72.14 (C-3, C-3′, C-5, C-5′), 96.85 (C-1, C-1′, C-2, C-2′). The NMR signals of **2a** and **2b** were assigned based on ^{1}H,^{1}H and ^{1}H,^{13}C COSY spectra and NOE experiments.

[10] Correct elemental analyses were obtained from all compounds described.

[11] **2a** ($C_{14}H_{14}Fe$, M_r = 238.11) crystallizes from *n*-pentane at −40 °C in the monoclinic space group $P2_1/n$ with a = 1207.9(4), b = 758.9(1), c = 1228.1(4) pm, β = 112.19(2)°, Z = 4, V = 1042.4 × 10^6 pm^3, ρ_{calcd} = 1.52 g cm^{-3}, $Mo_{K\alpha}$ radiation, 25 °C, CAD-4 Enraf-Nonius diffractometer, $\omega/2\theta$ scans, 2293 measured reflections, of which 1449 with $|F| \geq 4\sigma$ were used for refinement. Structure solution by direct methods, no intensity or absorption correction. R = 0.0830; R_w = 0.1656, residual electron density at Fe + 0.042 e Å^{-3}. – **2b** ($C_{14}H_{14}Cl_2Zr$; M_r = 344.39) crystallizes from *n*-hexane/dichloromethane (3:2) at 25 °C in the monoclinic space group $P2_1/n$ with a = 820.0(4), b = 1182.8(3), c = 1342.9(5) pm; β = 91.39(4)°, Z = 4, V = 1302.1 × 10^6 pm^3, ρ_{calcd} = 1.76 g cm^{-3}; $Mo_{K\alpha}$ radiation, 25 °C, CAD-4 Enraf-Nonius diffractometer, $\omega/2\theta$ scans, 1941 measured reflections, of which 1797 with $|F| \leq 4\sigma$ were used for refinement. Structure solution by direct methods, no intensity or absorption correction. R = 0.0399; R_w = 0.0955. Programs: SHELXS-86 and SHELXL-93. Further details of the crystal structure investigations may be obtained from the Fachinformationszentrum Karlsruhe, D-76344 Eggenstein-Leopoldshafen (FRG) on quoting the depository number CSD-58249.

[12] H. L. Lentzner, W. E. Watts, *Chem. Commun.* **1970**, 26–27.

[13] C. H. Winter, X.-X. Zhou, D. A. Dobbs, M. J. Heeg, *Organometallics* **1991**, *10*, 210–214, and references therein.

[14] MS (70 eV): *m/z* (%): 344(72) (M^+), 309(40) (M^+ − Cl), 270(24) (M^+ − 2Cl), 227(33), 91 (100) (Zr^+), 65(92) ($C_5H_5^+$), 39(70); UV (*n*-hexane): λ_{max} (lg ε) = 256 (3.53) (sh), 306 (3.36), 339 nm (2.98) (sh); ^{1}H NMR (300 MHz, $CDCl_3$): δ = 3.28, 3.36 (AA′BB′, J_1 = 2.5, J_2 = 11.7 Hz, 8H, $4CH_2$), 6.01 (t, J = 3.3 Hz, 2H, 4,4′-H), 6.48 (d, J = 3.3 Hz, 4H, 3,3′-H, 5,5′-H); ^{13}C NMR (75.47 MHz, $CDCl_3$): δ = 29.98 (CH_2), 110.42 (C-4, C-4′), 121.63 (C-3, C-3′, C-5, C-5′), 132.06 (C-1, C-1′, C-2, C-2′).

[15] S. Collins, B. A. Kuntz, N. J. Taylor, D. G. Ward, *J. Organomet. Chem.* **1988**, *342*, 21–29; S. Gutmann, P. Burger, H.-U. Hund, J. Hofmann, H. H. Brintzinger, *ibid.* **1989**, *369*, 343–357, and references therein.

[16] M. E. Maier, *Nachr. Chem. Tech. Lab.* **1993**, *41*, 811–823.

[17] E. B. Tjaden, J. M. Stryker, *J. Am. Chem. Soc.* **1993**, *115*, 2083–2085.

Heterodimetal–Betaine Chemistry: Catalytic and Stoichiometric Coupling of Alkynyl Ligands under the Joint Influence of Zirconium and Boron Centers**

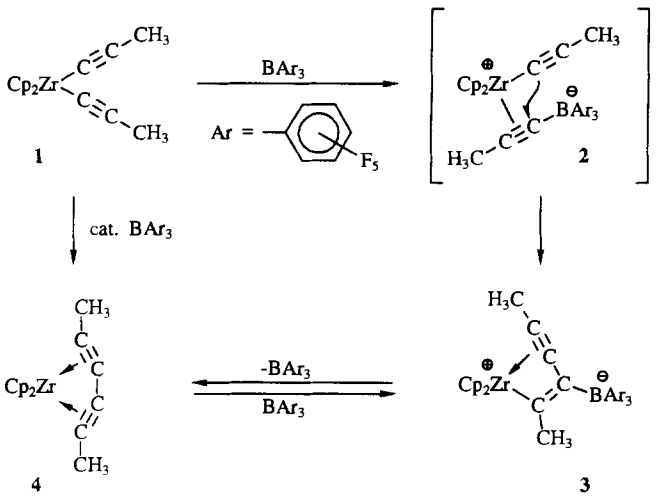
Bodo Temme, Gerhard Erker,* Roland Fröhlich, and Matthias Grehl

We have recently shown that the joint influence of zirconium and boron centers can be used for C–H activation in (μ-hydrocarbon)Zr–B complexes.[1] Beyond this there is evidence that $[Cp_2ZrR]^+/BR_4^-$ ion pairs and betaines are of significance in homogeneous Ziegler–Natta polymerization.[2, 3] We therefore wanted to investigate the previously poorly developed chemistry of Zr–B-containing heterodimetallic betaine complexes.[2] It was found that such $[\{Cp_2ZrR\}^+\{(\mu\text{-}R)BR_3^-\}]$ betaine complexes (to date hardly known) form very easily and that they readily rearrange under carbon–carbon coupling in a way that is typical for this class of compounds, to form an interesting heterodimetal-substituted organic skeleton. In this communication we describe a typical example.

Bis(propynyl)zirconocene (**1**) was obtained by the reaction of $[Cp_2ZrCl_2]$ with two molar equivalents of propynyllithium.[4] The reaction of **1** with tris(pentafluorophenyl)borane in a 1:1 molar ratio in toluene at room temperature rapidly gave the (μ-R)Zr–B betaine complex **3** in 83% yield. The ^{1}H and ^{13}C NMR spectra of complex **3** show resonance signals at δ = 5.32 and 116.3, respectively, for the Cp rings, as well as two singlets at δ = 2.26, 1.04 and 29.7, 10.7, respectively, for the methyl groups. The ^{13}C NMR resonances of the μ-2,4-hexadiyne ligand, which is unsymmetrically coordinated to the participating metal centers, appear at δ = 255.0, 108.5, and 105.0 (the B–*C* signal was not observed).

[*] Prof. Dr. G. Erker, Dipl.-Chem. B. Temme, Dr. R. Fröhlich, Dr. M. Grehl
Organisch-chemisches Institut der Universität
Corrensstrasse 40, D-48149 Münster (FRG)
Telefax: Int. code + (251)83-9772

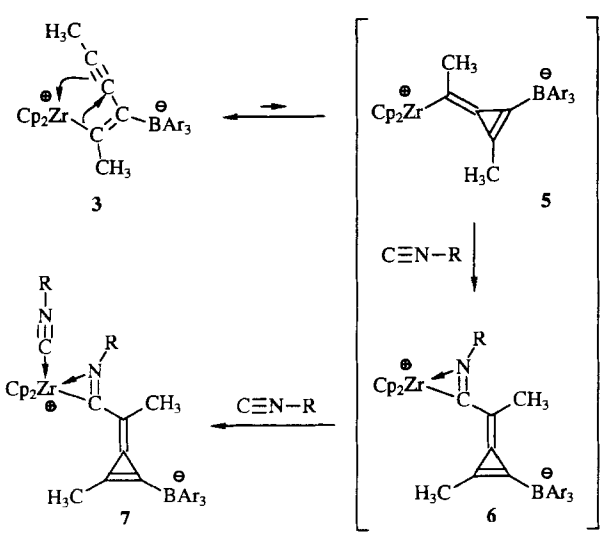
[**] This work was supported by the Fonds der Chemischen Industrie and the Alfried-Krupp-von-Bohlen-und-Halbach-Stiftung.



The formation of the organometallic betaine **3** can be rationalized by a simple reaction sequence. We assume that the first step involves a transfer of a σ ligand from the zirconium center to the boron atom.[5] Subsequently the insertion of the newly formed boron-substituted alkyne into the remaining metal–carbon σ bond at the zirconium atom presumably leads to the direct formation of **3**.[6]

The reaction takes a different course if **1** is treated with less than one equivalent of $B(C_6F_5)_3$. Thus the reaction of **1** with less than 1 mol% of this borane (room temperature, toluene) leads to C–C coupling of the alkynyl ligands and formation of the isomeric product (η^4-2,4-hexadiyne)zirconocene **4**. Presumably this triarylborane-catalyzed reaction proceeds via **3** as an intermediate, from which the rearranged zirconium complex **4** is liberated by transfer of $B(C_6F_5)_3$ to **1**. As expected, complex **3** also catalyzes the conversion of **1** to **4**.

We treated the (μ-2,4-hexadiyne)zirconium–boron betaine complex **3** with *tert*-butyl isonitrile and discovered a surprising reaction pathway. A simple CNR insertion into the reactive zirconium–carbon σ bond of **3** does not take place. Rather, we obtained the product **7** in good yield through a rearrangement



of the framework and a subsequent reaction with two isonitrile units. An isonitrile building block has been incorporated under C–C coupling and the formation of a cationic ZrNC three-membered ring;[7] for stabilization a second isonitrile then attached itself to the very electrophilic Zr^+ center.[8]

Compound **7** was characterized by an X-ray crystal structure analysis (Fig. 1). The metal complex **7** contains a Cp_2Zr^+ structural unit to which an iminomethyl ligand is η^2-coordinated. Furthermore a $C{\equiv}N{-}CMe_3$ ligand is bonded in a lateral position to the $(\eta^2\text{-}C{=}NR)ZrCp_2^+$ subunit. The nitrogen atom of the iminomethyl ligand occupies the central position in the plane of the σ ligands at the bent metallocene unit. The most remarkable structural feature in **7** is the substituted methylenecyclopropene unit, which is bound to the C5 atom of the ZrNC three-membered ring. The atoms C4 and C2 bear methyl substituents, and the $B(C_6F_5)_3$ unit is bound to C1. This boron-substituted methylenecyclopropene framework was formed by rearrangement of the BAr_3-substituted μ-2,4-hexadiyne ligand of the starting material **3**. Compound **7**, like **3**, is an organometallic betaine complex; the boron atom formally carries the negative charge, and consequently the zirconium center is positively charged. The C1–C2 bond of the central methylenecyclopropene unit of **7** is short [1.326(10) Å]. Its neighboring carbon–carbon bonds in the strained three-membered ring are clearly longer [1.417(10)Å C1–C3; 1.392(10)Å C2–C3], and also the adjacent C3–C4 double bond is only a little shorter [1.389(19)Å]. We assume that the regioselective incorporation into the betaine system stabilizes the very strained hydrocarbon framework in this case.[9] The whole $B^-(\mu\text{-organo})Zr^+$ betaine unit is planar [*0*(C3-C4-C5-N6) 178.5(9)°] and lies in the the σ-ligand plane of the bent metallocene.

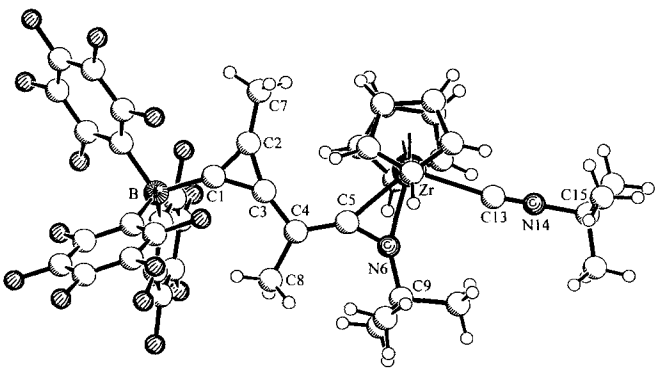


Fig. 1. Molecular geometry of **7**. Selected bond lengths [Å] and bond angles [°]: B-C1 1.627(11), B-C(Ar) (average value) 1.646(11), C1-C2 1.326(10), C1-C3 1.417(10), C2-C3 1.392(10), C2-C7 1.465(10), C3-C4 1.389(10), C4-C8 1.510(10), C4-C5 1.426(10), C5-N6 1.292(9), C5-Zr 2.217(8), N6-Zr 2.177(6), Zr-C13 2.377(9), C13-N14 1.133(9); B-C1-C3 147.5(7), B-C1-C2 151.1(7), C2-C1-C3 60.9(5), C1-C2-C3 62.7(6), C1-C2-C7 146.4(8), C3-C2-C7 150.7(7), C1-C3-C2 56.4(5), C1-C3-C4 143.7(7), C2-C3-C4 160.0(8), C3-C4-C8 115.6(7), C3-C4-C5 117.0(7), C8-C4-C5 127.4(7), C4-C5-N6 139.4(7), C4-C5-Zr 149.4(6), Zr-C5-N6 71.2(4), C5-N6-Zr 74.6(4), C5-N6-C9 133.1(6), C9-N6-Zr 152.3(5), C5-Zr-N6 34.2(2), C5-Zr-C13 121.0(3), Zr-C13-N14 172.0(7), C13-N14-C15 175.6(8).

It was noticed from the formation of **3** from **1** and $B(C_6F_5)_3$ that the alkyne insertion into the Zr–C(sp) σ bond proceeds rapidly in a Zr–B-containing betaine.[10] We therefore assume that, analogously to the above, a betaine-assisted insertion of an alkyne into a Zr–C(sp^2) σ bond is possible. Under these conditions it is apparent that the formation of the Zr–B-substituted methylenecyclopropene framework in the above-mentioned reaction can be taken as an intramolecular alkyne insertion. Compound **3** is possibly in equilibrium with the three-membered ring isomer **5**, though the equilibrium lies almost completely on the side of **3**. Only on addition of the isonitrile does the coordina-

tively unsaturated equilibrium partner **5** react preferentially and thus open the way for the formation of **7** from **3** and *tert*-butyl isonitrile.

These examples show that organometallic betaine compounds with a combination of transition metal and main group metal are easily accessible and that they make characteristic carbon–carbon coupling reactions possible. These variants in the chemistry of heterodimetallic complexes could open interesting routes to new stoichiometric reactions and catalytic processes.

Experimental Procedure

3: Precooled toluene was added at −78 °C to a mixture of **1** (1.50 g, 5.0 mmol) and tris(pentafluorophenyl)borane (2.56 g, 5.0 mmol). The mixture was then slowly warmed to room temperature with stirring and stirred for a further 4 h. The yellow precipitate which formed was filtered off, washed with toluene (30 mL), and dried under vacuum. Yield of **3**: 3.75 g, 81%; m.p. = 74 °C (decomp.). ^{1}H NMR ([D$_6$]benzene): δ = 5.32 (s, 10H, Cp), 2.26 (s, 3H, CH$_3$), 1.04 (s, 3H, CH$_3$); ^{13}C NMR (CD_2Cl_2): δ = 255.0, 151.2 (^1J(CF) = 232 Hz), 142.0 (^1J(CF) = 242 Hz), 140.1 (^1J(CF) = 240 Hz), B(C_6F_5)$_3$, 116.3 (Cp), 108.5, 105.0, 29.7 (CH$_3$), 10.7 (CH$_3$), B–*C* not observed; IR (KBr): $\tilde{\nu}$ = 3120, 2970, 2929, 1644, 1516, 1461, 1376, 1276, 1092, 1018, 977, 815, 761, 694 cm^{-1}. The corresponding hafnium–boron compound **8** was prepared analogously and isolated in 82% yield. M.p. = 78 °C (decomp.). ^{1}H NMR ([D$_6$]benzene): δ = 5.27 (s, 10H, Cp), 2.34 (s, 3H, CH$_3$), 1.00 (s, 3H, CH$_3$); IR (KBr): $\tilde{\nu}$ = 3118, 2967, 2927, 1646, 1517, 1463, 1381, 1279, 1094, 1017, 980, 806, 772, 697 cm^{-1}. Correct elemental analysis for $C_{34}H_{16}BF_{15}Hf\cdot C_7H_8$. The ($\mu$-hexadiyne)Hf–B betaine structure was confirmed for **8** by an X-ray structure analysis, which was, however, not discussed here in detail due to its high *R* value of 0.096.

4: Compound **1** (570 mg, 1.9 mmol) in toluene (30 mL) was stirred with tris(pentafluorophenyl)borane (6 mg, 12 μmol, 0.6 mol%) for 3 d at room temperature. Subsequently the solvent was removed under vacuum, and the resulting complex **4** was washed with pentane (20 mL). M.p. = 105 °C (decomp.). ^{1}H NMR ([D$_6$]benzene): δ = 5.09 (s, 10H, Cp), 2.83 (s, 6H, CH$_3$); ^{13}C NMR ([D$_6$]benzene): δ = 171.7, 132.5, 104.2 (Cp), 18.5 (CH$_3$); IR (KBr): $\tilde{\nu}$ = 3092, 2967, 2900, 1439, 1362, 1263, 1098, 1012, 797, 540, 456 cm^{-1}. We had already prepared the analogous (η^2-2,4-hexadiyne)hafnocene compound **9** earlier by photolysis (HPK 125, pyrex filter, toluene) of bis(propynyl)hafnocene [11]: isolated yield 2.5 g (66%), m.p. = 103 °C (decomp.). ^{1}H NMR ([D$_6$]benzene): δ = 5.04 (s, 10H, Cp), 2.86 (s, 6H, CH$_3$); ^{13}C NMR ([D$_6$]benzene): δ = 173.1, 105.8, 103.4 (Cp), 19.3 (CH$_3$); IR (KBr): $\tilde{\nu}$ = 3100, 2900, 1440, 1360, 1260, 1010, 800 cm^{-1}. Correct analysis for $C_{16}H_{16}Hf$.

7: Compound **3** (200 mg, 0.22 mmol) was suspended in toluene (5 mL), *t*-BuN≡C (0.16 mg, 1.9 mmol) was added, and the mixture stirred for 30 min at room temperature. After cooling to −20 °C complex **7** precipitated in the form of fine needles (210 mg, 91% yield). Crystals suitable for X-ray analysis were obtained by recrystallization from hot toluene (m.p. = 59 °C). ^{1}H NMR ([D$_8$]THF): δ = 5.73 (s, 10H, Cp), 2.52 (s, 6H, CH$_3$), 2.03 (s, 3H, CH$_3$), 1.69 (s, 9H, *t*Bu), 1.28 (s, 9H, *t*Bu); ^{13}C NMR ([D$_8$]THF): δ = 204.0, 169.0 (^1J(BC) = 63.7 Hz), 158.1, 152.3, 146.9, 84.5; B(C_6F_5)$_3$: 149.1 (^1J(CF) = 233 Hz), 139.7 (^1J(CF) = 246 Hz), 137.7 (^1J(CF) = 251 Hz), 106.2 (Cp), 60.0 ($C(CH_3)_3$), 57.5 ($C(CH_3)_3$), 31.6 ($C(CH_3)_3$), 29.3 ($C(CH_3)_3$), 23.4 (CH$_3$), 12.0 (CH$_3$); *ipso*-B(C_6F_5)$_3$ carbon not observed; IR (KBr): $\tilde{\nu}$ = 2986, 2932, 2873, 2195, 1809, 1642, 1580, 1513, 1495, 1465, 1374, 1277, 1188, 1092, 1045, 1013, 978, 893, 801, 731, 686 cm^{-1}. Correct analysis for $C_{44}H_{34}BF_{15}N_2Zr\cdot C_7H_8$.

Data for the X-ray structure analysis of **7**: Formula $C_{44}H_{34}BF_{15}N_2Zr\cdot 3C_7H_8$, M = 1254.2, crystal size 0.15 × 0.1 × 0.1 mm, a = 13.354(4), b = 14.778(5), c = 17.269(5) Å, α = 65.31(1), β = 73.08(2), γ = 89.95(2)°, V = 2934(2) Å^3, $\rho_{calcd.}$ = 1.420 gcm^{-3}, μ = 2.78 cm^{-1}, Z = 2, triclinic, space group $P\bar{1}$ (no. 2), Enraf–Nonius CAD 4 diffractometer, λ = 0.71073 Å, (ω − 2θ) scan, 8229 measured reflections ($\pm h$, $\pm k$, $-l$), [sinθ/λ]$_{max}$, 0.55 Å^{-1}, 7915 independent and 3693 observed reflections [$F \geq 4\sigma(F)$], 725 refined parameters, R = 0.063, wR^2 = 0.135, max. residual electron density 0.63(−0.50) e Å^{-3}, direct methods, H-atom positions calculated. Programs used: SHELX 93, SCHAKAL. Further details of the crystal structure investigation may be obtained from the Fachinformationszentrum Karlsruhe, D-76344 Eggenstein-Leopoldshafen (FRG) on quoting the depository number CSD-400795, the names of the authors, and the journal citation.

Received: April 6, 1994 [Z.6827IE]
German version: *Angew. Chem.* **1994**, *106*, 1570

[1] G. Erker, R. Noe, D. Wingbermühle, J. L. Petersen, *Angew. Chem.* **1993**, *105*, 1216; *Angew. Chem. Int. Ed. Engl.* **1993**, *32*, 1213.
[2] G. G. Hlatky, H. W. Turner, R. R. Eckman, *J. Am. Chem. Soc.* **1989**, *111*, 2728.
[3] M. Bochmann, G. Karger, A. J. Jaggar, *J. Chem. Soc. Chem. Commun.* **1990**, 1038; G. Erker, M. Albrecht, S. Werner, C. Krüger, *Z. Naturforsch. B* **1990**, *45*, 1205; A. D. Horton, J. H. G. Frijns, *Angew. Chem.* **1991**, *103*, 1181; *Angew. Chem. Int. Ed. Engl.* **1991**, *30*, 1152; D. M. Amorose, R. A. Lee, J. L. Petersen, *Organometallics* **1991**, *10*, 2191; G. Erker, M. Albrecht, C. Psiorz, *Z. Naturforsch. B* **1991**, *46*, 1571; G. G. Hlatky, R. R. Eckman, H. W. Turner, *Organometallics* **1992**, *11*, 1413; C. J. Schaverien, *ibid.* **1992**, *11*, 3476; C. Pellecchia, A. Grassi, A. Immirzi, *J. Am. Chem. Soc.* **1993**, *115*, 1160; D. J. Gillis, M.-J. Tudoret, M. C. Baird, *ibid.* **1993**, *115*, 2543; C. Pellecchia, A. Immirzi, A. Grassi, A. Zambelli, *Organometallics* **1993**, *12*, 4473; see also: G. Erker, R. Noe, D. Wingbermühle, *Chem. Ber.* **1994**, *127*, 805.
[4] G. Erker, W. Frömberg, R. Benn, R. Mynott, K. Angermund, C. Krüger, *Organometallics* **1989**, *8*, 911.
[5] Similar reactions were often observed in the generation of stable [$Cp_2Zr(R)L$]$^+$ complexes: X. Yang, C. L. Stern, T. J. Marks, *J. Am. Chem. Soc.* **1991**, *113*, 3623; C. Sishta, R. M. Hathorn, T. J. Marks, *ibid.* **1992**, *114*, 1112.
[6] M. Bochmann, L. M. Wilson, M. B. Hursthouse, M. Motevalli, *Organometallics* **1988**, *7*, 1148; C. S. Christ, Jr., J. R. Eyler, D. E. Richardson, *J. Am. Chem. Soc.* **1990**, *112*, 4778; S. L. Borkowsky, R. F. Jordan, G. D. Hinch, *Organometallics* **1991**, *10*, 1268; A. S. Guram, R. F. Jordan, D. F. Taylor, *J. Am. Chem. Soc.* **1991**, *113*, 1833; S. L. Borkowsky, N. C. Baenziger, R. F. Jordan, *Organometallics* **1993**, *12*, 486; Y. W. Alelyunas, Z. Guo, R. E. La Pointe, R. F. Jordan, *ibid.* **1993**, *12*, 544.
[7] R. D. Adams, D. F. Chodosh, *Inorg. Chem.* **1978**, *17*, 41. Review: L. D. Durfee, I. P. Rothwell, *Chem. Rev.* **1988**, *88*, 1059.
[8] R. F. Jordan, *Adv. Organomet. Chem.* **1991**, *32*, 325, and references therein; A. S. Guram, R. F. Jordan, *J. Org. Chem.* **1993**, *58*, 5595; G. Erker, R. Zwettler, C. Krüger, *Chem. Ber.* **1989**, *122*, 1377; G. Erker, R. Zwettler, *J. Organomet. Chem.* **1991**, *409*, 179; see also: D. M. Antonelli, E. B. Tjaden, J. M. Stryker, *Organometallics* **1994**, *13*, 763; Z. Guo, D. C. Swenson, A. S. Guram, R. F. Jordan, *ibid.* **1994**, *13*, 766.
[9] W. E. Billups, L.-J. Lin, E. W. Casserly, *J. Am. Chem. Soc.* **1984**, *106*, 3698; S. W. Staley, T. D. Norden, *J. Am. Chem. Soc.* **1984**, *106*, 3699; T. D. Norden, S. W. Staley, W. H. Taylor, M. D. Harmony, *ibid.* **1986**, *108*, 7912; substituted methylenecyclopropenes: W. E. Billups, A. J. Blakeney, N. A. Rao, J. D. Buynak, *Tetrahedron* **1981**, *37*, 3215; W. E. Billups, L.-J. Lin, *Tetrahedron Lett.* **1983**, *24*, 1683; Review: D. Wendisch, *Methoden Org. Chem. (Houben-Weyl)* **1971**, Vol. IV/3, pp. 749–763.
[10] J. J. Eisch, A. M. Piotrowski, S. K. Brownstein, E. J. Gabe, L. L. Florence, *J. Am. Chem. Soc.* **1985**, *107*, 7219; A. D. Horton, A. G. Orpen, *Angew. Chem.* **1992**, *104*, 912; *Angew. Chem. Int. Ed. Engl.* **1992**, *31*, 876; *Organometallics* **1992**, *11*, 8; A. D. Horton, *J. Chem. Soc. Chem. Commun.* **1992**, 185.
[11] W. Frömberg, Dissertation, Universität Bochum, **1986**.

Chlorine Trioxide: Spectroscopic Properties, Molecular Structure, and Photochemical Behavior**

Hinrich Grothe and Helge Willner*

Several years ago the symmetric ClO_3 radical was postulated as intermediate in the formation of chloryl perchlorate $O_2ClOClO_3$ from ClO_2 and O_3[1, 2] and in the gas-phase photolysis of ClO_2.[3] Despite its key role for the understanding of the chemistry of binary chlorine oxides and its potential significance for the chemistry of the stratosphere,[4] its existence could not yet be established. The determination of the molecular weight of gaseous Cl_2O_6[6] and the molecular magnetic properties of liquid Cl_2O_6[6] led to the formulation of the equilibrium $Cl_2O_6 \rightleftharpoons 2ClO_3$, which found its way into many textbooks. A few years ago, however, we showed that such an equilibrium does not exist.[2] Since experimental evidence was lacking, comprehensive ab initio calculations have been undertaken for different isomers to predict the physical molecular properties of the

[*] Prof. Dr. H. Willner, Dipl.-Chem. H. Grothe
Institut für Anorganische Chemie der Universität
Callinstrasse 9, D-30167 Hannover (FRG)
Telefax: Int. code + (511)762-3006

[**] This work was supported by the Bundesministerium für Forschung und Technologie (project 01VOZ08/8), the Deutsche Forschungsgemeinschaft, and the Fonds der Chemischen Industrie.

ClO_3 radical,[7, 8] and in this way the structure and infrared spectrum of the ClO_3 radical were calculated.[8] Now we describe the first experimental evidence for ClO_3 through vacuum flash pyrolysis of chlorine perchlorate Cl_2O_4 and matrix isolation of the products.

Vacuum flash pyrolysis of thermolabile compounds generates transient species, which can easily be trapped in a matrix and characterized by spectroscopy. By this method the $CH_3C(O)OO$ radical, for example, was synthesized by pyrolysis of peroxyacetyl nitrate and detected by IR spectroscopy.[9] We have now studied the pyrolysis products of chlorine perchlorate[10] (diluted in neon, argon, or oxygen in the ratio 1:400). At a pyrolysis temperature of 400 °C, a Cl_2O_4 partial pressure of 10^{-3} mbar, and a residence time of the Cl_2O_4 molecules in the pyrolysis zone of a few ms, 50% of the Cl_2O_4 decomposes into ClO and a new chlorine oxide. The proportion of the decomposed Cl_2O_4 can be determined by comparison of the IR spectra of the matrix-isolated starting compounds (that is, without pyrolysis). ClO was identified through the UV spectrum of the matrix-isolated products (Fig. 1). As in the gas phase, ClO in the matrix also

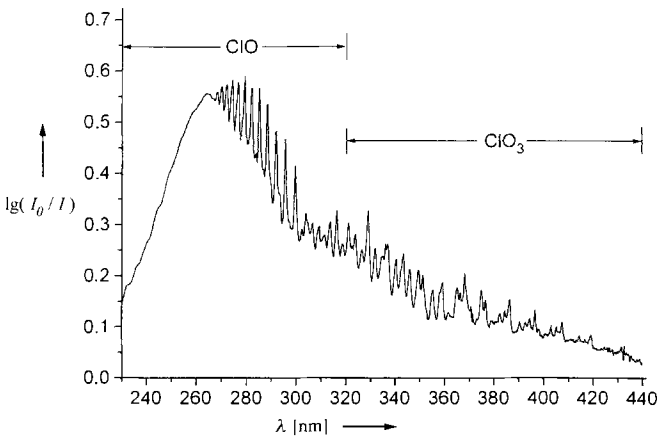


Fig. 1. UV spectrum of the products of the vacuum flash pyrolysis of $ClOClO_3$ in a neon matrix. Below 250 nm unchanged $ClOClO_3$ distorts the band profile of ClO in this region.

absorbs between 230 and 330 nm; the absorption band displays vibrational fine structure.[11] Furthermore, the values of the weak IR absorptions at 843.76 (^{35}ClO) and 836.57 cm^{-1} (^{37}ClO) in the neon matrix agree well with those recorded in the gas phase ($v_0, {}^2\Pi_{3/2}$) of 844.199 and 837.106 cm^{-1}.[12] Figure 2 shows the complete IR spectrum of the new chlorine oxide, and the vibrational wavenumbers are listed in Table 1. The ratio of the intensities of these bands was unchanged in several experiments. The intensity decreases monotonically during the photolysis of the matrix, which suggests that the bands stem from one species. The threshold for the photodissociation lies at 530 nm, and the photolysis product shows bands at $\tilde{\nu}(OO) = 1549.1$ and $\tilde{\nu}(^{35}ClO) = 839.4\ cm^{-1}$ (neon matrix). In contrast, the photolysis of the new chlorine oxide in an O_2 matrix yields ClO_2 and O_3.

The IR bands of the new chlorine oxide display an isotope pattern consistent with a molecule containing one chlorine atom. In experiments with ^{18}O-enriched Cl_2O_4, four isotopomers were detected (Fig. 3), from which it is deduced that the molecule incorporates three oxygen atoms. These findings and the number of IR-active fundamental modes (four) prove unambiguously the presence of a ClO_3 species with C_{3v} symmetry, for which the irreducible representation (a) is valid.

$$\Gamma_{vib} = 2\ a_1\ (IR, Raman\ p) + 2e\ (IR, Raman\ dp) \qquad (a)$$

Finally the good agreement of the measured and calculated values (see Table 1) leaves no doubt about the detection of the ClO_3 radical and confirms the assignment of the vibrational bands.

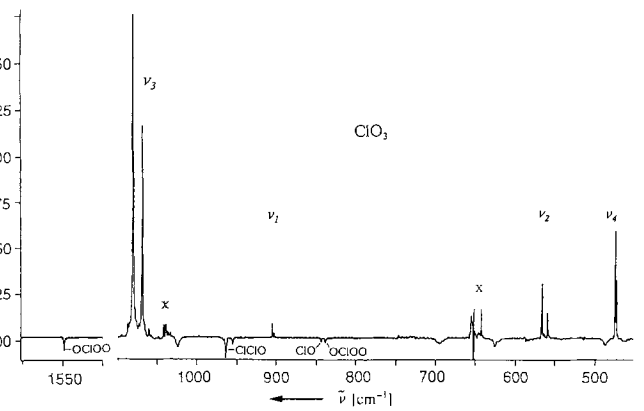


Fig. 2. Difference spectrum of the IR spectra of the pyrolysis products of Cl_2O_4 isolated in a neon matrix before and after the photolysis with light of wavelength greater than 420 nm. The bands of the ClO_3 point upwards and those of the OClOO isomer downwards. The bands of the photostable chlorine perchlorate that are not completely compensated are labeled X. ClClO is the photolysis product of ClOCl, which arises from the hydrolysis of chlorine perchlorate.

Table 1. Wavenumbers $\tilde{\nu}$ [cm^{-1}] of the fundamental frequencies of the chlorine trioxide radical isolated in a neon matrix, the relative band intensities I, and the assignment.

ab initio [c]	$\tilde{\nu}$ $^{35}Cl^{16}O_3$	$^{37}Cl^{16}O_3$	$^{35}Cl^{18}O_3$	$^{37}Cl^{18}O_3$	I [a]	Assignment [b]
1080 (77)	1081.27	1069.44	1047.06	1034.69	100	$\nu_3(e) = \nu_{as}(ClO)$
915 (2)	905.04	902.59	860.23	857.45	3.5	$\nu_1(a_1) = \nu_s(ClO)$
581 (21)	566.63	559.44	549.63	542.48	12	$\nu_2(a_1) = \delta_s(OClO)$
479 (16)	475.76	474.09	452.14	450.66	21	$\nu_4(e) = \delta_{as}(OClO)$

[a] $^{35}Cl^{16}O_3$ isotopomer, $I(\nu_3) = 100$. [b] Assignment to the point group C_{3v}. [c] Wavenumbers calculated for $^{35}Cl^{16}O_3$ with the RMP2/6-311G(2df) basis set [cm^{-1}], and intensities [km mol^{-1}] (in parentheses) [8].

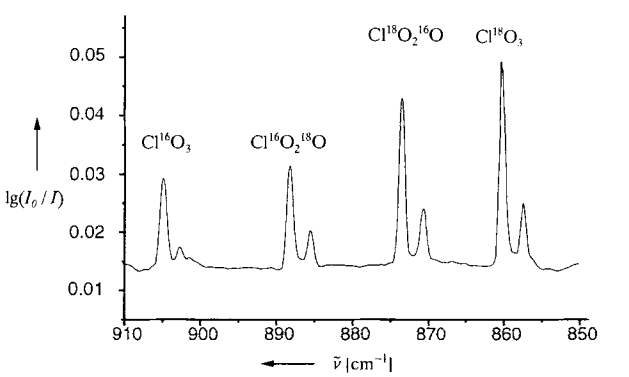


Fig. 3. IR bands of the symmetric Cl–O stretching band ν_1 of ^{18}O-enriched ClO_3, isolated in a Ne matrix.

The bond angle and harmonic force field were calculated from the analysis of the complete vibrational spectra of the four isotopomers of the ClO_3 radical. The required anharmonicity correction of the fundamental vibrations were performed according to Ref. [13]. Thus, the comparison of the isotope pairs $^{35}Cl^{16}O_3/^{37}Cl^{16}O_3$ and $^{35}Cl^{16}O_3/^{35}Cl^{18}O_3$ affords a O-Cl-O bond angle of $113.5 \pm 2^\circ$ (computed by ab initio methods: 114°[8]). The Cl–O force constant is $6.21 \times 10^2\ N\,m^{-1}$, and from a comparison of the corresponding force constants and bond lengths of ClO_2[13] (7.055 $N\,m^{-1}$, 146.98 pm) and ClO[12] (4.713 $N\,m^{-1}$, 156.96 pm), a ClO bond length of 150.0 ± 1 pm (calculated by ab initio methods: 144.5 pm[8]) is estimated. As anticipated, the O-Cl-O bond angle and the Cl–O force constant in the ClO_3 radical are both larger than in the ClO_3^- ion (106.6°, $5.87 \times 10^2\ N\,m^{-1}$).[14]

The UV spectrum of ClO_3 (Fig. 1) overlaps with that of ClO below 300 nm. Like the UV spectra of ClO and ClO_2,[11] it displays a pronounced vibrational fine structure, which, however, has a smaller absorption cross-section than ClO. The excitation of ClO_3 in a matrix with light of wavelength greater than 420 nm leads to OClO and O. In an O_2 matrix the O atom is trapped as O_3; in a neon matrix it reacts with OClO to OClOO, an unsymmetrical ClO_3 isomer. From the position of the O–O vibration and from the slight red shift of the Cl–O vibration relative to that of ClO in a neon matrix (see above), the bond between ClO and O_2 is deduced to be very weak. This isomer absorbs UV light below 295 nm. After photolysis the bands of OClOO disappear from the IR spectrum, and a van der Waals complex $[ClO/O_2]$ remains in the matrix cage with $\tilde{\nu}(^{35}ClO) = 844.4\ cm^{-1}$.

Received: March 5, 1994 [Z 6731 IE]
German version: *Angew. Chem.* **1994**, *106*, 1581

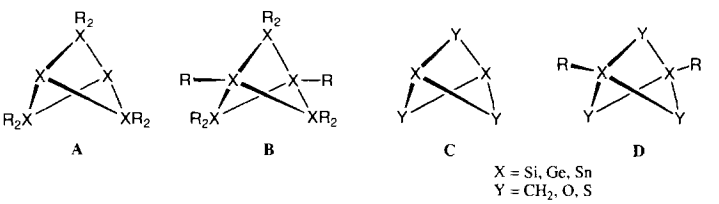
[1] H. J. Schumacher, G. Stieger, *Z. Anorg. Allg. Chem.* **1929**, *184*, 272.
[2] M. Jansen, G. Schatte, K. M. Tobias, H. Willner, *Inorg. Chem.* **1988**, *27*, 1703.
[3] a) F. Zabel, *Ber. Bunsenges. Phys. Chem.* **1991**, *95*, 893; b) A. J. Colussi, S. P. Sander, R. R. Fridl, *J. Phys. Chem.* **1992**, *96*, 4442.
[4] a) V. Handwerk, R. Zellner, *Ber. Bunsenges. Phys. Chem.* **1986**, *90*, 92; b) R. Simonaitis, J. Heicklen, *Planet. Space Sci.* **1975**, *23*, 1567.
[5] C. F. Goodeve, F. A. Todd, *Nature* **1933**, *132*, 514.
[6] J. Fargenharson, C. F. Goodeve, F. D. Richardson, *Trans. Faraday Soc.* **1936**, *32*, 790.
[7] a) T. Rathmann, R. N. Schindler, *Ber. Bunsenges. Phys. Chem.* **1992**, *96*, 421; b) *Chem. Phys. Lett.* **1992**, *190*, 539.
[8] A. Rauk, E. Tschnikow-Roux, Y. Chen, M. P. McGrath, L. Radom, *J. Phys. Chem.* **1993**, *97*, 7947.
[9] P. Bruckmann, H. Willner, *Environ. Sci. Technol.* **1983**, *17*, 352.
[10] Chlorine perchlorate was synthesized by treatment of an excess of $CsClO_4$ with $ClSO_3F$ for 5 days at -20°, as adapted from the method of K. O. Christe, C. J. Schack, E. C. Curtis, *Inorg. Chem.* **1971**, *10*, 1589. To prepare ^{18}O-enriched $CsClO_4$, CsCl was dissolved in $H_2{}^{18}O$ (Johnson Matthey) in a PFA flask (PFA = tetrafluoroethylene–perfluoro(propyl vinyl ether) copolymer) and oxidized first at room temperature and then for 2 h at $80^\circ C$ by an excess of XeF_2.
[11] W. B. Demore, D. M. Golden, R. F. Hampson, C. J. Howard, C. E. Kolb, N. J. Molina, A. R. Ravishankara, S. P. Sander, *Chemical Kinetics and Photochemical Data for Use in Stratospheric Modeling* (*JPL Publ.* **1992**, 122).
[12] J. B. Burkholder, P. D. Hammer, C. J. Howard, A. G. Maki, G. Thompson, C. Chackerian, Jr., *J. Mol. Spectrosc.* **1987**, *124*, 139.
[13] H. S. P. Müller, H. Willner, *J. Phys. Chem.* **1993**, *97*, 10589.
[14] H. Siebert in *Anwendungen der Schwingungsspektroskopie in der Anorganischen Chemie* (Ed.: M. Becke-Goehring), Springer, Berlin, **1966**.

$(t\mathrm{BuSi})_2(PC_6H_{11})_3$: A Propellane-Like Cyclosilaphosphane with Remarkable Structure**

Matthias Driess,* Rolf Gleiter, Rudolf Janoschek,* Hans Pritzkow, and Michael Reisgys

Dedicated to Professor Helmut Werner on the occasion of his 60th birthday

Since the synthesis of [1.1.1]propellane[1a] and because of its remarkable stability, the question of the existence of hetero-[1.1.1]propellanes **A** containing heavy elements of group 14 as framework atoms and of the related heterobicyclo[1.1.1]-pentanes **B** has become very topical. **A** and **B** possess remarkable electronic structures, which differ significantly from those



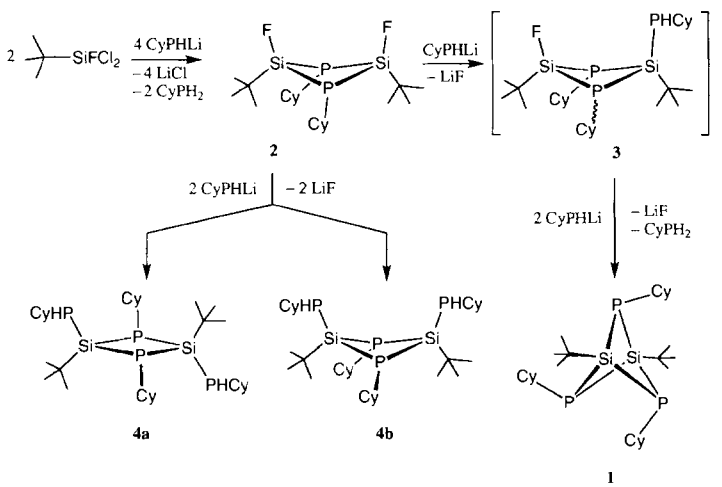
of the carbon compounds. For example, the bridged centers X1 and X3 are at almost the same distance from one another in each of the corresponding framework topologies **A** and **B**, and exhibit only a weak bonding interaction. This is substantiated by theoretical studies[1b] as well as by some structural data from corresponding pentasila[2a] and pentastanna compounds.[2b]

Interesting questions with regard to the chemical bonding also arise for structurally analogous compounds of the types **C** and **D**, in which the two centers X (X = Si, Ge, Sn) are bridged by three methylene groups or heteroatoms Y (Y = CH_2, O, S). Quantum chemical calculations for **C** and **D** gave unusually short X–X distances and an antibonding interaction between the two centers X; the difference in electronegativity between X and Y appears to play a key role.[3] Whereas a propellane analogue of type **C** has so far not been prepared, 2,4,5-triselena-1,3-disilabicyclo[1.1.1]pentane $[(Me_3Si)_3C-Si]_2Se_3$,[4] a compound of type **D**, was synthesized recently. We report here on the first 2,4,5-triphospha-1,3-disilabicyclo[1.1.1]pentane **1**, the electronic structure of which we have determined by photoelectron spectroscopy and quantum chemical calculations (MP2/6-31G*, RHF/DZ + POL). Its molecular structure can be explained simply with a consistent bonding model. Compound **1**[5] is formed by the reaction of tBuSiFCl$_2$ with CyPHLi (Cy = cyclohexyl) in the molar ratio 1:3 in THF in 33% yield. In this reaction the lithium phosphanide acts as a nucleophile and as an auxiliary base. Surprisingly, not only the kind of the *tert*-butyltrihalogensilane employed, but also the solvent used plays a

[*] Priv.-Doz. Dr. M. Driess, Dr. H. Pritzkow, Dipl.-Chem. M. Reisgys
Anorganisch-chemisches Institut der Universität
Im Neuenheimer Feld 270, D-69120 Heidelberg (FRG)
Telefax: Int. code + (6221)56-4197
Prof. Dr. R. Janoschek
Institut für Theoretische Chemie der Universität
Mozartstrasse 14, A-8010 Graz (Austria)
Telefax: Int. code + (316)38-2130
Prof. Dr. R. Gleiter
Organisch-chemisches Institut der Universität Heidelberg (FRG)

[**] This work was supported by the Deutsche Forschungsgemeinschaft (Dr 226/2-2, SFB 247) and the Fonds der Chemischen Industrie.

decisive role in the success of the synthesis: the desired bicyclic system was not obtained (^{31}P NMR) either with tBuSiCl$_3$ instead of tBuSiFCl$_2$ or with Et$_2$O instead of THF as solvent. The reaction mechanism for the formation of **1** is not yet known. We assume that the cyclocondensation of tBuSiFCl$_2$ and CyPHLi initially leads to the P$_2$Si$_2$ heterocyclobutane **2** as an intermediate. With additional phosphanide, **2** is converted into the *Si*-phosphanyl-substituted 1,3-diphospha-2,4-disilacyclobutane **3** and the diastereomeric *Si,Si'*-diphosphanyl-substituted derivatives **4** (Scheme 1).



Scheme 1. Postulated mechanism of the formation of **1**, **2**, **4a,b**. Cy = cyclohexyl.

Metalation of the exocyclic phosphorus atom in **3** with CyPHLi and subsequent cyclization with elimination of LiF leads to the formation of **1** (Scheme 1). In agreement with this mechanism is the fact that in addition to **1** only the compounds **4a,b** are formed. Compounds **4a,b** were characterized by NMR spectroscopy, mass spectrometry, and X-ray crystallography (Fig. 1a,b).[6, 7] Furthermore, **2** was isolated[6] and characterized by an X-ray crystal structure analysis.[7] Whereas a folded cycle is present in **2** and **4b**, the Si$_2$P$_2$ framework in **4a** possesses an inversion center.

The structure of **1** can be derived from the simple NMR spectra and its composition is confirmed by mass spectrometry and elemental analysis.[5] The ^{31}P NMR spectrum shows a singlet at $\delta = -69.7$ and the ^{29}Si NMR spectrum reveals a quartet at $\delta = -14.1$ with ^1J(Si, P) = 61.6 Hz. The value of the coupling constant ^1J(Si, P) is unexpectedly high for a four-membered cyclosilaphosphane and lies in the range normally associated with three-membered Si,P ring systems.[8] An X-ray crystal structure analysis of **1**[7] confirms that the bicyclic system has an unusual ring geometry (Fig. 2).

The endocyclic bond angles at the pyramidally coordinated P atoms lie between 66.7(1) and 67.4(1)°, that is they correspond to those in three-membered rings, whereas values between 82 and 85 are found in 1,3-diphospha-2,4-disilacyclobutanes (Fig. 1a,b).[9] Due to the acute inner angle at the phosphorus in **1**, the two Si atoms are remarkably close to each other (2.518(3) Å). This distance could imply a bonding interaction between the Si atoms, since it lies in the range for Si–Si single bond lengths (2.3–2.7 Å). Similar geometric relations were also observed for the Si$_2$Se$_3$ bicyclic system [(Me$_3$Si)$_3$CSi]$_2$Se$_3$.[4] A Si–Si bond strengthened by three-center bonds ("σ-bridging π orbitals") was proposed as an explanation for this extraordinary

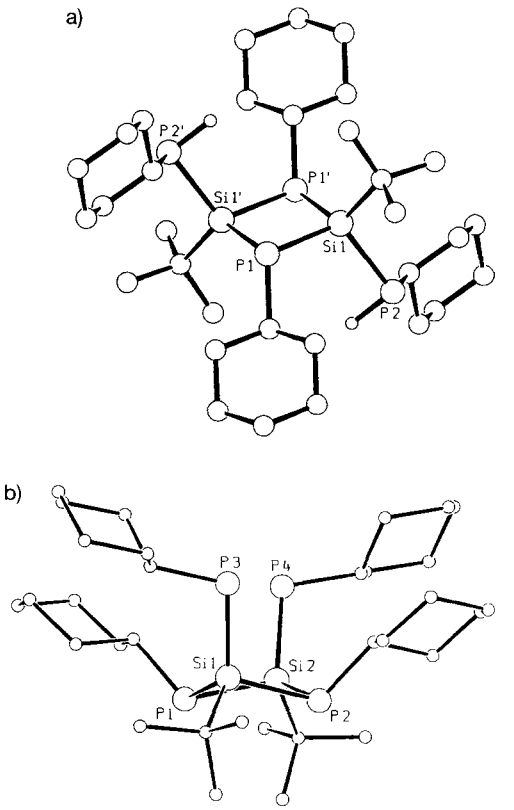


Fig. 1. a) Crystal structure of **4a**. Selected distances [Å] and angles [°]: Si1–P1 2.261(3), Si1–P2 2.278(4), Si1'–P1 2.274(4); Si1'-P1-Si1 83.86(12), P1'-Si1-P1 96.14(12), P2-Si1-P1 112.23(10), P2-Si1-P1' 107.56(12). b) Crystal structure of **4b**. Selected distances [Å] and angles [°]: Si1–P1 2.271(2), Si2–P1 2.272(1), Si1–P2 2.269(1), Si2–P2 2.269(2), Si1–P3 2.258(1), Si2–P4 2.269(1); Si2-P1-Si1 82.16(5), Si2-P2-Si1 82.28(5), P1-Si1-P2 92.71(5), P1-Si2-P2 92.67(5).

structure and thus an analogy to the bonding in chalcogen disiliranes was made. However, in this bonding model derived from calculations not all occupied orbitals were completely included.[4] Taking all the occupied orbitals into consideration, our calculations result in a net positive charge at the silicon atoms (0.665) and a total Si–Si bond order of −0.260, that is, in contrast to the proposed bonding model, an antibonding Si–Si interaction occurs. In comparison: the Si–Se bond order in the Si$_2$Se$_3$ bicyclic system is 0.323.[10]

Thus, what are the reasons for the unusual structure of **1**? We assume that geometric factors, in particular, are responsible for the short Si–Si distance and the small endocyclic angles at the phosphorus atoms. There is a tug-of-war between the three Si-P-Si and the six P-Si-P angles. Every increase of

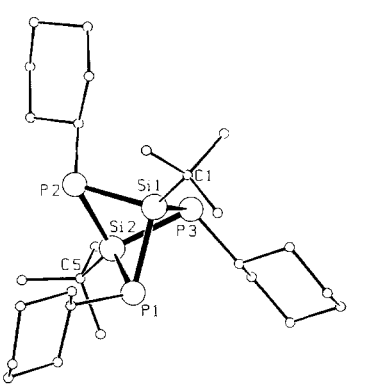


Fig. 2. Crystal structure of **1** (for the part with the higher occupation density). Selected distances [Å] and angles [°]: Si1–C1 1.906(6), Si1–P1 2.294(3), Si1–P2 2.274(3), Si1–P3 2.275(3), Si2–C5 1.900(5), Si2–P1 2.286(4), Si2–P2 2.267(3), Si2–P3 2.261(3); Si1-P1-Si2 66.7(1), Si1-P2-Si2 67.3(1), Si1-P3-Si2 67.4(1), P1-Si1-P2 91.0(1), P2-Si1-P3 93.6(1), P1-Si1-P3 91.7(1), P1-Si2-P2 91.4(1), P2-Si2-P3 94.2(1), P1-Si2-P3 92.3(1).

the Si–Si distance and thus the widening of the three Si-P-Si angles would lead to a reduction of the six already very small P-Si-P angles. A Si-P-Si inner angle of 82°, usual for Si_2P_2 cyclobutanes, would lead to a P-Si-P angle of 83° in **1**.[11] A reduction of the Si-P-Si angle to 67° lowers the angle strain at the silicon atoms (increase of the endocyclic P-Si-P angles to 93°). As a result of this the P-Si-P angles are approximately the same size as the endocyclic ones in **4b**, and somewhat smaller than those in **4a**. However, the Si–Si distance in **4a** is 3.02 Å and that in **4b** is 2.98 Å, and the mean exocyclic P-Si-P angles are 109.9 (**4a**, Fig. 1a) and 114° (**4b**, Fig. 1b), respectively.

MO calculations[12] on $(MeSi)_2(PMe)_3$ (Fig. 3, Table 1), as for the Si_2Se_3 bicyclic system, resulted in a Si–Si bond order of

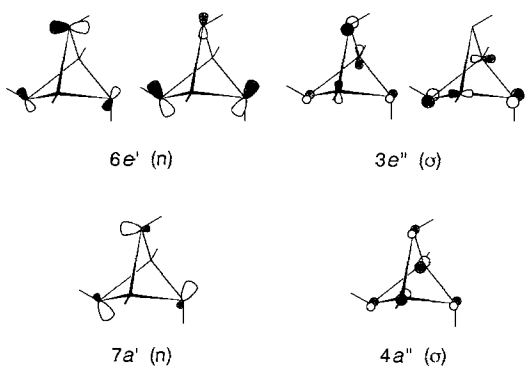


Fig. 3. Calculated frontier orbitals for the Si_2P_3 framework.

−0.300 and a Si–P bond order of 0.348. In the equilibrium structure the P atoms—like in the structure of **1**—are pyramidally coordinated (molecular symmetry C_{3h}). The calculated

Table 1. Comparison of several distances [Å] and angles [°] of **1** with the corresponding calculated values of $(MeSi)_2(PMe)_3$ (RHF/DZ + POL) [12].

	1	$(MeSi)_2(PMe)_3$
Si-Si	2.518(3)	2.548
P-Si	2.261(3)–2.294(3)	2.262
Si-C	1.900(5), 1.907(7)	1.870
Si-P-Si	66.7(1), 67.3(1)	68.5
P-Si-P	91.7(1)–94.2(1)	91.4

orbital energies were correlated (Koopmans theorem,[13] Table 2) with the measured ionization energies (vertical transitions) from the photoelectron spectrum of **1**.

Table 2. Experimental ionization energies I_{vi} (vertical transitions) of **1** [eV] and calculated orbital energies $-\varepsilon_i$ [12] of $(MeSi)_2(PMe)_3$ [C_{3h}].

Assignment	I_{vi} (**1**)	$-\varepsilon_i$ ($(MeSi)_2(PMe)_3$)
6e' (n)	7.3	8.3
7a' (n)	8.2	9.6
3e" (σ)	8.4	9.7

The comparison of the results of the MO calculation and photoelectron spectroscopy shows that the highest occupied orbitals (Fig. 3, Table 2) are of the n_P type (lone pair of electrons at phosphorus). The first n_P ionization energy is about 0.5 and the σ_{SiP} energy is about 1 eV lower than that in other silylphosphanes.[14] Interestingly, the calculated inversion barriers at the phosphorus atoms[15] in $(HSi)_2(PH)_3$ are 41.2 (MP2/6-31G*) and in $(MeSi)_2(PMe)_3$ 43.3 kcal mol^{-1} (RHF/DZ + POL) per P atom, compared with 35.4 kcal mol^{-1} in PH_3 (MP2/6-31G*) and 13.4 kcal mol^{-1} in $MeP(SiMe_3)_2$ (RHF/DZ + POL). A lower P inversion barrier (15–20 kcal mol^{-1}) was calculated for P_2Si_2 heterocyclobutanes, like for $MeP(SiMe_3)_2$, due to the σ donor effect ($Si^{\delta+}-P^{\delta-}$).[9] The inversion barriers for $(HSi)_2(PH)_3$ and $(MeSi)_2(PMe)_3$, which are spectacularly high for silylphosphanes, can be explained by the strongly antibonding interactions between the pure p-like lone pairs of electrons at the trigonal-planar configurated phosphorus atoms (molecular symmetry D_{3h}). According to MP2/6-31G* calculations the D_{3h} structure of $(HSi)_2(PH)_3$ is that of the triplet state, which lies even lower—by 1.9 kcal mol^{-1}—than that in the D_{3h} optimized singlet state.[12] We are currently investigating whether it is possible to synthesize a compound containing a trigonal-planar coordinated phosphorus by using suitable bulky electropositive substituents.

Experimental Procedure

$C_6H_{11}PH_2$ (5.3 g, 45.7 mmol) dissolved in THF (150 mL) was monolithiated at −70 °C with *n*BuLi (18.3 mL, 2.5 M solution in hexane). *t*BuSiFCl$_2$ (2.65 g, 15.2 mmol) dissolved in THF (50 mL) was added dropwise to this solution over an hour. After the pale red solution had been allowed to warm slowly to room temperature, the solvent was removed under vacuum (10^{-2} Torr) and the pale yellow, solid residue was taken up in toluene (50 mL). LiCl was removed by filtration and the solvent was removed again under vacuum. Compound **1** was isolated by crystallization from hexane. Yield: 1.3 g (2.54 mmol; 33%), colorless crystals, m.p. 211–213 °C.

2 and **4a, b** were obtained from the mother liquor after several fractionating crystallizations [6].

Received: March 2, 1994, [Z 6723 IE]
German version: *Angew. Chem.* **1994**, *106*, 1548

[1] a) K. B. Wiberg, *Chem. Rev.* **1989**, *89*, 975, and references therein; b) P. von R. Schleyer, R. Janoschek, *Angew. Chem.* **1987**, *99*, 1312; *Angew. Chem. Int. Ed. Engl.* **1987**, *26*, 1267; D. B. Kitchen, J. E. Jackson, L. C. Allen, *J. Am. Chem. Soc.* **1990**, *112*, 3408, and references therein; M. S. Gordon, K. A. Nguyen, M. T. Carroll, *Polyhedron* **1991**, *10*, 1247; C. Liang, L. C. Allen, *J. Am. Chem. Soc.* **1991**, *113*, 1878.

[2] a) Y. Kabe, T. Kawase, J. Okada, O. Yamashita, M. Goto, S. Masamune, *Angew. Chem.* **1990**, *102*, 823; *Angew. Chem. Int. Ed. Engl.* **1990**, *29*, 794; b) L. R. Sita, R. D. Bickerstaff, *J. Am. Chem. Soc.* **1989**, *111*, 6454; L. R. Sita, J. Kinoshita, *ibid.* **1990**, *112*, 8839.

[3] K. A. Nguyen, M. T. Carroll, M. S. Gordon, *J. Am. Chem. Soc.* **1991**, *113*, 7924; S. Nagase, T. Kudo, T. Kurakake, *J. Chem. Soc. Chem. Commun.* **1988**, 1063; A. Streitwieser, *ibid.* **1989**, 1261; see also ref. [1].

[4] H. Yoshida, Y. Takahara, T. Erata, W. Ando, *J. Am. Chem. Soc.* **1992**, *114*, 1098.

[5] ^{1}H NMR (200 MHz, C_6D_6, 25 °C): δ = 1.0–2.0 (m, 30H, CH_2), 1.33 (s, 18H, *t*Bu), 3.09 (m, 3H, PCH); ^{31}P NMR (81 MHz, C_6D_6, 25 °C): δ = −69.7 (s); ^{29}Si NMR (39 MHz, C_6D_6, Insensitive Nuclei Enhanced by Polarization Transfer (INEPT)): δ = −14.1 (q, ^1J(Si,P) = 61 Hz); EI-MS: *m/z* = 512 (M^+, 8%), 429 ($(M^+ - C_6H_{11})^+$, 100%), 347 ($(M - C_6H_{11} - C_6H_{10})^+$, 21%); correct elemental analysis.

[6] The NMR spectra and the molecular structures of **2**, **4a,b**, and related compounds will be discussed in detail in a future publication: M. Driess, M. Reisgys, H. Pritzkow, unpublished results.

[7] Crystal structure analyses (four-circle diffractometer, $Mo_{K\alpha}$ radiation, ω scan). a) **1**: triclinic, $P\bar{1}$, a = 10.524(10), b = 11.073(12), c = 15.967(15) Å, α = 107.94(8), β = 89.98(8), γ = 115.89(8)°, Z = 2, V = 1573 Å^3, 4084 measured reflections ($2\theta_{max}$ = 47°), 2882 of which observed ($I > 2\sigma(I)$). The molecule is disordered, the phosphorus atoms with the cyclohexyl groups occupy two positions (ratio ca. 4:1), in addition, one *t*Bu group is disordered. Refinement with all reflections against F^2 [16], cyclohexyl groups as rigid groups, Si and P atoms anisotropic, similarly the C atoms of the higher occupied positions, C atoms of the other positions isotropic, H atoms in calculated positions, 335 parameters. $R1$ = 0.068 (observed reflections only), $wR2$ = 0.192 (all reflections). b) **4a**: triclinic, $P\bar{1}$, a = 9.708(12), b = 10.641(15), c = 11.010(14) Å, α = 62.62(9), β = 74.59(9), γ = 70.24(10)°, Z = 1, V = 942.2 Å^3, 3896 measured reflections ($2\theta_{max}$ = 53°), 3251 of which observed ($I > 2\sigma(I)$). Refinement with all reflections against F^2 [16], non-hydrogen atoms anisotropic, H atoms

given in calculated positions, 184 parameters. $R1 = 0.037$, $wR2 = 0.101$ (all reflections). c) **4b**: monoclinic, $P2_1/a$, $a = 11.233(5)$, $b = 16.578(8)$, $c = 20.256(10)$ Å, $\beta = 94.61(4)°$, $Z = 4$, $V = 3760$ Å^3, 6628 measured reflections ($2\theta_{max} = 50°$), 4354 of which observed ($I > 2\sigma(I)$). Refinement with all reflections against F^2 [16], non-hydrogen atoms anisotropic, methyl groups treated as rigid groups, remaining H atoms given in calculated positions, 421 parameters. $R1 = 0.050$ (observed reflections only), $wR2 = 0.121$ (all reflections). d) **2**: orthorhombic, *Imam*, $a = 12.799(6)$, $b = 13.175(6)$, $c = 14.898(7)$ Å, $Z = 4$, $V = 2512$ Å^3, 1549 measured reflections ($2\theta_{max} = 55°$), 916 of which observed ($I > 2\sigma(I)$). Refinement with all reflections against F^2 [16], non-hydrogen atoms anisotropic, H atoms given in calculated positions, 76 parameters. $R1 = 0.049$, $wR2 = 0.125$ (all reflections). e) Further details of the crystal structure investigations may be obtained from the Fachinformationszentrum Karlsruhe, D-76344 Eggenstein-Leopoldshafen (FRG), on quoting the depository numbers CSD-400853 (**1**), 400856 (**2**), 400854 (**4a**), and 400855 (**4b**).

[8] M. Baudler, J. Jongebloed, *Z. Anorg. Allg. Chem.* **1979**, *458*, 9; M. Driess, A. D. Fanta, D. Powell, R. West, *Angew. Chem.* **1989**, *101*, 1087; *Angew. Chem. Int. Ed. Engl.* **1989**, *28*, 1038; M. Driess, H. Pritzkow, M. Reisgys, *Chem. Ber.* **1991**, *124*, 1923.

[9] U. Klingebiel, N. Vater, W. Clegg, M. Haase, G. M. Sheldrick, *Z. Naturforsch. B* **1983**, *38*, 1557; W. Clegg, M. Haase, U. Klingebiel, G. M. Sheldrick, *Chem. Ber.* **1983**, *116*, 146; M. Driess, H. Pritzkow, M. Reisgys, *ibid.* **1991**, *124*, 1931; M. Driess, U. Winkler, W. Imhof, L. Zsolnai, G. Huttner, *ibid.*, **1994**, *127*, 1031.

[10] In ref.[4] a net negative charge at the silicon atom is given (−0.18), although silicon shows a significantly smaller spectroscopic electronegativity than selenium: L. C. Allen, *J. Am. Chem. Soc.* **1989**, *111*, 9003.

[11] The endocyclic angle at the silicon atoms (α_{Si}) and at the phosphorus atoms (β_P) are linked to one another in a first approximation by the relationship $\sin(\alpha_{Si}/2) = \sin 60° \cos(\beta_P/2)$.

[12] All the calculations were carried out with the Gaussian 92 Revision C4 program. M. Frisch, G. W. Trucks, M. Head-Gordon, P. M. W. Gill, M. W. Wong, J. B. Foresman, B. G. Johnson, H. B. Schlegel, M. A. Robb, E. S. Replogle, R. Gomperts, J. L. Andres, K. Raghavachari, J. S. Binkley, C. Gonzales, R. L. Martin, D. J. Fox, D. J. Defrees, J. Baker, J. J. P. Stewart, J. A. Pople, Gaussian Inc., Pittsburg, PA, **1992**. The calculations labeled with RHF/DZ + POL refer to ab initio pseudo-potential calculations with sets of 5d functions for Si (0.45), P (0.55), Se (0.35). All net charges and bond orders (overlap populations) were calculated within the frame of the Mulliken population analysis.

[13] T. Koopmans, *Physica* **1934**, *1*, 104.

[14] S. Cradock, E. A. V. Ebsworth, W. J. Savage, R. A. Whiteford, *J. Chem. Soc. Faraday Trans. 2* **1972**, *68*, 934; H. Bock, B. Solouki, G. Fritz, W. Hölderich, *Z. Anorg. Allg. Chem.* **1979**, *458*, 53; R. Gleiter, K.-H. Pfeifer, M. Baudler, G. Scholz, T. Wettling, M. Regitz, *Chem. Ber.* **1990**, *123*, 757; M. Driess, U. Winkler, H. Pritzkow, R. Gleiter, unpublished results.

[15] Although the structure with a planar configurated phosphorus atom is irrelevant for the singlet state, the relative energy with respect to that of the minimum, divided by three, can be defined as the "average inversion barrier" at the phosphorus atoms.

[16] G. M. Sheldrick, SHELXL93, Universität Göttingen, **1993**.

A Highly Distorted and an Undistorted Borirane, C-B-H Hyperconjugation Induced by C-Si-H Hyperconjugation**

Christian Balzereit, Claudia Kybart, Heinz-Jürgen Winkler, Werner Massa, and Armin Berndt*

The methyleneborane **1**[1] adds trimethylsilylacetylene (**2**) at −30 °C to give the 1,4-diboraspiro[2.3]hex-5-ene **3**, whose four-membered ring is extended already at this temperature by the addition of another molecule of **2** to form the six-membered ring of the 1,4-diboraspiro[2.5]octa-5,7-diene **4** (Dur = 2,3,5,6-tetramethylphenyl). Some physical data of **3** and **4** are given in Table 1; Figure 1 shows the crystal structures of **3** and **4**.[2] The four-membered ring in **3** is folded by 30° along the short[3] (186.9 pm) B–C diagonal. This was to be expected because of the shielding of the boron atom ($\delta(^{11}B) = 32$) and the deshielding of the neighboring tricoordinate C atom ($\delta(^{13}C) = 176.1$), which indicate a strong 1,3 interaction.[4]

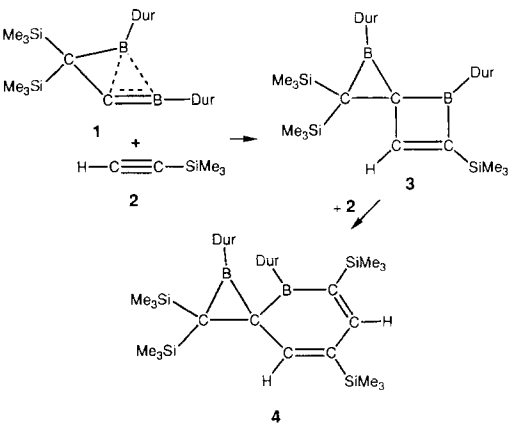


Table 1. Some physical data of **3**, **4**, and **8**.

3: Colorless crystals, m.p. 100 °C (decomp), yield (NMR spectroscopic): quantitative. ^{1}H NMR (400 MHz, $CDCl_3$, −30 °C): $\delta = 0.02, 0.39$, (each s, each 9H, $SiMe_3$ on the three-membered ring, 0.23 (s, 9H, $SiMe_3$ on the four-membered ring), 2.28, 2.35, 2.38, 2.39, 2.49, 2.77 (each s, in total 24H, *o*- and *m*-CH_3), 7.05, 7.44 (each s, each 1H, *p*-H), 8.11 (s, 1H, CH in the four-membered ring); ^{13}C NMR (100 MHz, $CDCl_3$, −30 °C): $\delta = -1.3$ (q, 3C, $SiMe_3$ on the four-membered ring), 2.1, 3.0 (each q, each 3C, $SiMe_3$ on the three-membered ring), 19.3, 19.5, 19.95, 20.0, 20.5, 20.8 (each q, in total 8C, *o*- and *m*-CH_3), 24.7 (s, 1C, CSi_2), 53.1 (s, 1C, CB_2), 129.9 (d, 1C, *p*-C), 131.7 (s, 1C, *i*-C), 132.3, 132.5, 133.7, 134.5 (each s, each 1C, *o*- and *m*-C), 137.5 (d, 1C, *p*-C), 138.4 (s, 1C, *i*-C), 146.0 (br. s, 2C, *o*-C in the three-membered ring), 154.3 (d, $^1J(C,H) = 168$ Hz, 1C, CH in the four-membered ring), 176.1 (s, 1C, =CB in the four-membered ring); ^{11}B NMR (96 Hz, pentane, −10 °C): $\delta = 32, 69$.

4: Colorless crystals, m.p. 143 °C (conversion into **8**), yield 60%. ^{1}H NMR (300 MHz, $CDCl_3$, 25 °C): $\delta = -0.23, -0.03, 0.21, 0.29$ (each s, each 9H, $SiMe_3$), 1.40, 1.44, 1.79, 2.03, 2.13, 2.18, 2.26, 2.49 (each s, each 3H, *o*- and *m*-CH_3), 6.79, 7.16 (each s, each 1H, *p*-H), 7.12, 7.91 (each d, $^4J(H,H) = 0.7$ Hz, each 1H, CH in the six-membered ring); ^{13}C NMR (100 MHz, $CDCl_3$, −30 °C): $\delta = -0.8, 0.5, 3.8, 4.0$ (each q, each 3C, $SiMe_3$), 17.7, 19.8, 20.0, 20.2, 20.3, 20.8, 21.5, 23.1 (each q, each 1C, *o*- and *m*-CH_3), 42.3 (s, 1C, CSi_2), 71.7 (s, 1C, CB_2), 129.4, 136.4 (each d, each 1C, *p*-C), 130.9 (s, 1C, BCSi), 131.8, 132.5, 132.8, 133.0, 133.3, 134.1, 136.1, 142.2, 143.6 (each s, each 1C, *o*- and *m*-C and CSi in the six-membered ring), 143.9, 147.2 (each s, each 1C, *i*-C), 152.5 (d, $^1J(C,H) = 148$ Hz, 1C, CH in the six-membered ring), 161.4 (d, $^1J(C,H) = 152$ Hz, 1C, CH in the six-membered ring); ^{11}B NMR (96 Hz, $CDCl_3$, 25 °C): $\delta = 57, 69$.

8: Colorless crystals, m.p. 134 °C, yield: quantitative. ^{1}H NMR (500 MHz, $CDCl_3$, −30 °C): $\delta = -0.34, 0.04, 0.16, 0.31$ (each s, each 9H, $SiMe_3$), 1.68, 2.02, 2.16, 2.26, 2.28, 2.29, 2.46, 2.51 (each s, each 3H, *o*- and *m*-CH_3), 4.01 (d, $^3J(H,H) = 4.6$ Hz, 1H, HCSi), 6.95, 7.02 (each s, each 1H, *p*-H), 7.23 (d, $^3J(H,H) = 4.6$ Hz, 1H, =CH in the six-membered ring; ^{13}C NMR (125 MHz, $CDCl_3$, −30 °C): $\delta = -0.9, 0.6, 1.1, 3.6$ (each q, each 3C, $SiMe_3$), 19.8, 20.1, 20.4, 21.0, 21.1, 22.2, 25.5 (each q, in total 8C, *o*- and *m*-CH_3), 48.6 (s, 1C, CSi_2), 62.6 (d, $^1J(C,H) = 117$ Hz, 1C, CHSi), 130.5, 130.9 (each d, each 1C, *p*-C), 132.2, 132.51, 132.54, 132.8, 133.6, 133.9, 134.2, 134.9, 135.5, 136.0 (each s, each 1C, *o*- and *m*-C and =CSi), 138.5 (s, 1C, $BCCSi_2$), 146.0, 146.7 (each s, 1C, BCCSi); ^{11}B NMR (96 MHz, $CDCl_3$, 25 °C): $\delta = 43, 72$.

HF/STO-3G or 6-31G* and MP2/6-31G* calculations on the unsubstituted 1,4-diboraspiro[2.3]hex-5-ene and on boracyclobutene, respectively, had given fold angles of 13, and 28°[5] and 33°[6], respectively. The B–C distances in the borirane ring of **3** (151.9 and 154.4 pm) correspond to those calculated for

[*] Prof. Dr. A. Berndt, Dipl.-Chem. C. Balzereit, Dipl.-Chem. C. Kybart, Dipl.-Chem. H.-J. Winkler, Prof. Dr. W. Massa
Fachbereich Chemie der Universität
D-35032 Marburg (FRG)
Telefax: Int. code + (6421)28-8917

[**] This work was supported by the Deutsche Forschungsgemeinschaft and the Fonds der Chemischen Industrie.

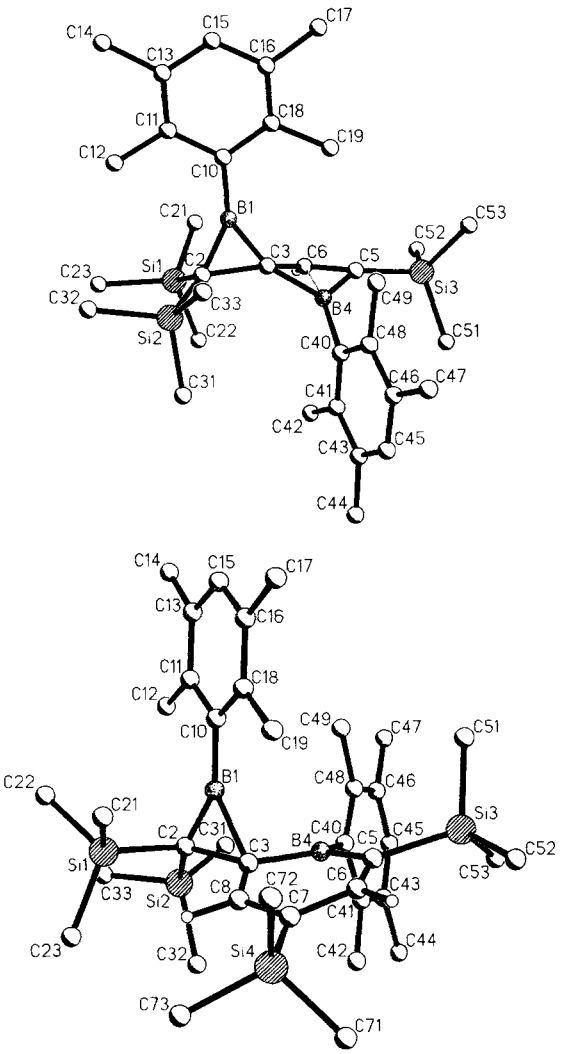
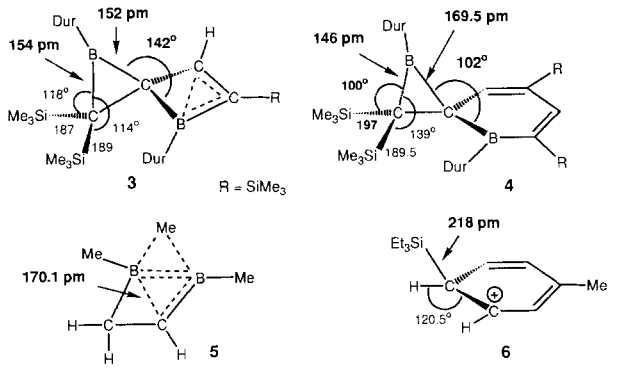


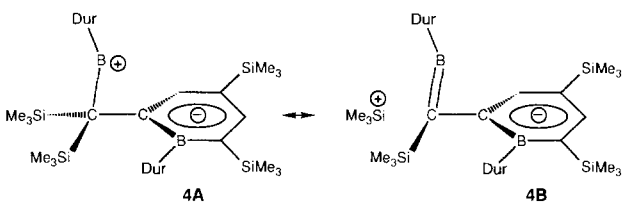
Fig. 1. Crystal structures of **3** (top) and **4** (bottom). Important distances [pm] and angles [°]: **3**: B1-C2 154.4(7), C2-C3 160.7(6), B1-C3 151.9(7), C3-B4 162.0(7), B4-C5 153.4(7), C5-C6 137.7(6), C6-C3 151.1(7), C6-B4 186.9(7), B1-C10 153.9(7), C2-Si1 188.8(4), C2-Si2 187.1(5), B4-C40 157.6(7), C5-Si3 184.3(5); B1-C3-C2 59.1(3), B4-C3-C6 73.2(3), B1-C3-B4 141.7(4), C2-C3-B4 139.5(4), B1-C3-C6 126.4(4), C2-C3-C6 128.2(4), B1-C2-Si1 118.3(3), B1-C2-Si2 114.4(3). **4**: B1-C2 146.0(10), C2-C3 163.4(10), B1-C3 169.5(11), C3-B4 157.0(12), B4-C5 155.9(11), C5-C6 132.6(10), C6-C7 145.5(11), C7-C8 138.2(10), C8-C3 144.5(10), B1-C10 152.1(11), C2-Si1 197.1(8), C2-Si2 189.5(7), B4-C40 158.4(11), C5-Si3 188.9(8), C7-Si4 184.5(8); B1-C3-C2 52.0(4), B4-C3-C8 115.4(6), B1-C3-B4 102.3(6), C2-C3-B4 126.4(6), B1-C3-C8 121.9(6), C2-C3-C8 118.0(6), B1-C2-Si1 100.1(5), B1-C2-Si2 139.5(6).

1-methylborirane (153.0 pm[7]). The C2–C3 and the B1–C3 bonds of the three-membered ring bend similarly with respect to the B4-C3-C6 plane of the four-membered ring (by 29.9 and 29.2°, respectively); the B1-C3-B4 angle (141.7°) is similar in size to the C2-C3-B4 angle (139.5).

In contrast, in **4** the C2–C3 bond lies almost in the B4-C3-C8 plane of the six-membered ring (deviation 4.7°), that is, C3 resides in an almost trigonal-planar environment formed by C2, B4, and C8. The B1-C3-B4 angle (102.3°) differs significantly from the C2-C3-B4 angle (126.4°). The plane of the borirane ring forms an angle of 72.5° with the B4-C3-C8 plane of the six-membered ring, that is, it is tilted by 17.5° toward the boron atom B4. The angle between the corresponding planes in **3** is 87.6°. The B1–C3 bond in **4** (169.5 pm) is 17 pm longer than that in **3**. A B–C bond (170.1 pm) of similar length was calculated for the nonclassical borylborirane **5**;[8] B–C distances of up to ≤158.0 pm have been determined experimentally for boriranes.[8]



The distortions in **4** are indicative of strong C–B hyperconjugation of the B1–C3 bond of the three-membered ring with the boracyclohexa-2,4-diene ring corresponding to the resonance structure **4A**. The formation of the 6π electron arene probably

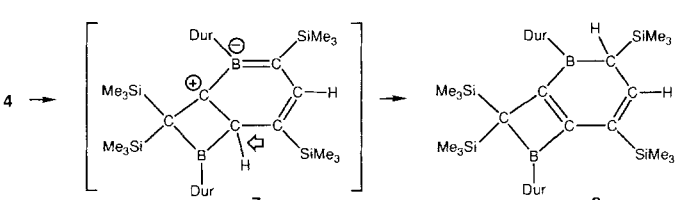


makes a major contribution to the strength of this effect. In **3** the electron deficiency of the boron atom of the four-membered ring is overcome by the formation of the 2π electron homoarene.

Distortions similar to those in **4** were recently described for the cyclohexadienyl cation **6**, isoelectronic with respect to the six-membered ring, with a C–Si instead of the strained C–B bond as σ donor.[9]

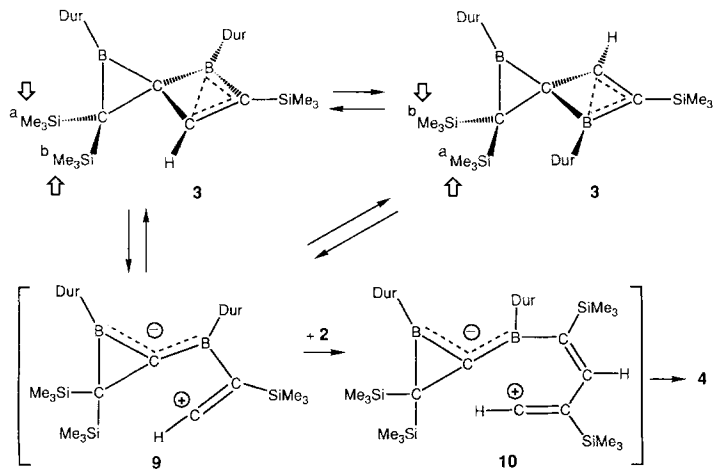
The increased electron deficiency at the boron atom of the three-membered ring (cf. **4A**) caused by the strong C–B hyperconjugation in **4** leads to strong C–Si hyperconjugation with the C2–Si1 bond (cf. **4B**), as indicated by a remarkably long C2–Si1 bond (197.1 vs. 189.5 pm for C2–Si2), a small B1-C2-Si1 angle (100.0° vs. 139.5° for B1-C2-Si2), and a very short C2–B1 distance (146.0 pm). In **3**, C–Si hyperconjugation with B1 as the electron-deficient center plays no significant role, as is apparent from the undistorted structure. The prerequisite for significant C–Si hyperconjugation in boriranes is evidently pronounced electron deficiency at the boron atom, which in **4** is caused by C–B hyperconjugation (resonance structure **4A**).

The weak B1–C3 bond in **4** is broken in solution even at room temperature: **4** rearranges within several days into the isomeric 2,7-diborabicyclo[4.2.0]octa-4,6-diene **8** (Table 1). Compound **8** forms as the only product when **4** melts. The constitution of **8** was confirmed by an X-ray structure analysis.[10]



The zwitterion **7** is probably the intermediate in this rearrangement; **7** can be considered as a σ complex of an intramolecular electrophilic substitution of **4A**. Migration of the proton to the carbanionic C atom bound to the boron atom in the six-membered ring gives **8**.

The ^1H and the ^{13}C NMR spectra show two sharp signals for the geminal trimethylsilyl groups in **3** only below $-30\,^\circ C$. These signals broaden at higher temperatures and coalesce at 30 and 20 °C, respectively. The barrier for the exchange was estimated to be 14 kcal mol^{-1}. We propose the zwitterion **9** as an intermediate. In **9** the negative charge is stabilized by π–π delocalization in a 1,3-diboraallyl anion and the positive charge of the vinyl cation[11] is stabilized by C–Si and C–B hyperconjugation. The formation of **4** can be readily explained by the addition of **2** to **9** and the cyclization of the resulting compound **10**.



Experimental Procedure

3: **2** (0.46 mL, 3.3 mmol) was added dropwise to **1** (1.53 g, 3.3 mmol) in pentane (20 mL) at −78 °C. The reaction mixture was slowly warmed to −30 °C and concentrated under vacuum at this temperature until crystallization began. Compound **3** crystallized at −30 °C overnight. The crystals were separated by filtration (D3 frit) and washed with pentane.

4: **2** (1.0 mL, 7.24 mmol) was added dropwise to a solution of **1** (1.66 g, 3.62 mmol) in pentane (20 mL) at −78 °C. After the mixture had been allowed to warm to −10 °C, it was concentrated and crystals of **4** were separated by filtration (D3 frit).

8: **4** was converted quantitatively into **8** by heating for 5 min at 143 °C.

Received: March, 17 1994 [Z6771IE]
German version: *Angew. Chem.* **1994**, *106*, 1579

[1] A. Berndt, *Angew. Chem.* **1993**, *105*, 1034-1058; *Angew. Chem. Int. Ed. Engl.* **1993**, *32*, 985-1009, and references therein.

[2] Crystal structure analyses: colorless crystals of **3** and **4** were investigated on a four-circle diffractometer (CAD4, Enraf-Nonius) at −80 °C with $Cu_{K\alpha}$ radiation ($\lambda = 154.178$ pm). **3**: $C_{33}H_{54}B_2Si_3$, crystal dimensions $0.3 \times 0.3 \times 0.5$ mm, monoclinic, space group $P2_1/c$, $Z = 4$, $a = 895.5(2)$, $b = 2088.4(4)$, $c = 1901.2(4)$ pm, $\beta = 95.01(3)^\circ$, $V = 3542.0 \times 10^{-30}$ m^3, $\rho_{calcd} = 1.044$ g cm^{-3}; 4954 measured reflections in the range up to $2\theta_{max} = 110^\circ$ (ω scans), 4446 of which were independent, 3341 reflections with $F_0 > 3\sigma(F_0)$ were used for the further calculations after Lorentz and polarization correction; no absorption correction ($\mu = 13.6$ cm^{-1}). The structure was solved by direct methods and refined against the F_0 data with full matrix. All hydrogen atoms were located by difference Fourier syntheses and were included in the calculation riding on their bonding partners and refined groupwise with isotropic temperature factors. Anisotropic temperature factors were used for all the remaining atoms except boron. $R = 0.056$, $wR = 0.049$ ($w = 1/\sigma^2(F_0)$), maximal residual electron density 0.33 eÅ^{-3}. **4**: $C_{38}H_{64}B_2Si_4$, crystal dimensions $0.6 \times 0.6 \times 0.3$ mm, monoclinic, space group $P2_1/c$, $Z = 4$, $a = 1226.0(2)$, $b = 1361.3(3)$, $c = 2545.3(5)$ pm, $\beta = 102.09(3)^\circ$, $V = 4153.8 \times 10^{-30}$ m^3, $\rho_{calcd} = 1.047$ g cm^{-3}; 5860 measured reflections in the range up to $2\theta_{max} = 110^\circ$ (ω scans), 5219 of which were independent, 3760 reflections with $F_0 > 3\sigma(F_0)$ were used for further calculations after Lorentz and polarization correction; the structure solution and refinement as for **3** led to $R = 0.080$, $wR = 0.063$, and a maximal residual electron density of 0.54 eÅ^{-3}. Further details of the crystal structure investigations may be obtained from the Fachinformationszentrum Karlsruhe, D-76344 Eggenstein-Leopoldshafen (FRG) on quoting the depository number CSD-58199.

[3] A B1–C3 distance of 205.5 pm was determined for a boracyclobutene without a strong 1,3-interaction: B. Glaser, E. P. Mayer, H. Nöth, W. Rattay, U. Wietelmann, *Z. Naturforsch. B* **1988**, *43*, 449-456.

[4] R. Wehrmann, H. Klusik, A. Berndt, *Angew. Chem.* **1984**, *96*, 369–370; *Angew. Chem. Int. Ed. Engl.* **1984**, *23*, 369–370.

[5] D. Cremer, J. Gauss, P. von R. Schleyer, P. H. M. Budzelaar, *Angew. Chem.* **1984**, *96*, 370–371; *Angew. Chem. Int. Ed. Engl.* **1984**, *23*, 370–371.

[6] P. Willershausen, C. Kybart, N. Stamatis, W. Massa, M. Bühl, P. von R. Schleyer, A. Berndt, *Angew. Chem.* **1992**, *104*, 1278–1280; *Angew. Chem. Int. Ed. Engl.* **1992**, *31*, 1238–1240.

[7] M. Bühl, P. von R. Schleyer, M. A. Ibrahim, T. Clark, *J. Am. Chem. Soc.* **1991**, *113*, 2466–2471.

[8] P. Willershausen, G. Schmidt-Lukasch, C. Kybart, J. Allwohn, W. Massa, M. L. McKee, P. von R. Schleyer, A. Berndt, *Angew. Chem.* **1992**, *104*, 1417–1420; *Angew. Chem. Int. Ed. Engl.* **1992**, *31*, 1384–1386.

[9] P. von R. Schleyer, P. Buzek, T. Müller, Y. Apeloig, H.-U. Siehl, *Angew. Chem.* **1993**, *105*, 1558–1561; *Angew. Chem. Int. Ed. Engl.* **1993**, *32*, 1471–1473; J. B. Lambert, S. Zhang, C. L. Stern, J. C. Huffman, *Science* **1993**, *260*, 1917–1918.

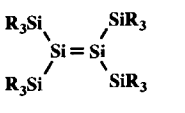
[10] The 1,3-distance in the four-membered ring of **8** is 189.9(11) pm and the fold angle along this diagonal is 31°. The formal C–C double bond (139.2(8)) common to both rings is remarkably long. Complete data for the crystal structure analysis: H.-J. Winkler, C. Balzereit, W. Massa, A. Berndt, unpublished results.

[11] H.-U. Siehl, F.-P. Kaufmann, Y. Apeloig, V. Braude, D. Danovich, A. Berndt, N. Stamatis, *Angew. Chem.* **1991**, *103*, 1546–1549; *Angew. Chem. Int. Ed. Engl.* **1991**, *30*, 1479–1482.

Stable Tetrakis(trialkylsilyl)disilenes; Synthesis, X-Ray Structures, and UV/VIS Spectra**

Mitsuo Kira,* Toyotaro Maruyama, Chizuko Kabuto, Keisuke Ebata, and Hideki Sakurai*

The chemistry of stable disilaethenes (disilenes) has been the subject of extensive studies since the first isolation of tetramesityldisilene in 1981 by West et al.[1] However, the variety in substituents of the disilenes whose structures have been determined by X-ray crystallography is rather limited; the substituents include alkyl, aryl, $(Me_3Si)_2N$, and very recently Me_3Si groups, but in addition these disilenes bear at least two aromatic groups.[2] Recent theoretical studies have shown that the geometry, stability, and electronic structure of disilenes should be affected significantly by substituents.[3] One of the most fascinating theoretical findings is that silyl substituents should increase the bond dissociation energy of disilenes; tetrasilyldisilenes have been suggested as interesting goals for synthesis.[3a] We report herein the isolation and characterization of tetrakis(trialkylsilyl)disilenes **1a**–**1c**,[4] which show unexpected features in their X-ray structures and NMR and UV/VIS spectra in comparison with previously isolated disilenes.



1a, $R_3Si = iPr_2MeSi$
1b, $R_3Si = tBuMe_2Si$
1c, $R_3Si = iPr_3Si$

[*] Prof. Dr. M. Kira, Prof. Dr. H. Sakurai, Dr. T. Maruyama, Dr. C. Kabuto, Dr. K. Ebata
Department of Chemistry, Faculty of Science
Tohoku University, Aoba-ku, Sendai 980-77 (Japan)
Telefax: Int. code + (22)268-9544

[**] Chemistry of Organosilicon Compounds, Part 313. This work was supported by the Japanese Ministry of Education, Science, and Culture (no. 02102004 and 05236203). Part 312: K. Sakamoto, M. Yoshida, H. Sakurai, *Macromolecules*, **1994**, *27*, 811.

 © VCH Verlagsgesellschaft mbH, D-69451 Weinheim, 1994 0570-0833/94/1414-1489 $ 10.00+.25/0

Disilene **1a** was prepared by refluxing a mixture of bis(diisopropylmethylsilyl)dibromosilane and sodium (2.6 equiv) in toluene for 6 h. After filtration of sodium bromide, the filtrate was condensed in vacuo and cooled to −20 °C to give yellow crystals of **1a**, which were isolated in 27% yield after filtration under argon. Disilene **1c** was obtained in 11% yield by reductive coupling of bis(triisopropylsilyl)dibromosilane with lithium naphthalene (2.3 equiv) in THF at −78 °C. Disilene **1b** was prepared by photolysis[5b, 6] of the corresponding cyclic trisilane, which was obtained in 47% yield by reductive coupling of bis(*tert*-butyldimethylsilyl)dibromosilane with lithium naphthalene in THF at −78 °C.[7] Disilenes **1a**–**1c** are highly air- and moisture-sensitive in solution but survived for a day in the solid state exposed to air. Physical data of these compounds are summarized in Table 1.

Table 1. Physical data of **1a**–**c**.

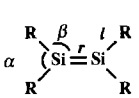
1a: yellow crystals; m.p. 142 °C; ^{1}H NMR (300 MHz, C_7D_8, TMS): δ = 0.38 (s, 12H, CH_3Si), 1.20 (d, ^3J(H,H) = 7.1 Hz, 24H, CH_3C), 1.27 (d, ^3J(H,H) = 7.2 Hz, 24H, CH_3C), 1.35–1.47 (m, 8H, CH); ^{13}C NMR (75.5 MHz, C_7D_8, TMS): δ = −6.8 (CH_3Si), 16.4 (CH), 19.3 (CH_3C), 21.3 (CH_3C); ^{29}Si NMR (59.6 MHz, C_7D_8, TMS): δ = 11.7 (Si2), 144.5 (^1J(Si,Si) = 50.3 Hz, Si1); UV/VIS (hexane): λ_{max} (ε) = 293 (2100), 357 (1400), 412 nm (7600); MS: *m/z* (%): 572 (2) [M^+], 129 (14), 73 (59), 59 (100); HRMS calcd for $C_{28}H_{68}Si_6$ 572.3969, found 572.3947.

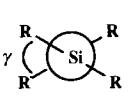
1b: light orange crystals; ^{1}H NMR (300 MHz, C_6D_6, TMS): δ = 0.44 (s, 24H, CH_3Si), 1.07 (s, 36H, CH_3C); ^{13}C NMR (75.5 MHz, C_6D_6, TMS): δ = 0.97 (CH_3Si), 19.6 ($(CH_3)_3C$), 28.4 (CH_3C); ^{29}Si NMR (59.6 MHz, C_6D_6, TMS): δ = 6.04 (Si2), 142.1 (^1J(Si,Si) = 51.5 Hz, Si1); MS: *m/z* (%): 516 (0.5) [M^+], 287 (7), 73 (100); UV/VIS (hexane): λ_{max} (ε) = 290 (2500), 361 (1700), 424 nm (2600); HRMS calcd for $C_{24}H_{60}Si_6$ 516.3311, found 516.3309.

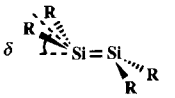
1c: yellow crystals; ^{1}H NMR (300 MHz, C_6D_6, TMS): δ = 1.35 (d, ^3J(H,H) = 7.3 Hz, 72H, CH_3), 1.61 (sept, ^3J(H,H) = 7.3 Hz, 12H, CH); ^{13}C NMR (75.5 MHz, C_6D_6, TMS): δ = 17.4 (CH_3), 21.4 (CH); ^{29}Si NMR (59.6 MHz, C_6D_6, TMS): δ = 16.4 (Si2), 154.5 (^1J(Si,Si) = 48.3 Hz, Si1); MS: *m/z* (%): 684 (0.4) [M^+], 303 (36), 129 (22), 101 (19), 87 (35), 73 (68), 59 (100); UV/VIS (hexane): λ_{max} (ε) = 296 (5400), 370 (2400), 425 (1300), 484 nm (1900); HRMS calcd for $C_{36}H_{84}Si_6$ 684.5189, found 684.5194.

The structures of **1a**–**1c** were determined by single-crystal X-ray diffraction studies.[8] Important structural parameters for **1a**–**1c** are summarized in Table 2. The ORTEP drawing for **1c** is shown in Figure 1. The spatial arrangement at the Si=Si bond depends significantly on the alkyl substituents at the saturated silicon atoms. Thus, in both **1a** and **1c** the substituents at central silicon atoms are *trans* to each other and bent out of the plane of the double bond (bend angle δ) by 5.4 and 10.2°, respectively; in **1b** the double bond is twisted by 8.9° (γ), but the substituents are not bent. The Si=Si bonds in **1a**–**1c** are roughly 0.1 Å longer than those in other known disilenes (2.14–2.16 Å).[2, 10] Theoretical calculations had predicted that the introduction of a silyl group into disilene would force a planar arrangement around the Si=Si bond, and that the Si=Si bond length would not be significantly different from that in the parent disilene.[3] Our experimental results are apparently not in accord with this prediction. The trialkylsilyl groups do not exert only electronic effects; severe steric repulsion among the trialkylsilyl groups could be responsible for the deformation from planarity and elongation of the Si=Si bond in the solid state. It is suggested that the potential energy surfaces are rather flat not only for twisting and bending but also stretching of the double bond; the disilene double bond could be referred to a *soft* double bond compared with the *hard* double bond of a simple olefin. The difference in the deformation mode among **1a**–**1c** may originate in the symmetry operation in the crystal structure.[8]

Table 2. Comparison of structural parameters of disilenes [a].







Disilene	r/Å	l/Å	α/°	β/°	γ/° [b]	δ/° [c]
1a (R = *i*Pr$_2$MeSi)	2.228(2)	2.374(2) 2.366(4)	115.3(1)	120.3(1) 124.1(1)	0	5.4(0)
1b (R = *t*BuMe$_2$Si)	2.202(1)	2.377(2) 2.383(2)	112.5(0)	122.9(0) 124.5(0)	8.9(1)	0.1(0)
1c (R = *i*Pr$_3$Si)	2.251(1)	2.400(2) 2.411(2)	114.9(0)	126.3(0) 117.5(0)	0	10.2(0)
Mes$_2$Si=SiMes$_2$ [13b]	2.143	1.879	116.8	120.7	3	13

[a] Standard deviations in parentheses. [b] γ = dihedral angle. [c] δ = bend angle.

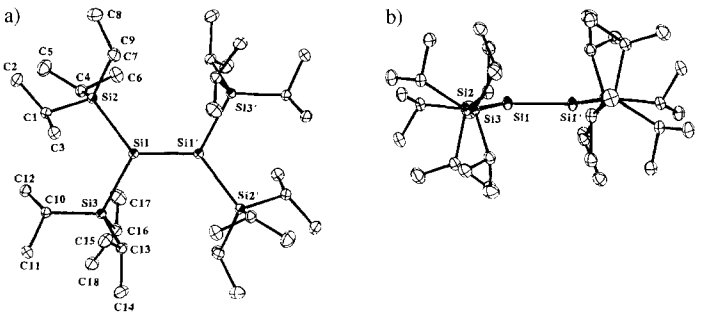


Fig. 1. Crystal structure of **1c** (ORTEP plot). a) Top view; b) side view.

The structures determined in the solid state may not be retained in solution, as shown in the unusual substituent effects in the UV/VIS spectra of **1a**–**1c** (vide infra).

The ^{29}Si NMR resonances for the tricoordinate silicon atoms in **1a**–**1c** (δ = 144.5, 142.1, and 154.5, respectively) appear at remarkably lower fields than those in the known disilenes, which lie between + 49 and + 98.[2a, 5c] These unusually low-field resonances may be compared with the corresponding ^{13}C NMR signals for tetrakis(trimethylsilyl)ethylene (δ = 195.3) and related silylethylenes[11a] which all appear at much lower fields than the corresponding signals of the parent ethylene (δ = 122.8). The origin of the effects of the trialkylsilyl substituents remains open.[11b]

While **1a**–**1c** are yellow to light orange in the solid state,[12] their solutions are quite different in color: the solutions in hexane at room temperature are yellow, orange, and dark red, respectively. The electronic spectra for the three disilenes were also very different, as shown in Figure 2. Since the bands for the π–π^* transition appear near 400 nm for the known disilenes,[2c] the absorption maxima observed at 412, 424, and 425 nm for **1a**, **1b**, and **1c**, respectively, are assigned to the π–π^* transition. Interestingly, the absorption coefficients of these maxima decrease significantly in this order; in the spectrum of **1c** there is a unique broad band at around 480 nm besides the low-intensity band for the π–π^* transition at 425 nm. The disilenes **1a** and **1b** show reversible thermochromism in hexane from light yellow (< 0 °C) to dark red (> 50 °C), as was also found for tetramesityldisilene.[13] The origin of the thermochromism may be attributed to a thermal equilibrium between the bent and twisted conformations, in analogy to the classical thermochromic olefins like bianthrones.[14] In contrast, the color of **1c** in solu-

 © VCH Verlagsgesellschaft mbH, D-69451 Weinheim, 1994 0570-0833/94/1414-1490 $ 10.00+.25/0

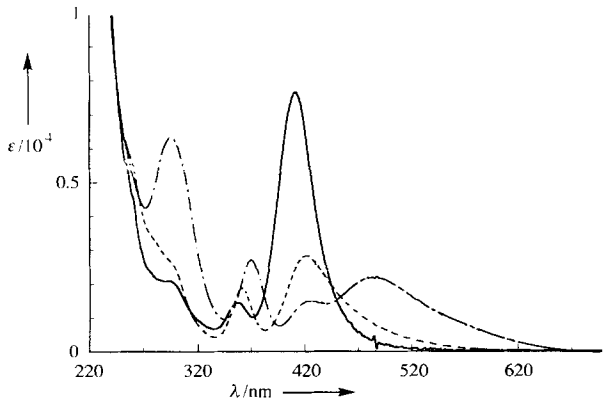


Fig. 2. UV/VIS spectra of **1a**–**1c** in hexane at room temperature: **1a** (—); **1b**, (- - -); **1c**, (· –·).

tion is apparently temperature independent. The extraordinary color change for this most crowded disilene from yellow in the solid state to dark red in solution suggests that in solution **1c** assumes a twisted form as the most stable conformation to relieve steric strain.

Received: February 24, 1994 [Z 6711 IE]
German version: *Angew. Chem.* **1994**, *106*, 1575

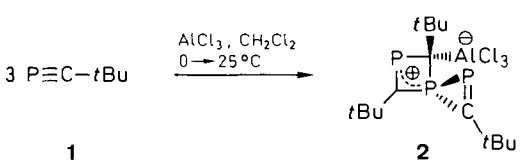
[1] R. West, M. J. Fink J. Michl, *Science (Washington)* **1981**, *214*, 1343.
[2] For reviews on stable disilens, see: a) R. West, *Angew. Chem.* **1987**, *99*, 1231; *Angew. Chem. Int. Ed. Engl.* **1987**, *26*, 1201; b) G. Raabe, J. Michl in *The Chemistry of Organosilicon Compounds, Part 2* (Eds.: S. Patai, Z. Rappoport), Wiley, Chichester, **1989**, Chap. 17; c) T. Tsumuraya, S. A. Batcheller, S. Masamune, *Angew. Chem.* **1991**, *103*, 916; *Angew. Chem. Int. Ed. Engl.* **1991**, *30*, 902.
[3] a) M. Karni, Y. Apeloig, *J. Am. Chem. Soc.* **1990**, *112*, 8589; b) C. Liang, L. C. Allen, *ibid.* **1990**, *112*, 1039.
[4] Although tetrakis[bis(trimethylsilyl)methyl]disilene was isolated as the first stable tetraalkyldisilene, no X-ray analysis was reported [5a]. Tetrakis(triethylsilyl)disilene was first detected by UV spectroscopy during photolysis of hexakis(triethylsilyl)cyclotrisilane but was not isolated [5b]. In 1992 West et al. isolated (*E*)- and (*Z*)-1,2-bis(2,4,6-triisopropylphenyl)disilenes; in these compounds the trimethylsilyl groups exert no remarkable effects on the structure [5c].
[5] a) S. Masamune, Y. Eriyama, T. Kawase, *Angew. Chem.* **1987**, *99*, 601; *Angew. Chem. Int. Ed. Engl.* **1987**, *26*, 584; b) H. Matsumoto, A. Sakamoto, Y. Nagai, *J. Chem. Soc. Chem. Commun.* **1986**, 1768; c) R. S. Archibald, Y. van den Winkel, A. J. Millevolte, J. M. Desper, R. West, *Organometallics* **1992**, *11*, 3276.
[6] a) S. Masamune, Y. Hanzawa, S. Murakami, T. Bally, J. F. Blount, *J. Am. Chem. Soc.* **1982**, *104*, 1150; b) S. Masamune, H. Tobita, S. Murakami, *ibid.* **1983**, *105*, 6524.
[7] Disilene **1a** was obtained also by the photolysis of the corresponding cyclotrisilane, which was prepared by the reductive coupling of the corresponding dibromosilane with lithium naphthalene in THF at −78 °C in 35% yield.
[8] The following holds for all the structure determinations. The reflection intensities were collected on a Rigaku AFC-5PR diffractometer with a rotating anode (45 kV, 200 mA) using graphite-monochromated $Mo_{K\alpha}$ radiation (λ = 0.71069 Å). Since the peak profiles for **1b** were broad at low temperatures, **1b** was measured at room temperature; **1a** and **1c** were measured at low temperature. Crystal data for **1a** (150 K): triclinic, space group $P\bar{1}$, a = 11.225(10), b = 11.651(7), c = 8.571(8) Å, α = 103.20(7), β = 111.03(8), γ = 105.22(6)°, V = 942.6(17) Å^3, Z = 1, ρ_{calcd} = 1.01 g cm^{-3}. A total of 5157 reflections were measured, of which 2655 [$F_0 > 3\sigma(F_0)$] were used in refinement. R = 0.105, R_w = 0.105. – Crystal data for **1b** (286 K): monoclinic, space group $C2/c$, a = 22.585(4), b = 7.988(1), c = 20.778(4) Å, β = 108.84(1)°, V = 3548.0(11) Å^3, Z = 4, ρ_{calcd} = 0.968 g cm^{-3}. A total of 5243 reflections were measured, of which 2866 [$F_0 > 3\sigma(F_0)$] were used in refinement. R = 0.060, R_w = 0.057. Crystal data for **1c** (170 K): monoclinic, space group $C2/c$, a = 19.220(3), b = 14.384(1), c = 17.089(2) Å, β = 110.88(1)°, V = 4414.5(11) Å^3, Z = 4, ρ_{calcd} = 1.03 g cm^{-3}. A total of 4973 reflections were measured, of which 3593 [$F_0 > 3\sigma(F_0)$] were used in refinement. R = 0.055, R_w = 0.076. The molecules of **1a** and **1c** have a crystallographic center of symmetry, while **1b** has a twofold symmetry axis. All calculations were performed with an ACOS-2000 computer at Tohoku University with the UNICS III system and the RANTAN81 program. Whereas the R values for **1b** and **1c** were rather reasonable, **1a** gave a relatively high R value. The final electron density map for **1a** showed a few of meaningful residual peaks near the Si=Si bond. These peaks are explainable by assuming a similar phenomenon to that observed in (*E*)-1,2-di(1-adamantyl)dimesityldisilene [9]. By including only three Si atoms of the minor component with the occupancy of 15%, the R value dropped by 0.04. Further details of the crystal structure investigation are available on request from the Director of the Cambridge Crystallographic Data Centre, 12 Union Road, GB-Cambridge CB21EZ (UK), on quoting the full journal citation.
[9] B. D. Shepherd, D. R. Powell, R. West, *Organometallics* **1989**, *8*, 2664.
[10] Very recently, Okazaki et al. reported an exceptionally long Si Si double bond [2.228(2) Å] in (*E*)-Tb(Mes)Si=Si(Mes)Tb (Tb = 2,4,6-tris[bis(trimethylsilyl)methyl]phenyl, Mes = 2,4,6-trimethylphenyl): N. Tokitoh, H. Suzuki, R. Okazaki, K. Ogawa, *J. Am. Chem. Soc.*, **1993**, *115*, 10428.
[11] a) H. Sakurai, H. Tobita, Y. Nakadaira, *Chem. Lett.* **1982**, 1251; b) the comparison between ^{29}Si and ^{13}C NMR chemical shifts may not be completely reliable, since the hybridization at the unsaturated silicon atoms deviates substantially from sp^2 as pointed out by a referee, cf. W. Kutzelnigg, *Angew. Chem.* **1984**, *96*, 262; *Angew. Chem. Int. Ed. Engl.* **1984**, *23*, 272.
[12] The solid-state UV/VIS spectra of **1a**–**1c** in KBr pellets are similar to one another and both have an absorption maximum at around 420 nm.
[13] a) M. J. Fink, M. J. Michalczyk, K. J. Haller, R. West, J. Michl, *Organometallics* **1984**, *3*, 793; b) B. D. Shepher, C. F. Campana, R. West, *Hetroat. Chem.* **1990**, *1*, 1.
[14] a) H. Meyer, *Monatsh. Chem.* **1909**, *30*, 165; b) *Ber. Dtsch. Chem. Ges.* **1909**, *42*, 143; c) Y. Tapuhi, O. Kalisky, I. Agranat, *J. Org. Chem.* **1979**, *44*, 1949, and references therein.

The First Carbon–Phosphorus–Aluminum Cage Compounds: Cyclooligomerization of Phosphaalkynes with Trialkylaluminum Compounds**

Bernhard Breit, Andreas Hoffmann, Uwe Bergsträsser, Louis Ricard, François Mathey, and Manfred Regitz*

Dedicated to Professor Reinhard Schmutzler on the occasion of his 60th birthday

Recently we found that the phosphaalkyne **1** can be spirocyclotrimerized with aluminum trichloride in the molar ratio 3:1 with the incorporation of the Lewis acid to give the stable complex **2**. Removal of the metal halide by addition of dimethyl



sulfoxide in the presence of a further equivalent of **1** leads to the desired formation of a cagelike phosphaalkyne cyclotetramer.[11]

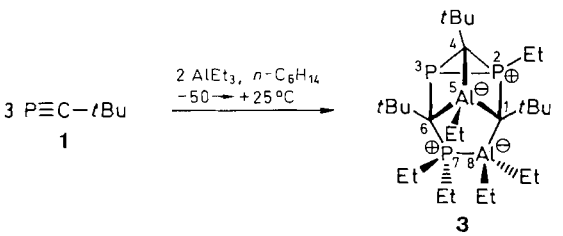
In the present communication we report on completely different cyclooligomerization reactions of **1** with triethylaluminum: surprisingly, polycycles are obtained highly selectively with the

[*] Prof. Dr. M. Regitz, Dr. B. Breit, Dipl.-Chem. A. Hoffmann, Dr. U. Bergsträsser
Fachbereich Chemie der Universität
Erwin-Schrödinger-Strasse, D-67663 Kaiserslautern (FRG)
Telefax: Int. code + (631)205-2187
Dr. L. Ricard, Prof. Dr. F. Mathey
Ecole Polytechnique, Département de Chimie, D. C. F. G. (France)
F-91128 Palaiseau (France)

[**] Phosphorus Compounds, Part 77. This work was supported by the Volkswagen-Stiftung and the Fonds der Chemischen Industrie. Part 76: W. Eisfeld, U. Bergsträsser, M. Slany, M. Regitz, *Tetrahedron Lett.* **1994**, *35*, 1527-1530.

incorporation of the Lewis acid, the composition of which depends on the solvent chosen.

If the reaction mixture containing the phosphaalkyne **1** and triethylaluminum (molar ratio 3:2) in *n*-hexane is allowed to warm up from −50 °C to room temperature, the carbon–phosphorus–aluminum compound **3** can be isolated in 91% yield;



polycycles comprising this combination of elements were hitherto unknown.[2]

The composition of **3** is apparent from the ^{1}H NMR spectrum: it is made up from three *tert*-butyl groups and six ethyl groups, which are magnetically inequivalent (Table 1). Also in agreement with the structure of **3** is the ^{31}P NMR spectrum which exhibits three high field absorptions,[3] which show $\lambda^3\sigma^3$ and $\lambda^4\sigma^4$ phosphorus with the mutual couplings (Table 1). In the ^{13}C NMR spectrum of the same compound, absorptions are found for the framework carbon atoms between $\delta = 32.8$ and 68.3, and the high-field signal with its two ^1J(P,C) couplings (51.8 and 23.4 Hz) is assigned unequivocally to C4. The migration of three *Al*-ethyl groups to phosphorus atoms is indicated by significant low field shifts and the occurrence of ^1J(P,C) couplings for the corresponding methylene carbon atoms.

Confirmation of the structure of the cage compound **3** was achieved by an X-ray crystal structure analysis (Fig. 1).[4, 5] Almost all the structural data including the P15–Al28 distance (2.4538 Å) lie in the expected range.[6] The only exceptions are the bond lengths P7–C8 (1.757 Å) and P7–C2 (1.770 Å), which are comparatively short.[7]

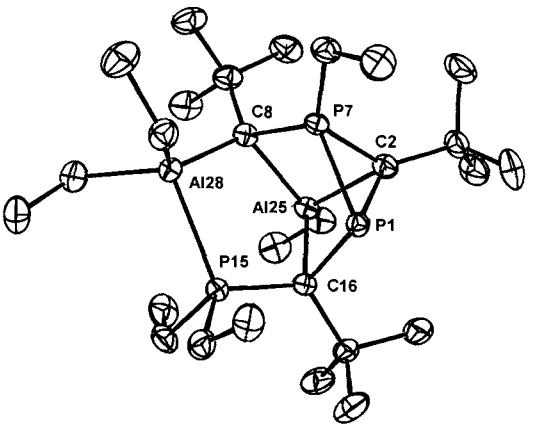


Fig. 1. Crystal structure of **3** (ORTEP). Selected bond lengths [Å] and angles [°]: P1–P7 2.1672(6), P1–C2 1.905(2), P1–C16 1.903(2), P7–C2 1.770(2), P7–C8 1.757(2), P15–Al28 2.4538(7), P15–C16 1.816(2), Al25–C2 2.115(2), Al25–C8 2.105(2), Al25–C16 2.075(2), Al28–C8 2.035(2); P7-P1-C2 51.04(6), P7-P1-C16 102.26(6), C2-P1-C16 97.71(8), P1-P7-C2 56.79(6), P1-P7-C8 111.05(6), C2-P7-C8 108.95(8), Al28-P15-C16 107.60(6), C2-Al25-C8 85.76(7), C2-Al25-C16 86.37(7), P1-C2-P7 72.17(7), P1-C2-Al25 84.83(7), P7-C2-Al25 80.65(7), P7-C8-Al25 81.22(7), P7-C8-Al28 103.18(8), Al25-C8-Al28 114.29(8), P1-C16-P15 107.66(9), C8-Al25-C16 100.91(7), P15-Al28-C8 94.67(5), P1-C16-Al25 85.98(7), P15-C16-Al25 108.59(8).

Table 1. Selected spectroscopic data of the cage compounds **3** and **4** [a].

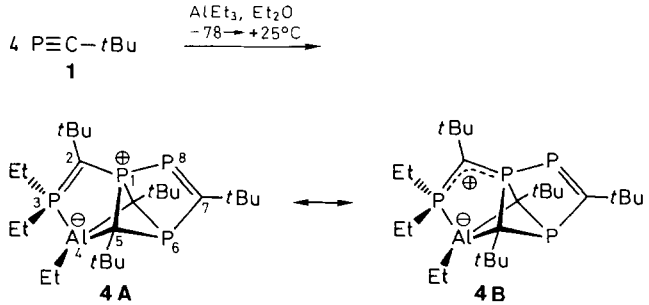
3: ^{1}H NMR (400.1 MHz): $\delta = 0.47$–0.66 (m, 6H, AlCH_2CH$_3$), 1.02–2.30 (m, 24H, AlCH$_2$CH_3/PCH_2CH_3), 1.41, 1.54 (each s, each 9H, C(CH$_3$)$_3$), 1.66 (d, ^4J(P,H) = 0.6 Hz, 9H, C(CH$_3$)$_3$); ^{13}C NMR: $\delta = 4.2$ (m, broad, 2 × AlCH$_2$CH$_3$), 8.2 (s, broad, AlCH$_2$CH$_3$), 8.8 (dd, ^2J(P,C) = 13.2, ^3J(P,C) = 7.6 Hz, PCH$_2$CH$_3$), 10.0, 10.2 (each s, AlCH$_2$CH$_3$), 10.9 (d, ^2J(P,C) = 5.1 Hz, PCH$_2$CH$_3$), 11.1 (d, ^2J(P,C) = 4.9 Hz, PCH$_2$CH$_3$), 11.3 (s, AlCH$_2$CH$_3$), 20.3 (d, ^1J(P,C) = 17.6 Hz, PCH$_2$CH$_3$), 20.8 (d, ^1J(P,C) = 8.3 Hz, PCH$_2$CH$_3$), 24.2 (pseudo-t, ^1J(P,C) = 12.3 Hz, PCH$_2$CH$_3$), 32.8 (dd, ^1J(P,C) = 51.8 and 23.4 Hz, C4), 34.6 (dd, ^3J(P,C) = 8.3, ^4J(P,C) = 3.8 Hz, C(CH$_3$)$_3$), 34.8 (dd, ^3J(P,C) = 8.4 and 5.0 Hz, C(CH$_3$)$_3$), 35.2 (d, ^2J(P,C) = 6.1 Hz, C(CH$_3$)$_3$), 36.6 (d, ^3J(P,C) = 13.7 Hz, C(CH$_3$)$_3$), 37.0 (dd, ^2J(P,C) = 9.7 and 3.3 Hz, C(CH$_3$)$_3$), 40.3 (d, ^2J(P,C) = 7.9 Hz, C(CH$_3$)$_3$), 45.8 (m, C1), 68.3 (m, C6); ^{31}P NMR: $\delta = -147.3$ (dd, ^1J(P,P) = 162.9, ^2J(P,P) = 21.7 Hz, P3), −61.6 (d, ^1J(P,P) = 162.9 Hz, P2), −1.2 (d, ^2J(P,P) = 21.7 Hz, P7).

4: ^{1}H NMR (400.1 MHz): $\delta = 0.55$ (q, ^3J(H,H) = 8.1 Hz, 2H, AlCH_2CH$_3$), 0.97–1.06 (m, 6H, 2 × PCH$_2$CH_3), 1.22 (s, 18H, 2 × C(CH$_3$)$_3$), 1.40 (s, 9H, C(CH$_3$)$_3$), 1.43 (t, ^3J(H,H) = 8.1 Hz, 3H, AlCH$_2$CH_3), 1.47 (d, ^4J(P,H) = 0.9 Hz, 9H, C(CH$_3$)$_3$), 1.69–1.78 (m, 4H, 2 × PCH_2CH$_3$); ^{13}C NMR: $\delta = 0.8$ (m, broad, AlCH$_2$CH$_3$), 10.3 (d, ^3J(P,C) = 2.6 Hz, AlCH$_2$CH$_3$), 12.8 (d, ^2J(P,C) = 4.1 Hz, 2 × PCH$_2$CH$_3$), 26.6 (dd, ^1J(P,C) = 22.0, ^3J(P,C) = 2.2 Hz, 2 × PCH$_2$CH$_3$), 32.4 (dd, ^3J(P,C) = 11.4 and 7.2 Hz, C(CH$_3$)$_3$), 33.4 (d, ^2J(P,C) = 4.8 Hz, C(CH$_3$)$_3$), 35.2–35.4 (m, 3 × C(CH$_3$)$_3$), 35.6 (d, ^2J(P,C) = 12.1 Hz, C(CH$_3$)$_3$), 36.4 (dd, ^2J(P,C) = 8.8 and 3.8 Hz, 2 × C(CH$_3$)$_3$), 44.0–44.6 (m, broad, C5/C9), 59.3 (d, broad, ^1J(P,C) = 39.8 Hz, C2), 108.0 (d, broad, ^1J(P,C) = 40.9 Hz, C7); ^{31}P NMR: $\delta = -32.8$ (m, P6), −1.0 (d, broad, ^2J(P,P) = 122.0 Hz, P3), + 87.1 (ddd, ^1J(P,P) = 320.6, ^2J(P,P) = 122.0 and 14.4 Hz, P1), + 208.0 (dd, ^1J(P,P) = 320.6, ^2J(P,P) = 10.8 Hz, P8).

[a] ^{1}H (TMS), ^{13}C (100.6 MHz, TMS) and ^{31}P NMR spectra (80.8 MHz, 85% of H_3PO_4) in C_6D_6. Numbering of the atoms as in the formula.

most all the structural data including the P15–Al28 distance (2.4538 Å) lie in the expected range.[6] The only exceptions are the bond lengths P7–C8 (1.757 Å) and P7–C2 (1.770 Å), which are comparatively short.[7]

If **1** is allowed to react with AlEt$_3$ in the molar ratio 4:1 in diethyl ether instead of in *n*-hexane, the carbon–phosphorus–aluminum polycycle **4** is obtained in 74% yield; there is no evidence in the ^{31}P NMR spectrum for the formation of **3** as a by-product.



The same ratio of the reaction partners is also apparent from in the ^{1}H NMR spectrum of **4** (Table 1). In contrast to **3** at least one phosphorus atom has a $\lambda^3\sigma^2$ configuration ($\delta = 208.0$);[8] it is split into a double doublet by both ^1J(P,P) and ^2J(P,P) coupling (320.6 and 10.8 Hz, respectively). This is in correspondence with the resonance of C7 at $\delta = 108.0$ with a typical P coupling of 40.9 Hz. The second P–C double bond of **4** has methylenephosphorane character; the fact that the resonance for the ylidic carbon appears at $\delta = 59.3$ is acceptable.[9] The relatively high field position of P3 ($\delta = -1.0$) results from the shielding effect of the neighboring aluminate group. The onium phosphorus P1 ($\delta = 87.1$) shows the expected couplings to P8 and P3[10] (Table 1). The $\lambda^3\sigma^3$ phosphorus P6 absorbs at high field ($\delta = -32.8$) as expected. For the tetracycle **4**, as in the case of **3**, a low-field shift and ^1J(P,C) couplings for the methylene carbon atoms originally bound to Al indicate ethyl migration to

the phosphorus. The latter and also the constitution of the reaction product were confirmed by an X-ray crystal structure analysis (Fig. 2).[5, 11] This analysis shows that the aluminum and all

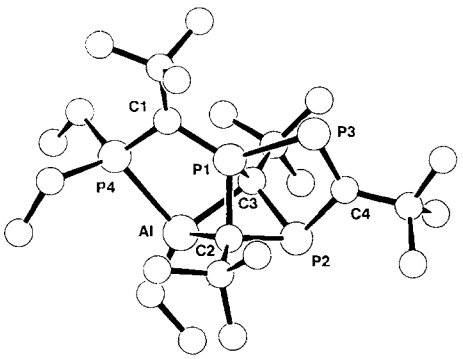


Fig. 2. Crystal structure of **4** (SCHAKAL-Plot). Selected bond lengths [Å] and angles [°]: P4–Al 2.441(3), C3–Al 2.038(6), P1–C1 1.713(6), P2–C2 1.853(6), P1–C3 1.813(6), P3–C4 1.651(6), P3–P1 2.235(2), C2–Al 2.039(6), P4–C1 1.743(6), P1–C2 1.834(6), P2–C3 1.868(6), P2–C4 1.917(6); C1-P1-P3 122.2(2), C3-P2-C2 78.2(3), C4-P2-C3 98.8(3), C1-P4-Al 95.5(2), C3-Al-P4 95.5(2), P2-C2-P1 86.1(3), Al-C2-P2 89.5(3), Al-C3-P2 89.1(3), P3-C4-P2 116.9(3), C2-P1-P3 103.5(2), C2-P1-C1 120.1(3), C3-P1-P3 103.1(2), C3-P1-C1 119.3(3), C4-P2-C2 100.2(3), C4-P3-P1 88.6(2), C2-Al-P4 96.7(2), C3-Al-C2 70.2(2), P4-C1-P1 105.0(3), Al-C2-P1 81.8(2), Al-C3-P1 82.3(2).

the phosphorus atoms as well as the carbon atoms C1 and C4 lie in one plane.[12] The P3–C4 distance (1.651 Å) lies in the range expected for P–C double bonds.[13] However, the very similar bond lengths P4–C1 and P1–C1 (1.743 and 1.713 Å, respectively) are indicative of an extensive delocalization of the positive charge over the PCP unit according to **4A**↔**4B**; they lie in the range between those of P–C single[6] and P–C double bonds.[14]

The question of the formation mechanism of the two completely different products **3** and **4** cannot be answered conclusively. However, it is assumed that the Lewis acid initially attacks at the phosphaalkyne carbon of **1**.[1] Then Et–P=C(*t*Bu)($AlEt_2$) is formed by a [1,2]-ethyl shift. Not later than after the analogous 1,2 addition of Et–P=C(*t*Bu)($AlEt_2$) to a further equivalent of **1**, the reaction must branch out. That compound **4** contains one equivalent, whereas **3** contains two equivalents of Lewis acid, must be due to the blocking effect of the Lewis base diethyl ether.

Experimental Procedure

3: A solution of the phosphaalkyne **1** [15] (0.35 g, 3.5 mmol) in *n*-hexane (3 mL) was added dropwise to a solution of triethylaluminum (0.23 g, 2.0 mmol) in *n*-hexane (3 mL) and stirred at −50 °C (exclusion of oxygen and moisture). After the reaction mixture had been allowed to warm to 25 °C over the course of 12 h, the solvent was removed at 25 °C/10^{-3} mbar and the residue was left to crystallize at −78 °C in a little *n*-hexane. Yield: 0.48 g (91%) colorless crystals; m.p. 175 °C.

4: A solution of the phosphaalkyne **1** [15] (0.40 g, 4.0 mmol) in diethyl ether (3 mL) was added dropwise to a solution of triethylaluminum (0.11 g, 1.0 mmol) in diethyl ether (3 mL) and stirred −78 °C (exclusion of air and moisture). After the reaction mixture had been allowed to warm to 25 °C over the course of 12 h, the solvent was removed at 25 °C/10^{-3} mbar to yield a red-brown oil after a further 36 h. Yield: 0.38 g (74%); red-brown crystals obtained from little *n*-hexane or diethyl ether; m.p. 168 °C.

Received: February 12, 1994 [Z6688IE]
German version: *Angew. Chem.* **1994**, *106*, 1541

[1] B. Breit, U. Bergsträsser, G. Maas, M. Regitz, *Angew. Chem.* **1992**, *104*, 1043-1046; *Angew. Chem. Int. Ed. Engl.* **1992**, *31*, 1055-1058.
[2] 2-(1-Adamantyl)-1-phosphaacetylene (**1**, 1-Ad instead of *t*Bu) reacts analogously with triethylaluminum; this is also true for reactions of **1** with trimethyl- and tri-*n*-propylaluminum: ^{31}P NMR(C_6D_6): $\delta = -151.0$ to -136.8 (dd, ^1J(P,P) = 152.4–162.8, ^2J(P,P) = 21.9–33.4 Hz, P3), −75.0 to −59.9 (d, ^1J(P,P) = 152.4–162.8 Hz, P2), −27.9 to +0.6 (d, ^2J(P,P) = 21.9–33.4 Hz, P7).
[3] J. G. Verkade, L. D. Quin, *Phosphorus-31-NMR-Spectroscopy in Stereochemical Analysis*, VCH, Deerfield Beach, **1987**.
[4] Enraf Nonius CAD4 diffractometer, $Cu_{K\alpha}$ radiation, graphite monochromator; **3**: $C_{27}H_{57}Al_2P_3$; M = 528.6 (recrystallized from *n*-hexane): monoclinic, space group $P2_1/c$ (no. 14), a = 11.433(1), b = 17.290(2), c = 15.830(2) Å, β = 96.48(1)°, V = 3109(1) Å^3, Z = 4, ρ_{calcd} = 1.129 g cm^{-1}, μ = 23.8 cm^{-1}; F(000) = 1088; measurement temperature T = −150 °C; 4615 independent reflections were measured, 4152 of which were observed with $F^2 \geq 3.0\sigma(F^2)$ and were used for structure refinement. Number of parameters 289. The final structural model converges at R = 0.033 and R_w = 0.061 and showed a maximum of 0.31(5) eÅ^{-3} and a minimum of 0.00(5) eÅ^{-3} in the difference Fourier synthesis. The positions of the H atoms were calculated geometrically and taken into consideration in the final cycle of the least squares refinement.
[5] Further details of the crystal structure investigations may be obtained from the Fachinformationszentrum Karlsruhe, D-76344 Eggenstein-Leopoldshafen (FRG) on quoting the depository number CSD-58074.
[6] A. H. Cowley, R. A. Jonas, M. A. Mardones, J. L. Atwood, S. C. Bott, *Angew. Chem.* **1990**, *102*, 1504-1505; *Angew. Chem. Int. Ed. Engl.* **1990**, *29*, 1409-1410; J. F. Janik, E. N. Duebler, W. F. McNamura, M. Westerhausen, R. T. Paine, *Organometallics* **1989**, *8*, 506-514.
[7] F. H. Allen, O. Kennard, D. G. Watsen, L. Brammer, A. G. Orpen, R. Taylor, *J. Chem. Soc. Perkin Trans. 2* **1987**, 1-19.
[8] For more information concerning the NMR spectroscopy of phosphaalkenes see K. Karaghiosoff in *Multiple Bonds and Low Coordination in Phosphorus Chemistry* (Eds.: M. Regitz, O. J. Scherer), 1st ed., Thieme, Stuttgart, **1990**, p. 463ff.
[9] E. Breitmeier, W. Voelter, *Carbon-13 NMR Spectroscopy*, VCH, Weinheim, **1987**, p. 247ff.
[10] R. Appel, U. Baumeister, F. Knoch, *Chem. Ber.* **1983**, *116*, 2275-2284; H. Schmidbaur, T. Costa, B. Milewski-Mahrla, *ibid.* **1981**, *114*, 1428-1441.
[11] Enraf-Nonius-CAD4-diffractometer, $Mo_{K\alpha}$ radiation, full-matrix refinement; **4**: $C_{30}H_{51}AlP_4$; M = 514.8: monoclinic, space group $P2_1/c$ (no. 14), a = 10.10(1), b = 16.58(1), c = 18.31(3) Å; β = 92.32(7)°, V = 3063(6) Å^3, μ = 2.9 cm^{-1}; F(000) = 1216; ρ_{calcd} = 1.220 g cm^{-3}; 5371 reflections were measured, 3210 of which were observed with $I > 2\sigma(I)$ and were used for structure refinement. Number of parameters 343. The final structural model converges at R = 0.0852 and R_w = 0.0662 and showed a maximum of 0.41 eÅ^{-3} and a minimum of −0.37 eÅ^{-3} in the difference Fourier synthesis. The positions of the H atoms were calculated with a fixed C–H distance of 1.08 Å and with groupwise identical temperature factors. The largest effective standard deviation was found at 0.206.
[12] Deviations from a least squares plane defined by the atoms mentioned earlier are smaller than 0.011 Å.
[13] R. Hoffmann, D. B. Boyd, S. Z. Goldberg, *J. Am. Chem. Soc.* **1970**, *92*, 3929-3936.
[14] R. Appel in ref. [8], p. 160, and references therein.
[15] Syntheses of **1** in ref. [8], pp. 59-63; optimal yields are obtained by using the method of W. Rösch, U. Hees, M. Regitz, *Chem. Ber.*, **1987**, *120*, 1645-1652.

Synthesis and Molecular Structure of Calcium Bis(trimethylstannanide)·4THF**

Matthias Westerhausen*

In the cocondensation of calcium with trimethylsilyltrimethylstannane and the subsequent reaction with bromobenzene and water, Mochida and Yamanishi[1] isolated hydrolysis products of $Me_3Si–Ca–SnMe_3$, in particular hexamethyldisiloxane, trimethylstannane, hexamethyldistannane, and hydroxy(trimethyl)stannane. However, the authors also ob-

[*] Dr. M. Westerhausen
Institut für Anorganische Chemie der Universität
Pfaffenwaldring 55, D-70569 Stuttgart (FRG)
Telefax: Int. code + (711)685-4241

[**] This work was supported by the Deutsche Forschungsgemeinschaft and the Fonds der Chemischen Industrie. We thank Prof. Dr. J. Weidlein for helpful discussions and Dr. W. Schwarz for the collection of the data set.

tained hexamethyldisiloxane, hexamethyldistannane, and hydroxy(trimethyl)stannane in a control experiment performed in the absence of calcium. Calcium stannanides have already proved themselves as polymerization initiators in the synthesis of polyacrylonitrile;[2] spectroscopic proof has as yet, however, only been obtained for calcium bis{tris[bis(trimethylsilyl)-methyl]stannanide}·2DME (DME = dimethoxyethane) with ions separated by solvent.[3]

After stirring for three days at room temperature, the insertion product calcium bis(trimethylstannanide)·4THF (**1**) can be isolated from the heterogeneous reaction of calcium with hexamethyldistannane in THF according to Equation (a). Compound **1** is recrystallized from a solvent mixture of THF and *n*-pentane.

$$Ca + Me_3Sn{-}SnMe_3 \xrightarrow{THF} \underset{\mathbf{1}}{[(Me_3Sn)_2Ca]\cdot 4\,THF} \quad (a)$$

A small amount of calcium bis[tris(trimethylstannyl)stannanide]·4THF (**2**) is also formed in this reaction in accordance with Equation (b), because both the calcium and the compound **1** already formed compete for the hexamethyldistannane still remaining. (The analogous reaction of lithium trimethylstannanide with $Me_3Sn{-}SnMe_3$ has already been resolved mechanistically.[4]) The NMR data of the $(Me_3Sn)_3Sn$ fragment bonded to calcium in **2** listed in Table 1 are remarkable, especially because of the large ^1J(Sn–Sn) and ^2J(Sn–Sn) coupling constants of 5806 and 873 Hz, respectively. By the use of an approximately seven-fold excess of hexamethyldistannane over calcium, compound **2** can be isolated nearly quantitatively.

$$[(Me_3Sn)_2Ca]\cdot 4\,THF + 6\,Me_3Sn{-}SnMe_3 \longrightarrow \underset{\mathbf{2}}{[\{(Me_3Sn)_3Sn\}_2Ca]\cdot 4\,THF} + 6\,SnMe_4 \quad (b)$$

The calcium bis(stannanide) **1** also shows characteristic spectroscopic parameters. The ^1J(Sn–C) coupling constant in the $^{13}C\{^1H\}$ NMR spectrum is extraordinarily small (106 Hz). The singlet at $\delta(^{119}Sn\{^1H\}) = -203$ is shifted upfield relative to that of lithium trimethylstannanide.[5]

Table 1. NMR spectroscopic data of the compounds **1** and **2**.

1: ([D$_8$]THF, 30 °C): ^{1}H: $\delta = -0.36$. ^{13}C: $\delta(SnMe_3) = -5.00$ (^1J(Sn-C) = 106.3 Hz, ^1J(C-H) = 122.4 Hz, ^3J(C-H) = 2.9 Hz). ^{119}Sn{^{1}H}: $\delta = -203.32$
2: ([D$_8$]THF, 30 °C): ^{1}H: $\delta = -0.25$. ^{13}C{^{1}H}: $\delta = -3.05$ (^1J(Sn-C) = 116.1 Hz, ^2J(Sn-C) = 11.0 Hz. ^3J(Sn-C) = 19.9 Hz). ^{119}Sn{^{1}H}: $\delta(SnMe_3) = -100.75$, $\delta(SnSn_3) = -1071.52$ (^1J(Sn-Sn) = 5806.2 Hz, ^2J(Sn-Sn) = 873.0 Hz)

Calcium bis(stannanide) **1** crystallizes from THF/*n*-pentane in the form of colorless cuboids in the centrosymmetric space group $P\bar{1}$.[6] The calcium atom lies on the crystallographic center of inversion. In Figure 1, the second half of the molecule indicated by primed numbers is generated from the point symmetry. The calcium atom is coordinated in a distorted octahedral fashion by two tin atoms and four oxygen atoms of the THF ligands in the *trans* configuration. The stereoscopic representation in Figure 2 of a projection along the Sn–Ca–Sn′ axis shows that the plane described by the oxygen atoms is tipped slightly from an orientation perpendicular to this axis (Sn–Ca–O1 87.5°, Sn–Ca–O2 90.8°) due to the steric repulsion between the methyl group with C1 and the THF ligand

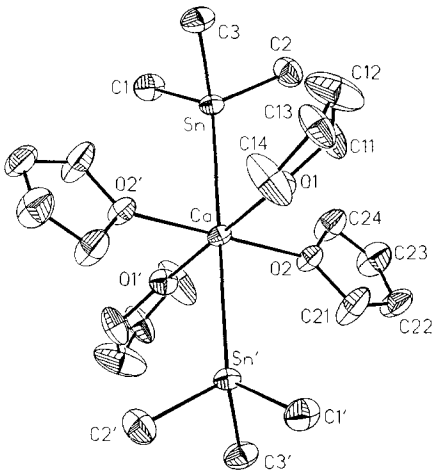


Fig. 1. Structural model of calcium bis(trimethylstannanide)·4THF (**1**); the numbering can be completed accordingly. The ellipsoids represent 30% probability. Selected distances [pm] and angles [°]: Ca-O1 236.3(3), Ca-O2 239.4(3), Ca-Sn 327.21(3), Sn-C1 219.6(5), Sn-C2 219.7(6), Sn-C3 220.1(5); C1-Sn-C2 96.4(3), C1-Sn-C3 97.9(2), C2-Sn-C3 95.2(3), Ca-Sn-C1 124.6(2), Ca-Sn-C2 120.5(2), Ca-Sn-C3 116.1(2), Sn-Ca-O1 87.52(8), Sn-Ca-O2 90.78(8).

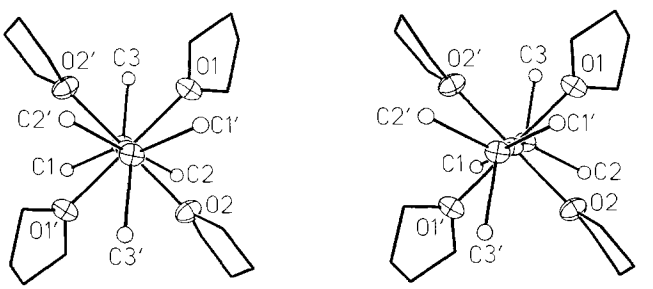


Fig. 2. Stereoscopic projection along the Sn–Ca–Sn axis in **1**; the carbon atoms have a randomly chosen radius.

with O1′ (torsional angle C1–Sn–Ca–O1′ 19.0(2)°). At the same time, the Ca–Sn–C1 angle is widened to 124.6°. The Ca–Sn bond length of 327 pm lies within the broad range of lengths observed in binary Ca–Sn phases, which increase with increasing tin content (Ca_2Sn 318 pm,[7] $Ca_{31}Sn_{20}$ 307–366 pm,[8] CaSn 327 pm,[9] and $CaSn_3$ 334 pm [10]).

The average C–Sn–C bond angle of 96.5° found in the trimethylstannanide substituent can be explained by the almost exclusive participation of p orbitals on the tin atom; the lone pair of electrons thus shows predominantly s character. This finding is confirmed by the unusually small ^1J(Sn–C) coupling constant. In comparison to Me_3Sn substituents bonded to transition metal elements, such as in, for example, $Me_3Sn{-}Mo(H)Cp_2$ (Sn–C 217 pm, C–Sn–C 102°[11]) $Me_3Sn{-}Mn(CO)_5$ (Sn–C 213 pm, C–Sn–C 107°[12]), and $[Me_3Sn{-}Ru(CO)_4]_2$ (Sn–C 215 pm, C–Sn–C 107°[13]), as well as in tetramethylstannane,[14] remarkably long Sn–C bonds in conjunction with small C–Sn–C angles appear in the calcium derivative **1**. Similar structural parameters may be observed in the triphenylstannanides of lithium[15] and potassium,[16] although the latter is built up of separate ions in the solid due to the complexation of the cation with 18-crown-6.

The THF ligands coordinated to the calcium atom are in the *envelope* (n = 1) or in the *twist* (n = 2) conformation, although the atoms C11/C11a, C13/C13a, and C14/C14a of one of the

THF molecules are disordered and have occupancies of 6/4 for two sites. The atoms O1 and C12 are common to both partial structures. The surface normals of the planes C(n1), O(n), C(n4) form angles of 41.8° (n = 1) and 78.6°(n = 2) to the surface normals of the plane calculated from the oxygen atoms. Both the large displacement of the THF ligand labeled n = 1 from the orthogonal arrangement of the CaO_4 plane and the realization of the *envelope* conformation are based on the interaction with the trimethylstannanide substituents already mentioned above. The Ca–O bond lengths of 236 and 239 pm lie within the characteristic range.

The vibrational spectra can be interpreted with the knowledge of the D_{3d} symmetry of the $(Me_3Sn)_2Ca$ fragment. The asymmetric stretching vibration $\nu_{as}(CaSn_2)$ is found at 231 cm^{-1} and is only observed in the IR spectrum. The exclusively Raman active symmetric vibration $\nu_s(CaSn_2)$ occurs at 69 cm^{-1}, which results in an estimated force constant of 53 Nm^{-1}. The $\nu(SnC_3)$ vibrations (463 cm^{-1}) are in agreement with the findings commented on above, and have clearly lower wavenumbers than those of organo(trimethyl)stannanes.

Calcium bis(stannanide) **1** is obtained in good yield, is soluble in the usual organic solvents, and forecasts a rapid development of the organometallic chemistry of the heavy alkali earth metal calcium, which until now was only accessible with difficulty; the successful investigation of lithium trimethylstannanide is referred to at this point.[17]

Experimental Procedure

All manipulations were carried out in purified anhydrous argon (BTS catalyst, P_4O_{10}). Distilled calcium (0.4 g, 10 mmol, 24% excess) and hexamethyldistannane (2.5 g, 7.6 mmol) were stirred for three days at room temperature in THF (30 mL). After removing all solids (excess calcium), all volatile components were removed under vacuum at room temperature. The residue was dissolved in a THF/*n*-pentane mixture. Compound **1** crystallized at −60 °C in the form of colorless cuboids. Yield: 3.0 g (4.6 mmol) 61%. M.p. 92–93 °C (decomposition, in argon). IR (nujol mull between CsBr plates): ν = 1309 (w), 1295 (w), 1245 (vw), 1172 (w), 1149 (w), 1074 (w), 1032 (vs), 918 (s), 878 (vs), 722 (vs), 678 (m), 463 (vs), 231 (s), 210 (m), 175 cm^{-1} (m).—Raman (on a single crystal): ν = 1034 (w), 920 (w), 889 (w), 723 (m), 678(vw), 472 (s), 463 (vs), 175 (s), 69 cm^{-1} (m).—Correct C,H analysis.

Received: February 6, 1994 [Z 6680 IE]
German version: *Angew. Chem.* **1994**, *106*, 1585

[1] K. Mochida, T. Yamanishi, *Bull. Chem. Soc. Jpn.* **1987**, *60*, 3429.
[2] S. Oda, K. Hisatani, *Jpn. Kokai Tokkyo Koho JP 03 68.606* **1991**; *Chem. Abstr.* **1991**, *115*, 233143g.
[3] M. Westerhausen, T. Hildenbrand, *J. Organomet. Chem.* **1991**, *411*, 1.
[4] K. Kobayashi, M. Kawanisi, T. Hitomi, S. Kozima, *J. Organomet. Chem.* **1982**, *233*, 299.
[5] a) P. G. Harrison, S. E. Ulrich, J. J. Zuckerman, *J. Am. Chem. Soc.* **1971**, *93*, 5398; b) J. D. Kennedy, W. McFarlane, *J. Chem. Soc. Chem. Commun.* **1974**, *983*, c) K. Kobayashi, M. Kawanisi, S. Kozima, T. Hitomi, H. Iwamura, T. Sugawara, *J. Organomet. Chem.* **1981**, *217*, 315; d) B. Mathiasch, U. Kunze, *Inorg. Chim. Acta* **1983**, *75*, 209.
[6] Crystal structure analysis of **1**: $CaSn_2O_4C_{22}H_{50}$, M = 656.08 $g\,mol^{-1}$; colorless cuboid (0.45 × 0.45 × 0.35 mm); triclinic, space group $P\bar{1}$ (No. 2), a = 943.0(1), b = 991.3(1), c = 1053.3(1) pm, α = 62.75(1), β = 71.09(1), γ = 63.58(1)°, V = 0.7749(1) nm^3, Z = 1, ρ_{calcd} = 1.406 $g\,cm^{-3}$, $F(000)$ = 334, μ = 1.797 mm^{-1}; Siemens P4 four-circle diffractometer. 4133 intensities were collected at −100 °C with graphite monochromated $Mo_{K\alpha}$ radiation (λ = 0.71073 nm, ω scan, 4.4 < 2θ < 58.0), 3896 symmetry-independent reflections ($R_{int.}$ = 0.026) were used in the solution (Patterson synthesis, difference Fourier syntheses) and in the refinement (least-squares refinement with full matrix on F^2 values, SHELXL-93 [18], neither extinction nor absorption corrections used) of the structure. All non-hydrogen atoms were refined anisotropically, the hydrogen atom positions were calculated using predefined tetrahedral angles on the carbon atoms. The calculations converged at $wR2$ = 0.1254 for 3895 reflections and 167 variables ($R1$ = 0.0489 for 3331 reflections with $I > 2\sigma(I)$). A difference Fourier synthesis calculated in conclusion indicated a residual electron density of +1661 and −1882 $e\,nm^{-3}$ in the vicinity of the tin atom. Further details of the crystal structure investigation may be obtained from the Fachinformationszentrum Karlsruhe, D-76344 Eggenstein-Leopoldshafen (FRG) on quoting the depository number CSD-58218, the names of the authors, and the journal citation.
[7] P. Eckerlin, E. Leicht, E. Wölfel, *Z. Anorg. Allg. Chem.* **1960**, *307*, 145.
[8] M. L. Fornasini, E. Franceschi, *Acta Crystallogr. Sect. B* **1977**, *33*, 3476.
[9] P. Eckerlin, H. J. Meyer, E. Wölfel, *Z. Anorg. Allg. Chem.* **1955**, *281*, 322.
[10] a) E. Zintl, S. Neumayr, *Z. Elektrochem. Angew. Phys. Chem.* **1933**, *39*, 86; b) K. Schubert, *Z. Metallkd.* **1955**, *46*, 43.
[11] A. N. Protsky, B. M. Bulychev, G. L. Soloveichik, V. K. Bel'skii, *Inorg. Chim. Acta* **1986**, *115*, 121.
[12] R. F. Bryan, *J. Chem. Soc. A* **1968**, 696.
[13] J. A. K. Howard, S. C. Kellett, P. Woodward, *J. Chem. Soc. Dalton Trans.* **1975**, 2332.
[14] a) L. O. Brockway, H. O. Jenkins, *J. Am. Chem. Soc.* **1936**, *58*, 2036; b) A. F. Wells, *J. Chem. Soc.* **1949**, 55; c) R. K. Sheline, *J. Chem. Phys.* **1950**, *18*, 602; d) M. Nagashima, H. Fujii, M. Kimura, *Bull. Chem. Soc. Jpn.* **1973**, *46*, 3708.
[15] D. Reed, D. Stalke, D. S. Wright, *Angew. Chem.* **1991**, *103*, 1539; *Angew. Chem. Int. Ed. Engl.* **1991**, *30*, 1459.
[16] T. Birchall, J. A. Vetrone, *J. Chem. Soc. Chem. Commun.* **1988**, 877.
[17] a) D. D. Davis, C. E. Gray, *Organomet. Chem. Rev. Sect. A* **1970**, *6*, 283; b) T. Sato, *Synthesis* **1990**, 259; c) M. Pereyre, J.-P. Quintard, A. Rahm, *Tin in Organic Synthesis*, Butterworths, London, **1987**; d) P. G. Harrison, *Chemistry of Tin*, Chapman & Hall, London, **1989**.
[18] G. M. Sheldick, *SHELXL-93*, Universität Göttingen, **1993**.

Keronopsins A and B, Chemical Defence Substances of the Marine Ciliate *Pseudokeronopsis rubra* (Protozoa): Identification by Ex Vivo HPLC

Gerhard Höfle,* Silke Pohlan, Gotram Uhlig, Karin Kabbe, and Dorothee Schumacher

The ciliate *Pseudokeronopsis rubra* lives in the shallow regions of the world's oceans, and is notable for its deep red color and its deterrent effect on predators and competitors for food supplies.[1, 2a] The orange, aqueous extracts of this organism are not merely antibiotic, but also display a variety of other biological activities.[2b, c] Thus, other ciliates and flagellates are paralyzed or even killed by these extracts,[2d] the cleavage divisions of sea urchin eggs are inhibited, and larval morphogenesis is greatly disturbed.[2e] In *Euplotes* (Ciliate), an inhibition of the inward calcium transport through the cell membrane has been reported.[3] It is also remarkable that an albino mutant of *P. rubra* takes up the yellow pigment from the extracts and then displays the negative phototactic behavior which is typical of this species.[2a] Till now, attempts to purify the toxins that are responsible for these effects, and that presumably also act as photoreceptors, have been unsuccessful.

Using HPLC analysis, we found that the composition and stability of aqueous and aqueous-methanolic extracts vary considerably depending on their history. Four main components were usually present in approximately equal amounts; we named them keronopsin A_1, A_2 (λ_{max} = 440 nm), B_1, and B_2 (λ_{max} = 420 nm) (Fig. 1). Although methanolic extracts of lyophilized cells were stable, the content of A_1 and A_2 decreased rapidly in aqueous extracts of fresh cells, with a concomitant

[*] Prof. Dr. G. Höfle, S. Pohlan
Gesellschaft für Biotechnologische Forschung mbH
Mascheroderweg 1, D-38124 Braunschweig (FRG)
Telefax: Telefax: Int. code + (531)6181-515
Dr G. Uhlig, K. Kabbe, D. Schumacher,
Biologische Anstalt Helgoland, Meeresstation

[**] This work was supported by the Fonds der Chemischen Industrie. We thank Dr. H.-M. Schiebel (Braunschweig) and Dr. K. D. Klöppel for the recording and discussion of the mass spectra, and Dr. V. Wray for recording the NMR spectra.

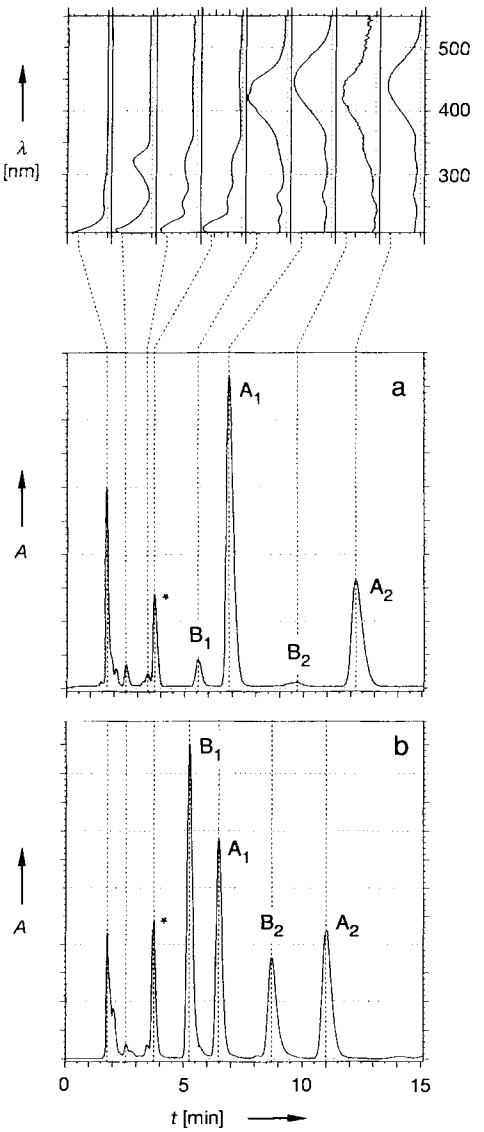
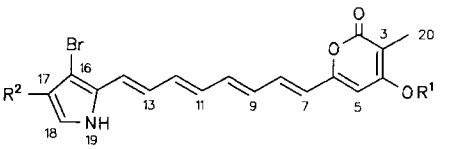


Fig. 1. Analytical HPLC of *Pseudokeronopsis rubra* constituents with the keronopsins A_1, A_2, B_1, and B_2, and pseudokeronopsin A(*): a) 300 living organisms in 20 μL water, b) methanol extract of lyophilized cells (Nucleosil RP-18, 7 μm, 4 × 25 cm, methanol/0.05 M ammonium acetate buffer = 68:32, pH = 8.2, 1.2 mL min^{-1}, diode array detection at 210–550 nm.

increase in B_1 and B_2 (τ about 10–20 min). However, a minor component called pseudokeronopsin A, which absorbs at considerably shorter wavelength, was stable.[4]

In order to determine the keronopsin composition in living organisms with as little change as possible, we applied a known number of organisms directly from a culture onto the HPLC column (ex vivo HPLC). The extremely fragile cells were lyzed on contact with the eluent, releasing their contents for immediate separation. A usable chromatogram could be obtained with as few as ten organisms (corresponding to about 1 μg fresh weight); with 100–300 organisms even trace components could be determined, without significantly affecting the peak widths and retention times. Besides pseudokeronopsin, the living cells contained almost exclusively keronopsins A_1 and A_2 (Fig. 1). Keronopsins B_1 and B_2 were present in low (and variable) amounts, and apparently arose from mechanically damaged cells.

To isolate these compounds, methanolic cell extracts were first subjected to a crude fractionation over Sephadex in methanol and then chromatographed on RP-18 silica gel with the eluent used for analytical HPLC. After freeze-drying of the aqueous methanolic fractions, keronopsins A_1 (**1a**) and B_1 (**1c**) were obtained as brick red, amorphous powders, whereas A_2 (**1b**) and B_2 (**1d**) were brown-red (Table 1). Components A_1 and



Keronopsin A_1 (**1a**), $R^1 = SO_3Na$, $R^2 = H$
Keronopsin A_2 (**1b**), $R^1 = SO_3Na$, $R^2 = Br$
Keronopsin B_1 (**1c**), $R^1 = H$, $R^2 = H$
Keronopsin B_2 (**1d**), $R^1 = H$, $R^2 = Br$

A_2 were unstable, as in the crude extract. Traces of acid led to their conversion into B_1 and B_2, respectively; in the dry state A_1 may also polymerize spontaneously to yield a black solid. Both reactions could be effectively prevented by addition of a small amount of sodium hydrogen carbonate before workup.

Table 1. Selected physical data of **1a–d**.

1a: $R_f = 0.57$ (silica gel, ethyl acetate/methanol/water = 16/3/2); IR (KBr): $\tilde{\nu}$ = 1685 (st), 1630 (st), 1575 (sst), 1534 (sst), 1278 (st), 1259 (st) cm^{-1}; UV/VIS (CH_3OH): λ_{max} = 221, 267, 325, 339, 439 nm; negative-ion FAB-MS (matrix: 3-nitrobenzyl alcohol (3-NBA)): *m/z*(%): 454 (32), 452 (29) [$M - Na^+$], 199 (95), 168 (100).

1b: $R_f = 0.57$ (silica gel, ethyl acetate/methanol/water = 16/3/2) IR (KBr): $\tilde{\nu}$ = 684 (st), 1635 (st), 1575 (sst), 1538 (sst), 1276 (st), 1261 (st) cm^{-1}; UV/VIS (CH_3OH): λ_{max} = 222, 269, 326, 434 nm; negative-ion FAB-MS (matrix: 3-NBA): *m/z* (%): 534 (9), 532 (17), 530 (9) [M-Na^+], 223 (100).

1c: black crystals, m.p. 135–139 °C (acetone); $R_f = 0.60$ (silica gel, dichloromethane/acetone/methanol 15/4/1); IR (KBr): $\tilde{\nu}$ = 1670 (st), 1648 (st), 1575 (m), 1544 (sst) cm^{-1}; UV/VIS (CH_3OH): λ_{max} (log ε) = 229 (4.16), 266 (4.27), 321 sh (4.03), 340 sh (4.16), 399 sh (4.71), 421 (4.84) 441 sh (4.80) nm; negative-ion DCI-MS (NH_3): *m/z* (%): 375 (100), 373 (99) [M^-], 295 (12), 293 (6), 81 (36), 79 (32); EI-MS (70 eV) *m/z* (%): 375 (22), 373 (22) [M^+]. 82 (99), 80 (100); ^{1}H NMR ([D_6]DMSO): δ = 1.84 (s, 20-H), 6.04 (s, 5-H), 6.09 (dd, 17-H), 6.12 (d, 7-H), 6.33 (dd, 11-H), 6.36 (dd, 9-H), 6.42 (d, 14-H), 6.49 (dd, 12-H), 6.55 (dd, 10-H), 6.73 (dd, 13-H), 6.78 (dd, 18-H), 6.94 (dd, 8-H), 11.20 (sbr, OH), 11.37 (s, NH); J-values [Hz]: J(7,8) = 15.0, J(8,9) = 11.5, J(9,10) = 14.6, J(10,11) = 11.5, J(11,12) = 14.5, J(12,13) = 11.0, J(13,14) = 15.5, J(17,18) = 2.5, J(17,19) = 2.5, J(18,19) = 2.5; ^{13}C NMR ($CDCl_3$/[D_6]DMSO): δ = 8.7 (C-20), 98.2 (C-3), 98.3 (C-16), 102.1 (C-5), 111.4 (C-17), 120.7 (C-18), 121.3 (C-14), 122.1 (C-7), 124.9 (C-13), 127.7 (C-15), 130.6 (C-9), 131.0 (C-11), 133.3 (C-8), 135.9 (C-12), 137.3 (C-10), 155.4 (C-6), 164.6 (C-2), 166.5 (C-4).

1d: $R_f = 0.62$ (silica gel, dichloromethane/acetone/methanol = 15/4/1); IR (KBr): $\tilde{\nu}$ = 1650 (sst), 1575 (sh), 1544 (sst) cm^{-1}; UV/VIS (CH_3OH): λ_{max} (log ε) = 229 (4.20), 397 sh (4.70), 419 (4.84), 439 sh (4.79) nm; FD-MS: *m/z* (%): 456 (54), 454 (100), 452 [$M + H^+$].

According to the ^{1}H and ^{13}C NMR spectra, the keronopsins are closely related, highly unsaturated compounds containing a 1,8-disubstituted octatetraene moiety. From the isotope pattern of the M^+ signal (*m/z*: 375/373) in the EI-mass spectrum, keronopsin B_1 (**1c**) contains a bromine atom; together with the elemental analysis this affords the molecular formula $C_{18}H_{16}BrNO_3$. By analysis of the 1D and 2D NMR spectra it was possible to assign a singlet at δ = 1.84 to a methyl group and two signals at δ = 11.20 and 11.37 to exchangeable protons. In addition, 6 quaternary and 11 methine C atoms in the sp^2 region

 © VCH Verlagsgesellschaft mbH, D-69451 Weinheim, 1994 0570-0833/94/1414-1496 $ 10.00+.25/0

were assigned. From the chemical shifts and the coupling constants of 2.5 Hz, 17-H, 18-H, and 19-H were assigned to the protons of a pyrrole ring. This pyrrole ring carries the octatetraenyl and bromo substituents in the 2- and 3-positions, respectively, as confirmed by the chemical shifts in the ^{13}C spectrum and by the COLOC spectrum (COLOC = correlation by long-range couplings). This substitution pattern is also apparent from the strong NOEs (NOE = nuclear Overhauser enhancement effect) between 19-H and 13-H/18-H, and between 17-H and 18-H. The remaining $C_6H_4O_3$ fragment is a 4-hydroxy-2-pyrone, which is connected to the octatetraenyl residue at C-6, and carries a methyl group in the 3-position. This assignment was confirmed by the COLOC spectrum and by a strong NOE between 5-H and 7-H. Keronopsin B_1 therefore has structure **1c**, and is present predominantly in the conformation depicted.

From the isotope pattern of the M^+ signal in the FD mass spectrum (m/z:456/454/452), keronopsin B_2 (**1d**) contains a second bromine atom. This is found at C-17, since the ^1H and ^{13}C NMR spectra of the two compounds were identical, apart from the absence of the 17-H signal. The same is true for keronopsins A_1 (**1a**) and A_2 (**1b**), which also have one and two bromo substituents, respectively, at C-16 and C-17 of the pyrrole ring. Keronopsins A_1 and A_2 differ from B_1 and B_2 only in the pyrone ring. The signal for the 4-hydroxy group is missing, the signal for 5-H is shifted by $\Delta\delta = 0.6$ downfield, and the signal for C-3 is moved by $\Delta\delta = 5$ downfield—the signals for C-2 and C-4 are shifted by $\Delta\delta = 4-6$ upfield, which suggests the presence of a 4-acyloxy substituent. From elemental analysis and negative-ion FAB-MS, keronopsins A_1 and A_2 are the sodium salts of sulfates **1a** and **1b**, which explains both their ready solubility in water and their hydrolysis by acid to **1c** and **1d**, respectively. In addition this latter reaction is accelerated by the sodium hydrogen sulfate which it releases. In organic solvents and during lyophilization, small amounts of sodium hydrogen sulfate can also induce polymerization; **1a** and **1c** are particularly susceptible to this, due to their free α- and β-positions in the pyrrole residue.

The hydrolysis of **1a** and **1b** in crude extracts, in contrast to that of the pure substances, cannot be stopped by addition of sodium hydrogen carbonate, but can be inhibited by high methanol concentrations or by brief boiling. Clearly the organism possesses a thermolabile sulfatase, which only comes into contact with keronopsins A when the cells are disrupted, and converts them into the more toxic[5] B compounds. This reaction may possibly also take place after uptake into the cellular food vacuole or in the stomach of predators, crippling or killing them, thus reducing the number of victims in the total population.

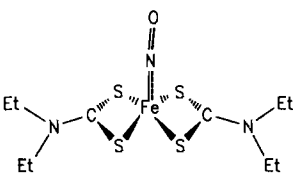
Received February 8, 1994 [Z 6679 IE]
German version: *Angew. Chem.* **1994**, *106*, 1561

[1] E. Wirnsberger, H. F. Larsen, G. Uhlig, *Eur. J. Protistol.* **1987**, *23*, 76–88.
[2] a) G. Uhlig, D. Schumacher, K. Kabbe, *Biologische Anstalt Helgoland, Jahresbericht*, **1991**, 72–75; b) G. Uhlig, *ibid.* **1987**, 45–48; c) G. Uhlig, D. Schumacher, *ibid.* **1989**, 51–52; d) G. Uhlig, S. Moschny, *ibid.* **1988**, 56–57; e) G. Uhlig, K. Kabbe, D. Schumacher, *ibid.* **1990**, 47–49.
[3] W. Lueken, G. Uhlig, T. Krüppel, *J. Protozool.* **1989**, *36* (4), 350–353.
[4] G. Höfle, H. Lautenbach, G. Uhlig, unpublished results.
[5] G. Uhlig, F. Sasse, unpublished results.

Single-Crystal EPR Spectroscopy on $[^{57}Fe(NO)(S_2CNEt_2)_2]$: The "Triplet Signal" in the EPR Spectrum of $[Fe(S_2CNEt_2)_3]$**

Reinhard Kirmse,* Simone Saluschke, Einar Möller, Eduard J. Reijerse, Edward Gelerinter, and Norman V. Duffy

Tris(diethyldithiocarbamato)iron(III) $[Fe(S_2CNEt_2)_3]$ is a classical spin-crossover system and a typical textbook example.[1a,b] The results of the first EPR investigation on the spin equilibrium $S = 1/2 \rightleftharpoons S = 5/2$ of $[Fe(S_2CNEt_2)_3]$ in solution (both spin states are EPR active) were reported by Cotton and Gibson in 1971.[2] In the EPR spectra besides the $S = 5/2$ and $S = 1/2$ signals for Fe^{III}, an additional triplet of lines near $g = 2.0$ was observed, originating from the interaction of an unpaired electron with the ^{14}N nucleus (nuclear spin $I = 1$). The question whether this signal could be assigned to the complex $[Fe^{I}(NO)(S_2CNEt_2)_2]$ (**1**)[3a,b] was, at that time, only shortly discussed.



1

In our investigation of $[Fe/In(S_2CNEt_2)_3]$ single crystals we also observed this triplet of lines together with the signals for $S = 5/2$ and $S = 1/2$. The assignment of the triplet to a Fe^{II}

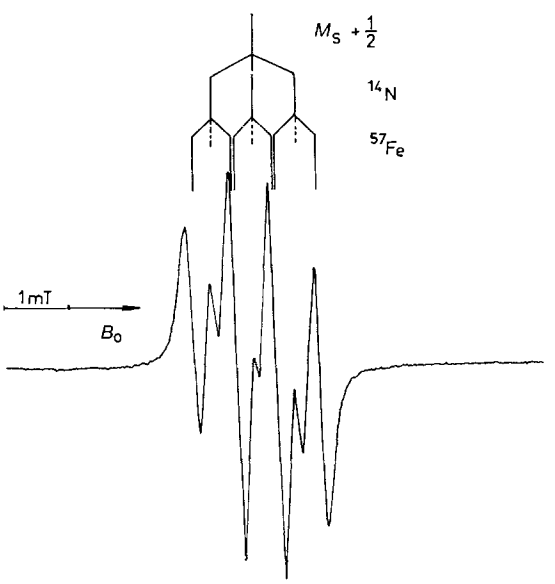


Fig. 1. The single-crystal EPR spectrum of **1** in $[In(S_2CNEt_2)_3]$. For this B_0 field direction $A^{Fe} = A^N$.

[*] Prof. Dr. R. Kirmse, Dipl.-Chem. S. Saluschke, Dipl.-Chem. E. Möller
Institut für Anorganische Chemie der Universität
Talstrasse 35, D-04103 Leipzig (FRG)
Telefax: Int. code + (3741)209325
Dr. E. J. Reijerse
Abteilung Molekülspektroskopie der Universität, Nijmegen (The Netherlands)
Dr. E. Gelerinter, Prof. Dr. N. V. Duffy
Departments of Physics and Chemistry, Kent State University, Ohio (USA)

[**] This work was supported by the Deutsche Forschungsgemeinschaft and the Fonds der Chemischen Industrie. Our thanks goes to Dr. W. Dietzsch (Leipzig) for his helpful discussions and interest in this work.

radical complex of the type $[(S_2CNEt_2)_2Fe^{II}(S_2CNEt_2)^{\cdot}]$ seemed obvious,[4] but could be excluded based on the results reported here.

To assure reliable interpretation we prepared $[^{57}Fe(NO)(S_2CNEt_2)_2]$ (^{57}Fe enrichment $\approx 80\%$) and performed a single-crystal EPR investigation on the magnetically diluted system $[^{57}Fe(NO)(S_2CNEt_2)_2/In(S_2CNEt_2)_3]$ to determine the structure and bonding. The diamagnetic host complex $[In(S_2CNEt_2)_3]$ crystallizes in the space group $A2/a$ with two nonequivalent molecule positions; the molecules themselves have approximately D_3 symmetry.[5] For the incorporation of the "pyramidal" $[Fe(NO)(S_2CNEt_2)_2]$[6] a maximum of six magnetically nonequivalent sites are feasible.[7a] However, first ENDOR spectra (ENDOR = electron nuclear double resonance) reveal that only two of the six sites are occupied by the guest complex $[Fe(NO)(S_2CNEt_2)_2]$.[7b]

Figure 1 shows a single-crystal EPR spectrum for a particular magnetic field orientation, and Figure 2 an anglular dependence

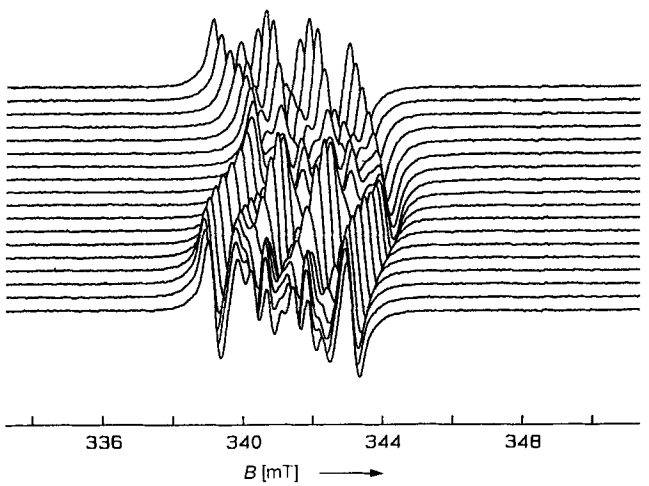


Fig. 2. Stack plot of the deppendence of the EPR spectrum of **1** on the angle in the x,y plane of the laboratory coordinate system.

as well as the complexity of the EPR spectra. The spectra reveal a very well resolved $^{14}N(NO)$ and ^{57}Fe hyperfine structure; parameters for the tensors g, A^{Fe} and $A^{N}(NO)$ obtained from the spectral analysis[8] are summarized in Table 1. Figure 3 illustrates the orientation of the principal tensor axes in the molecule studied. For reasons of symmetry a principal ^{14}N tensor axis is expected to fall along the bond vector of the N–O multiple bond.[9] The angle of 8° between the z axis of the molecule and the tensor component A_1^N corresponds surprisingly well with

Table 1. Principal values [a] of the tensors g, A^{Fe}, and A^{N} and the angles between the principal tensor axes.

Principal tensor values			Angle [°]			
g	$g_1 = 2.049$			g_1	g_2	g_3
	$g_2 = 2.044$		A_1^{Fe}	90	0	90
	$g_3 = 2.036$		A_2^{Fe}	0	90	90
			A_3^{Fe}	90	90	0
A^{Fe}	$A_1^{Fe} = 17.9$					
	$A_2^{Fe} = 12.6$			A_1^{N}	A_2^{N}	A_3^{N}
	$A_3^{Fe} = 1.9$		A_1^{Fe}	83	66	25
			A_2^{Fe}	87	25	115
A^{N}	$A_1^{N} = 13.8$		A_3^{Fe}	8	84	85
	$A_2^{N} = 12.0$					
	$A_3^{N} = 11.5$					

[a] Coupling constants in 10^{-4} cm^{-1}; exp. error: $g_i \pm 0.001$, A_i^{Fe}, $A_i^{N} \pm 0.2$.

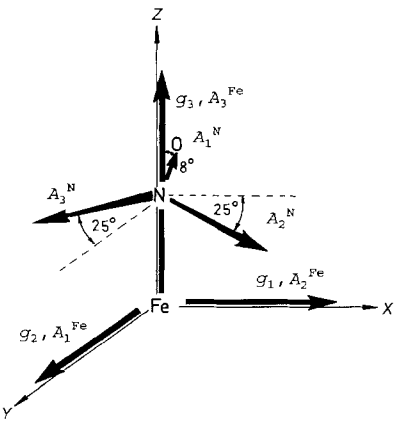


Fig. 3. The orientation of the principal axes of the tensors g, A^{Fe}, and $A^{N}(NO)$ in the molecular coordinate system.

with the Fe-N-O angle determined by X-ray crystal structure analysis.[6] Furthermore, the orientation of the other two principal ^{14}N tensor axes shows that the projection of the NO bond axis on the x,y plane of the molecular coordinate system (according to the crystallographic results) does not fall along the axis bisecting the S_2CNEt_2 ligand (= x axis). Rather, an angle of $\approx 20°$ with respect to the x axis was found. Accordingly, upon incorporation into $[In(S_2CNEt_2)_3]$, **1** maintains its geometry to the greatest possible extent.

For the molecular orbital with the unpaired electron [Eq. (a)],[3a,10] the following values for the spin density distribution in

$$\Psi(A_1) = \alpha\phi(\mathrm{Fe}) \pm \alpha'\phi(\mathrm{N^{NO}}) - (\alpha''/2)(\sum\phi_i(S_i)) \qquad \text{(a)}$$

the first coordination sphere are obtained from the observed hyperfine structure interaction (^{57}Fe, ^{14}N) by using standard formalism:[11] $\alpha^2(Fe) \approx 52\%$, $(\alpha')^2 \approx 6\%$. Thus about 58% of the spin density is located in the Fe–NO unit. Interactions with other nuclei were not observed in the EPR experiment.

The EPR parameters obtained indicate clearly that the triplet of the earlier investigation originates from the ^{14}N nucleus of the NO ligand and not from a radical complex of the type $[(S_2CNEt_2)_2Fe^{II}(S_2CNEt_2)^{\cdot}]$, for which the ^{14}N coupling would be attributed to the ^{14}N nucleus of the $S_2CNEt_2^-$ ligand. Furthermore, for the latter compound a different "pattern" for the principal axis system of the ^{14}N tensor would be expected,[12] and the ^{57}Fe hyperfine structure splitting should be hardly detectable. In contrast to earlier investigations on $[^{57}Fe(NO)(S_2CNEt_2)_2]$[3c] a pronounced rhombic symmetry of the A tensor of ^{57}Fe was expected and verified.

Possible nitrogen sources for the complex **1**, which forms spontaneously in the preparation of $[Fe^{III}(S_2NCEt_2)_3]$, include the nitrogen atom of the $S_2CNEt_2^-$ ligand, the protective gas (N_2) employed during the preparation, or a small amount of NO_3^- ion present in starting materials. The nitrogen in the $S_2CNEt_2^-$ ligand could be excluded through ^{15}N labeling, since a ^{15}N hyperfine structure doublet was not observed.[13] The subsitution of Ar for N_2 as the protective gas did not lead to any change in the intensity of the triplet signal. On the other hand, a very clear reduction in the EPR signal intensity (signal still however detectable) was found when analytical pure $FeCl_3$ (NO_3^- content $< 0.01\%$) was used. Obviously traces of NO_3^- in the starting material are responsible for the spontaneous formation of **1**. The high detection sensitivity of EPR spectroscopy (concentrations of ≈ 0.001 mol% are detectable when line widths are narrow) confirms this conclusion.

Experimental Procedure

$[In(S_2CNEt_2)_3]$ was synthesized by treating $Na(S_2CNEt_2)$ with $InCl_3$ [14]; ^{57}Fe labeled $[Fe(NO)(S_2CNEt_2)_2]$ was prepared in a one pot reaction employing $^{57}FeSO_4 \cdot 7H_2O$ (prepared from ^{57}Fe), NO, and $Na(S_2CNEt_2)$ [15]. Yield: 50%.

Magnetically diluted $[Fe(NO)(S_2CNEt_2)_2/In(S_2CNEt_2)_3]$ single crystals were obtained after about 6 weeks by slowly crystallizing a benzene solution containing both components in the ratio of 0.5% (Fe complex) to 99.5% (In complex) under a controlled N_2 stream. The edges of the crystals were up to 5 mm long.

EPR spectra: The spectra were recorded in X Band ($\nu \approx 9.7$ GHz) at $T = 295$ K with a spectrometer of the type ESP 300 E (Bruker). For the measurement of the angular dependence, the spectra were collected in three planes normal to each other in 10° divisions at 5° intervals. The data was evaluated with the program "MAGRES" [8].

To establish the N_2 source for the formation of **1** during the preparation of $[Fe/In(S_2CNEt_2)_3]$ crystals and powders, $[Fe(S_2CNEt_2)_3]$ prepared from analytically pure $FeCl_3$ (Fluka, NO_3 content < 0.01%) was used. Either N_2 or Ar was applied as the protective gas for the synthesis.

Received: January 19, 1994 [Z 6534 IE]
German version: *Angew. Chem.* **1994**, *106*, 1546

[1] a) L. Gambi, L. Szego, *Ber. Dtsch. Chem. Ges.* **1931**, *64*, 2591–2598; b) R. L. Martin, A. H. White, *Transition Met. Chem.* **1968**, *4*, 113–198; N. N. Greenwood, A. Earnshaw, *Chemie der Elemente*, corrected print of the 1st ed., VCH, Weinheim, **1990**, p. 1396–1398.

[2] S. A. Cotton, J. F. Gibson, *J. Chem. Soc. Dalton Trans.* **1971**, 803–809.

[3] a) Nitrosyl–Fe^I–dithiocarbamate was investigated in detail in solution, see J. H. Enemark, R. D. Feltham, *Coord. Chem. Rev.* **1974**, *13*, 339–406, and references therein; b) $[Fe^I(NO)(S_2CNMe_2)_2/Co(NO)(S_2CNMe_2)_2]$ was studied by single crystal EPR spectroscopy: R. D. Feltham, H. Crain, *Inorg. Chim. Acta* **1980**, *40*, 37–42. c) ^{57}Fe enriched $[Fe(NO)(S_2CNMe_2)_2]$ was analyzed in frozen solution in two studies: B. A. Goodman, J. B. Raynor, M. C. R. Symons, *J. Chem. Soc. A* **1969**, 2572–2575; N. D. Yordanov, Y. Iliev, D. Shopov, A. Jezierski, B. Jezowska-Trzebiatowska, *Inorg. Chim. Acta* **1982**, *60*, 9–15. The ^{57}Fe tensor given here has axial symmetry: $A_x^{Fe} = A_y^{Fe} \approx 1.5$ mT, $A_z^{Fe} \approx 0$ mT; this is in contrast to the low symmetry of the molecule investigated.

[4] E. Gelerinter, N. V. Duffy, St. S. Yarish, W. Dietzsch, R. Kirmse, *Chem. Phys. Lett.* **1991**, *184*, 375–378.

[5] K. Dymock, G. J. Palemik, J. Slezak, C. L. Raston, A. H. White, *J. Chem. Soc. Dalton Trans.* **1976**, 28–32.

[6] Crystal structure data have been reported for a) $[Fe^I(NO)(S_2CNMe_2)_2]$ by G. R. Davies, J. A. J. Jarvis, B. T. Kilbourn, R. H. B. Mais, P. G. Owston, *J. Chem. Soc. A* **1970**, 1275–1283; and b) $[Fe^I(NO)(S_2CNEt_2)_2]$ by M. Colapeitro, A. Domenicano, L. Scaramuzza, A. Vaciago, L. Zambonelli, *Chem. Commun.* **1967**, 583–584. The two structures are very similar: Fe-N-O angle (T = 295 K) ≈ 174°; the projection of the N–O vector onto the x,y plane of the molecule gives an angle of ≈ 20° to the x axis.

[7] a) Statistically the NO ligand could replace every ligand of the $[In(S_2CNEt_2)_3]$ molecule, which would then lead to three structurally different and simultaneously to three magnetically different sites per In complex. Thus for the unit cell with two nonequivalent molecule positions, there are six sites in total. The same number of nonequivalent magnetic sites also exists for O_h symmetry (for monodentate ligands). Since 180° symmetry can not be distinquished in an EPR experiment, of the six different sites in this case only three magnetic nonequivalent sites per molecule, as for D_3 symmetry, are possible. b) ENDOR investigation: S. Saluschke, R. Böttcher, R. Kirmse, unpublished results. Why only two insertion positions are occupied cannot be solved by this investigation.

[8] The EPR spectra were described with the spin Hamiltonian operator $H_{sp} = \beta_e B_0 \cdot g \cdot S + S \cdot A^{Fe} \cdot I^{Fe} + S \cdot A^{N} \cdot I^{N}$. The analysis was performed with the program "MAGRES": C. P. Keijzers, E. J. Reijerse, P. Stam, M. F. Dumont, M. C. M. Gribnau, *J. Chem. Soc. Faraday Trans. 1* **1987**, *83*, 3493–3503.

[9] R. Kirmse, R. Böttcher, J. P. Willems, E. J. Reijerse, E. de Boer, *J. Chem. Soc. Faraday Trans. 1* **1991**, *87*, 3105–3111.

[10] $\phi(Fe)$, $\phi(N^{NO})$, $\phi(S_i)$ denote the given sequence of the linear combination of the functions Fe–$3d_{z^2}$/Fe–4s, N–2s/2p (NO ligand), and S–3s/2p; the molecular orbital coefficients α, α', α'' are a measure of the spin density delocalization.

[11] J. R. Morton, K. S. Preston, *J. Magn. Reson.* **1978**, *30*, 577–582.

[12] R. Böttcher, R. Kirmse, J. Stach, E. J. Reijerse, C. P. Keijzers, *Chem. Phys.* **1986**, *107*, 145–157.

[13] N. V. Duffy, Kent State University, personal communication.

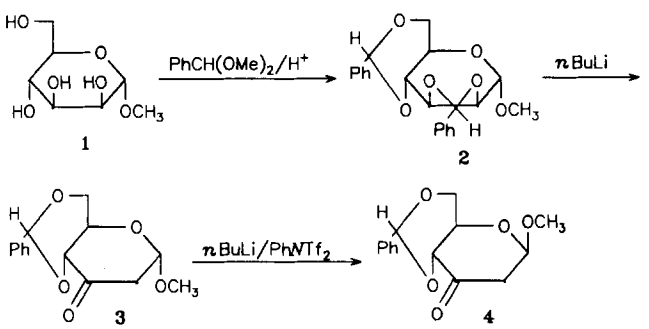
[14] D. Coucouvanis, *Prog. Inorg. Chem.* **1970**, *11*, 233–371.

[15] O. A. Ileperuma, R. D. Feltham, *Inorg. Synth.* **1976**, *16*, 5–7.

Enol Triflate Pyranoses, Versatile Reagents for the Formation of Conjugated Systems on Pyranoses**

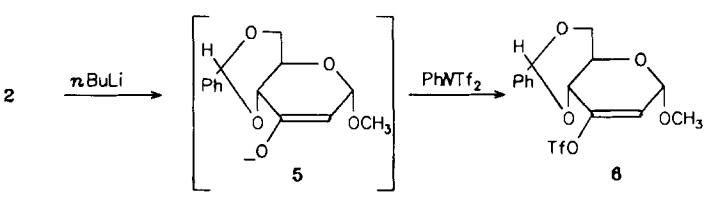
Yousef Al-Abed, Taleb H. Al-Tel, Christoph Schröder, and Wolfgang Voelter*

Over the last few years a whole series of synthetic routes have been described in which conjugated enals and dienes derived from carbohydrates are used in Diels–Alder reactions to obtain chiral carbocyclic systems as starting materials for the synthesis of natural products.[1] Thus, methyl-4,6,-*O*-benzylidene-2,3-dideoxy-3-C-vinyl-α-D-*erythro*-hex-2-enopyranoside (**14**) has finally been synthesized, after a less successful attempt,[1a] from methyl-α-D-glucopyranoside in seven[1i] or six[1j] steps in an overall yield of about 15%, based on the starting material. These multistep syntheses of diene **14** should be shortened drastically by the use of the enol triflate **6**. The synthesis of **6** from **3**, which is produced in two steps from commercially available **1** via **2**,[2] was unsuccessful: after a 10 to 15 h reaction at −78 to −30 °C with *n*BuLi and *N*-phenyltrifluoromethanesulfonimide ($PhNTf_2$),[3] only anomerization to **4** was observed.



With trifluoromethanesulfonic anhydride as reagent instead of trifluoromethanesulfonimide the reaction solution turned black when the temperature was increased from −78 to −30 °C; numerous decomposition products could be detected by thin-layer chromatography.

However, treatment of **2** with *n*BuLi in THF, at −40 °C for 30 min (formation of the enolate **5** is indicated by red coloration

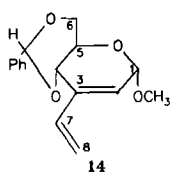
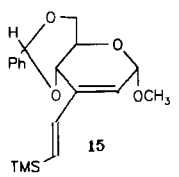
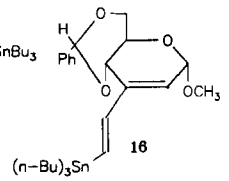
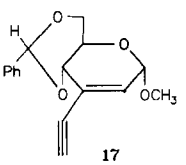
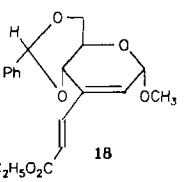
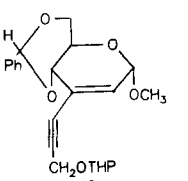
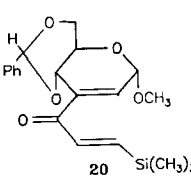


and disappearance of the starting material as shown by thin-layer chromatography), reaction of the resulting enolate solution with four equivalents of $PhNTf_2$ at −78 °C over 30 min, and then at −20 °C for 6 h gave the desired enol triflate **6** in 85%

[*] Prof. Dr. W. Voelter, Dr. Y. Al-Abed, T. H. Al-Tel, C. Schröder
Abteilung für Physikalische Biochemie des Physiologisch-chemischen Instituts der Universität
Hoppe-Seyler-Strasse 4, D-72076 Tübingen (FRG)
Telefax: Int. code + (7071)29-3361

[**] This work was supported by the Fonds der Chemischen Industrie and by the Deutschen Akademischen Austauschdienst (doctoral stipendia for Y. A.-A. and T. H. A.-T.)

Table 1. Products and yields from the reaction of vinyl triflate **6** with unsaturated tributylstannyl derivatives or Michael acceptors.

Reagent	Product	Yield [%]	Selected ^{1}H NMR data (250 MHz, $CDCl_3$)
Bu_3Sn (**7**)	 **14**	100	δ = 6.21 (dd, J = 17.7, 11.4 Hz, H-7), 5.60 (d, J = 17.8 Hz, H-8), 5.57 (br. s, H-2), 5.15 (dd, J = 11.2, 1.4 Hz, H-8), 4.89 (d, J = 2.1 Hz, H-1)
Bu_3Sn, $SiMe_3$ (**8**)	 **15**	100	δ = 6.32 (d, J = 19.3 Hz, H-7), 6.40 (d, J = 19.3 Hz, H-8), 5.60 (br. s, H-2), 4.88 (br. s, H-1)
Bu_3Sn, $SnBu_3$ (**9**)	 **16**	75	δ = 6.41 (d, J = 19.7 Hz, H-7), 6.70 (d, J = 19.7 Hz, H-8), 5.61 (br. s, H-2), 4.91 (br. d, J = 2.1 Hz, H-1)
$HC\equiv CSnBu_3$ (**10**)	 **17**	80	δ = 5.90 (s, H-2), 4.86 (br. s, H-1)
Bu_3Sn, CO_2Et (**11**)	 **18**	80	δ = 7.12 (d, J = 16.1 Hz, H-7), 6.29 (d, J = 16.1 Hz), 5.59 (br. s, H-2), 4.91 (br. d, J = 2.1 Hz, H-1)
$HC\equiv CCH_2OTHP$ (**12**)	 **19**	87	δ = 5.93 (br. s, H-2), 4.87 (br. s, H-1), 4.32 (s, 2H, H-9)
$H_2C=CCO_2Et$ (**13**)	**18**	83	see above
Bu_3Sn, $SiMe_3$ (**8**) + CO	 **20**	60	δ = 6.68 (d, J = 18.8 Hz, H-8), 7.12 (d, J = 18.9 Hz, H-9), 6.24 (t, J = 2.5 Hz, H-2), 4.89 (dd, J = 2.6, 1.1 Hz, H-1)

isolated yield after workup (the temperature should not be allowed to rise above 5 °C).

Compound **6** has shown itself to be a versatile reagent for the synthesis of pyranosides containing conjugated units, as already described for carbocyclic systems.[4] Reaction of **6** with tributylvinylstannane (**7**), tetrakis(triphenylphosphane)palladium(0) and lithium chloride according to Scott and Stille,[5] gave compound **14**, described by López et al.,[1a] in almost quantitative yield. With the same method, the conjugated compounds **15**–**18** are obtained from **6** in 80 to 100% yield by reaction with *trans*-1-tri-*n*-butylstannyl-2-trimethylsilylethylene (**8**),[6] *trans*-1,2-bis(tri-*n*-butylstannyl)ethylene (**9**),[6] ethynyltributylstannane (**10**), or *trans*-2-tributylstannylethyl acrylate[7] (**11**) (Table 1). The dienes **14**–**16** are chiral starting materials for the formation of carbocyclic systems that contain other reactive centers for further reactions by the Diels–Alder reaction. For example, the enyne **17** can be used as starting material for a regiospecific 1,2-functionalization of the olefinic double bond.[8] The conjugated systems can be synthesized easily by treating olefins with Michael acceptor properties or acetylenes with the enol triflate **6**.[9] Thus, the diene **18** and the enyne **19** are prepared in 80–85% yield from **6** by reaction with ethyl acrylate (**13**) or 2-propargyloxytetrahydropyran (**12**), respectively, in the presence of bis(triphenylphosphane)dichloropalladium(II) and triethylamine at 70 °C in dimethylformamide in 10 h.

Divinyl ketones can be prepared from the vinyl triflate **6** by a palladium-catalyzed reaction with **8** and carbon monoxide, as shown by the example of **20**. The successful insertion of CO is, however, strongly dependent on the temperature. If compound **6** is, according the literature,[10] treated with **8** at 55–60 °C, diene **15** is the predominant product. After a 10 h reaction at 20 °C only the starting material could be isolated. Even increasing the CO pressure from 1 to 3 atm did not lead to an improvement in the yield of **20**. On the other hand, when the reaction was carried out for 12 h at 50 °C, **20** could be obtained in 60% yield, together with 25% of **15**. Chiral divinylketones such as **20** could be used as Michael acceptors for numerous nucleophiles[11] or for the synthesis of optically active cyclopentenones by the Nazarov reaction.[12]

Received: February 14, 1994 [Z 6690 IE]
German version: Angew. Chem. **1994**, *106*, 1568

[1] a) J. C. López, E. Lameignère, C. Burnouf, A. A. Laborde, A. A. Ghini, A. Olesker, G. Lukacs, *Tetrahedron* **1993**, *49*, 7701–7722; b) R. M. Giuliano, A. D. Jordan, Jr., A. D. Gauthier, K. Hoogsteen, *J. Org. Chem.* **1993**, *58*, 4979–4988; c) R. Tsang, B. Fraser-Reid, *ibid.* **1992**, *57*, 1065–1067; d) K. S. Kim, I. H. Cho, Y. H. Joo, I. Y. Yoo, J. H. Song, J. H. Ko, *Tetrahedron Lett.* **1992**, *33*, 4029–4032; e) J. Herscovici, S. Delatre, K. Antonakis, *ibid.* **1991**, *32*, 1183–1186; f) R. M. Giuliano, J. H. Buzby, N. Macropulos, J. P. Springer, *J. Org. Chem.* **1990**, *55*, 3555–3562; g) C. Burnouf, J. C. López, F. G. Calvo-Flores, M. A. Laborde, A. Olesker, G. Lukacs, *J. Chem. Soc. Chem. Commun.* **1990**, 823–825; h) A. Mukhopadhyay, S. M. Ali, M. Husain, S. N. Suryawanshi, D. S. Bhakuni, *Tetrahedron Lett.* **1989**, *30*, 1853–1856; i) J. C. López, E. Lameignère, G. Lukacs, *J. Chem. Soc. Chem. Commun.* **1988**, 514–515; j) B. H. Lipshutz, S. L. Nguyen, T. R. Elworthy, *Tetrahedron* **1988**, *44*, 3355–3364; k) J. C. López, E. Lameignère, G. Lukacs, *J. Chem. Soc. Chem. Commun.* **1988**, 706–707; l) Y. Chapleur, M.-N. Euvard, *ibid.* **1987**, 884–885; m) M. Brehm, W. G. Dauben, P. Köhler, F. W. Lichtenthaler, *Angew. Chem.* **1987**, *99*, 1318–1319; *Angew. Chem. Int. Ed. Engl.* **1987**, *26*, 1271–1273; n) R. M. Giuliano, J. H. Buzby, *Carbohydr. Res.* **1986**, *158*, c1–c4.
[2] D. Horton, W. Weckerle, *Carbohydr. Res.* **1975**, *44*, 227–240.
[3] J. E. McMurry, W. J. Scott, *Tetrahedron Lett.* **1983**, *24*, 979–982.
[4] K. Kondo, M. Sodeoka, M. Mori, M. Shibasaki, *Synthesis* **1993**, 920–930; b) K. Ritter, *ibid.* **1993**, 735–762; c) T. N. Mitchell, *ibid.* **1992**, 803–815; d) V. N. Kalinin, *ibid.* **1992**, 413–432; W. J. Scott, J. E. McMurry, *Acc. Chem. Res.* **1988**, *21*, 47–54.
[5] W. J. Scott, J. K. Stille, *J. Am. Chem. Soc.* **1986**, *108*, 3033–3040.
[6] D. Seyferth, S. C. Vick, *J. Organomet. Chem.* **1978**, *144*, 1–12.
[7] A. J. Leusink, H. A. Budding, J. W. Marsman, *J. Organomet. Chem.* **1967**, *9*, 285–294.

[8] a) A. S. Gybin, W. A. Smit, R. Caple, A. L. Veretenov, A. S. Shashkov, L. G. Vorontsova, M. G. Kurella, V. S. Chertkov, A. A. Carapetyan, A. Y. Kosnikov, M. S. Alexanyan, S. V. Lindeman, V. N. Panov, A. V. Maleev, Y. T. Struchkov, S. M. Sharpe, *J. Am. Chem. Soc.* **1992**, *114*, 5555–5566; b) G. S. Mikaelian, A. S. Gybin, W. A. Smit, R. Caple, *Tetrahedron Lett.* **1985**, *26*, 1269–1272; c) A. A. Schegolev, W. A. Smit, Y. B. Kalyan, M. Z. Krimer, R. Caple, *ibid.* **1982**, *23*, 4419–4422.
[9] W. J. Scott, M. R. Peña, K. Swärd, S. J. Stoessel, J. K. Stille, *J. Org. Chem.* **1985**, *50*, 2303–2308.
[10] G. T. Crisp, W. J. Scott, J. K. Stille, *J. Am. Chem. Soc.* **1984**, *106*, 7500–7506.
[11] E. D. Bergman, D. Ginsburg, R. Pappo, *Org. React.* **1959**, *10*, 179–555.
[12] a) S. E. Denmark, K. L. Habermas, G. A. Hite, T. K. Jones, *Tetrahedron* **1986**, *42*, 2821–2829; b) M. Ramaiah, *Synthesis* **1984**, 529–570; C. Santelli-Rouvier, M. Santelli, *ibid.* **1983**, 429–442.

Luminescent Eu^{3+} and Tb^{3+} Complexes of a Branched Macrocyclic Ligand Incorporating 2,2′-Bipyridine in the Macrocycle and Phosphinate Esters in the Side Arms**

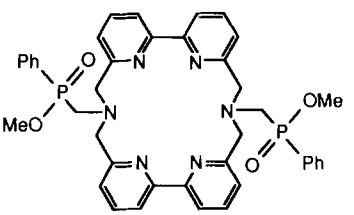
Nanda Sabbatini,* Massimo Guardigli, Fabrizio Bolletta, Ilse Manet, and Raymond Ziessel*

Lanthanide ions, in particular Eu^{3+} and Tb^{3+}, are interesting luminescent species for fluoroimmunoassay (FIA) because of the long lifetimes of their emitting states, which allow enhancement of the sensitivity by time-resolved measurements.[1] However, the Eu^{3+} and Tb^{3+} ions are characterized by low absorption coefficients;[2] consequently, direct excitation of the ion results only in low luminescence intensity. To overcome this problem, complexes of these ions with efficient chromophores have been prepared in order to obtain intense emission after an energy transfer from the excited ligand to the metal ion.

The first type of lanthanide complexes studied for application in FIA are the Eu^{3+} chelates.[3] These complexes are widely used in commercial kits, but the procedure is complicated because of a) the use of two chelates, b) the insolubility of the luminescent chelate in water, which is the solvent of interest in FIA, and c) the need to protect the chelated ion from interaction with the solvent.[3]

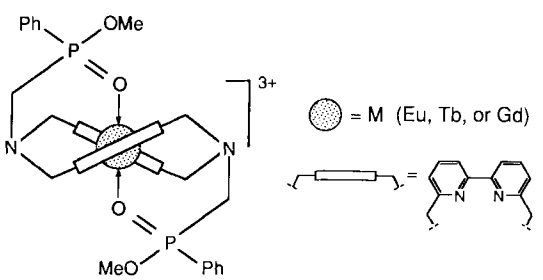
More recently, a different approach to the use of lanthanide ions in FIA, based on their complexation with cage-type ligands incorporating chromophoric groups, aims at simplified procedures by using compounds that simultaneously show solubility and kinetic inertness in water, shielding of the enclosed ion, and intense metal luminescence. Among the species studied, complexes of branched macrocyclic ligands incorporating the 2,2′-bipyridine (bpy) and the 1,10-phenanthroline chromophoric groups have drawn special attention because of their high molar extinction coefficients and efficient shielding of the enclosed metal ion.[4] For this class of compounds, only the Eu^{3+} complex of the ligand incorporating two bpy units in the macrocycle and two bpy units in the branches shows a luminescence intense enough to be interesting for application in FIA,[4a, 5] but the complex undergoes decomposition when used in immunological analyses, most likely because of weak coordination of the ion by the bpy units in the side arms. Research is therefore directed at introducing groups into the branches that are known to have better ligating properties towards lanthanide ions.

In this paper we present the novel, branched macrocyclic ligand **1**, which contains two bpy moieties in the macrocycle and phosphinate ester groups in the branches. The syntheses of the ligand **1** and the $[M \subset \mathbf{1}]^{3+}$ complexes (M = Eu, Tb, or Gd) are reported as well as their photophysical properties.



1

Ligand **1** has been synthesized as a mixture of diastereoisomers in a straightforward manner by treating the bpy · bpy macrocycle[6] (that is, H at the positions of the phosphinate ester groups) with paraformaldehyde and dimethylphenylphosphonite under anhydrous conditions, in a procedure adapted from the method described in the literature[7] (yield 45%, FAB-MS 731 $[M^+ + H]$). The $[M \subset \mathbf{1}]^{3+}$ complexes (M = Eu, Tb, or Gd) have been prepared as previously described:[8] $[Eu \subset \mathbf{1}]Cl_3 \cdot 3H_2O$ (yield 78%, FAB-MS 953 $[M^+ - Cl]$); $[Tb \subset \mathbf{1}]Cl_3 \cdot 2H_2O$ (yield 76%, FAB-MS 959 $[M^+ - Cl]$); $[Gd \subset \mathbf{1}]Cl_3 \cdot 3H_2O$ (yield 79%, FAB-MS 958 $[M^+ - Cl]$). Interestingly, the FT-IR spectra of these complexes display a significant shift (17 cm^{-1}) to lower frequency of the P–O stretching frequency indicating, as expected, strong coordination of this group to the metal.[9]



$[M \subset \mathbf{1}]^{3+}$

All the photophysical properties of solutions of the Eu^{3+}, Tb^{3+}, and Gd^{3+} complexes in water were unchanged for several days; these complexes are thus kinetically inert in this solvent. The absorption spectra of the complexes (Fig. 1) are characterized by intense bands in the UV region. By analogy with other lanthanide complexes of bpy-based ligands,[4a] these bands are attributed to bpy $\pi-\pi^*$ transitions which undergo some red shift upon complexation (Table 1). The shoulders in the 250–280 nm region correspond to the weak absorption of the phenyl moiety. Comparison of the absorption spectrum with the luminescence excitation spectrum of the metal obtained upon excitation of the ligand (Fig. 1) indicates that energy transfer from the excited ligand to the emitting metal ion takes place; the emitting state

[*] Prof. Dr. N. Sabbatini, Dipl.-Chem. M. Guardigli, Prof. Dr. F. Bolletta, Dipl.-Chem. I. Manet
Dipartimento di Chimica "G. Ciamician", Università degli Studi di Bologna
Via Selmi 2, I-40126 Bologna (Italy)
Telefax: Int. code + (51)259-456
Dr. R. Ziessel
Ecole Européenne des Hautes Etudes des Industries Chimiques de Strasbourg
IPCMS, UMR n° 46
1, rue Blaise Pascal, F-67008, Strasbourg Cedex (France)

[**] This work was supported by the Ministero dell'Università e della Ricerca Scientifica e Tecnologica (Italy) and the Centre National de la Recherche Scientifique (France).

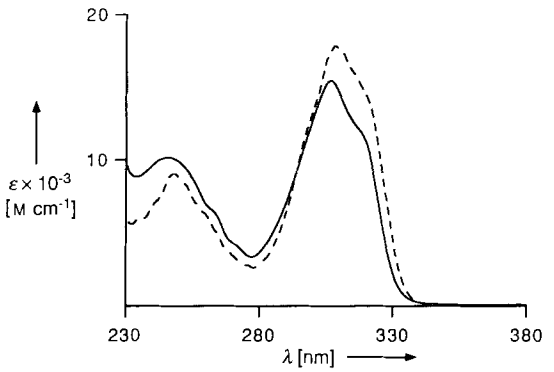


Fig. 1. Absorption (—) and luminescence excitation (- - -) spectra of the $[Eu \subset \mathbf{1}]^{3+}$ complex in water (similar absorption spectra were obtained for $[Tb \subset \mathbf{1}]^{3+}$ and $[Gd \subset \mathbf{1}]^{3+}$, and a similar luminescence excitation spectrum for $[Tb \subset \mathbf{1}]^{3+}$).

of the metal is clearly populated through absorption by the bpy unit, while the involvement of the phenyl moiety cannot be unequivocally assessed.

To study the behavior of the ligand-centered excited states in the energy transfer, the properties of the lowest singlet and triplet excited states belonging to the bpy moiety have been investigated. The lifetimes of the singlet excited state of the ligand and the fluorescence quantum yields of the ligand in the Gd^{3+}, Tb^{3+}, and Eu^{3+} complexes have been measured (Table 1). Comparison of the results obtained shows that $[Tb \subset \mathbf{1}]^{3+}$ and $[Eu \subset \mathbf{1}]^{3+}$ exhibit fluorescence quantum yields respectively about two times and fifty times lower than that of $[Gd \subset \mathbf{1}]^{3+}$. This might imply an energy transfer from the lowest singlet excited state of the ligand to the Eu^{3+} and Tb^{3+} emitting states. Such a process should take place with a rate constant greater than $10^9\ s^{-1}$ and $10^{10}\ s^{-1}$ for $[Tb \subset \mathbf{1}]^{3+}$ and $[Eu \subset \mathbf{1}]^{3+}$, respectively (calculated from the fluorescence quantum yield values in Table 1). It is not possible to decide whether the rate constant values are reasonable, because the only value available for an analogous process refers to an energy transfer from the ligand-centered triplet excited state.[10] Finally, it is worthwhile noting that the lower quantum yield of $[Eu \subset \mathbf{1}]^{3+}$ relative to that of $[Tb \subset \mathbf{1}]^{3+}$ may be due to nonradiative deactivation of the singlet excited state of the ligand to low-lying metal states (ligand-to-metal charge transfer, LMCT).[4, 11]

The lowest triplet excited state of the ligand has been investigated by studying the bpy phosphorescence and triplet–triplet absorption in the $[Eu \subset \mathbf{1}]^{3+}$, $[Tb \subset \mathbf{1}]^{3+}$, and $[Gd \subset \mathbf{1}]^{3+}$ complexes. Both these quantities could be measured for $[Gd \subset \mathbf{1}]^{3+}$ but not for $[Eu \subset \mathbf{1}]^{3+}$ or $[Tb \subset \mathbf{1}]^{3+}$ (Table 1). Since the energy of the lowest triplet excited state of 21 500 cm^{-1}, obtained from the highest energy feature of the phosphorescence of the $[Gd \subset \mathbf{1}]^{3+}$ complex (Table 1), lies above the Eu^{3+} $^5D_0$ and Tb^{3+} $^5D_4$ emitting states and below the first excited state of the Gd^{3+} ion, the behavior observed is ascribed to deactivation of the ligand triplet excited state by energy transfer to the Eu^{3+} or Tb^{3+} ions. An analogous conclusion was drawn for other Eu^{3+} and Tb^{3+} complexes of ligands containing bpy units.[4a]

Metal luminescence lifetime and quantum yields, obtained upon ligand excitation under various experimental conditions, are collated in Table 2. For both the $[Tb \subset \mathbf{1}]^{3+}$ and $[Eu \subset \mathbf{1}]^{3+}$ complexes comparison of the lifetimes and quantum yields in H_2O and D_2O solutions indicates that nonradiative deactivation through the O–H vibrations[12] occurs. By using the Horrocks and Sudnick equation[13] 1.3 and 1.4 water molecules are estimated to coordinate the metal ion in the $[Tb \subset \mathbf{1}]^{3+}$ and $[Eu \subset \mathbf{1}]^{3+}$ complexes, respectively. In the $[Tb \subset \mathbf{1}]^{3+}$ complex, the strong temperature dependence of the lifetimes indicates that an important role in the decay of the Tb^{3+} emitting state is played by a thermally activated process. As previously suggested for Tb^{3+} complexes of other ligands incorporating bpy units,[4a] such a process most likely involves the bpy lowest triplet excited state. In fact, as mentioned above, this level lies at 21 500 cm^{-1}, that is, 1100 cm^{-1} above the Tb^{3+} emitting level, and therefore it may be thermally populated at room temperature. Moreover, the quenching of the Tb^{3+} luminescence by oxygen ($k_q = 1.1 \times 10^6\ M^{-1}\ s^{-1}$, obtained from the values in Table 2) suggests that the Tb^{3+} $^5D_4$ level is in equilibrium with the bpy lowest triplet excited state. In fact, the luminescent states of the lanthanide ions are not quenched by oxygen;[10] thus quenching of the Tb^{3+} luminescence reasonably involves the bpy lowest triplet excited state. This hypothesis is supported by the observation that the bpy lowest triplet excited state in $[Gd \subset \mathbf{1}]^{3+}$ is quenched by oxygen ($k_q = 5.0 \times 10^8\ M^{-1}\ s^{-1}$, obtained from the lifetime values in Table 1). The same behavior has previously been found for analogous lanthanide complexes.[4a]

Table 2. Luminescence data of the metal ions [a].

Complex	Lifetime [ms] [b]				Quantum yield [c]	
	$\tau_{H_2O}^{300K}$	$\tau_{H_2O}^{77K}$	$\tau_{D_2O}^{300K}$	$\tau_{D_2O}^{77K}$	$\Phi_{H_2O}^{300K}$	$\Phi_{D_2O}^{300K}$
$[Tb \subset \mathbf{1}]^{3+}$	0.43	1.8	0.50	2.4	0.08	0.09
	0.53 [d]		0.62 [d]		0.10 [d]	0.11 [d]
$[Eu \subset \mathbf{1}]^{3+}$	0.60	1.2	2.1	2.0	0.08	0.30

[a] In aerated solution unless otherwise noted. Excitation in the ligand absorption band at 306 nm. [b] Experimental error ≤10%. [c] Experimental error ≈30%. [d] In deaerated solution.

Table 1. Absorption, fluorescence, and phosphorescence data of the ligand **1** and its complexes with lanthanide ions [a].

Compound	Ground state absorption	Fluorescence			Triplet–triplet absorption		Phosphorescence	
	λ_{max}, ε_{max} [nm, $M^{-1}cm^{-1}$]	λ_{max} [nm]	τ [b] [ns]	Φ [c]	λ_{max} [nm]	τ [b] [s]	λ_{max} [nm]	τ [b] [s]
1 [d]	299, 21 200	396	4	1×10^{-2}	360 [e]	1.6×10^{-5} [e]	475 [f] (445 [g])	1.6 [f]
	245, 16 100							
$[Gd \subset \mathbf{1}]^{3+}$	306, 14 200	353	~1	5×10^{-3}	375	0.36×10^{-5}	493 [h] (465 [g])	1×10^{-3} [h]
	245, 9800					1.5×10^{-5} [e]	495 [e]	1.8×10^{-5} [e]
$[Tb \subset \mathbf{1}]^{3+}$	306, 15 300	350	<1	2×10^{-3}	[i]		[i]	
	246, 10 100							
$[Eu \subset \mathbf{1}]^{3+}$	307, 15 100	≈360	<1	$\approx 10^{-4}$	[i]		[i]	
	246, 9900							

[a] In aerated water at 300 K unless otherwise noted. [b] Experimental error ≤10%. [c] Experimental error ≈30%. [d] In aerated methanol at 300 K, unless otherwise noted. [e] In deaerated solution. [f] In butyronitrile at 77 K. [g] Highest energy feature in the phosphorescence spectrum. [h] At 77 K. [i] Not observed.

In conclusion, the $[Eu \subset \mathbf{1}]^{3+}$ and $[Tb \subset \mathbf{1}]^{3+}$ complexes show interesting properties for applications in FIA. They are kinetically stable in water, and the metal ions are well protected against deactivation of the luminescent excited states by water. Moreover, the luminescence intensity is rather high, in spite of the relatively low molar extinction coefficients resulting from the presence in the ligand **1** of only two efficient chromophores. Substitution of the weakly absorbing phenyl units in the phosphinate groups by efficient chromophores should result in an even more intense luminescence, if absorption is followed by efficient energy transfer to the metal ion. As mentioned in the discussion of the luminescence excitation spectra of the metal, the involvement of the phenyl moiety in the energy transfer to the metal ion cannot be proved. However, for lanthanide complexes containing phosphinic or phosphonic groups incorporating benzyl or phenyl units a quite efficient energy transfer has recently been reported.[14]

Experimental Procedure

1: A suspension of the bpy · bpy macrocycle (200 mg, 0.51 mmol) and anhydrous paraformaldehyde (350 mg) in THF (100 mL) was heated at 60 °C for 2 h. Then, dimethylphenylphosphonite (0.24 mL, 1.52 mmol) was added under argon, and the mixture was heated at reflux for 24 h in a Soxhlet apparatus containing 3 Å molecular sieves (10 g). After cooling to room temperature the solvent was evaporated, and the residue was dissolved in the minimal amount of CH_2Cl_2 (about 20 mL). After filtration over celite, hexane (about 35 mL) was added as a counter solvent. Slow evaporation of the solvent caused the precipitation of the pure, white polymethylenephosphinate ester **1** as a diastereoisomeric mixture (yield 45%). UV/VIS (MeOH): λ_{max} [nm] (ε) = 299 (21 200), 245 (16 100). ^{1}H NMR (200.1 MHz, $CDCl_3$, 25 °C): δ = 8.33 (d, 4H, ^3J(H, H) = 8.1 Hz), 7.83 – 7.41 (m, 14H), 7.23 (d, 4H, ^3J(H, H) = 7.5 Hz), 3.71 (d, 6H, ^3J(P, H) = 11.6 Hz, OCH_3), 3.93 (s, 8H, CH_2-bpy), 3.03 (d, 4H, ^2J(P, H) = 6.5 Hz, CH_2P). $^{13}C\{^1H\}$ NMR (50.3 MHz, $CDCl_3$, 25 °C): δ = 156.33 (quart. C), 151.93 (quart. C), 148.76 (CH), 133.30 (CH), 132.35 (d, ^3J(P, C) = 10 Hz, *m*-Ar), 131.56 (CH), 130.30 (d, ^1J(P, C) = 120 Hz, C(Ar)(P)), 129.63 (CH), 128.05 (d, ^2J(P, C) = 13 Hz, *o*-Ar), 61.73 (CH_2-bpy), 59.40 (d, ^1J(P, C) = 123 Hz, CH_2P), 53.04 (d, ^2J(P, C) = 7 Hz, OCH_3). $^{31}P\{^1H\}$ NMR (81.0 MHz, $CDCl_3$, 25 °C): δ = 41.76 (s). MS (FAB$^+$ in *m*-nitrobenzylalcohol (*m*-NBA) as matrix): *m/z* 731 (M^+ + H). FT-IR (KBr pellet): $\tilde{\nu}$[cm^{-1}] = 2927, 2857, 1730, 1595, 1577, 1439, 1176 (P=O), 1122, 1035, 796. Anal. Calcd. for $C_{40}H_{40}N_6O_4P_2$ (Mr = 730.75).

Lanthanide complexes: To a solution of **1** (30 mg, 0.04 mmol) in CH_2Cl_2 (2 mL) an equimolar quantity of the lanthanide salt ($MCl_3 \cdot 6H_2O$, M = Eu, Tb or Gd), dissolved in methanol (3 mL) was added. After 2 h heating at 60 °C, the solvent was removed under reduced pressure, and the residue was recrystallized twice by slow diffusion of diethyl ether into an ethanol solution. $[Eu \subset \mathbf{1}]Cl_3 \cdot 3H_2O$ (yield 78%). UV/VIS (H_2O): λ_{max}[nm] (ε) = 307 (15 100), 246 (9900). MS (FAB$^+$ in *m*-NBA): *m/z* 953 (M^+ – Cl), 918 (M^+ – 2Cl) FT-IR (KBr pellet): $\tilde{\nu}$ = 1159 cm^{-1} (P=O). Anal. Calcd. for $C_{40}H_{40}N_6O_4P_2EuCl_3 \cdot 3H_2O$ (Mr = 989.07 + 54.05): $[Tb \subset \mathbf{1}]Cl_3 \cdot 2H_2O$ (yield 76%). UV/VIS (H_2O): λ_{max}[nm] (ε) = 306 (15 300), 246 (10 100). MS (FAB$^+$ in *m*-NBA): *m/z* 959 (M^+ – Cl), 924 (M^+ – 2Cl). FT-IR (KBr pellet): $\tilde{\nu}$ = 1159 cm^{-1} (P → O). Anal. Calcd. for $C_{40}H_{40}N_6O_4P_2TbCl_3 \cdot 2H_2O$ (Mr = 996.03 + 36.06): $[Gd \subset \mathbf{1}]Cl_3 \cdot 3H_2O$ (yield 79%). UV/VIS (H_2O): λ_{max}[nm] (ε) = 306 (14 200), 245 (9800). MS (FAB$^+$ in *m*-NBA): *m/z* 958 (M^+ – Cl), 923 (M^+ – 2Cl). FT-IR (KBr pellet): $\tilde{\nu}$ = 1159 cm^{-1} (P → O). Anal. Calcd. for $C_{40}H_{40}N_6O_4P_2GdCl_3 \cdot 3H_2O$ (Mr = 994.36 + 54.05).

Received: December 27, 1993
Revised version: March 18, 1994 [Z 6579 IE]
German version: *Angew. Chem.* **1994**, *106*, 1543

[1] E. Soini, I. Hemmilä, *Clin. Chem.* **1979**, *25*, 353–361; J.-C. G. Bünzli in *Lanthanide Probes in Life, Chemical and Earth Sciences* (Eds. J.-C. G. Bünzli, G. R. Choppin), Elsevier, Amsterdam, **1989**, Chap. 7.

[2] B. R. Judd, *Phys. Rev.* **1962**, *127*, 750–761; G. S. Ofelt, *J. Chem. Phys.* **1962**, *37*, 511–520.

[3] I. Hemmilä, S. Dakubu, US-B 4565790, **1986**; I. Hemmilä, *Anal. Chem.* **1985**, *57*, 1676–1681; I. Hemmilä, S. Dakubu, V.-M. Mukkala, H. Siitari, T. Lövgren, *Anal. Biochem.* **1984**, *137*, 335–343; T. Taketasu, *Talanta* **1982**, *29*, 397–400; T. Shigematsu, M. Matsui, R. Wake, *Anal. Chim. Acta* **1969**, *46*, 101–106.

[4] a) N. Sabbatini, M. Guardigli, J.-M. Lehn, *Coord. Chem. Rev.* **1993**, *123*, 201–228, and references therein. b) N. Sabbatini, M. Guardigli, F. Bolletta, I. Manet, R. Ziessel, *New J. Chem.* **1993**, *17*, 323–324; N. Sabbatini, M. Guardigli, I. Manet, F. Bolletta, R. Ziessel, *Inorg. Chem.*, **1994**, *33*, 955–959.

[5] V. Balzani, J.-M. Lehn, J. van de Loosdrecht, A. Mecati, N. Sabbatini, R. Ziessel, *Angew. Chem.* **1991**, *103*, 186–187; *Angew. Chem. Int. Ed. Engl.* **1991**, *30*, 190–191.

[6] G. R. Newkome, S. Papalardo, V. K. Gupta, F. R. Fronczek, *J. Org. Chem.* **1983**, *48*, 4848–4851, and references therein.

[7] C. J. Broan, E. Cole, K. J. Jankowski, D. Parker, E. Pulukkody, B. A. Boyce, N. R. A. Beeley, K. Miller, A. T. Millican, *Synthesis* **1982**, 63–68.

[8] V. Balzani, E. Berghmans, J.-M. Lehn, N. Sabbatini, R. Terörde, R. Ziessel, *Helv. Chim. Acta* **1990**, *73*, 2083–2089.

[9] A. D. Buss, W. B. Cruse, O. Kennard, S. Warren, *J. Chem. Soc. Perkin Trans.* **1992**, 675–681; R. Babecki, A. W. G. Platt, J. Fawcett, *J. Chem. Soc. Dalton Trans.* **1984**, 243–247.

[10] B. Alpha, R. Ballardini, V. Balzani, J.-M. Lehn, S. Perathoner, N. Sabbatini, *Photochem. Photobiol.* **1990**, *52*, 299–306.

[11] G. Blasse, *Struct. Bonding (Berlin)* **1976**, *26*, 43–79.

[12] G. Stein, E. Wurzberg, *J. Chem. Phys.* **1975**, *62*, 208–213; Y. Haas, G. Stein, *J. Phys. Chem.* **1971**, *75*, 3677–3681.

[13] W. DeW. Horrocks, D. R. Sudnick, *Acc. Chem. Res.* **1981**, *14*, 384–392.

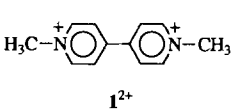
[14] M. Murru, D. Parker, G. Williams, A. Beeby, *J. Chem. Soc. Chem. Commun.* **1993**, 1116–1118; N. Sato, M. Goto, S. Matsumoto, S. Shinkai, *Tetrahedron Lett.* **1993**, *34*, 4847–4850.

A New Class of Novel Macrocyclic Mesogens**

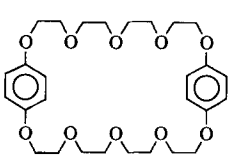
Peter R. Ashton, Detlev Joachimi, Neil Spencer, J. Fraser Stoddart,* Carsten Tschierske, Andrew J. P. White, David J. Williams, and Kerstin Zab

Since Pedersen[1] announced his discovery of the crown ethers in 1967, the amazing ability of these compounds to form complexes with a wide range of species, including alkali metal and alkaline earth metal cations and ammonium and alkylammonium ions, has had a widespread influence on the subsequent development of supramolecular chemistry.[2] In retrospect, therefore, it is hardly surprising that crown ethers, and the structurally related aza-crown ethers, have also been used[3] as building blocks in liquid crystal chemistry.

More recently we have shown[4a] that π-electron-deficient aromatic dications such as paraquat $\mathbf{1}^{2+}$ can be complexed, as its bis(hexafluorophosphate) salt, by crown ethers containing π-electron-rich arenes. Indeed, the macrocyclic polyether **2** proved



$\mathbf{1}^{2+}$



2

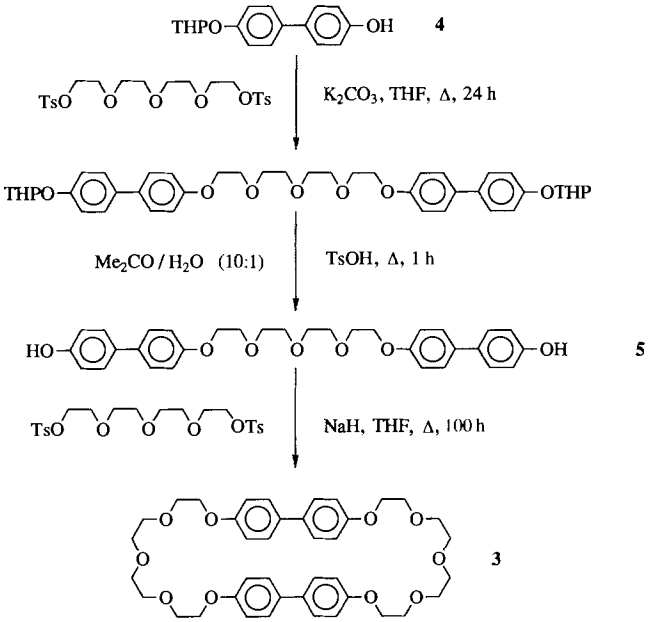
to be one of the most efficient molecular receptors for bipyridinium dications. These adducts—sustained by π–π aromatic stacking and electrostatic interactions, including hydrogen

[*] Prof. J. F. Stoddart, P. R. Ashton, Dr. D. Joachimi, Dr. N. Spencer
School of Chemistry, University of Birmingham
Edgbaston, Birmingham B15 2TT (UK)
Telefax: Int. code +(21) 414-3531
Dr. C. Tschierske, K. Zab
Institut für Organische Chemie, Martin-Luther-Universität Halle-Wittenberg
Halle/Saale (FRG)
Dr. A. J. P. White, Dr. D. J. Williams
Chemical Crystallography Laboratory
Department of Chemistry, Imperial College, London, SW7 2AY (UK)

[**] This work was supported by the German Academic Exchange Service (DAAD) and by the Science and Engineering Council (SERC) in the United Kingdom.

bonding—became[4b] subsequently the basis for the template-directed synthesis[5] of numerous catenanes and rotaxanes.

As part of our early investigations on the complexation behavior of **1** · $2PF_6$ with crown ethers like **2**, we had anticipated that replacement of the paraphenylene units in **2** by 4,4′-biphenyl units might enhance complexation between host and guest species. 1,4,7,10,13,26,29,32,35,38-Decaoxa[13.0.13.0]paracyclophane **3**[6] was synthesized in three steps (Scheme 1) starting from 4′-(2-tetrahydropyranyloxy)-4-dihydroxybiphenyl (**4**).[7] The X-ray crystal structure[8] of **3** shows (Fig. 1) that the macrocycle, in contrast with **2**, is self-filling; the two biphenyl units (twist angle, 11°) are aligned parallel and staggered with respect to each other about a crystallographic center of symmetry. The benzene rings are close enough for partial overlap (interplanar separation of 3.41 Å between rings A and A′, and a centroid–centroid separation of 4.78 Å). This geometry is commensurate with conventional parallel π–π stacking.[9] The molecules pack to form chevron-like sheets (Fig. 2) that have adjacent layers oriented to optimize T-type edge-to-face interactions[10] between the aromatic components with centroid–centroid separations between interacting rings of 4.96 Å: the centroid–centroid vectors are inclined by about 73° to the ring planes.



Scheme 1. Synthesis of **3**. THP = tetrahydropyranyl.

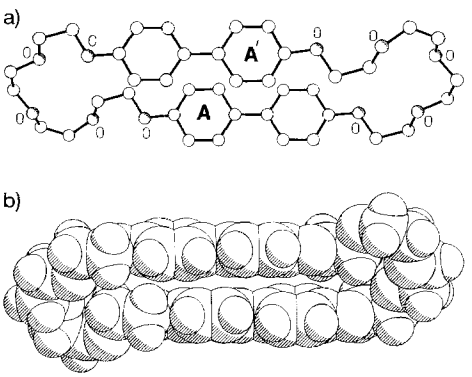


Fig. 1. a) Structure of **3** (crystallized from Et_2O) in the crystal showing the staggered parallel arrangement of the biphenyldiyl units, and b) a space-filling representation of the side view of the framework representation. Crystal data: orthorhombic, $a = 16.492(7)$, $b = 8.405(4)$, $c = 25.880(9)$ Å, $V = 3587$ Å^3, space group *Pbca*, $Z = 4$, $\rho_{calcd} = 1.275$ g cm^{-3}, 2746 independent measured reflections, 1309 with $|F_o| > 4\sigma(|F_o|)$, $2\theta \leq 125°$, Siemens P4/PC diffractometer, ω scans, $Cu_{K\alpha}$ radiation, graphite monochromator, solved by direct methods and refined anisotropically to $R = 0.064$, $R_w = 0.064$.

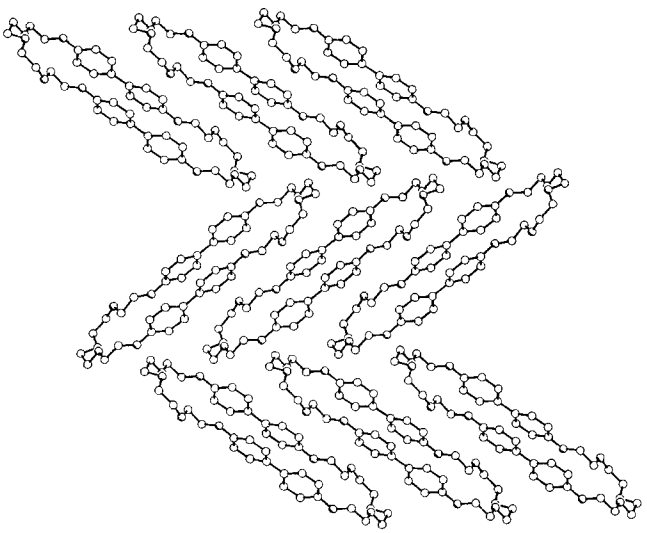


Fig. 2. The packing of molecules of **3** in two dimensions in the solid state.

Unfortunately, **3** is almost insoluble in solvents such as Me_2CO and MeCN, which we employ[4] routinely in complexation studies with bipyridinium salts. However, **3** includes two rigid biphenyl systems which are typical mesogenic structural elements of liquid crystals. Since the molecules of **3** have a rodlike shape (Fig. 1) in the solid state, arranging themselves (Fig. 2) in a smectic-like manner, we decided to investigate the compound for possible mesomorphic properties. Polarizing microscopy and differential scanning calorimetry established that **3** is indeed a thermotropic mesogen, showing enantiotropic smectic phases[11] with an unexpectedly high mesophase stability, as indicated by the high clearing temperature (Table 1). On cooling the isotropic liquid to 209 °C, a rapid formation of batonnets can be observed, which coalesce to a focal-conic fanlike texture with pseudotropic areas typical of a smectic A-type mesophase.[11] At 196 °C, the focal-conic fan texture changes to an arced focal-conic texture,

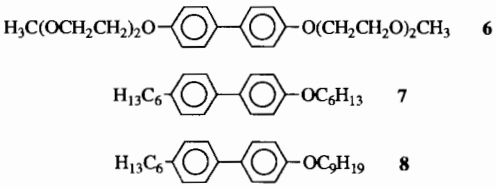
Table 1. Phase transitions [a] and associated temperatures (°C) of the compounds discussed in this paper.

Compound	Phase transitions [b]
3	cr 193 S_E 196 S_A 209 is
6	cr 87 is
7 [12a]	cr 9 S_E 68 S_B 84 is
8 [12b]	cr 34 S_B 82 is
9	cr 212 S_E (212) S_P 217 is
10	cr 182 S_E 185 S_P 189 is
11	cr 173 S_E 176 S_A 186 is
12	cr 156 S_E 161 S_P 167 is
13	cr 160 S_1 166 S_2 172 S_3 176 S_A 192 is
16	cr 168 S 173 S_A 196 is

[a] Determined by means of a hot-stage polarizing microscope. [b] Abbreviations: cr = crystalline; S_E = smectic E phase; S_A = smectic A phase; S_B = smectic B phase; is = isotropic liquid; S, S_1, S_2, S_3 = unidentified smectic phases.

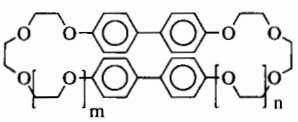
while the homeotropic areas, which appeared dark originally, start to show birefringent platelet areas with overlapping transparent platelets. This feature is unique to the smectic E phase.[11] Further cooling leads to crystallization at 190 °C. Reheating gives a melting point of 193 °C.

Unlike the polyether cyclophane **3**, its acyclic counterpart, 4,4′-bis[2-(2-methoxyethoxy)ethoxy]biphenyl (**6**), which has a molecular structure very similar to that of a typical conventional liquid crystal, does not form an enantiotropic mesophase at all. On supercooling to room temperature, not even a monotropic mesophase could be detected. However, biphenyl derivatives, for example, **7** and **8** with aliphatic side chains of comparable length to the oligoethylene glycol chains in **6** are known[12] to exhibit



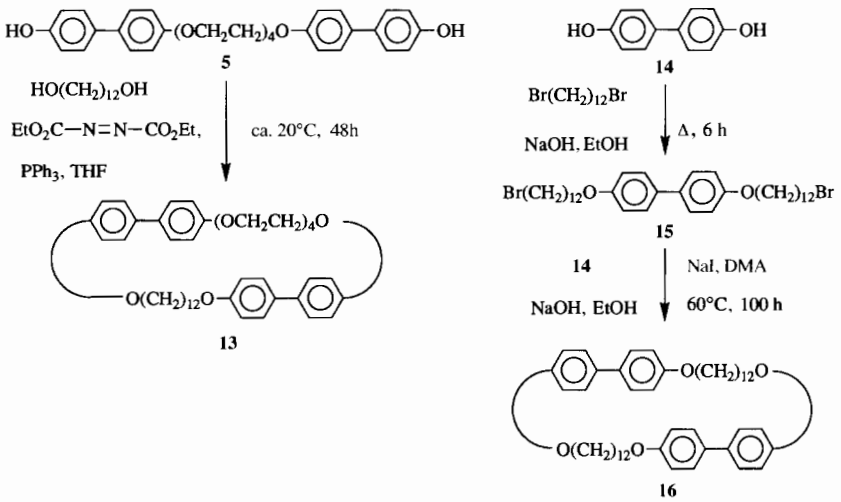
liquid crystalline behavior. Nevertheless, their clearing temperatures are below 100 °C, just as one would expect[13] for a mesogen with only one biphenyl unit in its rigid core.

Thus, in the case of **3**, not only are liquid crystalline properties present, but the clearing temperature is a lot higher than one anticipates[13] from a mesogen with only one biphenyl unit in its rigid core. The coupling of two appropriate rigid units[14] by flexible terminal chains seems to constitute a new and powerful approach towards mesophase induction and stabilization. This realization immediately poses several questions. For example, how does the length of the polyether chains linking the two aromatic units influence the mesomorphic behavior? Is this new principle of mesophase stabilization unique for compounds with polyether chains as linking units or does it also occur in compounds which contain aliphatic side chains? To answer these questions, we have synthesized compounds with structures related to **3**, but having polyether and aliphatic chains of differing lengths (**9**–**12** and **13** and **16**).



3, m = n = 2
9, m = 1, n = 2 **11**, m = 2, n = 3
10, m = 1, n = 3 **12**, m = n = 3

The comparison of **3** and **9**–**12** in Table 1 shows how the mesophase behavior is influenced by varying the length of the polyether chains. The type of mesophase exhibited is not affected: all the compounds show S_E and S_A mesophases. The shortening of one bridging chain by one ethyleneglycol unit (for instance, **9** compared to **3**) increases the melting as well as the clearing temperature. However, **9** exhibits slightly anomalous behavior in having only a monotropic smectic E phase, that is, the melting point increases beyond the smectic E/smectic A temperature and so the smectic E phase for this compound can only be observed on supercooling. The smectic E mesophase of all these other compounds shows enantiotropic behavior. Compound **10** is a constitutional isomer of **3**, containing one longer and one shorter polyether chain. "Desymmetrization" leads, as expected, to a lower melting and clearing temperature and a smaller range of enantiotropic mesomorphic properties. Lengthening of the polyether chains (**11** and **12** compared to **3**) also lowers the clearing and melting temperatures. This effect is well-known for conventional, acyclic, rodlike liquid crystals.[13]



Scheme 2. Synthesis of paracyclophanes **13** and **16**. The reaction giving **13** was performed at higher dilution. DMA = dimethylacetamide.

To gauge how important polyether bridging chains are for the mesophase stabilization effect, we substituted one or both polyether chains of **3** with aliphatic chains in the syntheses of the biphenylophanes **13** and **15**, respectively (Scheme 2). The phase transitions for **3**, **13** and **16**, listed in Table 1, reveal that the influence of the type of linking chain on the mesophase stability, that is, on the clearing temperatures, is not very strong. In fact, the replacement of *both* polyether chains by aliphatic chains (**16**) leads to a decrease in the clearing temperature of 13 K. The replacement of only one polyether link by an aliphatic chain (**13**) leads to a slightly larger decrease in mesophase stability. Interestingly, however, as the nature of the bridging links becomes more aliphatic, the type of smectic mesophase changes. Smectic A is still evident, but the smectic E phase is no longer observed.

We may conclude that linking rigid mesogenic groups in macrocycles with flexible units has a mesophase stabilizing effect. The type of mesophase formed by macrocycles is also likely to depend on the structure of the incorporated rigid aromatic units. We are now constructing cyclophane derivatives with different mesogenic units to investigate this dependence.

Experimental Procedures

3: A solution of **5** (0.53 g, 1.0 mmol) and tetraethyleneglycol bistosylate (0.60 g, 1.2 mmol) in dry THF (250 mL) was added to a stirred suspension of NaH (0.05 g, 1.2 mmol) in dry THF (100 mL) under reflux over 4 h. The mixture was stirred for a further 96 h under reflux. The solvent was evaporated off, and the residue partitioned between $CHCl_3$ and dilute HCl. The organic layer was separated and, after washing with H_2O and saturated aqueous NaCl solution, dried over Na_2SO_4. Removal of the solvent in vacuo gave a solid, which was purified by chromatography on SiO_2 (CH_2Cl_2:Et_2O, 4:1). Further purification by several recrystallizations from EtOAc gave pure **3** (0.03 g, 4.1%). M.p. 193 °C; ^{1}H NMR (300 MHz, $CDCl_3$): δ = 7.28 (m, 8H), 6.82 (m, 8H), 4.05 (m, 8H), 3.91 (m, 8H), 3.75 (m, 16H); ^{13}C NMR (75.5 MHz, $CDCl_3$): δ = 157.9, 133.2, 127.5, 114.8, 71.0, 70.8, 69.8, 67.6; positive ion FAB-MS: m/z = 727 ($[M + K]^+$, 13%), 711 ($[M + Na]^+$, 31%), 688 ($[M]^+$, 100%), 613 (26), 593 (9), 576 (7). Single crystals suitable for X-ray crystallography were grown from Et_2O.

9–**12**: These compounds were prepared analogously to **3** (Scheme 1) by using the appropriate ethyleneglycol bistosylates. **9**: (0.01 g, 1.5%), m.p. 212 °C; ^{1}H NMR (300 MHz, $CDCl_3$): δ = 7.39–7.21 (m, 8H), 6.82 (m, 8H) 4.10–4.02 (m, 8H),

 © *VCH Verlagsgesellschaft mbH, D-69451 Weinheim, 1994* *0570-0833/94/1414-1505 $ 10.00+.25/0*

3.94–3.84 (m, 8H), 3.80–3.71 (m, 12H); ^{13}C NMR (75.5 MHz, $CDCl_3$): δ = 158.0, 157.9, 133.2, 127.5, 115.1, 114.8, 71.2, 71.0, 70.8, 69.9, 69.8, 67.7; FAB-MS: *m/z* = 644 ($[M]^+$, 100%), 613 (7), 460 (51), 424 (11), 391 (15); **10**: 0.09 g (21.1%), m.p. 182 °C; ^{1}H NMR (300 MHz, $CDCl_3$): δ = 7.37–7.23 (m, 8H), 6.90–6.79 (m, 8H) 4.11–4.02 (m, 8H), 3.94–3.83 (m, 8H), 3.80–3.69(m, 16H); ^{13}C NMR (75.5 MHz, $CDCl_3$): δ = 158.0, 157.9, 133.3, 133.2, 127.5, 115.1, 114.8, 71.1, 71.0, 70.9, 69.9, 69.8, 67.6; FAB-MS: *m/z* = 711 ($[M + Na]^+$, 6.1%), 688 ($[M]^+$, 100), 460 (11); **11**: 0.01 g (2.1%), m.p. 172 °C; ^{1}H NMR (300 MHz, $CDCl_3$): δ = 7.35–7.26 (m, 8H), 6.89–6.80 (m, 8H) 4.10–4.03 (m, 8H), 3.93–3.85 (m, 8H), 3.78–3.68 (m, 20H); ^{13}C NMR (75.5 MHz, $CDCl_3$): δ = 157.9, 133.3, 127.5, 114.9, 71.0, 70.9, 70.8, 69.8, 67.6; FAB-MS: *m/z* = 732 ($[M]^+$, 48%), 257 (24), 239 (51), 185 (81), 169 (66), 152 (100), 136(95), 107 (61); **12**: m.p. 156 °C; ^{1}H NMR (300 MHz, $CDCl_3$): δ = 7.34 (m, 8H), 6.86 (m, 8H), 4.08 (t, *J* = 4.7 Hz, 8H), 3.87 (t, *J* = 4.7 Hz, 8H), 3.76–3.66 (m, 24H); ^{13}C NMR (75.5 MHz, $CDCl_3$): δ = 157.9, 133.4, 127.6, 114.9, 71.0, 70.8, 69.8, 67.6; FAB-MS: *m/z* = 777 ($[M + H]^+$).

13: At 0 °C, a solution of **5** (0.45 g, 0.9 mmol) and 1,12-dodecanediol (0.20 g, 1.0 mmol) in dry THF (250 mL) was added dropwise to a solution of diethyl azodicarboxylate (0.63 g, 3.6 mmol) and triphenylphosphane (0.94 g, 3.6 mmol) in dry THF (75 mL) over 5 h. The solution was allowed to warm up to room temperature, and stirring was continued for 48 h. Removal of the solvent in vacuo gave an oily residue to which $MeOH/H_2O$ (10:1) was added. The mixture was heated at reflux for 1 min before being allowed to cool to room temperature. The precipitated material was separated from the supernatant (containing mainly triphenylphosphane oxide) and purified by chromatography on SiO_2 (CH_2Cl_2:Et_2O, 4:1). Further purification by several recrystallizations from EtOAc finally gave pure **13** as a white crystalline solid (0.03 g, 5.1%). M.p. 166 °C; ^{1}H NMR (300 MHz, $CDCl_3$): δ = 7.42–7.38(m, 8H), 6.93–6.83 (m, 8H), 4.07 (t, *J* = 4.8 Hz, 4H), 3.97 (t, *J* = 7.5 Hz, 4H), 3.88 (t, *J* = 4.8 Hz, 4H), 3.77–3.66 (m, 8H), 1.86–1.72 (quint. *J* = 7.5 Hz, 4H), 1.54–1.25 (m, 16H); ^{13}C NMR (75.5 MHz, $CDCl_3$): δ = 158.2, 157.9, 133.5, 133.1, 127.6, 114.9, 114.8, 70.9, 69.8, 67.9, 67.6, 28.9, 28.7, 28.4, 28.3, 25.5; positive ion-FAB-MS: *m/z* = 696 ($[M]^+$, 100%), 613 (6), 460 (50), 440 (14).

16: Solutions of **15** (0.68 g, 1.0 mmol) and the disodium salt of **14** (0.25 g, 1.1 mmol) in dimethylacetamide (200 mL each) were added simultaneously to a solution of NaI (2.0 g, 13.3 mmol) in dimethylacetamide (80 mL) over 90 min at 60 °C. Stirring was continued for a further 100 h. The light green reaction mixture was allowed to cool to room temperature before being poured into ice/H_2O (1500 mL). The white precipitate was filtered off and partitioned between $CHCl_3$ and dilute HCl (100 mL). Insoluble material was removed by filtration. The organic layer was washed with H_2O, saturated aqueous $NaHCO_3$, H_2O, and saturated aqueous NaCl solution. After drying over Na_2SO_4, the solvent was removed by evaporation, and the residue was purified by chromatography on SiO_2 ($CHCl_3$). This product was recrystallized from EtOAc to give pure **16** as white shining needles. (0.02 g, 2.6%). M.p. 168 °C; ^{1}H NMR (300 MHz, $CDCl_3$): δ = 7.43 (m, 8H), 6.91 (m, 8H), 3.98 (t, *J* = 6.5 Hz, 8H), 1.78 (quint, *J* = 6.7 Hz, 8H), 1.52–1.22 (m, 32H); ^{13}C NMR (75.5 MHz,$CDCl_3$): δ = 158.2, 133.3, 127.6, 114.9, 67.9, 29.1, 28.9, 28.8, 28.7, 25.7; FAB-MS: *m/z* = 704 ($[M]^+$, 9%), 460 (100), 440 (30), 391 (22), 351 (12).

Received: February 15, 1994 [Z 6695 IE]
German version: *Angew. Chem.* **1994**, *106*, 1563

[1] C. J. Pedersen, *J. Am. Chem. Soc.* **1967**, *89*, 7017; *Angew. Chem.* **1988**, *100*, 1053; *Angew. Chem. Int. Ed. Engl.* **1988**, *27*, 1021.

[2] a) J.-M. Lehn, *Angew. Chem.* **1988**, *100*, 91; *Angew. Chem. Int. Ed. Engl.* **1988**, *27*, 89; b) D. J. Cram, *Science* **1988**, *240*, 760; *Angew. Chem.* **1988**, *100*, 1041; *Angew. Chem. Int. Ed. Engl.* **1988**, *27*, 1009.

[3] a) J.-M. Lehn, J. Malthete, A. M. Levelut, *J. Chem. Soc. Chem. Commun.* **1985**, 1795; b) G. X. He, D. Wada, K. Kikukawa, T. Matsuda, *ibid.* **1987**, 1294; c) M.-G. Xie, Y.-Y. Chenand, Y.-E. He, *Mol. Cryst. Liq. Cryst.* **1991**, *209*, 213; d) Z. Minggui, Q. Jun, H. Feng, *ibid.* **1991**, *209*, 309; e) A. Liebmann, C. Mertesdorf, T. Plesnivy, H. Ringsdorf, J. H. Wendorff, *Angew. Chem.* **1991**, *103*, 1358; *Angew. Chem. Int. Ed. Engl.* **1991**, *30*, 1375; f) S. H. J. Idziak, N. C. Maliszewskyj, P. A. Heiney, J. P. McCauley, Jr., P. A. Sprengeler, A. B. Smith III, *J. Am. Chem. Soc.* **1991**, *113*, 7666; g) S. Shinkai, T. Nishi, T. Matsuda, *Chem. Lett.* **1991**, 437; h) R. Rodenhouse, V. Percec, *Adv. Mater.* **1991**, *3*, 101; i) V. Percec, G. Johansson, *J. Mater. Chem.* **1993**, *3*, 83; j) V. Percec, G. Johansson, J. Heck, G. Ungar, S. V. Batty, *J. Chem. Soc. Perkin Trans. 1* **1993**, 1411.

[4] a) B. L. Allwood, N. Spencer, H. Shahriari-Zavareh, J. F. Stoddart, D. J. Williams, *J. Chem. Soc. Chem. Commun.* **1987**, 1064; b) P. L. Anelli, P. R. Ashton, R. Ballardini, V. Balzani, M. Delgado, M. T. Gandolfi, T. T. Goodnow, A. E. Kaifer, D. Philp, M. Pietraskiewicz, L. Prodi, M. V. Reddington, A. M. Z. Slawin, N. Spencer, J. F. Stoddart, C. Vicent, D. J. Williams, *J. Am. Chem. Soc.* **1992**, *114*, 193.

[5] S. Anderson, H. L. Anderson, J. K. M. Sanders, *Acc. Chem. Res.* **1993**, *26*, 469.

[6] Although various syntheses of biphenylophanes with structures related to **3** have been reported previously, liquid crystalline properties have not yet, to our knowledge, been noted. See, for example, a) H. Stetter, E.-E. Roos, *Chem. Ber.* **1955**, *88*, 1390; b) M. Haenel, H. A. Staab, *Tetrahedron Lett.* **1970**, 3585; c) H. A. Staab, M. Haenel, *Chem. Ber.* **1973**, *106*, 2190; d) R. Nagano, J. Nishiikido, T. Inazu, T. Yoshino, *Bull. Chem. Soc. Jpn.* **1973**, *46*, 653; e) R. Hilgenfeld, W. Saenger, *Angew. Chem.* **1982**, *94*, 788; *Angew. Chem. Int. Ed. Engl.* **1982**, *21*, 787.

[7] Compound **4** (m.p. 147 °C) has only been described previously as sodium salt (T. D. Shaffer, M. Jamaludin, V. Percec, *J. Polym. Sci. Polym. Chem. Ed.* **1986**, *24*, 15; E. Chiellini, G. Galli, F. Cioni, E. Dossi, B. Gallot, *J. Mater. Chem.* **1993**, *3*, 1065). We obtained **4** in a pyridinium-*p*-tosylate-catalyzed reaction between 4,4'-dihydroxybiphenyl **14** and dihydropyran in THF/$CHCl_3$ at room temperature and subsequent workup under neutral conditions.

[8] Details of the crystal structure investigation can be obtained from the Cambridge Crystallographic Data Centre, 12 Union Road, Cambridge CB2 1EZ (UK) on quoting the full journal citation.

[9] a) W. L. Jorgensen, D. L. Severance, *J. Am. Chem. Soc.* **1990**, *112*, 4768; b) C. A. Hunter, J. K. M. Sanders, *ibid.* **1990**, *112*, 5525.

[10] M. C. Grossel, A. K. Cheetham, D. A. O. Hope, S. C. Weston, *J. Org. Chem.* **1993**, *58*, 6654, and references therein.

[11] a) D. Demus, L. Richter, *Textures of Liquid Crystals*, Verlag Chemie, Weinheim, **1978**; b) G. W. Gray, J. W. Goodby, *Smectic Liquid Crystals–Textures and Structures*, Leonhard Hill, Glasgow, **1984**.

[12] a) C.-E. Rürup, Dissertation, Universität Halle, **1971**; b) D. Demus, L. Richter, C.-E. Rürup, H. Sackmann, H. Schubert, *J. Physiol. (Paris) Suppl.* **1975**, *36* (C1), 349.

[13] V. Vill in *Landolt Börnstein, New Series, Vol. IV/7a* (Eds.: O. Madelung, J. Thiem), Springer, Heidelberg, **1992**.

[14] A similar observation has been reported recently by Percec and Kawasumi for macrocycles incorporating conformationally flexible rodlike mesogens. They demonstrated that low molecular weight macrocycles based on 1-(4'-hydroxybiphenyl-4-yl)-2-(4-hydroxyphenyl)butane and flexible spacers "exhibit a higher ability to generate liquid crystalline phases than do their low-molar mass linear and both their linear and cyclic high-relative-molecular-mass homologues". However, the observed mesophase stabilization by cyclization is much less pronounced than in the examples reported here—probably as a result of the steric bulk of the branched mesogenic systems employed in these investigations. See V. Percec, M. Kawasumi, *Adv. Mater.* **1992**, *4*, 572; *J. Mater. Chem.* **1993**, *3*, 725; *J. Chem. Soc. Perkin Trans. 1* **1993**, 1319.

1,3-Dialkoxycalix[4]arenecrowns-6 in 1,3-Alternate Conformation: Cesium-Selective Ligands that Exploit Cation–Arene Interactions**

Rocco Ungaro,* Alessandro Casnati, Franco Ugozzoli, Andrea Pochini, Jean-François Dozol, Clement Hill, and Hélène Rouquette

Calixarene and particularly calix[4]arene derivatives have recently attracted considerable attention, since they can bind alkali and alkaline earth metal cations selectively with an efficiency comparable to that of cryptands.[1] Their complexation properties seem to be highly dependent not only on the nature of the donor groups but also on their stereochemical arrangement, which is determined by the conformation of the calix: cone, partial cone, 1,3-alternate, or 1,2-alternate (Fig. 1).[2] The 1,3-

[*] Prof. Dr. R. Ungaro, Dr. A. Casnati, A. Pochini
Dipartimento di Chimica Organica e Industriale
Università degli Studi di Parma
Viale delle Scienze 78, I-43100 Parma (Italy)
Telefax: Int. code + (521)905-472

Dr. F. Ugozzoli
Dipartimento di Chimica Generale ed Inorganica, Analitica, Chimica Fisica e
Centro di Studio per la Strutturistica Diffrattometrica del CNR
Università degli Studi di Parma

Dr. J.-F. Dozol, C. Hill, H. Rouquette
S.E.P./S.E.T.E.D., Centre d'Etudes de Cadarache
Commisariat a l'Energie Atomique, C.E.A. (France)

[**] This work was supported by the European Commission in the framework of the research program "Management and Storage of Radioactive Waste" (grant no. F12W-CT90-0062 (TSTS)).

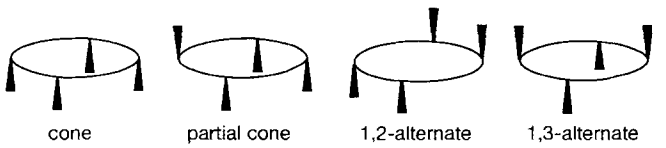
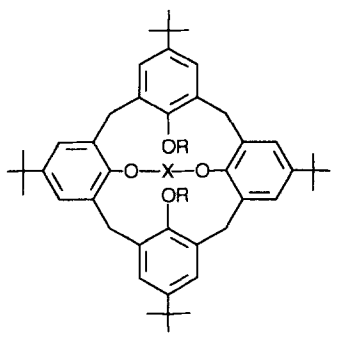


Fig. 1. Schematic representations of the four possible conformations of calix[4]-arenes. Filled triangles represent the arene rings; the ellipses represent the best plane containing the methylene bridges.

dialkoxy-*p*-*tert*-butylcalix[4]arenecrowns-5 **I**, for example, especially when fixed in the partial cone conformation, exhibit an exceptionally high selectivity for potassium ions over other alkali metal ions.[3, 4] This has led to their use in ion-sensitive field effect

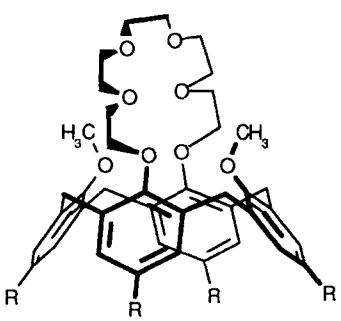


I: X = $(CH_2CH_2O)_3CH_2CH_2$
R = alkyl

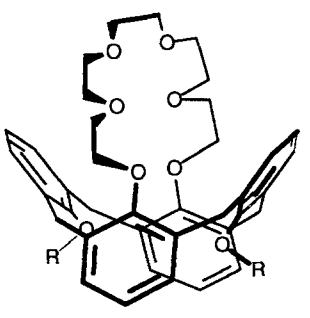
transistors (ISFETs)[5] and in supported liquid membranes[6] for the detection and separation, respectively, of alkali metal ions. The results are comparable to those obtained with the best potassium ionophore known so far, valinomycin.

Recently we have addressed the important problem of the removal of cesium and actinides from medium-level radioactive waste.[7, 8] The long-lived ^{137}Cs must be extracted from an aqueous solution which is 1 M in HNO_3 and 4 M in $NaNO_3$.[7] Here we report on calix[4]arenecrowns-6 which, when fixed in the 1,3-alternate conformation, are extremely selective in the extraction of cesium over sodium ions from an acidic aqueous phase containing metal nitrates. Studies of both solutions and solids point to the decisive role of cesium–arene interactions in determining the properties of such ligands.

We first synthesized the 1,3-dimethoxycalix[4]arenecrown-6 **1** (see Table 1), because we previously observed that 1,3-dimethoxy-*p*-*tert*-butylcalix[4]arenecrown-6 **2** had a slight binding preference for cesium ions in chloroform solution.[3]



1: R = H
2: R = *t*Bu



3: R = *i*Pr
4: R = *n*Oct
5: R = *n*Pr

Table 1. Selected physical data for compounds **1** and **3**–**5** [9].

1: M.p. 180–181 °C; ^1H NMR (400 MHz, $CDCl_3$, TMS): $\delta = 7.15$ (d, $^3J = 6.5$ Hz, 4H; ArH *meta*), 6.93 (t, $^3J = 6.5$ Hz, 2H; ArH *para*), 6.33 (s, 6H; ArH), 4.43 (d, $^2J = 12.9$ Hz, 4H; $ArCH_2Ar$), 4.05 (s, 4H; $ArO(CH_2CH_2O)_2CH_2$), 3.89 (s, 6H; OCH_3), 3.8–3.5 (m, 16H; $ArO(CH_2CH_2O)_2CH_2$), 3.15 (d, $^2J = 12.9$ Hz, 4H; $ArCH_2Ar$)

3: M.p. 197–198 °C; ^1H NMR (400 MHz, $CDCl_3$, TMS): $\delta = 7.07$ (d, $^3J = 7.5$ Hz, 4H; ArH *meta*), 7.03 (d, $^3J = 7.4$ Hz, 4H; ArH *meta*), 6.84–6.79 (m, 4H; ArH *para*), 4.23 (sept. $^3J = 6.3$ Hz, 2H; $OCH(CH_3)_2$), 3.83 (d, $^2J = 15.7$ Hz, 4H; $ArCH_2Ar$), 3.77 (d, $^2J = 15.7$ Hz, 4H; $ArCH_2Ar$), 3.73 (s, 4H; $ArO(CH_2CH_2O)_2CH_2$), 3.68 (t, $^3J = 4.1$ Hz, 4H; $ArOCH_2CH_2OCH_2CH_2OCH_3$), 3.53 (t, $^3J = 4.1$ Hz, 4H; $ArOCH_2CH_2OCH_2CH_2OCH_3$), 3.47 (t, $^3J = 6.0$ Hz, 4H; $ArOCH_2CH_2OCH_2CH_2OCH_3$), 3.34 (t, $^3J = 6.0$ Hz, 4H; $ArOCH_2CH_2OCH_2CH_2OCH_3$), 0.91 (d, $^3J = 6.3$ Hz, 12H; $OCH(CH_3)_2$)

4: M.p. 94–95 °C; ^1H NMR (400 MHz, $CDCl_3$, TMS): $\delta = 7.12$ (d, $^3J = 7.5$ Hz, 4H; ArH *meta*), 7.08 (d, $^3J = 7.5$ Hz, 4H; ArH *meta*), 6.83 (t, $^3J = 7.5$ Hz, 2H; ArH *para*), 6.77 (t, $^3J = 7.5$ Hz, 2H; ArH *para*), 3.78 (s, 8H; $ArCH_2Ar$), 3.71 (s, 4H; $ArO(CH_2CH_2O)_2CH_2$), 3.66 (t, $^3J = 4.6$ Hz, 4H; $ArOCH_2CH_2OCH_2CH_2OCH_3$), 3.60 (t, $^3J = 6.0$ Hz, 4H; $OCH_2(CH_2)_6CH_3$), 3.49 (t, $^3J = 4.6$ Hz, 4H; $ArOCH_2CH_2OCH_2CH_2OCH_3$), 3.40 (m, 8H; $ArOCH_2CH_2OCH_2CH_2OCH_3$), 1.36–1.15 (m, 24H; $OCH_2(CH_2)_6CH_3$), 0.92 (t, $^3J = 7.1$ Hz, 6H; $OCH_2(CH_2)_6CH_3$)

5: M.p. 140–141 °C; ^1H NMR (400 MHz, $CDCl_3$, TMS): $\delta = 7.10$ (d, $^3J = 7.2$ Hz, 4H; ArH *meta*), 7.03 (d, $^3J = 7.6$ Hz, 4H; ArH *meta*), 6.84 (t, $^3J = 7.2$ Hz, 2H; ArH *para*), 6.80 (t, $^3J = 7.6$ Hz, 2H; ArH *para*), 3.78 (s, 8H; $ArCH_2Ar$), 3.73 (s, 4H; $ArO(CH_2CH_2O)_2CH_2$), 3.68 (t, $^3J = 4.5$ Hz, 4H; $ArOCH_2CH_2OCH_2CH_2OCH_2CH_2OCH_3$), 3.62 (t, $^3J = 6.0$ Hz, 4H; $OCH_2CH_2CH_3$), 3.52 (t, $^3J = 4.5$ Hz, 4H; $ArOCH_2CH_2OCH_2CH_2OCH_2CH_2OCH_3$), 3.45–3.40 (m, 8H; $ArOCH_2CH_2OCH_2CH_2OCH_2CH_2OCH_3$), 1.32 (m, 4H; $OCH_2CH_2CH_3$), 0.73 (t, $^3J = 7.2$ Hz, 6H; $OCH_2CH_2CH_3$)

A titration experiment of **1** with cesium picrate in CD_3CN revealed some interesting features. Free **1** exists in solution mainly (>50%) in the cone conformation, which can be recognized in ^1H NMR spectra (Fig. 2a) by the doublets at $\delta \approx 3.2$ and 4.4 for the protons in the methylene bridge ($ArCH_2Ar$). In the corresponding cesium complex (Fig. 2b) the AX system coalesces to a singlet at $\delta \approx 3.7$, which indicates the rearrangement of **1** into the 1,3-alternate conformation. This conformation, which can be indicated as C_1 + +, − −, + +, − − according to a recently proposed notation,[10] is clearly shown in the X-ray crystal structure of the cesium picrate complex (Fig. 3). It crystallizes in the triclinic system ($P\bar{1}$) and shows two independent complexes in the asymmetric unit.[11] In both, the cesium ion appears to be coordinated by eight oxygen atoms (six from the calixcrown, two from the picrate ion, which acts as bidentate ligand), and by two opposite arene rings. To maximize the cesium–arene interaction the ligand changes its conformation into 1,3-alternate. The Cs^+ ion interacts in η^3 fashion with C(3B), C(4B), and C(5B), and in η^2 fashion with C(3D) and C(4D) of the arene ring. The Cs–C contacts range from 3.431(10) to 3.684(8) Å in one independent unit of the complex and from 3.354(7) to 3.588(8) Å in the second. These values compare with

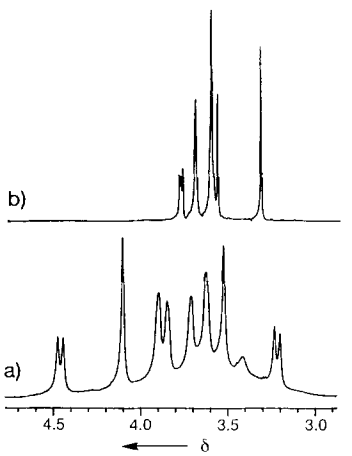


Fig. 2. ^1H NMR spectra (CD_3CN, 400 MHz) of a) free **1** and b) its cesium picrate complex.

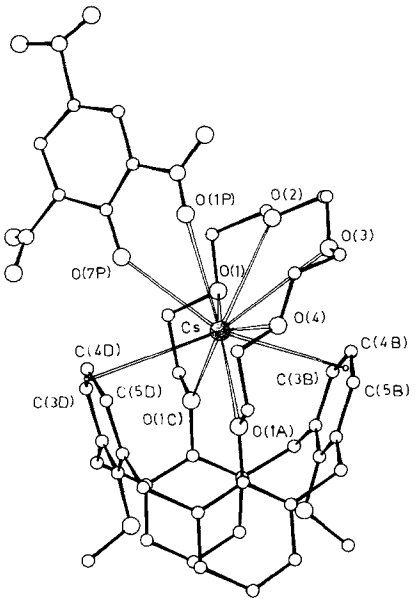


Fig. 3. X-ray crystal structure of the complex of **1** and cesium picrate. PLUTO plot of one of the two independent complexes. Selected distances [Å] in the two molecules: Cs-O (1A) 3.319(5) [3.468(5)], Cs-O(1C) 3.300(5) [3.269(9)], Cs-O(1) 3.212(5) [3.294(5)], Cs-O(2) 3.333(6) [3.398(6)], Cs-O(3) 3.670(10) [3.401(7)], Cs-O(4) 3.265(9) [3.196(7)], Cs-O(1P) 3.413(9) [3.360(10)], Cs-O(7P) 3.094(6) [3.147(6)], Cs-C(3B) 3.649(9) [3.588(8)], Cs-C(4B) 3.431(10) [3.354(7)], Cs-C(5B) 3.548(9) [3.566(7)], Cs-C(3D) 3.684(8) [3.549(7)], Cs-C(4D) 3.568(7) [3.422(7)], Cs-C(5D) 3.864(7) [3.807(8)].

those reported[12, 13] for systems for which cesium–arene interactions have been documented. The low-field shifts (0.1–0.7 ppm) in the ^{1}H NMR spectrum experienced by the arene protons of **1** upon complexation of cesium can be due to the presence of such interactions also in solution. However, the profound changes in the NMR spectra owing to the conformational rearrangement of the ligand complicate the analysis.

These observations, which clearly suggest that in this class of ionophores the preferred conformation to bind cesium is the 1,3-alternate, led us to synthesize preorganized ligands having this structure. It is known that substituents bulkier than ethyl block the interconversion between conformational isomers in tetraalkoxycalix[4]arenes.[14] Therefore, the reaction of the diametrically substituted 1,3-dialkoxycalix[4]arenes[4, 14b] with pentaethylene glycol di-*p*-toluenesulfonate in the presence of Cs_2CO_3 in CH_3CN[15] provided compounds **3**–**5** in good yields (>80%) in the fixed 1,3-alternate conformation (see Table 1). Probably in this case the cesium ion acts as template in determining the stereochemical outcome of the cyclization reaction. The binding abilities of compounds **1** and **3**–**5** have been tested by extraction of the ions from an aqueous solution 1 M in nitric acid and 5×10^{-4} M in ^{137}Cs or ^{22}Na nitrate into a 10^{-2} M solution of the ligand in hexyl 2-nitrophenyl ether. The amount of ^{137}Cs or ^{22}Na extracted into the organic phase was measured by γ spectrometry. These values were used to calculate the distribution coefficients $D_{(M^+)}$ as the ratio of the metal ion concentration in the organic phase versus the metal ion concentration in the aqueous phase.[16] Table 2 gives the technically important Cs^+/Na^+ selectivities as $\alpha = D_{(Cs^+)}/D_{(Na^+)}$.

As expected ligands **3**–**5** fixed in the 1,3-alternate conformation show much higher efficiency and selectivity than the conformationally flexible compound **1**. This is explained by the preorganization of the ligand[3] and by the fact that the less polar 1,3-alternate conformation[17] prefers cesium over sodium and

Table 2. Selectivities and extraction percentages of cesium and sodium nitrates. For details see text.

Compound	% Cs extracted	% Na extracted	α
1	3.78	0.27	14.4
3	96.6	<0.1	>28500
4	97.0	<0.1	>33000
5	95.0	0.18	10650

allows the interaction of the cesium ion with the π-electron cloud of the arene rings. The complexation properties of these ligands are the result of the simultaneous operation of several effects: the size of the crown ether ring, the polarity of the calix conformation, and the strength of the cation/π-electron interactions.[18] The easy removal of cesium cation from the complexes by stripping[16] and the consequent possibility of recycling the ligands, as well as their high lipophilicity, which allows their use in supported liquid membranes,[6] make these new cesium-selective ionophores highly attractive for treatment of radioactive waste.

Received: February 19, 1994 [Z 6697 IE]
German version: *Angew. Chem.* **1994**, *106*, 1551

[1] a) *Calixarenes, a Versatile Class of Macrocyclic Compounds* (Eds.: J. Vicens, V. Böhmer), Kluwer, Dordrecht, **1991**; b) R. Ungaro, A. Pochini in ref. [1a], pp. 127–147; c) M. A. McKervey, M.-J. Schwing in ref. [1a], pp. 149–172.

[2] A. Arduini, A. Casnati, M. Fabbi, P. Minari, A. Pochini, A. R. Sicuri, R. Ungaro in *Supramolecular Chemistry* (Eds.: V. Balzani, L. De Cola), Kluwer, Dordrecht, **1992**, pp. 31–50.

[3] P. J. Dijkstra, J. A. J. Brunink, K.-E. Bugge, D. N. Reinhoudt, S. Harkema, R. Ungaro, F. Ugozzoli, E. Ghidini, *J. Am. Chem. Soc.* **1989**, *111*, 7567–7575.

[4] E. Ghidini, F. Ugozzoli, R. Ungaro, S. Harkema, A. A. El-Fadl, D. N. Reinhoudt, *J. Am. Chem. Soc.* **1990**, *112*, 6979–6985.

[5] Z. Brzozka, B. Lammerink, D. N. Reinhoudt, E. Ghidini, R. Ungaro, *J. Chem. Soc. Perkin Trans. 2* **1993**, 1037–1040.

[6] W. F. Nijenhuis, E. G. Buitenhuis, F. de Jong, E. J. R. Sudhölter, D. N Reinhoudt, *J. Am. Chem. Soc.* **1991**, *113*, 7963–7968.

[7] *Radioactive Waste Management and Disposal* (Ed.: L. Cecille), Elsevier, London, **1991**.

[8] W. J. McDowell, G. N. Case, J. A. McDonough, R. A. Bartsch, *Anal. Chem.* **1992**, *64*, 3013–3017.

[9] All compounds provided satisfactory elemental analyses and M^+ peaks (100%) in the CI mass spectra.

[10] F. Ugozzoli, G. D. Andreetti, *J. Inclusion Phenom. Mol. Recognit. Chem.* **1992**, *13*, 337–348.

[11] X-ray structure analysis: $Cu_{K\alpha}$ radiation, graphite monochromator, data collection at room temperature, θ,2θ scan; intensities from profile analysis. Structure determination by direct methods with SIR92 and refinement with SHELX76; non-hydrogen atoms with anisotropic thermal parameters; H atoms in their calculated positions with geometrical constraint C–H = 0.96 Å; two independent complex molecules and one chloroform solvent molecule in the asymmetric unit. $C_{46}H_{48}CsN_3O_{15}\cdot0.5CHCl_3$ M_r = 1075.49, triclinic, a = 17.363(3), b = 26.590(5), c = 11.005(4) Å, α = 80.00(2), β = 88.11(2), γ = 93.80(2)°, V = 4987(2) Å^3, space group $P\bar{1}$ (No. 2), Z = 4, ρ_{calcd} = 1.432 g cm^{-3}, Siemens AED diffractometer, 2θ range 6–140°, 19934 reflections measured ($\pm h$, $\pm k$, $+l$), scan width from [θ – 0.65] to [θ + 0.65 + $\Delta\lambda\lambda^{-1}$ tgθ]°, scan rate 3–12° min^{-1}, 12235 observed reflections ($I \geq 2\sigma(I)$), 1178 parameters, R = 0.066, R_w = 0.073. The extremely disordered chloroform molecule was refined with geometrical constraints. Further details of the crystal structure investigation are available on request from the Director of the Cambridge Crystallographic Data Centre, 12 Union Road, GB-Cambridge CB2 1EZ, UK, on quoting the full journal citation.

[12] K. Gregory, M. Bremer, P. von R. Schleyer, P. A. A. Klusener, L. Brandsma, *Angew. Chem.* **1989**, *101*, 1261–1263; *Angew. Chem. Int. Ed. Engl.* **1989**, *28*, 1224–1226.

[13] J. M. Harrowfield, M. I. Ogden, W. R. Richmond, A. H. White, *J. Chem. Soc. Chem. Commun.* **1991**, 1159–1161.

[14] a) K. Iwamoto, K. Araki, S. Shinkai, *J. Org. Chem.* **1991**, *56*, 4955–4962; b) A. Casnati, E. Comelli, M. Fabbi, V. Bocchi, G. Mori, F. Ugozzoli, A. M. Manotti Lanfredi, A. Pochini, R. Ungaro, *Recl. Trav. Chim. Pays-Bas* **1993**, *112*, 384–392.

[15] W. Verboom, S. Datta, Z. Asfari, S. Harkema, D. N. Reinhoudt, *J. Org. Chem.* **1992**, *57*, 5394–5398.
[16] J.-F. Dozol, H. Rouquette, R. Ungaro, A. Casnati, FR-B 9304566, **1993**.
[17] J. de Mendoza, P. Prados, N. Campillo, P. M. Nieto, C. Sánchez, J.-P. Fayet, M. C. Vertut, C. Jaime, J. Elguero, *Recl. Trav. Chim. Pays-Bas* **1993**, *112*, 367–369, and references therein.
[18] Cation/π-electron interactions in 1,3-alternate calix[4]arenes have been also suggested by A. Ikeda, S. Shinkai, *Tetrahedron Lett.* **1992**, *33*, 7385–7388.

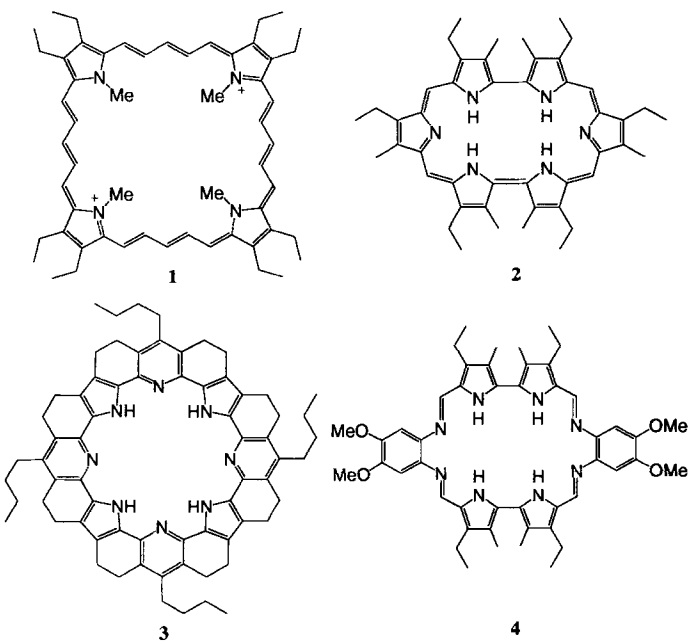
Turcasarin, the Largest Expanded Porphyrin to Date**

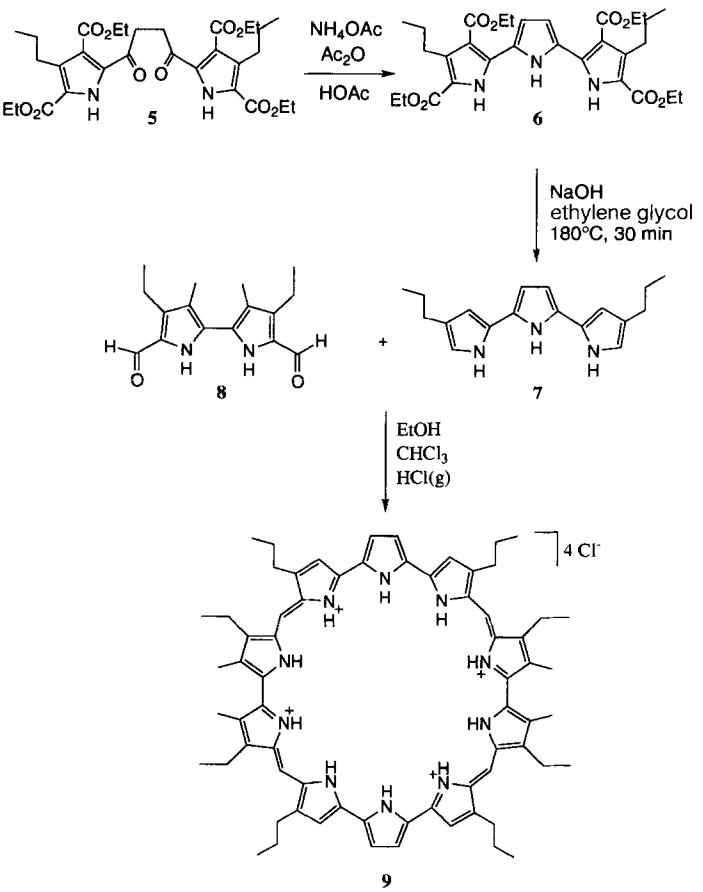
Jonathan L. Sessler,* Steven J. Weghorn, Vincent Lynch, and Martin R. Johnson

Dedicated to Professor Emanuel Vogel on the occasion of his 65th birthday

In recent years, the chemistry of large pyrrole-containing macrocycles has been receiving increasing attention.[1–6] Much of this interest reflects the fact that these compounds, known generically as "expanded porphyrins", bear analogies to the well-studied porphyrins, yet display chemical properties such as anion binding, which have no parallel in the chemistry of porphyrins or other naturally occurring tetrapyrrolic macrocycles. Further interest in expanded porphyrins is derived from the study of extended conjugated π-electron systems. Indeed, much recent attention has been devoted to making ever larger conjugated π-electron systems that absorb in the far-red region of the visible spectrum. For instance, the octavinylogous porphyrin **1** prepared by Franck et al. is a conjugated 34 π-electron system.[2] Also in the all-pyrrole category, expanded porphyrins with as many as six pyrrole subunits have been prepared.[3, 6b] One example is rubyrin **2**, which has a conjugated system with 26 π-electrons.[3] Other even larger expanded porphyrins that rely on additional non-pyrrole subunits to define the macrocycle core have also been prepared. For instance, torrand **3**[4] with eight nitrogen atoms and the Schiff base derived macrocycle **4**[5] each have extended π-conjugation pathways with visible absorptions considerably red-shifted relative to those of the porphyrins.

In spite of these successes, however, the need to prepare other new systems for the study of aromaticity and π-conjugation remains.[6] We therefore wish to report here the synthesis of a new class of expanded porphyrins, namely the ten pyrrole containing macrocycle **9**[7] ([40]decaphyrin-[0.0.1.0.1.0.0.1.0.1]-[8]). This system, which to the best of our knowledge is the highest order expanded porphyrin characterized to date, is prepared by the acid-catalyzed condensation of 4,4′-diethyl-5,5′-diformyl-3,3′-dimethyl-2,2′-bipyrrole (**8**)[9] with 2,5-bis(4-propyl-2-pyrrolyl)pyrrole (**7**) (Scheme 1). After purification, one obtains a 20% yield of a compound that formulates as **9** and, depending on its degree of protonation, displays an intense purple to blue to green color in organic solvents. Thus, in view of its color, we have assigned the trivial name turcasarin to this macrocycle (from Middle English "turcas").





Scheme 1. Synthesis of **9**.

Turcasarin **9** may be considered a 40 π-electron annulene. Thus, turcasarin should not be aromatic according to the (4*n* +

[*] Prof. J. L. Sessler, S. J. Weghorn, V. Lynch
Department of Chemistry and Biochemistry, University of Texas
Austin, TX 78712 (USA)
Telefax: Int. code + (512) 471-7550
Dr. M. R. Johnson
Department of Chemistry, The George Washington University

[**] This research was supported by the National Science Foundation (grant CHE 919122161 to J.L.S). Dr. Johnson thanks Prof. James Ibers, Northwestern University, and the National Institutes of Health (grant HL 13157).

 © VCH Verlagsgesellschaft mbH, D-69451 Weinheim, 1994 0570-0833/94/1414-1509 $ 10.00+.25/0

2) rule for aromatic systems. However, like its smaller aromatic congeners pentaphyrin[6a] and rubyrin, it displays a rather intense absorption in the visible portion of the electronic spectrum that is considerably red-shifted compared to that of the porphyrins. On the other hand, no evidence of ring current effects are seen for the pyrrolic proton resonances in the ^{1}H NMR spectrum. Thus, **9** can be considered a nonaromatic compound with a delocalized π system.

In addition to providing a test of aromaticity, NMR studies were also used to obtain solution-state structural information. The ^{13}C NMR spectrum indicates, for instance, that the frame of the macrocycle has apparent C_2 symmetry, as judged by the number of observable peaks. The ^{1}H NMR spectrum (Table 1)

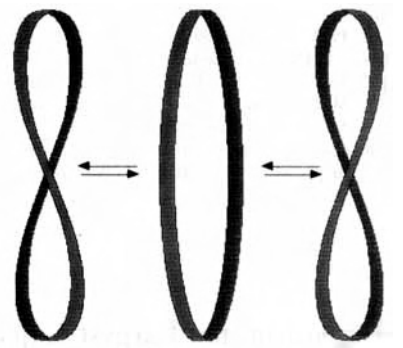


Fig. 1. Schematic representation showing the interconversion between the two limiting enantiomeric conformations of macrocycle **9**. These conformations may be considered as left- or right-handed twists along the long axis of a presumed open, pseudo-circular intermediate.

Table 1. Characterization data for new compounds.

6: M.p. 150 152 °C. ^{1}H NMR (300 MHz, $CDCl_3$): $\delta = 0.99$ (t, J(H,H) = 7.4 Hz, 6H, $CH_2CH_2CH_3$), 1.36 (t, J(H,H) = 7.1 Hz, 6H, OCH_2CH_3), 1.40 (t, J(H,H) = 7.1 Hz, 6H, OCH_2CH_3), 1.62 (sextet, J(H,H) = 7 Hz, 4H, $CH_2CH_2CH_3$), 3.06 (m, 4H, $CH_2CH_2CH_3$), 4.37 (q, J(H,H) = 7.1 Hz, 8H, OCH_2CH_3), 6.61 (d, J(H,H) = 2.5 Hz, 2H, pyrrole CH), 9.05 (bs, 2H, NH), 9.10 (bs, 1H, NH); ^{13}C NMR (75.5 MHz, $CDCl_3$): δ = 14.2, 14.3, 14.4, 24.5, 28.0, 60.5, 109.4, 111.9, 119.0, 124.3, 132.2, 135.7, 161.3, 166.0. MS ($CHCl_3$): 569 (100%), 523 (83), 477 (64). HRMS: calculated for $C_{30}H_{36}N_3O_8$: m/z 569.2337; found: 569.2720.

7: M.p. (sealed tube) 141–144 °C. ^{1}H NMR (300 MHz, [D$_6$]DMSO: $\delta = 0.91$ (t, J(H,H) = 7.4 Hz, 6H, $CH_2CH_2CH_3$), 1.53 (sextet, J(H,H) = 7.4 Hz, 4H, $CH_2CH_2CH_3$), 2.35 (t, J(H,H) = 7.4 Hz, 4H, $CH_2CH_2CH_3$), 6.13 (m, 2H, CHC(*n*Pr)C*H*nH), 6.44 (s, 2H, CH), 10.47 (s, 2H, NH), 10.56 (s, 1H, NH); ^{13}C NMR (75.5 MHz, [D$_6$]DMSO): δ = 14.0, 23.9, 28.9, 103.1, 103.3, 114.1, 123.3, 125.5, 125.7. MS ($CHCl_3$): 281 (100%), 252 (25), 238 (8). HRMS: calculated for $C_{18}H_{23}N_3$: m/z 281.1892; found: 281.1878.

9: M.p. >215 °C (decomp.); ^{1}H NMR (500 MHz, $CDCl_3$): $\delta = 0.99$ (t, J(H,H) = 7 Hz, 6H, CH_2CH_3), 1.05 (t, J(H,H) = 7 Hz, 6H, CH_2CH_3), 1.08 (t, J(H,H) = 7 Hz, 6H, $CH_2CH_2CH_3$), 1.27 (t, J(H,H) = 7 Hz, 6H, $CH_2CH_2CH_3$), 1.77 (m, 2H, $CH_2CH_2CH_3$), 1.85 (s, 6H, CH_3), 1.89 (m, 2H, $CH_2CH_2CH_3$), 2.06 (s, 6H, CH_3), 2.10 (m, 2H, $CH_2CH_2CH_3$), 2.19 (m, 2H, $CH_2CH_2CH_3$), 2.25 (q, J(H,H) = 7 Hz, 4H, CH_2CH_3), 2.36 (m, 4H, CH_2CH_3), 2.64 (m, 2H, $CH_2CH_2CH_3$), 2.87 (m, 2H, $CH_2CH_2CH_3$), 2.89 (m, 2H, $CH_2CH_2CH_3$), 6.73 (s, 2H, *meso*-H), 6.84 (s, 2H, *meso*-H), 7.00 (s, 2H, pyrrole CH), 7.65 (bs, 2H, pyrrole CH), 8.68 (s, 2H, pyrrole CH), 9.73 (bs, 2H, pyrrole CH), 14.32 (s, 2H, NH), 14.56 (s, 2H, NH), 14.75 (s, 2H, NH), 15.37 (s, 2H, NH), 15.74 (s, 2H, NH); ^{13}C NMR (75.5 MHz, $CDCl_3$): δ = 11.4, 11.5, 14.1, 14.4, 14.9, 15.0, 18.0, 18.2, 23.0, 23.2, 28.2, 28.9, 119.1, 119.7, 121.4, 122.8, 123.7, 124.7, 125.1, 127.0, 128.6, 132.7, 133.0, 133.9, 136.4, 137.2, 137.6, 139.6, 141.6, 143.1, 147.8, 148.17, 149.0, 151.3; UV/VIS (CH_2Cl_2): λ_{max} [nm] (ε) = 369 (46500), 399 (49000), 445 (51500), 642 (312500); HRMS (FAB): calculated for $C_{68}H_{79}N_{10}$: m/z 1035.6489; found: 1035.6505 ($(M+1)^+ - 4HCl$); correct C, H, N, Cl analysis for $C_{68}H_{82}Cl_4N_{10} \cdot H_2O$.

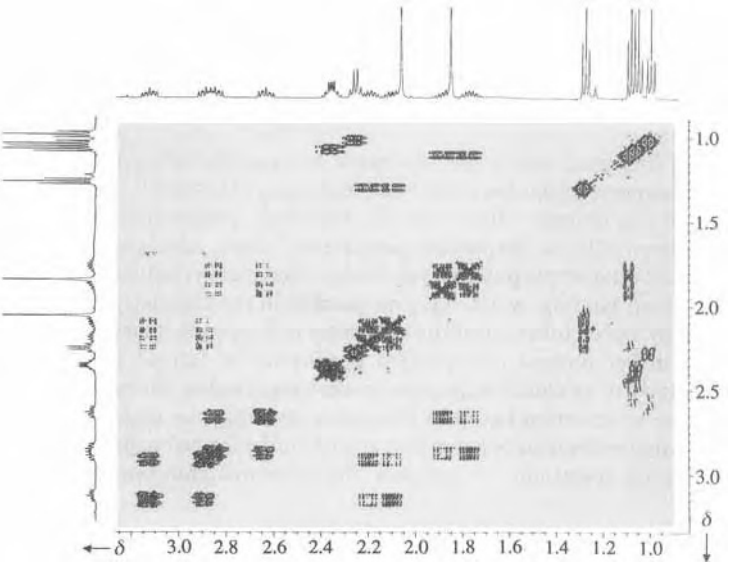


Fig. 2. Two-dimensional H,H-correlated spectrum (H,H COSY) of the alkyl region of macrocycle **9** that allowed definitive peak assignments to be made. Paired sets of crosspeaks indicate near C_2 symmetry in the molecule and provide evidence for diastereotopic protons in the propyl side chains.

is also consistent with C_2 symmetry as judged by the number of signals in the interior NH and exterior β-pyrrolic and *meso*-proton region. The signals in the alkyl region, on the other hand, prove more complex; no clear assignment of symmetry or structure is possible from immediate inspection. In fact, complex splitting patterns for the methylene protons of the alkyl side chains are observed.[10]

These complex splitting patterns led us to suggest that the macrocycle may exist in two limiting conformations. These two conformations result from a twist along a long axis of the molecule as shown in Figure 1. Molecule **9** could therefore exist as a pair of enantiomers. It would thus be disymmetric even though it possesses no formal stereogenic centers. Such a postulate of conformational chirality, even though unexpected for a fully conjugated macrocycle, would, of course, account for the observed complex splitting patterns, which arise as the result of an imposed diastereotopicity on the alkyl side chains.

Definitive assignments of the ^{1}H NMR signals were made based on COSY (Fig. 2) and NOESY experiments. The NOESY spectrum also shows significant exchange crosspeaks in all regions, indicating that the two enantiomers can readily interconvert, at least on the timescale of such experiments. However, variable-temperature ^{1}H NMR spectra ($CDCl_3$, -50 °C to $+50$ °C), by virtue of displaying very little change in the chemical shifts, indicate that this interconversion is slow on the NMR timescale at room temperature. This slow interconversion could reflect conformational stabilization imposed by the presumably strong hydrogen bonding interactions between the macrocycle and the chloride anions which are observed in the solid state (vide infra).

Solid-state structural information was obtained from a single-crystal X-ray structure of the tetrahydrochloride salt of **9** (Fig. 3).[11] In accord with what was found in the solution-phase NMR experiments, the tetraprotonated form of macrocycle **9** is found to adopt a nearly C_2-symmetric, twisted "figure-eight" conformation in the solid state, and not an open "circular" conformation. This twisted conformation serves to define two enantiomers (both of which are seen in the X-ray structure) such that the structure of **9** in the solid state more closely resembles the "twisted ribbons" in Figure 1, rather than the open, circle-like "loop".

As can be seen in Figure 3, the twist observed in the solid state also serves to define two pentaphyrin-like "hemi-macrocycles" as well as four smaller "pockets". Occupying each of these pockets is a chloride anion which is close enough to form a hydrogen

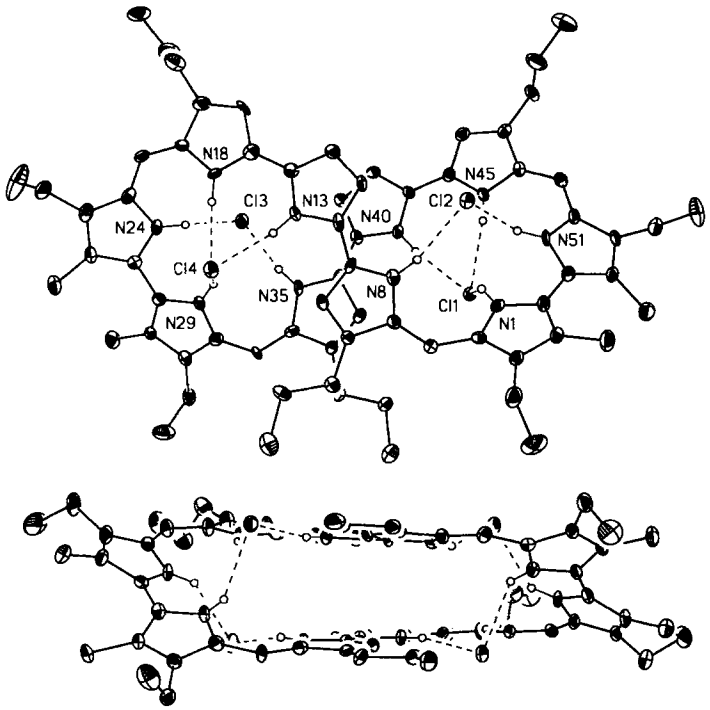


Fig. 3. Top and side views of the tetraprotonated form of **9** ($(C_{68}H_{74}N_{10})^{4+}$ $(Cl^-)_4$) with partial labeling showing the conformation of the macrocycle and the binding of the Cl^- ions. At the point of "ribbon crossing" the interplane separation is 3.268 Å. Further important distances [Å] and angles [°] N1-H1a···Cl1, N···Cl 3.133(11), H···Cl 2.442(11), N-H···Cl 133.9(10); N40-H40a···Cl1, N···Cl 3.054(10), H···Cl 2.178(10), N-H···Cl 164.3(11); N45-H45a···Cl1, N···Cl 3.194(10), H···Cl 2.370(10), N-H···Cl 152.4(11); N8-H8a···Cl2, N···Cl 3.190(10), H···Cl 2.353(10), N-H···Cl 154.8(11); N51-H51a···Cl2, N···Cl 3.116(11), H···Cl 2.334(11), N-H···Cl 145.2(11); N24-H24a···Cl3, N···Cl 3.133(11), H···Cl 2.349(11), N-H···Cl 145.5(11); N35-H35a···Cl3, N···Cl 3.161(11), H···Cl 2.280(11), N-H···Cl 166.0(11); N13-H13a···Cl4, N···Cl 3.069(10), H···Cl 2.183(10), N-H···Cl 167.8(11); N18-H18a···Cl4, N···Cl 3.194(11), H···Cl 2.375(11), N-H···Cl 151.4(11); N29-H29a···Cl4, N···Cl 3.132(10), H···Cl 2.459(10), N-H···Cl 131.9(10). Because the hydrogen atoms are at idealized positions, the resulting estimated standard deviations for quantities involving them are underestimated. Thermal ellipsoids were scaled to the 30% probability level. For clarity, only N–H hydrogen atoms are shown.

bond with the N–H group. These hydrogen bonding interactions are currently considered to account for the slow conformational interconversion observed at room temperature in solution on the NMR timescale. However, it is of interest to note that at the point of "ribbon crossing" the two pyrrole-containing π systems are separated from one another by a van der Waals distance of 3.268 Å.

The presence of four pockets binding chloride anions in the tetraprotonated form of **9** leads us to predict that this macrocycle, in analogy to several other expanded porphyrins,[1] could serve as an anion binding and transport agent in solution. Further, the observation that the twisting present in this decapyrrolic system serves to define two "hemipentaphyrins" leads us to suggest that system **9**, like pentaphyrin itself,[13] could chelate uranyl ions.[14] Of greatest interest, however, is perhaps the simple finding that conjugated, polypyrrolic macrocycles need not be flat or nearly flat but can adopt conformations that make them potentially chiral. To the best of our knowledge, such a conceptualization is new within the context of the expanded porphyrins.

Experimental Procedure

6: Dipyrrylbutanedione **5** (23.54 g, 40 mmol) [15], ammonium acetate (vacuum dried at 50 °C, 91.1 g, 1 mol), acetic anhydride (32 mL, 0.33 mol), and glacial acetic acid (150 mL) were held at reflux under argon for 18 h, poured into stirred ice water (400 mL), and stirred for 1 h. The solid was collected by filtration, washed with water, and dissolved in CH_2Cl_2. The CH_2Cl_2 solution was washed with water, diluted with methanol, and concentrated on the rotary evaporator until the volume was roughly 50 mL. The flask contents were cooled in ice for 1 h, and the solid was collected by filtration, washed (MeOH, Et_2O), and dried to give the pure product as light yellow needles or powder (17.85 g, 31.3 mmol, 78%).

7: Terpyrrole tetraester **6** (5.7 g, 10 mmol), NaOH (10 g, 400 mmol), and ethylene glycol (100 mL) were stirred under argon and heated at reflux. When the solution reached a temperature of 180 °C, it was heated for another 30 min and cooled. When the solution reached 100–120 °C, the flask contents were diluted with water (70 mL, degassed by the freeze-pump-thaw method) and allowed to cool to room temperature. The mixture was diluted to 400 mL with ice water. The solid obtained was separated by filtration under argon (an aluminum foil cover and a pipette as the gas inlet is fine), washed with water, and dried in vacuo to give the pure product as a tan to light green powder (2.62 g, 9.3 mmol, 93%).

9: Bipyrrole **8** (72.5 mg, 2.67×10^{-4} mol) was dissolved in 20 mL absolute ethanol with the aid of a heat gun. $CHCl_3$ was added (500 mL), followed by terpyrrole **7** (74.9 mg, 2.67×10^{-4} mol). HCl gas was bubbled into the stirred reaction mixture for 5 min. The reaction was then stirred under argon for 4 h. The $CHCl_3$ was removed with a rotary evaporator. The ethanolic residue was treated with concentrated aqueous $NaHCO_3$ until effervescence ceased and then extracted into $CHCl_3$. The organic layer was separated, dried over Na_2SO_4, and concentrated to dryness in vacuo. The residue was taken up in a minimum amount of CH_2Cl_2, and NH_3 gas was bubbled into the solution for 1 min. The resulting solution was purified by chromatography on a pretreated column (2 cm × 20 cm) of silica gel (before the column was packed, NH_3 was bubbled through a slurry of CH_2Cl_2 and silica gel). The first major purple band (CH_2Cl_2 eluent) was collected, and washed with water (2 × 25 mL) and 1 N HCl (3 × 25 mL). The organic layer was then separated, dried over Na_2SO_4, and concentrated to dryness in vacuo. Recrystallization from CH_2Cl_2 layered with hexanes gave pure **9** as shiny green metallic crystals (62.9 mg, 5.34×10^{-5} mol, 20%).

Received: January 17, 1994 [Z 6625 IE]
German version: *Angew. Chem.* **1994**, *106*, 1572

[1] J. L. Sessler, A. K. Burrell, *Top. Curr. Chem.* **1991**, *161*, 177–273.
[2] G. Knübel, B. Franck, *Angew. Chem.* **1988**, *100*, 1203–1211; *Angew. Chem. Int. Ed. Engl.* **1988**, *27*, 1170–1172.
[3] J. L. Sessler, T. Morishima, V. Lynch, *Angew. Chem.* **1991**, *103*, 1018–1021; *Angew. Chem. Int. Ed. Engl.* **1991**, *30*, 977–980.
[4] T. W. Bell, P. J. Cragg, M. G. B. Drew, A. Firestone, A. D.-I. Kwok, J. Liu, R. T. Ludwig, A. T. Papoulis, *Pure Appl. Chem.* **1993**, *65*, 361–366.
[5] J. L. Sessler, T. D. Mody, V. Lynch, *J. Am. Chem. Soc.* **1993**, *115*, 3346–3347.
[6] Other expanded porphyrins: a) H. Rexhausen, A. Gossauer, *J. Chem. Soc. Chem. Commun.* **1983**, 275; b) A. Gossauer, *Bull. Soc. Chim. Belg.* **1983**, *92*, 793–795; R. Charriere, T. Jenny, H. Rexhausen, A. Gossauer, *Heterocycles* **1993**, *36*, 1561–1575; c) M. Gosmann, A. Vogt, B. Franck, *Liebigs Ann. Chem.* **1990**, 163–168; d) H. König, C. Eickemeier, M. Möller, U. Rodewald, B. Franck, *Angew. Chem.* **1990**, *102*, 1437–1439; *Angew. Chem. Int. Ed. Engl.* **1990**, *29*, 1393–1395; e) S. Beckmann, T. Wessel, B. Franck, W. Hönle, H. Borrmann, G. H. von Schnering, *ibid.* **1990**, *102*, 1439–1441 and **1990**, *29*, 1395–1397; f) M. Gosmann, B. Franck, *ibid.* **1986**, *98*, 1107–1108 and **1986**, *25*, 1100–1101; g) T. Wessel, B. Franck, M. Möller, U. Rodewald, M. Läge, *ibid.* **1993**, *25*, 1100–1101; g) T. Wessel, B. Franck, M. Möller, U. Rodewald, M. Läge, *ibid.* **1993**, *105*, 1201–1204 and **1993**, *32*, 1148–1151; h) N. Lux, P. Koch, H. Schmickler, J. Lex, E. Vogel, *ibid.* **1990**, *102*, 1429–1431 and **1990**, *29*, 1385–1387; i) E. Vogel, N. Lux, E. Rodriguez-Val, J. Lex, H. Schmickler, *ibid.* **1990**, *102*, 1431–1434 and **1990**, *29*, 1387–1390; j) D. Dolphin, S. J. Rettig, H. Tang, T. Wijesekera, L. Y. Xie, *J. Am. Chem. Soc.* **1993**, *115*, 9301–9302; k) F. H. Carre, R. J. P. Corriu, G. Bolin, J. J. E. Moreau, C. Vernhet, *Organometallics* **1993**, *12*, 2478–2486; l) G. Märkl, U. Striebl, *Angew. Chem.* **1993**, *105*, 1387–1389; *Angew. Chem. Int. Ed. Engl.* **1993**, *32*, 1333–1335; m) J. L. Sessler, S. J. Weghorn, T. Morishima, M. Rosingana, V. Lynch, V. Lee, *J. Am. Chem. Soc.* **1992**, *114*, 8306–8307; n) Z. Hu, C. Scordilis-Kelley, M. P. Cava, *Tetrahedron Lett.* **1993**, *34*, 1879–1882; see also ref. [1], and references therein.
[7] The systematic name for **9** is 15,20,37,42-tetraethyl-16,19,38,41-tetramethyl-2,11,24,33-tetrapropyl-45,46,47,48,49,50,51,52,53,54-decaazaundecacyclo-[40.2.1.1^{5,8}.1^{9,12}.1^{14,17}.1^{18,21}.1^{23,26}.1^{27,30}.1^{31,34}.1^{36,39}.1^{40,43}]-tetrapentaconta-1,3,5,7,9(47),10,12,14,16,18(49),19,21,23,25,27,29,31(52),32,34,36,38,40(54),41,43-tetracosaene.
[8] a) Based on the naming system of Franck; see ref. [6f]. b) Because of the six direct pyrrole connections in the macrocycle, turcasarin **9** may alternatively be thought of as an "expanded corrole".
[9] J. L. Sessler, M. J. Cyr, V. Lynch, E. McGhee, J. A. Ibers, *J. Am. Chem. Soc.* **1990**, *112*, 2810–2813.
[10] 15,20,37,42-Tetraethyl-2,11,16,19,24,33,38,41-octamethylturcasarin has also recently been prepared. In the ^{1}H NMR spectrum of this newer system the NH, β-pyrrolic, and *meso* proton resonances are essentially the same as those of **9**; however as expected, the signals in the alkyl region are less complex. Charac-

terization data: ^{1}H NMR (300 MHz, $CDCl_3$): $\delta = 1.03$ (t, J(H,H) = 7 Hz, 6H, CH_2CH_3), 1.09 (t, J(H,H) = 7 Hz, 6H, CH_2CH_3), 1.67 (s, H_2O), 1.90 (s, 6H, CH_3), 2.09 (s, 6H, CH_3), 2.33 (q, J(H,H) = 7 Hz, 4H, CH_2CH_3), 2.39 (q, J(H,H) = 7 Hz, 4H, CH_2CH_3), 2.45 (s, 6H, CH_3), 2.80 (s, 6H, CH_3), 6.76 (s, 2H, *meso*-H), 6.95 (s, 2H, *meso*-H), 7.04 (s, 2H, pyrrole CH), 7.62 (d, 2H, pyrrole CH), 8.60 (s, 2H, pyrrole CH), 9.68 (d, 2H, pyrrole CH), 14.23 (s, 2H, NH), 14.44 (s, 2H, NH), 14.67 (s, 2H, NH), 15.21 (s, 2H, NH), 15.58 (s, 2H, NH); UV/VIS (CH_2Cl_2): $\lambda_{max} = 644$ nm; HRMS (FAB): calculated for $C_{60}H_{63}N_{10}$: m/z 923.5237; found: 923.5252 $(M+1)^+ - 4HCl$).

[11] Crystallographic data for **9** $(C_{68}H_{74}N_{10})^{4+}(Cl^-)_4 - 3CH_2Cl_2 - 3/2(C_6H_{14})$, $M_r = 1557.29$; crystallized as dark green blocks from methylene chloride layered with *n*-hexane in the triclinic space group $P\bar{1}$ (no. 2), with $a = 14.221(6)$, $b = 15.374(3)$, $c = 20.531(5)$ Å, $\alpha = 100.03(2)$, $\beta = 101.71(3)$, $\gamma = 106.23(3)°$, $V = 4091(2)$ Å^3, $\rho_{calcd} = 1.26$ g cm^{-3} for $Z = 2$, F(000) = 1642, $\mu(Mo_{K\alpha}) = 3.888$ cm^{-1}, $\lambda = 0.71073$ Å. Data were collected at −90 °C on a Nicolet R3 diffractometer equipped with a Nicolet LT-2 low-temperature device, ω-scans, 5–12° min^{-1}, $2\theta_{max} = 45°$. A total of 12144 reflections were collected, of which 10699 were unique. The R for averaging symmetry-equivalent reflections was equal to 0.034. Data were corrected for Lorentz and polarization effects, and for decay but not for absorption. The structure was solved by direct methods and refined by full-matrix least-squares using SHELXTL-Plus [12]. The hydrogen atoms were calculated in ideal positions, with $U_{iso} = 1.2 \times U_{eq}$ of the relevant atom. One molecule of *n*-hexane and one of dichloromethane are disordered. A total of 853 parameters were refined to a final $R = 0.0825$, $wR = 0.100$, and GOF = 2.607 using 4869 reflections having $F > 4\sigma(F)$. Further details of the crystal structure investigation are available upon request from the Director of the Cambridge Crystallographic Data Centre, 12 Union Road, GB-Cambridge CB2 1EZ (UK), on quoting the full journal citation.

[12] G. M. Sheldrick, SHELXTL-Plus, Siemens Analytical X-ray Instruments, Madison, WI, USA, **1991**.

[13] A. K. Burrell, G. Hemmi, V. Lynch, J. L. Sessler, *J. Am. Chem. Soc.* **1991**, *113*, 4690–4692.

[14] The bis-uranyl chelate of **9** has recently been prepared in our laboratory: J. L. Sessler, E. Brucker, S. Weghorn, unpublished results. Characterization data: UV/VIS (CH_2Cl_2): λ_{max} [nm] = 445, 682; LRMS (FAB): Calculated for $C_{68}H_{74}N_{10}U_2O_4$: m/z 1570; found 1570; The ^{1}H NMR spectrum is similar to that of the parent compound **9**, including diastereotopic splitting patterns in the alkyl region.

[15] M. R. Johnson, D. C. Miller, K. Bush, J. J. Becker, J. A. Ibers, *J. Org. Chem.* **1992**, *57*, 4414–4417.

Nonreactive Interactions between Ethene and Halogens: Detection of a π-Donor Complex $C_2H_4 \cdots BrCl$ by Rotational Spectroscopy**

Hannelore I. Bloemink, Kelvin Hinds, Anthony C. Legon,* and Joanna C. Thorn

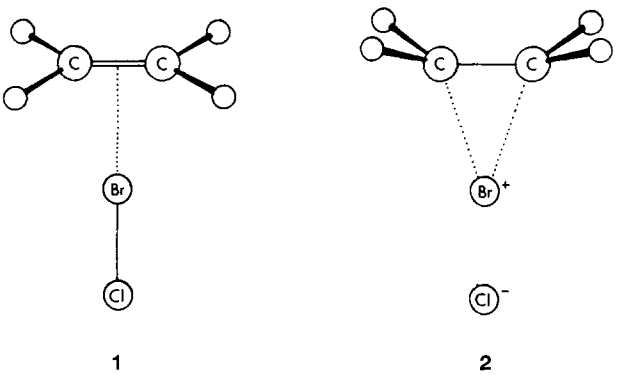
We report the first characterization of a molecular π-donor complex formed by ethene with a halogen or interhalogen in the gas phase. The microwave spectrum of $C_2H_4 \cdots BrCl$ was observed by employing a fast-mixing nozzle to keep the chemically reactive components separate until the point at which they expanded simultaneously into the evacuated Fabry–Pérot cavity of a Fourier transform (FT) microwave spectrometer. Complexes formed where the gases met had very low internal energies and underwent collisionless expansion before further progress along the reaction coordinate could occur. Properties of frozen species were then determined from an analysis of the rotational spectrum.

[*] Prof. A. C. Legon, Dr. H. I. Bloemink, K. Hinds, J. C. Thorn
Department of Chemistry
University of Exeter
Stocker Road, Exeter EX4 4QD (UK)
Telefax: Int. code +(392) 263-434

[**] This work was supported by a research grant and a studentship (for K. H.) from the Science and Engineering Research Council and a studentship (for J. C. T.) from the Ruth King Trust of the University of Exeter.

The addition reaction of, for example, molecular bromine to an alkene under "dark" conditions, that is, in the absence of radical initiation, and in a polar environment has been thoroughly investigated.[1] It is assumed to proceed through an intermediate formed when electrophilic Br_2 first encounters the nucleophilic alkene.[2] If the electrophile is BrCl, the addition reaction is about 400 times faster,[1, 2] in accordance with the idea that the polar interhalogen $^{\delta+}BrCl^{\delta-}$ is a better electrophilic halogenating agent than Br_2.

Two types of reactive intermediate can be envisaged for a halogen and a π donor such as ethene. Following the proposal of Mulliken,[3] we refer to an "outer" (weak) complex of the type **1**, and an "inner" complex **2** in which there is significant charge transfer. Under dark, polar conditions, one mechanism proposed[4, 5] for the addition of a halogen to an alkene proceeds from the initial pre-equilibrium complex of type **1** to the halogenium ion of type **2**, which subsequently suffers nucleophilic attack by, for example, Cl^-. Other, similar mechanisms are discussed in reference [1]. Although reactive intermediates of types **1** and **2** have been much invoked, they are difficult to characterize experimentally, particularly for the prototype alkene C_2H_4 because of rapid subsequent reaction. It is therefore of interest to isolate any molecular complex formed by ethene with, for example, BrCl and to determine its properties. What is the geometry of the complex? What is the extent of electric charge redistribution when it is formed? Is **1** or **2** the more appropriate description in the gas phase?



1 **2**

While rotational (microwave) spectroscopy has proved a powerful method for observing molecular complexes isolated in the gas phase,[6] it is usually conducted with premixed components in contact with surfaces, particularly those of metals. Since even so-called gaseous additions of chlorine and bromine to ethene are reactions on polar surfaces,[1] premature reaction of the premixed gases occurs. The problem of reaction has been overcome here by carrying out rotational spectroscopy on a jet of the gas mixture supersonically expanded from a fast-mixing nozzle[7] into the spacious Fabry–Pérot cavity of a FT microwave spectrometer. The essential feature of the fast-mixing nozzle is that the reactive components mix only as they expand simultaneously from a pair of coaxial and coterminal tubes into the evacuated cavity. Complexes of C_2H_4 and BrCl are formed only at the interface of the concentric gas flows, in the absence of surfaces. Moreover, they are in collisionless expansion within a few nozzle diameters (after about 10 μs in our experiment) and are then frozen at a very low effective temperature until they encounter a wall of the vacuum chamber.

The ground-state rotational spectrum of (C_2H_4, BrCl) observed in this way was that of a nearly prolate asymmetric-top

molecule with a nonzero a component of the electric dipole moment.[8] Each transition carried a nuclear quadrupole hyperfine structure characteristic of the presence of two nuclei of spin $I = {}^3/_2$. A detailed analysis of the $J = 5 \leftarrow 4$ and $4 \leftarrow 3$ transitions with the Watson A reduction[9] led to the ground-state rotational constants A_0, B_0, and C_0, the centrifugal distortion constants Δ_J and Δ_{JK}, the halogen nuclear quadrupole coupling constants $\chi_{aa}(X)$ and $\chi_{bb}(X) - \chi_{cc}(X)$, and the bromine spin-rotation constant $M_{bb}(Br)$, listed in Table 1 for the isotopomers (C_2H_4, $^{79}Br^{35}Cl$) and (C_2H_4, $^{81}Br^{35}Cl$). By using BrCl as the halogen we ensured that any species of type **1** had a significant electric dipole moment and hence a spectrum of reasonable intensity. The spectroscopic constants of Table 1 allow several conclusions about the nature of the observed complex to be drawn.

Table 1. Ground-state spectroscopic constants of two isotopomers of (C_2H_4, BrCl) [a].

Spectroscopic constant	(C_2H_4, $^{79}Br^{35}Cl$)	(C_2H_4, $^{81}Br^{35}Cl$)
A_0 [MHz]	25114(95)	25016(99)
B_0 [MHz]	1228.2834(2)	1228.3003(2)
C_0 [MHz]	1188.2822(2)	1188.2984(2)
Δ_J [kHz]	0.682(5)	0.679(5)
Δ_{JK} [kHz]	21.4(3)	21.5(3)
χ_{aa}(Br) [MHz]	882.54(3)	737.34(3)
χ_{aa}(Cl) [MHz]	− 94.71(2)	− 94.72(2)
$\{\chi_{bb}(Br) - \chi_{cc}(Br)\}$ [MHz]	12.88(5)	10.75(5)
$\{\chi_{bb}(Cl) - \chi_{cc}(Cl)\}$ [MHz]	− 0.21(4)	− 0.25(4)
M_{bb}(Br) [kHz]	− 3.4(3)	− 4.0(3)
P_b [uÅ^2] [b]	16.98(4)	17.03(4)
P_c [uÅ^2]	3.13(4)	3.17(4)
σ_f [kHz] [c]	2.3	2.3

[a] Numbers in parentheses are standard errors in units of the least significant digit. [b] $P_\alpha = \frac{1}{2}(I_\beta + I_\gamma - I_\alpha)$; α, β, γ to be permuted over a, b, c. [c] Standard deviation of the fit.

First, the value of A_0 for both isotopomers is only slightly larger than the rotational constant $C_0 = 24824.17(5)$ MHz of free ethene.[10] This provides strong evidence that the BrCl subunit lies along the c axis of ethene, that is, along the C_2 axis perpendicular to the ethene plane, as in **1**. The small increase almost certainly arises from zero-point effects.[11] The difference $B_0 - C_0$ is also consistent with the arrangement in **1** and the $^{79}Br/^{81}Br$ isotopic invariance of the rotational constants establishes that the Br atom lies close to the complex's center of mass. The planar moments P_b and P_c (see Table 1) are almost unchanged from $P_a = 16.8665(1)$ uÅ^2 and $P_b = 3.49188(2)$ uÅ^2, respectively, of free ethene.[10] Not only does this confirm that the angular geometry is that of type **1**; it also shows that the dimensions of ethene are at most weakly perturbed by complex formation.

Second, the assumption of weak interaction is reinforced when the nuclear quadrupole coupling constants are considered. For both isotopomers, χ_{aa}(Br) and χ_{aa}(Cl) are little changed from the corresponding values $\chi_0(X)$ for free BrCl.[12] This suggests only small changes in the electric field gradient along the BrCl axis when the diatomic molecule takes up its equilibrium position along the ethene c axis. Moreover, the difference $\chi_{bb}(X) - \chi_{cc}(X)$ is a small fraction of $\chi_0(X)$[12] for both X = Br and Cl, so demonstrating that the axial symmetry of the BrCl electric charge distribution is only slightly perturbed. Likewise, the value $k_\sigma = 10.5(1)$ Nm^{-1} for the intermolecular stretching force constant, as determined[13] from Δ_J, also suggests a weak interaction. It is similar in magnitude to those of many hydrogen-bonded complexes[14] and in particular that of the isostructural analogue (C_2H_4, HCl).[15] Significant charge transfer to give a complex of the inner type **2** would be expected to lead to a stronger interaction through the incipient chemical bonds. The parallelism of the properties of (C_2H_4, HCl) and (C_2H_4, BrCl) makes it likely that electrostatic interpretations[16, 17] of the properties of the former (especially the angular geometry) also apply to the latter.

Finally, the rotational constants B_0 and C_0 of (C_2H_4, BrCl) lead, under the assumption of unchanged component geometries,[18, 19] to 2.979(1) Å for the distance of the midpoint of the C=C bond to the Br atom in **1**.

Experimental Procedure

Rotational spectra of (C_2H_4, BrCl) were observed with a pulsed-nozzle FT microwave spectrometer [20] fitted with a fast-mixing nozzle [7]. A mixture of approximately 2% ethene (Argo International) in argon was pulsed through the outer of the two concentric tubes of the nozzle at a rate of 2 Hz from a pressure of 3 atm and mixed with a continuous flow of an equimolar mixture of chlorine and bromine (Aldrich) issuing from the exit of the inner tube. The halogen mixture flow rate was adjusted to give a steady pressure of 1×10^{-4} Torr in the vacuum chamber of the spectrometer. Spectra were observed in the range of frequencies 8–13 GHz. For each isotopomer approximately 75 hyperfine components associated with six rotational transitions were measured with an estimated accuracy of 2 kHz.

Received: March 15, 1994 [Z 6762 IE]
German version: *Angew. Chem.* **1994**, *106*, 1577

[1] C. K. Ingold, *Structure and Mechanism in Organic Chemistry*, 2nd ed., G. Bell, London, **1969**, Chapter XIII, pp. 964–982, and references therein.
[2] P. B. D. de la Mare, R. Bolton, *Electrophilic Additions to Unsaturated Systems*, Monograph 4 (Eds.: C. Eaborn, E. D. Hughes), Elsevier, London, **1966**, Chapter 6, pp. 71–112, and references therein.
[3] R. S. Mulliken, *J. Phys. Chem.* **1952**, *56*, 801–822.
[4] I. Roberts, G. E. Kimball, *J. Am. Chem. Soc.* **1937**, *59*, 947–948.
[5] A. J. Downs, C. J. Adams in *Comprehensive Inorganic Chemistry*, *Vol. 2* (Ed.: A. F. Trotman-Dickenson), Pergamon, New York, **1971**, Chapter 26, pp. 1216.
[6] A. C. Legon, *Chem. Soc. Rev.* **1990**, *19*, 197–237.
[7] A. C. Legon, C. A. Rego, *J. Chem. Soc. Faraday Trans.* **1990**, *86*, 1915–1921.
[8] W. Gordy, R. L. Cook, *Microwave Molecular Spectra* [*Techniques of Organic Chemistry*, *Vol. 9* (Ed.: A. Weissberger)], Interscience, New York, **1970**.
[9] J. K. G. Watson, *J. Chem. Phys.* **1968**, *48*, 4517–4524.
[10] F. Herlemont, M. Lyszyk, J. Lemaire, C. Lambeau, M. de Vleeschouwer, A. Fayt, *J. Mol. Spectrosc.* **1982**, *94*, 309–315.
[11] A. C. Legon, P. D. Aldrich, W. H. Flygare, *J. Chem. Phys.* **1981**, *75*, 625–630.
[12] A. C. Legon, J. C. Thorn, *Chem. Phys. Lett.* **1993**, *215*, 554–560.
[13] D. J. Millen, *Can. J. Chem.* **1985**, *63*, 1477–1479.
[14] A. C. Legon, D. J. Millen, *J. Am. Chem. Soc.* **1987**, *109*, 356–358.
[15] P. D. Aldrich, A. C. Legon, W. H. Flygare, *J. Chem. Phys.* **1981**, *75*, 2126–2134.
[16] A. C. Legon, D. J. Millen, *Faraday Discuss. Chem. Soc.* **1982**, *73*, 71–77; *Chem. Soc. Rev.* **1987**, *16*, 467–498.
[17] A. D. Buckingham, P. W. Fowler, *Can. J. Chem.* **1985**, *63*, 2018–2025.
[18] E. Hirota, Y. Endo, S. Saiko, K. Yoshida, I. Yamaguchi, K. Machida, *J. Mol. Spectrosc.* **1981**, *89*, 223–231.
[19] The value $r_0 = 2.1388$ Å used for BrCl was calculated from $r_0 = (h/8\pi^2\mu B_0)^{1/2}$, where the B_0 value came from ref. [10].
[20] A. C. Legon, *Annu. Rev. Phys. Chem.* **1983**, *34*, 275–300.

 © *VCH Verlagsgesellschaft mbH, D-69451 Weinheim, 1994* *0570-0833/94/1414-1513 $ 10.00+.25/0*

Stable Flexible Fibers and Rigid Tubules Made from Single-Chain Perfluoroalkylated Amphiphiles**

Françoise Giulieri, Marie-Pierre Krafft, and Jean G. Riess*

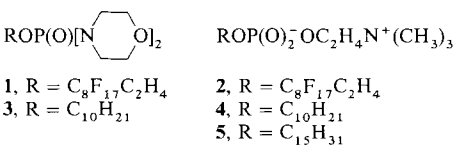
Supramolecular assemblies of amphiphiles have raised considerable interest at the crossroads of chemistry, physics, and biology. Vesicles, for example, are being intensively investigated as models of membranes and as drug carriers.[1] More recently, much attention has been given to a variety of microstructures with cylindrical geometry such as rods, tubules, and ribbons.[2, 3] Some of these structures have potential as building blocks in biomolecular engineering (delivery vehicles, microsurgery materials, etc.) or as novel elements of molecular devices for information processing and signal generation in material sciences (composites, liquid crystal media for electrooptics and microelectronics).[4] As the latter structures are more organized than vesicles, their study can also provide further insight into the molecular basis of the evolution of life with the use of self-organizational principles.[3]

One of the key driving forces for the formation of elongated structures appears to be the hydrophobic interactions between the amphiphiles' hydrophobic chains. Previously, these interactions were, however, not considered to be sufficient. They had to be supplemented by other intermolecular interactions such as hydrogen bonding, polymerization or metal coating, the introduction of rigid rodlike segments in the structure, and usually by the use of chiral molecules in order to achieve such cylindrical microstructures.[2, 3, 5] A stabilizing agent such as sodium dodecylsulfate is often required to avoid crystallization. Helical fibers have been obtained from dispersions of chiral amphiphiles derived from alkylaldonamides,[6, 7] amino acids,[8] and conjugated phospholipid nucleosides.[9] Cochleate lipid cylinders (formed by fusion of unilamellar vesicles into bilayer sheets which then fold spirally) have been reported to form with the addition of Ca^{2+} ions to phospholipids.[10] Ultrathin hollow capillaries made from polymerizable diacetylenic phosphatidycholines and stabilized by polymerization, which can be metalated, were also reported.[3, 11]

We have recently reported the formation of highly stable, heat-sterilizable vesicles from single-chain fluorinated amphiphiles without any additives.[12] Extended aggregates were then observed to form upon sonication of dispersions of these vesicles. The use of highly fluorinated compounds in medicine and biology has been reviewed lately.[13]

We report here that stable cylindrical aggregates including both flexible long fibers and rigid hollow tubules can be formed spontaneously at room temperature from unsonicated dilute dispersions of nonchiral fluorinated single-chain amphiphiles without requiring hydrogen bonding, polymerization, or any stabilizing additives. This shows that the strong hydrophobic forces developed by the fluorinated chains alone can suffice for the formation of microstructures more organized than vesicles. These supramolecular assemblies can have different morphologies and different rates of growth depending on the surfactant's polar head. We also found that the use of mixtures of two fluorinated surfactants can accelerate the growth of the flexible fibers.

Two perfluoroalkylated single-chain surfactants were used: a neutral one, dimorpholinophosphoramidate **1**,[14] and a zwitterionic one, phosphocholine **2**.[15] The hydrogenated analogues decyldimorpholinophosphoramidate **3**, decylphosphocholine **4**, and pentadecylphosphocholine **5** were prepared for comparative studies.



These fluorinated surfactants have no chiral center to stabilize their assemblies; there is no rigid segment to promote molecular alignment, nor is there any possibility of specific intermolecular binding. The behavior of **1** and **2** compared to that of their hydrogenated analogues **3** and **4**, and to that of the hydrogenated the surfactant **5**, whose hydrophobicity is equivalent to that of **2**,[16] clearly shows the impact of the fluorinated chain on the aggregation and organization of these amphiphiles.

Fibers were observed to form readily from unsonicated dispersions of both **1** and **2**, in other words with little or no energy input. The required 6% w/v dispersions are prepared simply by formation of thin films of the amphiphiles and hydration at 50 °C with gentle swirling by hand.

Rigid tubule-like aggregates (Fig. 1a, b) were observed by phase contrast optical microscopy within hours after preparation of dispersions of **1**. The aggregates then have a length of typically 10 to 50 μm and a diameter of 0.1 to 0.5 μm. A tubule structure consisting of wrapped bilayer sheets[2] is supported by the reversible transformation of these structures into large vesicles, which can be observed by optical microscopy at 40 °C.[11b]

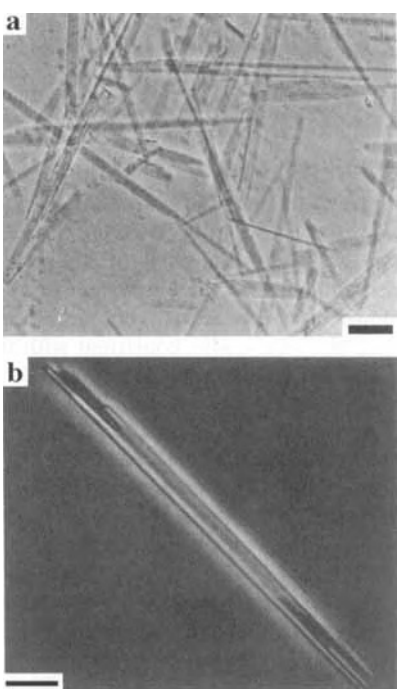


Fig. 1. Phase contrast optical micrographs of a) tubules obtained from **1**, b) an isolated tubule of 1. The length of the bars corresponds to 8 μm (a) and 4 μm (b).

[*] Prof. J. G. Riess, F. Giulieri, Dr. M.-P. Krafft
Unité de Chimie Moléculaire, associée au CNRS
Université de Nice-Sophia Antipolis, Faculté des Sciences
F-06108 Nice Cedex 2 (France)
Telefax: Int. code + 9352-9020

[**] This work was supported by the Centre National de la Recherche Scientifique and ATTA. We thank the Centre Commun de Microscopie Appliquée (CCMA, Prof. G. Nicaise, S. Pagnotta, J. P. Laugier) of the University of Nice-Sophia Antipolis.

Above 40 °C, optical polarization microscopy shows the presence of characteristic defects of a lamellar phase (maltese crosses) which are not present in the more organized tubular structures. These tubules are hollow, as can be seen in Figure 1 b, and break easily when manipulated. The fluorinated tubules are stable at room temperature with no significant modification of their size nor growth of three-dimensional crystals for at least six months at 20 °C.[17]

Fibers formed from **2** were found to be macroscopically completely different from those formed from **1**. Whereas **1** formed rigid linear hollow tubules, curved flexible filaments slowly appeared in unsonicated dispersions of **2**. After one month these fibers (ca. 10 μm in length and 0.1 μm in diameter) could be observed by transmission electron microscopy (Fig. 2a). After four months at a storage temperature not exceeding 20 °C, they had grown enough that they were visible by phase contrast and Nomarsky optical microscopy. These fibers are then very long (50–500 μm) and thin (1–5 μm in diameter) and can be branched. With time they start forming networks. When manipulated, these fibers are flexible and do not break. Their curved and branched structure, their flexibility, and the fact that they tend to form networks indicate that their microstructure is probably different from that of the tubules formed from **1**. They are not crystalline, as evidenced by polarization optical microscopy and the absence of electronic diffraction when observed by negative staining electron microscopy.

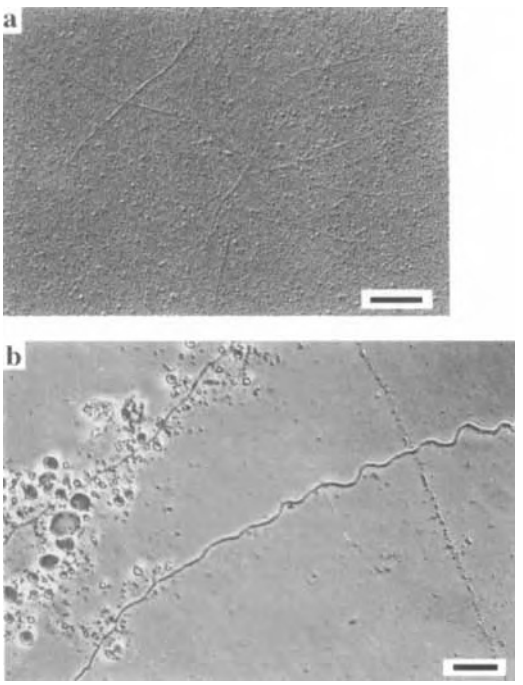


Fig. 2. a) Au/C shadowed transmission electron micrograph of the flexible fibers of **2**; b) phase contrast electron micrograph showing the reversible transformation at 50 °C of the flexible fibers of **2** into large vesicles. The length of the bars is 0.5 μm (a) and 8 μm (b).

The fluorinated fibers formed from **2** are reversibly transformed into larger vesicles at temperatures above 50 °C (Fig. 2b). These fibers are likely to be an intermediate state in the evolution of the supramolecular assemblies towards a tubular organization. A few similar flexible and branched fibers were transiently observed in dispersions of **1**; they are, however, transformed into tubules within hours, an observation that is in line with the above hypothesis. No crystallization was observed under these conditions, by contrast with the typical behavior of hydrocarbon amphiphiles.[5]

The rate of formation of the long flexible and branched fibers can be increased significantly by using equimolar mixtures of the fluorinated amphiphiles **1** and **2**. The resulting fibers have the same appearance as those prepared from dispersions of **2**, but they grow much more rapidly. Thus, fibers 50-μm long visible by optical microscopy were obtained after only two weeks. No tubules were observed in the optical micrographs.

In contrast, the hydrogenated analogues **3** and **4** (up to 20% w/v dispersions) did not form supramolecular assemblies of any sort, either spherical or elongated, according to electron or optical microscopy. Fibers were also not found in dispersions of **5**, the amphiphile whose CMC is comparable to that of **2**. This indicates the decisive strong effect of the fluorinated chain on the structuring of the amphiphiles into supramolecular assemblies.

The driving force of the formation of fibers and tubules from fluorinated amphiphiles reported here contrasts with that of bolaamphiphiles (the arborols), which also form fibers and in which the interactions between a multitude of amide groups bind the polar heads together so tightly that the hydrophobic effect is negligible.[18] The arborol-based fibers are formed by favored head-group interactions, while contact between the hydrophobic oligomethylene chains becomes almost impossible. The opposite situation is found with the amphiphiles investigated here, their interactions occur primarily between the fluorinated chains.

In addition to their strong hydrophobic character, the all-*trans* conformation of the fluorinated chains[19] may also play a role in favoring the formation of fibers, as is supposed to be the case for polymerizable phospholipids.[3]

Received: January 27, 1994 [Z 6650 IE]
German version: *Angew. Chem.* **1994**, *106*, 1583

[1] J. H. Fendler, *Membrane Mimetic Chemistry*, Wiley-Interscience, New York, **1982**; G. Gregoriadis, *Liposomes as Drug Carriers. Recent Trends and Progress*, Wiley, Chichester, **1988**; H. Ringsdorf, B. Schlarb, J. Venzmer, *Angew. Chem.* **1988**, *100*, 117–162; *Angew. Chem. Int. Ed. Engl.* **1988**, *27*, 113–158; G. Gregoriadis, *Liposome Technology, Vol I, II, III*, 2nd ed., CRC, Boca Raton, FL. **1993**.
[2] J. H. Fuhrhop, *Chem. Rev.* **1993**, *93*, 1565–1582; T. Kunitake, *Angew. Chem.* **1992**, *104*, 692–709; *Angew. Chem. Int. Ed. Engl.* **1992**, *31*, 709–726.
[3] J. M. Schnur, *Science* **1993**, *262*, 1669–1675.
[4] J. M. Lehn, *Angew. Chem.* **1990**, *102*, 1347–1362; *Angew. Chem. Int. Ed. Engl.* **1990**, *29*, 1304–1319.
[5] J. H. Fuhrhop, P. Schnieder, J. Rosenberg, E. Boekma, *J. Am. Chem. Soc.* **1987**, *109*, 3387–3390.
[6] J. H. Fuhrhop, S. Svenson, *Surfactant Science Series Vol. 23*, Dekker, New York, **1991**, pp. 273–299.
[7] J. H. Fuhrhop, P. Schnieder, E. Boekema, W. Helfrich, *J. Am. Chem. Soc.* **1988**, *110*, 2861–2867.
[8] N. Nakashima, S. Asakuma, T. Kunitake, *J. Am. Chem. Soc.* **1985**, *107*, 509–510; T. Imae, Y. Takahashi, H. Muramatsu, *ibid.* **1992**, *114*, 3414–3419.
[9] H. Yanagawa, Y. Ogawa, H. Furuta, K. Tsuno, *J. Am. Chem. Soc.* **1989**, *111*, 4567–4570.
[10] P. Papahadjopoulos, W. J. Vail, K. Jacobson, G. Poste, *Biochim. Biophys. Acta* **1975**, *394*, 483–491.
[11] a) P. Yager, P. E. Schoen, *Mol. Cryst. Liq. Cryst.* **1984**, *106*, 371–381; b) J. M. Schnur, R. Price, P. Schoen, P. Yager, J. M. Calvert, J. Georger, A. Singh, *Thin Solid Films* **1987**, *152*, 181–206.
[12] M. P. Krafft, F. Giulieri, J. G. Riess, *Angew. Chem.* **1993**, *105*, 783–785; *Angew. Chem. Int. Ed. Engl.* **1993**, *32*, 741–743.
[13] J. G. Riess, *Colloids Surf.* **1994**, *84*, 33–48.
[14] M. P. Krafft, P. Vierling, J. G. Riess, *Eur. J. Med. Chem.* **1991**, *26*, 545–550.
[15] M. P. Krafft, J. P. Rolland, P. Vierling, J. G. Riess, *New J. Chem.* **1990**, *14*, 869–875.
[16] The critical micellar concentrations (CMCs) were 9×10^{-5} M at 25 °C for **2** and 3×10^{-5} M at 50 °C for **5**. M. P. Krafft, F. Giulieri, *Colloids Surf.* **1994**, *84*, 121–127; F. Giulieri, M. P. Krafft, *Colloids Surf.* **1994**, *84*, 121–127.
[17] Additional evidence for the presence of an internal aqueous domain was provided by carboxyfluorescein encapsulation and release experiments.
[18] G. R. Newkome, G. R. Barker, S. Arai, M. J. Saunders, P. S. Russo, K. J. Theriot, C. N. Moorefield, L. E. Rogers, J. E. Miller, T. R. Lieux, M. M. R. Murray, B. Philipps, L. Pascal, *J. Am. Chem. Soc.* **1990**, *112*, 8458–8465.
[19] C. W. Bunn, E. R. Howells, *Nature* **1954**, *174*, 549–551.

 © VCH Verlagsgesellschaft mbH, D-69451 Weinheim, 1994 0570-0833/94/1414-1515 $ 10.00+.25/0

Metal Complexes of Marine Peptide Metabolites: A Novel Ag_4 Cluster**

Peter Wipf,* Srikanth Venkatraman, Chris P. Miller, and Steven J. Geib

The structural variety of oxazole- and thiazole-containing alkaloids that have recently been isolated from marine as well as terrestrial microorganisms is astounding.[1] The spectrum of pharmacological properties of these natural products includes exceedingly high cytotoxic and antiviral activities. In many cases, metal ion chelation has been postulated to be at least partly responsible for the biological activity.[2] However, there is a dearth of experimental evidence for metal binding that would support these hypotheses.[2]

We have recently completed the total synthesis of the highly modified cyclopeptide westiellamide (**1**).[3] Watters et al. isolated this marine cytotoxin from the ascidian *Lissoclinum bistratum*,[4] which has been the source of a wide variety of biologically active compounds.[5] We now report the structure of a novel $[Ag_4(\mathbf{1})_2]$ complex that is formed by addition of silver salts to a solution of the natural product.

The X-ray structure of **1** (Fig. 1) reveals that all N–H bonds and the lone pairs of the other nitrogen atoms are directed

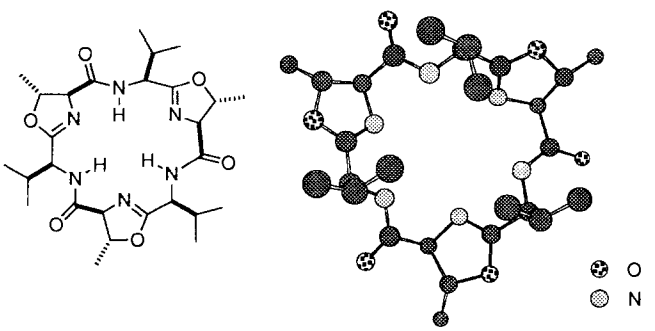


Fig. 1. Structural formula and the crystal structure of westiellamide (**1**).

towards the interior of the 18-membered macrocycle.[4a] This topology is quite common for a range of *Lissoclinum* peptides and appears suitable for metal ion chelation.[2, 6] However, there is only one report on the solid-state structure of a carbonate-bridged binuclear copper(II) complex of the related 24-membered ascidiacyclamide.[7] The conspicuous lack of data on metal chelation properties of cyclopeptides from ascidians can be explained, at least in part, by the problem of isolating sufficient quantities of material from natural sources. Our approach to the synthesis of dihydrooxazole-containing peptides by means of cyclooligomerization provides a convenient source of synthetic **1** and related macrocyclic ring systems.[3, 8] Whereas only weak interactions between **1** and gold(III), cadmium(II), cerium(III), copper(I), copper(II), iron(II), iron(III), mercury(II), potassium(I), lithium(I), magnesium(II), sodium(I), nickel(II), and zinc(II) salts were detected in screening studies, we observed a remarkable affinity of **1** toward silver(I) ions. NMR titration experiments in [D_4]methanol indicated the formation of a C_3-symmetric silver–**1** complex with a 2:1 stoichiometry and an association constant of $>10^5$. An X-ray analysis of a crystal obtained from an aqueous solution of **1** and $AgClO_4$, $[Ag_4(\mathbf{1})_2](ClO_4)_4$ (**2**), revealed the presence of a unique Ag_4 cluster sandwiched between two neutral macrocyclic ligands (Fig. 2a).[9]

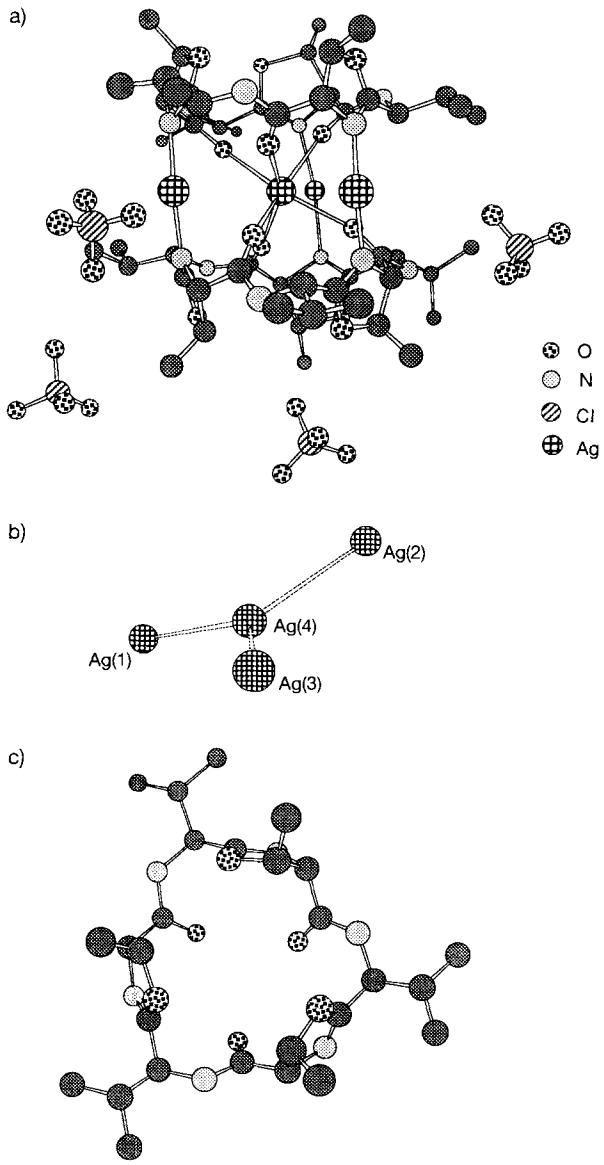


Fig. 2. Crystal structure of **2**. a) Complete salt (without hydrogen atoms). b) Ag_4 cluster. Selected distances [Å] and angles [°]: Ag(1)-Ag(4) 3.44, Ag(2)-Ag(4) 4.00, Ag(3)-Ag(4) 3.25, Ag(1)-Ag(2) 6.47, Ag(1)-Ag(3) 5.78; Ag(1)-Ag(4)-Ag(3) 118.9, Ag(1)-Ag(4)-Ag(2) 120.7, Ag(1)-Ag(2)-Ag(3)-Ag(4) 0.0. c) Cyclopeptide ligand.

Several features of this complex are noteworthy. The silver atoms of the tetranuclear cluster assume a novel distorted trigonal-planar arrangement (Fig. 2b). In contrast, numerous Ag_4 clusters[10] with tetrahedral[10] or distorted square-planar geometries have been found in silver thiolate and halide complexes.[11] The Ag(4)–Ag distances in **2** range from 3.25 to 4.00 Å. This is long compared to the distance in elemental silver (2.89 Å) and, with the exception of the Ag(4)–Ag(2) distance, similar to those in other Ag_3 and Ag_4 clusters, for example in cobalt–and

[*] Prof. Dr. P. Wipf, S. Venkatraman, C. P. Miller, Dr. S. J. Geib
Department of Chemistry
University of Pittsburgh
Pittsburgh, PA 15260 (USA)
Telefax: Int. code + (412)624-8606

[**] This work was supported by the National Institutes of Health (R01 AI34914). We thank Profs. N. John Cooper and Andrew D. Hamilton for stimulating discussions.

rhodium–silver complexes (2.83, 3.00 Å),[12, 13] silver–phosphane complexes (3.22, 3.36 Å),[14, 15] organotelluride–silver ions (3.13 Å),[10d] and piperazine–silver iodide (3.29 Å).[16] Since any bonding interactions between silver atoms in these metallic clusters are considered weak at best,[17] we conclude that the $[Ag_4]^{4+}$ unit in **2** is probably exclusively stabilized by coordination to the neutral macrocyclic ligands. The four perchlorate anions are noncoordinating; the shortest silver–oxygen contact is 2.95 Å.

Interestingly, the central silver ion, Ag(4), is coordinated to six carbonyl oxygen atoms that form a slightly distorted trigonal prism with an average twist angle of 22°.[18] The Ag(4)–O distances range from 2.41 to 2.55 Å, with an average length of 2.47 Å. In comparison, the Ag–O distance in a peptide–silver complex was found to be 2.57 Å.[19] In **2**, Ag(1), Ag(2), and Ag(3) are linearly coordinated to the nitrogen atoms of two dihydrooxazoles with bond lengths of 2.10 to 2.15 Å and N-Ag-N angles of 163.6 to 168.2°. The Ag–N distances are indicative of strong binding and are among the closest Ag–N contacts yet observed.[20] This unique inclusion is able to overcome the substantial electrostatic repulsion of the four Ag^+ ions.

The structure of the 18-membered macrocycle undergoes drastic changes upon binding silver ions. Both in solution and in the solid state,[21] uncomplexed **1** assumes the rather flat conformation shown in Figure 1 with planar dihydrooxazoles and axially oriented side chains and with all nitrogen atoms pointing inwards. As a consequence of metal chelation, the 18-membered macrocycles basically turn inside out and the side chains assume equatorial positions (Fig. 2c). The carbonyl groups point inwards and the dihydrooxazole rings are close to orthogonal to the macrocyclic ring. N_{oxaz}-C-C-N_{amide} and ϕ_{Val} dihedral angles, for example, change from a mean of 20.4° and −144.0°, respectively, in **1**, to a mean of 133.8° and −64.0°, respectively, in **2**.

The association constant of **2** in [D_4]methanol was too high to be determined by NMR spectroscopy. In [D_4]methanol/D_2O (9:1), an average K_a of $2.8 \times 10^{13}\ M^{-5}$ was determined by titration of **1** with silver perchlorate or silver triflate and integration of the ^1H NMR signals for **2**. Interestingly, the complexation seems to be highly cooperative; only uncomplexed ligand and the 4:2 complex are evident in the spectrum.[22] The rate of decomplexation appears to be slow in the (300 MHz) NMR timescale; no line broadening due to dynamic effects is observed.

Determination of the temperature dependence of the association constant in [D_4]methanol/D_2O (8:2) between 304 and 325 K allowed the calculation of the free enthalpy (ΔH^0) and entropy (ΔS^0) of formation of the complex as $-123\ kJ\,mol^{-1}$ and $-191\ J\,K^{-1}\,mol^{-1}$, respectively. The large negative entropy value leads to a considerable decrease of the association constant when the temperature of the solution is increased. All solution NMR data are in agreement with the solid-state structure of **2**.

We propose the following mechanistic scheme to explain both the observed high cooperativity and Ag^I selectivity. An initial weak association of a silver ion to the carbonyl groups of two molecules of **1** induces a ring inversion of the macrocycles and establishes an octahedral coordination sphere around Ag^+. The major energy barrier in the complexation is the formation of this labile complex, and subsequent rapid stabilization is achieved by the energetically very favorable linear complexation of silver ions to the nitrogen atoms of the dihydrooxazole rings. In order for a metal ion to be complexed in this way, it has to be stable in both octahedral and linear coordination geometries and its charge may not exceed +1, since otherwise the electrostatic repulsion within the complex becomes too large. Only silver(I) fulfills all these requirements.

Our studies have established first direct evidence for the interaction of marine *Lissoclinum* peptides with metal ions. The molecular structure of the westiellamide–silver complex **2** is unique; no analogous complexes are known in silver cluster or natural products chemistry. We will now investigate the biological role of metal chelation in the cytotoxic activity of **1** and its analogues.

Received: February 25, 1994 [Z 6705 IE]
German version: *Angew. Chem.* **1994**, *106*, 1554

[1] For a recent review, see: J. R. Lewis, *Nat. Prod. Rep.* **1993**, *10*, 29.
[2] a) G. Pattenden, *J. Heterocycl. Chem.* **1992**, *29*, 607; b) D. M. James, E. Wintner, D. J. Faulkner, J. S. Siegel, *Heterocycles* **1993**, *35*, 675. c) The facts and fantasies of metal ion chelation of marine metabolites have recently been nicely reviewed: J. P. Michael, G. Pattenden, *Angew. Chem.* **1993**, *105*, 1; *Angew. Chem. Int. Ed. Engl.* **1993**, *32*, 1.
[3] P. Wipf, C. P. Miller, *J. Am. Chem. Soc.* **1992**, *114*, 10975.
[4] a) T. W. Hambley, C. J. Hawkins, M. F. Lavin, A. L. van den Brenk, D. J. Watters, *Tetrahedron* **1992**, *48*, 341. b) Interestingly, this compound was also isolated from a terrestrial cyanophyte: M. R. Prinsep, R. E. Moore, I. A. Levine, G. M. L. Patterson, *J. Nat. Prod.* **1992**, *55*, 140.
[5] B. S. Davidson, *Chem. Rev.* **1993**, *93*, 1771.
[6] B. M. Degnan, C. J. Hawkins, M. F. Lavin, E. J. McCaffrey, D. L. Parry, A. L. van den Brenk, D. J. Watters, *J. Med. Chem.* **1989**, *32*, 1349.
[7] L. R. Gahan, University of Queensland, personal communication. Solution studies of this complex reveal the presence of complex equilibria. We thank Dr. Gahan for a preprint of his work.
[8] P. Wipf, C. P. Miller, S. Venkatraman, S. J. Geib, unpublished.
[9] X-ray crystallographic data for **2**: orthorhombic, $P2_12_12_1$, $a = 13.739(3)$, $b = 20.864(5)$, $c = 28.778(6)$ Å, $V = 8249(3)$ Å^3, $Z = 4$, $\varrho_{calcd} = 1.581\ g\,cm^{-3}$, 23 °C. A Siemens P3 diffractometer was used to collect 11426 reflections ($4° \le 2\theta \le 45°$), 7691 of which with $F_o > 6\sigma(F_o)$ were used in the solution and refinement. A semiempirical absorption correction (XEMP) was applied to all data ($\mu(Mo_{K\alpha}) = 1.139\ mm^{-1}$). Structure was solved by direct methods which located the four Ag ions; remaining non-hydrogen atoms were located from subsequent difference Fourier syntheses and refined anisotropically. Hydrogen atom positions were calculated (d(C H) = 0.96 Å). Structure refined to $R_F = 0.0642$ and $R_{wF} = 0.0790$; GOF = 1.71; greatest residual electron density $1.13\ e\,Å^{-3}$ (near Ag(2)). Further details of the crystal structure investigation are available on request from the Director of the Cambridge Crystallographic Data Centre, 12 Union Road, GB-Cambridge CB2 1EZ (UK), on quoting the full journal citation. Complex **2** is slightly photosensitive.
[10] a) G. B. Ansell, L. A. Burkardt, W. G. Finnegan, *Chem. Commun.* **1969**, 459; b) G. Henkel, P. Betz, B. Krebs, *Angew. Chem.* **1987**, *99*, 131; *Angew. Chem. Int. Ed. Engl.* **1987**, *26*, 145; c) M. G. Kanatzidis, S.-P. Huang, *ibid.* **1989**, *101*, 1556 and **1989**, *28*, 1513; d) J. Zhao, D. Adcock, W. T. Pennington, J. W. Kolis, *Inorg. Chem.* **1990**, *29*, 4358, and references therein.
[11] a) J. Estienne, *Acta Crystallogr. Sect. C* **1986**, *42*, 1512; b) K. Tang, M. Aslam, E. Block, T. Nicholson, J. Zubieta, *Inorg. Chem.* **1987**, *26*, 1488; c) J. A. Schuerman, F. R. Fronczek, J. Selbin, *Inorg. Chim. Acta* **1989**, *160*, 43; d) A. N. Nesmeyanov, N. N. Sedova, Y. T. Struchkov, V. G. Andrianov, E. N. Stakheeva, V. A. Sazonova, *J. Organomet. Chem.* **1978**, *153*, 115.
[12] P. A. Leach, S. J. Geib, N. J. Cooper, *Organometallics* **1992**, *11*, 4367.
[13] F. Bachechi, J. Ott, L. M. Venanzi, *J. Am. Chem. Soc.* **1985**, *107*, 1760.
[14] C.-M. Che, H.-K. Yip, V. W.-W. Yam, P.-Y. Cheung, T.-F. Lai, S.-J. Shieh, S.-M. Peng, *J. Chem. Soc. Dalton Trans.* **1992**, 427.
[15] A. A. M. Aly, D. Neugebauer, O. Orama, U. Schubert, H. Schmidbaur, *Angew. Chem.* **1978**, *90*, 125; *Angew. Chem. Int. Ed. Engl.* **1978**, *17*, 125.
[16] G. B. Ansell, W. G. Finnegan, *Chem. Commun.* **1969**, 1300.
[17] a) F. A. Cotton, F. Xuejun, M. Matusz, R. Poli, *J. Am. Chem. Soc.* **1988**, *110*, 7077, b) ref. [11c]; c) N. Rösch, A. Görling, D. E. Ellis, H. Schmidbaur, *Angew. Chem.* **1989**, *101*, 1410; *Angew. Chem. Int. Ed. Engl.* **1989**, *28*, 1357.
[18] F. A. Cotton, G. Wilkinson, *Advanced Inorganic Chemistry*, Wiley, New York, **1980**.
[19] J. F. Modder, G. van Koten, K. Vrieze, A. L. Spek, *Angew. Chem.* **1989**, *101*, 1723; *Angew. Chem. Int. Ed. Engl.* **1989**, *28*, 1698.
[20] a) G. C. van Stein, G. van Koten, K. Vrieze, A. L. Spek, E. A. Klop, C. Brevard, *Inorg. Chem.* **1985**, *24*, 1367; b) H. Adams, N. A. Bailey, W. D. Carlisle, D. E. Fenton, G. Rossi, *J. Chem. Soc. Dalton Trans.* **1990**, 1271; c) M. Ghosh, A. K. Basak, S. K. Mazumdar, *Acta Crystallogr. Sect. C* **1990**, *46*, 1223; d) S.-B. Silong, L. M. Engelhardt, A. H. White, *Aust. J. Chem.* **1989**, *42*, 1381; e) J. de Mendoza, E. Mesa, J.-C. Rodriguez-Ubis, P. Vázquez, F. Vögtle, P.-M. Windscheif, K. Rissanen, J.-M. Lehn, D. Lilienbaum, R. Ziessel, *Angew. Chem.* **1991**, *103*, 1365; *Angew. Chem. Int. Ed. Engl.* **1991**, *30*, 1331; f) T. G. Rich-

mond, E. P. Kelson, A. T. Patton, *J. Chem. Soc. Chem. Commun.* **1988**, 96; g) B. F. Hoskins, R. Robson, G. A. Williams, J. C. Wilson, *Inorg. Chem.* **1991**, *30*, 4160; h) K. Hirotsu, I. Miyahara, T. Higuchi, M. Toda, H. Tsukube, K. Matsumoto, *Chem. Lett.* **1992**, 699.

[21] The ^{1}H NMR coupling constants ($^3J_{HH}$) of a solution of **1** in $CDCl_3$ are in agreement with the conformation found in the solid state. Additionally, the C_3 symmetry is conserved, and no conformers are frozen out at $-25\,^\circ C$.

[22] **2**: ^{1}H NMR (300 MHz, CD_3OD/D_2O, 9/1): $\delta = 4.72$ (br. s, 2H), 4.28 (d, 1H, $J = 9.0$ Hz), 2.20–2.09 (m, 1H), 1.52 (d, 3H, $J = 5.0$ Hz), 1.09 (d, 3H, $J = 6.5$ Hz), 1.02 (d, 3H, $J = 6.7$ Hz).

Synthesis and Structure of the First Titanium(IV) α-Amino Acid Complexes**

Thomas M. Klapötke, Hartmut Köpf, Inis C. Tornieporth-Oetting,* and Peter S. White*

Metallocene dichlorides $[Cp_2MCl_2]$ (M = Ti, V, Nb, Mo) and *cis*-diamminedichloroplatinum(II) complexes have been of great interest owing to their antitumor properties.[1] Although numerous experiments indicate that metallocene dichlorides inhibit DNA synthesis, it has not been possible to synthesize titanium model complexes containing biologically important ligands under physiological conditions.[2] Only in nonaqueous solvents like THF or toluene has the synthesis of a few titanium(IV) model complexes and some titanium(III) complexes starting from $[Cp_2TiCl_2]$ succeeded, but the latter complexes are less important, because the reduction of titanium(IV) to titanium(III) in biological systems is not very likely.[1–5] Nevertheless, quite recently DNA–metal binding by Cp_2Ti complexes has been established by inductively coupled plasma (ICP) spectroscopy analysis.[6] In contrast, numerous stable Pt^{II} model complexes have been synthesized in aqueous solution.[7] Some authors claimed that the active antitumor species is not the titanocene complex but rather the cyclopentadiene released during the decomposition of Cp_2Ti compounds.[8] Later it was shown by in vivo experiments that neither cyclopentadiene (C_5H_6) nor its dimer ($C_{11}H_{12}$) are the active antiproliferative moieties in antitumor non-platinum complexes.[9] Because the pronounced antitumor properties of $[Cp_2TiCl_2]$ have been confirmed (e.g. against Ehrlich ascites tumor, sarcoma 180, melanoma B16, colon carcinoma 38, as well as several human tumors grafted onto athymic mice),[1, 9] the well-planned synthesis of a titanocene model complex containing a naturally occurring ligand is of great importance. The coordination behavior of $[Cp_2TiCl_2]$ towards α-amino acids has not been thoroughly investigated, and until now no titanium α-amino acid complex has been synthesized and structurally characterized.[10] In contrast, the coordination chemistry of Pt^{II} and Pd^{II} compounds towards amino acids is well understood and has been investigated by multinuclear NMR spectroscopy.[11, 12] It has been established that the coordination of amino acids to Pt^{II} and Pd^{II} compounds through a nitrogen or an oxygen atom or as a chelating ligand through nitrogen and oxygen atoms simultaneously depends on the pH of the aqueous reaction medium.[11, 12] The structures of many Pd^{II} amino acid chelate complexes have been determined by X-ray diffraction methods.[13]

Here we report for the first time on titanocene α-amino acid complexes $[Cp_2Ti(aa)_2]^{2+}[Cl]_2^-$ (aa = α-amino acid) which were prepared from biologically active $[Cp_2TiCl_2]$. Whereas $[Cp_2TiCl_2]$ hydrolyzes slowly in aqueous systems and does not react with amino acids like glycine to give the desired titanocene amino acid complex,[14, 15] the reaction of $[Cp_2TiCl_2]$ with stoichiometric amounts of an amino acid in the waterlike solvent MeOH (not necessarily anhydrous) afforded the shiny orange complexes **1**–**3** in good yields [Eq. (a)].

$$[Cp_2TiCl_2] + 2\,aa \xrightarrow{MeOH} [Cp_2Ti(aa)_2]^{2+}[Cl]_2^- \qquad (a)$$

1: aa = $^-O_2CCH_2NH_3^+$ = glycine
2: aa = $^-O_2CCH(CH_3)NH_3^+$ = L-alanine
3: aa = $^-O_2CC(CH_3)_2NH_3^+$ = 2-methylalanine

Complexes **1**–**3** are stable solids at room temperature and not sensitive towards air and moisture. The ^{1}H NMR spectra were recorded in D_2O. In **1** the protons bound to the α-C atom of the coordinated amino acid are shifted to significantly lower field in comparison with those of the free amino acid (**1**: $\delta(CH_2) = 3.68$, glycine: $\delta(CH_2) = 3.38$). Whereas the proton at the α-C atom of **2** also shows a significant shift to lower field, the methyl protons in **2** and **3** are only slightly shifted to lower field (**2**: $\delta(CH) = 3.87$, $\delta(CH_3) = 1.40$, L-alanine: $\delta(CH) = 3.63$, $\delta(CH_3) = 1.35$, **3**: $\delta(CH_3) = 1.52$, 2-methylalanine: $\delta(CH_3) = 1.47$). The signals of the NH_3^+ groups are observed neither in the ^{1}H NMR spectra of **1**–**3** nor in the spectra of the free amino acids but can be observed as expected in the ^{14}N NMR spectra. A noteworthy feature in the IR spectra of **1**–**3** is a very strong absorption due to the asymmetric ν(COO) stretching vibration and a strong band that can be assigned to the symmetric ν(COO) stretching vibration. In line with the observations of Nakamoto et al. concerning the vibrational data of metal amino acid complexes, the ν_{as}(COO) bands in the spectra of **1**–**3** are shifted to higher wavenumbers and ν_s(COO) modes are shifted to lower wavenumbers compared with the corresponding bands of the free amino acids.[16] A detailed discussion of the vibrational data (IR, Raman) and further experimental data (MS, UV) will be published shortly.

Slow evaporation of the solvent from an aqueous solution of **3** yielded orange-red crystals suitable for X-ray structure determination.[17] The structure of the cation in **3** is presented in Figure 1. The cation in **3** has approximately C_2 symmetry and a titanium center with distorted tetrahedral coordination sphere. The Cp rings are eclipsed. The Ti–O distance of 1.961 Å agrees with the expected value for a Ti–O single bond ($\sum r_{cov}$(TiO) = 1.98 Å)[18] and compares well with that of other O-coordinated titanocene complexes.[19] Moreover, the C2–O3 bond length (1.21 Å) compares nicely with the length of the double bond in R_2CO (R = H, CH_3),[20] but the O1–C2 bond length of 1.286 Å is significantly shorter than the length of C–O single bonds in alcohols (d(C–O) = 1.42 Å).[21] Along with a recently reported gold(I) complex[22] containing an O-coordinated hippurato amino acid ligand, compound **3** is one of the few ex-

[*] Dr. I. C. Tornieporth-Oetting, Priv.-Doz. Dr. T. M. Klapötke, Prof. Dr. H. Köpf
Institut für Anorganische und Analytische Chemie
der Technischen Universität Berlin, Sekr. C2
Strasse des 17. Juni 135, D-10623 Berlin (FRG)
Telefax: Int. code +(30) 314-22168
Dr. P. S. White
Department of Chemistry, University of North Carolina
Chapel Hill, NC 27599 (USA)
Telefax: Int. code +(919) 962-2388

[**] This work was supported by the Deutsche Forschungsgemeinschaft, the Fonds der Chemischen Industrie, and by NATO (CRG 920034). We thank Prof. Dr. J. Passmore for providing ^{14}N/^{15}N NMR facilities and Dipl.-Chem. M. Kempf for recording the DCI mass spectrum. We also thank both referees for valuable suggestions.

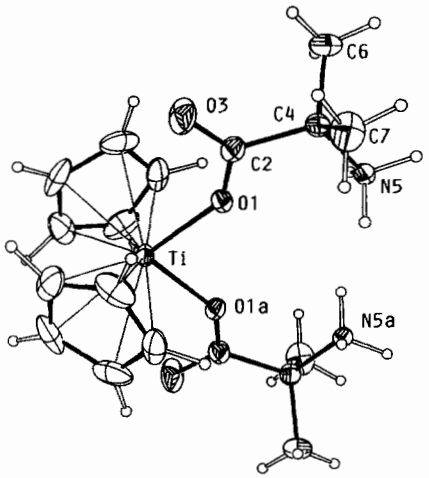


Fig. 1. Structure of the cation in **3** [17]. Important bond lengths [Å] and angles [°]: Ti-O1 1.9610(19), O1-C2 1.286(4), C2-O3 1.210(4); O1-Ti-O1a 90.75(8), Ti-O1-C2 141.21(19), O1-C2-O3 125.1(3). Hydrogen atom positions calculated [17].

amples of a complex in which the amino acid coordinates solely through the carboxylato group.[23]

Complexes **1**–**3** are the first titanocene α-amino acid complexes to be prepared and characterized. Polymeric titanocene and Pt^{II} complexes with amino acids have been reported;[24] however, their structures have not yet been determined by diffraction methods. Because of the very good solubility of these complexes in water and the likely low toxicity, we will investigate their antitumor properties.

Experimental Procedure

$[Cp_2TiCl_2]$ (8 mmol, 2.0 g) was stirred with the relevant amino acid (16 mmol; glycine: 1.20 g, L-alanine: 1.43 g, 2-methylalanine: 1.65 g) in 10 mL MeOH at room temperature. The precipitated orange red solid **1**, **2**, and **3**, respectively, was filtered off and dried in vacuo (**1**: 2.65 g, 83%, $T_{decomp} > 160$ °C; **2**: 1.43 g, 38%, $T_{decomp.} > 100$ °C; **3**: 3.30 g, 93%, $T_{decomp} > 240$ °C).

1: ^{1}H NMR (60 MHz, D_2O, 25 °C, D_2O int.): $\delta = 6.57$ (s, 10H, Cp), 3.68 (s, 4H, CH_2); ^{14}N NMR (28.90 MHz, D_2O, 25 °C, $MeNO_2$): $\delta = -352.1$ (s, NH_3^+); IR (KBr pellet): $\tilde{\nu}$[cm^{-1}] = 1655 vs ($\nu_{as}(COO^-)$), 1368/1362 s ($\nu_s(COO^-)$), 523 ms (ν(TiO)); Raman (60 mW, 25 °C): $\tilde{\nu}$[cm^{-1}] = 1443 (1) (ω(CC), Cp, δ(CH_2)), 1131 (6) (δ(CH), Cp, γ(NH_3^+)), 425 (3) (ν(TiCp)), 360 (6) (ν(TiCp)), 307 (2), 265 (10), 154 (1).

2: ^{1}H NMR (60 MHz, D_2O, 25 °C, D_2O int.): $\delta = 6.62$ (s, 10H, Cp), 3.87 (q, ^3J(H,H) = 7.6 Hz, 2H, CH), 1.40 (d, ^3J(H,H) = 7.6 Hz, 6H, CH_3); ^{14}N NMR (28.90 MHz, D_2O, 25 °C, $MeNO_2$): $\delta = -339.8$ (s, NH_3^+); IR (KBr pellet): $\tilde{\nu}$[cm^{-1}] = 1660 vs ($\nu_{as}(COO^-)$), 1375 ($\nu_s(COO^-)$); Raman (60 mW, 25 °C): $\tilde{\nu}$[cm^{-1}] = 1133 (5) (δ(CH), Cp, ν(CCN)), 828 (1) (γ(CH), Cp), 425 (3) (ν(TiCp)), 366 (5) (ν(TiCp)), 261 (10), 143 (3).

3: ^{1}H NMR (60 MHz, D_2O, 25 °C, D_2O int.): $\delta = 6.62$ (s, 10H, Cp), 1.52 (s, 12H, CH_3); ^{14}N NMR (28.90 MHz, D_2O, 25 °C, $MeNO_2$): $\delta = -327.9$ (s, NH_3^+); ^{15}N NMR (40.54 MHz, D_2O, 25 °C, $MeNO_2$): $\delta = -329.5$ (q, ^1J(N,H) = 18 Hz, NH_3^+); IR (KBr pellet): $\tilde{\nu}$[cm^{-1}] = 1655 vs ($\nu_{as}(COO^-)$), 1383 ($\nu_s(COO^-)$); Raman (60 mW, 25 °C): $\tilde{\nu}$[cm^{-1}] = 1132 (2) (δ(CH), Cp), 425 (2) (ν(TiCp)), 385 (2), 363 (5) (ν(TiCp)), 266 (10); DCI-MS *m/z*: 384, $[Cp_2Ti(2\text{-methylalanine})_2]^+$. – All compounds gave correct elemental analyses (C,H,N,Cl: **1**, **3**; C,H,N: **2**).

Received: March 7, 1994 [Z 6734 IE]
German version: *Angew. Chem.* **1994**, *106*, 1587

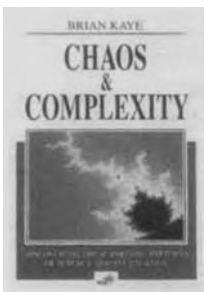
[1] P. Köpf-Maier, H. Köpf in *Structure and Bonding*, Springer, Berlin, **1988**, and references therein.
[2] D. Cozak, A. Mardhy, A. Morneau, *Can. J. Chem.* **1986**, *64*, 751.
[3] C. J. Cardin, A. Roy, *Inorg. Chim. Acta* **1985**, *107*, L33.
[4] A. Beauchamp, D. Cozak, A. Mardhy, *Inorg. Chim. Acta* **1984**, *92*, 191.
[5] *Metal Ions in Biological Systems, Vol. 30* (Eds.: H. Sigel, A. Sigel), Dekker, New York, **1994**.
[6] M. L. McLaughlin, J. M. Cronan, Jr., T. R. Schaller, R. D. Snelling, *J. Am. Chem. Soc.* **1990**, *112*, 8949.
[7] a) S. J. Lippard, *Science* **1982**, *218*, 1075; b) Review: *Pure Appl. Chem.* **1987**, *59*, 731, and references therein.; c) M. E. Howe-Grant, S. J. Lippard in *Metal Ions in Biological Systems, Vol. 11* (Ed.: H. Sigel), Dekker, New York, **1980**, p. 63.
[8] K. Döppert, *J. Organomet. Chem.* **1987**, *319*, 351.
[9] P. Köpf-Maier, H. Köpf, *J. Organomet. Chem.* **1988**, *342*, 167.
[10] U. Thewalt in *Gmelin Handbook of Inorganic Chemistry, Ti, Organotitanium Compounds, Part 3* (Ed.: A. Slowisch), 8th ed., Springer, Berlin, **1984**.
[11] T. G. Appleton, J. R. Hall, S. F. Ralph, *Inorg. Chem.* **1985**, *24*, 673.
[12] T. G. Appleton, A. J. Bailey, D. R. Bedgood, Jr., J. R. Hall, *Inorg. Chem.* **1994**, *33*, 217.
[13] L. D. Pettit, M. Bezer, *Coord. Chem. Rev.* **1985**, *61*, 97, and references therein.
[14] a) H. Köpf, S. Grabowski, R. Voigtländer, *J. Organomet. Chem.* **1981**, *216*, 185; b) J. H. Toney, T. J. Marks, *J. Am. Chem. Soc.* **1985**, *107*, 947.
[15] H. Köpf, unpublished.
[16] K. Nakamoto, *Infrared and Raman Spectra of Inorganic and Coordination Compounds*, Wiley, New York, **1986**, Chapter 3, and references therein.
[17] a) Crystal structure data of **3**: $M_r = 455.23$, monoclinic, $C2/c$, $a = 9.0630(11)$, $b = 28.173(3)$, $c = 8.8967(9)$ Å, $\beta = 96.379(9)°$, $V = 2257.5(4)$ Å^3, $Z = 4$, ρ_{calcd} 1.399 g cm^{-3}, $F(000) = 954.38$, $Mo_{K\alpha}$ radiation, $\lambda = 0.70930$ Å, $\mu = 0.64$ mm^{-1}, 3253 reflections, 2006 independent reflections and 1487 with $I_{net} > 2.5\sigma$. Measurement conditions: $T = 25(3)$ °C, $\theta/2\theta$ mode, $2\theta_{max.} = 49.9°$, Rigaku AFC 6S diffractometer. The structure was solved and refined with 28 atoms, 123 parameters, and 1487 out of the 2006 reflections with NRCVAX [17b–f]. All non-hydrogen atoms were refined anisotropically. $R_F = 0.042$, $R_w = 0.052$, GOF = 1.67, $F_o > 2.5\sigma$ (F), $R_F = \sum(F_o - F_c)/\sum F_o$, $R_w = [\sum(w(F_o - F_c)^2)/\sum w(F_o^2)]^{0.5}$, GOF = $[\sum(w(F_o - F_c)^2)/$(number of reflections − number of parameters)$]^{0.5}$. Further details of the crystal structure investigation may be obtained from the Fachinformationszentrum Karlsruhe, D-76344 Eggenstein-Leopoldshafen (FRG), on quoting the deposition number CSD-58138; b) E. J. Gabe, Y. Le Page, J.-P. Charland, F. L. Lee, P. S. White, *J. Appl. Cryst.* **1989**, *22*, 384; c) *International Tables for X-ray Crystallography, Vol. IV*, Kynoch, Birmingham, **1974**; d) C. K. Johnson, *Ortep – A Fortran Thermal Ellipsoid Plot Program*, Technical Report ORNL-5138, Oak Ridge, **1976**; e) Y. Le Page, *J. Appl. Crystallogr.* **1988**, *21*, 983; f) Y. Le Page, E. J. Gabe, *ibid.* **1979**, *12*, 464.
[18] J. E. Huheey, *Anorganische Chemie*, de Gruyter, Berlin, **1988**.
[19] A. Schäfer, E. Karl, L. Zsolnai, G. Huttner, H.-H. Brintzinger, *J. Organomet. Chem.* **1987**, *328*, 87.
[20] R. J. Gillespie, I. Hargittai, *The VSEPR Model of Molecular Geometry*, Allyn and Bacon, Boston, **1991**.
[21] D. A. Johnson, *Some Thermodynamic Aspects of Inorganic Chemistry*, Cambridge University Press, Cambridge, **1982**.
[22] P. G. Jones, R. Schelbach, *J. Chem. Soc. Chem. Commun.* **1988**, 1338.
[23] *Metal Ions in Biological Systems, Vol. 8* (Ed.: H. Sigel), Dekker, New York, **1979**.
[24] a) C. E. Carraher, Jr., L. G. Tisinger, *Polym. Mater. Sci. Eng.* **1991**, *65*, 29; b) C. E. Carraher, Jr., L. G. Tisinger, I. Lopez, M. Williams, *Biomimetic Polym.* **1990**, 71; c) C. E. Carraher, Jr., L. G. Tisinger, W. H. Tisinger, *Polym. Sci. Technol. (Plenum)* **1986**, *33*, 225.

 © *VCH Verlagsgesellschaft mbH, D-69451 Weinheim, 1994* *0570-0833/94/1414-1519 $ 10.00+.25/0*

Probability, Fractals and the Physical World

Chaos and Complexity. By *B. Kaye*. VCH Verlagsgesellschaft, Weinheim/VCH Publishers, New York, 1993. XXII, 593 pp., paperback DM 78.00.—ISBN 3-527-29007-9/1-56081-798-4

This book is intended as a popular introduction to some modern interdisciplinary ideas of chaos, fractals, and scaling. It is addressed mainly to a readership of high-school students and university beginners. The main content of the book is well described by its subtitle: "Discovering the Surprising Patterns of Science and Technology". The main goal of the book is stated in the last paragraph of the author's introduction: its readers should "gain a new appreciation of the physical significance of the theorems of probability theory and also grasp the significance of fractal structures manifest in the physical world around us". This is the main idea of the book, and therefore its title "Chaos & Complexity" is misleading.



Starting from some preliminary explanations of the concepts of dynamical chaos, the author switches to a very necessary introductory discussion of classical probability problems, including Buffon's needle and the Poisson distribution (although there are mistakes in both equations representing the Poisson distribution, on pp. 209 and 210) and others of a less classical nature, such as hyperbolic (scaling) probability distributions. This introduction is very interesting and motivating, and also provides young readers with ideas for simple experiments they can do by themselves in order to become familiar with the concepts and methods of probability theory and applied statistics, and to appreciate their relevance in science and everyday life. According to the classification adopted on page 7, all the cases described here are random rather then chaotic.

The greater part of the book is devoted to consideration of different fractal sets and objects. The concepts of fractal geometry leading to the notion of fractal dimension(s) form an important part of modern material and geological sciences and engineering, and also find applications in other fields, such as biology and social science. This notion gives us an important and experimentally measurable characteristic of rough lines and surfaces, such as coastlines and landscapes, catalyst surfaces, dusts, etc. The author is an expert in this field of characterization of fractal objects, and therefore the chapters devoted to the properties and characterization of real systems, such as aerosols, powders, aggregates, and mixtures are not only brilliantly written but also very interesting, even for a specialist.

Here I would like to stress once more that these topics are mostly classified by the scientific community as belonging to the fields of random (or stochastic) processes, fractals, scaling, growth or roughening phenomena, etc., which normally implies an "external" source of randomness, such as thermal Brownian motion, quenched disorder, and so on. This can be easily seen by comparing the titles of numerous conferences on these topics. Therefore, the greater part of the book is devoted to something other than the subject of its title. Only a small part of the book treats what scientists normally refer to as dynamical chaos. The only problems that can be considered as such are the logistic map (May's equation) discussed in Chapter 12 and parts of Chapters 2 and 14 on iteration of maps and the form of basins of attractors. The main questions of stability, sensitivity to initial conditions, and predictability are only briefly mentioned in the introductory Chapter 1 (see the discussion of the butterfly effect).

Although the author has a good habit of using a dictionary to explain the etymology and meanings of terms he uses and provides us with much interesting information in many other cases, the word "complex" is an unfortunate exception, being used more or less as a synonym for the word "complicated". The notion of complexity is not even analyzed (for a deeper discussion see, e.g., *Applied Chaos Theory. A Paradigm for Complexity*, by A. B. Çambel, Academic Press, 1993), and consequently many interesting points, such as hierarchical and algorithmic definitions of complexity, or problems of evolution of complex systems, which can be useful for an introductory text, remain unexplained.

Unfortunately some statements are unclear or vague, and some citations are inaccurate: e.g., the attribution of the uncertainty principle to Karl Heisenberg instead of Werner Heisenberg (p. 4), a reference to "Peratoe" (instead of V. Pareto) on page 442, and the three times erroneously transcribed name of N. Ya. Vilenkin.

Overall, the book is a very interesting introductory text which is more suitable for inspiration than for learning. It can serve as a source of additional material and fresh jokes and anecdotes concerning the whole field of probability and fractal geometry, and as a brilliant advertisement for this new field of science and new way of thinking. If this advertisement works, the reader will then turn to other texts that are more accurate and precise (see the discussion of these two concepts on p. 134).

Igor M. Sokolov
Institut für Theoretische Polymerphysik
der Universität Freiburg (FRG)

This section contains book reviews and a list of new books received by the editor. Book reviews are written by invitation from the editor. Suggestions for books to be reviewed and for book reviewers are welcome. Publishers should send brochures or (better) books to Dr. Ralf Baumann, Redaktion Angewandte Chemie, Postfach 101161, D-69451 Weinheim, Federal Republic of Germany. The editor reserves the right of selecting which books will be reviewed. Uninvited books not chosen for review will not be returned.

Too chaotic, too complex! In the book review section in issue 12 the cover of the book "Chaos and Complexity" was incorrectly depicted with the review of the book "Chemistry Imagined. Reflections on Science." The correct picture is shown here.



 © VCH Verlagsgesellschaft mbH, D-69451 Weinheim, 1994 0570-0833/94/1414-1521 $ 10.00+.25/0

New Books

Oxford Chemistry Primers: Chemical Bonding. By **M. J. Winter.** Oxford University Press, Oxford, **1994.** 90 pp., paperback, £ 4.99.—ISBN 0-19-855694-2; **Organometallics 1.** Complexes with Transition Metal-Carbon σ-Bonds. By **Manfred Bochmann.** Oxford University Press, Oxford, **1994.** 91 pp., paperback, £ 4.99.—ISBN 0-19-855751-5; **Organometallics 2.** Complexes with Transition Metal-Carbon π-Bonds. By **Manfred Bochmann.** Oxford University Press, Oxford, **1994.** 89 pp., paperback, £ 4.99.—ISBN 0-19-855813-2; **Bifunctional Compounds.** By **R. S. Ward.** Oxford University Press, Oxford, **1994.** 90 pp., paperback, £ 4.99.—ISBN 0-19-855808-2

Three-Dimensional Chemical Similarity Searching. (Research Studies Press). By **C. Pepperrell.** John Wiley, Chichester, Great Britain, **1994.** 304 pp., hardcover, £ 57.50.—ISBN 0-86380-145-5

Struktur der Materie: Grundlagen, Mikroskopie und Spektroskopie. By **W. Göpel, C. Ziegler.** B. G. Teubner, Leipzig, **1994.** 668 pp., paperback, DM 59.80.—ISBN 3-8154-2110-1

Computer-Enhanced Analytical Spectroscopy, Vol. 4. (Modern Analytical Chemistry). Plenum Press, New York, **1993.** 308 pp., hardcover, $ 89.50.—ISBN 0-306-44456-9

The Raman Spectra of Polymers. By **P. J. Hendra, J. K. Agbenyega.** John Wiley, Chichester, Great Britain, **1993.** Loose-Leaf Edition, £ 85.00.—ISBN 0-471-93837-8

Laboratory Waste Management. A Guidebook. By **ACS Task Force on Laboratory Waste Management.** American Chemical Society, Washington, **1994.** 222 pp., paperback, $ 16.95.—ISBN 0-8412-2849-3

Environmental Catalysis. (ACS Symposium Series No. 552). Edited by **J. N. Armor.** American Chemical Society, Washington, **1994.** 500 pp., hardcover, $ 99.95.—ISBN 0-8412-2851-5

Interpenetrating Polymer Networks. (Advances in Chemistry Series No. 239). Edited by **D. Klempner, L. H. Sperling, L. A. Utracki.** American Chemical Society, Washington, **1993.** 638 pp., hardcover, $ 139.95.—ISBN 0-8412-2528-1

Natural and Engineered Pest Management Agents. (ACS Symposium Series No. 551). Edited by **P. A. Hedin, J. J. Menn, R. M. Hollingworth.** American Chemical Society, Washington, **1994.** 752 pp., hardcover, $ 109.95.—ISBN 0-8412-2773-X

Environmental Geochemistry of Sulfide Oxidation. (ACS Symposium Series No. 550). Edited by **C. N. Alpers, D. W. Blowes.** American Chemical Society, Washington, **1993.** 752 pp., hardcover, $ 139.95.—ISBN 0-8412-2772-1

Macro-Ion Characterization. From Dilute Solutions to Complex Fluids. (ACS Symposium Series No. 548). Edited by **K. S. Schmitz.** American Chemical Society, Washington, **1993.** 640 pp., hardcover, $ 129.95.—ISBN 0-8412-2770-5

Environmental Chemistry of Lakes and Reservoirs. (Advances in Chemistry Series No. 237). Edited by **L. A. Baker.** American Chemical Society, Washington, **1993.** 627 pp., hardcover, $ 149.95.—ISBN 0-8412-2526-5

Time-of-Flight Mass Spectrometry. (ACS Symposium Series No. 549). Edited by **R. J. Cotter.** American Chemical Society, Washington, **1993.** 233 pp., hardcover, $ 59.95.—ISBN 0-8412-2771-3.

Food Phytochemicals for Cancer Prevention I. Fruits and Vegetables. (ACS Symposium Series No. 546). Edited by **M.-T. Huang, T. Osawa, C.-T. Ho, R. T. Rosen.** American Chemical Society, Washington, **1993.** 423 pp., hardcover, $ 99.95.—ISBN 0-8412-2768-3

Food Phytochemicals for Cancer Prevention II. Teas, Spices, and Herbs. (ACS Symposium Series No. 547). Edited by **C.-T. Ho, T. Osawa, M.-T. Huang, R. T. Rosen.** American Chemical Society, Washington, **1993.** 367 pp., hardcover, $ 89.95.—ISBN 0-8412-2769-1

Advances in Strain in Organic Chemistry, Vol. 3. Edited by **B. Halton.** JAI Press, London, **1994.** 300 pp., hardcover, £ 58.00.—ISBN 1-55938-554-5

Advances in Carbene Chemistry, Vol. 1. Edited by **U. H. Brinker.** JAI Press, London, **1994.** 291 pp., hardcover, £ 58.00.—ISBN 1-55938-545-6

Organized Assemblies in Chemical Analysis, Vol. 1. Reversed Micelles. Edited by **W. L. Hinze.** JAI Press, London, **1994.** Hardcover, £ 58.00.—ISBN 1-55938-336-4

Chemistry. The Central Science, 6/E. By **T. L. Brown, H. E. Lemay Jr., B. E. Bursten.** Prentice Hall, London, **1994.** 1152 pp., paperback, £ 24.95.—ISBN 0-13-176652-X

Comprehensive Organic Chemistry. Edited by **H. Beyer, W. Walter.** Ellis Horwood, New York, **1994.** 1015 pp., paperback, $ 42.00.—ISBN 0-13-010364-0

Ultrafast Dynamics of Chemical Systems. Understanding Chemical Reactivity, 7. Edited by **J. D. Simon.** Kluwer Academic Publishers Group, Dordrecht, **1994.** 392 pp., hardcover, $ 179.00.—ISBN 0-7923-2489-7

Anorganische Chemie, Chemie-Basiswissen I. By **H. P. Latscha, H. A. Klein.** Springer, Berlin, **1994.** 499 pp., hardcover, DM 49.80.—ISBN 3-540-56390-3

Biochemie, Eine Einführung. By **K. Dose.** Springer, Berlin, **1994.** 261 pp., hardcover, DM 49.50.—ISBN 3-540-56752-6

Basic Concepts in Organic Chemistry. A Programmed Learning Approach. By **P. Simpson.** Chapman & Hall, London, **1993.** 124 pp., paperback, £ 12.99.—ISBN 0-412-55830-0

Handbook on Metals in Clinical and Analytical Chemistry. Edited by **H. G. Seiler, A. Sigel, H. Sigel.** Marcel Dekker, New York, **1993.** 753 pp., hardcover, $ 195.00.—ISBN 0-8247-9094-4

Betäubungsmittelrecht Suchtbekämpfung. By **P. V. Lundt, P. Schiwy.** R. S. Schulz, Starnberg, **1993.** 238 pp., paperback, DM 98.00.—ISBN 3-7962-0361-2

Solvent Safety Sheets. Edited by **H. Henning.** Royal Society of Chemistry, Cambridge, **1993.** 243 pp., paperback, £ 39.95.—ISBN 0-85186-471-6

From Chemical Philosophy to Theoretical Chemistry. Dynamics of Matter and Dynamics of Disciplines, 1800-1950. By **M. J. Nye.** University of California Press, Berkeley (USA), **1994.** 328 pp., hardcover, $ 48.00.—ISBN 0-520-08210-9

Encyclopedia of Chemical Technology. Volume 9 plus Index Volumes 5 to 8. Edited by **J. I. Kroschwitz, M. Howe-Grant.** John Wiley, Chichester, **1994.** 1112 pp./172 pp., hardcover/paperback, £ 185.00.—ISBN 0-471-52677-0

Clusters and Colloids. From Theory to Applications. Edited by **G. Schmid.** VCH, Weinheim/New York, **1994.** 555 pp., DM 248.00/$ 145.00 (subscription price: DM 198.00/$ 115.00).—ISBN 3-527-29043-5/1-56081-753-4

Integrierte Pflanzenproduktion II. Forschungsbericht. Deutsche Forschungsgemeinschaft. VCH, Weinheim, **1994.** 296 pp. DM 86.00.—ISBN 3-527-27132-5

Biomembrane Electrochemistry. (Advances in Chemistry Series No. 235). Edited by **M. Blank, I. Vodyanoy.** American Chemical Society, Washington (USA), **1994.** 616 pp., hardcover, $ 139.95.—ISBN 0-8412-2525-7

Polymeric Drugs and Drug Administration. (ACS Symposium Series No. 545). Edited by **R. M. Ottenbrite.** American Chemical Society, Washington (USA), **1994.** 278 pp., hardcover, $ 69.95.—ISBN 0-8412-2744-6

Inorganic Fluorine Chemistry. Toward the 21st Century. (ACS Symposium Series No. 555). Edited by **J. S. Thrasher, S. H. Strauss.** American Chemical Society, Washington (USA), **1994.** 437 pp., hardcover, $ 109.95.—ISBN 0-8412-2869-8

Diagnostic Biosensor Polymers. (ACS Symposium Series No. 556). Edited by **A. M. Usmani, N. Akmal.** American Chemical Society, Washington (USA), **1994.** 368 pp., hardcover, $ 89.95.—ISBN 0-8412-2908-2

Prediction of the Deformation Properties of Polymeric and Composite Materials. By **A. Y. Goldman.** American Chemical Society, Washington (USA), **1993.** 360 pp., hardcover, $ 59.95.—ISBN 0-8412-2504-4

Time-of-Flight Mass Spectrometry and its Applications. Edited by **E. W. Schlag.** Elsevier, Amsterdam, **1994.** 420 pp., paperback, Dfl. 215.00.—ISBN 0-444-81875-8

Separation Technology. (Process Technology Proceedings, Vol. 11). Edited by **E. F. Vansant.** Elsevier, Amsterdam, **1994.** 994 pp., hardcover, Dfl. 700.00.—ISBN 0-444-89977-4

Supplements to the 2nd Edition of Rodd's Chemistry of Carbon Compounds. (Vol. IV: Heterocyclic Compounds, Part C and D). Edited by **M. F. Ansell.** Elsevier, Amsterdam, **1994.** 476 pp., hardcover, Dfl. 475.00.—ISBN 0-444-89932-4

Organic Reactions. Equilibria, Kinetics and Mechanism. (Studies in Organic Chemistry, Vol. 50). By **F. Ruff, I. G. Csizmadia.** Elsevier, Amsterdam, **1994.** 480 pp., hardcover, Dfl. 380.00.—ISBN 0-444-88174-3

Point-Group Theory Tables. By **S. L. Altmann, P. Herzig.** Clarendon Press/Oxford University Press, Oxford, **1994.** 704 pp., hardcover, £ 90.00.—ISBN 0-19-855226-2

The Chemical Synthesis of Peptides. By **J. Jones.** Clarendon Press/Oxford University Press, Oxford, **1994.** 230 pp., paperback, £ 18.50.—ISBN 0-19-855839-2

The Colloid Chemistry of Silica. (Advances in Chemistry Series No. 234). Edited by **H. E. Bergna.** American Chemical Society, Washington (USA), **1994.** 450 pp., hardcover, $ 129.95.—ISBN 0-8412-2103-0

Nitrosamines and Related *N*-Nitroso Compounds. Chemistry and Biochemistry. (ACS Symposium Series No. 553). Edited by **R. N. Loeppky, C. J. Michejda.** American Chemical Society, Washington (USA), **1994.** 381 pp., hardcover, $ 89.95.—ISBN 0-8412-2856-6

Emerging Technologies in Hazardous Waste Management IV. (ACS Symposium Series No. 554). Edited by **D. W. Tedder, F. G. Pohland.** American Chemical Society, Washington (USA), **1994.** 378 pp., hardcover, $ 89.95.—ISBN 0-8412-2857-4

Working Safely in the Chemistry Laboratory. Edited by **H. G. Hajian Sr., R. L. Pecsok.** American Chemical Society, Washington (USA), **1994.** 250 pp., hardcover, $ 59.95.—ISBN 0-8412-2706-3

Advances in Steroid Analysis '93. (Proceedings of the 5th Symposium on the Analysis of Steroids, Szombathely, Hungary, May 3-5, 1993). Edited by **S. Görög.** Akadémiai Kiadó, Budapest, **1994.** 623 pp., hardcover, $ 85.00.—ISBN 963-05-6721-0

Polymers and Neutron Scattering. By **J. S. Higgins, H. C. Benoit.** Oxford University Press, Oxford, **1994.** 436 pp., hardcover, £ 65.00.—ISBN 0-19-851003-9

Bond Carbohydrates in Nature. By **L. Warren.** Cambridge University Press, Cambridge, **1994.** 113 pp., paperback, £ 11.95.—ISBN 0-521-44231-1

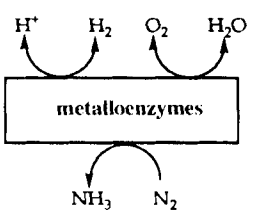
Molecular Catalysts for Multielectron Redox Reactions of Small Molecules: The "Cofacial Metallodiporphyrin" Approach**

James P. Collman,* Paul S. Wagenknecht, and James E. Hutchison

The role of metalloenzymes in important biological transformations has attracted increasing attention over the past several decades. Of the many chemical transformations mediated by enzymes, few are as challenging as multielectron redox reactions. Recent studies have revealed a partial structural and mechanistic description of these redox-active metalloenzymes, but there is much still to be learned regarding the mechanisms of substrate transformation. Due to the complexity of the metalloenzyme systems, simplified model systems are employed to mimic structural or functional features of the enzyme. In multielectron redox enzymes, several metals are probably involved in both substrate binding and the subsequent redox reactions. Thus, functional mimics of multielectron redox enzymes might also need two or more metal centers to be efficacious. The roles of multiple metal centers are to 1) increase the substrate's affinity for the catalyst, 2) increase the rate of electron transfer to the bound substrate, 3) increase the reactivity of the bound substrate, and 4) inhibit deleterious side reactions. Determining the importance of each factor may help in the development of these catalysts. Cofacial metallodiporphyrins, because of the control they provide over the geometric and electronic properties of the synthetic reaction center, are ideal bimetallic model complexes. The knowledge gained from model studies will help in understanding the mechanisms of metalloenzymes and can be used to design new homogeneous catalysts to effect multielectron transformations.

1. Introduction

In the regime of redox chemistry there is an important, general problem which has been resolved in nature and certain heterogeneous catalysts: the catalysis of multielectron redox reactions involving small gaseous molecules (O_2, H_2, and N_2) (Scheme 1). Catalysis of such redox reactions is extraordinarily challenging from a kinetic point of view despite the fact that the thermodynamic potentials for the overall multielectron change may be favorable. In nature metalloenzymes facilitate these transformations. In certain cases, heterogeneous catalysts have been developed to effect the same reactions, although not necessarily by the same mechanisms.



Scheme 1. Selected redox transformations catalyzed by metalloenzymes.

Many examples of multielectron redox reactions are found in enzymatic systems[1] such as sulfite reductase,[2] nitrate reductase,[3] cytochrome *c* oxidase,[4, 5] blue copper oxidases,[6, 7] pseudocatalase,[8] photosystem II,[9] nitrogenase,[10, 11] and hydrogenase.[12] In each case, the enzyme is thought to have one or more metals at the active site and in many cases the enzyme may also include active peripheral metal sites. Mechanisms for these multielectron transformations are largely obscure and form a major research theme in bioinorganic chemistry.[13] The present review discusses recent progress toward development of functional, synthetic models for redox processes involving $O_2 \rightleftharpoons H_2O$, $H_2 \rightleftharpoons H^+$, and $N_2 \rightleftharpoons NH_3$.

These transformations are extremely important in biology and technology. For example, the key step in life-sustaining, aerobic respiration is the four-electron reduction of O_2 to H_2O. This reduction is catalyzed by the membrane-associated, multimetalloenzyme, cytochrome *c* oxidase. The energy derived from O_2 reduction is used by a proton pump to establish a membrane potential.[14] This membrane potential drives the synthesis of the energy-rich molecule, ATP. In heterogeneous catalysis, the electrochemical reduction of dioxygen to water assumes a major role in the cathode of fuel cells. In fact, the efficiency of power production by fuel cells is limited by the efficiency of the best catalyst (Pt) for this transformation.

[*] Prof. J. P. Collman
Department of Chemistry, Stanford University
Stanford, CA 94305-5080 (USA)
Telefax: Int. code + (415)725-0259
Dr. P. S. Wagenknecht
Department of Chemistry, Occidental College (USA)
Dr. J. E. Hutchison
Department of Chemistry, University of Oregon (USA)

[**] Nearly 30 years ago Professor Henry Taube introduced this subject to Professor James Collman and encouraged his study of catalytic dioxygen reduction. Thus this article is dedicated to him.

Even the simplest multielectron redox reaction, oxidation of H_2 to $2H^+$ or its reverse, reduction of H^+, is kinetically challenging. In nature hydrogenase enzymes contained in a variety of bacterial and algal species catalyze this transformation in both directions and utilize the electronic energy in hydrogen for redox transformations within the cells of the organism.[12] In fact, hydrogenase enzyme-catalyzed CO_2 fixation supplies the sole carbon source for growth for several organisms.[15] Many heterogeneous catalysts promote this $H^+ \rightleftharpoons H_2$ transformation; the best studied is Pt, which is used to set the standard potential for the normal hydrogen electrode (NHE).

The reduction of molecular N_2 to NH_3 plays a major role in the biosphere because the inert atmospheric gas, N_2, must be fixed (i.e. converted into nutrients such as NH_3 usable by plants) before plants can perform the biosynthesis of proteins required by animals. The enzymes that carry out this transformation, the nitrogenase enzymes, are indeed famous. All nitrogenase enzymes have several metals, most commonly Fe and Mo, at their active sites. Until recently, the conventional (Fe/Mo) nitrogenase system was presumed to bind N_2 at the Mo site. Crystallographic work on *Azotobacter vinelandii*[16] by Rees et al. indicates that as many as three Fe atoms may be engaged in binding N_2; Mo appears to be coordinatively saturated. Despite this new information, the mechanism of biological reduction of nitrogen remains unknown. The commercial reduction of N_2 by the famous Haber–Bosch hydrogenation catalyst is well-developed and has played a major role in world history by providing economical sources of fixed nitrogen for use especially in agriculture (fertilizer) and military applications (munitions).

In each of the enzymatic examples cited in this section, multiple metal centers a) bind and alter the reactivity of the substrate and/or b) direct the timing and redox potential of the redox equivalents. This review focuses on the design and implementation of molecular, multielectron catalysts based primarily on cofacial metallodiporphyrins. In Section 2, the energetic constraints of these transformations and the analytical techniques used in these studies are examined. Sections 3 and 4 describe the structural properties of a select number of cofacial diporphyrins and the application of the cofacial metallodiporphyrin approach to preparing multielectron redox catalysts, respectively. Detailed accounts of the application of this strategy to redox transformations of O_2/H_2O, H_2/H^+, and N_2/NH_3 complete this review.



J. P. Collmann



P. S. Wagenknecht



J. E. Hutchison

James P. Collman was born in Beatrice, Nebraska, USA, in 1932 and received B. S. and M. S. degrees from the University of Nebraska in 1954 and 1956 and then a Ph.D. from the University of Illinois in 1958 under the supervision of R. C. Fuson. From 1958–1967 he was on the faculty of the University of North Carolina at Chapel Hill; in 1967 he moved to Stanford University where he is Daubert Professor of Chemistry. His research interests are very broad extending across inorganic and organic chemistry but also including superconductivity. His principal research is directed toward the invention and study of functional synthetic mimics of heme protein active sites. His work has been recognized by many awards, the most recent being the American Society Award for Distinguished Service to Inorganic Chemistry. He is a member of the National Academy of Sciences USA.

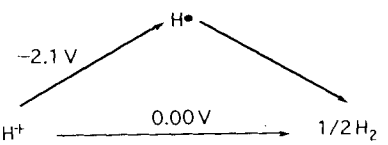
Paul S. Wagenknecht, born in 1964, studied chemistry until 1986 at Furman University where he performed undergraduate research with Noel Kane-Maguire. He then attended Stanford University as a National Science Foundation Predoctoral Fellow where he worked with James P. Collman and Nathan Lewis. His thesis research was concerned with utilizing dihydrogen complexes as functional models of hydrogenase enzymes. After receiving his Ph.D. in September 1991, he worked with Jack Norton at Colorado State University on the mechanism of proton transfer to and from tungsten hydrazido complexes relevant to nitrogen fixation. His current research interests include preparing and studying new crown and cryptand compounds as functional models of metalloenzymes.

James E. Hutchison was born in 1962 and raised in Oregon, USA. He studied chemistry until 1986 at the University of Oregon with Richard G. Finke and received his Ph.D. in 1991 under the supervision of James P. Collman for work on the binding of dihydrogen, dioxygen, and dinitrogen by cofacial metallodiporphyrins in the context of preparing multielectron redox catalysts. He is a National Science Foundation Postdoctoral Fellow and worked with Royce W. Murray at the University of North Carolina at Chapel Hill on the synthesis and electrochemistry of new redox-active self-assembled monolayers and highly concentrated redox liquids. He is now a member of the chemistry faculty at the University of Oregon where his research interests involve synthetic and mechanistic studies and electron transport.

2. General Principles

2.1. Thermodynamic and Kinetic Limitations

At the heart of this general problem is the fact that when one considers the multielectron redox reactions as a series of single-electron/single-proton transfer steps, one or more of the redox potentials are highly unfavorable, even though the overall multielectron redox process is thermodynamically favorable. For example, the reduction of two protons to dihydrogen occurs at 0.00 V vs. NHE, whereas the reduction of a single proton to a highly unstable hydrogen atom requires an extra two volts driving force[17] (Scheme 2). There are analogous thermodynamic impediments along other multielectron redox pathways involving a series of single-electron steps. For this reason, it is not feasible to carry out these reactions by outer-sphere electron transfer processes at an otherwise inert electrode. Catalysts are required to facilitate these transformations.



Scheme 2. Proton reduction to dihydrogen.

Possible catalysts will bind gaseous substrate molecules thereby providing lower energy pathways by stabilizing the intermediates relative to the substrate. This catalysis may be brought about either by raising the energy of the substrate or by lowering the energy of the transition states and/or intermediates. Another important feature of the binding is substrate specificity. A catalyst should bind the substrate but exclude inhibiting ligands. Because N_2, O_2, and H_2 are small molecules, catalysts with small pockets for substrate binding can exclude larger competitive inhibitors.

Another important issue concerns the role of protons in each of the catalytic cycles. Coordination of a ligand such as O_2 or N_2 may render the substrate a stronger Brønsted base. Protonation of the coordinated ligand makes the substrate more susceptible to reduction. Conversely, the binding of H_2 by a metal atom can make that ligand much more acidic. Deprotonation of the bound H_2 facilitates oxidation. For these reasons, the properties of coordination compounds formed between pairs of metals and these gaseous molecules in various oxidation states and over particular pH ranges are of great interest.

Microscopic reversibility is a useful principle in the analysis of certain redox processes. In a model for N_2 fixation it has been possible to observe the *reverse* of certain stages in the overall six-electron transformation (see Section 7.3). According to microscopic reversibility, these paths are theoretically available in the reductive direction; the same E^0 and pH values must be applicable, although the sequence of electron addition/removal, proton addition/removal will be the exact reverse when traversed in the opposite direction (see Section 7.4).

In examining an electrocatalyst two criteria are used to define its efficiency: overpotential and catalyst turnover rate. Recall that most multielectron processes require additional energy input if they are to proceed through several uncatalyzed single-electron transfer steps. The overpotential is the extra voltage that must be applied to overcome this "impediment". This means that for reductions, voltages more negative than the overall thermodynamic potential (for the multielectron change) must be applied; for oxidations, voltages more positive than the overall thermodynamic potential must be applied. We are interested here in preparing efficient catalysts with little to no overpotential, that is, the substrate transformation should occur at or near the thermodynamic potential. The second characteristic of catalyst efficiency is the turnover rate. If the substrate transformation within the catalyst is efficient, electrons can be transferred at a high rate, resulting in high current densities. Possible kinetic bottlenecks in the catalytic cycle, include substrate binding, proton transfer, electron transfer, and product release; these are discussed below.

2.2. Catalyst Screening and Electrochemical Methods

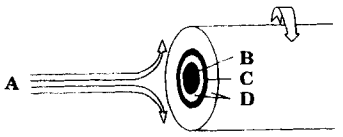
Electrochemical methods are essential in assaying the electrocatalytic properties of cofacial metallodiporphyrins. Cyclic voltammetry, rotating disk and rotating ring-disk electrochemical techniques are the most frequently used techniques in these studies. In the case of a slower reaction, current densities may be too low to be measured by these electrochemical methods. Slower reactions may be easier to monitor in solution by following product formation using NMR spectroscopy, gas or liquid chromatography, or ion- or molecule-selective electrodes. When feasible, spectroelectrochemical methods can be used to detect intermediates. The electrochemical methods are discussed briefly below. More detailed discussions appear in Section 5.

Normally when screening porphyrinic electrocatalysts they are first adsorbed onto an edge-plane graphite (EPG) electrode. Adsorption onto EPG offers advantages over solution catalysis because less catalyst is needed ($< 10^{-9}$ mol cm^{-2}) and electron transfer to the electrode-confined species is very fast. EPG is inexpensive, has a high surface area and, most importantly, adsorbs porphyrins strongly. Adsorption is performed by briefly dipping an EPG electrode into a nonaqueous, dilute solution of the catalyst. The porphyrins have been shown to adsorb in the form of islands up to 30 monolayers thick.[18] Assays of catalytic activity are performed with these porphyrin-modified electrodes.

Cyclic voltammetry is a rapid and easy method to screen these catalyst electrodes. Cyclic voltammograms of a solution containing the substrate are performed with the modified EPG electrode and an unmodified "control" EPG electrode. A catalytic effect can be seen as a decrease in the substrate transformation overpotential or an increase in the current density for the catalyst-coated electrode relative to the bare electrode.

To obtain more information about the kinetics of substrate transformation rotating disk electrode (RDE) experiments are performed.[19] In the typical experiment the EPG electrode is rotated at 100 rpm, while the potential is scanned through the region of interest. The plateau or limiting current is readily determined from the resulting sigmoidal voltammogram. Rotating the electrode replenishes the substrate at the electrode surface, resulting in higher limiting currents as the rotation rate is increased. An analysis of the limiting current versus the rotation rate allows a determination of the number of electrons transferred as well as the limiting rate constant.

A modification of the rotating disk electrode is the rotating ring-disk electrode (RRDE).[20] In this variation of the RDE experiment the disk is encircled by a platinum ring which is separated from the disk by an insulating layer. The potentials of the two electrode surfaces can be controlled independently. As the RRDE is rotated, solution flows first past the disk, and then past the ring (Scheme 3). The electrode products from the disk are uniformly swept past the ring where electroactive products can be detected. Thus, the ring monitors the formation of products at the disk.



Scheme 3. Schematic of rotating ring-disk experiment. A) Electrolyte and substrate flow. B) Edge-plane graphite disk. C) Platinum ring. D) Teflon shrouding.

Now that the energetic concerns governing the multielectron reductions and the tools available to examine the efficacy of possible catalysts have been presented, we next discuss the application of cofacial metallodiporphyrins to the multielectron redox reactions.

3. Cofacial Metallodiporphyrins

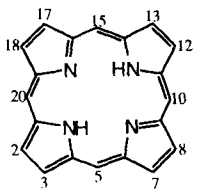
3.1. History

Cofacial diporphyrins (defined here as molecular assemblies in which two porphyrins are held in a stacked orientation) have a rich history that began two decades ago with simple covalently linked diporphyrins. Research into the area of covalently linked diporphyrins was initiated by Schwarz et al.[21] in order to study energy transfer between adjacent chromophores. Their first diporphyrin was covalently linked at the β-pyrrollic position by a single amide linkage. In this predecessor of the cofacial diporphyrin, however, the two porphyrins were not constrained to a stacked geometry.

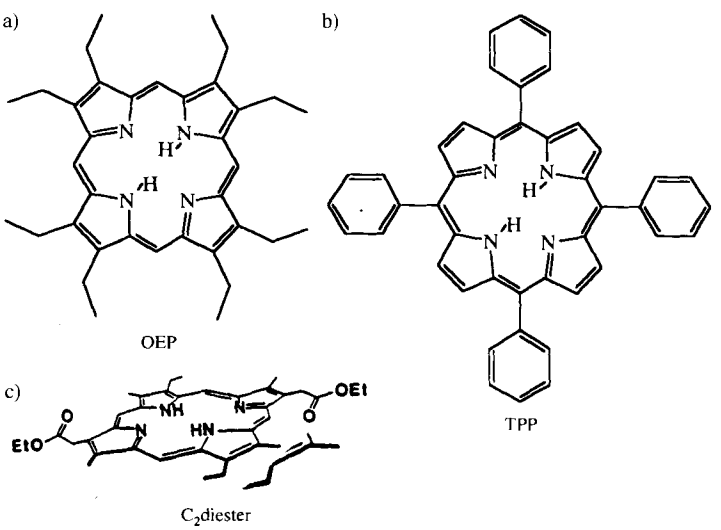
The first reports of cofacial diporphyrins were presented by Kagan[22] and Ogoshi et al.[23] at symposia in the mid 1970s. In 1977 the first published articles on cofacial diporphyrins appeared nearly contemporaneously by Collman et al.,[24] Ogoshi et al.,[25] Chang et al.,[26] and Kagan et al.[27] Most of this work still focused on the chemical relevance of these assemblies to the energy transfer process in chlorophylls. In our first article,[24] however, we proposed the use of these porphyrin dimers as catalysts for the four- and six-electron reductions of O_2 and N_2, respectively. Therein we stated "We have approached this problem by constructing a new class of so-called 'face-to-face porphyrins' in which two porphyrin rings are held in parallel conformation. Thus, two metal atoms might act in concert to bind and reduce dioxygen (or dinitrogen) in the gap between the porphyrin rings. Eventually these binuclear, cyclophane porphyrin complexes are to be attached to graphite to be tested as electrode catalysts." Though considerable effort has been expended on the syntheses of these ligands for different purposes by Sanders et al.[38] and others,[37] we will focus our discussion on the cofacial diporphyrins which have been central to the development of electrocatalysts.

3.2. Nomenclature

Since that initial burst of activity, a great number of cofacial diporphyrins have been synthesized. These assemblies have an extensive trivial nomenclature but as a class have been referred to as "cofacial", "*strati*", "face-to-face", and "stacked". The diporphyrins have been linked by one to four linkers at the *meso*-positions (5, 10, 15, or 20 positions, Scheme 4) or by two linkers at the 2 and 12 (β-pyrrollic) positions. Scheme 5 shows several of the most utilized diporphyrin ligands with their trivial names.[37] Several monoporphyrins which will be discussed in Section 5 are shown in Scheme 6. Within this review, ovals or linked ovals will be used to depict porphyrins or cofacial diporphyrins, respectively. The figure captions will indicate the specific porphyrin employed.



Scheme 4. Porphine with numbering of the centers.



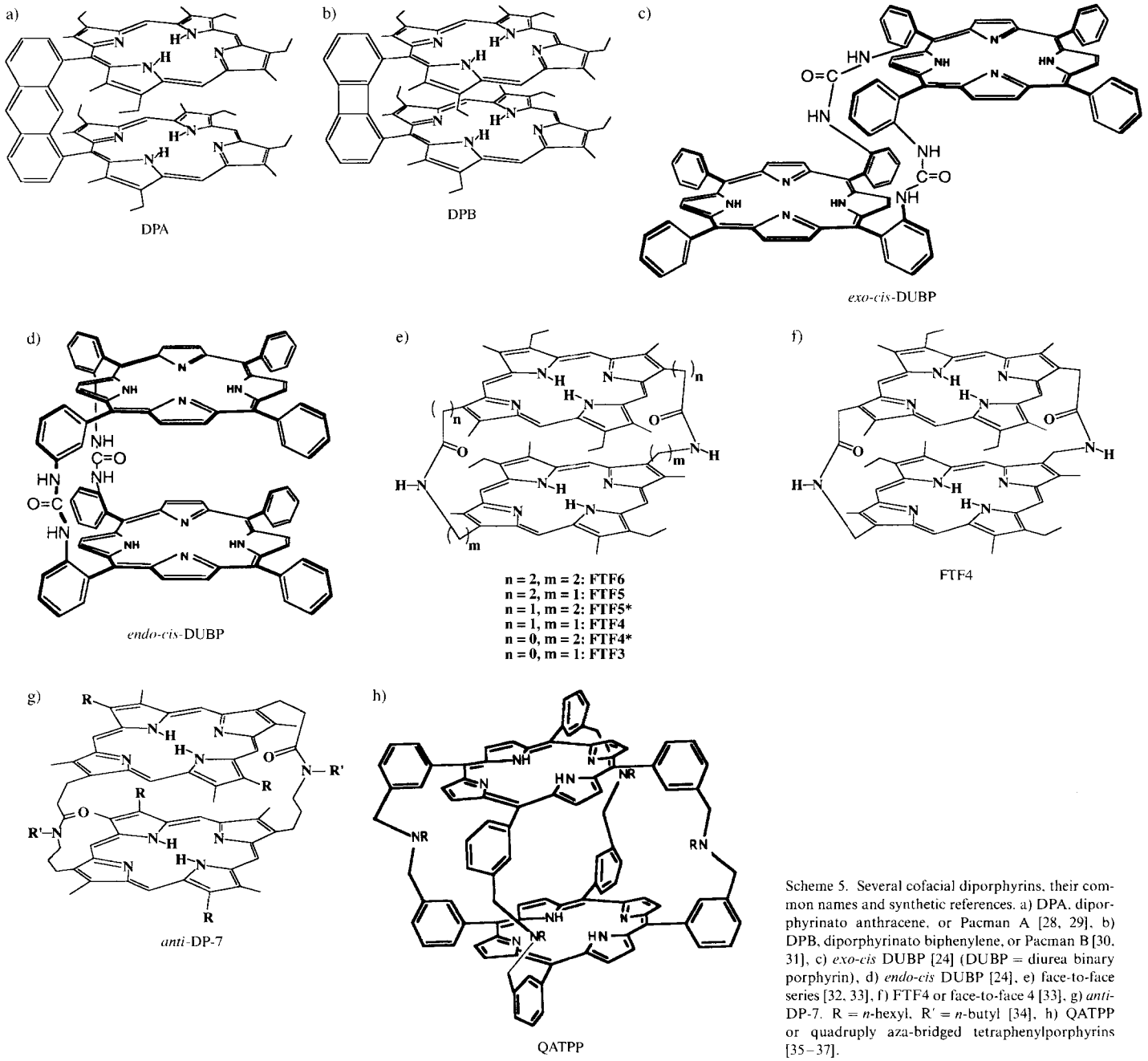
Scheme 6. Monomeric porphyrins discussed in this review. a) OEP or octaethylporphyrin, b) TPP or tetraphenylporphyrin, c) mesoporphyrin diethyl ester.

3.3. Structure

The initial goal of preparing the face-to-face porphyrins was to hold two porphyrins rigidly together in a coplanar arrangement. Several spectral features initially confirmed this arrangement and eventually crystallographic data was obtained as proof of structure. The spectroscopic means of determining the arrangement of the porphyrins is still quite important in characterizations and is explained below.

3.3.1. UV/VIS Spectroscopy

An important feature of porphyrin spectra is the Soret band, an intense band usually appearing between 389 and 440 nm of the UV/VIS spectrum.[39] Three of the early papers on cofacial diporphyrins report a blue shift and/or broadening of the Soret band of the diporphyrin relative to the Soret of the correspond-



Scheme 5. Several cofacial diporphyrins, their common names and synthetic references. a) DPA, diporphyrinato anthracene, or Pacman A [28, 29], b) DPB, diporphyrinato biphenylene, or Pacman B [30, 31], c) *exo-cis* DUBP [24] (DUBP = diurea binary porphyrin), d) *endo-cis* DUBP [24], e) face-to-face series [32, 33], f) FTF4 or face-to-face 4 [33], g) *anti*-DP-7. R = *n*-hexyl, R' = *n*-butyl [34], h) QATPP or quadruply aza-bridged tetraphenylporphyrins [35–37].

ing monomeric porphyrin halves.[24, 26, 27] Especially noteworthy is the comparison of *exo-cis* DUBP with *endo-cis* DUBP,[24] two diporphyrins which differ only in that the *endo* isomer is arranged with the porphyrins stacked on top of each other, whereas the *exo* isomer has the porphyrins arranged in an "anti" conformation (Scheme 5c and d). The Soret band of the *endo-cis* DUBP shows a 15–17 nm shift to shorter wavelength, whereas the Soret band of the *exo-cis* DUBP remains unshifted. This blue shift and the broadening of the Soret band appear to be peculiar to the cofacial diporphyrins and not to diporphyrins in general. Chang correlated this behavior of the Soret band with an exciton coupling between the two coplanar porphyrin rings.[40] These characteristic Soret bands are routinely used for initial structural determinations of cofacial diporphyrins. Such shifts in the Soret band are also seen in porphyrins linked by coordinate bonds; these compounds are not discussed here because they do not exhibit electrocatalytic activity. This is because the required coordination sites are blocked by the bridging ligand.

3.3.2. ^1H NMR Spectroscopy

The ^{1}H NMR spectra of porphyrins reflect the strong ring current of the aromatic porphyrin macrocycle. This ring current imparts an upfield shift to signals of the NH protons of free base porphyrins. In a true "face-to-face" porphyrin, the chemical shifts of protons on one porphyrin ring should be affected by the ring current of the second porphyrin as well. Thus, the NH proton signals should be shifted even further upfield for the cofacial diporphyrins relative to the corresponding monomer halves. In-

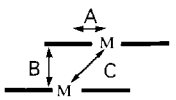
deed, two early papers reported an upfield shift of approximately 2 ppm for the NH protons of the diporphyrin relative to those of the monomer.[24, 26] The magnitude of this shift was also correlated with the length of the linker. Chang[40] found that diporphyrins linked by two five-atom bridges displayed a larger upfield shift of NH protons (4.7 ppm) relative to the corresponding monomer than a diporphyrin linked by two seven-atom bridges (2.4 ppm). We[33] and Bruice[35] have synthesized series of porphyrins which show the same trends, though we found instances where the nature of the linker upsets this correlation between linker length and NH resonance.[32]

3.3.3. EPR Spectroscopy

Distances between the metal centers in dimetalated diporphyrins have been determined by studying the dipolar interaction of two Cu^{II} or two Co^{II} paramagnetic centers.[24, 40, 41] The most noteworthy study is that of Eaton et al.[41] who used EPR spectroscopy to determine metal–metal distances and interplanar separations for several compounds with known crystal structures. Good agreement (± 0.4 Å) between EPR spectroscopic data and crystallographic data was demonstrated.

3.3.4. Crystallographic Data

The desired face-to-face geometry, supported by the above spectroscopic data, is confirmed by crystallographic data. The structures of these diporphyrins have several unique characteristics as outlined in Scheme 7. The two porphyrin rings are generally displaced relative to an eclipsed geometry by a distance known as the lateral shift.[45] The inter-ring separation is defined as the perpendicular distance between the pair of best planes of the macrocycles. Ct represents the center of the porphyrin with respect to the four nitrogen atoms and many studies report Ct–Ct distances for free base porphyrins. Table 1 displays the crystallographic M–M distances, the distance between two metals bound by the porphyrin cores, and the interplanar separations for all crystallographically characterized cofacial metallodiporphyrins.



Scheme 7. Structural parameters for cofacial diporphyrins. A) Lateral slip, B) inter-ring separation, and C) Ct Ct or M M distance.

The crystallographic data indicate a similarity amongst the inter-ring separations, that is, most of the values are approximately 3.5 Å. This distance is due in part to the $\pi-\pi$ interactions between the aromatic macrocycles as suggested by Scheidt's systematic evaluation of solid-state interactions between porphyrin rings.[45] The magnitude of this attraction between rings is evident in the case of $[Cu_2(DPB)]$. This diporphyrin with the biphenylene linker was synthesized to hold the two porphyrins perpendicular to the backbone in an eclipsed geometry approximately 3.8 Å apart. Regardless, the two porphyrins undergo a lateral shift of 1.52 Å to achieve optimum $\pi-\pi$ overlap with an inter-ring separation of 3.45 Å (Fig. 1).[43]

Table 1. X-ray crystallographic data for cofacial metallodiporphyrins.

Compound	M–M [Å]	Interring separation [Å]	Ref.
$[Cu_2(FTF6)]$	6.33	3.87	[42]
$[Ni_2(DPA)]$	4.57	3.9	[43]
$[Cu_2(DPB)]$	3.81	3.45	[43]
[CoAl(OEt)(DPB)]	4.37	3.54	[29]
$[Co_2(DPB)]$	3.73		[31]
$[Co_2(FTF4)]$	3.42	3.54	[44]
$[Cu_2(DP\text{-}7)]$	5.22	3.52	[34]

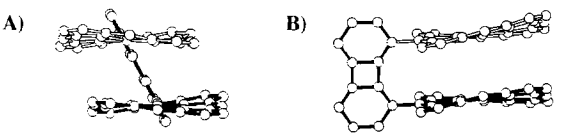


Fig. 1. Structural distortion of $[Cu_2(DPB)]$. A) Front view, and B) side view.

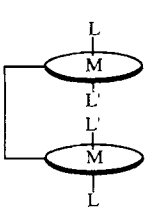
Initially, we suggested that such flexibility of the diporphyrin unit would be of importance in the accommodation of and chemical transformation of small molecules within the "face-to-face" porphyrin cavity.[24] However, the synthesis and structural analysis of $[Cu_2(FTF6)]$, a cofacial metallodiporphyrin linked at the *meso*-positions, demonstrated otherwise.[42] Because of the strong $\pi-\pi$ interactions, this complex distorts to achieve optimum $\pi-\pi$ overlap, resulting in a lateral shift of 5 Å. Apparently the linkers in this system are too flexible to constrain the porphyrins to a true "face-to face" geometry, thus the two metals are not arranged to act in concert on a small molecule. To ensure the close and truly "face-to-face" approach of two metalloporphyrins, only the shortest and most rigid linkers are appropriate. Consequently, most catalysis has been performed with the FTF4, DPB, and DPA derivatives.

3.3.5. Molecular Modeling

Recently, Bruice et al.[35–37, 46] have utilized molecular modeling to determine Ct–Ct distances for the quadruply (Scheme 5h) and triply aza-bridged cofacial tetraphenylporphyrins. These investigations suggested that these diporphyrins are very flexible and the Ct–Ct distance for a single diporphyrin can fluctuate by over 2 Å.

3.4. General Properties of Diporphyrins

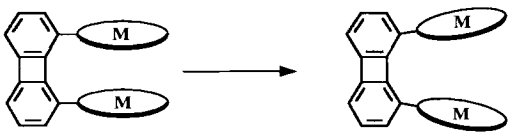
In order to understand substrate binding within the metallodiporphyrin cavity, its coordination sphere needs to be considered. Each porphyrin ring is a tetradentate ligand capable of binding a metal center, leaving two axial coordination sites on each metal (Scheme 8). The substrates that can bind to the inner coordination sites are limited by the size of the cavity between the porphyrins, whereas the outer coordination sites should coordinate any ligand capable of binding to metalloporphyrins.



Scheme 8. Generic ligated cofacial metallodiporphyrin. The ligands L are ligated to the outer coordination sites. The ligands L' occupy the inner coordination sites or "pocket".

Typically, catalysts are prepared by blocking the outside coordination sites with axial ligands leaving the coordination sites in the pocket open for substrate binding.

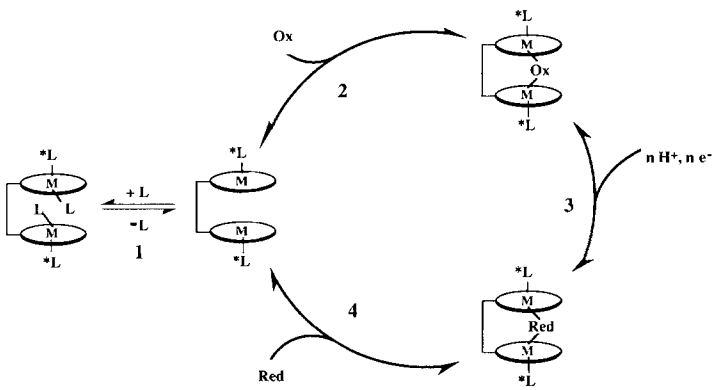
To control the size of the inner coordination pocket, several linkers have been utilized to attach the two porphyrins of the diporphyrin. The most robust and chemically inert of these are the anthracene and biphenylene bridges of the DPA and DPB ligands, respectively. Additionally, because of the rigidity of these linkers, the DPB and DPA ligands display small lateral shift parameters[4,5] and therefore most closely approximate a true face-to-face geometry. However, some flexibility is desired because during the transformation of a substrate bound in the pocket, the geometric binding constraints of the modified substrate will unavoidably change. The DPB and DPA ligands are capable of such flexibility because only one linker connects the diporphyrin unit. Thus, the diporphyrin can open its "bite" as shown in Scheme 9.[4,7] These geometric factors will be important in the binding and transformation of the substrate in each of the examples shown in Sections 5–7.



Scheme 9. Distortion of the DPB ligand to create a larger binding pocket.

4. The Invention of Cofacial Metallodiporphyrin Electrode Catalysts for Multielectron Redox Processes

Careful analysis of a generic multielectron redox cycle based on cofacial metallodiporphyrins can be useful in designing a possible catalyst. In Scheme 10, clockwise rotation through the



Scheme 10. Cofacial metallodiporphyrin approach to multielectron redox catalysis. Ox = oxidized form of the substrate/product pair and Red = the reduced form. 1 = "Formation of the active site", 2, 4 = substrate binding or product release depending upon whether the transformation is oxidizing or reducing, 3 = the multielectron transfer steps.

cycle corresponds to substrate reduction, whereas counterclockwise rotation involves substrate oxidation. There are principally four steps in the cycle: 1) creation of the active site, 2) substrate binding and activation, 3) addition or removal of electrons and protons, and 4) liberation of the product.

In order to bind one (or two) substrate molecules in the pocket of the catalyst, there must be open, interior coordination sites. Practically, this means that if interior inhibiting ligands are present, the substrate must be able to displace them. In some cases it is necessary to block the outer coordination sites with strong axial ligands so that substrate binding is required to occur within the cavity. If the catalyst precursor contains a metal–metal bond bridging the two inner coordination sites, a *trans* ligand is required to weaken or break this bond thus creating the active site. In the cases where outer axial ligands are employed, care must be taken to ensure that they are bulky enough to be excluded from the active site cavity.

All of the multielectron redox transformations involve bond formation or rupture in the substrate; therefore, the cofacial metallodiporphyrin must bring reactants together to facilitate bond formation or weaken the substrate bond to be broken. Both of these processes begin with substrate binding. Although *strong* binding of the substrate to the active site is not a prerequisite for catalysis, some affinity of the catalyst for the substrate is required. The affinity of the catalyst for the substrate relative to its affinity for other competing substrates determines the specificity or selectivity of the catalyst.

In the third phase of catalysis, electron and proton transfers occur. The cofacial metallodiporphyrin can facilitate these transformations because a) the catalyst acts as an electron reservoir mediating the timing and potential of electron transfers between the electrode and the substrate and/or b) the catalyst/substrate complex is more easily oxidized/reduced than the free substrate. During these steps, protons must be added to or removed from the substrate/catalyst complex. Because the catalyst affects the pK_a of the bound substrate, it may affect the order of electron/proton transfers.

The final step in the cycle is release of product from the catalyst. This stage can be problematic if the product binds too tightly to the catalyst. Frequently this step can be assisted by protonation of the bound product or replacement of bound product by incoming substrate.

This analysis reveals that there are structural and electronic parameters that are important in designing a functional catalyst. The principal controllable parameters are the spacial position of the two metal centers and the nature of each metal center. The position of the metals can be controlled in a cofacial diporphyrin by varying the number and type of bridges between the two porphyrin rings. The reactivity of the metal centers is varied by changing the metal, the electron richness of the porphyrin ring, or the nature of the axial ligands *trans* to the active site. Cofacial metallodiporphyrins allow for a great deal of control over many of the geometric and electronic features of the synthetic reaction center. Systematic manipulation of the geometric parameters was illustrated in the discussion of the variety of cofacial diporphyrins in Section 3.

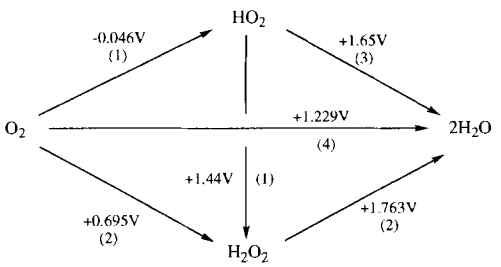
5. The Four-Electron Reduction of Dioxygen

5.1. Background

Electrode materials that catalyze the four-electron reduction of dioxygen at or near its thermodynamic reduction potential

(+1.23 V vs. NHE) would be ideal fuel-cell cathodes and would allow maximal energy conversion in these cells. All known electrodes catalyze the reduction of dioxygen at more negative potentials, that is with some overpotential. For example, metallic platinum, the most efficient fuel-cell cathode known, operates at an overpotential of nearly 600 mV.[48-50] The limiting potential for a given electrode will be governed primarily by the reduction pathway.

Scheme 11 shows the reversible standard electrode potentials connecting O_2 and its reduction products: hydroperoxyl, hydrogen peroxide, and water.[51] The one-electron change connecting O_2 with HO_2 (hydroperoxyl) is quite unfavorable. In fact, this one-electron change is more than one volt more negative than the $E_{1/2}$ connecting O_2 directly with $2H_2O$—the desired four-electron change. This means that an otherwise catalytically inert electrode acting as a simple source of electrons for outer-sphere electron transfer would produce an infinitesimally small quantity of HO_2 at the thermodynamic potential for the overall four-electron transformation. It is therefore not possible to reduce O_2 to $2H_2O$ at this four-electron thermodynamic potential by an initial one-electron change. The thermodynamic potential for the two-electron change occurs at about + 0.7 V. Thus hydrogen peroxide cannot be a free intermediate if an oxygen-reducing electrode is to operate at or near the thermodynamic potential for four-electron dioxygen reduction (+1.23 V).[33] In designing a four-electron dioxygen reduction catalyst, the one- and two-electron paths must be avoided.



Scheme 11. Dioxygen reduction to water. The number of electrons transferred is given in parentheses.

Our approach to this problem was based on the knowledge that various monomeric transition metal macrocyclic complexes (phthalocyanines and porphyrins) catalyze the reduction of dioxygen to H_2O_2.[52] Cobalt is the metal with the most positive M^{II}/M^{III} redox potential[53] that still binds O_2 with measureable affinity.[54] Thus, we first considered that the two Co^{II} sites of cofacial diporphyrins could collectively bind and reduce O_2 to the peroxide stage. Intuition suggested that further reduction of the peroxide group might take place, especially in the presence of sufficient proton flux. In addition, it had been suggested that two metals might favor a four-electron reduction by minimizing the energy costs arising from spin, ligand, and solvent reorganization associated with a four-electron change.[24]

5.2. Four-Electron Reduction of Dioxygen by Cofacial Bis(Cobalt) Diporphyrins

After a great deal of experimentation,[48] a particular cofacial bis(cobalt) diporphyrin, $[Co_2(FTF4)]$,[55] adsorbed on an EPG electrode was found to catalyze the reduction of O_2 by an overall four-electron change—without the intermediacy of free H_2O_2. By exploring a range of cofacial diporphyrins possessing different linking groups, containing different metal centers, and having diverse metal–metal separations, we found that only special situations would promote this four-electron change—most other cofacial metallodiporphyrins catalyze the two-electron reduction to H_2O_2.

Nearly contemporaneously, others reported similar four-electron reductions of O_2. One notable class of four-electron O_2 reduction catalysts is the bis(cobalt) complexes of biphenylene- and anthracene-bridged diporphyrins, $[Co_2(DPB)]$ and $[Co_2(DPA)]$, respectively.[56] Other metal complexes of these arene-bridged ligands proved useful in our studies of redox reactions involving H_2 (Section 6) and N_2 (Section 7). To date a wide variety of cofacial diporphyrins have been prepared. Their electrochemical and catalytic dioxygen reduction properties are summarized in Table 2. The remainder of Section 5 describes what is known about the dioxygen reduction mechanism, the factors that determine two- versus four-electron reduction pathways, and the future development of this class of catalysts.

5.2.1. *Rotating Disk Electrochemical Studies*

The ring-disk experiment[19, 20, 57] shown in Figure 2 illustrates the successful four-electron reduction of O_2 for $[Co_2(FTF4)]$ (analogous experiments with $[Co_2(DPB)]$ and $[Co_2(DPA)]$ yield similar results). The rotating ring-disk electrode (RRDE, see Scheme 3) is placed in contact with an oxygenated aqueous electrolyte solution, and variable potential is applied to the disk, starting from a high, positive potential. The rotation of the electrode assembly causes the electrode products (water and hydrogen peroxide) to be ejected radially across the ring while bringing fresh solution vertically to the disk. As the disk potential is made

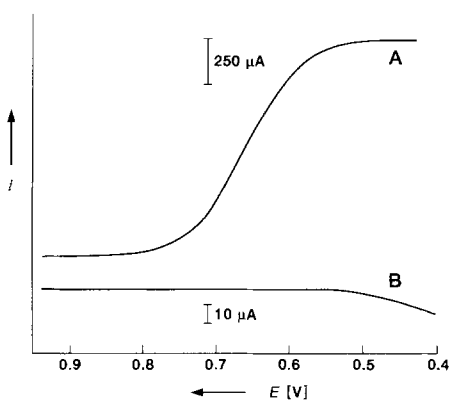


Fig. 2. Rotating ring-disk voltammogram for the reduction of dioxygen by $[Co_2(FTF4)]$. A) Disk current and B) ring current.

more reducing, the ring potential is held at +1.4 V where any catalytically produced hydrogen peroxide is oxidized back to dioxygen thus allowing sensitive detection of the two-electron product. Note that with the most effective four-electron catalyst, $[Co_2(FTF4)]$, the ring shows no oxidation of H_2O_2 at the platinum ring; thus the 2e product, H_2O_2, is not released to the solution.[33, 55, 58, 59] When the disk potential is scanned more negative than + 0.55 V vs. NHE, the electrode ring begins to sense the production of H_2O_2. Thus $[Co_2(FTF4)]$ catalyzes the four-electron process only over a limited potential range.

The RRDE was used to determine the product distribution and kinetic parameters of these electroreductions.[19, 33, 57] It is possible to quantify the production of hydrogen peroxide using the collection efficiency, N_0,[19, 65] and the ratio of the currents at the ring and disk. However, the magnitudes of the ring currents are often low and irreproducible.[58, 63, 66] The dependence of the disk currents upon the rotation rate ω often yields more quantitative information. As the ring-disk assembly is rotated more rapidly, the rate of delivery of the substrate from solution to the disk is increased. Correspondingly, the overall rate of the catalytic reduction of O_2 is increased as manifested by increased disk currents. The limiting current is proportional to $\omega^{1/2}$ and to the number of electrons (n) in the reduction as described by the Levich equation.[67]

Figure 3 shows the experimental and calculated Levich[67] and Koutecky–Levich plots[68] for RDE voltammograms of dioxygen reduction by $[Co_2(FTF4)]$ on EPG at increasing rotation rates. At higher rotation rates the experimental Levich curve increasingly deviates from the calculated line because the reaction rate is no longer limited simply by the rate of dioxygen delivery to the electrode. This curvature is consistent with a rate-limiting chemical step preceeding the electron transfer step(s) and likely reflects the rate of either dioxygen binding to the catalyst and/or protonation of the bound substrate.[33, 58] The experimental Koutecky–Levich (K–L) plots are linear and have the same slopes as the calculated four-electron line. From the intercept of the K–L plot and the surface coverage, the rate of dioxygen reduction can be determined (ca. 400 s^{-1} for $[Co_2(FTF4)]$).[58] Through the use of the RRDE, a number of cofacial metallodiporphyrins have been screened for four-electron reduction activity and these results are summarized in Table 2.

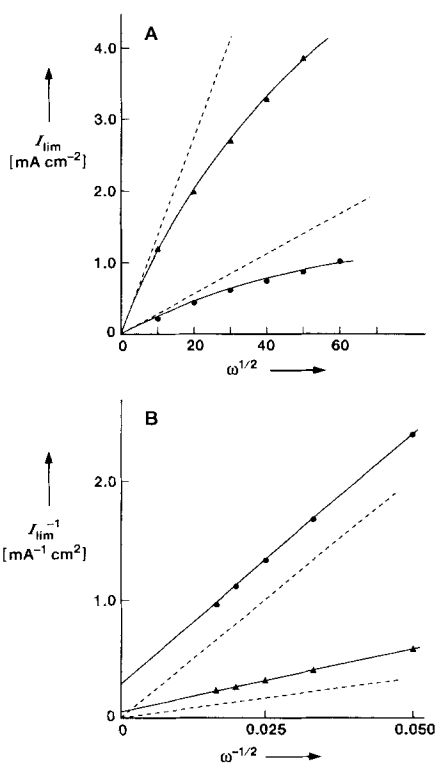


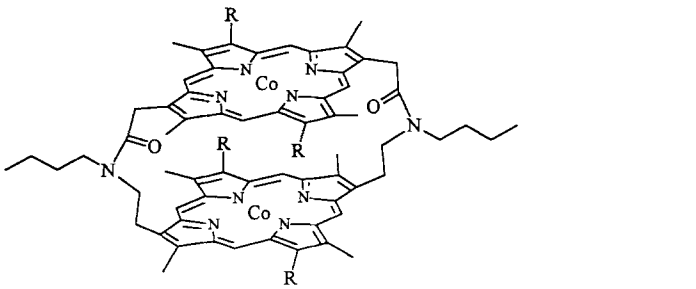
Fig. 3. Levich (A) and Koutecky–Levich (B) plots of rotating disk limiting currents in air (●) and dioxygen saturated (▲) 1 M CF_3COOH (TFA). The dashed lines represent the calculated responses for the mass transfer limited, four-electron reductions of dioxygen in air- and dioxygen-saturated solutions. ω in rpm.

5.2.2. *Fundamental Characteristics of the Dioxygen Electroreduction*

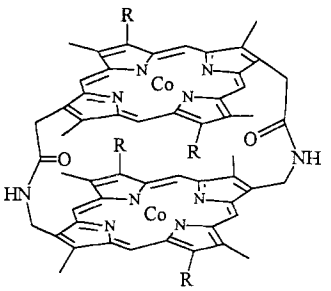
A series of cofacial bis(cobalt)-substituted diporphyrin catalysts were systematically examined for their activity in the four-electron reduction of O_2. As shown in Table 2, only three catalysts show excellent four-electron activity (FTF4, DPB, and DPA); the others vary from pure two-electron activity to intermediate values. The extent of four-electron activity depends both on the nature of the two metal centers and the distance between them. The distance dependence is more pronounced in the FT*Fn* series[58] than in the related DPB, DPA family.[61] Apparently, a preferred orientation of the two metal sites is necessary to stabilize intermediates and guide the reaction along the four-electron path. The fact that complexes $[Co_2(DPB)]$ and $[Co_2(DPA)]$ with arene bridges have Co–Co separations that vary by nearly an Ångstrom,[43] yet have identical catalytic activities,[56] implies that the geometric requirement is less strict in this series. These singly bridged molecules may be flexible enough to adopt the optimum metal–metal distance (see Section 3.4).

The $[Co_2(FTF4)]$ complex mentioned above does not form hydrogen peroxide as a free intermediate in the four-electron reduction of dioxygen.[33, 55, 58] One line of evidence that hydrogen peroxide is not an intermediate is that the ratio of the disk-to-ring current in the RRDE experiment is independent of the rotation rate. If free hydrogen peroxide were produced, at higher rotation rates it would be swept from the electrode surface before it could be further reduced to water and would result in increased ring currents.[69] These complexes do catalyze the reduction of free hydrogen peroxide in the absence of dioxygen,[18, 62] however, the rate is 30-fold slower (the rate constants of the heterogeneous reaction being 0.003 vs. 0.98 cm s^{-1} for the $[Co_2(FTF4)]$[18] catalyst) than the rate of dioxygen reduction.

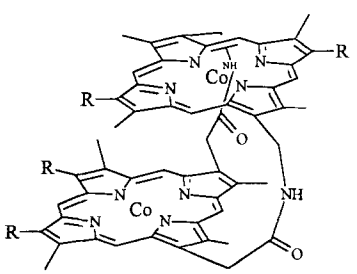
A more detailed understanding of the mechanism of the four-electron reduction can be obtained by reexamining the thermodynamic potentials of overall redox transformations of O_2 to H_2O (see Scheme 11). Note that the thermodynamic potential for the two-electron change occurs at about 0.7 V (at pH = 0). It is significant that all of the overall four-electron catalysts thus far discovered begin the electrocatalytic reduction of O_2 at values near 0.7 V. A logical interpretation of this result is that all of these reactions proceed through an intermediate which has the character of H_2O_2. This peroxide probably remains bound due to kinetic factors such as decreased lability due to chelation by two metals and more rapid subsequent reduction to H_2O compared with hydrolysis, which would release free H_2O_2.



Co-Co-5



Co-Co-4



slipped Co-Co-4

R = $(CH_2)_4CH_3$

Table 2. Dioxygen reduction by cofacial metallodiporphyrins [a].

Compound	$E_{surface}$ [b]	$E_{1/2}(O_2)$ [b]	I_{lim} (ω)	Supporting electrolyte	n	Ref.
[Co_2(FTF4)]	0.86/0.51	0.71	1.3 (100)	1 M TFA	3.9	[33, 55, 58, 60]
[Co(C_2diester)]	0.78	0.44	0.8 (100)	1 M TFA	2.5	[33, 55, 58, 60]
[Co_2(FTF3)]	0.88/0.58	0.64	0.8 (100)	1 M TFA	ca. 2	[58]
[Co_2(FTF4*)]	0.88/0.59	0.68	0.8 (100)	1 M TFA	ca. 2	[58]
[Co_2(FTF5)]	0.84	0.62	1.1 (100)	1 M TFA	ca. 3	[58]
[Co_2(FTF6)]	0.83	0.56	0.8 (100)	1 M TFA	ca. 2	[33, 55, 58]
[CoFe(FTF4)]	0.84	0.49/ 0.17	0.7/1.2 (100)	1 M TFA	2/4	[58]
[CoAl(FTF4)]		0.46		0.1 M TFA	3.0	[60]
[CoCu(FTF4)]				0.1 M TFA	1.8	[60]
[CuCo(FTF4)]				0.1 M TFA	1.9	[60]
[CoMn(FTF4)]		0.47	0.8 (100)	1 M TFA	ca. 2	[58]
[CoPd(FTF4)]		0.56		0.5 M TFA	ca. 2.9	[33, 55]
[CoH_2(FTF4)]	0.84	0.44	0.8 (100)	1 M TFA	2.9	[58, 60]
Co-Co-4	0.93/0.60	0.69		0.5 M TFA	3.2–3.7	[56, 61]
"slipped" Co-Co-4	0.92/0.52	0.48		0.5 M TFA	2.3	[61]
Co-Co-5	0.87/0.54	0.38		0.5 M TFA	2.4	[61]
[Co_2(DPB)]	0.88/0.58	0.70		0.5 M TFA	3.7–3.8	[50, 56]
[Co_2(DPA)]	0.87/0.57	0.67		0.5 M TFA	3.7–3.8	[56, 62]
[Co(TPP)]	0.90	0.51		0.5 M TFA	ca. 2	[56]
[CoH_2(DPA)]	0.59	0.55		1 M TFA [c]	ca. 3.5	[62]
[CoCu(DPA)]	0.53	0.52		1 M TFA [c]	ca. 2	[63]
[FeH_2(DPA)]	0.00	0.16		1 M TFA [c]	ca. 2/ca. 4	[63]
[Fe_2(DPA)]	0.00	0.35		1 M TFA [c]	3.8/4	[63]
[CoFe(DPA)]	−0.02	0.47		1 M TFA [c]	3.6/4.1	[63]
[Ir(OEP)H]	0.48	0.72		0.1 M TFA	3.9	[50]
Pt/C		0.79		0.1 M TFA	4.0	[50]
[Co_2(QATPP)] (**2** in ref. [35])			1.06 (100)	0.1 N H_2SO_4	3.3	[35]
[$Ru(NH_3)_5]_4$	0.46			0.5 M NH_4PF_6/ 0.1 M $HClO_4$ [c]	ca. 3.6	[64]
[Co(*p*TPyrP)] [d]						

[a] For compound abbreviations see Schemes 5 and 6. $E_{surface}$ is the $E_{1/2}$ value determined for the surface adsorbed porphyrin from cyclic voltammetry. $E_{1/2}(O_2)$ is the half-wave potential for dioxygen reduction found from the RDE experiments. I_{lim} is the limiting current from the RDE experiement at the designated rotation rate ω. All electrolyte solutions are saturated with dioxygen unless otherwise noted. The number of electrons, n, transferred in the dioxygen reduction is determined by Koutecký–Levich analysis or estimated from the data given in the indicated references. All potentials given are vs. NHE. Those originally reported vs. SCE were converted using NHE = SCE + 0.242 V. [b] When two values are given, they are for the two distinct surface waves or dioxygen reduction waves. [c] Air-saturated electrolyte. [d] *p*TPyrP = *meso*-tetrakis(4-pyridyl)porphyrin.

The distribution of two- and four-electron products is strongly dependent on the pH of the oxygenated electrolyte solution.[33, 58, 62] For [Co_2(FTF4)], below pH = 3.5 little or no H_2O_2 is detected by the Pt ring, indicative of a four-electron process. Reductions carried out at pH values above 4.5 yield predominantly hydrogen peroxide, the product of the two-electron reduction. These results suggest that a relatively strong acid ($pK_a < 4.5$) is needed to promote subsequent reduction of intermediates by an apparent heterolytic O–O bond cleavage reaction. Above pH = 6, surface voltammetry of the catalyst under N_2 suggests that oxo or hydroxo ligands bind to the cobalt centers, possibly blocking the active site of the catalyst so that two-electron reduction occurs at the exterior cobalt site in the same manner as for monomeric cobalt porphyrins.[70]

5.2.3. *The Mechanism of Dioxygen Reduction in Catalysis by Cofacial Bis(Cobalt) Diporphyrins*

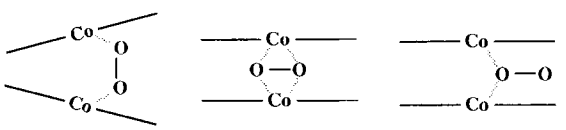
Next, consider the probable "activated complex" that is the structure of the electrocatalytic system that initiates the kinetically slow step in four-electron reduction. First it has been demonstrated that the rate of O_2 reduction is linearly related to the cofacial diporphyrin catalyst concentration.[18] Second the limiting current and therefore the reaction rate is proportional to the partial pressure of O_2. This suggests that the catalyst becomes oxygenated before or during the rate-limiting step. Finally, the pH dependence indicates that bound O_2 is probably protonated giving a conjugate acid with a pK_a value of about 4.0. Thus, it seems probable that binding/protonation of O_2 to the catalyst site is rate-limiting; this leaves in question the oxidation state of the bis(cobalt) complex that binds O_2.

Initially, we assigned the most active form of the catalyst by examining the cyclic voltammetry of the catalytic electrode in the absence of O_2; a surface wave was found close to the potential at which the four-electron reduction of O_2 begins.[33] The active form of the catalyst was first assigned to the $Co^{II}Co^{II}$ state. Subsequently, solution studies[71, 72] showed that the mixed-valence form of the catalyst, $Co^{II}Co^{III}$, exhibits a very high affinity for O_2, much more so than the $Co^{II}Co^{II}$ state. The intermediate complex can be thought of as a μ-superoxo complex, in which an O_2 ion is simultaneously bound to two equivalent Co^{III} sites. This hypothesis is well supported by equilibrium binding studies,[72] as well as isolation and full characterization[31] of the intermediate. Differential pulse polarographic investigations of [Co_2(FTF4)] surface waves over a wide pH range and in the presence of axial ligands suggest that the surface wave associated most closely with dioxygen reduction is a $Co^{III}Co^{III}$ to $Co^{II}Co^{III}$ process.[18, 73] We conclude that the mixed-valence complex is the active form of the catalyst. This idea is reinforced by the observation that when the electrocatalytic reaction is performed at more reducing (lower) potentials, the rotating ring-disk experiment shows some production of H_2O_2.[33] At these more reducing potentials the $Co^{II}Co^{II}$ form of the catalyst would be present on the electrode. Apparently, it is less effective in promoting the four-electron pathway.

Additional evidence for the mixed-valence hypothesis comes from the fact that only one redox-active metal, Co, need be present to catalyze the four-electron reduction. When one Co atom is substituted by a redox-inactive metal having the same

charge, Al^{III}, a four-electron reduction of O_2 is observed in parallel to the two-electron reduction.[60] In fact, it was found that only a single cobalt atom need be present in the cofacial porphyrin system with the other ring in its protonated "free base" form.[60, 62] This protonated form can serve as a Lewis acid effecting four-electron reduction of O_2. Thus, in the mixed-valence complex, $Co^{II}Co^{III}$, the Co^{III} is probably serving as a Lewis acid site. If, however, the other porphyrin ring is substituted with a metal such as Cu (which has no affinity for any axial ligand), only two-electron reduction of O_2 is observed.[60] A Lewis acid is probably required to hold the partially reduced substrate in the diporphyrin cavity so that it does not dissociate before complete reduction.

The efficiency of catalysis is controlled not only by the choice of metals, but also by the M–M distance of the cofacial metallodiporphyrin (see Section 3 and Table 2). Structural and spectroscopic studies to elucidate the geometry and reactivity of the μ-superoxo complex (a putative intermediate along the catalytic pathway) have been attempted. Based upon X-ray crystal structures of the bis(cobalt) derivatives[31, 44] and EPR[31, 33, 71, 74] and Raman studies[75] of μ-superoxo complexes of the bis(cobalt) compound, plausible geometries of the transition state incorporating the proton have been proposed (Scheme 12).[31, 44, 75] The precise geometry remains a matter of speculation. The proton is not shown in Scheme 12



Scheme 12. Proposed dioxygen binding modes for $[Co_2(FTF4)]$.

5.3. Recent Developements and Future Challenges

Recently other catalysts have been shown to promote the four-electron reduction of O_2. A remarkable example, which is still not well understood mechanistically, is the catalysis by the monoporphyrin [Ir(OEP)H].[50] This system is as good a four-electron catalyst as the previous, best bis(cobalt) complexes (Table 2). Catalysis is also observed when [Ir(OEP)I] or [Ir(OEP)OOH] is initially deposited on the electrode, but only after an activation process at a reducing potential. The dimer, $[Ir(OEP)]_2$, exhibits good catalytic activity without any activation. Whether or not the Ir–Ir bond of the dimer reacts directly with O_2 is a major question. This Ir catalyst shows similarities to the bis(cobalt) complexes. Its activity is also pH dependent, but not as dramatically as that of the bis(cobalt) systems; both have the same initial limiting potential, 0.7 V. In contrast, the [Ir(OEP)] system does not reduce free H_2O_2 and sustains four-electron reduction over a greater potential range than the bis(cobalt) systems (Fig. 4). Despite its greater potential range for pure four-electron reduction, the [Ir(OEP)] catalyst becomes almost inactive at potentials more reducing than 0.2 V vs. NHE.

Another important but poorly understood aspect of the electrocatalytic reduction of O_2 is the apparent requirement for

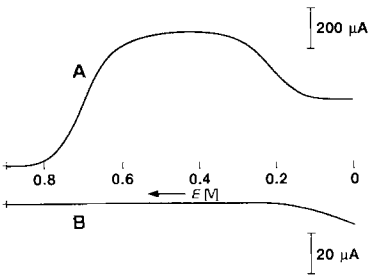


Fig. 4. Rotating ring-disk voltammogram of [Ir(OEP)H] in O_2-saturated solution. A) Disk current and B) ring current. The potential is given relative to the standard hydrogen electrode (SHE).

catalyst adsorption on EPG electrodes. Attempts to bind these catalysts to other electrodes while preserving their four-electron activity have been unsuccessful. For example, experiments in which these catalysts were either in solution or bound to acidic polymers (Nafion) near non-graphitic electrode surfaces failed. Although the underlying reasons for this requirement are not clear, one can speculate about probable causes. It seems likely that the intermediate stages in the four-electron reduction of O_2 are unstable towards hydrolysis. Thus, if electrons are not delivered rapidly enough to these systems, the intermediate H_2O_2 will leach into solution. There may be surface groups on the EPG electrodes[76] that facilitate electron transfer to the cobalt centers or the cobalt–oxygen complex. Another possibility is that there may be some kind of special additional association (axial coordination) with the EPG electrode surface perhaps through a quinone or phenol function associated with the metal sites. There is a very strong association between EPG and these catalysts which seem to bind in tight clusters.[18] More weakly bound catalyst layers are not effective in promoting the four-electron reduction of O_2.[18]

This electrode association phenomenon has one possible exception. Anson et al. found that a special monomeric cobalt (tetrakis(4-pyridyl)porphyrin), with four $[Ru(NH_3)_5]^{2+}$ groups around the porphyrin periphery, can effect the four-electron reduction of O_2 when this complex is incorporated in a Nafion layer next to an EPG electrode surface.[77] Given the strong adsorption of porphyrins to graphite, some or all of the observed catalysis in Nafion may be due to surface-adsorbed porphyrins. Subsequent studies of analogous cobalt porphyrins possessing one to four peripheral ruthenium centers adsorbed directly on to the EPG electrode show that three or more ruthenium centers are required to obtain the four-electron reduction.[64, 78]

The potential at which four-electron reduction occurs for the above ruthenated cobalt porphyrins is much lower than that for the best bis(cobalt) catalyst; furthermore, a two-electron path is always observed (15%). Additionally, the activity of this catalyst is particularly dependent on the method of electrode surface preparation. Although the mechanism of this catalysis is unknown, these results suggest that the Ru centers become fully reduced (to Ru^{II}) and then, in concert with the EPG electrode, deliver all four electrons to the Co-O_2 center. There is a similarity between these results and that of cytochrome *c* oxidase, in which all four electrons must be loaded before the four-electron reduction of O_2 is achieved. The rates of these intramolecular electron transfers are apparently sufficiently rapid to effect four-electron reduction.

Another recent, related application of cofacial metallodiporphyrins is a functional analogue of manganese catalase (pseudo-

catalase).[8] Because the active site of pseudocatalase is thought to consist of two closely spaced manganese centers Naruta et al.[79] employed a cofacial bis(manganese) diporphyrin, [Mn_2(DPB)], to effect the disproportionation of hydrogen peroxide to oxygen and water. In this case the cofacial diporphyrin system appears to create an active reaction center that is bimetallic yet avoids a deleterious side reaction (μ-oxo complex formation).

Dioxygen reduction by mono- and cofacial diporphyrins continues to attract interest. In addition to attempts to develop new, more efficient catalysts, there is considerable interest in elucidating the role of the EPG electrode in these electroreductions. Work is in progress to attach cofacial diporphyrins to different electrode surfaces that are more amenable to spectroscopic studies of the catalytic species in situ. Covalent attachment of catalysts to such electrodes should reduce leaching of the catalyst from the electrode surface. The most significant challenge is to try to break the 0.7 V barrier by employing new heterobimetallic systems or through the use of peripherally substituted cofacial diporphyrins. Such peripheral substitution with electronegative groups might also protect the porphyrin ligand from decomposition due to the reduction by-product, H_2O_2.

6. The Reduction of Protons and Oxidation of Hydrogen

6.1. Background

The discovery and understanding of molecular electrode catalysts for the hydrogen electrode reaction have captured the attention of chemists for the last century. Efficient catalysts for this reversible two-electron conversion occur naturally in the hydrogenase enzymes; the mechanism is not yet understood.

At several metal surfaces the hydrogen electrode reaction is fully reversible. It thus occurs at the thermodynamic potential, determined by the solution pH according to the Nernst equation specific to this reaction:

$$2\,H^+ + 2\,e^- \rightleftharpoons H_2$$
$$E_{1/2} = 0.00\ V - 0.059\ V \times pH$$

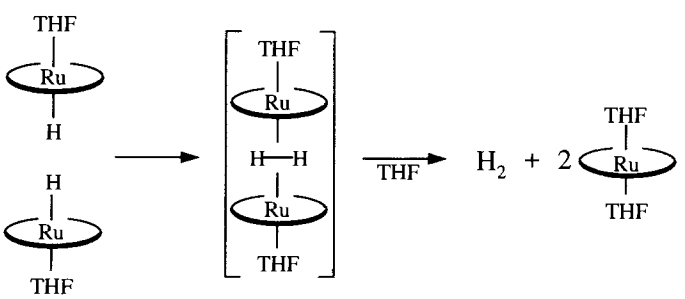
At many other metal surfaces, however, an overpotential is required to reduce protons or to oxidize hydrogen. As stated in Section 2, this overpotential arises because the reduction of a single proton by one electron, which results in the formation of an unstable hydrogen atom [Eq. (a)], occurs at -2.10 V vs. NHE.[17]

$$H^+ + e^- \longrightarrow H^\bullet \qquad \text{(a)}$$

The oxidation of dihydrogen must also proceed along extremely unfavorable pathways: either the initial oxidation of H_2 to H_2^+ if oxidation occurs first, or the deprotonation of H_2 to H^- if deprotonation occurs first. Lowering the barrier of these high-energy pathways allows certain metal surfaces to catalyze the hydrogen electrode reaction. Presumably, hydrogenase enzymes utilize the iron or nickel present in the active site to stabilize high-energy intermediates or destabilize the substrate. One of the long-term goals of research into the hydrogen electrode reaction has been to synthesize bimetallic complexes which will show the same catalytic activity as metal surfaces and hydrogenase enzymes.

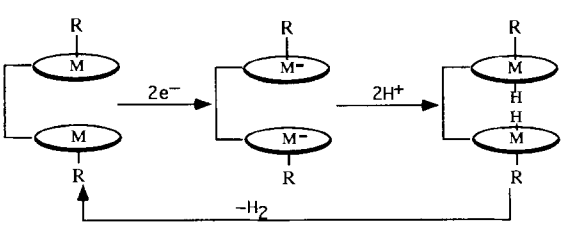
6.2. Proton Reduction Catalysts

Spiro et al.[80] and Espenson et al.[81] independently developed Co^I complexes which catalytically evolve dihydrogen at relatively low overpotentials. In both systems H_2 production was shown to proceed in part by a mechanism involving both metal centers in which two cobalt hydrides eliminate one molecule of dihydrogen. In order to facilitate hydrogen elimination from two metal hydrides, both Bitterwolf et al.[82] and Mueller-Westerhoff et al.[83] have prepared bridged bis(metallocenes) in which the two metal hydrides are held in close proximity. These systems catalytically reduce protons to hydrogen as well, presumably through a dinuclear elimination of hydrogen from the two linked metal hydrides. Research in our own laboratories has demonstrated that ruthenium(III) and osmium(III) octaethylporphyrin hydrides also eliminate hydrogen by an analogous mechanism[84] (Scheme 13). These results suggested that cofacial metallodiporphyrins might act as efficient electrocatalysts for proton reduction.

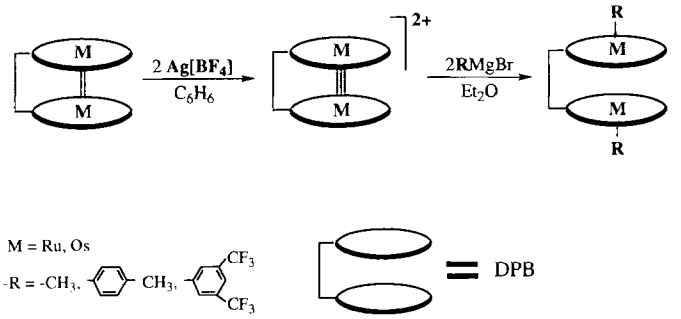


Scheme 13. Schematic illustration for the reductive elimination of dihydrogen from [Ru(OEP)(thf)H].

The challenge of this research was to synthesize a cofacial metallodiporphyrin with the outer faces blocked by axial ligands so that two protons could react with the metals only on the inside of the pocket. The resulting metal hydrides would then be in the ideal geometry to eliminate dihydrogen. The desired catalytic cycle is shown in Scheme 14. The catalysts shown in Scheme 15 were prepared by alkylation of [Ru_2(DPB)] and [Os_2(DPB)]. These complexes proved to be moderate catalysts (two to three turnovers in 20 minutes) for the reduction of protons at mercury pool electrodes in THF.[85]



Scheme 14. Catalytic cycle for proton reduction using cofacial metallodiporphyrins.



Scheme 15. Synthesis of proton reduction catalysts.

Varying the central metal and axial ligands (Scheme 15) changed the reduction potentials by approximately 600 mV (Table 3). Complexes with more positive reduction potentials may also have lower overpotentials for proton reduction. Unfortunately, the reduced forms of these catalysts become less basic as their reduction potentials become more positive. Thus, stronger acids are needed to carry out the catalysis shown in Scheme 14 for the compounds having more positive reduction potentials. The variation of basicity with reduction potential is that expected from the Nernst equation. Consequently, though cofacial metallodiporphyrin catalysts for proton reduction were prepared, the overpotential was not significantly affected by varying the reduction potential of closely related catalysts. These catalysts are furthermore handicapped by slow reaction kinetics; apparently solvent molecules competitively inhibit the reaction site by coordination with the metal centers.[85]

Table 3. Reduction potentials of cofacial bisorganometallic diporphyrin complexes $[M_2R_2(DPB)]$ from Scheme 15.

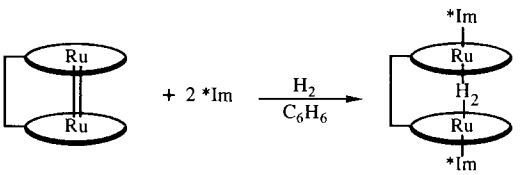
M	R	exp. $E_{1/2}$ [V] [a] (III)(III)	(III)(II)	(III)(II)	(II)(II)	Estimated $E_{1/2}$ [V] [b] (III)(III)	(III)(II)	(III)(II)	(II)(II)
Ru	3,5-$(CF_3)_2C_6H_3$	−0.94		−1.38		−0.39		−0.83	
Ru	4-$CH_3C_6H_4$	−1.26		−1.45		−0.71		−0.90	
Ru	CH_3	−1.38		−1.72		−0.83		−1.17	
Os	3,5-$(CF_3)_2C_6H_3$	−1.18		−1.58		−0.63		−1.03	
Os	4-$CH_3C_6H_4$	−1.47		−1.69		−0.92		−1.14	
Os	CH_3	−1.55		−1.97		−1.00		−1.42	

[a] Based on $FeCp_2^+/FeCp_2$. The cyclic voltammograms of the complexes were obtained in freshly distilled THF containing 0.2 M tetra-*n*-butylammonium hexafluorophosphate. The data were recorded at a scan rate of 100 mVs^{-1}. [b] Conversions used: $FeCp_2^+/FeCp_2 = +0.31$ V vs. SCE; SCE = +0.24 V vs. NHE.

6.3. Hydrogen Oxidation

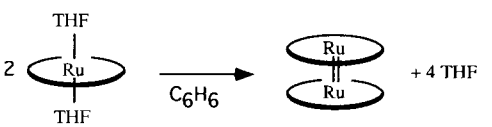
Oxidation of dihydrogen occurs at its thermodynamic potential at metal surfaces such as platinum. To our knowledge, however, no molecular catalysts for the oxidation of dihydrogen were previously known. Monomeric $[Ru(OEP)(thf)_2]$ is capable of binding dihydrogen which in turn is readily deprotonated. The resulting hydride is capable of reducing NAD^+ analogues and has been invoked in a scheme for H_2O/D_2O exchange.[86] This reactivity is quite reminiscent of hydrogenase enzyme reactivity and suggests that cofacial metallodiporphyrins might be useable as hydrogen oxidation catalysts.

Our approach to this problem[87] was to bind bulky axial ligands to the outer faces of a $[Ru_2(DPB)]$ complex in the presence of 1 atm of dihydrogen. The H_2 could then bind only inside the pocket of the bis(ruthenium) complex. Two equivalents of the bulky imidazole ligand 1-*tert*-butyl-5-phenylimidazole, *Im, were added to $[Ru_2(DPB)]$ in the presence of 1 atm of dihydrogen. The reaction forming $[Ru_2(DPB)(*Im)_2(H_2)]$ (Scheme 16) is quantitative. The dihydrogen molecule is bound as molecular hydrogen with the H–H axis parallel to the porphyrin planes as determined by the dipole–dipole coupling constant in a 620 MHz ^1H NMR experiment.[88] Our hope was that we could readily deprotonate the dihydrogen complex and that the resulting anion would undergo subsequent oxidation. Unfortunately, the complex does not deprotonate even with very strong bases such as NaH. This compound also proved to be incapable of hydrogen oxidation or proton reduction catalysis when adsorbed onto an EPG electrode.



Scheme 16. Preparation of the bridged dihydrogen complex $[Ru_2(DPB)(*Im)_2(H_2)]$.

Earlier success with the $[Ru(OEP)(thf)_2]$ monomer[86] suggested that it may be a good hydrogen electrode catalyst. When $[Ru(OEP)(thf)_2]$ is adsorbed onto an EPG electrode moderate hydrogen oxidation activity is found with an overpotential of 0.15 V. Further experiments demonstrated that the active form of the catalyst was actually the "cofacial dimer" $[Ru(OEP)]_2$ resulting from dimerization of two $[Ru(OEP)(thf)_2]$ molecules to form a Ru–Ru double bond. Such a dimerization has also been observed in solution (Scheme 17).[89] Rotating disk experiments with $[Ru(OEP)]_2$ adsorbed onto an EPG electrode in a basic aqueous solution saturated with both argon and hydrogen are shown in Figure 5. Note the significant oxidation wave in the hydrogen-saturated solution (Fig. 5b) which is not present under argon (Fig. 5a). The catalytic wave was also absent if no catalyst was adsorbed onto the electrode.[88]



Scheme 17. Dimerization reaction of $[Ru(OEP)(thf)_2]$.

Curiously, there is an absence of a steady-state current (i.e. the i-V curve has a peak rather than a steady-state plateau) in the slow scan rotating disk experiment under hydrogen. (Note the similarity between this behavior and that discussed earlier for dioxygen reduction, Sections 5.2 and 5.3.) The decrease in the oxidation current after the plateau indicates that the dihydrogen oxidation process is being inactivated at more positive

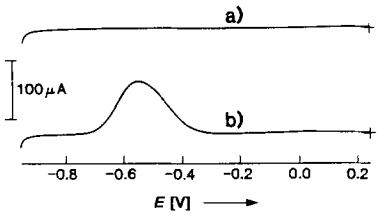


Fig. 5. Rotating disk voltammograms of a $[Ru(OEP)]_2$-modified EPG electrode in a basic aqueous solution (pH = 13). Scan rate = $5\,mVs^{-1}$, $\omega = 100$ rpm. a) Argon-saturated solution, b) hydrogen-saturated solution.

potentials. This is strictly an inactivation of the catalyst and *not* a destruction of the catalyst; subsequent scans through the wave show identical behavior. This decrease in oxidation current as the electrode is biased more positive suggests that the binding of dihydrogen occurs only within a certain potential window. At more positive potentials, the catalyst may be in an oxidized form which does not bind dihydrogen.[88]

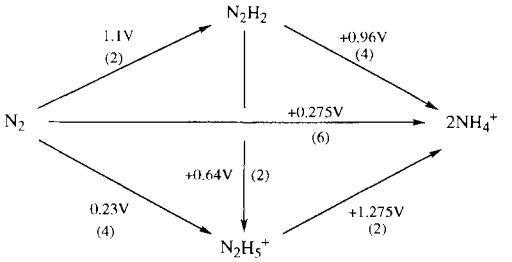
The oxidation current for dihydrogen is also pH dependent. (Again, this behavior parallels the case for the diporphyrin catalyzed oxygen reduction discussed in Section 5.) When identical experiments were performed in solutions in the pH range 10–13, the oxidation wave was found to move to a more positive potential and the current to decrease in intensity with decreasing pH, until the oxidation is nearly unobservable at pH = 10. Presumably, bound dihydrogen cannot be deprotonated when the pH of the solution is less than 10. Additionally, there is a decrease in the oxidation current when the solution pH is changed from 13 to 14. Addition of 1 M KBr to solutions at pH 13 also suppressed the oxidation current. Addition of 1 drop of pyridine (< 0.1% v/v) to the pH 13 solution completely suppressed the oxidation current. These experiments suggest that other ligands (OH^-, Br^- and pyridine) compete for the binding site of dihydrogen.[88]

Though the mechanism for this hydrogen oxidation remains largely unknown, the above experiments suggest that the binding of dihydrogen to a metal and the deprotonation are important steps. Unfortunately, these two requirements oppose each other. Binding of dihydrogen requires electron density on the metal to be donated into the antibonding orbitals of dihydrogen. Unfortunately, this renders the bound dihydrogen less acidic. Too little electron donation from the metal to dihydrogen renders the dihydrogen complex too short-lived to be deprotonated. On the other hand too much electron donation renders the bound dihydrogen too hydridic to be deprotonated. This latter phenomenon is responsible for the catalytic impotence of the $[Ru_2(DPB)(*Im)_2(H_2)]$ complex. Such a dilemma demonstrates the tightrope that must be traversed in designing these electrocatalysts.

7. The Interconversion of Dinitrogen and Its Nitrogen Hydrides

7.1. Background

Dinitrogen is perhaps the most challenging substrate to reduce electrocatalytically. Rupture of the first π bond of the N–N triple bond requires 130 kcal mol^{-1}, and the first ionization potential (15.6 eV) of the N_2 molecule rivals that of argon.[90] Various multielectron pathways linking dinitrogen with ammonia are shown in Scheme 18. Although the initial electron transfers are difficult, the overall thermodynamics of four- and



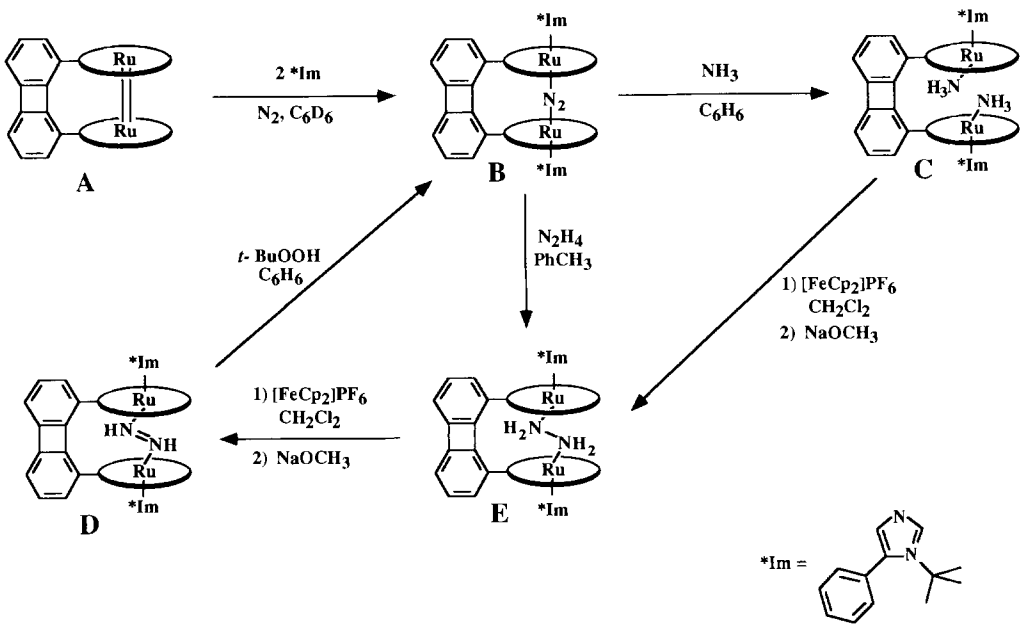
Scheme 18. Reduction of dinitrogen to ammonia.

six-electron reductions are exergonic. As was the case for dioxygen reduction (Section 5.1), the key to successful catalyst design is to avoid the initial one- or two-electron paths.

Although we proposed in 1977 that the cofacial metallodiporphyrin approach might also be applied to the electroreduction of dinitrogen,[24] progress toward this goal has been much slower than the development of the four-electron dioxygen catalysts. Although we were drawn initially toward early transition metal and certain heterobimetallic complexes of cofacial diporphyrins,[91] our primary target was a bis(ruthenium) compound because of the known dinitrogen coordination chemistry of ruthenium porphyrins.[92] The limited reactivity of known, bridged dinitrogen complexes[93] suggested that a bis(ruthenium) diporphyrin would not be a good dinitrogen electrode catalyst. However, through the study of the bis(ruthenium) dinitrogen complex and its nitrogen hydride analogues we hoped to learn which factors were important in designing better catalysts. Although the goal of electroreduction of dinitrogen to hydrazine (four electrons) or ammonia (six electrons) has still not been achieved, the information from these solution studies is being applied toward developing a functional electroreduction catalyst.

7.2. Stable Nitrogen and Nitrogen Hydride Complexes

The first step toward developing a dinitrogen electroreduction catalyst was to find a cofacial bis(ruthenium) diporphyrin that has a reasonable dinitrogen affinity and binds dinitrogen *between* the two metals. Initially, bis(ruthenium) complexes of FTF4, DPB, and DPA with exterior axial triphenylphosphane ligands and open internal coordination sites inside were prepared.[91] Although these complexes bind hydrazine within the cavity, they have no affinity for dinitrogen. After some experimentation, it was found that use of a nitrogenous axial ligand, 1-*tert*-butyl-5-phenylimidazole, provides a bis-five-coordinate complex that has a substantial dinitrogen affinity[94] (see Scheme 19). In fact, this N_2 complex, $[(\mu\text{-}N_2)Ru_2(DPB)(Im^*)_2]$, is substantially more stable than corresponding ruthenium monoporphyrin N_2 complexes (perhaps because of the "chelate" effect of the two metal centers).[47] The dinitrogen complex has been well-characterized[47] and seems to have the properties of a linear, bridged dinitrogen complex such as $[\{Ru(NH_3)_5\}_2N_2]$.[93] That the DPB framework can accomodate this geometry is unexpected given its dimensions (Section 3.3.4). There must be considerable flexibility in the porphyrin rings and/or displacement of the metal centers from the planes of the porphyrin rings. Given the bridging nature of this dinitrogen complex, one would



Scheme 19. Synthetic interconversions of dinitrogen and nitrogen hydride complexes of $[Ru_2(DPB)]$. **A**) The metal–metal bonded dimer, $[Ru_2(DPB)]$, **B**) the bridged dinitrogen complex, $[(\mu\text{-}N_2)Ru_2(DPB)(*Im)_2]$, **C**) the bis(ammine) complex, $[(NH_3)_2Ru_2(DPB)(*Im)_2]$, **D**) the bridged diazene complex, $[(\mu\text{-}N_2H_2)Ru_2(DPB)(*Im)_2]$, and **E**) the bridged hydrazine complex, $[(\mu\text{-}N_2H_4)Ru_2(DPB)(*Im)_2]$.

predict that it is not easily protonated.[47] Indeed, a very strong acid is required to protonate this complex (Section 7.4).

In hope of learning the requirements for a successful dinitrogen reduction catalyst, the plausible two-electron/two-proton intermediates (diazene, hydrazine, and bis(ammine) complexes) along the multielectron reduction pathway were prepared and characterized.[94] The synthetic methodology is shown in Scheme 19. The process of developing synthetic, oxidative conversions between these species led to a more detailed examination of these oxidations to determine whether the nature of these transformations could yield information about catalytic conversions between dinitrogen and ammonia.

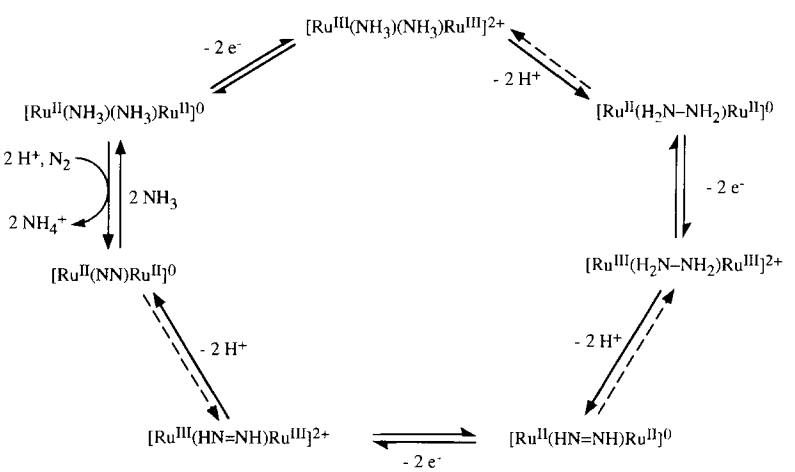
7.3. Oxidative Interconversions and Ammonia Oxidation

Oxidation of the bis(ammine) complex **C** with *tert*-butylhydroperoxide led not only to formation of the bridged hydrazine-complex **E**, but also to formation of the bridged diazene and dinitrogen complexes (**D** and **B**, respectively). Subsequent electrochemical oxidations as well as chemical oxidations employing either atom-transfer reagents such as *tert*-butylhydroperoxide or a combination of an outer-sphere oxidant (ferricinium) and a base were investigated to understand the redox and acid-base chemistry of each of the two-electron/two-proton steps. All of these intermediates have now been connected by oxidation, deprotonation, and ligand replacement reactions which describe a cycle (Scheme 20) for ammonia oxidation and provide insight into the reverse process, dinitrogen reduction.

The redox potential and a limiting pK_a of the base required for deprotonation in each of the oxidation steps has been determined.[95] Because the bis(ammine) complex **C** and the bridged hydrazine complex **E** could not be deprotonated (over the pH range studied) prior to oxidation,[95] the order of removal of electrons and protons from the complexes is known. In the pH range of the experiments ($pH \leq 16$), it appears that oxidation must occur prior to deprotonation in all steps. The most difficult oxidation and deprotonation of these conversions set pH and potential limits on this ammonia oxidation cycle ($+0.71$ V vs. NHE for the second oxidation of the diazene complex and a pK_a of about 16 for the deprotonation of the dicationic diruthenium bis(ammine) complex). Thus, for the cycle to proceed, the potential must be $\geq +0.71$ V and the pH of the solution ≥ 16.

A key transformation that cannot be controlled by pH or electrode potential is the N–N bond forming step ($[Ru^{III}(NH_3)(NH_3)Ru^{III}]^{2+} \rightleftharpoons [Ru^{II}(NH_2\text{–}NH_2)Ru^{II}]$). This thermally controlled step proceeds rapidly during oxidation, however, its reverse, an endothermic bond cleavage reaction, is likely to impede possible reduction cycles.

A possible kinetic limitation for the ammonia oxidation cycle involves replacement of the product (dinitrogen) by reactant (ammonia). The dinitrogen ligand is replaced slowly by ammo-



Scheme. 20. Catalytic oxidation (and reduction) cycle linking NH_3 and N_2. The bold arrows represent steps which have been accomplished.

nia in the neutral $Ru^{II}Ru^{II}$ complex; however, under the conditions required for ammonia oxidation catalysis, the complex should exist in the $Ru^{II}Ru^{III}$ state where the dinitrogen ligand would be much more easily replaced.[95]

Attempts to observe ammonia oxidation catalysis utilizing the dinitrogen complex adsorbed on EPG electrodes were unsuccessful, since uncoated EPG itself is a reasonable oxidation catalyst. Future research will be directed at attaching these catalysts to less active electrode materials.

7.4. Prospects for a Dinitrogen Reduction Catalyst

Our initial goal was to try to develop a dinitrogen reduction catalyst. Based on the oxidation chemistry described in Section 7.3, we can comment on the requirements for such a catalyst. Considering the reverse reaction of each oxidation step in the context of microscopic reversibility, it is predicted that the reductions will occur by first proton, then electron, addition. The limiting conditions for dinitrogen reduction can also be estimated (-0.22 V vs. NHE to reduce the diazene complex monocation and an acid stronger than trifluoroacetic acid to protonate the dinitrogen ligand). It is unlikely that any catalyst based on this system could reduce dinitrogen beyond the hydrazine intermediate due to the apparent required thermal N–N bond cleavage (see Section 7.3).[95]

In order to design a catalyst that can carry out the reduction of nitrogen to ammonia, a different reaction pathway may be required. In particular, metals having a lower d-electron count that favor formation of metal nitrides may be necessary. Possible catalysts employing cofacial diporphyrins containing transition metals found in the nitrogenase enzymes such as molybdenum, vanadium and iron are presently being studied.

8. Summary and Outlook

Some general principles of catalyst design can be gleaned from the results obtained with cofacial diporphyrin catalysts for multielectron redox reactions. The engineered cofacial diporphyrins provide a powerful framework for developing constrained bimetallic reaction centers. The multielectron catalytic pathways can be broken down into individual steps, which often can be studied independently. Additionally, using the principle of microscopic reversibility, the reverse catalytic cycle can be used to gain insight into the forward process.

A strong connection exists between the coordination and reactivity of the bound substrate. The chemical properties of the catalyst/substrate complex are perhaps more important than the catalyst's affinity for the substrate. For example, coordination of O_2 leads immediately to a partially reduced substrate (O_2^-). Conversely, coordination of H_2 renders this ligand acidic and facilitates deprotonation and subsequent oxidation. Coordination of N_2 by certain metal complexes, on the other hand, renders this ligand basic, facilitating protonation and further reduction.

Electrochemical limitations of a pathway derive from the most reducing or most oxidizing potential required for a catalytic reduction or oxidation, respectively. For example, the potential necessary for the catalytic reduction of dioxygen must be more negative than the most reducing potential for any single step. However, if the electrode potential is made too negative, the oxidation state of the catalyst will change and the activity of the catalyst may decrease. Similar potential dependencies are apparent for dihydrogen oxidation and dinitrogen reduction. *Thus, these molecular catalysts are active only within a well-defined potential range.*

Limiting pH ranges can be predicted from the Brønsted acidities of intermediates. Dihydrogen oxidation is a good example. This oxidation requires a deprotonation of bound dihydrogen, and thus the pH of the solution must be near or greater than the pK_a of bound dihydrogen. Again, similar behavior in proton reduction, oxygen reduction, and nitrogen reduction is observed.

Taken together, these considerations lead to an understanding of the limiting potential for the overall electrocatalytic reaction and the pH range under which this will function. From the overall limiting potential, one sees that most catalysts operate at an overpotential. One important caveat stems from this fact: *if there is an overpotential for the catalytic system in one direction, it is thermodynamically impossible for that catalyst to work using the microscopic reverse of the forward pathway.* Performing such a process would mean operating at an "underpotential". All of the catalysts surveyed here operate with an overpotential. Thus, it appears that most successful electrocatalysts will be useful in only one direction; a different or modified catalyst must be discovered for the reverse reaction.

Cofacial metallodiporphyrin catalysts appear to be most efficient when they are intimately associated with the electrode. This suggests rapid electron transfer is necessary, so that the desired electrocatalytic transformation occurs more rapidly than deleterious side reactions not involving electron transfer (such as hydrolysis or dissociation). In one case, a catalyst previously loaded with all four electrons required for O_2 reduction gives some four-electron reaction.[79] This system is reminiscent of enzymes such as cytochrome *c* oxidase, which are only effective when all four reducing equivalents are loaded.

Finally, the product of an electrocatalytic transformation must be labile; otherwise this product will inhibit further electrocatalytic cycling. For example, the two NH_3 molecules in nitrogenase enzymes must be replaced by N_2. It is interesting to note that this is possible in the bis(ruthenium) system that we have studied.

The role of a second metal (when required) varies. Both metals may be redox-active (as in the case of the bis(cobalt) catalyst for the reduction of O_2). Alternatively, the second metal may serve as a Lewis acid which both activates substrate and intermediates towards further reduction and kinetically stabilizes these intermediates, preventing undesirable side reactions along the multielectron path.

Examination of these electrocatalysts reveals similarities between the metallodiporphyrin catalysts and the respective enzyme systems, even though they are structurally different. One example of this is found in the overpotential for cytochrome *c* oxidase compared with the overpotential for the four-electron O_2 reducing catalysts (when these are adjusted for differences in pH). Apparently, both systems go through the same thermodynamic barrier, involving the intermediacy of bound peroxide. Parallels also exist between the H_2 oxidizing system and hydro-

genases. Experiments have shown that the [Ru(OEP)] catalyst is capable of activating dihydrogen to deprotonation, affording a hydride which is capable of reactivity similar to that manifested by the hydrogenase systems.[86] It is also curious that nitrogenase enzymes produce H_2 during nitrogen fixation. The bis(ruthenium) cofacial diporphyrin system described in Section 7, which binds dinitrogen tenaciously, forms a stable H_2 complex, which can be displaced by N_2. It is tempting to suggest nitrogenase enzymes carry out a prior reduction of H^+ and that the resulting H_2 complex "reserves" a coordination site for the incoming N_2 ligand.[111]

Systematic investigation has allowed us to break down the multielectron redox transformations into a series of steps. Many of the problems in these simple steps have not been solved but rather defined. Solutions to the overpotential and reversibility problems are still actively being sought. Searches are not confined to the substrates mentioned above, but include methane activation, water oxidation, CO_2 and CO reduction, and others. The search for new and better catalysts continues to be guided by the desire for a deeper understanding of how the natural enzymes solve such seemingly complex problems with relative ease.

The work described in this review was the result several important collaborations. The collaborative efforts of Prof. Fred Anson, Carl Koval, Richard Durand, and Prof. Nate Lewis at Cal Tech; Howard Tennent at Hercules Powder Co; Prof. Maurice L'Her and Yves LeMest at Université de Bretagne Occidentale, Brest, France; and Prof. Roger Guilard and Michel Angel Lopez at Université de Bourgogne, Dijon, France were most crucial. For the results obtained at Stanford, the creativity and hard work of a number of past students and research associates are most appreciated. The contributions of these associates are included in the reference section of this review. Among the key contributors to these projects are: Carmen Susanna Bencosme, Craig Barnes, Leng Leng Chng, Peter J. Denisevich, Eric Evitt, Michael Elliot, Matthew Ennis, Robert Gagne, Yunkyoung Ha, Thomas R. Halbert, Neil Hendricks, Kimoon Kim, Yutaka Konai, Charles Leidner, Matthew Marrocco, Brian Miller, Lisa McElwee White, Kurt Meier, Bryan D. Miller, Eric Schmittou, and Ben Tovrog. We thank Prof. Royce Murray (University of North Carolina), and Prof. Robert Hembre (University of Nebraska), for critical discussions and suggestions, and Hilary Arnold, Leng Leng Chng, H. T. Fish, and David Tyvoll for proofreading. Financial support from the NSF and NIH is gratefully acknowledged.

Received: September 6, 1993 [A 231E]
German version: *Angew. Chem.* **1994**, *106*, 1620

[1] *Metalloproteins: Chemical Properties and Biological Effects* (Eds.: S. Otsuka, T. Yamanaka), Elsevier, Amsterdam, **1988**.
[2] J. Tan, J. A. Cowan, *Biochemistry* **1991**, *30*, 8910–8917.
[3] M. W. W. Adams, L. E. Mortenson in *Molybdenum Enzymes* (Ed.: T. G. Spiro), Wiley-Interscience, New York, **1985**, pp. 519–593.
[4] M. Wikström, K. Krab, M. Saraste, *Cytochrome Oxidase: A Synthesis*, Academic Press, London, **1981**.
[5] G. T. Babcock, M. Wikström, *Nature* **1992**, *356*, 301–309.
[6] *Copper Proteins and Copper Enzymes, Vol. III* (Ed.: R. Lontie), CRC, Boca Raton, Fl, USA, **1984**.
[7] *The Biochemistry of Copper* (Eds.: J. Peisach, P. Aisen, W. E. Blumberg), Academic Press, New York, **1966**.
[8] K. Wieghardt, *Angew. Chem.* **1989**, *101*, 1179–1198; *Angew. Chem. Int. Ed. Engl.* **1989**, *28*, 1153–1172.
[9] R. Debus, *Biochim. Biophys. Acta* **1992**, *1102*, 269–352; *Manganese Redox Enzymes* (Ed.: V. Pecararo), VCH, New York, **1992**.
[10] R. N. F. Thorneley, D. J. Lowe in *Molybdenum Enzymes* (Ed.: T. G. Spiro), Wiley-Interscience, New York, **1985**, pp. 221–341.
[11] B. K. Burgess, *Chem. Rev.* **1990**, *90*, 1377–1406; W. Orme-Johnson, *Annu. Rev. Biophys. Biophys. Chem.* **1985**, *14*, 419–459; E. I. Stiefel, H. Thomann, H. Jin, R. E. Bare, T. V. Morgan, S. J. N. Burgmayer, C. L. Coyle, *ACS Symp. Ser.* **1987**, *372*, 372–389; R. H. Burris, *J. Biol Chem.* **1991**, *266*, 9339–9342; B. E. Smith, R. R. Eady, *Eur. J. Biochem.* **1992**, *205*, 1.
[12] M. W. W. Adams, *Biochim. Biophys. Acta* **1990**, *1020*, 115–145; a) *The Bioinorganic Chemistry of Nickel* (Ed.: J. R. Lancaster, Jr.), VCH, New York, **1988**; b) R. Cammack, V. M. Fernandez, K. Schneider in [12a], pp. 167–190; c) J. J. G. Moura, M. Teixeira, I. Moura, J. LeGall in [12a], pp. 191–226; M. W. W. Adams, L. E. Mortenson, J. S. Chen, *Biochim. Biophys. Acta* **1981**, *594*, 105–176.
[13] S. J. Lippard, *Science* **1993**, *261*, 699–700; K. D. Karlin, *ibid.* **1993**, *261*, 701–708.
[14] B. G. Malmström, *Chem. Rev.* **1990**, *90*, 1247–1260.
[15] J. H. Klemme, *Arch. Mikrobiol.* **1968**, *64*, 29–42; K. Schneider, H. G. Schlegel, *ibid.* **1977**, *112*, 229–238.
[16] M. M. Georgiadis, H. Komiya, P. Chakrabarti, D. Woo, J. J. Kornuc, D. C. Rees, *Science* **1992**, *257*, 1653–1659; J. Kim, D. C. Rees, *Nature* **1992**, *360*, 553–560.
[17] W. M. Latimer, *Oxidation Potentials*, 2nd ed., Prentice Hall, New York, **1952**, pp. 29–37.
[18] J. P. Collman, N. H. Hendricks, C. R. Leidner, E. Ngameni, M. L'Her, *Inorg. Chem.* **1988**, *27*, 387–393.
[19] H. R. Thirsk, J. A. Harrison in *A Guide to the Study of Electrode Kinetics*, Academic Press, New York, **1972**.
[20] W. J. Albery, M. L. Hitchman, *Ring-Disc Electrodes*, Clarendon, Oxford, **1971**.
[21] F. P. Schwarz, M. Gouterman, Z. Muljiani, D. Dolphin, *Bioinorg. Chem.* **1972**, *2*, 1–32.
[22] N. E. Kagan, *Brookhaven Symp. in Biol.* **1976**, *28*, 371.
[23] H. Ogoshi, H. Sugimoto, Z.-I. Yoshida, *Hukusokan Kagaku Toronkai Koen Yoshishu 8th 1975* **1975**, 239–243; *Chem. Abstr.* **1975**, *84*, 82897u.
[24] J. P. Collman, C. M. Elliott, T. R. Halbert, B. S. Tovrog, *Proc. Natl. Acad. Sci. USA* **1977**, *74*, 18–22.
[25] H. Ogoshi, H. Sugimoto, Z. I. Yoshida, *Tetrahedron Lett.* **1977**, *2*, 169–172.
[26] C. K. Chang, M.-S. Kuo, C.-B. Wang, *J. Heterocycl. Chem.* **1977**, *14*, 943–945.
[27] N. E. Kagan, D. Mauzerall, R. B. Merrifield, *J. Am. Chem. Soc.* **1977**, *99*, 5484–5486.
[28] C. K. Chang, I. Abdalmuhdi., *J. Org. Chem.* **1983**, *48*, 5388–5390.
[29] R. Guilard, M. A. Lopez, A. Tabard, P. Richard, C. Lecomte, S. Brandes, J. E. Hutchison, J. P. Collman, *J. Am. Chem. Soc.* **1992**, *114*, 9877–9890.
[30] C. K. Chang, I. Abdalmuhdi, *Angew. Chem.* **1984**, *96*, 154–155; *Angew. Chem. Int. Ed. Engl.* **1984**, *23*, 164–165.
[31] J. P. Collman, J. E. Hutchison, M. A. Lopez, A. Tabard, R. Guilard, W. K. Seok, J. A. Ibers, M. L'Her, *J. Am. Chem. Soc.* **1992**, *114*, 9869–9877.
[32] J. P. Collman, C. S. Bencosme, C. E. Barnes, B. D. Miller, *J. Am. Chem. Soc.* **1983**, *105*, 2704–2710.
[33] J. P. Collman, P. Denisevich, Y. Konai, M. Marrocco, C. Koval, F. C. Anson, *J. Am. Chem. Soc.* **1980**, *102*, 6027–6036.
[34] M. H. Hatada, A. Tulinsky, C. K. Chang, *J. Am. Chem. Soc.* **1980**, *102*, 7115–7116.
[35] R. Karaman, S. Jeon, O. Almarsson, T. C. Bruice, *J. Am. Chem. Soc.* **1992**, *114*, 4899–4905.
[36] R. Karaman, A. Blasko, O. Almarsson, R. Arasasingham, T. C. Bruice, *J. Am. Chem. Soc.* **1992**, *114*, 4889–4898.
[37] For an extensive listing of cofacial diporphyrin ligands, see: B. C. Bookser, T. C. Bruice, *J. Am. Chem. Soc.* **1991**, *113*, 4208–4218.
[38] H. L. Anderson, C. A. Hunter, M. N. Meah, J. K. M. Sanders, *J. Am. Chem. Soc.* **1990**, *112*, 5780–5789, and references therein.
[39] Y. P. Myer, A. Pande in *The Porphyrins, Vol. III* (Ed.: D. Dolphin), Academic Press, New York, **1978**, p. 286.
[40] C. K. Chang, *J. Heterocycl. Chem.* **1977**, *14*, 1285–1288.
[41] S. S. Eaton, G. R. Eaton, C. K. Chang, *J. Am. Chem. Soc.* **1985**, *107*, 3177–3184.
[42] J. P. Collman, A. O. Chong, G. B. Jameson, R. T. Oakley, E. Rose, E. R. Schmittou, J. A. Ibers, *J. Am. Chem. Soc.* **1981**, *103*, 516–533.
[43] J. P. Fillers, K. G. Ravichandran, I. Abdalmuhdi, A. Tulinsky, C. K. Chang, *J. Am. Chem. Soc.* **1986**, *108*, 417–424.
[44] K. Kim, J. P. Collman, J. A. Ibers, *J. Am. Chem. Soc.* **1988**, *110*, 4242–4246.
[45] W. R. Scheidt, Y. J. Lee in *Struct. Bonding (Berlin)*, **1987**, *64*, 1.
[46] R. Karaman, O. Almarsson, A. Blasko, T. C. Bruice, *J. Org. Chem.* **1992**, *57*, 2169–2173.
[47] J. P. Collman, J. E. Hutchison, M. A. Lopez, R. Guilard, *J. Am. Chem. Soc.* **1992**, *114*, 8066–8073.
[48] J. P. Collman, F. C. Anson, S. Bencosme, A. Chong, T. Collins, P. Denisevich, E. Evitt, T. Geiger, J. Ibers, G. Jameson, Y. Konai, C. Koval, K. Meier, R. Oakley, R. B. Pettman, E. Schmittou, J. Sessler in *Organic Synthesis Today and Tomorrow* (Eds.: B. M. Trost, C. R. Hutchinson), Pergamon, Oxford, **1981**, pp. 29–45.
[49] A. Damjanovic, M. A. Genshaw, J. O'M. Bockris, *J. Electrochem. Soc.* **1967**, *114*, 466–472.
[50] J. P. Collman, K. Kim, *J. Am. Chem. Soc.* **1986**, *108*, 7847–7849.

[51] *Standard Potentials in Aqueous Solution*, (Eds.: A. J. Bard, R. Parsons, J. Jordan), Marcel Dekker, New York, **1985**.
[52] J. Zagel, R. K. Sen, E. Yeager, *J. Electroanal. Chem. Interfacial Electrochem.* **1977**, *83*, 207–213.
[53] R. D. Jones, D. A. Summerville, F. Basolo, *Chem. Rev.* **1979**, *79*, 139–179.
[54] The binding of O_2 is, itself, a redox reaction in which simultaneously the metal center undergoes a one-electron oxidation and O_2 undergoes a one-electron reduction in the formation of the metal-dioxygen complex. There is a strong correlation between the $E_{1/2}$ value for M^{II}/M^{III} reduction and the affinity for O_2: lower $E_{1/2}$ values result in greater O_2 equilibrium affinities.
[55] J. P. Collman, M. Marrocco, P. Denisevich, C. Koval, F. C. Anson, *J. Electroanal. Chem. Interfacial Electrochem.* **1979**, *101*, 117–122.
[56] C. K. Chang, H. Y. Liu, I. Abdalmuhdi, *J. Am. Chem. Soc.* **1984**, *106*, 2725–2726.
[57] A. C. Riddiford, *Adv. Electrochem. Electrochem. Eng.* **1966**, 4, 47–116.
[58] R. R. Durand Jr., C. S. Bencosme, J. P. Collman, F. C. Anson, *J. Am. Chem. Soc.* **1983**, *105*, 2710–2718.
[59] J. P. Collman, F. C. Anson, C. E. Barnes, C. S. Bencosme, T. Geiger, E. R. Evitt, R. P. Kreh, K. Meier, R. B. Pettman, *J. Am. Chem. Soc.* **1983**, *105*, 2694–2699.
[60] J. P. Collman, N. H. Hendricks, K. Kim, C. S. Bencosme, *J. Chem. Soc., Chem. Commun.* **1987**, 1537–1538.
[61] H. Y. Liu, M. J. Weaver, C. B. Wang, C. K. Chang, *J. Electroanal. Chem. Interfacial Electrochem.* **1983**, *145*, 439–447.
[62] H. Y. Liu, I. Abdalmuhdi, C. K. Chang, F. C. Anson, *J. Phys. Chem.* **1985**, *89*, 665–670.
[63] C. L. Ni, I. Abdalmuhdi, C. K. Chang, F. C. Anson, *J. Phys. Chem.* **1987**, *91*, 1158–1166.
[64] C. Shi, F. C. Anson, *Inorg. Chem.* **1992**, *31*, 5078–5083.
[65] The RRDE can be calibrated by oxidizing a well-behaved redox probe (ferro/ferricyanide, for example) at the disk and rereducing it at the ring. The collection efficiency is the ratio of I_r/I_d for the reversible redox couple.
[66] T. Geiger, F. C. Anson, *J. Am. Chem. Soc.* **1981**, *103*, 7489–7496.
[67] V. G. Levich, *Physiochemical Hydrodynamics*, Prentice-Hall, Englewood Cliffs, NJ, **1962**.
[68] J. Koutecký, V. G. Levich, *Zh. Fizi. Khim.* **1958**, *32*, 1565–1575.
[69] A. Damjanovic, M. A. Genshaw, J. O'M. Bockris, *J. Chem. Phys.* **1966**, *45*, 4057–4059.
[70] R. R. Durand, F. C. Anson, *J. Electroanal. Chem. Interfacial Electrochem.* **1982**, *134*, 273–289.
[71] Y. Le Mest, M. L'Her, J. Courtot-Coupez, J. P. Collman, E. R. Evitt, C. S. Bencosme, *J. Chem. Soc., Chem. Commun.* **1983**, 1286–1287.
[72] Y. Le Mest, M. L'Her, J. P. Collman, N. H. Hendricks, L. McElwee-White, *J. Am. Chem. Soc.* **1986**, *108*, 533–535.
[73] E. Ngameni, Y. Le Mest, M. L'Her, J. P. Collman, N. H. Hendricks, K. Kim, *J. Electroanal. Chem. Interfacial Electrochem.* **1987**, *220*, 247–257.
[74] C. K. Chang, *J. Chem. Soc. Chem. Commun.* **1977**, 800–801.
[75] L. M. Proniewicz, J. Odo, J. Goral, C. K. Chang, K. Nakamoto, *J. Am. Chem. Soc.* **1989**, *111*, 2105–2110.
[76] B. R. Puri, *Chem. Phys. Carbon* **1970**, *6*, 191–282.
[77] C. Shi, F. C. Anson, *J. Am. Chem. Soc.* **1991**, *113*, 9564–9570.
[78] B. Steiger, C. Shi, F. C. Anson, *Inorg. Chem.* **1993**, *32*, 2107–2113.
[79] Y. Naruta, K. Maruyama, *J. Am. Chem. Soc.* **1991**, *113*, 3595–3597.
[80] R. M. Kellett, T. G. Spiro, *Inorg. Chem.* **1985**, *24*, 2373–2377; 2378–2382.
[81] P. Connolly, J. H. Espenson, *Inorg. Chem.* **1986**, *25*, 2684–2688; T.-H. Chao, J. H. Espenson, *J. Am. Chem. Soc.* **1978**, *100*, 129–133.
[82] T. E. Bitterwolf, A. C. Ling, *J. Organomet. Chem.* **1973**, *57*, C15–C18; *ibid.* **1981**, *215*, 77–86; T. E. Bitterwolf, *ibid.* **1983**, *252*, 305–316; T. E. Bitterwolf, W. C. Spink, M. D. Rausch, *ibid.* **1989**, *363*, 189–195.
[83] U. T. Mueller-Westerhoff, A. Nazzal, *J. Am. Chem. Soc.* **1984**, *106*, 5381–5382.
[84] J. P. Collman, P. S. Wagenknecht, N. S. Lewis, *J. Am. Chem. Soc.* **1992**, *114*, 5665–5673.
[85] J. P. Collman, Y. Ha, P. S. Wagenknecht, M. A. Lopez, R. Guilard, *J. Am. Chem. Soc.* **1993**, *115*, 9080–9088.
[86] J. P. Collman, P. S. Wagenknecht, R. T. Hembre, N. S. Lewis, *J. Am. Chem. Soc.* **1990**, *118*, 1294–1295.
[87] J. P. Collman, J. E. Hutchison, P. S. Wagenknecht, N. S. Lewis, M. A. Lopez, R. Guilard, *J. Am. Chem. Soc.* **1990**, *112*, 8206–8208.
[88] J. P. Collman, P. S. Wagenknecht, J. E. Hutchison, N. S. Lewis, M. A. Lopez, R. Guilard, M. L'Her, A. A. Bothner-By, P. K. Mishra, *J. Am. Chem. Soc.* **1992**, *114*, 5654–5664.
[89] G. D. Venburg, Ph.D. Thesis, Stanford University, Stanford CA, **1990**.
[90] G. J. Leigh in *The Chemistry and Biochemistry of Dinitrogen Fixation* (Ed.: J. R. Postgate), Plenum, London, **1971**, pp. 19–56.
[91] J. P. Collman, K. Kim, C. R. Leidner, *Inorg. Chem.* **1987**, *26*, 1152–1157.
[92] B. R. James, S. R. Mikkelson, T. W. Leung, G. M. Williams, R. Wong, *Inorg. Chim. Acta* **1984**, *85*, 209–213; C. Shista, M. J. Camenzind, B. R. James, D. Dolphin, *Inorg. Chem.* **1987**, *26*, 1181–1182; J. P. Collman, J. I. Brauman, J. P. Fitzgerald, J. W. Sparapany, J. A. Ibers, *J. Am. Chem. Soc.* **1988**, *110*, 3486–3495; B. R. James, A. W. Addison, M. Cairns, D. Dolphin, N. P. Farrell, D. R. Paulson, S. Walker in *Fundamental Research in Homogeneous Catalysis, Vol. 3* (Ed.: M. Tsutsui), Plenum, New York, **1979**, pp. 751–752; M. J. Camenzind, B. R. James, D. Dolphin, *J. Chem. Soc. Chem. Commun.* **1986**, 1137–1139; M. J. Camenzind, B. R. James, D. Dolphin, J. W. Sparapany, J. A. Ibers, *Inorg. Chem.* **1988**, *27*, 3054–3057.
[93] I. M. Treitel, M. T. Flood, R. E. Marsh, H. B. Gray *J. Am. Chem. Soc.* **1969**, *91*, 6512–6513; J. Chatt, A. B. Nikolsky, R. L. Richards, J. R. Sanders, *Chem. Commun.* **1969**, 154–155.
[94] J. P. Collman, J. E. Hutchison, M. A. Lopez, R. Guilard, R. A. Reed, *J. Am. Chem. Soc.* **1991**, *113*, 2794–2796.
[95] J. P. Collman, J. E. Hutchison, M. S. Ennis, M. A. Lopez, R. Guilard, *J. Am. Chem. Soc.* **1992**, *114*, 8074–8080.

Synthesis and Reactions of Optically Active Cyanohydrins

Franz Effenberger*

Cyanohydrins have always held a place of importance both as technical products and as reagents in organic chemistry. It is surprising, therefore, that optically active cyanohydrins have been extensively investigated and employed for syntheses relatively recently. This can be explained by the fact that only in the past few years have enzymatic methods made chiral cyanohydrins readily available in high optical purity. Chiral cyanohydrins are widespread in nature in the form of the respective glycosides and serve roughly 3000 plants and many insects as antifeedants. For the preparative organic chemist, this class of compounds offers an enormous synthetic potential for making other chiral compounds accessible. In a few instances, the pharmacological principle of a drug also incorporates a chiral cyanohydrin as constitutive structural element. In the development of novel, physiologically active compounds all possible stereoisomers must be synthesized and investigated with respect to their activity range and the pathway of their metabolic transformations and/or degradation. The development of simple synthetic procedures for such compounds, which also entail a high degree of stereoselectivity, therefore has prime importance. To this end chiral cyanohydrins may serve as stereochemically pure starting materials.

In the present review, the following topics will be addressed: enantioselective addition of hydrogen cyanide (HCN), catalyzed by the enzymes (*R*)- and (*S*)-oxynitrilase, to aldehydes and ketones yielding (*R*) and (*S*) cyanohydrins, respectively; enantioselective addition of HCN to aldehydes catalyzed by cyclic dipeptides; enantioselective esterification of racemic cyanohydrins and enantioselective hydrolysis of cyanohydrin esters catalyzed by lipases and esterases, respectively; transformation of the nitrile group of chiral cyanohydrins to provide optically active α-hydroxycarboxylic acids, aldehydes, and ketones, as well as 2-amino alcohols; sulfonylation of the OH group of chiral cyanohydrins to furnish optically active α-sulfonyloxynitriles which undergo S_N2 displacement of the activated OH group yielding α-azido-, α-amino, and α-fluoronitriles with inverted configuration.

1. Introduction

A whole series of procedures has been developed in the last few years for preparing optically active cyanohydrins as precursors for α-hydroxycarboxylic acids, α-hydroxy aldehydes, and vicinal amino alcohols, which have thus become accessible in stereochemically pure form.[1–3]

The stereoselective syntheses of cyanohydrins can be classified into chemical and enzymatic (enzyme-catalyzed) procedures. The most important chemical methods are the diastereoselective addition of trimethylsilyl cyanide[4] and related cyanide-transfer agents[5] to chiral aldehydes, and the enantioselective addition of trimethylsilyl cyanide to aldehydes in the presence of chiral catalysts.[6, 7] Enzymatic procedures leading to optically active cyanohydrins include the oxynitrilase-catalyzed enantioselective addition of HCN to aldehydes, the enantioselective hydrolysis of cyanohydrin ester racemates with esterases, and the enantioselective esterification of cyanohydrin racemates with lipases.

In special cases cyclic dipeptides also catalyze the enantioselective addition of HCN to aldehydes;[8] this procedure does not fit into the chemical/enzymatic classification. Formally, cyclic dipeptides can be considered chiral catalysts; however, structural similarities to the active center of oxynitrilases, the structure of which is not yet known, cannot be ruled out completely.

If one weighs the advantages and disadvantages of the chemical and enzymatic methods for preparing optically active cyanohydrins, the scales tip in favor of enzyme-catalyzed processes as general techniques, both with respect to the *ee* values attainable and possible adaptation for the preparation of cyanohydrins on a technical scale. This does not exclude the possibility, though, that other processes might be more advantageous in special cases.

This review focuses on the enzyme-mediated procedures and the use of cyclic dipeptide catalysts for the synthesis of optically active cyanohydrins, in particular aldehyde cyanohydrins, because of their practical importance. In addition, the tremendous potential of optically active cyanohydrins for the synthesis of other important chiral compounds will be discussed.

[*] Prof. Dr. F. Effenberger
Institut für Organische Chemie der Universität
Pfaffenwaldring 55, D-70569 Stuttgart (FRG)
Telefax: Int. code + (711)685-4269

 © VCH Verlagsgesellschaft mbH, D-69451 Weinheim, 1994 0570-0833/94/1515-1555 $ 10.00+.25/0

2. (*R*)-Oxynitrilase-Mediated Addition of HCN to Aldehydes

One of the first asymmetric synthesis effected by enzymes ("durch Enzyme bewirkte asymmetrische Synthese"[9]), published by L. Rosenthaler in 1908, concerns the preparation of mandelonitrile from benzaldehyde and HCN, with emulsin as source of the enzymatic catalyst. Rosenthaler gave detailed information on the course of the reaction and the effect of the reaction conditions on the optical yield, but this interesting example of an enzyme-catalyzed asymmetric synthesis was not followed up for many years.[10]

More than fifty years later E. Pfeil et al. took up the idea and developed it into a more general procedure. The enzyme (*R*)-oxynitrilase [EC 4.1.2.10], which actually catalyzes the addition of HCN to benzaldehyde, was isolated from bitter almonds (*Prunus amygdalus*), purified, and characterized.[11] It was shown that (*R*)-oxynitrilase accepts other aromatic aldehydes besides its natural substrate benzaldehyde, as well as saturated and unsaturated aliphatic and heterocyclic aldehydes; in each case, the enzyme catalyzes the formation of the corresponding (*R*) cyanohydrin.[12] (*R*)-Mandelonitrile was prepared with 86% *ee* (determined from the specific rotation), which was very high for that time. For less reactive aldehydes, however, the optical yield decreased dramatically; thus, this simple procedure for the preparation of (*R*) cyanohydrins found virtually no practical application for the next two decades.

All efforts failed to improve the optical yields under the conditions used by Pfeil et al. (solvent: water or water/ethanol; pH 5–6 corresponding to the activity optimum of the enzyme).[12b, 13a] Under these conditions the chemical addition of HCN to aldehydes leading to racemic products cannot be suppressed and prevails especially when the enzyme-catalyzed reaction is slow.

The decisive breakthrough for this process came when it was discovered that the undesirable chemical addition is more or less suppressed in organic solvents that are not miscible with water, for example ethyl acetate or diisopropyl ether (Fig. 1).[13] As Figure 1 shows, the uncatalyzed addition of HCN to benzaldehyde is very slow indeed in ethyl acetate. Thus even for aldehydes that are poor substrates for the enzyme, the enzymatic process predominates over the chemical addition in these media, and products with high *ee* values result (see Scheme 1, Table 1).[13] In contrast to most other enzyme-catalyzed reactions, (*R*)-oxynitrilase combines low substrate specificity with high enantioselectivity; for example, it accepts aromatic and aliphatic aldehydes and converts them to the respective cyanohydrins with high enantioselectivity (Table 1). Even with sterically demanding substrates such as isopentyl aldehyde, high

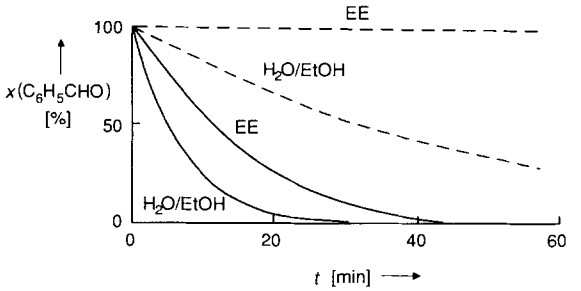
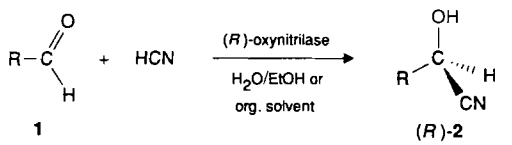


Fig. 1. Comparison of the rate of addition of HCN to benzaldehyde (x = mol fraction) in H_2O/EtOH and in ethyl acetate (EE) without enzyme (- - -) and with enzyme (—).



Scheme 1. Preparation of (*R*) cyanohydrins by (*R*)-oxynitrilase-catalyzed addition of HCN to aldehydes.

Table 1. Synthesis of (*R*) cyanohydrins (*R*)-**2** by enzyme-catalyzed addition of HCN to aldehydes **1** in H_2O/EtOH and in organic solvents [13].

R	in H_2O/EtOH			in EtOAc/Avicel [a]			in iPr_2O/Avicel [a]		
	t [h]	Yield [%]	*ee* [b] [%]	t [h]	Yield [%]	*ee* [b] [%]	t [h]	Yield [%]	*ee* [b] [%]
C_6H_5	1	99	86	2.5	95	99	3	96	>99
3-C_6H_5O-C_6H_4	5	99	11	192	99	98	–	–	
2-furyl	2	86	69	4	88	99	–		–
3-thienyl	–		–	–		–	6	95	>99
3-pyridyl	2.5	78	7	4.5	89	14	3	97	82
$H_3CCH{=}CH$	1.5	68	76	3	68	97	–	–	
$H_3CS(CH_2)_2$	3	87	60	6.5	97	80	16	98	96
C_3H_7	2	75	69	–	–	–	16	98.6	98
$C_6H_5(CH_2)_3$	–	–	–	–	–		45	94	90
$(H_3C)_3C$	2.5	56	45	4.5	78	73	4.5	84	83

[a] The enzymes were bound to crystalline cellulose (Avicel). [b] Determined by gas chromatography after either reaction with (*R*)-α-methoxy-α-trifluoromethylphenylacetoyl chloride [(*R*)-(+)-MTPA chloride] to provide the diastereomeric (*R*)-(+)-MTPA esters, or after acetylation with acetic anhydride [13].



Franz Effenberger was born in 1930 in Goldenstein (North Moravia), studied chemistry from 1951 to 1956 at the Technische Hochschule in Stuttgart, and received his PhD in 1959 with H. Bredereck. He completed his "Habilitation" in Stuttgart in 1964 and spent a year at the University of Michigan, Ann Arbor, with P. A. S. Smith. He was a Winnacker Fellow from 1964 to 1969. In 1972 he succeeded H. Bredereck at the University of Stuttgart. He was a guest professor in 1977 at Cornell University in Ithaca and in 1989 at the Ecole Supérieure de Physique et Chimie Industrielles in Paris. He received the Alexander-von-Humboldt-Forschungspreis in 1991. He is interested in preparative and mechanistic aspects of electron-rich π systems (enol ethers, aminobenzenes, donor–acceptor substituted polyenes, and oligothiophenes), synthesis and reactions of α-amino acids, and applications of enzyme reactions in organic synthesis with emphasis on stereoselective C–C bond formation.

ee values (83%) are obtained. The reaction of 3-phenoxybenzaldehyde strikingly illustrates the advantage of the organic compared to the aqueous reaction medium: the uncatalyzed reaction is suppressed to the extent that even after 192 h the corresponding (*R*) cyanohydrin is obtained with 98% *ee* (Table 1). Only the reaction of pyridine-3-carbaldehyde gives an unsatisfactory optical yield (14% *ee*) in ethyl acetate. A change of the organic medium to diisopropyl ether suffices to raise the *ee* value once more to a satisfactory 82% (Table 1).

The use of organic solvents in enzyme-catalyzed reactions has been widely reported,[14] especially for such processes where water is the actual reagent. Among these are ester-, amide-, and peptide-forming or -cleaving reactions catalyzed by lipases, amidases, and proteases.[14] Water does not actually take part in the (*R*)-oxynitrilase-catalyzed cyanohydrin formation, but it probably promotes the chemical addition of HCN to the carbonyl double bond.

Of the many organic solvents that have been tested for oxynitrilase-mediated reactions,[15] diisopropyl ether has proven especially advantageous with respect to the *ee* values obtained. This is illustrated strikingly by a number of reactions listed in Table 1 which were carried out in both ethyl acetate and diisopropyl ether. Moreover, enzyme activity in diisopropyl ether can be maintained even over a period of several weeks (Fig. 2). In ethyl acetate, in contrast, (*R*)-oxynitrilase activity is diminished by more than 50% within a few hours (Fig. 2). The lower water content in diisopropyl ether compared to that in ethyl acetate[16] apparently affects both (*R*)-oxynitrilase activity and stability very favorably.

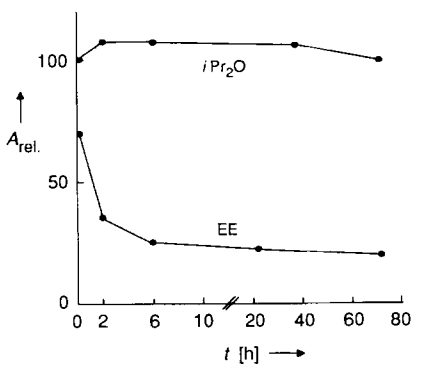


Fig. 2. Plot of the relative activity A of (*R*)-oxynitrilase on a crystalline cellulose support (Avicel) in ethyl acetate (EE) and diisopropyl ether (iPr_2O) [15].

For the reactions carried out in organic solvents it is particularly advantageous to employ enzymes bound to a suitable support, for example a crystalline cellulose material such as Avicel. Thus, the "support-bound" enzyme may be filtered off after the reaction is complete and reused as catalyst. (*R*)-Oxynitrilase in organic solvents also accepts rather high substrate concentrations (up to 2 mol L^{-1}) without decreasing the *ee* values; thus, product formation is characterized by a highly favorable space–time yield.[16] The reaction may even be run in a continuous mode: the starting materials are dissolved in the organic solvent and then passed over a column loaded with the support-bound enzyme,[15a] or alternatively, kept in a membrane reactor whence the products are separated from unreacted starting materials and the catalyst by evaporation.[15b]

In aqueous medium the oxynitrilase-catalyzed addition of HCN to aldehydes may be carried out with high selectivity also by simply lowering the pH of the reaction medium below 4.0, where the chemical addition is largely suppressed.[17] Enzyme activity, however, is also reduced at such low pH values. This may be compensated for by employing higher enzyme concentrations; still, reactions with the less reactive aldehyde substrates have poor selectivity. Also, this process is not conductive to the reaction of aldehydes that are poorly or not at all soluble in water.

Many attempts have been reported to avoid the use of the highly toxic, free hydrogen cyanide in the synthesis of cyanohydrins. For instance, aldehydes in water/ethanol have been treated with potassium cyanide and acetic acid in the presence of (*R*)-oxynitrilase; the respective (*R*) cyanohydrins were obtained, though with lower optical yields.[18] Transcyanation with acetone cyanohydrin as HCN donor in the presence of (*R*)-oxynitrilase has been reported to give (*R*) aldehyde cyanohydrins and acetone;[19] however, the selectivities claimed by the authors could not be reproduced.[20]

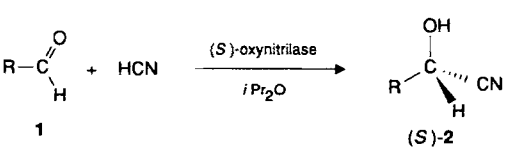
3. (*S*)-Oxynitrilase-Mediated Addition of HCN to Aldehydes

An enzyme that preferentially cleaves (*S*) cyanohydrins into aldehydes and HCN, and thus may also be expected to catalyze the reverse reaction, was first isolated from *Sorghum bicolor* and characterized by Conn and Bové in 1961.[21a] This (*S*)-oxynitrilase [EC 4.1.2.11] and the (*R*)-oxynitrilase [EC 4.1.2.10] from bitter almonds differ in both structure[11b, 21b, 22] and catalytic properties. The most striking structural difference is that (*R*)-oxynitrilase has a prosthetic group (flavine adenine dinucleotide, FAD) which is missing in (*S*)-oxynitrilase. Removal of the FAD moiety from the (*R*)-oxynitrilase results in complete loss of the catalytic activity.

It is substantially more time-consuming to isolate amounts of (*S*)-oxynitrilase sufficient for preparative purposes from *Sorghum bicolor* than it is to isolate (*R*)-oxynitrilase from bitter almonds. Consequently, this enzyme has been applied in organic syntheses only very recently.[23, 24]

(*S*)-Oxynitrilase from *Sorghum* catalyzes exclusively addition of HCN to aromatic and heteroaromatic aldehydes to yield the respective (*S*) cyanohydrins (Scheme 2), but it does not accept aliphatic aldehydes as substrates.[23, 24] The selectivities in organic solvents are comparable for the two enzymes (Tables 1, 2).

For the synthesis of (*S*) cyanohydrins, reactions in organic solvents rather than in aqueous medium are particularly advantageous since much smaller amounts of the poorly accessible



Scheme 2. Preparation of (*S*) cyanohydrins.

Table 2. Synthesis of (*S*) cyanohydrins (*S*)-**2** by enzyme-catalyzed addition of HCN to aldehydes **1** in diisopropyl ether [23].

R	(*S*) Cyanohydrin **2**			R	(*S*) Cyanohydrin **2**		
	t [h]	Yield [%]	*ee* [a] [%]		*t* [h]	Yield [%]	*ee* [a] [%]
C_6H_5	3	91	97	3-$F_3CC_6H_4$	20	87	52
4-ClC_6H_4	48	87	54	3-$H_3COC_6H_4$	20	93	89
4-$H_3CC_6H_4$	32	78	87	3-$C_6H_5OC_6H_4$	144	93	96
3-HOC_6H_4	24	97	91	2-furyl	9	80	80
3-BrC_6H_4	18	94	92	3-thienyl	20	85	97
3-ClC_6H_4	48	95	91				

[a] Determined by gas chromatography of the (*R*)-MTPA esters as described in Table 1.

enzyme are required. In addition some technically interesting (*S*) cyanohydrins, such as those from 3-phenoxybenzaldehyde and various heteroaromatic aldehydes, are difficult to prepare in an aqueous system owing to the low solubility of the respective aldehydes.[24]

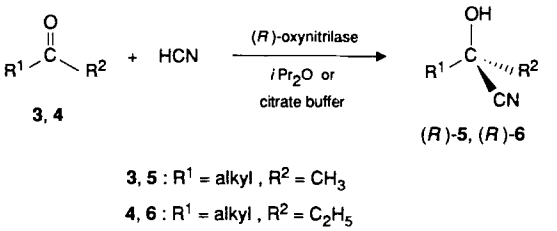
Recently, the catalytic activity of another (*S*)-oxynitrilase, isolated from the leaves of the rubber plant (*Hevea brasiliensis*), was investigated.[25] In contrast to (*S*)-oxynitrilase from *Sorghum*, this enzyme was found to accept both aliphatic and aromatic aldehydes; however, the enantioselectivity of the reaction proved to be unsatisfactory for a number of substrates tested.[25]

Despite all improvements in the isolation of (*S*)-oxynitrilase from *Sorghum bicolar* L.,[26] industrial application of this enzyme requires the respective gene to be cloned in pro- or eucaryotic organisms and overexpressed. So far, 90% of the native hydroxynitrile lyase (HNL) has in fact been cloned.[26b]

4. (*R*)-Oxynitrilase-Mediated Addition of HCN to Ketones

The few optically active ketone cyanohydrins described in the literature have as a rule been obtained by stereoselective addition of HCN or of cyanides to ketones that already have a stereogenic center. Thus, addition of HCN to 17-oxosteroids proceeds with very high diastereoselectivity.[27] Comparable optical induction is observed for the addition of $Me_2Si(CN)_2$ to chiral β-hydroxyketones,[28] of Et_2AlCN to chiral β-ketosulfoxides,[29] and of trimethyl-(2-propenyl)silane to chiral acyl cyanides.[30] The enantioselective hydrolysis of racemic esters of cyanohydrins with yeast cells from *Pichia miso* gives only poor chemical yield.[31]

The defense mechanism in which HCN is released from *O*-glycosyl cyanohydrins (cyanogenesis) by enzymes, is effective with both aldehyde and ketone cyanohydrins;[32] thus, ketones are likewise expected to be substrates for oxynitrilases. For the (*R*)-oxynitrilase from bitter almonds [EC 4.1.2.10] the natural substrate is benzaldehyde; surprisingly, this enzyme also catalyzes the addition of HCN to ketones (Scheme 3),[33] and (*R*) cyanohydrins are formed from 2-alkanones in good chemical yield and with excellent *ee* values.[33a] 3-Alkanones are much less suitable substrates; the respective cyanohydrins are obtained only with unsatisfactory chemical yield and also much lower optical purity (Table 3).[33] The best results for the synthesis of (*R*) ketone cyanohydrins are again obtained in organic



Scheme 3. Preparation of (*R*) ketone cyanohydrins.

Table 3. Synthesis of (*R*) ketone cyanohydrins (*R*)-**5** ($R^2 = CH_3$) and (*R*)-**6** ($R^2 = C_2H_5$) by enzyme-catalyzed addition of HCN to ketones **3** ($R^2 = CH_3$) and **4** ($R^2 = C_2H_5$), respectively, in diisopropyl ether [33a] and in aqueous citrate buffer [33b].

R^1	in iPr_2O/Avicel [a]				in citrate buffer [b]	
	(*R*)-**5** [c]		(*R*)-**6** [d]		(*R*)-**5** [c]	
	Yield [%]	*ee* [%]	Yield [%]	*ee* [%]	Yield [%]	*ee* [%]
nC_3H_7	70	97	33	85	78	95
nC_4H_9	90	98	21	90	94	98
nC_5H_{11}	88	98	7	66	56	96
$(H_3C)_2CHCH_2$	57	98	–	–	40	98

[a] 20 U enzyme per mmol ketone. [b] 50 U enzyme per mmol ketone. [c] Enantiomeric excesses of the diastereomeric (*R*)- or (*S*)-MTPA esters determined by gas chromatography [33]. [d] Enantiomeric excesses determined by gas chromatography on β-cyclodextrin columns after saponification to give the corresponding carboxylic acids and esterification with diazomethane [33b].

solvents; the *ee* values for reactions in citrate buffer (pH ≤ 4) are comparable if at least double the amount of enzyme is employed (Table 3).[33b] (*S*)-Oxynitrilase from *Sorghum bicolor* does not accept ketones as substrates.[24]

5. Cyclodipeptides as Catalysts for the Enantioselective Addition of HCN to Aldehydes

Inoue et al. showed that cyclic dipeptides (1,4-dioxopiperazines) containing a histidine moiety also catalyze the asymmetric addition of HCN to benzaldehyde to provide optically active mandelonitrile.[8, 34] The highest selectivity (87% *ee* of (*R*)-mandelonitrile) was obtained with the cyclic dipeptide from (*S*)-histidine and (*S*)-phenylalanine (Table 4).[34c] The reaction is not restricted to benzaldehyde. It has been extended to other aromatic aldehydes and numerous heterocyclic and aliphatic aldehydes; in most cases, though, the selectivity was unsatisfactory (Table 5).[34c, 35, 36] With ketones, the corresponding cyanohydrins are obtained with very low enantioselectivi-

Table 4. Cyclic dipeptides as catalysts for the enantioselective addition of HCN to benzaldehyde.

Catalyst	Mandelonitrile			Ref.
	Yield [%]	Config.	*ee* [%]	
cyclo[(*S*)-Ala-(*S*)-His]	50	*R*	9.9	[8a, 34a]
cyclo[(*R*)-Ala-(*S*)-His]	90	*R*	7.5	[8a, 34a]
cyclo[(*S*)-His-(*S*)-His]	50	*R*	2.5	[8a, 34a]
cyclo[(*S*)-His-(*S*)-Leu]	85	*S*	55	[34b]
cyclo[(*S*)-His-(*S*)-Phe]	40	*R*	90	[8b]
cyclo[(*S*)-His-(*S*)-Phe]	97	*R*	97	[34c]
cyclo[(*R*)-His-(*R*)-Phe]	86	*S*	79	[36a]

Table 5. Enantioselective addition of HCN to aldehydes **1** catalyzed by *cyclo*[(*S*)-His-(*S*)-Phe] to give (*R*) cyanohydrins (*R*)-**2**.

R	(*R*)-**2** Yield [%]	*ee* [%]	Ref.	R	(*R*)-**2** Yield [%]	*ee* [%]	Ref.
3-$C_6H_5OC_6H_4$	97	92	[34c]	4-$F_3CC_6H_4$	90	80	[36b]
2-$H_3COC_6H_4$	45	84	[34c]	4-$(CH_3)_2NC_6H_4$	50	53	[36b]
3-$H_3COC_6H_4$	97	90	[36b]	2-naphthyl	100	86	[36b]
4-$H_3COC_6H_4$	85	83	[36b]	2-furyl	76	93	[36b]
4-$H_3CC_6H_4$	91	92	[36b]	2-pyrrolyl	31	0	[36b]
4-$O_2NC_6H_4$	77	29	[36b]	2-thienyl	70	58	[36b]
3-HOC_6H_4	75	67	[35b]	3-pyridyl	89	0	[36b]
4-HOC_6H_4	86	35	[36b]	C_3H_7	100	26	[36b]
4-ClC_6H_4	96	66	[36b]	$C_6H_5CH_2$	100	14	[36b]
4-NCC_6H_4	100	32	[34c]	$(H_3C)_2CH$	79	71	[34c]
4-$C_6H_5OC_6H_4$	100	81	[36b]	*c*-C_6H_{11}	96	58	[34c]

ties.[36b] In virtually all cases examined so far, cyclic dipeptide catalysts with (*S*,*S*) configuration favor the formation of (*R*) cyanohydrins. Only with *cyclo*[(*S*)-His-(*S*)-Leu] are (*S*) cyanohydrins formed preferentially.[34b] The dipeptide catalyst *cyclo*[(*R*)-His-(*R*)-Phe] gives an excess of the (*S*) product, the respective *cyclo*[(*S*)-His-(*S*)-Phe] an excess of the (*R*) cyanohydrin (Table 4).[36a] This possibility of inverting the product configuration by simply changing the catalyst was employed in the synthesis of (*S*)-3-phenoxybenzaldehyde cyanohydrin,[36, 37] the alcohol component of a commercially important pyrethroid.[38]

The mechanism of the enantioselective addition of HCN to aldehydes under cyclic dipeptide catalysis still remains to be unraveled. Nothing definite is known yet, for instance, of the structure of the transition state or of intermediates, despite many efforts.[36a, 39]

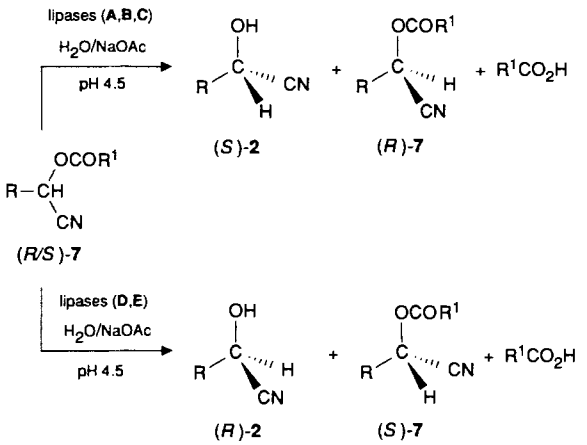
Acyclic dipeptides also show limited catalytic activity for enantioselective HCN addition to aldehydes; however, acceptable selectivities were obtained only in the presence of certain titanium complexes.[40]

6. Preparation of (*R*) and (*S*) Cyanohydrins by Kinetic Resolution with Esterases and Lipases

Aldehyde cyanohydrins are secondary alcohols and thus may form esters with carboxylic acids. Esterase-catalyzed hydrolysis or lipase-catalyzed esterification thus might be utilized to separate the enantiomers of either racemic cyanohydrins or cyanohydrin esters.[41]

6.1. Enantioselective Hydrolysis of Racemic Cyanohydrin Esters

If saponification of cyanohydrin acetate racemates catalyzed by ester hydrolases from *Pseudomonas sp.* is carried out in a phosphate buffer at pH 7, only the unreacted cyanohydrin acetates are isolated in stereochemically pure form. Under the reaction conditions the chiral cyanohydrins apparently are racemized.[42] Only in a few cases are the free cyanohydrins isolated as more or less pure enantiomers.[43] Hydrolysis with lipases in a sodium acetate buffer at pH 4.5 without exception affords both cyanohydrin esters and cyanohydrins in optically active form.[41] Lipases from *Pseudomonas fluorescens* (**A**), lipase PS (**B**) and lipase P (**C**), preferentially cleave the (*S*) cyanohydrin acetates; with lipases from *Candida cylindracea* (**D**) and with lipase AY (**E**), on the other hand, the (*R*) cyanohydrins are formed (Scheme 4).[41] For the lipases **A**, **B**, and **C**, aromatic



Scheme 4. Enantioselective hydrolysis of racemic cyanohydrin esters (R = C_3H_7, C_6H_5; R^1 = CH_3, C_3H_7, C_5H_{11}, $C_6H_5CH_2$) with various lipases to give (*R*) cyanohydrins and (*S*) cyanohydrin esters, and (*S*) cyanohydrins and (*R*) cyanohydrin esters; lipase from *Pseudomonas fluorescens* (**A**), lipase PS (**B**), lipase P (**C**), lipase from *Candida cylindracea* (**D**), and lipase AY (**E**).

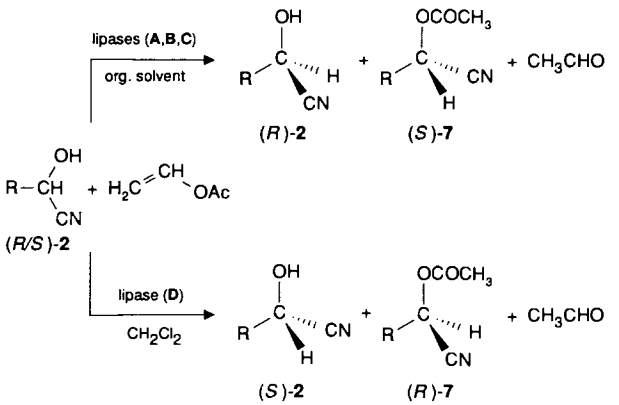
cyanohydrin esters are good substrates (R = C_6H_5), but aliphatic derivatives (R = C_3H_7) are not. Butyrates (R^1 = C_3H_7) yield (*S*) cyanohydrins with the highest selectivities (97% *ee*). The situation is reversed for lipases **D** and **E**; for these enzymes, the aliphatic cyanohydrin esters (R = C_3H_7) are good substrates, and the butyrates (R^1 = C_3H_7) once again give (*R*) cyanohydrins with the highest selectivities (up to 86% *ee*).

6.2. Enantioselective Esterification of Cyanohydrin Racemates

Chiral cyanohydrins do not racemize to any significant extent in organic solvents. Lipase-catalyzed enantioselective esterification of a cyanohydrin racemate in organic solvents thus appears especially suitable for racemate resolution when the unprotected optically active cyanohydrin is desired.[41, 43] With vinyl acetate, for which acylation is not reversible,[44] and in dichloromethane as solvent,[41] the lipases **A**–**D** exhibit the same configurational specificity as that observed in the enantioselective hydrolysis of the ester racemates described in Section 6.1 (Scheme 5).

The highest optical yields for the (*S*) acetates (*S*)-**7**, up to 98% *ee*, for aromatic cyanohydrins have been obtained with *Pseudomonas fluorescens* lipase (**A**),[41] which also catalyzes the acetylation of aliphatic cyanohydrins yielding the acetates (*S*)-**7**.

One principal disadvantage of kinetic resolution is that at most 50% of the racemic material can be obtained as the desired enantiomer. It is generally necessary, therefore, to subsequently racemize the remaining undesired enantiomer and to return the resulting racemate to the process. The enantioselective acetylation of a cyanohydrin racemate may also be carried out with



Scheme 5. Enantioselective esterification of cyanohydrin racemates (R = C_3H_7, C_6H_5, $C_6H_5CH_2CH_2$, 4-HOC_6H_4, 3-$CH_3OC_6H_4$, etc.) with vinyl acetate in organic solvents with various lipases (cf. Scheme 4).

isopropenyl acetate in an organic solvent and in the presence of a basic ion exchange resin that is sufficiently basic to cause racemization of the cyanohydrin, but not of the optically active cyanohydrin acetate formed.[45] Thus, a subsequent, separate racemization is no longer required, and the racemic substrate can be completely converted into one enantiomer. The subsequent hydrolysis of the enantiomerically pure cyanohydrin acetates can be conducted under nonracemizing conditions.

Apart from the enantioselective hydrolysis of cyanohydrin ester racemates (Section 6.1) and the enantioselective esterification of such racemic cyanohydrins (Section 6.2), racemic mixtures of cyanohydrin esters can be resolved by lipase-catalyzed transesterification with high-boiling alcohols in organic solvents.[41, 46]

7. Stereoselective Reactions of Optically Active Cyanohydrins

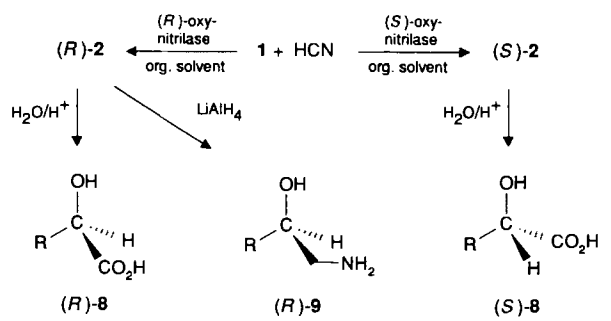
Since chiral cyanohydrins as α-substituted carboxylic acid derivatives have considerable synthetic potential, subsequent stereoselective reactions should lead to other important classes of compounds with stereogenic centers. Two types of reactions of cyanohydrins can be differentiated: reactions of the CN function which do not involve the α-hydroxyl moiety, and those in which reaction occurs at the OH group. Application of either reaction type in general synthesis requires racemization-free processes.

7.1. Reactions of the Nitrile Group

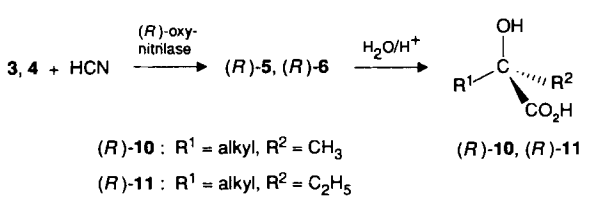
In contrast to α-amino acids, only a few optically active α-hydroxycarboxylic acids are found in nature. General processes for the preparation of chiral α-hydroxycarboxylic acids therefore had to be developed. Today, they are accessible by straightforward chemical synthesis,[47] by fermentation,[48] and by enzymatic processes.[49, 50] Specific (*S*) α-hydroxycarboxylic acids may be obtained by diazotization of natural L α-amino acids in aqueous medium. The diazonium salts formed initially undergo intramolecular substitution to the respective α-lactones with inversion of configuration; these are hydrolyzed, again with inversion, to give α-hydroxycarboxylic acids with a configuration identical to that of the starting α-amino acid. The (*S*) enantiomers thus obtained may be converted into the corresponding (*R*)-2-hydroxycarboxylic acids by activation of the OH group followed by S_N2 displacement with an oxygen nucleophile.[51]

The racemization-free hydrolysis of chiral cyanohydrins offers an interesting general route to (*R*) and (*S*) 2-hydroxycarboxylic acids. Hydrolysis of an optically active cyanohydrin with concentrated hydrochloric acid was first described for mandelonitrile where it was used to probe for the optical purity of the nitrile.[10a] Other authors later on assumed that in some cases acid-catalyzed hydrolysis of unprotected cyanohydrins resulted in partial racemization.[31, 35a] O-protected cyanohydrins, on the other hand, are hydrolyzed with a high degree of retention of configuration to the respective α-hydroxycarboxylic acids in both acidic[52] and basic media.[44a] Since both the formation of a cyanohydrin and its cleavage to the aldehyde and HCN are base catalyzed, one might expect that the acid-catalyzed hydrolysis of unprotected cyanohydrins would proceed without racemization.

(*R*) and (*S*) cyanohydrins derived from aldehydes[13c, 23] and (*R*) ketone cyanohydrins[33] are indeed hydrolyzed by concentrated hydrochloric acid to give the corresponding (*R*) and (*S*) hydroxycarboxylic acids, respectively, in excellent chemical yield and with complete retention of configuration (Schemes 6, 7; Tables 6, 7). Actually, such hydrolyses can be carried out quite simply. In the first step, the optically active cyanohydrins are prepared from the parent carbonyl compound and HCN in an organic solvent under enzyme catalysis. The Avicel-bound enzyme is filtered off, the solvent removed, and the cyanohydrin residue hydrolyzed with concentrated hydrochloric acid directly and without any additional purification step. The HCl is removed, and the α-hydroxycarboxylic acids are extracted with



Scheme 6. Acid-catalyzed hydrolysis of (*R*) and (*S*) cyanohydrins to give (*R*) and (*S*) 2-hydroxycarboxylic acids, respectively, and racemization-free hydrogenation of (*R*) cyanohydrins to give (*R*) 2-amino alcohols.



Scheme 7. Acid-catalyzed hydrolysis of (*R*) ketone cyanohydrins to give (*R*) 2-hydroxycarboxylic acids.

Table 6. Acid-catalyzed hydrolysis of the (*R*) and (*S*) cyanohydrins **2** [a] (prepared in situ by enzyme-catalyzed addition of HCN to aldehydes **1**) to give (*R*) and (*S*) α-hydroxycarboxylic acids **8**, respectively.

R	(*R*)-**2** *ee* [%]	(*S*)-**2** *ee* [%]	(*R*)-**8** Yield [%]	(*R*)-**8** *ee* [b] [%]	(*S*)-**8** Yield [%]	(*S*)-**8** *ee* [b] [%]
C_6H_5	99	97	82	99	77	98
4-$H_3CC_6H_4$	98	78	82	98	75	78
4-ClC_6H_4	99	54	71	99	63	54
3-$C_6H_5OC_6H_4$	97	96	72	97	70	96
3-$O_2NC_6H_4$	89	–	81	87	–	–
$C_6H_5CH_2$	74	–	90	74	–	–
c-C_6H_{11}	99	–	88	97	–	–
3-BrC_6H_4	–	92	–	–	76	90
3-ClC_6H_4	–	91	–	–	69	91
3-$H_3COC_6H_4$	–	89	–	–	67	90
$H_3C(CH_3)_2$	96	–	85	96	–	–
2-$H_3CS(CH_2)_2$	98		87	98		–

[a] Crude product. [b] Determined by gas chromatography after formation of the isopropyl ester (treatment with HCl-saturated isopropanol) and subsequent derivatization to the diastereomeric (*R*)-MTPA esters [13, 23].

Table 7. Acid-catalyzed hydrolysis of the (*R*) ketone cyanohydrins (*R*)-**5** and (*R*)-**6** (prepared in situ by enzyme-catalyzed addition of HCN to ketones **3** and **4**, respectively) to α-hydroxycarboxylic acids (*R*)-**10** and (*R*)-**11**, respectively [33].

R^1	R^2	(*R*)-**5**, (*R*)-**6** *ee* [%]	(*R*)-**10**, (*R*)-**11** Yield [%]	(*R*)-**10**, (*R*)-**11** *ee* [a] [%]
C_2H_5	CH_3	76	85	76
nC_3H_7	CH_3	97	64	99
nC_4H_9	CH_3	98	72	98
nC_5H_{11}	CH_3	98	78	98
$(H_3C)_2CH$	CH_3	90	76	90
$(H_3C)_2CHCH_2$	CH_3	98	89	96
$(H_3C)_2CH(CH_2)_2$	CH_3	98	88	99
nC_3H_7	C_2H_5	85	82	85
nC_4H_9	C_2H_5	90	89	90

[a] Determined by gas chromatography on β-cyclodextrin columns after esterification with diazomethane [33].

diethyl ether, isolated, and characterized. Comparison of the optical purity of the crude cyanohydrins with that of the isolated and purified α-hydroxycarboxylic acids shows hydrolysis to proceed virtually without racemization in all cases investigated (Tables 6, 7).

A wide spectrum of cyanohydrins is easily accessible by the enzymatic procedure outlined above. The acid-catalyzed hydrolysis of the optically active cyanohydrins, which can be conducted without racemization, thus represents a general route for the preparation of chiral α-hydroxycarboxylic acids.

Optically active α-hydroxy aldehydes are also important structural elements in natural products and thus might also be employed as chiral starting materials in asymmetric syntheses.[52] Direct conversion of optically active cyanohydrins into the corresponding α-hydroxy aldehydes would make this class of compounds easily accessible. Cyanohydrin racemates in fact have been hydrogenated with Raney nickel in acidic medium to α-hydroxy aldehydes.[53a] When this procedure was extended to optically active cyanohydrins, the configuration of the isolated products indicated that hydrogenation occurs with a high degree of retention of configuration.[53b] Because of the moderate yields and the difficult product isolation, however, selective hydrogenation of α-hydroxycarboxylic acids (see above) appears a much more favorable route to chiral α-hydroxy aldehydes.[52d, 54]

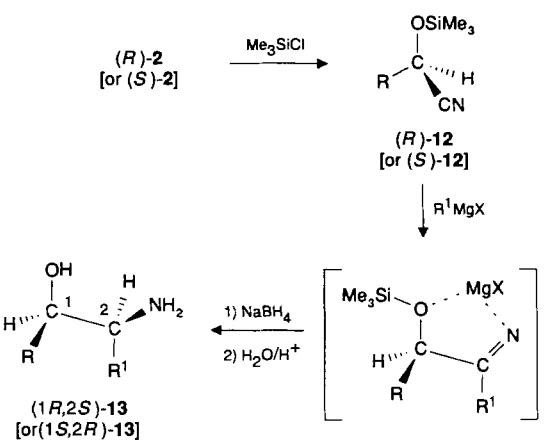
Hydrogenation of chiral cyanohydrins to 2-amino alcohols is also of considerable preparative interest, since these compounds have a wide spectrum of biological activity.[55] They may be categorized as adrenalin-type derivatives (amino function at a primary carbon atom) or ephedrin-type derivatives (amino function at a secondary carbon atom). Adrenalin-type 2-amino alcohols can be prepared from O-protected chiral cyanohydrins by various hydrogenating procedures without any trace of racemization.[4a, 43a, 56] Interestingly, free chiral cyanohydrins may also be hydrogenated directly and without racemization to the corresponding amino alcohols.[13c] Here, as in the synthesis of α-hydroxycarboxylic acids, the chiral cyanohydrins obtained from enzyme-catalyzed HCN addition in organic solvents can be applied directly, without any specific purification, for the hydrogenation process (Scheme 6, Table 8).[13c]

Table 8. Hydrogenation of (*R*) cyanohydrins (*R*)-**2** (prepared in situ by enzyme-catalyzed addition of HCN to aldehydes **1**) with $LiAlH_4$ to give amino alcohols (*R*)-**9** [13c].

R	(*R*)-**2** *ee* [%]	(*R*)-**9** Yield [%]	(*R*)-**9** *ee* [a] [%]	R	(*R*)-**2** *ee* [%]	(*R*)-**9** Yield [%]	(*R*)-**9** *ee* [a] [%]
C_6H_5	99	92	99	2-$H_3CS(CH_2)_2$	98	31	98
3-$C_6H_5OC_6H_4$	98	97	95	nC_3H_7	96	99	89
4-$H_3CC_6H_4$	99	100	>98	2-furyl	98	71	98
c-C_6H_{11}	91	94	80	$(H_3C)_3C$	93	70	>90

[a] Determined by gas chromatography on Chiracil-Val columns after conversion into the corresponding (*R*)-β-*N*,*O*-bis(trifluoroacetyl)amino alcohols by treatment with trifluoroacetic acid [13c].

Preparation of 2-amino alcohols of the ephedrin type starting from cyanohydrins was first described by Krepski et al.; O-protected racemic cyanohydrins were reacted with Grignard reagents, and the resulting imino intermediates were subsequently hydrogenated with $NaBH_4$.[57] This method was also applied successfully to (*R*) and (*S*) cyanohydrins.[58, 59] Investigation of the stereochemistry of this reaction for both (*R*) and (*S*) cyanohydrins established that the Grignard addition pro-



Scheme 8. Stereoselective synthesis of 2-amino alcohols. R = C_3H_7, C_6H_5; R^1 = CH_3, C_2H_5, C_6H_5; X = Br, I.

ceeds without any racemization at C-1. The hydrogenation at C-2 is highly diastereoselective owing to chelate control; *erythro* products are formed almost exclusively (Scheme 8, Table 9).[59] On the other hand, the *threo* compounds are formed predominantly when *N*-diisobutylaluminum hydride is added to the O-protected cyanohydrin before the organolithium reagent is added.[60] This procedure, however, is decidedly less diastereoselective.[60]

Table 9. Synthesis of 2-amino alcohols (1*R*,2*S*)- and (1*S*,2*R*)-**13** from the respective cyanohydrins (*R*)- and (*S*)-**2** (crude products) by formation of the trimethylsilyl ethers (*R*)- and (*S*)-**12**, Grignard reaction, and subsequent hydrogenation of sodium borohydride [59].

R	Cyanohydrin **2**		2-Amino alcohol (1*R*,2*S*)- or (1*S*,2*R*)-**13**					
	ee [%]	Config.	R^1	Yield [a] [%]	*ee* [b] [%]	*de* [b] [%]	*ee* [c] [%]	*de* [c] [%]
C_6H_5	>99	(*R*)	C_6H_5	83	99	99	100	100
C_6H_5	>99	(*R*)	C_2H_5	53	97	94	>99	>99
C_6H_5	>99	(*R*)	CH_3	50	99	92	99	>99
C_3H_7	95	(*R*)	C_6H_5	93	92	93	>99	>99
C_3H_7	95	(*R*)	CH_3	44	93	63	–	63
C_6H_5	>99	(*S*)	C_6H_5	95	99	99	100	100
C_6H_5	>99	(*S*)	CH_3	66	99	90	>99	>99

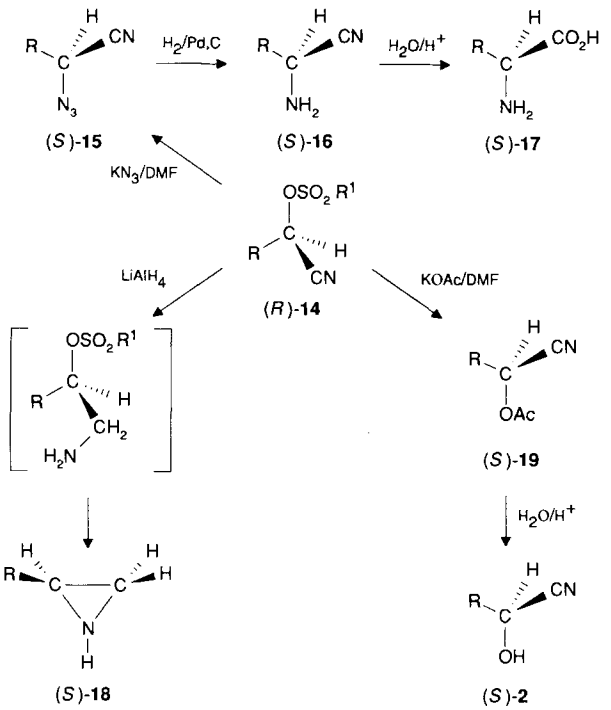
[a] As the hydrochloride. [b] Determined by gas chromatography after treatment of the crude products with pivaloyl chloride and filtration through silica gel. [c] Determined after one recrystallization.

In both hydrogenation[61a] and Grignard reaction[61b] with O-protected cyanohydrins, imines are formed initially; these may be subjected to transimination with primary amines to furnish biologically interesting N-substituted amino alcohols. Addition of HCN to the imino compounds affords β-hydroxy α-amino acids stereoselectively, if one starts out with a chiral cyanohydrin.[62] Hydrolysis of the imino compounds formed by addition of Grignard reagents to O-protected chiral cyanohydrins yields optically active acyloins.[18a, 63]

7.2. Reactions of the Hydroxyl Group

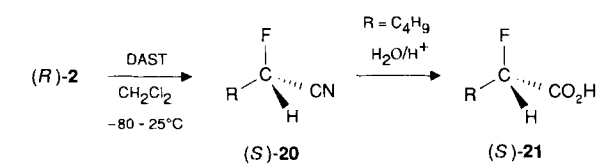
The synthetic potential of optically active cyanohydrins can be extended tremendously if the OH group is converted into a good leaving group which may be exchanged stereoselectively with a wide range of nucleophiles.[64] Nucleophilic substitution reactions with activated α-hydroxycarboxylic acids and esters are well established,[51a, 65] but little is known about the analogous reactions of α-hydroxynitriles.[66] So far only α-halonitriles have been prepared in optically pure form.[66] The halide ion released upon reaction of these compounds is a good nucleophile and leads to partial racemization of the chiral α-halonitriles during nucleophilic substitution.[66] α-Sulfonyloxynitriles (*R*)-**14**, which are easily accessible from chiral cyanohydrins (*R*)-**2** by sulfonylation, have a much higher configurational stability than the α-halonitriles (Scheme 9).[64] α-Sulfonyloxynitriles derived from aliphatic cyanohydrins are considerably more stable than those from aromatic cyanohydrins.[64] Under mild conditions aliphatic α-sulfonyloxynitriles (*R*)-**14** react with nucleophiles with complete inversion of configuration; the aromatic analogues react with weak nucleophiles with at least partial racemization.[64]

Nucleophilic substitution of optically active α-sulfonyloxynitriles (*R*)-**14** allows access to a great variety of interesting compounds, such as α-azidonitriles (*S*)-**15**, α-aminonitriles (*S*)-**16**, α-amino acids (*S*)-**17**, and aziridines (*S*)-**18** in optically pure form (Scheme 9).[64] Aliphatic cyanohydrins (*S*)-**2**, which are not accessible by the (*S*)-oxynitrilase-catalyzed addition of HCN to aldehydes,[23, 24] may be prepared by S_N2 reactions of the stable (*R*) 2-sulfonyloxynitriles (*R*)-**14** with acetates.[64b] The resulting cyanohydrin esters (*S*)-**19** then are hydrolyzed to the cyanohydrins (*S*)-**2**.



Scheme 9. Stereoselective reactions of sulfonyl-activated (*R*) cyanohydrins with nucleophiles with inversion of configuration. $R^1 = CH_3$, CF_3, 4-$CH_3C_6H_4$.

Sulfonyl-activated cyanohydrins are often employed in synthesis, since both the cyanohydrin and the nucleophile can be varied. In addition, direct stereoselective reactions of the cyanohydrin OH group are also feasible with special reagents. (*S*) Fluoronitriles (*S*)-**20**, for instance, may be prepared directly and in good optical yield from the (*R*) cyanohydrins (*R*)-**2** by reaction with diethylaminosulfur trifluoride (DAST).[67] These α-fluoronitriles (*S*)-**20** then are hydrolyzed to the α-fluorocarboxylic acids (*S*)-**21** without notable racemization (Scheme 10).[67]



$R = C_3H_7$, C_4H_9, $(H_3C)_2CHCH_2$, *c*-C_6H_{11}, C_6H_5

Scheme 10. Preparation of (*S*) 2-fluoronitriles and (*S*)-2-fluorocarboxylic acids from (*R*) cyanohydrins.

Another example of a stereoselective reaction in this context is the Mitsunobu reaction of optically active cyanohydrins in the presence of carboxylic acids, which takes place with inversion of configuration, thus permitting preparation of (*S*) cyanohydrins directly from their (*R*) isomers.[68]

8. Summary and Outlook

The enzyme-catalyzed asymmetric synthesis of cyanohydrins known for close to ninety years has only in the last decade turned into an important instrument for organic synthesis. The markedly improved enantioselectivities are possible primarily by suppression of the chemical cyanohydrin formation. This can be achieved either by employing an organic solvent or by working at low pH values.

(*R*) Cyanohydrins in particular have become easily accessible by this procedure, and their considerable synthetic potential as α-substituted carboxylic acid derivatives has been firmly established within a few years. Reactions of optically active cyanohydrins can be conducted with retention of chirality, and further stereogenic centers can be introduced diastereoselectively. Thus chiral cyanohydrins open up routes to other important classes of compounds with stereogenic centers. The synthetic potential of chiral cyanohydrins appears particularly important for the diastereoselective synthesis of drugs with stereogenic centers. Even if drugs like 2-amino alcohols are still applied in racemic form today, all stereoisomers are required for registration, since the activity spectrum and metabolism of each isolated stereoisomer must be established. Chiral cyanohydrins frequently open simple and direct routes to the individual stereoisomers.

The (*R*)-oxynitrilase from bitter almonds has a broad substrate spectrum and can be obtained readily in industrial quantities. In contrast, the substrate spectrum of (*S*)-oxynitrilase from *Sorghum* is restricted mainly to aromatic aldehydes, and the poor availability of this enzyme is more or less prohibitive for industrial applications. Future developments in the synthesis of optically active cyanohydrins are thus expected primarily in extending the substrate spectrum of (*S*)-oxynitrilases and in improving their availability. (*S*)-oxynitrilases from other organisms (plants, insects) may extend and improve the substrate spectrum. The poor accessibility of (*S*)-oxynitrilases, however, will be overcome only by cloning and overexpression in a sufficiently efficient production organism.

Modification of the active center(s) of the oxynitrilases, which is prerequisite for further optimization of the substrate selectivity, requires knowledge of the complete enzyme structure. Currently, little or rather almost nothing is known about the three-dimensional structure of oxynitrilases. If this deficit can be overcome, oxynitrilases will gain even more importance in the synthesis of chiral compounds.

The enthusiastic commitment of my co-workers, who are cited in the references, has helped to bridge the gap between organic synthesis and enzymology which has been decisive for our successful exploitation of chiral cyanohydrins in synthesis. My special gratitude is due to Drs. Thomas Ziegler and Siegfried Förster who played a major role from the beginning in the development of the work described in this review. Dr. Angelika Baro was strongly engaged in the drafting of this article, for which I am very grateful. Generous financial support of this work by the Bundesministerium für Forschung und Technologie (BMFT) under the auspices of the "Zentrales Schwerpunktprogramm Bioverfahrenstechnik Stuttgart" is gratefully acknowledged, as is the constant support by the Fonds der Chemischen Industrie.

Received: October 25, 1993 [A 33 IE]
German version: *Angew. Chem.* **1994**, *104*, 1609

[1] a) F. Effenberger, *NATO ASI Ser. Ser. C* **1992**, *381*, 25–33 [*Chem. Abstr.* **1993**, *118*, 254088v]; b) F. Effenberger in *Enzyme Catalysis in Organic Synthesis* (Eds.: K. Drauz, H. Waldmann), VCH, Weinheim, in press.
[2] a) C. G. Kruse, J. Brussee, A. van der Gen, *Spec. Chem.* **1992**, *12*, 184–192 [*Chem. Abstr.* **1992**, *117*, 150273q]; b) C. G. Kruse, H. W. Geluk, G. J. M. van Scharrenburg, *Chim. Oggi* **1992**, *10*, 59–63 [*Chem. Abstr.* **1992**, *117*, 113935m]; c) C. G. Kruse in *Chirality in Industry* (Eds.: A. N. Collins, G. N. Sheldrake, J. Crosby), Wiley, New York, **1992**, pp. 279–299.
[3] W. R. Jackson, H. A. Jacobs, G. S. Jayatilake, B. R. Matthews, K. G. Watson, *Aust. J. Chem.* **1990**, *43*, 2045–2062.
[4] a) J. D. Elliott, V. M. F. Choi, W. S. Johnson, *J. Org. Chem.* **1983**, *48*, 2294–2295; b) M. T. Reetz, M. W. Drewes, K. Harms, W. Reif, *Tetrahedron Lett.* **1988**, *29*, 3295–3298; c) M. T. Reetz, M. W. Drewes, A. Schmitz, X. Holdgruen, T. Wuensch, J. Binder, *Philos. Trans. R. Soc. London A* **1988**, *326*, 573–578 [*Chem. Abstr.* **1989**, *111*, 77550x].
[5] a) R. Herranz, J. Castro-Pichel, T. Garcia-Lopez, *Synthesis* **1989**, 703–706; b) J. L. Garcia Ruano, A. M. Martin Castro, J. H. Rodriguez, *Tetrahedron Lett.* **1991**, *32*, 3195–3198.
[6] a) M. Hayashi, T. Matsuda, N. Oguni, *J. Chem. Soc. Chem. Commun.* **1990**, 1364–1365; b) M. Hayashi, T. Matsuda, N. Oguni, *J. Chem. Soc. Perkin Trans. 1*, **1992**, 3135–3140; c) M. Hayashi, Y. Miyamoto, T. Inoue, N. Oguni, *J. Org. Chem.* **1993**, *58*, 1515–1522; d) K. Narasaka, T. Yamada, H. Minamikawa, *Chem. Lett.* **1987**, 2073–2076; e) H. Minamikawa, S. Hayakawa, T. Yamada, N. Iwasawa, K. Narasaka, *Bull. Chem. Soc. Jpn.* **1988**, *61*, 4379–4383.
[7] a) H.-J. Altenbach in *Organic Synthesis Highlights* (Eds.: J. Mulzer, H.-J. Altenbach, M. Braun, K. Krohn, H.-U. Reissig), **1991**, pp. 66–70; b) D. M. Dalton, C. M. Garner, J. M. Fernández, J. A. Gladysz, *J. Org. Chem.* **1991**, *56*, 6823–6829; c) S. Kobayashi, Y. Tsuchiya, T. Mukaiyama, *Chem. Lett.* **1991**, 541–544; d) E. J. Corey, Z. Wang, *Tetrahedron Lett.* **1993**, *34*, 4001–4004.
[8] a) J. Oku, N. Ito, S. Inoue, *Makromol. Chem.* **1979**, *180*, 1089–1091; b) J. Oku, S. Inoue, *J. Chem. Soc. Chem. Commun.* **1981**, 229–230; c) M. North, *Synlett* **1993**, 807–820.
[9] L. Rosenthaler, *Biochem. Z.* **1908**, *14*, 238–253.
[10] a) V. K. Krieble, W. A. Wieland, *J. Am. Chem. Soc.* **1921**, *43*, 164–175; b) H. Albers, K. Hamann, *Biochem. Z.* **1932**, *255*, 44–65; c) H. Albers, K. Hamann, *ibid.* **1934**, *269*, 14–25.
[11] a) W. Becker, U. Benthin, E. Eschenhof, E. Pfeil, *Biochem. Z.* **1963**, *337*, 156–166; b) W. Becker, E. Pfeil, *ibid.* **1966**, *346*, 301–321.
[12] a) W. Becker, H. Freund, E. Pfeil, *Angew. Chem.* **1965**, *77*, 1139; *Angew. Chem. Int. Ed. Engl.* **1965**, *4*, 1079; b) W. Becker, E. Pfeil, *J. Am. Chem. Soc.* **1966**, *88*, 4299–4300; c) E. Pfeil, W. Becker, DE-B 1300111, **1969** [*Chem. Abstr.* **1970**, *72*, P3061t].
[13] a) F. Effenberger, T. Ziegler, S. Förster, *Angew. Chem.* **1987**, *99*, 491–492; *Angew. Chem. Int. Ed. Engl.* **1987**, *26*, 458–460; b) F. Effenberger, T. Ziegler, S. Förster (Degussa AG), DE-B 3701383, **1988** [Chem. Abstr. **1989**, *110*, 74845r]; c) T. Ziegler, B. Hörsch, F. Effenberger, *Synthesis* **1990**, 575–578.
[14] a) C. Laque, J. Tramper, M. D. Lilly, *Biocatalysis in Organic Media*, Studies in Organic Chemistry, vol. 29, Elsevier, Amsterdam, **1987**; b) S. Fukui, A. Tanaka, *Endeavour* **1985**, *9*, 10–17 [*Chem. Abstr.* **1985**, *103*, 33788m]; c) A. M. Klibanov, *Acc. Chem. Res.* **1990**, *23*, 114–120; d) K. R. Natarajan, *J. Chem. Educ.* **1991**, *68*, 13–16; e) K. Faber, *Biotransformations in Organic Synthesis*, Springer, Berlin, **1992**, pp. 248–282.
[15] a) F. Effenberger, B. Spachmann, S. Förster, B. Bauer, J. Wonner, unpublished results; b) B. Bauer, H. Strathmann, F. Effenberger, DE-B 4041896, **1991** [*Chem. Abstr.* **1992**, *116*, 150138d].
[16] E. Wehtje, P. Adlercreutz, B. Mattiasson, *Biotechnol. Bioeng.* **1990**, *36*, 39–46.
[17] a) U. Kragl, U. Niedermeyer, M.-R. Kula, C. Wandrey, *Ann. N. Y. Acad. Sci.* **1990**, *613*, 167–175 [*Chem. Abstr.* **1991**, *115*, 181477x]; b) U. Niedermeyer, U. Kragl, M.-R. Kula, C. Wandrey, K. Makryaleas, K. Drauz (Degussa AG), *Eur. Pat. Appl.* EP 0326063 A2, **1989** [*Chem. Abstr.* **1990**, *112*, 234012p].
[18] a) J. Brussee, E. C. Roos, A. van der Gen, *Tetrahedron Lett.* **1988**, *29*, 4485–4488; b) J. Brussee, W. T. Loos, C. G. Kruse, A. van der Gen, *Tetrahedron* **1990**, *46*, 979–986; c) P. Zandbergen, J. van der Linden, J. Brussee, A. van der Gen, *Synth. Commun.* **1991**, *21*, 1387–1391.
[19] a) V. I. Ognyanov, V. K. Datcheva, K. S. Kyler, *J. Am. Chem. Soc.* **1991**, *113*, 6992–6996; b) T. T. Huuhtanen, L. T. Kanerva, *Tetrahedron Asymmetry* **1992**, *3*, 1223–1226.
[20] F. Effenberger, J. Eichhorn, unpublished results.

[21] a) C. Bové, E. E. Conn, *J. Biol. Chem.* **1961**, *236*, 207–210; b) M. K. Seely, R. S. Criddle, E. E. Conn, *ibid.* **1966**, *241*, 4457–4462.
[22] a) I. Jansen, R. Woker, M.-R. Kula, *Biotechnol. Appl. Biochem.* **1992**, *15*, 90–99; b) H. Wajant, K.-W. Mundry, *Plant Sci. Limerick Irel.* **1993**, *89*, 127–133; c) E. Smitskamp-Wilms, J. Brussee, A. van der Gen, G. J. M. van Scharrenburg, J. B. Sloothaak, *Recl. Trav. Chim. Pays-Bas* **1991**, *110*, 209–215.
[23] F. Effenberger, B. Hörsch, S. Förster, T. Ziegler, *Tetrahedron Lett.* **1990**, *31*, 1249–1252.
[24] U. Niedermeyer, M.-R. Kula, *Angew. Chem.* **1990**, *102*, 423–424; *Angew. Chem. Int. Ed. Engl.* **1990**, *29*, 386–387.
[25] N. Klempier, H. Griengl, M. Hayn, *Tetrahedron Lett.* **1993**, *34*, 4769–4772.
[26] a) S. Förster, F. Effenberger, unpublished results; b) H. Wajant, H. Böttinger, K.-W. Mundry, *Biotechnol. Appl. Biochem.* **1993**, *18*, 75–82.
[27] D. A. Livingston, J. E. Petre, C. L. Bergh, *J. Am. Chem. Soc.* **1990**, *112*, 6449–6450.
[28] N. S. Batra, E. Brunet, *Tetrahedron Lett.* **1993**, *34*, 711–714.
[29] J. L. Garcia Ruano, A. M. Martin Castro, J. H. Rodriguez, *J. Org. Chem.* **1992**, *57*, 7235–7241.
[30] M. T. Reetz, K. Kesseler, A. Jung, *Angew. Chem.* **1985**, *97*, 989–990; *Angew. Chem. Int. Ed. Engl.* **1985**, *24*, 989–990.
[31] H. Ohta, Y. Kimura, Y. Sugano, T. Sugai, *Tetrahedron* **1989**, *45*, 5469–5476.
[32] A. Nahrstedt, *Biol. Unserer Zeit* **1988**, *18*, 105–109.
[33] a) F. Effenberger, B. Hörsch, F. Weingart, T. Ziegler, S. Kühner, *Tetrahedron Lett.* **1991**, *32*, 2605–2608; b) S. Heid, Diplomarbeit, Universität Stuttgart, **1991**.
[34] a) J. Oku, N. Ito, S. Inoue, *Makromol. Chem.* **1982**, *183*, 579–586; b) A. Mori, Y. Ikeda, K. Kinoshita, S. Inoue, *Chem. Lett.* **1989**, 2119–2122; c) K. Tanaka, A. Mori, S. Inoue, *J. Org. Chem.* **1990**, *55*, 181–185.
[35] a) S. Asada, Y. Kobayashi, S. Inoue, *Makromol. Chem.* **1985**, *186*, 1755–1762; b) Y. Kobayashi, S. Asada, I. Watanabe, H. Hayashi, Y. Motoo, S. Inoue, *Bull. Chem. Soc. Jpn.* **1986**, *59*, 893–895.
[36] a) W. R. Jackson, G. S. Jayatilake, B. R. Matthews, C. Wilshire, *Aust. J. Chem.* **1988**, *41*, 203–213; b) B. R. Matthews, W. R. Jackson, G. S. Jayatilake, C. Wilshire, H. A. Jacobs, *ibid.* **1988**, *41*, 1697–1709; c) W. Dong, W. L. Petty (Shell Oil Co.), US-A 535500, **1983** [*Chem. Abstr.* **1985**, *103*, 196420z].
[37] a) H. Danda, H. Nishikawa, K. Otaka, *J. Org. Chem.* **1991**, *56*, 6740–6741; b) H. Danda, *Synlett* **1991**, 263–264; c) S. D. Rychnovsky, *Chemtracts: Org. Chem.* **1992**, *5*, 102–105 [*Chem. Abstr.* **1992**, *117*, 150608c].
[38] K. Naumann, *Chemistry of Plant Protection, 5: Synthetic Pyrethroid Insecticides: Chemistry and Patents*, Springer, Berlin, **1990**, pp. 110–141.
[39] a) M. North, *Tetrahedron* **1992**, *48*, 5509–5522; b) D. Callant, B. Coussens, T. v. d. Maten, J. G. de Vries, N. Koen de Vries, *Tetrahedron Asymmetry* **1992**, *3*, 401–414; c) H. J. Kim, W. R. Jackson, *ibid.* **1992**, *3*, 1421–1430; d) D. J. P. Hogg, M. North, *Tetrahedron* **1993**, *49*, 1079–1090.
[40] a) A. Mori, H. Ohno, H. Nitta, K. Tanaka, S. Inoue, *Synlett* **1991**, 563–564; b) H. Ohno, H. Nitta, K. Tanaka, A. Mori, S. Inoue, *J. Org. Chem.* **1992**, *57*, 6778–6783.
[41] F. Effenberger, B. Gutterer, T. Ziegler, E. Eckhardt, R. Aichholz, *Liebigs Ann. Chem.* **1991**, 47–54, and references therein.
[42] a) N. Matsuo, N. Ohno, *Tetrahedron Lett.* **1985**, *26*, 5533–5534; b) A. van Almsick, J. Buddrus, P. Hönicke-Schmidt, K. Laumen, M. P. Schneider, *J. Chem. Soc. Chem. Commun.* **1989**, 1391–1393.
[43] a) H. Ohta, Y. Miyamae, G. Tsuchihashi, *Agric. Biol. Chem.* **1986**, *50*, 3181–3184; *ibid.* **1989**, *53*, 215–222; b) H. Hirohara, S. Mitsuda, E. Ando, R. Komaki, *Stud. Org. Chem. (Amsterdam)* **1985**, *22*, 119–134.
[44] a) Y. F. Wang, S. T. Chen, K. K. C. Liu, C. H. Wong, *Tetrahedron Lett.* **1989**, *30*, 1917–1920; b) S. H. Hsu, S. S. Wu, Y. F. Wang, C. H. Wong, *ibid.* **1990**, *31*, 6403–6406.
[45] a) M. Inagaki, J. Hiratake, T. Nishioka, J. Oda, *J. Am. Chem. Soc.* **1991**, *113*, 9360–9361; b) M. Inagaki, A. Hatanaka, M. Mimura, J. Hiratake, T. Nishioka, J. Oda, *Bull. Chem. Soc. Jpn.* **1992**, *65*, 111–120; c) M. Inagaki, J. Hiratake, T. Nishioka, J. Oda, *J. Org. Chem.* **1992**, *57*, 5643–5649.
[46] H. S. Bevinakatti, A. A. Banerji, R. V. Newadkar, *J. Org. Chem.* **1989**, *54*, 2453–2455.
[47] a) D. A. Evans, M. M. Morrissey, R. L. Dorow, *J. Am. Chem. Soc.* **1985**, *107*, 4346–4348; b) H. C. Brown, J. Chandrasekharan, P. V. Ramachandran, *J. Org. Chem.* **1986**, *51*, 3394–3396; c) E. J. Corey, J. O. Link, *Tetrahedron Lett.* **1992**, *33*, 3431–3434; d) K. Mikami, M. Terada, T. Nakai, *J. Am. Chem. Soc.* **1990**, *112*, 3949–3954.
[48] a) S. Servi, *Synthesis* **1990**, 1–25; b) S. Tsuboi, E. Nishiyama, H. Furutani, M. Utaka, A. Takeda, *J. Org. Chem.* **1987**, *52*, 1359–1362.
[49] a) M.-J. Kim, G. M. Whitesides, *J. Am. Chem. Soc.* **1988**, *110*, 2959–2964; b) M.-R. Kula, C. Wandrey, *Methods Enzymol.* **1987**, *136*, 9–21; c) M.-J. Kim, J. Y. Kim, *J. Chem. Soc. Chem. Commun.* **1991**, 326–327.
[50] a) P. Kalaritis, R. W. Regenye, J. J. Partridge, D. L. Coffen, *J. Org. Chem.* **1990**, *55*, 812–815; b) T. Sugai, H. Ohta, *Tetrahedron Lett.* **1991**, *32*, 7063–7064.
[51] a) U. Burkard, F. Effenberger, *Chem. Ber.* **1986**, *119*, 1594–1612; b) H. Kunz, H.-G. Lerchen, *Tetrahedron Lett.* **1987**, *28*, 1873–1876.
[52] a) S. K. Massad, L. D. Hawkins, D. C. Baker, *J. Org. Chem.* **1983**, *48*, 5180–5182; b) J.-R. Schwark, D. Hoppe, *Synthesis* **1990**, 291–294; c) Y. Kobayashi, M. Takase, Y. Ito, S. Terashima, *Bull. Chem. Soc. Jpn.* **1989**, *62*, 3038–3040; d) M. Larcheveque, Y. Petit, *Bull. Soc. Chim. Fr.* **1989**, 130–139; e) E. J. Corey, G. B. Jones, *Tetrahedron Lett.* **1991**, *32*, 5713–5716.
[53] a) W. Althoff, R. Karsdorf, P. Tinapp, *Arch. Pharm. (Weinheim Ger.)* **1981**, *314*, 518–524; b) B. R. Matthews, H. Gountzos, W. R. Jackson, K. G. Watson, *Tetrahedron Lett.* **1989**, *30*, 5157–5158.
[54] F. Effenberger, M. Hopf, T. Ziegler, J. Hudelmayer, *Chem. Ber.* **1991**, *124*, 1651–1659.
[55] a) J. Engel, *Chem.-Ztg.* **1982**, *106*, 169–183; b) A. Kleemann, J. Engel, *Pharmazeutische Wirkstoffe, Synthesen, Patente, Anwendungen*, 2nd ed., Thieme, Stuttgart, **1982**, and **1987** supplement; c) E. J. Corey, J. O. Link, *Tetrahedron Lett.* **1990**, *31*, 601–604; d) *J. Org. Chem.* **1991**, *56*, 442–444; e) M. T. Reetz, M. W. Drewes, A. Schmitz, *Angew. Chem.* **1987**, *99*, 1186–1188; *Angew. Chem. Int. Ed. Engl.* **1987**, *26*, 1141–1143; f) M. T. Reetz, M. W. Drewes, K. Lennick, A. Schmitz, X. Holdgrün, *Tetrahedron Asymmetry* **1990**, *1*, 375–378; g) T. Ishizuka, S. Ishibuchi, T. Kunieda, *Tetrahedron* **1993**, *49*, 1841–1852.
[56] N. Matsuo, N. Ohno, *Tetrahedron Lett.* **1985**, *26*, 5533–5534.
[57] L. R. Krepski, K. M. Jensen, S. M. Heilmann, J. K. Rasmussen, *Synthesis* **1986**, 301–303.
[58] a) J. Brussee, F. Dofferhoff, C. G. Kruse, A. van der Gen, *Tetrahedron* **1990**, *46*, 1653–1658; b) W. R. Jackson, H. A. Jacobs, B. R. Matthews, G. S. Jayatilake, K. G. Watson, *Tetrahedron Lett.* **1990**, *31*, 1447–1450.
[59] F. Effenberger, B. Gutterer, T. Ziegler, *Liebigs Ann. Chem.* **1991**, 269–273.
[60] G. Cainelli, E. Mezzina, M. Panunzio, *Tetrahedron Lett.* **1990**, *31*, 3481–3484.
[61] a) P. Zandbergen, A. M. C. H. van den Nieuwendijk, J. Brussee, A. van der Gen, *Tetrahedron* **1992**, *48*, 3977–3982; b) J. Brussee, A. van der Gen, *Recl. Trav. Chim. Pays-Bas* **1991**, *110*, 25–26.
[62] P. Zandbergen, J. Brussee, A. van der Gen, C. G. Kruse, *Tetrahedron Asymmetry* **1992**, *3*, 769–774.
[63] J. Brussee, R. A. T. M. van Benthem, C. G. Kruse, A. van der Gen, *Tetrahedron Asymmetry* **1990**, *1*, 163–166.
[64] a) F. Effenberger, U. Stelzer, *Angew. Chem.* **1991**, *103*, 866–867; *Angew. Chem. Int. Ed. Engl.* **1991**, *30*, 873–874; b) F. Effenberger, U. Stelzer, *Chem. Ber.* **1993**, *126*, 779–786.
[65] a) F. Effenberger, U. Burkard, J. Willfahrt, *Liebigs Ann. Chem.* **1986**, 314–333; b) U. Azzena, G. Delogu, G. Melloni, O. Piccolo, *Tetrahedron Lett.* **1989**, *30*, 4555–4558; c) P. R. Fleming, K. B. Sharpless, *J. Org. Chem.* **1991**, *56*, 2869–2875.
[66] a) I. A. Smith, *Ber. Dtsch. Chem. Ges. B* **1938**, *71*, 634–643; b) K. Ichimura, M. Ohta, *Bull. Chem. Soc. Jpn.* **1970**, *43*, 1443–1450.
[67] U. Stelzer, F. Effenberger, *Tetrahedron Asymmetry* **1993**, *4*, 161–164.
[68] E. G. J. C. Warmerdam, J. Brussee, C. G. Kruse, A. van der Gen, *Tetrahedron* **1993**, *49*, 1063–1070.

Ligands as "Compass Needles": How Orientations of Alkene, Alkyne, and Alkylidene Ligands Reveal π-Bonding Features in Tetrahedral Transition Metal Complexes

Vernon C. Gibson*

This article outlines the strikingly simple structural pattern to which transition metal complexes containing π-bonding ligands conform, and suggests simple rules (and ligand classifications) by which the pattern can be understood, and by which individual structures can be rationalized or predicted. Alkenes, alkynes, and alkylidene ligands adopt distinct orientations with respect to other ligands attached to a transition metal because of competition between the various ligand types for metal–ligand π bonds, whatever the coordination geometry. However, a particularly interesting feature of the tetrahedral geometry is that "single-faced" π ligands can function as "sensors" of relative ligand π-donor capacities for all other groups attached to the metal. Here, using simple "triad representations" of tetrahedral complexes, a simple qualitative analysis is presented that builds on calculations by Hoffmann et al. and which allows preferred ligand orientations and relative ligand π-bond strengths to be deduced for a wide variety of these transition metal complexes.

1. Introduction

Ligands that are capable of forming only a single π interaction with a metal center often adopt distinct orientations with respect to other ligands attached to a metal center. Provided there is no steric conflict, such orientation effects are a consequence of the competition that arises between the different ligands for π bonding to the metal and are relatively well understood for octahedral complexes where the alignment of the ligands along the coordinate axes allows a clear distinction between the d orbitals responsible for forming π bonds (the t_{2g} set) and σ bonds (the e_g set). The situation is much less clear for structures where the orbitals are no longer directed along, or perpendicular to, the metal-ligand axes. A good example is the tetrahedral geometry whose traditional representation within a cube (with the x, y, and z axes emerging from the centers of the faces) is shown in Figure 1.

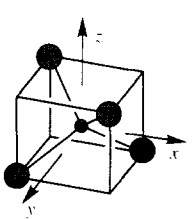


Fig. 1. Relationship of ligand positions with respect to x, y, z axes in a tetrahedral complex.

Competitive effects are, therefore, not so readily assessed for tetrahedral species and it is often necessary to resort to quantum chemical calculations. However, complexes with tetrahedral geometry are particularly attractive for the study of competitive ligand π bonding due to the ability of metal centers with this coordination geometry to accommodate up to four multiply bonded ligands all of which necessarily engage in competition for the available p and d metal orbitals capable of π bonding.[1]

Here, we shall examine a series of tetrahedral and pseudo-tetrahedral complexes containing either alkene, alkyne, or alkylidene ligands and exploit their orientation preferences to evaluate the relative π-donor capacities of the other attendant ligands. This task is facilitated by many recent additions to the family of pseudo-tetrahedral four-coordinate transition metal complexes, particularly examples containing relatively hard, strong π donors such as oxo and imido ligands, and these will be highlighted during the subsequent discussion. We shall also include within the definition of tetrahedral complexes those containing polyene or polyenyl ligands which are considered to occupy a single coordination site. Such systems were the basis of extended Hückel calculations by Hoffmann et al.[2, 3] which first laid the foundations for an understanding of the factors influencing the preferred orientations of carbene, alkene, alkyne, and allyl ligands L with respect to the ancillary Cp ligands in these pseudo-tetrahedral environments. We shall not dwell on the details of MO calculations here but rather call on their qualitative findings to draw together these seemingly quite different yet structurally related systems, to assess the influence of different π-bonded ligands on the structural patterns observed, and to develop a simple unified approach to predicting ligand orientations and relative π-bond strengths in these tetrahedral and pseudo-tetrahedral environments.

[*] Prof. V. C. Gibson
Department of Chemistry, University Science Laboratories,
South Road, Durham DH1 3LE (UK)
Telefax: Int. code + (91)386-1127

 © VCH Verlagsgesellschaft mbH, D-69451 Weinheim, 1994 0570-0833/94/1515-1565 $ 10.00+.25/0

2. A Triad Representation of Tetrahedral and Pseudo-Tetrahedral Complexes

To assist the analysis, a simple triad representation of a tetrahedral complex will be used (related to Newman projections for organic systems). If we consider a tetrahedral complex containing the four ligands A, B, C, D, and the metal atom M, and view the molecule along the A–M axis, then the three ligands B, C, and D present a triad which is conveniently represented by the triangle notation shown in Figure 2a. Here, the metal atom lies

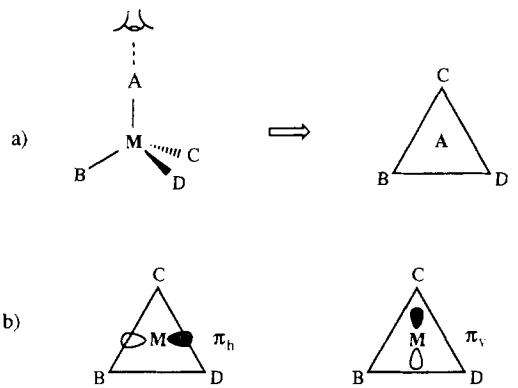


Fig. 2. A triad representation of a tetrahedral complex. a) View along the A–M axis. b) The metal orbitals with π symmetry (π_v and π_h) which are available for interaction with the ligand A.

above the plane defined by B, C, and D and directly beneath the ligand A which lies at the center of the triangle along the normal to the BCD plane. If the ligand A is capable of π bonding to the metal center, it could interact with either (or both) of the metal orbitals with π symmetry (π_h or π_v) shown in Figure 2b which illustrate the MBCD pyramid as viewed from A. Note that the metal orbitals π_h and π_v are represented as p-type orbitals lying parallel to the BCD plane, but they could equally be forward-projecting lobes of dπ orbitals or, as is more likely the case hybrids of both p and d orbitals. This representation captures the essence of MO calculations[2, 3] in which the authors aligned the z axis along the A–M vector and where ligand C is Cp and B and D are carbonyl or nitrosyl ligands.

Note that the metal orbitals have been shown aligned (for convenience) with respect to the M–C axis, but it is evident that the orbitals could also be orientated with respect to either the M–B or M–D axes. Since the π bonding ligands compete for the available metal orbitals with dπ symmetry in a tetrahedral environment, the orientation of the available π symmetry orbitals for ligand A will in effect depend on which of ligands B, C, or D can form the strongest π bonds.

3. Ligand Types

Before proceeding further, we first need to consider the electronic and orbital characteristics of the types of ligands. Table 1 shows the frontier orbitals of a variety of ligands, classified as σ, π, or δ according to their potential for bonding to the metal; the π symmetry orbitals are assigned h or v subscripts depending on whether they align with the "horizontal" or "vertical" metal π orbitals in the diagrams shown in Figure 2b.

The ligands are grouped according to the number of orbitals with π symmetry available for bonding to the metal atom:

1. Π_1-type ligands; these have only one π symmetry orbital and therefore can form at most a double bond to the metal atom consisting of a sigma and pi interaction (1σ, 1π). Such ligands have, on occasion, been referred to as "single-faced" π ligands.
2. Π_2- and $\Pi_{2'}$-type ligands; these possess two π symmetry orbitals and thereby can form two equivalent π bonds potentially giving rise to a triple bond to the metal (1σ, 2π). It is helpful to make a distinction between ligands with degenerate π levels and those with π orbitals differing in energy, since for the latter, one of the π orbitals becomes energetically more accessible to the metal. These latter ligands with non-degenerate π orbitals we shall denote as $\Pi_{2'}$ ligands.

Figure 3 shows the principal s and p (or σ and π) ligand orbitals for each ligand type with accompanying energy level diagrams to emphasize the similarities and differences within, and between, categories. Thus, for the Π_1 ligands, the singlet carbene has a vacant p orbital and so is able to accept π-electron density from the metal, while the amido ligand has three electrons distributed between its two available orbitals and so will



Vernon C. Gibson born in 1958 in Grantham, England, studied chemistry at the University of Sheffield before moving to the University of Oxford where he was awarded a D. Phil. in 1983 for work on the coordination and organometallic chemistry of the early transition metals carried out in the group of M. L. H. Green. He then spent two years as a NATO post-doctoral researcher at the California Institute of Technology with J. E. Bercaw before returning to England to take up a lectureship in chemistry at Durham University in 1986, where he is now a full Professor of Chemistry. His interests lie in synthetic, structural, and mechanistic inorganic and organometallic chemistry, with a particular emphasis on transition-metal compounds containing metal–ligand multiple bonds and their applications in polymer synthesis.

Table 1. Classification of ligands by the number and type of their frontier orbitals.

Ligand A	Electrons available	Frontier orbitals
1) Π_1-ligands		
R, C, H	2	σ, p_h
R, N, H	3	σ, p_h
>C=C<	2	σ, π^*_h
–C≡C–	2	σ, π^*_h
2) Π_2-ligands		
CO	2	σ, π^*_h, π^*_v
NO	3	σ, π^*_h, π^*_v
R, C	3	σ, p_h, p_v
R, N	4	σ, p_h, p_v
O	4	σ, p_h, p_v
R, O	5	σ, p_h, p_v
Cl	5	σ, p_h, p_v
	3	σ, π_h, π_v
	4	σ, π_h, π_v, δ^*
	5	σ, π_h, π_v, δ^*_1, δ^*_2
3) $\Pi_{2'}$-ligands		
	3	σ, π_h, π^*_v
–C≡C–	4	σ, π^*_h, π_v, δ^*
	4	σ, π_h, π^*_v, δ^*

act as a net π donor to the metal. Simple energy level diagrams can be derived for the cyclic Π_2 ligands, C_nH_n, by standing the ring on an apex. It can be seen that the π levels are

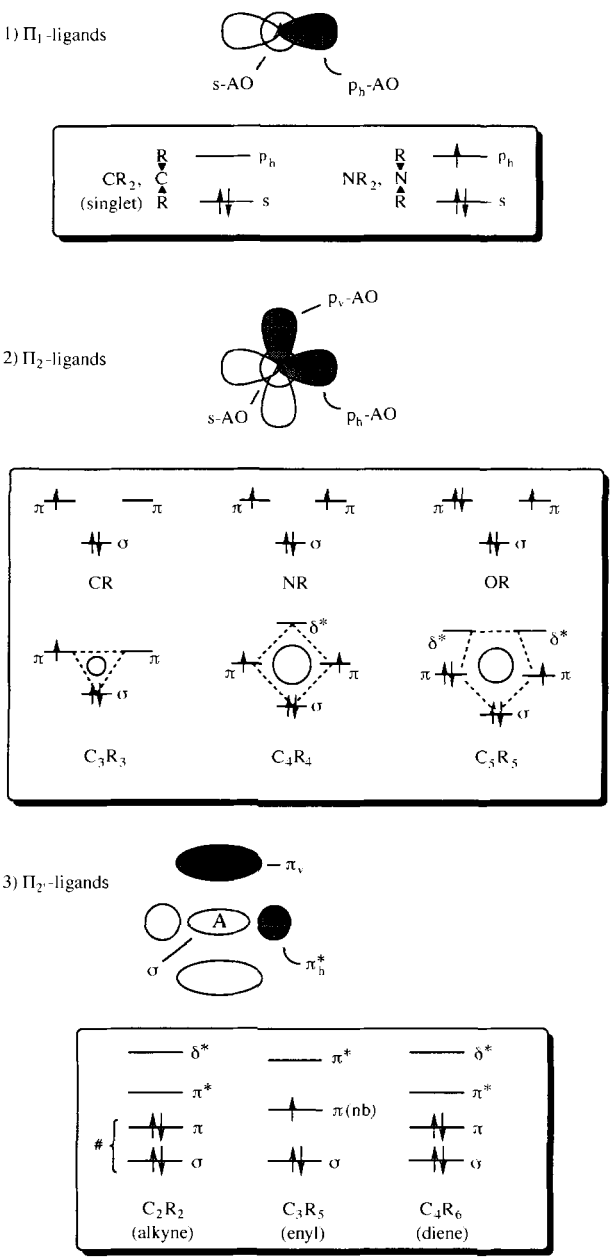


Fig. 3. Frontier orbitals of some representative ligands. The two orbitals indicated by # are the degenerate pair of filled alkyne C–C π-bonding MOs, but are shown as non-degenerate because of their different orientations with respect to the metal ligand axis. The MOs of $\Pi_{2'}$ ligands are represented by a four-electron alkyne ligand.

degenerate[*] in each case and therefore directly comparable with CR, NR, and OR. By contrast, it can be seen that the π levels for $\Pi_{2'}$ ligands are non-degenerate.

Of particular interest to this study are the Π_1 ligands such as alkylidene (CHR), amido (NHR), alkene (C_2R_4), and the "two-electron" alkyne ligand (C_2R_2), which have available only one π orbital for interaction with a metal center and so an orientation preference should be observed depending upon which of the

[*] It should be noted that a Jahn–Teller distortion would remove the degeneracy for an isolated fragment. The view shown in Figure 3 is adopted to assist comparisons between the different ligand types and for the purpose of electron "book-keeping".

metal π_h or π_v orbitals is the most accessible. In the following sections, we shall examine the effect of either one or two of the three ligands in the triad dominating the π-donor bonding.

4. Complexes Possessing Two Dominant Π_2-Donor Ligands

Let us first consider triad representations for complexes containing cyclopentadienyl (Cp) or imido (NR) groups in combination with ancillary alkene ligands (Fig. 4). Figure 4a shows a typical triad representation for a zirconocene alkene complex of the type $[Cp_2Zr(H_2C{=}CHR)(PMe_3)]$.[4] Here, the C=C bond of the alkene ligand orientates in the plane that contains the Zr–P bond, the so-called equatorial binding plane or binding wedge of the metallocene fragment. This is, of course, the well-established bent metallocene geometry for which the electronic constraints are well-documented both through their extensive derivative chemistry[5] and through detailed quantum chemical calculations.[6] The frontier orbitals of the bent $[Cp_2M]$ unit are shown in Figure 5, which illustrates their shapes and projections in the *yz* plane. Thus, if we consider a triad representation for a $[Cp_2ML]$ fragment (Fig. 6), we find that it is only the π_v orbital (with respect to L) that is accessible to a fourth π-bonding ligand. It is also worth noting that, since this ligand approaches in the *yz* plane but *between* the *y* and *z* axes, the π interaction will largely consist of a "side-on" interaction with the "d_{yz}" $1a_1$ orbital of the metal atom (Fig. 7).

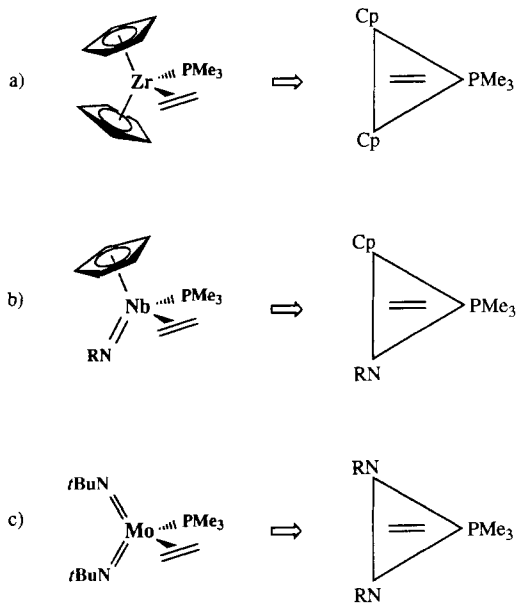


Fig. 4. Triad representations of complexes containing cyclopentadienyl and imido ligands in combination with alkene ligands: a) bent metallocene derivatives; b) half-sandwich imido complexes; c) bis(imido) complexes.

According to this description the π_h orbital is virtually inaccessible to a fourth π-bonding ligand since it is heavily involved in π bonding to the Cp rings, and therefore any interaction with the π_h orbital would necessarily weaken the π bonds between the Cp ligands and the metal center. The orientation preference would be expected to be lost only if the π_v orbital is filled (i.e. a d^2 metal center) and the Π_1 ligand is a π donor such as an amide.

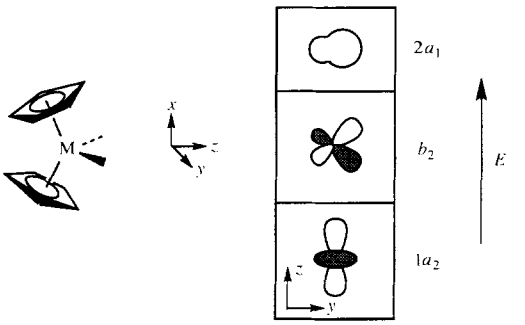


Fig. 5. The frontier orbitals of the bent $[Cp_2M]$ metallocene fragment illustrating their shapes and orientations with respect to the *y* and *z* axes.

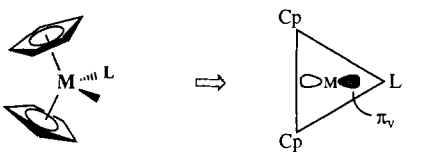


Fig. 6. A triad representation illustrating the orientation of the π-symmetry orbital available for bonding to a fourth ligand in a $[Cp_2ML]$ fragment. The π_v orbital is vertical with respect to the ligand L.

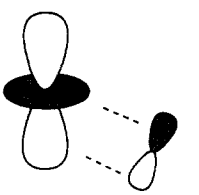


Fig. 7. The side-on π interaction between a d_{z^2}-type metal orbital and a π-symmetry ligand orbital.

More recently, a related series of half-sandwich niobium imido complexes has been synthesized;[7] these show a similar alignment of the alkene C=C bond, orientated towards the phosphane ligand when viewed as a triad representation (see Fig. 4b). Precisely the same "metallocene-like" orientation is found for the alkene ligand in $[Mo(NtBu)_2(H_2C{=}CHMe)(PMe_3)]$[8] (see Fig. 4c). At first sight the close relationship apparent between bent metallocenes, half-sandwich imido, and bis(imido) systems may not seem at all obvious. However, when the symmetry properties of the frontier orbitals for the Cp and NR units are taken into consideration, the situation becomes much clearer, since both of these fragments are seen to bind to a metal using a combination of 1σ and 2π interactions (see Table 1); the Cp group of course also has two δ-symmetry acceptor orbitals available for back-donation but provided these δ-bonding interactions are weak, they will have minimal impact on the metal–ligand bonding. The alkene ligand, then, effectively orientates towards the σ-bonded phosphane group so as to avoid direct competition with the dominant Π_2-donor groups for metal–ligand π bonds.

An analogous situation is found for the alkylidene derivatives $[Cp_2Ta(CHPh)(CH_2Ph)]$[9] and $[Cp^*Nb\{N(2,6\text{-}iPr_2C_6H_3)\}(CHPh)(PMe_3)]$[10] ($Cp^* = C_5Me_5$) (Fig. 8). Here, the p orbital of the benzylidene ligands is orientated with one lobe pointing in the direction of the σ-bonded group and with the other lobe bisecting the Π_2-donor groups (the orientations of the alkylidene substituents are indicated by wedge lines); this again avoids competition with the Cp and NR ligands for π bonds.

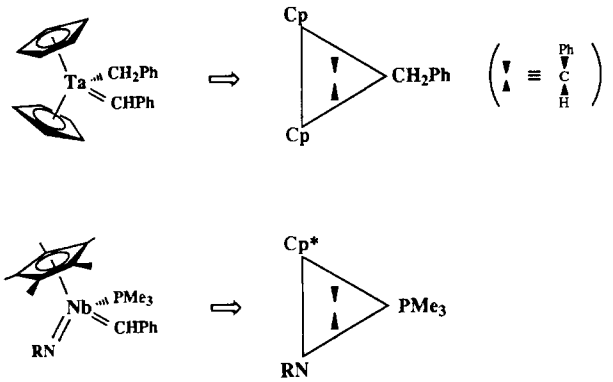


Fig. 8. Triad representations showing alkylidene ligand orientations in $[Cp_2Ta(CHPh)(CH_2Ph)]$ and $[Cp^*Nb(NR)(CHPh)(PMe_3)]$.

Thus the alignments of the alkene double bond and the alkylidene substituents differ by 90°.

The OR ligand can also act as a Π_2 donor (see Table 1) and therefore, as far as the symmetries of its frontier orbitals are concerned, it can be regarded as being pseudo-isolobal with the Cp ligand. It should come as little surprise, then, that the two substituted phenolato complexes, $[Ta\{O(2,6\text{-}tBu_2C_6H_3)\}_2(CHSiMe_3)(CH_2SiMe_3)_2]$[11] and $[Ti\{O(2,6\text{-}Ph_2C_6H_3)\}_2(C_2H_4)(PMe_3)]$[12] shown in Figure 9 also display related orientation preferences to those seen in the cyclopentadienyl and imido systems.

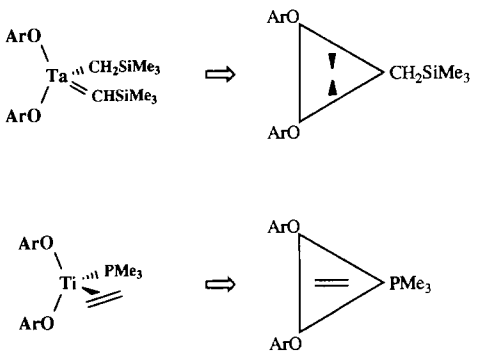


Fig. 9. Triad representations showing alkene and alkylidene ligand orientations in substituted bis(phenolato) complexes.

5. Complexes Possessing One Dominant Π_2-Donor Ligand

Now, if we bear in mind the orientation preferences we have just witnessed for bis(phenolato) complexes in Section 4, we can then examine the effect of placing a very strong NR donor group in competition with the two alkoxo ligands through the four-coordinate alkylidene(imido) complexes $[M\{N(2,6\text{-}iPr_2C_6H_3)\}(CHCMe_3)(OtBu)_2]$ (M = Mo, W)[13] and $[Mo(NtBu)(CHCMe_3)\{OCH(CF_3)_2\}_2]$.[14] The triad representation of a structurally characterized derivative shown in Figure 10a reveals that the alkylidene ligand now bisects the R'O–OR' edge of the triangle and aligns in the direction of the NR group.

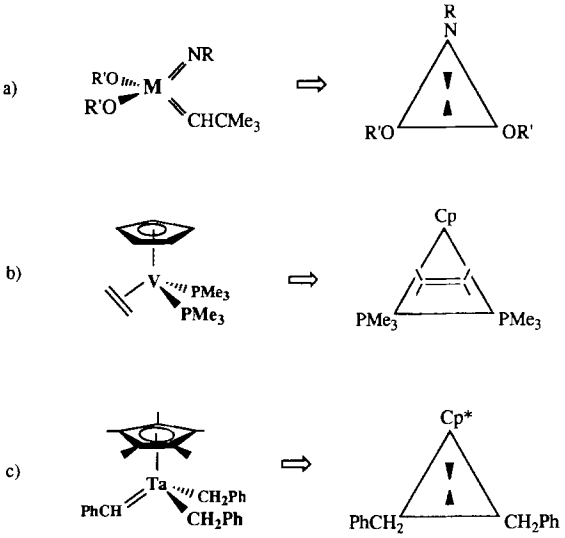


Fig. 10. Examples of complexes possessing a single dominant Π_2-donor ligand: a) $[M\{N(2,6\text{-}iPr_2C_6H_3)\}(CHCMe_3)(OtBu)_2]$ (M = Mo, W); b) $[CpV(PMe_3)_2(C_2H_4)]$; c) $[Cp^*Ta(CHPh)(CH_2Ph)_2]$.

This orientation is consistent with the imido ligand now dominating the π-donor bonding, a point the alkylidene ligand neatly emphasizes by pointing towards it in each of the complexes. A related alkene complex of the type $[Mo(NR)(H_2C{=}CH_2)(OR')_2]$, not to our knowledge synthesized to date, would be anticipated to align its alkene π-acceptor orbital with the π_h orbital of the metal atom, resulting in the alkene orientation illustrated in Figure 11.

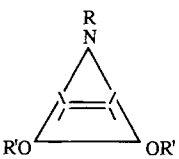


Fig. 11. The anticipated orientation of an ethene ligand in a hypothetical complex of the type $[Mo(NR)(H_2C{=}CH_2)(OR')_2]$.

An analogous orientation effect is found in the cyclopentadienyl vanadium complex $[CpV(PMe_3)_2(C_2H_4)]$[15] (see Fig. 10b). Here, since the PMe_3 ligands cannot function as π donors, the cyclopentadienyl ligand dominates the bonding, a point the alkene ligand helpfully "underlines" by its orientation. The dominance of the cyclopentadienyl ligand is also apparent in the complex $[Cp^*Ta(CHPh)(CH_2Ph)_2]$[16] (see Fig. 10c) in which the plane of the alkylidene substituents aligns with the metal-ring centroid vector, so pointing to the Cp ligand as the dominant π-bonding ligand. If the π system in the ligand is extended, for example, in $[CpTiCl_2\{{=}N{=}C(tBu)_2\}]$,[17] the preferred orientation of the substituents changes by a 90° twist, as expected in this complex for alignment of the nitrogen p orbital with the π_h orbital. Similar "twists" are found in complexes containing cumulene-type ligands such as vinylidene and allenylidene.

The origin of the orientation effect in "tetrahedral" complexes possessing a single dominant Π_2-donor ligand can be seen by considering the d orbital splitting diagram in Figure 12: for convenience and clarity this is derived unconventionally with the z axis aligned along the Π_2-ligand–metal axis. Here, instead of the usual "3 over 2" pattern, the degeneracy of the upper triplet is split into an e and a_1 set. There are now two sets of

doubly degenerate orbitals, the upper set (d_{xz}, d_{yz}) allowing π-interactions with the π donor to be maximized, while the lower *e* set ($d_{x^2-y^2}$, d_{xy}) aligns orthogonal to the M–Π_2 ligand bond thereby minimizing interactions with the Π_2 ligand. Since we are now viewing the molecule side-on to the M ; (Fig. 12), it is apparent that d_{xy} effectively correspon ıe π_h orbital viewed from A, while both d_{xz} and d_{z^2} can interactions with A in the vertical plane (π_v). Note that d_{xz} is already engaged in π bonding with the "axial" Π_2-ligand and that the d_{z^2} orbital is σ bonding with respect to the Π_2 ligand whilst also being capable of forming a π interaction with the ligand A of the type illustrated in Figure 7. This provides a simple pictorial illustration of the competition for ligand–metal π bonds in "tetrahedral" complexes.

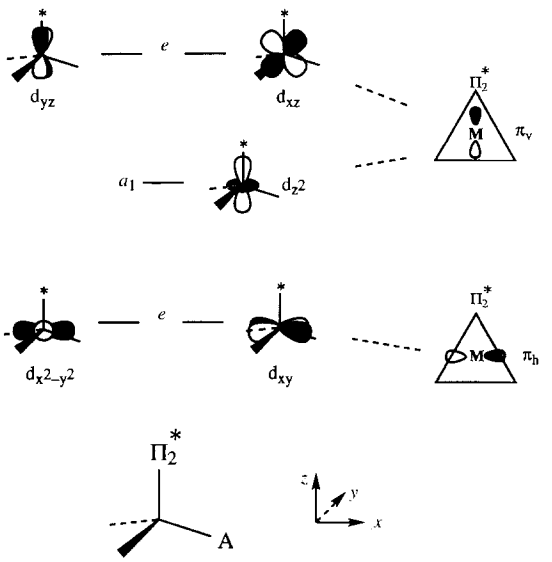


Fig. 12. Splitting diagram for the d orbitals of the metal atom in a tetrahedral complex possessing a single dominant Π_2-donor ligand (derived with the *z* axis aligned in the direction of the Π_2-ligand).

An interesting situation arises when the strongly π-donating NR unit is in competition with a strong polyenyl π donor such as the cyclopentadienyl ligand. A series of half-sandwich niobium,[18] molybdenum,[19] and rhenium[20] compounds of general formula [CpM(NR)Cl_2] shows a significant ring-slippage along with an orientation preference for the C_5R_5 ring such that one of the ring carbon atoms eclipses the M–NR bond (the ring is orientated so as to "point" to the NR group). This is illustrated in Figure 13a for [CpNb(NR)Cl_2] by using the triad notation viewed down the ring centroid-metal axis.

The ring-slippage has been attributed in general terms to the strong *trans* influence of the imido ligand leading to a weakening of the two metal–carbon bonds *trans* to the NR group and a consequent adjustment towards an allyl-ene Cp bonding situation.[18–20] However, the ring distortion also follows from our previous observations for complexes with a "single dominant" NR π-donor ligand. For the two π-type interactions of the cyclopentadienyl group, it is expected that the interaction perpendicular to the M–N bond (**I** in Fig. 13b), that is the one with the π_h orbital, will be stronger than that with the metal π-symmetry orbital (π_v) nearly parallel to the M–N bond (**II** in

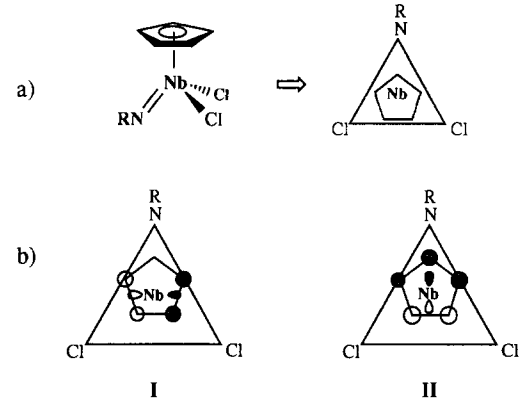


Fig. 13. A triad representation of half-sandwich imido complexes of the type [CpNb(NR)Cl_2]: a) orientation of the Cp ligand; b) π interactions between the orbitals of the Cp ligands and the π_v and π_h orbitals of the metal atom.

Fig 13b). Consequently, the filled π-level of the Cp ligand in **II** will remain largely ligand centered and give rise to the allyl-ene distortion.

6. Complexes Containing Π_2' Ligands

Orientation effects are also often seen for Π_2' ligands in competition with strong Π_2 donors. The strongest π interaction might again be expected to be with the π_h orbital, but the orientation of the Π_2' ligand is less easily predicted since their frontier π-symmetry orbitals are non-degenerate (see Fig. 3) and either of the π interactions could dominate. Just which will dominate will depend on a number of factors including i) the relative energies of the π and π* levels of the ligand orbitals relative to π_h and π_v orbitals of the metal fragment, and ii) the directional properties of the ligand π orbitals (with respect to the metal). We shall not elaborate on these factors here, but the structures of the acetylene complex [Cp*Ta(PhC≡CPh)Cl_2][21] and the benzyne complex [Cp*Ta(C_6H_4)Me_2][22] should be noted (Fig. 14). In both complexes the alkyne ligand functions as a four-electron donor. The orientation of the diphenylacetylene is the same as that expected for a Π_1 ligand, indicating that the π bonding may be dominated by alignment of the π*-acceptor orbital with the π_h orbital. However, steric factors have also been suggested to play a role since the less bulky benzyne ligand is found to align in a perpendicular orientation. The alignment of the butadiene ligand in [CpTa(butadiene)Cl_2][23a] (Fig. 14c) is consistent with the butadiene π-donor orbital interacting with the π_h orbital, the π*-acceptor orbital then aligning with the π_v orbital.

A useful illustration of how the π-bonding capacities of Π_2 and Π_2' ligands can be compared in a complex is provided by the example, [CpNb(η^4-butadiene)(η^2-PhC≡CMe)(PMe_3)][23b] which, in addition to possesing a Π_2 Cp ligand, has two different Π_2' ligand systems (the butadiene and alkyne groups) attached to the metal center (Fig. 14d). Without knowing anything about the detailed MO description of the complex, the orientation of the alkyne indicates that the π-donor bonding is dominated by the Cp and butadiene ligands, a point reinforced by low-frequency ^{13}C NMR shifts for the acetylenic carbon atoms which reflect little or no donation of electron density from the alkyne's orthogonal π system.

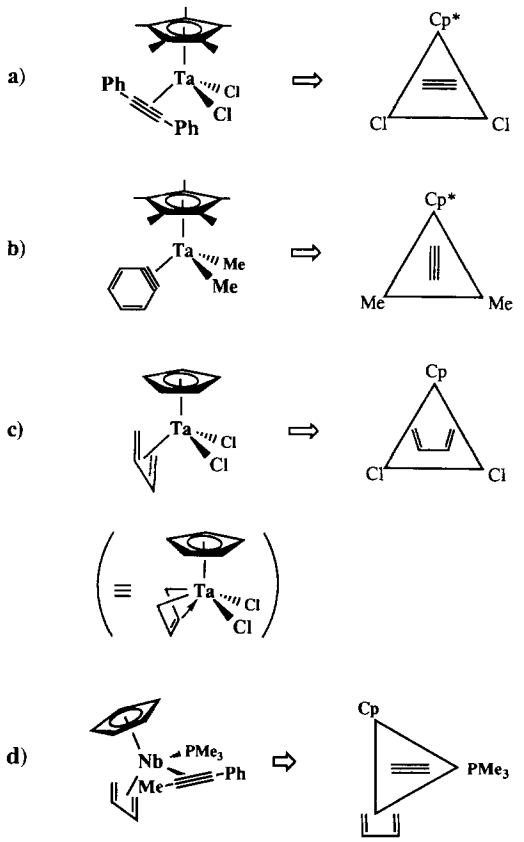


Fig. 14. Triad representations for complexes possessing Π_2 ligands in competition with Π_2 donors: a) [Cp*Ta(PhC≡CPh)Cl_2]; b) [Cp*Ta(C_6H_4)Me_2]; c) [CpTa(C_4H_6)Cl_2]; d) [CpNb(C_4H_6)(PhC≡CMe)(PMe_3)].

7. Low-Valent Systems

Although the analysis presented so far has largely focused on high-valent complexes (i.e. those with metal centers in high oxidation states) where π-donor interactions are of overriding significance, the first detailed MO studies of the factors influencing the orientations of Π_1 ligands were carried out by Hoffmann et al.[2, 3] on low-valent complexes of the type [CpM($CO)_2$L] and [CpM(CO)(NO)(L)] (where L is a Π_1 ligand such as carbene, alkene, or alkyne). For the non-symmetrical nitrosyl case, the orientation preference of the carbene ligand in, for example, [CpCr(CO)(NO)(CPh_2)][24] has been interpreted in terms of the relative π-acidities of the CO and NO^+ groups.

How does this description compare with the treatment we have adopted for the complexes with π-donor ligands and metal atoms in high oxidation states described in the previous sections? Qualitatively, we would expect very little difference: the MO descriptions of the fragments [CpM($CO)_2$] and [CpM(CO)(NO)] also apply to high-valent transition metal systems, since irrespective of whether the ligands are π donors or π acceptors (e.g. NR, Cl, vs. CO etc.) they bind to the metal using similar combinations of σ and π symmetry orbitals (see Table 1). It is only the relative energies of the orbitals and the localization of the electrons ultimately in ligand- or metal-centered MOs that distinguish the situations in high- and low-valent systems.

Thus, in accord with a π-donor approach, CO and NO could be considered to lie at the weak end of a π-donor scale. It then

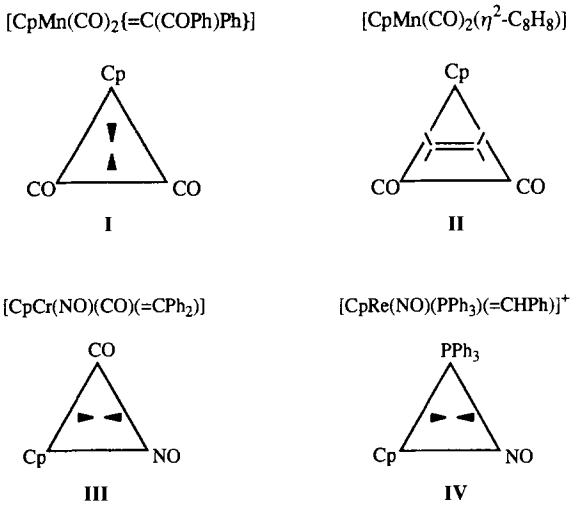


Fig. 15. Triad representations of some low-valent complexes containing Π_1 ligands.

follows that the symmetrical dicarbonyl complexes [CpMn($CO)_2$(L)] (L = Π_1 ligand, e.g. carbene, alkene, alkyne etc.) would be expected to show an alignment of their Π_1 ligands with respect to the single dominant π-donor, the cyclopentadienyl group. This is indeed the case as exemplified by complexes **I**[25] and **II**[26] in Figure 15.

For the mixed carbonyl(nitrosyl) complex [CpCr(CO)(NO)(CPh_2)],[24] (**III**) and the related rhenium phosphane complex [CpRe(NO)(PPh_3)(=CHPh)][PF_6][27] (**IV**) the relative donor capacities of CO in comparison to those of NO are seen to be important. If NO is considered as a neutral ligand (rather than as the nitrosonium ion), it may be regarded as a better π-donor than CO and the alignment of the p orbital of the carbene ligand with the weaker π donor ligands CO and PPh_3 can be ascribed to the Cp and NO ligands dominating the π-donor bonding resulting in an orientation preference reminiscent of the type seen in bent metallocene derivatives.

Finally, perhaps one of the best illustrations of a Π_1 ligand acting as a molecular sensor of π-donor capacity can be found in the complexes [CpMo(O)($CF_3C{\equiv}CCF_3$)(SC_6F_5)] and [CpMo(CO)($CF_3C{\equiv}CCF_3$)(SC_6F_5)][28] (Fig. 16). In the oxo derivative, an 18 electron count is achieved with the acetylene acting as a two-electron (Π_1) ligand and the acetylene is directed towards the SC_6F_5 group showing that the cyclopentadienyl and oxo ligands dominate the π-donor bonding. However, when the oxo ligand is replaced by a carbonyl group, the Cp and SC_6F_5 ligands now dominate the π-donor bonding, and the acetylene responds like a compass needle, reorientating towards the CO ligand. Thus, here the Π_1-acetylene is clearly acting as an indica-

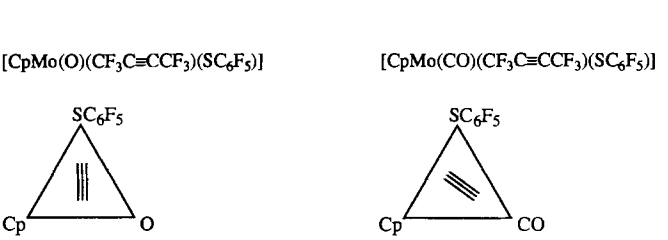


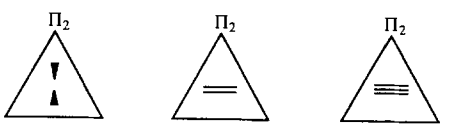
Fig. 16. Triad representations of [CpMo(O)($CF_3C{\equiv}CCF_3$)(SC_6F_5)] and [CpMo(CO)($CF_3C{\equiv}CCF_3$)(SC_6F_5)] illustrating how the alkyne ligand acts as a sensor of π-donor capacity.

tor of relative ligand π-donor strength. Analogous orientation effects are also seen in the tungsten complexes [CpW(O)(PhC≡CPh)(Ph)][29] and [CpW(O)(PhC≡CH)(CH_2CO_2Et)],[30] where the acetylene aligns with the Ph and CH_2CO_2Et groups, respectively, and even in heterobimetallic systems such as [Cp(O)(PhC≡CPh)MoRu(CO)$_2$Cp][31] where the molybdenum-bound acetylene aligns with the Mo–Ru bond.

8. Summary

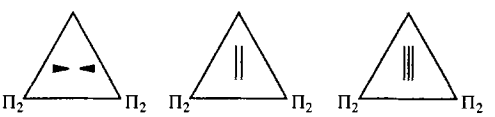
Ligands capable of forming two strong π bonds to a metal atom dominate the bonding in tetrahedral and pseudo-tetrahedral complexes allowing ligands capable of forming only one π interaction to be exploited as sensors to identify the dominant π-bonding groups. These observations lead to some general rules that (in the absence of overriding steric influences) govern the preferred orientations of Π_1 ligands in the presence of strong Π_2 donor groups:

1. For "tetrahedral" species containing a single dominant Π_2-donor, if a triad notation is employed, the substituents of an ancillary carbene or alkylidene ligand will point to the strongest π donor **A**, while an alkene or alkyne ligand will doubly or triply "underline" it (**B** and **C**, respectively).



A **B** **C**

2. For complexes containing two strong Π_2-donor ligands, the alkene and alkyne groups point to the weakest π donor (**E** and **F**, respectively), the alkylidene substituents "underline" it (or provide it with a bow tie!) (**D**).



D **E** **F**

By comparing a series of complexes, it is thereby possible to derive a qualitative ordering of ligand π-bond strengths. For example, from the limited range of examples outlined here the imido group is seen to π bond more effectively than OR, Cp, and Cl ligands, whereas the Cp ligand π bonds more strongly than Cl and SR ligands. All of these ligands of course dominate the solely σ-bonding groups such as PMe_3 and alkyl and π-acceptors such as CO, CHR, and alkenes.

We have found it useful to highlight relationships between complexes containing ligands of a similar class (Π_1, Π_2, Π_2, etc.). Such relationships should not be regarded as rigid, but rather as an aid for understanding stoichiometry and structural patterns in new and seemingly unrelated systems, while at the same time providing a useful basis for evaluating their likely reactions.[32]

Professor Ken Wade is thanked for many helpful and stimulating discussions.

Received: November 16, 1993 [A 37IE]
German version: *Angew. Chem.* **1994**, *106*, 1640

[1] W. A. Nugent, J. M. Mayer, *Metal-Ligand Multiple Bonds*, Wiley-Interscience, New York, **1988**, Chapter 2.
[2] B. E. R. Schilling, R. Hoffmann, D. L. Lichtenberger, *J. Am. Chem. Soc.* **1979**, *101*, 585.
[3] B. E. R. Schilling, R. Hoffmann, J. W. Faller, *J. Am. Chem. Soc.* **1979**, *101*, 592.
[4] H. G. Alt, C. E. Denner, U. Thewalt, M. D. Rausch, *J. Organomet. Chem.*, **1988**, *356*, C83; P. Binger, P. Müller, R. Benn, A. Rufinska, B. Gabor, C. Krüger, P. Betz, *Chem. Ber.* **1989**, *122*, 1035.
[5] For leading references see: *Comprehensive Organometallic Chemistry*, (Eds.: G. Wilkinson, F. G. A. Stone, E. W. Abel) Pergamon, New York, **1982**; *Principles and Applications of Organotransition Metal Chemistry*, (Eds.: J. P. Collman, L. S. Hegedus, J. R. Norton, R. G. Finke), University Science Books, Mill Valley, CA, **1987**.
[6] J. W. Lauher, R. Hoffmann, *J. Am. Chem. Soc.* **1976**, *98*, 1729; L. Zhu, N. M. Kostic, *J. Organomet. Chem.* **1987**, *335*, 395.
[7] A. D. Poole, V. C. Gibson, W. Clegg, *J. Chem. Soc. Chem. Commun.* **1992**, 237.
[8] P. W. Dyer, V. C. Gibson, J. A. K. Howard, B. Whittle, C. Wilson, *J. Chem. Soc. Chem. Commun.* **1992**, 1666.
[9] R. R. Schrock, L. W. Messerle, C. D. Wood, L. J. Guggenberger, *J. Am. Chem. Soc.* **1978**, *100*, 3793.
[10] J. K. Cockcroft, V. C. Gibson, J. A. K. Howard, A. D. Poole, U. Siemeling, C. Wilson, *J. Chem. Soc. Chem. Commun.* **1992**, 1668.
[11] L. Chamberlain, I. P. Rothwell, J. C. Hoffman, *J. Am. Chem. Soc.* **1982**, *104*, 7338.
[12] J. E. Hill, P. E. Fanwick, I. P. Rothwell, *Organometallics*, **1992**, *11*, 1771.
[13] C. J. Schaverien, J. C. Dewan, R. R. Schrock, *J. Am. Chem. Soc.* **1986**, *108*, 2771; J. S. Murdzek, R. R. Schrock, *Organometallics* **1987**, *6*, 1373.
[14] G. Schoettel, J. Kress, J. A. Osborn, *J. Chem. Soc., Chem. Commun.* **1989**, 1062.
[15] B. Hessen, A. Meetsma, J. H. Teuben, *J. Am. Chem. Soc.* **1988**, *110*, 4860; B. Hessen, A. Meetsma, F. van Bolhuis, J. H. Teuben, G. Helgesson, S. Jagner, *Organometallics* **1990**, *9*, 1925.
[16] L. W. Messerle, P. Jennische, R. R. Schrock, G. Stucky, *J. Am. Chem. Soc.* **1978**, *100*, 3793.
[17] I. A. Latham, G. J. Leigh, G. Huttner, I. Jibril, *J. Chem. Soc. Dalton Trans.* **1986**, 377.
[18] V. C. Gibson, D. N. Williams, W. Clegg, D. C. R. Hockless, *Polyhedron*, **1989**, *8*, 1819; D. N. Williams, J. P. Mitchell, A. D. Poole, U. Siemeling, W. Clegg, D. C. R. Hockless, P. A. O'Neil, V. C. Gibson, *J. Chem. Soc. Dalton Trans.*, **1992**, 739.
[19] M. L. H. Green, P. C. Konidaris, P. Mountford, S. J. Simpson, *J. Chem. Soc. Chem. Commun.* **1992**, 256.
[20] W. A. Herrmann, G. Weichselbaumer, R. A. Paciello, R. A. Fischer, E. Herdtweck, J. Okuda, D. W. Marz, *Organometallics* **1990**, *9*, 489.
[21] G. Smith, R. R. Schrock, M. R. Churchill, W. J. Youngs, *Inorg. Chem.* **1981**, *20*, 387.
[22] S. J. McLain, R. R. Schrock, P. R. Sharp, M. R. Churchill, W. J. Youngs, *J. Am. Chem. Soc.* **1979**, *101*, 263.
[23] a) H. Yasuda, K. Tatsumi, T. Okamoto, K. Mashima, K. Lee, A. Nakamura, Y. Kai, N. Kanehisa, N. Kasai, *J. Am. Chem. Soc.* **1985**, *107*, 2410; b) G. E. Herberich, U. Englert, K. Linn,. P. Roos, J. Runsink, *Chem. Ber.*, **1991**, *124*, 975.
[24] W. A. Herrmann, J. L. Hubbard, I. Bernal, J. D. Korp, B. L. Haymore, G. L. Hillhouse, *Inorg. Chem.* **1984**, *23*, 2978.
[25] A. D. Redhouse, *J. Organomet. Chem.* **1975**, *99*, C29.
[26] I. B. Benson, S. A. R. Knox, R. D. Stansfield, P. Woodward, *J. Chem. Soc. Chem. Commun.* **1977**, 404.
[27] W. A. Kiel, G-Yu Lin, A. G. Constable, F. B. McCormick, C. E. Strouse, O. Eisenstein, J. A. Gladysz, *J. Am. Chem. Soc.* **1982**, *104*, 4865.
[28] P. S. Braterman, J. L. Davidson, D. W. A. Sharp, *J. Chem. Soc. Dalton Trans.* **1976**, 241; J. A. K. Howard, R. F. D. Stansfield, P. Woodward, *ibid.* **1976**, 246.
[29] N. G. Bokiy, Yu. V. Gatilov, Yu. T. Struchkov, N. A. Ustynyuk, *J. Organomet. Chem.* **1973**, *54*, 213.
[30] E. R. Burkhardt, J. J. Doney, R. G. Bergman, C. H. Heathcock, *J. Am. Chem. Soc.* **1987**, *109*, 2022.
[31] J. S. Drage, M. Tilset, P. C. Vollhardt, T. W. Weidman, *Organometallics* **1984**, *3*, 812.
[32] For a more detailed outline of the arguments presented here see V. C. Gibson, *J. Chem. Soc. Dalton Trans.* **1994**, 1607.

Binary Encoding of Compound Libraries

Peter Eckes*

During the last decade supramolecular chemistry has developed into a new area of chemical research. Thinking in terms of supramolecular functional units has also influenced current views of biological processes. Modern methods in molecular biology, genetic engineering, and structure analysis have provided the information necessary to understand supramolecular interactions in biological systems. Despite these findings, the rational de novo design of drugs and pesticides that interfere in biological processes by means of supramolecular interactions is still in its infancy.

Random screening remains an important component in the search for biologically active compounds which has also profited from recent developments in the life sciences. Efficient testing systems make it possible to study the activity of thousands of compounds with a molecular target annually. In addition to individual synthesized compounds, mixtures of substances like those in plant extracts, marine organisms, and fermentation broths can also be tested.

Inspired by the tremendous diversity of molecules active in biological systems, chemists have recently developed methods for the synthesis of libraries of compounds for the rapid identification of molecules with biological activity. This research appears to have altered prototypical synthetic chemistry by the introduction of concepts from biology. The result is combinatorial chemistry aimed at the preparation of many structurally diverse compounds.

Research in combinatorial chemistry has been summarized in a series of review articles.[1] Most of the published work describes the synthesis and application of libraries of biooligomers. The preference of peptide and oligonucleotide libraries can be explained by two points: 1) Since the pioneering work of Merrifield and Letsinger, the synthesis of these compounds has been constantly improved. 2) Established methods exist for the determination of the molecular structure even of miniscule samples. The particular challenge in the application of the concepts of peptide and oligonucleotide libraries to libraries of smaller organic molecules is identifying the components in the mixtures prepared by combinatorial methods that participate in supramolecular interactions.

Brenner and Lerner suggested the first solution to this problem.[2] They proposed generating an encoded compound library by combining the split method[3] (see Scheme 2) with two sequential combinatorial steps. In this approach the information for the starting material for the second combinatorial step in the synthesis is stored in the first combinatorial step, the coding step. If a product is deemed "active" in a later test, the encoded sequence information indicates the structure of the active compound independent of the chemistry used in the synthesis.

The viability of the approach was proved with a peptide library. Whereas Nielsen et al.[4] relied on an oligonucleotide code analogous to that in nature, Kerr et al.[5] employed an amino acid code. Despite the independence of synthesis and analysis, both approaches appear to have intrinsic problems: 1) The synthetic sequence of two combinatorial reaction steps requires the development of an orthogonal protecting group strategy for the compound library and the code. 2) In the generation of the diversity of molecules in the two combinatorial steps a tag molecule may also take part in supramolecular interactions. 3) With oligonucleotides in particular the number of possible reactions is limited owing to their chemical lability.

Still et al.[6] have developed an interesting new concept based on the approach of Lerner et al.[2] which appears to solve the aforementioned problems and thus opens up new perspectives for combinatorial chemistry. In two recent papers they describe encoding peptide libraries with a binary code.[6,7] In this approach the tag molecules are not linked to each other sequentially. Thus decoding does not result from the determination of the sequence information but from the formal assignment of the binary code for individual tag molecules and their mixtures. The principle of the encoding is represented in Table 1.

Table 1. Coding compound libraries with a binary code. The letters A–E represent the starting compounds employed, T_1–T_4 the tag molecules.

Starting cmpd.	Step	Binary code	Tag molecule
A	1	10	T_1
B	1	01	T_2
C	1	11	$T_1 + T_2$
D	2	10	T_3
E	2	01	T_4
F	2	11	$T_3 + T_4$

The efficiency of this encoding strategy can be demonstrated with a hypothetical example. X tag molecules can be used to encode $2^X - 1$ starting compounds per reaction step. Thus in an N-step reaction sequence the application of combinatorial principles makes it possible to encode a compound library with

[*] Dr. P. Eckes
BASF AG, Hauptlaboratorium, ZH/W
D-67056 Ludwigshafen (FRG)
Telefax: Int. code + (621)60-21236

 © VCH Verlagsgesellschaft mbH, D-69451 Weinheim, 1994 0570-0833/94/1515-1573 $ 10.00+.25/0

$(2^X - 1)^N$ components with only $X \cdot N$ types of tag molecules. For example, 20 code molecules can be used to code 923 521 compounds prepared in a four-step process.

A series of homologous chlorofluoroarenes serve as tag molecules, which can be separated by capillary gas chromatography. The code molecules can be detected even in attomolar concentrations with electron capture detectors.

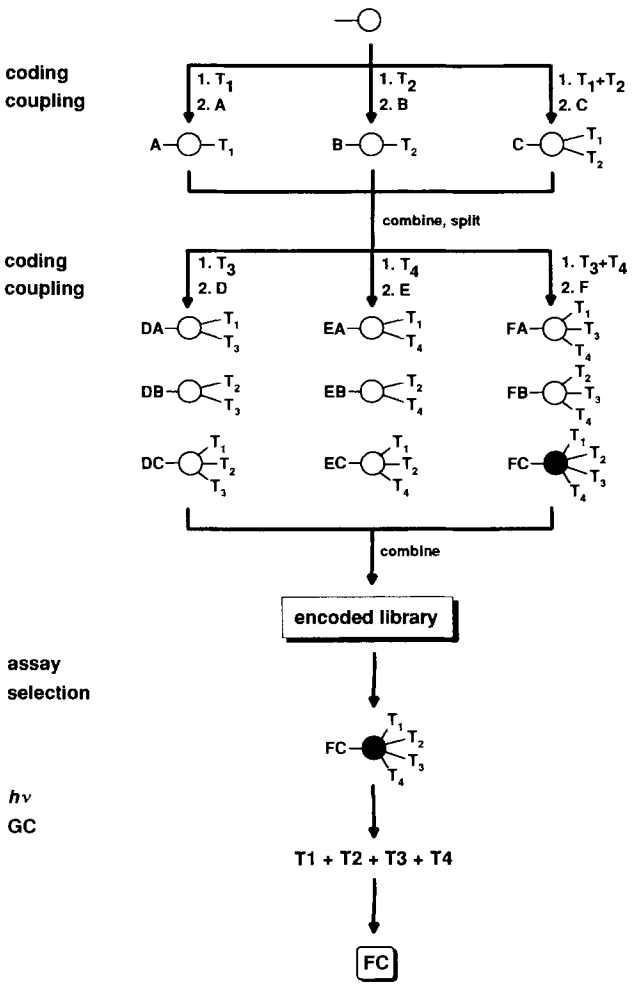
The tag molecules are synthesized according to a simple building block principle shown in Scheme 1. The code molecules are bound to the polymeric support through amide bonds; only a small proportion (< 1 %) of the free amino groups are used in each coding step. The tags are released later by photochemical cleavage of the *o*-nitrobenzyl linker.

In Scheme 2 the construction of a peptide library with a binary code is illustrated. The polymeric support is labeled with the molecular "bar code" in separate reaction flasks. Then the actual coupling reaction with the different amino acids is conducted, still in the separate flasks. Thus the tag molecule and the starting compound have a one-to-one correspondence. By combining and splitting the support particles, defined mixtures are obtained, which can be encoded and coupled in the same way.

The resulting compound library is screened in functional assays, and the support particles linked to "active" molecules are identified. After selection of a particle, photochemical cleavage of the support-bound tag molecules, and silylation of the tag molecules, the code can be read by gas chromatography, and thus the compound that participates in supramolecular interactions can be identified.

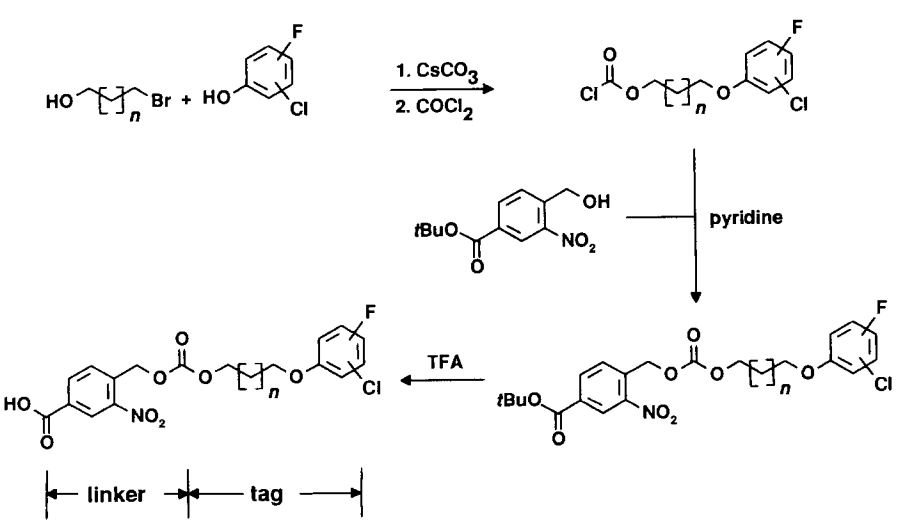
One drawback of the new coding strategy is that in the published procedure[6,7] the assay is still conducted with support-bound compounds. Thus undesired interactions with the support that may lead to changes in conformation affecting binding cannot be ruled out.

As a first test[6] Still et al. screened a encoded peptide library theoretically composed of 117649 14-mers against a monoclonal murine anti-c-MYC antibody. In this peptide library the six N-terminal amino acids were varied (H_2N-XXXXXXEEDLGGGG-support; X can be amino acids D, E, I, K, L, Q, or S). To distinguish the particles to which the anti-c-MYC antibodies bind, the authors employed the color reaction of a second antibody coupled to alkaline phosphatase. All peptide sequences that were determined by decoding the stained particles had a high degree of homology to the MYC epitope. Deviations in the sequence occurred in at most two positions. As a control the affinity of five peptides in solution was determined. All of the IC_{50} values measured were in the lower micromolar range.

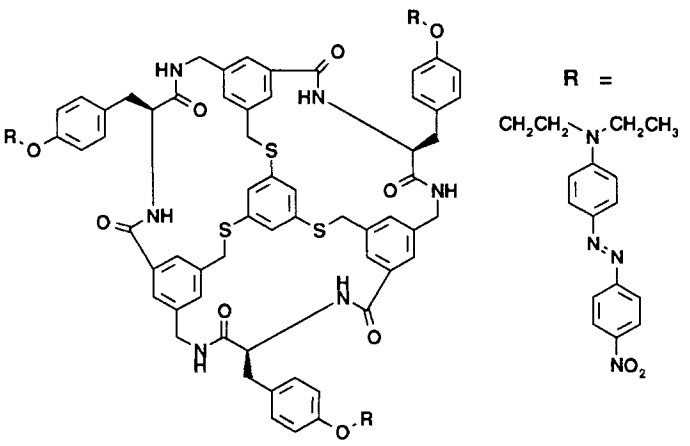


Scheme 2. Schematic description of the construction of a compound library encoded by a binary code, and of the selection of structures from this library that interact in a supramolecular ensemble. —○ denotes the support.

In the second example[7] a peptide ligand was identified which binds selectively to the synthetic receptor **1** (Scheme 3), which is labeled with a red azo dye. The encoded tripeptide library used by Still et al. in their screening included L- and D-amino acids and had various acylated N termini. It was possible here, too, to identify a series of sequences whose marked affinity to the synthetic receptor **1** was confirmed by synthesis and tests in solution.



Scheme 1. Synthesis of the tag molecules. TFA = trifluoroacetic acid.



1

Scheme 3. The synthetic receptor 1 labeled with an azo dye R.

Still et al. have proved the viability of their concept with these two examples,[6,7] and have shown that combinatorial chemistry is a useful tool for the study of supramolecular interactions. Certainly the advantages of binary coding will first be realized fully in the synthesis of compound libraries of small organic molecules.[8] The future of combinatorial chemistry promises to be interesting.

German version: *Angew. Chem.* **1994**, *106*, 1649

[1] Peptide libraries: G. Jung, A. G. Beck-Sickinger, *Angew. Chem.* **1992**, *104*, 357; *Angew. Chem. Int. Ed. Engl.* **1992**, *31*, 375; phage libraries: J. A. Wells, H. B. Lowman, *Curr. Opin. Biotechnol.* **1992**, *3*, 355; libraries of peptidomimetics: R. N. Zuckermann, *Curr. Opin. Struct. Biol.* **1993**, *3*, 580; oligonucleotide libraries: M. Famulok, J. W. Szostak, *Angew. Chem.* **1992**, *104*, 1001; *Angew. Chem. Int. Ed. Engl.* **1992**, *31*, 979; molecular diversity: M. R. Pavia, T. K. Sawyer, W. H. Moss, *Bioorg. Med. Chem. Lett.* **1993**, *3*, 387; W. H. Moos, G. D. Green, M. P. Pavia, *Annu. Rep. Med. Chem.* **1993**, *28*, 315.
[2] S. Brenner, R. A. Lerner, *Proc. Natl. Acad. Sci. USA* **1992**, *89*, 5381.
[3] A. Furka, F. Sebestyen, M. Asgedom, G. Dibo, *Int. J. Pept. Protein Res.* **1991**, *37*, 487; K. S. Lam, S. E. Salmon, E. M. Hersh, V. J. Hruby, W. M. Kazmierski, R. J. Knapp, *Nature* **1991**, *354*, 82.
[4] J. Nielsen, S. Brenner, K. D. Janda, *J. Am. Chem. Soc.* **1993**, *115*, 9812.
[5] J. M. Kerr, S. C. Banville, R. N. Zuckermann, *J. Am. Chem. Soc.* **1993**, *115*, 2529.
[6] M. H. J. Ohlmeyer, R. N. Swanson, L. W. Dillard, J. C. Reader, G. Asouline, R. Kobayashi, M. Wigler, W. C. Still, *Proc. Natl. Acad. Sci. USA* **1993**, *90*, 10922.
[7] A. Borchardt, W. C. Still, *J. Am. Chem. Soc.* **1994**, *116*, 373.
[8] C. Chen, L. A. A. Randall, R. B. Miller, A. D. Jones, M. J. Kurth, *J. Am. Chem. Soc.* **1994**, *116*, 2661.

New Ionic, Isoelectronic Analogues of CO_2 and CS_2

Thomas M. Klapötke*

Several isoelectronic analogues of CO_2 have been known for a long time and are well characterized. These include neutral N_2O ($C_{\infty v}$) and the ionic species N_3^- ($D_{\infty h}$), CN_2^{2-} ($D_{\infty h}$), and NO_2^+ ($D_{\infty h}$).[1] In the last few years, in particular, great progress has been made in the area of these simple 22-electron (16-valence-electron) X=Y=Z species. Thus, all of the possible $X{=}Y{=}Z^n$ systems that contain X, Y, and Z elements of the second period and net charges ($-4 \leq n \leq +4$) have been computed by ab initio methods and many ions were predicted to be locally stable.[2] In meantime several of these unknown species have been prepared and characterized, for example CBN^{4-} and C_3^{4-}, and these species together with their heavier CS_2 analogues are highlighted here.

The structurally well-characterized ionic, isoelectronic analogues of CO_2 known to date are summarized in Table 1 together with three isoelectronic ions of CS_2, the heavier homologue of CO_2. Furthermore, the BAs_2^{3-} anion, which is isoelectronic to CSe_2, has been reported ($d_{BAs} = 186.8$ pm).[3]

In all cases the bond lengths in the ions isoelectronic to CO_2 and CS_2 are appropriate for bond orders greater than unity, and therefore significant $(p\text{-}p)_\pi$ bonding has to be considered. Even in the recently published PCS^- ion the C–S bond length (162 pm) is significantly shorter than the value expected for a typical single bond (cf. d_{CS} (thioether) $\approx$ 182 pm).[7] However, the NBO (NBO = natural bond orbitals) analysis for the PCS^- ion based on an ab initio calculation (HF 6-31 + G*), $d_{PC} = 157$ pm, $d_{CS} = 164$ pm) clearly indicates that $P{\equiv}C - S^-$ is the most favored Lewis structure (NBO charges [e]: P −0.03, C −0.63, S −0.34).[15]

Table 1. Bond lengths of CO_2 and CS_2 and their ionic, isoelectronic analogues [a].

X=Y=Z	d_{XY} [pm]	d_{YZ} [pm]	Ref.	X=Y=Z	d_{XY} [pm]	d_{YZ} [pm]	Ref.
OCO(g)	116.3		[4]	SCS(g)	155		[4]
ONO^+	115		[4]	SNS^+	146		[5, 6]
NNN^-	118		[4]				
NCO^-	121	113	[4] [b]	PCS^-	155.5	162.0	[7]
NCN^{2-}	123.0		[8]				
NBN^{3-}	135.8		[9, 10]	PBP^{3-}	176.7		[3]
CBN^{4-}	144	138	[11, 12]				
CCC^{4-}	134.6		[13]				

[a] Ions that are isoelectronic or isovalence-electronic to OCS, for example $SeCN^-$ [1] are also known; however, they are not discussed here. Polymeric structures have been proposed for the compounds Li_3AlN_2, Li_3GaN_2, Li_3AlP_2, and Li_3AlAs_2 [3]. Formally isosteric transition metal species (e.g. $[FeN_2]^{4-}$ isosteric to SiS_2) have been described see ref. [14]. [b] The fulminate ion CNO^- isomeric to the cyanate ion is also known [1].

[*] Priv.-Doz. Dr. T. M. Klapötke
Institut für Anorganische und Analytische Chemie der
Technischen Universität
Strasse des 17. Juni 135, D-10623 Berlin (FRG)
Telefax: Int. code + (30)314-22168

 © VCH Verlagsgesellschaft mbH, D-69451 Weinheim, 1994 0570-0833/94/1515-1575 $ 10.00+.25/0

With the exception of the C_3^{4-} ion all species quoted in Table 1 can be regarded as linear within the reported standard deviations. Interestingly, the C_3^{4-} ion exhibits C_{2v} symmetry with a C-C-C bond angle of 169.0(6)°; the C–C distances of 134.6(4) pm are consistent with the expected value for C–C double bonds of 135 pm.[13] A comparison of the experimentally determined structural parameters of the C_3^{4-} ion with those computed by ab initio methods showed that the unusual deviation from linearity can be explained by matrix effects caused by the trigonal prismatic coordination of the C_3^{4-} ion by Ca^{2+} ions.

In all ions isoelectronic to CO_2 the most electropositive atom always occupies the central Y position in the X=Y=Z species. This is consistent with theoretical calculations which predict that this isomer will always be the most stable.[16]

Most of the anionic 16-valence-electron species that are isoelectronic to CO_2 and CS_2 were synthesized by high-temperature solid-state reactions in sealed niobium or tantalum ampoules. For example, the compounds $Sr_3(BN_2)_2$[10] and K_3BP_2[3] were prepared at 1000 °C from strontium nitride and BN or from K and BP, respectively. Ca_3Br_2CBN and Sr_3Cl_2CBN were synthesized at 950 °C from the corresponding metal, its dihalide, boron nitride, and graphite.[11] In analogy, $Ca_3Cl_2C_3$ was formed from calcium, $CaCl_2$, and graphite at 900 °C.[13] The synthesis of the first compound containing an isolated PCS^- ion was achieved in solution by treatment of lithium bis(trimethylsilyl)phosphanide with equimolar amounts of *O,O'*-diethyl thiocarbonate [Eq. (a)].[7]

$$S{=}C(OC_2H_5)_2 + [(CH_3)_3Si]_2P\text{-}Li \xrightarrow{\text{DME, } -50\,^\circ C} [Li(dme)_3][PCS] + 2\,H_5C_2OSi(CH_3)_3 \quad (a)$$

(dme = 1,2-dimethoxyethane)

The SNS^+ ion is classically obtained by oxidation of a mixture of tetrasulfurtetranitride and sulfur with AsF_5 [Eq. (b)];[6] however, two new laboratory syntheses are more convenient and do not involve the use of explosive S_4N_4 [Eqs. (c) and (d)].[17]

$$S_4N_4 + \tfrac{1}{2}S_8 + 6\,AsF_5 \longrightarrow 4[SNS][AsF_6] + 2\,AsF_3 \quad (b)$$

$$S_8[AsF_6]_2 + NaN_3 \longrightarrow [SNS][AsF_6] + NaAsF_6 + N_2 + \tfrac{3}{4}S_8 \quad (c)$$

$$[N(SCl)_2][AlCl_4] + SnCl_2 \longrightarrow [SNS][AlCl_4] + SnCl_4 \quad (d)$$

Of all the ions considered here so far, the SNS^+ cation has attracted the most interest as a starting material in preparative inorganic chemistry. The preparation of new pseudoaromatic S–N heterocycles [Eq. (e)], unusual, thermally stable radicals [Eq. (f)], and polymeric sulfur nitride, $(SN)_x$, [Eq. (g)] demonstrate the synthetic potential of the SNS^+ cation in main group chemistry.[6]

$$S_2N^+ + SN^+ \longrightarrow \overline{[N\text{-}S\text{-}N\text{-}S\text{-}S]}^{2+} \quad (6\pi \text{ aromatic}) \quad (e)$$

$$S_2N^+ + F_3C\text{-}C{\equiv}C\text{-}CF_3 \longrightarrow [(F_3C)\overline{C\text{-}S\text{-}N\text{-}S\text{-}C}(CF_3)]^+ \xrightarrow{\text{red.}} [(F_3C)\overline{C\text{-}S\text{-}N\text{-}S\text{-}C}(CF_3)]^{\bullet} \quad (7\pi \text{ radical}) \quad (f)$$

$$S_2N^+ + N_3^- \longrightarrow 2/x(SN)_x + N_2 \quad (g)$$

Earlier this year the synthesis, isolation and characterization of the CBN^{4-} ion, an additional molecule isoelectronic to CO_2, was achieved. It had been predicted for many years on the basis of quantum mechanical calculations that this anion should be stable. This result should encourage the synthesis of new analogues of CO_2 and CS_2. The most likely possible new anions include: NCB^{4-} isomeric to the experimentally characterized CBN^{4-},[11] NCC^{3-} and OBC^{3-} isoelectronic with NBN^{3-},[10] and OBN^{2-} analogous to the known NCN^{2-}.[8] One particularly exciting challenge in this field that remains is the synthesis of the highly charged cations analogous to CO_2, namely O_3^{2+} and FNF^{3+}; these are predicted to be locally stable.[2]

German version: *Angew. Chem.* **1994**, *106*, 1651

[1] N. N. Greenwood, A. Earnshaw, *Chemistry of the Elements*, Pergamon, Oxford, **1984**, p. 337, 509; *Chemie der Elemente*, VCH, Weinheim, **1988**, p. 375, 567.

[2] P. Pyykkö, Y. Zhao, *J. Phys. Chem.* **1990**, *94*, 7753.

[3] H. G. von Schnering, M. Somer, M. Hartweg, K. Peters, *Angew. Chem.* **1990**, *102*, 63; *Angew. Chem. Int. Ed. Engl.* **1990**, *29*, 65; and references therein.

[4] A. F. Wells, *Structural Inorganic Chemistry*, 5th ed., Clarendon, Oxford, **1984**.

[5] R. Faggiani, R. J. Gillespie, C. J. L. Lock, J. D. Tyrer, *Inorg. Chem.* **1978**, *17*, 2975.

[6] S. Parsons, J. Passmore, *Acc. Chem. Res.* **1994**, *27*, 101.

[7] G. Becker, K. Hübler, *Z. Anorg. Allg. Chem.* **1994**, *620*, 405.

[8] M. G. Down, M. J. Haley, P. Hubberstey, R. J. Pulham, A. E. Thunder, *J. Chem. Soc. Dalton Trans.* **1978**, 1407.

[9] H. Yamane, S. Kikkawa, H. Horiuchi, M. Koizumi, *J. Solid State Chem.* **1986**, *65*, 6.

[10] H. Womelsdorf, H.-J. Meyer, *Z. Anorg. Allg. Chem.* **1994**, *620*, 262.

[11] H. Womelsdorf, H.-J. Meyer, *Z. Anorg. Allg. Chem.* **1994**, *620*, 258.

[12] H.-J. Meyer, *Z. Anorg. Allg. Chem.* **1991**, *594*, 113.

[13] H.-J. Meyer, *Z. Anorg. Allg. Chem.* **1991**, *593*, 185.

[14] N. Jansen, H. Spiering, P. Gütlich, D. Stahl, R. Kniep, V. Eyert, J. Kübler, P. C. Schmidt, *Angew. Chem.* **1992**, *104*, 1632; *Angew. Chem. Int. Ed. Engl.* **1992**, *31*, 1624; A. Gudat, S. Haag, P. Höhn, R. Kniep, W. Milius, A. Rabenau, *J. Alloys Compd.* **1991**, *177*, L 17.

[15] A. Schulz, T. M. Klapötke, unpublished.

[16] B. M. Gimarc, *J. Am. Chem. Soc.* **1970**, *92*, 266; J. K. Burdett, N. J. Lawerence, J. J. Turner, *Inorg. Chem.* **1984**, *23*, 2419.

[17] B. Ayres, A. J. Banister, P. D. Coates, M. I. Hansford, J. M. Rawson, C. E. F. Rickard, M. B. Hursthouse, K. M. Abdul Malik, M. Motevalli, *J. Chem. Soc. Dalton Trans.* **1992**, 3097; A. J. Banister, R. G. Hey, G. K. MacLean, J. Passmore, *Inorg. Chem.* **1982**, *21*, 1679.

Template Effects in New Self-Replicating Molecules**

M. Morgan Conn, Edward A. Wintner, and Julius Rebek, Jr.*

Template effects, the enhancement of reactions by complementary surfaces, lie at the heart of many chemical and biological processes.[1] A special form of templating occurs when two complementary molecules are covalently bound.[2] If the product enhances its own formation, replication is possible. This has been shown to be the case for short nucleic acids[3] and other self-complementary structures.[4, 5] We describe here a new replicating system which, by its geometry, minimizes the effects of the inevitable background reactions associated with such systems. We give evidence that the autocatalysis that is observed arises from template effects, and suggest an advantage of replication by these means.

The carbazole derivative **1** is a nearly ideal complement to the purine unit of adenine.[6, 7] The imides can chelate the purine unit through simultaneous Watson–Crick and Hoogsteen base-pairing, and stacking interactions are possible between the extended surface of the carbazole and the purine moieties. The result is high binding affinity in $CDCl_3$ ($K_a \approx 10^5$), MeOH ($K_a = 130$), and even H_2O ($K_a = 150$).[8] The tight binding also provides unambiguous positioning of the two complementary components.[7] The new replicator utilizes these features and contains a biphenyl spacer between the carbazole nitrogen atom and an electrophilic component (structure 7). The complementary structure for the replication experiments is the 5′-amino-5′-deoxy-2′,3′-*O*-isopropylideneadenosine **2**.

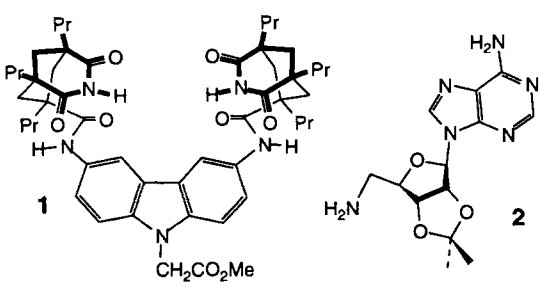


Figure 1 shows the geometry predicted in a modeling study[9] for a bimolecular complex between **2** and the biphenylcarbazole as the methyl ester **6**. The amine and ester groups are separated by a significant distance, at least 5.8 Å. This distance is well enforced; the diimide-bound adenine has only limited motion within the complex. Since the two reactive centers cannot approach each other within the complex, covalent bond formation between the amine and ester groups must occur in an intermolecular sense.

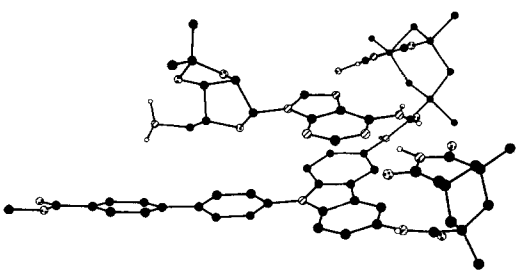
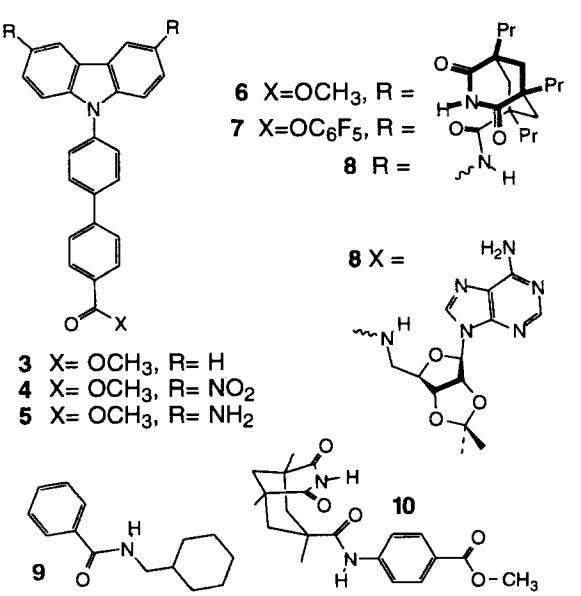


Fig. 1. Structure of a complex of **2** and **6** as predicted by molecular modeling [9].

Synthesis of the biphenylcarbazole derivative **6** proceeded through Ullmann coupling[10] of methyl 4′-iodobiphenyl-4-carboxylate and carbazole to give **3**, followed by nitration (HNO_3/HOAc) to **4**, and reduction (H_2/Pd-C, THF) to the diamine **5**.[11] Condensation of **5** with the tripropyl derivative of Kemp's triacid as the imide acid chloride gave the methyl ester **6**.[12] Demethylation of **6** was achieved by S_N2 dealkylation with thiolate anion,[13] and condensation of the corresponding acid chloride (prepared by reaction with oxalyl chloride) with adenosine **2** produced the self-complementary amide **8**. Demethylated **6** was also used to give **7** through coupling with pentafluorophenol (1-ethyl-3-(3-dimethylamino)carbodiimide (EDC), 4-dimethylaminopyridine (DMAP), THF).



[*] Prof. Dr. J. Rebek, Jr., M. M. Conn, E. A. Wintner
Department of Chemistry, Massachusetts Institute of Technology
Cambridge, MA 02139 (USA)
Telefax: Int. code + (617)253-7929

[**] This work was supported by the National Science Foundation (NSF) (Grant No. 9119995-CHE). M. M. C. thanks the National Science and Engineering Research Council (NSERC) and E. A. W. the NSF for predoctoral fellowships.

As anticipated, compound **6** has very high affinity for adenine. The slow exchange processes of the molecule lead to highly broadened ^{1}H NMR spectra during titration in $CDCl_3$, and the binding constant can only be estimated as $10^5\ M^{-1}$. In the more competitive [D_8]THF, the association constant between **6** and 2′,3′-isopropylidene adenosine was found by ^{1}H NMR titration to be $570\ M^{-1}$ at 298 K. This value is based on the downfield shift of the imide proton from $\delta = 9.65$ to $\delta = 12.87$ during titration.

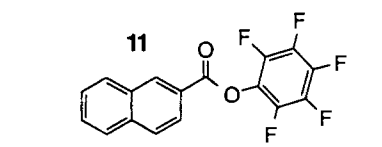
Kinetic studies of the coupling reactions[14] were performed in $CHCl_3$/THF mixtures using the pentafluorophenyl active ester **7** and amine **2**. Appearance of the amide product **8** was followed by high-performance liquid chromatography (HPLC) with various additives as controls. For example, the benzoyl derivative **9** presents a secondary amide function in a steric environment similar to that of **8**, but the structure lacks recognition elements. The results are summarized in Table 1 and reveal the following:

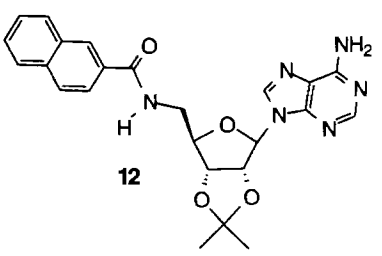
Table 1. Average initial rates v for the reaction of **2** with **7** and **11** [14].

Reactants	Additive (0.5 equiv.)	v [$\mu M\,min^{-1}$], ±5%	Reactants	Additive (0.5 equiv.)	v [$\mu M\,min^{-1}$]
2 + **7**	–	1.71 ± 0.06	**2** + **7**	**6**	1.18 ± 0.10
2 + **7**	**8**	2.63 ± 0.11	**2** + **11**	–	3.78 ± 0.06
2 + **7**	**10**	1.72 ± 0.02	**2** + **11**	**12**	4.08 ± 0.03
2 + **7**	**9**	1.56 ± 0.08			

1) *Autocatalysis occurs in the complementary system.* Addition of the product **8** increases the rate of the coupling reaction of ester **7** with **2**. Experiments with **7** and **2** at concentrations of 6.2 mM show a 54% increase in initial rate with 0.5 equivalents of added **8** (Table 1). This enhancement is comparable to that observed with our original replicators.[5]

2) *The benzoyl amide does not catalyze the reaction.* The coupling rate of **7** with **2** is not increased by the addition of the secondary amide **9**. Furthermore, the coupling of **2** with **11** under identical conditions is not significantly enhanced by addition of amide **12**; under these conditions, the general formation of secondary amides is not appreciably autocatalytic. These results are consistent with those of other self-replicating systems involving adenine recognition.[5]





3) *The adenosine moiety is not an effective catalyst for the formation of secondary amides.* This is shown by the failure of product **12** to catalyze the coupling of **2** with **11** significantly.

4) *The imide function alone is not responsible for the autocatalysis.* This was established by control experiments with the methyl ester **6**. This molecule does not catalyze the reaction of **7** with **2**; rather, some inhibition results as a consequence of its sequestering the adenosine amine in an unproductive complex. Additional experiments with **10**, which competes only poorly for adenosines, further support the conclusion that the imide group is an ineffective catalyst.

5) *Self-replication is the result.* Separated, the individual features and functionalities of **8** are unable to account for the autocatalysis observed. Instead, the effect of the whole molecule is greater than the sum of the effects of its parts. The most elegant explanation for the autocatalytic nature of **8** is that the molecule serves as a template for its own formation: the reaction between **2** and **7** or between two complexes of **2**·**7** is slow, but once formed, template **8** can bring together **2** and **7** in a productive termolecular complex. Within the complex, functional groups are presented is such a way that a tetrahedral intermediate is easily reached. The intermediate is modeled[9] in Fig. 2.

What are the consequences of complexation for replicators? The rate of formation of **8** compared with that of **12** under these conditions reveals that recognition *slows* the rate of coupling by a factor of two; in the presence of **2**, pentafluorophenyl esters such as **11** which are unable to complex **2** are twice as reactive toward amines than is ester **7**. For the same reasons, however, noncomplexed esters are also more exposed to side reactions. Structures that recognize each other and form complexes become stabilized; the surfaces in contact are protected from external, often harmful reagents, and the protected structures react primarily with molecules that are specifically complexed with them.[15] Accordingly, molecular recognition offers advantages for evolution at the molecular level; survival as well as replication is enhanced.

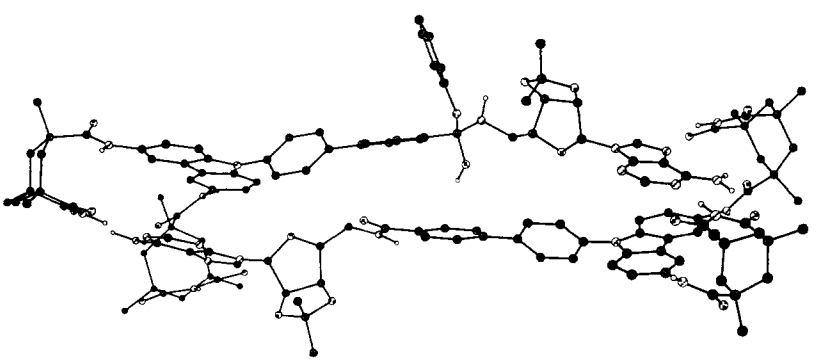


Fig. 2. Structure of the tetrahedral intermediate in a termolecular complex of **2**, **7**, and **8** as predicted by molecular modeling [9].

Our current targets are molecules in which functional groups are incorporated into the template for *chemical catalysis* of the replication step.[16] These include functions that can enhance proton transfers in the tetrahedral intermediates which are formed and destroyed along the coupling pathway. In addition, these high-affinity molecules augur well for the synthesis of structures capable of replication in aqueous media.

Received: March 4, 1994 [Z 6727 IE]
German version: *Angew. Chem.* **1994**, *106*, 1665

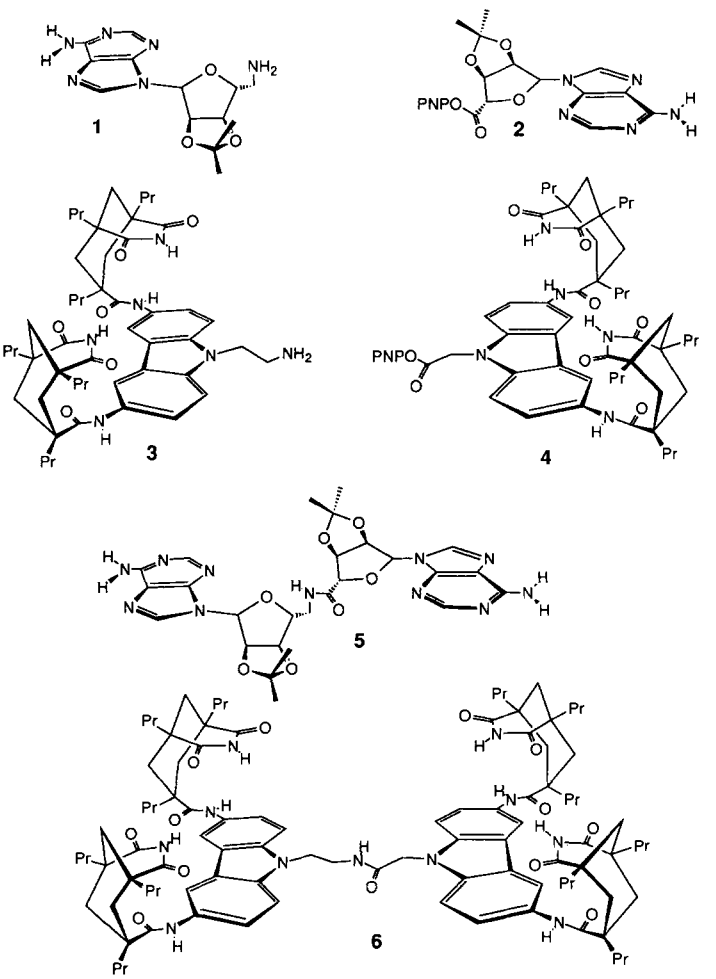
[1] S. Anderson, H. L. Anderson, J. K. M. Sanders, *Acc. Chem. Res.* **1993**, *26*, 469–475; T. R. Kelly, G. J. Bridger, C. Zhao, *J. Am. Chem. Soc.* **1990**, *112*, 8024–8034.
[2] J. Rebek, Jr., *Chem. Ind.* **1992**, 171–174.
[3] G. von Kiedrowski, B. Wlotzka, J. Helbing, M. Matzen, S. Jordan, *Angew. Chem.* **1991**, *103*, 456–459; *Angew. Chem. Int. Ed. Engl.* **1991**, *30*, 423–426; L. E. Orgel, *Nature* **1992**, *358*, 203–209.
[4] A. Terfort, G. von Kiedrowski, *Angew. Chem.* **1992**, *104*, 626–628; *Angew. Chem. Int. Ed. Engl.* **1992**, *31*, 654–656.
[5] T. Tjivikua, P. Ballester, J. Rebek, Jr., *J. Am. Chem. Soc.* **1990**, *112*, 1249–1250; J. S. Nowick, Q. Feng, T. Tjivikua, P. Ballester, J. Rebek, Jr., *ibid.* **1991**, *113*, 8831–8839; V. Rotello, J. I. Hong, J. Rebek, Jr., *ibid.* **1991**, *113*, 9422–9423.
[6] A. Galán, J. de Mendoza, C. Toiron, M. Bruix, G. Deslongchamps, J. Rebek, Jr., *J. Am. Chem. Soc.* **1991**, *113*, 9424–9425; G. Deslongchamps, A. Galán, J. de Mendoza, J. Rebek, Jr., *Angew. Chem.* **1992**, *104*, 58–60; *Angew. Chem. Int. Ed. Engl.* **1992**, *31*, 61–63.
[7] M. M. Conn, G. Deslongchamps, J. de Mendoza, J. Rebek, Jr., *J. Am. Chem. Soc.* **1993**, *115*, 3548–3557.
[8] Y. Kato, M. M. Conn, J. Rebek, Jr., *J. Am. Chem. Soc.*, in press.
[9] MacroModel 3.5X. F. Mohamadi, N. G. Richards, W. C. Guida, R. Liskamp, M. Lipton, C. Caufield, G. Chang, T. Hendrickson, W. C. Still, *J. Comput. Chem.* **1990**, *11*, 440–467.
[10] For a review on the Ullmann coupling see: J. Lindley, *Tetrahedron* **1984**, *40*, 1433–1456.
[11] K. S. Jeong, A. V. Muehldorf, J. Rebek, Jr., *J. Am. Chem. Soc.* **1990**, *112*, 6144–6145.
[12] All new compounds were characterized by standard spectroscopic techniques (^{1}H NMR, IR) and by high-resolution mass spectrometry.
[13] For a review of ester dealkylation, see: J. McMurry, *Org. React.* **1976**, *24*, 187–224.
[14] Kinetic studies: Averages represent four runs in the reactions of **2** + **7** and three runs in the reactions of **2** + **11**. Rates were obtained from the slope of the curve for the coupling reaction up to 5% conversion. All reactions were performed at 6.2 mM initial concentrations of reactants in 13% THF/$CHCl_3$ with 1% triethylamine. Formation of products was followed by HPLC with UV detection at 270 nm on a Waters 600E instrument equipped with a Waters 717 autosampler and a Waters 490E UV detector. The temperature inside the autosampler was constant at 22 ± 1 °C. Analytical separation of the reaction products was achieved using a Beckman Ultrasphere SI column (4.6 mm × 25 cm) with gradient elution from 1% to 5% MeOH/$CHCl_3$.
[15] There are earlier examples of a template slowing down a reaction but improving the yield of the desired molecule; see C. Dietrich-Buchecker, J. P. Sauvage, *New J. Chem.* **1992**, *16*, 277–285.
[16] C. Andreu, R. Beerli, N. Branda, M. M. Conn, J. de Mendoza, A. Galán, I. Huc, Y. Kato, M. Tymoschenko, C. Valdez, E. A. Wintner, R. Wyler, J. Rebek, Jr., *Pure Appl. Chem.* **1993**, *65*, 2313–2318.

Reciprocal Template Effects in a Replication Cycle**

Roland J. Pieters, Ivan Huc, and Julius Rebek, Jr.*

The enhancement of chemical reactions by complementary surfaces—template effects—is widespread in biological and chemical processes.[1] Nucleic acid replication is the typical example: one strand acts as a template for the other's formation. We have earlier described self-complementary structures[2] and their ability to act as templates in self-replicating systems and as subunits for molecular assemblies. Here we show that template effects operating in a reciprocal sense, in a replication cycle, can be even more efficient than the self-replicating systems.

The molecular recognition involved is the chelation of the purine nucleus of adenine by two imides attached to a carbazole surface. The imides provide simultaneous Watson–Crick and Hoogsteen base pairing, while the carbazole and the purine interact by π stacking. High binding affinities between these two components ($K_a = 10^4$–10^5 M^{-1}) are observed in organic solvents.[3] We have now outfitted the two components with complementary chemically reactive functions, nucleophilic amines and electrophilic activated esters, for covalent coupling reactions. Specifically, amines **1** and **3** and *p*-nitrophenyl esters **2** and **4** were prepared (Scheme 1). The slow reaction of amine **1** with



Scheme 1. Amines (**1** and **3**), esters (**2** and **4**), and their coupling products (templates) **5** and **6**. PNP = *p*-nitrophenyl.

were prepared (Scheme 1). The slow reaction of amine **1** with ester **2** (each 0.05 mM) in chloroform in the presence of triethylamine produced **5**.[4] The initial rate was 1.5×10^{-8} M min^{-1} (Table 1). Likewise, amine **3** and ester **4** gave **6** at an initial rate of 4.3×10^{-9} M min^{-1} under the same conditions.

The accelerating effects of templates in these bisubstrate reactions were observed as follows: in the presence of the receptor **6**, **1** and **2** reacted to give **5** at a rate up to 12 times that of the background reaction.[5] As shown in Table 1, the acceleration was reduced by the competitive binding partner 9-ethyladenine and by the actual product **5**. Maximum rate acceleration was observed when two equivalents of the template **6** were used (Fig. 1).[6] Addition of further amounts of template led to lower coupling rates; the two reactive components form complexes on different template molecules and become increasingly separated. In control experiments with one equivalent of **7** (Scheme 2), a molecule that bears many of the structural and functional

[*] Prof. J. Rebek, Jr., R. J. Pieters, I. Huc
Department of Chemistry, Massachusetts Institute of Technology
Cambridge, MA 02139 (USA)
Telefax: Int. code + (617)253-7929

[**] This research was supported by the National Institutes of Health, the National Science Foundation, and Rhône-Poulenc (predoctoral fellowship to I. H).

Table 1. Initial rates v_0 of amide formation.

Reaction[a]	c(5) [mM]	c(6) [mM]	c(7) [mM]	c(8) [mM]	c(9-Et-Ad) [mM]	v_0[b] [10^{-9} M min^{-1}]
1 + 2						15
1 + 2		0.05				150
1 + 2	0.05	0.05				42
1 + 2		0.05			0.5	30
1 + 2			0.05			14
1 + 2				0.05		11
3 + 4						4.3
3 + 4	0.05					23
3 + 4	0.05	0.05				13
3 + 4	0.05				0.5	15
3 + 2						53000
1 + 4						2200

[a] $c(1) = c(2) = c(3) = c(4) = 0.05$ mM, $c(Et_3N) = 4$ mM, Solvent: $CHCl_3$, $T = 25$ °C. [b] Averaged values from multiple independent runs; standard deviations ±15%.

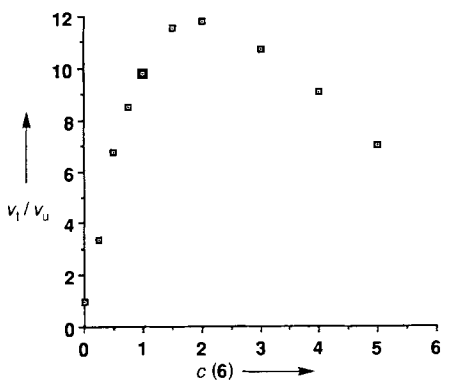
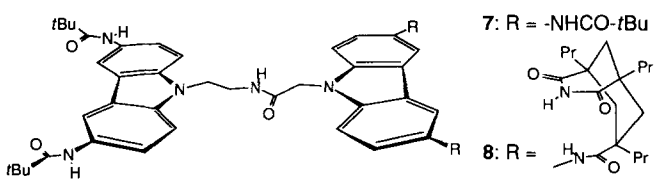


Fig. 1. The acceleration of the initial rate of the reaction between **1** and **2** (template catalyzed rate: v_t; uncatalyzed rate: v_u) as a function of the concentration of **6** (in equivalents). $c(1) = c(2) = 5 \times 10^{-5}$ M, $c(NEt_3) = 4 \times 10^{-3}$ M, solvent: $CHCl_3$, $T = 25$ °C.

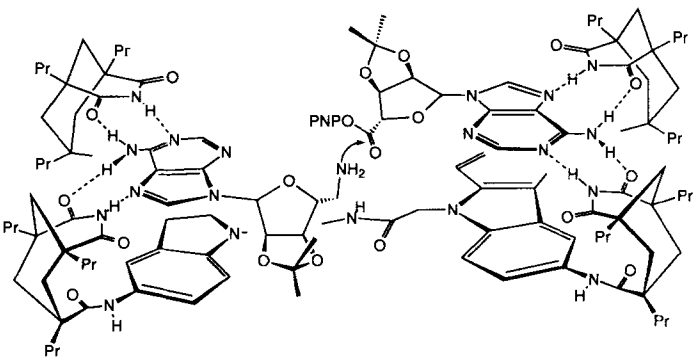


Scheme 2. Structures of molecules used as controls.

features of the template but lacks the recognition elements, no rate enhancement in the reaction of **1** with **2** was observed. Similarly, addition of one equivalent of **8**, containing one binding site, did not increase the coupling rate. These observations can be explained by the formation of a termolecular complex (Scheme 3).[7]

The reciprocal template, product **5**, proved capable of catalyzing the coupling of **3** and **4**. The observed rate enhancement over the uncatalyzed reaction was fivefold, and again, product inhibition with **6** and competitive inhibition with 9-ethyladenine was observed.

The rate enhancements here are comparable to those observed by Kelly[1d, e] for templates for bimolecular S_N2 reactions and are considerably larger (by an order of magnitude) than those observed for template effects involving *self*-complementary structures.[2a, b] The reciprocal templating effects of **5** and **6** formally represent a replication cycle. Whether these cycles are generally more efficient than the minimalist self-complementary replicators is the subject of ongoing research.



Scheme 3. The proposed termolecular complex responsible for the enhanced rates for the reaction of **1** with **2**.

In the meantime, we note that large rate accelerations can be achieved in complexes of a bimolecular sort.[8] Thus, reaction of amine **3** with active ester **2** at concentrations of 0.05 mM was 3500 times faster than the reaction of **1** with **2**. The reaction of amine **1** with ester **4** was 500 times faster than the reaction of **3** with **4**. In both cases, the products are self-complementary, but due to the flexibility of the spacers between the reactive functions, they remain folded shut in intramolecular complexes.[9]

Received: April 21, 1994 [Z 6866 IE]
German version: *Angew. Chem.* **1994**, *106*, 1667

[1] a) R. Hoss, F. Vögtle, *Angew. Chem.* **1994**, *106*, 389; *Angew. Chem. Int. Ed. Engl.* **1994**, *33*, 375, and references therein.; b) S. Anderson, H. L. Anderson, J. K. M. Sanders, *Acc. Chem. Res.* **1993**, *26*, 469, and references therein.; c) C. J. Walter, H. L. Anderson, J. K. M. Sanders, *J. Chem. Soc. Chem. Commun.* **1993**, 458; d) T. R. Kelly, C. Zhao, G. J. Bridger, *J. Am. Chem. Soc.* **1989**, *111*, 3744; e) T. R. Kelly, G. J. Bridger, C. Zhao, *ibid.* **1990**, *112*, 8024; f) C. O. Dietrich-Buchecker, J. P. Sauvage, J. M. Kern, *ibid.* **1984**, *106*, 3043; g) W. L. Mock, T. A. Irra, J. P. Wepsiec, M. Adhya, *J. Org. Chem.* **1989**, *54*, 5302; h) G. von Kiedrowski, B. Wlotzka, J. Helbing, M. Matzen, S. Jordan, *Angew. Chem.* **1991**, *103*, 456; *Angew. Chem. Int. Ed. Engl.* **1991**, *30*, 423; i) A. Terfort, G. von Kiedrowski, *ibid.* **1992**, *104*, 626 and **1992**, *31*, 654; j) J. T. Goodwin, D. G. Lyn, *J. Am. Chem. Soc.* **1992**, *114*, 9197; k) for a system with multiple reaction see: T. Achilles, G. von Kiedrowski, *Angew. Chem.* **1993**, *105*, 1225; *Angew. Chem. Int. Ed. Engl.* **1993**, *32*, 1198.

[2] a) J. S. Nowick, Q. Feng, T. Tjivikua, P. Ballester, J. Rebek, Jr., *J. Am. Chem. Soc.* **1991**, *113*, 8831; b) T.-K. Park, Q. Feng, J. Rebek, Jr., *ibid.* **1992**, *113*, 4529; c) R. Wyler, J. de Mendoza, J. Rebek, Jr., *Angew. Chem.* **1993**, *105*, 1820; *Angew. Chem. Int. Ed. Engl.* **1993**, *32*, 1699.

[3] a) M. M. Conn, G. Deslongchamps, J. de Mendoza, J. Rebek, Jr., *J. Am. Chem. Soc.* **1993**, *115*, 3448; b) R. J. Pieters, J. Rebek, Jr., *Recl. Trav. Chim. Pays-Bas*, **1993**, 330.

[4] The rate was determined by monitoring the release of *p*-nitrophenolate spectrophotometrically at 330 nm. Typically reactions were monitored to at least 30% conversion, and initial rates were obtained for up to 10% conversion.

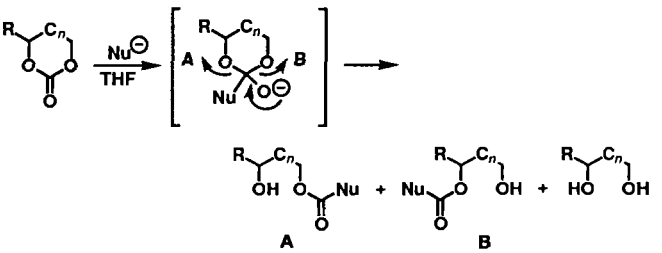
[5] The products were analyzed as follows: two solutions were prepared both 0.1 mM **1** and **2** and 8 mM NEt_3 (in 20 mL $CHCl_3$). One of these also contained 0.1 mM **6**, which led to an initial rate eight times faster than that without **6** (determined spectrophotometrically). After 72 h the solvent and NEt_3 were removed, and the residues were redissolved in [D_6]DMSO and analyzed by ^{1}H NMR spectroscopy. In both cases **5** was the only observed product.

[6] Due to the low concentrations of the reagents used and binding constants of $K_a = 10^4 - 10^5$ M^{-1}, the receptors are not fully saturated with guests. Therefore the maximum is not at one equivalent of template **6**.

[7] A referee suggested that these control experiments show that catalysis by simple amides as proposed by Menger et al. (F. M. Menger, A. V. Eliseev, N. A. Khanjin, *J. Am. Chem. Soc.* **1994**, *116*, 3613) can be excluded. Menger's experiments showed that high concentrations (generally 30 mM) are required for simple amides to exert their (small) catalytic effects, whereas accelerations due to a template in the same system are operative at concentrations as low as 0.33 mM [2a]. Template effects are highly dependent on the magnitude of the association constants of the species involved and, as the present work shows, can be observed at concentrations orders of magnitude lower than required for simple amide catalysis.

[8] For related systems see: a) P. Tecilla, A. D. Hamilton, *J. Chem. Soc. Chem. Commun.* **1990**, 1232; b) M. W. Göbel, J. W. Bats, G. Dürner, *Angew. Chem.* **1992**, *104*, 217; *Angew. Chem. Int. Ed. Engl.* **1992**, *31*, 207; b) J.-M. Lehn, C. Sirlin, *J. Chem. Soc. Chem. Commun.* **1978**, 949; d) D. J. Cram, H. E. Katz, *J. Am. Chem. Soc.* **1983**, *105*, 135; e) G. L. Trainor, R. Breslow, *ibid.* **1981**, *103*, 154.

[9] M. M. Conn, PhD Thesis, Massachusetts, Institute of Technology, **1994**. We thank Dr. Conn for his conformational analysis of these products.

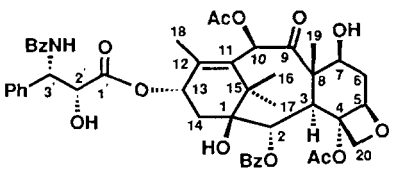


Scheme 1.

Synthesis of C-2 Taxol Analogues**

Kyriacos Costa Nicolaou,* Elias A. Couladouros, Phillipe G. Nantermet, Joanne Renaud, Rodney Kiplin Guy, and Wolfgang Wrasidlo

Taxol (**1**)[1, 2] is currently of substantial interest due to its exceptional chemistry,[3] biology,[3a, 4] and medical applications.[3, 4] Researchers in both academic and industrial laboratories have been devoting considerable time and effort to the



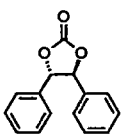
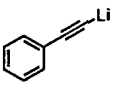
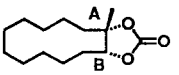
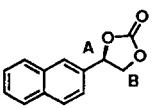
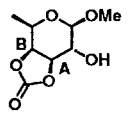
1 Taxol

design, synthesis, and biological evaluation of taxol analogues[3, 5] with the aim of attaining pharmacological properties superior to those exhibited by the parent compound. In this communication we report a general method for the regioselective functionalization of cyclic carbonates by nucleophilic ring opening and its application in the synthesis of a series of new taxoids functionalized at C-2; a family of compounds hitherto difficult to obtain.[6]

A key observation made during the total synthesis of taxol (**1**)[2a] involved the opening of a five-membered cyclic carbonate with PhLi. This reaction proceeded with exquisite regio- and chemoselection and gave a high yield of the desired product. The addition of nucleophiles to carbonates to provide esters has seen only rare use[7] and reports of such regioselective manipulation of a cyclic carbonate are rather scarce.[8] Expanding the scope of this reaction and demonstrating its wide applicability in the taxol field were the objectives of this program.

Scheme 1 shows the general strategy for the regioselective functionalization of cyclic carbonates by ring opening with nucleophilic reagents. The examples listed in Table 1 demonstrate

Table 1. Regioselective synthesis of esters through nucleophilic addition to cyclic carbonates.

Entry	Carbonate	Nucleophile	No. of equivalents	T [°C]	t [min]	Yield [%] (A:B:diol)
1a			1.5 1.25	−100 −78	25 30	70:0:26 78 [a]:0:15
1b			1.3	−78	30	98:0:0
1c			1.1	0	15	87:0:0
1d			1.5	−78, then −45	60 30	100:0:0
2a			1.5	−78	30	85:0:12
2b			1.3	−78	30	94:0:3
3			1.5	−78	30	67:17:0
4			3.5	−78	30	93 [a]:0:0

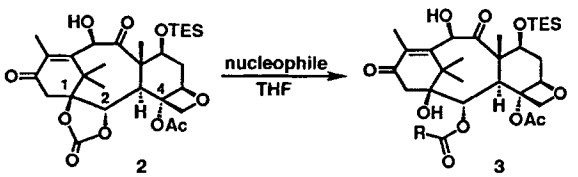
[a] Yield based on 70–90% conversion.

the wide range of both substrates and nucleophiles that undergo this reaction and the considerable selectivities attained. The predominant product in each reaction was the ester; the only side product detected in several cases was the diol. In all cases except the primary/secondary, the exclusive product was the less substituted ester **A**. In the primary/secondary cases, the regioselectivity was about 4:1 in favor of **A**.

When applied to taxoid **2**, available from both total synthesis[2a] and semisynthesis,[9] this ring-opening process produced a number of novel taxoids **3** (Table 2). The remarkable selectivity of this reaction was quite striking, particularly in view of the three additional carbonyl groups present in the substrate **2**. Steric shielding must be largely responsible for the protection of the latter sites against the reactive nucleophiles employed. Products obtained by this method are particularly interesting in that they provide access to taxols with additional functionalities at C-2.

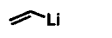
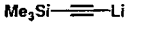
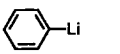
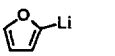
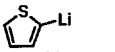
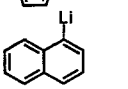
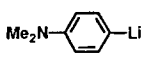
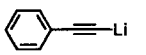
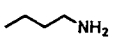
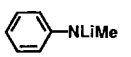
[*] Prof. Dr. K. C. Nicolaou, E. A. Couladouros, P. G. Nantermet, J. Renaud, R. K. Guy, W. Wrasidlo
Department of Chemistry, The Scripps Research Institute
10666 North Torrey Pines Road, La Jolla, CA 92037 (USA)
and
Department of Chemistry, University of California
San Diego, 9500 Gilman Drive, La Jolla, CA 92093 (USA)
Telefax: Int. code + (619)554-6738

[**] We thank E. Bombardelli for 10-deacetylbaccatin III, K. B. Sharpless for a series of diols, and I. Ojima for the β-lactam **6**. This work was supported by The Scripps Research Institute, National Institutes of Health (USA), Office of Naval Research (USA) (R. K. G.), Natural Sciences and Engineering Research Council (Canada) (J. R.), the Agricultural University of Athens (E. A. C.), and Rhone-Poulenc Rorer (P. G. N.).



TES=Triethylsilyl

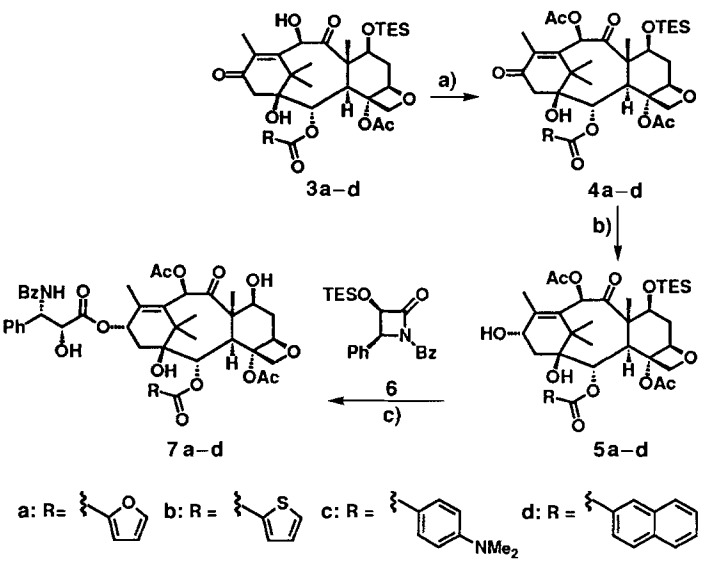
Table 2. Nucleophilic ring opening of cyclic carbonates to give C-2 taxol analogues **3**.

Entry	Nucleophile RX	No. of equivalents	*t* [min]	*T* [°C]	Yield [%]
1		1.1	30	−78	72 [a]
2		15	90	−78	74 [b]
3		20	90	−20	60 [b]
4		20	10	0	60 [a, c]
5		10	30	−78	85
6		15	10	−78	78
7		15	30	−78	96 [b]
8		15	10	−78	89
9		5	30	−78	42 [a]
10		15	30	−78	95 [d]
11		20	15	25	92
12		10	60	25	93 [d]

[a] Reaction also produced variable amounts of the C-4 hydroxy and C1-C2 dihydroxy compounds. [b] Yield based on 50–80% conversion. [c] Yield based on desilylated acetylenic compound obtained after workup. [d] 10–20% conversion only.

This position has been recognized as important for biological activity.[3] To explore such structure–activity relationships we have undertaken the conversion of compounds **3a–d** to taxoids (**7a–d**).

Several compounds of type **3** have previously been converted to taxoids.[2a] Thus acetylation of **3a–d** (Scheme 2) provided



Scheme 2. Synthesis of novel taxoids **7** [11]. a) Ac_2O/CH_2Cl_2 (1/4), Et_3N (5 equiv), 4-dimethylaminopyridine (cat.), 75–85%; b) $NaBH_4$ (10 equiv), MeOH, 0 → 25 °C, 80–90%; c) 1. $NaN(SiMe_3)_2$ (2.5 equiv), **6** (2 equiv), THF, 0 °C; 2. HF · py, THF, 25 °C, 65–85%. TES = triethylsilyl.

the corresponding 10-acetyl compounds **4** in high yield. Stereocontrolled sodium borohydride reduction of the enone carbonyl of compounds **4** led to the desired 13-α-hydroxyl compounds **5a–d** in excellent yields. Finally, coupling of these baccatin III analogues with the side-chain β-lactam **6** using Ojima's protocol,[10] followed by deprotection resulted in the formation of the new taxoids **7a–d** in high overall yields (Scheme 2).

Preliminary biological evaluation of selected compounds from this series (Table 3) revealed cytotoxicities comparable to that of taxol for the thiophene analogue **7b** and the furanyl analogue **7a**, a cytoxicity considerably less than that of taxol for the *p*-dimethylaminophenyl taxoid **7c**, and essentially no activity for the naphthalene compound **7d**. These results suggest rather well-defined demands by the taxol receptor for the C-2 ester group.[6]

The chemistry described above opens a practical approach to previously inaccessible C-2 taxol analogues and provides new opportunities for drug design and development in the taxol field. Studies directed at further refinement of the characteristics of the binding domain for taxol are currently underway in this laboratory.

Received: March 21, 1994 [Z 6783 IE]
German version: *Angew. Chem.* **1994**, *106*, 1669

Table 3. Cytotoxicities of C-2 taxol analogues **7** [a].

Cell type	Cell line	**1**	**7a**	**7b**	**7c**	**7d**
Human T-cell leukemia	MOLT-4	5.3×10^{-10}	4.5×10^{-8}	3.7×10^{-9}	2.2×10^{-6}	$>1\times10^{-4}$
Mouse leukemia	L1210	1.1×10^{-9}	4.7×10^{-7}	1.8×10^{-8}	1.6×10^{-6}	2.9×10^{-5}
Melanoma	SK-MEL 28	2.8×10^{-9}	8.4×10^{-8}	1.2×10^{-8}	1.2×10^{-4}	$>1\times10^{-4}$
Lung adenocarcinoma	UCLA-P3	2.7×10^{-9}	6.9×10^{-8}	9.3×10^{-9}	9.8×10^{-6}	$>1\times10^{-4}$
Human promyelocytic leukemia	HL-60	1.8×10^{-9}	2.5×10^{-8}	1.2×10^{-8}	1.3×10^{-5}	$>1\times10^{-4}$
Human prostate adenocarcinoma	PC-3	5.6×10^{-9}	1.0×10^{-7}	1.8×10^{-8}	3.4×10^{-5}	$>1\times10^{-4}$
Human ovarian carcinoma	OVCAR-3	6.9×10^{-9}	9.9×10^{-9}	5.8×10^{-9}	1.1×10^{-5}	$>1\times10^{-4}$
Human perirenal cell carcinoma	786-O	9.8×10^{-9}	5.2×10^{-6}	4.3×10^{-7}	5.0×10^{-5}	$>1\times10^{-4}$

[a] Data were obtained in the concentration range from 1×10^{-13} to 1×10^{-4} M by 1:10 direct aqueous dilutions of dimethylsulfoxide solutions of the compounds.

 © VCH Verlagsgesellschaft mbH, D-69451 Weinheim, 1994 0570-0833/94/1515-1582 $ 10.00+.25/0

[1] Isolation: M. C. Wani, H. L. Taylor, M. E. Wall, P. Coggon, A. T. McPhail, *J. Am. Chem. Soc.* **1971**, *93*, 2325–2327.
[2] Synthesis: a) K. C. Nicolaou, Z. Yang, J.-J. Liu, H. Ueno, P. G. Nantermet, R. K. Guy, C. F. Claiborne, J. Renaud, E. A. Couladouros, K. Paulvannan, E. J. Sorensen, *Nature* **1994**, *367*, 630–634; b) R. A. Holton, C. Somoza, H.-B. Kim, F. Liang, R. J. Biediger, P. D. Boatman, M. Shindo, C. C. Smith, S. Kim, H. Nadizadeh, Y. Suzuki, C. Tao, P. Vu, S. Tang, P. Zhang, K. K. Murthi, L. N. Gentile, J. H. Liu, *J. Am. Chem. Soc.* **1994**, *116*, 1597–1598; c) R. A. Holton, H.-B. Kim, C. Somoza, F. Liang, R. J. Biediger, P. D. Boatman, M. Shindo, C. C. Smith, S. Kim, H. Nadizadeh, Y. Suzuki, C. Tao, P. Vu, S. Tang, P. Zhang, K. K. Murthi, L. N. Gentile, J. H. Liu, *ibid.* **1994**, *116*, 1599–1600.
[3] a) K. C. Nicolaou, W.-M. Dai, R. K. Guy, *Angew. Chem.* **1994**, *106*, 38–69; *Angew. Chem. Int. Ed. Engl.* **1994**, *33*, 15–44. b) D. G. I. Kingston, *Fortschr. Chem. Org. Naturst.* **1993**, *61*, 1–192; c) D. Guenard, F. Gueritte-Voegelein, P. Potier, *Acc. Chem. Res.* **1993**, *26*, 160–166.
[4] E. K. Rowinsky, N. Onetto, R. M. Canetta, S. G. Arbuck, *Semin. Oncol.* **1992**, *19*, 646–662.
[5] a) S.-H. Chen, J.-M. Wei, V. Farina, *Tetrahedron Lett.* **1993**, *34*, 3205–3206; b) J. M. Rimoldi, D. G. I. Kingston, A. G. Chaudhary, G. Samaranayake, S. Grover, E. Hamel, *J. Nat. Prod.* **1993**, *56*, 1313–1330; c) A. G. Chaudhary, D. G. I. Kingston, *Tetrahedron Lett.* **1993**, *34*, 4921–4924; D. M. Vyas, H. Wong, A. R. Crosswell, A. M. Casazza, J. O. Knipe, S. W. Mamber, T. W. Doyle, *Bioorg. Med. Chem. Lett.* **1993**, *3*, 1357–1360.
[6] S.-H. Chen, V. Farina, J.-M. Wei, B. Long, C. Fairchild, S. W. Mamber, J. F. Kadow, D. Vyas, T. W. Doyle, *Bioorg. Med. Chem. Lett.* **1994**, *4*, 479–482.
[7] G. Satyanarayana, S. Sivaram, *Synth. Commun.* **1990**, *20*, 3273–3276.
[8] P. A. Wender, H. Kogan, H. Y. Lee, J. D. Munger, R. S. Wilhelm, P. D. Williams, *J. Am. Chem. Soc.* **1989**, *111*, 8957–8958.
[9] K. C. Nicolaou, P. G. Nantermet, H. Ueno, R. K. Guy, *J. Chem. Soc. Chem. Commun.* **1994**, 295–296.
[10] I. Ojima, C. M. Sun, M. Zucco, Y. H. Park, O. Duclos, S. Kuduk, *Tetrahedron Lett.* **1993**, *34*, 4149–4152; I. Ojima, I. Habus, M. Zaho, M. Zucco, Y. H. Park, C. M. Sun, T. Brigaud, *Tetrahedron* **1992**, *48*, 6985–7012; R. A. Holton, EP-B 400971, **1990** [*Chem. Abstr.* **1990**, *114*, 164568q].
[11] Selected physical data of the compounds **3b**, **4b**, **5b**, and **7b**.—**3b**: Amorphous solid: $R_f = 0.56$ (silica, ethyl acetate/hexanes 1/1); IR (film): $\tilde{\nu} = 3403, 2945, 2881, 1717, 1669, 1520, 1413, 1360, 1248, 1078\ cm^{-1}$; ^1H NMR (500 MHz, $CDCl_3$): $\delta = 7.84$ (dd, $J = 1.0, 3.5$ Hz, 1H, thiophene), 7.64 (dd, $J = 1.0, 5.0$ Hz, 1H, thiophene), 7.14 (dd, $J = 3.5, 5.0$ Hz, 1H, thiophene), 5.53 (d, $J = 6.5$ Hz, 1H, 2-H), 5.29 (d, $J = 2.5$ Hz, 1H, 10-H), 4.90 (br d, $J = 7.5$ Hz, 1H, 5-H), 4.44 (A of AB, d, $J = 8.5$ Hz, 1H, 20-H), 4.35 (dd, $J = 6.5, 10.5$ Hz, 1H, 7-H), 4.29 (d, $J = 2.5$ Hz, 10-OH), 4.19 (B of AB, d, $J = 8.5$ Hz, 1H, 20-H), 3.90 (d, $J = 6.5$ Hz, 1H, 3-H), 2.89 (A′ of A′B′, d, $J = 19.5$ Hz, 1H, 14-H), 2.62 (B′ of A′B′, d, $J = 19.5$ Hz, 1H, 14-H), 2.43–2.49 (m, 1H, 6-H), 2.15 (s, 3H, OAc), 2.07 (s, 3H, 18-CH_3), 1.85–1.91 (m, 1H, 6-H), 1.73 (s, 1H, 1-OH), 1.54 (s, 3H, 19-CH_3), 1.21 (s, 3H, 16-CH_3), 1.13 (s, 3H, 17-CH_3), 0.91 (t, $J = 8.0$ Hz, 9H, $Si(CH_2CH_3)_3$), 0.49–0.56 (m, 6H, $Si(CH_2CH_3)_3$); FAB-HRMS ($C_{33}H_{46}O_{10}SSi$ [$M + H^+$]): calcd: 663.2659; found: 663.2655.—**4b**: Amorphous solid; $R_f = 0.56$ (silica, ethyl acetate/hexanes 1/1); IR (film): $\tilde{\nu} = 3456, 2956, 1711, 1669, 1525, 1413, 1376, 1264, 1227, 1073\ cm^{-1}$; ^1H NMR (500 MHz, $CDCl_3$): $\delta = 7.84$ (dd, $J = 1.5, 4.0$ Hz, 1H, thiophene), 7.63 (dd, $J = 1.5, 5.0$ Hz, 1H, thiophene), 7.13 (dd, $J = 4.0, 5.0$ Hz, 1H, thiophene), 6.56 (s, 1H, 10-H), 5.58 (d, $J = 6.5$ Hz, 1H, 2-H), 4.90 (br d, $J = 8.0$ Hz, 1H, 5-H), 4.44 (dd, $J = 7.0, 10.5$ Hz, 1H, 7-H), 4.42 (A of AB, d, $J = 8.5$ Hz, 1H, 20-H), 4.18 (B of AB, d, $J = 8.5$ Hz, 1H, 20-H), 3.85 (d, $J = 6.5$ Hz, 1H, 3-H), 2.91 (A′ of A′B′, d, $J = 19.5$ Hz, 1H, 14-H), 2.64 (B′ of A′B′, dd, $J = 1.0, 19.5$ Hz, 1H, 14-H), 2.48–2.55 (m, 1H, 6-H), 2.20 (s, 3H, OAc), 2.15 (s, 3H, OAc), 2.14 (s, 3H, 18-CH_3), 1.83–1.88 (m, 1H, 6-H), 1.65 (s, 3H, 19-CH_3), 1.23 (s, 3H, 16-CH_3), 1.16 (s, 3H, 17-CH_3), 0.88 (t, $J = 8.0$ Hz, 9H, $Si(CH_2CH_3)_3$), 0.53–0.59 (m, 6H, $Si(CH_2CH_3)_3$); FAB-HRMS ($C_{35}H_{48}O_{11}SSi$ [$M + Cs^+$]): calcd: 837.1741; found: 837.1736.—**5b**: Amorphous solid; $R_f = 0.34$ (silica, ethyl acetate/hexanes 1/1); IR (film): $\tilde{\nu} = 3478, 2945, 2892, 1717, 1519, 1365, 1238, 1083\ cm^{-1}$; ^1H NMR (500 MHz, $CDCl_3$): $\delta = 7.85$ (dd, $J = 1.5, 3.5$ Hz, 1H, thiophene), 7.61 (dd, $J = 1.5, 5.0$ Hz, 1H, thiophene), 7.12 (dd, $J = 3.5, 5.0$ Hz, 1H, thiophene), 6.43 (s, 1H, 10-H), 5.51 (d, $J = 7.0$ Hz, 1H, 2-H), 4.94 (br d, $J = 7.5$ Hz, 1H, 5-H), 4.78–4.83 (m, 1H, 13-H), 4.45 (dd, $J = 7.5, 10.5$ Hz, 1H, 7-H), 4.41 (A of AB, d, $J = 8.0$ Hz, 1H, 20-H), 4.19 (B of AB, d, $J = 8.0$ Hz, 1H, 20-H), 3.82 (d, $J = 7.0$ Hz, 1H, 3-H), 2.48–2.54 (m, 1H, 6-H), 2.24 (s, 3H, OAc), 2.21–2.26 (m, 2H, 14-CH_2), 2.16 (d, $J = 1.0$ Hz, 3H, 18-CH_3), 2.15 (s, 3H, CH_3), 2.00 (d, $J = 5.0$ Hz, 1H, OH), 1.85–1.89 (m, 1H, 6-H), 1.66 (s, 1H, 19-CH_3), 1.58 (s, 1H, 1-OH), 1.15 (s, 3H, 16-CH_3), 1.02 (s, 3H, 17-CH_3), 0.90 (t, $J = 8.0$ Hz, 9H, $Si(CH_2CH_3)_3$), 0.55–0.59 (m, 6H, $Si(CH_2CH_3)_3$); FAB-HRMS ($C_{35}H_{50}O_{11}SSi$ [$M + Cs^+$]): calcd: 839.1897; found: 839.1893.—**7b**: Amorphous solid: $R_f = 0.44$ (silica, ethyl acetate/hexanes 3/1); IR (film): $\tilde{\nu} = 3417, 2929, 1715, 1649, 1521, 1460, 1417, 1368, 1247, 1076\ cm^{-1}$; ^1H NMR (500 MHz, $CDCl_3$): $\delta = 7.90$ (dd, $J = 1.0, 4.0$ Hz, 1H, thiophene), 7.73 (d, $J = 7.0$ Hz, 2H, NBz), 7.63 (dd, $J = 1.0, 5.0$ Hz, 1H, thiophene), 7.32–7.51 (m, 8H, Ar), 7.14 (dd, $J = 4.0, 5.0$ Hz, 1H, thiophene), 6.96 (d, $J = 9.0$ Hz, 1H, NH), 6.24 (s, 1H, 10-H), 6.19 (br t, 1H, $J = 9.0$ Hz, 13-H), 5.75 (dd, $J = 2.5$ Hz, 9.0 Hz, 1H, 3′-H), 5.55 (d, $J = 7.0$ Hz, 1H, 2-H), 4.94 (br d, $J = 8.0$ Hz, 1H, 5-H), 4.76 (dd, $J = 2.5, 5.0$ Hz, 1H, 2′-H), 4.41 (A of AB, d, $J = 8.5$ Hz, 1H, 20-H), 4.32–4.40 (m, 1H, 7-H), 4.24 (B of AB, d, $J = 8.5$ Hz, 1H, 20-H), 3.73 (d, $J = 7.0$ Hz, 1H, 3-H), 3.52 (d, $J = 5.0$ Hz, 1H, 2′-OH), 2.50–2.56 (m, 1H, 6-H), 2.44 (d, $J = 4.0$ Hz, 1H, 7-OH), 2.35 (s, 3H, OAc), 2.29 (d, $J = 9.0$ Hz, 2H, 14-CH_2), 2.22 (s, 3H, OAc), 1.84–1.90 (m, 1H, 6-H), 1.76 (s, 3H, 18-CH_3), 1.66 (s, 3H, 19-CH_3), 1.23 (s, 3H, 16-CH_3), 1.10 (s, 3H, 17-CH_3); FAB-HRMS ($C_{45}H_{49}NO_{14}S$ [$M + Cs^+$]): calcd: 992.1928; found: 992.1952 (the experimental error (0.0024) lies within the accepted limits.).

A Water-Soluble Prodrug of Taxol with Self-Assembling Properties**

Kyriacos Costa Nicolaou,* Rodney Kiplin Guy, Emmanuel Nicolauo Pitsinos, and Wolfgang Wrasidlo

Taxol (**1**, Fig. 1) is a novel anticancer agent, originally isolated from the American Pacific yew tree (*Taxus brevifolia*)[1] which, due to its important in vivo biological activity,[2] has elicited much research effort from chemists,[3–7] biologists,[2, 6] and clinicians.[2] Despite its current usage in the clinic for treatment of ovarian cancer and its much celebrated status as a major advance in cancer chemotherapy, taxol suffers from extremely low solubility in water ($< 5 \times 10^{-6}$ M). Thus taxol is applied clinically in a mixture of Cremaphor (a polyoxyethylated castor oil) and ethanol. Unfortunately this formulation often induces significant side effects, including strong hypersensitivity reactions.[8] Although premedication and slow administration of the drug can circumvent some of these problems clinically,[9] the entire protocol is rather cumbersome and requires extensive monitoring of procedures and patients.[10] While taxol's impressive efficacy has driven clinical usage of the drug forward despite these shortcomings, a water-soluble form of taxol could completely obviate these problems and both expand its usage and dramatically improve its pharmacological profile.

Numerous attempts have been made to improve the solubility and pharmacological properties of taxol.[11–17] Among the most notable taxol derivatives synthesized so far are those in which the C-2′ and C-7 hydroxyl groups of the molecule are engaged in a functional group that collapses, upon in vivo activation, releasing taxol. Conjugates of this type are termed prodrugs. Owing to persisting problems with solubility and bioavailability, none of these prodrugs have been applied successfully in the clinic. Successful application of these compounds requires that their properties be finely balanced. On the one hand, they must be hydrophilic for formulation purposes, while on the other, they must be lypophilic for therapeutic purposes. Furthermore, to avoid execretion through the kidneys they must rapidly convert from the hydrophilic to lypophilic form.

[*] Prof. Dr. K. C. Nicolaou, R. K. Guy, E. N. Pitsinos, W. Wrasidlo
Department of Chemistry, The Scripps Research Institute
10666 North Torrey Pines Road, La Jolla, CA 92037 (USA)
and
Department of Chemistry
University of California, San Diego
9500 Gilman Drive, La Jolla, CA 92093 (USA)
Telefax: Int. code + (619)554-6738

[**] This work was supported by the National Institutes of Health, the Office of Naval Research (a predoctoral fellowship to R.K.G.), and The Scripps Research Institute. We thank Drs. R. Milligan and X. Chan for the TEM studies, S. Mauch for the in vivo animal studies, and R. Merlock for development and execution of HPLC and tubulin experiments, Gary Siuzdak for assistance with mass spectrometry, and D.-H. Huang for his help with the NMR studies.

In pursuing a program directed at the design and chemical synthesis of novel derivatives of taxol in which the C-2′ and C-7 hydroxyl groups are functionalized, we prepared taxol-2′-methylpyridinium acetate (taxol-2′-MPA **2**; Fig. 1a), a compound that was expected to be quite reactive towards nucleophilic displacement.[18] Compound **2** was prepared by the method of Mukaiyama et al.[19] from taxol (**1**) and 2-fluoro-1-methylpyridinium tosylate (1.2 equiv) in the presence of triethylamine (1.5 equiv) in dichloromethane (25 °C, 0.5 h). Purification by reversed-phase high-pressure liquid chromatography (RP-HPLC) followed by ion exchange (tosylate for acetate) and lyophilization gave pure taxol-2′-MPA (**2**) in 90% yield as an amorphous white solid (Fig. 1b). Spectroscopic and analytical data were in accord with structure **2**. Preliminary investigations (vide infra) revealed that this compound has a number of important properties, including hydrolytic stability, high solubility in water, the ability to release taxol rapidly in human plasma, cytotoxicity and antitumor properties similar to those of taxol, and aggregation behavior.

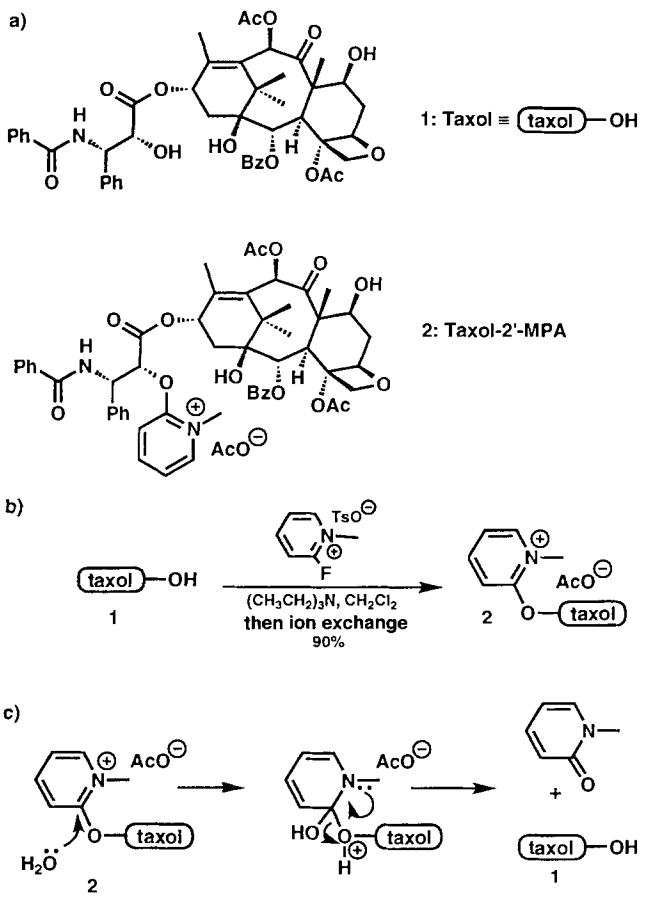


Fig. 1. a) Molecular formulas of taxol (**1**) and taxol-2′-MPA (**2**); b) synthesis of **2**; c) possible mechanism for release of **1** from **2**.

Taxol-2′-MPA (**2**) exhibits high stability both in the solid state and in aqueous solutions. In all studies carried out, the only degradation products detected were taxol (**1**) and the pyridinone that results from hydrolysis of the pyridinium salt (Fig. 1c). Owing to differences in retention times under the HPLC conditions used and differing ultraviolet (UV) absorption maxima ($\lambda_{280}/\lambda_{254} = 1.6$ for **2** and 0.3 for **1**), the stability of **2** was easily assayed by HPLC using UV detection. Taxol-2′-MPA (**2**) appears to be completely stable in the solid state at ambient temperatures for at least 30 days. In water, 5% dextrose, or 0.9% saline solution, **2** is stable for several days at ambient temperatures (Fig. 2) but begins to exhibit slow degradation after four days. In phosphate-buffered saline (PBS) or ammonium acetate buffers of

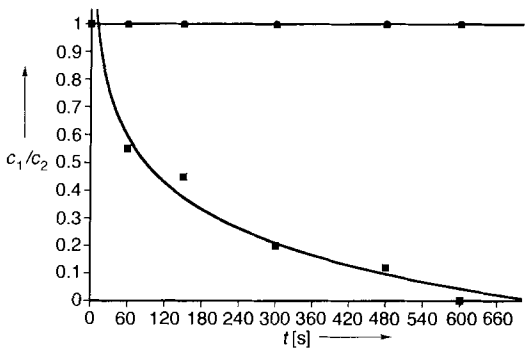


Fig. 2. Rates of taxol release from taxol-2′-MPA (**2**) in aqueous solutions at 25 °C. Although **2** is stable in water and aqueous buffer solutions (horizontal line), extraction with CH_2Cl_2 of plasma treated with **2** showed complete conversion of **2** into taxol (**1**) within 10 min (curve, 20% of total recovered). c_1 is the concentration of free **2**; c_2 is the concentration of free taxol.

pH 6.0 to 7.3, **2** is stable at ambient temperatures for at least 21 days. However, taxol-2′-MPA (**2**) shows limited and varying stability in 5% aqueous HCl (pH 1.1), brine (ca. 6 M aqueous NaCl), and aqueous ethanolic solutions. Most significantly, **2** rapidly converts to taxol (**1**) when incubated at 37 °C with human plasma (< 10 min, Fig. 2). In experiments with pure albumin taxol (**1**) was also rapidly released. Furthermore, in studies with tritiated **2** in mice, only 5% of the compound was excreted through the kidneys as taxol, a result that is in complete accord with the behavior of taxol.[20] These results strongly suggest that **2** functions in vivo as a prodrug to taxol. It should be noted that the excellent bioavailability of **2** stands in contrast to a number of previously synthesized protaxols,[16] which are rapidly excreted through the kidneys.[21] The release of taxol from **2** is presumed to be the result of a nucleophilic attack by water or another nucleophile at the 2-position of the pyridinium moiety as indicated in Figure 1c. Whether this rapid reaction in human plasma is enzyme-assisted remains to be clarified.

The solubility and partition coefficient data for taxol-2′-MPA (**2**) and taxol (**1**) were determined using HPLC. In 100 mM PBS **2** exhibited asolubility of 1.5 mM and a partition coefficient (octanol/water) of 50; the corresponding values for taxol were < 0.0015 mM and 10000. It should be noted that the solubility of taxol is at the detection limit of the HPLC instrument used and thus represents an upper limit. The solubility of **2** was determined at a concentration at which the solution was clear and noncolloidal and thus represents a lower limit. Compound **2** demonstrated similar solubilities in various buffer systems in the pH range 6.2 to 7.4. In pure water the solubility appears limited only by the formation of clear colorless gels at high concentrations (> 20 mM). These data clearly show that **2** is orders of magnitude more soluble in water than the parent taxol (**1**). The solubility exhibited by **2** in a range of aqueous systems is significantly higher than taxol's clinically relevant dosages (3–30 μM).

Microtubule polymerization–depolymerization experiments[22] with taxol-2′-MPA (**2**) revealed very similar effects to those observed with guanosine-5′-triphosphate (GTP)/saline controls and drastically different from those elicited by taxol. Thus, **2** demonstrated no stabilization of microtubules upon

$CaCl_2$ addition, which reflects the compound's lack of intrinsic activity and its chemical stability in the medium used for this assay. This result is in accord with the behavior of other 2'-substituted derivatives.[23-25] Taxol (**1**), recovered from human plasma to which compound **2** was added, exhibited the expected stabilization of microtubules, which again indicates that **2** acts as a prodrug for taxol.

Taxol-2'-MPA (**2**) was tested for its cytotoxicity against a series of cell lines that included leukemia, ovarian, lung, breast carcinoma, and melanoma cells (Fig. 3). The cytotoxicity profiles for **2** were compared to those of taxol and found to be quite similar, although some differences were noted. Both compounds exhibited IC_{50} values ranging from 10^{-5} to 10^{-12} M with means close to 1 nM. Extremely high cytotoxicity levels were recorded for human leukemia, metastatic melanoma, and cervical carcinoma cells. Overall, and as expected for a taxol prodrug, **2** shows the same remarkable tumor cell selectivity and cell line specificity as taxol.

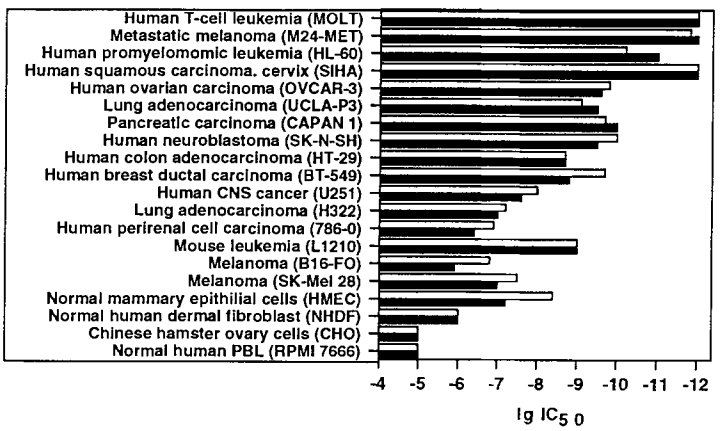


Fig. 3. Cytotoxicities of taxol-2'-MPA (**2**, white bar) and taxol (**1**, black bar) against a series of cell lines.

The promising in vitro results and solubility profile of taxol-2'-MPA (**2**) prompted us to study its in vivo action and compare it with that of taxol by using nude mice inflicted with human prostate carcinoma xenografts (Fig. 4). In contrast to taxol (**1**), compound (**2**) was formulated in sterile 5% aqueous dextrose solution without Cremaphor, which demonstrates the suitability of **2** for simple bolus administration and its first advantage over the parent compound. Several experiments with mice revealed that taxol-2'-MPA exhibits tumor growth inhibition equal to that of taxol at the same molar concentration; both compounds demonstrated impressive antitumor properties as compared to controls (Fig. 4). Most impressively, in studies in which **1** and **2** were both applied at the maximum tolerated dose (MTD) of taxol, taxol showed significant toxicity (four of eight animals died before the study's end), while taxol-2'-MTA showed no visible toxicity (four of eight animals were also tumor free at the end of this study).

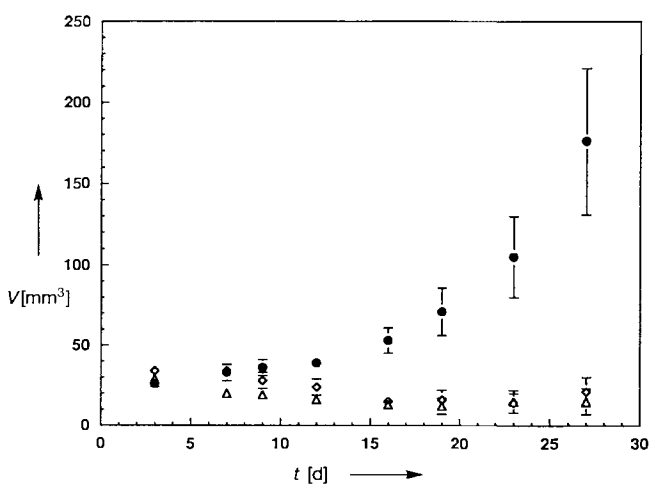


Fig. 4. In vivo efficacy of taxol-2'-MPA (**2**) in prostate tumor xenograft nude mouse model: 5% dextrose (●), taxol (△), and taxol-2'-MPA (◇).

The novel molecular structure of taxol-2'-MPA and its high solubility in aqueous media prompted us to investigate its self-assembly properties. Molecular self-assembly is a phenomenon of considerable current interest. Much of the excitement is derived from the potential of this process to form nanostructures with possible applications in materials science and medicine.[26-28] Central to these investigations are the contributions from chemistry, which include the design and synthesis of self-assembling molecules such as lipid-based[29] and H-bonded structures.[30] Living systems also use extensively self-assembling processes to construct nanostructures; microtubules, taxol's cellular target,[31] are a prominent example.

Taxol-2'-MPA (**2**) was found to form several types of assemblies, including regular helices and micelles, depending on the nature of the media. This rather serendipitous finding is not that surprising, since the molecular structure of **2** is ideal for self-assembly processes.[32-34] It combines a highly hydrophobic segment (taxol skeleton) with a polar head (pyridinium moiety), a characteristic feature of many self-aggregating molecules. While self-assembly is known for planar amphiphiles such as the antiasthmatic cromolyn, it is, to our knowledge, unknown in such globular molecules. Furthermore, the chirality of the structure apparently induces helicity in long nanostructures formed by this building block.[35-38] Although aqueous solutions of **2** were optically clear at all concentrations examined ($< 1 \times 10^{-3}$ M), buffered solutions with concentrations exceeding 1×10^{-3} M exhibited a blue haze to the naked eye and diffuse scattering of monochromatic light, both characteristic properties of colloids. At higher concentrations colloidal gels form. UV absorption measurements at 340 nm, a wavelength at which **2** exhibits no absorption, showed an exponential increase in optical density (OD) above 4×10^{-4} M, a result also characteristic of colloid formation.

Transmission electron microscopy (TEM) confirmed the presence of supramolecular structures in these solutions. Thus, 1 mM solutions of **2** in PBS displayed uniform aggregates of fibrillar structure (Fig. 5A) with helical conformations. These nanostructures exhibited varying lengths up to 800 Å but a consistent diameter of roughly 80 Å with a helical twist of about seven units per turn (Fig. 5c). Additionally, in freshly sonicated aqueous solutions of **2** (1 mM) spherical structures (Fig. 5B) with a consistent diameter of about 50 Å were observed. Highly concentrated solutions (colloidal, ca. 2×10^{-3} M) revealed more complicated molecular architectures; meta tubules assembled from the original filaments (Fig. 6).

We described here the novel physical, chemical, and biological properties of taxol-2'-MPA (**2**), a compound obtained in one step and in high yield from taxol (**1**). Compound **2** appears to be superior to taxol (**1**) as an antitumor agent based on its aqueous solubility and in vivo action against tumor xenografts. The data presented in this paper suggest that taxol-2'-MPA (**2**) is a prime candidate for development as an anticancer agent. Other taxoids such as taxotere[39] may be similarly modified to afford more

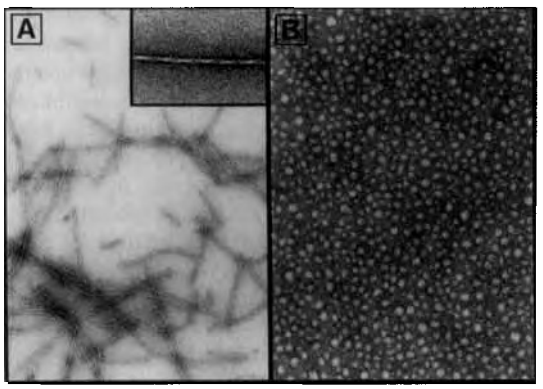


Fig. 5. A) TEM image of taxol-2′-MPA (**2**, 1 mM in 100 mM PBS) at a magnification of 25000× (negative phosphotungstate stain) showing the helical fibrous nanostructures present in buffered solutions of this compound above the critical aggregation concentration (CAC). The inset shows a magnified portion of one of the fibrils and the helical twist. B) TEM image of taxol-2′-MPA (**2**, 1 mM in H_2O) at a magnification of 45000-fold (negative uranyl acetate stain) showing the spherical nanostructures present in unbuffered solutions of this compound above the CAC.

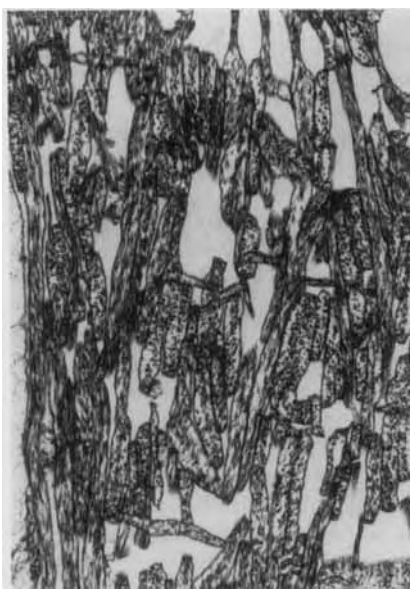


Fig. 6. TEM image of taxol-2′-MPA (**2**, 2 mM in 100 mM PBS) at a magnification of 10000×.

effective agents. Furthermore, other functional groups similar to the pyridinium moiety could be introduced at the 2′-, 7-, or other appropriate positions of taxoids to endow the new derivatives with such properties. The impressive properties of **2** may be attributable to its ability to self-assemble into nanostructures in aqueous media. Studies aimed at elucidating the relationship between such nanostructures and activity are currently under way.

Experimental Procedure

Synthesis of 2: Taxol (10.2 mg, 0.012 mmol) was dissolved in dichloromethane (0.4 mL) and treated sequentially at ambient temperature and under an atmosphere of dry argon with triethylamine (2 μL,1.3 equiv) and 2-fluoro-1-methylpyridinium tosylate (4.0 mg, 1.2 equiv). The clear colorless solution rapidly turned to a clear pale yellow. After stirring for 30 min at ambient temperature the reaction was judged complete, as no taxol remained and only one compound was apparent by HPLC (Vydak 22.5 mm × 250 mm C18 column, 10 mM NH_4OAc in 20% aq. methanol → methanol over 30 min, 9 mL min^{-1}. UV, *R*: **2**, 26.2 min; **1**, 28.8 min). The crude product was purified by HPLC, and solvent was removed in vacuo to give **2** (11 mg, 90%). ^1H NMR ($CDCl_3$, 500 MHz) δ = 1.07 (s, 3H, C16-H), 1.11 (s, 3H, C17-H), 1.62 (s, 3H, C19-H), 1.76 (s, 3H, C18-H), 1.85 (m, 1H, C6-βH), 2.00 (s, 3H, C10-OAc), 2.1–2.2 (br. m, 2H, C14-H), 2.2 (s, 3H, C4-OAc), 2.53 (overlapping s and m, 4H, C6-H, counterion OAc), 3.67 (d, 1H, *J* = 7.0 Hz, C3-H), 4.05 (s, 3H, N-CH3), 4.10 (d, 1H, *J* = 8.5 Hz, C20-H, A of AB), 4.22 (d, 1H, *J* = 8.5, C20-H, B of AB), 4.31 (dd, 1H, *J* = 8.7, 10.7 Hz, C7-H), 4.87 (dd, 1H, J = 1.0, 7.7 Hz, C5-H), 5.50 (d, 1H, J = 7.0 Hz, C2-H), 5.70 (br. t, 1H, *J* = 8.0 Hz, C2′-H), 5.95 (dd, 1H, *J* = 1.0, 8.0 Hz, C13-H), 6.20 (s, 1H, C10-H), 6.46 (br. d, 1H, *J* = 10.0 Hz, C3′-H), 7.08 (t, 1H, J = 7.5 Hz, NH), 7.33–7.45 (m, 7H, Ar-H), 7.57 (t, 2H, *J* = 8 Hz, Ar-H), 7.69 (d, 2H, *J* = 9.0 Hz, Ar-H), 7.79 (d, 1H, *J* = 9.0 Hz, Ar-H), 8.01 (dd, 2H, *J* = 1.0, 8.0 Hz,Ar-H), 8.14 (d, 1H, *J* = 8.0 Hz, Ar-H), 8.29 (d, 2H, *J* = 7.0 Hz, Ar-H), 8.41 (t, 1H, *J* = 7.0 Hz, Pyr-H), 10.48 (d, 1H, *J* = 7.0 Hz, Pyr-H). IR (neat, KCl) $\tilde{\nu}$[cm^{-1}]: 3640–3120 (bm), 3030–2870 (bm), 2320 (m), 1720 (s), 1630 (m), 1560 (m), 1500 (m), 1360 (s), 1160 (m), 1070 (m), 700 (m). UV/VIS ($CHCl_3$): λ_{max} [nm] = 254, 280. FAB-HRMS: calc for M^+ $C_{53}H_{57}O_{14}N_2$: 945.3810; found: 945.3810

Stability Studies: **2** was dissolved in the aqueous system with the aid of sonication for 5 min. Aliquots were removed at the times shown in Figure 2, partitioned into dichloromethane to quench the reaction, and analyzed by using a Waters Maxima HPLC instrument equipped with an autoinjector (3.9 × 300 mm C18 column equipped with a precolumn; flow rate 1.5 mL min^{-1}; eluent gradient A–B over 30 min where A is 80% 80 mM NH_4OAc (pH 6.0) and B is 100% methanol; UV diode-array detector). The ratio of **2** (c_1, R_f = 16.2 min) to taxol (c_2, R_f = 16.8 min) remaining was determined from the relative areas of the peaks after normalization with previously determined calibration curves. The stability studies in aqueous solutions were continued for more than two weeks; little degradation was exhibited by the buffered solutions of **2**.

Solubility Studies: Solubility was determined dissolving the compound in solvent with the aid of sonication (5 min), centrifuging the sample, and injecting the supernatant into an HPLC instrument (for conditions, see Stability Studies). The values reported were normalized using calibration curves constructed for both compounds by preparing solutions with known concentrations in the range 1×10^{-6} to 1×10^{-3} M in dichloromethane and subjecting to them HPLC analysis under the same conditions. Partition coefficients were determined by dissolving the compound in the organic phase, shaking the resulting solution with water for 10 min, and analyzing each phase by HPLC as described above. No degradation of **2** was noted during these studies.

Cytotoxicity Measurements: Cells were plated on 96 well plates with the following controls: no cells and toxic control (1×10^{-3} M sodium dodecyl sulfate (SDS)). The drug was added to the first set of wells and diluted according to standard dilution methods from these wells. Plates were incubated at 37 °C under 5% carbon dioxide in sterile air in an humidified incubator for 72 h. A solution (50 μL) of 2,3-bis-(methoxy-4-nitro-5-sulfophenyl)-5-[(phenylamino)carbonyl]-2*H*-tetrazolium hydroxide, XTT, 1 mg mL^{-1}) in PBS (100 mM) was added to each well. In the presence of viable cells, this colorless clear solution is enzymatically transformed to give a pink coloration. The plates were read at 450 nm using a microplate reader (Molecular Devices Thermomax).

In Vivo Efficacy: The tumor model was generated from an ATTC PC-3 prostate carcinoma cell line that was maintained under standard cell proliferation conditions (37 °C, 5% carbon dioxide in sterile air). Each cohort was comprised of eight randomly chosen, female athymic nude mice, for a total population size of 24. Hemocytometer-counted cells suspended in Hanks medium (Gibco, Grand Island, NY) were implanted subcutaneously (10^6 cells in 0.4 mL per mouse). Solid tumor growth was measured on each third day and tumor volume determined using the equation (length) × (width)^2(0.5). Equimolar amounts of the test compounds (1.0 μM) were injected intraperitoneally on days 1, 3, 5, 7, 9, and 11 using the following media: control, 5% dextrose in water (D5W); taxol, suspended in Cremaphor/D5W (5/95, 18.0 mg kg^{-1} of animal weight); taxol-2′-MPA, dissolved in D5W (23.9 mg kg^{-1} of animal weight). The procedures used for the maintenance of tumors and the experimental details were according to protocols set forth by the Developmental Therapeutics Program, National Cancer Institute (NCI). Inferences about efficacy were drawn by ANOVA followed by protected t-test. For example: day 9 (worst case); after ANOVA shows significant variance at the 0.06 level, t-test shows taxol and taxol-2′-MPA are significantly different from the control at the 0.04 level. After day 9, each data set is significantly different from the others at better than 0.05 confidence limit. Data shown as mean value with standard error.

Received: April 11, 1994 [Z 6838 IE]
German version: *Angew. Chem.* **1994**, *106*, 1672

[1] M. C. Wani, H. L. Taylor, M. E. Wells, P. Coggan, A. T. McPhail, *J. Am. Chem. Soc.* **1971**, *93*, 2325–2327.
[2] E. K. Rowinsky, N. Onetto, R. M. Canetta, S. G. Arburk, *Semin. Oncol.* **1992**, *19*, 646–662.
[3] P. Potier, *Chem. Soc. Rev.* **1992**, *21*, 113–119.
[4] D. G. I. Kingston, *Pharmacol. Ther.* **1991**, *52*, 1–34.

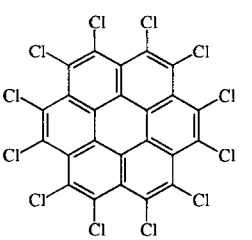
[5] C. S. Swindell, *Org. Prep. Proced. Int.* **1991**, *23*, 465–543.
[6] K. C. Nicolaou, W.-M. Dai, R. K. Guy, *Angew. Chem.* **1994**, *106*, 15–69; *Angew. Chem. Int. Ed. Engl.* **1994**, *33*, 15–44.
[7] K. C. Nicolaou, Z. Yang, J. J. Liu, H. Ueno, P. G. Nantermet, R. K. Guy, C. F. Claiborne, J. Renaud, E. A. Couladouros, K. Paulvannan, E. J. Sorensen, *Nature* **1994**, *367*, 630–634.
[8] R. Weiss, R. C. Donehower, P. H. Wiernik, T. Ohnuma, R. S. Gralla, D. L. Trump, J. R. Daker, D. A. von Echo, D. D. von Hoff, B. Leyland-Jones, *J. Clin. Oncol.* **1990**, *8*, 1263–1268.
[9] E. K. Rowisnky, E. E. Eisenhauer, V. Chaudhry, S. G. Arbuck, R. C. Donehower, *Semin. Oncol.* **1993**, *20 (4 Suppl. 3)*, 1–15.
[10] B. G. Lubejko, S. E. Sartorius, *Semin. Oncol.* **1993**, *20 (4 Suppl. 3)*, 26–30.
[11] H. M. Deutsch, J. A. Glinksi, M. Hernandez, R. D. Haugwitz, V. L. Narayanan, M. Suffness, L. H. Zalhow, *J. Med. Chem.* **1989**, *32*, 788–792.
[12] C. S. Swindell, N. E. Krauss, S. B. Horwitz, I. Ringel, *J. Med. Chem.* **1991**, *34*, 1176–1184.
[13] Z. Zhao, D. G. I. Kingston, A. R. Crosswell, *J. Nat. Prod.* **1991**, *54*, 1607–1611.
[14] A. M. Mathew, R. Mejillano, J. P. Nath, R. H. Himes, V. J. Stella, *J. Med. Chem.* **1992**, *35*, 145–151.
[15] D. M. Vyas, H. Wong, A. R. Crosswell, A. M. Casazza, J. O. Knipe, S. W. Mamber, T. W. Doyle, *Biomed. Chem. Lett.* **1993**, *3*, 1357–1360.
[16] K. C. Nicolaou, C. Riemer, M. A. Kerr, D. Rideout, W. Wrasidlo, *Nature* **1993**, *364*, 464–466.
[17] D. G. I. Kingston, Z. Y. Zhao, *Eur. Patent Appl.* EP 537905 A1 (21 April **1993**).
[18] T. Mukaiyama, *Angew. Chem.* **1979**, *91*, 798–812; *Angew. Chem. Int. Ed. Engl.* **1979**, *18*, 707–721.
[19] S. Kobayashi, M. Tsutsui, T. Mukaiyama, *Chem. Lett.* **1976**, 373–374.
[20] E. K. Rowinsky, R. C. Donehower, *Semin. Oncol.* **1993**, *20 (4 Suppl. 3)*, 16–25.
[21] W. Wrasidlo, K. C. Nicolaou, unpublished results.
[22] R. Merlock, W. Wrasildo, *Anal. Biochem.*, in press.
[23] J. Parness, D. G. I. Kingston, R. G. Powell, C. Harracksingh, S. B. Horwitz, *Biochem. Biophys. Res. Commun.* **1982**, *105*, 1082–1089.
[24] W. Mellado, N. F. Magri, D. G. I. Kingston, R. Garcia-Arenas, G. A. Orr, S. B. Horwitz, *Biochem. Biophys. Res. Commun.* **1984**, *124*, 329–336.
[25] H. Lasaste, H. Senilh, M. Wright, D. Guenard, P. Potier, *Proc. Natl. Acad. Sci. USA* **1984**, *81*, 4090–4094.
[26] H. Ringsdorf, B. Schlar, J. Venzmer, *Angew. Chem.* **1988**, *100*, 117–162; *Angew. Chem. Int. Ed. Engl.* **1988**, *27*, 113–158.
[27] Special section: A. S. Rudolph, J. M. Calvert, P. E. Schoen, J. M. Schnur in *Biotechnological Applications of Lipid Microstructures* (Eds.: B. P. Gaber, J. M. Schnur, D. Chapman), Plenum, New York, **1988**, pp. 320–325.
[28] "Engineering a Small World", *Science* **1991**, *254*, 1300–1335.
[29] J. M. Schnur, *Science* **1993**, *262*, 1669–1676.
[30] M. R. Ghadiri, J. R. Granja, R. A. Milligan, D. E. McRee, N. W. Khazanovich, *Nature* **1993**, *366*, 324–327.
[31] S. B. Horwitz, J. Fant, P. B. Schiff, *Nature* **1979**, *277*, 665–667.
[32] F. Vögtle, *Supramolecular Chemistry*, Wiley, New York, **1991**.
[33] J. H. Fuhrhop, G. Penzlin, *Organic Synthesis Concepts, Methods and Starting Materials*, 2nd ed., VCH, New York, **1993**, pp. 350–356.
[34] G. M. Whitesides, J. P. Mathias, C. T. Seto, *Science* **1993**, *254*, 1312–1319.
[35] J. H. Fuhrhop, P. Schnieder, J. Rosenberg, E. Boekema, *J. Am. Chem. Soc.* **1987**, *109*, 3387–3390.
[36] J. H. Fuhrhop, P. Schnieder, E. Boekema, W. Helfrich, *J. Am. Chem. Soc.* **1988**, *110*, 2861–2867.
[37] J. H. Fuhrhop, S. Svenson, C. Boettcher, E. Rossler, H.-M. Vieth, *J. Am. Chem. Soc.* **1990**, *112*, 4307–4312.
[38] J. H. Fuhrhop, C. Boettcher, *J. Am. Chem. Soc.* **1990**, *112*, 1768–1776.
[39] R. Pazdur, R. A. Newman, B. M. Newman, A. Fuentes, J. Benvenuto, B. Bready, D. Moore, I. Jaiyesimi, F. Vreeland, M. M. G. Bayssas, M. N. Rader, *J. Natl. Cancer Inst.* **1992**, *84*, 1781–1788.

Trigonal Symmetry as a Host Design Element: Novel Conformation of Dodecakis(3,5-dimethylphenylthio)coronene in its 1,4-Dioxane Clathrate**

Gary A. Downing, Christopher S. Frampton, David D. MacNicol,* and Paul R. Mallinson

It is becoming increasingly apparent that the rotational symmetry of the individual host molecule is a key strategic design factor for the discovery and development of new series of host compounds capable of forming crystalline inclusion compounds.[1] The significance of a C_2 axis is highlighted by design of hosts related to *exo*-2, *exo*-6-dihydroxy-2,6-dimethylbicyclo[3.3.1]nonane,[2] tetraphenylene-derived hosts,[3] roof- and scissor-type hosts,[4] and naphthalene-based spider hosts;[5] whilst the crucial importance of a C_3 axis is well represented by hosts of the cyclotriphosphazene type,[6] cyclododecatriene-based hosts,[7] racemic and optically resolved *trans,anti,trans, anti,trans*-perhydrotriphenylene,[8] cyclotriveratrylene and related hosts,[9] and hexa-hosts (i.e. hexasubstituted benzenes designed to produce cavities)[10] along with their Piedford counterparts.[11]

The hexa-host series,[10] members of which typically display an *ababab* conformation with regular alternation of side-chain units above and below the central benzene core, suggested to us an analogous series of hosts possessing *six pairs* of side-chain units corresponding to a dodecasubstituted coronene nucleus. To explore the possibility of synthesizing such novel hosts, the suitable precursor perchlorocoronene **1** was prepared in high yield by perchlorination of coronene under $SO_2Cl_2/S_2Cl_2/AlCl_3$ conditions.[12] The molecular structure of **1**, determined by single-crystal X-ray analysis[12] and electron microscopy[13] at 1 Å resolution, was found to be markedly nonplanar, reflecting pronounced *peri* interactions, and to have symmetry close to D_{3d}. The molecule displays two concave faces and its conformation was found to be, in an extension of our earlier nomenclature,[14] of the highly promising *aabbaabbaabb* type with pairs of chlorine atoms alternating regularly above and below the mean plane of the coronene nucleus. The presence of this conformation in related molecules should enhance host characteristics, not only because of the C_3 axis normal to the central coronene core, but also because of the favorable overall molecular shape reminiscent of a higher order hexa-host (vide infra). Preliminary studies[12] indicated that persubstitution of **1** with arenethiolate nucleophiles was readily achieved at ambient temperature, employing 1,3-dimethylimidazolidin-2-one (DMEU) as solvent. The resulting dodecasubstituted coronenes were, however, found to display rather limited host properties indicating that design of the side-chain unit would be of critical importance.



1

[*] Dr. D. D. MacNicol, Dr. G. A. Downing, Dr. C. S. Frampton, Dr. P. R. Mallinson
Department of Chemistry
University of Glasgow
Glasgow G128QQ (UK)
Telefax: Int. code + (41)3304888

[**] This work was supported by the Science and Engineering Research Council (SERC). We wish to thank BASF AG for a generous gift of coronene.

 © VCH Verlagsgesellschaft mbH, D-69451 Weinheim, 1994 0570-0833/94/1515-1587 $ 10.00+.25/0

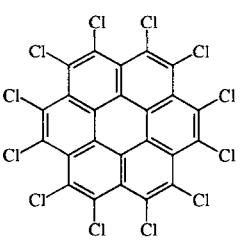
[5] C. S. Swindell, *Org. Prep. Proced. Int.* **1991**, *23*, 465–543.
[6] K. C. Nicolaou, W.-M. Dai, R. K. Guy, *Angew. Chem.* **1994**, *106*, 15–69; *Angew. Chem. Int. Ed. Engl.* **1994**, *33*, 15–44.
[7] K. C. Nicolaou, Z. Yang, J. J. Liu, H. Ueno, P. G. Nantermet, R. K. Guy, C. F. Claiborne, J. Renaud, E. A. Couladouros, K. Paulvannan, E. J. Sorensen, *Nature* **1994**, *367*, 630–634.
[8] R. Weiss, R. C. Donehower, P. H. Wiernik, T. Ohnuma, R. S. Gralla, D. L. Trump, J. R. Daker, D. A. von Echo, D. D. von Hoff, B. Leyland-Jones, *J. Clin. Oncol.* **1990**, *8*, 1263–1268.
[9] E. K. Rowisnky, E. E. Eisenhauer, V. Chaudhry, S. G. Arbuck, R. C. Donehower, *Semin. Oncol.* **1993**, *20 (4 Suppl. 3)*, 1–15.
[10] B. G. Lubejko, S. E. Sartorius, *Semin. Oncol.* **1993**, *20 (4 Suppl. 3)*, 26–30.
[11] H. M. Deutsch, J. A. Glinksi, M. Hernandez, R. D. Haugwitz, V. L. Narayanan, M. Suffness, L. H. Zalhow, *J. Med. Chem.* **1989**, *32*, 788–792.
[12] C. S. Swindell, N. E. Krauss, S. B. Horwitz, I. Ringel, *J. Med. Chem.* **1991**, *34*, 1176–1184.
[13] Z. Zhao, D. G. I. Kingston, A. R. Crosswell, *J. Nat. Prod.* **1991**, *54*, 1607–1611.
[14] A. M. Mathew, R. Mejillano, J. P. Nath, R. H. Himes, V. J. Stella, *J. Med. Chem.* **1992**, *35*, 145–151.
[15] D. M. Vyas, H. Wong, A. R. Crosswell, A. M. Casazza, J. O. Knipe, S. W. Mamber, T. W. Doyle, *Biomed. Chem. Lett.* **1993**, *3*, 1357–1360.
[16] K. C. Nicolaou, C. Riemer, M. A. Kerr, D. Rideout, W. Wrasidlo, *Nature* **1993**, *364*, 464–466.
[17] D. G. I. Kingston, Z. Y. Zhao, *Eur. Patent Appl.* EP 537905 A1 (21 April **1993**).
[18] T. Mukaiyama, *Angew. Chem.* **1979**, *91*, 798–812; *Angew. Chem. Int. Ed. Engl.* **1979**, *18*, 707–721.
[19] S. Kobayashi, M. Tsutsui, T. Mukaiyama, *Chem. Lett.* **1976**, 373–374.
[20] E. K. Rowinsky, R. C. Donehower, *Semin. Oncol.* **1993**, *20 (4 Suppl. 3)*, 16–25.
[21] W. Wrasidlo, K. C. Nicolaou, unpublished results.
[22] R. Merlock, W. Wrasildo, *Anal. Biochem.*, in press.
[23] J. Parness, D. G. I. Kingston, R. G. Powell, C. Harracksingh, S. B. Horwitz, *Biochem. Biophys. Res. Commun.* **1982**, *105*, 1082–1089.
[24] W. Mellado, N. F. Magri, D. G. I. Kingston, R. Garcia-Arenas, G. A. Orr, S. B. Horwitz, *Biochem. Biophys. Res. Commun.* **1984**, *124*, 329–336.
[25] H. Lasaste, H. Senilh, M. Wright, D. Guenard, P. Potier, *Proc. Natl. Acad. Sci. USA* **1984**, *81*, 4090–4094.
[26] H. Ringsdorf, B. Schlar, J. Venzmer, *Angew. Chem.* **1988**, *100*, 117–162; *Angew. Chem. Int. Ed. Engl.* **1988**, *27*, 113–158.
[27] Special section: A. S. Rudolph, J. M. Calvert, P. E. Schoen, J. M. Schnur in *Biotechnological Applications of Lipid Microstructures* (Eds.: B. P. Gaber, J. M. Schnur, D. Chapman), Plenum, New York, **1988**, pp. 320–325.
[28] "Engineering a Small World", *Science* **1991**, *254*, 1300–1335.
[29] J. M. Schnur, *Science* **1993**, *262*, 1669–1676.
[30] M. R. Ghadiri, J. R. Granja, R. A. Milligan, D. E. McRee, N. W. Khazanovich, *Nature* **1993**, *366*, 324–327.
[31] S. B. Horwitz, J. Fant, P. B. Schiff, *Nature* **1979**, *277*, 665–667.
[32] F. Vögtle, *Supramolecular Chemistry*, Wiley, New York, **1991**.
[33] J. H. Fuhrhop, G. Penzlin, *Organic Synthesis Concepts, Methods and Starting Materials*, 2nd ed., VCH, New York, **1993**, pp. 350–356.
[34] G. M. Whitesides, J. P. Mathias, C. T. Seto, *Science* **1993**, *254*, 1312–1319.
[35] J. H. Fuhrhop, P. Schnieder, J. Rosenberg, E. Boekema, *J. Am. Chem. Soc.* **1987**, *109*, 3387–3390.
[36] J. H. Fuhrhop, P. Schnieder, E. Boekema, W. Helfrich, *J. Am. Chem. Soc.* **1988**, *110*, 2861–2867.
[37] J. H. Fuhrhop, S. Svenson, C. Boettcher, E. Rossler, H.-M. Vieth, *J. Am. Chem. Soc.* **1990**, *112*, 4307–4312.
[38] J. H. Fuhrhop, C. Boettcher, *J. Am. Chem. Soc.* **1990**, *112*, 1768–1776.
[39] R. Pazdur, R. A. Newman, B. M. Newman, A. Fuentes, J. Benvenuto, B. Bready, D. Moore, I. Jaiyesimi, F. Vreeland, M. M. G. Bayssas, M. N. Rader, *J. Natl. Cancer Inst.* **1992**, *84*, 1781–1788.

Trigonal Symmetry as a Host Design Element: Novel Conformation of Dodecakis(3,5-dimethylphenylthio)coronene in its 1,4-Dioxane Clathrate**

Gary A. Downing, Christopher S. Frampton, David D. MacNicol,* and Paul R. Mallinson

It is becoming increasingly apparent that the rotational symmetry of the individual host molecule is a key strategic design factor for the discovery and development of new series of host compounds capable of forming crystalline inclusion compounds.[1] The significance of a C_2 axis is highlighted by design of hosts related to *exo*-2, *exo*-6-dihydroxy-2,6-dimethylbicyclo[3.3.1]nonane,[2] tetraphenylene-derived hosts,[3] roof- and scissor-type hosts,[4] and naphthalene-based spider hosts;[5] whilst the crucial importance of a C_3 axis is well represented by hosts of the cyclotriphosphazene type,[6] cyclododecatriene-based hosts,[7] racemic and optically resolved *trans,anti,trans, anti,trans*-perhydrotriphenylene,[8] cyclotriveratrylene and related hosts,[9] and hexa-hosts (i.e. hexasubstituted benzenes designed to produce cavities)[10] along with their Piedford counterparts.[11]

The hexa-host series,[10] members of which typically display an *ababab* conformation with regular alternation of side-chain units above and below the central benzene core, suggested to us an analogous series of hosts possessing *six pairs* of side-chain units corresponding to a dodecasubstituted coronene nucleus. To explore the possibility of synthesizing such novel hosts, the suitable precursor perchlorocoronene **1** was prepared in high yield by perchlorination of coronene under $SO_2Cl_2/S_2Cl_2/AlCl_3$ conditions.[12] The molecular structure of **1**, determined by single-crystal X-ray analysis[12] and electron microscopy[13] at 1 Å resolution, was found to be markedly nonplanar, reflecting pronounced *peri* interactions, and to have symmetry close to D_{3d}. The molecule displays two concave faces and its conformation was found to be, in an extension of our earlier nomenclature,[14] of the highly promising *aabbaabbaabb* type with pairs of chlorine atoms alternating regularly above and below the mean plane of the coronene nucleus. The presence of this conformation in related molecules should enhance host characteristics, not only because of the C_3 axis normal to the central coronene core, but also because of the favorable overall molecular shape reminiscent of a higher order hexa-host (vide infra). Preliminary studies[12] indicated that persubstitution of **1** with arenethiolate nucleophiles was readily achieved at ambient temperature, employing 1,3-dimethylimidazolidin-2-one (DMEU) as solvent. The resulting dodecasubstituted coronenes were, however, found to display rather limited host properties indicating that design of the side-chain unit would be of critical importance.



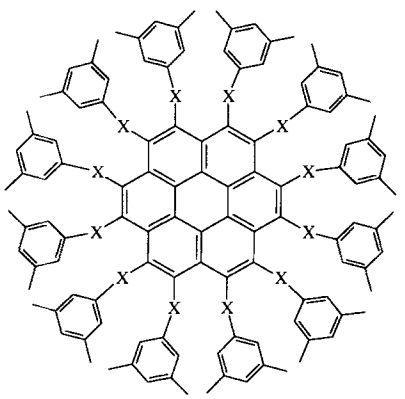
1

[*] Dr. D. D. MacNicol, Dr. G. A. Downing, Dr. C. S. Frampton, Dr. P. R. Mallinson
Department of Chemistry
University of Glasgow
Glasgow G128QQ (UK)
Telefax: Int. code + (41)3304888

[**] This work was supported by the Science and Engineering Research Council (SERC). We wish to thank BASF AG for a generous gift of coronene.

 © VCH Verlagsgesellschaft mbH, D-69451 Weinheim, 1994 0570-0833/94/1515-1587 $ 10.00+.25/0

We now report the synthesis of the versatile coronene-based host dodecakis(3,5-dimethylphenylthio)coronene **2** with an optimized side chain. Host **2** was found to form stable crystalline inclusion compounds with many guests, for example, *N*-methylmorpholine, 1,4-dioxane, 1,4-thioxane, THF, tetrahydrothiophene, cyclohexanone, cycloheptanone, and DMEU, all with a common host–guest ratio of 1:2. In addition, we describe results of a detailed single-crystal X-ray analysis of the 1,4-dioxane adduct of **2**, undertaken to elucidate the structure and conformation of host **2** as well as the host–guest packing in this highly crystalline inclusion compound. Also, briefly reported is the synthesis of the dodecaether host dodecakis(3,5-dimethylphenoxy)coronene **3**, the first member of a new class of molecule, featuring the same favored 3,5-dimethyl substitution pattern in the side-chain moiety.



2, X = S

3, X = O

The 1,4-dioxane inclusion compound of **2** is triclinic,[15] space group $P\bar{1}$, with two host and four 1,4-dioxane guest molecules per unit cell. Interestingly, the well-formed crystals of this adduct are weakly diffracting at room temperature, so X-ray data had to be collected at low temperature (120 K). The stereoview shown in Figure 1 illustrates the molecular structure of **2**. As can be seen the molecule's coronene core is markedly nonplanar. A key feature of the molecule is an approximate C_3 axis normal to the central coronene core. Since the molecule occupies a general position in the unit cell, this is not required by the crystallographic symmetry. Corresponding to this noncrystallographic C_3 axis, there are two types of pairs of side chain moieties, splayed or parallel, respectively above and below the coronene nucleus. Satisfyingly, the host molecule possesses the *aabbaabbaabb* conformation, alternating pairs of sulfur atoms being displaced above and below the mean plane of the twelve most central carbon atoms (see Fig. 2 and legend). The six carbon atoms of the central benzene ring and the carbon atoms directly attached to it, whilst close to planarity,

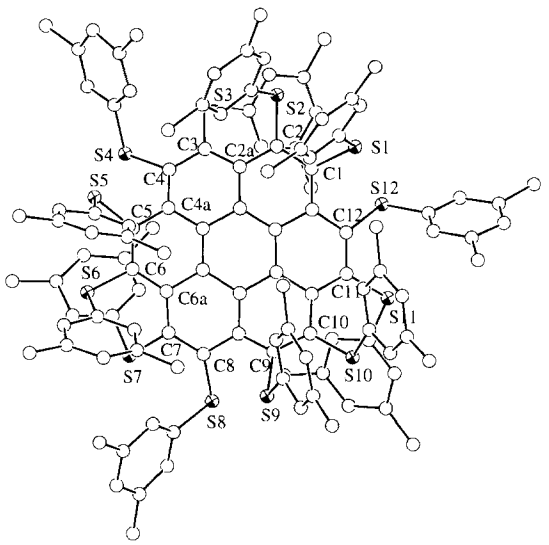


Fig. 2. A view of **2** in its 1,4-dioxane adduct, illustrating the host's atomic numbering scheme. Displacements of approximately C_3-related pairs of sulfur atoms from the mean plane of the central twelve carbon atoms are: S1,S2: −1.12, −0.85; S5,S6: −1.20, −0.78; S9,S10: −1.26, −0.90. − S3,S4: +1.28, +1.14; S7,S8: +1.50, +1.25; S11,S12: +1.20, +1.25. From the same mean plane, related displacements of the C atoms are: C1,C2: −0.38, −0.34; C5,C6: −0.42, −0.34; C9,C10: −0.44, −0.39. − C3,C4: 0.49, +0.40; C7,C8: +0.57, +0.47; C11,C12: +0.50, +0.45. Carbon atoms C6a,C2a, and C4a show respective displacements of +0.06, +0.04, and −0.03 Å from this plane. The remaining nine central carbon atoms are coplanar to within ± ca. 0.02 Å. Estimated standard deviations for S and C, 0.002 and 0.007 Å, respectively.

are not so accurately planar as in the perchlorocoronene precursor.[12]

Figure 3 illustrates the host–guest packing in 1,4-dioxane · **2** viewed along the *a* axis. There are two crystallographically independent 1,4-dioxane guest molecules, both occupying general positions. A pair of well-ordered molecules of the first type may be seen close to $\frac{1}{2}, \frac{1}{2}, \frac{1}{3}$ and $\frac{1}{2}, \frac{1}{2}, \frac{2}{3}$, straddling the center of the cell; whilst the second type of guest, close to 0,0,1, is incompletely located. The corresponding (isostructural)[15] 1,4-thioxane adduct of **2** also exhibits two similar guest sites, with apparent interchange of order and disorder for the two sites.

The above-noted approximate C_3 symmetry does not arise purely from chance, but reflects approximate trigonal packing of the molecules of **2**. This is, perhaps, best appreciated from Figure 4 which corresponds to the view along the rhomb diagonal of a cell approximating to $R\bar{3}$; however, the guests' orientation pattern (only well-ordered guest shown) does not conform to the approximate trigonal packing. The outline of the true triclinic cell (viewed approximately normal to its *ab* plane) is also shown in Figure 4 for comparison.

The dodecaether host compound **3** analogous to **2** forms light yellow crystals of a 1,4-dioxane adduct on recrystallization from the same solvent. However, in this case the crystals are monoclinic, not triclinic, and a host–guest ratio of about 1:6 has been established by ^{1}H NMR. A single-crystal X-ray analysis of this 1,4-dioxane adduct of **3** is currently underway.

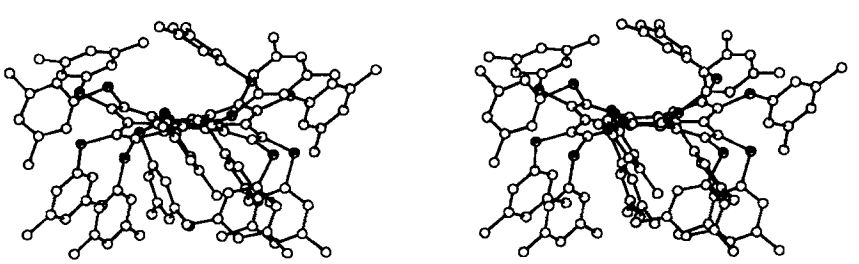


Fig. 1. A stereoview of the molecular structure and conformation of **2** in its 1,4-dioxane adduct.

Experimental Procedure

Synthesis of **2**: **1** [12] (0.25 g, 0.3 mmol) and sodium 3,5-dimethylbenzenethiolate (1.15 g, 7.2 mmol), prepared from 3,5-dimethylbenzenethiol and sodium in absolute ethanol, were stirred in 20 mL of dry, degassed DMEU for two days at ambient temperature, under N_2. The mix-

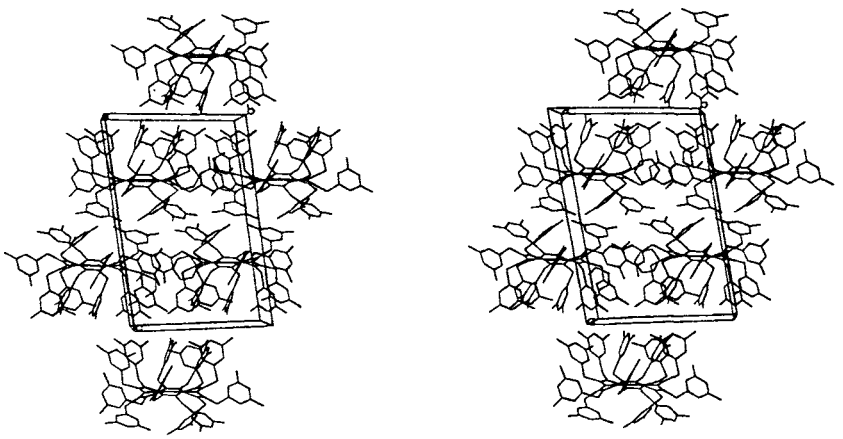


Fig. 3. A stereoview of the host–guest packing in the 1,4-dioxane clathrate of **2**. Two well-ordered 1,4-dioxane guest molecules may be seen around $\frac{1}{2}, \frac{1}{2}, \frac{1}{3}$ and $\frac{1}{2}, \frac{1}{2}, \frac{2}{3}$, whilst the second guest type, represented by only five atoms, is shown close to two cell corners.

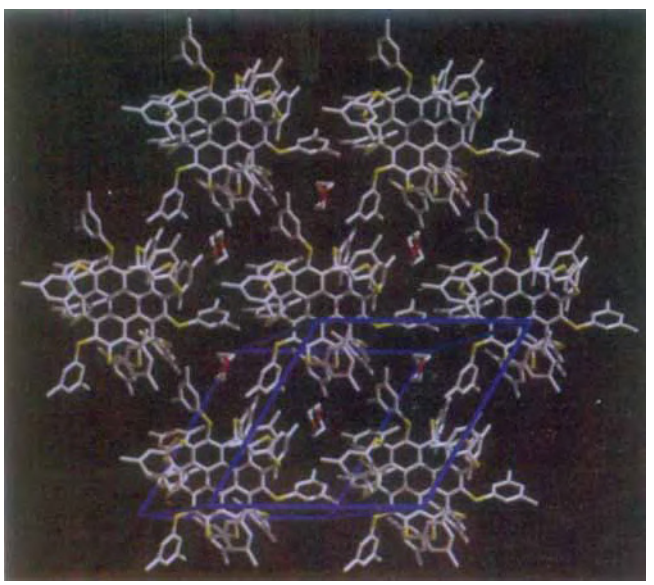


Fig. 4. A view of the approximate trigonal packing of the host molecules of **2** in its 1,4-dioxane adduct (only well-ordered type of 1,4-dioxane guest shown).

ture was then added to toluene (250 mL), washed with water (250 × 10 mL), and evaporation of the solvent gave a red oil, from which compound **2** was obtained (as its 1,4-dioxane adduct) on recrystallization from 1,4-dioxane/methanol; yield 0.52 g (90%), purple crystals, m.p. 275–278 °C (1,4-dioxane adduct). ^{1}H NMR (200 MHz, $CDCl_3$): $\delta = 1.89$ (s, 72H), 6.25 (s, 24H), 6.55 (s, 12H); ^{13}C NMR (50 MHz, $CDCl_3$): $\delta = 21.1$, 123.6, 124.4, 127.1, 134.4, 137.5, 138.8, 139.7; FAB MS: *m/z*: 1933.52 (±0.17) [M^+ + H]; $C_{120}H_{109}S_{12}$ requires 1933.52.

Synthesis of **3**: **1** [12] (0.2 g, 0.28 mmol) and sodium 3,5-dimethylphenolate (1.20 g, 9.8 mmol), prepared from 3,5-dimethylphenol and sodium in absolute ethanol, were stirred in 20 mL of dry hexamethylphosphoric acid triamide for seven weeks at 90 °C, under N_2. The mixture was then added to toluene (350 mL), washed with water (350 × 10 mL), and evaporation of the solvent gave a brown oil which was chromatographed (dry column) on silica gel (97/3, 40–60 °C petrol/diethyl ether) to afford 88 mg (18%) of **3** as a yellow powder, m.p. 291–292 °C. ^{1}H NMR (200 MHz, $CDCl_3$): $\delta = 2.00$ (s, 72H), 6.04 (s, 24H), 6.40 (s, 12H); FAB MS: *m/z*: 1741 [M^+ + H].

Received: February 15, 1994 [Z 6693 IE]
German version: *Angew. Chem.* **1994**, *106*, 1653

[1] See for example: a) *Inclusion Compounds, Vol. 1–3* (Eds.: J. L. Atwood, J. E. D. Davies, D. D. MacNicol), Academic Press, London, **1984**; b) *Inclusion Compounds, Vol. 4 + 5* (Eds.: J. L. Atwood, J. E. D. Davies, D. D. MacNicol), Oxford University Press, Oxford, **1991**.

[2] R. Bishop, I. G. Dance, in ref. [1 b], Vol. 4, Chap. 1; *Top. Curr. Chem.* **1988**, *149*, 137.

[3] T. C. W. Mak, H. N. C. Wong, *Top. Curr. Chem.* **1987**, *140*, 141; *Acc. Chem. Res.* **1989**, *22*, 148.

[4] E. Weber in ref. [1 b], Vol. 4, Chap. 5; E. Weber, M. Czugler, *Top. Curr. Chem.* **1988**, *149*, 45; see also F. Toda in ref. [1 b], Vol. 4, Chap. 4.

[5] D. D. MacNicol, P. R. Mallinson, C. D. Robertson, *J. Chem. Soc. Chem. Commun.* **1985**, 1649.

[6] H. R. Allcock in ref. [1 a], Vol. 1, Chap. 8.

[7] D. D. MacNicol, S. Swanson, *Tetrahedron Lett.* **1977**, 2969.

[8] M. Farina in ref. [1 a], Vol. 2, Chap. 3.

[9] A. Collet in ref. [1 a], Vol. 2, Chap. 4.

[10] D. D. MacNicol in ref. [1 a], Vol. 2, Chap. 5, p. 132; see also A. A. Freer, D. D. MacNicol, P. R. Mallinson, *Tetrahedron Lett.* **1992**, *33*, 261.

[11] A. S. Jessiman, D. D. MacNicol, P. R. Mallinson, I. Vallance, *J. Chem. Soc. Chem. Commun.* **1990**, 1619.

[12] T. Baird, J. H. Gall, D. D. MacNicol, P. R. Mallinson, C. R. Michie, *J. Chem. Soc. Chem. Commun.* **1988**, 1471.

[13] W. Dong, T. Baird, J. R. Fryer, C. J. Gilmore, D. D. MacNicol, G. Bricogne, D. J. Smith, M. A. O'Keefe, S. Hövmoller, *Nature (London)* **1992**, *355*, 605.

[14] D. D. MacNicol, P. R. Mallinson, C. D. Robertson, *J. Chem. Soc. Chem. Commun.* **1985**, 1649.

[15] **2** · 2 (1,4-dioxane): Crystal data: $C_{120}H_{108}S_{12} \cdot 2C_4H_8O_2$, $M = 2111.1$, triclinic, space group $P\bar{1}$, $a = 17.094(6)$, $b = 17.489(6)$, $c = 23.987(6)$ Å, $\alpha = 74.63(2)$, $\beta = 71.72(3)$, $\gamma = 60.53(3)°$, $V = 5874(3)$ Å^3, $Z = 2$, $\rho_{calcd} = 1.193$ g cm^{-3}, $Mo_{K\alpha}$ radiation, $\lambda = 0.71069$ Å, cell parameters from 25 reflections, $\theta = 11$–$15°$, $\mu = 2.63$ cm^{-1}, $T = 120$ K, deep purple rhomb 0.5 × 0.5 × 0.4 mm. Data collection: Enraf-Nonius CAD-4 diffractometer, $\theta_{max} = 27°$, $\omega - 2\theta$ scans, absorption correction: none, 25554 independent reflections, 14741 observed reflections [$I > 2\sigma(I)$]. The structure was solved by direct methods by using SHELXS-86 [16] and refined on F to $R = 0.097$, $R_w = 0.129$ for the 14741 observed reflections. $w = 1/\sigma^2(F)$. Hydrogen atoms were placed in calculated positions and not refined. Oxygen atoms of the dioxane guest molecules were treated as carbon atoms. One ring atom of one of the dioxane molecules was not located. Hydrogen atoms of the dioxane were not included in the calculations. Least squares refinement was carried out using the NRC package [17]. Other calculations used GX [18], which incorporates a locally modified version of ORTEP [19]. Further details of the crystal structure investigations are available on request from the Director of the Cambridge Crystallographic Data Centre, 12 Union Road, GB-Cambridge CB2 1EZ (UK), on quoting the full journal citation. **2** · 2 (1,4-thioxane): Crystal data: $C_{120}H_{108}S_{12} \cdot 2C_4H_8OS$, $M = 2143.3$, triclinic, space group $P\bar{1}$, $a = 17.250(4)$, $b = 17.461(11)$, $c = 24.046(10)$ Å, $\alpha = 74.32(4)$, $\beta = 72.02(3)$, $\gamma = 60.03(4)°$, $V = 5908(5)$ Å^3, $Z = 2$, $\rho_{calcd} = 1.204$ g cm^{-3}.

[16] G. M. Sheldrick, *SHELXS-86. Program for solution of crystal structures*, Universität Göttingen, **1986**.

[17] A. C. Larson, F. L. Lee, Y. Le Page, M. Webster, J. P. Charland, E. J. Gabe, *The NRCVAX Crystal Structure System*, Chemistry Division, NRC, Ottawa, Canada.

[18] P. R. Mallinson, K. W. Muir, *J. Appl. Crystallogr.* **1985**, *18*, 51.

[19] C. K. Johnson, *ORTEP II*. Report ORNL-3794, 2nd revision, and supplementary instructions, Oak Ridge National Laboratory, TN, 1970.

A General Synthetic Strategy for Neutral Phosphorus-Containing Dendrimers

Nathalie Launay, Anne-Marie Caminade, Roger Lahana, and Jean-Pierre Majoral*

Dendrimers, highly branched functionalized molecules formed by iterative reaction sequences, are attracting considerable attention in organic, supramolecular, and polymer chemistry.[1] Until now few of these macromolecules have contained main group

[*] Dr. J.-P. Majoral, N. Launay, Dr. A.-M. Caminade
Laboratoire de Chimie de Coordination du CNRS
205, Route de Narbonne, F-31077 Toulouse Cédex (France)
Telefax: Int. code +61 553003
Dr. R. Lahana
Oxford Molecular SA, X-Pole, Ecole Polytechnique
Palaiseau (France)

elements such as silicon[2] or phosphorus.[3] Only phosphorus dendrimers having charges within the cascade structure and elaborated to three generations have been reported,[3] and no example of neutral phosphorus dendrimers has yet been described.

We report here on the easy, high-yielding preparation of up to fourth-generation neutral cascade molecules in which the core and subsequent branch points are pentavalent phosphorus atoms. These dendrimers possess at the periphery up to 48 of two of the most reactive functional groups in organic and main group element chemistry—aldehyde groups and phosphorus–chlorine bonds.

The first step consists of the reaction of trichlorothiophosphorous(V) (1 equiv) with the sodium salt of 4-hydroxybenzaldehyde **1** (3 equiv) to give **2**. Subsequent addition of the hydrazine derivative **3** leads quantitatively to **4a**, a first-generation dendrimer possessing six P–Cl bonds (Scheme 1). Further elaboration to second-, third-, and fourth-generation cascade molecules is accomplished by repetition of these two steps (Scheme 1). In each reaction cycle terminal aldehyde groups and then terminal dichlorothiophosphoryl groups are introduced quantitatively and remain available for continued reactions. No protection/deprotection procedure is necessary, and the only by-products are sodium chloride and water! All the compounds, including those of the fourth generation, **7a** ($M = 11269$) and **7b** ($M = 15381$), are stable and remain perfectly soluble in a variety of organic solvents (chloroform, THF, etc.). All the dendrimers were characterized by NMR and IR spectroscopy, and elemental analysis (Table 1). Mass spectrometry (FAB or electron spray) is useful for dendrimers up to the second generation (**5b**: m/z: 3418 $[M+1]^+$).

Remarkably the construction of each generation can be easily followed by ^{31}P NMR spectroscopy: all phosphorus sites are distinguishable at each generation by their ^{31}P NMR chemical shifts and by the intensities of the different signals (Fig. 1 and Table 2).

Table 1. Selected physical and spectroscopic data of compounds **4**–**7** [a,b].

4a: white powder; m.p. 70–71 °C (decomp). ^1H NMR ($CDCl_3$): $\delta = 3.5$ (d, $^3J_{HP_1} = 14$ Hz, 9H, P_1-N-Me), 7.1 (dd, $^3J_{HH} = 8.6$, $^4J_{HP_0} = 1.6$ Hz, 6H, H-C_2), 7.7 (d, $^4J_{HP_1} = 2.5$ Hz, 3H, CH=N), 8.0 (d, $^3J_{HH} = 8.6$ Hz, 6H, H-C_3); $^{13}C\{^1H\}$ NMR ($CDCl_3$): $\delta = 31.2$ (d, $^2J_{CP_1} = 13.2$ Hz, P_1-N-CH_3), 120.9 (d, $^3J_{CP_0} = 5.1$ Hz, C_2), 128.3 (s, C_3), 131.4 (s, C_4), 139.8 (d, $^3J_{CP_1} = 18.7$ Hz, CH=N), 151.0 (d, $^2J_{CP_0} = 7$ Hz, C_1)

4b: white powder; m.p. 74–75 °C (decomp). ^1H NMR ($CDCl_3$): $\delta = 3.4$ (d, $^3J_{HP_1} = 10.9$ Hz, 9H, P_1-N-Me), 7.3 (dd, $^3J_{HH} = 8.6$, $^4J_{HP_0} = 1.5$ Hz, 6H, C_2-H), 7.4 (dd, $^3J_{HH} = 8.6$, $^4J_{HP_1} = 1.5$ Hz, 12H, C_2'-H), 7.6 (s, 3H, CH=N), 7.7 (d, $^3J_{HH} = 8.6$ Hz, 6H, C_3-H), 7.8 (d, $^3J_{HH} = 8.6$ Hz, 12H, C_3'-H), 9.9 (s, 6H, CHO); $^{13}C\{^1H\}$ NMR ($CDCl_3$): $\delta = 32.3$ (d, $^2J_{CP_1} = 13.9$ Hz, P_1-N-CH_3), 120.9 (d, $^3J_{CP_0} = 5.0$ Hz, C_2), 121.3 (d, $^3J_{CP_1} = 5.4$ Hz, C_2'), 127.8 (s, C_3), 130.8 (s, C_3'), 131.7 (s, C_4), 133.0 (s, C_4'), 138.6 (d, $^3J_{CP_1} = 13.3$ Hz, CH=N), 150.6 (d, $^2J_{CP_0} = 7.3$ Hz, C_1), 154.4 (d, $^2J_{CP_1} = 7.3$ Hz, C_1'), 190.1 (s, CHO)

5a: yellow powder; m.p. 81 °C (decomp). ^1H NMR ($CDCl_3$): $\delta = 3.40$ (d, $^3J_{HP_1} = 11.6$ Hz, 9H, P_1-N-Me), 3.45 (d, $^3J_{HP_2} = 14.1$ Hz, 18H, P_2-N-Me), 7.0–8.0 (m, 45H, C_6H_4, CH=N); $^{13}C\{^1H\}$ NMR ($CDCl_3$): $\delta = 31.2$ (d, $^2J_{CP_2} = 13.1$ Hz, P_2-N-CH_3), 32.5 (d, $^2J_{CP_1} = 13.6$ Hz, P_1-N-CH_3), 120.9 (d, $^3J_{CP_0} = 4.1$ Hz, C_2), 121.3 (d, $^3J_{CP_1} = 4.1$ Hz, C_2'), 127.8 (s, C_3), 128.1 (s, C_3'), 127.8 (s, C_3), 128.1 (s, C_3'), 130.9 (s, C_4'), 131.9 (s, C_4), 138.1 (d, $^3J_{CP_1} = 13.1$ Hz, CH=N), 140.0 (d, $^3J_{CP_2} = 19.1$ Hz, CH=N), 150.5 (d, $^2J_{CP_0} = 11.6$ Hz, C_1), 151.2 (d, $^2J_{CP_1} = 8.7$ Hz, C_1')

5b: yellow powder; m.p. 111 °C (decomp). ^1H NMR ($CDCl_3$): $\delta = 3.7$ (d, $^3J_{HP_{1,2}} = 10.9$ Hz, 27H, $P_{1,2}$-N-Me), 7.2–8.0 (m, 93H, C_6H_4, CH=N), 9.9 (s, 12H, CHO); $^{13}C\{^1H\}$ NMR ($CDCl_3$): $\delta = 32.3$ (d, $^2J_{CP_2} = 13.2$ Hz, P_2-N-CH_3), 32.4 (d, $^2J_{CP_1} = 13.1$ Hz, P_1-N-CH_3), 120.9 (d, $^3J_{CP_0} = 4.8$ Hz, C_2), 121.3 (d, $^3J_{CP_{1,2}} = 4.6$ Hz, C_2' and C_2''), 127.6 (s, C_3'), 127.8 (s, C_3), 130.8 (s, C_3''), 131.2 (s, C_4'), 132.0 (s, C_4), 133.0 (s, C_4''), 138.2 (d, $^3J_{CP_1} = 16$ Hz, CH=N), 138.9 (d, $^3J_{CP_2} = 14.6$ Hz, CH=N), 150.5 (d, $^2J_{CP_0} = 7.3$ Hz, C_1), 150.9 (d, $^2J_{CP_1} = 8.7$ Hz, C_1'), 154.4 (d, $^2J_{CP_2} = 7$ Hz, C_1''), 190.1 (s, CHO)

6a: yellow powder; m.p. 131–132 °C (decomp). ^1H NMR ($CDCl_3$): $\delta = 3.35$ (d, $^3J_{HP_{1,2}} = 11.5$ Hz, 27H, $P_{1,2}$-N-Me), 3.40 (d, $^3J_{HP_3} = 14.2$ Hz, 36H, P_3-N-Me), 7.2–7.8 (m, 105H, C_6H_4, CH=N); $^{13}C\{^1H\}$ NMR ($CDCl_3$): $\delta = 31.2$ (d, $^2J_{CP_3} = 13.1$ Hz, P_3-N-CH_3), 32.4 (d, $^2J_{CP_{1,2}} = 13.0$ Hz, $P_{1,2}$-N-CH_3), 121.2 (d, $^3J_{CP_{0,1,2}} = 4.9$ Hz, C_2, C_2', C_2''), 127.7 (s, C_3, C_3'), 128.1 (s, C_3''), 130.9 (s, C_4''), 131.5 (s, C_4'), 132.0 (s, C_4), 138.5 (d, $^3J_{CP_{1,2}} = 13.5$ Hz, CH=N), 140.2 (d, $^3J_{CP_3} = 18.5$ Hz, CH=N), 150.5 (d, $^2J_{CP_{0,1}} = 6.9$ Hz, C_1, C_1'), 151.3 (d, $^2J_{CP_2} = 7.5$ Hz, C_1'')

6b: yellow powder; m.p. 121 °C (decomp). ^1H NMR ($CDCl_3$): $\delta = 3.3$ (d, $^3J_{HP_{1,2,3}} = 10.8$ Hz, 63H, $P_{1,2,3}$-N-Me), 7.2–7.8 (m, 201H, C_6H_4, CH=N), 9.9 (s, 24H, CHO); $^{13}C\{^1H\}$ NMR ($CDCl_3$): $\delta = 32.3$ (d, $^2J_{CP_{1,2,3}} = 13.8$ Hz, $P_{1,2,3}$-N-CH_3), 121.3 (d, $^3J_{CP_{0,1,2,3}} = 4.9$ Hz, C_2, C_2', C_2'', C_2'''), 127.6 (br. s, C_3, C_3', C_3''), 130.7 (s, C_3'''), 131.1 (s, C_4''), 131.5 (s, C_4'), 132.0 (s, C_4), 133.0 (s, C_4'''), 138.5–139.3 (m, CH=N), 150.5 (d, $^2J_{CP_{0,1}} = 6.1$ Hz, C_1, C_1'), 150.9 (d, $^2J_{CP_2} = 6.2$ Hz, C_1''), 154.6 (d, $^2J_{CP_3} = 7.4$ Hz, C_1'''), 189.9 (s, CHO)

7a: yellow powder; m.p. 124 °C (decomp). ^1H NMR ($CDCl_3$): $\delta = 3.30$ (d, $^3J_{HP_{1,2,3}} = 10.9$ Hz, 63H, $P_{1,2,3}$-N-Me), 3.40 (d, $^3J_{HP_4} = 13.4$ Hz, 72H, P_4-N-Me), 7.2–7.7 (m, 225H, C_6H_4, CH=N); $^{13}C\{^1H\}$ NMR ($CDCl_3$): $\delta = 31.2$ (d, $^2J_{CP_4} = 13.1$ Hz, P_4-N-CH_3), 32.4 (d, $^2J_{CP_{1,2,3}} = 13.1$ Hz, $P_{1,2,3}$-N-CH_3), 121.2 (br. s, C_2, C_2', C_2'', C_2'''), 127.7 (s, C_3, C_3', C_3''), 128.0 (s, C_3'''), 130.8 (s, C_4'''), 131.4 (s, C_4''), 131.6 (s, C_4, C_4'), 138–138.5 (CH=N), 140.1 (d, $^3J_{CP_4} = 18.1$ Hz, CH=N), 150.5–151.0 (m, C_1, C_1', C_1''), 151.2 (d, $^2J_{CP_3} = 7.2$ Hz, C_1''')

7b: white powder; m.p. 131–132 °C (decomp). ^1H NMR ($CDCl_3$): $\delta = 3.3$ (d, $^3J_{HP_{1,2,3,4}} = 8.9$ Hz, 135H, $P_{1,2,3,4}$-N-Me), 7.2–7.7 (m, 417H, C_6H_4, CH=N), 9.9 (s, 48H, CHO); $^{13}C\{^1H\}$ NMR ($CDCl_3$): $\delta = 32.1$–32.4 (m, $P_{1,2,3,4}$-N-CH_3), 121.2 (d, $^3J_{CP_{0,1,2,3,4}} = 4.3$ Hz, C_2, C_2', C_2'', C_2''', C_2''''), 127.6 (s, C_3, C_3', C_3'', C_3'''), 130.8 (s, C_3''''), 131.1 (s, C_4''), 131.5 (s, C_4, C_4', C_4''), 132.9 (s, C_4''''), 138.0–140.0 (m, CH=N), 150.0–150.5 (m, C_1, C_1', C_1''), 150.8 (d, $^2J_{CP_3} = 6.2$ Hz, C_1'''), 154.4 (d, $^2J_{CP_4} = 7.4$ Hz, C_1''''), 190.0 (s, CHO)

[a] Correct C,H,N,P analyses were obtained for all compounds. [b] C_1 (= *ipso*), C_2 (= *ortho*), C_3 (= *meta*), C_4 (= *para*): carbon atoms of the phenoxy group linked to the phosphorus core. C_1', C_2', C_3', C_4': carbon atoms of the phenoxy groups linked to P_1 (first generation). C_1'', C_2'', C_3'', C_4'', C_1''', C_2''', C_3''', C_4''' and C_1'''', C_2'''', C_3'''', C_4'''': carbon atoms of phenoxy groups linked to P_2 (second generation), P_3 (third generation) and P_4 (fourth generation), respectively.

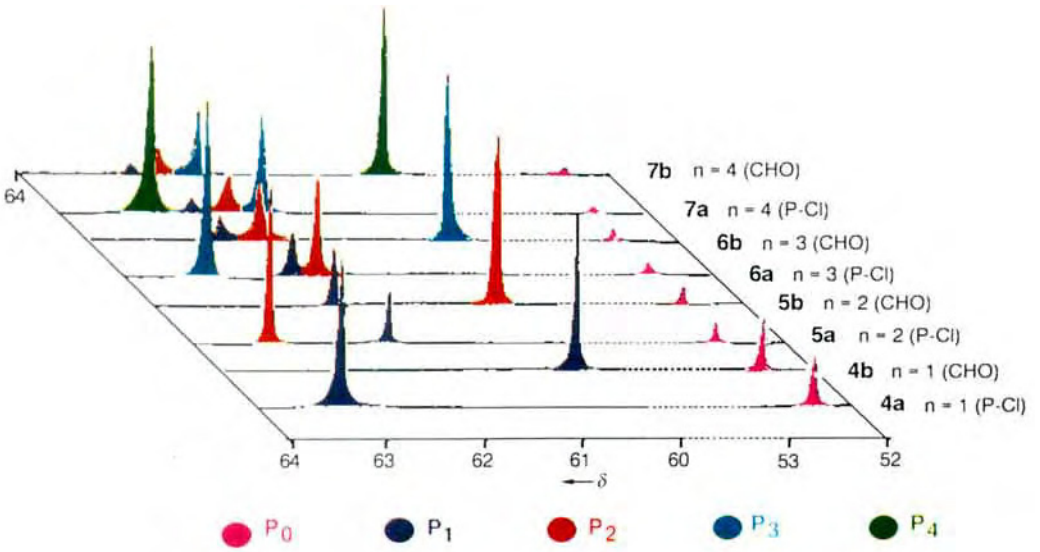


Fig. 1. ^{31}P NMR spectra (81.01 MHz) of dendrimers **4**–**7** in $CDCl_3$. n = Generation.

Table 2. ^{31}P NMR chemical shifts and molecular weights M of dendrimers **4**–**7**.

Cmpd.	n	No. of terminal functions PCl/CHO	$\delta(^{31}P)$ [a] P_0	P_1	P_2	P_3	P_4	M
4a	1	6/-	52.3	63.1				909
4b	1	-/6	52.5	60.4				1423
5a	2	12/-	52.6	62.0	63.2			2389
5b	2	-/12	52.7	62.2	60.6			3417
6a	3	24/-	52.7	62.3	62.0	63.2		5349
6b	3	-/24	52.7	62.7	62.3	60.4		7405
7a	4	48/-	52.5	62.7	62.3	62.0	63.1	11269
7b	4	-/48	52.5	62.9	62.7	62.3	60.4	15381

[a] P_0: phosphorus core; P_1, P_2, P_3 and P_4: phosphorus atoms of the first, second, third, and fourth generations, respectively.

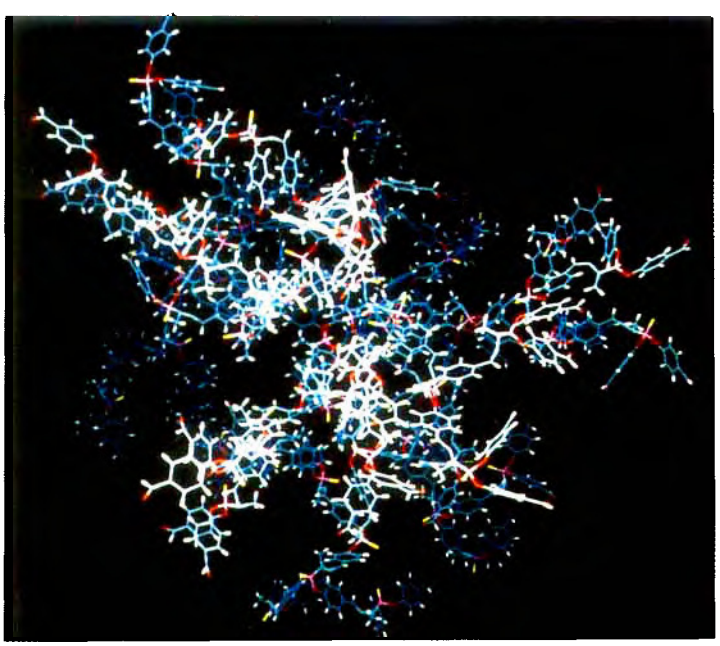


Fig. 2. Structure of dendrimer **7b** from molecular modeling.

The structure of compound **7b** was calculated using the molecular modeling package MAD[4a] on an SGI Indigo XS24 R4000. The basic template $N-N(CH_3)-P(S)[O-p-(C_6H_4)-CH=O]_2$ was constructed and minimized; in the conformational analysis a tree searching algorithm[4b] with an extended MM2 force field and a Newton-Raphson minimizer was used. The force field was tuned using results from X-ray structure analyses. Four iterative three-step procedures were then used to build the full molecule from the external ends to the core phosphorus. Finally, the template obtained was grafted three times on the phosphorus core $(S)P[O-p(C_6H_4)CHO]_3$ resulting in the whole dendrimer, which was given a final check to avoid steric contacts. The resulting structure is shown in Figure 2.

Our synthetic approach appears to be also effective for the formation of dendrimers having alternating thiophosphoryl and phosphoryl groups, or phosphoryl groups exclusively, since analogous reactions can be conducted with either $H_2NN(CH_3)P(O)Cl_2$ (**8**), then **3** (or vice versa), or with **8** only.[5] Introduction of other functional groups (amino, phosphino, vinylic, allylic, acidic groups, (etc.) is in progress,[6] and applications of these cascade molecules in catalysis and coordination chemistry are being investigated.

Experimental Procedure

7a: A solution of polyaldehyde **6b** (0.0166 mmol, 0.123 g) in 4 mL of $CHCl_3$ was added at 25 °C to a solution of the freshly prepared hydrazine derivative **3** (0.4 mmol, 0.072 g) in 4 mL of $CHCl_3$ containing 4 Å molecular sieves. The resulting mixture was stirred 12 h then filtered. The solvent was removed to give a yellow powder which was washed with 10 mL of ether.

7b: A solution of **7a** (0.01 mmol, 0.113 g) in 5 mL of THF was added dropwise at 25 °C to a suspension of the sodium salt **1** (0.48 mmol, 0.069 g) in 5 mL of THF. After 12 h of stirring at 25 °C, the resulting mixture was filtered. The solvent was removed to give a white powder which was washed with 10 mL of ether.

Received: February 12, 1994 [Z 6689IE]
German version: *Angew. Chem.* **1994**, *106*, 1682

[1] Reviews: D. A. Tomalia, A. M. Naylor, W. A. Goddart III, *Angew. Chem.* **1990**, *102*, 119; *Angew. Chem. Int. Ed. Engl.* **1990**, *29*, 138; H. B. Mekelburger, W. Jaworek, F. Vögtle, *ibid.* **1992**, *104*, 1609 bzw. **1992**, *31*, 1571; M. F. Ottaviani, S. Bossmann, N. J. Turro, D. A. Tomalia, *J. Am. Chem. Soc.* **1994**, *116*, 661, and references therein.

[2] H. Uchida, Y. Kabe, K. Yoshino, A. Kawamata, T. Tsumuraya, S. Masamune, *J. Am. Chem. Soc.* **1990**, *112*, 7077; L. J. Mathias, T. W. Carothers, *ibid.* **1991**, *113*, 4043; E. A. Rebrov, A. M. Muzafarov, V. S. Papkov, A. A. Zhdanov, *Dokl.*

Akad. Nauk SSSR **1989**, *309*, 376; A. W. van der Made, P. W. N. M. van Leeuwen, *J. Chem. Soc. Chem. Commun.* **1993**, 1400.
[3] K. Rengan, R. Engel, *J. Chem. Soc. Chem. Commun.* **1990**, 1084; *J. Chem. Soc. Perkin Trans. 1* **1991**, 987; R. Engel, K. Rengan, C. S. Chan, *Phosphorus Sulfur Silicon Relat. Elem.* **1993**, *77*, 221.
[4] a) MAD is available from Oxford Molecular Ltd., Oxford Science Park, The Magdalen Centre, Sandford on Thames, OX4 4GA Oxford, UK. b) M. Lipton, C. Still, *J. Comput. Chem.* **1988**, *9*, 343.
[5] N. Launay, A.-M. Caminade, J.-P. Majoral, unpublished.
[6] According to the systematic nomenclature proposed by Newkome et al. [7] **7a** and **7b** can be named as follows: **7a**: [48-cascade:thiophosphate[3]:{(phenoxy-4-(thiophosphonomethylhydrazino)methylene}^{4}:chloride]; **7b**: [48-cascade:thiophosphate[3]:{(phenoxy-4-(thiophosphonomethylhydrazino)methylene}^{4}-phenoxy-4-aldehyde].
[7] G. R. Newkome, G. R. Baker, J. K. Young, J. G. Traynham, *J. Polym. Sci. Part A Polym. Chem.* **1993**, *31*, 641.

Ferromagneto-Structural Correlations in $[Mn(OC_6X_3H_2)_2(bipy)]_2$ Compounds, X = Cl, Br**

Marcel Wesolek, Daniel Meyer, John A. Osborn,* André De Cian, Jean Fischer,* Alain Derory, Patrick Legoll, and Marc Drillon*

The search for ferromagnetic molecular materials continues apace.[1] Ideally in such structures the spin carriers (e.g. organic radicals,[2] transition metal ions,[3] or their hybrids[4]) need to be incorporated into molecules which are functionalized so that when these molecules assemble into a two- (or preferably three-) dimensional network, the resulting supramolecular structure should also provide ferromagnetic interactions between the constituent molecules. However, the factors that determine such desired intermolecular magnetic effects in the solid state are not well understood although an orbital approach would seem the most attractive.[1d] An initial objective for the synthetic chemist is the discovery of molecules which display the appropriate magnetic properties and to attempt to correlate these effects with detailed structural features. We present here the syntheses, X-ray crystal structures, and magnetic studies on two new dinuclear manganese(II) complexes which, although possessing rather simply functionalized ligands, are found to exibit both intramolecular and intermolecular ferromagnetic interactions.

The complexes **1** and **2** are formed in two steps by treatment of $MnBr_2(CH_3CN)_2$ with two equivalents of the sodium salt of

$Mn_2(OC_6X_3H_2)_4(bipy)_2$ **1**, X = Cl; **2**, X = Br; bipy = bipyridine

the corresponding 2,4,6-trisubstituted phenol in THF and, after filtration of NaBr, the addition of one equivalent of bipyridine. Crystals suitable for X-ray structure analysis and magnetic measurements were obtained after recrystallization from hot CH_3CN.

The X-ray crystal structures[5] of both **1** and **2** (Fig. 1) show an essentially identical dimeric core, in which two identical Mn^{II} ions are symmetrically bridged by two phenoxy ligands. The

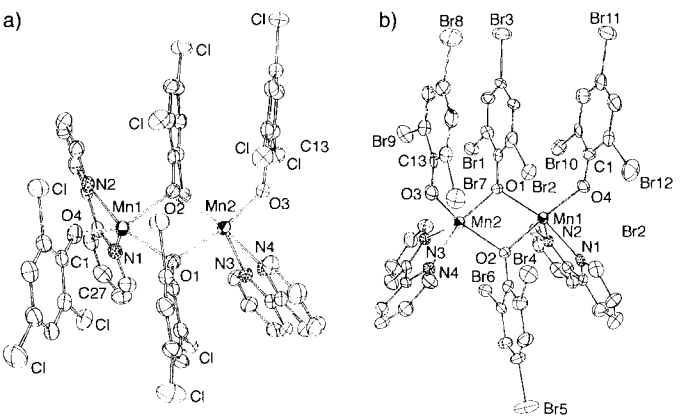


Fig. 1. Crystal structures of **1**(a) and **2**(b). Selected bond lengths [Å] and angles [°]: **1** (**2**): Mn1-N1 2.232(4) (2.241(7)), Mn1-N2 2.250(4) (2.218(6)), Mn2-N3 2.209(4) (2.235(6)), Mn2-N4 2.248(4) (2.248(6)), Mn1-O1 2.123(3) (2.160(5)), Mn1-O2 2.139(3) (2.198(5)), Mn1-O4 1.996(3) (2.039(5)), Mn2-O1 2.173(3) (2.178(5)), Mn2-O2 2.125(3) (2.120(5)), Mn2-O3 2.045(3) (2.024(5)), C-X between 1.727(5) and 1.748(5) (1.875(7) and 1.921(8)), average values 1.737(5) (1.896(7)). Mn···Mn 3.369(1) (3.424(2)), Mn1-O2-Mn2 104.8(1) (104.9(2)), Mn1-O1-Mn2 103.7(1) (104.2(2)), O1-Mn1-O2 75.3(1) (74.6(2)), O1-Mn2-O2 74.5(1) (75.8(2)), Mn1-O4-C1 137.0(1) (138.4(5)), Mn2-O3-C13 132.4(3) (137.9(5)), N1-Mn1-N2 73.5(1) (73.7(2)), N3-Mn2-N4 74.1(1) (73.1(2)), N1-Mn1-O4 114.9(1) (85.7(2)), N2-Mn1-O4 87.4(1) (103.7(2)), N3-Mn2-O3 90.1(1) (110.0(2)), N4-Mn2-O3 102.4(1) (86.0(2)).

Mn–Mn distances and internal core angles Mn-O-Mn in the two complexes are very similar. Each Mn ion is further bound to a terminal phenoxy ligand and a bipyridine ligand, leading to a highly distorted trigonal bipyramidal geometry about each Mn ion. However, the arrangement of the ligands in **1** and **2** differ markedly. In **1** each terminal phenoxy ligand is involved in a stacking interaction with one of the bridging phenoxy groups: the dihedral angles φ formed between the the aromatic planes are 7.3(8)° and 12.7(5)°, and the neighboring C–C separations vary from 3.26 to 3.79 Å. In **2**, however, the two terminal phenoxy ligands and one of the bridging phenoxy ligands form an intramolecular triple stack of phenyl units on one side of the dimer, creating dihedral angles of 0.6 and 6.9° and proximate C–C separations varying from 3.27 to 3.51 Å.

In the crystal both **1** and **2** form chains in which the bipyridine ligands of each dimer are involved in intermolecular π-π interactions with the bipyridine ligands of the neighboring dimers in the chain (Fig. 2). In both **1** and **2** two different bpy–bpy separations are found in which the intermolecular C–C distances vary from 3.29 to 3.43 Å and 3.58 to 3.89 Å, respectively for **1** and from 3.11 to 3.52 Å and 3.25 to 3.61 Å for **2**. The major difference between the two structures is that in **1** no interchain contacts are observed: the 2,4,6-trichlorophenoxy ligands show no intermolecular π-π interactions or Cl–Cl contacts. However in **2**, although no intermolecular π-π interactions are observed between the 2,4,6-tribromophenoxy ligands, a direct interchain Br^3–Br^6 contact is observed at 3.615 Å (0.3 Å shorter than a van der Waals contact).

Magnetic measurements were carried out in the temperature range 1.7–300 K with a SQUID magnetometer at an applied

[*] Prof. Dr. J. A. Osborn, Dr. M. Wesolek, Dr. D. Meyer
Laboratoire de Chimie des Métaux de Transition et de Catalyse, U.R.A. 424 CNRS
Institut Le Bel, Université Louis Pasteur
4, rue Blaise Pascal, F-67070 Strasbourg (France)
Telefax: Int. code +88 416171
Prof. Dr. J. Fischer, Dr. A. De Cian
Laboratoire de Cristallochimie et de Chimie Structurale
Institut Le Bel, Université Louis Pasteur (France)
Dir. Dr. M. Drillon, Ing. A. Derory, Dr. P. Legoll
IPCMS, Groupe de Chimie des Matériaux Inorganiques
UM-380046-EHICS, 1 rue Blaise Pascal, F-67008 Strasbourg (France)

[**] We thank Prof. Dr. A. Herr and Ing. R. Poinsot for measurements on the SQUID magnetometer and Tech. J.-P. Lambour for the specific heat measurements. bpy = bipyridine.

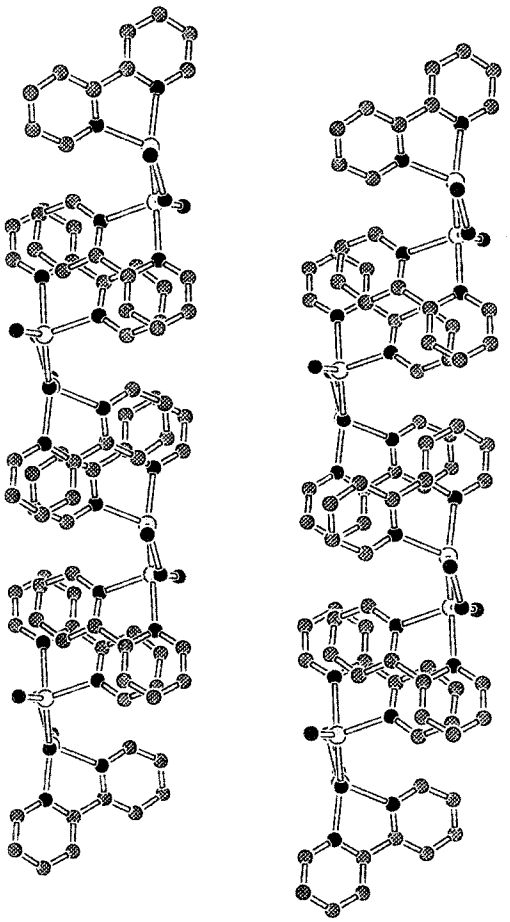


Fig. 2. Packing of **2** in the crystal. The substituted rings of the phenoxy ligands are omitted for clarity. Yellow: Mn; red: O; blue: N.

field $H = 300$ Oe. Figure 3 shows the temperature dependence of the $\chi_M T$ product for both **1** and **2**. Above 100 K, the magnetic behavior obeys a Curie–Weiss law in agreement with two isolated manganese(II) ions per molecule; the effective magnetic moment at 300 K is 5.93 μ_B per manganese atom for **1** and 5.67 μ_B per manganese atom for **2**. Upon cooling, $\chi_M T$ increases, which

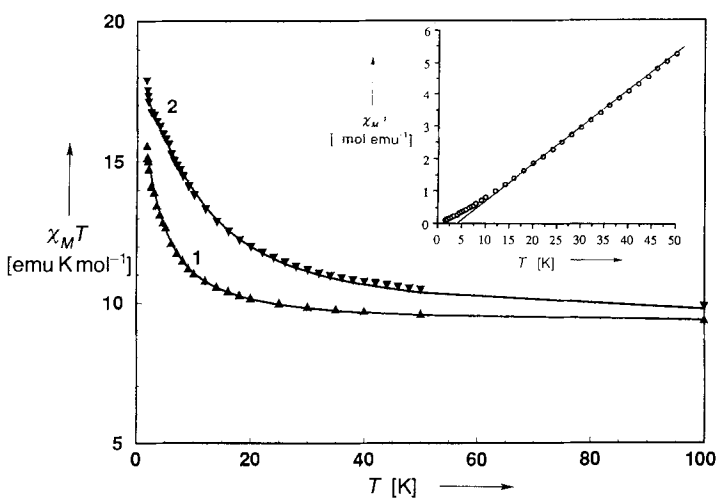


Fig. 3. Temperature-dependence of the product of the molar susceptibility and temperature for **1** and **2**. The inset represents the thermal variation of χ_M^{-1} for **2** and gives a Curie–Weiss temperature of 3.6 K.

is the signature of intramolecular ferromagnetic interactions within the dimeric manganese(II) units. At very low temperatures $\chi_M T$ exceeds the value predicted ($\chi_M T = 15$) for an $S = 5$ ferromagnetic ground state, reflecting the influence of intermolecular ferromagnetic correlations between neighboring Mn^{II} dimers which are more significant in **2** than in **1**. Specific heat capacities were determined in the temperature range 1.1–20 K, in zero magnetic field (Fig. 4). A minimum of C_p is observed around 2 K, whose width and height differ for both compounds, followed by a noticeable increase at higher temperature which is mainly related to the lattice contribution. At very low temperature (ca. 1 K), the divergence of C_p is probably due to the onset of a long-range magnetic ordering.

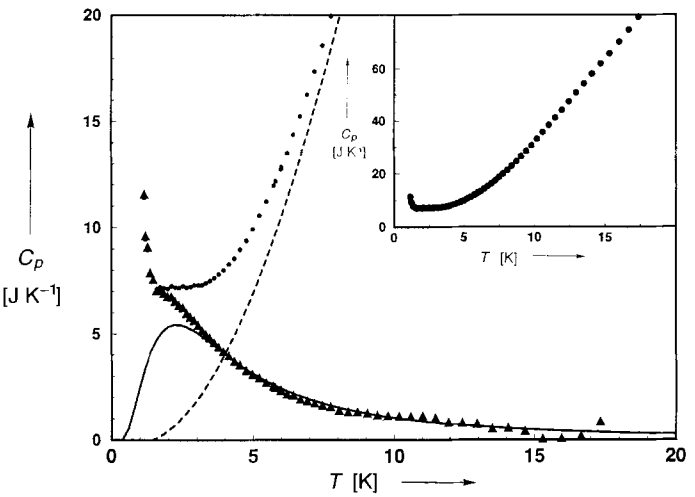


Fig. 4. Temperature-dependence of the specific heat C_p (exp., •), the lattice contribution (calcd. – – –), and the magnetic contribution (calcd. —); ▲ is the difference between the experimental values and the lattice contribution. The inset shows the variation of C_p in the 1.1–17.4 K range.

The magnetic properties of both compounds can be analyzed by considering the isotropic model of $S = 5/2$ dimeric units, described by the Hamiltonian (a). The influence of the interac-

$$\hat{H} = -J\,\hat{S}_1\,\hat{S}_2 - g\mu_B\hat{H}\,(S_1^z + S_2^z) \qquad \text{(a)}$$

tions between the dimers is taken into account through a molecular field contribution θ within the expression[6] of χ_M. In addition, the diamagnetic contribution is estimated from Pascal's values (-680×10^{-6} for **1** and -800×10^{-6} for **2**). Such a model leads to very good fits of the experimental values of $\chi_M T$ (Fig. 3). The calculated values for the intra-(J) and intermolecular(θ) ferromagnetic interactions (expressed in K) are +0.74, $+8.7\times10^{-3}$ for **1** and +2.25, +0.19 for **2**, respectively. In both cases g has a value of 2.04. Using the above results, the magnetic contribution to the specific heat, namely the Schottky-type anomaly[6] can be readily deduced. A maximum of C_p is predicted at 2.2 K for **1** and at 6.8 K for **2**. As displayed in Figure 4 for compound **1**, the theoretical curve agrees well with the experimental one deduced from raw data by substraction of the lattice contribution, approximated to be 0.024 T^3.

An intramolecular ferromagnetic interaction between the Mn^{II} ions in these complexes was somewhat unexpected since dimeric Mn^{II} compounds bridged by phenoxy ligands are generally either paramagnetic or antiferromagnetic,[7] although one complex[8] shows weak ferromagnetism ($J = +0.2$ cm^{-1} or 0.29 K for comparison with our values). However, there ap-

pears to be no simple relation between the magnetism and observed Mn-O-Mn angles[4] which varied from 82.2 to 115.8°. This ferromagnetic effect in **1** and **2** may result from the distorted trigonal bipyramidal field about the Mn^{II} ions, an explanation offered to interpret similar behavior in phenoxy-bridged complexes[9] of Fe^{III} and Fe^{II}. However, although the Mn_2O_2 core geometries are very similar in **1** and **2**, the intramolecular ferromagnetic interaction is three times larger for the latter. Although small differences in stereochemical or electronic effects may be responsible, we suggest that the triple stack structure of the phenoxy ligands in **2** could offer further spin exchange through π-π interactions across the dimer. For **1**, in which only pairwise stacking of phenoxy ligands occurs, this effect may be smaller or indeed cause diminution of the overall ferromagnetism. Calculations will be necessary to clarify this point.

The intermolecular ferromagnetic effect can also be related to structural features. The π-π interaction between bipyridine ligands in the chains would appear to offer an important junction for the transmission of magnetic effects, possibly by a McConnell spin polarization mechanism. However, this interaction in **1** alone does not give rise to appreciable ferromagnetism. Hence the 20-fold increase in θ in **2** would appear to indicate that the interchain Br–Br contacts are crucial in greatly increasing the correlation length. The onset of a long-range ordering below 1 K indicated by the specific heat measurements may also result from this mechanism.

In conclusion the dimeric Mn^{II} compounds **1** and **2** form ferromagnetic chain structures in the crystalline state; however, additional interchain interactions appear to be needed to achieve significant ferromagnetic effects. The π-π stacking interactions responsible for the chain structure thus may only play a significant role in the magnetism by a further increase in the dimensionality of the overall structure.[3d] Although the effects in these systems are as yet modest, research is currently underway in which such magneto-structural features will be incorporated in the design of magnetic molecular materials.

Received: January 17, 1994
Revised: May 5, 1994 [Z 6624IE]
German version: *Angew. Chem.* **1994**, *106*, 1660

[1] For recent reviews see: a) *Molecular Magnetic Materials* (Eds.: D. Gatteschi, O. Kahn, J. S. Miller, F. Palacio, Kluwer, London, **1991**, *E198*; b) J. S. Miller, A. J. Epstein, W. M. Reiff, *Chem. Rev.* **1988**, *88*, 201–220; c) O. Kahn, Y. Pei, Y. Journaux in *Inorganic Materials* (Eds.: D. W. Bruce, D. O'Hare), Wiley, Chichester, **1992**, p. 59–114; d) C. Kollmar, O. Kahn, *Acc. Chem. Res.* **1993**, *26*, 259–262. e) J. S. Miller, A. J. Epstein, *Angew.* **1994**, *106*, 399–432; *Angew. Chem. Int. Ed. Engl.* **1994**, *33*, 385–415.

[2] Recent examples: a) P. Turek, K. Nozawa, D. Shiomi, K. Awaga, T. Inabe, Y. Maruyama, M. Kinoshita, *Chem. Phys. Lett.* **1991**, *180*, 327; b) M. Tamura, Y. Nakazawa, D. Shiomi, K. Nozawa, Y. Hosokoshi, M. Ishikawa, M. Takahashi, M. Konoshita, *ibid.* **1991**, *186*, 401; c) R. Chiarelli, A. Rassat, P. Rey, *J. Chem. Soc. Chem. Commun.* **1992**, 1081–1082; d) R. Chiarelli, M. A. Novak, A. Rassat, J. L. Tholence, *Nature* **1993**, *363*, 147; e) E. Hernàndez, M. Mas, E. Molins, C. Rovira, J. Veciana, *Angew. Chem.* **1993**, *105*, 919–921; *Angew. Chem. Int. Ed. Engl.* **1993**, *32*, 882–884.

[3] Recent examples: a) O. Kahn, Y. Pei, M. Verdaguer, J. P. Renard, J. Sletten, *J. Am. Chem. Soc.* **1988**, *110*, 782; b) K. Nakatani, P. Y. Carriat, Y. Journaux, O. Kahn, F. Lloret, J. P. Renard, Y. Pei, J. Sletten, M. Verdaguer, *ibid.* **1989**, *111*, 5739–5748; c) K. Nakatani, P. Bergerat, E. Codjovi, C. Mathonière, Y. Pei, O. Kahn, *Inorg. Chem.* **1991**, *30*, 3977; d) H. O. Stumpf, Y. Pei, O. Kahn, J. Sletten, J. P. Renard, *J. Am. Chem. Soc.* **1993**, *115*, 6738–6745.

[4] Recent examples: a) A. Caneschi, D. Gatteschi, R. Sessoli, P. Rey, *Acc. Chem. Res.* **1989**, *22*, 392; b) J. S. Miller, J. C. Calabrese, R. S. McLean, A. J. Epstein, *Adv. Mater.* **1992**, *4*, 498.

[5] Crystal data for **1**: $C_{44}H_{24}N_4Cl_{12}Mn_2$, $M = 1208.0$, yellow, triclinic $P\bar{1}$, $a = 14.055(5)$, $b = 14.519(5)$, $c = 12.473(4)$ Å, $\alpha = 92.23(2)$, $\beta = 110.79(2)$, $\gamma = 95.47(2)$, $V = 2361.5$ Å^3, $Z = 2$, $\rho_{calcd} = 1.699$, μ ($Cu_{K\alpha}$) = 33.755 cm^{-1}, 4921 reflections ($3° < \theta < 51°$, $\pm h + k + l$) were collected at -100 °C on a crystal of $0.26 \times 0.20 \times 0.09$ mm, empirical absorption correction were applied, 3950 reflections with $I > 3\sigma(I)$ were used in the refinements (full matrix) $R = 0.033$, $Rw = 0.049$, GOF = 1.10, final residual electron density = 0.32 e Å^{-3}. Crystal data for **2**: $C_{44}H_{24}N_4Br_{12}Mn_2$, $M = 1741.5$, yellow, monoclinic $P2_1/n$, $a = 13.910(4)$, $b = 20.590(6)$, $c = 17.412(5)$ Å, $\beta = 91.91(2)°$, $V = 4983.6$ Å^3, $Z = 4$, $\rho_{calcd} = 2.321$, μ ($Cu_{K\alpha}$) = 33.755 cm^{-1}, 6027 reflections ($3° < \theta < 52°$, $\pm h + k + l$) were collected at -100 °C on a crystal of $0.28 \times 0.24 \times 0.26$ mm, empirical absorption corrections were applied, 4385 reflections with $I > 3\sigma(I)$ were used in the refinements (full matrix) $R = 0.033$, $Rw = 0.051$, GOF = 1.112, final residual electron density = 0.23 eÅ^{-3}. Further details of the crystal structure investigations are available on request from the Director of the Cambridge Crystallographic Data Centre, 12 Union Road, GB-Cambridge CB 21EZ (UK), on quoting the full journal citation.

[6] The expressions of the susceptibility and specific heat are derived as follows: $\chi_M = N\mu_B^2 g^2 [K(T-\theta)]^{-1} A B^{-1}$ and $C_p = NKx^2[CZ^{-1} - D^2Z^{-2}]$ with $A = 55 + 30\,e^{5x} + 14\,e^{9x} + 5\,e^{12x} + e^{14x}$, $B = 11 + 9\,e^{5x} + 7\,e^{9x} + 5\,e^{14x} + 3\,e^{14x} + e^{15x}$, $C = 225e^{5x} + 567\,e^{9x} + 720\,e^{12x} + 588\,e^{14x} + 225\,e^{15x}$, $D = 45\,e^{5x} + 63\,e^{9x} + 75\,e^{12x} + 42\,e^{14x} + 15\,e^{15x}$, $x = -J[kT]^{-1}$, Z is the partition function.

[7] a) Y. Gultneh, A. Farooq, S. Liu, K. D. Karlin, J. Zubieta, *Inorg. Chem.* **1992**, *31*, 3607–3611; b) R. A. Barlett, J. J. Ellison, P. P. Power, S. C. Shoner, *ibid.* **1991**, *30*, 2888–2894; c) S.-B. Yu, C.-P. Wang, E. P. Day, R. H. Holm, *ibid.* **1991**, *30*, 4067–4074; d) R. A. Jones, S. U. Koschmieder, C. M. Nunn, *ibid.* **1988**, *27*, 4524–4526.

[8] L. Lambert, D. N. Hendrickson, *Inorg. Chem.* **1979**, *18*, 2683–2686; H.-R. Chang, S. K. Larsen, P. D. W. Boyd, C. G. Pierpont, D. N. Hendrickson, *J. Am. Chem. Soc.* **1988**, *110*, 4565–4576.

[9] S. Snyder, G. S. Patterson, A. J. Abrahamson, R. H. Holm, *J. Am. Chem. Soc.* **1989**, *111*, 5214–5223.

Preparation and Preliminary Characterization of a Covalently Pillared Zirconium Phosphate–Diphosphonate with Interlayer Microporosity**

Giulio Alberti,* Fabio Marmottini, Sonia Murcia-Mascarós, and Riccardo Vivani

The recent progress in the chemistry of the γ-M^{IV} phosphates (compounds which were for many years formulated as $M^{IV}(HPO_4)_2 \cdot 2H_2O$ and now as $M^{IV}PO_4(H_2PO_4) \cdot 2H_2O$[1] and our improved knowledge of the structures of γ-layers of these compounds[2] has renewed the interest in these materials. Many organic derivatives, prepared in topotactic reactions similar to those initially proposed by Yamanaka,[3] have recently been obtained and characterized.[4] Furthermore, our recent successful synthesis of a microporous pillared zirconium diphosphonate with layers of α-type[5] has stimulated our interest in the preparation of microporous γ-compounds.

We found that, whereas pillared compounds of the α-type can only be prepared by direct synthesis, the covalent pillaring for the γ-type can be achieved more readily by a topotactic reaction between γ-zirconium phosphate (γ-ZrP, **1**) and a suitable diphosphonic acid.[6] No appreciable porosity was found in the first pillared γ-compounds; however, it was immediately recognized that the lack of interlayer microporosity very probably had to be ascribed either to the short length of the diphosphonate groups employed, or to their excessive crowding in the interlayer region. Therefore, a longer rigid diphosphonate group, such as biphenyldiphosphonate, was chosen as the pillar and a systematic study of the gradual replacement of the origi-

[*] Prof. Dr. G. Alberti, Dr. F. Marmottini, Dr. S. Murcia-Mascarós, Dr. R. Vivani
Dipartimento di Chimica, Università di Perugia,
via Elce di Sotto 8, I-06123 Perugia (Italy)
Telefax: Int. code + (75)585 5566

[**] This work was supported by Ministero Università Ricerca Scientifica e Tecnologica (MURST).

nal $H_2PO_4^-$ ions was performed. The hope was to find some stable phases with a concentration of pillars sufficiently low for the creation of interlayer microporosity. Therefore, many samples with an increasing percentage of pillars were prepared from **1**, and characterized by chemical analysis[7] and X-ray powder diffraction.[8] The results obtained for a selected number of samples, **2a**–**2e**, are summarized in Table 1. The following gen-

Table 1. Experimental data for selected samples with the general formula $ZrPO_4(H_2PO_4)_{1-x}[C_{12}H_8(PO_2OH)_2]_{x/2}$ **2**.

Product	Volume [a] [mL]	Moles taken up [b] [%]	x	n [c]	d [d] [Å]	d [e] [Å]
2a	94	94	0.28	3.1	16.4	16.3
2b	113	96	0.33	3.4	16.4	16.4
2c	126	90	0.34	3.1	16.7	16.4
2d	156	81	0.39	2.5	16.7	16.4
2e	188	77	0.44	2.7	17.0	16.7

[a] Volume of the 0.005 M solution of the diphosphonic acid used in the topotactic reaction for 1 g of γ-ZrP **1**. [b] Percent of moles of diphosphonate groups in the initial solution taken up by 1 g of **1**. [c] Moles of water per mol of Zr in samples conditioned at 90% r.h. [d] Interlayer distance of samples conditioned at 90% r.h. [e] Interlayer distance of anhydrous samples at 200 °C.

eral trends were observed: 1) If the topotactic replacement is less than 50%, a large proportion of the diphosphonate ions initially present in the solution is taken up by the solid, while an equivalent number of $H_2PO_4^-$ groups is released into the solution; in this respect this topotactic reaction is similar to an anion-exchange process in which monovalent anions are exchanged, with very high selectivity, by bivalent anions [Eq. (a)]. In accordance

$$ZrPO_4(H_2PO_4)\cdot 2H_2O + x/2\ R(PO_2OH)_2^{2-} \rightleftarrows ZrPO_4(H_2PO_4)_{1-x}[R(PO_2OH)_2]_{x/2}\cdot nH_2O + x\ H_2PO_4^- \quad (a)$$

with this exchange reaction the expression "percentage of pillaring" is equivalent to "percentage of topotactic replacement of $H_2PO_4^-$ with diphosphonate groups"; the x values reported in Table 1 are related, by the factor 100, to these percentages.

2) The characteristic peak at 12.25 Å, corresponding to the interlayer distance of γ-$ZrPO_4(H_2PO_4)\cdot 2H_2O$[9], disappears completely for very low percentages of pillaring ($\leq$10%) with the introduction of the diphosphonate groups; correspondingly, a hydrated phase of composition $ZrPO_4(H_2PO_4)_{1-x}[R(PO_2OH)_2]_{x/2}\cdot nH_2O$, in which x ranges from less than 0.1 to 0.58, was formed (the interlayer distances of wet samples range between 17.0 and 18.0 Å).

The samples were conditioned at room temperature over a saturated $BaCl_2$ solution at about 90% relative humidity (r.h.) and the water content (nH_2O) was determined by dehydration at 200 °C. The stability of the pillared compounds to dehydration was then studied by determining the variation of their X-ray patterns at 200 °C. In the pillaring range 28–44% the interlayer distance was found not to change appreciably with dehydration. On the other hand, an increase in the intensity of a peak at 9.4 Å, characteristic of anhydrous **1**, together with a decrease in the intensity of the peak corresponding to the anhydrous pillared phase (16.0–16.3 Å), was found at pillaring percentages < 25%. In other words, when less than a quarter of the original $H_2PO_4^-$ ions are replaced, the pillared phase seems to be stable only in the presence of intercalated solvent; when the water is removed, a segregation into two immiscible solid phases (the anhydrous **1** and the anhydrous pillared phase) is observed. In contrast at pillaring percentages $\geq$ 25%, stable phases can be obtained even in the absence of interlayer water.

Thus, taking into account that the microporosity should increase with the dilution of the pillars, the maximum interlayer microporosity must be expected at the minimum concentration of pillars that assures the stability of the anhydrous phase, that is 25–28% pillaring. The determination of the volume of the micropores and the specific surface area of anhydrous samples at different pillaring percentages showed that their maximum (ca. 0.12 $cm^3 g^{-1}$ and ca. 320 $m^2 g^{-1}$, respectively) is obtained at the value expected (Fig. 1). Furthermore, the Horvath–Kawazoe[10] differential pore volume plot of sample **2a** (Fig. 2) showed a narrow micropore size distribution with an average diameter of 5.8 Å.[11]

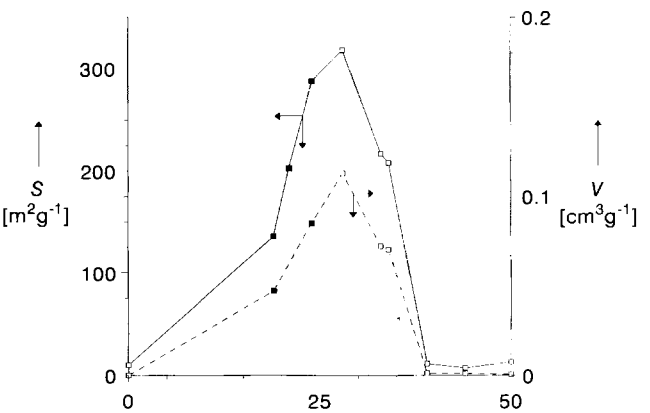


Fig. 1. Specific surface area S, and volume of the micropores V of anhydrous samples as a function of the pillaring percentages. □ and ■ refer to monophasic and biphasic systems, respectively.

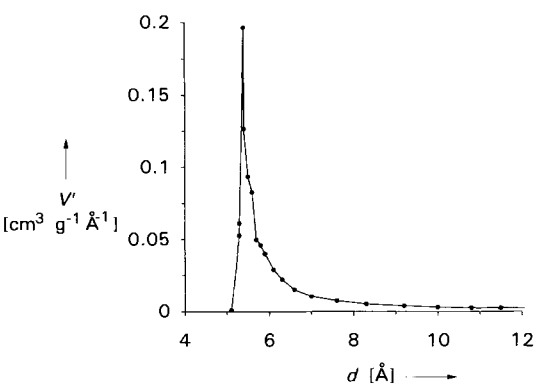


Fig. 2. Differential pore volume V' as a function of the pore diameter d of sample **2a**.

The thermal stability was determined by thermogravimetry and evolved gas analysis (EGA) as well as by X-ray powder diffraction with a high-temperature camera. The weight loss at temperatures lower than 200 °C was attributed to hydration water only. At temperatures higher than 220 °C, as confirmed by EGA, the organic pillars decompose even in inert atmosphere. In each case, the final product in air is cubic ZrP_2O_7 so that the total weight loss of the samples can be calculated from their initial composition. In general, the agreement between calculated and experimental values was good. As an example, the thermogravimetric curve of sample **2a** is shown in Figure 3. Unfortunately, the degree of crystallinity of sample **2a** was not sufficient for the unambiguous determination of the cell parameters. We therefore attempted to recrystallize this sample in a hydrothermal bomb at 215 °C for six days, but unambigu-

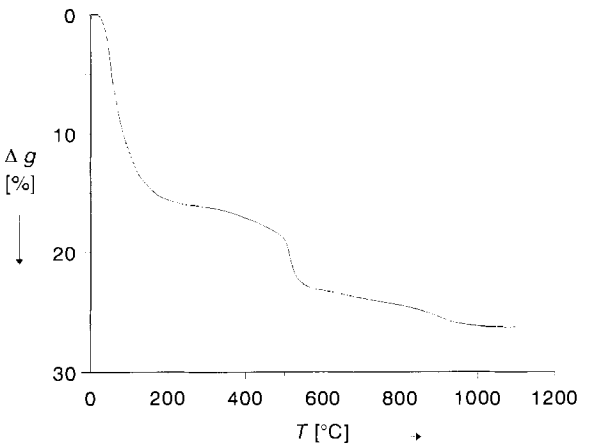


Fig. 3. Thermogravimetric curves (heating rate: 5 K min^{-1}; air flow) of sample **2a** (previously conditioned over a saturated $BaCl_2$ solution to 90% r.h.). The total weight loss Δg (25.9%) is in good agreement with the value expected from its composition (25.4%).

ous cell parameters were still not obtained. Thus, we tried to recrystallize a more thermally stable pillared derivative of **1** such as the previously described $ZrPO_4(H_2PO_4)_{0.06}[C_4H_8(PO_2OH)_2]_{0.47}\ 1.3H_2O$.[16] In this case, since it was possible to operate at 250 °C for six days, a considerable increase of the degree of crystallinity was achieved and the following cell parameters were obtained: orthorhombic, $a = 5.382$, $b = 6.625$, $c = 13.017$ Å. Since the a and b parameters were very similar to those of the original γ-ZrP ($a = 5.386$, $b = 6.636$ Å), it can be deduced that the inorganic backbone of the γ-layer remains practically unaltered; this is true not only after the replacement of the original $H_2PO_4^-$ with monophosphonate[4] but even after pillaring with diphosphonate groups.

Based on this result, some computer structural models were generated (Fig. 4). These models used: a) the original a and b parameters of the γ-layer, b) the regular distribution of pillars that have replaced up to 25% of the $H_2PO_4^-$ groups, c) the calculated length of the diphosphonate groups, and d) the interlayer distance of sample **2a** determined experimentally. The distance between adjacent pillars is in good agreement with the value derived from the surface analysis of the pores. Furthermore, all the X-ray reflections of sample **2a** can be indexed for a monoclinic unit cell which is similar to that derived from the model: $a = 10.750$, $b = 13.220$, $c = 16.723$ Å, $\beta = 98.451°$. Together with the microporous pillared compounds of α-type obtained recently,[5] the covalent pillaring of layered structures with organic groups presented here opens an alternative route for the preparation of new molecular sieves and/or "shape-selective" catalysts.

Experimental Procedure

2a–**2e**: In each experiment γ-$ZrPO_4(H_2PO_4)\cdot 2H_2O$ (1 g) (particle size: 0.5–10 μm) was treated, under shaking at 75 °C for four days, with different volumes (see Table 1) of a 0.005 M solution of 4,4'-biphenyldiphosphonic acid (**3**) in water acetone (1/1). The solids were separated by centrifugation and washed twice with water/acetone (75 mL).

1 and **3** were prepared as described in refs. [9] and [12], respectively. ^{31}P NMR (200 MHz, 50 mg of compound dissolved in 1 mL of 2 M HF in [D_6] DMSO, 25 °C): δ (**3**) = 19.5 (m, br. PCH(Ar)), δ (**1**) = 4.3 (s); the shifts are relative to D_3PO_4 in D_2O, external.

The surface analysis was carried out with the Micromeritics ASAP 2010 Micropore System, the EGA with a Stanton thermobalance coupled with a quadrupole mass Spectrometer (Thermolab-Fisons).

Received: November 12, 1993
Revised: March 18, 1994 [Z 6496IE]
German version: *Angew. Chem.* **1994**, *106*, 1655

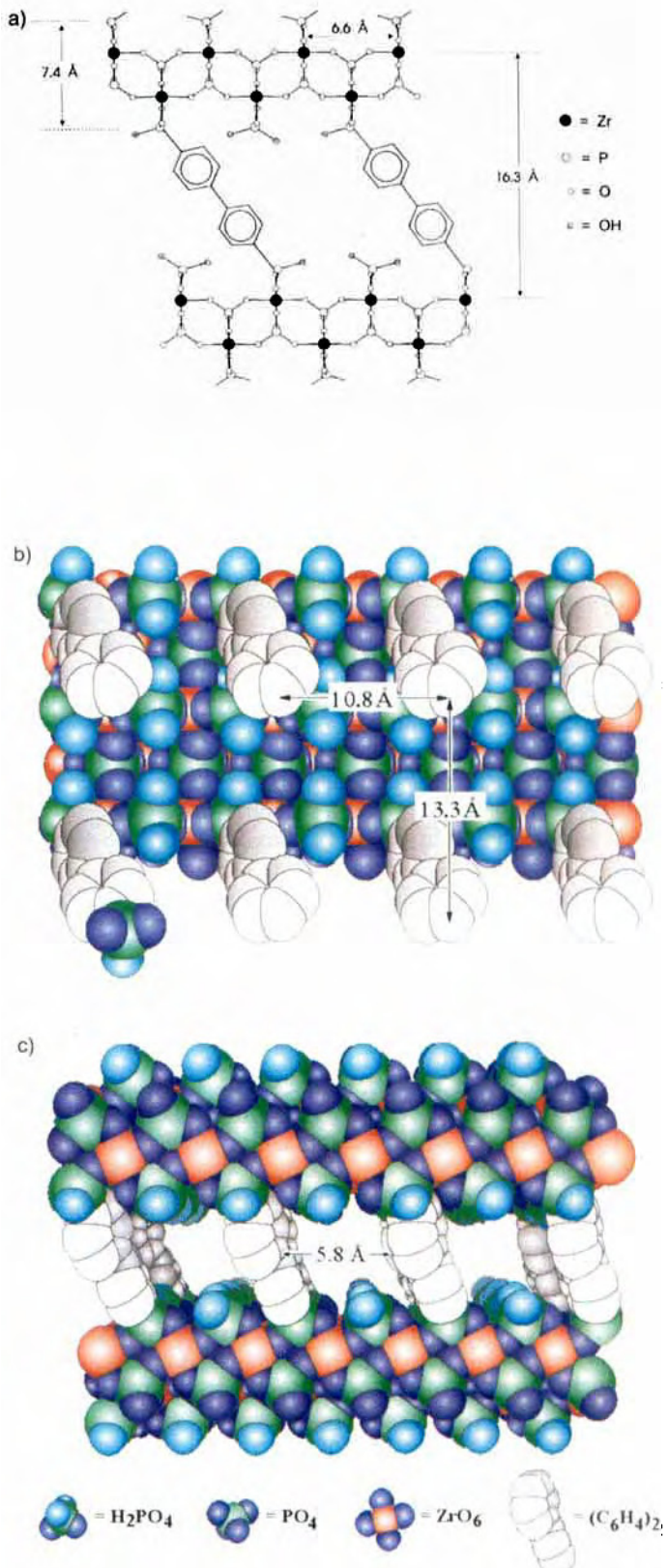


Fig. 4. Computer-generated models: a) Schematic representation of two γ-layers covalently pillared by 4,4'-biphenyldiphosphonate groups. The experimentally determined basal spacing of sample **2a** (16.3 Å) is consistent with that derived from this model if the diphosphonate groups are inserted between the layers with an angle of about 60°. b) View of a side of a γ-layer in which 25% of the $H_2PO_4^-$ groups have been replaced (regular distribution) by 4,4'-biphenyldiphosphonate groups. The majority of the O_2POH groups which belong to biphenyl groups are omitted for clarity. c) A lateral view of the pillared γ-compound of ideal composition $ZrPO_4^-(H_2PO_4)_{0.75}[R(PO_2OH)_2]_{0.125}$ showing intercolumnar free spaces.

 © VCH Verlagsgesellschaft mbH, D-69451 Weinheim, 1994 0570-0833/94/1515-1596 $ 10.00+.25/0

[1] A. Clearfield, R. H. Blessing, J. A. Stynes, *J. Inorg. Nucl. Chem.* **1968**, *30*, 2249; S. Yamanaka, M. Tanaka, *ibid.* **1979**, *41*, 45.
[2] N. J. Clayden, *J. Chem. Soc. Dalton Trans.* **1987**, 1877; A. Christensen, E. K. Andersen, I. G. K. Andersen, G. Alberti, N. Nielsen, M. S. Lehmann, *Acta Chem. Scand.* **1990**, *44*, 865.
[3] S. Yamanaka, *Inorg. Chem.* **1976**, *15*, 2811; S. Yamanaka, K. Sakamoto, M. Hattori, *J. Phys. Chem.* **1984**, *88*, 2067.
[4] G. Alberti, M. Casciola, R. K. Biswas, *Inorg. Chim. Acta* **1992**, *201*, 207; G. Alberti, U. Costantino, R. Vivani, R. K. Biswas, *React. Polym.* **1992**, *17*, 245; G. Alberti, R. Vivani, R. K. Biswas, S. Murcia-Mascarós, *ibid.* **1993**, *19*, 1; G. Alberti, M. Casciola, R. Vivani, R. K. Biswas, *Inorg. Chem.* **1993**, *32*, 4250.
[5] G. Alberti, U. Costantino, R. Vivani, P. Zappelli, *Angew. Chem.* **1993**, *105*, 1396; *Angew. Chem. Int. Ed. Engl.* **1993**, *32*, 1357.
[6] G. Alberti, S. Murcia-Mascarós, R. Vivani, *Mater. Chem. Phys.* **1993**, *35*, 187.
[7] Average values (NMR, elemental analysis) were used for the determination of the compositions as previously reported [6].
[8] The interlayer distances were derived from the first reflection in the X-ray powder diffraction patterns.
[9] G. Alberti, M. G. Bernasconi, M. Casciola, *React. Polym.* **1989**, *11*, 245.
[10] G. Horvath, K. Kawazoe, *J. Chem. Eng. Jpn.* **1983**, *16*, 470.
[11] Surface areas were investigated by BET analysis. The presence of mesopores was excluded by the reversibility of the adsorption isotherms. Information on the volume of the micropores was derived from both the t-plot and the Horvath–Kawazoe analysis; the samples were previously degassed at 10^{-5} Torr. Crystalline α-ZrP **1** was used as a nonporous reference material.
[12] G. Alberti, U. Costantino, R. Vivani, P. Zappelli, *Mat. Res. Soc. Symp. Proc.* **1991**, *233*, 95.

Molecular Recognition of C_{60} with γ-Cyclodextrin**

Zen-ichi Yoshida,* Hideko Takekuma, Shin-ichi Takekuma, and Yoshiharu Matsubara

Based on the superaromaticity concept we predicted that C_{60} was a soccerball-type molecule.[1a] Since C_{60} has been available on a preparative scale,[1b] one of our big concerns associated with biomimetic studies on enzymes[2, 3] has been the molecular recognition of C_{60} at active sites in the hydrophobic pocket of enzymes and the resulting biological functions.[4]

Very recently such an exciting example was reported for the inhibition of HIV-1 protease by C_{60} derivatives;[5] we were interested in the fundamental problem of how C_{60} interacts with the cylindrical hydrophobic cavity of γ-cyclodextrin (γ-CyD) in the complex formed on recognition of C_{60} by γ-CyD in water. Such a host–guest interaction is generally investigated in the equilibrium system in solution, in which, however, other complexes of different compositions can exist. To avoid this problem, the stable inclusion complex of defined composition should be studied. For this reason we have tried to prepare a stable C_{60}/γ-CyD complex; an unstable complex of nondefined composition has already been reported.[7] The preliminary examination of the complex formation in the two phase solution system (fullerenes in toluene, γ-CyD in water) demonstrated that, firstly, among α-, β- and γ-cyclodextrins only γ-CyD formed the complex and, secondly, γ-CyD recognized only C_{60} in the solution of C_{60} and C_{70}. The latter observation is particularly interesting because, judging from the cavity size of γ-CyD (9 Å circular opening) and the size of soccerball C_{60} (7 Å diameter) and rugbyball C_{70} (7 Å diameter at the equator, 8 Å between poles), γ-CyD can accommodate both C_{60} and C_{70}.

Here we report the first preparation of the stable, water-soluble C_{60}/γ-CyD (1:2) complex ("bicapped buckminsterfullerene") and the spectral investigation for elucidation of the molecular recognition of C_{60} by γ-CyD.

The synthesis of the stable complex (samples **A**, **B**, and **C**) (see Experimental[6, 7]) has the following features: 1) efficient formation of the complex by expelling C_{60} from toluene solution into the aqueous γ-CyD solution, utilizing the anomalously large solubility decrease of C_{60} in toluene at 118 °C,[8, 9] and 2) strengthening of the interaction between C_{60} and γ-CyD by dehydration of the hydrated complex by heating under vacuum. The obtained samples **A**, **B**, and **C** can be stored in crystalline form without decomposition. However, they differ in their stability in aqueous solution. At room temperature, sample **A** commences to eliminate C_{60} from the complex in solution after 10 h. On the other hand samples **B** and **C** are stable in aqueous solution at least for one and three days, respectively. These samples, and sample **C** in particular, can therefore be employed to investigate the molecular recognition of C_{60} with γ-CyD.

Although X-ray diffraction of the C_{60}/γ-CyD (1:2) complex ($[\alpha]_D^{20}$: +126° for sample **C**) has not yet been accomplished because of difficulty in growing single crystals for this purpose, a bicapped structure (Fig. 1) is deduced on the basis of the ^1H and ^{13}C NMR and elemental analyses.

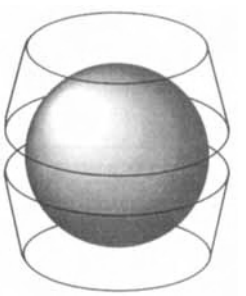


Fig. 1. Model of the C_{60}/γ-CyD (1:2) complex (bicapped buckminsterfullerene).

Evidence for molecular recognition is obtained from the CD spectra (Fig. 2) for the C_{60}/γ-CyD complex (samples **A**, **B**, and **C**) in aqueous solution (pH 6.8, 25 °C). Since C_{60} is chromophoric but achiral and γ-CyD is chiral but nonchromophoric, this indicates induction of chirality by the host (γ-CyD) in the guest (C_{60}). It is worth noting that increasing dehydration gives rise to more intense negative (in particular at 230 nm) and positive (in particular at 258 nm) CD bands which suggests increas-

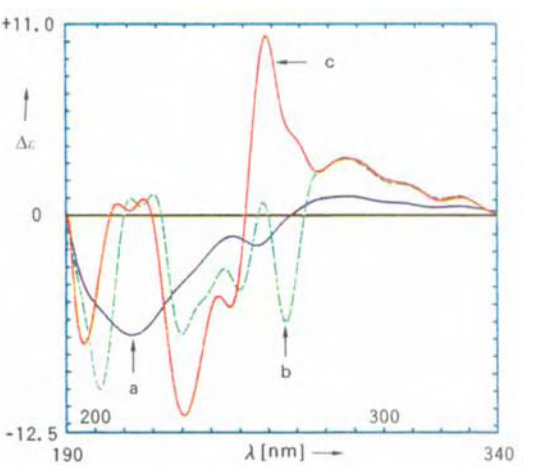


Fig. 2. CD spectra of the C_{60}/γ-CyD complex in aqueous solution at 25 °C (pH 6.8, concentration: 1.0 mg mL^{-1} each, length of the cell: 1 mm); a) sample **A** (without freeze-drying): λ_{max} [nm] = 212.4, 255.2, 287.4, 305.6, 326.2; b) sample **B** (after freeze-drying): λ_{max} [nm] = 201.4, 211.8, 219.6, 229.6, 238.4 sh, 249.8, 257.6, 265.8, 276.2 sh, 286.2, 307.6, 326.0; c) sample **C** (after freeze-drying and drying at 55 °C for 24 h): λ_{max} [nm] = 195.6, 207.0, 216.0, 230.5, 246.0, 257.9, 268.8 sh, 287.3, 307.6, 327.2.

[*] Prof. Dr. Z. Yoshida, H. Takekuma, Prof. Dr. S. Takekuma, Prof. Dr. Y. Matsubara
Department of Applied Chemistry, Faculty of Science and Engineering
Kinki University
3-4-1, Kowakae, Higashi-Osaka 577 (Japan)
Telefax: Int. code + (6) 727-4301

[**] This work was partially supported by the Ministry of Education, Science and Culture (Grant-in-Aids for Scientific Research No. 05453131).

ing interaction due to orbital steering between C_{60} and the functional groups (active sites -O- and OH) of γ-CyD as these become increasingly exposed.

This interaction (recognition) is elucidated by NMR spectroscopy. The chemical shifts of the ^1H NMR spectrum (500 MHz) and ^{13}C NMR spectrum (125 MHz) for γ-CyD and the C_{60}/γ-CyD complex (sample **C**) are shown in Tables 1 and 2,

Table 1. ^1H NMR (500 MHz, D_2O) chemical shifts δ for the protons of the glucose units in γ-CyD and C_{60}/γ-CyD [a] complex.

	δ						
	H-1	H-2	H-3	H-4	H-5	H-6a	H-6b
γ-CyD	5.155	3.698	3.980	3.631	3.907	3.915	3.910
C_{60}/γ-CyD	5.084	3.634	4.220	3.611	3.823	3.980	3.975
difference	−0.071	−0.064	+0.240	−0.020	−0.084	+0.065	+0.065

[a] Sample **C**. [b] $J(1,2) = 4.0$ Hz, $J(2,3) = J(3,4) = J(4,5) = 10.0$ Hz, $J(5,6a) = J(5,6b) = 3.0$ Hz, $J(6a,6b) = 15.0$ Hz, $J(4,6a) = J(4,6b) = 1.0$ Hz.

Table 2. ^{13}C NMR (125 MHz) chemical shifts δ for the C atoms in C_{60} and in the glucose unit of γ-CyD and C_{60}/γ-CyD [a] complex.

	δ						
	C_{60}	C-1	C-2	C-3	C-4	C-5	C-6
C_{60} [b]	143.23						
γ-CyD [c]		102.64	72.76	73.92	81.43	73.30	61.23
C_{60}/γ-CyD [c]	144.05	104.59	73.55	74.21	83.38	73.64	61.45
difference	+0.82	+1.95	+0.79	+0.29	+1.95	+0.34	+0.22

[a] Sample **C**. [b] In [D_6]benzene. [c] In D_2O.

respectively. From the substantially low-field shifts of $\delta = 0.24$ for C3-*H*,[10, 11] $\delta = 1.95$ for C1 and $\delta = 1.95$ for C4, we conclude that the specific interaction leading to chirality induction and the stability of the complex is the charge transfer from the n-donor (the hydroxy oxygen atom bound to C_3 and the ether oxygen between adjacent glucose units) to C_{60}, as shown in Figure 3. The reasons are following: 1) C_{60} does not behave as

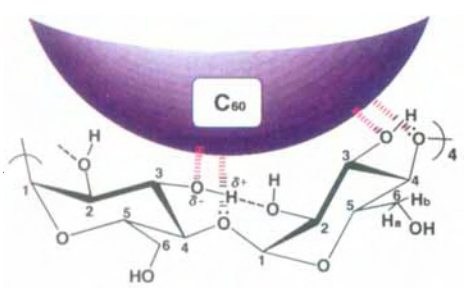


Fig. 3. Mode of interaction in the C_{60}/γ-CyD complex based on the HGS stereochemical molecular model (HGS = Hinomoto Gouseijushi Seisakujo) and X-ray crystal structure of γ-CyD and C_{60}.

a π base like benzene but as an extremely strong electron acceptor (electron affinity: 2.7 eV),[12, 13] and ether oxygen and alcoholic oxygen functions are known to serve as the n-donor in charge-transfer complex formation with iodine (electron affinity: 2.5 eV);[14] 2) intermolecular hydrogen bonding between OH groups and π-electron systems is not observed even for electronegative, substituted benzenes (like benzonitrile) and alkenes (like acrylonitrile);[15] 3) molecular models and X-ray structures of γ-CyD and C_{60} indicate that the ether oxygen atom and the strongly hydrogen-bonded oxygen atom at C3 (C3-OH···OH-C2) between adjacent glucose units are favorably situated for charge transfer to C_{60}.[16, 17] Since the characteristic NIR and ESR spectra[18, 19] of the anions of C_{60} were not observed, the amount of the charge transfer is considered to be smaller than one elementary charge.

The specific interaction due to such a charge transfer in addition to size and shape recognition between C_{60} and biological systems (for example, enzymes like HIV-1 protease where the active site is a carboxylate n-donor[5, 20]) should presumably be reflected in the specific biological functions of C_{60}.

Experimental Procedure

The mixture of two liquid phases consisting of a solution of γ-CyD (67 mg, 52 μmol) in water (10 mL) and a solution of C_{60} (or C_{60}/C_{70} mixture, 92/8) (20 mg) in toluene (10 mL) was refluxed at 118 °C for 30 h under vigorous magnetic stirring. After cooling to room temperature, the aqueous layer containing precipitated C_{60}/γ-CyD complex was centrifuged. The purple crystals were washed with cold water (10 mL) and dried in vacuo (sample **A**). The obtained crystals were dissolved in warm (50–60 °C) water (200 mL), and filtered to remove the insoluble materials (C_{60} eliminated from unstable complexes). The filtrate was freeze-dried to give 40 mg of stable C_{60}/γ-CyD complex (sample **B**, HPLC purity > 99.8%). These crystals were then recrystallized from water and dried at 55 °C for 24 h to provide the purple plates (sample **C**, the most stable complex). A similar result was obtained by using an efficient freeze-dry system (e.g. Labconco LL-6). Sample **C**: M.p. > 290 °C; $[\alpha]_D^{20}$: +126° (c = 0.1 in water) [compare $[\alpha]_D^{20}$ (γ-CyD): +177°, (c = 0.1 in water)]; UV/VIS (water): λ_{max} [nm] (log ε) = 214 (5.10), 231 sh (4.83), 260 (5.08), 332 (4.63), 408 (3.24), 493 sh (2.73), 536 (2.81), 574 sh (2.70), 601 (2.73), 629 sh (2.46); IR (KBr): $\tilde{\nu}$ [cm^{-1}] (bands that are not assigned to γ-CyD or C_{60}) = 1641, 1430 sh, 1410, 1369, 1335, 1101 sh, 1078, 1026, 937, 731, 581, 527; C, H analysis for $C_{156}H_{190}O_{95}$ ($C_{60} \cdot 2$ γ-CyD $\cdot 15$ H_2O): calcd. C, 52.26; H, 5.30; found: C, 52.23 H, 4.88. The 1:2 composition of C_{60} and γ-CyD was confirmed from the ratio of the areas of the corresponding ^{13}C NMR spectral peaks to C_{60} and γ-CyD (analytical mode: single pulse with heterogated decoupling without NOE). The ^1H and ^{13}C NMR spectral data of this complex suggest a symmetric structure for C_{60}/γ-CyD (1:2) complex (see Figure 1), because the signals for the two γ-CyD units were not split.

Received: March 17, 1994 [Z 6767 IE]
German version: *Angew. Chem.* **1994**, *106*, 1658

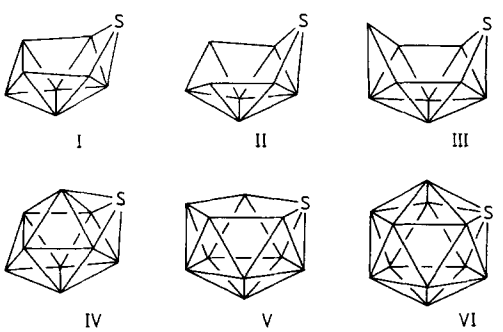
[1] a) Z. Yoshida, E. Osawa, *Aromaticity*, Kagakudojin, Kyoto, **1970**, p. 74 (in Japanese); b) W. Krätschmer, L. D. Lamb, K. Fostiropoulos, D. R. Huffman, *Nature (London)* **1990**, *347*, 354.
[2] a) Z. Yoshida, M. Kato, *J. Am. Chem. Soc.* **1954**, *76*, 311; b) *Nippon Kagaku Zasshi* **1954**, *75*, 109.
[3] Z. Yoshida, in *Biomimetic Chemistry* (Eds.: D. Dolphin, C. Mckenna, Y. Murakami, I. Tabushi), American Chemical Society, Washington, **1980**, p. 307.
[4] Recently we detected herbicide activity with C_{60}.
[5] S. H. Friedman, D. L. DeCamp, R. P. Sijbesma, G. Srdanov, F. Wudl, G. L. Kenyon, *J. Am. Chem. Soc.* **1993**, *115*, 6506.
[6] Our procedure of heating of an aqueous solution of sample **A** to obtain pure C_{60} as crystals is considered to be a better purification method for C_{60} from toluene extract of soots than the method proposed by Wennerström et al. [7].
[7] T. Andersson, K. Nilsson, M. Sundahl, G. Westman, O. Wennerström, *J. Chem. Soc. Chem. Commun.* **1992**, 604.
[8] R. S. Ruoff, R. Malhotra, D. L. Huestis, D. S. Tse, D. C. Lorents, *Nature (London)* **1993**, *362*, 140.
[9] Efficient complex formation is demonstrated by a color change (purple to colorless) of the toluene layer after refluxing.
[10] The low-field shift is not to the ring current of C_{60}; its value is negligible because the diamagnetic and paramagnetic ring currents cancel [11].
[11] R. C. Haddon, *Science* **1993**, *261*, 1545.
[12] Z. Yoshida, *Petrotech (Tokyo)* **1992**, *15*, 396.
[13] Z. Yoshida, I. Dogane, H. Ikehira, T. Endo, *Chem. Phys. Lett.* **1992**, *201*, 4816.
[14] P. A. D. de Maine, *J. Chem. Phys.* **1957**, *26*, 1192.
[15] a) Z. Yoshida, E. Osawa, *J. Phys. Chem.* **1964**, *68*, 2895; b) *J. Am. Chem. Soc.* **1965**, *37*, 1467; c) *Nippon Kagaku Zasshi* **1966**, *87*, 509; d) E. Osawa, T. Kato, Z. Yoshida, *J. Org. Chem.* **1967**, *32*, 2803; e) Z. Yoshida, N. Ishibe, H. Ozoe, *J. Am. Chem. Soc.* **1972**, *94*, 4948.
[16] The cyclodextrin macrocycle is stabilized by intramolecular hydrogen bonds O3–H···O2 between secondary OH groups of adjacent glucose units.
[17] a) K. Lindner, W. Saenger, *Biochem. Biophys. Res. Commun.* **1980**, *92*, 933; b) J. M. Maclennan, J. J. Stezowski, *ibid.* **1980**, *92*, 926; Review: c) W. Saenger, *Angew. Chem.* **1980**, *92*, 343. *Angew. Chem. Int. Ed. Engl.* **1980**, *19*, 344.

[18] a) T. Kato, T. Kodama, M. Oyama, S. Okazaki, T. Shida, T. Nakagawa, Y. Matsui, S. Suzuki, H. Shiromaru, K. Yamauchi, Y. Achiba, *Chem. Phys. Lett.* **1991**, *186*, 35; b) M. A. Greaney, S. M. Gorun, *J. Phys. Chem.* **1991**, *95*, 7142.
[19] D. R. Lawson, D. L. Feldheim, C. A. Foss, P. K. Dorhout, C. M. Elliot, *J. Electrochem. Soc.* **1992**, *139*, L68.
[20] M. V. Hosur, T. N. Bhat, D. J. Kempf, E. T. Baldwin, B. Liu, S. Gulnik, N. E. Wideburg, D. W. Norbeck, K. Appelt, J. W. Erickson, *J. Am. Chem. Soc.* **1994**, *116*, 847.

Macropolyhedral Boron-Containing Cluster Chemistry: Isolation and Characterization of the First Macropolyhedral Thiaborane, the *arachno*-Type $[9,9'\text{-}S_2B_{17}H_{18}]^-$ Ion**

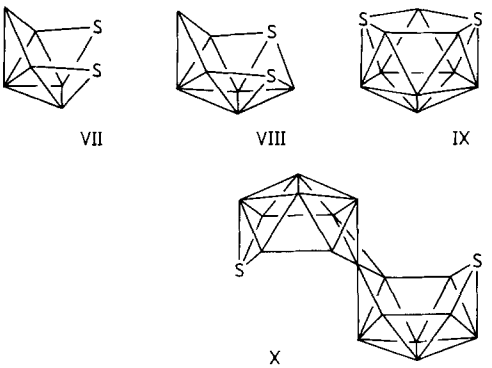
Tomáš Jelínek, John D. Kennedy,* Bohumil Štíbr, and Mark Thornton-Pett

The structural variety of polyhedral boron hydride chemistry is in principle also available to any combinations of main-group elements that have the same numbers of valence electrons. However, heteroborane chemistry, other than that of the carbaboranes,[1] is surprisingly limited. Apart from the carboboranes, the best-exemplified and most diverse main-group polyhedral heteroboranes are the thiaboranes. However, only seven basic contiguous monothiaborane building blocks are available (cluster geometries I–VI, Scheme 1).[2–19]



Scheme 1.

These comprise the nine-vertex *nido*[2] and *arachno*[3–6] $\{SB_8\}$ systems (I and II, respectively), the ten-vertex *closo* $\{SB_9\}$ system (IV),[3, 7–11] the ten-vertex *nido*[4, 11–14] and *arachno*[11, 14–17] $\{SB_9\}$ systems (both of gross geometry III), the eleven-vertex *nido* $\{SB_{10}\}$ system (V),[3, 12, 18] and the twelve-vertex *closo* $\{SB_{11}\}$ system (VI).[3, 10, 12, 19] In contrast to the very extensive known dicarbaborane chemistry,[1] only three dithiaborane building blocks (geometries VII–IX, Scheme 2) are known.[20–22] These comprise the eight-vertex *hypho* $\{S_2B_6\}$ system (VII),[20] the nine-vertex *arachno* $\{S_2B_7\}$ system (VIII),[20, 21] and the eleven-vertex *nido* $\{S_2B_9\}$ system (IX).[22]



Scheme 2.

There is current interest in large macromolecular units based on assemblies of heteroborane clusters with twelve vertices and fewer.[23] The individual clusters of reported assemblies are however generally linked together by a single two-electron two-center σ bond, or by a single common atom, generally of a metallic element. An alternative approach to large boron-based molecules is to use larger contiguous heteroborane building blocks that are based upon the fusion of smaller polyhedral clusters rather than upon clusters that are joined by single linkages. Here there is value in the discovery and delineation of new intercluster bonding modes that will facilitate the development of this new area of "macropolyhedral" heteroborane chemistry.

We now report our preliminary results on the isolation and characterization of the presently unique large nineteen-vertex macropolyhedral dithiaborane anion, $[S_2B_{17}H_{18}]^-$ (cluster connectivity as in X, Scheme 2). This is the first structurally characterized macropolyhedral heteroborane, and it also demonstrates for the first time a structure in which two *arachno*-type subclusters are fused to form a boron macropolyhedron. Previous macropolyhedral structures have been limited to fusions among *nido*- and *closo*-type clusters.

The $[S_2B_{17}H_{18}]^-$ ion, isolated in 48% yield as its $[PPh_4]^+$ salt, is obtained by the action of elemental sulfur on a solution of the *anti*-$[B_{18}H_{20}]^{2-}$ ion (formed from *anti*-$B_{18}H_{22}$ and NaH in THF),[24, 25] followed by chromatographic separation of the products. It was identified and characterized by X-ray diffraction analysis (Fig. 1) and NMR spectroscopy (Fig. 2). The principal other product is the known[3, 12, 18] *nido*-$[7\text{-}SB_{10}H_{11}]^-$ ion (45%), identified by NMR spectroscopy. The formation of the $[S_2B_{17}H_{18}]^-$ ion from the *anti*-$\{B_{18}\}$ skeleton involves a marked change in structure: incorporation of the two sulfur atoms is accompanied by loss of one boron center and there is an interesting reduction in the intimacy of the intercluster fusion. From two boron atoms held in common in $[B_{18}H_{20}]^{2-}$ there is a conversion to a somewhat more open structure that has one boron atom in common and has the interboron linkage B(8)–B(8′) (Scheme 3; open circles represent BH units).

The structure of this $[B_2B_{17}H_{18}]^-$ ion (Fig. 1) derives formally from the fusion, with two common vertices, between a ten-vertex *arachno* $\{SB_9\}$ cluster and an eleven-vertex *arachno* $\{SB_{10}\}$ cluster, although a useful alternative model consistent with the inherent twofold symmetry consists of two ten-vertex *arachno* $\{SB_9\}$ clusters fused with one common boron atom (B(9)) and with one additional intercluster link (B(8)–B(8′)). The *arachno* nature of the two $\{SB_9\}$ subclusters is readily apparent: a) the similarity of the NMR properties with those of the *arachno*

[*] Dr. J. D. Kennedy, Dr. M. Thornton-Pett
School of Chemistry of the University of Leeds
Leeds LS2 9JT (UK)
Telefax: Int. code + (532)336565
Dr. T. Jelínek, Dr. B. Štíbr
Institute of Inorganic Chemistry of the Academy of Sciences of the Czech Republic

[**] Contribution no. 44 from the Řež-Leeds Anglo-Czech Polyhedral Collaboration (ACPC). We thank the Royal Society (London), The Academy of Sciences of the Czech Republic (grant no. 43204), and Borax Research Ltd for support, and Dr. R. A. Walker and Dr. D. M. Wagnerová for helpful cooperation. The work by T. Jelínek was carried out in the Leeds laboratories during the tenure of a Royal Society Fellowship.

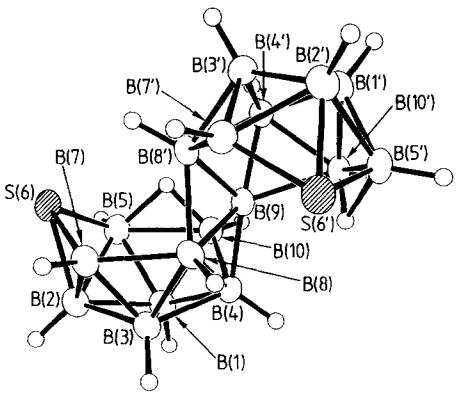


Fig. 1. Molecular structure (ORTEP) of the $[S_2B_{17}H_{18}]^-$ ion in $[PPh_4][S_2B_{17}H_{18}]$. In the solid state the anion approximates closely to the twofold rotational symmetry implicit in its liquid-state NMR properties. Selected interatomic distances: B(5)-S(6) 1.905(3), B(7)-S(6) 1.886(3), B(5')-S(6') 1.901(3), B(7')-S(6') 1.878(2), B(7)-B(8) 1.896(4), B(8)-B(9) 1.788(3), B(5)-B(10) 1.858(3), B(9)-B(10) 1.873(3), B(7')-B(8') 1.904(3), B(5')-B(10') 1.858(3) and B(9)-B(10') 1.873(3) Å. The dihedral angles B(9)B(4)B(2)S(6)/B(9)B(4')B(2')S(6') and B(5)B(7)B(8)B(10)/B(5')B(7')B(8')B(10') are 112.1(1) and 16.92(1)°, respectively, and the intercluster linkage B(8)-B(8') is 1.874(3) Å.

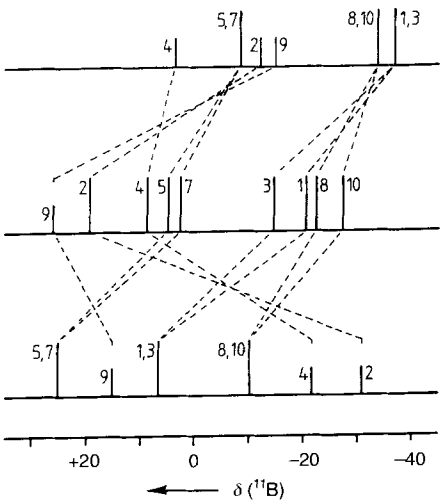
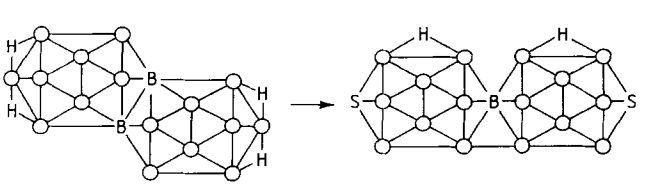


Fig. 2. Stick diagram of the chemical shifts and relative intensities in the ^{11}B NMR spectra of (top) the *arachno* $[6\text{-}SB_9H_{12}]^-$ ion [14], (center) the $[S_2B_{17}H_{18}]^-$ ion, and (bottom) *nido* $[6\text{-}SB_9H_{11}]$ [14]. Hatched lines join equivalent cluster positions in the three compounds. The B(9) position is that involved in the common vertex, and the B(2) position is antipodal to B(9). The typical *arachno* ten-vertex chemical-shift ordering [26, 27] is retained in $[S_2B_{17}H_{18}]^-$, although there is a general decrease in cluster shielding compared to the single-cluster *arachno* monoanion $[SB_9H_{12}]^-$. The typical *arachno* → *nido* inversion of shielding order [14, 26, 27], in particular the shift of $\delta(^{11}B(2))$ and $\delta(^{11}B(4))$ from low to extreme high field, is readily seen in the comparison with *nido*-SB_9H_{11}.

$\{SB_9\}$ cluster model of *arachno*-$[6\text{-}SB_9H_{12}]^-$ itself (Fig. 2) is confirmatory; in particular, the general NMR diagnostic ten-vertex *arachno* versus ten-vertex *nido* shielding characteristics,[26, 27] and also those specifically established for the $\{SB_9\}$ system,[14] are clearly *arachno*; b) the *arachno*-type bridging hydrogen atom at the (5,10) position is also diagnostic of ten-vertex *arachno* character; in particular, this position is occupied in preference to the (9,10) position that is specific to *nido*-type cluster behavior, both in single-cluster species[27] and in fused-cluster macropolyhedral species.[25] The similarities of the NMR spectra also suggest that the origin of the cluster bonding orbital associated with the (7,8) bridging hydrogen in *arachno*-$[6\text{-}SB_9H_{12}]^-$ is closely related to that involved in the (8,8') linkage in the $\{S_2B_{17}\}$ species, and that the overall ten-vertex $\{$*arachno*-$SB_9\}$ cluster electronic structure is thereby not drastically perturbed by the fusion. This is of interest because there was previously no precedent for how two *arachno*-type ten-vertex clusters might fuse, if at all.

The convenient preparation of the $[S_2B_{17}H_{18}]^-$ ion in reasonable yield provides an entry into the chemistry of macropolyhedral thiaboranes. Further work on these and related systems, as well as on the extension to macropolyhedral boron species containing heteroatoms other than sulfur, is in progress.[28]



Scheme 3.

Experimental Procedure

$[PPh_4][S_2B_{17}H_{18}]$: *anti*-$B_{18}H_{22}$ (300 mg; 1.36 mmol) and NaH (120 mg; 5.0 mmol) were stirred in THF (30 mL) for 2 h, filtered, and elemental sulfur (500 mg, 15.6 mg-atoms of S) added to the filtrate. The mixture was stirred at about 20 °C (4 h), then heated at reflux (8 h), cooled, and filtered. The yellow filtrate was evaporated to dryness, and extracted with CH_2Cl_2/aqueous HCl (1:3). The CH_2Cl_2 layer was separated and evaporated, and the resulting yellow viscous residue was dissolved in aqueous K_2CO_3 (95% solution, 30 mL). This solution was filtered, aqueous $[PPh_4]Cl$ (1 M; 10 mL) was added, and the resulting precipitate filtered off, washed with H_2O, and dried in vacuo. The precipitate was separated chromatographically [silica gel: CH_2Cl_2/C_6H_{14} (3:1)], yielding two main fractions. The first [R_f(anal.) 0.35 in CH_2Cl_2] was crystallized from CH_2Cl_2/hexane as yellow crystals and identified as $[PPh_4][S_2B_{17}H_{18}]$ (400 mg; 0.66 mmol; 48%), and the second [R_f(anal.) 0.23 in CH_2Cl_2] was identified as $[PPh_4]$[*nido*-7-$SB_{10}H_{11}$] (300 mg; 0.61 mmol; 45% by NMR spectroscopy) [25].

X-ray diffraction analysis: $[PPh_4][S_2B_{17}H_{18}]$, $M = 605.4$, triclinic, $a = 11.042(2)$, $b = 11.242(2)$, $c = 14.425(4)$ Å, $\alpha = 67.102(12)$, $\beta = 86.137(12)$, $\gamma = 81.521(12)°$, $V = 1631.4(5)$ Å^3, space group $P\bar{1}$ (no. 2), $Z = 2$, $\rho_{calcd} = 1.232$ g cm^{-3}, $\mu(Mo_{K\alpha}) = 0.231$ mm^{-1}, $F(000) = 628$. 8402 reflections (5744 were unique) were measured on a Stoe STAD14 diffractometer ($2\theta_{max} = 50°$) using ω-θ scans and on-line profile fitting. The structure was solved by direct methods [SHELXS-86] and refined on F^2 using all 5744 independent reflections [SHELXL-93] with anisotropic displacement parameters for non-hydrogen atoms, freely refined borane H atoms and constrained phenyl H atoms. $wR_2 = [\Sigma w(F_o^2 - F_c^2)/\Sigma F_o^2]^{1/2} = 0.1161$, $R_1 = \Sigma \| F_o| - |F_c\| / \Sigma F_o = 0.0404$ [on 5141 F values with $F_o^2 > 2.0\sigma(F_o^2)$], goodness of fit on $F^2 = 1.047$ on 477 parameters. Further details of the crystal structure investigation are available on request from the Director of the Cambridge Crystallographic Data Centre, 12 Union Road, GB-Cambridge, CB2 1EZ (UK), on quoting the full journal citation.

NMR spectra: ^1H and ^{11}B NMR data for $[PPh_4][S_2B_{17}H_{18}]$ in $(CD_3)_2CO$, 294 303 K; $\delta(^{11}B)$ [approximate coupling constant $^1J(^{11}B\text{-}^1H)$ [Hz] in square brackets] $\delta(^1H)$: BH(1) −20.5 [145] +1.83, BH(2) +19.3 [157] +4.34, BH(3) −14.7 [170] +1.86, BH(4) +8.6 [145] +3.56, BH(5) +4.9 [154 (coupling to μ-H not resolved, <ca. 10 Hz] +3.20, BH(7) +2.6 [145] +2.84, BH(8) −22.4 [137] −0.52, B(9) +26.2, BH(10) −27.2 [147/44] +1.34; assignments by $[^{11}B\text{-}^{11}B]$-COSY and $^1H\{^{11}B\}$ NMR experiments; there is a minor uncertainty among the 2, 3, and 7 positions due to weak COSY cross-peaks; $\delta(\mu\text{-}H)(5,10) - 0.64$; $\delta(^1H)[PPh_4]^+$ between +7.4 and +8.2 (400 MHz). ^1H and ^{11}B NMR data for $[PPh_4][SB_{10}H_{11}]$, measured and ordered as above: BH(1) −36.3 [143] +1.02, BH(2,3) −17.9 [J obscured] +1.60, BH(4,6) −5.8 [148] +2.18, BH(5) −17.1 [J obscured] +1.38, BH(8,11) −11.9 [140] +1.76, BH(9,10) −17.3 [J obscured] +1.28; $\delta(\mu\text{-}H)$ (9,10) − 3.95; $\delta(^1H)[PPh_4]^+$ between +7.4 and +8.2 (400 MHz).

Received: December 11, 1993 [Z 6556 IE]
German version: *Angew. Chem.* **1994**, *106*, 1663

[1] See for example B. Štíbr, *Chem. Rev.* **1992**, *92*, 225–250, and references therein.; A. K. Saxena, N. S. Hosmane, *ibid.* **1993**, *93*, 1081–1124, and references therein.
[2] J. Holub, J. D. Kennedy, B. Štíbr, *Collect. Czech. Chem. Commun.*, **1994**, *59*, 367–373.
[3] W. R. Pretzer, R. W. Rudolph, *J. Am. Chem. Soc.* **1976**, *98*, 1441–1447.
[4] K. Baše, S. Heřmánek, V. Gregor, *Chem. Ind. (London)* **1979**, 743–744.
[5] K. Baše, X. L. R. Fontaine, N. N. Greenwood, J. H. Jones, J. D. Kennedy, B. Štíbr, M. G. H. Wallbridge, *Polyhedron* **1989**, *8*, 2089–2090.

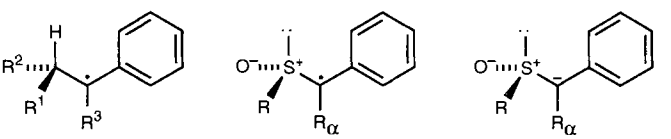
[6] J. Holub, J. D. Kennedy, B. Štíbr, M. Thornton-Pett, T. Jelinek, *Inorg. Chem.*, **1994**, in press.
[7] W. R. Pretzer, R. W. Rudolph, *J. Am. Chem. Soc.* **1973**, *95*, 931–932.
[8] W. L. Smith, B. J. Meneghelli, N. McClure, R. W. Rudolph, *J. Am. Chem. Soc.* **1976**, *98*, 624–626.
[9] W. L. Smith, B. J. Meneghelli, D. A. Thompson, P. Klymko, N. McClure, M. Bower, R. W. Rudolph, *Inorg. Chem.* **1977**, *16*, 3008–3012.
[10] S. Heřmánek, D. Hnyk, Z. Havlas, *J. Chem. Soc. Chem. Commun.* **1989**, 1859–1861.
[11] R. W. Rudolph, W. R. Pretzer, *Inorg. Synth.* **1983**, *22*, 226–231.
[12] W. R. Hertler, F. Klanberg, E. L. Muetterties, *Inorg. Chem.* **1967**, *6*, 1696–1706.
[13] B. J. Meneghelli, M. Bower, N. Canter, R. W. Rudolph, *Organometallics* **1983**, *2*, 569–570.
[14] M. Bown, X. L. R. Fontaine, J. D. Kennedy, *J. Chem. Soc. Dalton Trans.* **1988**, 1467–1473.
[15] A. R. Siedle, G. M. Bodner, A. R. Garber, L. J. Todd, *Inorg. Chem.* **1974**, *13*, 1756–1760.
[16] L. J. Guggenberger, *J. Organomet. Chem.* **1974**, *81*, 271–280.
[17] K. Nestor, X. L. R. Fontaine, N. N. Greenwood, J. D. Kennedy, M. Thornton-Pett, *J. Chem. Soc. Dalton Trans.* **1991**, 2657–2667.
[18] D. A. Thompson, W. R. Pretzer, R. W. Rudolph, *Inorg. Chem.* **1976**, *15*, 2948–2950.
[19] J. Plešek, S. Heřmánek, *J. Chem. Soc. Chem. Commun.* **1975**, 127–128.
[20] S. O. Kang, L. G. Sneddon, *J. Am. Chem. Soc.* **1989**, *111*, 3281–3289.
[21] J. Plešek, S. Heřmánek, Z. Janoušek, *Collect. Czech. Chem. Commun.* **1977**, *42*, 785–792.
[22] G. D. Friesen, A. Barriola, P. Daluga, P. Ragatz, J. C. Huffman, L. J. Todd, *Inorg. Chem.* **1980**, *19*, 458–462.
[23] R. N. Grimes, *Angew. Chem.* **1993**, *105*, 1350–1352; *Angew. Chem. Int. Ed. Engl.* **1993**, *32*, 1289–1290; I. T. Chizhevsky, S. E. Johnson, C. B. Knobler, F. A. Gomez, M. F. Hawthorne, *J. Am. Chem. Soc.* **1993**, *115*, 6981–6982; W. Clegg, W. R. Gill, J. A. H. MacBride, K. Wade, *Angew. Chem.* **1993**, *105*, 1402–1404; *Angew. Chem. Int. Ed. Engl.* **1993**, *32*, 1328–1329; W. Siebert, *Pure Appl. Chem.* **1987**, *59*, 947–954; R. N. Grimes, *Chem. Rev.* **1992**, *92*, 251–268; X. Meng, M. Sabat, R. N. Grimes, *J. Am. Chem. Soc.* **1993**, *115*, 6143–6151.
[24] *anti*-$B_{18}H_{22}$ is also known by the trivial name of *n*-$B_{18}H_{22}$; its formal name is *nido*-decaborano-(6′,7′:5,6)-*nido*-decaborane [25]. Its isomer *syn*-$B_{18}H_{22}$, known by the trivial name of *iso*-$B_{18}H_{22}$, is *nido*-decaborano-(5′,6′:5,6)-*nido*-decaborane; this latter species is enantiomeric, the second enantiomer being formally *nido*-decaborano-(6′,7′:6,7)-*nido*-decaborane.
[25] X. L. R. Fontaine, N. N. Greenwood, J. D. Kennedy, P. MacKinnon, *J. Chem. Soc. Dalton Trans.* **1988**, 1785–1793.
[26] See for example J. D. Kennedy in *Multinuclear NMR* (Ed.: J. Mason), Plenum, London and New York, **1987**, p. 221–258, and references therein.
[27] See for example M. A. Beckett, J. D. Kennedy, *J. Chem. Soc. Chem. Commun.* **1983**, 575–576.
[28] Note added in proof (July 8, 1994): See now T. Jelínek, J. D. Kennedy, B. Štíbr, *J. Chem. Soc. Chem. Commun.* **1994**, 677–678 (for $NB_{11}H_{20}$) and 1415–1416 (for $S_2B_{16}H_{16}$).

Stereoselective Reactions of Sulfinylated Benzyl Radicals: Effects of Solvents and Lewis Acids**

Philippe Renaud,* Thierry Bourquard, Michèle Gerster, and Nadira Moufid

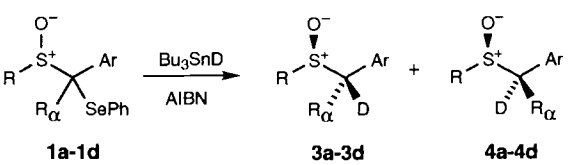
Dedicated to Professor M. Schlosser on the occasion of his 60th birthday

The control of the stereoselectivity in the reactions of acyclic radicals is presently a field of intensive research.[1] The 1,2-transfer of chirality has attracted a great deal of attention, and different models have been proposed to account for the observed diastereoselectivities. Substituted benzyl radicals of type **I** have been reported to react with good diastereoselectivity, and a model based on allylic 1,3-strain was proposed to explain the stereochemical outcome.[2] We are presently interested in using easily accessible and highly versatile sulfoxides for the control of 1,2-induction in reactions of acyclic radicals.[3, 4] We report here a study of sulfinylated radicals of type **II**, for which an unusual influence of the solvent on the diastereoselectivity was observed. Moreover, an exceptional degree of inversion of the stereoselectivity was obtained in the presence of bulky Lewis acids such as Yamamoto's methylaluminum diphenoxide derivatives. A comparison with the deuteration of deprotonated sulfoxides of type **III** is also presented.

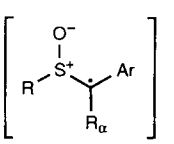


I **II** **III**

The radical precursors **1a–1d** have been prepared from the corresponding benzyl sulfoxides by selenenylation using LiHMDS/PhSeCl (HMDS = hexamethyldisilazane). Radical deuteration of these compounds with Bu_3SnD/azobisisobutyronitrile (AIBN)[5] gave the corresponding α-deuterosulfoxides **3** and **4** (for the definition of the substituents see Table 1).



1a-1d **3a-3d** **4a-4d**



2a-2d

The influence of the solvent is summarized in Table 1. With the exception of **1d** (entry 12) low to medium stereoselectivities were observed in CH_2Cl_2 (entries 1,7, and 9). A pronounced increase of the diastereoselectivity in favor of compound **3** was observed by running the deuteration in benzene (entries 2, 8, 10,

Table 1. Effect of solvent on the deuteration of **1a–1d** [5].

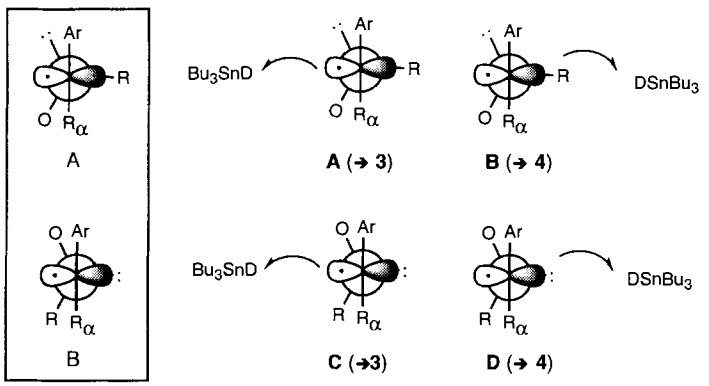
Entry	Cmpd.	R	R_α	Ar	Solvent	Yield [%]	3:4
1	**1a**	Ph	H	Ph	CH_2Cl_2	87	66:34
2	**1a**	Ph	H	Ph	C_6H_6	93	82:18
3	**1a**	Ph	H	Ph	THF	51	82:18
4	**1a**	Ph	H	Ph	mesitylene	66	85:15
5	**1a**	Ph	H	Ph	CH_3CH_2CN	58	69:31
6	**1a**	Ph	H	Ph	CF_3CH_2OH	79	35:65
7	**1b**	Me	H	Ph	CH_2Cl_2	59	50:50
8	**1b**	Me	H	Ph	C_6H_6	74	77:23
9	**1c**	Ph	H	2,6-$Cl_2C_6H_3$	CH_2Cl_2	75	59:41
10	**1c**	Ph	H	2,6-$Cl_2C_6H_3$	C_6H_6	92	86:14
11	**1c**	Ph	H	2,6-$Cl_2C_6H_3$	THF	95	72:28
12	**1d**	Ph	Me	Ph	CH_2Cl_2	59	93:7
13	**1d**	Ph	Me	Ph	C_6H_6	67	96:4

[*] Prof. P. Renaud, T. Bourquard, M. Gerster, Dr. N. Moufid
Université de Fribourg
Institut de Chimie Organique
Pérolles, CH-1700 Fribourg (Switzerland)
Telefax: Int. code + (37)82 64 72

[**] This work was supported by Swiss National Science Foundation (project no. 20-30'891.91 and project CHiral2 no. 21-36750.92). P. R. thanks also the Stiftung für Stipendien auf dem Gebiete der Chemie for the Alfred Werner stipend. T. B. is very grateful to the Stipendienfonds der Chemischen Industrie Basel for funding. We thank Dr. P.-A. Carrupt (Ecole de Pharmacie, Lausanne) for performing the calculations.

and 13) or THF (entries 3 and 11). For compound **1a**, the highest selectivity (entry 4, **3a**:**4a** 85:15) was obtained in mesitylene, which demonstrates that the steric bulk of the aromatic solvent is an important factor. Interestingly, we observed a partial inversion of stereoselectivity for **1a** in 2,2,2-trifluoroethanol (entry 6, **3a**:**4a** 35:65). Compound **1d** which possesses a methyl substituent in α-position gave **3d** with diastereoselectivities of 93% *ds* in CH_2Cl_2 and 96% *ds* in benzene (entries 12 and 13, respectively).

All these results may be rationalized by considering the two calculated minimum energy conformations A and B of the radical type **2** (Scheme 1).[6, 7] In noncoordinating solvents such as



Scheme 1. Conformations A and B of the radical type **2**, and models **A**–**D** for possible approaches of Bu_3SnD.

CH_2Cl_2, both conformers of **2a** and **2b** have similar energies; thus, attack from either face leading to **3** and **4** is possible (models **A**–**D**). Radical **2c** exists almost exclusively in conformation A due to strong allylic 1,3-interactions caused by the presence of the *ortho*-chlorine atoms. The low selectivity in dichloromethane may be interpreted by attack of A from either face (models **A** and **B**). For the deuteration of **1d** (R_x = Me), the role of the methyl substituent may be explained by a destabilization of conformer B due to *gauche* interactions with the group R bound on the sulfur atom (1,2-allylic interactions); thus, the preferred pathway leads almost exclusively to **3** through the transition state depicted in model **A**.[8] The solvent effect may also be explained by looking at the different models. Aromatic solvents are known to complex efficiently sulfoxides at the sulfur atom *anti* to the S–O bond.[9] For both conformers A and B, this type of complexation results in a shielding of the face, leading to the minor diastereoisomer **4** (models **B** and **D**, respectively), and thus reactions leading to **3** according to model **A** and **C**, respectively, are favored. The effect of THF is certainly similar to that of benzene, as already demonstrated in cyclic systems. 2,2,2-Trifluoroethanol has an opposite effect because of hydrogen bonding with the oxygen atom.[10]

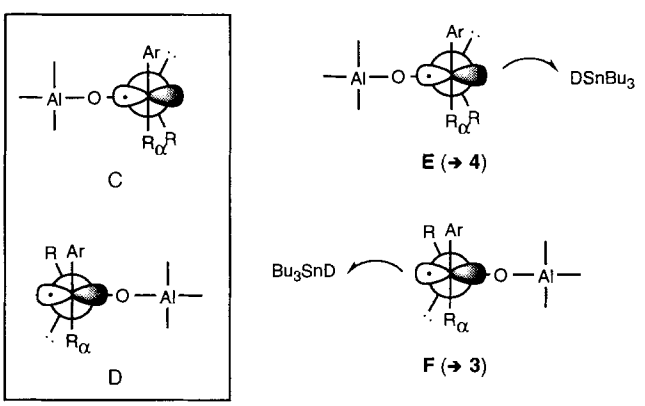
Next, we investigated the effect of Lewis acids[11] on the stereoselectivity of the deuteration of **1a**, **1b**, and **1d**. The results are summarized in Table 2. Lithium perchlorate and [Eu(dpm)$_3$] (dpm = 2,2,6,6-tetramethylheptane-3,5-dionato), which are very efficient for the control of the stereoselectivity in cyclic systems,[4d, 4e] reduced strongly the diastereoselectivity of the deuteration. However, the main isomer formed was still **3** (entries 1 and 2). With the very bulky and oxophilic methylaluminum di(2,6-di-*tert*-butyl-4-methylphenoxide) (MAD) and methylaluminum di(4-bromo-2,6-di-*tert*-butylphenoxide) (MABR),[12] an excellent selectivity (>97% *ds*, entries 3 and 5)

Table 2. Effect of Lewis acids on the deuteration of **1a**, **1b**, and **1d** (Ar = Ph) [5].

Entry	Cmpd.	R	R_x	Solvent	Lewis acid (equiv.)	Yield [%]	**3**:**4**
1	**1a**	Ph	H	CH_3CH_2CN	$LiClO_4$ (1.2)	51	58:42
2	**1a**	Ph	H	CH_2Cl_2	[Eu(dpm)$_3$] (1.1)	95	54:46
3	**1a**	Ph	H	CH_2Cl_2	MAD (1.1)	85	2.5:97.5
4	**1a**	Ph	H	CH_2Cl_2	MAD (0.1)	89	62:38
5	**1a**	Ph	H	CH_2Cl_2	MABR (1.1)	84	<3:97
6	**1a**	Ph	H	CH_2Cl_2	MABR (0.1)	91	52:48
7	**1b**	Me	H	CH_2Cl_2	MAD (1.1)	77	4.3:95.7
8	**1d**	Ph	Me	C_6H_6	MAD (1.1)	86	42:58
9	**1d**	Ph	Me	CH_2Cl_2	MAD (1.1)	73	14:86

was obtained for **1a** with preferential formation of **4a**. Deuteration of **1b**, which was unselective in CH_2Cl_2 gave also preferentially **4b** with 95% *ds* (entry 7). The inversion was also observed with **1d** but to a lesser degree (entry 9, 86% *ds*). Unlike what we observed in cyclic systems,[4e] the effect of the Lewis acid is not catalytic. In the presence of 10 mol% of MAD or MABR, a nearly 1:1 mixture of isomers was formed (entries 4 and 6, respectively).

The effect of methylaluminum diphenoxides can be understood by considering two conformations C and D of the radical type **2** (Scheme 2). Conformation C corresponds to a minimum



Scheme 2. Conformations **C** and D of the radical type **2** complexed with MAD and MABR, and models **E** and **F** for possible approaches of Bu_3SnD.

1,3-allylic strain situation, where the $OAlR_3$ group plays the role of the largest substituent. Preferential attack of the radical *anti* to the bulky $OAlR_3$ group of the most stable conformer C gives **4** (model **E**). The lower selectivity observed for **1d** may be explained by destabilizing *gauche* interactions (1,2-allylic strain) caused by the presence of an α-methyl group in C; thus, the contribution of conformer D (model **F**) to the stereoselectivity becomes more important.

Finally, for comparison purposes, we carried out the ionic deuteration ($LiNiPr_2$/BuLi/D_2O, −78 °C) of benzyl phenyl sulfoxide and 2,6-dichlorobenzyl phenyl sulfoxide. These reactions yielded **3a**:**4a** (54:46) and **3c**:**4c** (> 98:2), respectively. The ionic deuteration of benzyl methyl sulfoxide has been reported previously and affords **3b**:**4b** as a 94:6 mixture of isomers.[13] Thus, the same diastereoisomer is preferentially formed for both ionic deuterations and radical deuterations without added Lewis acids. However, no inversion of the diastereoselection has ever been reported for the ionic deuteration.

In conclusion, we have demonstrated that sulfinylated benzyl radicals may be used for highly stereoselective reactions. The sense and the degree of stereoselectivity can be controlled by proper choice of the solvent and by the adjunction of Lewis acids. In the presence of the latter, the radical method is complementary to the ionic reaction. Our simple model for the stereoselectivity, which is based on conformational analysis of the radical intermediate, has good predicting power and will be further investigated by examining directly the possible transition states with computational techniques.

Received: March 18, 1994 [Z 6774IE]
German version: *Angew. Chem.* **1994**, *106*, 1680

[1] For recent reviews on this subject, see: N. A. Porter, B. Giese, D. P. Curran, *Acc. Chem. Res.* **1991**, *24*, 296–303; W. Smadja, *Synlett* **1994**, 1–26.

[2] a) B. Giese, M. Bulliard, H.-G. Zeitz, *Synlett* **1991**, 425–427; b) D. P. Curran, G. Thoma, *Tetrahedron Lett.* **1991**, *32*, 6307–6310; c) D. P. Curran, G. Thoma, *J. Am. Chem. Soc.* **1992**, *114*, 4436–4437.

[3] For 1,2-induction with sulfinylated radicals, see: a) Y.-M. Tsai, B.-W. Ke, C.-H. Lin, *Tetrahedron Lett.* **1990**, *31*, 6047–6050; b) A. L. J. Beckwith, R. Hersperger, J. M. White, *J. Chem. Soc. Chem. Commun.* **1991**, 1151–1152; c) B. B. Snider, B. Yu-Fong Wan, B. O. Buckman, B. M. Foxman, *J. Org. Chem.* **1991**, *56*, 328–334; d) A. De Mesmaeker, A. Waldner, P. Hoffmann, T. Mindt, *Synlett* **1993**, 871–874; e) P. Renaud, *Tetrahedron Lett.* **1990**, *31*, 4601–4604; f) P. Renaud, P.-A. Carrupt, M. Gerster, K. Schenk, *ibid.* **1994**, *35*, 1703–1706; g) P. Renaud, T. Bourquard, *ibid.* **1994**, *35*, 1707–1710.

[4] Cyclic sulfinylated radicals have been investigated: a) A. Waldner, A. De Mesmeaker, P. Hoffmann, T. Mindt, T. Winkler, *Synlett* **1991**, 101–104; b) T. Toru, Y. Watanabe, M. Tsusaka, Y. Ueno, *J. Am. Chem. Soc.* **1993**, *115*, 10464–10465; c) P. Renaud, *Helv. Chim. Acta* **1991**, *74*, 1305–1313; d) P. Renaud, M. Ribezzo, *J. Am. Chem. Soc.* **1991**, *113*, 7803–7804; e) P. Renaud, N. Moufid, L. H. Chen, D. P. Curran, *J. Org. Chem.* **1994**, *59*, 3547–3552.

[5] Typical procedure: A solution of the sulfoxide (2 mmol), Bu_3SnD (2.2 mmol), and AIBN (15 mg) in the indicated solvent was irradiated (sunlamp 300 W), in the presence of or without a Lewis acid, for 12 h at 10 °C. (δ) ^1H NMR: H_α: **3a** (3.96), **4a** (4.08); **3b** (3.90), **4b** (4.00); **3c** (4.35), **4c** (4.65); Me_α: **3d** (1.58), **4d** (1.70).

[6] The minimum energy conformations A and B have been deduced from semiempirical AM1 calculations for radical **2a**. Full details of these calculations will be published separately in due time. A strong analogy between the structure of the radicals and the one of vinyl sulfoxides has been found: S. D. Kahn, W. J. Hehre, *J. Am. Chem. Soc.* **1986**, *108*, 7399–7400.

[7] We assume in this discussion that transition states are reactant-like. Such approaches were very successful in numerous cases, see examples in refs. [1,2].

[8] A similar explanation was put forward by Hart et al. to explain the effect of the α-methyl group in the case of alkoxycarbonyl-substituted radicals: D. J. Hart, R. Krishnamurthy, *J. Org. Chem.* **1992**, *57*, 4457–4470.

[9] T. Ledaal, *Tetrahedron Lett.* **1968**, 1683–1688.

[10] A similar role of THF and trifluoroethanol in cyclic systems has already been reported in refs. [4a,4d,4e].

[11] Recently, Lewis acids have been used to control the stereoselectivity of radical reactions, see refs. [4a,4b,4d,4e] and: Y. Guindon, J. F. Lavallée, M. Llinas-Brunet, G. Horner, J. Rancourt, *J. Am. Chem. Soc.* **1991**, *113*, 9701–9702; K. S. Feldman, A. L. Romanelli, R. E. Ruckle, Jr., R. F. Miller, *ibid.* **1988**, *110*, 3300–3302; Y. Yamamoto, S. Onuki, M. Yumoto, N. Asao, *ibid.* **1994**, *116*, 421–422.

[12] K. Maruoka, T. Itoh, H. Yamamoto, *J. Am. Chem. Soc.* **1985**, *107*, 4573–4576; K. Ishihara, N. Hanaki, H. Yamamoto, *ibid.* **1991**, *113*, 7074–7075; K. Maruoka, T. Ooi, H. Yamamoto, *ibid.* **1990**, *112*, 9011–9013; K. Maruoka, A. B. Concepcion, N. Hirayama, H. Yamamoto, *ibid.* **1990**, *112*, 7422–7423; T. Hirukawa, T. Shudo, T. Kato, *J. Chem. Soc. Perkin Trans. 1* **1993**, 217–225.

[13] K. Nakamura, M. Higaki, S. Adachi, S. Oka, A. Ohno, *J. Org. Chem.* **1987**, *52*, 1414–1417.

Functionalization of Aromatic Azo Compounds by the Cobalt-Catalyzed, Regioselective Double Addition of Tolane: 2,6-Distilbenylazobenzenes and 2,3-Dihydrocinnolines**

Günther Halbritter, Falk Knoch, Alexander Wolski, and Horst Kisch*

Dedicated to Professor Borislav Bogdanović on the occasion of his 60th birthday

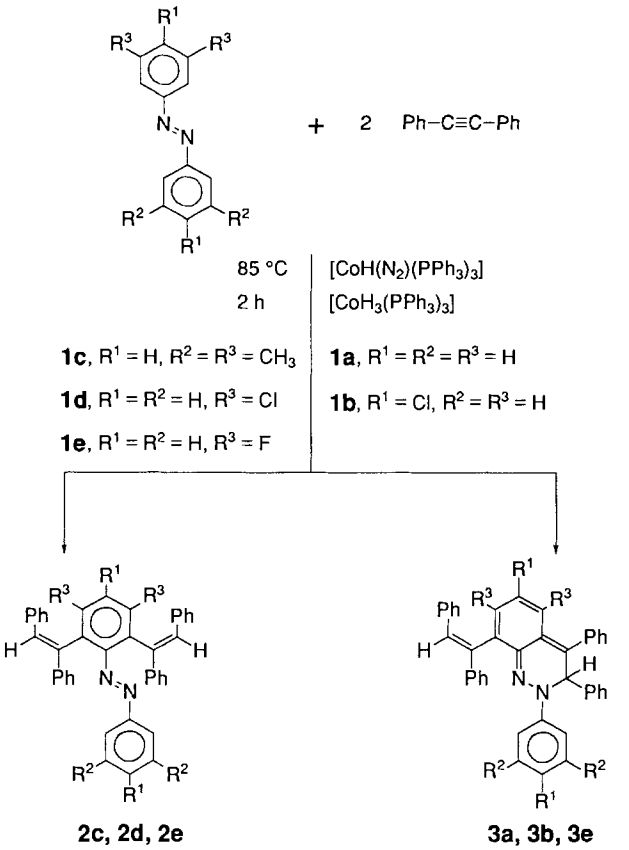
Easily accessible aromatic azo compounds can, as a rule, only be utilized in the synthesis of heterocycles if they are activated by transition metal carbonyls (M = Co, Ru). Thus, C–N coupling can be achieved with carbon monoxide,[1] alkynes,[2] amines, and alcohols.[3] A generally unwanted side reaction is the *ortho*-semidine rearrangement, which usually is accompanied by N=N cleavage, and which is also observed in the presence of iron carbonyls.[4] On the other hand, in the presence of $[CoClL_3]$ (L = PPh_3)[5] or $[Pd(pap)(CH_3CN)_2]^+$ (pap = *ortho*-(phenylazo)phenyl)[6] and tolane, *N*-arylaminoindole or 2-arylcinnolinium salts are formed in a stoichiometric reaction with retention of the N–N bond, as a result of a 1:1 addition. We have now found that, when $[CoH_3L_3]$ or $[CoH(N_2)L_3]$ is used, a catalytic, regioselective 2:1 addition of tolane takes place to give the previously unknown 2,6-di-(*trans*-stilbenyl)azobenzene derivatives and 2,3-dihydrocinnolines.

When $[CoH(N_2)(PPh_3)_3]$ or $[CoH_3(PPh_3)_3]$ is added to a molten mixture of diphenylacetylene (tolane) and azobenzene **1a** or its derivative **1b** at 85 °C, a vigorous evolution of gas and a red coloration occurs instantly. The products **3a** or **3b**, respectively, are obtained as red powders, which can be purified by column chromatography (Scheme 1).

The X-ray crystal structure analysis[7, 8] of **3b** indicated that an alkyne molecule had been inserted into each of the *ortho*-C–H bonds of one of the benzene rings, and that one of the so formed *trans*-stilbene groups was bonded to the N atom of the N=N bond attached to the other benzene ring, to form a previously unknown 2,3-dihydrocinnoline ring (Fig. 1).[9] The *ortho*-quinoid system is characterized by the alternating C–C bond lengths in the ring of approximately 135 and 143 pm and the short C10–N1 and C15–C1 distances of about 132 and 137 pm, respectively. The nitrogen atom N2 lies only 1.6 pm above the plane defined by the N1, C2, and C20 atoms. That this allows a conjugation of the quinoid system with the 4-chlorophenyl substituent is indicated by the shortened bonds between N1 and N2 (135 pm) and N2 and C20 (141 pm). In general, the aromatic character of the benzenoid ring of the dihydrocinnoline system remains intact. Accordingly, only the 1,2- and the more stable 1,4-dihydro derivatives have been previously described in the literature.[10] The few known examples, in which an *ortho*-quinoid system forms part of the cinnoline framework, 4-phenyl-4*H*-cyclopentacinnoline,[11] 3(2*H*)-cinnoline,[12] and a pyrrolo[1,2*b*]cinnoline derivative,[13] always have an sp^2 hybridized C atom in the 3-position, allowing the formation of planar systems which are stabilized by conjugation. However, in **3b** this atom is sp^3 hybridized.

[*] Prof. Dr. H. Kisch, Dipl.-Chem. G. Halbritter, Dr. F. Knoch, Dr. A. Wolski, Institut für Anorganische Chemie der Universität Erlangen-Nürnberg, Egerlandstrasse 1, D-91058 Erlangen (FRG)
Telefax: Int. code + (9131)857363

[**] Transition Metal Complexes of Diazenes, Part 32. This work was supported by the Volkswagen-Stiftung. Part 31: D. Garn, F. Knoch, H. Kisch, *J. Organomet. Chem.* **1993**, *444*, 155.



Scheme 1. Synthesis of 2,6-distilbenylazobenzenes **2** and 2,3-dihydrocinnolines **3**.

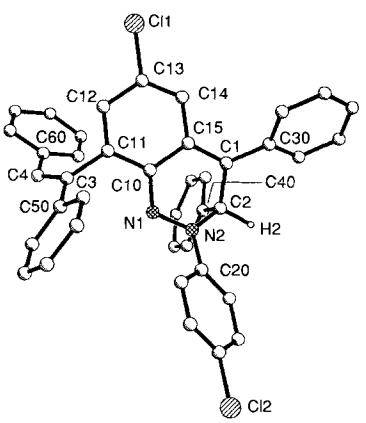


Fig. 1. Crystal structure of **3b**. With the exception of H2 the hydrogen atoms have been omitted for clarity. Selected distances [pm] and angles [°]: N1-N2 135.1(7), N2-C2 147.0(8), C2-C1 152.8(9), C1-C15 137.5(8), C15-C14 143.3(9), C14-C13 134.9(9), C13-C12 142.2(9), C12-C11 136.2(9), C11-C10 143.8(9), C10-N1 132.4(8), C20-N2 141.2(8); N2-C2-C1 104.3(5), C2-C1-C15 113.9(5), C1-C15-C14 125.1(5), C15-C14-C13 119.2(5), C14-C13-C12 124.7(6), C13-C12-C11 118.7(5), C12-C11-C10 119.9(5), C11-C10-N1 117.0(5), N2-N1-C10 115.7(5), N1-N2-C20 115.7(5), N1-N2-C2 120.0(4), C2-N2-C20 124.3(5), C1-C2-C40 114.5(5), N2-C2-C40 112.4(5).

When 3,5,3′,5′-tetramethylazobenzene (**1c**) is used as the azo component, the reaction mixture turns orange, and **2c** is obtained as an orange powder, which can be purified by extraction with ether. As can be seen from its crystal structure analysis,[14, 8] a regioselective insertion of an alkyne in each of the *ortho*-C–H bonds of one of the benzene rings has also taken place; however, without the simultaneous formation of a C–N bond (Fig. 2).[15] These products, the 2,6-di-(*trans*-stilbenyl)-azobenzene derivatives, are also not described in the literature. 3,5-Dichloroazobenzene (**1d**) similarly yields only the distilbenyl product **2d**, while **2e** and **3e** are both formed with 3,5-difluoroazobenzene (**1e**). Single-crystal X-ray structure analyses have been carried out for both compounds.[16, 8] In each case the yields are between 70 and 80%, the turnover number varies from 3–15 mmol product/mmol catalyst.

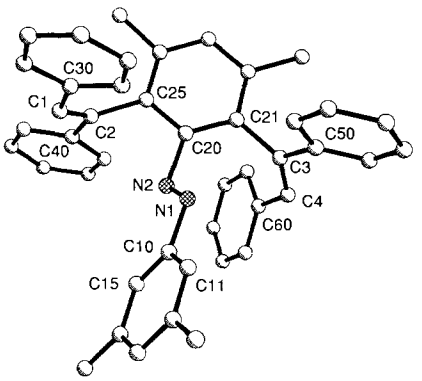


Fig. 2. Crystal structure of **2c**. The hydrogen atoms have been omitted for clarity. Selected distances [pm] and angles [°]: N1-N2 119.5(10), N2-C20 150.6(12), N1-C10 150.0(12), C1-C2 131.1(11), C1-C30 149.1(14), C2-C40 152.5(14), C3-C4 129.1(13), C3-C50 153.4(15), C4-C60 149.4(13), C2-C25 152.9(10; C21-C3 153.3(9); N2-C20-C21 124.4(6), N2-C20-C25 113.0(6), N1-N2-C20 107.9(7), N2-N1-C10 112.5(7), N1-C10-C15 123.7(8), N1-C10-C11 113.0(8), C3-C4-C60 128.8(7), C4-C3-C50 121.4(7), C21-C3-C50 116.7(8), C2-C1-C30 128.9(8), C1-C2-C40 121.2(7), C25-C2-C1 122.8(9).

We have assumed the following mechanism for the formation of distilbenylbenzenes **2**: Firstly the initial complex [CoH(ArN=NAr)L_3] is formed by the substitution of N_2 or H_2, respectively, in the catalyst precursor; the subsequent orthometalation to give the dihydrido complex presumably proceeds by a nucleophilic attack of the cobalt center, since both 3,5-dihalogenoazobenzenes **1d** and **1e** are attacked regioselectively at the substituted benzene nucleus,[17] as can be concluded from the structures of **2d** and **2e**. Insertion of the alkyne in a Co–H bond[18] yields a *trans*-stilbenyl ligand whose subsequent migration to the metalated C atom leads to the 2-(*trans*-stilbenyl)azobenzene complex. Renewed attack of the Co center on the stilbenylphenyl nucleus[19] and repetition of the above reaction steps yields a 2,6-di(*trans*-stilbenyl)azobenzene complex, which is transformed to the product **2** and the initial complex by the entrance of a new azo compound.

The 2,3-dihydrocinnolines **3** are formed in an uncatalyzed reaction starting from **2**, as the experiments with 3,5-difluoroazobenzene **1e** indicate [Eq. (a)]. When the mixture **2e**/**3e**, prepared by chromatographic work-up,[20] is irradiated in dichloromethane at −30 °C, an orange powder precipitates. The X-ray diffraction pattern of this material indicates the presence of only **2e**.[21] On warming to room temperature the solution turns red and, according to the UV/Vis spectrum, the mixture is again present. UV/Vis spectroscopy for **3a**, **3b**, and **3e** shows that a uniform reaction sequence occurs in this photochromic system because at 355, 375, and 346 nm, respectively, there is an isosbestic point. The *ortho*-quinoid system of **3e** has

$$\mathbf{2e} \underset{h\nu,\ -30\ ^\circ C}{\overset{\text{ca. } 20\ ^\circ C}{\rightleftharpoons}} \mathbf{3e} \qquad \text{(a)}$$

an intense band at 515 nm ($\varepsilon \approx 10000\ M^{-1}cm^{-1}$), while **2e** absorbs only weakly in this region (490 nm, $\varepsilon \approx 1000\ M^{-1}cm^{-1}$). The absence of ring closure in the case of the 3,5-disubstituted azobenzene derivatives **1c** and **1d** could be due to the greater spatial requirements of the substituents (R^3 = Me, Cl) in comparison to those of **1a** and **1b** (R^3 = H), which should make the formation of a planar transition state more difficult. Accordingly, only the 2,3-dihydrocinnoline derivative is formed from 3,3'-dimethylazobenzene.

Experimental Procedure

All operations were carried out under an atmosphere of nitrogen, and with anhydrous, N_2-saturated solvents.

General procedure: To a melt of two parts tolane and one part of the azo compound **1** at 85 °C was added, in portions, the appropriate amount of catalyst (in the case of **1a**, **1b**, and **1d** 0.25 equivalents, for **1c** 0.066 equivalents and for **1e** 0.33 equivalents). The mixture was then stirred for two hours at 85 °C. For **1a**, **1b**, and **1e**, the resultant material was dissolved in CH_2Cl_2, alumina added, and the mixture evaporated to dryness. The resulting powder was chromatographed on alumina (neutral, activity I, ICN) with petroleum ether/THF 10/1 (v/v). For **1c**, the reaction mixture was stirred with petroleum ether and the remaining solid extracted with ether in a Soxhlet extractor. For **1d**, dissolution in CH_2Cl_2, filtration through alumina, and evaporation to dryness gave a solid which was dissolved in a minimum amount of CH_2Cl_2 and overlayered with twice the volume of methanol to precipitate the product.

All compounds gave correct C,H,N analyses and the corresponding molecular ion peaks in their mass spectra (EI, 70eV).

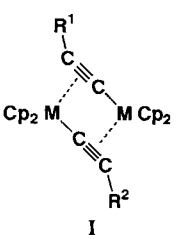
Received: February 24, 1994 [Z 6709 IE]
German version: *Angew. Chem.* **1994**, *106*, 1676

[1] a) S. Horiie, S. Murahashi, *J. Am. Chem. Soc.* **1956**, *78*, 4816; b) *Bull. Chem. Soc. Jpn.* **1960**, *33*, 88; c) T. Ioh, N. Hagihara, S. Murahashi, ibid. **1967**, *40*, 661.
[2] M. I. Bruce, B. L. Goodall, F. G. A. Stone, *J. Chem. Soc. Dalton Trans.* **1975**, 1651.
[3] a) A. Spencer, *J. Organomet. Chem.* **1985**, *294*, 357; b) *ibid.* **1985**, *295*, 199.
[4] a) M. I. Bruce, B. L. Goodall in *The Chemistry of the Hydrazo, Azo and Azoxy Groups* (Ed.: S. Patai), Wiley, New York, **1975**, p. 259; b) H. Kisch, P. Reisser, F. Knoch, *Chem. Ber.* **1991**, *124*, 1143.
[5] H. Gstach, H. Kisch, *Z. Naturforsch. B* **1983**, *38*, 251.
[6] a) G. Wu, A. L. Rheingold, R. F. Heck, *Organometallics* **1987**, *6*, 2386; b) *ibid.* **1986**, *5*, 1922.
[7] Crystal structure analysis of **3b**: $0.7 \times 0.3 \times 0.2$ mm, triclinic, $P\bar{1}$, $a = 1030.6(4)$, $b = 1245.8(6)$, $c = 1264.6(5)$ pm, $\alpha = 94.56(3)$, $\beta = 90.62(3)$, $\gamma = 101.42(3)°$, $V = 1.586(1)$ nm^3, $\rho_{calcd} = 1.27$ g cm^{-3}, $2\theta_{max} = 54°$, $Mo_{K\alpha}$ radiation, $\lambda = 71.073$ pm, ω scan, $T = 293$ K, 7608 measured reflections, of which 6994 were independent and 2132 observed, $F > 4\sigma(F)$, SHELXTL-PLUS, direct method, full-matrix least-squares, 397 refined parameters, H atoms were taken from the difference Fourier synthesis and were not refined, $R = 0.048$, $R_w = 0.040$, refinement against $|F|$, residual electron density 0.18 eÅ^{-3} [8].
[8] Further details of the crystal structure investigations can be obtained from the Fachinformationszentrum Karlsruhe, D-76344 Eggenstein-Leopoldshafen, on quoting the deposition number CSD-400708 (**3b**), CSD-400709 (**2c**), CSD-400711 (**2e**) and CSD-380041 (**3e**).
[9] The measured and the simulated powder diffraction diagrams coincide completely; XPOW, program for the prediction of powder diagrams, SHELXTL-PC 4.1 Siemens X-Ray Analytical Instruments Inc. **1990**, USA.
[10] G. M. Singerman in *The Chemistry of Heterocyclic compounds, Vol. 27* (Eds.: A. Weissberger, E. C. Taylor), Wiley, New York, **1973**, p. 300.
[11] Y. A. Ustynyuk, I. V. Barinov, *J. Organomet. Chem.* **1970**, *23*, 551.
[12] a) M. H. Elngadi, F. A. M. Abdul-Aal, N. M. Taha, Y. M. Yassin, *Z. Naturforsch. B* **1990**, *45*, 389; b) M. G. Hutchings, D. P. Devonald, *Tetrahedron Lett.* **1989**, *30*, 3715; c) R. L. Zey, M. L. Gross, G. S. Groenewold, *J. Heterocycl. Chem.* **1990**, *27*, 209.
[13] W. Flitsch, J. Lauterwein, M. Leimkühler, D. Leaver, U. Lewinski, R. Mattes, R. Temme, B. Wibbeling, *Liebigs Ann. Chem.* **1990**, 627.
[14] Crystal structure analysis of **2c**: $0.6 \times 0.5 \times 0.5$ mm, triclinic, $P\bar{1}$, $a = 1224.5(2)$, $b = 1290.2(3)$, $c = 1296.6(2)$ pm, $\alpha = 103.64(2)$, $\beta = 102.82(1)$, $\gamma = 113.38(2)°$, $V = 1.708(1)$ nm^3, $\rho_{calcd} = 1.16$ g cm^{-3}, $2\theta_{max} = 54°$, $Mo_{K\alpha}$ radiation, $\lambda = 71.073$ pm, ω scan, $T = 293$ K, 7672 measured reflections, of which 7440 were independent and 2203 observed, $F > 4\sigma(F)$, SHELXTL-PLUS, direct method, full-matrix least-squares, 415 refined parameters, H atoms wree taken from the difference Fourier synthesis and were not refined, $R = 0.063$, $R_w = 0.052$, refinement against $|F|$, residual electron density 0.19 eÅ^{-3} [8].
[15] In this case the powder diffraction diagram contains more than the calculated reflections. Possibly, **2c** crystallizes in two different modifications, only one of which yielded crystals capable of delivering an X-ray structure. TLC, HPLC, and UV/Vis spectroscopy could not provide any evidence for the existence of isomers.
[16] a) Crystal structure analysis of **2e**: G. Halbritter, F. Knoch, H. Kisch, *Z. Kristallogr.* in press; b) X-ray structure analysis of **3e**: G. Halbritter, F. Knoch, D. Fenske, H. Kisch, unpublished results.
[17] This is also observed in the orthometalation with $[MeMn(CO)_5]$: M. I. Bruce, B. L. Goodall, F. G. A. Stone, *J. Chem. Soc. Chem. Commun.* **1973**, 558.
[18] In analogy to the indium and rhodium complexes, the alternative insertion into a Co–C bond should also be disfavored on thermodynamic grounds: a) H. E. Selnau, J. S. Merola, *Organometallics* **1993**, *12*, 3800; b) *J. Am. Chem. Soc.* **1991**, *113*, 4008; c) W. T. Boese, A. S. Goldman *Organometallics* **1991**, *10*, 782.
[19] The lower lying LUMO (in comparison with the other N-aryl group) could explain the regioselectivity of this second nucleophilic attack.
[20] The powder diffraction diagram contains the reflections from both compounds.
[21] The possibility that traces of isomers with *cis*-stilbenyl groups exist in solution cannot be excluded.

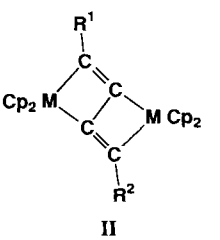
Synthesis and Structure of the Smallest Cyclic Cumulene; Reaction of 1,3-Diynes with Zirconocene Complexes**

Uwe Rosenthal,* Andreas Ohff, Wolfgang Baumann, Rhett Kempe, Annegret Tillack, and Vladimir V. Burlakov

For some time now we have been studying the interaction of disubstituted butadiynes with Group 4 metallocenes "Cp_2M" as a function of the metal M and the substituents of the diyne. For M = Ti the central C–C single bond of $Me_3Si-C\equiv C-C\equiv C-SiMe_3$ is cleaved, and a dimeric complex $[Cp_2Ti(\mu\text{-}\eta^1\text{:}\eta^2\text{-}C\equiv CSiMe_3)]_2$[1] containing bridged σ-π acetylide groups (type **I**) is formed. This cleavage was found to be dependent on the nature of the diyne substituents. For all other investigated disubstituted butadiynes $R^1C\equiv C-C\equiv CR^2$ ($R^1 = R^2$ = Ph, *t*Bu; $R^1 = SiMe_3$, R^2 = Ph, *t*Bu) the C_4 unit remains intact for M = Ti. This affords binuclear complexes with tetradehydro-*trans*, *trans*-butadiene moieties (μ-η(1–3), η(2–4)-*trans*,*trans*-butadiene or "zigzag butadiyne") between the Ti centers (type **II**).[2]



I



II

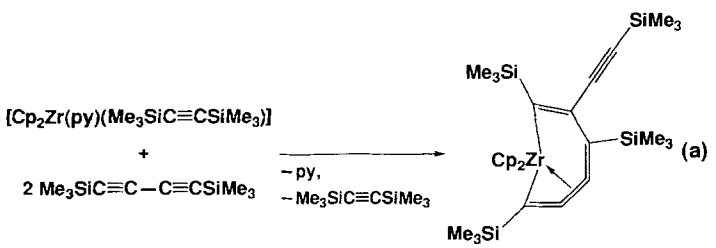
[*] Prof. Dr. U. Rosenthal, Dipl.-Chem. A. Ohff, Dr. W. Baumann, Dr. R. Kempe, Dr. A. Tillack, Dr. V. V. Burlakov[+]
Max-Planck-Gesellschaft, Arbeitsgruppe "Komplexkatalyse"
an der Universität Rostock
Buchbinderstrasse 5–6, D-18055 Rostock (FRG)
Telefax: Int. code + (381)4669369
[+] Permanent address:
Institute of Organoelement Compounds of the Russian Academy of Sciences, Moscow (Russia)

[**] This work was supported by the Max-Planck-Gesellschaft and the Fonds der Chemischen Industrie. We thank Prof. Dr. G. Oehme for the reception of the research group at the Institut für Organische Katalyseforschung in Rostock.

In contrast, cleavage of the diyne appears to be favored for M = Zr. When using the zirconocene synthon $[Cp_2Zr(thf)(Me_3SiC_2SiMe_3)]$[3] all butadiynes, except $tBuC{\equiv}C{-}C{\equiv}CtBu$, undergo cleavage. For $R^1 = R^2 = SiMe_3$, the reaction yields the complex $[Cp_2Zr(\mu\text{-}\eta^1{:}\eta^2\text{-}C{\equiv}CSiMe_3)]_2$, which has recently also been prepared by a different route.[4] By using unsymmetrically substituted butadiynes ($R^1 = SiMe_3$, R^2 = Ph, tBu) we were able to prepare the first complexes of type $[Cp_2Zr(\mu\text{-}\eta^1{:}\eta^2\text{-}C{\equiv}CR^1)(\mu\text{-}\eta^1{:}\eta^2\text{-}C{\equiv}CR^2)ZrCp_2]$. Notably, the σ-π acetylide bridges connecting the two Zr centers differ in these complexes.[5] Reaction with di-*tert*-butyl-1,3-butadiyne yields product mixtures that are difficult to separate and do not contain any product due to cleavage.

Employing the alkyne zirconocene complex $[Cp_2Zr(py)(Me_3SiC_2SiMe_3)]$[6] (py = pyridine) as a zirconocene synthon yielded novel zirconocene complexes in a surprising array of reactions. These transformations clearly show that in treating complexes of type $[Cp_2Zr(L)(Me_3SiC_2SiMe_3)]$ (L = thf or py) with diynes the nature of the ligands L has a decisive influence on the course of the reaction.

When using $Me_3Si{-}C{\equiv}C{-}C{\equiv}C{-}SiMe_3$ the binuclear complex $[Cp_2Zr(\mu\text{-}\eta^1{:}\eta^2\text{-}C{\equiv}CSiMe_3)]_2$ is formed only as a by-product. Zirconocene complex **1** is the main product, which results from the unusual coupling of two diyne molecules [Eq. (a)]. It was also recently obtained by treating the same

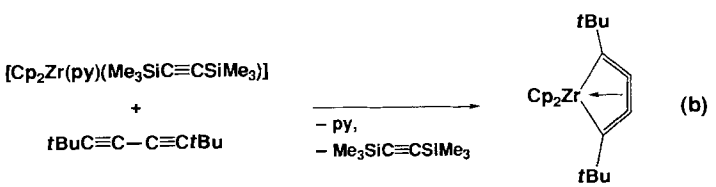


1

butadiyne with di-*n*-butylzirconocene (precursor to the Cp_2Zr synthon $[Cp_2Zr(n\text{-butene})]$[8]).[9] It crystallizes as yellow prisms that melt in an argon atmosphere at 187–188 °C.[7]

The 2,4,7-tris(trimethylsilyl)-3-(trimethylsilylethynyl)zircona cyclohepta-2,4,5,6-tetraene **1** contains the smallest cyclic cumulene yet synthesized (seven-membered).[10] Previously only the organic cumulene cyclonona-1,2,3-triene[11] had been isolated and a cyclohexa-1,2,3-triene detected in situ.[12]

On treatment of $[Cp_2Zr(py)(Me_3SiC_2SiMe_3)]$ with $tBuC{\equiv}C{-}C{\equiv}CtBu$, the complex **2**, in which only one diyne is complexed by zirconocene, is formed instead of the expected cleavage or coupling product [Eq. (b)].



2

Complex **2** crystallizes as light green needles, which melt with decomposition at 190–192 °C. They are sensitive to oxygen and moisture. In the IR spectrum of **2**, no absorption is observed in the region characteristic of the stretching vibrations for coordinated (1700–1800 cm^{-1}) or free C–C triple bonds (2050–2200 cm^{-1}). The ^1H and ^{13}C NMR spectra of **2** confirm a highly symmetrical coordination of the butadiyne.[13] Relative to the free diyne (δ = 86.2 ($C{\equiv}\underline{C}tBu$), 65.2 ($\underline{C}{\equiv}CtBu$), the signals for the alkyne C atoms in **2** are shifted downfield (δ = 186.4 and 105.5, respectively); they are also not as prominent as those in the binuclear Ti complex of type **II** (δ = 234.4 and 125.3, respectively).[2] The mass spectrum shows a molecular ion peak (M^+) at m/z = 382, indicative of a mononuclear complex.

The result of the X-ray structure analysis[14] for **2** is shown in Figure 1 and identifies the compound as a highly strained cumulene. The bond lengths for C1–C2 (1.28(1) Å), C2–C3 (1.31(1) Å), and C3–C4 (1.29(1) Å) are equivalent and confirm an identical bond order (double bond[15]). The atoms Zr, C1, C2, C3, and C4 are almost perfectly coplanar, and even the tertiary C atoms of the tBu substituents are bent out-of-plane by only 0.02(1) Å. Accordingly, all four ring C atoms possess p orbitals perpendicular to the plane of cumulene; in addition, the sp-hybridized C atoms (C2, C3) also possess p orbitals lying in-plane. The C2=C3 double bond is therefore suitable for coordination by the zirconium center. This results in a shortening of the distance between the β-C atoms and the zirconium center, which reduces the deviation of the cumulene unit in **2** from linearity. Nevertheless, the cumulene remains highly strained (the bond angles C1–C2–C3 of 150.0(5)° and C2–C3–C4 of 147.2(5)° differ markedly from 180°) and is coordinated to the zirconium center by σ bonds to carbon atoms C1 and C4.

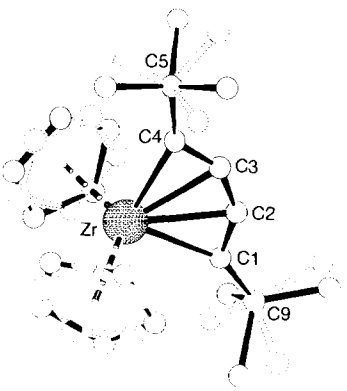


Fig. 1. Structure of **2** in the crystal.

A comparison of the data listed in Table 1 supports the description of **2** as a cyclic cumulene. Distances and angles of the

Table 1. Distances and angles of comparable structural elements in selected cyclic cumulenes X–C(1)=C(2)=C(3)=C(4)–Y [a].

	A [b]	**B** [b]	**C** [b]	**1** [9]	**2**
X	CH_2	CH_2	CH_2	Zr	Zr
Y	–	CH_2	CH_2CH_2	C≡C	
Distances [Å]					
C1–C2	1.335	1.317	1.316	1.279(6)	1.28(1)
C2–C3	1.312	1.292	1.278	1.298(6)	1.31(1)
C3–C4	1.335	1.317	1.316	1.337(6)	1.29(1)
Angles [°]					
C1–C2–C3	116.37	132.23	145.04	148.8(5)	150.0(5)
C2–C3–C4	116.37	132.23	145.04	160.1(5)	147.2(5)

[a] **A** = 1,2,3-cyclopentatriene, **B** = 1,2,3-cyclohexatriene, C = 1,2,3-cycloheptatriene. [b] Calculated [11].

ZrC_4 unit in **2** are comparable to those reported for the cumulene unit in **1** and are also in accord with values calculated for cyclic cumulenes (**A**, **B**, and **C**).[11]

The cyclic structure of **2**, in principal, resembles that found in metallacyclopentadienes (for example, as reported for zirconi-

um),[16] in which the ring atoms are also coplanar. However, in **2** the ring strain is increased by the central double bond.

In summary, *t*BuC≡C–C≡C*t*Bu and $Me_3SiC{\equiv}C{-}C{\equiv}CSiMe_3$ react completely differently with zirconocene complexes. The latter cleaves[5] or couples [Eq. (a), ref. [9]] when treated with "Cp_2Zr". In contrast, the less reactive *t*BuC≡C–C≡C*t*Bu remains intact to yield the mononuclear complex **2**. One possible explanation for these differences in reactivity lies in the different electronic influences the substituents exert on the butadiyne system. For R = $SiMe_3$ a withdrawal of electron density from the central C atoms through dπ(Si)–pπ(C) interactions is conceivable; this situation is described by the limiting structure $Me_3\overset{(-)}{Si}{=}C{=}\overset{(+)}{C}{-}\overset{(+)}{C}{=}C{=}\overset{(-)}{Si}Me_3$. For R = *t*Bu the central double bond (essential for coordination as a cumulene) is stabilized in the complex. Coordination is therefore favored over cleavage or coupling (as observed for R = $SiMe_3$).

Experimental Procedure

All reactions were conducted under anaerobic and anhydrous conditions.

1: To an orange solution of [$Cp_2Zr(py)(Me_3SiC_2SiMe_3)$] (400 mg, 0.85 mmol) in *n*-hexane (20 mL) was added a solution of bis(trimethylsilyl)-1,3-butadiyne (330 mg, 1.7 mmol) in *n*-hexane (10 mL), and the mixture was stirred for 48 h at room temperature. The solvent was removed under vacuum, the residue redissolved in *n*-hexane and filtered through a frit, and the filtrate was then allowed to crystallize in the cold. Yellow crystals of **1** formed and were washed with cold *n*-hexane and dried under vacuum. Yield: 210 mg (51%), m.p. 187–188 °C, correct elemental analysis.

2: At room temperature, a solution of di-*tert*-butyl-1,3-butadiyne (183 mg, 1.13 mmol) in *n*-hexane (10 mL) was added to a stirred solution of [$Cp_2Zr(py)(Me_3SiC_2SiMe_3)$] (532 mg, 1.13 mmol) in *n*-hexane (15 mL). The solution's color changed from dark red to green. After 24 h all volatile components were removed under vacuum and *n*-hexane was added. Following filtration, **2** crystallized upon cooling in form of light green needles; these were washed with cold *n*-hexane and dried under vacuum. Yield: 281 mg (65%, m.p. 190–192 °C (decomp.), correct elemental analysis.

Received: March 10, 1994
Revised: April 14, 1994 [Z 6747 1E]
German version: *Angew. Chem.* **1994**, *106*, 1678

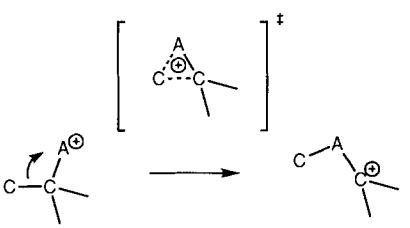
[1] U. Rosenthal, H. Görls, *J. Organomet. Chem.* **1992**, *439*, C36–C41.
[2] U. Rosenthal, A. Ohff, A. Tillack, W. Baumann, H. Görls, *J. Organomet. Chem.* **1994**, *468*, C4–C8.
[3] U. Rosenthal, A. Ohff, M. Michalik, H. Görls, V. V. Burlakov, V. B. Shur, *Angew. Chem.* **1993**, *105*, 1228–1230; *Angew. Chem. Int. Ed. Engl.* **1993**, *32*, 1193–1195.
[4] N. Metzler, H. Nöth, *J. Organomet. Chem.* **1993**, *454*, C5–C7.
[5] U. Rosenthal, A. Ohff, W. Baumann, R. Kempe, A. Tillack, V. V. Burlakov, *Organometallics*, **1994**, *13*, 2903–2906.
[6] U. Rosenthal, A. Ohff, A. Tillack, W. Baumann, H. Görls, V. V. Burlakov, V. B. Shur, *Z. Anorg. Allg. Chem.*, in press.
[7] **1** (cf. ref. [9]): IR (Nujol): $\tilde{\nu}$ = 1650, 1874, 2122 cm^{-1}; MS: *m/z* = 608 (M^+); ^1H NMR (C_6D_6, Bruker ARX 300, 30 °C): δ = 0.31, 0.35, 0.57, 0.66 (s, 9H, $SiMe_3$), 5.38 (s, 10H, Cp); $^{13}C\{^1H\}$ NMR: δ = −0.3, −0.1, 1.3, 3.2 (CH_3), 105.3 (Cp), 91.6, 161.2, 162.8, 229.3 ($CCSiMe_3$), 101.1, 110.1, 152.3, 187.9 ($CCSiMe_3$).
[8] E. Negishi, F. E. Cederbaum, T. Takahashi, *Tetrahedron Lett.* **1986**, *27*, 2829–2832.
[9] D. P. Hsu, W. M. Davis, S. L. Buchwald, *J. Am. Chem. Soc.* **1993**, *115*, 10394–10395.
[10] Review on cyclic cumulenes: R. P. Johnson, *Chem. Rev.* **1989**, *89*, 1111–1124.
[11] R. O. Angus, Jr., R. P. Johnson, *J. Org. Chem.* **1984**, *49*, 2880–2883.
[12] W. C. Shakespeare, R. P. Johnson, *J. Am. Chem. Soc.* **1990**, *12*, 8578–8579.
[13] **2**: $C_{22}H_{28}Zr$, M_r = 383.66 g mol^{-1}, MS: *m/z* = 382 (M^+); ^1H NMR (C_6D_6, Bruker ARX 300, 30 °C): δ = 1.52 (s, 18H, CH_3), 5.23 (s, 10H, Cp); $^{13}C\{^1H\}$ NMR: δ = 33.2 (CH_3), 37.4 ($C(CH_3)_3$), 103.7 (Cp), 105.5 (*C* = C*t*Bu), 186.4 (C = *C*t*Bu*).
[14] CAD 4 diffractometer with graphite monochromator, $Mo_{K\alpha}$-radiation, structure solution with direct methods SHELXS-86 (G. M. Sheldrick, *Acta Crystallogr. Sect. A* **1990**, *46*, 467–473), refinement with SHELXL-93 on full matrix by the least squares method for F^2 (G. M. Sheldrick, unpublished), structural drawings generated with SCHAKAL 92 (E. Keller, Universität Freiburg, 1992). Space group $P2_12_12_1$, *a* = 9.2279(6), *b* = 14.357(1), *c* = 15.059(2) Å, V = 1995.1(3) $Å^3$, *Z* = 4, ρ = 1.277 $g\,cm^{-3}$, 6480 measured reflections at 293 K, 3439 symmetry-independent reflections of which 2879 were observed ($I > 2\sigma(I)$), disordered atoms isotropic, all other non-hydrogen atoms anisotropic, *R*1 = 0.040, *wR*2 = 0.101, ($I > 2\sigma(I)$) for 193 parameters and no boundary constraints. Further details of the crystal structure investigation are available upon request from the Director of the Cambridge Crystallographic Data Centre, 12 Union Road, GB-Cambridge CB21EZ (UK), on quoting the full journal citation.
[15] In general, double bonds between sp- and/or sp^2-hybridized carbon atoms are 1.28–1.31 Å in length (F. H. Allen, O. Kennard, D. G. Watson, L. Brammer, A. G. Orpen, R. Taylor, *J. Chem. Soc. Perkin Trans. 2* **1987**, S1–S19).
[16] W. A. Nugent, D. L. Thorn, R. L. Harlow, *J. Am. Chem. Soc.* **1987**, *109*, 2788–2796.

An Antibody-Catalyzed 1,2-Rearrangement of Carbon–Carbon Bonds**

Yuanwei Chen, Jean-Louis Reymond,* and Richard A. Lerner*

Catalytic antibodies are generated by immunization with stable transition state analogues of a chemical reaction. This technique provides rapid and practical access to new protein catalysts, and has been successfully applied to a number of chemical transformations.[1] However, only a few reactions involving C–C bonds have been catalyzed by antibodies.[2] These include the Diels–Alder reaction,[3] the Claisen and the oxy-Cope rearrangements,[4] and decarboxylations.[5] Herein we report on the first antibody-catalyzed 1,2-rearrangement of C–C bonds, namely the dienone–phenol rearrangement.

Many rearrangements of C–C bonds are nucleophilic 1,2-shifts, in which an electronic sextet formed on an atom A attached to a carbon atom induces an adjacent C–C bond to move with its electron pair to that center to fill its valence shell. A carbenium ion is left behind, which is then stabilized by donation of an electron pair from one of its substituents (Scheme 1).



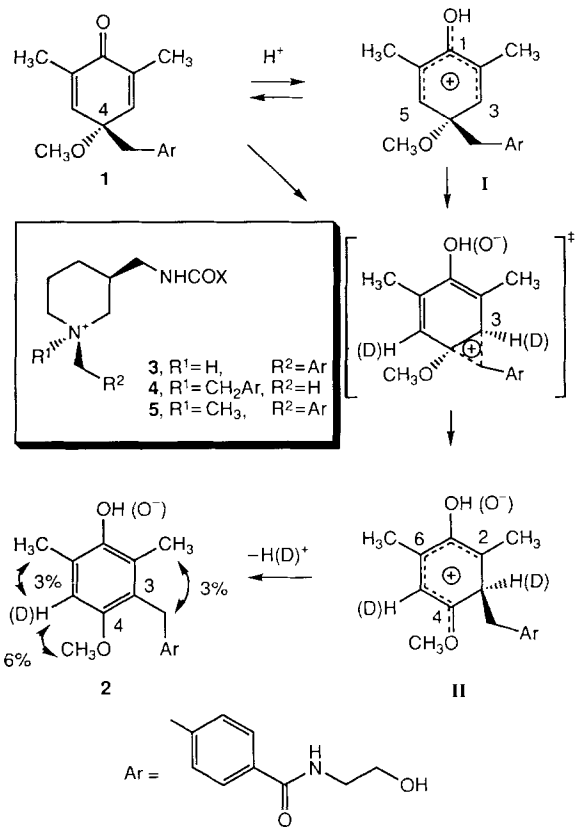
Scheme 1. Nucleophilic 1,2-shift of a C–C bond. The atom A has an electronic sextet and may be positively charged (A = carbon, oxygen) or neutral (A = nitrogen).

This mechanism is of extremely broad scope and encompasses many important synthetic transformations.[6] When A is oxygen or nitrogen, the reaction is an oxidation. Examples of this are the Baeyer–Villiger and Beckmann rearrangements of ketones and oximes, or the Curtius and Hofmann degradations of carboxylic acids. When A is carbon, the reaction is a rearrangement, as is the case in the pinacol, dienone–phenol, or Wagner–Meerwein reactions.

[*] Prof. J.-L. Reymond, Prof. R. A. Lerner, Dr. Y. Chen
Departments of Molecular Biology and Chemistry
The Scripps Research Institute
10666 North Torrey Pines Road, La Jolla, CA 92037 (USA)
Telefax: Int. code + (619) 554-9899

[**] We thank the National Institutes of Health (GM 49736 to J.-L. R.) for financial support.

The dienone–phenol rearrangement is the acid-catalyzed transformation of a 4,4-disubstituted cyclohexadienone into a 3,4-disubstituted phenol.[7] In the case of compound **1**, the benzyl group migrates preferentially to give phenol **2** (Scheme 2).



Scheme 2. Mechanism of dienone–phenol rearrangement of **1** to **2**; transition state analogues **3**–**5** were used as haptens. Nuclear Overhauser effects observed for **2** confirm that the benzyl group migrated to C-3. X represents the link to the carrier protein.

The reaction mechanism involves preequilibrium protonation of the carbonyl oxygen by the acid catalyst to form **I**, followed by rate-determining migration of the benzyl group to form **II**. Proton abstraction from C-3 finally leads to aromatization and regeneration of the acid catalyst. Two important structural and electronic changes occur during the benzyl group migration: 1) carbon atoms C-3 and C-4 change their hybridization, forming a three-membered ring with the migrating group in the transition state; 2) the positive charge, which is delocalized at C-1, C-3, C-5, and the carbonyl oxygen atom in intermediate **I**, becomes localized within the three-membered ring of the transition state. We reasoned that the piperidinium haptens **3**–**5** could be considered as analogues of the transition state in this reaction, because, with the ammonium center in the position corresponding to the homobenzylic position of the migrating group, they mimic the charge distribution in the transition state. The structural features common to both haptens and transition state are the most strongly immunogenic elements of haptens **3**, **4**, and **5** and were thus expected to shape the immune response. It was hoped that the resulting antibodies might catalyze the rearrangement of **1** to **2**.

Dienone **1** was obtained as a minor product in the alkylation of 4-methoxy-2,6-dimethylphenol.[8] When treated with aqueous acid, **1** was quantitatively converted to phenol **2**. Fourteen anti-**3**, twenty-two anti-**4**, and twenty-one anti-**5** antibodies[9] were assayed for catalysis of the rearrangement of **1** to **2** at pH 5.75 and 37 °C. One anti-**3** and one anti-**4** antibody were found to catalyze the reaction. Catalysis followed Michaelis–Menten kinetics. Quantitative inhibition was observed on addition of the respective haptens, thus confirming that the catalytic reaction was taking place at the antibody binding site. Antibody 62C7 (anti-**3**) was characterized in detail (Fig. 1, Table 1).

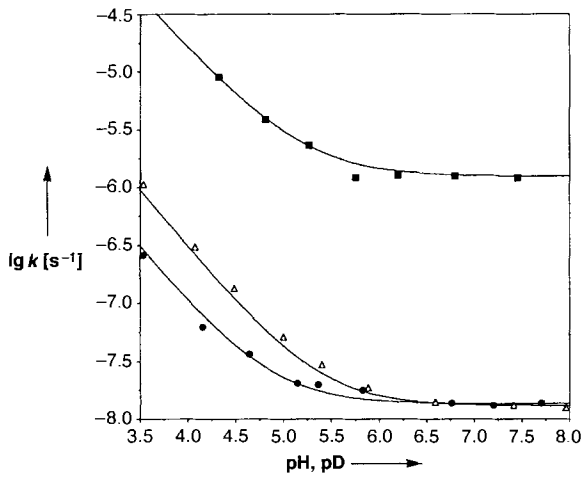


Fig. 1. Plot of lg$k$ vs. pH for the rearrangement of **1** to **2**: catalyzed by antibody 62C7 (anti-**3**) (■), and background reactions in H_2O (●) and D_2O (△). The lines were calculated from the equations $k_{cat} = k^0_{cat} + k_{cat,H}\cdot[H_3O^+]^{0.92}$; $k(H_2O) = k^0 + k_H\cdot[H_3O^+]$; $k(D_2O) = k^0 + k_D\cdot[D_3O^+]$.

Table 1. Isotope effects in antibody-catalyzed and background rearrangements of **1** to **2** [10].

Substrate	pH	K_m [μM]	$k_{cat.}$ [s^{-1}]	$k_{uncat.}$ [s^{-1}]	$k_{cat.}/k_{uncat.}$
1	5.75	670	1.22×10^{-6}	1.51×10^{-8}	80
[D_2] **1**	5.75	770	1.37×10^{-6}	1.71×10^{-8}	80
1	7.07	1200	1.25×10^{-6}	1.38×10^{-8}	90
1 (D_2O)	7.07 (pD)	1300	1.25×10^{-6}	1.31×10^{-8}	90

Below pH 5.75, both the 62C7-catalyzed and background reactions proceed with hydronium catalysis ($k_{cat,H^+} = 0.176\ M^{-1}s^{-1}$, $k_{H^-} = 1.51\times10^{-3}\ M^{-1}s^{-1}$). The latter exhibits a large inverse-solvent isotope effect ($k_{H^+}/k_{D^+} = 0.32$), consistent with preequilibrium protonation of **1** to form **I**.[10, 11] Above pH 5.75, a pH-independent pathway with a solvent isotope effect of about 1 predominates ($k^0_{cat} = 1.23\times10^{-6}\ s^{-1}$, $k^0 = 1.33\times10^{-8}\ s^{-1}$; Fig. 1, Table 1).[10, 12] These results point to a spontaneous rearrangement **1** to the conjugate base of intermediate **II** and of the complex [Ab·**1**] (Ab = antibody) to the conjugate base of the complex [Ab·**II**]. Importantly, a small inverse secondary isotope effect is observed in all cases at C-3 of the dienone ($k_{cat,H}/k_{cat,D} = 0.89$ at pH = 5.75, $k_H/k_D = 0.88$–0.94 from pH = 2.93 to 9.54). This indicates that the rate-determining step is the C–C bond migration itself involving rehybridization from sp^2 to sp^3 at C-3.[11] The C-3–H bond is ultimately broken during the formation of phenol **2**. This step is however not rate determining, since a large primary isotope effect at C-3 would then have been expected.[10]

The pH profile and isotope effects described above demonstrate that the antibody 62C7 catalyzes both the oxonium-promoted and the spontaneous rearrangement of **1** to **2** with similar efficiency and without altering the mechanism. Here, 62C7 is

clearly not acting as a simple acid catalyst. Since both pathways involve the localization of a positive charge near the rearranging C–C bond, the catalytic effect of 62C7 might result from selective stabilization of the charge distribution in the transition state.[13] The catalytic effect does not change significantly between pH 5 and 8. Stabilization of a positive charge could be mediated either by a carboxylate with a pK_a of less than 5 or by aromatic residues.[14]

Using electrostatic complementarity to the transition state as a guiding principle for hapten design, we have developed the first antibody-catalyzed 1,2-rearrangement of C–C bonds. Since formation of a transient positive charge in the migrating bond is a general feature of nucleophilic 1,2-shifts, the same principle should be applicable to the design of transition state analogues for other rearrangement reactions. We are now investigating improved haptens containing additional features of the transition state, such as a cyclopropane moiety which mimics the geometry of the bond migration.

Experimental Procedure

4-Methoxy-2,6-dimethylphenol was obtained in 87% yield by heating 2,6-dimethylhydroquinone with conc. H_2SO_4 in methanol at reflux [8a]. 4-Methoxy-2,6-dimethyl[3,5-D_2]phenol (96% D_2, 85% yield) was obtained by using D_2SO_4 and [D_1]methanol. Treatment with *N*-hydroxyethyl-4-chloromethylbenzamide and sodium hydroxide in refluxing water gave **1** (2.5%) [8b], and the O-alkylation (38%) and 2-alkylation (25%) products. Compound **1** was purified by preparative HPLC (>98% purity, reverse-phase C-18, H_2O/CH_3CN gradient). **1**: M.p. 130.0–131.0 °C; ^{1}H NMR (500 MHz, $CDCl_3$): δ = 7.66, 7.16 (2d, ^3J = 8.2 Hz, 2 × 2H), 6.88 (t, ^3J = 5.3 Hz, 1H), 6.45 (s, 2H), 3.78 (t, ^3J = 4.7 Hz, 2H), 3.58 (dt, ^3J = 4.7 Hz, 5.3 Hz, 2H), 3.15 (s, 3H), 2.97 (s, 2H), 1.84 (s, 6H); ^{13}C NMR (125 MHz, $CDCl_3$): δ = 186.4, 168.3, 145.4, 139.5, 137.9, 132.5, 130.8, 126.5, 75.4, 62.1, 52.8, 46.3, 42.7, 15.8, 15.7.

2: M.p. 147.0–148.0 °C; ^{1}H NMR (500 MHz, CD_3CN): δ = 7.66, 7.16 (2d, ^3J = 8.3 Hz, 2 × 2H), 7.08 (bs, 1H), 6.67 (s, 1H), 5.64 (s, 1H), 4.03(s, 2H), 3.70 (s, 3H), 3.59(m, 2H), 3.41 (m, 2H), 3.15 (t, ^3J = 4.5 Hz, 1H), 2.21, 2.06 (2s, 2 × 3H); ^{13}C NMR (125 MHz, CD_3CN): δ = 168.6, 152.1, 147.6, 146.2, 132.8, 129.1, 128.0, 126.1, 125.7, 123.8, 112.0, 61.6, 56.6, 43.1, 32.2, 17.0, 12.9.

Assay conditions: 50–1500 μM substrate **1**, 8 μM antibody in 100 mM NaCl, 50 mM either bis-tris(bis(hydroxyethyl)iminotris(hydroxymethyl)methane) or 1,3-bis-[tris(hydroxymethyl)methylamino]propane, 37 °C. Product formation was followed by reverse-phase HPLC (Vydac C-18 218TP54, 0.45 × 22 cm, 1.5 mL min^{-1}, t_R(**1**) = 5.02 min, t_R(**2**) = 7.14 min; 28% CH_3CN, 72% H_2O, and 0.1% CF_3COOH). The pD (98% D_2O) values were obtained by adding 0.4 to the pH-electrode reading.

Received: March 28, 1994 [Z6807IE]
German version: *Angew. Chem.* **1994**, *106*, 1694

[1] a) R. A. Lerner, S. J. Benkovic, P. G. Schultz, *Science* **1991**, *252*, 659–667; b) P. G. Schultz, R. A. Lerner, *Acc. Chem. Res.* **1993**, *26*, 391.
[2] D. Hilvert, *Acc. Chem. Res.* **1993**, *26*, 552.
[3] a) D. Hilvert, K. W. Hill, K. D. Nared, M.-T. M. Auditor, *J. Am. Chem. Soc.* **1989**, *111*, 9261; b) A. C. Braisted, P. G. Schultz, *ibid.* **1990**, *112*, 7430; c) V. E. Grouverneur, K. N. Houk, B. de Pacual-Teresa, B. Beno, K. D. Janda, R. A. Lerner, *Science* **1993**, *262*, 204.
[4] a) D. Hilvert, K. D. Nared, *J. Am. Chem. Soc.* **1988**, *110*, 5593; b) D. Y. Jackson, J. W. Jacobs, R. Sugasawara, S. H. Reich, P. A. Bartlett, P. G. Schultz, *ibid.* **1988**, *110*, 4841; c) D. Y. Jackson, M. N. Liang, P. A. Bartlett, P. G. Schultz, *Angew. Chem.* **1992**, *104*, 196; *Angew. Chem. Int. Ed. Engl.* **1992**, *31*, 182; e) A. C. Braisted, P. G. Schultz, *J. Am. Chem. Soc.* **1994**, *116*, 2211.
[5] a) C. Lewis, T. Kramer, S. Robinson, D. Hilvert, *Science* **1991**, *253*, 1019; b) J. A. Ashley, C.-H. L. Lo, G. P. McElhaney, P. Wirshing, K. D. Janda, *J. Am. Chem. Soc.* **1993**, *115*, 2515.
[6] For general discussion, see: J. March, *Advanced Organic Chemistry*, 4th ed., Wiley, New York, **1992**, pp. 1051–1156.
[7] For review, see: B. Miller, *Acc. Chem. Res.* **1975**, *8*, 245; applications: R. Cassis, M. Scholz, R. Tapia, J. A. Valderrama, *Tetrahedron Lett.* **1985**, *26*, 6281; F. M. Hauser, K.-H. Park, *J. Org. Chem.* **1978**, *43*, 113; S. M. Kupchan, C.-K. Kim, K. Miyano, *Heterocycles* **1976**, *4*, 235; U. Eder, G. Haffer, G. Neef, K. Prezewowsky, G. Sauser, R. Wiechert, *Chem. Ber.* **1978**, *111*, 939; D. J. Hart, A. Kim, R. Krishnamurthy, G. H. Merriman, A. M. Waltos, *Tetrahedron* **1992**, *48*, 8179.
[8] a) H. Greuter, H. Schmid, *Helv. Chim. Acta.* **1972**, *55*, 2382; b) J. Borgulya, R. Madeja, P. Fahrni, H. J. Hansen, H. Schmid, *ibid.*, **1973**, *56*, 34.
[9] J.-L. Reymond, K. D. Janda, R. A. Lerner, *Angew. Chem.* **1991**, *103*, 1690, *Angew. Chem. Int. Ed. Engl.* **1991**, *30*, 1711.
[10] K. B. Wiberg, *Chem. Rev.* **1955**, *55*, 713.
[11] V. P. Vitullo, N. Grossman, *J. Am. Chem. Soc.* **1974**, *94*, 3844.
[12] A. R. Becker, D. J. Richardson, J. C. Brown, *J. Am. Chem. Soc.* **1977**, *99*, 5058.
[13] Other anti-**3**, anti-**4**, and anti-**5** antibodies might fail to catalyze the reaction because they bind intermediate **I** equally or better than the transition state.
[14] S. K. Burley, G. A. Petsko, *FEBS Lett.* **1986**, *203*, 139; M. Levitt, M. F. Perutz, *J. Mol. Biol.* **1988**, *201*, 751.

Oxidation of Metal-Coordinated Thioethers with Dimethyldioxirane—A New Stereoselective Synthesis of Chiral Sulfoxides**

Wolfdieter A. Schenk,* Jürgen Frisch, Waldemar Adam,* and Frank Prechtl

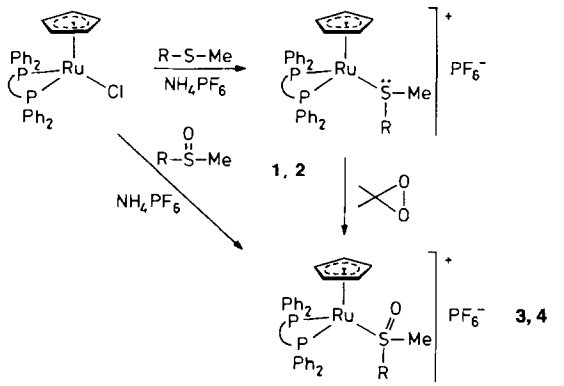
Dedicated to Professor Helmut Werner on the occasion of his 60th birthday

Enantiomerically pure sulfoxides RS(O)R′ play an eminent role as intermediates and final products.[1] Nucleophilic substitution at diastereomerically pure sulfinic acid esters or amides is especially suitable for their synthesis;[2] the stereoselective oxidation of prochiral thioethers is another attractive method. When microorganisms or isolated enzymes are employed, high expectations regarding yield and selectivity are often not fulfilled.[3] However, oxidation of alkyl aryl sulfides with enantiomerically pure oxaziridines[4] and especially with *t*BuOOH in the presence of asymmetric titanium catalysts, methods developed by Kagan et al.[5] and Uemure et al.[6] are well proven. Dialkyl sulfides, on the other hand, are generally oxidized with only poor enantioselectivity.[4–6] We report here on a new methodology for solving this selectivity problem. The prochiral thioether is first coordinated to an enantiomerically pure transition metal complex fragment, which is then oxidized with a reactive oxygen transfer reagent.

It has been known for some time that the three-coordinate sulfur in thioether complexes is still susceptible to electrophilic attack, for example, by $[Me_3O]^+$.[7] Dimethyldioxirane (DMD) has proven to be an exceptionally effective, predominantly electrophilic oxygen transfer reagent,[8] which can also be used in the oxidation of organometallic substrates.[9] Therefore, we first tested whether the readily available thioether complexes **1a**, **b** and **2a**, **b** can be oxidized by DMD in acetone (Scheme 1).[10] Indeed, the sulfoxide complexes **3a**, **b** and **4a**, **b** were obtained in high yields. The identity of the products was established spectroscopically and by independent synthesis. By crossover experiments it was shown that the reaction does *not* proceed according to the following reaction sequence: a) dissociation of the thioether, b) oxidation of the uncoordinated thioether, and c) coordination of the resulting sulfoxide. Thus, oxidation of an

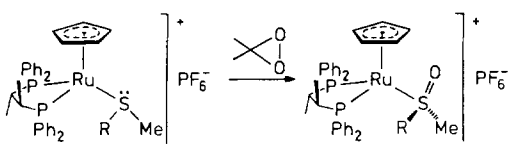
[*] Prof. Dr. W. A. Schenk, Dipl.-Chem. J. Frisch
Institut für Anorganische Chemie der Universität
Am Hubland, D-97074 Würzburg (FRG)
Telefax: Int. code +(931)888-4605
Prof. Dr. W. Adam, Dr. F. Prechtl
Institut für Organische Chemie der Universität
Am Hubland, D-97074 Würzburg (FRG)
Telefax: Int. code +(931)888-4606

[**] Sulfur(IV) Compounds as Ligands, Part 21. This work was supported by the Deutsche Forschungsgemeinschaft (SFB 347 "Selective Reactions of Metal-Activated Molecules") and the Fonds der Chemischen Industrie. Part 20: W. A. Schenk, A. Khadra, C. Burschka, *J. Organomet. Chem.* **1994**, *468*, 75.



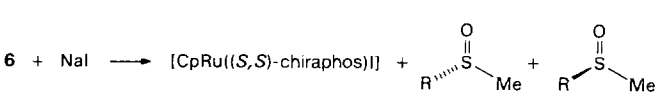
Scheme 1. **1a**–**4a**: R = Ph; **1b**–**4b**: R = CH_2Ph. The bidentate phosphane ligand is bis(diphenylphosphino)methane (dppm) in **1** and **3**, and bis(diphenylphosphino)ethane (dppe) in **2** and **4**.

equimolar mixture of **1a** and **2b** with DMD gave the sulfoxide complexes **3a** and **4b**. No crossover products **3b** and **4a** were formed. Similarly only **3b** and **4a** were obtained from a mixture of **1b** and **2a**, and no detectable amounts ($\leq 2\%$, ^{31}P NMR spectrum) of the crossover products **3a** and **4b** were found.



Scheme 2. **5a**, **6a**: R = Ph; **5b**, **6b**: R = CH_2Ph; **5c**, **6c**: R = *i*Pr.

The oxidation with DMD can be applied without problems to the (*S*,*S*)-chiraphos (chiraphos = 1,2-dimethyl-1,2-ethanediyl-bis[(diphenyl)phosphane]) complexes **5a–c** (Scheme 2). The sulfoxide complexes **6a–c** were thus obtained in nearly quantitative yields, and their identity was corroborated by independent synthesis from [CpRu{(*S*,*S*)-chiraphos}Cl].



	R	*R* (%)	*S* (%)
a	Ph	27 (+)	73 (-)
b	CH_2Ph	≤1 (+)	≥99 (-)
c	*i*Pr	93 (+)	7 (-)

Scheme 3.

The bound sulfoxides were decomplexed in quantitative yields with sodium iodide in acetone. The chiral metal fragment was recovered in a form which would allow it to be recycled (Scheme 3). Separation of the sulfoxides by HPLC on a chiral column confirmed the diastereoselectivities determined by NMR spectroscopy and the stereospecificity of the cleavage reaction. Thus, for example, enantiomerically pure (*S*)-**7b** was obtained from (R_S)-**6b** with retention of configuration at sulfur. The absolute configurations of **7a**[5a] and **7b**[2a] follow from the sign of the specific rotation. The positive sign of the specific rotation for **7c** indicates an *R* configuration by analogy with (*S*)-MeS(O)*n*Pr ($[\alpha]_D = -139$) and (*R*)-MeS(O)*i*Bu ($[\alpha]_D = +138$).[2a]

The high diastereoselectivity of the oxygen transfer is kinetic in origin. The sulfur atom in thioether complexes usually undergoes rapid pyramidial inversion;[11] for example, only at −40 °C can separate NMR signals be observed for the two diastereoisomers of **5b**, which are nearly equal in energy (18% *de*). Each diastereoisomer can exist as three different rotamers with respect to the Ru–S bond. According to the NOE difference spectra (NOE = nuclear Overhauser effect; irradiation of the Cp resonance frequencies causes comparable enhancement of the SCH_3 and SCH_2 signals for both diastereomers of **5b**), the energetically preferred rotamer is that with both substituents at sulfur oriented towards the cyclopentadienyl ring. In this orientation, the lone pair at sulfur is sterically shielded by the aryl groups of the chelating phosphane.[12] As a result, the oxygen atom must be preferentially transferred to one of the other two rotamers of (R_S)-**5b**. The diastereoselectivity of the oxidation therefore depends on the difference in energy between the two higher energy rotamers, which were not observed in the NMR spectra, as well as on the difference in their reactivities. Since a large number of C_2-symmetric bidentate phosphane ligands are known, many of which are commercially available, our results open up a novel route for the enantioselective oxidation of thioethers.

Experimental Procedure

All experiments were carried out with purified solvents and under an inert atmosphere. ^{31}P NMR spectra were recorded at 162 MHz in [D_6]acetone at 25 °C, using 85% H_3PO_4 as the reference.

1, **2**: A solution of 0.25 mmol [CpRu (dppm)Cl] or [CpRu(dppe)Cl], 50 mg NH_4PF_6 (0.30 mmol), and 1.00 mmol thioether in 10 mL of methanol was heated for 3–4 h under reflux. The mixture was then concentrated to dryness and the residue recrystallized twice from dichloromethane/diethyl ether. The products were thus obtained as yellow crystalline powders in about 90% (**1a, b**) and 75% (**2a, b**) yield (correct elemental analyses). **1a**: M.p. 173–175 °C; ^{31}P NMR: $\delta = 7.7$. **1b**: M.p. 192–197 °C; ^{31}P NMR: $\delta = 8.8$. **2a**: M.p. 164–167 °C; ^{31}P NMR: $\delta = 73.7$. **2b**: M.p. 218–220 °C; ^{31}P NMR: $\delta = 72.8$.

3, **4**: a) The independent synthesis of **3** and **4** was achieved by an analogous procedure starting from the chloro complex and sulfoxide in 80–85% yield. b): To a solution of 0.15 mmol thioether complex in 3 mL of acetone at 0 °C was added slowly a solution of 0.60 mmol DMD in acetone [10]. After 45 min all volatiles were removed under vacuum and the residue recrystallized from acetone/diethyl ether. The products were thus obtained as light yellow crystalline powders (correct elemental analyses) in yields >90%. No thioether complex could be detected in the NMR spectra of the crude products. **3a**: M.p. 120–124 °C; ^{31}P NMR: $\delta = 8.5, 5.0$, J (P,P) = 85 Hz. **3b**: M.p. 214–217 °C; ^{31}P NMR: $\delta = 8.0, 7.7$, J (P,P) = 85 Hz. **4a**: M.p. 171–175 °C; ^{31}P NMR: $\delta = 78.9, 69.9$, J (P,P) = 20 Hz. **4b**: M.p. 162–165 °C; ^{31}P NMR: $\delta = 73.6, 72.9$, J (P,P) = 22 Hz.

5: The synthesis was achieved following the procedure given for **1** and **2**; the products were obtained as yellow crystalline powders in >95% yield (correct elemental analyses). **5a**: M.p. 148–153 °C; ^{31}P NMR: $\delta = 82.1, 63.8$, J (P,P) = 41 Hz. **5b**: M.p. 212–217 °C; ^{31}P NMR: $\delta = 82.2, 66.8$, J (P,P) = 40 Hz. **5c**: M.p. 187–189 °C; ^{31}P NMR: $\delta = 81.4, 64.4$, J (P,P) = 41 Hz.

6: a) The independent synthesis was achieved starting from the chloro complex and sulfoxide and following the procedure given for **1** and **2**; **6a–c** were thus obtained as pale yellow crystalline powders in 85–90% yield (correct elemental analyses). (R_S)-**6a**: (S_S)-**6a** = 93:7 (86% *de*); (R_S)-**6a**: ^{31}P NMR: $\delta = 81.8, 60.3$, J (P,P) = 36 Hz; (S_S)-**6a**: ^{31}P NMR: $\delta = 79.1, 62.3$, J (P,P) = 36 Hz. (R_S)-**6b**: (S_S)-**6b** = 50:50 (0% *de*); (R_S)-**6b**: ^{31}P NMR: $\delta = 80.9, 61.2$, J (P,P) = 37 Hz; (S_S)-**6b**: ^{31}P NMR: $\delta = 80.9, 61.8$, J (P,P) = 36 Hz. (R_S)-**6c**: (S_S)-**6c** = 12:88 (76% *de*). R_S-**6c**: ^{31}P NMR: $\delta = 78.6, 60.4$, J (P,P) = 37 Hz; (S_S-**6c**): ^{31}P NMR: $\delta = 80.6, 57.8$, J (P,P) = 37 Hz. b) The oxidation of **5a–c** to **6a–c** with DMD was carried out as described above. The extent of reaction and the diastereoisomeric ratios were determined from the NMR spectra of the crude reaction mixtures. **6a**: Yield 95%, (R_S)-**6a**: (S_S)**6a** = 73:27 (46% *de*). **6b**: Yield 90%, (R_S)-**6b**: (S_S)-**6b** ≥99:1 (98% *de*). **6c**: Yield 95%, (R_S)-**6c**: (S_S)-**6c** = 7:93 (86% *de*).

Removal of the sulfoxide: The sulfoxide complex (0.10 mmol) and 75 mg sodium iodide (0.50 mmol) were heated for 15 h under reflux in 5 mL of acetone. The mixture was then concentrated. The residue was taken up into 2 mL of dichloromethane and chromatographed on silica. [CpRu{(S,S)-chiraphos}I] was

eluted first with dichloromethane and then the sulfoxide with acetone. Upon removal of the solvent, the product was obtained in pure form and in quantitative yield (NMR). The enantiomeric ratio was determined by HPLC (Chiracel OD column, hexane/2-propanol 9:1, UV and optical rotation detector).

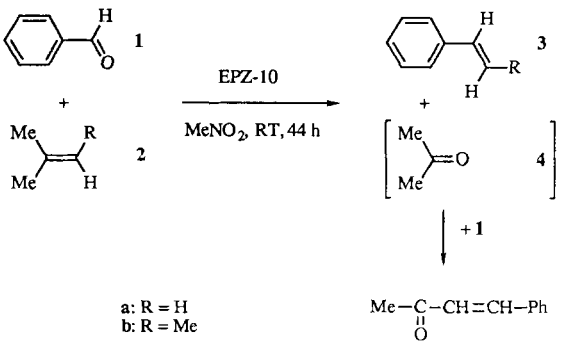
Received: December 2, 1993
Revised version: March 3, 1994 [Z 6532 IE]
German version: *Angew. Chem.* **1994**, *106*, 1699

[1] a) T. Durst in *Comprehensive Organic Chemistry, Vol. 3* (Eds.: D. Barton, D. Ollis), Pergamon, Oxford, **1979**, p. 121; b) G. Solladie, *Synthesis* **1981**, 185; c) G. H. Posner, *Acc. Chem. Res.* **1987**, *20*, 72; d) *The Chemistry of Sulfones and Sulfoxides* (Eds.: S. Patai, Z. Rappoport, C. Stirling), Wiley, New York, **1988**; e) K. K. Andersen in [1d], p. 55; f) G. H. Posner in [1d], p. 823.
[2] a) K. K. Andersen, B. Bujnicki, J. Drabowicz, M. Mikolajczyk, J. B. O'Brien, *J. Org. Chem.* **1984**, *49*, 4070; b) F. Rebiere, O. Samuel, L. Ricard, H. B. Kagan, *ibid.* **1991**, *56*, 5991; c) D. A. Evans, M. M. Faul, L. Colombo, J. J. Bisaha, J. Clardy, D. Cherry, *J. Am. Chem. Soc.* **1992**, *114*, 5977; d) I. Fernandez, N. Khiar, J. M. Llera, F. Alcudia, *J. Org. Chem.* **1992**, *57*, 6789.
[3] H. L. Holland, *Chem. Rev.* **1988**, *88*, 473.
[4] a) F. A. Davis, R. T. Reddy, W. Han, P. J. Carroll, *J. Am. Chem. Soc.* **1992**, *114*, 1428; b) V. Meladinis, U. Verfürth, R. Herrmann, *Z. Naturforsch. B* **1990**, *45*, 1689.
[5] a) P. Pitchen, E. Dunach, M. N. Deshmukh, H. B. Kagan, *J. Am. Chem. Soc.* **1984**, *106*, 8188; b) H. B. Kagan, F. Rebiere, O. Samuel, *Phosphorus Sulfur Silicon Relat. Elem.* **1991**, *58*, 89.
[6] N. Komatsu, M. Hashizume, T. Sugita, S. Uemura, *J. Org. Chem.* **1993**, *58*, 4529.
[7] a) R. D. Adams, D. F. Chodosh, *J. Am. Chem. Soc.* **1978**, *100*, 812; b) R. D. Adams, C. Blankenship, B. E. Segmüller, M. Shiralian, *ibid.* **1983**, *105*, 4319.
[8] W. Adam, D. Golsch, *Angew. Chem.* **1993**, *105*, 771; *Angew. Chem. Int. Ed. Engl.* **1993**, *32*, 737, and references therein.
[9] a) S. Wolowiec, J. K. Kochi, *Inorg. Chem.* **1991**, *30*, 1215; b) W. A. Schenk, J. Frisch, W. Adam, F. Prechtl, *ibid.* **1992**, *31*, 3329; c) W. Adam, U. Azzena, F. Prechtl, K. Hindahl, W. Malisch, *Chem. Ber.* **1992**, *125*, 1409; d) A. Perez-Encabo, S. Perrio, A. M. Z. Slawin, S. E. Thomas, A. T. Wierzchleyski, D. J. Williams, *J. Chem. Soc. Chem. Commun.* **1993**, 1059; e) M. C. Fermin, J. W. Bruno, *J. Am. Chem. Soc.* **1993**, *115*, 7511.
[10] W. Adam, J. Bialas, L. Hadjiarapoglou, *Chem. Ber.* **1991**, *124*, 2377.
[11] E. W. Abel, K. G. Orrell, S. K. Bhargava, *Prog. Inorg. Chem.* **1984**, *32*, 1.
[12] a) J. I. Seeman, S. G. Davies, *J. Chem. Soc. Chem. Commun.* **1984**, 1019; b) S. G. Davies, J. I. Seeman, *Tetrahedron Lett.* **1984**, *25*, 1845; c) J. I. Seeman, *Pure Appl. Chem.* **1987**, *59*, 1661.

Acid-Catalyzed Olefination of Benzaldehyde

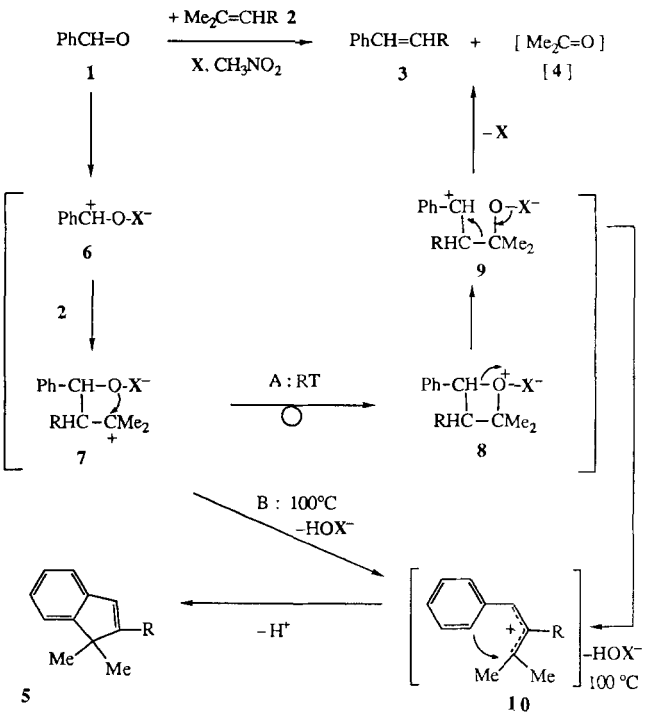
Henk-Peter van Schaik, Robert-Jan Vijn, and Friedrich Bickelhaupt*

Olefinations of carbonyl compounds are usually performed under alkaline conditions. The reaction starts with the nucleophilic attack of a negative carbon atom on a carbonyl group. This applies to the classical Wittig[2] reaction and its variants.[2] We present here an acid-catalyzed olefination, namely the reaction of benzaldehyde with olefins catalyzed by a solid Lewis acid. This reaction is particularly interesting not only because of the acid catalysis. First, it is a one-pot reaction with a surprising, and to our knowledge hitherto unknown, reaction mechanism. Second, in spite of having certain inherent limitations, this reaction is attractive from a preparative point of view because the carbon atom used for the olefination of the carbonyl group comes from a simple olefin, that is, from an inexpensive raw material. The principle of this reaction is shown in Scheme 1. In



Scheme 1. Reaction of benzaldehyde (**1**) with **2a** (15% **3a** at 60% aldehyde conversion) and **2b** (30% **3b** at 25% aldehyde conversion). RT=room temperature.

a typical experiment, benzaldehyde (**1**), one equivalent of alkene **2**, and the solid Lewis acid catalyst EPZ-10[3] were stirred in nitromethane for 44 hours at room temperature. From this reaction styrene (**3a**) (15%) or β-methylstyrene (**3b**) (30%) were obtained; these yields are based on conversion rates of 60 and 25%, respectively. At higher temperatures or longer reaction times, better conversions were obtained; however, the formation of by-products also increased. As known from the literature,[4] **3a** dimerized to (*E*)-1,3-diphenylbut-1-ene. At higher temperature (100 °C) indenes **5a** (< 1%) or **5b** (10%) and increased amounts of polymeric products were formed (Scheme 2).

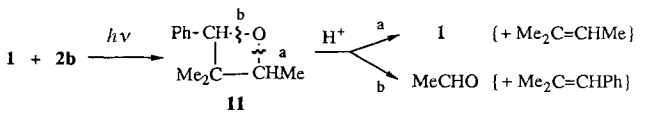


Scheme 2. Postulated mechanism of product formation. X corresponds to the catalyst EPZ-10.

The, at first glance, surprising formation of **3** can easily be explained by using well-known mechanistic principles (Scheme 2). It is assumed that the acidic catalyst **X** and **1** generate the intermediate **6**, which adds to **2** leading to the formation of **7**; this corresponds to the first step of the Prins reaction.[5] In the continuation of the Prins reaction, except for some special

[*] Prof. Dr. F. Bickelhaupt, Drs. H.-P. van Schaik
Scheikundig Laboratorium, Vrije Universiteit
De Boelelaan 1083, NL-1081 HV Amsterdam (The Netherlands)
Telefax: Int. code +(20)6461479
Dr. R.-J. Vijn
DSM Research B. V., Department Fine Chemical Intermediates
NL-6160 MD Geleen (The Netherlands)

cases,[6] the ring closure to give the oxetane does not seem to play a major role; however, in the case of **7** the formation of the (complexed) oxetane **8** (Scheme 2, route A) is the simplest hypothesis.[7] There are some examples[8] in the chemistry of oxetanes[6] for the subsequent acid-catalyzed ring opening. They show, as expected, that the most stable carbocation is formed after the cleavage of the four-membered ring. Accordingly, **8** should open to give the intermediate **9** with a cationic benzylic group, which produces **3a** or **3b** by a Grob fragmentation.[9] The majority of these reaction steps are probably reversible. Thus, for example, it is known that oxetane **11**, which is made by photoaddition of **1** to **2b** and whose structure is regioisomeric with that of **8b**, can be cleaved by acid to give acetaldehyde as well as **1**[8a] (Scheme 3). The olefination is, however, not



Scheme 3. Fragmentation of oxetane **11** [8a].

dominated exclusively by the thermodynamically determined position of equilibrium, since model calculations for the reaction **1** + **2** → **3** + **4** (Scheme 1) indicate strongly negative reaction enthalpies (ΔH_R) and Gibbs energies (ΔG_R) (with **2a**: $(\Delta H_R) = -4.5$; with **2b**: $(\Delta H_R) = -5.2$; $(\Delta G_R) = -4.6$ kcal mol^{-1}) that should lead to an almost complete displacement of the equilibrium to the right-hand side. The formation of **5** under extreme conditions seems to proceed via the allyl cation **10**, which can be generated (in a multistep process) from **7** (Scheme 2, route B) or from **9**.

Acetone (**4**), which along with **3** was expected to be the second fragmentation product, was not detected, presumably because under these reaction conditions acetone rapidly reacts to form the aldol condensation product, benzalacetone, which has been identified in the reaction mixture (Scheme 1). From this, the first limitation of the new olefination process can be derived directly: the carbonyl compound to be olefinated may not contain any α-hydrogen atoms, since otherwise, the aldol condensation dominates. Furthermore, the cation formed by protonation of the carbonyl compound must not be *too* stable; for instance, no reaction was observed between benzophenone and **2a** even at 100 °C, presumably because the reaction corresponding to the conversion **6** → **7** would be thermodynamically unfavorable for the intermediate with a cationic diphenylhydroxymethyl unit. The same applies to the olefin **2** used in the process whose nucleophilicity may be neither too low nor too high. We draw this conclusion from the observation that benzaldehyde did not react either with 1-octene or with 1,1-diphenylethene. In the case of 1-octene, the attack of the olefin on **6** leading to the formation of **7** is probably too unfavorable; for 1,1-diphenylethene, the Lewis acid could either react directly with the olefin to form a stable zwitterion, or **7** (with the cationic diphenylmethyl group!) is so stable that ring closure to give the oxetane **8** does not occur.

Further studies on the mechanism, as well as the optimization and limitations of the new reaction sequence, are in progress.

Experimental Procedure

In a typical experiment **1** (20 mmol) and EPZ-10 (1 g) [3] (heated for about 15 h in an oven at 130 °C) were stirred in nitromethane (20 mL) under nitrogen at room temperature. **2** (20 mmol) was added and the mixture stirred for an additional 44 h; in the case of **2a**, a reflux condenser filled with acetone/dry ice was applied. After completion of the reaction, the catalyst was separated by filtration. The yield in the filtrate was determined by GC/MS analysis with nitrobenzene as an internal standard. The identity of the products was confirmed by ^{1}H NMR spectroscopy of samples purified by preparative gas chromatograhy: **3a** (authetic sample); **3b** [10]. **5a** [11] (because the yield was less than 1% identification by mass spectrometry only was possible); **5b** [12], (*E*)-1,3-diphenyl-1-butene [4a], benzalacetone (authetic sample).

Received: March 14, 1994 [Z 6757IE]
German version: *Angew. Chem.* **1994**, *106*, 1703

[1] a) G. Wittig, G. Geissler, *Liebigs Ann. Chem.* **1953**, *580*, 44–57; b) G. Wittig, U. Schöllkopf, *Chem. Ber.* **1954**, *87*, 1318–1330; c) B. E. Maryanoff, A. B. Reitz, *Chem. Rev.* **1989**, *89*, 863–927.
[2] S. H. Pine, G. S. Shen, H. Hoang, *Synthesis* **1991**, 165–167.
[3] a) The best results were obtained by using the zinc chloride containing clay catalyst Envirocat EPZ-10 from Contract Chemicals, Prescot, England. We would like to thank Contract Chemicals for supplying the catalyst free of charge. b) Further applications of EPZ-10: T. W. Bastock, J. H. Clark in *Speciality Chemicals, Innovations in Industrial Synthesis and Applications* (Ed.: B. Pearson), Elsevier, London, **1991**, pp. 383–396; c) Nafion-H (further applications of Nation-H: G. S. Olah, P. S. Iyer, G. K. S. Prakash, *Synthesis* **1986**, 513–531) zinc chloride and *p*-toluenesulfonic acid have similar product mixtures; however, the yields of **3** were lower.
[4] a) A. R. Taylor, G. W. Keen, E. J. Eisenbraun, *J. Org. Chem.* **1977**, *42*, 3477–3480; b) M. J. Climent, A. Corma, H. Garcia, S. Iborra, J. Primo, *Rec. Trav. Chim. Pays-Bas* **1991**, *110*, 275–278.
[5] D. R. Adams, S. P. Bhatnagar, *Synthesis* **1977**, 661–672.
[6] a) H. W. Scheeren, R. W. M. Aben, P. H. J. Ooms, R. J. F. Nivard, *J. Org. Chem.* **1977**, *42*, 3128–3132; b) J. W. Scheeren, *Recl. Trav. Chim. Pays-Bas* **1986**, *105*, 71–84; c) J. Mattay, K. Buchkremer, *Heterocycles* **1988**, *27*, 2153–2165; d) H. Sugimura, K. Osumi, *Tetrahedron Lett.* **1989**, *30*, 1571–1574.
[7] A closely related mechanistic variant would be, for example, the reaction of **7** with a second benzaldehyde molecule to give 1,3-dioxane, which is often found in Prins reactions, and its fragmentation to **3** and **4**. This would, however, not affect the important aspects of the reaction.
[8] a) G. Büchi, C. G. Inman, E. S. Lipinsky, *J. Am. Chem. Soc.* **1954**, *76*, 4327–4331; b) D. Scharf, F. Korte, *Tetrahedron Lett.* **1963**, 821–823; c) S. A. Carr, W. P. Weber, *J. Org. Chem.* **1985**, *50*, 2782–2785.
[9] C. A. Grob, *Angew. Chem.* **1969**, *81*, 543–554; *Angew. Chem. Int. Ed. Engl.* **1969**, *8*, 535–546.
[10] C. L. Bumgardner, *J. Am. Chem. Soc.* **1961**, *83*, 4420–4423.
[11] *EPA/NIH Mass Spectral Data Base: Vol. 1* [*Natl. Stand. Ref. Data Ser. U.S. Natl. Bur. Stand* NSRDS-NBS *63*, **1978**, 403].
[12] R. Gelin, B. Chantegrel, *Bull Soc. Chim. Fr.* **1971**, 2527–2544.

Lewis Acid Promoted [2+2] Cycloaddition of Allylsilanes and Unsaturated Esters: A Novel Method for Cyclobutane Construction**

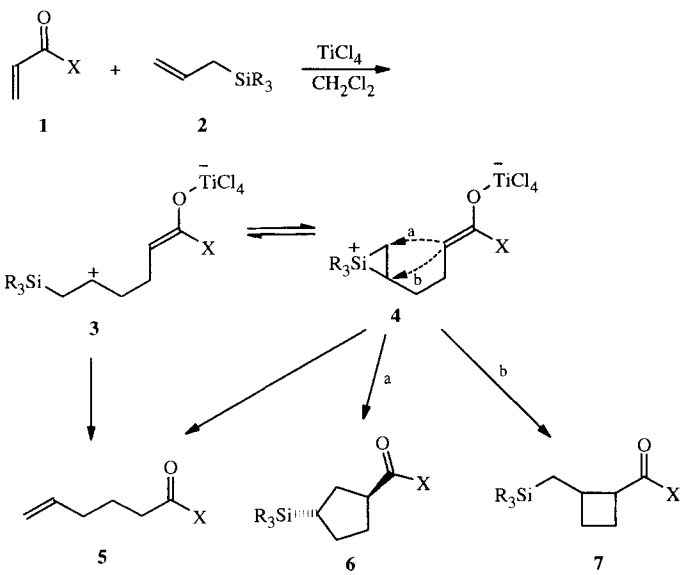
Hans-Joachim Knölker,* Gerhard Baum, and Regina Graf

The [3+2] cycloaddition of allylsilanes, which was first described by us four years ago,[1] has been established as an efficient method for the stereoselective construction of five-membered ring systems.[2–4] The major achievement was the suppression of the classical Sakurai reaction[5] by using bulky substituents at the silicon atom of the allylsilane.[2] We report herein a novel mode of reactivity for allylsilanes and α,β-unsaturated carbonyl compounds in the presence of a Lewis acid, the

[*] Prof. Dr. H.-J. Knölker, Dipl.-Chem. R. Graf
Institut für Organische Chemie der Universität
Richard-Willstätter-Allee, D-76131 Karlsruhe (FRG)
Telefax: Int. code +(721)698-529
G. Baum
Institut für Anorganische Chemie der Universität Karlsruhe (FRG)

[**] Cycloadditions of Allylsilanes, Part 6. This work was supported by the Deutsche Forschungsgemeinschaft (Gerhard-Hess-Förderpreis) and the Fonds der Chemischen Industrie. Part 5: [13].

[2+2] cycloaddition of allylsilanes and α,β-unsaturated esters. The three types of reactions of allylsilanes with unsaturated carbonyl compounds can be rationalized as presented in Scheme 1.



Scheme 1. Possible reactions for the α,β-unsaturated carbonyl compound **1** and allylsilanes **2** in the presence of $TiCl_4$: Sakurai reaction (product **5**; R = Me; X = H, alkyl), [3+2] cycloaddition (product **6**; R = Ph, *i*Pr; X = alkyl), and [2+2] cycloaddition (product **7**; R = Ph, *i*Pr; X = Oalkyl).

Nucleophilic attack of the allylsilane **2** is initiated by the Lewis acid and takes place at the β position of the conjugated carbonyl system **1**. The positive charge of the resulting β-silyl cation **3** is stabilized by internal nucleophilic neighboring group participation of the silicon atom, and a bridged nonclassical pentavalent silicon cation (= siliranium ion) **4** is generated. The pentavalency of silicon in the siliranium ion is possible because of its d orbitals.[6] This contribution to the β-effect of silicon has been termed "non-vertical stabilization" by Traylor.[7] Intermolecular nucleophilic attack at the silicon atom of the cationic intermediate either in its open form **3** or in the form of the siliranium ion **4** provides the Sakurai product **5** after hydrolysis and workup.[5] Sterically demanding substituents inhibit the nucleophilic attack at the silicon atom of either cationic species and thus favor cyclization by intramolecular nucleophilic attack of the titanium enolate. In the case of α,β-unsaturated ketones nucleophilic attack of the titanium enolate occurs at the primary carbon atom of the siliranium ion **4** (pathway a, 5-*exo-tet* cyclization)[8] and thus results in a [3+2] cycloaddition of the allylsilane involving a cationic 1,2-silyl shift to the silylcyclopentane **6**.

Herein we describe cyclizations that are inititated by nucleophilic attack of the titanium enolate at the secondary carbon atom of the intermediate siliranium cation (pathway b, 4-*exo-tet* cyclization)[8] which afford the silylmethylcyclobutanes **7**. Two points are worth noting in this context and should be mentioned in order to avoid any confusion. First, allyltrimethylsilanes failed to give conjugate additions in the Lewis acid ($TiCl_4$) promoted reaction with α,β-unsaturated carboxylic acid esters.[5a] Secondly, all proposed silylmethylcyclobutanes reported as by-products from the Lewis acid promoted reaction of conjugated enones[9] were reassigned as silylcyclopentanes.[10] These reassignments are not challenged by the present findings, which describe for the first time[11] that allylsilanes having bulky substituents at the silicon atom undergo Lewis acid promoted [2+2] cycloadditions with α,β-unsaturated esters leading to silylmethylcyclobutanes.

Initially, we investigated the [2+2] cycloaddition of the allylsilanes **2** and the methyl acrylates **8**. The cycloadditions of allyltriphenylsilane (**2a**) and allyltriisopropylsilane (**2b**) with methyl acrylate (**8a**) afforded irrespective of the temperature a mixture of the diastereomeric silylmethylcyclobutanes *anti*-**9** and *syn*-**9** (*syn* and *anti* specify the position of the silylmethyl side chain relative to the methoxycarbonyl group) and minor amounts of silylcyclopentane **10** (Table 1). However, the range of products

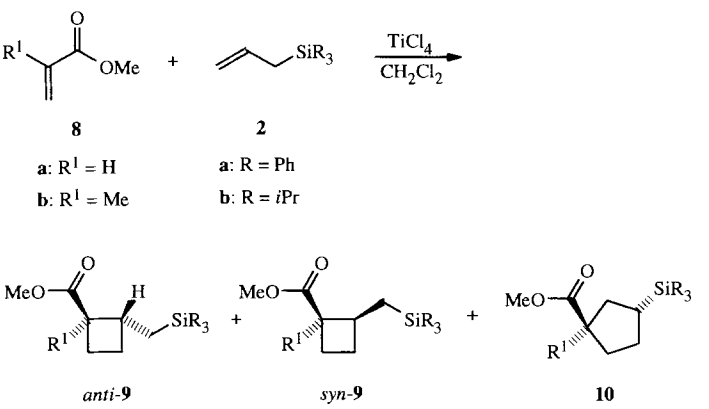


Table 1. Results of the cycloadditions of allylsilanes **2** and methyl acrylates **8**.

Products	R^1	R	Reaction conditions	Yield [%]	Product ratio [a] *anti*-**9**:*syn*-**9**:**10**
9a, **10a**	H	Ph	25 °C, 1 d → 40 °C, 1 d	46	9.8:12:1
9b, **10b**	H	*i*Pr	−40 °C → 0 °C, 19 h	100	9.5:11.9:1
9b, **10b**	H	*i*Pr	40 °C, 3 h	97	1.7:6.3:1
9c, **10c**	Me	Ph	25 °C → 40 °C, 4 d	69	9:2.5:1
9d, **10d**	Me	*i*Pr	−78 °C → −20 °C, 19 h	40	8.6:1:1.1
9d, **10d**	Me	*i*Pr	−78 °C → 40 °C, 19 h	57	5.4:1:13

[a] The product ratios were determined by NMR spectroscopy.

in the reaction of **8a** with allyltriisopropylsilane (**2b**) was significantly dependent on the temperature during the cycloaddition. Addition of **2b** to the titanium tetrachloride complex of **8a** at −40 °C and subsequent reaction at 0 °C for 19 h quantitatively provided the diastereomers *anti*-**9b** and *syn*-**9b** (1:1.25) together with small amounts of **10b**. When the reaction was performed in refluxing dichloromethane, a mixture of *anti*-**9b**, *syn*-**9b**, and **10b** was obtained in a ratio of 1.7:6.3:1 (97% yield). Therefore, it can be concluded that higher reaction temperatures favor both the cyclization of intermediate **4** (X = Oalkyl) to the *syn*-configurated silylmethylcyclobutane over the *anti* product, and the formation of the silylcyclopentane product (cyclization according to pathway a). The same trend was observed in the cycloaddition of allyltriisopropylsilane (**2b**) and methyl methacrylate (**8b**). In this case the regioselectivity for the cyclization of the intermediate siliranium ion is reversed in favor of the cyclization leading to the corresponding cyclopentane derivative (path a). Reaction at 40 °C provided the silylcyclopentane **10d** and the two diastereomers of silylmethylcyclobutane **9d** in a ratio of 2:1. Also for this example a higher proportion of the *syn*-silylmethylcyclobutane isomer was obtained at a higher temperature.

Structural assignments of the silylmethylcyclobutanes **9** and the silylcyclopentanes **10** are based on the ^{13}C NMR data (Table 2). The signals for the C atom α to the silicon atom (αSi-CH) appear for the silylcyclopentanes **10** at roughly $\delta = 23$.

Table 2. Selected ^{13}C NMR data (100 MHz, $CDCl_3$, δ values) of the silylmethylcyclobutanes **9**, **12**, and **15** [a].

	anti		*syn*	
Cyclobutane	αSi-CH_2	βSi-CH	αSi-CH_2	βSi-CH
9a	16.0	34.3	20.3	36.3
9b	11.9	34.7	17.3	37.1
9c	14.9	37.6	16.2	42.6
9d	9.9	37.7	[b]	43.1
12	11.6	49.4	17.3	49.7
15	10.2; 13.3 [c]	31.4; 35.2 [c]	13.6 [d]	40.7 [d]

[a] Relevant ^{13}C NMR data of further products for comparison: **10a**: 22.9 (αSi-CH); **10b**: 22.4 (αSi-CH); **10c**: 23.3 (αSi-CH); **10d**: 23.5 (αSi-CH); acid of *anti*-**9c**: 14.7 (αSi-CH_2), 37.6 (βSi-CH); **14**: 12.6 (αSi-CH_2), 38.8 (βSi-CH). [b] No assignment possible because of overlap with the signal of the triisopropylsilyl group. [c] *anti,syn*-**15** (major isomer). [d] *syn,syn*-**15** (minor isomer).

The NMR signals of αSi-CH groups in this type of compound generally show up in the region of $\delta = 20-25$.[2, 3, 10] The ^{13}C NMR signals of the αSi-CH_2 groups in the silylmethylcyclobutanes described here are, as expected, significantly shifted to higher field, while the signal of the βSi-CH group appears in the normal region. As anticipated, the signals of the *anti*-silylmethylcyclobutanes are shifted towards higher field relative to their *syn* isomers, in which the silylmethyl group is on the same side of the four-membered ring as the methoxycarbonyl group. For an unambiguous confirmation of the relative configuration we required an X-ray analysis. In contrast to the triphenylsilylcyclopentanes, which crystallize very easily,[2] most of the silylmethylcyclobutanes described here were obtained as oils. However, saponification of the triphenylsilylmethylcyclobutanes **9c** (KOH, H_2O, reflux, 1 d, 92%) afforded the corresponding acids from which the major diastereoisomer exhibiting the *anti* orientation was easily crystallized. Single crystals of the acid of *anti*-**9c** were suitable for an X-ray crystal structure determination, and the four-membered ring with the *anti* configuration of the side chain was unequivocally confirmed (Fig. 1).[12] The racemic acid of *anti*-**9c** crystallized diastereospecifically; dimers formed by hydrogen bonding are composed exclusively of the two opposite enantiomers (Fig. 2). Comparison of the ^{13}C NMR data of the acid of *anti*-**9c** with those of the other silylmethylcyclobutane derivatives confirms the structural assignments made above (cf. Table 2).

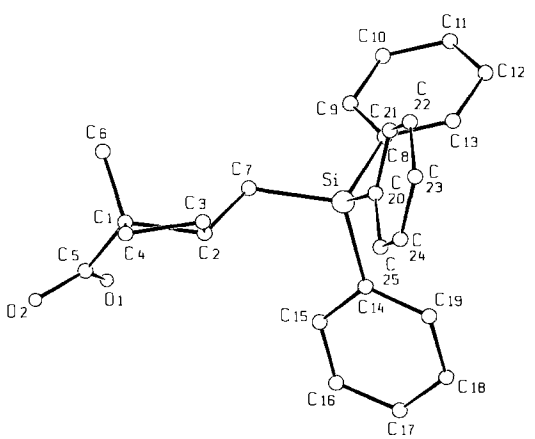


Fig. 1. Molecular structure of the acid of *anti*-**9c** in the crystal. Selected bond lengths [Å]: C1-C2 1.571(4), C2-C3 1.544(4), C3-C4 1.536(5), C1-C4 1.541(4), C1-C5 1.486(4), C1-C6 1.531(4), C2-C7 1.518(3), C7-Si 1.874(3), C8-Si 1.873(3), C14-Si 1.867(3), C20-Si 1.875(3), C5-O1 1.304(3), C5-O2 1.227(3).

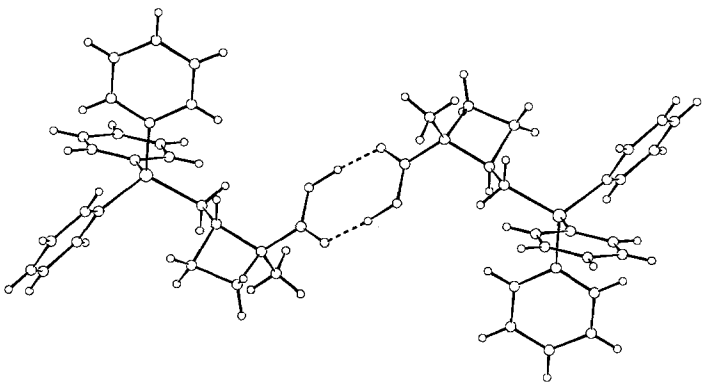
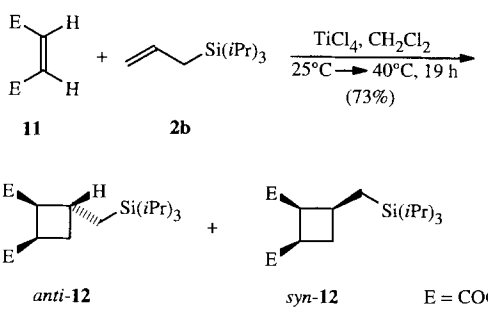


Fig. 2. Arrangement of the dimer formed by the acid of *anti*-**9c** in the crystal. Selected distances [Å] and angles [°]: O1-H1 1.16(6), O2-H1 1.47(6), O1-O2 2.619(3); O1-H1-O2 173(5).

Addition of allyltriisopropylsilane (**2b**) to the titanium tetrachloride complex of dimethyl maleate (**11**) at room temperature and subsequent reaction at 40 °C for 19 h afforded in 73% yield a mixture of the diastereomers *anti*-**12** and *syn*-**12** in a ratio of



4:1. In this case lower reaction temperatures favored the formation of the *syn* diastereomer (25 °C, 5 d, 61% yield; *anti*-**12**/*syn*-**12** = 1:1.3). Structural assignments were again based on the ^{13}C chemical shift of the CH_2 group α to silicon, which is significantly shifted downfield for the *syn* diastereomer (Table 2).

We recently described a remarkable extension of the [3+2] cycloaddition methodology of allylsilanes—the direct synthesis of bicyclo[3.3.0]octanes by the domino [3+2] cycloaddition of allylsilanes and 3-butyn-2-one.[13] This process generates four C–C σ-bonds in a one-pot reaction. Thus we expected that direct access to the bicyclo[2.2.0]hexane framework should be feasible by a domino [2+2] cycloaddition of allyltriisopropylsilane (**2b**) and propynoic ester **13**. In this reaction the two four-membered rings would be formed sequentially, the first by a [2+2] cycloaddition of **2b** to the Lewis acid complex of **13**, and the second by a [2+2] cycloaddition to the Lewis acid complex of the intermediate cyclobutenecarboxylic acid ester formed in the first step.

Addition of three equivalents of allyltriisopropylsilane (**2b**) to the titanium tetrachloride complex of methyl propynoate (**13**) at −78 °C and subsequent reaction at −20 °C for 19 h selectively provided the cyclobutene **14** in 98% yield (Table 3). After reac-

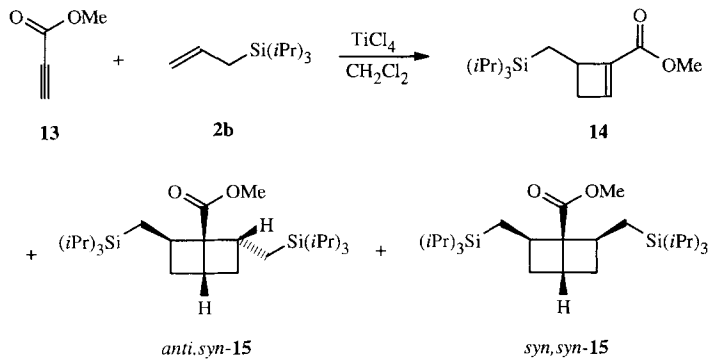


Table 3. Cycloaddition of allylsilane **2b** and methyl propynoate (**13**).

Reaction conditions	**14**, Yield [%]	**15**, Yield [%]
3 equiv **2b**, −78 °C → −20 °C, 19 h	98	–
4 equiv **2b**, −78 °C → 25 °C, 5 d	45	46 [a]
3 equiv **2b**, 25 °C → 40 °C, 19 h	34	64 [a]

[a] *anti,syn*-**15**: *syn,syn*-**15** = 3:1. Traces of the Sakurai product and a cyclopentane derivative were also detected.

tion at room temperature for five days, **14** and the bicyclo[2.2.0]hexane **15**, the product of the domino reaction, were formed in approximately equal amounts. Cycloaddition of **2b** with **13** in dichloromethane at reflux for 19 h provided **15** and **14** in yields of 64% and 34%, respectively. Bicyclo[2.2.0]hexane **15** was obtained as a mixture of the *anti,syn* and the *syn,syn* diastereomers in a 3:1 ratio. The two diastereomers are easily distinguished by their ^{13}C NMR spectra. The major isomer *anti,syn*-**15** shows two signals for the αSi-CH_2 groups, one *anti* to the methoxycarbonyl group at $\delta = 10.2$ and one *syn* at $\delta = 13.3$. The minor isomer *syn,syn*-**15** is symmetrical and therefore exhibits only one signal for the αSi-CH_2 group in the region typical for the *syn* diastereoisomer ($\delta = 13.6$). Thus, this product was assigned the *syn,syn* configuration with both silylmethyl groups on the same side as the methoxycarbonyl group.

Experimental Procedure

15: A solution of methyl propynoate (**13**) (337 μL, 339 mg, 4.03 mmol) in dry dichloromethane (5 mL) was added to a stirred solution of titanium tetrachloride (490 μL, 840 mg, 4.43 mmol) in dry dichloromethane (5 mL) at room temperature. To this mixture was added a solution of allyltriisopropylsilane (**2b**) (2.92 mL, 2.40 g, 12.08 mmol) in dry dichloromethane (5 mL). The reaction mixture was refluxed for 19 h and then quenched by addition of an aqueous solution of ammonium chloride. The organic layer was separated, the aqueous layer was extracted three times with dichloromethane, and the combined organic layers were dried over magnesium sulfate. Evaporation of the solvent and flash chromatography (hexane/ether 15:1) of the residue on silica gel provided the bicyclo[2.2.0]hexane **15** (1.24 g, 64%) and the cyclobutene **14** (387 mg, 34%) both as colorless oils.

Received: March 15, 1994 [Z 6760 IE]
German version: *Angew. Chem.* **1994**, *106*, 1705

[1] H.-J. Knölker, P. G. Jones, J.-B. Pannek, *Synlett* **1990**, 429; H.-J. Knölker in *Organic Synthesis via Organometallics* (Eds.: K. H. Dötz, R. W. Hoffmann), Vieweg, Braunschweig, **1991**, p. 119; H.-J. Knölker, P. G. Jones, J.-B. Pannek, A. Weinkauf, *Synlett* **1991**, 147; H.-J. Knölker, *ibid.* **1992**, 371.

[2] H.-J. Knölker, N. Foitzik, H. Goesmann, R. Graf, *Angew. Chem.* **1993**, *105*, 1104; *Angew. Chem. Int. Ed. Engl.* **1993**, *32*, 1081. This work was presented at the 8th ORCHEM meeting in Bad Nauheim (Germany), September 24–26, 1992.

[3] H.-J. Knölker, R. Graf, *Tetrahedron Lett.* **1993**, *34*, 4765.

[4] a) K. Ohkata, K. Ishimaru, Y.-G. Lee, K.-Y. Akiba, *Chem. Lett.* **1990**, 1725; b) S. Imazu, N. Shimizu, Y. Tsuno, *ibid.* **1990**, 1845; c) Y.-G. Lee, K. Ishimaru, H. Iwasaki, K. Ohkata, K.-Y. Akiba, *J. Org. Chem.* **1991**, *56*, 2058; d) G. Majetich, J.-S. Song, C. Ringold, G. A. Nemeth, M. G. Newton, *ibid.* **1991**, *56*, 3973; e) B. B. Snider, Q. Zhang, *ibid.* **1991**, *56*, 4908; f) J. Ipaktschi, A. Heydari, *Angew. Chem.* **1992**, *104*, 335; *Angew. Chem. Int. Ed. Engl.* **1992**, *31*, 313; g) R. L. Danheiser, B. R. Dixon, R. W. Gleason, *J. Org. Chem.* **1992**, *57*, 6094; h) J. S. Panek, N. F. Jain, *ibid.* **1993**, *58*, i) 2345; R. L. Danheiser, T. Takahashi, B. Bertók, B. R. Dixon, *Tetrahedron Lett.* **1993**, *34*, 3845; j) M.-J. Wu, J.-Y. Yeh, *Tetrahedron* **1994**, *50*, 1073.

[5] a) A. Hosomi, H. Sakurai, *J. Am. Chem. Soc.* **1977**, *99*, 1673; G. Majetich, A. M. Casares, D. Chapman, M. Behnke, *Tetrahedron Lett.* **1983**, *24*, 1909; b) T. A. Blumenkopf, C. H. Heathcock, *J. Am. Chem. Soc.* **1983**, *105*, 2354. Reviews: H. Sakurai, *Pure Appl. Chem.* **1982**, *54*, 1; A. Hosomi, *Acc. Chem. Res.* **1988**, *21*, 200; D. Schinzer, *Synthesis* **1988**, 263.

[6] M. R. Ibrahim, W. L. Jorgenson, *J. Am. Chem. Soc.* **1989**, *111*, 819; J. B. Lambert, *Tetrahedron* **1990**, *46*, 2677; J. B. Lambert, E. C. Chelius, *J. Am. Chem. Soc.* **1990**, *112*, 8120; J. M. White, G. B. Robertson, *J. Org. Chem.* **1992**, *57*, 4638; J. B. Lambert, R. W. Emblidge, S. Malany, *J. Am. Chem. Soc.* **1993**, *115*, 1317.

[7] W. Hanstein, H. J. Berwin, T. G. Traylor, *J. Am. Chem. Soc.* **1970**, *92*, 829; T. G. Traylor, W. Hanstein, H. J. Berwin, N. A. Clinton, R. S. Brown, *ibid.* **1971**, *93*, 5715.

[8] J. E. Baldwin, *J. Chem. Soc. Chem. Commun.* **1976**, 734.

[9] R. Pardo, J.-P. Zhara, M. Santelli, *Tetrahedron Lett.* **1979**, 4557; A. Hosomi, H. Kobayashi, H. Sakurai, *ibid.* **1980**, *21*, 955; S. Danishefsky, M. Kahn, *ibid.* **1981**, *22*, 485; H. O. House, P. C. Gaa, D. VanDerveer, *J. Org. Chem.* **1983**, *48*, 1661; G. Majetich, J. Defauw, C. Ringold, *ibid.* **1988**, *53*, 50; K. Nickisch, H. Laurent, *Tetrahedron Lett.* **1988**, *29*, 1533; G. Majetich, K. Hull, D. Lowery, C. Ringold, J. Defauw in *Selectivities in Lewis Acid Promoted Reactions* (Ed.: D. Schinzer), Kluwer, Dordrecht, **1989**, p. 169; G. Majetich, J.-S. Song, C. Ringold, G. A. Nemeth, *Tetrahedron Lett.* **1990**, *31*, 2239.

[10] H.-J. Knölker, N. Foitzik, R. Graf, J.-B. Pannek, P. G. Jones, *Tetrahedron* **1993**, *49*, 9955.

[11] a) Photochemical [2+2] cycloaddition of allyltrimethylsilanes and 1,4-naphthoquinones: M. Ochiai, M. Arimoto, E. Fujita, *J. Chem. Soc. Chem. Commun.* **1981**, 460; b) [2+2] cycloaddition of allyltrimethylsilanes and tetracyanoethylene: G. D. Hartmann, T. G. Traylor, *Tetrahedron Lett.* **1975**, 939 and ref. [4b]; c) Lewis acid mediated [2+2] cycloaddition of 3-methylthio-4-trimethylsilyl-1,2-butadiene and alkenes: M. Hojo, K. Tomita, Y. Hirohara, A. Hosomi, *Tetrahedron Lett.* **1993**, *34*, 8123.

[12] Crystal structure analysis of the acid of *anti*-**9c**: $C_{25}H_{26}O_2Si$, monoclinic, space group $P2_1/n$, $a = 9.445(3)$, $b = 19.035(7)$, $c = 12.235(5)$ Å, $\beta = 96.90(3)°$, $V = 2183.7(14)$ Å^3, $Z = 4$, $\rho_{calcd} = 1.176$ g cm^{-3}, $T = 200(1)$ K, $\mu = 0.124$ mm^{-1}; $\lambda = 0.71069$ Å; $2\theta_{max} = 52°$; 4009 independent reflections; refinement method: full-matrix least squares on F^2; $R_1 = 0.0507$, $wR_2 = 0.1226$; maximal residual electron density: 0.477 eÅ^{-3}. Programs: G. M. Sheldrick, SHELXS-86 (Göttingen **1986**), SHELXL-93 (Göttingen **1993**); E. Keller, SCHAKAL-92 (Freiburg i.Br., **1992**). Further details of the crystal structure investigation may be obtained from the Fachinformationszentrum Karlsruhe D-76344 Eggenstein-Leopoldshafen, on quoting the depository number CSD-58304.

[13] H.-J. Knölker, R. Graf, *Synlett* **1994**, 131.

The Formation and an Unusual Dimerization of 2-Mesityl-1,1-bis(trimethylsilyl)silene**

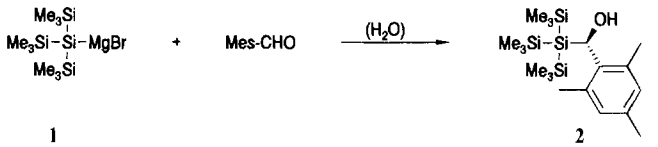
Clemens Krempner, Helmut Reinke, and Hartmut Oehme*

The reaction of tris(trimethylsilyl)silylmagnesium bromide **1** with aldehydes and ketones makes accessible 1-hydroxyalkyltris(trimethylsilyl)silanes, which have proven useful as precursors for the synthesis of silenes by a modified Peterson mechanism. Recently we have reported the formation of 2-*tert*-butyl-1,1-bis(trimethylsilyl)silene by the base-initiated elimination of trimethylsilanolate from 2,2-dimethyl-1-tris(trimethylsilyl)silylpropanol and its head-to-head cyclodimerization to the corresponding 1,2-disilacyclobutane.[1]

[*] Prof. Dr. H. Oehme, Dipl.-Chem. C. Krempner, Dr. H. Reinke
Fachbereich Chemie der Universität
D-18051 Rostock (FRG)
Telefax: Int. code + (381)498-1763

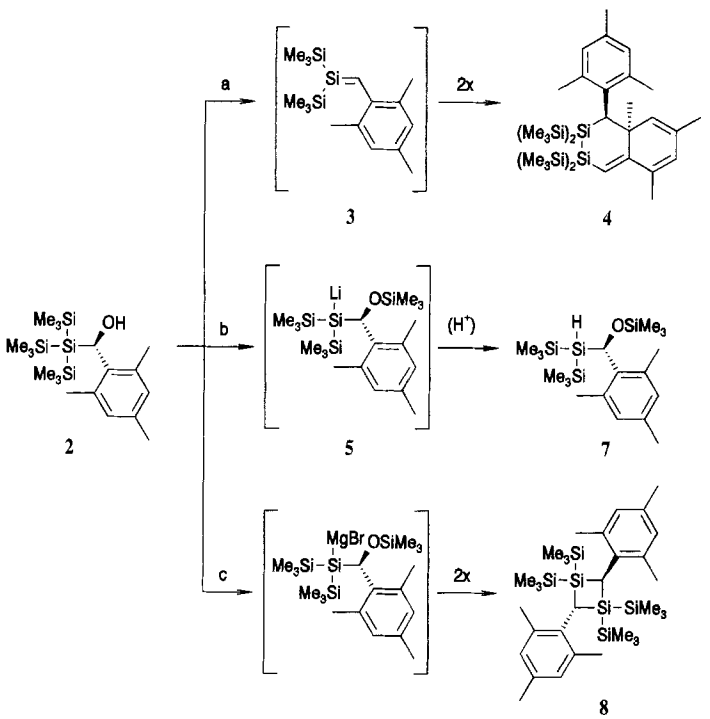
[**] This work was supported by the Deutsche Forschungsgemeinschaft and the Fonds der Chemischen Industrie.

The reaction of 2,4,6-trimethylbenzaldehyde and **1**, which is prepared from $(Me_3Si)_3SiLi \cdot 3THF$[2] and magnesium bromide in ether and is used in situ, yields mesityltris(trimethylsilyl)silylmethanol **2**. The identity of **2** has been established by spectroscopic and mass spectrometric means.



1 2

If strong bases are added to **2**, trimethylsilanolate is eliminated which, after aqueous workup, can be identified by gas chromatography as hexamethyldisiloxane. The result of this reaction is strongly dependent on the base used for deprotonation, the solvent employed, and the reaction conditions. For example, the deprotonation of **2** with methyllithium in ether at $-78\,^{\circ}C$ leads to a colorless, crystalline, air-stable compound, which was identified by ^1H, ^{13}C, and ^{29}Si NMR spectroscopy, mass spectrometry, and an X-ray crystal structure analysis as (*E*)-1,2,3,8a-tetrahydro-1-mesityl-5,7,8a-trimethyl-2,2,3,3-tetrakis(trimethylsilyl)-2,3-disilanaphthalene **4** (see Scheme 1, Fig. 1).[3] The crystal



Scheme 1. Deprotonation of **2**: a) by MeLi in Et_2O at $-78\,^{\circ}C$, elimination of Me_3SiOLi; b) by MeLi in THF at $-70\,^{\circ}C$; c) by MeMgBr in Et_2O at $0\,^{\circ}C$, elimination of $Me_3SiOMgBr$.

structure analysis yielded an interesting boat conformation for the disilacyclohexene fragment, in which the plane defined by Si1, Si2, and C8 is tilted by 16.8° and the plane defined by C1, C2, and C7 by 43.6° with respect to the plane defined by Si1, C1, C7, and C8.

We interpret the formation of **4** as the result of a head-to-head cyclodimerization of the unstable silaethene (silene) **3**, which undergoes an unusual [2+4] reaction in which the silene acts as

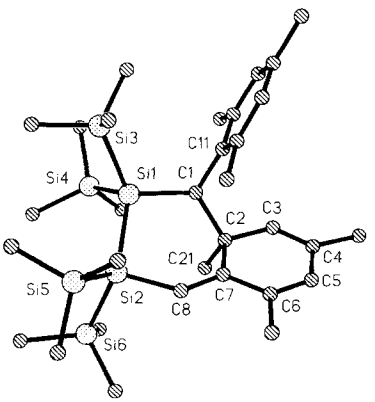
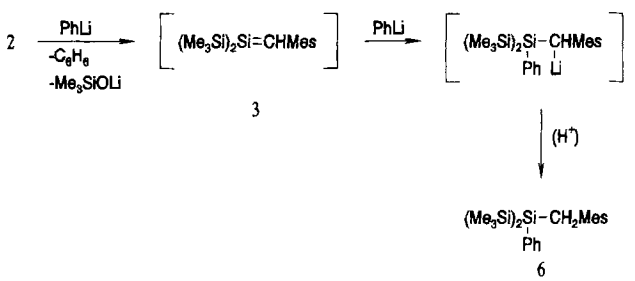


Fig. 1. Structure of **4** in the crystal (H atoms omitted for clarity). Selected bond lengths [pm] and angles [°]: Si1-Si2 236.9(1), Si1-Si3 237.6(1), Si1-Si4 238.4(1), Si2-Si5 237.1(1), Si2-Si6 238.0(1), Si1-C1 195.6(2), C1-C2 159.0(2), C2-C3 150.7(3), C2-C21 154.9(2), C2-C7 154.6(3), C7-C8 134.8(3), C8-Si2 187.3(2); Si1-Si2-C8 101.18(7), Si2-Si1-C1 104.01(6), Si1-C1-C2118.52(12), C1-C2-C3 118.84(14), C2-C7-C8 122.46(16), C7-C8-Si2 131.82(15), C21-C2-C7 105.03(15), Si3-Si1-Si4 101.62(4), Si5-Si2-Si6 104.68(4).

the monoene as well as by utilizing the aromatic substituent the diene (see Scheme 1). The groups of Brook[4] and Ishikawa[5] have identified radical intermediates for the dimerization of similar silenes. Based on these results we assume an initial Si–Si linkage and the formation of a diradical, which then stabilizes and yields **4**. The current results do not allow the exclusion of an alternative mechanism, namely the addition of the lithium silanide **5** to the Si=C bond of silene **3** and subsequent ring formation in the sense of a nucleophilic substitution of the trimethylsiloxy unit. The intermediate formation of the silene **3** can be proven by the reactions of **2** with an excess of organolithium compounds, which yield the corresponding 2-alkyl- or 2-aryltrisilanes. For instance, the reaction of **2** with an excess of phenyllithium leads to 1,1,1,3,3,3-hexamethyl-2-(2,4,6-trimethylphenylmethyl)-2-phenyltrisilane **6** in 92% yield. The nucleophilic addition of phenyllithium to **3** leads to an organolithium intermediate, which is transformed into **6** by the aqueous workup.



The dimerization behavior of **3** is unusual insofar as, in the absence of scavenger reagents, sterically encumbered unstable silenes usually dimerize in a head-to-head fashion, yielding 1,2-disilacyclobutanes.[6] Silene **3** is therefore also fundamentally different from the 2-mesityl-2-trimethylsiloxy-1,1-bis(trimethylsilyl)silene prepared by Brook and co-workers.[7] This compound is stable in solution for extended periods and reacts under photolysis conditions to yield a substituted dihydrobenzocyclobutene. A [2+4] reaction similar to the synthesis of **4** has been discussed by Fink et al. for the dimerization of 1-mesityl-2,3,4-tri-*tert*-butyl-1-silacyclobutadiene.[8]

The initially unexpected [2+4] reaction of **3** becomes more obvious when one considers the steric demands of the mesityl group and the weak C–C bonds in the 1,2-disilacyclobutanes formed by the dimerization of sterically hindered silenes.[9] Silenes with allyl groups avoid the formation of four-membered rings and prefer a linear dimerization by a H transfer.[5, 10] For many silenes, for example 2-*tert*-butyl-1,1-bis(trimethylsilyl)silene,[1] there is apparently no alternative to the [2+2] cyclodimerization. For **3** the [2+4] addition is a viable pathway to avoid the steric hindrance stemming from the formation of a four-membered ring, while dimerization would lead to a 1,2-disilacyclobutane with a sterically congested C–C bond.

A completely different scenario is found for the reaction of **2** in THF. The addition of MeLi to a THF solution of **2** at −70 °C leads to a rapid 1,3-Si,O-trimethylsilyl migration, forming the lithium silanide **5**, which yields mesityltrimethylsiloxybis(trimethylsilyl)silylmethane (**7**) upon protonation (see Scheme 1). This transformation proceeds particularly smoothly, in THF as well as ether, when sodium hydride is used as base, yielding **7** quantitatively. Compound **5** and its sodium analogue are apparently unable to form a silene in THF; compound **4** could not be found in the reaction mixture.

If **2** is deprotonated with MeMgBr in THF 2,4-dimesityl-1,1,3,3-tetrakis(trimethylsilyl)-1,3-disilacyclobutane **8** is formed in addition to **7** (see Scheme 1). Dimer **8** can also be prepared by the in situ reaction of **1** and mesitylaldehyde in THF. The proposed structure is supported by NMR and mass spectrometry data and an X-ray crystal structure analysis, which showed the presence of a slightly bent four-membered ring (see Fig. 2).[11]

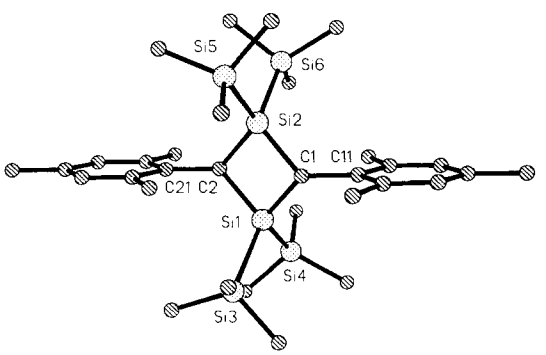


Fig. 2. Structure of **8** in the crystal (H atoms omitted for clarity). Selected bond lengths [pm] and angles [°]: Si1-C1 194.3(4), Si1-C2 194.3(4), Si1-Si3 239.2(2), Si1-Si4 237.7(2), Si2-C1 194.1(3), Si2-C2 194.5(4), Si2-Si5 238.3(2), Si2-Si6 238.1(2), C1-C11 151.6(5), C2-C21 151.1(5); C2-Si1-C1 90.11(15), C2-Si2-C1 90.10(15), Si1-C1-Si2 89.91(15), Si1-C2-Si2 89.79(15).

The two planes each containing the Si atoms and one C atom of the ring intersect at an angle of 3°. This four-membered ring structure leads to a relatively short distance between Si1 and Si2 (274.4 pm).

The cyclobutane **8** is formally the head-to-tail cyclodimerization product of the silene **3**. Apparently the change of solvent for the deprotonation of **2** from ether to THF also leads to a fundamental change in the course of the reaction. The formation of **4** from **2** and MeLi in ether is likely to proceed through an intermediate silene. As will be reported elsewhere, this intermediate leads to the expected products upon reaction with 2,3-dimethylbutadiene and nucleophiles. On the other hand, we assume that **8** is the result of an intermolecular elimination of trimethylsilanolate from a magnesium silanide similar to **5**. Bimolecular reactions of this type have been identified in similar cases.[12]

Experimental Procedure

2: Within 30 minutes a solution of 2.37 g (0.016 mol) of 2,4,6-trimethylbenzaldehyde in 30 mL of ether was added dropwise, at −70 °C, to a solution of **1**, prepared from 7.3 g (0.016 mol) of $(Me_3Si)_3SiLi \cdot 3THF$ and an equimolar amount of $MgBr_2$ in 80 mL of ether. The mixture was stirred for 3 h at −70 °C and subsequently subjected to an aqueous workup. After solvent removal, volatile impurities were removed from the crude product by vacuum sublimation. The residue was recrystallized twice from acetonitrile. Yield 4.06 g (66%); m.p. 119–120 °C; IR (Nujol mull): $\tilde{\nu}_{OH} = 3507.2\ cm^{-1}$; ^1H NMR (250 MHz, [D$_6$]acetone): $\delta = 0.12$ (s, $SiCH_3$, 27H), 2.17 (s, Ar-*p*-CH_3), 3H), 2.35 (br s, Ar-*o*-CH_3, 6H), 3.72 (d, $^3J = 4.1$ Hz, OCH, 1H), 5.64 (d, $^3J = 4.4$ Hz, COH, 1H), 6.75 (br s, ArH, 2H); ^{13}C NMR (62.9 MHz, [D$_6$]acetone): $\delta = 2.13$ ($SiCH_3$), 20.76 (Ar-*p*-CH_3), 21.53, 23.44 (Ar-*o*-CH_3), 62.75 (COH), 129.34, 131.02, 133.45, 135.61, 137.89, 140.99 (aromatic C); ^{29}Si NMR (59.6 MHz, $CDCl_3$): $\delta = -11.94$ ($SiCH_3$), −71.26 (*Si*($SiMe_3$)$_3$); MS (CI, isobutane): *m/z* (%): 397 (1.5) [$M^+ - 1$], 379 (100) [$M^+ - OH$], 307 (7) [$M^+ - Me_3SiOH$].

4: To a solution of 0.5 g (1.26 mmol) of **2** in 20 mL of ether at −78 °C was added an equimolar amount of MeLi (1.6 M). The mixture was stirred at −78 °C for 1 h and subsequently allowed to warm to room temperature over a period of 2 h. After hydrolytic workup and solvent removal, a residue was obtained that was recrystallized twice from acetone. Yield 0.27 g (70%); m.p. 152–154 °C; ^1H NMR ([D$_6$]benzene): $\delta = 0.07$ (s, $SiCH_3$, 9H), 0.52, 0.52, 0.55 (3s, $SiCH_3$, 27H), 1.49, 1.56, 2.06, 2.16, 2.34, 2.47 (6s, CH_3, 6 × 3H), 3.87 (s, Si*CH*Mes, 1H), 5.14, 5.65, 6.37 (3s, olefinic H, 3 × 1H), 6.76, 6.82 (2s, aromatic H, 2 × 1H); ^{13}C NMR ([D$_6$]benzene, DEPT, C,H-COSY): $\delta = 1.93$, 2.33, 2.56, 3.04 ($SiCH_3$), 20.67, 21.09, 21.14, 23.14, 26.02, 37.94 (CCH_3), 37.53 (SiCHMes), 45.21 (8a-C), 119.61, 125.31, 136.15 (olefinic CH), 129.36, 130.92 (aromatic CH), 125.46, 133.14, 134.18, 135.51, 137.43, 141.63, 160.93 (quarternary, olefinic, and aromatic C); ^{29}Si NMR ([D$_6$]benzene): $\delta = -94.70$, −87.10 (*Si*$SiMe_3$), −12.44, −11.83, −11.26, −10.22 ($SiMe_3$); MS (70 eV): *m/z* (%): 612 (7) [M^+], 597 (4) [$M^+ - CH_3$], 539 (14) [$M^+ - SiMe_3$], 348 (100) {[$Me_3Si]_2Si)_2$}$^+$.

6: A solution of 0.5 g (1.26 mmol) of **2** in 20 mL of ether was added dropwise to a five-fold molar excess of PhLi in 10 mL of ether at room temperature. After 4 h of stirring the solution was worked up hydrolytically. Compound **6** was obtained from the organic phase by Kugelrohr distillation (0.1 Torr, 175 °C). Yield 0.45 g (92%); m.p. 76 °C; ^1H NMR ($CDCl_3$): $\delta = 0.02$ (s, $SiCH_3$, 18H), 2.02 (s, Ar-*o*-CH_3, 6H), 2.18 (s, Ar-*p*-CH_3, 3H), 2.49 (s, $SiCH_2$, 2H), 6.70 (s, Mes-H, 2H), 7.20–7.24, 7.37–7.41 (2m, Ph-H, 5H); ^{13}C NMR ($CDCl_3$, DEPT): $\delta = -0.18$ ($SiCH_3$), 13.75 ($SiCH_2$), 20.70 (Ar-*p*-Me), 21.56 (Ar-*o*-Me), 127.72, 127.80, 128.63, 135.04 (aromatic CH), 133.24, 134.78, 135.88, 138.58 (aromatic C); ^{29}Si NMR ($CDCl_3$): $\delta = -42.56$ (Ph-Si), −15.38 ($SiMe_3$); MS (70 eV): *m/z* (%): 383 (8) [$M^+ - H$], 369 (10) [$M^+ - CH_3$], 307 (100) [$M^+ - Ph$].

7: To a solution of 0.5 g (1.26 mmol) of **2** in 25 mL of THF were added 0.06 g (2.5 mmol) of NaH, and the mixture was stirred for 1 h at room temperature. After aqueous workup and solvent removal, an oil was obtained that was purified by Kugelrohr distillation (0.1 Torr, 140 °C). Yield 0.47 g (93%); IR (capillary): $\tilde{\nu}_{SiH} = 2043.4$, 2088.4 cm^{-1}; ^1H NMR ([D$_6$]benzene): $\delta = 0.01$, 0.11, 0.26 (3s, $SiCH_3$, 3 × 9H), 2.10 (s, Ar-*p*-CH_3, 3H), 2.25 (s, Ar-*o*-CH_3, 3H), 2.69 (s, *o*-CH_3, 3H), 3.97 (d, $^3J = 5.43$ Hz, SiH, 1H), 5.55 (d, $^3J = 5.9$ Hz, CH, 1H), 6.67, 6.78 (2s, aromatic H, 2H); ^{13}C NMR ([D$_6$]benzene, DEPT): $\delta = 0.94$, 1.22, 1.33 ($SiCH_3$), 21.54, 21.76, 22.85 (Ar-CH_3), 63.83 (CHOSi), 129.80, 132.03 (aromatic CH), 132.75, 136.26, 138.90, 139.60 (aromatic C); ^{29}Si NMR ([D$_6$]benzene): $\delta = -58.4$ (SiH, $J_{SiH} = 162.8$ Hz), −14.61, −15.33 (Si*Si*Me_3), 17.09 ($OSiMe_3$); MS (CI, isobutane): *m/z* (%): 395 (0.2) [$M^+ - 1$], 381 (0.6) [$M^+ - CH_3$], 307 (4) [$M^+ - OSiMe_3$], 221 (100) [$Me_3SiOCHMes^+$].

8: To a solution of 0.5 g (1.26 mmol) of **2** in 10 mL of THF at 0 °C was added an equimolar amount of methylmagnesium bromide (prepared from MeLi and $MgBr_2$). The mixture was stirred for 5 h while cooling on ice and subsequently subjected to an aqueous workup. After solvent removal an oil was obtained that was dissolved in acetone. Cyclobutane **8** slowly crystallized from this solution and was recrystallized once from acetone. Yield 0.053 g (14%); m.p. 240–241 °C; ^1H NMR ($CDCl_3$): $\delta = 0.07$ (s, $SiCH_3$, 36H), 2.18 (s, Ar-*p*-CH_3, 6H), 2.45 (s, Ar-*o*-CH_3, 12H), 3.87 (s, ring CH, 2H), 6.70 (s, Ar-H, 4H); ^{13}C NMR ($CDCl_3$, DEPT): $\delta = 0.68$ ($SiCH_3$), 14.91 (Ar-*p*-CH_3), 20.59 (ring C), 24.25 (Ar-*o*-CH_3), 128.74 (Ar-*o*-*C*), 132.29, 134.46, 136.09 (Ar-*ipso*-*C*, Ar-*m*-*C*, Ar-*p*-*C*); ^{29}Si NMR ($CDCl_3$): $\delta = -12.25$ (Si*Si*Me_3), −6.10 (*Si*$SiMe_3$); MS (CI, isobutane): *m/z* (%): 613 (60) [$M^+ - H$], 612 (28) [M^+], 597 (8) [$M^+ - CH_3$], 539 (72) [$M^+ - SiMe_3$], 493 (100) [$M^+ - Mes$].

Received: February 19, 1994 [Z6698IE]
German version: *Angew. Chem.* **1994**, *106*, 1709

[1] C. Krempner, H. Oehme, *J. Organomet. Chem.* **1994**, *464*, C7.
[2] G. Gutekunst, A. G. Brook, *J. Organomet. Chem.* **1982**, *225*, 1.
[3] Crystal structure analysis of **4**: space group *P*1, $a = 1027.5(2)$, $b = 1093.4(2)$, $c = 2007.2(4)$ pm, $\alpha = 97.84(3)$, $\beta = 98.66(3)$, $\gamma = 114.36(3)°$, $V = 1.9809\ nm^3$, $Z = 2$, $\mu = 0.23\ mm^{-1}$ ($Mo_{K\alpha}$). 7683 measured reflections, $2\theta_{max} = 52°$, structure solution by direct methods [13] 7650 independent reflections used for refinement on F^2 [14]. The Si and C atoms were refined anisotropically, H atoms were calculated from electron density difference maps and refined by

using a riding model, 361 parameters, $R1$ for 6670 reflections with $F_0 > 4\sigma(F_0)$ was 0.0444, and 0.0509 for all data, $wR2$ for all data was 0.1325, GOF = 1.061; cf. [11b].
[4] A. G. Brook, J. W. Harris, J. Lennon, M. ElSheikh, *J. Am. Chem. Soc.* **1979**, *101*, 83; A. G. Brook, K. M. Baines, *Adv. Organomet. Chem.* **1986**, *25*, 26.
[5] J. Ohshita, Y. Masaoka, M. Ishikawa, *Organometallics* **1991**, *10*, 3775.
[6] G. Raabe, J. Michl in *The Chemistry of Organic Silicon Compounds* (Eds.: S. Patai, Z. Rappoport), Wiley, New York, **1989**, p. 1100.
[7] A. G. Brook, H.-J. Wessely, *Organometallics* **1985**, *4*, 1487.
[8] D. B. Puranik, M. P. Johnson, M. J. Fink, *J. Chem. Soc. Chem. Commun.* **1989**, 706.
[9] A. G. Brook, S. C. Nyburg, W. F. Reynolds, Y. C. Poon, Y.-M. chang, J.-S. Lee, J. P. Picard, *J. Am. Chem. Soc.* **1979**, *101*, 6750; D. Bravo-Zhivotovskii, V. Braude, A. Stanger, M. Kapon, Y. Apeloig, *Organometallics* **1992**, *11*, 2326.
[10] K. M. Baines, A. G. Brook, *Organometallics* **1987**, *6*, 692.
[11] a) Crystal structure analysis of **8**: space group $P2_1/c$, $a = 1026.6(2)$, $b = 2055.7(4)$, $c = 1836.7(4)$ pm, $\beta = 97.14(3)^\circ$, $V = 3.8461$ nm^3, $Z = 4$, $\mu = 0.24$ mm^{-1} ($Mo_{K\alpha}$). 7558 measured reflections, $2\theta_{max} = 52^\circ$, structure solution by direct methods [13], 7450 reflections used for refinement on F^2 [14]. The Si and C atoms were refined anisotropically, H atoms were calculated from electron density difference maps and refined by using a riding model, 343 parameters, $R1$ for 4246 reflections with $F_0 > 4\sigma(F_0)$ was 0.0672, and 0.1347 for all data, $wR2$ for all data was 0.1903, GOF = 1.040. b) Further details of the crystal structure investigation may be obtained from the Fachinformationszentrum Karlsruhe, D-76344 Eggenstein-Leopoldshafen (FRG) on quoting the depository number CSD-58237.
[12] N. Wiberg, *J. Organomet. Chem.* **1984**, *273*, 141.
[13] G. M. Sheldrick, SHELXS 86, Universität Göttingen, **1986**.
[14] G. M. Sheldrick, SHELXL-93, Universität Göttingen, **1993**.

An Efficient Access to Organocerium(IV) Complexes: Synthesis and Structure of Bis[1,3,6-tris(trimethylsilyl)cyclooctatetraene]cerium(IV)**

Ulrike Kilimann, Regine Herbst-Irmer, Dietmar Stalke, and Frank T. Edelmann*

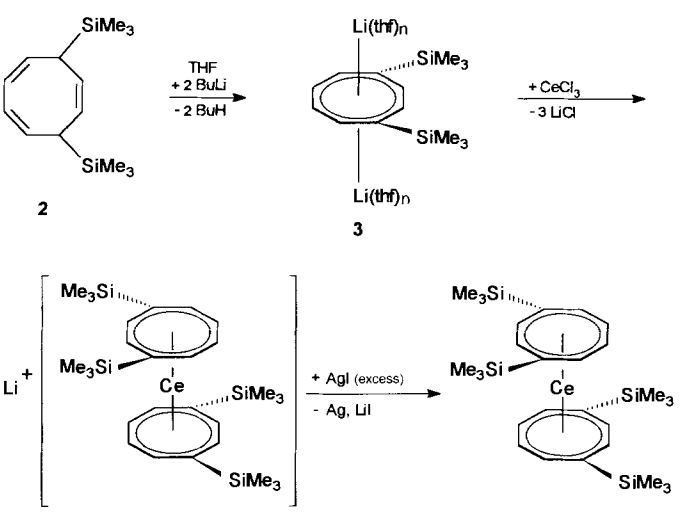
Dedicated to Professor Wolfgang Lüttke on the occasion of his 75th birthday

The synthesis of stable organometallic compounds containing tetravalent cerium is one of the challenges in the field of preparative organo-f-element chemistry.[1] The main reason why numerous attempts at the synthesis of organocerium(IV) complexes have failed is the strong oxidizing effect of the cerium(IV) ion (E^0 for Ce^{3+}/Ce^{4+} in HCl: +1.28 V; in 8 M $HClO_4$: +1.87 V[2]). Thus, in reactions with organometallic reagents such as NaC_5H_5, the cerium(IV) reagents $(NH_4)_2[Ce(NO_3)_6]$ or $[pyH]_2[CeCl_6]$ (pyH = pyridinium cation) are reduced without exception to cerium(III) products. A series of complexes of the type $[(C_5H_5)_3CeX]$ and $[(C_9H_7)_2CeX_2]$ (X = H, BH_4, Cl, N_3, CN, NCO, NO_2, NO_3, OR, O_2CR, SR, NH_2, alkyl, aryl) described in the 1970s[3–6] were all found to have been wrongly characterized.[1] Also, for "$[(C_5H_5)_4Ce]$"[3] it was demonstrated that this compound was in fact $[(C_5H_5)_3Ce(thf)]$.[7] Bis(cyclooctatetraene)cerium(IV) (**1**), also known as bis([8]annulene)-cerium(IV) or "cerocene", which is of considerable theoretical interest,[8, 9] and its 1,1′-dimethyl derivative $[Ce(C_8H_7Me)_2]$[10] are among the few fully characterized organocerium(IV) complexes. Complex **1** was discovered in 1976 by Cesca et al.;[11] however, because of its pyrophoric nature and its poor solubility in organic solvents, unsubstituted **1** is not very attractive for reactivity studies. We describe here an efficient entry to soluble bis(cyclooctatetraene)cerium(IV) complexes, which for the first time allows an extensive study of this interesting class of compounds.

$[Ce(\eta^8\text{-}C_8H_8)_2]$ **1**

For the reasons mentioned above the controlled oxidation of cerium(III) precursors appeared to be a more suitable route for the synthesis of new cerium(IV) complexes than starting from $(NH_4)_2[Ce(NO_3)_6]$ or $[pyH]_2[CeCl_6]$. In our synthesis concept substituted cyclooctatetraene ligands should sterically shield the cerium atom and thus protect it from decomposition reactions. As in many cyclopentadienyl complexes, for example those with 1,3-bis(trimethylsilyl)cyclopentadienyl ligands,[12, 13] bulky trimethylsilyl substituents should be particularly suitable for this purpose.

Following a suggestion by Cloke et al.,[14] initially the dianion of 1,4-bis(trimethylsilyl)cyclooctatetraene was prepared. Its lithium salt **3** is readily accessible by metalation of 1,4-bis(trimethylsilyl)cyclooctatriene (**2**) with *n*-butyllithium.[13] The starting material **2** can be obtained in a one-pot reaction from 1,5-cyclooctadiene.[15] The reaction of **3** with anhydrous cerium trichloride in a molar ratio of 2:1 leads to the bright green anionic sandwich complex **4**, which because of its extreme sensitivity to oxidation was not isolated but immediately converted to the neutral cerium(IV) derivative. The desired oxidation to yield **5** occurs smoothly and under mild conditions with



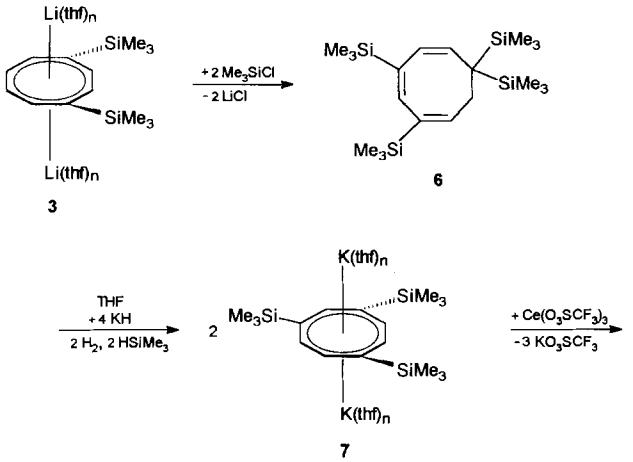
an excess of silver iodide as oxidizing agent. Bis[1,4-bis-(trimethylsilyl)cyclooctatetraene]cerium(IV) (**5**) is the first readily accessible derivative of **1**, which is sufficiently soluble to allow reactivity studies. Spectroscopically pure, diamagnetic **5** is obtained as a deep purple oil, which thermally decomposes only above 226 °C. In contrast to the pyrophoric parent compound **1**,[11] compound **5** can be handled in air for short periods of time. In the EI mass spectrum the molecular ion appears as the highest mass peak with 6% relative intensity.

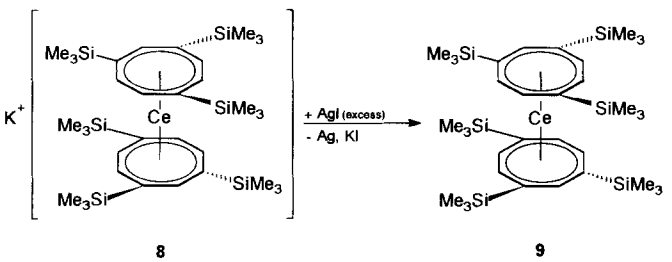
The synthesis of a crystalline derivative of **1** was achieved by using the new sterically demanding ligand 1,3,6-$(Me_3Si)_3C_8H_5^{2-}$. Compound **3** prepared in situ reacted with two

[*] Priv.-Doz. Dr. F. T. Edelmann, Dr. U. Kilimann, Dr. R. Herbst-Irmer, Priv.-Doz. Dr. D. Stalke
Institut für Anorganische Chemie der Universität
Tammannstrasse 4, D-37077 Göttingen (FRG)
Telefax: Int. code + (551)39-3373

[**] This work was supported by the Fonds der Chemischen Industrie, by the Deutsche Forschungsgemeinschaft, and by the BASF AG.

equivalents of chlorotrimethylsilane in Et_2O/THF selectively to give 1,3,6,6-tetrakis(trimethylsilyl)cyclooctatriene (**6**),[15] which can be isolated as colorless, sublimable needles in 52% yield. The substitution pattern of **6** is confirmed unequivocally by the NMR data. The presence of two trimethylsilyl groups on one carbon atom of the cycle initially made the desired derivatization to give the substituted cyclooctatetraene dianion appear impossible (1,2,4,4-tetrakis(trimethylsilyl)cyclopentadiene cannot be metalated at the cyclopentadiene ring[16]).





Indeed, **6** proved to be completely inert towards *n*-butyllithium. Surprisingly, the metalation was achieved with potassium hydride; however, a notable reaction was only observed in boiling THF. In addition to the expected deprotonation, a trimethylsilyl group is eliminated in the form of trimethylsilane. This leads to the dipotassium salt of the 1,3,6-*tris*(trimethylsilyl)cyclooctatetraene dianion **7** (37%). The latter is isolated as a colorless, microcrystalline powder of the composition $[K_2(thf)_3][C_8H_5(SiMe_3)_3]$ and spectroscopically characterized. Subsequent reaction with cerium triflate (molar ratio 2:1) led to the extremely air-sensitive dark green anionic complex **8**, which was oxidized in situ with silver iodide to give bis[1,3,6-tris(trimethylsilyl)cyclooctatetraene]cerium(IV) (**9**). This forms permanganate-colored crystals with a low melting point (m.p. = 38 °C), which are stable in air for a short period of time and very soluble in nonpolar solvents such as pentane, hexane, or toluene. Complex **9** can be vaporized without decomposition; in the EI mass spectrum it exhibits the molecular peak with 14% relative intensity.

Deep purple single crystals of **9** were obtained from acetonitrile. The single-crystal X-ray structure analysis[17] confirms the presence of a neutral cerium(IV) complex (Fig. 1). The two annulene rings are η^8-coordinated to the cerium atom. The Ce1–C distances range from 267.0 to 275.1 pm and are comparable with those of related complexes.[10] The two C_8 rings in **9** are not coplanar. The ring centroid-Ce-ring centroid angle is

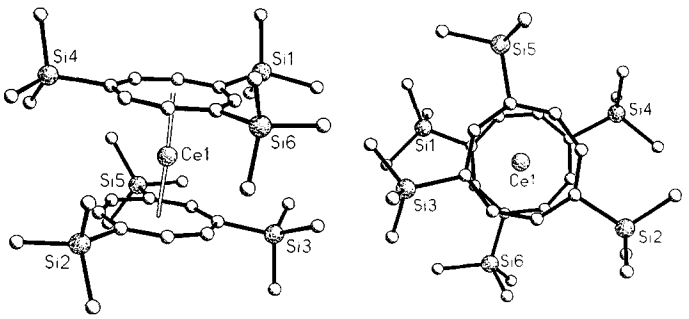


Fig. 1. Side view (left) and top view (right) of **9**; mean bond lengths [pm] and bond angles [°]: Ce1–C (mean) 270.4(7) (267.0(6)–275.1(7)), Ce1–ring centroid 197.6(6) and 197.7(6); ring centroid-Ce1-ring centroid 176.1(3).

176.1° and is thus almost identical with the corresponding value in the anionic Yb^{II} derivative $[Yb(C_8H_8)_2]^{2-}$ (177°).[18] The nonlinear coordination of the metal atom in **9** is probably due to steric reasons. The more open side of **9** is the one at which the Me_3Si groups of Si1 and Si3 (Fig. 1 right) are closest to each other (521.4 pm). In comparison, for example, the Si2···Si4 distance on the closed side is 30 pm longer. All other Si···Si distances range from 570 to 590 pm.

The high solubility of **9** can be attributed to the Me_3Si groups, which interlock like a set of cog wheels (Fig. 2) and surround the metal atom with an organic shell.

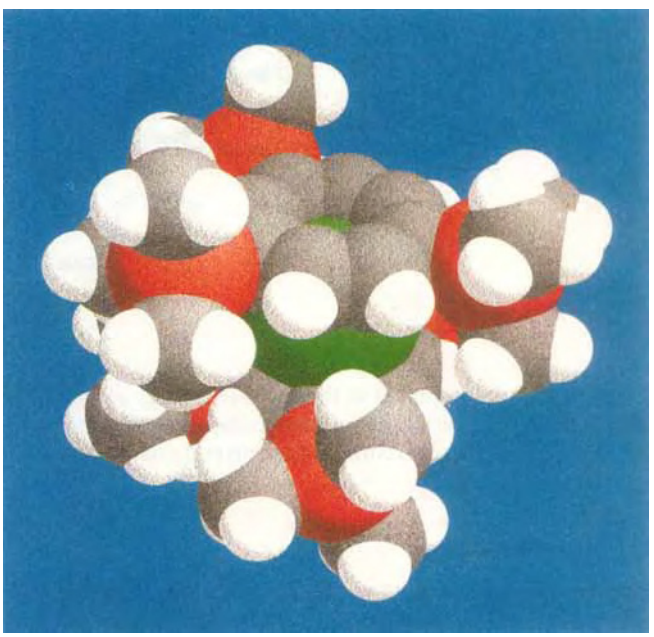
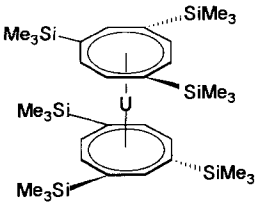


Fig. 2. Space-filling model of **9**.

In order to determine the rotation barrier in sandwich complexes with the 1,3,6-$(Me_3Si)_3C_8H_5^{2-}$ ligand, the uranium complex **10**, analogous to **9**, was synthesized and its variable-temperature ^1H NMR spectra were analyzed. Dark green **10** is readily obtained from the reaction of anhydrous uranium tetrachloride with two equivalents of **7**. This complex is also stable in air for a short period of time, whereas the unsubstituted parent compound $[U(C_8H_8)_2]$ is highly pyrophoric.[19] In the EI mass spectrum of **10** the molecular peak appears with 100% relative intensity. The energy barrier for the rotation of the two sub-

 © VCH Verlagsgesellschaft mbH, D-69451 Weinheim, 1994 0570-0833/94/1515-1619 $ 10.00+.25/0



10

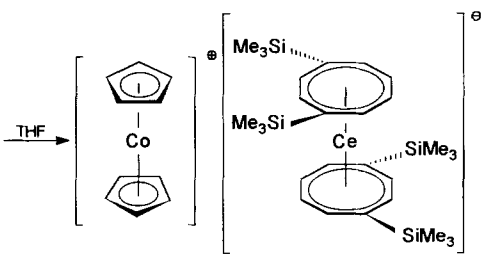
stituted cyclooctatetraene rings can be determined ($\Delta G^{\neq} = 18\ kJ\,mol^{-1}$) from the coalescence of the $SiMe_3$ signals in the temperature-dependent ^1H NMR spectrum of **10**.

This value seems surprisingly low when compared with the rotation barrier of $34.7\ kJ\,mol^{-1}$, which was determined by Streitwieser et al. for bis[1,4-bis(*tert*-butyl)cyclooctatetraene]-uranium.[20] Our explanation for this difference is that the substituted cyclooctatetraene ligands in **10** do not undergo a complete rotation but only oscillate. The same phenomenon was already detected by NMR spectroscopy by Okuda for 1,1′,2,2′,4,4′-hexakis(trimethylsilyl)ferrocene.[21, 22] The rotation barrier here is as high as that for 1,1′,3,3′-tetrakis-(trimethylsilyl)ferrocene ($11.0\ kJ\,mol^{-1}$), which contains only four silyl groups.

The ready availability of soluble cerium(IV) complexes opens up very promising perspectives for novel electron transfer reactions. The redox reaction of **5** with cobaltocene serves as a first example. This reduction leads to the saltlike Ce^{III} compound **11**, in which both the cation and the anion are sandwich complexes. The green cobaltocenium salt **11** can be characterized spectroscopically without any problems.

$$[\{1,4\text{-}(Me_3Si)_2C_8H_6\}_2Ce] \;+\; [(C_5H_5)_2Co]$$

5



11

The further development of the redox chemistry of **5** and **9** as well as possible applications of these complexes as soluble oxidizing agents in organic synthesis are currently under investigation.

Experimental Procedure

Synthesis and characterization: All work was carried out under a purified N_2 atmosphere.

5: **2** (6.1 g, 24.4 mmol) [14] in THF (50 mL) was treated dropwise with *n*BuLi (48.8 mmol) at −30 °C. The mixture was allowed to warm to room temperature and stirred for 1 h. To the resulting brown solution was added a suspension of $CeCl_3$ (3.0 g, 12.2 mmol) [23] in THF (30 mL) at 0 °C. This led to a dark green solution which was again allowed to warm to room temperature, stirred for two days, filtered through a layer of Celite, and the filtrate was treated with AgI (5.6 g, 24.0 mmol). In addition to the formation of elemental Ag, the solution immediately turned deep purple. The reaction mixture was stirred for 12 h with exclusion of light, and evaporated. The residue was treated with hexane (50 mL), and carefully filtered. Removal of the solvent under vacuum afforded **5** (3.1 g, 40%) as a deep purple, oily product. Correct elemental analysis; m.p. 226 °C (decomp), ^1H NMR (250.1 MHz, C_6D_6): $\delta = 6.13$ (m, $^3J(H,H) = 7$ Hz, 2H, ring-H), 5.98 (m, 2H, ring-H), 5.92 (m, $^3J(H,H) = 11$ Hz, $^4J(H,H) = 3$ Hz, 2H, ring-H), 5.88 (m, $^3J(H,H) = 7$ Hz, 2H, ring-H), 5.83 (m, 2H, ring-H), 5.72 (m, $^3J(H,H) = 11$ Hz, $^4J(H,H) = 3$ Hz, 2H, ring-H), 0.08 (s, 18H, $SiMe_3$), 0.07 (s, 18H, $SiMe_3$); ^{29}Si NMR (49.7 MHz, [D$_8$]toluene): $\delta = -5.44$ (s), −5.43 (s); MS (EI): *m/z*: 636 ([M^+], 6%), 388 ([$Ce[C_8H_6(1,4\text{-}SiMe_3)_2^+]$], 52%), 249 ([$C_8H_6(1,4\text{-}SiMe_3)_2^+$], 4%), 73 ([$SiMe_3^+$], 100%); IR (KBr, pure substance): $\tilde{\nu}[cm^{-1}] = 1578$ m, 1310 m, 1249 vs, 1102 s, 1080 m, 1004 m, 975 m, 929 s, 880 s, 839 vs, 751 s, 715 m, 633 s, 565 m, 511 m, 447 m, 372 m.

6: *n*BuLi (239.6 mmol) was added dropwise to a solution of **2** (30 g, 119.8 mmol) [14] in THF (200 mL) at −30 °C. Subsequently the solution was allowed to warm to room temperature and stirred for a further 12 h. The resulting deep brown solution was added dropwise to a solution of Me_3SiCl (26.0 g, 239.6 mmol) in Et_2O (150 mL) at −10 °C. The mixture was allowed to react at −10 °C for 10 min, then for 12 h at room temperature, filtered carefully, and the filtrate was evaporated to dryness under vacuum. The crude product was treated with dry MeOH (250 mL) and filtered while hot to remove the insoluble material. Cooling to −20 °C afforded pale yellow, needlelike crystals of **6** (24.7 g, 52%), m.p. 87 °C, correct elemental analysis; ^1H NMR ($CDCl_3$, 400.1 MHz): $\delta = 6.15$ (ddd, $^3J(H,H) = 9$ Hz, $^4J(H,H) = 1$ Hz, $^4J(H,H) = 1$ Hz, 1H, ring-H), 5.51 (dd, $^3J(H,H) = 11$ Hz, $^3J(H,H) = 9$ Hz, 1H, ring-H), 5.43 (dd, $^3J(H,H) = 13$ Hz, $^4J(H,H) = 1$ Hz, 1H, ring-H), 5.22 (ddd, $^3J(H,H) = 11$ Hz, $^4J(H,H) = 1$ Hz, $^4J(H,H) = 1$ Hz, 1H, ring-H), 5.18 (ddd, $^3J(H,H) = 13$ Hz, $^4J(H,H) = 1$ Hz, $^5J(H,H) = 1$ Hz, 1H, ring-H), 4.27 (ddd, $^3J(H,H) = 9$ Hz, $^3J(H,H) = 9$ Hz, $^4J(H,H) = 1$ Hz, 1H, ring-H), 0.10 (s, 9H, $SiMe_3$), 0.04 (s, 9H, $SiMe_3$), 0.03 (s, 9H, $SiMe_3$), −0.03 (s, 9H, $SiMe_3$); ^{13}C NMR ($CDCl_3$): $\delta = 145.6$ (s, ring-C), 143.1 (t, $^1J(^{13}C,^{29}Si) = 66$ Hz, ring-C), 133.1 (s, ring-C), 131.0 (s, ring-C), 129.0 (s, ring-C), 126.2 (s, ring-C), 37.4 (t, $^1J(^{13}C,^{29}Si) = 43$ Hz, ring-C), 29.9 (t, $^1J(^{13}C,^{29}Si) = 53$ Hz, ring-C), −1.3 (t, $^1J(^{13}C,^{29}Si) = 52$ Hz, $SiMe_3C$), −1.4 (t, $^1J(^{13}C,^{29}Si) = 52$ Hz, $SiMe_3C$), −1.5 (t, $^1J(^{13}C,^{29}Si) = 52$ Hz, $SiMe_3C$), −3.1 (t, $^1J(^{13}C,^{29}Si) = 51$ Hz, $SiMe_3C$); ^{29}Si NMR ($CDCl_3$): $\delta = -5.3$ (s, $SiMe_3$), 2.0 (s, $SiMe_3$), 2.4 (s, $SiMe_3$), 2.6 (s, $SiMe_3$); MS (EI): *m/z*: 394 ([M^+], 34%), 321 ([$M-SiMe_3^+$], 60%), 233 ([$M-2SiMe_3CH_3^+$], 54%), 73 ([$SiMe_3^+$], 100%); IR (KBr, Nujol): $\tilde{\nu}[cm^{-1}] = 1578$ m, 1310 m, 1249 vs, 1102 s, 1080 s, 1004 m, 975 m, 929 s, 880 s, 839 vs, 751 s, 715 s, 686 s, 633 s, 565 m, 511 m, 447 m, 372 m.

7: **6** (2.5 g, 6.3 mmol) and KH (0.8 g, 20.0 mmol) were heated under reflux in THF (50 mL) for 2 days. Subsequently, excess KH was filtered off, the orange solution evaporated to dryness, and the residue taken up in hexane (40 mL) and stirred for for 3 h. The solid precipitate was separated and dried under vacuum. A white, microcrystalline powder **7** (1.57 g, 37%) was obtained. Correct elemental analysis; m.p. 247 °C (decomp); ^1H NMR (250.1 MHz, [D$_8$]THF): $\delta = 6.39$ (m, 1H, ring-H), 6.34 (m, 1H, ring-H), 6.30 (m, 1H, ring-H), 6.23 (m, 1H, ring-H), 6.18 (m, 1H, ring-H), 3.62 (m, 12H, THF), 1.79 (m, 12H, THF), 0.32 (s, 18H, $SiMe_3$), 0.27 (s, 9H, $SiMe_3$); ^{29}Si NMR ([D$_8$]THF): $\delta = -2.3$ (s), −3.2 (s, half intensity); MS (EI): *m/z*: 320 ([$C_8H_5(SiMe_3)_3^+$], 8%), 247 ([$C_8H_5(SiMe_3)_2^+$], 42%), 73 ([$SiMe_3^+$], 100%); IR (KBr, Nujol): $\tilde{\nu}[cm^{-1}] = 1734$ m, 1532 m, 1304, 1240 vs, 1216 m, 1081 vs, 1046 vs, 975 s, 924 m, 889 m, 870 s, 824 vs, 740 vs, 672 m, 633 m, 567 m, 511 m.

9: 7 (2.5 g, 3.6 mmol) in THF (50 mL) was treated with a suspension of $Ce(O_3SCF_3)_3$ (1.1 g, 1.8 mmol) [24] in THF (30 mL) at 0 °C and stirred. The solution turned bright green. Subsequently, the mixture was allowed to react for a further 12 h under reflux, then AgI (0.9 g, 3.8 mmol) was added at room temperature, which caused an immediate color change to purple. After stirring the mixture for 1 h with exclusion of light, the solvent was evaporated, the residue taken up in hexane (50 mL) and filtered. The filtrate was evaporated to dryness and the residue was treated with MeCN (50 mL). Crystallization at room temperature afforded **9** (0.5 g, 33%) as a microcrystalline, deep purple solid. Correct elemental analysis; m.p. 38 °C; ^1H NMR (250.1 MHz, C_6D_6): $\delta = 6.43$ (d, $^3J(H,H) = 12$ Hz, 4H, ring-H), 6.00 (d, $^3J(H,H) = 12$ Hz, 4H, ring-H), 5.61 (s, 2H, ring-H), 1.11 (s, 18 H, $SiMe_3$), 0.99 (s, 36H, $SiMe_3$); ^{29}Si NMR (C_6D_6): $\delta = -1.74$ (s), −3.09 (s, half intensity); MS (EI): *m/z*: 780 ([M^+], 14%), 708 ([$M-SiMe_3^+$], 2%), 460 ([$CeC_8H_5(SiMe_3)_3^+$], 100%), 386 ([$CeC_8H_5(SiMe_3)_2^+$], 8%), 73 ([$SiMe_3^+$], 38%).

10: UCl_4 (0.7 g, 1.8 mmol) [25] in THF (30 mL) was added to a solution of **7** (2.5 g, 3.6 mmol) in THF (50 mL) at 0 °C. The solution was then stirred for 3 h at room temperature, concentrated, treated with hexane (30 mL), and stirred for a further 12 h. Subsequently, the mixture was filtered while hot and concentrated to 10 mL. Cooling to −20 °C afforded green crystals of **10** (0.4 g, 28%). Correct elemental analysis; m.p. 110 °C (decomp); ^1H NMR (250.1 MHz, [D$_8$]THF): $\delta = 0.03$ (m, 10H, ring-H), −7.30 (br. s, 36H, $SiMe_3$), −9.10 (s, 18H, $SiMe_3$); ^{29}Si NMR ([D$_8$]THF): $\delta = -120.7$ (s); MS (EI): *m/z*: 878 ([M^+], 100%), 806 ([M^+-SiMe_3], 3%), 732 ([$M^+-2SiMe_3$], 5%), 558 ([$UC_8H_5(SiMe_3)_3^+$], 51%), 73 ([$SiMe_3^+$], 44%); IR (KBr, Nujol): $\tilde{\nu}[cm^{-1}] = 1260$ vs, 1249 s, 1090 vs, 1019 vs, 836 s, 801 vs, 747 m, 638 m.

11: **5** (2.0 g, 3.1 mmol) and Cp_2Co (0.6 g, 3.1 mmol) [26] were dissolved in THF (40 mL) and stirred for 3 h. The initially purple solution turned red-brown. The mixture was filtered over a thin layer of Celite and the filtrate was evaporated to dryness. The residue taken up in hexane (50 mL), and the green precipitate was isolated and dried. Compound **11** (0.2 g, 7%) was obtained as a pyrophoric, extremely air-sensitve solid. Correct elemental analysis; m.p. 142 °C (decomp); ^1H (250.1 MHz, [D$_8$]THF): $\delta = 6.21-5.79$ (m, 12H, ring-H), 1.30 (s, 5H, C_5H_5), 1.05 (s, 18H, $SiMe_3$), 0.90 (s, 5H, C_5H_5), 0.08 (s, 18H, $SiMe_3$); ^{29}Si NMR ([D$_8$]THF): $\delta = -2.4$ (s), −5.3 (s); MS (EI): *m/z*: 248 ([$C_8H_6(1,4\text{-}SiMe_3)_2^+$], 16%), 189 ([$Co(C_5H_5)^+_2$], 50%), 124 ([$Co(C_5H_5)^+$], 11%), 73 ([$SiMe_3^+$], 100%); IR (KBr, Nujol): $\tilde{\nu}[cm^{-1}] = 1413$ m, 1306 m, 1261 vs, 1248 m, 1092 vs, 1037 vs, 980 m, 937 m, 861 m, 836 s, 800 vs, 750 m, 688 m, 637 m, 436 m.

Received: March 26, 1994 [Z 6800 IE]
German version: *Angew. Chem.* **1994**, *106*, 1684

[1] H. Schumann, *Angew. Chem.* **1984**, *96*, 475; *Angew. Chem. Int. Ed. Engl.* **1984**, *23*, 484.
[2] D. A. Johnson, *Adv. Inorg. Chem. Radiochem.* **1977**, *20*, 1.
[3] B. L. Kalsotra, S. P. Anand, R. K. Multani, B. D. Jain, *J. Organomet. Chem.* **1971**, *28*, 87.
[4] B. L. Kalsotra, R. K. Multani, B. D. Jain, *J. Inorg. Nucl. Chem.* **1972**, *34*, 2265.
[5] S. Kapur, B. L. Kalsotra, R. K. Multani, B. D. Jain, *J. Inorg. Nucl. Chem.* **1973**, *35*, 1689.
[6] S. Kapur, B. L. Kalsotra, R. K. Multani, *J. Inorg. Nucl. Chem.* **1973**, *35*, 3966.
[7] G. B. Deacon, T. D. Tuong, D. G. Vince, *Polyhedron* **1983**, *2*, 969.
[8] N. Rösch, A. Streitweiser, *J. Am. Chem. Soc.* **1983**, *2*, 969; N. Rösch, *Inorg. Chim. Acta* **1984**, *94*, 297..
[9] M. Dolg, P. Fulde, W. Küchle, C.-S. Neumann, H. Stoll, *J. Chem. Phys.* **1991**, *94*, 3011.
[10] T. R. Boussie, D. C. Eisenberg, J. Rigsbee, A. Streitwieser, A. Zalkin, *Organometallics* **1991**, *10*, 1922.
[11] A. Greco, S. Cesca, G. Bertolini, *J. Organomet. Chem.* **1976**, *113*, 321.
[12] M. F. Lappert, A. Singh, J. L. Atwood, W. E. Hunter, *J. Chem. Soc. Chem. Commun.* **1981**, 1190.
[13] M. F. Lappert, A. Singh, J. L. Atwood, W. E. Hunter, *J. Chem. Soc. Chem. Commun.* **1981**, 1191.
[14] N. C. Burton, F. G. N. Cloke, P. B. Hitchcock, H. C. de Lemos, A. A. Sameh, *J. Chem. Soc. Chem. Commun.* **1989**, 1463.
[15] After the completion of our work compound **6** was also published by Cloke et al.: N. C. Burton, F. G. N. Cloke, S. C. P. Joseph, H. Karamallakis, A. A. Sameh, *J. Organomet. Chem.* **1993**, *462*, 39.
[16] P. Jutzi, R. Sauer, *J. Organomet. Chem.* **1973**, *50*, C29.
[17] Crystal data of **9**: $[(Me_3Si)_3C_8H_5]_2Ce$, $M = 781.51$, orthorhombic, space group $Pna2_1$, $a = 2232.2(4)$, $b = 1647.6(3)$, $c = 1132.3(2)$ pm, $V = 4.163(1)$ nm^3, $Z = 4$, $\rho_{calcd} = 1.247$ Mg m^{-3}, $F(000) = 1640$, $\lambda = 71.073$ pm, $T = -120$ °C, $\mu(Mo_{K\alpha}) = 1.286$ mm^{-1}, crystal dimensions: $0.6 \times 0.6 \times 0.4$ mm, $4° < 2\theta \leq 50°$; of 5491 measured reflections, 5084 were independent and 5080 were used for the refinement of 388 paramters; maximum residual electron density: 1572 e nm^{-3}, $R1(F > 4\sigma(F)) = 0.039$, $wR2 = 0.115$ (all data) with $R1 = \Sigma||F_o| - |F_c||/\Sigma|F_o|$ and $wR2 = (\Sigma w(F_o^2 - F_c^2)^2/\Sigma w(F_o^2)^2)^{0.5}$. The data were collected on a Stoe-Huber diffractometer. The intensity measurements were carried out on a rapidly cooled crystal in the oil drop [26] by the $2\theta/\omega$ method. Semiempirical absorption corrections were carried out on all data. The structure was solved by Patterson and Fourier methods (SHELXS-90) [27] and refined with the least squares method on F^2 [28]. The refinement of the inversion twin parameter [29] ($x = 0.00(2)$ for $x = 0$ for the correct absolute structure and $x = +1$ for the inverted structure) confirmed the absolute structure of **9**. Further details of the crystal structure investigation are available on request from the Director of the Cambridge Crystallographic Data Centre, 12 Union Road, GB-Cambridge CB2 1EZ (UK), on quoting the full journal citation.
[18] S. A. Kinsley, A. Streitwieser, A. Zalkin, *Acta Crystallogr. Sect. C* **1979**, *35*, 1068.
[19] A. Steitwieser, U. Müller-Westerhoff, *J. Am. Chem. Soc.* **1968**, *90*, 7364.
[20] W. D. Luke, A. Streitwieser, *J. Am. Chem. Soc.* **1981**, *103*, 3241.
[21] J. Okuda, *Top. Curr. Chem.* **1992**, *160*, 97.
[22] J. Okuda, E. Herdtweck, *Chem. Ber.* **1988**, *121*, 1899.
[23] J. H. Freeman, M. L. Smith, *J. Inorg. Nucl. Chem.* **1958**, *7*, 224.
[24] F. E. Hahn, J. Mohr, *Chem. Ber.* **1990**, *123*, 481.
[25] J. A. Herrmann, J. F. Suttle, *Inorg. Synth.* **1957**, *5*, 143.
[26] T. Kottke, D. Stalke, *J. Appl. Crystallogr.* **1993**, *26*, 615.
[27] G. M. Sheldrick, *Acta Crystallogr. Sect. A* **1990**, *46*, 467.
[28] G. M. Sheldrick, SHELXL-93, program for crystal structure refinement, Göttingen, **1993**.
[29] H. D. Flack, *Acta Crystallogr. Sect. A* **1983**, *39*, 876.

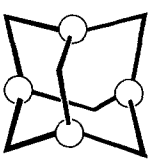
Mixed-Valence, Tetranuclear Iron Chelate Complexes as Endoreceptors: Charge Compensation Through Inclusion of Cations**

Rolf W. Saalfrank,* Roman Burak, Alexandra Breit, Dietmar Stalke, Regine Herbst-Irmer, Jörg Daub, Michael Porsch, Eckhard Bill, Markus Müther, and Alfred X. Trautwein

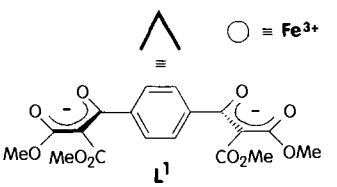
Dedicated to Professor Helmut Ringsdorf on the occasion of his 65th birthday

An essential prerequisite for the rapid development of endohedral chemistry, that is chemistry within cages, is easy access to host molecules of variable internal diameter.[2] In this context we have recently reported the tetranuclear adamantanoid Fe^{III} spacer-complex $[Fe_4L^1{}_6]$ **1**.[1] Complex **1** is endowed with a substantial cavity, which should, in principle, be suitable for the uptake of guest molecules. Our attempts to obtain the spacer-free metallospherand core unit $[Fe_4L^2_6]$ in analogous manner have thus far given rise to products which could not be characterized unambiguously.

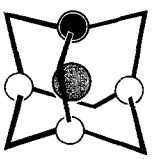
In contrast, we have obtained for the first time, the tetranuclear, mixed-valence ammonium inclusion complexes $[NH_4 \subset Fe_4L^2_6]$ **2** and $[NH_4 \subset Fe_4L^3_6]$ **3** in a one-pot reaction.[3] Complexes **2** and **3** are formed by spontaneous self-assembly[1, 4–7] from the reaction of dialkyl malonates with methyllithium/iron(II) chloride and oxalyl chloride at −78 °C in tetrahydrofuran, followed by workup with aqueous ammonium



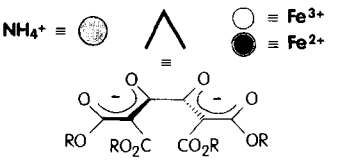
1



L1



2, 3



L2: R = Me ; L3: R = Et

[*] Prof. Dr. R. W. Saalfrank, Dr. R. Burak, Dipl.-Chem. A. Breit, Institut für Organische Chemie der Universität Erlangen-Nürnberg Henkestrasse 42, D-91054 Erlangen (FRG)
Telefax: Int. code + (9131)85-6864
Priv.-Doz. Dr. D. Stalke, Dr. R. Herbst-Irmer[+]
Institut für Anorganische Chemie der Universität Göttingen (FRG)
Prof. Dr. J. Daub, Dipl.-Chem. M. Porsch[++]
Institut für Organische Chemie der Universität Regensburg (FRG)
Dr. E. Bill, Dipl.-Phys. M. Müther, Prof. Dr. A. X. Trautwein[+++]
Institut für Physik der Medizinischen Universität Lübeck (FRG)

[+] Single-crystal X-ray diffraction analyses.

[++] Electrochemistry.

[+++] Mössbauer spectra.

[**] "Adamantanoid" Chelate Complexes, Part 4. This work was supported by the Deutsche Forschungsgemeinschaft and by the Fonds der Chemischen Industrie. We thank Prof. Dr. F. Vögtle and Dr. S. Schuth, Universität Bonn, and Prof. Dr. K.-P. Zeller, Universität Tübingen for the measurement of the FAB mass spectra. Part 3: ref. [1].

chloride. The bis(bidentate), spacer-free bridging ligands L^2 and L^3 are formally obtained by coupling of two dialkyl malonate monoanions with oxalyl chloride to form H_2L^2 and H_2L^3, respectively, followed by double deprotonation.

The microanalytical data and FAB mass spectra of **2** and **3** gave the first indications that these products might constitute host–guest systems. The molecular- and fragment ion peaks of **2** and **3** are, in each case, 18 mass units greater, as expected for the inclusion of an ammonium ion.

For a definitive characterization of **2** and **3**, we have carried out crystal structure analyses on both complexes.[8] The results of these show that **2** and **3** are present in the crystal as neutral, tetranuclear, mixed-valence chelate complexes with an endohedrally complexed cation for charge compensation (Fig. 1). The

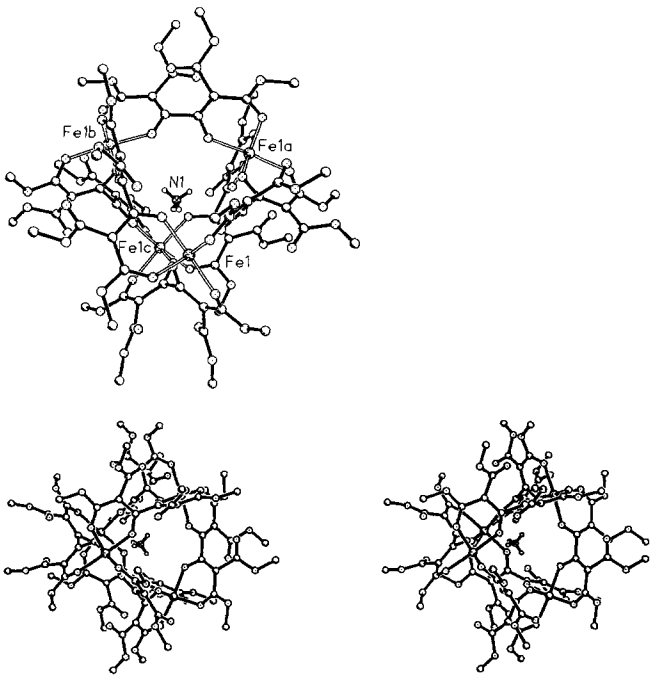


Fig. 1. Top: Structure of **2** in the crystal (view along the crystallographic C_3 axis: H atoms of the NH_4^+ ion plain, O atoms dotted, C atoms shaded). Bottom: Stereoview of **2** along the crystallographic C_3 axis. Water of crystallization is not depicted for reasons of clarity.

receptor nucleus of **2** and **3** consists in each case of a regular tetrahedron with corners defined by one Fe^{II} and three Fe^{III} ions. The six edges of the tetrahedron are each formed by the bis(bidentate), doubly negatively charged bridging ligands L^2 or L^3. Each of the four iron ions is octahedrally coordinated by six oxygen atoms.[13] In the center of the iron tetrahedron there is an ammonium ion which serves presumably as a template for the formation of **2** and **3**, thereby becoming enclosed during the construction of these systems.

Two pairs of enantiomers [(Δ)-, (Λ)-*fac* and (Δ)-, (Λ)-*mer*] are principally possible for octahedral complexes of type MA_3B_3 [for bidentate ligands: $M(AB)_3$]. The chiral racemic complexes **2** and **3** crystallize in the cubic space group $Fd\bar{3}$. All four iron centers in **2** and **3** are identically coordinated, hence the complexes are present as either ($\Delta,\Delta,\Delta,\Delta$)-*fac* or as ($\Lambda,\Lambda$, Λ,Λ)-*fac* stereoisomers.[1] With an idealized representation, (the Fe–Fe distances differ from one another in both cases by less than 1.3%), **2** and **3** are shown to have approximately *T*-molecular symmetry (characterized by three C_2 and four C_3 axes).[5, 15] This contrasts with the spacer-complex $[Fe_4L_6^1]$ **1**, which is exactly S_4 symmetric and thus achiral (*meso*-form). In **1**, the ligands L^1 are arranged facially about the four iron centers; however, in this case two of the four iron centers have the same configuration [(Δ,Δ)- and (Λ,Λ)-*fac*].[14]

The mixed-valence character of **2** and **3** was established unambiguously from their Mössbauer spectra. Powder samples of complexes **2** and **3** each show, in a temperature range of 4.2–300 K, a virtually temperature independent triplet, arising from the overlap of two quadrupolar doublets [one high-spin Fe^{II} center: quadrupolar splittings $\Delta E_Q(4.2\ K) = 2.90$ (**2**), 2.79 (**3**) $mm\,s^{-1}$, isomeric shifts $\delta(4.2\ K) = 1.29$ (**2**), 1.29 (**3**) $mm\,s^{-1}$; three Fe^{III} centers: quadrupolar splittings $\Delta E_Q(4.2\ K) = 0.71$ (**2**), 0.84 (**3**) $mm\,s^{-1}$, isomeric shifts $\delta(4.2\ K) = 0.56$ (**2**), 0.55 (**3**) $mm\,s^{-1}$] (Fig. 2, left). The observation of distinct Mössbauer

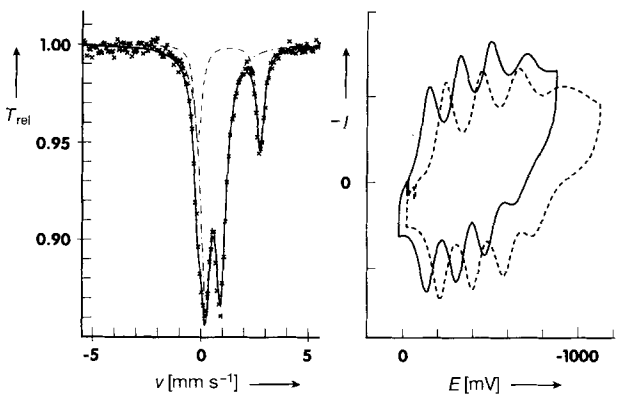


Fig. 2. Left: Mössbauer spectra of a powder sample of **2**, recorded at 4.2 K. The connecting line is the result of a two-doublet adjustment of the Lorentz line. Subspectra: Fe^{II} (- - -), $\Delta E_Q = 2.90\ mm\,s^{-1}$, $\delta = 1.29\ mm\,s^{-1}$, $\Gamma = 0.42\ mm\,s^{-1}$, 24% rel. intensity; Fe^{III} (- · - · -), $\Delta E_Q = 0.71\ mm\,s^{-1}$, $\delta = 0.56\ mm\,s^{-1}$, $\Gamma = 0.59\ mm\,s^{-1}$, 76% rel. intensity. Right: Pseudo-thin layer cyclic voltammogram of **2** (——) and **3** (····) in acetonitrile/0.1 M tetrabutylammonium hexafluorophosphate, scan rate $2\ mV\,s^{-1}$ (**2**), $5\ mV\,s^{-1}$ (**3**). Ordinate scale: one unit corresponds to 0.05 μA (**2**), 0.1 μA (**3**), negative current plotted upwards, potentials vs. ferrocene/ferrocenium (Fc/Fc^+).

subspectra for the Fe^{II} and Fe^{III} centers in complexes **2** and **3** indicates localized valences, at least on the Mössbauer timescale (ca. 10^{-7} s). Even at room temperature, no significant line-broadening occurs, which would point to a dynamic valence process. The seemingly contradictory results of the X-ray analyses of **2** and **3**, in which there were no apparent differences in the coordination spheres of the Fe^{II} and Fe^{III} centers are attributed to a statistical disordering of the Fe^{II} loci. For complexes **2** and **3**, no exchange interactions between the mixed-valence iron centers could be observed from temperature-dependent susceptibility measurements in the range 1.5–300 K. On the basis of the EPR spectroscopic results, it must, however, be assumed that a weak coupling ($J < 1\ cm^{-1}$) between these centers does exist, because only a single, very broad resonance signal at $g = 2$ is observed.

The redox-active iron centers of the mixed-valence complexes **2** and **3** are located in fairly inaccessible sites within these compounds, and possess very similar electrochemical properties. The cyclic voltammograms of these compounds under aprotic conditions[16] show an extreme dependency on the scan rate. Consequently, meaningful spectra of **2** and **3** could only be obtained under pseudo-thin-layer conditions[17] with a very slow scan rate. With these preconditions, cyclic voltammograms are observed which display four[18] quasi-reversible redox steps (Fig. 2, right). The recorded potentials are listed in Table 1. Notably, **3** is reduced at more negative potentials than **2**. As for

Table 1. Peak potentials for **2** and **3**, given in mV against Fc/Fc^+, derived from thin-layer cyclic voltammograms in acetonitrile/0.1 M tetrabutylammonium hexafluorophosphate with a scan rate of 2 mVs^{-1} (**2**) or 5 mVs^{-1} (**3**) (see Fig. 2, right).

		E^I	E^{II}	E^{III}	E^{IV}
2	E_{pc} [a]	−150	−330	−510	−700
	E_{pa} [b]	−130	−310	−470	−640
3	E_{pc} [a]	−240	−450	−660	−910
	E_{pa} [b]	−210	−390	−570	−720

[a] E_{pc}: cathodic peak potential. [b] E_{pa}: anodic peak potential.

the spacer complex **1**, only a very slight electronic interaction exists between the tetrahedrally arranged iron centers of compounds **2** and **3**. In contrast to complex **1**, which shows a one-potential four-electron transfer, a four-potential four-electron transfer is observed for **2** and **3**. These findings are probably due to the shorter iron–iron distances in **2** and **3** (compared to **1**); this gives rise to a stronger coulombic interaction between the metal centers, leading to a splitting of the redox potentials.

All in all, the compounds obtained, **2**[19] and **3**, may be viewed as neutral fragments. Species of this type are of considerable interest because of their analogies with the series metal atom $\{Na\}$, cryptatium $\{[Na^+ \subset (bpy)_3]e^-\}$, and electride $\{[K^+ \subset [2.2.2]cryptand],\ e^-\}$. Preliminary FAB mass spectrometric results confirm the assumption that inclusion complexes of type $[M \subset Fe_4L_6^3]$ (molecular zeolites, M = Na, K, Rb, Cs) may also be prepared by the method described above. A decisive advantage of the synthetic strategy utilized here is that complex structures with defined architecture and specific properties are accessible by spontaneous self-assembly and without the inconvenience associated with multistep synthesis.

Experimental Procedure

General procedure: Methyllithium solution (1.6 M in diethyl ether, 30 mmol) diluted with dry THF (10 mL) was added dropwise to a solution of the dialkyl malonate (30 mmol) in dry THF (50 mL) (N_2, −78 °C) over 30 min. The mixture was stirred for 1 h at −78 °C and then $FeCl_2 \cdot 4H_2O$ (5.96 g, 30 mmol) was added. After stirring for 1 h, a cooled (−78 °C) solution of oxalyl chloride (freshly distilled, 0.95 g, 0.65 mL, 7.5 mmol) in dry THF (20 mL) was added dropwise to the suspension, which was then warmed to 20 °C during 18 h and the resulting clear, deep red solution treated with saturated aqueous ammonium chloride solution (100 mL). The two phases were separated, the aqueous layer extracted three times with an alkyl halide (70 mL, trichloromethane for **2**, dichloromethane for **3**), and the combined organic phases dried over anhydrous sodium sulfate. After concentration to small volume (5 mL), the reaction product was crystallized by the addition of diethyl ether/hexane (1:1, 50 mL, 0 °C). Occasionally, black-red octahedra are formed (R = Me), which, on the basis of Mössbauer spectra (300 K), are shown to have a Fe^{II}/Fe^{III} ratio of 1:1 (Fe^{II}: $\Delta E_Q = 2.69\ mm\,s^{-1}$, $\delta = 1.20\ mm\,s^{-1}$, Fe^{III}: $\Delta E_Q = 0.55\ mm\,s^{-1}$, $\delta = 0.46\ mm\,s^{-1}$). Likewise, ruby-red octahedra (R = Et), which, on the basis of Mössbauer spectra (300 K), contain exclusively Fe^{III} ($\Delta E_Q = 0.77\ mm\,s^{-1}$, $\delta = 0.44\ mm\,s^{-1}$).

2: Ruby-red crystals from chloroform, by diffusion of diethyl ether. Yield: 1.47 g (55%); m.p. > 200 °C (decomp.); IR (KBr): $\tilde{\nu} = 1730\ cm^{-1}$ (C=O, broad); FAB MS (3-nitrobenzylalcohol matrix): *m/z* 2138 $[NH_4 \subset Fe_4L_6^2]$.

3: Ruby-red crystals from dichloromethane, by diffusion of diethyl ether. Yield: 1.23 g (40%); m.p. > 200 °C (decomp.); IR (KBr): $\tilde{\nu} = 1700\ cm^{-1}$ (C=O, broad). FAB-MS (3-nitrobenzylalcohol matrix): *m/z* 2475 $[NH_4 \subset Fe_4L_6^3]$.

Received: February 15, 1994 [Z 6694 IE]
German version: *Angew. Chem.* **1994**, *106*, 1697

[1] R. W. Saalfrank, B. Hörner, D. Stalke, *Angew. Chem.* **1993**, *105*, 1223–1225; *Angew. Chem. Int. Ed. Engl.* **1993**, *32*, 1179–1182.

[2] Highlights on this topic: *Frontiers in Supramolecular Organic Chemistry and Photochemistry* (Eds.: H.-J. Schneider, H. Dürr), VCH, Weinheim, **1991**; T. Weiske, T. Wong, W. Krätschmer, J. K. Terlouw, H. Schwarz, *Angew. Chem.* **1992**, *104*, 242–244; *Angew. Chem. Int. Ed. Engl.* **1992**, *31*, 183–185; M. T. Pope, A. Müller, *ibid.* **1991**, *103*, 56–70 and **1991**, *30*, 34–48; A. Müller, R. Rohlfing, E. Krickemeyer, H. Bögge, *ibid.* **1993**, *105*, 916–918 and **1993**, *32*, 909–912; M. I. Khan, A. Müller, S. Dillinger, H. Bögge, Q. Chen, J. Zubieta, *ibid.* **1993**, *105*, 1811–1814 and **1993**, *32*, 1780–1782; A. Müller, K. Hovemeier, R. Rohlfing, *ibid.* **1992**, *104*, 1214–1216 and **1992**, *31*, 1192–1194; A. Müller, E. Krickemeyer, M. Penk, R. Rohlfing, A. Armatage, H. Bögge, *ibid.* **1991**, *103*, 1720–1722 and **1991**, *30*, 1674–1677; H. Hopf, *ibid.* **1991**, *103*, 1137–1139 and **1991**, *30*, 1117–1118; C. Seel, F. Vögtle, *ibid.* **1992**, *104*, 542–563 and **1992**, *31*, 528–549; K. Worm, F. P. Schmidtchen, A. Schier, A. Schäfer, M. Hesse, *ibid.* **1994**, *106*, 360–362 and **1994**, *33*, 327–329; Y. D. Chang, J. Salta, J. Zubieta, *ibid.* **1994**, *106*, 347–350 and **1994**, *33*, 325–327.

[3] For a definition of endohedral inclusion complexes [σ⊂ρ (σ = substrate, ρ = receptor) see ref. [6a].

[4] R. W. Saalfrank, A. Stark, K. Peters, H. G. von Schnering, *Angew. Chem.* **1988**, *100*, 878–880; *Angew. Chem. Int. Ed. Engl.* **1988**, *27*, 851–853.

[5] R. W. Saalfrank, A. Stark, M. Bremer, H.-U. Hummel, *Angew. Chem.* **1990**, *102*, 292–294; *Angew. Chem. Int. Ed. Engl.* **1990**, *29*, 311–314.

[6] Reviews: a) J.-M. Lehn, *Angew. Chem.* **1988**, *100*, 91–116; *Angew. Chem. Int. Ed. Engl.* **1988**, *27*, 89–112; b) *ibid.* **1990**, *102*, 1347–1362 and **1990**, *29*, 1304–1319.

[7] I. Cragg-Hine, M. G. Davidson, O. Kocian, F. S. Mair, E. Pohl, P. R. Raithby, R. Snaith, N. Spencer, J. F. Stoddart, *Angew. Chem.* **1993**, *105*, 1254–1256; *Angew. Chem. Int. Ed. Engl.* **1993**, *32*, 1182–1184; M. Simard, D. Su, J. D. Wuest, *J. Am. Chem. Soc.* **1991**, *113*, 4696–4698.

[8] Crystal data for **2**: $[NH_4 \subset C_{72}H_{72}O_{60}Fe_4] \cdot 15.88\,H_2O$, $M = 2424.82$, cubic space group $Fd\bar{3}$, $a = b = c = 3132.7(4)$ pm, $V = 30.744(7)\ nm^3$, $Z = 8$, $\rho_{calcd} = 1.048\ Mgm^{-3}$, F(000) = 10062, $\lambda = 71.073$ pm, $T = 153$ K, $\mu(Mo_{K\alpha}) = 0.451\ mm^{-1}$, crystal dimensions: $1.0 \times 0.5 \times 0.5$ mm, $6 \le 2\theta \le 50$°; from the 9825 collected reflections 2277 were independent, 2273 of which were used for the refinement of 156 parameters with 102 restraints; maximum residual electron density 272 $e\,nm^{-3}$, $R1\ [F > 4\sigma(F)] = 0.062$, $wR2 = 0.200$ (all data).
Crystal data for **3**: $[NH_4 \subset C_{96}H_{120}O_{60}Fe_4] \cdot 4\,CH_2Cl_2 \cdot 15\,H_2O$, $M = 3085.31$, cubic space group $Fd\bar{3}$, $a = b = c = 3216.9(4)$ pm, $V = 33.290(7)\ nm^3$, $Z = 8$, $\rho_{calcd} = 1.231\ Mgm^{-3}$, F(000) = 12872, $\lambda = 71.073$ pm, $T = 153$ K, $\mu(Mo_{K\alpha}) = 0.555\ mm^{-1}$, crystal dimensions: $0.8 \times 0.6 \times 0.6$ mm, $4 \le 2\theta \le 50$°; from the 5105 collected reflections 2460 were independent, 2450 of which were used for the refinement of 164 parameters with 39 restraints; maximum residual electron density 526 $e\,nm^{-3}$, $R1[F > 4\sigma(F)] = 0.069$, $wR2 = 0.210$ (all data) with $R1 = \Sigma\|F_o| - |F_c\|/\Sigma|F_o|$, $wR2 = [\Sigma w(F_o^2 - F_c^2)^2/\Sigma w(F_o^2)^2]^{0.5}$. The data for both structures were collected on a Stoe-Huber diffractometer. Intensity measurements were performed on a rapidly cooled crystal in an oil drop [9] according to a $2\theta/\omega$ scan. All data were subjected to semiempirical absorption correction. The structures were solved by direct methods (SHELXS-90) [10] and refined by least-squares relative to F^2 [11]. The structure of **2** was successfully refined ($Fd\bar{3}/Fd\bar{3}m$) as a twin. The twinning factor *B* refined to 0.474(4) [12]. The disorder of the CH_2Cl_2 solvent molecules of **3** could not be resolved completely. One CCl_2 unit was refined with distance restraints. Further details of the crystal structure investigations may be obtained from the Director of the Cambridge Crystallographic Data Center, 12 Union Road, GB-Cambridge CB2 1EZ on quoting the literature citation.

[9] T. Kottke, D. Stalke, *J. Appl. Crystallogr.* **1993**, *26*, 615–619.

[10] G. M. Sheldrick, *Acta Crystallogr. Sect. A* **1990**, *46*, 467–473.

[11] G. M. Sheldrick, SHELXL-93, Program for structure refinement, Göttingen, **1993**.

[12] C. S. Pratt, B. A. Coyle, J. A. Ibers, *J. Chem. Soc. A* **1971**, 2146–2151.

[13] For the topology of the tetranuclear chelate complexes **1**–**3** (bridgehead: Fe ions) c.f. also the conditions for spherical tricycles (bridgehead: N atoms): ref. [6]; F. P. Schmidtchen, *Angew. Chem.* **1977**, *89*, 751-752; *Angew. Chem. Int. Chem. Ed. Engl.* **1977**, *16*, 720-721; J.-M. Lehn, *Pure Appl. Chem.* **1977**, *49*, 857-870; E. Graf, J.-M. Lehn, *J. Am. Soc. Chem.* **1975**, *97*, 5022-5024.

[14] M. Becke-Goehring, H. Hoffmann, *Komplexchemie*, Springer, Berlin, **1970**, p. 26ff; see also *Nomenclature of Inorganic Chemistry* (Ed.: G. J. Leigh), Blackwell, Oxford, **1991**, p. 179ff. (For octahedral complexes of type $MA^1B^1A^2B^2A^3B^3$ five enantiomeric pairs occur: J. Leong, K. N. Raymond, *J. Am. Chem. Soc.* **1975**, *97*, 293-296). cf. also the IUPAC recommended nomenclature OC-6-22 (for facial) and OC-6-21 (for meridional).

[15] R. S. Cahn, C. K. Ingold, V. Prelog, *Angew. Chem.* **1966**, *78*, 413–447; *Angew. Chem. Int. Ed. Engl.* **1966**, *5*, 385-415; G. Haas, V. Prelog, *Helv. Chim. Acta* **1969**, *52*, 1202-1218.

[16] Amel System 5000. Ungraduated cell with Pt plate electrodes and pseudoreference electrode. Potential measured vs. Fc/Fc^+.

[17] Pseudo thin-layer signifies that the working electrode is mounted on the glass head of the CV cell. CV = cyclovoltametry.

[18] The starting point for the CV experiments was at + 250 mV (**2**) and + 200 mV (**3**) vs Ag/AgCl pseudoreference electrodes. Thus, for the compounds under study, which contain one Fe^{II} and three Fe^{III} centers, the remaining Fe^{II} center is first oxidized before commencement of the potential cycle, allowing four sequential reduction signals to be observed.

[19] An alternative way of writing $[NH_4 \subset Fe_4L_6^2]$ **2** is $\{[NH_4^+ \subset Fe_4L_6^2]e^-\}$ **2**.

[20] The series alkali metal atom, cryptatium ("expanded atom" or radical contact ion pair), and electride (Rydberg-atom or electron salt) exemplifies systems in which formally, the electron is progressively further removed from the atom. For comparison see: L. Echegoyen, A. DeCian, J. Fischer, J. M. Lehn, *Angew. Chem.* **1991**, *103*, 884-886; *Angew. Chem. Int. Ed. Engl.* **1991**, *30*, 838-840.

Effects of $^{35}Cl/^{37}Cl$, ^{13}C Residual Dipolar Coupling on the Variable-Temperature ^{13}C CP/MAS NMR Spectra of Solid, Chlorinated Sodium Acetates**

Sergio H. Alarcón, Alejandro C. Olivieri,* Stephen A. Carss, and Robin K. Harris

The effects of combined residual dipolar and scalar coupling between spin 1/2 nuclei and a large variety of quadrupolar nuclei have been recently reviewed.[1] Interest from organic chemists in this phenomenon has been usually restricted to the (^{14}N, ^{13}C) case,[2] whose manifestation has almost disappeared from the literature due to the use of high-field NMR spectrometers.[1] Very recently, however, ^{13}C CP/MAS NMR spectra (CP = cross polarization, MAS = magic angle spinning) of solid chlorine-containing organic compounds have been shown to display splittings arising from residual coupling (mostly dipolar in nature) between the observed spin 1/2 ^{13}C nucleus and the $^{35,37}Cl$ isotopes ($S = 3/2$ in both cases) at bonding distances.[3] In all cases reported so far, carbon atoms bonded to a single chlorine atom were studied.[3] We report here on the effects of residual dipolar ($^{35}Cl/^{37}Cl$, ^{13}C) coupling at both bonding and nonbonding distances in compounds containing CH_2Cl, $CHCl_2$, and CCl_3 groups.

Detailed theory has been produced on this subject, including a fully computational solution of the (spin 1/2, spin 3/2) dipolar coupling under MAS conditions,[4, 5] first-order perturbation theory (valid when $|\chi/\nu_S| < 1$; χ is the quadrupole coupling constant and ν_S is the resonance frequency for the quadrupolar S nuclei),[2, 5, 6] and a polynomial fit to the exact solution (valid for $1 < |\chi/\nu_S| < 3$).[5] According to first-order perturbation theory,[6] the ^{13}C CP/MAS NMR signal of a carbon atom affected by a single chlorine nucleus at a distance r should give a symmetric doublet with a splitting $s = 6D_\chi(3\cos^2\beta^D - 1)/20\nu_S$ [$D = (\mu_0/4\pi)\gamma_I\gamma_S h/4\pi^2 r^3$; β^D is the angle between the vector $\boldsymbol{r}$ and the z_{EFG} axis of the quadrupole tensor at the $^{35,37}Cl$]. Since χ is substantial for the $^{35,37}Cl$ isotope bonded to the carbon nucleus, deviations are expected from the first-order regime even at high fields, in which case Equation (a) can be used (in the range $1 < |\chi/\nu_S| < 3$),[5] where s is still a symmetric splitting. It

$$s = D[(3\cos^2\beta^D - 1)/2](0.581|\chi/\nu_S| + 0.033|\chi/\nu_S|^2 - 0.021|\chi/\nu_S|^3) \quad \text{(a)}$$

should be noted that the ^{35}Cl and ^{37}Cl isotopes have similar nuclear properties, and their separate effects are thus difficult to detect. This means that the calculated effect on the observed carbon nucleus should be the weighted average of those corresponding to the individual isotopes.

Values of $\chi(^{35}Cl)$ for chlorinated organic compounds usually lie in the vicinity of -70 MHz,[7] so that $|\chi/\nu_S|$ is about 2.4 at 7.05 T [and thus Eq. (a) can be used] and 3.6 at 4.7 T. Therefore, in this latter case one has to resort to exact calculations, which predict a broad triplet with intensities in the ratio 1:1:2 (in the direction of increasing frequencies; the intrinsic asymmetry of these triplets depends on the sign of χ). [5] These results have been experimentally confirmed in organic compounds for carbon atoms directly bonded to a single chlorine.[3] The ^{13}C NMR signal resulting from coupling to two and three equivalent chlorine atoms is expected to be a 1:2:1 triplet and a 1:3:3:1 quartet, respectively, at high fields ($|\chi/\nu_S| < 3$), whereas more complex line shapes are predicted at lower fields. Figure 1 shows the experimental results obtained for sodium monochloro-(**1**), dichloro-(**2**), and trichloroacetate (**3**); the relevant chemical shift information is presented in Table 1. At ambient probe temperature, compound **1** gives, for both the carbon of the CH_2Cl group and for that of the carboxyl group, the expected 1:1 doublets at 7.05 T and 1:1:2 triplets at 4.7 T. Using

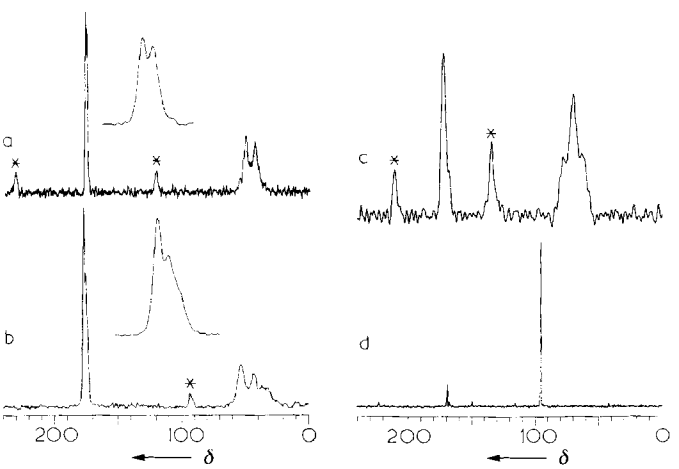


Fig. 1. ^{13}C CP/MAS NMR spectra for the compounds **1**–**3** in the solid state. a) Spectrum of **1** at ambient probe temperature, $B_0 = 7.05$ T, $\nu(^{13}C) = 75.4$ MHz. b) Spectrum of **1** at ambient probe temperature, $B_0 = 4.7$ T, $\nu(^{13}C) = 50.3$ MHz. c) Spectrum of **2** at 158 K (nominal temperature), $B_0 = 7.05$ T. d) Spectrum of **3** at ambient probe temperature, $B_0 = 7.05$ T. The low-temperature spectra (down to 163 K) of **3** were essentially identical to that shown in this figure. The inserts in spectra a) and b) show expansions of the carboxyl region. Asterisks denote spinning side bands.

Table 1. Chemical shifts observed for **1**–**3** in the ^{13}C MAS NMR spectra.

Compound		δ values			
		7.05 T		4.7 T	
	T [K]	C1	C2	C1 [b]	C2 [b]
1	293	175.7 [a]	42.2 [a]	174.0 [c]	33.9
		176.7	50.0	175.7	43.3
				177.7	53.2
2	163	172.3	61.8 [d]		
		($w_{1/2} = 4.0$)	69.8		
			77.8		
3	163	168.0	95.4		
		($w_{1/2} = 0.4$)			

[a] 1:1 Doublets. [b] 1:1:2 Triplets. [c] Shoulder of the signal at $\delta = 175.7$. [d] 1:2:1 Triplet.

[*] Prof. A. C. Olivieri, S. H. Alarcón
Departamento de Química Analítica
Facultad de Ciencias Bioquímicas y Farmacéuticas
Universidad Nacional de Rosario
Suipacha 531, Rosario (2000) (Argentina)
Telefax: Int. code +(41) 395980
S. A. Carss, Prof. R. K. Harris
Department of Chemistry
University of Durham
South Road, Durham DH1 3LE (UK)

[**] This work was supported by the University of Rosario, Consejo Nacional de Investigaciones Científicas y Técnicas, Argentina, (CONICET) and Fundación Antorchas (A.C.O., S.H.A.) We thank the U.K. Science and Engineering Research Council (SERC) for access to the Varian VXR 300 spectrometer under the National Solid-State NMR Service arrangements, and for provision of the Chemagnetics CMX 200 system (research grant GR/H96096). We are grateful to R. Challoner, B. J. Say, and D. C. Apperley for assistance with spectrometer operation. S.A.C. thanks the University of Durham for a Research Studentship.

$\chi(^{35}Cl) = -67.8$ MHz[8] [$\chi(^{37}Cl) = -53.4$ MHz; $Q(^{37}Cl)/Q(^{35}Cl) = 0.788$][9], $\nu_S(^{35}Cl) = 29.4$ MHz (24.5 MHz for ^{37}Cl), and a typical chloroacetate geometry ($r = 1.77$ Å, $\beta^D = 0$ for C2; $r = 2.74$ Å, $\beta^D = 30°$ for C1, see Fig. 2),[10] first-order per-

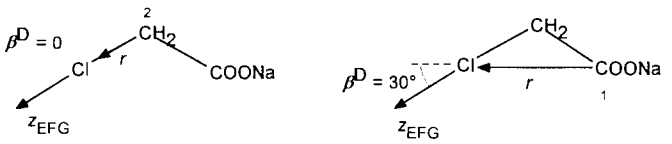


Fig. 2. Relative orientation of the internuclear vector r and the $^{35}Cl/^{37}Cl$ z_{EFG} axis for the carbon atoms C1 and C2 in **1**. EFG = electric field gradient

turbation theory in a magnetic field of 7.05 T gives symmetric splittings s of 9.2 ppm for the doublet of C2 and 1.6 ppm for the doublet of C1 (averaged in both cases according to the natural abundances of the Cl isotopes, ^{35}Cl, 75.5%; ^{37}Cl, 24.5%). On the other hand, if Equation(a) ($|\chi/\nu_S| = 2.31$ for ^{35}Cl; 2.18 for ^{37}Cl at 7.05 T) is used to calculate the splittings, one obtains values of s of 8.4 ppm and 1.4 ppm for the C2 and the C1 doublet, respectively, which are in better agreement with the experimental data (Table 1, $s = 7.8$ ppm for C2 and 1.0 ppm for C1 at 7.05 T). At 4.7 T neither first-order perturbation theory nor Equation (a) are appropriate. In this case a broad 1:1:2 triplet is expected on the basis of the exact calculations.[4, 5] Using the quadrupole data for **1**, $\nu_S = 19.6$ MHz for ^{35}Cl (16.3 MHz for ^{37}Cl) at 4.7 T, the exact calculation gives the following shifts of the signals relative to the isotropic ^{13}C frequency: -12.9; -2.8; $+7.8$ ppm for the C2 atom and -2.0; -0.4; $+1.2$ ppm for the C1 atom. These values are in excellent agreement with experimental ones: -12.2; -2.8; $+7.1$ ppm for the C2 triplet and -2.2; -0.5; $+1.1$ ppm for the C1 triplet (Fig. 1 and Table 1; values measured from the center of the 7.05 T doublets). In the case of compound **2**, the expected 1:2:1 triplet is only observed for the C2 signal in the low-temperature spectrum recorded at 7.05 T. The distance between adjacent peaks of this C2 triplet (8.0 ppm, Table 1) is very similar to that observed in the corresponding doublet for **1** at the same field. The expected long-range effect on C1 (a 1:2:1 triplet with interpeak distances of about 1 ppm) may be lost within the experimental line width (Table 1). Quadrupole data are not known for **2** but information is available on the corresponding acids;[8] this shows that all three compounds have similar $\chi(^{35}Cl)$ values. Thus, the ^{13}C NMR data for the C2 nucleus in compound **2** shown in Figure 1 and Table 1 are readily explained. Interestingly, the C2 triplet collapses into a broad singlet at room temperature, indicating that the reorientation of the $CHCl_2$ segment (or an overall molecular motion) may be able to induce an efficient $^{35}Cl/^{37}Cl$ longitudinal relaxation which causes the ^{13}C nucleus to be self-decoupled.[11] This effect has also been reported in other cases,[12] and is very pronounced in compound **3**; thus even at low temperatures (down to 163 K) two sharp ^{13}C singlets (Fig. 1 and Table 1) occur. The easier rotation of the threefold symmetric CCl_3 group in the solid is expected to lead to an even faster quadrupole relaxation than in the $CHCl_2$ case.

In summary, ^{13}C CP/MAS NMR spectra of chlorinated organic compounds recorded at high fields are expected to reveal complex line shapes, if the molecular motions are slow enough to prevent self-decoupling by fast quadrupole relaxation of the chlorine nuclei. However, the effects can be conveniently explained by the existing theory.

Experimental Procedure

^{13}C NMR spectra at 75.4 MHz were recorded with a Varian VXR 300 NMR spectrometer equipped with a Doty 7 mm probe; spectral width, 30 kHz; acquisition time, 39.4 ms (**1** and **2**), 59.7 ms (**3**); relaxation delay, 30 s (**1** and **3**), 300 s (**2**); contact time, 3 ms (**1**), 1 ms (**2**); memory, 8 K; number of acquisitions, 1840 (**1** and **2**), 84 (**3**); spinning speed, 4200 Hz (**1**), 2850 Hz (**2**), 4050 Hz (**3**). Spectra for compounds **1** and **2** were recorded in the CP mode, whereas compound **3** was studied by single-pulse acquisition. The CP spectrum for **2** was recorded at 50.3 MHz on a Chemagnetics CMX 200 NMR spectrometer equipped with a Bruker 7 mm probe; spectral width, 20 kHz; acquisition time, 20 ms; relaxation delay, 30 s; contact time, 3.5 ms; memory, 8 K; number of acquisitions, 2040; spinning speed, 4200 Hz. The temperature was lowered by cooling the driving gas in liquid N_2.

Received: March 11, 1994 [Z 6750 IE]
German version: *Angew. Chem.* **1994**, *106*, 1708

[1] R. K. Harris, A. C. Olivieri, *Prog. Nucl. Magn. Reson. Spectrosc.* **1992**, *24*, 435.
[2] A. C. Olivieri, L. Frydman, L. E. Diaz, *J. Magn. Reson.* **1987**, *75*, 50.
[3] A. C. Olivieri, P. Cabildo, R. M. Claramunt, J. E. Elguero, *J. Phys. Chem.* **1994**, *98*, 5207; R. K. Harris, M. Sünnetçioğlu, K. S. Cameron, F. G. Riddell, *Magn. Reson. Chem.* **1993**, *31*, 963; R. M. Cravero, C. Fernandez, M. Gonzalez-Sierra, A. C. Olivieri, *J. Chem. Soc. Chem. Commun.* **1993**, 1253.
[4] E. M. Menger, W. S. Veeman, *J. Magn. Reson.* **1982**, *46*, 257.
[5] S. H. Alarcón, A. C. Olivieri, R. K. Harris, *Solid State Nucl. Magn. Reson.* **1993**, *2*, 325.
[6] A. C. Olivieri, *J. Magn. Reson.* **1989**, *81*, 201; *ibid.* **1993**, *101 A*, 313; *Solid State Nucl. Magn. Reson.* **1992**, *1*, 345.
[7] E. A. C. Lucken, *Nuclear Quadrupole Coupling Constants*, Academic Press, London, **1969**, p. 187.
[8] H. C. Allen, *J. Am. Chem. Soc.* **1952**, *74*, 6074.
[9] P. Pyykko, *Z. Naturforsch. A* **1992**, *47*, 189.
[10] M. Ichikawa, *Acta Crystallogr. Sect. B* **1974**, *30*, 651; D. Hadzi, I. Leban, B. Orel, M. Iwata, J. M. Williams, *J. Cryst. Mol. Struct.* **1979**, *9*, 117.
[11] The relevant relaxation rate in this case is the one connecting the $|\pm 3/2\rangle$ and $|\pm 1/2\rangle$ ^{35}Cl states, since these are responsible for each of the components of the symmetric doublets observed at high fields.
[12] A. C. Olivieri, *J. Chem. Soc. Perkin Trans. 2* **1990**, 85; H. W. Spiess, U. Haeberlen, H. Zimmermann, *J. Magn. Reson.* **1977**, *25*, 55; R. K. Harris, A. Root, *Mol. Phys.* **1989**, *66*, 993; S. H. Alarcón, A. C. Olivieri, P. Jonsen, *J. Chem. Soc. Perkin Trans. 2* **1993**, 1783.

Dissolution of Cholesterol in Water by a Synthetic Receptor**

Blake R. Peterson and François Diederich*

Dedicated to Professor C. Rüchardt on the occasion of his 65th birthday

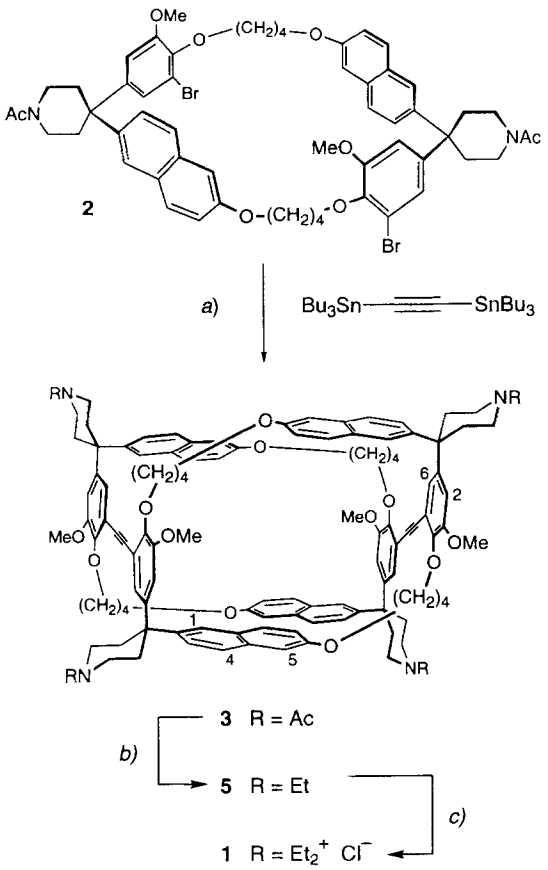
Cholesterol is an essential component of animal cells. This highly water-insoluble steroid serves as both a modulator of membrane fluidity and as a raw material for the production of steroid hormones and bile acids.[1] The hydrophobic properties of cholesterol, which make it an essential component of cell membranes, also make it lethal when deposited on arterial walls. The deposition of cholesterol-containing plaque in blood vessels, known as atherosclerosis,[2] is a leading cause of death in western industrialized societies. While current drug therapies focus on enzyme inhibition of endogenous cholesterol biosynthesis[3] or bile acid depletion[4] to reduce blood cholesterol

[*] Prof. Dr. F. Diederich, B. R. Peterson
Laboratorium für Organische Chemie, ETH-Zentrum
Universitätstrasse 16, CH-8092 Zürich (Switzerland)
Telefax: Int. code + (1)261-3524

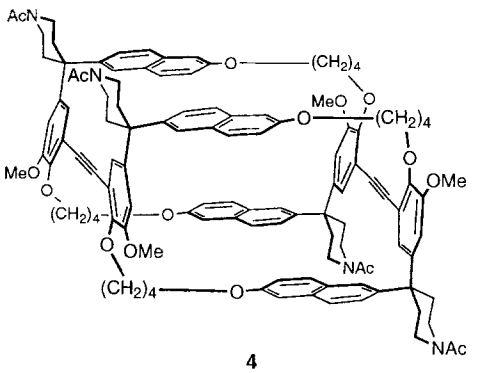
[**] This work was supported by ETH Zürich. We thank Dr. B. Jaun for his assistance in obtaining and interpreting the 2D NMR spectra of the macrotricyclic compounds and Drs. W. Amrein and P. James for recording the mass spectra.

levels, the selective dissolution of cholesterol deposits by strongly binding synthetic receptors could provide a new alternative therapeutic strategy. Naturally occurring cyclodextrins[5, 6] could be used in such treatments, since they are known to form inclusion complexes with cholesterol in aqueous solution, but a lack of selectivity limits their scope as specific cholesterol-binding agents. Although a few synthetic cyclophane receptors have been used in studies of steroid recognition phenomena,[7-11] complexation of highly insoluble steroids such as cholesterol in aqueous solution has previously remained elusive. We describe herein the synthesis of a novel water-soluble tricyclic cyclophane receptor **1** which binds strongly and selectively to cholesterol in water.

The key step in the synthesis of **1** was the Pd^0-catalyzed Stille-type coupling[12] of equimolar amounts of bis(tributylstannyl)acetylene and dibromocyclophane **2** (Scheme 1), which can be prepared in multigram quantities in six steps starting from 2-bromo-6-ethoxynaphthalene.[11] This remarkable cyclization reaction produced the chiral D_2-symmetrical macrotricycle **3** selectively in 14% yield and none of the possible achiral isomer **4** with C_{2h} symmetry. Reduction of **3** with $LiAlH_4$ to tetramine **5** followed by quaternization with ethyl iodide and ion exchange chromatography (Cl^-) afforded the water-soluble receptor **1**.



Scheme 1. Synthesis and analytical data of receptor **1**. Reagents and yields: a) $[Pd(PPh_3)_4]$, 2,6-di-*tert*-butyl-*p*-cresol, dimethylformamide, 110 °C, pressure bottle, 2 d, 14%; b) $LiAlH_4$, Et_2O, 20 °C, 12 h, 59%; c) C_2H_5I, $CHCl_3$, 20 °C, 4 d, followed by ion exchange on Dowex resin (Cl^-) eluting with H_2O/CH_3OH 1:1, 78%. Analytical data for **1**: m.p. 250–252 °C (decomp). ^1H NMR (500 MHz, $(CD_3)_2SO$, 400 K, see formula **3** for numbering of atoms) $\delta = 1.22-1.33$ (m, 24 H, NCH_2CH_3), 1.92–2.05 (2 × m, 16 H, CH_2CH_2), 2.55–2.91 (br. 3 × m, 16 H, NCH_2CH_2), 3.13–3.52 (br. 5 × m, 32 H, NCH_2CH_2, NCH_2CH_3), 3.88 (*s*, 12 H, OCH_3), 4.08–4.14 (2 × m, 16 H, $PhOCH_2$, $NaphOCH_2$), 6.87 (br. s, 8 H, Ph H-C(6), Ph H-C(2)), 7.06 (br. s, 4 H, Naph H-C(5)), 7.14 (br. s, 4 H, Naph H-C(8)), 7.21 (br. s, 4 H, Naph H-C(3)), 7.39–7.48 (m, 8 H, Naph H-C(4), Naph H-C(7)), 7.49–7.63 (m, 4 H, Naph H-C(1)); ^{13}C NMR (125.8 MHz, CD_3OD, 300 K) $\delta = 7.27$, 7.51, 7.83, 7.90, 26.90, 27.67, 29.82, 30.72, 44.61, 52.78, 56.85, 59.04, 68.68, 74.05, 91.16, 107.44, 112.88, 119.51, 120.44, 124.32, 125.24, 126.09, 129.01, 130.16, 130.75, 134.61, 141.68 (2 ×), 148.95, 154.51, 158.58. Matrix-assisted laser desorption ionization time-of-flight mass spectrometry (MALDI-TOF, sinapic acid): *m/z* 2029 (M^+, $C_{124}H_{148}N_4O_{12}Cl_4$), calc. 2027. Correct elemental analysis for $C_{124}H_{148}N_4O_{12}Cl_4 \cdot 8H_2O$ (2172.52).



The formation of only one isomer in the Pd^0-mediated macrocyclization was evident from the one spot for the product in the thin-layer chromatogram ($R_f = 0.15$, SiO_2, CH_2Cl_2/CH_3OH 20:1) and the presence of only one set of corresponding resonances in the ^1H and ^{13}C NMR spectra. Two-dimensional NMR spectra of **5** demonstrated that the chiral D_2-symmetrical isomer **3** was formed exclusively. ROESY spectroscopy provided evidence of intramolecular aliphatic–aromatic $^1H\{^1H\}$ nuclear Overhauser effects (NOEs) which are only possible in the D_2-symmetrical compound (Fig. 1). In addition, molecular dynamics simulations with MacroModel[13] (Fig. 2) showed the D_2-symmetrical isomer **3** to be more stable than the C_{2h}-symmetrical isomer **4** by 6 kcal mol^{-1}, which would explain the exclusive formation of **3**.

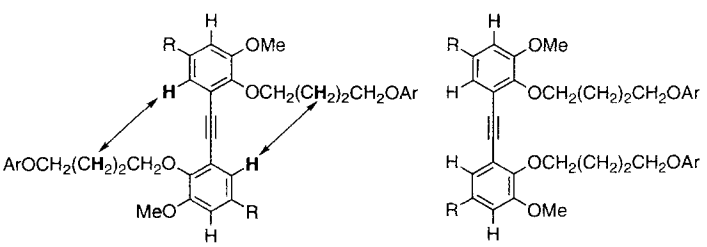


Fig. 1. Aromatic–aliphatic $^1H\{^1H\}$ nuclear Overhauser effects (NOEs) observed by ROESY spectroscopy of **5** support the D_2-symmetric structure. Irradiation at the frequency of the aromatic signal leads to approximately equal NOE enhancements for the two CH_2 groups shown. The alternative C_{2h}-symmetrical isomer cannot exhibit the observed NOE enhancements. Shown are only the fragments of the two isomers that are relevant to the NOE discussion. The D_2-symmetric isomer is represented on the left, the C_{2h}-symmetric on the right.

Receptor **1** is highly soluble in water (6 mg mL^{-1}, 3.0 mM) and does not aggregate appreciably at concentrations below 2.5 mM, as determined by ^1H NMR dilution experiments. This relatively high critical aggregation concentration (CAC) is due in part to the presence of the four peripheral CH_3O substituents, which have been shown to significantly increase the CAC values of other water-soluble cyclophanes.[14] When two cyclophanes **2** are connected by two acetylene bridges, the depth of the cavity increases from approximately 5 Å (in **2**) to roughly 11 Å (in **1**) (Fig. 2), which provides a nearly perfect environment, both in terms of space and hydrophobicity, for complete encapsulation

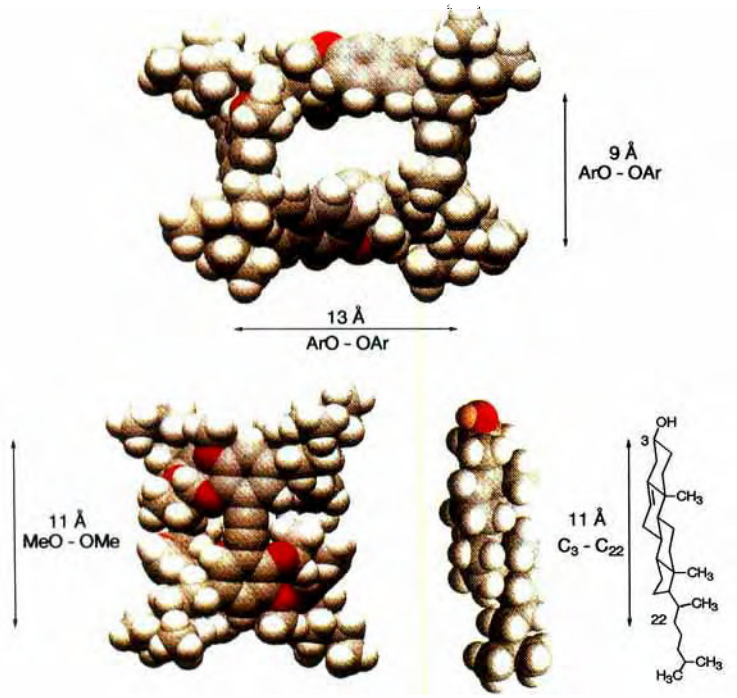


Fig. 2. Comparison of minimum-energy structures of **1** (top and bottom left) and cholesterol (bottom right) [13]. The top view shows the dimensions of the cavity entrance in **1** (9 × 13 Å). The bottom view of **1** shows the depth of the cavity (11 Å) which is sufficient to incorporate all four rings A–D of axially included cholesterol and parts of the hydrophobic side chain.

of a hydrophobic steroid like cholesterol in an axial orientation. Since the receptor has a cavity opening with dimensions of 9 × 13 Å, steroids can penetrate without significant steric hindrance.

Table 1. Association constants K_a and binding free energies ΔG° for steroid complexes of **1** determined by solid–liquid extraction in H_2O at 295 K [a].

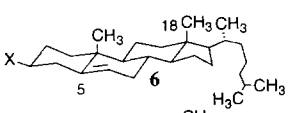
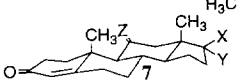
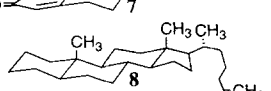
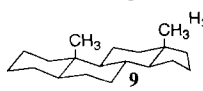
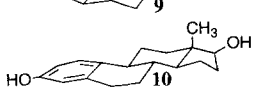
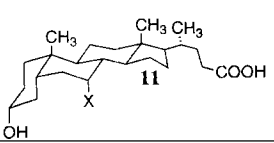
Steroid	K_a [L mol^{-1}]	$-\Delta G^\circ$ [b] [kcal mol^{-1}]	Solubility [M]
cholesterol	1.1×10^6	8.2	4.7×10^{-6} [c]
testosterone	6.8×10^4	6.5	8.3×10^{-5} [d]

[a] Solutions of **1** (1–2 mM) in H_2O were sonicated for 45 min in the presence of excess solid steroid and allowed to equilibrate at 295 K for 2 h. The suspension was centrifuged and the supernatant liquid filtered through a 0.45 μm cellulose acetate filter. Removal of water under reduced pressure was followed by addition of CD_3OD, which allowed determination of percent steroid extracted by integration of the ^{1}H NMR signals. For the calculation of K_a, see ref.[15]. The association constants given are average values for two diastereomeric complexes, which are of similar stability (see Table 2). [b] Data from triplicate runs. Reproducibility of ΔG° values: ±0.4 kcal. [c] Ref.[16]. [d] Ref.[17].

The complexation of two of the least water-soluble steroids, cholesterol and testosterone, by **1** in water was evaluated using the solid–liquid extraction method[15] (Table 1). The maximum solubility of cholesterol in pure water is 4.7×10^{-6} M.[16] Upon extraction of an excess of solid cholesterol with a 1.0 mM aqueous solution of **1**, a 8.5×10^{-4} M solution of cholesterol is obtained. This corresponds to a complexation-mediated increase in solubility by a factor of 190. The association constant for the **1**·cholesterol complex in pure water can then be calculated as $K_a = 1.1 \times 10^6$ L mol^{-1} (295 K). Solid testosterone is also extracted into water through complexation by **1**, although, at $K_a = 6.8 \times 10^4$ L mol^{-1}, its binding affinity is much lower. This can be readily explained by the higher affinity of the more polar testosterone to the aqueous phase, which is reflected in its higher solubility in water compared to that of cholesterol.[16, 17]

A more detailed analysis of the steroid-binding properties of **1** was obtained by ^{1}H NMR binding titrations in CD_3OD, in which all steroids and their complexes with **1** form homogenous

Table 2. Association constants K_a and binding free energies $-\Delta G^\circ$ from ^{1}H NMR binding titrations for 1:1 complexes of steroids and receptor **1** in CD_3OD at 298 K. Also shown are the complexation-induced changes in chemical shift of the protons of the CH_3 group at position 18 at saturation binding $\Delta\delta_{sat}$, which were evaluated in the titration [a].

		Steroid	X	Y	Z	K_a [L mol^{-1}]	$-\Delta G^\circ$ [kcal mol^{-1}]	$\Delta\delta_{sat}$ CH_3(18)
	**6a**	cholesteryl acetate	$OCOCH_3$			4800	5.0	1.95
	6b	5-cholestene	H			3200	4.8	1.19
	6c	cholesterol	OH			1500	4.3	1.70
	**7a**	testosterone	OH	H	H_2	2100	4.5	1.69
	7b	cortisone	$COCH_2OH$	OH	O	150	3.0	2.16
	7c	hydrocortisone	$COCH_2OH$	OH	α-H, β-OH	110	2.8	0.60
	**8**	5-α-cholestane				870	4.0	1.57
	**9**	5-α-androstane				500	3.7	1.74
	**10**	β-estradiol				390	3.5	2.04
	**11a**	lithocholic acid	H			310	3.4	0.57
	11b	chenodeoxycholic acid	OH			40	2.2 [b]	

[a] Association constants determined by nonlinear least squares curve fitting of 500 MHz ^{1}H NMR titrations. The resonances of the methyl groups at position 18 for the two diastereomeric complexes were not resolved, and the association constants given are an average value. This approximation is justified by the absence of significant differential complexation-induced shifts for the diastereomeric complexes. Reproducibility of K_a values: ±10%. [b] Estimated upper limit.

 © VCH Verlagsgesellschaft mbH, D-69451 Weinheim, 1994 0570-0833/94/1515-1627 $ 10.00+.25/0

solutions in the desired concentration ranges. Similar highly accurate binding assays were not possible in D_2O owing to slow exchange kinetics and low steroid solubilities.

Although the hydrophobic driving force for complexation is much weaker in CD_3OD than in D_2O,[18] cholesterol and its derivatives **6a,b** and testosterone (**7a**) form stable complexes with **1** in the organic solvent (Table 2). The relatively high stability of the testosterone complex in CD_3OD may be explained by favorable electrostatic $\pi-\pi$ interactions between the electron-deficient α,β-unsaturated ketone moiety in ring A with the electron-rich aryl ether cavity walls of the receptor.[19] The complexes of other steroids studied are substantially less stable. The comparison between the binding of **6b** and **8** [$\Delta(\Delta G^\circ)_{\mathbf{6b}-\mathbf{8}} = 0.8$ kcal mol^{-1}] indicates that the unsaturation at C(5) of the steroid ring system contributes significantly to complex stability, although it is uncertain whether this effect is a result of favorable attractive interactions of the polarizable double bond with the receptor or due to differences in the steric fit inside the cavity. Unlike other cyclophanes that preferentially bind aromatic steroids,[9, 10] receptor **1** only forms a weak complex with **10**. Contributions of the aliphatic steroid side chain to complex stability are significant but small [$\Delta(\Delta G^\circ)_{\mathbf{8}-\mathbf{9}} = 0.3$ kcal mol^{-1}], which implies that this hydrophobic residue is only partially encapsulated. Increasing steroid polarity rapidly decreases binding affinity. Comparison of binding affinities of bile acids **11a** and **11b** indicates that a single highly solvated OH group on the steroid B ring substantially inhibits stable complex formation.

Steroid binding studies with **1** indicate that this receptor exhibits sufficient binding affinity and specificity to warrant further exploration as an agent for solubilizing solid cholesterol deposits under biological conditions. These studies may result in a new, receptor-based strategy for the dissolution of cholesterol deposits.

Received: April 6, 1994 [Z 6829 IE]
German version: *Angew. Chem.* **1994**, *106*, 1688

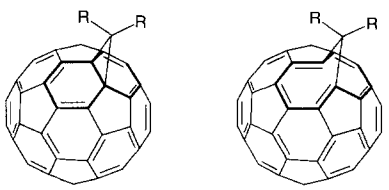
[1] M. S. Brown, J. L. Goldstein, *Angew. Chem.* **1986**, *98*, 579–599; *Angew. Chem. Int. Ed. Engl.* **1986**, *25*, 583–602.
[2] R. Ross, *Nature* **1993**, *362*, 801–809.
[3] A. Endo, *J. Med. Chem.* **1985**, *28*, 401–405.
[4] H. R. Casdorph in *Lipid Pharmacology, Vol. 2(2)* (Eds.: R. Paoletti, C. J. Glueck), Academic Press, New York, **1976**, pp. 222–256.
[5] P. Claudy, J. M. Létoffé, P. Germain, J. Bastide, A. Bayol, S. Blasquez, R. C. Rao, B. Gonzalez, *J. Therm. Anal.* **1991**, *37*, 2497–2506.
[6] F. Djedaïni, B. Perly, *J. Pharm. Sci.* **1991**, *80*, 1157–1161.
[7] H. Kawakami, O. Yoshino, K. Odashima, K. Koga, *Chem. Pharm. Bull.* **1985**, *33*, 5610–5613.
[8] D. R. Carcanague, F. Diederich, *Angew. Chem.* **1990**, *102*, 836–838; *Angew. Chem. Int. Ed. Engl.* **1990**, *29*, 769–771.
[9] S. Kumar, H.-J. Schneider, *J. Chem. Soc. Perkin Trans. 2* **1989**, 245–250.
[10] C. S. Wilcox, T. H. Webb, F. J. Zawacki, N. Glagovich, H. Suh, *Supramol. Chem.* **1993**, *1*, 129–137.
[11] B. R. Peterson, P. Wallimann, D. R. Carcanague, F. Diederich, *Tetrahedron*, in press.
[12] K. C. Nicolaou, T. K. Chakraborty, A. D. Piscopio, N. Minowa, P. Bertinato, *J. Am. Chem. Soc.* **1993**, *115*, 4419–4420.
[13] MacroModel V.4.0; F. Mohamadi, N. G. J. Richards, W. C. Guida, R. Liskamp, M. Lipton, C. Caufield, G. Chang, T. Hendrickson, W. C. Still, *J. Comput. Chem.* **1990**, *11*, 440-467. Equilibration of the D_2 and C_{2h} isomers **3** and **4** for 500 ps (AMBER*, 300 K, $CHCl_3$) was followed by repeated 200 ps simulations until the total energies converged.
[14] S. B. Ferguson, E. M. Seward, F. Diederich, E. M. Sanford, A. Chou, P. Inocencio-Szweda, C. B. Knobler, *J. Org. Chem.* **1988**, *53*, 5593–5595.
[15] F. Diederich, K. Dick, *J. Am. Chem. Soc.* **1984**, *106*, 8024–8036.
[16] M. E. Haberland, J. A. Reynolds, *Proc. Natl. Acad. Sci. USA* **1973**, *70*, 2313–2316.
[17] E. B. Kabasakalian, M. D. Yudis, *J. Pharm. Sci.* **1966**, *55*, 642.
[18] D. B. Smithrud, F. Diederich, *J. Am. Chem. Soc.* **1990**, *112*, 339–343.
[19] S. B. Ferguson, E. M. Sanford, E. M. Seward, F. Diederich, *J. Am. Chem. Soc.* **1991**, *113*, 5410–5419.

61,61-Bis(trimethylsilylbutadiynyl)-1,2-dihydro-1,2-methanofullerene[60]: Crystal Structure at 100 K and Electrochemical Conversion to a Conducting Polymer**

Harry L. Anderson, Corinne Boudon, François Diederich*, Jean-Paul Gisselbrecht, Maurice Gross*, and Paul Seiler*

Methanofullerenes are among the most thoroughly explored types of covalent fullerene derivatives.[1] Methano bridging may either occur at the junction between two six-membered rings (6-6 methano-bridged) or at the junction between a five- and a six-membered ring (6-5 methano-bridged). Further, by analogy with methanoannulenes,[2] methanofullerenes could occur as four possible valence isomers (closed 6-6, open 6-6, closed 6-5, and open 6-5 methano-bridged structures), depending on whether there is a transannular bond in the methanoannulene subunit (Scheme 1).

Scheme 1. The two possible isomeric methanofullerenes bridged at the 6-6 ring junction: the closed (left, observed) and open (right, not observed) 6-6 structures. The methanoannulene type substructures are highlighted.

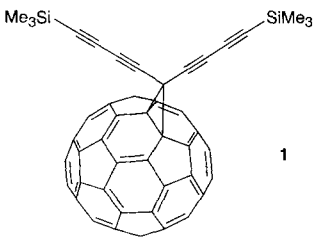


Ever since the synthesis of the first methanofullerenes by Wudl et al.,[3] there has been controversy about their structure. Originally, the 6-6 methano-bridged derivatives were thought to have an open 6-6 structure. This conclusion was based on a low-quality and therefore not necessarily conclusive X-ray crystal structure analysis of 61,61-bis(4-bromophenyl)-1,2-dihydro-1,2-methanofullerene[60].[4] A transannular distance between the bridgehead atoms C(1) and C(2) of about 1.84 Å is observed, a value similar to that found for some partially open 1,6-methano[10]annulenes.[5] However, NMR evidence[6, 7] and theoretical calculations[8] strongly imply that 6-6 methano-bridged fullerenes have a closed 6-6 structure containing a cyclopropane ring. The preference for the closed over the open 6-6 structure, which seems to be independent of the nature of the substituents at the methano C atom,[8b] was explained in terms of the favorable [5]radialene-type bonding pattern observed in C_{60}. The shorter bonds with higher double bond character are located exocyclic to the pentagons.[6c, 8b]

We report here on the low-temperature (100 K) crystal structure analysis of 61,61-bis(trimethylsilylbutadiynyl)-1,2-dihydro-1,2-methanofullerene (**1**).[9] The first accurate X-ray data for

[*] Prof. Dr. F. Diederich, P. Seiler, Dr. H. L. Anderson
Laboratorium für Organische Chemie, ETH Zentrum
Universitätstrasse 16, CH-8092 Zürich (Switzerland)
Telefax: Int. code + (1) 261-3524
Prof. M. Gross, C. Boudon, J.-P. Gisselbrecht
Laboratoire d'Electrochimie et de Chimie Physique du
Corps Solide U. R. A. au C. N. R. S. n° 405
Faculté de Chimie, Université Louis Pasteur
1 et 4, rue Blaise Pascal, B. P. 296
F-67008 Strasbourg Cedex (France)

[**] This work was supported by the Schweizerische Nationalfonds zur Förderung der wissenschaftlichen Forschung. H. L. A. thanks the Engineering and Physical Science Research Council (UK) for a postdoctoral research fellowship.



1

a 6-6 methano-bridged fullerene definitively confirm the preference for a closed 6-6 structure.[*] This paper also presents evidence that electrochemical polymerization of **1** yields an air-stable, electrically conducting film.

Two ordered crystal modifications of **1**, referred to as **1a** and **1b**, were obtained from CS_2 and toluene solutions, respectively.[10] Modification **1a** crystallized in the monoclinic space group $P2_1/c$ with four molecules of **1** and two CS_2 molecules in the unit cell; **1b** has a triclinic space group $P\bar{1}$, with two molecules of **1** and four toluene molecules. Here we mainly discuss the molecular geometry of the more accurate structure **1b**;[11] the geometry of **1a** is practically identical within the estimated standard deviations.

As expected, the butadiynyl substituents of **1b** (Fig. 1) are in a nearly symmetrical arrangement. Approximate C_{2v} symmetry

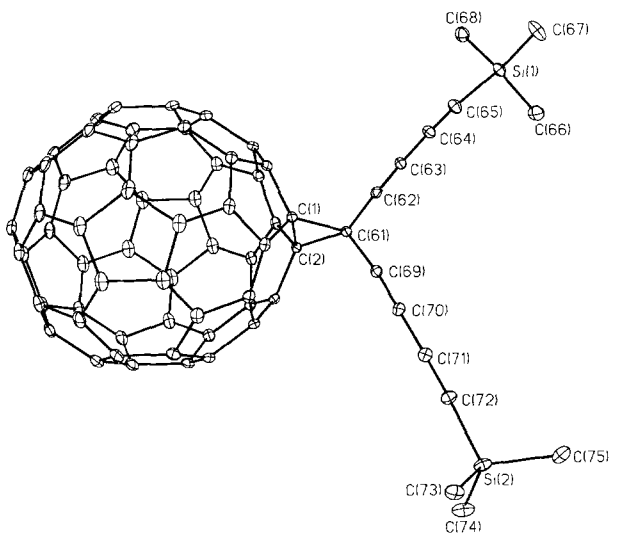


Fig. 1. Molecular structure of **1b**. Vibrational ellipsoids are shown at the 30% probability level. Selected bond lengths [Å] and angles [°] [11]: C(1)–C(61) 1.536, C(2)–C(61) 1.542, Si(1)–C(65) 1.849, C(65)–C(64) 1.210, C(64)–C(63) 1.372, C(63)–C(62) 1.201, C(62)–C(61) 1.440, C(61)–C(69) 1.440, C(69)–C(70) 1.207, C(70)–C(71) 1.372, C(71)–C(72) 1.212, C(72)–Si(2) 1.852; C(2)-C(1)-C(61) 59.4, C(1)-C(2)-C(61) 59.1, C(1)-C(61)-C(2) 61.5, C(62)-C(61)-C(69) 116.7.

is thus adopted. Bond lengths and angles are given in Figure 2.[4] The crucial 6-6 bond length C(1)–C(2) is 1.574(3) Å, which is close to the calculated value of 1.55(1) Å for a closed 6-6 structure.[8b] Except for the three-membered ring, the geometry of the bridged pyracylene (Fig. 2) is, on the whole, in good agreement with recent X-ray results obtained for dibenzohomopyracylene **2** (Fig. 3).[2c,12] The C–C bonds in the cyclopropane ring of **1b** are about 0.02–0.04 Å longer than those in the corresponding ring of **2**. The geometry of the three-membered ring in **1b** closely resembles that in some accurate structures of strained [n.1.1] propellanes,[13] which exhibit C–C bond lengths of about 1.58 Å for the central bond and 1.52 Å for the other cyclopropane bonds.

The strain at the bridgehead atoms C(1) and C(2) is evident from an analysis of the bond angles, which deviate significantly

[*] Addition in proof (August 9, 1994): Recently the X-ray structure analysis of another methanofullerene was reported: J. Osterodt, M. Nieger, F. Vögtle, *J. Chem. Soc. Chem. Commun.* **1994**, 1607.

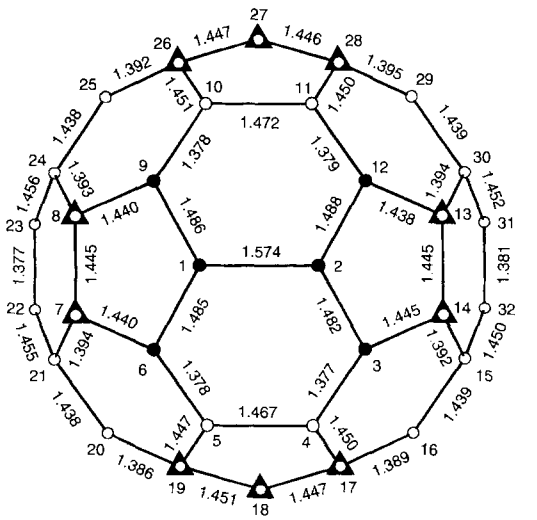


Fig. 2. Detail of structure **1b**; the methano bridge at C(1)–C(2) is omitted for clarity. Atoms nearest and furthest from the centroid Z_0 are marked with triangles and filled-in circles, respectively. Selected bond angles [°] [11]: C(2)-C(1)-C(6) 115.8, C(2)-C(1)-C(9) 116.4, C(6)-C(1)-C(9) 106.0, C(1)-C(2)-C(3) 116.6, C(1)-C(2)-C(12) 116.1, C(3)-C(2)-C(12) 105.9, C(2)-C(3)-C(4) 122.6, C(2)-C(3)-C(14) 108.0, C(4)-C(3)-C(14) 120.0, C(1)-C(6)-C(5) 122.6, C(1)-C(6)-C(7) 108.0, C(5)-C(6)-C(7) 119.9, C(1)-C(9)-C(8) 107.6, C(1)-C(9)-C(10) 122.6, C(8)-C(9)-C(10) 119.9, C(2)-C(12)-C(11) 122.6, C(2)-C(12)-C(13) 107.8, C(11)-C(12)-C(13) 119.7. Centroid–C distances [Å]: C(1) 3.726, C(2) 3.722, C(3) 3.557, C(4) 3.538, C(5) 3.532, C(6) 3.557, C(7) 3.519, C(8) 3.520, C(9) 3.567, C(10) 3.542, C(11) 3.541, C(12) 3.564, C(13) 3.515, C(14) 3.521, C(15) 3.532, C(16) 3.534, C(17) 3.523, C(18) 3.514, C(19) 3.519, C(20) 3.537, C(21) 3.536, C(22) 3.546, C(23) 3.539, C(24) 3.536, C(25) 3.540, C(26) 3.528, C(27) 3.520, C(28) 3.527, C(29) 3.536, C(30) 3.528, C(31) 3.541, C(32) 3.543.

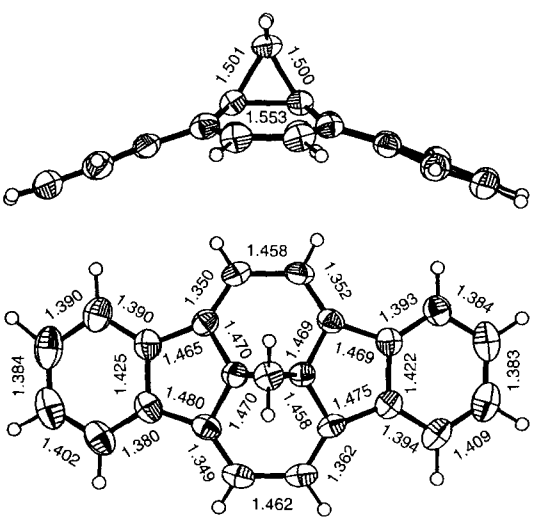


Fig. 3. Crystal structure of **2** [2c,12].

from ideal tetrahedral geometry. The three bond angles in the fullerene shell range from 105.9 to 116.6°, and the sums of these angles at C(1) and C(2) are 338.2 and 338.6°, respectively (about 10° larger than the ideal value of 328°). The bond angles at the other fullerene C atoms are 107.1–108.7° (mean 108.0°) in the pentagons and 119.3–120.9° (mean 120.0°) in the hexagons, values which are within the normal range.

The lengths of the 5-6 bonds within the C_{60} skeleton, excluding the bonds in rings containing C(1) or C(2), range from 1.438 to 1.457 Å (mean 1.449(5) Å);[11] the lengths of the 6-6 bonds range from 1.377 to 1.397 Å (mean 1.391(5) Å). This demonstrates that the [5]radialene-type bonding structure of C_{60} is preserved. The shortest 6-6 bonds are those on the edges of the bridged pyracylene moiety (mean 1.378 Å) and those in two of

the four equatorial positions (C(22)–C(23) and C(31)–C(32); mean 1.379 Å). These bonds have the highest double bond character and should have the highest reactivity towards nucleophiles.[14] The lengths of the 6-6 bonds in the rear hemisphere (not shown in Fig. 2) range from 1.383 to 1.395 Å.

Most of the five- and six-membered rings are planar with deviations from least-squares planes of less than 0.003 Å; the largest deviations (of up to about 0.06 Å) occur in the five-membered rings containing C(1) or C(2). The distances between the fullerene C atoms, excluding C(1) and C(2), and the centroid Z_o of the C_{60} ball range from 3.514 to 3.567 Å, the average being 3.539(11) Å. The C(1)–Z_o and C(2)–Z_o distances of 3.726 and 3.722 Å, respectively, are considerably longer than the average value; thus, as observed in other fullerene derivatives, C(1) and C(2) protrude from the C_{60} skeleton.[15] Atoms nearest to and furthest from the centroid Z_o are marked on Figure 2 by triangles and filled-in circles, respectively. The fullerene shell is slightly compressed along the axis perpendicular to the plane of the cyclopropane ring.

In the crystal packing of **1b** (Fig. 4), the fullerene molecules near the corners of the triclinic unit cell are related by a center of inversion. The shortest intermolecular C(60)···C(60) distance through the inversion center is 3.30 Å. There are two different types of toluene molecules in the unit cell. One ordered toluene molecule lies between two fullerenes with its molecular plane roughly perpendicular to the $Z_o \cdots Z_o$ axis (not indicated). Two short C···C distances (3.24 and 3.28 Å) separate this molecule from C(17) of one C_{60} sphere and one short distance (3.34 Å) from C(44) of another sphere. A slightly disordered toluene molecule lies parallel to the *b*,*c* plane between acetylenic substituents and does not have short contacts.

The more interesting crystal packing of **1a** is shown in Figure 5 as a projection onto the *b*,*c* plane of the monoclinic unit cell. Two fullerene molecules are related by a center of inversion occupied by the C atom of a CS_2 molecule. The shortest distances between solvent and C_{60} sphere are those between the central carbon atom of the CS_2 molecule and the atoms of the 5-6 bond C(44)–C(57) (3.24 and 3.36 Å, respectively). The intermolecular distances along the *c* axis between the electron-rich

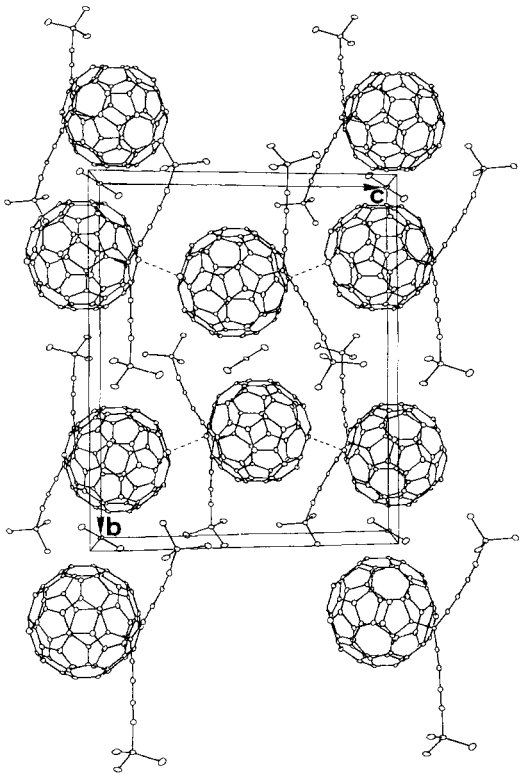


Fig. 5. Crystal packing in **1a** viewed along the *a* axis.

6-6 bonds C(8)–C(24) and the electron-deficient 5-6 bonds C(33)–C(34) of adjacent C_{60} spheres are remarkably short (four short C···C distances, 3.04–3.32 Å; only the shortest C(8)···C(33) distances are shown in Fig. 5).

Many butadiynes polymerize in the solid state to give polydiacetylenes.[16] In this case, the butadiyne moieties in the crystals **1a** and **1b** are too far apart to undergo this topochemical reaction. In solution, however, **1** does appear to undergo reductive electrochemical polymerization to give an insoluble, electrically conducting film on the surface of the platinum cathode.

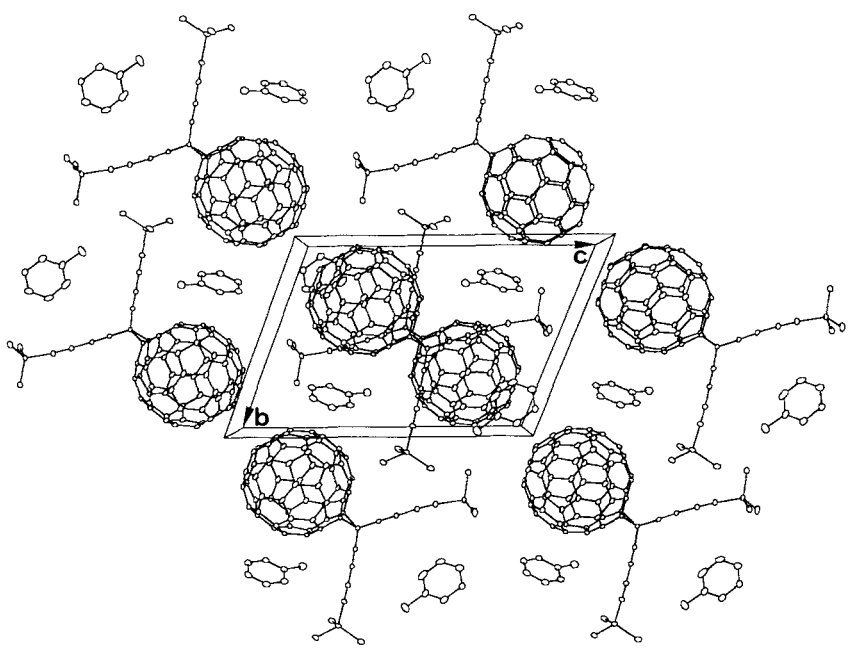


Fig. 4. Crystal packing in **1b** viewed along the *a* axis.

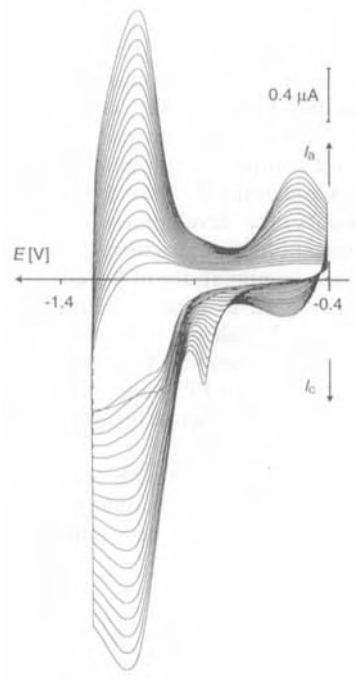


Fig. 6. Iterative cyclic voltammogram of **1** in $Bu_4N^+PF_6^-/CH_2Cl_2$ (0.1 M), Pt electrode, sweep rate 0.1 Vs^{-1} (19 cycles, vs. ferrocene).

Cyclic voltammograms of solutions of C_{60} in CH_2Cl_2 show three reversible one-electron reductions at −0.98, −1.37, and −1.83 V (vs. ferrocene). Only one well-defined reduction peak at −1.00 V (vs. ferrocene) is observed for **1** during the first scan.[17] Repeated potential cycling at 0.1 Vs^{-1} for this first reduction step (−0.40 to −1.30 V, vs. ferrocene) gives a voltammetric peak current which builds up with the number of scans (Fig. 6). During this reduction an insoluble, probably polymeric material accumulates on the platinum surface and forms a highly adhesive film, which is bright gold when thin (20–50 cycles) and orange when thicker (100–200 cycles). If the coated electrode is carefully rinsed and then reintroduced into a fresh solution containing only $Bu_4N^+PF_6^-$ in CH_2Cl_2 (0.1 M), the electrochemical response is still observed at the same potential and amplitude as for the last cycle in the original solution. This result confirms that an immobilized electroactive coating is formed on the electrode.

The morphology of the film was investigated with a scanning electron microscope (Fig. 7). The structure of the film appears to be homogeneous, with small ball-like features, resembling those previously observed in cathodic electropolymerized ruthenium bis(4-pyridyl)acetylene complexes.[18]

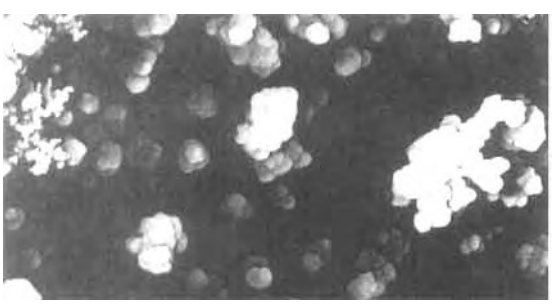


Fig. 7. Scanning electron micrograph of a film formed by polymerization of **1** on a Pt cathode (100 cycles), magnification: 3×10^3; 3 mm ≈ 1 μm.

The fact that the film continues to build up during electrolysis of **1**, even after it has covered the electrode, implies that it is electrically conducting. This conclusion is supported by the observation that film-covered electrodes give an essentially normal electrochemical response with known redox systems.[19] The C_{60} polymer is chemically stable in air and can be used as a material in electrodes with a reasonably wide electroactivity range (e.g., −0.8 to + 0.6 V, vs. ferrocene, 0.1 M solution of $Bu_4N^+PF_6^-$ in CH_2Cl_2).[20]

Reductive electrochemical polymerization has previously been reported for some simple alkynes,[21] as well as for a few metal complexes containing alkynyl pyridine ligands.[18,22] But in general, this type of electropolymerization has received little attention.[23]

Received: June 7, 1994 [Z 7010 IE]
German version: *Angew. Chem.* **1994**, *106*, 1691

[1] F. Diederich, L. Isaacs, D. Philp, *Chem. Soc. Rev.* **1994**, in press.
[2] a) E. Vogel, *Isr. J. Chem.* **1980**, *20*, 215–224; b) *Pure Appl. Chem.* **1969**, *20*, 237–262; c) *ibid.* **1993**, *65*, 143–152.
[3] a) T. Suzuki, Q. Li, K. C. Khemani, F. Wudl, Ö. Almarsson, *Science (Washington D. C., 1883-)* **1991**, *254*, 1186–1188; b) F. Wudl, *Acc. Chem. Res.* **1992**, *25*, 157–161; c) S. Shi, K. C. Khemani, Q. C. Li, F. Wudl, *J. Am. Chem. Soc.* **1992**, *114*, 10656–10657.
[4] For the numbering, see: R. Taylor, *J. Chem. Soc. Perkin Trans. 2* **1993**, 813–824.
[5] a) E. Vogel, T. Scholl, J. Lex, G. Hohlneicher, *Angew. Chem.* **1982**, *94*, 878–879; *Angew. Chem. Int. Ed. Engl.* **1982**, *21*, 869–870; b) H. B. Bürgi, E. Shefter, J. D. Dunitz, *Tetrahedron*, **1975**, *31*, 3089-3092; c) R. Bianchi, T. Pilati, M. Simonetta, *J. Am. Chem. Soc.* **1981**, *103*, 6426–6431.
[6] a) A. Vasella, P. Uhlmann, C. A. A. Waldraff, F. Diederich, C. Thilgen, *Angew. Chem.* **1992**, *104*, 1383–1385; *Angew. Chem. Int. Ed. Engl.* **1992**, *31*, 1388–1390; b) L. Isaacs, A. Wehrsig, F. Diederich, *Helv. Chim. Acta* **1993**, *76*, 1231–1250; c) L. Isaacs, F. Diederich, *ibid* **1993**, *76*, 2454–2464.
[7] M. Prato, V. Lucchini, M. Maggini, E. Stimpfl, G. Scorrano, M. Eiermann, T. Suzuki, F. Wudl, *J. Am. Chem. Soc.* **1993**, *115*, 8479–8480.
[8] a) K. Raghavachari, C. Sosa, *Chem. Phys. Lett.* **1993**, *209*, 223–228; b) F. Diederich, L. Isaacs, D. Philp, *J. Chem. Soc. Perkin Trans. 2* **1994**, 391–394.
[9] H. L. Anderson, R. Faust, Y. Rubin, F. Diederich, *Angew. Chem.* **1994**, *106*, 1427–1429; *Angew. Chem. Int. Ed. Engl.* **1994**, *33*, 1366–1368.
[10] We first attempted an X-ray structure analysis of 61,61-bis(trimethylsilylethynyl)-1,2-dihydro-1,2-methanofullerene[60]. Large cubic single crystals were grown from cyclohexane, but these crystals were highly disordered and scattered to a resolution of only about 2.5 Å, so an accurate structure could not be obtained. Orientational disorder is common in such compounds. We sought to circumvent this problem by increasing the length of the acetylenic substituents, and suitable crystals of **1** were grown. Crystal data at 100 K for **1a** $[(C_{75}H_{18}Si_2)\cdot 1/2(CS_2), M_r = 1031.2]$: monoclinic, space group $P2_1/c$ (no. 14), $\rho_{calcd} = 1.57\ g\,cm^{-3}$, $Z = 4$, $a = 10.230(3)$, $b = 22.720(12)$, $c = 19.316(11)$ Å, $\beta = 103.37(4)°$, $V = 4368(4)$ Å^3. Enraf-Nonius CAD4 diffractometer, $Cu_{K\alpha}$ radiation, $\lambda = 1.5418$ Å. Crystal specimens of **1a** were obtained by slow evaporation of a CS_2 solution. At room temperature, the crystals lost their solvent very quickly in air, so they were cut and mounted at about 250 K. All investigated crystals were more or less twinned. To reduce the effect of this systematic error, all reflections were measured in at least two crystal orientations. Some of the strongly contaminated reflections were reexamined on the diffractometer after data collection. In most cases, the error could be reduced substantially. For 15 reflections no satisfactory correction could be made, and they were excluded from the analysis. The structure was solved by direct methods and refined by full-matrix least-squares analysis (SHELXTL PLUS), using an isotropic extinction correction and an exponentially modified weight factor $r = 4$ Å^2. $R(F) = 0.053$, $wR(F) = 0.068$ for 722 variables and 2872 observed reflections with $F > 4\sigma(F)$ and $\theta < 55°$ (heavy atoms, anisotropic; H atoms, isotropic; H positions based on stereochemical considerations). Crystal data at 100 K for **1b** $[(C_{75}H_{18}Si_2)\cdot 2(C_7H_8), M_r = 1159.3]$: triclinic, space group $P\bar{1}$ (no. 2), $\rho_{calcd} = 1.42\ g\,cm^{-3}$, $Z = 2$, $a = 12.580(1)$, $b = 13.547(2)$, $c = 17.984(2)$ Å, $\alpha = 109.08(1)$, $\beta = 90.37(1)$, $\gamma = 109.16(1)°$, $V = 2714(1)$ Å^3. Enraf-Nonius CAD4 diffractometer, $Cu_{K\alpha}$ radiation, $\lambda = 1.5418$ Å. Single crystals of **1b** were obtained by slow evaporation of a toluene solution. To avoid evaporation of the solvent molecules, a single crystal was cut and mounted at about 250 K. The structure was solved by direct methods and refined by full-matrix least-squares analysis (SHELXTL PLUS), using an isotropic extinction correction and an exponentially modified weight factor $r = 5$ Å^2. Final $R(F) = 0.049$, $wR(F) = 0.052$ for 857 variables and 8722 observed reflections with $F > 6\sigma(F)$ and $\theta < 75°$ (heavy atoms, anisotropic; H atoms, isotropic; H positions based on stereochemical considerations). Further details of the crystal structure investigations are available on request from the Director of the Cambridge Crystallographic Data Centre, 12 Union Road, GB-Cambridge CB2 1EZ (UK), on quoting the full journal citation.
[11] Estimated standard deviations are 0.002–0.004 Å for bond lengths and atom centroid distances, and 0.1–0.3° for bond angles in **1b**. The standard deviation s of the mean values (given in parentheses) was calculated according to the equation $s = [\Sigma_m(x_m - \langle x \rangle)^2/(m-1)]^{1/2}$.
[12] We are grateful to Prof. E. Vogel, Dr. J. Lex, H. Wrubel, and C. König (Cologne) for permitting us to present unpublished results on the structure of **2**.
[13] P. Chakrabarti, P. Seiler, J. D. Dunitz, A.-D. Schlüter, G. Szeimies, *J. Am. Chem. Soc.* **1981**, *103*, 7378–7380; P. Seiler, J. Belzner, U. Bunz, G. Szeimies, *Helv. Chim. Acta* **1988**, *71*, 2100–2110.

[14] a) A. Hirsch, I. Lamparth, H. R. Karfunkel, *Angew. Chem.* **1994**, *106*, 453–455; *Angew. Chem. Int. Ed. Engl.* **1994**, *33*, 437–439; b) C. C. Henderson, C. M. Rohlfing, R. A. Assink, P. A. Cahill, *ibid* **1994**, *106*, 803–805 and **1994**, *33*, 786–788.

[15] a) J. M. Hawkins, A. Meyer, T. A. Lewis, S. Loren, F. J. Hollander, *Science (Washington D. C., 1883-)* **1991**, *252*, 312–313; b) H. Irngartinger, C.-M. Köhler, U. Huber-Patz, W. Krätschmer, *Chem. Ber.* **1994**, *127*, 581–584.

[16] a) G. Wegner, *Pure Appl. Chem.* **1977**, *49*, 443–454; b) J. D. Wright, *Molecular Crystals*, Cambridge University Press, **1987**, p. 116.

[17] All electrochemical measurements were carried out with a 0.1 M solution of $Bu_4N^+PF_6^-$ in anhydrous dichloromethane as the supporting electrolyte. A potentiostat (Bruker EI30M) connected to an x-y plotter (Ifélec IF3802) was used. Electrolysis was performed in a classical three-electrode cell. The working electrode was a platinum disk electrode, the counter electrode a platinum wire, and the reference an aqueous Ag/AgCl electrode. Potentials were referenced to the internal ferrocene.

[18] J. M. Calvert, D. L. Peebles, R. J. Nowak, *Inorg. Chem.* **1985**, *24*, 3111–3119.

[19] For example, with a film-covered Pt electrode, the cyclic voltammograms of the ferrocene/ferricinium couple in $Bu_4N^+PF_6^-/CH_2Cl_2$ (0.1 M) exhibited peaks at + 0.44 V with respect to Ag/AgCl [$(E_{pa} + E_{pc})/2$], and a ΔE_p of 100 mV ($= E_p^{ox} - E_p^{red}$) at a sweep rate of 0.1 Vs^{-1}; with a bare Pt electrode, peaks were located at + 0.41 V with a ΔEp of 60 mV.

[20] For previous modifications of electrodes with unpolymerized C_{60}, see a) C. Jehoulet, Y. S. Obeng, Y. T. Kim, F. Zhou, A. J. Bard, *J. Am. Chem. Soc.* **1992**, *114*, 4237–4247; b) W. Koh, D. Dubois, W. Kutner, M. T. Jones, K. M. Kadish, *J. Phys. Chem.* **1992**, *96*, 4163–4165; c) R. G. Compton, R. A. Spackman, D. J. Riley, R. G. Wellington, J. C. Eklund, A. C. Fisher, M. L. H. Green, R. E. Doothwaite, A. H. H. Stephens, J. Turner, *J. Electroanal. Chem.* **1993**, *344*, 235–247.

[21] C. I. Simionescu, M. Grovu, *Angew. Macromol. Chem.* **1983**, *111*, 149–163; C. I. Simionescu, M. Grovu, A. Duca, *ibid.* **1983**, *115*, 47–59.

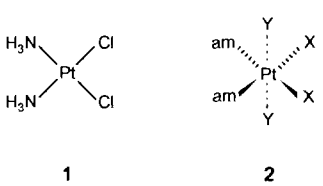
[22] P. D. Beer, O. Kocian, R. J. Mortimer, C. Ridgway, *J. Chem. Soc. Chem. Commun.* **1991**, 1460–1463.

[23] J. Simonet, J. Rault-Berthelot, *Prog. Solid St. Chem.* **1991**, *21*, 1–48.

An Unusual Route to Potential Platinum Antitumor Compounds: Synthesis, Reactivity, and Spectroscopic Properties of the Pt^{IV} Complex *fac*-$[PtCl_3(NH_3)_2L]Cl$**

Ulrich Bierbach* and Jan Reedijk*

The clinical successes in the treatment of malignant tumors with cisplatin (*cis*-diamminedichloroplatinum(II) **1**, Scheme 1), particularly in the urogenital and gynecological areas,[1] are

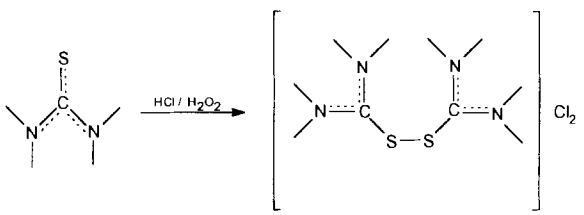


1 **2**

Scheme 1. Cisplatin (**1**) and general formula **2** for potentially active, second-generation Pt^{II} and Pt^{IV} antitumor compounds: am = nonleaving groups (am(m)ine ligands). X = leaving groups (Cl^-, RCO_2^-), Y = axial ligands in Pt^{IV} complexes (Cl^-, OH^-).

counterposed by drastic side effects in the digestive tract and in the kidney region. In attempts to reduce the toxic side effects, coordinatively saturated, kinetically inert Pt^{IV} antitumor compounds have been prepared. Iproplatin, *cis,trans,cis*-$[PtCl_2(OH)_2(iPrNH_2)_2]$,[2] and tetraplatin, $[PtCl_4(dach)]$ (dach = *d,l-trans*-1,2-diaminocyclohexane),[3] are currently undergoing clinical trials. Acid-stable, lipophilic Pt^{IV} complexes with carboxylato ligands (in the *trans* positions, instead of OH^- or Cl^-) are possibly the first active antitumor compounds based on platinum that can be administered orally.[4] Apart from minimization of the undesired toxicity, the development of substances with different activity spectra (tumor specificity) is also important.[5] For this purpose new combinations of ligands are needed, which do not necessarily need to exactly follow the structure–activity relationship (see **2**, Scheme 1) for second-generation Pt^{II} and Pt^{IV} antitumor compounds. We have now expanded the spectrum of the ligands Y in Pt^{IV} compounds of type **2** by an S-donor ligand with the regioselective introduction of a thiourea derivative.

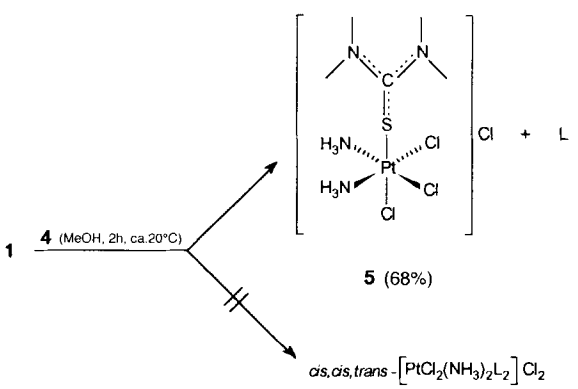
The oxidative dimerization of 1,1,3,3-tetramethylthiourea (**3**) leads to a doubly positively charged bis(formamidinium) ion with a central disulfide bridge (Scheme 2). Its synthetic potential



3 **4**

Scheme 2. Oxidative dimerization of **3** (L) to **4** ($[L-L]Cl_2$).

was first demonstrated by redox substitutions in Fe^{II} complexes, in which the thiolato ligands (under maintenance of the oxidation state of the central ion) were oxidized to the corresponding disulfide, which could be replaced by thiourea.[6] The 1:1 reaction of **4** with cisplatin yields **5**[7] (Scheme 3), the parent com-



Scheme 3. *fac*-$[PtCl_3(NH_3)_2L]Cl$ (**5**), the product of the oxidative addition of **4** to cisplatin (**1**). A chloride counterion from **4** becomes a ligand in **5**. The following mechanism seems plausible: 1. electrophilic attack of $[L-L]^{2+}$ on the Pt d_{z^2} orbital with 2e oxidation of the central ion; 2. square-pyramidal, positively charged Pt^{IV} transition state with thiourea coordination; 3. completion of the octahedral geometry and reduction of the charge by addition of Cl^- *trans* to sulfur.

pound of a new group of cationic, water-soluble Pt^{IV} complexes (the reaction with $[PtCl_2(en)]$ and other cisplatin derivatives leads to analogous complexes).[8] The overall reaction can be described as an oxidative *trans* addition of a thiourea ligand and

[*] Dr. U. Bierbach, Prof. Dr. J. Reedijk
Leiden Institute of Chemistry, Gorlaeus Laboratories
Leiden University, P. O. Box 9502
NL-2300 RA Leiden (The Netherlands)
Telefax: Int. code + (71) 274451

[**] L = 1,1,3,3-tetramethylthiourea. This research was supported by the Deutsche Forschungsgemeinschaft. We thank Johnson Matthey Ltd. (Reading, England) for the generous loan of platinum.

a chloro ligand. The desired *trans* addition of two thiourea ligands was not observed. Consequently the anions in **4** were exchanged by noncoordinating tetrafluoroborate (BF_4^-) to avoid an excess of anionic ligands in solution that compete with L. However, no reaction occurred, even after heating at reflux for several hours. Thus free chloride in solution must probably play a role in the mechanism of the oxidative addition (for details see the legend of Scheme 3).

Complex **5** is unusually acidic in aqueous solution: a 0.01 M solution has a pH value of 2, which is reached within 10 minutes after dissolution of the Pt^{IV} complex. A linear relationship was observed between the pH value and $\lg c_{Pt^{IV}}$, which indicates that independent of the degree of dilution one proton is released per complex cation, and **5** is thus a strong acid. This hypothesis can be explained as follows: hydrolysis occurs owing to the labilizing influence of the S donor on the Pt–Cl bond in *trans* position, and subsequently the aqua ligand is deprotonated to give a hydroxo ligand.

In the IR spectrum of **5** the broad stretching bands ν_{as}(NH) and ν_{sym}(NH) of the ammine ligands at $\tilde{\nu} = 3270$ and 3010 cm^{-1}, respectively, lie at unusually low wavenumbers. This observation indicates that hydrogen bonds of the NH–Cl type exist in the solid state. These have previously only been observed in antitumor complexes of Pt^{IV}, in which the N–H bond is strongly polarized, as confirmed by an X-ray structural analysis.[9] The band of the ν_{as}(CN) stretching vibration of the thiourea ligand (C = thiocarbonyl carbon) at $\tilde{\nu} = 1586$ cm^{-1} is shifted to higher wavenumbers by 80 cm^{-1} relative to the corresponding band of free **3**. This leads to the conclusion that the ligand coordinates through the sulfur atom, and consequently the bond order of the C–N bond in the thiourea ligand increases. Three intense vibrational bands in the far-IR spectrum are assigned as follows: $\tilde{\nu}_{as}$(PtCl) = 341 cm^{-1}, $\tilde{\nu}_{sym}$(PtCl) = 326 cm^{-1} for chloride *trans* to NH_3, corresponding to *a'* and *a''* assuming C_s symmetry for the complex, and $\tilde{\nu}$(PtCl) = 309 cm^{-1} for chloride *trans* to the S-donor ligand.

The ^{1}H NMR spectrum of **5** in [D_4]methanol shows, apart from a singlet for the methyl protons of the thiourea ligand at $\delta = 3.35$, an unusually well-resolved nine-line pattern for the ammine protons centered at $\delta = 5.82$ (Fig. 1). This is due to ^{195}Pt–^{1}H coupling, $^2J = 48$ Hz ("platinum satellites"), and ^{14}N–^{1}H coupling, $^1J = 53$ Hz. This latter quadrupole coupling is observed only in Pt^{IV} complexes.[10] Integration of the signals indicates that the ratio of NH_3 to CH_3 protons is 1:2 and consequently confirms the presence of only one thiourea ligand in **5**. Significant H,D exchange was not observed for the signal of the ammine protons, even after several hours in anhydrous [D_4]methanol. The ^{1}H-decoupled ^{195}Pt NMR spectrum of **5** in [D_4]methanol shows a quintet at $\delta = 910$ (ext. standard $K_2[PtCl_4]$), which corresponds to $\delta = -721$ when $[PtCl_6]^{2-}$ is used as a standard.[11] The splitting is due to the coupling of the two equivalent ^{14}N nuclei of the NH_3 ligands ($I = 1$) with the platinum isotope ^{195}Pt ($I = 1/2$, natural abundance 34%) (Fig. 2). The coupling constant $^1J(^{195}Pt,^{14}N) = 173$ Hz lies in a region characteristic for Pt^{IV} complexes with ammine ligands *trans* to chloro ligands. This value also points to the *cis* influence of the axial S donor on the ^{195}Pt–^{14}N coupling.[12] The introduction of a S-donor ligand, in other words the formal replacement of a chloro ligand in *cis*-$[(NH_3)_2PtCl_4]$ ($\delta_{Pt} = -145$ relative to $[PtCl_6]^{2-}$)[12] with a tetramethylthiourea ligand in **5**, leads, as expected, to a greater shielding of the Pt nucleus and thus to an upfield shift of the ^{195}Pt resonance.

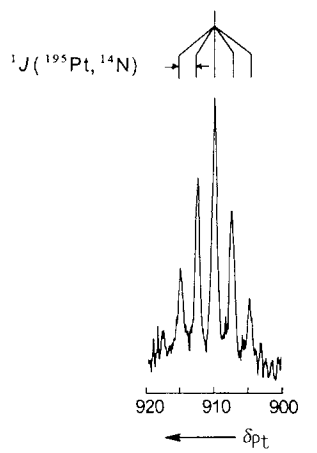


Fig. 2. ^{195}Pt{^{1}H} NMR spectrum of **5** (64 MHz, [D_4]methanol, $c = 10^{-2}$ M, 298 K, ext. standard $K_2[PtCl_4]$ (aq)) with a scheme of the heteronuclear coupling.

The primary target molecule in the mechanism of action of Pt antitumor compounds is chromosomal DNA.[13] In a model reaction we treated **5** with 5'-guanosine monophosphate (5'-GMP), a simple monomeric nucleic acid fragment, under physiological conditions. We will report on the preliminary results of these studies as well as on current in vivo investigations with **5** on P388 leukemia elsewhere.

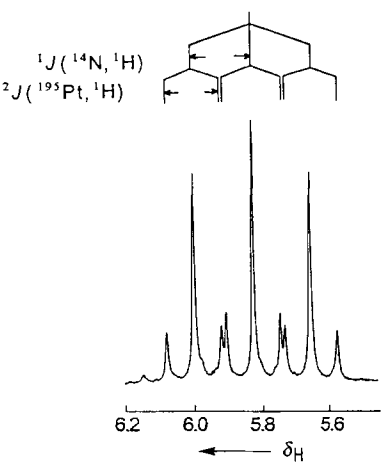


Fig. 1. ^{1}H NMR signal of the ammine ligands in **5** (300 MHz, [D_4]methanol, $c = 10^{-2}$ M, 298 K, TMS) with a scheme of the heteronuclear couplings.

Experimental Procedure

The ^{1}H and ^{195}Pt NMR measurements were conducted on a Bruker WM300 NMR spectrometer at 300 and 64 MHz respectively; the IR and far-IR spectra (KBr and polyethylene pellets, respectively) were recorded on a Bruker IFS 113v FT-IR spectrometer.

Synthesis of **5**: To a solution of 0.167 g (0.5 mmol) **4** [6] in 5 mL anhydrous methanol was added 0.15 g (0.5 mmol) cisplatin (**1**) [14]. The suspension was stirred at room temperature under exclusion of light for 2 h. Diethyl ether was added to the resultant orange-yellow solution until it became cloudy, and the mixture was stored for several days in a refrigerator. The resulting orange microcrystalline precipitate was filtered off and washed with diethyl ether to give 0.176 g (68%) of **5**. The complex crystallized as **5**·0.5CH_3OH, which was confirmed by C,H,N analysis.

Received: March 19, 1994 [Z6777IE]
German version: *Angew. Chem.* **1994**, *106*, 1701

[1] L. R. Kelland, S. J. Clarke, M. J. McKeage, *Platinum Met. Rev.* **1992**, *36*, 178.
[2] V. H. C. Bramwell, D. Crowther, S. O'Malley, R. Swindell, R. Johnson, E. Creaven, *Cancer Treat. Rep.* **1985**, *69*, 409.
[3] Y. Kido, A. R. Khokhar, Z. H. Siddik, *Anti Cancer Drugs* **1993**, *4*, 251.
[4] L. R. Kelland, G. Abel, M. J. McKeage, M. Jones, P. M. Goddard, M. Valenti, B. A. Murrer, K. R. Harrap, *Cancer Res.* **1993**, *53*, 2581.
[5] B. K. Keppler in *Metal Complexes in Cancer Chemotherapy* (Ed.: B. K. Keppler), VCH, Weinheim, **1993**, p. 1.
[6] U. Bierbach, W. Barklage, W. Saak, S. Pohl, *Z. Naturforsch. B* **1992**, *47*, 1593.
[7] Systematic name of **5**: (*OC*-6-33)-diamminetrichloro(1,1,3,3-tetramethylthiourea-κ*S*)platinum(IV) chloride.

 © *VCH Verlagsgesellschaft mbH, D-69451 Weinheim, 1994* *0570-0833/94/1515-1633 $ 10.00+.25/0*

[8] U. Bierbach, J. Reedijk, unpublished results.
[9] R. Kuroda, S. Neidle, I. M. Ismail, P. J. Sadler, *Inorg. Chem.* **1983**, *22*, 3620.
[10] G. Müller, J. Riede, R. Beyerle-Pfnür, B. Lippert, *J. Am. Chem. Soc.* **1984**, *106*, 7999.
[11] S. J. S. Kerrison, P. J. Sadler, *J. Magn. Reson.* **1978**, *31*, 321.
[12] I. M. Ismail, P. J. Sadler in *Platinum, Gold and Other Metal Chemotherapeutic Agents* (*ACS Symp. Ser.* **1983**, *209*, 171).
[13] J. Reedijk, *Inorg. Chim. Acta* **1992**, *198–200*, 873.
[14] S. C. Dhara, *Indian J. Chem.* **1970**, *8*, 193.

Monomer–Dimer Equilibria in Homo- and Heterodinuclear Cationic Alkylzirconium Complexes and Their Role in Polymerization Catalysis**

Manfred Bochmann* and Simon J. Lancaster

Base-free cationic Group 4 metal alkyl complexes of the general formula $[Cp_2M\text{-}R]^+$ (R = alkyl, M = Ti, Zr, Hf) are highly active catalysts for the polymerization of olefins.[1–3] In conventional homogeneous Ziegler catalyst systems cationic species of this kind are formed by the reaction of metallocenes with alkylaluminum activators such as methylaluminoxane.[1c, 4, 5] Aluminum-free complexes are best prepared by reacting dialkylated metallocenes $[Cp_2MR_2]$ with triphenylcarbenium salts of "noncoordinating" anions,[6] such as $[CPh_3][B(C_6F_5)_4]$ (**2** in Scheme 1). It is generally assumed that these reactions lead to monomeric cationic 14-electron complexes [Eq. (a)].[7] This reaction has found widespread application for the generation of cationic polymerization catalysts.[3, 8–11]

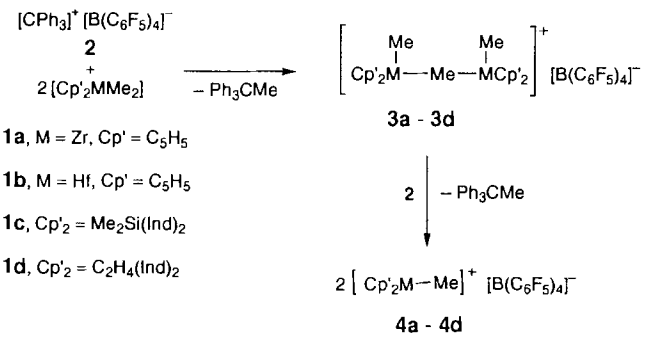
$$[Cp_2MR_2] + [CPh_3][B(C_6F_5)_4] \longrightarrow [Cp_2M\text{-}R][B(C_6F_5)_4] + Ph_3CR \qquad (a)$$

As part of our continuing interest in the characterization of homogeneous polymerization systems based on cationic alkyl metal complexes[2, 10, 12] we have shown recently that monomeric alkyl cations $[Cp_2ZrR]^+$ are indeed the only products if $R = CH_2Ph$, even in the presence of an excess of $[Cp_2ZrR_2]$, since the electron deficiency of the metal center is alleviated by the η^2-coordination of the benzyl ligand.[3, 13] However, we noted earlier in the case of methyltitanium complexes the appearance of a short-lived dimeric intermediate, $[(Ind_2TiMe)_2(\mu\text{-}Me)]^+$ (Ind = indenyl).[10, 14] Following the reaction of methylzirconium and -hafnium complexes with $[CPh_3][B(C_6F_5)_4]$ (**2**) at low temperature has now shown that the formulation of Equation (a) does not adequately describe the course of the reaction and that stable dimeric complexes may be the major products, depending on the reaction conditions.

The reaction of the methyl complexes $[Cp'_2MMe_2]$ (**1a–1d**) with **2** at −60 °C in CD_2Cl_2 led to the formation of dinuclear methyl-bridged complexes **3** (Scheme 1). The reaction is essentially quantitative. Evidently adduct formation with a neutral dialkylmetallocene stabilizes the 14-electron cation $[Cp'_2MMe]^+$ more effectively than a solvent molecule or anion coordination.

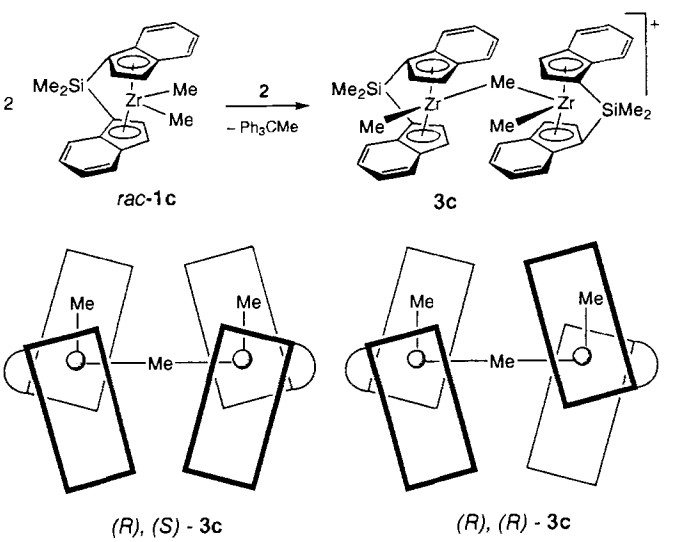
[*] Dr. M. Bochmann, S. J. Lancaster
School of Chemical Sciences, University of East Anglia
GB-Norwich NR4 7TJ (UK)
Telefax: Int. code + (603)259396

[**] This work was supported by the Science and Engineering Research Council. We thank Dr. S. Holding (RAPRA Technology Ltd.) for GPC molecular weight measurements.



Scheme 1. Counterion of the complexes **3** and **4** is $[B(C_6F_5)_4]^-$.

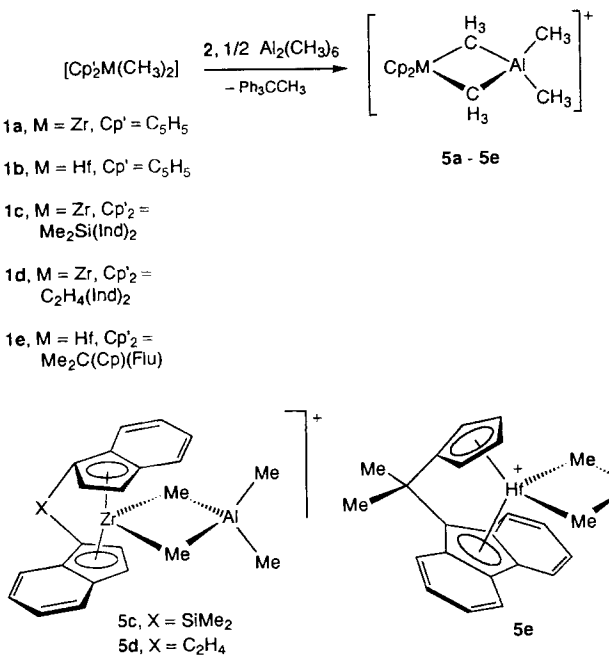
Compounds **3a**-$[B(C_6F_5)_4]$ and **3b**-$[B(C_6F_5)_4]$ are obtained from dichloromethane/hexane mixtures as off-white, very hydrolysis-sensitive needlelike crystals, while the attempted isolation of **3c** led to the precipitation of a red oil which could not be crystallized. For spectroscopic examination the compounds are generated in situ in CD_2Cl_2. Since *rac*-**1c** consists of a mixture of (*R*) and (*S*) enantiomers, the formation of a cationic dimer results in two diastereomers in a ratio of 2:1 (Scheme 2). The cation **3d** forms a pair of diastereomers in a ratio of 1.7:1.



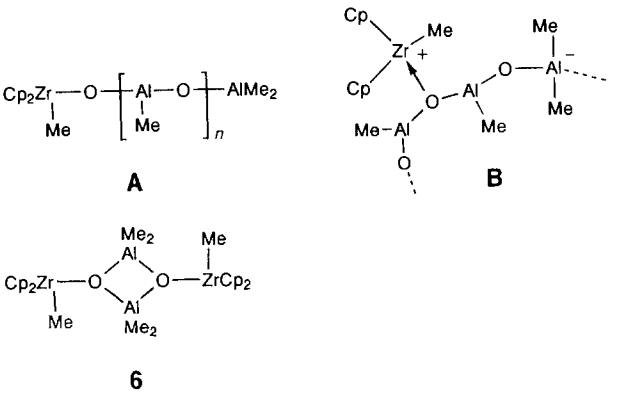
Scheme 2. Counterion is $[B(C_6F_5)_4]^-$.

The stability of the dimers and the rate of reaction with excess CPh_3^+ depends on the nature of the Cp ligands. The reaction of **3a** with **2** is essentially complete on warming a solution to −40 °C; this gives the monomeric cation **4a**.[15] By contrast, **3c** persists even in the presence of an excess of the triphenylcarbenium salt up to a temperature of about 20 °C. Although at that stage further reaction with **2** does take place, presumably with formation of **4c**, this is quickly followed by decomposition since **4c** is not stable in chlorinated solvents under these conditions. The cation **3d** is slightly less stable than **3c**, and conversion to **4d** begins already at 0 °C.[16] As in the case of **4c**, an unambiguous assignment of the Zr–Me ^{1}H NMR signal of **4d** was not possible.[17] The compounds are insufficiently soluble for NMR studies in toluene.

In the presence of trimethylaluminum the cations $[Cp'_2MMe]^+$ form preferentially the heterodinuclear complexes $[Cp'_2M(\mu\text{-}Me)_2AlMe_2]^+$ (**5a–5e**) (Scheme 3). The reaction of a



Scheme 3. Counterion of complex **5** is $[B(C_6F_5)_4]^-$. Flu = fluorenyl.

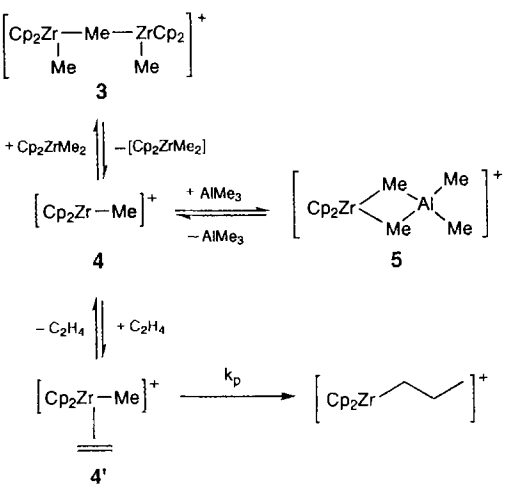


mixture of **1a**, Al_2Me_6, and **2** in CD_2Cl_2 at $-50\,^{\circ}C$ gave **5a**-$[B(C_6F_5)_4]$ as the main product, characterized in the ^1H NMR spectrum by two sharp singlets at $\delta = -0.48$ and $\delta = 0.68$, besides small quantities of **3a**-$[B(C_6F_5)_4]$ and residual Al_2Me_6. In the absence of **1a** there is no reaction between Al_2Me_6 and $[CPh_3]^+$ below $20\,^{\circ}C$. In contrast to Al_2Me_6, **5a** does not show fluctuating behavior in CD_2Cl_2 up to a temperature of $25\,^{\circ}C$. There is no evidence for an intramolecular exchange process between bridging and terminal methyl ligands of **5a**, or for an intermolecular exchange between **5a**, **3a**, and Al_2Me_6. The fluxional behavior of the latter is not influenced by the presence of the zirconium complexes. Whereas monomeric alkyl cations such as $[Cp_2Zr(\eta^2\text{-}CH_2Ph)]^+$ decompose slowly in CD_2Cl_2 above $-40\,^{\circ}C$ and more rapidly on warming to $20\,^{\circ}C$,[3] **5a** is stable in dichloromethane at $20\,^{\circ}C$ for several hours. The analogous hafnium complex **5b** shows similar behavior. Both complexes are isolated as colorless, pyrophoric needles in 90 and 74% yield, respectively. Once crystallized the complexes are only sparingly soluble in dichloromethane or toluene.

The *ansa*-metallocene complexes **5c**–**5e** were obtained similarly and have been characterized in CD_2Cl_2. They are stable in chlorinated solvents. On cooling to $-20\,^{\circ}C$ **5c**-$[B(C_6F_5)_4]$ precipitates as an oil which could not be crystallized.

The nature of the interaction between alkylaluminum compounds, such as methylaluminoxane (MAO), and metallocene catalysts has been the subject of much debate. While it could be shown that the reaction of $[Cp_2ZrMe_2]$ with solid MAO generated $[Cp_2ZrMe]^+$ on the surface,[5] the structure of the cationic species and the nature of the interaction between the catalyst and MAO under catalytic conditions, in other words in solution, remains uncertain. For example, coordination of an MAO oxygen atom to the metal center has been suggested, as in **A** or **B**,[18, 19] and Erker et al. were able to isolate complex **6**, formally an adduct between $[Cp_2ZrMe]^+$ and $[Al_2O_2Me_4]^{2-}$, which may be regarded as a model for such an interaction.[19] However, **6** does not possess any readily accessible coordination sites and is not catalytically active in the absence of excess MAO. Since MAO always contains significant amounts of $AlMe_3$ ($3.5 \pm 1\%$ have been estimated[20]) and is usually employed at Al/Zr ratios of 10^3 to 10^4,[21] it seems likely that the cationic zirconium species formed under these conditions is not $[Cp_2ZrMe]^+$ but the alkylaluminum adduct **5**. This assumption is supported by the finding that a large proportion of MAO can be replaced by $AlMe_3$ without loss of productivity.[22, 23] Catalysts generated from $[Cp'_2ZrX_2]$/**2** mixtures in the presence of excess AlR_3 have recently been reported (X = Cl, Me; R = Me, Et), although the resulting zirconium complexes have not been identified.[7g, 24]

According to the current mechanistic concept olefin polymerizations with the dimeric complexes **3** are only possible if **3** dissociates partially to **1** and the active species **4** (Scheme 4). The



Scheme 4.

catalytic activity should therefore decrease with increasing concentration of **1**, since the equilibrium is shifted towards **3** at the expense of the productive complex **4'**. However, ethylene polymerizations with 1:1 mixtures of **1a** and **2** in toluene produce only traces of polymer, whereas a ratio of 3:1 gives a productivity of 0.5×10^6 g PE(mol Zr +)$^{-1}$bar^{-1}h^{-1}. We explain this anomaly by the lack of stability of the unsubstituted cation **4a**. By contrast, complex **4c**, generated from a 1:1 mixture of *rac*-**1c** and **2**, polymerizes propene with excellent activities (Table 1) which decrease with increasing **1c**/**2** ratio, as expected (Fig. 1). Increasing the metallocene excess from 1:1 to 16:1 reduces the productivity at $20\,^{\circ}C$ by about one order of magnitude.[25] Since higher temperatures favor dissociation, this effect is less pronounced at $60\,^{\circ}C$ but still significant.

Similarly, alkylaluminum adducts **5** are coordinatively saturated and lack a vacant orbital suitable for binding the olefinic substrate. Initiation of chain growth requires therefore the dis-

Table 1. Propene polymerizations with *rac*-**1c**/**2** in a molar ratio of 1:1 [a].

Temperature [°C]	Polymer yield [g]	Productivity [b] 10^6 g PP(mol Zr^+)$^{-1}$ $[C_3H_6]^{-1}$ h^{-1}	M.p. [°C]	M_w	M_w/M_n
60	0.336	98.7 ± 0.7	107.5	13000	2.0
21	0.635	45.0 ± 0.01	144.3	48600	2.4
0	0.049	1.75 ± 0.45	151.8	75500	2.1
−20	0.026	0.97 ± 0.13	155.8	76300	2.2
−55	0.018	0.21 ± 0.1	158.6	121000	2.3

[a] At 1 bar C_3H_6 pressure, **1c** (5.0 μmol), **2** (5.0 μmol) in toluene (20 mL), stirring speed 1000 rpm. Polymerizations were terminated by methanol injections after 30 s. [b] Productivities at 0 °C and below were calculated under the assumption of the formation of dimeric complexes, that is $[Zr^+] = 0.5[CPh_3^+]_0$.

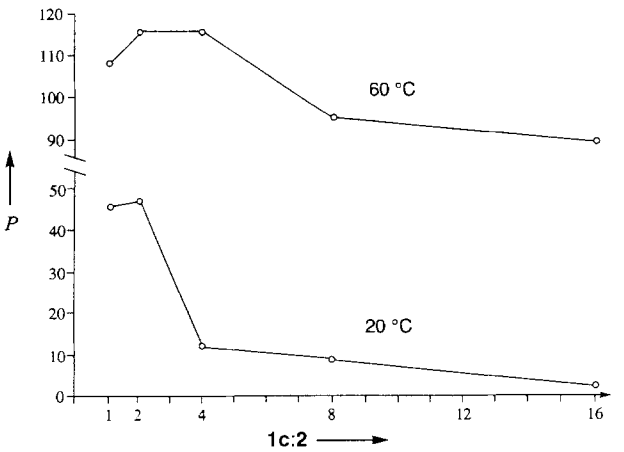


Fig. 1. Productivity P [10^6 g PP (mol Zr^+)$^{-1}$ $[C_3H_6]^{-1}$ h^{-1} of propene polymerizations with *rac*-**1c**/**2** catalysts as a function of the **1c**/**2** ratio at 20 and 60 °C (1 bar propene pressure).

sociation of the alkylaluminum (Scheme 4) and should be inhibited by an increase in the concentration of $AlMe_3$. Propene polymerizations with 1:1 mixtures of *rac*-**1c** and **2** in toluene in the presence of 1, 10, 50, and 100 equivalents of $AlMe_3$ confirm this assumption (Table 2). The highest productivities are found

Table 2. Propene polymerizations with *rac*-$[Me_2Si(Ind)_2Zr(\mu\text{-}Me_2)AlMe_2]$-$[B(C_6F_5)_4]$ (**5c**)/$AlMe_3$ [a].

1c [μmol]	$AlMe_3$ [μmol]	Temperature [°C]	PP yield [g]	Productivity [b] 10^6 g PP(mol Zr^+)$^{-1}$ $[C_3H_6]^{-1}$ h^{-1}	M.p. [°C]	M_w	M_w/M_n
5	5	20	0.547	39.7 ± 4.2	144.3	51000	2.1
5	50	20	0.163	11.9 ± 0.7	149.0	49100	1.6
5	250	20	0.027	1.95 ± 0.23			
5	500	20	0.013	0.94 ± 0.01	145.4	7400	1.2
5	5	60	0.383	107.0 ± 1.0	121.1	18200	2.2
5	50	60	0.336	94.2 ± 3.5	114.3	14900	1.9
5	250	60	0.271	75.6 ± 0.64	113.2		
5	500	60	0.204	56.9 ± 2.7	116.1	9800	1.9

[a] Polymerization conditions as given in Table 1. Polymerizations were terminated by methanol injection after 30 s. [b] Under the assumption that $[CPh_3^+]_0$ = maximum $[Zr^+]$ concentration.

for an Al/Zr ratio of only 1:1; at 20°C the addition of a 100-fold excess of $AlMe_3$ lowers the productivity by about a factor of 40. Higher aluminum concentrations also reduce the polymer molecular weight, probably as the result of chain-transfer reactions. Ethylene polymerizations with **5a** and **5b** show a similar trend. Large excesses of alkylaluminum are evidently not an essential requirement for high catalytic activity and may indeed be counterproductive.

Experimental Procedure

All manipulations were carried out under dry argon.

3a-$[B(C_6F_5)_4]$: **1a** (300 mg, 1.2 mmol) and **2** (400 mg, 0.43 mmol) were dissolved in CH_2Cl_2 (10 mL) at −78 °C. The pale yellow solution was layered with hexane (10 mL) and left to crystallize at −16 C. Off-white, very air-sensitive needles of **3a**-$[B(C_6F_5)_4]$ were obtained (150 mg, 0.13 mmol, 30%). The elemental analysis of the compond was low in C due to the sensitivity to hydrolysis ($C_{47}H_{29}BF_{20}Zr_2$, calcd. C, 48.4; H, 2.5; found C, 46.9; H, 2.3). The crystalline compound was only sparingly soluble in cold dichloromethane.

The procedure for generating solutions of **3**-$[B(C_6F_5)_4]$ in situ is exemplified below for **3a**-$[B(C_6F_5)_4]$. **1a** (100 mg, 0.39 mmol) and **2** (153 mg, 0.16 mmol) were each dissolved in CD_2Cl_2 (0.4 mL), cooled to −78 °C, and transferred to an NMR tube to give a yellow solution on mixing. The sample was inserted into a JEOL EX270 spectrometer at −60 °C. The triphenylcarbenium salt was consumed quantitatively under these conditions, and **3a**-$[B(C_6F_5)_4]$ was observed besides residual unconverted **1a**. **3c**-$[B(C_6F_5)_4]$ was obtained as a dark red oily precipitate. In all cases the assignment of the NMR signals was confirmed by 2D $^1H/^{13}C$ COSY experiments. **3a**-$[B(C_6F_5)_4]$: ^1H NMR (CD_2Cl_2, −60 °C): δ = −0.76 (s, 3 H, Zr-(CH_3)-Zr), 0.28 (s, 6 H, Zr-CH_3 terminal), 6.30 (s, 20 H, Cp); ^{13}C NMR (CD_2Cl_2, −60 °C): δ = 23.81 (q, ^1J(C,H) = 135.5 Hz, Zr-(CH_3)-Zr), 38.81 (q, ^1J(C,H) = 120.2 Hz, Zr-CH_3 terminal), 113.06 (Cp). **3b**-$[B(C_6F_5)_4]$: ^1H NMR (CD_2Cl_2, −20 °C): δ = −0.72 (s, 3 H, Hf-(CH_3)-Hf), 0.09 (s, 6 H, Hf-CH_3 terminal), 6.24 (s, 20 H, Cp); ^{13}C NMR (CD_2Cl_2, −20 °C): δ = 24.42 (q, ^1J(C,H) = 134 Hz, Hf-(CH_3)-Hf), 40.93 (q, ^1J(C,H) = 118 Hz, Hf-CH_3 terminal), 112.43 (Cp). **3c**-$[B(C_6F_5)_4]$: Only the Zr-CH_3 and Si-CH_3 signals were assigned. Signals in the indenyl region overlap because of the presence of two isomers as well as triphenylethane. ^1H NMR (CD_2Cl_2, −60 °C): isomer A: δ = −2.75 (s, 3 H, Zr-(CH_3)-Zr), −0.89 (s, 6 H, Zr-CH_3 terminal), 0.99 (s, 3 H, Si-CH_3), 1.11 (s, 3 H, Si-CH_3). Isomer B: δ = −2.93 (s, 3 H, Zr-(CH_3)-Zr), −0.88 (s, 6 H, Zr-CH_3 terminal), 0.98 (s, 3 H, Si-CH_3), 1.08 (s, 3 H, Si-CH_3). ^{13}C NMR (CD_2Cl_2, −60 °C) (isomer A): δ = −3.05 (Si-CH_3), −1.96 (Si-CH_3), 25.43 (q, ^1J(C,H) = 136.1 Hz, Zr-(CH_3)-Zr), 46.40 (q, ^1J(C,H) = 115.8 Hz, Zr-CH_3 terminal). **3d**: ^1H NMR (CD_2Cl_2, −60 °C): isomer A: δ = −2.99 (s, 3 H, Zr-(CH_3)-Zr), −0.87 (s, 6 H, Zr-CH_3 terminal). Isomer B: δ = −3.10 (s, 3 H, Zr-(CH_3)-Zr), −0.96 (s, 6 H, Zr-CH_3 terminal).

5a-$[B(C_6F_5)_4]$: Al_2Me_6 (0.7 mmol, 0.7 mL of a 1 mM solution in dichloromethane) was added to a solution of **1a** (0.18 g, 0.67 mmol) and **2** (0.8 g, 0.87 mmol) in dichloromethane (15 mL) at −70 °C. The resulting suspension was warmed to −20 °C with stirring until the yellow-orange color of **2** faded. Addition of cyclopentane (10 mL) produced a white precipitate which was filtered off, washed with cyclopentane, and dried in vacuo. Yield 0.6 g (0.60 mmol, 90%). The product contained traces of **3a**. Crystalline **5a** was only sparingly soluble in dichloromethane and could not be recrystallized without decomposition. ^1H NMR (270 MHz, CD_2Cl_2, −60 °C): δ = −0.48 (s, 6 H, terminal Al-CH_3), 0.68 (s, 6 H, μ-CH_3), 6.62 (s, 10 H, Cp). ^{13}C NMR (67.8 MHz, CD_2Cl_2, −60 °C): δ = −6.76 (q, ^1J(C,H) = 115.4 Hz, Al-CH_3), 38.51 (q, ^1J(C,H) = 113.5 Hz, μ-CH_3), 115.96 (Cp).

5b-$[B(C_6F_5)_4]$: **1b** (0.35 g, 1.0 mmol), **2** (0.92 g, 1.0 mmol), and Al_2Me_6 (1 mmol) were treated similarly in dichloromethane at −78 °C to −20 °C to give white, finely crystalline **5b** (0.80 g, 74%). Elemental analysis: calcd. $C_{38}H_{22}AlBF_{20}Hf$: C, 42.46; H, 1.75; found C, 43.46; H, 1.75. ^1H NMR (270 MHz, CD_2Cl_2, −20 °C): δ = −0.44 (s, 6 H, Al-CH_3), 0.98 (s, 6 H, μ-CH_3), 6.49 (s, 10 H, Cp). ^{13}C NMR (67.8 MHz, CD_2Cl_2, −60 °C): δ = −6.31 (q, ^1J(C,H) = 114 Hz, Al-CH_3), 38.20 (q, ^1J(C,H) = 114 Hz, μ-CH_3), 114.43 (Cp).

5c-$[B(C_6F_5)_4]$: **1c** (50 mg, 0.12 mmol) and **2** (120 mg, 0.13 mmol) were each dissolved in CD_2Cl_2 (0.4 mL). The solution of **1c** was transferred into an NMR tube, cooled to −78 °C, and treated with Al_2Me_6 (1 mL of a 0.05 mM solution), followed by the cold (−78 °C) solution of **2**. Spectra were recorded between −60 °C and 20 °C. ^1H NMR (270 MHz, CD_2Cl_2, −20 °C): δ = −0.81 (s, 6 H, μ-CH_3), −0.61 (s, 6 H, Al-CH_3), 1.29 (s, 6 H, Si-CH_3), 5.91 (d, 2 H, ^3J(H,H) = 3.3 Hz, Ind-C_5), 6.92 (d, 2 H, ^3J(H,H) = 3.3 Hz, Ind-C_5), 7.08–7.34 (m, 4 H, Ind-C_6, partially obscured by Ph_3CMe), 7.58 (d, 2 H, ^3J(H,H) = 8.6 Hz, Ind-C_6), 7.77 (d, 2 H, ^3J(H,H) = 8.6 Hz, Ind-C_6). ^{13}C NMR (67.8 MHz, CD_2Cl_2, −60 °C): δ = −7.12 (q, ^1J(C,H) = 115 Hz, Al-CH_3), −2.34 (Si-CH_3), 35.27 (q, ^1J(C,H) = 113.5 Hz, μ-CH_3), 85.16 (Si-C_5), 116.05 (C_5), 119.33 (C_5), 124.98, 125.84, 126.41, 128.91, 129.45, 132.65 (C_6).

5d-$[B(C_6F_5)_4]$: ^1H NMR (270 MHz, CD_2Cl_2, −20 °C): δ = −0.63 (s, 6 H, μ-CH_3), −0.58 (s, 6 H, Al-CH_3), 4.04 (s, 4 H, -C_2H_4-), 6.20 (d, 2 H, ^3J(H,H) = 3.3 Hz, Ind-C_5), 6.44 (dd, 2 H, J = 3.3 and 0.7 Hz, Ind-C_5), 7.07–7.35 (m, 4 H, Ind-C_6, partially obscured by Ph_3CMe), 7.58 (m, 2 H, Ind-C_6), 7.90 (dd, 2 H, J = 8.6 and 1.0 Hz, Ind-C_6). ^{13}C NMR (67.8 MHz, CD_2Cl_2, −60 °C): δ = −7.03 (q, ^1J(C,H) = 116.4 Hz, Al-CH_3), 30.93 (C_2H_4), 37.32 (q, ^1J(C,H) = 113.7 Hz, μ-CH_3), 108.30 (C_5), 117.05 (C_5), 122.68 (bridgehead-C of C_5) 124.49, 125.25, 127.44, 128.82, 129.00, 131.00 (C_6).

5e-$[B(C_6F_5)_4]$: ^{1}H NMR (270 MHz, CD_2Cl_2, 25°C): $\delta = -0.72$ (s, 3 H, Al-CH_3 terminal), -0.63 (s, 3 H, Al-CH_3 terminal), -0.57 (s, 6 H, μ-CH_3), 2.49 (s, 6 H, Me_2C), 5.58 (t, 2 H, ^3J(H,H) = 2.6 Hz, C_5), 6.32 (t, 2 H, ^3J (H,H) = 2.6 Hz, C_5); Flu: 7.75 (t, 2 H, ^3J (H,H) = 8.58 Hz), 7.34 (t, 2 H, ^3J(H,H) = 8.91 Hz), 7.96 (d, 2 H, ^3J(H,H) = 8.91 Hz), 8.22 (d, 2 H, ^3J(H,H) = 8.58 Hz). ^{13}C NMR (67.8 MHz, CD_2Cl_2, 25 °C): $\delta = -7.13$ (Al-CH_3 terminal), -7.01 (Al-CH_3 terminal), 28.55 (Me_2C), 28.63 (Me_2C), 29.02 (μ-CH_3); C_5H_4: 74.14, 102.75, 117.63; Flu: 111.95, 121.29, 121.94, 124.76, 125.12, 127.22, 131.41. The resonances of the anion are identical to those of noncoordinated $[B(C_6F_5)_4]^-$ and have not been listed.

Olefin polymerizations: low-sulfur toluene (20 mL) was equilibrated at the stated temperature with the olefin under 1 bar pressure. The appropriate amount of a standard solution of the dialkyl metallocene (and of Al_2Me_6 where applicable) was injected, followed by a solution of **2** in toluene. Immediate rapid polymerization was observed. The reactor was stirred magnetically at 1000 rpm. The reactions were terminated by the injection of methanol (2 mL). The polymer was precipitated with methanol/HCl, washed with methanol, and dried at 70 °C to a constant weight. The productivities given in the Tables are the averages of at least two independent experiments per data point and were calculated by using the propene solubilities in toluene given in [21b]. Melting points of polymers were determined with a DuPont DSC 10 differential scanning calorimeter. Polymers have not been fractionated. Molecular weights and polydispersities were determined by gel permeation chromatography (polystyrene standard, PLgel-column, 1,2-dichlorobenzene, 140 °C).

Received: March 4, 1994 [Z 6729/6730 IE]
German version: *Angew. Chem.* **1994**, *106*, 1715

[1] Review articles: a) F. S. Dyachkovskii in *Coordination Polymerization*, (Ed.: J. C. W. Chien), Academic Press, New York, **1975**, p. . 199; b) R. F. Jordan, *Adv. Organomet. Chem.* **1991**, *32*, 325; c) T. J. Marks, *Acc. Chem. Res.* **1992**, *25*, 57; d) M. Bochmann, *Nachr. Chem. Tech. Lab.* **1993**, *41*, 1220.
[2] M. Bochmann, A. J. Jaggar, J. C. Nicholls, *Angew. Chem.* **1990**, *102*, 830; *Angew. Chem. Int. Ed. Engl.* **1990**, *29*, 780.
[3] M. Bochmann, S. J. Lancaster, *Organometallics* **1993**, *12*, 633, and references therein.
[4] H. Sinn, W. Kaminsky, *Adv. Organomet. Chem.* **1980**, *18*, 99.
[5] C. Sishta, R. M. Hathorn, T. J. Marks, *J. Am. Chem. Soc.* **1992**, *114*, 1112.
[6] a) M. Bochmann, *Angew. Chem.* **1992**, *104*, 1206; *Angew. Chem. Int. Ed. Engl.* **1992**, *31*, 1181; b) H. W. Turner (Exxon), EPA. 0277004, **1988** [*Chem. Abstr.* **1989**, *110*, 58290a]; c) A. R. Siedle, W. M. Lamanna, R. A. Newmark, *Makromol. Chem. Macromol. Symp.* **1993**, *66*, 215.
[7] See for example: a) K. Hortmann, H. H. Brintzinger, *New J. Chem.* **1992**, *16*, 51; b) P. Burger, K. Hortmann, H. H. Brintzinger, *Makromol. Chem. Macromol. Symp.* **1993**, *66*, 127; c) M. H. Prosenc, C. Janiak, H. H. Brintzinger, *Organometallics* **1992**, *11*, 4036; d) L. Cavallo, G. Guerra, M. Vacatello, P. Corradini, *Macromolecules* **1991**, *24*, 1784; e) L. A. Castonguay, A. K. Rappé, *J. Am. Chem. Soc.* **1992**, *114*, 5832; f) J. R. Hart, A. K. Rappé, *ibid.* **1993**, *115*, 6159; g) J. A. Ewen, M. J. Elder, *Makromol. Chem. Macromol. Symp.* **1993**, *66*, 179; h) A. R. Siedle, W. M. Lamanna, R. A. Newmark, *ibid.* **1993**, *66*, 215.
[8] J. A. Ewen, M. J. Elder (Fina Technology Inc.), EPA 0426637, **1990** [*Chem. Abstr.* **1991**, *115*, 136988d].
[9] J. C. W. Chien, W. M. Tsai, M. D. Rausch, *J. Am. Chem. Soc.* **1991**, *113*, 8570.
[10] M. Bochmann, S. J. Lancaster, *J. Organomet. Chem.* **1992**, *434*, C1.
[11] a) J. A. Ewen, M. J. Elder, *Makromol. Chem. Macromol. Symp.* **1993**, *66*, 179; b) J. C. W. Chien, W. M. Tsai, *ibid.* **1993**, *66*, 141; c) J. C. W. Chien, B. Xu, *Makromol. Chem. Rapid Commun.* **1993**, *14*, 109.
[12] a) M. Bochmann, A. J. Jaggar, L. M. Wilson, M. B. Hursthouse, M. Motevalli, *Polyhedron* **1989**, *8*, 1838; b) M. Bochmann, G. Karger, A. J. Jaggar, *J. Chem. Soc. Chem. Commun.* **1990**, 1038; c) M. Bochmann, A. J. Jaggar, *J. Organomet. Chem.* **1992**, *424*, C5.
[13] Mixtures of $[Cp_2Zr(CH_2Ph)_2]$ and $[Cp_2Zr(CH_2Ph)]^+$ in ratios from 2:1 to 11:1 between -20 °C and -60 °C in CD_2Cl_2 fail to provide evidence for the formation of dimeric complexes: M. Bochmann, S. J. Lancaster, *Organometallics*, **1994**, *13*, 2235.
[14] A related dimeric thorium complex is known: X. Yang, C. L. Stern, T. J. Marks, *Organometallics* **1991**, *10*, 840.
[15] The Zr-CH_3 resonance signals of the monomeric complex **4a** could not be assigned with certainty. Singlets at $\delta = 0.76$ and 0.77 and a weaker signal at $\delta = 0.66$ are replaced on addition of $[D_5]$pyridine by a single signal at $\delta = 0.35$ (-50 °C). The signals at $\delta = 0.76$ and 0.77 remain unchanged on warming, whereas the signal at $\delta = 0.66$ broadens.
[16] The stability of dimeric methyl complexes of *ansa*-zirconocenes has consequences for the evaluation of the catalytic activity of these species at low temperatures. The stability of **3c** and **3d** at low temperature suggests that only half as many cationic centers are formed as are expected on the basis of Equation (a).
[17] The ^{1}H NMR spectrum of **4c** at -30 °C shows signals for Zr-Me at $\delta = -0.47$ and -0.61 which broaden on cooling. This finding may be consistent with the presence of solvent and anion adducts of **4c**, an unambiguous assignment was, however, not possible.
[18] E. Giannetti, G. M. Nicoletti, R. Mazzocchi, *J. Polym. Sci. Part A: Polym. Chem.* **1985**, *23*, 2117.
[19] G. Erker, M. Albrecht, S. Werner, C. Krüger, *Z. Naturforsch. B* **1990**, *45*, 1205.
[20] L. Resconi, S. Bossi, L. Abis, *Macromolecules* **1990**, *23*, 4489.
[21] See for example: a) N. Herfert, G. Fink, *Makromol. Chem. Macromol. Symp.* **1993**, *66*, 157; b) B. Rieger, X. Mu, D. T. Mallin, M. D. Rausch, J. C. W. Chien, *Macromolecules* **1990**, *23*, 3559; c) W. A. Herrmann, J. Rohrmann, E. Herdtweck, W. Spalek, A. Winter, *Angew. Chem.* **1989**, *101*, 1536; *Angew. Chem. Int. Ed. Engl.* **1989**, *28*, 1511; d) W. Spalek, M. Antberg, J. Rohrmann, A. Winter, B. Bachmann, P. Kiprof, J. Behm, W. A. Herrmann, *ibid.* **1992**, *104*, 1373 and **1992**, *31*, 1347.
[22] J. C. W. Chien, B. P. Wang, *J. Polym. Sci. Part A: Polym. Chem.* **1988**, *26*, 3089.
[23] The formation of **5** does not exclude the possibility of Zr-O coordination like that in **6**. It is conceivable, however, that this side reaction may contribute to the deactivation of the catalyst.
[24] J. C. W. Chien, W. M. Tsai, *Makromol. Chem. Macromol. Symp.* **1993**, *66*, 141. Heterobimetallic lanthanide complexes $[Cp_2M(\mu\text{-}Me)_2AlMe_2]$ (M = Sc, Y, Gd, Dy, Ho, Er, Tm, Yb) which are isostructural to **5a** are known: J. Holton, M. F. Lappert, D. G. H. Ballard, R. Pearce, J. L. Atwood, W. E. Hunter, *J. Chem. Soc. Dalton Trans.* **1979**, 45.
[25] By contrast, Fink et al. found for ethylene polymerizations with the system **1c**/$[HNnBu_3][B(C_6F_5)_4]$ an activity increase with increased **1c**/$[HNnBu_3]^+$ ratio, whereas propene polymerizations showed a maximum at a ratio of 1:1: N. Herfert, G. Fink, *Makromol. Chem. Rapid Commun.* **1993**, *14*, 91.

The First Decaisopropylmetallocene: One-Pot Synthesis of $[Rh(C_5iPr_5)_2]PF_6$ from $[Rh(C_5Me_5)_2]PF_6$ by Formation of 20 Carbon–Carbon Bonds**

Dirk Buchholz and Didier Astruc*

Dedicated to Dr. Françoise Moulines on the occasion of her 60th birthday

Decamethylmetallocenes $[MCp^*_2]$ ($Cp^* = C_5Me_5$)[1–3] have proven highly valuable as magnetic materials[1] and catalysts.[2] Transition metal complexes with pentaisopropylcyclopentadienyl ligands show a unique directionality,[4, 5] and form a new type of chiral metallocene.[6] The remarkable robustness of these metallocenes suggests their application in chemotherapy and catalysis. Sitzman et al.[4, 7] have shown that the reaction of pentaisopropylcyclopentadienylsodium with iron chloride does not lead to decaisopropyl ferrocene, but electron transfer takes place to give the C_5iPr_5 radical.[7] We now report the synthesis of the first decaisopropylmetallocene and compare the "built-from-inside" route starting from decamethylcobaltocenium and decamethylrhodocenium.

The homologation of permethylated ligands in cationic 18-electron complexes by using excess CH_3I and *t*BuOK has been shown to work with first-row transition metal sandwich complexes containing only one permethylated ring [Eqs. (1) and (2)].

$$[Fe(C_6Me_6)Cp]PF_6 \xrightarrow[\text{THF, 25 °C}]{\text{MeI + } t\text{BuOK}} [Fe(C_6Et_6)Cp]PF_6 \quad (1)$$

$$[CoCp^*Cp]PF_6 \xrightarrow[\text{THF, 60 °C}]{\text{MeI + } t\text{BuOK}} [Co(C_5iPr_5)Cp]PF_6 \quad (2)$$

Attempts to extend this route to first-row transition metal sandwich complexes in which both rings are permethylated

[*] Prof. D. Astruc, Dr. D. Buchholz
Laboratoire de Chimie Organique et Organométallique
Université Bordeaux I, URA CNRS 35
351, cours de la Libération, F-33405 Talence Cédex (France)
Telefax: Int. code + 56846646

[**] This work was supported by the CNRS, the University Bordeaux I, and the Région Aquitaine. D. B. thanks the Deutsche Forschungsgemeinschaft for a postdoctoral grant.

have not been successful. Starting from the complex $[FeCp^*(C_6Me_6)]PF_6$, a mixture of partially ethylated complexes is obtained, even under forcing conditions.[8] Similarly, $[CoCp^*_2]PF_6$[9] is incompletely permethylated on reaction with excess MeI and *t*BuOK in THF or with MeI and KOH in dimethoxyethane (DME) at 60 °C. The resulting mixture was treated again under similar conditions, and further methylation took place. After seven successive reactions, 69% permethylation was obtained, which appears to be the limit of steric saturation, and corresponds to roughly 14 added methyl groups per complex (Fig. 1).

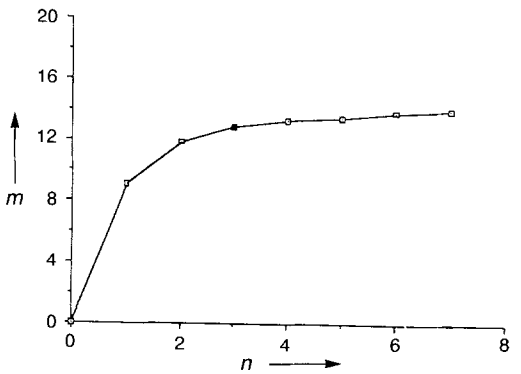
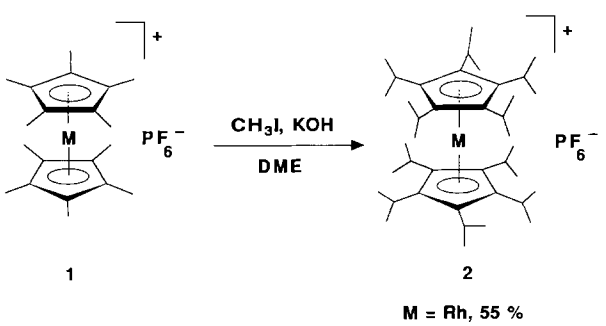


Fig. 1. Number of methyl groups *m* introduced in $[CoCp^*_2]PF_6$ as a function of the number of successive reactions *n* with excess KOH and MeI in DME at 60 °C.

We then reasoned that more space would be available between the two rings in decamethylrhodocenium since the atomic radius of Rh is greater than that of Co. Treatment of $[\{RhCp^*_2Cl_2\}_2]$ with Cp*Li in THF at −10 °C for 12 hours, followed by metathesis with aqueous HPF_6 and recrystallization from acetone/alcohol led to decamethylrhodocenium hexafluorophosphate **1** in 42% yield.[10, 11]. The reaction of $[RhCp^*_2]PF_6$ (**1**) with excess KOH and MeI in DME for two days at 60 °C afforded $[Rh(C_5iPr_5)_2]PF_6$ (**2**) in 55% yield after recrystallization from acetone/alcohol (Scheme 1).[12]



Scheme 1. Synthesis of **2**. An excess of CH_3I is used. For M = Co the reaction does not go to completion.

The ^1H NMR spectrum of **2** at 200 MHz in $C_6D_5NO_2$ shows a single septet for the ten equivalent methine protons at $\delta = 2.88$, and two doublets at $\delta = 1.17$ and 1.34 for the *endo* and *exo* methyl groups, as expected from the directionality of the *i*Pr groups in the C_5iPr_5 complexes. The signals of the methyl groups coalesce at 135 °C at which temperature no decomposition of the complex is observed. The rotation barrier of the ten *i*Pr groups in **2** is $\Delta G^{\neq} = 85.5 \pm 0.8$ kJ mol^{-1}.[13] If **3**[14] is allowed to react with excess KOH and MeI at 60 °C for three hours, **4** is obtained in 80% yield after recrystallization from acetone/alcohol.[15] In the ^1H NMR spectrum of **4** at 200 MHz in $C_6D_5NO_2$ the signals coalesce at 60 °C ($\Delta G^{\neq} = 70.3 \pm 0.8$ kJ mol^{-1}). Under these conditions, the signals for **5**[5] coalesce at 77 °C ($\Delta G^{\neq} = 71.3 \pm 0.8$ kJ mol^{-1}).

$[RhCp^*Cp]PF_6$ **3**

$[Rh(C_5iPr_5)Cp]PF_6$ **4**

$[Co(C_5iPr_5)Cp]PF_6$ **5**

The $\Delta G^{\neq}$ values for the coalescence of **4** and **5** thus differ very little from each other, which indicates that the interaction between the C_5iPr_5 ring and the Cp ring is not significant. On the other hand, the rotation barrier is higher in **2** than in **4** and **5**, as expected from the mutual steric hindrance of the two C_5iPr_5 rings. Note that, at low temperature, the single directionality of each C_5iPr_5 ring gives the possibility of obtaining two diastereoisomers of **2** (Fig. 2; **A**: clockwise/clockwise and **B**: clockwise/counterclockwise). Molecular models[15] of **2** show that **B** is considerably favored. Indeed, only the more favored diastereoisomer is detected by ^1H and ^{13}C NMR spectroscopy.[12]

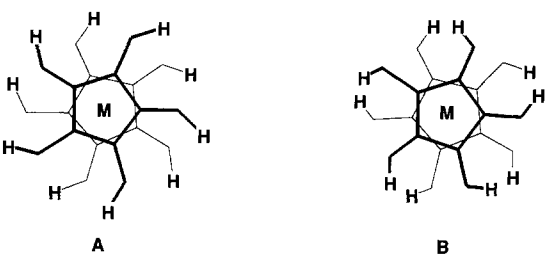


Fig. 2. The two possible conformations of decaisopropylmetallocenes. **A**: clockwise/clockwise, **B**: clockwise/counterclockwise. In the present case M = Rh^+.

In conclusion, in synthesizing the first decaisopropylmetallocene, we have shown that the permethylation of both rings in fully permethylated cationic 18-electron sandwich complexes is possible for complexes with second-row transition metals, but not for complexes of the first-row metals.

Experimental Procedure

2: **1** (518 mg, 1 mmol) and powdered KOH (5.6 g, 100 mmol) were dried in vacuo at 60 °C for 3 h, then CH_3I (14.2 g, 100 mmol) in degassed DME (20 mL) in was added by cannula. The reaction mixture was heated at 60 °C for 1 day. After the volatiles had been removed in vacuo, the solid residue was dissolved in CH_2Cl_2 and water. The aqueous phase was neutralized with HCl and washed with CH_2Cl_2. The combined aqueous extracts were shaken with an aqueous HPF_6 solution (5%), filtered over Na_2CO_3, and dried over Na_2SO_4. After removal of the solvent in vacuo, the residue was recrystallized from acetone/ethanol at −20 °C to give yellow crystals of **2** (440 mg, 55% yield). Correct C,H analysis; ^1H and ^{13}C NMR spectra see ref. [12].

4: Complex **4** was synthesized analogously from **3** (reaction time 3 h, 80% yield, see ref. [15]).

Received: February 25, 1994 [Z 6714 IE]
German version: *Angew. Chem.* **1994**, *106*, 1721

[1] a) J. S. Miller, A.-J. Epstein, *Angew. Chem.* **1994**, *106*, 399; *Angew. Chem. Int. Ed. Engl.* **1994**, *33*, 385; b) W. E. Broderik, J. A. Thomson, E. P. Day, B. M. Hoffman, *Science* **1990**, *249*, 401.

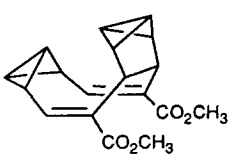
[2] a) P. L. Watson, G. W. Parshall, *Acc. Chem. Res.* **1985**, *18*, 51; b) T. J. Marks, *Science* **1982**, *217*, 989.

[3] a) P. Jutzi, *Pure Appl. Chem.* **1989**, *61*, 1731; b) R. B. King, *Coord. Chem. Rev.* **1976**, *20*, 155; c) G. P. Pez, J. N. Armor, *Adv. Organomet. Chem.* **1981**, *19*, 1; d) for a recent review on bulky cyclopentadienyl complexes, see: J. Okuda, *Top. Curr. Chem.* **1991**, *160*, 97; C. Janiak, H. Schumann, *Adv. Organomet. Chem.* **1991**, *33*, 291.
[4] H. Sitzmann, *Chem. Ber.* **1990**, *123*, 2311.
[5] B. Gloaguen, D. Astruc, *J. Am. Chem. Soc.* **1990**, *112*, 4607.
[6] H. Brunner, *Adv. Organomet. Chem.* **1980**, *18*, 151.
[7] a) H. Sitzmann, R. Boese, *Angew. Chem.* **1991**, *103*, 1027; *Angew. Chem. Int. Ed. Engl.* **1991**, *30*, 971; b) H. Sitzmann, H. Bock, R. Boese, T. Dezember, Z. Havlas, W. Kaim, M. Moscherosch, L. Zanathy, *J. Am. Chem. Soc.* **1993**, *115*, 12003.
[8] a) D. Astruc, J.-R. Hamon, G. Althoff, E. Román, P. Batail, P. Michaud, J.-P. Mariot, F. Varret, D. Cozak, *J. Am. Chem. Soc.* **1979**, *101*, 5445; b) J.-R. Hamon, J.-Y. Saillard, A. Le Beuze, M. McGlinchey, D. Astruc, *ibid.* **1982**, *104*, 7549; c) D. Astruc, *Top. Curr. Chem.* **1991**, *160*, 47.
[9] U. Kolle, F. Khouzami, *Angew. Chem.* **1980**, *92*, 658; *Angew. Chem. Int. Ed. Engl.* **1980**, *19*, 640.
[10] In the meantime an alternative synthesis of $[RhCp_2^*]PF_6$ has been published: U. Kölle, W. Klaui, *Z. Naturforsch. B* **1991**, *46*, 75.
[11] a) The X-ray crystal structure of **1** shows a perfectly staggered conformation [11b]; b) L. Zsolnai, G. Huttner, D. Buchholz, D. Astruc, unpublished results.
[12] **2**: ^{1}H NMR (200 MHz, $C_6D_5NO_2$, 25 °C, TMS): δ = 1.17 (d, 30H, ^3J(H,H) = 7.6 Hz), 1.34 (d, 30H, ^3J(H,H) = 7.6 Hz), 2.88 (sept, 10H, ^3J(H,H) = 7.6 Hz); ^{13}C NMR (50.3 MHz): δ = 24.4 (s), 26.2 (s), 26.7 (s), 114.8 (d, ^1J(Rh,C) = 8 Hz). Correct C,H analysis. Several attempts to solve the X-ray crystal structure of **2** have been unsuccessful; however, the available X-ray data are in accord with the form **B** (Fig. 2) [11b].
[13] For a discussion of the errors on the NMR determination of ΔG^+, see for instance D. Kost, E. H. Carlson, M. Raban, *J. Chem. Soc. Chem. Commun.* **1971**, 656.
[14] B. L. Both, R. N. Haszeldine, M. Hill, *J. Chem. Soc. A* **1969**, 1299.
[15] **4**: ^{1}H NMR (250 MHz, $CDCl_3$, 25 °C, TMS): δ = 1.24 (d, 15H, ^3J(H,H) = 7.3 Hz), 1.30 (d, 15H, ^3J(H,H) = 7.3 Hz), 2.90 (sept, 1H, ^3J(H,H) = 7.3 Hz), 5.78 (s, 5H); ^{13}C NMR (62.38 MHz): δ = 20.3 (s), 24.5 (s), 27.0 (s), 87.8 (d, ^1J(Rh,C) = 6.7 Hz), 112.8 (d, ^1J(Rh,C) = 8.1 Hz). Correct C,H analysis. The X-ray crystal structure of **5** shows the single directionality of the five isopropyl groups: M. Cotrait, D. Buchholz, D. Astruc, unpublished results.

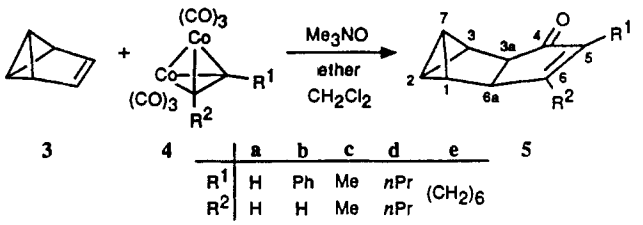
Octahydro-1,2,3:4,5,6-dimethenopentalene-2-carbonitrile, the First Derivative of a Yet-Unknown $(CH)_{10}$ Hydrocarbon**

Manfred Christl,* Michael Türk, Eva-Maria Peters, Karl Peters, and Hans Georg von Schnering

The "nonconjugated" bisbicyclobutane **1** has interesting reactivity. Owing to the proximity of the two bicyclobutane units, they interact either directly or after an external reagent has attacked either of the two.[1] In this context we have been interested in the synthesis of compounds in which two bicyclobutane units are next to one another but not linked directly. We report here on our first goal achieved in this area, the synthesis of the title compound **9**.

1  **2** 

In analogy to the synthesis of octabisvalenecarbonitrile (pentacyclo[5.1.0.0^{2,4}.0^{3,5}.0^{6,8}]octane-3-carbonitrile) by Prinzbach et al.,[2] the cyclopentenone derivative **5a** can be considered the key compound in the synthesis of **9**. We first contemplated a route starting with the allylic oxidation of hexahydro-1,2,3-methenopentalene **2**. In fact, compound **2** is known, but two preparations proceed in very low yields;[3,4] a third, a six-step sequence starting with benzvalene (**3**), has an overall yield of roughly 10% and is also quite time-consuming.[5]

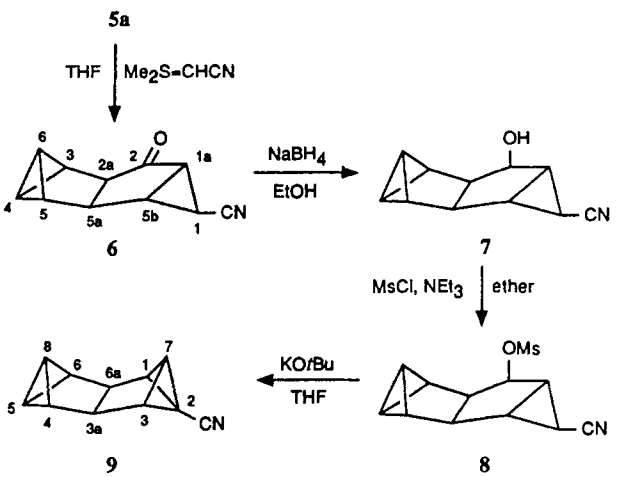


3 **4**

	a	b	c	d	e
R^1	H	Ph	Me	*n*Pr	$(CH_2)_6$
R^2	H	H	Me	*n*Pr	

5

The construction of cyclopentenones from olefins by the Pauson–Khand reaction[6] seemed to be ideal for the one-step conversion of **3** into **5a**. Thus we treated **3** with the dicobalt complex **4a**, but thereby only isomerized **3** into benzene. The intended reaction proceeded readily, however, when trimethylamine oxide, a reagent known for accelerating such reactions,[7] was added, and the desired product **5a** was isolated in 30–51% yield (see Experimental Procedure). Analogously, the derivatives **5b–e** were obtained in unoptimized yields of 33, 40, 43, and 35%, respectively.



By applying the reaction sequence recently used to transform tricyclo[4.1.0.0^{2,7}]hept-4-en-3-one into octabisvalenecarbonitrile,[2] we converted **5a** into the target compound **9** in four steps. Treatment of **5a** with dimethylsulfonium cyanomethanide provided oxonitrile **6** and its diastereomer with the opposite configuration at C1 in a 1:1 ratio (54% yield). After separation by flash chromatography (basic Al_2O_3, activity IV, diethyl ether), **6** was reduced with sodium borohydride to give hydroxynitrile **7** and its diastereomer (opposite configuration at C2) in a ratio of 4:1. Separation by flash chromatography (basic Al_2O_3, activity IV, dichloromethane) provided the pure compounds in yields of 48 and 16%, respectively. Treatment of

[*] Prof. Dr. M. Christl, Dipl.-Chem. M. Türk
Institut für Organische Chemie der Universität
Am Hubland, D-97074 Würzburg (FRG)
Telefax: Int. code + (931)888-4606
E.-M. Peters, Dr. K. Peters, Prof. Dr. H. G. von Schnering
Max-Planck-Institut für Festkörperforschung, Stuttgart

[**] This work was supported by the Deutsche Forschungsgemeinschaft and the Fonds der Chemischen Industrie. We thank CHEMETALL GmbH, Union Rheinische Braunkohlen Kraftstoff AG, and Hoechst AG for donating chemicals.

7 with methanesulfonyl chloride gave mesylate **8** (98%), which was converted into bisbicyclobutane **9** (83%) by reaction with potassium *tert*-butoxide in tetrahydrofuran. Compound **9** is the first derivative of the yet-unknown $(CH)_{10}$ hydrocarbon[8] octahydro-1,2,3:4,5,6-dimethenopentalene (hexacyclo[4.4.0.0^{2,4}.0^{3,5}.0^{7,9}.0^{8,10}]decane).

The structures of **8** and **9** were confirmed by X-ray structure analyses.[9] It is evident in Figure 1 that the cyclopropanecar-

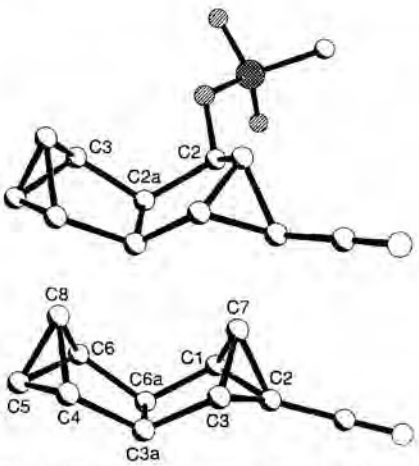
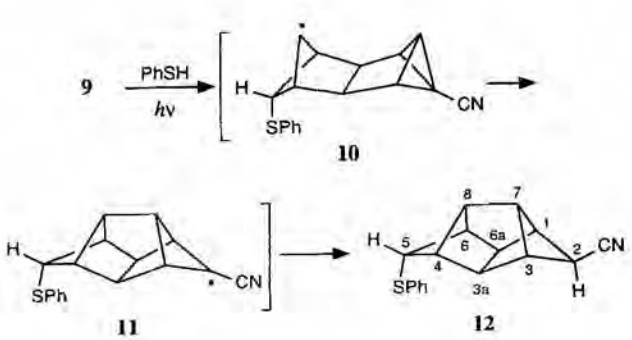


Fig. 1. X-ray crystal structures of **8** (top) and **9** (bottom) [9]. The central bonds in the bicyclobutane units have different lengths (143.6 (**8**), 145.6 (**9**, C5–C8), and 148.3 pm (**9**, C2–C7)), even though the flap angles of the bicyclobutane units are almost identical (111.1° (**8**), 110.5° (**9**, C4,5,6,8), and 111.7° (**9**, C1,2,3,7)). Thus the correlation between these bond lengths and flap angles [10] holds only for the unsubstituted bicyclobutane unit in **9**. The nitrile group in **9** causes the bonds of C2 within the three-membered rings [11] to be particularly long [C2–C1 (150.8 pm), C2–C3 (151.8 pm), and C2–C7]. The configuration of C2 is an inverted tetrahedron. The inversion parameter (angle between the bond vector C2–CN and the plane through C1,C2,C3) [12] is 174.6°. The *cis* annelation of the two five-membered rings in both **8** and **9** leads to relatively small distances between atoms that are not directly bonded [e.g. between C3 and the oxygen atom at C2 in **8** (280 pm) and between C7 and C8 in **9** (312 pm)], which results in large bond angles [C2-C2a-C3 (118.4°) in **8** and C1-C6a-C6 (116.4°) in **9**].

bonitrile unit and the mesylate group in **8** are *trans*. Thus the stereochemical prerequisite for the 1,3-elimination, in which the mesylate group is removed with inversion, is fulfilled. In **9** the distance between the bicyclobutane bridgehead atoms C7 and C8 is 312 pm.

This distance is small enough for a transannular reaction: irradiation of a solution of **9** and thiophenol in benzene furnished a 6:1 mixture of 1,3:4,6-ethane-1,2-diylidenepentalene (pentacyclo[5.3.0.0^{2,5}.0^{4,10}.0^{6,9}]decane) derivative **12** and its diastereomer (opposite configuration at C2) in 70% yield. This reaction is most likely a radical chain process analogous to the corresponding reaction of **1**.[11] The cyclobutyl radicals **10** and **11** are assumed to occur as intermediates.



The IR, NMR, and mass spectra, as well as elemental analyses, obtained for all new compounds are in agreement with the assigned structures. Selected physical data are given in Table 1.

Table 1. Selected physical data for **5a**, **6**–**9**, and **12**; 200 or 400 MHz ^{1}H NMR spectra, 50, 63, or 100 MHz ^{13}C NMR spectra, measured in $CDCl_3$; the assignments given in the NMR spectra are based on decoupling experiments, NOE effects, and ^{1}H,^{1}H COSY spectra.

5a: B.p. 50–55 °C/0.15 mbar; IR (neat): $\tilde{\nu}$ = 1703 cm^{-1} (C=O), 1582 (C=C); MS (70 eV), *m/z* (%): 132 (29) [*M*$^+$], 131 (100), 104 (42), 103 (60), 78 (42), 77 (22), 51 (21); ^{1}H NMR: δ = 1.91 (dtt, J(2,7) = 9.2, J(1,7) = J(3,7) = 1.7, J(3a,7) = J(6a,7) = 1.3 Hz; H7), 2.16 (dt, J(1,2) = J(2,3) = 1.7 Hz; H2), 2.23 (≈dq, J(1,3) = 4.9 Hz; H1), 2.27 (≈dqd, J(3,6) = 0.3 Hz; H3), 2.50 (dt, J(3a,6a) = 5.4, J(3,3a) = 1.3 Hz; H3a), 3.13 (ddq, J(6,6a) = 2.5, J(1,6a) = J(5,6a) = 1.2 Hz; H6a), 5.94 (dd, J(5,6) = 5.8 Hz; H5), 7.42 (ddd; H6); ^{13}C NMR: δ = −0.5 (dtd, J(C,H) = 219, 8, 6 Hz; C7), 10.5 (dd, 217, 6 Hz; C2), 35.1 (ddq, 170, 14, 4 Hz; C3), 37.5 (ddq, 168, 13, 4 Hz; C1), 49.7 (ddq, 140, 9, 5 Hz; C6a), 51.4 (dquint, 140, 5 Hz; C3a), 134.2 (dt, 170, 4 Hz; C6), 164.3 (dq, 164, 3 Hz; C5), 210.7 (dm, 13 Hz; C4)

6: M.p. 112–113 °C; IR (KBr): $\tilde{\nu}$ = 2243 cm^{-1} (C≡N), 1718 (C=O); ^{13}C NMR: δ = −0.3 (C6), 5.3 (C4), 8.9 (C1), 30.3 (C1a), 35.2 (C5b), 35.8, 37.5 (C3,5), 45.6 (C2a), 51.1 (C5a), 117.7 (CN), 210.5 (C2)

7: M.p. 56–57 °C; IR (KBr): $\tilde{\nu}$ = 3220 cm^{-1} (broad, O-H), 2235, 2243 (C≡N); ^{13}C NMR: δ = 1.3 (C6), 4.2 (C4), 6.1 (C1), 29.5, 33.3 (C1a,5b), 36.6, 37.2 (C3,5), 50.5 (C2a), 51.9 (C5a), 73.2 (C2), 120.1 (CN)

8: M.p. 127–128 °C; IR (KBr): $\tilde{\nu}$ = 2238 cm^{-1} (C≡N); ^{13}C NMR: δ = 2.5 (C6), 4.9 (C4), 7.0 (C1), 30.2, 33.6 (C1a,5b), 34.4, 37.0 (C3,5), 38.1 (CH_3), 51.4 (C2a), 52.3 (C5a), 80.9 (C2), 119.1 (CN)

9: M.p. 78–79 °C; IR (KBr): $\tilde{\nu}$ = 2220 cm^{-1} (C≡N); MS (70 eV), *m/z* (%): 155 (14) [*M*$^+$], 154 (76), 153 (21), 140 (59), 128 (44), 127 (100), 126 (15), 115 (29), 78 (14), 77 (40), 76 (15), 63 (18), 52 (25), 51 (24), 50 (20), 39 (13); ^{1}H NMR: δ = 1.78 (dt, J(5,8) = 9.2, J(4,5) = 1.8 Hz; H5), 1.83 (dtt, J(4,8) = 1.7, J(3a,8) = 1.3 Hz; H8), 1.89 (m; H4,6), 2.34 (m; H3a,6a), 2.56 (dm; H1,3), 2.83 (tt, J(1,7) = 2.2, J(3a,7) = 1.5 Hz; H7); ^{13}C NMR: δ = 0.3 (dtd, J(C,H) = 215, 8, 4 Hz; C8), 0.9 (s; C2), 7.0 (dd, 214, 4 Hz; C5), 15.7 (dt, 216, 8 Hz; C7), 34.6 (ddt, 165, 14, 4 Hz; C4,6), 43.5 (ddd, 169, 12, 5 Hz; C1,3), 48.5 (dquintd, 141, 6, 2 Hz; C3a,6a), 118.9 (d, 7 Hz; CN)

12: M.p. 91–92 °C; IR (KBr): $\tilde{\nu}$ = 2237 cm^{-1} (C≡N); ^{1}H NMR: δ = 2.35 (qt, J(4,8) = J(7,8) = 3.2, J(3a,8) = 1.6 Hz; H8), 2.67 (s; H2), 2.75 (br. s; H3a,6a), 3.00 (qt, J(1,7) = 3.5, J(3a,7) = 1.6 Hz; H7), 3.12 (br. d; H1,3), 3.15 (br. t; H4,6), 3.82 (t, J(4,5) = 2.8 Hz; H5), 7.15–7.32 (m; C_6H_5); ^{13}C NMR: δ = 31.5 (C2), 43.9 (C3a,6a), 48.6 (C5), 50.0 (C8), 51.8 (C7), 55.4 (C1,3), 57.4 (C4,6), 121.4 (CN), 125.8 (*p*-C), 128.8, 129.1 (*m*-,*o*-C), 136.4 (*i*-C)

Experimental Procedure

5a: A moderate stream of acetylene (passed through a trap at −78 °C to remove acetone) was bubbled through a stirred, ice-cooled solution of octacarbonyldicobalt (82.0 g, 240 mmol) in dichloromethane (700 mL) under nitrogen until release of CO could no longer be detected (ca. 5 h). The solution was transferred to an addition funnel and added dropwise under nitrogen within 45 min to a stirred suspension of anhydrous trimethylamine *N*-oxide (135 g, 1.80 mol) in a solution of benzvalene (**3**) [13] (19.0 g, 243 mmol) in diethyl ether (300–450 mL) cooled to −75 °C. The mixture was stirred and allowed to warm to 20 °C over 2 h. Then a gentle stream of oxygen was passed through the mixture for 4 h. Diethyl ether was added repeatedly to replace the solvent that evaporated, such that the original volume was maintained. The brown precipitate was filtered off, the filtrate extracted with water (4 × 100 mL), the organic phase dried with K_2CO_3, and the solvent removed by distillation. Distillation of the yellow-brown residue at 50–55 °C/0.15 mbar gave 9.5–16.1 g (30–51%) **5a**, which was pale blue in the cooled (−30 °C) receiving flask but turned yellow-brown upon warming to 20 °C. Trace amounts of volatile cobalt-containing compounds were probably the source of these colors. Impurities are not evident in the NMR spectra. Compound **5a** purified by preparative gas chromatography (1.5 m column, 20% EGA on Volaspher® A2, 90 °C) was colorless. Spectroscopic data are given in Table 1.

Received: March 17, 1994 [Z 6768 IE]
German version: *Angew. Chem.* **1994**, *106*, 1719

[1] M. Christl, S. Freund, H. Henneberger, A. Kraft, J. Hauck, H. Irngartinger, *J. Am. Chem. Soc.* **1988**, *110*, 3263–3271.
[2] B. Trupp, D.-R. Handreck, H.-P. Böhm, L. Knothe, H. Fritz, H. Prinzbach, *Chem. Ber.* **1991**, *124*, 1757–1775.
[3] U. Burger, B. Bianco, *Helv. Chim. Acta* **1983**, *66*, 60–67.
[4] The synthesis of **2** from the adduct of dibromocarbene and tetrahydropentalene following the procedure in ref.[3] gives only a 5% yield: A. Mentzschel, Diplomarbeit, Universität Würzburg, **1989**.
[5] F. Lanzendörfer, Dissertation, Universität Würzburg, **1984**.

[6] P. L. Pauson, *Tetrahedron* **1985**, *41*, 5855–5860; N. E. Schore, *Org. React.* **1991**, *40*, 1–90.
[7] S. Shambayati, W. E. Crowe, S. L. Schreiber, *Tetrahedron Lett.* **1990**, *31*, 5289–5292; M. Thommen, P. Gerber, R. Keese, *Chimia* **1991**, *45*, 21–24; N. Jeong, Y. K. Chung, B. Y. Lee, S. H. Lee, S.-E. Yoo, *Synlett* **1991**, 204–206; M. E. Krafft, I. L. Scott, R. H. Romero, S. Feibelmann, C. E. Van Pelt, *J. Am. Chem. Soc.* **1993**, *115*, 7199–7207.
[8] A. T. Balaban, M. Banciu, V. Ciorba, *Annulenes, Benzo-, Hetero-, Homo-Derivatives and their Valence Isomers, Vol. II*, CRC, Boca Raton, FL, **1987**, pp. 40–62.
[9] **8**: Monoclinic, $P2_1/c$; $a = 1379.1(5)$, $b = 826.0(4)$, $c = 1088.5(5)$ pm, $\beta = 108.87(3)$; 2992 measured reflections, of which 2641 with $F > 3\sigma(F)$ were considered independent; $R = 0.125$, $R_w = 0.120$. **9**: Monoclinic, $P2_1/n$; $a = 685.8(2)$, $b = 1796.7(4)$, $c = 662.1(1)$ pm, $\beta = 90.08(2)$; 2090 measured reflections, of which 1080 with $F > 3\sigma(F)$ were considered independent; $R = 0.055$, $R_w = 0.041$. Further details of the crystal structure investigations may be obtained from the Fachinformationszentrum Karlsruhe, D-76344 Eggenstein-Leopoldshafen (FRG) on quoting the depository numbers CSD-400696 (**8**) and CSD-400697 (**9**).
[10] H. Irngartinger, K. L. Lukas, *Angew. Chem.* **1979**, *91*, 750; *Angew. Chem. Int. Ed. Engl.* **1979**, *18*, 694–695; M. N. Paddon-Row, K. N. Houk, P. Dowd, P. Garner, R. Schappert, *Tetrahedron Lett.* **1981**, *22*, 4799–4812; M. Eisenstein, F. L. Hirshfeld, *Acta Crystallogr. Sect. B* **1983**, *39*, 61–75; P. G. Gassman, M. L. Greenlee, D. A. Dixon, S. Richtsmeier, J. Z. Gougoutas, *J. Am. Chem. Soc.* **1983**, *105*, 5865–5874.
[11] R. Hoffmann, *Tetrahedron Lett.* **1970**, 2907–2909; H. Günther, *ibid.* **1970**, 5173–5176.
[12] H. Irngartinger, W. Reimann, R. Lang, M. Christl, *Acta Crystallogr. Sect. B* **1990**, *46*, 234–238, and references therein.
[13] T. J. Katz, E. J. Wang, N. Acton, *J. Am. Chem. Soc.* **1971**, *93*, 3782–3783; T. J. Katz, R. J. Roth, N. Acton, E. J. Carnahan, *Org. Synth.* **1973**, *53*, 157.

The Use of Heterometallic Bridging Moieties To Generate Tractable Lanthanide Complexes of Small Ligands**

William J. Evans,* Reiner Anwander, Robert J. Doedens, and Joseph W. Ziller

Dedicated to Professor M. Frederick Hawthorne on the occasion of his 65th birthday

Lanthanide chemistry is dominated by large, anionic ligands which meet the steric and electronic demands of these large electropositive metals. On the other hand, the chemistry of simple lanthanide complexes of general formula LnZ_3 in which Z is a small anionic ligand such as methanide, methanolate, ethanolate, or dimethylamido, is poorly developed since these complexes are either unstable or insoluble.[1, 2] The only homoleptic lanthanide complexes with small ligands which are tractable enough to be definitively characterized by X-ray crystallography are the hexamethyl "ate" complexes $[LnMe_6]^{3-}$ of the late lanthanides Ho, Er, and Lu.[2]

We describe here a method for the synthesis of isolable, soluble lanthanide complexes of small ligands Z (Z = NMe_2, Me) which also provides a convenient route to heterometallic complexes which have component combinations of interest with respect to polymerization catalysis[3] and the formation of materials from molecular precursors.[4] We also report details of the first structurally characterized molecular complexes containing a lanthanide metal and gallium.[5]

[*] Prof. W. J. Evans, Dr. R. Anwander, Prof. R. J. Doedens, Dr. J. W. Ziller
Department of Chemistry, University of California
Irvine, CA 92717 (USA)
Telefax: Int. code + (714) 725-2210

[**] We thank the Division of Chemical Sciences of the Office of Basic Energy Sciences of the Department of Energy for support for this research and the Deutsche Forschungsgemeinschaft for a Postdoctoral Fellowship (to R. A.).

For many years it has been known that trialkylaluminum complexes will add to lanthanide complexes containing bulky stabilizing co-ligands to form bridged heterometallic species such as those given in Scheme 1.

$[(C_5H_5)_2Yb(\mu\text{-}Me)_2Al(Me)_2]$[6]

$[Yb\{[\mu\text{-}N(SiMe_3)_2](\mu\text{-}Me)_2AlMe\}_2]$[7]

$[(C_5Me_5)_2Ln(\mu\text{-}Me)_2AlMe_2]_n$[5, 8b]

$[(C_5Me_5)_2Sm(\mu\text{-}C_2H_5)_2Al(C_2H_5)_2]$[8a]

Scheme 1. Examples of lanthanide heterometallic complexes.

Recently, we have shown that $AlMe_3$ will also bridge and stabilize metal ligand combinations such as $Y(OCMe_3)_3$ in $[Y\{(\mu\text{-}OCMe_3)(\mu\text{-}Me)AlMe_2\}_3]$[9] and $[(C_5H_4SiMe_3)Y(OCMe_3)_2]$ in $[(C_5H_4SiMe_3)Y\{(\mu\text{-}OCMe_3)(\mu\text{-}Me)AlMe_2\}_2]$.[10] We now report that $AlMe_3$ will not only react with soluble reagents containing bulky ligands, but that it will also react with and solubilize the insoluble materials formed from reactions of lanthanide halides with small anionic ligands.

The reaction of anhydrous $NdCl_3$ with three equivalents of $LiNMe_2$ (Z = NMe_2) in THF at room temperature formed a blue material which was identified as **1a** [Eq. (a)]. Reaction of $AlMe_3$ or $GaMe_3$ with a suspension of **1a** in hexane yielded the hexane-soluble products **2a** (violet-blue) and **2b** (blue), respectively.

$$NdCl_3 + 3\,LiNMe_2 \longrightarrow \underset{\mathbf{1a}}{[Nd(NMe_2)_3(LiCl)_3]} \xrightarrow{3\,MMe_3} [Nd(NMe_2)_3(MMe_3)_3] + 3\,LiCl \quad \text{(a)}$$

2a, M = Al; **2b**, M = Ga

The intensely colored solutions of **2** are stable at room temperature. Evaporation of the solvent results in oily residues which solidify at −35 °C. These solids slowly decompose at room temperature to form large colorless crystals of $[\{Me_2NMMe_2\}_2]$ (M = Al, Ga (**4**))[11] which sublime to the top of the container. Compounds **2a** and **2b** can be isolated in 80% yield by crystallization of the initially isolated solids from hexane at −35 °C; the molecular structure of **2b** is shown in Figure 1.[12]

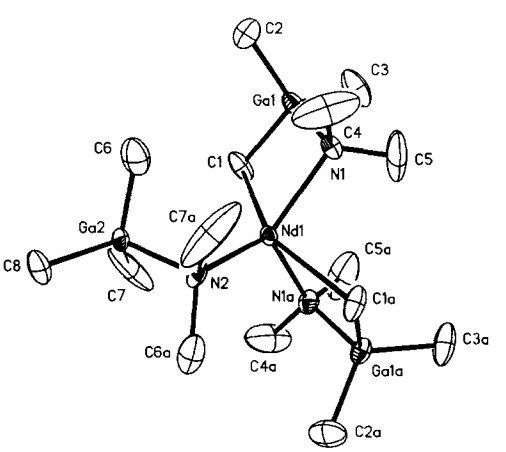


Fig. 1. Molecular structure of **2b**; the numbering is identical to that of isostructural **2a**. Thermal ellipsoids are drawn at the 50% probability level. Selected distances [Å] and angles [°] for **2b** are as follows (**2a** in brackets): Nd1-N1 2.395(5) [2.435(4)], Nd1-N2 2.362(10) [2.433(8)], Nd1-C1 2.749(7) [2.708(5)], Nd1-C6 3.28 [3.39], Nd1-C7 3.35 [3.21], Nd1-M1 3.276(1) [3.274(2)], Nd1-M2 3.242(1) [3.191(3)]; Nd1-N1-M1 94.7(2) [96.0(1)], Nd1-C1-M1 84.3(2) [85.7(1)], N1-Nd1-C1 77.3(2) [74.7(1)], N1-M1-C1 103.0(3) [102.5(2)], Nd1-N2-M2 94.5(4) [92.6(3)].

X-ray crystallography revealed that compounds **2a** and **2b** are isostructural, which is somewhat surprising considering the structural differences of the aluminum and gallium starting reagents and their different bonding patterns towards transition metal centers.[13] The overall structure shown in Figure 1 lacks the threefold symmetry found in $[Y\{(\mu\text{-}OCMe_3)(\mu\text{-}Me)AlMe_2\}_3]$.[9] Instead, there are only two symmetrically identical $[(\mu\text{-}NMe_2)(\mu\text{-}Me)MMe_2]$ chelating units (involving N1 and N1a) which have planar four-membered Nd-C-M-N metallacyclic rings. The third NMe_2MMe_3 unit involving N2 is disordered about the twofold symmetry axis and the methyl groups attached to aluminum or gallium in this unit are not as close to the Nd center as those in the other two units. A planar four-membered ring is not formed because neither of the two closest carbon atoms, C6 and C7, lie in a plane with Nd1, N2, and M.

The five ligands directly bound to Nd in **2** describe a distorted square pyramid in which N2 is slightly disordered. The Nd1–N1 distances of the bridges (**2a**, 2.435(4); **2b**, 2.395(5) Å) are longer than the terminal Nd–N(silylamido) distances in five-coordinate $[Nd\{N(SiHMe_2)_2\}_3(thf)_2]$ (2.343(5) Å)[14] and lie in the range found for terminal Nd–N(pyrazolato) bond lengths in the eight-coordinate complex $[Nd\{3,5\text{-di}(tert\text{-butyl})pyrazolato\}_3(thf)_2]$ (2.443(9) Å).[15] The Nd1–N2 distances are similar to the Nd1–N1 lengths (**2a**, 2.433(8); **2b**, 2.362(10) Å). The Nd1–C1 distances (**2a**, 2.708(5); **2b**, 2.749(7) Å) are similar to the Sm–C(μ-Me) distances in $[\{(C_5Me_5)_2Sm(\mu\text{-}Me)AlMe_2(\mu\text{-}Me)\}_2]$ (2.743(16) and 2.750(16) Å).[8b] In contrast, the Nd1–C6 and Nd1–C7 distances are more in the range of agostic interactions.[16] The bridging M1–C(methyl) distances (**2a**, 2.056(4); **2b** 2.073(6), Å) the M–N bond lengths (**2a**, 1.950(5) and 1.955(8) Å; **2b**, 2.048(6) and 2.043(11) Å), and the terminal M1–C(methyl) distances (average: **2a**, 1.958(9); **2b**, 1.984(11) Å) are not unusual.[7, 8, 13b]

Although solvent-free heterometallic peralkyl compounds like $NaBMe_4$ and $LiAlMe_4$ (Z = Me) have been very common reagents for a long time,[17] compounds of the type $M_xM'_yR_z$ containing a transition metal and a main group metal are very rare.[18] Furthermore, the above-mentioned "-ate" derivatives like $[Ln\{(\mu\text{-}Me)_2Li(tmeda)\}_3]$[2] are known only in the presence of coordinating donor solvents and are more stable for the late lanthanide elements.

$$\underset{\mathbf{1a}}{} \xrightarrow{GaMe_3} \underset{\mathbf{2b}}{[Nd(NMe_2)_3(GaMe_3)_3]} \longrightarrow [Nd\{(\mu\text{-}Me)_2GaMe_2\}_3] + [\{Me_2NGaMe_2\}_2] \quad \text{(b)}$$
$$\mathbf{3} \qquad \mathbf{4}$$

The reaction of **1a** with six equivalents or an excess of $GaMe_3$ under mild conditions (room temperature, hexane) afforded the heterometallic peralkyl complex **3** in 84% yield [Eq. (b)].

The formation of **3** is likely to occur through an intermediate **2b**, which can be seen clearly by the disappearance of M-NMe_2 vibrational modes in the IR spectra. The formation of the very stable **4**[11] undoubtedly helps drive the reaction to completion. Complex **3** is not sublimable and decomposes above 50 °C under high vacuum. Both **3** and **4** are very soluble in hexane and can be separated by fractional crystallization at −35 °C. Complex **3** crystallizes first as large blue pyramids (edge lengths ca. 5 mm), after which **4** crystallizes as colorless cubes. Complex **3** was characterized by IR spectroscopy, elemental analysis, and X-ray structural analysis (Fig. 2).[19]

The methyl groups in **3** are arranged in an octahedral geometry around Nd and a tetrahedral geometry around Ga. Each Nd-C-Ga-C ring is planar to within <0.07 Å. The fact that octahedral lanthanide complexes exist which contain larger bridging groups, for example **2a**, and smaller metals, for example $[Y\{(\mu\text{-}OCMe_3)_3(\mu\text{-}Me)AlMe_2\}_3]$,[9] suggests that the coordination environment around neodymium in **3** is sterically unsaturated. Complex **3** differs from the -ate complexes mentioned earlier in that the lanthanide metal is more electropositive than the other metallic component (electronegativities: Nd ≈ 1.1, Ga ≈ 1.8[20]). Therefore **3** is better described as a gallate ($[GaMe_4]^-$) rather than a neodymate ($[NdMe_6]^{3-}$) complex, although the most important aspect of this difference will be in the reactivity.

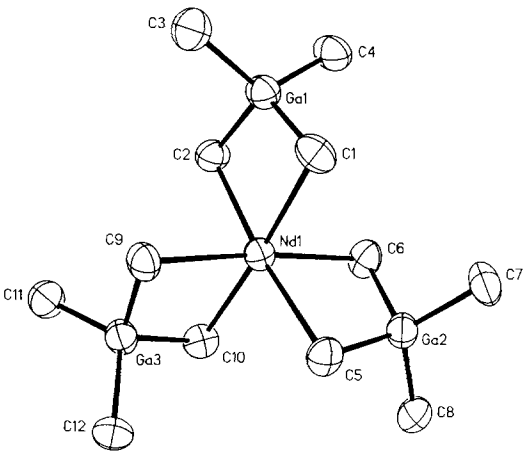


Fig. 2. Molecular structure of **3** with probability ellipsoids drawn at the 50% level. Selected distances [Å] and angles [°]: Nd1-C1 2.605(10), Nd1-C2 2.591(11), Nd1-C5 2.619(10), Nd1-C6 2.597(11), Nd1-C9 2.581(10), Nd1-C10 2.599(10), Ga-(μ-C) 2.115(11), Ga-(C_t) 1.989(13), Nd1-Ga1 3.129(1), Nd1-Ga2 3.136(1), Nd1-Ga3 3.117(1); Ga1-Nd1-Ga2 116.7(1), Ga2-Nd1-Ga3 121.1(1), Ga1-Nd1-Ga3 122.0(1), C1-Nd1-C2 84.5(3), Nd1-C1-Ga1 82.0(3), C1-Ga1-C2 110.7(4).

The Nd–C distances in **3** are close to that of the Nd–C bond length of 2.65 Å expected in the unknown $[Nd\{(\mu\text{-}Me)_2Li(tmeda)\}_3]$ on the basis of Shannon radii[21] and the known Ho and Er structures.[2a, b] Other relevant Nd–C distances are 2.53(2) and 2.70(2) Å in $[\{(C_5H_4CMe_3)_2Nd(\mu\text{-}Me)\}_2]$,[22] 2.517(7) Å in $[\{(C_5Me_5)_2Nd[CH(SiMe_3)_2]\}]$,[23a] and 2.506(7) Å in $[Me_2Si(C_5Me_4)_2Nd\{CH(SiMe_3)_2\}]$.[23b] The Ga–C distances in **3** are similar to those in **2b**.

The exchange of NMe_2 groups for methyl in reaction (b) is likely to occur in a stepwise fashion; examination of the analogous lanthanum system **1b** with four equivalents of $GaMe_3$ provided the partially exchanged complex **5** [Eq. (c)], which was characterized by elemental analysis, NMR spectroscopy, IR spectroscopy, and X-ray structural analysis (Fig. 3).[24]

$$\underset{\mathbf{1b}}{[La(NMe_2)_3(LiCl)_3]} + 4\,GaMe_3 \longrightarrow \underset{\mathbf{2c}}{[La(NMe_2)_3(GaMe_3)_3]} \longrightarrow [La\{(\mu\text{-}Me)_2GaMe_2\}\{(\mu\text{-}Me)(\mu\text{-}NMe_2)GaMe_2\}_2] + 0.5\,\mathbf{4} \quad \text{(c)}$$
$$\mathbf{5}$$

In complex **5**, the La–C distances in the two heteroleptic bridging units La(μ-Me)(μ-NMe_2) are rather long (2.891(5) and 2.992(5) Å) and are similar to those in $[La\{(Ph_2P)_2CH\}_3]$ (2.890(5), 2.790(4), 2.908(5) Å)[25] and even resemble the agostic La···C interactions in $[(C_5Me_5)La\{CH(SiMe_3)_2\}_2(thf)_x]$ (x = 0, 1; 2.978(6)–3.265(14) Å).[16] The La–C distances in the homoleptic bridging unit La(μ-$Me)_2$ are also relatively long in comparison to the Nd–C distances in **3**. In comparison, La–C (terminal alkyl) distances of 2.515(9) and 2.537(5)–2.651(8) Å are found in $[La\{CH(SiMe_3)_2\}_3]$[26] and $[(C_5Me_5)La\{CH(SiMe_3)_2\}_2(thf)_x]$,[16] respectively. The La–N bond lengths (2.451(4), 2.444(4) Å) are in the range of those found for terminal

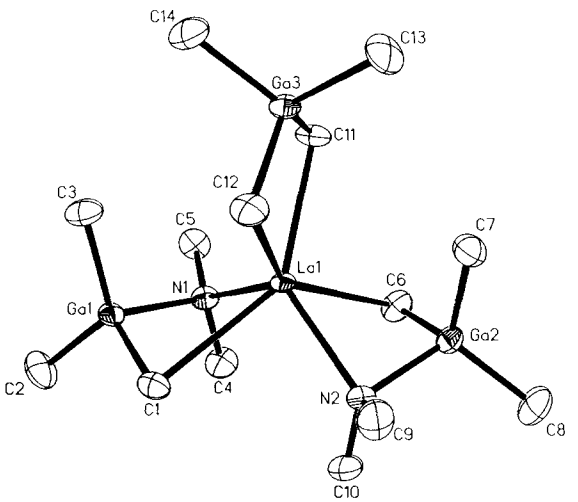


Fig. 3. Molecular structure of **5** with probability ellipsoids drawn at the 50% level. Selected distances [Å] and angles [°]: La1-C1 2.891(5), La1-C6 2.992(5), La1-C11 2.776(5), La1-C12 2.742(5), La1-N1 2.451(4), La1-N2 2.444(4), La1-Ga1 3.187(1), La1-Ga2 3.112(1), La1-Ga3 3.291(1), Ga1-C1 2.058(5), Ga2-C6 2.033(5), Ga3-C11 2.084(5), Ga3-C12 2.096(5), Ga-C, 1.978(7); C11-La1-C12 78.4(2), C1-La1-N1 71.2(1), C6-La1-N2 68.9(1).

La–N bonds in $[La\{N(SiMe_3)_2\}_3(PPh_3O)]$ (2.41(2) Å)[27a] and $[(C_5Me_5)_2La(NHMe)(H_2NMe)]$ (2.323(10) Å).[27b] A consequence of this irregular bonding pattern is that Ga1 and Ga2 lie closer to the La center than Ga3, and the La-C-Ga-N rings are nonplanar. The orientation of Ga1 and Ga2 toward the Ga3 unit and the arrangement of the methyl groups of the amido ligands with respect to the other methyl moieties appear to optimize the steric packing.

The isolation and characterization of complexes **2**, **3**, and **5** demonstrates that insoluble, oligomeric lanthanide complexes of small ligands can be "cracked" under very mild conditions (room temperature, hexane) by the attack of strong, soluble Lewis acids to form alkane-soluble, tractable compounds. This approach to developing the chemistry of lanthanide complexes of small ligands should be general; preliminary results show that species such as "$Ln(OMe)_3$" and InR_3 fit in this scheme.

Experimental Procedure

1: Addition of $LiNMe_2$ (2.22 g, 43.5 mmol) under nitrogen in a glovebox to a suspension of $NdCl_3$ (3.63 g, 14.5 mmol) in THF (50 mL) caused a spontaneous reaction indicated by a color change from pink to violet. After stirring the mixture at room temperature for two days, the solvent was removed to give a powder of composition **1a**. IR (Nujol): $\tilde{\nu}$ = 1205 m, 1126 s, 1113 s, 1052 m, 973 w, 893 vs, 459 m cm^{-1}. **1b** is prepared similarly.

2: Addition of MMe_3 (3 mmol) to a pink suspension of **1a** (0.40 g, 0.99 mmol) in hexane resulted in the extraction of soluble products into the hexane phase; this steadily darkened in color. After 12 h, the mixtures were centrifuged, concentrated, and crystallized. Analytical and spectroscopic data were collected on crystals grown from hexane solutions. **2a** (0.39 g, 80%): IR (Nujol): $\tilde{\nu}$ = 1220 sh, 1193 vs, 1145 w, 1113 s, 1091 w, 1043 s, 1024 w, 901 s, 695 vs, 580 vs, 537 m, 510 m, 480 m, 423 m, 311 m cm^{-1}. **2b** (0.51 g, 83%): IR (Nujol): $\tilde{\nu}$ = 1218 m, 1196 s, 1140 w, 1116 s, 1086 w, 1040 s, 971 w, 901 s, 724 s, 675 w, 650 w, 590 m, 556 s, 532 m, 495 w, 456 m, 411 s, 265 m cm^{-1}. Reaction of **1a** with one or two equivalents of MMe_3 also gave the homoleptic compounds **2**, but in lower yield.

3: To a suspension of **1a** (0.43 g, 1.05 mmol) in hexane (20 mL) was added $GaMe_3$ (0.63 mL, 6.30 mmol). After stirring this mixture for 36 h at room temperature, a white precipitate was separated from a blue hexane soluble product by centrifugation. After stirring for an additional 48 h, **3** can be separated from **4** by fractional crystallization at −35 °C as blue pyramidal crystals. **3** (0.47 g, 84%): IR (Nujol): $\tilde{\nu}$ = 1413 m, 1191 s, 736 s, 716 s, 582 s, 564 s, 527 s, 416 s, 289 s cm^{-1}.

5: A suspension of **1b** (0.75 g, 1.88 mmol) in hexane (20 mL) was extracted with $GaMe_3$ (0.75 mL, 7.52 mmol). The mixture was stirred overnight and centrifuged. Crystallization of the solution at −35 °C provided **5** as colorless crystals in 65% yield. IR (Nujol): $\tilde{\nu}$ = 1221 m, 1199 m, 1193 m, 1187 m, 1142 w, 1121 s, 1090 w, 1044 s, 904 s, 724 s, 664 m, 621 (sh) m, 598 m, 561 m, 530 m, 476 m, 408 s, 272 m cm^{-1}. ^1H NMR (300 MHz, C_6D_6, 25 °C): δ = 2.19 (s, 12H, NMe_2), 2.10 (s, 6H, μ-CH_3), 2.06 (s, 6H, μ-CH_3), −0.19 (s, 6H, $GaMe_2$), −0.23 (s, 12h, $GaMe_2$). $^{13}C\{^1H\}$ NMR (300 MHz, C_6D_6, 25 °C): δ = 42.7 (μ-CH_3), 41.8 (NMe_2), 41.3 (μ-CH_3), −3.1 ($GaMe_2$), −4.1 ($GaMe_2$).

Elemental analysis [%]: **1a**: Calcd for $NdLi_3Cl_3N_3C_6H_{18}$: C 17.85, H 4.49, N 10.41, Nd 35.73; found: C 16.42, H 4.26, N 10.96, Nd 35.0. – **2a**: Calcd for $NdAl_3N_3C_{15}H_{45}$: C 36.56, H 9.21, N 8.53; found: C 35.86, H 9.41, N 6.61. – **2b**: Calcd for $NdGa_3N_3C_{15}H_{45}$: C 29.01, H 7.30, N 6.77, Nd 23.23; found: C 27.50, H 7.25, N 5.44, Nd 22.3. – **3**: Calcd for $C_{12}H_{36}Ga_3Nd$: C 27.00, H 6.80, Nd 27.0; found: C 26.81, H 6.54, Nd 26.5. – **5**: Calcd for $C_{14}H_{42}Ga_3LaN_2$: C 28.67, H 7.22, N 4.78, La 23.7; found: C 27.16, H 7.00, N 4.82, La 21.8.

Received: February 3, 1994 [Z 6666 IE]
German version: *Angew. Chem.* **1994**, *106*, 1725

[1] a) D. C. Bradley, R. C. Mehrotra, D. P. Gaur, *Metal Alkoxides*, Academic Press, London, **1978**; b) M. F. Lappert, P. P. Power, A. R. Sanger, R. C. Srivastava, *Metal And Metalloid Amides*, Ellis Horwood, Chichester, **1980**.
[2] a) H. Schumann, J. Pickardt, N. Bruncks, *Angew. Chem.* **1981**, *93*, 127; *Angew. Chem. Int. Ed. Engl.* **1981**, *20*, 120; b) H. Schumann, J. Müller, N. Bruncks, H. Lauke, J. Pickardt, *Organometallics* **1984**, *3*, 69; c) H. Schumann, H. Lauke, E. Hahn, J. Pickardt, *J. Organomet. Chem.* **1984**, *263*, 29.
[3] M. Bruzzone in *Fundamental and Technological Aspects of Organo-f-Element Chemistry* (Eds.: T. J. Marks, I. L. Fragalà), Reidel, Dordrecht, **1985**, p. 387.
[4] H. D. Kaesz, R. S. Williams, R. F. Hicks, J. I. Zink, Y.-J. Chen, H.-J. Müller, Z. Xue, D. Xu, D. K. Shuh, Y. K. Kim, *New J. Chem.* **1990**, *14*, 527.
[5] Few gallium lanthanide compounds have been reported. M. A. Busch, R. Harlow, P. L. Watson, *Inorg. Chim. Acta* **1987**, *140*, 15.
[6] J. Holton, M. F. Lappert, D. G. H. Ballard, R. Pearce, J. L. Atwood, W. E. Hunter, *J. Chem. Soc. Dalton Trans.* **1979**, 45.
[7] J. M. Boncella, R. A. Andersen, *Organometallics* **1985**, *4*, 205.
[8] a) W. J. Evans, L. R. Chamberlain, J. W. Ziller, *J. Am. Chem. Soc.* **1987**, *109*, 7209; b) W. J. Evans, L. R. Chamberlain, T. A. Ulibarri, J. W. Ziller, *ibid.* **1988**, *110*, 6423.
[9] W. J. Evans, T. J. Boyle, J. W. Ziller, *J. Am. Chem. Soc.* **1993**, *115*, 5084.
[10] W. J. Evans, T. J. Boyle, J. W. Ziller, *J. Organomet. Chem.* **1993**, *462*, 141.
[11] a) The compounds $[Me_2NMMe_2]_2$ [11 b, c] were identified by mass spectrometry and ^1H NMR and IR spectroscopy; b) O. T. Beachley, G. E. Coates, G. Kohnstam, *J. Chem. Soc.* **1965**, 3248; c) H. Hess, A. Hinderer, S. Steinhauser, *Z. Anorg. Allg. Chem.* **1970**, *377*, 1; d) B. A. Amero, E. P. Schram, *Inorg. Chem.* **1976**, *15*, 2842; e) L. K. Krannich, C. L. Watkins, D. K. Srivastava, *Polyhedron* **1990**, *9*, 289.
[12] a) The complexes **2** crystallize from hexane in the monoclinic space group *C2/c*. **2a** (−110 °C): a = 16.437(4), b = 11.194(2), c = 15.219(3) Å, β = 116.38(2)°, V = 2508.8(10) Å^3, ρ_{calcd} = 1.304 gcm^{-3} for Z = 4; 2743 reflections ($I \geq 4\,\sigma(I)$), R_F = 0.037. – **2b** (−110 C): a = 16.215(3), c = 11.2890(10), C = 15.221(2) Å, β = 116.760(10)°, V = 2487.8(6) Å^3, ρ_{calcd} = 1.537 g cm^{-3} for Z = 4; 3167 reflections ($I \geq 4.0\,\sigma(I)$), R_F = 0.061. Both molecules lie on a twofold axis and are disordered. b) Further details of the crystal structure investigations may be obtained from the Fachinformationszentrum Karlsruhe, D-76344 Eggenstein-Leopoldshafen (FRG), on quoting the depository number CSD-58236. c) The SmGa analogue was prepared similarly and is isostructural with **2a** and **2b**.
[13] a) R. A. Fischer, J. Behm, T. Priermeier, W. Scherer, *Angew. Chem.* **1993**, *105*, 776; *Angew. Chem. Int. Ed. Engl.* **1993**, *32*, 746; b) G. Erker, M. Albrecht, C. Krüger, S. Werner, *J. Am. Chem. Soc.* **1992**, *114*, 8531.
[14] W. A. Herrmann, R. Anwander, F. C. Munck, W. Scherer, V. Dufaud, N. W. Huber, G. R. J. Artus, *Z. Naturforsch. B*, in press.
[15] J. E. Cosgriff, G. B. Deacon, B. M. Gatehouse, H. Hemling, H. Schumann, *Angew. Chem.* **1993**, *105*, 906; *Angew. Chem. Int. Ed. Engl.* **1993**, *32*, 874.
[16] H. Heijden, C. J. Schaverien, A. G. Orpen, *Organometallics* **1989**, *8*, 255.
[17] a) C. Elschenbroich, A. Salzer, *Organometallics*, VCH, Weinheim, **1992**; b) J. L. Atwood, G. D. Stucky, *J. Am. Chem. Soc.* **1969**, *91*, 2538; c) R. L. Gerteis, R. E. Dickerson, T. L. Brown, *Inorg. Chem.* **1964**, *3*, 872.
[18] S. K. Boocock, S. G. Shore in *Comprehensive Organometallic Chemistry*, *Vol. 6*, (Eds.: G. Wilkinson, F. G. A. Stone, E. W. Abel), **1982**, Chap. 41.2, p. 947.
[19] **3** crystallizes from hexane in tetragonal the space group $I4_1/a$ with (T = −110 °C) a = 17.665(2), c = 26.652(4) Å, Z = 16, V = 8317(2) Å^3, ρ_{calcd} = 1.705 gcm^{-3}, $F(000)$ = 4176; 3538 reflections ($|F_0| > 4.0\,\sigma(|F_0|)$), R_1 = 0.056 [12 b].
[20] L. Pauling, *The Nature of the Chemical Bond*, 3rd ed., Cornell University Press, Ithaca, NY, **1960**.
[21] R. D. Shannon, *Acta Crystallogr. Sect. A* **1976**, *32*, 751.
[22] Q. Shen, Y. Cheng, Y. Lin, *J. Organomet. Chem.* **1991**, *419*, 293.
[23] a) G. Jeske, H. Lauke, H. Mauermann, P. N. Swepston, H. Schumann, T. J. Marks, *J. Am. Chem. Soc.* **1985**, *107*, 8091; b) G. Jeske, L. E. Schock, P. N. Swepston, H. Schumann, T. J. Marks, *ibid.* **1985**, *107*, 8103.

[24] **5** crystallizes from hexane in the space group $P\bar{1}$ with ($T = -110$ C) $a = 7.976(3)$, $b = 10.590(4)$, $c = 14.414(5)$ Å, $\alpha = 84.87(3)$, $\beta = 84.46(3)$, $\gamma = 86.69(3)°$, $Z = 2$, $V = 1205.5(7)$ Å^3, $\rho_{calcd} = 1.616$ g cm^{-3}, $F(000) = 5444$; 5179 reflections ($|F_o| > 3.0\,\sigma(|F_o|)$), $R_F = 0.044$.

[25] H. H. Karsch, A. Appelt, G. Müller, *Angew. Chem.* **1986**, *98*, 832; *Angew. Chem. Int. Ed. Engl.* **1986**, *25*, 823.

[26] P. B. Hitchcock, M. F. Lappert, R. G. Smith, R. A. Bartlett, P. P. Power, *J. Chem. Soc. Chem. Commun.* **1988**, 1007.

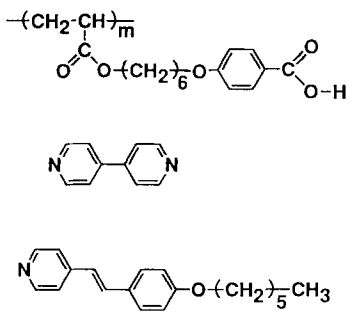
[27] a) D. C. Bradley, J. S. Ghotra, F. A. Hart, M. B. Hursthouse, P. R. Raithby, *J. Chem. Soc. Dalton Trans.* **1977**, 1166; b) M. R. Gagne, C. L. Stern, T. J. Marks, *J. Am. Chem. Soc.* **1992**, *114*, 275.

A Liquid-Crystalline Polymer Network Built by Molecular Self-Assembly through Intermolecular Hydrogen Bonding**

Takashi Kato,* Hideyuki Kihara, Uday Kumar, Toshiyuki Uryu, and Jean M. J. Fréchet*

The use of noncovalent interactions such as hydrogen bonds for materials design has attracted much attention.[1] Mesogenic structures can be obtained by self-assembly of two different components by means of selective hydrogen bond formation.[2-5] This concept has been extended to side-chain[3] and main-chain[4, 5] liquid-crystalline polymers.

We demonstrate here that a mesogenic three-dimensional network can be constructed by self-assembly through noncovalent interactions. Hydrogen-bonded cross-linked polymers were prepared by complexation of a polyacrylate (**1**) containing a benzoic acid moiety (H-bond donor) with various ratios of bifunctional 4,4′-bipyridine (**2**) and the monofunctional stilbazole **3** as



1

2

3

H-bond acceptors.[6] Compound **2** is capable of recognizing and binding carboxylic acid fragments of the polymer at each of its pyridyl ends and functions as a cross-linker. The hydrogen-bonded complexes were prepared by the evaporation method,[2, 3] and the stoichiometry of the H-bond donor and H-bond acceptors was maintained. For the ternary complex of **1**, **2**, and **3**, a mixture of H-bond acceptors (x/2 mol of **2** corresponding to x mol of the pyridyl unit, and y mol of **3**) was complexed with an amount of **1** containing $x + y$ mol of the H-bond donor moiety. The mol fraction of the pyridyl moiety of **2** relative to the all of the pyridyl units in the complex is represented as $\bar{x} = x/(x + y)$.

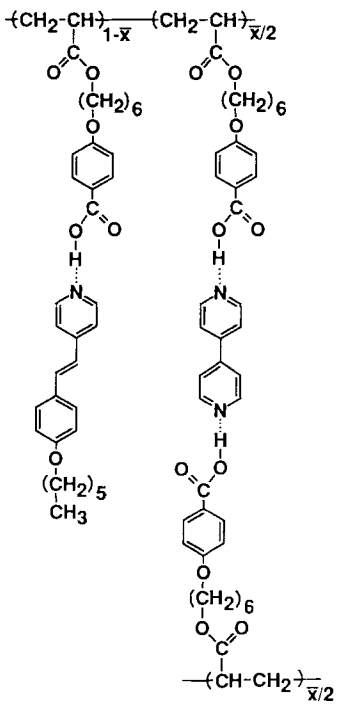


Fig. 1. Proposed molecular structure of the polymeric complex consisting of **1**, **2**, and **3**.

The proposed structure of the hydrogen-bonded 1:1 complex (containing an equimolar amount of H-bond donor and acceptor) prepared from H-bond donor polymer **1** and H-bond acceptors **2** and **3** is shown in Figure 1. The self-assembly of a cross-linked mesogen for the polymeric networks was expected.

Differential Scanning Calorimetry (DSC) thermograms of the polymeric complexes containing various ratios of **2** and **3** on heating scans are shown in Figure 2. Plots of transition temperatures of the polymeric complexes against $\bar{x}$, the mol fraction of pyridyl units of **2** in the mixture of **2** and **3**, are shown in Figure 3. The 1:1 complex of **1** and **3** behaves like a side-chain liquid-crystalline polymer[3d, 7] and exhibits

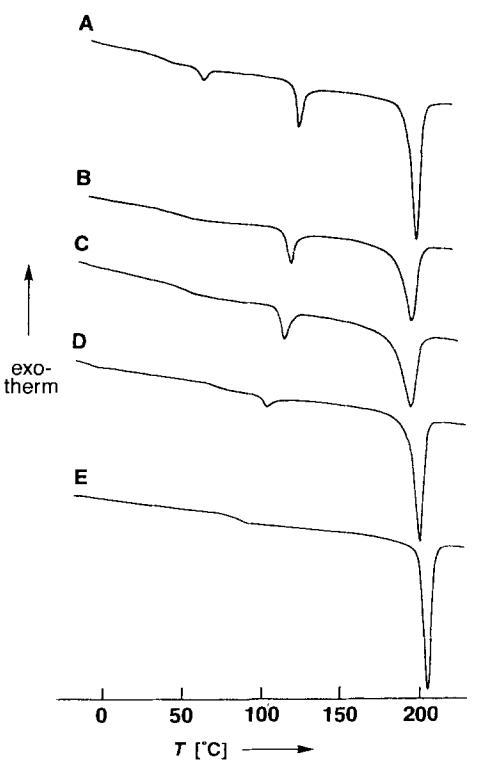


Fig. 2. DSC thermograms of polymeric complexes: A: $\bar{x} = 0$; B: $\bar{x} = 0.3$; C: $\bar{x} = 0.5$; D: $\bar{x} = 0.7$; E: $\bar{x} = 1.0$.

[*] Dr. T. Kato, H. Kihara, Prof. T. Uryu
Institute of Industrial Science, The University of Tokyo
Roppongi, Minato-ku, Tokyo 106 (Japan)
Telefax: Int. code + (3)3402-6350
Prof. J. M. J. Fréchet, Dr. U. Kumar
Department of Chemistry, Baker Laboratory, Cornell University
Ithaca, NY 14853-1301 (USA)

[**] This work was supported by the Asahi Glass Foundation and the National Science Foundation (DMR 91 21654). We thank Dr. S. Ujiie and Prof. K. Iimura for the X-ray measurements and helpful discussions.

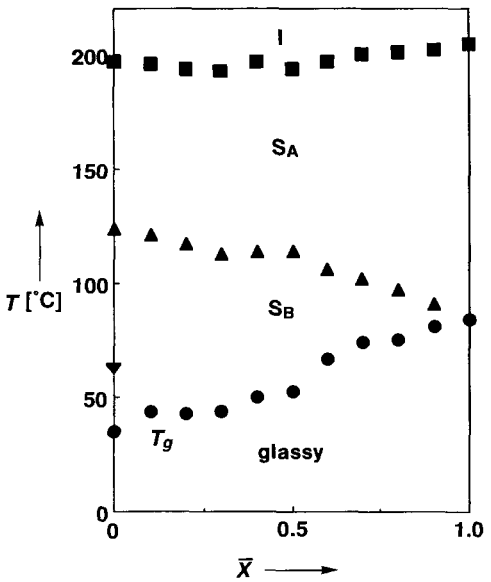


Fig. 3. Phase diagram of the polymeric complexes of **1** and mixtures of **2** and **3**.

and exhibits a smectic A phase from 124 to 197 °C (Fig. 2, curve A; Fig. 3, $\bar{x} = 0$). The enthalpy change of the smectic–isotropic transition is 20.2 $J\,g^{-1}$.

As the proportion of **2** in the polymeric complex increases, the glass transition temperature increases. Liquid-crystalline behavior is observed up to about 200 °C for the complexes in the whole composition range of the H-bond acceptor mixture. For example, the polymeric complex having a larger fraction of the cross-linking H-bond acceptor (Fig. 2, curve D; Fig. 3, $\bar{x} = 0.7$) shows smectic phases from 74 to 200 °C.

It is noteworthy that the binary 1:1 complex of **1** and **2** (Fig. 2, curve E; Fig. 3, $\bar{x} = 1.0$) exhibits a smectic phase up to 205 °C. The melt of the complex of **1** and **2** is viscous but shows shear flow between glass plates. The enthalpy change on transition to the isotropic phase on heating is 24.9 $J\,g^{-1}$. The smectic–isotropic transition occurs reversibly for these complexes. A focal conic fan texture develops when the complex is cooled from an isotropic phase. The X-ray diffraction pattern for the mesophase at 170 °C consists of one sharp inner peak at 39.8 Å and one diffused halo at 4.5 Å. The length of the fully stretched conformation between two polymer backbones that form the complex with **2** is estimated to be 41 Å by molecular modeling. These results indicate that the network complex retains a smectic A phase structure as shown in Figure 4. The phase transition curves change continuously as the proportion of the bifunctional moiety increases (Fig. 3). This phase diagram also supports the finding that the noncovalently cross-linked complex consisting of only **1** and **2** exhibits a smectic A phase. The X-ray diffraction pattern for the complex of $\bar{x} = 0.5$ at 70 °C above the glass transition temperature shows only two sharp reflections at 38.7 and 4.2 Å, which suggests the existence of a liquid-crystalline smectic B phase.[8] One sharp inner peak at 38.7 Å and one broad halo at 4.4 Å are observed when the sample forms a smectic A phase at 140 °C. The layer spacing is constant in the two mesophases for this sample.

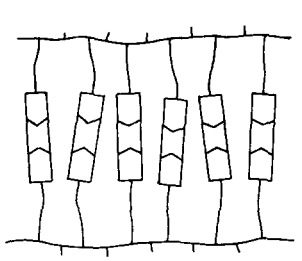


Fig. 4. Schematic illustration of the liquid-crystalline network structure formed by self-assembly of **1** and **2**. The rectangles in the middle made up of three components represent the hydrogen-bonded mesogenic unit.

In the self-assembled structure shown in Figure 4 liquid crystallinity is induced by the interaction between the pyridyl units of **2** and two benzoic acid moieties of **1**, which results in the formation of the hydrogen-bonded intermolecular mesogen. Moreover, the dynamic nature of the hydrogen bonding of the mesogen should contribute to the induction of a fluid mesomorphic phase and the reversibility of the cross-linking. When the sample is heated to the isotropic state, some of the hydrogen bonds between the carboxylic acid and bipyridyl moieties should break to form a disordered state. Upon cooling from the isotropic state, the intermolecular hydrogen bonds form again, which results in the smectic A phase.

Covalently cross-linked network based on liquid-crystalline polymers have been reported previously[9] for side-chain and main-chain polymers. In the case of the polymer containing a high density of covalent cross-links, molecular orientations were preserved in the solid state and no thermotropic liquid-crystalline behavior was observed for the polymers.[9]

The formation of a hydrogen-bonded mesogen in the polymer side-chain was first reported by Blumstein et al.[10] Solid-state mesomorphic order was observed for poly[(*p*-acryloyloxy)benzoic acid] and poly[(*p*-methacryloyloxy)benzoic acid] owing to the formation of a benzoic acid dimer. However, these H-bonded polymers did not show a liquid-crystalline state because of the lack of flexibility resulting from the absence of methylene spacers.

The system reported here is a novel polymeric network that exhibits liquid-crystalline behavior by self-assembly of polymers and small molecules by means of noncovalent interactions.

Received: January 8, 1994 [Z 6605 IE]
German version: *Angew. Chem.* **1994**, *106*, 1728

[1] For example: J.-M. Lehn, *Angew. Chem.* **1990**, *102*, 1347; *Angew. Chem. Int. Ed. Engl.* **1990**, *29*, 1304; M. C. Etter, G. M. Frankenbach, *Chem. Mater.* **1989**, *1*, 10.

[2] T. Kato, J. M. J. Fréchet, *J. Am. Chem. Soc.* **1989**, *111*, 8533; T. Kato, A. Fujishima, J. M. J. Fréchet, *Chem. Lett.* **1990**, 919; M. Fukumasa, T. Kato, T. Uryu, J. M. J. Fréchet, *ibid.* **1993**, 65; T. Kato, T. Uryu, F. Kaneuchi, C. Jin, J. M. J. Fréchet, *Liq. Cryst.* **1993**, *14*, 1311; T. Kato, J. M. J. Fréchet, P. G. Wilson, T. Saito, T. Uryu, A. Fujishima, F. Kaneuchi, C. Jin, *Chem. Mater.* **1993**, *5*, 1094; T. Kato, H. Kihara, T. Uryu, S. Ujiie, K. Iimura, J. M. J. Fréchet, U. Kumar, *Ferroelectrics*, **1993**, *148*, 161.

[3] a) T. Kato, J. M. J. Fréchet, *Macromolecules* **1989**, *22*, 3818; b) U. Kumar, T. Kato, J. M. J. Fréchet, *J. Am. Chem. Soc.* **1992**, *114*, 6630; c) U. Kumar, J. M. J. Fréchet, T. Kato, S. Ujiie, K. Iimura, *Angew. Chem.* **1992**, *104*, 1545; *Angew. Chem. Int. Ed. Engl.* **1992**, *31*, 1531; d) T. Kato, H. Kihara, T. Uryu, A. Fujishima, J. M. J. Fréchet, *Macromolecules* **1992**, *25*, 6836.

[4] M.-J. Brienne, J. Gabard, J.-M. Lehn, I. Stibor, *J. Chem. Soc. Chem. Commun.* **1989**, 1868; C. Fouquey, J.-M. Lehn, A.-M. Levelut, *Adv. Mater.* **1990**, *2*, 254; J.-M. Lehn, *Makromol. Chem. Makromol. Symp.* **1993**, *69*, 1.

[5] C. Alexander, C. P. Jariwala, C.-M. Lee, A. C. Griffin, *Polym. Prep. Am. Chem. Soc. Div. Polym. Chem.* **1993**, *34*(1), 168.

[6] The synthesis and characterization of polyacrylate **1** and stilbazole **3** are described in ref.[3d].

[7] In a previous paper [3d] we reported that the 1:1 polymeric complex of **1** and **3** showed a crystal melting at 124 °C. However, a further X-ray diffraction study has suggested that the complex forms an ordered smectic phase from 35 to 64 °C and a subsequent smectic B phase up to 124 °C. The details of these investigations will be reported elsewhere.

[8] G. W. Gray, J. W. Goodby, *Smectic Liquid Crystals*, Leonard Hill, Glasgow, 1984, p. 23.

[9] For example: J. Kupfer, H. Finkelman, *Makromol. Chem. Rapid Commun.* **1991**, *12*, 717; D. J. Broer, J. Boven, G. N. Mol, G. Challa, *Makromol. Chem.* **1989**, *190*, 2255; G. G. Barclay, C. K. Ober, K. I. Papathomas, D. W. Wang, *J. Polym. Sci. Part A: Polym. Chem.* **1992**, *30*, 1831; T. Uryu, K. Sato, T. Kato, *Polym. Prep. Jpn.* **1988**, *37*, 217.

[10] A. Blumstein, S. B. Clough, L. Patel, R. B. Blumstein, E. C. Hsu, *Macromolecules* **1976**, *9*, 243.

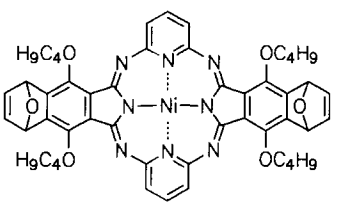
Ladder Polymers and Oligomers Based on Hemiporphyrazine**

Michael Rack and Michael Hanack*

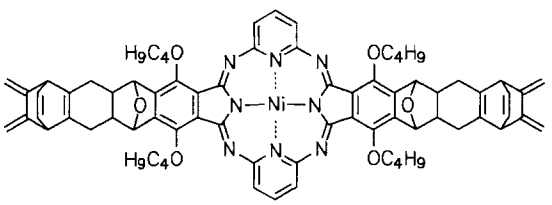
Conjugated polymers with ladder structure have received increasing attention over the last several years, as topics of both preparative and theoretical studies.[1] These structures are expected to have interesting electronic, optical, and magnetic properties. Repetitive Diels–Alder reactions have proved effective for synthesizing this type of polymer as well as its precursors.[2] The dienophilic and enophilic monomers used to date do not contain metallomacrocycles as structural fragments.[3]

Ladder polymers that contain phthalocyanines as stabilizing units are not easily accessible, because an unsymmetrically substituted phthalocyanine is required for their preparation.[4] Hemiporphyrazinatometal(II) compounds[5] that have D_{2h} symmetry are easier to synthesize. With appropriate peripheral substitution one can obtain monomer precursors with good solubility, which can in turn be converted to ladder polymers.

We report on the synthesis of oligomers **5**–**9** (Scheme 1) using repetitive Diels–Alder reactions at standard pressure based on the hemiporphyrazinatonickel(II) compounds **1** and **2**[6] and pentaene **3**[7] (C_4H_9 = *n*-butyl).



1



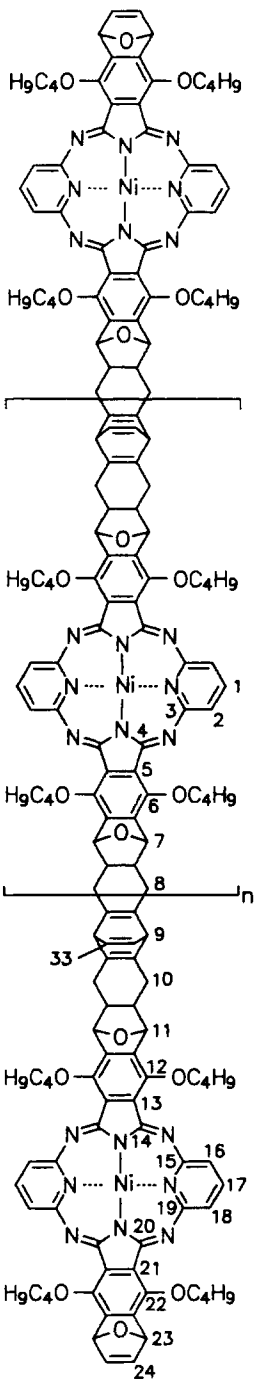
2



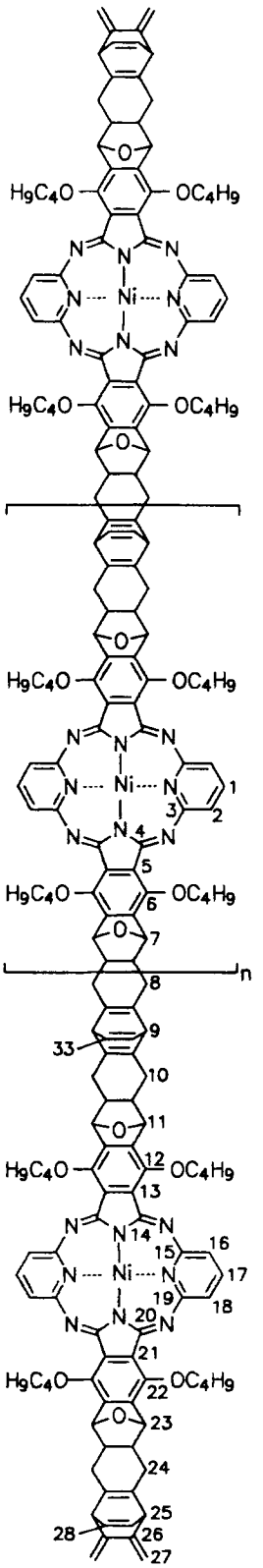
3

We first heated the dienophilic hemiporphyrazine **1** (*syn, anti*) with an equimolar amount of the enophilic hemiporphyrazine **2** (*syn, anti*)[6] in refluxing toluene for seven days. (The notation *syn* and *anti* denotes the position of the oxygen bridges in **1** and **2**.) This reaction yielded a solid that is practically insoluble in typical organic solvents. The ^{13}C-CP/MAS NMR spectrum in Figure 1 shows characteristic signals consistent with the structure of polymer **4**.

The insolubility of **4** made it impossible to determine its molecular weight distribution. This fact, combined with the lack of spectroscopic data for the polymer, led us to conduct a systematic synthesis of model oligomers in order to characterize **4** by spectroscopy. In addition, the solubility limit of the oligomers was determined in stepwise fashion, in order to obtain



4 (n ≥ 7)
5 (n = 1)
7 (n = 3)
9 (n = 5)



6 (n = 1)
8 (n = 3)

[*] Prof. Dr. M. Hanack, Dipl.-Chem. M. Rack
Institut für Organische Chemie
Lehrstuhl für Organische Chemie II der Universität
Auf der Morgenstelle 18, D-72076 Tübingen (FRG)
Telefax: Int. code + (7071)29-5244

[**] This research was supported by the Bundesministerium für Forschung und Technologie (Projekt Nr. 03M4045-8) and BASF AG. We thank Dr. C. Maichle-Mössmer and Dr. R. Schlichenmaier, Institut für Anorganische Chemie der Universität Tübingen, for conducting the crystal structure analysis, Dipl.-Chem. K. Schmeer, Institut für Organische Chemie der Universität Tübingen, for obtaining the ion spray mass spectra, and Dr. D. Waidelich, GSG Mess- und Analysengeräte Vertriebsgesellschaft mbH, Karlsruhe, for obtaining the laser desorption mass spectra.

information about the number of repeat units in **4**. To achieve these objectives, we used a two-step reaction starting with compounds **1**, **2**, and **3** to synthesize the trimers **5** and **6**, the pentamers **7** and **8**, and the heptamer **9** (Scheme 1). All oligomers were fully characterized by spectroscopic methods.[8]

2.5 **1** + **2** $\xrightarrow{73\%}$ **5** (n = 1)

2.5 **3** + **5** $\xrightarrow{80\%}$ **6** (n = 1)

2.5 **2** + **6** $\xrightarrow{65\%}$ **7** (n = 3)

2.5 **3** + **7** (n = 3) $\xrightarrow{81\%}$ **8** (n = 3)

2.5 **1** + **8** (n = 3) $\xrightarrow{36\%}$ **9** (n = 5)

Scheme 1. Synthesis scheme for oligomers **5**–**9**.

The trimer **5** was obtained by reaction of **1** (*syn, anti*) and **2** (*syn, anti*) (molar ratio 2.5:1) in refluxing toluene over seven days. The workup was accomplished by precipitation followed by chromatography on neutral alumina/5% H_2O (CH_2Cl_2/MeOH 20:1), to give **5** in 73% yield (see Scheme 1).[9] Trimer **6** was obtained by treating **5** with pentaene **3** (molar ratio 1:2.5) in refluxing toluene for 48 h. The crude product was purified by the same procedures as in the preparation of trimer **5**. Synthesis of the higher molecular weight oligomers **7**, **8**, and **9** was carried out analogously as for compounds **5** and **6** (see Scheme 1).[10] All oligomers are readily soluble in CH_2Cl_2 and $CHCl_3$ and exhibit nearly identical ^1H and ^{13}C NMR spectra. The ^{13}C NMR spectra of **5**, **7**, and **9** are depicted in Figure 1 (see the formulas for the numbering of the carbon atoms). Signals at $\delta = 80.7$ (C-23) and 142.5 (C-24) are attributed to the end groups, while the macrocyclic groups give rise to signals at $\delta = 158.5$ (C-4, 20), 155.7 (C-3, 19), 120.1 (C-2, 16, 18), and 139.7 (C-1, 17). The signals for the ladder-type structure fragments occur at $\delta = 31$ (C-8, 10), 42 (C-7a, 10a), 56.2 (C-9), and 82.7–83.8 (C-7, 11). The vinylene bridging atoms (C-33) yield the signal at $\delta = 139.8$.

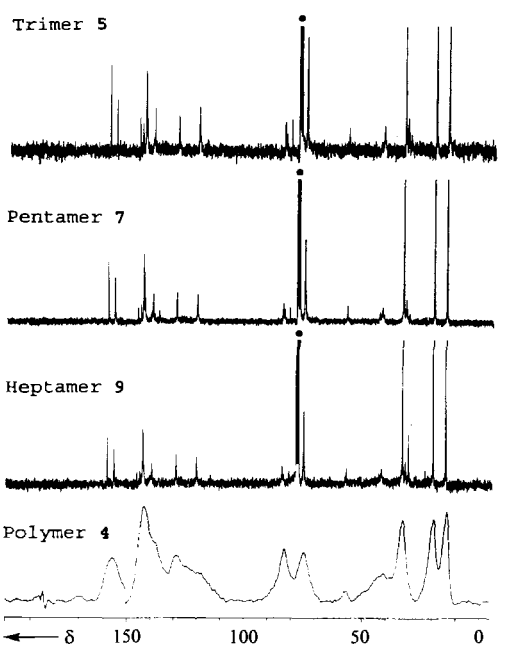


Fig. 1. ^{13}C NMR spectra of **5**, **7**, and **9**, 62.9 MHz, $CDCl_3$; •: signal from $CDCl_3$; ^{13}C CP/MAS NMR spectrum of polymer **4**.

The ^{13}C NMR spectra of **6** and **8** show characteristic peaks at $\delta = 41.9$–42.5 (C-23a), 53.3–53.5 (C-25), 101.4 (C-27), and 137.2 (C-24a) originating from the diene end groups. The positions of the signals for the carbon atoms of the macrocyclic moiety as well as the ladder-type structure fragments correspond to those observed for oligomers **5**, **7**, and **9**. The ^1H NMR spectra of oligomers **5**–**9** exhibit the expected signals.

The molecular weights of oligomers **5**–**9** were determined by ion spray and laser desorption mass spectrometry (LD-MS). For oligomers **5** and **6** molar masses of 3064.7 (calculated: 3065.3) and 3378.0 (calculated: 3377.8), respectively, were determined by the ion spray method.[11] The LD-MS method for determining the molecular weights of oligomers **7**–**9** yielded the following values: pentamer **7**: 5208.1 (calculated: 5213.1), pentamer **8**: 5526 (calculated: 5526), and heptamer **9**: 7393 (calculated 7361).

Oligomers **5**–**9** exhibit differences in their IR spectra only in the fingerprint region from 600 to 900 cm^{-1}. For oligomers **6** and **8** with diene end groups, a band at $\nu = 655$ cm^{-1} appears, whereas no absorption is observed in this region for oligomers **5**, **7**, and **9**. Oligomer **4** also shows no IR absorption at 655 cm^{-1}, which leads to the conclusion that its end groups are epoxynaphthalene fragments.

The ^{13}C CP/MAS NMR spectrum of polymer **4** is in agreement with the high-resolution ^{13}C NMR spectra of oligomers **5**, **7**, and **9** (Fig. 1), which provides additional support for the epoxynaphthalene end groups in **4**.

Oligomers **5**–**9** are formed as mixtures of isomers on account of the mixtures of *syn, anti* isomers of **1** and **2** employed, and the possible stereoisomers that form in Diels–Alder reactions. The NMR spectra of **5**–**9** therefore contain multiple peaks that are difficult to assign to the individual isomers. In order to obtain products with fewer isomers, **1** was treated with thin-layer chromatography on neutral alumina (eluting with CH_2Cl_2/MeOH 250:1), and **2** was subjected to column chromatography on alumina (eluting with ethyl acetate/hexane 1:3). Following separation of the *syn* and *anti* isomers, *anti*-**1** and *anti*-**2** were converted to trimer **5** (hereafter denoted as *anti*-**5**).[13]

The two configurational isomers of **1** cannot be distinguished by NMR spectroscopy. Therefore, an X-ray structure analysis of the bispyridine complex of *anti*-**1** was performed (Fig. 2).[14] Because the rings are rotating, only the average electron density distribution of the pyridine rings is shown in Figure 2.[15]

The two-configurational isomers of **2** could be distinguished by NMR spectroscopy.[16] As expected, the ^1H and ^{13}C NMR spectra of the *anti*-**5** trimer provides better resolution. Despite

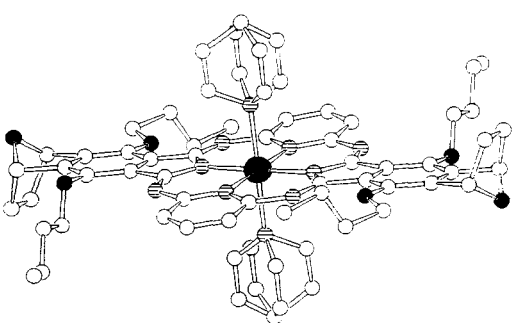
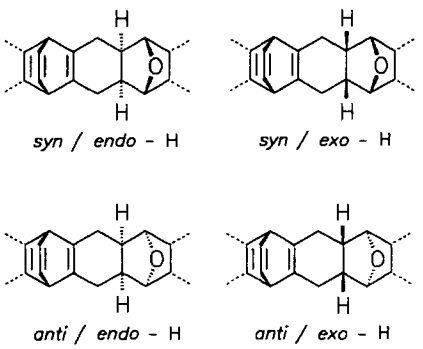


Fig. 2. Crystal structure of the bispyridine complex of *anti*-**1** [15].

 © VCH Verlagsgesellschaft mbH, D-69451 Weinheim, 1994 0570-0833/94/1515-1647 $ 10.00+.25/0

the use of the stereochemically pure compounds *anti*-**1** and *anti*-**2**, a large number of stereoisomers of *anti*-**5** are possible. These isomers are only in part due to the *exo*/*endo* attack that occurs in the Diels–Alder reaction. In our case, the adducts are solely bicyclic compounds, with possible formation of the isomers shown in Scheme 2. Here the *syn* and *anti* designations indicate the relative positions of the oxygen and vinylene bridges.



Scheme 2. Possible stereoisomers formed in the Diels–Alder reaction of bicyclic enophile **2** and dienophile **1**.

In comparable cycloaddition reactions the primary products obtained are solely the *syn*/*endo*-H isomers.[17] In our case, only a single isomer of *anti*-**5** should therefore be obtained; however, there are more peaks in the NMR spectra of *anti*-**5** than would be expected from a single isomer. Based on the signal doubling in the ^{13}C NMR spectrum of *anti*-**5**, we conclude that at least two isomers are formed. Determination of the exact structure of these isomers would require that they be separated, crystallized, and subjected to X-ray structure analysis. For the exact assignment of the ^{13}C NMR signals of *anti*-**5**, C/H-COSY and C/H-correlated long range coupled NMR spectra were obtained.[18]

We are presently working on aromatization procedures for the oligomers described here.

Experimental Procedure

5: 150 mg (0.16 mmol) of **1** and 80 mg (0.07 mmol) of **2** were dissolved in 20 mL of toluene and stirred 7 d under reflux. After the reaction mixture had cooled, the toluene was removed under vacuum. The green residue was taken up in a small amount of CH_2Cl_2, precipitated by addition of hexane, and centrifuged. This process was repeated twice in order to remove residual **1** and **2**. Further purification was accomplished by column chromatography on alumina (deactivated with 5% H_2O) eluting with $CHCl_3$. After chromatographic purification the compound was again precipitated in CH_2Cl_2/hexane and dried under vacuum at 75 °C. Compound **5** was obtained as an olive-green powder (145 mg, 73%).

6: 80 mg (0.26 μmol) of **5** and 12 mg (77 μmol) of **3** were dissolved in 10 mL of toluene and stirred 48 h under reflux. The workup proceeded analogously as in the preparation of **5**. Compound **6** was obtained as an olive-green powder (70 mg, 87%).

7–**9**: Reaction and workup were analogous to those described for **5** and **6**, with yields of 65, 81, and 36%, respectively.

4: Reaction procedure identical to that for **5**, except that equimolar amounts of **1** and **2** were used. Purification was possible by continuous extraction with CH_2Cl_2, after which the solvent was removed under vacuum.

Received: March 3, 1994 [Z 6725 IE]
German version: *Angew. Chem.* **1994**, *106*, 1712

[1] S. Kivelson, O. L. Chapman, *Phys. Rev. B: Condens, Matter* **1983**, *28*, 7263; J. L. Bredas, R. H. Baughman, *J. Chem. Phys.* **1985**, *83*, 1316–1322; A. K. Bakhshi, J. Ladik, *Synth. Met.* **1989**, *30*, 115–121; P. Gomez-Romero, Y.-S. Lee, M. Kertezs, *Inorg. Chem.* **1988**, *27*, 3672–3675; K. Müllen, *Pure Appl. Chem.* **1993**, *65* (1), 89–96.

[2] J. K. Stille, K. Plummer, *J. Org. Chem.* **1961**, *26*, 4026–4029; M. Wagner, W. Wohlfahrt, K. Müllen, *Chimia* **1988**, *42*, 377–379; A. D. Schlüter, *Nachr. Chem. Tech. Lab.* **1990**, *38*, 8–13; W. Christophel, L. C. Miller, *J. Org. Chem.* **1986**, *51*, 4160–4175.

[3] S. Wegener, K. Müllen, *Chem. Ber.* **1991**, *124*, 2101–2103; *Macromolecules* **1993**, *26*, 3037–3040; T. Horn, K. Müllen, *ibid.* **1993**, *26*, 3472–3475.

[4] H. Schultz, H. Lehmann, M. Rein, M. Hanack, *Struct. Bonding (Berlin)* **1991**, *74*, 41; C. Feucht, T. Linssen, M. Hanack, *Chem. Ber.* **1994**, *127*, 113–117.

[5] M. Hanack, K. Haberroth, M. Rack, *Chem. Ber.* **1993**, *126*, 1201–1204; A. Ferencz, R. Ries, G. Wegner, *Angew. Chem.* **1993**, *105*, 1251–1253; *Angew. Chem. Int. Ed. Engl.* **1993**, *32*, 1184–1187.

[6] M. Rack, M. Hanack, unpublished; M. Rack, Dissertation, Universität Tübingen, **1994**.

[7] R. Gabioud, P. Vogel, *Tetrahedron* **1980**, *36*, 149–154.

[8] The measured UV/VIS spectra of oligomers **5**–**9** are equivalent to those of the starting monomers **1** and **2**. Aggregation of **5**–**9** was not observed.

[9] In all reactions only a single product was obtained. The decrease in the yield can be attributed to the formation of higher molecular weight oligomers, which remain on the column during chromatographic purification.

[10] Formation of ring structures was not observed in any of the conversions. The direct reaction of the *syn* isomers of **1** and **2** (equimolar) at ambient pressure also did not lead to the formation of ring structures.

[11] Determination of the molar masses was conducted using an API III TAGA 6000E mass spectrometer from the company Sciex. Samples in MeOH/CH_2Cl_2 (1:1) were injected with an injection pump at a continuous flow rate of 5 μL min^{-1}.

[12] Molecular weights were determined by matrix-supported laser desorption mass spectrometry using a VESTEC Laser-Tec focus (BenchTop II) instrument. Measurement conditions: positive ion mode, 26 KV acceleration current; matrix: sinapic acid and 2,5-dihydroxybenzoic acid.

[13] Assuming ideal stereochemistry in the Diels–Alder reaction for *anti*-**5** (*syn*-*endo*-H), the molecule would have a length of approximately 6.3 nm.

[14] E. Agostinelli, D. Attanasio, I. Collamati, V. Fares, *Inorg. Chem.* **1984**, *23*, 1162–1165.

[15] X-ray structure data of *anti*-**1**: Enraf–Nonius CAD-4 diffractometer, room temperature, $Cu_{K\alpha}$ radiation, $\lambda = 1.5405$ Å, structure solution with SHELX 86; triclinic, space group $P\bar{1}$, $a = 9.324(1)$, $b = 12.381(2)$, $c = 12.720(2)$ Å, $\alpha = 72.90(1)$, $\beta = 73.92(1)$, $\gamma = 85.05(1)°$, $V = 1348.66$ Å^3, $Z = 2$, $\rho_{calcd} = 1.395$ g cm^{-3}, 6002 reflections of which 4878 with $I > 3\rho(I)$ were observed, $R = 0.055$, $R_w = 0.056$. Further details of the crystal structure investigation may be obtained from the Fachinformationszentrum Karlsruhe, D-76344 Eggenstein-Leopoldshafen (FRG), on quoting the depository number CSD-58252.

[16] Assignment of the two configurational isomers of **2** was verified by comparing the ^1H NMR spectra of *anti*-**2** and the product of the reaction of *anti*-**1** with **3**.

[17] P. R. Ashton, G. R. Brown, N. S. Isaacs, D. Giufrida, F. H. Kohnke, J. P. Mathias, A. M. Z. Slawin, D. R. Smith, J. F. Stoddart, D. J. Williams, *J. Am. Chem. Soc.* **1992**, *114*, 6330–6353.

[18] A. Bax, M. F. Summers, *J. Am. Chem. Soc.* **1986**, *108*, 2093–2094.

Biosynthetic Investigations on Pyridazomycin**

Heike Bockholt, John M. Beale, and Jürgen Rohr*

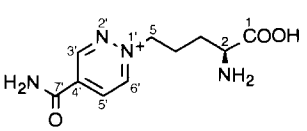
Dedicated to Professor Heinz G. Floss on the occasion of his 60th birthday

The antifungal antibiotic Pyridazomycin **1**, produced by the soil bacterium *Streptomyces violaceoniger* ssp. *griseofuscus* (strain Tü 2557), is the only natural product containing a pyridazine ring.[1] The biosyntheses of this unusual nitrogen heterocyclic compound is of interest because of the features of the

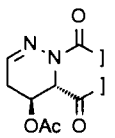
[*] Priv.-Doz. Dr. J. Rohr, Dr. H. Bockholt
Institut für Organische Chemie der Universität
Tammannstrasse 2, D-37077 Göttingen (FRG)
Telefax: Int. code + (551)39-9660
Prof. Dr. J. M. Beale
Institute for Medicinal and Natural Product Chemistry
College of Pharmacy, University of Texas,
Austin, TX, 78712 (USA)

[**] This work was supported by the Deutsche Forschungsgemeinschaft, the Fonds der Chemischen Industrie, and NATO.

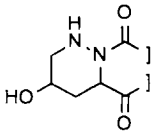
N–N bond and the amino acid side chain linked to a quaternary positively charged nitrogen atom. Structurally related compounds with partially or fully saturated pyridazine rings occur in biologically active cyclopeptides, for example the moiety **2** in luzopeptin A,[2] and piperazic acid (**3**) in citropeptin, himastatin, variapeptin, and others.[3] An N–N bond also appears in the pyrimidine nucleotide biosynthesis inhibitor pyrazofurin (**4**)[4] as well as in several noncyclic azoxy compounds, such as valanimycin (**5**).[5–9] Because of the N^+-bound side



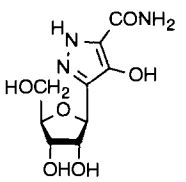
1



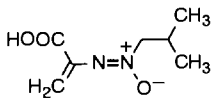
2



3



4

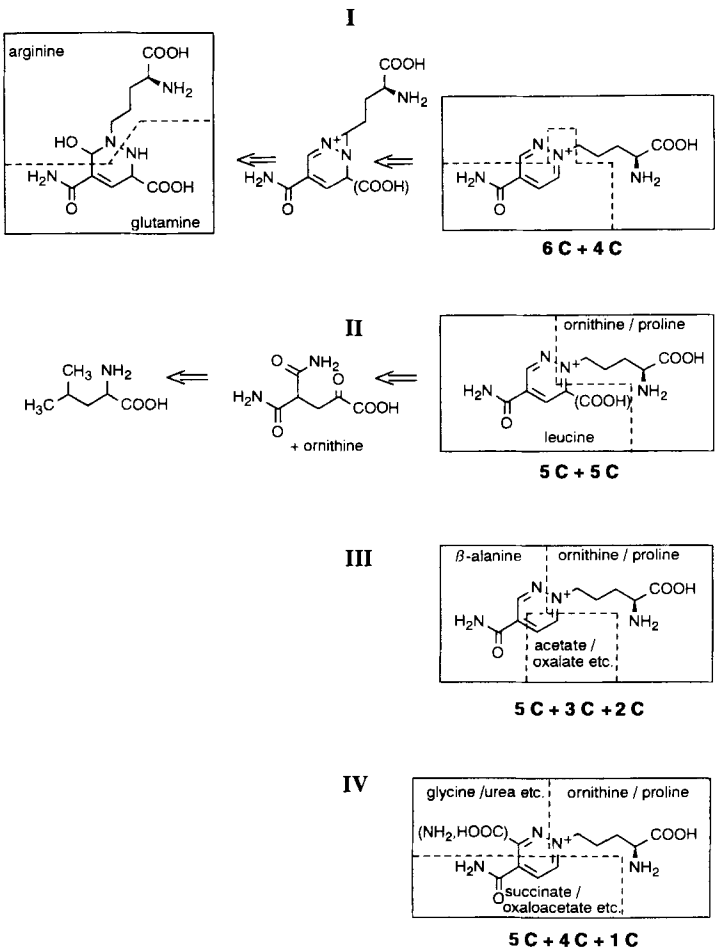


5

chain, **1** exhibits chemical lability at a pH >6.5, limiting chemical derivatization approaches to improve the biological activity. Thus, we expected to gain information from the biosynthetic studies which allowed selective biological derivatization approaches, such as precursor-directed biosynthesis.[10] Here we present the results of our initial feeding experiments from which emerges an interesting novel biosynthetic pathway of general significance.

For the biogenetic origin of all carbon and heteroatoms in pyridazomycin **1** from building blocks of the primary metabolism, four principal working hypotheses were considered, in which I and II each require two, and III and IV, three building blocks, preferably amino acids (Scheme 1). A seemingly insurmountable microbiological problem, namely the low production of pyridazomycin by *Streptomyces violaceoniger* of 0.75 mg L^{-1}, was solved by strain selection experiments, extensive studies of the fermentation process (using a 1 L-fermentor), and, in particular, by avoiding an alkaline pH during the isolation procedure.[11] This finally enabled us to isolate pyridazomycin **1** in amounts of 20–30 mg L^{-1}.

The above-mentioned four hypotheses were examined by a series of feeding experiments with stable, isotopically labeled precursors in such a way that basic information was made available quickly (Table 1). Feeding experiments with ^{13}C-labeled acetate (universal precursor of the intermediates of the citric acid cycle and putative direct precursor of the C_2 building block in hypothesis III) and [1,3-$^{13}C_2$]glycerol (universal precursor of the carbohydrate metabolism and of amino acids deriving from pyruvate, such as alanine, valine, or leucine) provided "scrambling", in other words unspecific, indirect enrichments of several carbon atoms of **1**, in particular C-4′, C-5′, C-6′, and C-7′. Both precursors are definitely not immediately incorporated.



Scheme 1. Hypothetical precursors I–IV of pyridazomycin **1**. The numbers refer to the remaining carbon atoms of a precursor in **1**.

The C_5 amino acid glutamic acid serves as a metabolic precursor of the four amino acids ornithine, glutamine, proline, and arginine, in other words it has also the characteristic of a general precursor.

The feeding experiment with [5-^{13}C]glutamic acid showed a weak, but significant ^{13}C enrichment in the C-5 position of the pyridazomycin side chain. Since C-7′ of the carboxamide side chain was not enriched, and consecutive feeding experiments

Table 1. Incorporation experiments on pyridazomycin **1** with *Streptomyces violaceoniger* [a].

Precursor	Specific incorporation [%][12]	Enrichment in positions
[1,2-$^{13}C_2$]acetate [b]	0.7–3.7	C-4′, C-5′, C-6′, C-7′
[1,3-$^{13}C_2$]glycerol [c]	0.5–0.9	C-4′, C-5′, C-6′, C-7′
[5-^{13}C]glutamic acid [d]	0.6	C-5
[5-^{13}C]ornithine [e]	10.4	C-5
[5-^{15}N]ornithine [f]		N-1′
[2-^{13}C]glycine [g]	9.8	C-3′
[2-^{13}C,^{15}N]glycine [h]	11.5	C-3′, N-2′

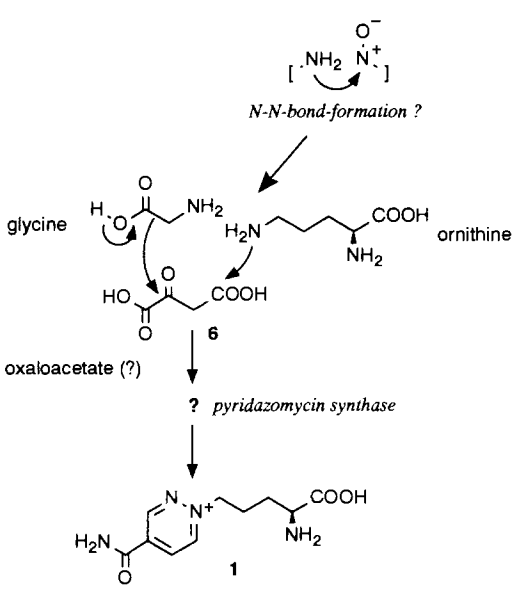
[a] Additionally, feeding experiments with [3-^{13}C]-β-alanine, L-[2-^{13}C]leucine, [1-^{13}C]glycine, D,L-[4-^{13}C]aspartic acid, [^{13}C]urea, [*S*-$^{13}CH_3$]methionine, L-[5-^{15}N]glutamine, [2-^{15}N]glutamine, and [2,3-$^{2}H_4$]succinic acid, respectively, did not result in the enrichment of any of the atoms of **1**; [b] 12.2 mmol (99% ^{13}C); [c] 2.7 mmol (50% ^{13}C); [d] 3.4 mmol (99% ^{13}C); [e] 5.9 mmol (99% ^{13}C); [f] 3.0 mmol (99% ^{15}N); due to poor yield, the only signal observable in the ^{15}N NMR spectrum is N-1′; [g] 6.7 mmol (99% ^{13}C); [h] 3.3 mmol (99% ^{13}C, 99% ^{15}N); $^1J(C,N) = 2.6$ Hz.

 © VCH Verlagsgesellschaft mbH, D-69451 Weinheim, 1994 0570-0833/94/1515-1649 $ 10.00+.25/0

with differently ^{15}N-labeled glutamine samples gave no incorporations, hypotheses I (or IV) for glutamine as one of the building blocks of the aromatic ring had to be rejected.

Feeding experiments with [5-^{13}C]- and [5-^{15}N]ornithine, however, confirmed the apparent idea that this amino acid serves directly as the immediate building block of the side chain. The former showed a significantly better incorporation than [5-^{13}C]glutamic acid. The ^{15}N NMR spectrum of **1** isolated after the experiment with [5-^{15}N]ornithine shows that the nitrogen atom N-1′ of the pyridazine ring derives directly from the 5-NH_2 group of this amino acid. These incorporation experiments along with several additional negative results (see Table 1, footnote [a]) finally ruled out the hypotheses I–III, thus, the [5C + 4C + 1C] hypothesis (IV) was favored and examined with regard to the C_1 pool. Within this phase of the studies a feeding experiment with [2-^{13}C]glycine (also useful as source of the tetrahydrofolic acid C_1-metabolism) gave a high specific incorporation (ca. 10%) into the expected position, namely C-3′ of **1**. Thus glycine is the second biosynthetic building block of pyridazomycin **1**. An additional feeding experiment with [2-^{13}C,^{15}N]glycine confirmed this conclusion and furthermore proved that N-2′ also derives from this amino acid (^{15}N NMR) and that the C–N bond of glycine remains intact, proven by the observed coupling ($^1J_{C,N}$ = 2.6 Hz) in the ^{13}C NMR spectrum of **1**. Since the feeding experiment with [1-^{13}C]glycine did not yield a ^{13}C-enriched sample of **1**, the origin of C-4′ from the carboxyl group of glycine was ruled out.

The results of the three feeding experiments with labeled glycine also allow a conclusion about the remaining building block of **1**: The incorporation of glycine is performed under decarboxylation, that is, under release of an electron pair. This requires an electrophilic carbon, preferably a carbonyl group, of the remaining building block to serve as an acceptor. Thus, we assume that oxaloacetate **6** is the most likely candidate for the remaining building block, because its functionalities permit both necessary bond formations, an aldol condensation of its carbonyl group with glycine (→ C-3′–C-4′ bond of **1**) and an amide bond formation of its (activated) γ-carboxyl group with the δ-NH_2 of ornithine (→ C-6′–N-1′ bond of **1**, Scheme 2). Even though an incorporation experiment with D,L-[4-^{13}C]-aspartate, which we expected to be transaminated into oxaloacetate **6**, failed, we still favor the [5C + 4C + 1C] hypothesis with **6** as the most likely third building block of pyridazomycin. The negative result may be caused by membrane permeability problems or the inability of the organism to transaminate aspartate into oxaloacetate. Thus, the formation of **6** in *Streptomyces violaceoniger* may be performed only by the citric acid cycle, whose metabolization into the uncertain carbon atoms of **1** is indicated by the feeding experiments with [1,2-$^{13}C_2$]acetate and [1,3-$^{13}C_2$]glycerol. Both compounds can serve as sources of the citric acid cycle, the former directly and thus more immediate than the latter, which has to be metabolized by glycolysis and the pyruvate decarboxylase complex. The specific incorporation rates[1,2] (Table 1) reflect these circumstances. Presently we are working on a synthesis of ^{13}C-labeled oxaloacetate parallel to the establishment of a cell-free system to examine **6** directly as a precursor. We are also looking for the stereochemical course of the glycine incorporation into **1**. Future aspects of our biosynthesis studies on **1** will focus on the N–N bond formation mechanism,[1,3] the order of the bond connection between the given biosynthetic building blocks as well as on the enzymes involved ("pyridazomycin synthase", see Scheme 2).



Scheme 2. Proposed mechanism of the biosynthesis of pyridazomycin **1**.

Experimental Procedure

Cultivation of the microorganism: *Streptomyces violaceoniger* (Tü 2557) was cultivated on slants (20% agar–agar, 10% malt extract, 4% glucose, 4% yeast extract, pH 7.0, adjusted before autoclaving) at 28 °C until sporulation occurred, then stored at 4 °C (for max. four months). The preculture for the fermentations was inoculated directly from the slants and shaken on a rotary shaker (type BS 4, B. Braun, Melsungen, FRG) in 250 mL Erlenmeyer flasks fitted with three baffles, filled with 100 mL medium (2.5% soybean meal, 2.5% mannitol, pH 6.8 before autoclaving) for 48 h at 28 °C and 250 rpm. 100 mL of the preculture was used to inoculate the 1 L fermentor (type ISF 100, Infors GmbH, Basel, Switzerland, filled with 1 L of the same medium as used for the preculture plus additional 30 mmol L^{-1} ornithine hydrochloride, except the feeding experiments with labeled ornithine and glutamic acid, respectively, 28 °C, aeration: 1.6 L min^{-1}, 700 rpm), harvesting about 64 h after inoculation.

Isolation of pyridazomycin **1**: The culture filtrate of the fermentations was exposed to an acidic ion exchange resin (Dowex 50) and washed with about 1.8 L demineralized water, elution with $NH_4^+HCOO^-$ (pH 5; gradient 0.3 M (1.5 L), 0.5 M (0.7 L), and 0.7 M (1 L). The fractions containing **1** were evaporated in vacuo at 40 °C and chromatographed on silica gel (column 60 × 3 cm, *n*BuOH:CH_3COOH:H_2O = 3:2:2), followed by chromatography on Sephadex G-10 (column 100 × 2.5 cm, MeOH:H_2O = 8:2, pH 4.0, adjusted with 0.1 M HCl) and lyophilization of the pyridazomycin-containing fractions.

Feeding experiments: The labeled compounds were dissolved in sterile water (100 mL) and added in four equal portions every six hours or continuously beginning at 25 h (after inoculation) to the growing 1 L-culture (1 L-fermentor) of *S. violaceoniger* (Tü 2557).

Labeled compounds: All the ^{2}H-, ^{13}C-, and/or ^{15}N-labeled compounds, if not synthesized (see below), were obtained from the Cambridge Isotope Laboratories, Cambridge, MA, USA. The variously labeled ornithine samples were synthesized according to Gould et al. [14] from 2-chloroethanol, K^{13}CN (99% ^{13}C) and K^{15}N (99% ^{15}N), respectively, and diethylacetamido malonate. The labeled glycerol was synthesized from bromoacetic acid and K^{13}CN (99% ^{13}C) via cyanoacetic acid, diethyl malonate, and diethyl 2-acetoxy malonate (oxidation with $PbOAc_4$). The [3-^{13}C]β-alanine was synthesized by hydrogenation (12 h, 25 °C, 90 mg Pt as catalyst, in ethanol (30 mL), acidified with concentrated HCl (0.2 mL)) of the previously mentioned labeled cyanoacetic acid (1.5 g) and purified by chromatography on silica gel (column, 30 × 2 cm, 1-propanol:H_2O = 4:1, yield: 0.3 g).

Received: February 26, 1994 [Z 6715 IE]
German version: *Angew. Chem.* **1994**, *106*, 1733

[1] R. Grote, Y. Chen, A. Zeeck, Z. Chen, H. Zähner, P. Mischnick-Lübbecke, W. A. König, *J. Antibiot.* **1988**, *41*, 595–601.
[2] P. Hughes, J. Clardy, *J. Org. Chem.* **1989**, *54*, 3260-3264, and references therein.
[3] a) M. Nakagawa, Y. Hayakawa, K. Furihata, H. Seto, *J. Antibiot.* **1990**, *43*, 477-484; b) K. Isshiki, T. Sawa, H. Naganawa, Y. Koizumi, N. Matsuda, M. Hamada, T. Takeuchi, M. Iijima, M. Osono, T. Masuda, M. Ishizuka, *ibid.* **1990**, *43*, 1195-1198; c) J. E. Leet, D. R. Schroeder, B. S. Krishnan, J. A. Matson, *ibid.* **1990**, *43*, 961-966; d) O. D. Hensens, R. P. Borris, L. R. Koupal, C. G. Caldwell, S. A. Currie, A. A. Haidri, C. F. Homnick, S. S. Honeycutt, S. M. Lindenmayer, C. D. Schwartz, B. A. Weissberger, H. B. Woodruff, D. L.

Zink, L. Zitano, J. M. Fieldhouse, T. Rollins, M. S. Springer, J. P. Springer, *ibid.* **1991**, *44*, 249–254.
[4] a) J. G. Buchanan, M. R. Hamblin, G. S. Sood, R. H. Wightman, *J. Chem. Soc. Chem. Commun.* **1980**, 917-918; b) C. S. J. Walpole, R. Wrigglesworth, *Nat. Prod. Rep.* **1989**, *6*, 311–346.
[5] a) M. Yamato, T. Takeuchi, H. Umezawa, N. Sakata, H. Hayashi, M. Hori, *J. Antibiot.* **1986**, *39*, 1263-1269, and references therein; b) R. J. Parry, Y. Li, F.-L. Lii, *J. Am. Chem. Soc.* **1992**, *114*, 10062–10064.
[6] Y. Takahashi, M. Nakayama, I. Watanabe, T. Deushi, H. Ishiwata, M. Shiratsuchi, G. Otani, *J. Antibiot.* **1989**, *42*, 1541–1546, and references therein.
[7] a) T. Kameyama, A. Takahashi, H. Matsumoto, S. Kurasawa, M. Hamada, Y. Okami, M. Ishizuka, T. Takeuchi, *J. Antibiot.* **1988**, *41*, 1561-1567; b) A. Takahashi, H. Nakamura, D. Ikeda, H. Naganawa, T. Kameyama, S. Kurasawa, Y. Okami, T. Takeuchi, Y. Iitaka, *ibid.*, 1568–1574.
[8] a) C. L. Stevens, B. T. Gillis, J. C. French, T. H. Haskell, *J. Am. Chem. Soc.* **1958**, *80*, 6088–6092; b) R. J. Parry, H. S. P. Rao, J. Mueller, *ibid.* **1982**, *104*, 339–340; c) R. J. Parry, J. V. Mueller, *ibid.* **1984**, *106*, 5764–5765.
[9] a) N. Imamura, H. Kuga, K. Otoguro, H. Tanaka, S. Ōmura, *J. Antibiot.* **1989**, *42*, 156–158; b) W. Giencke, O. Ort, H. Stark, *Liebigs Ann. Chem.* **1989**, 671–676.
[10] R. Thiericke, J. Rohr, *Nat. Prod. Rep.* **1993**, *10*, 265–289, and references therein.
[11] a) D. Hege, H. Zähner, personal communication; b) D. Hege, Diplomarbeit **1988**, Universität Tübingen, FRG; c) H. Bockholt, Diplomarbeit **1989**, Universität Göttingen, FRG.
[12] A. I. Scott, C. A. Townsend, K. Okada, M. Kajiwara, R. J. Cushley, P. J. Whitman, *J. Am. Chem. Soc.* **1974**, *96*, 8069–8080.
[13] We assume an N–N bond formation by an N-oxidation of ornithine, for example, initiated through an ornithine-N^5-hydroxylase [5b].
[14] J. Wityak, V. I. Palaniswamy, S. J. Gould, *J. Labelled Compd.* **1985**, *22*, 1155–1157.

Preparation and Structure of $C_{76}(S_8)_6$: A First Step in the Crystallographic Investigation of Higher Fullerenes**

Rudi H. Michel, Manfred M. Kappes, Peter Adelmann, and Georg Roth*

"Higher fullerenes"—those molecular allotropes of carbon with more than 70 atoms per molecule—have recently become of great interest to preparative chemists and theoreticians. They are minor constituents of the "Krätschmer–Huffman soot"[1] which contains predominantly C_{60} and C_{70}. C_{76} is the smallest among the more abundant (C_{76}, C_{78}, C_{82}, C_{84}) "higher fullerenes" and small quantities of it have been separated chromatographically by a number of groups.[2–6] The topology and molecular structure of C_{76} has been studied theoretically by various methods.[7–10] A detailed prediction of C–C bond lengths in the C_{76} molecule based on ab initio SCF–Hartree–Fock calculations has been published by Colt and Scuseria.[9] There are two possible isolated pentagon ring isomers of C_{76}; these have D_2 and Jahn–Teller distorted T_d symmetry. The most stable isomer of C_{76} is predicted to be the D_2 form. Ettl et al.[5] confirmed this molecular symmetry by ^{13}C NMR measurements on C_{76} in solution. As a chiral species, C_{76} exists as a "right-handed" and a "left-handed" form. These are energetically degenerate and expected to occur in equal proportions (racemic mixture). Very recently, the kinetic resolution of the two chiral isomers has been demonstrated.[11] Effort has also been invested in the prediction of the electronic structure of the molecule.[12, 13]

Owing to the scarcity of the material—the total worldwide production of pure C_{76} is probably in the 10–100 mg range few computational predictions have ever been checked experimentally. In particular, very little information is currently available on solid-state and structural properties of C_{76} or C_{76}-containing compounds.[14] In a scanning tunneling microscopy (STM) study of various higher fullerenes, Li et al.[15] have shown that pure C_{76} appears to form closely packed layers. A crystal structure determination of either pure C_{76} or of any C_{76}-containing compound has, however, not yet been reported.

In this paper we describe the preparation and structure determination of the first C_{76}-containing van der Waals compound, $C_{76}(S_8)_6$. This material is a further representative of the family of fullerene–sulfur adducts, which have the general formula $C_{2n}(S_8)_m$,[16–19] and which are formed by a combination of fullerene molecules with S_8 rings. Its structure is closely related to that of the compound $C_{70}(S_8)_6$.[18] Just as in the C_{70} compound, which in the absence of a well-ordered C_{70} single crystal allowed the first molecular structure study of C_{70} in the solid state, $C_{76}(S_8)_6$ permits the determination of C–C bond lengths in an only weakly (van der Waals) matrix-perturbed fullerene molecule by diffraction methods. The material also offers, for the first time, the chance to perform macroscopic measurements on a structurally well-defined C_{76}-containing crystalline solid.

C_{76} was isolated from fullerene-containing soot prepared by the Krätschmer–Huffman method (electric arc evaporation of graphite in an inert gas atmosphere).[1] Toluene soot extract was coarsely separated by liquid chromatography on an activated alumina column with 5% and 15% toluene in hexane as eluent. Amount and composition of the resulting C_{76}-enriched starting material used for further purification by high-performance liquid chromatography (HPLC) has already been described elsewhere,[20] together with a more quantitative discussion of the whole procedure. Briefly, HPLC isolation of C_{76} was carried out with a Buckyclutcher column.[21] Three consecutive purification cycles were performed with a three-component eluent (50% toluene, 40% hexane, and 10% dichloromethane, 6 mL min^{-1}) in the first cycle and a different composition (28% toluene, 55% hexane, and 17% dichloromethane, 6 mL min^{-1}) optimized for C_{76}/C_{78} resolution in the second and third cycle. The resulting purity was better than 99% C_{76}.[22] Exposure to light was minimized during the whole separation process. Exposure to air was minimized in the third separation stage by purging with nitrogen. Third stage C_{76} solutions, once separated, were stored at below 0 °C prior to eluent removal during which heating above 40 °C was avoided. The solid material was recrystallized from CS_2, stored under nitrogen, and kept/transferred at low temperature prior to use.

Given the very small amount of material available—a few hundred μg in the present case—the growth of $C_{76}(S_8)_6$ single crystals of appreciable size and quality poses quite a challenge. The following procedure finally proved to be successful:

Crystals were grown by slow evaporation (under vacuum) of a solution of C_{76} and sulfur (in excess) in CS_2 at room temperature. A capillary (1 mm internal diameter, one end open) containing about 1 mm^3 of the solution was dipped with the closed end into a "CS_2-heat bath" and the total pressure adjusted such that the CS_2 bath was gently boiling. This stabilizes both the temperature and the CS_2 vapour pressure above the solution. The outer container was slightly heated from below to introduce a small temperature gradient. This helps to avoid unwanted

[*] Dr. G. Roth, Dr. P. Adelmann
Kernforschungszentrum Karlsruhe
Institut für Nukleare Festkörperphysik
Postfach 3640, D-76021 Karlsruhe (FRG)
Telefax: Int. code + (7247)82-4624
R. H. Michel, Prof. M. M. Kappes
Institut für Physikalische Chemie der Universität Karlsruhe (FRG)

[**] M. M. K. acknowledges support from the Bundesministerium für Forschung und Technologie under "Pilotprogramm Fullerene".

supersaturation of the solution at the surface and the container walls. The crystals obtained this way are isometric with linear dimensions of up to 0.5 mm. CCl_4 may be used to remove excess sulfur from the crystals. As an additional complication, the crystals are often twinned (rotation twin around the c axis).

Temperature-dependent X-ray diffraction measurements[23] show no evidence for a structural phase transformation between room temperature and 180 K. We concentrate on the low temperature data here, because they offer better $\sin\theta/\lambda$ resolution.

The structure (Fig. 1) was solved in space group Cm[24] by direct methods for the positions of the 26 symmetry independent

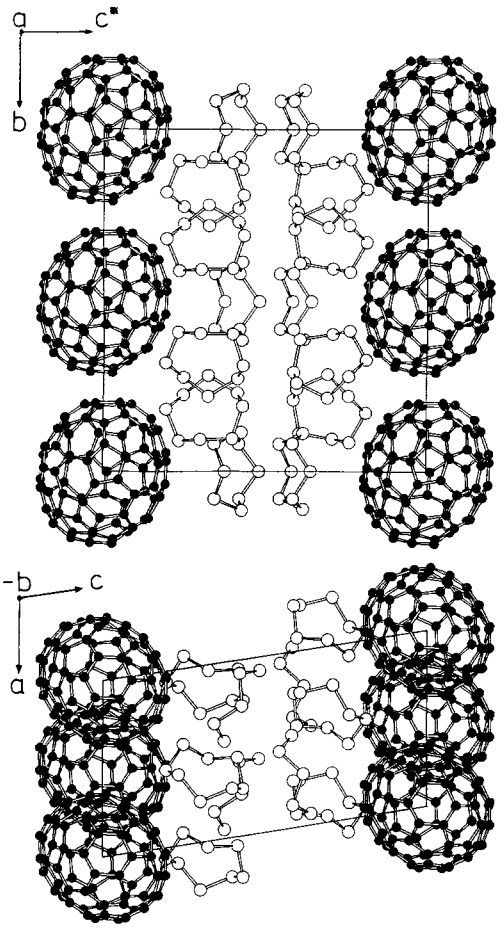


Fig. 1. The structure of $C_{76}(S_8)_6$ projected along the a (top) and b axis (bottom), black circles: carbon, open circles: sulfur atoms. For clarity, only one enantiomer in orientation I is drawn.

sulfur atoms. The arrangement of the sulfur atoms is similar to that in $C_{70}(S_8)_6$;[18] the sulfur atoms form layers (here: in the a-b plane) consisting of a rather complex array of four symmetrically distinct S_8 rings (in the usual "crown" configuration), two of them symmetry-restrained by the mirror plane of space group Cm. Sulfur–sulfur bond lengths range from 2.038 Å to 2.056 Å (average: 2.046(4) Å) and bond angles are close to 108°, in good agreement with the corresponding values observed in the various allotropes of elemental sulfur.[25] Also just as in $C_{70}(S_8)_6$, the fullerenes in $C_{76}(S_8)_6$ form planes between these sulfur sheets consisting of a pseudo-hexagonal arrangement of closely packed fullerene molecules. The center-to-center "packing distance" amounts to 10.4 Å along a and 11.5 Å along the diagonal in the a-b plane (at 180 K). The compound is a typical van der Waals solid with shortest carbon–sulfur distances on neighboring molecules ranging from 3.3 Å upwards. Also in analogy to $C_{70}(S_8)_6$, thin sections of $C_{76}(S_8)_6$ show a pronounced pleochroism (green/yellow) in the plane of closely packed fullerene molecules.

The optimum orientations of the C_{76} molecule were found by systematic, stepwise orientational search.[26] Figure 2 shows two one-dimensional sections through parameter space at the optimum orientations for the D_2 isomers along with a similar plot

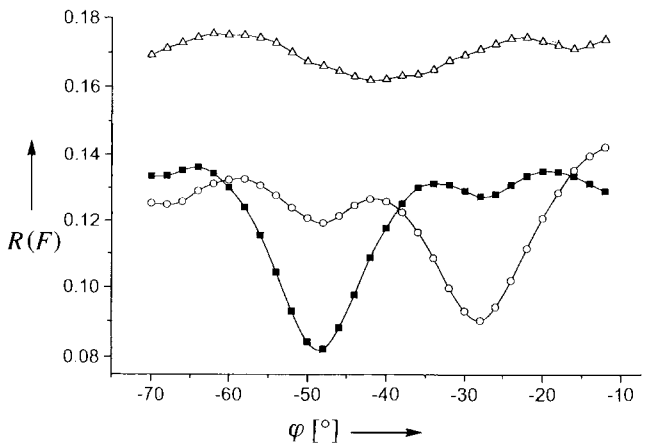


Fig. 2. $R(F)$ value ($|F| > 2\sigma(|F|)$) for C_{76} isomers plotted vs. rotation angle around the longest molecular axis. ■ D_2 isomer close to orientation I, ○ close to orientation II. All other angles and the center of gravity were fixed to their optimum values; △ representative plot for T_d isomer for comparison (rotation around a fivefold molecular axis oriented perpendicular to the mirror plane).

for the T_d isomer. The latter clearly does not fit the data nearly as well as the D_2 isomer and we take this as direct evidence for the overriding dominance of the D_2 isomer. We have found two differently oriented enantiomeric pairs of D_2-C_{76} molecules sharing the same site in $C_{76}(S_8)_6$. Their centers of gravity coincide and are situated on the mirror plane, but the three molecular twofold rotation axes of each of the four molecules are not aligned with any of the crystallographic axes. Starting from a reference orientation with the longest, second longest, and shortest molecular axis oriented along the b_f, a_f, and c_f axis of a fixed orthogonal coordinate system (with a_f, b_f, c_f parallel to the a, b, and c^* axis of the crystallographic unit cell), rotation angles of approximately $-48°$ around b_f, $+17°$ around a_f, and $-7°$ around c_f (in the sequence b_f, a_f, c_f) are necessary to arrive at the first optimum orientation (I). The second, slightly less favorable minimum of the R value occurs for rotation angles $-32°$, $-17°$, and $+6°$ (orientation II). The enantiomers are then generated by the mirror plane of the space group. Owing to the general orientation of the C_{76} molecules the "envelopes" of the two enantiomers do not coincide.[27] All four molecules appear to occupy the same site in a (spatially) random fashion. The occupancies are equal (by symmetry) for the two members of each enantiomeric pair but the first pair has a slightly higher occupation number. The resulting populations (2×0.28 and 2×0.22) and the rotation angles of the two enantiomeric pairs are temperature independent. Presumably, these orientations and their proportions are "frozen in" already during crystal growth and there appears to be no dynamic equilibrium between them at low temperature.

Despite the frequent overlap of many of the carbon atom positions, the resolution of the data[23] at 180 K is sufficient not only to identify the two pairs of orientations but also to extract

 © VCH Verlagsgesellschaft mbH, D-69451 Weinheim, 1994 0570-0833/94/1515-1652 $ 10.00+.25/0

some semiquantitative bond length data from it. For this purpose, a number of bond length restraints[28] were used during structure refinement.[29, 30] These restraints were chosen such that they do not put any bias onto the resulting *average* bond lengths of the "idealized" C_{76} molecule.[31] Figure 3 shows the C_{76} molecule in projections along the three molecular twofold axes.

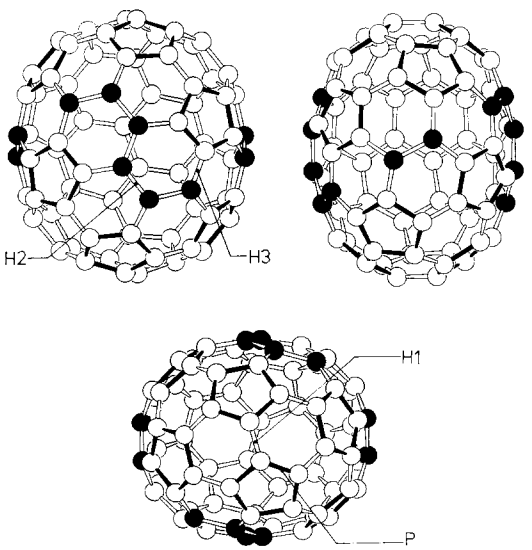


Fig. 3. D_2-C_{76} (one enantiomer) projected along the three principal axes of the molecule. Bonds of type "P" on the front of the molecule are drawn with solid lines, C atoms on "pyrene-type" sites as black spheres.

The overall dimensions of the C_{76} molecule[32] are 8.77(1), 7.77(1), and 6.92(1) Å, in fair agreement with the predicted ones (8.79, 7.64, 6.68 Å;[5] 8.82, 7.71, 6.83 Å[9]). Also, the "bond ordering" which has been predicted by SCF-HF[9] is confirmed experimentally: Bonds shared by a pentagon and a hexagon ("P") are long bonds (exp.: 1.436(4) Å, calcd: 1.453 Å,[9] solid lines in Fig. 3), those connecting the tips of two pentagons and joining two hexagons ("H1") are the shortest bonds in the molecule (exp.: 1.376(7) Å; calcd: 1.370 Å[9]). Near the "pole-caps" of C_{76} (viewed along the longest twofold molecular axis) this leads to the well-known "bond alternation" in the hexagons, most clearly seen in C_{60}[33] but also on the "pole-caps" of C_{70}.[18] Close to the equator this ordering is not possible for topological reasons both in C_{70} and C_{76}. In C_{76}, this leads (to a good approximation) to two additional groups of bonds, 12 bonds of type "H2" connecting the 16 atoms (per molecule) on "pyrene-type"[3] sites, which belong to three hexagons—these are the longest C–C bonds in the molecule (exp.: 1.485(8) Å, calcd: 1.482 Å[9])—and bond type "H3", (topologically similar to "H1") connecting the corners of the pentagons with the "pyrene-type" sites (exp.: 1.409(6) Å, calcd: 1.404 Å[9]). Due to the pronounced disorder[34] of the C_{76} molecule in $C_{76}(S_8)_6$, a more detailed comparison of calculated and individual experimental bond lengths cannot be performed.[28]

A note on the principal limitations of this work seems appropriate at this stage: The structure has been "solved" (in the classical crystallographic sense) only for the sulfur atoms. The orientational disorder of the C_{76} molecule prohibits such an approach (with no reference to the expected molecular shape) for the fullerene molecule. Even more important, crystal chemical knowledge, usually very helpful—if not decisive—in judging the correctness of a structure solution, is of very little help in this case. The superposition of more than one C_{76} molecule on the same site inevitably leads to "unreasonably short" apparent *intramolecular* C–C distances. Previous knowledge about *intermolecular* distances (of the van der Waals type), on the other hand, is not sufficient to favor (a priori) any orientation over the other. We are therefore left with the problem that neither the correctness nor the uniqueness of the present structural model can be proven rigorously.[35] This problem is intrinsic to cases where a major part of the structure is partially disordered and it gets worse with increasing size and decreasing symmetry of the disordered group. In this sense, such structural models with pronounced molecular disorder—among them the present one—should not be taken as "the final word" on the respective structures.

We have been able to show that the diffraction data measured for $C_{76}(S_8)_6$ are compatible with the postulated chiral D_2 structure of C_{76} and also to establish some basic semiquantitative aspects of its bond ordering by diffraction methods. Under crystal chemical aspects it is interesting to note that, just as in the case of $C_{70}(S_8)_6$, the combination of the larger fullerene C_{76} with the "bulky" S_8 rings leads to a structurally very similar and also comparatively well-defined heteromolecular van der Waals solid which, although intrinsically disordered, again offers atomic resolution of the fullerene molecule even at room temperature. The reason why most of the fullerene–sulfur adducts show no cage rotation at room temperature presumably lies in the specific interaction of fullerenes with the S_8 rings (possibly due to the nucleophilicity of sulfur as proposed in ref. [36]), a point which is, however, not sufficiently understood as yet.

A really substantial improvement of the quality of the bond length data for C_{76} can be expected from diffraction experiments on corresponding compounds with only one enantiomer. The kinetic resolution of the two chiral isomers of C_{76} by asymmetric osmylation, which has recently been demonstrated by Hawkins and Meyer,[11] has now opened a possible synthetic path to such compounds.

Received: December 3, 1993 [Z6536IE]
German version: *Angew. Chem.* **1994**, *106*, 1742

[1] W. Krätschmer, L. D. Lamb, K. Fostiropoulos, D. R. Huffman, *Nature* **1990**, *347*, 354.
[2] H. Aije, L. D. Alvarez, S. J. Anz, R. D. Beck, F. Diederich, K. Fostiropoulos, D. R. Huffman, W. Krätschmer, Y. Rubin, K. E. Schriver, D. Sensharma, R. L. Whetten, *J. Phys. Chem.* **1990**, *94*, 8630–8633.
[3] F. Diederich, R. L. Whetten, *Acc. Chem. Res.* **1992**, *25*, 119–126.
[4] F. Diederich, R. Ettl, Y. Rubin, R. L. Whetten, R. Beck, M. Alvarez, S. Anz, D. Sensharama, F. Wudl, K. C. Khemani, A. Koch, *Science* **1992**, *252*, 548–551.
[5] R. Ettl, I. Chao, F. Diederich, R. L. Whetten, *Nature* **1991**, *353*, 149–153.
[6] K. Kikuchi, N. Nakahara, M. Honda, S. Suzuki, K. Saito, H. Shiromaru, K. Yamauchi, I. Ikemoto, T. Kramochi, S. Hino, Y. Achiba, *Chem. Lett.* **1991** 1607–1610.
[7] D. E. Manolopoulos, *J. Chem. Soc. Faraday Trans.* **1991**, *87*, 2861–2862.
[8] B. L. Zhang, C. Z. Wang, K. M. Ho, *Chem. Phys. Lett.* **1992** *193*, 225–230.
[9] J. R. Colt, G. E. Scuseria, *J. Phys. Chem.* **1992** *96*, 10265–10268.
[10] O. Ori, M. D'Mello, *Chem. Phys. Lett.* **1992**, *197*, 49–54.
[11] J. M. Hawkins, A. Meyer, *Science* **1993**, *260*, 1918–1920.
[12] H. P. Cheng, R. L. Whetten, *Chem. Phys. Lett.* **1992**, *197*, 44–48.
[13] G. Orlandi, F. Zerbetto, P. W. Fowler, D. E. Manolopoulos, *Chem. Phys. Lett.* **1993**, *208*, 441–445.
[14] S. Hino, K. Matsumoto, D. Hasegawa, H. Inokuchi, T. Morikawa, T. Takahashi, K. Seki, K. Kikuchi, S. Suzuki, I. Ikemoto, Y. Achiba, *Chem. Phys. Lett.* **1992**, *197*, 38–42.
[15] Y. Z. Li, J. C. Patrin, M. Chander, J. H. Weaver, K. Kikuchi, Y. Achiba, *Phys. Rev. B* **1993**, *47*, 10867–10872.
[16] G. Roth, P. Adelmann, *Appl. Phys. A* **1993**, *56*, 169–174.
[17] G. Roth, P. Adelmann, R. Knitter, *Mater. Lett.* **1993** *16*, 357–363.
[18] G. Roth, P. Adelmann, *J. Phys. I* **1992**, *2*, 1541–1548; H. B. Bürgi, P. Venugopalan, D. Schwarzenbach, F. Diederich, C. Thilgen, *Helv. Chim. Acta* **1993**, *76*, 2155–2159.
[19] N. D. Kushch, *J. Phys. I* **1993**, *3*, 1987–1991.

[20] R. Michel, H. Schreiber, R. Gierden, F. Hennrich, J. Rockenberger, R. D. Beck, C. Lehner, P. Adelmann, J. F. Armbruster, *Ber. Bunsen Ges. Phys. Chem.* **1994**, *98*, 7.

[21] Regis Chemical Company, 5μm particle size, 10 mm × 250 mm.

[22] The purity was estimated by mass spectrometry. HPLC analysis showed 5% impurities at longer retention times. Since the mass spectra did not show any evidence for fullerenes higher than C_{76}, the impurity might be due to C_{76} oxide.

[23] Untwinned single crystal, dimensions 0.08 × 0.09 × 0.36 mm^3, four-circle diffractometer, $Mo_{K\alpha}$ radiation, graphite monochromator, N_2-cryostat, lattice parameters: 295 K: $a = 10.506(2)$, $b = 20.624(4)$, $c = 19.563(3)$ Å, $\beta = 98.8(1)^\circ$, 180 K: $a = 10.410(3)$, $b = 20.500(6)$, $c = 19.480(5)$ Å, $\beta = 98.8(1)^\circ$, thermal expansion coefficients $(-1/\Delta T)\Delta d/d$ just below room temperature: 9.3×10^{-5}, 6.1×10^{-5}, and 4.4×10^{-5} K^{-1} along a, b, and c respectively. Data collection at 180 K: Full sphere 0–20°, half sphere 20–40°, asymmetric unit 40–55° 2θ, $\sin\theta/\lambda = 0$–0.65 Å^{-1}, 4830 symmetry independent reflections, 3487 with $|F|^2 > 2\sigma_{|F|}^2$, $\mu = 12.9$ cm^{-1}, $R_{int} = 0.03$, $R_{sigma} = 0.048$.

[24] Among the three possible space groups consistent with the systematic extinctions, $C2$ and $C2/m$ could be ruled out because the final arrangement of the sulfur atoms does not comply with these symmetries. Atomic displacement ellipsoids of some of the sulfur atoms are elongated along b. Comparison of the 295 K with the 180 K data suggests that these displacements are dominated by static positional disorder, probably reflecting the fact that the C_{76} part of the structure obeys the mirror symmetry only in a statistical sense but not locally. Efforts to refine the structure in space group $C1$ (including pseudomeroedric and racemic twinning) failed. Also, there is no indication (from line splitting or intensity symmetry) for a deviation from the average monoclinic symmetry over the whole temperature range studied.

[25] R. Steudel in *Studies in Inorganic Chemistry, Vol.5*, (Eds.: A. Müller, B. Krebs), Elsevier, Amsterdam, **1984**, pp. 3–37.

[26] A single C_{76} molecule (D_2 as well as T_d isomer) was used as a "probe". Approximate atomic coordinates for the free molecule were kindly provided by the authors of ref. [8]. The parameter space is six-dimensional, with three orientational variables (Euler angles) plus three translational variables specifying the center of gravity which is, however, approximately known, once the sulfur arrangement has been determined. $R(F)$ values (4197 reflections) for rigid group refinement of C_{76}: Sulfur only: 0.20, with orientation I: 0.078, orientation I + II: 0.06. The fact that these R values are already not too far from the internal consistency R value of 0.03 suggests that the experimental molecular shape is quite close to the predicted one. It was also tried to directly build up the molecule by collecting the individual carbon atoms from successive Fourier syntheses. The resulting list of peaks contained most of the actual atom positions generated by the orientational search. Due to the superposition of four molecules on the same site, it is, however, almost impossible to unambiguously assign the Fourier peaks to the four individual (two symmetry independent) C_{76} molecules without a reference to the molecular shape.

[27] In the second orientation, the superposition of the enantiomeric pair results in almost the same "envelope" as for the first orientation, but the local arrangement of the carbon atoms is different and it is clearly not just the arrangement that would have been obtained by applying a local twofold axis to the C_{76} molecule or by interchanging the two enantiomers. This "correct orientation but wrong isomer" case is responsible for the shallow side minima in Figure 2. Besides these, there is a large number of additional, shallow local minima.

[28] The ideal symmetry of the "free" molecule was imposed by restraining distances equivalent under the idealized symmetry of tbe free molecule to be equal to each other within an estimated standard deviation of 0.01 Å. These restraints make groups of four atoms (related by the three twofold molecular axes) equivalent to each other, thus reducing the number of independent carbon atoms on the C_{76} molecule from 76 to 19 and the number of different C C bonds from 114 to 30. Equivalent bonds on the two differently oriented molecules were also tied together. If all variables were refined freely under these restraints, the resulting 30 C–C bond lengths ranged from 1.25 to 1.55 Å. This broad range reflects the high overlap of atoms on different molecules sharing the same site. Therefore, the 30 independent bonds on the idealized molecule were further grouped into four classes of topologically equivalent bonds (see text) which were restrained to have equal lengths within an estimated standard deviation of 0.03 Å. These average distances themselves were refined freely. The restraints are treated by the refinement program [30] as additional "soft data". This also helps to avoid singularities in the least squares calculations. The relative weighting of the diffraction data and the restraints, however, is quite a delicate problem. In detail, the bond lengths actually depend on this weighting (as well as on the type of restraints chosen), the estimated standard deviations probably underestimate the actual errors and the figures we give should therefore be considered approximate.

[29] Full matrix least squares [30], anisotropic displacement parameters for sulfur, one common isotropic displacement factor ($u = 0.044(1)$ Å^2) for all carbons, 692 variables, $R(F) = 0.0395$ for 3487 observed, $R(F) = 0.0634$ for all data, see [30] for definitions; goodness of fit (GOF) for all data: 1.055, restrained GOF: 0.941. Largest peak in a final Fourier synthesis below 0.49 electrons per Å^3, located on the envelope of the C_{76} molecule. Further details of the crystal structure determination may be obtained from the Fachinformationszentrum Karlsruhe Gesellschaft für wissenschaftliche Information mbH, D-76344 Eggenstein-Leopoldshafen (FRG), on quoting the depository number CSD-380024.

[30] G. M. Sheldrick, Program system Shelxl-93, unpublished.

[31] They do imply, however, that the influence of the van der Waals bonding on individual bond lengths of the C_{76} molecule can be neglected, a fair assumption for the present purpose, because the experimental accuracy for individual bond lengths is far from being sufficient to identify the expected small distortions on the order of 0.01 Å, see Q. M. Zhang, J. Y. Yi, J. Bernholc, *Phys. Rev. Lett.* **1991**, *66*, 2633–2636.

[32] Defined here as twice the average distance from the center of gravity of the molecule to the atom pairs close to the three twofold molecular axes; it is not quite clear, which definitions are used in refs. [5] and [9].

[33] W. I. F. David, R. M. Ibberson, J. C. Mathewman, K. Prassides, T. J. Dennis, J. P. Hare, H. W. Kroto, R. Taylor, P. R. M. Walton, *Nature* **1991**, *353*, 147–149; S. Liu, Y. Lu, M. M. Kappes, J. A. Ibers, *Science* **1991**, *254*, 408–410; H. B. Bürgi, E. Blanc, D. Schwarzenbach, S. Liu, Y. Lu, M. M. Kappes, J. Ibers, *Angew. Chem.* **1992**, *104*, 667–669; *Angew. Chem. Int. Ed. Engl.* **1992**, *31*, 640–643.

[34] Presumably, this disorder is intrinsic to this compound: A second, much smaller crystal from a different batch, studied at room temperature, showed qualitatively similar disorder phenomena.

[35] Once the existence of a second pair of enantiomers has been established, the dimensionality of the relevant parameter space more than doubles (six rotations, six translations, one additional occupancy). A "verified solution" of this disorder problem would require the evaluation of the R value on a sufficiently closely spaced grid in this 13-dimensional space—given the size of the structure, this is nearly impossibly. What we have actually done is to seek the solution in a six-dimensional section through the 13-dimensional space. Nothing guarantees that the solution in this subspace is also the global optimum in the true 13-dimensional parameter space.

[36] R. Taylor, D. R. M. Walton, *Nature* **1993**, *363*, 685–693.

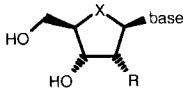
Synthesis of an Azathymidine and Its Incorporation into Oligonucleotides**

Karl-Heinz Altmann,* Susan M. Freier, Uwe Pieles, and Tammo Winkler

The inhibition of protein synthesis by antisense oligonucleotides is a fundamentally new approach in medicinal chemistry research.[1] The concept is based on the very specific rules that govern the mutual recognition of nucleic acids (Watson–Crick base pairing) and aims to exploit the selective hybridization of an (antisense) oligonucleotide to a complementary base sequence on the appropriate messenger RNA in order to block the expression of a disease-related protein. The general viability of this strategy has been proven in a large number of in vitro experiments; however, these experiments have also demonstrated that the antisense oligonucleotide should be sufficiently stable towards enzymatic degradation in order to achieve significant inhibitory effects on protein synthesis.[1] Since natural oligonucleotides are rapidly degraded under physiological conditions, the quest for metabolically more stable compounds has led to the design and investigation of various types of sugar-, base-, and backbone-modified oligonucleotides or oligonucleotide analogues.[1, 2] These include oligonucleotides containing carbocyclic nucleosides **1** (Fig. 1)[3, 4] and thia analogues of

[*] Dr. K.-H. Altmann, Dr. U. Pieles
CIBA, Central Research Laboratories, R-1060.2.34
CH-4002 Basel (Switzerland)
Telefax: Int. code + (61)697-9267
Dr. S. M. Freier
ISIS Pharmaceuticals, Carlsbad, CA, (USA)
Dr. T. Winkler
CIBA, Research Services, Physics Department

[**] We thank Dr. H.-P. Buser for the determination of the enantiomeric purity of **6** by chiral HPLC.



1 X = CH_2, R = H
2 X = S, R = H, OH
3 X = NR', R = H
4 X = $NCOCH_3$, R = H
base = thymine

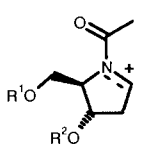
thymidine[6] and ribothymidine **2**[7] (base = thymine). In contrast, no oligonucleotides are known so far that incorporate pyrrolidine-based nucleoside analogues **3**.

Compounds of type **3** with R' = H can be expected to be chemically too unstable to be incorporated into antisense oligonucleotides,[8] but the corresponding acetylated derivatives (R' = Ac) could be interesting building blocks for antisense molecules. While the exact hybridization properties of these modified oligomers for complementary RNA are difficult to predict, molecular models indicate that acetylated building blocks of type **3** can be accomodated within standard nucleic acid duplex structures without major distortions. Moreover, it appears likely that the increased steric bulk of the acetamido group (as compared to the furanose oxygen atom) may impede recognition of the corresponding oligonucleotides by nucleolytic enzymes and therefore lead to improved metabolic stability.

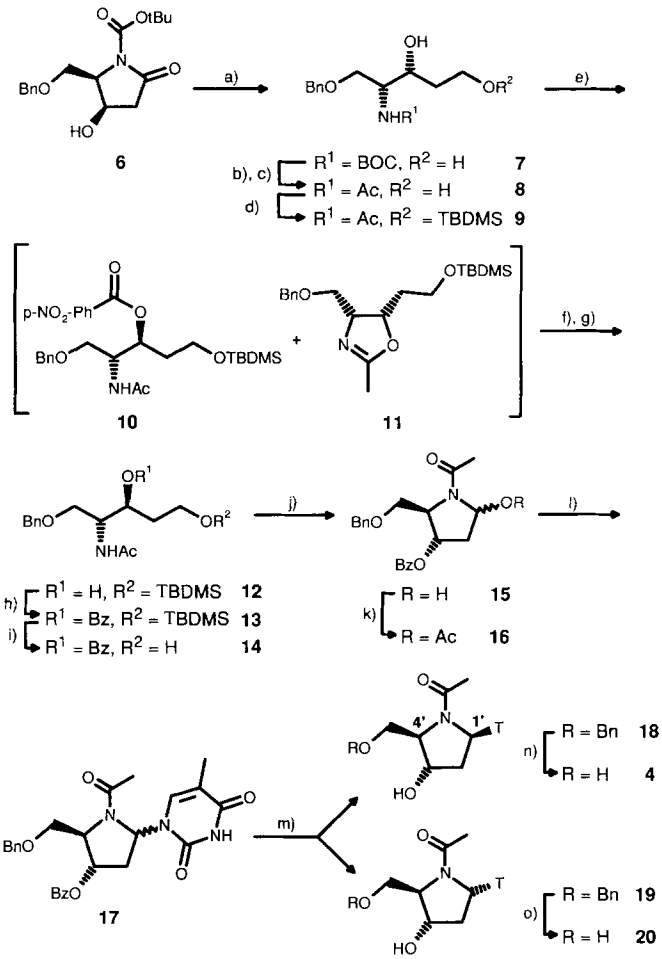
These considerations led us to investigate the properties of modified oligonucleotides containing nucleoside analogues of type **3** with R' = Ac. We first focused our attention on azathymidine **4**, an analogue in which the oxygen atom of the ribofuranosyl unit is replaced by an *N*-acetyl group. A 13-step synthesis of compound **4** starting from 2-deoxyribose has recently been reported.[9] In this paper we now describe a different approach to the synthesis of **4**, the incorporation of this building block into selected oligonucleotide sequences, and the hybridization properties and nuclease resistance of these oligomers.

Our strategy for the synthesis of **4** relies on the Lewis acid catalyzed generation of a suitably protected *N*-acyliminium ion **5** as the key reactive intermediate.[10] In situ trapping of **5** with silylated thymine as a nucleophile and subsequent protecting group manipulations should then lead to the target compound **4**.

As shown in Scheme 1 the synthesis started from optically active pyrrolidine **6**, which can be prepared in three steps from BOC-D-Ser(OBn)-OH (BOC = *tert*-butoxycarbonyl) according to literature procedures.[11] Treatment of **6** with $NaBH_4$/EtOH in the presence of catalytic amounts of HCl gave partially protected amino triol **7** in practically quantitative yield. Compound **7** was directly converted into the crystalline *N*-acetylated compound **8** by acid-catalyzed removal of the BOC protecting group and subsequent acylation with *N*-acetoxysuccinimide (AcONSu). Selective silylation of the primary hydroxyl group of **8** with *tert*-butyldimethylsilyl chloride (TBDMS-Cl)[12] furnished **9**, whose elaboration into **4** required inversion of the configuration at the secondary hydroxyl group. Mitsunobu reaction of **9** with *p*-nitrobenzoic acid as the external nucleophile[13] produced a roughly 1:1 mixture of the desired *p*-nitrobenzoate **10** and oxazoline **11**. No reaction occurred under standard Mitsunobu conditions[14] with either benzoic or formic acid as external nucleophiles. The mixture of **10** and **11** was converted to the desired amino triol **12** by saponification with NaOH/THF and subsequent opening of the oxazoline ring with NaOAc/dimethoxyethane (DME)/H_2O at 125 °C in 60% overall yield (based on **9**). Benzoylation followed by TBDMS removal with NH_4F/MeOH[15] then gave **14** as the immediate precursor of acetal **15**. In contrast, TBDMS cleavage from *rac*-**13** with tetrabutylammonium fluoride (TBAF) resulted in quantitative migration of



5



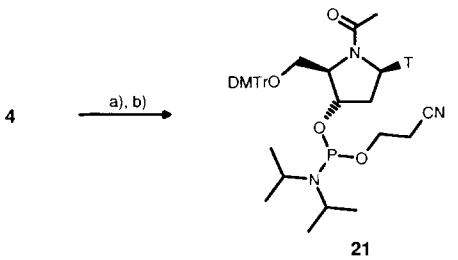
Scheme 1. a) $NaBH_4$ (9 equiv), EtOH, H^+ (cat.), 0 °C, 20 h, quant.; b) HCl/MeOH, room temperature (RT), 1 h; c) AcONSu, Hünig's base, THF/*N*,*N*-dimethylformamide (DMF) 1/1, 4 h, 45% (2 steps); d) TBDMS-Cl, Et_3N, 4-dimethylaminopyridine (DMAP), CH_2Cl_2/DMF 2/1, RT, 7 h, 94%; e) diethylazodicarboxylate (DEAD), Ph_3P, *p*-NO_2-C_6H_4-COOH, benzene, RT, 22 h; f) 2 N NaOH/THF 1/5, RT, 4.5 h; g) AcONa, DME/H_2O 12.5/1, 125 °C, 24 h, 60% (3 steps); h) Bz-Cl, pyridine, RT, 5 h, 74%; i) NH_4F (15 equiv), MeOH, 60 °C, 8 h, 82%; j) TPAP (0.1 equiv), NMMO · H_2O (1.2 equiv), AcOH (1 equiv), CH_2Cl_2, RT, 1.5 h and 4 h, 41%; k) Ac_2O, DMAP, CH_2Cl_2/pyridine 4/1, RT, 3 h, quant.; l) $(TMS)_2$-thymine (2.5 equiv), $SnCl_4$ (1.3 equiv), CH_3CN, −15 °C, 1 h, 93%; m) 1. NaOMe (1.1 equiv), MeOH, RT, 1.5 h, 86%; 2. flash-chromatography in CH_2Cl_2/MeOH 12.5/1: **18**: 33%, **19**: 48%; n) H_2, 10% Pd-C, MeOH, RT, 1.25 h, quant.; o) H_2, 10% Pd-C, MeOH, RT, 1.25 h, quant.

the benzoyl group to the primary hydroxyl group. Oxidation of **14** with tetra-*n*-propylammonium perruthenate (TPAP)/*N*-methylmorpholine *N*-oxide (NMMO)[16] furnished acetal **15** in 41% yield. The moderate yield is mainly caused by rapid further oxidation of **15** to the corresponding lactam. For this reason the reaction mixture was worked up after 1.5 h, the product was isolated, and recovered **14** was resubjected to oxidation. Compound **15** was converted into acetate **16**, the immediate precursor of *N*-acyliminium ion **5**. Treatment of **16** with $SnCl_4$ in the presence of $(TMS)_2$-thymine at −15 °C for 1 h gave a 93% yield of **17** as a mixture of diastereomers which could not be separated at this stage. Transesterification with NaOMe/MeOH and subsequent chromatographic separation then gave **18** and **19** in 33% and 48% yield, respectively. The identity of **18** and **19** was determined by NOE difference spectroscopy (NOE = nuclear Overhauser enhancement). While a strong NOE was observed between H-4' and H-6 of the base in **19**, no such NOE was detectable in **18**. Instead, an NOE between H-1' and H-4' in **18**

 © VCH Verlagsgesellschaft mbH, D-69451 Weinheim, 1994 0570-0833/94/1515-1655 $ 10.00+.25/0

clearly indicated a *cis* relationship for these two protons. The synthesis of **4** as well as its diastereomer **20** were completed by benzyl ether cleavage by catalytic hydrogenation in essentially quantitative yield.[17] According to their ^{1}H NMR spectra each of these compounds exists in MeOH solution as an approximately 1:1 mixture of rotamers.

For the oligonucleotide synthesis **4** was converted into the protected phosphoramidite **21** according to standard methodology[18a] (Scheme 2). Compound **21** was used for the preparation



Scheme 2. a) 4,4'-Dimethoxytrityl chloride (DMTr-Cl), Et_3N, DMAP, RT, 27 h, 70%; b) $NCCH_2CH_2OP[N(i\text{-}C_3H_7)_2]_2$, diisopropylammonium tetrazolide, CH_2Cl_2, RT, 23 h, 70%.

of four oligonucleotides containing between one and four azathymidine residues (vide infra). The oligonucleotides were synthesized according to standard solid-phase procedures,[18b] and no special problems were encountered in the coupling of **21**.[19] The 5'-4,4'-dimethoxytrityl (DMTr) protected oligonucleotides were purified by reversed-phase high-performance liquid chromatography (RP-HPLC), and the DMTr group was subsequently removed by treatment with 80% AcOH for 20 min at room temperature. Capillary electrophoresis (CE) indicated that the fully deprotected compounds were at least 95% pure.[20]

The data for the hybridization of three of these four oligonucleotides with complementary RNA (as the target of antisense oligonucleotides) are summarized in Table 1. It is evident that

Table 1. Hybridization of oligodeoxynucleotides containing azathymidine **4** with complementary RNA sequences (oligoribonucleotides).

Oligonucleotide [a]	T_m [b, e]	T_m(WT) [c, e]	ΔT_m/mod. [d]
d(**t**CC AGG **t**G**t** CCG CA**t** C)	57.4	62.3	−1.2
d(CTC GTA CC**t** TTC CGG TCC)	62.8	63.3	−0.5
d(CTC GTA C**tt** **tt**C CGG TCC)	55.8	61.8	−1.5

[a] **t** = azathymidine **4**. [b] Melting temperature of the duplex between the modified oligodeoxynucleotide and the corresponding complementary oligoribonucleotide (RNA) in °C. [c] Melting temperature of the unmodified wild-type (WT) duplex in °C. [d] $T_m - T_m$(WT) per modified building block. [e] Determined in 10 mM phosphate buffer, pH 7, containing 100 mM Na^+ and 0.1 mM ethylenediaminetetraacetic acid (EDTA) [22].

the incorporation of azathymidine causes a modest destabilization of the DNA/RNA heteroduplex (as compared to the unmodified wild-type duplex), which is reflected in an average decrease of the T_m-value of 1.3 °C per modification. The destabilizing effect may arise from distortions of the normal duplex structure caused by the acetyl substituent on nitrogen, although this is not obvious from molecular models (vide supra). In addition, different rotamers about the tertiary amide bond may affect binding in a different manner.

In contrast to the destabilizing effect of **4** on overall binding affinity incorporation of **4** into an oligonucleotide does not lead to any adverse effects on the specificity of hybridization with complementary RNA. As shown in Table 2 the differences in

Table 2. Hybridization of d(CTC GTA CCt TTC CGG TCC) with r(GGA CCG GAA **Y**GG UAC GAG) [a].

Y	T_m [b, e]	ΔT_m [c, e]	ΔT_m(WT) [d, e]
rA	62.8	–	–
rC	53.1	−9.7	−8.9
rG	54.9	−7.9	−1.7
rU	51.1	−11.7	−7.5
average	–	−9.7	−6.0

[a] **t** = **4**. [b] Melting temperature of the modified DNA/RNA heteroduplex in °C. [c] Difference in melting temperature between the fully matched (**Y** = rA) and the respective mismatched duplex in °C. [d] Difference in melting temperature between the fully matched (**Y** = rA) and the respective mismatched wild-type (WT) duplex (i.e. all hybrids contain natural thymidine in place of **4**). [e] Determined in 10 mM phosphate buffer, pH 7, containing 100 mM Na^+ and 0.1 mM EDTA [22].

melting temperature between the fully matched DNA/RNA duplex containing a single azathymidine residue ("**t**") as part of the DNA strand (**t**:A base pair) and the various mismatched hybrids (containing **t**:C, **t**:G, and **t**:U base pairs, respectively) in all three cases even exceed the corresponding temperature differences for the parent duplexes containing natural thymidine in place of **4**. In view of the very limited data base this apparent enhancement of hybridization specificity by the incorporation of **4** should not be overinterpreted, but the data presented in Table 2 certainly indicate that oligodeoxynucleotides containing **4** should hybridize to complementary RNA with similar specificity as the corresponding wild-type oligodeoxynucleotides.

To evaluate the nuclease resistance of oligonucleotides containing azathymidine **4** we investigated the stability of TCC AGG TGT CCG **ttt** C to degradation by 3'-exonucleases in 10% heat-inactivated fetal calf serum (FCS).[1] Not considering loss of the natural 2'-deoxycytidine residue at the 3'-end, the half-life of this oligonucleotide in FCS has been determined to be $\gg$48 h.[23] Under the same experimental conditions the unmodified wild-type oligonucleotide has a half-life of only 2 h. Thus, the modified oligonucleotide displays a >20-fold increase in nuclease resistance.

In view of these results pyrrolidino nucleosides of type **3** with R' = Ac should be excellent tools for the stabilization of antisense oligonucleotides against degradation by 3'-exonucleases. However, additional experiments are required to determine whether the hybridization affinity of fully modified sequences (containing only building blocks of type **3** with R' = Ac) would still suffice for biological applications.

Received: January 8, 1994
Revised version: March 29, 1994 [Z 6607 IE]
German version: *Angew. Chem.* **1994**, *106*, 1735

[1] a) E. Uhlmann, A. Peyman, *Chem. Rev.* **1990**, *90*, 543–584; b) S. T. Crooke, *Annu. Rev. Pharmacol. Toxicol.* **1992**, *32*, 329–376; c) J. F. Milligan, M. D. Matteucci, J. C. Martin, *J. Med. Chem.* **1993**, *36*, 1923–1937.
[2] P. D. Cook, *Anticancer Drug. Des.* **1991**, *6*, 585–607.
[3] a) M. Perbost, M. Lucas, C. Chavis, A. Pompon, H. Baumgartner, B. Rayner, H. Griengl, J.-L. Imbach, *Biochem. Biophys. Res. Commun.* **1989**, *165*, 742–747; b) J. Sagi, A. Szemzo, J. Szécsi, L. Ötvös, *Nucleic Acids Res.* **1990**, *18*, 2133–2140; c) H. E. Moser, *Perspectives in Medicinal Chemistry* **1993** (Eds.: B. Testa, E. Kyburz, W. Fuhrer, R. Giger) Verlag Helvetica Chimica Acta, Basel, **1993**, pp. 275–297.
[4] Compounds of type **1** with R = OH are also known [5], but no corresponding oligonucleotides have been reported.

[5] For a review see: A. D. Borthwick, K. Biggadike, *Tetrahedron* **1992**, *48*, 571–623.
[6] E. L. Hancox, B. A. Connolly, R. T. Walker, *Nucleic Acids Res.* **1993**, *21*, 3485–3491.
[7] a) L. Bellon, J.-L. Barascut, G. Maury, G. Divita, R. Goody, J.-L. Imbach, *Nucleic Acids Res.* **1993**, *21*, 1587–1593; b) L. Bellon, F. Morvan, J.-L. Barascut, J.-L. Imbach, *Biochem. Biophys. Res. Commun.* **1992**, *184*, 797–803.
[8] K.-H. Altmann, *Tetrahedron Lett.* **1993**, *34*, 7721–7724.
[9] B. Huang, B. Chen, Y. Hui, *Synthesis* **1993**, 769–771.
[10] For a review on *N*-acyliminium ion mediated reactions see: H. Hiemstra, W. N. Speckamp in *Comprehensive Organic Synthesis, Vol. 2* (Eds.: B. M. Trost, I. Fleming), Pergamon, Oxford, **1991**, pp. 1047–1082.
[11] P. Jouin, B. Castro, D. Nisato, *J. Chem. Soc. Perkin Trans. 1* **1987**, 1177–1182. **6** was purified by flash chromatography and then recrystallized from acetone. In contrast to what might be implied from the above literature report, optically active material had to be recovered from the mother liquor of the recrystallization mixture, while the crystalline precipitate consisted mainly of the racemate. The $[\alpha]_D^{25}$ value of **6** was −65.5 ($c = 1.01$ in MeOH), m.p. 99–100 °C (ref. (+)-**6**: $[\alpha]_D^{20} = +59$ ($c = 1.0$ in MeOH), m.p. 100–101 °C), and its *ee* was determined as 96% by chiral HPLC. BOC-D-Ser(OBn)-OH was synthesized from BOC-D-Ser-OH according to H. Sugano, M. Miyoshi, *J. Org. Chem.* **1976**, *41*, 2352–2353.
[12] S. K. Chaudhary, O. Hernandez, *Tetrahedron Lett.* **1979**, 99–102.
[13] S. F. Martin, J. A. Dodge, *Tetrahedron Lett.* **1991**, *32*, 3017–3020.
[14] O. Mitsunobu, *Synthesis* **1981**, 1–28.
[15] W. Zhang, M. J. Robins, *Tetrahedron Lett.* **1992**, *33*, 1177–1180.
[16] W. P. Griffith, S. V. Ley, G. P. Whitcombe, A. D. White, *J. Chem. Soc. Chem. Commun.* **1987**, 1625–1627.
[17] **4**: ^{1}H NMR (250 MHz, CD_3OD, TMS): $\delta = 8.05$ (s, 0.45H; H-6 (minor rotamer (min.)), 7.60 (s, 0.55H; H-6 (major rotamer (maj.)), 6.40 (dd, $^3J(H,H) = 7$ Hz, $^3J(H,H) = 7$ Hz, 0.45H; H-1′ (min.)), 6.20 (dd, $^3J(H,H) = 8$ Hz, $^3J(H,H) = 8$ Hz, 0.55H; H-1′ (maj.)), 4.30 (s, br, 0.45H; H-3′ (min.)), 4.25 (d, $^3J(H,H) = 5$ Hz, 0.55H; H-3′ (maj.)), 4.00–3.65 (m, 3H; H-5′ (2), H-4′), 2.40–2.15 (m, 2H; H-2′-α, H-2′-β), 2.10 (s, 1.65H; CH_3 (Ac) (maj.)), 1.85 (s, 1.35H; CH_3(Ac) (min.)), 1.89, 1.86 (2 × s, 3H; CH_3 (thymine)). FAB-MS: ($C_{12}H_{17}N_3O_5$ (283.116)): 284 (45, $[M + H]^+$). **20**: ^{1}H NMR (250 MHz, CD_3OD, TMS): $\delta = 7.55$ (s, 0.45H; H-6 (min.)), 7.50 (s, 0.55H; H-6 (maj.)), 6.30 (d, $^3J(H,H) = 8$ Hz, 0.55H; H-1′ (maj.)), 6.20 (d, $^3J(H,H) = 8$ Hz, 0.45H; H-1′ (min.)), 4.30 (m, 1H; H-3′), 4.15 (s, br, 0.55H; H-4′ (maj.)), 4.05 (t, br, 0.45H; H-4′ (min.)), 3.70–3.45 (m, 2H; H-5′), 2.30–2.10 (m, 1H; H-2′-β), 2.15 (s, 1.35H; CH_3(Ac) (min.)); 1.95–1.75 (m, 5.65H; incl. s, 1.90, CH_3(Ac) (maj.): s, 1.78; s, 1.74, CH_3(thymine); H-2′-α). FAB-MS ($C_{12}H_{17}N_3O_5$ (283.116)): 284 (56, $[M + H]^+$).
[18] a) N. D. Sinha, J. Biernat, J. McManus, H. Köster, *Nucleic Acids Res.* **1984**, *12*, 4539–4557; b) *Oligonucleotide synthesis – a practical approach* (Ed.: M. J. Gait) IRL, Oxford, **1984**.
[19] Coupling times of 10 min were routinely employed for the incorporation of **21**.
[20] Compound **4** is completely stable under the conditions of oligonucleotide synthesis. In addition, incorporation of **4** as an intact unit into the various oligonucleotides was ascertained by matrix-assisted laser desorption time-of-flight (MALDI-TOF) mass spectrometry [21].
[21] U. Pieles, W. Zürcher, M. Schär, H. E. Moser, *Nucleic Acids Res.* **1993**, *21*, 3191–3196.
[22] E. A. Lesnik, C. J. Guinosso, A. M. Kawasaki, H. Sasmor, M. Zounes, L. L. Cummins, D. J. Ecker, P. D. Cook, S. M. Freier, *Biochemistry* **1993**, *32*, 7832–7838.
[23] The natural nucleotide building block at the 3′-end of the oligonucleotide is present only for synthetic convenience, as it allows solid-phase oligonucleotide synthesis to be conducted starting from a commercially available support. This residue is removed from the oligonucleotide by the action of 3′-exonucleases rather rapidly, independent of the nature of the adjacent building blocks. The degree of protection against degradation by 3′-exonucleases conferred by the modified building blocks **4** in TCC AGG TGT CCG **ttt** C is therefore determined by the half-life of the $(n-1)$ species generated by removal of the 3′-terminal cytidine residue.

Active Surface Carbon—A Reactive Intermediate in the Production of Synthesis Gas from Methane and Carbon Dioxide

Michael F. Mark and Wilhelm F. Maier*

An efficient use of the climatically relevant gases CH_4 and CO_2 (greenhouse effect) as a source of carbon is a central issue in heterogeneous catalysis.[1] The reaction (a) of CO_2 with CH_4 to give a mixture of CO and H_2 (synthesis gas), so-called dry or CO_2 reforming, is a particularly elegant way to utilize both gases directly.[2, 3] The synthesis gas resulting from reaction (a) has a

$$CH_4 + CO_2 \rightleftharpoons 2\,CO + 2\,H_2 \quad \Delta H_{R298} = 261\ kJ\ mol^{-1} \qquad (a)$$

lower H_2/CO ratio than that produced by the cleavage of CH_4 with steam (steam reforming[4]), which is advantageous for hydroformylations and Fischer–Tropsch processes. CO_2 reforming was exploited[5] industrially in the USA already in 1948 and is still used today in the Calcor process, mainly for the manufacture of CO.[6] Renewed interest has been shown in this conversion because of its potential use as an effective reaction for energy storage,[7, 8] and because it allows a carbonization (coking)-free utilization of CO_2.[2]

Rh, Ir, and Ru support catalysts have proved particularly useful in the case of the extremely endothermic equilibrium reaction (a). A coking-free conversion on Rh, Ru,[2, 3, 8] and Ir[2, 3] catalysts has been reported. In contrast Ni, Pt, and Pd catalysts are less suited for CO_2 reforming, since they are not as active as Rh, Ru, or Ir catalysts. Furthermore, Ni and Pd catalysts are prone to deactivation caused by carbonization.[2, 3, 9] At the expense of a loss in activity Ni catalysts can be used after passivation with H_2S.

Although Fischer and Tropsch[11] reported the reaction of natural gas with carbon dioxide already in 1928, even today the reaction mechanism has not been completely clarified. On account of kinetic investigations Bodrov and Apel'baum postulated the formation of water as an important intermediate.[12] The basis of the presently accepted mechanism[3] is the dissociative adsorption of CO_2 and the stepwise dissociation of CH_4 at active metal centers (Scheme 1). In 1991 the observed activity order of the catalyst metals was correlated with the CO_2 dissociation activity.[9]

$$CH_4 + s \rightleftharpoons [CH_{xs} + (4-x)H_s] \rightleftarrows C_s + 2\,H_2$$
$$CO_2 + 2\,s \rightleftharpoons CO_s + O_s$$
$$C_s + O_s \rightleftharpoons CO_s + s$$
$$CO_s \rightleftharpoons CO + s$$

Scheme 1. Currently accepted mechanism for the formation of synthesis gas [3]. The support is indicated by 's' (surface); thus C_s corresponds to a carbon atom adsorbed on the surface (surface carbon).

The detection of small amounts of ethane in the decomposition of methane on Rh/SiO_2 catalysts at 250 °C was interpreted as evidence for the formation of CH_x units on the surface.[13, 14] Solymosi et al.[14] observed the formation of C species of differing reactivity on Rh catalysts; the most reactive form of these C species reacts with H_2 to give methane even at 80 °C. The same

[*] Prof. Dr. W. F. Maier, Dipl.-Chem. M. F. Mark
Max-Planck-Institut für Kohlenforschung
Kaiser-Wilhelm-Platz 1, D-45466 Mülheim an der Ruhr (FRG)
Telefax: Int. code + (208)306-2987

authors discussed an alternative mechanism for the conversion of active surface carbon C_s with CO_2[14] for the first time in 1993 (Scheme 2).

$$CH_4 + Rh_s \cdots\rightarrow C_s{-}Rh_s + 2H_2\uparrow$$

$$C_s - Rh_s + CO_2 \longrightarrow 2\,CO\uparrow + Rh_s$$

Scheme 2. Alternative mechanism for the formation of synthesis gas [14].

The mechanism of this reaction was of particular interest to us because of the effective utilization of CO_2. In the preceeding investigations under gas phase flow conditions we were able to confirm the exceptional activity and selectivity of Rh and Ir on Al_2O_3. Since an almost linear relationship exists between conversion and the size of the active metal surface for both support catalysts, the influence of particular surface structures on the mechanism can be excluded. The reaction of CH_4 with CO_2 is not limited by diffusion under the chosen reaction conditions (35 mL min^{-1}, CH_4:CO_2 = 1:1) up to 800 °C, and is first order in CO_2 and CH_4, confirming the participation of both reactants in the rate-determining step.

The interaction of the starting materials CH_4 and CO_2 with a Rh(5%)/Al_2O_3 catalyst was investigated in detail by pulse chemisorption under the reaction conditions used in CO_2 reforming (700 °C). An exclusively mesoporous γ-Al_2O_3 (CONDEA pural, S_{BET} = 78 m^{2}g^{-1}, pore diameter ca. 20 nm) was used as the support. After just a few experiments at 700 °C this catalyst displayed a constant activity over many weeks, as well as a stable dispersion (CO chemisorption) of 3.25% (active metal surface 0.8 m^{2}g^{-1}). The sizes of the Rh crystallites range from 10–30 nm; TEM studies confirm the stable, relatively low dispersion (Fig. 1). Under steady state conditions at 700 °C, 150 mg catalyst, and a volume flow of 35 mL min^{-1} CH_4/CO_2, more than 90% of the equilibrium conversion [conversion (CH_4) = 70%; conversion (CO_2) = 88.5%] can be achieved. In control experiments the pure Al_2O_3 support proved to be completely inactive for CO_2 reforming.

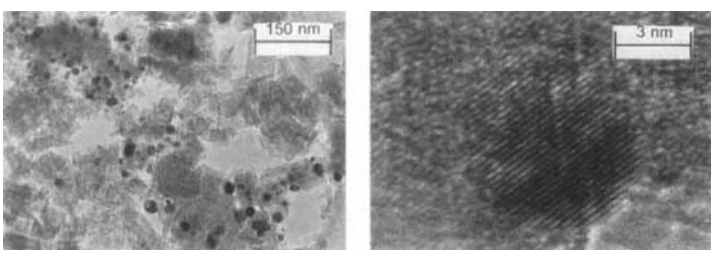


Fig. 1. A transmission electron micrograph (TEM) of the used Rh/Al_2O_3 catalyst; Overview showing Rh particles (left), and a high resolution picture of a small Rh particle with atomic resolution of the crystal lattice (right). The identity of rhodium was confirmed by X-ray scattering (EDX) analysis using an electron beam of 2 nm diameter.

In CO_2-pulsed chemisorption studies on a Rh/Al_2O_3 catalyst at 200–400 °C Solymosi et al.[13] were only able to detect the formation of less than 0.1% CO. When CO_2 pulses (0.33 monolayers C_s/Rh_s) are applied to a pre-reduced and flushed Rh catalyst (reduction: 1 h, 30 mL min^{-1} H_2 at 600 °C; flushing: 30 min 30 mL min^{-1} He at reaction temperature) there is no detectable amount of CO produced [error < 3%, Eq. (b)]. This confirms the results of Solymosi et al. and indicates an extremely small interaction between CO_2 and the reduced Rh.

$$CO_2 + Rh_s \longrightarrow CO + O{-}Rh_s \qquad (b)$$

When the first CH_4 pulse (0.33 monolayers C_s/Rh_s) is applied to the pre-reduced and flushed Rh catalyst sample at 700 °C, a quantitative decomposition of CH_4 is observed. The detection of CO_2 and CO in the product pulse in addition to H_2 is due to unavoidable residual oxygen on the catalyst surface. After the second pulse the formation of hydrogen dominates clearly, and a total amount of carbon remains which corresponds to a third of a monolayer. When the catalyst is now subjected to CO_2 pulses at the same temperature, 72% and 18% of the CO_2 will be converted exclusively into two equivalents of CO after the first and second pulses, respectively. This corresponds to a 90% conversion of the surface carbon. During additional CO_2 pulses no further CO formation is detectable. The residual carbon (approximately 0.03 monolayers) is obviously not reactive and could be detected as CO_2 released above 400 °C during a temperature-programmed oxidation. This shows that 90% of the surface carbon arising from the decomposition of methane on a Rh catalyst reacts extremely fast with CO_2 to give CO, and must therefore be highly reactive.

The question can then be asked whether this reactive surface carbon C_s is present in some form in a stoichiometric relationship at the Rh surface, for instance as a sort of surface carbide. Thus, the decomposition of methane was carried out repeatedly on a pre-reduced catalyst with up to 80 methane pulses (about 25 carbon monolayers).

The degree of CH_4 dissociation decreases with increasing coverage of the catalyst surface (encapsulating carbon), presumably since the catalytically active centers become inaccessible or deactivated.[13, 14] Methane is decomposed many times over in relation to the Rh surface. Even with a coverage of more than 15 monolayers it is still possible to observe a dissociation of about 50% of the pulsed methane. In contrast to the results of Solymosi et al., who studied the CH_4 decomposition on a Rh catalyst at lower temperatures (200–400 °C),[13, 14] we were able to detect H_2 in the product gas but no ethane. After exposure of the carbon coated Rh catalyst to CO_2 pulses, an almost quantitative conversion of a limited number of CO_2 pulses into 2 CO can be detected depending on the amount of CH_4 previously dissociated (Figs. 2 and 3). Figure 2 shows the mass-spectrometric response signal at *m/z* values of 28 and 44 from identical CO_2 pulses on a catalyst previously coated with carbon, and from the empty catalysis tube (calibration pulse). The calibration pulse documents the CO formation through fragmentation in the mass spectrometer.

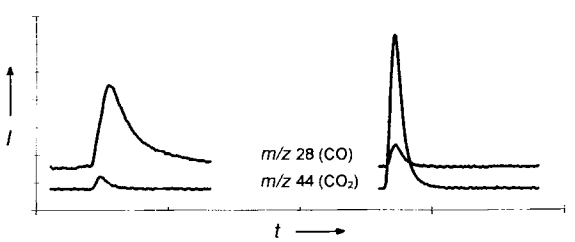


Fig. 2. Signal intensities at *m/z* = 44 and 28 of the product after identical CO_2 pulses in an empty tube (calibration pulse, right) and over the Rh(5%)/Al_2O_3 catalyst coated with 2.5 monolayers of preadsorbed carbon by prior decomposition of methane. One division on the time axis represents 50 s.

Figure 3 shows the typical rapid decay of the CO_2 conversion after seven CO_2 pulses on a Rh catalyst coated with 2.5 monolayers of carbon by CH_4 decomposition. The amount of surface carbon which is transformed by CO_2 into CO is determined by the amount of CH_4 dissociated and the CO produced. From the

 © VCH Verlagsgesellschaft mbH, D-69451 Weinheim, 1994 0570-0833/94/1515-1658 $ 10.00+.25/0

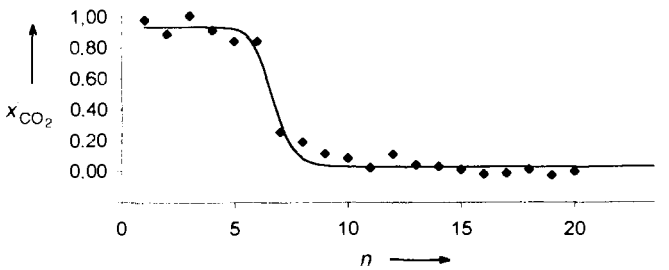


Fig. 3. CO_2 conversion x (entirely to 2 equivalents CO) as a function of increasing CO_2 pulse count n over a Rh(5%)/Al_2O_3 catalyst coated with about 2.5 monolayers of carbon (determined from the peak areas at mass 44).

plot of preadsorbed monolayers of carbon against monolayers of CO_2 released (with 2 CO as the only product) (see Fig. 4) it is evident that at lower carbon coverages the surface carbon reacts almost quantitatively. However, as the coverage increases, an increasingly large proportion of unreactive carbon remains on the surface of the catalyst. Even with a coating of 13 monolayers there are still 9 monolayers of active carbon present, which are transformed spontaneously and quantitatively by CO_2 to CO. This is inconsistent with the formation of defined surface species, and suggests the formation of highly reactive carbon as the active center for the CO_2 transformation. Possibly rhodium does not participate in the conversion of CO_2 and is soley responsible for the activation of methane and the formation of active surface carbon.

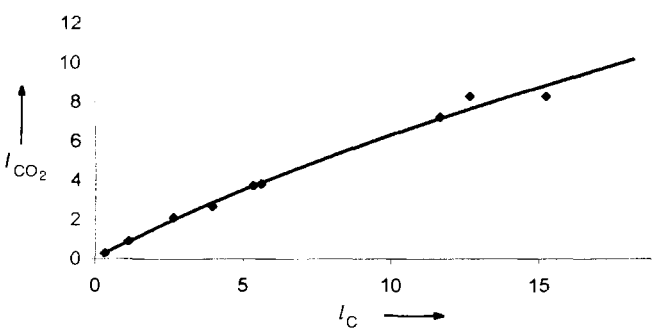


Fig. 4. Dependence of the amount of CO_2 (I_{CO_2}) converted (to 2 equivalents CO) in monolayers CO_2/Rh_s on the amount of preadsorbed carbon I_c in monolayers C_s/Rh_s.

Even though hydrogen is the only detectable product from methane decomposition in the stepwise CO_2 reforming, the question remains whether this reactive surface carbon contains any hydrogen-containing CH_x species. Since the release of hydrogen proceeds stoichiometrically within experimental error—two equivalents of H_2 are released per equivalent of CH_4 converted the concentration of partially dissociated methane (CH_x) species must be lower than the experimental error of about 5%. This was confirmed by deuteration experiments. At 700 °C the surface carbon can be effectively hydrogenated to methane by using pulses of hydrogen. If a catalyst previously coated with carbon is flushed at 700 °C with D_2 (30 mL min^{-1}), the deposited carbon is deuterated exclusively to CD_4. A significant amount to the partly deuterated methane was not detectable. This confirmed the investigations of Solymosi et al.,[14] who could not find any CH_x intermediates in in situ IR studies of the CH_4 decomposition on a Rh/Al_2O_3 catalyst.

After it was shown that the stepwise catalytic conversion of CH_4 with CO_2 in the presence of rhodium proceeds nearly quantitatively, it can be assumed that the same reaction mechanism as in Scheme 2 is operative in the continuous reaction process at identical reaction conditions.

Decisive for carbonization-free CO_2 reforming is a rapid reaction of the active carbon with CO_2, which avoids a high surface coverage of carbon. Such conditions can, of course, only be achieved when both reactants are added simultaneously, which corresponds to the well-known reaction conditions of the CO_2 reforming process. That this is the case with Rh/Al_2O_3 catalysts is shown by our results as well as those of Richardson et al.,[8] who were able to carry out the reaction under steady-state conditions (CH_4:CO_2 = 1:1, 500–800 °C) without deactivation, and who failed to observe any C deposition on the Rh catalyst even after longer reaction times.

The mechanism of the related reaction for production of syngas from methane and oxygen on Rh and Pt catalysts also appears to proceed via a reactive surface carbon intermediate. On account of the high selectivity of hydrogen in this reaction, Hickman and Schmidt[15] postulated that the complete decomposition of CH_4 with associated desorption of H_2 occurs as a preliminary step, prior to the selective oxidation of the resulting surface carbon with O_2 to give CO. Similar behavior in the CO_2 and steam reforming processes suggests that the reaction of CH_4 with H_2O proceeds by the same mechanism. The same stepwise mechanism may possibly form the basis of all these reactions of methane for the production of syngas. The exact characterization of the reactive carbon and its structural difference to unreactive carbon still remains to be clarified.

Experimental Procedure

The pulse experiments were carried out by using a catalyst characterization unit AMI 1 (Altamira Instruments). Gas pulses with a volume of 50 μL (ca. 2 μmol) were passed over the catalyst sample using helium carrier gas (30 mL min^{-1}). The interval between consecutive pulses was about 4 min. The gas flow containing products was monitored on-line with a thermal conductivity detector and a mass spectrometer (Ametek M200 M). The sampling for the mass spectrum was achieved by a quartz capillary located directly behind the catalyst sample, which was positioned in a heated, U-shaped quartz tube (internal diameter 4 mm). The temperature of the catalyst bed was monitored by a thermocouple attached to the outside—calibration experiments confirmed the outside to be at the same temperature as the catalyst bed. Rh(5%)/Al_2O_3 (390 mg) was used as catalyst. This was produced by an impregnation process from $RhCl_3 \cdot H_2O$ and Al_2O_3 Condea Pural 200 (S_{BET} = 78 m^2 g^{-1}). In order to ensure the reproducibility of the CH_4 and CO_2 chemisorption studies, the catalyst was subjected to an oxidation–reduction cycle between individual CH_4 and CO_2 chemisorption measurements (in each case 30 mL min^{-1}, O_2/30 min/600 °C, H_2/2 h/600 °C). The metal dispersion, that is the ratio of Rh atoms at the surface (Rh_s) to the total number of Rh atoms, was determined by CO-pulsed chemisorption, with an adsorption stoichiometry CO:Rh_s = 1:1, and yielded 3.25%. This dispersion remained constant throughout the studies. Before starting the pulse sequences the catalyst was reduced at 600 °C for 1 h in a flow of H_2 (30 mL min^{-1}) and then brought up to the desired reaction temperature of 700 °C by using a ramp rate of 10 K min^{-1} and a flow of He (30 mL min^{-1}). Finally the pulses of reactant gases CH_4 or CO_2 were applied. The TEM studies were obtained at 200 KeV on a field emission electron microscope (Hitachi HF2000).

Received: March 3, 1994 [Z 6726 IE]
German version: *Angew. Chem.* **1994**, *106*, 1738

[1] *Studies in Surface Science and Catalysis, Vol. 36* (Eds.: D. M. Bibby, C. D. Chang, R. F. Howe, S. Yurchak), Elsevier, Amsterdam, **1988**; J. M. Fox III, *Catal. Rev. Sci. Eng.* **1993**, *35*(2), 169.
[2] A. T. Ashcroft, A. K. Cheetham, M. L. H. Green, P. D. F. Vernon, *Nature* **1991**, *352*, 225.
[3] J. R. Rostrup-Nielsen, J.-H. Bak Hansen, *J. Catal.* **1993**, *144*, 38.
[4] J. R. Rostrup-Nielsen in *Catalysis Science and Technology, Vol. 5* (Eds.: J. R. Anderson, M. Boudart), Springer, Berlin, **1984**, p. 1; J. R. Rostrup-Nielsen, *Catal. Today* **1993**, *18*, 305.
[5] R. E. Reitmeier, K. Atwood, H. A. Bennett, H. M. Baugh, *Ind. Eng. Chem.* **1948**, *40*, 620.

[6] S. Teuner, *Hydrocarbon Proc.*, **May 1985**, 106; G. Kurz, S. Teuner, *Erdöl Kohle Erdgas, Petrochem.* **1990**, *32*, 171.
[7] O. Tokunaga, Y. Osada, S. Ogasawara, *Fuel* **1989**, *68*, 990; J. S. H. Q. Perera, J. W. Couves, G. Sankar, J. M. Thomas, *Catal. Lett.* **1991**, *11*, 219.
[8] J. T. Richardson, S. A. Paripatyadar, *Appl. Catal.* **1990**, *61*, 293.
[9] F. Solymosi, G. Kutsán, A. Erdhöhelyi, *Catal. Lett.* **1991**, *11*, 149.
[10] J. R. Rostrup-Nielsen, *J. Catal.* **1984**, *85*, 31.
[11] F. Fischer, H. Tropsch, *Brennstoffchemie* **1928**, *9*, 39.
[12] I. M. Bodrov, L. O. Apelbaum, *Kinet. Katal.* **1967**, *8*, 326.
[13] F. Solymosi, A. Erdöhelyi, J. Cserényi, *Catal. Lett.* **1992**, *16*, 399.
[14] A. Erdöhelyi, J. Cserényi, F. Solymosi, *J. Catal.* **1993**, *141*, 287.
[15] D. A. Hickmann, L. D. Schmidt, *Science* **1993**, *259*, 343.

Carboxylatoiron(II) Aggregates: A Novel Fe^{II}_4 Complex with Threefold Symmetry**

Stéphane Ménage, Hiroshi Fujii, Michael P. Hendrich, and Lawrence Que, Jr.*

Studies on the coordination chemistry of carboxylatoiron(II) complexes have recently been stimulated by the emergence of a new subclass of metalloproteins with nonheme diiron sites,[1] including hemerythrin (Hr),[2] the R 2 protein of ribonucleotide reductase (RNR),[3] and methane monooxygenase (MMO).[4] The diiron oxidation state is strongly implicated in the dioxygen binding and activation chemistry found for these proteins, and crystallographic studies show that carboxylato ligands bridge the divalent metal centers in hemerythrin and ribonucleotide reductase.[2a, 3b] As a result of efforts to model such protein sites, a number of bis(μ-carboxylato-*O*,*O'*)diiron complexes have been characterized, including $[Fe_2(\mu\text{-}O_2CCH_3)_2(tpa)_2](BPh_4)_2$[5, 6] $[Fe_2(\mu\text{-}OH)(\mu\text{-}O_2CCH_3)_2(Me_3tacn)_2]X$,[7] and $[Fe_2(\mu\text{-}H_2O)(O_2CCH_3)_4(tmen)_2]$;[8] the latter two complexes have additional μ-hydroxo and μ-aqua bridges. Furthermore, a new bridging motif, the monodentate carboxylate bridge supported by two other bidentate carboxylate bridges, has been found in $[Fe_2(biPhMe)_2(O_2CH)_4]$[9] and $[Fe_3(biPhMe)_2(O_2CCH_3)_6]$.[10] Using the carboxylate-containing tetradentate tripodal ligand bpg, we have synthesized a novel Fe^{II}_4 aggregate with crystallographic threefold symmetry; this is the largest carboxylatoiron(II) aggregate structurally characterized to date.

The combination of $Fe(ClO_4)_2\cdot 6H_2O$, Hbpg, $C_6H_5CO_2H$, and Et_3N in a molar ratio 1:1:1:2 in MeOH under argon engenders a light yellow precipitate which affords hexagonal crystals of **1** upon crystallization from CH_3CN/Et_2O. X-ray diffraction studies[11] show a tetrairon aggregate (Fig. 1), which consists of three crystallographically identical $Fe(bpg)(O_2CC_6H_5)$ units coordinated to a central Fe^{II} ion. The central iron ion (Fe 1) has a slightly distorted octahedral coordination environment formed by three benzoate oxygen atoms and three bpg carboxylate oxygen atoms; the Fe–O distances are 2.026(7) and 2.182(6) Å, respectively. The face consisting of the benzoate oxygen atoms spans a larger area than the corresponding face consisting of the bpg oxygen atoms, as indicated by respective O-Fe-O angles of 93.7 (4)° and 83.9(2)° within each face.

$[Fe_4(bpg)_3(O_2CC_6H_5)_3](ClO_4)_2$ **1**

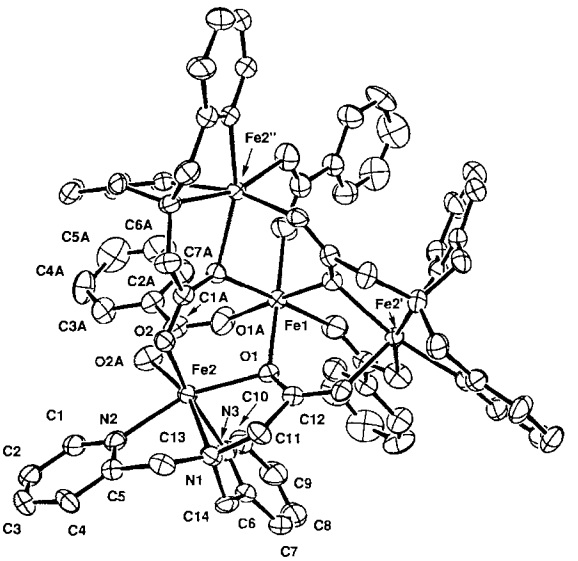


Fig. 1. Crystal structure of the $[Fe_4(bpg)_3(O_2CC_6H_5)_3]^{2+}$ cation in **1** (ORTEP plot, view down the threefold axis; 50% probability ellipsoids). Hydrogen atoms are omitted for clarity. Selected bond lengths [Å] and angles [°]: Fe1-O1 2.182(6), Fe1-O1A 2.026(7), Fe2-O1 2.168(6), Fe2-O2 2.143(6), Fe2-O2A 1.999(7), Fe2-N1 2.278(8), Fe2-N2 2.177(9), Fe2-N3 2.128(8), Fe1-Fe2 3.393(7), Fe2-Fe2' 5.484(7); Fe1-O1-Fe2 102.5(3), O1-Fe2-O2A 122.2(3), O1-Fe2-N1 75.4(2), O1-Fe2-N2 148.3(3), O1-Fe2-N3 82.8(2).

The aggregate is assembled as a trio of (μ-carboxylato-*O*)bis(μ-carboxylato-*O*,*O'*)diiron(II) pairs. Benzoate bridges between Fe 1 and the peripheral Fe 2 ions in a bidentate manner using the O1A *anti* lone pair for Fe 1 and the O2A *syn* lone pair for Fe 2. One bpg carboxylate oxygen atom acts as an monodentate bridge between Fe 1 and one Fe 2 ion and at the same time serves as part of a bidentate bridge between Fe 1 and a second Fe 2 center. Thus, the bpg carboxylate groups serve to hold three metal ions together, and the long Fe–O distances reflect this trinuclear bridging mode. Such a trinuclear arrangement with a monodentate bridge between one pair of metal centers and a bidentate bridge for another pair has been previously observed in $[Mn(O_2CCH_3)_2(H_2O)_4]$[12] and demonstrates the versatility of lone pairs on carboxylate oxygen atoms in bridging metal centers.[13] The Fe 1–Fe 2 distance of 3.393(7) Å compares favorably with the corresponding Fe–Fe distance of 3.325(1) Å found for $[Fe_3(biPhMe)_2(O_2CCH_3)_6]$, which also consists of a central iron ion connected to the terminal iron centers by this triply bridging motif.

The peripheral iron centers have N_3O_3 coordination environments derived from the nitrogen atoms of bpg and oxygen atoms from one benzoate and carboxylates of two different bpg ligands. The O1-Fe2-O2A angle of 122.2(3)° deviates most strongly from an ideal octahedral arrangement, no doubt a result of the *syn*, *anti* bridging mode of the benzoate ligand. The Fe 2–O 2A bond is the shortest (1.999(7) Å) of the complex and is *trans* to the expectedly long $Fe-N_{amine}$ bond (2.278(8) Å). The $Fe-N_{py}$ distances (2.177(9) and 2.138(8) Å) are typical of $Fe^{II}-N_{py}$ bonds. The peripheral Fe 2 centers are separated from each other by a distance of 5.484(7) Å.

The NMR spectrum of **1** exhibits a number of well-resolved isotropically shifted resonances that indicate an intact tetranuclear aggregate in solution (Fig. 2). The signals have been assigned on the basis of their relative intensities, T_1 values, COSY

[*] Prof. L. Que, Jr., Dr. H. Fujii, Dr. M. P. Hendrich
Department of Chemistry, University of Minnesota
Minneapolis, MN 55455 (USA)
Telefax: Int. code + (612)626-7541
Dr. S. Ménage
L.E.D.S.S. Université Joseph Fourier (France)

[**] This work was supported by a grant from the National Institutes of Health (GM-38767).

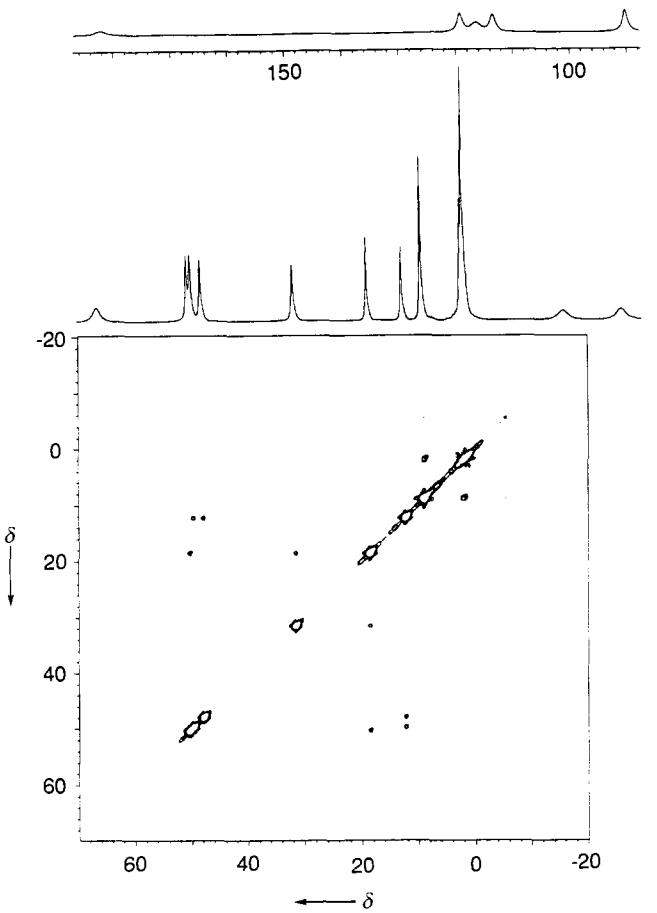


Fig. 2. 1D- and 2D (COSY) ^{1}H NMR spectra of **1** obtained at 300 MHz in CD_3CN.

connectivities, and comparisons with other high-spin iron(II) pyridine complexes.[14] Two sets of pyridine resonances are observed, each resonance corresponding to a proton per bpg unit, consistent with the distinct environments found for each of the pyridine units on the individual bpg ligands. The benzoate protons are also paramagnetically shifted (*m*: $\delta = 9.9$; *p*: $\delta = 4.2$), demonstrating that the carboxylato ligands remain coordinated in solution.

The EPR spectrum of **1** as a solid and dissolved in acetonitrile exhibits a signal at $g = 21$ which is enhanced in parallel mode ($H_1 \parallel H$) and increases in intensity as the temperature is lowered to 2 K (Fig. 3). These properties indicate that the signal arises from the ground doublet of an integer spin system.[15] Uncoupled Fe^{II} centers ($S = 2$) are expected to exhibit signals near $g = 8$, while a tetrairon(II) cluster with strong ferromagnetic coupling ($S = 8$) would result in a signal near $g = 32$. Thus, the position of the EPR signal of **1** indicates the presence of weak ferromagnetic interactions within the tetrairon aggregate. However, the complexity of the energy levels associated with a tetrairon species with weak ferromagnetic coupling does not allow us at present to pinpoint the origin of this signal without further investigation.

The temperature dependence of the magnetic moment of **1** at 0.31 T applied field is consistent with the EPR data. From 300 to 150 K its μ_{eff} value remains relatively constant at 10.4 μ_B (or 5.2 μ_B per Fe center), increases to a maximum of 10.8 μ_B (or 5.4 μ_B per Fe center) at 10 K, and then decreases dramatically below 10 K. The high temperature value suggests that the four iron centers are effectively uncoupled at high temperature, since it is

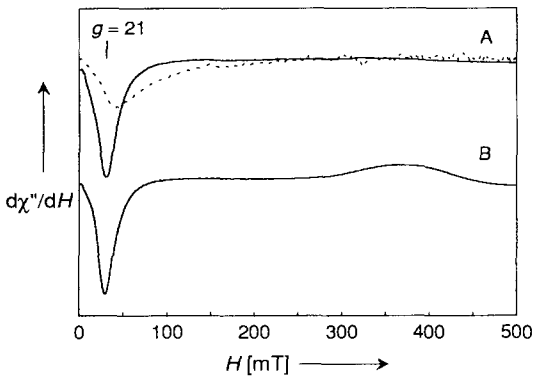


Fig. 3. EPR spectra of **1** in acetonitrile (A), $H_1 \parallel H$ (——), $H_1 \perp H$ (· · ·), and (B) 9 mg solid, $H_1 \parallel H$. The feature at $H = 375$ mT in (B) is not observed in solution and is of uncertain origin. Instrumental parameters: microwaves, 0.2 mW at 9.1 GHz, modulation, 0.1 mTpp at 100 kHz; gain for (A), 5000; gain for (B), 350.

only slightly higher than the spin-only value calculated for the uncoupled aggregate (9.8 μ_B per Fe_4 unit or 4.9 per Fe center). The value observed would be consistent with an uncoupled aggregate, when the spin-orbit coupling effects of high spin Fe^{II} centers are considered. The increase in magnetic moment at lower temperatures suggests the presence of weakly ferromagnetic coupling interactions, while the dramatic decrease of μ_{eff} below 10 K is attributed to zero-field splitting effects. A more detailed description of the magnetic properties of **1** is unavailable due to the complexity of the tetranuclear spin system. Given the large differences in the Fe1–Fe2 and the Fe2–Fe2 distances, the dominant magnetic interaction likely occurs between the central ion and the peripheral ions.

We have reported the structure and properties of a novel carboxylatotetrairon(II) aggregate. As carboxylato ligands are proposed as the initial binding loci for iron(II) ions in the threefold symmetric channels of the iron storage protein ferritin,[16] it is possible that aggregates similar to **1** may form in such channels.[17] If weak ferromagnetic interactions occur among these iron(II) centers, their presence in ferritin may be discerned by integer spin EPR spectroscopy.

Experimental Procedure

1: Treatment of $Fe(ClO_4)_2 \cdot 6H_2O$ (180 mg, 0.5 mmol) in MeOH (5 mL) with Hbpg (130 mg, 0.5 mmol), $HO_2CC_6H_5$ (61 mg, 0.5 mmol), and Et_3N (0.14 mL, 1 mmol) in MeOH (10 mL) under argon afforded a light yellow precipitate after stirring for 10 min. Recrystallization with CH_3CN/Et_2O afforded hexagonally shaped crystals suitable for X-ray diffraction. Correct C,H,N analysis.

Caution! Metal complexes with organic ligands and perchlorate anions are potentially explosive. Care should be exercised in handling these complexes, and they should be prepared in small amounts.

Received: March 10, 1994 [Z 6748 IE]
German version: *Angew. Chem.* **1994**, *106*, 1730

[1] L. Que, Jr., A. E. True, *Prog. Inorg. Chem.* **1990**, *37*, 97–200.
[2] a) M. A. Holmes, I. L. Trong, S. Turley, L. C. Sieker, R. E. Stenkamp, *J. Mol. Biol.* **1991**, *218*, 583–593; b) S. Sheriff, W. A. Hendrickson, J. L. Smith, *ibid.* **1987**, *197*, 273–296; c) R. E. Stenkamp, L. C. Sieker, L. H. Jensen, J. D. McCallum, J. Sanders-Loehr, *Proc. Natl. Acad. Sci. USA* **1985**, *82*, 713–716.
[3] a) P. Nordlund, B.-M. Sjöberg, H. Eklund, *Nature* **1990**, *345*, 593–598; b) M. Atta, R. Nordlund, A. Åberg, H. Eklund, M. Fontecave, *J. Biol. Chem.* **1992**, *267*, 20682–20688.
[4] A. C. Rosenzweig, C. A. Frederick, S. J. Lippard, P. Nordlund, *Nature (London)* **1993**, *366*, 537–543; b) J. G. DeWitt, J. G. Bensten, A. C. Rosenzweig, B. Hedman, J. Green, S. Pilkington, G. C. Papaefthymiou, H. Dalton, K. O. Hodgson, S. J. Lippard, *J. Am. Chem. Soc.* **1991**, *113*, 9219–9235; c) B. G. Fox, W. A. Froland, J. E. Dege, J. E. Lipscomb, *J. Biol. Chem.* **1989**, *264*, 10023–10033.
[5] S. Ménage, Y. Zang, M. P. Hendrich, L. Que, Jr., *J. Am. Chem. Soc.* **1992**, *114*, 7786–7792.

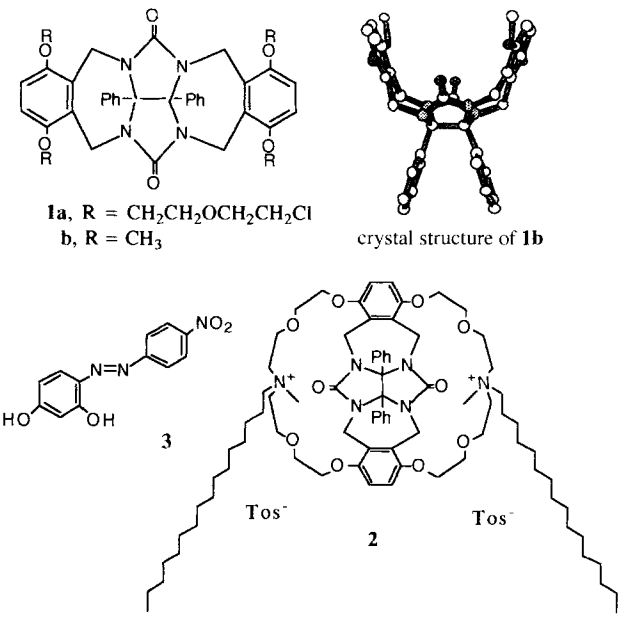
[6] Abbreviations used: biPhMe: 2,2'-bis(1-methylimidazolyl)phenylmethoxymethane; Hbpg, *N*,*N*-bis(2-pyridylmethyl)glycine; Me_3tacn: 1,4,7-trimethyl-1,4,7-triazacyclononane; tmen: *N*,*N*,*N'*,*N'*-tetramethylethylenediamine; tpa: tris(2-pyridylmethyl)amine.
[7] a) P. Chaudhuri, P. K. Wieghardt, B. Nuber, J. Weiss, *Angew. Chem.* **1985**, *97*, 774; *Angew. Chem. Int. Ed. Engl.* **1985**, *24*, 778–779; b) J. R. Hartman, R. L. Rardin, P. Chaudhuri, K. Pohl, K. Wieghardt, B. Nuber, J. Weiss, G. C. Papaefthymiou, R. B. Frankel, S. J. Lippard, *J. Am. Chem. Soc.* **1987**, *109*, 7387–7396.
[8] K. S. Hagen, R. Lachicotte, *J. Am. Chem. Soc.* **1992**, *114*, 8741–8742.
[9] a) W. B. Tolman, A. Bino, S. J. Lippard, *J. Am. Chem. Soc.* **1989**, *111*, 8522–8523; b) W. B. Tolman, S. Liu, J. G. Bentsen, S. J. Lippard, *ibid.* **1991**, *113*, 152–164.
[10] a) R. L. Rardin, A. Bino, P. Poganiuch, W. B. Tolman, S. Liu, S. J. Lippard, *Angew. Chem.* **1990**, *102*, 842–844; *Angew. Chem. Int. Ed. Engl.* **1990**, *29*, 812–814; b) R. L. Rardin, P. Poganiuch, A. Bino, D. P. Goldberg, W. B. Tolman, S. Liu, S. J. Lippard, *J. Am. Chem. Soc.* **1992**, *114*, 5240–5249.
[11] X-ray diffraction studies were carried out at 172 K on an Enraf-Nonius diffractometer on a crystal with dimensions $0.50 \times 0.45 \times 0.30$ mm and the following crystallographic parameters: space group, $P6_3$ (no. 173); $a = b = 13.129(5)$, $c = 25.413(7)$ Å; $V = 3794(4)$ Å^3; $Z = 2$. 9733 reflections were measured and combined to give 3144 ($R_{int} = 0.063$) unique reflections. All calculations were performed by using 2077 reflections ($I > 3.00\sigma(I)$) with 306 parameters (data/parameter = 6.79) to afford $R = 0.050$ and $R_w = 0.067$. The Texsan-Texray Structure Analysis Package from Molecular Structure Corporation (1985) was used. Further details of the crystal structure investigation are available on request from the Director of Cambridge Crystallographic Data Centre, 12 Union Road, GB-Cambridge CB21EZ (UK), on quoting the full journal citation.
[12] E. F. Bertaut, Q. D. Tran, P. Burlet, M. Thomas, J. M. Moreau, *Acta Crystallogr. Sect. B* **1974**, *30*, 2234.
[13] R. L. Rardin, W. B. Tolman, S. J. Lippard, *New J. Chem.* **1991**, *15*, 417–430.
[14] L.-J. Ming, H. G. Jang, L. Que, Jr., *Inorg. Chem.* **1992**, *31*, 359–364.
[15] a) M. P. Hendrich, L. L. Pearce, L. Que, Jr., N. D. Chasteen, E. P. Day, *J. Am. Chem. Soc.* **1991**, *113*, 3039–3044; b) M. P. Hendrich, E. Münck, B. G. Fox, J. D. Lipscomb, *ibid.* **1990**, *112*, 5861–5865.
[16] a) J. G. Wardeska, B. Viglione, N. D. Chasteen, *J. Biol. Chem.* **1986**, *261*, 6677–6683; b) D. Jacobs, G. D. Watt, R. B. Frankel, G. C. Papaefthymiou, *Biochemistry* **1989**, *28*, 9216–9221; c) G. D. Watt, R. B. Frankel, D. Jacobs, H. Huang, G. C. Papaefthymiou, *ibid.* **1992**, *31*, 5672–5679.
[17] Interestingly, when exposed to O_2, **1** converts to a (μ-oxo)diiron species with an NMR spectrum identical to that of the previously reported $[Fe_2O(O_2CC_6H_5)(bpg)_2](ClO_4)$ (S. Ménage, L. Que, Jr., *New. J. Chem.* **1991**, *15*, 431–438).

Molecular Golf Balls: Vesicles from Bowl-Shaped Host Molecules**

Albertus P. H. J. Schenning, Bas de Bruin, Martinus C. Feiters,* and Roeland J. M. Nolte*

Synthetic molecules containing a hydrophilic head group and one or two hydrophobic tails are known to form a great variety of supramolecular structures such as micelles, multilayers, rods, and vesicles.[1] It has been proposed that the type of aggregate structure depends on the shape of the amphiphile, as characterized by the so-called "packing parameter".[2] Recent studies, however, indicate that other factors are important. For example, single-tail surfactants with a large rigid segment[3, 4] or surfactants with a hyperextended chain[5] form vesicles instead of micelles, as predicted by the shape–structure concept. Vesicular structures are also formed by two-headed single-chain surfactants, for instance the lariat ether bolaamphiphiles.[6] We report here that bowl-shaped host **2**, which has two tails, two head groups, and a rigid cleft, forms vesicles upon dispersal in water.

Amphiphile **2**[7] was synthesized in two steps (Scheme 1): first **1a**[8] was treated with hexadecylamine in acetonitrile under Finkelstein conditions[9] (60%) and subsequently the product was methylated with methyl tosylate in toluene (80%).



Scheme 1.

When **2** (10 mmol) was dissolved in methanol (50 µL) and injected in water (3 mL) vesicles were formed, as could be deduced from electron microscopy.

As can be seen in Figure 1, the application of both the freeze-fracture and the negative staining technique show the presence of spherical vesicles with a diameter of approximately 4000 Å. These aggregates have a closed structure, as deduced from subsequent encapsulation experiments[1] with the fluorescent dye ethidium bromide.[10] Conductivity measurements revealed that the critical aggregation concentration (CAC) of **2** is 2×10^{-5} M. A vesicle dispersion of the amphiphile was dried on a glass plate in vacuo to give a cast film which was examined by X-ray diffraction. The diffraction patterns displayed a clear periodicity of 53 Å up to the 10th order reflection.

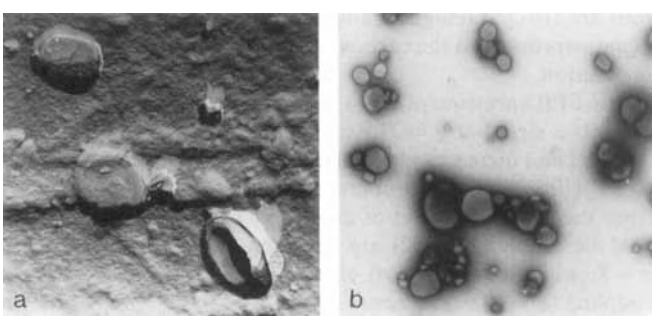


Fig. 1. Electron micrographs of a 0.02 M dispersion of **2**. Freeze-fracture (magnification 28000 ×) (a) and negative staining technique (magnification 9000 ×) (b).

[*] Prof. Dr. R. J. M. Nolte, Dipl.-Chem. A. P. H. J. Schenning, B. de Bruin, Dr. M. C. Feiters
Department of Organic Chemistry, NSR Center, University of Nijmegen
Toernooiveld, NL-6525 ED Nijmegen (The Netherlands)
Telefax: Int. code + (31)80-55-34-50

[**] This work was supported by Netherlands Foundation for Chemical Research (SON) with financial aid from the Netherlands Organization for Scientific Research (NWO).

Based on these data, we propose that the vesicles have a structure similar to that of a golf ball (Fig. 2). The thickness of the bilayer is 53 Å, which corresponds to two fully extended hexadecylamine chains. The host amphiphiles are aligned with their concave binding moieties facing the aqueous phases.

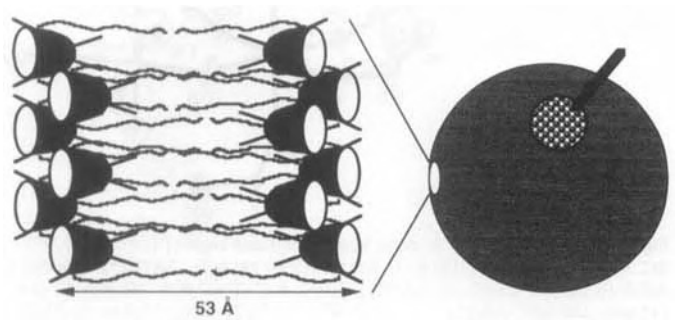


Fig. 2. Schematic representation of a vesicle formed by **2**.

We previously showed[11] that molecular clips such as **1b** can bind aromatic substrates in chloroform, for example resorcinol and its derivative **3**. Binding occurs by π-π stacking interactions with the two aromatic "walls" of **1b** and by hydrogen bonding with the urea carbonyl groups, as determined by IR and ^{1}H NMR spectroscopy.

The binding properties of **2** were determined in chloroform and water by NMR and UV/Vis titration experiments.[12] In chloroform, resorcinol and resorcinol derivative **3** form 1:1 inclusion complexes with **2**; the corresponding association constants are $K_a = 3400$ and 500 M^{-1}, respectively. These values are similar to those measured for these guests with **1b** ($K_a = 2600$ and 700 M^{-1}, respectively). In water, under the CAC of **2**, compound **3** is bound in a 1:1 host–guest ratio with an association constant of $K_a = 3 \times 10^5$ M^{-1}. This value is very high when compared to that in chloroform, but is of the same order of magnitude as that found for amphiphilic cyclophanes[13] with nonionic guests. Titration experiments with **2** in concentrations above the CAC indicated that only 50% of the molecular bowls are capable of binding a guest molecule. In a separate experiment we checked with electron microscopy that the vesicle structure is not destroyed by guest binding. The titration curve could only be fitted by assuming that half of the host molecules are involved in the binding process. In this case, we obtained a good correlation for a 1:1 complex with a binding constant of $K_a = 4 \times 10^5$ M^{-1}. This result suggests that only the dimples on the outer surface of the molecular golf balls are accessible to guest molecules and that the inner part of the aggregates cannot be reached.

In summary, we have shown that molecular objects with high binding affinities can be formed from rigid host molecules that have two tails and two ammonium groups. Further studies are aimed at stabilizing the aggregates by polymerization. Application of the polymerized structures can be conceived in the field of chromatographic separation of organic molecules. To this end the synthesis of chiral derivatives of **2** is currently in progress.

Received: February 19, 1994 [Z 6699 IE]
German version: *Angew. Chem.* **1994**, *106*, 1741

[1] J. H. Fendler, *Membrane Mimetic Chemistry*, Wiley, New York, **1982**.
[2] J. N. Israelachvili, D. J. Mitchell, B. W. Ninham, *J. Chem. Soc. Faraday Trans. 2* **1976**, *72*, 1525.
[3] T. Kunitake, Y. Okahata, M. Shimomura, S. Yasunami, K. Takarabe, *J. Am. Chem. Soc.* **1981**, *103*, 5401.
[4] A. P. H. J. Schenning, M. C. Feiters, R. J. M. Nolte, *Tetrahedron Lett.* **1993**, 7077.
[5] F. M. Menger, Y. Yamasaki, *J. Am. Chem. Soc.* **1993**, *115*, 3840.
[6] S. Muñoz, J. Mallén, A. Nakano, Z. Chen, I. Gay, L. Echegoyen, G. W. Gokel, *J. Am. Chem. Soc.* **1993**, *115*, 1705.
[7] **2**: M.p. 210 °C; ^{1}H NMR (90 MHz, $CDCl_3$, 25 °C, TMS): $\delta = 0.86$ (t, 6H, CH_2CH_3), 1.24 (s, 52H, CH_2),1.80 (m, 4H, CH_2CH_2N), 2.30 (s, 6H, CH_3 tosylate), 4.6 3.2 (m, 42H, CH_2N, CH_3N, CH_2O, NCH_2Ar), 5.61 (d, 4H, NCH_2Ar), 6.58 (s, 4H, ArH), 7.13 (m, 14H, ArH, ArH tosylate), 7.81 (d, 4H, ArH tosylate); IR (KBr): $\tilde{\nu}$[cm^{-1}] = 3080 2980 (ArH), 2960–2820 (CH_2 and CH_3), 1707 (C=O), 1640–1590 (C=C), 1480 1420 (CH_2 and CH_3), 1350 (C–N), 1150–1050 (C-O-C); IR (D_2O, 5×10^{-3} M): $\tilde{\nu} = 1692$ cm^{-1} (C=O); FAB-MS (nitrobenzyl alcohol) *m/z* (%): 1525 (50) [*M* – Tos], 1339 (100) [*M* – Me – 2Tos]. Correct elemental analysis (C,H,N,S) for $C_{96}H_{140}N_6O_{16}S_2 \cdot 3H_2O$.
[8] R. P. Sijbesma, R. J. M. Nolte, *J. Org. Chem.* **1991**, *56*, 3122.
[9] *Methoden Org. Chem. (Houben-Weyl) 4th ed. 1952–*, Vol. V/4, **1952**, p. 595.
[10] R. P. Haugland, *Molecular Probes, 5th ed. 1992–1994*, Molecular Probes, Eugene, **1992**.
[11] R. P. Sijbesma, A. P. M. Kentgens, E. T. G. Lutz, J. H. van der Maas, R. J. M. Nolte, *J. Am. Chem. Soc.* **1993**, *115*, 8899.
[12] Binding constants in chloroform were determined by ^{1}H NMR by following the chemical shift of appropriate host and guest protons and by UV/Vis by following the absorption of the guest **3** at 438 nm as a function of its concentration ($0-2 \times 10^{-4}$ M). For both types of experiments the same constant host concentration was used (5×10^{-4} M). In water, NMR measurements could not be applied for this purpose because of the occurrence of broad lines due to aggregation of **2**. Under the CAC of **2** the absorbance of **3** was monitored at 450 nm as a function of the guest concentration ($0-1.8 \times 10^{-5}$ M) with a constant host concentration of 2.5×10^{-6} M. At a concentration above the CAC of **2** the absorbance of **3** was monitored at 534 nm as a function of the guest concentration ($0-5 \times 10^{-4}$ M), with a constant host concentration of 2.5×10^{-6} M. The errors in the binding constants are approximately 10% and 50% for the experiments in chloroform and water, respectively.
[13] Y. Murakami, J. Kikuchi, T. Ohno, O. Hayashida, M. Kojima, *J. Am. Chem. Soc.* **1990**, *112*, 7672.

Synthesis and Structure of $[Ni(SO_2)_6](AsF_6)_2$ and $[Fe(SO_2)_4(FAsF_5)_2]$**

Enno Lork, Jan Petersen, and Rüdiger Mews*

The chemistry of SO_2 as a ligand[1] and solvent[2] has been studied in great detail. The coordination behavior of this three-atom molecule is remarkably versatile: Six different bonding modes are known;[1] this figure does not take into account insertion products obtained from organometallic reactions.[3] Vibrational spectra and/or stability criteria allow predictions to be made on the nature of the metal–ligand linkage;[1] these predictions are often, but not always, correct.

The most common modes of coordination for SO_2 ligands in transition metal chemistry are η^1-S and side-on η^2-SO; however, examples of S- or SO-bound bridging ligands are also known. Only three complexes (Ni^{II} and Mn^{II} chemistry[4–7]) in which the SO_2 ligands are exclusively O-bound, as determined by X-ray structure analysis, have been reported to date. In these complexes a maximum of two SO_2 ligands in a *trans* arrangement are attached to a six-coordinate metal center.

The oxidation of Ni powder with AsF_5 in liquid SO_2 yields $[Ni(SO_2)_n](AsF_6)_2$.[8] Accounts in the literature regarding the nature of the Ni–ligand bond and the number *n* of coordinated SO_2 molecules differ. Passmore and Desjardins[8] have suggest-

[*] Prof. Dr. R. Mews, E. Lork, J. Petersen
Institut für Anorganische und Physikalische Chemie der Universität
Postfach 330440, D-28334 Bremen (FRG)
Telefax: Int. code + (421)218-4267

[**] This work was supported by the Fonds der Chemischen Industrie.

ed that $n = 2$. From the IR spectrum they concluded that SO_2 is O-coordinated; the tetrahedral environment of the central Ni atom followed from magnetic measurements. However, the similarity of the IR spectrum to that obtained for $[Mg(OSO)_2(\mu\text{-}F_2AsF_4)_2]_n$,[9] which was unambiguously characterized by X-ray structure analysis, is indicative of a six-coordinate environment.

We report here on the observation that the bis(sulfur dioxide) complex **2**, isolated as a yellow powder, is a degradation product of the green, crystalline six-coordinate complex **1**, the first characterized homoleptic SO_2 complex. Complex **1** is only stable in

$$Ni + 3\,AsF_5 \xrightarrow{SO_2} \underset{\mathbf{1}}{[Ni(SO_2)_6](AsF_6)_2} + AsF_3$$

$$\xrightarrow{-4\,SO_2} \underset{\mathbf{2}}{[Ni(SO_2)_2](AsF_6)_2}$$

the presence of an excess pressure of SO_2 or in contact with liquid SO_2; rapid decomposition even occurs under an SO_2 atmosphere. The X-ray structure analysis of **1** at $-100\,^{\circ}C$ shows that the Ni^{II} center is octahedrally coordinated with O-bound SO_2 ligands (Fig. 1).[10] The Ni–O bond lengths are 203.3(3)–204.3(4) pm, and the Ni–O–S angles range from 139.8(2) to 145.6(2)°. The distance between S and the coordinating oxygen atom ($d(O_\mu\text{–}S)$, 144.3(4)–145.0(4) pm) is slightly greater than that in free SO_2 ($d(SO) = 143.1$ pm[13]); the bond between S and the noncoordinated oxygen atom is, on the other hand, markedly shortened ($d(S\text{–}O_t)$, 140.5(4)–141.8(4) pm). These results are consistent with previously established bonding models.[14]

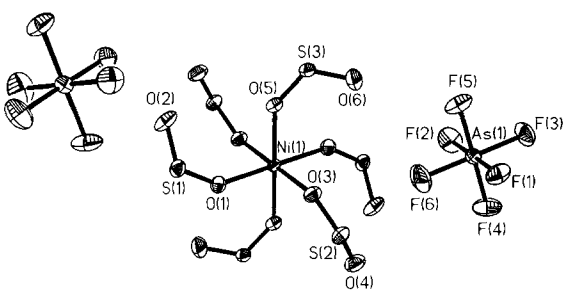


Fig. 1. Crystal structure of **1**; bond lengths [pm] and angles [°]: Ni-O 203.3(3)–204.4(3), O_μ-S144.3(4)–145.0(4), S-O_t 140.5(4)–141.8(4), As-F 169.6(4)–173.3(3); Ni-O-S 139.8(2)–145.6(2), O-S-O 116.2(2)–117.5(2), F-As-F 89.2(2)–90.7(2).

From these studies we conclude that O-coordination of SO_2 in transition metal chemistry is not as uncommon as previously thought and that it occurs for metal centers with oxidation states $\geq$ II. The lability of these complexes has prevented their characterization by X-ray structure analysis. The number of isolable, homoleptic SO_2 complexes is expected to be very limited, but this structural type is certainly quite common for compounds of the general formula $[ML_m(SO_2)_n]^{2+}$ with $n = 1, 2$, in which SO_2 is present as coligand.

In his report on the oxidation of iron with AsF_5 in liquid SO_2, P. A. W. Dean did not explicitly state how many SO_2 ligands were present in the product.[15] An X-ray structure analysis of the product **3** shows that four SO_2 ligands are attached to the

$$Fe + 3\,AsF_5 \xrightarrow{SO_2} \underset{\mathbf{3}}{[Fe(SO_2)_4(AsF_6)_2]}$$

central Fe atom; two $FAsF_5$ ligands in a *cis* relationship complete the octahedral coordination geometry (Fig. 2).[16] At

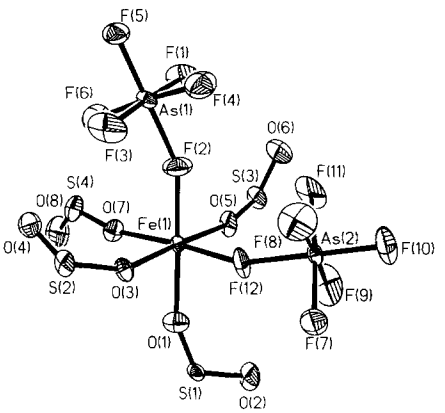


Fig. 2. Crystal structure of **3**; bond lengths [pm] and angles [°]: Fe-O 207.5(7)–212.3(6), O_μ-S 141.4(7)–144.4(7), S-O_t 137.3(9)–141.8(7), As(1)-F(2) 180.2(6), As1-F 167.6(6)–171.6(6), As(2)-F(12) 176.3(5), As(2)-F 167.9(7)–169.9(6); Fe-O-S 142.6(4)–164.5(5), O-S-O 117.2(5)–119.4(5), Fe-Fe(2)-As(1) 155.7(4), Fe-F(12)-As(2) 148.2(3).

room temperature complex **3** rapidly loses some of the SO_2 ligands.

Experimental Procedure

Complex **1** was prepared according to the literature [8] by oxidation of Ni powder with AsF_5 in liquid SO_2 at room temperature. The reaction was carried out in a high-pressure Schlenk vessel [17], which was equipped with a porcelain frit. After filtration of the reaction solution, the solvent was transfered into the ice-cooled side arm of the reaction vessel. Green crystals of **1** were formed. The solvent SO_2 was removed by evaporation under normal pressure at 0 °C.

The synthesis [14], isolation, and preparation of single crystals of **3** was achieved in an analogous fashion [18].

Received: March 16, 1994 [Z.6766IE]
German version: *Angew. Chem.* **1994**, *106*, 1724

[1] R. R. Ryan, G. J. Kubas, D. C. Moody, P. G. Eller, *Struct Bonding (Berlin)* **1981**, *46*, 47–100; W. A. Schenk, *Angew. Chem.* **1987**, *99*, 101–112; *Angew. Chem. Int. Ed. Engl.* **1987**, *26*, 98–109.
[2] For example: D. F. Burow in *Nonaqueous Solvents, Vol. 3* (Ed.: J. J. Lagowski), Academic Press, New York, **1970**, p. 138; R. Mews, *J. Chem. Soc. Chem. Commun.* **1979**, 278–279.
[3] A. Wojcicki, *Adv. Organomet. Chem.* **1974**, *12*, 31–81.
[4] R. Hoppfenheit, R. Mews, M. Noltemeyer, G. M. Sheldrick, *Chem. Ber.* **1983**, *116*, 874–881.
[5] R. Maggiulli, R. Mews, W.-D. Stohrer, M. Noltemeyer, *Chem. Ber.* **1990**, *123*, 29–34.
[6] G. A. Gott, J. Fawcett, C. A. McAuliffe, D. R. Russel, *J. Chem. Soc. Chem. Commun.* **1984**, 1283–1284.
[7] SO_2 is also O-bound in $[Cd\{(CN)_2\}_2SO_2]$, H. W. Roesky, M. Noltemeyer, J. Schimkowiak, G. M. Sheldrick, *Z. Naturforsch. B* **1988**, *43*, 949–951.
[8] C. D. Desjardins, J. Passmore, *J. Fluorine Chem.* **1975**, *6*, 379–388.
[9] R. Hoppenheit, W. Isenberg, R. Mews, *Z. Naturforsch. B* **1982**, *37*, 1116–1121.
[10] X-ray structure analysis of **1** ($As_2F_{12}NiS_6O_{12}$): $M = 820.9$; crystal dimensions $0.8 \times 0.4 \times 0.3$ mm^3, space group $P2_1/c$, $a = 785.3(2)$, $b = 870.2(2)$, $c = 1513.6(3)$ pm, $\beta = 93.51(3)^{\circ}$, $V = 1032.4(4) \times 10^6$ pm^3, $Z = 2$, $\rho_{calcd} = 2.641$ Mgm^{-3}, $\mu = 4.884$ mm^{-1}. A crystal suitable for X-ray structure analysis was mounted with Kel-F oil on a glass thread. X-ray data was collected using a Siemens-P4 diffractometer equipped with a graphite monochromator ($Mo_{K\alpha}$ radiation) at $-100\,^{\circ}C$. 5752 measured reflections in $\omega/2\theta$ scan mode ($5.0^{\circ} < 2\theta < 55^{\circ}$) of which 2379 were symmetry-independent after averaging. Structure solution by direct methods. After an empirical absorption correction was applied [11], refinement of F converged for $R = 0.0570$, $wR = 0.0449$ for 1765 reflections with $F_0 > 4\sigma(F_0)$ and 152 parameters. All calculations were carried out using the SHELXTL program package [12] (cf. [16b]).
[11] N. Walker, D. Stuart, *Acta Crystallogr. Sect. A* **1983**, *39*, 158–166.
[12] Siemens SHELXTL PLUS: Release for Siemens R3 Cristallographic Research Systems, Siemens Analytical X-Ray Instruments Inc., Madison, WI, USA, 1989.
[13] B. Post, R. S. Schwartz, J. Fankuchen, *Acta Crystallogr.* **1952**, *5*, 372–374; C. H. Holder, Jr., M. Fink, *J. Chem. Phys.* **1981**, *75*, 5323–5325.
[14] R. J. Gillespie, F. G. Riddell, D. R. Slim, *J. Am. Chem. Soc.* **1976**, *98*, 8069–8072; W. J. Moore, H. W. Baird, H. B. Miller, *J. Am. Chem. Soc.* **1968**, *90*, 1358–1359.

[15] P. A. W. Dean, *J. Fluorine Chem.* **1975**, *5*, 499–507.
[16] a) X-ray structure analysis of **3** ($As_2F_{12}FeO_8S_4$): $M = 689.93$, crystal dimensions $1.0 \times 0.8 \times 0.4$ mm^3, space group $P2_1/c$, $a = 858.1(2)$, $b = 1358.2(3)$, $c = 1481.8(3)$ pm, $\beta = 99.66(2)^\circ$, $V = 1702.5(6) \times 10^6$ pm^3, $Z = 4$, $\rho_{calcd} = 2.692$ Mg m^{-3}, $\mu = 5.389$ mm^{-1}. X-ray data collection as described above for **1**. 3988 measured reflections in $\omega/2\theta$ scan mode ($5.0^\circ < 2\theta < 50^\circ$). Empirical absorption correction by ψ-scans for 16 reflections; 2971 independent reflections remained after averaging. Structure solution by direct methods. Refinement of F^2 converged for $wR2 = 0.1621$ for all data and 244 parameters ($R1 = 0.0588$ for 2157 reflections with $F_0 > 4\sigma(F_0)$). Structure solution with the SHELXTL program package [12]; for refinement SHELXL-93 [19] was used. b) Further details of the crystal structure investigation may be obtained from the Fachinformationszentrum Karlsruhe, D-76344 Eggenstein-Leopoldshafen (FRG), on quoting the depository number CSD-58197.
[17] G. Hartmann, R. Fröböse, R. Mews, G. M. Sheldrick, *J. Naturforsch. B* **1982**, *37*, 1234–1240.
[18] We thank H. Gillandt and M. Plikat for the preparation of compound **3**.

Three-Dimensional Interpenetrating Double and Triple Framework Structures in $[Cd(bpy)_2\{Ag(CN)_2\}_2]$ and $[Cd(pyrz)\{Ag_2(CN)_3\}\{Ag(CN)_2\}]$

Takayoshi Soma, Hidetaka Yuge, and Toschitake Iwamoto*

By replacing CN bridges in multidimensional CN-linked metal complexes by NC-Ag-CN or NC-Ag-(CN)-Ag-CN units, we have obtained **1** (bpy = 4,4′-bipyridine) and **2** (pyrz = pyrazine), which are composed of double and triple interpenetrating frameworks, respectively. In both compounds the three-dimensional frameworks are constructed entirely by coordinative linkages. The interpenetrating triple framework of **2** is unprecedented.

$[Cd(bpy)_2\{Ag(CN)_2\}_2]$ **1** $[Cd(pyrz)\{Ag_2(CN)_3\}\{Ag(CN)_2\}]$ **2**

A number of the topologically different multidimensional structures with M-CN-Cd links have been developed using $[M(CN)_4]^{2-}$ moieties (M = Ni, Pd, Pt: square planar; M = Cd, Hg, Zn: tetrahedral) as building blocks.[1–5] We have recently replaced the CN group in the M-CN-Cd link (5.5 Å long) with the bidentate linear NC-Ag-CN and NC-Ag-(CN)-Ag-CN groups to extend the bridge to 10.5 Å and 16 Å, respectively. In this way we obtained in the first case, [Cd(4-methylpyridine)$_2\{Ag(CN)_2\}_2$] · 4-methylpyridine, a compound with an interwoven double network, and in the second case, the polymeric complex $[Cd(4\text{-methylpyridine})_4\{Ag_2(CN)_3\}][Ag(CN)_2]$, which is composed of linear chains,[6] in which only the unidentate 4-methylpyridine completes the octahedral coordination of the Cd atoms. Novel supramolecular structures may be generated by using extended linear bridging ligands as spacers between the Cd atoms.

Colorless crystals of **1** formed in the reaction of $CdCl_2$ and $K[Ag(CN)_2]$ (1:2 molar ratio) and a small excess of bipyridine in aqueous solution; the pH of the solution was adjusted to 10 with $NH_2CH_2CH_2OH$ and $CH(OH)CO_2H(CH_2CO_2H)_2$. Crystals of **2** were obtained from an aqueous solution of $K_2[Cd(CN)_4]$, $AgNO_3$, and pyrazine (1:2:1 molar ratio) under the same basic conditions. The postulated compositions were confirmed by elemental analysis, and the structures were determined by single-crystal X-ray diffraction.[7]

In the structure of **1** the Cd atoms are located at the origin and equivalent positions in the $P2_1/c$ space group and are each linked by four *catena*-μ-$[Ag(CN)_2]^-$ ligands to four further Cd atoms (Fig. 1 top). A two-dimensional network along the *bc* plane results with an approximately rhombic mesh (edge length

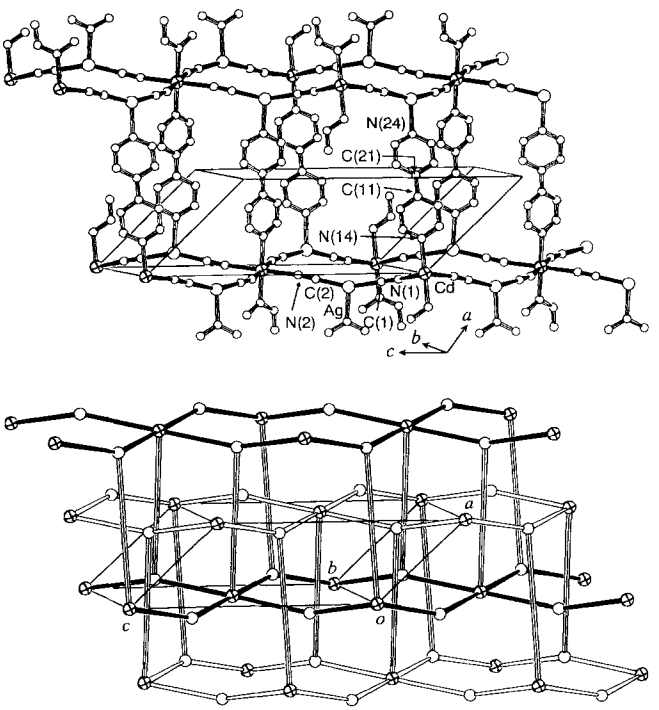


Fig. 1. Top: One of the 3D frameworks observed in **1**; view along the *b* axis; the unit cell is sketched in with the thin lines. Bottom: View of the interpenetrating double framework structure of **1**. Cd: balls with crosses; Ag: white balls; CN: white sticks; bpy: lined sticks.

of $(b + c)/2 \approx 10.5$ Å, acute angle of roughly 66°). The Cd-NC-Ag-CN-Cd bridge in **1** is about twice the length of the Hofmann-type Cd-NC-Ni bridge.[1] The Cd atoms in the network coordinate to two bpy ligands in a *trans* arrangement to attain octahedral coordination. The Cd-NC-Ag units deviate from linearity (Cd-N(2)-C(2) 157.9(4)°). The network puckers such that the $Ag(CN)_2$ moieties shift alternately upwards and downwards out of the *bc* plane. The bpy ligands are "threaded" through the meshes of the immediately adjacent networks and bound to the Ag atoms in subsequent network (Fig. 1 bottom). The Ag atoms are three-coordinate, the Ag–N(24) distance is 2.463(3) Å, and the C-Ag-C units are bent out of the *bc* plane (C(1)-Ag-C(2) 153.6(2)°). The threaded network generated by translation along the *a* axis is thus completely independent; no direct covalent bonds link the interpenetrating networks. Owing to the puckering of the network, the Cd-(bpy)-Ag distance of 11.93(2) Å is shorter than $2a \sin\beta = 12.85(1)$ Å. The dihedral angle between the pyridine rings of the bpy ligands is 27.5°.

The hexacoordinate Cd atoms in **2** are located on the twofold axes of the $P2/c$ space group and are interconnected to form a three-dimensional framework (Fig. 2). The Cd···Cd distance in the Cd(*catena*-μ-pyrz)-Cd unit along the C_2 axis parallel to the *b* axis is 7.560(3) Å, in the Cd-(*catena*-μ-NC-Ag(CN)Ag-

[*] Prof. Dr. T. Iwamoto, T. Soma, Dr. H. Yuge
Department of Chemistry, College of Arts and Sciences
University of Tokyo
Komaba, Meguro, Tokyo 153 (Japan)
Telefax: Int. code + (3)3485-2904

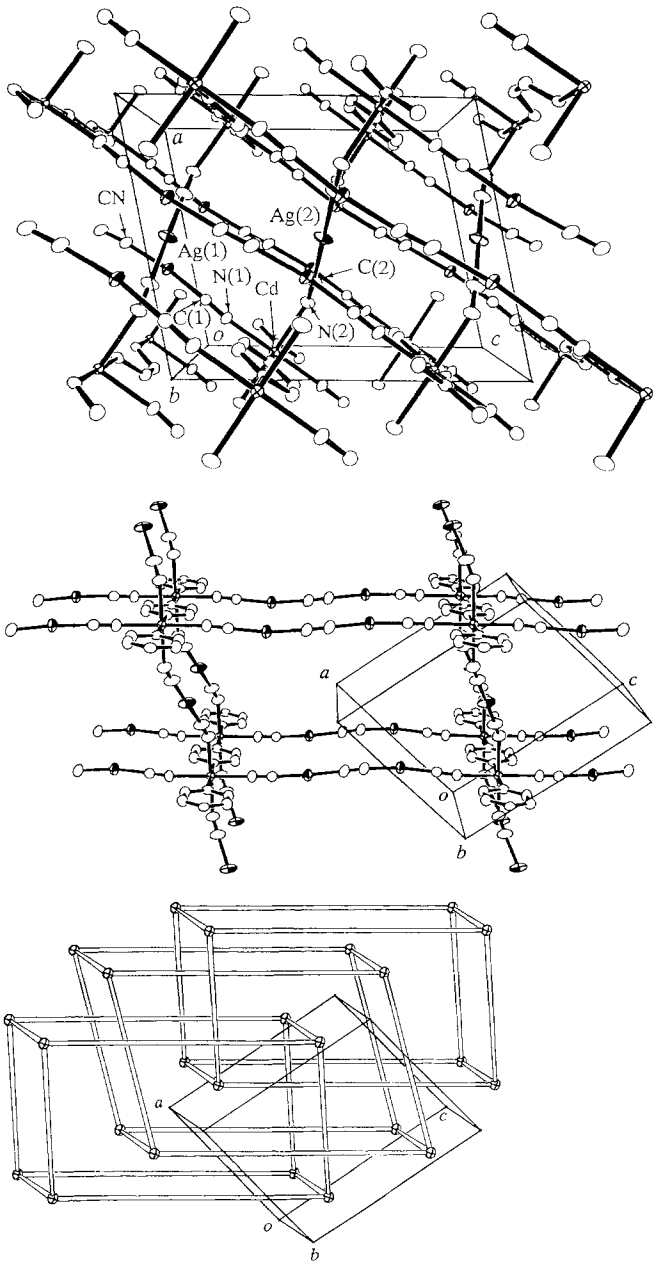


Fig. 2. Top: Unit cell structure of **2** viewed along the *b* axis; the unit cell is sketched in with thin lines. Middle: View of one of the three frameworks. Bottom: Representation of the interpenetrating triple framework structure along with a sketch of the unit cell; Cd atoms: balls with crosses; pyrz, $Ag(CN)_2$, and $Ag_2(CN)_3$ units: sticks.

CN)-Cd unit parallel to the [101] roughly 16 Å, and in the Cd-(*catena*-μ-NC-Ag-CN)-Cd unit parallel to [121] or [1$\bar{2}$1] approximately 9.6 Å. Because of the C_2 symmetry, crystallographic discrimination between the C and N atoms of the central CN group in the NC-Ag-(CN)-Ag-CN unit is impossible. The two-dimensional networks formed by the Cd-pyrz-Cd and Cd-NC-Ag-(CN)-Ag-CN-Cd links (horizontal layers in Fig. 2 middle) are stacked along [101] with a separation of roughly 3.2 Å. Two such layers are connected by perpendicular Cd-NC-Ag-CN-Cd bridges to form a three-dimensional framework structure. These links "thread" the meshes of adjacent networks such that the first and fourth are coordinatively connected. In this way three sets of interpenetrating frameworks are formed which give an unprecedented triple framework structure without any direct chemical bonds. The layers (horizontal in Fig. 2 middle and bottom) have a zigzag arrangement since the direction of the Cd-NC-Ag-CN-Cd bridge changes alternately from [121] to [1$\bar{2}$2] in a set of the framework. The Ag–Ag distance between the NC-Ag-CN and NC-Ag-(CN)-Ag-CN linkages is 3.144(1) Å, only slightly longer than that in Ag metal (2.89 Å).

Extended linear structures with $Ag(CN)_2$ bridges have been observed in $[Zn(en)_2][\{Ag(CN)_2\}_2]$ (en = ethylenediamine)[8a] and in $[Cu(2,2'\text{-bpy})_2][\{Ag(CN)_2\}_2]$.[8b] Compounds with multiple, three-dimensional, interpenetrated structures are also known: two interpenetrated 3D frameworks linked by coordinative bonds occur in the anticuprite-type $M(CN)_2$ (M = Cd, Zn)[2d, 4a] and in $[Zn(H_2O)_2(bpy)_2] \cdot SiF_6$.[9] in the latter the monodentate aqua ligands do not participate in bridging. Six three-dimensional interpenetrated diamondlike frameworks exist in $[Cu\{NC(CH_2)_4CN\}_2]_n \cdot nNO_3^-$.[10] The adiponitrile bridge between the Cu^I atoms is about 12 Å long, and the NO_3^- ions do not participate in the bridging. Five interpenetrated framework structures were found in the diamondlike 3D framework formed by the hydrogen bonds between adamantane-1,3,5,7-tetracarboxylic acid molecules.[11]

The individual frameworks in **1** and **2** may be considered 2D networks supported by bpy or NC-Ag-CN pillars. Crystal structures with such large cavities are stabilized either by inclusion of suitable guests or by interpenetrating lattices. The difference in the span length of the bridging moieties (bpy, pyrz, NC-Ag-CN, and -NC-Ag-(CN)-Ag-CN) is an important factor in determining the multiplicity of the framework.

Received: March 21, 1994 [Z 6780 IE]
German version: *Angew. Chem.* **1994**, *106*, 1746

[1] T. Iwamoto in a) *Inclusion Compounds, Vol. 5* (Eds.: J. L. Atwood, J. E. D. Davies, D. D. MacNicol), Oxford University Press, Oxford, **1991**, p. 177; b) *Chemistry of Microporous Crystals* (Eds.: T. Inui, S. Namba, T. Tatsumi), Kodansha/Elsevier, Tokyo, **1991**, p. 1.

[2] a) T. Kitazawa, S. Nishikiori, R. Kuroda, T. Iwamoto, *Chem. Lett.* **1988**, 459 and 1729; b) T. Kitazawa, S. Nishikiori, T. Iwamoto, *Mater. Sci. Forum* **1992**, *91–93*, 257; c) T. Kitazawa, S. Nishikiori, A. Yamagishi, R. Kuroda, T. Iwamoto, *J. Chem. Soc. Chem. Commun.* **1992**, 413; d) T. Kitazawa, S. Nishikiori, R. Kuroda, T. Iwamoto, *J. Chem. Soc. Dalton Trans.*, **1994**, 1029.

[3] K.-M. Park, T. Iwamoto, *J. Inclusion Phenom.* **1991**, *11*, 397; *J. Chem. Soc. Dalton Trans.* **1993**, 1875; S. Nishikiori, C. I. Ratcliffe, J. A. Ripmeester, *J. Am. Chem. Soc.* **1992**, *114*, 8590; H. Yuge, T. Iwamoto, *J. Chem. Soc. Dalton Trans.* **1993**, 2841.

[4] a) B. F. Hoskins, R. Robson, *J. Am. Chem. Soc.* **1990**, *112*, 1546; b) B. F. Abrahams, B. F. Hoskins, J. Liu, R. Robson, *ibid.* **1991**, *113*, 3045; c) B. F. Abrahams, M. J. Hardie, B. F. Hoskins, R. Robson, G. A. Williams, *ibid.* **1992**, *114*, 10641.

[5] J. Černák, I. Potočňák, J. Chomič, M. Duraj-Jurčo, *Acta Crystallogr. Sect. C* **1990**, *46*, 1098; J. Černák, J. Chomič, P. Domiano, O. Ori, G. D. Andreetti, *ibid.* **1990**, *46*, 2103; J. Černák, I. Potočňák, J. Chomič, M. Dunaj-Jurčo, *ibid.* **1991**, *47*, 1088; J. Černák, I. Potočňák, V. Petříček, K. Kalý, *J. Inclusion Phenom.* **1992**, *14*, 73.

[6] T. Soma, T. Iwamoto, *Chem. Lett.* **1994**, 821.

[7] Crystal data: **1**: $Ag_2CdC_{24}H_{16}N_8$, $M = 744.66$, monoclinic, $P2_1/c$, $a = 8.891(4)$, $b = 11.464(3)$, $c = 17.656(4)$ Å, $\beta = 133.73(2)°$, $V = 1300.3(7)$ Å^3, $Z = 2$, $\rho_{exp} = 1.92(1)$, $\rho_{calcd} = 1.90$ g cm^{-3}, $R = 0.039$, $R_w = 0.040$ and GOF = 1.61 for 168 parameters using 3461 ($> 3\sigma(F_o)$) reflections. **2**: $Ag_3CdC_9H_4N_7$, $M = 646.19$, monoclinic, $P2/c$, $a = 9.235(2)$, $b = 7.560(3)$, $c = 11.274(1)$ Å^3, $\beta = 101.71(2)°$, $V = 770.7(6)$ Å^3, $Z = 2$, $\rho_{exp} = 2.78(1)$ g cm^{-1}, $\rho_{calcd} = 2.78$ g cm^{-3}, $R = 0.038$, $R_w = 0.041$, and GOF = 1.52 for 95 parameters using 1864 ($> 3\sigma(F_o)$) reflections. In common for **1** and **2**: Rigaku AFC5S diffractometer, $Mo_{K\alpha}$ radiation, 2θ-ω scan in $4° < 2\theta < 60°$. SHELX76 anisotropic refinement for all non-hydrogen atoms. Further details of the crystal structure investigation are available on request from the Director of the Cambridge Crystallographic Data Centre, 12 Union Road, GB-Cambridge CB2 1EZ (UK) on quoting the full journal citation.

[8] a) C. Kappenstein, A. Ouli, M. Guerin, J. Černák, J. Chomič, *Inorg. Chim. Acta* **1988**, *147*, 189; b) J. Černák, F. Gerard, J. Chomič, *Acta Crystallogr. Sect. C* **1993**, *49*, 1294.

[9] R. W. Gable, B. F. Hoskins, R. Robson, *J. Chem. Soc. Chem. Commun.* **1990**, 1677.

[10] Y. Kinoshita, I. Matsubara, T. Higuchi, Y. Saito, *Bull. Chem. Soc. Jpn.* **1959**, *32*, 1221.

[11] O. Ermer, *J. Am. Chem. Soc.* **1988**, *110*, 3747.

Octaplane: A Saturated Hydrocarbon with a Remarkably Low Ionization Energy Leading to a Cation with a Planar Tetracoordinate Carbon Atom**

Jennifer E. Lyons, Danne R. Rasmussen, Mark P. McGrath, Ross H. Nobes, and Leo Radom*

We have recently suggested the *alkaplane* family of molecules as a new class of saturated hydrocarbons containing a potentially planar tetracoordinate carbon atom.[1] The alkaplanes consist essentially of a $C^q(CH)_4$ unit containing the target quaternary carbon atom (C^q), capped above and below by cycloalkane moieties. Examples characterized in detail through ab initio calculations include octaplane (**1**), hexaplane (**2**), and biheptaplane (**3**).[1, 2] Our calculations for octaplane show a structure



1 **2** **3**

with S_4 symmetry (Fig. 1) and the closest approach to planarity reported to date for a tetracoordinate carbon atom in a neutral saturated hydrocarbon.[3] The $C^1C^qC^2$ angle that would be 180° in an exactly planar arrangement is found to be 168.8° in octaplane (**1**).

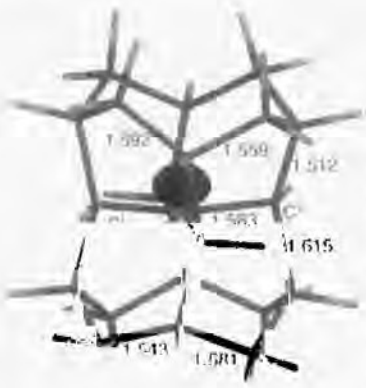


Fig. 1. Selected C–C bond lengths [Å] calculated at the HF/6-31G* level and highest occupied molecular orbital (HOMO) for **1** (symmetry S_4). The $C^1C^qC^2$ bond angle is 168.8°. The HOMO is largely a p-type lone pair orbital localized on the central carbon atom. Some distortion from radial symmetry can be seen. The orbital surface was drawn at a value corresponding to a density of 0.15 eÅ^{-3}.

One striking feature of the electronic structure of the alkaplanes is the highest occupied molecular orbital (HOMO) which is basically a p-type lone pair orbital localized on the quaternary carbon atom, as shown in Figure 1 for octaplane. This is likely to lead to interesting chemical and physical properties. In particular, one might expect ionization energies for alkaplanes to be substantially lower than for other saturated hydrocarbons. In the present paper, we explore this point for the octaplane molecule (**1**) and examine the effect of ionization on the structure.

The structures and energies of octaplane (**1**) and the octaplane radical cation (**1**$^{\bullet+}$) were determined by standard ab initio calculations,[4–6] carried out with the TURBOMOLE,[7] GAUSSIAN 92,[8] and CADPAC 5[9] programs. The structures of **1** and **1**$^{\bullet+}$ shown in Figures 1 and 2 were characterized as equilibrium structures through HF/6-31G* geometry optimizations and HF/3-21G frequency calculations.[10]

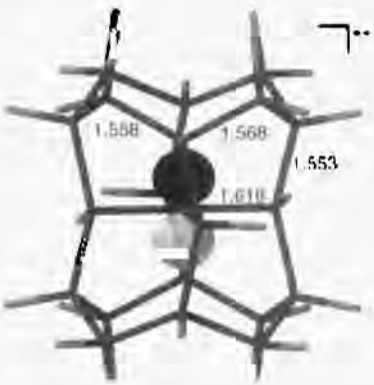


Fig. 2. Selected C–C bond lengths [Å] calculated at the HF/6-31G* level and singly occupied molecular orbital (SOMO) for **1**$^{\bullet+}$ (symmetry C_{4h}). The SOMO is a half-filled p-type orbital localized on the central carbon atom. The orbital surface was drawn at a value corresponding to a density of 0.15 eÅ^{-3}.

All C–C bonds in the structures of **1** and **1**$^{\bullet+}$ calculated at the HF/6-31G* level are in the range 1.51–1.62 Å. Some of these bonds are long but they are not unusual for strained hydrocarbons (cf. bond lengths of 1.53–1.61 Å in the diterpene lauren-1-ene).[3g] The C–C bond lengths in the cyclooctane rings appear to be relatively unaffected by ionization of octaplane (all are about 1.56–1.59 Å) although they are somewhat longer than those in free crown cyclooctane (1.535 Å at HF/6-31G*). The four central C–C bonds, on the other hand, are lengthened on ionization from 1.583 Å in neutral octaplane to 1.618 Å in the radical cation. The most striking effect of ionization of octaplane, however, is a significant reduction in the out-of-plane distortion forces present in the central five-carbon moiety of neutral octaplane. This results in a singly charged octaplane radical cation (**1**$^{\bullet+}$) with C_{4h} symmetry and a *planar tetracoordinate carbon atom* (see Fig. 2). Although planar tetracoordinate carbon has been found in hydrocarbon dications (e.g. CH_4^{2+}),[11] octaplane cation is the first reported *singly charged* saturated hydrocarbon containing a planar quaternary carbon atom.

The adiabatic ionization energy for octaplane was calculated at the MP2/6-31G*//HF/6-31G* level and is found to be 4.63 eV (Table 1). Test calculations for a selection of molecules for which experimental data are available[12] and/or for which accurate (G2) calculations[13] can be performed (e.g. NH_3, CH_2, CH_4) show that the ionization energies at the MP2/6-31G* level are generally too low by about 0.3–0.7 eV. On this basis, we estimate that the ionization energy for octaplane is approximately 5 eV. This is strikingly low, comparable in fact to the experimental values for the alkali metals lithium and sodium (5.39 and 5.14 eV, respectively)! In comparison, the lowest experimental value[12] for a neutral saturated hydrocarbon is 7.1 eV for tetra-*tert*-butyltetrahedrane.[14]

[*] Prof. L. Radom, J. E. Lyons, D. R. Rasmussen, Dr M. P. McGrath
Research School of Chemistry, Australian National University
Canberra, ACT 0200 (Australia)
Telefax: Int. code + (62)49-0750

Dr R. H. Nobes
Australian National University Supercomputer Facility
Australian National University (Australia)

[**] The award of an Australian National University Vacation Scholarship to J. E. L. and a generous allocation of time on the Fujitsu VP2200 of the Australian National University Supercomputer Facility are gratefully acknowledged.

The orbital depicted in Figure 2 is the singly occupied molecular orbital (SOMO) of the octaplane radical cation $\mathbf{1}^{\bullet+}$, corresponding to the removal of one electron from the HOMO of octaplane (**1**). Whereas the SOMO in $\mathbf{1}^{\bullet+}$ has almost radial symmetry, the HOMO in **1** shows some distortion towards the neighboring C–C bonds (see Fig. 1). It is thus not a pure p-type lone pair orbital but includes some bonding contributions between the central carbon atom and its four neighboring carbon atoms. This is allowed because of the lower (S_4) symmetry. The weakening of the four central C–C bonds and the reduction in the out-of-plane distortion forces following ionization can be rationalized in terms of this small degree of participation in bonding, seen in the HOMO of octaplane but not in the SOMO of octaplane cation.

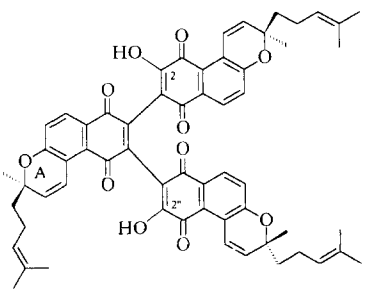
The remarkably low ionization energy predicted for octaplane (**1**) is likely to result in properties quite distinct from those of other neutral saturated hydrocarbons. We believe that the octaplane radical cation, a singly charged saturated hydrocarbon containing a planar tetracoordinate carbon atom, may be isolable as a salt[15] and formed from the oxidation of octaplane.[16] These and other intriguing features may provide added impetus to attempts at its challenging synthesis.

Received: February 26, 1994 [Z 6707 IE]
German version: *Angew. Chem.* **1994**, *106*, 1722

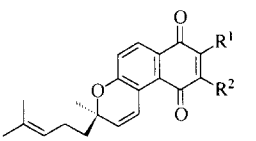
[1] M. P. McGrath, L. Radom, *J. Am. Chem. Soc.* **1993**, *115*, 3320.
[2] M. P. McGrath, D. R. Rasmussen, L. Radom, unpublished results.
[3] For leading references to previous studies related to planar tetracoordinate carbon, see, for example, a) R. Hoffmann, *Pure Appl. Chem.* **1971**, *28*, 181; b) J. B. Collins, J. D. Dill, E. D. Jemmis, Y. Apeloig, P. von R. Schleyer, R. Seeger, J. A. Pople, *J. Am. Chem. Soc.* **1976**, *98*, 5419; c) J. F. Liebman, A. Greenberg, *Chem. Rev.* **1976**, *76*, 311; d) A. Greenberg, J. F. Liebman: *Strained Organic Molecules*, Academic Press, New York, **1978**; e) R. Keese, *Nachr. Chem. Tech. Lab.* **1982**, *30*, 844; f) B. R. Venepalli, W. C. Agosta, *Chem. Rev.* **1987**, *87*, 399; g) W. C. Agosta in *The Chemistry of Alkanes* (Eds.: S. Patai, Z. Rappoport), Wiley, Chichester, **1992**, pp. 927–962, and references therein.
[4] Structures were obtained at the Hartree–Fock level with a modified 6-31G* basis set in which five pure *d* functions are used instead of the set of six second-order cartesian gaussians of the standard basis. Vibrational frequencies were determined at the HF/3-21G level and, after scaling by 0.9, were used to obtain zero-point vibrational energies. Improved relative energies were obtained through calculations on the HF/6-31G* optimized structures using second-order Møller-Plesset (MP2) perturbation theory (MP2/6-31G*), employing the frozen-core approximation.
[5] Open-shell systems were examined throughout using restricted (ROHF, RMP2) theory. See P. J. Knowles, J. S. Andrews, R. D. Amos, N. C. Handy, J. A. Pople, *Chem. Phys. Lett.* **1991**, *186*, 130.
[6] For a description of the basis sets and theoretical methods used, see W. J. Hehre, L. Radom, P. von R. Schleyer, J. A. Pople: *Ab Initio Molecular Orbital Theory*, Wiley, New York, **1986**.
[7] a) M. Haser, R. J. Ahlrichs, *J. Comput. Chem.* **1989**, *10*, 104; b) R. Ahlrichs, M. Bar, M. Haser, H. Horn, C. Kolmel, *Chem. Phys. Lett.* **1989**, *162*, 165.
[8] M. J. Frisch, G. W. Trucks, M. Head-Gordon, P. M. W. Gill, M. W. Wong, J. B. Foresman, B. G. Johnson, H. B. Schlegel, M. A. Robb, E. S. Replogle, R. Gomperts, J. L. Andres, K. Raghavachari, J. S. Binkley, C. Gonzalez, R. L. Martin, D. J. Fox, D. J. DeFrees, J. Baker, J. J. P. Stewart, J. A. Pople, GAUSSIAN 92, Revision E, Gaussian Inc., Pittsburgh PA, **1992**.
[9] R. D. Amos, I. L. Alberts, J. S. Andrews, S. M. Colwell, N. C. Handy, D. Jayatilaka, P. J. Knowles, R. Kobayashi, N. Koga, K. E. Laidig, P. E. Maslen, C. W. Murray, J. E. Rice, J. Sanz, E. D. Simandiras, A. J. Stone, M. D. Su, CADPAC 5: The Cambridge Analytic Derivatives Package, Cambridge, **1992**.
[10] Evidence that the structures calculated at the HF/6-31G* level are indeed equilibrium structures was gained from geometry optimizations performed on distorted structures of **1** and $\mathbf{1}^{\bullet+}$. These were all found to collapse back to higher symmetry. Further evidence comes from HF/3-21G frequency calculations on the S_4 and C_{4h} structures of **1** and $\mathbf{1}^{\bullet+}$, respectively, which give all real frequencies. For related systems in which it has been possible to carry out both HF/6-31G* and HF/3-21G vibrational analyses, we have found that the results are in very close agreement with one another.
[11] a) J. B. Collins, P. von R. Schleyer, J. S. Binkley, J. A. Pople, L. Radom, *J. Am. Chem. Soc.* **1976**, *98*, 3436; b) J. A. Pople, B. Tidor, P. von R. Schleyer, *Chem. Phys. Lett.* **1982**, *88*, 533; c) P. E. M. Siegbahn, *Chem. Phys.* **1982**, *66*, 443; d) D. Stahl, F. Maquin, T. Gaumann, H. Schwarz, P. A. Carrupt, P. Vogel, *J. Am. Chem. Soc.* **1985**, *107*, 5049; e) M. W. Wong, L. Radom, *ibid.* **1989**, *111*, 1155.
[12] S. G. Lias, J. E. Bartmess, J. F. Liebman, J. L. Holmes, R. D. Levin, W. G. Mallard, *J. Phys. Chem. Ref. Data Suppl.* **1988**, *17*, 1.
[13] L. A. Curtiss, J. A. Carpenter, K. Raghavachari, J. A. Pople, *J. Chem. Phys.* **1992**, *96*, 9030.
[14] E. Heilbronner, T. B. Jones, A. Krebs, G. Maier, K.-D. Malsch, J. Pocklington, A. Schmelzer, *J. Am. Chem. Soc.* **1980**, *102*, 564.
[15] For the isolation of stable salts formed from radical cations, see for example a) R. W. Alder, A. G. Orpen, J. M. White, *J. Chem. Soc. Chem. Commun.* **1985**, 949; b) F. Gerson, J. Knöbel, U. Buser, E. Vogel, M. Zehnder, *J. Am. Chem. Soc.* **1986**, *108*, 3781.
[16] The oxidation of saturated hydrocarbons, olefins, arenes, and amines whose ionization energy in the gas phase is below 8 eV can be achieved by using $AlCl_3/CH_2Cl_2$: see P. Vogel, *Carbocation Chemistry*, Elsevier, Amsterdam, **1985**, 112, and references therein.

Corrigenda

In the Highlight "Conocurvone – Prototype of a New Class of Anti-HIV Active Compounds?" by H. Laatsch (*Angew. Chem. Int. Ed. Engl.* **1994**, *33*, 422), some of the structural formulas have been incorrectly depicted. The following are correct:



1a
1b: H instead of ring



2a: R^1 = H, R^2 = OH
2b: $R^1 = R^2$ = H
2c: R^1 = H, R^2 = *p*-$OCOC_6H_4Br$
2d: $R^1 = R^2 = SC_6H_5$

The title of the communication by C. Balzereit, C. Kybart, H.-J. Winkler, W. Massa, A. Berndt (*Angew. Chem. Int. Ed. Engl.* **1994**, *33*, 1487) should read "A Highly Distorted and an Undistorted Borirane, C–B Hyperconjugation induced by C–Si Hyperconjugation".

In the communication "A New Class of Novel Macrocyclic Mesogens" by P. R. Ashton, D. Joachimi, N. Spencer, J. F. Stoddart, C. Tschierske, A. J. P. White, D. J. Williams, and K. Zab (*Angew. Chem. Int. Ed. Engl.* **1994**, *33*, 1503), the phase S_p for compounds **9**, **10**, and **12** in Table 1 should be replaced by S_A.

A Broad Base from Theory to Applications

Cluster Ions. (Wiley Series in Ion Chemistry and Physics.) Edited by *C-Y. Ng, T. Baer* and *I. Powis*. Wiley, Chichester, 1993. 479 pp., hardcover £ 80.00—ISBN 0-471-93830-0

This book contains a survey of recent developments in fundamental research on cluster ions. It consists of seven chapters, mostly concerned with van der Waals clusters, although carbon and silicon clusters are also included. The title is in fact too broad, suggesting to the reader that metal clusters are also covered.



First W. Kamke describes cluster studies using the photoelectron–photoion coincidence (PEPICO) technique, dealing both with the experimental aspects and with applications to van der Waals systems. This method is very effective for recording photoelectron spectra of size-selected neutral clusters, especially when applied with electrons of zero kinetic energy (threshold photoelectrons, TPE). The use of the technique is illustrated by examples, such as studies of the unimolecular decay of noble gas clusters, charge transfer in mixed clusters, and ion–molecule reactions in ammonia clusters. The next chapter by C. Lifshitz is concerned with the unimolecular and collision-induced decomposition of proton-bound clusters and carbon cluster ions. For the first of these ion types, with the general formula $H^+(M_n)$, excitation typically results in a solvent molecule M being "evaporated" off within a few microseconds. By measuring the kinetic energies of the ejected molecules one can determine bond energies, and collision-induced dissociation reveals isomeric structures. The section on carbon clusters deals particularly with the currently fashionable fullerenes C_{60}^+, C_{70}^+, and C_{84}^+ and their novel chemistry. In Chapter 3 M. F. Jarrold describes the many unique features of the physics and chemistry of positive and negative silicon cluster ions. The author has worked intensively in this field, using a variety of experimental methods to obtain the fullest possible information. Some of his results from drift-tube measurements are in striking disagreement with those obtained by Smalley's group using Fourier transform ion cyclotron resonance; the reason for this discrepancy is not yet known.

The fourth chapter by J. M. Lisy describes vibrational spectroscopic studies of solvated proton and metal ion clusters which serve as models for dilute electrolyte solutions. An interesting result is that proton clusters generated in a corona discharge are relatively cold, and consequently more than one infrared photon is needed for dissociation, whereas the metal ion clusters, which are produced by association and are relatively warm, are dissociated by only one CO_2 laser photon. Next (Ch. 5) J. M. Farrar reports on the electronic photodissociation of mass-selected van der Waals clusters, mainly with regard to the influence of solvation on this process. The closer one approaches to the condensed phase, i.e. the greater the number of solvent molecules attached to the central ion, the further the absorption is shifted towards the infrared. Measurements of this effect are reported for several systems; for example, the addition of up to six ammonia molecules to Sr^+ shifts the absorption maximum from about 400 nm to about 1400 nm. However, the number of ligands is still insufficient to simulate the transition from gas phase clusters to the liquid phase. Noble gas clusters are the subject of Chapter 6, by I. Last and T. F. George, then in the final chapter B. G. Brunetti and F. Vecchiocattivi report on autoionization dynamics of collision complexes. In a typical experiment noble gas atoms are excited into metastable states by electron impact, then atoms of a single metastable species are selected by optical excitation and are allowed to collide with a reaction partner under thermal conditions. Whereas the average time needed for a collision is about 10^{-12} s, autoionization takes place in about 10^{-15} s. After describing the experimental technique the authors discuss applications involving hydrogen, mercury, alkali metal, and noble gas atoms, and molecules such as N_2, CO, Cl_2, H_2O, and even CF_3Cl.

The individual chapters are carefully written, and the authors are acknowledged experts in the areas covered. I greatly enjoyed reading the book and can recommend it unreservedly to other physical chemists in the field.

Manfred P. Irion
Institut für Physikalische Chemie
der Technischen Hochschule
Darmstadt (FRG)

Phase Transfer Catalysis. 3rd Revised and Enlarged Edition. By *E. V. Dehmlow* and *S. S. Dehmlow*. VCH Verlagsgesellschaft, Weinheim/VCH Publishers, New York, 1993. 499 pp., hardcover DM 188.00, $ 125.00—ISBN 3-527-28408-7/1-56081-206-0

Phase Transfer Catalysis. Selected Problems and Applications. By *Y. Goldberg*. Gordon and Breach, Longhorne, PA, 1993. 456 pp., hardcover $ 170.00 ($ 95.00 if ordered from the publishers by private individuals).—ISBN 2-88124-870-5

Phase transfer catalysis (PTC) has nowadays become an indispensable tool for organic synthesis. Many reactions can be carried out more efficiently and selectively by this method, and others for which it has been used were not even possible previously.

The above book by Dehmlow and Dehmlow replaces the second edition published ten years ago, having been updated and, where necessary, revised. It includes many new developments in PTC.

This section contains book reviews and a list of new books received by the editor. Book reviews are written by invitation from the editor. Suggestions for books to be reviewed and for book reviewers are welcome. Publishers should send brochures or (better) books to Dr. Ralf Baumann, Redaktion Angewandte Chemie, Postfach 101161, D-69451 Weinheim, Federal Republic of Germany. The editor reserves the right of selecting which books will be reviewed. Uninvited books not chosen for review will not be returned.

 © *VCH Verlagsgesellschaft mbH, D-69451 Weinheim, 1994* *0570-0833/94/1515-1669 $ 10.00+.25/0*

The literature coverage now extends to mid-1990, while at the same time some outdated references have been dropped. There are 1700 new literature citations, bringing the total to over 3600, now listed (unlike the earlier editions) in alphabetical order. The subject index too is a valuable aid when working with this book.

Goldberg's book on the same subject is based on one originally published in Russian in 1989, which has been revised and updated for this English version. It contains about 1300 literature references extending up to 1991. The subject index, which is mainly substance-orientated, is a useful working aid.

The book by Dehmlow and Dehmlow begins with two chapters of more than 60 pages altogether on the theoretical basis of PTC. The first chapter is mainly concerned with the principles underlying the effectiveness of the most important types of catalysts, while the second deals with the mechanistic aspects of the different variants of the PTC method. Chapter 3 (over 300 pages long) is concerned with synthetic applications of PTC. It begins with a section on the choice of reaction conditions, such as the type and quantity of catalyst, the solvent, and the stirring rate. Particular attention is given to enantioselective PTC, describing its applications, problems, and the many potential sources of error. Next the authors describe various practical applications of PTC, arranged so far as possible according to reaction types. These include substitutions leading to alkyl halides, nitriles, esters, thiols, sulfides, and ethers, *N*- and *C*-alkylations, alkylations and acylations of ambidentate anions, isomerizations, H/D exchange reactions, and additions at C=O and C=N bonds. Also treated in detail are α-, β-, and γ-elimination reactions, the preparation of phosphonium and sulfonium ylides, nucleophilic aromatic substitutions, applications of PTC to organometallic compounds, and reductions and oxidations. It is pleasing to find that as well as giving well-proven synthetic recipes the authors include general principles that have been derived for carrying out various types of transformations under phase transfer conditions. The large amount of factual information is very clearly presented, often in the form of tables, enabling the reader not only to quickly find specific details but also to get an overview of a chosen area.

Goldberg's book differs considerably from that of Dehmlow and Dehmlow, both in emphasis and in structure. A first chapter (24 pp.) dealing with the theoretical fundamentals is followed by several chapters describing some selected areas of application of PTC. Chapter 2, the longest in the book with about 100 pages, is concerned with PTC in the chemistry of N-heterocycles. Alkylations and acylations of compounds of this class are described, as also are reactions of halogenated N-heterocycles with nucleophiles. Reactions of N-heterocycles with carbenes are treated next, followed by oxidations and reductions, as well as the use of PTC in the preparation of such compounds. In Chapter 3 (about 50 pp.), on PTC in organometallic chemistry, much attention is devoted to reactions involving organosilicon compounds; other reactions discussed include those of mercury, molybdenum, tungsten, iron, cobalt, and platinum compounds. Chapter 4 (about 70 pp.) is devoted to catalysis by metal complexes under phase transfer conditions, including reductions, oxidations, dehydrogenations, and carbonylations. Chapter 5, on three-phase catalytic reactions (about 30 pp.), discusses the advantages and disadvantages of using quaternary onium salts, crown ethers, or open-chain polyethers immobilized on polymers or other substrates for a variety of reactions. In Chapter 6, on asymmetric phase transfer catalysis (about 50 pp.), Goldberg discusses in great detail a number of types of reactions for which PTC has proved more or less successful. He also analyzes a number of experiments that failed completely and were thus of no interest for synthetic purposes, and identifies the factors that previously led to wrong interpretations. These latter discussions are extremely valuable for any chemist intending to apply PTC to asymmetric syntheses for the first time. However, reactions giving optical purities of 15–19% should not be regarded as satisfactory, as is implied on page 299. Chapter 7 (about 40 pp.) is concerned with less common variants of PTC; here the author discusses cationic reactions, reactions at phase boundaries between neutral species, inverse PTC, electron phase transfer, and reactions under the influence of ultrasonic excitation at phase boundaries.

The book by Dehmlow and Dehmlow is a standard work on PTC, affording the reader a comprehensive overview ranging from the theoretical fundamentals to the diverse wealth of practical applications of this useful method in synthetic chemistry. It is an indispensable monograph for every chemist, being suitable not only for organic chemists with experience of PTC but also for those about to use this method of synthesis for the first time. Goldberg's book does not give such a comprehensive picture, nor was that the author's aim. Instead it is intended for specialists. Because of this quite different approach it may be regarded as complementary to the Dehmlow and Dehmlow monograph, extending the subject and treating it in greater depth, with detailed discussions of many applications of PTC. At some points one might say that it gives too much information—for example, the details given beside the reaction arrows of the synthesis schemes. In both books the subject matter is clearly arranged, in a readable style, and in a sturdy binding. No library should be without them.

Fritz Theil
Institut für Angewandte Chemie
Berlin-Adlershof (FRG)

Fundamentals of Nuclear Magnetic Resonance. By *J. W. Hennel* and *J. Klinowski*. Longman, Harlow (UK), 1993. 288 pp., paperback £ 22.50.—ISBN 0-582-06703-0

In their preface the authors formulate their aim: it is to explain the physical and mathematical basis of NMR *simply* but *exactly*. In a certain sense they succeed. However, the question is: what *are* the fundamentals of nuclear magnetic resonance? In the opinion of the authors they are the magnetic dipole moment (of a compass needle, a current loop, an orbiting electron, or a nucleus with a spin), the magnetization of a macroscopic sample in thermodynamic equilibrium, the Larmor precession of an isolated spin, Bloch's equations, the Fourier transformation, the Zeeman and dipolar parts of the Hamiltonian, the method of (second) moments, and the spin-echo and COSY experiments.

Sure, all these topics *are* fundamentals of NMR, and I would regard it as almost a moral obligation of all those who practise NMR to be thoroughly familiar with fundamentals of this kind. It may well be the experience of Jacek Hennel and Jacek Klinowski that only too many are not. And I must admit that the authors' overview and judgement are very likely quite correct. Therefore, let us admit that there is a need to explain such fundamentals simply and exactly. Does the book fulfill the promise?

It starts with a chapter of 42 pages on the "Elements of Quantum Mechanics". It is supplemented by five appendices explaining topics from "Complex Numbers" to "Sinusoidal Operators." This is now the third recent book on NMR which I have read in which the authors assume, on the one hand, that they must provide an introduction to complex numbers and,

on the other, that their readers should master quantum mechanics up to the (spin) density matrix, the Hilbert space and the like. In my opinion it is a complete illusion to hope that someone who needs an introduction to complex numbers is able to appreciate any exposition of quantum mechanics. I am afraid, therefore, that Hennel's and Klinowski's book is of little help to those who have *not* previously followed a course in quantum mechanics. For those who have done so (and have worked through their homework problems) the book may be a useful revision, and they may like to see how quantum mechanics is applied *exactly* and *simply* and at great length to practical cases. However, a major problem is that the book does not lead the reader far enough. Almost all the fundamentals remain on an educational, a cultural level. They do not open the door to practical modern NMR. On the whole the book breathes the air of the fifties, maybe sixties. Pake's ingenious but hopelessly obsolete "high frequency bridge" is described to illustrate how NMR is detected. Pulse and FT NMR are discussed but no modern probehead or related instrumentation is shown. Of the total of 54 references no less than 37 appeared in or before 1967, and 19 of these are from the fifties. All those from after 1980 are monographs and textbooks. Abragam appears under 1983, whereas I bought my copy of his book in 1961.

The final chapter is on "Nuclear Magnetic Relaxation". It brought me an almost nostalgic re-encounter with Gierer and Wirtz (1953) and their microviscosity coefficients. I had hoped for a more up-to-date climax. I recommend the book for introductory NMR teaching, either in a class or in a laboratory course, and to all those who do practical NMR work and desperately feel that they do not really understand the fundamentals of their experimental tool. But they should not expect a link between these fundamentals and their own work.

U. Haeberlen
Max-Planck-Institut
für medizinische Forschung
Heidelberg (FRG)

Neural Networks for Chemists. An Introduction. By *J. Zupan* and *J. Gasteiger*. VCH Verlagsgesellschaft, Weinheim/VCH Publishers, New York, 1993. 305 pp., hardcover DM 138.00, paperback DM 68.00. —ISBN 3-527-28592-X/1-56081-791-7 (hardcover), 3-527-28603-9/1-56081-793-3 (paperback)

To explain precisely the basic concepts of a new interdisciplinary area of research and communicate them to a wide readership is a difficult task. Jure Zapan and Johann Gasteiger have managed to do this very successfully. This book offers a sound introduction to artificial neural networks, with insights into their architecture, functioning, and applications, which is intended not only for chemists but also for scientists from other disciplines. The capabilities and limitations of different systems are compared and evaluated. The authors have sensibly limited their treatment to a few carefully chosen and clearly distinguished types of networks, explaining how they are used for classifying, modeling, and analyzing molecules and their properties, for evaluating visual images (e.g., to interpret spectra or to analyze structure–activity relationships), and for controlling chemical reactions. The book is written in a readable style and is well structured. The reader's task is made easier by providing a short summary of the main learning objectives at the start of each chapter, and by the use of easily remembered mnemonics. The treatment is divided into two parts, one concerned with theory and the other with describing different types of applications. This arrangement means that, after studying the clear and very informative introduction to the topic, the reader can look at the examples of applications and assess the suitability of the chosen method in each case, possibly even suggesting an alternative solution. The chapters on Kohonen networks and counterpropagation systems are especially good. The examples of applications, such as the representation of the three-dimensional electrostatic potential of a molecule in the form of a two-dimensional map using the Kohonen approach, surprise one at first by the simplicity of the concepts, but this is in itself an illustration of one of the strengths of artificial neural networks. The authors explain clearly and concisely how these principles can be applied in order to make an appropriate selection of representative data for an analysis using neural networks. The reader is not distracted from the core issues by too many literature references in the text; instead the authors give a useful selection at the end of each chapter.

In our view there are only a few aspects of neural networks that have not been fully covered in the book. The authors have not discussed effective algorithms for the systematic optimization of network architectures—for example, genetic algorithms. Also, in restricting the discussion to the back-propagation algorithm for multipositional networks the authors have covered only a part (admittedly by far the largest) of the range of reliable strategies for supervised learning. A similar criticism applies to the choice of applications. In particular, the analysis of biological macromolecules receives only marginal treatment, being limited to predicting the three-dimensional structures of proteins from their amino acid sequences. Here it would have been desirable to include some more examples—e.g., the use of neural networks to analyze data banks—as these methods have already advanced considerably and much effort is being put into further developments. However, additional topics such as these can no doubt be included in a second edition. This is a very well-written guide for anyone who wants to make greater use of information theories in chemistry. The excellent quality of the contents and the presentation should ensure that it reaches a wide international readership.

Gisbert Schneider, Paul Wrede
Institut für Medizinische/
Technische Physik und Lasermedizin
der Freien Universität Berlin (FRG)

Homogeneous Transition Metal Catalyzed Reactions. Edited by *W. R. Moser* and *D. W. Slocum*. (Series: Advances in Chemistry, Vol. 230.) American Chemical Society, Washington, DC, 1992. 625 pp., hardcover $ 139.95.—ISBN 0-8412-2007-7

This book contains a substantial number of the presentations from the symposium on "New Science in Homogeneous Transition Metal Catalyzed Reactions", held during the 199th National Meeting of the American Chemical Society, in Boston, Massachusetts, April 22–27, 1990.

About one third of the chapters have been written by chemists working in industrial laboratories. The authors are in general very well known for their contributions to the field. The fact that the papers are subjected to the editorial standards of the ACS is a further warranty for the high quality of the book.

The book has been organized in six chapters: Spectroscopy and Mechanism, 7 papers; Asymmetric Induction and Shape Selectivity, 4 papers; C–H Activation, 4 papers; Carbonylation and Synthesis Gas Conversion, 13 papers; General Functionalization, 9 papers; Oligomerization and Polymerization, 4 papers. Some of the contributions are written in the style of a review article, while others report original research.

The first chapter concerns the application of spectroscopic techniques (such as IR, NMR, flash photolysis) to the identification and study of catalytic intermediates. Chaos in catalytic oxidations and a theoretical study related to intermediates in the cobalt catalyzed hydroformylation are also discussed.

In the second chapter enantioselective hydrogenation (mainly by ruthenium systems), homo-Diels–Alder reactions, and hydroboration are discussed. One paper describes a remarkable substrate selectivity in the epoxidation of olefins by manganese porphyrin catalysts.

In the third chapter a review article describes various catalytic functionalizations of hydrocarbons under irradiation. Examples related to the mercury photosensitized activation of C–H bonds and to the conversion of ethanol to ethylene glycol are then presented. Model stoichiometric reactions using rhodium and iridium complexes are also included.

In the chapter involving the chemistry of carbon monoxide six papers are dedicated to hydroformylation (or related chemistry) with different metal catalysts (rhodium, ruthenium, platinum, and cobalt). Carbonylations of olefinic substrates to amino acid precursors and to azacyclic compounds are also described. Three papers deal with the carbonylation of oxygenated compounds and one with the water-gas shift reaction. The activation of carbon monoxide by 17-electron porphyrin complexes of cobalt, rhodium, and iridium(II) is also discussed.

In the chapter on general functionalization, reactions leading to cyclic and macrocyclic compounds through intermolecular insertion reactions of diazo compounds or through palladium catalyzed allylic alkylation are discussed. Palladium catalysis, as well as model nickel chemistry, is also described in some examples of conjugated addition reactions. One paper relates to new applications of so-called "classic process chemistry" (such as hydrocyanation or cyclopropanation) to the manufacture of commodity chemicals. Evidence of the heterogeneous nature of the catalysis in the hydrosilylation of olefin substrates promoted by the "Karstedt" catalyst [i.e. platinum bis(divinyltetramethyldisiloxane)] is presented. The catalytic and noncatalytic hydrosilylation of acetyl metal complexes is also described. Other papers report on the amination of ethylene glycol, the deoxygenation of platinum allyl oxides and aryl oxides by carbon monoxide as a model for the catalytic deoxygenation of phenols, and the reduction of methanol by the tetracarbonylcobalt anion assisted by carbon dioxide and cobalt cation.

The polymer chemistry chapter contains papers on the catalytic synthesis of polymethylsilsesquioxanes, on the ionic nature of Ziegler–Natta catalysts derived from titanocene halides and organoaluminum Lewis acids ($RAlCl_2$), and on catalysis by half-sandwich chromium compounds (model for Phillips catalysts) in ethylene polymerization and in the ring-opening metathesis polymerization of norbornene. A proposal for a new mechanism of the Fischer–Tropsch synthesis based on model organometallic chemistry is also presented here.

Although the arrangement of the subject matter seems a little arbitrary, the book presents an overview of different aspects of homogeneous catalysis by transition metal complexes which is comprehensive enough to give a rough idea of the scope of applications of this type of catalysis. Moreover, the book is mainly directed to specialists in the field. However, some of its interest has perhaps been "diluted" due to the very long editorial time. For this reason, and due to the rather high price of the volume, I do not think that many people or institutions will acquire it. This is really a pity since I find it a very good, useful, and stimulating "pot-pourri" of themes related to homogeneous catalysis by transition metal complexes.

Giambattista Consiglio
Laboratorium für Technische Chemie
Eidgenössische Technische Hochschule
Zürich (Switzerland)

Metal Complexes in Cancer Chemotherapy. Edited by *B. K. Keppler*. VCH Verlagsgesellschaft, Weinheim/VCH Publishers, New York, 1993. 436 pp., hardcover DM 196.00, $ 125.00.—ISBN 3-527-28425-7/1-56081-216-8

This book contains 17 articles reporting on the present state of knowledge in the area of metal complexes with cytostatic activity. The metallic elements concerned range through the alphabet from A (e.g., Au) to V (vanadium). Although clinical success has so far been convincingly demonstrated only for platinum compounds (cisplatin, carboplatin), it is now recognized that a wide variety of other metal complexes offer promising possibilities, even though it is not yet possible to fully evaluate their real effectiveness, nor have they been proved in clinical use. Nevertheless, we know that even during the development of cisplatin there was a stage when its usefulness was seriously questioned. As the editor points out in the introduction to this book, one of the main driving forces for research in this field is the hope of discovering metal complexes with modes of action different from those of the platinum cytostatic agents.

The elements platinum, ruthenium, and tin each occupy three chapters of the book. Another four chapters are devoted to complexes of gold, gallium, and titanium and to cyclopentadienyl complexes of various metals. A further four are concerned with general aspects, namely the present clinical status of metal compounds (M. E. Heim), the stages in the development of an antitumor agent from initial testing to final release (F. T. Saur), the current situation in the treatment of colon and rectal tumors with special reference to metal complexes (M. R. Berger, M. H. Seelig, A. Galeano), and a possible novel therapeutic approach based on reactions of metal complexes with serum proteins (F. Kratz).

The most comprehensive articles are those on platinum compounds. E. von Angerer reports on the state of development of platinum complexes for the treatment of hormone-dependent tumors, T. Klenner and coworkers on the activity of various platinum phosphonate complexes in the treatment of bone tumors, and E. Holler on the mode of action of carcinostatic platinum complexes. The articles on ruthenium are concerned with the basic features of the interaction of ruthenium with biomolecules (M. J. Clarke), and with new developments in cytostatic ruthenium complexes with DMSO or N-heterocycles as ligands (G. Mestroni et al. and B. K. Keppler et al., respectively). Two chapters, by F. Huber and R. Barbieri and by M. Gielen et al., respectively, describe organotin compounds with various ligands (dipeptides, mercapto amino acids, salicylic acid). J. Crowe then attempts to define the extent and limitations of the analogy between tin compounds and cisplatin. The remaining four articles are concerned with tumor-inhibiting gold and gallium compounds (by O. M. Di Dhubhghaill and P. J. Sadler,

and by P. Collery and C. Pechery, respectively), the current state of development of budotitan (B. K. Keppler et al.), and progress on cytostatic metallocene compounds (P. Köpf-Maier).

The editor's attempt to provide an up-to-date standard work on the rapidly growing subject of cytostatic metal complexes is to be welcomed. The most recent previous monograph of this kind (*Platinum, Gold, and Other Metal Chemotherapeutic Agents*, edited by S. J. Lippard) is already ten years old. The more recent book *Transition Metal Complexes as Drugs and Chemotherapeutic Agents*, by N. Farrell, is not directly comparable as its aims are different. However, the rapid pace of developments has already made Keppler's book out of date in a few places. For example, in the field of platinum cytostatic agents such important developments as the work on bis-platinum complexes and the orally effective platinum(IV) compounds have not been included. This could be a consequence of the selection of authors: apart from one exception all the contributions are from European laboratories and medical institutes. This latter fact is in itself a positive sign, as it reflects the increased interest in this field in Europe, but the two new developments mentioned above have both come from the USA.

Most of the articles, though unfortunately not all, are of a quality and comprehensiveness that one expects in a standard work. I did not like the fact that too many of the contributions contain a mini-review of the history of tumor-inhibiting metal complexes, as this leads to a good deal of repetition. The standard of production is on the whole good. There are few errors and faults of presentation, and the fact that in the last article Figures 18 and 24 are not in color, as they were claimed to be, is not a disaster.

Specialists in the field, whether they are bioinorganic chemists with medical interests or medical scientists interested in chemical aspects, will probably buy the book without even examining its contents beforehand. Every library concerned with this area of science should have the book in its collection.

Bernhard Lippert
Fachbereich Chemie
der Universität Dortmund (FRG)

Fluorescence Spectroscopy. New Methods and Applications. Edited by *O. S. Wolfbeis*. Springer, Heidelberg, 1993. XX, 310 pp., hardcover DM 168.00.—ISBN 3-540-55281-2

Fluorescence is increasingly an "in" topic! Anyone who takes up this little book edited by Wolfbeis will certainly agree that much progress is being made in the application of fluorescence spectroscopy.

In this book of 21 chapters Wolfbeis, an analytical chemist, has succeeded in putting together a thoroughly up-to-date picture of the wide variety of ways in which fluorescence processes can be used in qualitative and quantitative analysis. The authors, well-known experts in the field, each present their own view of the situation. Schulman leads off with a critical overview of the subject. Rigles and coworkers then describe a relatively unfamiliar application of fluorescence correlation spectroscopy which allows one to observe individual fluorophore molecules. MacKay describes the application of a digitalized two-dimensional detector array utilizing luminescence phenomena for rapid imaging of processes that emit fluorescence.

Rettig reports on kinetic studies using fluorescence probes that are excited using synchrotron radiation. Bastiaens and Visser describe the use of fluorescence relaxation spectroscopy to observe rapid conformational changes in dimeric flavoproteins. Oelkrug and coworkers have carried out surface microstructure studies into the interaction of adsorbed fluorophore molecules with the substrate. Trettnak then reports on a purely analytical topic, namely the application of fluorescence quenching in optical sensor technology.

Beginning the next topic area, "Applications of Fluorimetry", Schneckenburger and Schmidt describe how pollution damage to forests has been studied by in situ measurements of the laser-induced time-resolved fluorescence of NADH and photopigments on leaves and branches. Riegler and Möhwald have used fluorescence microscopy to study the formation of structures and domains in Langmuir–Blodgett films, by incorporating fluorescence probes into the film. Applications of time-resolved fluorescence to the imaging of concentration distributions in cell biology studies are reported by Lakowicz and coworkers. Hermetter et al. use phase-modulated fluorescence spectroscopy to obtain insights into the structures of cell membranes, in particular the arrangement of ether phospholipid molecules. Pyrene labeling is a very useful way of introducing a fluorescence probe, and Kinnunen et al. describe the use of this method to study biomembranes. Slavik shows how suitable fluorescence labels can be used to observe intracellular processes.

In the area of the more conventional analytical applications of fluorescence, the current trend is towards the use of near infrared fluorescence. Miller et al. discuss the choice of suitable fluorophores for such work. Valcárcel and Lúque de Castro describe the use of flow injection analysis with coupled detection of a fluorescent product. The use of fluorescent tracer compounds in environmental analysis and hydrogeology is already a well established method. Goldberg and Weiner report on further extensions of fluorescent tracer techniques based on multidimensional analysis of spectra.

The fourth topic area is the application of fluorescence methods to immunological analysis. Klein and coworkers describe the wide variety of ways in which fluorescence can be used in immunoassay as a very sensitive labeling method. By labeling with rare earth complexes in conjunction with time-resolved luminescence measurements Hemmilä has achieved extremely low levels of detectability. Jansen reports on the use of similar techniques to analyze environmental samples. The monograph ends with contributions on the use of time-resolved fluorescence measurements in physiology, to reveal discontinuities in the potential and in the concentrations of sodium and calcium ions in nerve fibers (by Ross and by Kamino et al., respectively).

Altogether this is a worthwhile excursion into the world of fluorescence applications, which Wolfbeis has selected and presented very successfully. Despite the rather high price, it is well worth buying!

Reinhard Nießner
Institut für Wasserchemie
und Chemische Balneologie
der Technischen Universität München
(FRG)

 © VCH Verlagsgesellschaft mbH, D-69451 Weinheim, 1994 0570-0833/94/1515-1673 $ 10.00+.25/0

New Books

Oxford Chemistry Primers: Periodicity and the p-Block Elements. By **N. C. Norman.** Oxford University Press, Oxford, **1994.** 90 pp., paperback, £ 4.99.—ISBN 0-19-855763-9

Chemical Technology in Printing and Imaging Systems. Edited by **J. A. G. Drake.** Royal Society of Chemistry, Cambridge, **1993.** 188 pp., hardcover, £ 39.50.—ISBN 0-85186-655-7

Organic Materials for Non-Linear Optics III. Edited by **G. J. Ashwell, D. Bloor.** Royal Society of Chemistry, Cambridge, **1993.** 362 pp., hardcover, £ 59.50. ISBN 0-85186-625-5

The Chemistry and Physics of Coatings. Edited by **A. R. Marrion.** Royal Society of Chemistry, Cambridge, **1994.** 206 pp., paperback, £ 15.00.—ISBN 0-85186-994-7

Band Theory of Solids. An Introduction from the Point of View of Symmetry. By **S. L. Altmann.** Oxford University Press, Oxford, **1994.** 304 pp., paperback, £ 19.50.—ISBN 0-19-855866-X

Anwendung des Modells CoTAM zur Simulation von Stofftransport und geochemischen Reaktionen. By **K. Hamer, R. Sieger.** Ernst & Sohn, Berlin, **1994.** 208 pp., hardcover, DM 118.00.—ISBN 3-433-01544-9

Fractionation by Packed-Column SFC and SFE. Principles and Applications. Edited by **M. Saito, Y. Yamauchi, T. Okuyama.** VCH, Weinheim/New York/Cambridge, **1994.** 276 pp., hardcover, DM 198.00/$ 80.00.—ISBN 1-56081-591-4

Electron Transfer, Vol. I. (Topics in Current Chemistry, Vol. 169). Edited by **J. Mattay.** Springer, Heidelberg, **1994.** 371 pp., hardcover, DM 248.00.—ISBN 3-540-57565-0

The Biosynthesis of the Tetrapyrrole Pigments. Edited by **D. J. Chadwick, K. Ackrill.** John Wiley, Chichester, Great Britain, **1994.** 360 pp., £ 47.50.—ISBN 0-471-93947-1

Fachwörterbuch Physik-Basiswortschatz, Englisch-Deutsch. By **R. Sube.** Alexandre Hatier, Berlin, **1994.** 452 pp., paperback, ca. DM 69.00.—ISBN 3-86117-057-4

Introduction to Surface Chemistry and Catalysis. By **G. A. Somorjai.** John Wiley, Chichester, Great Britain, **1994.** ca. 500 pp., £ 24.95.—ISBN 0-471-03192-5

Oxford Chemistry Primers: Cluster Molecules of the *p*-Block Elements. By **C. E. Housecroft.** Oxford University Press, Oxford, **1994.** 91 pp., paperback, £ 4.99.—ISBN 0-19-855698-5

Atoms, Molecules, and Reactions, An Introduction to Chemistry. By **R. J. Gillespie, D. R. Eaton, D. A. Humphreys, E. A. Robinson.** Prentice Hall, New Jersey (USA) **1994.** 747 pp., hardcover, $ 49.95.—ISBN 0-13-088790-0

Principles of Electron Spin Resonance. (Physical Chemistry Series). By **N. M. Atherton.** Ellis Horwood, Chichester, Great Britain, **1994.** 585 pp., hardcover, $ 127.00.—ISBN 0-13-721762-5

Second Supplements to the 2nd Edition of Rodd's Chemistry of Carbon Compounds. (Vol. II: Alicyclic Compounds. Part B-C-D-E). Edited by **M. Sainsbury.** Elsevier, Amsterdam, **1994.** 672 pp., hardcover, Dfl. 660.00.—ISBN 0-444-81483-3

Handbook of Natural Products Data. (Vol. 2: Pentacyclic Triterpenoids). By **V. U. Ahmad, A. U. Rahman.** Elsevier, Amsterdam, **1994.** 1564 pp., hardcover, Dfl. 1200.00.—ISBN 0-444-88200-6

Synthetic Diamond. Emerging CVD Science and Technology. By **K. E. Spear, J. P. Dismukes.** Wiley, Chichester, Great Britain, **1994.** 600 pp., £ 69.95.—ISBN 0-471-53589-3

Intermediate Organic Chemistry, 2nd Ed. By **J. Stowell.** Wiley, Chichester, Great Britain, **1994.** 250 pp., £ 41.50.—ISBN 0-471-57456-2

Kurzes Lehrbuch der Biochemie. Für Mediziner und Naturwissenschaftler, 14th Ed. By **P. Karlson, D. Doenecke, J. Koolman.** Thieme, Stuttgart, **1993.** 552 pp., paperback, DM 68.00.—ISBN 3-13-357814-6

Sekundärionenmassenspektrometrie an molekularen Oberflächenstrukturen. By **B. Hagenhoff.** Deutscher Universitäts-Verlag, Leverkusen, **1994.** 179 S., paperback, DM 48.00.—ISBN 3-8244-2052-X

Dynamische Analyse elektrochemischer Reaktionssysteme. By **J. Braunsburger.** Deutscher Verlag für Grundstoffindustrie, Leipzig, **1994.** 196 pp., paperback, DM 48.00.—ISBN 3-342-00373-1

Liquid Crystals. (Topics in Physical Chemistry, Vol. 3). Edited by **H. Stegemeyer.** Steinkopff Verlag, Darmstadt, **1994.** 250 pp., hardcover, DM 64.00/reduced price for members of the Deutsche Bunsen-Gesellschaft DM 44.80.—ISBN 3-7985-0924-7

New Chemical Index Guide. Featured in **AIChE Publication.** American Institute of Chemical Engineers, New York, **1994.** For AIChE members $ 24.00/for nonmembers $ 30.00.

Advances in Chromatography, Vol. 34. Edited by **P. R. Brown, E. Grushka.** Marcel Dekker, New York, **1994.** 456 pp., hardcover, $ 165.00.—ISBN 0-8247-9087-1

Molekülphysik und Quantenchemie, 2nd Edited by Einführung in die experimentellen und theoretischen Grundlagen. By **H. Haken.** Springer, Heidelberg, **1994.** 429 pp., hardcover, DM 74.00.–ISBN 3-540-57460-3

New Gmelin Volumes:

Ni Organonickel Compounds. Suppl. Vol. 1. By **P. W. Jolly.** Springer, Heidelberg, **1993.** 381 pp., hardcover, DM 2160.00.—ISBN 3-540-93681-5

P Phosphorus. Suppl. Vol. C, Part 1. Edited by **D. Koschel et al.** Springer, Heidelberg, **1993.** 326 pp., hardcover, DM 1940.00.—ISBN 3-540-93680-7

Th Thorium. Suppl. Vol. C, Part 8. By **M. Bickel, H. Wedemeyer.** Springer, Heidelberg, **1993.** 301 pp., hardcover, DM 1800.00.—ISBN 3-540-93675-0

W Tungsten. Suppl. Vol. A, Part 4. Edited by **W. Huisl, W. Kurtz, F. Stein.** Springer, Heidelberg, **1993.** 277 pp., hardcover, DM 1590.00. ISBN 3-540-93677-7

W Tungsten. Suppl. Vol. A, Part 5/b. Edited by **J.v. Jouanne, E. Koch, E. Koch.** Springer, Heidelberg, **1993.** 196 pp., hardcover, DM 1190.00.—ISBN 3-540-93676-9

A Random Walk Through Fractal Dimensions, 2nd Ed. By **Brian H. Kaye.** VCH, Weinheim, **1994.** 427 pp., paperback, DM 78.00.—ISBN 3-527-29078-8

The Protection of Technical Innovations and Designs in Germany. Obtainment - Exploitation - Enforcement. By **W. Stockmair.** VCH, Weinheim, **1994.** 265 pp., paperback, DM 128.00.—ISBN 3-527-28656-X

Nuclear Materials. Materials Science and Technology, Vol. 10A. Edited by **B. R. T. Frost.** VCH, Weinheim, **1994.** 557 pp., hardcover, DM 450.00.—ISBN 3-527-26823-5

Nuclear Materials. Materials Science and Technology, Vol. 10B. Edited by **B. R. T. Frost.** VCH, Weinheim, **1994.** 454 pp., hardcover, DM 450.00.—ISBN 3-527-29236-5

Vom Wasser, Vol. 82. Edited by **Fachgruppe Wasserchemie in der Gesellschaft Deutscher Chemiker.** VCH, Weinheim, **1994.** 425 pp., hardcover, DM 268.00.—ISBN 3-527-28650-0

Primary Cereal Processing. A Comprehensive Sourcebook. Edited by **B. Godon, C. Willm.** VCH, Weinheim, **1994.** 544 pp., hardcover, DM 234.00.—ISBN 1-56081-609-0

Introduction to Modern Colloid Science. By **R. J. Hunter.** Oxford University Press, Oxford, **1993.** 338 pp., paperback, £ 14.95.—ISBN 0-19-855386-2

Introduction to Synthetic Polymers. By **I. M. Campbell.** Oxford University Press, Oxford, **1994.** 213 pp., paperback, £ 13.95.—ISBN 0-19-855398-6

Analytical Chemistry, 5th Ed. By **G. D. Christian.** Wiley, Chichester, Great Britain, **1994.** 812 pp., paperback, £ 18.95.—ISBN 0-471-30582-0

Molecular Aspects of Enzyme Catalysis. Edited by **T. Fukui, K. Soda.** VCH, Weinheim, New York, Tokyo, **1994.** 244 pp., hardcover, DM 208.00—ISBN 3-527-30017-1/1-56081-771-9/4-06-206497-9

Inorganic Chemistry. By **D. F. Shriver, P. W. Atkins, C. H. Langford.** Oxford University Press, Oxford, **1994.** 819 pp., paperback, £ 19.50.—ISBN 0-19-855396-X

Biotechnologie in der Lebensmittelindustrie. By **M. P. Tombs.** Springer, Berlin, **1994.** 241 pp., paperback, DM 49,80.—ISBN 3-540-57452-2

Group Theory in Chemistry and Spectroscopy. A Simple Guide to Advanced Usage. By **B. S. Tsukerblat.** Academic Press, London, **1994.** 430 pp., hardcover, £ 40.00.—ISBN 0-12-702285-6

Grundlagen elektrischer Maschinen. By **G. Müller.** VCH, Weinheim, **1994.** 594 pp., paperback, DM 78.00.—ISBN 3-527-28390-0

Encyclopedia of Chemical Technology, Vol. 10. Edited by **J. I. Kroschwitz, M. Howe-Grant.** Wiley, Chichester, Great Britain, **1993.** 1022 pp., hardcover, £ 185.00.—ISBN 0-471-52678-9

Topics in Stereochemistry, Vol. 21. Edited by **E. L. Eliel, S. H. Wilen.** Wiley, Chichester, Great Britain, **1994.** 533 pp., hardcover, £ 111.00.—ISBN 0-471-52120-5

Fundamentals of Organic Chemistry. By **T. W. G. Solomons.** Wiley, Chichester, Great Britain, **1994.** 1047 pp., paperback, £ 22.50.—ISBN 0-471-30562-6

Fundamentals of General, Organic, and Biological Chemistry. By **J. R. Holum.** Wiley, Chichester, Great Britain, 1994. 800 pp., paperback, £ 19.95.—ISBN 0-471-59981-6

Basic Concepts of Chemistry. By **L. J. Malone.** Wiley, Chichester, Great Britain, **1994.** 684 pp., paperback, £ 24.95.—ISBN 0-471-02019-2

Homogeneous Hydrogenation. By **P. A. Chaloner, M. A. Esteruelas, F. Joó, L. A. Oro.** Kluwer Academic Publishers, Dordrecht, Niederlande **1994.** 288 pp., hardcover, $ 118.50.—ISBN 0-7923-2474-9

Modern Chromatographic Analysis of Vitamins. Edited by **A. P. De Leenheer, W. E. Lambert, H. J. Nelis.** Marcel Dekker, New York, **1992.** 592 pp., hardcover, $ 175.00.—ISBN 0-8247-8626-2

Wörterbuch Bibliotheks- und Informationswissenschaft/Dictionnaire des sciences de l'information, de la bibliotheque et de la documentation. By **S. von Keitz, W. von Keitz.** VCH, Weinheim **1994.** 327 pp., hardcover, DM 108.00.—ISBN 3-527-29237-3

Von CA bis CAS online. Datenbanken in der Chemie. By **H. Schulz, U. Georgy.** Springer, Berlin, **1994.** 321 pp., hardcover, DM 98.00.—ISBN 3-540-57482-4

Sterically Stabilized Vesicles

Danilo D. Lasic*

After significant developments in liquid crystal and polymer research, scientists became interested in lyotropic systems containing polymers. These studies investigated, for instance, phase behavior and stability characteristics of suspensions of colloidal particles containing water-soluble or surface-adsorbed polymers or block copolymers. The most frequently studied were micelles, latex particles, and lipid vesicles (liposomes). Liposomes aggregate and fuse in the presence of hydrophilic polymers but their properties were difficult to explain when block copolymers were adsorbed or surfactants with larger polymeric polar heads were inserted into the liposome membrane, because such systems are inherently ill defined. Liposomes containing diacyl surfactants with covalently linked, longer polymer chains display many new properties with very important consequences for both basic and applied research. They stimulate fundamental studies on phase behavior and polymer conformation, scaling laws, colloidal and surface properties, and cell function; applications deal predominantly with liposomes as drug delivery systems. While in basic research theory is currently more advanced than experiment, in medical applications theoretical understanding lags behind experimental achievements. It was discovered only relatively late that liposomes with an appropriate polymer coating are significantly more stable in a biological milieu, a necessary condition for their utility as drug carriers. In particular in medical applications, this practice has rejuvenated the field of anticancer therapy and targeted drug delivery. All these advances were made possible by an effective and synergistic overlap of many different disciplines.

1. Introduction

Matter in nature occurs, in general, in three states. Certain substances, however, behave under special conditions neither as a gas, nor as a liquid, nor as a solid. Liquid crystals, for instance, simultaneously exhibit some properties of liquids (including low viscosity and tendency to form droplets) as well as of solids (anisotropy of optical, mechanical, electrical, and magnetic properties).[1,1] The liquid-crystalline state of matter has several important properties which enable, and may be necessary for, biological processes and life: at relatively high diffusion and permeability rates it offers certain organizational ordering and barrier properties, and serves to store information.[2] In the lipid bilayer, the most common mesophase found in living cells, lipid molecules self-organize into large sheets which close to form membranes. They can be either in the fluid or solid state. The temperature of the phase transition from crystal to liquid crystal, that is, at which the two dimensional solid fluidizes (T_c), is an important parameter in liposome as well as biomembrane behavior.

In addition to thermotropic liquid crystals in which properties depend on temperature, some molecules form ordered structures by interactions with various solvents. In most cases, these molecules are amphiphiles, containing a hydrophilic and hydrophobic group in the same molecule. They can form various lyotropic liquid crystalline phases whose structures are determined by polar and nonpolar interactions of molecules that contain both groups. Examples of these amphiphilic molecules include some proteins, polypeptides, and predominantly, polar lipids in mixtures with water.[3-5]

Polar lipids aggregate in aqueous solutions into ordered structures in a variety of liquid crystalline phases (Fig. 1). Although phase diagrams can be calculated in some cases on the basis of molecular geometry and intermolecular interactions, we shall simply state that self-organization of these systems is due to the tendency of hydrophilic parts of the molecules to be in contact with water while the nonpolar parts prefer an apolar environment. The topology of various liquid crystalline phases and colloid aggregates offer exactly this molecular organization.[1-5]

Liquid crystals are characterized by long-range order and, depending on the temperature, short-range order or disorder. With respect to the symmetry of a particular phase, the order may include zero-, one-, or two-dimensional positional periodicity and some degree of orientational order. The phases, with the exception of some nonequilibrium cubic phases,[6] are thermodynamically stable, and molecules can reversibly self-organize into various structures upon appropriate changes in concentration(s), temperature, pressure, ionic strength, or pH.

[*] Dr. D. D. Lasic
Mega Bios Corp.
871-J Industrial Road, San Carlos
CA 94070 (USA)
Telefax: Int. + (415)802-0355

 © VCH Verlagsgesellschaft mbH, D-69451 Weinheim, 1994 0570-0833/94/1717-1685 $ 10.00+.25/0

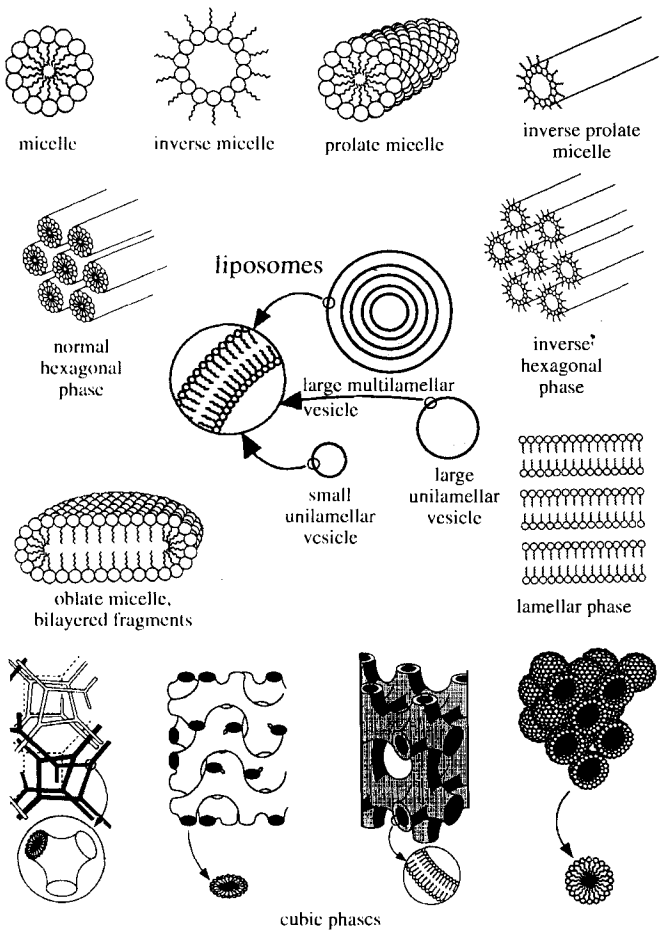


Fig. 1. Schematic representation of aggregates and phases formed by different amphiphiles at different concentrations in mixtures with water. Under these conditions spherical inverse micelles occur only with some charged single-chain surfactants at higher temperatures; they are, however, found frequently in ternary mixtures with a nonpolar phase. In aqueous suspensions the inverse hexagonal phase is coated with a lipid monolayer. The sphere represents the hydrophilic part of the molecule, while the hydrophobic tail is shown as a wavy line.

Upon the dilution of lyotropic liquid crystalline phases, the periodic lipid water structure can disintegrate into colloidal particles, especially if the dilution is accompanied by an input of (mechanical) energy, such as agitation or shaking. The molecular assembly and local molecular symmetry is retained in the small and intermediate range, while the long-range order is lost. Another possibility is that the homogeneous, lyotropic, liquid crystalline phase disproportionates upon dilution into a heterogeneous system comprising a fully swollen liquid crystalline phase in excess water.[4] An example of the former process is the disintegration of large micelles of normal hexagonal phase of single-chain polar lipids into small micelles;[4] the breakdown of lamellar phases of diacyl lipids normally results in the formation of liposomes.[7] With the exception of simple micelles, the loss of long-range order in systems after dispersing the liquid crystalline phases into colloidal particles normally results in the loss of thermodynamic stability.[8]

Liposomes are spherical, self-closed vesicles of colloidal dimensions with phospholipid bilayers that sequester part of the solvent in which they are suspended in their interior.[9, 10] According to size and number of lamellae, small or large unilamellar vesicles or, in the case of many concentric bilayers, large multilamellar vesicles may be defined (Fig. 1).[11]

Because of their structure, chemical composition, and colloidal size, which can be well controlled during preparation, liposomes possess several useful properties. The most important features are small size, for instance, rather uniform particle size distributions in the range from 20 nm to 500 nm (some methods allow formation of larger liposomes with diameters up to 50 μm), and special membrane and surface characteristics, which include bilayer phase behavior, its mechanical properties and permeability, charge density, presence of surface-bound or grafted polymers, or attachment of special ligands. Additionally, due to their amphiphilic character and very large surface-to-volume ratio, liposomes form powerful solubilizing or dispersing systems for a wide range of compounds. Apart from these physico-chemical properties, liposomes from natural lipids exhibit many special biological characteristics, including biocompatibility, biodegradability, and (specific) interactions with biological membranes and cells.[2]

Based on these properties, liposomes are used in several applications, for example, as solubilizers or dispersants for sparingly soluble substances, as sustained release and delivery systems for the micro-encapsulated substances, and as stabilizers, protective agents, and microreactors. All living cells on the planet are surrounded by a membrane in which various proteins are embedded into the lipid bilayer. This bilayer is analogous to the liposome bilayer and similarly represents a mechanical, chemical, and electrical barrier between exterior and interior. There-



Danilo D. Lasic was born in Ljubljana, Slovenia in 1952, where he studied Chemistry and completed his PhD on lyotropic liquid crystals at the Department of Solid State Physics at Institute J. Stefan in Ljubljana in 1979. He was a post-doctoral research fellow with Charles Tanford at Duke University and Helmut Hauser at the ETH Zurich, and visiting scientist at the Physics Department of the University of Waterloo, Ontario, Canada. From 1988 to 1993 he worked at Liposome Technology, Inc. (LTI) in the San Francisco Bay Area. Since the beginning of this year he has been employed by MegaBios, where he is studying cationic liposomes for gene therapy. His academic research on thermodynamics and mechanism of vesicle formation was an excellent preparation for his active participation in the development of Stealth liposomes at LTI. His book on this subject, Liposomes: from Physics to Applications, was published in 1993.

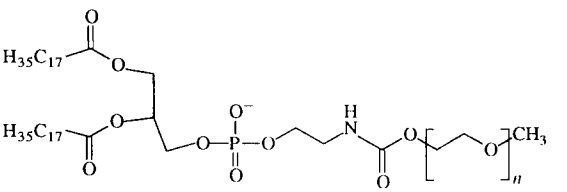
fore, in addition to the above-mentioned applications, which have had significant impact in several industries, the unique properties of liposomes offer a very useful model system in many fundamental studies on topology, membrane biophysics, photophysics and photochemistry, colloidal interactions, cell function, signal transduction (including traffic of synaptic vesicles with encapsulated neurotransmitters), secretion and many others.[2, 5, 11-16]

Bilayers can be made entirely from naturally occurring substances and are therefore nontoxic, biodegradable, and practically nonimmunogenic. This makes them ideal candidates for drug delivery systems. Apart from these well-known endeavors, liposomes are also employed in industry as adjuvants in vaccination, signal enhancers or carriers in medical diagnostics and analytical biochemistry, and transfection vectors in genetic engineering. Currently, however, the largest marked is in cosmetics, in which liposomes serve as dispersants or support matrices for various ingredients and, according to some reports, as penetration enhancers. Although some of the claims of cosmetics producers are not supported by rigorous scientific tests, liposomes, at the very least, represent an improvement simply because hydrophobic substances are suspended in an aqueous and biocompatible matrix as opposed to creams and gels that use skin-irritating oils, alcohols, and surfactants.[2]

2. Liposomes in Drug Delivery

The optimistic expectations for liposomes as drug delivery systems have not been met, mostly because of stability problems. Although the problems with shelf-life were successfully solved in most cases, the stability of liposomes in liposomicidal environments of biological systems presented a greater challenge that was only recently solved.[17, 18]

Intravenously administered liposomes quickly release the encapsulated or membrane-bound molecules. The leakage can be greatly reduced by the inclusion of cholesterol into their membranes,[19] but this did not help much in the fast sequestration and clearance of liposomes by the mononuclear phagocytic (MP) cells of the immune system located mostly in liver and spleen, which is the major drawback in most applications. First attempts to alter their biodistribution by either surface ligands or membrane composition were undertaken in the late seventies. The results showed that liposome disposition can be changed, but predominantly within the mononuclear phagocytic system itself. To prolong the circulation time of liposomes in the blood without recourse to undesired methods such as presaturation, suppression, or impairment of the MP system, small, neutral liposomes composed of rigid lipids and cholesterol were used. The first substantial improvements, however, were achieved by the incorporation of ganglioside G_{M1} or phosphatidylinositol at between 5 and 10 mol% into the bilayer.[20] The best results were obtained by substituting a synthetic polymer-containing lipid for these two lipids. The longest circulation times were achieved with polyethylene glycol covalently bound to the phospholipid (Fig. 2). Intermediate molecular weights (1500–5000 Da) at a concentration of about 5 mol% in the bilayer gives rise to the longest liposome circulation times.[18] Figure 3 shows blood clearance profiles of several different formulations.



DSPE, $n \approx 16, 45, 113$

Fig. 2. Structural formula of the poly(ethylene glycol)-lipid mPEG-DSPE. They are normally applied as the sodium salt. Usually molecular weights of poly(ethylene glycol) (PEG) are 750, 1000, 2000, 3000, 5000, and 12000. Commercial grade PEG has a polydispersity index p of 1.1, while that of BioTech grade is 1.05; p does not change after linkage.

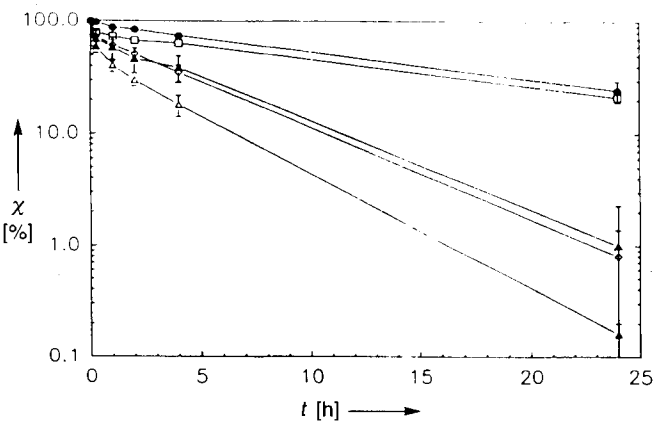


Fig. 3. Blood clearance profiles of several liposome formulations as percentage of the injected dose χ as a function of time t. From top to bottom: ^{2000}mPEG-DSPE/EPC/Chol (●), ^{5000}mPEG-DSPE/EPC/Chol (□), ^{120}mPEG-DSPE/EPC/Chol (▲), EPC/Chol (2/1) (○), and EPG/EPC/Chol (△); formulations with molar ratio 0.15/1.85/1. Abbreviations: mPEG = methoxy poly(ethylene glycol), DSPE = distearoyl phosphatidylethanolamine, EPC = partially hydrogenated egg phosphatidylcholine (iodine value 40), Chol = cholesterol, EPG = egg phosphatidylglycerol. The 100-nm liposomes were labeled with ^{67}Ga-desferal (from ref. [67]).

Similar approaches have been tried with other colloidal particles, from micelle-forming block copolymers[11] to latex particles.[22] Whereas latex particles with adsorbed block copolymers such as PEG–PPO (polyethyleneglycol–polypropyleneoxide) showed changes in pharmacokinetics similar to those of PEG-grafted liposomes;[2] the block copolymer micelles containing PEG chains were taken up rapidly by macrophages by pinocytosis.[21]

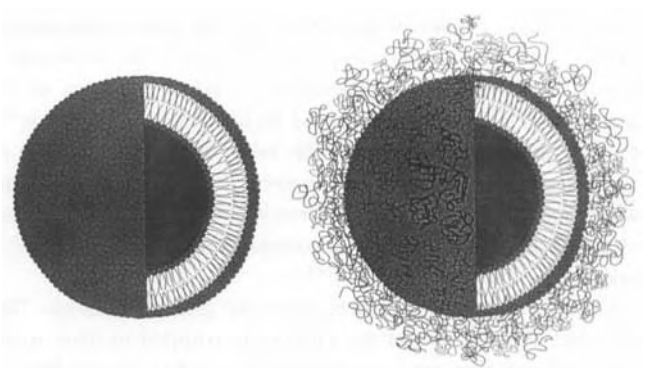


Fig. 4. Schematic representation of conventional (left) and Stealth liposomes (right). Polymer chains can be attached to one or both sides of the vesicle. By courtesy of Phillip Le Roy Carter, Liposome Technology, Inc. (LTI).

In general, however, surface grafting of polymers offers much better control over the colloidal properties. Furthermore, surface adsorption of polymers onto liposomes normally leads to leakage of the encapsulated molecules,[23] and liposomes can often aggregate.

In our opinion the enhanced liposome stability in the biological milieu is due to the steric barrier that the surface-attached polymer presents to the interacting macromolecules. For this reason they are often called sterically stabilized liposomes;[24] commercially they are often referred to as Stealth* liposomes because of their invisibility to the body's immune system (Fig. 4).

3. Stability of Liposomes

In liposome research and applications the term stability is used rather vaguely and is often not properly defined. In the broadest sense it refers to the stability of the particle and its constituents, including the entrapped molecules, in any, including liposomicidal, environment. This general definition of stability contains various aspects which can be defined separately but often act synergistically.

I shall arbitrarily define stability as a sum and product of physical, chemical, and colloidal stability. In addition to these inherent stability components, the definition must also include the stability of liposomes under the conditions of the application, which is often in liposomicidal environment. Since most of them are of pharmaceutical nature, one can define biological and shelf-life stabilities, which are each a cumulative property of several of these stabilities.

3.1. Physical Stability

This aspect mostly involves preservation of the liposome structure and entrapment, that is, the stability of liposome size and shape (size distribution of the sample), and of the barrier properties of the bilayers for the encapsulated or membrane-bound molecule.

Both the preservation of the size as well as encapsulation depends on the mechanical properties of the bilayers and the thermodynamics of the systems.

Vesicles are thermodynamically unstable because the symmetric membrane is curved, and the low energy conformation of membranes is, in general, planar (that is, the spontaneous curvature $C'_0 = 0$). The excess energy of each vesicle due to its curvature is $8\pi K$, where K is the elastic bending modulus of the membrane.[12, 25, 26] Vesicles could be formed spontaneously[27] only in the case of bilayers with very low values of K[28] or asymmetric bilayers with nonzero spontaneous curvature, which may originate from differences in internal and external phase, from nonbalanced lipid compositions, or from the use of asymmetric bipolar lipids.[29–35]

Once the liposome is formed, however, it is rather stable. This indicates that liposomes are kinetically trapped in their structures, because they are formed in an irreversible nonequilibrium process during which excesses of energy are high;[2, 8, 26, 36] the energy needed to open or break them can be 50 kT.[2, 37] The above analysis shows that part of the energy input during liposome formation becomes stored in the conformational energy of the bilayer–bilayer curvature[38] and is responsible for their metastability.

A simple Gedanken (thought) experiment shows the advantage of kinetically trapped systems over systems in thermodynamic equilibrium for applications such as microencapsulation. A system at equilibrium quickly adjusts to the external change (for instance, dilution, change in concentration(s), temperature, pressure, presence of other substances, or injection into body fluids) by changing phase. For instance, micelles or microemulsion droplets quickly disintegrate upon dilution (that is, move into a different region of the phase diagram), while liposomes made from phospholipids with very low values of critical micelle concentration (cmc) are stable against dilution. This simple analysis can explain many of the unexpected findings on drug delivery with colloidal carriers.

It is also interesting to note that liposomes can be stabilized against some phase transitions, such as freeze-thawing and freeze-drying by the addition of water-soluble cryoprotectants like sucrose. This enables manufacturing of freeze-dried (lyophilized) liposome formulations with improved shelf-life stabilities.[39]

Liposome integrity also depends strongly on the mechanical properties of the bilayer. Mechanically stronger (more cohesive) bilayers are expected to resist external perturbations better. Measurements with micropipette manipulations allow the determination of stretching moduli of a particular membrane [isotropic dilatation modulus ($K_{d/c}$) and critical areal strain (τ) of various bilayers],[40, 41] and these values correlate with the stability of liposomes. Table 1 shows the values of $K_{d/c}$ and τ for various bilayers. A general observation is that cholesterol makes bilayers more cohesive by inducing the ordered fluid phase.[41, 42]

Bilayers can also be mechanically stabilized by polymerization[43–48] or by using lipids with fluorocarbon chains.[49–51] Despite reduced van der Waals attraction between the carbon chains, these lipids form stronger and less permeable bilayers due to stronger hydrophobic interaction.[2]

Table 1. Mechanical properties of bilayers as measured by the micropipette manipulation technique. The compressibility modulus $K_{d/c}$ and tensile strength τ of various liposome bilayers are shown. From *Biochemistry* **1988**, *27*, 8261 and **1992**, *31*, 2017; *Biophys. J.* **1990**, *58*, 997.

Composition [mol mol^{-1}] [a]	$K_{d/c}$ [dyn cm^{-1}]	τ [dyn cm^{-1}]
SOPC	193	5.7
SOPC/Chol (ca. 86/14)	216	8.7
SOPC/Chol (ca. 50/50)	≈1200	24.9
DMPC	145	
DMPC/Chol (67/33)	559	
DMPC(Chol (50/50)	633	
DMPC (L_β)	855	
DPPC/Chol	2235	
BSM/Chol (ca. 50/50)	≈1720	23.2
DAPC	57	2.3
DAPC/Chol (ca. 50/50)	102	4.5

[a] Abbreviations: SOPC: stearoyloleoyl phosphatidylcholine; Chol: cholesterol; DMPC: dimiristoyl PC; DPPC: dipalmitoyl PC; BSM: bovine sphingomyelin; DAPC: diarachidonoyl PC.

[*] Stealth is a registered trade name by Liposome Technology, Inc.

3.2. Chemical Stability

Most biomolecules are degraded in a variety of ways, and lipids are one of the most sensitive naturally occurring substances. The most common degradation pathways are oxidation and hydrolysis (Fig. 5). In general, the polar heads are much more stable than the hydrocarbon chains. Hydrocarbon chains, especially unsaturated ones, are subject to oxidation, whereas hydrolysis pinches off one or both hydrocarbon chains from the backbone of lipid molecule. Because the reaction is acid- and base-catalyzed, it exhibits a strong pH dependence (Fig. 5, top left).[52, 53] The protective measures therefore include optimization of pH, normally around 6.5, and, preferentially, freezing or drying the sample in the presence of cryoprotectants.

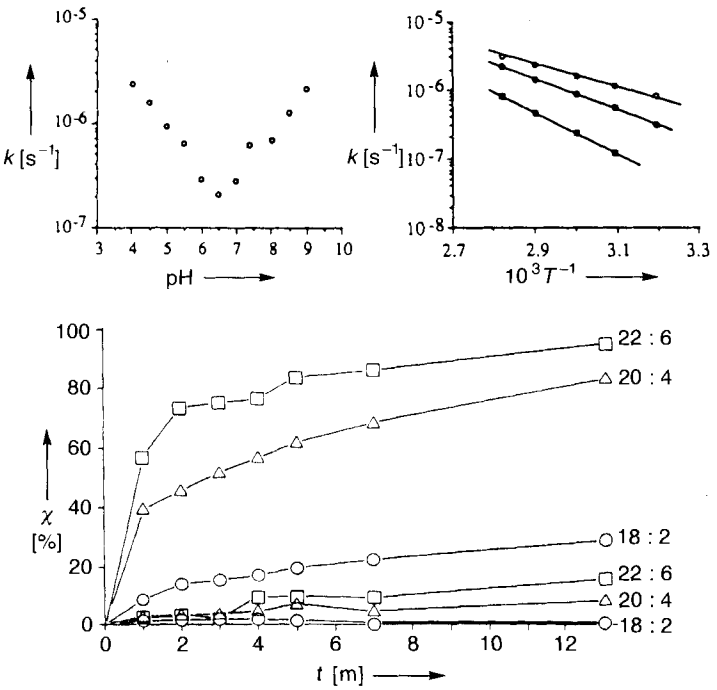


Fig. 5. The chemical stability of liposomes. Top: hydrolysis rate of soybean lecithin in liposomes as a function of pH (left) and temperature (right); the temperature dependence was performed at pH 4.0 (○), 6.5 (□), and 8.0 (●) (by courtesy of M. Grit and D. Crommelin, Utrecht University). Bottom: oxidation of polyunsaturated fatty acids in egg lecithin liposome at 38 °C in vented vials as a function of time (in months). The lower three curves show the reduction in oxidation rate due to the presence of 1 mol% antioxidant 2,6-di-*tert*-butyl-4-methylphenol (BHT). The information to the right of each curve gives the chain length and degree of unsaturation. For example, 22:6 indicates a C_{22} chain with 6 double bonds (by courtesy of Frank Martin, LTI).

Oxidation is a radical reaction that ultimately results in the breakage of chains or, in the case of two adjacent double bonds, formation of cyclic peroxides. Protective measures, which include the use of saturated lipids and addition of antioxidants such as vitamin E (α-tocopherol) or BHT (butylated hydroxytoluene), reduce the oxidation rate substantially, and samples can be stable, within tight specifications (normally the maximum allowable change in chemical composition is 2%), for years.[54]

Several synthetic lipids, including those with fatty acids linked to the glycerol backbone through an ether linkage, are chemically more stable;[35] they are, however, not biodegradable by mammalian enzymes. That limits their use in parenteral drug delivery, although they are often used in chemical or cosmetic applications.

3.3. Colloidal Stability

In phospholipid liposome preparations the particle size increases mainly as a result of particle aggregation, because size growth due to Ostwald ripening is negligible.[2, 55] Aggregation is the first step in vesicle–vesicle fusion[56] and depends on the thermodynamic stability of the sample, crystal defects, and the presence of intrinsic or exogeneous, fusogenic substances or vectors. Fusion is practically an irreversible process (liposome fission is rarely spontaneous) while aggregation can be reversible.

There are several attractive and repulsive forces which act between colloidal particles. Ubiquitous is the van der Waals attraction that acts between all particles separated by a medium with different polarizing properties. Particles bearing the same charge experience an electrostatic repulsion. These two forces are the basis of the DLVO theory (DLVO = Derjaguin, Landau, Verwey, Overbeek) of the stability of colloidal particles in which a colloidal system is defined as stable if a minimum (with a depth of approximately $\Delta E < 10$ kT) exists on the graph of potential energy vs distance.[57] In many cases, however, this theory could not predict the stability of liposomes against aggregation. To elucidate why colloidal suspensions have a lower stability than expected, additional attractive forces between colloidal particles, such as hydrophobic attraction or ion–ion correlation attraction were introduced,[58–60] while the stability of uncharged liposomes and liposomes in media of high ionic strength, could only be explained after other repulsive forces between two liposomes such hydration[61] and undulation[62] were recognized.

The origin of some of these forces is not known yet, and they are still controversial. For instance, recently hydration as source of a repulsive force was questioned, and the protrusion repulsive force, a steric repulsion caused by the vertical motion of polar heads, was proposed.[63] The situation is even less clear with respect to the attractive long-range hydrophobic force between two liposomes.[55, 58, 64] Qualitatively, however, this attraction can be explained as a consequence of the perturbation of the water structure. Bulk water molecules have directed hydrogen bonds; this three-dimensional network of hydrogen bonds is highly perturbed near molecules with a hydrophobic surface.[65, 66] The formation of additional H-bonds between water molecules which form the cage around the hydrophobic surface may not compensate the entropy loss and/or the loss of electrostatic contribution in this two-dimensional surface of water molecules relative to that in the three-dimensional arrangement of bulk water molecules. A tension is created, which results in a location that has an unfavorable free energy. Because water molecules tend to leave these positions an attractive force is created. However, their long-range character still cannot be satisfactorily explained.

These forces provide a basis to explain the stability of liposomes. Predominantly, surface charge density, zeta potential,

size distribution and homogeneity, as well as ionic strength and pH of the medium determine colloidal stability in vitro. In biological systems, however, the behavior is completely different because of the presence of active liposomicidal substances.

Additional repulsive interactions emanate from molecules attached to the surface (see Section 4.1). Since Egyptian times it has been known that lyophobic colloids, such as pigments in inks, can be stabilized by natural polymers such as arabic gum, starch, or cellulose. This gives rise to the so-called steric repulsion, which will be discussed in Section 4.

3.4. Biological Stability

Even the most stable conventional liposomes are rather unstable in a biological milieu. In addition to interactions with various plasma components and enzymes, they are actively taken up by the body's immune system (Fig. 6). Mechanical stability can help to reduce the interactions in vitro and reduce leakage in vivo but cannot slow down appreciably the uptake of liposomes by phagocytic cells upon parenteral administration.

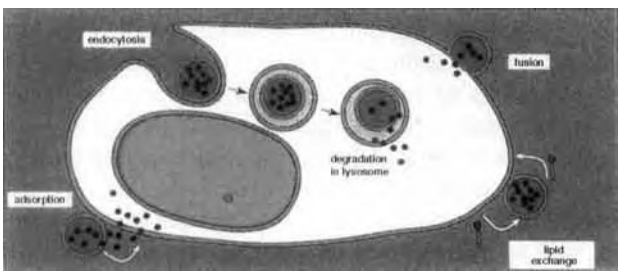


Fig. 6. Interactions of liposomes with cells. The four most important interactions are adsorption, lipid exchange, fusion, and endocytosis (from ref. [82]).

The predominant mechanisms of liposome clearance from blood[2, 24] are 1) opsonization (= preparation for phagocytosis) by immune and nonimmune components in blood such as immunoglobulins, complement factors, and fibronectin, which trigger subsequent macrophage uptake and 2) reaction with plasma (lipo)proteins.

In order for effective opsonization to take place it was hypothesized that a macromolecule has to bind to the liposome surface.[24] This absorption can be either chemi- or physisorption; the total adsorption energy W_{tot} contains contributions from electrostatic W_{est}, hydrophobic W_{hfo}, van der Waals W_{vdW}, hydrogen bonding W_{Hbond}, and specific interactions W_{spec} [Eq. (a)]. Specific interactions occur mostly when antibodies, antigens, or haptens are attached. Obviously, an ideal targeting system for drugs would eliminate all contributions to W_{tot} with exception of W_{spec}. In addition, the adsorption or adhesion probably requires conformational change in some proteins to trigger subsequent macrophage uptake.

$$W_{tot} = -W_{est} - W_{hfo} - W_{vdW} - W_{Hbond} - W_{spec} \quad (a)$$

Similar conclusions may be drawn for interaction with plasma proteins. More cohesive bilayers interact with plasma components less avidly and exchange lipid molecules with the surroundings more slowly. Very cohesive bilayers in the gel state, however, contain too many hydrophobic defects to be stable.[2]

Uncharged liposomes should be more stable, because any strong ionic binding is absent ($W_{est} = 0$). For mechanically stronger (that is, more cohesive) bilayers, hydrophobic binding, for example, the penetration of a segment of the macromolecule into the bilayer, should also be reduced (reduction of W_{hfo}). Physisorption, however, is not prevented (that is, W_{vdW} and W_{Hbond} are negative, and this may explain the lower stability of such bilayers in vivo and their macrophage uptake. Physisorption can be greatly reduced by the presence of a steric shield of an inert, nonimmunogenic ($W_{spec} = 0$), nonionic ($W_{est} = 0$) polymer (see Fig. 4 right). Surface-grafted polymers can prolong blood circulation times for fluid and less cohesive or charged liposomes.[66] This property is important for designing cholesterol-free liposomes with well-defined leakage characteristics as well as for improving their encapsulation efficiency for hydrophobic molecules.

In contrast to electrostatic stabilization, which was effective in many in vitro applications, steric stabilization is a suitable way of stabilizing particles in biological systems and in media with high or variable salinity.

4. Theoretical Understanding of Steric Stabilization of Liposomes

4.1. Two Specific Models for Steric Stabilization

The repulsive forces between two particles can be greatly increased by coating the surface of the particle with appropriate molecules.[68] Natural and synthetic polymers are the most common materials used. They must be inert, well solvated, compatible with the solvent, and have a polarizability close to that of water. Steric stabilization can be induced by attaching polymers to the surface, either by adsorption, hydrophobic insertion, electrostatic binding, or, preferentially, by grafting through covalent bonding. Nonionic, water-compatible, flexible, and well-hydrated polymers are preferred. The repulsion between surfaces with attached polymers was shown to be dependent on the density of grafting and degree of polymerization. For low grafting densities, that is, in the region where the polymer chains cannot interact among themselves, the so-called mushroom model was defined. Conformational entropy of the mushroom is reduced upon approach of other surfaces, and steric repulsion in this model at a distance h[69] is defined according to Equations (b) and (c). D is the average distance between adjacent grafting points, a the size of the segment, and N the degree of polymerization. At higher densities where the interaction of the polymers causes their extension, the so-called brush model can be applied [Eq. (d)].[68]

$$F_{st}^{m} = \frac{kT}{D^2 h_c}\left(\frac{h_c}{h}\right)^{8/3} \quad (b)$$

$$h_c = Na\left(\frac{a}{D}\right)^{2/3} \quad (c)$$

$$F_{st}^{br} = \frac{kT}{D^3}\left[\left(\frac{h_c}{h}\right)^{9/4} - \left(\frac{h}{h_c}\right)^{3/4}\right] \quad (d)$$

The repulsion in the brush regime is determined by the competition between an elastic force associated with the conformational entropy of the chains and an osmotic force related to the monomer-monomer interactions. These equations describe the repulsion between liposomes when the polymers on their surface form a depletion or an adsorption layer.[70] In the case of polymers forming depletion layers, the polymer conformation in the mushroom regime probably looks more like an inverse droplet or pear (rather than a hemisphere of polymers forming the adsorption layer). This conformation alters the density profile on the surface, but leaves the scaling laws unchanged.[71] Theoretical analysis of this case predicted that the chains will be 40% longer than in the case of a mushroom of an adsorption-layer-forming polymer,[72] that is, the polymer extension is larger than the Flory radius (defined as $R_F = aN^{3/5}$), namely 7/5 R_F.

4.2. An Extended DLVO Interparticle Potential

For the most general case the total potential between the particles should include all the above-mentioned forces, including the steric factor (st) [Eq. (e)]. A treatment analogous to the

$$V_{tot} = -V_{vdW} - V_{hfo} + V_{est} + V_{hyd} + V_{und} + V_{st} \qquad (e)$$

DLVO model for two potentials[57] should be performed to find the stability of the system. In a first approximation potentials could be treated as additive. For rigorous treatment, however, possible interdependence of various terms should be taken into account. It is reasonable to expect that the electrostatic, hydration, and steric interactions are interrelated when surfaces are charged or polymers are covalently bound, because of different water structure at the surface.[73]

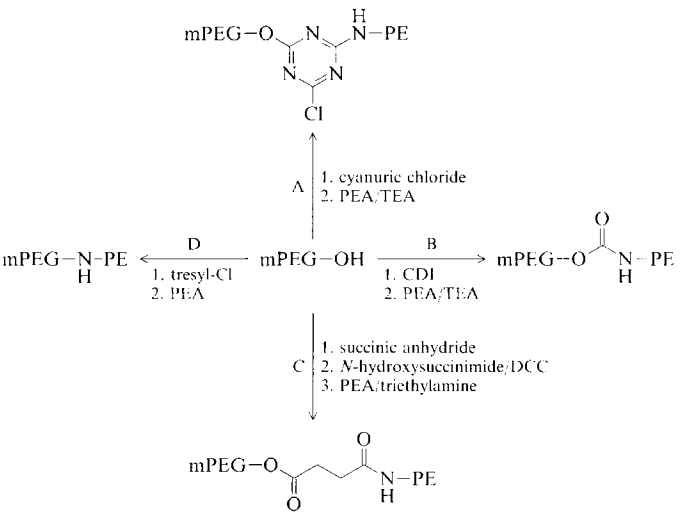
In the case of grafted polyelectrolyte chains, however, the conformation of chains themselves is a function of electrostatic interactions and surface charge. Obviously detailed analyses should be performed.[73, 74]

5. Coupling of Poly(ethylene glycol) to Lipids

PEG polymer chains of various lengths can be covalently coupled to lipids by means of several different coupling agents. Although shorter oligoethyleneoxide spacers have been coupled to many different lipids,[75] the only lipid used for the attachment of longer PEG chains was phosphatidylethanolamine (PE) with different chain lengths and degrees of saturation, because of the reactivity of the amino group. The reactivity of this group is further enhanced by deprotonation by triethylamine. Several researchers also attached PEG chains on cholesterol, but results in general do not show prolonged blood circulation times.[76] Since molecules like cholesterol-O-$(CH_2$-CH_2-$O)_{24}$-H are commercially available surfactants, this is not unexpected, because due to their high cmc values, PEG–lipid molecules can be quickly lost, especially after dilution, from the bilayer. For instance, in the amphotropic cholesterol derivative tetraoxycholesteryl hemisuccinate, a cmc of 1.6 mM was measured.[77]

Synthesis with other phospho- or sphingolipids has either not yet been performed or yielded products with rather unstable and hydrolyzable ester bonds. PEGs of different chain lengths, for instance, with a degree of polymerization $n = 3$, 8, 17, 45, 115, and 270, and polydispersities have been attached. The polydispersity of the polymer depends on the polydispersity index p (defined as the weight average molecular weight divided by the number average molecular weight) of the starting material and virtually does not change during the synthesis (see also legend to Fig. 2).

All coupling strategies are adopted from protein-chemistry.[78] They start with methoxy-PEG (mPEG) and use phosphatidylethanolamine as lipid. Three different synthetic routes (Scheme 1) were employed yielding ester (route C), secondary amine (routes A and D), and uretane (route B) linkages.[18] Although the hydrolysis of the ester linkage formed in route C is probably too slow to contribute significantly to the liposome uptake (e.g. in cells), this linkage is less stable than the urethane bond.[79] The coupling in route A, however, uses a toxic reagent, which is undesirable for in vivo applications.



Scheme 1. Four different synthetic routes to link the polymer PEG to the lipid PE. Most frequently used is route B. Abbreviations: mPEG methoxy poly(ethylene glycol), PE phosphatidylethanolamine, TEA triethylamine, CDI carbonyldiimidazole, DCC dicyclohexylcarbodiimide. By courtesy of Samuel Zalipsky, LTI.

From the above considerations the following synthetic route was developed: The reaction of mPEG (1) and carbonyl diimidazole (CDI) in a molar ratio of 1:1.1 in dried benzene under a nitrogen atmosphere at 75 °C for 16 hours yielded the carbamate of mPEG ether. Coupling of this carbamate to phosphatidylethanolamine was achieved by heating with triethylamine in a 1:2:2 molar ratio at reflux in benzene at 95 °C for 6 hours. The resulting PEG-PE was purified by reverse-phase silica gel chromatography by eluting with chloroform/methanol or water/ethanol mixtures. Because PEG-PE forms micelles in aqueous solutions, it can be purified simply by dialyzing the micellar solution against water or, preferably, against saline. PEG-lipids behave as ionic surfactants in aqueous solutions, and addition of electrolytes appreciably reduces their cmc values; according to preliminary measurements, the cmc of ^{2000}PEG-DSPE decreases from mM to 30 μM upon addition to salt.

Recently the synthesis was further improved. The coupling reaction can be performed at 45 °C in 10 minutes if succinimidyl carbonate of PEG is used rather than PEG activated by car-

bonyl diimidazole. The high rate of this reaction allows polymer to be coupled to the preformed liposomes in aqueous phase[80] and probably makes this method more advantageous than the use of PEG activated by tresyl chloride.

With heterobifunctional PEG chains antibodies can be subsequently attached to the far end of the grafted polymer chain.[80] Because all the above syntheses use unreactive mPEG on one side, a heterobifunctional polymer derivative was prepared that carried the reactive succinimidyl carbonate for the attachment to the amino group of phosphatidylethanolamine on one side and a tertbutyloxycarbonyl(Boc)-protected hydrazine group on the other. The chemical versatility of the hydrazide group[80] enables various ligands including monoclonal or polyclonal antibodies to be linked to preformed functionalized liposomes containing this conjugate.

Preliminary results with several other polymers did not match the prolongation of blood circulation as achieved by PEG-modified liposomes. It seems that poly(acrylamide) and poly(vinylpyrrolidone) do not combine the hydrophilicity and flexibility of PEG. The same was true for oligo- and polysaccharides such as glucuronic acid, dextrans, cellulose derivatives, and copolymers of glucuronic acid with simple sugars. These polymers can form stronger and denser steric shields (possibly with more hydrogen bonding sites), but mobility of the chains is reduced. Furthermore, there are many specific receptors for various sugars in the body. I am sure, however, that there are other polymers that can impose the same effect.

Liposomes containing PEG-lipid can be prepared by using virtually all the standard preparation methods. Hydration of thin films improves the dispersal, and liposomes have fewer lamellae. Unilamellar liposomes are generally characterized by enhanced stability. During formation the PEG-lipid is possibly unevenly distributed in the two monolayers. In addition to steric (colloidal) stabilization, this could enhance thermodynamic stability by generating nonzero spontaneous curvature. Additionally, as suggested by a referee, PEG-lipid can be distributed unevenly with respect to the chain length: lower degrees of polymerization may tend to accumulate in the inner monolayer. The argument of nonzero spontaneous curvature is definitely true for the liposomes with polymers attached only on the outer surface. In fact, at an appropriate grafting density a condition $C_0 = 1/R$, meaning that the spontaneous curvature is inversely proportional to the liposome radius, can be achieved.

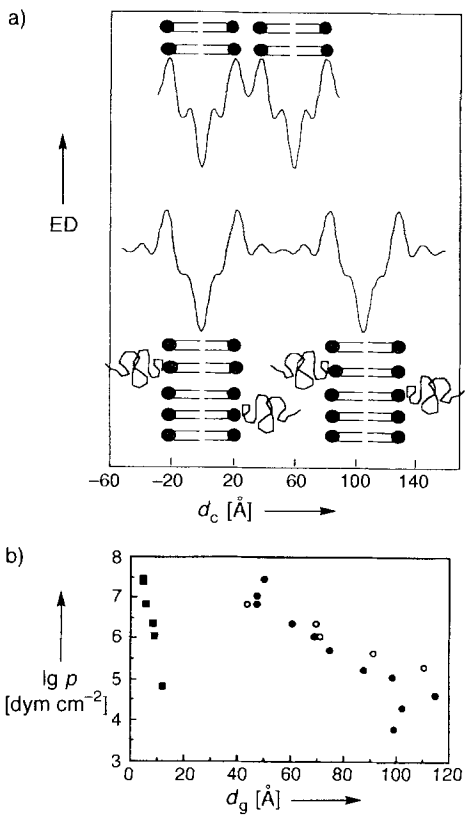


Fig. 7. a) Electron density (E.D.) in arbitrary units as a function of distance from bilayer center (d_c) of bilayers with (bottom) and without (top) ^{2000}PEG-lipid, as determined by small-angle X-ray scattering (SAXS) measurements on multilamellar vesicles. Two bilayers are shown, and it can be clearly seen that the presence of polymer increases the gap between the bilayers. Furthermore, increased electron density in the aqueous gap may indicate that the polymer, which is known to form the depletion layer, is stretched away from the bilayer. b) Dependence of the gap (distance between bilayer surfaces, d_g) between adjacent lamellae on pressure. ■: stearoyloleoyl phosphatidylcholine/cholesterol (2/1) bilayers, ● and ○: same bilayers with 4 mol% of ^{2000}PEG-lipid in 100 mM and 1 mM NaCl, respectively. At all pressures the presence of polymer-bearing lipid markedly increases the aqueous gap between the bilayers (from ref. [80]).

6. Discussion of Some Experimental Results

The effect of increased repulsive pressure above the membrane and reduced adsorption of macromolecules recognized by the immune system on the blood circulation lifetimes was tested by measuring the repulsive pressure between membranes with and without incorporated polymer-bearing lipid. Figure 7a shows that in multilamellar vesicles bilayers containing PEG-lipid the interbilayer spacings are much larger, and even upon strong compression (Fig. 7b) the bilayers are still 4 nm apart, whereas surface-unmodified bilayers show practical collapse to the hard wall repulsion.[80, 81]

The interbilayer repulsion was calculated from the repulsive pressure exerted by the surface-attached polymer in the mushroom model [dotted line, Eq. (f)]. When $N = 44$, $a = 0.35$ nm, $D = 3.57$ nm, the calculated value agrees with experimental data.[82] For distances smaller than h_c, the repulsive pressure is zero.

$$P = \frac{5\,kTNa}{2(D^2/a)}\left(\frac{a}{(h/2)}\right)^{8/3} \qquad \text{(f)}$$

Similar results were obtained by measurement of the surface force.[83] Incorporation of PEG-lipids gives rise to a repulsive force between the two bilayers at all separations. Equilibrium force profiles were reversible and practically insensitive to changes in temperature and ionic strength. The thickness of the steric barrier could be controlled by adjusting the concentration of PEG-lipids and was found to be in agreement with theoretical predictions.[83] These results show increased repulsion with increasing amount of PEG polymer, though biological data give optimal circulation times at lower surface coverages or a saturation-like behavior at grafting densities that ensure complete coating of the surface. Whether this is due to the dynamics of the system, phase transition, phase segregation, increased lateral

pressure, induction of defects, or simply to the oversimplified model will be discussed later.

The presence of surface-attached polymers was confirmed by the measurements of zeta potential.[84] Decreased mobility of PEG-coated liposomes relative to the conventional sample with the same surface charge was attributed to the hydrodynamic drag exhibited by the polymer. The estimated thickness of 5 nm was in agreement with the extension obtained both by measurement of the osmotic stress and the surface force[83] and by theoretically predicted values.[82]

More direct evidence for the hypothesis that reduced interactions lead to increased stability comes from protein adsorption studies on the PEG-coated surfaces. The preliminary investigations demonstrated that on the PEG-lipid containing BLM (black lipid membranes) less protein was adsorbed, and interactions with lipoproteins were reduced.[85] To elucidate the importance of the chain density and flexibility on the uptake of liposomes in the bloodstream, similar studies are being performed at higher grafting densities.

Similarly, reduced protein adsorption and a concomitant 40-fold increase in blood circulation times were seen in the case of polystyrene latex particles (75 nm) coated with polyethylene oxide (>5000 Da)–polypropylene oxide (>3000 Da) block copolymers.[86] Here too, the protein adsorption rate decreased, and the circulation times increased only up to a certain critical density,[87] and as for liposomes (see Table 2 and Fig. 8), optimal stability was found near the mushroom–brush transition.[87]

The simple theory presented above states that higher grafting densities of longer chains result in stronger repulsion and, presumably, better stabilization and longer circulation times. Accordingly, in vitro studies have shown increased repulsion with increasing grafting density and chain length.[83, 88] In vivo experiments, however, do not exhibit this behavior. The longest circulation times were obtained when the PEG contained about 5–10 mol% of relatively short chains ($N = 40–130$); the optimum seems to lie at 5% of PEG-lipids with chains of length $N = 40–70$.

Table 2 shows the stability of liposomes in blood circulation. These studies are very difficult to compare because researchers use different labels, lipid compositions and concentrations, liposomes of different size distributions, and different animals. They also do not report the plasma-induced leakage from the sample (that is, the fraction of the label released through leakage during circulation and not on liposome uptake). This may result in underestimates as high as 30–40%. Nevertheless I have compiled data of comparable studies. If not indicated otherwise in Table 2, small vesicles at unsaturated lipid doses were used. Researchers report mostly the percentage of the dose remaining in circulation at a particular time, or the ratio of the remaining label and the amount taken up by liver and spleen (B/RES). More confusion arises because researchers normalize this either to the starting dose or dose recovered at particular time point. High ratios therefore do not necessarily mean long circulation times but could be an artifact of label losses, for instance. Being aware of these pitfalls I tried to define a single quantity to correlate and unify these numbers. For qualitative discussion we shall rely on the "stealthiness factor" arbitrarily defined at time t after injection [Eq. (g)].

$$SF = \{t_{1/2}[h] - 3\} + (B/RES)[t] \times F[t] \qquad (g)$$

Table 2. Stability of 100-nm liposomes in the blood circulatory system as a function of grafting density and polymer chain length. Various physico-chemical parameters of the systems are also shown. M_{PEG} = molecular weight of poly(ethylene glycol). Mol% = percentage of PEG-lipid in the bilayer. $t_{1/2}$ = half-life of the liposomes in the blood. B/RES ratio of the amount of liposome label present in blood to that in the reticuloendothelial system (liver and spleen) 24 hours after injection. SF = stealth factor. n = degree of polymerization. R_F = Flory radius, R_g = radius of gyration. D = average distance between grafting points as based on the square lattice. ρ = density of monomers per lipid area in the bilayer. Conf: conformation of the polymer as mushroom (m) or brush (br). Δ = the difference between the size of the polymer and their separation. Negative values of Δ infer overlap and zero indicates the transition to the brush conformation.

M_{PEG} [Da]	Mol%	$t_{1/2}$ [h]	c^{24h}_{blood} [%]	B/RES	Comment	SF	n	R_F [Å]	R_g [Å]	D [Å]	ρ	Conf.	Δ D-R_F	Ref.
120	5	3.6	1	0.08		3	2.7	6.5		34.7	0.135	–	28.2	[67]
120	10	5.44	4.7	0.33		4.65	2.7	6.5		24.5	0.27		18	[67]
120	15	8.49	14.1				2.7	6.5				–		[76]
350	33.3	6.92	9	0.52		6.6	7.95	12.35		13.4	2.65		1.05	[a]
750	5	4.86	3.2	0.33		5	17.04	19.5	5.3	34.7	0.85	m	15.2	[b]
750	8		16				17.04	19.5	5.3					[76]
750	33.3	8.5	12.3	0.9		10	17.04	19.5	5.3	13.4	5.68	b	−6.1	[a]
1000	6	≈4	49.5	4.4	4 h, 200 nm		22.7	23.1	6.7		1.36			[c]
1000	6	≈4	49	4.4	4 h, 200 nm		22.7	23.1	6.7					[c]
1000	6		13.7	3.0	4 h, fluid, 200 nm		22.7	23.1	6.7					[c]
2000	5	10.67–13.5	21–29	1.5–2.7	solid; fluid	15–24	45.4	35.1	10.1	34.7	2.27	m-b	−0.4	[18, 24]
2000	5	18.5	40	4	negative charge (PG)	35.5	45.4	35.1	10.1					[18, 24]
2000	6	15.8	35				45.4	35.1	10.1					[76]
2000	7.5	5	50		5 h	12	45.4	35.1	10.1	28.3	3.40		−6.8	[d]
2000	6		47–49	4.8–5	4 h		45.4	35.1	10.1	30.2	2.72	b	−4.9	[c]
3000	5	17.94	34	4		35	68.2	44.1	12.9	34.7	3.41	m	−9.4	[a]
5000	5	10.98	33	2.2		19	113.6	60.9	17.8	34.7	5.68	b	−26.2	[d]
5000	5		21	2.17			113.6	60.9	17.8					[c]
5000	7		28.3				113.6	60.9	17.8	35		b	−25	[76]
5000	6		32.2	2.05	4 h, 200 m		113.6	60.9	17.8					[c]
5000	10	3.5	45		4 h	6.7	113.6	60.9	17.8	23.4	11.36	b	−40.5	[91] [e]
5000	10			1.56		6.7	113.6	60.9	17.8					[91] [e]
12000	6	2.44	34	1.8	4 h, 200 nm		272.7	103	29.4					[c]

[a] M. Newman, M. C. Woodle, personal communication. [b] M. C. Woodle, D. D. Lasic, C. Redemann, M. Newman, S. Babbar, F. Martin, *Period. Biol.* **1991**, *93*, 349. [c] K. Maruyama, T. Yuda, A. Okamoto, S. Kojima, A. Suginaka, H. Twatsuru, *Biochim. Biophys. Acta* **1992**, *1128*, 44. [d] A. L. Klibanov, K. Maruyama, V. P. Torchillin, L. Huang, *FEBS Lett.* **1991**, *286*, 235. [e] G. Blume, G. Cevc, *Biochim. Biophys. Acta* **1990**, *1029*, 91.

Mostly I will use $t = 24$ hours and numerical factor $F[t = 24\ \text{h}] = 5$. Because the blood/RES ratio is less characteristic than blood levels its weighting is, empirically, smaller than that of the blood circulation halflife $t_{1/2}$ (normally 2/3 of the value); the halflife is not used as a sole parameter because the value of $t_{1/2}$ can be too low as a result of leaky liposomes, not well purified samples, and anatomical disorders than can cause liposomes to be lost by leakage into extravascular space and not by endocytosis. Furthermore, the background noise and secondary clearance (the so-called β clearance) of the label can contribute $<1\%$ to the fractions in the blood a day after injection; this corresponds to a halflife of 3 h, and therefore 3 h are empirically subtracted. SF values below 5 characterize conventional liposomes, while for Stealth liposomes SF $>10-15$. These numbers are also sensitive to the type of the label. In the experiments whose results are listed in Table 2, predominantly water-soluble liposome markers were employed.

The best results, as judged from $t_{1/2}$, B/RES, and SF values, are associated with Δ values around 0, where Δ is defined as the difference between the average distance between attachment points of the polymer chains and the size of polymer as defined by Flory radius. At large Δ values the coverage is incomplete. Separate mushrooms start to interact and overlap at $\Delta = 0$, while for $\Delta < 0$ a polymer brush is formed. There is not much correlation between SF and n, the monomer density per site above the bilayer. At shorter chain lengths and very high grafting densities there is no effect, probably because the too thin surface barrier cannot prevent van der Waals binding.[18] When the chains are longer, the correlation may follow the Δ dependence, that is, SF is sensitive to the mushroom–brush transition of the polymer conformation.

Qualitatively, three reasons why SF does not increase with Δ and n above a certain optimal level, as expected from Equation (g) are possible: 1) flexibility of the polymer chains, 2) phase segregation and/or collapse of a polyoxyethylene brush, and 3) reduced solubility of the PEG-lipid in the bilayer due to the increased lateral pressure of the polymer above the surface of the bilayer or additional surface tension. Or in other words, our assumption that blood circulation times are inversely proportional to the protein adsorption, which is again inversely proportional to the repulsive pressure above the membrane, must be refined.

Flexibility of the surface-attached polymer chains is important in reducing the adsorption of blood components on biocompatible surfaces.[89] It was speculated that correlation times of chain motion (that is, the inverse of the frequency of conformational changes in the chains) should be greater than the contact times of molecules for bonding to occur. Although NMR relaxation studies of the polymer chains grafted to liposomes have not been performed yet, similar work in PEG polymers showed the correlation between molecular motion and adsorption rates.[90] The importance of chain mobility, that is, ever changing molecular conformation, and its effect on adsorption[18] was recently termed mobile steric hindrance.[91] It is reasonable to expect that the mobility and flexibility of polymer chains decrease with grafting density. Increased polymer concentration at the surface may have, however, two other effects as well. At higher local PEG concentration the polymer chains may undergo intra- and intermolecular reactions, which may lead to condensation of the chains and thereby the collapse of the brush.[92] The process is analogous to the phase segregation of aqueous PEG polymer solutions at higher concentrations and ionic strengths[93] (above the ϑ temperature). The incorporation of PEG-lipid into the bilayer at higher mol fractions may be reduced, and polymer molecules form a separate mixed micellar phase which may be difficult to detect in the presence of liposomes.[94] Even higher PEG-lipid concentrations lead to the dissolution of liposomes.[94] Alternatively, high lateral pressure between polymer chains may affect the stability of the bilayer, and the formation of various defects within the bilayer surface may lead to the exposure of hydrophobic groups and protein adsorption.[83] Various studies, including measurements of protein adsorption, blood circulation times, liposome stability and leakage in vitro, as well as spectroscopic and scattering studies of polymer conformation and dynamics may resolve this question. It seems that both mushroom and brush arrangements of polymer have advantages and disadvantages: both reduce protein adsorption, but the mushroom shape cannot protect the surface from smaller macromolecules, while the brush form either causes bilayer defects and phase changes, or allows weak protein adsorption. This may be tested experimentally: liposome covered simultaneously with a brush of shorter polymer and a mushroom of a longer one (for example 4–6 mol% of PEG 2000 and 2 mol% of PEG 5000) should exhibit the highest biological stability.

All these models assume complete inertness of the PEG chains. The assumption that the adsorption enthaply ΔH for protein binding onto PEG can be (slightly) negative can, however, explain qualitatively the difference between in vitro measured repulsive pressure and biological stability. A simple model of adsorption rate in the absence of PEG (K) and on the PEG chains (k), in which ϑ is the fraction of the surface coated by polymer, yields adsorption rate according to Equation (h).

$$A = K(1 - \vartheta) + k\vartheta \qquad \text{(h)}$$

The postulate that biological stability is the reciprocal of the protein adsorption rate gives maximum stability if the first term becomes zero at complete coverage, and in the brush regime, A is proportional to $k\vartheta'$, where ϑ' is proportional to PEG concentration on the surface. In other words, simultaneous binding to two or more chains may be implied.[95] Figure 8 shows data from Table 2 and theoretical curve from Equation (h), assuming that biological stability is inversely proportional to A, that is, stability $= A^{-1}$, for $K = 0.033$ and $k = K/10$. Of course, this simple picture gives no insights on the molecular level.

Yet another unanswered question is why the blood circulation times decrease with increasing liposome size. The liver hardly takes up liposomes larger than 200 nm, but uptake by the spleen increases, which suggests a different mechanism and/or mediator for these two organs. It is possible that small proteins of the complement system still bind to the liposome surface but that their interactions with the receptors in the spleen are compromised by the steric barrier, and that this interaction is size dependent. Alternatively, the binding of the protein may simply depend on the curvature of the liposome (which also defines the interactions between polymer chains and their mobility) or on

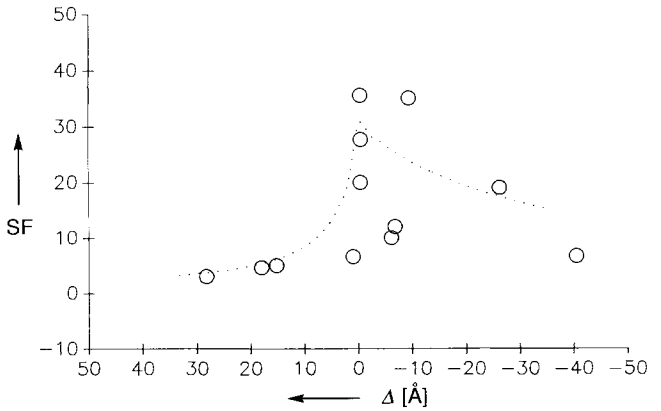


Fig. 8. Stealth factor SF as a function of the difference between the average separation of polymer grafting points D and the Flory radius R_F. Data points are from Table 2 and unpublished data from M. Newman and M. C. Woodle. The dotted line is a fit from the simple empirical equation, Equation (h).

rotational diffusion rate of the particle, and is therefore size-dependent.

This brings us to the final question: can we make an artificial colloidal particle comparable to erythrocytes, which circulate for 100 days and have SF values larger than 2000. Specific interactions, including those with molecules such as dysopsonins or histocompatibility complexes, must play a role, because, despite their sophisticated steric stabilization by glycocalyx, erythrocytes from one person cannot circulate in a person with a different blood group. A thick brush of 7.5 kDa polysaccharides on the red blood cell seems to be much more rigid and dense than the artificial polymer coatings.

7. Applications of Sterically Stabilized Liposomes

Sterically stabilized vesicles are suitable models for studies of polymers and scaling laws, colloid stability, and cell biology. Apparently in cells specific attraction and nonspecific repulsion play an important function, as in these vesicles. Therefore, sterically stabilized liposomes offer a much better model for the study of cell function and interactions than conventional liposomes, which can exhibit many nonspecific attractive interactions. In addition, the nonspecific repulsion of sterically stabilized liposomes offers several useful applications, mostly in diagnostics and drug delivery.

In addition to liposomes and other lyotropic colloidal particles, PEG-lipid molecules can stabilize other lipid structures as well. A typical example are foams. Due to the bulky polar heads, PEG-lipids in pure form do not form very stable foams. However, foams made from lecithins containing 5–10 mol% of PEG-lipids are extremely stable and refractory to the addition of the defoaming agent ethanol. While typical lecithin foams collapse within minutes, these foams can be stable for months. The stability is probably due to the reduced drainage of water because of the presence of well-swollen and immobilized polymer in the aqueous layer. At present, however, it is still too early to speculate on potential applications, such as coating of various surfaces with PEG-lipid-containing monolayers.

7.1. Medical Applications of Sterically Stabilized Liposomes

Stealth liposomes provide an entirely new and unique drug delivery vehicle because of their ability to evade quick clearance by the immune system. With such liposomes Ehrlich's idea (now almost one century old) of a magic bullet—a drug delivery system that would target only diseased cells—became practically possible. Indeed, early studies have shown increased delivery of antibody-labeled stealth liposomes to the target tissue in accessible sites. The accessible sites upon system administration are in vascular compartments,[96] at sites of increased vascular permeability (which occurs naturally at the sites of infections, inflammations, tumors, and other traumatic conditions, or can be induced artificially)[97–100] and upon localized administration in the peritoneal cavity and in the central nervous system compartment.[101] This is also the case in nontargeted stealth liposomes, which represent the majority of applications and will be discussed below. An unresolved problem is the delivery of the encapsulated drug into the cell, because most cells are not phagocytic, and fusion of liposomes and cells is a very rare phenomenon. One approach to overcome this difficulty is to promote fusion by surface-attached fusogenic proteins. Simpler ways include attempts to induce leakage of liposomes by changes in temperature or pH, or the preparation of liposomes with compromised stability.

Although this is one of the current hot issues in liposome research, several applications are not affected by lack of drug bioavailability.[2] For instance, the anthracycline anticancer drugs can be loaded at very high concentrations (normally 1 g drug per 7.5 g lipid, see Figure 9) and have elicited great improvements in therapeutic efficacy upon encapsulation into stealth liposomes. According to current understanding,[117] the prolonged presence of liposomes in blood allows them to extravasate into sites where the vasculature is leaky. This is often

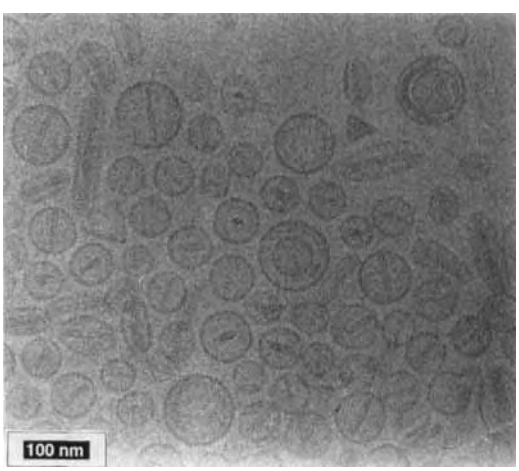


Fig. 9. Cryoelectron micrograph image of unilamellar vesicles with encapsulated drug. Doxorubicin can be encapsulated at very high lipid concentrations by using various gradients. We used an ammonium sulfate gradient in which weak base NH_3 (pK = 9.3) exchanges with weak base doxorubicin · HCl (pK = 8.3). When doxorubicin enters the liposome, its charged form precipitates with sulfate as counterion, and this molecular sink keeps the chemical potential gradient of doxorubicin unchanged until most of the drug is precipitated. This results in very high concentrations in the liposome interior. Solidification of the drug gives rise to peculiar changes in liposome shapes. I thank P. Frederik, University of Limburg, Maastricht for this picture.

the case in tumors,[97-99] and indeed, experiments with animals and humans have shown that the drug concentration in tumors on delivery with liposomes is ten times higher than on administration of the free drug.[102-105] In these cases, it seems that liposomes are trapped in the tissue, where they slowly release their contents either by leakage or upon degradation by enzymes such as phospholipases. This agrees with the observation that peak drug levels in tumors are observed three to four days after liposome administration as compared to a few hours for the free drug.[98] The peak concentration of the drug can be 10–30 times higher when the drug is encapsulated in stealth liposomes.[106]

Figure 10 shows the effect of various treatments on the tumor size in a C26 solid tumor mouse model, which is virtually insensitive to treatment with free adriamycin (= doxorubicin, "S-Dox") or with conventional liposomes containing the drug.[107] Animals treated with placebo liposomes and their mixture with free drug as controls did not show any significant effect over the untreated (that is, saline injected) animals. The administration of stealth liposomes containing adriamycin, however, resulted in complete remission of tumors on early treatment and in significant improvements on delayed treatment. Virtually identical results were obtained with the very similar drug epirubicin.[108]

Improvements were also achieved in other resistant tumor models, such as mammary carcinoma (Fig. 11). Adriamycin formulation was substantially more effective not only in curing mice with recent implants from various tumors but also in reducing the incidence of metastases originating from these intramammary implants.[109] The growth of human lung tumor xenografts in scid (scid = severe combined immunodeficient) mice was completely arrested by adriamycin formulation, while free drug and drug encapsulated in conventional liposomes were ineffective.[110]

The same extravasation mechanism of small liposomes at sites of leaky vasculature can be used in the treatment of inflammations and infections, which are also characterized by enhanced vascular permeability.[111]

While many new drugs are currently being monitored and tested for encapsulation into sterically stabilized liposomes, phase I and II clinical trials of doxorubicin encapsulated into stealth liposomes in humans have yielded very encouraging results. It was found that blood circulation times in humans, as measured by the plasma concentration of the drug, are around 45 hours. This results in reduced bone marrow suppression, neutropenia, and leucopenia, as well as shifted biodistribution of doxorubicin from the body into tumors, as in AIDS patients with Kaposi sarcoma.[103, 112] The measured concentrations of doxorubicin in these lesions were 11.4-, 5.2-, and 9.9-fold higher for injected doses of 10, 20, and 40 mg m^{-2}, respectively.[103] In contrast to the free drug for which the dose-limiting factors are acute myelosuppression (reduction of white blood cell count) and cumulative cardiotoxicity, the dose-limiting factor of the stealth liposome encapsulated drug is stomatitis, a skin disease—in this case lesions—inside the mouth.

As mentioned above, the property of sterically stabilized vesicles to avoid rapid uptake by liver and spleen made the concept of targeted liposomes feasible for in vivo applications. Currently much effort is devoted to this area in order that these vesicles containing drugs or markers and labeled with appropriate anti-

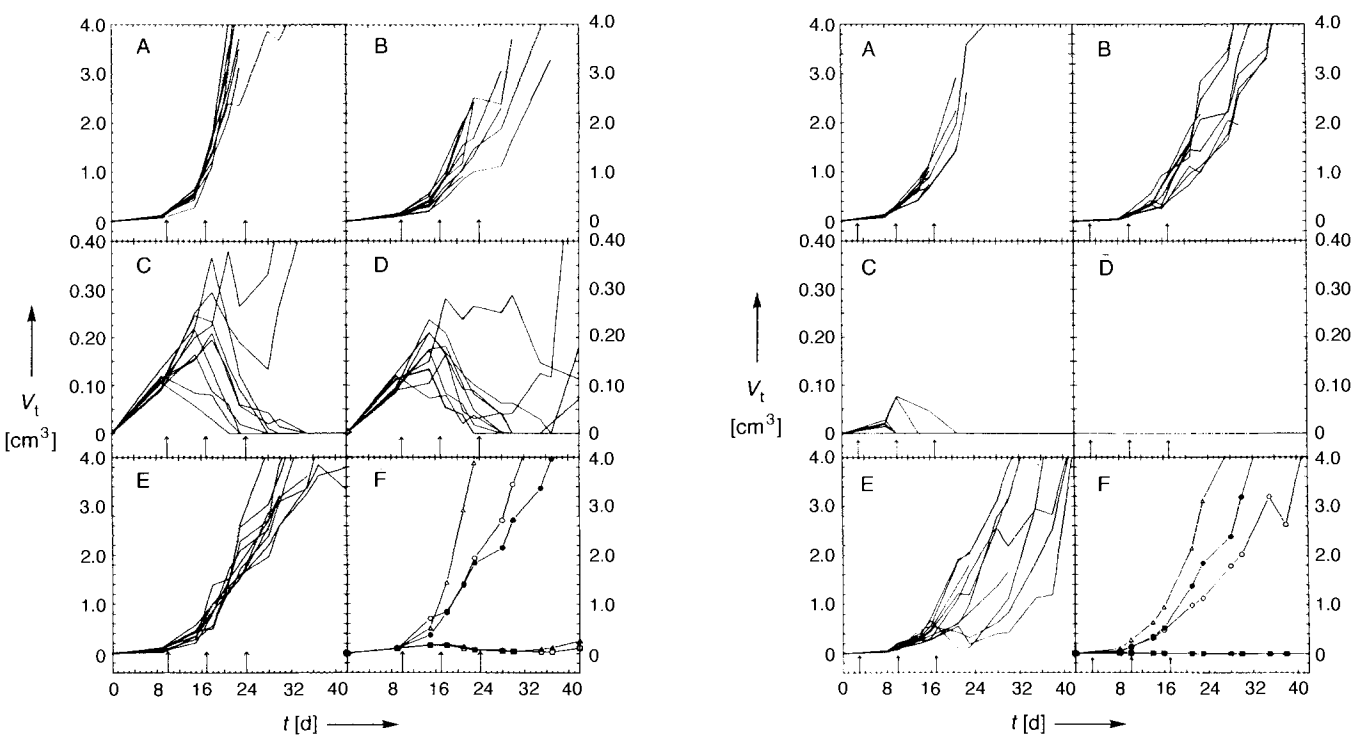


Fig. 10. The effect of the anticancer drug epirubicin on the growth of solid C26 tumor, which is practically resistant to conventional therapies: the graph shows the tumor volume (V_t) as a funtion of time t. Mice were injected with 10^6 C26 cells on day zero. Treatments were conducted (arrows) on days 3, 10, and 17 (left), or 10, 17, and 24 (right). Panels A–E show the tumor growth of ten animals for different treatments. A: saline (control); B: free epirubicin at 6 mg per kilogram body weight; C and D: epirubicin in Stealth liposomes at 6 mg kg^{-1} and 9 mg kg^{-1}, respectively; E: control (mixture of Placebo liposomes and free drug); F: averages of all these treatments—from left to right: saline, free drug, mixture, and overlapping the two liposome encapsulated drugs. (Note the different scale for C and D.) From ref. [102]. Virtually identical results were obtained with doxorubicin-containing Stealth liposomes [103].

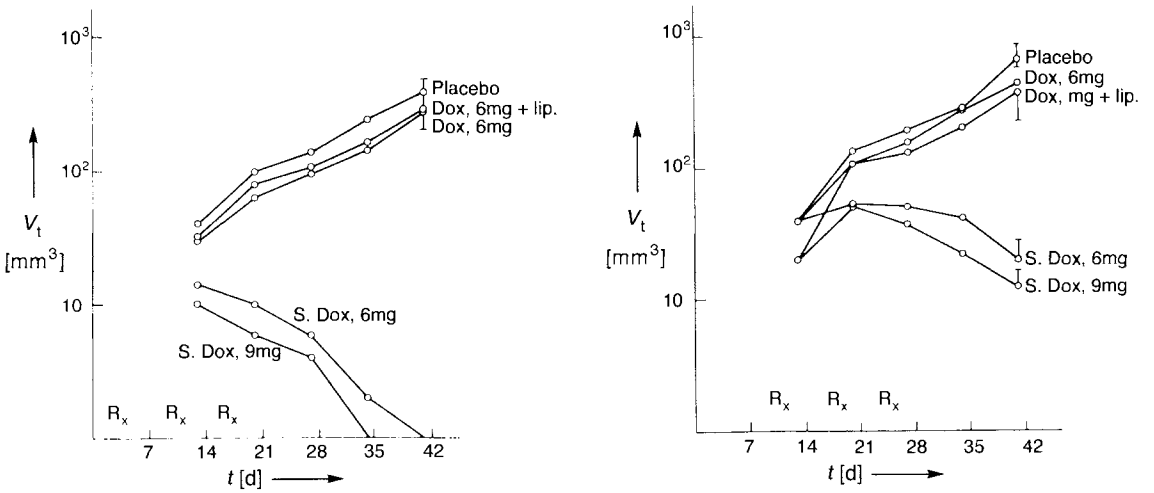


Fig. 11. Dependence of the tumor sizes (V_t) on time in mice with implanted mammary MC2B tumors (1 mm^3). The treatment (R_x) in the left-hand graph was on days 3, 10, and 17. For the right-hand graph treatment was delayed by one week (days 10, 17, and 24). The treatment included (from top to bottom) saline, mixture of free doxorubicin and placebo liposomes (6 mg kg^{-1}), free drug at 6 mg kg^{-1}, and doxorubicin encapsulated in Stealth liposomes at 6 and 9 mg kg^{-1} (from ref. [104]).

bodies and other ligands target cancer cells, atherosclerotic lesions and plaques, sites of ischemia, and some other traumatic areas.

8. Concluding Remarks

In conclusion, polymer-grafted liposomes and their applications show an interplay of various sciences, from theoretical polymer physics, colloid and interface science, organic chemistry, to biology, immunology, pharmacology, medicine, anatomy, and oncology. As a result very stable liposomes in biological environments were designed and showed remarkable therapeutic potential. The next goals are now to improve spatial and temporal control of the release of the encapsulated drug. Targeting can be improved in physically accessible sites by the attachment of antibodies to the far end of polymer chains. Better control of the temporal release of the drug will be tackled mostly by three routes: physical approaches use temperature, pH, or (target) binding-sensitive induced phase change, chemical approaches try to destabilize liposomes at a particular location by a chemical change of membrane-forming lipid and the formation of bilayers with fusogenic ability, and biological approaches employ surface-attached fusogenic molecules or stimulate internalization. For such a rational liposome design, of course, liposomes must be made from an appropriate bilayer matrix. We dare to conclude that sterically stabilized vesicles are an example of how complex and elusive problems can be solved by a multidisciplinary approach. For the continuation of this development even broader interdisciplinary work will be required.

Received: June 28, 1993
Revised version: October 25, 1993 [A 7 IE]
German version: *Angew. Chem.* **1994**, *106*, 1765

[1] P. G. deGennes, *Physics of Liquid Crystals*, Oxford Univ. Press, Oxford, **1974**.
[2] D. D. Lasic, *Liposomes: From Physics to Applications*, Elsevier, Amsterdam, **1993**.
[3] V. Luzzati, H. Mustachi, A. Skoulios, R. Husson, *Acta Crystallogr.* **1960**, *13*, 660–667.
[4] G. H. Brown, J. W. Doane, V. D. Noff, *Structure and Properties of Liquid Crystals*, CRC, Boca Raton, FL, USA, **1970**.
[5] H. Ringsdorf, B. Schlarb, J. Venzmer, *Angew. Chem.* **1988**, *100*, 117–162; *Angew. Chem. Int. Ed. Engl.* **1988**, *27*, 113–158.
[6] J. Charvolin, J. F. Sadoc, *Colloid Polym. Sci.* **1990**, *268*, 190–195.
[7] D. D. Lasic, *J. Theor. Biol.* **1987**, *124*, 35–41.
[8] D. D. Lasic, *J. Colloid Interface Sci.* **1990**, *140*, 302–304.
[9] A. D. Bangham, R. W. Horne, *J. Mol. Biol.* **1964**, *8*, 660–668.
[10] A. D. Bangham, M. M. Standish, J. C. Watkins, *J. Mol. Biol.* **1965**, *13*, 238–252.
[11] *Ann. NY Acad. Sci.* **1978**, *308*, 1–412. (Ed.: D. Papahadjopoulos).
[12] S. Leibler, *Phys. Today* **1988**, *41* (2), 25.
[13] R. Lipowsky, *Nature* **1991**, *349*, 475–481.
[14] J. Kas, E. Sackmann, R. Podgornik, S. Svetina, B. Zeks, *J. Phys. II* **1993**, *3*, 631–645.
[15] *Handbook on Membranes* (Eds.: R. Lipowsky, E. Sackmann), Elsevier, Amsterdam, in press.
[16] J. Maddox, *Nature* **1993**, *363*, 205.
[17] D. Papahadjopoulos, D. T. Allen, A. Gabizon, E. Mayhew, S. K. Huang, K. Lee, M. C. Woodle, D. D. Lasic, C. Redemann, F. J. Martin, *Proc. Natl. Acad. Sci. USA* **1991**, *88*, 11460–11464.
[18] M. C. Woodle, D. D. Lasic, *Biochim. Biophys. Acta* **1992**, *1113*, 171–199.
[19] G. Gregoriadis, *News Physiol. Sci.* **1989**, *4*, 146–151.
[20] A. Gabizon, D. Papahadjopoulos, *Proc. Natl. Acad. Sci. USA* **1988**, *85*, 6949–6953.
[21] M. K. Pratten, J. B. Lloyd, G. Horpel, H. Ringsdorf, *Makromol. Chem.* **1985**, *186*, 725–733.
[22] L. Illum, S. S. Davis, R. H. Muller, E. Mak, P. West, *Life Sci.* **1987**, *40*, 367–374.
[23] M. C. Woodle, M. S. Newman, F. J. Martin, *Int. J. Pharm.* **1992**, *88*, 327–334.
[24] D. D. Lasic, F. J. Martin, A. Gabizon, S. K. Huang, D. Papahadjopoulos, *Biochim. Biophys. Acta* **1991**, *1070*, 187–192.
[25] W. Helfrich, *Phys. Lett. A* **1974**, *50*, 115–116.
[26] D. D. Lasic, *Biochim. Biophys. Acta* **1982**, *692*, 501–502.
[27] D. D. Lasic, *Nature* **1992**, *355*, 279–280.
[28] L. Cantu, M. Corti, M. Musolino, P. Salina, *Europhys. Lett.* **1990**, *13*, 1655–1657.
[29] J. M. Gebicki, M. Hicks, *Nature* **1973**, *243*, 232–234.
[30] E. W. Kaler, A. K. Murthy, B. E. Rodriguez, J. A. N. Zasadzinski, *Science* **1989**, *245*, 1371–1374.
[31] Y. Talmon, D. F. Evans, B. W. Ninham, *Science* **1983**, *221*, 1047–1048.
[32] B. Z. Lin, C. C. Yin, H. Hauser, *Biochim. Biophys. Acta* **1993**, *1147*, 237–244.
[33] D. D. Lasic, *J. Colloid Interface Sci.* **1988**, *124*, 428–435.
[34] P. Mariani, V. Luzzati, H. Delacroix, *J. Mol. Biol.* **1988**, *204*, 165–189.
[35] J. H. Fuhrhop, D. Fritsch, *Acc. Chem. Res.* **1986**, *19*, 130–137.
[36] D. D. Lasic, *Biochem. J.* **1988**, *252*, 1–11.
[37] K. H. Klotz, M. Winterhalter, R. Benz, *Biochim. Biophys. Acta* **1993**, *1147*, 161–164.
[38] D. D. Lasic, *Nature* **1991**, *351*, 613.
[39] J. A. Crowe, L. M. Crowe, D. Chapman, *Science* **1984**, *223*, 201–203.
[40] E. Evans, R. Skalak, *CRC Crit. Rev. Bioeng.* **1979**, *3*, 181–330.
[41] D. Needham, R. Nunn, *Biophys. J.* **1990**, *58*, 997–1009.

[42] M. Bloom, O. Mouritsen, E. Evans, *Q. Rev. Biophys.* **1991**, *24*, 293–397.
[43] S. L. Regen, B. Czech, A. Singh, *J. Am. Chem. Soc.* **1980**, *102*, 6638–6671.
[44] J. H. Fendler, *Science* **1984**, *223*, 888–894.
[45] H. H. Hüb, B. Hupfer, H. Koch, H. Ringsdorf, *Angew. Chem.* **1980**, *92*, 962–964; *Angew. Chem. Int. Ed. Engl.* **1980**, *19*, 938–940.
[46] W. Reed, D. Lasic, H. Hauser, J. H. Fendler, *Macromolecules* **1985**, *18*, 2005–2012.
[47] D. S. Johnston, S. Sanghera, M. Pons, D. Chapman, *Biochim. Biophys. Acta* **1980**, *602*, 57–69.
[48] B. Hupfer, H. Ringsdorf, H. Schupp, *Chem. Phys. Lipids* **1983**, *33*, 355–374.
[49] T. Kunitake, *Angew. Chem.* **1992**, *104*, 692–710; *Angew. Chem. Int. Ed. Engl.* **1992**, *31*, 709–726.
[50] C. Santaella, P. Vierling, J. G. Riess, *Angew. Chem.* **1991**, *103*, 584–586; *Angew. Chem. Int. Ed. Engl.* **1991**, *30*, 567–568.
[51] H. Bader, H. Ringsdorf, *J. Polym. Sci. Polym. Chem. Ed.* **1982**, *20*, 1623–1628.
[52] M. Grit, J. H. deSmit, A. Struijke, D. J. A. Crommelin, *Int. J. Pharm.* **1989**, *50*, 1–6.
[53] M. Grit, D. J. A. Crommelin, *Chem. Phys. Lipids* **1992**, *62*, 113–122.
[54] F. J. Martin in *Specialized Drug Delivery Systems* (Ed.: E. Tyle), M. Dekker, New York, **1990**, p. 267–316.
[55] J. N. Israelachvili, *Intermolecular and Surface Forces*, Academic Press, New York, **1985**.
[56] S. Nir, J. Bentz, J. Wilschut, N. Duzgunes, *Prog. Surf. Sci.* **1983**, *13*, 1–124.
[57] E. J. Verwey, J. Th. G. Overbeek, *The Theory of the Stability of Lyophobic Colloids*, Elsevier, Amsterdam, **1948**.
[58] C. Helm, J. N. Israelachvili, P. M. McGuiggan, *Science* **1989**, *246*, 919–921.
[59] A. M. Carmona-Ribeiro, *J. Phys. Chem.* **1992**, *96*, 9555–9557.
[60] S. I. Leon, J. H. Lee, J. D. Andrade, P. G. deGennes, *J. Colloid Interface Sci.* **1991**, *142*, 149–158.
[61] A. C. Crowley, N. L. Fuller, R. P. Rand, V. A. Parsegian, *Biochemistry* **1978**, *17*, 3163–3168.
[62] W. Helfrich, *Z. Naturforsch. A* **1978**, *33*, 305–315.
[63] J. N. Israelachvili, H. Wennerstrom, *Langmuir* **1990**, *6*, 837–876.
[64] R. Podgornik, V. A. Parsegian, *Chem. Phys.* **1991**, *154*, 477–483.
[65] S. Svetina, B. Zeks, *Croat. Chem. Acta* **1987**, *60*, 505–516.
[66] S. Svetina, B. Zeks, *Stud. Biophys.* **1986**, *111*, 127–134.
[67] M. C. Woodle, K. K. M. Atthay, M. S. Newman, J. Hidayat, L. Collins, C. Redemann, F. Martin, D. Papahadjopoulos *Biochim. Biophys. Acta* **1992**, *1105*, 193–200.
[68] D. H. Naper, *Polymeric Stabilization of Colloidal Dispersions*, Academic Press, New York, **1983**.
[69] P. G. deGennes, *Adv. Colloid Interface Sci.* **1987**, *27*, 189–209.
[70] P. G. deGennes, *Macromolecules* **1981**, *14*, 1637–1644.
[71] P. G. deGennes, personal communication, **1992**.
[72] a) *Stealth Liposomes* (Eds: D. D. Lasic, F. J. Martin), CRC, in press; b) K. Hristova, D. Needham, in [72a].
[73] J. N. Israelachvili, personal communication, **1993**.
[74] R. S. Ross, P. Pincus, *Macromolecules* **1992**, *25*, 2177–2183.
[75] G. Vanlerberghe, R. M. Handjani-Villa, A. Ribier, *Coll. Nationaux. CNRS* **1978**, *938*, 303–311.
[76] T. M. Allen, C. Hansen, F. Martin, C. Redemann, Y. Y. Yang, *Biochim. Biophys. Acta* **1991**, *1066*, 29–36.
[77] G. Decher, H. Ringsdorf, *Liq. Cryst.* **1993**, *13*, 57–69.
[78] S. Zalipsky, C. Lee in *Poly(ethylene) Glycol Chemistry* (Ed.: J. M. Harris), Plenum, New York, **1992**, p. 347–370.
[79] S. Zalipsky, R. Seltzer, S. Menon-Rudolph, *Biotechnol. Appl. Biochem.* **1992**, *15*, 100–114.
[80] S. Zalipsky, *Bioconjugate Chem.* **1993**, *4*, 296–299.
[81] D. Needham, T. J. McIntosh, D. D. Lasic, *Biochim. Biophys. Acta* **1992**, *1108*, 40–48.
[82] D. Needham, K. Hristova, T. J. McIntosh, M. Dewhirst, N. Wu, D. D. Lasic, *J. Liposome Res.* **1992**, *2*, 411–430.
[83] T. L. Kuhl, D. E. Leckband, D. D. Lasic, J. N. Israelachvili, *Biophys. J.* **1994**, *66*, 1479–1488.
[84] M. C. Woodle, L. R. Collins, E. Sponsler, N. Kossovsky, D. Papahadjopoulos, F. Martin, *Biophys. J.* **1992**, *61*, 902–910.
[85] R. Benz, K. H. Klotz, D. D. Lasic, M. Winterhalter, unpublished.
[86] J. S. Tan, D. E. Butterfield, C. L. Voycheck, K. D. Caldwell, J. T. Li, *Biomaterials*, in press.
[87] K. D. Caldwell, personal communication, **1993**.
[88] T. J. McIntosh, D. Needham, personal communication, **1992**.
[89] J. D. Andrade, S. Nagaoka, S. Cooper, T. Okano, S. W. Kim, *ASAIO Trans.* **1987**, *33*, 75–78.
[90] E. Bayer, W. Rapp in *Poly(ethylene glycol) Chemistry* (Ed.: M. Harris), Plenum, New York, **1992**, p. 325–340.
[91] G. Blume, G. Cevc, *Biochim. Biophys. Acta* **1993**, *1146*, 157–168.
[92] P. G. deGennes, *C. R. Seances Acad. Sci. Ser.* ■ **1991**, *313*, 1117–1122.
[93] P. Molyneux, *Water Soluble Synthetic Polymers*, CRC, Boca Raton, FL, USA, **1990**.
[94] D. D. Lasic, M. C. Woodle, F. Martin, T. Valentincic, *Period. Biol.* **1991**, *93*, 287–291.
[95] I thank P. G. de Gennes, H. Wennerstrom, J. N. Israelachvili, G. Tiddy, J. Andrade, K. Caldwell, E. Evans, L. Auvray, O. Borisov, E. Sackmann, D. Papahadjopoulos, D. Needham and M. C. Woodle for stimulating discussions.
[96] J. Connel, T. M. Allen, *Cancer Res.* **1993**, *53*, 1484–1488.
[97] H. F. Dvorak, A. J. Nagy, J. T. Dvorak, A. M. Dvorak, *Am. J. Pathol.* **1988**, *133*, 95–108.
[98] J. A. Nagy, ■other authors■, *Biochim. Biophys. Acta* **1988**, *948*, 305–326.
[99] R. K. Jain, *Cancer Metastasis Rev.* **1987**, *6*, 559–593.
[100] Z. Ning, D. Da, T. L. Rudoll, D. Needham, A. Whorton, M. W. Dewhirst, *Cancer Res.* **1993**, *53*, 3765–3770.
[101] U. K. Nassander, A. Steereberg, H. Poppe, G. Prels, W. DeJong, D. J. A. Crommelin, *Cancer Res.* **1992**, *52*, 646–653.
[102] A. Gabizon, *Cancer Res.* **1992**, *52*, 891–896.
[103] D. Northfelt, L. Kaplan, J. Russell, P. A. Volberding, F. Martin in *VIII Int. Conf. AIDS*, Amsterdam, **1992**, Abstracts; see also D. Northfelt, in [72a].
[104] D. D. Lasic, *Am. Sci.* **1992**, *80*, 20–31.
[105] D. D. Lasic in *Structure and Dynamics of Membranes* (Eds.: R. Lipowsky, E. Sackmann), Elsevier, in press.
[106] P. W. Working, M. S. Newman, K. Huang, E. Mayhew, J. Vaage, D. D. Lasic, *J. Liposome Res.* **1994**, *4*, 667–687.
[107] E. Mayhew, D. D. Lasic, S. Babbar, F. J. Martin, *Int. J. Cancer* **1992**, *51*, 302–309.
[108] S. K. Huang, E. Mayhew, S. Gilani, D. D. Lasic, F. Martin, D. Papahadjopoulos, *Cancer Res.* **1992**, *52*, 6774–6781.
[109] J. Vaage, E. Mayhew, D. D. Lasic, F. J. Martin, *Int. J. Cancer* **1992**, *51*, 942–948.
[110] S. S. Williams, T. R. Alosco, E. Mayhew, D. D. Lasic, F. J. Martin, R. B. Bankert, *Cancer Res.* **1993**, *53*, 3964–3967.
[111] I. A. J. M. Bakker-Woudenberg, A. F. Lokersee, M. T. ten Kate, J. W. Mouton, M. C. Woodle, G. Storm, *J. Infect. Dis.* **1993**, *168*, 164–171.
[112] J. R. Bogner, F. Göbel, *VIII Int. Conf. AIDS*, Amsterdam, **1992**, Abstracts; J. R. Bogner, F. D. Goetzel in [72a].

Peptidomimetics—Tailored Enzyme Inhibitors

Joachim Gante*

Dedicated to Professor Hans Joachim Langmann on the occasion of his 70th birthday

Peptides and proteins (there is no clear boundary between the two classes of compounds) are absolutely essential components of organisms in many ways. While proteins have biocatalytic functions and are important components of tissues, peptides play an important role in the organism as hormones, neurotransmitters, and neuromodulators. Peptides and their analogues have long been used in medicinal chemistry as therapeutic agents for pathological conditions generally characterized by a disruption of the interplay between messenger molecules or enzyme substrates and their targets, the receptors and enzymes. For various biochemical and biophysical reasons there is an increasing tendency towards the use of chemical "Trojan horses" known as peptidomimetics. The chances that such agents are active generally increase with the magnitude of the "deceptive effect", in other words in proportion to the degree of conversion of a peptide into a non-peptide. Rational design has become a catchphrase which is at present applied frequently to the development of peptidomimetics. New computer programs are invaluable tools in such design processes. However, in spite of the many advances already made, we are still far from the final goal, the de novo design of peptidomimetics. Rational design is nonetheless advancing rapidly, and it is already clear that developments in the area of peptidomimetics have given a great boost to peptide chemistry as a whole. This can be expected to continue, so that in future peptide chemistry may be characterized by a type of symbiotic alliance between peptides and non-peptides.

1. Introduction

Over the years peptidomimetics[1] have become immensely important for both organic and medicinal chemists. In the biological, chemical, and pharmaceutical areas they offer interesting advantages over physiologically active peptides, which as active substances are crucial for the organism. Apart from increasing the effectivity and selectivity of peptides, which may decrease side effects, improving oral bioavailability and prolonging the activity by hindering enzymatic degradation within the organism are of particular importance.[2]

It is possible by combining computer graphics, modern NMR techniques, and X-ray structural analysis to design drugs by constructing and synthesizing tailor-made molecules, the structural spectrum of which lies between slightly modified peptides on the one side and pure non-peptides on the other. "Browsing" in peptide libraries[3] and the discovery of completely new non-peptidic structures in the course of empirical mass screening often provide new lead structures, which can in turn be subjected to structural variation in order to optimize the required properties of the active substance.

[*] Prof. Dr. J. Gante
E. Merck
Präklinische Pharmaforschung, Medizinische Chemie
D-64271 Darmstadt (FRG)
Telefax: Int. code + (6151) 72-2000

The synthesis of such compounds can require the use of the complete arsenal of synthetic organic chemistry. Thus modern peptide chemistry (which includes that of the mimetics) cannot rely only on traditional synthetic methods.

The generation of peptidomimetics is based primarily on the knowledge of the conformational, topochemical, and electronic properties of the native peptide and that of its address, in other words, the receptor or the active site of the enzyme with which it interacts. The design of peptidomimetics as potential bioactive substances must take particular account of two structural factors: 1) a favorable fit (total conformation) with respect to the corresponding complementary spatial situation at the active site; if necessary the conformation can be stabilized by the introduction of elements conferring rigidity; 2) the placement of certain structural elements (e.g. functional groups, polar and hydrophobic regions) in defined positions so that the required interactions (e.g. hydrogen bonds, electrostatic or hydrophobic interactions) can occur.

Thus for example in the case of enzyme inhibition both prerequisites require knowledge of the corresponding steric features of the enzyme–substrate complex and the mechanism of enzyme catalysis, that is, its modus operandi. The latter is a precondition for a specific course of action, since it may indicate which reactants are involved at which sites in the complex in a certain reaction. In addition the knowledge of the bioactive

conformation of an active substance is essential in drug design. Apart from spectroscopic methods (NMR) and X-ray structural analysis, computer modeling is an important tool in such studies.

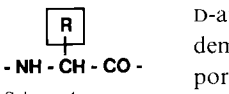
This review has been written with the goal of further clarifying the basic features of drug design. The immense amount of material available makes it necessary to limit the discussion to a few characteristic and important examples. After discussing general structural and synthetic aspects, we will examine some current examples of the application of peptidomimetics in the area of therapeutically relevant enzyme inhibition. The effect of such active substances (e.g. CCK antagonists, angiotensin II receptor antagonists) on receptors has been described very recently in a review in this journal.[2b]

2. Structural Possibilities

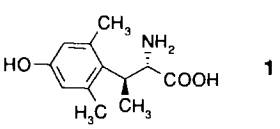
From a structural point of view peptidomimetics can be prepared by approaches ranging from the slight modification of the initial structure to the generation of a pure nonpeptide.

2.1. Modification of the Side Chains of Amino Acid Residues

One possible strategy for modifying the side chains of amino acids is the well-known practice of replacing natural by unnatural side chains and the exchange of L- for D-amino acids (Scheme 1). A recent example demonstrates that this procedure is still important today: modification of the tyrosine side chain by introducing methyl groups in the 2′-, 6′-, and β-positions hinders free rotation about the $C^{\beta}-C^{\gamma}$ bond and can thus favor the formation of bioactive conformations (**1**).[4]



Scheme 1.

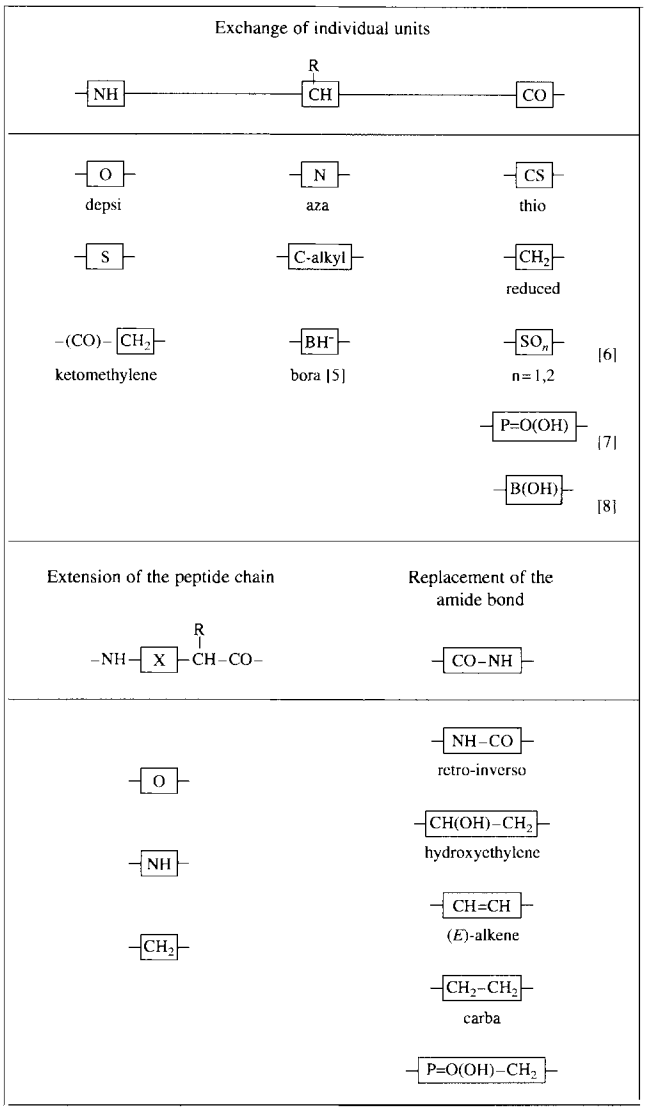


1

2.2. Modification of the Peptide Backbone

Modification of the peptide backbone refers to the generally isosteric or isoelectronic exchange of units in the peptide chain and the introduction of additional fragments.[2c] The most general modifications are listed in Table 1.

Table 1. The most frequent modifications to the peptide backbone.

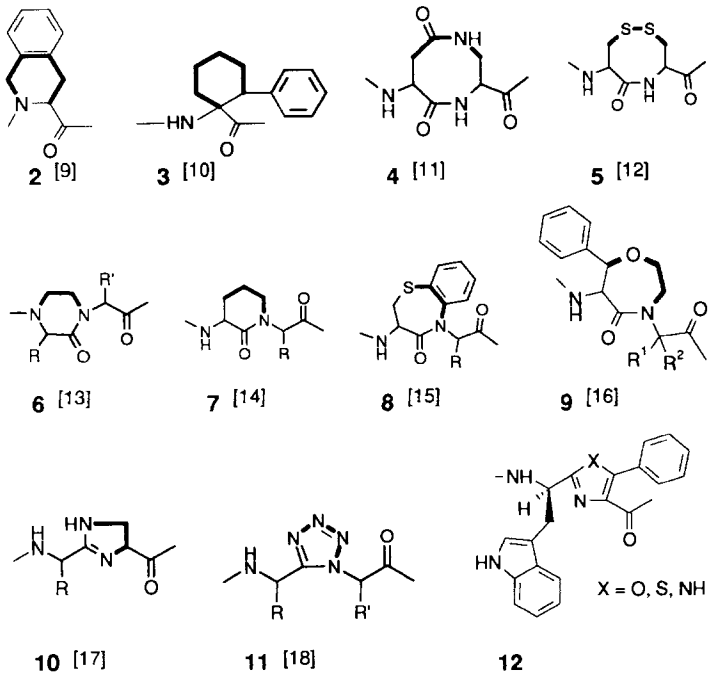




Joachim Gante was born in 1933 in Berlin and studied chemistry at the Freie Universität in Berlin. He received his Ph.D. and "Habilitation" for his research on peptide-analogous azapeptides. In 1968 he joined E. Merck in Darmstadt, where he has directed research on peptidomimetics as potential pharmaceuticals and developed fundamental methods of peptide synthesis. He also has a professorship at the Technische Hochschule in Darmstadt, where he lectures on peptide chemistry.

2.3. Conformation-Stabilizing Rings (Bridging)

The conformation of a peptide can be stabilized or fixed by the introduction of bridges of various lengths between different parts of the molecule; such elements make the molecule more rigid (Scheme 2). The bridging can either occur within a single amino acid residue as in **2** and **3**, or may involve several amino acid residues; in general two amino acid residues take part (dipeptide analogues). Bridges can be introduced at various sites and involve various backbone regions. The bridge can be a link between two side chains (as in **4** and **5**), between two backbone units (**6**), or between a side chain and backbone unit (**7**–**9**). In addition the peptide bond can be completely or exclusively incorporated into the ring (**10** and **11**).

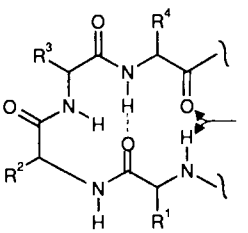


Scheme 2. Bridging in peptidomimetics.

Mimetics in which the peptide bond is involved also include peptide azoles like **12**, which have recently been the subject of an interesting article.[19] Hexapeptide analogues containing such units show a substance P antagonistic activity up to ten times higher than that of the original peptide.

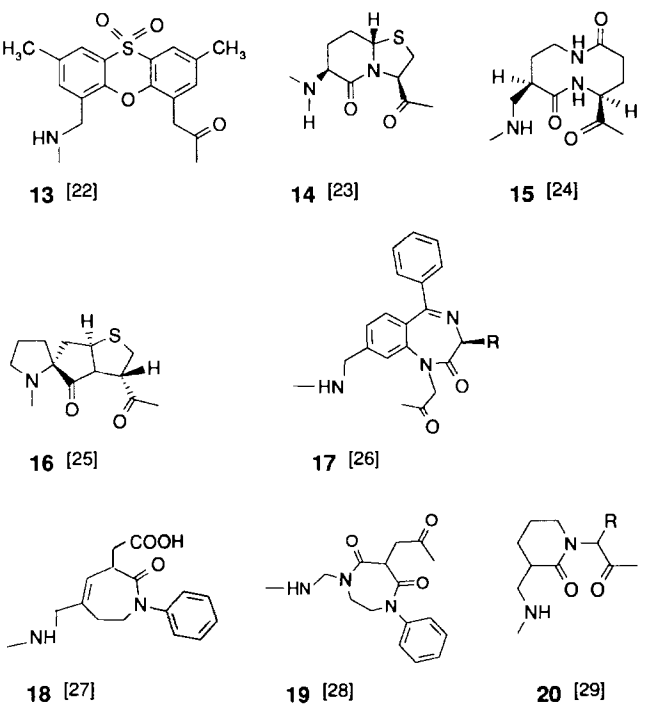
2.4. Induction and Stabilization of Secondary Structures (β Turns, γ Turns, α Helices)

The retention of peptide secondary structures by mimetism is an important tool in drug research which is applied with the goal of fixing those bioactive conformations characterized to a high degree by such structural elements. In addition to α-helix and β-sheet structures, turns and loops are essential conformational components for peptides and proteins.[20] The apparently most important "turning point", the β turn, is formed from four amino acids and is stabilized by a hydrogen bond between the carbonyl group of the first amino acid and the NH group of the fourth (Scheme 3). A second hydrogen bond can further stabilize the β turn. A γ turn is formed in a similar manner from three amino acids.



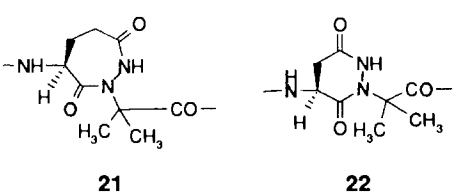
Scheme 3. Structure of a typical β turn.

A few examples from the tremendous amount of available material (which has been surveyed in recent reviews[2a, 2b, 21]) demonstrate that the structural motifs range from still recognizable peptide chains to completely non-peptidic components (**13**–**20** in Scheme 4).



Scheme 4. Characteristic β- (**13**–**17**) and γ-turn mimetics (**18**–**20**).

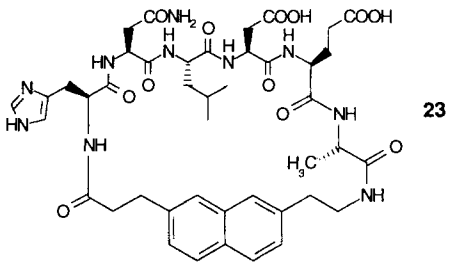
Whereas structure **13** can be used to produce two antiparallel peptide chains,[22a] the same tricyclic system has also recently been employed in the construction of β-sheet mimetics with corresponding parallel chains simply by changing the anchor groups.[22b] α-Helix initiators of the cyclic hydrazide type (**21** and **22**, Scheme 5) have recently been described.[30]



Scheme 5. α-Helix initiators.

A new Ω-loop mimetic has also been described recently.[31] Ω loops are larger, conformationally stabilized curves in a peptide chain which involve 6–16 amino acid residues. The Ω-loop

mimetic **23** mimics the sequence 41–48 in interleukin-1α, an important mediator in immunological and inflammatory processes.[32] Ω Loops are found in many proteins, where they can for example link β strands, and are generally anchored securely to the protein surface. They are considered to play an important role in biological recognition. It has been demonstrated that Ω loops are also involved (by complexation) in trypsin inhibition.[33]



23

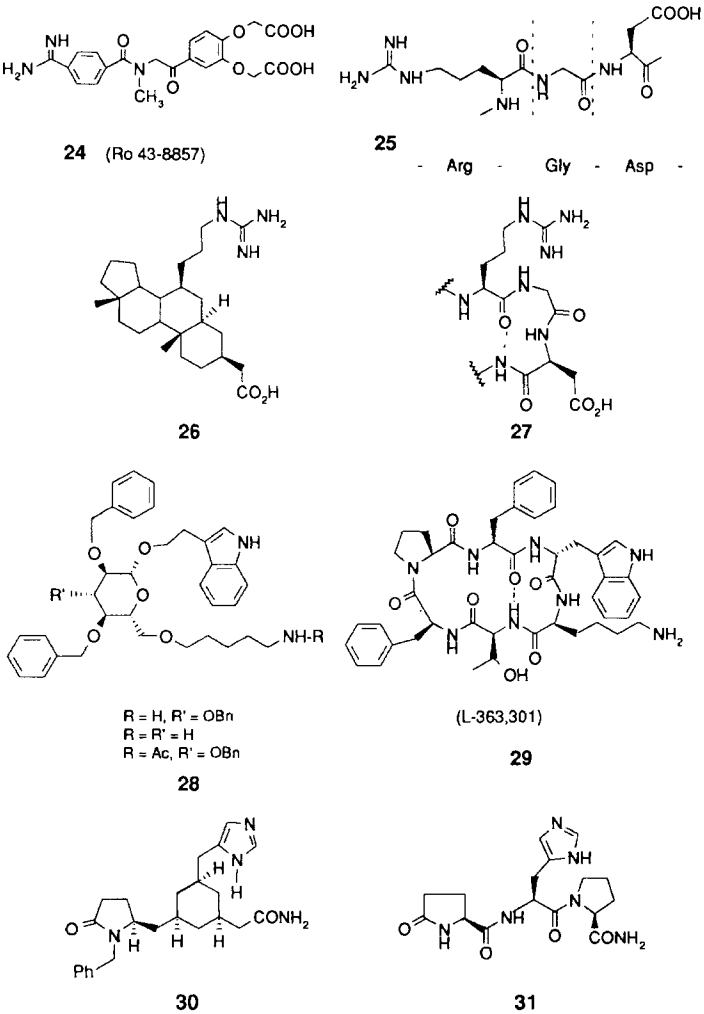
2.5. Scaffold Peptidomimetics

In scaffold mimetics a completely unnatural framework is used to support those side-chain elements of the original peptide which are responsible for its effectiveness. Compounds of this type appear particularly interesting with regard to their potential oral bioavailability, which is a serious general problem for peptides. It is therefore only logical to use frameworks or structural elements based on natural products or drugs whose oral resorption is established. The relative conformational rigidity of such systems is also important, as it often prevents the hydrophobic collapse[34] of a partial structure to afford an inactive conformation (see Section 6).

A number of important scaffold mimetics are shown in Scheme 6. Compound **24**, a mimetic of the partial sequence Arg-Gly-Asp (RGD) (**25**) in fibrinogen, is a potent adhesion receptor (GpIIb/IIIa) antagonist (it prevents thrombocyte aggregation), and carries the end groups vital for its activity (amidine, carboxyl substituents) in the correct positions.[35] While in **24** the framework still shows peptidic features, compound **26** is a typical scaffold mimetic, whose steroid skeleton bears the appropriate groups. Interestingly, it does indeed show GpIIb/IIIa-antagonistic activity, albeit weak.[36] As is evident in Scheme 6, this mimetic is able to imitate an β turn in the area of the RGD sequence of **27** apparently relevant for activity.

β-D-Glucose serves as the scaffold for mimetics such as **28** of the cyclic hexapeptide **29**, which has been known for some time to bind to the somatostatin receptor.[37] A remarkable feature of these β-turn mimetics is that changes in their concentration cause them to function as either agonists or antagonists towards the relevant receptor. Amazingly, acetylation leads to an umpolung, giving a selective substance P (SP) antagonist, which is the very first neutral effector of this type to be described.[38]

Compound **30**[39] is an effective analogue of the tripeptide thyreotropin releasing hormone (TRH) **31**.

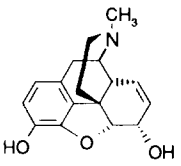


Scheme 6. Characteristic scaffold mimetics (left) and the original peptides (right).

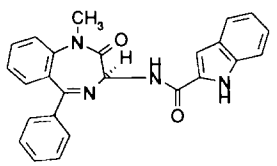
2.6. Non-Peptide Mimetics

Non-peptide mimetics have generally been discovered in the course of random screening of large numbers of substances, which include culture filtrates of microorganisms and fungus metabolites. These mimetics belong to various classes of organic compounds and have no apparent structural relationship with the natural peptide ligands. The term limetics (from ligand mimetics) has been coined for this group of peptidomimetics.[40] The wide variety of structures is demonstrated by compounds **32**–**36** (Scheme 7).

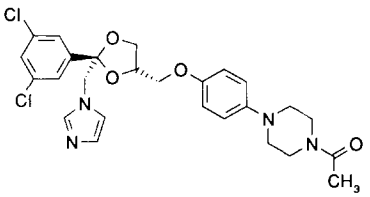
Extremely successful drug design was carried out with the help of computer modeling for the series of angiotensin II antagonists of the type DuP 753 (**36**).[45] The highly active structure **37** was optimized systematically from a series of similar compounds by superposition on the presumed bioactive conformation of angiotensin II (AII, **38**) (Scheme 8). For example, the suggested superposition of the structures indicated that the butyl group in **37** corresponds spatially to the Ile^5 side chain of **38**. The N-C-N unit of the imidazole and the acrylate double bond in **37** both mimic peptide bonds, while the thienyl group takes the place of the Phe^8 phenyl ring. Compared with the corresponding mimetic containing a phenyl ring, this hetero-



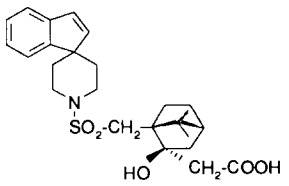
32



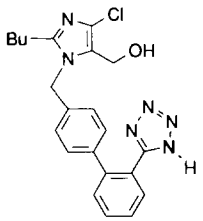
33 [41]



34 [42]

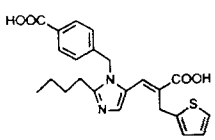


35 [43]



36 [44]

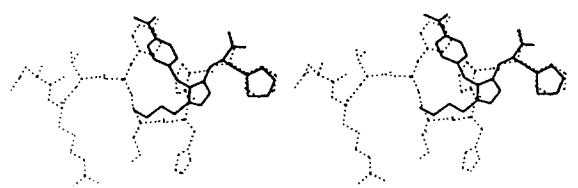
Scheme 7. Peptidomimetics with completely non-peptidic structures: the analgesic morphine (**32**), the CCK antagonist **33**, the antimycotic ketoconazole (**34**), the oxytocin antagonist **35**, and the angiotensin II antagonist DuP 753 (**36**).



37

Asp-Arg-Val-Tyr-Ile-His-Pro-Phe

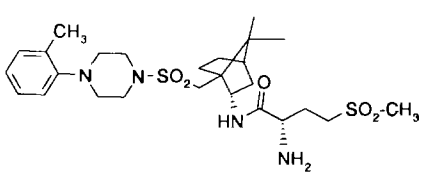
angiotensin II **38**



Scheme 8. Superposition of the calculated conformation of **37** and that of angiotensin II (**38**).

cyclic compound leads to an increase in the binding strength by a factor of 5 and to an increase in the activity subsequent to oral administration. More recently it has been possible on the basis of the data referred to above to develop a refined angiotensin II model with a greater congruence of structurally more diverse A II antagonists.[46]

The further development of the oxytocin antagonists related to compound **35** (cf. Scheme 7) has led to a number of compounds including **39**, which has an IC_{50}-value of less than 10 nM.[47]



39

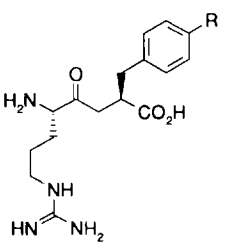
3. Synthesis of Peptidomimetics

The synthesis of peptidomimetics is often much more complicated than peptide synthesis especially as the degree of mimetism increases. On the one hand, it is not generally as simple to increase the chain length of the mimetics as that of peptides, and on the other, it is no longer possible to take advantage of the chiral pool of optically active amino acids. Instead the defined stereochemistry corresponding to the endogenous peptide must be set. The complete arsenal of methods provided by organic chemistry is required for the variety of structures of peptidomimetics. The synthetic possibilities will be demonstrated below with some examples from the area of backbone-modified peptides.

3.1. Carbapeptides

One of the classes of backbone-modified peptides most often studied is the carbapeptides. Strictly speaking carbapeptides are those in which the NH unit of the amide bond is replaced by a CH_2 group (ketomethylene, (Ψ(CO-CH_2)). According to a broader definition this class also includes hydroxyethylene (Ψ(CHOH-CH_2)) and carba (Ψ(CH_2-CH_2)) modifications (see Table 1). Ketomethylene[48] and hydroxyethylene[49] peptide analogues play a role particularly in the chemistry of enzyme inhibitors;[50] compounds containing dipeptide-analoguous hydroxyethylene groups are among the most active inhibitors of renin[51] and HIV-1 protease[52] (see Sections 5.2.1 and 5.5).

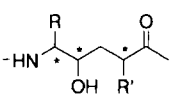
Ketomethylene analogues have in fact even been found to occur naturally! Umezawa et al. have isolated the arphenamines A (**40**) and B (**41**), potent inhibitors of arginyl aminopeptidase, from *Chromobacterium violaceum*, determined their structures, and recently synthesized them.[53] These compounds are of considerable therapeutic interest, for example as immunomodulators, opioid peptide degradation inhibitors, and carcinostatics.[54]



40 (R = H)

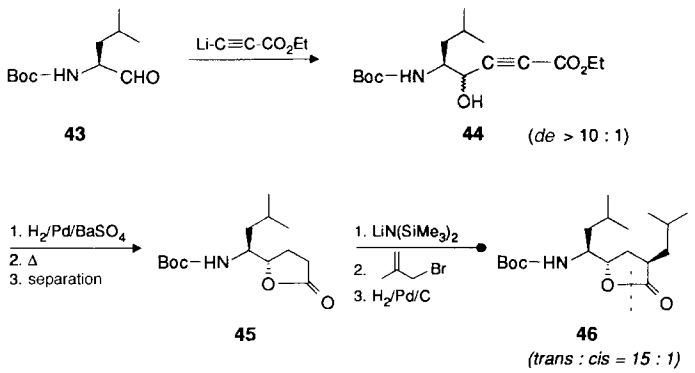
41 (R = OH)

Synthetic approaches for Ψ(CHOH-CH_2) dipeptide analogues have been described in a recent review.[49] In the construction of the the α-substituted hydroxyethylene unit **42**, controlled stereochemistry at all three stereocenters is of particular importance. The starting material is an enantiomerically pure amino acid derivative (from the chiral pool), so that stereoselectivity is preprogrammed.[49, 55]



42

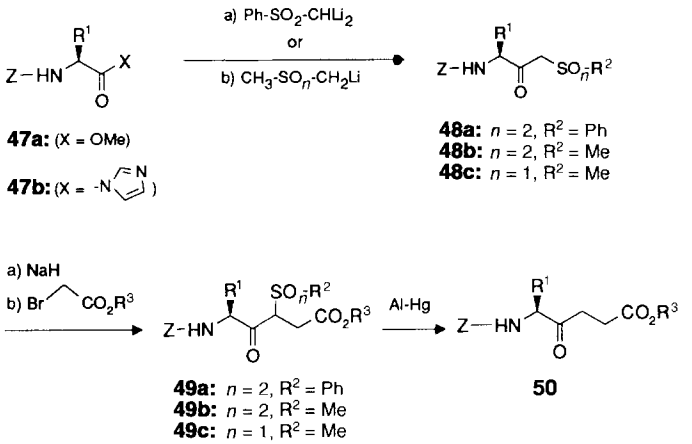
A relatively elegant synthesis (Scheme 9) starts from the Boc-protected amino aldehyde **43**, which is treated with the lithium derivative of ethyl propynoate to give **44**. Hydrogenation gives lactone **45**, which in turn is metalated and treated with methallyl bromide. Final hydrogenation affords the α-substituted lactone **46**,[56] which can undergo ring-opening with nucleophiles (OH^-, NHR) to give the linear peptide analogues. In a more



Scheme 9. Synthesis of hydroxyethylene dipeptide units according to Fray et al. [56]. Boc = *tert*-butoxycarbonyl.

recent synthesis, which also starts with aldehydes but leads only to the α-unsubstituted products, titanated propionates are used as homoenolate components.[57]

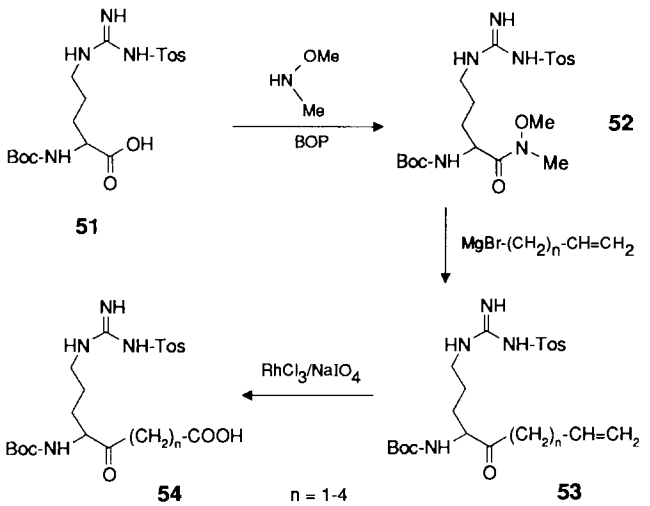
Interesting new aspects of the synthesis of ketomethylene peptide analogues have resulted from the use of β-ketosulfones **48a,b** and -sulfoxides **48c**, which can be obtained from the respective reactions of protected amino acid esters and imidazolides **47** with lithiated phenyl methyl sulfone[58] or with lithiated dimethyl sulfone and dimethyl sulfoxide[59] (Scheme 10). Metalation of **48** and reaction with bromoacetates yields **49**, and subsequent reductive desulfurization affords the corresponding carba-Gly dipeptide analogues **50**.



Scheme 10. Synthesis of ketomethylene dipeptide units according to Lygo [58] and Gante et al. [59]. Benzyloxycarbonyl (Z) or Boc groups are used as protecting groups.

It has been shown[59] that an α substituent can be introduced by using a branched α-bromocarboxylate. With enantiomerically pure halogen compounds, which are readily available from the chiral pool of amino acids, it should be possible to obtain stereoisomerically pure analogues of almost all the natural amino acids. This approach has also been shown to be suitable for the preparation of $\Psi(CH_2\text{-}CH_2)$ and $\Psi(CH{=}CH)$ dipeptide analogues.[58]

A different procedure is employed for the synthesis of ketomethylene analogues of arginyl dipeptide derivatives, which have been shown to be extremely efficient and protease-resistant thrombin inhibitors (see Section 5.3)[60] (Scheme 11). The *N,O*-

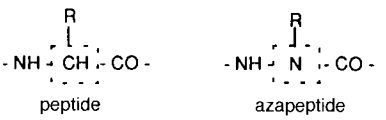


Scheme 11. Synthesis of ketomethylene analogues of arginyl dipeptide derivatives according to DiMaio et al. [60]. Tos = tosyl.

dimethylhydroxamic acid derivative **52**[61] prepared from the protected amino acid **51** was converted by a Grignard reaction into **53**, and subsequent Sharpless oxidation[62] provided the required carboxylic acid **54**. An improved synthesis of the precursors for arginyl dipeptidomimetics using N-α-Boc-Arg-Z_2 has recently been reported.[63]

3.2. Azapeptides

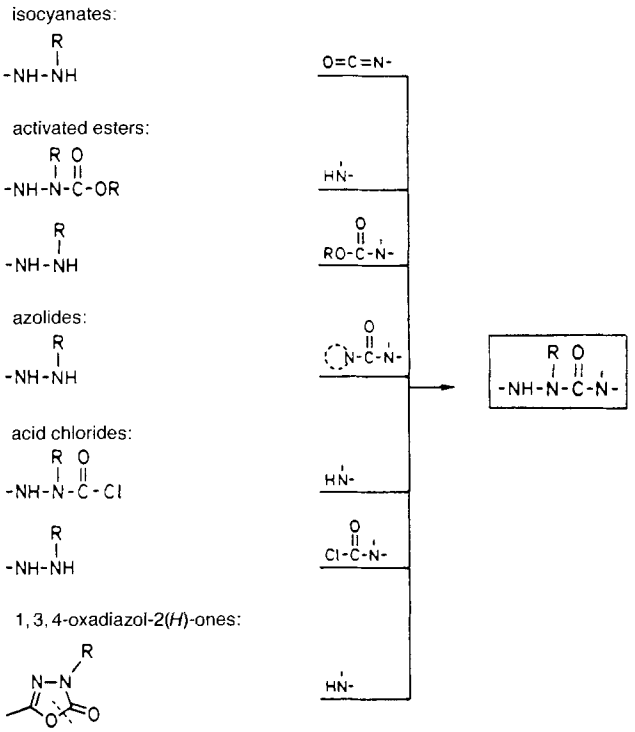
Another class of backbone-modified peptides that has become important in pharmaceutical chemistry is the azapeptides.[64] In these peptide analogues the α-CH group of one or more amino acid residues in a peptide chain is replaced isoelectronically by a nitrogen atom with retention of the original side chain (Scheme 12).



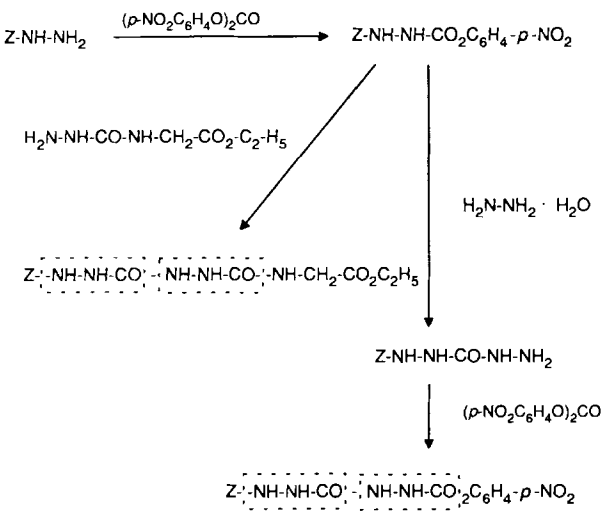
Scheme 12. Azapeptides formed by the isoelectronic exchange of an α-CH group in a peptide chain by an N atom.

Since N-N(R)CO units are generally components of substituted semicarbazides (C-terminal azaamino acid esters are exceptions), the construction of azapeptides from substituted hydrazines or hydrazides by the formal introduction of a carbonyl group between two nitrogen atoms can be carried out very simply. The various possibilities for the synthesis of these azaamino acid residues[64] are shown schematically in Scheme 13. Azapeptides can also be prepared by the direct linkage of azaamino acids in any particular order, such that in principle any "pure" azapeptide should be available by repetitive synthetic sequences, as shown in Scheme 14 for C-terminal activated esters.[65]

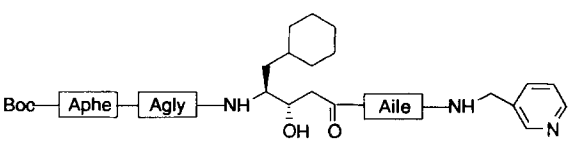
The first analogue of this type of a biologically active compound (**55**, Scheme 15) has recently been described; here all the



Scheme 13. Synthetic strategies for azapeptides.



Scheme 14. Direct linkage of azaamino acid residues.

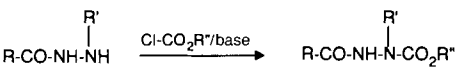


55

Scheme 15. The three-letter code for the amino acid is preceded by an A to denote the corresponding azaamino acid [67].

aza groups were connected by use of the nitrophenyl ester method.[66] In contrast to the native peptide, which is a highly active renin inhibitor,[68] and the previously synthesized compounds with only one azaamino acid residue (Aphe,[69] Agly,[70] or Aile[71]), this all-azapeptide **55** has no inhibitory effect on renin, probably for conformational reasons.

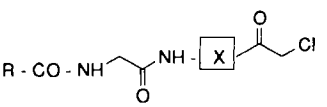
Gray et al. recently showed that longer chain azapeptides can also be obtained by solid-phase synthesis by incorporation of azaglutamine residues into poliovirus and adenovirus polyprotein sequences.[72] C-terminal azaamino acid esters **57** can be readily obtained by reaction of the corresponding hydrazides **56** with chloroformates[64b, 65, 67, 73] (Scheme 16). Aza-



56 **57**

Scheme 16. Synthesis of C-terminal azaamino acid residues. R = amino acid or peptide residue, R′ = H, alkyl, benzyl, R″ = alkyl, aryl.

peptides of this type are extremely interesting and therapeutically relevant inhibitors of serine and cysteine proteases.[67] The same is true for the aza analogues **58** of the amino acid chloromethyl ketones **59**, which in analogy with the aza esters **57** can be prepared by simple hydrazine acylation.[74]



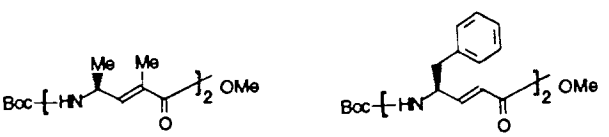
58: X = NH
59: X = CH_2

4. Recent Modification Principles

In the study of peptidomimetics three newer directions of development are worthy of mention because of their interesting application possibilities, in particular for backbone-modified peptides; these are the use of vinylogous amino acids as building blocks, special oligopyrrolinones, and the novel peptoid principle.

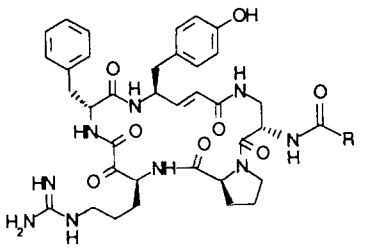
4.1. Vinylogous Peptides

Vinylogous peptides, which are not true peptide isosteres and are conceptionally related to hexose-DNA, can form secondary structures similar to those of peptides. This makes them interesting as potential receptor and enzyme ligands. Thus the X-ray crystal structure of **60**, which contains α-methyl groups, exhibits an antiparallel β-sheet structure, whereas **61** has a corresponding parallel structure.[75]



60 **61**

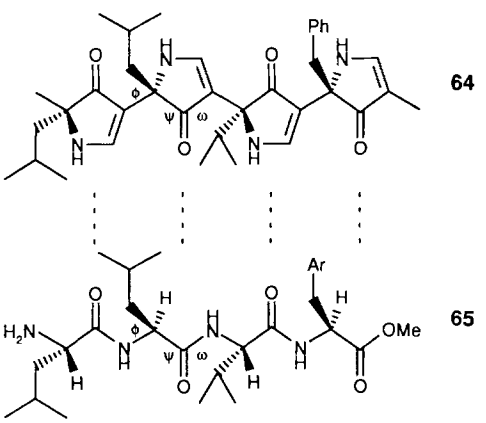
Such peptide analogues do indeed occur naturally: the marine sponge *Theonella* was found to have the cyclic peptidic structures cyclotheonamides A (**62**) and B (**63**), which contain vinylogous tyrosine, and a further unusual amino acid, α-ketoarginine.[76] These natural products inhibit thrombin, an important enzyme in the blood coagulation cascade, and are thus of interest in medicinal chemistry as potential antithrombotics (see Section 5.3).



62 R = H
63 R = Me

4.2. Oligopyrrolinones

Observations on the relevance of β-strand conformations for the binding of inhibitors to proteolytic enzymes and molecular modeling studies have led recently to the concept of a new type of peptidomimetic system in which a greatly modified backbone is integrated into cyclic structures (which are again vinylogous amino acids) to produce oligopyrrolinones.[77] Scheme 17

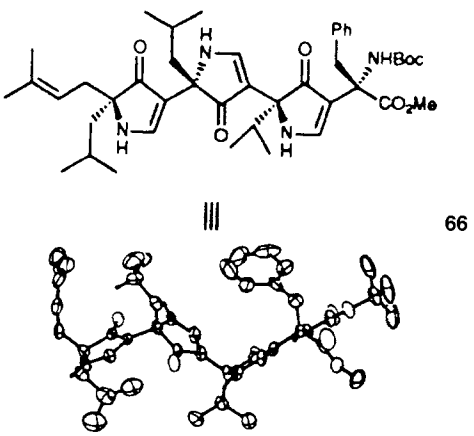


Scheme 17. Comparison of the structures of oligopyrrolinone **64** and peptide **65**. Ar = aryl.

shows a section (**64**) of the chain of such a compound and a corresponding tetrapeptide fragment from equine angiotensinogen (**65**), which has been demonstrated to have a parallel β-sheet structure in the crystalline state. The mimetic contains all the features necessary for the formation of an analogous secondary structure: not only the dihedral angles ϕ, ψ, and ω, and the orientation of the side chains are completely appropriate, the structural preconditions for the formation of the hydrogen bonds necessary for the construction of β-strand conformations are also present.

Although the chain is completely atypical and the various amino acid residues are arranged orthogonal to the chain, the orientation of the amine and carbonyl groups in the vinylogous peptide corresponds almost exactly to that in the peptide. In addition, even though the vinylogous pyrrolinone NH groups do not form part of the backbone, they are about as basic as the amide group, and are thus able to stabilize β conformations by intra- and intermolecular hydrogen bonds.

The results of model studies were confirmed to a large extent by the synthesis of compound **66** (Scheme 18). The X-ray structures of **65** and **66** confirm the spatial overlap between the side chains and the carbonyl groups. It is also evident that **66** forms an antiparallel β-sheet structure, which demonstrates clearly that the pyrrolinone N atoms act as H-bond donors between the strands of the desired β conformations.



66

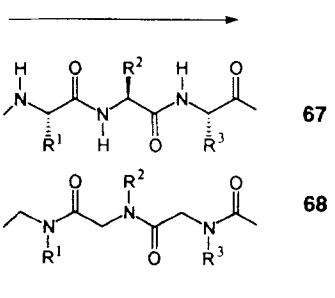
Scheme 18. Structural formula and X-ray crystal structure of **66**, an oligopyrrolinone unit.

The synthesis of these peptidomimetics is particularly relevant, because the iterative construction of the chain by a repetitive reaction sequence is thus possible.

4.3. Peptoids

The recently described oligomeric peptide analogues called peptoids are extremely interesting.[78] These compounds contain *N*-alkylated glycines joined together in a peptide-like manner, in which the α-CHR groups have been replaced by NR units (the aza principle), and conversely, the NH groups (of the peptide bond) by CH_2 units (the carba principle). The positions of the side chains and carbonyl groups of the original peptide chain **67** remains unchanged, as can be seen from the comparison with the peptoid chain **68** (Scheme 19).

The amino acid sequence in the peptoids is opposite to that in the peptides. This aspect of the peptoids is reminiscent of the retro-inverso peptidomimetics, which have been known for some time and which have recently been reviewed in detail.[79] Peptoids are not chiral, since the side chains corresponding to the normal amino acids are attached

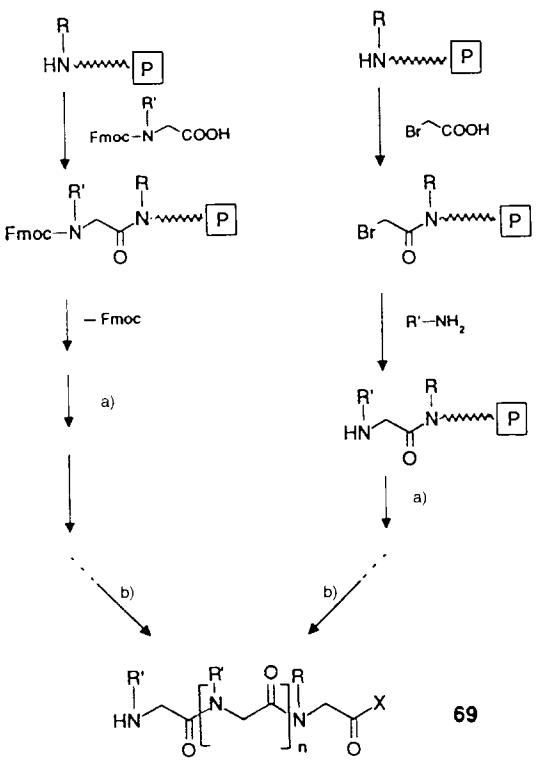


67

68

Scheme 19. Comparison of segments of peptide (**67**) and peptoid chains (**68**).

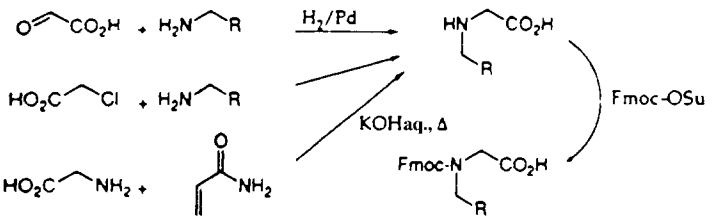
to the N atoms and only achiral CH_2 groups are present instead of NH groups. Most of the peptoid amino acids have been prepared; the oligomers can be obtained from the corresponding monomers in any required chain length by using the solid-phase method with Rink amide resin.[80] Two procedures are used: *N*-alkyl glycines protected at the amino group and side chain functionalities (e.g. by 2-fluorenylmethoxycarbonyl (Fmoc) or *t*Bu) are coupled, either automatically or manually, to the NH_2 groups at the end of the polymer by using the coupling reagents benzotriazol-1-yloxy-tris-(pyrrolidino)phosphonium hexafluorophosphate (PyBOP) or bromo-tris(pyrrolidino)phosphonium hexafluorophosphate (pyBrOP);[78a] alternatively, the corresponding polymeric bromoacetyl compounds undergo repetitive reactions with the necessary amines (submonomer solid-phase synthesis) to give **69**[78b] (Scheme 20).



Scheme 20. Solid-phase synthesis of peptoids. R = R′ = H or protected side chain; X = NH_2, OH; $n \leq 23$; P = polymer resin. a) The reaction sequence is repeated n times; b) the peptoid is deprotected and cleaved from the resin.

With the newer procedure protecting groups for the NH_2 functions are not required and the monomer does not have to be prepared in advance, since the subunits are generated directly on the resin. The protected monomeric glycines can be obtained readily (Scheme 21).

Conformational studies (Ramachandran plot,[81] molecular modeling) show that peptoids have much greater conformational flexibility than the peptides. The absence of CO–HN hydrogen bonds (no NH groups are present in the peptoid chain!) naturally affects secondary structures. As experiments have demonstrated, peptoids are not degraded by important proteolytic enzymes such as papain, chymotrypsin, and thermolysin. This has important implications for the development of orally active drugs.



Scheme 21. Synthesis of peptoid monomers [78a]. The residue R is protected.

Initial studies showed that peptoid analogues of biologically active peptides can be as effective enzyme inhibitors as the original peptides. Thus the activity of analogues of Ac-Trp-Arg-Tyr-OMe (inhibition constant $K_i = 100$ μM), an α-amylase inhibitor, is comparable with that of the native compound, but the retro sequence Ac-Nhtyr-Narg-Nhtrp-NH_2 ($K_i = 200$ μM) shows a higher activity than the "forward" sequence Ac-Nhtry-Narg-Nhtyr-NH_2 ($K_i = 350$ μM).[*]

As another example, the peptoid sequence analogous to the peptide Ac-Glu-Leu-Ala-Thr-Gln-Ser-Phe-Ser-NH_2, which inhibits the 3C-protease of hepatitis A virus, shows inhibition only if the retro sequence is used; the magnitude of the inhibition is approximately the same as that of the original peptide. The observation that peptoid analogues of peptide sequences from the HIV tat protein also bind to TAR-RNA may have ramifications for AIDS research.

The greatest potential of the peptoids may however lie in peptoid libraries, analogous to peptide libraries, which may be prepared by automated multiple syntheses. These libraries should facilitate the discovery of new non-peptidic lead structures by simultaneous screening.

5. Enzyme Inhibition by Peptidomimetics

5.1. Introduction

As already mentioned, enzyme inhibition[82] is another highly topical area of application for peptidomimetics in addition to interactions with receptors.[2b] Proteases[83] naturally offer an attractive field of study for peptide analogues because of the sequential structure of their substrates. Proteases are essential to numerous biological processes and have a wide variety of functions. Thus certain proteases can liberate peptide hormones and neuromodulators from inactive precursor molecules (e.g. renin, angiotensin converting enzyme (ACE)), others activate other enzymes (e.g. blood clotting factors), and still other peptidases (e.g. enkephalinase) repress biological response by degrading the corresponding messenger peptide.

It is not surprising that such enzymes are regulated by endogeneous protease inhibitors to ensure optimal performance.[84] It is clear that it may be possible with the aid of exogeneous inhibitors of such enzymes to intervene when the biological equilibrium of this kind is pathologically disturbed. The goal is to construct inhibitors that exhibit a strong (reversible or irreversible) binding to the enzyme and thus compete with the nat-

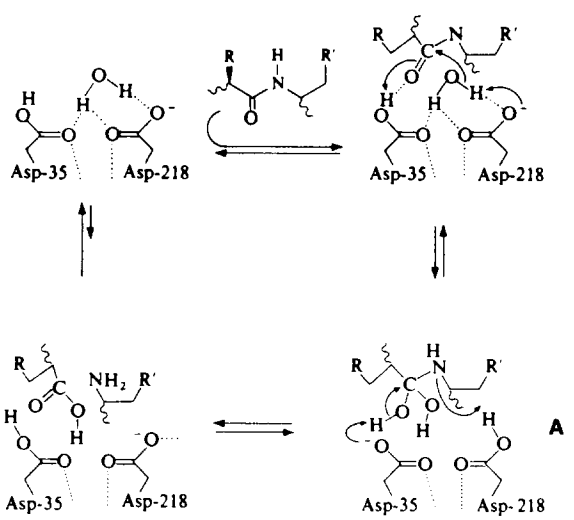
[*] Peptoid nomenclature: the three-letter code for the relevant amino acid is preceded by N or Nh for the (side-chain) homologue.

ural substrate. The activity of an inhibitor is due to the degree of the displacement of the substrate from the active site.

Since detailed knowledge of the way the enzyme works is often extremely important for the design of effective peptidomimetics of this type, we will briefly give a classification of the proteases according to their mechanism of action. Proteases can be divided into four groups; in Table 2 several examples are given for each case.[82b] In serine proteases the hydroxyl group in the side chain of a serine residue acts as a nucleophile in the active site.[85] Cysteine proteases contain a cysteine SH group near a histidine imidazole ring as a mechanistically essential element of the active site.[86] Aspartyl proteases use the β-carboxyl groups of two aspartic acid residues at the catalytic center to stabilize the tetrahedral transition state for the hydrolytic cleavage of a peptide bond[87] (Scheme 22). A tetrahedral transition state is also involved in the mechanism of action of certain metalloproteases that have a Zn ion at the binding site. The Zn ion complexes a molecule of water and and also acts as a Lewis acid in the activation of the NH–CO bond to be cleaved.[88]

Table 2. Classification of the proteases based on their mechanism of action.

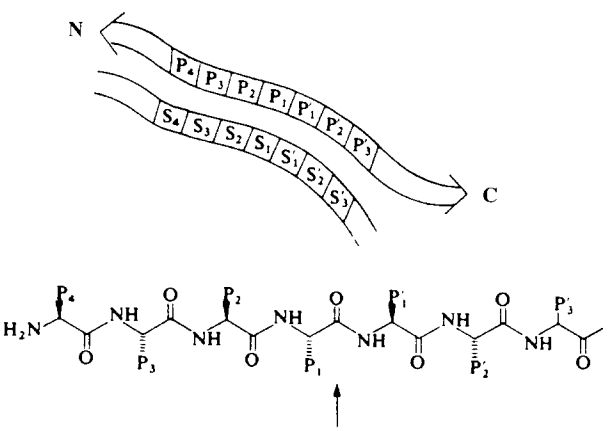
1. *Serine proteases*	2. *Cystein proteases*
chymotrypsin	cathepsins B, C, HL
kallikrein	papain
elastase	
plasmin	
subtilisin	
thrombin	
trypsin	
3. *Aspartyl proteases*	4. *Metalloproteases*
HIV protease	ACE
cathepsins D, E	collagenase
pepsin	enkephalinase
renin	



Scheme 22. Mechanism of catalysis for aspartyl proteases. A denotes the tetrahedral transition state.

Proteases are also classified according to their substrate specificity, in other words, their ability to recognize and cleave peptide bonds either adjacent to certain amino acids or within certain characteristic amino acid sequences.[82b] For this purpose recognition sites exist within the enzyme which correspond to certain positions in the substrate or inhibitor.

To characterize the cleavage site of a substrate, the amino acid sequences are numbered starting from this site in the direction of both the N-terminus and the C-terminus, according to a scheme proposed by Schechter and Berger.[89] The cleavage site is denoted as the P_1-P'_1 position and corresponds to the S_1-S'_1 position of the enzyme (Scheme 23).



Scheme 23. Definition of the nomenclature used to describe the specificity of a protease according to Schechter and Berger [89]. The amino acid residues of the substrate are designated P or P', the corresponding residues in the enzyme S or S'. In the structural formula the cleavage site is marked by an arrow and is the starting point for the numbering of the sequence. The N-terminus of the substrate is labeled with an N, the C-terminus with a C.

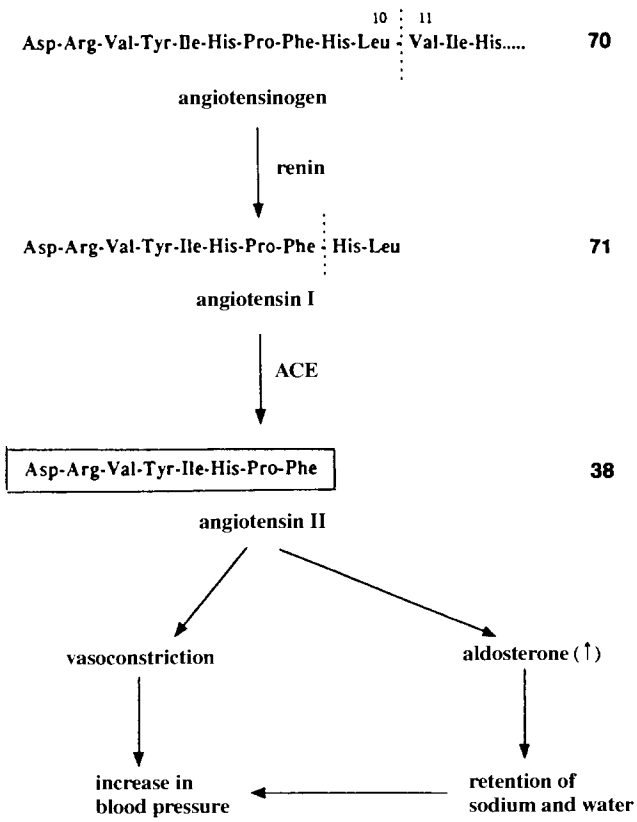
5.2. Influencing the Renin–Angiotensin System

One of the most important therapeutic applications for enzyme inhibitors is influencing the renin–angiotensin system (RAS). This complex includes both the renin inhibitors[90] and the inhibitors of the angiotensin converting enzyme (ACE).[91]

The RAS is characterized by a sequence of enzymatic reactions, the last of which releases the octapeptide angiotensin II (A II, **38**)), which has strongly hypertensive properties. Therapeutic efforts are targeted towards lowering the A II level in order to reduce an A II-dependent, pathologically increased blood pressure to a normal value. As can be seen from Scheme 24, this goal can be achieved by intervention at various positions.

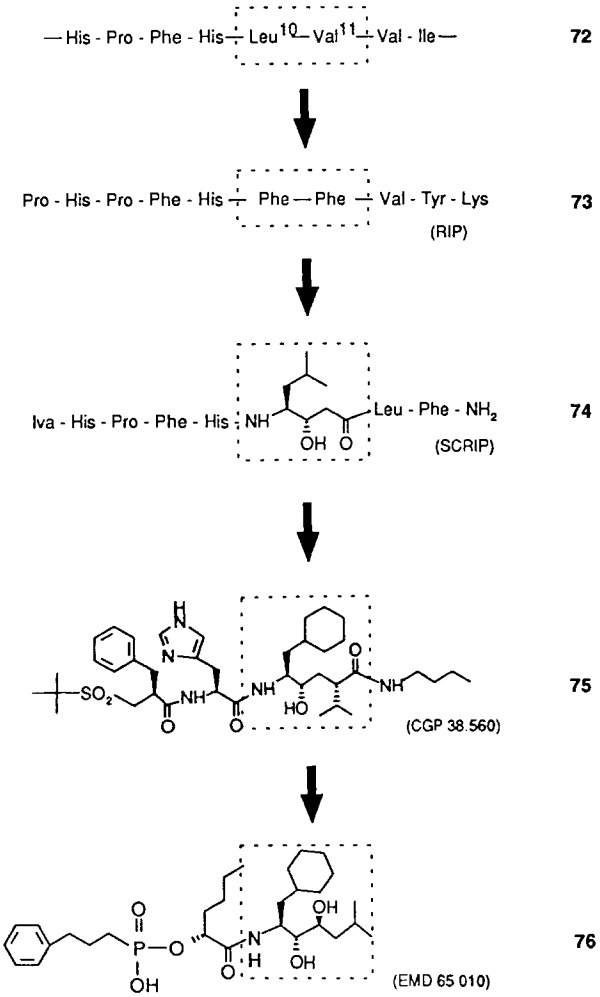
First the globular protein angiotensinogen (**70**) is cleaved by renin, an aspartyl protease that occurs mainly in the kidneys, between the amino acid residues Leu^{10} and Val^{11} to give the biologically inactive decapeptide angiotensin I (A I, **71**). Thus inhibition of this enzyme makes it possible to influence the formation of A II as early as this point in the cascade.

In a second step A I (**71**) is cleaved by the metalloprotease ACE; a dipeptide unit is split off to give the octapeptide angiotensin II (**38**). This is the stage at which the ACE inhibitors intervene to lower the A II level.



Scheme 24. RAS cascade: release and physiological effects of angiotensin II (**38**).

A completely different method of influencing A II is blockage of the A II receptor by A II antagonists; the formation of A II is not influenced here (see Section 2.6).



Scheme 25. The development of renin inhibitors.

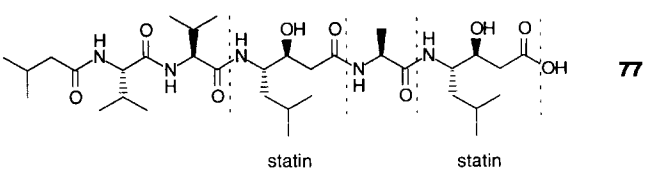
5.2.1. Renin Inhibitors

The continuous development of renin inhibitors based on the natural substrate angiotensinogen (**72**) starting from a pure peptide and progressing to true peptidomimetics is demonstrated by the compounds shown in Scheme 25. This sequence of structures shows the course of development starting from an analogue of the substrate angiotensinogen, **73** (RIP = renin inhibiting peptide),[92] to the transition state analogue **76**,[93] which has almost nothing in common with the original peptide structure.

The inhibitor properties of compound **73** are caused by the exchange of the Leu-Val fragment in the P_1-P'_1 position of the human angiotensinogen fragment **72** by Phe-Phe, which renders the octapeptide no longer cleavable by renin.

A considerable increase in the activity of the renin inhibitors was made possible by the application of the transition state analogy principle.[94] In such analogues the P_1-P'_1 position is modified by replacing the two amino acids by a dipeptide-analogous unit containing an sp^3 hydroxymethylene group in place of the carbonyl group of the amide bond in the center (**74**, SCRIP = statin containing renin inhibiting peptide).[95] This group thus mimics the tetrahedral transition state for the hydrolysis of the natural substrate (see Scheme 22).

The idea of using such residues arose from the observation made by Umezawa et al.[96] that the peptidic aspartyl protease inhibitor pepstatin (**77**) isolated from microorganism culture filtrates can interfere in the RAS mechanistically because of the γ-amino-β-hydroxycarboxylic acid statin it contains. The transition state analogue binds much more effectively to the enzyme, and the persistence of the inhibitor at the binding site is increased by its enzymatic inertness.



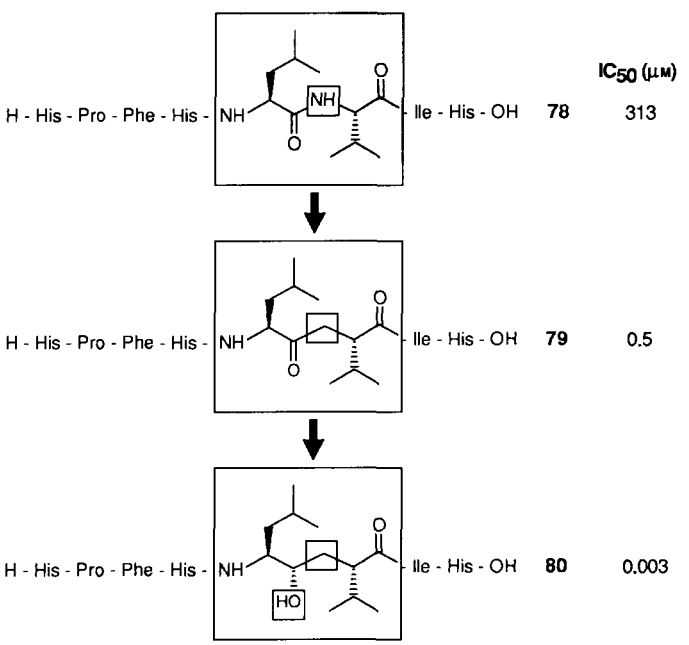
Like **75**, such dipeptide-analogous units can contain an additional carbon atom in the peptide backbone (hydroxyethylene modification, see Section 3.1), in which case they have a chain length corresponding to that of a dipeptide.[97]

It can also be seen from structures in Scheme 25 that the number of amino acid residues in the molecule can be considerably reduced without any negative effect on the high inhibitory activity of these compounds (the IC_{50} values all lie in the nanomolar range). It is hoped that renin inhibitors with reduced

peptide character and molecular weight will have an increased oral bioavailability, which has been unsatisfactory so far.

A further development in this direction is the use of C-terminal dihydroxyl components, as found in compound **76**, as a mimetic surrogate for the normal peptide bond in this section of the molecule.[93] As is evident from Scheme 25, it is also possible to use components at the N-terminus which resemble the original amino acid only in terms of their backbone length and side chain (**75**) or are totally different (**76**). Apart from the structures shown, a large variety of similar compounds has been developed,[98] some of which exhibit marked oral bioavailability.

The increase in activity brought about by mimetism at only a single position in the backbone can be demonstrated very well by a renin inhibitor of the carba type[94] (Scheme 26). The transition from a purely peptidic inhibitor (**78**) to the carbapeptide **79** leads to an increase in the activity by a factor of about 600, while further modification to give the dihydrocarbapeptide **80** affords a further increase by a factor of about 170.

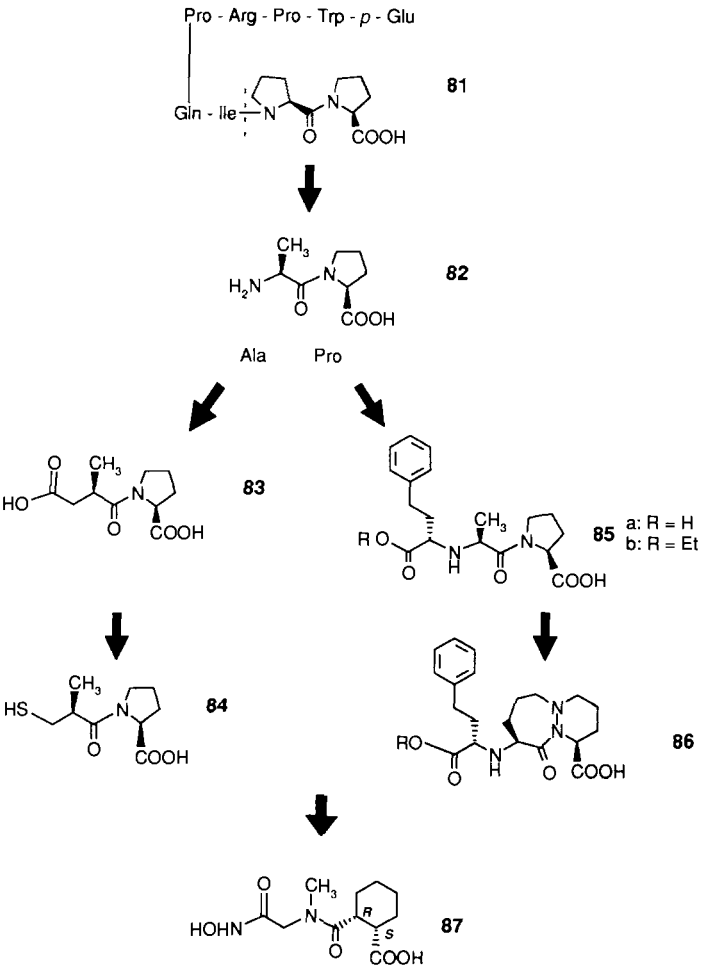


Scheme 26. Results of carba-type mimetism on the activity of a renin inhibitor.

In both modifications the site of biochemical attack can be demonstrated very clearly. In **79** the resistance of the isosteric peptide bond surrogate to cleavage prevents the subsequent liberation from the active site which normally occurs when the cleavage products diffuse. The change to compound **80** additionally introduces the transition state effect, in which further interactions lead to an even stronger binding to the enzyme.

5.2.2. *ACE Inhibitors*

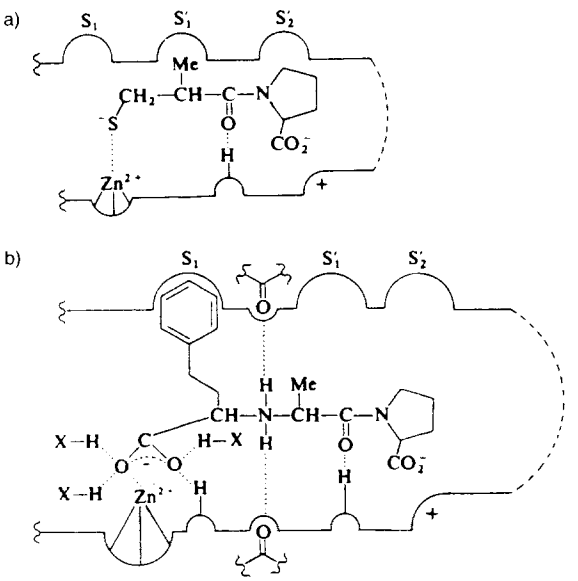
The starting point for the synthesis of mimetics of inhibitors of the angiotensin converting enzyme (ACE), a metalloprotease with a Zn ion at the active site, is the nonapeptide teprotide (**81**) (Scheme 27). It has been shown that the observed bradykinin-potentiating property of this substance, which was originally isolated from snake venom, is due to the inhibition of ACE.[99]



Scheme 27. Development of ACE inhibitors.

It was later observed that even the modified C-terminal fragment Ala-Pro (**82**) inhibits ACE, if only very weakly. At that time it was known[100] that benzylsuccinic acid has a blocking effect on carboxypeptidase A (CPA), which is mechanistically closely related to ACE; thus α-methylsuccinylproline **83** was synthesized.[101] It was expected that the carboxyl group would coordinate with the Zn ion and thus strengthen the enzyme binding, and indeed **83** was found to be more effective than **82** by a factor of 100. The replacement of the carboxyl group by the more strongly Zn-coordinating mercapto group led finally to captopril (**84**), the activity of which is yet 1000 times greater. This ACE inhibitor has been on the market for years as a very successful orally active drug for reducing high blood pressure and is also effective against heart failure.[101]

Another approach, in which the alanine residue of **82** was retained, led to enapril (**85**), another extremely successful blood pressure reducing drug.[102] In this case the strength of the enzyme binding is apparently due not only to the extra carboxyl group but in particular to the phenylethyl side chain; in comparison with captopril (**84**), **85** is able to undergo an additional hydrophobic interaction with the S_1 subsite of the enzyme (Scheme 28). It is evident in Scheme 28b that, as in the case of captopril, a cationic group of the enzyme forms an ionic bond with the proline carboxyl group of **85**, while a hydrogen bond donor from the enzyme interacts with the carbonyl group of

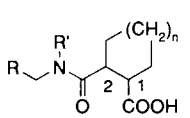


Scheme 28. Binding interactions between the active site of ACE and captopril (**84**) (a) [103] and enapril (**85**) (b) [102a,104].

alanine and the *N*-carboxyalkyl group binds to the Zn ion of the enzyme.

In fact only the ethyl ester derivative **85b** is suitable for oral application, since the free acid **85a** is not resorbed.[82b] In the organism the ester is cleaved enzymatically to give the active acid, such that it can be considered as a prodrug. The further development of this principle led eventually to cilazapril (**86**),[105] a compound with a high degree of mimetism.

A completely new class of ACE inhibitors, in which the peptoid principle was applied for the first time (inadvertently?) to a group of known drugs, has recently been described.[106] These structures contain 1,2-cycloalkane dicarboxylic acid residues as proline equivalents; one carboxyl group is linked by an amide bond to an aminoalkyl group, which in turn bears the Zn-coordinating substituent in the form of a mercapto, carboxyl, or hydroxamic acid group (**88**). Although the 2*R* configuration is



88

R = -CH_2-CH_2-SH, -CH_2-COOH, -CH_2-CONHOH
R' = H, alkyl
n = 1, 2

essential for the activity of such compounds, position 1 can have either *S* or *R* configuration. In contrast, in the classical ACE inhibitors an *S* configuration at the C-terminal carboxyl group is absolutely necessary.

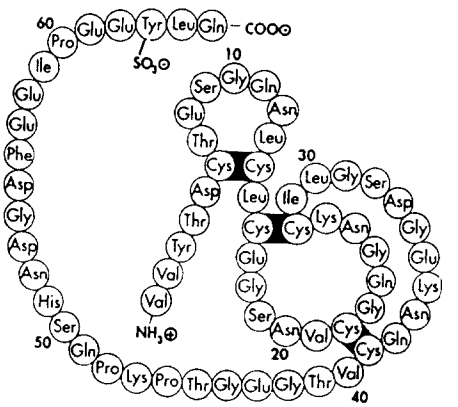
The most active compound, with an IC_{50} of 7 nM (comparable to that of captopril), is hydroxamic acid **87** (1*S*,2*R* *cis* form, see Scheme 27).[106] It is described as showing in vitro and in vivo activity in various animal species and has a very low toxicity; it is at present undergoing clinical trials. Many other highly potent analogues of both captopril and enapril have also been synthesized by variations at many different sites in the molecules.[107]

5.3. Thrombin Inhibitors

Thrombin, a serine protease similar to trypsin, is a key enzyme in the blood clotting system.[108] It promotes coagulation in many ways, mainly by cleaving fibrinogen to give fibrin, but also by activating factors V, VIII, and XIII, and by activating protein C at the surface of endothelial cells with the help of thrombomodulin.[109] Thrombin also induces platelet aggregation and promotes the proliferation of endothelial cells, the liberation of the plasminogen activator, and contraction and dilation of the blood vessels.[110] Because of these properties, selective inhibition of thrombin may result in efficient control of various pathophysiological states such as thrombosis and arteriosclerosis, and prevention of myocardial infarction.

The possibilities for thrombin inhibition, including that by non-peptidic compounds, are many. For example, thrombin is inhibited by heparin, a mixture of sulfated polysaccharides. Heparin functions indirectly on the enzyme by influencing various activity-regulating factors.[111] Thrombin is also inhibited indirectly by vitamin K antagonists such as warfarin.[112]

Since such drugs have serious side effects, mainly because of a lack of specificity, there has long been interest in the development of more specific thrombin inhibitors that work directly. One of these is hirudin (**89**), a polypeptide isolated from the leech (*Hirudo medicinalis*) containing 65 amino acid residues (Scheme 29), from which various analogues have been developed.[113]



89

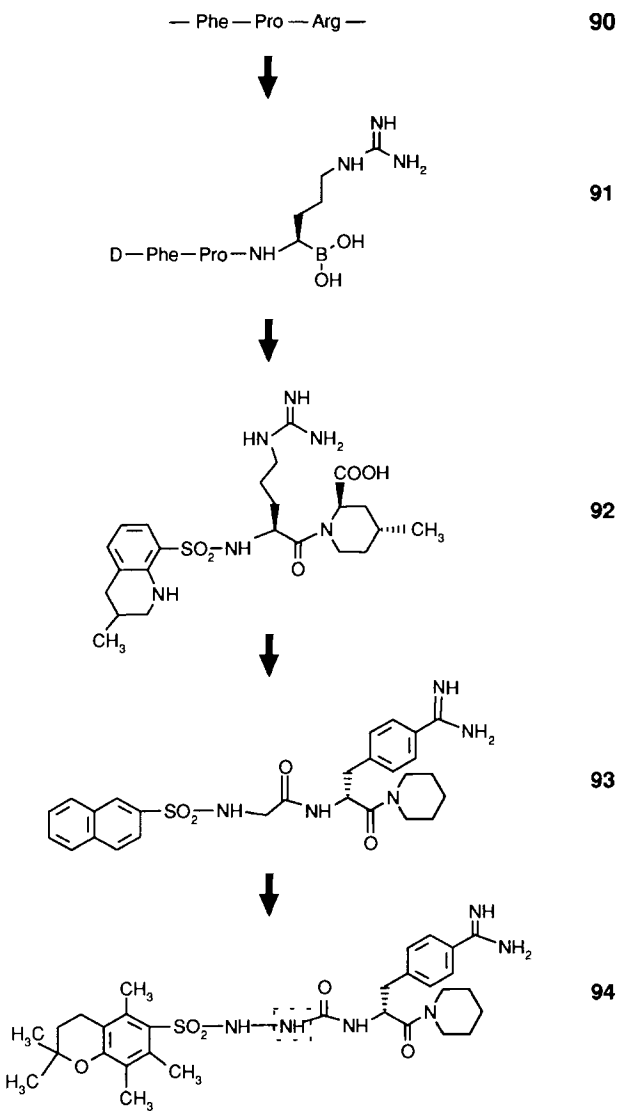
Scheme 29. Structure of hirudin (**89**).

Hirudin forms a noncovalent, high-affinity complex with thrombin and hinders the approach of substrate molecules sterically by binding to various fixation points of the enzyme.[114] Hirudin, with an inhibition constant K_i of 20 fM, is the strongest known thrombin inhibitor.[115] For a long time it was available only with difficulty and in small amounts, but hirudin can now be obtained in large amounts and with a high degree of purity by expression in yeast or *E. coli*. The rec-hirudin obtained in this way lacks the sulfate group at Tyr^{63}, but the reduction in activity is small. The Ciba-Geigy product CGP 39393 with a K_i value of 230 fM is highly active and is at an advanced stage of clinical evaluation.[116]

Hirudin fragments, for example deca- and dodecapeptides from the C-terminus, have also been shown to be active.[117]

Thrombin inhibition by the natural products cyclotheonamide A and B (**62** and **63**)[76] has already been mentioned (see Section 4.1).

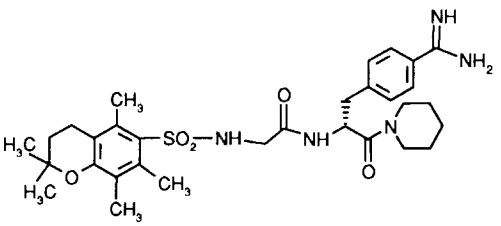
The development of an extremely interesting series of peptidomimetics for influencing thrombin activity was based on substrate analogues. These inhibitors occupy the active site rather than fibrinogen and thus block the normal function of the enzyme. This class of substances is based on the sequence Phe-Pro-Arg (**90**) in fibrinogen (Scheme 30), which is adjacent to the peptide bond to be cleaved.[118] The development from the peptide to the "complete" peptidomimetic, which contains no natural amino acids, can be demonstrated clearly by the compounds shown in Scheme 30.



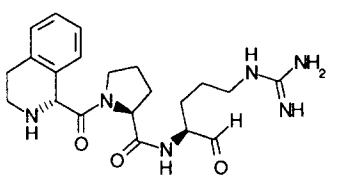
Scheme 30. Development of thrombin inhibitors.

The exchange of D-Phe for Phe and the additional replacement of the carboxyl group in Arg by various residues gave the corresponding chloromethyl ketone,[119] aldehyde,[120] and nitrile;[121] however, the most effective analogue was the boroarginine derivative **91** which has an extremely high activity (K_i = 3.6 pM!).[122] This compound has been found to mimic the tetrahedral transition state of the catalyzed reaction.[123] Recently the *N*-acetyl derivative of **91** was shown to be active in vivo and to influence both venous and arterial thrombosis.[124]

The next step in mimetism, which was based on the observation that even the simple methyl ester of tosylarginine is a thrombin inhibitor, led to the highly active sulfonamide derivative **92** (argatroban, MD 805).[125] Replacement of the arginine by the unnatural amino acid *p*-amidinophenylalanine and introduction of a glycine residue into the molecule led among others to compound **93** (NAPAP);[126] the derivative having the modified phenylalanine residue with the unnatural D configuration is 1000 times more active than that with the L isomer.[127] The final molecule in this series is compound **94**,[128] the azaglycine analogue of the highly active compound **95**,[129] a further development of the NAPAP principle. A considerable increase in activity has been reported for compound **94**. Since such azapeptides also show resistance to enzymatic degradation, they should have improved stability within the organism as well as increased activity.



Further developments of the principles discussed above which have led to compounds with improved properties include the replacement of D-Phe by the corresponding rigidified amino acid D-Tic (tetrahydroisoquinolinecarboxylic acid) in the tripeptidealdehyde **96**.[130] and combinations with the hirudin motif

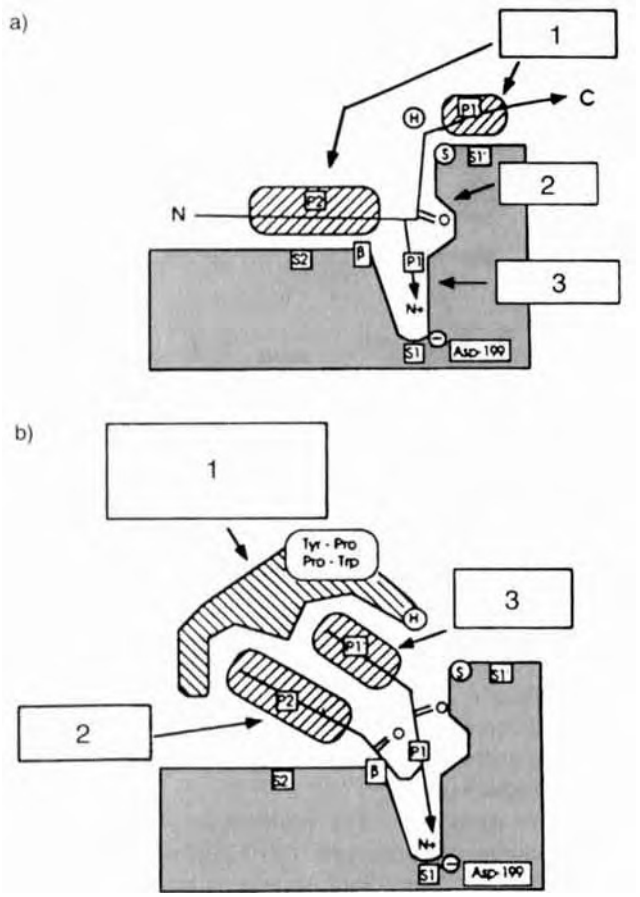


(hirulog 1 and hirulog 4), in which D-Phe-Pro-Arg is attached to the hirudin sequence 53–64 by means of spacers of different lengths composed of glycine residues.[131] The replacement of the spacer by a variable number of ω-aminopentenoyl residues in this series leads to products with improved activity.[132] Other newer variations make use of ketomethylene arginyl dipeptide residues[133] and diphenylmethyl residues instead of the Phe side chain.[134]

The nature of the binding of the thrombin inhibitors to the enzyme has been the subject of many detailed studies. It has recently been observed that intramolecular hydrophobic interactions which had previously been neglected may be essential in the binding of argatroban- and NAPAP-type inhibitors.

Although it had been supposed earlier that thrombin inhibitors generally bind in the the same manner as the substrate (substrate-like binding),[135] X-ray structural studies have

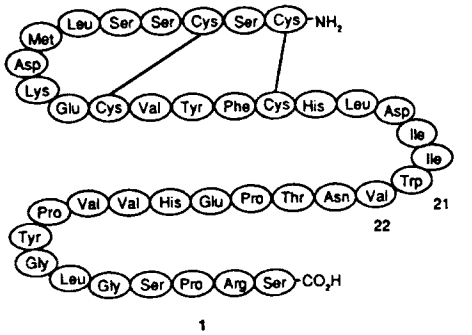
shown a different type of binding (inhibitor-like) for inhibitors of the types mentioned.[127,136] Hydrophobic interactions are found in the bioactive conformations of argatroban (**92**) (between the tetrahydroquinolyl and piperidine groups) and of NAPAP (**93**) (between the naphthyl and piperidine groups; Scheme 31), and the conformations are thus subject to so-called hydrophobic collapse (for an explanation see Section 6). As shown in Scheme 31, the hydrophobic residues interact solely with hydrophobic pockets formed by the amino acid residues 47–50 (Tyr-Pro-Pro-Trp) of the enzyme.



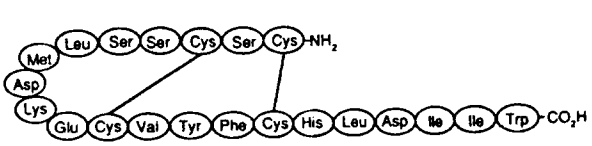
Scheme 31. a) Binding of a substrate to a trypsin-like serine protease. 1: hydrophobic groups, 2: pocket for an oxy group, 3: recognition pocket, C: C-terminus, N: N-terminus, H: His^{43}, S: Ser^{205}, β: β-autocatalytic site. b) Hydrophobic collapse during the binding of the inhibitor to thrombin. 1: extra loop, residues 47–50 containing two pockets, the P pocket (proximal to Ser^{205}) and the D pocket (distal to Ser^{205}). This loop is not present in trypsin. 2: hydrophobic group in the D pocket, 3: hydrophobic group in the P pocket.

5.4. ECE Inhibitors

The use of inhibitors of the endothelin converting enzyme (ECE) in the treatment of cardiovascular disorders has recently become a subject of great interest. Endothelin-1 (ET-1, **98**), a peptide containing 21 amino acids with two disulfide bridges, can be isolated from endothelial cells and shows a strongly vasoconstricting and hypertensive activity. This peptide is liberated from a precursor peptide, the big ET-1 (**97**) with 38 amino acids, by an ECE-mediated hydrolytic cleavage of the Trp^{21}-Val^{22} bond (Scheme 32).[137]



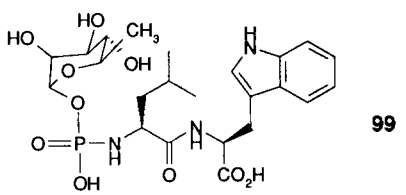
97



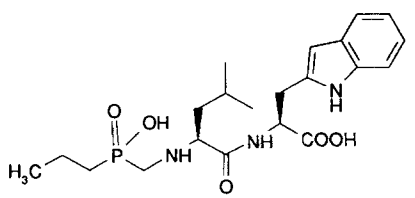
98

Scheme 32. Big endothelin-1 (**97**) and endothelin-1 (**98**).

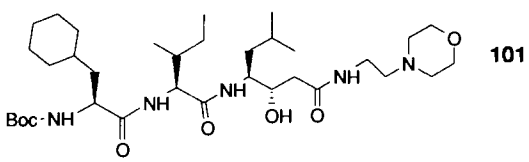
Endothelin exists in several forms, ET-1 (**98**), ET-2, and ET-3. Since ET-1 seems to play the dominant role in humans, all the pharmacological studies so far have been concerned with this particular isoform. A high ET level seems to play an important role in pathophysiological conditions such as high blood pressure,[138] acute kidney failure,[139] and coronary and cerebral vasospasm.[140] Accordingly, lowering an extreme ET level by inhibiting the enzymatic release of ET appears to be an attractive therapeutic goal. Other attempts to reach this goal have



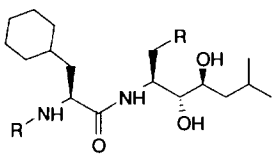
99



100



101



102

Scheme 33. ECE inhibitors. **102**: R = 1-naphthyl, $K_i = 2.3 \times 10^{-8}$ M; R = 2-naphthyl, $K_i = 3.1 \times 10^{-9}$ M.

involved the blockage of the endothelin receptor by corresponding antagonists.[2b]

Since the structure of the ECE is still relatively unclear, the conception and synthesis of antagonists is presently still in its initial stages. On the one hand ECE is inhibited by inhibitors of the metalloprotease neutral endopeptidase (NEP) such as phosphoramidon (**99**)[141] and more simple analogues such as **100**[142a] as well as by the chelating agents EDTA and *o*-phenanthroline. This suggests that ECE is a metalloprotease[142b] (Scheme 33). On the other hand there is evidence that ECE activity is possibly due to the aspartyl proteases cathepsin D and/or cathepsin E.[143] Further evidence for an aspartyl protease comes from the recent discovery that an enzyme activity isolated from rat lung is very effectively inhibited by pepstatin (**77**), a potent pepsin inhibitor.[144] This provided the stimulus for optimizing certain structural principles known from transition state analogues of renin inhibitors (see Section 5.2.1) for ECE inhibition. The result was two groups of inhibitors of the statin (**101**) and diol (**102**) types,[144] which in some cases show high specificity for ECE over renin and cathepsin D.

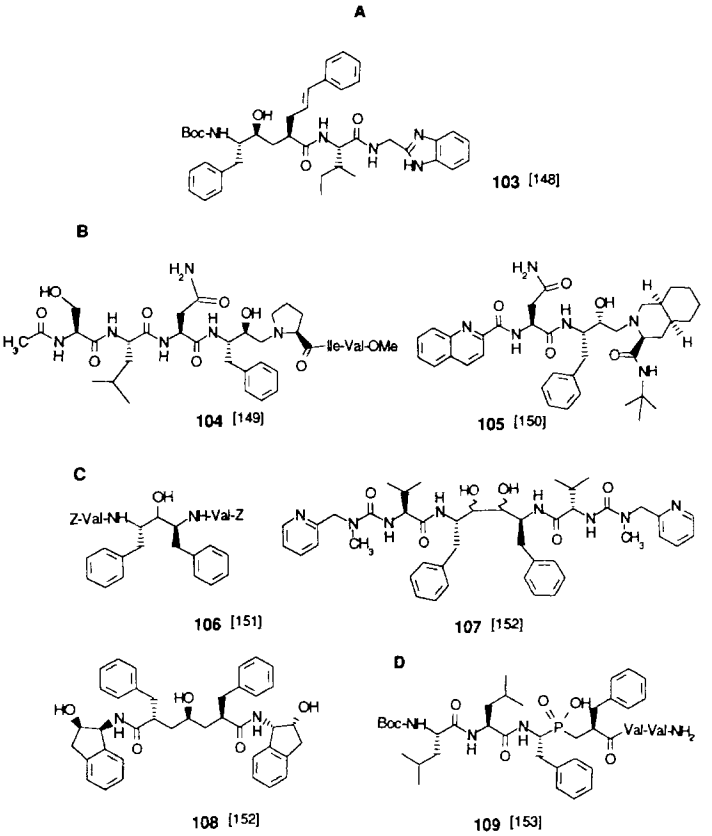
5.5. Inhibitors of Other Proteases

The detailed discussion of inhibitors of therapeutically relevant enzymes will now be followed by a short treatment of some other recent developments in this area.

In addition to some completely different approaches[145] the development of inhibitors of the HIV-1 protease has become an interesting target in AIDS therapy.[2c,146] This aspartyl protease, which is vital for the replication of the virus, is responsible for the proteolytic processing of the gag and gag-pol polyproteins to give infectious virions.[147] As an aspartyl protease, the HIV-1 protease can in principle be influenced by substances of the renin-inhibitor type containing statin or hydroxyethylene units (**103**, Scheme 34).[148] Other highly active inhibitors are of the hydroxyethylamine type (**104** and **105**).[149,150] More recent developments are based on the observation that the HIV-1 protease crystallizes as a C_2-symmetric homodimer, in which each chain provides one aspartate residue which plays an important role in the catalysis.[151] On the basis of this result various types of inhibitors have been synthesized in which the peptide bond is replaced by C_2-symmetric and C_2-pseudosymmetric units (**106**–**108**).[151a,152]

Phosphinic acid derivatives such as **109**, in which the central CHOH group has been replaced isosterically, have also proved to be highly active.[153] Further developments of the principles discussed here are described in the recent literature.[154–161]

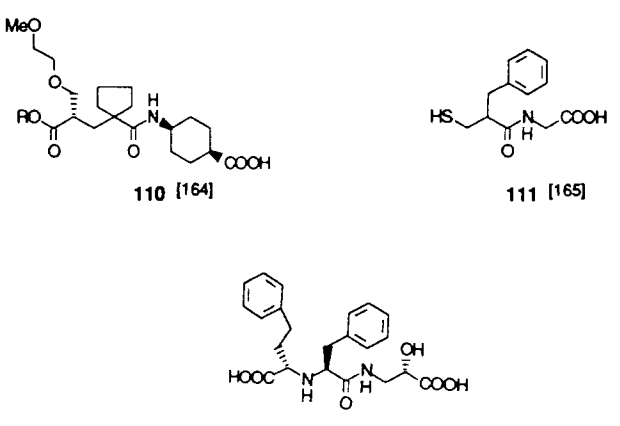
Inhibitors of the neutral endopeptidase (NEP), a Zn metalloprotease, have been the subject of increasing interest. NEP has two physiological functions: in the central nervous system it inactivates the enkephalins, endogeneous opioid peptides,[162] and it also mediates the proteolytic degradation of the atrial natriuretic peptide (ANP), a peptidic vasodilator secreted by atrial tissue which has a blood pressure regulating function.[163] The inhibition of this enzyme can thus have both pain-relieving and blood pressure reducing effects. It is not surprising that the inhibitors of this metalloprotease developed so far are structurally similar to ACE inhibitors, as ACE belongs to the same



Scheme 34. Inhibitors of HIV-1 protease. **A**: renin inhibitor type (**103**); **B**: hydroxyethylamine type (**104**, **105**); **C**: C_2-(pseudo)symmetric type (**106**–**108**); **D**: phosphinic acid type (**109**).

class of proteases. Characteristic compounds that have been developed as ANP degradation inhibitors primarily for cardiovascular indication are candoxatril (**110**),[164] thiorphan (**111**),[165] and Sch 39370 (**112**)[166] (Scheme 35). New developments, mainly analogues of these compounds, can be found in the more recent literature.[167–170]

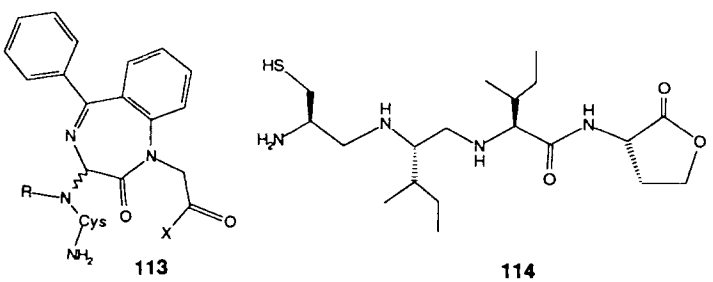
Inhibitors of elastase, a serine protease, are of interest for combating pulmonary emphysema.[2c,171] It is hoped that inhibition of collagenase, a metalloprotease, may lead in particular



Scheme 35. ANP degradation inhibitors. Candoxatril: **110**, R = 5-indanyl; candoxatrilat: **110**, R = H.

to drugs for combating rheumatoid arthritis, a pathological condition in which this enzyme is involved by excessive proteolysis.[82b,172] Inhibitors of peptidyl-prolyl *cis/trans* isomerases (PPIases), a group of enzymes involved in protein folding which can influence the immune system, are also of current interest.[2c,173] Inhibitors of cysteine proteases, which include papain, can influence pathological conditions caused by defective functions of such proteases in processing biologically active peptides.[82b,174] Inhibitors of enzymes that degrade the neuropeptides neurotensin and neuromedin could lead to effective treatment of pain.[175]

The efficiency of different forms of peptidomimetism cannot be more clearly demonstrated than by the example of two compounds recently described independently, which as inhibitors of the enzyme farnesyl protein transferase (FPT) may lead to highly interesting possibilities for cancer therapy. Both **113**, which has a novel cyclic dipeptide-analogous unit of the benzodiazepine type,[176] and the tetrapeptide-analogous lactone **114**,[177] characterized by two reduced amide bonds at the N-terminus, can inhibit the growth of certain types of tumor cells very effectively (Scheme 36).



113 **114**

Scheme 36. X = Met-COOH, Ser-COOH, Leu-COOH, Met-COOMe, Met-$CONH_2$.

These substances are directed against oncogenic ras proteins, which play a decisive role in the formation of most human pancreas and colon tumors. These oncogenic ras proteins, which are formed by point mutations, require the linkage of a farnesyl group to a cysteine SH group of the C-terminal tetrapeptide group of the protein so that they can adhere to the inner side of the cell membrane. Only in this state are they able to induce uninhibited cell division. The goal of this protein deactivation approach is preventing the transfer of the farnesyl residue by inhibiting the farnesyl protein transferase that catalyzes this process.[178]

In contrast to other approaches of this type[178,179] (in some cases with appropriate tetrapeptides analogous to the C-terminus[179,180]), the mimetics of the peptides described above are able to penetrate the cell membrane and are also much more resistant towards degrading enzymes.

It has been shown that these compounds are able to inhibit the coupling of the farnesyl group to the mutated ras protein (and thus its adherence to the cell membrane) even at a very low concentration, thus leading to cell growth inhibition. In cell cultures these substances show high selectivity and extremely low toxicity.

6. Conclusions and Future Prospects: Hydrophobic Collapse, De Novo Design

New impulses for the rational design of new drugs may come from the information available on the apparently quite general phenomenon known as hydrophobic collapse. Because of its potential importance in the planning of new peptidomimetics, we shall present a short description of this phenomenon and its consequences.

When the whole spectrum of presently known peptidomimetics is considered, it becomes clear that they have one structural feature in common with many pharmacophores of known drugs: they contain hydrophobic groups that are either conformatively rigid or at least limited in their flexibility. This reduction in conformational mobility hinders intramolecular hydrophobic interactions, which in aqueous media (i.e. also at the receptor and the active site) would lead to a collapse of a bioactive conformation with concomitant loss of activity. This phenomenon is referred to as hydrophobic collapse.[181]

The basis for this phenomenon is the hydrophobic effect,[182] which plays an important role in all biological processes. This effect is used to explain the observation that when complicated molecules are dissolved in water the interactions between hydrophobic groups and the solvent are reduced to a minimum. Thus because of this effect proteins have, for example, developed develop structures that make use of hydrophobic interactions for binding ligands to receptors. In enzymes such hydrophobic pockets are important in binding substrates and inhibitors. The "construction blueprint" of proteins seems ideal for the stabilization of such hydrophobic pockets, for example at active sites of enzymes, and the hydrophobic collapse in the absence of the ligand is thus prevented.

For the ligands, too, this type of conformational stabilization often appears to be necessary for the effective presentation of the hydrophobic groups required for an interaction with the active site of the enzyme. Without this stabilization, which can for example be achieved by rigidifying scaffolds, the active substance would undergo hydrophobic collapse to give an inactive conformation. On the other hand, the hydrophobic collapse of a ligand can also be advantageous, since in some cases only the collapsed conformation is bioactive. This can be shown, for example, for cyclosporin A[183] and for thrombin inhibitors (see Section 5.3).

The design of peptidomimetics must always take into account whether a hydrophobic collapse is to be prevented or induced. Thus in the future it will generally continue to be important for the discovery of new lead peptidomimetic structures to look for scaffolds, whose rigidity would prevent the hydrophobic collapse of essential groups in an aqueous medium. The scaffolds previously identified, such as the sugar or steroid scaffolds (see Section 2.5) appear to fulfill these conditions.

A goal that has not yet been achieved is the de novo design of peptidomimetics. At present, natural substrates, inhibitors, or a lead structure identified by screening (plant or animal extracts, substances isolated from microorganisms, compound libraries) are required as the starting point for a development sequence. In contrast, de novo design implies development without such a starting point. Thus for example the structure of an inhibitor

would be developed based only on the known amino acid sequence of an enzyme or the natural interaction partner.

Attaining the final goal of de novo design would have immense practical value in medicinal chemistry. Consider the extremely labor-intensive research in drug development, in which the conventional approach still relies primarily on empirical findings. This investment of time and effort is the obvious result of the statistical fact that thousands of compounds must be synthesized and tested before one of them is deemed marketable; the other compounds are weeded out in stringent pharmacological, toxicological, and clinical tests. Certainly with the help of de novo development this rejection rate could be drastically reduced.

A step in the direction of de novo design has been taken by various computer programs such as CAVEAT[184] which have the goal of calculating new active structures based only on the active site of the enzyme. The program DESIGN has recently been introduced[185] and used for designing a template for mimicking the enzyme thioredoxin.

The rational design of peptidomimetics is, however, already possible to a certain extent even today, as we hope to have shown in this review. Highly refined methods of conformational analysis (e.g. NMR, X-ray structural analysis) and the new computer programs have made an important contribution to the current state of the art. Rational design has already proved to be very useful in translating peptide structures with their biological information content into low molecular weight non-peptidic molecules.

Synthetic chemistry has also made great progress. Without the modern methods developed by organic chemists the construction of complex, stereochemically defined molecules with particular functional groups and hydrophobic elements attached to a non-peptidic scaffold would hardly have been possible.

Further progress in this area depends on the combined efforts of organic and medicinal chemists, as well as contributions from other disciplines concerned with the chemistry of biological systems. The goal of this effort is the design of compounds that are compatible with living systems, as well as the development of synthetic methods producing compounds that satisfy specific chemical, structural, conformational, topographical, and dynamic requirements on the one hand and are biologically active on the other. Research on peptidomimetics illustrates this trend, and on the basis of what has been achieved so far and the justified hope of further progress, the realization of the goal of tailor-made peptidomimetic enzyme inhibitors certainly appears within reach.

Received: August 6, 1993 [A 13 E]
German version: *Angew. Chem.* **1994**, *106*, 1780
Translated by Dr. T. N. Mitchell, Dortmund (FRG)

[1] A peptidomimetic is defined as a substance having a secondary structure as well as other structural features analogous to that of the original peptide, which allows it to displace the original peptide from receptors or enzymes. As a result the effects of the original peptide are inhibited (antagonist, inhibitor) or duplicated (agonist).

[2] Reviews: a) R. M. J. Liskamp, *Recl. Trav. Chim. Pays-Bas* **1994**, *113*, 1; b) A. Giannis, T. Kolter, *Angew. Chem.* **1993**, *105*, 1303; *Angew. Chem. Int. Ed. Engl.* **1993**, *32*, 1244; c) R. A. Wiley, D. H. Rich, *Med. Res. Rev.* **1993**, *13*, 327; d) G. L. Olson, D. R. Bolin, M. P. Bonner, M. Bös, C. M. Cook, D. C. Fry, B. J. Graves, M. Hatada, D. E. Hill, M. Kahn, V. S. Madison, V. K. Rusiecki, R. Sarabu, J. Sepinwall, G. P. Vincent, M. E. Voss, *J. Med. Chem.* **1993**, *36*, 3039; e) A. F. Spatola in *Methods in Neurosciences, Vol. 13* (Ed.: P. M. Conn), Academic Press, San Diego, **1993**, p. 19; f) B. A. Morgan, J. A. Gainor, *Annu. Rep. Med. Chem.* **1989**, *24*, 244; g) A. F. Spatola in *Chemistry and Biochemistry of Amino Acids, Peptides, and Proteins, Vol. VII*, (Ed.: B. Weinstein), Marcel Dekker, New York, **1983**, p. 267; h) V. J. Hruby, *Biopolymers* **1993**, *33*, 1073; i) *Nachr. Chem. Tech. Lab.* **1994**, *42*, 164; j) M. Kahn, *Synlett* **1993**, 821; k) A. E. P. Adang, P. H. H. Hermkens, J. T. M. Linders, H. C. J. Ottenheijm, C. J. van Staveren, *Recl. Trav. Chim. Pays-Bas* **1994**, *113*, 63.

[3] a) G. Jung, A. G. Beck-Sickinger, *Angew. Chem.* **1992**, *104*, 375; *Angew. Chem. Int. Ed. Engl.* **1992**, *31*, 367; b) H. E. Radunz, *GIT Fachz. Lab.* **1992**, *36*, 869.

[4] D. Jiao, K. C. Russell, V. J. Hruby, *Tetrahedron* **1993**, *49*, 3511.

[5] a) A. Sood, C. K. Sood, B. F. Spielvogel, I. H. Hall, *Eur. J. Med. Chem.* **1990**, *25*, 301; b) A. Sood, C. K. Sood, B. F. Spielvogel, I. H. Hall, O. T. Wong, M. Mittakanti, K. Morse, *Arch. Pharm. (Weinheim, Ger.)* **1991**, *324*, 423; c) M. Mittakanti, D. A. Feakes, K. W. Morse, *Synthesis* **1992**, 380.

[6] a) W. J. Moree, L. C. van Gent, G. A. van der Marel, R. M. J. Liskamp, *Tetrahedron* **1993**, *49*, 1133; b) D. Merricks, P. G. Sammes, E. R. Walker, K. Henrick, M. M. McPartlin, *J. Chem. Soc. Perkin Trans. 1* **1991**, 2169; c) W. J. Moree, G. A. van der Marel, R. M. J. Liskamp, *Tetrahedron Lett.* **1991**, *32*, 409; d) *ibid.* **1992**, *33*, 3689.

[7] a) D. A. McLeod, R. I. Binkworth, J. A. Ashley, K. D. Janda, P. Wirsching, *Bioorg. Med. Chem. Lett.* **1991**, *1*, 653; b) P. Coutrot, C. Grison, C. Charbonnier-Gerardin, *Tetrahedron* **1992**, *48*, 9841.

[8] a) C. A. Kettner, L. Mersinger, R. Knabb, *J. Biol. Chem.* **1990**, *265*, 18289; b) D. H. Kinder, J. A. Katzenellenbogen, *J. Med. Chem.* **1985**, *28*, 1917; c) C. A. Kettner, A. B. Shenvi, *J. Biol. Chem.* **1984**, *259*, 15106.

[9] W. Kazmierski, V. J. Hruby, *Tetrahedron* **1988**, *44*, 697.

[10] C. C. Cativiela, M. D. Diaz de Villegas, A. Avenoza, J. M. Peregrina, *Tetrahedron* **1993**, *49*, 10987.

[11] a) R. Rone, N. Manesis, M. Hassan, M. Goodman, A. T. Hagler, D. H. Kitson, V. A. Roberts, *Tetrahedron* **1988**, *44*, 895; b) N. Manesis, M. Goodman, *J. Org. Chem.* **1987**, *52*, 5331; c) N. Manesis, M. Hassan, R. Glaser, M. Goodman, *Biopolymers* **1986**, *25* (Suppl.), 97.

[12] D. K. Suumaran, M. Prorok, D. S. Lawrence, *J. Am. Chem. Soc.* **1991**, *113*, 706.

[13] J. Di Maio, B. Bellau, *J. Chem. Soc. Perkin Trans. 1* **1989**, 1687.

[14] a) R. M. Freidinger, D. F. Veber, D. S. Perlow, J. R. Brooks, R. Saperstein, *Science* **1980**, *210*, 656; b) R. M. Freidinger, D. S. Perlow, D. F. Veber, *J. Org. Chem.* **1982**, *47*, 104; c) Z. Procházka, M. Lebl, T. Barth, J. Hlaváček, A. Trka, M. Budešinsky, K. Jošt, *Collect. Czech. Chem. Commun.* **1984**, *49*, 642; d) R. M. Freidinger, *J. Org. Chem.* **1985**, *50*, 3631; e) T. M. Zydowsky, J. F. Dellaria, Jr., H. N. Nellans, *ibid.* **1988**, *53*, 5607; f) S. Thaisrivongs, D. T. Pals, S. R. Turner, L. T. Kroll, *J. Med. Chem.* **1988**, *31*, 1369; g) J. D. Aebi, D. Guillaume, B. E. Dunlap, D. H. Rich, *ibid.* **1988**, *31*, 1805; h) J. P. Wolf, H. Rapoport, *J. Org. Chem.* **1989**, *54*, 3164; i) G. Valle, M. Crisma, C. Toniolo, K.-L. Yu, R. L. Johnson, *J. Chem. Soc. Perkin Trans. 2* **1989**, 83; k) D. S. Garvey, P. D. May, A. M. Nadzan, *J. Org. Chem.* **1990**, *55*, 936.

[15] J. Gante, R. Weitzel, *Tetrahedron Lett.* **1988**, *29*, 181.

[16] T. P. Burkholder, E. W. Huber, G. A. Hynn, *Bioorg. Med. Chem. Lett.* **1993**, *3*, 231.

[17] R. C. F. Jones, G. F. Ward, *Tetrahedron Lett.* **1988**, *29*, 3853.

[18] J. Zabrocki, G. D. Smith, J. B. Dunbar, Jr., K. W. Marshall, M. Toth, G. R. Marshall, *Pept. Proc. Eur. Pept. Symp. 20th 1988* **1989**, 295.

[19] T. Gordon, P. Hansen, B. Morgan, J. Singh, E. Baizman, S. Ward, *Bioorg. Med. Chem. Lett.* **1993**, *3*, 915; see further R. Jones, G. Ward, *Tetrahedron Lett.* **1988**, *29*, 3858; C. I. Fincham, M. Higginbottom, D. R. Hill, D. C. Horwell, J. C. O'Toole, G. S. Ratcliffe, D. C. Rees, E. Roberts, *J. Med. Chem.* **1992**, *35*, 1472; I. Gilbert, D. C. Rees, R. S. Richardson, *Tetrahedron Lett.* **1991**, *32*, 2277.

[20] a) B. Gardner, H. Nakanishi, M. Kahn, *Tetrahedron* **1993**, *49*, 3433; b) J. B. Ball, R. A. Hughes, P. F. Alewood, P. R. Andrews, *ibid.* **1993**, *49*, 3467.

[21] G. Hölzemann, *Kontakte (Darmstadt)* **1991** (1), 3; *ibid.* **1991** (2), 55; b) P. D. Bailey, *Peptide Chemistry*, Wiley, New York, **1990**, p. 182.

[22] a) M. Feigel, *J. Am. Chem. Soc.* **1986**, *108*, 181; b) G. Wagner, M. Feigel, *Tetrahedron* **1993**, *49*, 10831; c) V. Brandmeier, W. H. B. Sauer, M. Feigel, *Helv. Chim. Acta* **1994**, *77*, 70.

[23] a) K. Sato, U. Nagai, *J. Chem. Soc. Perkin Trans. 1* **1986**, 1231; b) U. Nagai, K. Sato, R. Nakamura, R. Kato, *Tetrahedron* **1993**, *49*, 3577.

[24] D. S. Kemp, W. E. Stites, *Tetrahedron Lett.* **1988**, *29*, 5057.

[25] M. J. Genin, R. L. Johnson, *J. Am. Chem. Soc.* **1992**, *114*, 8778.

[26] W. C. Ripka, G. V. DeLucca, A. C. Bach II, R. S. Pottorf, J. M. Blaney, *Tetrahedron* **1993**, *49*, 3593, 3609.

[27] J. F. Callahan, J. W. Bean, J. L. Burgess, D. S. Eggleston, S. M. Hwang, K. D. Kopple, P. F. Koster, A. Nichols, C. E. Peishoff, J. M. Samanen, J. A. Vasko, A. Wong, W. F. Huffman, *J. Med. Chem.* **1992**, *35*, 3970.

[28] J. F. Callahan, K. A. Newlander, J. L. Burgess, D. S. Eggleston, A. Nichols, A. Wong, W. F. Huffman, *Tetrahedron* **1993**, *49*, 3479.

[29] M. Sato, J. Y. H. Lee, H. Nakanishi, M. E. Johnson, R. A. Chrusciel, M. Kahn, *Biochem. Biophys. Res. Commun.* **1992**, *187*, 1000.

[30] M. Kahn, M. Lee, H. Nakanishi, J. Urban, B. Gardner, *Proc. Am. Pept. Symp. 13th 1993*, in press; see also K. Müller, D. Obrecht, A. Knierzinger, C. Stankovic, C. Spiegler, W. Bannwarth, A. Trzeciak, G. Englert, A. M. Labhadt, P. Schönholzer in *Perspectives in Medicinal Chemistry* (Eds.: B. Testa, W. Fuhrer, E. Kyburz, R. Giger), Helvetica Chimica Acta, Basel/VCH, Weinheim, **1993**, p. 513; D. S. Kemp, T. P. Curran, W. M. Davis, J. G. Boyd, C. Muendel, *J. Org. Chem.* **1991**, *56*, 6672; D. S. Kemp, T. P. Curran, J. G. Boyd, T. J. Allen, *ibid.* **1991**, *56*, 6683.

[31] R. Sarabu, K. Lovey, V. S. Madison, D. C. Fry, D. W. Greeley, C. M. Cook, G. L. Olson, *Tetrahedron* **1993**, *49*, 3629.

[32] C. A. Dinarello, *Adv. Immunol.* **1989**, 153.

[33] R. M. Sweet, H. T. Wright, J. Janin, C. H. Chotki, D. M. Blow, *Biochemistry* **1974**, *13*, 4212.

[34] a) D. H. Rich, *Med. Res. Rev.* **1993**, *13*, 368; b) C. Tanford, *The Hydrophobic Effect: Formation of Micelles and Biological Membranes*, Wiley-Interscience, New York, **1980**.

[35] L. Alig, A. Edenhofer, P. Hadvary, M. Hürzeler, D. Knopp, M. Müller, B. Steiner, A. Trzeciak, T. Weller, *J. Med. Chem.* **1992**, *35*, 4393.

[36] a) R. Hirschmann, P. A. Sprengeler, T. Kawasaki, J. W. Leahy, W. C. Shakespeare, A. B. Smith III, *J. Am. Chem. Soc.* **1992**, *114*, 9699; b) *Tetrahedron* **1993**, *49*, 3665.

[37] R. Hirschmann, K. C. Nicolaou, S. Pietranico, E. M. Leahy, J. Salvino, B. Arison, M. A. Cichy, P. G. Spoors, W. C. Shakespeare, P. A. Sprengeler, P. Hamley, A. B. Smith III, T. Reisine, K. Raynor, L. Maechler, C. Donaldson, W. Vale, R. M. Freidinger, M. R. Cascieri, C. D. Strader, *J. Am. Chem. Soc.* **1993**, *115*, 12550.

[38] R. Hirschmann, K. C. Nicolaou, S. Pietranico, J. Salvino, E. M. Leahy, P. A. Sprengeler, G. Furst, A. B. Smith III, C. D. Strader, M. A. Cascieri, M. R. Candelore, C. Donaldson, W. Vale, L. Maechler, *J. Am. Chem. Soc.* **1992**, *114*, 9217.

[39] a) G. R. Marshall, *Tetrahedron* **1993**, *49*, 3547; b) R. Hirschmann, *Angew. Chem.* **1991**, *103*, 1305; *Angew. Chem. Int. Ed. Engl.* **1991**, *30*, 1278.

[40] D. F. Veber in *Peptides: Chemistry and Biology* (Eds.: J. A. Smith, J. E. Rivier), Escom, Leiden, **1992**, p. 3.

[41] B. E. Evans, M. G. Bock, K. E. Rittle, R. M. Di Pardo, W. L. Whitter, D. F. Veber, P. S. Anderson, R. M. Freidinger, *Proc. Natl. Acad. Sci. USA* **1986**, *83*, 4918.

[42] D. Biswanath, J. J. Plattner, E. N. Bush, H. Jae, G. Diaz, E. S. Johnson, T. J. Perun, *J. Med. Chem.* **1989**, *32*, 2036.

[43] a) B. E. Evans, J. L. Leighton, K. E. Rittle, K. F. Gilbert, G. F. Lundell, N. P. Gould, D. W. Hobbs, R. M. Di Pardo, D. F. Veber, D. J. Pettibone, B. V. Clineschmidt, P. S. Anderson, R. M. Freidinger, *J. Med. Chem.* **1992**, *35*, 3919; b) B. E. Evans, G. F. Lundell, K. F. Gilbert, M. G. Bock, K. E. Rittle, L. A. Carroll, P. D. Williams, J. M. Pawluczyk, J. L. Leighton, M. B. Young, J. M. Erb, D. W. Hobbs, N. P. Gould, R. M. DiPardo, J. B. Hoffman, D. S. Perlow, W. L. Whitter, D. F. Veber, D. J. Pettibone, B. V. Clineschmidt, P. S. Anderson, R. M. Freidinger, *ibid.* **1993**, *36*, 3993.

[44] J. V. Duncia, A. T. Chiu, D. J. Carini, G. B. Gregory, A. L. Johnson, W. A. Price, G. J. Wells, P. C. Wong, J. C. Calabrese, P. B. Timmermans, *J. Med. Chem.* **1990**, *33*, 1312.

[45] J. Weinstock, R. M. Keenan, J. Samanen, J. Hempel, J. A. Finkelstein, R. G. Franz, D. E. Gaitanopoulos, G. R. Girard, J. G. Gleason, D. T. Hill, T. M. Morgan, C. E. Peishoff, N. Aiyar, D. P. Brooks, T. A. Fredrickson, E. H. Ohlstein, R. R. Ruffolo, Jr., E. J. Stack, A. C. Sulpizio, E. F. Weidley, R. M. Edwards, *J. Med. Chem.* **1991**, *34*, 1514.

[46] J. M. Samenen, C. E. Peishoff, R. M. Keenan, J. Weinstock, *Bioorg. Med. Chem. Lett.* **1993**, 909.

[47] P. D. Williams, P. S. Anderson, R. G. Ball, M. G. Bock, L. A. Carroll, S.-H. Lee Chiu, B. V. Clineschmidt, J. C. Culberson, J. M. Erb, B. E. Evans, S. L. Fitzpatrick, R. M. Freidinger, M. J. Kaufman, G. F. Lundell, J. S. Murphy, K. L. Thompson, D. F. Veber, *J. Med. Chem.* **1994**, *37*, 565.

[48] a) R. G. Almquist, W.-R. Chao, M. E. Ellis, H. L. Johnson, *J. Med. Chem.* **1980**, *23*, 1392; b) H. Ewenson, R. Laufer, M. Chorev, Z. Selinger, C. Gilon, *ibid.* **1988**, *31*, 416; c) R. G. Almquist, W.-R. Chao, A. K. Judd, C. Mitoma, D. J. Rossi, R. E. Panasevich, R. J. Matthews, *ibid.* **1988**, *31*, 561.

[49] Review: R. Henning, *Nachr. Chem. Tech. Lab.* **1990**, *38*, 460.

[50] S. L. Harbeson, D. H. Rich, *J. Med. Chem.* **1989**, *32*, 1378.

[51] P. Bühlmayer, A. Caselli, W. Fuhrer, R. Göschke, V. Rasetti, H. Rüeger, J. L. Stanton, L. Criscione, J. M. Wood, *J. Med. Chem.* **1988**, *31*, 1839.

[52] G. B. Dreyer, B. W. Metcalf, T. A. Tomaszek, Jr., T. J. Carr, A. C. Chandler, L. Hyland, S. A. Fakhoury, V. W. Magaard, M. L. Moore, J. E. Strichler, C. Debouck, T. D. Meek, *Proc. Natl. Acad. Sci. USA* **1989**, *86*, 9752.

[53] a) H. Umezawa, T. Nakamura, S. Fukatsu, T. Aoyagi, K. Tatsuka, *J. Antibiot.* **1983**, *36*, 1787; b) S. Ohuchi, A. Okuyama, K. Kawamura, T. Aoyagi, H. Umezawa, *Agric. Microbiol. Chem.* **1984**, *48*, 1661.

[54] K. Miusa, T. Sawa, T. Takeuchi, H. Umezawa, *J. Antibiot.* **1986**, *39*, 734.

[55] B. K. Evans, C. Rittle, J. Homnick, J. Springer, J. Hirshfield, D. Veber, *J. Org. Chem.* **1985**, *50*, 4615.

[56] A. H. Fray, R. L. Kaye, E. F. Kleinman, *J. Org. Chem.* **1986**, *51*, 4828.

[57] A. E. De Camp, A. T. Kawaguchi, R. P. Volante, I. Shinkai, *Tetrahedron Lett.* **1991**, *32*, 1867.

[58] B. Lygo, *Synlett* **1992**, 793.

[59] J. Gante, U. Anlauf, R. Weitzel, *Pept. Proc. Eur. Pept. Symp. 21st 1992* **1993**, 605.

[60] a) J. Di Maio, B. Gibbs, J. Lefebvre, Y. Konishi, D. Munn, S. Y. Yue, W. Hornberger, *J. Med. Chem.* **1992**, *35*, 3331; J. DiMaio, F. Ni, B. Gibbs, Y. Konishi, *FEBS Lett.* **1991**, *282*, 47.

[61] a) S. Nahm, S. M. Weinreb, *Tetrahedron Lett.* **1981**, *22*, 3815; b) Y. A. Fehrentz, B. Castro, *Synthesis* **1983**, 676.

[62] P. H. J. Carlsen, T. Katsuki, V. S. Martin, K. B. Sharpless, *J. Org. Chem.* **1981**, *46*, 3939.

[63] G. Guichard, J. P. Briand, M. Friede, *Pept. Res.* **1993**, *6*, 121.

[64] a) Review: J. Gante, *Synthesis* **1989**, 405; b) A. S. Dutta, J. S. Morley, *J. Chem. Soc. Perkin Trans. 1* **1975**, 1712.

[65] J. Gante, *Chem. Ber.* **1965**, *98*, 3340.

[66] J. Gante, M. Krug, G. Lauterbach, R. Weitzel, *Proc. Am. Pept. Symp. 13th 1993*, **1994**, 299.

[67] J. Magrath, R. H. Abeles, *J. Med. Chem.* **1992**, *35*, 4279.

[68] P. Raddatz, A. Jonczyk, K.-O. Minck, C. J. Schmitges, J. Sombroek, *J. Med. Chem.* **1991**, *34*, 3267.

[69] J. Gante, H. Kahlenberg, *Liebigs Ann. Chem.* **1989**, 1085.

[70] J. Gante, R. Weitzel, *Liebigs Ann. Chem.* **1990**, 349.

[71] J. Gante, H. Kahlenberg, *Chem. Ztg.* **1991**, *115*, 215.

[72] C. J. Gray, M. Quibell, K. L. Jiang, N. Bagett, *Innovation Perspect. Solid Phase Synth. Collect. Pap. Int. Symp. 2nd 1991* **1992**, 295.

[73] J. Gray, J. C. Ireson, R. C. Parker, *Tetrahedron* **1977**, *33*, 739.

[74] T. L. Graybill, M. J. Ross, B. R. Gauvin, J. S. Gregory, A. L. Harris, M. A. Ator, J. M. Rinker, R. E. Dolle, *Bioorg. Med. Chem. Lett.* **1992**, *2*, 1375.

[75] a) T. Kolter, A. Klein, A. Giannis, *Angew. Chem.* **1992**, *104*, 1394; *Angew. Chem. Int. Ed. Engl.* **1992**, *31*, 1391; b) M. Hagihara, N. J. Anthony, T. J. Stout, J. Clardy, S. L. Schreiber, *J. Am. Chem. Soc.* **1992**, *114*, 6568.

[76] a) M. Hagihara, S. L. Schreiber, *J. Am. Chem. Soc.* **1992**, *114*, 6570; b) P. Wipf, H. Kim, *J. Org. Chem.* **1993**, *58*, 5592; c) B. E. Maryanoff, X. Qiu, K. P. Padmanabhan, A. Tulinsky, H. R. Almond, Jr., P. Andrade-Gordon, M. N. Greco, J. A. Kauffmann, K. C. Nicolaou, A. Liu, P. H. Brungs, N. Fusetani, *Proc. Natl. Acad. Sci. USA* **1993**, *90*, 8048.

[77] A. B. Smith III, T. P. Keenan, R. C. Holcomb, P. A. Sprengeler, M. C. Guzman, J. L. Wood, P. C. Carroll, R. Hirschmann, *J. Am. Chem. Soc.* **1992**, *114*, 10672.

[78] a) R. J. Simon, R. S. Kania, R. N. Zuckermann, V. D. Huebner, D. A. Jewell, S. Banville, S. Wang, S. Rosenberg, C. K. Marlowe, D. C. Spellmeyer, R. Tan, A. D. Frankel, D. V. Santi, F. E. Cohen, P. A. Bartlett, *Proc. Natl. Acad. Sci. USA* **1992**, *89*, 9367; b) R. N. Zuckermann, J. M. Kerr, S. B. H. Kent, W. H. Moos, *J. Am. Chem. Soc.* **1992**, *114*, 10646; c) *Chemtracts: Macromol. Chem.* **1993**, *4*, 80; d) H. Kessler, *Angew. Chem.* **1993**, *105*, 572; *Angew. Chem. Int. Ed. Engl.* **1993**, *32*, 543.

[79] M. Chorev, M. Goodman, *Acc. Chem. Res.* **1993**, *26*, 266.

[80] H. Rink, *Tetrahedron Lett.* **1987**, *28*, 3787.

[81] G. N. Ramachandran, V. Sasisekharan, *Adv. Protein Chem.* **1968**, *23*, 283.

[82] a) M. I. Page, *Compr. Med. Chem.* **1990**, *2*, 61; b) D. H. Rich, *ibid.* **1990**, *2*, 391, 402.

[83] Collective term for enzymes that catalyze the hydrolytic cleavage of the peptide bond in proteins and peptides: *Römpp Chemie-Lexikon*, Thieme, Stuttgart, **1992**, p. 3647.

[84] See Chapters 7–20 in *Proteinase-Inhibitors* (Eds.: A. J. Barrett, G. Salvesen), (*Res. Monogr. Cell Tissue Physiol.* **1986**, *13*, 301).

[85] a) Review: D. Banner, J. Ackermann, A. Gast, K. Gubernator, P. Hadváry, K. Hilpert, L. Labler, K. Müller, G. Schmid, T. Tschopp, H. van de Waterbeemd, B. Wirz in *Perspectives of Medicinal Chemistry* (Eds.: B. Testa, W. Fuhrer, E. Kyburz, R. Giger), Helvetica Chimica Acta, Basel/VCH, Weinheim, **1993**, p. 27; b) J. Kraut, *Annu. Rev. Biochem.* **1977**, *46*, 331.

[86] D. H. Rich, *Res. Monogr. Cell Tissue Physiol.* **1986**, *12*, 153.

[87] a) D. H. Rich, *Res. Monogr. Cell Tissue Physiol.* **1986**, *12*, 179; b) K. Suguma, E. A. Padlan, C. W. Smith, W. D. Carlson, D. R. Davies, *Proc. Natl. Acad. Sci. USA* **1987**, *84*, 7009; c) T. Hofmann, B. M. Dunn, A. L. Fink, *Biochemistry* **1984**, *23*, 5253; see also S. S. Abdel-Mequid, *Med. Res. Rev.* **1993**, *13*, 731.

[88] D. G. Hangauer, A. F. Monzingo, B. W. Matthews, *Biochemistry* **1984**, *23*, 5730.

[89] I. Schechter, A. Berger, *Biochem. Biophys. Res. Commun.* **1967**, *27*, 157; *ibid.* **1968**, *32*, 898.

[90] Review: D. H. Rich, *Compr. Med. Chem.* **1990**, *2*, 414.

[91] Review: D. H. Rich, *Compr. Med. Chem.* **1990**, *2*, 400.

[92] a) J. Burton, R. J. Cody, Jr., J. A. Herd, E. Haber, *Proc. Natl. Acad. Sci. USA* **1980**, *77*, 5476; b) R. J. Cody, J. Burton, G. Evin, K. Poulson, J. A. Herd, E. Haber, *Biochem. Biophys. Res. Commun.* **1980**, *97*, 230.

[93] P. Raddatz, K.-O. Minck, F. Rippmann, C.-J. Schmitges, *J. Med. Chem.* **1994**, *37*, 486.

[94] a) M. Szelke, D. M. Jones, B. Atrash, A. Hallett, B. J. Leckie, *Pept. Struct. Funct. Proc. Am. Pept. Symp. 8th 1983*, **1983**, 579; b) M. Tree, J. J. Brown, B. J. Leckie, A. F. Lever, P. Manhem, J. J. Morton, J. I. Robertson, M. Szelke, D. Webb, *Biochem. Soc. Trans.* **1984**, *12*, 948.

[95] D. F. Veber, M. G. Bock, S. F. Brady, E. H. Ulm, D. W. Cochran, G. M. Smith, B. I. Lamont, R. M. Di Pardo, M. Poe, R. M. Freidinger, B. E. Evans, J. Boger, *Biochem. Soc. Trans.* **1984**, *12*, 956.

[96] a) H. Umezawa, T. Aoyagi, H. Morishima, M. Hamada, T. Takeuchi, *J. Antibiot.* **1970**, *23*, 259; b) H. Umezawa, *Annu. Rev. Microbiol.* **1982**, *36*, 75.

[97] X. Jeunemaitre, J. Menard, J. Nussberger, T. T. Guyenne, H. R. Brunner, *Am. J. Hypertens.* **1988**, *2*, 819.

[98] a) J.-P. Clozel, W. Fischli, *Arzneim. Forsch.* **1993**, *43*, 260; b) T. Ogihara, J. Higaki, M. Nagano, K. Higashimori, K. Masuo, H. Mikami, *Hypertension* **1992**, *20*, Abstr. P16; c) W. C. Patt, H. W. Hamilton, M. D. Taylor, M. J. Ryan, D. G. Taylor, Jr., C. J. Connolly, A. M. Doherty, S. R. Klutchko, I. Sircar, B. A. Steinbaugh, *J. Med. Chem.* **1992**, *35*, 2562; d) S. F. Martin, R. E. Austin, C. J. Valman, W. R. Baker, S. L. Condon, E. de Lara, S. H. Rosenberg, K. P. Spina, H. H. Stein, J. Cohen, *ibid.* **1992**, *35*, 1710; e) K. M. Verburg, J. S. Polakowski, P. J. Kovar, V. Klinghofer, J. L. Barlow, H. H. Stein, R. A. Manti, A. K. Fung, S. A. Boyd, W. R. Baker, H. D. Kleinert, *J. Cardiovasc. Pharmacol.* **1993**, *21*, 149.

[99] a) S. H. Ferreira, D. C. Bartelt, L. J. Greene, *Biochemistry* **1970**, *9*, 2583; b) M. A. Ondetti, N. J. Williams, E. F. Sabo, J. Pluscec, E. R. Weaver, O. Kocy, *ibid.* **1971**, *10*, 4033.

[100] a) L. D. Byers, R. Wolfenden, *J. Biol. Chem.* **1972**, *247*, 606; b) L. D. Byers, R. Wolfenden, *Biochemistry* **1973**, *12*, 2070.

[101] M. A. Ondetti, B. Rubin, D. W. Cushman, *Science* **1977**, *196*, 441.

[102] a) M. J. Wyvratt, A. A. Patchett, *Med. Res. Rev.* **1985**, *5*, 483; b) A. A. Patchett, E. Harris, E. W. Tristram, M. J. Wyvratt, M. T. Wu, D. Taub, E. R. Peterson, T. J. Ikeler, J. ten Broeke, L. G. Payne, D. L. Ondeyka, E. D. Thorsett, W. J. Greenlee, N. S. Lohr, R. D. Hoffsommer, H. Joshua, W. V. Ruyle, J. W. Rothrock, S. D. Aster, A. L. Maycock, F. M. Robinson, R. Hirschmann, C. S. Sweet, E. H. Ulm, D. M. Gross, T. C. Vassil, C. A. Stone, *Nature (London)* **1980**, *288*, 280.

[103] M. A. Ondetti, D. W. Cushman, *Crit. Rev. Biochem.* **1984**, *16*, 381.

[104] A. A. Patchett, E. H. Cordes, *Adv. Enzymol. Relat. Areas Mol. Biol.* **1985**, *57*, 1.

[105] a) C. H. Hassall, A. Krohn, C. J. Moody, W. A. Thomas, *FEBS Lett.* **1982**, *147*, 175; b) C. H. Hassall, A. Krohn, C. J. Moody, W. A. Thomas, *J. Chem. Soc. Perkin Trans. 1* **1984**, 155.

[106] L. Turbanti, G. Cerbai, C. Di Bugno, R. Giorgi, G. Garzelli, M. Criscuoli, A. R. Renzetti, A. Subissi, G. Bramante, *J. Med. Chem.* **1993**, *36*, 699.

[107] a) D. H. Rich, *Compr. Med. Chem.* **1990**, *2*, 400 (Review); b) M. A. Wyvratt, A. A. Patchett, *Med. Res. Rev.* **1985**, *5*, 483 (Review); c) R. D. Carr, L. Higgs, P. G. Killingback, A. K. Nikoi, S. E. O'Connor, A. Robson, E. Wells, W. T. Simpson, *Br. J. Pharmacol.* **1990**, *100*, 83; d) T. Ando, S. Okada, I. Uchida, K. Hemmi, M. Nishikawa, Y. Tsurumi, A. Fuji, K. Yoshida, M. Okuhara, *J. Antibiot.* **1987**, *40*, 468; e) M. Shirota, H. Inoue, T. Yamamoto, Y. Kajiwara, K. Kitabatake, *Arzneim. Forsch.* **1992**, *42*, 1430; f) S. S. Ghosh, O. Said-Nejad, J. Roestamadji, S. Mobashery, *J. Med. Chem.* **1992**, *35*, 4175.

[108] a) R. A. Wiley, D. H. Rich, *Med. Chem. Rev.* **1993**, *13*, 350; b) A. Hijikata-Okunomiya, S. Okamoto, *Semin. Thromb. Hemostasis* **1992**, *18*, 135; c) J. A. Jakubowski, G. F. Smith, D. J. Sall, *Annu. Rep. Med. Chem.* **1992**, *27*, 99.

[109] a) J. W. Fenton II, *Ann. N. Y. Acad. Sci.* **1981**, *370*, 468; b) F. J. Walker, P. W. Sexton, C. T. Esmon, *Biochem. Biophys. Acta* **1979**, *571*, 333; c) A. Hijikata-Okumoniya, S. Okamoto, *Semin. Thromb. Hemostasis* **1992**, *18*, 135.

[110] a) J. F. Mustard, M. A. Packham, *Phamacol. Rev.* **1970**, *22*, 97; b) D. Gospodarowicz, K. D. Brown, C. R. Birdwell, B. R. Zetter, *J. Cell Biol.* **1978**, *77*, 774.

[111] L. B. Jaques, *Pharmacol. Rev.* **1980**, *31*, 99.

[112] J. Hirsch, *Sem. Thromb. Hemostasis* **1986**, *12*, 1.

[113] a) F. Markwardt, *Biomed. Biochim. Acta* **1985**, *44*, 1007; b) J. M. Maraganore, P. Bourdon, J. Jablonski, K. L. Ramachandran, J. W. Fenton, *Biochemistry* **1990**, *29*, 7095.

[114] J.-Y. Chang, *Biochemistry* **1991**, *30*, 6656.

[115] S. Stone, J. Hofsteenge, *Biochemistry* **1986**, *25*, 4622.

[116] M. D. Talbot, *Sem. Thromb. Hemostasis* **1989**, *15*, 293.

[117] M. D. Talbot, K. D. Butler, *Drugs News Perspect.* **1990**, *3*, 357.

[118] G. Claeson, L. Aurell, *Ann. N. Y. Acad. Sci.* **1981**, *370*, 798.

[119] S. R. Hanson, L. A. Harker, *Proc. Natl. Acad. Sci. USA* **1988**, *85*, 3184.

[120] S. Bajusz, E. Szell, D. Bagdy, E. Barbas, G. Horvath, M. Dioszegi, Z. Zittler, G. Szabo, A. Juhasz, E. Tomori, G. Szilagyi, *J. Med. Chem.* **1990**, *33*, 1729.

[121] a) B. Kaiser, M. Richter, J. Hauptmann, F. Markwardt, *Pharmazie* **1991**, *46*, 128; b) W. Bode, J. Mayr, U. Baumann, R. Huber, S. R. Stone, J. Hofsteenge, *EMBO J.* **1989**, *8*, 3467.

[122] C. Kettner, L. M. Mersinger, R. Knabb, *J. Biol. Chem.* **1990**, *30*, 18289.

[123] a) W. W. Bachovchin, W. Y. Wong, S. Farr-Jones, A. B. Shenvi, C. A. Kettner, *Biochemistry* **1988**, *27*, 7689; b) R. Bone, D. Frank, C. A. Kettner, D. A. Agard, *ibid.* **1989**, *28*, 7600.

[124] a) M. S. Lim, E. R. Johnston, C. A. Kettner, *J. Med. Chem.* **1993**, *36*, 1831; b) R. M. Knabb, C. A. Kettner, P. B. Timmermans, T. M. Reilly, *Thromb. Haemostasis* **1992**, *67*, 56.

[125] a) S. Okamoto, A. Hijikata, R. Kikumoto, S. Tonomura, H. Hara, K. Ninomiya, A. Maruyama, M. Sugano, Y. Tamao, *Biochem. Biophys. Res. Commun.* **1981**, *101*, 440; b) R. Kikumoto, Y. Tamao, T. Tezuka, S. Tonomura, H. Hara, K. Ninomiya, A. Heijikata, S. Okamoto, *Biochemistry* **1984**, *23*, 85; c) M. Heras, J. H. Chesebro, M. W. Webster, J. S. Mruk, D. E. Grill, W. J. Penny, E. J. Bowie, L. Badimon, V. Fuster, *Circulation* **1990**, *82*, 1476; d) M. J. Mellott, T. M. Connolly, S. J. York, L. R. Bush, *Thromb. Haemostasis* **1990**, *64*, 526.

[126] J. Stürzebecher, F. Markwardt, B. Voigt, G. Wagner, P. Walsmann, *Thromb. Res.* **1983**, *29*, 635.

[127] D. W. Banner, P. Hadvary, *J. Biol. Chem.* **1991**, *266*, 20085.

[128] W. Stüber (Behringwerke AG), EP-B 508220, **1992**.

[129] W. Stüber, unpublished, see also ref. [128].

[130] R. T. Shuman, R. B. Rothenberger, C. S. Campbell, G. F. Smith, D. S. Gifford-Moore, P. D. Gesellchen, *J. Med. Chem.* **1993**, *36*, 314.

[131] J. M. Maraganore, P. Bourdon, J. Jablonski, K. L. Ramachandran, J. W. Fenton, *Biochemistry* **1990**, *29*, 7095.

[132] J. DiMaio, B. Gibbs, D. Munn, J. Lefebvre, F. Ni, Y. Konishi, *J. Biol. Chem.* **1990**, *265*, 21698.

[133] J. DiMaio, B. Gibbs, J. Lefebvre, Y. Konishi, D. Munn, S. Y. Yue, *J. Med. Chem.* **1992**, *35*, 3331.

[134] L. Cheng, L. A. Goodwin, M. F. Schully, V. V. Kakkar, G. Claeson, *J. Med. Chem.* **1992**, *35*, 3364.

[135] T. J. Owen, J. L. Krstenansky, M. J. Yates, S. J. Mao, *J. Chem. Chem.* **1988**, *31*, 1009.

[136] W. Bode, D. Turk, J. Stürzebecher, *Eur. J. Biochem.* **1990**, *193*, 175.

[137] a) M. Yanagisawa, H. Kurihara, S Kimura, Y. Tomobe, M. Kobayashi, Y. Mitsui, Y. Yazaki, K. Goto, T. Masaki, *Nature (London)* **1988**, *332*, 411; b) T. J. Opgenoth, J. R. Wu-Wong, K. Shiosaki, *FASEB J.* **1992**, *6*, 2653; c) A. M. Doherty, *J. Med. Chem.* **1992**, *35*, 1493.

[138] L. H. Mortensen, C. M. Pawlowski, N. L. Kanagy, G. D. Fink, *Hypertension* **1990**, *15*, 729.

[139] a) P. Nambi, M. Pullen, L. C. Contino, D. P. Brooks, *Eur. J. Pharmacol.* **1990**, *187*, 113; b) Y. Shibouta, N. Suzuki, A. Shino, H. Matsumoto, Z. J. Terashita, K. Kondo, K. Nishikawa, *Life Sci.* **1990**, *46*, 1611.

[140] a) Y. Matsumura, R. Ikegawa, Y. Suzuki, M. Takaoka, T. Uchida, H. Kido, H. Shinyama, K. Hayashi, M. Watanabe, S. Morimoto, *Life Sci.* **1991**, *49*, 841; b) T. Asano, I. Ikegawa, Y. Suzuki, S.-I. Satoh, M. Shibuya, *Biochem. Biophys. Res. Commun.* **1989**, *159*, 1345.

[141] a) E. G. McMahon, M. A. Palomo, W. M. Moore, J. F. McDonald, M. K. Stern, *Proc. Natl. Acad. Sci. USA* **1991**, *88*, 703; b) T. Fukuroda, K. Noguchi, S. Tsuchida, M. Nishikibe, F. Ikemoto, K. Okada, M. Yano, *Biochem. Biophys. Res. Commun.* **1990**, *172*, 390; c) Y. Tsukahara, Y. Matsumura, K. Kuninobu, T. Kojima, M. Takaoka, S. Morimoto, *Life Sci.* **1993**, *53*, 465; d) E. G. McMahon, M. A. Palomo, M. A. Brown, S. R. Bertenshaw, J. S. Carter, *Am. J. Hypertens.* **1993**, *6*, 667.

[142] a) S. R. Bertenshaw, R. S. Rogers, M. K. Stern, B. H. Norman, W. M. Moore, G. M. Jerome, L. M. Branson, J. F. McDonald, *J. Med. Chem.* **1993**, *36*, 173; b) Review: A. J. Turner, *Biochem. Soc. Trans.* **1993**, *21*, 697.

[143] a) R. Ikegawa, Y. Matsumura, M. Takaoka, S. Morimoto, *Biochem. Biophys. Res. Commun.* **1990**, *167*, 860; b) T. Sawamura, S. Kimura, O. Shinmi, Y. Sugida, M. Kobayashi, Y. Mitsui, M. Yanagisawa, K. Goto, J. Masaki, *ibid.* **1990**, *169*, 1138; c) T. Sawamura, O. Shinmi, N. Kishi, Y. Sugita, M. Yanagisawa, K. Goto, T. Masaki, S. Kimura, *ibid.* **1990**, *172*, 883; d) W. E. Lees, S. Kalinka, J. Meech, S. J. Capper, N. D. Cook, J. Kay, *FEBS Lett.* **1990**, *273*, 99.

[144] K. Shiosaki, A. S. Tasker, G. M. Sullivan, B. K. Sorensen, T. W. von Geldern, J. R. Wu-Wong, C. A. Marselle, T. J. Opgenorth, *J. Med. Chem.* **1993**, *36*, 468.

[145] a) H. Mitsuya, S. Broder, *Proc. Natl. Acad. Sci. USA* **1986**, *83*, 1911; b) H. Mitsuya, S. Broder, *Nature* **1987**, *325*, 773.

[146] a) A. Wlodawer, J. W. Erickson, *Annu. Rev. Biochem.* **1993**, *62*, 543 (review); b) J. W. Erickson, *Perspect. Drug. Discovery Des.* **1993**, *1*, 109 (review); c) J. R. Huff, *J. Med. Chem.* **1991**, *34*, 2305; d) T. D. Meek, *J. Enzyme Inhib.* **1992**, *6*, 65; e) R. M. Williams, *Biomed. Appl. Biotechnol.* **1993**, *1*, 204; f) S. K. Grant, T. D. Meek, B. W. Metcalf, S. R. Pettway, Jr., *ibid.* **1993**, *1*, 349.

[147] a) R. A. Kramer, M. D. Schaber, A. M. Skalka, K. Ganguly, F. Wong-Staal, E. P. Reddy, *Science* **1986**, *231*, 1580; b) N. E. Kohl, E. A. Emini, W. A. Schleif, L. J. Davis, J. C. Heimbach, R. A. Dixon, E. M. Scolnick, I. S. Sigal, *Proc. Natl. Acad. Sci. USA* **1988**, *85*, 4686.

[148] S. J. de Solms, E. A. Giulani, J. P. Guare, J. P. Vacca, W. M. Sanders, S. L. Graham, J. M. Wiggins, P. L. Darke, J. S. Sigal, J. A. Zugay, E. A. Emini, W. A. Schleif, J. C. Quintero, P. S. Anderson, J. R. Huff, *J. Med. Chem.* **1991**, *34*, 2852.

[149] D. R. Rich, C. Q. Sun, J. V. Vara Prasad, A. Pathiasseril, M. V. Toth, G. R. Marshall, M. Clare, R. A. Mueller, K. Houseman, *J. Med. Chem.* **1991**, *34*, 1222.

[150] N. A. Roberts, J. A. Martin, D. Kinchington, A. V. Broadhurst, J. C. Craig, I. B. Duncan, S. A. Galpin, B. K. Handa, J. Kay, A. Krohn, R. W. Lambert,

J. H. Merrett, J. S. Mills, K. E. Parkes, S. Redshaw, A. J. Ritchie, D. L. Taylor, G. J. Thomas, P. J. Machin, *Science* **1990**, *248*, 358.

[151] a) D. J. Kempf, *J. Med. Chem.* **1990**, *33*, 2687; b) A. Wlodawer, M. Miller, M. Jakolski, B. Sathyanaryama, E. Baldwin, I. T. Weber, L. M. Selk, L. Schneider, S. B. Kent, *Science* **1989**, *245*, 616; c) A. M. Navia, P. M. Fitzgerald, B. M. McKeever, C. T. Leu, J. C. Heimbach, W. K. Herber, J. S. Segal, P. L. Darke, *Nature* **1989**, *337*, 615; d) K. L. Yu, W. E. Harte, P. Spinazze, J. C. Martin, M. M. Mansuri, *Bioorg. Med. Chem. Lett.* **1993**, *3*, 535.

[152] R. Bone, J. P. Vacca, P. A. Anderson, M. K. Holloway, *J. Am. Chem. Soc.* **1991**, *113*, 9382.

[153] a) D. Grobelny, E. M. Wondrak, R. E. Galardy, S. Oroszlan, *Biochem. Biophys. Res. Commun.* **1990**, *169*, 1111; b) A. Peyman, K.-H. Budt, J. Spanig, D. Ruppert, *Angew. Chem.* **1993**, *105*, 1852; *Angew. Chem., Int. Ed. Engl.* **1993**, *32*, 1720; c) S. S. Abdel-Meguid, B. Zhao, K. H. M. Murthy, E. Winborne, J. K. Choi, R. L. DesJarlais, M. D. Minnich, J. S. Culp, C. Debouck, *Biochemestry* **1993**, *32*, 7972.

[154] D. H. Rich, J. V. Vara Prasad, C.-Q. Sun, J. Green, R. Mueller, K. Houseman, D. MacKenzie, M. Malkowsky, *J. Med. Chem.* **1992**, *35*, 3803.

[155] A. Spaltenstein, J. L. Leban, E. S. Furfine, *Tetrahedron Lett.* **1993**, *34*, 1457.

[156] A. K. Ghosh, W. J. Thompson, H. Y. Lee, S. P. McKee, P. M. Munson, T. T. Duong, P. L. Darke, J. A. Zugay, E. A. Emini, W. A. Schleif, J. R. Huff, P. S. Anderson, *J. Med. Chem.* **1993**, *36*, 924.

[157] W. J. Thompson, A. K. Ghosh, M. K. Holloway, H. Y. Lee, P. M. Munson, J. E. Schwering, J. Wai, P. L. Darke, J. Zugay, E. A. Emini, W. A. Schleif, J. R. Huff, P. S. Anderson, *J. Am. Chem. Soc.* **1993**, *115*, 801.

[158] A. K. Gosh, W. J. Thompson, S. P. McKee, T. T. Duong, T. A. Lyle, J. C. Chen, P. L. Darke, J. A. Zugay, E. A. Emini, W. A. Schleif, J. R. Huff, P. S. Anderson, *J. Med. Chem.* **1993**, *36*, 292.

[159] H. L. Sham, D. A. Betebenner, C. Zhao, N. E. Wideburg, A. Saldivar, D. J. Kempf, J. J. Plattner, D. W. Norbeck, *J. Chem. Soc. Chem. Cummun.* **1993**, 1052.

[160] T. K. Sawyer, J. F. Fisher, J. B. Hester, C. W. Smith, A. G. Tomasselli, W. G. Tarpley, P. S. Burton, J. O. Hui, T. J. MacQuade, R. A. Conradi, V. S. Bradford, L. Liu, J. H. Kinner, J. Tustin, D. L. Alexander, A. W. Harrison, D. E. Emmert, D. J. Staples, L. L. Maggiora, Y. Z. Zhang, R. A. Poorman, B. M. Dunn, C. Rao, P. E. Scarborough, W. T. Lowther, C. Craik, D. DeCamp, J. Moon, W. J. Howe, R. L. Heinrikson, *Bioorg. Med. Chem. Lett.* **1993**, *3*, 819.

[161] I. S. Thaisrivongs, S. R. Turner, J. W. Strohbach, R. E. Ten Brink, W. G. Tarpley, T. J. McQuade, R. L. Heinrikson, A. G. Tomasselli, J. O. Hui, W. J. Howe, *J. Med. Chem.* **1993**, *36*, 941.

[162] B. P. Roques, M. C. Fournié-Zoluski, *NIDA Res. Monogr.* **1986**, *70*, 128.

[163] a) P. Needleman, S. P. Adams, B. R. Cole, M. G. Currie, D. M. Geller, M. L. Michener, C. B. Saper, D. Schwartz, D. G. Standaert, *Hypertension* **1985**, *7*, 469; b) A. S. Hollister, T. Inagami, *Am. J. Hypertens.* **1991**, *4*, 850; c) H. Ruskoako, *Pharmcol. Rev.* **1992**, *44*, 479.

[164] a) D. B. Northbridge, A. G. Jardine, C. T. Alabaster, J. McConnell, S. G. Dilly, A. G. Lever, *Lancet* **1989**, 8663, 591; b) J. E. O'Connell, A. G. Jardine, G. Davidson, J. M. Connell, *J. Hypertens.* **1992**, *3*, 271.

[165] a) B. P. Roques, M.-C. Fournié-Zaluski, E. Soroca, J. M. Lecompte, B. Malfroy, C. Llorens, J.-C. Schwartz, *Nature* **1980**, *288*, 286; b) C. Llorens, G. Gacel, J.-P. Swerts, R. Perdrisot, M.-C. Zournié-Zaluski, J. C. Schwartz, B. P. Roques, *Biochem. Biophys. Res. Commun.* **1980**, *96*, 1710.

[166] E. J. Sybertz, P. J. Chiu, S. Vemulapalli, B. Pitts, C. J. Foster, R. W. Watkins, A. Barnett, M. F. Haslanger, *J. Pharmacol. Exp. Ther.* **1989**, *250*, 624.

[167] J. Gomez-Monterrey, S. Turcaud, E. Lucas, L. Bruetschy, B. P. Roques, M.-C. Fournié-Zaluski, *J. Med. Chem.* **1993**, *36*, 87.

[168] M. C. Chappell, W. R. Welches, K. B. Brosnihan, C. M. Ferrario, *Peptides* **1992**, *13*, 943.

[169] S. M. Gardiner, P. A. Kemp, T. Bennett, *Br. J. Pharmacol.* **1992**, *106*, 180.

[170] K. James, M. J. Palmer, *Bioorg. Med. Chem. Lett.* **1993**, *3*, 825.

[171] a) P. D. Edwards, P. R. Bernstein, *Med. Res. Rev.* **1994**, *14*, 127; b) R. L. Stein, A. M. Strimpler, P. D. Edwards, J. J. Lewis, R. C. Manger, J. A. Schwartz, M. M. Stein, D. A. Trainor, R. A. Wildonger, M. A. Zottola, *Biochemistry* **1987**, *26*, 2682.

[172] a) J. F. Woessner, Jr. in *Collagenases in Normal and Pathological Tissue* (Eds.: D. E. Wooley, J. J. Evanson), Wiley, Chichester, **1980**, p. 223; b) B. Beszant, J. Bird, L. M. Gaster, G. P. Harper, I. Hughes, E. H. Karran, R. E. Markwell, A. J. Miles-Williams, S. A. Smith, *J. Med. Chem.* **1993**, *36*, 4030; c) J. Bird, R. C. DeMello, G. P. Harper, D. J. Hunter, E. H. Karran, R. E. Markwell, A. J. Miles-Williams, S. S. Rahman, R. W. Ward, *ibid.* **1994**, *37*, 158.

[173] a) G. Fischer, B. Wittmann-Liebold, K. Lang, T. Kiefhaber, F. X. Schmid, *Nature* **1989**, *337*, 476; b) E. R. Schoenbrunner, S. Mayer, M. Tropschug, G. Fischer, N. Takahashi, F. X. Schmid, *J. Biol. Chem.* **1991**, *266*, 3630; G. Fischer, *Angew. Chem.* **1994**, *106*, 1479; *Angew. Chem. Int. Ed. Engl.* **1994**, *33*, 1415; c) D. K. Donald, M. E. Cooper, M. Furber, E. Wells, R. Hutchinson, F. M. Black, *Tetrahedron Lett.* **1991**, *32*, 1375; d) B. E. Bierer, P. K. Somers, T. J. Wandless, S. J. Burakoff, S. L. Schreiber, *Science* **1990**, *250*, 556.

[174] a) R. Ando, Y. Morinaka, H. Tokuyama, M. Isaka, E. Nakamura, *J. Am. Chem. Soc.* **1993**, *115*, 1174; b) T. Murachi, *Trends Biochem. Sci.* **1983**, *8*, 295; c) A. J. Barrett, J. K. McDonald, *Mammalian Proteinases: A Glossary and Bibliography, Vol. 1*, Endopeptidases, Academic Press, New York, **1980**.

[175] S. Doulut, I. Dubuc, M. Rodriguez, F. Vecchini, H. Fulcrand, H. Barelli, F. Checker, E. Bourdel, A. Aumelas, J. C. Lallement, P. Kitabgi, J. Costentin, J. Martinez, *J. Med. Chem.* **1993**, *36*, 1369.

[176] G. L. James, J. L. Goldstein, M. S. Brown, T. E. Rawson, T. C. Somers, R. S. McDowell, C. W. Crowley, B. K. Lucas, A. D. Levinson, J. C. Marsters, Jr., *Science* **1993**, *260*, 1937.

[177] a) S. L. Graham, S. J. deSolms, E. A. Giuliani, N. E. Kohl, S. D. Mosser, A. I. Oliff, D. L. Pompliano, E. Rands, M. J. Breslin, A. A. Deana, V. M. Garsky, T. H. Scholz, J. B. Gibbs, R. L. Smith, *J. Med. Chem.* **1994**, *37*, 725; b) N. E. Kohl, S. D. Mosser, S. J. de Solms, E. A. Giuliani, D. L. Pompliano, S. L. Graham, R. L. Smith, E. M. Scolnick, A. Oliff, J. B. Gibbs, *Science* **1993**, *260*, 1934; c) see also A. M. Garcia, C. Rowell, K. Ackermann, J. J. Kowalcyk, M. D. Lewis, *J. Biol. Chem.* **1993**, *268*, 18415.

[178] a) B. M. Willumsen, K. Norris, A. G. Papageorge, N. L. Hubbert, D. R. Lowy, *EMBO J.* **1984**, *3*, 2581; b) J. F. Hancock, A. J. Magee, J. E. Childs, C. J. Marshall, *Cell* **1989**, *57*, 1167; c) J. B. Gibbs, D. L. Pompliano, S. D. Mosser, E. Rands, R. B. Lingham, S. B. Singh, E. M. Scolnick, N. E. Kohl, A. Oliff, *J. Biol. Chem.* **1993**, *268*, 7617.

[179] a) D. L. Pompliano, E. Rands, M. D. Schaber, S. D. Mosser, N. J. Anthony, J. B. Gibbs, *Biochemistry* **1992**, *31*, 3800.

[180] a) J. L. Goldstein, M. S. Brown, S. J. Stradley, Y. Reiss, L. M. Gierasch, *J. Biol. Chem.* **1991**, *266*, 15575; b) M. S. Brown, J. L. Goldstein, K. J. Paris, J. P. Burnier, J. C. Masters, Jr., *Proc. Natl. Acad. Sci. USA* **1992**, *89*, 8313.

[181] D. H. Rich in *Perspectives in Medicinal Chemistry* (Eds.: B. Testa, W. Fuhrer, E. Kyburz, R. Giger), Helvetica Chimica Acta, Basel/VCH, Weinheim, **1993**, p. 15; see also ref. [2a], p. 268.

[182] C. Tanford, *The Hydrophobic Effect: Formation of Micelles and Biological Membranes*, Wiley-Interscience, New York, **1980**.

[183] a) M. Kock, H. Kessler, D. Seebach, A. Thaler, *J. Am. Chem. Soc.* **1992**, *114*, 2676; b) D. Altschuh, O. Vix, B. Rees, J.-C. Thierry, *Science* **1992**, *256*, 92.

[184] a) J. B. Moon, J. Howe, *Proteins: Struct. Funct. Genet.* **1991**, *11*, 314; b) P. A. Bartlett, G. T. Shea, S. T. Telfer, S. Waterman in *Molecular Recognition: Chemical and Biochemical Problems* (Ed.: S. M. Roberts), Royal Society, London, **1989**, p. 182.

[185] S. R. Wilson, W. K. Tam, M. J. Di Grandi, W. Cui, *Tetrahedron* **1993**, *49*, 3655.

[186] **Addendum**: Many publications on the topics in this review have appeared since the submission of this manuscript. A selection (up to April 1994) are listed here.

Structure: a) M. Quibell, W. G. Turnell, T. Johnson, *J. Chem. Soc. Perkin Trans. 1* **1993**, 2843; b) J. A. Robl, M. P. Cimarusti, *Tetrahedron Lett.* **1994**, *35*, 1393; c) N. K. Harn, S. J. Cripps, G. M. Rishton, *ibid.* **1994**, *35*, 1389; d) E. Graf von Roedern, H. Kessler, *Angew. Chem.* **1994**, *106*, 684; *Angew. Chem. Int. Ed. Engl.* **1994**, *33*, 687; e) J. A. Robl, M. P. Cimarusti, L. M. Simpkins, H. N. Weller, Y. Y. Pan, M. Malley, J. D. DiMarco, *J. Am. Chem. Soc.* **1994**, *116*, 2348; f) K. Burgess, K.-K. Ho, *ibid.* **1994**, *116*, 799; g) P. P. Mager, *Med. Res. Rev.* **1994**, *14*, 75 (review); h) C. Aleman, J. J. Perez, *Int. J. Pept. Protein Res.* **1994**, *43*, 258; i) M. Marraud, V. Dupont, V. Grand, S. Zerkout, A. Lecoq, G. Boussard, J. Vidal, A. Collet, A. Aubry, *Biopolymers* **1993**, *33*, 1135.

ACE/NEP inhibition: a) J. L. Stanton, D. M. Sperbeck, A. J. Trapani, D. Cote, Y. Sakane, C. J. Berry, R. D. Ghai, *J. Med. Chem.* **1993**, *36*, 3829; b) G. A. Flynn, D. W. Beight, S. Mehdi, J. R. Koehl, E. L. Giroux, J. F. F. French, P. W. Hake, R. C. Dage, *ibid.* **1993**, *36*, 2420; c) A. Patel, H. J. Smith, R. D. E. Sewell, *Prog. Med. Chem.* **1993**, *30*, 328; d) S. DeLombaert, M. D. Erion, J. Tan, L. Blanchard, L. El-Chehabi, R. D. Ghai, Y. Sakane, C. Berry, A. J. Trapani, *J. Med. Chem.* **1994**, *37*, 498; e) J. L. Stanton, G. M. Ksander, R. deJesus, D. M. Sperbeck, *Bioorg. Med. Chem. Lett.* **1994**, *4*, 539; f) J. French, G. A. Flynn, E. L. Giroux, S. Mehdi, B. Anderson, D. C. Beach, J. R. Koehl, R. C. Dage, *J. Pharmacol. Exp. Ther.* **1994**, *268*, 180; g) M.-C. Fournié-Zaluski, P. Coric, S. Tucaud, N. Rousselet, W. Gonzalez, B. Barbe, I. Pham, N. Jullian, J.-B. Michel, B. P. Roques, *J. Med. Chem.* **1994**, *37*, 1070.

Inhibition of aspartyl proteases: a) S. S. Abdel-Meguid, *Med. Res. Rev.* **1993**, *13*, 731 (review).

Inhibition of HIV-1 protease: a) H. L. Sham, D. A. Betebenner, C. Zhao, N. E. Wideburg, A. Saldivar, D. J. Kempf, J. J. Plattner, D. W. Norbeck, *J. Chem. Soc. Chem. Commun.* **1993**, *13*, 1052; b) D. S. Holmes, I. R. Clemens, K. N. Cobley, D. C. Humber, J. Kitchin, D. C. Orr, P. Binakumari, I. L. Paternoster, R. Storer, *Bioorg. Med. Chem. Lett.* **1993**, *3*, 503; c) K. T. Chong, M. J. Ruwart, R. R. Hinshaw, K. F. Wilkinson, B. D. Rush, M. F. Yancey, J. W. Strohbach, S. Thaisrivongs, *J. Med. Chem.* **1993**, *36*, 2575; d) D. S. Holmes, R. C. Bethell, N. Cammack, I. R. Clemens, J. Kitchin, P. McMeekin, C. L. Mo, D. C. Orr, B. Patel, *ibid.* **1993**, *36*, 3129; e) A. Wonacott, R. Cooke, F. R. Hayes, M. M. Hann, H. Jhoti, P. McMeekin, A. Mistry, P. Murray-Rust, O. M. P. Singh, M. P. Weir, *ibid.* **1993**, *36*, 3113; f) M. Vaillancourt, B. Vanasse, E. Cohen, G. Sauve, *Bioorg. Med. Chem. Lett.* **1993**, *3*, 1169; g) K. A. Newlander, J. F. Callahan, M. L. Moore, T. A. Tomaszek, Jr., W. F. Huffman, *J. Med. Chem.* **1993**, *36*, 2321; h) H. L. Sham, D. A. Betebenner, N. Wideburg, A. C. Saldivar, W. E. Kohlbrenner, A. Craig-Kennard, S. Vasavanonda, D. J. Kempf, J. J. Clement, *FEBS Lett.* **1993**, *329* (1, 2), 144; i) A. K. Ghosh, W. J. Thompson, M. K. Holloway, S. P. McKee, T. T. Duong,

H. Y. Lee, P. M. Munson, A. M. Smith, J. M. Wai, *J. Med. Chem.* **1993**, *36*, 2300; j) A. Kiriyama, T. Mimoto, S. Kisanuki, Y. Kiso, K. Takada, *Biopharm. Drug Dispos.* **1993**, *14*, 697; k) M. T. Konieczny, P. H. Toma, M. Cushman, *J. Org. Chem.* **1993**, *58*, 4619; l) W. R. Baker, J. K. Pratt, *Tetrahedron* **1993**, *49*, 8739; m) D. C. Humber, M. J. Bamford, R. C. Bethell, N. Cammack, K. Cobley, D. N. Evans, N. M. Gray, M. M. Hann, D. C. Orr, J. Saunders, B. E. V. Shenoy, R. Storer, G. G. Weingarten, P. G. Wyatt, *J. Med. Chem.* **1993**, *36*, 3120; n) A. B. Smith, R. Hirschmann, A. Pasternak, R. Akaishi, M. C. Guzman, D. R. Jones, T. P. Keenan, A. P. Sprengeler, P. L. Darke, *ibid.* **1994**, *37*, 215; o) S. Y. S. Cho, L. N. Jungheim, A. J. Baxter, *Bioorg. Med. Chem. Lett.* **1994**, *4*, 715; p) R. E. Babine, N. Zhang, S. R. Schow, Z. Xu, R. A. Byrn, R. C. Hastings, M. F. Semmelhack, M. M. Wick, S. S. Kerwar, *ibid.* **1994**, *4*, 583; q) J. P. Vacca, P. M. D. Fitzgerald, M. K. Holloway, R. W. Hungate, K. E. Starbuck, L. J. Chen, P. L. Darke, P. S. Anderson, J. R. Huff, *ibid.* **1994**, *4*, 449; r) M. V. Hosur, T. N. Bhat, D. J. Kempf, E. T. Baldwin, B. Liu, S. Gulnik, N. E. Widebug, D. W. Norbeck, K. Appelt, J. W. Erickson, *J. Am. Chem. Soc.* **1994**, *116*, 847; s) B. Kammermeier, G. Beck, D. Jacobi, H. Jendralla, *Angew. Chem.* **1994**, *106*, 719; *Angew. Chem. Int. Ed. Engl.* **1994**, *33*, 685; t) A. B. Smith III, R. Hirschmann, A. Pasternak, R. Akaishi, M. C. Guzman, D. R. Jones, T. P. Keenan, P. A. Sprengeler, *J. Med. Chem.* **1994**, *37*, 215.

Thrombin inhibition: S. Okamoto, A. Hijikata-Okunomiya, *Methods Enzymol.* **1993**, *222*, 238 (review); b) S. R. Stone, J. M. Maraganore, *ibid.* **1993**, *223*, 312 (review); c) C. Tapparelli, R. Metternich, C. Ehrhardt, N. S. Cook, *Trends Pharmacol. Sci.* **1993**, *14*, 366 (Review); d) C. Thurieau, S. Simonet, J. Paladino, J.-F. Prost, T. Verbeuren, J.-L. Fauchère, *J. Med. Chem.* **1994**, *37*, 625; e) J. Oleksyszyn, B. Boduszek, C.-M. Kam, J. C. Powers, *ibid.* **1994**, *37*, 226.

A stop-gap solution?



If the latest library copy of Angewandte spends more time off the shelf than on, stop the gap with a personal subscription.

Just call or fax

VCH

USA: Tel. 1-(800) 422-8824; Fax (305) 428-8201
UK: Tel. (0223) 321111, Fax (0223) 313221

Mills–Nixon Effect: Wherefore Art Thou?

Jay S. Siegel*

The structural chemistry conundrum known as the Mills–Nixon effect is a progeny of the empirical successes of van't Hoff and Kekulé. The proposed effect states that small ring annelation onto benzene would induce significant bond length alternation within the benzene nucleus;[1] a reasonable postulate if benzene existed as an equilibrium mixture of Kekulean valence tautomers. Indeed, at the time of the conception of the Mills–Nixon hypothesis, the details of benzene's structure as resonance hybrid or tautomeric equilibrium were still in debate. Although the debate has been essentially resolved in favor of a single D_{6h} benzene,[2] the remnants of predictions based on the antiquated equilibrating model linger as a provocative postulate without structural experimental backing. Recent advances in organic structural chemistry are bringing the geometric aspects of this problem to a close. It is instructive, however, to follow this "garden path" from its beginnings.

The work of the Palermo school in general and Koerner's study of the isomers of halogenated benzenes in particular spawned a dichotomy in the conceptualization of molecular structure that discriminated between static and dynamic (permutation) symmetry.[3] In order to account for Koerner's observations, a high symmetry structure for benzene appeared to be necessary, and many chemist's searched for this in the form of a single ideal valence structure.[4] Kekulé's original structure failed Koerner's test in that two *ortho*-chlorobenzenes were predicted.[5] however, its salvation materialized in the idea of a time-averaged structural equilibration which Kekulé called the oscillation theory.[6] In this proposal, the structure of benzene had alternate double and single bonds in a D_{3h} structure that was in equilibrium with another equivalent structure, where the double and single bonds had traded places. Kekulé demonstrated that the oscillation of the bonds exchanged the identity of the two *ortho*-dichlorobenzene isomers and thus created a dynamic permutational symmetry. This idea of a dynamic structure for benzene was considered ludicrous by the community and was heartily ridiculed by "Findig" in 1886.[7] Nonetheless, Kekulé's proposal marks the beginning of the problem of single versus double energy minima in structural chemistry.[8]

In 1887, van't Hoff's "Dix Années dans l'Histoire d'une Theorie" expanded upon and generalized his 1874 observations that carbon should have four valences radiating toward the corners of a regular tetrahedron.[9] From this spatial imperative, he formulated a tetrahedral theory for carbon–carbon bonding where the number of juxtaposed vertices represented the order of the bond: point–point (single); edge–edge (double); face–face (triple). Due to the great success of the model in predicting the isomers of saturated and unsaturated compounds, van't Hoff's tetrahedra were applied to gauge the structural details of the Kekulé forms of benzene. Each valence structure was viewed as three (van't Hoff) double bonds grouped to form a six-atom ring. Each double bond comprised two regular tetrahedra connected edge to edge; the terminal angle having a magnitude of 109.5° as dictated by the tetrahedral elements. Thus, the Kekulé forms possessed alternating bond lengths and external angles α and β of about 110 and 125°, respectively (Fig. 1).

Even with the backing of the highly successful tetrahedral theory, Kekulé's proposal was considered to have received "a death-blow" in 1888.[10] Despite this premature epitaph, the germ of Kekulé's oscillating benzene structure remained fertile, and the advent of the concept of tautomerism gave his idea new life.[11] It reappeared in the work of Reddelien in 1915, when he suggested that it should be experimentally possible to test for the two forms, and indicated that the action of ozone on benzene might serve this purpose.[12] Indeed, in 1932, Levine and Cole ozonolyzed *o*-xylene and found glyoxal, methylglyoxal, and dimethylglyoxal as products.[13] No single Kekulé form could give rise to this mixture and therefore they concluded that the single isomer of *o*-xylene was actually a rapidly equilibrating mixture of the two Kekulé forms, each susceptible to attack by ozone.

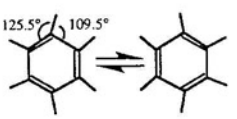


Fig. 1. Kekulé's view of the oscillating structure of benzene; quantitative structural aspects were derived from the tetrahedral construction of van't Hoff. This is the model accepted by chemists circa 1930 and upon which Mills and Nixon made their postulate.

The concept of the rapidly equilibrating Kekulé forms also captured the imagination of Mills and Nixon in 1930.[1] They proposed a structure perturbation approach to test for the oscillation hypothesis. Given that there really were two distinct forms of benzene and two distinct external angles α and β, then controlled annelation should favor either α or β as the angle within the annelation and therefore "freeze-out" one Kekulé form. The "ideal" angle α of 109.5° matched well with that of the 108° angle of a five-membered ring; therefore, indan and tetralin became the chosen test structures. Lacking the necessary structural tools to observe the actual bond alternation in the isomer, they pursued the regioselective reactivity of hydroxyindan and tetralin.

[*] Prof. Dr. J. S. Siegel
Department of Chemistry, University of California
San Diego, La Jolla, CA 92093-0358 (USA)
Telefax: Int. code + (619) 534-5838

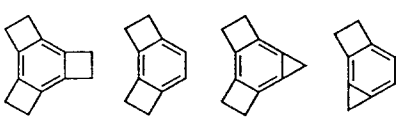
 © VCH Verlagsgesellschaft mbH, D-69451 Weinheim, 1994 0570-0833/94/1717-1721 $ 10.00+.25/0

During the years immediately following Mills and Nixon's article, Pauling published his seminal works on the Nature of the Chemical Bond and the concept of resonance.[14] Shortly after his work on resonance, Pauling and L. E. Sutton addressed the possible structural ramifications of ring annelations a la Mills and Nixon.[15] Unlike Mills and Nixon's view of benzene as a tautomeric equilibrium, Pauling's resonance hybrid ideas depicted benzene as a single symmetrical form, not a time average between two Kekulé forms.[16] Sutton and Pauling concluded that the stabilization due to resonance was so great as to be only slightly perturbed by any annelations. Nonetheless, they admitted that the energy differences necessary to account for the observed selectivity would not mandate experimentally detectable changes in goemetrical structure. Coulson and Longuet-Higgins also investigated the Mills–Nixon effect and concluded that it would be at best small, but in the opposite direction (a "reversed" Mills–Nixon effect).[25]

The ensuing 60-year period has been replete with computational and experimental investigations of the Mills–Nixon proposal, however, none of these studies has been conclusive and often they arrive at divergent conclusions.[17] Recently, tricyclobutabenzene (**1**) has emerged as the "touchstone" for evaluating the structural aspects of the Mills–Nixon effect, and finally the result of ab initio HF/6-31G(D) calculations and density functional theory (DFT) and experiment (low-temperature high-accuracy X-ray crystallography) have converged harmoniously.

Three groups collaborating among Berkeley, Essen, and Rice[18] have crystallographically confirmed computational predictions first made specifically by Stanger (3-21G)[19] and later more generally by Baldridge and Siegel (6-31G(D))[20] that **1** adheres more closely to the Pauling model than the Longuet-Higgins model, or more importantly that "benzene, even if distorted in the σ-plane, simply wants to remain 'aromatic'." The Berkeley and Rice groups (W. E. Billups, M. M. Haley, D. L. Mohler, and K. P. C. Vollhardt) prepared four highly strained annelated benzenes and determined their structures crystallographically in a collaboration with R. Boese, D. Bläser, and A. H. Maulitz in Essen, Germany. The crystals of **1** were grown, using Boese's exceptionally elegant sublimation technique, from material prepared by the method of Randy P. Thummel (University of Houston).[21]

All four of the structures determined by Boese's team (**1**–**4**) show characteristic features of small strained rings, such as elec-

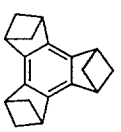


1 **2** **3** **4**

tron density deformations consistent with "bent bonds."[22] *In no case is any appreciable bond alternation observed*; specifically, the bond lengths in the central ring of **1** are 1.40 and 1.38 Å as compared to 1.50 and 1.33 Å for a standard C_{sp^2}–C_{sp^2} single and double bond, respectively.[23] Additional ab initio computations by these researchers corroborated the crystallographic findings.

The elegant work of these three research groups conclusively brings to a close an important chapter of the Mills–Nixon story, with Pauling's predictions surfacing as quite general among simple annelated benzenes. Questions still remain, however, about the feasibility of inducing bond alternation purely through sigma strain.

In contrast to the present experimental data, Stanger demonstrated that computations on an artificially constrained benzene structure with the C-C-H angles crimped to 90° yield a central ring with a bond length alternant geometry (1.52 and 1.33 Å).[19] Empirically, strain induced by bicyclic annelations gives rise to anomalous effects (e.g. the bicyclic effect proposed by Lehn for pyramidal inversion at nitrogen). Structural predictions by ab initio calculations (HF/6-31G(D) and DFT) on bicyclic annelated benzenes point to a new class of strained benzenoids, for example **5**, with significant bond length alternation (0.06–0.1 Å).[20] Experimental investigations on this series of structures related to **5** will either finally uncover a Mills–Nixon distorted benzene or identify a serious shortcoming of split-valence level HF theory for the prediction of strained hydrocarbon structure.



5

In hindsight, one can discuss the Mills–Nixon effect from the point of view of how a given perturbation will alter the average structure of a species described by a double-well versus, a single-well potential. The isotopic perturbation work of Saunders et al. most clearly illustrates this principle.[24] The average position in a double-well structure is defined by the relative population of the two wells. A small energy change in either well leads to a large change in population and therefore a large shift in the average structure, in other words double-well equilibria should be quite sensitive to small perturbations. The average position in a single-well potential, however, is related to the anharmonicity of the well, which is normally less sensitive to such perturbations. This simple hindsight can not fully explain why such draconian perturbations lead to such minor effects on the delocalized structure of benzene, but it definitely illuminates to the modern chemist the origins of this anachronistic structural proposal called the Mills–Nixon effect.

German version: *Angew. Chem.* **1994**, *106*, 1808

[1] W. H. Mills, I. G. Nixon, *J. Chem. Soc.* **1930**, 2510.

[2] Concerns about closing this debate prematurely have been raised as late as 1987, but the preponderance of evidence clearly favors the D_{6h} structure, see: a) O. Ermer, *Angew. Chem.* **1987**, *99*; 791–793; *Angew. Chem. Int. Ed. Engl.* **1987**, *26*, 782–784; b) M. Oldani, R. Widmer, G. Grassi, A. Bauder, *J. Mol. Struct.* **1988**, *190*, 31.

[3] Here I generalize to the Palermo school because the work of Paternó in 1868 on halogenated ethanes preceded van't Hoff. Though Paternó neglected chirality per se, he was inspired to postulate the tetrahedral carbon atom but not the dynamic conformational averaging of free rotation to account for the number of isomers, see: E. Paternò, *Gior. Sci. Nat. Econ. (Palermo)* **1869**, *5*, 117 (cited in E. Paternò, *Gazz. Chim. Ital.* **1893**, *23*, 35).

[4] For a superb discussion of Koerner's proof see: J. M. McBride, *J. Am. Chem. Soc.* **1980**, *102*, 4134–4137.

[5] F. A. Kekulé, *Justus Liebigs Ann. Chem.* **1866**, *137*, 158.

[6] F. A. Kekulé, *Justus Liebigs Ann. Chem.* **1872**, *162*, 77.

[7] A humorous account of this is presented in E. Heilbronner, J. D. Dunitz, *Reflections on Symmetry in Chemistry ... and Elsewhere*, VHCA and VCH, Basel and Weinheim, **1993**, chap. VI.

[8] The historical impact of this proposal can been seen in the comments of Arndt in 1924: Kekule's idea of the oscillating double bonds in benzene was the closest approximation to the resonance interpretation of benzene ... up to 1924, and Longuet-Higgins in 1957: The revolutionary nature of Kekule's descrip-

tion of benzene consisted in his recognition that the second half of the double bond, unlike the single bond, is a nomadic entity which cannot always be assigned a unique position in the molecule. ... The electronic theory of valency ... shed a flood of light on structural chemistry and revealed the fundamental distinction between localized and non-localized electrons. a) C. A. Russell, *The History of Valency*, Humanities, New York, **1971**; b) F. G. Arndt, in a letter see: E. Campaigne, *J. Chem. Educ.* **1959**, *36*, 336; c) H. C. Longuet-Higgens, *Proc. Chem. Soc.*, London, **1957**, 157.
[9] J. H. van't Hoff, *Dix Années dans l'Histoire d'une Théorie*, P. M. Bazebdijk, Rotterdam, **1887**; *Chemistry in Space*, Clarendon, Oxford, **1891**.
[10] J. E. Marsh, *Philos. Mag.* **1888**, *26*, 426.
[11] See: L. Pauling, *Nature of the Chemical Bond*, 3rd ed., Cornell University Press, Ithaca, NY, **1964**, chap. 14.
[12] G. Reddelien, *J. Prakt. Chem.* **1915**, 213.
[13] a) A. A. Levine, A. G. Cole, *J. Am. Chem. Soc.* **1932**, *54*, 338; b) similar results were later published, see: J. P. Wibaut, P. W. Haayman, *Science* **1941**, *94*, 49.
[14] a) L. Pauling, *J. Am. Chem. Soc.* **1931**, 1367; b) L. Pauling, *ibid.* **1932**, *54*, 988; c) L. Pauling, G. W. Wheland, *J. Chem. Phys.* **1933**, *1*, 362.
[15] L. E. Sutton, L. Pauling, *Trans. Faraday Soc.* **1935**, *31*, 939.
[16] This distinction of single versus double minima is clearly stated by Sutton and Pauling. "It appears very definitely that benzene is a single molecular species and ... we can say that it is a hybrid of the two Kekulé structures ... and that the angles between pairs of external valencies are all 60°. ... Our procedure here is different from that of Mills and Nixon, for they assumed that the molecule had either structure I or structure II, whereas we consider that initially it has the symmetrical resonating structure and then calculate how much it is distorted when a ring is attached."
[17] N. Frank, J. S. Siegel, unpublished.
[18] R. Boese, D. Bläser, W. E. Billups, M. M. Haley, A. H. Maulitz, D. L. Mohler, K. P. C. Vollhardt, *Angew. Chem.* **1994**, *106*, 321–325; *Angew. Chem. Int. Ed. Engl.* **1994**, *33*, 313–17.
[19] A. Stanger, *J. Am. Chem. Soc.* **1991**, *113*, 8277.
[20] K. K. Baldridge, J. S. Siegel, *J. Am. Chem. Soc.* **1992**, *114*, 9583.
[21] W. Natakul, R. P. Thummel, A. D. Taggart, *J. Am. Chem. Soc.* **1979**, *101*, 770.
[22] a) R. Neidlein, D. Christen, V. Poignée, R. Boese, D. Bläser, A. Gieren, C. Ruiz-Pérez, T. Hübner, *Angew. Chem.* **1988**, *100*, 292–293; *Angew. Chem. Int. Ed. Engl.* **1988**, *27*, 294–295; b) R. Boese, D. Bläser, *ibid.* **1988**, *100*, 293–295 and **1988**, *27*, 304–305.
[23] In this regard, perfluoro-**1** serves as a good model for these strained monocyclic annelated benzenes in general, see: R. P. Thummel, J. D. Korp, I. Bernal, R. L. Harlow, R. L. Soulen, *J. Am. Chem. Soc.* **1977**, *99*, 6916.
[24] M. Saunders, M. R. Kates, *J. Am. Chem. Soc.* **1980**, *102*, 6867.
[25] H. C. Longuet-Higgins, C. A. Coulson, *Trans. Faraday Soc.* **1946**, *42*, 746.

Detection and Imaging of Single Molecules by Optical Near-Field Microscopy

Thomas Basché

„... we never experiment with just one electron or atom or molecule. In thought experiments we sometimes assume we do; this invariably entails ridiculous consequences."
Erwin Schrödinger, 1952

The successful storage and spectroscopic characterization of individual atoms in electromagnetic traps and the development of microscopic techniques with atomic resolution such as scanning tunneling microscopy (STM) and atomic force microscopy (AFM) are two examples that make us realize that Schrödinger's notion has been outpaced by reality. One should, however, bear in mind that the observation of single particles, as commonplace as it may seem today, has only become possible within the past 10–15 years, regardless of the technique. This Highlight deals with new developments in the field of optical detection of single molecules; other methods of detection are not covered.

The first optical detection of a single molecule in the condensed phase was achieved in 1989 with the spectroscopic characterization of an individual pentacene molecule in an organic mixed crystal at low temperatures (T = 1.5 K).[1] Not much later, and independent of the research on solids, efforts to detect individual dye molecules in a liquid were successful.[2]

A single molecule in a solid at low temperature is a very sensitive spectroscopic probe for the properties of its local environment, owing to its extremely narrow optical linewidth. In contrast, for single-molecule detection (SMD) in liquids or, more general, for all techniques that can be performed at room temperature, analytical aspects are as important as the measurement of spectroscopic details. SMD represents the ultimate limit in chemical trace analysis and has been proposed as a realistic method for sequencing the DNA of the human genome within a reasonable period of time. In molecular biology the detection of single fluorescence-labeled species (proteins, viruses) is a foreseeable and increasingly important development.

Optical spectroscopy of single molecules has already given rise to a host of new experimental results, including the development of techniques for the optical characterization of individual molecules with ever increasing sensitivity. Ultrasensitive fluorescence detection is ideally suited for the optical observation of single molecules. The experimental challenge here lies in the discrimination of the weak fluorescence of a single molecule from the matrix background light (Rayleigh and Raman scattering, matrix luminescence). Since the signal of the molecule is proportional to the intensity of the incident radiation (power/area), and since the background light and the concomitant background noise level increase with the power, enhanced sensitivity is achieved by decreasing the area of illumination. Consequently, tight focusing of the exciting laser light is essential. Focusing with lenses, however, invariably involves the fundamental Abbe diffraction limit to resolution, which states that foci of dimensions less than the wavelength of the light used are not possible. Fortunately, the method of near-field scanning optical microscopy (NSOM) developed during the last few years

[*] Dr. T. Basché
Institut für Physikalische Chemie der Universität
Sophienstrasse 11, D-80333 München (FRG)
Telefax: Int. code + (89) 590-2602

 © VCH Verlagsgesellschaft mbH, D-69451 Weinheim, 1994 0570-0833/94/1717-1723 $ 10.00+.25/0

circumvents this limit and is therefore ideally suited for fluorescence detection of single molecules. Recently, using this new microscopic technique, Betzig et al.[3] and Ambrose et al.[4] independently succeeded in imaging individual dye molecules on the surface of a substrate at room temperature. Before these experiments are described, let us first look at the principles and potential applications of near-field optical microscopy.

Conventional optical microscopy has a limited resolution of about $\lambda/2$ of the optical wavelength employed. This theoretical resolution limit is a consequence of diffraction effects due to the wave characteristics of light; for green light under ideal conditions this limit is roughly 0.3 μm, and with good optical microscopes it can in fact be reached. (However, even in confocal microscopy resolution better than $\lambda/2$ can be achieved using special "tricks".) When light is passed through a small aperture, whose diameter is less than the wavelength, the dimensions of the light beam at a distance close to the aperture are nearly unchanged. This area is called the optical near field. Such an aperture can be scanned raster fashion across the surface of a close-lying object. Many recorded points can then be combined to reconstruct an image of the surface. The resolution of this microscopy is not limited by the wavelength of light, but only by the size of the aperture and its distance from the object.

Near-field microscopy in the visible regime was first demonstrated independently by Pohl et al.[5] and Lewis et al.[6] Since then, several optical near-field probes have been developed. In most cases the light is directed from the light source to the aperture by a some sort of wave guide. To collect images quickly and with a good signal-to-noise ratio, it is of special importance to pass as much light as possible through the miniscule aperture. To this end, the tips of tapered optical fibers and micropipettes with dimensions on the order of 10 nanometers turned out to be ideal apertures. Other aperture geometries have also been proposed and were recently successfully employed, for example, a partially metal-coated tetrahedral tip.[7] The aperture can also be used to collect light from the object and to scatter evanescent waves from the near field into propagating modes of the optical wave-guide.

We will next describe a schematic setup of a near-field microscope in the so-called illumination (or transmission) mode (Fig. 1). Here the tip of a tapered optical fiber is used as an aperture and scanned raster fashion across the object of interest. The light is coupled into the fiber through an objective. The fiber tapers from the original fiber diameter to a tip having a flat face perpendicular to the fiber axis. The tip is produced by simultaneously heating the fiber with a CO_2 laser and pulling the ends apart. This process leads to apertures from 20 to 500 nm with high reproducibility. Finally, the tip is vapor-coated with a metal film (Al) to prevent the light from leaking out at the sides. The sample is placed within about 10 nm of the fiber tip and is moved in the x,y direction with a piezoelectric transducer. The signal is detected at each point, and the image is generated pixel by pixel. During the scan the distance between the fiber tip and the object must be kept constant by using an active feedback mechanism. An elegant approach to this is shear force feedback detection (not included in Fig. 1), in which the fiber tip is excited at one of its a high-quality mechanical resonance frequencies. The damping of the vibration as the object approaches the tip is then recorded as a distance-dependent

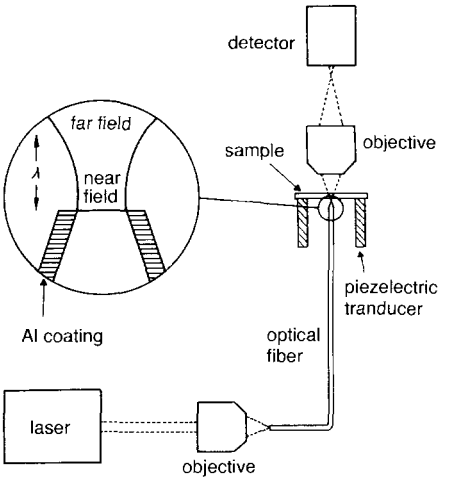


Fig. 1. Schematic setup of a scanning near-field microscope. The inset (middle left) shows the fiber tip with the near-field and far-field regions. For details see text.

signal. A lateral resolution (x,y) of about 12 nm (or $\lambda/43$) could be demonstrated with a setup similar to that shown in Figure 1.[8]

The best resolution currently possible in NSOM is roughly two to three orders of magnitude less than that of other scanning microscopic techniques like STM and AFM. Yet NSOM offers some highly interesting possibilites: 1) All contrast mechanisms known in conventional optical (far-field) microscopy can be employed, e.g. polarization, refractive index, and fluorescence. 2) NSOM is possible under ambient conditions, and light has only a weak disturbing effect on samples – an important prerequisite for the study of biomolecules. 3) Specific interactions in the optical near field (evanescent modes) can, for example, lead to local amplifications of the fluorescence. 4) NSOM can be combined with other optical spectroscopies without loss of its high local resolution. A good review of the latest, in part spectacular research in near-field microscopy, frequently conducted on biological systems, is presented in the conference proceedings[9] of the Second Near-Field Optics Conference, Raleigh, NC, USA, 1993. In addition to NSOM images of blood cells or DNA, images of, for example, quantum layers are shown. First investigations on magnetooptical data storage with NSOM have yielded storage densities of 7 Gbit cm^{-2} at a local resolution of 30–60 nm.[10]

Figure 2 shows an NSOM image (Betzig et al.) of lipophilic carbocyanine molecules spread with high dilution (about 23 molecules per μm^2) over a thin poly(methyl methacrylate) (PMMA) film.[3] High dilution ensures a mean distance between the dye molecules which is larger than the diameter of the aperture – this condition is necessary for the distinction of individual molecules. The setup of the near-field microscope was as shown in Figure 1. The excited, fluorescing single molecules, which appeared as microscopic points of light, were detected with a lateral resolution of 50 nm and a vertical resolution of 5 nm. The view that the emissions indeed arise from individual molecules is supported by a number of arguments. Most convincing is the fact that photoinduced bleaching, which happens to some of the molecules after longer illumination, does not lead to the gradual decrease of the signals, but to the discrete and total extinction of individual emissions. The very good signal-to-

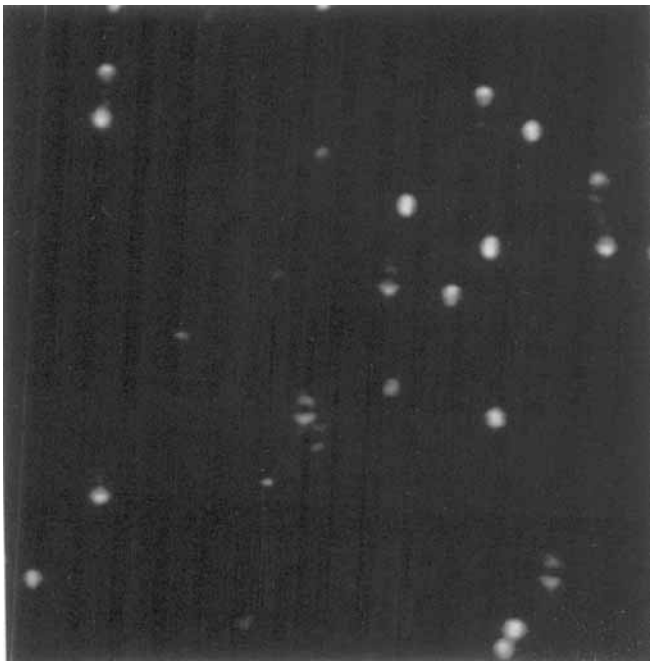


Fig. 2. Near-field microscopic picture of fluorescent single carbocyanine dye molecules on the surface of a PMMA substrate (from ref. [3]).

noise ratio in Figure 2 is attributed to the low background signal in the NSOM technique; as already discussed, only a very small sample volume is illuminated with high intensity. It is not yet clear if fluorescence amplification by evanescent fields in the optical near field contributes to the signal. At closer inspection, different geometric shapes of the structures in Figure 2 are apparent. They result from different orientations of the molecular transition dipoles. From an analysis of these shapes, the authors could determine the arrangement of the individual molecular transition dipoles, in other words of the individual molecules, on the surface. Moreover, by reverse reasoning, Betzig et al. were also able to use the molecular point dipole to map the optical near field of their fiber tip.

Ambrose et al. succeeded in imaging the fluorescence of single rhodamine 6G molecules on a silica surface using basically the same NSOM setup.[4] An interesting result of their investigation is the observation of reversible photobleaching of individual molecular chromophores. The authors attribute this effect to hopping motions that change the molecular orientation and consequently the excitation probability of the molecules. In a sense, this implies that a photoinduced reaction of a single molecule at room temperature has been observed.

We can expect that near-field microscopy will lead to many fascinating experiments with individual molecules in the near future. These include investigations on the conditions for light-induced photobleaching of individual chromophores, an unwanted effect that limits all sensitive fluorescence measurements at room temperature. Time-resolved measurements after excitation with picosecond pulses or by analysis of the fluorescence autocorrelation function are also just being tackled.[11] New perspectives of special interest are offered by investigations of single molecules at low temperatures with a combination of NSOM and optical spectroscopy. Here, an extremely high spectral resolution can be used additional to the high local resolution in NSOM.

German version: *Angew. Chem.* **1994**, *106*, 1805

[1] W. E. Moerner, L. Kador, *Phys. Rev. Lett.* **1989**, *62*, 2535; M. Orrit, J. Bernard, *ibid.* **1990**, *65*, 2716; W. E. Moerner, T. Basché, *Angew. Chem.* **1993**, *105*, 537; *Angew. Chem. Int. Ed. Engl.* **1993**, *32*, 457.
[2] E. B. Shera, N. K. Seitzinger, L. M. Davis, R. A. Keller, S. A. Soper, *Chem. Phys. Lett.* **1990**, *174*, 553; R. Rigler, J. Widengren, Ü. Mets in *Fluorescence Spectroscopy: New Methods and Applications* (Ed.: O. S. Wolfbeis), Springer, Berlin, **1993**, p. 13.
[3] E. Betzig, R. J. Chichester, *Science* **1993**, *262*, 1422.
[4] W. P. Ambrose, P. M. Goodwin, J. C. Martin, R. A. Keller, *Phys. Rev. Lett.* **1994**, *72*, 160.
[5] D. W. Pohl, W. Denk, M. Lanz, *Appl. Phys. Lett.* **1984**, *44*, 651.
[6] A. Lewis, M. Isaacson, A. Harootunian, M. Muray, *Ultramicroscopy* **1984**, *13*, 227.
[7] U. C. Fischer in *Near Field Optics* (Eds.: D. W. Pohl, D. Courjon), Kluwer, Dordrecht, **1993**, p. 255.
[8] E. Betzig, J. K. Trautman, T. D. Harris, J. S. Weiner, R. L. Kostelak, *Science* **1991**, *251*, 1468.
[9] See *Second Near-Field Optics Conference* (Raleigh, NC, October 1993), special issue *Ultramicroscopy* **1994**, in press.
[10] E. Betzig, J. K. Trautman, R. Wolfe, E. M. Gyorgy, P. L. Finn, M. H. Kryder, C.-H. Chang, *Appl. Phys. Lett.* **1992**, *61*, 142.
[11] See, for example, W. P. Ambrose, P. M. Goodwin, J. C. Martin, R. A. Keller, *Science* **1994**, *265*, 364.

Blue-Violet Pentamethylbismuth

Bernhard Neumüller and Kurt Dehnicke*

Pentavalent bismuth has such a high oxidation potential in acidic solution that manganese metal can be oxidized to manganate(VII) and water to oxygen. Thus, for a long time only bismuth(V) compounds with highly electronegative partners, such as fluorine and oxygen, were considered as isolable solids. Examples include BiF_5, which forms linear chains of edge-linked octahedra,[1] and hexafluorobismutates such as $NaBiF_6$ derived from it.[2] The synthesis of defined oxo compounds of pentavalent bismuth is already far more difficult. The well-known "Bi_2O_5" has still not been prepared in a pure form. In contrast, several mixed-valent bismutates(III)/(V), such as $(Ba,K)BiO_3$[3] or the high-temperature superconductors of the copper–bismuth family $Bi_2Sr_2CaCu_2O_{8+x}$,[4] have been obtained as stoichiometric compounds; however, the positions of Bi^{III} and Bi^{V} could not be identified either by spectroscopy or by crystallography. The locations of Bi^{3+} and Bi^{5+} in the crystal lattice were clearly assigned for the first time recently, based on the Bi–O distances, in the mixed-valent silver bismutate $Ag_{25}Bi_3O_{18}$ obtained by high-pressure synthesis from Ag_2O, "Bi_2O_5", and oxygen.[5]

Under these circumstances it was very surprising that pentaphenylbismuth (**1**)[6] and the complex ions tetraphenylbismutonium[6] and hexaphenylbismutate[7, 8] derived from it were prepared readily. Hexaphenylbismutate was recently structurally characterized in $[Li(thf)_4][BiPh_6]\cdot 2THF$.[9] Because of the relatively large group electronegativities of phenyl groups and their substituted derivatives,[10] these appear, among organic ligands, to be particularly suitable for the stabilization of Bi^{V}. In the meantime, several more pentaarylbismuth(V) compounds have been prepared and structurally characterized (Table 1). All

Table 1. Structurally characterized pentaorganobismuth compounds.

Compound	No.	Color solution	Color solid	Local symmetry in the solid	Ref.
$BiPh_5$	**1**	violet	violet	C_{4v}	[11]
$(4\text{-}MeC_6H_4)_3Bi(C_6F_5)_2$	**2**	yellow	yellow	C_{4v}	[12]
$(4\text{-}FC_6H_4)_3Bi(C_6F_5)_2$	**3**	yellow	yellow	C_{4v}	[12]
$Ph_3Bi(2,6\text{-}F_2C_6H_3)_2$	**4**	orange-red	orange-red	C_{4v}	[12]
$Bi(4\text{-}MeC_6H_4)_5\cdot Li(THF)_2Cl$	**5**	violet-red	violet-red	D_{3h}/C_{4v}	[13]
$(4\text{-}MeC_6H_4)_3Bi(2,6\text{-}F_2C_6H_3)_2$	**6**	orange-red	orange-red	C_{4v}	[13]
$Ph_3Bi(C_{12}H_8)$	**7**	orange-red	orange-red	C_{4v}	[13]
$Ph_3Bi(2\text{-}FC_6H_4)_2$	**8**	red	violett	C_{4v}	[14]
$(4\text{-}MeC_6H_4)_3Bi(2\text{-}FC_6H_4)_2$	**9**	red	orange	D_{3h}	[14]
$BiMe_5$	**10**	blue-violet	violet	D_{3h}	[15]

of these compounds have monomeric molecular structures, in which the square-pyramidal arrangement (local symmetry C_{4v}) predominates. Exceptions are **9**, in which the Bi atom is trigonal-bipyramidally surrounded (local symmetry D_{3h}), and **5**, which possesses a local symmetry between C_{4v} and D_{3h}.

Taking all these findings into consideration the possibility of preparing methylbismuth(V) compounds had to be regarded as highly unlikely, since the CH_3 group with 2.472 has the lowest group electronegativity of all organic groups (cf. phenyl: 2.717).[10] However, Seppelt et al. have recently successfully synthesized pentamethylbismuth (**10**) by treatment of dichlorotrimethylbismuth, which in turn was accessible from trimethylbismuth and sulfuryl chloride, with methyllithium in diethyl ether at −95 °C according to Equation (a):[15]

$$Bi(CH_3)_3Cl_2 + 2\,LiCH_3 \xrightarrow[-95\,^\circ C]{Et_2O} \underset{\mathbf{10}}{Bi(CH_3)_5} + 2\,LiCl \qquad (a)$$

Violet crystals of **10**, which were suitable for an X-ray structure analysis at −163 °C, were isolated from the blue-violet solution at −110 °C. According to this structure analysis **10** is trigonal bipyramidal; its Bi–C distances are equal within the standard deviations (227 and 230(2) pm). This finding is in accordance with the large atomic radius of the Bi atom, which leads to only small ligand–ligand interactions; thus, there are no measureable differences between the axial and the equatorial position.[16]

Compound **10** is very unstable, in solution it decomposes, probably with evolution of ethane, to give trimethylbismuth; in the crystalline state it explodes on rapid warming to room temperature. All the methyl groups are equivalent in the ^1H NMR spectrum even at −90 °C. This suggests that the CH_3 groups change places by way of a Berry mechanism, during which the tetragonal pyramid is an intermediate state.[17]

In contrast, the salt containing the tetramethylbismutonium cation, prepared by a quaternization reaction from trimethylbismuth and methyl trifluoromethanesulfonate [Eq. (b)], is thermally stable up to 150 °C.

$$Bi(CH_3)_3 + CH_3OSO_2CF_3 \longrightarrow [Bi(CH_3)_4]^+SO_3CF_3^- \qquad (b)$$

The structure of the cation fits perfectly into the series of tetramethylelement compounds of N to Sb, which are also tetrahedral. There were indications of the existence of the $[Bi(CH_3)_4]^+$ ion previously, however, in the β decay of $^{210}Pb(CH_3)_4$.[18]

When reaction (a) was carried out with excess methyllithium and in the presence of tetrahydrofuran at −78 °C, hexamethylbismutate, which is isoelectronic with hexamethyltellurium,[19] can be isolated as yellow crystals [Eq. (c)].[15]

$$Bi(CH_3)_3Cl_2 + 3\,LiMe \xrightarrow{THF} [Li(THF)_4]^+[Bi(CH_3)_6]^- \qquad (c)$$

As expected, the octahedral hexamethylbismutate is only stable at low temperatures. Its Bi–C bonds of 230 to 236(2) pm are slightly longer than those in **10**.

[*] Prof. Dr. K. Dehnicke, Dr. B. Neumüller
Fachbereich Chemie der Universität
Hans-Meerwein-Strasse, D-35032 Marburg (FRG)
Telefax: Int. code + (6421)28-8917

A fascinating, but still not fully answered question is the relationship between the color and the structure of pentaorganobismuth compounds. Ab initio calculations on the hypothetical BiH_5 reveal that the HOMO–LUMO separation is only about half as large for tetragonal symmetry as it is for trigonal-bipyramidal symmetry, when relativistic effects are taken into consideration.[14] A charge transfer transition explaining the blue color of pentaphenylbismuth could thus be easily deduced from its tetragonal-pyramidal structure. A look at Table 1 shows, however, that this is only valid for **5**, whereas all other arylbismuth(v) derivatives are yellow to orange-red despite having tetragonal-pyramidal structures. The packing effects[14] and electron-withdrawing effects of substituents, above all for those derivatives with fluoro-substituted phenyl groups, were put forward to explain this behavior.[12] In contrast, the + I effect of the methyl groups is used to explain the blue color of **10**. This effect should ease the charge transfer transition despite the trigonal-bipyramidal structure.[15]

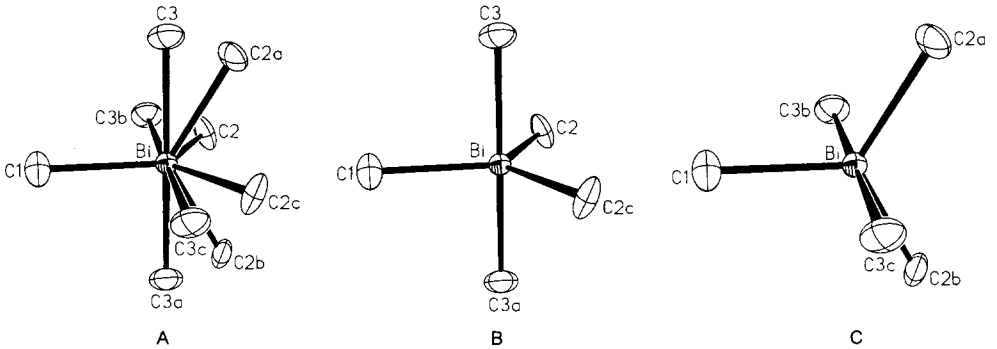


Fig. 2. Structure of the molecule of **10** with **A** as the resultant of the two disordered units B and C. Only the C atoms 2 and 3 participate in the disorder (50% probability for the thermal ellipsoids; in the original publication [15] two thermal ellipsoids, ((3a) or (3b), (2a) or (2b)) were drawn with the wrong spatial orientation).

To assess the possible influence of special features of the packing effects on the blue-violet color of pentamethylbismuth, we drew the unit cell using the atomic coordinates that were made available to us.[20] The view along the crystallographic *b* axis is shown in Figure 1. The atoms Bi and C1 lie on the section line

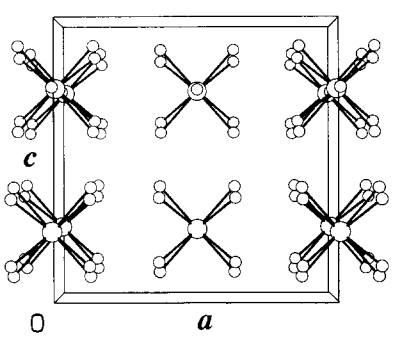


Fig. 1. Illustration of the unit cell of **10** showing the disorder. View along the crystallographic *b* axis.

intersecting mirror planes (cf. also Fig. 2). The chosen view of the unit cell of **10** gives the impression of tetragonal symmetry for the individual molecules, as is the case in the structure of BiF_5 along the needle axis.[1] Unlike the latter example, in **10** this impression is simulated by a disorder of the $Bi(CH_3)_5$ molecules, as it results (form **A**) from the superposition of two trigonal-bipyramidal units (**B** and **C** in Fig. 2). In the solid-state structure of **10** at −163 °C there are no indications of a conceivable dynamic process involving a Berry pseudorotation, contrary to what was detected for **10** in solution even at −90 °C.[15] Such indications would be expressed by special features of the thermal ellipsoids of C2 and C3. Thus, there is no doubt about the trigonal-bipyramidal structure of **10**.

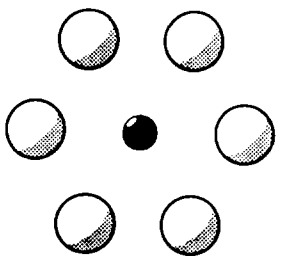
However, on the otherhand, the unit cell would allow installation of single $Bi(CH_3)_5$ molecules with tetragonal symmetry along the *b* axis, which as "coloring centers" might then be responsible for the blue-violet color. The occasional occurrence of such tetragonal units, which are intermediates in the pseudorotation process, cannot be ruled out without further investigation because pseudorotation is still to be expected at the melting point of **10** at −110 °C .[21] An ab initio calculation at a very high level of theory will be required before a definitive explanation of the correlation between the color and the structure of pentamethylbismuth can be made.

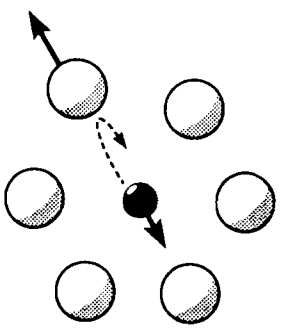
German version: *Angew. Chem.* **1994**, *106*, 1803

[1] C. Hebecker, *Z. Anorg. Allg. Chem.* **1971**, *384*, 111.
[2] C. Hebecker, *Z. Anorg. Allg. Chem.* **1971**, *376*, 236.
[3] R. J. Cava, B. Batlogg, J. J. Krajewski, R. C. Farrow, L. W. Rupp, Jr., A. E. White, K. T. Short, W. F. Peck, Jr., T. Y. Kometani, *Nature* **1988**, *332*, 814.
[4] H. Maeda, Y. Tanaka, M. Fukutomi, T. Asano, *Jpn. J. Appl. Phys. Part 2* **1988**, *27*, 209.
[5] M. Bortz, M. Jansen, *Z. Anorg. Allg. Chem.* **1992**, *612*, 113.
[6] G. Wittig, K. Clauß, *Justus Liebigs Ann. Chem.* **1952**, *578*, 136.
[7] D. Hellwinkel, G. Kilthau, *Justus Liebigs Ann. Chem.* **1967**, *705*, 66.
[8] D. Hellwinkel, M. Bach, *Justus Liebigs Ann. Chem.* **1968**, *720*, 198.
[9] S. Wallenhauer, D. Leopold, K. Seppelt, *Inorg. Chem.* **1993**, *32*, 3948.
[10] P. R. Wells, *Prog. Phys. Org. Chem.* **1968**, *6*, 111.
[11] A. Schmuck, J. Buschmann, J. Fuchs, K. Seppelt, *Angew. Chem.* **1987**, *99*, 1206; *Angew. Chem. Int. Ed. Engl.* **1987**, *26*, 1180.
[12] A. Schmuck, K. Seppelt, *Chem. Ber.* **1989**, *122*, 803.
[13] A. Schmuck, D. Leopold, S. Wallenhauer, K. Seppelt, *Chem. Ber.* **1990**, *123*, 761.
[14] A. Schmuck, P. Pyykkö, K. Seppelt, *Angew. Chem.* **1990**, *102*, 211; *Angew. Chem. Int. Ed. Engl.* **1990**, *29*, 213.
[15] S. Wallenhauer, K. Seppelt, *Angew. Chem.* **1994**, *106*, 1044; *Angew. Chem. Int. Ed. Engl.* **1994**, *33*, 976.
[16] In contrast, in the structure of pentamethylantimony, which crystallizes in the same space group *Cmcm*, the Sb–C distances of the axially arranged methyl groups are 7 pm longer than the Sb–C bonds of the equatorially arranged methyl groups. C. Pulham, A. Haaland, A. Hammel, K. Rypdal, H. P. Verne, H. V. Volden, *Angew. Chem.* **1992**, *104*, 1534; *Angew. Chem. Int. Ed. Engl.* **1992**, *31*, 1464; S. Wallenhauer, D. Leopold, K. Seppelt, *Inorg. Chem.* in press.
[17] T. Auf der Heyde, *Angew. Chem.* **1994**, *106*, 871; *Angew. Chem. Int. Ed. Engl.* **1994**, *33*, 823
[18] J. C. Duncan, F. G. Thomas, *J. Inorg. Nucl. Chem.* **1967**, *29*, 869.
[19] L. Ahmed, J. A. Morrison, *J. Am. Chem. Soc.* **1990**, *112*, 7911.
[20] We thank Prof. Dr. K. Seppelt for providing us with the structure data. The structure of **10** was solved in the non-conventional setting *Ccnm* by the authors [15]. Our Figures are based on the conventional setting *Cmcm*.
[21] Based on the structure data available to us a twinning of the crystals for **10** is difficult to imagine. Unlike in the case of a superstructure, which, for example, would lead to the doubling of one of the lattice constants. However, this would mainly affect the positions of the C atoms. As a result of the high scattering factor of the bismuth atoms, superstructure reflections, which might occur, could only be detected with low-temperature measurements.

Handbook of Hot Atom Chemistry

Edited by J.-P. Adloff et al.



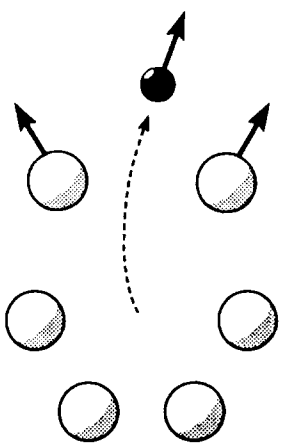


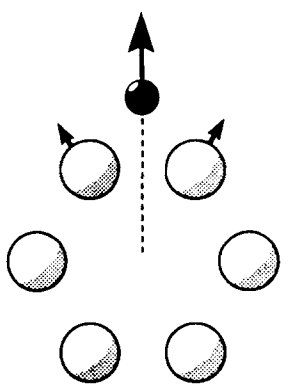
1992. XIII, 702 pages.
Hardcover. DM 345.00.
ISBN 3-527-29001-X

Hot atom chemistry is an increasingly important field, which has contributed significantly to our understanding of many fundamental processes and reactions. Its techniques have become firmly entrenched in numerous disciplines, such as applied physics, biomedical research, and all fields of chemistry.

Written by leading experts, this comprehensive handbook encompasses a broad range of topics. Each chapter comprises a collection of stimulating essays, giving an in-depth account of the state-of-the-art of the field, and stressing opportunities for future work.

An extensive introduction to the whole area, this book provides unique insight into a vast subject, and a clear delineation of its goals, techniques, and recent findings. It also contains detailed discussions of applications in fields as diverse as nuclear medicine, geochemistry, reactor technology, and the chemistry of comets and interstellar grains.





To order please contact your bookseller or:

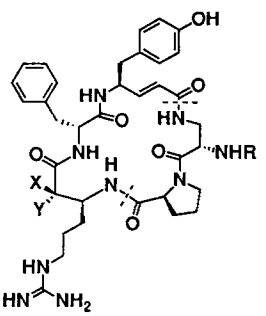
VCH, P.O. Box 10 11 61, D-69451 Weinheim
VCH, Hardstrasse 10, P.O. Box, CH-4020 Basel
VCH, 8 Wellington Court, Cambridge CB1 1HZ, UK
VCH, 220 East 23rd Street, New York, NY 10010-4606, USA
(toll free: 1-800-367-8249)

VCH

Synthesis of Cyclotheonamide B and Its Derivatives**

Jingen Deng, Yasumasa Hamada, Takayuki Shioiri,* Shigeki Matsunaga, and Nobuhiro Fusetani

Cyclotheonamides A (**1**: R = CHO; X, Y = O) and B (**2a**: R = Ac; X, Y = O) have been isolated from a marine sponge of the genus *Theonella* collected off Hachijo-jima Island, Japan.[1] These macrocyclic pentapeptides strongly inhibit various proteinases, particularly thrombin, and are the first macrocyclic thrombin inhibitors having two novel amino acid residues: a vinylogous tyrosine and an arginine extended by a carbonyl group in the α-position (α-carbonyl homologue of arginine) (Scheme 1). Their structural uniqueness as well as intriguing biological activities motivated their total synthesis[2–5] and determination of their mechanism of serine protease inhibition.[4, 6]



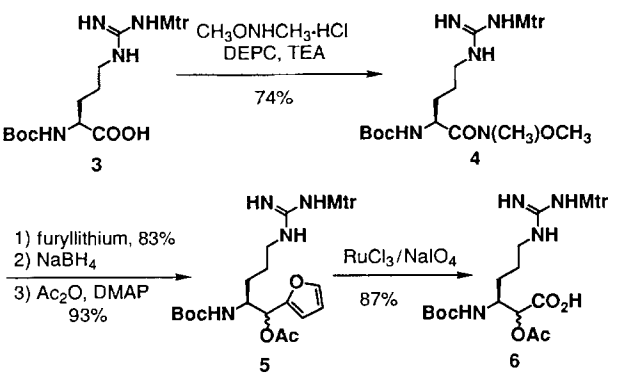
cyclotheonamide A **1**, R = CHO, X, Y = O
cyclotheonamide B **2a**, R = Ac, X, Y = O
2b, R = Ac, X = H, Y = OH
2c, R = Ac, X = OH, Y = H

Scheme 1. The macrocyclic pentapeptides **1** and **2** and the disconnections crucial for the convergent synthesis.

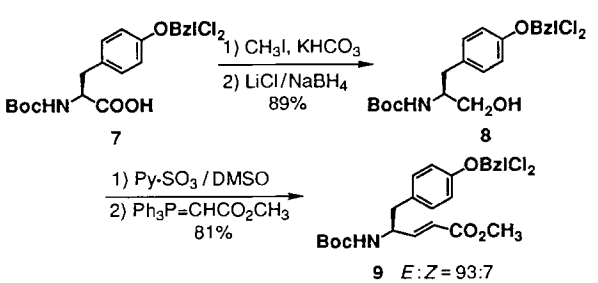
Herein, we report on an effective total synthesis of cyclotheonamide B (**2a**) and its derivatives **2b** and **2c**, in which the α-carbonyl group of the arginine homologue is reduced. In our strategy, the organophosphorus reagents diethylphosphonocyanidate ($(C_2H_5O)_2P(O)CN$, DEPC)[7] and pentafluorophenyldiphenylphosphinate ($Ph_2P(O)OC_6F_5$, FDPP),[8] were used for formation of the peptide bond with satisfactory efficiency. A convergent strategy was adopted (Scheme 1), and coupling of the two fragments was accomplished at the position at which no epimerization can occur. The noteworthy features are the high-yielding (>80%) final macrolactamization with FDPP and the utilization of the 2-furyl group as the synthetic equivalent of the carbonyl group.[9]

Since the α-carbonylamide function was reported to form tetrahedral hemiketals with serine proteases[4, 6] and play a main role in the enzyme affinity of cyclotheonamide A (**1**), we expected to use the two dihydro analogues **2b** and **2c** to confirm the biological importance of the α-carbonylamide moiety.

Synthesis of the western part started from N^{α}-*tert*-butoxycarbonyl-N^{ω}-(4-methoxy-2,3,6-trimethylbenzenesulfonyl)-(*S*)-arginine (**3**, Boc-(*S*)-Arg(Mtr)-OH), which was coupled with *N*,*O*-dimethylhydroxylamine (DEPC, triethylamine (TEA), dimethylformamide (DMF), room temperature (RT), 4 h). The resultant Weinreb amide **4** was condensed with 2-furyllithium, generated from furan (*t*BuLi, THF, −78 °C, 1 h; 0 °C, 4 h), followed by reduction ($NaBH_4$, MeOH, −10 °C, 0.5 h) and then acetylation (Ac_2O, DMAP, CH_2Cl_2, RT, 12 h) to give the furan derivative **5** as a mixture of the *syn* and *anti* isomers in a ratio of 61:39).[10] The ruthenium-catalyzed oxidation ($RuCl_3$/$NaIO_4$, $CH_3CN/CCl_4/H_2O$, 1.5 h)[9, 11] smoothly afforded the α-acetoxycarboxylic acid **6**, a precursor of the α-carbonyl homologue of arginine.



Synthesis of the (*E*)-vinylogous (*S*)-tyrosine derivative **9** was achieved stereoselectively and in good yield from the amino alcohol **8** in a one-pot reaction.[12] *N*-*tert*-Butoxycarbonyl-*O*-2,6-dichlorobenzyl-(*S*)-tyrosine (**7**, Boc-(*S*)-Tyr(Cl_2Bzl)-OH) was converted into **8** by synthesis of the methyl ester (CH_3I, $KHCO_3$, DMF, RT, 4 h) and subsequent reduction (LiCl/$NaBH_4$, THF/EtOH, RT, 12 h) according to our method.[13] Oxidation of **8**

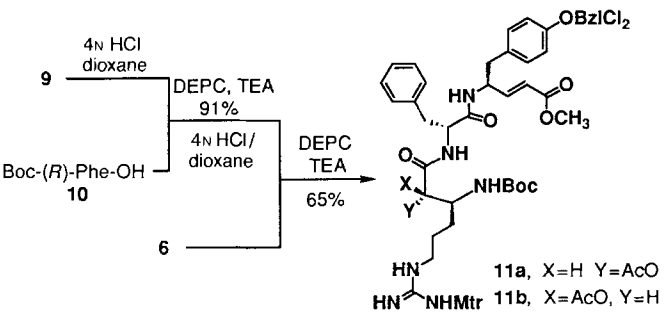


[*] Prof. Dr. T. Shioiri, J. Deng, Prof. Dr. Y. Hamada
Department of Synthetic Organic Chemistry
Faculty of Pharmaceutical Sciences, Nagoya City University
Tanabe-dori, Mizuho-ku, Nagoya 467 (Japan)
Telefax: Int. code + (52)834-4172
Dr. S. Matsunaga, Prof. Dr. N. Fusetani
Laboratory of Marine Biochemistry, Faculty of Agriculture
The University of Tokyo
Yayoi, Bunkyo-ku, Tokyo 113 (Japan)

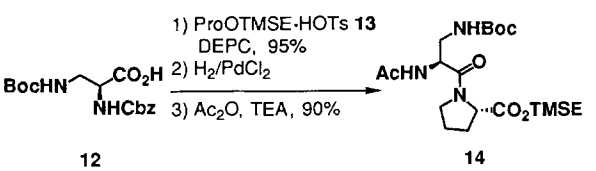
[**] This work was supported in part by the Ministry of Education, Science and Culture, Japan. One of the authors (J. D.) is grateful to the Japan Society for the Promotion of Science for the postgraduate fellowship.

(dimethyl sulfoxide (DMSO), sulfur trioxide/pyridine complex, TEA, 0.5 h) followed by Wittig reaction with methoxycarbonylmethylenetriphenylphosphorane afforded the (*E*)-vinylogous tyrosine derivative **9** (m.p. 125–126 °C, $[\alpha]_D^{25} = +4.3$ ($c = 1.03$ in MeOH) as the major product together with a small amount of the corresponding (*Z*) isomer (*E*:*Z* = 93:7).

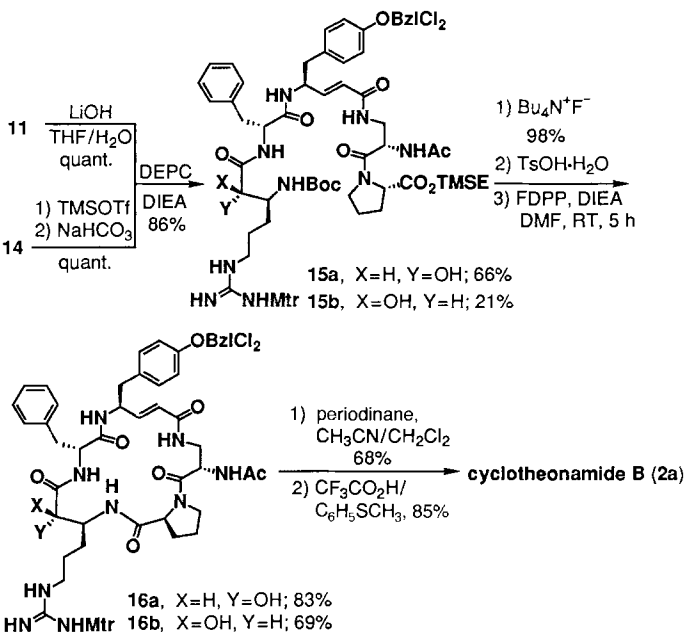
The required western fragment **11** was prepared from **9** by attachment of Boc-(*R*)-phenylalanine (**10**, Boc-(*R*)-Phe-OH) and then the arginine derivative **6** through acidic deprotection of the N-terminal Boc group (4N HCl/dioxane, 0 °C, 2 h then RT, 0.5 h) and coupling by use of DEPC (TEA, DMF, 0 °C, 12 h). Compound **11** was obtained as a mixture of the *syn* and *anti* isomers, **11a** and **11b**, in a ratio of 69:31.



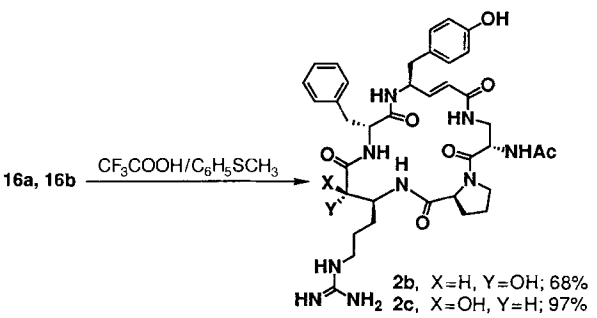
The eastern fragment **14** (m.p. 88–89 °C, $[\alpha]_D^{22} = -42.3$ ($c = 1.05$ in $CHCl_3$) was synthesized by condensation of N^{α}-Cbz-N^{β}-Boc-(*S*)-2,3-diaminopropionic acid (**12**)[14] (Cbz = carbobenzoxy) with the salt of (*S*)-proline trimethylsilylethyl (TMSE) ester and toluenesulfonic acid (**13**) in the presence of of DEPC (TEA, DMF, 0 °C, 12 h), subsequent hydrogenolytic removal of the Cbz group (H_2, $PdCl_2$, MeOH, 0.5 h), and acetylation of the free amino group (Ac_2O, TEA, CH_2Cl_2, RT, 12 h).



Before the convergent construction of the whole carbon skeleton of cyclotheonamide B (**2a**), the protecting group at the C-terminus of **11** was removed under alkaline conditions (LiOH, THF/H_2O, 0 °C, 3.5 h then RT, 3.5 h), and the protecting group at the N^{β}-terminus of **14** was cleaved by treatment with trimethylsilyl triflate (TMSOTf) in CH_2Cl_2 and then saturated aqueous $NaHCO_3$. TMSOTf was more effective than CF_3CO_2H or *p*-TsOH. Coupling of the two deprotected fragments (DEPC, diisopropylethylamine (DIEA), DMF, 0 °C, 12 h) afforded the linear pentapeptides **15a** and **15b**, which were easily separated by column chromatography on silica gel[15] in yields of 66 and 21%, respectively. After removal of the protecting group at the C-terminus ($Bu_4NF \cdot 3H_2O$, THF, 0 °C, 3.5 h then RT, 1.5 h) and then at the N-terminus (*p*-TsOH·H_2O, CH_2Cl_2, RT, 12 h), the macrolactamization was efficiently achieved by use of FDPP in the presence of DIEA in DMF to give **16a** and **16b** in 83 and 69% yield, respectively. The major isomer **16a** was oxidized with the Dess–Martin periodinane[16] (CH_3CN/CH_2Cl_2 (1:2), 50 °C, 6 h) to give the oxo compound. Subsequent removal of both the 2,6-dichlorobenzyl and the 4-methoxy-2,3,6-trimethyl-



benzenesulfonyl groups with trifluoroacetic acid/thioanisole (RT, 20 h) followed by purification with preparative HPLC afforded cyclotheonamide B (**2a**) ($[\alpha]_D^{24} = -13.1$ ($c = 0.2$ in MeOH), which was identified by comparison of its spectra with those of the natural product. Analogously, deprotection of **16a** and **16b** and then purification by HPLC afforded the hydroxy derivatives of cyclotheonamide B, **2b** and **2c**, in 68 and 97% yield, respectively (**2b**: $[\alpha]_D^{25} = -7.9$ ($c = 0.21$ in MeOH); **2c**: $[\alpha]_D^{25} = -4.2$ ($c = 0.22$ in MeOH)).



The enzyme inhibiting activities of the synthetic cyclotheonamide B (**2a**) and its hydroxy derivatives **2b** and **2c** were evaluated against thrombin and trypsin in comparison with natural cyclotheonamide A (**1**). Although **2a** showed full activity against thrombin and trypsin,[17] **2b** and **2c** exhibited little or no activity. These results clearly indicate that the α-carbonylamide portion dominates the enzyme inhibiting action of cyclotheonamides. A more detailed investigation of the inhibiting action and the synthesis of analogues of cyclotheonamide B are in progress.

Received: March 24, 1994 [Z 6797 IE]
German version: *Angew. Chem.* **1994**, *106*, 1811

[1] N. Fusetani, S. Matsunaga, H. Matsumoto, Y. Takebayashi, *J. Am. Chem. Soc.* **1990**, *112*, 7053.
[2] For reassignment of stereochemistry and total synthesis of cyclotheonamide B, see: M. Hagihara, S. L. Schreiber, *J. Am. Chem. Soc.* **1992**, *114*, 6570.
[3] For the total synthesis of cyclotheonamide A, see: P. Wipf, H. Kim, *J. Org. Chem.* **1993**, *58*, 5592; Corrigendum: *ibid.* **1994**, *59*, 2914.

[4] For X-ray crystallographic studies of a human α-thrombin complex, biological activities, and total synthesis of cyclotheonamide A, see: B. E. Maryanoff, X. Qiu, K. P. Padmanabhan, A. Tulinsky, H. R. Almond, Jr., P. Andrade-Gordon, M. N. Greco, J. A. Kauffman, K. C. Nicolaou, A. Liu, P. H. Brungs, N. Fusetani, *Proc. Natl. Acad. Sci. USA* **1993**, *90*, 8048.

[5] For the synthesis of fragments of cyclotheonamides: a) P. Roth, R. Metternich, *Tetrahedron Lett.* **1992**, *33*, 3993; b) P. Wipf, H. Kim, *Tetrahedron Lett.* **1992**, *33*, 4275; c) J. Deng, Y. Hamada, T. Shioiri in *Peptide Chemistry 1992* (Proc. 2nd Jpn. Symp. Peptide Chem.) (Ed.: N. Yanaihara), Escom, Leiden, **1993**, 72.

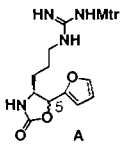
[6] A. Y. Lee, M. Hagihara, R. Karmacharya, M. W. Albers, S. L. Schreiber, J. Clardy, *J. Am. Chem. Soc.* **1993**, *115*, 12619.

[7] S. Takuma, Y. Hamada, T. Shioiri, *Chem. Pharm. Bull.* **1982**, *30*, 3147, and references therein.

[8] S. Chen, J. Xu, *Tetrahedron Lett.* **1991**, *32*, 6711; J. Dudash, Jr., J. Jiang, S. C. Mayer, M. M. Joullié, *Synth. Commun.* **1993**, *23*, 349.

[9] For aryl groups as the synthetic equivalent of carboxyl groups, see: F. Matsuura, Y. Hamada, T. Shioiri, *Tetrahedron*, **1994**, *50*, 265; *Tetrahedron Lett.* **1994**, *35*, 733, and references therein.

[10] The configurations of **5** were determined by the ^{1}H NMR spectra of the corresponding oxazolinones **A**: major isomer (*syn*): δ(5-H) = 5.58 (J = 8.25 Hz); minor isomer (*anti*): δ(5-H) = 5.09 (J = 6.59 Hz): M. A. Poss, J. A. Reid, *Tetrahedron Lett.* **1992**, *33*, 1411.



A

[11] P. H. J. Carlsen, T. Katsuki, V. S. Martin, K. B. Sharpless, *J. Org. Chem.* **1981**, *46*, 3936; M. T. Nuñez, V. S. Martín, *ibid.* **1990**, *55*, 1928.

[12] The corresponding vinylogous (*R*)-tyrosine ester was obtained analogously in 89% yield (*E*:*Z* = 95:5). See also ref.[5c].

[13] Y. Hamada, M. Shibata, T. Sugiura, S. Kato, T. Shioiri, *J. Org. Chem.* **1987**, *52*, 1252.

[14] M. Waki, Y. Kitajima, N. Izumiya, *Synthesis* **1981**, 266.

[15] **15a**: m.p. 87–88 °C, $[\alpha]_D^{25} = -43.4$ (c = 1.06 in $CHCl_3$); **15b**: m.p. 105–106 °C, $[\alpha]_D^{25} = -19.0$ (c = 1.09 in $CHCl_3$). The configurations of the hydroxyl functions in **15a** and **15b** were deduced from those of their precursors **5**; see also ref.[10].

[16] D. B. Dess, J. C. Martin, *J. Am. Chem. Soc.* **1991**, *113*, 7277.

[17] The IC_{50} values for our synthetic cyclotheonamide B (**2a**) against thrombin and trypsin are 7.2 and 17 ng mL^{-1}, respectively, while those for natural cyclotheonamide A (**1**) are 7.2 and 10 ng mL^{-1} under the same conditions. Since cyclotheonamide B was not available, the comparative study of the enzyme inhibition was not possible.

Decaphenylferrocene and Decaphenylferrocenium Tetrafluoroborate**

Herbert Schumann,* Alexander Lentz, Roman Weimann, and Joachim Pickardt

In memory of J. J. Zuckerman

Although decaphenylferrocene (**1**) was first described in 1983 by Slocum et al.,[1] a symmetrical sandwich structure has not to date been established for this metallocene. The NMR spectra of **1**, obtained from $[Fe(CO)_5]$ and C_5Ph_5Br, were interpreted by Masters et al. in terms of a zwitterionic complex $[(\eta^5\text{-}C_5Ph_5)Fe]^+[(\eta^6\text{-}C_6H_5\text{-}C_5Ph_4]^-$.[2] The proposed structure could not however be confirmed by X-ray structure analysis. One argument in favor of this zwitterionic structure arises from the considerable spatial requirements of the five phenyl groups, whose coplanar arrangement about the cyclopentadienyl anion is therefore hindered. A propeller-like structure, analogous to that observed for decaphenylstannocene,[3] is adopted. It is argued that the short Fe–Cp_z distance of 170 pm (Cp_z = center of cyclopentadienyl ligand),[4] which has been shown to be necessary for additional π-bond stabilization of ligand–iron bonding in symmetric sandwich compounds, can no longer be achieved. However, in octaphenylferrocene,[5] which has only two fewer phenyl groups, an Fe–Cp_z distance well within that required for stabilization is observed. The same holds for the recently described pentaphenylferrocene[6] and for decabenzylferrocene,[7, 8] in which all the benzyl groups point away from the metal, in contrast to all other previously known pentabenzylcyclopentadienyl complexes.[9]

At first our investigations confirmed the argument based on bond-length criterion presented above. Thus, reaction of $[(C_5Ph_5)Fe(CO)_2Br]$[10] in xylene at 80 °C yielded, after hydrolysis with conc. HCl, only the orange-red salt **2**. In the complex

$[Fe(\eta^6\text{-}C_6H_4Me_2)(\eta^5\text{-}C_5Ph_5)]^+[FeCl_4]^-$ **2**

cation of **2**, a sterically less demanding xylene molecule was found to replace the second C_5Ph_5 ligand.[11] Also, the metathesis and metal-vapor methods successfully employed in the synthesis of decaphenylstannocene could not be applied to decaphenylferrocene. However, when $[(C_5Ph_5)Fe(CO)_2Br]$ was heated for two days in boiling xylene [Eq. (a)], **1** was isolated in 30% yield as a pink, microcrystalline powder, insoluble in all common solvents. Complex **1**, which is inert to 0.1 N HCl and is stable up to 400 °C, was also formed when **2** was heated to 350 °C [Eq. (b)].

$$2[(C_5Ph_5)Fe(CO)_2Br] \xrightarrow{130\,^\circ C} \underset{\mathbf{1}}{[Fe(C_5Ph_5)_2]} + FeBr_2 + 4\,CO \qquad (a)$$

The single crystal X-ray structure analysis of **1** (Fig. 1)[12] performed on the microcrystals obtained could only be refined to R = 0.159. An in-depth discussion of the bonding in **1** is therefore not possible. However, like the ^{13}C solid-state NMR, IR, and Raman spectra,[13] the structure analysis also confirms the presence of a symmetric sandwich complex, isostructural with decaphenylstannocene.[14] Oxidation of **1** with $NOBF_4$ yielded

$$\underset{\mathbf{2}}{[Fe(\eta^6\text{-}C_6H_4Me_2)(\eta^5\text{-}C_5Ph_5)]^+[FeCl_4]^-} \xrightarrow{350\,^\circ C} \underset{\mathbf{1}}{[Fe(C_5Ph_5)_2]} \qquad (b)$$

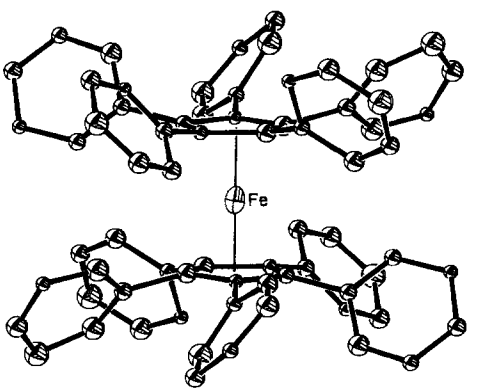


Fig. 1. ORTEP diagram of a molecule of **1** (ellipsoids at the 50% probability level). The average distance between the Fe atom and the C atoms of the Cp ligand is 211 pm.

[*] Prof. Dr. H. Schumann, Dr. A. Lentz, Dr. R. Weimann, Prof. Dr. J. Pickardt
Institut für Anorganische und
Analytische Chemie der Technischen Universität
Strasse des 17. Juni 135, D-10623 Berlin (FRG)
Telefax: Int. code + (30) 314-22168

[**] This work was supported by the Deutsche Forschungsgemeinschaft (SFB "Anisotropic Fluids") and the Bundesministerium für Bildung und Wissenschaft through the Graduiertenkolleg "Synthese und Strukturaufklärung niedermolekularer Verbindungen".

decaphenylferrocenium tetrafluoroborate **3** [Eq. (c)] in 81% yield as dark, reddish brown crystals, which were extremely soluble in polar solvents.

$$\underset{\mathbf{1}}{[Fe(C_5Ph_5)_2]} + [NO]^+[BF_4]^- \longrightarrow \underset{\mathbf{3}}{[Fe(C_5Ph_5)_2]^+[BF_4]^-} + NO \qquad (c)$$

Cyclic voltammetric investigations (Fig. 2) show that **3** is reversibly reduced to **1** in CH_3CN. Precipitation of **1**, which is

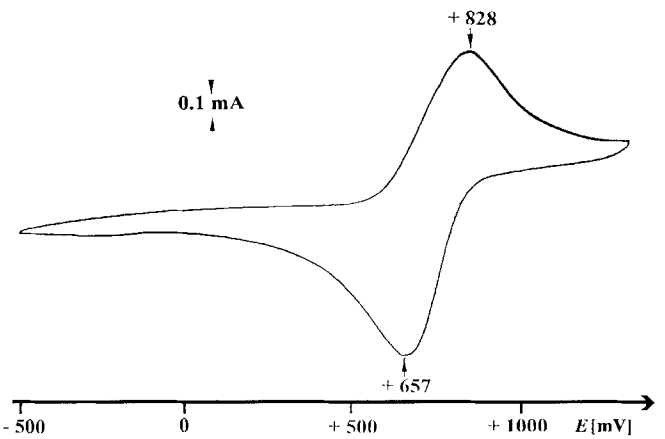


Fig. 2. Cyclic voltammogram of $[Fe(C_5Ph_5)_2]$ / $[Fe(C_5Ph_5)_2]^+[BF_4]^-$ [4.4 mg of **3** per mL of CH_3CN solvent; supporting electrolyte Bu_4NBF_4 (0.1 M); Pt/Pt electrodes (0.56 cm^2); Ag/AgCl reference electrode (Metrohm); salt bridge agar-agar/sat. KCl solution; potential scanned at 200 mVs^{-1}; room temperature; E_0 = +743 mV (Ag/AgCl)]. We thank Dr. Miklautz, Schering AG, Berlin, for the cyclic voltammetric measurements.

only sparingly soluble in CH_3CN, is observed. The redox potential [mV] for the one-electron oxidation of **1** is +743 (Ag/AgCl) and is therefore of the same order of magnitude as the values obtained for the parent compound ferrocene (+493[15] and +433[16] in CH_3CN, +593 in THF[16]), decabenzylferrocene (+333 in CH_3CN, +563 in THF),[16] pentabenzylferrocene (+443 in CH_2Cl_2),[16] and benzylferrocene (+403 in CH_3CN)[17] (all vs. Ag/AgCl).

The salt **3** crystallizes from CH_2Cl_2 with two molecules of solvent in the crystal lattice.[18] Two independent $[Fe(C_5Ph_5)_2]^+$

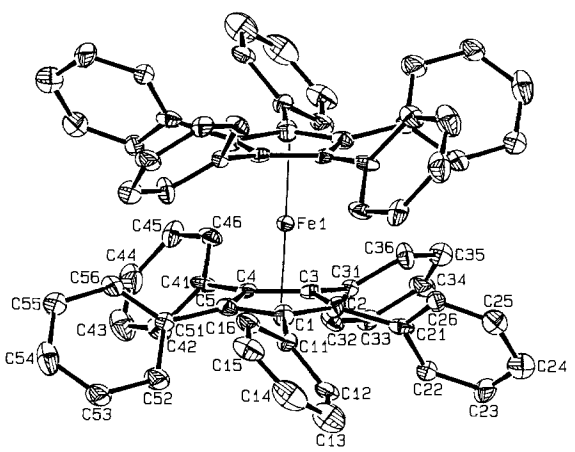


Fig. 3. ORTEP diagram of one of the two cations of **3** (ellipsoids at the 50% probability level). Selected bond lengths, deviations [pm] and interplanar angles [°]. Fe-C1 217(1), Fe-C2 215(1), Fe-C3 213(1), Fe-C4 216(1), Fe-C5 221(1), Cp-C11 18(6), Cp-C21 34(6), Cp-C31 23(6), Cp-C41 19(6), Cp-C51 24(6); Cp-Ph1 43.7(7), Cp-Ph2 57.6(6), Cp-Ph3 47.2(7), Cp-Ph4 50.9(7), Cp-Ph5 48.8(7).

ions are located within the unit cell. The positions occupied by the Fe atoms are related by a crystallographic center of inversion. One of the two cations is shown in Figure 3. The sandwich structure of the symmetrically disposed cyclopentadienyl ligands can be clearly seen. The cyclopentadienyl ligands are separated by distances of 358.6 (Fe1) and 358.0 pm (Fe2). The Fe^{3+} ions are shifted by 6.7 (Fe1) and 4.7 pm (Fe2) from the Cp_z-Cp_z line. The phenyl substituents bound to the planar cyclopentadienyl ligands are not only twisted out of the plane of the cyclopentadienyl ligands in a propeller-like arrangement, but also point away from the metal center. The two cyclopentadienyl ligands are therefore able to approach the Fe^{3+} ion more easily. Although the interplanar distance is 27 pm greater than that observed for decabenzylferrocene (331.3 pm[7]), it is, nonetheless, clearly shorter than that for decaphenylstannocene (480.2 pm[3]). In the latter, molecular stabilization through π interactions between the central tin atom and the cyclopentadienyl ligands is not possible, but also not necessary.

Experimental Procedure

1: A blue solution of $[(C_5Ph_5)Fe(CO)_2Br]$ (2.5 g, 3.9 mmol) in xylene (100 mL) was heated under reflux for 48 h. The mixture was acidified to pH 1 with conc. HCl and ice water. A reddish brown precipitate was collected and combined with the organic phase from the filtrate. The mixture was concentrated and the solid obtained extracted for 24 h with toluene, 2 d with THF, and then 5 h with CH_2Cl_2. The product **1** was obtained from the residue and dried at 10^{-3} Torr. Correct C,H analysis; MS (70 eV, 370 °C): *m/z* (%): 948 (32) $[M^+ + H]$, 947 (56) $[M^+]$, 946 (100) $[M^+ - H]$, 501 (23) $[M^+ - C_5Ph_5]$, 446 (2) $[C_5Ph_5^+]$.

3: To a suspension of **1** (0.60 g, 0.63 mmol) in CH_2Cl_2 (20 mL) was added rapidly $NOBF_4$ (0.12 g, 1.00 mmol). After it had been stirred for 12 h at room temperature, the mixture was filtered. The solution was treated with ether (20 mL) and cooled to −30 °C. Reddish brown crystals of **3** were obtained (0.53 g, 81%). M.p. 315 °C (dec.); correct C,H analysis; ^1H NMR (270 MHz, CD_2Cl_2, TMS): δ = 5.9–6.6 (Ph-H); MS (70 eV, 360 °C): *m/z* (%): 948 (15) $[M^+ + H]$, 947 (33) $[M^+]$, 946 (44) $[M^+ - H]$, 502 (13) $[M^+ - C_5Ph_5 + H]$, 501 (25) $[M^+ - C_5Ph_5]$, 446 (13) $[C_5Ph_5^+]$.

Received: February 8, 1994
Revised version: April 21, 1994 [Z6677IE]
German version: *Angew. Chem.* **1994**, *106*, 1827

[1] D. W. Slocum, S. Johnson, M. Matusz, S. Duraj, I. L. Cmarik, K. M. Simpson, D. A. Owen, *Polym. Mater. Sci. Eng.* **1983**, *49*, 353–357; D. W. Slocum, S. Duraj, M. Matusz, I. L. Cmarik, K. M. Simpson, D. A. Owen in *Metal Containing Polymeric Systems* (Eds.: J. E. Sheats, C. E. Carraher, C. U. Pittmann), Plenum, New York, **1985**, p. 59.

[2] K. N. Brown, L. D. Field, P. A. Lay, C. M. Lindall, A. F. Masters, *J. Chem. Soc. Chem. Commun.* **1990**, 408–410.

[3] M. J. Heeg, C. Janiak, J. J. Zuckerman, *J. Am. Chem. Soc.* **1984**, *106*, 4259–4261.

[4] D. Seiler, J. D. Dunitz, *Acta Crystallogr. Sect. B* **1979**, *35*, 1068–1074; Yu. T. Struchkov, V. G. Andrianov, T. N. Salnikova, I. R. Lyatifov, R. B. Materikova, *J. Organomet. Chem.* **1978**, *145*, 213–223; D. P. Freyberg, J. L. Robbins, K. N. Raymond, J. C. Smart, *J. Am. Chem. Soc.* **1979**, *101*, 892–897; J. Okuda, E. Herdtweck, *Chem. Ber.* **1988**, *121*, 1899–1905.

[5] M. P. Castellani, J. M. Wright, S. J. Geib, A. L. Rheingold, W. C. Trogler, *Organometallics* **1986**, *5*, 1116–1122.

[6] M. J. Aroney, I. E. Buys, G. D. Dennis, L. D. Field, T. W. Hambley, P. A. Lay, A. F. Masters, *Polyhedron* **1993**, *12*, 2051–2056.

[7] H. Schumann, C. Janiak, R. D. Köhn, J. Loebel, A. Dietrich, *J. Organomet. Chem.* **1989**, *365*, 137–150.

[8] M. D. Rausch, W. M. Tsai, J. W. Chambers, R. D. Rogers, H. G. Alt, *Organometallics* **1989**, *8*, 816–821.

[9] C. Janiak, H. Schumann, *Adv. Organomet. Chem.* **1992**, *33*, 291–393.

[10] S. McVey, P. L. Pauson, *J. Chem. Soc.* **1965**, 4312–4318.

[11] A. Lentz, Dissertation, Technische Universität Berlin, **1993**.

[12] $C_{50}H_{50}Fe$ (**1**): M = 947.01, crystal dimensions 0.03 × 0.03 × 0.23 mm^3, monoclinic, $P2_1/n$ (no. 14); a = 2115.7(8), b = 1313.9(8), c = 941.4(8) pm, β = 114.22(6)°, V = 2386(3) × 10^{-30} m^3, Z = 2, ρ_{calcd} = 1.32 gcm^{-3}, μ = 6.03 cm^{-1}, Enraf-Nonius CAD4 diffractometer, $Cu_{K\alpha}$ radiation, λ = 71.069 pm, graphite monochromator, T = 230 K, $1 \le 2\theta \le 48°$, 3992 measured reflections, of which 1794 were independent (R_{int} = 0.0447), 1231 observed reflections with $(F_o) \ge 4\sigma(F_o)$, solution by direct methods and structure refinement with SHELX76, absorption correction (DIFABS, min. 0.785, max. 1.265), R = 0.159, Rw = 0.166 ($w = 1/\sigma^2(F_o)$), anisotropic refinement of heavy atom, isotropic refinement of all other non-hydrogen atoms, the positions of the H atoms were calculated [18b].

[13] In the IR and Raman spectra, apart from the typical bands for C_5Ph_5 ligands, only three additional bands are observed: $\nu_{as}(FeCp_2)$ 425 cm^{-1} (IR), $\nu_s(FeCp_2)$ 290 cm^{-1} (IR), $\delta(FeCp_2)$ 170 cm^{-1} (Raman) [11].
[14] M. J. Heeg, R. H. Herber, C. Janiak, J. J. Zuckerman, H. Schumann, W. F. Manders, *J. Organomet. Chem.* **1988**, *346*, 321–332.
[15] S. P. Gubin, S. A. Smirnova, L. I. Denisovich, A. A. Lubovich, *J. Organomet. Chem.* **1971**, *30*, 243–255.
[16] P. Zanello, A. Cinquantini, S. Mangani, G. Opromolla, L. Pardi, C. Janiak, M. D. Rausch, *J. Organomet. Chem.*, in press; C. Janiak, personal communication.
[17] G. L. K. Hoh, W. E. McEwen, J. Kleinberg, *J. Am. Chem. Soc.* **1961**, *83*, 3949.
[18] a) $C_{70}H_{50}BF_4Fe \cdot C_2H_4Cl_4$ (**3**): $M = 1203.68$, crystal dimensions $0.23 \times 0.10 \times 0.10$ mm^3, triclinic, $P\bar{1}$ (no. 2), $a = 1346.7(7)$, $b = 1732.2(5)$, $c = 1322.1(3)$ pm, $\alpha = 107.00(2)$, $\beta = 100.80(3)$, $\gamma = 74.00(4)^\circ$, $V = 2815(2) \times 10^{-30}$ m^3, $Z = 2$, $\rho_{calcd} = 1.42$ $g\,cm^{-3}$, $\mu = 4.51$ cm^{-1}, Enraf-Nonius CAD4 diffractometer, $Cu_{K\alpha}$ radiation, $\lambda = 71.069$ pm, graphite monochromator, $T = 190$ K, $1 \leq 2\theta \leq 45$, 7681 measured reflections, of which 6131 were independent ($R_{int} = 0.0280$), 3756 observed reflections with $(F_o) \geq 4\sigma(F_o)$, solution by direct methods and structure refinement with SHELX76, absorption correction (DIFABS, min. 0.733, max. 1.369), $R = 0.086$, $Rw = 0.094$ ($w = 1/\sigma^2(F_o)$), refinement of all non-hydrogen atoms mostly anisotropic, otherwise isotropic, the positions of the H atoms were calculated [18]. Rotational disorder of the F atoms F2, F3, and F4 in the BF_4 anion could be established by refinement of the population factors F2, F3, F4 and F2a, F3a, F4a with approximately 0.49/0.51. b) Further details of the crystal structure investigation may be obtained from the Fachinformationszentrum Karlsruhe, D-76344 Eggenstein-Leopoldshafen (FRG) on quoting the depository number CSD-58235.

Organolanthanoid–Carbene-Adducts**

Herbert Schumann*, Mario Glanz, Jörn Winterfeld, Holger Hemling, Norbert Kuhn,* und Thomas Kratz

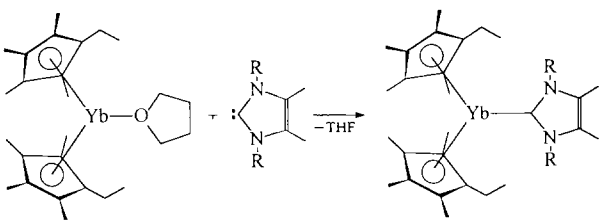
Dedicated to Professor Ekkehardt Lindner on the occasion of his 60th birthday

Carbenes usually exhibit acceptor properties as ligands and are most often dependent on classic backbonding for the formation of stable metal complexes. For this reason lanthanoid metals with their 4f electrons, which lie deep in the inside of the electron shell and thus hardly participate in bonding, are considered to be very poor coordination partners for carbenes. The reports that have recently appeared on stable derivatives of imidazol-2-ylidene[1] open up new possibilities due to the nucleophilic character of these compounds. The successful synthesis of stable adducts with iodine,[2] tellurium,[3] selenium,[4] and, in particular, the bond formation to electron-deficient centers such as GeI_2,[5] AlH_3,[6] and BH_3[7] gave the impression that it should also be possible to prepare lanthanoid carbene complexes.[8] Particularly suitable for this should be oligomethylated bis(cyclopentadienyl)samarium(II), -europium(II), and -ytterbium(II) derivatives, which can not only alter the oxidation state,[9–11] but also have enough space for a sterically demanding third ligand because of their bent structure.

[*] Prof. Dr. H. Schumann, Dr. M. Glanz, Dr. J. Winterfeld, Dr. H. Hemling
Institut für Anorganische und
Analytische Chemie der Technischen Universität
Strasse des 17. Juni 135, D-10623 Berlin (FRG)
Telefax: Int. code + (30)314-22168
Prof. Dr. N. Kuhn, Dipl.-Chem. T. Kratz
Institut für Anorganische Chemie der Universität
Auf der Morgenstelle 18, D-72076 Tübingen (FRG)

[**] Organometallic Compounds of Lanthanoids, Part 86. This work was supported by the Deutsche Forschungsgemeinschaft, the Fonds der Chemischen Industrie, and the Bundesministerium für Bildung und Wissenschaft (Graduiertenkolleg „Synthese und Strukturaufklärung niedermolekularer Verbindungen"). Part 85: H. Schumann, J. Winterfeld, M. Glanz, R. D. Köhn, H. Hemling, *J. Organomet. Chem.*, in press.

Thus, treatment of the bis(ethyltetramethylcyclopentadienyl)ytterbium complex **1** with the imidazol-2-ylidenes **2** leads to the corresponding organolanthanoid–carbene adducts **3** in good yields. Compounds **3** are thermally very stable (decomposition temperature at 0.1 mbar for **3a** is 229 °C and 155 °C for **3b**) and can be isolated as black crystals. They are soluble in relatively polar and aromatic solvents such as tetrahydrofuran, diethyl ether, toluene, and benzene. In contrast, they are only sparingly soluble in hexane or pentane. Both products **3** are considerably more stable to air and moisture than **1**.



1 **2a**: R = Me **3a**: R = Me
2b: R = *i*Pr **3b**: R = *i*Pr

The chemical shifts in the ^1H and ^{13}C NMR spectra of **3a** and **3b** are as expected and are not significantly different from the data of complex **1** and those of the carbenes **2**. These results and the intense dark color of the isolated adducts clearly show that quasi-coordinative Yb^{II}–C bonds are present in **3** and that **3a** and **3b** are not paramagnetic Yb^{III} compounds. The ^{13}C NMR spectrum also indicates a new quality of the metal carbene interactions, since in **3**, in contrast to the ylidene complexes of I_2, Se, Te, GeI_2, BH_3, and AlH_3,[2–7] the carbene carbon atom is slightly shifted for the first time to higher field by about 8 ppm.

The electron impact (70 eV) mass spectra of **3a** and **3b** show no peak for the molecular ion; only several peaks for metal–carbene fragments occur in addition to the expected signals for $[(C_5Me_4Et)Yb]^+$ and $[(C_5Me_4Et)_2Yb]^+$.

In the crystal the ylidene forms a planar five-membered ring, the plane of which to a good approximation also contains all the atoms bound to the heterocycle (Fig. 1). Alternating bond lengths, which are also observed in other complexes, occur within the carbene ring; however, here they are not so pronounced.[7] Whereas the C13–N (1.387(5) Å) distance indicates

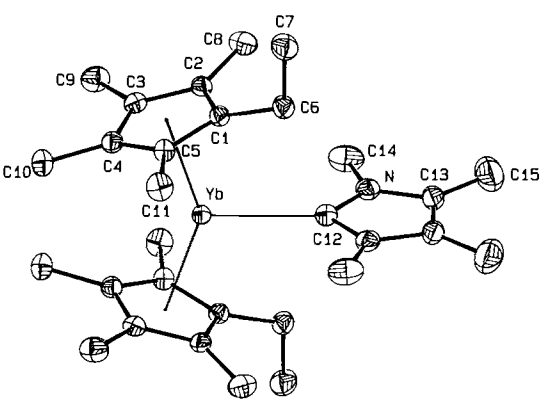


Fig. 1. Crystal structure of **3a** (ORTEP [12], thermal ellipsoids drawn at 50% probability level (the atom positions produced by symmetry operations [−x, y, 1.5−z] are not shown). Selected distances [Å] and angles [°] (standard deviations are given in parentheses) [13]: Yb–C1 2.669(4), Yb–C2 2.692(4), Yb–C3 2.688(4), Yb–C4 2.671(4), Yb–C5 2.648(3), Yb–C12 2.552(4); Cp-Yb-Cp 144.0(4), Cp-Yb-C12 107.5(4).

a formal single bond, the distances C13–C13′ (1.358(11) Å) and C12–N (1.362(4) Å) are shorter and lie in the range expected for double bonds. The exocyclic C–C (1.489(6) Å) and N–C bonds (1.453(6) Å) of the ylidene,[7] and the Yb–C distances to the cyclopentadienyl ligand[9] (average 2.674(4) Å) as well as the Cp-Yb-Cp and Cp-Yb-C12 angles[9] correspond to the expected values. The Yb–C12 bond length is appropriate for an extended single bond and is slightly longer than the corresponding distances in $[\{Cp_2Yb(\mu\text{-Me})\}_2]$ (2.49 Å, 2.54 Å);[16] however, it is significantly shorter than the corresponding bonds in $[Cp^*_2Yb(\mu\text{-Me})BeCp^*]$ (2.77 Å)[17] or $[Cp^*_2Yb(\mu\text{-Et})AlEt_2(thf)]$ (2.85 Å).[18] This illustrates the problems associated with the discussion of the structure in comparison to classic carbene complexes. Whereas the nearly trigonal-planar configuration of the C12 atom, which almost corresponds to sp^2 hybridization, and the p_π-p_π interactions in the bonds C12–N can be interpreted as characteristic features of a carbene complex, the Yb–C12 distance does not fit into the range expected for a double bond. As a consequence of the lack of Yb–C backbonding, **3a** and **3b** can be considered as Fischer-type carbene adducts of organolanthanoid(II) compounds.

Experimental Procedure

Compound **1** was obtained analogously to Cp^*_2Yb [9], and **2a, b** were prepared according to literature [1]. The NMR spectra were recorded with a Bruker AMX 200 spectrometer at 200 MHz (^1H) or 50.32 MHz (^{13}C).

3a: **2a** (0.16 g, 1.3 mmol) in THF (5 mL) was added dropwise to a solution of **1** (0.68 g, 1.2 mmol) in THF (40 mL) at −30 °C and stirred for 12 h at 25 °C. The solvent was removed under vacuum, the residue washed with hexane (15 mL) and suspended in toluene (40 mL). The clear solution was concentrated to 20 mL from which black crystals of **3a** were obtained at −25 °C.

Yield 0.63 g (80%); m.p. (0.1 mbar) 229 °C. ^1H NMR ([D$_8$]THF): δ = 3.37 (s, 6H, NCH_3), 2.48 (q, 4H, $C_5CH_2CH_3$), 2.08 (s, 6H, CCH_3), 1.84 (s, 12H, C_5CH_3), 1.82 (s, 12H, C_5CH_3), 0.86 (t, 6H, $C_5CH_2CH_3$); ^{13}C NMR ([D$_8$]THF): δ = 205.0 (:C), 125.8 (CCH_3), 119.0 ($C_5CH_2CH_3$), 111.8 (C_5CH_3), 111.1 (C_5CH_3), 35.9 (NCH_3), 19.8 ($C_5CH_2CH_3$), 16.7 ($C_5CH_2CH_3$), 10.9 (C_5CH_3), 10.8 (C_5CH_3), 8.6 (CCH_3). Correct elemental analysis for $C_{20}H_{46}N_2Yb$ (595.74).

3b: Analogously to **3a**, **1** (0.31 g, 0.6 mmol) was treated with **2b** (0.10 g, 0.6 mmol) and black crystals of **3b** were obtained at −25 °C. Yield 0.29 g (78%); m.p. (0.1 mbar) 155 °C. ^1H NMR (C_6D_6): δ = 3.67 (sept, 2H, $NCHCH_3$), 2.57 (q, 4H, $C_5CH_2CH_3$), 2.18 (s, 12H, C_5CH_3), 2.12 (s, 12H, C_5CH_3), 1.55 (s, 6H, CCH_3), 1.22 (t, 6H, $C_5CH_2CH_3$), 1.17 (d, 12H, $NCHCH_3$); ^{13}C NMR (C_6D_6): δ = 198.1 (:C), 124.8 (CCH_3), 118.9 ($C_5CH_2CH_3$), 111.9 (C_5CH_3), 111.0 (C_5CH_3), 49.7 ($NCHCH_3$), 21.0 ($NCHCH_3$), 20.5 ($C_5CH_2CH_3$), 16.8 ($C_5CH_2CH_3$), 12.0 (C_5CH_3), 11.7 (C_5CH_3), 8.9 (CCH_3). Correct elemental analysis for $C_{33}H_{54}N_2Yb$ (651.85).

Received: April 2, 1994 [Z68211E]
German version: *Angew. Chem.* **1994**, *106*, 1829

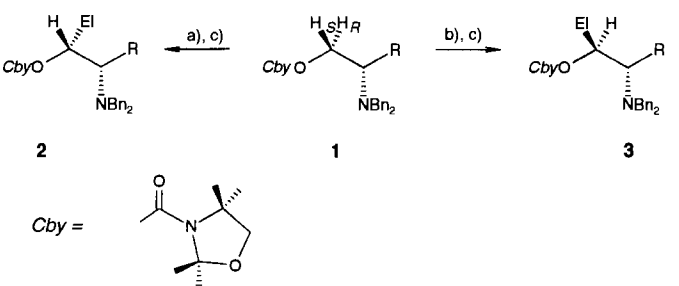
[1] A. J. Arduengo III, R. L. Harlow, M. Kline, *J. Am. Chem. Soc.* **1991**, *113*, 361–363; A. J. Arduengo III, H. V. R. Diaz, R. L. Harlow, M. Kline, *ibid.* **1992**, *114*, 5530–5534; N. Kuhn, T. Kratz, *Synthesis* **1993**, 561–562.
[2] N. Kuhn, T. Kratz, G. Henkel, *J. Chem. Soc. Chem. Commun.* **1993**, 1778–1779.
[3] N. Kuhn, G. Henkel, T. Kratz, *Chem. Ber.* **1993**, *126*, 2047–2049.
[4] N. Kuhn, G. Henkel, T. Kratz, *Z. Naturforsch. B* **1993**, *48*, 973–977.
[5] A. J. Arduengo III, H. V. R. Diaz, J. C. Calabrese, F. Davidson, *Inorg. Chem.* **1993**, *32*, 1541–1542.
[6] A. J. Arduengo III, H. V. R. Diaz, J. C. Calabrese, F. Davidson, *J. Am. Chem. Soc.* **1992**, *114*, 9724–9725.
[7] N. Kuhn, G. Henkel, T. Kratz, J. Kreutzberg, R. Boese, A. H. Mautlitz, *Chem. Ber.* **1993**, *126*, 2041–2045.
[8] For the coordination of imidazol-2-ylidenes to centers of d-block elements cf. K. Öfele, W. A. Herrmann, D. Mihalios, M. Elison, E. Herdtweck, W. Scherer, J. Mink, *J. Organomet. Chem.* **1993**, *459*, 177-184; N. Kuhn, T. Kratz, R. Boese, D. Bläser, *ibid.* **1994**, *470* C8-C11, and references therein.
[9] T. D. Tilley, R. A. Andersen, B. Spencer, H. Ruben, A. Zalkin, D. H. Templeton, *Inorg. Chem.* **1980**, *19*, 2999–3003.
[10] W. J. Evans, L. A. Hughes, T. Hanusa, *J. Am. Chem. Soc.* **1984**, *106*, 4270–4272.
[11] W. J. Evans, L. A. Hughes, T. Hanusa, *Organometallics* **1986**, *5*, 1285–1291.
[12] C. K. Johnson, ORTEP-II, Report ORNL-5138, Oak Ridge National Laboratory, TN, USA, 1976.
[13] Crystal data: 0.6 × 1.5 × 1.5 mm, orthorhomic, $C222_1$, a = 11.366(3), b = 15.953(4), c = 14.990(4) Å, V = 2718.0(12) Å^3, Z = 4, ρ_{calcd} = 1.451 g cm^{-3}, measurement parameters: Enraf-Nonius CAD-4 diffractometer, T = 150(2) K, λ = 71.069 pm ($Mo_{K\alpha}$), graphite monochromator, μ = 3.323 mm^{-1}, Ω–2θ, $4 \le 2\theta \le 65°$; 2690 measured, 2689 independent (R_{int} = 0.0063), 2639 observed reflections ($|F_o| > 4\sigma|F_o|$), corrections: Lorentz, polarization, decay (min: 1.000, max: 1.010), DIFABS (min: 0.819, max: 1.256), solution: Patterson (SHELX-86 [14]), difference Fourier (SHELX-93 [15]) all non-hydrogen atoms anisotropic, all hydrogen positions calculated isotropically ($u_{iso,H}$ = 0.08 Å^2), e_o: max 0.609, min −0.857 Å^3; refined parameters: 146, $R1 = \Sigma||F_o| - |F_c||/\Sigma|F_o| = 0.0175$, $wR2 = [\Sigma w(F_o^2 - F_c^2)^2/\Sigma w(F_o^2)^2]^{1/2} = 0.0424$. Further details of the crystal structure investigation may be obtained from the Fachinformationszentrum Karlsruhe, D-76344 Eggenstein-Leopoldshafen (FRG) on quoting the depository number CSD-58277.
[15] G. M. Sheldrick, SHELX-93, Program for Crystal Structure Determination, Univesität Göttingen, **1993**.
[16] J. Holton, M. F. Lappert, D. G. H. Ballard, R. Pearce, J. L. Atwood, W. E. Hunter, *J. Chem. Soc. Chem. Commun.* **1976**, 480–481.
[17] C. J. Burns, R. A. Andersen, *J. Am. Chem. Soc.* **1987**, *108*, 5853–5855.
[18] H. Yamamoto, H. Yasuda, K. Yokota, A. Nakamura, Y. Kai, N. Kasai, *Chem. Lett.* **1988**, 1963–1966.

Regio- and Stereoselective Electrophilic C-Substitution of 2-(*N*,*N*-Dibenzylamino)-1,ω-alkanediols by Lithiation of Their Carbamates**

Walter Guarnieri, Matthias Grehl, and Dieter Hoppe*

Dedicated to Professor Werner Tochtermann on the occasion of his 60th birthday

Enantiomerically pure β-amino-α-hydroxy acids and aminopolyols are becoming increasingly important for the synthesis of enzyme inhibitors.[1] We report here on a simple and very flexible approach to these classes of compounds. The carbamate derivatives **1** of (*S*)-2-(*N*,*N*-dibenzylamino)-1-alkanols can be deprotonated at C-1 by *sec*-butyllithium to give the configurationally stable ion pairs **2** (El = Li) or **3** (El = Li), which react with electrophiles stereospecifically with retention of configuration (Scheme 1).[2] Deprotonation in the presence of the achiral additive *N*,*N*,*N*′,*N*′-tetramethylethylenediamine (TMEDA, variant A) is directed by the stereogenic center at C-2 and favors the removal of the (*pro-R*) proton H_R; in contrast, in the presence of (−)-sparteine (variant B) H_S is abstracted.[3, 4]



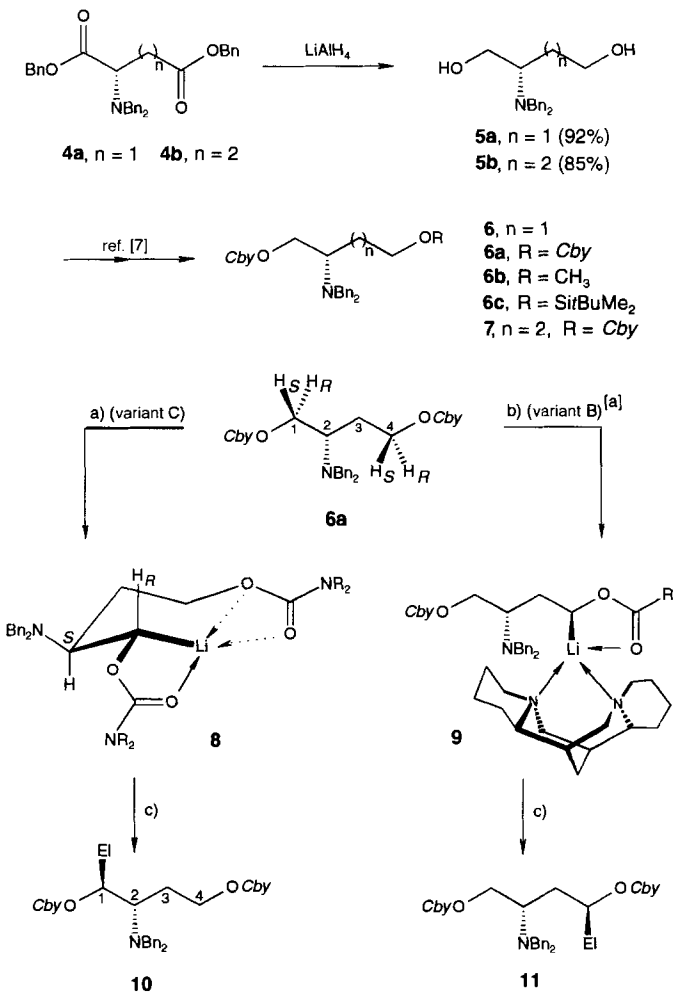
Scheme 1. Variant A: a) *s*BuLi, TMEDA, Et_2O, −78 °C; Variant B: b) *s*BuLi, (−)-sparteine, Et_2O, −78 °; c) electrophile ElX.

[*] Prof. Dr. D. Hoppe, W. Guarnieri, Dr. M. Grehl[+]
Organisch-chemisches Institut der Universität
Corrensstrasse 40, D-48149 Münster (FRG)
Telefax: Int. code + (251)83-9772

[+] X-ray structure analysis

[**] This research was supported by the Deutsche Forschungsgemeinschaft, the Fonds der Chemischen Industrie, and the Pharma Research Center of Bayer AG, Wuppertal.

When we applied this method to dicarbamate **6a**,[7, 8] which was prepared from (*S*)-aspartic acid via diol **5a**,[5, 6] we observed that the reaction following variant A was completely unselective: the four possible products **10**, 1-*epi*-**10**, **11**, and 4-*epi*-**11** formed in roughly equal amounts (Scheme 2). Variant



Scheme 2. a) 1.5 equiv *s*BuLi, Et_2O, 5 h at −78 °C. b) 1.5 equiv *s*BuLi, 1.5 equiv (−)-sparteine, Et_2O, 5 h at −78 °C. c) Electrophile EIX (see Table 1). −78 → 20 °C. [a] Side reaction.

B with sparteine provided the diastereomerically pure substitution products **10** and **11** in varying proportions.[9] Since exclusive formation of regioisomers **10** occurred only with especially reactive electrophiles like CH_3OD and CO_2, we suspected that the 4-carbamoyloxy group is involved in the rapid formation of a bicyclic chelate[10, 11] such as **8**, which is in a slow equilibrium with the sparteine complex[12] **9**. This hypothesis was confirmed convincingly when we conducted the lithiation in the absence of an external complexing agent (variant C).[3] Trapping the intermediate lithium compound with diverse electrophiles gave exclusively the diastereomerically pure regioisomers **10** (Table 1).[8, 14] The proposed intermediate **8** is characterized by high reactivity and low basicity; even the bulky electrophile diisopropyl ketone added readily to give **10k**. Acylation of **10f–h** with acid chlorides also proceeded smoothly without epimerization.[15]

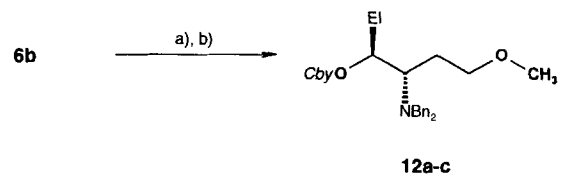
The following control experiments underline the importance of a second complexing group in the 4-position in determining the course of the reaction.[16] The 4-silyl ether[4, 6] **6c** is inert

Table 1. Aminoalkanediol derivatives **10** and **12–16**.

Starting Material	Variant	EIX	Product [a]	El	Yield [%]	$[\alpha]_D^{20}$ [b]
6a	C	MeOD	**10a**	D	95	−29.2
6a	C	CH_3I	**10b**	CH_3	93	+14.3
6a	C	CO_2	**10c**	CO_2Me [c]	92	−20.2
6a	C	Me_3SiCl	**10d**	Me_3Si	73	+17.3
6a	C	Me_3SnCl	**10e**	Me_3Sn	75	+19.4
6a	C	*t*BuC(=O)Cl	**10f**	*t*BuC(=O)	81	−40.2
6a	C	[d]	**10g**	[f]	83	−51.8
6a	C	EtC(=O)Cl	**10h**	EtC(=O)	80	−33.0
6a	C	$Me_2C=O$	**10i**	$Me_2C(OH)$	85	+11.3
6a	C	$iPr_2C=O$	**10k**	$iPr_2C(OH)$	75	+14.6
6a	C	EtCH=O	**10l**	EtCH(OH) [e]	80	–
6b	C	CH_3I	**12a**	CH_3	69	+18.4
6b	C	CO_2	**12b**	CO_2Me [c]	74	−27.3
6b	C	[d]	**12c**	[f]	71	−64.6
10b	B	CO_2	**13**	CH_3	90	−12.5
10a	B	CH_3I	**14**	CO_2Me [c]	88	+4.7
7	B	CO_2	**15**	CO_2Me [c]	78	−1.3
7	C	CO_2	**16**	CO_2Me [c]	61	−21.4

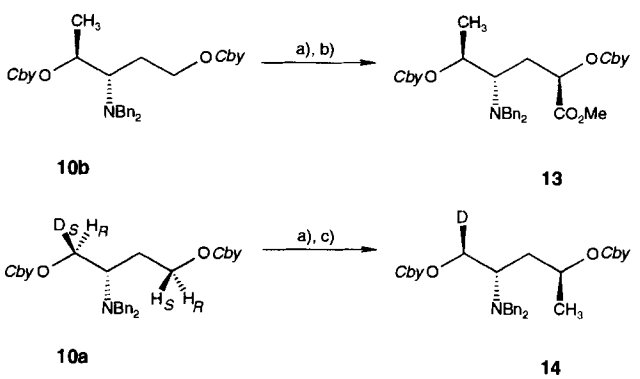
[a] All products were obtained in diastereomeric and regioisomeric purity of ≥97 %. [b] $c = 0.8–1.2$ in $CHCl_3$. [c] After esterification of the acid with diazomethane. [d] (*E*)-$CH_3CH=CHC(=O)Cl$. [e] Mixture of epimers, (1*R*):(1*S*) = 85:15. [f] (*E*)-$CH_3CH=CHC(=O)$.

even at −40 °C under the conditions for variant C (and also B); however, the 4-methyl ether[6, 8] **6b** was deprotonated readily at −78 °C and yielded the diastereomerically pure substitution products **12a–c** (Scheme 3, Table 1).



Scheme 3. a) 1.5 equiv *s*BuLi, Et_2O, 5 h at −78 °C. b) EIX, −78 → 0 °C. **12a**: El = CH_3; **12b**: El = CO_2Me; **12c**: El = (*E*)-$CH_3CH=CHC(=O)$.

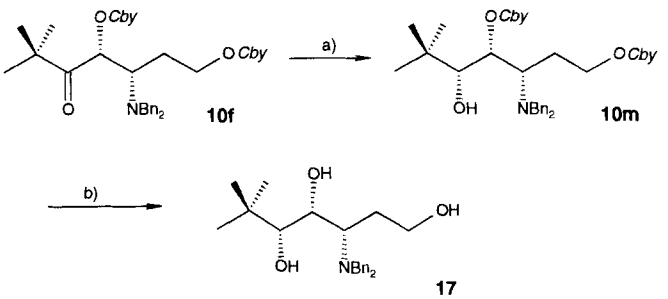
Directed substitution at C-4 is possible by a second deprotonation step following variant B; this was demonstrated by the conversion of the 1-methyl derivative **10b** into ester **13** (Scheme 4).[8, 19] The 1-H_S atom can also be protected against deprotonation by deuteriation, owing to the extraordinarily large H/D kinetic isotope effect.[20] When the (1*S*) deuterio derivative



Scheme 4. a) 1.5 equiv (−)-sparteine, 1.5 equiv *s*BuLi, Et_2O, 5 h at −78 °C. b) 1. CO_2, 2. CH_2N_2; 90 %. c) CH_3I, −78 → 0 °C; 86 %.

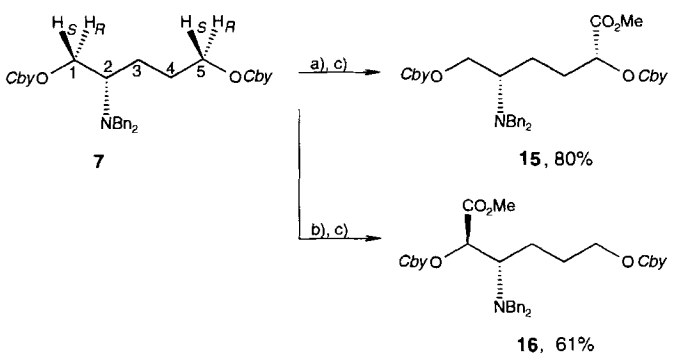
10a was deprotonated in the presence of (−)-sparteine (variant B), exclusively 4-H_S was abstracted. Subsequent methylation led to pure diol **14**[8, 19] with an extended carbon chain.

The configuration of adducts **10** was established by the X-ray structure analysis[17] of triol **17**,[18] which was obtained from ketone **10f** (Scheme 5).



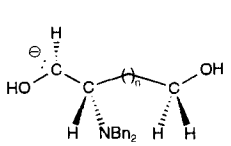
Scheme 5. a) $NaBH_4$, Et_2O, 0 °C, 2 h; *ds* = 5:1; separation by chromatography (diethyl ether/pentane (1:5) on silica gel), 70% **10m**. b) $LiAlH_4$, Et_2O, 12 h reflux, 65%.

In contrast, (*S*)-2-(*N*,*N*-dibenzylamino)-1,5-pentanediyl dicarbamate (**7**),[7, 8] which was prepared in three steps from (*S*)-glutamic acid, was lithiated selectively at C-5 when variant B was employed. The analogous reaction according to variant C, though sluggish, proceeded at C-1. Carboxylation and esterification provided the pure isomers **15** and **16**,[8] respectively (Scheme 6, Table 1). This result indicates that a sterically less favorable homologue of the bicyclic chelate of type **8** is involved.

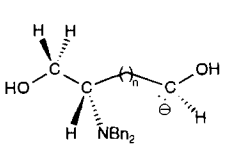


Scheme 6. a) 1.5 equiv (−)-sparteine, 1.5 equiv *s*BuLi, Et_2O, 5 h at −78 °C. b) 1.5 equiv *s*BuLi, Et_2O, 5 h at −78 °C. c) 1. CO_2, 2. CH_2N_2, −78 → 0 °C.

The procedure described here offers a simple, direct approach to synthetic equivalents of essentially stereohomogeneous aminodihydroxyalkanides like **18** and **19**. As demonstrated,



18 (n = 1,2)



19 (n = 1,2)

the cleavage of the carbamate group is possible reductively or hydrolytically under acid catalysis.[3b, 11a]

Experimental Procedure

Variant C: A solution of dicarbamate **6a** (595 mg, 1.00 mmol) in diethyl ether (6 mL) was cooled in a dry ice/acetone bath while 1.5 mmol of a ca. 1.4 M solution of *sec*-butyllithium in isopentane/cyclohexane was added dropwise. The reaction mixture was stirred for 5 h at −78 °C. Then 1.70 mmol of the electrophile was added, and the reaction mixture was allowed to warm slowly (14 h) to room temperature. The reaction mixture was worked up by the addition of 6 mL of water. The aqueous phase was extracted with diethyl ether, and the combined organic phases were dried and concentrated under vacuum. The crude products were purified by column chromatography on silica gel eluting with diethyl ether/pentane. In variants A and B TMEDA (174 mg, 1.50 mmol) and (−)-sparteine (351 mg, 1.5 mmol), respectively, were added to the solution of dicarbamate **6a**.

Received: March 23, 1994 [Z6789IE]
German version: *Angew. Chem.* **1994**, *106*, 1815

[1] D. H. Rich in *Comprehensive Medicinal Chemistry*, *Vol. 2* (Eds: C. Hansch, P. G. Sammes, J. B. Taylor), Pergamon, Oxford, **1990**, Chapter 8.
[2] J. Schwerdtfeger, D. Hoppe, *Angew. Chem.* **1992**, *104*, 1547; *Angew. Chem. Int. Ed. Engl.* **1992**, *31*, 1505.
[3] a) D. Hoppe, F. Hintze, P. Tebben, *Angew. Chem.* **1990**, *102*, 1457; *Angew. Chem. Int. Ed. Engl.* **1990**, *29*, 1422; b) F. Hintze, D. Hoppe, *Synthesis* **1992**, 1216.
[4] a) O. Zschage, D. Hoppe, *Angew. Chem.* **1989**, *101*, 67; *Angew. Chem. Int. Ed. Engl.* **1989**, *28*, 69; b) P. Beak, L. G. Carter, *J. Org. Chem.* **1981**, *46*, 2363; c) S. T. Kerrick, P. Beak, *J. Am. Chem. Soc.* **1991**, *113*, 9708; d) P. Beak, S. T. Kerrick, S. Wu, J. Chu, *ibid.* **1994**, *116*, 3231; e) short overview: P. Knochel, *Angew. Chem.* **1992**, *104*, 1486; *Angew. Chem. Int. Ed. Engl.* **1992**, *31*, 1459.
[5] Diols **5a** [6d] and **5b** were obtained by $LiAlH_4$ reduction of dibenzyl esters **4a** and **4b**, respectively, which were prepared from (*S*)-aspartic and (*S*)-glutamic acid, respectively, in analogy to the procedure of L. Velluz et al. [6c]. **5a**: $[\alpha]_D^{20} = +17.4$ (*c* = 1.9 in $CHCl_3$); **5b**: $[\alpha]_D^{20} = +69.5$ (*c* = 1.2 in $CHCl_3$).
[6] a) M. T. Reetz, M. T. Drewes, A. Schmitz, *Angew. Chem.* **1987**, *99*, 1186; *Angew. Chem. Int. Ed. Engl.* **1987**, *26*, 1141; b) Review: M. T. Reetz, *ibid.* **1991**, *103*, 1559 bzw. **1991**, *30*, 1531; c) L. Velluz, G. Amiard, R. Heymes, *Bull. Soc. Chim. Fr.* **1954**, 1012; d) P. Gmeiner, A. Kärtner, D. Junge, *Tetrahedron Lett.* **1993**, *34*, 4325.
[7] Dicarbamates **6a** (75%) and **7** (79%) were obtained from the reactions of **5a** and **5b**, respectively, with 2,2,4,4,-tetramethyl-1,3-oxazolidin-3-carbonyl chloride and NaH [3b]. For the synthesis of silyl ether **6c**, **5a** was silylated selectively at the 4-OH group with *tert*-butyldimethylsilyl chloride and then carbamoylated according to [3b]. Methyl ether **6c** was obtained by desilylation of **6c** (with tetrabutylammonium fluoride) and subsequent O-methylation (methyl iodide, sodium hydride). $[\alpha]_D^{20}$ (*c* = 1.0–1.3 in $CHCl_3$): **6a** = −40.9; **6b** = −28.5; **6c** = −14.4; **7** = −11.8.
[7] Dicarbamates **6a** (75%) and **7** (79%) were prepared by reaction of **5a** and **5b**, respectively, with 2,2,4,4,-tetramethyl-1,3-oxazolidine-3-carbonyl chloride according to the sodium hydride method. The silyl ether **6c** was obtained by selective silylation of **5a** (4-OH group) with *tert*-butyldimethylsilyl chloride and subsequent carbamoylation [3b]. For the preparation of the methyl ether **6b**, compound **6c** was desilylated with tetrabutylammonium fluoride and then *O*-methylated (methyl iodide, sodium hydride). $[\alpha]_D^{20}$ (*c* = 1.0–1.3 in $CHCl_3$): **6a** = −40.9; **6b** = −28.5; **6c** = −14.4; **7** = −11.8.
[8] Satisfactory C,H analyses (C ± 0.3, H ± 0.3) were obtained for all new compounds.
[9] Reaction of **6a** with CO_2 under the conditions of variant B gave only regioisomer **10c**; reaction with $(CH_3)_3SnCl$ yielded products **10e** and **11e** in a 7:3 ratio; **11e**: $[\alpha]_D^{20} = -37.8$ (*c* = 2.0 in $CHCl_3$).
[10] The structure of the bicyclic chelate is not yet known; formula **8** offers only a plausible explanation of its role in the reaction. It is not known whether the lithium cation is complexed by the more basic oxo group, the ester oxygen atom, or both [11–13].
[11] References to related bicyclic chelates of 1,3- and 1,4-dicarbamates: a) M. Paetow, H. Ahrens, D. Hoppe, *Tetrahedron Lett.* **1992**, *33*, 5327; b) *ibid.* **1992**, *33*, 5323.
[12] X-ray structure analysis of a lithiated carbamate, see: M. Marsch, K. Harms, O. Zschage, D. Hoppe, G. Boche, *Angew. Chem.* **1991**, *103*, 338; *Angew. Chem. Int. Ed. Engl.* **1991**, *30*, 321.
[13] The *N*,*N*-dibenzylamino group is a poor coordinating function for Li^+, see: P. Sommerfeld, D. Hoppe, *Synlett* **1992**, 764.
[14] The ratios of isomers were determined by ^1H NMR spectroscopy. The detection limit for the minor diastereomers and regioisomers was roughly 3%. The enantiomeric purity of the substitution products was > 98% *ee*. Diol **5a** served as the standard in the purity determinations: *ent*-**5a** was not found as an impurity [GC analysis of alcohol **6c** in the form of *N*-(*S*)-(1-phenylethyl)urethane]. Racemization during the lithiation can be excluded, since the very improbable deprotonation at the stereogenic center C-2 of **6** or **7** would lead to degradation or elimination.

[15] In general the acylation of primary and secondary alkyllithium compounds is problematic because of the deprotonation and addition reactions of the ketone formed.

[16] For the chelate effect of carbamoyloxy groups in lithiation, see: a) D. Hoppe, *Angew. Chem.* **1984**, *96*, 930; *Angew. Chem. Int. Ed. Engl.* **1984**, *23*, 932; b) J. E. Resek, P. Peak, *J. Am. Chem. Soc.* **1994**, *116*, 405; c) V. Snieckus, *Chem. Rev.* **1990**, *90*, 879; d) P. Beak, A. I. Meyers, *Acc. Chem. Res.* **1986**, *19*, 356.

[17] X-ray structure analysis of **17**: Enraf-Nonius CAD4 diffractometer, $Mo_{K\alpha}$ radiation ($\lambda = 0.71069$ Å), graphite monochromator, $T = 20$ °C, crystal dimensions $0.63 \times 0.31 \times 32$ mm, $C_{23}H_{33}NO_3$, orthorhombic, space group $P2_12_12_1$, $a = 9.357(1)$, $b = 10.931(1)$, $c = 22.109(2)$ Å, $V = 2261.3(3)$ Å^3, $\rho_{calcd} = 1.09$ g cm^{-3}, $m(Mo_{K\alpha}) = 0.7$ cm^{-1}, $Z = 4$, 2180 measured reflections, 2180 independent reflections, 984 reflections with $I \geq 2\sigma(I)$, ω-2θ scans, $2\theta_{max} = 50.2$°, scan rate 5.5–16.5° min^{-1}. The structure was solved by direct methods with the program SHELXS-86. The non-hydrogen atoms were refined based on F_o^2 with the program SHELXL-93. The positions of the hydrogen atoms were calculated. Weighting scheme: $wR^2 = [\Sigma[w(F_o^2 - F_c^2)^2]/[\Sigma[w(F_o^2)^2]]^{1/2}$, $R(R^2w) = 0.055$ (0.119), residual electron density 0.30 e Å^{-3}. Further details of the crystal structure investigation may be obtained from the Fachinformationszentrum Karlsruhe, D-76344 Eggenstein-Leopoldshafen (FRG) on quoting the depository number CSD-58248.

[18] **17**: ^{1}H NMR (300 MHz, $CDCl_3$, TMS): $\delta = 0.90$ (s, 1-CH_3), 2.10 (m, 5-H), 3.04 (dt, $^3J(H_3,H_4) = 4.9$ Hz, 2H, $^3J(H_4,H_5) = 8.7$ Hz, 3H), 3.30 (d, 2-H), 3.63–3.75 (dd, 3-H; m, 6-H), 3.82 (m, $^3J(H_5,H_6) = 10.6$ Hz, 6-H); ^{13}C NMR ($CDCl_3$): $\delta = 26.23$ (C-1-CH_3), 28.95 (C-5), 34.87 (C-1), 56.80 (C-4), 61.73 (benzyl), 54.82 (C-6), 72.42 (C-3), 76.95 (C-2).

[19] **13**: ^{1}H NMR (300 MHz, $CDCl_3$, TMS): $\delta = 1.10$–1.80 (m, Ox-CH_3), 1.40 (d, $^3J(H_1,H_2) = 6.4$ Hz, 2H), 2.15 (m, 4-H), 3.05 (m, 3-H), 3.60 (s, 7-H), 3.61–3.79 (m, 10-H, 14-H, 17-H), 3.95 (d, 16-H), 5.18 (dd, $^3J(H_4,H_5) = 6.6$ Hz, 3H), 5.41 (dq, $^3J(H_2,H_3) = 3.8$ Hz, 4H); ^{13}C NMR ($CDCl_3$): $\delta = 18.23$ (C-1), 27.98 (C-4), 52.15 (C-7), 54.88 (C-14, C-15), 57.50 (C-3), 70.28, 70.39 (C-2 and C-5), 127.23, 128.51, 129.02, 139.84 (Ph), 171.94 (C-6). **14**: ^{1}H NMR (300 MHz, $CDCl_3$, TMS): $\delta = 1.10$–1.80 (m, Ox-CH_3), 1.55 (d, 5-H), 2.15 (m, 3-H), 3.20 (m, 2-H), 3.62–3.90 (m, 9-H, 13-H, 15-H, 16-H), 4.27 (d, $^3J(H_1,H_2) = 4.7$ Hz, 2H), 5.25 (tq, $^3J(H_3,H_4) = 6.8$ Hz, 3H, $^3J(H_4,H_5) = 6.2$ Hz, 4H), 7.21–7.42 (Ph); ^{13}C NMR ($CDCl_3$): $\delta = 19.56$ (C-5), 31.83 (C-3), 53.74 (C-2), 54.41 (C-15, C-16), 61.23 (t, C-1), 70.14 (C-4), 127.26, 128.44, 129.33, 139.73 (Ph).

[20] D. Hoppe, M. Paetow, F. Hintze, *Angew. Chem.* **1993**, *105*, 430; *Angew. Chem. Int. Ed. Engl.* **1993**, *32*, 394.

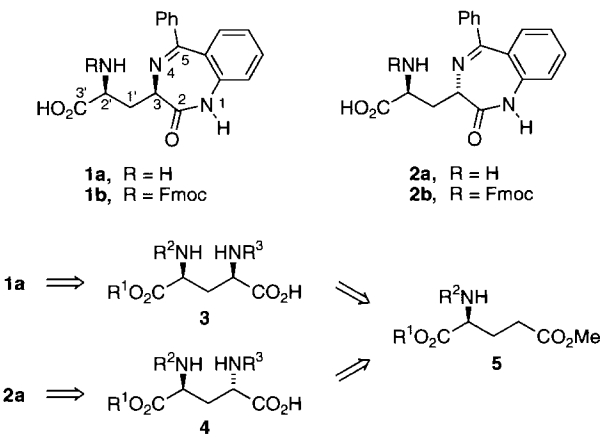
Synthesis of a New Unnatural Amino Acid with a Benzodiazepine-Containing Side Chain and Incorporation into a Tripeptide

Johann Mulzer,* Fridtjof Schröder, Alessandro Lobbia, Jürgen Buschmann, and Peter Luger

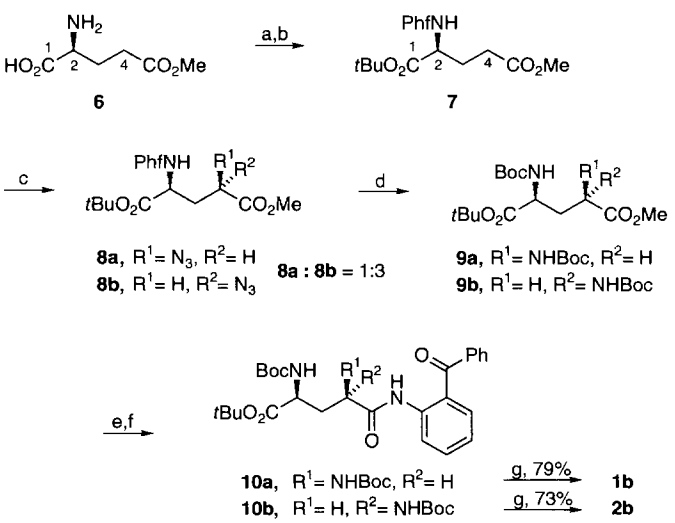
Owing to the constantly growing therapeutic importance of new physiologically active peptidomimetics,[1] the pool of available unnatural amino acids must be continually increased.[2] Of particular interest are the α-amino acids, which have side chains with a functional group that can act as a receptor ligand. In this case the peptidomimetic formed from these amino acids can behave as both a peptide and non-peptide receptor ligand.

Various hydrogenated forms of benzodiazepine have proved themselves to be good receptor ligands.[3] The amino acids **1a** and **2a** appear to be particularly attractive building blocks for peptidomimetics. Owing to the 1,3-substitution of the amino functions on the peptide, the benzodiazepine and peptide chain should be sufficiently far apart; however, a certain degree of mutual interaction is still maintained. The form of functionalization in **1a** and **2a** is analogous to that in the arylalanines histidine and trytophan. Little is known about the synthesis of 2,4-diaminoglutaric acids: Belokon et al. successfully synthesized the *anti*-(2*S*,4*S*)-diaminoglutaric acid via a stabilized asymmetric nickel complex;[4] the corresponding *syn* compound is unknown. The synthesis of the target compounds **1a** and **2a** is essentially a question of differentiating between the two amino acid groups. This is especially so for the *syn*-diaminoglutaric acid because of its *meso* symmetry.

Our retrosynthetic analysis showed that **1** and **2** could be made by a half-side Sternbach cyclization[5] of the *syn*- (**3**) and *anti*-2,4-diaminoglutaric acid derivatives (**4**), respectively. These in turn could be formed from the regioselective amination of N-protected (*S*)-glutamate (**5**).



The synthesis is shown in Scheme 1. Use of Rapoport's 9-phenylfluoren-9-yl (Phf) protecting group[6] and the C-1 *tert*-butyl ester completely blocked the 2-position in glutamate **7**, leading to selective formation of the 4-enolate upon treatment



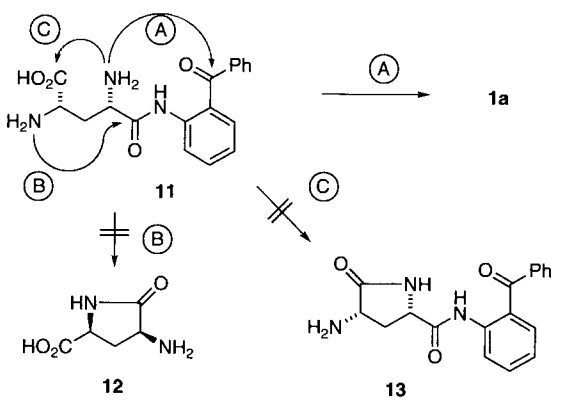
Scheme 1. Synthesis of **1b** and **2b**. a) Trimethylsilyl chloride, 9-phenylfluoren-9-yl bromide, $Pb(NO_3)_2$, 80%. b) *N*,*N*′-Dicyclohexyl-*O*-*tert*-butylisourea, CH_2Cl_2, 25 °C, 2 d, 76%. c) 1. KHDMS, THF, −60 °C; 2. 2,4,6-Triisopropylbenzenesulfonyl azide, −78 °C, 50 min, 54%. d) Boc_2O, 10% Pd/C, H_2 (4 bar), MeOH, 91%. e) LiOH, THF, 91%. f) *N*-Methylpiperidine, isobutyl chloroformate, CH_2Cl_2, −10 °C, 30 min, then 2-aminobenzophenone, 25 °C, 72 h, 78%. g) 1. EtOAc, HCl (pH = 4.5), 25 °C, 90 min; 2. H_2O, Na_2CO_3 (pH = 8.5), 3 h, then acetone, Fmoc-*O*-succinimide, 25 °C, 20 h.

[*] Prof. J. Mulzer, Dr. F. Schroeder
Institut für Organische Chemie der Freien Universität
Takustrasse 3, D-14195 Berlin (FRG)
Telefax: Int. code + (30)838-5163
Dr. A. Lobbia
Schering AG, Berlin (FRG)
J. Buschmann, P. Luger
Institut für Kristallographie der Freien Universität Berlin (FRG)

with potassium hexamethyldisilazide (KHDMS). Quenching this enolate with 2,4,6-triisopropylbenzenesulfonyl azide (trisyl-azide)[7] gave a 1:3 mixture of diastereomeric azides, **8a** and **8b**. Use of a chiral auxiliary on the neighboring carboxyl group would certainly have led to a better selectivity, but, as the diastereomers could be easily separated at a later stage, this complication was avoided. Catalytic hydrogenation of **8** in the presence of *tert*-butoxycarbonyl(Boc) anhydride led, in one step, to removal of the Phf protecting group, hydrogenation of the azide to the amine, and protection of both amine groups with Boc groups. The two ester groups in **9** are easily differentiable: the methyl ester can be selectively hydrolyzed with lithium hydroxide and subsequently transformed into the amide **10** with aminobenzophenone. The diastereomers **10a** and **10b** were easily separated at this stage by column chromatography.

Cyclization of **10a** and **10b** gave, after removal of the Boc groups with gaseous HCl in ethyl acetate, the benzodiazepines **1a** and **2a**, respectively. The solvent and the isobutene produced were removed under vacuum. The reaction was completed by addition of aqueous sodium carbonate until the pH value reached 8.5. Because of the instability of the free amino acids, they were immediately converted into their crystalline fluoren-9-ylmethoxycarbonyl (Fmoc) derivatives **1b** and **2b**.[9]

Cyclization of the aminoketones to the seven-membered ring compound **1** (Scheme 2, pathway A) proceeded smoothly, which



Scheme 2. Cyclization of **11**.

is surprising as two competing cyclizations to γ-lactams **12** (pathway B) and **13** (pathway C) are conceivable. Since the reaction takes place also in the solid phase, the crystal structure of the cyclization substrate **10b** (Fig. 1) may indicate the reasons for the conformational preference of one pathway over another. If the conformation in the section C-2 to C-5 determines the reaction pathway (numbering as in Fig. 1) and the NH-Boc and CO_2t-Bu groups are less important, then N-2 and C-12 are brought sufficiently close for a nucleophilic attack by their cisoid conformation. The 12-CO group is twisted in the benzophenone unit, thus allowing attack of N-2 on the π* CO orbital; in contrast, N-1 and C-5 (pathway B) are transoid, as are N-2 and C-1 (pathway C), which makes the reaction impossible. The structures of **10a**, **10b**, and the products of their reactions were established on the basis of the crystal structure of **10b**.

To prove that the new amino acids can be incorporated into peptides, **2b** was coupled in a stepwise fashion with (*S*)-Fmoc-alanine and (*S*)-Fmoc-leucine using the Merrifield solid-phase method to give the tripeptide, whose free NH_2 group was subse-

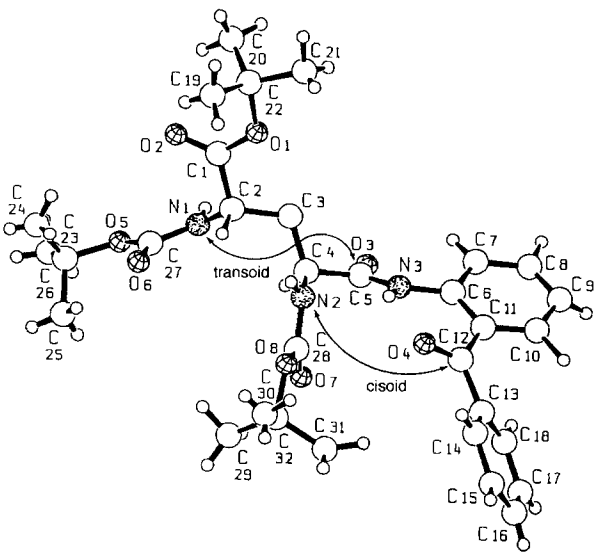
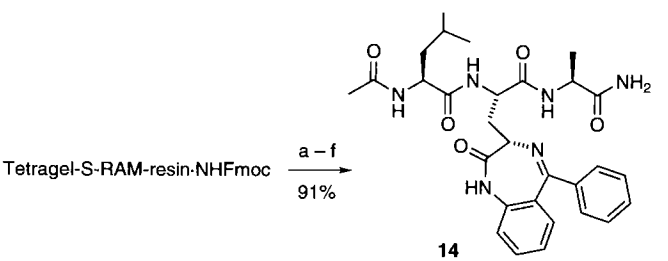


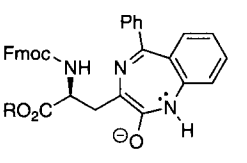
Fig. 1. Crystal structure of **10b** [11].

quently acetylated (Scheme 3). After separation from the resin, amide **14** was obtained in diastereomerically pure form (HPLC, 500 MHz ^{1}H NMR, 125 MHz ^{13}C NMR), indicating the enan-



Scheme 3. a) Piperidine (20% in DMF), 4 min. b) L-Fmoc-Ala-OH, TBTU [10], iPr$_2$EtN, CH_2Cl_2, 15 min. c) **2b**, TBTU, iPr$_2$EtN, CH_2Cl_2, 15 min. d) L-Fmoc-Leu-OH, iPr$_2$EtN, CH_2Cl_2, 15 min. e) 10% Ac_2O in DMF, 30 min. f) 96% CF_3CO_2H, 35 °C, 2.5 h.

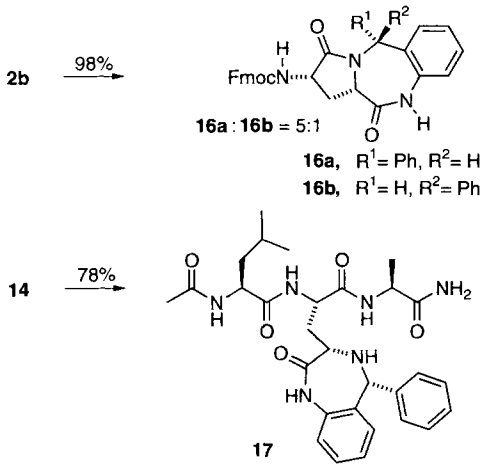
tiomeric and diastereomeric purity of the amino acid **2b**. Despite the activation from the C=N bond **2** cannot racemize, as deprotonation to **15** would lead to an antiaromatic 8π electron system.



15

To study the question of how much the diastereofacial shielding of functional groups is affected by their incorporation into peptide chains, the C=N bonds in **2b** and in **14** were hydrogenated under identical conditions (Scheme 4). In the first case a diastereomeric mixture of **16a** and **16b** (5:1) was formed; in the second case the tripeptide **17** was obtained diastereomerically pure (500 MHz ^{1}H NMR). Higher selectivities are therefore obtainable in peptide chains than with isolated amino acids. The configuration of the newly formed stereocenters in **16** and **17** was determined by difference NOE (nuclear Overhauser enhancement) experiments.

In conclusion α-amino acids with benzodiazepine-containing side chains have been prepared for the first time and their suitability for peptide coupling has been demonstrated. The synthe-



Scheme 4. Reduction of the C=N bond in **2b** and **14** ($Na[BH_3CN]$, AcOH, H_2O, 22 °C).

sis is applicable to all stereoisomers of the 1,3-diamino system and can probably be extended to other 1,*n*-diamino systems. The physiological properties of **1a** and **2a** and their incorporation into peptidomimetics is currently under investigation.

Received: March 12, 1994 [Z 6755 IE]
German version: *Angew. Chem.* **1994**, *106*, 1813

[1] A. Giannis, T. Kolter, *Angew. Chem.* **1993**, *105*, 1303; *Angew. Chem. Int. Ed. Engl.* **1993**, *32*, 1244.
[2] R. O. Duthaler, *Tetrahedron* **1994**, *50*, 1539.
[3] Anxiolytic activity: S. H. Snyder, *Chemie der Psyche*, Heidelberg, Spektrum der Wissenschaft, **1988**, p. 155; for the activity of asperlicine and related compounds as cholecystokinin antagonists see ref. [1]. For the use of benzodiazepine as an inhibitor of the human immunodeficiency virus (HIV) reverse transcriptase see: V. J. Merluzzi, *Science* **1990**, *250*, 1411; R. Pauwels, *Nature* **1991**, *343*, 470. Benzodiazepines as anticancer agents: N. E. Kohl, S. D. Mosser, S. J. deSolms, E. A. Giuliani, D. L. Pompliano, S. L. Graham, R. L. Smith, E. M. Scolnick, A. Oliff, J. B. Gibbs, *Science* **1993**, *260*, 1934; G. L. James, J. L. Goldstein, M. S. Brown, T. E. Rawson, T. C. Somers, R. S. McDowell, C. W. Crowley, B. K. Lucas, A. J. Levinson, J. C. Masters, Jr., *ibid.* **1993**, 1937.
[4] J. N. Belokon, N. I. Chenroglazova, A. S. Batsanov, N. S. Carbalinskaya, V. I. Bakhmutov, Y. T. Struchkov, V. M. Belikov, *Izv. Akad. Nauk. SSSR Ser. Khim.* **1987**, 852. For the synthesis of *syn*- and *anti*-2,6-diaminopimelic acids see G. Bold, T. Allmendinger, P. Herold, L. Moesch, H. P. Schar, R. Duthaler, *Helv. Chim. Acta* **1992**, *75*, 865; R. M. Williams, Ch. Yuan, *J. Org. Chem.* **1992**, *57*, 6519.
[5] B. E. Evans, K. E. Rittle, M. G. Bock, R. M. DiPardo, *J. Med. Chem.* **1987**, *30*, 1229; D. Kolbah, N. Blazevic, M. Hannoun, F. Kajfez, T. Kovac, S. Rendic, V. Sunjic, *Helv. Chim. Acta* **1977**, *60*, 265; V. Sunjic, F. Kajfez, I. Stromar, N. Blazevic, *J. Heterocycl. Chem.* **1973**, *10*, 591; A. Walser, A. Szente, J. Hellerbach, *J. Org. Chem.* **1973**, *38*, 449; T. Sugasawa, M. Adachi, T. Toyoda, *J. Heterocycl. Chem.* **1979**, *16*, 445.
[6] P. Gmeiner, P. L. Feldman, M. J. Chu-Moyer, H. Rapoport, *J. Org. Chem.* **1990**, *55*, 3068, and references therein; see also M. M. Paz, F. J. Sardina, *ibid.* **1993**, *58*, 6990.
[7] J. E. Leffler, Y. Tsuno, *J. Org. Chem.* **1963**, *28*, 902; R. E. Harmon, G. Wellman, S. K. Gupta, *ibid.* **1973**, *38*, 11.
[8] D. A. Evans, T. C. Britton, J. A. Ellman, R. L. Dorow, *J. Am. Chem. Soc.* **1990**, *112*, 4011.
[9] **1b**: $[\alpha]_D^{22} = -54.6$ ($c = 1.0$ in DMSO); m.p. 108 °C (decomp); ^{1}H NMR (250 MHz, [D$_6$]DMSO, 25 °C, TMS): δ = 2.3–2.5, (m, 1H; 3-H), 2.65–2.78 (m, 1H; 3'-H), 3.75 (t, J = 6.3 Hz; 4-H), 4.0–4.3 (m, 4H; Fmoc-C*H*$_2$-C*H*, NH), 4.4 (dd, J(3,2) = 6.2 Hz, J(3',2) = 12.6 Hz; 2-H), 7.1–7.77, 7.78 (m, d, 17H; 2-aminobenzophenone-H, Fmoc-H), 10.65 (s, 1H, benzodiazepine-NH), 12.9 (s, br, 1H; COOH); ^{13}C NMR (63 MHz, [D$_6$]DMSO, 25 °C): δ = 33.2, 46.6, 51.3, 59.7, 65.7, 120.0, 121.1, 122.7, 125.1, 126.5, 127.0, 127.6, 128.1, 129.4, 130.2, 131.6, 138.8, 139.0, 140.7, 143.5, 143.7, 143.8, 156.0, 168.1, 170.0, 173.6. – **2b**: $[\alpha]_D^{22} = +39.7$ ($c = 1.0$ in DMSO); m.p. 140 °C (decomp); ^{1}H NMR (250 MHz, [D$_6$]DMSO, 25 °C, TMS): δ = 2.0–2.15 (ddd, 1H, J(3,3') = 12.5 Hz, J(3,2) = 3.2 Hz, J(3,4) = 10 Hz; 3-H), 2.5–2.65 (ddd, 1H, J(3,3') = 12.5 Hz, J(3',2) = 11.6, J(3',4) = 2.5 Hz; 3'-H), 3.51 (dd, J(3,4) = 10 Hz, J(3',4) = 2.5 Hz; 4-H), 3.9–4.25 (m, 4H; Fmoc-CH$_2$-CH, NH), 4.4 (ddd, J(3,2) = 3.2 Hz, J(3',2) = 11.6 Hz, J(2,NH) = 7.5 Hz; 2-H), 7.0–7.6, 7.78 (m, d, 17H; 2-aminobenzophenone-H, Fmoc-H), 10.6 (s, 1H, benzodiazepine-NH), 12.7 (s, br., 1H; COOH); ^{13}C NMR (63 MHz, [D$_6$]DMSO, 25 °C): δ = 32.2, 46.6, 50.7, 59.5, 65.5, 120.0, 121.2, 122.8, 125.0, 126.6, 127.0, 127.6, 128.2, 129.4, 130.5, 131.7, 139.1, 140.6, 140.7, 143.6, 143.8, 156.0, 168.7, 170.5, 174.5.
[10] *O*-(1*H*-Benzotriazol-1-yl)-*N*,*N*,*N*',*N*'-tetramethyluroniumtetrafluoroborate (TBTU): R. Knorr, A. Trzeciak, W. Bannwarth, D. Gillessen, *Tetrahedron Lett.* **1989**, *30*, 1927.
[11] Further details of the crystal structure investigation may be obtained from the Fachinformationszentrum Karlsruhe, D-76344 Eggenstein-Leopoldshafen (FRG) on quoting the depository number CSD-58198, the names of the authors, and the journal citation.

Dendritic Porphyrins: Modulating Redox Potentials of Electroactive Chromophores with Pendant Multifunctionality**

Peter J. Dandliker, François Diederich,* Maurice Gross,* Carolyn B. Knobler, Alain Louati, and Elizabeth M. Sanford

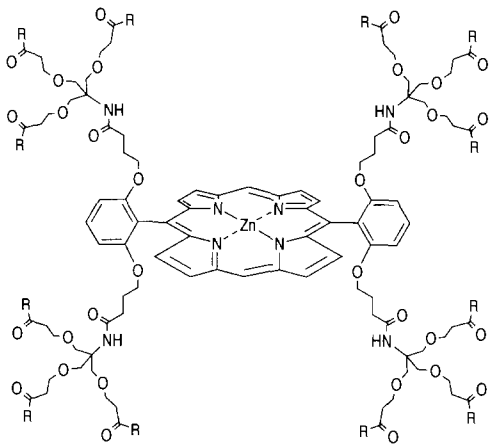
Dedicated to Professor Helmut Ringsdorf on the occasion of his 65th birthday

The synthesis[1] of cascade polymers has recently sparked much interest.[2] Efficient nonlinear growth schemes quickly provide high molecular weight, monodisperse globular structures with unique properties. A considerable body of work has focused on changing functional groups on the outer surface of dendrimers;[3] however, the idea of incorporating initiator cores with well-defined functional properties is less well explored.[4] Recent work has shown that the polarity in the interior of dendrimers changes markedly with increasing cascade generation.[4b] Constructing a dendrimer around a porphyrin core could alter the polarity of the surroundings of the electrophore and modify its electrochemical behavior. Dendritic porphyrins could therefore be regarded as models for electron-transfer proteins like cytochrome c, which exhibits oxidation potentials in aqueous solution 300–400 mV more positive than those of similarly ligated heme model systems that lack the hydrophobic peptide shell.[5, 6] We report here on the synthesis of the porphyrin compounds **1**–**3** using cascade polymer methodology. Preliminary electrochemical studies on **1**–**3** suggest that the environment of redox-active chromophores can be controlled through encapsulation in dendrimers; this opens up a method for the selective synthesis of redox catalysts.

The starting point for the synthesis of the cascade molecules **1a**–**3** through to the third generation was the tetraacid **7** pre-

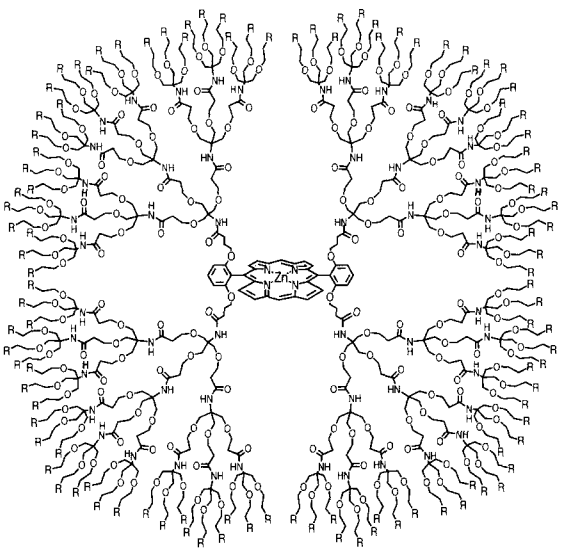
[*] Prof. Dr. F. Diederich, P. J. Dandliker
Laboratorium für Organische Chemie, ETH-Zentrum
Universitätstrasse 16, CH-8092 Zürich (Switzerland)
Telefax: Int. code + (1)261-3524
Prof. Dr. M. Gross, Dr. A. Louati
Laboratoire d'Electrochimie et de
Chimie Physique du Corps Solide
Université de Strasbourg
4 rue Blaise Pascal, F-67000 Strasbourg (France)
Dr. C. B. Knobler, Dr. E. M. Sanford
Department of Chemistry and Biochemistry, University of California
Los Angeles

[**] This work was supported by a grant by the research council of ETH Zürich and by the Office of Naval Research. We thank Prof. U. Suter and Dr. M. Colussi for the GPC data, Dr. W. Amrein, Dr. M. M. Ross, and Mr. L. Isaacs for mass spectrometric data, and Dr. D. Philp for the computer modeling of **3**.



1a, R = OCH_3
1b, R = OH

2a, R = $NHC(CH_2OCH_2CH_2CO_2CH_3)_3$
2b, R = $NHC(CH_2OCH_2CH_2COOH)_3$

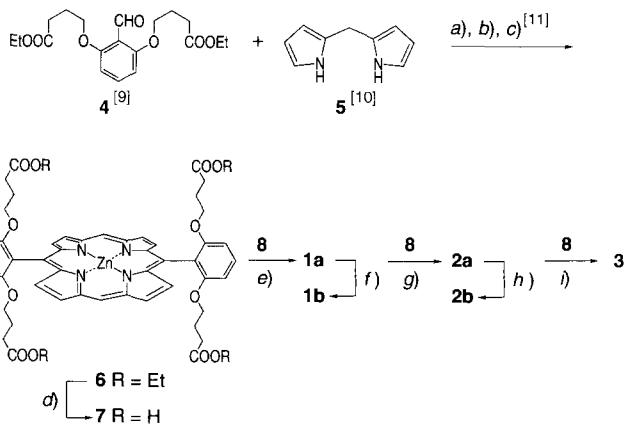


3 R = $COOCH_3$

pared from ester **6** (Scheme 1). The X-ray crystal structure of **6** shows that the four linkers for dendritic arm attachment have the desired spatial arrangement above and below the zinc porphyrin plane.[7]

The polyether–amide cascade described by Newkome et al.[8] was chosen to generate the cascade polymers **1a**/**b**, **2a**/**b**, and **3** (Scheme 1). Thus, the first generation dendritic zinc porphyrin **1a** (Table 1) was obtained in 75% yield from **7** and **8** by using the peptide coupling methodology, followed by purification by preparative gel permeation chromatography (GPC, Biorad Biobeads SX-3, toluene). Subsequent hydrolysis of **1a** with LiOH in $MeOH/H_2O$ smoothly afforded the first generation dodecacarboxylic acid **1b**.

A repeat of this reaction sequence gave the second generation compounds **2a** and **2b** bearing 36 methyl esters and 36 carboxylic acids, respectively. The structures of these compounds were confirmed by ^1H and ^{13}C NMR spectroscopy and mass spectrometric (MS) analysis. The fast atom bombardment (FAB) mass spectrum of **2a** shows the protonated molecular ion peak as the base peak at $m/z = 6547$ (calcd 6547) in addition to a peak at $m/z = 6167$ assigned to a fragment formed by loss of a single



Scheme 1. Synthesis of cascade polymers **1a–3**. a) CF_3COOH, CH_2Cl_2, 20 °C, 18 h. b) Chloranil, CH_2Cl_2, reflux, 1 h. c) $Zn(OAc)_2$, $CHCl_3/CH_3OH$ 1:1, reflux, 18% (steps a–c). d) Na_2CO_3, $EtOH/H_2O$ 1:1, reflux, 2 d, 93%. e) *N,N'*-dicyclohexyl carbodiimide (DCC), 1-hydroxybenzotriazole (HOBT), THF, 20 °C, 43 h, 75%. f) LiOH, CH_3OH/H_2O 1:1, 20 °C, 48 h, 81%. g) DCC, HOBT, THF, 20 °C, 18 h, 83%. h) LiOH, CH_3OH/H_2O 1:1, 20 °C, 48 h, 96%. i) DCC, HOBT, THF, 20 °C, 48 h, 51%.

Table 1. Selected physical data for compounds **1–3** [a].

1a: Viscous, red oil. FT-IR($CHCl_3$): 1743, 1672 ($\tilde{\nu}$(C = O)) cm^{-1}; ^1H NMR (300 MHz, $CDCl_3$): δ = 1.04–1.19 (m, 8H, $OCH_2CH_2CH_2$), 1.21–1.30 (m, 8H, $OCH_2CH_2CH_2$), 2.17 (t, J = 6.2 Hz, 24H, OCH_2CH_2), 3.15–3.40 (m, 84H, OCH_3, CH_2O, OCH_2CH_2), 3.89 (t, J = 5.4 Hz, 8H, $OCH_2CH_2CH_2$), 4.87 (s, 4H, NH), 7.04 (d, J = 8.3 Hz, 4H, *m*-aryl H), 7.70 (t, J = 8.3 Hz, 2H, *p*-aryl H), 9.00 (d, J = 4.3 Hz, 4H, β_2H), 9.31 (d, J = 4.5 Hz, 4H, β_1H), 10.13 (s, 2H, *meso*-H); ^{13}C NMR (75 MHz, $CDCl_3$): δ = 172.5, 171.9, 159.8, 150.4, 148.9, 131.6, 131.2, 129.9, 121.1, 111.8, 105.4, 104.9, 68.9, 67.6, 66.7, 59.5, 51.4, 34.4, 32.4, 24.6; UV/VIS($CDCl_3$): $\lambda_{max}(\varepsilon)$ = 415 (448000), 545 (42000); FAB-MS: *m/z* 2379 (100%, M^+ + H, $C_{112}H_{153}N_8O_{44}Zn$), calcd 2379.

1b: Red powder, m.p. 94–95 °C. FT-IR(KBr): 1717, 1639 ($\tilde{\nu}$(C = O)) cm^{-1}; ^{13}C NMR (125 MHz, [D$_8$]THF): δ = 173.0, 172.6, 161.1, 151.3, 149.9, 132.2, 132.1, 131.7, 122.2, 112.2, 105.9, 105.5, 69.9, 68.4, 67.8, 60.7, 35.1, 32.6, 25.6; UV/VIS(THF): $\lambda_{max}(\varepsilon)$ = 415 (370000), 545 (13000); FAB-MS: *m/z* 2211 (100%, M^+ + H, $C_{100}H_{129}N_8O_{44}Zn$). Correct C,H,N analysis.

2a: Viscous, red oil. FT-IR($CHCl_3$): 1733, 1667 ($\tilde{\nu}$(C = O)) cm^{-1}; ^1H NMR (200 MHz, $CDCl_3$): δ = 1.1–1.3 (br.s, 8H, $OCH_2CH_2CH_2$), 1.4–1.6 (br.s, 8H, $OCH_2CH_2CH_2$), 1.9–2.2 (br.s, 24H, OCH_2CH_2, first generation), 2.25–2.50 (br.s, 72H, OCH_2CH_2, second generation), 3.1–3.6 (br.m, 300H, OCH_2CH_2, CCH_2O, OCH_3), 3.65–3.85 (br.s, 8H, $OCH_2CH_2CH_2$), 5.8–6.1 (br.s, 16H, NH), 6.97 (d, J = 7.9 Hz, 4H, *m*-aryl H), 7.61 (t, J = 7.9 Hz, 2H, *p*-aryl H), 8.85 (d, J = 4.1 Hz, 4H, β_2H), 9.18 (d, J = 4.1 Hz, 4H, β_1H), 9.98 (s, 2H, *meso*-H); ^{13}C NMR (125 MHz, $CDCl_3$): δ = 172.3, 172.0, 170.7, 159.6, 150.2, 148.8, 131.4, 131.0, 129.7, 121.2, 111.4, 105.3, 104.6, 68.9 (2×), 67.5, 66.6 (2×), 59.6 (2×), 51.4, 36.8, 34.5, 32.2, 24.5; UV/VIS($CHCl_3$): $\lambda_{max}(\varepsilon)$ = 415 (346000), 545 (30000); FAB-MS: *m/z* 6547 (100%, M^+ + H, $C_{292}H_{453}N_{20}O_{140}Zn$), calcd: 6547; 6167 ($M^+$ – $NHC(CH_2OCH_2CH_2CO_2CH_3)_3$).

2b: Red powder, m.p. 64–65 °C. FT-IR(KBr): 1722, 1644 ($\tilde{\nu}$(C = O)) cm^{-1}; ^{13}C NMR (125 MHz, [D$_8$]THF): δ = 173.9, 173.3, 172.4, 160.9, 151.2, 149.8, 132.0, 131.8, 130.7, 122.2, 112.3, 106.1, 105.4, 69.8, 69.6, 68.4, 67.8 (2×), 60.9 (2×), 37.6, 35.2, 32.8, 25.7; UV/VIS(THF): $\lambda_{max}(\varepsilon)$ = 415 (333000), 545 (11000); MALDI-TOF-MS (linear mode): *m/z*(%): 6043 (M^+, $C_{256}H_{380}N_{20}O_{140}Zn$), and fragments formed by loss of $NHC(CH_2OCH_2CH_2COOH)_3$. Correct C,H,N analysis.

3: Viscous, red oil. FT-IR($CHCl_3$): 1733, 1667 ($\tilde{\nu}$(C = O)) cm^{-1}; ^1H NMR (500 MHz, $CDCl_3$): δ = 1.30–1.40 (br.s, 8H, $OCH_2CH_2CH_2$), 1.55–1.65 (br.s, 8H, $OCH_2CH_2CH_2$), 1.70–2.00 (br.s, 96H, OCH_2CH_2, first and second generation), 2.15–2.65 (br.m, 216H, OCH_2CH_2, third generation), 3.35–3.85 (br.m, 956H, $OCH_2CH_2CH_2$, OCH_2CH_2, CCH_2O, OCH_3), 6.05–6.35 (br.m, 52H, NH), 7.07 (s, 4H, *m*-aryl H), 7.68 (br.s, 2H, *p*-aryl H), 8.91 (br.s, 4H, β_2H), 9.20 (br.s, 4H, β_1H), 10.00 (s, 2H, *meso*-H); ^{13}C NMR (125 MHz, $CDCl_3$): δ = 172.0, 170.9, 69.0, 67.5, 66.7, 59.8, 51.6, 37.0, 34.7; UV/VIS($CHCl_3$): $\lambda_{max}(\varepsilon)$ = 415 (346000), 545 (30000); MALDI-TOF-MS (linear mode): *m/z*(%): 18900 (broad, 100%, M^+, $C_{832}H_{1352}N_{56}O_{428}Zn$), calcd 19044; 37000 (broad); 54000 (broad).

[a] The matrices for FAB- and MALDI-TOF-MS determinations were 3-nitrobenzyl alcohol and 2,4,6-trihydroxyacetophenone, respectively.

monomeric fragment $NHC(CH_2OCH_2CH_2CO_2CH_3)_3$. The matrix-assisted laser desorption ionization time-of-flight (MALDI TOF) mass spectrum of **2b** shows the molecular ion peak as base peak at $m/z = 6043$ (calcd 6041) and peaks corresponding to fragment ions resulting from successive loss of $NHC(CH_2OCH_2CH_2COOH)_3$ moieties.

Finally, coupling of **2b** with **8** gave the third generation dendrimer **3** bearing 108 methyl esters (51% yield). The integrity of the zinc porphyrin core in **3** was confirmed by the ^1H NMR and UV VIS spectroscopic studies (Table 1). As expected, the ^{13}C NMR spectrum shows only a single set of peaks for the outer cascade layer. The MALDI-TOF mass spectrum shows the molecular ion peak as the base peak at m/z 18900 (calcd 19044) together with minor peaks at around m/z 37000 and m/z 54000 corresponding to ionic, gas-phase complexes of two and three molecules of **3**, respectively. The dendritic zinc porphyrins **1a**, **2a**, and **3** are red, viscous oils; the polycarboxylic acids **1b** and **2b** are red, low-melting solids (Table 1).

The GPC chromatograms of esters **1a**, **2a**, and **3** show a single sharp peak for each compound and thus provide further confirmation that the cascade molecules are monodisperse. The results of detailed GPC and light-scattering studies will be published in due course.

Computer-generated models of **3** predict a globular molecule, approximately 4 nm in diameter (Fig. 1).[12] The densely packed structure of **3** resembles in size and shape the electron-transfer protein cytochrome c, which also has an encapsulated porphyrin core, (Fig. 1).[13, 14]

The influence of the close-packed dendritic branches on the redox properties of the central zinc porphyrin unit was studied by cyclic voltammetry in THF and CH_2Cl_2 with $Bu_4N^+PF_6^-$ (0.1 M) as the supporting electrolyte (Table 2).

Esters **1a** and **2a** exhibit two reversible one-electron reduction processes at the Hg electrode in the explored potential range (from -1 to -2.5 V vs. SCE) (Fig. 2, top). The absolute potential difference between the first and second reduction potentials is 0.49 and 0.46 V, respectively. These values agree well with the range of 0.35 to 0.40 V typically observed for ring-centered reductions of metalloporphyrin complexes.[15] The third generation compound **3** shows a less well defined wave for a single irreversible reduction process, which is located at approximately -1.9 V in dilute solutions (Fig. 2 top). Control experiments with **9** suggest that signals for the electrochemical reduction of the zinc porphyrin in **3** overlap with signals produced by irreversible multielectron transfers involving the dendritic branches. The region of overlap is between -1.6 V and the accessible potential limit of the solvent.

Table 2. Redox potentials for the zinc porphyrins [a]

Porphyrin	$E^{1,2}_{red}$(I) [b]	$E^{1,2}_{red}$(II) [b]	$E^{1,2}_{ox}$(I) [b]	$E^{1,2}_{ox}$(I) [c]	$E^{1,2}_{ox}$(II) [c]
ZnTPP [d]	−1.50	−1.94	+1.08		
6	−1.60	−2.01	+0.85	+0.63	+1.04
1a	−1.69	−2.18	+0.87	+0.71	+1.09
2a	−1.72	−2.18	+0.65	+0.63	+1.07
3	−1.90 [e, g]		+0.55 [f, g]	+0.54 [g]	+1.00 [g]

[a] Redox potentials as determined by cyclic voltammetry: $E^{1,2}$ (approximated by $(E^c_p + E^a_p)/2$) in V vs. SCE; supporting electrolyte $Bu_4N^+PF_6^-$ (0.1 M), reductions performed at the Hg electrode (dropping mercury electrode), scan rate 5 Vs^{-1}; oxidations performed at the Pt electrode, scan rate 50 mV s^{-1}; $T = 298$ K. [b] Solvent THF. [c] Solvent CH_2Cl_2, scan rate 100 mV s^{-1}. [d] Zinc *meso*-tetraphenylporphyrin (ZnTPP). [e] Poorly resolved signal. [f] Broad signal. [g] Irreversible transfer, peak potential from CV measurements.

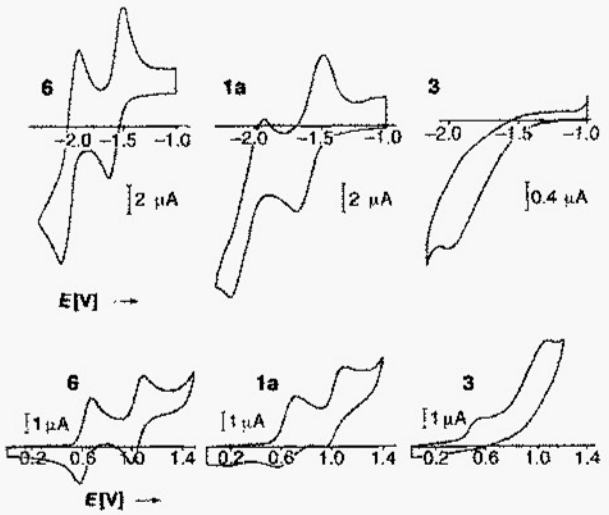
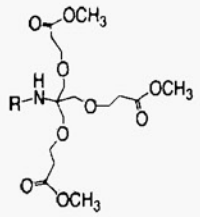


Fig. 2. Top: Reduction cyclic voltammograms in THF (0.1 M $Bu_4N^+PF_6^-$). Working electrode: Hg drop. Scan rate = 5 V s^{-1}, $T = 298$ K. Bottom: Oxidation cyclic voltammograms in CH_2Cl_2 (0.1 M $Bu_4N^+PF_6^-$). Working electrode: Pt. Scan rate = 0.10 Vs^{-1}, $T = 298$ K.

The first reduction potential of the zinc porphyrin unit becomes more negative with increasing dendrimer generation. The values obtained obtained are more negative than the potential for the reduction of the central unit **6** by 90 to 300 mV. This trend can be explained by the increasingly electron-rich microenvironment created by the dendritic branches around the porphyrin core. Because the microenvironment of the porphyrin core becomes increasingly electron rich on moving from **1a** to **3**, electron addition becomes energetically more difficult.



8 R = H
9 R = CH_3CO

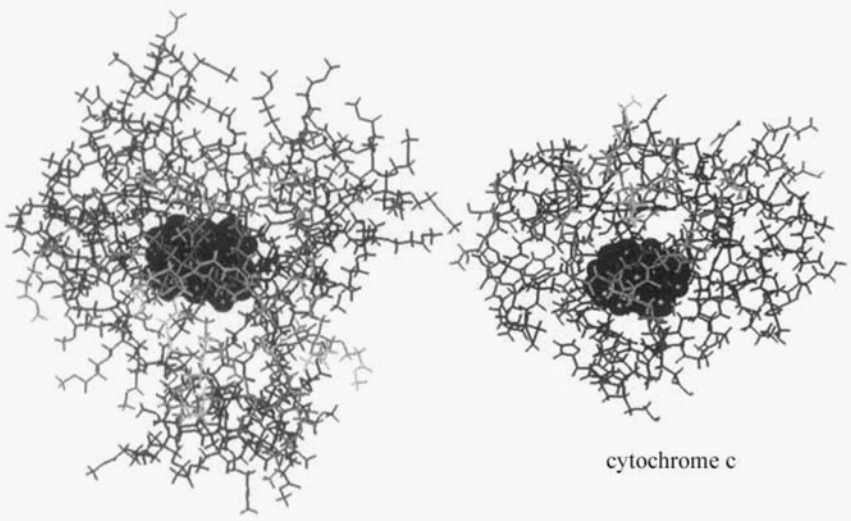


Fig. 1. Computer-generated model of the dendritic zinc porphyrin **3** [12]. For comparison, the X-ray crystal structure of cytochrome c (bonita) at 2.3 Å resolution [14].

A similarly strong microenvironmental effect on the electrochemical properties was observed when the oxidation of **1a**, **2a**, and **3** was compared to that of **6**. Between 0 and 1.2 V, the complexes **1a** and **2a** display two reversible oxidation steps at the platinum electrode in CH_2Cl_2 (Fig. 2 bottom). In THF, on the other hand, only one oxidation step is observed before reaching the anodic solvent-accessible potential limit. For compound **3**, the two oxidation processes that are observed in THF become completely irreversible in CH_2Cl_2 (Fig. 2 bottom). Control compound **9** does not show any sign of oxidation in THF or CH_2Cl_2 up to the anodic potential limit. In all the dendritic systems described above, electrochemical oxidation is expected to generate a monocation by removal of an electron from the porphyrin π system. Evidence for this comes from the potential difference between the first reduction and the first oxidation, which ranges from 2.37 to 2.56 V. These values are comparable to the separation of 2.25 ± 0.15 V reported for other metalloporphyrin complexes.[15] In the dendritic complexes, the first oxidation potentials are up to 300 mV (THF) less positive than the value for zinc porphyrin **6**. This can again be explained by the increasingly electron-rich microenvironment provided by the dendritic branches, which favors the generation of the porphyrin radical cation.

Rather than using traditional through-bond substituent effects to influence the electrochemical behavior of metalloporphyrins, we have modulated the redox characteristics of **1a**, **2a**, and **3** with a through-space mechanism, namely, the control of the electrophore's environment.[16] Electrochemical studies into the potential of water-soluble iron porphyrin analogues of **1a**–**3** as mimics of cytochrome c are currently in progress.

Received: April 6, 1994 [Z 6830 IE]
German version: *Angew. Chem.* **1994**, *106*, 1821

[1] a) E. Buhleier, W. Wehner, F. Vögtle, *Synthesis* **1978**, 155–158; b) H.-B. Mekelburger, W. Jaworek, F. Vögtle, *Angew. Chem.* **1992**, *104*, 1609–1614; *Angew. Chem. Int. Ed. Engl.* **1992**, *31*, 1571–1576; c) D. A. Tomalia, A. M. Taylor, W. A. Goddard III, *ibid.* **1990**, *102*, 119–157 and **1990**, *29*, 138–175; d) D. A. Tomalia, H. D. Durst, *Top. Curr. Chem.* **1993**, *165*, 193–313; e) G. R. Newkome in *Proceedings of the II NATO Science Forum on Supramolecular Chemistry* (Eds.: V. Balzani, L. De Cola), Kluwer, Dordrecht, **1992**, pp. 145–155.

[2] a) C. J. Hawker, J. M. J. Fréchet, *J. Am. Chem. Soc.* **1990**, *112*, 7638–7647; b) Z. Xu, J. S. Moore, *Angew. Chem.* **1993**, *105*, 1394–1396; *Angew. Chem. Int. Ed. Engl.* **1993**, *32*, 1354–1357; c) E. M. M. de Brabander-van den Berg, E. W. Meijer, *ibid.* **1993**, *105*, 1370–1372 and **1993**, *32*, 1308–1311; d) C. Wörner, R. Mülhaupt, *ibid.* **1993**, *105*, 1367–1370 and **1993**, *32*, 1306–1308; e) L.-L. Zhou, J. Roovers, *Macromolecules* **1993**, *26*, 963–968; f) E. W. Kwock, T. X. Neenan, T. M. Miller, *Chem. Mater.* **1991**, *3*, 775–777; g) A. W. van der Made, P. W. N. M. van Leeuwen, *J. Chem. Soc. Chem. Commun.* **1992**, 1400–1401; h) G. R. Newkome, C. N. Moorefield, G. R. Baker, R. K. Behera, G. H. Escamilla, M. J. Saunders, *Angew. Chem.* **1992**, *104*, 901–903; *Angew. Chem. Int. Ed. Engl.* **1992**, *31*, 917–919; i) S. Serroni, G. Denti, S. Campagna, A. Juris, M. Ciano, V. Balzani, *ibid.* **1992**, *104*, 1540–1542 and **1992**, *31*, 1493–1495.

[3] a) Y.-H. Liao, J. R. Moss, *J. Chem. Soc. Chem. Commun.* **1993**, 1774–1777; b) C. J. Hawker, J. M. J. Fréchet, *J. Chem. Soc. Perkin Trans. 1* **1992**, 2459–2469; c) K. L. Wooley, C. J. Hawker, J. M. J. Fréchet, *ibid.* **1991**, 1059–1076.

[4] a) R.-H. Jin, T. Aida, S. Inoue, *J. Chem. Soc. Chem. Commun.* **1993**, 1260–1262; b) C. J. Hawker, K. L. Wooley, J. M. J. Fréchet, *J. Am. Chem. Soc.* **1993**, *115*, 4375–4376; c) K. L. Wooley, C. J. Hawker, J. M. J. Fréchet, F. Wudl, G. Srdanov, S. Shi, C. Li, M. Kao, *ibid.* **1993**, *115*, 9836–9837.

[5] a) S. K. Panicucci, J. Bixler, G. Bakker, F. Sherman, G. McLendon, *J. Am. Chem. Soc.* **1992**, *114*, 5443–5445; b) K. L. Bren, H. B. Gray, *ibid.* **1993**, *115*, 10382–10383; c) M. T. Cruañes, K. K. Rodgers, S. G. Sligar, *ibid.* **1992**, *114*, 9660–9661.

[6] a) V. T. Taniguchi, W. R. Ellis, Jr., V. Cammarata, J. Webb, F. C. Anson, H. B. Gray, *Adv. Chem. Ser.* **1982**, *201*, 51–68; b) T. Flatmark, K. Dus, H. deKlerk, M. D. Kamen, *Biochemistry* **1970**, *9*, 1991–1996; c) T. Daido, T. Akaike, *J. Electroanal. Chem. Interfacial Electrochem.* **1993**, *344*, 91–106; d) K. B. Koller, F. M. Hawkridge, *J. Am. Chem. Soc.* **1985**, *107*, 7412–7417; e) W. J. Alberty, M. J. Eddowes, H. A. O. Hill, A. R. Hillman, *ibid.* **1981**, *103*, 3904–3910; f) H. A. Harbury, J. R. Cronin, M. W. Fanger, T. P. Hettinger, A. J. Murphy, Y. P. Myer, S. N. Vinagradov, *Proc. Natl. Acad. Sci. USA* **1965**, *54*, 1658–1664; g) P. K. Warme, L. P. Hager, *Biochemistry* **1970**, *9*, 1606–1614; h) G. R. Moore, G. W. Pettigrew, *Cytochromes c. Evolutionary, Structural, and Physicochemical Aspects*, Springer, New York, **1990**.

[7] X-ray crystal data for **6** ($C_{56}H_{60}N_4O_{12}Zn$): $M_r = 1046.5$, monoclinic space group $P2_1/c$, $Z = 2$ (centrosymmetric molecule); $a = 14.697(8)$, $b = 12.298(9)$, $c = 9.051(4)$ Å, $\beta = 94.38(2)^\circ$, $V = 2520$ Å^3, $Mo_{K\alpha}$ radiation, $2\theta = 43^\circ$, 2887 unique reflections; the structure was solved by heavy-atom methods, yielding $R = 0.091$, $R_w = 0.102$ for 1359 independent reflections with $I > 3\sigma(I)$. Further details of the crystal structure investigation are available on request from the Director of the Cambridge Crystallographic Data Centre, 12 Union Road, GB-Cambridge CB2 1EZ (UK), on quoting the full journal citation.

[8] a) G. R. Newkome, X. Lin, *Macromolecules* **1991**, *24*, 1443–1444; b) G. R. Newkome, X. Lin, C. D. Weis, *Tetrahedron: Asymmetry* **1991**, *2*, 957–960.

[9] Ester **4** was synthesized in 65% yield by alkylation of 2,6-dihydroxybenzaldehyde with ethyl 4-bromobutyrate and K_2CO_3 in DMF at 80 °C for 8 h.

[10] R. Chong, P. S. Clezy, A. J. Liepa, A. W. Nichol, *Aust. J. Chem.* **1969**, *22*, 229–238.

[11] J. S. Manka, D. S. Lawrence, *Tetrahedron Lett.* **1989**, *30*, 6989–6992.

[12] The program Insight II (version 2.3.0, Biosym Technologies, Inc., San Diego, CA, 1993) was used for the computer simulation of **3**. Steric clashes in the initial input structure were removed by performing an energy minimization (DISCOVER, Biosym Technologies) first with steepest descents and then with conjugate gradient methods to an RMS gradient (RMS = root mean square) of less than 0.1 with the CVFF force field.

[13] T. Takano, O. B. Kallai, R. Swanson, R. E. Dickerson, *J. Biol. Chem.* **1973**, *248*, 5234–5255.

[14] N. Tanaka, T. Yamane, T. Tsukihara, T. Ashida, M. Kudoko, *J. Biochem. (Tokyo)* **1975**, *77*, 147–161.

[15] J.-H. Fuhrhop, K. M. Kadish, D. G. Davis, *J. Am. Chem. Soc.* **1973**, *95*, 5140–5147.

[16] a) H. L. Chen, P. E. Ellis, Jr., T. Wijesekera, T. E. Hagan, S. E. Groh, J. E. Lyons, D. P. Ridge, *J. Am. Chem. Soc.* **1994**, *116*, 1086–1089; b) P. E. Ellis, Jr., J. E. Lyons, *Coord. Chem. Rev.* **1990**, *105*, 181–193; c) T. Wijesekera, A. Matsumoto, D. Dolphin, D. Lexa, *Angew. Chem.* **1990**, *102*, 1073–1074; *Angew. Chem. Int. Ed. Engl.* **1990**, *29*, 1028–1030; d) T. G. Traylor, S. Tsuchiya, *Inorg. Chem.* **1987**, *26*, 1338–1339.

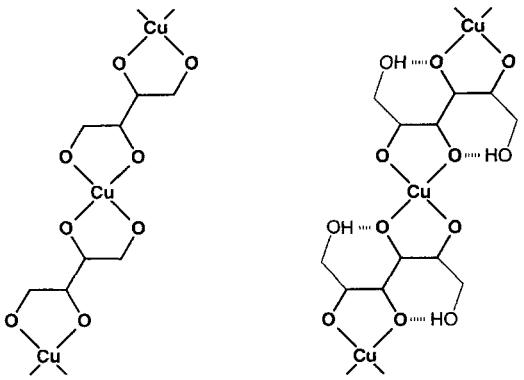
Linear Coordination Polymers of Copper(II) and Fourfold Deprotonated Sugar Alcohols**

Peter Klüfers* and Jörg Schuhmacher

In the presence of Cu^{II} or Pd^{II} ions, polyols are multiply deprotonated, even in aqueous solution, and bind as chelate ligands to the metal ion.[1] Because of the structural variety of polyols—diols, triols, and sugar alcohols, but also low molecular weight carbohydrates, oligo- and polysaccharides—they are versatile building blocks for the systematic synthesis of complex structures. Metal-containing polymers are, for example, obtained by using polysaccharides as ligands. Simple polyols should be suitable as building blocks for coordination polymers in which metal ions combine with polyolato ligands to form extended structures. Polymer chains are expected when difunctional metal building blocks are used. This principle is illustrated on the left side of Scheme 1 for a deprotonated bisdiol and Cu^{II} ions, which are generally difunctional towards diolato(2−) ligands.

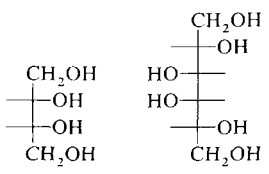
[*] Prof. Dr. P. Klüfers, Dipl.-Chem. J. Schuhmacher
Institut für Anorganische Chemie der Universität
Engesserstrasse, Gebäude 30.45, D-76128 Karlsruhe (FRG)
Telefax: Int. code + (721) 608-4290

[**] Polyol–Metal Complexes, Part 9. This work was supported by the Bundesministerium für Forschung und Technologie (grant no. 0319368A) and by Akzo AG, Wuppertal. Part 8: M. Klaassen, P. Klüfers, *Z. Anorg. Allg. Chem.*, in press.



Scheme 1. The polymeric cuprate ions (without charges) in **1** (left) and **2** (right).

We report here on the successful crystallization from aqueous solution and the structure determination[2] of two linear polyolato cuprates containing one-dimensional polymeric anions based on two different sugar alcohols, the simplest bisdiol, erythritol (Eryt), and the trisdiol, dulcitol = galactitol (Dulc).



Eryt Dulc

Crystals of $Na_2[Cu(ErytH_{-4})]\cdot Eryt\cdot 12H_2O$ **1** contain the fully deprotonated form of erythritol as the building block of the coordination polymer (Scheme 1 left and Fig. 1 bottom). The structure analysis shows that both the complexed tetraanion and the free, nondeprotonated erythritol exist side by side in the crystal. We had not expected to obtain this structure. Our original aim was the synthesis of a mononuclear complex of the same stoichiometry but with two dianionic ligands per copper ion. When the reaction is expressed as equilibrium (a), it becomes clear that the acidity constants for the four protolysis steps of the polyol must be very similar in order

$$[Cu(ErytH_{-2})_2]^{2-} \rightleftharpoons [Cu(ErytH_{-4})]^{2-} + Eryt \qquad (a)$$

to achieve a bias towards the right-hand side. The nondeprotonated erythritol molecules in the crystal are an essential component in the structure; they form short (but asymmetric), chelate-like hydrogen bonds with the cuprate chains, which thus leads to extensive crosslinking of the polymer chains (Fig. 1 bottom: $d(O\cdots O^-) = 258.0(5)$ and 252.8(6) pm).

In basic solutions of the trisdiol dulcitol and an excess of copper did not yield a complex containing $DulcH_{-6}$ ligands. Instead, a tetraanionic ligand is found in $Li_2[Cu(DulcH_{-4})]\cdot 10H_2O$ (**2**)—the primary OH groups are not deprotonated. The coordination polymer formed has the same topology as **1**, but is more rigid (Scheme 1 right). Despite the large stability constants of polyolato–copper complexes,[1a] the hexaol is not completely deprotonated. A structural feature, which we first observed when using β-cyclodextrin as the polyol component[3] and then with the polysaccharide cellulose,[1a] competes with complexation: whenever possible, the polyolate adopts a conformation which allows formation of short intramolecular hydrogen bonds of the type $O-H\cdots O^-$. Dulcitol is no exception to this rule; the C_6 chain adopts a centrosymmetric S-shaped conformation in which the two terminal O-H groups act as intramolecular hydrogen-bond donors to the third nearest oxygen atom in the chain. The donor–acceptor distance of 248.2(5) pm is unusually short for a polyolate. The hydrogen bond is "compressed" because, with its formation, angular strain builds up in the C_6 chain, and all C–C–C angles are greater than 120° (Fig. 2). This explains why intramolecular hydrogen bonds are not observed in the crystal structures of dulcitol itself and all other sugar alcohols, since these contain only hydroxy groups and no strongly binding alkoxide functions, which could act as acceptors.[4]

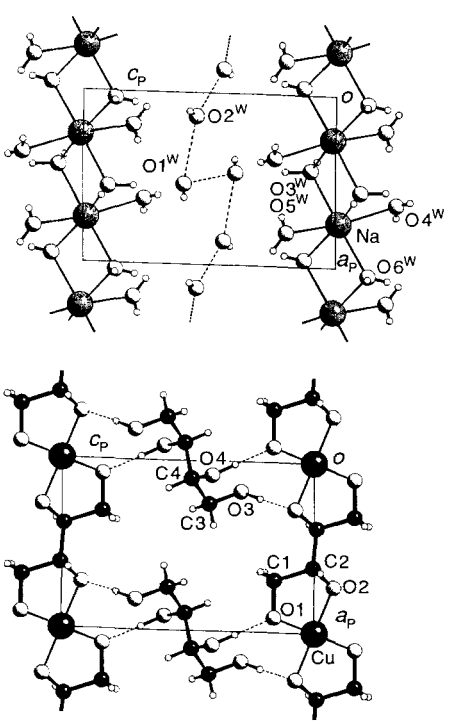


Fig. 1. Projection along [0$\bar{1}$0]. Top: Section at $y = 0$; $[Na(H_2O)_4]_2\cdot 4H_2O$ with disordered hydrogen bonds [2]; water O atoms are indicated with O^w. Bottom: Section around $y = 1/2$; $[Cu(ErytH_{-4})]\cdot$ Eryt, selected distances [pm] and angles [°]: Cu–O1 191.2(4), Cu–O2 192.2(4); O1-Cu-O2 87.2(2), O1-C1-C2-O2 47.6(5), O3-C3-C4-O4 −69.5(5).

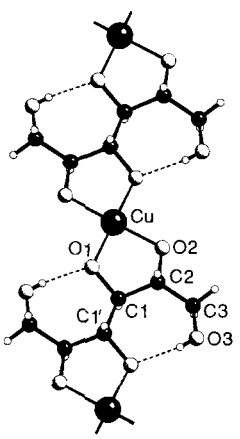


Fig. 2. Cuprate ion in **2**, selected distances [pm] and angles [°]: Cu–O1 195.2(3), Cu–O2 193.8(3); O1-Cu-O2 84.52(12), C2-C1-C1' 120.3(4), C1-C2-C3 122.0(4), O3-C3-C2 116.1(4), O1-C1-C2-O2 47.7(5).

In the crystals of both **1** and **2**, further structural fragments are responsible for the lateral arrangement of the anionic rods in a three-dimensional structure. Fragments of this type also lead to formation of extended structures in other crystals, even in the absence of a polymeric motif. In **1**, chains of edge-sharing hexaaquasodium octahedra[5a] and cooperative associations of water molecules[5b] serve this purpose (Fig. 1 top). In **2**, a homodromic[4] helix of water molecules winds round the 2_1 axis along [010]. The water molecules organize the three-dimensional crystalline structure by binding directly to both the lithium cations and the cuprate ions, which are arranged parallel to the water helices. The significance of this endless, one-dimensional cooperative system in the structure is emphasized by the fact that further cooperative sequences run in and out of the helix; the characteristic intramolecular $O-H\cdots O^-$ bond also does not exist in isolation, but is embedded in this system (Fig. 3).

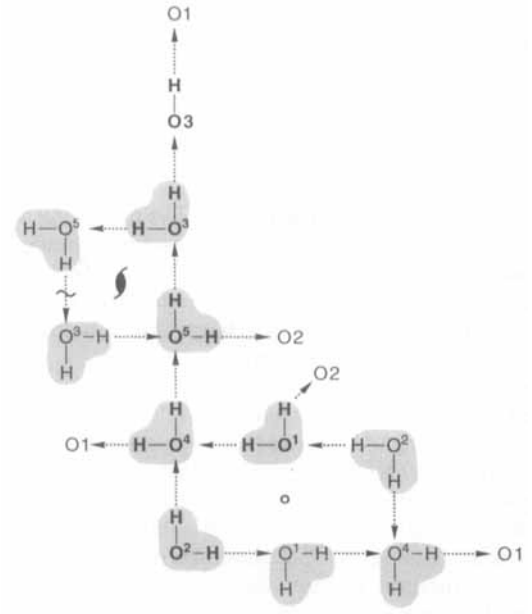


Fig. 3. Section of the cooperative hydrogen bonding system in **2**. The O atoms of water molecules are designated by O^n; the hydrogen bonding surrounding the atoms in bold print is given in full: O3, O^1, O^2, and O^3 are also ligands at Li. The crystallographic symmetry elements 2_1 and $\bar{1}$ are denoted by the appropriate symbols. The start of a new turn in the homodrome helix around 2_1 is marked by a wavy line.

Both of the coordination polymers introduced here belong to a class of materials, the metal-containing polymers, that are of interest because of their (potential) properties as materials (e.g., special magnetic effects, formation of nematic phases).[6] The polyolato complexes are, in addition, made from alkoxides which are readily accessible from inexpensive starting materials and are stable towards protolysis in alkaline aqueous media. In the design of a target complex, it should be taken into account that the sequence of the acidity constants is not comparable with that found for mineral acids. The acidity constants for the individual steps seem to differ only slightly. *Multiple* deprotonation to form polyolato ligands, even in aqueous solution is typical for the complex chemistry of polyols. Only the protons embedded in the intramolecular $O-H\cdots O^-$ structural fragments are not easily accessible.

Received: March 2, 1994 [Z 67201E]
German version: *Angew. Chem.* **1994**, *106*, 1839

[1] a) W. Burchard, N. Habermann, P. Klüfers, B. Seger, U. Wilhelm, *Angew. Chem.* **1994**, *106*, 936–939; *Angew. Chem. Int.* Ed. Engl. **1994**, *33*, 884–887; b) M. Achternbosch, P. Klüfers, *Acta Crystallogr. Sect. C*, **1994**, *50*, 175–178.

[2] **1**: Blue, needle-shaped fragment from a fibrous aggregate, obtained by evaporation of a stoichiometric solution. $0.32\times0.07\times0.04$ mm^3, triclinic, $P\bar{1}$; a = 680.9(5), b = 946.9(8), c = 950.0(9) pm, α = 95.04(7), β = 90.57(7), γ = 106.76(6)°, $V = 583.8(9)\times10^6$ pm^3, ρ_{calcd} = 1.604(2) g cm^{-3}; $2\theta_{max} = 0°$, STOE-IPDS area detector, $Mo_{K\alpha}$ (graphite monochromator, λ = 71.069 pm), T = 200 K; 4047 *hkl* measured, 1912 *hkl* independent and taken into account, 1440 *hkl* with $|F_0| \geq 4\sigma(F_0)$, Lp correction, no absorption correction, μ = 1.058 mm^{-1}, direct methods (SHELXS), refinement with full matrix based on F^2 (SHELXL), 180 parameters, H atoms at C in calculated positions with common U, position parameter free at O, common U, refinement with "antibumping constraint" (d(O–H)$_{min}$ = 64 pm); for the water molecules not bound to Na, O1, and O2 (Fig. 1 top), only the H atom directed towards an alkoxide O atom was located; the second H atom is clearly part of a cooperative hydrogen-bonding system whose ordered arrangement is not compatible with the symmetry of the space group; an ordering in the sense of an isomorphous transition would be possible by doubling c; however, the crystal quality did not allow an X-ray diffraction investigation; $R(F)_{obs}$ = 0.057, $wR(F^2)$ = 0.151, S = 1.081, $\Delta\rho_{max} = 0.71\times10^{-6}$ e pm^{-3}. - **2**: Crystallization as for **1**: blue platelets, $0.20\times0.20\times0.03$ mm^3, monoclinic, $C2/c$; a = 1505.6(6), b = 691.7(2), c = 1823.5(9) pm, β = 104.06(4)°, $V = 1842.1(13)\times10^6$ pm^3, ρ_{calcd} = 1.5711(9) g cm^{-3}; $2\theta_{max}$ = 50°, T = 200 K; 3594 *hkl* measured, 1493 *hkl* independent and taken into account, 1235 *hkl* with $|F_0| \geq 4\sigma(F_0)$, μ = 1.258 mm^{-1}, 150 parameters, $R(F)_{obs}$ = 0.052, $wR(F^2)$ = 0.153, S = 1.111, $\Delta\rho_{max} = 0.78\times10^{-6}$ e pm^{-3}, all other data as for **1**. Further details of the crystal structure investigations may be obtained from the Fachinformationszentrum Karlsruhe, D-76344 Eggenstein-Leopoldshafen (FRG), on quoting depository numbers CSD-400680 (**1**) and CSD-400683 (**2**).

[3] R. Fuchs, N. Habermann, P. Klüfers, *Angew. Chem.* **1993**, *105*, 895–897; *Angew. Chem. Int. Ed. Engl.* **1993**, *32*, 852–854.

[4] G. A. Jeffrey, W. Saenger, *Hydrogen Bonding in Biological Structures*, Springer, Berlin, **1991**, p. 176 (pp. 38–39 explains the term homodromic).

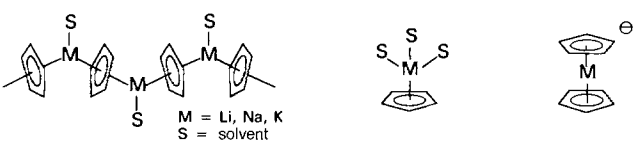
[5] Examples of low molecular weight polyolato complexes: a) N. Habermann, G. Jung, M. Klaassen, P. Klüfers, *Chem. Ber.* **1992**, *125*, 809–814; b) see ref. [1b].

[6] C. U. Pittman, C. E. Carraher, J. E. Sheats, M. D. Timken, M. Zeldin in *Inorganic and Metal-Containing Polymeric Materials* (Eds.: J. E. Sheats, C. E. Carraher, C. U. Pittman, M. Zeldin, B. Curell), Plenum, New York, **1990**, pp. 1–27.

The Simplest Metallocene Sandwich: the Lithocene Anion**

Sjoerd Harder* and Marc Heinrich Prosenc

Metallocenes of alkali metals were the first known organometallic cyclopentadienyl compounds.[1] Their versatility in the syntheses of cyclopentadienyl transition metal complexes led to a widespread interest in their structures.[2–4] A structural form commonly observed is a polymeric chain of bridging η^5-cyclopentadienyl rings alternating with alkali metal cations, with or without solvation (**1**).[2] Additional solvation of the metal cation may break the polymer chain into smaller oligomers or monomeric units (**2**).[3]



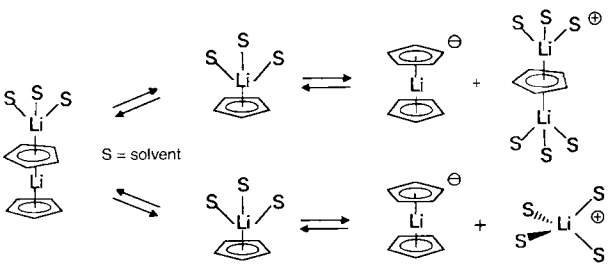
1 **2** **3**

The possible existence of alkali metal cyclopentadienides (**3**) with a sandwich structure in solution has been discussed previously,[5] and recently new evidence for such sandwich complexes was obtained.[6] Results of a cryoscopic molecular weight determination for cyclopentadienyllithium ([CpLi]) in liquid ammonia, suggested an equilibrium between the monomer and a higher species.[6a] This could be either a stacked dimer or a combination of an anionic $[Cp_2Li]$ sandwich complex with an inverse sandwich cation (Scheme 1, top).[7]

A recent extensive NMR study shows that, at low temperature, monomeric [CpLi] dissolved in THF is in equilibrium with a metallocene anion with a sandwich structure and a THF-solvated Li cation (Scheme 1, bottom).[6b] Though some crystal structures of Li^+ sandwiched between π-electron systems are known,[8] definite structural proof of the simplest metallocene, the lithocene anion, was still lacking. We here describe the syn-

[*] Dr. S. Harder, Dipl.-Chem. M. H. Prosenc
Universität Konstanz
Postfach 5560, M 738, D-78434 Konstanz (FRG)
Telefax: Int. code +(7531)883137

[**] This work was supported by the Alexander-von-Humboldt foundation (fellowship for S. H.). Prof. Dr. H.-H. Brintzinger and Prof. Dr. G. Müller are thanked for helpful discussions and for providing laboratory facilities.



Scheme 1.

thesis and solid-state structure of the dicyclopentadienyllithium anion (**3**, M = Li).

Mixing [CpLi] and Ph_4PCl (molar ratio 2/1) in THF results in the formation of large yellow-brown crystals of $[Ph_4P]^+[Cp_2Li]^-$, suitable for an X-ray structure determination.[9] Figure 1 shows a plot of the monoclinic unit cell with

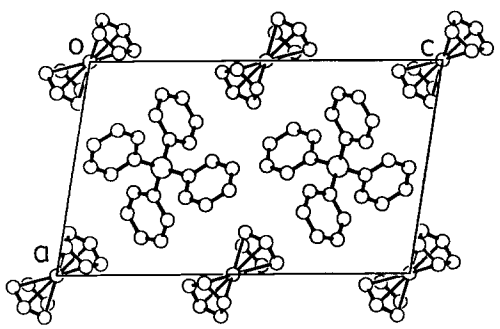


Fig. 1. Crystal structure of $[Ph_4P]^+[Cp_2Li]^-$: view of the monoclinic unit cell along the *b* axis (space group: $P2/c$).

$P2/c$ symmetry. The Ph_4P cations show C_2 symmetry; the phosphorus atoms are located on crystallographic two fold axes. The $[Cp_2Li]$ anions are positioned on crystallographic inversion centers. In this respect, the crystal structure of the $[Cp_2Li]$ anion is comparable to those of magnesocene, chromocene, ferrocene, cobaltocene and nickelocene.[10] All these compounds crystallize in centrosymmetric monoclinic spacegroups in which metals are located on inversion centres.

The structure of the $[Cp_2Li]$ anion is shown in Figure 2. The Cp rings are perfectly planar (max. deviation from least-squares plane: 0.001 Å). The coplanarity of the Cp rings is inherent to

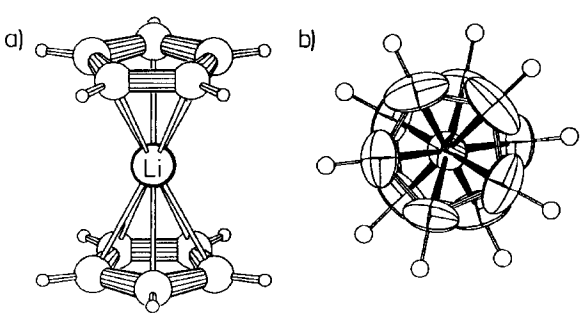


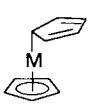
Fig. 2. a) Molecular structure of the $[Cp_2Li]$ anion. C–Li-bond distances [Å]: C1-Li 2.362(3), C2-Li 2.366(4), C3-Li 2.303(3), C4-Li 2.262(3), C5-Li 2.298(4), average (2.318(4)). C C-bond distances vary from 1.340(5) to 1.387(5), average 1.362(5) Å. b) ORTEP plot showing disorder within the planes of the cyclopentadienyl rings (top view; ellipsoids represent 50% probability).

the centrosymmetric nature of this metallocene anion. The $Cp_{centroid}$–Li distance of 2.008(4)Å is at the high end of the 1.79–2.06 Å range previously observed in [CpLi] compounds like **2**, and also slightly longer than the comparable distance of 1.967 Å in polymeric unsolvated $[Me_3SiCpLi]$ (type **1** wihout solvation).[2c] In the $[Cp_2Li]$ anion the C–Li bond distances vary only slightly 2.262(3) to 2.366(4) Å, average 2.318(4) Å),[21] and the angle between the $Cp_{centroid}$–Li axis and the Cp plane is 87.1(3)°. Therefore, the Cp–Li interaction can be regarded as η^5-coordination of a ring that has hardly slipped. η^5-Coordination has been calculated to be the most stable interaction for Cp–Li bonding[11] and is commonly observed in structures of [CpLi] compounds.[2c, 3] Bonding in [CpLi] is regarded to be highly ionic,[12] similarly, the bonding in the $[Cp_2Li]$ anion should be considered ionic.

The Cp rings in the $[Cp_2Li]$ anion are almost perfectly staggered. However, high anisotropy in the ring thermal parameters indicates substantial disorder in the positions of the Cp carbon atoms (see Fig. 2b).[13] This is most likely due to small energy differences between staggered and eclipsed conformations. Recent MNDO calculations on the $[Cp_2Li]$ anion do indeed indicate essentially free rotation of the Cp rings around the longitudinal axis.[6b]

In the context of the theoretical discussion on out-of-plane bending of the hydrogen atoms in cyclopentadienyl–metal species, that is, bending away from or toward the metal,[6b, 11, 14, 15] it would be interesting to determine the Cp-hydrogen positions. Unfortunately, the Cp hydrogens in the crystal structure of the $[Cp_2Li]$ anion could not be exactly located. Attempts to localize and refine hydrogen atoms were severely hindered by the large thermal parameters of atoms in the Cp ring (Fig. 2b).

The $[Cp_2Li]$ anion is isoelectronic with its first-row relatives $[Cp_2Be]$[16] and the $[Cp^*_2B]$ cation ($Cp^* = \eta^5$-C_5Me_5).[17] However, the latter compounds are not isostructural with the $[Cp_2Li]$ anion but are of the slipped sandwich type with one η^1- and one η^5-coordinated Cp ligand (**4**). Preference for this geometry has been discussed in terms of three-dimensional aromaticity,[14, 18] but can also be explained by simple size arguments. The very short (η^5-Cp_{plane})–Be distance of 1.505(6) Å does not favor a symmetrical D_{5d} sandwich complex in which the Cp···Cp distance (3.01 Å) would be shorter than the interlayer distance in graphite,[19] the Cp···Cp distance in a D_{5d} $[(\eta^5\text{-}Cp^*)_2B]$ complex would be even shorter. The D_{5d} sandwich structures observed for the isovalent second-row relatives $[Cp_2Mg]$ and the $[Cp^*_2Al]$ cation,[20] on the other hand, exhibit relatively long Cp···Cp distances of 3.96(1) and 3.67(1) Å, respectively. As in these compounds, the long Cp···Cp distance of 4.012(8) Å in the Cp_2Li-anion apparently does not induce substantial ring slippage.



4

In summary, the $[Cp_2Li]$ anion has a staggered sandwich structure with D_{5d} symmetry (average C–Li bond distance of 2.318(4) Å) and shows a striking similarity with the structure of $[Cp_2Mg]$ (staggered D_{5d} conformation, average C–Mg bond distance of 2.304(8) Å).

Experimental Procedure

$[Ph_4P]^+$ $[Cp_2Li]^-$: (the synthesis was carried out under argon with normal Schlenk techniques and predried solvents). Addition of CpLi (0.30 g, 4.16 mmol) dissolved in 15 mL of THF to a suspension of anhydrous Ph_4PCl (0.78 g, 2.08 mmol) in 15 mL of THF results in immediate formation of a slightly turbid orange-red solution. The reaction mixture was centrifuged, and the clear solution decanted. After 12 h at room temperature, large yellow-brown crystals of $[Ph_4P]^+$ $[Cp_2Li]^-$ were isolated and washed with THF (yield 0.76 g, 76%). The crystals are very slightly soluble in THF. ^{1}H NMR (250 MHz, [D$_8$]THF, 25 °C, TMS): δ = 5.37 (s, 10 H,

CpH), 7.50–7.80 (m, 20 H, Ph_4P). ^{13}C NMR: δ = 104.1 (Cp), 118.7 (d, ^1J(C,P) = 353 Hz, Ph_{ipso}), 131.1 (d, ^2J(C,P) = 50 Hz, Ph_{ortho}), 135.7 (Ph_{para}), 135.8 (Ph_{meta}).

Received: April 29, 1994 [Z 6878 IE]
German version: *Angew. Chem.* **1994**, *106*, 1830

[1] J. Thiele, *Ber. Dtsch. Chem. Ges.* **1901**, *34*, 68.
[2] a) T. Aoyagi, H. M. M. Shearer, K. Wade, G. Whitehead, *J. Organomet. Chem.* **1979**, *175*, 21; b) P. Jutzi, W. Leffers, B. Hampel, S. Pohl, W. Saak, *Angew. Chem.* **1987**, *99*, 563; *Angew. Chem. Int. Ed. Engl.* **1987**, *26*, 583; c) W. J. Evans, T. J. Boyle, J. W. Ziller, *Organometallics* **1992**, *11*, 3903; d) E. Weiss, *Angew. Chem.* **1993**, *105*, 1565; *Angew. Chem. Int. Ed. Engl.* **1993**, *32*, 1501.
[3] a) M. F. Lappert, A. Singh, L. M. Engelhardt, A. H. White, *J. Organomet. Chem.* **1984**, *262*, 271; b) P. Jutzi, E. Schlüter, S. Pohl, W. Saak, *Chem. Ber.* **1985**, *118*, 1959; c) A. Hammel, W. Schwarz, J. Weidlein, *Acta Crystallogr. Sect. C* **1990**, *46*, 2337; d) H. Chen, P. Jutzi, W. Leffers, M. M. Olmstead, P. Power, *Organometallics* **1991**, *10*, 1282.
[4] Reviews on main group metallocenes: a) P. Jutzi, *Adv. Organomet. Chem.* **1986**, *26*, 217; b) *J. Organomet. Chemistry* **1990**, *400*, 1.
[5] $[Cp_2Li]^-$, was postulated on the basis of conductivity measurements: W. Strohmeier, H. Lansfeld, F. Gernert, *Z. Elektrochem.* **1962**, *66*, 823.
[6] a) R. den Besten, S. Harder, L. Brandsma, *J. Organomet. Chem.* **1990**, *385*, 153; b) L. A. Paquette, W. Bauer, M. R. Sivik, M. Bühl, M. Feigel, P. von R. Schleyer, *J. Am. Chem. Soc.* **1990**, *112*, 8776; c) M. Eiermann, K. Hafner, *ibid.* **1992**, *114*, 135.
[7] An analogous inverse sandwich structure has been confirmed by X-ray diffraction: S. S. Stults, R. Andersen, A. Zalkin, *J. Am. Chem. Soc.* **1989**, *111*, 4507.
[8] a) D. Bladauski, W. Broser, H. J. Hecht, D. Rewicki, H. Dietrich, *Chem. Ber.* **1979**, *112*, 1380; b) H.-D. Hausen, J. Tödtmann, J. Weidlein, *J. Organomet. Chem.* **1994**, *466*, C1.
[9] Crystal structure data for $[Ph_4P]^+[Cp_2Li]^-$: monoclinic, a = 10.770(3), b = 6.965(2), c = 17.654(5) Å, β = 99.25(2)°, V = 1307.1(6) Å^3, space group $P2/c$, $\{(C_{24}H_{20}P)(C_{10}H_{10}Li)\}$, M = 476.5, Z = 2, ρ_{calcd} = 1.211 g cm^{-3}, $\mu(Mo_{K\alpha})$ = 0.12 mm^{-1}; 5202 reflections were measured on a Siemens R 3m/V diffractometer ($Mo_{K\alpha}$, graphite monochromator, T = −40 °C), 2578 unique reflections after merging (R_{int} = 0.021), 1960 observed reflections with $F > 4.0\,\sigma(F)$. Solution by direct methods with the (SHELXTL) program, refinement by minimization of $\Sigma w(|F_o| - |F_c|)^2$ to $R(F)$ = 0.048, $wR(F)$ = 0.046 (165 parameter, 1960 data observed) with $w = 1/(\sigma^2(F) + 0.0001(F)^2)$. Non-hydrogen atoms were refined anisotropically; all hydrogen atoms were assigned to calculated positions and refined with an overall isotropic thermal parameter. Further details of the crystal structure investigation may be obtained from the Fachinformationszentrum Karlsruhe, D-76344 Eggenstein-Leopoldshafen (FRG) on quoting the depository number CSD-58 375.
[10] $[Cp_2Mg]$: W. Bünder, E. Weiss, *J. Organomet. Chem.* **1975**, *92*, 1; $[Cp_2Cr]$: E. Weiss, E. O. Fischer, *Z. Anorg. Allg. Chem.* **1956**, *284*, 69; $[Cp_2Fe]$: J. D. Dunitz, L. E. Orgel, A. Rich, *Acta Crystallogr.* **1956**, *9*, 373; $[Cp_2Co]$: W. Bünder, E. Weiss, *J. Organomet. Chem.* **1975**, *92*, 65; $[Cp_2Ni]$: P. Seiler, J. D. Dunitz, *Acta Crystallogr. Sect. B* **1980**, *36*, 2255.
[11] S. Alexandratos, A. Streitwieser, Jr., H. F. Schaefer III, *J. Am. Chem. Soc.* **1976**, *98*, 7959.
[12] NPA charges (NPA = natural population analysis) calculated for CpLi: Cp −0.91/Li +0.91; C. Lambert, P. von R. Schleyer, *Organometallics* **1993**, *12*, 853.
[13] The X-ray measurement at −40 °C suggests a static disorder model. Since the temperature dependence of the thermal ellipsoids has not been studied, the nature of this disorder could be either static or dynamic.
[14] a) E. D. Jemmis, P. von R. Schleyer, *J. Am. Chem. Soc.* **1982**, *104*, 4781; b) E. D. Jemmis, S. Alexandratos, P. von R. Schleyer, A. Streitwieser, Jr., H. F. Schaefer III, *ibid.* **1978**, *100*, 5695.
[15] K. C. Waterman, A. Streitwieser, Jr., *J. Am. Chem. Soc.* **1984**, *106*, 3138.
[16] K. W. Nugent, J. K. Beattie, T. W. Hambley, M. R. Snow, *Aust. J. Chem.* **1984**, *37*, 1601.
[17] P. Jutzi, A. Seufert, *J. Organomet. Chem.* **1978**, *161*, C5.
[18] A total of 12 interstitial electrons in species $[Cp_2Be]$ and $[Cp_2B]^+$ with D_{5d}-symmetry, would result in occupation of the degenerated $(Cp_2)e_{1g}$ orbitals for which no bonding combination with metal s- and p-orbitals is possible. The alternative slipped sandwich complex (**4**), with 6 interstitial electrons, satisfies the rules for three-dimensional aromaticity in such species. J. B. Collins, P. von R. Schleyer, *Inorg. Chem.* **1977**, *16*, 152. See also ref. [14].
[19] The interlayer distance of 3.35 Å in graphite is commonly regarded as the equilibrium distance between two non-bonded aromatic carbon atoms. This is approximately twice the van der Waals radius for carbon.
[20] C. Dohmeier, H. Schnöckel, C. Robl, U. Schneider, R. Ahlrichs, *Angew. Chem.* **1993**, *105*, 1714; *Angew. Chem. Int. Ed. Engl.* **1993**, *32*, 1655.
[21] While in press, the structure of the (isodicyclopentadiene)$_2$Li anion with C–Li bond lengths in a similar range was published: F. Zaegel, J. C. Galluci, P. Meunier, B. Gautheron, M. R. Sivik, L. A. Paquette, *J. Am. Chem. Soc.* **1994**, *116*, 6466.

The Structures of Two Lithium Hydrazides: Is There Electron-Deficient Bonding?

Nils Metzler, Heinrich Nöth,* and Hermann Sachdev

Dedicated to Professor Michael F. Lappert on the occasion of his 65th birthday

N-Lithiohydrazides are useful synthetic reagents.[1] However, their structures have not been investigated until very recently,[2] in contrast to the well-developed chemistry and structural chemistry of alkali metal amides, aldimides, and ketimides.[3] Also, our knowledge of the state of lithium hydrazides in solution is negligible,[4] although anionic rearrangements of several lithium bis(organosilyl)hydrazides have been investigated thoroughly by NMR methods.[5]

In the course of our studies related to the synthesis of borylated hydrazines from lithium hydrazides and diorganylboron halides we obtained the compounds **1** and **2**[6] as single crystals, which we studied by X-ray structure analysis.

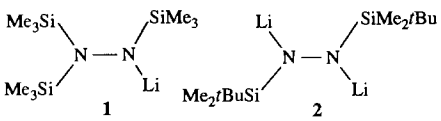


Figure 1 depicts an ORTEP diagram of one of the two crystallographically independent molecules of **1**.[7] Both show very similar bonding parameters. The most noticeable feature of **1** is

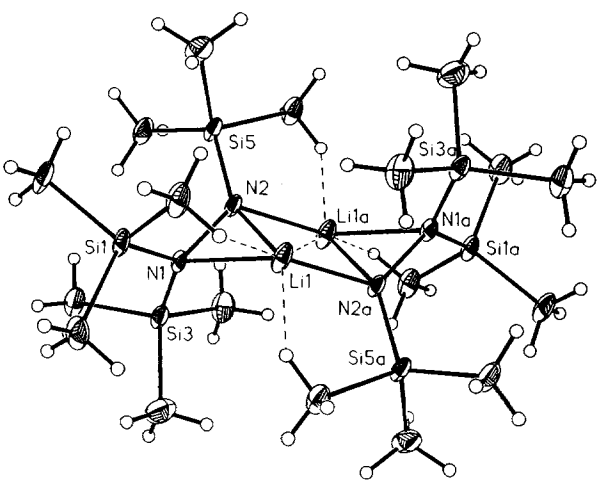


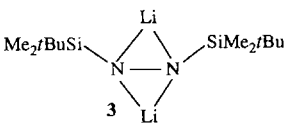
Fig. 1. ORTEP representation of the molecular structure of one of the two crystallographically independent $(\mathbf{1})_2$ molecules. Thermal ellipsoids represent 25% probability. Selected bond lengths [Å]: N1–Si1 1.744(4), N1–Si3 1.767(5), N2–Si5 1.712(4), N1–Li1 2.15(1), N1–N2 1.509(6), N2–Li1 1.925(9), Li1–Li1a 2.28(2). Selected bond angles [°]: Si1-N1-Si3 125.3(2), Li1-N1-N2 60.5(3), Si1-N1-Li1 96.6(3), Si3-N1-Li1 125.1(3), Si1-N1-N2 116.8(3), Si3-N1-N2 114.3(3), Si5-N2-N1 124.7(3), Si5-N2-Li1 147.6(4), Si5-N2-Li1a 108.2(3), N2-Li1-N2a 108.2(4), N1-Li1-N2 43.1(2), Li1-N2-Li1a 71.8(4).

its centrosymmetric *dimeric* nature which can be perceived as being formed from two three-membered LiN_2 rings. The Li···Li distances (2.28, 2.32 Å) are short. The skeleton is composed of tricoordinated Li and tetracoordinated N atoms. The

[*] Prof. Dr. H. Nöth, Dr. N. Metzler, Dipl.-Chem. H. Sachdev
Institut für Anorganische Chemie der Universität
Meiserstrasse 1, D-80333 München (FRG)
Telefax: Int. code + (89)590-2451

Li–N distances fall into two groups: two are short (1.93(1) Å) and one is longer (2.15(1) Å). This corresponds with the structural features of lithium amides.[3] The angles N-Li-N′ range from 43.1(2)° to 129.7(5)° and those at N2 from 71.8(4) to 147.6(4)°. In contrast, bond angles subtended at atom N1 are closer to a tetrahedral angle. The Si–N2 bond length is significantly shorter (1.712(4) Å) than Si–N1 bond lengths (1.744 and 1.767(5) Å); the latter compare well with those observed for $(t\mathrm{BuMe_2SiNH-NHLi})_6$.[2] More important, however, is the rather long N1–N2 bond. Although the Li atoms in $(\mathbf{1})_2$ are tricoordinated (by N atoms) the two short Li···H contacts (2.27 Å and 2.31 Å) suggest agostic interactions, which contribute to the steric shielding of the Li centers.

Compound **2** proved to be a *trimer* in the solid state and cocrystallizes with one molecule of hexane.[8] Figure 2 presents a view of the molecular structure at the top and the architecture of the skeletal atoms in more detail at the bottom. The molecule possesses a crystallographically imposed C_2 symmetry. The monomeric unit in **2** is represented by **3**; this Li_2N_2 bicyclic skeleton is also the energy minimum on the potential energy surface according to HF/6-31G** calculations for the model compound $Li_2N_2H_2$.[9] The side-on coordination of Li atoms has also been predicted by ab initio calculations for $H_2N-NHLi$[10] as well as for the isoelectronic species $ONHLi_2$ and $ONLi_3$.[11] Three monomeric $Li_2N_2R_2$ units associate as shown at the bottom of Figure 2, and the resulting Li_6N_6 skeleton is composed of pentacoordinated N atoms and tetracoordinated Li centers, which also feature two agostic Li···H contacts.



The Li–N bond lengths in $(\mathbf{2})_3$ fall within a much narrower range than those in $(\mathbf{1})_2$. There are three different sizes of Li-N-Li′ bond angles: close to 70°, close to 95° and close to 108°. Moreover, the structure reveals two types of N′-N-Li bond angles: two are close to 66.5° and the third at 123°. Si-N-Li bond angles can be as large as 135°.

The N–N bonds in $(\mathbf{2})_3$ (1.556(3), 1.563(4) Å) are longer than in $(\mathbf{1})_2$ which are in turn longer than in $(\mathrm{LiHN-NHSiMe_2}t\mathrm{Bu})_6$ (1.49 Å).[2] All exceed those found for hydrazine itself or organylhydrazines (1.45–1.48 Å). This points to an increasing charge transfer from Li to N as one moves from neutral hydrazines to (formal) hydrazide(2−) units.

The pentacoordinated nitrogen atoms in $(\mathbf{2})_3$ as well as electron-counting according to Wade's rules suggest that it is a bicapped distorted hexagonal antiprism in which two vertices are missing, resulting in an *arachno* type of compound.[12] As shown at the bottom of Figure 2, the skeleton is indeed built from deltohedra, as is typical for electron-deficient compounds. A molecule with a geometriy similar to $(\mathbf{2})_3$ is Bürger's $[\mathrm{PhSi(NLi}\cdot t\mathrm{Bu})_3]_2$,[13] which has also been considered an electron-deficient cluster.

Wiberg et al.[4] have pointed out that **1** is dimeric in solution. This has now been verified for the solid state as well as in solution (C_6D_6) which also contains monomeric **1**, as multinuclear NMR spectra show.[14] Moreover, the NMR data of **2** are consistent with its trimeric nature in deuterobenzene solution. There is only one signal for the Li atoms, and all silyl groups are equivalent as demonstrated by four ^{13}C NMR signals for $SiMe_2CMe_3$ substituent. Therefore, the structure of $(\mathbf{2})_3$ is obviously more symmetrical in the solution than in the solid state.

Present evidence suggests that the degree of association of metalated silyl and organyl hydrazines[5] will not only depend on the ratio of the number of N atoms to the number of metal centers, but also on the steric demand of the substituents as well as on the absence or presence of donor molecules that interact with the metal centers.[3, 15] It appears that lithium and other metal hydrazides may be an exceptionally interesting and suitable class of compounds with which to study the degree of association and bonding along the series of oligomeric species from R_3N_2M through $R_2N_2M_2$ and RN_2M_3 to N_2M_4.

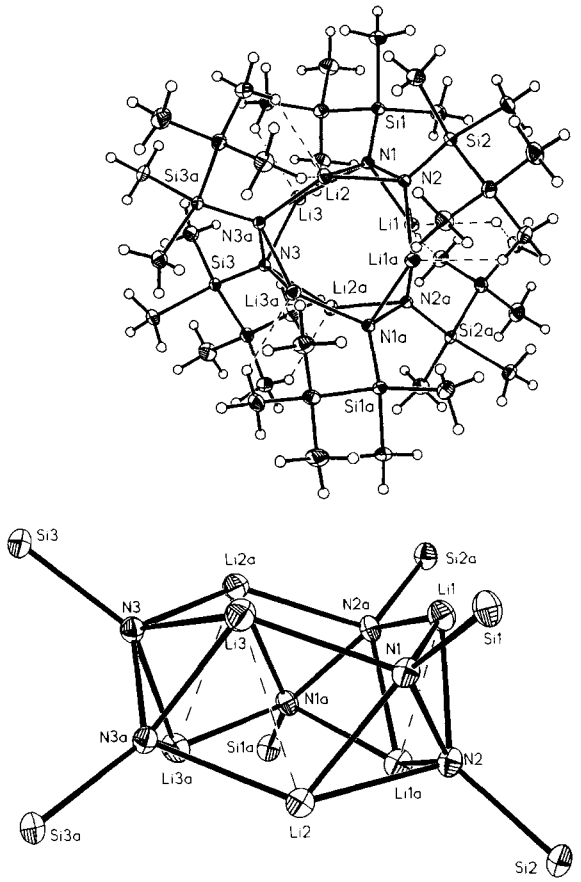


Fig. 2. Top: ORTEP representation of $(\mathbf{2})_3$. Thermal ellipsoids represent 25% probability. Note the two agostic Li···H interactions for each Li atom (represented by dotted lines). Selected bond lengths [Å]: N2–Si2 1.715(2), N1–Si1 1.716(2), N3–Si3 1.715(2), Li1–N1 1.939(5), Li1–N1a 2.000(5), Li2–N2 1.948(5), Li2–N1 1.940(5), Li3–N3a 1.950(5), Li3–N3 1.954(5), Li2–Li3 2.279(6), Li1–Li2a 2.908(6), Li2-Li3 2.279(6), Li2–Li3a 2.904(6), Li1–Li1a 2.277(9), Li1–Li3 2.906(7), N1–N2 1.556(3), N3–N3a 1.563(4). Selected bond angles [°] (standard deviations are 0.1 to 0.2°): N2-N1-Li1 65.9, N2-N1-Li2 66.7, N2-N1-Li3 123.0, Li3-N1-Li1 94.8, Si1-N1-Li1 116.2, Si1-N1-Li2 135.0, N1-N2-Li2 66.2, N1-N2-Li1a 123.1, Li1-N2-Li1a 70.6, Si3-N3-Li2a 110.5, N3a-N3-Si3 126.54, Si3-N3-Li3a 134.6, N3a-N3-Li3 66.3. Bottom: "Side" view on the core of $(\mathbf{2})_3$ to demonstrate the deltohedral array of the skeleton.

Received: December 11, 1993
Revised version: April 16, 1994 [Z 6555 IE]
German version: *Angew. Chem.* **1994**, *106*, 1837

[1] C. Drost, U. Klingebiel, M Noltemeyer, *J. Organomet. Chem.* **1991**, *414*, 307.
[2] U. Klingebiel, S. Dielkus, C. Drost, R. Herbst-Irmer, *Angew. Chem.* **1993**, *105*, 1689; *Angew. Chem. Int. Ed. Engl.* **1993**, *32*, 1625.
[3] a) R. E. Mulvey, *Chem. Soc. Rev.* **1991**, *20*, 167; b) P. von R. Schleyer, *Adv. Organomet. Chem.* **1985**, *24*, 353; c) C. Schade, P. von R. Schleyer, *ibid.* **1987**, *27*, 169; d) K. Gregory, P. von R. Schleyer, R. Snaith, *ibid.* **1991**, *37*, 48.
[4] N. Wiberg, E. Weinberg, W.-C. Joo, *Chem. Ber.* **1974**, *107*, 1664.
[5] R. West, B. Bichlmeir, *J. Am. Chem. Soc.* **1972**, *94*, 1649.
[6] $(\mathbf{1})_2$: $(\mathrm{Me_3Si})_3N_2H$ (8.00 g, 32.2 mol) was dissolved with stirring in 100 mL of *n*-hexane. A solution of LiBu in hexane (20.6 mL, 1.56 M) was added. After heating at reflux for 2 h, crystals of $(\mathbf{1})_2$ separated on cooling. Yield 93%, m.p.

183–185 °. Correct elemental analysis. ^{1}H NMR (270.17 MHz, C_6D_6, 28 °C): $\delta = 0.24$ (broad, dimer, 85% intensity), 0.13 (broad, $NLiSiMe_3$), 0.11 (s, $N(SiMe_3)_2$). The last two signals are assigned to monomeric **1**. Their intensity ratio is 2:1 and their total intensity is 15%; ^{6}Li NMR (39.76 MHz, C_6D_6): $\delta = 1.10$ (s, sharp); ^{7}Li NMR (105.01 MHz, C_6D_6): $\delta = 1.76$ (s, sharp); ^{13}C NMR (67.94 MHz, C_6D_6): a) of $(\mathbf{1})_2$: $\delta = 3.80$ (broad, $N(Li)SiMe_3$), 2.84 ($NSiMe_3$); b) of **1**: $\delta = 1.98$ (s, $N(Li)SiMe_3$), 1.29 (s, $N(SiMe_3)_2$), 0.91 (s, $N(SiMe_3)_2$. ^{29}Si NMR (53.67 MHz, C_6D_6): a) of $(\mathbf{1})_2$: $\delta = 6.76$ (broad); b) of **1**: $\delta = 6.93$ (broad), 6.52 (broad).

$(\mathbf{2})_3 \cdot C_6H_{14}$: $(t\mathrm{BuMe_2Si})_2N_2H_2$ (7.82 g) dissolved in *n*-hexane (100 mL) was allowed to react with a 1.56 M solution of LiBu in hexane at ambient temperature and with stirring. After heating the mixture for 1 h at reflux, followed by cooling, to −20 °C, crystals including single crystals of $(\mathbf{2})_3$ separated. Yield: 86%, m.p. 73–76 °C, correct elemental analysis. All NMR data were recorded in C_6D_6. ^{1}H NMR (270 MHz): $\delta = 0.98$ (s, $SiMe_2CMe_3$), 0.93 (s, $SiMe_2CMe_3$), 0.23 (s, $SiMe_2CMe_3$); ^{6}Li NMR (39.76 MHz): $\delta = 1.10$ (sharp); ^{7}Li NMR (105.01 MHz): $\delta = 1.44$ (s, sharp); ^{13}C NMR (67.94 MHz): $\delta = 0.55$ ($SiMe_2CMe_3$), 1.84 ($SiMe_2CMe_3$), 18.59 ($SiMe_2CMe_3$), 28.88 ($SiMe_2CMe_3$), 14.25 (CH_2), 22.67 (CH_2), 38.78 (CH_3). The latter three signals result from hexane. ^{29}Si NMR (53.67 MHz): $\delta = -0.47$.

[7] a) X-ray structure determination of $(\mathbf{1})_2$. Crystal size = 0.3 × 0.4 × 0.5 mm, $(C_9H_{27}LiN_2Si_3)_2$, $M_r = 254.54$ g mol^{-1}, colorless prism, $a = 8.85(1)$, $b = 9.598(9)$, $c = 21.98(2)$ Å, $\alpha = 100.62(7)$, $\beta = 91.9(1)$, $\gamma = 115.90(8)$°, $V = 1636$ Å^3, triclinic, space group = $P\bar{1}$, $Z = 2$, $\rho_{calcd} = 1.033$ g cm^{-3}, $F(000) = 560$. Data collection: Nicolet R3m four-circle diffractometer, $Mo_{K\alpha}$ radiation, graphite monochromator, $T = 173$ K, 2θ-range = 3.8–48° in h, $-/+k$, $-/+l$, scan speed = 1.8 to 29.3° min^{-1}, ω scans, scan width = 1.4°, 5489 data collected, 5110 independent reflections, 3708 considered observed ($F > 3\sigma(F)$). Structure solution: SHELXTL PLUS (VMS), non-hydrogen atoms anisotropic, H atoms in calculated positions, riding model, 271 refined parameters, ratio of observed data to no. of variables = 13.6:1, $R = 0.095$, $R_w = 0.11$, $1/w = \sigma^2(F) + 0.0004\,F^2$, wR_2 (on F^2) = 0.2466, GOF = 2.21, largest diff. peak/hole = 0.79/−1.09 e Å^{-3}. The crystal of $(\mathbf{1})_2$ was only weakly diffracting, which may account for the fairly high R values. b) Further details of the structure determination are deposited at the Fachinformationszentrum Karlsruhe, Gesellschaft für wissenschaftliche Information, D-76344 Eggenstein-Leopoldshafen and may be obtained by quoting the depository number CSD-58392 and the literature citation.

[8] X-ray structure determination of $(\mathbf{2})_3$. Crystal size: 0.4 × 0.45 × 0.55 mm, colorless prism, $a = 21.782(5)$, $b = 12.465(3)$, $c = 21.839(4)$ Å, $\beta = 101.71(1)$°, $V = 5806(2)$ Å^3, $Z = 4$, monoclinic, space group $C2/c$, $\rho_{calcd} = 1.034$ g cm^{-3}, $\mu = 1.75$ cm^{-1}, $F(000) = 2000$. Data collection: Siemens P4 diffractometer, $Mo_{K\alpha}$ radiation, $T = 173$ K, 2θ-range = 3.8–48° in h: −1 to 23, k: 0 to 13, l: −24 to 24, ω scans, scan speed = 3° min^{-1}, scan range = 1.2°, 4634 reflection collected, 4137 independent reflections ($R_{int.} = 0.035$), 2317 observed ($4\sigma(F)$). Structure solution: Siemens SHELXTL PLUS PC. Refinement: SHELX93 PC, direct methods, non-hydrogen atoms refined anisotropically, H atoms freely refined except the hydrogen atoms of the CH_2 groups of hexane, $R = 0.0448$ (with data $I > 4\sigma(I)$), $R = 0.0625$ (all data), $wR_2 = 0.1154$ (F^2!). Data to parameter ratio = 10:1. $1/w = \sigma^2(F_0)^2 + (0.0486P)^2 + 12.0653P$ where $P = (F_o^2 + 2F_c^2)/3$, GOF = 1.029 on F^2, largest difference peak/hole = 0.59/−0.58 e Å^{-3}. See also [7b].

[9] Ab initio HF/6-31G** calculations on $Li_2N_2H_2$ showed that a bicyclic structure like **3** with C_2, symmetry is the most stable one. Calculated bond lengths [Å]: N–N = 1.529, N–Li = 1.828, Li···Li′ = 3.030; calculated bond angles [°]: Li-N-Li′ = 111.94, Li-N-N′ = 63.87, N-Li-N′ = 52.26, N-Li-Li′ = 34.03. The population analysis according to Mulliken resulted in the following partial charges [e]: H = 0.233, N = −0.726, Li = 0.492 and indicates electron density between Li and N atoms. However, it is known for any population analysis that the charges are likely to be overestimated. In addition, the calculation suggests (very) weak Li···Li′ interaction ($p_{\mu\nu} = 0.045$). This lies on the borderline for a meaningful interpretation. The long Li···Li′ distance corresponds with the long Li···Li distances in $(\mathbf{2})_3$. However, it should been noted that the Li···Li′ distances between the two sets of six membered rings in $(\mathbf{2})_3$ are much shorter than in the monomeric model.

[10] J. R. Dilworth, A. Rodriguez, G. L. Leigh, J. N. Murrell, *J. Chem. Soc. Dalton Trans.* **1983**, *2*, 455.

[11] D. R. Armstrong, P. G. Pelter, G. T. Walter, *J. Mol. Struct.* **1985**, *122*, 189.

[12] G. A. Olah, K. Wade, R. E. Williams, *Electron Deficient Boron and Carbon Clusters*, Wiley, New York, **1991**.

[13] D. J. Brauer, H. Bürger, G. R. Liewald, *J. Organomet. Chem.* **1986**, *308*, 119.

[14] ^{1}H NMR spectra for $(\mathbf{1})_2$ show three broad signals due to the presence of dimer and monomer in an approximate 89:11 ratio. There is only one signal for the dimer, but the expected three signals were observed in the ^{13}C NMR spectra, and only two rather broad signals for the monomer. We could not resolve the broad signals by changing the resonance frequencies, solvent, and temperature.

[15] N. Veith, *Chem. Rev.* **1990**, *90*, 3.

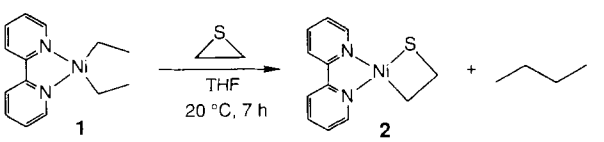
Thianickelacycles by Ring-Opening Reactions of Cyclic Thioethers and Their Subsequent Carbonylation to Thioesters**

Phillip T. Matsunaga and Gregory L. Hillhouse*

In the pathway of CO_2 fixation in anaerobic bacteria, nickel is believed to play a key role in the synthesis of acetyl coenzyme A (acetyl-CoA) by the metalloenzyme carbon monoxide dehydrogenase. Although the majority of studies on CO-dehydrogenase have been performed on the acetogenic bacteria *Clostridium thermoaceticum* and *Autobacterium woodii*, this enzyme is also found in some methanogenic, sulfate-reducing, and photosynthetic bacteria.[1] EPR data indicate that Ni is involved in the binding of CO, which is incorporated as the C-1 carbon of acetyl-CoA, and EXAFS data suggest that the Ni atom is four-coordinate with N- and S-donor ligands in the coordination sphere. Although the biosynthesis of acetyl-CoA is probably effected at multiple sites and not at a single Ni center in the native enzyme, we report herein the preparation of simple Ni complexes containing N-donor ligands (bipyridine (bpy)) as well as alkyl and thiolate ligands. One such complex reacts with CO to give a thioester in a transformation analogous to that involved in acetyl-CoA biosynthesis. Holm and co-workers have reported a series of Ni complexes that model the Ni site in CO-dehydrogenase and demonstrate an alternate route to the synthesis of thioesters.[2]

We recently showed that the O atom of N_2O can be abstracted by Ni alkyl complexes, which enabled us to prepare stable examples of otherwise inaccessible Ni alkoxides containing β-H atoms.[3] The unavailability of N_2S as an S-atom source led us to investigate the use of cyclic thioethers as precursors to thiolatenickel complexes. This strategy seemed attractive since reactions involving sulfur-atom abstraction from ethylene sulfide and ring-opening of thietane and tetrahydrothiophene by transition-metal cluster complexes have been described.[4, 5]

The Ni^{II} complex **1** [6] reacts with ethylene sulfide (THF solution, 20 °C) to effect reductive elimination of butane and



addition of the ring-opened episulfide to give the monomeric thiametallacycle **2** in 30% yield as the only soluble complex; the remainder of the Ni precipites as NiS (see Table 1 for spectroscopic data).[7] Although a number of Ni thiolates are known,[8] cyclic derivatives like **2** have not been previously reported.

Since the conversion **1** → **2** probably requires rate-limiting reductive elimination of butane from **1**, we investigated the reaction of the Ni^0 complex **3** (cod = 1,5-cyclooctadiene)[9] with ethylene sulfide. The conversion **3** → **2** proceeds under much milder conditions (0 °C, 30 min) to give **2** in 21% isolated yield.

[*] Prof. G. L. Hillhouse, Dr. P. T. Matsunaga
Searle Chemistry Laboratory, Department of Chemistry
The University of Chicago
5735 S. Ellis Avenue, Chicago, IL 60637 (USA)
Telefax: Int. code + (312) 702-0805

[**] This work was supported by a U. S. National Science Foundation grant (CHE-9200943 to G. L. H.).

Table 1. Physical data for complexes **2**, **4**, and **6** [a].

2: Blue crystals. ^{1}H NMR: δ = 0.93 (t, 2 H, NiCH_2), 4.18 (t, 2 H, SCH_2), 6.34 (t, 1 H, bpy), 6.39 (t, 1 H, bpy), 6.65 (t, 2 H, bpy), 6.78 (t, 1 H, bpy), 6.87 (t, 1 H, bpy), 8.10 (d, 1 H, bpy), 8.77 (d, 1 H, bpy). ^{13}C{^{1}H} NMR: δ = -19.0, 33.0, 119.3, 120.5, 125.4, 125.9, 133.1, 135.3, 146.0, 146.7. Correct elemental analysis for $C_{12}H_{12}N_2SNi$. Molecular weight: M_{calcd} = 275. M_{found} = 260.

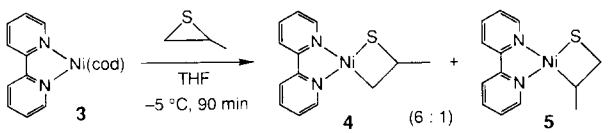
4: Blue crystals. ^{1}H NMR: δ = 0.53 (t, 1 H, NiCH*H*), 1.26 (dd, 1 H, NiC*H*H), 1.87 (d, 3 H, CH_3), 4.41 (m, 1 H, SC*H*), 6.38 (t, 2 H, bpy), 6.74 (t, 2 H, bpy), 6.81 (t, 1 H, bpy), 6.92 (t, 1 H, bpy), 8.11 (d, 1 H, bpy), 8.74 (d, 1 H, bpy). ^{13}C{^{1}H} NMR: δ = -5.1, 31.3, 43.0, 119.4, 120.6, 125.4, 125.9, 133.1, 135.3, 146.0, 146.9. Correct elemental analysis for $C_{13}H_{14}N_2SNi$. Molecular weight: M_{calcd} = 289. M_{found} = 260.

6: Blue crystals. ^{1}H NMR: δ = 2.29-2.36 (m, 4 H, CH_2), 3.10 (t, 2 H, SCH_2), 6.31 (t, 1 H, bpy), 6.34 (t, 1 H, bpy), 6.63 (d, 2 H, bpy), 6.72 (t, 1 H, bpy), 6.84 (t, 1 H, bpy), 8.42 (d, 1 H, bpy), 9.40 (d, 1 H, bpy). ^{13}C{^{1}H} NMR: δ = 29.4, 32.2, 42.3, 119.5, 120.5, 125.0, 125.7, 133.5, 135.4, 147.6, 150.6. Correct elemental analysis for $C_{13}H_{14}N_2SNi$. Molecular weight: M_{calcd} = 289. M_{found} = 313.

[a] ^{1}H NMR spectra recorded at 500 MHz, ^{13}C{^{1}H} NMR spectra recorded at 125.8 MHz, C_6D_6 solutions, 20 °C. Molecular weights were determined in THF solution by the Signer method [14].

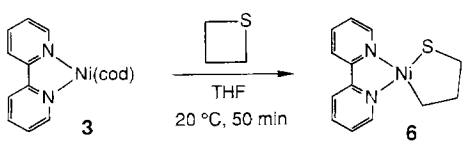
Here again, most of the Ni precipitates as NiS (with ethylene as a by-product), consistent with other studies in which **3** has been shown to extract sulfur from dibenzothiophene to give NiS as the metal-containing product.[10]

Propylene sulfide reacts with **3** to give a 6:1 mixture of **4** and **5** in an overall yield of 22%. Steric factors appear to



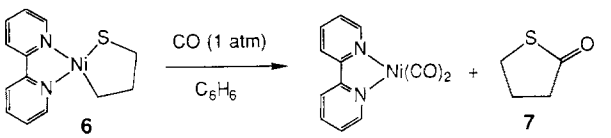
dictate the product distribution in this reaction in which insertion occurs preferentially at the least substituted S–C bond to give **4** as the major product.

The four-membered cyclic thioether, thiethane, reacts with **3** to produce the thiametallacyclopentane complex **6** in 47% yield. Tetrahydrothiophene, however, is unreactive toward **3**.



The five-membered ring thus seems not to possess sufficient ring strain to promote C–S bond cleavage. Moreover, **3** is unreactive toward oxygen analogues such as propylene oxide, oxetane, and tetrahydrofuran. These observations probably reflect the greater C–O bond strengths in cyclic ethers relative to the C–S bonds in cyclic thioethers. More reactive cyclic substrates (for example, cyclic anhydrides), however, do give rise to C–O bond cleavage.[11]

The [(bpy)Ni(R)(OR)] complexes undergo carbonylation reactions to give [(bpy)Ni(CO)$_2$] and esters.[3, 12] In an analogous reaction, carbon monoxide (1 atm, 20 °C) reacts with **6** to give [(bpy)Ni(CO)$_2$] and γ-thiobutyrolactone (**7**).[13] No intermediates were detected by spectroscopy in this transformation, and we have no mechanistic basis for differentiating between initial CO insertion into the Ni–S or the Ni–C bond of **6** prior to reductive elimination of the thiolactone. The 28% isolated yield of **7** is relatively low, possibly a consequence of the tendency



of thiolactones, particularly those of small ring size, to polymerize. Under similar conditions, the reaction of **2** with CO does not give a clean product, possibly because of excessive ring strain in the expected thioester.

We are continuing to investigate the chemistry of these thiametallacyclic complexes, and are examining other cyclic substrates to evaluate the extent of substrate compatibility with this ring-opening methodology.

Experimental Procedure

All reactions were carried out under argon with standard Schlenk and high-vacuum techniques and dry, air-free solvents.

2: (Method A) To a solution of **1** (0.250 g, 0.916 mmol) in THF (10 mL) was added, dropwise, ethylene sulfide (54.5 µL, 0.916 mmol) by syringe. The solution was stirred at ambient temperature for 7 h, during which time the color changed from green to blue. The solution was filtered, and the residue was washed with THF (3 × 5 mL). The filtrate was concentrated to 5 mL, and pentane (5 mL) was added to precipitate the product. The solid was filtered and washed with pentane (3 × 5 mL). The residual solvent was removed under reduced pressure to yield 0.076 g (0.28 mmol, 30%) of **2** as dark blue microcrystals.
Method B: **2** was synthesized in 21% yield from **3** with a modified procedure described above—the reaction was carried out at 0 °C over a 30 min period.

4, **5**, **6**: Analogous procedures to that described for **2** were used for all compounds. Reaction conditions are given in the reaction equations, yields in the text.

7: A solution of **6** (0.050 g, 0.17 mmol) in C_6D_6 (1 mL) was exposed to carbon monoxide (1 atm). After 30 min, the excess CO was removed and the volatiles were separated from [(bpy)Ni(CO)$_2$] by vacuum transfer. Analysis by ^{1}H NMR spectroscopy (internal standard: ferrocene) gave a yield of 0.047 mmol (28%) for **7**. The product was identified by spectral comparison with an authentic sample.

Received: March 22, 1994
Revised version: May 13, 1994 [Z 6785 IE]
German version: *Angew. Chem.* **1994**, *106*, 1841

[1] S. W. Ragsdale, H. G. Wood, T. A. Morton, L. G. Ljungdahl, D. V. DerVartanian in *The Bioinorganic Chemistry of Nickel* (Ed.: J. R. Lancaster), VCH, Weinheim, **1988**, Ch. 14.
[2] P. Stavropoulos, M. Carrie, M. C. Muetterties, R. H. Holm, *J. Am. Chem. Soc.* **1990**, *112*, 5385; P. Stavropoulos, M. C. Muetterties, M. Carrie, R. H. Holm, *ibid.* **1991**, *113*, 8485.
[3] P. T. Matsunaga, G. L. Hillhouse, A. L. Rheingold, *J. Am. Chem. Soc.* **1993**, *115*, 2075.
[4] R. D. Adams, J. E. Babin, *Inorg. Chem.* **1986**, *25*, 3418; R. D. Adams, J. E. Babin, M. Tasi, *ibid.* **1986**, *25*, 4514.
[5] R. D. Adams, M. P. Pompeo, *Organometallics* **1990**, *9*, 1718; *ibid.* **1992**, *11*, 2281; R. D. Adams, M. P. Pompeo, W. Wu, J. H. Yamamoto, *J. Am. Chem. Soc.* **1993**, *115*, 8207.
[6] T. Saito, Y. Uchida, A. Misono, A. Yamamoto, K. Morifuji, S. Ikeda, *J. Am. Chem. Soc.* **1966**, *88*, 5198.
[7] Compound **2** can also be isolated from the reaction of [(bpy)Ni(*i*Bu)$_2$] with ethylene sulfide, which indicates that the ethylene backbone of the metallacycle does not originate from one of the ethyl groups of **1**.
[8] L. Sacconi, F. Mani, A. Bencini in *Comprehensive Coordination Chemistry, Vol. 5* (Ed.: G. Wilkinson), Pergamon, Oxford, **1987**, Ch. 50; B. Krebs, G. Henkel, *Angew. Chem.* **1991**, *103*, 785; *Angew. Chem. Int. Ed. Engl.* **1991**, *30*, 769.
[9] K. I. Han, A. M. Piotrowski, J. J. Eisch in *Organometallic Syntheses, Vol. 3* (Eds.: R. B. King, J. J. Eisch), Elsevier, Amsterdam, **1986**, p. 112.
[10] J. J. Eisch, L. E. Hallenbeck, K. I. Han, *J. Org. Chem.* **1983**, *48*, 2963.
[11] E. Uhlig, G. Fehske, B. Nestler, *Z. Anorg. Allg. Chem.* **1980**, *465*, 141; K. Sano, T. Yamamoto, A. Yamamoto, *Chem. Lett.* **1983**, *115*; R. Fischer, B. Nestler, H. Schutz, *Z. Anorg. Allg. Chem.* **1989**, *577*, 111; R. Fischer, D. Walther, G. Braunlich, B. Undeutsch, W. Ludwig, H. Bandmann, *J. Organomet. Chem.* **1992**, *427*, 395.
[12] S. Komiya, Y. Akai, K. Tanaka, T. Yamamoto, A. Yamamoto, *Organometallics* **1985**, *4*, 1130.
[13] A mixture of [$Co_2(CO)_8$] and [$Ru_3(CO)_{12}$] catalyzes the carbonylation of thietane to γ-thiobutyrolactone (60 atm CO, 125 °C, 2 days). M.-D. Wang, S. Calet, H. Alper, *J. Org. Chem.* **1989**, *54*, 20.
[14] R. Signer, *Justus Liebigs Ann. Chem.* **1930**, *478*, 246; E. P. Clark, *Ind. Eng. Chem. Anal. Ed.* **1941**, *13*, 820.

Redox Control for the Recognition of Ag^+ Ions in a Macrocycle Containing Two SH Groups or an S–S Bridge inside the Cavity**

Tatsuya Nabeshima,* Hiroyuki Furusawa, and Yumihiko Yano

An advanced and challenging target in host–guest chemistry is the construction of a host molecule having the ability of specific recognition regulated in a similar fashion to that observed, for example, in allostery or in cooperative effects.[1] The external stimulus or effector may be a molecule, ion, electron, etc.[2] We have been interested in an electron as an effector, because the redox reaction between thiols and disulfides controls perfectly the enzymatic activity of ribonuclease.[3] However, perfect and facile regulation using the reaction has been extremely difficult because of some drawbacks in the artificial systems:[4] quantitative interconversion between redox forms could not be performed,[5] or the reduced form is somewhat difficult to treat without oxidation owing to its high sensitivity to molecular oxygen.[6] Additionally, a more critical problem is that a recognition site could not be made to vanish completely despite a large conformational change induced by the redox reactions.

In this paper we provide a new concept of gating, the interconversion of an open and a closed state of a recognition site (Fig. 1) that uses the redox reactions between thiols and disulfides for regulation, and report novel artificial ionophores **1** (**1**(red), the reduced form for the open state; **1**(ox), the oxidized form for the closed state) designed on the basis of this concept. Host molecules **1** are novel macrocyclic polyethers with a redox gate containing sulfur atoms inside the binding cavity. This system solved all problems mentioned above and regulates remarkably high Ag^+ affinity. To the best of our knowledge, this is the first example of gating to control ion recognition.

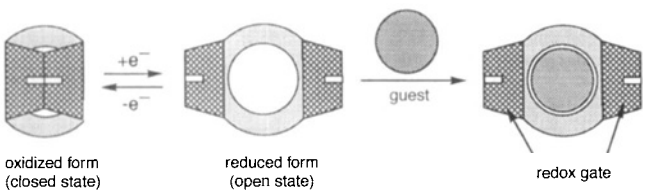
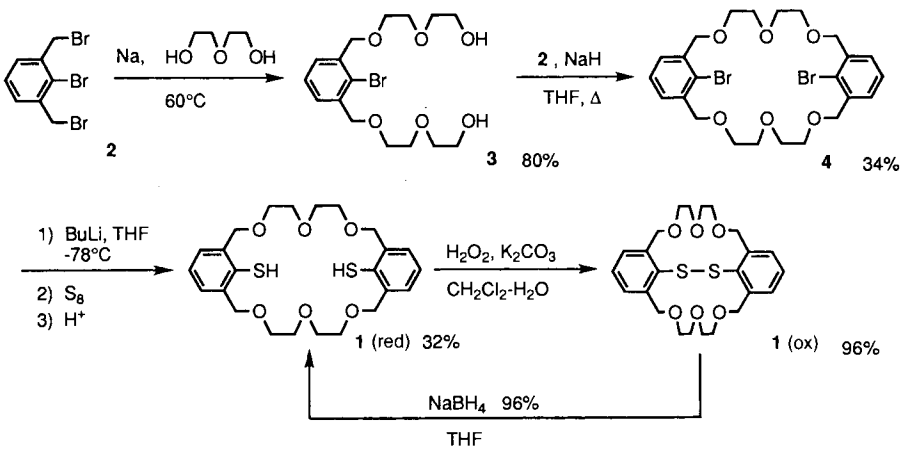


Fig. 1. Principle of molecular recognition controlled by a redox gate.

Tribromide **2**[7] was treated with an excess of diethylene glycol to give diol **3** (Scheme 1). Cyclic dibromide **4** was obtained in 34% yield by the reaction of **2** and **3**. Lithiation of **4**, followed by treatment with elemental sulfur, afforded **1**(red) bearing two thiol groups, in 32% yield as colorless crystals after recrystallization from EtOAc. The form **1**(red) was oxidized by iodine or peroxide such as hydrogen peroxide to yield **1**(ox) quantitatively. The proximate and inward arrangement of the thiol groups in the **1**(red) ring should prevent generation of polymeric compounds. Importantly, **1**(red) is very stable under aerobic conditions: no detectable amount of **1**(ox) was observed by ^1H NMR spectroscopy after bubbling oxygen through a solution of **1**(red) in chloroform for several hours. The oxidized form **1**(ox) was



Scheme 1. Synthesis of **1**.

reverted by $NaBH_4$ to **1**(red) in 96% yield, thus confirming the quantitative interconversion.

Solvent extraction (3×10^{-5} M metal picrate and 0.1 M metal chloride in H_2O; 3×10^{-4} M **1** in 1,2-dichloroethane) showed that both **1**(red) and **1**(ox) exhibit almost no affinity toward alkali metals.[8] Inspection of CPK models suggests that the sulfur atoms permit coordination of only two oxygen atoms in the ring, which is not sufficient for the recognition of alkali metals. On the other hand, **1**(red) extracts several soft heavy metals (0.01 M metal nitrate and 3×10^{-5} M picric acid in H_2O; 3×10^{-4} M **1** in 1,2-dichloroethane): 44, 36, and 13% of the initial amount of the picrate were extracted for Pb^{2+}, Cu^{2+}, and Cd^{2+}, respectively. The best recognition was for Ag^+ (ca. 100%). However, very little, if any, Cr^{3+}, Mn^{2+}, Fe^{3+}, Co^{2+}, Ni^{2+}, and Zn^{2+} was extracted (0, 1, 0, 3, 0, and 3%, respectively). Without picric acid (3.0 mM metal nitrate solutions), remarkably high Ag^+ selectivity was observed by atomic absorption spectroscopy (extractability:[9] 216, 8, and 8% for Ag^+, Cu^{2+}, and Pb^{2+}, respectively). Furthermore, Ag^+ was specifically extracted (extractability: 175, 0, and 0% for Ag^+, Cu^{2+}, and Pb^{2+}, respectively) from a mixture of Ag^+, Cu^{2+}, and Pb^{2+} (3.0 mM each). The extractability for Ag^+ suggests that **1**(red) can capture at least two Ag^+ ions. A 1:2 complexation between **1**(red) and Ag^+ was also implied by UV/VIS titration by monitoring at 295 nm.[10]

Specific Ag^+ binding by **1**(red) was also observed in a transport experiment through a liquid membrane of 1,2-dichloroethane in a dual cylindrical apparatus.[2d] As seen in Figure 2, Ag^+ was exclusively transported by **1**(red). In contrast, Cu^{2+}, Pb^{2+}, Zn^{2+}, Cd^{2+}, Na^+, and K^+ were not transported at all within experimental error, although **1**(red) exhibits a low affinity for some of the metals. In the case of **1**(ox), Ag^+, Pb^{2+}, and Cu^{2+} were not detected in the receiving phase. These facts reveal that Ag^+ is bound only when the gate is open, as also seen in the extraction. In competitive transport ($[Ag^+] = [Pb^{2+}] = [Cu^{2+}] = 0.01$ M in the source phase), the high Ag^+ selectivity

[*] Prof. Dr. T. Nabeshima, H. Furusawa, Prof. Dr. Y. Yano
Department of Chemistry, Gunma University
Kiryu, Gunma 376 (Japan)
Telefax: Int. code + (277)30-1300

[**] This work was supported by the Gunma University Foundation for Science and Technology.

of **1**(red) was not changed. Addition of *m*-chloroperbenzoic acid (*m*-CPBA) to the transport system 8 h after the start caused an abrupt increase of Ag^+ transported and subsequent termination of the transport (Fig. 2). This phenomenon can be rationalized by the closing of the gate to release Ag^+ bound to the **1**(red) and by the lack of Ag^+ binding of **1**(ox). Although the structure of **1**(red)-Ag^+ is unclear,[11] these results explicitly show that the sulfur atoms of **1** function very efficiently as a redox gate to regulate selectivity as well as binding strength to metal ions.

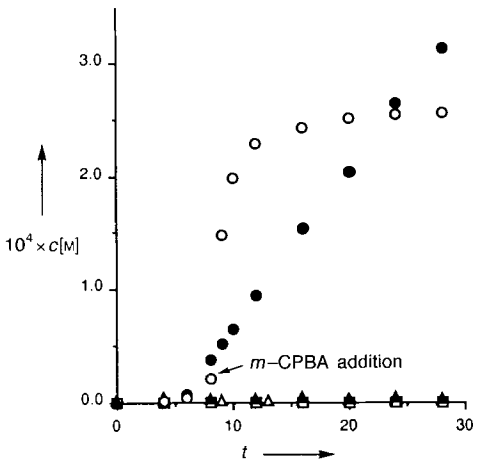


Fig. 2. Transport of Ag^+ (●), Cu^{2+} (□), and Pb^{2+} (▲) by **1**(red) and Ag^+ by **1**(ox) (△) through a liquid membrane, and the effect of *m*-CPBA on the transport (○). The concentration of **1** in the organic phase (1,2-dichloroethane) was 2×10^{-4} M. The initial concentration of metal nitrate in the aqueous source phase was 0.01 M, the receiving phase was deionized water. The concentrations of the metal ion in the receiving phase were determined by atomic absorption spectroscopy.

Many artificial systems for regulation of ion and molecular recognition reported so far could not achieve complete elimination of the recognition site; all-or-nothing regulation was extremely difficult. Without doubt the gating reported here is one of the most convenient and capable methodologies for such regulation and, therefore, will be useful and important for the construction of various sophisticated recognition systems (artificial systems for transport and modulation of molecular information [2d, 12] such as systems combining molecular recognition and other molecular functions, and regulated by some external conditions.

Experimental Procedure

3: Under N_2 **2** (9.06 g, 26.4 mmol) was added in several portions to a solution of Na (2.80 g, 0.122 mol) dissolved in diethylene gylcol (84 g). The mixture was heated at 60 °C for 2 days. After cooling, 3 N HCl (50 mL) was added, followed by extraction with CH_2Cl_2 (2×100 mL). The organic layer was washed with H_2O (2×150 mL), then dried over $MgSO_4$, and concentrated in vacuo. The residue was purified on a silica gel column, by elution with EtOAc/*n*-hexane/ethanol (5:4:1, v/v) to give a pale yellow oil **3** (8.35 g, 80% yield). ^{1}H NMR (200 MHz, $CDCl_3$): $\delta = 2.17$ (br. s, 2H; OH), 3.55–3.85 (m, 16H), 4.66 (s, 4H; $ArCH_2$), 7.25–7.50 (m, 3H, ArH); HRMS (EI): *m/z* 392.08548 (calcd 392.08345) $[M^+]$.

4: Under N_2 a solution of **2** (5.31 g, 15.5 mmol) and **3** (6.08 g, 15.5 mmol) in THF (40 mL) was added very slowly to a refluxed suspension of NaH (1.51 g, 55% in oil, 34.6 mmol) in THF (900 mL). The mixture was then heated at reflux for three days. After the reaction had been quenched by the addition of H_2O, the solvent was removed in vacuo. The residue was diluted with CH_2Cl_2 (150 mL), washed with 3 N HCl (100 mL), H_2O (100 mL), and brine (100 mL), and subsequently dried with $MgSO_4$. The residue obtained after concentration of the solvent was extracted with hot *n*-hexane to give crude **4**, which was purified by recrystallization from EtOAc. Yield: 3.00 g, 34%. M.p. 108–110 °C; ^{1}H NMR (200 MHz, $CDCl_3$): $\delta = 3.74$ (s, 16H), 4.61 (s, 8H; $ArCH_2$), 6.90–7.45 (m, 6H; ArH); MS(EI): *m/z* 576 ($[M+4]$, 2.4%), 574 ($[M+2]$, 4.7%), 572 ($[M^+]$, 2.5%).

1(red): A solution of *n*BuLi (1.54 M) in *n*-hexane (1.30 mL, 2.00 mmol) under N_2 was added at −78 °C to a solution of **4** (401 mg, 0.698 mmol) in THF (100 mL). The mixture was stirred for 4.5 h at −78 °C, and then S_8 (69 mg, 2.15 mmol) was added. After further stirring at −78 °C for 1 h, the mixture was gradually warmed to about 5 °C, and then 3 N HCl (1 mL) was added. The solvent was removed in vacuo, and the residue thus obtained was diluted with CH_2Cl_2 (50 mL), washed with H_2O (30 mL), dried over $MgSO_4$, and concentrated in vacuo. Recrystallization from EtOAc gave **1**(red). Yield: 108 mg, 32%. M.p. 160–163 °C; ^{1}H NMR (200 MHz, $CDCl_3$): $\delta = 3.60$–3.85 (m, 16H), 4.61 (s, 8H, $ArCH_2$), 4.82 (s, 2H; ArSH), 7.00–7.35 (m, 6H; ArH); ^{13}C NMR (50 MHz, $CDCl_3$): $\delta = 69.89$, 70.62, 73.16, 124.86, 129.45, 134.30, 136.06; IR (KBr) 2532(SH) cm^{-1}; HRMS (FAB): *m/z* 503.1553 (calcd 503.1538) $[M+Na]^+$.

1(ox): A solution of **1**(red) (24. mg, 0.050 mmol) in CH_2Cl_2 (30 mL) was mixed with 30% H_2O_2 (5 mL) and K_2CO_3 (50 mg) in H_2O (25 mL) for 15 min at room temperature. The organic layer was washed with H_2O (20 mL) and brine (20 mL), dried over $MgSO_4$, and then concentrated in vacuo to afford **1**(ox) (23 mg, 96%). No by-product was detected by ^{1}H NMR (200 MHz) and TLC analysis. M.p. 139–142 °C; ^{1}H NMR (200 MHz, $CDCl_3$): $\delta = 3.60$–3.85 (m, 16H), 4.71 (s, 8H; $ArCH_2$), 7.30–7.45 (m, 6H; ArH); ^{13}C NMR (50 MHz, $CDCl_3$): $\delta = 70.55$, 71.85, 72.21, 127.79, 129.74, 130.62, 143.69; HRMS (FAB) *m/z* 479.1576 (calcd 479.1562) $[M+H]^+$.

Reduction of **1**(ox) to **1**(red) with $NaBH_4$: To a solution of **1**(ox) (140 mg, 0.29 mmol) in THF (40 mL) at room temperature was added $NaBH_4$ (25 mg, 0.66 mmol). The mixture was stirred for 30 min. After addition of 3 N HCl (5 mL), concentration in vacuo, and dilution with CH_2Cl_2 (30 mL), the residue was washed with H_2O (25 mL), dried over $MgSO_4$, and then concentrated in vacuo to afford crude product, which was recrystallized from EtOAc to give **1**(red) (134 mg, 96%).

Received: March 22, 1994 [Z 6784 IE]
German version: *Angew. Chem.* **1994**, *106*, 1849

[1] Reviews: a) J. J. Rebek, *Acc. Chem. Res.* **1984**, *17*, 258–264; b) I. Tabushi, *Pure Appl. Chem.* **1988**, *60*, 581–586.
[2] a) T. Nabeshima, T. Inaba, N. Furukawa, *Tetrahedron Lett.* **1987**, *28*, 6211–6214; b) T. Nabeshima, T. Inaba, T. Sagae, N. Furukawa, *ibid.* **1990**, *31*, 3919–3922; c) T. Nabeshima, T. Inaba, N. Furukawa, S. Ohshima, T. Hosoya, Y. Yano, *ibid.* **1990**, *31*, 6543–6546; d) T. Nabeshima, T. Inaba, N. Furukawa, T. Hosoya, Y. Yano, *Inorg. Chem.* **1993**, *32*, 1407–1416, and references therein.
[3] C. R. Cantor, P. R. Schimmel, *Biophysical Chemistry, Part I*. Freeman, New York, **1980**, p. 293–295.
[4] Other redox systems: a) T. Saji, I. Kinoshita, *J. Chem. Soc. Chem. Commun.* **1986**, 716–717; b) L. Echeverria, M. Delgado, V. J. Gatto, G. W. Gokel, L. Echegoyen, *J. Am. Chem. Soc.* **1986**, *108*, 6825–6826; c) L. E. Echegoyen, K. Y. Hyunsook, V. J. Gatto, G. W. Gokel, L. Echegoyen, *ibid.* **1989**, *111*, 2440–2443.
[5] a) M. Raban, J. Greenblatt, F. Kandil, *J. Chem. Soc. Chem. Commun.* **1983**, 1409–1411; b) S. Shinkai, K. Inuzuka, O. Manabe, *Chem. Lett.* **1983**, 747–750; c) S. Shinkai, K. Inuzuka, K. Hara, T. Sone, O. Manabe, *Bull. Chem. Soc. Jpn.* **1984**, *57*, 2150–2155; d) S. Shinkai, K. Inuzuka, O. Miyazaki, O. Manabe, *J. Am. Chem. Soc.* **1985**, *107*, 3950–3955.
[6] T. Nabeshima, A. Sakiyama, A. Yagyu, N. Furukawa, *Tetrahedron Lett.* **1989**, *30*, 5287–5288.
[7] a) F. Vögtle, *Chem. Ber.* **1969**, *102*, 1784–1788; b) M. Newcomb, S. S. Moore, D. J. Cram, *J. Am. Chem. Soc.* **1977**, *99*, 6405–6410.
[8] 1.6(1.6), 1.6(3.8), and 1.9(2.2) % of the initial amount of the picrate were extracted by **1**(red) (**1**(ox)) for Li^+, Na^+, and K^+, respectively.
[9] Extractability [%] = ([metal ion]$_{org}$/3×10^{-4} M) × 100.
[10] λ_{max} of **1**(red) (249 nm, CH_3CN) was shifted to about 300 nm in the presence of $AgNO_3$.
[11] Partial dissociation of the thiol groups of **1**(red) is suggested by fall in pH (5.2 → 3.3) of the aqueous Ag^+-solution after reaching the equilibrium for the extraction.
[12] a) J.-M. Lehn, *Angew. Chem.* **1990**, *102*, 1347–1362; *Angew. Chem. Int. Ed. Engl.* **1990**, *29*, 1304–1319; b) F. Stoddart, *Chem. Britain* **1991**, 714–718.

 © VCH Verlagsgesellschaft mbH, D-69451 Weinheim, 1994 0570-0833/94/1717-1751 $ 10.00+.25/0

The First Metal Complexes with a Doubly S_3-Bridged Ferrocene Ligand**

Scott L. Ingham and Nicholas J. Long*

During the past two decades, polythioether macrocycles have been extensively studied because of their potential as ligands for the coordination of heavy metals in unusual oxidation states and geometries.[1-8] The flexibility of the macrocycles and the stability of the complexes formed has resulted in their use in nuclear medicine,[9] organometallic chemistry,[6] and the design of ion-selective receptors.[8, 10, 11] These macrocyclic compounds have also been modified in order to develop new functionalities. One such modification is the incorporation of a metallocene unit into a crown ether ring.[12, 1] This system contains both a redox function and a fragment able to bind a metal cation, and has been shown to possess useful electrochemical and chromogenic properties.[14] The compounds can be designed to recognize electrochemically the binding of a charged guest and, as such, are thought to have immense potential as chemical sensors, redox-switchable ligands, and catalytic systems.[15, 6]

We recently synthesized and characterized the first doubly chalcogen-bridged metallocenophane, 1,1′,2,2′-bis(1,2,3-trithia-1,3-propanediyl)ferrocene (**1**).[17] This molecule possesses the aforementioned, potentially useful attributes of a redox-active center and a metal binding site. We now report on the first metal (copper) complexes of this doubly S_3-bridged ferrocene **1**.

The 1,2-arrangement of the S_3 chains on the cyclopentadienyl rings results in the formation of a "basket-shaped" ligand, which potentially offers different modes of coordination (Fig. 1). Binding of the four central sulfur atoms results in tetradentate arrangement, linking of one atom from each S_3 bridge in a bidentate structure. Depending on the size of the metal species, bidentate coordination could occur on each side of the ligand system or involve more than one ferrocenophane **1** (see later). Although the chair–chair form is most favored and is adopted in the solid state,[17] the chair–boat conformer is also observed in solution.[18] Because of the orientation of the sulfur lone pairs, the sulfur bridges in the latter conformer would be expected to act as a tridentate ligand. It should be noted that Rauchfuss et al. have utilized **1** and analogous systems to form disulfide-bridged ferrocene polymers.[19]

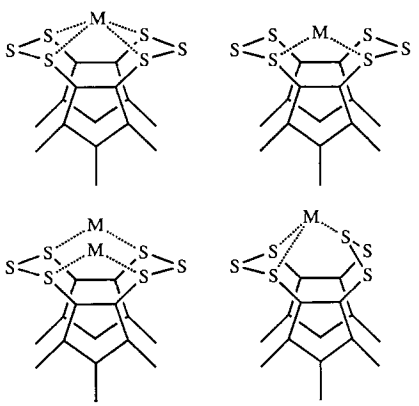
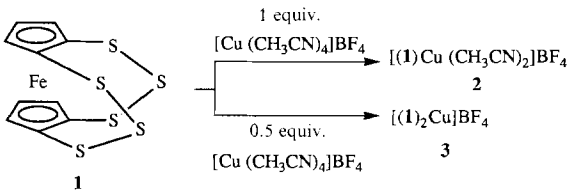


Fig. 1. A representation of the possible metal complexes formed by the ferrocenophane **1**.

Because soft metals preferentially bind to sulfur, we chose to use the copper complex $[Cu(CH_3CN)_4]^+$ in our initial investigations into the coordination properties of **1**. Depending on how many of the weakly bound acetonitrile molecules it displaces, **1** could potentially act as mono-, bi-, tri-, or tetradentate ligand. A solution of **1** in CH_2Cl_2 was treated with $[Cu(CH_3CN)_4]BF_4$ (1 equiv), and almost immediately an orange solution of **2** was formed (Scheme 1). From the experimental data, it was clear



Scheme 1. Reactions of **1** with $[Cu(CH_3CN)_4]BF_4$.

that two acetonitrile molecules had been displaced. Apparently, the copper-to-ligand bonding is not as strong in **2** as in other copper–thioether complexes, since filtration through silica or alumina resulted in decomposition and regeneration of **1**. Heating or prolonged stirring of the reaction mixture resulted in formation of an insoluble, presumably polymeric, species.

Treatment of **1** with 0.5 equivalents of $[Cu(CH_3CN)_4]BF_4$ (Scheme 1) led to instantaneous formation of a reasonably air-stable, orange-red complex **3**, which analyzed as $[(\mathbf{1})_2Cu]BF_4$, formed with loss of all acetonitrile ligands from copper (yield = 0.030 g, 62%; FAB$^+$-MS: m/z 813 $[M^+ - BF_4]$). Again, filtration of the solution led to decomposition, but dilution with diethyl ether resulted in the formation of orange-red crystals, which were then subjected to an X-ray structure analysis.[20]

It is interesting to note that there is very little difference between the ^{1}H NMR spectra of the ligand **1** and the complexes **2** and **3** (chair–chair and chair–boat conformations are again observed). This is presumably due to the very similar geometry of these compounds and, less importantly, to the weak coordination of the copper ion, which is thus distant from the cyclopentadienyl rings. Sato et al.[13] also found only small changes in IR, NMR, and electronic spectral data on going from analogous free ligands to the corresponding metal complexes. They suggested that the ferrocene moiety of the complexes is little influenced by coordination of a metal to the sulfur atoms of the crown ether. These conclusions were backed up by preliminary electrochemical data.[21]

The Cu complex **3** crystallized in the space group $I2(1)/a$ with 1.5 molecules per asymmetric unit. The structure of the cation is illustrated in Figure 2. The two ferrocenophane ligands form a distorted tetrahedral arrangement around the copper(I) ion. Distortion is manifested in a large angle for S(4a)-Cu(1)-S(4) (145.4(2)°); however, all Cu–S distances are around 2.35 Å, a value comparable to those in analogous Cu complexes with thioether macrocycles.[22, 23] As expected from models showing the orientation of the lone pairs on the sulfur atoms, each ferrocenophane acts as a bidentate ligand; one sulfur from each S_3 bridge is involved in coordination. Generally, there is not much change in the structure of the ferrocenophane when it is trans-

[*] Dr. N. J. Long, Dr. S. L. Ingham
University Chemical Laboratories
Lensfield Road, GB-Cambridge, CB21EW (UK)
Telefax: Int. code + (223)336-362

[**] We wish to thank Michael Colbert for carrying out the electrochemical experiments.

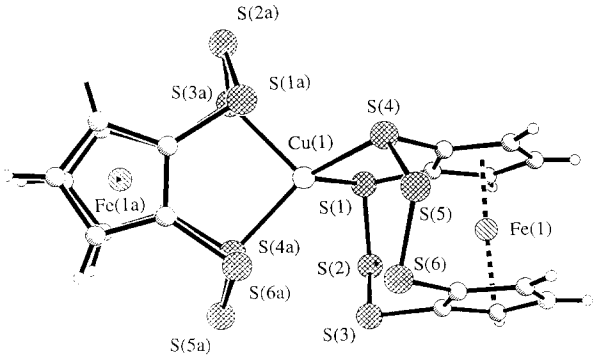


Fig. 2. Molecular structure of the cation in **3**. Selected bond lengths [Å] and angles [°]: Cu(1)–S(1) 2.358(3), Cu(1)–S(4) 2.347(3), S(1)–S(2) 2.088(4), S(4)–S(5) 2.088(4), S(2)–S(3) 2.037(4), S(5)–S(6) 2.038(4); S(1)-S(2)-S(3) 105.3(2), S(4)-S(5)-S(6) 103.9(2), C(12)-S(4)-S(5) 101.8(4), C(11)-S(1)-S(2) 103.0(4), C(22)-S(6)-S(5) 104.5(4), C(21)-S(3)-S(2) 103.7(4), S(4a)-Cu(1)-S(4) 145.4(2), S(4a)-Cu(1)-S(1) 106.64(10), S(1)-Cu(1)-S(4) 92.46(11).

formed from the free state[17] to being part of a complex. However, it is worth noting that the S–S bond lengths involving the copper-coordinated sulfur atoms (e.g., S(1)–S(2) 2.088(4) and S(4)–S(5) 2.088(4) Å) are noticeably greater than those involving uncoordinated sulfur atoms (S(2)–S(3) 2.037(4) and S(5)–S(6) 2.038(4) Å) (cf., the average S–S bond length in S_3-bridged ferrocenes[17, 24] and osmocenes[25] of 2.054(4) Å). The increase in bond length is presumably due to a removal of electron density from the sulfur to the copper atom.

The cyclopentadienyl rings are virtually parallel and eclipsed (which is to be expected, since all reported structures for trichalcogen-bridges metallocenes show this eclipsed conformation[17, 24, 25–28]). The fact that sulfur atoms are only slightly displaced from the ring planes indicates that there is virtually no strain within the structure. There is also very little difference between the bond angles around the bridgehead and the analogous angles in the free ferrocenophane. The bridges are, as expected, in the chair–chair conformation, which is the most populous form of **1** in solution.

We are currently investigating the coordination of various transition metals with differing geometries and oxidation states to the ligand system **1**.

Experimental Procedure

2: To a yellow solution of **1** (0.050 g, 0.13 mmol) in dichloromethane (25 mL) was added $[Cu(CH_3CN)_4]BF_4$ (0.042 g, 0.13 mmol). The solution immediately turned orange and was stirred at room temperature for 30 min. Dilution of the solution with diethyl ether (25 mL) resulted in formation of two layers and crystallization of orange crystals of **2** (0.037 g, 47%, m.p. 120–122 °C). Satisfactory elemental analysis. FAB$^+$-MS: *m/z* $[M^+ - (CH_3CN)_2]$; ^{1}H NMR ($CDCl_3$): δ = 2.00 (s, 6H; CH_3CN), 4.09 (dd, 1H; C_5H_3), 4.14 (d, 2H; C_5H_3), 4.62 (t, 1H; C_5H_3), 4.69 (m, 2H; C_5H_3).

3: A solution of **1** (0.040 g, 0.107 mmol) in dichloromethane (25 mL) was treated with $[Cu(CH_3CN)_4]BF_4$ (0.017 g, 0.053 mmol). The resultant red solution was stirred for 1 h or heated to 50 °C for 5 min. Dilution of the solution with diethyl ether (20 mL) and crystallization of 0 °C overnight gave orange-red crystals of **3** (0.030 g, 62%, m.p. 135–137 C). Satisfactory elemental analysis. FAB$^+$-MS: *m/z* 813 $[M^+ - BF_4]$; ^{1}H NMR ($CDCl_3$), δ = 4.09 (m, 1H; C_5H_3), 4.14 (d, 2H; C_5H_3), 4.62 (t, 1H; C_5H_3), 4.69 (m, 2H; C_5H_3).

Received: January 4, 1994
Revised: March 22, 1994 [Z 6599 IE]
German version: *Angew. Chem.* **1994**, *106*, 1847

[1] M. Schroder, *Pure Appl. Chem.* **1988**, *60*, 517; A. J. Blake, M. Schroder, *Adv. Inorg. Chem.* **1990**, *35*, 1; G. Reid, M. Schroder, *Chem. Soc. Rev.* **1990**, *19*, 239; A. J. Blake, D. Collison, R. O. Gould, G. Reid, M. Schroder, *J. Chem. Soc. Dalton Trans.* **1993**, 521, and references therein.

[2] S. R. Cooper, *Acc. Chem. Res.* **1988**, *21*, 141; S. C. Rawle, S. R. Cooper, *Struct. Bonding (Berlin)* **1991**, *72*, 1.

[3] D. Sellman, F. Knoch, C. Wronna, *Angew. Chem.* **1988**, *100*, 710; *Angew. Chem. Int. Ed. Engl.* **1988**, *27*, 691.

[4] J. J. H. Edema, H. T. Stock, J. Bater, R. M. Kellogg, W. J. J. Smeets, A. L. Spek, F. van Bolhuis, *Angew. Chem.* **1993**, *105*, 448; *Angew. Chem. Int. Ed. Engl.* **1993**, *32*, 436.

[5] D. W. Stephan, *J. Chem. Soc. Chem. Commun.* **1991**, 129.

[6] N. W. Alcock, J. C. Cannadine, G. R. Clark, A. F. Hill, *J. Chem. Soc. Dalton Trans.* **1993**, 1131; J. Cannadine, A. Hector, A. F. Hill, *Organometallics* **1992**, *11*, 2323.

[7] F. Demirhan, A. Gelling, S. Irisli, J. C. Jeffery, S. N. Salek, O. S. Senturk, M. J. Went, *J. Chem. Soc. Dalton Trans.* **1993**, 2765.

[8] B. de Groot, H. A. Jenkins, S. J. Loeb, *Inorg. Chem.* **1992**, *31*, 203.

[9] R. J. Smith, G. D. Adams, A. P. Richardson, H. J. Kuppers, P. J. Blower, *J. Chem. Soc. Chem. Commun.* **1991**, 475.

[10] J. Casabo, L. Mestres, L. Escriche, F. Teixidor, C. Perez-Jimenez, *J. Chem. Soc. Dalton Trans.* **1991**, 1969.

[11] A. J. Blake, E. C. Pasteur, G. Reid, M. Schroder, *Polyhedron* **1991**, 1546.

[12] G. De Santis, L. Fabbrizzi, M. Licchelli, P. Pallavicini, A. Perotti, *J. Chem. Soc. Dalton Trans.* **1992**, 3283.

[13] M. Sato, S. Tanaka, S. Akabori, Y. Habata, *Bull. Chem. Soc. Jpn.* **1986**, *59*, 1515; M. Sato, K. Suzuku, S. Akabori, *ibid.* **1986**, *59*, 3611; M. Sato, M. Katada, S. Nakashima, H. Sano, S. Akabori, *J. Chem. Soc. Dalton Trans.* **1990**, 1979.

[14] C. D. Hall, N. W. Sharpe, I. P. Danks, Y. P. Sang, *J. Chem. Soc. Chem. Commun.* **1989**, 419; C. D. Hall, I. P. Danks, N. W. Sharpe, *J. Organomet. Chem.* **1990**, *390*, 227; C. D. Hall, J. H. R. Tucker, S. Y. F. Chu, *ibid.* **1993**, *448*, 175.

[15] G. W. Gokel, *Crown Ethers and Cryptands*, Royal Society of Chemistry, Letchworth, **1991**.

[16] P. D. Beer, *Chem. Soc. Rev.* **1989**, *18*, 409, and references therein.; P. D. Beer, D. B. Crowe, M. I. Ogden, M. G. B. Drew, B. Main, *J. Chem. Soc. Dalton Trans.* **1993**, 2107; P. D. Beer, J. E. Nation, M. E. Harman, M. B. Hursthouse, *J. Organomet. Chem.* **1992**, *441*, 465; P. D. Beer, Z. Chen, M. G. B. Drew, J. Kingston, M. Ogden, P. Spencer, *J. Chem. Soc. Chem. Commun.* **1993**, 1047.

[17] N. J. Long, S. J. Sharkey, M. B. Hursthouse, M. A. Mazid, *J. Chem. Soc. Dalton Trans.* **1993**, 23.

[18] E. W. Abel, N. J. Long, K. G. Orrell, V. Sik, G. N. Ward, *J. Organomet. Chem.* **1993**, *462*, 287.

[19] P. F. Brandt, T. B. Rauchfuss, *J. Am. Chem. Soc.* **1992**, *114*, 1926; C. P. Galloway, T. B. Rauchfuss, *Angew. Chem.* **1993**, *105*, 1407; *Angew. Chem. Int. Ed. Engl.* **1993**, *32*, 1319.

[20] Crystal data for **3**: $CuFe_2S_{12}F_4BC_{20}H_{12}$; M = 899.07; monoclinic space group $I2_1a$, a = 24.816(5), b = 12.634(1), c = 27.250(4) Å, β = 90.95(2)°, V = 8542(2) Å^3, Z = 12, ρ_{calcd} = 2.097 g cm^{-3}, $\mu(Mo_{K\alpha})$ = 2.688 mm^{-1}, T = 293 K. Data were collected on a Rigaku AFC7R diffractometer ($Mo_{K\alpha}$, graphite monochromator, θ_{max} = 22.5°) with an orange, lamellar single crystal. The structure was solved by a combination of Patterson and Fourier techniques. The positions of hydrogen atoms were calculated. Absorption corrections with semiempirical ψ scans (minimum and maxium transmission coefficients 0.8465 and 0.9989, respectively). Full matrix least-squares refinement on F_o^2 for 5584 reflections, 520 parameters, and 10 restraints converged to $wR2$ = 0.1947 (all data), conventional $R1$ = 0.0591 (observed data, 3911 reflections with $F_o^2 > 2\sigma(F_o^2)$), $(\Delta/\sigma)_{max}$ = −0.015, GOF (all data) = 1.109. Residual electron density = 1.917, −0.656 e Å^{-3}. Further details of the crystal structure investigation are available on request from the Director of the Cambridge Crystallographic Data Centre, 12 Union Road, GB-Cambridge CB2 1EZ, on quoting the full journal citation.

[21] The electrode potentials of **1** and **3** differ by only 0.02 V for the ferrocene redox center, indicating that copper coordination has little influence on the electrochemical properties. Complex **3** also decomposes over a short period of time during the electrochemical experiment. Full electrochemical discussion on doubly trichalcogen-bridged ferrocenes will be included in a forthcoming publication: N. J. Long, P. R. Raithby, P. Zanello, *J. Chem. Soc. Dalton Trans.*, in press.

[22] N. Atkinson, A. J. Blake, M. G. B. Drew, G. Forsyth, R. O. Gould, A. J. Lavery, G. Reid, M. Schroder, *J. Chem. Soc. Dalton Trans.* **1992**, 2993.

[23] M. Melnik, L. Macaskova, C. E. Holloway, *Coord. Chem. Rev.* **1993**, *126*, 71.

[24] B. R. Davis, I. Bernal, *J. Cryst. Mol. Struct.* **1972**, *2*, 107.

[25] E. W. Abel, N. J. Long, A. G. Osborne, M. B. Hursthouse, M. A. Mazid, *J. Organomet. Chem.* **1992**, *430*, 117.

[26] A. G. Osborne, R. E. Hollands, R. F. Bryan, J. A. K. Howard, *J. Organomet. Chem.* **1981**, *205*, 395.

[27] A. J. Blake, R. O. Gould, A. G. Osborne, *J. Organomet. Chem.* **1986**, *308*, 297.

[28] M. Herberhold, P. Leitner, U. Thewalt, *Z. Naturforsch. B* **1990**, *45*, 1503.

Donor-Stabilized Aluminum(I) Bromide**

Mario Mocker, Christian Robl, and Hansgeorg Schnöckel*

Dedicated to Professor Nils Wiberg on the occasion of his 60th birthday

The structures of gaseous monohalides of the monovalent elements of Group 3 have been extensively studied as high-temperature species by spectroscopy.[1] The information available about the structures of these compounds in the solid state varies considerably: for the heavy homologues In and Tl, monohalides can be stabilized as ionic compounds. For the lightest homologue, BX compounds are found with interesting polyhedral structures and B–B bonds;[2] however, these are metastable towards disproportionation to elemental boron and boron trihalide. We are not aware of any structurally characterized solid monohalides of aluminum and gallium.[3] Recently, however, we obtained a metastable solution of AlCl[6] by condensing the high-temperature species AlCl with toluene/ether.[7] However, to date the structure of AlCl in these solutions still remains unclear. From solutions prepared analogously by cocondensation of AlBr with triethylamine we have isolated an aluminum(I) halide as a solid for the first time; we report here on its preparation and structure.

The cocondensation of AlBr (35 mmol, prepared from aluminum and HBr at about 1000 °C) and a mixture of NEt_3 (0.25 mol) and toluene (0.5 mol) afforded a dark red solution on thawing of the condensate at about −100 °C, from which a yellow solid slowly precipitated (yield ca. 50%). The ^{27}Al NMR spectrum of the red solution shows a broad signal at $\delta = 120$.[8] When the solution is warmed to 110 °C, the solid formed originally decomposes completely in about a week, and an aluminum mirror is deposited.[9] Only one sharp signal for $AlBr_3 \cdot NEt_3$ at $\delta = 102$ can still be recognized in the ^{27}Al NMR spectrum of the solution that has been heated for a week.

The yellow solid obtained directly after the cocondensation precipitates as fine needles after washing with toluene/pentane.[10] These needles decompose above about 95 °C under disproportionation to give metallic Al and $AlBr_3 \cdot NEt_3$.[11] The analysis of the solid (Al, Br content) and the determination of the oxidation number of aluminum ($Al^+ + 2H^+ \rightarrow H_2 + Al^{3+}$) support the composition **1**. The Raman spectrum of the solid,

$(AlBr \cdot NEt_3)_n$ **1**

which contains very few bands, indicates that the compound obtained is highly symmetrical.[12] No details about the structure of the compound can be deemed from the IR spectroscopic results, since traces of hydrolysis products ($NEt_3 \cdot HBr$) always occur even if the most extreme care is taken during the preparation of the compound in a glove box (under argon).

Crystals suitable for the structure analysis are obtained by recrystallization of the yellow precipitate in benzene. The result of the X-ray structure analysis is illustrated in Figure 1.[13] The four bromine atoms bound to a square Al_4 ring alternate above and below the plane of the ring. The vacant fourth coordination site at each of the aluminum atoms is occupied by a triethylamine ligand, resulting in an approximate D_{2d}-symmetric structure. The Al–Al distance (264 pm) lies in the range expected for single bonds. This is also confirmed by quantum chemical calculations on a model compound for **1**, $Al_4Br_4 \cdot 4NH_3$:[14] The calculated Al–Al distance here is 264 pm, and the SEN (shared electron number)[18] is 1.3. A value of 380 kJ mol^{-1} was calculated for the tetramerization energy [$4(AlBr \cdot NH_3) \rightarrow Al_4Br_4 \cdot 4NH_3$]. Thus, as expected, the Al–Al interaction is stronger than that in the donor-free electron-deficient compound Al_4Cl_4 with T_d symmetry ($\Delta E_{SCF} = E_{SCF}(Al_4Cl_4) - 4E_{SCF}(AlCl) = 145$ kJ mol^{-1}), although the Al–Al bond (263 pm) in this case is not shortened significantly. However, the tetramerization energy increases drastically to 363 kJ mol^{-1}, when the electron correlation (here MP2) is taken into consideration and by the use of larger basis sets.[19]

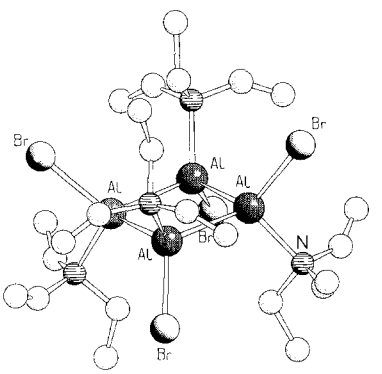


Fig. 1. Crystal structure of **1** (hydrogen atoms not shown). Selected bond lengths [pm] and angles [°] (standard deviations in parentheses): Al–Al 264.3(3), Al–Br 241.7(2), Al–N 209.5(6); Al-Al-Al 90.0(1), Br-Al-N 101.7(2), N-Al-Al 114.8(2), Br-Al-Al 118.4(1).

Significantly shorter Al–Al bonds occur in $Al_2Br_4 \cdot 2D$.[20] This shortening of the bonds is plausible also as a result of a simple estimation: $d(Al^{2+}) < d(Al^+)$.[21] The dissociation energy for the corresponding donor-free chloride Al_2Cl_4 to give two molecules of $AlCl_2$ of 100 kJ mol^{-1} is additional evidence for the notable strength of such Al–Al bonds.[22]

In comparison to the Al–Br distances in $AlBr_3$ (220 pm)[24] and $Al_2Br_4 \cdot 2$anisole (230 pm),[20] that in **1** (242 pm) is particularly long. This stepwise increase in the Al–Br distances is plausible because of the increasing size of the relevant ions $Al^{3+} < Al^{2+} < Al^+$. In agreement with this argumentation, the Al–N distance (209 pm) in **1** is particularly long: in comparison, for the NH_3 adduct of $AlCl_3$ and $AlBr_3$ an Al–N distance of 200 pm[27] was measured and for $NMe_3 \cdot AlCl_3$ even a distance of 196 pm.[28]

Subsequently a Raman spectrum was recorded of the single-crystal studied by X-ray crystallography. According to this spectrum the fine crystalline yellow precipitate, which occurs directly after the cocondensation, is the same compound as that on which the X-ray structure analysis was also carried out. Thus, sufficient solid is available for further reactions of **1** ($n = 4$), for example for the preparation of new organoaluminum(I) compounds.

Received: April 2, 1994 [Z68201E]
German version: *Angew. Chem.* **1994**, *106*, 1860

[*] Prof. Dr. H. Schnöckel
Institut für Anorganische Chemie der Universität
Engesserstrasse, Geb. 30.45, D-76128 Karlsruhe (FRG)
Telefax: Int. code + (721)608-4854
Dipl.-Chem. M. Mocker
Institut für Anorganische Chemie der Universität München (FRG)
Prof. Dr. C. Robl
Institut für Anorganische und Analytische Chemie der Universität Jena (FRG)

[**] This work was supported by the Deutsche Forschungsgemeinschaft and the Fonds der Chemischen Industrie. We thank G. Stösser for performing numerous quantum chemical calculations.

[1] K. P. Huber, G. Herzberg, *Molecular Spectra and Molecular Structure, IV Constants of Diatomic Molecules*, Van Nostrand Reinold, New York, **1979**.

[2] See for example A. G. Massey, *Adv. Inorg. Chem. Radiochem.* **1983**, *26*, 1.

[3] There are, however, several gallium halides, in which in addition to gallium(I), gallium is also present in other oxidations states, for example Ga_4Cl_6 [4] and $Ga_5Cl_9 \cdot 5Et_2O$ [5].

[4] $Ga_2[Ga_2Br_6]$ and $Ga_2[Ga_2I_6]$: W. Hönle, G. Gerlach, W. Weppner, A. Simon, *J. Solid State Chem.* **1986**, *61*, 171; G. Gerlach, W. Hönle, A. Simon, *Z. Anorg. Allg. Chem.* **1982**, *486*, 7.

[5] D. Loos, H. Schnöckel, D. Fenske, *Angew. Chem.* **1993**, *105*, 1124; *Angew. Chem. Int. Ed. Engl.* **1993**, *32*, 1059.

[6] M. Tacke, H. Schnockel, *Inorg. Chem.* **1989**, *28*, 2895.

[7] These solutions open the way to other Al^I compounds such as AlCp*: C. Dohmeier, C. Robl, M. Tacke, H. Schnöckel, *Angew. Chem.* **1991**, *103*, 594; *Angew. Chem. Int. Ed. Engl.* **1991**, *30*, 564.

[8] NMR spectra (C_6D_6, 25 C): Jeol GSX-270 or Bruker EX-400 spectrometer, TMS or external $[Al(H_2O)_6]^{3+}$ as standard. ^{27}Al NMR: $\delta = 120$. After dissolution of the yellow crystals: ^1H NMR: $\delta = 0.93$ (t), 1.18 (t), 2.40 (g), 3.08 (g); ^{13}C NMR: $\delta = 9.80$, 12.46, 46.82, 49.05.

[9] At approximately 50 C, a slow decomposition can be observed first after one week.

[10] If attempts are made to dissolve the yellow solid in C_6D_6 the majority of the solid remains undissolved. The ^{27}Al NMR spectrum of the remaining solution shows only a weak broad signal at $\delta = 120$, which is difficult to differentiate from the background noise. Signals for two (on raising the temperature to 60 C also for more than two) different ethyl groups are observed in the ^1H and ^{13}C NMR spectra [8]. The elucidation of the structure present in solution is a focus of current investigations.

[11] On warming, $AlBr_3 \cdot NEt_3$ can be detected in the mass spectrometer.

[12] Raman spectrum: Bruker FRA-106 spectrometer; Nd: YAG, 1064 nm, $\tilde{\nu}$ [cm^{-1}] (rel. int.) = 2936 (10), 2884 (5), 1452 (3), 1297 (1.5), 1044 (1), 895 (0.5), 734 (0.5), 571 (0.5), 442 (1.5), 410 (1.5), 315 (1), 152 (6). We assign the band at 410 or 442 cm^{-1} to the totally symmetric stretch (a_1). As a consequence of the strong couplings between some of these stretches, the reliable assignment of the remaining a_1 stretches is only possible with the help of extensive quantum chemical calculations, which are the subject of current investigations.

[13] X-ray structure analysis: $C_{24}H_{60}N_4Al_4Br_4$; $M = 832.3$, tetragonal, space group $P4_2/n$, $a = b = 1247.2(2)$, $c = 1267.2(3)$ pm, $V = 1971.1 \times 10^6$ pm^3, $Z = 2$, $\rho_{calcd} = 1.402$ $g\,cm^{-3}$, $F(000) = 848$, $\mu = 41.5$ cm^{-1} (Mo_α), 295 K, ω scan, $\theta_{max} = 25$°, measurement rate 2.44–14.65° min^{-1}, scan width 1.3°, Siemens R3m/V diffractometer, graphite monochromator; of 7255 measured reflections, 1742 are symmetry independent; $R_{int} = 0.0098$; 1350 reflections with $|F| > 3\sigma_{|F|}$ were classified as observed. Calculations with SHELXTL-Plus, 83 parameters, H atoms geometrically positioned; non-hydrogen atoms refined anisotropically, empirical absorption correction; $R = 0.1020$, $R_w = 0.0490$, $R_g = 0.0272$; $w = \sigma_{|F|}^{-2}$. Limits of the final difference Fourier synthesis +1.06/−1.01 e × 10^{-6} pm^3. Further details of the crystal structure investigation may be obtained from the Fachinformationszentrum Karlsruhe, D-76344 Eggenstein-Leopoldshafen (FRG), on quoting the depository number CSD-58231.

[14] The calculations were carried out with the Turbomole program [15] on an IBM-RISC 6000 workstation. Basis sets: Al: ECP-10 dz + p [16] (η(d): 0.300); Br: ECP-28 dz + p (η(d): 0.389); N: SVP (split valence polarization) [17]; H: SVP. d(Al–Al): 264.0 pm; d(Al–Br): 242.4 pm; d(Al–N): 209.2 pm; ∢ (Br-Al-N): 95.8°; out-of-plane Al_4: 11.6°. SCF energy: −284492940 a.u.; ΔE for the planar configuration (saddle point): 7.6 kJ mol^{-1}.

[15] R. Ahlrichs, M. Bär, M. Häser, H. Horn, C. Kölmel, *Chem. Phys. Lett.* **1989**, *162*, 165.

[16] P. H. Hay, W. R. Wadt, *J. Chem. Phys.* **1985**, *892*, 284.

[17] A. Schäfer, H. Horn, R. Ahlrichs, *J. Chem. Phys.* **1991**, 97, 2571.

[18] C. Ehrhardt, R. Ahlrichs, *Theor. Chim. Acta* **1985**, *68*, 231; R. Ahlrichs, C. Ehrhardt, *Chem. Unserer Zeit* **1985**, *19*, 120.

[19] R. Ahlrichs, M. Ehrig, H. Horn, *Chem. Phys. Lett.* 1991, *183*, 227.

[20] M. Mocker, C. Robl, H. Schnöckel, *Angew. Chem.* **1994**, *106*, 946; *Angew. Chem. Int. Ed. Engl.* **1994**, *33* 862.

[21] With anisole as donor, the distance determined experimentally (253 pm) corresponds to that from quantum chemical calculations, from which a SEN of 1.4 was calculated for the Al–Al bond, which can be interpreted as a π contribution resulting from Br → Al back bonds.

[22] This energy value is based on a combination of quantum chemical calculations (in order to prevent open-shell systems) with experimental thermodynamic values: $2AlCl_3 \rightarrow 2AlCl_2 + Cl_2$; $\Delta H_R = 608$ kJ mol^{-1} [23]. Since ab initio calculations for the reaction $2AlCl_3 \rightarrow Cl_2Al-AlCl_2 + Cl_2$ give a value of $\Delta H_R = 510$ kJ mol^{-1}, the dissociation energy for $Cl_2Al-AlCl_2 \rightarrow 2AlCl_2$ is about 100 kJ mol^{-1}.

[23] M. W. Chase, Jr. C. A. Davies, J. R. Downey, Jr., D. J. Frurip, R. A. McDonal, A. N. Syverud, *JANAF Thermochemical Tables*, 3rd ed., ACS, AIP, NBS, Midland, MI, **1985**.

[24] The structure of $AlBr_3$ in the gas phase has still not been studied. The Al–Br distance is expected, however, correspond to that of the terminal Al–Br bond of Al_2Br_6 (222 pm [25]): also the terminal Al–Cl distance of Al_2Cl_6 corresponds to that of $AlCl_3$ [26].

[25] P. A. Akishin, N. G. Rambidi, E. Z. Zasovin, *Sov. Phys. Crystallogr. Engl. Transl.* **1959**, *4*, 167.

[26] I. Hargittai, M. Hargittai, *J. Chem. Phys.* **1974**, *60*, 2563.

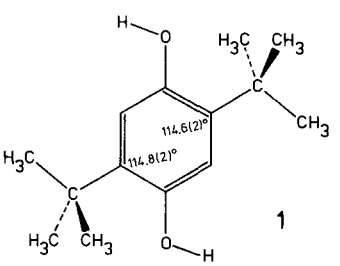
[27] M. Hargittai, I. Hargittai, V. P. Spiridonov, M. Pellisier, J. F. Labarre, *J. Mol. Struct.* **1975**, *24*, 27; M. Hargittai, I. Hargittai, V. P. Spiridonov, A. A. Ivanov, *ibid.* **1977**, *39*, 225.

[28] D. F. Grant, R. C. G. Killean, J. L. Lawrence, *Acta Crystallogr. Sect. B.* **1969**, *25*, 377.

Crystal Structure of 2,5-Di-*tert*-butylhydroquinone: Polar Stacking of Nonpolar Hydrogen-Bonded Sheets with Trigonal Symmetry**

Otto Ermer* and Christof Röbke

While the title compound **1** is a rather trivial and cheap substance, its crystal structure[1] involves unusual features worth reporting. In the crystal, **1** forms trigonal, puckered sheets held together by hydrogen bonds. The topology of the sheets is analogous to that of elemental (gray) arsenic with chair conformations of *trans*-fused six-membered rings (α-As). It may be developed from α-As through replacement of the As atoms by H-bonded three-membered rings of oxygen atoms, and the As–As bonds by covalent 2,5-di-*tert*-butyl-*p*-phenylene links (Figs. 1, 2). We are not aware of another published example of H-bonded sheet architecture with this super-arsenic connectivity pattern. The H bonds (O···O distances: 2.832(3) and 2.878(3) Å) are bent outward (Fig. 1), because of the small size of the O_3 ring and probably also because of electrostatic repulsions between the bridging H atoms. Three-membered rings of H-bonded oxygen atoms are rare and only a few other examples could be retrieved from the literature.[2] Like **1**, these cases are bulky (tertiary) alcohols, which is not surprising since the small intraannular angles of the H-bonded O_3 rings lead to large extraannular space. Interestingly, the best structure of the water trimer $(H_2O)_3$ also involves a H-bonded O_3 ring,[4] the geometry of which is very similar to that in the crystals of **1**.



1

Centrosymmetric molecules usually crystallize in centrosymmetric space groups, and in many cases even retain the molecular center of symmetry in the crystal.[4] The hydroquinone **1** is a rare example of a centrosymmetric, nonpolar molecule with a noncentrosymmetric, polar crystal structure.[5, 7] The space group of **1**, $P31c$, is trigonal with six molecules in the cell.[1] The

[*] Prof. Dr. O. Ermer, C. Röbke
Institut für Organische Chemie der Universität
Greinstrasse 4, D-50939 Köln (FRG)
Telefax: Int. code + (221)470-5151

[**] This work was supported by the Fonds der Chemischen Industrie.

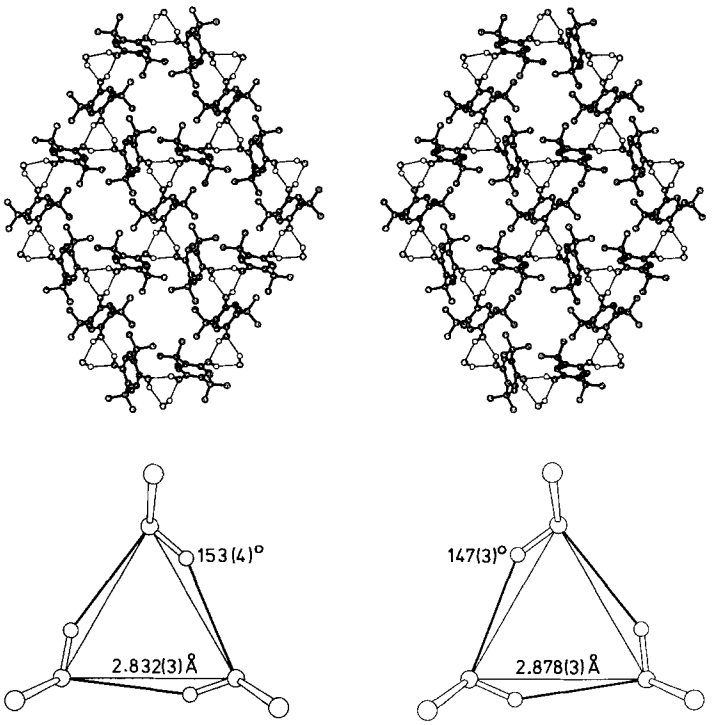


Fig. 1. Top: Stereoview (approximately along the c axis) of a section of a trigonal H-bonded sheet of **1**; H atoms omitted, except alcoholic ones; thin lines represent H bonds. Note the effective centrosymmetry and nonpolarity of the sheet. Bottom: The two independent H-bonded O_3 rings with O···O distances and O–H···O angles; standard deviations in parentheses; crystallographic C_3 symmetry.

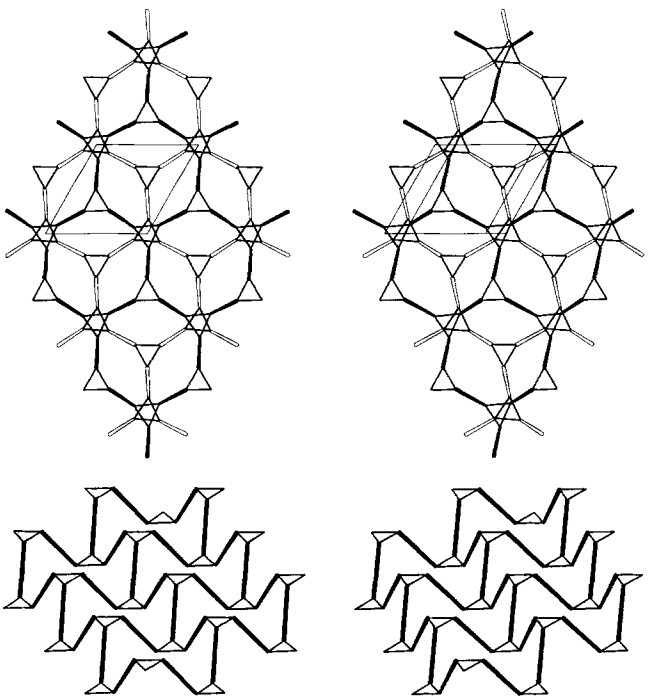


Fig. 2. Top: Diagrammatic stereoview (along c axis for left member of the pair) of two adjacent H-bonded sheets of **1**. The unit cell edges are indicated. Only the oxygen positions are drawn. The equilateral triangles (C_3 symmetry) represent the H-bonded O_3 rings, and the interconnecting rods (solid in the upper, outlined in the lower sheet) symbolize the di-*tert*-butyl-*p*-phenylene links. Note the polarity of the stacking pattern (layer sequence ABAB...) despite the virtually centrosymmetric and nonpolar individual sheets. Bottom: Oblique diagrammatic stereoview of a single sheet to highlight its super-arsenic topology.

molecules of **1** thus have no crystallographic symmetry although their conformation in the crystal is centrosymmetric to a very good approximation (see structural formula and Fig. 1; even the higher symmetry C_{2h} is still well approximated). Moreover, this non-crystallographic local center of symmetry is maintained throughout the puckered H-bonded trigonal sheets. The entire sheets are thus centrosymmetric and consequently nonpolar. The polarity of the overall three-dimensional crystal structure of **1** arises from the polar stacking of the nonpolar sheets along the trigonal crystal axis c (layer sequence ABAB...). Figure 2 shows a diagrammatic representation of this remarkable stacking pattern. Its polarity is immediately evident since one-third of the H-bonded O_3 rings are stacked at a distance of $c/2$ with their emanating *p*-phenylene links oriented pyramidally in one direction, while the other two-thirds of the O_3 rings are stacked at a distance c with the pyramidal orientation of their links in the opposite direction (c, trigonal cell edge length).[8] It would be interesting, at least from a theoretical point of view, to measure nonlinear optical properties of **1**. Such phenomena should be rather weak as a result of the large, almost perfectly centrosymmetric substructures, that is, the individual H-bonded sheets.

Remarkably, the crystal structure of **1** appears to be completely ordered, probably because steric congestion pretty much locks the conformation of **1** (see structural formula and Fig. 1). This follows simply from the repulsion between the *ortho*-positioned hydroxyl and *tert*-butyl groups, which prevents orientational disorder by rotation around the C–O and C(sp^2)–C(sp^3) bonds. (Note that the preferred orientation of a phenolic OH group is coplanar with the aromatic ring;[10] the alternative coplanar orientation of OH in **1** would be rather unfavorable because of the bulky *ortho*-positioned *tert*-butyl group.) Evidence for the steric hindrance of **1** is seen in the compressed angles of the six-membered ring shown in the structural formula (114.6(2), 114.8(2)°).

Received: January 27, 1994 [Z 6648 IE]
German version: *Angew. Chem.* **1994**, *106*, 1832

[1] Large crystals shaped like truncated hexagonal pyramids were obtained from a 2:1 acetone/toluene mixture. Polar trigonal space group $P31c$ (No. 159), $Z = 6$, $a = 11.430(3)$, $c = 18.198(3)$ Å; $\rho_{calcd} = 1.076$, $\rho_{exp.} = 1.081$ g cm^{-3}; intensity measurements at room temperature on a four-circle diffractometer ($\lambda_{Mo} = 0.71069$ Å, $\theta_{Mo}(max) = 30°$); structure solution with direct methods; C, O refined (on F^2) anisotropically, H isotropically, including 2090 reflections (88 reflections with very negative F^2 not considered); $R(F) = 0.041$, $wR(F^2) = 0.114$ (1737 reflections with $F > 4\sigma(F)$); $w = 1/[\sigma(F_o^2)^2 + 0.01p^2]$, where $p = [\max f(F_o^2, 0) + 2F_c^2]/3$; maximum residual electron density, 0.20 e Å^{-3}. The centrosymmetric space group $P\bar{3}1c$, which is also compatible with diffraction symmetry and systematic extinctions, was discarded: Attempts to solve the structure in this space group by direct methods did not lead to a refinable model that makes sense structurally. Trial refinements in $P\bar{3}1c$ with a structural model derived by translating the trigonal H-bonded layers so that the molecules of **1** occupy inversion centers gave R values of about 0.40. Moreover, this model in $P\bar{3}1c$ involves unacceptably short atomic contacts between neighboring layers. It is noted that statistical indicators of the intensity distribution lie about midway between the expectation values for centrosymmetric and noncentrosymmetric structures. Finally, it is noteworthy that in the full-matrix refinements in the correct polar space group $P31c$ no serious correlations related to the pseudo centrosymmetry occurred (program SHELXL93; G. M. Sheldrick, University of Göttingen, 1993). Further details of the crystal structure analysis may be obtained from the Fachinformationszentrum Karlsruhe, D-76344 Eggenstein-Leopoldshafen, on quoting th depository number CSD-58130 and the journal citation.

[2] P. G. Jones, D. Schomburg, H. Hopf, V. Lehne, *Acta Crystallogr. Sect. C* **1992**, *48*, 2203; D. R. Bruss, R. Larsen, R. J. Walsh, J. Fait, B. P. Mundy, R. A. Ekeland, A. Fitzgerald, *ibid.* **1987**, *43*, 1932; W. Herz, N. Kumar, J. F. Blount, *J. Org. Chem.* **1982**, *47*, 1785. Possibly, H-bonded O_3 rings are also present in crystalline triphenylmethanol (trityl alcohol) built up from tetrahedral tetramers with tetrahedra of closely approaching oxygen atoms; the alcoholic H atoms of this structure could, however, not be located reliably (probable disorder): G. Ferguson, J. F. Gallagher, C. Glidewell, J. N. Low, S. N. Scrimgeour, *Acta Crystallogr. Sect. C* **1992**, *48*, 1272.

[3] N. Pugliano, R. J. Saykally, *Science* **1992**, *257*, 1937; K. Liu, J. G. Loeser, M. J. Elrod, B. C. Host, J. A. Rzepiela, N. Pugliano, R. J. Saykally, *J. Am. Chem. Soc.* **1994**, *116*, 3507; D. J. Wales, *J. Am. Chem. Soc.* **1993**, *115*, 11180; F. B. van Duijneveldt, M. de Groot-den Hartogh, J. G. C. M. Duijneveldt-van de Rijdt, *Croat. Chim. Acta* **1992**, *65*, 1; E. Honegger, S. Leutwyler, *J. Chem. Phys.* **1988**, *88*, 2582; J. C. Owicki, L. L. Shipman, H. A. Scheraga, *J. Phys. Chem.* **1975**, *79*, 1794.

[4] A. I. Kitaigorodsky, *Molecular Crystals and Molecules*, Academic Press, New York, **1973**, Chapter IA.6.

[5] In a wider sense, all noncentrosymmetric crystal structures are polar; in a more restricted sense, this applies only to those permitting a permanent dipole moment. The latter comprise the 10 crystal classes C_1, C_s, C_2, C_{2v}, C_3, C_{3v}, C_4, C_{4v}, C_6 and C_{6v} [6]. The crystal structure of **1** is thus polar also in the restricted sense (crystal class C_{3v}, crystallographic three-fold axis is the polar axis).

[6] *International Tables for Crystallography, Vol. A, Space Group Symmetry* (Ed.: T. Hahn), Reidel, Dordrecht, **1987**, p. 788.

[7] Quantitative information about the frequency of centrosymmetric molecules crystallizing in noncentrosymmetric space groups would require the tedious inspection of all known noncentrosymmetric crystal structures. To get a preliminary lead, we selected the noncentrosymmetric space group $Pna2_1$ (No. 33) and with the help of the *Cambridge Structural Database*, CSD (F. H. Allen, O. Kennard, R. Taylor, *Acc. Chem. Res.* **1983**, *16*, 146), inspected all published crystal structures of this symmetry. This space group was chosen since it occurs fairly frequently (1834 entries in the CSD up to January 4, 1994), and is achiral (avoidance of chiral natural products). With some reliability, eleven virtually centrosymmetric molecular structures in $Pna2_1$ could be identified (frequency 0.6%; CSD codes: DIBXIV, DMXPCR10, DMXPMO10, FAHNOR05, FETCOW, FUYMIV, IMZNCU, KILWOR, SIKRIN, SIWDEH01, THUPDC01). A purely organic example is the β form of 9,9'-anthril (H.-D. Becker, B. W. Skelton, A. H. White, *Austr. J. Chem.* **1991**, *44*, 181). Interestingly, in addition to these cases, 35 noncentrosymmetric, polar molecular structures that form almost ideally centrosymmetric, weakly bound dimers (H-bonds, dipole and van der Waals forces) could be retrieved in $Pna2_1$ (frequency 1.9%; CSD codes: BAAANL10, BDMGCO10, BEPPUH, BOTYUE, BZCBAP, DAFPUV, DUMTAG, FAWTAY10, FAYGAN01, FOPMOM, GAXJIY, GESCAI, GIKDIN, HXMHCH10, JOXDAB, JUJXUH, JUJYAO, JUNFUT, KACDOH, KEDDIG, KEVFUM, KOCYIK, KOYHEL, KUFHIC, MAMBRF, SEPPIM, SLFNMA02, SUCHED, TMPSUL10, TOLDIN, TORDAZ, VAVKEI, VOVRED, VOVTEF, VOYJUO); the unit cells contain eight molecules, that is, one centrosymmetric dimer per asymmetric unit. An example of such a H-bonded, centrosymmetric dimer in $Pna2_1$ is a diphenyltriazolone (A. D. Rae, C. G. Ramsay, P. J. Steel, *Austr. J. Chem.* **1988**, *41*, 419). Caution is required when analysing and evaluating crystal structures of this nature: Often the noncentrosymmetric space groups concerned may not be derived unambiguously through the systematic absences of reflections, and the centrosymmetric choice then has to be reliably excluded by other means (cf. R. E. Marsh, *Acta Crystallogr. Sect. B* **1986**, *42*, 193). In the present example of space group $Pna2_1$ the centrosymmetric alternative with the same systematic extinctions is *Pnam* (or *Pnma*, No. 62). Furthermore, the influence of crystal twinning, disorder effects, and poor data quality must be considered, as well as the possibility of not clearly recognizable solvent molecules built into the crystal lattice. About 85% of all commonly used solvents consist of noncentrosymmetric, polar molecules! Finally, when pseudosymmetry is present, strong parameter correlations usually ensue from pseudosymmetry in the structure refinements; see, however, ref. [1].

[8] The stacking pattern of hexagonal graphite (layer sequence ABAB...) is comparable to that of **1**. However, since the carbon sheets are planar, the space group symmetry of hexagonal graphite, $P6_3/mmc$, is much higher, but nonpolar, and centrosymmetric. The space group of **1**, $P31c$, is a subgroup of $P6_3/mmc$. The stacking pattern of (gray) α-arsenic is different from **1** and is nonpolar and centrosymmetric (layer sequence ABCABC..., rhombohedral space group $R\bar{3}m$); this holds similarly for rhombohedral graphite (again space group $R\bar{3}m$) [9].

[9] J. Donohue, *The Structures of the Elements*, Wiley, New York, **1974**; Krieger, Malabar, Florida, **1982** (reprinted).

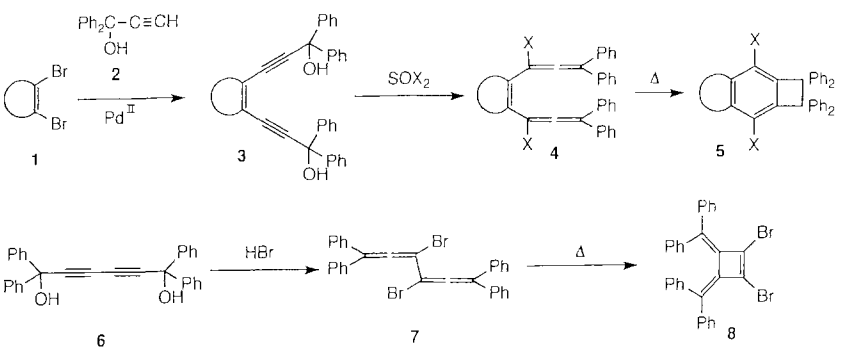
[10] N. W. Larsen, *J. Mol. Struct.* **1979**, *51*, 175.

A New Synthetic Route to 1,2-Dihydrocyclobutaarenes**

Fumio Toda,* Koichi Tanaka, Isao Sano, and Toru Isozaki

Highly strained aromatic compounds such as benzocyclobutene, naphthocyclobutene, and anthrodicyclobutene[***] have long been considered interesting from the point of view of structural[1] and synthetic organic chemistry.[2] For example, 1,2-dimethylenecyclohexa-3,5-diene, which is easily derived from benzocyclobutene by thermolysis, is a useful intermediate for the synthesis of various organic compounds in Diels–Alder reactions.[2] However, in many cases, preparation of benzocyclobutenes is not easy. For example, the synthesis of naphthodicyclobutene from 1,2-dimethylenecyclobutane and dimethyl cyclobutene-1,2-dicarboxylate requires six reaction steps.[3]

We now report on a very simple synthetic route to benzocyclobutene derivatives **5** starting from enediynediols **3**, which can easily be prepared by Pd-catalyzed condensation of 1,2-dihalogenocycloalkenes **1** with 1,1,-diphenyl-2-propyn-1-ol (**2**),[4] by thermal cyclization of the diallene intermediates octa-1,2,4,6,7-pentaenes **4** derived from **3** by a propargyl rearrangement (Scheme 1). The idea for this synthesis came from the well-known thermal cyclization of diallene derivatives to 3,4-dimethylene-1,2-cyclobutenes.[5, 6] For example, 3,4-dibromo-1,1,6,6-tetraphenyl-1,2,4,5-hexatetraene (**7**), which can easily be derived by reaction of 1,1,6,6,-tetraphenyl-2,4-hexadiyne-1,6-diol (**6**) with hydrobromic acid, cyclizes to 1,2-dibromo-3,4-bis-(diphenylmethylene)cyclobutene (**8**) (Scheme 1 bottom).[6, 7] Applying the same principle, compounds **11**, **14**, and **17** (Scheme 2) as well as **20** and **23** (Scheme 3) were synthesized.



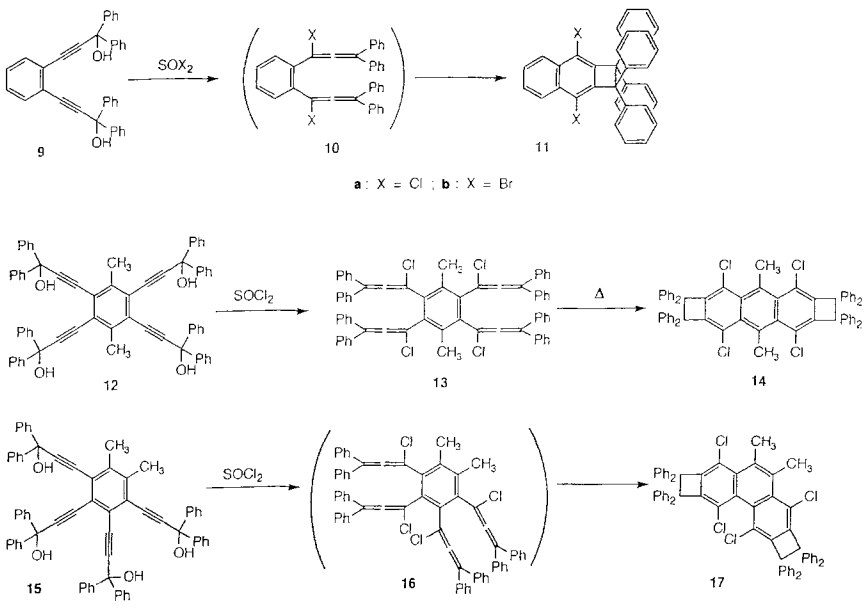
Scheme 1.

The acetylenic alcohols substituted with a bulky *tert*-butyl group instead of Ph reacted only as far as the thermally stable diallene intermediate. For example, treatment of 1,2-bis(3,3-di-*tert*-butyl-3-hydroxy-1-propynyl)benzene (**24**), prepared from *o*-dibromobenzene and 1,1-di-*tert*-butyl-2-propynol (colorless prisms, 48% yield, m.p. 167–169 °C), with $SOCl_2$ in THF gave 1,2-bis(3,3-di-*tert*-butyl-1-chloro-1,2-propadienyl)benzene (**25**) as colorless prisms (53% yield, m.p. 158–159 °C); IR: $\tilde{\nu}$ = 1950,

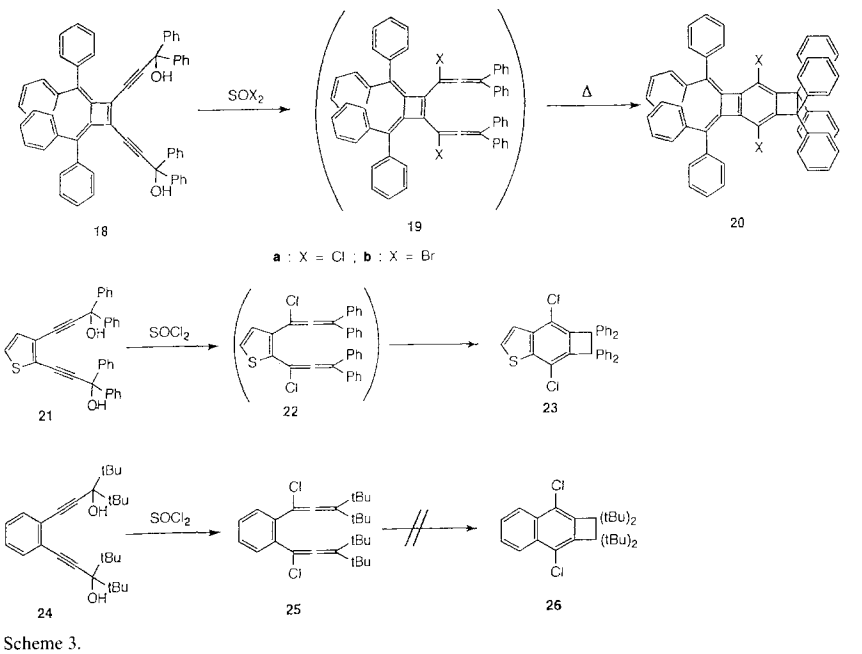
[*] Prof. Dr. F. Toda, Prof. Dr. K. Tanaka, I. Sano, T. Isozaki
Department of Applied Chemistry, Faculty of Engineering
Ehime University
Matsuyama, Ehime 790 (Japan)
Telefax: Int. code + (899)23-0672

[**] This work was supported by the Ministry of Education, Science, and Culture of the Japanese government.

[***] According to IUPAC nomenclature, these compounds should be referred to as 1,2-dihydrocyclobutaarenes. The names used here are however more common.



Scheme 2.



Scheme 3.

1920 cm^{-1} (C=C=C); ^1H NMR: δ= 1.3 (*t*Bu, 36H) 7.3 (Ph, 4H); UV: λ_{max} (ε) = 240 (22000), 288 nm (11000). After it had been heated in toluene under reflux for 4 h, **25** was recovered unchanged.

Experimental Procedure

3,8-Dichloro-1,1,2,2,-tetraphenylnaphthocyclobutene (**11a**): A mixture of *o*-dibromobenzene (10 g, 42 mmol), **2** (36 g, 170 mmol), CuI (0.1 g), $[(Ph_3P)_2PdCl_2]$ (0.1 g), PPh_3 (0.52 g), and NEt_3 (200 mL) was heated under reflux for 44 h. After filtration, the organic layer was evaporated to give, after recrystallization from EtOAc/hexane, 1,2-bis(3-hydroxy-3,3-diphenyl-1-propynyl)benzene (**9**) as colorless prisms (16.3 g, 79% yield, m.p. 152–154 °C); IR [8]: $\tilde{\nu}$ = 3270 cm^{-1} (OH). After a solution of **9** (0.5 g), pyridine (0.2 mL), and $SOCl_2$ (0.2 g, 2.7 mmol) in THF (50 mL) had been stirred at room temperature for 5 h, the solution was extracted with toluene. The toluene solution was worked up by the usual method to give **11a** as colorless prisms (0.26 g, 40% yield, m.p. 200–201 °C). The ^1H NMR spectrum [8] shows a sharp singlet at δ = 7.0 corresponding to 20 shielded aromatic protons in addition to the normal aromatic proton signal at δ = 7.7 corresponding to four protons. Treatment of **9** with $SOBr_2$ gave the dibromo analogue **11b** as colorless prisms in 47% yield (m.p. 229–231 °C); ^1H NMR: δ = 7.0 (20H), 7.7 (4H). In both cases, the diallene intermediate **10** was too labile to be isolated.

Anthrodicyclobutene (**14**): Tetrakis(3-hydroxy-3,3-diphenyl-1-propynyl)-*p*-xylene (**12**) was prepared from tetrabromo-*p*-xylene and **2** as colorless prisms (85% yield, m.p. 281–283 °C); IR: $\tilde{\nu}$ = 3350, 3480 cm^{-1} (OH); ^1H NMR: δ = 2.6 (Me, 6H), 5.9 (OH, 4H), 7.6–7.2 (Ph, 40H). Compound **12** was treated with $SOCl_2$ in THF as described above to give the tetraallene derivative **13** as colorless prisms (95% yield); IR: $\tilde{\nu}$ = 1940 cm^{-1} (C=C=C); ^1H NMR: δ = 2.5 (Me, 6H), 7.3 (Ph, 40H). (200 °C, 10 min). However, the crystal of **13** did not have a sharp melting point and transformed to **14** on heating (200 °C, 10 min). Heating of **13** (0.2 g) in toluene (20 mL) under reflux for 1 h gave **14** as yellow prisms (0.19 g, 95% yield, m.p. >300 °C): ^1H NMR: δ = 3.3 (Me, 6H), 7.0 (Ph, 40H); UV [8]: λ_{max} (ε) = 237 (81000), 297 (53000), 398 (2200), 425 (2900), 451 nm (3100).

Phenanthrodicyclobutene **17**: Tetrakis(3-hydroxy-3,3-diphenyl-1-propynyl)-*o*-xylene (**15**) was prepared from tetrabromo-*o*-xylene and **2** as colorless prisms (69% yield, m.p. 215–218 °C); IR: $\tilde{\nu}$ = 3320 cm^{-1} (OH); ^1H NMR: δ = 2.4 (Me, 6H), 3.1 (OH, 4H), 7.5–7.2 (Ph, 40H). Compound **15** was treated with $SOCl_2$ in THF. The tetraallene derivative **16** was obtained as an oil (IR: $\tilde{\nu}$ = 1940 cm^{-1} (C=C=C)), which gradually cyclized to 4,5,8,11-tetrachloro-9,10-dimethyl-1,1,2,2,6,6,7,7,-octaphenyl-phenanthrodicyclobutene (**17**). Recrystallization from toluene yielded **17** as pale yellow prisms (59% yield based on **15**, m.p. >300 °C); ^1H NMR: δ = 3.0 (Me, 6H), 7.0 (Ph, 40H); UV: λ_{max} (ε) 232 (64000), 269 (22000), 297 (47000), 345 nm (19000).

3,6-Dichloro-4,5-bis(diphenylmethylene)-1,1,2,2,-tetraphenylbenzodicyclobutene **20a**: 3,4-Bis(diphenylmethylene)-1,2-bis(3-hydroxy-3,3-diphenyl-1-propynyl)cyclobutene (**18**) was prepared from **8** [6,7] and **2** as colorless needles (94% yield, m.p. 195 °C). Reaction of **18** with $SOCl_2$ gave 1,2-bis(1-chloro-3,3-diphenyl-1,2-propadienyl)-3,4-bis(diphenylmethylene)cyclobutene (**19a**) as red prisms (65% yield, m.p. not sharp); IR: $\tilde{\nu}$ = 2000, 1930 cm^{-1} (C=C=C); UV: λ_{max} (ε) = 279 (25000), 365 (14000), 468 nm (8100). After it had been heated in toluene under reflux for 1 h, **19a** gave **20a** as yellow prisms (70% yield, m.p. 259–260 °C); ^1H NMR: δ = 6.9 (Ph, 30H), 7.3 (Ph, 10H); UV: λ_{max} (ε) = 236 (44000), 261 (34000), 312 (50000), 373 nm (15000). Bromo analogue **20b** was prepared with $SOBr_2$ (54% yield, m.p. >300 °C).

3,7-Dichloro-1,1,2,2,-tetraphenylbenzothiophenocyclobutene (**23**): 2,3-Bis(3-hydroxy-3,3-diphenyl-1-propynyl)thiophene (**21**) was obtained from 2,3-dibromothiophene and **2** as colorless prisms (45% yield, m.p. 166–168 °C) and treated with $SOCl_2$ in THF to give **23** via the diallene intermediate **22**. After recrystallization from EtOAc, colorless prisms were obtained (97% yield, m.p. 214–216 °C): ^1H NMR: δ = 6.8 (Ph, 20H), 7.6 (thiophene, 2H); UV: λ_{max} (ε) = 239 (20800), 269 (3700), 308 nm (1200).

Received: March 28, 1994 [Z 6808IE]
German version: *Angew. Chem.* **1994**, *106*, 1856

[1] M. P. Cava, M. J. Mitchell, *Cyclobutadiene and Related Compounds*, Academic Press, New York, **1967**; R. Boese, D. Blaser, W. E. Billups, M. M. Haley, A. H. Maulitz, D. L. Mohler, K. P. C. Vollhardt, *Angew. Chem.* **1994**, *106*, 321; *Angew. Chem. Int. Ed. Engl.* **1994**, *33*, 313, and references therein.
[2] T. Kametani, M. Tsubuki, H. Nemoto, *J. Org. Chem.* **1980**, *45*, 4391.
[3] R. P. Thummel, W. Nutakul, *J. Am. Chem. Soc.* **1978**, *100*, 6171.
[4] K. Sonogashira, Y. Tohda, N. Hagihara, *Tetrahedron Lett.* **1975**, 4467.
[5] H. Hopf, F. Lenich, *Chem. Ber.* **1973**, *106*, 3461.
[6] F. Toda, H. Ishihara, K. Akagi, *Tetrahedron Lett.* **1969**, 2531; F. Toda, K. Kumada, N. Ishiguro, K. Akagi, *Bull. Chem. Soc. Jpn.* **1970**, *43*, 3535.
[7] F. Toda, P. Garratt, *Chem. Rev.* **1993**, *92*, 1685.
[8] IR, ^1H NMR, and UV spectra were measured in nujol, $CDCl_3$, and hexane, respectively. For all new compounds, satisfactory elemental analyses were obtained.

Two-Dimensional Sheets of Tetragonal Copper(II) Lattices: X-Ray Crystal Structure and Magnetic Properties of $[Cu(C_6O_4Cl_2)(C_4H_4N_2)]_n$

Satoshi Kawata, Susumu Kitagawa,* Mitsuru Kondo, Isamu Furuchi, and Megumu Munakata

Transition metal coordination polymers have been the subject of intensive research in the last few decades, and major advances have been made in both their theoretical description and their applications as new materials.[1] The most remarkable developments are perhaps the preparation and characterization of molecular-based magnets and oxide superconductors.[2] Some of these compounds are considered as two-dimensional (2D) systems having interesting cooperative effects. We were thus interested in novel 2D compounds based on transition metal complexes.

Transition metal complexes can form various kinds of assemblies. Two-dimensional coordination polymers having coupled localized metal d electrons and delocalized ligand π electrons are of substantial interest owing to their anticipated cooperative magnetic behavior and conductive properties. In particular, 2D copper polymers are the preferred systems for the realization of a new conductive and magnetic phase as an extreme case of the Hubbard model, in which a single electron spin is arranged on each corner of a square lattice.[3] Many inorganic metal halides, calcogenides, and hydroxides have layered structures.[2c] But molecular-based layer compounds, in which spins on metals are coupled over a sheet, are still rare, on account of the lack of methods for linking monomer units. Fortunately, there are many 1D coordination polymers,[2c, 4] and cooperative phenomena have been observed in several 1D polymers containing bridging organic ligands such as oxalate,[5] squarate,[6] and 3,6-substituted 2,5-dihydroxy-*p*-benzoquinones ($H_2(R_2$-DHBQ)).[7] A useful approach to 2D coordination polymers is to fabricate "woven" 2D coordination polymers from 1D polymers as the warp and additional ligands as the woof, which bridge the linear chains. A key point here is the choice of bridging ligands, which should link the 1D polymers without breaking the chain structures.

Chloranilic acid (H_2CA, which corresponds to $H_2(R_2$-DHBQ) with R = Cl) forms 1D chains with Ca^{II}, Sr^{II}, and Y^{III} ions, which are interlinked by CA^{2-} or another bridging ligands such as water molecules.[7h, i] These results encouraged us to utilize CA chains of transition metals as the warp in a 2D polymer. We have succeeded in synthesizing and characterizing a 2D polymer **1** (pz = pyrazine), where pz is used as the woof in the

$[Cu(CA)(pz)]_n$ **1**

woven coordination polymer. The structure and magnetic properties of the corresponding 1D polymer, $[Cu(CA)]_n$, were first reported in 1962.[7b, g] Although the X-ray structure has not been published, EXAFS studies and the magnetic properties imply one-dimensional ribbon structures for $[Cu(CA)]_n$ and $[Cu(CA)L_2]_n$, where L is a nitrogen-containing ligand such as pyridine.[7k]

The crystal structure of **1** shows parallel sheets, which consist of square arrays of Cu^{II} ions bridged by CA^{2-} ions and pyrazine ligands (Fig. 1).[8] The repeating unit Cu(CA)(pz) develops along the *bc* plane. All copper atoms of **1** are linked by coordination bonds giving a 2D structure essential to a 2D band structure. The sheets are well separated from each other: the shortest interlayer metal–metal distance is 9.785(2) Å, while within the layer the distances between the nearest neighbors Cu-CA-Cu and Cu-pz-Cu are 7.993(1) and 6.977(2) Å, respectively. In contrast, zigzag chains are found in $\{[Y_2(CA)_3(H_2O)_6] \cdot 6.6H_2O\}_n$,[7i] and $\{Na_2[M(H_2\text{-DHBQ})_3] \cdot (H_2O)_{24}\}_n$ (M = Mn^{II}, Cd^{II}),[9a] and additional H_2-$DHBQ^{2-}$ ions link these chains to afford large cavities available for building zeolite- or clathrate-like structures.[9]

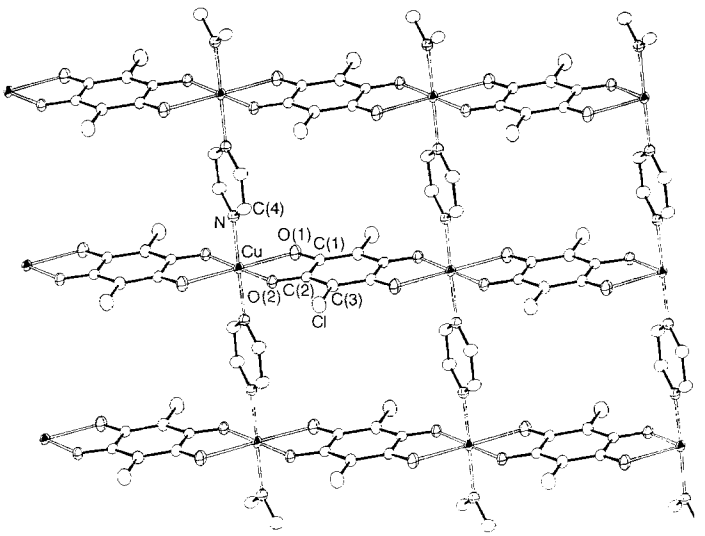


Fig. 1. Crystal structure of **1**; view onto the *bc* plane. Important bond lengths [Å] and angles [°]: Cu-O(1) 2.290(2), Cu-O(2) 1.955(2), Cu-N 2.091(2), Cl-C(3) 1.729(3), O(1)-C(1) 1.233(3), O(2)-C(2) 1.281(3), N-C(4) 1.338(2), C(1)-C(2) 1.537(4), C(2)-C(3) 1.369(3); O(1)-Cu-O(2) 77.23(7), Cu-O(1)-C(1) 109.9(2), Cu-O(2)-C(2) 119.7(2), C(1)-C(2)-C(3) 119.5(2), Cu-N-C(4), 121.7(2).

The geometry around the copper atom is a distorted elongated octahedron. All of the CA^{2-} ligands and the copper atoms sit on the crystallographic mirror plane, and the line connecting the copper and nitrogen atoms of the pz ligands coincides with the crystallographic twofold axis perpendicular to the mirror plane, which indicates that the Cu–N bonds are perpendicular to the CA^{2-} plane. The Cu–N distance (2.091(2) Å) is slightly longer than those for usual bridging pz ligands in Cu^{II} complexes.[10] The pz ligand is also planar, and the Cu-pz-Cu distance falls within the range reported for pz-bridged complexes.[10] The twist angle ($\theta = 14.7°$) of the pz ring out of the plane CuN_2O_2 is small compared with that in other pz-bridged polymers. Interestingly, the Cu–O distances are not identical: one (1.955(2) Å) is similar to that found in the corresponding linear chains (EXAFS study),[7k] whereas the other (2.290(2) Å) is longer than the C–O separations reported for typical Cu^{II} complexes.[11] The effect of the asymmetrical coordination is also found in the different C–O distances in the CA^{2-} ion, 1.233(3) and 1.281(3) Å. One of the distances is shorter than those reported for the free chloranilate ion (1.243(7), 1.253(7) Å),[12] and the other is longer, which indicates that the ligand has a *p*-quinone form[7, 9, 13] like that in $[Cu_2(terpy)_2(CA)]^{2+}$

[*] Prof. Dr. S. Kitagawa, Dr. S. Kawata, Dr. M. Kondo
Department of Chemistry, Tokyo Metropolitan University
Minami Ohsawa
Hachiouji, Tokyo, 192-03 (Japan)
Telefax: Int. code + (426)77-2525
I. Furuchi, Prof. Dr. M. Munakata
Department of Chemistry, Kinki University, Kowakae
Higashi-Osaka (Japan)

 © VCH Verlagsgesellschaft mbH, D-69451 Weinheim, 1994 0570-0833/94/1717-1759 $ 10.00+.25/0

(terpy = 2,2′:6′,2″-terpyridine),[13a] but is dissimilar to the ligands in $\{[Y_2(CA)_3(H_2O)_6]\cdot 6.6H_2O\}_n$[7i] and $\{[Pr_2(CA)_3(C_2H_5OH)_6]\cdot 2C_2H_5OH\}_n$,[9b] in which CA^{2-} has a delocalized electron system. Therefore the environment of the Cu^{II} ion consists of four short in-plane bonds and two longer out-of-plane bonds, giving rise to a distorted tetragonal "4 + 2" configuration.

The ESR spectrum consists of three signals (g values 2.304, 2.082, and 2.068) indicating that magnetic orbital is formed mainly by the $d_{x^2-y^2}$ orbital. No hyperfine structure was observed; however, the linewidth appeared to be extremely narrow, which suggests significant exchange coupling. The magnetic susceptibilities χ_M were measured over temperatures of 2–300 K. $\chi_M T$ decreases at lower temperatures, indicative of weak antiferromagnetic exchange coupling leading to a singlet ground state. The data were analyzed by using the Heisenberg linear chain theory with a mean field approximation[14] to give $J = -2.86\ cm^{-1}$, $zJ' = -1.05\ cm^{-1}$, $g = 2.09$, and $\rho = 7.12\%$.[15] The absolute values of the exchange coupling constants are smaller than that for $[Cu(CA)]_n$, which has a planar ribbon structure ($-24.5\ cm^{-1}$), and are comparable to that for $[Cu(CA)L_2]$,[7k] which suggests that the magnetic orbital $d_{x^2-y^2}$ of **1** is no longer simply parallel to chloranilate plane but a plane formed by Cu–N(pz) and Cu–O(CA) vectors. The absolute values of J and zJ' are also smaller than those for pz-bridged coordination polymers.[10] These differences in the exchange parameters are attributed to the interaction of the magnetic orbital and pyrazine π orbital, which is greatly associated with the twist angle θ of the pz ring. The θ angles for $[Cu(pz)_2(ClO_4)_2]_n$ and $[Cu(pz)_2(CH_3SO_3)_2]_n$ are 66.1° ($J = -5.3\ cm^{-1}$), and 28.5° ($J = -3.82\ cm^{-1}$), respectively,[10e,f] while in **1** the pz ring is tilted by 14.7°. Thus the smaller twist angle of **1** makes antiferromagnetic interaction smaller.

The hydrogen-bond donor CH_3OH also served as the woof in the synthesis of a woven polymer.[7l,m,16] Single crystals of **2** also afford the 2D layers in which the straight 1D $[Cu(CA)(CH_3OH)_2]$ chains are linked by two hydrogen bonds

$[Cu(CA)(CH_3OH)_2]_n$ **2**

(O···O distance: 2.845(3) Å) between the apically coordinated CH_3OH ligand and the oxygen atom of CA^{2-} in the nearest neighbor chain (Fig. 2).[17] A similar hydrogen bond is also found between oxygen atoms of aqua ligands and Et_2DHBQ^{2-} in $\{[Ca(Et_2DHBQ)_2]\cdot 3H_2O\}_n$, where the corrugated chains are linked by hydrogen bonds (3.094(7) Å) longer than those in **2**.[7l] The repeating unit of $Cu(CA)(CH_3OH)_2$ develops along the *ac* plane. The geometry around the copper atom is a distorted elongated octahedron. The four chloranilate oxygen and the copper atoms form a basal plane, because the Cu–O distances are shorter than the two apical $Cu-O(CH_3OH)$ distances, which results in the Cu-CA-Cu distance (7.672(1) Å) being shorter than that of **1** by about 0.3 Å. Therefore the magnetic orbital in **2** lies on the basal plane, in contrast to **1**. The interchain hydrogen bonds lead to short nearest neighbor Cu–Cu distances (5.108(1) Å), and the geometry of the 2D sheet can be regarded as a rectangular array of copper atoms.

Complexes **1** and **2** are good examples of lattice structures formed by coordination and/or hydrogen bonds. The fabrication of 2D polymers from warp and woof components has been shown to be quite useful in the construction of tetragonal copper lattices. This concept can also be applied to a wide variety of compounds having square lattices.

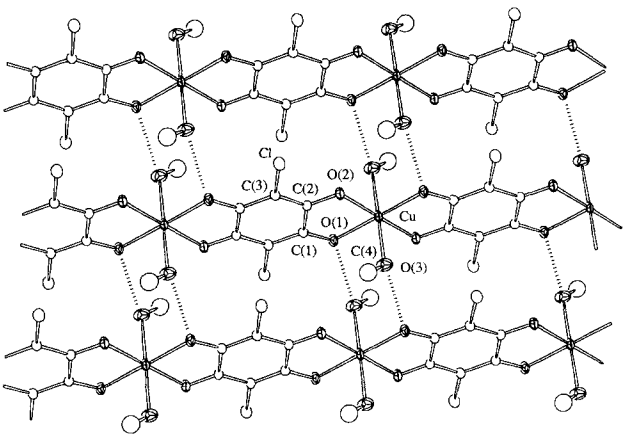


Fig. 2. Crystal structure of **2**: view onto the *ac* plane. Important bond lengths [Å] and angles [°]: Cu-O(1) 2.006(2), Cu-O(2) 1.963(2), Cu-O(3) 2.278(3), Cl-C(3) 1.727(3), O(1)-C(1) 1.262(3), O(2)-C(2) 1.258(3), O(3)-C(4) 1.392(5), C(1)-C(2) 1.530(4), C(2)-C(3) 1.394(3); O(1)-Cu-O(2) 82.41(8), Cu-O(1)-C(1) 112.7(2), Cu-O(2)-C(2) 113.7(2), C(1)-C(2)-C(3) 119.6(2), Cu-O(3)-C(4) 132.8(3). The dashed lines denote the hydrogen bonds; O(1)---O(3′), 2.845(3).

Experimental Procedure

Syntheses of the Complexes: **1**: An aqueous solution (10 mL) of $Cu(NO_3)_2$ (6×10^{-5} mol), CH_3COOH (25×10^{-5} mol), and CH_3COONa (50×10^{-5} mol) was transferred to a test tube, then an aqueous solution (10 mL) of pz (6×10^{-5} mol) and H_2CA (6×10^{-5} mol) was poured into the tube without mixing the two solutions. Dark green platelets began to form within a week. One of these crystals was used for X-ray crystallography. Correct C,H,N analysis. IR (KBr pellet): $\tilde{\nu}[cm^{-1}] = 3117m$, 1634m, 1534s, 1416m, 1373m, 1277m, 1161w, 1119m, 1090w, 1065m, 997w, 851m, 615w, 575w, 473w.

2: The very slow growth of the crystals is essential to obtaining single crystals for X-ray structure determination. Oxidation of copper(I) complexes was used. A methanol solution (20 mL) of chloranil (6×10^{-5} mol) and $[Cu(CH_3CN)_4]PF_6$ (6×10^{-5} mol) was added to a methanol solution (10 mL) of thiochrome (6×10^{-5} mol). The clear yellow solution was transferred to a test tube and kept at room temperature. A small amount of black platelets formed over two months. One of these crystals was used for X-ray crystallography.

Physical Measurements: IR spectra were measured on a Jasco FT/IR-8000 or Hitachi I-5040FT-IR spectrophotometer. KBr discs were prepared for measurements. ESR spectra were recorded at X-band frequency with a JEOL RE-3X spectrometer operating at 9.1–9.5 GHz. Resonance frequencies were measured on an Anritsu MF76A microwave frequency counter. Magnetic fields were calibrated with an Echo Electronics EFM-2000AX NMR field meter. The magnetic susceptibility data were recorded over the temperature range from 2 to 300 K at 1 T with a SQUID susceptometer (Quantum Design, San Diego, CA) interfaced with an HP Vectra computer system. All data were corrected for diamagnetism which was calculated from Pascal's table. The temperature-independent paramagnetism was assumed to be $60\times10^{-6}\ cm^3 mol^{-1}$. Least-squares fittings of the magnetic susceptibility to approximate equations for the antiferromagnetic chain were performed with the least-squares program NGRAPH on a NEC PC9801 computer.

Received: December 17, 1993
Revised version: February 21, 1994 [Z 6567 IE]
German version: *Angew. Chem.* **1994**, *106*, 1861

[1] *Organic and Inorganic Low Dimensional Crystalline Materials* (Eds.: P. Delhaes, M. Drillon), Reidel, Dordrecht, **1987**; *Magnetic Molecular Materials* (Eds.: D. Gatteschi, O. Kahn, J. S. Miller, F. Palacio), Reidel, Dordrecht, **1991**.
[2] a) *Magneto-Structural Correlation in Exchange-Coupled Systems* (Eds.: R. D. Willet, D. Gatteschi, O. Kahn), Reidel, Dordrecht, **1985**; b) A. Caneschi, D. Gatteschi, R. Sessoli, P. Rey, *Acc. Chem. Res.* **1989**, *22*, 392; c) *Inorganic Materials* (Eds.: D. W. Bruce, D. O'Hare), Wiley, Chichester, **1992**.
[3] Y. Nagaoka, *Phys. Rev.* **1966**, *147*, 392.
[4] *Extended Linear Chain Compounds* (Ed.: J. S. Miller), Plenum, New York, **1983**.
[5] A. Michalowicz, J. J. Girerd, J. Goulon, *Inorg. Chem.* **1979**, *18*, 3004; J. J. Girerd, O. Kahn, M. Verdaguer, *ibid.* **1980**, *19*, 274; K. T. Mcgregor, Z. Soos, *ibid.* **1976**, *15*, 2159; A. Gleizes, F. Maury, J. Galy, *ibid.* **1981**, *20*, 2074; M. Melnik, M. Langfelderova, J. Garay, J. Gazo, *Inorg. Chim. Acta* **1973**, *7*, 669.
[6] R. West, H. Y. Niu, *J. Am. Chem. Soc.* **1963**, *85*, 2589; M. Habenschuss, B. Gerstein, *J. Chem. Phys.* **1974**, *61*, 852; M. Benetó, L. Soto, J.-G. Lozano, E. Escrivá, J.-P. Legros, F. Dahan, *J. Chem. Soc. Dalton Trans.* **1991**, 1057; J. A. C. van Ooijen, J. Reedijk, A. L. Spek, *Inorg. Chem.* **1979**, *18*, 1184; G. R. Frauen-

hoff, F. Takusagawa, D. H. Busch, *ibid.* **1992**, *31*, 4002; G. Bernardinelli, D. Deguenon, R. Soules, P. Castan, *Can. J. Chem.* **1989**, *67*, 1158; C. Robl, A. Weiss, *Z. Naturforsch. B* **1986**, *41*, 1341; I. Castro, J. Faus, M. Julve, M. Verdaguer, A. Monge, E. G-Puebla, *Inorg. Chim. Acta* **1990**, *170*, 251.

[7] a) S. Kanda, *Nippon Kagaku Zasshi* **1960**, *81*, 1347; b) H. Kobayashi, T. Haseda, E. Kanda, *J. Phys. Soc. Jpn.* **1963**, *18*, 349; c) R.S. Bottei, D. L. Greene, *J. Inorg. Nucl. Chem.* **1968**, *30*, 1469; d) H. D. Coble, J. H. F. Holtzclaw, *ibid.* **1974**, *36*, 1049; e) R. Sartene, F. H. Boutron, *Mol. Phys.* **1970**, *18*, 825; f) J. T. Wrobleski, D. B. Brown, *Inorg. Chem.* **1979**, *18*, 2738; g) S. Kanda, *Nippon Kagaku Zasshi* **1962**, *83*, 282; h) C. Robl, A. Weiss, *Mater. Res. Bull.* **1987**, *22*, 497; i) C. Robl, *ibid.* **1987**, *22*, 1483; j) C. Robl, A. Weiss, *Z. Naturforsch. B* **1986**, *41*, 1495; k) M. Verdaguer, M. Michalowicz, J. J. Girerd, N. Alberding, O. Kahn, *Inorg. Chem.* **1980**, *19*, 3271; l) C. Robl, W. F. Kuhs, *J. Solid State Chem.* **1989**, 79, 46; m) *ibid.* **1988**, *74*, 21.

[8] X-ray analysis: A suitable crystal was chosen and mounted on a glass fiber with epoxy resin. Cell constants and the orientation matrix for collection of intensity data for each crystal were based on the setting angles of 21 carefully centered reflections with 2θ values in the range of $48.10^\circ < 2\theta < 49.90^\circ$. The structures were solved by direct methods (Rigaku TEXSAN crystallographic software package of Molecular Structure Corporation). Full-matrix least-squares refinement was carried out with anisotropic thermal parameters for all non-hydrogen atoms. After anisotropic least-squares refinement for non-hydrogen atoms, all hydrogen atoms were located in the difference Fourier map, but their parameters were not refined. The final cycle of full-matrix least-squares refinement was based on N_o and n variable parameters and converged with unweighted R-factors of $R = \sum||F_o| - |F_c||/\sum|F_o|$, $Rw = [\sum|F_o| - |F_c|)^2/\sum w|F_o|^2]^{1/2}$ where $w = 4F_o^2/\sigma^2(F_o^2)$. Crystal data: $CuCl_2O_4N_2C_{10}H_4$, $M = 350.60$, monoclinic, space group $C2/m$, $a = 9.785(2)$, $b = 6.977(2)$, $c = 7.993(1)$ Å, $\beta = 97.26(1)^\circ$, $V = 541.3(2)$ Å^3, $Z = 2$, $\varrho_{calcd} = 2.151$ g cm^{-3}, $\lambda(Mo_{K\alpha}) = 0.71069$ Å, $F(000) = 346$, $\mu(Mo_{K\alpha}) = 25.26$ cm^{-1}, $T = 23^\circ$C. Crystal dimensions: $0.05 \times 0.05 \times 0.10$ mm. $2\theta_{max} = 55.0^\circ$; N_o, $N = 715$, 603; $n = 55$; R, $R_w = 0.020$, 0.027 [18].

[9] a) C. Robl, A. Weiss, *Z. Naturforsch. B.* **1986**, *41*, 1501; b) P. E. Riley, S. F. Haddad, K. N. Raymond, *Inorg. Chem.* **1983**, *22*, 3090.

[10] a) J. S. Haynes, S. J. Rettig, R. C. Thompson, J. Trotter, *Can. J. Chem.* **1987**, *65*, 420; b) A. Santro, A. D. Mighell, C. W. Reimann, *Acta Crystallogr. Sect. B* **1970**, *26*, 979; c) R. C. E. Belford, D. E. Fenton, M. R. Truter, *J. Chem. Soc. Dalton Trans.* **1974**, 17; d) B. Morosin, R. Hughes, Z. G. Soos, *Acta Crystallogr. Sect. B* **1975**, *31*, 762, e) J. Darriet, M. S. Haddad, E. N. Duesler, D. N. Hendrickson, *Inorg. Chem.* **1979**, *18*, 2679; f) H. W. Richardson, J. R. Wasson, W. E. Hatfield, *ibid.* **1977**, *16*, 484; g) P. D. Boyd, S. Mitra, *ibid.* **1980**, *19*, 3547; h) T. Otieno, S. J. Rettig, R. C. Thompson, J. Trotter, *ibid.* **1993**, *32*, 4384.

[11] B. J. Hathaway, *Coord. Chem. Rev.* **1983**, *52*, 87.

[12] E. K. Andersen, *Acta Crystallogr.* **1967**, *22*, 191.

[13] a) J. V. Folgado, R. Ibáñez, E. Coronado, D. Beltrán, J. M. Savariault, J. Galy, *Inorg. Chem.* **1988**, *27*, 19; b) W.-Y. Jeong, R. A. Holwerda, *ibid.* **1988**, *27*, 2571; c) M. A. Calvo, A. M. M. Lanfredi, L. A. Oro, M. T. Pinillos, C. Tejel, A. Tiripicchio, F. Ugozzoli, *ibid.* **1993**, *32*, 1147; d) F. Tinti, M. Verdaguer, O. Kahn, J.-M. Savariault, *ibid.* **1987**, *26*, 2380.

[14] W. E. Hatfield, *J. Appl. Phys.* **1981**, *52*, 1985.

[15] This may indicate that the 2D exchange interaction spreads over the polymer sheet. However, we cannot determine if the effective exchange pathway is over pz or CA. We have also analyzed the data with the 1D model an obtained the exchange parameter $J = -2.99$ cm^{-1}, $g = 2.08$, $\rho = 7.68\%$. The dimensionality of the interaction is uncertain.

[16] C. Robl, S. Hentschel, G. J. McIntyre, *J. Solid State Chem.* **1992**, *96*, 318; S. R. Breeze, S. Wang, *Inorg. Chem.* **1993**, *32*, 5981.

[17] The data collection and refinement was done in analogy to **1**. Crystal data for **2**: $CuCl_2O_6C_8H_8$, $M = 334.60$, triclinic, space group $P\bar{1}$, $a = 7.672(1)$, $b = 7.780(2)$, $c = 5.108(1)$ Å, $\alpha = 99.89(2)^\circ$, $\beta = 98.41(1)^\circ$, $\gamma = 100.25(2)^\circ$, $V = 290.63(9)$ Å^3, $Z = 1$, $\varrho_{calcd} = 1.912$ g cm^{-3}, $\lambda(Mo_{K\alpha}) = 0.71069$ Å, $F(000) = 167$, $\mu(Mo_{K\alpha}) = 23.56$ cm^{-1}, $T = 23^\circ$C. Crystal dimensions: $0.15 \times 0.15 \times 0.10$ mm. $2\theta_{max} = 55.0^\circ$; N_o, $N = 1422$, 1049; $n = 80$; R, $R_w = 0.029$, 0.037 [18].

[18] Further details of the crystal structure investigations may be obtained from the Fachinformationszentrum Karlsruhe, D-76344 Eggenstein-Leopoldshafen (FRG), on quoting the depository number CSD-58273.

Dendritic Macromolecules Incorporating Tetrathiafulvalene Units**

Martin R. Bryce,* Wayne Devonport, and Adrian J. Moore

A burgeoning topic at the interface of supramolecular and polymer chemistry is the synthesis and characterization of dendritic macromolecules (also termed "starburst polymers" or "cascade molecules").[1-12] These macromolecules comprise a polyfunctional core surrounded by covalently linked layers of monomers, with a branch occurring at each monomer unit. This structure gives rise to a hyperbranched polymer possessing a high level of three-dimensional order; control over molecular weight, topology, interior cavity size, and surface functionality can be achieved. Current interest in these materials stems from the fundamental synthetic challenges they pose and the range of properties they may display, such as, self-assembly, molecular recognition, and catalysis, and their potential applications in molecular electronic devices. The incorporation of redox-active molecular units into a dendrimer structure is essentially unexplored. In this context, organometallic systems with arene–iron[10] and ruthenium–terpyridine monomers[11] elaborated into dendrimer structures have recently been reported, and dendritic polyradicals have been prepared.[12]

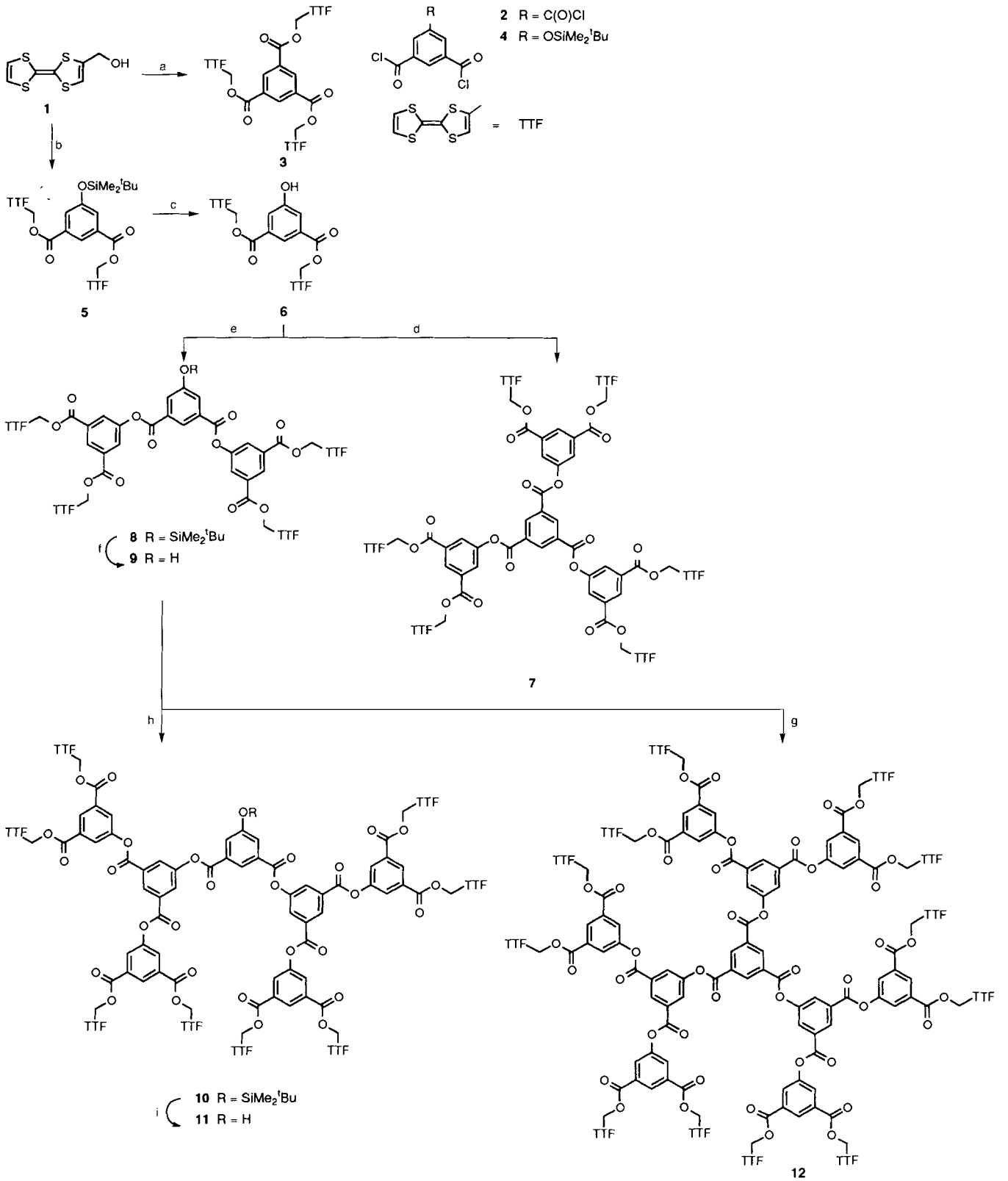
We now describe the first examples of dendritic macromolecules that contain redox-active tetrathiafulvalene (TTF) units. The incorporation of TTF into hyperbranched structures presents a fascinating prospect for the following reasons:[13] 1) oxidation of TTF to the cation radical and dication species occurs sequentially and reversibly at relatively low potentials (for unsubstituted TTF, $E^{1/2} = +0.34$ and $+0.74$ V, vs. Ag/AgCl); 2) the oxidation potentials can be finely tuned by the attachment of appropriate substituents; 3) the TTF cation radical is thermodynamically very stable; and 4) oxidized TTF units are key components of molecular conductors, because of their propensity to form highly-ordered stacks.

The starting TTF monomer unit for the present synthesis is 4-(hydroxymethyl)tetrathiafulvalene (**1**).[14] By a convergent synthetic strategy based on a repetitive coupling/deprotection sequence, we have assembled the symmetrical dendrimer **12** which contains 12 TTF units at the periphery of the macromolecule. The key functionalized reagent for the esterification reactions that build up successive generations is 5-(*tert*-butyldimethylsiloxy)isophthaloyl chloride (**4**).[15] In an initial model experiment we established that TTF derivative **1** could be readily esterified by reaction with 1,3,5-benzenetricarbonyl chloride (**2**) to yield the tris(TTF) derivative **3** in 83% yield. The analogous reaction of **1** with the silyl-protected diacid dichloride **4** gave compound **5** (92% yield), deprotection of which gave the dendrimer arm **6** (85% yield) (Scheme 1).

Reaction of compound **6** with triacid trichloride **2** in the presence of 4-dimethylaminopyridine (DMAP) as base gave the hexakis(TTF) dendrimer **7** (75% yield). No reaction occurred when triethylamine was used instead of DMAP. Following the same procedure, reaction of **6** with reagent **4** yielded compound **8** (85% yield), which was desilylated to give the phenol derivative **9** (95% yield). Compounds **9** and **4** reacted in the presence of a

[*] Dr. M. R. Bryce, W. Devonport, Dr. A. J. Moore
Department of Chemistry, University of Durham
GB-Durham DH1 3LE (UK)
Telefax: Int. code + (91) 384-4737.

[**] We thank the SERC for financial support for this work and the Department of Molecular Biology at the University of Odense for obtaining the plasma desorption mass spectra.



Scheme 1. a) **2**, CH_2Cl_2, Et_3N, 18 h, 20 °C, 83%; b) **4**, CH_2Cl_2, Et_3N, 18 h, 20 °C, 92%; c) Bu_4NF, THF, 12 h, 20 °C, 85%; d) **2**, CH_2Cl_2, DMAP, 18 h, 20 °C, 75%; e) **4**, CH_2Cl_2, DMAP, 18 h, 20 °C, 85%; f) Bu_4NF, THF, 12 h, 20 °C, 95%; g) **2**, CH_2Cl_2, *N*,*N*-dimethylaniline, 56 h, 20 °C, 48%; h) **4**, CH_2Cl_2, *N*,*N*-dimethylaniline, DMAP, 56 h, 20 °C, 76%; i) Bu_4NF, THF, 56 h, 20 °C, 50%.

mixture of *N*,*N*-dimethylaniline and DMAP (optimum ratio 1/1 v/v) to yield octakis(TTF) derivative **10** (76% yield, no product was obtained when either triethylamine, *N*,*N*-dimethylaniline, or DMAP were used as the sole base). Desilylation of **10** yielded phenol derivative **11** (50% yield). Compound **9** reacted, as expected, with **2** to give the dendrimer **12** decorated with twelve peripheral TTF units (48% yield). A notable feature of the above iterative esterification reactions is the need to select care-

fully the correct base for the reaction; this is in accord with previous observations of Miller et al.[15] Dendrimers **3**, **7**, and **12** are stable when stored below 0 °C; after seven days at room temperature in the dark and under an argon atmosphere, notable decomposition is observed (Table 1).

Table 1. Selected characteristic data for compounds **3** and **5**–**12** [a].

3: Orange solid; m.p. 37–38 °C; PDMS: *m/z*: 859.3 (M^+, calcd: 859.24 for $C_{30}H_{18}O_6S_{12}$); ^{1}H NMR ($CDCl_3$): δ = 8.85 (s, 3H), 6.45 (s, 3H), 6.29 (s, 6H), 5.10 (s, 6H); UV (CH_2Cl_2): λ_{max} = 220, 307, 365 nm (after addition of an excess of I_2: 225, 363, 439, 590 nm).

5: Yellow solid; m.p. 45–46 °C; ^{1}H NMR [$(CD_3)_2CO$]: δ = 8.26 (t, J = 1.5 Hz, 1H), 7.74 (d, J = 1.5 Hz, 2H), 6.85 (s, 2H), 6.63 (s, 4H), 5.21 (s, 4H), 1.03 (s, 9H), 0.30 (s, 6H).

6: Yellow solid; m.p. 76–77 °C; PDMS: *m/z*: 614.7 (M^+, calcd: 614.9 for $C_{22}H_{14}O_2S_8$); ^{1}H NMR [$(CD_3)_2CO$]: δ = 9.24 (s, 1H), 8.16 (t, J = 1.5 Hz, 1H), 7.73 (d, J = 1.5 Hz, 2H), 6.85 (s, 2H), 6.63 (s, 4H), 5.19 (s, 4H).

7: Yellow solid; m.p. 80–81 °C; PDMS: *m/z*: 2000.6 (M^+, calcd: 2000.7 for $C_{75}H_{42}O_{18}S_{24}$); ^{1}H NMR ([D$_6$]DMSO): δ = 9.10 (s, 3H), 8.44 (s, 3H), 8.32 (s, 6H), 7.00 (s, 6H), 6.70 (s, 12H), 5.20 (s, 12H); UV (CH_2Cl_2): λ_{max} = 220, 263, 305, 360 nm (after addition of an excess of I_2: 222, 294, 363, 590 nm).

8: Yellow solid; m.p. 85–86 °C; PDMS: *m/z*: 1490.0 (M^+, calcd: 1490.1 for $C_{58}H_{44}O_{13}S_{16}Si$); ^{1}H NMR [$(CD_3)_2CO$]: δ = 8.61 (t, J = 1.5 Hz, 1H), 8.55 (t, J = 1.5 Hz, 2H), 8.25 (d, J = 1.5 Hz, 4H), 7.95 (d, J = 1.5 Hz, 2H), 6.84 (s, 4H), 6.58 (s, 8H), 5.22 (s, 8H), 1.04 (s, 9H), 0.32 (s, 6H).

9: Yellow oil; ^{1}H NMR [$(CD_3)_2CO$]: δ = 9.30 (br. s, 1H), 8.15 (t, J = 1.5 Hz, 3H), 7.73 (d, J = 1.5 Hz, 6H), 6.86 (s, 4H), 6.63 (s, 8H), 5.20 (s, 8H).

10: Orange oil; PDMS: *m/z*: 1505.0 (M^{2+}/2, calcd: 3011.9 for $C_{118}H_{76}O_{24}S_{32}Si$); ^{1}H NMR [$(CD_3)_2CO$]: δ = 8.62 (t, J = 1.5 Hz, 1H), 8.56 (t, J = 1.5 Hz, 2H), 8.25 (d, J = 1.5 Hz, 12H), 7.94 (d, J = 1.5 Hz, 6H), 6.81 (s, 8H), 6.58 (s, 16H), 5.18 (s, 16H), 1.03 (s, 9H), 0.32 (s, 6H).

11: Orange oil; ^{1}H NMR [$(CD_3)_2CO$]: δ = 9.30 (br. s, 1H), 8.14 (t, J = 1.5 Hz, 7H), 7.78 (d, J = 1.5 Hz, 14H), 6.83 (s, 8H), 6.58 (s, 16H), 5.15 (s, 16H).

12: Orange oil; ^{1}H NMR [$(CD_3)_2CO$]: δ = 8.54 (s, 3H), 8.17 (t, J = 1.5 Hz, 9H), 7.73 (d, J = 1.5 Hz, 18H), 6.84 (s, 12H), 6.61 (s, 24H), 5.19 (s, 24H); UV (CH_2Cl_2): λ_{max} = 220, 296, 363 nm (after addition of an excess of I_2: 223, 262, 291, 363, 590 nm).

[a] All the new compounds were isolated pure (as judged either by C,H combustion analysis or analysis by gel permeation chromatography) after column chromatography on silica; PDMS = plasma desorption mass spectroscopy.

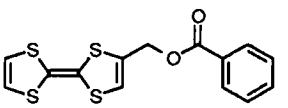
The redox behavior of the dendrimers **3**, **7**, and **12** was investigated by cyclic voltammetry (CV) (Table 2). The dendrimers **3**, **7**, and **12** exhibit the characteristic redox behavior typical of the TTF system: they show two quasi-reversible redox couples at

Table 2. Cyclic voltammetry data (in volts). Experimental conditions: sweep rate 100 mVs^{-1}, 0.1 M Bu_4NPF_6, Ag/AgCl reference electrode, platinum working and counter electrodes, 20 °C.

	$E_1^{1/2}$	$E_2^{1/2}$
TTF [a]	0.34	0.74
3 [a]	0.42	0.84
7 [b]	0.45	0.86
12 [a]	0.43	0.81
13 [a]	0.48	0.86

[a] Solvent: MeCN. [b] Solvent: MeCN/CH_2Cl_2 (1/1 v/v).

approximately $E_1^{1/2} \approx +0.45$ and $E_2^{1/2} \approx +0.85$ V. The results of classical CV, chronoamperometry, and CV with ultramicroelectrodes clearly show that for the dendrimers **3**, **7**, and **12** each couple involves a simultaneous multielectron transfer; at least five electrons are transferred for compound **12** in each redox couple. Formation of these species bearing a multiple positive charge produces no significant perturbation from the redox behavior of the parent TTF phenyl ester **13**. It can thus be concluded that there is no significant interaction between the charged TTF units in the dendrimer derivatives **3**, **7**, and **12**.[16] Oxidation of the TTF units in dendrimers **3**, **7**, and **12** has also been achieved by reaction with an excess of iodine in dichloromethane solution. After addition of iodine, the UV spectra show the presence of a new broad absorption band centered at λ_{max} 590 nm, which is consistent with the formation of the TTF cation radical.[17]



13

In summary, we have established an efficient methodology for the assembly of the first TTF dendrimers; these materials provide unprecedented scope for the study of charge-transfer interactions involving functionalized dendrimers.

Received: December 28, 1993
Revised: May 4, 1994 [Z6588IE]
German version: *Angew. Chem.* **1994**, *106*, 1862

[1] Reviews: a) D. A. Tomalia, A. M. Naylor, W. A. Goddard III, *Angew. Chem.* **1990**, *102*, 119; *Angew. Chem. Int. Ed. Engl.* **1990**, *29*, 138; b) G. R. Newkome, C. N. Moorefield, *Aldrichimica Acta* **1992**, *25*, 31; c) H.-B. Mekelburger, W. Jaworek, F. Vögtle, *Angew. Chem.* **1992**, *104*, 1609; *Angew. Chem. Int. Ed. Engl.* **1992**, *31*, 1571; d) D. A. Tomalia, *Aldrichimica Acta* **1993**, *26*, 91.
[2] I. Gitsov, K. L. Wooley, J. M. J. Fréchet, *Angew. Chem.* **1992**, *104*, 1282; *Angew. Chem. Int. Ed. Engl.* **1992**, *31*, 1200.
[3] R.-H. Jin, T. Aida, S. Inoue, *J. Chem. Soc. Chem. Commun.* **1993**, 1260.
[4] Z. Xu, J. S. Moore, *Angew. Chem.* **1993**, *105*, 1394; *Angew. Chem. Int. Ed. Engl.* **1993**, *32*, 1354.
[5] T. M. Miller, T. X. Neenan, E. W. Kwock, S. M. Stein, *J. Am. Chem. Soc.* **1993**, *115*, 356.
[6] C. Wörner, R. Mülhaupt, *Angew. Chem.* **1993**, *105*, 1367; *Angew. Chem. Int. Ed. Engl.* **1993**, *32*, 1306.
[7] E. M. M. de Brabander-van den Berg, E. W. Meijer, *Angew. Chem.* **1993**, *105*, 1370; *Angew. Chem. Int. Ed. Engl.* **1993**, *32*, 1308.
[8] K. L. Wooley, C. J. Hawker, J. M. Fréchet, F. Wudl, G. Srdanov, S. Shi, C. Li, M. Kao, *J. Am. Chem. Soc.* **1993**, *115*, 9836.
[9] Y.-H. Liao, J. R. Moss, *J. Chem. Soc. Chem. Commun.* **1993**, 1774.
[10] F. Moulines, L. Djakovitch, R. Boese, B. Gloaguen, W. Thiel, J.-L. Fillaut, M.-H. Delville, D. Astruc, *Angew. Chem.* **1993**, *105*, 1132; *Angew. Chem. Int. Ed. Engl.* **1993**, *32*, 1075.
[11] a) S. Serroni, G. Denti, S. Campagne, A. Juris, M. Ciano, V. Balzani, *Angew. Chem.* **1992**, *104*, 1540; *Angew. Chem. Int. Ed. Engl.* **1992**, *31*, 1493; b) G. R. Newkome, F. Cardullo, E. C. Constable, C. N. Moorefield, A. M. W. Cargill Thompson, *J. Chem. Soc. Chem. Commun.* **1993**, 925.
[12] A. Rajca, S. Utamapanya, *J. Am. Chem. Soc.* **1993**, *115*, 10688.
[13] For alternative approaches to multi(TTF) systems, see: a) M. L. Kaplan, R. C. Haddon, F. Wudl, *J. Chem. Soc. Chem. Commun.* **1977**, 338; b) M. Adam, P. Wolf, H. J. Räder, K. Müllen, *ibid.* **1990**, 1624; c) F. Bertho-Thoroval, A. Robert, A. Souizi, K. Boubekeur, P. Batail, *ibid.* **1991**, 843; d) M. Jørgensen, K. A. Lerstrup, K. Bechgaard, *J. Org. Chem.* **1991**, *56*, 5684; e) M. R. Bryce, G. J. Marshallsay, A. J. Moore, *ibid.* **1992**, *57*, 4859; f) M. Fourmigué, Y.-S. Huang, *Organometallics*, **1993**, *12*, 797.
[14] D. C. Green, *J. Org. Chem.* **1979**, *44*, 1476; for an improved method for the preparation of compound **1**, see: J. Garin, J. Orduna, S. Uriel, A. J. Moore, M. R. Bryce, S. Wegener, D. S. Yufit, J. A. K. Howard, *Synthesis* **1994**, 489.
[15] T. M. Miller, E. W. Kwock, T. X. Neenan, *Macromolecules* **1992**, *25*, 3143.
[16] Detailed electrochemical experiments on **3**, **7**, and **12**, performed in collaboration with Professor M. Jubault, Université d'Angers, will be reported elsewhere.
[17] J. B. Torrance, B. A. Scott, B. Welber, F. B. Kaufman, P. E. Seiden, *Phys. Rev. B* **1979**, *19*, 730.

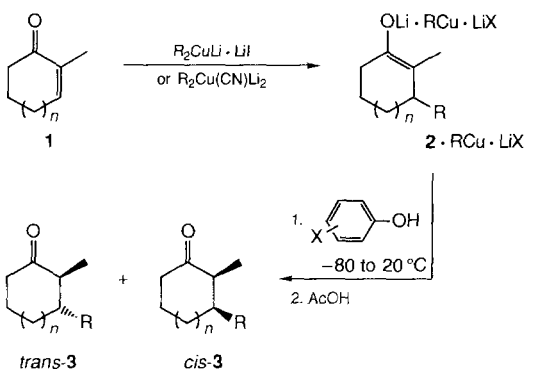
 © VCH Verlagsgesellschaft mbH, D-69451 Weinheim, 1994 0570-0833/94/1717-1763 $ 10.00+.25/0

Substituent Effects and Complexation Phenomena in the Diastereoselective Protonation of Chiral Enolates**

Norbert Krause*

In contrast to alkylation and acylation, protonation at carbanionic carbon centers in stereoselective syntheses has received little attention. Some successes with enantioselective protonation of prochiral enolates have been achieved in recent years.[1, 2] However, little is still known about diastereoselective protonation of chiral enolates,[3] despite the fact that it is a frequently used reaction in areas such as the synthesis of natural products.[4] Up until now, it has not been possible to systematically develop methods for *reagent-controlled diastereoselective or enantioselective protonation* which could be applied to a range of compounds. In other words, suitable proton sources for particular compounds have had to be found only by trial and error.[1-4] Only in two cases[2b, f] could the observed stereoselectivity be explained (assumed chelate-type interactions between "carbanion" and protonating agent). There is therefore a need for a systematic study into the steric and electronic influence of the starting material and the proton source on the stereoselectivity of protonation reactions. We now report on the diastereoselective protonation of chiral lithium enolates of type **2**.

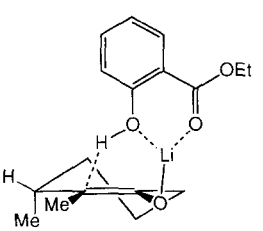
Cyclic enolates of this type are, depending on their ring size, conformationally more or less strongly fixed and can only exist as (*E*) isomers. They are obtained by 1,4-addition of organocuprates[5] to readily available 2-methyl-2-cycloalkenones **1**.[6] The



use of a range of cuprates allows various residues R to be introduced at C-3 of the enolate. However, by analogy with the enolization of carbonyl compounds with lithium diisopropylamide (LDA),[7] it must be assumed that the organocopper compound formed in the Michael addition is bound to the lithium enolate[8] and influences its protonation.

A prerequisite for high stereoselectivity in protonation reactions is that the acidity of the proton source is markedly higher than that of the protonated product, so that complete protonation is achieved.[9] The reaction must also proceed with C-protonation and not O-protonation, since the stereochemistry of the tautomerization of the enol formed in the latter case is probably beyond the influence of the protonating agent. Conditions favorable to C-protonation are achieved in kinetically controlled protonations with weak organic acids.[10] In addition, the rate of protonation of the enolate by the proton source must be considerably higher than the rate of proton exchange between the enolate and the protonation product, since the latter can lead to epimerization of the chiral product. It is therefore essential that the proton source be available in large excess *at all times during reaction* (addition of the enolate to the proton source and not vice versa). To avoid epimerization of the protonation product, basic metallic salts present in the reaction mixture must be trapped during workup (e.g., with acetic acid).

In the case of the chiral enolate **2a**, prepared by 1,4-addition of lithium dimethylcuprate to **1** ($n = 1$), the kinetically controlled diastereoselective protonation to give *cis*-**3a** was of interest, since thermodynamic control favored the *trans* product (equilibrium ratio 81:19,[11] see Table 1). In the protonation with phenols a marked substituent effect was observed: phenols substituted with donor groups preferentially yielded *trans*-**3a**, whereas phenols substituted with acceptor groups largely yielded *cis*-**3a**.[12, 13] This substituent effect, observed for the first time in stereoselective protonation, implies that charge separation in the transition state leading to *trans*-**3a** is greater than in that leading to *cis*-**3a**. The substituent effects were particularly marked in *ortho*-substituted phenols, which possess the structural prerequisites for the formation of chelate complexes (*cis* protonation was favored with salicyl alcohol, 2-hydroxyacetophenone, and salicylaldehyde[12]). By far the highest selectivity towards *cis*-**3a** (96:4) resulted from protonation with ethyl salicylate. Here, a comparatively rigid chelate complex (e.g., **4**) is probably formed as a result of interactions between the lithium ion of the enolate and the carbonyl and hydroxyl oxygen atoms of the salicylate (the fourth coordination point of the lithium ion is assumed to be occupied by the copper species formed by cuprate addition[8]). Clearly, this type of chelation reduces the degrees of freedom of the system to such an extent that the difference in the activation barriers for the transition states leading to *cis*- and *trans*-**3a** reaches a preparatively useful magnitude (a product ratio of 96:4 corresponds to a difference in the Gibbs activation energy of about 5 kJ mol^{-1}).



4

Table 1. Equilibrium ratios for ketones **3** [a] and product ratios for their syntheses by protonation of enolate **2** with ethyl salicylate (X = 2-CO_2Et).

Product	*n*	R	Equilibrium ratio *trans*:*cis*	Product ratio *trans*:*cis*
3a	1	Me	81:19	4:96
3b	1	*n*Bu	76:24	3:97
3c	1	$(CH_2)_3CH=CH_2$	78:22	3:97
3d	0	Me	87:13	17:83
3e	2	Me	55:45	1:99

[a] By base-catalyzed equilibration.

Such high stereoselectivities could only be achieved by the addition of the enolate to an excess of the salicylate. With reverse addition, proton exchange between the enolate and the protonation product clearly occurs, which leads to a drastic reduction in the diastereoselectivity (a *cis*:*trans* ratio of 69:31 was observed). The influence of temperature was, on the other hand, small

[*] Dr. N. Krause
Institut für Organische Chemie der Technischen Hochschule
Petersenstrasse 22, D-64287 Darmstadt (FRG)
Telefax: Int. code + (6151)163-374

[**] This work was supported by the Deutsche Forschungsgemeinschaft and the Fonds der Chemischen Industrie. I thank Markus Oberthür for carrying out some of the experiments.

(protonation at $-20\,^{\circ}C$ instead of $-80\,^{\circ}C$: *cis*:*trans* = 92:8). Similarly, changes in the ester function of the salicylate hardly affected the selectivity.[12] The introduction of a methyl group at C-3 of the salicylate, on the other hand, led to the loss of *cis* selectivity (*cis*:*trans* = 53:47). Clearly, a type **4** chelate cannot be formed here because of the steric interactions between the additional methyl group and the enolate. Finally, in order to investigate the effect on the stereoselectivity of protonation exerted by the copper cluster coordinated to the lithium enolate **2a**,[8a] the copper-free enolate was prepared by transmetalation of the corresponding silyl enol ether with MeLi. Protonation with ethyl salicylate resulted in a *cis*/*trans* ratio of 86:14 in diethyl ether and 92:8 in THF. The formation of complex **4** therefore also occurs in the absence of copper; in this case, the fourth coordination site of the lithium ion is probably occupied by solvent, which hardly influences the diastereoselectivity of the proton transfer.

The *cis*-selective protonation with salicylates can be extended to numerous chiral five-, six-, and seven-membered ring enolates with various substituents (see Table 1).[14] Thus, with six-membered ring enolates having *n*-butyl or 4-penten-1-yl residues at C-3, the protonation products **3b** and **3c** were formed with a *cis* selectivity of 97:3. Protonation of the methyl-substituted, five-membered ring enolate yielded a product ratio of 83:17 and that of the corresponding seven-membered ring enolate **3e** a ratio of 99:1. Thus, *cis* selectivity increases with increasing ring size. Interestingly, the same trend is also observed for the equilibrium ratios[11] (see Table 1). The kinetically controlled protonation with ethyl salicylate therefore "works against" the increasing thermodynamic preference for the *trans* product with decreasing ring size.

In summary, marked substituent effects and complexation phenomena have been observed for the first time in the diastereoselective protonation of type **2** chiral enolates with phenols. High *cis* selectivities were obtained by protonation with ethyl salicylate. The application of this concept to the diastereoselective protonation of other cyclic and acyclic enolates with chiral centers or axes is the subject of current investigations.

Experimental Procedure

MeLi (20.0 mL, 30.0 mmol, 1.5 M in diethyl ether) was added, dropwise at $-10\,^{\circ}C$ to a suspension of CuI (2.86 g, 15.0 mmol) in diethyl ether (100 mL). The clear cuprate solution was cooled to $-80\,^{\circ}C$ and treated with 2-methyl-2-cyclohexenone (1.10 g, 10.0 mmol) in diethyl ether (20 mL). After the mixture had been stirred for 30 min at $-80\,^{\circ}C$, a yellow suspension was formed. This was transferred through a Teflon tube under nitrogen pressure and added dropwise to a solution of ethyl salicylate (6.65 g, 40.0 mmol) in diethyl ether (50 mL) also cooled to $-80\,^{\circ}C$. The mixture was warmed to room temperature and treated with acetic acid (2.3 mL, 40.0 mmol). After filtration through celite the filtrate was washed once with saturated $NaHCO_3$ solution and three times with water. After the solvent had been removed, the crude product was purified by column chromatography (silica gel, diethyl ether/hexane 1:20). Ethyl salicylate (6.02 g) and *cis*-2,3-dimethylcyclohexanone (*cis*-**3a**) (0.96 g, 76%, colorless liquid, d.s. = 96:4) were obtained. ^1H NMR (300 MHz, $CDCl_3$): $\delta = 0.76$ (d, $J = 7.1$ Hz, 3H; 3-Me), 0.91 (d, $J = 6.9$ Hz, 3H; 2-Me), 1.53–1.66 (m, 1H), 1.72–1.89 (m, 3H), 2.10–2.33 (m, 3H), 2.47–2.56 (m, 1H); ^{13}C NMR (75.5 MHz, $CDCl_3$): $\delta = 11.9$ (3-Me), 14.6 (2-Me), 23.4 (C-5), 31.2 (C-4), 37.4 (C-3), 40.7 (C-6), 49.3 (C-2), 214.3 (C-1)

Received: March 12, 1994 [Z 6753 IE]
German version: *Angew. Chem.* **1994**, *106*, 1845

[1] Overview: a) L. Duhamel, P. Duhamel, J.-C. Launay, J.-C. Plaquevent, *Bull. Soc. Chim. Fr.* **1984**, II-421–II-430; b) H. Waldmann, *Nachr. Chem. Tech. Lab.* **1991**, *39*, 413–418.

[2] Most recent work: a) J. Reymond, K. D. Janda, R. A. Lerner, *J. Am. Chem. Soc.* **1992**, *114*, 2257–2258; b) T. Haubenreich, S. Hünig, H.-J. Schulz, *Angew. Chem.* **1993**, *105*, 443–445; *Angew. Chem. Int. Ed. Engl.* **1993**, *32*, 398–400; c) T. Yasukata, K. Koga, *Tetrahedron: Asymmetry* **1993**, *4*, 35–38; d) K. Fuji, K. Tanaka, H. Miyamoto, *ibid.* **1993**, *4*, 247–259; e) C. Fehr, I. Stempf, J. Galindo, *Angew. Chem.* **1993**, *105*, 1091–1093, 1093–1095; *Angew. Chem. Int. Ed. Engl.* **1993**, *32*, 1042–1044, 1044–1046; f) A. Yanagisawa, T. Kuribayashi, T. Kikuchi, H. Yamamoto, *ibid.* **1994**, *106*, 129–130 and **1994**, *33*, 107–108.

[3] a) E. J. Panek, T. J. Rodgers, *J. Am. Chem. Soc.* **1974**, *96*, 6921–6928; b) S. Takano, W. Uchida, S. Hatakeyama, K. Ogasawara, *Chem. Lett.* **1982**, 733–736; c) S. Takano, J. Kudo, M. Takahashi, K. Ogasawara, *Tetrahedron Lett.* **1986**, *27*, 2405–2408; d) D. Awandi, F. Henin, J. Muzart, J.-P. Pete, *Tetrahedron: Asymmetry* **1991**, *2*, 1101–1104; e) R. Tamura, K. Watabe, A. Kamimura, K. Hori, Y. Yokomori, *J. Org. Chem.* **1992**, *57*, 4903–4906; f) U. Gerlach, S. Hünig, *Tetrahedron Lett.* **1987**, *28*, 5805–5808; g) U. Gerlach, T. Haubenreich, S. Hünig, Y. Keita, *Chem. Ber.* **1993**, *126*, 1205–1215.

[4] For example, a) C. H. Heathcock, E. Kleinman, E. S. Binkley, *J. Am. Chem. Soc.* **1978**, *100*, 8036–8037; b) C. H. Heathcock, C. M. Tice, T. C. Germroth, *ibid.* **1982**, *104*, 6081–6091; c) F. E. Ziegler, J. J. Piwinski, *ibid.* **1982**, *104*, 7181–7190; d) F. Rehders, D. Hoppe, *Synthesis* **1992**, 859–864; e) S. G. Davies, O. Ichihara, I. A. S. Walters, *Synlett* **1993**, 461–462; f) R. Tamura, K. Watabe, N. Ono, Y. Yamamoto, *J. Org. Chem.* **1993**, *58*, 4471–4472; g) W. R. Baker, J. K. Pratt, *Tetrahedron* **1993**, *49*, 8739–8756.

[5] B. H. Lipshutz, S. Sengupta, *Org. React.* **1992**, *41*, 135–631.

[6] Chlorination of 2-methylcyclohexanone with SO_2Cl_2 and HCl elimination with LiCl according to a literature method (E. W. Warnhoff, D. G. Martin, W. S. Johnson, *Org. Synth. Collect. Vol. IV* **1963**, 162–166) yielded a 9:1 mixture of 2-methyl-2-cyclohexenone and 6-methyl-2-cyclohexenone. Pure 2-methylcycloalkenones were obtained by the addition of chloroethylcarbene to silyl enol ethers (L. Blanco, P. Amice, J.-M. Conia, *Synthesis* **1981**, 289–291).

[7] The diisopropylamine formed during the enolization of carbonyl compounds with LDA is bound to the enolate and plays an important role in its protonation: T. Laube, J. D. Dunitz, D. Seebach, *Helv. Chim. Acta* **1985**, *68*, 1373–1393; overview of enolate structures: D. Seebach, *Angew. Chem.* **1988**, *100*, 1685–1715; *Angew. Chem. Int. Ed. Engl.* **1988**, *27*, 1624–1654.

[8] a) N. Krause, *Chem. Ber.* **1990**, *123*, 2173–2180; b) A. Haubrich, M. van Klaveren, G. van Koten, G. Handke, N. Krause, *J. Org. Chem.* **1993**, *58*, 5849–5852.

[9] Equilibrium acidities in dimethyl sulfoxide: cyclohexanone: $pK_a = 26.4$; phenol: $pKa = 18.0$ (F. G. Bordwell, *Acc. Chem. Res.* **1988**, *21*, 456–463.

[10] a) H. E. Zimmerman, *Acc. Chem. Res.* **1987**, *20*, 263–268; b) S. Arndt, G. Handke, N. Krause, *Chem. Ber.* **1993**, *126*, 251–259.

[11] Cf.: P. E. Pfeffer, S. F. Osman, *J. Org. Chem.* **1972**, *37*, 2425–2428.

[12] Ratio *trans*-**3a** : *cis*-**3a** (determined by GC; OV-1701, H_2) in the protonation with substituted phenols: X = 2-CN: 78:22; 2-CONHPh: 72:28; 4-COMe: 67:33; 4-NH_2: 65:35; 4-OH: 62:38; 3-CO_2Et: 53:47; 3-NO_2: 53:47; 2-NO_2: 52:48; 4-OMe: 52:48; 3-Cl: 51:49; 4-CO_2Et: 50:50; 4-NO_2: 50:50; 4-Me: 48:52; 4-F: 48:52; H: 47:53; 4-Br: 44:56; 3-CF_3: 42:58; 4-Cl: 41:59; 4-I: 41:59; 4-CN: 40:60; 2-Cl: 39:61; 2-CH_2OH: 30:70; 2-COMe: 16:84; 2-CHO: 13:87; 2-CO_2Ph: 11:89; 2-CO_2tBu: 6:94; 2-CO_2Me: 4:96; 2-CO_2Et: 4:96.

[13] The use of the Hammett equation on the values obtained for the *meta*- and *para*-substituted phenols bearing donors and weak acceptors yields an approximately straight line plot ($\rho = +0.46$, $r = 0.94$). This means that the reactions with these proton sources probably have a common mechanism. Large deviations occur with nitrophenols and carbonyl-substituted phenols; this indicates that a different mechanistic pathway is followed.

[14] Collidinium trifluoroacetate, recently used for the *cis*-selective protonation of a cyclic titanium enolate [4f], is not suitable for *cis*-selective protonation of lithium enolate **2a** (product ratio: *trans*-**3a** : *cis*-**3a** = 73:27)

A Novel Approach to the Stereoselective Synthesis of β-Mannosides

Yukishige Ito and Tomoya Ogawa*

Among several problems in oligosaccharide synthesis, the formation of β-mannoside has been considered to be one of the most challenging. Since a β-mannose residue linked to the C-4 position of *N*-acetylglucosamine (GlcNAc) represents the "core" structure of asparagine (Asn)-linked oligosaccharides,[1]

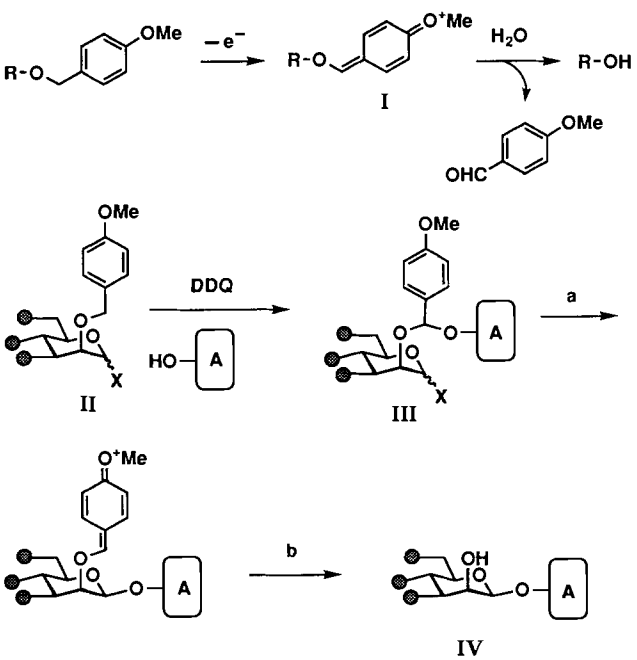
[*] Prof. Dr. T. Ogawa,[+] Dr. Y. Ito
The Institute of Physical and Chemical Research (RIKEN)
Wako-shi, Saitama 351-01 (Japan)
Telefax: Int. code + (48)462-4680

[+] Alternative address: Department of Cellular Biochemistry
Faculty of Agriculture, The University of Tokyo
Yayoi, Bunkyo-ku, Tokyo 113 (Japan)

the formation of this type of glycosidic linkage is of general significance in the field of glycoconjugate synthesis. Due to its 1,2-*cis*-arrangement, and the stereoelectronically disfavored anomeric equatorial C–O linkage, construction of β-mannosides based on conventional technology is difficult to achieve.[2] Although the "insoluble silver catalyst" (i.e. Ag silicate or zeolite) method serves as the practical approach,[3] the degree of β-selectivity is highly dependent on the reactivity of substrates. As a consequence, the proper choice of protecting groups both on the glycosyl donor and the acceptor (aglycon) is critical for substantial selectivity.[4] In addition, this method requires a highly unstable bromide as a donor. Thus, the use of modern glycosylation technologies,[5] which are now considered to be more well-adapted to complex oligosaccharide synthesis than the halide-based conventional approach, has been essentially eliminated.

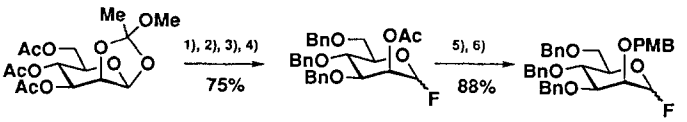
A new concept, the so-called "aglycon delivery" method has been reported by Barresi and Hindsgaul,[6] and later by Stork and Kim.[7, 8] Although complete stereochemical control could be realized, both of these approaches seem to require the manipulation of rather sensitive intermediates (isopropenyl ether or alkoxychlorosilane). Furthermore, the whole sequence is quite probably compatible only with severely limited range of protecting groups.

Taking these results into consideration, we turned our attention to *p*-methoxybenzyl (PMB) ether as a stereocontrolling element. The PMB group is frequently employed as a protecting group for an alcohol group in organic synthesis. It can be deprotected oxidatively by using 2,3-dichloro-5,6-dicyano-*p*-benzoquinone (DDQ)[9] or cerium(IV) ammonium nitrate (CAN),[10] presumably via the intermediacy of oxocarbenium species **I** (Scheme 1). Thus, starting from the mannosyl donor **II**, which



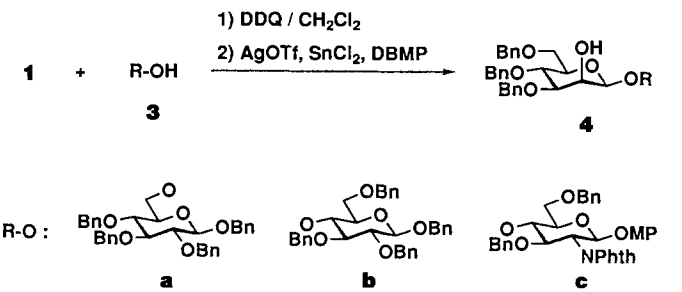
Scheme 1. Use of 2-*O*-PMB derivative for β-mannosidation. a: activation; b: workup. A = aglycon; Ac = acetyl; Bn = benzyl.

carries a PMB group at the C-2 position, we expected that treatment with alcohol in the presence of DDQ and under anhydrous conditions would give the mixed acetal **III**.[11] After subsequent activation at the anomeric position, β-mannoside (**IV**) should be formed. To examine such a possibility, mannosyl fluoride **1**[12] was synthesized in six steps from the known orthoester **2** (Scheme 2) in 65% overall yield.



Scheme 2. Preparation of mannosyl fluoride **1**. 1) NaOMe/MeOH, room temperature; 2) benzyl chloride, NaH/DMF, 0 °C → room temperature; 3) 70% AcOH, room temperature; 4) Et_2NSF_3/toluene, 0 °C; 5) iBu_2AlH/THF, −40 °C; 6) PMBCl, NaH/DMF, 0 °C → room temperature.

Compound **1** served as glycosyl donor in the β-mannosidation; its reaction with alcohols **3a–c** in CH_2Cl_2 in the presence of DDQ and molecular sieves (4 Å) proceeded smoothly to give the corresponding mixed acetal, which was treated, without purification, with $AgOSO_2CF_3$ (AgOTf) and $SnCl_2$ in the presence of 2,6-di-*tert*-butyl-4-methylpyridine (DBMP) and molecular sieves (4 Å) (Scheme 3). The disaccharides **4a–c** were obtained stereoselectively (Table 1).[13]



Scheme 3. Stereoselective mannosidation. Step 2) was performed in a solvent specified in Table 1. Phth = phthaloyl.

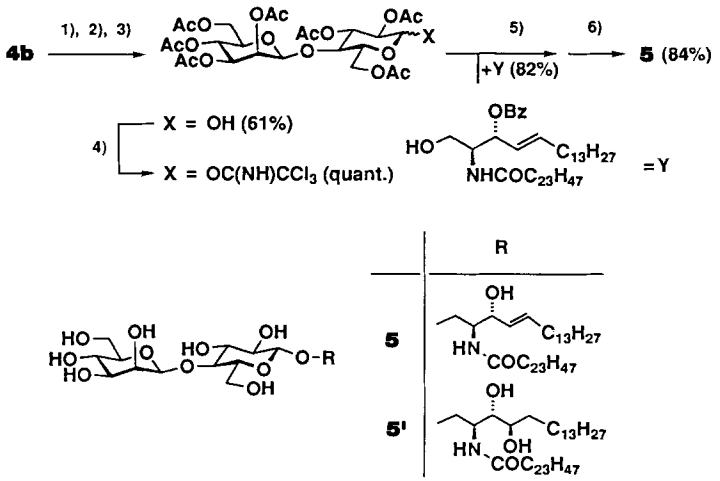
Table 1. Results of stereoselective mannosidation.

Entry	ROH	Solvent [a]	Product	Yield [%]	$[\alpha]_D$ [b]
1	**3a** [c]	Et_2O	**4a**	74	
2	**3a**	CH_2Cl_2	**4a**	65	−4.7 ($c = 1.1$)
3	**3a**	MeCN	**4a**	67	
4	**3b** [c]	CH_2Cl_2	**4b**	52	
5	**3b**	Et_2O	**4b**	45	+3.0 ($c = 0.8$)
6	**3c** [d]	CH_2Cl_2	**4c**	40	+45.2 ($c = 1.4$)

[a] Indicates the solvent used for the treatment with AgOTf/$SnCl_2$/DBMP. [b] Measured in $CHCl_3$ at 20 ± 3 °C. [c] See ref. [19a]. [d] See ref. [19b].

Although the effect of solvent seems to be minimal (entries 1–3, 4 and 5 in Table 1), the reaction in toluene was quite sluggish and resulted in an intractable mixture, presumably due to poor stabilization of the cationic intermediate. Also to be noted is that the GlcNAc derivative **3c**, which contains a *p*-methoxyphenyl (MP) group known to be sensitive under oxidative conditions,[14] could be used as a substrate.

To confirm the stereoselectivity of this transformation unambiguously, disaccharide **4b** was converted into the mannose-containing glycosphingolipid **5**[15] (Scheme 4). Synthetic **5** was compared with **5′** derived from wheat flour. The synthesis of the latter as well as that of the α-Man isomer **5′α** was reported by



Scheme 4. Synthesis of glycosphingolipid **5**. 1) H_2, $Pd(OH)_2$/C/MeOH, 45 °C; 2) Ac_2O/pyridine/DMAP, room temperature; 3) NH_2NH_2/AcOH/DMF, 50 °C; 4) CCl_3CN, 1,8-diazabicyclo[5.4.0]undec-7-ene./CH_2Cl_2, 0 C → room temperature; 5) Me_3Si-OTf, molecular sieves 4 Å/$CHCl_3$, 0 C; 6) NaOMe/THF/MeOH.

Koike et al.[16] The chemical shifts of carbohydrate portions of **5** and **5′** in the ^1H NMR spectrum were essentially identical[17] and clearly distinguishable from those of **5′α**.[18]

The method described here can be carried out simply and, more importantly, it is expected to be compatible with a variety of manipulations encountered in oligosaccharide synthesis. We are currently trying to use this approach to stereoselectively synthesize Asn-linked oligosaccharides.

Experimental Procedure

Synthesis of **4a**: To an ice-water cold mixture of DDQ (42 mg, 0.19 mmol) and powdered molecular sieves (4 Å, 0.3 g) in CH_2Cl_2 (0.5 mL) was added with stirring a solution of **1** (102.7 mg, 0.179 mmol) and **3a** (65.9 mg, 0.121 mmol) in CH_2Cl_2 (2.5 mL). After being stirred at room temperature for 3 h, the mixture was quenched by stirring with a solution of ascorbic acid (0.7%), citric acid, (1.3%), and NaOH (0.9%) in water (3 mL), diluted with ethyl acetate, and filtered through Celite. The filtrate was washed with water, aqueous $NaHCO_3$, and brine, successively, dried (Na_2SO_4), and evaporated in vacuo. After evacuation at high vacuum for 1 h the crude acetal was obtained.

The solution of the acetal in ether (8 mL) was added dropwise to an ice-water cold mixture of AgOTf (62 mg, 0.24 mmol), $SnCl_2$ (46 mg, 0.24 mmol), DBMP (59 mg, 0.24 mmol), and powdered molecular sieves (4 Å, 0.3 g) in ether (2 mL), and the mixture was stirred at room temperature for 2.5 h. After being stirred with aqueous $NaHCO_3$, the mixture was diluted with ethyl acetate, filtered through Celite, and the filtrate was washed with brine, dried ($MgSO_4$), and evaporated in vacuo. The residue was purified by silica gel column chromatography (hexane/ethyl acetate 2:1) to afford **4a** (87.1 mg, 74%): m.p. 115–117 °C (from ether/hexane); ^1H NMR (CD-Cl_3) δ = 4.50 (d, ^3J(H,H) = 8 Hz, 1H, H-1′), 4.32 (s, 1H, H-1²); ^{13}C NMR (CD-Cl_3) δ = 102.3 (^1J(C,H) = 160 Hz, C-1′), 100.2 (^1J(C,H) = 156 Hz, C-1²).

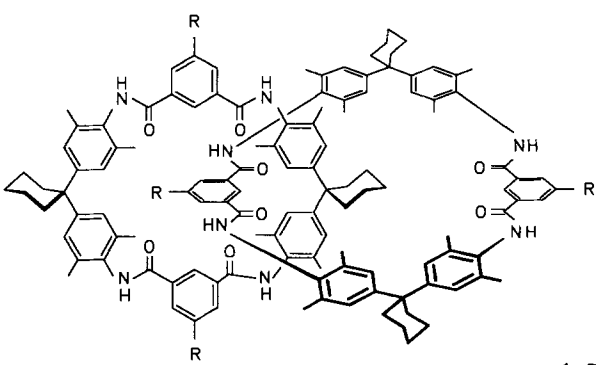
Received: April 12, 1994 [Z 6840 IE]
German version: *Angew. Chem.* **1994**, *106*, 1843

[1] J. C. Paulson, *Trends Biochem. Sci.* **1989**, *14*, 272–276.
[2] H. Paulsen, *Angew. Chem.* **1982**, *94*, 184–201; *Angew. Chem. Int. Ed. Engl.* **1982**, *21*, 155–173.
[3] P. J. Garegg, T. Iversen, *Carbohydr. Res.* **1979**, *70*, C13–C14; P. J. Garegg, C. Henrichson, T. Norberg, P. Ossowski, *ibid.* **1983**, *119*, 95–100; H. Paulsen, O. Lockhoff, *Chem. Ber.* **1981**, *114*, 3102–3114.
[4] H. Paulsen, R. Lebuhn, O. Lockhoff, *Carbohydr. Res.* **1982**, *103*, C7–C11; C. A. A. van Boeckel, T. Beetz, S. F. van Aelst, *Tetrahedron* **1984**, *40*, 4097–4107.
[5] Recent review: K. Toshima, K. Tatsuta, *Chem. Rev.* **1993**, *93*, 1503–1531.
[6] F. Barresi, O. Hindsgaul, *J. Am. Chem. Soc.* **1991**, *113*, 9376–9377; *Synlett* **1992**, 759–761.
[7] G. Stork, G. Kim, *J. Am. Chem. Soc.* **1992**, *114*, 1087–1088.
[8] Similar strategy for stereoselective α-glucosidation: M. Bols, *Tetrahedron* **1993**, *49*, 10049–10060; *Acta Chem. Scand.* **1993**, *47*, 829–834.
[9] Y. Oikawa, T. Yoshioka, O. Yonemitsu, *Tetrahedron Lett.* **1982**, *23*, 885–888.
[10] R. Johansson, B. Samuelsson, *J. Chem. Soc. Chem. Commun.* **1984**, 201–202.
[11] For cyclic *p*-methoxybenzlidene acetal by DDQ: Y. Oikawa, T. Yoshioka, O. Yonemitsu, *Tetrahedron Lett.* **1982**, *23*, 889–892.
[12] NMR data of **1** ($CDCl_3$): ^1H NMR: δ = 5.55 (dd, ^3J(H,F) = 50 Hz, ^3J(H,H) = 1.5 Hz, 0.8H; H-1α), 5.32 (d, ^3J(H,F) = 50 Hz, 0.2H; H-1β), 3.77 (s, 3H; OMe); ^{13}C NMR: δ = 107.0 (d, ^1J(C,F) = 220 Hz; C-1β), 106.5 (d, ^1J(C,F) = 222 Hz; C-1α)), 79.1, 75.0, 74.1, 74.0, 73.4, 73.2, 72.8, 72.7, 72.4, 68.6, 55.2.
[13] NMR data ($CDCl_3$): **4b**: ^1H NMR: δ = 4.62 (s, 1H; H-1²), 4.53 (d, ^3J(H,H) = 8 Hz, 1H; H-1′); ^{13}C NMR: δ = 102.6 (^1J(C,H) = 161 Hz; C-1′), 99.8 (^1J(C,H) = 159 Hz; C-1²). – **4c**: ^1H NMR: δ = 5.61 (d, ^3J(H,H) = 8 Hz, 1H; H-1′), 4.67 (s, 1H; H-1²); ^{13}C NMR: δ = 100.4 (^1J(C,H) = 157 Hz; C-1²), 97.8 (^1J(C,H) = 162 Hz; C-1′). – Data of **4a** see Experimental Procedure. All assignments were made based on an C-H COSY experiment.
[14] T. Fukuyama, A. A. Laird, L. M. Hotchkiss, *Tetrahedron Lett.* **1985**, *26*, 6291–6292.
[15] T. Hori, O. Itasaka, M. Kamimura, *J. Biochem. (Tokyo)* **1968**, *64*, 125–128; M. Sugita, S. Shirai, O. Itasaka, T. Hori, *ibid.* **1975**, *77*, 125–130.
[16] K. Koike, M. Mori, Y. Ito, Y. Nakahara, T. Ogawa, *Agric. Biol. Chem.* **1990**, *54*, 2931–2939.
[17] **5**: ^1H NMR ([D_5]pyridine/D_2O, 80 °C): δ = 5.12 (d, ^3J(H,H) = 1 Hz, 1H; H-1²), 4.72 (d, ^3J(H,H) = 8 Hz, 1H; H-1′), 4.44 (dd, ^3J(H,H) = 3 and 1 Hz, 1H; H-2²), 3.93 (dd, ^3J(H,H) = 9 and 3 Hz; H-3³), 3.86 (dd, ^3J(H,H) = 9 and 8 Hz; H-2′), 3.77 (m, 1H; H-5²), 3.67 (m, 1H; H-5′).
[18] The ^1H NMR signals of H-1² and H-2² of compound **5α′** appear at δ = 6.12 and 4.60 respectively [16].
[19] a) J.-M. Petit, J.-C. Jaquinet, P. Sinaÿ, *Carbohydr. Res.* **1980**, *82*, 130; b) T. Nakano, Y. Ito, T. Ogawa, *Tetrahedron Lett.* **1990**, *31*, 1597.

Isomeric Lactam Catenanes and the Mechanism of their Formation

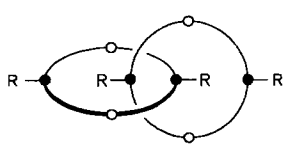
Stephan Ottens-Hildebrandt, Stephan Meier, Wolfgang Schmidt, and Fritz Vögtle*

The increasing interest in catenanes during the last years is documented by a rising number of publications.[1] Through the outstanding work of Sauvage et al.[2] and Stoddart et al.,[3] certain catenane types have been made accessible. High yields were obtained by skillful use of supramolecular template effects.[4] Likewise, the one-[5] and two-step[6] syntheses of neutral catenanes of type **1**, **2** described in 1992 were achieved with



1: R = OCH_3
2: R = H

≙



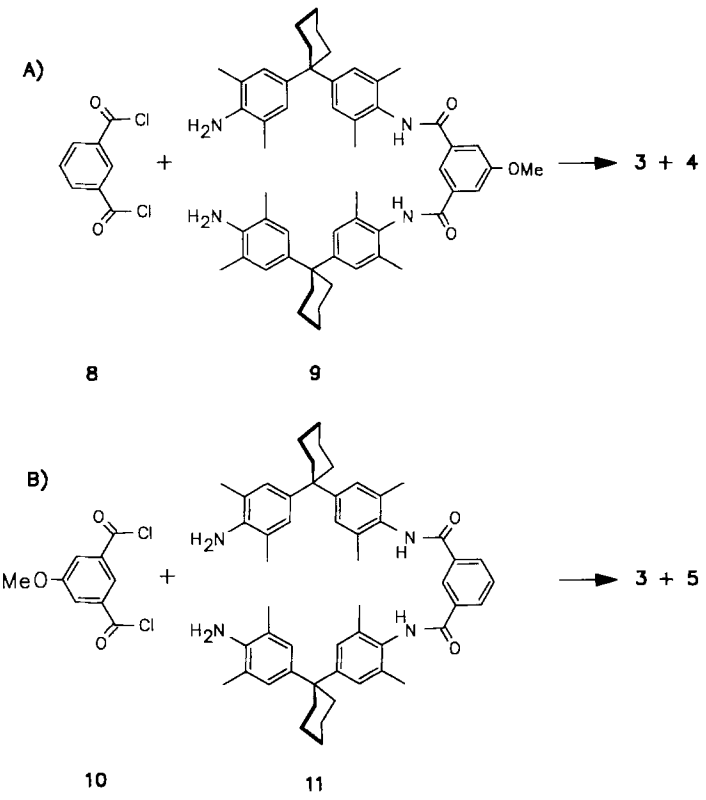
[*] Prof. Dr. F. Vögtle, Dipl.-Chem. S. Ottens-Hildebrandt, Dipl.-Chem. S. Meier, Dipl.-Chem. W. Schmidt
Institut für Organische Chemie und Biochemie der Universität
Gerhard-Domagk-Strasse 1, D-53121 Bonn (FRG)
Telefax: Int. code + (228)73-5662

amazingly simple building blocks and remarkably high yields. The question concerning the mechanism of formation of these octalactam catenanes and, in particular, the underlying template interaction has not, however, been adequately addressed. Until now it has been assumed that "orthogonalization", the perpendicular preorganization of the catenane building blocks, is based on three effects: steric complementarity, hydrogen bonding between carbonyl oxygen atoms and amide protons, and $\pi-\pi$ interactions[7] between the benzene rings of host and guest subunits.[5, 6]

Herein we report on the syntheses of the isomeric [2]catenanes **3**–**5** and of **6** (Scheme 1), and on our conclusions concerning their mechanism of formation. The synthetic strategy which leads to the monomethoxy-substituted catenane **6** makes it possible, for the first time, to obtain lactam catenanes with two different interlocking macrocycles. In this synthesis, formation of the catenanes can be detected by mass spectrometry.[8]

The isomeric [2]catenanes **3**–**5** and **6** were synthesized by three different routes (Scheme 2, A and B; Scheme 4, C). The isomers **3** and **4** were prepared by a method developed by Hunter (route A);[6] instead of the unsubstituted diamine **11**, the methoxy-substituted diamine **9** was used in the reaction with isophthaloyl dichloride (**8**). The resulting mixture contained the substituted macromonocycles **12** and **13** (Scheme 4), and the isomeric dimethoxy catenanes **3** and **4** (17 and 23% yield, respectively).[9] The products were separated by column chromatography and show characteristic differences in their NMR spectra.[10]

In an attempt to synthesize the third dimethoxy-substituted catenane isomer **5**, we performed the reaction with starting materials having a reversed substitution pattern: 5-methoxyisophthaloyl dichloride (**10**) and the diamine **11** were employed (route B). Besides the monocycles **12** and **13**, the isomers **3** and **5** were formed exclusively (2.7 and 1.4% yield, respectively). Isomer **5** was isolated by column chromatography. As expected, important portions of its NMR spectra resemble that of catenane **1**.

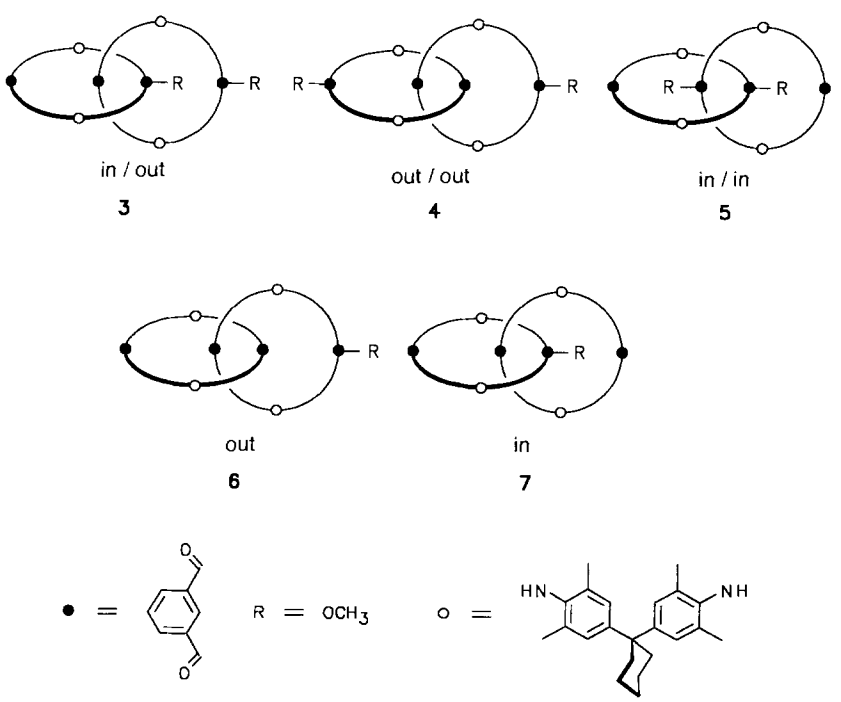


Scheme 2. Route A leads to a different set of dimethoxy-substituted catenanes (**3**, **4**) than route B (→ **3**, **5**).

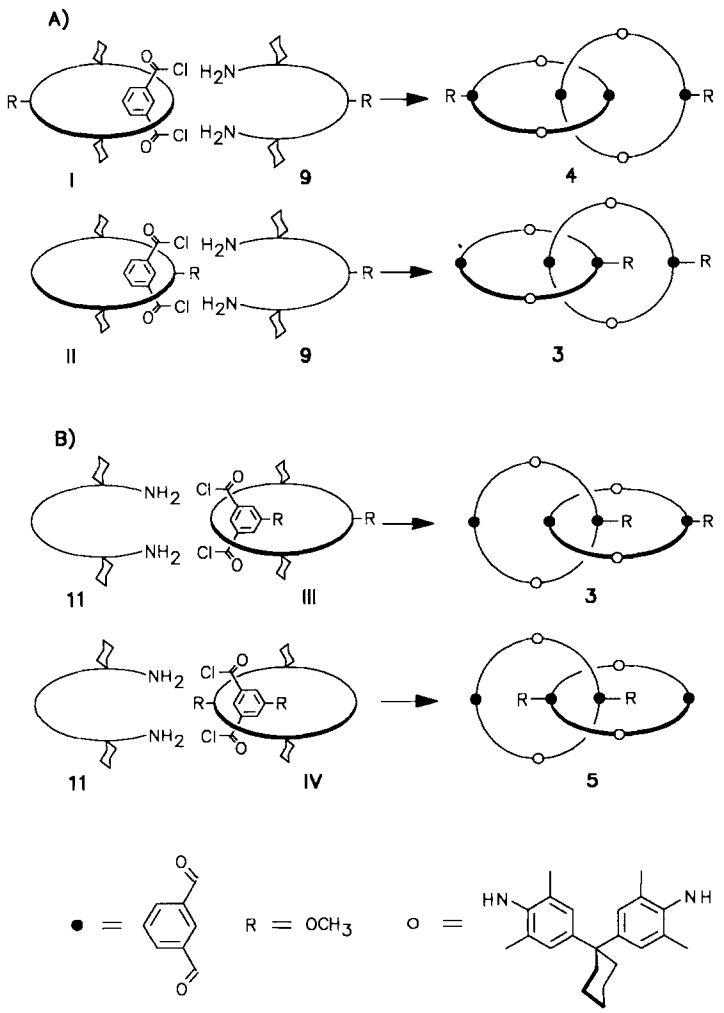
The route-dependent, selective formation of the stable isomers **4** and **5**[11] allows conclusions to be drawn about the mechanism of ring interlocking. We assume that the supramolecular template effect, which is responsible for catenation, results from the respective diacid dichlorides (**8**, **10**) "lodging" as guests in the host, the intermediate macromonocycle **12**, in such a way that the metaphenylene ring of the guest is orthogonal to the ring plane of the host (Scheme 3).[12] Because of the two isophthaloyl binding sites in the host cycle, there are two possible orientations (I, II and III, IV, respectively) for each acid chloride (**8** and **10**). Routes A and B thus lead to selective formation of isomers **4** and **5**, respectively, in addition to **3**.

This mechanism provides an explanation for the significantly different yields obtained in routes A and B: In the case of route B, the methoxy substituent on the diacid dichloride may cause steric hindrance in the host–guest complexes. Catenanes **3** and **5** in route B should thus be formed in lower yields than **3** and **4** in route A.

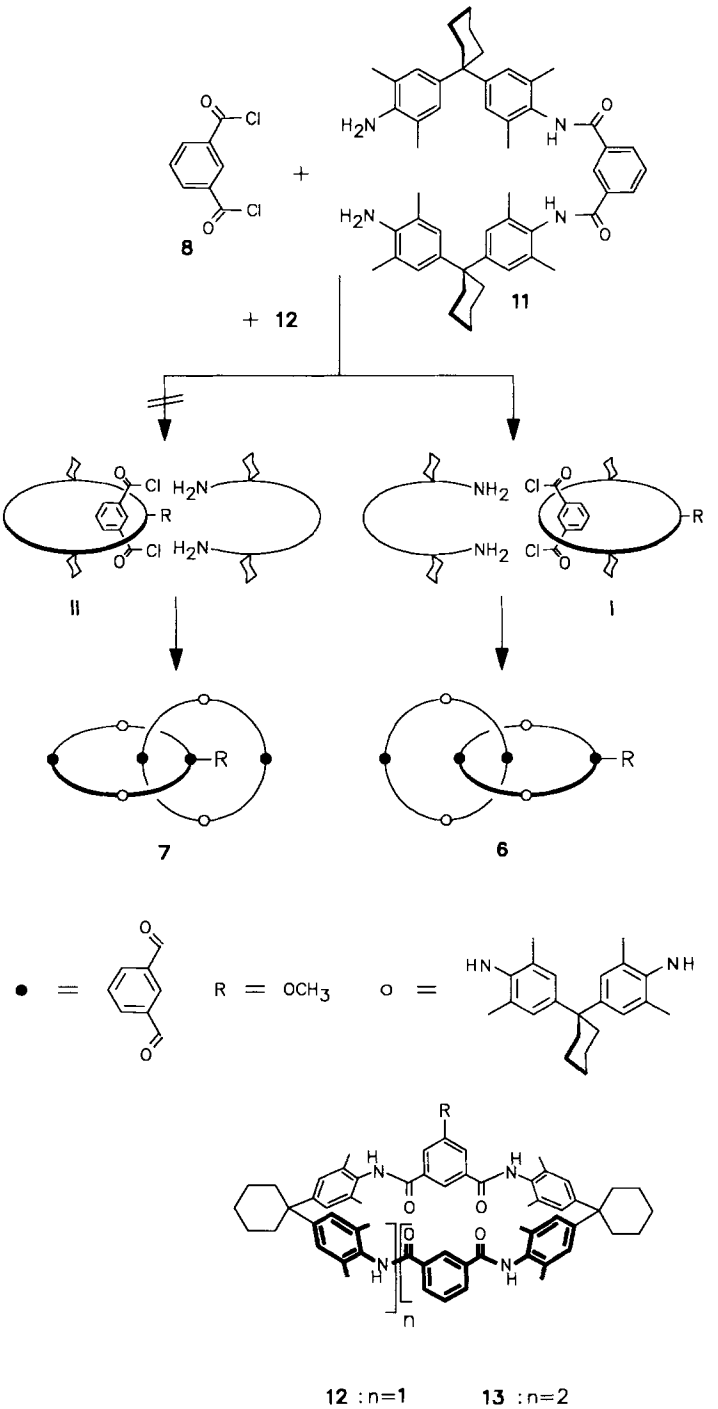
To provide further evidence for the hypothesis that the reaction proceeds via an intermediate monocycle of type **12**, we carried out a synthesis following route C (Scheme 4). Building blocks **8** and **11**, which have already been used by Hunter et al. for other targets,[6] were mixed in the presence of macrocycle **12**, obtained as a byproduct in routes A and B. Of the two possible monomethoxy-substituted isomers **6** and **7**, only **6** was formed in 3%



Scheme 1. The three isomeric disubstituted catenanes **3**–**5** and the isomeric monosubstituted catenanes **6** and **7**.



Scheme 3. The proposed template and orthogonalization mechanism (cf. I–IV) provides an explanation for the formation of different catenane isomers (**3**, **4** and **3**, **5**) in routes A and B.



12 : n=1 **13** : n=2

Scheme 4. Route C. The "catenation" of the macromonocycle **12** with **8** and **11** leads to formation of catenane **6**. The guest diacid dichloride **8** and the host **12** are locked in an orthogonal arrangement (**I**). The functional groups are fixed and thus preorganized for reaction with the diamine **11**.

yield. The combination of the three reaction components **8**, **11**, and **12** to form a single product is consistent with our proposed orthogonalization and interlocking mechanism shown in Schemes 3 and 4. Other mechanisms, in particular the interlocking of two open-chain fragments such as **8** with **9** or **9** with **9**, do not appear to be significant.

An advantage of route C lies in the fact that the catenane **6** formed from the monocycle **12** can be identified unambiguously from the molecular peak in the mass spectrum, because the isomeric macromonocycle (identical molecular mass) cannot be formed in route C.

The orthogonalization and interlocking mechanism has far-reaching consequences: In future more reagents of types I–IV will become available, in which a host cavity (e.g., **12**) and a (di)functionalized guest (e.g., **8**, **10**) are bound together by macromolecular interactions in an orthogonalized precatenane (prerotaxane, cf. I–IV) bearing two reactive groups. The synthesis of a variety of other catenanes by reaction with other partners and the formation of rotaxanes have now become feasible.

Experimental Procedure

Route A: 1.04 g (1.29 mmol) **9** mixed with 0.4 mL triethylamine and 0.26 g (1.29 mmol) **8**, each dissolved in 250 mL anhydrous dichloromethane, were added simultaneously over 24 h under argon to 1 L of stirred anhydrous dichloromethane. The solvent was evaporated in vacuo and the residue dissolved in 300 mL chloroform. The organic layer was washed with 50 mL water, dried over $MgSO_4$, filtered, and concentrated in vacuo. The residue was purified by column chromatography (SiO_2, 40–60 μm; dichloromethane/ethyl acetate 7:1). Four fractions were isolated: First fraction (catenane isomer **4**): Yield 300 mg (23%); thin-layer chromatography (TLC): $R_f = 0.58$ (SiO_2, dichloromethane/ethyl acetate 7/1); m.p. >300 °C (decomp.); ^{1}H NMR (400 MHz, $CDCl_3/CD_3OD$ 95/5): $\delta = 0.37$ (s, 6H; Ar-CH_3), 0.72 (s, 6H; Ar-CH_3), 1.00–2.40 (m, 76H; Ar-CH_3 and aliphatic CH_2), 3.64 (s, 6H; OCH_3), 6.02, 6.06 (broad, 4H; arom. H), 6.45–6.60 (broad, 4H; arom. H), 6.78, 6.84 (broad, 4H; arom. H), 7.00–7.10 (broad, 4H; arom. H), 7.13 (dt, $^3J = 8$, $^4J = 1.5$ Hz, 2H; arom. H), 7.17 (t, $^3J = 8$ Hz, 2H; arom. H), 7.31 (pseudo-t;

$^4J = 1.5$, $^4J = 1.5$ Hz, 2H; arom. H), 7.60 (pseudo-t, $^4J = 1.5$, $^4J = 1.5$ Hz, 2H; arom. H), 7.78 (dt, $^3J = 8$, $^4J = 1.5$ Hz, 2H; arom. H), 7.88 (t, $^4J = 1.6$ Hz, 2H; arom. H), 8.26 (t, $^4J = 1.5$ Hz, 2H; arom. H); ^{13}C NMR (62.9 MHz, $CDCl_3$/CD_3OD 95/5): δ = 16.71, 17.90, 18.20, 18.32, (Ar-CH_3), 22.81, 26.18, 34.24, 34.52, 35.93, 36.23 (CH_2), 44.62, 45.11 (C_q), 55.42 (OCH_3), 116.85, 117.37, 122.85, 125.03, 127.42, 127.68, 128.37, 129.52, 130.75 (CH), 125.50, 130.08, 130.21, 130.83, 130.88, 130.95, 132.62, 133.70, 134.15, 134.29, 134.72, 134.79, 135.70, 135.81, 136.06, 146.15, 146.36, 148.56, 149.44, 160.48, 163.20, 163.98, 164.04, 166.27, 166.34, 168.75 (C_q); FAB-MS: *m/z*: 1871.0 [$(M + H)^+$] ($C_{122}H_{132}N_8O_{10}$: 1870.43).

Second fraction (catenane isomer **3**): Yield 220 mg (17%); TLC (SiO_2): R_f = 0.32 (dichloromethane:ethyl acetate 7:1); m.p. > 300 °C (decomp.); ^{1}H NMR (250 MHz, CD_2Cl_2/CD_3OD 95/5): δ = 0.61 (s, 6H; Ar-CH_3), 0.90–2.70 (m, 82H; Ar-CH_3 and aliphatic CH_2), 3.85, 3.90 (s, 6H; OCH_3), 6.29, 6.32 (broad, 4H; arom. H), 6.79 (broad, 4H; arom. H), 6.97 (broad, 1H; arom. H), 7.05, 7.12 (broad, 4H; arom. H), 7.20–7.36 (broad, 4H; arom. H), 7.42 (broad, 2H; arom. H), 7.51 (broad, 1H; arom. H), 7.60–7.70 (m, 3H; arom. H), 7.80–7.95 (m, 2H; arom. H), 8.08 (d, $^3J = 8$ Hz, 1H; arom. H), 8.09 (broad, 1H; arom. H), 8.32 (d, $^3J = 8.2$ Hz, 1H; arom. H), 8.34, 8.47 (s, 2H; amide H), 8.55 (broad, 1H; arom. H), 8.77 (broad, 1H; arom. H), 8.91 (broad, 1H; arom. H), 8.93, 9.08, 9.14, 9.22, 9.28 (s, 5H; amide H); ^{13}C NMR (62.9 MHz, $CDCl_3$/CD_3OD 95/5): δ = 17.01, 18.12, 18.34, 18.53, 18.66 (Ar-CH_3), 23.31, 26.61, 34.67, 34.90, 36.30, 36.64 (CH_2), 45.08, 45.12, 45.52 (C_q), 55.93, 56.32 (OCH_3), 112.09, 117.22, 117.43, 118.10, 123.41, 123.68, 125.06, 125.53, 127.96, 128.57, 131.15, 132.32 (CH), 129.67, 130.90, 131.09, 131.33, 131.39, 131.55, 132.21, 132.32, 133.14, 133.51, 134.26, 134.70, 134.84, 134.95, 135.07, 135.32, 136.17, 136.24, 136.34, 136.51, 137.58, 146.43, 146.57, 149.05, 149.89, 160.68, 160.86, 163.54, 163.63, 164.26, 166.41, 166.78, 168.91, 169.20 (C_q); FAB-MS: *m/z*: 1869.8 [$(M + H)^+$].

Third fraction (dimer **12**): Yield 370 mg (28%); TLC (SiO_2): R_f = 0.28 (dichloromethane:ethyl acetate 7:1); m.p. > 300 °C (decomp.); ^{1}H NMR (400 MHz, $CDCl_3$/CD_3OD 95/5): δ = 1.51 (broad, 4H; aliphatic CH_2), 1.63 (broad, 8H; aliphatic CH_2), 2.16 (s, 24H; Ar-CH_3), 2.32 (broad, 8H; aliphatic CH_2), 3.92 (s, 3H; OCH_3), 6.98 (s, 8H; arom. H) 7.63 (d, $^4J = 1.5$ Hz, 2H; arom. H), 7.64 (t, $^3J = 5$ Hz, 1H; arom. H), 7.92 (t, $^4J = 1.5$ Hz, 1H; arom. H), 8.09 (dd, $^3J = 5$, $^4J = 1.5$ Hz, 2H; arom. H), 8.33 (t, $^4J = 1.5$ Hz, 1H; arom. H); ^{13}C NMR (62.9 MHz, $CDCl_3$/CD_3OD 95/5): δ = 17.85 (Ar-CH_3), 22.52, 25.92, 34.97 (CH_2), 44.80 (C_q), 55.17 (OCH_3), 116.33, 118.50, 125.97, 129.10, 130.98 (CH), 130.74, 130.93, 134.64, 134.66, 135.50, 147.79, 160.41, 166.37, 166.67 (C_q); FAB-MS: *m/z*: 935.5 [$(M + H)^+$] ($C_{61}H_{66}N_4O_5$: 935.22).

Fourth fraction (tetramer **13**): Yield 100 mg (7.7%); TLC (SiO_2): R_f = 0.1 (dichloromethane:ethanol 50:1); m.p. > 300 °C (decomp.); IR (KBr): $\tilde{\nu}$[cm^{-1}] = 3288 (br), 2925 (s), 2855 (s), 1656 (s), 1593 (m), 1500 (vs), 1372 (m), 1361 (s), 1252 (s), 1170 (m), 1051 (m), 856 (m), 752 (m), 723 (m); FAB-MS: *m/z*: 1870.9 [$(M + H)^+$].

Route B: Analogous to route A, but with 1.00 g (1.29 mmol) **11** and 0.30 g (1.29 mmol) **10**. The residue was chromatographed on silica gel (40–60 μm) (dichloromethane:ethyl acetate 7:1). Four fractions were isolated:

First fraction (catenane isomer **3**): Yield 35 mg (2.7%).
Second fraction (catenane isomer **5**): Yield 18 mg (1.4%); TLC (SiO_2): R_f = 0.22 (dichloromethane:ethyl acetate 50:1); m.p. > 300 °C (decomp.): ^{1}H NMR (250 MHz, $CDCl_3$/CD_3OD 95/5): δ = 0.35, 0.77 (s, 12H; Ar-CH_3), 1.00–2.50 (m, 76H; Ar-CH_3 and aliphatic CH_2), 3.63 (s, 6H; OCH_3), 6.06, 6.09 (broad, 4H; arom. H), 6.45–6.55 (broad, 4H; arom. H), 6.65 (broad, 2H; arom. H), 6.8 (broad, 2H; arom. H), 6.86 (broad, 2H, arom. H) 6.95–7.15 (broad, 4H, arom. H), 7.36 (t, $^3J = 7.7$ Hz, 2H; arom. H), 7.40, 7.45 (broad, 4H; arom. H), 7.8 (t, $^3J = 7.7$ Hz, 2H; arom. H), 8.10 (t, $^3J = 7.7$ Hz, 2H; arom. H), 8.65 (broad, 2H; arom. H); ^{13}C NMR (62.9 MHz, $CDCl_3$/CD_3OD 95/5): δ = 16.39, 17.84, 18.07, 18.13, 18.06 (Ar-CH_3), 22.66, 26.05, 34.20, 34.50, 35.99, 36.21 (CH_2), 44.49, 44.96 (C_q), 55.55 (OCH_3), 111.26, 117.38, 122.75, 123.22, 124.70, 124.92, 127.30, 128.28, 129.13, 131.67, 131.84 (CH), 130.26, 130.67, 130.74, 130.80, 130.96, 132.47, 133.18, 133.80, 134.04, 134.43, 134.66, 135.82, 135.57, 136.86, 146.21, 145.97, 148.32, 149.33, 160.07, 163.11, 164.01, 167.07, 168.62 (Cq); FAB-MS: *m/z*: 1869.9 [$(M + H)^+$].
Third fraction (dimer **12**): Yield 310 mg (23%).
Fourth fraction (tetramer **13**): Yield 120 mg (9.2%).

Route C: 200 mg **12** (0.21 mmol) was dissolved in 1 L anhydrous $CHCl_3$, 1.00 g (1.29 mmol) **11** mixed with 0.4 mL triethylamine and 0.26 g (1.29 mmol) **8**, each dissolved in 250 mL anhydrous $CHCl_3$, were added simultaneously to the first solution over 24 h under an argon atmosphere. The solvent was evaporated in vacuo, and the residue dissolved in 300 mL chloroform. The organic layer was washed with 50 mL water, dried over $MgSO_4$, filtered, and concentrated in vacuo. The residue was purified by column chromatography (SiO_2, 40 60 μm; dichloromethane/ethyl acetate 7/1). One fraction was isolated (catenane isomer **6**): Yield 40 mg (3%): TLC (SiO_2): R_f = 0.73 (dichloromethane: acetone 10:1); m.p. > 300 °C (decomp.); ^{1}H NMR (400 MHz, $CDCl_3$/CD_3OD 95/5): δ = 0.28, 0.61 (s, 12H, Ar-CH_3), 0.70–2.25 (m, 76H, Ar-CH_3 and aliphatic CH_2), 3.52 (s, 3H; OCH_3), 5.91, 5.96 (broad, 4H; arom. H), 6.40–6.50 (broad, 4H; arom. H), 6.69, 6.73 (broad, 4H; arom. H), 6.90–6.99 (broad, 4H; arom. H), 6.99–7.02 (m, 2H; arom. H) 7.08 (t, $^3J = 3$ Hz, 2H; arom. H), 7.20 (broad, 1H; arom. H), 7.28 (t, $^3J = 8$ Hz, 1H; arom. H), 7.50 (broad, 1H; arom. H), 7.68 (d, $^3J = 7$ Hz, 2H; arom. H), 7.70 (d, $^3J = 7$ Hz, 1H; arom. H), 7.78 (broad, 2H; arom. H), 7.97 (d, $^3J = 8$ Hz, 1H; arom. H) 8.14 (s, 1H; arom. H), 8.53 (s, 1H; arom. H); ^{13}C NMR (62.9 MHz, $CDCl_3$/CD_3OD 95/5): δ = 17.18, 17.89, 18.39, 18.59, 18.73, 19.10 (Ar-CH_3), 23.41, 26.74, 34.74, 35.05, 36.46, 36.78 (CH_2), 45.23, 45.68 (C_q), 56.03 (OCH_3), 117.63, 123.48, 125.04, 125.71, 126.98, 127.98, 128.26, 128.73, 128.88, 130.23, 131.31, 132.28 (CH), 129.82, 131.10, 131.44, 131.63, 131.75, 132.56, 133.24, 134.39, 134.85, 135.22, 135.45, 136.36, 136.57, 146.64, 147.00, 149.17, 150.10, 161.04, 163.84, 164.40, 164.50, 164.90, 169.40 (C_q); FAB-MS: *m/z*: 1840.41 [$(M + H)^+$] ($C_{121}H_{130}N_8O_6$: 1840.41); calcd: N 6.09, found: N 6.14%.

Received: March 30, 1994 [Z 6814 IE]
German version: *Angew. Chem.* **1994**, *106*, 1818

[1] Overview: G. Schill, *Catenanes, Rotaxanes, and Knots*, Academic Press, New York, **1971**; D. Philp, J. F. Stoddart, *Synlett* **1991**, 445–458; G. Schill, N. Schweickert, H. Fritz, W. Vetter, *Angew. Chem.* **1983**, *95*, 909–911; *Angew. Chem. Int. Ed. Engl.* **1983**, *22*, 889; *Chem. Ber.* **1988**, *121*, 961; D. M. Walba, R. M. Richards, M. Hermsmeier, R. C. Haltiwanger, *J. Am. Chem. Soc.* **1987**, *109*, 7081–7087, and references therein; cf. also G.-J. M. Gruter, F. J. J. de Kanter, P. R. Markies, T. Nomoto, O. S. Akkerman, F. K. Bickelhaupt, *J. Am. Chem. Soc.* **1993**, *115*, 12179–12180; M. Fujita, F. Ibukuro, H. Hagihara, K. Ogura, *Nature* **1994**, *367*, 723.

[2] See for example: C. O. Dietrich-Buchecker, J. P. Sauvage, *Bioorg. Chem. Front.* **1991**, *2*, 195–248; C. O. Dietrich-Buchecker, B. Frommberger, I. Lüer, J.-P. Sauvage, F. Vögtle, *Angew. Chem.* **1993**, *105*, 1526–1529; *Angew. Chem. Int. Ed. Engl.* **1993**, *32*, 1434, and references therein.

[3] D. Armspach, P. R. Ashton, C. P. Moore, N. Spencer, J. F. Stoddart, T. J. Wear, D. J. Williams, *Angew. Chem.* **1993**, *105*, 944–948; *Angew. Chem. Int. Ed. Engl.* **1993**, *32*, 854; D. B. Amabilino, P. R. Ashton, M. S. Tolley, J. F. Stoddart, D. J. Williams, *ibid.* **1993**, *105*, 1358–1362 or **1993**, *32*, 1297, and references therein; cf. also F. Vögtle, W. M. Müller, U. Müller, M. Bauer, K. Rissanen, *ibid.* **1993**, *105*, 1356–1358 and **1993**, *32*, 1295.

[4] F. Vögtle, R. Hoss, *Angew. Chem.* **1994**, *106*, 389; *Angew. Chem. Int. Ed. Engl.* **1994**, *33*, 375–384; S. Anderson, H. L. Anderson, J. K. M. Sanders, *ibid.* **1992**, *104*, 921–924 and **1992**, *31*, 907; *Acc. Chem. Res.* **1993**, *26*, 469–475.

[5] F. Vögtle, S. Meier, R. Hoss, *Angew. Chem.* **1992**, *104*, 1628–1631; *Angew. Chem. Int. Ed. Engl.* **1992**, *31*, 1619–1622.

[6] C. A. Hunter, *J. Am. Chem. Soc.* **1992**, *114*, 5303–5311.

[7] C. A. Hunter, *Angew. Chem.* **1993**, *105*, 1653–1655; *Angew. Chem. Int. Ed. Engl.* **1993**, *32*, 1584; C. A. Hunter, J. K. M. Sanders, *J. Am. Chem. Soc.* **1990**, *112*, 5525–5534.

[8] Reported partly at GDCh lectures in Constance (December 8, 1993), Cologne, Münster, Tübingen, and Krefeld as well as at lectures in Ravello and Stockholm.

[9] The remaining products from routes A–C consisted of mixtures of open-chain and monocyclic higher oligomers, which were not separated chromatographically.

[10] The structures of the various isomers were confirmed by the ^{1}H NMR, ^{13}C NMR (see *Experimental Procedure*), and, in particular, NOESY spectra. Using electrospray mass spectrometry, Prof. Dr. M. Przybylski, Universität Konstanz, is attempting to distinguish between catenane isomers **3**–**5**.

[11] No interconversion or equilibration of the isomeric catenanes could be observed even at higher temperature (300 °C). The translation of the rings seems to be hindered by the cyclohexyl residues, as proposed in earlier publications [6, 7].

[12] We do not exclude the possibility that the isopthaloyl dichloride (**8** or **10**) already forms *one* amide bond with the corresponding diamine (**9** or **11**) before "lodging" in the host.

Synthesis and Characterization of the First Thiaselanes**

Josef Hahn* and René Klünsch

Until now selanes H_2Se_x and the thiaselanes $H_2S_ySe_{x-y}$ derived from them by selenium–sulfur exchange were only known in the form of organo[1] and chloro derivatives.[2] We report here on the synthesis and NMR spectroscopic characterization of thiaselanes with the general formula $H_2S_mSe_n$, as well as on the isolation of

[*] Prof. Dr. J. Hahn, Dipl.-Chem. R. Klünsch
Institut für Anorganische Chemie der Universität
Greinstrasse 6, D-50939 Köln (FRG)
Telefax: Int. code + (221)470-5196

[**] This work was supported by the Deutsche Forschungsgemeinschaft (SFB 301).

1,3-dithiatriselane H-S-Se-S-H (**1**), a solid which melts at −40 °C. It is surprising that attempts to synthesize thiaselanes have been unsuccessful so far, since binary sulfur–hydrogen compounds H_2S_x with chain lengths of up to $x = 35$ are known.[3] The conversion of sulfanes into thiaselanes according to the general reaction (a)

$$-S-S- + Se-Se- \longrightarrow 2\,S-Se- \quad (a)$$

should, on the basis of calculations,[4] be exothermic. Furthermore, on the basis of these calculations, as well as from a simple comparison of the stability of thiols and selenols, it is expected that isomers containing SH groups are favored over those with SeH groups. Therefore, our first efforts concentrated on the synthesis of α,ω-dithiaselanes.

Initial attempts to produce thiaselanes using a method based on a gentle synthesis of sulfanes[5] by protolysis of silylated selenium–sulfur chains of the general formula $(MePh_2Si)_2S_2Se_n$ and $(Ph_3Si)_2S_2Se_n$ failed owing to the instability of the starting materials.[6] However, the desired products were obtained by condensing hydrogen sulfide and dichlorodiselane [Eq. (b)].

$$2\,H_2S + Se_2Cl_2 \longrightarrow \underset{\mathbf{2}}{H-S-Se\ Se-S-H} + 2\,HCl \quad (b)$$

Because the starting materials as pure substances react very vigorously with each other even at low temperatures, liquid hydrogen sulfide (in excess) was treated at −78 °C with a very dilute solution of dichlorodiselane (ca. 6 wt% in CS_2). Under these conditions an orange-yellow solution and a small amount of an orange-red solid is formed. In the orange-red solution remaining after evaporation of the hydrogen sulfide at −40 °C only thiaselanes of differing composition could be detected by NMR spectroscopy (Table 1).

Table 1. ^1H and ^{77}Se NMR parameters (δ(Se) relative to Me_2Se) of the thiaselanes from reaction (b); saturated solution in CS_2/[D_6]-benzene 6/1 at 295 K.

	δ(H) [a]	δ(Se) [a]	^2J	^3J(Se,H)[Hz] [b]	^4J
H–S, Se, H–S **1**	3.43	527	3.53	–	–
H–S–Se, H–S–Se **2**	3.52	729	3.65	2.60	–
$H-S^1-Se^2$, $H-S^5-Se^4$, Se^3 **3**	3.59	685 (2, 4) 918 (3)	3.49	2.10	1.10
$H-S^1-Se^2$, $H-S^6-Se^5$, Se^3, Se^4 **4**	3.66	682 (2, 5) 887 (3, 4)	3.53	2.54	1.66
H–S–Se, S, H–S–Se **5**	3.62	750	3.65	–	1.32
$H^a-S^1-Se^2-S^3$, $H^b-S^6-Se^5-Se^4$ **6**	3.69 (a) 3.68 (b)	749 (2) 954 (4) 690 (5)	3.65 (a, 2) 3.60 (b, 5)	– 2.32 (b, 4)	1.94 (a, 4) –

[a] The atoms which correspond to the δ-values are given in brackets. [b] The coupling atoms are given in brackets.

1,4-Dithiatetraselane **2**, the expected product according to Equation (b), was not the major product even under optimum reaction conditions. Due to a disproportionation reaction it was obtained along with 1,3-dithiatriselane **1** in the molar ratio 1:1.7 to 1:3. Further disproportionation products were disulfane and dithiaselanes with more than four chalcogen atoms. Disproportionation is fast during the condensation reaction; afterwards it is notably slower. Disproportionation of the product mixture was almost halted at −78 °C, and could be forced back into the above range during the reaction by a high concentration of HCl (saturation of the liquid hydrogen sulfide with HCl prior to the start of the reaction). At room temperature (Ar atmosphere) the half-life of dithiatetraselane **2** in dilute CS_2 solution is about 20 h, whereas that of the more stable dithiatriselane **1** is roughly 5 d. From changes in concentration in the CS_2 solution it is concluded that there is a stepwise disproportionation in which one selenium atom is transferred at a time [Eq. (c)]. Because of their low solubility, the higher thiaselanes precipitated and could no longer be detected by NMR spectroscopy.

$$H-S-Se_o-S-H + H-S-Se_p-S-H \longrightarrow H-S-Se_{o-1}-S-H + H-S-Se_{p+1}-S-H \quad (c)$$

1,3,5-Trithiapentaselane **5** and 1,3,6-trithiahexaselane **6** are derived formally from 1,4,7-trithiaheptaselane (not detected) by the cleavage of two and one selenium atoms, respectively. In spite of the large excess of H_2S, compounds of this type can arise directly from the secondary reaction (d), or by subsequent disproportionation (for $n = 2$).

$$H_2S_2Se_n + Se_2Cl_2 + H_2S \longrightarrow H-S-Se_n-S-Se_2-S-H + 2\,HCl \quad (n = 1.2) \quad (d)$$

After removal of the solvent at −50 °C a mixture of thiaselanes was obtained as an orange-red solid which turns into a dark red oil above −40 °C. The solid was no longer completely soluble in CS_2; however, the soluble fraction contained approximately the original distribution of thiaselanes. 1,3-Dithiatriselane **1** could be sublimed in vacuo (10^{-5} mbar) at −45 °C from the orange-red solid. It could be trapped at −78 °C without other more volatile disproportionation reaction products, and could be isolated as a pale yellow solid which melts at −40 °C with decomposition. The only impurity was the less volatile 1,4-dithiatetraselane **2** (3–5 mol%).

Mixtures of thiaselanes containing more sulfur could also be obtained in a synthesis analogous to that above. The tetrathiaselanes **7**–**9** (Table 2) arise in the synthesis of 1,2,5,6-tetrathiahexaselane **8** by dropwise addition of a solution of Se_2Cl_2 (ca. 4 wt% in CS_2) into solvent-free disulfane saturated with HCl (molar ratio 1:100) at −78 °C [Eq. (e)]. This condensation reaction is also accompanied by disproportionation, and the tetrathiaselanes with one, two, and three Se atoms **7**, **8**, and **9**, respectively, were present in the molar ratio 1.5:1:0.5.

$$2\,H_2S_2 + Se_2Cl_2 \longrightarrow H-S-S-Se-Se-S-S-H + 2\,HCl \quad (e)$$

Table 2. ^1H and ^{77}Se NMR parameters (δ(Se) relative to Me_2Se) of the thiaselanes from reaction (e); reaction solution/[D_6]benzene 6/1 at 295 K; $\delta(Se)_{calcd}$ was estimated using the equation in Scheme 1.

	δ(H)	$\delta(Se)_{exp.}$ [a]	$\delta(Se)_{calcd}$	^3J(Se,H)[Hz]	^4J
H–S–S, Se, H–S–S **7**	4.20	1059	1055	2.49	
H–S–S–Se, H–S–S–Se **8**	4.23	967	955	2.84	1.54
$H-S^1-S^2-Se^3$, $H-S^7-S^6-Se^5$, Se^4 **9**	4.25	948 (3, 5) 834 (4)	945 855	[b]	[b]

[a] See Table 1. [b] Not determined.

The conclusive identification of the thiaselanes in the mixtures was achieved by ^1H and ^{77}Se NMR spectroscopy. The most impor-

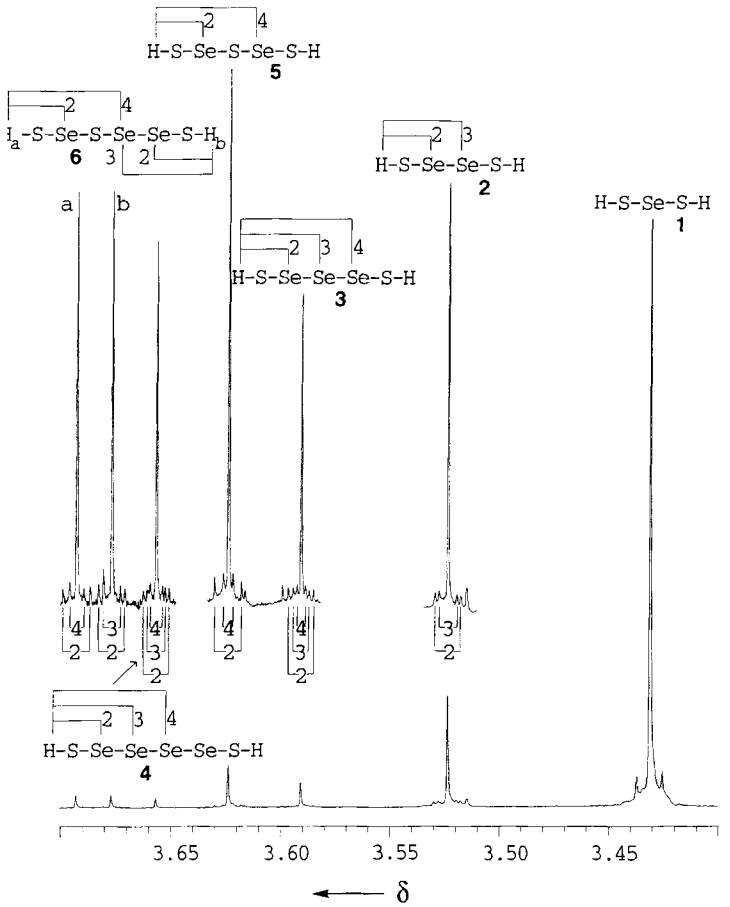


Fig. 1. ^{1}H NMR spectrum of the thiaselanes from reaction (b). The labels on the signals indicate the satellites due to ^{77}Se,^{1}H coupling. Additionally, the number of bonds is given through which the nuclei are coupled; this number is repeated in the structural formulae; frequency 300.13 MHz; temperature 295 K.

tant relationships between the structure and NMR parameters are summarized here.

1. The number of Se atoms in a molecule can be derived from the number of ^{77}Se satellite pairs[7] in the ^{1}H NMR spectrum (Fig. 1). Within a molecule, the value of the coupling constant decreases with the number of bonds separating the coupling nuclei.

2. The δ(H) values[8] increase with increasing chain length (**1** → **2** → **3** → **4**, **5** → **6**, Table 1; **7** → **8** → **9**, Table 2). A downfield shift also results, to a lesser extent, when one selenium atom is exchanged for one sulfur atom while the chain length remains constant (**3** → **5**, **4** → **6**, Table 1).

3. The environment of the ^{77}Se nuclei has, as expected, a very strong influence on their magnetic shielding. According to the equation in Scheme 1, δ(Se) of a given Se atom is dependant on the number of Se and S atoms in the α-, β-, and γ-positions. As is found for alkanes[9] and phosphanes,[10] the neighboring atoms in the α- and β-positions cause a downfield shift and those in γ-positions an upfield shift. Consistent with the greater electronegativity, the constants for sulfur are always more positive (stronger downfield shifts).

The constitution of the thiaselanes **1**–**9** follows unequivocally from the structural dependence of the NMR parameters (points 1–3). This means that in addition to the known interchalcogen–hydrogen compounds of oxygen and sulfur, H-S-O-H[11] and H-O-S-S-O-H,[12] those of sulfur and selenium have now been synthesized. In contrast to the former compounds, the oxasulfanes, which have only been detected by matrix or neutralization–reionization mass spectrometry, the thiaselanes can be obtained on a preparative scale. Thus, in addition to the isolation of H-S-Se-S-H **1**, the separation of the higher homologues as pure compounds and the investigation of their chemical reactions looks promising.

$\delta(\mathrm{Se}) = -227 + i\,\alpha_X + j\,\beta_X + k\,\gamma_X \pm 5$; X = S, Se

i, j, k = number of S or Se atoms in α, β, and γ positions, respectively

$\alpha_S = 377$, $\beta_S = 264$, $\gamma_S = -34$, $\alpha_{Se} = 311$, $\beta_{Se} = 254$, $\gamma_{Se} = -36$

Scheme 1. Calculation of δ(Se) with chemical shift increments.

Experimental Procedure

The thiaselanes were synthesized under inert conditions (argon atmosphere). All glassware used must be completely free of grease, and acidified by boiling in concentrated hydrochloric acid.

$H_2S_2Se_n$: Hydrogen sulfide (300 mL, 280 g, 4.2 mol), dried over P_4O_{10}, was condensed into a reaction flask at −78 °C, and dried (P_4O_{10}) HCl gas was added until saturation. With continued cooling and vigorous stirring, a solution of Se_2Cl_2 (5 g, 22 mmol) in CS_2 (70 mL) was added from a dropping funnel cooled to −78 °C. The mixture was stirred for 1 h and subsequently excess H_2S condensed off. For complete removal of H_2S, the mixture was warmed to −50 °C in vacuo (1 mbar).

$H_2S_4Se_n$: H_2S_2 and Se_2Cl_2 were reacted analogously to the synthesis given above. A solution of Se_2Cl_2 (0.92 g, 4 mmol) in CS_2 (20 mL) was added dropwise to H_2S_2 (20 mL, 27 g, 0.4 mol) saturated with HCl gas. H_2S_2, which is less volatile than H_2S, could not be completely removed by the low temperatures required.

Received: March 18, 1994 [Z6773IE]
German version: *Angew. Chem.* **1994**, *106*, 1824

[1] H. J. Möckel, F. Höfler, H. Melzer, *Chromatographia* **1985**, *20*, 471–476; M. Pridöhl, R. Steudel, F. Baumgart, *Polyhedron* **1993**, *12*, 2577–2585.
[2] M. Pridöhl, R. Steudel, F. Baumgart, *Phosphorus Sulfur Silicon Relat. Elem.* **1992**, *65*, 169–172; M. Lamoureux, J. Milne, *Polyhedron* **1990**, *9*, 589–595; J. Milne, A. J. Williams, *Inorg. Chem.* **1992**, *31*, 4534–4538.
[3] J. Hahn, *Z. Naturforsch. B* **1985**, *40*, 263–272.
[4] R. Laitinen, T. Pakkanen, *J. Mol. Struct. THEOCHEM* **1983**, *91*, 337–352.
[5] J. Hahn, K. Altenbach, *Z. Naturforsch. B* **1986**, *41*, 675–679.
[6] J. Hahn, A. Dolgner, unpublished results.
[7] The characteristic values of the Se,H coupling constants were used to identify the signals in the ^{1}H-coupled ^{77}Se NMR spectrum for compounds **1**, **2**, **5**, **7**, and **9**.
[8] The ^{1}H chemical shifts of the thiaselanes were very dependent on the solvent and on the concentration. Thus, the δ-values in Tables 1 and 2 are useful only for comparison within a particular mixture.
[9] D. M. Grant, E. G. Paul, *J. Am. Chem. Soc.* **1964**, *86*, 2984–2990.
[10] M. Baudler, U. M. Krause, J. Hahn, R. Riekehof-Böhmer, *Z. Anorg. Allg. Chem.* **1986**, *543*, 35–44.
[11] R. R. Smardzewski, M. C. Lin, *J. Chem. Phys.* **1977**, *66*, 3197.
[12] H. Schmidt, R. Steudel, D. Sülzle, H. Schwarz, *Inorg. Chem.* **1992**, *31*, 941–944.

Magnetic Spin Effects on Photooxidation Quantum Yields of Ru^{II}-tris(bipyridine) Type Complexes in Magnetic Fields up to 17.5 Tesla**

Dieter Bürßner, Hans-Joachim Wolff, and Ulrich E. Steiner*

Today a large number of magnetic field and magnetic isotope effects on the rates and yields of chemical reactions are known.[1] Their mechanisms are closely related to electronic- and nuclear-spin polarization effects arising from chemical reac-

[*] Prof. Dr. U. E. Steiner, D. Bürßner, H.-J. Wolff
Fakultät für Chemie der Universität
D-78434 Konstanz (FRG)
Telefax: Int. code + (7531)88-3014

[**] This work was supported by the Deutsche Forschungsgemeinschaft and the Fonds der Chemischen Industrie. Thanks are also due to the Centre National de la Recherche Scientifique and the Max-Planck-Gesellschaft for allowing the use of their high magnetic field facility, and to Prof. G. Maret and A. Klaschka for their help in organizing the experiment at Grenoble.

tions. The acronyms CIDEP and CIDNP have become established for these effects. The systematic study of all these effects is the object of *spin chemistry*.[2] For magnetic field effects to influence chemical reaction rates, processes of electron spin must be kinetically coupled to processes of chemical change. In a magnetic field, the Larmor precession of the unpaired electron spins will modify the spin processes and thereby possibly alter the overall reaction kinetics. As a general rule, the magnetic field dependence of the observed kinetic effect reflects the ratio between the rates of inherent processes (spin processes and connected chemical processes) and the frequency of Larmor precession. Typically, the magnetic field effect has its strongest dependence on the relative change of the field at the point where both spin precession and internal processes occur at about the same rate (note that at a field of 1 Gauss (0.1 mT) the Larmor precession period is 0.36 μs). The effect approaches a saturation value at field strengths several times higher. Most spin chemical experiments reported so far have been conducted in fairly weak magnetic fields (several 100 Gauss) for the obvious reason that this is sufficient if the internal spin processes are governed by hyperfine coupling. The field strength has, at least, been limited by the usual laboratory equipment for generating variable magnetic fields, that is, electromagnets which can only provide several Tesla of magnetic induction. Few investigations have utilized the fields of superconducting solenoids[3] or have applied pulsed magnetic fields.[4, 5] In one paper[6] magnetic field effects at one high-field value of 14.5 T, produced by a Bitter type magnet, have been compared to effects at low fields; however, rather small effects were seen. In this communication we report the first investigations[7] where the field is gradually varied from zero field to the highest field of 17.5 Tesla. Magnetic field dependent reaction kinetics could be measured for a system exhibiting the highest saturation fields observed so far and allowing determination of the fastest chemical and spin processes investigated so far by spin chemical methods.

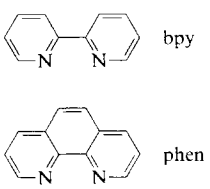
The reaction we studied is the photooxidation of Ru^{II}-tris-(bipyridine) type complexes **1a**–**1d** by methylviologen (MV^{2+}).

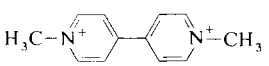
$[Ru^{II}(bpy_3)]^{2+}$ **1a**

$[Ru^{II}(bpy)_2(phen)]^{2+}$ **1b**

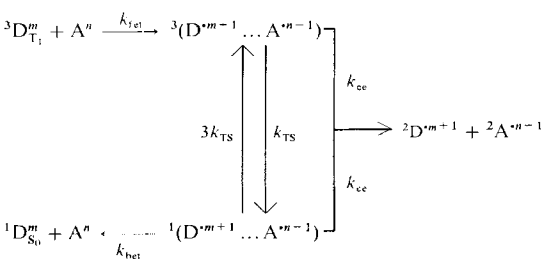
$[Ru^{II}(bpy)(phen)_2]^{2+}$ **1c**

$[Ru^{II}(phen)_3]^{2+}$ **1d**





The relevant reaction steps (Scheme 1) apply in general to electron transfer reactions with photoexcited triplet states. A triplet excited electron donor $^3D^m$ ($^3[Ru^{II}L_3]^{2+}$) undergoes electron *forward* transfer in a diffusion-controlled reaction (rate constant k_{fet}) with a singlet ground state electron acceptor $A^n(MV^{2+})$ to generate a radical-ion pair $D^{\bullet m+1}\ldots A^{\bullet n-1}$ ($[Ru^{III}L_3]^{3+}\ldots MV^{\bullet+}$), which may dissociate (with rate constant k_{ce} of cage escape) to form the free radical ions, or else can undergo a *backward* electron transfer in the solvent cage to regenerate the ground-state reactants. The reaction scheme assumes conservation of spin multiplicity during the electron transfer steps. Thus the primary radical-ion pair (RIP) forms as a triplet spin state, and backward electron transfer (with rate constant k_{bet}) is only possible after a spin-flip transition to the corresponding singlet RIP state, occurring with a rate constant of k_{TS} and, for spin statistical reasons, of $3k_{TS}$ for the reverse process. An external magnetic field modifies the *rate* of spin equilibration in the RIP (for details see below) and thereby affects the overall efficiency of backward electron transfer and, indirectly, of cage escape (η_{ce}). The latter quantity is measured in our experiments.



Scheme 1.

The sources, preparation, and purification of the compounds employed in this investigation are described in Refs. [8,9]. The experiments were carried out with a Bitter magnet at the High Magnetic Field Laboratory of MPI/CNRS at Grenoble. The magnetic field effect on the formation of free radicals was investigated by photostationary illumination in a continuous flow system.[10, 11] The $MV^{\bullet+}$ radicals produced in the photoreaction were protected against reoxidation through Ru^{III} complexes in the bulk by adding 2×10^{-2} M EDTA as a sacrificial donor to reduce Ru^{III} to Ru^{II}. The experiments were carried out in aqueous solutions with concentrations of 2×10^{-5} M for the complexes and 3×10^{-3} M for MV^{2+}. Further experimental details can be found in ref. [9].

The observed magnetic field dependence of the cage escape efficiency η_{ce} (which corresponds to the measured magnetic field effect on the quantum yield of photoinduced $MV^{\bullet+}$ radical production) with the four complexes **1a**–**1d** is depicted in Figure 1.

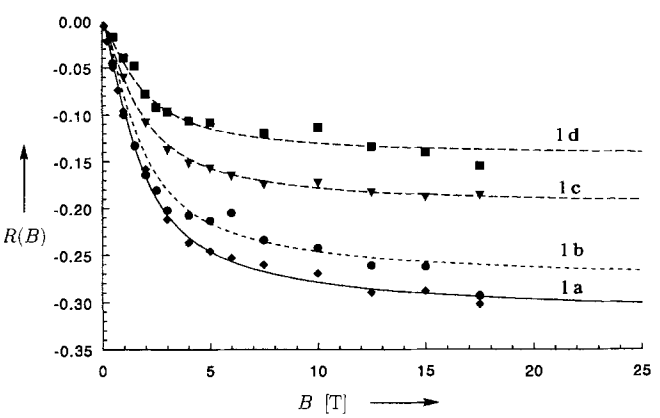


Fig. 1. Relative magnetic field effect $R(B) = (\eta_{ce}(B) - \eta_{ce}(0))\eta_{ce}(0)^{-1}$ on the quantum yield of $MV^{\bullet+}$ radical production in the photoreaction with complexes **1a**–**1d**. The curves are results of theoretical simulations of the magnetic field dependence of η_{ce} using the parameters given in Table 1.

There is a pronounced ligand effect on the magnetic field sensitivity, which decreases regularly for every replacement of a bipyridine ligand by a phenanthroline ligand. In the low-field region the values measured with the Bitter magnet are in very good agreement with the results previously obtained up to 3.3 Tesla with the electromagnet in our laboratory.[9] However, the new experiments with the fivefold extended field range clearly exhibit saturation behavior of the field effect above fields of about 5 Tesla.

 © VCH Verlagsgesellschaft mbH, D-69451 Weinheim, 1994 0570-0833/94/1717-1773 $ 10.00+.25/0

The observed magnetic field dependence can be excellently reproduced by theoretical simulations based on our recently reported theoretical model,[9, 12] which may be briefly summarized as follows: In the description of the spin state of the primary RIP ($[Ru^{III}L_3]^{3+} \cdots MV^{\bullet+}$) we make use of the concept of *effective spin* in order to account for the strongly spin-orbit-coupled nature of the Ru^{III} ground state in its low-spin d^5 electron configuration. The changes of the RIP spin state are governed by the fast relaxation of the effective spin at Ru^{III} described by a magnetic field independent relaxation time $\tau_S = T_1 = T_2$ (at zero field, k_{TS} in Scheme 1 is equal to $(4\tau_s)^{-1}$) and by the Zeeman interaction which, due to the strongly anisotropic g-tensor of Ru^{III}, enforces a fast loss of spin correlation between the effective spin at the complex and the spin at $MV^{\bullet+}$. Cage escape of the RIP and backward electron transfer are treated as first-order chemical rate processes with rate constants k_{ce} and $k_{bet,i}$, respectively; individual rate constants of backward electron transfer are employed for the four spin substates (denoted by index i) of the pair. These individual rate constants correspond to the products of the rate constant k_{bet} of the hypothetically spin-allowed process with the individual singlet characters $p_{S,i}$ of the respective spin states, one of them being essentially of singlet, three of them essentially of triplet nature. The efficiency of cage escape and its magnetic field dependence are calculated by numerically solving the pertinent stochastic Liouville equation and averaging the result over all orientations of the Ru^{III} complex.

In the simulation of the observed magnetic field effect, the values of the g-tensor components of the Ru^{III} complexes were taken from ESR spectra measured at low temperature in a solid matrix of acetonitrile/sulfuric acid,[13] whereas the rate constants τ_S^{-1}, k_{ce}, and k_{bet} were treated as empirical fit parameters. As it turned out, in order to reproduce the absolute values of η_{ce} (0) (the cage escape efficiency at zero field) and the full magnetic field effect curves within the bounds of experimental error, all three parameters of the set could be fixed with certainty within a margin of $\pm 20\%$ for each of the complexes. Thus a fairly precise, *absolute* determination of τ_S^{-1}, k_{ce}, and k_{bet} is possible with our method. No supplementary information on these parameters is needed beforehand. The values determined for the four complexes are listed in Table 1.

Since the four spin substates of the primary RIP exhibit kinetic differences the overall kinetics of the RIP decay is not truly monoexponential. An effective overall decay time may be defined, however, as in Equation (a). As can be seen from Table 1,

$$\tau_{eff} = \frac{\eta_{ce}}{k_{ce}} \qquad (a)$$

τ_{eff} lies around 100 ps. Under conditions of diffusion-controlled formation of the RIPs in a homogeneous reaction, as in our experiment, it would be impossible to observe the RIPs directly with ps time-resolution, since even with the highest acceptor concentration the time of formation of the RIP cannot be decreased below several ns. Direct observation of the RIP is, however, feasible and has been reported for a number of chemically linked systems of electrons donor and acceptor (dyads) where the forward electron transfer step is not limited by diffusion (cf. Ref. [14]). In a ps time-resolved study of dyads composed of a Ru^{II}-tris(bipyridine) type electron donor and a methylviologen type electron acceptor connected by a covalent spacer of one or two CH_2 links, Yonemoto et al.[15] observed RIP lifetimes between 8.5 and 70 ps, depending on the number n of links and the thermodynamic driving force of backward electron transfer ΔG^0_{bet}. For $n = 2$ and $\Delta G^0_{bet} = -1.65$ eV, a situation that can be considered as corresponding closely to the case of the RIPs formed in our free diffusion reaction, the observed value is 70 ps, which indeed comes rather close to the values determined by our spin chemical approach. Thus, while the ps time-resolved studies of the dyads corroborate the conclusions from our spin chemical investigations, the spin chemical approach yields additional, highly relevant information on the nature of the process that, in fact, determines the *observable* effective decay time of the RIP, not only in our freely diffusing systems but, of course, also in the dyads. The magnetic field effects described here give unequivocal evidence that the overall backward electron transfer is a two-step process involving spin conversion followed by spin-conserving electron transfer. Using relation (b) we can predict from our results the lifetimes $\tau_{bet,eff}$ (cf. Table 1) that would

$$\tau_{bet,eff} = \frac{\eta_{ce}}{(1-\eta_{ce})}\frac{1}{k_{ce}} \qquad (b)$$

be observed for our RIPs if cage escape could be excluded. On comparison of these values with $\tau_{bet} = k_{bet}^{-1}$, the time constant of the spin-allowed backward transfer, it becomes clear that the $\tau_{bet,eff}$ values are significantly longer which implies that the observed lifetime must be strongly controlled by the spin relaxation process. This conclusion suggests that before discussing lifetimes of the RIP derived from the ps experiment in terms of electron transfer theory, the observed time constants must be decomposed into a spin conversion part and an electron transfer part. The spin chemical approach, as applied here, seems the only way to achieve such a kinetic separation. Hence, it should be a great experimental challenge to verify our conclusions by *directly* observing the magnetic field effect on the decay time of dyadic RIPs in ps time-resolved experiments.

For k_{ce} a value of 5×10^9 s^{-1} based on an estimation using the Eigen–Debye equation is usually referred to in the literature.[16] The k_{ce} values resulting from our analysis are of the same order of magnitude. A deviation by a factor of 2–3 seems acceptable in view of the assumptions in the diffusional model. Further-

Table 1. Characteristic reaction parameters for the primary Ru^{III} complex/$MV^{\bullet+}$ radical pair.

Ligands	Parameters									
	ΔG^0_{bet} [eV] [a]	η_{ce} [a]	$g_\perp$ [b]	$g_\parallel$ [b]	k_{ce} [ns^{-1}] [c]	k_{bet} [ns^{-1}] [c]	τ_S [ps] [c]	τ_{eff} [ps] [d]	τ_{bet} [ps] [e]	$\tau_{bet,eff}$ [ps] [f]
$(bpy)_3$	−1.70	0.19	2.60	1.18	2.3 [g]	78 [g]	26.7 [g]	83	12.8	102
$(bpy)_2$ (phen)	−1.70	0.19	2.60	1.18	2.2	66	23.5	86	15.2	107
(bpy) $(phen)_2$	−1.71	0.18	2.54	0.95	1.9	46	21.3	95	21.7	116
$(phen)_3$	−1.71	0.19	2.53	0.90	1.5	32 [g]	19.2 [g]	127	31.2	156

[a] Data from ref. [9]. [b] Data for ref. [13]. [c] From a simulation of the magnetic field dependence of η_{ce}. [d] Equation (a). [e] $\tau_{bet} = k_{bet}^{-1}$. [f] Equation (b). [g] Minor deviations from our preliminary values in [7] are due to more precise values of the g-tensor components employed in the present calculations. Here we use individual experimental values for each complex, whereas in [7] for both the $(bpy)_3$ and the $(phen)_3$ complex only a common, approximate set of values for the g-tensor components was used.

 © VCH Verlagsgesellschaft mbH, D-69451 Weinheim, 1994 0570-0833/94/1717-1774 $ 10.00+.25/0 Angew. Chem. Int. Ed. Engl. 1994, 33, No. 17

more, we note that the slight decrease of k_{ce} observed as bipyridine ligands are replaced by the somewhat larger phenanthroline ones is in agreement with the prediction of diffusion theory, according to which the rate constant of dissociation of a pair of reactants should decrease with increasing reaction distance. Taking into account that the backward electron transfer is a nonadiabatic process that depends on the value of the electronic coupling matrix element, the fact that k_{bet}, too decreases by such a type of ligand substitution seems to support an assumption of increasing reaction distance because a concomitant decrease of the electronic coupling matrix element is expected for increasing separation. Since ΔG^0_{bet} is constant, only a change in the coupling matrix element or in the internal reorganization energy associated with electron backward transfer or in both may account for a change of k_{bet}. Which of these two possibilities applies on substituting bipyridine by phenanthroline ligands cannot be decided at present.

The parameter τ_S is the paramagnetic relaxation time of the Ru^{III} complex in the RIP. It seems unlikely that the presence of the $MV^{\bullet+}$ radical near the Ru^{III} complex has a significant effect on τ_S, and thus it may be conveniently compared to the corresponding value in the free Ru^{III} complex. Because of the short relaxation time and the large g-tensor anisotropy, an ESR signal of the present type of Ru^{III} complexes is not detectable in liquid solutions. However, indirect experimental access to τ_S is possible through the linewidth of ^1H resonances in NMR spectra.[17, 18] Actually a value of $\tau_S \approx 20$ ps was evaluated by Doddrell et al.[19] for $[Ru(acac)_3]$ in a field range from 0.2 to 6 T. We have measured the ^1H-T_1 times for $[Ru(bpy)_3]^{3+}$, from which the electronic relaxation times 25 ps and 9 ps, respectively, have been determined.[20] These values are in rather good agreement with the spin chemical τ_S values. In particular these data confirm that our spin chemical inference of a decrease of τ_S on replacing bipyridine by phenthroline ligands is correct.

In conclusion, we have shown that the spin chemical modeling of the magnetic field effects observed over a large range of magnetic fields allows an excellent simulation of the experimental data with a minimum of parameters. There is a substantial amount of evidence that the determined parameters represent reliable physical information that is not easily, if at all, available otherwise. This renders the method most valuable for a deep look into the details of fast backward electron transfer kinetics and paramagnetic relaxation occuring on a time scale of several tens of ps, with strongly spin–orbit coupled paramagnetic intermediates.

Received: March 8, 1994 [Z 6736 IE]
German version: *Angew. Chem.* **1994**, *106*, 1834

[1] U. E. Steiner, T. Ulrich, *Chem. Rev.* **1989**, *89*, 51; U. E. Steiner, H.-J. Wolff in *Photochemistry and Photophysics, Vol. IV* (Ed.: J. F. Rabek), CRC, Boca Raton, FL, **1991**, Chap. 1, p. 1; I. V. Khudyakov, Yu. A. Serebrennikov, N. J. Turro, *Chem. Rev.* **1993**, *93*, 537; H. Hayashi in *Photochemistry and Photophysics, Vol. I* (Ed.: J. F. Rabek), CRC, Boca Raton, FL, **1990**, Chap. 2, p. 59; K. M. Salikhov, Yu. N. Molin, R. Z. Sagdeev, A. L. Buchachenko, *Spin Polarization and Magnetic Effects in Radical Reactions*, Elsevier, Amsterdam, **1984**.
[2] Cf. recent journal volumes devoted to spin chemistry: *Chem. Phys.* **1992**, *162*, 1–234; *Z. Phys. Chem. Munich* **1993**, *180*; *ibid.* **1993**, *182*.
[3] Y. Nakamura, M. Igarashi, Y. Sakaguchi, H. Hayashi, *Chem. Phys. Lett.* **1994**, *217*, 387; Y. Sakaguchi, H. Hayashi, *Chem. Lett.* **1993**, 1183.
[4] M. Mukai, Y. Fujiwara, Y. Tanimoto, M. Okazaki, *J. Phys. Chem.* **1993**, *97*, 12660.
[5] G. Ferraudi, G. A. Argüello, *J. Phys. Chem.* **1988**, *92*, 1846.
[6] N. J. Turro, C.-J. Chung, G. Jones II, W. G. Becker, *J. Phys. Chem.* **1982**, *86*, 3677.
[7] We communicated part of these results in preliminary form at the 10th International Symposium on the Photophysics and Photochemistry of Coordination Compounds, July 1993, Sendai, Japan. The papers of this meeting are published in *Coord. Chem. Rev.* **1994**, *132*.
[8] H.-J. Wolff, U. E. Steiner, *Z. Phys. Chem. Munich* **1990**, *169*, 147.
[9] D. Bürßner, H.-J. Wolff, U. E. Steiner, *Z. Phys. Chem. Munich* **1993**, *182*, 297.
[10] W. Schlenker, U. E. Steiner, *Ber. Bunsenges. Phys. Chem.* **1985**, *89*, 1041.
[11] U. E. Steiner, H.-J. Wolff, T. Ulrich, T. Ohno, *J. Phys. Chem.* **1989**, *93*, 5147.
[12] U. E. Steiner, D. Bürßner, *Z. Phys. Chem. Munich* **1990**, *169*, 159.
[13] H.-J. Wolff, *Dissertation*, Universität Konstanz, **1994**.
[14] V. Balzani, F. Scandola, *Supramolecular Photochemistry*, Ellis Horwood, New York, **1991**.
[15] E. H. Yonemoto, R. L. Riley, Y. Il Kim, S. J. Atherton, R. H. Schmehl, T. E. Mallouk, *J. Am. Chem. Soc.* **1992**, *114*, 8081.
[16] M. Z. Hoffman, *J. Phys. Chem.* **1988**, *92*, 3458; C. Chiorboli, M. T. Indelli, M. A. R. Scandola, F. Scandola, *ibid.* **1988**, *92*, 156.
[17] *NMR of Paramagnetic Molecules* (Eds.: G. N. LaMar, W. DeW. Horrocks, Jr., R. H. Holm), Academic Press, New York, **1973**; L. Banci, I. Bertini, C. Luchinat, *Nuclear and Electron Relaxation*, VCH, Weinheim, **1991**.
[18] K. V. Vasavada, B. D. Nageswara Rao, *J. Magn. Reson.* **1989**, *81*, 275; I. Bertini, F. Briganti, K. V. Vasavada, *ibid.* **1990**, *89*, 243.
[19] D. M. Doddrell, D. T. Pegg, M. R. Bendall, A. K. Gregson, *Aust. J. Chem.* **1977**, *30*, 1635.
[20] D. Bürßner, Dissertation, Universität Konstanz, **1994**.

Pronounced Electronic Coupling in Rigidly Connected N,C,N-Coordinated Diruthenium Complexes over a Distance of Up to 20 Å**

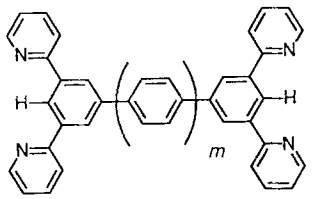
Marc Beley, Sandrine Chodorowski-Kimmes, Jean-Paul Collin, Philippe Lainé, Jean-Pierre Launay,* and Jean-Pierre Sauvage*

Molecular systems able to ensure fast long-range electron transfer are an essential requirement for the application of thermal or photoinduced charge separation in artificial photosynthesis[1] and in molecular electronics.[2] Mixed-valence complexes are the prototypes of molecules able to undergo fast electron transfer usually between two metals and through a bridging ligand.[3–11] We recently reported that a bridging ligand consisting of two cyclometalating bipyridylbenzenes connected back-to-back (**1**) affords diruthenium ($\mathbf{5}^{3+}$)[12, 13] and diosmium[13] complexes displaying intense communication between both metal centers at a M–M distance of roughly 11 Å. (Strong intervalence coupling over this distance has also been recently observed in the "[Ru(pincer–pincer)Ru]" systems[14]). In the present paper, we describe extended systems with two N,C,N coordination sites connected by various aromatic spacers, and show that strong communication can occur in diruthenium compounds with much longer bridging ligands. These ligands contain up to four phenyl rings and thus lead to a Ru–Ru distance of around 20 Å.

The synthesis of the ligand precursors **2**-H_2 and **3**-H_2, as well as their diruthenium(II) complexes $\mathbf{6}^{2+}$ and $\mathbf{7}^{2+}$, was described recently.[15] In these complexes the metals are connected by a 4,4″-terphenyldiyl and 4,4‴-quaterphenyldiyl ligand, respec-

[*] Dr. J.-P. Sauvage, Dr. M. Beley, S. Chodorowski-Kimmes, Dr. J.-P. Collin
Laboratoire de Chimie Organo-Minérale, UA 422 du CNRS
Institut de Chimie, Université Louis Pasteur
F-67008 Strasbourg (France)
Telefax: Int. code +88607312
Dr. J.-P. Launay, Dr. P. Lainé
CEMES-LOE, CNRS
29 rue Jeanne Marvig
F-31055 Toulouse (France)
Telefax: Int. code +62257999

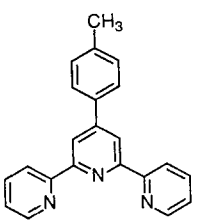
[**] This work was supported by the Centre National de la Recherche Scientifique. We thank Patrice Staub for his technical assistance.



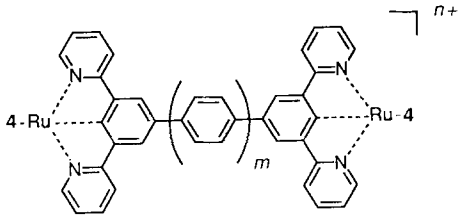
1-H_2 : $m = 0$

2-H_2 : $m = 1$

3-H_2 : $m = 2$



4



$\mathbf{5}^{n+}$: $m = 0$

$\mathbf{6}^{n+}$: $m = 1$

$\mathbf{7}^{n+}$: $m = 2$

tively, and the whole edifice is stabilized by the four additional pyridine units bonded to the metal centers.

The UV/VIS data for the diruthenium(II) complexes and some of their most significant electrochemical parameters are given in Table 1. All three compounds show an intense absorption band in the visible region (500–550 nm), which corresponds to a metal-to-ligand charge transfer transition. As expected, UV bands originating from ligand-centered transitions are also present. The reduction potentials of the compounds are much lower (< -1.5 V) than those of classical ruthenium complexes with six coordinating N atoms such as $[Ru(terpy)]^{2+}$ [16] (terpy = 2,2′,6′,2″-terpyridine, $E = -1.25$ V). It should be stressed that the reduction is very likely to be ligand localized. As already observed,[12, 13] the N_5C coordination polyhedron makes the complexes much weaker electron acceptors than their N_6 congeners because of the strong donating character of the σC–Ru bond. Accordingly, oxidation of Ru^{II} to Ru^{III} is very easy, occurring at potentials from +0.34 to +0.52 V, that is, about 0.8 V less anodic than for noncyclometalated complexes of the $[RuN_6]^{2+}$ family. The electron-rich character of the cyclometalating N,C,N fragment is so pronounced that the Ru^{III}/Ru^{IV} couple can even be clearly detected.

Table 1. UV/VIS data, electrochemical parameters, and comproportionation constants K_c for the diruthenium complexes $\mathbf{5}^{2+}$, $\mathbf{6}^{2+}$, and $\mathbf{7}^{2+}$.

Complex	Absorption [a] λ_{max} [nm] ($\varepsilon \times 10^{-4}$ [M^{-1} cm^{-1}])	$E_{1/2}$ [b] Oxidation	Reduction	K_c [d]
$\mathbf{5}^{2+}$	543 (3.06), 516 (3.06) 287 (11.29), 220 (6.75)	0.505, 0.340	−1.55	690
$\mathbf{6}^{2+}$	513 (3.53), 369 (5.65), 287 (12.7), 243 (7.12), 223 (7.13)	1.39 [c], 0.510	< −1.5	16
$\mathbf{7}^{2+}$	511 (3.50), 374 (5.77), 288 (13.23), 243 (8.11), 228 (8.44)	1.39 [c], 0.515	< −1.5	6

[a] In CH_3CN. [b] [V] vs. SCE in CH_3CN. [c] Irreversible two-electron wave corresponding to the reaction Ru^{III}, $Ru^{III} \rightarrow Ru^{IV}$, Ru^{IV} + 2 e. [d] From spectroelectrochemical titration. The uncertainty is ±2.

The comproportionation constant K_c corresponding to equilibrium (a) can be obtained by analyzing the cyclic voltammetry

$$Ru^{II}, Ru^{II} + Ru^{III}, Ru^{III} \rightleftharpoons 2Ru^{II}, Ru^{III} \quad (a)$$

data for the two electrochemical processes in Scheme 1 or by equilibrium studies.[6] In the case of $\mathbf{5}^{n+}$, both potentials are

$$Ru^{II}, Ru^{II} \rightleftharpoons Ru^{II}, Ru^{III} + e$$

$$Ru^{II}, Ru^{III} \rightleftharpoons Ru^{III}, Ru^{III} + e$$

Scheme 1.

sufficiently different to allow a direct determination of K_c.[12] However in the case of $\mathbf{6}^{n+}$ and $\mathbf{7}^{n+}$, a single electrochemical wave is observed, which precludes a similar determination of K_c. Nevertheless, this is possible by using a redox titration, in which the optical density ($\log I_o/I$) is plotted as a function of the amount of oxidant or the quantity of electricity in an electrolysis. This is basically the procedure described by Taube et al. some years ago[6] but with a least squares refinement of the comproportionation constant, as described elsewhere.[17] The values obtained in this way are collected in Table 1. As could be anticipated, for the longer system $\mathbf{7}^{2+}$ the K_c value approaches the statistical value of 4.

The spectra of the mixed-valence complexes are depicted in Figure 1. In the case of $\mathbf{5}^{3+}$, the directly recorded spectrum is shown, because the comproportionation constant is large enough; the corrected spectra given for $\mathbf{6}^{3+}$ and $\mathbf{7}^{3+}$ were obtained by subtracting the contribution of the homovalent species. All complexes display an intense intervalence transfer (IVT) band in the near-infrared (NIR) region (Table 2). This band is exceptionally intense for $\mathbf{5}^{3+}$. It decreases with intermetallic distance but remains strong even for $\mathbf{7}^{3+}$.

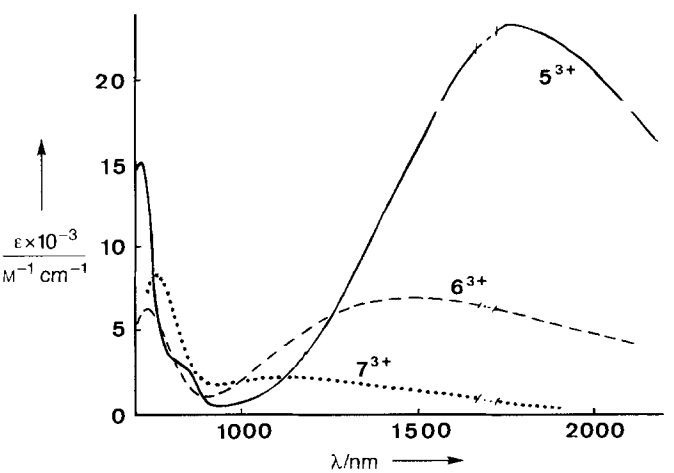


Fig. 1. Corrected spectra of the mixed-valence dinuclear complexes $\mathbf{5}^{3+}$, $\mathbf{6}^{3+}$, and $\mathbf{7}^{3+}$ showing the intervalence transitions.

There is some overlap of the intervalence band with the nearby charge transfer band in the case of $\mathbf{6}^{3+}$ and especially of $\mathbf{7}^{3+}$. Nevertheless, this does not preclude a quantitative evaluation of

Table 2. IVT bands in the NIR region [a] and calculated matrix elements V_{ab} for the diruthenium complexes 5^{3+}, 6^{3+}, 7^{3+} and 8^{5+}.

Complex	Ru–Ru [b] [Å]	λ_{max} [nm]	$\Delta\tilde{\nu}_{1/2}$ [cm^{-1}]	ε_{max} [M^{-1} cm^{-1}]	V_{ab} [eV]
5^{3+}	11	1936	2660	22000	0.127
6^{3+}	15.5	1650	5112	6600	0.074
7^{3+}	20	1214	5714	2200	0.041
8^{5+} [c]	11	1580	4008	1620	0.047

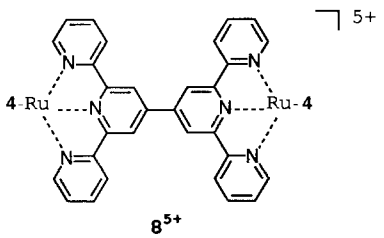
[a] In CH_3CN. [b] Approximate distances. [c] Ref. [11].

the data. We have deconvoluted the spectra into a sum of Gaussian components using a method already proposed by Reimers and Hush[9] and described elsewhere.[17]

The intervalence band parameters allow the determination of the metal–metal coupling parameter V_{ab}, according to the Hush formula [Eq. (b)], where V_{ab} is the coupling in cm^{-1}, ε_{max} the

$$V_{ab} = 2.05 \times 10^{-2} (\varepsilon_{max} \tilde{\nu}_{max} \Delta\tilde{\nu}_{1/2})^{1/2} / R_{MM} \quad \text{(b)}$$

maximum extinction coefficient, $\tilde{\nu}_{max}$ the band position in cm^{-1}, $\Delta\tilde{\nu}_{1/2}$ the full-width at half-maximum in cm^{-1}, and R_{MM} the metal–metal distance in Å. For comparison, the same set of data for the dinuclear complex 8^{5+} containing two RuN_6 moieties is also included in Table 2.



8^{5+}

From the V_{ab} values of Table 2 it is obvious that the biscyclometalated complexes 5^{3+}, 6^{3+}, and 7^{3+} are very strongly coupled, considering the large metal–metal separations, (11–20 Å). Noteworthy is the dramatic difference between the isoelectronic complexes 5^{3+} and 8^{5+}, which have a very similar Ru–Ru distance. In fact, the electronic coupling in the noncyclometalated system 8^{5+} is similar to that in compound 7^{3+} (comparable V_{ab} values), despite the much longer bridge in 7^{3+} (four aromatic rings as opposed to two in the connecting rod).

It is interesting to search for the theoretical reasons for these differences. We have thus determined the V_{ab} couplings by Extended Hückel calculations.[19] First we compared the bis(N_6) complex 8^{5+} with the bis(N_5C) complex 5^{3+}. Even though the crystal structure of 5^{3+} (with PF_6^- as counterion) shows a small dihedral angle (22°) between the two halves of the molecule,[12] the calculation was made for a planar conformation, which greatly simplifies the discussion. (An investigation of the angle influence shows a decrease of only 7% of the coupling between 0 and 20°). The values thus obtained are reasonably close to the experimental ones (Table 3) and confirm the higher coupling of the cyclometalated species. Analysis of the energy levels and eigenvectors shows that on passing from 8^{5+} to 5^{3+} there is a general increase in the energy of the ligand levels, which induces a stronger mixing with the metal orbitals. (This effect is also apparent in a theoretical comparison of N,N and C,N donors using the Fenske–Hall method.[20]) Since furthermore the Ru–C bond is shorter than the Ru–N bond by 0.1 Å,[12] it is not surprising that stronger coupling results.

Table 3. Experimental and calculated values (from Extended Hückel calculations with planar conformation of the bridging ligand) of the metal–metal couplings (in eV) for complexes of the type [(terpy)Ru–bridging ligand–Ru(terpy)]$^{n+}$; comparison of 5^{3+} and 8^{5+}.

Bridging ligand	Complex	V_{ab}, expt.	V_{ab}, calcd.
bis(terpy)	8^{5+}	0.047	0.047
1^{2-}	5^{3+}	0.127	0.090

Thus the higher coupling through bis(N,C,N) ligands can be mainly explained by their strong electron-donating character. Clearly, the charge transfer from the bridging ligand to Ru^{III} is much more favorable for 5^{3+}, 6^{3+}, and 7^{3+} than for 8^{5+}, in agreement with orbitals with matching energies. This energy matching principle has recently been applied to diruthenium compounds with terminal cyclometalating ligands and a normal bis(terpy) bridge and also leads to high coupling.[21] However, in the present study the influence of the N/C exchange is not correctly reproduced by the Extended Hückel method. Calculational work with more advanced methods is in progress to improve our description of these systems. Another open problem is the more rapid decrease of the metal–metal coupling with distance in the case of the bis(N,C,N) complexes (see Fig. 2). This seems to confirm an earlier prediction that it is difficult to obtain simultaneously both strong coupling and a low decay rate.[22]

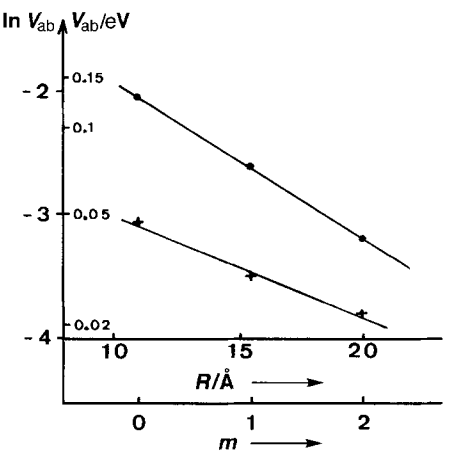


Fig. 2. Decrease in the metal–metal coupling for the isoelectronic series: bis(terpyridyl) (+) and biscyclometalated complexes (●).

In conclusion, the present series of dinuclear complexes displays intense electronic coupling over up to 20 Å in their mixed-valence forms. This reflects a favorable ligand-to-metal charge transfer interaction owing to the strong reducing character of the bis(cyclometalated) bridging systems.

Experimental Procedure

The synthesis of 5^{2+}, 6^{2+}, and 7^{2+} has been reported elsewhere [12,13,15]. The complexes were electrolyzed in acetonitrile containing 0.1 M NBu_4PF_6. The complex concentration was in the range 5×10^{-5} to 1×10^{-4} M, and the progress of the oxidation was followed coulometrically. UV/VIS/NIR spectra were recorded during the electrolysis with 1 cm cells and a Shimadzu UVPC 3101 spectrophotometer. The determination of comproportionation constant and the deconvolution of intervalence and charge transfer bands have been described elsewhere [17].

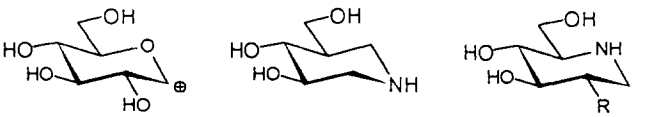
Received: March 3, 1994 [Z 6724 IE]
German version: *Angew. Chem.* **1994**, *106*, 1854

[1] V. Balzani, F. Scandola in *Supramolecular Photochemistry* (Ed.: T. J. Kemp), Ellis Horwood, London, **1991**.
[2] *Molecular Electronics* (Ed.: G. J. Ashwell), RSP, Taunton, **1991**.
[3] C. Creutz, H. Taube, *J. Am. Chem. Soc.* **1969**, *91*, 3988.
[4] W. H. Callahan, F. R. Keene, T. J. Meyer, D. J. Salmon, *J. Am. Chem. Soc.* **1977**, *99*, 1064.
[5] C. A. Stein, N. A. Lewis, G. Seitz, *J. Am. Chem. Soc.* **1982**, *104*, 2596.
[6] D. E. Richardson, H. Taube, *J. Am. Chem. Soc.* **1983**, *105*, 40; *Coord. Chem. Rev.* **1984**, *60*, 107; J. E. Sutton, P. M. Sutton, H. Taube, *Inorg. Chem.* **1979**, *18*, 1017.
[7] S. Woitellier, J.-P. Launay, C. W. Spangler, *Inorg. Chem.* **1989**, *28*, 758.
[8] Y. Kim, C. M. Lieber, *Inorg. Chem.* **1989**, *28*, 3990.
[9] J. R. Reimers, N. S. Hush, *Inorg. Chem.* **1990**, *29*, 3686.
[10] M. A. S. Aquino, F. L. Lee, E. J. Gabe, C. Bensimon, J. E. Greedan, R. J. Crutchley, *J. Am. Chem. Soc.* **1992**, *114*, 5130.
[11] J.-P. Collin, P. Lainé, J.-P. Launay, J.-P. Sauvage, A. Sour, *J. Chem. Soc. Chem. Commun.* **1993**, 434.
[12] M. Beley, J.-P. Collin, R. Louis, B. Metz, J.-P. Sauvage, *J. Am. Chem. Soc.* **1991**, *113*, 8521.
[13] M. Beley, J.-P. Collin, J.-P. Sauvage, *Inorg. Chem.* **1993**, *32*, 4539.
[14] J.-P. Sutter, D. M. Grove, M. Beley, J.-P. Collin, N. Veldman, A. L. Spek, J.-P. Sauvage, G. van Koten, *Angew. Chem.* **1994**, *106* 1359; *Angew. Chem. Int. Ed. Engl.* **1994**, *33*, 1282.
[15] M. Beley, S. Chodorowski, J.-P. Collin, J.-P. Sauvage, *Tetrahedron Lett.* **1993**, *34*, 2933.
[16] N. E. Tokel-Takvoryan, R. E. Hemingway, A. J. Bard, *J. Am. Chem. Soc.* **1973**, *95*, 6582.
[17] A.-C. Ribou, J.-P. Launay, K. Takahashi, T. Nihira, S. Tarutani, C. W. Spangler, *Inorg. Chem.* **1994**, *33*, 1325.
[18] N. S. Hush, *Prog. Inorg. Chem.* **1967**, *8*, 391. The formula is given in: N. S. Hush, *Coord. Chem. Rev.* **1985**, *64*, 135.
[19] Calculations performed with the Extended Hückel program ICON 8 with ruthenium parameters given by Tatsumi and Hoffmann (K. Tatsumi, R. Hoffmann, *J. Am. Chem. Soc.* **1981**, *103*, 3328).
[20] E. C. Constable, C. E. Housecroft, *Polyhedron* **1990**, *9*, 1939.
[21] E. C. Constable, A. M. W. Cargill Thompson, S. Greulich, *J. Chem. Soc. Chem. Commun.* **1993**, 1444.
[22] C. Joachim, J.-P. Launay, S. Woitellier, *Chem. Phys.* **1990**, *147*, 131.

Isofagomine, a Potent, New Glycosidase Inhibitor**

Tina M. Jespersen, Wenling Dong, Michael R. Sierks,* Troels Skrydstrup, Inge Lundt, and Mikael Bols*

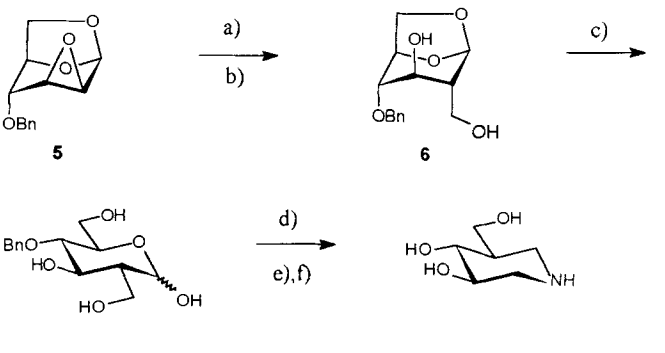
Glycosidases are an important group of enzymes that have been the subject of intense research.[1] The strong interest in the development of glycosidase inhibitors in the last decade was stimulated by the isolation of potent, naturally occurring inhibitors.[2] However, there is still much debate about the exact steric and electronic nature of the transition state for enzymatic glycoside cleavage.[3] We rationalized that since the enzymatic glycoside cleavage would result in formation of carbocation **1**, a good mimic of the transition state would be a compound able to accept a positive charge at the anomeric position. In this paper we report the synthesis of such a compound, isofagomine (**2**) and a disaccharide analogue of **2**. These compounds appear to be good transition state mimics, as both compounds are strong inhibitors of several glucosidases; indeed, isofagomine is the most potent β-glucosidase inhibitor reported so far.



1 **2** **3**, R=H **4**, R=OH

A large number of sugar analogues having a nitrogen atom in place of the oxygen atom in the ring, such as fagomine (**3**)[4] and deoxynojirimycin (**4**)[5], have been reported to be glycosidase inhibitors.[6] Surprisingly no sugar analogues with a nitrogen in place of the anomeric carbon have ever been prepared. In an attempt to design a good transition state mimic, we chose glucose analogue **2**, in which the oxygen atom in the ring has been replaced by carbon, the anomeric carbon replaced with nitrogen, and the 2-hydroxyl group removed. Compound **2** should have the general structure of glucose, be stable, and be able to accept a positive charge at the anomeric position.

The synthesis of **2** started from known epoxide **5**,[7] a compound that can be prepared in four steps from levoglucosane (Scheme 1). Opening of the epoxide by reaction with ten equiv-



Scheme 1. a) CH_2=CHMgBr, THF, 87%; b) 1. O_3; 2. $NaBH_4$, 96%; c) 1 M H_2SO_4, reflux, 1 h, 97%; d) $NaIO_4$, MeOH/H_2O 1:1, 45 °C, 5 h, 72–87%; e) NH_3/H_2O, H_2 (5000 kPa), Pd/C, 86%; f) H_2 (101 kPa), Pd/C, HCl, 71%.

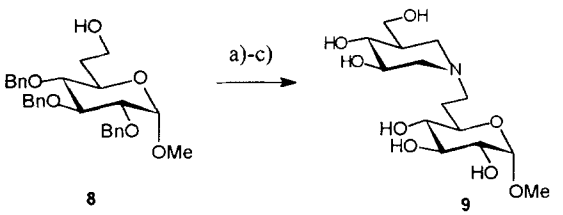
alents of vinyl magnesium bromide in refluxing THF[8] gave the corresponding 2-*C*-vinyl compound in 87% yield, which upon ozonolysis[9] in ethanol at 0 °C and subsequent reduction with $NaBH_4$ was converted into the 2-*C*-hydroxymethyl derivative **6** in 63% yield. Hydrolysis of this 1,6-anhydride in refluxing 1 M sulfuric acid gave 4-*O*-benzyl-2-deoxy-2-*C*-hydroxymethyl-D-glucose (**7**) in 97% yield. Treatment of **7** with five equivalents of $NaIO_4$ at 45 °C resulted in slow cleavage of the bond between C-5 and C-6 to give the resulting dialdehyde, which was isolated in yields from 72 to 87%. This reaction is sluggish compared to other similar cleavages with periodate, because only the open-chain form of the compound reacts. Hydrogenation[10] of the dialdehyde in 0.23 M ammonia in EtOH gave the piperidine in 86% yield, surprisingly with the 4-*O*-benzyl group intact. It was important to have a low concentration of ammonia during the

[*] Dr. M. R. Sierks, W. Dong
University of Maryland Baltimore County
Chemical and Biochemical Engineering
Baltimore, MD 21228-5398 (USA)
Telefax: Int. code + (410)455 1049
Dr. M. Bols, T. M. Jespersen, Dr. I. Lundt
Department of Organic Chemistry, The Technical University of Denmark, B201, DK-2800 Lyngby (Denmark)
Telefax: Int. code + (45)93-3968
Dr. T. Skrydstrup
Laboratoire de Biochimie Structurale, Université d'Orleans

[**] This work was supported by NATO (grant CRG 930718).

ring closure to avoid formation of a 1,5-diamino compound. The benzyl group was removed by hydrogenation in the presence of hydrochloric acid to give the hydrochloride of isofagomine (**2**) in 71% yield.[11] Isofagomine is clearly in the $^4C_1$ conformation, as apparent from the large coupling constants (11–13 Hz) of the axial protons adjacent to the nitrogen atom, H-2ax and H-6ax, with H-3 and H-5, respectively. The hydrochloride salt could be converted to the free amine **2** by chromatography on silica gel (EtOH/25% NH_4OH, 10:1).

We also prepared a transition state analogue for enzymatic cleavage of the 1,6-linked disaccharide isomaltose. The sugar derivative **8**,[12] which has a hydroxyl group at C-7, was subjected to Swern oxidation[13] to give the corresponding aldehyde in 85% yield (Scheme 2). Reductive coupling[10] of the aldehyde



8 **9**

Scheme 2. a) $(COCl)_2$, DMSO, Et_3N, $-70 \rightarrow 20$ °C, 85%; b) **2**, H_2 (5000 kPa), Pd/C, 84%; c) H_2 (101 kPa), Pd/C, HCl, 94%.

with **2** in the ratio 1:1 by hydrogenation with palladium on carbon gave the tertiary amine in 84% yield, again with the benzyl groups intact. The benzyl groups were removed by hydrogenation in the presence of hydrochloric acid to give the isomaltose analogue **9** in 94% yield.[14]

To evaluate how well **2** and **9** mimic the transition state for glycoside hydrolysis, the inhibition constants of these compounds were determined for a number of glycosidases, α-glucosidase (yeast), β-glucosidase (almonds), and isomaltase (baker's yeast), with *p*-nitrophenylglycosides as substrates; the inhibition constants are listed with those of the known inhibitor deoxynojirimycin (**4**) in Table 1. Enzyme assays were performed at 37 °C in phosphate buffer (0.05 M, pH 6.8) as described in the literature.[15, 16] The constant K_m was calculated with the program Grafit;[17] the K_i values were calculated by plotting the apparent K_m values versus inhibitor concentration.

Table 1. K_i values for glycosidase inhibition [μM].

Enzyme [a]	**4**	**2**	**9**
α-glucosidase (yeast)	25.4	85.9	58.8
β-glucosidase (almonds)	47.5	0.11	2.32
isomaltase (baker's yeast)	11.2	7.23	103

[a] The enzymes were purchased from Sigma Chemical Co., St. Louis, MO (USA).

Isofagomine (**2**) is a better inhibitor than **4** against two of the three glucosidases, but shows the strongest inhibition against β-glucosidase; in this case its K_i value is 440 times lower than that obtained for **4**. In fact **2** is the most potent inhibitor of β-glucosidase from sweet almond known. The disaccharide analogue **9** has generally weaker inhibition, but is still a very potent inhibitor. It is not surprising that the K_i values for **9** are lower than those of isofagomine for the α- and β-glucosidase, because these enzymes are fairly nonspecific. Thus mimicking the aglycon group should not provide any additional binding. The poorer inhibition constant obtained with isomaltase is more surprising, but is probably because the glucoside substituent on nitrogen is equatorial for steric reasons and thus mimics a β-1,6 linkage more closely than an α-1,6 linkage. We are currently investigating this hypothesis.

In view of the many piperidine and pyrrolidine sugar analogues that have been prepared and tested for glucosidase inhibition, the strong inhibition of isofagomine is quite surprising, especially considering the high K_i values previously observed for fagomine (**3**). With all the recent work on glycoside inhibitors the structural features for a good azasugar inhibitor were considered to be well defined;[18, 19] one group even derived an equation to predict inhibition constants of compounds against β-glucosidases.[15] This equation implies that the K_i of isofagomine should be approximately 1 mM. Since the experimental value is 0.1 μM, this represents an error of 10^4. Apparently sugar analogues with a nitrogen atom in place of the anomeric carbon have not been accounted for in the structural analysis of glycoside inhibitors. The strong inhibition of compound **2** may arise from a specific interaction between the positively charged NH group in the anomeric position and a negatively charged carboxylate group. Apparently the structure for electrostatic interaction in the active site is more favorable in the β-glucosidase than in the α-glucosidase, which thus accounts for the large difference in inhibition contants beteen the two enzymes. Our findings imply that azasugars such as **4** may inhibit by the same mechanism. Apparently the geometric features do not favor this interaction, since **4** is a poorer inhibitor than **2**.

Received: March 29, 1994 [Z 6809 IE]
German version: *Angew. Chem.* **1994**, *106*, 1858

[1] M. L. Sinnott, *Chem. Rev.* **1990**, *90*, 1171; G. Legler, *Adv. Carbohydr. Chem. Biochem.* **1990**, *48*, 319.
[2] B. Junge, F.-R. Heiker, J. Kurz, L. Müller, D. D. Schmidt, C. Wuensche, *Carbohydr. Res.* **1984**, *128*, 235; N. Ishida, K. Kumagai, T. Niida, T. Tsuruoka, H. Yumoto, *J. Antibiot.* **1967**, *20*, 66; L. P. Hohenschutz, E. A. Bell, P. J. Jewess, D. P. Leworthy, R. J. Pryce, E. Arnold, J. Clardy, *Phytochemistry* **1981**, *20*, 811.
[3] For recent articles on this topic see: R. W. Franck, *Bioorg. Chem.* **1992**, *20*, 77; M. L. Sinnott, *ibid.* **1993**, *21*, 34; R. R. Schmidt, H. Dietrich, *Angew. Chem.* **1991**, *103*, 1348; *Angew. Chem. Int. Ed. Engl.* **1991**, *30*, 1328; P. Ermert, A. Vasella, M. Weber, K. Rupitz, S. G. Withers, *Carbohydr. Res.* **1993**, *250*, 113.
[4] M. Koyama, T. Aijima, S. Sakamura, *Agric. Biol. Chem.* **1974**, *38*, 1467.
[5] S. Murao, S. Miyata, *Agric. Biol. Chem.* **1980**, *44*, 219.
[6] B. Winchester, G. W. J. Fleet, *Glycobiology* **1992**, *2*, 199.
[7] T. Trnka, M. Černý, *Collect. Czech. Chem. Commun.* **1971**, *36*, 2216.
[8] I. Inghardt, T. Freid, *Synthesis* **1990**, 285.
[9] J. A. Sousa, A. L. Bluhm, *J. Org. Chem.* **1960**, *25*, 108.
[10] M. Bols, I. Lundt, C. Pedersen, *Tetrahedron* **1992**, *48*, 319.
[11] Data for **2** (as hydrochloride salt): $[\alpha]_D^{20} = +19.6$ ($c = 0.85$, EtOH); ^{13}C NMR (D_2O): δ=70.7, 68.1 (C-3, C-4), 58.6 (CH_2OH), 46.2, 44.4 (C-2, C-6) 40.6 (C-5); ^1H NMR (500 MHz, D_2O): $\delta = 3.72$ (dd, $J_{5b',5a'} = 11.5$, $J_{5b',5} = 3.3$ Hz, 1H, H-5b'), 3.67 (ddd, $J_{3,2ax} = 11.2$ Hz, $J_{3,4} = 8.9$, $J_{3,2eq} = 4.9$ Hz, 1H, H-3), 3.64 (dd, $J_{5a',5} = 6.2$ Hz, 1H, H-5a'), 3.43 (ddd, $J_{2eq,2ax} = 12.7$, $J_{2eq,6} = 2.0$ Hz, 1H,H-2eq), 3.42 (dd, $J_{4,5} = 10.5$ Hz, 1H, H-4), 3.41 (ddd, $J_{6eq,6ax} = 13.4$ Hz, $J_{6eq,5} = 3.8$ Hz, 1H, H-6eq), 2.87 (dd, $J_{6ax,5} = 12.2$ Hz, 1H, H-6ax), 2.78 (dd, 1H, H-2ax), 1.86 (ddddd, 1H, H-5).
[12] J. B. Ducep, C. Danzin, Merrell Dow Pharmaceuticals, Inc. EP-B 389723, **1990**; [*Chem. Abstr.* **1991**, *114*, 247673W].
[13] A. J. Mancuso, S.-L. Huang, D. Swern, *J. Org. Chem.* **1978**, *43*, 2480.
[14] Data for **9** (as the hydrochloride salt): $[\alpha]_D^{20} = +36.7$ ($c = 0.85$, MeOH); ^{13}C NMR (D_2O): δ = 98.6 (C-1), 72.3, 72.2 (C-3, C-4), 70.0 (2C, C-2, C-4'), 68.0 (C-5), 67.9 (C-3'), 58.2 (CH_2OH), 54.6 (OCH_3), 54.0 (C-2'), 53.5 (C-7), 53.0 (C-6'), 40.3 (C-5'), 25.1 (C-6).
[15] H. O. Halvorson, *Methods Enzymol.* **1966**, *8*, 559.
[16] J. Gorman, H. O. Halvorson, *Methods Enzymol.* **1966**, *8*, 562.
[17] Program Grafit from Erichaecus Software.
[18] M. K. Tong, G. Papandreou, B. Ganem, *J. Am. Chem. Soc.* **1990**, *112*, 6137; B. Ganem, G. Papandreou, *ibid.* **1991**, *113*, 8984; G. Papandreou, M. K. Tong, B. Ganem, *ibid.* **1993**, *115*, 11682.
[19] T. Kajimoto, K. K.-C. Liu, R. L. Pederson, Z. Zhong, Y. Ichikawa, J. A. Porco, C.-H. Wong, *J. Am. Chem. Soc.* **1991**, *113*, 6187; K. K.-C. Liu, T. Kajimoto, L. Chen, Z. Zhong, Y. Ichikawa, C.-H. Wong, *J. Org. Chem.* **1991**, *56*, 6280.

Human Oxalate—Really Just an End-Product of Metabolism?

Steffen Albrecht,* Herbert Brandl, and Christoph Schönfels

Oxalate is a product of human metabolism which is not currently considered to have any physiological importance. Gall stone and kidney stone complaints and calcification of organs are, of course, often caused by crystallization of calcium oxalate. Only plant cells[1] and certain bacteria (*Oxalobacter formigenes, Pseudomonas oxalaticus*) are known to metabolize oxalate [Eqs. (a), (b)].

$$HOOCCOOH + O_2 \xrightarrow{\text{oxalate oxidase}} 2CO_2 + H_2O_2 \quad (a)$$

$$HOOCCOOH \xrightarrow{\text{oxalate decarboxylase}} HCOOH + CO_2 \quad (b)$$

A highly sensitive and specific chemiluminometric method was developed to determine oxalate in body fluids.[2] It is based on the rapid oxidation of oxalate by H_2O_2 in the presence of carbodiimide and a suitable fluorophore at a low pH. The resulting intermediate, monoperoxyoxalic acid, breaks down into CO_2 and O_2 by exciting the fluorophore. The overall reaction is described by Equation (c) and the light emission by Equation (d). The emitted light can be measured with sensitive luminometers to detect very small oxalate concentrations to 200 nmol L^{-1}. Since interference from other organic molecules does not occur, the method is suitable for oxalate determination in biological samples.

$$(HOOC)_2 + H_2O_2 + R\text{-}N{=}C{=}N\text{-}R + F \xrightarrow{H^+} H_2O + 2CO_2 + R\text{-}NH\text{-}C(O)\text{-}NH\text{-}R + F^* \quad (c)$$

$$F^* \longrightarrow F + h\nu \quad (d)$$

(R = cyclohexyl; F = 9,10-diphenylanthracene; F* = fluorophore in first excited singlet state)

The determination of the oxalate content of human serum and plasma samples gave reproducible values which were different for the two media[3] and confirmed by data in recent literature.[4] Our experiments gave average values of 4.0 μmol L^{-1} for oxalate in plasma and 12.3 μmol L^{-1} for oxalate in serum—a result which was difficult to interpret at first.

During the examination of hemodialysis patients another noteworthy result appeared: The total amount of oxalic acid precipitated in the dialyzate significantly exceeded the amount that was calculated from the difference in oxalate concentration in the plasma before and after dialysis, taking the total blood volume into account. Possibly high intracellular oxalate concentrations are the cause of this discrepancy. It is known that partial lesion of human blood cells occurs, both during the coagulation process and high-speed centrifugation, and during the blood flow in the capillary tubes of the dialysis capsules. Hence intracellular oxalate concentrations were determined in erythrocytes, thrombocytes, granulocytes, and monocytes, since no reliable data was available.

These blood cells were obtained from 60 adults aged 20 to 40 years and separated using known methods (see Experimental Procedure). After a final washing step with physiological NaCl solution, the cell suspensions, which contained 10^5 to 10^6 cells per mL, were quick-frozen three times in liquid nitrogen, and 100 μL 15% HCl was added per mL cell suspension, which resulted in complete lesion of the cells. Next the oxalate concentration in the supernatant was determined by chemiluminometric measurements. Values between 0.1 and 10 mg L^{-1} were obtained. The average erythrocyte and thrombocyte volumes were determined using differential blood cell counting devices. Average volumes of 1100 and 3100 fL were assumed for granulocytes and monocytes, respectively, based on literature values.[5]

The oxalate concentrations summarized in Table 1 were calculated taking into account the relevant cell counts and volumes. The intracellular oxalate concentration exceeds that in the plasma by at least two orders of magnitude, independent of the cell type. The question of whether the oxalate is produced extra- or intracellularly cannot be answered at present. There is no evidence of active ATP-dependent transport processes for oxalate, as are known for alkaline and alkaline earth metal ions. It is likely that intracellular formation of oxalate is enzyme catalyzed from the precursors serine, L-hydroxyproline, tyrosine, phenylalanine, tryptophan, and L-ascorbic acid.[4] The intracellular oxalate concentrations are similar to the known concentrations of other substances in human cells. For example, the concentration of 2,3-diphosphoglycerate in erythrocytes is 4720 μmol L^{-1}.[5] Of course, the oxalate concentrations given in Table 1 have to be taken as total oxalate. It is not possible to state how the oxalate is present in vivo. Because oxalate is a small mono- or dianion, most of it should be bound, that is, complexed with transition metal cations. Since with our method the oxalate concentrations are measured at pH 1, the majority of the oxalate is present as the free monoanion or as the neutral acid; even calcium oxalate microcrystallites would dissolve under these conditions. The following questions thus arise: Is oxalate really just an end-product of human metabolism? If it is, what purpose do the high intracellular oxalate concentrations have?

Table 1. Average intracellular oxalate concentration in human blood cells and extracellular oxalate concentration in heparin plasma.

Cell type	No. of samples	Oxalate conc. [μmol L^{-1}]	2 SD [μmol L^{-1}] [a]
erythrocytes	60	615	±183
thrombocytes	36	890	±223
granulocytes	60	1830	±411
monocytes	26	2910	±638
heparin plasma	60	3.98	±1.68

[a] Standard deviation.

The enzyme-catalyzed oxalate metabolism known in the plant kingdom [Eq. (a)] could indicate that an oxalate oxidase pathway may also be important in human metabolism. A human enzyme with oxalate oxidase activity and the genetic determination of this enzyme would be prerequisite; we are currently conducting preliminary investigatious is this direction. The reaction products H_2O_2 and CO_2 have important biochemical functions: H_2O_2 forms a substantial component of the "respira-

[*] Dr. rer. nat. habil. S. Albrecht
Universitätsklinikum der Technischen Universität
Institut für Klinische Chemie und Laboratoriumsmedizin
Fetscherstrasse 74, D-01307 Dresden (FRG)
Telefax: Int. code + (351)458-4340
StR H. Brandl
Gymnasium Kaltenkirchen (FRG)
Dipl.-Biochem. C. Schönfels
Medizinisches Labor Dr. Schottmann, Freiburg (FRG)

tory burst" of cells capable of phagocytosis and is generated mainly from O_2 during inflammatory processes [Eq. (e)].

$$2H^+ + 2O_2^{\cdot-} \xrightarrow{\text{superoxide dismutase}} H_2O_2 + O_2 \qquad \text{(e)}$$

The oxalate oxidase pathway may be an alternative to Equation (e). It was recently confirmed experimentally that mechanisms should exist by which oxalate can be enzymatically converted in human blood cells. When separated human neutrophilic granulocytes are stimulated with endogenic noxious substances such as zymosan or endotoxin, the intracellular oxalate concentration, in comparison to unstimulated cells, is only 60 to 65% of the values given in Table 1. If investigations using molecular biology demonstrate the existence and genetic determination of one or more enzymes with oxalate oxidase activity, this would be the first time that it was shown that oxalate is not just a useless end-product of human metabolism. From our results it is not possible to state how oxalate exists in human blood cells, only that it is present in considerable amounts.

Experimental Procedure

Cell separation: The separation of the erythrocytes was performed by dextran sulfate sedimentation. Granulocytes were isolated from the supernatant by density gradient centrifugation, according to the method of Eckert [6]. Thrombocytes were separated by centrifugation, according to the method of Kazemi et al. [7]. Monocytes were isolated according to Hamid [8]. All cell counts were performed on a differential blood cell counting device from Coulter (Krefeld).

Chemiluminometric measurements: After centrifugation the cell-lysate superantants were measured with a luminometer LB 9503 from Berthold, Wildbad (100 µL sample volume, measuring time 4 s). Further details are given in ref. [2]. Duplicate measurements were performed, and the standard deviation was always less than 4%.

Received: March 17, 1994 [Z 6769 IE]
German version: *Angew. Chem.* **1994**, *106*, 1864

[1] B. G. Lane, J. M. Dunwell, J. A. Ray, M. R. Schmitt, A. C. Cuming, *J. Biol. Chem.* **1993**, *268*, 12239–12242.
[2] S. Albrecht, H. Hornak, T. Freidt, W. D. Böhm, K. Weis, A. Reinschke, *J. Biolumin. Chemilumin.* **1993**, *8*, 21–24.
[3] S. Albrecht, A. Reinschke, W. D. Böhm, A. Blatter, K. Weis, J. U. Leititis, *Z. Urol. poster* **1993**, 22–24.
[4] S. Albrecht, "*Zur Anwendung moderner Chemilumineszenzmethoden in der biochemischen Analytik*", Habilitationsschrift, Technische Universität Dresden, **1993**, pp. 28–60.
[5] H. Arnold, K. Hass in *Praktische Blutzelldiagnostik* (Eds.: I. Boll, S. Heller), Springer, Berlin, **1991**, pp. 101–108.
[6] R. Eckert in *Immunologische Arbeitsmethoden* (Ed.: H. Friemel), Fischer, Jena, **1984**, pp. 252–254.
[7] A. Kazemi, A. K. Singh, N. G. P. Slater, *Br. J. Haematol.* **1991**, *79*, 624–627.
[8] A. Hamid, "*Monozytenfunktionen and Immunstatus at Patienten with Non-Hodgkin-Lymphomen*", Dissertation, Medizinische Akademie, Dresden, **1992**, pp. 32–33.

An Overall Picture of Biomembranes from the Mosaic of Data

Biomembranes. Physical Aspects. Edited by *M. Shimitzky*. VCH Verlagsgesellschaft, Weinheim/VCH Publishers, New York, 1993. 371 pp., hardcover DM 198.00, $ 135.00.—ISBN 3-527-30021-X/1-56081-771-2

This book is the first volume in a series that aims to provide a structure for the many-faceted subject of biological membranes; it is concerned with the physical phenomena that result from the integrity and fluidity of lipid double layers. This is a well-chosen topic to begin the series, as it introduces the basic principles for later discussions of membrane functions.

Although the present picture of lipid membrane structures is fairly clear, it is a mosaic made up of many thousands of publications. Does this book fulfill its claim to provide the picture with a structure? In my view it mainly does; three of the chapters achieve this especially well, and these will be described first. In Chapter 4 on "Fluidity, Dynamics, Order", B. Wieb van der Meer defines in a brief and simple way six types of dynamic processes in lipid membranes, then treats these in a textbook style, comparing and evaluating their importance. Molecular alignment, domain formation, and asymmetry in membranes are thoroughly discussed, as also are basic concepts, methods, and current problems. The bibliography to this chapter is systematically arranged and includes full titles, enabling the reader to quickly find material on topics of particular interest. Chapter 7 on the electrical properties of membranes (L. M. Loew) is much shorter, but this too strikes me as perfect in its way. Here again one finds an easily readable text, with illustrations that are precisely in harmony with it, and the titles of the most important publications are given. Also very pleasing is Chapter 6, in which Y. I. Henis gives a detailed description, with up-to-date illustrations, of the interesting method of "fluorescence photobleaching recovery".

On the other hand, the remaining four chapters are competently written surveys of particular topic areas, rather than attempts at providing a structure. In Chapter 1 D. Marsh summarizes the thermodynamic equations from the more extensive treatment in his book *Phospholipid Bilayers*, but a clear physical model fails to emerge from the illustrations or from the qualitative descriptions of the forces that are at work. Chapter 2, by D. Chapman, is concerned with phase transformations in lamellar, hexagonal, and cubic phases. In my view this does not really fit into the subject of biomembranes, despite the inclusion of a section entitled "Biological Relevance" which introduces comparisons with cell partitioning, domain formation, etc. The same comment applies to the topic of micelles in Chapter 3 by D. Lichtenberg, since to my knowledge micelles in the usual sense do not occur in biological systems. In contrast liposomes are not treated in sufficient detail. There are no electron micrographs of these, nor is there anything on fusion models or undulations. Most of the figures are more likely to mislead than to elucidate the text (examples: Figs. 8 and 9 show micelles that are not curved, which is very untypical; Fig. 4 shows turbidity occurring as a result of micelle formation, despite the fact that micellar solutions are nearly always quite clear; Fig. 2 shows molecular models that are cone-shaped, even though there are no examples of these). That leaves only Chapter 5 on lipid–protein interactions, by A. H. Parola, which is by far the longest in the book. I feel that the content of this chapter is well summarized by the author's comment on page 221 that "...work on membrane protein purification and reconstitution leaves very limited evidence of specific lipid requirements for membrane protein reactivation...". The listing of the many proteins whose interactions with liposomes have been investigated makes boring reading for the nonspecialist, and the discussion of the results yields few surprises. On the other hand, a novel idea that could be important is the model of malignant plasma membranes with intercalated domains of electroneutral lipids (also containing DNA?—this point is not made clear). The comprehensive survey of protein–lipid interactions is, of course, of central interest to the specialist reader.

The book is undoubtedly an important addition to the literature for the reader envisaged in the preface, who is engaged in research in this field. He or she will find here comprehensive information on membrane fluidity, membrane proteins, and electrical properties. However, this thorough coverage extends only up to 1988; beyond that it becomes thin. For the students also envisaged as potential users, I recommend Chapters 4, 6, and 7 as readable introductions; they will also find Chapter 5 useful, although much of it can be skipped over. With regard to the introductory Chapters 1–3, the student would be better served by other books, such as *Phospholipid Bilayers*, by G. Cevc and D. Marsh, *Membrane Mimetic Chemistry*, by J. H. Fendler, and *Intermolecular and Surface Forces*, by J. N. Israelachvili. It is not until Chapter 4 when the focus turns to biological aspects that the book begins to fulfill its special objective. One must therefore hope for the best in the volumes that are to follow.

Jürgen-H. Fuhrhop
Institut für Organische Chemie
der Freien Universität Berlin (FRG)

Medicinal Chemistry. The Role of Organic Chemistry in Drug Research. Edited by *C. R. Ganellin* and *S. M. Roberts*. Academic Press, London, 1993. 302 pp., hardcover £ 29.00.—ISBN 0-12-274120-X

Eight years after the publication of the first edition of this book, this new edition has appeared. It consists of 14 chapters with 17 authors, offering the reader an excellent survey of the pharmacological aspects and the synthesis, development, and medical importance of new pharmaceutical products. The descriptions of pharmacologically active compounds and their meth-

This section contains book reviews and a list of new books received by the editor. Book reviews are written by invitation from the editor. Suggestions for books to be reviewed and for book reviewers are welcome. Publishers should send brochures or (better) books to Dr. Ralf Baumann, Redaktion Angewandte Chemie, Postfach 101161, D-69451 Weinheim, Federal Republic of Germany. The editor reserves the right of selecting which books will be reviewed. Uninvited books not chosen for review will not be returned.

ods of preparation are illustrated throughout by structural formula diagrams.

Seven of the chapters are revised and updated treatments of topics that were included in the first edition, and these appear at the beginning and end of the new version, as follows: Chapter 1, "Introduction to Receptors and the Action of Drugs"; Chapter 2, "Structure and Catalytic Properties of Enzymes"; Chapter 3, "Receptor Pharmacology"; Chapter 10, "Beta Blockers"; Chapter 11, "Salbutamol: A Selective β_2-Stimulant Bronchodilator"; Chapter 12, "Discovery of Cimetidine, Ranitidine and other H_2-Receptor Histamine Antagonists"; Chapter 14, "Clavulanic Acid and Related Compounds: Inhibitors of β-Lactamase Enzymes". The new chapters that have been added are: Chapter 4, "Drug Access and Prodrugs"; Chapter 5, "QSAR and the Role of Computers in Drug Design"; Chapter 6, "The Current Status and Future Impact of Molecular Biology in Drug Discovery"; Chapter 7, "General Approaches to Discovering New Drugs: A Historical Perspective"; Chapter 8, "Discovery and Development of Cromakalim and Related Potassium Channel Activators"; Chapter 9, "Angiotensin-Converting Enzyme (ACE) Inhibitors and the Design of Cilazapril"; Chapter 13, "Fluconazol, an Orally Active Antifungal Agent".

Following the introduction to the general principles of pharmacology in the first half of the book, the emphasis in the second half is on the practical importance of pharmaceutical compounds in areas where there is likely to be impressive progress in the age of our modern industrial society. Chapter 8 describes a new therapeutic principle for the treatment of cardiac and circulatory disorders and bronchial asthma, which is becoming increasingly important with the discovery of the mechanism whereby cromakalim acts as a potassium channel activator. Chapter 9 is concerned with ACE inhibitors, which are now the most favored agents for the treatment of hypertension and cardiac degeneration. The development of ACE inhibitors such as captopril, enalapril, and cilazapril is described, together with their biological properties. Chapter 10 discusses the chemistry, pharmacology, and clinical effects of beta blockers, which competitively and reversibly inhibit the positive inotropic and chronotropic effects of catecholamines on the heart (by blocking the β_1 receptors), and also inhibit bronchospasmolysis by blocking the β_2 receptors. Chapter 11 is concerned with salbutamol and analogous compounds derived from adrenalin and isoprenalin, which are used in the treatment of bronchial asthma. Chapter 12 is devoted to cimetidine and ranitidine, two compounds that rank as milestones in the development of H_2-receptor histamine antagonists and are used in the treatment of gastritis and ulcers; their preparation is described in detail and structure–activity relationships are discussed. Chapters 13 and 14 are concerned with antiinfectives, in particular with the widely used orally active antifungal agent fluconazol and with clavulanic acid which is used as an inhibitor of β-lactamase enzymes. A combination of clavulanic acid with amoxicillin has proved successful as a further development in the penicillins field.

This altogether excellent book, an enlarged revision of the edition published in 1985, is a valuable addition to other recently published books on medicinal chemistry (R. B. Silverman, *The Organic Chemistry of Drug Design and Drug Action*; B. Testa, W. Fuhrer, E. Kyburz, and R. Giger, *Perspectives in Medicinal Chemistry*; both published in 1992). *Medicinal Chemistry* contains many valuable articles which help the reader to understand important concepts of pharmacology and molecular biology, and describe new developments in pharmacological agents.

Gunter Schmidt
Bayer AG
Wuppertal (FRG)

2D NMR. Density Matrix and Product Operator Treatment. By *G. D. Mateescu* and *A. Valeriu*. PTR Prentice Hall, Englewood Cliffs, 1993. 200 pp., hardcover $ 50.00.—ISBN 0-13-013368-X

This book aims to provide the reader with a detailed guide to analyzing multiple-pulse NMR experiments, using the density matrix and product operator approaches. The text is deliberately and unashamedly didactic in its approach, and the calculations are set out step-by-step without leaving out any intermediate results. In addition, the manipulations by which a result is simplified and interpreted are also set out in some detail.

The first section of the book is devoted to examples of the use of the density matrix approach, the first such example being an analysis of the HETCOR experiment whereby one observes ^{13}C and obtains a two-dimensional $^{13}C-^{1}H$ shift correlation spectrum. The authors introduce the concept of the density matrix, explaining how to set up the equilibrium conditions, the effect of pulses, how to calculate evolution, and finally how to calculate observables. Each of these ideas is introduced as it is needed in deducing the effect of the pulse sequence, and so there is a natural flow to the discussion, with the concepts appearing in context. Having completed the analysis, the authors then compare this with an attempt at a vector analysis of the sequence, showing that the vector method is at best cumbersome, and at its worst extremely confusing. The reader is left with the impression that multiplying matrices together is preferable to trying to understand the apparently random rules that govern these vectors.

The main criticism of this opening section is that it rather fudges the important issue of the connection between the terms one sees at the end of a calculation and the appearance of a two-dimensional spectrum. The authors do not make a clear distinction between terms which simply affect the amplitude or phase of a peak and those which contain the information about the frequencies present in the F_1 spectrum. Further, the connection between the form of these terms and the phase (or even sign) of the peaks in the spectrum is not well described.

The density matrix section goes on to cover the INADEQUATE and COSY procedures. As before, the issues of phase and lineshapes are somewhat lost, and the difference between the phase properties of the cross and diagonal peaks in COSY spectra receives scant attention. The section closes with a discussion of "phase cycling" in the COSY experiment; in fact the topic covered is frequency discrimination, which is rather a different matter.

The second section of the book goes on to introduce the product operator formalism, again using the approach of showing how a calculation is done and highlighting the rules by which these operators are manipulated. Some time is spend on establishing the relationship between the operators, their matrix representations, and observable signals; this is a welcome discussion. Once again HETCOR is used as the first example but, incredibly, this is the only *two-dimensional* experiment analyzed using product operators. The remainder of the examples are all one-dimensional experiments, such as DEPT; in these cases the analysis is extended to include magnetic equivalence. It is very unfortunate that the authors did not include COSY and double-quantum-filtered COSY as examples, as these both provide excellent vehicles for explaining the usefulness and properties of product operators. Generally speaking, this section on product operators does not read well; the overall impression is one of confusion, and a lack of structure and authority.

 © VCH Verlagsgesellschaft mbH, D-69451 Weinheim, 1994 0570-0833/94/1717-1784 $ 10.00+.25/0

The book closes with a series of appendices which bring together the concepts used in the rest of the book, i.e., listings of matrix representations of rotation operators, properties of operators, rotations, etc. In addition some of the quantum-mechanical background is given in more detail, together with discussions of the more formal aspects of the theory.

This book has a thoroughly laudable aim — to show the reader exactly how to do density matrix and product operator calculations. There are few texts available which seek to do this and so, despite its less than ideal presentation of the subject, some will no doubt find this book a helpful guide.

J. H. Keeler
University of Cambridge
(United Kingdom)

Comprehensive Dictionary of Physical Chemistry. Edited by *L. Ulický* and *T. J. Kemp*. Ellis Horwood/PTR Prentice Hall, New York, 1992. 472 pp., hardcover $ 45.00.—ISBN 0-13-151747-3

Physical chemistry has grown by leaps and bounds in recent years. In the past dozen years alone, dramatic progress has been witnessed in areas as diverse as the imaging of atoms and molecules by scanning tunneling microscopy, the discovery and characterization of a host of new cluster molecules such as the fullerenes, the imaginative practical applications that have been found for theoretical concepts such as chirality or similarity, the breakthroughs in molecular recognition studies with the mapping of biological receptors and other species, the realization of the role played by chaos in chemical systems, and the rapidly developing uses of fuzzy logic and neural networks in the solution of a wide range of chemical problems. It has certainly been an exciting time and there can be little doubt that physical chemistry today is one of the most vibrant and dynamic areas of chemistry. Keeping pace with this exciting whirl of activity has not been easy, and so there is ample scope for review works such as dictionaries and encyclopedias to expound and elucidate what has been going on. Indeed, one turns to such works with a certain sense of relief to guide one through the intricate maze of development that is current physical chemistry.

Thus it was with eager anticipation that I embarked on reading the *Comprehensive Dictionary of Physical Chemistry*. My expectations were further heightened as I read on the opening pages that this work is to form part of a series that will "encompass outstanding works by world-class chemists" and moreover that the series as a whole is intended to "become a by-word for quality". Imagine then my disappointment when I discovered that not one of the research areas enumerated above had even been mentioned in this "comprehensive" dictionary! As I delved deeper into this work, my sense of frustration was compounded when it became apparent that this work not only failed to reflect the dynamism and energy of modern physical chemistry but that it also succeeded in making the physical chemistry of yesteryear uninspiring and boring. This double whammy set me to wondering how a book that was announced with so much fanfare could make an exciting subject seem so insipid. I eventually came to the conclusion that this work fails for three major reasons.

First, this dictionary was not originally written in English but is a translation from the Slovak. A team of eight translators were involved in this project, and differences in approach and style are all too evident. In some parts of the dictionary British English is used whereas American English is used in other parts. Worse yet, the language is often stilted and in some instances just plain wrong. Thus, we read on page 343 that radioactive elements are "chemical elements whose all isotopes are radioactive", and on page 193 that "although it is impossible to materialize a model of an ideal crystal, it represents an abstraction which is very useful mainly to explain laws governing crystal forms"; again on page 262 a molecule is defined as "the smallest stable particle constituting matter which is composed of atomic nuclei and electrons bound by chemical bonds and which exhibits its specific chemical properties". On occasion, the English thoroughly confuses the reader, as in the definition of the point group of a molecule on page 317: "a symmetry group that characterizes the symmetric properties of molecules", or when we are told that "the Schrödinger equation, just as the other postulates of quantum mechanics, cannot be derived" (p. 323).

Secondly, the dictionary contains more than a fair share of factually inaccurate or, at the very least, highly misleading statements. For instance, on page 27 the planetary model of the atom is ascribed to Rutherford, whereas this model was first put forward by the Japanese physicist Nagaoka. In the discussion on quantum chemistry on page 174, we are informed that the Hamiltonian of a molecule is "an operator of the total energy Born–Oppenheimer approximation". In fact, the Hamiltonian of a molecule and the Born–Oppenheimer approximation are two quite separate matters that should not be mixed up with one another. The treatment of symmetry (p. 412) becomes almost hilarious when it is stated that the human body consists of two halves, one being the mirror image of the other. One can only wonder where the authors imagine the human heart to be located! In spite of statements in the preface to this work that "entries were required to be factual" and that all entries were "scrutinized by readers, discussed by the specialist commission and approved by the editorial board" such errors are to be found in many entries in this dictionary.

Thirdly, the entire work is seriously out of date and is written in a style very reminiscent of the 1970s. This impression is reinforced by the 6-page bibliography at the end of the book; this lists references dating mainly from the 1960s and 1970s and earlier. Moreover, the presentation of the material is dry and unimaginative. The figures and diagrams are particularly poor, and when one thinks of some of the highly imaginative uses made of illustrations in many modern American technical books it is surprising that the publisher would want to put something so dreary on the market. Particularly when the work is billed as "a very direct source of contemporary physical chemistry"! All of which is most unfortunate, for there is presently a very real need for good guides to the current physical chemistry landscape. Whereas there are many encyclopedias and dictionaries of chemistry as a whole, there is precious little devoted specifically to physical chemistry. The work under review will not be able to fulfill the need, and so for the time being the gap will remain. Those on the cutting edge of physical chemistry who fancy themselves as budding lexicographers should please take note!

Dennis H. Rouvray
University of Georgia
Athens, Georgia (USA)

 © *VCH Verlagsgesellschaft mbH, D-69451 Weinheim, 1994* *0570-0833/94/1717-1785 $ 10.00+.25/0*

New Books

Polymer Analysis and Characterization. Advances in Polymer Science, Vol. 114. By **V. A. Bershtein, G. C. Berry, J. Lesec, H. Matsuoka, I. Norio, I. S. Osad'ko, V. Ryzhov, J. L. Viovy.** Springer, Berlin. **1994.** 299 pp., hardcover, DM 228.00.—ISBN 3-540-57238-4

Photoconducting Polymers/Metal-Containing Polymers. Advances in Polymer Science, Vol. 115. By **M. Biswas, A. Mukherjee, V. Mylnikov.** Springer, Berlin. **1994.** 132 pp., hardcover, DM 128.00. —ISBN 3-540-57476-X

Regulation and Control of Complex Biological Processes by Biotransformation. Frontiers in Biotransformation, Vol. 9. Edited by **K. Ruckpaul, H. Rein.** Akademie Verlag, Berlin. **1994.** 253 pp., hardcover, DM 228.00.—ISBN 3-05-501367-0

Studienführer Chemie. Edited by **Gesellschaft Deutscher Chemiker.** VCH, Weinheim. **1994.** 405 pp., paperback, DM 29.80.—ISBN 3-527-29226-8

Chemie in Haus und Garten. By **G. Vollmer, M. Franz, I. Hestermann.** Thieme, Stuttgart, **1994.** 287 pp., paperback, DM 22.90.—ISBN 3-13-767501-4

Chromatographische Trennmethoden. Theoretische Grundlagen, Techniken und analytische Anwendungen. By **G. Schwedt.** Thieme, Stuttgart, **1994.** 224 pp., paperback, DM 42.00. —ISBN 3-13-576403-6

Organische Chemie I. Grundlagen, Stoffklassen, Reaktionstypen. By **E. Breitmaier, G. Jung.** Thieme, Stuttgart, **1993.** 480 pp., hardcover, DM 75.00.—ISBN 3-13-541503-1

NMR-Spektroskopie von Nichtmetallen. By **S. Berger, S. Braun, H.-O. Kalinowski.** Thieme, Stuttgart, **1993.** 240 pp., hardcover, DM 286.00.—ISBN 3-13-769301-2

Membrane-Mimetic Approach to Advanced Materials. Advances in Polymer Science, Vol. 113. By **J. H. Fendler.** Springer, Berlin. **1994.** 236 pp., hardcover, DM 168.00.—ISBN 3-540-57237-6

Oberflächentechnologie mit Niederdruckplasmen. Beschichten und Strukturieren in der Mikrotechnik. By **G. Franz.** Springer, Berlin, **1994.** 434 pp., hardcover, DM 148.00.—ISBN 3-540-57360-7

Properties of Liquids and Solutions, 2nd Edition. By **J. N. Murrell, A. D. Jenkins.** Wiley, Chichester, Great Britain, **1994.** 303 pp., paperback, £ 16.95.—ISBN 0-471-94419-X

Chemical Group Theory. Introduction and Fundamentals. Edited by **D. Bonchev, D. H. Rouvray.** Gordon and Breach, Reading, Great Britain, **1994.** 262 pp., hardcover, £ 78.00.—ISBN 2-88124-959-0

Emeriti erinnern sich. Rückblicke auf die Lehre und Forschung in Heidelberg. Edited by **O. M. Marx, A. Moses.** VCH, Weinheim, **1994.** 508 pp., hardcover, DM 88.00.—ISBN 3-527-29221-7

Mathematik für Chemiker. 5th Ed. By **H. G. Zachmann.** VCH, Weinheim, **1994.** 700 pp., hardcover, DM 84.00.—ISBN 3-527-29224-1

Flüssigkeitsring-Vakuumpumpen, -Kompressoren und -Anlagen. Technisches Handbuch. Grundlagen - Berechnung - Planung. By **H. Bannwarth.** VCH, Weinheim, **1994.** 494 pp., hardcover, DM 228.00.—ISBN 3-527-28670-5

Transition Metal Chemistry. The Valence Shell in d-Block Chemistry. By **M. Gerloch, E. C. Constable.** VCH, Weinheim/New York, **1994.** 211 pp., paperback, DM 58.00/$ 35.00. ISBN 3-527-29219-5/1-56081-884-0

Nanoscale Characterization of Surfaces and Interfaces. By **N. J. DiNardo.** VCH, Weinheim, **1994.** 163 pp., DM 128.00.— ISBN 3-527-29247-0

Highlights of Chemistry as Mirrored in Helvetica Chimica Acta. Edited by **M. V. Kisakürek, E. Heilbronner.** VCH, Weinheim, Helvetica Chimica Acta, Basel. **1994.** 985 pp., hardcover, DM 248.00.—ISBN 3-527-29238-1/3-906390-08-X

Fundamentals of Polymer Science. By **M. M. Coleman, P. C. Painter.** Technomic Publ. Co., Lancaster, **1994.** 441 pp., hardcover, $ 75.00.—ISBN 1-56676-152-2

Chemie der Heterocyclen. Struktur, Reaktionen und Synthesen. By **T. Eicher, S. Hauptmann.** Thieme, Stuttgart. **1994.** 504 pp., paperback, DM 76.00.—ISBN 3-13-135401-1

Advanced Instrumental Methods of Chemical Analysis. Edited by **J. Churácek.** Ellis Horwood, New York, **1993.** 486 pp., hardcover, $ 152.00. ISBN 0-13-913195-7

Statistics for Analytical Chemistry. By **J. C. Miller, J. N. Miller.** Ellis Horwood, New York. **1992.** 227 pp., paperback, $ 64.55.—ISBN 0-13-845421-3

Radical Polymerization in Disperse Systems. By **J. Barton, I. Capek.** Ellis Horwood, New York, **1994.** 352 pp., hardcover, $ 120.00.—ISBN 0-13-752353-X

Electrochemistry of Novel Materials. Edited by **J. Lipkowski, P. N. Ross.** VCH, New York, **1994.** 387 pp., hardcover, DM 245.00/$ 145.00.—ISBN 0-89573-788-4

Plants and the Chemical Elements. Biochemistry, Uptake, Tolerance and Toxicity. Edited by **M. E. Farago.** VCH, Weinheim/New York, **1994.** 292 pp., hardcover, DM 198.00/$ 115.00.—ISBN 3-527-28269-6/1-56081-135-8

Das chemisch-technische Praktikum für Berufsausbildung und Studium. By **V. Hopp, H. Heinz.** VCH, Weinheim, **1994.** 411 pp., hardcover, DM 78.00.—ISBN 3-527-28625-X

Circular Dichroism. Principles and Applications. Edited by **K. Nakanishi, N. Berova, R. W. Woody.** VCH, New York, **1994.** 570 pp., hardcover, DM 209.00/$ 125.00.—ISBN 1-56081-618-X

Optische Spektroskopie. Eine Einführung für Naturwissenschaftler und Techniker. By **W. Schmidt.** VCH, Weinheim, **1994.** 426 pp., paperback, DM 68.00.—ISBN 3-527-29035-4

Quantenchemie. Zweite, erweiterte Auflage. By **H.-H. Schmidtke.** VCH, Weinheim, **1994.** 324 pp., paperback, DM 68.00.—ISBN 3-527-29240-3

Advanced Organic Chemistry of Nucleic Acids. By **Z. Shabarova, A. Bogdanov.** VCH, Weinheim, **1994.** 588 pp., hardcover, DM 248.00/$ 145.00.—ISBN 3-527-29021-4

Azeotropic Data. Part I and Part II. By **J. Gmehling, J. Menke, K. Fischer, J. Krafczyk.** VCH, Weinheim, **1994.** 1729 pp., hardcover, DM 698.00 (subscription price: 598.00). DM 698.00/$ 410.00 (subscription price: DM 598.00/$ 350.00).—ISBN 3-527-28671-3

Nitroalkenes. Conjugated Nitro Compounds. By **V. V. Perekalin, E. S. Lipina, V. M. Berestovitskaya, D. A. Efremov.** Wiley, Chichester, **1994.** 256 pp., hardcover, £ 60.00.—ISBN 0-471-94318-5

The Chemistry of **Organic Arsenic, Antimony and Bismuth Compounds.** Edited by **S. Patai.** Wiley, Chichester. **1994.** 962 pp., hardcover, £ 250.00.—ISBN 0-471-93044-X

The Surface Science of Metal Oxides. By **V. E. Henrich, P. A. Cox.** Cambridge University Press, Cambridge. **1994.** 464 pp., hardcover, £ 55.00.—ISBN 0-521-44389-X

Flame Chemiluminescence Analysis by Molecular Emission Cavity Detection. Edited by **D. A. Stiles, A. C. Calokerinos, A. Townshend.** Wiley, Chichester, **1994.** 193 pp., hardcover, £ 50.00.—ISBN 0-471-94340-1

Basic Mathematics for Chemists. By **P. Tebbutt.** Wiley, Chichester, **1994.** 244 pp., paperback, £ 15.95.—ISBN 0-471-94371-1

Photosynthesis. Fifth edition. By **D. O. Hall, K. K. Rao.** Cambridge University Press, Cambridge. **1994.** 211 pp., £ 9.95. ISBN 0-521-43622-2

IIC Studies, Vol. 14. Copyright and the Public Interest. By **G. Davies.** VCH, Weinheim, **1994.** 220 pp., paperback, DM 118.00.—ISBN 3-527-28638-1

Namen- und Schlagwort-Reaktionen der Organischen Chemie. By **T. Laue, A. Plagens.** Teubner, Stuttgart, **1994.** 338 pp., paperback, DM 36.80.—ISBN 3-519-03526-X

Characterization of Solid Polymers. New Techniques and Developments. Edited by **S. J. Spells.** Chapman & Hall, London, **1994.** 368 pp., hardcover, £ 69.00.—ISBN 0-412-58490-5

Rubber Toughened Engineering Plastics. Edited by **A. A. Collyer.** Chapman & Hall, London, **1994.** 366 pp., hardcover, £ 85.00.— ISBN 0-412-58380-1

Concise Encyclopedia of **Composite Materials.** Revised edition. Edited by **A. Kelly.** Elsevier Science Ltd., Oxford, **1994.** 349 pp., paperback, £ 38.00.—ISBN 0-08-042300-0

Oxford Chemistry Primers: Modern Liquid Phase Kinetics. By **B. G. Cox.** Oxford University Press, Oxford, **1994.** 92 pp., paperback, £ 4.99.—ISBN 0-19-855744-2

Chemical Dynamics at Low Temperatures. By **V. A. Benderskii, D. E. Makarov, C. A. Wight.** Wiley, Chichester, **1994.** 385 pp., hardcover, £ 66.00.—ISBN 0-471-58585-8

Liquid Crystalline Polymers. Edited by **C. Carfagna.** Elsevier Science Ltd., Oxford, **1994.** 257 pp., £ 80.00.—ISBN 0-08-042149-0

Aromaticity and Antiaromaticity. Electronic and Structural Aspects. By **V. I. Minkin, M. N. Glukhovtsev, B. Y. Simkin.** Wiley, Chichester, **1994.** 313 pp., £ 66.00.—ISBN 0-471-59382-6

Angular Momentum. An Illustrated Guide to Rotational Symmetries for Physical Systems. By **W. J. Thompson.** Wiley, Chichester, **1994.** 461 pp., hardcover, £ 54.00.—ISBN 0-471-55264-X

Quantum Field Theory. By **L. S. Brown.** Cambridge University Press, Cambridge, **1994.** 542 pp., paperback, £ 22.95.—ISBN 0-521-46946-5

Structural Biology: The State of the Art. Vol. 1.. Edited by **R. H. Sarma, M. H. Sarma.** Adenine Press, New York, **1994.** 338 pp., hardcover, $ 125.00.—ISBN 0-940030-43-8

Structural Biology: The State of the Art. Vol. 2. Edited by **R. H. Sarma, M. H. Sarma.** Adenine Press, New York, **1994.** 380 pp., hardcover, $ 125.00.—ISBN 0-940030-44-6

Catalyst Characterization. Physical Techniques for Solid Materials. Edited by **B. Imelik, J. C. Vedrine.** Plenum Press, New York, **1994.** 702 pp., hardcover, £ 125.00.—ISBN 0-306-43950-6

Plastics from Microbes. Microbial Synthesis of Polymers and Polymer Precursors. Edited by **D. P. Mobley.** Carl Hanser Verlag, München, **1994.** 269 pp., hardcover, DM 128.00.—ISBN 3-446-17367-6

Introduction to Surface Chemistry and Catalysis. By **G. A. Somorjai.** Wiley, Chichester, **1994.** 667 pp., hardcover, £ 24.95.—ISBN 0-471-03192-5

Destruction of Hazardous Chemicals in the Laboratory, Second Edition. By **G. Lunn, E. B. Sansone.** Wiley, Chichester, **1994.** 501 pp., hardcover, £ 66.00.—ISBN 0-471-57399-X

Ligand Effects on the Chemoselectivity of Transition Metal Catalyzed Reactions of α-Diazo Carbonyl Compounds**

Albert Padwa* and David J. Austin

The transition metal catalyzed reaction of α-diazo carbonyl compounds has found numerous applications in organic synthesis, and its use in either heterocyclic or carbocyclic ring formation is well precedented. Early work in this area made use of insoluble copper catalysts. Although these catalysts are still employed today, their use has decreased significantly with the advent of homogeneous copper catalysts and catalysts based on other metals. The discovery that Rh^{II} carboxylates facilitate nitrogen loss from diazo compounds rekindled significant interest in the field of diazo/carbenoid chemistry. Since the realization that Rh^{II} carboxylates are superior catalysts for the generation of transient electrophilic metal carbenoids from α-diazo carbonyl compounds, intramolecular carbenoid addition and insertion reactions have assumed strategic importance in C–C bond-forming reactions in organic synthesis. In contrast to other catalysts that are suitable for carbenoid reactions of diazo compounds, those constructed with the dirhodium(II) framework are most amenable to ligand modifications that, in turn, can influence reaction selectivity. This article will emphasize the chemical behavior of transition metal carbenoid complexes that are greatly affected by the nature of the ligand groups attached to the metal center. Much of the discussion will center on the ability of the dirhodium(II) ligands to determine reaction preference toward different functional groups on the same molecule.

1. Introduction

Catalytic methods for the generation of metallocarbenes have attracted a great deal of attention in recent years.[1–6] The early investigations of diazo compounds revealed that the problems of selectivity and reactivity could be significantly reduced by using transition metals for their decomposition.[7] The first example of a metal-mediated reaction of an α-diazo carbonyl compound was described by Silberrad and Roy in 1906.[8] Copper dust was added to accelerate the decomposition of ethyl diazoacetate yielding triethyl 4,5-dihydropyrazole-3,4,5-tricarboxylate and was described as follows: "When the diazoacetate is added to copper dust, no reaction appears to take place below 80°, but above that temperature the addition of the first drop of ester is accompanied by an explosion of sufficient violence to shatter the flask". From that time forward, a wide range of transition metal complexes have been used for α-diazo carbonyl decomposition. The most common transition metals include complexes of Cu^{II},[2] Rh^{II},[3] Mn^{II},[9] Fe^{II},[9] Co^{II},[9] Ni^{0},[10] Ni^{II},[11] Zn^{II},[12] Mo^{II},[13, 14] Ru^{II},[13, 15] Ru^{III},[13, 15] and Pd^{II}.[16] Many carbonyl[14, 15] and porphyrin[17] complexes, and to a lesser extent, Brønsted and Lewis acids have also been utilized.[18]

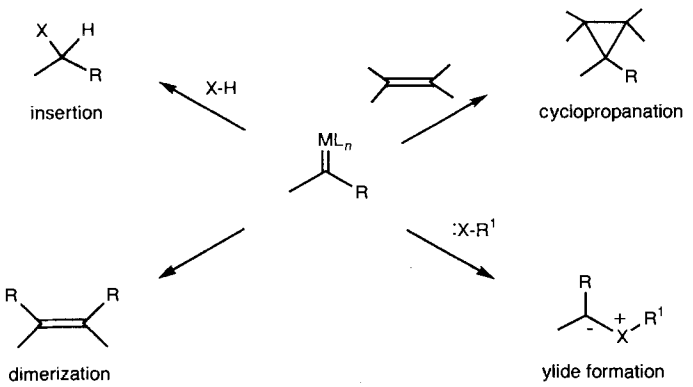
The metal-catalyzed reactions of α-diazo carbonyl compounds is not limited to cyclopropanation, even though the focus of many studies has centered on this transformation.[19] Metallocarbenoid reactions involving either X–H insertions (X = C, O, N)[20] or ylide generation[21] have also been used to prepare complex synthetic targets. Copper and rhodium complexes are particularly effective catalysts for reactions of diazo compounds, and an increasing number of chemical syntheses are based on this catalytic methodology.[3, 4] Some of the common reactions of metallocarbenes are given in Scheme 1.

Although many recent reports deal with the control of stereoselectivity[1–4] and—in particular with chiral catalysts—enantioselectivity[22] of metal-catalyzed α-diazo carbonyl reactions, a growing number of examples also addresses the question of chemoselectivity. Regioselectivity not only depends on the type of α-diazo carbonyl compound used, but is also governed by steric, conformational, and electronic factors. In certain cases, the nature of the solvent and the oxidation state of the metal can also play an important role. This review broadly defines the boundaries of our present knowledge in this field. Such an

[*] Prof. A. Padwa, Dr. D. J. Austin
Department of Chemistry
Emory University, Atlanta, GA 30322 (USA)
Telefax: Int. code + (404)727-0283

[**] The following abbreviations are frequently used in this review: acac = acetylacetonate, acm = acetamidate, bnp = 1,1'-binaphthyl-2,2'-diylphosphate, cap = caprolactamate, diphos = ethylene bis(diphenylphosphane), fmd = di(*para*-tolyl)formamidinate, hfacac = hexafluoroacetylacetonate, man = mandelate, oct = octanoate, pfb = perfluorobutyrate, piv = pivalate, py = pyridine, tcap = thiocaprolactamate, tfa = trifluoroacetate, tfacac = trifluoroacetylacetonate, tfm = trifluoroacetamidate, tpa = triphenylacetate, tpiv = thiopivalate, tpp = tetraphenylporphyrin.

 © VCH Verlagsgesellschaft mbH, D-69451 Weinheim, 1994 0570-0833/94/1818-1797 $ 10.00+.25/0

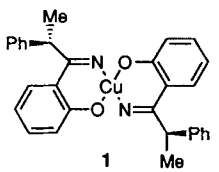


Scheme 1. Typical reactions of metallocarbenes. R = alkyl, aryl, or carbonyl.

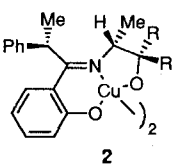
overview will put in perspective what has been accomplished. We hope it will provide impetus for further investigation of metal-catalyzed reactions of diazo carbonyl compounds.

2. Enantioselectivity in Carbenoid-Mediated Reactions

The ability of transition metal catalysts to induce asymmetry in catalytic cyclopropanation has attracted a great deal of attention recently.[22] The first report of cyclopropanation involving a chiral transition metal catalyst was described by Nozaki et al., who used the Cu^{II} complex **1**.[23] The enantiomeric excess (*ee*) obtained with this catalyst for the reaction of styrene with ethyl diazoacetate was only 10%. Aratani et al.[24] were able to increase the enantioselectivity of the cyclopropanation reaction greatly by using a different Cu^{II} complex (**2**) as the catalyst.

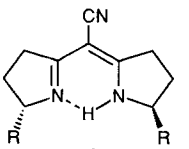


1

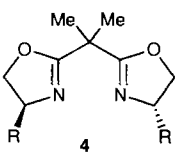


2

Further improvement in the enantioselectivity of cyclopropanation by using a copper catalyst containing the chiral semicorrin ligand **3**, R = alkyl, was reported by Pfaltz et al.[25] who later changed the ligand to the bis(oxazoline) ligands **4** and **5**;[26] these catalysts were studied independently by Evans et al.,[27] and Masamune et al.[28] The same catalysts also proved to be quite effective for aziridination[29, 30] and Diels–Alder[31] cycloadditions. Complexes containing other metals such as Fe^{III} and Mg^{II} with the same ligands are also effective catalysts for Diels–Alder reactions.[32] Other catalysts that show good

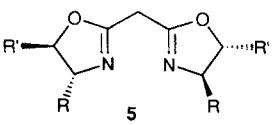


3



4

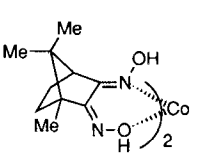
R = Ph, CHMe$_2$, CMe$_3$



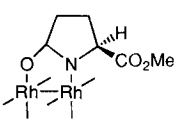
5

R = Me; R' = Ph
R = CH$_2$OH; R' = H
R = CH$_2$CH$_3$; R' = H

enantioselectivity for cyclopropanation include Nakamura's bis(1,2-dioximato)cobalt(II) (**6**),[33] Doyle's dirhodium(II) tetrakis(methyl 2-pyrrolidone-5-carboxylate) complex (**7**),[34] as well as (tribornylphosphito)copper(I) chloride,[35] copper(II) tartrate,[36] a trifluoroacetylcamphor complex of copper(II),[37] chiral iodoporphyrinrhodium(III) complexes,[38] and a variety of other rhodium(II) carboxylates,[39] carboxamides,[40] and binaphthylphosphonates.[41] Enantiomeric excesses are generally moderate to excellent, and this represents an area of intense current research and the subject of several timely reviews.[1, 22]



6



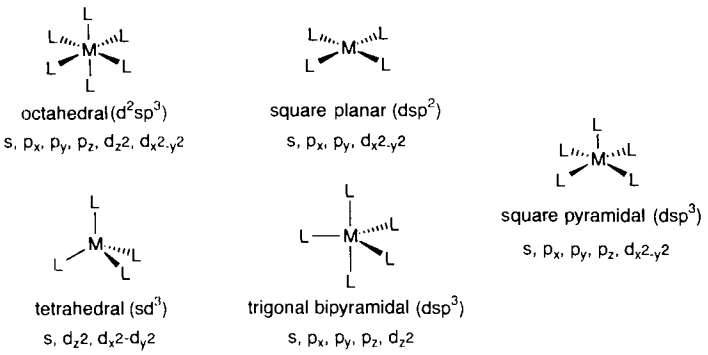
7



Albert Padwa was born in 1937 in New York City. He studied chemistry at Columbia University and received his Ph.D. in 1962 for his work with Cheves Walling on reactions of organic hypohalites. He spent a year (1962–1963) as a NSF postdoctoral research associate at the University of Wisconsin working with Howard E. Zimmerman on cyclohexenone photochemistry. In 1963 he was appointed Assistant Professor of chemistry at the Ohio State University. After three years he moved to the State University of New York, Buffalo, as an Associate Professor and was promoted to full professor in 1969. Since 1979 he has been the William P. Timmie Professor of Chemistry at Emory University in Atlanta. His research interest centers on heterocyclic chemistry, synthetic methodology using cycloadditions, the chemistry of small rings, photochemistry, and the utilization of transition metal carbene complexes for organic synthesis.

3. Copper Catalysts for Carbenoid Generation

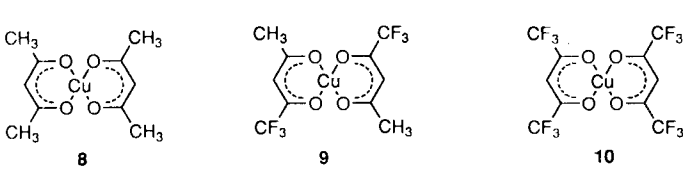
Copper is a group IB (Group 11) element in the first transition series with atomic number 29, a relative atomic mass of 63.546, and an electron configuration of $1s^2 2s^2 2p^6 3s^2\ 3p^6 3d^{10} 4s^1$ for its neutral metal Cu^0. The more common oxidation states of copper include 0, I, II, III, and IV. Copper(I) is a d^{10} transition metal that shares formal stoichiometry with the alkali metals, but retains its transition metal character. Two-coordinate copper forms linear complexes, while three-coordinate copper has a planar geometry. Complexes of four-coordinate copper are most often tetrahedral, but can also be square-planar. Six-coordinate copper complexes are octahedrally disposed. An example of some transition metal geometries and their respective d-orbital hydridizations are given in Scheme 2.



Scheme 2. Geometries of the complexes, the hybridization of the central metal atom, and the orbitals of the metal participating in hybridization.

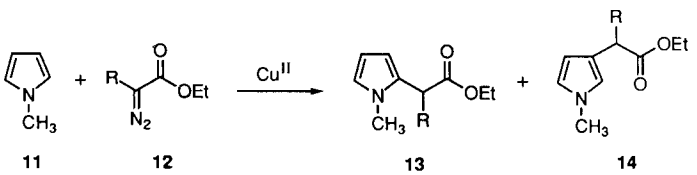
Copper(II) is a d^9 transition metal with a trigonal-planar geometry in three-coordinate complexes, while four-coordinate species have been found in both distorted tetrahedral and square-planar geometries. Five-coordinate systems are trigonal-bipyramidal, and six-coordinate complexes are commonly octahedral. In addition to copper metal, both Cu^I and Cu^{II} complexes can decompose α-diazo ketones. Copper catalysts for α-diazo ketone decomposition are traditionally classified as either heterogeneous or homogeneous. Some examples of heterogeneous copper catalysts are Cu powder,[42] Cu_2O,[43] $CuSO_4$,[44] and CuX (X = Cl, Br).[45] Homogeneous copper catalysts such as trifluoromethanesulfonatocopper(I) (copper(I) triflate)[46] and $Cu^I(PR_3)$[47] were developed later and have since played a major role.[48] Because Cu^{II} is reduced to Cu^I by the diazo functionality,[46, 49] Cu^I is probably the active catalytic species. Since copper(II) triflate is much easier to handle, it is often employed in place of copper(I) triflate.[50] Another homogeneous catalyst, $[Cu(acac)_2]$ (**8**), has also been used for cyclopropanation,[39] heteroatom insertions into X–H (X = N, O) bonds,[40] and ylide formation.[41] Products derived from carbon–hydrogen insertions are less prevalent, but have been reported as side products in moderate yield.[51, 52] Of all the copper catalysts, $[Cu(acac)_2]$ has the unique ability to be altered electronically without changing the overall geometry. The complexes [Cu(tfacac)$_2$] (**9**) and [Cu(hfacac)$_2$] (**10**) are conveniently prepared reagents that are useful for exploring the effect of electronically different ligands on the reactivity of copper carbenoids.

X-ray crystallographic data shows that the $[Cu(acac)_2]$ complex **8** has a Cu–O bond length of 1.90 Å,[53] while that of the hexafluoroacetylacetonate complex **10** is slightly longer (1.96 Å).[54] The complexes are both square planar, but [Cu(hfacac)$_2$] is often isolated in an octahedral geometry with axially disposed dative ligands.[55] Many perfluorinated copper(II) acetylacetonate complexes have been synthesized,[56] and the effects of the electron-withdrawing groups on their Lewis acidity and thermodynamic behavior have been reported.[57] The fluorinated copper compounds **9** and **10** are commercially available, as is the $[Cu(acac)_2]$ complex **8**.



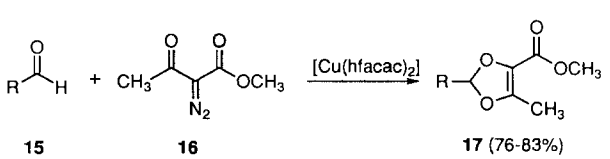
4. Chemoselectivity of Copper Carbenoid Mediated Reactions

One of the first studies on the effect of ligands on the reactivity of Cu^{II} catalysts was reported by Maryanoff,[58] who examined the insertion of the carbenoid derived from diazoester **12** into an aromatic *N*-methyl pyrrole. Thus, treatment of pyrrole **11** with either ethyl diazoacetate or ethyl diazomalonate in the presence of catalytic $[Cu(acac)_2]$ gave mainly the 2-substituted pyrrole **13** and a minor amount of the 3-substituted isomer **14**. When treated under identical conditions with [Cu(hfacac)$_2$], an overall increase in the yield of **13** was noted.



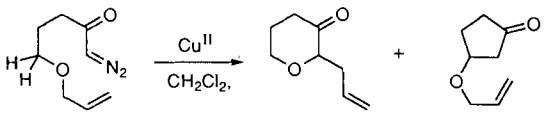
R = H	[Cu(acac)$_2$]	33%	3%
	[Cu(hfacac)$_2$]	45%	12%
R = CO_2Me	[Cu(acac)$_2$]	58%	7%
	[Cu(hfacac)$_2$]	73%	10%

Alonso and Garcia[59] reported on the efficient use of [Cu(hfacac)$_2$] in the reaction of 2-diazo-3-oxobutyrate (**16**) with aldehydes (**15**, R = alkyl, alkenyl, aryl) to give substituted 1,3-dioxole carboxylates (**17**). The reaction is high-yielding and free of the side products encountered with $[Cu(acac)_2]$, such as epoxidation, insertion, dimerization, and Wolff rearrangement. This



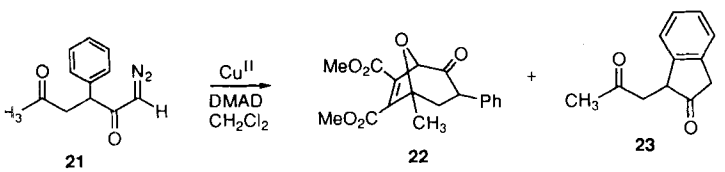
transformation was also adapted to electron-rich alkenes and alkynes with much success.[60]

An interesting example of the influence of the ligand of the copper catalyst on chemoselectivity was recently reported by Clark et al.,[52] who examined the use of several copper catalysts for the formation of oxonium ylides. When α-diazo ketone **18** was treated with a catalytic amount of $[Cu(acac)_2]$ in dichloromethane under reflux, the oxonium ylide rearranges to form pyran **19** and a small amount of insertion product **20**. $[Cu(hfacac)_2]$ as catalyst increases the yield of **19**, and no pentanone **20** was detected. Oxonium ylides with seven- and eight-membered rings were also synthesized selectively.



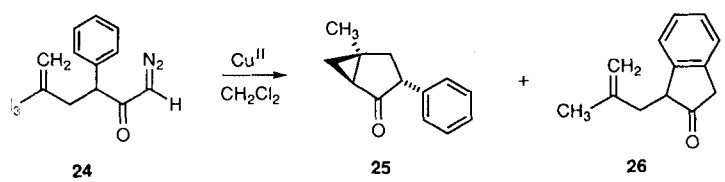
$[Cu(acac)_2]$	61%	12%
$[Cu(hfacac)_2]$	83%	0%

We encountered another example of an interesting chemoselectivity effect using Cu(II) catalysts in a study of the reaction of α-diazo ketone **21** in which carbonyl ylide formation (**22**) competed with aromatic C–H insertion (**23**).[61] In general,



$[Cu(acac)_2]$	71%	19%
$[Cu(tfacac)_2]$	77%	0%
$[Cu(hfacac)_2]$	29%	0%

copper catalysts show a preference for cyclopropanation and ylide formation over C–H insertion. In the competitive copper-mediated reaction of α-diazo ketone **24**, all of the copper catalysts showed a preference for intramolecular cyclopropanation (**25**) to the total exclusion of aromatic C–H insertion (**26**).[61]

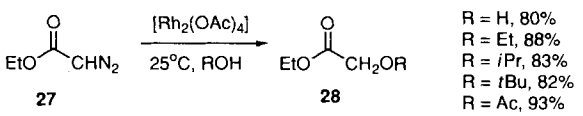


$[Cu(acac)_2]$	86%	0%
$[Cu(tfacac)_2]$	75%	0%
$[Cu(hfacac)_2]$	50%	0%

$[Cu^{II}(hfacac)_2]$ has also been used for the formation of arsonium, stibonium, bismuthonium, selenonium, and telluronium ylides.[62] These ylides could not be obtained by thermal or $[Cu(acac)_2]$ decomposition of the starting diazo compounds because the ylides were unstable under the harsh reaction conditions. The fluorinated catalyst exhibited much greater reactivity and allowed the generation of the ylides at significantly lower temperatures.

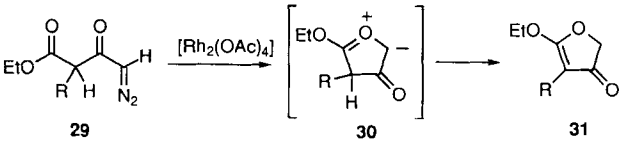
5. Rhodium Catalysts for Carbenoid Generation

The enormous utility of rhodium(II) carboxylates in the catalytic decomposition of diazo compounds has become apparent over the last decade.[1–6] Rhodium-mediated carbenoid reactions generally proceed under much milder conditions than is common for classical synthetic methodology with copper or its complexes.[7] In 1973 Teyssié et al. described the decomposition of ethyl diazoacetate (**27**) with $[Rh_2(OAc)_4]$[63] via a rhodium carbenoid intermediate and subsequent intermolecular O–H insertion with alcohols to produce ethers (**28**). Later they reported



the ability of the rhodium catalyst to induce insertion of the diazo compound into N–H and S–H bonds. Insertion into C–H bonds was originally reported to occur only with $[Rh_2(tfa)_4]$,[64] but it is now widely accepted that all of the rhodium(II) carboxylates can induce this insertion reaction.[3]

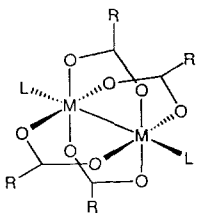
In the same year that Teyssié et al. described the first example of cyclopropanation using a rhodium catalyst (1976),[65] Bien et al. reported on the decomposition of an α-diazo ketone (**29**, R = alkyl) with formation of a carbonyl ylide intermediate (**30**) using $[Rh_2(OAc)_4]$.[66] Although the 1,3-dipole ultimately underwent a hydrogen shift to produce furanone **31**, the system was later modified to allow for intramolecular cycloaddition.[67] Since this early report, rhodium(II) has become the premier catalyst for α-diazo carbonyl decomposition.[1–4] Consequently, interest in the synthesis and chemical behavior of new Rh^{II} dimers has significantly increased in recent years.[68–70]



Rhodium is a Group VII (Group 9) element in the second transition series with atomic number 45, a relative atomic mass of 102.9055, and an electron configuration of $1s^2 2s^2 2p^6 3s^2 3p^6 3d^{10} 4s^2 4p^6 4d^8 5s^1$ for its neutral metal Rh(0). Known oxidation states of rhodium include −I, 0, I, II, III, IV, V, and VI, but much of the chemistry of rhodium centers about the oxidation states I, II, and III. Rhodium(I), a d^8 transition metal, forms planar complexes when its coordination number is 3 or 4, although some four-coordinate rhodium complexes

are tetrahedral. Five-coordinate rhodium species are in trigonal bipyramidal environments. The most common Rh^{I} complexes in organic chemistry are Wilkinson's catalyst[71] $[Rh(PPh_3)_3]Cl$ and $[Rh(diphos)(thf)_2]^+$[72], both having been widely used in catalytic hydrogenation. Instead of diphos, chiral phosphane ligands have been employed with some success.[73] Monsanto's carbonylation of methanol to acetic acid[74] is an extremely successful commercial process involving homogeneous catalysis that proceeds through an anionic Rh^{I} complex, $[Rh(CO)_2I_2]^-$.

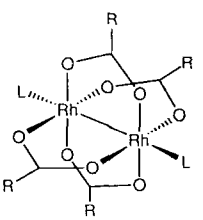
Rhodium(III) is a d^6 transition metal whose five-coordinate complexes can be either trigonal-bipyramidal or square-pyramidal. Six-coordinate Rh^{III} complexes such as the very useful $RhCl_3 \cdot 3H_2O$ are octahedral. Both Rh^{I} and Rh^{III} complexes have been shown to decompose diazo compounds,[63] but neither proved as efficient as Rh^{II}.



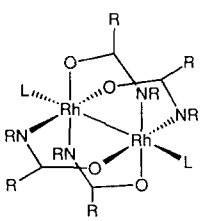
32

Rhodium(II) is a d^7 transition metal that has a propensity to form Rh–Rh metal bonds. The first reported rhodium dimer, the acetate **32** (M = Rh, $R = CH_3$) was initially described by Chernyaev et al.[75] as a rhodium(I) formate, but later its structure was corrected on the basis of single crystal X-ray diffraction studies.[76] $[Rh_2(OAc)_4]$ is the most common and best studied Rh^{II} catalyst.[68, 69]

Other transition metals that form metal–metal bonds centered within carboxylate bridging ligands include Re,[77] Tc,[78] Mo,[79] W,[80] Cr,[81] Ru,[82] Os,[83] Pt,[84] Cu,[85] and mixed Cr–Mo complexes.[86] $[Mo_2(OAc)_4]$[87] decomposes α-diazo ketones with limited success, but less is known about the other catalysts. The ligands associated with rhodium(II) dimers can be categorized as bridging (RCO_2 in **32**) or axial (L in **32**). The bridging ligands, by convention, are used to categorize the rhodium dimers into seven different types. Dimers like **33**, with bridging carboxylic acid ligands, are known as rhodium(II) carboxylates. Amides and 2-oxypyridines are commonly used to form rhodium(II) carboxamides such as **34**. The analogous thio-



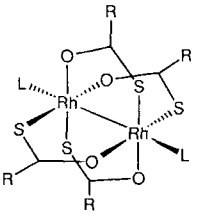
33



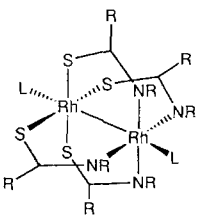
34

carboxylate (**35**) and thioamidate (**36**) complexes are much less common, but have also been prepared. Some additional species include the rhodium(II) phosphonates **37**, sulphonates **38**, and dirhodium complexes without bridging ligands (**39**).

Axial ligands (L in **33**–**39**) form a much weaker bond to rhodium than bridging ligands,[88] and are easily removed by photolysis or by heating the complex under vacuum.[89] Some of the axial ligands found in complexes of rhodium(II) acetate are

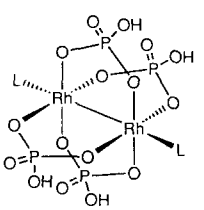


35

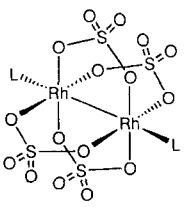


36

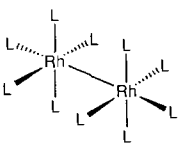
water,[90] thiol,[91] tetrahydrothiophene,[92] phosphane,[93] acetonitrile,[94] amine,[95] pyridine,[96] carbonyl,[97] formate,[98] thioformate,[99] halogen (X = Cl[100] and Br[101]), arsenic,[102] and antimony.[102] Since the axial position is believed to be the site of binding with the carbene center, these ligands are usually absent when the dimers are used for catalytic processes. Nevertheless, these ligands do influence the Rh–Rh distance, which in turn may be partially responsible for the reactivity of the carbenoid.



37

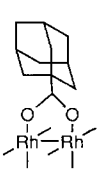


38

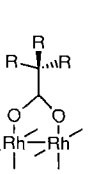


39

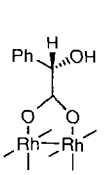
Rhodium(II) carboxylates containing a large variety of alkyl or aryl substituents have been prepared. Rhodium(II) acetate is readily made by heating $[Rh^{III}Cl_3 \cdot 3H_2O]$ with sodium acetate and glacial acetic acid in ethanol under reflux.[103] Complexes containing carboxylate ligands with lower pK_a values can be formed simply by treating rhodium trichloride with the appropriate carboxylate salt in ethanol.[104] Ligand exchange is another method of synthesis: Rhodium(II) acetate or octanoate is heated with a carboxylate salt in chlorobenzene. For acetate exchange, the solution is heated at reflux in a Soxhlet extraction apparatus which contains a 1:1 mixture of Na_2CO_3 and sand. This serves to remove acetic acid and drives the equilibrium toward completion. The types of complexes with bridging carboxylates that have been used include the adamantane-1-carboxylate (**40**),[105] the pivalate (**41**),[92] the triphenyl acetate (**42**),[105] the mandelate (**43**),[106] and the salicylate (**44**).[107] (Only one of the four bridging ligands has been depicted in the structural formulas in each case.)



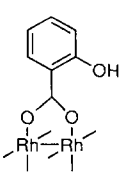
40



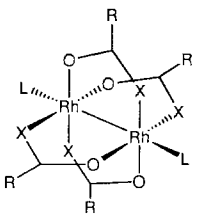
41, R = CH_3
42, R = Ph



43



44



45

Rhodium(II) carboxylate complexes with ligands that have different electronic properties to acetate are most commonly those with perfluorinated substituents, for example, the trifluoroacetate complex $[Rh_2(tfa)_4]$ (**45**, R = CF_3; X = O) or the perfluorobutyrate complex $[Rh_2(pfb)_4]$ (**45**, R = C_3F_7; X = O). Although formally considered carboxylates, both the geometry and reactivity of these catalysts differ greatly from that of the rhodium alkyl carboxylates.

All of the rhodium(II) carboxylates that have been structurally investigated exist in the lantern arrangement, both with and without axially bound ligands (L). Changes in the length of the Rh–Rh bond of the dimer are directly related to its reactivity.[68] The Rh–Rh bond length for $[Rh_2(OAc)_4 \cdot 2H_2O]$ (**46**) was initially reported to be 2.45 Å,[76] but later corrected to 2.38 Å.[82, 90] The distance anticipated for a normal Rh–Rh single bond is on the order of 2.7–2.8 Å. This shorter distance originally led to the postulate of a Rh–Rh triple bond, which became the subject of much controversy, since the spectral evidence pointed to a single Rh–Rh bond. Theoretical calculations,[108] spectral measurements,[109] and ESR studies[88] have subsequently demonstrated that the Rh–Rh bond of the dimer is best described as a single bond. The Rh–Rh lengths of some typical complexes of type **45** are given in Table 1.

Table 1. Bond lengths for some typical Rh^{II} catalysts

Complex	X	R	L	Rh–Rh bond length [Å]
46	O	CH_3	H_2O	2.38
47	O	$C(CH_3)_3$	H_2O	2.37
48	O	CF_3	H_2O	2.41
49	S	CH_3	$CH_3C(S)OH$	2.55
50	S	$C(CH_3)_3$	PPh_3	2.58
51	O	C_3H_7	none	2.36
52	O	CH_3	MeOH	2.37
53	O	CH_3	$PhCH_2SH$	2.40
54	O	CH_3	pyridine	2.39
55	O	CH_3	PPh_3	2.45
62	NH	CH_3	none	—
63	NH	CH_3	DMSO	2.44
64	NH	CF_3	pyridine	2.47

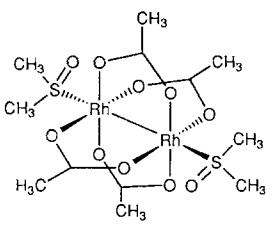
The Rh–Rh bond of the carboxylates generally falls within the range of 2.37 to 2.49 Å. Standard alkyl and aryl carboxylates have the shorter bond lengths, while those of the perfluorinated type are longer. The electronic effect of the bridging ligand on the Rh–Rh bond is easily noted by a comparison of the pivalate $[Rh_2(piv)_4 \cdot 2H_2O]$ (**47**) with the trifluoroacetate $[Rh_2(tfa)_4 \cdot 2H_2O]$ (**48**). The effect of the electron-donating trimethylacetate ligand is to shorten the Rh–Rh bond (2.37 Å),[92] while the electron-withdrawing trifluoroacetate ligand has the opposite effect (length: 2.41 Å).[110]

Rhodium(II) thiocarboxylates are much less common and characteristically less stable.[111] $[Rh_2(SAc)_4]$ (**49**)[112] and rhodium(II) thiopivalate $[Rh_2(tpiv)_4]$ (**50**)[113] possess long Rh–Rh bond lengths of 2.55 and 2.58 Å, respectively.

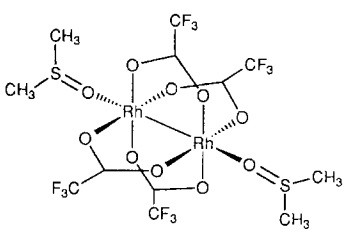
Axial ligands can significantly influence the length of the Rh–Rh bond.[88, 92] X-ray crystal structure analysis of rhodium(II) dimers without axially bound ligands are rare. Rhodium(II) butyrate (**51**) has no axial substituents and a Rh–Rh bond length of 2.36 Å.[114] As described earlier, the Rh–Rh bond of $[Rh_2(OAc)_4 \cdot 2H_2O]$ (**46**) is 2.38 Å long.[82, 90] When the water ligands are replaced with methanol (**52**), this distance shortens slightly to 2.37 Å.[114] The effect of the two benzylthiol groups in **53** is a lengthening of the Rh–Rh bond to 2.40 Å.[115]

Nitrogen ligands are common in Rh^{II} complexes and tend to lengthen the Rh–Rh distance to essentially the same value as in the thiol complexes. The Rh–Rh bond length in compound **54** (with pyridine ligands) was determined to be 2.39 Å.[116] A more dramatic bond lengthening is seen by the addition of triphenylphosphane at the axial position, giving rise to complex **55** which contains a Rh–Rh bond of 2.45 Å.[93]

Perhaps the most interesting axial ligand effect noted involves dimethyl sulfoxide (DMSO). As axial ligand in $[Rh_2(OAc)_4 \cdot 2dmso]$ (**56**),[92] DMSO bonds to rhodium through the sulfur atom. However, in $[Rh_2(tfa)_4 \cdot 2dmso]$ (**57**),[117, 118] the oxygen atom of the sulfoxide moiety is attached to the rhodium center.



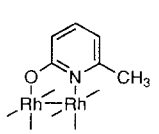
56



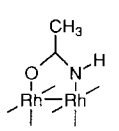
57

Sulfur is also the preferred ligating atom in rhodium(II) propionate[117] and rhodium(II) benzoate.[119] The ambidentate character of DMSO is well known, but a different site of attachment on the same metal within the same oxidation state is unusual.[120] This effect is not completely understood but is believed to be related to the greater Lewis acidity of $[Rh_2(tfa)_4]$ (caused by its electron-withdrawing ligands) than $[Rh_2(OAc)_4]$ (containing the more electron-donating alkyl ligands). In addition to influencing the distance between the Rh atoms, both the bridging and axial ligands can also alter the spectral properties of the rhodium dimers.[68] The clearest evidence is seen in the colors of complexes: $[Rh_2(OAc)_4(H_2O)_2]$ (**46**) and $[Rh_2(tfa)_4(H_2O)_2]$ (**48**) are emerald green and $[Rh_2(OAc)_4(PPh_3)_2]$ (**55**) deep red;[121] $[Rh_2(OAc)_4(dmso)_2]$ (**56**) exists as orange prisms, and $[Rh_2(tfa)_4(dmso)_2]$ (**57**) as dark blue needles.[117]

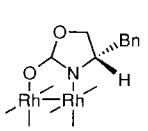
Another important class of rhodium(II) dimers are those in which one oxygen and one nitrogen atom are the ligating atoms of the bridging ligand instead of two oxygen atoms. A typical example of such a dimer is the 2-oxypyridine system (**58**).[122]



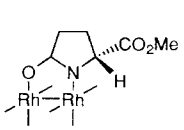
58



59



60



61

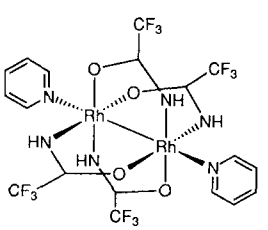
(For compounds **58**–**61** only one of the ligands are depicted). Other rhodium(II) carboxamides that have been prepared incorporate, for instance, acetamide (**59**),[123] or the chiral oxazolidinone (**60**)[124] and pyrrolidinone (**61**) ligands.[125] Catalysts **60** and **61** have become extremely important in enantioselective cyclopropanations.[22]

The oxypyridine rhodium(II) complexes, like the carboxamides, are structurally related to the carboxylates in that they both adopt the lantern structure. The Rh–Rh bond length for the oxypyridine system ranges from 2.35 to 2.36 Å and for the carboxamides from 2.39 to 2.45 Å. The absence of axial ligands has been proposed to account for the shorter Rh–Rh distance in the oxypyridine complexes. The substituent on the 6-position of the pyridine ring is located directly over the axial position, thus preventing coordination.[122]

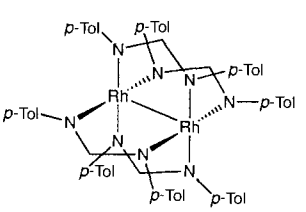
The effect of axial ligands on the carboxamide systems is not so clear, since fewer X-ray crystal structures have been performed on these complexes. The acetamidate $[Rh_2(acm)_4]$ (**62**, of type **59**) without axial ligands has been characterized, but no atomic parameters are available.[123] In the complex with DMSO in the axial position, $[Rh_2(acm)_4(dmso)_2]$ (**63**), the interrhodium distance is 2.44 Å.[126] The DMSO ligands bind to the Rh atom through sulfur, as in the alkyl carboxylates. This is consistent with a relatively electron-rich rhodium atom and is undoubtedly related to the electron-donating character of the nitrogen atom.

The trifluoroacetamide $[Rh_2(tfm)_4]$ is the only example of a perfluorinated carboxamide that has been reported to date. The complex containing axial pyridine ligands (**64**) has a Rh–Rh bond length of 2.47 Å,[127] which is slightly longer than that of a nonfluorinated carboxamide. The binding mode of DMSO with this complex would be worth investigating, since the bridging ligands contain both an electron-donating nitrogen atom and an inductively withdrawing trifluoromethyl group.

Only one example of a rhodium dimer with ligands bridging through two nitrogen atoms has been described: the Rh–Rh bond length in this *p*-tolylformamidinate $[Rh_2(fmd)_4]$ (**65**) is 2.43 Å.[128]

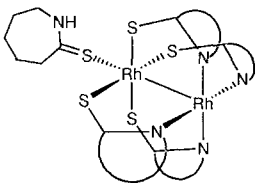


64

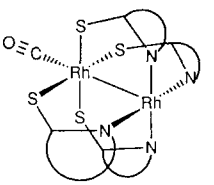


65

Structural studies on rhodium(II) thiocarboxamides indicate that these complexes exhibit some interesting geometric features. Unlike the thiocarboxylate and carboxamides, the thiocarboxamide ligands do not coordinate to the rhodium metal with a *trans* arrangement of S and N ligating atoms. Two thiocaprolactam complexes have been examined: each contain only one axial ligand, namely monodentate thiocaprolactam ($[Rh_2(tcap)_4(Htcap)]$ **66**) or carbonyl ($[Rh_2(tcap)_4CO]$ **67**).[129] In addition to the unique orientation of the bridging ligands, the single axial ligand coordinates to the Rh atom bearing only sulfur as ligating atom. The Rh–Rh bond in these complexes is rather long (2.49 Å).

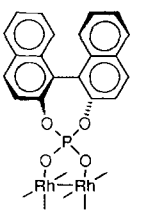


66

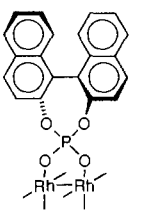


67

Sulfonate[130] and phosphonate[131] complexes were among the first noncarboxylate Rh^{II} catalysts to be prepared. The sulfonate complex was never structurally investigated, but rhodium(II) phosphonate $[Rh_2(HPO_3)_4(H_2O)_2]$ displays a 2.48 Å Rh–Rh bond.[132] These bridging ligands have not been extensively utilized, but the unusually long Rh–Rh bond of the phosphonate prompted the synthesis rhodium(II) complexes of (*S*)-(+)-1,1′-binaphthyl-2,2′-diylphosphate ($[Rh_2\{(S)\text{-bnp}\}_4]$[133] (**68a**)) from $Na_4[Rh_2(CO_3)_4]\cdot 2.5H_2O$ and of the (*R*)-(−) isomer ($[Rh_2\{(R)\text{bnp}\}_4]$[134] (**68b**)) by ligand substitution of $[Rh_2(OAc)_4]$. (In the structural formulas only one of the four ligands is depicted.)

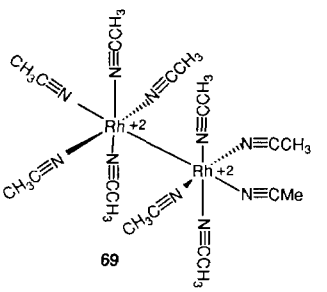


68a



68b

Two types of substituent commonly encountered in nonbridged rhodium(II) dimers are alkyl- or aryl-substituted cyano or isocyano ligands. An example of such a complex is the acetonitrile $[Rh_2(CH_3CN)_{10}(BF_4)_4]$ (**69**).[135] This field is a relatively new and growing area of research. Bond lengths in the nonbridged systems are the longest encountered: 2.62 Å for compound **69**,[135] and values ranging from 2.78 to 2.83 Å for the isocyanides.[136] Interestingly, these bonds more closely approximate a Rh–Rh single bond length of 2.7–2.8 Å.



69

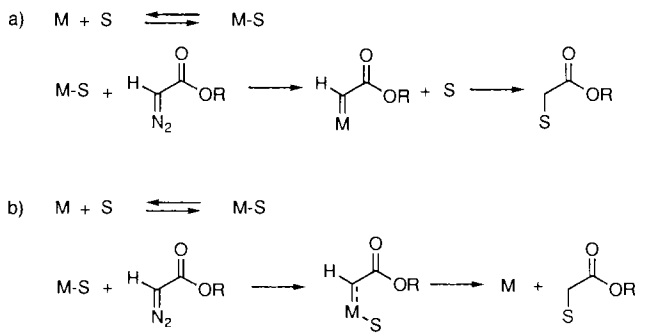
6. Chemoselectivity of Rhodium(II)-Mediated Reactions

6.1. Mechanism

Structural studies of the rhodium(II) dimers with their characteristic axial binding may ultimately provide insight into the structure of the carbenoid intermediate. A particularly interesting example reported by Doyle et al.[137] indicated that

$[Rh_2(pfb)_4]$ can form π complexes with olefins, while none of the unactivated carboxylates or carboxamides exhibit this type of behavior. Unfortunately, no spectroscopic or crystallographic data is available for these π-bonded carbenoids. Proof of their existence and insight into the nature of the intermediate is obtained through reactivity–selectivity correlations with known, stable Fischer carbenes.[138]

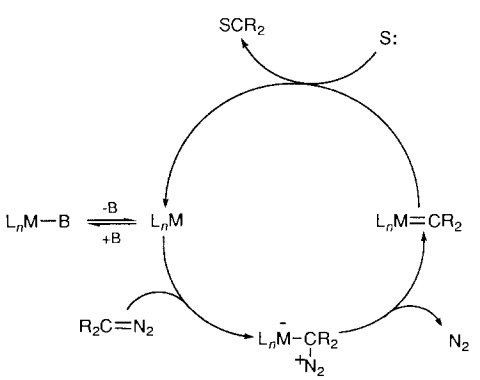
The first detailed description of a mechanism for the rhodium(II)-mediated decomposition of an α-diazo ketone was postulated by Teyssié et al. (Scheme 3).[63] In the first step a metal–



Scheme 3. Mechanism of the transition metal catalyzed reaction of α-diazocarbonyl compounds according to Teyssié et al. a) Carbenoid mechanism. b) Coordination mechanism.

substrate complex (M–S) is formed, which subsequently dissociates when the metal is attacked by the α-diazo ester. Extrusion of nitrogen results in formation of the metal–carbene complex. This complex then reacts with the substrate in what has been described as an attack from outside the coordination sphere of the metal (carbenoid mechanism). Teyssié proposed a mechanism, in which the metal–substrate complex remained intact during the formation of the metallocarbenoid (coordination mechanism). The substrate and carbene then react within the coordination sphere of the metal. Rhodium carbenoids are believed to react by the carbenoid mechanism and palladium carbenoids by the coordination mechanism.

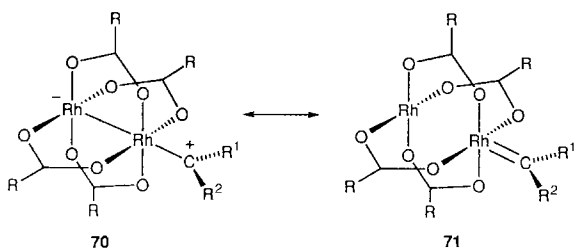
Somewhat later Doyle proposed the catalytic cycle of Scheme 4 to explain the course of the reaction between an α-diazo carbonyl compound and a transition metal such as rhodium.[1] The first step of the sequence is decomplexation of the



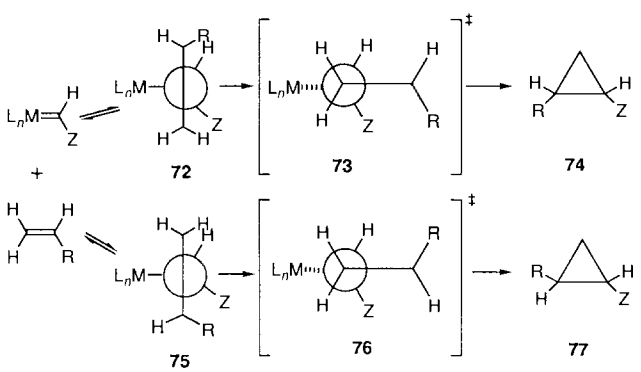
Scheme 4. Mechanism of the transition metal catalyzed reaction of α-diazocarbonyl compounds according to Doyle et al. S = substrate; M = metal; R = alkyl, aryl; B = Lewis base

metal from the Lewis base (that is, the solvent). This is followed by attack of the diazo functionality at the metal to form a zwitterionic metallo intermediate. At this point nitrogen is extruded, presumably through some sort of π backbonding, to form the metal carbenoid. The carbenoid can then react with the various substrates present (alkene, C–H bond, etc.), ultimately producing the observed product. The initial catalyst is regenerated to complete the catalytic cycle.

The resonance structures **70** and **71** have been proposed to describe the rhodium(II) carbenoid species.[1, 22] It should be noted, however, that no rhodium carbenoid has ever actually been isolated or observed by spectroscopy.



As the resonance structures **70** and **71** suggest, the carbenoid intermediate should behave as a metal-stabilized carbocation. Doyle has used this representation of the rhodium carbenoid in his proposed mechanism of cyclopropanation (Scheme 5).[1]



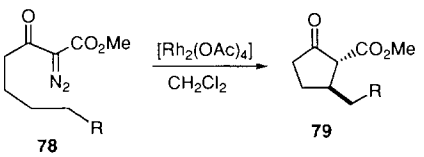
Scheme 5. Mechanism of cyclopropanation according to Doyle et al. Z = CO_2Et; R = alkyl.

First, coordination of the rhodium carbenoid with the alkene leads to complexes **72** or **75**. The orientation of the alkene substituent R can be either *syn* or *anti* to the carbene substituent Z; the initial relationship is expressed in the cyclopropane products **74** and **77**, respectively. The σ bond forms at the least substituted C atom of the alkene, which enables better stabilization of the positive charge developed in the transition state (**73** and **76**) at the more highly substituted C atom. Backside displacement of the metal results in collapse of the complex with concomitant cyclopropane formation (**74** and **77**). Interaction of the R and Z groups in both the π complex and transition state were thought to be important in determining the relative amounts of the diastereomeric cyclopropanes produced.[139]

6.2. C–H Insertion Reactions

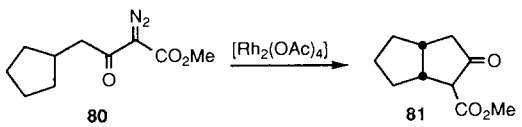
6.2.1. Steric Factors

Much of what is known today about intramolecular insertions into C–H bonds of carbenoids has come from independent studies by Taber et al.[140] and Doyle et al.[141] Initial reports involved the reaction of α-diazo-β-ketoester **78** with rhodium(II) acetate as the catalyst.[140] The major product isolated from this reaction was the 2-carboalkoxy-substituted cyclopentanone system **79**. This seminal report clearly demonstrated that with freely rotating acyclic systems C–H insertion can be an efficient process.[140]



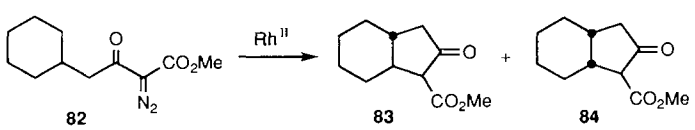
78 **79**

Steric factors may play an important role in determining the ratio of potential insertion products. Thus, insertion into C–H bonds of cyclopentane[142] gives only the *cis*-substituted products (example: **80** → **81**). However, when this insertion occurs



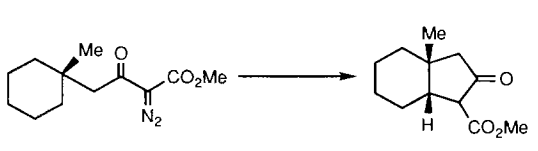
80 **81**

with a cyclohexane, the observed *cis* to *trans* ratio depends on the nature of the catalyst. For example, treatment of the diazo ketone **82** with $[Rh_2(OAc)_4]$ acetate led to a 3:1 mixture of the *trans* and *cis* insertion products **83** and **84**, respectively. Changing the catalyst to the octanoate $[Rh_2(oct)_4]$ increased the ratio to 5:1. With the even larger tetraphenylporphyrin rhodium chloride ([Rh(tpp)]Cl), the ratio increased to 15:1 in favor of the *trans* product. In contrast, when the methylcyclohexyl compound **85** was used as substrate, only *cis*-octahydro-1*H*-indole **86** was obtained. In this case, the methyl group blocks the approach of the rhodium carbenoid to the equatorial hydrogen that is responsible for the formation of the *trans* product.



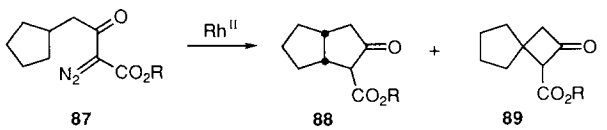
82 **83** **84**

$[Rh_2(OAc)_4]$	3:1
$[Rh_2(oct)_4]$	5:1
$[Rh_2(tpp)]$ Cl	15:1



85 **86**

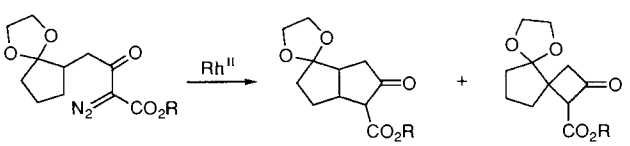
Cyclization of electrophilic rhodium–carbene complexes of conformationally mobile acyclic compounds results in the preferential formation of five-membered rings.[140] The order of reactivity of the target C–H site is methine > methylene > methyl.[140] Recently, Ikegami et al. have reported that triphenylacetate $[Rh_2(tpa)_4]$, which features a bulky bridging ligand on the rhodium metal, exhibits an exceptionally high order of selectivity for insertion into a methylene C–H bond rather than into a methine C–H bond in the catalytic decomposition of α-diazo-β-keto esters appended to cyclic systems.[143] The original papers by Taber et al.[140] and Cane and Thomas[142] reported that the reaction of diazo ester **87** (R = alkyl) with $[Rh_2(OAc)_4]$ yielded a 2:1 mixture of **88** and **89**. In contrast, the reaction of **87** with $[Rh_2(tpa)_4]$ led to the smooth formation of **88** (R = alkyl) with no detectable amounts of **89**. The virtually complete selectivity for insertion into the



87 **88** **89**

$[Rh_2(OAc)_4]$	2:1
$[Rh_2(tpa)_4]$	>30:1

methylene C–H bond was ascribed to the steric bulk of the bridging ligand on the rhodium. This catalyst is superior to $[Rh_2(OAc)_4]$ for C–H insertion in a cyclic system. Also worthy of mention is the tetraacetamidate[144] $[Rh_2(acm)_4]$, which resulted predominantly in insertion into the methine C–H bond rather than into the methylene C–H bond because this catalyst discriminates on the grounds of electronic factors[145, 146] (see the reaction **90** → **91** + **92**). Hence, $[Rh_2(tpa)_4]$, for which steric factors control the regioselectivity, can be complementary to $[Rh_2(NHAc)_4]$ for site-selective C–H insertion reactions.

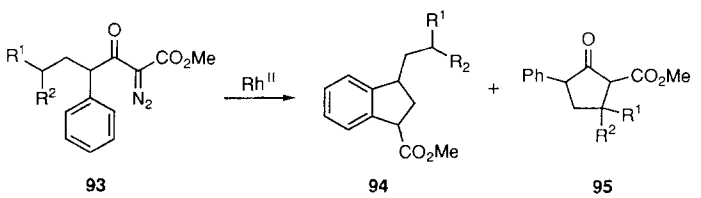


90 **91** **92**

$[Rh_2(OAc)_4]$	37:63
$[Rh_2(tfa)_4]$	56:44
$[Rh_2(acm)_4]$	14:86
$[Rh_2(piv)_4]$	37:63
$[Rh_2(OBz)_4]$	54:46
$[Rh_2(OCOCHPh_2)_4]$	64:36
$[Rh_2(OCOCMePh_2)_4]$	82:18
$[Rh_2(tpa)_4]$	96: 4

Rhodium(II) triphenylacetate, which features a bulky bridging ligand, has also been shown by the Ikegami group to be very much more selective for insertion into aryl C–H bonds than for insertion into aliphatic C–H bonds or for cyclopropanation in Rh^{II}-catalytic reactions with α-diazo carbonyl compounds.[147]

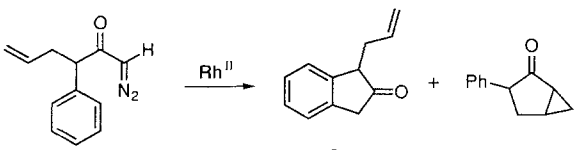
Taber and Ruckle had initially demonstrated that the energy requirements for aryl insertion were approximately the same as those for methylene insertion in the $[Rh_2(OAc)_4]$-induced reaction of α-diazo ketone **93**.[140] When $[Rh_2(tpa)_4]$ or the diphenylmethylpropionate $[Rh_2(O_2CCMePh_2)]$ was used, insertion into the aryl C–H bond (formation of **94**) predominated over methylene C–H insertion (formation of **95**). It was suggested that the larger steric bulk of the bridging ligand on the rhodium retards the methylene C–H insertion process.



93 **94** **95**

R^1, R^2 = H, CH_3		
	$[Rh_2(OAc)_4]$	85:15
	$[Rh_2(OCOCHPh_2)_4]$	54:46
	$[Rh_2(tpa)_4]$	96: 4

$[Rh_2(tpa)_4]$ catalysis also favors aryl insertion over cyclopropanation. Thus, the $[Rh_2(tpa)_4]$-catalyzed cyclization of **96** led to the formation of indan-2-one **97** in 83% yield, with no trace of the cyclopropane **98**, whereas $[Rh_2(OAc)_4]$ catalysis of **96** gave **97** and **98** in 26 and 63% yield, respectively.[147] It would seem that the steric bulk of the triphenylacetate ligand does not interfere at all with the insertion into aryl C–H bonds.

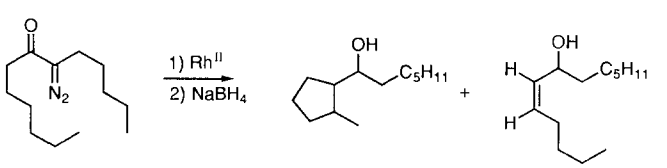


96 **97** **98**

$[Rh_2(OAc)_4]$	26%	63%
$[Rh_2(tpa)_4]$	83%	0%

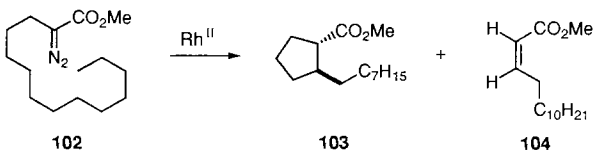
6.2.2. *Electronic Factors*

The Taber group recently noted that the ligand on the rhodium(II) carboxylate catalyst plays an important role in the cyclization of α-diazo ketone **99**.[148] Strong electron-withdrawing ligands favor β-hydride elimination (to form **101**), while the 1,5-insertion reaction (→ **100**) is favored by electron-donating ligands. The more reactive rhodium carbenoid derived from the trifluoroacetate catalyst favors the entropically less demanding pathway (β-hydride elimination). A similar trend was noted with α-diazo ester **102**, which forms **103** and **104**.



99 **100** **101**

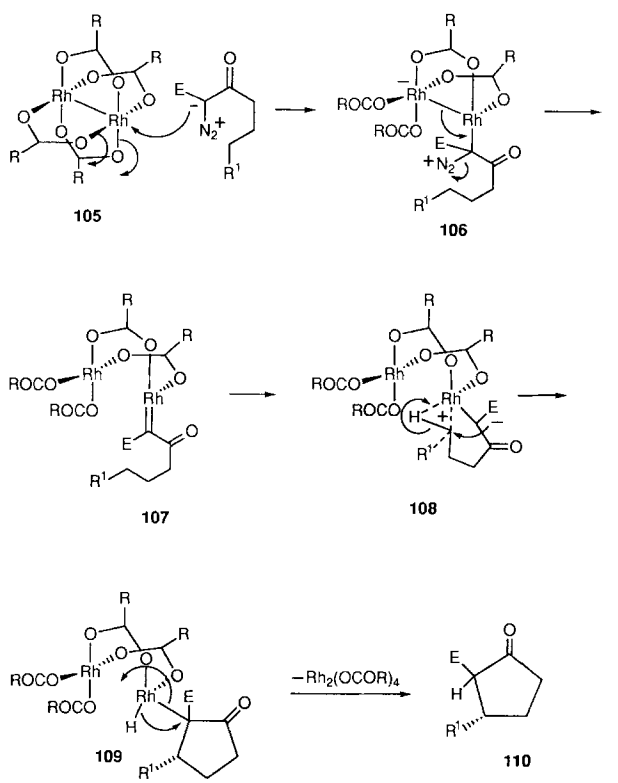
$[Rh_2(OAc)_4]$	70:30
$[Rh_2(OBz)_4]$	60:40
$[Rh_2(OCO\text{-}p\text{-}ClC_6H)_4]$	40:60
$[Rh_2(tfa)_4]$	38:62



102 **103** **104**

$[Rh_2(piv)_4]$	85:15
$[Rh_2(OCO\text{-}n\text{-}C_8H_{17})_4]$	78:22
$[Rh_2(OBz)_4]$	78:22
$[Rh_2(OAc)_4]$	66:34
$[Rh_2(tfa)_4]$	52:48

A detailed mechanism describing the role of the metal in the C–H insertion reaction was proposed by Taber et al. (Scheme 6):[140] Initial attack of the α-diazo carbonyl at the axial position of the rhodium dimer **105** gives intermediate **106**. This is followed by cleavage of the Rh–Rh bond with concomitant loss of nitrogen to generate **107**. At this point the rhodium metal needs to be electrophilic enough to coordinate with a C–H sigma bond in a three-centered arrangement (**108**). Electronic reorganization ultimately results in carbon–carbon bond formation **109**. A subsequent elimination of the rhodium hydride produces the C–H insertion product **110** and recovered catalyst. This highly speculative mechanism raises a number of

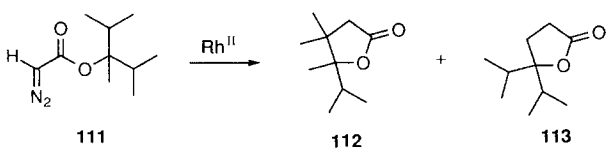


105 **106** **107** **108** **109** **110**

Scheme 6. Mechanism of C–H insertion according to Taber et al. R = alkyl, aryl; E = CO_2R'; R' = alkyl, aryl.

interesting issues. Cleavage of the Rh–Rh single bond is most unusual considering the high degree of stereoselectivity generally encountered in these reactions. According to the above suggestion, the electronic nature of the bridging ligand should have an effect on lability of the Rh–Rh bond and thereby influence the mechanism of the insertion reaction.

Carbenoid formation with α-diazo esters provides a convenient method for synthesizing highly substituted γ-lactones. Doyle's group has shown that treatment of 2,3,4-trimethyl-3-pentyl diazoacetate (**111**) with $[Rh_2(OAc)_4]$ in dichloromethane at 25 °C resulted in the formation of nearly equal amounts of the γ-lactones **112** and **113**.[141, 146] In the $[Rh_2(OAc)_4]$-catalyzed

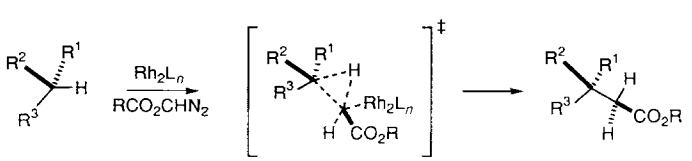


111 **112** **113**

$[Rh_2(OAc)_4]$	53:47
$[Rh_2(pfb)_4]$	32:68
$[Rh_2(acm)_4]$	99: 1

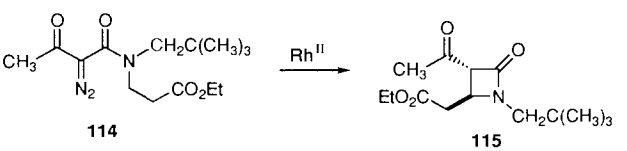
reaction, an approximately statistical distribution of C–H insertion products results. By changing the ligand on the catalyst, significant manipulation of the product ratio was achieved. While $[Rh_2(pfb)_4]$ afforded a mixture of lactones, use of the catalyst $[Rh_2(acm)_4]$ led to the exclusive formation of lactone **112**. Thus, regiocontrol in these reactions can clearly be achieved by ligand variation. The results also emphasize that the C–H insertion reaction occurs from a metal–carbene rather than a free carbene intermediate. The enhanced regioselectivity with donor ligands implies a tighter transition state for insertion reactions catalyzed by $[Rh_2(acm)_4]$.

Metal–carbene reactions catalyzed by dirhodium(II) carboxylates and carboxamides are electrophilic in character, resembling those of a metal-stabilized carbocation more than those of a metal–carbene.[1] Furthermore, the C–H insertion occurs with retention of configuration at the carbon–hydrogen bond undergoing reaction, and the high degree of enantioselectivity that is achieved with chiral dirhodium(II) carboxamides suggests that the ligands remain intact on the dirhodium framework during the insertion process. To account for these observations Doyle et al. suggested a mechanism for C–H insertion (Scheme 7)[141] that is fundamentally different from Taber's proposal.[140] The Doyle mechanism involves overlap of the p orbital of the carbene carbon with the σ orbital of the reacting C–H bond. C–C and C–H bond formation takes place concertedly as the metal–carbene dissociates. Electron-withdrawing ligands will increase the electrophilicity of the carbene thereby causing bond formation to take place at a greater distance from the reacting C–H bond (earlier transition state) with a resulting decrease in selectivity. Ligands with decreased electron-withdrawing ability, such as carboxamides, will result in a later transition state and greater selectivity.

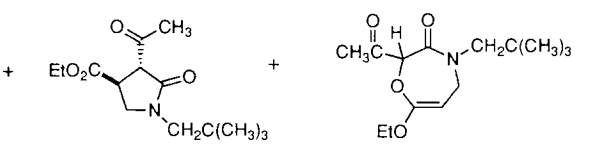


Scheme 7. Mechanism of C–H insertion according to Doyle et al. R, R^1, R^2, R^3 = alkyl, aryl.

The importance of conformational factors in the intramolecular carbenoid reactions of α-diazoacetoacetamides has also been established by the Doyle group.[149] A series of diazoacetoacetamides, when treated with a catalytic quantity of a rhodium(II) carboxylate, afforded a product derived from a carbonyl ylide intermediate as well as those derived from intramolecular C–H insertion. Decomposition of **114** in refluxing benzene gave rise to a mixture of β- and γ-lactams (**115** and **116**) and, in addition, **117** arising from a carbonyl ylide. Changing the catalyst from $[Rh_2(pfb)_4]$ through $[Rh_2(OAc)_4]$ to $[Rh_2(acm)_4]$ yielded significant differences in the product distribution. The major



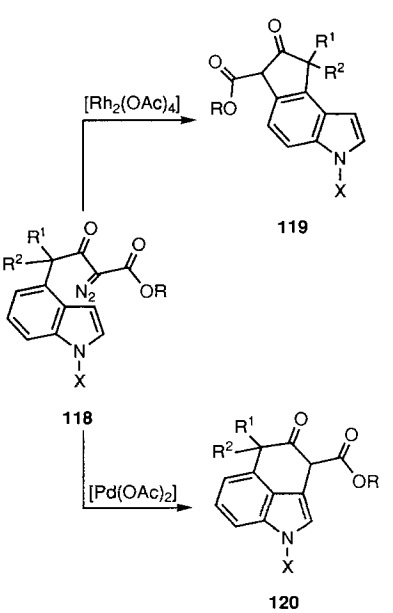
114 **115**



116 **117**

$[Rh_2(pfb)_4]$	22 : 17 : 61
$[Rh_2(OAc)_4]$	59 : 10 : 30
$[Rh_2(acm)_4]$	64 : 26 : 10

product from the $[Rh_2(pfb)_4]$-catalyzed reaction of **114** is **117**, which arises from ester carbonyl entrapment of the intermediate metal–carbene. This is undoubtedly related to the fact that this Rh^{II} complex possesses the highest oxophilicity of the three catalysts. Dominant formation of the β-lactam ring was attributed to a conformational preference that juxtaposes the carbenoid center and the less sterically encumbered amide substituent, which activates the C–H bond adjacent to the amide nitrogen atom.

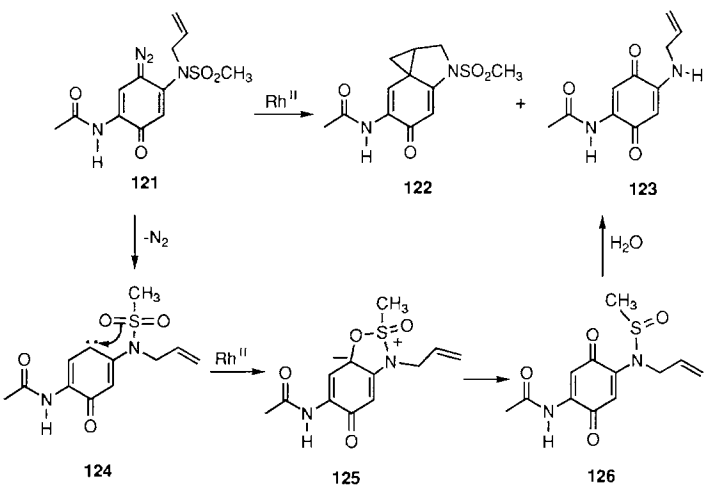


118 **119** **120**

The hapalindole family of alkaloids was prepared in high yield through an intramolecular indole C–H insertion reaction.[150]

When $[Cu(acac)_2]$ was used as the catalyst, only the tricyclic structure **119** was formed in 20% yield. This compound resulted from insertion of the carbenoid into the 5-position of the indole ring in **118**. Switching the catalyst to rhodium(II) acetate still afforded the undesired adduct **119**, but in much higher yield (89%). On the other hand, palladium(II) acetate catalysis in methanol gave the desired compound **120** in 71% yield. The postulated mechanism of the palladium-catalyzed reaction proceeds through a zwitterionic intermediate which is favored in polar solvents and results in cyclization at the 3-position of the indole. The rhodium-catalyzed reaction takes place preferentially through a five-membered transition state.

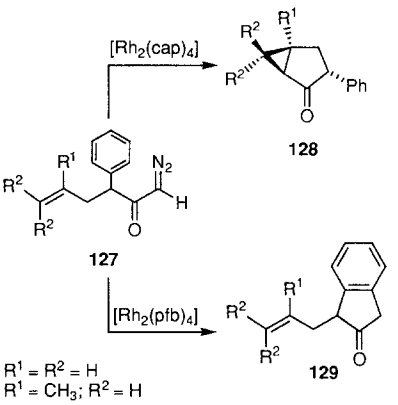
The synthesis of spirocyclopropyl quinone **122**, which serves as the precursor to the A-ring of the antitumor antibiotic CC-1065, by an intramolecular carbenoid addition was investigated by Sundberg et al.[151] Catalytic decomposition of diazo ketone **121** with $[Rh_2(piv)_4]$ at 40 °C for 2 h proved to be the most effective conditions for cyclopropanation. The desulfonylated quinone **123** was also formed in varying yields depending on the particular catalyst and conditions used. Whereas reaction with



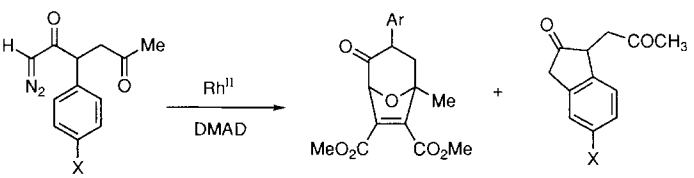
$[Rh_2(OAc)_4]$ was rather slow, the more soluble $[Rh_2(oct)_4]$ and $[Rh_2(piv)_4]$ led to a faster reaction and improved the cyclopropane to quinone ratio. The origin of the desulfonylated quinone **123** was traced to an intramolecular oxygen transfer to the carbenoid carbon producing **126**, which was hydrolyzed to **123** under the reaction conditions.

6.3. Competition Experiments

Carboxylate and carboxamide ligands of dirhodium(II) catalysts were also found to influence chemoselectivity in metal-mediated transformations of α-diazo carbonyl compounds.[152] The choice of catalyst exerted effective control on competitive intramolecular cyclopropanation and intramolecular aromatic substitution with 1-diazo-3-aryl-5-hexen-2-ones **127**. Use of $[Rh_2(OAc)_4]$ yielded products from both transformations (**128** and **129**) in nearly equal amounts, but $[Rh_2(pfb)_4]$ catalyzed only the aromatic substitution, and $[Rh_2(cap)_4]$ only the cyclopropanation. Similar results were obtained from dirhodium(II) catalysts in competition between intramolecular cyclopropanation and insertion into tertiary C–H bonds, aromatic cycloaddition and C–H insertion, cyclopropanation and aromatic cycloaddition, and C–H insertion and aromatic substitution. What is so remarkable is the degree to which chemoselectivity can be achieved over such a broad spectrum of carbene reactions by simply changing the ligands on the catalyst from perfluorobutyrate to carboxamide. The significant difference in chemical behavior between $[Rh_2(tfa)_4]$ and $[Rh_2(cap)_4]$ has been attributed to the large differences in charge and in frontier orbital properties. With certain substrates conformational effects may also play a dominant role in product formation.[152]



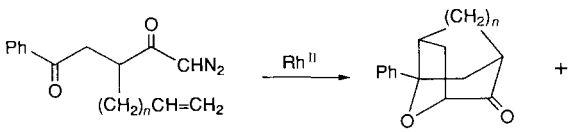
The choice of catalyst also exerted a dramatic effect on the product distribution in reactions with diazo compounds **130** and **133**, substrates in which intramolecular aromatic substitution competes with carbonyl ylide formation.[153] Thus, the $[Rh_2(OAc)_4]$-catalyzed decomposition of **130** in the presence of dimethyl acetylenedicarboxylate (DMAD) gave rise to a mixture of oxabicyclooctanone **131** (60%) and the 2-indanone **132** (20%); carbonyl ylide formation predominated over attack on the aromatic ring. However, on changing the catalyst to $[Rh_2(cap)_4]$, only the carbonyl ylide cycloadduct **131** was formed (90%). In contrast, use of the more electrophilic $[Rh_2(pfb)_4]$ resulted in exclusive formation of the aromatic substitution product **132** (85%). Diazo compound **133** showed a similar pattern of reactivity (formation of **134** and **135**).



$[Rh_2(OAc)_4]$	60%	20%
$[Rh_2(cap)_4]$	90%	0%
$[Rh_2(pfb)_4]$	0%	85%

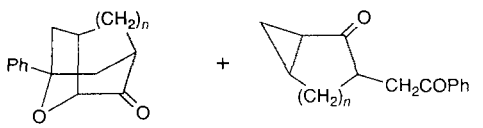
The reactions of 3-allyl-1-diazopentane-2,5-dione (**136**) and 3-butenyl-1-diazopentane-2,5-dione (**140**) with a Rh^{II} catalyst

were also studied.[154] The three major products corresponded to the intramolecular reaction of a carbonyl ylide intermediate (products **137** + **138** and **141** + **142**, respectively) and intramolecular cyclopropanation (products **139** and **143**, respectively). Changing the catalyst from $[Rh_2(OAc)_4]$ to $[Rh_2(tfa)_4]$ caused a rather startling and unexpected alteration in product distribution with diazo dione **136**: cycloadduct **137** was the major product isolated when $[Rh_2(tfa)_4]$ was used, whereas cycloadduct **138** was the major regioisomer formed with the other two catalysts. No such regiochemical crossover was observed with the three catalysts for the butenyl-substituted **140**. Intramolecular cyclopropanation occurs to a considerable extent with all catalysts in systems where a bicyclo[3.1.0] ring system is produced (**139**; $n = 1$). The importance of this pathway diminishes when a bicyclo[4.1.0] ring system (**143**; $n = 2$) is formed, presumably as a result of conformational and entropic factors.



136, $n = 1$ **140**, $n = 2$

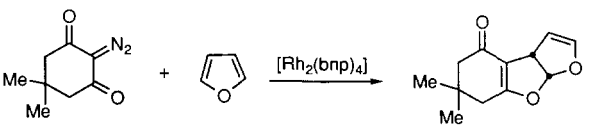
	137, $n = 1$	**141**, $n = 2$
$[Rh_2(OAc)_4]$	10%	60%
$[Rh_2(tfa)_4]$	34%	67%
$[Rh_2(cap)_4]$	12%	70%



	138, $n = 1$	**142**, $n = 2$	**139**, $n = 1$	**143**, $n = 2$
$[Rh_2(OAc)_4]$	47%	11%	37%	13%
$[Rh_2(tfa)_4]$	12%	0%	30%	0%
$[Rh_2(cap)_4]$	52%	11%	32%	17%

The regiochemical differentiation for diazo dione **136** by the rhodium catalyst is most remarkable. Regiochemical control in [3 + 2] dipolar cycloaddition reactions has generally been rationalized on the basis of FMO considerations (FMO = frontier molecular orbital).[155] Cyclization by overlap of the lone pair of electrons of the more remote carbonyl group and an orbital of the reactive α-keto metallocarbene intermediate is believed to be followed by dissociation of the catalyst and generation of a dipole not complexed to the metal.[21] However, to explain the results with diazo dione **136**, the mechanism needs to be modified. One possibility is that immediately after dipole generation, the $[Rh_2(tfa)_4]$ catalyst coordinates to the nearby olefinic π bond.[156] This complexation may very well lower the LUMO energy of the tethered alkene and consequently shift the cycloaddition from a LUMO- to a HOMO-controlled process. Alternatively, the $[Rh_2(tfa)_4]$ catalyst may still be coordinated (η^2 or η^3) to the dipole, and this complex could undergo a subsequent intramolecular cycloaddition with a different regiochemical profile. Further work is necessary before one can distinguish between these two possibilities.

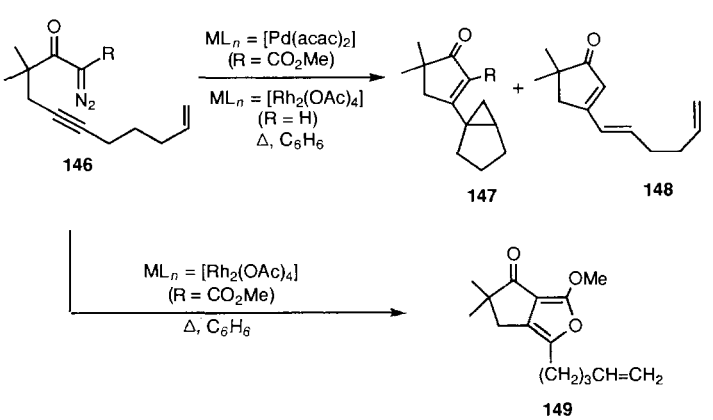
Recently Pirrung and Zhang explored the asymmetric dipolar cycloaddition reactions of diazo compounds mediated by tetrakis(binaphthyldiylphosphate)dirhodium ($[Rh_2(bnp)_4]$).[134] The interrhodium distance in this catalyst is 0.1 Å longer than in the corresponding carboxylates,[157] which should have an effect on its catalytic properties. Interestingly, the cycloaddition of diazo dimedone (**144**) to furan catalyzed by $[Rh_2(bnp)_4]$ provided **145** in 50% yield and with 49% *ee*. The working hypothesis for the above cycloaddition reaction involves an initial cyclopropanation,[158] and this model was used to rationalize the asymmetric induction observed. However, this hypothesis was difficult to reconcile with all of the experimental observations.



144 **145**

6.4. Alkyne Metathesis Reaction

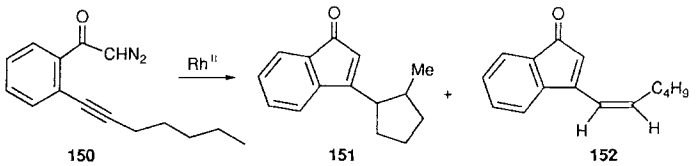
The insertion of alkynes into transition metal–carbon bonds is a well-documented reaction and has been observed in nearly all of the triads of transition metals.[159] The Rh^{II}-catalyzed reaction of α-diazo ketones bearing tethered alkyne units has recently been used for the construction of polycyclic skeletons. Hoye and Dinsmore et al. examined the intramolecular carbenoid additions to acetylenes.[160] Their results indicated that the product distribution was markedly dependent upon the nature of the catalyst. For example, treatment of α-diazo ketone **146** with catalytic $[Pd(acac)_2]$ produced cyclopropane **147** (R = CO_2Me) in 78% yield. However, when $[Rh_2(OAc)_4]$ was used as the catalyst, **147** was not formed. Instead, furan **149** was isolated in 65% yield. This compound arose by a 1,5-electrocyclization reaction of the initially produced vinyl carbenoid. Removal of the stabilizing ester carbonyl gave both **147** (R = H) and the 1,2-hydrogen shift product **148**. The ratio of products also varied on changing the ligands on the rhodium atom.



146 **147** **148** **149**

An analogous set of results were encountered in a study of the Rh^{II}-catalyzed reaction of *o*-alkynyl-substituted α-diazo-

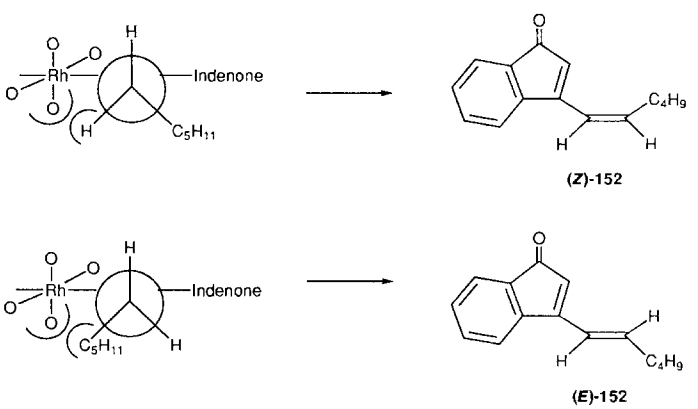
acetophenone derivatives.[161] Several structural influences were observed by varying the nature of the substituent group attached to the alkyne carbon atom. In the cyclization reaction a rhodium-stabilized carbenoid added to the acetylenic π bond to generate a vinyl carbenoid. The vinyl carbenoid underwent both CH and CC migration (**151**), as well as δ-CH insertion into the alkyl backbone (**152**). The α-diazo alkyne insertion reactions



150 151 152

$[Rh_2(man)_4]$	50:50
$[Rh_2(OAc)_4]$	66:33
$[Rh_2(oct)_4]$	80:20
$[Rh_2(pfb)_4]$	10:90

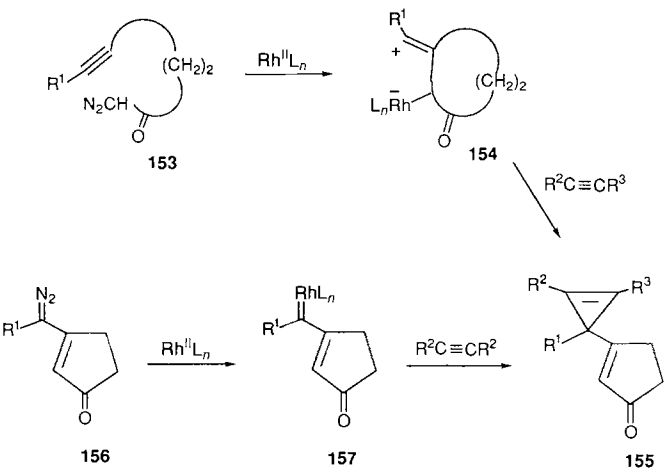
in this system were ligand dependent, which implies that a metalated species is involved in the product-determining step. By choice of the catalyst, the product distribution could be manipulated. The more electron-withdrawing perfluorobutyrate ligand favors β-hydride elimination, while 1,5-insertion is favored by the more electron-donating ligands. The rhodium carbenoid intermediate is highly electron-deficient at the carbon center and is further destabilized by an electron-withdrawing ligand. With this more reactive intermediate, the entropically less demanding β-hydride elimination pathway is favored as noted earlier. Another point worth noting is the preferential formation of the thermodynamically less stable *Z* isomer **152** as product of the 1,2-hydrogen shift. The rhodium carboxylate restricts the orientation of the alkyl chain in the metal carbene intermediate (Scheme 8), and thus directs the hydrogen migration.[162–164]



Scheme 8. Stereochemical considerations in the preferred formation of (*Z*)-**152**.

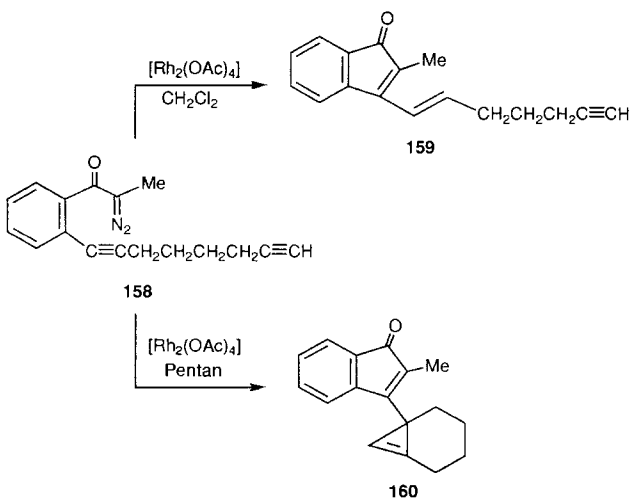
An added complication is the marked influence of the solvent on the mechanism as well as on the chemoselectivity of the reactions (see Section 6.5). Many intermediates may be envisioned along the pathway from **150** to **152**, and it is not an easy task to identify the mechanistic differences.

In another study of the rhodium(II)-catalyzed alkyne insertion reaction, Hoye and Dinsmore reported on the Rh^{II}-catalyzed double *internal–external* alkyne insertion reaction of an acetylenic α-diazo ketone.[165] The initially formed rhodium carbenoid intermediate apparently underwent internal insertion into the tethered alkyne unit followed by a second external addition to produce a cyclopropenyl-substituted cyclopentenone derivative (**155**). Migration of the rhodium metal to the remote alkyne carbon by a [2 + 2] cycloaddition/cycloreversion path (**153**–**157**) was discounted on the basis that the distribution of products derived from **153** differed significantly from that obtained from the rhodium carbenoid species **157** generated from the vinylogous diazo ketone precursor **156**. Instead, the results were rationalized by proposing the intermediacy of zwitterion **154**.



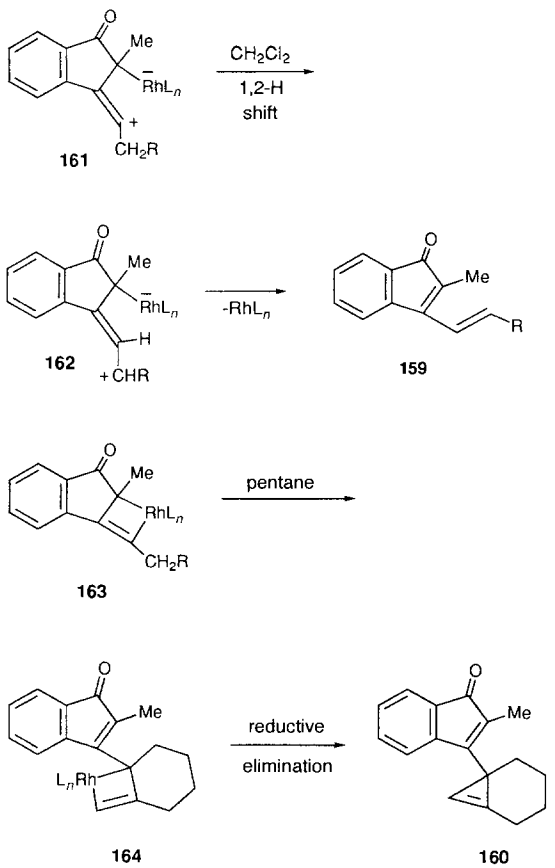
153 154 156 157 155

Our subsequent work[166] showed that the reaction mechanism was markedly dependent on the solvent employed in the Rh^{II}-catalyzed insertion reactions. The treatment of α-diazo ketone **158** with a catalytic quantity of $[Rh_2(OAc)_4]$ at 25°C in CH_2Cl_2 afforded a 2:1 mixture of the *cis* and *trans* alkenyl-substituted indenones **159** (R = $(CH_2)_3C{\equiv}H$) in 85% combined yield, whereas $[Rh_2(oct)_4]$ as catalyst in this solvent furnished a 2:3 mixture of cyclopropene **160** and indenone **159**. Use of pentane instead of CH_2Cl_2 with $[Rh_2(OAc)_4]$ resulted in the exclusive formation of cyclopropene **160** (80%). The degree



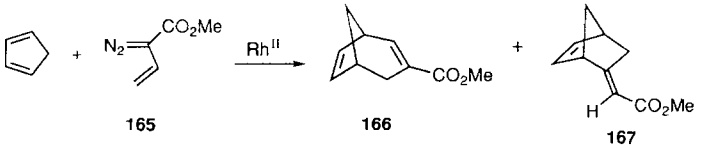
to which chemoselectivity can be achieved by simply changing the solvent from CH_2Cl_2 to pentane is extremely unusual.

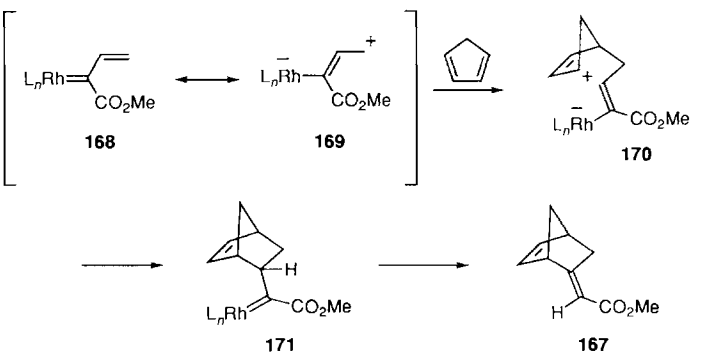
In the mechanism proposed to account for the formation of indenone **159**, the initially formed carbenoid cyclizes stepwise in accord with the Hoye–Dinsmore proposal.[165] A 1,2-hydrogen shift from **161** (R = $(CH_2)_3C{\equiv}H$) yielding **162** is followed by dissociation to **159** and regeneration of the rhodium catalyst. The intermediates en route to **159** are dipolar, which would explain why the generation of **159** is strongly inhibited in pentane. Metal migration occurs via the metallocyclobutene intermediates **163** (R = $(CH_2)_3C{\equiv}H$) and **164** in pentane so as to avoid charge buildup.



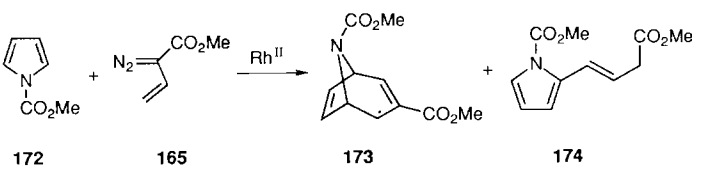
6.5. Solvent Effects on Chemoselectivity

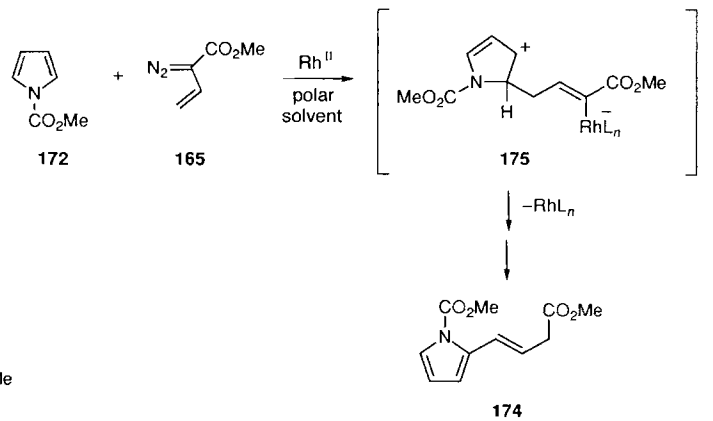
Davies et al. showed that the rhodium(II)-catalyzed decomposition of vinyldiazomethanes in the presence of dienes represents a direct and stereoselective method for the construction of seven-membered rings.[167] For example, the rhodium(II)-catalyzed reaction of vinyldiazomethane **165** with cyclopentadiene resulted in a mixture of **166** and **167**.[168] Both the solvent and the ligands on the catalyst had a major effect on the product distribution. The formation of **166** through a tandem cyclopropanation/Cope rearrangement[167] was greatly enhanced in less polar solvents. Electron-withdrawing ligands (such as trifluoroacetate) on the rhodium facilitated formation of **167**, by stabilizing the dipolar resonance structure **169** of the metal–vinylcarbenoid **168**; thus the vinyl terminus acts as a competing electrophilic center generating the dipolar structure **170** which then undergoes ring closure followed by a 1,2-hydrogen shift. Nonpolar solvents as well as electron-releasing ligands severely retard this reaction, which accounts for the variation in product ratio.





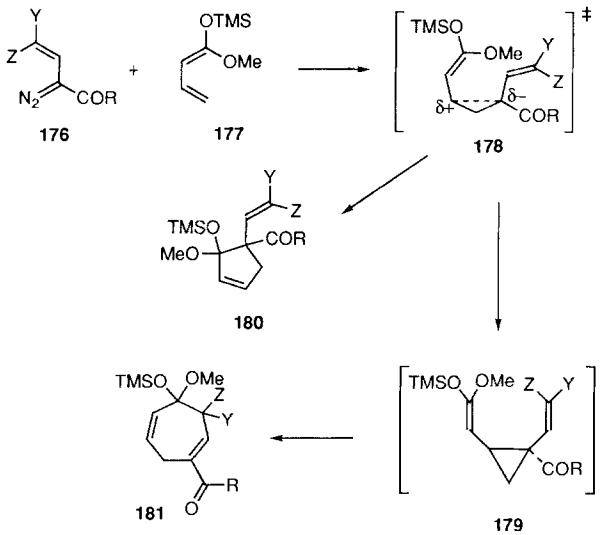
The reaction of **165** with *N*-methoxycarbonyl-substituted pyrrole (**172**) also gave a mixture of two products, **173** and **174**.[168, 169] Once again, the distribution of products could be controlled through the use of an appropriate solvent and catalyst. Electron-withdrawing ligands on the rhodium such as trifluoroacetate strongly enhanced the formation of the alkylated product **174**. On changing to nonpolar solvents, the formation of **174** was totally suppressed, since polar intermediates are involved in its production. The results encountered with pyrrole





172 are very similar to those found in the reaction of **165** with cyclopentadiene.[166] More than likely the formation of **174** proceeds through intermediate **175** by pyrrole attack at the vinyl terminus of the resulting carbenoid derived from **165**. Rearomatization of **175** is facilitated intramolecularly with the generation of a rhodium hydride species which undergoes reductive elimination and double-bond isomerization producing pyrrole **174**.

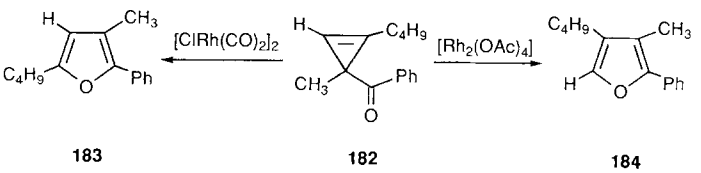
Still another example of a catalyst/solvent effect on the product distribution in this [3 + 4] annulation reaction was described by Davies et al. in the context of their approach to the tropane ring skeleton.[170] The Rh^{II}-catalyzed reaction of vinyldiazo methanes (**176**, Y = CO_2Et, Ph; Z = H, OMe) in the presence of diene **177** afforded both five- and seven-membered rings (**180** and **181**) depending on the choice of catalyst and solvent.



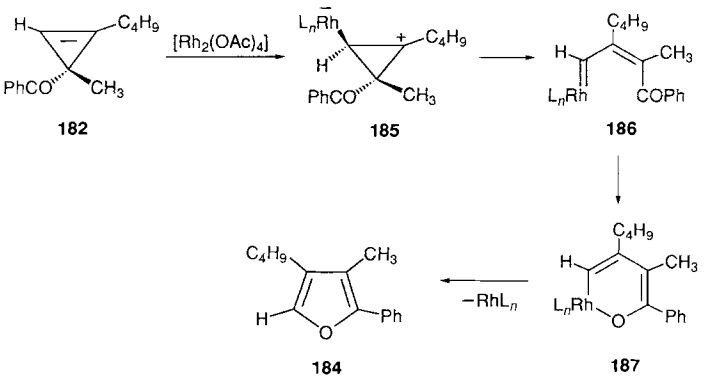
The occurrence of a partially dipolar transition state caused by a nonsynchronous cyclopropanation step explained the results: if the cyclopropanation step were not completed, side products from the dipolar structure **178** would be observed. Nonpolar solvents did destabilize the polar transition state, and formation of the five-membered ring **180** was totally suppressed. Under these conditions the normal cyclopropanation/Cope rearrangement product (**181**) was isolated in high yield.

6.6. Effect of the Oxidation State of the Metal on the Chemoselectivity

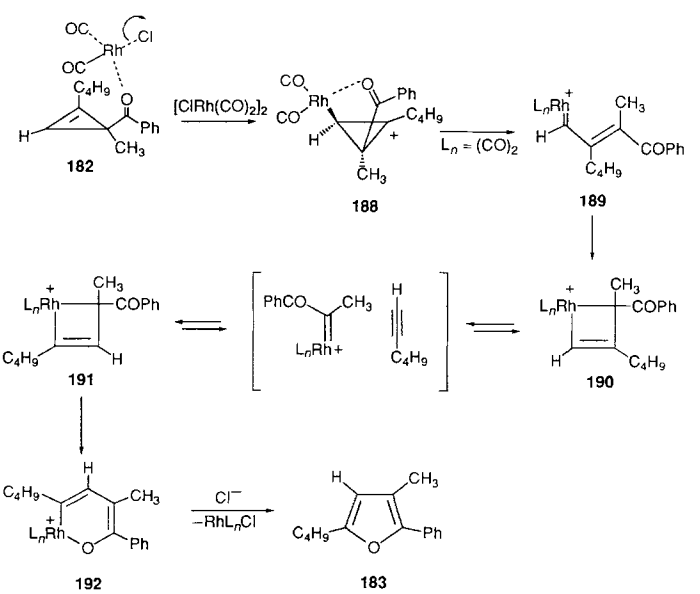
The interaction of transition metal complexes with strained carbocyclic compounds has been a subject of considerable interest in recent years.[171] These metals catalyze a variety of rearrangements, the course of which depends on the nature of both the substrate and the metal complex.[172] Due to both synthetic and theoretical aspects, the rhodium(II)-catalyzed ring opening of cyclopropene derivatives is particularly important.[173, 174] Our research has demonstrated an unusual effect on the regioselectivity of ring opening of the cyclopropene by the oxidation state of the metal:[175] catalysis by the Rh^{II} compound $[Rh_2(OAc)_4]$ of the reaction of an unsymmetrically substituted cyclopropene such as **182** gave a substituted furan (**184**) derived from cleavage of the less substituted σ bond. In contrast, Rh^{I} catalysis with $[ClRh(CO)_2]_2$ resulted in cleavage of the more substituted σ bond producing the regioisomeric furan **183**.



The model of Doyle, Müller et al.[176] readily accounts for the Rh^{II} results: a preferential electrophilic attack by the Rh^{II} catalyst *trans* to the ketone moiety produces the more substituted cyclopropyl cation **185**. Disrotatory ring opening of **185** leads to the carbene complex **186**. Electrocyclization of the vinyl carbenoid to **187** followed by reductive elimination eventually affords furan **184**.



The mechanistic rationale for the formation of the other regioisomeric furan **183** with a Rh^{I} catalyst proposes electrophilic attack of $[ClRh(CO)_2]_2$ on the less substituted carbon



of the cyclopropene π bond to give the tertiary cyclopropyl carbocation **188**. Ring opening followed by a rapid electrocyclization reaction produces the metallocyclobutene **190**. Equilibration of **190** with the thermodynamically more stable 1,3-disubstituted isomer **191** proceeds by a cycloreversion–cycloaddition pathway.[177, 178] Rhodium migration from carbon to oxygen followed by reductive elimination produces the observed furan. The different reactivity of the catalysts can be explained by the fact that the formal increase in oxidation state from Rh^{I} to Rh^{III} which accompanies the conversion **189** → **190** is a much more facile process than the comparable $Rh^{II} \rightarrow Rh^{IV}$ formal oxidation.[171]

7. Summary and Outlook

Dirhodium(II) acetate and related carboxylates react with α-diazo carbonyl compounds to form metal carbenes, which undergo a broad spectrum of chemical transformations, including cyclopropanation, carbon–hydrogen insertion, ylide generation, and aromatic cycloaddition. The carboxylate and carboxamide ligands of dirhodium(II) catalysts can cause chemoselectivity in competitive metal carbene transformations of diazo compounds to switch between competitive transformation. Although $[Rh_2(OAc)_4]$ is most often used to test the feasibility of metal carbene transformations, chemoselectivity with this catalyst generally falls between those of $[Rh_2(pfb)_4]$ and $[Rh_2(cap)_4]$. Either charge control or HOMO/LUMO control or both may be operating in these transformations, and with certain substrates, conformational effects play a dominant role in product formation.

In the future, ligands with different backbones containing chiral groups will be developed. Many different Rh^{II} complexes containing a wide assortment of bidendate ligands can be envisaged. The investigation of the catalytic behavior of transition metal complexes for organic synthesis is at its very beginning. Consequently, our understanding of the role that ligands play in influencing diastereo- and chemoselectivity with transition metal complexes is still in a primitive state. As is the case in all new areas of research using catalysts, investigation of the chemistry of these transition metal complexes in the near future will be dominated by the search for asymmetric synthesis.

We are indebted to our excellent co-workers for their commitment and considerable contributions in the form of ideas and experiments. Their names can be found in the references. We are particularly grateful to the National Institutes of Health and the National Science Foundation for generous support. Some aspects of the research were only possible through the cooperation of other groups, in particular those of Professors Michael P. Doyle at Trinity University and Chris Moody at Loughborough University.

Received: October 25, 1993 [A321E]
German version: *Angew. Chem.* **1994**, *106*, 1881

[1] M. P. Doyle, *Chem. Rev.* **1986**, *86*, 919; *Acc. Chem. Res.* **1986**, *19*, 348.
[2] G. Maas, *Top. Curr. Chem.* **1987**, *137*, 75.
[3] J. Adams, D. M. Spero, *Tetrahedron* **1991**, *47*, 1765.
[4] A. Padwa, K. E. Krumpe, *Tetrahedron* **1992**, *48*, 5385.
[5] K. H. Dötz, *Angew. Chem.* **1975**, *87*, 672; *Angew. Chem. Int. Ed. Engl.* **1975**, *14*, 644.
[6] W. D. Wulff in *Comprehensive Organic Synthesis, Vol. 5* (Eds.: B. M. Trost, I. Fleming), Pergamon, New York, **1990**.
[7] Review: D. S. Wulfman, G. Linstrumelle, C. F. Cooper in *The Chemistry of Diazonium and Diazo Groups, Part 2* (Ed.: S. Patai), Wiley Interscience, New York, **1978**, Chap. 18.
[8] O. Silberrad, C. S. Roy, *J. Chem. Soc.* **1906**, *89*, 179.
[9] G. V. Pazynina, E. A. Luk'yanets, I. G. Bolesov, *Zh. Org. Chim.* **1984**, *20*, 802.
[10] A. Nakamura, T. Yoshida, M. Cowie, S. Otsuka, J. A. Ibers, *J. Am. Chem. Soc.* **1977**, *99*, 2108; H. Werner, J. H. Richards, *ibid.* **1968**, *90*, 4976; B. Bogdanović, M. Kröner, G. Wilke, *Justus Liebigs Ann. Chem.* **1966**, *699*, 1; C. Rüchardt, G. Schrauzer, *Chem. Ber.* **1960**, *93*, 1840.
[11] A. K. Chakraborti, J. K. Ray, K. K. Kundu, S. Chakrabarty, D. Mulkherjee, U. R. Ghatak, *J. Chem. Soc. Perkin Trans. 1* **1984**, 261; A. K. Chakraborti, B. Saha, U. R. Ghatak, *Indian J. Chem. Sect. B* **1981**, *20*, 911.
[12] D. S. Crumrine, H.-H. B. Yen, *J. Am. Chem. Soc.* **1976**, *98*, 297; D. S. Crumrine, T. J. Haberkamp, D. J. Suther, *J. Org. Chem.* **1975**, *40*, 2274.
[13] A. J. Anciaux, A. J. Hubert, A. F. Noels, N. Petiniot, P. Teyssié, *J. Org. Chem.* **1980**, *45*, 695.
[14] M. P. Doyle, R. L. Dorow, W. H. Tamblyn, *J. Org. Chem.* **1982**, *47*, 4059; M. P. Doyle, J. G. Davidson, *ibid.* **1980**, *45*, 1538.
[15] W. H. Tamblyn, S. R. Hoffmann, M. P. Doyle, *J. Organomet. Chem.* **1981**, *216*, C64.
[16] A. Nakamura, T. Koyama, S. Otsuka, *Bull. Chem. Soc. Jpn.* **1978**, *51*, 593; A. J. Hubert, A. F. Noels, A. J. Anciaux, P. Teyssié, *Synthesis* **1976**, 600; R. Paulissen, A. J. Hubert, P. Teyssié, *Tetrahedron Lett.* **1972**, 1465.
[17] H. J. Callot, F. Metz, C. Piechocki, *Tetrahedron* **1982**, *38*, 2365; H. J. Callot, E. Schaeffer, *Nouv. J. Chim.* **1980**, *4*, 311; H. J. Callot, C. Piechocki, *Tetrahedron Lett.* **1980**, *21*, 3489.
[18] A. B. Smith III, R. K. Dieter, *Tetrahedron* **1981**, *37*, 2407.
[19] S. D. Burke, P. A. Grieco, *Org. React. (NY)* **1979**, *26*, 361.
[20] D. F. Taber, *Comprehensive Organic Synthesis, Vol. 3*, (Eds.: B. M. Trost, I. Fleming), Pergamon, New York, **1991**, p. 1045.
[21] A. Padwa, S. F. Hornbuckle, *Chem. Rev.* **1991**, *91*, 263.
[22] M. P. Doyle, *Recl. Trav. Chim. Pays-Bas* **1991**, *110*, 305.
[23] H. Nozaki, H. Takaya, S. Moriuti, R. Noyori, *Tetrahedron* **1968**, *24*, 3655; H. Nozaki, S. Moriuti, H. Takaya, R. Noyori, *Tetrahedron Lett.* **1966**, 5239; R. Noyori, *Science* **1990**, *248*, 1194.
[24] T. Aratani, Y. Yoneyoshi, T. Nagase, *Tetrahedron Lett.* **1982**, *23*, 685; *ibid.* **1977**, 2599.
[25] F. Hugo, U. Leutenegger, K. Siegmann, A. Pfaltz, W. Keller, C. Kratky, *Helv. Chim. Acta* **1988**, *71*, 1541; F. Hugo, U. Leutenegger, A. Pfaltz, *ibid.* **1988**, *71*, 1553.
[26] D. Müller, G. Umbricht, B. Weber, A. Pfaltz, *Helv. Chim. Acta* **1991**, *74*, 232.
[27] D. A. Evans, K. A. Woerpel, M. M. Hinman, M. M. Faul, *J. Am. Chem. Soc.* **1991**, *113*, 726.
[28] a) R. E. Lowenthal, A. Abiko, S. Masamune, *Tetrahedron Lett.* **1990**, *32*, 6005; b) R. E. Lowenthal, S. Masamune, *ibid.* **1991**, *32*, 7373.
[29] a) D. A. Evans, M. M. Faul, M. T. Bilodeau, B. A. Anderson, D. M. Barnes, *J. Am. Chem. Soc.* **1993**, *115*, 5328; b) For another example of copper-mediated chiral catalytic aziridination, see Z. Li, K. R. Conser, E. N. Jacobsen *ibid.* **1993**, *115*, 5326.
[30] A footnote in the second paper of ref. [28b] describes a high-yielding, highly enantioselective aziridination with a chiral bis(oxazoline)copper complex as catalyst. See also citation 9 from ref. [29a].
[31] D. A. Evans, S. J. Miller, T. Lectka, *J. Am. Chem. Soc.* **1993**, *115*, 6460.
[32] E. J. Corey, N. Imai, H.-Y. Zhang, *J. Am. Chem. Soc.* **1991**, *113*, 728; E. J. Corey, K. Ishihara, *Tetrahedron Lett.* **1992**, *33*, 6807.
[33] A. Nakamura, A. Konishi, Y. Tatsuno, S. Otsuka, *J. Am. Chem. Soc.* **1978**, *100*, 3443; A. Nakamura, A. Konishi, R. Tsujitani, M. Kudo, S. Otsuka, *ibid.* **1978**, *100*, 3449; A. Nakamura, *Pure Appl. Chem.* **1978**, *50*, 37.
[34] M. P. Doyle, B. D. Brandes, A. P. Kazala, R. J. Pieters, M. B. Jarstfer, L. M. Watkins, C. T. Eagle, *Tetrahedron Lett.* **1990**, *31*, 6613.
[35] W. R. Moser, *J. Am. Chem. Soc.* **1969**, *91*, 1135.
[36] A. R. Daniewski, T. Kowalczyk-Przewloka, *Tetrahedron Lett.* **1982**, 23, 2411; *J. Org. Chem.* **1985**, *50*, 2976.
[37] S. A. Matlin, W. J. Lough, L. Chan, D. M. H. Abram, Z. Zhou, *J. Chem. Soc. Chem. Commun.* **1984**, 1038.
[38] H. Brunner, H. Kluschanzoff, K. Wutz, *Bull. Soc. Chim. Belg.* **1989**, *98*, 63.
[39] S.-I. Hashimoto, N. Watanabe, T. Sato, M. Shiro, S. Ikegami, *Tetrahedron Lett.* **1993**, *34*, 5109; B. Kojic-Prodic, R. Marcec, B. Nigovic, Z. Raza, V. Sunjic, *Tetrahedron: Asymmetry* **1992**, *3*, 1; M. P. Doyle, R. L. Dorrow, W. E. Buhro, J. H. Griffin, W. H. Tamblyn, M. L. Trudell, *Organometallics* **1984**, *3*, 44; S. Danishefsky, J. Regan, R. Doehner, *J. Org. Chem.* **1981**, *46*, 5255; T. Hudlicky, F. J. Koszyk, T. M. Kutchan, J. P. Sheth, *ibid.* **1980**, *45*, 5020.
[40] K. N. Mehrotra, G. S. Singh, *Indian J. Chem. Sect. B* **1982**, *21*, 672; S. Kulkowit, M. A. McKervey, *J. Chem. Soc. Chem. Commun.* **1981**, 616; S. B. Singh, K. N. Mehrotra, *Can. J. Chem.* **1981**, *59*, 2475.
[41] P. de March, M. Moreno-Mañas, I. Ripoll, *Synth. Commun.* **1984**, *14*, 521; T. Ibata, J. Toyoda, *Chem. Lett.* **1983**, 1453.
[42] E. Vogel, A. Vogel, H.-K. Kübbeler, W. Sturm, *Angew. Chem.* **1970**, *82*, 512; *Angew. Chem. Int. Ed. Engl.* **1970**, *9*, 514; Z. Arnold, *J. Chem. Soc. Chem.*

Commun. **1967**, 299; W. von E. Doering, B. M. Ferrier, E. T. Fossel, J. H. Hartenstein, M. Jones, Jr., G. Klumpp, R. M. Rubin, M. Saunders, *Tetrahedron* **1967**, *23*, 3943.
[43] T. Nakata, A. Tahara, *Tetrahedron Lett.* **1976**, 1515; F. Greuter, J. Kalvoda, O. Jeger, *Proc. Chem. Soc. London* **1958**, 349.
[44] W. Kreiser, P. Below, *Liebigs Ann. Chem.* **1985**, 203; K. Saigo, H. Kurihara, H. Miura, A. Hongu, N. Kubota, H. Nohira, M. Hasegawa, *Synth. Commun.* **1984**, *14*, 787.
[45] O. M. Nefedov, I. E. Dolgii, Y. V. Tomilov, V. G. Bordakov, *Izv. Akad. Nauk SSSR Ser. Khim.* **1984**, 119; D. S. Wulfman, B. G. McGibboney, E. K. Steffen, N. V. Thinh, R. S. McDaniel, Jr., B. W. Peace, *Tetrahedron* **1976**, *32*, 1257; D. S. Wulfman, B. W. Peace, E. K. Steffen, *J. Chem. Soc. Chem. Commun.* **1971**, 1360; E. Müller, H. Kessler, B. Zech, *Fortschr. Chem. Forsch.* **1966**, *7*, 128.
[46] R. G. Salomon, J. K. Kochi, *J. Am. Chem. Soc.* **1973**, *95*, 3300.
[47] W. R. Moser, *J. Am. Chem. Soc.* **1969**, *91*, 1141.
[48] H. O. House, C. J. Blankley, *J. Org. Chem.* **1968**, *33*, 47; R. K. Armstrong, *ibid.* **1966**, *31*, 618; I. A. D'yakonov, O. V. Guseva, *J. Gen. Chem. USSR (Engl. Transl.)* **1952**, *22*, 1355.
[49] G. Wittig, K. Schwarzenbach, *Justus Liebigs Ann. Chem.* **1961**, *650*, 1.
[50] R. G. Salomon, M. F. Salomon, T. R. Heyne, *J. Org. Chem.* **1975**, *40*, 756; R. G. Salomon, J. K. Kochi, *J. Am. Chem. Soc.* **1973**, *95*, 1889.
[51] M. C. Pirrung, J. A. Werner, *J. Am. Chem. Soc.* **1986**, *108*, 6060.
[52] J. S. Clark, S. A. Krowiak, L. J. Street, *Tetrahedron Lett.* **1993**, *34*, 4385.
[53] Z. A. Starikova, E. A. Shugman, *J. Struct. Chem. (Engl. Transl.)* **1969**, *10*, 290.
[54] R. C. E. Belford, D. E. Fenton, M. R. Truter, *J. Chem. Soc. Dalton Trans.* **1972**, 2208.
[55] T. Kogane, M. Ishii, K. Harada, R. Hirota, M. Nakahara, *Bull. Chem. Soc. Jpn.* **1990**, *63*, 1005; D. Gatteschi, J. Laugier, P. Rey, C. Zanchini, *Inorg. Chem.* **1987**, *26*, 938; J. Pradilla-Sorzano, J. P. Fackler, *ibid.* **1973**, *12*, 1174.
[56] R. L. Belford, A. E. Martell, M. Calvin, *J. Inorg. Nucl. Chem.* **1956**, *2*, 11, and references therein.
[57] D. P. Graddon, S. Rochani, H. Way, *Inorg. Chim. Acta* **1985**, *104*, 87; T. M. Shepherd, *J. Chem. Soc. Dalton Trans.* **1972**, 813.
[58] B. E. Maryanoff, *J. Org. Chem.* **1982**, *47*, 3000; *ibid.* **1979**, *44*, 4410.
[59] M. E. Alonso, G. M. C. Garcia, *J. Org. Chem.* **1985**, *50*, 988.
[60] M. E. Alonso, A. Morales, A. W. Chitty, *J. Org. Chem.* **1982**, *47*, 3747; M. E. Alonso, A. W. Chitty, *Tetrahedron Lett.* **1981**, *22*, 4181.
[61] A. Padwa, D. J. Austin, unpublished results.
[62] C. Glidewell, D. Lloyd, S. Metcalfe, *Synthesis* **1988**, 319; J. N. C. Hood, D. Lloyd, W. A. MacDonald, T. M. Shepherd, *Tetrahedron* **1982**, *38*, 3355.
[63] R. Paulissen, E. Reimlinger, E. Hayez, A. J. Hubert, P. Teyssié, *Tetrahedron Lett.* **1973**, 2233; *ibid.* **1974**, 607.
[64] N. Petinoit, A. F. Noels, A. J. Anciaux, A. J. Hubert, P. Teyssié in *Fundamental Research in Homogeneous Catalsis, Vol. 3* (Ed.: M. Tsutsui), Plenum, New York, **1979**, p. 421.
[65] A. J. Hubert, A. F. Noels, A. J. Anciaux, P. Teyssié, *Synthesis* **1976**, 600.
[66] S. Bien, A. Gillon, S. Kohen, *J. Chem. Soc. Perkin Trans. 1* **1976**, 489.
[67] A. Gillon, D. Ovadiva, M. Kapon, S. Bien, *Tetrahedron* **1982**, *38*, 1477.
[68] T. R. Felthouse, *Prog. Inorg. Chem.* **1982**, *29*, 73.
[69] E. B. Boyar, S. D. Robinson, *Coord. Chem. Rev.* **1983**, *50*, 109.
[70] F. A. Cotton, R. A. Walton, *Multiple Bonds Between Metal Atoms*, 2nd ed., Clarendon, Oxford, **1982**, Chap. 7; M. H. Chisholm, I. P. Rothwell, *Prog. Inorg. Chem.* **1982**, *29*, 1.
[71] B. R. James, *Homogeneous Hydrogenation*, Wiley, New York, **1974**; A. D. Birch, D. H. Williamson, *Org. React.* **1976**, *24*, 1.
[72] R. R. Schrock, J. A. Osborn, *J. Am. Chem. Soc.* **1976**, *98*, 2134.
[73] K. E. Koenig, *Asymmetric Synthesis, Vol. 5* (Ed.: J. D. Morrison), Academic Press, New-York, **1985**, Chap. 3; W. S. Knowles, *Acc. Chem. Res.* **1983**, *16*, 106.
[74] D. Forster, *Adv. Organomet. Chem.* **1979**, *17*, 255.
[75] I. I. Chernyaev, E. V. Shenderetskaya, A. A. Karyagina, *Russ. J. Inorg. Chem. (Engl. Transl.)* **1960**, *5*, 559.
[76] M. A. Porai-Koshits, A. S. Antsyshkina, *Dokl. Chem.* **1962**, *146*, 902.
[77] D. M. Collins, F. A. Cotton, L. D. Gage, *Inorg. Chem.* **1979**, *18*, 1712.
[78] F. A. Cotton, L. D. Gage, *Nouv. J. Chim.* **1977**, *1*, 441.
[79] F. A. Cotton, Z. C. Mester, T. R. Webb, *Acta Crystallogr. Sect. B* **1974**, *30*, 2768.
[80] M. H. Chisholm, H. T. Chiu, J. C. Huffman, *Polyhedron* **1984**, *3*, 759.
[81] F. A. Cotton, G. W. Rice, *Inorg. Chem.* **1978**, *17*, 2004.
[82] M. J. Bennett, K. G. Caulton, F. A. Cotton, *Inorg. Chem.* **1969**, *8*, 1.
[83] F. A. Cotton, A. R. Chakravarty, D. A. Tocher, T. A. Stephenson, *Inorg. Chim. Acta* **1984**, *87*, 115.
[84] T. Yamaguchi, Y. Sasaki, T. Ito, *J. Am. Chem. Soc.* **1990**, *112*, 4038.
[85] V. M. Rao, H. Manohar, *Inorg. Chim. Acta* **1979**, *34*, L213.
[86] C. D. Garner, R. G. Senior, T. J. King, *J. Am. Chem. Soc.* **1976**, *98*, 3526.
[87] M. P. Doyle, R. L. Dorow, W. H. Tamblyn, *J. Org. Chem.* **1982**, *47*, 4059.
[88] G. G. Christoph, Y. B. Koh, *J. Am. Chem. Soc.* **1979**, *101*, 1422.
[89] J. L. Bear, J. Kitchens, M. R. Willcott, *J. Inorg. Nucl. Chem.* **1971**, *33*, 3479.
[90] F. A. Cotton, B. G. DeBoer, M. D. LaPrade, J. R. Pipal, D. A. Ucko, *Acta Crystallogr. Sect. B* **1971**, *27*, 1664.
[91] G. G. Christoph, M. Tolbert, *Am. Crystallogr. Assoc. Ser. 2*, **1980**, *7*, 39.
[92] F. A. Cotton, T. R. Felthouse, *Inorg. Chem.* **1980**, *19*, 323.
[93] G. G. Christoph, J. Halpern, G. P. Khare, Y. B. Koh, C. Romanowski, *Inorg. Chem.* **1981**, *20*, 3029.
[94] F. A. Cotton, J. L. Thompson, *Acta Crystallogr. Sect. B* **1981**, *37*, 2235.
[95] Y.-B. Koh, G. G. Christoph, *Inorg. Chem.* **1979**, *18*, 1122.
[96] F. A. Cotton, T. R. Felthouse, *Acta Crystallogr. Sect. C* **1984**, *40*, 42.
[97] G. G. Christoph, Y.-B. Koh, *J. Am. Chem. Soc.* **1979**, *101*, 1422.
[98] M. Moszner, T. Glowiak, J. J. Ziolkowskii, *Polyhedron* **1985**, *4*, 1413.
[99] G. Faraglia, R. Graziani, L. Volponi, U. Casellato, *Inorg. Chim. Acta* **1988**, *148*, 159.
[100] L. M. Dikareva, G. G. Sadikov, I. B. Baranovskii, M. A. Porai-Koshits, *Russ. J. Inorg. Chem. (Engl. Trans.)* **1980**, *25*, 1725.
[101] L. M. Dikareva, *Acta Crystallogr. Sect. A* **1966**, *21*, 140.
[102] R. J. H. Clark, A. J. Hempleman, H. M. Dawes, M. B. Hursthouse, C. D. Flint, *J. Chem. Soc. Dalton Trans.* **1985**, 1775.
[103] G. A. Rempel, P. Legzdins, H. Smith, G. Wilkinson, *Inorg. Synth.* **1972**, *13*, 90; P. Legzdins, R. W. Mitchell, G. L. Rempel, J. D. Ruddick, G. Wilkinson, *J. Chem. Soc. A* **1970**, 3322.
[104] J. Kitchens, J. L. Bear, *Thermochim. Acta* **1970**, *1*, 537; G. Winkhaus, P. Ziegler, *Z. Anorg. Allg. Chem.* **1967**, *350*, 51.
[105] F. A. Cotton, J. L. Thompson, *Inorg. Chim. Acta* **1984**, *81*, 193.
[106] P. A. Agaskar, F. A. Cotton, L. R. Falvello, S. Han, *J. Am. Chem. Soc.* **1986**, *108*, 1214.
[107] D. P. Bancroft, F. A. Cotton, S. Han, *Inorg. Chem.* **1984**, *23*, 2408.
[108] B. E. Bursten, F. A. Cotton, *Inorg. Chem.* **1981**, *20*, 3042; J. G. Norman, Jr., G. E. Renzoni, D. A. Case, *J. Am. Chem. Soc.* **1979**, *101*, 5256; J. G. Norman, Jr., H. J. Kolari, *ibid.* **1978**, *100*, 791.
[109] G. Bienek, W. Tuszynski, G. Gliemann, *Z. Naturforsch. B* **1978**, *33*, 1095; D. S. Martin, Jr., T. R. Webb, G. A. Robbins, F. E. Fanwick, *Inorg. Chem.* **1979**, *18*, 475.
[110] F. A. Cotton, T. R. Felthouse, *Inorg. Chem.* **1982**, *21*, 2667.
[111] I. K. Kireeva, G. Ya. Mazo, R. N. Shchelokov, *Russ. J. Inorg. Chem. (Engl. Transl.)* **1979**, *24*, 220; L. M. Dikareva, M. A. Porai-Koshits, G. G. Sadikov, I. B. Baranovski, M. A. Golubnichaya, R. N. Shchelokov, *ibid.* **1977**, *22*, 1093.
[112] L. M. Dikareva, M. A. Porai Koshits, G. G. Sadikov, I. B. Baranovskii, M. A. Golubnichaya, R. N. Shelokov, *Russ. J. Inorg. Chem. (Engl. Transl.)* **1978**, *23*, 578.
[113] E. C. Morrison, D. A. Tocher, *Inorg. Chim. Acta* **1989**, *156*, 99.
[114] F. A. Cotton, K.-B. Shiu, *Rev. Chim. Miner.* **1986**, *23*, 14.
[115] G. G. Christoph, M. Tolbert, 7th Meeting of the American Crystallographic Association, Abstracts, Eufaula, AL, **1980**, p. 6.
[116] Y.-B. Koh, G. G. Christoph, *Inorg. Chem.* **1978**, *17*, 2590.
[117] F. A. Cotton, T. R. Felthouse, *Inorg. Chem.* **1980**, *19*, 2347.
[118] F. A. Cotton, T. R. Felthouse, *Inorg. Chem.* **1982**, *21*, 431.
[119] C. J. Simmons, A. Clearfield, Y. Sun, *Inorg. Chim. Acta* **1986**, *121*, L3.
[120] F. A. Cotton, R. Francis, *J. Am. Chem. Soc.* **1960**, *82*, 2986; F. A. Cotton, R. Francis, W. D. Horrocks, Jr., *J. Phys. Chem.* **1960**, *64*, 1534.
[121] F. A. Cotton, G. Wilkinson, *Advanced Inorganic Chemistry*, 5th ed., Wiley Interscience, New York, **1988**, Chap. 19, p. 913.
[122] F. A. Cotton, T. R. Felthouse, *Inorg. Chem.* **1981**, *20*, 584.
[123] T. P. Zhu, M. Q. Ahsan, T. Malinski, K. M. Kadish, J. L. Bear, *Inorg. Chem.* **1984**, *23*, 2.
[124] M. P. Doyle, B. D. Brandes, A. P. Kazala, R. J. Pieters, M. B. Jarstfer, L. M. Watkins, C. T. Eagle, *Tetrahedron Lett.* **1990**, *31*, 6613.
[125] M. P. Doyle, R. J. Pieters, S. F. Martin, R. E. Austin, C. J. Oalmann, P. Müller, *J. Am. Chem. Soc.* **1991**, *113*, 1423.
[126] M. Y. Chavan, X. Q. Lin, M. Q. Ahsan, I. Bernal, J. L. Bear, K. M. Kadish, *Inorg. Chem.* **1986**, *25*, 1281.
[127] A. M. Dennis, J. D. Korp, I. Bernal, R. A. Howard, J. L. Bear, *Inorg. Chem.* **1983**, *22*, 1522.
[128] P. Piraino, G. Bruno, S. L. Schiavo, F. Laschi, P. Zanello, *Inorg. Chem.* **1987**, *26*, 2205.
[129] R. S. Lifsey, M. Y. Chavan, L. K. Chau, M. Q. Ahsan, K. M. Kadish, J. L. Bear, *Inorg. Chem.* **1987**, *26*, 822.
[130] S. I. Ginzburg, N. N. Chalisova, O. N. Eustaf'eva, *Russ. J. Inorg. Chem. (Engl. Transl.)* **1966**, *11*, 404.
[131] I. B. Baranovski, N. N. Chalisova, G. Y. Mazo, *Russ. J. Inorg. Chem. (Engl. Transl.)* **1979**, *24*, 1893.
[132] L. M. Dikareva, G. G. Sadikov, M. A. Porai-Koshits, I. B. Baranovski, S. S. Abdullaev, *Russ. J. Inorg. Chem. (Engl. Transl.)* **1980**, *25*, 488.
[133] N. McCarthy, M. A. McKervey, T. Ye, M. McCann, E. Murphy, M. P. Doyle, *Tetrahedron Lett.* **1992**, *33*, 5983.
[134] M. C. Pirrung, J. Zhang, *Tetrahedron Lett.* **1992**, *33*, 5987.
[135] K. R. Dunbar, *J. Am. Chem. Soc.* **1988**, *110*, 8247.
[136] H. Endres, N. Gottstein, H. J. Keller, R. Martin, W. Rodemer, W. Steiger, *Z. Naturforsch. B* **1979**, *34*, 827; M. M. Olmstead, A. L. Balch, *J. Organomet. Chem.* **1978**, *148*, C15.

[137] M. P. Doyle, S. N. Mahapatro, A. C. Caughey, M. S. Chinn, M. R. Colsman, N. K. Harn, A. E. Redwine, *Inorg. Chem.* **1987**, *26*, 3070.
[138] M. P. Doyle, J. H. Griffin, V. Bagheri, R. L. Dorow, *Organometallics* **1984**, *3*, 53; M. P. Doyle, J. H. Griffin, J. Conceičo, *J. Chem. Soc. Chem. Commun.* **1985**, 328.
[139] It was pointed out by one of the reviewers that the interaction of the *R* and *Z* groups in the π complexes **72** and **75** are irrelevant for the stereoselectivity of this reaction, based on the Curtin–Hammet principle. For additional discussion, see M. Brookhart, W. B. Studabaker, *Chem. Rev.* **1987**, *87*, 411.
[140] D. F. Taber, E. H. Petty, *J. Org. Chem.* **1982**, *47*, 4808; D. F. Taber, J. C. Amedio, Jr., R. G. Sherill, *ibid.* **1986**, *51*, 3382; D. F. Taber, R. E. Ruckle, Jr., *Tetrahedron Lett.* **1985**, *26*, 3059; D. F. Taber, J. C. Amedio, Jr., K. Raman, *J. Org. Chem.* **1988**, *53*, 2984; D. F. Taber, M. J. Hennessy, R. S. Hoerrner, K. Raman, R. E. Ruckle, Jr., J. S. Schuchardt, *Catalysis of Organic Reactions* (Ed.: D. W. Blackburn), Dekker, New York, **1988**, Chap. 4, p. 43; D. F. Taber, R. E. Ruckle, Jr., *J. Am. Chem. Soc.* **1986**, *108*, 7686.
[141] M. P. Doyle, L. J. Westrum, N. E. Wolthuis, M. M. See, W. P. Boone, V. Bagheri, M. M. Pearson, *J. Am. Chem. Soc.* **1993**, *115*, 958.
[142] D. E. Cane, P. J. Thomas, *J. Am. Chem. Soc.* **1984**, *106*, 5295.
[143] S.-I. Hashimoto, N Watanabe, S. Ikegami, *Tetrahedron Lett.* **1992**, *33*, 2709.
[144] M. P. Doyle, V. Bagheri, T. J. Wandless, N. K. Harn, D. A. Brinker, C. T. Eagle, K.-L. Loh, *J. Am. Chem. Soc.* **1990**, *112*, 1906.
[145] M. P. Doyle, J. Tauton, H. Q. Pho, *Tetrahedron Lett.* **1989**, *30*, 5397.
[146] M. P. Doyle, V. Bagheri, M. M. Pearson, J. D. Edwards, *Tetrahedron Lett.* **1989**, *30*, 7001.
[147] S.-I. Hashimoto, N. Watanabe, S. Ikegami, *J. Chem. Soc. Chem. Commun.* **1992**, 1508.
[148] D. F. Taber, M. J. Hennessy, J. P. Louey, *J. Org. Chem.* **1992**, *57*, 436.
[149] M. P. Doyle, M. S. Shanklin, S. M. Oon, H. Q. Pho, F. R. Van der Heide, W. R. Veal, *J. Org. Chem.* **1988**, *53*, 3384; M. P. Doyle, J. Tauton, H. Q. Pho, *Tetrahedron Lett.* **1989**, *30*, 5397; M. P. Doyle, R. J. Pieters, J. Tauton, H. Q. Pho, A. Padwa, D. L. Hertzog, L. Precedo, *J. Org. Chem.* **1991**, *56*, 820.
[150] M. Matsumoto, N. Watanabe, H. Kobayashi, *Heterocycles* **1987**, *26*, 1479.
[151] R. J. Sundberg, E. W. Baxter, W. J. Pitts, R. Ahmed–Schofield, T. Nishiguchi, *J. Org. Chem.* **1988**, *53*, 5097.
[152] A. Padwa, D. J. Austin, S. F. Hornbuckle, M. A. Semones, M. P. Doyle, M. N. Protopopova, *J. Am. Chem. Soc.* **1992**, *114*, 1874; A. Padwa, D. J. Austin, A. T. Price, M. A. Semones, M. P. Doyle, M. N. Protopopova, W. R. Winchester, A. Tran, *ibid.* **1993**, *115*, 8669.
[153] C. G. Cox, C. J. Moody, D. J. Austin, A. Padwa, *Tetrahedron* **1993**, *49*, 5109.
[154] A. Padwa, D. J. Austin, S. F. Hornbuckle, A. T. Price, *Tetrahedron Lett.* **1992**, *33*, 6427.
[155] R. Huisgen, *1,3-Dipolar Cycloaddition Chemistry, Vol. 1* (Ed.: A. Padwa), Wiley Interscience, New York, **1984**.
[156] M. P. Doyle, M. R. Colsman, M. S. Chinn, *Inorg. Chem.* **1984**, *23*, 3684.
[157] L. B. Baranovski, S. S. Abduullaev, R. N. Shchelokov, *Russ. J. Inorg. Chem. (Engl. Transl.)* **1979**, *24*, 1753.
[158] M. C. Pirrung, J. Zhang, A. T. McPhail, *J. Org. Chem.* **1991**, *56*, 6269.
[159] D. F. Harvey, M. F. Brown, *J. Am. Chem. Soc.* **1990**, *112*, 7806; D. F. Harvey, K. P. Lund, *ibid.* **1991**, *113*, 5066.
[160] T. R. Hoye, C. J. Dinsmore, D. S. Johnson, P. F. Korkowski, *J. Org. Chem.* **1990**, *55*, 4518; T. R. Hoye, C. J. Dinsmore, *J. Am. Chem. Soc.* **1991**, *113*, 4343; *Tetrahedron Lett.* **1992**, *33*, 169.
[161] A. Padwa, K. E. Krumpe, J. M. Kassir, *J. Org. Chem.* **1992**, *57*, 4940.
[162] B. K. R. Shankar, H. Shechter, *Tetrahedron Lett.* **1982**, *23*, 2277.
[163] N. Ikota, N. Takamura, S. D. Young, B. Ganem, *Tetrahedron Lett.* **1981**, *22*, 4163.
[164] M. P. Doyle, K. G. High, S. M. Oon, A. K. Osborn, *Tetrahedron Lett.* **1989**, *30*, 3049.
[165] T. R. Hoye, C. J. Dinsmore, *Tetrahedron Lett.* **1991**, *32*, 3755.
[166] A. Padwa, D. J. Austin, S. L. Xu, *J. Org. Chem.* **1992**, *57*, 1330.
[167] H. M. L. Davies, M. J. McAfee, C. E. M. Oldenburg, *J. Org. Chem.* **1989**, *54*, 930; H. M. L. Davies, W. B. Young, H. D. Smith, *Tetrahedron Lett.* **1989**, *30*, 4653; H. M. L. Davies, H. D. Smith, O. Korkor, *ibid.* **1987**, *28*, 1853; H. M. L. Davies, D. M. Clark, D. B. Alligood, G. R. Eiband, *Tetrahedron* **1987**, *43*, 4265; H. M. L. Davies, D. M. Clark, T. K. Smith, *Tetrahedron Lett.* **1985**, *26*, 5659.
[168] H. M. L. Davies, E. Saikali, T. J. Clark, E. H. Chee, *Tetrahedron Lett.* **1990**, *31*, 6299.
[169] H. M. L. Davies, E. Saikali, W. B. Young, *J. Org. Chem.* **1991**, *56*, 5696.
[170] H. M. L. Davies, T. J. Clark, G. Kimmer, *J. Org. Chem.* **1991**, *56*, 6440.
[171] J. P. Collman, L. S. Hegedus, J. R. Norton, R. G. Finke, *Principles and Applications of Organotransition Metal Chemistry*, University Science Books, Mill Valley, CA, **1987**.
[172] *Tetrahedron Symposia in Print* (Ed.: M. F. Semmelhack), **1985**, *42*, 5741.
[173] K. C. Bishop, *Chem. Rev.* **1976**, *76*, 461.
[174] M. L. Deem, *Synthesis* **1982**, 701; *ibid.* **1972**, 675.
[175] A. Padwa, J. M. Kassir, S. L. Xu, *J. Org. Chem.* **1991**, *56*, 6971.
[176] P. Müller, N. Pautex, M. P. Doyle, V. Bagheri, *Helv. Chim. Acta* **1990**, *73*, 1233.
[177] F. N. Tebbe, R. L. Harlow, *J. Am. Chem. Soc.* **1980**, *102*, 6149.
[178] S. K. Cho, L. S. Liebeskind, *J. Org. Chem.* **1987**, *52*, 2631.

Recycling in the Earth's Atmosphere: The OH Radical—Its Importance for the Chemistry of the Atmosphere and the Determination of Its Concentration

Franz Josef Comes*

The troposphere, the part of the earth's atmosphere which is closest to the surface, harbors important life processes. This important part of our environment contains primarily nitrogen and oxygen. In addition, it comprises a number of other substances, which are generally present in low concentrations. The primary reason for the low content of these trace components is the activity of a diatomic radical, namely the hydroxyl radical. OH is the main constituent of the oxidizing potential of the troposphere and causes the transformation of many trace components into water-soluble forms, which can then rain out and be removed from the troposphere. OH has therefore acquired the title "detergent of the atmosphere". The knowledge of local hydroxyl radical concentrations is therefore an important piece of information, especially with respect to model calculations for atmospheric chemistry. The OH concentration is very low and its determination represents a significant analytical challenge. It is controlled in a delicate manner by chemical formation and decomposition reactions, which interact to create a recycling process in the troposphere.

1. Introduction

When talking about the earth's atmosphere and its chemistry, one thinks primarily of the gas envelope covering the globe. This is an incomplete view, a fact which is demonstrated nearly daily by the presence of clouds. Hence, there are also liquid components of the atmosphere, but in addition, there also exist solid ones (e.g., aerosols). These additional components play a role in the chemistry of the atmosphere which must not be neglected. In spite of the fact, that the earth's atmosphere is not a single phase, this article will primarily focus on the gaseous phase, as the processes to be discussed here are basically pure gas-phase processes. On the other hand, our knowledge of processes in the other phases of the atmosphere is still very fragmentary.

The atmosphere is bound to the earth by gravity, which leads to an atmospheric density distribution that can be described well by the barometric equation. According to this equation, density decreases roughly exponentially with increasing altitude. If the entire mass of the atmosphere were condensed to the pressure found at the earth's surface, we obtain the so-called scale height, about 8 km. In a liquefied state, the same quantity would only be a few meters. Compared to the diameter of our planet of about 13000 km, these values indicate the comparatively small total mass of the atmosphere.

The atmosphere has a characteristic temperature profile. Beginning at the surface, there is a nearly linear decrease in temperature with increasing altitude up to the tropopause, at an average altitude of 10–15 km. The tropopause is the region where the temperature ceases to decrease; in the beginning of the stratosphere the temperature begins to increase again. The part of the atmosphere from the surface to the tropopause is called the troposphere. Due to the physically unstable layering of the air in the troposphere, turbulent mixing of the gases takes place. About 80% of the total mass of the atmosphere is present in the troposphere. Even though the troposphere can be considered as quasi-closed due to the temperature inversion in the tropopause, there are several important possible exchange processes, such as the transport of ozone from the stratosphere into the troposphere.[1] The transport in the reverse direction is also possible; a fact illustrated by many reports about the transport of chlorofluorocarbons (CFCs) into the stratosphere.

Our interest in the atmosphere and especially the troposphere stems from the fact that it is the region in which human life on earth is taking place. It therefore represents an important aspect of our environment. The impact on this environment caused by human activity is increasing considerably. The world's population is increasing rapidly, and encroachments on nature, caused by industrial and agricultural developments, are becoming more numerous. These interventions also have effects on the upper layers of the atmosphere. The reports on the Antarctic ozone hole have demonstrated how vulnerable this part of our environment turns out to be. It is therefore of vital interest to understand precisely those processes that primarily determine the behavior of the atmosphere. This includes above all the processes connected with the hydroxyl radical. The cleansing action of the OH radical controls the content of trace components in our

[*] Prof. Dr. F. J. Comes
Institut für Physikalische und Theoretische Chemie der Universität
Marie-Curie-Strasse 11, D-60439 Frankfurt (FRG)
Telefax: Int. code + (69)5800-9484

 © VCH Verlagsgesellschaft mbH, D-69451 Weinheim, 1994 0570-0833/94/1818-1816 $ 10.00+.25/0 Angew. Chem. Int. Ed. Engl. 1994, 33, 1816–1826

atmosphere. These trace species include, for example, poisonous carbon monoxide, the greenhouse gas methane, sulfur dioxide, and the nitrogen oxides.[2]

1.1. Fundamental Photochemical Processes

The atmosphere can be viewed as a chemical reactor filled to a large extent with gaseous substances and "heated" by the sun. The solar spectrum is that of a black body at nearly 6000 K. The incident solar power on the earth is described by the solar constant, which gives the incident energy on the outer edge of the atmosphere at vertical irradiation per m^2 per second, $S = 1.368\ Wm^{-2}$. Absorption in the atmosphere changes this radiation, especially in the UV region.

The most important components of the atmosphere, such as nitrogen and oxygen, completely absorb the short wavelength UV radiation ($\lambda < 200$ nm) at high altitudes, so that this radiation cannot reach the surface. The penetration of lower wavelength radiation, between about 200–300 nm, to the ground would, however, be fatal for organic life. Nature has provided an additional shield against this, resulting from the photochemical decomposition of the oxygen molecule. In the lower, and hence more dense, layers of the stratosphere the decomposition of O_2, which here only occurs partially, leads to the formation of a new oxygen species, namely ozone. Newly formed oxygen atoms can react with the oxygen molecules still present in a ternary collision to form O_3 [Eq. (1) where M = third collision partner e.g. O_2, N_2].[3]

$$O + O_2 \xrightarrow{M} O_3 \qquad (1)$$

This reaction leads to the stratospheric ozone layer, or just ozone layer for short, which is often discussed in the media.[4] This layer contains about 90–95% of the total ozone and is centered at around 25 to 30 km in altitude, depending on season and geographic location. The remaining 5–10% of the ozone are located in the troposphere and there fulfill an important function.[5]

The stratospheric ozone layer is of interest to us primarily due to its absorption of UV radiation. Ozone absorbs very strongly between 200 and 300 nm, leading, with a quantum yield of about 0.9–1.0, to a molecular fragmentation into metastable products [Eq. (2a)]. The other process leads to products in their ground states [Eq. (2b)].[6]

$$O_3 + h\nu \longrightarrow \begin{cases} O(^1D) + O_2(^1\Delta_g) & (2a) \\ O(^3P) + O_2(^3\Sigma_\sigma^-) & (2b) \end{cases}$$

The stated quantum yields are correct as long as the wavelengths in question are below 306 nm. For longer wavelengths the quantum yield for the formation of singlet species [Eq. (2a)] decreases and, in the troposphere, vanishes completely above 330 nm.[7] The presence of ozone as a very effective absorber of UV radiation leads to the fact that solar radiation reaching the earth's surface has a lower wavelength limit of about 300 nm. This assures sufficient protection for organic life on earth. Radiation above this limit is increasingly less absorbed and, hence, reaches the surface in increasing proportions.

The problems connected with the shielding effect of ozone and anthropogenic influences thereupon are well known[8] and will not be further discussed here. The photochemical limit for reaction (2a), which is of great importance for the following discussion, lies at 310 nm. This value can be modified by the internal energy content, that is the thermal energy of the ozone molecule. Measurements at this limit and the determination of the quantum yield for the process (2a) are very important and have shown that above about 330 nm, there is no more photochemical production of singlet oxygen species by the sun in the troposphere.[7]

Until now, only the processes themselves, but not their relevance, have been discussed; this will be done now. Both dissociation products, $O(^1D)$ and $O_2(^1\Delta_g)$, from reaction (2a) are metastable because of their electronic states. They have large radiative lifetimes of 148 s and 65 min,[9] respectively, and have a significant energy content of 189 and 94 $kJ\,mol^{-1}$, respectively. Since ozone does exist in the troposphere, and solar radiation below 330 nm can penetrate into the troposphere, singlet oxygen is produced in the troposphere. Of the two particles, primarily the $O(^1D)$ atom is photochemically active as it is extraordinarily reactive. The rate constants of $O(^1D)$ for many of its relevant



Franz Josef Comes, born in 1928, obtained his Diplom in Physics in Mainz, and his doctorate at the Max-Planck-Institut für Chemie (Otto-Hahn-Institut) in Mainz working with Paneth on the study of meteorites by mass spectrometry. After this excursion into geophysics and cosmochemistry, he worked on problems of molecular spectroscopy and reaction kinetics at the University of Bonn with Groth where he obtained his habilitation in 1964 and became Professor in 1969. In 1970 he was awarded the Fritz-Haber prize of the Deutsche Bunsengesellschaft for fundamental work on photodissociation, photoionization, and molecular and photoelectron spectroscopy. After a guest professorship at the University of Southern Carolina, Los Angeles, followed by a period as guest in the synchrotron group of Desy in Hamburg, he accepted the chair of Physical Chemistry at Frankfurt University in 1972. His interests include the application of lasers in chemistry, in particular in studies on reaction dynamics. Other fields of research are atmospheric chemistry and applications of the photovoltaic effect, in particular for the development of solar cells from amorphous silicon and germanium.

reactions are nearly equal and frequently gas kinetic, so that its further reactions in the atmosphere are essentially controlled by the concentration of the reaction partners.[10] In our geographic latitudes, water vapor is the third most common atmospheric component, after N_2 and O_2. $O(^1D)$ reacts exceptionally well with H_2O, with a temperature-independent rate constant of 2.02×10^{-10} molecules $cm^{-3}s^{-1}$, leading to the formation of hydroxyl radicals [Eq. (3)].[11]

$$O(^1D) + H_2O \longrightarrow 2OH \quad (3)$$

This indicates that water vapor is the most important reaction partner of $O(^1D)$ and reaction (3) is the most significant process for the initial formation of OH in the troposphere.

The reaction dynamics of reaction (3) is very interesting because the energy is distributed unequally between the two OH products; thus, one of the two OH radicals can be identified as stemming from the water molecule and the other one as coming from the reaction with $O(^1D)$. This indicates that a very fast chemical process without a longer lived transition complex is occurring.[12]

The production of $O(^1D)$ during the UV photolysis of ozone leads to the formation of hydroxyl radicals. The chemical activity of these OH radicals leads to their role as the "detergent of the atmosphere".[13] The process of OH formation itself, however, possesses a certain dramatic element as well. In general, it would be expected that the absorption by stratospheric ozone removes all solar radiation that can act in the photolysis of tropospheric ozone, as is the case for the absorption by N_2 and O_2. This is, however, not the full story. On the long wavelength side of the O_3 UV absorption, in other words, in a region with decreasing absorptivity, a certain fraction of the solar radiation can penetrate to the ground. On the other hand, the intensity of the solar radiation increases with increasing wavelength. The result of these dueling effects is depicted in Figure 1, which shows the course of the O_3 absorption cross section (dotted line) and the transmission of sunlight to the surface (heavy dashed line).[14] Of special interest is the region around 310 nm, the photochemical limit for the $O(^1D)$ formation (this limit refers to O_3 at 0 K!). Ozone also absorbs at longer wavelengths, but this leads primarily to the formation of $O(^3P)$ atoms [Eq. (2b)], which cannot initiate the relevant reaction (3). The third curve in Figure 1 (thinly dashed) shows the portion of the absorption cross section which can induce process (2a). This leads to the dotted area in Figure 1, which indicates the overlap crucial to $O(^1D)$ formation. Only in this region is tropospheric $O(^1D)$ formation, and subsequent OH production possible. The initial photochemical step of OH formation by ozone photolysis through sunlight turns out to be a very selective overall process, which is only active in a very narrow window.

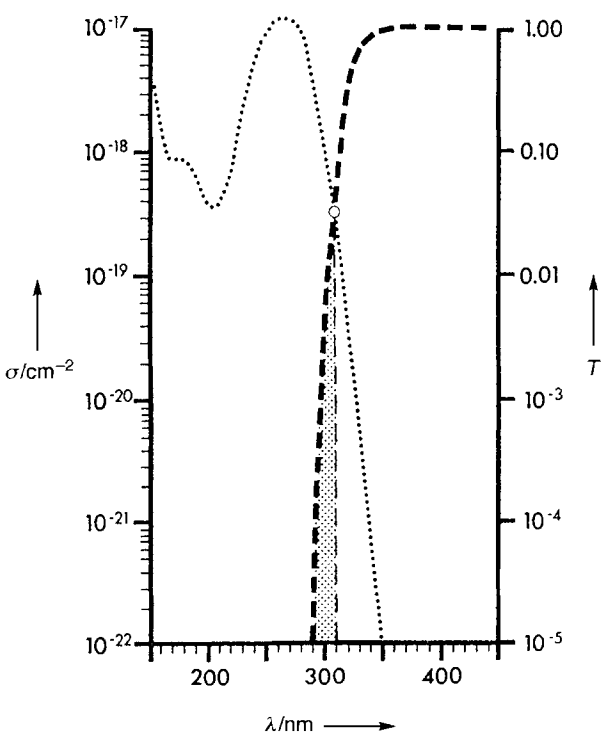


Fig. 1. ·····: UV absorption cross section σ of ozone; - - - - - -: transmitted sunlight after passage through the upper atmosphere; – – – – –: $O(^1D)$-producing absorption cross section of ozone. Dotted area: region where tropospheric $O(^1D)$ formation is possible.

1.2. Atmospheric Recycling Processes

Radicals are known throughout chemistry primarily as short-lived intermediates in complex chemical processes. Due to their high reactivity, their chemical lifetime is usually short and their stationary concentration is low. This is particularly true for tropospheric OH radicals, for which, according to recent model calculations, the stationary concentration in our latitudes on summer middays is about 10^6 particles per cubic centimeter (3×10^6 particles $cm^{-3} \triangleq 0.1$ pptv (parts per trillion (10^{12})in volume units).[15] As their existence is directly linked with the UV activity of the sun, they should be tied to a daily cycle which approximately reflects the solar incidence. In Section 1.1 the cleansing function of OH radicals was mentioned. What is the nature of this function?

OH radicals are reactive. Many of their reactions with atmospheric gases have been examined and measured. The first notable result of these investigations is that hydroxyl radicals do *not* react with the most common components of the troposphere. In decreasing order of abundance, these are nitrogen, oxygen, water vapor, argon, and carbon dioxide. OH radicals only react readily with so-called tropospheric trace components, which have abundances of 1 ppmv or even significantly below that. As an oxidizing agent, OH frequently transforms these trace gases into water-soluble chemical species. Subsequent raining out removes these trace components from the atmosphere, a process we have described as the cleansing effect. It causes the atmospheric content of trace components to be low, even though these components are continuously released into the atmosphere even by non-anthropogenic, that is, natural, sources. Hydroxyl radicals are therefore important reaction partners in many processes in atmospheric chemistry and, hence, their concentration is a crucial parameter for the chemistry of the atmosphere.

The thus far described aspect of tropospheric photochemistry is therefore an extremely selective overall process: the upper atmosphere only permits the penetration of a small fraction of

high-energy UV radiation into the troposphere, which leads to the release of excited, hence reactive, oxygen atoms from the ozone present in trace quantities. These oxygen atoms then react almost exclusively with water vapor to give OH radicals, which in turn selectively choose trace components as reaction partners, which establishes the prerequisites for the cleansing process.

The discussion thus far has dealt with the initial formation of hydroxyl radicals by ozone photolysis and their further chemical actions. The ozone content of the troposphere played a significant role in this context. A question now arises: why does the troposphere contain ozone at all? There are two possible sources for this ozone. For one, there is the possibility that stratospheric ozone is transported into the lower layers of the atmosphere. A second potential source is chemical events in the troposphere, which are closely linked to the OH radical.

In terms of quantity, the most important reaction partner for the OH radical is carbon monoxide, CO. It is present in the troposphere with nearly 0.1 ppmv. Even though methane, another important reaction partner for the OH radical, is about tenfold more abundant than CO, it reacts slower with OH, putting it in second place. These two species contribute about 90% of the entire OH removal. Their reactions with OH determine its atmospheric lifetime of about one second. Even though OH radicals react with many other trace components, such as SO_2 and other hydrocarbons, these do not significantly influence the total OH budget. On the other hand, however, OH has an often crucial role in the atmospheric balance of these trace species.

The reaction of OH with CO leads to a very interesting result [Eq. (4)]. CO is oxidized to CO_2, and a hydrogen atom is formed. The reaction proceeds via an intermediate that yields a temperature dependence different from the typical Arrhenius behavior.[16] The H atoms thus formed can now initiate an important event in the atmosphere, since they react with atmospheric oxygen. This reaction (5) exhibits another characteristic of

$$OH + CO \longrightarrow CO_2 + H \quad (4)$$

$$H + O_2 \xrightarrow{M} HO_2 \quad (5)$$

of tropospheric reactions. In order for an HO_2 molecule to form from the reactants H and O_2, the excess energy, which is the binding energy, must be carried off by a third collision partner (M). Ternary collisions are notably less frequent than bimolecular reactions and become more probable only in denser media, such as the troposphere. Reaction (5) re-establishes the oxidizing potential which was temporarily lost by the reaction of OH in (4). In clean air above continents, the main reaction partner of HO_2 is the nitrous oxide molecule NO, which is oxidized to NO_2 [Eq. (6)]. This oxidation has two remarkable products.

$$HO_2 + NO \longrightarrow NO_2 + OH \quad (6)$$

NO_2 is formed, a member of the NO_x family, which, at higher NO_x concentrations, reacts primarily with OH according to Equation (7) to yield HNO_3, and thus represents a significant sink for the OH radical. On the other hand, (6) also regenerates OH. Hence OH has completed a cycle in the reactions (4)–(6), which corresponds to the formal reaction $CO + NO + O_2 \rightarrow CO_2 + NO_2$, and one can talk about OH recycling. Cycles such as this one are typical for atmospheric chemistry and determine the equilibria which result from the interaction of sources and sinks.

$$OH + NO_2 \xrightarrow{M} HNO_3 \quad (7)$$

Connected with NO_2 is a further characteristic phenomenon of atmospheric chemistry, namely the fact that the chemical processes occur in a radiation field. In this field, many compounds, for example, ozone, are not stable, because they can decompose by photodissociation. This is also the case for the NO_2 molecule due to its reaction (8).[17]

$$NO_2 + h\nu(\lambda \leq 430\ nm) \longrightarrow NO + O \quad (8)$$

Solar irradiation in this wavelength region reaches the troposphere in sufficient intensity, therefore a photochemical equilibrium between NO and NO_2 is rapidly established. The oxygen atoms created in this way react, owing to the high O_2 content of the troposphere, to directly yield O_3. This represents an important source of ozone in the troposphere.

Reactions (4)–(8) are important steps in the recycling mechanisms for the OH radical. Their individual importance in this recycling process is determined by atmospheric conditions governing their chemistry. This means simply that their contribution to the total process varies with the concentrations of the reactants involved. This principle will be demonstrated by using the photochemical formation of ozone as an example. If, for instance, there is sufficient NO present in the atmosphere, it is transformed to NO_2, and subsequent photolysis yields O_3. The sequence of reactions (4)–(6), (8), and (1) adds up to the following stoichiometry:

$$CO + 2O_2 \longrightarrow CO_2 + O_3.$$

One ozone molecule is formed for each oxidized CO molecule. If, on the other hand, the NO concentration is very small, reaction (6) becomes correspondingly slower, and two other processes begin to become more important [Eqs. (α) and (β)]:

$$HO_2 + HO_2 \longrightarrow H_2O_2 + O_2 \quad (\alpha)$$

$$HO_2 + O_3 \longrightarrow OH + 2O_2 \quad (\beta)$$

$$H_2O_2 + h\nu \longrightarrow 2OH \quad (\gamma)$$

As H_2O_2 is cleaved by UV light [Eq. (γ)],[18] the reaction sequence (4), (5), (α), and (γ) leads to

$$2CO + O_2 \longrightarrow 2CO_2,$$

which does not cause a change in the O_3 content by CO oxidation. HO_2 can also react with O_3, which gives, according to (4), (5), and (β), and an overall loss of ozone.

$$CO + O_3 \longrightarrow CO_2 + O_2,$$

The reactions (4)–(8) describe only the subsequent reactions of OH radicals initiated by CO. Methane is a second important

reaction partner for OH. During this reaction [Eq. (9)], OH is

$$CH_4 + OH \longrightarrow CH_3 + H_2O \quad (9)$$

converted to H_2O, and a methyl radical is formed. The further reactions in the oxidation mechanism of CH_4 are heavily influenced by a ternary collision process [Eq. (10)], which becomes rather likely under troposphere conditions.

$$CH_3 + O_2 \xrightarrow{M} CH_3O_2 \quad (10)$$

Reaction (10) leads to the peroxy radical, which upon contact with NO converts it into NO_2 [Eq. (11)]. This in turn can yield

$$NO + CH_3O_2 \longrightarrow NO_2 + CH_3O \quad (11)$$

O atoms by photolysis [Eq. (8)] and hence is a precursor for O_3. The methoxy radical CH_3O reacts rapidly with O_2 to yield formaldehyde and one molecule of HO_2 [Eq. (12)]. The HO_2

$$CH_3O + O_2 \longrightarrow HCHO + HO_2 \quad (12)$$

from (12) can yield OH by reaction (6), which means that methane oxidation can also lead to OH recycling.

The intermediates in reactions (9)–(11) are short-lived, while formaldehyde is a longer lived species, which, however, also decomposes upon solar irradiation. Its atmospheric lifetime of several hours leads to concentrations of the order of 1 ppbv, even in non-polluted air. The most important further reaction of HCHO is its photodissociation [Eq. (13)], which can proceed by two pathways. The onset of cleavage into H and HCO, however, is below 335 nm.[19]

$$HCHO + h\nu(\lambda \leq 370\ nm) \longrightarrow H_2 + CO \quad (13a)$$

$$HCHO + h\nu(\lambda \leq 335\ nm) \longrightarrow H + HCO \quad (13b)$$

Pathway (13b) is important, because H and HCO react rapidly with O_2 [Eqs. (5) and (14)] to yield HO_2, which in turn is converted into OH by NO.

$$HCO + O_2 \longrightarrow HO_2 + CO \quad (14)$$

The quantum yields for reactions 13a and 13b are strongly wavelength dependent, in addition, above 330 nm the quantum yields are also dependent on pressure.[1]

Apart from methane, there is a multitude of other hydrocarbons in the troposphere. Their concentrations, however, are very much lower under normal circumstances. These hydrocarbons are classified in the literature as NMHC (non-methane hydrocarbons). The majority of them react readily with OH, which generally makes them an initial OH sink. In combination with the chemistry of NO_x, however, many of them are potential sources for HO_2 by subsequent peroxide formation [see Eq. (10)]. This couples them with the OH recycling mechanism. For one group of hydrocarbons, there are, apart from the man-made sources, significant natural sources, stemming from biogenic processes. For isoprene and monoterpenes, the important sources come from the tree and bush vegetation, with isoprene stemming primarily from deciduous and monoterpenes from coniferous trees. The oceans are also significant sources of hydrocarbons formed by biogenic processes.

In a recent study on the mountain station of Izana on Tenerife, there were indications that more consideration has to be given to these biogenic substances in future field measurements of OH.[20] Even though these substances can play special roles in local situations, their influence on the OH content in the normal troposphere is generally small.

The two examples of CO and CH_4, which are the most important reaction partners for OH in the "normal", in other words, nonpolluted troposphere, allowed the demonstration of a recycling process for OH. The extent of OH regeneration is dependent on the actual concentrations of the reactants. The measured stationary OH concentration in the troposphere is therefore the result of a sensitive equilibrium, which is controlled to a significant extent by these recycling mechanisms.

2. Results of Model Calculations and Conditions for their Verification

Models are an abstraction of reality. Results of model calculations can lead to important predictions. However, models always require experimental verification. In order to test models for the chemistry of the troposphere, an identification of all significant reaction partners, including the OH radical itself, is necessary, which must be as complete as possible. The comparison of measured and calculated concentrations can then serve to verify or falsify existing models. The fact that such a fundamental question like testing models for atmospheric chemistry is brought up in connection with measurements on the OH radical stems from the chemical properties of this molecule. It reacts with all relevant trace components, and does so rapidly. The latter implies that the formation and further reaction of individual OH radicals occur in a fairly small space. This has important consequences for the development of models, as it can be used to reduce the complexity of models in a reasonable way.

The rate at which substances in a reactive system appear and/or disappear is determined by the reactive properties of those substances and their concentration. The concentrations are given at the beginning of the reaction and after that are determined by the reactions themselves. Atmospheric reactions, however, occur in open systems. Air movements, that is transport, can also effect concentration changes. This transport is both turbulent and directional, which on one hand leads to good mixing, on the other to a certain wind velocity. It would therefore be very helpful if the quantities governing the transport could be neglected in the model calculations, as the main interest during model testing lies in the chemical aspect. This aspect consists of comparisons of measurement results from a single determination. If the transport term is to be neglected, it is necessary that the measurements satisfy certain conditions. As the measurements are performed in a system which is fixed in space, these conditions must include the maximum measurement volume and the time interval for the measurement. The conditions are always satisfied as long as the volumes are small and the time intervals short. But what is "small" and "short" in this context?

In order to estimate these quantities, a value for the air velocity is required. A moderate wind of 10–30 km h^{-1} (classified as a weak to moderate breeze) implies that the air moves about 3–9 m per second. A time interval of one second corresponds to the characteristic time for the chemical turnover of OH radicals in the atmosphere. Through transport, individual OH radicals would on average not exceed a volume extending over a few meters in diameter. A complete determination of all quantities relevant to the model calculations in a measurement volume that is restricted to a spatial extent of a few meters will therefore not lead to an incorrect spatial and temporal averaging of the desired measurement values. The mixing caused by the turbulence always present in air streams leads to an unavoidable natural averaging, which has the effect of making measurement conditions less stringent. This leads to air pockets with a certain spatial extent in which the approximation holds that the contained mass of air is homogeneously mixed. As long as the UV irradiation by the sun does not change over the course of a few seconds –which is unlikely even for a rapidly changing cloud cover—the measurement interval can be increased, with all other conditions remaining unchanged. For a wind velocity of 20 km h^{-1}, an air pocket of about 100 m, and a measurement cell size of 6 m, the time interval would be 20 seconds.

To determine the "local" concentrations of the relevant trace components in order to test models of the atmospheric chemistry, measurement intervals from a few seconds to one minute are permissible for measurement cells extending over a few meters. Measurements that do not fulfill these criteria, namely those which are not local and fast, lead to unacceptable averaging. Its extent depends on the lifetime of the components involved. Furthermore, the nonlinearity of the occurring processes significantly increases the error caused by this averaging.[21] This nonlinearity is especially noteworthy for the effect of the NO_x concentration on the stationary concentration of the OH radical. For low values of the NO_x concentration, the recycling of OH by reaction (6) dominates. If the NO_x concentration increases, however, process (7) becomes more significant and overall OH is lost. This creates a maximum in the OH concentration for the range of 1 to several ppbv NO_x, as long as other factors are held essentially constant.

The conclusions reached above are especially significant for techniques that require extended measurement pathlengths of several kilometers for the determination of tropospheric OH.[22] Another remark must be made here, which is based on the results of three studies by us in 1991, 1992, and 1993. In all cases, during the day there were severe variations in the measured OH concentrations. These occurred in a time frame from a few to tens of minutes.[20] Because the OH radical reacts with all relevant trace components and has a short lifetime (1 s), it simultaneously acts as a tracer which rapidly reacts to variations in the chemical composition of the atmosphere as well as the homogeneity of physical parameters (e.g., temperature, humidity). These brief variations can also be found in the results of another group of researchers, who also used a locally measuring detection method.[23] This indicates that homogeneity can only be assumed for smaller volumes of air. Absorption measurements that are done over extended pathlengths can lead to erroneous interpretations.

Since the hydroxyl radical is a key component in the chemistry of the troposphere, the determination of its local concentration therefore yields important information. The high reactivity, however, limits the measurement interval of the detection method. In combination with the movement of the air this determines the maximum size of the critical volume that can be used for the measurement. Together, both conditions define the quality of a local measurement. This determination yields a value $c_i(x,t)$, that is the concentration c of a atmospheric component i in location x at time t. The value of $c_i(x,t)$ is assumed to be representative for the given choice of x and t. Model calculations make use of continuity equations, which describe the temporal change of a component's concentration at a given location by the processes which effect these changes. Limited to gas-phase components, these are the sources Q, sinks S, and the effect of transport T. The equation can then be written as (15).

$$\frac{dc_i(x,t)}{dt} = Q_i(x,t) - S_i(x,t) + T_i(x,t) \tag{15}$$

There is such an equation for every component i. Since the terms Q, S, and T are also affected by other components j, (15) represents a system of coupled differential equations. The preceding discussion has shown that for a single measurement the T term can be neglected as long as a fast and local determination is performed. For this case, which is only valid for a time interval corresponding to the measurement interval, Equation (15) simplifies to include only the source and sink terms, which describe chemical events.

Even though many gas-phase reactions relevant to atmospheric processes have been quantitatively studied in the laboratory and the search for atmospheric trace components has yielded a considerable list of them, the total picture is still incomplete. It can therefore not be expected that there will be good agreement between the measured and calculated values for the OH concentration. The first goal will be to determine the discrepancy between these values and to show how it behaves over time. The time interval in question could be an hour or even a whole day. In this case, the studies of the temporal behavior are subject to the complete continuity equation, because for time intervals longer than minutes the transport term has to be taken into account. Fast local measurements of the above-mentioned quality within certain time intervals Δt will allow conclusions about the transport during Δt. Two important pieces of information can be expected from these efforts, namely the quality and completeness of the model calculations as well as the effect of transport. Only when these data have either led to a confirmation of the previous assumptions or to an improved new set of assumptions, will it be possible to address more fundamental questions of atmospheric chemistry. These could include the question whether the currently observable increase in the methane concentration is due to increased output by its sources or decreased activity by its sinks. A worldwide decrease in the OH concentration could be a reason for the latter effect.

Figure 2a shows the results of model calculations for clean continental air, which describe an atmospheric situation which is valid for the point in time that is characterized by the parameter set.[15] The picture shows the important steps in the OH budget and the percentage of the given particles which partici-

pate in that step. Therefore 70% of OH radicals react with CO to give CO_2 and H. For the selected situation, CH_4 contributes another 18% to the removal of OH. The OH recycling process contributes 54% of the OH formed, while 46% stem from $O(^1D)$ from the primary ozone photolysis. For Figure 2b the initial concentration of NO_x was increased to 2 ppbv. As expected, there is a definite increase in the contribution to OH recycling by the reaction of HO_2 with NO. This leads to a decrease of the percentage for the primary OH formation by ozone photolysis to now only 16%. The role of NO_2 as OH sink is indicated by its 13% share in the total OH removal process.

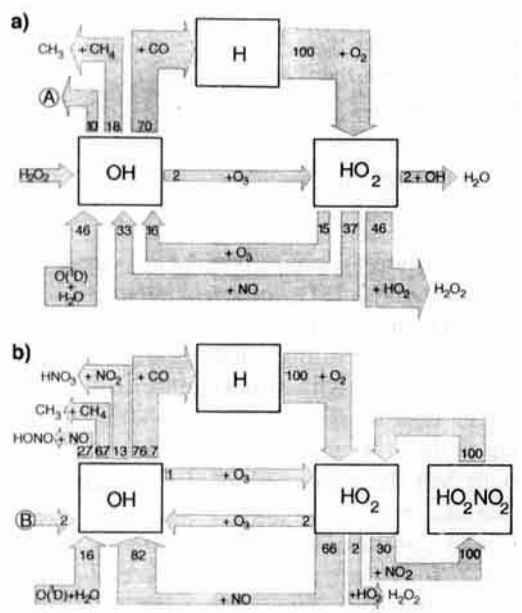


Fig. 2. Recycling mechanisms and circulation of OH. a) pure air conditions [CO]: 0.15 ppmv, $[NO_x]$: 0.01 ppbv, $[O_3]$: 20 ppbv, $[H_2O]$: 1.2%, $[CH_4]$: 1.64 ppmv, $T = 293$ K, [OH]: 9×10^5 cm^{-3}. Ⓐ stands for reactions with NO_2, H_2O, H_2O_2, and decomposition products of CH_4. b) Moderately polluted air [CO]: 0.37 ppmv, $[NO_x]$: 2 ppbv, $[O_3]$: 52 ppbv, $[H_2O]$: 1.2%, $[CH_4]$: 1.64 ppmv, $T = 293$ K. [OH]: 5×10^6 cm^{-3}. Ⓑ stands for other sources.

This example indicates that the OH lifecycle is very sensitive to the presence of NO_x. While Figure 2 shows the relative shifts in significance for the individual channels, it does not provide absolute values for the involved quantities. In connection with the NO_x contribution, these data would show that the OH concentration calculated by the model is not only dependent on the NO_x content in a nonlinear fashion, but also that the OH concentration as a function of the NO_x content, exhibits a definite maximum.[21] This leads to the interesting situation that "a little bit" of pollution is quite beneficial for the OH radical. Nitrogen oxides can therefore be both beneficial as well as detrimental to the OH concentration. For locations close to cities, which is the case for many areas in Western Germany, NO_x values are found that are usually beyond the maximum and therefore lead to a negative correlation between OH and NO_x (cf. Section 3).

3. Measurements in the Troposphere

It is necessary to find an appropriate technique to measure the OH radical concentration in order to do justice to its importance as a test substance for tropospheric models. The measurement volume and time interval must satisfy the criteria laid out above if a critical examination of the model is to be possible. The volume should not exceed a few cubic meters, and the interval should not be longer than a minute. Apart from the determination of the OH concentration, ancillary measurements are necessary to describe the conditions in the atmosphere which are relevant to the OH chemistry. As the OH concentration is directly related to ozone photolysis, the ozone concentration as well as the photolytically active solar irradiation are to be determined initially. In atmospheric chemistry, this active solar irradiation is described by the rate of ozone photolysis, $J(O_3)$. This quantity is defined by Equation (16),[5] where $\sigma(\lambda)$ is the absorp-

$$J(O_3) = \int_{\lambda_{min}}^{\lambda_{max}} \sigma(\lambda)\phi(\lambda)J(\lambda)\,d\lambda \qquad (16)$$

tion cross section of ozone, $\Phi(\lambda)$ the quantum yield of $O(^1D)$, and $J(\lambda)$ the photon flux. λ_{min} and λ_{max} are the lower and upper wavelength boundaries, respectively, between which tropospheric production of $O(^1D)$ from O_3 is possible. The wavelength interval for the measurement from λ_{min} to λ_{max} is given by the dotted region in Figure 1. The product of the ozone photolysis rate and the ozone concentration yields the $O(^1D)$ concentration. The measurement of the ozone photolysis rate places strict demands on the instrumentation. It is necessary to quantitatively detect the effective radiation, which is incident from all directions, at one point in space at all relevant wavelengths.

Other ancillary data required include the concentration of water vapor and NO_x (NO, NO_2), as well as another photolysis rate, namely that of NO_2, $J(NO_2)$, which is critical to the chemistry of the atmosphere due to the photodecomposition of NO_2 [Eq. (8)]. Together with the determination of the CO and CH_4 concentrations, this means that all significant components for the OH lifecycle are being recorded. The restriction of all concentration measurements to the same space and time conditions required for the OH determination is not necessary in all cases. This restriction helps, however, to minimize problems due to transport. A measurement setup capable of determining the concentration of all mentioned species simultaneously in the same volume would be ideal. The determination of the photolysis rates do not create any new problems with respect to spatial considerations, as they have to be performed as point measurements.

The most difficult aspect of the described measurement regime for testing tropospheric models is the determination of the OH concentration. It turns out that the technique employed here is capable of determining not only the OH concentration, but also that of other components, all in the same measurement step. The apparatus presented here is so far the only one with the necessary sensitivity and measurement speed capable of yielding absolute values for the local tropospheric OH concentration.[*] It should be noted that until recently there have been no known reports regarding measurements that satisfy these requirements for the verification of tropospheric models, even though this has been attempted for the last 25 years.[24]

[*] Recently, two reports were published (Mount [22b], Eisele et al. [23]) describing two methods which rely on UV long path absorption and chemical detection, respectively. The latter methods are local, but not absolute, and require subsequent calibration.

The basic idea for this instrument, which was developed in Frankfurt, is the absolute determination of concentrations of gases by the absorption of light. As the most intense absorption of the OH radical stems from the transition $A^2\Pi \leftarrow X^2\Sigma$ at 308 nm, the measurement has to be done in the UV. At surface temperatures, the molecule is present in the vibrational ground state, and here the lowest rotational states are excited. Figure 3 shows the most suitable portion of the absorption spectrum together with the spectroscopic terms for the transitions.[25] The

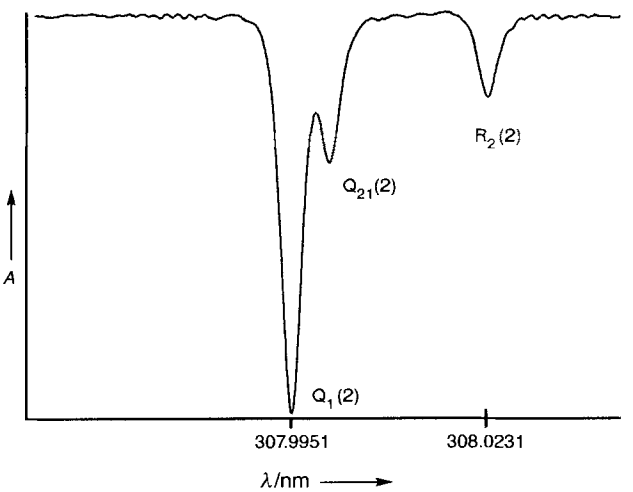


Fig. 3. OH spectrum at 308 nm under atmospheric conditions (1013 mbar, 293 K). A = OH absorption in arbitrary units.

transition probabilities for these line absorptions are known well enough to enable the calculation of the corresponding absorption cross sections for the transitions.[26] To determine the concentration from the absorption it is necessary to know the line width caused by the atmospheric pressure and the temperature, as well as the line width of the light source employed for the absorption measurement.[27] The intensity ratio of the three absorption lines shown in Figure 3 is determined by the surrounding temperature. The transitions $Q_1(2)$ and $Q_{21}(2)$ originate from the same spin system starting from the same ground state, which makes their intensity ratio temperature independent. This means that the same population can be assumed, with good accuracy, for the initial state. The $R_2(2)$ transition stems from a different spin system.[28] Its initial state differs energetically from that of the other two transitions, so that the line intensity ratio of $R_2(2)$ to $Q_1(2)$ and $Q_{21}(2)$ is temperature dependent. The expected atmospheric absorption spectrum can therefore vary with the external temperature. In order to obtain a measurable absorption ($\Delta I/I_0 = 1 \times 10^{-5}$) for the strongest line $Q_1(2)$ at an OH concentration of 5×10^5 cm^{-3}, a pathlength of 1.2 km is required.

Apart from this technique developed in Frankfurt, which relies on the measurement of the three mentioned absorption lines, another method has recently become known. It depends on a long-path absorption with a pathlength of 20.6 km and utilizes the three OH absorption lines above 308 nm, namely $P_1(1)$, $Q_{21}(3)$, and $Q_1(3)$. The method exploits the coincidence of these line positions with the emission of the XeCl eximer laser. Even though the averaging over long absorption pathlengths is expected to lead to some inaccuracies, there are additional errors in the corresponding publications, which question the value of this method. These errors stem mainly from the use of incorrect absorption cross sections, which were too large.[2b]

Absorption measurements are characterized by the fact that the total absorption is determined. If several species absorb in the same wavelength range, a further determination of their respective contributions to the total absorption is necessary. For this spectral data are required. In general, different species have different spectra, so that their contribution to the total can be determined by properly constructing the total spectrum from its constituent spectra. This is done by a fitting procedure. This basically simple procedure cannot be directly applied to atmospheric measurements as every attenuation of the light can be a priori interpreted as a molecular absorption. In the atmosphere, however, the intensity of a light beam can be changed not only by the desired molecular absorptions, but scattering processes (Rayleigh, Mie, etc.) also contribute to the attenuation. Since these processes are independent of each other, the well-known Lambert–Beer law can be used in the form described by Equation (17), which gives the light intensity I_L for a given wave-

$$I_L(\lambda) = I_0(\lambda) \exp(-L \sum_i N_i \sigma_i) \tag{17}$$

length after passage through a distance L in a medium with the absorption or scattering cross section σ_i for a gas mixture with the partial densities N_i. The scattering effects can be factored out using a factor A and one obtains Equation (18), in which σ_j

$$I_L(\lambda) = I_0(\lambda) A \exp(-L \sum_j N_j \sigma_j) \tag{18}$$

are now only the cross sections for the molecular absorptions. The factor A must be ≤ 1, because only the fraction A of the original light intensity I_0 can contribute to the molecular absorptions. The new baseline to which the atmospheric absorption is referred is now $A \times I_0$, where A is generally unknown. A can be assumed to be constant for the observed wavelength region. If a measurement is performed on an absorber that is characterized by an isolated absorption line, $A \times I_0$ can, in principle, be determined at two wavelengths, namely right at the position of the line and right next to it. This situation is generally not found for molecular gases under atmospheric conditions. The spectra are usually not fully resolved and there is a continuous baseline absorption. Therefore a spectral region should be recorded that allows the identification of the absorbing substance or substances. If the whole spectral region is recorded the determination of $A \times I_0$ can be avoided. For example, if the ratio of the measured light intensities at two different wavelength positions λ_1 and λ_2, $I(\lambda_1)$ and $I(\lambda_2)$, is formed, one obtains an expression which no longer contains $A \times I_0$, if I_0 is independent of wavelength for the respective interval [Eq. (19)]. The method

$$I(\lambda_1)/I(\lambda_2) = \exp\left\{-L \sum_j N_j [\sigma_j(\lambda_1) - \sigma_j(\lambda_2)]\right\} = \exp\left(-L \sum_j N_j \Delta\sigma_j\right) \tag{19}$$

is therefore a procedure that utilizes the differential absorption, that is, the structural component of the total absorption, to

determine the absolute quantities of the absorbing species. To fit the component spectra, it is necessary to measure them first in the laboratory, using the pure components. It is essential that these comparison spectra are recorded under atmospheric conditions, which means that the spectra are obtained in air at atmospheric pressure. This allows all of the effects caused by Doppler and pressure broadening, which change the spectra in characteristic ways, to be taken into account.

In atmospheric chemistry, OH concentrations of 5×10^5 cm^{-3} must be measured, therefore the detection limit for the absorption must be at around 1×10^{-5}–2×10^{-5}, as it is unrealistic to assume pathlengths of more than 2 km. This pathlength is currently the upper limit when the discussed measurement requirement for locality is to be satisfied. This pathlength of 2 km must be obtained by multiple reflections between mirrors of a suitable cell (e.g., according to White[29]). This cell has a small volume, and the distance between the mirrors, which determines the dimensions of the cell, is only a few meters. The Frankfurt setup has a mirror distance of 6 meters and hence requires about 300 reflections.[30]

The atmosphere is not optically homogeneous; the glimmering of air is well known. The intensity fluctuations in the light beam caused by this are big enough to make measurements impossible which attempt to quantify effects on the order of 10^{-5}. Studies of the temporal behavior of these effects, which are caused by density fluctuations in the air, have shown that they occur in a time frame that is longer than 100 μs.[31] If it were possible to obtain the entire desired spectral information in a time interval of less than 100 μs, the atmosphere could be considered as sufficiently stable. The spectrum obtained in this way would have a baseline that remains unchanged over this time period.

This baseline characterizes the continuous background underlying the structured absorption (given by $\Delta\sigma$). It is not a straight line over the entire spectral region of the absorption, but exhibits a structure with statistical fluctuations. The summation of many single spectra during the course of a measurement yields a total spectrum that is characteristic for the corresponding atmospheric situation, exhibiting an as yet unknown characteristic baseline. The spectrum is worked up, as was discussed above, by fitting the spectra of its components. After the contributions of all component spectra are removed, a residual spectrum remains, which, together with the continuous background, represents the baseline. Once the baseline is known, Equation (19) can be used to determine the absolute concentration of each absorber.

The basic principles for the determination of the local tropospheric OH concentration, as performed in Frankfurt, have now been described. Our field measurements in the Black Forest (1991)[32] and in the Taunus (1992)[33] have shown that the concentration of three additional gases could be measured in the wavelength range of the selected OH absorption, namely SO_2, $C_{10}H_8$ (naphthalene), and HCHO (formaldehyde). This transforms the absorption method into a multicomponent method in which the individual components are all measured under the same conditions, which is an ideal prerequisite for the testing of models.[34]

The measurements on SO_2 have another use as well. There are other, very sensitive nonoptical analytical methods available for this gas. These "conventional" methods must be calibrated before use. The optical method described herein can then be used for this calibration. The SO_2 measurements therefore act as a secondary standard, as SO_2 is nearly always present in measurable quantities.

The schematic setup of the apparatus in Frankfurt is shown in Figure 4.[35] A laser functions as primary light source; the beam quality is improved by an additional modulator which stabilizes the beam intensity. The beam passes through a 6m-long multireflection cell and reaches a total pathlength of 1.2 km before arriving at the detector. A newer version of the apparatus utilizes not only the UV light at 308 nm, which is obtained by frequency doubling, for the measurements, but also its first harmonic radiation at 616 nm. For this 616 nm beam, a second multireflection cell, identical to the first one except for a different mirror coating, is placed parallel to the UV cell. NO_2, which is so important for the chemistry of the atmosphere, absorbs in this wavelength region. The multicomponent system is hereby expanded by another interesting component.[36] As NO_2 is directly involved in OH recycling, and the measurements obtained in this apparatus are absolute, this expansion is especially valuable for the measurements on OH. As for SO_2, there are conventional techniques available for NO_2, which require additional calibration.

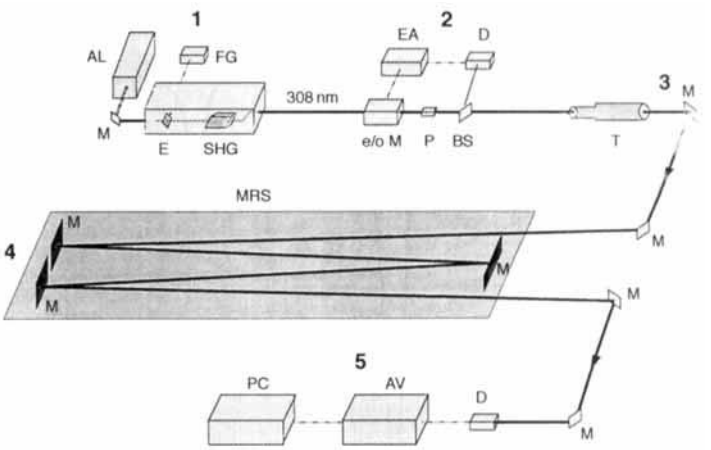


Fig. 4. Schematic representation of the measurement setup. 1) Components of the UV laser; AL: argon ion laser, M: mirror, E: etalon, SHG: frequency doubler (second harmonic generator), FG: function generator. 2) Components of the control and stabilizing unit; e/o M: electrooptic modulator, P: polarizer, BS: beam splitter, EA: error amplifier, D: photodiode. 3) T: telescope, M: mirror. 4) Shaded area: 6m-long multireflection cell (MRS) allowing a path length of 1.2 km in the free troposphere. 5) Components of the detection unit; D: photodiode, AV: averager, PC: computer.

Figure 5 shows the results of a measurement which was performed on September 7, 1992, on the Kleiner Feldberg in the Taunus mountains in Germany. The complete UV absorption spectrum is shown in Figure 5a. The contributing component spectra were sequentially subtracted from the total spectrum. For the sake of illustration, this was done in different orders. On that particular day, the concentration of formaldehyde was below the detection limit, therefore the spectrum contains "only" three components.

The success of this analysis of the atmospheric absorption spectrum is also a confirmation of the quality of the technique.

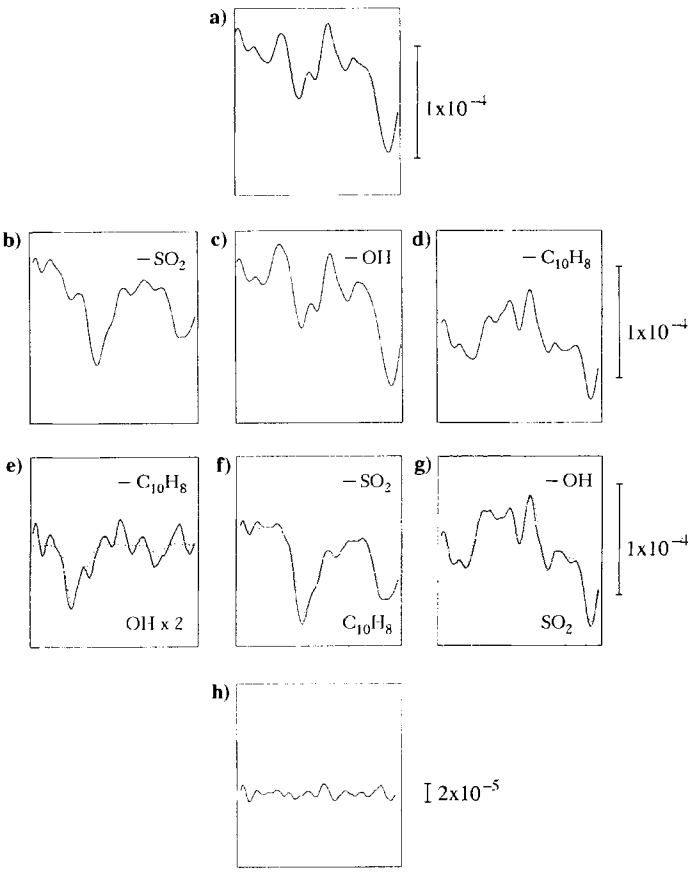


Fig. 5. Single measurement at 1:00 pm CET on September 7, 1992 at the Taunus Observatory of the University Frankfurt/Main, located on the Kleiner Feldberg (FRG) (800 m above sea level). a): Total tropospheric spectrum in the region of OH absorption; b)–d): Total spectrum corrected for the presence of SO_2, OH, and naphthalene, respectively; e)–g): Remaining spectrum after subtraction of SO_2/naphthalene, OH/SO_2, and naphthalene/OH, respectively. h): Residual spectrum. ·····: Reference, ——: Troposphere. The spectra shown correspond to the following concentrations of OH, naphthalene, and SO_2: [OH] = 0.05 pptv, [$C_{10}H_8$] = 40 pptv, [SO_2] = 3 ppbv.

In addition, the results were verified by further independent experiments, which can only be mentioned here.[33] This should satisfy the demand of analytical chemists that any single technique must be verified by independent procedures in order to receive a high degree of confidence. It remains to be noted that it is now finally possible to begin with the long-desired testing of models of the chemistry of the atmosphere.

4. Conclusion and Outlook

Atmospheric chemistry is the chemistry of atmospheric trace components. Hydroxyl radicals play a central role in this chemistry. Their reactions have a crucial influence on the chemistry of the trace species and thereby initiate the self-cleansing process of the atmosphere. That is why the OH radical is also called the detergent of the atmosphere. These molecules therefore also play an important role as a test substance for the verification of existing models.

The above discussion has shown that OH radicals in the troposphere are subjected to a recycling process. This recycling process is a very sensitive instrument in the maintenance of the balance between OH sources and sinks and thereby has a decisive influence on the oxidative potential of the troposphere. In the course of these cycles, the hydroperoxy radical HO_2 also occupies an important position, therefore the determination of its concentration is also an important goal. Due to its comparatively lower reactivity it is present in higher stationary concentrations than OH, but its spectroscopic properties have so far not allowed suitable in situ measurements. The transfer of the fast detection technique presented here to a spectral region suitable for HO_2 appears feasible, however. A new laser system would have to be developed for this application.

Due to the low tropospheric OH concentration, experimental tests of atmospheric models by field measurements are a significant challenge for analytical chemistry. The work summarized here is supposed to show that it is now possible to carry out this test and that a critical verification of atmospheric models can now be performed, something atmospheric chemists have waited a long time for. The developments in Frankfurt further permit measurements in which the absolute concentrations of other atmospheric components, which are used in the verification of the models as well, can be determined simultaneously with and at the same location as OH. The analytical technique described here is therefore a local multicomponent technique which has the required sensitivity as well as the necessary temporal and spatial resolution to enable the realization of such an important endeavor as the verification of models for the chemistry of the atmosphere.[37]

The experimental results described in this article were taken from several Ph.D. and Master's (Diplom) theses. My special gratitude goes to W. Armerding, A. Herbert, M. Spiekermann, J. Walter, and C. Rüger. This work was supported by the Bundesministerium für Forschung und Technologie and the Deutsche Forschungsgemeinschaft.

Received: May 3, 1993
Revised version: December 10, 1993 [A 940 IE]
German version: *Angew. Chem.* **1994**, *106*, 1900
Translated by Dr. W. C. Wilisch, Ansbach (FRG)

[1] P. Warneck, *Chemistry of the Natural Atmosphere*, Academic Press, New York, **1988**.
[2] D. J. Bates, A. E. Witherspoon, *Mon. Not. R. Astron Soc.* **1952**, *112*, 101; J. A. Logan, M. J. Prather, S. C. Wolfsky, M. B. McElroy, *J. Geophys. Res.* **1981**, *86*, 7210; A review on the transport and fate of organic compounds in the atmosphere and hydrosphere appeared in 1992: K. Ballschniter, *Angew. Chem.* **1992**, *104*, 501; *Angew. Chem. Int. Ed. Engl.* **1992**, *31*, 487.
[3] D. L. Baulch, R. A. Cox, P. J. Crutzen, R. F. Hampson, Jr., J. A. Kerr, J. Troe, R. T. Watson, *J. Phys. Chem. Ref. Data* **1982**, *11*, 351.
[4] S. Chapman, *Mem. R. Meteorol. Soc.* **1930**, *3*, 103.
[5] B. J. Finlayson-Pitts, J. M. Pitts, Jr., *Atmospheric Chemistry*, Wiley, New York, **1986**.
[6] C. E. Fairchild, E. J. Stone, G. M. Lawrence, *J. Chem. Phys.* **1978**, *69*, 3632.
[7] B. Schülke, Dissertation, Universität Frankfurt, **1992**; J. C. Brock, R. T. Watson, M. R. Troiier, J. R. Wiesenfeld *J. Geophys. Res. D* **1988**, *93*, 7119; W. Armerding, F. J. Comes, B. Schülke, *J. Phys. Chem.* submitted. *Chem. Phys.* **1980**, *46*, 477
[8] M. J. Molina, F. S. Rowland, *Nature* **1974**, *249*, 810.
[9] R. M. Badger, A. C. Wright, R. F. Whitlock, *J. Chem. Phys.* **1965**, *43*, 4345.
[10] J. Heicklen, *Atmospheric Chemistry*, Academic Press, New York, **1976**.
[11] K. H. Gericke, F. J. Comes, *Chem. Phys. Lett.* **1981**, *81*, 218.
[12] F. J. Comes, K. H. Gericke, J. Manz, *J. Chem. Phys.* **1981**, *75*, 2853.
[13] F. J. Comes, *Forschung Frankfurt* **1991**, *9*(4), 26.
[14] H. S. Johnston, *Acta Astronaut.* **1974**, *1*, 135.
[15] A. Herbert, Dissertation, Universität Frankfurt, **1993**.
[16] R. P. Wayne, *Chemistry of Atmospheres*, Clarendon Press, Oxford, **1985**.
[17] I. I. N. Jones, K. D. Bayes, *J. Chem. Phys.* **1973**, *59*, 4836.

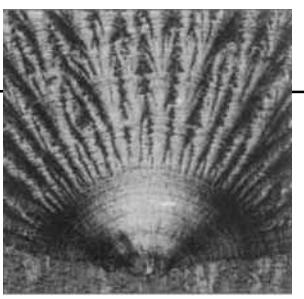
[18] R. Atkinson, A. C. Lloyd, *J. Phys. Chem. Ref. Data* **1984**, *13*, 315.
[19] G. K. Moortgat, P. Warneck, *J. Chem. Phys.* **1979**, *70*, 3639.
[20] F. J. Comes, W. Armerding, C. Rüger, M. Spiekermann, unpublished results.
[21] W. Armerding, A. Herbert, F. J. Comes, *Ber. Bunsenges. Phys. Chem.* **1991**, *95*, 1293.
[22] a) A. Hofzumahaus, H.-P. Dorn, J. Callies, U. Platt, D. H. Ehhalt, *Atmos. Environ. Part A* **1991**, *25*, 2017; G. H. Mount, *J. Geophys. Res. D* **1992**, *97*, 2427.
[23] F. L. Eisele, D. J. Tanner, *J. Geophys. Res. D.* **1991**, *96*, 9295.
[24] D. R. Crosley, Tech. Rep. SRI Int., MP-92-135, **1992**; b) G. H. Mount, *J. Geophys. Res. D.* **1992**, *97*, 2427.
[25] G. Ortgies, K. H. Gericke, F. J. Comes, *J. Mol. Struct.* **1980**, *61*, 239.
[26] G. N. Dieke, H. M. Crosswhite, *J. Quant. Spectrosc. Radiat. Transfer.* **1961**, *2*, 97.
[27] R. Engleman, *J. Quant. Spectrosc. Radiat. Transfer* **1969**, *9*, 3916; C. Leonard, Dissertation, Universität Hannover, **1990**.
[28] G. Herzberg, *Spectra of Diatomic Molecules*, Van Nostrand, New York, **1966**.
[29] J. U. White, *J. Opt. Soc. Am.* **1976**, *66*, 411; D. M. Bakalyar, J. V. James, C. C. Wang, *Appl. Opt.* **1982**, *21*, 2901.
[30] W. Armerding, J. Walter, F. J. Comes, *Fresenius J. Anal. Chem.* **1991**, *340*, 661.
[31] W. Armerding, A. Herbert, G. Mollekopf, T. Schindler, M. Spiekermann, F. J. Comes, *Bericht Projektträgerschaften*, GSF München, November 1988.
[32] F. J. Comes, W. Armerding, R. Grigonis, A. Herbert, M. Spiekermann, J. Walter, *Ber. Bunsenges. Phys. Chem.* **1992**, *96*, 284.
[33] W. Armerding, M. Spiekermann, F. J. Comes, *J. Geophys. Res. D* **1994**, *99*, 1225.
[34] F. J. Comes, W. Armerding, M. Spiekermann, J. Walter, C. Rüger, *Ber. Bunsenges. Phys. Chem.* **1993**, *97*, 1156.
[35] W. Armerding, A. Herbert, M. Spiekermann, J. Walter, F. J. Comes, *Fresenius J. Anal. Chem.* **1991**, *340*, 654.
[36] W. Armerding, J. Walter, C. Rüger, M. Spiekermann, F. J. Comes, *Ber. Bunsenges. Phys. Chem.* **1993**, *97*, 1440.
[37] Note added in proof (August 5, 1994): In the time which has elapsed between the submission and the publication of this review two extensive series of measurements have been carried out at the mountain station of Izana on Tenerife, by the German Sun Observatory and by the Spanish Weather Service with international collaboration. These studies reveal strong correlations between OH concentrations measured with short wave solar radiation and important trace components such as O_3, H_2O, NO_x, hydrocarbons. In certain cases the OH concentrations measured exceeded 1×10^7 cm^{-3}.

F. Cramer
Chaos and Order
The Complex Structure of Living Systems
With a foreword by I. Prigogine

1993. 250 pages with 89 figures. Hardcover.
DM 48.00.
ISBN 3-527-29067-2

What is life? How do ideas arise in our brain? Is there a vital force?
Recent progress in biological research has had a profound effect on our perception of nature. A deeper understanding of nonlinear systems far from equilibrium and of self-organization are no longer outside the scope of science. Professor F. Cramer, who is well known for his contributions in the field of molecular biology, uses his own insights as a starting point for developing an overall picture of the great questions that have always fascinated mankind.

'[Chaos and Order] is the work of a man who rejects a fragmented view of the universe, who refuses to be a prisoner of preconceived doctrines. There is a feeling of excitement, a feeling that we are living at a unique moment in the history of science. The world appears to us at the same time as more strange, but also as more connected and more harmonious, than to any of the generations which have preceded us. I can only hope that Cramer's book will inspire many readers and will receive the international acclaim that it fully deserves.'
Angewandte Chemie



SCIENCE

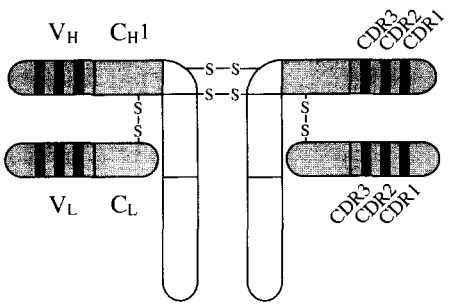
To order please contact your bookseller or:
VCH, P.O. Box 10 11 61, D-69451 Weinheim, Telefax (0) 62 01 - 60 61 84
VCH, Hardstrasse 10, P.O. Box, CH-4020 Basel
VCH, 8 Wellington Court, Cambridge CB1 1HZ, UK
VCH, 220 East 23rd Street, New York, NY 10010-4606, USA (toll free: 1-800-367-8249)
VCH, Eikow Building, 10-9 Hongo 1-chome, Bunkyo-ku, Tokyo 113, Japan

VCH

Specific Binding of Antibodies to DNA through Combinatorial Antibody Libraries

Michael Famulok* and Dirk Faulhammer

The immune system of a higher developed organism is probably the most potent system in nature for the highly specific recognition of all different kinds of molecular species. The antibody repertoire in man or mouse has a diversity between 10^7 and 10^{11}. The enormous number of antibody specificities is achieved by the combination of a relatively small number of incomplete genes (see e.g. immunoglobulin G1, Scheme 1). For



Scheme 1. Immunoglobulin G1. The regions shown in gray represent the Fabs. They consist of the variable (V_H) and the constant (C_H1) regions of the heavy chain, as well as the variable (V_L) and constant (C_L) regions of the light chain. The antigen is bound mainly in the complementarity-determining regions (CDR regions) within the V_H and V_L.

the variable region V_H of the heavy chain around 100 V_H genes combine with 30 diversity genes (D genes) and 6 joining genes (J genes) to yield about 18000 different complete V_H chains. Because of inaccuracies in connecting the genes and enzymatic treatment, this number can increase by three orders of magnitude. The variable region V_L of the light chain results from the combination of 100 V_L genes with 5 J genes. An antigen binding site consists of a V_L and a V_H chain; their random fusion increases the number of possible combinations to 10^{11}. Finally, somatic mutations in these gene regions can raise the number of different antibody specificities even further by several orders of magnitude. This diversity, however, is far from fully utilized by the organism. The actually existing repertoire is sufficient for the development of antibodies against an incredible number of possible antigens, and as a result it effectively protects an organism against pathogenic or otherwise harmful agents.

This natural process, however, has certain limitations. Overcoming them would be of great importance for the more extensive technical, therapeutic, and diagnostic application of antibody technology. For example, the generation of antibodies specific for nucleic acids, such as double-stranded DNA (dsDNA) or RNA, by classical immunization of animals is quite often difficult, because nucleic acids typically lead to an extremely weak immune response. Likewise, the generation of catalytic antibodies by immunization with transition state analogues (TSAs) does not always lead to results desirable for an effective catalyst. In addition, only a fraction of the antibodies isolated from TSA-immunized animals bind the immunogen. On the other hand, only a few binders obtained are catalytically active.

For these and other reasons, extensive effort has been devoted for some time to the generation of synthetic antibodies, whereby the natural process is not only copied, but even improved.[1] The goal is to use an antibody library with a huge number of binding specificities without relying on the immunization of animals or the employment of eukaryotic cells. A recent publication by Barbas et al. on the specific recognition of double-stranded DNA (dsDNA) by semisynthetic antibodies shows that these efforts are very promising.[2]

How is it possible to copy nature's combinatorial process of antibody formation in the laboratory? How can it be used successfully for the selection of antibodies with novel functionalities? More importantly, how can the selected functional molecules be traced back genetically and amplified?

Among the most decisive steps for the generation of antibody diversity in vitro is the expression of single antigen-binding fragments (Fabs) in the bacterium *Escherichia coli*.[3] The antigen-binding fragment is a heterodimer which consists of a light chain and a fragment of the heavy chain. Another crucial aspect is the amplification of V_H and V_L genes by the polymerase chain reaction (PCR).[4] This was employed in the straightforward construction of libraries from the genomic cDNA of antibody-producing cells (spleen, bone marrow, peripheric blood cells). Furthermore, in this step semisynthetic antibody genes can be used, in which a part of the complementarity-determining region (CDR) is substituted by a randomized oligonucleotide. Finally, a gene vehicle, a vector, is required which is suitable for cloning the largest possible number of antibody genes and for

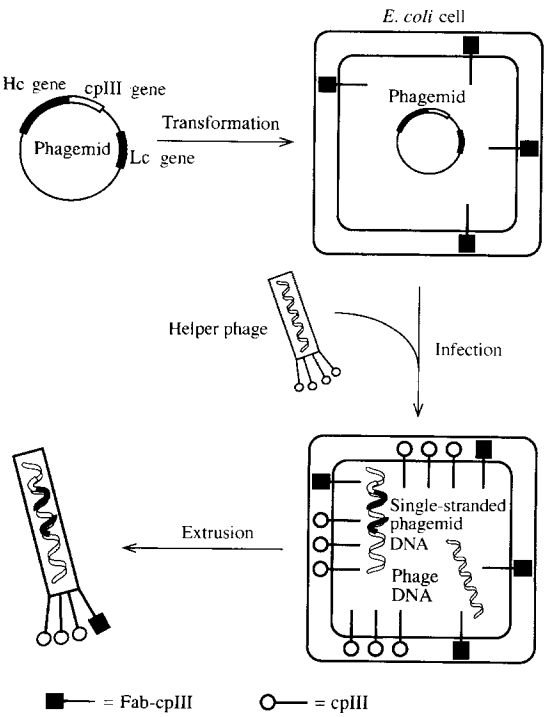
[*] Dr. M. Famulok, Dipl.-Chem. D. Faulhammer
Institut für Biochemie der Universität München
Am Klopferspitz 18a, D-82152 Martinsried (FRG)
Telefax: Int. code + (89)8578-2470

 © VCH Verlagsgesellschaft mbH, D-69451 Weinheim, 1994 0570-0833/94/1818-1827 $ 10.00+.25/0

multiplying the corresponding proteins in the foreign cells. For this purpose, a bacterial virus (phage) is used, which contains the genes for the heavy and light chain and which is able to specifically infect bacteria with high efficiency.[5] Another crucial advantage of phage was shown by G. P. Smith in 1985: any peptide can be exprimed on the phage surface.[6] This was achieved by cloning the peptide-encoding DNA into the phage in such a way that the resulting peptide is fused with either its N- or C-terminus to a phage protein called coat protein III (cpIII). The cpIII is responsible for the binding of the phage to the bacterium. For that purpose it is exprimed at the phage surface at about four copies per virion. Exactly the same fusion principle could be applied to the antibody genes.[7] For the construction of the antibody library a specially designed vector (fdCAT1) is used. This vector is constructed in such a way that owing to its fusion with cpIII the heavy chain can be anchored to the inner membrane of the bacterium, whereas the light chain is excreted into the periplasm, the space between the inner and outer bacterial membrane. Hence, the two chains assemble on the membrane to give the complete antibody. By this design it is possible to combine the genetic and the structural information: the interior of the phage contains the antibody genes which are expressed on the outside such that the antibody can interact with its antigen in solution. In addition, it is thus possible to select the phage by binding them to immobilized antigens, for example, by means of affinity chromatography. The phage selected in this way can then be used again to infect bacteria. This selection process can be repeated until a maximal enrichment of functional antigen-binding fragments (Fabs) is achieved.

However, this method still had two disadvantages: the phage requires cpIII on its surface to enter the bacterium. But after the direct cloning of the antibody genes into the phage, all four cpIII molecules on the "tip" of the phage contain a Fab, which leads to a dramatic reduction of infectivity. Futhermore, the four Fabs on the phage tip lead to an increase in binding capacity; in this way, weak binders can simulate low dissociation constants by chelatization effects.

This problem was circumvented by using a special cloning vector, the phagemid pComb3, in combination with a helper phage for the cloning of the antibody library (Scheme 2). A phagemid is a hybrid of phage and plasmid, which consists of parts of the genome of a single-stranded DNA phage and of double-stranded components of plasmid DNA. Phagemids can reproduce within a host cell just like double-stranded plasmids. The simultaneous infection of the cells by the helper phage (M13) results in the synthesis of the gene products required for the packaging of phage particles, including the phagemids. In this case the phagemids can reproduce just like single-stranded DNA phages. In addition to the coat proteins, both intact cpIII and the Fab–cpIII fusion protein are produced; their genetic information is contained in the DNA of the helper phage and phagmid, respectively. If the DNA of the helper phage is mutated in a special way, the phagemid DNA is packaged preferentially. When the assembled phage is excreted from the cell, its surface is usually supplied with three cpIIIs and one Fab–cpIII fusion protein. The excreted phage thus contains the genetic information for the antibody genes in the form of a single-stranded copy of the phagemid DNA, together with a Fab molecule at its surface as well as the cpIII molecules required for



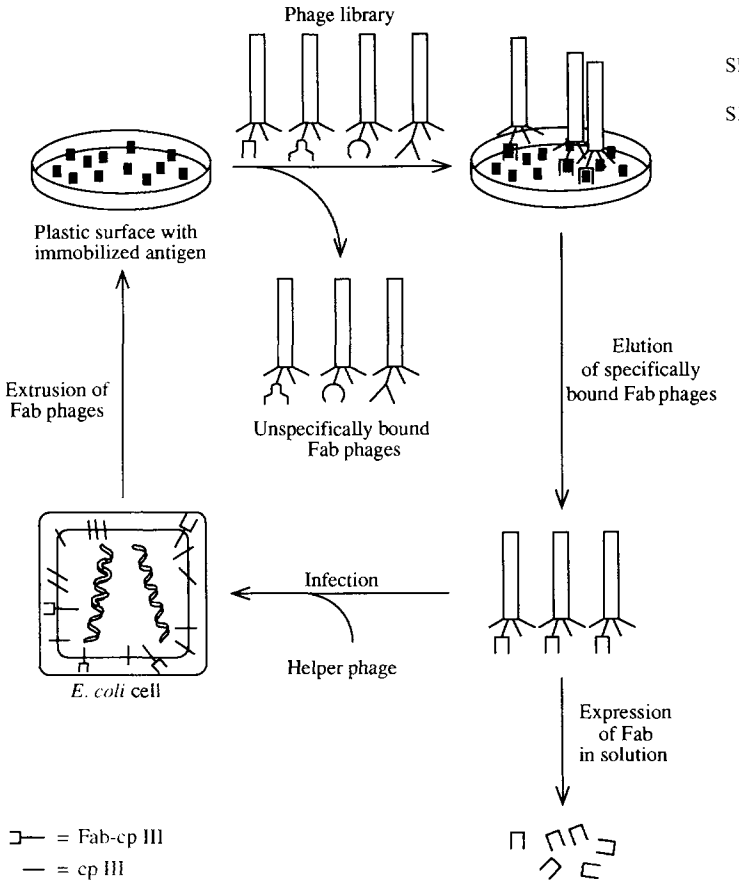
Scheme 2. Phagemid rescue of phagemid DNA by helper phages. The phagemid contains the genes for the light chain (Lc) and for the fusion protein, which consists of the cpIII and the heavy chain (Hc) of the Fab. Transformation into *E. coli* cells leads to the expression of the Fab–cpIII fusion protein in the periplasm (see text for details). The helper phage exprimes all the proteins required in the construction of the virus particle, including cpIII. Since the phagemid carries signals required for phage packaging, the phagemid DNA is packaged into the phage particle in single-stranded form.

efficient infection. In this way about 10^5 copies of each phage and of each set of antibody genes are produced.

The selection step, in technical terminology referred to as "panning", is represented in Scheme 3. The whole pool consisting of roughly 10^{12} Fab-containing phage (10^5 copies $\times$ 10^7 different phages in the library) is incubated with the antigen, which is immobilized on a plastic surface. Nonbinding phages are eluted with binding buffer, and the binding phages are thus enriched by about 100-fold. Specifically binding phages are then eluted, for example by affinity elution with the antigen or by lowering the pH. The isolated phages are used again to infect bacteria and amplify the phagemid DNA during cell growth. This DNA can then be packaged after addition of the helper phage, and the Fab can be exprimed at the surface, as described above. These steps are repeated until most of the phage of the enriched phage–Fabs of the pool bind to the antigen. The DNA is then isolated from the specifically binding phage–Fabs, the cpIII gene is removed by treatment with restriction enzymes, and the phagemid is regenerated by ligation. The phagemid can now be used to infect bacteria that do not exprime the Fab at their surface, because the cpIII part at the surface is missing. The unfused Fab is produced in soluble form, and the free antibody can be isolated from the bacterial cell extract. The antibodies can now be tested individually for their binding affinity to the antigen.

Barbas et al. used three antibody libraries each consisting of 10^9 different molecules,[2] in which certain regions in the V_H chain were randomized, to isolate specific DNA-binding anti-

 © VCH Verlagsgesellschaft mbH, D-69451 Weinheim, 1994 0570-0833/94/1818-1828 $ 10.00+.25/0



Scheme 3. The panning process for selection of antigen-specific Fabs (see text for details).

bodies. In one library 10 amino acids in the CDR-3 of the heavy chain were randomized, in the other two libraries 16 amino acids. In general the CDR-3 of the antibody contributes most significantly to antigen recognition, because this region is characterized by the highest diversity. For the first two libraries the V_L region was held constant; in the third library the V_L chain contained a short randomized portion. For the panning, dsDNA from human placenta was used, which was immobilized on a plastic surface. After four cycles of panning, individual Fabs were tested for their binding behavior by enzyme linked immunosorbent assay (ELISA). Two Fabs (SD1 and SD2) gave a strongly positive signal. Both Fabs, which were bound to the immobilized DNA, could be eluted with a DNA solution that was only 10^{-9} M, which indicates a dissociation constant between 10 and 100 nM. The antibody SD1 clearly binds preferentially to G-C-rich regions; increasing concentrations of poly(dG) · poly(dC) and poly(dG-dC) · poly(dG-dC) inhibit its binding to DNA, whereas poly(dA) · poly(dT) or poly(dA-dT) · poly(dA-dT) do not show such an effect.

The antibodies selected by Barbas et al. do not fulfil the demands for an immediate technical or therapeutic application. In order to do so, they would have to bind with much better sequence specificity. With their preference for G-C-rich regions, however, the selected Fabs provide the basis for a novel class of sequence-specific DNA-binding molecules. This becomes evident when the 16-mer V_H region of SD1 is compared to the 10-mer V_H region of SD2. The amino acid sequence of both initially randomized regions show considerable homologies:

SD1: Gly-Arg-Ala-Tyr-Gly-Gly-Asn-Gly-Leu-Lys-Met-Met-Ser-Leu-Asp-Asn

SD2: Gly-Arg-Gly-Trp-Ser-Gly——————————Ser-Leu-Asp-Ile

However, SD1 contains six additional amino acids. Since this is the most significant difference between the two Fabs, it is thought that this insertion of six amino acids might be responsible for the G-C preference of SD1. The effect of changes in this region on the sequence specificity of the antibody is being tested.

Antibodies tailored for the recognition of specific DNA sequences could be used in many different ways. In genome mapping, for example, specific DNA sequences could be blocked making them inaccessible to other enzymes. Synthetic DNA-binding Fabs could be used to interfere with the control of the expression of specific genes, which could be employed in a range of therapeutic applications. Sequence-specific antibodies might help to identify certain DNA sequences in gene diagnostics. But these are only a few of the potential applications. It is important to note that in principle the range of applications is unlimited whether for the generation of synthetic biocatalysts or for the neutralization of viruses or toxins. One of the most important prospects might be the selection and improvement of catalytic antibodies. The first promising results have already been reported.[8, 9] For example, Chen et al. showed that an antibody library from mice immunized with a TSA hapten could be transferred to phage.[8] From this phage library, hapten-binding clones were isolated, some of which were catalytically active. This result was the proof for the principal applicability of combinatorial Fab libraries for the generation of catalytic antibodies.

It can be expected that a broad spectrum of antibody chains with various binding motifs will soon be available. The corresponding genes could be used as building blocks for the construction of designer antibodies. Another emerging possibility is the selection of antibodies that function even under exotic conditions, for example in the presence of organic solvents or toxic compounds.

German version: *Angew. Chem.* **1994**, *106*, 1911

[1] R. A. Lerner, A. S. Kang, J. D. Bain, D. R. Burton, C. F. Barbas III, *Science* **1992**, *258*, 1313–1314; A. S. Kang, T. M. Jones, D. R. Burton, *Proc. Natl. Acad. Sci. USA* **1991**, *88*, 11120–11123; C. F. Barbas, III, E. Björling, F. Chiodi, N. Dunlop, D. Chababa, T. M. Jones, S. L. Zebedee, M. A. Persson, P. L. Nara, E. Norrby, D. R. Burton, *ibid.* **1992**, *89*, 9339–9343; D. R. Burton, *Acc. Chem. Res.* **1993**, *26*, 405–411.

[2] S. M. Barbas, P. Ghazal, C. F. Barbas III, D. R. Burton, *J. Am. Chem. Soc.* **1994**, *116*, 2161–2162.

[3] A. Skerra, A. Plückthun, *Science* **1988**, *240*, 1038–1041; M. Better, C. P. Chang, R. R. Robinson, A. H. Horvitz, *ibid.* **1988**, *240*, 1041–1043.

[4] J. W. Larrick, Y. L. Chiang, R. Cheng-Dong, G. Senyk, P. Casali, *Prog. Biotechnol.* **1988**, *5*, 231; R. Orlandi, D. H. Güssow, P. T. Jones, G. Winter, *Proc. Natl. Acad. Sci. USA* **1989**, *86*, 3833–3837.

[5] W. D. Huse, L. Sastry, S. A. Iverson, A. S. Kang, M. Alting-Mees, D. R. Burton, S. J. Benkovic, R. A. Lerner, *Science* **1989**, *246*, 1275–1281.

[6] G. P. Smith, *Science* **1985**, *228*, 1315–1316; J. K. Scott, G. P. Smith, *ibid.* **1990**, *249*, 386–390.

[7] J. McCafferty, A. D. Griffiths, G. Winter, D. J. Chiswell, *Nature* **1990**, *348*, 552–554; A. S. Kang, C. F. Barbas III, K. D. Janda, S. J. Benkovic, R. A. Lerner, *Proc. Natl. Acad. Sci. USA* **1991**, *88*, 4363–4366; C. F. Barbas III, A. S. Kang, R. A. Lerner, S. J. Benkovic, *ibid.* **1991**, *88*, 7978–7982; T. Clackson, H. R. Hoogenboom, A. D. Griffiths, G. Winter, *Nature* **1991**, *352*, 624–628.

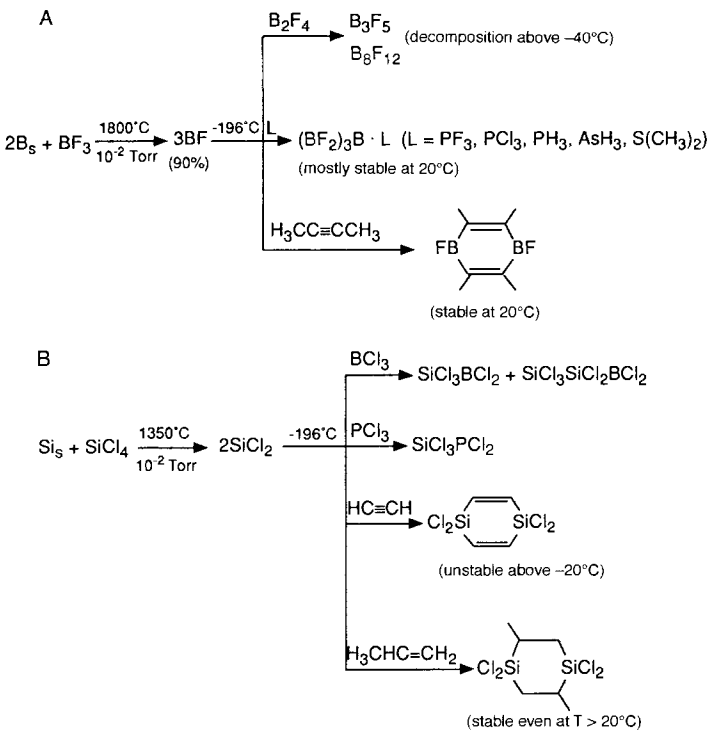
[8] Y.-C. J. Chen, T. Danon, L. Sastry, M. Mubaraki, K. D. Janda, R. A. Lerner, *J. Am. Chem. Soc.* **1993**, *115*, 357–358.

[9] B. Posner, J. Smiley, I. Lee, S. Benkovic, *Trends Biochem. Sci.* **1994**, *19*, 145–150; J. D. Stewart, S. J. Benkovic, *Int. Rev. Immunol.* **1993**, *10*, 229–240.

Subvalent Aluminum Halides as Examples of High-Temperature Species in Inorganic Syntheses

Jörg J. Schneider*

It is now 20 years since the pioneering work of P. L. Timms in the field of chemical synthesis with subvalent compounds EX_n of the third and fourth main group elements (especially with E = B and Si) (Scheme 1).[11] Subvalent in this context means



Scheme 1. Selected cocondensation reactions of the subvalent HT species BF (A) and $SiCl_2$ (B) with organic and inorganic compounds at −196 °C.

that the valence of the element E in these compounds is lower than the maximum valence allowed in the group. A variety of special handling techniques were developed to produce these compounds and to allow them to react with suitable partners, and, in particular, to have these high-temperature (HT) species available in preparative quantities on a laboratory scale.[1, 2] In the meantime, a large number of these molecules is experimentally accessible (Table 1).

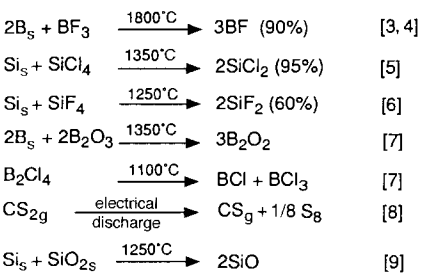
Disproportionation and comproportionation reactions are the most common synthesis routes (Scheme 2). In every case, as a second step after their actual synthesis (mostly at high temperatures), trapping of these species at low temperatures (e.g. at −196 °C) is essential to bridle their extraordinary reactivity.

[*] Priv.-Doz. Dr. J. J. Schneider
Max-Planck-Institut für Kohlenforschung
Kaiser-Wilhelm-Platz 1, D-45470 Mülheim an der Ruhr (FRG)
New address: Institut für Anorganische Chemie der Universität
Universitätsstrasse 3–5, D-45117 Essen (FRG)
Telefax: Int. code + (201)183-2402

Table 1. Selected examples of preparatively accessible subvalent HT species of main group elements [2b].

BF	CS	
BCl	CF_2	
BC_2	CBr_2	
B_2O_2		
AlCl	SiO	P_2
AlF	SiS	PF
	SiC	PN
	SiF_2	PF_2
	$SiCl_2$	

All HT molecules presented in Table 1 have coordination numbers far below the maximum possible numbers, which explains this high reactivity. Careful treatment of these molecules with suitable reactants between −196 °C and room temperature enables largely selective reactions. Once the researcher has mastered the hurdles associated with the challenging experimental conditions during the synthesis of such compounds, he is rewarded with attractive yields and the above-mentioned extraordinarily high reactivity of these molecules. This allows a rich synthetic chemistry even at very low temperatures. Recently, the potential of subvalent HT species, especially those of the aluminum species, has been rediscovered.



Scheme 2. Disproportionation and comproportionation reactions for the synthesis of subvalent HT compounds of the group 13 and group 14 elements with references. The pressure is less than 10^{-1} Torr for all reactions.

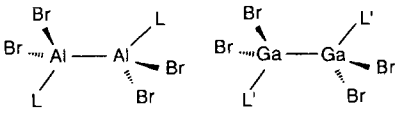
For some time, H. Schnöckel's research group has specialized in the preparation and investigation of the reaction behavior of subvalent EX (E = Al, Ga; X = Cl, Br) species. They have obtained AlX and GaX by cocondensation of atomic Al or Ga and gaseous HX in very good yields [Eq. (a)].[10]

$$E_s \xrightarrow[10^{-2}\ \text{Torr}]{\text{ca. } 1000\,^\circ\text{C}} E_g \xrightarrow[10^{-2}\ \text{Torr (90\%)}]{\text{HX, } -196\,^\circ\text{C}} EX + \tfrac{1}{2}H_2 \qquad \text{(a)}$$

E = Al, Ga; X = Cl, Br

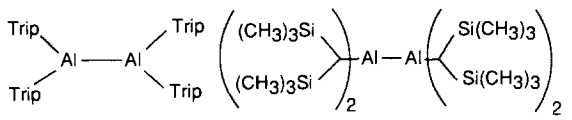
Initially, work centered on the actual synthesis, matrix isolation, and spectroscopic characterization of these HT species. Lately, more preparatively oriented work, especially on

alanediyl AlCl, has spawned important contributions to the chemistry of Al^{I} and, more recently, also to that of Al^{II}. Crucial to the preparative breakthrough in this sector of high-temperature chemistry was the observation that AlCl as well as its heavier homologue GaCl could be prepared as metastable molecules and stored in a mixture of toluene and diethyl ether at low temperature for quite some time. A spectacular result of these studies, for instance, was the synthesis of $[(\eta^5\text{-Cp*})Al]_4$,[11] the first homoleptic $(\eta^5\text{-Cp*})Al$ cluster, subject of an earlier Highlight.[12] Recently, again from H. Schnöckel's research group, the synthesis and characterization of donor-stabilized $AlBr_2$ (**1**) (Scheme 3) was reported.[13a] It is a subvalent aluminum(II)



2.527(6) 2.395(6)

1 [13a] **2** [14]



2.647(3) 2.660(1)

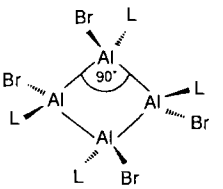
3 [15] **4** [16a]

Scheme 3. E–E distances [Å] in the subvalent compounds **1**–**4**. L = anisole, L' = 1,4-dioxane, Trip = 2,4,6-tri-isopropylphenyl.

halide stable at room temperature. The corresponding halide of the heavier homologue gallium (compound **2**) has been known for some time and its structure has been characterized.[14] Donor-stabilized $AlBr_2$ forms by comproportionation from a cocondensation solution of AlBr and anisole, in which $AlBr_3$ (10%) is also present. The actual primary product of the reaction $AlBr_2$ is trapped at $-30\,^{\circ}C$ by the donor solvent anisole (L) in the form of a stable complex $Al_2Br_4 \cdot L_2$ (**1**). The presence of $AlBr_3$ in the cocondensate as an "impurity" is thus essential for the in-situ formation of the new $Al^{II}Br_2$ species. The extended synthesis route to **1** via AlBr is necessary, since $AlBr_2$ cannot be made directly from Al atoms and HBr on a preparative scale.[13b] In the solid, **1** does not disproportionate into Al^{I} and Al^{III} compounds.

The Al–Al bond in **1** is noticeably shorter than that in other organoalanes such as **3** and **4**, and similar to the one found for the radical anion $\mathbf{3}^{\bullet -}$. One-electron reduction of **3** and **4** to $\mathbf{3}^{\bullet -}$ and $\mathbf{4}^{\bullet -}$, respectively, entails a significant shortening of the central Al–Al bond (Δd(Al–Al) = 0.17[15] and 0.13 Å, respectively).[16] Additional π bonding contributions in the radical anions are supposed to be responsible for this. If a—purely hypothetical—shortening of the Al–Al bond of the same order as upon reduction of **3** and **4** occurs on going from **1** to $\mathbf{1}^{\bullet -}$, an Al_2 system with an E–E bond even shorter than that found so far in $\mathbf{3}^{\bullet -}$ and $\mathbf{4}^{\bullet -}$ would result. H. Schnöckel et al. now have also succeeded in preparing Et_3N-donor-stabilized AlBr (**5**) and have characterized this species spectroscopically as well as structurally. This has just recently been reported in *Angewandte Chemie*.[17]

Unlike the donor-stabilized $AlBr_2$ **1**, **5** is tetrameric in the crystal ($[BrAl{\leftarrow}NEt_3]_4$) and features a square Al_4 unit. The Al–Al distances in **5** (2.643(3) Å) lie within the range of Al–Al single bonds.[11, 15, 16a] Similarly, in contrast to **1**, **5** already forms around $-100\,^{\circ}C$ from the cocondensate mixture of (AlBr/toluene and Et_3N). Accordingly, no efficient formation of $AlBr_2$ from AlBr and $AlBr_3$, as is supposed to happen during the synthesis of **1**, occurs under these reaction conditions, and consequently no formation of an aluminum(II) system is observed. Not until $-30\,^{\circ}C$ does the actual comproportionation reaction between AlBr and $AlBr_3$ set in leading to the formation of $AlBr_2$.[13] The trapping of the HT species AlBr with the appropriate donor solvent in the right temperature range is thus of prime importance for the formation of AlX or AlX_2 molecules in these syntheses. This has certainly to be taken into account during further studies of AlX and possibly GaX. The rather elongated Al–Br bonds (as compared to those in **1**[13] and $AlBr_3$[18]) in **5** support its formulation as an aluminum(I) bromide. The same holds for the Al–N bonds if one compares them to those found for the NH_3 and Me_3N adducts of $AlBr_3$.[19] These observations are in accord with an increasing ionic radius in the series $Al^{3+} < Al^{2+} < Al^{+}$.



5, L = Et_3N

The formation of **5** constitutes the second synthesis of a homonuclear Al_4 cluster from monomeric AlX. It remains to be seen if a conventional preparative route to these unusual Al^{I} and Al^{II} compounds (**5** and possibly **1**) can be found, as has already been the case for $[(\eta^5\text{-Cp*})Al]_4$.[20] Since the E–E bond is already present in **1**, and since halide substitution should be easy, **1** suggests itself as a starting material for the synthesis of other dialanes like **4**. For the heavier element homologues Ga and In this has already been illustrated by type **2** compounds.[21] This opens an alternative route to new dialane type molecules, a class of compounds which so far has only been accessible by reduction of dialkyl element halides.[22]

Preparative synthetic chemistry under extreme conditions, be it in the form of free-atom syntheses, or in the application of highly reactive subvalent molecules as shown in this Highlight, has once again proven its merits among other preparative methods. It continues to offer surprising results such as unexpected molecules like **1** and **5**.

In this context, a speculative glance at the neighbor of aluminum in group 14 should be permitted. Maybe for SiX_2[23] or even SiO (both preparatively quite accessible subvalent HT species) there exist unexpected ways of stabilizing them analogously to AlX or GaX. Then a complex-bound SiO, whether at a main group metallic center or at a transition metal center (analgous to CO?) could in this way become a reality in the future.

German version: *Angew. Chem.* **1994**, *106*, 1914

[1] a) P. L. Timms in *Cryochemistry* (Eds.: M. Moskovits, G. A. Ozin), Wiley, New York, **1976**, Chap. 2, p. 9, and references therein.; b) for boron and silicon subhalides see: P. L. Timms, *Acc. Chem. Res.* **1973**, *6*, 118.
[2] a) A. G. Massay, *Adv. Inorg. Chem. Radiochem.* **1983**, *26*, 1; b) a recent reviw of preparatively accessible HT species can be found in: W. W. Porterfield, *Inorganic Chemistry. A Unified Approach*, 2nd ed., Academic Press, New York, **1993**, p. 473.
[3] P. L. Timms, *J. Am. Chem. Soc.* **1968**, *90*, 4585.
[4] R. W. Kirk, P. L. Timms, D. L. Smith, W. Airey, *J. Chem. Soc. Dalton Trans.* **1972**, 1392.
[5] D. L. Smith, R. W. Kirk, P. L. Timms, *J. Chem. Soc. Chem. Commun.* **1972**, 295.
[6] P. S. Maddren, Dissertation, University of Bristol, England, **1975**.
[7] K. J. Klabunde, C. M. White, H.F. Efner, *Inorg. Chem.* **1974**, *13*, 1778.
[8] K. J. Klabunde, E. Moltzen, A. Senning, *Chem. Rev.* **1988**, *88*, 391.
[9] E. Schaschel, D. N. Gray, P. L. Timms, *J. Organomet. Chem.* **1972**, *35*, 69.
[10] a) H. Schnöckel, *Z. Naturforsch. B* **1976**, *31*, 1291; b) H. Schnöckel, *J. Mol. Struct.* **1978**, *50*, 275, 267; c) M. Tacke, H. Schnöckel, *Inorg. Chem.* **1989**, *28*, 2895; d) M. Tacke, H. Kreienkamp, L. Plaggenberg, H. Schnöckel, *Z. Anorg. Allg. Chem.* **1991**, *604*, 35; e) D. Loos, H. Schnöckel, D. Fenske, *Angew. Chem.* **1993**, *105*, 1124; *Angew. Chem. Int. Ed. Engl.* **1993**, *32*, 1059.
[11] C. Dohmeier, C. Robl, M. Tacke, H. Schnöckel, *Angew. Chem.* **1991**, *103*, 594; *Angew. Chem. Int. Ed. Engl.* **1991**, *30*, 564.
[12] P. Paetzold, *Angew. Chem.* **1991**, *103*, 559; *Angew. Chem. Int. Ed. Engl.* **1991**, *30*, 544.
[13] a) M. Mocker, C. Robl, H. Schnöckel, *Angew. Chem.* **1994**, *106*, 946; *Angew. Chem. Int. Ed. Engl.* **1994**, *33*, 862; b) the spectroscopic characterization of donor-free was already reported by G. A. Olah, O. Farooq, S. M. Farnia, M. R. Bruce, E. L. Clouet, P. M. Morton, G. K. S. Prakash, R. C. Stevens, R. Bau, K. Lammertsma, S. Suzer, L. Andrews, *J. Am. Chem. Soc.* **1988**, *110*, 3231.
[14] a) J. C. Beamish, R. W. H. Small, *Inorg. Chem.* **1979**, *18*, 220; b) R. W. H. Small, I. J. Worall, *Acta Crystallogr. Sect. B* **1982**, *38*, 250.
[15] R. J. Wehmschulte, K. Ruhlandt-Senge, M. M. Olmstead, H. Hope, B. E. Sturgeon, P. P. Power, *Inorg. Chem.* **1993**, *32*, 2983.
[16] a) W. Uhl, *Z. Naturforsch. B* **1988**, *43*, 1113; b) C. Pluta, K.-R. Pörschke, C. Krüger, K. Hildenbrand, *Angew. Chem.* **1993**, *105*, 451; *Angew. Chem. Int. Ed. Engl.* **1993**, *32*, 388.
[17] M. Mocker, C. Robl, H. Schnöckel, *Angew. Chem.* **1994**, *106*, 1860; *Angew. Chem. Int. Ed. Engl.* **1994**, *33*, 1754.
[18] P. A. Akishin, N. G. Rambidi, E. Z. Zasovin, *Sov. Phys. Crystallogr.* (*Engl. Transl.*) **1959**, *4*, 167.
[19] a) M. Hargittai, I. Hargittai, V. P. Spiridonov, M. Pellisier, J. F. Labarre, *J. Mol. Struct.* **1975**, *24*, 27; b) M. Hargittai, I. Hargittai, V. P. Spridonov, A. A. Ivanov, *ibid.* **1977**, *39*, 225; c) D. F. Grant, R. C. G. Killean, J. L. Lawrence, *Acta Crystallogr Sect. B* **1969**, *25*, 377.
[20] S. Schulz, H. W. Roesky, H. J. Koch, G. M. Sheldrick, D. Stalke, A. Kuhn, *Angew. Chem.* **1993**, *105*, 1828; *Angew. Chem. Int. Ed. Engl.* **1993**, *32*, 1729.
[21] a) W. Uhl, M. Layh, T. Hildenbrand, *J. Organomet. Chem.* **1989**, *364*, 289; b) W. Uhl, M. Layh, W. Hiller, *ibid.* **1989**, *368*, 139.
[22] W. Uhl, *Angew. Chem.* **1993**, *105*, 1449; *Angew. Chem. Int. Ed. Engl.* **1993**, *105*, 1386.
[23] Complexation of $SiCl_2$ by a classical route was first achieved by G. Schmid, H. J. Balk, *Chem. Ber.* **1970**, *103*, 2240.

The Search for Selective, Neutral Anion Receptors

Dieter E. Kaufmann* and A. Otten

The binding of guest to host molecule for selective activation for a subsequent reaction is an extremely successful principle in biological processes and in organic synthesis. Thus the synthesis of organic mono- or bicyclic host macrocycles has become established over the last 25 years for the selective complexation of cationic guests and opened diverse possibilities for applications.[1]

The synthesis of molecules for the selective recognition of anions is, in contrast, more difficult from the outset, because

- the anions are coordinatively saturated and therefore bind only sluggishly
- their size requires that the macrocycles that must be developed are significantly larger than those for cations, and
- the solvent-dependent formation of ion pairs or their very efficient solvation impede a selective complexation.

The rapid development—also stimulated by the huge significance of biological anion receptors –of supramolecular chemistry in the past decade has contributed to the increased efforts to synthesize molecules for the recognition of anions.[2] Interesting fields of application are molecular recognition, development of synthetic enzyme analogues, transport of anions, and homogeneous catalysis. In medical diagnosis the concentration of anions is already routinely determined with very ion-selective electrodes.[3]

Different structure and binding concepts have been investigated with the aim of recognizing anions selectively. At first it made sense to use the experience gained from the chemistry of cation receptors and to prepare, by addition of electrophiles, the electronic inverse and thus polyammonium macro- and oligocycles as well as guanidinium compounds fundamentally suitable for anion complexation. These macrocycles with protonated or quaternary nitrogen functions display high positive charge densities and a strong ability for complexation, and consequently also an often very small selectivity for the guest anions. Uncharged host molecules for anions should, in principle, provide a better chance for selectivity.

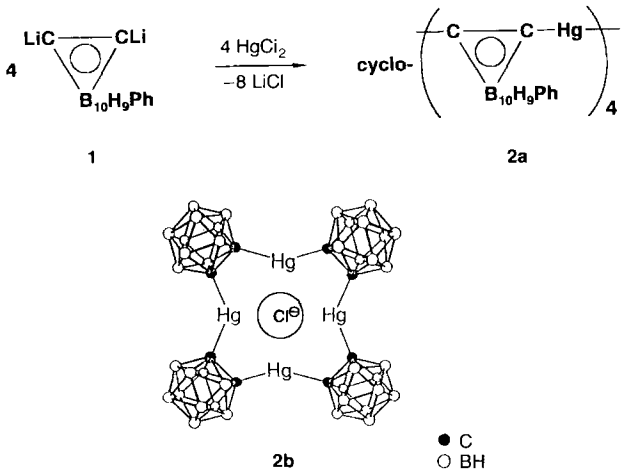
Very recently interesting syntheses of charged and neutral host molecules have been developed. In 1993 Stang and Zhdankin[4] reported a simple synthesis of macrocyclic tetrabiphenyldiyltetraiodium compounds that are unusual cationic molecular cages. Presently the selective complexation of anions and/or basic neutral molecules by these molecules is being investigated.

Covalently bound Lewis acid centers are suitable binding sites for coordinative complexation of anion and basic molecules according to another bonding concept: they invariably have lone electron pairs. The work of Jung et al.[5] on a macrocyclic

[*] Prof. Dr. D. E. Kaufmann, Dr. A. Otten
Institut für Organische Chemie der Technischen Universität
Leibnizstrasse 6, D-38678 Clausthal-Zellerfeld (FRG)
Telefax: Int. code + (5323)72-2834

trisilane as well as that of Newcomb et al.[6] and Kuivila et al.[7] on stanna-coronands and -cryptands fit into this concept. Ion transport studies gave strong evidence for the selective and reversible inclusion of a halide ion; this was proven by solid-state ^{119}Sn NMR spectroscopy and crystal structure analyses.

Hawthorne et al.[8] postulated that a kinetic template effect resulted in the exclusive formation of the tetradentate [12]mercuracarborand-4 on treatment of 1,2-dilithio-3-phenyl-*ortho*-carborane (**1**) with mercury halides, although on energetic considerations the trimeric [9]mercuracarborand-3 was the preferred product. These "anti-crown" complexes are accessible in good yields, soluble in polar organic solvents, and can bind halide guest anions reversibly (structure **2b** shows the results of the crystal structure analysis).



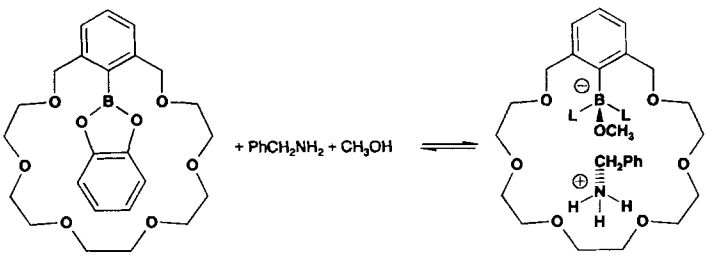
1 2a 2b

Simon et al.[9] developed electrodes with membranes incorporating the organomercury compounds and displaying a pronounced selectivity for chloride ions.

As early as 1985 Katz[10] reported on the cooperative binding of a hydride and a chloride ion by 1,8-diborylated naphthalene (hydride sponges). Oligoboron anticoronands or -cryptands are, on the other hand, as yet unknown. After a theoretical study by Jacobson and Pizer was published in 1993,[11] macrotricyclic host molecules with boron atoms in the four bridgehead positions are considered particularly promising synthetic targets because of their predicted strong binding to, and selectivity for, anions.

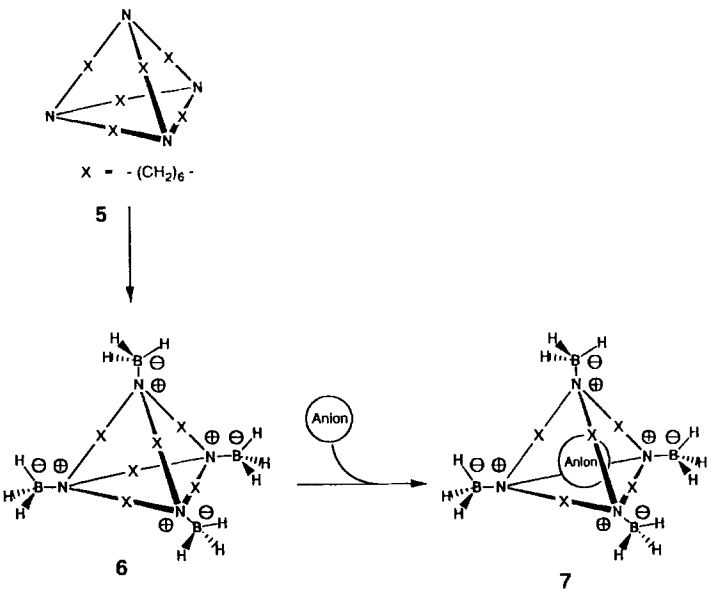
With the synthesis of the crown ethers **3** containing *one* Lewis acidic boryl substituent, Reetz et al.[12] opened the way to a new class of neutral host molecule that, depending on the anion, can bind either the anion or the cation of potassium salts monotopically, or both ions heterotopically. These host molecules can also recognize and incorporate two different organic guest molecules: an alcohol/amine mixture has indeed been shown to be bound heterotopically as in **4**. Steric factors are particularly important for the molecular recognition, so the host **3** can distinguish between methanol and ethanol.

Recently Schmidtchen et al.[13] were the first to report the synthesis and properties of an uncharged artificial anion host without Lewis acid character, thus demonstrating a third possibility for anion recognition: the borane/amine adduct **6**, which



3 4

is readily accessible by treatment of the known macrotricyclic amine **5** with BH_3·THF, can form a complex with anions through anion–dipole interaction with the strong B–N dipoles. For optimal stabilization of the anion, the orientation of the dipoles by a macrotricyclic framework like that of **6** is important.



5 6 7

This precise preorganization for the fixation of the negatively charged guest species brings both advantages and disadvantages. Problems lie in the often difficult syntheses of preorganized hosts, the subsequent changes in their structure that are always laborious to perform, and the often strong binding of the anion to the host that results in poor decomplexation and regenerability. Favorable aspects are the ability to fix the binding site of the guest quite precisely, the exact positioning of the anchor groups, and the choice of guest according to size. The crystal structure analysis shows that the cavity in **6** is smaller than that in the fourfold positively charged macrocyclic ammonium salt as a result of the distorted tetrahedral N atoms in the adduct. The α-CH_2 protons in the host molecule may be used as a ^{1}H NMR probe for conformational changes caused by anion complexation during the titration of **6** with ammonium or phosphonium salts. This experiment shows that large iodide and phosphorus hexafluoride anions are complexed only to a slight extent, and whereas the small chloride and cyanide anions are readily incorporated, binding to the bromide ion is virtually optimal. The exchange of the guest in a 1:1 host–guest complex

can also be achieved. Both the 1:1 host–chloride complex and the displacement of the chloride ion by a bromide or iodide ion was detected by electrospray mass spectrometry.

Interesting applications should be possible through the controlled change of the dipole strength by selection of the borane entity and through variation of the framework of the host molecule.

A long road lies ahead before the anion host molecules are as versatile as their cationic counterparts. Chemists wait in eager anticipation for these new approaches to lead to a breakthrough in the use of neutral anion receptors.

German version: *Angew. Chem.* **1994**, *106*, 1917

[1] J.-M. Lehn, *Angew. Chem.* **1988**, *100*, 92; *Angew. Chem. Int. Ed. Engl.* **1988**, *27*, 89; B. Dietrich, P. Viout, J. M. Lehn, *Macrocyclic Compounds Chemistry. Aspects of Organic and Inorganic Supramolecular Chemistry*, VCH, Weinheim, **1992**.

[2] a) F. P. Schmidtchen, *Nachr. Chem. Tech. Lab.* **1988**, *36*, 8; b) F. P. Schmidtchen, A. Gleich, A. Schummer, *Pure Appl. Chem.* **1989**, *61*, 1535; c) B. Dietrich, *ibid.* **1993**, *65*, 1457.

[3] U. Spichiger, W. Simon, E. Bakker, M. Lerchi, P. Buehlmann, J. P. Haug, M. Kuratli, S. Ozawa, S. West, *Sens. Actuators B* **1993**, *B11*, 1.

[4] P. J. Stang, V. V. Zhdankin, *J. Am. Chem. Soc.* **1993**, *115*, 9808.

[5] M. E. Jung, H. Xia, *Tetrahedron Lett.* **1988**, *29*, 297.

[6] M. T. Blanda, J. H. Horner, M. Newcomb, *J. Org. Chem.* **1989**, *54*, 4626.

[7] K. Jurkschat, H. G. Kuivila, S. Liu, J. A. Zubieta, *Organometallics* **1989**, *8*, 2755.

[8] Z. Zheng, X. Yang, C. B. Knobler, M. F. Hawthorne, *J. Am. Chem. Soc.* **1993**, *115*, 5320; X. Xang, C. B. Knobler, M. F. Hawthorne, *Angew. Chem.* **1991**, *103*, 1519; *Angew. Chem. Int. Ed. Engl.* **1991**, *30*, 1507.

[9] M. Rothmaier, W. Simon, *Anal. Chim. Acta* **1992**, *271*, 135.

[10] H. E. Katz, *Organometallics* **1987**, *6*, 1134.

[11] S. Jacobson, R. Pizer, *J. Am. Chem. Soc.* **1993**, *115*, 11216.

[12] M. T. Reetz, C. M. Niemeyer, K. Harms, *Angew. Chem.* **1991**, *103*, 1515; *Angew. Chem. Int. Ed. Engl.* **1991**, *30*, 1472; *ibid.* **1991**, *103*, 1517 and **1991**, *30*, 1474; M. T. Reetz, GDCh-Vortrag, Technische Universität Clausthal, January 21, 1994.

[13] K. Worm, F. P. Schmidtchen, A. Schier, A. Schäfer, M. Hesse, *Angew. Chem.* **1994**, *106*, 360; *Angew. Chem. Int. Ed. Engl.* **1994**, *33*, 360.

A stop-gap solution?



If the latest library copy of Angewandte spends more time off the shelf than on, stop the gap with a personal subscription.

Just call or fax

VCH

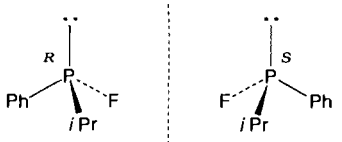
USA: Tel. 1-(800) 422-8824; Fax (305) 428-8201
UK: Tel. (0223) 321111, Fax (0223) 313221

First Resolution of a Free Fluorophosphane Chiral at Phosphorus

Michael Pabel, Anthony C. Willis, and S. Bruce Wild*

Dedicated to Professor Ekkehard Lindner on the occasion of his 60th birthday

Following the first resolution of a simple acyclic tertiary phosphane in 1961,[1] the question arose as to the suitability for resolution of other simple trivalent phosphorus compounds, especially halophosphanes of the type PXR^1R^2, which in optically active form would be valuable intermediates for subsequent syntheses. Calculations of the energy barrier for the pyramidal inversion of compounds of this type indicated that configurational stability at phosphorus increased with attachment of electronegative substituents, for example chlorine or especially fluorine atoms.[2] Nevertheless the first reported attempts at synthesizing optically active fluoro- and chlorophosphanes from optically active compounds of the type $P(NR_2)R^1R^2$ by cleavage of the amino group with acyl halides, hydrogen chloride, or phosphorus trichloride were unsuccessful.[3] In 1992, however, it was reported that (*S*)-(−)-[P(SMe)Cl*t*BuPh]CF_3SO_3 of 63% optical purity could be desulfurized with tris(dimethylamino)phosphane at −70 °C to give (*S*)-(+)-PCl*t*BuPh of 49.4% optical purity before purification.[4] The chlorophosphane lost its optical activity over 20 h in the polarimeter cell. In other work it has been shown that (±)-PClMePh and (±)-AsFMePh can be resolved as ligands in certain iron(II) complexes, but these halogen-containing ligands cannot be liberated from the metal.[5] Here we report that (±)-**1** can be readily resolved by the separation of diastereomers of certain optically active palladium(II) complexes containing the phosphane, and that free (S_P)-(−)-**1** can be liberated in optically pure form from the less soluble diastereomer.

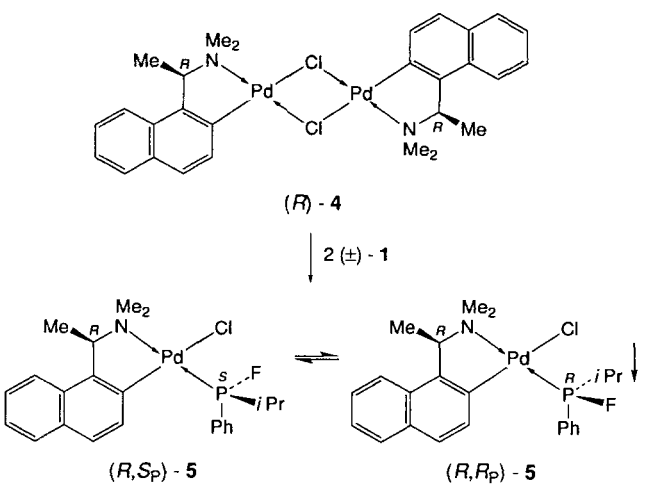


(±) - **1**

Based on the literature procedure for the synthesis of $PFtBu_2$,[6] (±)-**1** was isolated in 55% yield by heating a mixture of (±)-PClPh*i*Pr[7] and sodium fluoride in sulfolane and distilling with collection at −196 °C. The $^{31}P\{^1H\}$ NMR spectrum of the freshly thawed distillate in benzene at 25 °C indicated 86% of (±)-**1**, along with a number of minor impurities including the disproportionation product **2** [Eq. (a)]. A neat sample of (±)-**1**, after 16 h at 25 °C, had disproportionated into **2** and (*R**,*R**)/(*R**,*S**)-**3**. Thus, (±)-**1** is considerably less stable than $PFtBu_2$, which showed no evidence of decomposition when heated at 150 °C for 100 h, even in the presence of a trace of sodium fluoride.[6] It is noteworthy, however, that the disproportionation of (±)-**1** is slowed down dramatically in benzene.[8]

$$\underset{(\pm)\text{-}\mathbf{1}}{3\ \mathrm{PFPh}i\mathrm{Pr}} \longrightarrow \underset{\mathbf{2}}{\mathrm{PF_3Ph}i\mathrm{Pr}} + \underset{(R^*,R^*)/(R^*,S^*)\text{-}\mathbf{3}}{\mathrm{Ph}i\mathrm{PrP{-}PPh}i\mathrm{Pr}} \qquad \text{(a)}$$

The reaction of two equivalents of (±)-**1** with (*R*)-**4** in dichloromethane produced the pair of diastereomeric complexes (*R*,R_P)- and (*R*,S_P)-**5** in almost equal amounts (Scheme 1).



Scheme 1.

This was evidenced by a sharp doublet at $\delta = 185.14$ ($^1J(P,F) = 927.8$ Hz) and a broad doublet at $\delta = 181.36$ ($^1J(P,F) = 937.5$ Hz) in the $^{31}P\{^1H\}$ NMR spectrum. Interestingly, the relative intensity of the resonance at $\delta = 185.14$ increased to 75% over 18 h and then remained constant at this equilibrium value. Consistent with this observation, removal of solvent, followed by dissolution of the residue in diethyl ether, and subsequent filtration to remove a small quantity of solid impurity gave a colorless solution, which on concentration afforded the diastereomer having $\delta = 185.14$ in 64% combined yield in a typical second-order asymmetric transformation.[9] The final mother liquor was found to contain both diastereomers in the equilibrium 75:25 ratio. In pure form, (*R*,R_P)-**5** is kinetically stable in CD_2Cl_2.[10] The configurationally homogeneous product having $\delta = 185.14$, colorless prisms readily soluble in dichloromethane and benzene, and moderately soluble in diethyl ether, was identified as (*R*,R_P)-**5** by X-ray crystallography.[11]

The molecular structure of (*R*,R_P)-**5** is shown in Figure 1, together with selected bond lengths and angles. Compound (*R*,R_P)-**5** is the first alkylarylfluorophosphane complex to be isolated, and the structure determination performed is the first to our knowledge on an organofluorophosphane palladium

[*] Dr. S. B. Wild, Dr. M. Pabel, Dr. A. C. Willis
Research School of Chemistry, Institute of Advanced Studies
Australian National University
Canberra, ACT 0200 (Australia)
Telefax: Int. code + (6) 249-0750

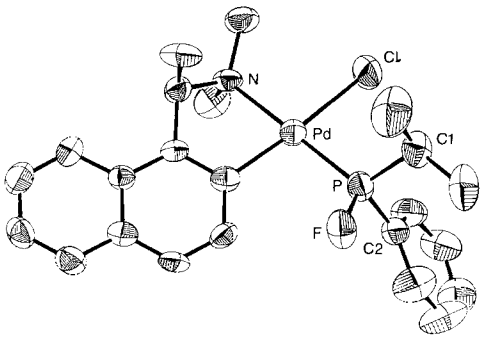
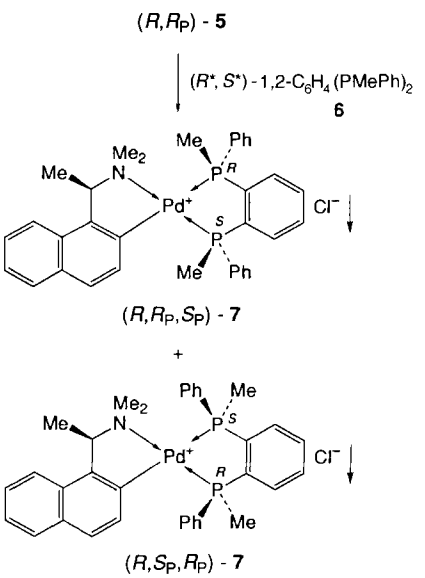


Fig. 1. Crystal structure of (R,R_P)-**5** (ORTEP diagram, thermal ellpsoids enclose 50% probability levels). Selected distances [Å] and angles [°]: P–F 1.589(5), P–Pd 2.215(3), P–C1 1.819(10), P–C2 1.786(9), Pd-P-F 117.1(2), Pd-P-C1 115.0(3), Pd-P-C2 115.3(3), F-P-C1 99.4(4), C1-P-C2 107.0(5), C2-P-F 100.9(4).

complex. The P–F distance in (R,R_P)-**5** is slightly longer than the P–F bonds in similar diarylfluorophosphane complexes,[12] but very similar to the corresponding distance in *trans*-[Ni-$Br_2(PF/Bu_2)_2$],[13] where the P–F bond was shortened by 4 pm upon complexation.[14] The coordination geometry around the palladium in the complex is slightly distorted from square-planar; the fluorophosphane is situated *trans* to the dimethylamino group, which is typical for such complexes.[15] The liberation of optically pure (S_P)-(−)-**1** from (R,R_P)-**5** was effected by treatment of the complex with achiral **6**[16] in benzene (Scheme 2).



Scheme 2.

The displacement proceeds with retention of configuration at phosphorus to give homochiral (S_P)-(−)-**1** as verified by the quantitative regeneration of the starting complex (R,R_P)-**5** from the free ligand and (*R*)-**4** (Scheme 1) in a rapid quenching experiment. A solution of (S_P)-(−)-**1** having $[\alpha]_D^{20} = -210$ ($c = 0.59$ in C_6H_6) was obtained within 30 min of liberation, the minimum period required to remove (R,R_P,S_P)- and (R,S_P,R_P)-**7** and prepare an accurate sample of the phosphane for measurement. Significantly, however, although the rotation of the solution increased to zero within 6 h (presumably by intermolecular fluorine exchange[3, 4]), the $^{31}P\{^1H\}$ NMR spectrum of a sample taken from the same solution showed no discernible disproportionation into **2** and $(R^*,R^*)/(R^*,S^*)$-**3** over 6 h.

Presently we are examining the stereochemistry of reactions of (S_P)-(−)-**1** in coordinated and free form.

Experimental Procedure

(±)-**1**: A mixture of chlorophenylisopropylphosphane (11.75 g, 63.0 mmol) and sodium fluoride (14.36 g, 342.0 mmol) in sulfolane (120 mL) was heated with stirring at 140 °C for 80 min. The product (b.p. 93 °C, 14 mmHg) was collected at −196 °C. Yield 6.09 g (55%). $^{31}P\{^1H\}$ NMR (121.42 MHz, CD_2Cl_2, 25 °C, H_3PO_4): $\delta = 183.10$ (d, $^1J(P,F) = 855.3$ Hz) (ca. 86%); ^1H NMR (299.95 MHz, CD_2Cl_2, 25 °C, TMS): $\delta = 0.91$ (ddd, $^3J(H,P) = 15.6$ Hz, $^3J(H,H) = 6.9$ Hz, $^4J(H,F) = 1.2$ Hz, 3 H; CH_3), 1.21 (ddd, $^3J(H,P) = 13.5$ Hz, $^3J(H,H) = 6.9$ Hz, $^4J(H,F) = 1.2$ Hz, 3 H; CH_3), 1.94–2.14 (m, 1 H; CH), 7.44–7.62 (m, 5 H; C_6H_5); $^{13}C\{^1H\}$ NMR (75.43 MHz, CD_2Cl_2, 25 °C, TMS): $\delta = 15.30$ (dd, $^2J(C,P) = 19.2$ Hz, $^3J(C,F) = 5.5$ Hz; CH_3), 16.85 (dd, $^2J(C,P) = 15.3$ Hz, $^3J(C,F) = 2.7$ Hz; CH_3), 34.09 (dd, $^1J(C,P) = 21.4$ Hz, $^2J(C,F) = 12.1$ Hz; CH), 128.71 (dd, $^3J(C,P) = 7.7$ Hz, $^4J(C,F) = 1.7$ Hz; *meta*-CH), 129.64 (dd, $^2J(C,P) = 23.1$ Hz, $^3J(C,F) = 8.2$ Hz; *ortho*-CH), 130.66 (s; *para*-CH), 140.66 (dd, $^1J(C,P) = 29.1$ Hz, $^2J(C,F) = 10.5$ Hz; *ipso*-C); ^{19}F NMR (282.20 MHz, $CDCl_3$, 25 °C, $CFCl_3$): $\delta = -208.44$ (dd, $^1J(F,P) = 857.5$ Hz, $^3J(F,H) = 13.7$ Hz). A sample of (±)-**1** after 16 h at 25 °C had the following $^{31}P\{^1H\}$ NMR spectrum in CD_2Cl_2: $\delta = -13.18$ (td, $^1J(P,F_{ax}) = 849.8$ Hz, $^1J(P,F_{eq}) = 979.6$ Hz) (**2**): −8.98 (s) and −15.30 (s), [$(R^*,R^*)/(R^*,S^*)$-**3**].

(R,R_P)-**5**: A solution of (*R*)-**4** (7.67 g, 10.0 mmol) in dichloromethane (200 mL) was added over 5 min to a solution of (±)-**1** (4.07 g of 86% purity, 20.3 mmol) in the same solvent (100 mL). After stirring for 18 h the solvent was removed from the reaction mixture in vacuo, and the residue was dissolved in diethyl ether (400 mL). The solution was filtered and concentrated to ca. 60 mL, whereupon a colorless microcrystalline solid precipitated. The crude product was washed with 25 mL of cold diethyl ether and dried in vacuo. Concentration of the mother liquor yielded additional product. Three recrystallizations of the combined crude material from diethyl ether gave the pure product. Yield 6.65 g (64%). M.p. 182 °C. $[\alpha]_D^{20} = +35.2$ ($c = 0.88$ in CH_2Cl_2). $^{31}P\{^1H\}$ NMR (121.42 MHz, $CDCl_3$, 25 °C, H_3PO_4): $\delta = 185.14$ (d, $^1J(P,F) = 927.8$ Hz); ^1H NMR (299.95 MHz, $CDCl_3$, 25 °C, TMS): $\delta = 1.00$ (dd, $^3J(H,P) = 14.3$ Hz, $^3J(H,H) = 7.1$ Hz, 3 H; *i*Pr-CH_3), 1.68 (dd, $^3J(H,P) = 20.3$ Hz, $^3J(H,H) = 7.4$ Hz, 3 H; *i*Pr-CH_3), 1.97 (d, $^3J(H,H) = 6.3$ Hz, 3 H; benzyl-CH_3), 2.58 (d, $^4J(H,P) = 1.8$ Hz, 3 H; N-CH_3), 2.90 (d, $^4J(H,P) = 3.9$ Hz, 3 H; N-CH_3), 2.92–3.06 (m, 1 H; *i*Pr-CH), 4.31 (d of quart., $^4J(H,P) = 6.8$ Hz, $^3J(H,H) = 6.3$ Hz 1 H; benzyl-CH), 7.20–8.20 (m, 11 H; aromatics); $^{13}C\{^1H\}$ NMR (50.31 MHz, $CDCl_3$, 25 °C, TMS): $\delta = 14.95$ (dd, $^2J(C,P) = 6.0$ Hz, $^3J(C,F) = 3.1$ Hz; *i*Pr-CH_3), 18.27 (d, $^2J(C,P) = 4.2$ Hz; *i*Pr-CH_3), 23.64 (s; benzyl-CH_3), 34.28 (dd, $^1J(C,P) = 28.5$ Hz, $^2J(C,F) = 12.5$ Hz; *i*Pr-CH), 47.66 (d, $^3J(C,P) = 2.7$ Hz; N-CH_3), 50.93 (d, $^3J(C,P) = 3.3$ Hz; N-CH_3), 72.60 (d, $^3J(C,P) = 3.5$ Hz; benzyl-CH), 123.09–148.94 (aromatics); ^{19}F NMR (282.20 MHz, $CDCl_3$, 25 °C, $CFCl_3$): $\delta = -185.08$ (dd, $^1J(F,P) = 927.8$ Hz, $^3J(F,H) = 24.4$ Hz); MS (70 eV: 511.1 [M^+]; correct elemental analyses were obtained.

(S_P)-(−)-**1**: A solution of **6** (67.5 mg, 209.4 μmol) in benzene (1 mL) was added to a stirred solution of (R,R_P)-**5** (106.8 mg, 209.3 μmol) in the same solvent (1 mL). The mixture was diluted immediately with benzene (4 mL) and centrifuged to give a colorless solution of (S_P)-(−)-**1**, $[\alpha]_D^{20} = -210$ ($c = 0.59$ in C_6H_6), and a sediment of (R,R_P,S_P)- and (R,S_P,R_P)-**7**. Treatment of this solution with (*R*)-**4** regenerated quantitatively (R,R_P)-**5** as shown by spectral comparisons.

Received: March 24, 1994
Revised version: May 19, 1994 [Z 6792 IE]
German version: *Angew. Chem.* **1994**, *106*, 1917

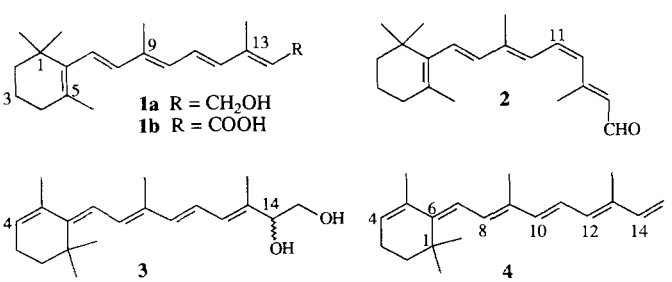
[1] L. Horner, H. Winkler, A. Rapp, A. Mentrup, H. Hoffmann, P. Beck, *Tetrahedron Lett.* **1961**, 161–166.
[2] R. D. Baechler, K. Mislow, *J. Am. Chem. Soc.* **1971**, *93*, 773–774.
[3] L. Horner, M. Jordan, *Phosphorus Sulfur Relat. Elem.* **1980**, *8*, 235–242.
[4] J. Omelańczuk, *J. Chem. Soc. Chem. Commun.* **1992**, 1718–1719.
[5] G. Salem, G. B. Shaw, A. C. Willis, S. B. Wild, *J. Organomet. Chem.* **1993**, *444*, 147–154; *ibid.* **1993**, *455*, 185–192.
[6] M. Fild, R. Schmutzler, *J. Chem. Soc. A* **1970**, 2359–2364; O. Stelzer, R. Schmutzler, *Inorg. Synth.* **1978**, *18*, 173–179.
[7] J. D. Mitchell, S. O. Grim, *Inorg. Synth.* **1976**, *16*, 195–197.
[8] A solution of (±)-**1** in benzene after several months had disproportionated according to Equation (a), but a trace of (±)-**1** was still evident in the $^{31}P\{^1H\}$ NMR spectrum.

[9] E. E. Turner, M. M. Harris, *Q. Rev. Chem. Soc.* **1947**, *1*, 299–330.
[10] The interconversion between (R,R_P)-**5** and (R,S_P)-**5** could be caused by ligand exchange involving traces of (±)-**1** or its decomposition products with one or both of the diastereomers and subsequent intermolecular racemization and recoordination of the fluorophosphane.
[11] X-ray structure analysis (Rigaku AFC6S diffractometer): (R,R_P)-**5** crystallized from benzene/diethyl ether, $C_{23}H_{28}ClFNPPd$, $M = 510.31$, crystal dimensions $0.20 \times 0.16 \times 0.13$ mm^3, space group $P2_12_12_1$, $a = 9.967(2)$, $b = 10.998(4)$, $c = 21.324(3)$ Å, $V = 2337.3(7)$ Å^3, $\rho_{calcd} = 1.450$ g cm^{-3}, $Z = 4$ (measurement temperaure 25 °C), $Mo_{K\alpha}$ radiation ($\mu = 9.93$ cm^{-1}), $2\theta = 4$–$46.4°$, total number of reflections 1923, number of reflections with $I \geq 3\sigma(I)$ 1528, refined parameters 253, analytical absorption correction, $R = 0.031$, $R_w = 0.020$, $S = 2.09$, residual electron density 0.37 e Å^3, solution and refinement with the teXsan computer program. H atoms were placed on idealized positions. Absolute configuration from known chirality of precursor and by analysis of pairs of Friedel opposites. Further details of the crystal structure investigation are available on request from the Director of the Cambridge Crystallographic Data Centre, 12 Union Road, GB-Cambridge CB2 1EZ (UK), on quoting the full journal citation.
[12] L. Heuer, P. G. Jones, R. Schmutzler, *J. Fluorine Chem.* **1990**, *46*, 243–254; T. G. Meyer, P. G. Jones, R. Schmutzler, *Z. Naturforsch. B* **1993**, *48*, 875–885.
[13] W. S. Sheldrick, O. Stelzer, *J. Chem. Soc. Dalton Trans.* **1973**, 926–929.
[14] H. Oberhammer, R. Schmutzler, O. Stelzer, *Inorg. Chem.* **1978**, *17*, 1254–1258.
[15] P. H. Leung, A. C. Willis, S. B. Wild, *Inorg. Chem.* **1992**, *31*, 1406–1410; P. Gugger, A. C. Willis, S. B. Wild, *J. Chem. Soc. Chem. Commun.* **1990**, 1169–1170.
[16] N. K. Roberts, S. B. Wild, *J. Am. Chem. Soc.* **1979**, *101*, 6254–6260.

Spectroscopic Studies of Anhydroretinol, an Endogenous Mammalian and Insect *retro*-Retinoid**

Fadila Derguini,* Koji Nakanishi, Jochen Buck, Ulrich Hämmerling, and Felix Grün

Carotenoids obtained through diet have been adapted for a wide variety of essential roles in animal physiology. The most commonly used primary metabolite, retinol (vitamin A1, **1a**), acts as the prohormone in at least three distinct effector pathways in mammals. The visual pigment rhodopsin uses *11-cis*-retinal (**2**) as its chromophore;[1] retinoic acid (**1b**) performs functions during cellular differentiation and morphogenesis[2] through the control of gene expression by ligand-dependent nuclear receptors. Retinol itself, or metabolites distinct from the retinoic acid series, is essential for regulation of spermatogenesis[3] and the immune system.[4] 14-Hydroxy-4,14-*retro*-retinol (14-HRR, **3**), the first bioactive *retro*-retinoid reported, functions as a potent intracellular agonist of retinol-dependent events in immune cells.[5] First isolated from mammalian cells, 14-HRR has also been identified in *Drosophila* and other insect cells. In addition, we found another naturally occurring *retro*-retinoid, anhydroretinol (AR, **4**), which reversibly inhibits retinol and 14-HRR dependent effects and blocks B lymphocyte proliferation as well as activation of resting T lymphocytes.[6] 14-HRR and AR constitute the first agonist/antagonist pair of lipid signaling molecules to be reported. Anhydroretinol, a physiological retinol derivative, was originally isolated from fish liver oils;[7] however, its biological role remained obscure, and until recently it was referred to as the "inactive retinoid".[8] More recently AR was characterized in a variety of mammalian cells, for example in liver and lung cells,[9a] in transformed mouse fibroblasts,[9b] and in insect cell lines such as *Drosophila* S2M3 cells and *Spodoptera frugiperda* SF 21 cells, where it is the predominent retinol metabolite. In contrast, a subclone of this latter line, SF 9, did not produce a detectable amount of AR.[6] Addition of [^{3}H]retinol to cell preparations followed by immediate extraction and analysis by high-pressure liquid chromatography (HPLC) does not lead to spontaneous formation of anhydroretinol. Moreover, AR is not detected when cells are kept at 4 °C, fixed with glutaraldehyde, or treated with sodium azide. Thus its synthesis is dependent on an active metabolic state. The newly discovered biological role of AR, as a naturally occurring 14-HRR antagonist, makes the study of anhydroretinol of special interest. We describe here the purification of AR from *Drosophila* Schneider S2M3 cells and the characterization of its synthetic isomers.



Insect S2M3 cells were grown in Schneider's medium. HPLC analysis of the lipid fraction (Fig. 1a) indicated the ability of the cells to metabolize retinol to various retinoids common both to mammalian and insects, as well as to insect-specific retinoids. On the basis of UV absorption spectra, retention times, and/or coelution studies with standards, the peak at 25 min was identified as 14-HRR ($\lambda_{max} = 324$, 348, 365 nm), and that at 18 min as a mixture of 3- and 4-hydroxyretinol (3/4-OH-Rol; $\lambda_{max} =$

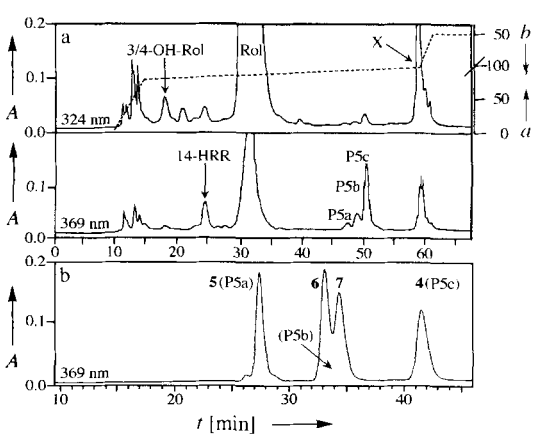


Fig. 1. HPLC profile of a) retinoid metabolites from a 4 g Schneider S2M3 cell pellet (X = retinyl ester; gradient elution: a = percentage of MeOH in MeOH/H_2O, b = percentage of MeOH in MeOH/$CHCl_3$; detection at 324 and 369 nm), and b) synthetic anhydroretinol isomers (isocratic elution H_2O/CH_3OH 14/86; detection at 369 nm).

[*] Dr. F. Derguini, Prof. K. Nakanishi
Department of Chemistry, Columbia University
New York, NY 10027 (USA)
Telefax: Int. code + (212)932-8273
Dr. J. Buck
Department of Pharmacology
Cornell University Medical College, New York, NY (USA)
Dr. U. Hämmerling, Dr. F. Grün
Department of Immunology
Memorial Sloan-Kettering Cancer Center, New York, NY (USA)

[**] This study was supported by the National Institutes of Health (grants CA-49933, CA-08748 (U. H.), and JM-47599 (U. H., K. N.)). We thank Dr. R. Delotto for providing the insect cell lines S2M3, and Dr. C. Cherapak for assistance in NMR measurements. J. B. is a Pew Scholar in the Medical Sciences.

325 nm).[10] Fractions eluting between 48 and 52 min (P5a, b, c) exhibit UV/VIS spectra with vibronic fine structure and maxima around 270, 348, 368, and 390 nm, characteristic of a *retro*-retinoid skeleton comprising six double bonds.[11] These fractions were shown by photoisomerization experiments to be isomers of the same chromophore.

The major isomer P5c was purified from bulk cultures of S2M3 by reversed-phase HPLC; a 180 g cell pellet yielded 60 absorbance units at 369 nm, which corresponds to 128 μg of pure P5c. The high-resolution electron ionization mass spectrum (EI-MS) gave *m/z* 268.2186 (calculated for $C_{20}H_{28}$: *m/z* 268.2191) indicative of loss of one molecule of water from the parent compound retinol (*m/z* 286 [M^+]). From these data and the characteristic UV/VIS spectrum P5c can be identified as anhydroretinol.[7, 12] This was confirmed by analysis of the ^{1}H NMR spectrum (Table 1), which was identical to that reported for synthetic all-*trans*-anhydroretinol.[13] In order to confirm these data and provide direct physical proof for the configurations of the anhydroretinol isomers, we measured the ^{1}H NMR and UV spectra of the four major anhydroretinol isomers obtained upon acid-catalyzed dehydration of retinol.

Table 1. Spectroscopic data of anhydroretinol isomers **4**–**7**.

all-*trans*-AR **4**: ^{1}H NMR ($CDCl_3$): δ = 1.3 (s, 6H; 1-Me_2), 1.51 (t, J = 1.5 Hz, 2H; 2-H_2), 1.92, 1.93, 1.96 (3 × s, each 3H; 5-, 9-, 13-Me), 2.13 (m, 2H; 3-H_2), 5.04 (d, J = 10.4 Hz, 1H; 15-H-*E*), 5.22 (d, J = 17 Hz, 1H; 15-H-*Z*), 5.79 (t, J = 3 Hz, 1H; 4-H), 6.20 (d, J = 11 Hz, 1H; 12-H), 6.39 (d, J = 12.5 Hz, 1H; 7-H), 6.46 (dd, J = 17, 10.4 Hz, 1H; 14-H), 6.45 (d, J = 15 Hz, 1H; 10-H), 6.60 (dd, J = 15, 11 Hz, 1H; 11-H), 6.78 (d, J = 12.5 Hz, 1H; 8-H); UV-VIS (MeOH): λ_{max} (ε) = 270, 348, 369 (125000), 390 nm; CI-MS: *m/z*: 269 [(M + H)$^+$].

(8*Z*)-AR **5**: ^{1}H NMR (CD_3OD): δ = 1.28 (s, 6H; 1-Me_2), 1.50 (t, J = 6 Hz, 2H; 2-H_2), 1.90, 1.92, 2.0 (3 × s, each 3H; 5-, 9-, 13-Me), 2.12 (m, 2H; 3-H_2), 5.04 (d, J = 11 Hz, 1H; 15-H-*E*), 5.24 (d, J = 17 Hz, 1H; 15-H-*Z*), 5.77 (t, J = 4 Hz, 1H; 4-H), 6.24 (d, J = 11 Hz; 12-H), 6.47, (dd, J = 17, 11 Hz, 1H; 14-H), 6.54 (d, J = 12.4 Hz, 1H; 7-H), 6.64 (d, J = 12.4 Hz, 1H; 8-H), 6.68 (dd, J = 15, 11 Hz, 1H; 11-H), 6.90 (d, J = 15 Hz, 1H; 10-H); UV-VIS (MeOH): λ_{max} (ε) = 273, 348, 365 (50000), 385 nm; CI-MS: *m/z*: 269 [(M + H)$^+$].

(12*Z*)-AR **6**: ^{1}H NMR (CD_3OD): δ = 1.30 (s, 6H; 1-Me_2), 1.52 (t, J = 6 Hz, 2H; 2-H_2), 1.89, 1.91, 1.93 (3 × s, each 3H; 5-, 9-, 13-Me), 2.13 (m, 2H; 3-H_2), 5.15 (d, J = 11 Hz, 1H; 15-H-*E*), 5.26 (d, J = 17 Hz, 1H; 15-H-*Z*), 5.78 (t, J = 4 Hz, 1H; 4-H), 6.12 (d, J = 11 Hz, 1H; 12-H), 6.36 (d, J = 15 Hz, 1H; 10-H), 6.40 (d, J = 12 Hz, 1H; 7-H), 6.78 (d, J = 12 Hz, 1H; 8-H), 6.80 (dd, J = 15, 11 Hz, 1H; 11-H), 7.07 (dd, J = 17, 11 Hz, 1H; 14-H); UV-VIS (MeOH): λ_{max} (ε) = 270, 348, 364 (50000), 383 nm; CI-MS: *m/z*: 269 [(M + H)$^+$].

(6*Z*)-AR **7**: ^{1}H NMR (CD_3OD): δ = 1.14 (s, 6H; 1-Me_2), 1.52 (t, J = 6 Hz, 2H; 2-H_2), 1.92, 1.95 (2 × s, each 3H; 9-, 13-Me), 2.08 (s, 3H; 5-Me), 2.21 (m, 2H; 3-H_2), 5.03 (d, J = 11 Hz, 1H; 15-H-*E*), 5.23 (d, J = 17 Hz, 1H; 15-H-*Z*), 5.67 (m, 1H; 4-H), 6.19 (d, J = 11 Hz, 1H; 12-H), 6.39 (d, J = 12 Hz, 1H; 7-H), 6.46 (d, J = 15 Hz, 1H; 10-H), 6.47 (dd, J = 17, 11 Hz, 1H; 14-H), 6.64 (dd, J = 15, 11 Hz, 1H; 11-H), 6.69 (d, J = 12 Hz, 1H; 8-H); UV-VIS (MeOH): λ_{max} (ε) = 270, 347, 364 (75000), 385 nm; CI-MS: *m/z*: 269 [(M + H)$^+$].

Various methods for the dehydration of vitamin A leading to anhydroretinol (10 to 30% yield) are described in the literature.[7, 12, 14] Figure 1 b shows the HPLC profile of synthetic AR isomers. Indeed, the fourth and major peak eluting at 41.2 min, which corresponds to P5c, was identified as all-*trans*-anhydroretinol **4**. The (6*E*) configuration was confirmed by the 10% nuclear Overhauser effect (NOE) observed between 1-Me_2 and 8-H. The chemical shifts of 4-H (δ = 5.79) and 1-Me_2 (δ = 1.3), both downfield compared to the analogous signals of (6*Z*)-*retro*-retinoids (δ = 5.63 and 1.11),[13, 15] provided corroboration.

The first peak eluting at 27.2 min (P5a) was shown to correspond to the (8*Z*) isomer **5** (Table 1). The (8*Z*), (10*E*), and (12*E*) configurations were deduced from the NOEs of –7, 14, and 11% observed for 7-H, 10-H, and 14-H respectively, upon irradiation of 12-H. The (10*E*) configuration was also supported by the observed coupling constant J(10,11) = 15 Hz.

The second compound eluting at 33 min exhibits a ^{1}H NMR spectrum characteristic of the (12*Z*) isomer **6** (Table 1). The (6*E*) configuration derives from the chemical shifts of 1-Me_2 (δ = 1.30) and 4-H (δ = 5.78). The *E* configuration of the C-8 C-9 double bond is evident from the upfield shift of 10-H (δ = 6.36) as compared the analogous signal of the (8*Z*) isomer (δ = 6.90). The (10*E*) configuration derives from the coupling constant J(10,11) = 15 Hz, and the (12*Z*) configuration from the chemical shifts of 12-H (δ = 6.12) and 14-H (δ = 7.07), which are upfield and downfield, respectively, of the corresponding signals (δ = 6.2, 6.46) of the all-*trans* isomer.

The compound eluting at 34.4 min has been characterized as the (6*Z*) isomer **7** based on the upfield chemical shifts of 1-Me_2 and 4-H, and the downfield chemical shift of 5-Me reported for (6*Z*)-*retro*-retinoids.[13, 15] Thus fraction P5b (cf. Fig. 1 a) contains both (12*Z*)- and (6*Z*)-anhydroretinol (**6** and **7**, respectively). (10*Z*)-AR and other possible di-*cis* isomers were not formed in sufficent amounts to be isolated and characterized.

Figure 2 shows the UV/VIS absorption spectra of (8*Z*)-, (12*Z*)-, and (6*Z*)-AR isomers as compared to that of all-*trans*-AR. Their absorption maxima and extinction coefficients are listed in Table 1. Because the compounds decompose slowly when kept dry, the extinction coefficient of each isomer was determined by directly computing the ratios of the integrated peaks from UV absorption and the ratios of the specific radioactivity of [^{3}H]retinol and [^{3}H]AR isomers prepared from [^{3}H]retinol.

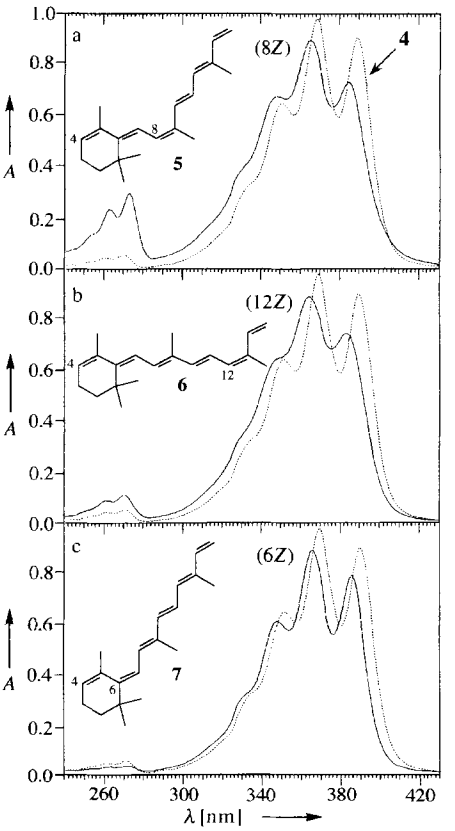


Fig. 2. UV/VIS absorption spectra (photodiode array detector) of (8*Z*)- **5** (a), (12*Z*)- **6** (b), (6*Z*)- **7** (c), and all-*trans*-anhydroretinol **4** (dotted line) in H_2O/CH_3OH 14/86.

 © VCH Verlagsgesellschaft mbH, D-69451 Weinheim, 1994 0570-0833/94/1818-1838 $ 10.00+.25/0

all-*trans*-Anhydroretinol exhibits a weak band for *cis* double bonds at 262 nm ("*cis* band"), a strong band at 369 nm ($\varepsilon = 125000$), and a well-resolved vibronic structure. Isomerization of a double bond is accompanied by a slight blue shift in the λ_{max}, an increase in the intensity of the *cis* band, and a more diffuse vibronic structure. Thus, the (8*Z*) isomer, in which the *cis* double bond is central, exhibits the strongest *cis* band.

Anhydroretinol, a good model for the study of polyenes by absorption spectroscopy,[11, 14] has received increasing attention because of its newly discovered biological role. Its antagonism to 14-HRR suggests that these *retro*-retinoids might function as ligands for cytoplasmic or nuclear receptors.[6] In the insect cell line SF21, AR is synthesized by a cytosolic enzyme with a molecular weight of 41 kDa.[16] Characterization of this enzyme and isolation of 14-HRR and AR binding proteins are currently being pursued.

Experimental Procedure

^{1}H NMR spectra were recorded on a Varian VXR-400 spectrometer in $CDCl_3$ or CD_3OD. The chemical shifts δ are relative to $\delta(CHCl_3) = 7.24$ or $\delta(CH_3OH) = 3.30$. High-resolution EI mass spectra were measured on a JEOL DX-303 HF spectrometer (matrix: perfluorokerosine, PFK). Chemical ionization mass spectra (CIMS) were measured on a NERMAG R1010 spectrometer (carrier gas: methane).

Isolation of anhydroretinol from insect cell culture: Schneider S2M3 cells were grown in Schneider's insect medium supplemented with 10% fetal bovine serum (FBS) or 10% horse serum (Gibco, Life Technologies Inc., Grand Island, NY, USA) in the exponential growth phase at a density of $2-4 \times 10^6$ cells per mL. Cells were treated with 10^{-5} M retinol 12 h prior to harvesting by centrifugation, and the pellets were worked up according to McClean's method [17]. Retinoids present in the acetonitrile/butanol phase were separated with a preparative C_{18} reversed-phase column (Vydac 218 TP, 22 mm × 30 cm; Vydac, Hesperia, CA, USA) with a water/methanol/chloroform gradient (cf. Fig. 1a, 100% H_2O → 100% MeOH → MeOH/$CHCl_3$ 1:1; flow rate 8 mL min); photodiode array detector (Waters 991).

Preparation of anhydroretinol isomers by acid dehydration [7a]: A solution of all-*trans*-retinol (20 mg, Sigma) in absolute ethanol (10 mL) was treated with anhydrous HCl to a final concentration of 0.3 M. After 15 min at room temperature the solution was neutralized by titration with a 10 M sodium hydroxide solution, and diluted with about 5 mL of water. The solution was extracted with hexane, the organic layer was washed with water and concentrated, and the residue was dissolved in methanol. The mixture of anhydroretinol isomers was isolated by preparative HPLC as described above. Further separation was achieved on an analytical C_{18} reversed-phase column by isocratic elution (Vydac 201 TP, 5.4 mm × 30 cm; H_2O/CH_3OH 14:86, flow rate 1 mL min^{-1}).

Received: January 17, 1994
Revised version: June 6, 1994 [Z 6620 IE]
German version: *Angew. Chem.* **1004**, *106*, 1954

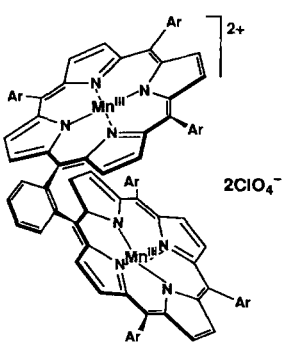
[1] G. Wald, *Science* **1968**, *162*, 230–239.
[2] a) C. Thaller, G. Eichele, *Nature* **1987**, *327*, 625–628; b) M. Wagner, C. Thaller, T. Jessell, G. Eichele, *ibid.* **1990**, *345*, 819–822; S. J. Collins, R. C. Gallo, R. E. Gallagher, *ibid.* **1977**, *270*, 347–349; T. R. Breitman, S. E. Selonick, S. J. Collins, *Proc. Natl. Acad. Sci. USA* **1980**, *77*, 2936–2940.
[3] a) C. Y. David, J. L. Sell, *J. Nutr.* **1983**, *113*, 1914–1919; b) G. Dennert in *The Retinoids, Vol. 2* (Hrsg.: M. B. Sporn, A. B. Roberts, D. W. Goodman), Academic Press, New York, **1984**, pp. 373–390.
[4] J. Buck, G. Ritter, L. Dannecker, V. Katta, B. Chait, U. Hämmerling, *J. Exp. Med.* **1990**, *171*, 1613–1624.
[5] J. Buck, F. Derguini, E. Levi, K. Nakanishi, U. Hammerling, *Science* **1991**, *254*, 1654–1656; F. Derguini, K. Nakanishi, U. Hämmerling, J. Buck, *Biochemistry* **1994**, *33*, 623–628.
[6] J. Buck, F. Grün, F. Derguini, Y. Chen, S. Kimura, N. Noy, U. Hämmerling, *J. Exp. Med.* **1993**, *178*, 675–680.
[7] a) J. R. Edisbury, A. M. Gillam, I. M. Heilbron, R. A. Morton, *Biochem. J.* **1932**, *26*, 1164–1173; b) N. D. Embree, *J. Biol. Chem.* **1939**, *128*, 187–198.
[8] H. J. Palmer, V. M. Mahler, J. J. McCormick, *In Vitro Cell. Dev. Biol.* **1989**, *25*, 1009–1015; T. N. R. Varma, P. Erdody, T. K. Murray, *J. Pharm. Pharmacol.* **1965**, *17*, 474–479.
[9] a) U. Hämmerling, unpublished; b) P. V. Bhat, L. M. Deluca, S. Adamo, I. Akalovsky, C. S. Silverman-Jones, G. L. Peck, *J. Lipid Res.* **1979**, *20*, 357–362.
[10] 11-*cis*-3-Hydroxyretinal is the chromophore in the visual pigment of flies, xanthopsin, whereas *all-trans*- or 13-*cis*-3-hydroxyretinol is bound to their "sensitizing pigment": a) K. Vogt, K. Kirschfeld, *Naturwiss.* **1984**, *71*, 211–213; b) M. Ito, N. Matsuoka, K. Tsukida, T. Seki, *Chem. Pharm. Bull.* **1988**, *36*, 78–86; c) J. Schwemer in *Proc. Yamada Conf. XXI* (Ed.: T. Hara), Yamada Science Foundation, Osaka, Japan, **1988**, pp. 299–304; d) K. Hamdorf, P. Hochstrate, G. Höglund, M. Moser, S. Sperber, P. Schlecht, *J. Comp. Physiol. A* or **1992**, *171*, 601–615.
[11] a) W. Oroshnik, G. Karmas, A. D. Mebane, *J. Am. Chem. Soc.* **1952**, *74*, 295–304; b) R. L. Christensen, B. E. Kohler, *Photochem. Photobiol.* **1973**, *18*, 293–301.
[12] E. M. Shantz, J. D. Cawley, N. D. Embree, *J. Am. Chem. Soc.* **1943**, *65*, 901–906.
[13] W. Vetter, G. Englert, N. Rigassi, U. Schweiter in *Carotenoids* (Ed.: O. Isler), Birkhauser, Basel, **1971**, pp. 204–243.
[14] a) P. E. Blatz, N. Baumgartner, V. Balasubramaniyan V., P. Balasubramaniyan, E. Stedman, *Photochem. Photobiol.* **1971**, *14*, 531–549; b) R. A. Auerbach, M. F. Granville, B. E. Kohler, *Biophys. J.* **1979**, *25*, 443–454.
[15] G. Englert, M. Vecchi M., *J. Chromatogr.* **1982**, *235*, 197–203.
[16] F. Grün, J. Buck, unpublished results.
[17] S. W. McClean, M. E. Rudel, E. G. Gross, J. J. DiGiovani, G. L. Pede, *Clin. Chem. (Winston-Salem NC)* **1982**, *28*, 693–696.

Oxygen Evolution by Oxidation of Water with Manganese Porphyrin Dimers**

Yoshinori Naruta,* Masa-aki Sasayama, and Takao Sasaki

A tetranuclear manganese cluster in the photosystem II (PS II) of higher plants and cyanobacteria catalyzes evolution of oxygen by four-electron oxidation of water.[1, 2] Owing to the instability of preparations of PS II, only a limited amount of information on this cluster is available.[2, 3] Extensive efforts have been made to synthesize *structural* models of water oxidation complex (WOC),[1a, 4–6] but evolution of oxygen by catalytic oxidation of water has never been attained with them.[7] We report herein the catalytic oxidation of water to molecular oxygen with rigidly linked manganese porphyrin dimers.

As a functional model complex, we used the dimanganese complexes **1**–**3** of dimers of triphenylporphyrin (TPP)[8] linked by an *o*-phenylene bridge. Cyclic voltammetry of dimers **1** and **2** in dry acetonitrile showed reversible waves.[10] In an aqueous



1 Ar = 4-*t*BuC$_6$H$_4$
2 Ar = 2,4,6-Me$_3$C$_6$H$_2$
3 Ar = C$_6$F$_5$

[*] Dr. Y. Naruta
Institute for Molecular Science
Myodaiji, Okazaki 444 (Japan)
Telefax: Int. code + (564) 54-2254
M. Sasayama, T. Sasaki
Department of Chemistry, Faculty of Science, Kyoto University

[**] This work was supported by the Japanese Ministry of Education, Science and Culture (Grant-in-Aid for Scientific Research grant nos. 05209214, 05453030, and 05235225.)

acetonitrile solution (5% v/v H_2O in CH_3CN) containing nBu_4NOH, all these Mn complexes showed a similar irreversible discharge current at ≥ 1.2 V (vs. Ag/Ag^+).[11] The anodic oxidation of the aqueous acetonitrile solution without the manganese porphyrin dimers did not evolve oxygen in the potential range up to + 2.3 V (vs. Ag/Ag^+). However, the electrochemical oxidation of a solution containing **2** (1.0 mM) showed oxygen evolution at the potential range + 1.2 – + 2.0 V with a faradaic efficiency of 5–17% (Fig. 1). The other dimanganese complex-

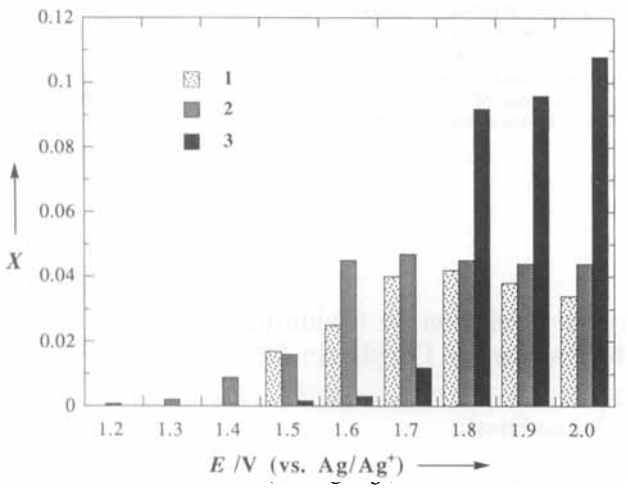


Fig. 1. Evolution of oxygen by catalytic oxidation of water at different anodic potentials [11]. X = mol O_2 per mol catalyst per min.

es, **1** and **3**, also produced O_2 at similar potentials, whereas the corresponding monomeric manganese porphyrin complexes[9] (2.0 mM) did not show O_2 evolution. Of the three dimers **3** showed the highest activity at rather high potential range, and its maximum turnover number (mol O_2/mol catalyst) was 9.2 in the presence of nBu_4NOH. The observed rate of oxygen evolution was proportional to the concentration of the applied complex. These results also indicate that the manganese porphyrin dimers are involved in the rate-determining step of O_2 evolution.

The evolved O_2 was analyzed during the reaction by a mass spectrometer with direct gas introduction through a Teflon membrane.[12] When a solution containing $H_2{}^{16}O$ and $H_2{}^{18}O$ (1:1) and the catalyst **3** underwent reaction at an anodic potential of + 1.8 V (vs. Ag/Ag^+), the isomeric ratio of the evolved O_2 was $^{16}O_2{:}^{16}O,^{18}O{:}^{18}O_2 = 1:2:1$, the same as the expected statistical distribution.[13]

According to the mechanism of this oxygen evolution, two possible electrochemical pathways can be considered. If the reaction proceeds through a two-electron pathway, although this has a higher oxidation potential ($E^0(H_2O/H_2O_2) = 1.78$ V vs. normal hydrogen electrode) than the four-electron oxidation process ($E^0(H_2O/O_2) = 1.23$ V),[14] H_2O_2 is produced. Oxygen could evolve even through this two-electron oxidation, because of the high catalase activity of the applied manganese dimers.[15, 16] To differentiate between these two pathways, we performed the anodic oxidation of the solvent at + 1.8 V for 8 min without any manganese complex, and then added the dimer **3** in the absence of current. Oxygen formation was not detected, and thus the oxygen evolved does not arise from H_2O_2. Independently, we confirmed the absence of H_2O_2 in the reaction mixture by means of a H_2O_2-sensitive electrode after the anodic oxidation of the solvent.

The number of electrons n involved in this reaction was determined by means of a rotating disk electrode. From the Levich plot of the dimer **3**, we obtained $n = 3.7$,[17] which is exactly twice that of the corresponding monomer [MnPFPP].[18] Thus, we can conclude that the O_2 evolution in the present case is based on a *four-electron* oxidation. Clarification of the detailed reaction mechanism is now under way, but since the two-electron oxidation of a $Mn^{III}(OH)$ complex can give the corresponding $Mn^{V}(=O)$,[19] the following mechanism is plausible for the present example: If HO^- ions coordinate to each Mn ion of the dimer inside the cavity, the resultant $Mn^{V}(=O)$ dimer could form a $Mn^{IV}-O-O-Mn^{IV}$ complex,[20] because of the proximity of the Mn ions. The peroxy bridge could be replaced by HO^- ions, and simultaneous decomposition would give O_2 and the Mn^{III} complex.

This is the first demonstration of oxygen evolution by the four-electron oxidation of water with structurally well-defined binuclear manganese complexes. These results are also very interesting in light of theoretical predictions.[21]

Received: June 2, 1994 [Z6988IE]
German version: *Angew. Chem.* **1994**, *106*, 1964

[1] a) G. Renger, *Angew. Chem.* **1987**, *99*, 660–678; *Angew. Chem. Int. Ed. Engl.* **1987**, *26*, 643–660; b) R. J. Debus, *Biochim. Biophys. Acta* **1992**, *1102*, 269–352; c) G. Renger, *Photosynthesis Res.* **1993**, *38*, 229–247. See also a recent Highlight: K. wieghardt, *Angew. Chem.* **1994**, *106*, 765; *Angew. Chem. Int. Ed. Engl.* **1994**, *33*, 725.

[2] K. Sauer, V. K. Yachandra, R. David Britt, M. P. Klein, *Manganese Redox Enzymes* (Ed.: V. L. Pecoraro), VCH, New York, **1992**, pp. 141–175.

[3] G. N. George, R. C. Prince, S. P. Cramer, *Science* **1989**, *243*, 789–791.

[4] K. Wieghardt, *Angew. Chem.* **1989**, *101*, 1179–1198; *Angew. Chem. Int. Ed. Engl.* **1989**, *28*, 1153–1172.

[5] G. Christou, *Acc. Chem. Res.* **1989**, *22*, 328–335.

[6] D. N. Hendrickson, G. Christou, E. A. Schmitt, E. Libby, J. S. Baskin, S. Wang, H.-L. Tsai, J. B. Vincent, P. D. Boyd, J. C. Huffman, K. Folting, Q. Li, W. E. Streib, *J. Am. Chem. Soc.* **1992**, *114*, 2445–2471.

[7] Oxygen evolution with a solid dinuclear manganese complex [7a] or a dispersed manganese oxide [7b] has been reported. However, neither the reaction mechanism nor the reactive complex has been elucidated. a) R. Ramaraj, A. Kira, M. Kaneko, *Angew. Chem.* **1986**, *98*, 824–825; *Angew. Chem. Int. Ed. Engl.* **1986**, *25*, 825–827; b) N. P. Luneva, E. I. Knerelman, V. Ya. Shafirovich, A. E. Shilov, *J. Chem. Soc. Chem. Commun.* **1987**, 1504–1505.

[8] *o*-Phenylene-linked porphyrin dimers **1**–**3** were prepared by the stepwise formation of the macrocycle under Lindsey conditions after major improvement of the synthetic route. Cf. J. S. Lindsey, R. W. Wagner, *J. Org. Chem.* **1989**, *54*, 828–836; H. Meier, Y. Kobuke, S. Kugimiya, *J. Chem. Soc. Chem. Commun.* **1989**, 923–924.

[9] The applied porphyrin monomers corresponding to the dimers **1**–**3** are the manganese complexes of 5,10,15,20-tetrakis(4-*tert*-butylphenyl)-21*H*,23*H*-porphin (*t*BuPP), 5,10,15,20-tetrakis(2,4,6-trimethylphenyl)-21*H*,23*H*-porphin (TMP), and 5,10,15,20-tetrakis(pentafluorophenyl)-21*H*,23*H*-porphin (PFPP), respectively.

[10] All the Mn complexes showed similar cyclic voltammograms in dry acetonitrile (scan rate 100 mVs^{-1}, supporting electrolyte 0.1 M nBu_4NClO_4). $E_{1/2}$ [V] vs. Ag/Ag^+: [Mn*t*BuPP] 0.89, 1.20; [MnTMP] 0.75, 0.94; **1** 0.81, 0.97, 1.30; **2** 0.86, 1.00. Clear reversible waves were not obtained for [MnPFPP] and **3**.

[11] Anodic oxidation was performed potentiostatically under the following conditions: A thermostated cell at 10.0 ± 0.2 °C equipped with Pt gauze working and counter electrodes was filled with an acetonitrile solution containing 1.0×10^{-4} M of the manganese porphyrin dimer (2.0×10^{-4} M for the monomer), 0.1 M nBu_4NClO_4, 5.0×10^{-6} M nBu_4NOH, 20% v/v sulfolane, and 2% v/v H_2O. Evolved oxygen was analyzed by a Clark-type oxygen electrode (YSI-5531).

[12] G. Hoch, B. Kok, *Arch Biochem. Biophys.* **1963**, *101*, 160–170.

[13] When $H_2{}^{18}O$ was used under the same anodic oxidation conditions without the dimer **3**, $^{18}O_2$ was not detected by mass spectrometry.

[14] D. T. Sawyer, *Oxygen Chemistry*, Oxford University Press, New York, **1991**.

[15] Y. Naruta, K. Maruyama, *J. Am. Chem. Soc.* **1991**, *113*, 3595–3596.

[16] Y. Naruta, M. Sasayama, K. Maruyama, *Chem. Lett.* **1992**, 1267–1270.

[17] From the Levich equation, $i_l = \Gamma n \omega^{1/2}$, $\Gamma = 0.62 FA D^{2/3} \nu^{-1/6} C^*$, where i_l and ω denote the limiting current and the angular velocity of the electrode, respectively. Γ is the constant term under the fixed conditions. F is the Faraday constant, A is the surface area (0.0314 cm^2) of the electrode, D is the diffusion

constant, ν is the kinematic viscosity, and C^* is the catalyst concentration (1.0×10^{-3} M). n was determined from the slope of Levich plot $I/n = 1.7 \times 10^{-5}$ A. The kinetic viscosity n was found to be 4.8×10^{-3} cm^{2}s^{-1}, and the diffusion constant $D = 2.4 \times 10^{-5}$ cms^{-1} for the observed solvent system with ferrocene as a standard compound. In consideration of the higher molecular weight of **3**, n and D for **3** should be smaller than those of ferrocene and the actual n should be larger than that estimated.

[18] Under the same conditions the Levich plot of the corresponding monomer [MnPFPP] gave $n = 1.8$.

[19] Similar oxidation of [MnTMP] through a one-electron oxidation process gives the corresponding stable $Mn^{IV}(=O)$ complex, see J. T. Groves, M. K. Stern, *J. Am. Chem. Soc.* **1987**, *109*, 3812–3814; R. S. Czernuszewicz, Y. Oliver Su, M. K. Stern, K. A. Macor, D. Kim, J. T. Groves, T. G. Spiro, *J. Am. Chem. Soc.* **1988**, *110*, 4158–4165.

[20] U. Bossek, T. Weyhermüller, K. Wieghardt, B. Nuber, J. Weiss, *J. Am. Chem. Soc.* **1990**, *112*, 6387–6388.

[21] D. M. Proserpio, R. Hoffmann, G. C. Dismukes, *J. Am. Chem. Soc.* **1992**, *114*, 4374–4382.

$[(C_6H_5)_4P]\,{}^1_\infty[Cu_3I_4]$—The First Compound with a Helical Chain of Face-Sharing Tetrahedra as a Structural Element**

Hans Hartl* and Farbod Mahdjour-Hassan-Abadi

The tremendous structural diversity of iodocuprates(I) $[Cu_xI_y]^{(y-x)-}$ can be explained firstly by the fact that Cu^I can have trigonal-planar as well as tetrahedral coordination in these compounds, and secondly, since in addition to the corner- and edge-sharing of CuI_4 tetrahedra, the unusual face-sharing of tetrahedra is also possible. It was long considered unlikely that MX_4 tetrahedra could be linked through common faces, since the centers of the tetrahedra would be quite close.[1] In undistorted CuI_4 tetrahedra with an average edge length of 4.4 Å the Cu–Cu distance would be only 1.81 Å. In the previously reported face-sharing iodocuprates(I) the Cu atoms are far enough from the centers of the tetrahedra that Cu–Cu distances of 2.45–2.53 Å are found (Cu–Cu distance in metallic copper: 2.56 Å). The first iodocuprates(I) with face-sharing tetrahedra may have been considered exotic exceptions,[2] but now it is apparent that this linkage mode is a special, though not uncommon feature of the structural chemistry of iodocuprates(I). Two, three, and five face-sharing CuI_4 tetrahedra[3] are known, as well as endless chains of face-sharing tetrahedra. In $[(C_2H_5)_4N]\,{}^1_\infty[Cu_2I_3]$ and $[(C_3H_7)_4N]\,{}^1_\infty[Cu_3I_4]$ units of two and three face-sharing CuI_4 tetrahedra, respectively, are linked through common edges to form chains.[3, 4] Besides the examples among the iodocuprates(I) only two anions with face-sharing MX_4 tetrahedra are known: heptabromopentacuprate(I) $[Cu_5Br_7]^{2-}$[5] and the dinuclear pentathiolatodicobaltate $[Co_2(SC_3H_7)_5]^-$.[6]

Scientists in various fields and even artists have puzzled over the linkage of tetrahedra through common faces. For example, a helical chain of face-sharing tetrahedra was described by A. H. Boerkijk[7] and by Buckminster-Fuller,[8] who named it a "tetrahelix" (see Fig. 1). In accordance with quasi-periodic structures this chain was called a "Bernal spiral", since it has an irrational twist angle (vide infra) and thus an infinite translation period in the direction of the chain. A few years ago band structure calculations for hypothetical compounds, including CuI, with this helical structure were conducted.[9] But an actual compound with this kind of tetrahedron chain was not known at that time. We were thus even more surprised when we found that the CuI_4 tetrahedra of the anion in $[(C_6H_5)_4P]\,{}^1_\infty[Cu_3I_4]$ occur in the form of a helix of face-sharing tetrahedra.

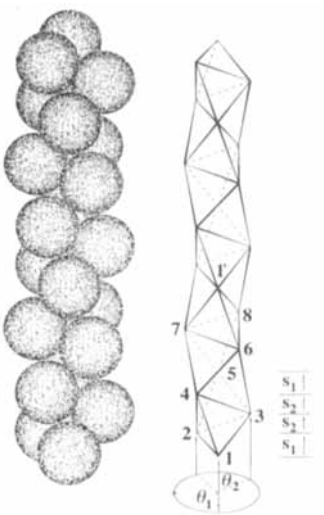


Fig. 1. Helix of iodine tetrahedra in $[(C_6H_5)_4P]\,{}^1_\infty[Cu_3I_4]$. Left: Sphere model. Right: Polyhedra representation; the twist angles θ_1 and θ_2 are 138.2 and 131.8°, respectively; the pitch parameters s_1 and s_2 have values of 0.348 and 0.309, respectively (for details see text).

The construction of the helix of tetrahedra can be described as follows (Fig. 1): If a vertex of a tetrahedron (in this case an iodine atom) is designated as the helical unit, then the other vertices are found by rotation about the axis of the chain by the twist angle θ and subsequent translation in the direction of the chain axis by $s \times$ edge length of the tetrahedron. In the ideal helix of tetrahedra the pitch parameter s has the value 0.3162. The twist angle θ, 131.81....°, is irrational, in other words, the helix does not repeat itself upon translation in the direction of the chain.[9]

In crystalline $[(C_6H_5)_4P]\,{}^1_\infty[Cu_3I_4]$ the chain achieves the translationally identical arrangement after eight turns (eight tetrahedra). This periodicity is possible owing to two different twist angles $\theta_1 = 138.2$ and $\theta_2 = 131.8°$ (average: 135°). The corresponding pitches of 1.533 and 1.359 Å and the average I–I edge length of 4.40 Å imply pitch parameters $s_1 = 0.348$ and $s_2 = 0.309$, respectively. The arrangement in the chain has the order $\ldots\theta_1,\theta_2,\theta_2,\theta_1$ with $\ldots s_1,s_2,s_2,s_1\ldots$.

Complete occupancy of the centers of the iodine tetrahedra with Cu^I would result in unrealistically short Cu–Cu distances. Thus in the COOP calculations (COOP = crystal overlap orbital population) for the hypothetical helix of CuI tetrahedra the Cu–I distances were set arbitrarily at 3.30 Å, and as a result the Cu–Cu distances increased to 2.20 Å, which is still short.[9] In the $\,{}^1_\infty[Cu_3I_4^-]$ helix this distance problem is solved by the occupancy of four centers of the iodine tetrahedra by only three Cu^I ions. The three copper atoms are distributed over the four centers of the tetrahedra and the centers of the face-sharing triangles such that realistic Cu–Cu distances of roughly 2.30 Å result.

X-ray structural investigations of $[(C_6H_5)_4P]\,{}^1_\infty[Cu_3I_4]$ at 22 and −145 °C (crystal 1) and at −140 °C (crystal 2)[10] showed that the occupancy parameters for the individual split atom positions are temperature dependent. At room temperature the Cu atoms Cu1, Cu2 had occupancies at the centers of the tetrahedra of 0.71(2) and 0.44(2), respectively, and the Cu atoms Cu3, Cu4, Cu5 occupancies at the centers of the triangles of 0.17(2), 0.19(2), and 0.06(1), respectively. When the crystal was cooled slowly to −145 °C, the occupancy parameters changed: Cu1, Cu2, and Cu3 were 0.50(2), 0.53(2), and 0.39(2), respec-

[*] Prof. Dr. H. Hartl, Dr. F. Mahdjour-Hassan-Abadi
Institut für Anorganische und Analytische Chemie
der Freien Universität
Fabeckstrasse 34/36, D-14195 Berlin (FRG)
Telefax: Int. code + (30)838-2424

[**] Synthesis and Structural Investigations of Iodocuprates(I), Part 16. This work was supported by the Deutsche Forschungsgemeinschaft and the Fonds der Chemischen Industrie. We thank Prof. Dr. Roald Hoffmann for a valuable tip and Dipl.-Chem. F. Schröder for conducting the DSC measurements. Part 15: M. Hoyer, H. Hartl, *Z. Anorg. Allg. Chem.* **1992**, *612*, 45–50.

tively, and positions Cu4 and Cu5 were no longer occupied. When crystal 2 was cooled rapidly to $-140\,^{\circ}C$, occupancy parameters for Cu1, Cu2, Cu3, and Cu4 of 0.60(1), 0.45(1), 0.36(1), and 0.06(1), respectively, were found. In this case position Cu5 remained unoccupied. The distribution of Cu^{I} in crystal 2 can be considered as a frozen intermediate of the high- and low-temperature structures of crystal 1.

The arrangement of the Cu^{I} ions (Fig. 2) and their temperature factors at room temperature are indicative of great mobility within the chain. The Cu^{I} ions change positions by moving through the shared faces of the coordination tetrahedra to the unoccupied center of a neighboring tetrahedron. This hypothesis is supported by the specific conductivity in the chain direction of roughly $10^{-7}\,S\,cm^{-1}$, which is greater than that perpendicular by a factor of 10^{3}.[11] On cooling, the conductivity decreases continuously and jumps at $-100\,^{\circ}C$. Differential thermal analysis and differential scanning calorimetry both show a reversible thermal process at $-100(\pm 2)\,^{\circ}C$, which can be interpreted as the freezing/thawing of the Cu^{I} motion ($\Delta H = \pm 0.21\,kJ\,mol^{-1}$; exothermic on cooling).

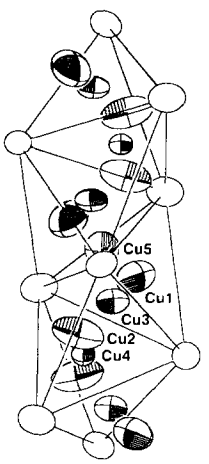


Fig. 2. Section of the helix of tetrahedra $^{1}_{\infty}[Cu_3I_4^-]$ at room temperature. (ORTEP plot at the 50% probability level; Cu atoms: hatched vibrational ellipsoids; I atoms: outlines of the vibrational ellipsoids.) On slow cooling to $-145\,^{\circ}C$ (crystal 1) only positions Cu1, Cu2, and Cu3 are occupied; on rapid cooling to $-140\,^{\circ}C$ (crystal 2) positions Cu1, Cu2, Cu3, and Cu4 are occupied. The Cu–I distances range from 2.417(2) to 3.09(1) Å at room temperature and from 2.525(6) to 3.216(8) Å at lower temperatures.

The individual $^{1}_{\infty}[Cu_3I_4^-]$ chains are chiral. In the crystal the chains are separated by the tetraphenylphosphonium ions and arranged in a rod packing parallel to the [100] direction. A racemic mixture of chains is required by symmetry (space group *Ccca*).

A definite answer to the question of why certain cations lead to specific types of iodocuprates(I) has not yet been possible. We can also not explain why tetraphenylphosphonium ions are accompanied by the formation of the unusual helical tetrahedron chains, whereas anions having the same composition form $[Cu_3I_4^-]$ chains with other linkage modes when the cation is methyltriphenylphosphonium, tetrapropylammonium, or bis(formamidium).[12]

Experimental Procedure

A mixture of tetraphenylphosphonium iodide (1.16 g, 2.5 mmol), iodine (1.27 g, 2.5 mmol), and Cu powder (1.27 g, 5 mmol) was heated in anhydrous acetone (50 mL) under a nitrogen atmosphere until the solution turned pale yellow and was filtered while hot. The cooled solution provided white, needle-shaped crystals with the composition $[(C_6H_5)_4P][Cu_3I_4]$. M.p. 254–256 °C. When the filtrate was allowed to stand for an extended time or petroleum ether was added, white flakes or prismatic crystals formed with the composition $[(C_6H_5)_4P][CuI_2]$-A and -B, respectively [13]. M.p. 210 °C.

Received: March 24, 1994 [Z 6793 IE]
German version: *Angew. Chem.* **1994**, *106*, 1929

[1] A. F. Wells, *Structural Inorganic Chemistry*, 5th ed., Clarendon, Oxford, **1984**, p. 191.
[2] H. Hartl, F. Mahdjour-Hassan-Abadi, *Angew. Chem.* **1981**, *93*, 804–805; *Angew. Chem. Int. Ed. Engl.* **1981**, *20*, 772–773.
[3] K. P. Bigalke, A. Hans, H. Hartl, *Z. Anorg. Allg. Chem.* **1988**, *563*, 96–104; H. Hartl, *Angew. Chem.* **1987**, *99*, 925–926; *Angew. Chem. Int. Ed. Engl.* **1987**, *26*, 927–928; H. Hartl, F. Mahdjour-Hassan-Abadi, *ibid.* **1984**, *96*, 359–360 and **1984**, *23*, 378–379.
[4] H. Hartl, F. Mahdjour-Hassan-Abadi, *Z. Naturforsch. B* **1984**, *39*, 149–156.
[5] S. Andersson, S. Jagner, *J. Crystallogr. Spectrosc. Res.* **1988**, *18*, 591.
[6] G. Henkel, S. Weissgräber, *Angew. Chem.* **1992**, *104*, 1382–1383; *Angew. Chem. Int. Ed. Engl.* **1992**, *31*, 1368–1369.
[7] A. H. Boerdijk, *Philips Res. Rep.* **1952**, *7*, 303–313.
[8] R. Buckminster-Fuller, *Synergetics*, 1st ed. (paperback), MacMillan, New York, **1982**, p. 520–522.
[9] C. Zheng, R. Hoffmann, D. R. Nelson, *J. Am. Chem. Soc.* **1990**, *112*, 3784–3791, and references therein for the helix of tetrahedra.
[10] Crystal structure data for $[(C_6H_5)_4P]^{1}_{\infty}[Cu_3I_4]$: $M = 1037.6$, orthorhombic, *Ccca*. Crystal 1: $T = -145$ and $20\,^{\circ}C$ (data for $20\,^{\circ}C$ in square brackets), $a = 11.559(3)$ [11.567(6)], $b = 20.917(4)$ [21.112(7)], $c = 22.983(9)$ [23.319(6)] Å, $V = 5556.8$ [5694.6] Å^3, $\rho_{calcd} = 2.48$ [2.42] g cm^{-3}; Enraf-Nonius CAD-4 four-circle diffractometer, $\omega/2\theta$ scans, $Mo_{K\alpha}$ radiation/graphite monochromator, $2\theta = 40$ [45]°, 1296 [1791] symmetry-independent reflections, of which 215 [454] had $I < 2\sigma(I)$; 165 [173] refined parameters (Cu5 isotropic, all other atoms anisotropic, no H atoms), isotropic extinction correction, absorption correction DIFABS [14], $R = 0.048$ [0.054] at uniform weights. Crystal 2: $T = -140\,^{\circ}C$, $a = 11.567(2)$, $b = 20.930(3)$, $c = 22.991(3)$ Å, $V = 5566.0$ Å^3, $\rho_{calcd} = 2.48$ g cm^{-3}; Enraf-Nonius CAD-4 four-circle diffractometer, $\omega/2\theta$ scans, $Mo_{K\alpha}$ radiation/graphite monochromator, $2\theta = 50°$, 1829 symmetry-independent reflections, of which 624 had $I < 3\sigma(I)$; 168 refined parameters (Cu4 isotropic, all other atoms anisotropic, no H atoms), isotropic extinction correction, absorption correction DIFABS [14], $R = 0.058$ at uniform weights. Further details of the crystal structure investigation may be obtained from the Fachinformationszentrum Karlsruhe, D-76344 Eggenstein-Leopoldshafen (FRG) on quoting the depository number CSD-58250.
[11] Direct current on single crystals, contact by means of a conducting paste (Hydrokollack), Cu electrodes.
[12] R. Frydrych, T. Muschter, I. Brüdgam, H. Hartl, *Z. Naturforsch. B* **1989**, *45*, 679–688.
[13] H. Hartl, I. Brüdgam, F. Mahdjour-Hassan-Abadi, *Z. Naturforsch. B* **1985**, *40*, 1032–1039.
[14] N. Walker, D. Stuart, *Acta Crystallogr. Sect. A* **1982**, *39*, 158–166.

Asymmetric Synthesis of Biaryls by Intramolecular Oxidative Couplings of Cyanocuprate Intermediates**

Bruce H. Lipshutz,* Frank Kayser, and Zi-Ping Liu

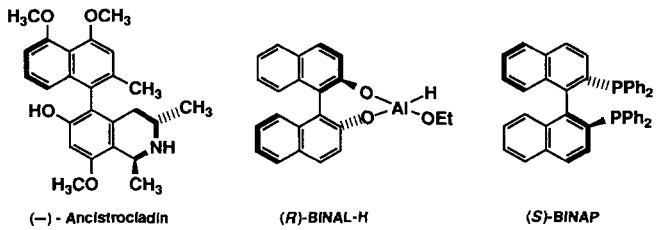
Dedicated to Professor Manfred Schlosser on the occasion of his 60th birthday

The biaryl nucleus is a key subunit associated with many natural products[1] (e.g., steganone, ancistrocladin, etc.) and forms the basis of several nonracemic reagents (e.g., BINAL-H, BINAP, etc.) of extraordinary value in synthetic chemistry (Scheme 1).[2] Owing to the substitution pattern on the ring(s) or other restraints, hindered rotation about the adjoining C–C bond gives rise to the stereochemical feature known as atropisomerism. Given the importance of this structural type, there are

[*] Prof. B. H. Lipshutz, Dr. F. Kayser, Dr. Z.-P. Liu
Department of Chemistry, University of California
Santa Barbara, CA 93106 (USA)
Telefax: Int. code + (805) 893-4120

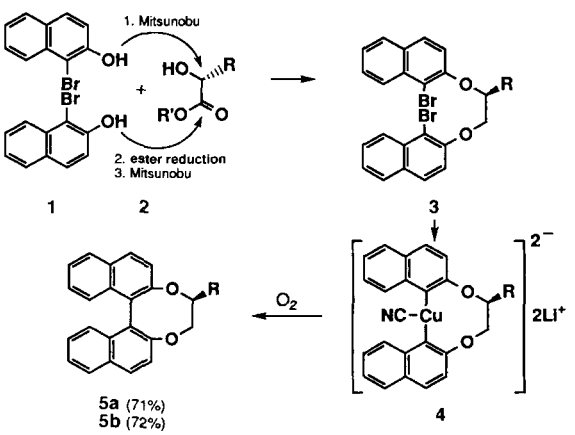
[**] This research was supported by the National Science Foundation (CHE-93-03883) and the Deutsche Forschungsgemeinschaft (fellowship to F. K.). We warmly thank Prof. K. B. Sharpless for a generous gift of nonracemic **14b** used in this study.

relatively few chemical methods that directly yield nonracemic biaryls.[3] Some rely on intermolecular coupling of organometallic compounds,[4] while others are based on intramolecular bond formation by the traditional Ullmann coupling.[5] Varying levels of generality and stereocontrol are observed. We now describe an experimentally straightforward, general method, which affords nonracemic biaryls with virtually complete stereoinduction.



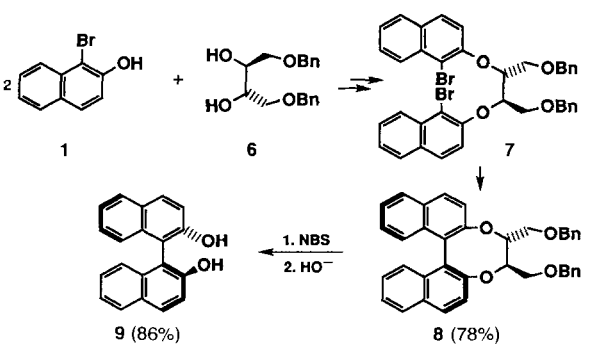
Scheme 1. Examples of binaphthyl derivatives.

In our approach to the well-known 2,2′-binaphthol system,[6] inexpensive 1-bromo-2-naphthol (**1**) was converted to dibromide **3a** with lactic acid ester **2a** (R′ = Me). Treatment of **3a** with *t*BuLi[7] followed by addition of solubilized CuCN[8] presumably led to formation in situ of a higher order cyanocuprate **4a**,[9] which produced the binaphthyl **5a** upon exposure to oxygen.[10] A ^{1}H NMR analysis (500 MHz) revealed an 83:17 ratio



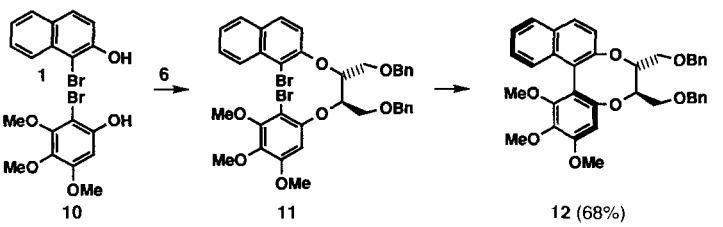
2-**5** : **a**, R = Me; **b**, R = Ph

of diastereomers (66% *de*). With the mandelic acid derivative **3b**, **5b** was obtained with 80–90% *de*. To increase the *gauche* interaction(s) assumed to be responsible for the induction,[11]

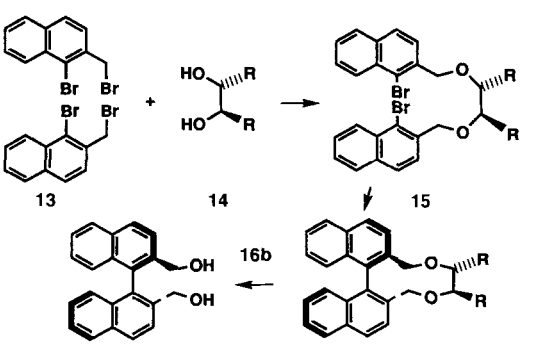


tartaric acid was converted to diol **6**. Consecutive Mitsunobu reactions of **6** with **1** yielded **7**.[12] Treatment of **7** in an analogous procedure to that used for **3** resulted in formation of a single binaphthyl derivative **8**. Removal of the tether could be accomplished in a one-pot process, by double benzylic oxidation with *N*-bromosuccinimide (NBS) followed by addition of aqueous KOH. (*S*)-2,2′-Binaphthol (**9**) was thus obtained directly. The identity of the product was confirmed by comparison with authentic material.[13]

In an identical procedure, linkage of **1** and **10** with tether **6** provided the mixed dibromide **11**. Dilithiation,[7] cyanocuprate formation, and oxidation of **11** at 0 °C afforded the nonracemic unsymmetrical biaryl **12**, again, as a single product (by NMR spectroscopy).



The method applies equally well to 2,2′-C-substituted binaphthyls such as **17**. In these cases, the simpler, more readily available nonracemic vicinal diols **14** served as tethers[14] in the formation of dibromodiethers **15** from **13** (2 equiv). Intramolecular biaryl coupling led in each case to a single diastereomer **16**, even though a ten- rather than an eight-membered ring was formed (cf. **16** vs. **8**).[15]

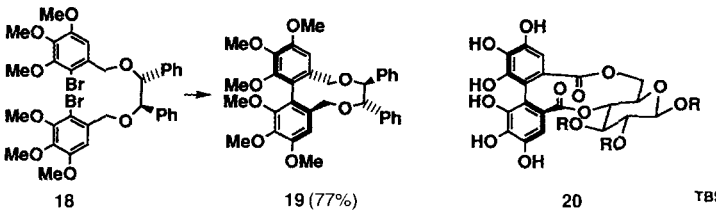


14-**16** : **a**, R = Me; **b**, R = Ph

Removal of the tether in **16b** was best effected by catalytic hydrogenation in HOAc over Pd on charcoal at room temperature. The resulting diol **17** was thus obtained in 90% yield. The specific rotation of the product compared quite favorably with the reported value.[16]

Finally, this method appears well-suited for use in the synthesis of the biaryl portion in several natural products of current interest, such as vancomycin,[17a] the michellamines,[17b] and the ellagitannins (e.g., tellimagrandin II (**20**), R = 3,4,5-trihydroxybenzoyl).[17c] A step towards target **20**[18] was achieved by subjecting dibromodiether **18** to cuprate-induced coupling. Biaryl **19** was obtained in 77% yield as the only observable isomer.[19]

In summary, a powerful new method for controlling axial chirality in numerous biaryl systems has been developed. This



18 19 (77%) 20

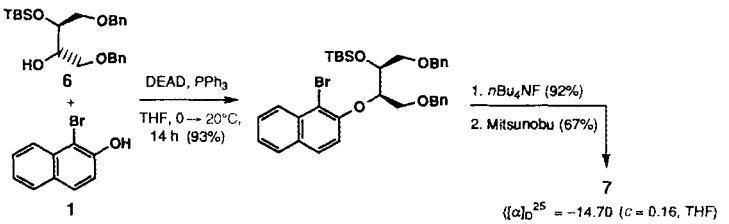
proceeds with oxidation of intramolecularly constructed cyanocuprates. The aryl bromide precursors are readily available; the nonracemic tethers are derived from inexpensive members of the "chiral pool"; and the couplings take place, unlike their intermolecular counterparts,[20] at practical temperatures and are thus expected to be more amenable to scale-up.

Experimental Procedure

16b: Copper cyanide (180 mg, 2.0 mmol) was placed in an oven- and flame-dried three-necked round-bottom flask (100 mL) equipped with a T-top (for argon/vacuum), a thermometer adapter fitted with a gas dispersion tube, and a rubber septum. The flask was once again gently dried with a heat gun under vacuum and allowed to cool to room temperature under argon. THF (35 mL) was added, and the resulting suspension cooled to $-78\,^{\circ}C$. In a round-bottom flask (50 mL), dibromodiether **15b** (1.31 g, 2.0 mmol) was dissolved in THF (35 mL). The flask was cooled to $-78\,^{\circ}C$, and 4.2 equiv of *tert*-butyllithium (4.98 mL, 8.4 mmol, 1.7 M in pentane) added dropwise to give a clear yellow solution. The reaction mixture was stirred at this temperature for 0.5 h. The dilithium compound was transferred with a cannula to the flask containing the CuCN suspension. The mixture was warmed to $-40\,^{\circ}C$ with gentle stirring. A clear yellow solution of the higher order cuprate was obtained. This was recooled to $-78\,^{\circ}C$. The argon flow was then stopped and dry oxygen (passed through a trap at $-78\,^{\circ}C$) was bubbled through the reaction mixture for 30 min, whereupon the solution turned dark. The mixture was allowed to warm to $0\,^{\circ}C$, and the oxygen flow was continued for 1.5 h. The reaction was then quenched with a solution of methanol and concentrated aqueous $NaHSO_3$ (2 mL). The mixture was allowed to warm to room temperature and poured into a solution of 10% NH_3 in concentrated NH_4Cl (100 mL). After it had been stirred for 0.5 h, the organic layer was separated. The aqueous phase was extracted three times with ether, and the combined extracts were subsequently washed with 5% HCl, saturated $NaHCO_3$, and brine. The organic phase was dried over $MgSO_4$ and filtered. The solvent was removed under reduced pressure. Chromatography of the crude mixture on silica gel (hexane/ethyl acetate 90/10) gave **16b** as a white crystalline product (720 mg, 73%). 0.48; IR (KBr): $\tilde{\nu}$ = 3030, 3020, 2835, 1455, 1340, 1090, 1070, 1030, 820, 750, 695 cm^{-1}; ^1H NMR (500 MHz, $CDCl_3$): δ = 4.35 (s, 2H, 2 × CH), 4.58 und 4.69 (AB, 4H, J = 10.7 Hz, 2 × CH_2), 6.88–7.03 (m, 12H, Ar-H), 7.17 (t, 2H, J = 7.6 Hz, Ar-H), 7.42 (t, 2H, J = 7.3 Hz, Ar-H), 7.90 (d, 2H, J = 8.4 Hz, Ar-H), 7.94 (d, 2H, J 8.4 Hz, Ar-H), 8.07 (d, 2H, J = 8.5 Hz, Ar-H); ^{13}C NMR (50 MHz, $CDCl_3$): δ = 70.5, 87.3, 125.8, 126.3, 126.9, 127.2, 127.3, 127.8, 127.9, 128.4, 133.0, 133.5, 134.3, 136.6, 139.3; EI-MS: *m/z* (%): 386 (6), 281 (23), 280 (100), 279(73), 276 (15), 265 (11); CI-MS (CH_4): *m/z* (%): 493 (1.5), 387 (10), 325 (15), 298 (22), 297 (90), 296 (19), 295 (31), 281 (56), 280 (44), 267 (99), 197 (100), 107 (71); high-resolution EI-MS: $C_{36}H_{29}O_2$ (M +1): calcd: 493.21674, found: 493.21676.

Received: April 14, 1994 [Z 6847 IE]
German version: *Angew. Chem.* **1994**, *106*, 1962

[1] a) G. Bringmann, R. Walter, R. Weirich, *Angew. Chem.* **1990**, *102*, 1006; *Angew. Chem. Int. Ed. Engl.* **1990**, *29*, 977; b) H.-J. Altenbach in *Organic Synthesis Highlights, Vol. 1* (Ed.: J. Mulzer), VCH, Weinheim, **1991**, p. 181.
[2] R. Noyori, *Chem. Rev.* **1989**, *18*, 187; S. Inoue, H. P. Takaya, K. Tani, S. Otsuka, T. Sato, R. Noyori, *J. Am. Chem. Soc.* **1990**, *112*, 4897.
[3] D. W. Knight in *Comprehensive Organic Synthesis, Vol. 3* (Ed.: B. Trost), Pergamon, New York, **1991**, p. 481.
[4] T. D. Nelson, A. I. Meyers, *J. Org. Chem.* **1994**, *59*, 2655; H. Moorlag, A. I. Meyers, *Tetrahedron Lett.* **1993**, *34*, 6989; K. Tomioka, M. Shindo, K. Koga, *ibid.* **1993**, *34*, 681; T. Hayashi, K. Hayashizaki, T. Kiyoi, Y. Ito, *J. Am. Chem. Soc.* **1988**, *110*, 8153; A. I. Meyers, K. A. Lutomski, *ibid.* **1982**, *104*, 879; M. Shindo, K. Koga, K. Tomioka, *ibid.* **1992**, *114*, 8732; ref. [1a]; A. I. Meyers, M. Reumann, *Tetrahedron* **1985**, *41*, 837.
[5] M. Takahashi, T. Ogiku, K. Okamura, T. Da-te, H. Ohmizu, K. Kondo, T. Iwasaki, *J. Chem. Soc. Perkin Trans. 1* **1993**, 1473; S. Miyano, H. Fukushima, S. Handa, H. Ito, H. Hashimoto, *Bull. Chem. Soc. Jpn.* **1988**, *61*, 3249; S. Miyano, S. Handa, K. Shimizu, K. Tagami, H. Hashimoto, *ibid.* **1984**, *57*, 1943.
[6] C. Rosini, L. Franzini, A. Raffaelli, P. Salvadori, *Synthesis* **1992**, 503.
[7] Only 1 equiv of *t*BuLi per aryl bromide unit is needed to effect dilithiation when performed at $-100\,^{\circ}C$.
[8] P. Knochel, M. C. P. Yeh, S. C. Berk, J. Talbert, *J. Org. Chem.* **1988**, *53*, 2390.
[9] B. H. Lipshutz, S. Sengupta, *Org. React.* **1992**, *41*, 325.
[10] All new compounds gave satisfactory IR, NMR, MS, and HRMS data.
[11] Further discussion is deferred to the full account of this work.
[12] The tether was attached as follows (TBS = *tert*-butyldimethylsilyl, Bn = benzyl, DEAD = diethyl azodicarboxylate):



[13] The isolated binaphthol **9** showed an $[\alpha]_D^{25}$ of -31 (c = 0.0125, THF). This confirms the sense of chiral induction in the cyclization (i.e., that the (*S*) isomer was formed). A scale-up of this reaction has not yet been attempted.
[14] Diol **14a** is commercially available, and **14b** can be obtained by Sharpless asymmetric dihydroxylation; cf. G. A. Crispino, K.-S. Jeong, H. C. Kolb, Z.-M. Wang, D. Xu, K. B. Sharpless, *J. Org. Chem.* **1993**, *58*, 3785.
[15] It should be noted that the sense of the asymmetric induction in the synthesis of **16** is opposite to that observed in that of **8**. This observation is in accord with the conformational requirements of an eight- versus a ten-membered ring [11].
[16] a) Observed $[\alpha]_{546}^{23}$ = + 82 (c = 0.056, THF); ref. [16b] $[\alpha]_{546}^{23}$ = + 86 (c = 1.0, acetone); b) S. Miyano, M. Tobita, H. Hashimoto, *Bull. Chem. Soc. Jpn.* **1981**, *54*, 3522.
[17] a) D. A. Evans, C. J. Dinsonore, *Tetrahedron Lett.* **1993**, *34*, 6029; J. Zhu, R. Beugelmans, A. Bigot, G. P. Singh, M. Bois-Choussy, *ibid.* **1993**, *34*, 7401; b) G. Bringmann, R. Zagst, M. Schäffer, Y. F. Hallock, J. H. Cardellina, M. R. Boyd, *Angew. Chem.* **1993**, *105*, 1242; *Angew. Chem. Int. Ed. Engl.* **1993**, *32*, 1190; c) D. E. Berry, L. MacKenzie, E. A. Shultis, J. A. Chan, S. M. Hecht, *J. Org. Chem.* **1992**, *57*, 420.
[18] K. S. Feldman, S. M. Ensel, R. D. Minard, *J. Am. Chem. Soc.* **1994**, *116*, 1742; T. D. Nelson, A. I. Meyers, *J. Org. Chem.* **1994**, *59*, 2577.
[19] B. H. Lipshutz, Z. Liu, F. Kayser, *Tetrahedron Lett.*, **1994**, *35*, 5567.
[20] B. H. Lipshutz, K. Siegmann, E. Garcia, F. Kayser, *J. Am. Chem. Soc.* **1993**, *115*, 9276.

The Trehalase Inhibitor Salbostatin, a Novel Metabolite from *Streptomyces albus*, ATCC 21838

László Vértesy,* Hans-Wolfram Fehlhaber, and Arno Schulz

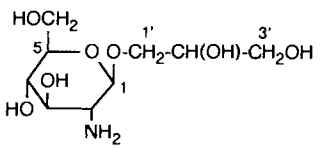
Although microbial cultures constitute an enormously rich source of the most varied secondary metabolites, there have till now been very few systematic studies of the metabolic products of any given organism. Usually, only those compounds that respond to specific biological or biochemical screening tests are isolated and characterized. So-called chemical screening has recently also come into use,[1] but this, too, yields only a random selection of metabolites.

High performance mutants of *Streptomyces albus*, ATCC 21838, are used for production of the polyether antibiotic salinomycin,[2] which is a coccidiostatic. Industrially, feed antibiotics are often not applied in a pure form, but as a dried

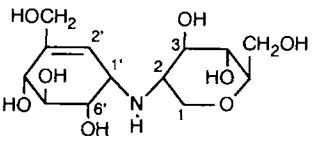
[*] Dr. L. Vértesy, Dr. H.-W. Fehlhaber
Allgemeine Pharma Forschung der Hoechst AG
D-65926 Frankfurt am Main (FRG)
Telefax: Int. code + (69) 305-16354
Dr. A. Schulz
Forschung Biochemie der AgrEvo, Frankfurt am Main

fermentation material—after digestibility has been checked—because of the good specific yields thus attained. In order to investigate the compounds produced by this strain, and to obtain a better understanding of its secondary metabolism, we studied the culture filtrate from a long-term fermentation (twelve days) of a salinomycin overproducer. The strain was grown in submerged culture, on a nutrient-rich, complex medium. Salinomycin and its by-products[2] were identified in a butanol extract of this medium, along with small amounts of $\Delta^{22(29)}$-hopene and several other hopanoids. The antibiotic elaiophylin,[3] which is produced by the wildtype strain ATCC 21838 at levels of up to 3%, was also detected at a concentration of less than 0.01% of the dry product.

The non-extractable residue was separated on an ion exchanger: the neutral fraction contained primarily α,α'-trehalose; nucleotide bases, mainly cytidine, and two novel natural products were isolated from the basic fraction. One of these was identified as 2',3'-dihydroxypropyl-(2-amino-2-deoxy)-β-D-*gluco*pyranoside (**1**) from its NMR data and from the mass spectrometric fragmentation of its peracetyl derivative. The physiological significance of **1** is unclear. A capsule biopolymer of *Actinobacillus pleuropneumoniae* that contains the phosphorylated *N*-acetyl derivative of **1** was recently described;[4] synthetically produced fatty acid esters of **1** displayed immunological activity.[4b]

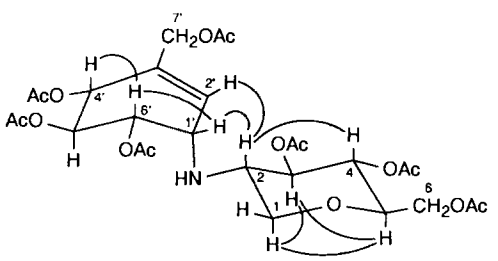


1



2

The main component of the basic fraction, which was present at a concentration of 1 mg L^{-1} in the culture supernatant, was assigned the structure **2**: The NMR spectra of **2** and of its peracetyl derivative **2'** (Scheme 1) were completely analyzed by H,H-correlation NMR spectroscopy (Table 1); selective NOE measurements (see Scheme 1) and high resolution mass spectrometry were also performed. We have named this unusual



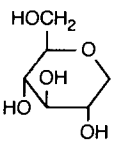
Scheme 1. Structure of the peracetyl derivative **2'**. The curved lines indicate the protons which gave rise to positive NOEs.

pseudodisaccharide salbostatin;[5] it consists of valienamine linked to 2-amino-1,5-anhydro-2-deoxyglucitol, which till now had not been reported as a natural product. Salbostatin has a specific rotation of $[\alpha]_D = +115$ and therefore, given the rotation values of valienamine (+ 48.6)[6a] and of 1,5-anhydroglucitol **3** (+ 42.3),[6b] which is isosteric to the second part of the molecule, presumably has the D-configuration shown in **2**.

Table 1. ^{1}H NMR data for salbostatin **2** and the peracetyl derivative **2'**.

Proton	δ	**2** in [D_6]DMSO patern (J/Hz)	δ	**2'** in $CDCl_3$ pattern (J/Hz)
1-H_{ax}	2.92	dd (11, 11)	3.13	dd (11, 11)
1-$H_{äq}$	3.87	dd (4.6, 11)	4.07	dd (5, 11)
2-H	2.59	ddd (4.6, 10, 11)	2.88	ddd (5, 9.5, 11)
3-H	3.01–3.06	m	4.86	dd (9.5, 9.5)
4-H			4.93	dd (9.5, 9.5)
5-H			3.53	ddd (2, 5, 9.5)
6-H_a	3.39	dd (5.8, 11.5)	4.09	dd (2, 12)
6-H_b	3.64	dd (5.6, 11.5)	4.18	dd (5, 12)
1'-H	3.17	dd (3, 5)	3.64	dd (5, 5)
2'-H	5.86	d (3.2)	5.86	d (5)
4'-H	3.69	d (5)	5.51	d (6.5)
5'-H	3.42	dd (5, 9)	5.46	dd (6.5, 10)
6'-H	3.30	dd (5, 9)	4.96	dd (4, 10)
7'-H_a	3.94	d (14)	4.36	d (13)
7'-H_b	4.00	d (14)	4.62	d (13)

Although the 1,5-anhydroglucitol **3** has been found in several organisms,[7] nothing is known about the function of this class of compounds. Valienamine is known as a component of the validamycin-type aminoglycoside antibiotics,[8a] and of α-glucosidase inhibitors. The latter are of pharmaceutical interest, because of their inhibitory action on intestinal enzymes.[8b]



3

Salbostatin (**2**) shows no antibiotic activity; it does not inhibit the enzymes saccharase and maltase (EC 3.2.1.26, EC 3.2.1.20, from the mucus of porcine small intestine), and it inhibits aldose reductase (EC 1.1.1.21, from murine liver) only weakly ($IC_{50} = 0.68$ mM L^{-1}).[9] However, it is an effective inhibitor of trehalase (EC 3.2.1.28, from porcine kidneys), with an inhibition constant $K_i = 1.8 \times 10^{-7}$ M. The inhibition is competitive with respect to trehalose. Since trehalose is the most important storage and transport form of glucose in many insects and fungi, and in several pollen bodies, trehalase inhibitors are sought-after compounds in the plant protection industry. Apart from the validamycins, known trehalase inhibitors include trehalostatin,[10] trehazolin,[10] and suidatrestin.[11] Salbostatin **2** could serve as a new lead structure for the design and production of novel active compounds.

Salbostatin is considered to play a role in the abundant trehalose production of the organism *Streptomyces albus*, ATCC 21838. The importance of trehalose metabolism in the sporulation of *Streptomyces griseus* and in the hydrobiosis and anhydrobiosis of yeast has been reported.[12]

We have not yet investigated the acidic fraction from *Streptomyces albus*. Amphoteric fructos-1-yl-dipeptides with strong inhibitory activity towards the endopeptidase EC 3.4.24.11 have been isolated; they are however present only at extremely low concentrations.[13] Salbostatin (**2**) is therefore quantitatively the most important metabolite of *Streptomyces albus*, ATCC 21838, after salinomycin.

Experimental Procedure

Instruments used: HR-EI mass spectrometer, Kratos MS-902S (70 eV, R. P. 10000); CI mass spectrometer, Kratos MS-80RFA (isobutane); ^{1}H NMR spectrometer, Brucker AX-270 and AM-400WB.

Isolation of **1** and **2**: The culture filtrate (1800 L) from a 12 day fermentation of a salinomycin-overproducing mutant of *Streptomyces albus*, ATCC 21838, was extracted with *n*-butanol (600 L). The nonpolar components of this extract were isolated by chromatography on silica gel. The aqueous phase was concentrated under vacuum (to 150 L), and diluted with CH_3OH (600 L). After separating the high molecular weight precipitate, the basic components were adsorbed on a cation

exchanger (Dowex 50WX2, acid form), and subsequently eluted with 0.5 M aqueous NH_3. The resulting product mixture was separated by chromatography on S-Sepharose and on Fractogel TSK HW-40 (monitored with iodine, Rydon–Smith, and α-naphthol/sulfuric acid staining, and by UV detection at 210 nm). Total yield of **1** and **2** was 0.9 g and 1.5 g, respectively.

Hexaacetyl derivative of **1**: Compound **1** (10 mg) was dissolved in anhydrous pyridine (3 mL) and acetic anhydride (1 mL). The solution was maintained at room temperature for 15 h. Ice was then added, and the reaction was extracted with $CHCl_3$. After chromatographic purification on silica gel with $CHCl_3/CH_3OH$ (99:1), 5 mg of hexaacetyl-**1** was isolated. HR-EI MS: *m/z* 506.1865 (0.2%), [$M + H^+$, calcd 506.1874 for $C_{21}H_{32}NO_{13}$], 446.1437 (3%), [$M - AcNH_2$, calcd 446.1425], 330.1193 (4%), [$M - OCH_2CH(OAc)CH_2OAc$, calcd 330.1188], 159.0662 (100%), [$^+CH_2CH(OAc)CH_2OAc$, ber. 159.0657], 143.0584 (40%), [$AcOCH{=}CHNHAc^+$; ber. 143.0582]; ^1H NMR ($CDCl_3$, 270 MHz): δ = 5.15, 5.10 (2 t, 9 Hz, 3α-H, 4β-H), 5.0 (d, 3.5 Hz, 1α-H), 4.1–4.4 (m, 7H), 3.65 (m, OCH_2), 2.0–2.1 (6 OAc).

Salbostatin **2**: $[\alpha]_D^{20} = +115$ ($c = 1$, H_2O); $C_{13}H_{23}NO_8$ (321); CI MS: *m/z* 322 (100%), [$M + H^+$], 304 (11%), [$MH^+ - H_2O$], 286 (9%), [$MH^+ - 2H_2O$], 164 (33%), [$^+H_3NC_6H_{11}O_4$]; ^1H NMR ([D$_6$]DMSO/D_2O, 400 MHz; see Table 1); ^{13}C NMR ([D$_6$]DMSO, 68 MHz): δ = 52.8 (d, C-1'), 57.6 (d, C-2), 61.4 (t, C-6, C-7'), 69.1 (t, C-1), 70.2, 70.5, 70.9, 72.9, 76.6, 81.7 (6 d, C-3, C-4, C-5, C-4', C-5', C-6'), 120.4 (d, C-2'), 140.5 (s, C-3').

Heptaacetyl derivative of **2**: salbostatin (50 mg) was dissolved in anhydrous pyridine (3 mL) and acetic anhydride (1 mL). The solution was maintained at room temperature for 15 h, treated with ice, and extracted with $CHCl_3$. Chromatographic purification on silica gel with $CHCl_3/CH_3OH$ (99:1) afforded 16.6 mg heptaacetyl salbostatin **2'**. HR-EI MS: *m/z* 615.2108 (4%), [M^+; calcd 615.2164 for $C_{27}H_{37}NO_{15}$], 555.1911 (25%), [M – AcOH, calcd 555.1952], 495.1698 (17%), [M – 2AcOH, calcd 495.1741], 471.1743 (22%), [M – AcOCH=CHOAc, calcd 471.1740], 231.0865 (100%), [$AcOCH_2CH_2CH(OAc)CH(OAc)^+$, calcd 231.0868]; ^1H NMR ($CDCl_3$, 400 MHz) see Table 1. NOE difference spectroscopy and Fig. 1.

Received: April 22, 1994 [Z 6869 IE]
German version: *Angew. Chem.* **1994**, *106*, 1936

[1] S. Umezawa, K. Tsuchiya, H. Umezawa, *J. Antibiot.* **1970**, *23*, 20–27; H. Zähner, H. Drautz, W. Weber in *Bioactive Microbial Products; Search and Discovery* (Ed.: J. D. Bu'Lock, L. J. Nisbet, D. J. Winstanley), Academic Press, New York, **1982**, pp. 51–70; S. Breiding-Mack, A. Zeeck, *J. Antibiot.* **1987**, *40*, 952–960.

[2] Y. Miyazaki, M. Shibuya, H. Sugawara, O. Kawaguchi, C. Hirose, J. Nagatsu, S. Esumi, *J. Antibiot.* **1974**, *27*, 814–821; J. W. Westley, J. F. Blount, R. H. Evans, C.-M. Liu, *ibid.* **1977**, *30*, 610–612.

[3] E. F. Paulus, L. Vértesy, G. M. Sheldrick, *Acta Crystallogr. Sect. C* **1984**, *40*, 700–703.

[4] a) J. A. F. Op den Kamp, P. P. M. Bonsen, L. L. M. Van Deenen, *Biochim. Biophys. Acta* **1969**, *176*, 298–305; E. Altmann, J. R. Brisson, M. B. Perry, *Carbohydr. Res.* **1988**, *183*, 321–331; b) N. C. Phillips, L. Chedid, J. M. Bernard, M. Level, P. Lefrancier, *J. Biol. Response Modif.* **1987**, *6*, 678–691.

[5] L. Vértesy, H.-W. Fehlhaber, A. Schulz (Hoechst AG), DE-A 3836675 A1, **1988**; [*Chem. Abstr.* **1989**, *113*, 96134 x].

[6] a) H. Paulsen, F. R. Heiker, *Angew. Chem.* **1980**, *92*, 930–931; *Angew. Chem. Int. Ed. Engl.* **1980**, *19*, 904–905; b) H. G. Fletcher, Jr., *J. Am. Chem. Soc.* **1947**, *69*, 706–707.

[7] Y. Shiga, H. Mizuno, H. Akanuma, *J. Bacteriol.* **1993**, *175*, 7138–41.

[8] a) Y. Kemada, S. Horii, *J. Chem. Soc. Chem. Commun.* **1972**, 746–747; b) E. Truscheit, W. Frommer, B. Junge, D. D. Schmidt, W. Wingender, *Angew. Chem.* **1981**, *93*, 738–755; *Angew. Chem. Int. Ed. Engl.* **1981**, *20*, 744–761.

[9] Dr. F. E. Beyhl (Hoechst AG), unpublished.

[10] S. Ogawa, C. Uchida, Y. Yuming, *J. Chem. Soc. Chem. Commun.* **1992**, 886–888.

[11] S. Murao, EP-A 0566275 A1, **1992**.

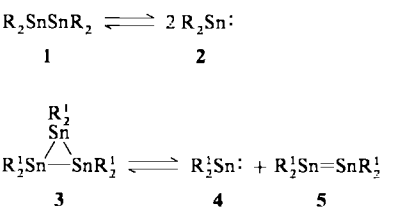
[12] M. J. McBride, J. C. Ensign, *J. Bacteriol.* **1990**, *172*, 3637–3643; C. Marino, M. Curto, R. Bruno, M. T. Rinaldo, *Int. J. Biochem.* **1989**, *21*, 1369–1375.

[13] L. Vértesy, P. Schindler, H. Kogler, H. W. Fehlhaber (Hoechst AG), EP-A 0288897, **1988**; [*Chem. Abstr.* **1989**, *110*, P193414j].

Bis(2,4,6-tri-*tert*-butylphenyl)stannanediyl: A Diarylstannylene without Donor Stabilization**

Manfred Weidenbruch,* Josephin Schlaefke, Annemarie Schäfer, Karl Peters, Hans Georg von Schnering, and Heinrich Marsmann

The nature of the tin–tin bonding in distannenes (distannaethenes) has not yet been completely rationalized. Thus, the distannene **1** of Lappert et al. is the sole structurally characterized compound of this type, and in the solid state is best described as a double donor–acceptor adduct of two stannylenes (stannanediyls) **2** (Scheme 1). Evidence for this includes the tin–tin interatomic distance,[1, 2] which is hardly shorter than that of tin–tin single bonds,[3] the results of quantum mechanical calculations,[2, 4] ^{119}Sn solid-state NMR data,[5] and the dissociation of **1** in solution into two stannylene molecules **2**.[6]



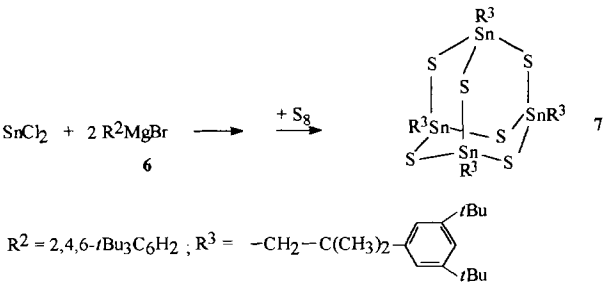
Scheme 1. R = $(Me_3Si)_2CH$; R^1 = 2,4,6-*i*$Pr_3C_6H_2$.

Different behavior is observed for the tetraaryldistannene **5**,[7] which, according to ^{119}Sn NMR data,[7, 8] retains its structural integrity even in solution. Moreover, trapping reactions with chalcogens[9] or phenylacetylene[8] indicate the likely presence of a double bond in **5**. The distannene **5** is formed together with the stannylene **4** upon photolysis or thermolysis of the cyclotristannane **3**, with which it exists in thermal equilibrium over a wide temperature range.[7] In the solid-state, however, only the three-membered ring **3** is present at room temperature;[10] hence no X-ray structure analysis on **5** has been possible.

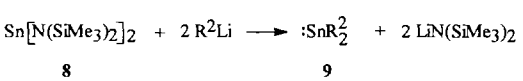
The replacement of the 2,4,6-triisopropylphenyl groups R^1 in **4** and **5** with the significantly bulkier 2,4,6-tri-*tert*-butylphenyl groups R^2, in order to suppress the formation of the analogous cyclotristannane, proved not possible at first. This was due not only to the aryl/alkyl isomerization ($R^2 \rightarrow R^3$) previously known for R^2 groups,[11, 12] but also to disproportionation reactions of the presumed tin(II) intermediate species. Thus, reaction of the Grignard reagent **6** with tin(II) chloride—which in the case of the corresponding 2,4,6-triisopropylphenyl compound had led smoothly to **3**[8, 9]—gave rise to a dark red solution, from which, upon addition of sulfur, the tin sesquisulfide **7** with rearranged alkyl groups was isolated, as well as tin(IV) compounds.

[*] Prof. Dr. M. Weidenbruch, Dipl.-Chem. J. Schlaefke, Dr. A. Schäfer
Fachbereich Chemie der Universität
Carl-von-Ossietzky-Strasse 9–11, D-26111 Oldenburg (FRG)
Telefax: Int. code + (441)798-3329
Dr. K. Peters, Prof. Dr. H. G. von Schnering,
Max-Planck-Institut für Festkörperforschung Stuttgart (FRG)
Prof. Dr. H. Marsmann
Fachbereich Chemie der Universität-Gesamthochschule Paderborn (FRG)

[**] Compounds of Germanium and Tin. Part 13. This work was supported by the Deutsche Forschungsgemeinschaft and by the Fonds der Chemischen Industrie. Part 12: M. Weidenbruch, A. Ritschl, K. Peters, H. G. von Schnering, *J. Organomet. Chem.* **1992**, *437*, C25.



Success was finally achieved by the reaction of the tin(II) amide **8**[13] with 2,4,6-tri-*tert*-butylphenyllithium,[14] from which highly air-sensitive, dark red crystals of **9** were obtained. The ^{1}H and ^{13}C NMR spectra clearly show that insertion of the unsaturated tin atom into one of the methyl C–H bonds of the *ortho-tert*-butyl substituents had not occurred. Furthermore, molecular mass determinations (cryoscopic in benzene) and the absence of $^1J(^{119}Sn,^{117}Sn)$ coupling in the ^{119}Sn NMR spectrum indicate the presence of monomeric stannylene molecules in solution.



A crystal structure analysis[15] (Fig. 1) established the composition of **9** and confirmed that this stannylene also exists in monomeric form in the crystal, since the shortest tin–tin distance (884 pm) lies outside of any bonding interaction. Whereas

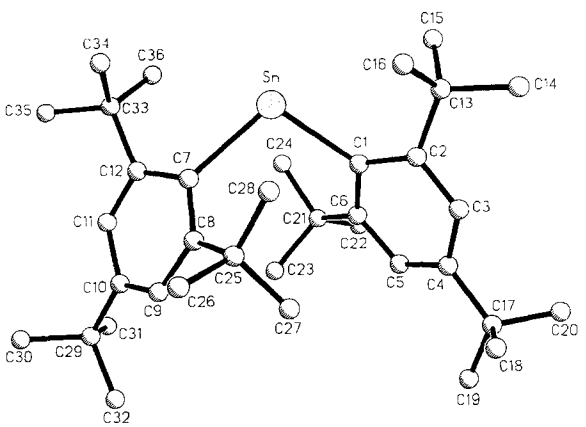


Fig. 1. Molecular Structure of **9** in crystal (without H atoms). Selected bond lengths [pm] and angles [ ]: Sn–C1 225.5(4), Sn–C7 226.7(4); C1-Sn-C7 103.6(1), C1-C2-C13 122.7(4), C1-C6-C21 124.2(4), C7-C8-C25 123.9(4), C7-C12-C33 122.7(3).

the tin–carbon interatomic distances correspond to those in **2**,[6] the C-Sn-C angle is widened by about 8°, presumably on account of the greater steric demands of the R^2 groups. The two phenyl rings are each twisted by 54° from the C1-Sn-C7 plane, forming an angle of 30° with respect to one another, thereby permitting optimal orientation for the bulky *ortho-tert*-butyl groups. Agostic interactions between the tin atom and the neighboring methyl C–H bonds were not observed, since all four *ortho-tert*-butyl groups point away from the tin atom. The carbon atom C24 does approach the tin atom at a distance of 312 pm, though this distance is still probably too great for an interaction between the C–H bond and the unsaturated tin atom.

Compound **9** is the first diarylstannylene which exists without intramolecular donor-stabilization.[16] The only other structurally characterized diarylstannylene $[2,4,6\text{-}(CF_3)_3C_6H_2]_2Sn$: (**10**) probably owes its stability to the close contact between the fluorine atoms of the *ortho*-CF_3 groups and the low-valent tin atom.[17] A recent report describes R^1R^4Sn: (**11**, $R^4 = 2,4,6\text{-}[(Me_3Si)_2CH]_3C_6H_2$), whose substituents show similar steric demands to **9**.[18] Isolation of **11** has not yet been accomplished.

Evidently, the bulky *ortho-tert*-butyl groups in **9** not only hinder cyclotristannane formation, but also destabilize a possible distannene. The ^{119}Sn NMR spectrum of **9** is unusual and shows, instead of the expected singlet, two signals at $\delta = 961$ and 1105 in an intensity ratio of about 4:1 at room temperature. These coalesce upon heating to 50 °C into a single signal at $\delta = 980$, which persists even after cooling. The obvious supposition is that a partial isomerization of **9** into the sterically less encumbered stanylene R^2R^3Sn: (**12**) takes place in solution; this is supported not only by the ^{13}C NMR spectrum, in which a CH_2 group at $\delta = 62.5$ is detected unambiguously, but also through trapping reactions, from which thus far only products with one aryl/alkyl isomerized R^3 group were isolable.

The positions of both signals is of interest since they are clearly distinct from that of molecule **2**,[5] as well as that of a structurally related compound in which both C-H hydrogen atoms of **2** are replaced with an ethylene bridge,[19] and that of **11**,[18] which display drastically deshielded tin nuclei ($\delta > 2200$). Rather, the chemical shifts observed for **9** and **12** lie in the region typical for hetero-substituted stannylenes,[20] for example **8**,[21] and also for **10**.[17] Whereas these stannylenes minimize their electron deficiency through interaction between free electron pairs and an unoccupied 5pπ-orbital at the tin center, the reason for the similar shielding of the tin nuclei in **9** and **12** is currently still obscure.

Experimental Procedure

A solution of 2,4,6-tri-*tert*-butylphenyllithium (14.7 g, 46 mmol) in toluene (70 mL) was added slowly dropwise, with the exclusion of air and moisture, to a solution of **8** (10.0 g, 23 mmol) in toluene (40 mL), and the dark red mixture stirred for about 3 h. After concentration of the solution to 80 mL, cooling to −30 °C afforded **9** (9.0 g, 64%) as dark red rectangular crystals. M.p. 125–130 °C. ^{1}H NMR (300 MHz, C_6D_6): $\delta = 1.16, 1.26, 1.33, 1.34, 1.38$ (each s, 9H), 1.68 (s, 6H), 7.41 (s, 1H), 7.44 (s, 1H), 7.46 (s, 1H), 7.57, 7.576; $^{13}C\{^1H\}$ NMR (75.44 MHz, C_6D_6): $\delta = 31.54, 31.64, 31.77, 31.86, 32.90, 33.23, 34.75, 35.09, 35.14, 38.80, 40.09, 62.50, 119.68, 120.02, 122.20, 125.65, 128.87, 129.28, 148.13, 150.34, 150.47, 150.93, 156.70$; $^{119}Sn\{^1H\}$ NMR (112.22 MHz, [D$_8$]toluene, Me_4Sn): $\delta = 950.6$, 1120.1 (270 K); 960.8, 1105.0 (293 K); 980.4 (323 K); UV/VIS (*n*-pentane): $\lambda_{max} = 476$ nm.

Received: April 6, 1994
Revised version: June 4, 1994 [Z6826IE]
German version: *Angew. Chem.* **1994**, *106*, 1938

[1] D. E. Goldberg, D. H. Harris, M. F. Lappert, K. M. Thomas, *J. Chem. Soc. Chem. Commun.* **1976**, 261.
[2] D. E. Goldberg, P. B. Hitchcock, M. F. Lappert, K. M. Thomas, A. J. Thorne, T. Fjeldberg, A. Haaland, B. E. R. Schilling, *J. Chem. Soc. Dalton Trans.* **1986**, 2387.
[3] A. Haaland, A. Hammel, H. Thomassen, H. V. Volden, H. B. Singh, P. K. Khanna, *Z. Naturforsch. B* **1990**, *45*, 1143.
[4] a) G. Trinquier, J.-P. Malrieu, *J. Am. Chem. Soc.* **1987**, *109*, 5303; b) A. Savin, A. D. Becker, J. Flad, R. Nesper, H. Preuss, H. G. von Schnering, *Angew. Chem.* **1991**, *103*, 421; *Angew. Chem. Int. Ed. Engl.* **1991**, *30*, 409; c) H. Jacobsen, T. Ziegler, *J. Am. Chem. Soc.* **1994**, *116*, 3667, and references therein.
[5] K. W. Zilm, G. A. Lawless, R. M. Merrill, J. M. Millar, G. G. Webb, *J. Am. Chem. Soc.* **1987**, *109*, 7236.
[6] P. J. Davidson, D. H. Harris, M. F. Lappert, *J. Chem. Soc. Dalton Trans.* **1976**, 2228; T. Fjeldberg, A. Haaland, M. F. Lappert, B. E. R. Schilling, R. Seip, A. J. Thorne, *J. Chem. Soc. Chem. Commun.* **1982**, 1407.
[7] S. Masamune, L. R. Sita, *J. Am. Chem. Soc.* **1985**, *107*, 6390.

[8] M. Weidenbruch, A. Schäfer, H. Kilian, S. Pohl, W. Saak, H. Marsmann, *Chem. Ber.* **1992**, *125*, 563.
[9] A. Schäfer, M. Weidenbruch, W. Saak, S. Pohl, H. Marsmann, *Angew. Chem.* **1991**, *103*, 873, 978; *Angew. Chem. Int. Ed. Engl.* **1991**, *30*, 834, 962.
[10] F. J. Brady, C. J. Cardin, D. J. Cardin, M. A. Convery, M. M. Devereux, G. A. Lawless, *J. Organomet. Chem.* **1991**, *421*, 199.
[11] M. Weidenbruch, K. Schäfers, S. Pohl, W. Saak, K. Peters, H. G. von Schnering, *J. Organomet. Chem.* **1988**, *346*, 171.
[12] J. Frey, D. A. Nugiel, Z. Rappoport, *J. Org. Chem.* **1991**, *56*, 466.
[13] M. J. S. Gyane, D. H. Harris, M. F. Lappert, P. P. Power, P. Rivière, M. Rivière-Baudet, *J. Chem. Soc. Dalton Trans.* **1977**, 2004.
[14] M. Weidenbruch, K. Kramer, *J. Organomet. Chem.* **1985**, *291*, 159.
[15] X-ray crystal structure analysis of **9**: $C_{36}H_{58}Sn$, $M_r = 609.57$, orthorhombic, space group *Pbca*, $a = 1767.3(4)$, $b = 1915.2(4)$, $c = 2059.6(5)$ pm, $V = 6971(3) \times 10^6$ pm^3, $Z = 8$, $\rho_{calcd} = 1.161$ g cm^{-3}, $Mo_{K\alpha}$ radiation, graphite monochromator, $2\theta_{max.} = 55°$, Wyckoff-scan, 8730 independent reflections, 5738 observed independent reflections ($F > 3\sigma(F)$), F_o/parameter ratio = 17.2. Solution by direct methods and refinement with the Siemens-SHELXTL-Plus program system, $R = 0.050$, $R_w = 0.046$. Further details of the crystal structure investigation may be obtained from the Fachinformationszentrum Karlsruhe, D-76344 Eggenstein-Leopoldshafen (FRG), upon quoting the depository number CSD-400727.
[16] The existence of (impure) **9** was presumed on the basis of its Mössbauer spectrum: M. P. Bigwood, P. J. Corvan, J. J. Zuckerman, *J. Am. Chem. Soc.*, **1981**, *103*, 7643.
[17] H. Grützmacher, H. Pritzkow, F. T. Edelmann, *Organometallics*, **1991**, *10*, 23. A second crystalline form of **10** with a weak tin–tin interaction is described: U. Lay, H. Pritzkow, H. Grützmacher, *J. Chem. Soc. Chem. Commun.* **1992**, 260.
[18] N. Tokitoh, M. Saito, R. Okazaki, *J. Am. Chem. Soc.* **1993**, *115*, 2065.
[19] M. Kira, R. Yauchibara, R. Hirano, C. Kabuto, H. Sakurai, *J. Am. Chem. Soc.* **1991**, *113*, 7785.
[20] M. Veith, O. Recktenwald, *Top. Curr. Chem.* **1982**, *104*, 1.
[21] B. Wrackmeyer, *J. Magn. Res.* **1985**, *61*, 536.

Optically Active Lactones from a Baeyer–Villiger-Type Metal-Catalyzed Oxidation with Molecular Oxygen**

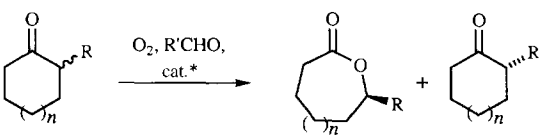
Carsten Bolm,* Gunther Schlingloff, and Konrad Weickhardt

Catalyzed asymmetric oxidations are of paramount importance for the synthesis of chiral building blocks. Enantioselectivities of over 90% have been achieved in the dihydroxylation of olefins[1] and in the epoxidation of allyl alcohols[2] and nonfunctionalized *cis* alkenes.[3] In general, highly oxidized reagents, such as peracids or other peroxy compounds, are employed as the source of oxygen. *Mukaiyama* et al. reported that molecular oxygen could also be used as a simple oxidizing agent in the asymmetric oxidation of olefins provided that an oxygen acceptor, such as an aldehyde, were present in stoichiometric quantities.[4] As part of our investigations into the activation and transfer of oxygen,[5] we have now developed an enantioselective, metal-catalyzed variant of the Baeyer–Villiger oxidation, a reaction which had previously only been achieved with the help of enzymes.[6]

[*] Prof. Dr. C. Bolm [+], Dipl.-Chem. G. Schlingloff [+], Dr. K. Weickhardt
Institut für Organische Chemie der Universität
St. Johanns-Ring 19, CH-4056 Basel (Switzerland)
[+] New address: Fachbereich Chemie der Universität
Hans-Meerwein-Strasse, D-35032 Marburg (FRG)
Telefax: Int. code + (6421)28-8917

[**] This research was supported by the Schweizerischer Nationalfonds and the Deutsche Forschungsgemeinschaft (project: oxygen transfer / peroxide chemistry). We thank Professors Pfaltz and Schiess, Universität Basel, for samples.

In the presence of an aldehyde and a metal catalyst, cyclic ketones are oxidized to lactones with molecular oxygen.[5, 7] We chose 2-phenylcyclohexanone (**1a**) as the model compound for our investigations into the asymmetric oxidation reaction, because **1a** is converted into lactone **2a** in high yields and with good regioselectivities in the reaction catalyzed by achiral nickel and copper complexes.[5] The enantiomeric excesses (*ee*) ob-

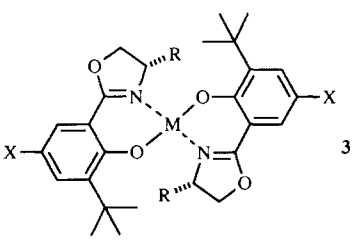


rac-**1** **a**: $n = 1$, R = Ph; **b**: $n = 1$, R = 4-Cl-Ph; **c**: $n = 1$, R = 4-MeO-Ph; **d**: $n = 0$, R = Ph; **e**: $n = 2$, R = Ph

(*R*)-**2** (*S*)-**1**

cat.* = Ni or Cu complex with chiral ligands

tained for lactone **2a** and ketone **1a** can be determined reliably and unambiguously by HPLC on a chiral column. With the optically active nickel(II) complex **3a**, *rac*-**1a** was converted to *rac*-**2a**, regardless of the reaction conditions employed; with the corresponding copper complex, **2a** was obtained with enantioselectivities of up to 69% *ee*.



3a: M = Ni, R = Alkyl, X = H
b: M = Cu, R = *t*Bu, X = NO_2
c: M = Cu, R = *t*Bu, X = H
d: M = Cu, R = *i*Pr, X = NO_2
e: M = Cu, R = *i*Pr, X = H

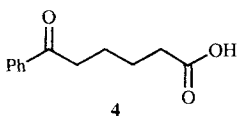
In order to achieve good reactivity and high asymmetric induction, several reaction parameters had to be optimized. The best results were obtained with *p*-nitro-substituted copper complex **3b** in water-saturated benzene and with pivalaldehyde as the oxygen acceptor (= coreducing agent) (Table 1). Use of 1 mol% of (*S,S*)-**3b** as catalyst at room temperature and under an oxygen atmosphere resulted in formation of lactone (*R*)-**2a** in 41% yield and 65% *ee* after 16 hours; at 6 °C, an increase in

Table 1. Enantioselective Baeyer–Villiger oxidation of cyclic ketones with (*S,S*)-**3b**.

Entry	Aldehyde	Ketone	Lactone	Yield [%]	*ee* [%] [a]
1	*t*BuCHO	**1a**	(*R*)-**2a**	41	65
2 [b]	*t*BuCHO	**1a**	(*R*)-**2a**	47	69
3 [c]	*m*-Cl-PhCHO	**1a**	(*R*)-**2a**	32	49
4	*p*-MeO-PhCHO	**1a**		–	–
5	*t*BuCHO	**1a**	(*R*)-**2a**	65	59
6	$C_6H_{11}CHO$	**1a**	(*R*)-**2a**	61	61
7	*t*BuCHO	**1b**	**2b** [d]	43	ca. 60 [e]
8	*t*BuCHO	**1c**	**2c** [d]	53	65
9	*t*BuCHO	**1d**	**2d** [d]	21	47

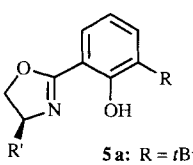
[a] Determined by HPLC on a chiral phase. [b] 6 d at 6 °C. [c] Reaction time 5 d. [d] The absolute configuration was not determined. [e] No base-line separation.

enantioselectivity was observed (69% *ee*). Since the unreacted ketone was enriched in enantiomer (*S*)-**1a**,[8] the lactone formation formally corresponds to a kinetic resolution. The "overoxidation" product, 6-oxo-6-phenylhexanoic acid (**4**), was isolated as a byproduct. In the absence of an aldehyde, copper-catalyzed oxidations with molecular oxygen also result in formation of **4**.[9–11] Lactone **2a** was found to be stable under the reaction conditions and was not oxidized to **4**. The reaction was suppressed when 5 mol% of catalyst, 2,6-di-*tert*-butylcresol as a radical trap, or an excess of the free ligand **5** were used.[12] Racemic lactone was obtained in the presence of molecular sieves (4 Å) or solid $NaHCO_3$. Only small or negligible quantities of lactone were formed in other solvents, such as, ethyl acetate, acetone, *tert*-butyl methyl ether, acetonitrile, cyclohexane, toluene, or 1,2-dichloroethane, which was the solvent used in the Ni-catalyzed reaction.[5] Aromatic aldehydes did not give satisfactory results as coreducing agents in the Cu-catalyzed reaction; even with longer reaction times, poorer yields and enantioselectivities were obtained (Table 1, entries 3 and 4).

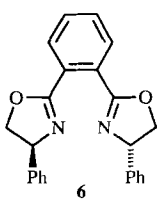


4

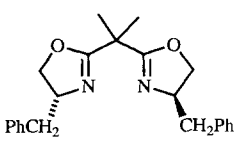
The 1:1 complexes obtained from copper(II) trifluoromethanesulfonate and the C_2-symmetric bisoxazolines **6**–**8**[13, 14a] also catalyzed the formation of optically active **2a**; the yields and enantioselectivities were however poor: with **6**, 39% yield (12% *ee*); with **7**, 39% yield (25% *ee*); and with **8**, 25% yield (12% *ee*).



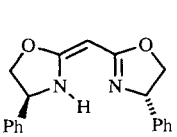
5a: R = *t*Bu, R' = *i*Pr
b: R = H, R' = *t*Bu
c: R = NO_2, R' = *t*Bu



6



7



8

The steric and electronic properties of the ligand influence the activity and enantioselectivity of the catalyst. Higher yields were obtained with the *p*-nitro-substituted complexes **3b** and **3d** than with the corresponding unsubstituted compounds **3c** and **3e**; the enantiomeric excesses obtained were not always higher: with **3b**, 41% yield (65% *ee*); with **3c**, 29% yield (57% *ee*); with **3d**, 57% yield (32% *ee*); and with **3e**, 34% yield (36% *ee*).

Without the *tert*-butyl substituent on the arene (**5b** and **5c**),[14] the ligand formed copper complexes which were only weakly active (yield < 10%). In the substrates, electronic effects play a secondary role. The *p*-chlorophenyl- and *p*-methoxyphenyl-substituted ketones **1b** and **1c** were transformed into lactones **2b** and **2c** with very similar enantioselectivities (Table 1, entries 7 and 8). The dependency of reactivity on ring size corresponds to that observed for peracids:[15, 16] **1a** was oxidized fastest, **1d** slower (Table 1, entry 9), and **1e** not at all. The alkyl-substituted cyclic ketone 2-cyclohexylcyclohexanone and the positional isomer 4-phenylcyclohexanone did not react.

We are currently working on elucidating the course of reaction and on other oxidation reactions with the new catalysts.[17]

Experimental Procedure

The ketone (1 mmol) and the catalyst (10 μmol) were dissolved in water-saturated benzene (2.5 mL) and treated with the aldehyde (0.5 mmol) and water (100 μL). The mixture was stirred under an oxygen atmosphere for 16–20 h, diluted with diethyl ether (150 mL), and washed with saturated aqueous $NaHCO_3$ solution (50 mL). The organic phase was dried over Na_2SO_4. After removal of the solvent, the crude product was chromatographed on silica gel. The enantiomeric excesses for **1** and **2** were determined by HPLC, when necessary, after bulb-to-bulb distillation under high vacuum [Chiracel ODH (Daicel); flow rate 0.5 mL min^{-1}; for **2a**: UV detector (254 nm), 2-propanol/hexane 1/3, retention times: (*S*)-**2a**: 12.4 min, (*R*)-**2a**: 16.0 min; for **1a**: UV detector (220 nm), 2-propanol/hexane 1/9, retention times: (*S*)-**1a**: 14.5 min, (*R*)-**1a**: 15.7 min].

Received: April 28, 1994 [Z 6876 IE]
German version: *Angew. Chem.* **1994**, *106*, 1944

[1] a) *Catalytic Asymmetric Synthesis* (Ed.: I. Ojima), VCH, Weinheim, **1993**; b) R. A. Johnson, K. B. Sharpless in ref. [1a], pp. 227–272.
[2] R. A. Johnson, K. B. Sharpless in ref. [1a], pp. 101–158.
[3] E. N. Jacobsen in ref. [1a], pp. 159–202.
[4] a) T. Yamada, K. Imagawa, T. Nagata, T. Mukaiyama, *Chem. Lett.* **1992**, 2231–2234; b) T. Mukaiyama, T. Yamada, T. Nagata, K. Imagawa, *ibid.* **1993**, 327–330.
[5] C. Bolm, G. Schlingloff, K. Weickhardt, *Tetrahedron Lett.* **1993**, *34*, 3405–3408.
[6] a) F. Petit, R. Furstoss, *Tetrahedron: Asymmetry* **1993**, *4*, 1341–1352; b) V. Alphand, R. Furstoss, *J. Org. Chem.* **1992**, *57*, 1306–1309; c) M. J. Taschner, L. Peddada, *J. Chem. Soc. Chem. Commun.* **1992**, 1384–1385; d) G. Grogan, S. M. Roberts, A. J. Willetts, *ibid.* **1993**, 699–701; e) O. Abril, C. C. Ryerson, C. Walsh, G. M. Whitesides, *Bioorg. Chem.* **1989**, *17*, 41–52; f) For reviews, see: C. T. Walsh, Y.-C. J. Chen, *Angew. Chem.* **1988**, *100*, 342–352; *Angew. Chem. Int. Ed. Engl.* **1988**, *27*, 333–343; and references therein.
[7] a) T. Yamada, K. Takahashi, K. Kato, T. Takai, S. Inoki, T. Mukaiyama, *Chem. Lett.* **1991**, 641–644; b) S.-I. Murahashi, Y. Oda, T. Naota, *Tetrahedron Lett.* **1992**, *33*, 7557–7560; c) M. Hamamoto, K. Nakayama, Y. Nishiyama, Y. Ishii, *J. Org. Chem.* **1993**, *58*, 6421–6425; d) K. Kaneda, S. Ueno, T. Imanaka, E. Shimotsuma, Y. Hishiyama, Y. Ishii, *ibid.* **1994**, *59*, 2915–2917.
[8] The enantiomeric excess obtained for the ketone after purification by chromatography on silica gel (46–75% yield) ranged between 10 and 30%, depending on the reaction conditions. For the absolute configuration of **1a**, see: G. Berti, B. Macchia, F. Macchia, L. Monti, *J. Chem. Soc. C* **1971**, 3371–3375. To establish the configuration of **2a**, (*S*)-**1a** was oxidized with *m*-chloroperbenzoic acid.
[9] In the Cu^{II}-catalyzed oxygenation of carbonyl compounds, copper enolates may also be involved: a) S.-J. Jin, P. K. Arora, L. M. Sayre, *J. Org. Chem.* **1990**, *55*, 3011–3018; b) L. M. Sayre, S.-J. Jin, *ibid.* **1984**, *49*, 3498–3503.
[10] Analogous products were obtained with other metal catalysts: a) S. Ito, M. Matsumoto, *J. Org. Chem.* **1983**, *48*, 1133–1135; b) T. Hirao, M. Mori, Y. Ohshiro, *Bull. Chem. Soc. Jpn.* **1989**, *62*, 2399–2400; c) A. Atlamsani, J.-M. Brégeault, M. Ziyad, *J. Org. Chem.* **1993**, *58*, 5663–5665.
[11] In the absence of aldehyde, the starting material isolated from the reaction of **1a** with **3e** in toluene (73% yield) was found to be enriched in (*R*)-**1a** (8% *ee*).
[12] Carried out with **3e** in benzene; inhibition with the free ligand **5a**.
[13] A. Pfaltz, *Acc. Chem. Res.* **1993**, *26*, 339–345.
[14] a) C. Bolm, K. Weickhardt, M. Zehnder, T. Ranff, *Chem. Ber.* **1991**, *124*, 1173–1180; b) C. Bolm, K. Weickhardt, M. Zehnder, D. Glasmacher, *Helv. Chim. Acta* **1991**, *74*, 717–726; c) C. Bolm, *Angew. Chem.* **1991**, *103*, 556–558; *Angew. Chem. Int. Ed. Engl.* **1991**, *30*, 542–543; d) H. Yang, M. A. Khan, K. M. Nicholas, *Organometallics* **1993**, *12*, 3485–3494.
[15] a) S. L. Friess, *J. Am. Chem. Soc.* **1949**, *71*, 2571–2575; b) G. R. Krow in *Comprehensive Organic Synthesis, Vol. 7* (Eds.: B. M. Trost, I. Fleming), Pergamon, Oxford, **1991**, pp. 671–688.
[16] After 15 h in benzene/water under argon and in the presence of 1 mol% (*S,S*)-**3b**, *rac*-**1a** was oxidized with peracetic acid (40% in acetic acid) to the lactone (*R*)-**2a** with 21% *ee* (46% yield). The ketone (*S*)-**1a** was isolated with 21% *ee* (36% yield).
[17] Cu^{II} catalyzes the epoxidation of olefins with RCHO and O_2: S.-I. Murahashi, Y. Oda, T. Naota, N. Komiya, *J. Chem. Soc. Chem. Commun.* **1993**, 139–140.

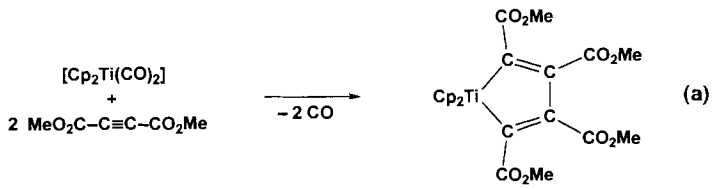
 © VCH Verlagsgesellschaft mbH, D-69451 Weinheim, 1994 0570-0833/94/1818-1849 $ 10.00+.25/0

Unexpected Reactions of Acetylenedicarboxylates with Zirconocene Complexes

Uwe Rosenthal,* Andreas Ohff, Wolfgang Baumann, Rhett Kempe, Annegret Tillack, and Vladimir V. Burlakov

In cyclizations of unsaturated compounds using the metallocene fragments "Cp_2M" (M = Ti or Zr), which are frequently employed preparatively, relatively little is known about competing reactions between double and triple bonds and other functional groups. For substrates in which a triple bond is present, coordination at the metal center leads to the initial formation of a metallacyclopropene complex.[1] This is normally followed by reaction with a further triple bond and the formation of metallacyclopentadiene complexes.[2] Alternatively, reaction of the metallocene alkyne complex with a carbonyl group, in place of the second triple bond, gives rise to a metalladihydrofuran.[2] We have recently reported a special example, in which the zirconocene alkyne complex $[Cp_2Zr(L)(Me_3SiC{\equiv}CSiMe_3)]$, L = THF (**I**),[3] pyridine (**II**),[4] reacts with acetone to give the zirconadihydrofuran $[Cp_2Zr{-}O{-}C(Me_2){-}C(SiMe_3){=}C(SiMe_3)]$ **1**.[5] Thus, whether the carbonyl group is tolerated by the metallocene unit, or instead becomes involved in the cyclization is of decisive importance for the use of unsaturated carboxylic esters in this synthesis.[6] Herein, we report on model reactions of metallocenes with acetylenedicarboxylates and their unexpected outcome.

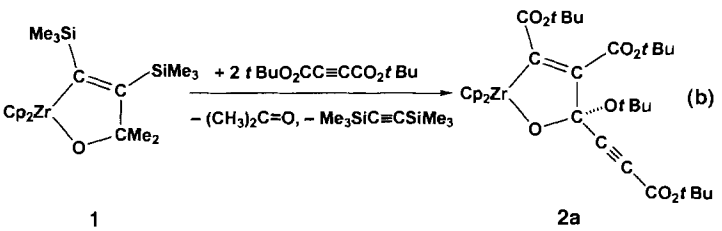
In the case of the titanocene complex, the reaction with dimethyl acetylenedicarboxylate is already known;[7] the expected metallacyclopentadiene is formed [Eq. (a)]. In contrast, analogous reactions with zirconocene are unknown.



(a)

With the recently synthesized and structurally characterized zirconocene alkyne complexes **I**[3] and **II**,[4] as well as the reactive zirconadihydrofuran **1**,[5] suitable precursors are available for the generation of the unstable zirconocene "Cp_2Zr" (c.f. ref. [2d]). This reacts under mild conditions with selected acetylenedicarboxylates to give unexpected products. For the reactions with the dicarboxylate diesters, the dihydrofuran **1** proved the most appropriate.

With dimethyl acetylenedicarboxylate, no defined products could be isolated from these reactions. Upon exposure of **1**, in *n*-hexane, to di-*tert*-butyl acetylenedicarboxylate, bis(trimethylsilyl)acetylene and acetone are cleaved, and the "Cp_2Zr" moiety reacts with two equivalents of acetylenedicarboxylate. This does not give rise to the substituted metallacyclopentadiene expected, as is the case, for example, with diphenylacetylene.[5] Instead, insertion of an ester carbonyl group from the second molecule of alkyne leads to the zirconadihydrofuran **2a** [Eq. (b)]. Complex **2a** crystallizes from *n*-hexane as colorless prisms, sensitive towards air and moisture, and melting with decomposition above 130 °C.



(b)

1 2a

Characterization of **2a** by IR and NMR spectroscopy confirms the unusual reaction depicted in Equation (b), in which zirconocene "Cp_2Zr" reacts with the acetylenedicarboxylate in a molar ratio of 1:2. For the crystal structure analysis of **2a**, suitable crystals could only be obtained from a THF/*n*-hexane mixture.[8] These crystals contain an additional molecule of solvent coordinated to **2a**, and are therefore present as the THF-adduct **2b**. The structure of **2b** in the crystal is shown in Figure 1.

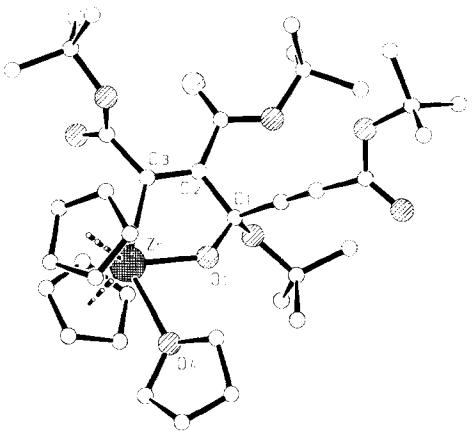


Fig. 1. Structure of **2b** in crystal, selected distances [Å] and angles[°]: Zr-O1 2.002(6), Zr-C3 2.391(8), Zr-O4 2.451(7), O1-C1 1.374(10), C1-C2 1.502(12), C2-C3 1.304(12); O1-Zr-C3 70.9(3), C1-O1-Zr 128.4(5), O1-C1-C2 109.5(7), C1-C2-C3 117.4(8), Zr-C3-C2 112.9(6).

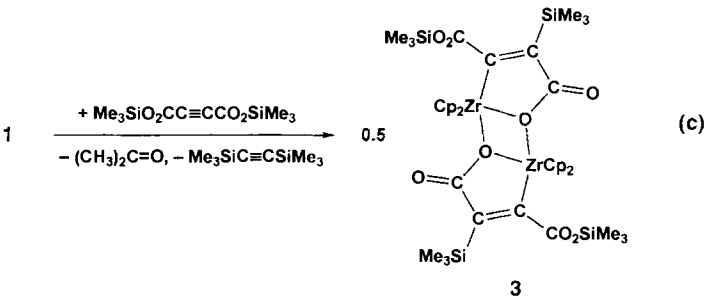
The central structural element is a nearly planar zirconadihydrofuran ring. Two Cp ligands are attached to the central metal atom, and in complex **2b**, unlike other metalladihydrofurans,[5] a THF molecule is coordinated in addition. The THF ligand (Zr–O 2.451(7) Å) is more weakly bound than in complex **1** or comparable compounds (Zr–O 2.122–2.390 Å[3]).

A completely different product was formed upon reaction of **1** with bis(trimethylsilyl) acetylenedicarboxylate. Here, the zirconocene unit reacts with only one alkyne molecule, which leads to the dimeric zirconadihydrofuranone complex **3**, following an unusual 1,3-migration of a trimethylsilyl group from an oxygen atom to a carbon atom [Eq. (c)]. Complex **3** crystallizes as colorless prisms, which are not sensitive towards oxygen and moisture, and melt with decomposition above 175 °C.

[*] Prof. Dr. U. Rosenthal, Dipl.-Chem. A. Ohff, Dr. W. Baumann, Dr. R. Kempe, Dr. A. Tillack, Dr. V. Burlakov,[+]
Max-Planck-Gesellschaft Arbeitsgruppe "Komplexkatalyse" an der Universität Rostock
Buchbinderstrasse 5–6, D-18055 Rostock (FRG)
Telefax: Int. code + (381)4669369

[+] Permanent address: Institute for Organoelement Compounds of the Russian Academy of Sciences Moscow (Russia)

[**] This work was supported by the Max-Planck-Gesellschaft and by the Fonds der Chemischen Industrie. We thank Prof. Dr. G. Oehme for the admission of our research group into the Institut für Organische Katalyseforschung.



(c)

A reaction of the zirconocene **1** with bis(trimethylsilyl) acetylenedicarboxylate in a 1:1 molar ratio and the formation of a symmetrical complex are confirmed by the spectroscopic data. In the ^{13}C NMR spectrum of **3**, signals arising from the alkyne C atoms occur at $\delta = 222.6$ (C_α) and 138.2 (C_β); the latter shows a $^1J_{(C-Si)}$ coupling of 64 Hz. Further proof of the unexpected location of the silyl group is the coupling of the $SiMe_3$ protons with C_β ($J \approx 1.5$ Hz) in the CH-coupled NMR spectrum. The ^{29}Si chemical shifts of the two differently bonded silyl groups are clearly distinguished ($\delta = 21.7$, -6.6); hence, the low-field signal of the CO_2SiMe_3 unit (free ester: $\delta = 29.1$) and the high-field signal of the sp^2-C-$SiMe_3$ group can be assigned.

The X-ray structure analysis of **3**[8] yielded a dimeric structure which is depicted in Figure 2. Molecule **3** is C_i-symmetric with the center of symmetry at the center of the four-membered Zr–O–Zr–O ring. This ring is planar; the O atoms simultaneously form part of a five-membered zirconafuranone. Each Zr center is coordinated as a distorted trigonal bipyramid; the Cp ring centroids and O1 are in equatorial positions, O1′ and C3 in axial positions. The structure of **3** is comparable to that of a dimeric zirconafuranone, which is formed by a completely different reaction from **1** and CO_2.[9]

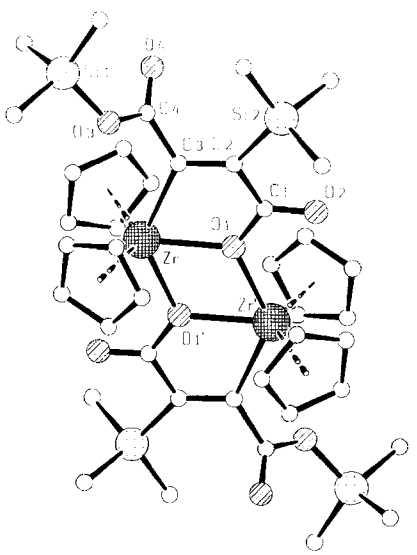
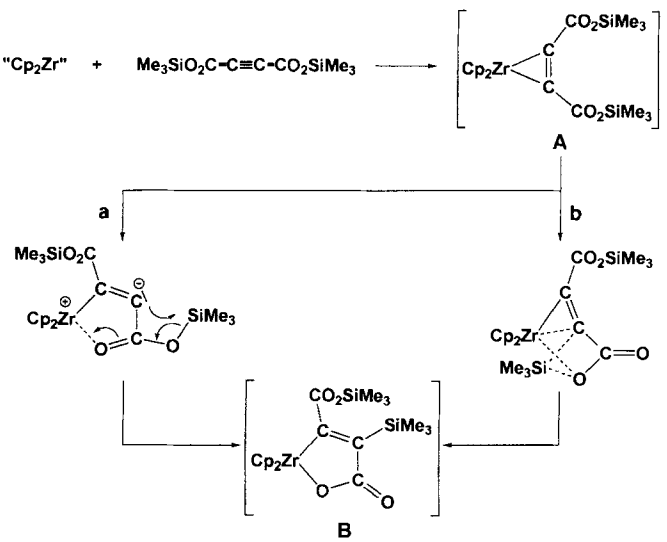


Fig. 2. Structure of **3** in crystal, selected distances [Å] and angles[ ]: Zr-O1 2.2213(14), Zr-O1′ 2.3073(14), Zr-C3 2.371(2), O1-C1 1.349(2), O2-C1 1.217(3), C1-C2 1.482(3), C2-C3 1.348(3), C3-C4 1.494(3); O1-Zr-O1′ 63.83(6), O1-Zr-C3 70.45(6), Zr-O1-Zr′ 116.17(6), C1-C2-C3 115.1(2), C3-C2-Si2 132.6(2), C2-C3-C4 118.1(2).

As the key step in the formation of **3**, the transition metal-induced 1,3-migration of the silyl group in bis(trimethylsilyl) acetylenedicarboxylate, from an oxygen atom to carbon, is surprising in view of the oxophilicity of silicon. Such O → C silyl migrations are very rare and were previously observed only in the rearrangement of silyl ketene acetals[10] and carbanion–oxyanion isomerizations.[11] Due to the high Si–O bond energy, trialkylsilyl groups in uncharged molecules normally only migrate from atoms other than oxygen. Thus, in the generation of **3**, the similarly high oxophilicity of zirconium and the simultaneous formation of the Zr–O bond and the Zr–O–Zr–O four-membered ring must play an important role.

The nature of the intermediate species in this reaction is not clear. As such, we would like to propose two possible mechanisms (Scheme 1), starting with coordination of the alkyne at the metal center and the formation of the metallacyclopropene **A**. The subsequent course of the reaction depends upon which



Scheme 1. Possible (unverified experimentally) reaction pathways for the intramolecular migration of a trimethylsilyl group from an oxygen atom to a carbon atom upon reaction of "Cp_2Zr" with bis(trimethylsilyl) acetylenedicarboxylate.

oxygen atom of the ester functionality interacts with the zirconium center. Rearrangement to **B** may be rationalized both as a 1,3 silyl group migration with an ionic transition state structure (path a, similar to a silyl-Wittig or retro-Brook rearrangement[12]) as well as in terms of a concerted mechanism (path b, formally comparable with a dyotropic rearrangement[13]). Both pathways are illustrated here in greatly simplified form, since **B**, of course, exists as a dimeric metallacycle, thus an intermolecular migration of the silyl group in the formation of **3** is likewise feasible. Experimental proof in favor of either mechanism is not yet at hand.

Overall, the varying course of the reaction of acetylenedicarboxylates with metallocenes "Cp_2M" is influenced both by the metal and by the alcohol component of the ester. Thus, in comparison to titanium, zirconium displays a pronounced tendency towards varied and unusual reactions of the ester group due to its greater oxophilicity and larger atomic radius.

Experimental Procedure

All manipulations were carried out with the exclusion of oxygen and moisture. Despite the relatively low yields for **2a** and **3**, no side-products could be isolated.

2a: A solution of di-*tert*-butyl acetylenedicarboxylate (492 mg, 2.18 mmol) in *n*-hexane (10 mL) was added to an orange solution of **1** [5] (0.49 g, 1.09 mmol) in *n*-hexane

(20 mL). The solution was filtered and allowed to stand at room temperature for 8 h without stirring. A yellow solid crystallized and was separated from the mother liquor and washed with *n*-hexane. Recrystallization from *n*-hexane gave **2a** (198 mg, 27%) as a colorless solid (m.p. > 130 °C (decomp), correct elemental analysis). $C_{34}H_{46}O_8Zr$, M_r = 674 g mol^{-1}; IR (Nujol): $\tilde{\nu}$ = 2216 cm^{-1} (ν(C≡C)), 1700, 1640, 1570 cm^{-1} (ν(C=O), ν(C=C)); NMR (C_6D_6, Bruker ARX 300, 30 °C): δ (^{1}H) = 1.29, 1.54, 1.57, 1.61 (s, 9H, CMe_3), 6.26, 6.27 (s, 5H, Cp); δ ($^{13}C\{^1H\}$) = 27.9, 28.5, 28.7, 30.8 (CCH_3), 76.2, 79.0, 79.7, 83.1 (CCH_3), 113.8, 114.1 (Cp), 77.8, 91.2, 99.6, 146.2, 155.0, 161.0, 172.9, 196.7 ($C_{quart.}$).

2b: The zirconocene complex **2a** was recrystallized from a THF/*n*-hexane mixture affording **2b** in the form of colorless needles (m.p. > 105 °C (decomp)). $C_{38}H_{54}O_9Zr$, M_r = 746.03 g mol^{-1}; IR (Nujol): $\tilde{\nu}$ = 2235, 2213 cm^{-1} (ν(C≡C)), 1697, 1669, 1574 cm^{-1} (ν(C=O), ν(C=C)); NMR ([D$_8$]THF, Bruker ARX 300, 30 °C): δ (^{1}H) = 1.35, 1.45, 1.48, 1.56 (s, 9H, CMe_3), 6.14, 6.30 (s, 5H, Cp), 1.78, 3.62 (m, 4H, THF); δ ($^{13}C\{^1H\}$): = 28.1, 28.5, 28.8, 31.0 (CCH_3), 75.6, 78.8, 79.1, 82.1 (CCH_3), 112.1, 112.8, (Cp), 76.6, 90.0, 102.9, 143.9, 153.8, 162.0, 175.0, 196.6 ($C_{quart.}$), 26.3, 68.1 (THF).

3: Complex **1** (586 mg, 1.3 mmol) was dissolved in *n*-hexane (25 mL). An equimolar quantity of bis(trimethylsilyl) acetylenedicarboxylate (0.34 mL, 1.3 mmol) was added at room temperature, and the orange solution was allowed to stand without stirring. After some time, the reaction mixture became orange-brown and a light yellow solid crystallized. After 12 h, the mother liquor was decanted and the residue washed with cold *n*-hexane and then recrystallized from THF/*n*-hexane (1/5). This yielded **3** (237 mg, 38%) as a colorless solid (m.p. > 175 °C (decomp), correct elemental analysis). $C_{40}H_{56}O_8Si_4Zr_2$, M_r = 959.64 g mol^{-1}; IR (Nujol): $\tilde{\nu}$ = 1660, 1651, 1528 cm^{-1} (ν(C=O), ν(C=C)); NMR (C_6D_6, Bruker ARX 300, 30 °C): δ (^{1}H) = 0.39, 0.55 (s, 9H, $SiMe_3$), 6.10 (s, 10H, Cp); δ($^{13}C\{^1H\}$) = 0.5, 0.7 (CH_3), 113.0 (Cp), 138.2 (ZrC=C), 176.7, 180.2 (C(O)O), 222.6 (ZrC=C); δ(^{29}Si) = − 6.6 ($CSiMe_3$), 21.7 ($OSiMe_3$).

Received: 13 May 1994 [Z 69291E]
German version: *Angew. Chem.* **1994**, *106*, 1946

[1] V. B. Shur, V. V. Burlakov, M. E. Vol'pin, *J. Organomet. Chem.* **1988**, *347*, 77-83; V. V. Burlakov, U. Rosenthal, R. Beckhaus, A. V. Polyakov, Y. T. Struchkov, G. Oehme, V. B. Shur, M. E. Vol'pin, *Metalloorg. Khim.* **1990**, *3*, 476 [English translation: *Organomet. Chem. USSR* **1990**, *3*, 237]; U. Rosenthal, H. Görls, V. V. Burlakov, V. B. Shur, M. E. Vol'pin, *J. Organomet. Chem.* **1992**, *426*, C53-C57; V. V. Burlakov, U. Rosenthal, P. V. Petrovski, V. B. Shur, M. E. Vol'pin, *Metalloorg. Khim.* **1988**, *1*, 953 [English translation: *Organomet. Chem. USSR* **1988**, *1*, 526].

[2] a) S. L. Buchwald, B. T. Watson, *J. Am. Chem. Soc.* **1987**, *109*, 2544–2546; b) S. L. Buchwald, R. B. Nielsen, *Chem. Rev.* **1988**, *88*, 1047–1058; c) G. Erker, R. Zwettler, *J. Organomet. Chem.* **1991**, *409*, 179–188; d) E. Negishi, T. Takahashi, *Acc. Chem. Res.* **1994**, *27*, 124–130.

[3] U. Rosenthal, A. Ohff, M. Michalik, H. Görls, V. V. Burlakov, V. B. Shur, *Angew. Chem.* **1993**, *105*, 1228–1230; *Angew. Chem. Int. Ed. Engl.* **1993**, *32*, 1193–1195.

[4] U. Rosenthal, A. Ohff, W. Baumann, A. Tillack, H. Görls, V. V. Burlakov, V. B. Shur, *Z. Anorg. Allg. Chem.*, in press.

[5] U. Rosenthal, A. Ohff, W. Baumann, A. Tillack, H. Görls, V. V. Burlakov, V. B. Shur, *J. Organomet. Chem.*, in press.

[6] P. A. Wender, F. E. McDonald, *Tetrahedron Lett.* **1990**, *31*, 3691–3694; A. M. Wilson, T. E. Waldman, A. L. Rheingold, R. D. Ernst, *J. Am. Chem. Soc.* **1992**, *114*, 6252–6254; R. B. Grossman, S. L. Buchwald, *J. Org. Chem.* **1992**, *57*, 5803–5805.

[7] B. Demerseman, P. H. Dixneuf, *J. Chem. Soc. Chem. Commun.* **1981**, 665–666.

[8] X-ray structure analyses: CAD4 diffractometer, graphite monochromated $Mo_{K\alpha}$ radiation, solution of structures by direct methods (SHELXS-86; G. M. Sheldrick, *Acta. Crystallogr. Sect. A.* **1990**, *46*, 467–473), refinement with full-matrix least squares against F^2 (SHELXL 93; G. M. Sheldrick, unpublished). Structural drawings generated with SCHAKAL 92 (E. Keller, Universität Freiburg, **1992**). **2b**: Space group *Ia*, a = 9.399(1), b = 41.89(1), c = 11.383(1) Å, β = 105.71(1)°, V = 4314(1) Å^3, Z = 4, ρ_{calcd} = 1.149 g cm^{-3}, 3881 measured reflections, 3880 symmetry independent reflections of which 3284 observed ($I > 2\sigma(I)$), R = 0.053, $wR2$ = 0.142 ($I > 2\sigma(I)$), 434 refined parameters. **3**: Space group $P\bar{1}$, a = 10.018(1), b = 10.716(1), c = 11.762(1) Å, α = 67.341(4)°, β = 76.202(5)°, γ = 84.259(6)°, V = 1131.6(2) Å^3, Z = 2, ρ_{calcd} = 1.408 g cm^{-3}, 4876 measured reflections, 4601 symmetry independent reflections of which 3937 observed ($I > 2\sigma(I)$), R = 0.025, $wR2$ = 0.063 ($I > 2\sigma(I)$), 244 refined parameters. Further details of the crystal structure investigations may be obtained from the Director of the Cambridge Crystallographic Data Centre, 12 Union Road, GB-Cambridge CB2 1EZ (UK), on quoting the journal citation.

[9] U. Rosenthal, A. Ohff, M. Michalik, H. Görls, V. V. Burlakov, V. B. Shur, *Organometallics* **1993**, *12*, 5016–5019.

[10] Y. Yamamoto, K. Maruyama, K. Matsumoto, *Organometallics* **1984**, *3*, 1583–1585; S. Raucher, D. C. Schindele, *Synth. Commun.* **1987**, *17*, 637; Y. Hong, D. J. Norris, S. Collins, *J. Org. Chem.* **1993**, *58*, 3591–3594; Y. Makioka, Y. Taniguchi, K. Takaki, Y. Fujiwara, *Chem. Lett.* **1994**, 645–648.

[11] Ausgewählte Beispiele: A. Wright, R. West, *J. Am. Chem. Soc.* **1974**, *96*, 3214–3222; E. J. Corey, C. Rücker, *Tetrahedron Lett.* **1984**, *25*, 4345–4348; A. G. Brook, P. Chiu, J. McClenaghnan, A. J. Lough, *Organometallics* **1991**, *10*, 3292–3301; B. Mergardt, K. Weber, G. Adiwidjaja, E. Schaumann, *Angew. Chem.* **1991**, *103*, 1679–1680; *Angew. Chem. Int. Ed. Engl.* **1991**, *30*, 1687–1688.

[12] T. Nakai, K. Mikami, *Chem. Rev.* **1986**, *86*, 885–902; R. J. Lindeman, A. Ghannam, *J. Am. Chem. Soc.* **1990**, *112*, 2392–2398.

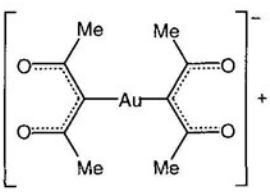
[13] M. T. Reetz, *Adv. Organomet. Chem.* **1977**, *16*, 33–65.

A Postulated Carrier of Gold in Hydrothermal Ore Solutions: Synthesis and Crystal Structure of $[(Ph_3P)_2N][Au(SH)_2]$, the First Homoleptic Hydrogensulfido Complex**

José Vicente,* María-Teresa Chicote,* Pablo González-Herrero, Peter G. Jones, and Birte Ahrens

It has been suggested that considerable quantities of gold may be transported in hydrothermal ore solutions as $[Au(SH)_2]^-$. Although solubility measurements of gold and Au_2S in aqueous sulfide or H_2S solutions indicate formation of this complex, it has never been isolated.[1] Interest in hydrogensulfido metal complexes stems from the reactivity they exhibit toward organic substrates,[2] their proposed role as intermediates in important industrial (hydrodesulfuration)[3] and biological catalytic processes,[4] and their use as models in theoretical studies.[5] However, although approximately one hundred such complexes have been reported, few have been fully characterized.[4, 6, 7] The majority of hydrogensulfido complexes involve the transition elements (we are aware of two exceptions, $[\{Ga(tBu)_2(\mu\text{-}SH)\}_2]$[7] and $[Mg\{\eta^3\text{-}HB(3\text{-}tBupyz)_3\}(SH)]$,[8] pyz = pyrazolyl), most commonly Mo[9] and Ru.[10] All these complexes are stabilized by auxiliary ligands (e.g., cyclopentadienyl,[11] carbonyl,[9b, 12] or phosphane[13]). We report here the synthesis and crystal structure of the first homoleptic hydrogensulfido metal complex.

Slow addition of a solution of $[(Ph_3P)_2N][Au(acac)_2]$[14] (Hacac = acetylacetone) to a saturated solution of H_2S (both in dichloromethane) gave the salt $[(Ph_3P)_2N]$-**1** in 91% yield [Eq. (a)]. Alternatively, **1** was obtained more directly by bubbling H_2S through a solution of $[(Ph_3P)_2N][AuCl_2]$ in Et_2NH



1 (a)

[*] Prof. Dr. J. Vicente, Dr. M.-T. Chicote, P. González-Herrero
Grupo de Química Organometálica
Departamento de Química Inorgánica
Facultad de Química, Universidad de Murcia
Aptdo. 4021, E-30071 Murcia (Spain)
Telefax: Int. code + (68)36-4143
Prof. Dr. P. G. Jones, B. Ahrens
Institut für Anorganische und Analytische Chemie
Technische Universität Braunschweig

[**] Complexes with S-donor Ligands, Part 1. This work was supported by Dirección General de Investigación Cientifica y Técnica (PB-92-0982-C) and the Fonds der Chemischen Industrie. P. G.-H. is grateful to Fundacion Cultural CAM for a grant.

(65% yield). Hydrogensulfido complexes have been prepared 1) by reaction of H_2S or HS^- with chloro,[15] hydroxo,[16] oxo,[17] hydrido,[18] or carbonyl[19] complexes; 2) by oxidative addition of H_2S to low-valent metal complexes;[20] 3) by insertion of sulfur into an M–H bond;[21] and 4) by reaction of sulfido complexes with H_2[22] or protic acids;[6d, 23] our method is a new example of the synthetic utility of acetylacetonatogold complexes.[14, 24]

The solid-state IR spectrum of $[(Ph_3P)_2N]$-**1** is almost identical to that of $[(Ph_3P)_2N][AuCl_2]$, except for the absence of the band at 350 cm^{-1} assigned to ν(AuCl) and the presence of a new band at 340 cm^{-1} that can reasonably be assigned to ν(AuS). The two IR-active bands in the 2300–2600 cm^{-1} region corresponding to ν(SH) vibration modes cannot be clearly assigned; however, these bands are generally not observed or are, at best, weak.[4, 6–23] The ^1H NMR spectrum of $[(Ph_3P)_2N]$-**1** in $CDCl_3$ shows the resonance from the SH protons at $\delta = -1.22$. In most hydrogensulfido complexes, this signal appears between $\delta = +4$ and $\delta = -4$.[4, 6–23]

The salt $[(Ph_3P)_2N]$-**1** crystallizes with two formula units in the asymmetric unit.[25] In the anion **1**, the gold atom shows essentially linear coordination (S-Au-S 176.7, 178.2(1)°) with Au–S bond lengths of 227.7(4), 227.8(4), 228.8(4), and 229.7(3) pm (cf. 226.2, 227.1(8) pm in the anion $[Au(S\text{-}Ph)_2]^-$).[26] There are no short Au···Au contacts.

The hydrogen atoms of the SH^- ligands could not be located in the X-ray analysis, despite the otherwise acceptable precision; use of a different counterion might prove more successful. There are no short S···N contacts that might indicate hydrogen bonds. Crystallographically, the $[Au(SH)_2]^-$ anion is thus essentially indistinguishable from $[AuCl_2]^-$. Nonetheless, we are confident that we have measured $[Au(SH)_2]^-$ for the following reasons: 1) $[AuCl_2]^-$ is not stable in the presence of H_2S, yet $[(Ph_3P)_2N]$-**1** was synthesized in and single crystals were grown from dichloromethane saturated with H_2S; 2) complex $[(Ph_3P)_2N]$-**1** and $[(Ph_3P)_2N][AuCl_2]$ react to give a brown precipitate, which has not yet been characterized; and 3) we have determined the unit cell of an authentic sample of $[(Ph_3P)_2N][AuCl_2]$: it is tetragonal, primitive, but with marked I-pseudocentering, and with cell constants of $a = 2947.1(3)$, $c = 1570.0(2)$ pm at -130 °C.[27]

Experimental Procedure

A solution of $[(Ph_3P)_2N][Au(acac)_2]$ (181 mg, 0.19 mmol) in dichloromethane (8 mL) was added dropwise to a saturated solution of H_2S in dichloromethane (4 mL). The resulting solution was stirred under an H_2S atmosphere for 15 min, filtered through celite, and concentrated (3 mL). Addition of diethyl ether (15 mL) gave a white precipitate that was filtered off and dried under vacuum to give $[(Ph_3P)_2N]$-**1**. Elemental analysis for $C_{36}H_{32}AuNP_2S_2$: calcd C 53.93, H 4.02, N 1.75, S 8.00, Au 24.57; found C 53.96, H 4.03, N 1.79, S 7.61, Au 25.04. M.p. 141 °C, $\Lambda_M = 111\ \Omega^{-1}\,cm^2\,mol^{-1}$ (4.4×10^{-4} M in acetone)].

Received: March 8, 1994 [Z 6739 IE]
German version: *Angew. Chem.* **1994**, *106*, 1966

[1] See, for example P. J. Renders, T. M. Seward, *Geochim. Cosmochim. Acta* **1989**, *53*, 245–253; D. M. Shenberger, H. L. Barnes, *ibid.* **1989**, *53*, 269–278; K. Hayashi, H. Ohmoto, *ibid.* **1991**, *55*, 2111–2116; H. Colley, *Chem. Br.* **1992**, *28*, 720–723, and references therein.

[2] D. Seyferth, G. B. Womack, R. S. Henderson, M. Cowie, B. W. Hames, *Organometallics* **1986**, *5*, 1568–1575, and references therein; W. Weigand, G. Bosl, C. Robl, J. Kroner, *Z. Naturforsch. B.* **1993**, *48*, 627–635, and references therein.

[3] H. Vahrenkamp, *Angew. Chem.* **1975**, *87*, 369–371; *Angew. Chem. Int. Ed. Engl.* **1975**, *14*, 322–329; M. Rakowski Dubois, *Chem. Rev.* **1989**, *89*, 1–9; R. J. Angelici, *Acc. Chem. Res.* **1988**, *21*, 387–394, and references therein.

[4] See, for example D. R. English, D. N. Hendrickson, K. S. Suslick, C. W. Eigenbrot, Jr., W. R. Scheidt, *J. Am. Chem. Soc.* **1984**, *102*, 7258–7259, and references therein.

[5] See, for example C. J. Adams, M. I. Bruce, M. J. Liddell, B. W. Skelton, A. H. White, *J. Chem. Soc. Chem. Commun.* **1992**, 1314–1318.

[6] a) F. Bottomley, D. F. Drummond, G. O. Egharevba, P. S. White, *Organometallics* **1986**, *5*, 1620–1625; b) M. DiVaira, M. Peruzzini, P. Stoppioni, *Inorg. Chem.* **1991**, *30*, 1001–1007; c) W. A. Howard, G. Parkin, *Organometallics* **1993**, *12*, 2363–2366; d) M. E. Noble, J. C. Huffman, R. A. D. Wentworth, *Inorg. Chem.* **1983**, *22*, 1756–1760; e) F. Secheresse, J. M. Manoli, C. Potvin, *ibid.* **1986**, *25*, 3967–3971; f) T. R. Gaffney, J. A. Ibers, *ibid.* **1982**, *21*, 2857–2859; g) A. M. Mueting, P. D. Boyle, R. Wagner, L. H. Pignolet, *ibid.* **1988**, *27*, 271–279; h) C. Bianchini, A. Meli, *ibid.* **1987**, *26*, 4268–4271.

[7] a) M. B. Power, A. R. Barron, *J. Chem. Soc. Chem. Commun.* **1991**, 1315–1317; b) M. B. Power, J. W. Ziller, A. N. Tyler, A. R. Barron, *Organometallics* **1992**, *11*, 1055–1063, and references therein.

[8] R. Han, G. Parkin, *J. Am. Chem. Soc.* **1992**, *114*, 748–757.

[9] See, for example a) J. Allshouse, B. B. Kaul, M. Rakowski DuBois, *Organometallics* **1994**, *13*, 28–36, and references therein; b) M. K. Cooper, P. A. Duckworth, K. Henrick, M. McPartlin, *J. Chem. Soc. Dalton Trans.* **1981**, 2357–2364; c) R. A. Fischer, W. A. Herrmann, *J. Organomet. Chem.* **1987**, *330*, 365–376.

[10] See, for example U. Kölle, A. Hörnig, U. Englert, *J. Organomet. Chem.* **1992**, *438*, 309–317; J. Amarasekera, T. Rauchfuss, *Inorg. Chem.* **1989**, *28*, 3875–3883, and references therein; A. Shaver, P.-Y. Plouffe, P. Bird, E. Livingstone, *ibid.* **1990**, *29*, 1826–1832, and references therein

[11] See, for example A. Shaver, J. M. McCall, *Organometallics* **1984**, *3*, 1823–1829; Y. Ozawa, A. Vazquez de Miguel, K. Isobe, *J. Organomet. Chem.* **1992**, *433*, 183–188.

[12] W. Beck, W. Danzer, R. Höfer, *Angew. Chem.* **1973**, *85*, 87–88; *Angew. Chem. Int. Ed. Engl.* **1973**, *12*, 77–78; M. Herberhold, G. Süss, *J. Chem. Res. Synop.* **1973**, 246; *J. Chem. Res Miniprint* **1973**, 2720–2743.

[13] See, for example K. Osakada, T. Yamamoto, A. Yamamoto, A. Takenaka, Y. Sasada, *Inorg. Chim. Acta* **1985**, *105*, L9–L10; C. Bianchini, C. Mealli, A. Meli, M. Sabat, *Inorg. Chem.* **1986**, *25*, 4617–4618.

[14] J. Vicente, M. T. Chicote, I. Saura-Llamas, M. C. Lagunas, *J. Chem. Soc. Chem. Commun.* **1992**, 915–916.

[15] See, for example M. Schmidt, G. G. Hoffmann, *J. Organomet. Chem.* **1977**, *124*, C5–C8; A. M. Mueting, P. Boyle, L. H. Pignolet, *Inorg. Chem.* **1977**, *23*, 44–48.

[16] See, for example R. Graves, J. M. Homan, G. L. Morgan, *Inorg. Chem.* **1970**, *9*, 1592–1593; H. E. Brynza, L. K. Fong, R. A. Pacciello, W. Tam, J. E. Bercaw, *J. Am. Chem. Soc.* **1987**, *109*, 1444–1456.

[17] See, for example E. Königer-Ahlborn, H. Schulze, A. Müller, *Z. Anorg. Allg. Chem.* **1977**, *428*, 5–15.

[18] See, for example K. Osakada, T. Yamamoto, A. Yamamoto, *Inorg. Chim. Acta* **1984**, *90*, L5–L6.

[19] See, for example R. G. W. Gingerich, R. Angelici, *J. Am. Chem. Soc.* **1979**, *101*, 5604–5608.

[20] See, for example F. Cecconi, P. Innocenti, S. Midollini, S. Moneti, A. Vacca, J. A. Ramirez, *J. Chem. Soc. Dalton Trans.* **1991**, 1129–1134.

[21] See, for example F. J. Garcia Alonso, M. Garcia Sanz, V. Riera, S. Garcia Granda, E. Perez Garreño, *J. Chem. Soc. Dalton Trans.* **1992**, 545–548.

[22] See, for example M. Rakowsky DuBois, M. C. VanDerveer, D. L. DuBois, R. C. Haltiwanger, W. K. Miller, *J. Am. Chem. Soc.* **1980**, *102*, 7456–7461.

[23] See, for example D. Seyferth, G. B. Womack, R. S. Henderson, M. Cowie, B. W. Hames, *Organometallics* **1982**, *1*, 125–133.

[24] J. Vicente, M. T. Chicote, M. C. Lagunas, *Inorg. Chem.* **1993**, *32*, 3748, and references therein; R. Usón, J. Vicente, M. T. Chicote, *J. Organomet. Chem.* **1981**, *209*, 271–279, and references therein; J. Vicente, M. D. Bermúdez, M. P. Carrillo, P. G. Jones, *J. Chem. Soc. Dalton Trans.* **1992**, 1975–1980, and references therein.

[25] Crystal data for $[(Ph_3P)_2N]$-**1**: $C_{36}H_{32}AuNP_2S_2$, monoclinic, $P2_1/n$, $a = 2511.9(9)$, $b = 992.9(4)$, $c = 2679.2(9)$ pm, $\beta = 94.42(3)°$, $V = 6.662(4)$ nm^3, $Z = 8$, $\mu = 4.7$ mm^{-1}, $T = -100$ °C. A colorless needle (ca. $0.8 \times 0.15 \times 0.1$ mm) was mounted in inert oil (type RS3000, Riedel de Haën). A total of 11994 intensities, of which 11489 were independent, were registered on a Siemens R3 diffractometer fitted with an LT-2 low-temperature attachment ($Mo_{K\alpha}$ radiation, $2\theta_{max}$ 50°, absorption correction based on ψ-scans). The structure was solved by the heavy-atom method and refined anisotropically on F^2 (program SHELXL-93, G. M. Sheldrick, University of Göttingen). H atoms were included using a riding model; however, H atoms of the anion could not be located even with high-angle refinement. The final $wR(F^2)$ value was 0.117, with conventional $R(F)$ 0.057, for 757 parameters and 762 restraints. Further details of the crystal structure investigation may be obtained from the Fachinformationszentrum Karlsruhe, D-76344 Eggenstein-Leopoldshafen (FRG), on quoting the deposition number CSD-401041.

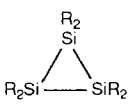
[26] P. A. Bates, J. M. Waters, *Acta Crystallogr. Sect. C* **1985**, *41*, 862–5.

[27] Note added in proof (3.8.1994): By chance we recently obtained the salt $[(Ph_3P)_2N][AuCl_2] \cdot CH_2Cl_2$ as a byproduct in another reaction; the compound crystallizes in the $P2_1/c$ space group with $a = 921.89(10)$, $b = 2381.5(2)$, $c = 1654.35(14)$ pm, $\beta = 102.551(8)°$ at -100 °C (P. G. Jones, *Z. Kristallogr.*, submitted).

Structures of 2-(Me_2NCH_2)C_6H_4-Substituted Oligosilanes**

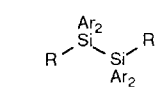
Johannes Belzner,* Nicola Detomi, Heiko Ihmels, and Matthias Noltemeyer

Isolable cyclotrisilanes[1] owe their existence to the stabilization of the strained three-membered ring by bulky substituents. Not only their stability, however, but also their formation through metal-mediated coupling of dihalosilanes is founded on the steric demands of the substituents at the silicon centers:[1,2] bulky groups force a conformation on the intermediate 3-halo-1-metallatrisilane in which the proximity of the termini of the acyclic trisilane favors an intramolecular ring closure (Thorpe–Ingold effect). Previously, bulky alkyl or aryl groups whose silyl substituents are blocked by alkyl groups in the *ortho* positions were used as suitable substituents for the synthesis of stable cyclotrisilanes. Against this background, the stability and the ready formation of the cyclotrisilane **1a**[3] by transformation of the appropriate diaryldihalosilane with magnesium is astounding; the 2-(dimethylaminomethyl)phenyl substituent introduced by Corriu et al.[4] into the chemistry of highly coordinated silicon compounds has only a relatively moderate steric effect and should actually favor the formation of larger rings. Also unusual is the reactivity of **1a**, which transfers all three diarylsilanediyl constituents of the ring to several substrates.[3,5]



1a: R = 2-(Me_2NCH_2)C_6H_4
1b: R = 2,6-$Me_2C_6H_3$
1c: R = H

Both the unexpected stability and the reactivity of **1a** made it desirable to investigate its structure in the crystal. An added goal was to gain more insight into the structural principles of 2-(dimethylaminomethyl)phenyl-substituted oligosilanes. We report here on the structures of the cyclotrisilane **1a** and the di- and tetrasilanes **2b** and **2c**, accessible from it.



Ar = 2-(Me_2NCH_2)C_6H_4

2a: R = Li
2b: R = H
2c: R = $SiMe_3$
2d: R = Cl

Cyclotrisilane **1a** crystallizes with two independent molecules in the asymmetric unit.[6] Neither in **1a** (**A**) (Fig. 1) nor in **1a** (**B**) is there a coordinative interaction between the amino and the silicon centers; moreover, the ^{29}Si NMR chemical shift of **1a**, which at $\delta = -64.7$ lies in the expected range for perarylated cyclotrisilanes, also precludes the formation of highly coordinated structures in solution. Though in the three-membered ring

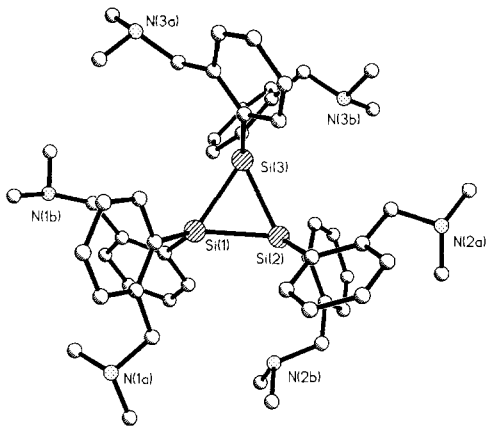


Fig. 1. Structure of the cyclotrisilane **1a** in the crystal (molecule **A**). Selected distances [pm] (the values in square brackets refer to molecule **B**): Si(1)–Si(2) 235.2(2) [236.4(2)], Si(2)–Si(3) 236.8(2) [235.7(2)], Si(3)–Si(1) 237.2(2) [235.6(2)], Si–C (averaged) 189.2(5) [189.2(5)].

of molecule **1a** (**A**) small deviations from the ideal geometry of an equilateral triangle are present, in **1a** (**B**) the Si–Si distances are identical, within experimental error. The endocyclic bonds (between 235 and 237 pm) are distinctly shorter than most experimentally determined bonds in other cyclotrisilanes.[7] The average Si–Si bond length in **1b**,[8] which was the only perarylated cyclotrisilane whose structure in the crystal had been studied previously, is 240.7 pm. In contrast, the average Si–Si bond length of 236.2 pm in **1a** approaches the value calculated for the parent compound (233–234 pm).[9] These observations show clearly that the 2-(dimethylaminomethyl)phenyl substituent does indeed have a relatively low steric demand, and class cyclotrisilane **1a** as a structurally hardly distorted member of this type of compound. The unusually facile cleavage of all three Si–Si bonds of **1a** cannot be predicted from its solid-state structure. Intramolecular stabilization of an intermediate silanediyl by the amino group of the aryl substituents cannot be excluded as reason for this reactivity.[10]

Cyclic trisilane **1a** can be converted by treatment with lithium into the vicinal dilithiodisilane,[11] whose reactions with electrophiles make many other disilanes accessible. Thus the protonation of **2a** with cyclopentadiene[12] yields the disilane **2b**,[13] which is moderately sensitive to hydrolysis. Figure 2 depicts one of the two independent molecules in the asymmetric unit

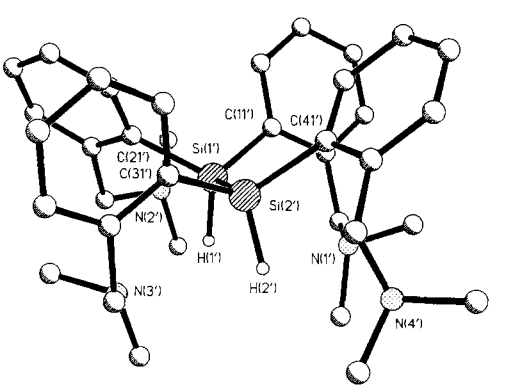


Fig. 2. Structure of the disilane **2b** in the crystal (molecule **A**). Selected distances [pm] and dihedral angles [°]: Si(1')–Si(2') 238.4(2), Si(1')–N(1') 309.8(3), Si(1')–N(2') 307.6(3), Si(1')···N(3') 338.0(2), Si(2')–N(1') 332.4(3), Si(2')–N(3') 312.9(2), Si–C (averaged) 189.3(4); H(1')-Si(1')-Si(2')-H(2') 10.1(20), C(11')-Si(1')-Si(2')-C(41') 8.3(3), C(21')-Si(1')-Si(2')-C(31') 9.8(2). Nonprimed atomic numbering is used for molecule **B**.

[*] Dr. J. Belzner, Dipl.-Chem. H. Ihmels
Institut für Organische Chemie der Universität
Tammannstrasse 2, D-37077 Göttingen (FRG)
Telefax: Int. code + (551)39-9475
N. Detomi
Dipartimento di Chimica Organica, Universitá di Padova (Italy)
Dr. M. Noltemeyer
Institut für Anorganische Chemie der Universität Göttingen (FRG)

[**] This work was supported by the Deutschen Forschungsgemeinschaft and the Fonds der Chemischen Industrie. N. D. was supported by an ERASMUS exchange grant form the European Community.

[**2b** (**A**)].[6] The inter-silicon distance of 238.4 pm in this compound is larger than that in **1a**.[14] Remarkable is the synperiplanar conformation about the Si–Si bond, since for tetraaryl-[15] and 2,2-dialkyl-1,1-diaryldisilanes,[16] antiperiplanar arrangements of the substituents were found. The eclipsed, sterically unfavorable conformation of **2b** is apparently adopted because of a coordinative interaction—which is, however, weak—between amino and silicon centers: the distances from the amino nitrogen atoms N(1′) and N(2′) to the silicon center Si(1′) and from N(3′) to Si(2′) are significantly smaller than the sum of the van der Waals radii of these elements (365 pm).[17, 18]

A completely different situation arises for tetrasilane **2c**, which is prepared by the reaction of **2a** with Me_3SiCl (Fig. 3):[6] Coordination between the amino and the silicon center no longer occurs. The additional steric congestion caused

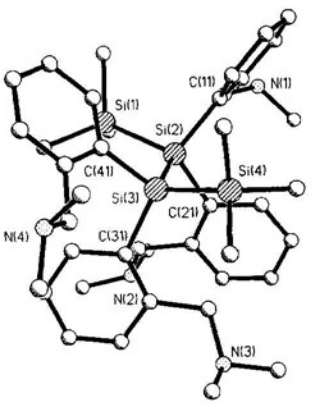


Fig. 3. Structure of the tetrasilane **2c** in the crystal. Selected distances [pm] and dihedral angles [°]: Si(1)-Si(2) 241.05(13), Si(2)-Si(3) 241.3(2), Si(3)-Si(4) 240.12(13), Si(2)-C(11) 191.2(3), Si(2)-C(21) 191.6(3), Si(3)-C(31) 192.0(3), Si(3)-C(41) 191.7(3); C(41)-Si(3)-Si(2)-Si(1) 35.3(2), Si(1)-Si(2)-Si(3)-C(31) 77.2(3), C(31)-Si(3)-Si(2)-C(21) 52.3(3), C(21)-Si(2)-Si(3)-Si(4) 77.3(2), Si(4)-Si(3)-Si(2)-C(11) 35.7(3), C(11)-Si(2)-Si(3)-C(41) 82.2(2).

by two trimethylsilyl groups results in an approximately antiperiplanar arrangement of the substituents about the central Si(2)–Si(3) bond. Despite this staggered conformation the system additionally relieves the steric pressure by a significant stretching of the Si(2)–Si(3) bond to 241.3 pm. The average C_{aryl}–Si bond length of 191.7 pm is also distinctly longer than that in **1a** ($\bar{d}_{Si-C} = 189.2$ pm) and **2b** ($\bar{d}_{Si-C} = 189.3$ pm) and reflects the steric strain in **2c**.

Apart from the diversity of their structures whose variety is certainly not exhausted by the three compounds described here, the 2-(dimethylaminomethyl)phenyl-substituted di- to tetrasilanes have large potential for application in synthesis. For instance, **2b** can be transformed quantitatively under mild conditions with *N*-chlorosuccinimide into the dichloro compound **2d**.[19] At present we are investigating whether **2d** and **2a** open preparative paths to the previously unknown class of base-coordinated disilenes.[10a]

Experimental Procedure

2b: Lithium turnings (30 mg, 4.36 mmol) were added to a solution of **1a** (647 mg, 0.73 mmol) in THF (11 mL). The mixture was stirred for 14 h at 20 °C, and the resulting deep red solution was filtered and treated at 0 °C with cyclopentadiene (290 mg, 4.39 mmol). THF was exchanged for 15 mL hexane. The suspension was filtered and concentrated. On cooling to −6 °C, 401 mg (92%) of **2b** crystallized as colorless crystals (m.p. 91–92 °C).

2c: To a solution of **2a**, prepared from **1a** (1.366 g, 1.54 mmol) and lithium (64 mg, 9.21 mmol) in THF (20 mL) and cooled at −10 °C, was added a solution of Me_3SiCl (1.17 mL, 9.21 mmol) in THF (5 mL). After stirring for two hours at 20 °C, the solvent was exchanged for 30 mL hexane, the resulting suspension filtered, and the filtrate evaporated to half its volume. On cooling to −6 °C 609 mg (54%) of **2c** precipitated as colorless crystals (m.p. 183–185 °C). ^{1}H NMR (C_6D_6, 72 °C, 300 MHz): $\delta = 0.35$ (s; 18 H, $SiMe_3$), 2.09 (s; 24 H, Me), 2.88, 3.31 (AB system, $J = 15$ Hz; 8 H, CH_2), 7.01, 7.26, 7.84 (3 mc (1:1:2); 16 arom. H); ^{13}C NMR ($CDCl_3$, 27 °C, 75.47 MHz): $\delta = 3.16$ ($SiMe_3$), 45.19 (NMe_2), 63.1 (CH_2), 125.24, 127.24, 129.22, 135.2, 139.18, 145.62 (arom. C); ^{29}Si NMR ($CDCl_3$, 27 °C; 59.63 MHz): $\delta = -13.6$ ($SiSiMe_3$), −26.8 ($SiSiMe_3$); MS (70 eV): *m/z* (%): 738 (3) [M^+], 369 (100) [$(M/2)^+$], 134 (15) [$Ar^+ - H$]; correct C,H,N analysis.

Received: March 28, 1994
Revised version: May 21, 1994 [Z 6801 IE]
German version: *Angew. Chem.* **1994**, *106*, 1949

[1] T. Tsumuraya, S. A. Batcheller, S. Masamune, *Angew. Chem.* **1991**, *103*, 916–944; *Angew. Chem. Int. Ed. Engl.* **1991**, *30*, 902–930, and references therein
[2] H. Watanabe, T. Muraoka, M. Kageyama, K. Yoshizumi, Y. Nagai, *Organometallics* **1984**, *3*, 141–147.
[3] J. Belzner, *J. Organomet. Chem.* **1992**, *430*, C51–C55.
[4] C. Chuit, R. J. P. Corriu, C. Reye, J. C. Young, *Chem. Rev.* **1993**, *93*, 1371–1448, and references therein.
[5] J. Belzner, H. Ihmels, *Tetrahedron Lett.* **1993**, *34*, 6541–6544.
[6] Crystal structure analysis of **1a** at 153 K: monoclinic, space group $P2_1/c$, $a = 1436.9(2)$, $b = 3211.2(4)$, $c = 2251.5(4)$ pm, $\beta = 90.86(2)°$, $V = 10.388(3)$ pm^3, $\rho_{calcd} = 1.137$ g cm^{-3}, 2θ range from 7.0 to 45.0° ($-15 \le h \le 15$, $0 \le k \le 34$, $-22 \le l \le 24$), $Mo_{K\alpha}$, $\lambda = 71.073$ pm, crystal dimensions: $0.60 \times 0.50 \times 0.50$ mm, 13567 reflections, 13499 independent, of which 13435 were used for the structure refinement on F^2 (SHELXL-93); final R_1 value [$I > 2\sigma(I)$] = 0.0779, $wR_2 = 0.2210$ (all data), residual electron density: +1208 and −670 e nm^{-3}. Crystal structure analysis of **2b** at 293 K: triclinic, space group $P\bar{1}$, $a = 1149.8(2)$, $b = 1847.7(4)$, $c = 1915.1(5)$ pm, $\alpha = 63.55(1)°$, $\beta = 83.01(1)°$, $\gamma = 79.75(1)°$, $V = 3.5804(14)$ pm^3, $\rho_{calcd} = 1.104$ g cm^{-3}, 2θ range from 7.0 to 45.0° ($-12 \le h \le 12$, $-17 \le k \le 19$, $-16 \le l \le 20$), $Mo_{K\alpha}$, $\lambda = 71.073$ pm, crystal dimensions: $0.5 \times 0.5 \times 0.5$ mm, 10780 reflections, 9352 independent, of which 9352 were used for the refinement on F^2 (SHELXL-93); the Si-bound hydrogen atoms were calculated from the difference Fourier map and freely refined; final R_1 value [$I > 2\sigma(I)$] = 0.0643, $wR_2 = 0.1867$ (all data), residual electron density: +442 and −333 e nm^{-3}. Crystal structure analysis of **2c** at 153 K: monoclinic, space group Cc, $a = 2528.9(5)$, $b = 917.6(2)$, $c = 2177.6(4)$ pm, $\beta = 116.74(3)°$, $V = 4.513(2)$ pm^3, $\rho_{calcd} = 1.088$ g cm^{-3}, 2θ range from 7.0 to 45.0° ($-26 \le h \le 27$, $-9 \le k \le 9$, $-23 \le l \le 23$), $Mo_{K\alpha}$, $\lambda = 71.073$ pm, crystal dimensions: $1.00 \times 1.00 \times 0.80$ mm, 4822 reflections, 4818 independent, of which 4817 were used for the structure refinement on F^2 (SHELXL-93); final R_1 value [$I > 2\sigma(I)$] = 0.0408, $wR_2 = 0.1132$ (all data), residual electron density: +374 and −245 e nm^{-3}. Further details of the crystal structure investigations may be obtained from the Fachinformationszentrum Karlsruhe, D-76344 Eggenstein-Leopoldshafen (FRG) on quoting the depository number CSD-58355, and the journal citation.
[7] Only in one case, that of an oxysubstituted cyclotrisilane, was a shorter Si–Si bond length determined (234.2 pm): G. R. Gillette, G. Noren, R. West, *Organometallics* **1990**, *9*, 2925–2933.
[8] S. Masamune, Y. Hanzawa, S. Murakami, T. Bally, J. F. Blount, *J. Am. Chem. Soc.* **1982**, *104*, 1150–1153.
[9] a) S. Nagase, M. Nakano, T. Kudo, *J. Chem. Soc. Chem. Commun.* **1987**, 60–62; b) W. W. Schoeller, T. Dabisch, *Inorg. Chem.* **1987**, *26*, 1081–1086; c) M. S. Gordon, D. Bartol, *J. Am. Chem. Soc.* **1987**, *109*, 5948–5950; d) R. S. Grev, H. F. Schaefer III, *ibid.* **1987**, *109*, 6569–6577.
[10] a) G. R. Gillette, G. H. Noren, R. West, *Organometallics* **1989**, *8*, 487–491; b) R. Corriu, G. Lanneau, C. Priou, F. Soulairol, N. Auner, R. Probst, R. Conlin, C. Tan, *J. Organomet. Chem.* **1994**, *466*, 55–68; c) R. T. Conlin, D. Laakso, P. Marshall, *Organometallics* **1994**, *13*, 838–842.
[11] J. Belzner, D. Stalke, unpublished.
[12] With H_2O or alcohols as proton sources, the cleavage of the Si–Si bond is also observed.
[13] **2b**, which has already been described as the hydrolysis product of **1a** [5], is also accessible through the potassium-induced coupling of the appropriate diaryl chlorosilane.
[14] The molecule of **2b** (**B**) that is not depicted differs from **2b** (**A**) mainly in a somewhat shorter Si–Si distance (236.4 pm).
[15] S. G. Baxter, K. Mislow, J. F. Blount, *Tetrahedron* **1980**, *36*, 605–616.
[16] M. Weidenbruch, K. Kramer, K. Peters, H. G. von Schnering, *Z. Naturforsch. B* **1985**, *40*, 601–606.
[17] A. Bondi, *J. Phys. Chem.* **1964**, *68*, 441–451.
[18] The distances between N(3′) and Si(1′) as well as between N(1′) and Si(2′) are also smaller than 365 pm; nevertheless, an additional coordinative interaction is not indicated, mainly because the lone pairs of the amino nitrogen atoms do not point towards the silicon centers.
[19] **2d** is also obtained by treatment of **1a** with $CHCl_3$.

Asymmetric Diels–Alder Reactions Catalyzed by a Chiral Iron Lewis Acid**

Ernst Peter Kündig,* Bernadette Bourdin, and Gérald Bernardinelli

Very impressive results have recently been reported for enantioselective Diels–Alder reactions catalyzed by chiral Lewis acids.[1, 2] Main group elements dominate in this chemistry, and aluminum- and boron-based catalysts with chiral ligands have produced the best results to date. We report here on a highly enantioselective Diels–Alder reaction catalyzed by a Lewis acid derived from an easily prepared and well-defined transition metal complex.

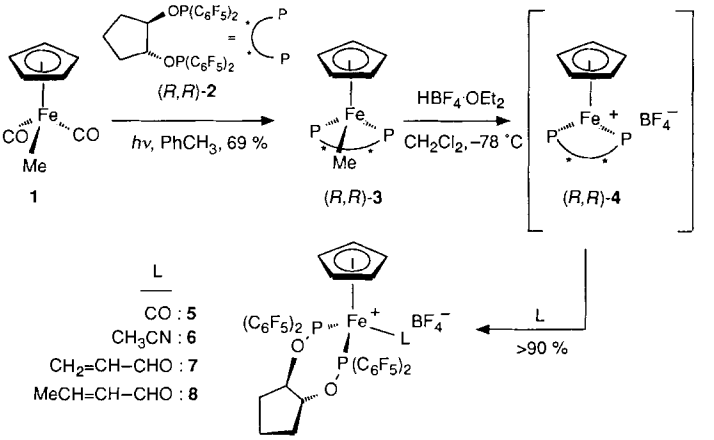
Titanium[2o] and copper[2k, l] complexes apart, only three examples of asymmetric transition-metal catalysts for the Diels–Alder reaction have been reported. An Fe^{III}-based Lewis acid, containing a C_2-chiral bis(oxazoline) ligand and generated in situ, catalyzed the reaction between cyclopentadiene and 3-acryloyl-1,3-oxazolidin-2-one to give the cycloadduct with 86% ee and 99:1 *endo/exo* selectivity.[3] Lower enantioselectivities (<60%) were observed for the same reaction with another Fe^{III} system with bis(sulfoxide) ligands,[4] which had also been generated in situ. The reactions between cyclopentadiene and the dienophiles acrolein, methacrolein, and methyl methacrylate, catalyzed by a chiral Lewis acid based on zirconium, also gave only modest enantioselectivities.[5]

Achiral transition-metal catalysts for the Diels–Alder reaction were investigated by several groups.[6–8] The complex $[CpFe(CO)_2(thf)]BF_4$ was one of a series of catalysts studied by Hersh et al. They found that the Diels–Alder reaction between acroleins and cyclopentadiene was accelerated in the presence of the iron(II) complex. The catalytic activity, however, was significantly greater than expected on the basis of stoichiometrically determined rate constants.[6a] This suggested that another catalyst, a Brønsted or Lewis acid impurity, was present and cast some doubt on the role of the iron complex in this process. According to these authors, the best evidence for involvement of the iron center would be to demonstrate that a chiral analogue is capable of asymmetric induction in this reaction. We here provide this evidence.

The Lewis acidity of the d^6 iron(II) center in the complex described above arises as a result of the overall positive charge of the complex and the presence of the two CO acceptor ligands. This effect is, however, attenuated by the donor ligand Cp, and $[CpFe(CO)]^{2+}$ is a weak Lewis acid as a result. The most direct way to asymmetrically modify this complex is by substituting one or both carbonyl ligands by a chiral ligand. It is readily apparent that Lewis acidity will only be preserved if the electronic characteristics of the new ligand resemble those of CO. In the search for a catalyst with chirality at the metal center, Hossain et al. found that substitution of one of the two CO ligands by PPh_3 completely suppressed activity in the Diels–Alder reaction. Some activity remained, however, with the less electron-rich complex $[CpFe(CO)\{P(OMe)_3\}(thf)]BF_4$.[8b]

We recently reported the synthesis of both enantiomers of several new C_2-chiral phosphorus ligands that, to a degree, emulate the bonding characteristics of CO.[9] We envisaged replacing the two *cis* carbonyl ligands of various transition-metal catalysts with these new ligands and using the resulting complexes in asymmetric reactions. For the investigations reported here, we chose to modify the Lewis acid $[CpFe(CO)_2]^+$ with the fluorophenyl ligand (*R,R*)-**2**.

Complex [CpFe(L)Me] (**3**) was readily prepared by photolytic ligand substitution in **1** (Scheme 1). Treatment of a CH_2Cl_2



Scheme 1. Synthesis of the chiral Lewis acid **4** and its complexes with CO, acetonitrile, acrolein, and crotonaldehyde.

solution of **3** with HBF_4 at −78 °C presumably generated the coordinatively unsaturated cationic intermediate **4**. Reaction of **4** with CO in situ afforded the carbonyl complex **5**, and reaction with MeCN gave complex **6**. The X-ray structure analysis of **6** shows the spatial arrangement of the four bulky pentafluorophenyl groups in the complex (Fig. 1).[10]

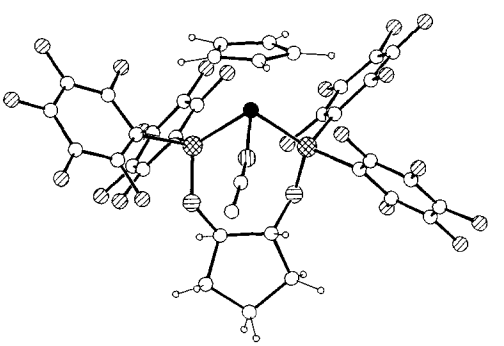


Fig. 1. Crystal structure of rac-**6**. The (*R,R*) enantiomer is shown. ● = Fe, ○ = N, ⊜ = O, ⊕ = P, ◎ = F.

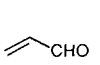
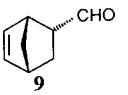
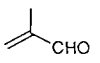
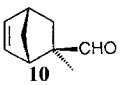
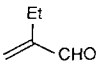
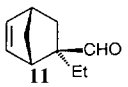
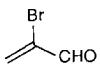
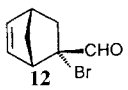
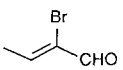
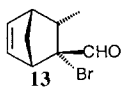
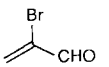
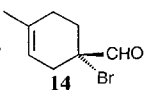
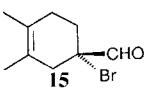
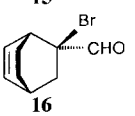
The deep green solution of **4** in CH_2Cl_2 turned dark red when acrolein was added. Addition of hexane resulted in precipitation of a brown solid **7**, which was found to be the acrolein complex with an η^1 M–O=C interaction.[11] Full characterization proved difficult because of the instability of **7** in solution and its high reactivity towards Lewis bases.

In the presence of 5 mol% of (*R,R*)-**7** and 2.5 mol% of 2,6-di-*tert*-butylpyridine, methacrolein reacted with cyclopentadiene to give (1*S*,2*R*,4*S*)-2-methylbicyclo[2.2.1]hept-5-ene-2-carbaldehyde (**10**) in 62% yield, 90% *ee*, and with an *exo/endo* formyl selectivity of 97/3. This and further examples of asymmetric

[*] Prof. Dr. E. P. Kündig, B. Bourdin
Département de Chimie Organique, Université de Genève
30 Quai Ernest Ansermet, CH-1211 Genève (Switzerland)
Telefax: Int. code + (22)329-6102
Dr. G. Bernardinelli
Laboratoire de Crystallographie, Université de Genève (Switzerland)

[**] We thank the Swiss National Science Foundation for support of this work (FNS grant 20-32672.91)

Table 1. Asymmetric Diels–Alder reactions catalyzed by (*R*,*R*)-7 [a].

Entry	Dienophile	Diene	T [°C]/*t* [h]	Product [b]	*exo*/*endo* [c]	Yield [d] [%]	*ee* [%] (configuration)
1			−30/16	 **9**	38/62	46	84 [e] (*R*) [f] *exo*: 64 [e]
2			−20/20	 **10**	97/3	62	90 [e] (*R*) [f]
3			−20/20	 **11**	98/2	55	94 [g]
4			−40/16	 **12**	95/5	87	95 [h] (*S*) [i]
5			−20/18	 **13**	97/3	12	88 [j]
6			−20/18	 **14**	[k]	88	96 [j], 97 [g]
7			−20/18	 **15**		92	97 [j], 98 [g]
8			−20/28	 **16**	10/90 [m]	88 [l]	>99 [h]

[a] The reactions were carried out in freshly distilled CH_2Cl_2 (1 M solution) with 5 mol% of catalyst, 2.5 mol% of 2,6-di-*tert*-butylpyridine, and equimolar portions of diene and dienophile (unless otherwise noted). [b] The structure shown is the major product. [c] The terms *exo* and *endo* refer to the position of the formyl group. [d] Isolated yield after flash chromatography. [e] Determined by GC analysis after conversion to the acetal derivative of (2*R*,4*R*)-pentanediol [14]. [f] The configuration was assigned by comparing the sign of $[\alpha]_D$ with that in the literature: (*R*)-**9** [1a], (*R*)-**10** [1a,14]. [g] Determined from the ^{1}H NMR spectrum after conversion to the acetal derivative of (2*R*,4*R*)-pentanediol. [h] Determined from the ^{1}H NMR spectrum in the presence of the chiral shift reagent Eu(hfc)$_3$. [i] Assignment after conversion to norbornen-2-one and comparison of the sign of $[\alpha]_D$ with that in the literature [13a,21]. [j] Determined by GC analysis on a chiral column (MN FS-Lipodex E). [k] A single regioisomer was observed. [l] 5 equiv of diene was used; yield with 1 equiv was 28%. [m] *endo*-Formyl assignment is based on ^{1}H NMR and GC comparison.

Diels–Alder reactions between α,β-enals and dienes are listed in Table 1. 2,6-Di-*tert*-butylpyridine was added to scavenge residual acid impurities. In the absence of a scavenger, the rate of reaction was found to vary; this is consistent with Hersh's findings.[6a] More importantly, enantioselectivities were lower (20–60% *ee*) and not reproducible. This behavior is expected if a competing achiral catalyst is present.[12]

The best results were obtained with the very reactive dienophile α-bromoacrolein. Corey et al. used this compound for the synthesis of versatile cycloaddition products.[2i, 13] As was observed with other Lewis acid catalysts, high *exo* selectivity was found for α-substituted enals. Yields were lower with other dienophiles, but enantioselectivities remained quite high. Thus, while the *ee* of the *endo* product **9** from the reaction with acrolein matched the best literature result,[14] yield and *exo*/*endo* selectivity were low. (*E*)-Crotonaldehyde did not react. Higher reaction temperatures proved impracticable because of slow decomposition of the catalyst above −20 °C. The yield for the reaction of α-bromoacrolein (entry 8) with cyclohexadiene was improved from 28 to 88% by increasing the proportion of diene from one equivalent to five. It is noteworthy that a single enantiomer of the *endo*-formyl diastereomer was formed in this reaction is and that diastereoselectivity is good.

A transition state, based on the solid state structure of **6**, that accounts for the observed stereoselectivity is shown in Figure 2. The diene approaches the olefin *si* face of the s-*trans* conformer

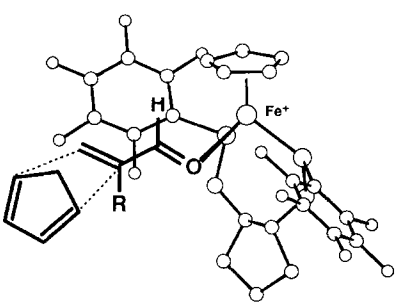


Fig. 2. Model of the transition state for the Diels–Alder reaction catalyzed by **7**. A partial structure of complex **6**, the coordinated α-substituted enal, and the cyclopentadiene are shown.

of the coordinated enal. The *re* face is shielded by a pentafluorophenyl ring of the ligand (*R*,*R*)-**2**.

In conclusion, despite the limitations that can be attributed to the weak Lewis acidity[15] and low thermal stability of **7**, these first results are highly encouraging. They confirm the hypothesis that chiral ligands that model the bonding properties of CO are attractive for asymmetric catalysis. Further studies will focus on understanding the transition state in these reactions and on improving the catalytic system for the Diels–Alder reaction and other Lewis acid catalyzed processes.[15]

Experimental Procedure

(*R,R*)-**3**: A N_2-saturated solution of **1** [16] (0.291 g, 1.5 mmol) and (*R,R*)-**2** (1.249 g, 1.5 mmol) [9] in toluene (90 mL) was irradiated at 15 °C with a 125 W high-pressure mercury lamp equipped with a pyrex filter. A slow stream of N_2 was maintained throughout the reaction, and progress was monitored by *IR* analysis (νCO) of samples taken from the reaction. When all starting material had been consumed, the mixture was filtered through Celite, and volatiles were removed under vacuum. Recrystallization from hexane at −20 °C afforded (*R,R*)-**3** (1.004 g, 69%). Enantiomeric purity was >99% as measured by HPLC (Daicel OD, eluent: hexane/*i*PrOH 400/1). M.p. 141 °C (decomp.); $[\alpha]_D^{20} = +1.83$ ($c = 0.2$ in $CHCl_3$); ^{1}H NMR (400 MHz, C_6D_6, 21 °C): $\delta = 0.37$ (br. t, ^3J(H,P) = 6.5 Hz, 3H; Me), 1.12–1.76 (m, 6H; CH_2), 3.87–4.02 (m, 1H; OCH), 3.97 (s, 5H; C_5H_5), 4.21–4.35 (m, 1H; OCH); ^{31}P NMR (162 MHz, C_6D_6, 21 °C, H_3PO_4): $\delta = 156.81$ (AB(bd), ^2J(P,P) = 82 Hz; P_1), 158.13 (AB(bd), ^2J(P,P) = 82 Hz; P_2); ^{13}C NMR (100 MHz, CD_2Cl_2, 21 °C): $\delta = -25.3$ (br. t, ^2J(C,P) = 28 Hz; CH_3), 18.8 (CH_2), 28.8 (d, J(C,P) = 7 Hz; CH_2), 29.2 (d, J(C,P) = 4 Hz; CH_2), 80.0 (OCH), 81.8 (d, J(C:P) = 5 Hz; OCH), 84.9 (C_5H_5), 136.4–137.5 (m, C_{arom}), 138.9–140.0 (m, C_{arom}), 140.4–145.2 (m, C_{arom}), 146.0–147.0 (m, C_{arom}), 148.7–149.5 (m, C_{arom}). Anal.: calcd for $C_{35}H_{16}F_{20}FeO_2P_2$ (966.28): C 43.50, H 1.67; found: C 43.36, H 1.81.

(*R,R*)-**7**: To a stirred solution of (*R,R*)-**3** (0.581 g, 0.6 mmol) in CH_2Cl_2 (60 mL) at −78 °C was added HBF_4 (90 µL of a 54% solution in ether, 1 equiv). After 15 min at −75 °C, the green solution was treated with acrolein (210 µL, 5 equiv) and an immediate color change to red was observed. The reaction mixture was allowed to warm up to −20 °C over a period of 3.5 h, and then concentrated to about 10 mL. The product was precipitated by addition of hexane (20 mL), isolated, and then washed several times with the same solvent. A red-brown powder (*R,R*)-**7** was obtained in 90% yield (0.591 g). ^{1}H NMR (400 MHz, CD_2Cl_2, −20 °C): $\delta = 9.79$ (br. s, 1H), 7.09–6.83 (br. d, 1H, $J = 15$ Hz), 6.82–6.60 (m, 1H), 6.35–6.10 (m, 1H), 4.47 (s, 5H), 4.23–4.02 (m, 1H), 3.90–3.70 (m, 1H), 2.15–1.25 (m, 6H); ^{31}P NMR (162 MHz, CD_2Cl_2, −20 °C, H_3PO_4): $\delta = 156.15$ (AB(bd), $J = 79$ Hz, P_1), 159.55 (AB(bd), $J = 79$ Hz, P_2).

Cycloaddition reactions: To freshly distilled CH_2Cl_2 (2 mL) was added at −40 °C (*R,R*)-**7** (110 mg, 0.1 mmol) and 2,6-di-*tert*-butylpyridine (12 µL, 0.05 mmol). The resulting dark red solution was then treated with methacrolein (170 µL, 2.0 mmol). After the mixture had been stirred for 15 min, freshly distilled cyclopentadiene (170 µL, 2.0 mmol) was slowly added (5 min). The reaction mixture was stirred at −20 °C for 20 h. The catalyst was precipitated by addition of hexane, and washed three times with the same solvent. The combined organic phase was exposed to air to remove traces of residual catalyst by oxidation. Filtration through Celite, solvent removal, and flash chromatography on silica gel (eluent hexane/ether 10/1) gave **10** in 62% (174 mg) with an *endo*/*exo* ratio of 3/97 (determined by GC before chromatography). The *ee* of *exo*-**10** was 90%.

Received: April 9, 1994 [Z 6835 IE]
German version: *Angew. Chem.* **1994**, *106*, 1931

[1] For the first successful asymmetric Lewis acid catalyzed Diels–Alder reaction, see a) S. Hashimoto, N. Komeshima, K. Koga, *J. Chem. Soc. Chem. Commun.* **1979**, *437*; for recent reviews, see b) U. Pindur, G. Lutz, C. Otto, *Chem. Rev.* **1993**, *93*, 741; c) H. B. Kagan, O. Riant, *Chem. Rev.* **1992**, *92*, 1007; d) K. Narasaka, *Synthesis* **1991**, 1.

[2] a) See [1c], and references therein; b) J. M. Hawkins, S. Loren, M. Nambu, *J. Am. Chem. Soc.* **1994**, *116*, 1657; c) K. Ishihara, H. Yamamoto, *ibid.* **1994**, *116*, 1561; d) J. Bao, W. D. Wulff, A. L. Rheingold, *ibid.* **1993**, *115*, 3814; e) K. Ishihara, Q. Gao, H. Yamamoto, *ibid.* **1993**, *115*, 10412; f) *J. Org. Chem.* **1993**, *58*, 6917; g) E. J. Corey, T. D. Roper, K. Ishihara, G. Sarakinos, *Tetrahedron Lett.* **1993**, *34*, 8399; h) E. J. Corey, Z. Wang, *ibid.* **1993**, *34*, 4001; i) E. J. Corey, T.-P. Loh, *ibid.* **1993**, *34*, 3979; j) K. Tanaka, H. Uno, H. Osuga, H. Suzuki, *Tetrahedron: Asymmetry* **1993**, *4*, 629; k) D. A. Evans, T. Lectka, S. J. Miller, *Tetrahedron Lett.* **1993**, *34*, 7027; l) D. A. Evans, S. J. Miller, T. Lectka, *J. Am. Chem. Soc.* **1993**, *115*, 6460; m) E. J. Corey, T.-P. Loh, T. D. Roper, M. D. Azimioara, M. C. Noe, *ibid.* **1992**, *114*, 8290; n) E. J. Corey, S. Sarshar, J. Bordner, *ibid.* **1992**, *114*, 7938; o) K. Narasaka, I. Yamamoto, *Tetrahedron* **1992**, *48*, 5743.

[3] E. J. Corey, N. Imai, H.-Y. Zhang, *J. Am. Chem. Soc.* **1991**, *113*, 728.

[4] N. Khiar, I. Fernández, F. Alcudia, *Tetrahedron Lett.* **1993**, *34*, 123.

[5] Y. Hong, B. A. Kuntz, S. Collins, *Organometallics* **1993**, *12*, 964.

[6] a) P. V. Bonnesen, C. L. Puckett, R. V. Honeychuck, W. H. Hersh, *J. Am. Chem. Soc.* **1989**, *111*, 6070; b) R. V. Honeychuck, P. V. Bonnesen, J. Farahi, W. H. Hersh, *J. Org. Chem.* **1987**, *52*, 5293.

[7] a) W. Odenkirk, A. L. Rheingold, B. Bosnich, *J. Am. Chem. Soc.* **1992**, *114*, 6392; b) T. K. Hollis, W. Odenkirk, N. P. Robinson, J. Whelan, B. Bosnich, *Tetrahedron* **1993**, *49*, 5415; c) T. K. Hollis, N. P. Robinson, B. Bosnich, *J. Am. Chem. Soc.* **1992**, *114*, 5464.

[8] a) A. K. Saha, M. M. Hossain, *Tetrahedron Lett.* **1993**, *34*, 3833; b) A. S. Olson, W. J. Seitz, M. M. Hossain, *ibid.* **1991**, *32*, 5299.

[9] E. P. Kündig, C. Dupré, B. Bourdin, A. Cunningham, Jr., D. Pons, *Helv. Chim. Acta* **1994**, *77*, 421.

[10] Crystallographic data for *rac*-**6**: Red crystals were grown from a CH_2Cl_2/hexane solution. $(C_{36}H_{16}NO_2P_2F_{20}Fe)(C_6H_{14})(PF_6)$, $M_r = 1223.4$; $\mu = 0.582$ mm^{-1}, $F(000) = 2440$, $\rho_{calcd} = 1.80$ g cm^{-3}, monoclinic, $P2_1/n$, $Z = 4$, $a = 11.893(5)$, $b = 16.213(8)$, $c = 23.402(8)$ Å, $\beta = 91.09(1)°$, $V = 4512(3)$ Å^3, from 25 reflections ($14 < 2\theta < 26°$). Cell parameters and intensities were measured at room temperature on a Nonius CAD4 diffractometer with graphite-monochromated $Mo_{K\alpha}$ radiation ($\lambda = 0.71069$ Å), ω–2θ scans, scan width $1.2° + 0.25 \tan\theta$, and scan speed 0.02–0.14° per s. Two reference reflections measured every 100 reflections showed variation less than $3.2\sigma(I)$. $-11 < h < 11$, $0 < k < 16$, $0 < l < 23$; 4978 measured reflections, 4838 unique reflections of which 2862 were observable ($|F_o| > 4\sigma(F_o)$). Data were corrected for Lorentz and polarization effects but not for absorption. The structure was solved by direct methods (MULTAN 87 [17]), all other calculations used XTAL [18] system and ORTEP [19] programs. Atomic scattering factors and anomalous dispersion terms were taken from ref. [20]. Full-matrix least-squares refinement based on F with weighting 1 gave final values $R = wR = 0.010$ for 656 variables. Hydrogen atoms were placed in calculated positions. Both the PF_6^- and hexane molecules are disordered. The fluorine atoms of PF_6^- were found at 13 sites with population parameters ranging between 0.25 and 1; the hexane molecules were entirely disordered. The disorder results in rather high residual R factors. Further details of the crystal structure investigation are available on request from the Director of the Cambridge Crystallographic Data Centre, 12 Union Road, GB-Cambridge CB2 1EZ (UK), on quoting the full journal citation.

[11] Complex **7** is stable in the solid state and can be handled in air. It reacts with CH_3CN to give **6** quantitatively. In CH_2Cl_2, **7** decomposes gradually above −20 °C. The ^{1}H NMR spectrum showed **7** to be a 1:1 complex of acrolein with **4**. Although signals were broad, the pattern is consistent with an M–O=C σ-bound acrolein. The IR spectrum of the more stable crotonaldehyde complex **8** showed an absorption at 1604 cm^{-1} (in KBr). Compared to free (*E*)-crotonaldehyde, the carbonyl band in the complex is shifted by 88 cm^{-1} to lower wavenumbers. This is consistent with the proposed mode of coordination of the Lewis acid. For important references on Lewis acid–carbonyl complexation, see a) Y.-H. Huang, J. A. Gladysz, *J. Chem. Educ.* **1988**, *65*, 298; b) S. Shambayati, S. L. Schreiber in *Comprehensive Organic Synthesis*, *Vol. 1* (Eds. B. M. Trost, I. Fleming), Pergamon, Oxford, **1991**, pp. 283–324; c) S. E. Denmark, N. G. Almstead, *J. Am. Chem. Soc.* **1993**, *115*, 3133, and references therein.

[12] Control experiments with the chiral ligand only (no iron) in combination with HBF_4 or BF_3 gave, at best, very low yields of racemic Diels–Alder products.

[13] a) E. J. Corey, T.-P. Loh, *J. Am. Chem. Soc.* **1991**, *113*, 8966; b) E. J. Corey, C. L. Cywin, *J. Org. Chem.* **1992**, *57*, 7372.

[14] K. Furuta, S. Shimizu, Y. Miwa, H. Yamamoto, *J. Org. Chem.* **1989**, *54*, 1481.

[15] Low Lewis acidity should be an asset in the hetero-Diels–Alder reaction and in the Mukaiyama reaction. For reports on the catalysis of the hetero-Diels–Alder reaction by $[CpRu(PPh_3)_2(C_2H_4)]^+$ and $[CpRu((S,S)\text{-chiraphos})(C_2H_4)]^+$ (25% *ee*), see J. W. Faller, C. J. Smart, *Tetrahedron Lett.* **1989**, *30*, 1189, and of the Mukaiyama aldol reaction by $[CpFe(dppe)]^+$, see T. Bach, D. N. A. Fox, M. T. Reetz, *J. Chem. Soc. Chem. Commun.* **1992**, 1634. For a review of transition metal Lewis acids see W. Beck, K. Sünkel *Chem. Rev.* **1988**, *88*, 1405.

[16] a) C. Roger, M.-J. Tudoret, V. Guerchais, C. Lapinte, *J. Organomet. Chem.* **1989**, *365*, 347; b) T. S. Piper, G. Wilkinson, *J. Inorg. Nucl. Chem.* **1956**, *3*, 104.

[17] P. Main, S. J. Fiske, S. E. Hull, L. Lessinger, G. Germain, J.-P. Declercq, M. M. Woolfson, *A System of Computer Programs for the Automatic Solution of Crystal Structures from X-Ray Diffraction Data*, University of York, England, and Louvain-la-Neuve, Belgium, **1987**.

[18] *XTAL3.2 User's Manual* (Eds.: S. R. Hall, H. D. Flack, J. M. Stewart), Universities of Western Australia and Maryland, **1992**.

[19] C. K. Johnson, *ORTEP II; Report ORNL-5138*, Oak Ridge National Laboratory, Oak Ridge, TN, **1976**.

[20] *International Tables for X-ray Crystallography, Vol. IV*, Kynoch, Birmingham, **1974**.

[21] L. A. Paquette, C. W. Doecke, F. R. Kearney, A. F. Drake, S. F. Mason, *J. Am. Chem. Soc.* **1980**, *102*, 7228.

Synthesis and Structure of $[WOTe_3]^{2-}$

Donna R. Gardner, James C. Fettinger, and Bryan W. Eichhorn*

In contrast to the large number of compounds containing terminal oxido,[1] sulfido,[2] and selenido[3] ligands, compounds containing terminal tellurido ligands are rare.[4] For example, the $[MQ_4]^{2-}$ ions are known for M = Mo, W; Q = O, S, and Se but not for Te.[5] The first compound with a terminal tellurido ligand, $[W(PMe_3)_4(Te)_2]$, was isolated only a few years ago.[6] Subsequently, several tellurido complexes of the early transition metals (Zr, Hf, Nb, Ta, W) have been prepared and characterized.[7-11] The methods for preparing tellurido species vary from direct oxidative additions of elemental Te to disilyltelluride elimination reactions. It is somewhat surprising that reactions between polytelluride anions and precursors of transition metal complexes have thus far not led to compounds containing terminal tellurido ligands; similar reactions involving the lighter polychalcogenides have been successful.[3, 12, 13]

We have been investigating the chemistry of the polychalcogenides with dinuclear Mo and W carboxylato complexes having metal–metal quadruple bonds. The reaction between $[Mo_2(O_2CMe)_4]$ and K_2Te_4 in ethylenediamine (en) that gave the unusual $\{[Mo_2(\mu\text{-}Te_2)_2(en)_2]_2(\mu\text{-}Te_3)_2(\mu\text{-}Te_2)\}^{2-}$ ion was described previously.[14] In an attempt to extend this chemistry to the dinuclear tungsten systems, we conducted similar experiments with $[W_2(O_2CC_3H_7)_4]$ and K_2Te_2. Herein we report the synthesis and characterization of a novel product from these reactions, $[WOTe_3]^{2-}$, which contains three terminal tellurido ligands. The existence of this compound suggests that homoleptic $[MTe_4]^{n-}$ ions may indeed be isolable in contrast to previous beliefs.[12]

The reaction of $[W_2(O_2CC_3H_7)_4]$ and K_2Te_2 in en gave low yields of the $[WOTe_3]^{2-}$ ion as the PPh_4^+ salt. The dark red-brown crystals have been characterized by single-crystal X-ray diffraction, IR spectroscopy, and energy dispersive X-ray analysis (EDX). The same crystalline compound[15] was also isolated in low yields from the reaction of WCl_4 and K_2Te_2 in en. The source of the oxygen atom in the product is not known for either reaction. The more reasonable reaction of $WOCl_4$ and K_2Te in en is complicated by the extensive aminolysis of $WOCl_4$, and $[WOTe_3]^{2-}$ is not detected. The same reaction conducted in *N*,*N*-dimethyformamide (DMF) gives the $[OW(Te_4)_2]^{2-}$ ion as originally reported by Kolis and Flomer.[16] The majority of the reactions between transition metal complexes and polytellurides reported thus far involve DMF solvent and give polytellurido complexes. For example, Kolis and Flomer have shown that reactions of WCl_6 and WCl_4 and solutions of polytelluride anions (Te_x^{2-}, where $x = 2-5$) in DMF lead to the W^{IV} compound $(PPh_4)_2[WO(Te_4)_2]$.[16] In contrast, numerous compounds containing terminal sulfido and selenido ligands have been prepared from polychalcogenide precursors in DMF (e.g. $[WSe_4]^{2-}$, $[Mo_2(S)_2(\mu\text{-}S)_2(\eta^2\text{-}S_2)_2]^{2-}$, and $[W_2Se_6]^{2-}$).[17-19]

The single-crystal X-ray structure[20] of $(PPh_4)_2[WOTe_3]\cdot 0.5en$ reveals that the C_{3v}-symmetrical $[WOTe_3]^{2-}$ ion is isostructural to $[WOS_3]^{2-}$ (Fig. 1).[22] The distortions from idealized tetrahedral symmetry arise from the differences in size between the Te^{2-} and O^{2-} ligands. The W–Te bond lengths (2.54(1) Å average) in $[WOTe_3]^{2-}$ are among the shortest M–Te contacts reported to date[6, 7, 9-11] but are best described as

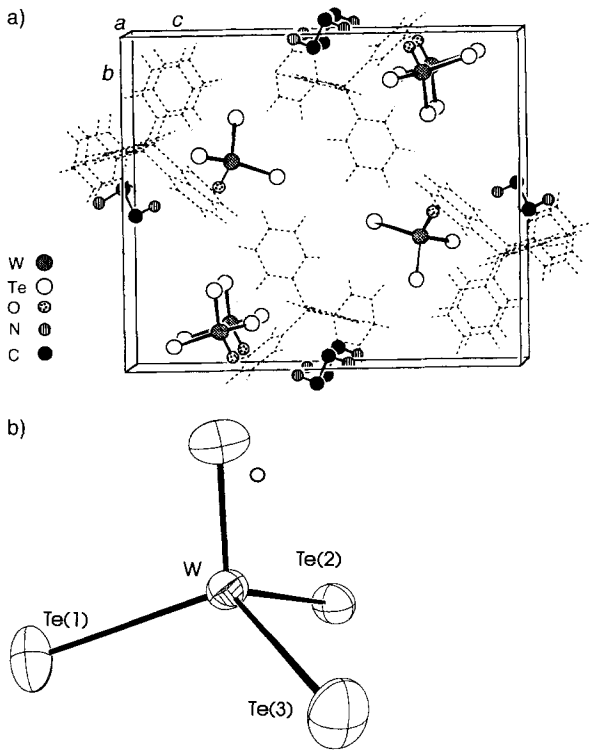


Fig. 1. a) Unit cell of $(PPh_4)_2[WOTe_3]\cdot 0.5en$ and b) ORTEP drawing of the $[WOTe_3]^{2-}$ anion. Selected interatomic distances [Å] and angles [°]: W–O 1.716(6), W–Te(1) 2.544(2), W–Te(2) 2.542(2), W–Te(3) 2.530(1); Te(1)-W-Te(2) 110.29(6), Te(1)-W-Te(3) 111.68(3), Te(1)-W-O 109.2(2), Te(2)-W-Te(3) 110.20(4), Te(2)-W-O 107.3(2), Te(3)-W-O 108.1(2).

double bonds (see below). The short bonds are consistent with the high oxidation state of W and the low coordination number of the metal ion relative to other known W compounds. The W–O bond length (1.716(6) Å) is within the range reported for other W^{VI} complexes (1.89–1.57 Å)[11b] and is shorter than the W–O contacts in the $[WO_4]^{2-}$ and $[WOS_3]^{2-}$ ions at 1.79 and 1.760 Å, respectively.[22] This apparent trend of decreasing W–O distance for the $[WOQ_3]^{2-}$ ions (where Q = O, S, and Te) is attributed to the decreasing π-donor ability of the heavier chalcogenides.[22] The ethylenediamine solvate molecule and the two PPh_4^+ ions are well separated from the anion and are crystallographically well behaved.

The IR spectrum of the $[WOTe_3]^{2-}$ ion (KBr pellet) shows bands associated with the PPh_4^+ ions, the en solvate molecule, and a strong ν_{W-O} band at 904 cm^{-1}. A summary of the structural and IR spectroscopic data for the $[WOQ_3]^{2-}$ ions is given in Table 1. The increase in W–O force constants (f_{W-O}) for the $[WOQ_3]^{2-}$ ions where Q = O, S, Se, and Te parallels the trend in decreasing W–O distances and W–Q π-bond orders (see below). In addition, the colors of the $[WOQ_3]^{2-}$ ions change

Table 1. Structural and IR spectroscopic data for the $[WOQ_3]^{2-}$ ions where Q = O, S, Se, Te.

Cmpd.	W–O [Å][a]	W–Q [Å][a]	$\tilde{\nu}_{W-O}$ [cm^{-1}]	f_{W-O} [mdyn $Å^{-1}$]	Ref.
$[WO_4]^{2-}$	1.79	1.79	931[b], 829	6.38	[23]
$[WOS_3]^{2-}$	1.76	2.20	878	6.66	[23]
$[WOSe_3]^{2-}$	–	–	878	6.66	[23]
$[WOTe_3]^{2-}$	1.716(6)	2.54(1)	904	7.09	[24]

[a] Averaged where appropriate. [b] Raman-active band.

[*] Prof. B. W. Eichhorn, D. R. Gardner, Dr. J. C. Fettinger
Department of Chemistry, University of Maryland
College Park, MD 20742 (USA)
Telefax: Int. code + (301)314-9121

 © VCH Verlagsgesellschaft mbH, D-69451 Weinheim, 1994 0570-0833/94/1818-1859 $ 10.00+.25/0

from colorless (Q = O) to yellow (Q = S) to orange-red (Q = Se) to dark red-brown (Q = Te) as expected from the decrease in energy of the $^1A \rightarrow {}^1E$ ligand-to-metal charge transfer transition (see below).

The maximum M–Q bond order in a tetrahedral $[MQ_4]^{2-}$ ion is 2.25, which gives a total of nine M–Q bonds ($4\sigma + 5\pi$).[25] When all four Q ligands are of equal π-donor ability (e.g. $[WO_4]^{2-}$) the π interactions transform under $e + t_2$ symmetry and are of course distributed equally among the four Q atoms (Fig. 2). When the Q ligands are of differing π-donor

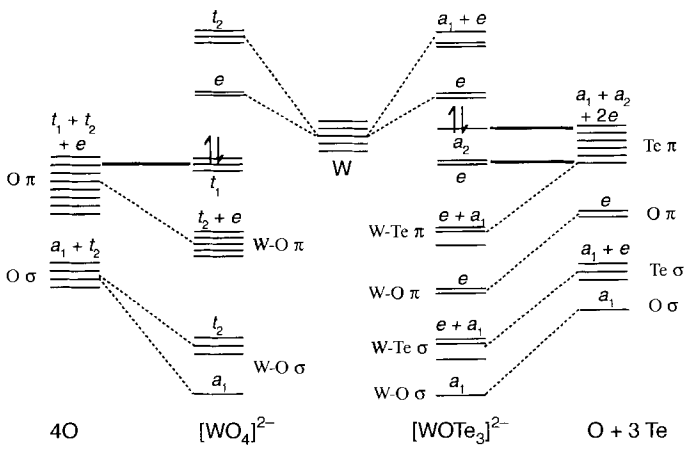


Fig. 2. Qualitative orbital interaction diagrams for $[WO_4]^{2-}$ and $[WOTe_3]^{2-}$. The latter illustrates the limiting valence description comprising $W^-{\equiv}O^+$ and W=Te interactions. The d orbitals for W are given in the middle.

ability, the individual bond orders may vary in order to attain the five strongest possible π bonds. For example, one could obtain a W–O bond order of three with W–Te bond orders of two for the $[WOTe_3]^{2-}$ ion in the limiting case (Fig. 2).[26] Due to the trends in bond lengths and f_{W-O} values in the $[WOQ_3]^{2-}$ series, it appears that $[WOTe_3]^{2-}$ is approaching this limit. One may therefore assign formal W–Te bond orders of two in this complex. The only reported metal–tellurido complexes that could potentially have W–Te bond orders of more than two are the *cis*-$[WTe_2(PMe_3)_2(\eta^2\text{-}OCR_2)]$ compounds where R = H, Ph.[11] The $[WOTe_3]^{2-}$ ion represents the limit of Te incorporation in the tetrahedral $[WQ_4]^{2-}$ ion that does not require a W–Q bond order of more than two. Attempts to prepare $[WTe_4]^{2-}$ are in progress.

Experimental Procedure

Method 1: With Schlenk techniques $[W_2(O_2CC_3H_7)_4]$ (100 mg, 0.14 mmol) and K_2Te_2 (54 mg, 0.16 mmol) were dissolved in approximately 8 mL of en. After the solution was stirred for 8 h at room temperature, $K(O_2CC_3H_7)$ was removed by filtration and solid PPh_4Br was added to induce crystallization. Red-brown needles of $(PPh_4)_2[WOTe_3]\cdot 0.5en$ were obtained after 6 d in low yield (ca. 8 mg, 6% yield based on Te).

Method 2: In a dry box, en (3 mL) was added to a vial containing WCl_4 (32.6 mg, 0.10 mmol). The green suspension was stirred for 30 min before K_2Te_x (20 mg, ≈0.10 mmol) and K_2Te_2 (20 mg, 0.06 mmol) were added as solids. The resulting red-brown solution was stirred for an additional 4.5 h. After the solution was filtered, solid PPh_4Br (84 mg, 0.20mmol) was added to induce crystallization. Red-brown needles of $(PPh_4)_2[WOTe_3]\cdot 0.5en$ were isolated after 8 d (ca. 6 mg, 5% based on W). Crystals were characterized by EDX, single-crystal X-ray diffraction (indexed cell) and IR ($\nu_{W-O} = 904\ cm^{-1}$).

$[W_2(O_2CC_3H_7)_4]$ was prepared according to published procedures [26] except $Na(O_2CC_3H_7)$ was used instead of $Na(O_2CtBu)$. ^1H NMR (400 MHz, [D$_6$]benzene): $\delta = 0.92$ (t, 12H), 1.80 (sextet, 8H), 3.12 (t, 8H). $^{13}C\{^1H\}$ NMR (100 MHz, [D$_6$]benzene): $\delta = 13.7, 21.6, 38.2, 183.6$. K_2Te_2 and K_2Te_x ($x \approx 1$) were prepared from stoichiometric amounts of K and Te in refluxing DMF.

Received: April 11, 1994 [Z6837IE]
German version: *Angew. Chem.* **1994**, *106*, 1973

[1] a) J. M. Mayer, *Inorg. Chem.* **1988**, *27*, 3899. b) W. A. Nugent, J. M. Mayer, *Metal-Ligand Multiple Bonds*, Wiley-Interscience: New York, **1988**, p. 173, and references therein.
[2] A. Müller, *Polyhedron* **1986**, *5*, 323, and references therein.
[3] M. A. Ansari, J. A. Ibers, *Coord. Chem. Rev.* **1990**, *100*, 223, and references therein.
[4] U. Siemeling, *Angew. Chem.* **1993**, *105*, 70; *Angew. Chem. Int. Ed. Engl.* **1993**, *32*, 67.
[5] A. Müller, E. Diemann, R. Jostes, H. Bögge, *Angew. Chem.* **1981**, *93*, 957; *Angew. Chem. Int. Ed. Engl.* **1981**, *20*, 934, and references therein.
[6] D. Rabinovich, G. Parkin, *J. Am. Chem. Soc.* **1991**, *113*, 9421.
[7] V. Christou, J. Arnold, *J. Am. Chem. Soc.* **1992**, *114*, 6240.
[8] U. Siemeling, V. C. Gibson, *J. Chem. Soc. Chem. Commun.* **1992**, 1670.
[9] V. Christou, J. Arnold, *Angew. Chem.* **1993**, *105*, 1551; *Angew. Chem. Int. Ed. Engl.* **1993**, *32*, 1450.
[10] W. A. Howard, G. Parkin, *J. Am. Chem. Soc.* **1994**, *116*, 606.
[11] D. Rabinovich, G. Parkin, *J. Am. Chem. Soc.* **1993**, *115*, 9822.
[12] J. W. Kolis, *Coord. Chem. Rev.* **1990**, *105*, 195.
[13] B. W. Eichhorn, D. R. Gardner, A. Nichols-Ziebarth, K. J. Ahmed, S. G. Bott, *Inorg. Chem.* **1993**, *32*, 5412.
[14] B. W. Eichhorn, R. C. Haushalter, F. A. Cotton, B. Wilson, *Inorg. Chem.* **1988**, *27*, 4084.
[15] The identity of the compound was confirmed by X-ray diffraction and IR spectroscopy.
[16] W. A. Flomer, J. W. Kolis, *Inorg. Chem.* **1989**, *28*, 2513.
[17] S. C. O'Neal, J. W. Kolis, *J. Am. Chem. Soc.* **1988**, *110*, 1971.
[18] W.-H. Pan, M. A. Harmer, T. R. Halbert, E. I. Steifel, *J. Am. Chem. Soc.* **1984**, *106*, 459.
[19] Y.-j. Lu, M. A. Ansari, J. A. Ibers, *Inorg. Chem.* **1989**, *28*, 4049.
[20] Crystal Data: Monoclinic, $P2_1/n$, $a = 14.290(5)$, $b = 16.693(4)$, $c = 19.75(2)$ Å; $\beta = 99.73(6)°$; $V = 4644(5)$ Å^3, $Z = 4$, $\rho_{calcd} = 1.855\ g\,cm^{-3}$. Data were collected at 20 °C [4491, $I > 2\sigma(I)$] on an Enraf-Nonius CAD4F diffractometer using $Mo_{K\alpha}$ radiation ($\lambda = 0.70930$ Å) and a $\theta/2\theta$ scan mode; $2\theta_{max} = 44.9°$; $\mu = 0.143\ mm^{-1}$; min./max. transmission = 0.723/1.00. Lorentz and polarization corrections were applied. A secondary extinction correction was also applied in the final stages of refinement. The structure was solved by direct methods and successive Fourier syntheses and refined against $|F^2|$ to $R(F) = 0.033$ and $R_w(F^2) = 0.077$ (unit weights) with the SHELXS solution package [21]. An empirical correction for absorption was made by using psi-scans. Maximum $\Delta/\sigma = 0.005$ for the last cycle with 509 parameters. Residual electron density ca. 2.4 Å from the W center (near the O atom) was observed in the later difference maps. The residual electron density could be refined as a Te atom with a partial occupancy of ca. 5% or a Br atom with a partial occupancy of ca. 7%. EDX analysis showed W, Te, and P in all samples and small amounts of Br in two of the crystals analyzed. For the final refinement, we assumed the chemical composition of $WTe_{3.05}O_{0.95}NP_2C_{49}H_{44}$ showing a 5% occupancy of Te near the O position. Further details of the crystal structure investigation may be obtained from the Fachinformationszentrum Karlsruhe, D-76344 Eggenstein-Leopoldshafen (FRG), on quoting the depository number CSD-58291.
[21] a) SHELXS-86 solution package, G. M. Sheldrick, *Acta. Crystallogr. Sect. A* **1990**, *46*, 467. b) SHELXL-93, G. M. Sheldrick, Siemens XRD, Madison, WI (USA).
[22] B. Krebs, B. Buss, A. Ferwanah, *Z. Anorg. Allg. Chem.* **1972**, *387*, 142.
[23] K. H. Schmidt, A. Müller, *Spectrochim. Acta Part A* **1972**, *28*, 1829.
[24] Data from this work. Force constants were calculated by using standard methods. R. S. Drago, *Physical Methods for Chemists*, 2nd ed., Saunders College Publishing, New York, **1972**, 151.
[25] Z. Lin, M. B. Hall, *Coord. Chem. Rev.* **1993**, *123*, 149.
[26] Formally, the W–O interaction must be described as either a single bond ($W^+\text{–}O^-$) or a triple bond ($W^-{\equiv}O^+$), because the W–O p interactions in the $[WOTe_3]^{2-}$ ion (C_{3v}) transform under *e* symmetry. However, linear combinations of the 3 Te π orbitals possess two π-type *e* combinations and can compete with O for the W-based *e* acceptor orbitals. For a bonding analysis of $[WOSe_3]^{2-}$, see A. Müller, E. Diemann, *Chem. Ber.* **1969**, *102*, 2044.
[27] D. J. Santure, A. P. Sattelberger, *Inorg. Synth.* **1989**, *26*, 219.

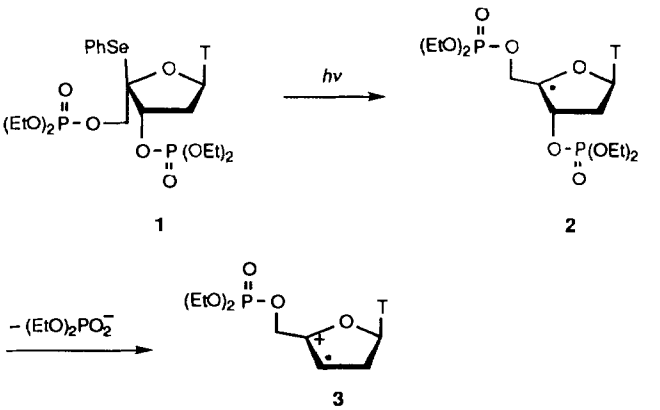
Synthesis and Selective Radical Cleavage of C-4′-Modified Oligonucleotides**

Bernd Giese,* Adrian Dussy, Cornelius Elie, Peter Erdmann, and Urs Schwitter

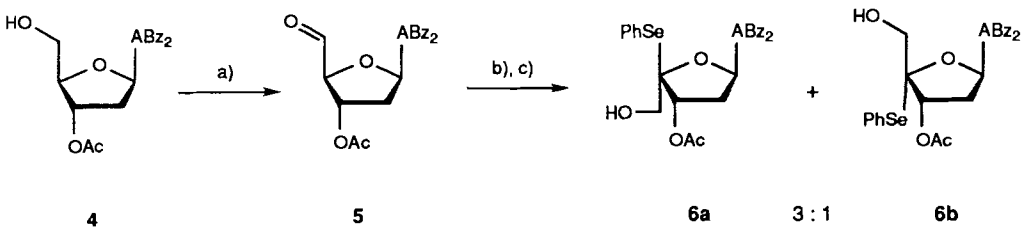
Dedicated to Professor Christoph Rüchardt on the occasion of his 65th birthday

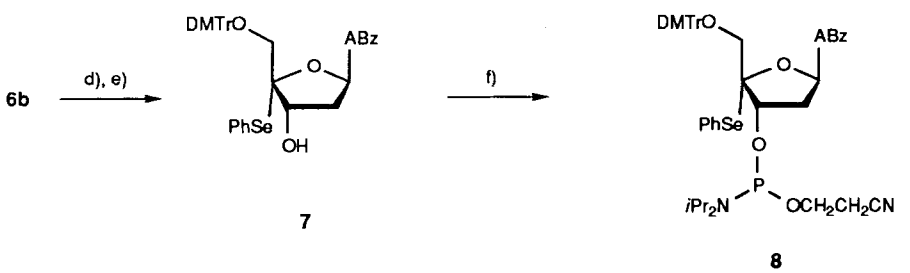
The chemotherapeutic action of the antibiotics bleomycin and neocarzinostatin is initiated by the abstraction of H atoms from the 4′- and/or 5′-position of the deoxyribose of DNA.[1] In studies with mononucleotides we recently found evidence for the Schulte-Frohlinde mechanism[2] for the anaerobic cleavage of the DNA strand.[3] Selenide **1** was photolyzed to generate the 4′-nucleotide radical **2**, which decays heterolytically to the radical cation **3**. Its occurrence was proven by chemical trapping experiments[3a] and by conductivity measurements.[3b]

However, since these experiments were conducted in nonaqueous solution on mononucleotides bearing phosphoric ester groups, conclusions regarding the radical reactions of oligonucleotides in water are problematic. We report here on the synthesis of 4′-deoxyribonucleotide radicals and studies of the strand scission of oligonucleotide radicals in aqueous solution.



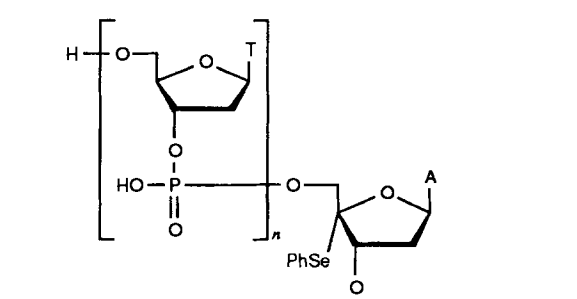
It was necessary to test whether selenide **8** could tolerate the oxidative, acidic, and basic conditions of the steps in oligonucleotide synthesis with the DNA synthesizer. Thus, we prepared dimer **9** as the triethylammonium salt both from **7** according to





Scheme 1. a) $(COCl)_2$, dimethyl sulfoxide (DMSO), NEt_3, CH_2Cl_2, −78 °C; b) PhSeCl, NEt_3, CH_2Cl_2, −78 to 0 °C, 87% (steps a + b); c) $Bu_4NBH_3(CN)$, THF, −78 to 0 °C, H^+/H_2O, 88%; d) *p*-dimethoxytrityl chloride (DMTrCl), pyridine, 20 °C, 85%; e) NaOMe, MeOH, 10 min, NH_3, MeOH, 50 min, 0 °C, 93%; f) $NC(CH_2)_2O(iPr_2N)PCl$, $NEtiPr_2$, CH_2Cl_2, CH_3CN, 20 °C, 90%. Bz = benzoyl, A = adenosyl.

The deoxythymidine derivative **1** has the wrong L-*lyxo* configuration at C-4′ for incorporation in oligonucleotides. However, selenation of deoxyadenosine **4** and subsequent reduction to the alcohol provides both the *lyxo* compound **6a** analogous to **1** and the *ribo* isomer **6b**, which were separated by flash chromatography (silica gel, ether:CH_2Cl_2 = 3:2).[4] Following appropriate protecting group manipulations (**6b** → **7**), the deoxyadenosyl derivative was converted into **8**,[5] the building block for the oligonucleotide synthesis (Scheme 1).



	n	m
9	0	1
10	4	7
11	8	7
12	12	7

[*] Prof. Dr. B. Giese, A. Dussy, Dr. C. Elie, P. Erdmann, U. Schwitter
Departement Chemie der Universität
St. Johanns-Ring 19, CH-4056 Basel (Switzerland)
Telefax: Int. code + (61)322-6017

[**] This work was supported by the Schweizerischen Nationalfonds zur Förderung der wissenschaftlichen Forschung.

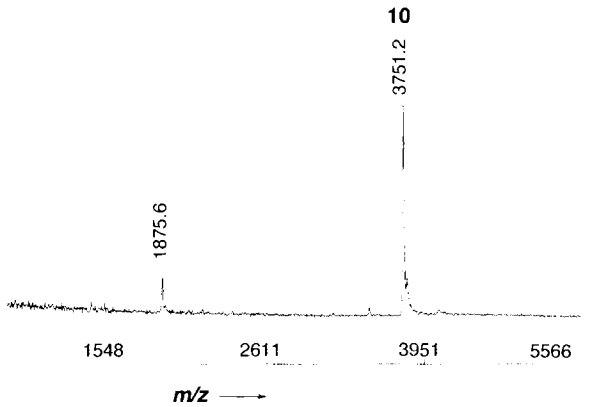


Fig. 1. MALDI-TOF mass spectrum (negative-ion mode) of the modified dodecamer **10**. The signal at *m/z* 1875.6 corresponds to the doubly deprotonated molecular ion of **10**.

the phosphotriester method,[6] and from phosphoramidite **8** with the DNA synthesizer.[7, 8] Thus deoxyadenosine derivative **8** is a nucleotide derivative that can be incorporated into oligonucleotides prepared with a synthesizer. Oligomers **10**–**12** were synthesized analogously; in each, the eighth nucleotide in the deoxythymidine chain is the precursor for the 4′-deoxyadenosyl radical.[9] Oligomers **10**–**12** were characterized by analytical gel electrophoresis and MALDI-TOF mass spectrometry[10] (Fig. 1).

An aqueous solution of the modified oligonucleotide **10** was irradiated with light having a wavelength >320 nm.[11] Within 60 min 90% of starting material **10** had reacted and given rise to predominantly the cleavage products **15** and **18** (Fig. 2a). When the photolysis experiment was conducted in the presence of an excess of glutathione,[11] then the H-trapping products **16** and **20** were formed in addition to **15** and **18** (Fig. 2b). The products were analyzed and assigned based on their MALDI-TOF mass spectra and by comparison of their HPLC retention times with those of the independently prepared compounds **15**, **16**, and **20**.

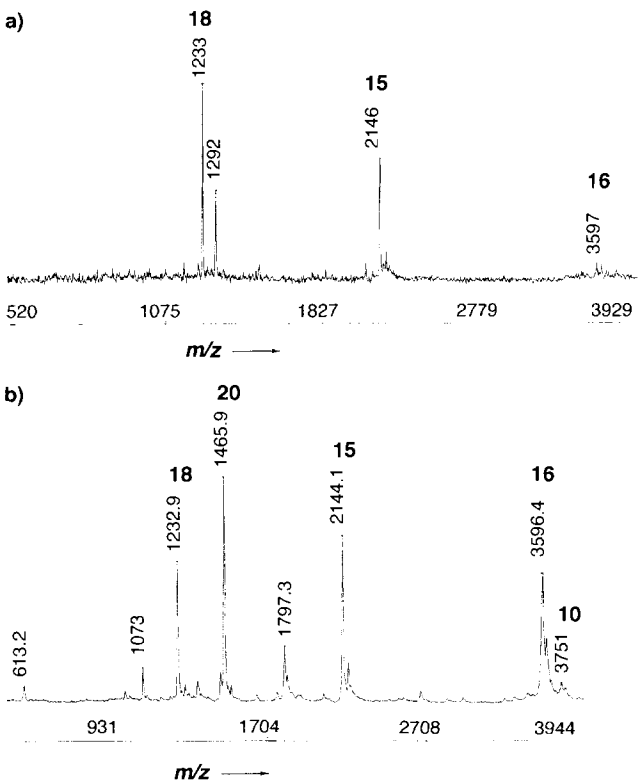
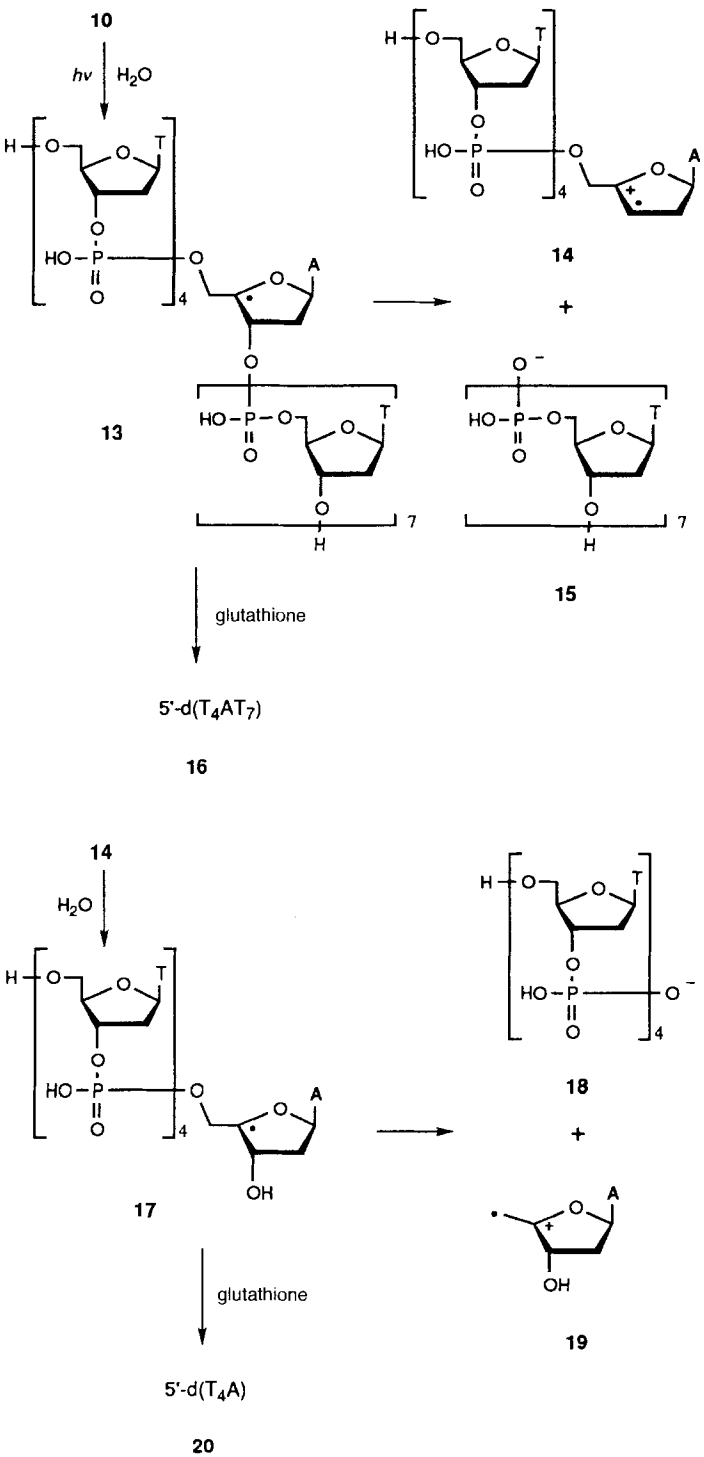


Fig. 2. MALDI-TOF mass spectrum (negative-ion mode) of the reaction mixture after irradiation (60 min) of a) an aqueous solution of **10** and b) an aqueous solution of **10** in the presence of glutathione. The signal at *m/z* 1292 is not yet assigned, but is thought to correspond to the glycolate of cleavage product **18**. The signals at *m/z* 1797.3 and 1073 correspond to the doubly deprotonated molecular ions of **16** and **15**, respectively. The dimer of glutathione gives rise to the peak at *m/z* 613.2.



The results of these experiments with oligodeoxyribonucleotides in water agreed remarkably well with the results of our

model studies.[3] The oligomeric 4′-deoxynucleotide radical **13** generated selectively from the radical precursor **10** is trapped as dodecamer **16** by H abstraction, or it decays heterolytically to the phosphorylated heptamer **15** and the radical cation **14**. Reaction of **14** with H_2O provides the pentanucleotide radical **17**, which is either converted into pentanucleotide **20** with glutathione, or cleaves off the phosphorylated tetramer **18**. The subsequent reactions of the reactive monomeric fragment **19** cannot be described in detail yet; however, the HPLC trace shows that adenine is released.

The reaction of the oligomeric 4′-deoxyribonucleotide radical **13** proceeds quite uniformly. The H-trapping products **16** and **20**, and the cleavage products **15** and **18** were formed in the presence of glutathione in a total yield of 80% (HPLC analysis). These experiments prove that under anaerobic conditions and in water 4′-oligonucleotide radicals cleave off the oligomeric phosphates at the 3′- and 5′-positions. The incorporation of radical precursors thus opens up new possibilities for the selective cleavage of DNA.

Received: April 27, 1994
Revised version: June 29, 1994 [Z 6874 IE]
German version: *Angew. Chem.* **1994**, *106*, 1941

[1] Leading reviews: J. Stubbe, J. W. Kozarich, *Chem. Rev.* **1987**, *87*, 1107; I. H. Goldberg, *Acc. Chem. Res.* **1991**, *24*, 191; K. C. Nicolaou, W.-M. Dai, *Angew. Chem.* **1991**, *103*, 1453; *Angew. Chem. Int. Ed. Engl.* **1991**, *30*, 1387.

[2] G. Behrens, G. Koltzenburg, D. Schulte-Frohlinde, *Z. Naturforsch. C.* **1982**, *37*, 1205; C. von Sonntag, *The Chemical Basis of Radiation Biology*, Taylor and Francis, London, **1987**, p. 167.

[3] a) B. Giese, X. Beyrich-Graf, J. Burger, C. Kesselheim, M. Senn, T. Schäfer, *Angew. Chem.* **1993**, *105*, 1850; *Angew. Chem. Int. Ed. Engl.* **1993**, *32*, 1742; b) B. Giese, P. Erdmann, L. Giraud, T. Göbel, M. Petretta, T. Schäfer, *Tetrahedron Lett.* **1994**, *35*, 2683.

[4] The new compounds were characterized by ^1H and ^{13}C NMR spectroscopy, mass spectrometry, and, when possible, by elemental analysis. The assignment of the configurations of isomers **6a** and **6b** was based on NOE experiments. Characteristic NMR data (300 MHz instrument) of **6b**: ^1H NMR ($CDCl_3$): $\delta = 2.66$ (ddd, 1H, H-2b′, $J(2b',3') = 4.3$, $J(2b',1') = 6.6$, $J(2b',2a') = 14.0$ Hz), 3.17 (ddd, 1H, H-2a′, $J(2a',1') = 7.0$, $J(2a',3') = 7.3$ Hz), 3.73 (dd, 1H, H-5b′, $J(5a',5b') = 3.2$, $J(5b',OH) = 10.4$ Hz), 3.92 (dd, 1H, OH), 4.11 (dd, 1H, H-5a′, $J(5a',OH) = 12.3$ Hz), 6.01 (dd, 1H, H-3′), 6.53 (dd, 1H, H-1′), 8.19 (s, 1H, H-8(adenine)), 8.61 (s, 1H, H-2(adenine)); ^{13}C NMR ($CDCl_3$): $\delta = 96.82$ (C-4′). NOE effects between H-5′ and H-3′, H-5′ and H-2(adenine), and H-1′ and *ortho*-H(PhSe).

[5] Owing to its chiral phosphorus center, building block **8** occurs as two diastereomers, which were separated by flash chromatography (silica gel, ethyl acetate:hexane:triethylamine = 6:4:0.5). Characteristic NMR data (300 MHz instrument) of **8**: ^1H NMR ($CDCl_3$): $\delta = 5.29$ (m, 1H, H-3′), 6.65 (dd, 1H, H-1′, $J(1',2a') = 4.9$, $J(1',2b') = 7.4$ Hz), 8.23 (s, 1H, H-8(adenine)), 8.80 (s, 1H, H-2(adenine)); ^{13}C NMR ($CDCl_3$): $\delta = 43.42$ (C-2′, $J(C,P) = 2.6$ Hz), 74.02 (C-3′, $J(C,P) = 16.5$ Hz), 98.24 (C-4′, $J(C,P) = 8.1$ Hz); ^{31}P NMR ($CDCl_3$, standard H_3PO_4): $\delta = 149.7$.

[6] J. B. Chattopadhyaya, C. B. Reese, *Tetrahedron Lett.* **1979**, 5059; G. Gosselin, J. L. Imbach, *ibid.* **1981**, *22*, 4699. Dimer **9** was obtained from **7** in four steps in 30% yield.

[7] J. Stollwerk, in *Gentechnische Methoden* (Eds.: S. Bertram, H. G. Gassen), Fischer, Stuttgart, **1991**, p. 201. The coupling efficiency for the synthesis of **9** from amidite **8** was 98% (measured according to the trityl method).

[8] Characteristic NMR data (300 MHz instrument) for the triethylammonium salt of **9**: ^1H NMR (CD_3OD): $\delta = 4.51$ (m, 1H, H-3′(thymidine)), 5.35 (m, 1H, H-3′(adenosine)), 6.28 (t, 1H, H-1′, $J(1',2') = 7.5$ Hz, thymidine), 6.57 (dd, 1H, H-1′, $J(1',2a') = 4.4$, $J(1',2b') = 7.5$ Hz, adenosine), 7.73 (s, 1H, H-6(thymidine)), 8.13 (s, 1H, H-2(Adenin)), 8.29 (s, 1H, H-8(Adenin)); ^{13}C NMR (CD_3OD): $\delta = 66.86$ ($J(C,P) = 4.3$ Hz, C-5′(thymidine)), 76.39 ($J(C,P) = 4.7$ Hz, C-4′(thymidine)), 87.33 ($J(C,P) = 8.6$ Hz, C-3′(adenosine)), 98.62 ($J(C,P) = 11.2$ Hz, C-4′(adenosine)); ^{31}P NMR (CD_3OD, standard H_3PO_4): $\delta = 0.184$.

[9] The synthesis of the oligonucleotides was conducted with an ABI 392 DNA synthesizer in batch sizes of 0.2 μmol. After seven thymidine units, building block **8** was introduced; the reaction time allowed for the coupling was 30 min. The coupling efficiency for this step was 98% (measured according to the trityl method). Then four, eight, or twelve thymidine units were added on, during which the coupling efficiency decreased to 92–95%. The samples were deprotected with ammonia, purified by passage through an OPC cartridge (MWG-Biotech), concentrated, purified by HPLC (Merck Lichrospher 10 RP-18,5 μm, eluent: linear gradient of 5–40% CH_3CN in aqueous 0.1 M triethylammonium acetate buffer over 20 min, pH 7), and then lyophilized.

[10] M. Karas, F. Hillenkamp, *Anal. Chem.* **1988**, *60*, 2299; E. Nordhoff, A. Ingendoh, R. Cramer, A. Overberg, B. Stahl, M. Karas, F. Hillenkamp, P. F. Crain, *Rapid Commun. Mass Spectrom.* **1992**, *6*, 771; U. Pieles, W. Zürcher, M. Schär, H. E. Moser, *Nucleic Acids Res.* **1993**, *14*, 3191. The experiments were conducted with a Vestec Benchtop II instrument in the negative-ion mode. Matrix solution: 2,4,6-trihydroxyacetophenone (0.3 M) in $CH_3CN:H_2O:EtOH = 50:45:5$; additional solution: ammonium tartrate (0.1 M) in H_2O. The aqueous solution of the sample (1 μL) was mixed with the matrix solution (1 μL) and the additional solution (0.5 μL). After the sample had dried the measurements were conducted with a laser intensity of 0.2 μJ per pulse (accumulation of 30–50 pulses per individual measurement; pulse length 3 ns). When the laser intensity was increased, fragmentation reactions of the starting compound **10** were evident in the MALDI spectrum. We are examining the effect of the matrix and the wavelength of the laser on this fragmentation.

[11] A degassed aqueous solution (pH 7) of **10** (100–200 μL; $A_{260} = 0.1$–0.2 optical density) was irradiated (Oriel Hg high-pressure lamp, 500 W, 320nm filter) at 20 °C. For the photolysis experiments in the presence of a H donor 2 mg of glutathione was added (pH 3). Samples were taken at 5, 10, 20, 40, and 60 min and analyzed by HPLC [9] and MALDI-TOF MS [10]. The peaks in the HPLC trace were assigned by comparison with those of the independently synthesized compounds **15**, **16**, and **20** and by HPLC enrichment and MALDI-TOF MS. The mass spectrum shown in Fig. 2 was recorded for the product mixture obtained by radiation for 60 min in the presence of glutathione. In the HPLC trace each of the H-trapping products **16** and **20** appear as two peaks, which indicates that as in the model experiments [3] the H trapping is not stereoselective.

Sixteenfold Deprotonated γ-Cyclodextrin Tori as Anions in a Hexadecanuclear Lead(II) Alkoxide**

Peter Klüfers* and Jörg Schuhmacher

Polyols (including carbohydrates) can, in the presence of suitable metal salts, be multideprotonated to polyolato ligands even in aqueous solution. Due to the large variety of available polyols, metal complexes having very differing structural characteristics can be obtained. For instance, polysaccharides can serve as a backbone for polymers containing metals,[1] and coordination polymers can be synthesized with sugar alcohols.[2] Multinuclear complexes which are similarly spatially extended, but of nonpolymeric character, can be conceived with oligosaccharides. Cyclodextrins are especially suitable for this purpose. However, the number of the metal ions that can be incorporated into a double torus at higher pH values is limited due to the high tendency of such systems to form intramolecular hydrogen bonds of the type $O-H\cdots O^-$. Four Cu^{2+} ions were thus incorporated between two multideprotonated β-cyclodextrin tori to form a polyolatometalate.[3] In contrast, in a simple metal polyolate, a metal polyolatometalate, which bears the same relationship to a polyolatometalate as a higher aggregated hydroxide to a hydroxometalate, it should be possible to obtain a greater metal-to-ligand ratio.

[*] Prof. Dr. P. Klüfers, Dipl.-Chem. J. Schubmacher
Institut für Anorganische Chemie der Universität
Engesserstrasse, Gebäude 30.45, D-76128 Karlsruhe (FRG)
Telefax: Int. code + (721)608-4290

[**] Polyol–Metal Complexes, Part 11. This work was supported by the Bundesministerium für Forschung und Technologie (grant no. 0319368A), Akzo AG, Wuppertal, and Wacker-Chemie, Munich (cyclodextrin donation). Part 10: [5].

Experiments based on this principle have now led to the first structurally characterized lead(II)–carbohydrate complex. These investigations have helped to answer several questions of current interest: The ability of polyols to undergo multiple deprotonation to give polyolato ligands in aqueous solution has been demonstrated. Equally impressively, it has been shown that new and unusual structures can be synthesized from polyols. The complex also appears to be an example of a multinuclear complex formed by a cooperative mechanism.

We used γ-cyclodextrin (cyclomaltooctaose, γ-CD) as the polyol component in the experiments described below. Highly refractive, colorless crystals of $[Pb_{16}(\gamma\text{-}CDH_{-16})_2]\cdot$ ca. $20\,H_2O$ (**1**) precipitate from hot aqueous solutions of the cyclodextrin containing substoichiometric quantities of lead(II) nitrate and NaOH in a ratio of 1:2. The X-ray structure analysis confirms the formation of a hexadecanuclear lead complex,[4] whose structure is shown in Figure 1. Both cyclodextrin tori in the complex are deprotonated sixteenfold, and each of the alkoxide O atoms is coordinated in a bridging fashion to two lead atoms. The unusual arrangement of the lead atoms in the form of an eight-point star can be understood by comparison with the structure of the coordination polymer $[Pb(C_4H_6O_3)]\cdot H_2O$ (**2**), in which the dianion of the simple diol anhydroerythritol (*meso*-oxolane-3,4-diol) is incorporated in a structure with an analogous topography.[5] Scheme 1 (top) shows a strip made from lead(II) cations and diolate dianions in **2**. If a strip of suitable length is closed to form a ring, the principle behind the construction of **1** (middle) can be recognized. The analogy is not perfect, however, since the metal-bonding diolate ligands are displaced with respect to one another in **2** (Scheme 1, bottom),

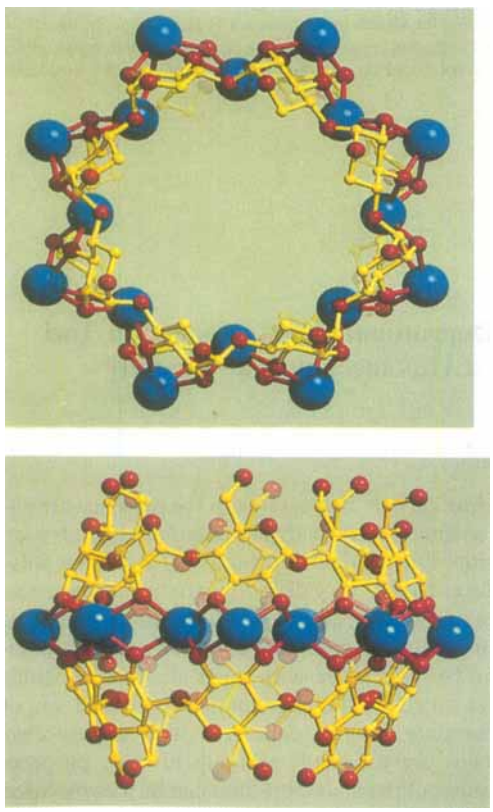
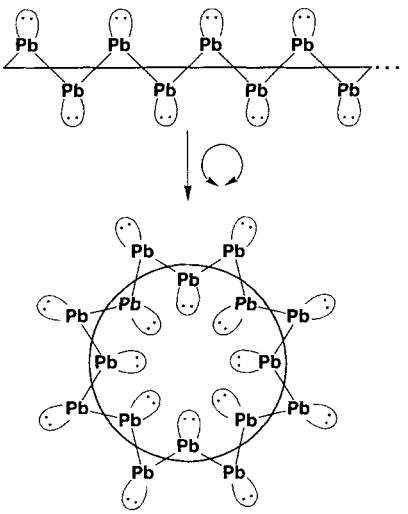
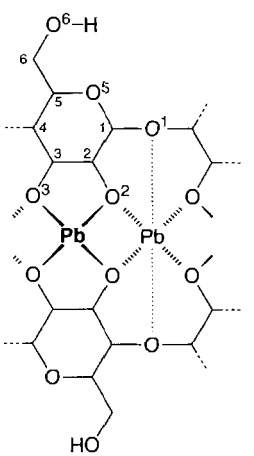


Fig. 1. Crystal structure of **1** (top: without C-6 and O^6 atoms of the anhydroglucose fragments, O^6 = O atom at C-6); blue: Pb, red: O, yellow: C. See Scheme 2 for the numbering of atoms. The distances to the nearest atoms of the given type (min/max/middle, in Å; the values in parentheses are the standard deviations of the last decimal place): Pb–O^2, O^3 2.212(15)/2.502(15)/2.37; Pb_{inner}–O^1 3.100(13)/3.273(13)/3.19; Pb···Pb (intramolecular) 3.7631(12)/3.9364(12)/3.829. Bottom: Projection of the structure perpendicular to the that in the upper picture.



Scheme 1. The relationship between the structure of the simple polymeric lead(II) diolate **2** [5] and that of **1**.

but are exactly opposite one another in the double torus in **1** (Scheme 2). The outer lead atoms (left in Scheme 2) are thus part of two five-membered chelate rings; they have the same environment as the copper atoms in the β-cyclodextrin salt. The inner Pb atoms are, on the other hand, in a more unusual environment: four alkoxide O atoms from four different anhydroglucose units and two additional O^1 atoms approximately 0.8 Å further away, which function as ligating atoms, combine to form a (4 + 2) coordination sphere (Scheme 2, right). The shape of the CD tori in **1** is different than usual; the cyclodextrin truncated cones are widened at the base by the large Pb_{16} ring (Fig. 1, bottom). The distance between opposing inner Pb atoms is 12.5 Å. The space within the double torus is therefore not constricted at the middle. For the purpose of its use as a host compound, it can be assumed that a channel with an almost constant diameter of approximately 8 Å runs through the double torus (assuming the van der Waals' radius of a Pb^{2+} ion including the lone pair to be 2 Å). Hydrogen bonds are less important in **1** than in polyolatocuprates. This can be understood in terms of the weaker acceptor



Scheme 2. The numbering of the C and O atoms of an anhydroglucose unit and the environment of the inner (right) and the outer lead atoms (left) in **1**.

 © VCH Verlagsgesellschaft mbH, D-69451 Weinheim, 1994 0570-0833/94/1818-1864 $ 10.00+.25/0

properties of μ_2-alkoxido O atoms compared to terminal O^- functions. The lead atoms also bind water molecules only very loosely, because the latter have to approach from the side of the stereochemically active lone pair. There are, therefore, only weak contacts between lead atoms and water molecules, mostly with a Pb–O distance >3.4 Å. The majority of the bonding intermolecular distances between lead and cyclodextrin O atoms are also found in this range.

Remarkably, **1** crystallizes from solutions with an excess of cyclodextrin. It is not, therefore, high lead concentrations which are the driving force for the incorporation of the 16 Pb atoms in the double torus. The behavior of this system rather indicates a cooperative mechanism which leads to the formation of **1** alongside lead-free tori.

It may at first seem surprising that all the protons in **1** from the α,β-diol groups are cleaved, although, in the aforementioned cuprates, protons remain tightly bound in hydrogen bonds, even at higher pH values. It should however be noted that a similar situation is observed with the aqua ligand, which can also undergo multideprotonation. In weakly acidic solution, double deprotonation to give a bridging oxo ligand can be observed, whereas in alkaline solution a terminal hydroxide ligand is formed after a single deprotonation.[6]

We then asked ourselves whether polyols can be deprotonated in aqueous solutions around pH = 7, or whether the competing reactions in the aqueous system determine the distribution of the products formed. Given the surprisingly high formation constants of polyolatometalates,[1a] it appears conceivable that metal polyolates could be formed in neutral solution. A counterargument, on the other hand, is the claim, also found in more recent overviews, that carbohydrates can only form complexes of weak stability in neutral solution;[7] here, the possibility of deprotonation was not considered. It should however be noted that dissolution of saccharides and numerous metal salts in water—and the comment refers to this typical experimental procedure—does not yield neutral, but distinctly acidic solutions. Adjustment of the pH to about 7 results in formation of precipitates from these metal salt–saccharide solutions, which, at first glance, could be taken for the corresponding metal hydroxides; however, in the case of Cu^{II}, for example, the color of the precipitate is turquoise and not the pure blue of the expected hydroxide. Subject to the determination of the formation constants, the conditions for the precipitation of **1** contribute to the clarification of the extent to which carbohydrates can be deprotonated in neutral aqueous solution: A solution of 0.107 M $Pb(NO_3)_2$ and 0.0154 (= 0.123/8) M γ-CD was found to have a pH of 3.4 at room temperature. On addition of NaOH, the colorless, gelatinous precipitate described above formed at around pH 5.7. After the addition of two molar equivalents of NaOH with respect to lead, the solution itself had a pH of 9.2; the neutral point was first crossed after the addition of nine tenths of this amount. A solution that was adjusted to the neutral point also formed crystals of **1** on heating. The homologous β-CD compound remained in solution under similar conditions, so that all protolysis equilibria were represented; after addition of two equivalents of NaOH, the pH of this system was also found to be 9.2.

These findings show that carbohydrates, ubiquitous in organisms, can form stable complexes in the form of deprotonated ligands in this pH range, which is of special interest in biochemistry. Their hydroxide-like, voluminous, gelatinous appearance seems to have detracted attention from these complexes until now. At lower temperatures, **1** also behaves in a typical fashion: The crystals obtained at 75 °C swell at room temperature in the then opalescent mother liquor within the course of an hour, without dissolving to any large extent; the X-ray reflections then disappear in the background noise. If the gelatinous precipitate is warmed to 75 °C, it recrystallizes in about the same time.

The structures of **1**, **2**, and a lead 1,2-glycerolate[8] with a structure analogous to that of **2** emphasize the possibility of manipulating building blocks based on oxide structures—here the PbO modifications—through the polyolato ligands. In the coordination polymer **2**, PbO layers are broken down into strips. In contrast, in **1** the building motif of the solid undergoes an ordering to form a ring, a variation which goes beyond the mere removal of a given linkage pattern present in the solid.[9]

Experimental Procedure

Lead(II) nitrate (3.31 g, 10.0 mmol) and γ-CD (2.00 g, 1.54 (= 12.3/8) mmol) were dissolved in water (15 mL). The addition of NaOH (20 mL, 1 M) led to the formation of a colorless gelatinous mass. On warming to 75 °C, a clear solution resulted, from which highly refractive colorless crystals of **1** precipitated. A dehydrated sample decomposed above 210 °C without melting.

Received: April 18, 1994 [Z 68571E]
German version: *Angew. Chem.* **1994**, *106*, 1925

[1] a) W. Burchard, N. Habermann, P. Klüfers, B. Seger, U. Wilhelm (*Angew. Chem.* **1994**, *106*, 936–939; *Angew. Chem. Int. Ed. Engl.* **1994**, *33*, 884–887) give an example with cellulose; b) *Inorganic and Metal-Containing Polymeric Materials* (Eds.: J. E. Sheats, C. E. Carraher, C. U. Pittman, M. Zeldin, B. Curell), Plenum, New York, **1990**, c) C. E. Carraher, D. Gill, Y. Naoshima, M. Williams in ref. [1 b], pp. 319–326, and Y. Naoshima, C. E. Carraher in ref. [1 b], pp. 327–334, describe metal-containing starch compounds.

[2] P. Klüfers, J. Schuhmacher, *Angew. Chem.* **1994**, *106*, 1839–1841; *Angew. Chem. Int. Ed. Engl.* **1994**, *33*, 1742–1744.

[3] R. Fuchs, N. Habermann, P. Klüfers, *Angew. Chem.* **1993**, *105*, 895–897; *Angew. Chem. Int. Ed. Engl.* **1993**, *32*, 852–854.

[4] $C_{96}H_{128}O_{80}Pb_{16}\cdot 20H_2O$, $M_r = 6237.5$, crystal dimensions $0.15\times 0.15\times 0.10\,mm^3$, monoclinic space group $P2_1$; $a = 20.309(2)$, $b = 18.884(2)$, $c = 21.647(2)$ Å, $\beta = 96.350(10)°$, $V = 8251.0(14)$ Å^3, $Z = 2$, $\rho_{calcd} = 2.5107(4)\,g\,cm^{-3}$; Stoe-IPDS area detector, $Mo_{K\alpha}$ radiation, (graphite monochromator, $\lambda = 0.71069$ Å), room temperature; $2\theta_{max} = 52°$, 62767 *hkl* measured, 31256 *hkl* independent and considered, 25762 *hkl* with $|F_o| \geq 4\sigma(|F_o|)$, Lp correction, no absorption correction ($\mu = 16.35\,mm^{-1}$), direct methods (SHELXS), refinement with full matrix against F^2 (SHELXL), 935 parameters, H atoms on C in calculated positions with common U, $wR(F^2) = 0.146$, $R(F)_{4\sigma} = 0.058$, $S = 1.095$, $\Delta\rho_{max} = 2.1\,e\,Å^{-3}$, analysis and depiction with PLATON and SCHAKAL. Water content according to the X-ray analysis: $19.3\,H_2O$ per formula unit on 21 positions, some of which were not fully occupied; analytical water content based on loss of mass after heating for 5 hours at 110 °C in an oil pump vacuum: $19.7\,H_2O$. Further details of the crystal structure investigation may be obtained from the Fachinformationszentrum Karlsruhe, D-76344 Eggenstein-Leopoldshafen (FRG) on quoting the depository number CSD-400811.

[5] P. Klüfers, J. Schuhmacher, *Z. Anorg. Allg. Chem.*, in press.

[6] J. Burgess (*Metal Ions in Solution*, Ellis Horwood, Chichester, **1978**, pp. 290–304) describes the formation of the $[AlO_4\{Al(OH)_2\}_{12}]^{7+}$ ion in weakly acidic solution as an example. After addition of a sufficient quantity of base, the μ-oxo ligands are present in the protonated form in the $[Al(OH)_4]^-$ ion.

[7] a) K. Burger, L. Nagy in *Biocoordination Chemistry* (Ed.: K. Burger), Ellis Horwood, Chichester, **1990**, p. 236–283, 236; b) D. M. Whitfield, S. Stojkovski, B. Sarkar, *Coord. Chem. Rev.* **1993**, *122*, 171–225, 178.

[8] H.-L. Keller, H.-J. Riebe, *Z. Anorg. Allg. Chem.* **1987**, *550*, 102–108.

[9] For an introduction to the use of lead alkoxides for the development of superconductors containing lead and to applications of other oxidic lead ceramics, see: S. C. Goel, M. Y. Chiang, W. E. Buhro, *Inorg. Chem.* **1990**, *29*, 4640–4646.

 © VCH Verlagsgesellschaft mbH, D-69451 Weinheim, 1994 0570-0833/94/1818-1865 $ 10.00+.25/0

On the Mechanism of Fullerene Formation**

Thilo Belz, Harald Werner, Friedrich Zemlin, Ursula Klengler, Michael Wesemann, Bernd Tesche, Elmar Zeitler, Armin Reller, and Robert Schlögl*

Dedicated to Professor Hans Bock on the occasion of his 65th birthday

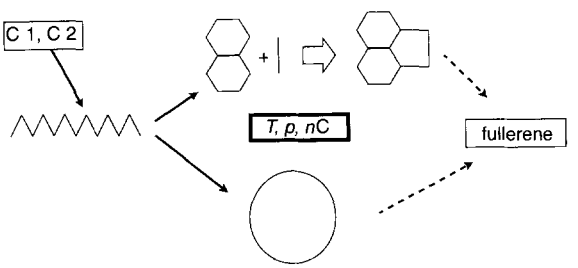
Fullerenes[1] differ in their molecular character from the currently known forms of elemental carbon such as graphite (including derived turbostratic variations) and diamond. They do not form extended two- or three-dimensional structures, but closed molecular systems based on sp^2-carbon atoms as the common building block. Fullerenes can currently be prepared by thermal treatment of graphite[2] and pyrolysis of arenes in flames.[3] Separation and purification techniques are also available.[4] Graphitic tubules[5] and onionlike spheres,[6] which are related to the fullerenes, have been structurally characterized and produced in microscopic quantities, but are not yet available in pure form and preparative amounts.[7] Given both the diversity of products and methods of production, and the necessity to develop generally applicable syntheses for novel carbon forms, the question arises as to the mechanism of formation of these compounds. Methods involving the thermal treatment of carbon in an electric arc, with fluxes of highly energetic electrons, or with a laser beam have the disadvantage that only limited control over the selectivity of formation of particular products has been possible up to now; the exact production parameters do, however, have a crucial influence on the product distribution.[8] We chose to investigate the formation of fullerenes in an electric arc despite the low degree of control over the course of the reaction, since this is now the most important method for the production of significant amounts of fullerenes. When more is known about the formation processes, this technique should also have considerable potential in the preparation of molecular forms of carbon other than soluble fullerenes.

The initial formation of C_x fragments containing no heteroatoms is the common step in all synthetic routes to fullerenes. According to numerous growth theories,[9] these fragments form small rings that combine with C_1 and C_2 units to give additional five- or six-membered rings and eventually fullerenes (Scheme 1). A second growth theory postulates that the first step is the formation of large monocyclic compounds. Shock annealing under certain conditions then results in the formation of numerous linkages between the carbon atoms in these monocycles to give carbon clusters. These then isomerize to fullerenes, which are thermodynamically stable under the reaction conditions. Evidence for this sequence was provided by mass-spectrometric experiments in the vapor phase under model conditions used for the synthesis of fullerenes.[10] The suggested mechanisms[11] differ on the question whether many small rings condense together and oligomerize via polycyclic arenes to form fullerenes, or whether a large carbon ring isomerizes to produce a fullerene molecule.

All reaction pathways leading to fullerene molecules require an atmosphere that is as inert as possible. This ensures that the lower chemical stability of five- compared to that of six-membered rings does not result in a decrease in concentration of the five-membered ring structures below a critical level. Furthermore, reactants which form stable carbon–heteroatom bonds under the reaction conditions should not be present, since they would prevent the formation of an all-carbon compound.

Previous investigations into the mechanism of formation relied on experiments carried out in the vapor phase with mass-selected sections of the primary product spectrum obtained from carbon vaporization. Due to a microstructure that is X-ray amorphous, fullerene black, which is the main product formed in the synthesis of fullerenes, has hardly been investigated structurally.[12] Studies in this area could provide significant clues on the mechanism of formation. Assuming that fullerene black arises from all the failed self-organization processes which lead to fullerenes, we would expect a microstructure consisting of platelets if the reaction proceeds by polycondensation of small rings and a three-dimensional, random microstructure if the isomerization process dominates.

The experiments were performed with an arc-discharge carbon vaporization apparatus,[13] which produces soluble fullerenes with a 10% selectivity. Using emission spectroscopy,[14] we were only able to observe the bands corresponding to C_1 and C_2 units. Figure 1 shows the low-resolution spectra with band assignments.[15] The substantial change in the partial pressure of helium, which causes an increase in yield from 0.025 to 10%, is clearly not accompanied by a change in the nature of the species in the plasma. The reactions in the graphite vaporization experiments leading to the formation of the C_x clusters and to fuller-



Scheme 1. Postulated mechanisms for the formation of fullerenes.

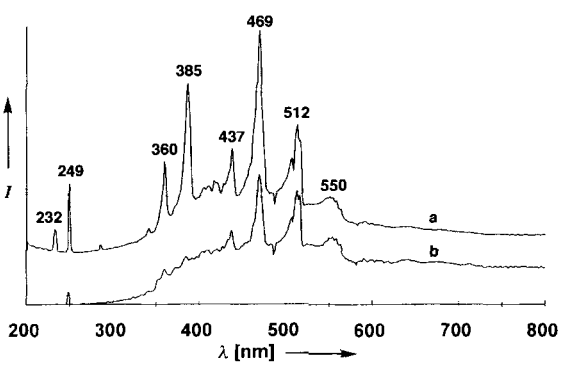


Fig. 1. Emission spectrum of an electric arc during fullerene synthesis. Discharge conditions: graphite rods for spectroscopy (Ringsdorf RW 4), diameter 6.15 mm, current 150 A, alternating current, distance between electrodes (regulated) 3.0 mm. The helium pressure during the measurement of spectra a and b (×4) was 10 and 2×10^4 Pa, respectively. The band at 249 nm is assigned to the C_1 fragment; all other bands belong to the transitions of singlet and triplet C_2 molecules (232: Mulliken system; 360, 385: Deslandres–d'Azambuja system; 437, 469, 512, 550: Swan system). Refer to the text for a discussion of those signals overlapping with bands of the CN molecule.

[*] Prof. Dr. R. Schlögl, Dipl.-Chem T. Belz, Dipl.-Chem. H. Werner, Dr. F. Zemlin, U. Klengler, M. Wesemann, Dr. B. Tesche, Prof. Dr. E. Zeitler
Fritz-Haber-Institut der Max-Planck-Gesellschaft
Faradayweg 4–6, D-14195 Berlin (FRG)
Telefax: Int. code + (30)8305-487
Prof. Dr. A. Reller
Institut für Anorganische Chemie der Universität Hamburg (FRG)

[**] This work was supported by the Fonds der Chemischen Industrie, the Hermann-Willkom-Stiftung and the Bundesministerium für Forschung und Technologie (Fullerene Pilot Project).

enes obviously proceed in the cool part of the carbon cloud outside the range accessible to emission spectroscopy (diffuse background in the visible region). The spectra thus give an insight into the initial precursors of fullerenes, but not into the formation of larger carbon frameworks. Even the small C_3 fragment with an expected principal band at 405 nm cannot be detected. This is consistent with earlier observations in laser vaporization experiments that C_3 fragments were detected by mass spectrometry in the cold region of the apparatus, but not in the plasma emission spectrum.[16] This evidence emphasizes the significance of the colder zones within the reaction chamber for the construction of larger frameworks. The hot zone is, in contrast, the source of building blocks.[17] The rate at which the building blocks are supplied is, however, fundamental to the whole process and is determined by the parameters in the hot zone, as can be seen from the spectra in Figure 1.

The different intensity ratios of the bands corresponding to the C_2 fragments in the spectra of Figure 1 arise because of overlap in the 360 and 385 nm regions with bands assigned to CN molecules, which dominate when traces of nitrogen are added to the quench gas. Their appearance at low partial pressures of helium (spectrum a) is explained by the fact that the carbon fragments react with residual air components in the absence of the inert quench gas. This has consequences for the growth mechanism.

A systematic investigation into the structural and chemical properties of conventional carbon black and fullerene black indicates that the two nanocrystalline carbon forms differ markedly. This can be deduced from the differing microstructure, which has been investigated by means of high-resolution transmission electron microscopy (TEM).[18] In the mesoscopic region both materials consist of spherical aggregates of many primary building blocks.[19]

Figure 2 clearly reveals that the spherical aggregates in conventional carbon black are formed from many planar basic structural units (BSU),[20] which are stacked in a parallel

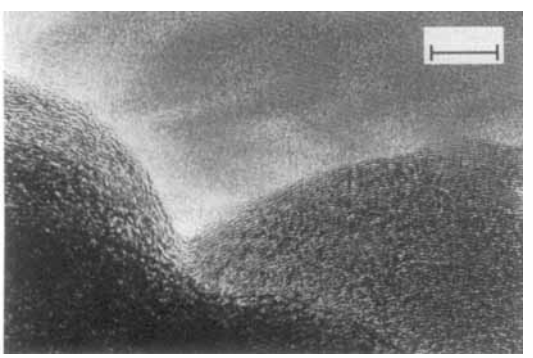


Fig. 2. High-resolution TEM image of carbon black (industrial sample FW-1 from Degussa). The spacing between the planar carbon platelets agrees with that between the layers in graphite (approximately 340 pm). The length of the bar represents 10 nm.

arrangement.[21] Stacking errors caused by platelets being tilted with respect to the stacking axis and by nonplanar objects (BSU of differing ring size) result in formation of the bent secondary structure in the carbon black particles. No in-plane correlation exists between the BSU (turbostratic arrangement).[20]

The microstructure of fullerene black is far more complex and depends to a large extent on the reaction conditions. Under conditions that give rise to high yields of C_{60}, the structures shown in Figure 3 have been observed. A network of continuously curved multilayers of carbon can be recognized inside the particle. The spacing of parallel layers is similar to that observed in conventional carbon black or graphite. The carbon layers are far more extended[22] than those in BSU of conventional carbon black. Large parts of the particles are composed of amorphous carbon that is not arranged in two-dimensional layers, but rather as a tangle of threadlike polymers.

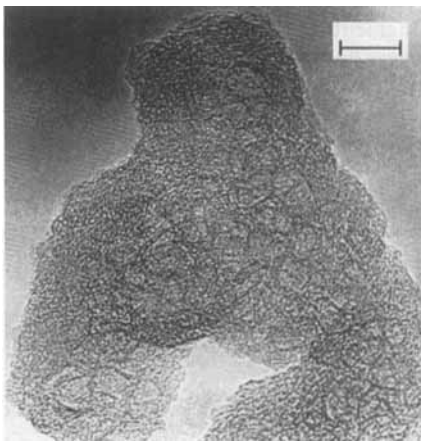


Fig. 3. High-resolution TEM image of fullerene black. The experimental conditions were adjusted to optimize the C_{60} yield. One can see the empty cavities inside the continuous carbon loops. The enhanced contrast of the loops suggests a two-dimensional structure of layered aggregates which are not quite parallel to one another. The length of the bar represents 10 nm.

If energy input and quench-gas pressure in the plasma chamber are reduced, the threadlike molecules can be observed directly on the periphery of the fullerene black particles. Figure 4 shows a single tangled cluster of these carbon threads. The fact that continuous curves of different radii are present both in and perpendicular to the plane of projection of the microscope explains the "interrupted contrast" (cf. "regular contrast" of the BSU in Fig. 2). A platelike primary structure can thus be ruled out. Figure 4 provides clear evidence for the formation of large (possibly irregularly) crosslinked rings of carbon atoms, which are required for fullerene formation. It also becomes clear why fullerene black is considerably more susceptible to oxidation and chlorination reactions than conventional carbon black.[12]

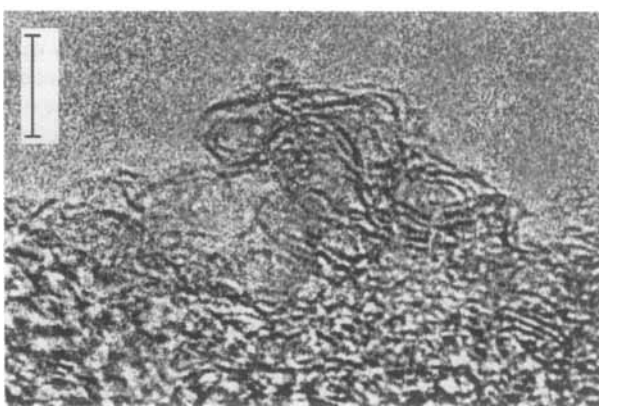


Fig. 4. Section of a high-resolution TEM image of fullerene black. The reaction conditions were chosen to maximize the ratio of higher fullerenes relative to C_{60}; this reduced the overall yield markedly. The length of the bar represents 5 nm.

 © VCH Verlagsgesellschaft mbH, D-69451 Weinheim, 1994 0570-0833/94/1818-1867 $ 10.00+.25/0

The growth of the carbon threads is largely suppressed if the plasma apparatus is operated without a quench gas at a residual pressure of about 10^{-4} bar.[23] In this case, the few remaining collision partners are no longer inert, and chain termination reactions by incorporation of a heteroatom from the residual gas occur very frequently (see also text to Fig. 1). This is also reflected in the extremely low rate of fullerene formation. A highly resolved TEM image of this product is shown in Figure 5. Color coding is used to depict a section through the projection plane of the microscope. The objects with a red border are short fragments of carbon threads. Their orientation is irregular, and a very hard but not very dense form of carbon that is completely amorphous to X-rays results.[24] The mechanical hardness of this material suggests that the units in Figure 5 are covalently bonded.

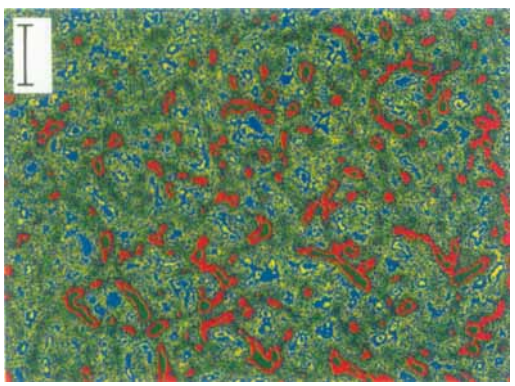


Fig. 5. Artificial color-coded representation of a highly resolved section of a TEM image of hard fullerene black. Under the conditions chosen, the yield of soluble fullerenes was less than 0.4%. The length of the bar represents 2 nm.

In summary, the microstructural analysis of different fullerene black samples clearly indicates that a significant proportion of the vaporized carbon atoms condenses to form threadlike molecules. These combine to ring systems, which either form intramolecular links, or fall apart if their energy content is too high. Intermolecular bonds are then formed when the density is sufficiently high. The proportion of ring growth and shock annealing determines the yield of soluble fullerenes. The majority of rings are apparently not able to react to form stable fullerenes, since either the ring size cannot be suitably adjusted, or bond formation releases too much energy and dissociation and polymerization results.

A portion of the vaporized carbon apparently reacts to form more or less planar layers. This can be explained by early ring closure and formation of C_x rings ($x = 5, 6, 7$). The conclusion that a range of ring sizes are formed follows from the observed continuous curvature of the resulting layers. This reaction pathway, which proceeds parallel to the linking up of larger monocycles, may be the mechanism for the formation of graphitic tubules and onionlike spheres. It is unlikely that such structures are formed by linking of monocycles; a condensation mechanism is much more probable.

The detrimental effect of heteroatoms acting as chain-terminating reagents was also clearly shown and is consistent with evidence from the synthesis of fullerenes.[25] It is known that linear or cyclic intermediates in the formation of complex carbon species can be trapped and thus detected by addition of heteroatoms to the quench gas. Our observations indicate that these products do not arise as a result of disruption of the main process, but rather from the increased frequency of side reactions.

Our findings complement those obtained in vapor phase experiments[26] and show that in the "caldron" of the plasma reactor both condensation and crosslinking reactions of macrocycles proceed side by side. At the same time, cyclic compounds are formed and fall apart, depending on the energy content of the molecule and its immediate environment. The "recipe" for the synthesis of fullerenes, fullerene black, and planar, layered structures is determined by the local properties of the vapor phase outside the plasma. These observations and the fundamentally different structures of the condensation products point to kinetic control of the overall reaction. The selectivity of the condensation of the small primary fragments produced in the plasma is determined by their concentration, by the efficiency of energy exchange,[27] and by heteroatoms disrupting growth and rearrangement of the carbon fragments.

Received: April 2, 1994 [Z 6822 IE]
German version: *Angew. Chem.* **1994**, *106*, 1919

[1] R. E. Smalley, *Acc. Chem. Res.* **1992**, *29*, 98.
[2] H. W. Kroto, J. R. Heath, S. C. O'Brien, R. F. Curl, R. E. Smalley, *Nature* **1985**, *318*, 162; W. Krätschmer, L. Lamb, K. Fostiropoulos, D. Huffman, *ibid.* **1990**, *347*, 354; G. Peters, M. Jansen, *Angew. Chem.* **1992**, *104*, 240; *Angew. Chem. Int. Ed. Engl.* **1992**, *31*, 223.
[3] T. Baum, S. Löffler, P. Löffler, P. Weilmünster, K. H. Homann, *Ber. Bunsenges. Phys. Chem.* **1992**, *96*, 841.
[4] A. Gügel, M. Becker, D. Hammel, L. Mindach, J. Räder, T. Simon, M. Wagner, K. Müllen, *Angew. Chem.* **1992**, *104*, 666; *Angew. Chem. Int. Ed. Engl.* **1992**, *31*, 644; H. Werner, D. Bublak, U. Göbel, B. Henschke, W. Bensch, R. Schlögl, *ibid.* **1992**, *104*, 909 and **1992**, *31*, 868.
[5] S. Iijma, *Nature* **1991**, *354*, 56; N. Hamada, S. Sawada, A. Oshiyama, *Phys. Rev. Lett.* **1992**, *68*, 1579.
[6] D. Ugarte, *Nature* **1992**, *359*, 707.
[7] This remains true despite the most recent reports on metal-catalyzed production processes, since a selective synthesis is still not possible. R. Dagani, *Chem. Eng. News* **1993**, *71*, 6.
[8] The yield of soluble fullerenes is a sensitive and complex function of the helium vapor pressure (used for quenching), the electrode diameter, and the distance between the electrodes, which also influences the selectivity of formation of the various fullerenes: hot plasmas with a small electrode separation give increased quantities of higher fullerenes at lower overall yields. Graphitic tubules can be found within the carbon slag formed on the negative electrode used in the arc discharge with direct current. Graphitic onionlike spheres apparently arise only when fullerene black is intensively bombarded with electrons; however, the desired structure is not obtained in every batch, even when conditions are identical. It has not been proved beyond doubt whether graphitic onionlike spheres can be produced by other thermal processes, since transmission electron microscopy has, up to now, been the only possible means of identification.
[9] R. F. Curl, *Philos. Trans. R. Soc. London A* **1993**, *343*, 19.
[10] G. van Helden, N. G. Gotts, M. T. Bowers, *J. Am. Chem. Soc.* **1993**, *115*, 4363; *Nature* **1993**, *363*, 60; G. van Helden, M.-T. Hsu, P. R. Kemper, M. T. Bowers, *J. Chem. Phys.* **1991**, *95*, 3835.
[11] H. Schwarz, *Angew. Chem.* **1993**, *105*, 1493; *Angew. Chem. Int. Ed. Engl.* **1993**, *32*, 1420.
[12] H. Werner, M. Wohlers, D. Herein, D. Bublak, J. Blöcker, A. Reller, R. Schlögl, *Fullerene Sci. Technol.* **1993**, *1*, 199; H. Werner, D. Herein, J. Blöcker, B. Henschke, U. Tegtmeyer, T. Schedel-Niedrig, M. Keil, A. M. Bradshaw, R. Schlögl, *Chem. Phys. Lett.* **1992**, *34*, 62.
[13] Modified ULVIC BUCKY II apparatus equipped with graphite rods for spectroscopy (6 mm, 3 mm apart); alternating current of 150 A; distance between electrodes adjusted to give a constant current.
[14] Diode array spectrophotometer BECKMANN DU 7000; spectra were recorded with the help of a quartz optical fiber and a quartz window directly in front of the center of the electric arc.
[15] E. A. Rohlfing, *J. Chem. Phys.* **1988**, *89*, 6103, and references therein.
[16] M. Jeunehomme, R. P. Schwenker, *J. Chem. Phys.* **1965**, *42*, 2406.
[17] In plasmas, a large number of charged particles are also formed. The electrical charge can influence the formation of fullerenes, and this source of building blocks could give rise to additional selectivity. However, the fact that fullerenes are also produced under conditions in which charged species are absent suggests that electrically charged building blocks are helpful but not essential.
[18] All samples were investigated supported on amorphous carbon films after deagglomeration in an ultrasonic bath of acetone. Siemens (Elmiskop 102,

120 kV, double tilt, side entry), Jeol (CX 200, 200 kV, double tilt, top entry), and Phillips (CM 20, modified with a cryoprojection lens, ultrahigh vacuum in the sample chamber, single tilt, side entry) instruments were used.
[19] F. Atamny, H. Kollmann, W. Bartl, R. Schlögl, *Ultramicroscopy* **1993**, *48*, 281.
[20] A. Oberlin, *Chem. Phys. Carbon* **1989**, *22*, 1.
[21] F. Atamny, R. Schlögl, A. Reller, *Carbon* **1992**, *30*, 1123.
[22] The layered character of the objects, shown with continuous contrast, also follows from powder X-ray diffraction data, which show a clear peak corresponding to the interlayer separation of 341 pm and a complex, modulated background [13]. This material can be distinguished from the electrode graphite, which may contaminate the product, by its much lower combustion temperature [12].
[23] Since the apparatus was designed for the manufacture of large amounts of fullerenes, we operated with a regulated electrode separation and continuous external adjustment of the graphite rods, which led to a leak rate of the same order as the residual pressure. This factor could only be eliminated if the whole apparatus was placed in a glove box with an inert atmosphere.
[24] Presumably, this material is always formed when the apparatus is in operation and acts as a "getter" to the vapor-phase contaminants (helium 5.0). Moreover, such particles may well act as nuclei for the condensation of large fullerenes. A. Goeres, E. Sedelmayer, *Chem. Phys. Lett.* **1991**, *184*, 310; H. W. Kroto, K. McKay, *Nature* **1988**, *331*, 328.
[25] T. Grösser, A. Hirsch, *Angew. Chem.* **1993**, *105*, 1390; *Angew. Chem. Int. Ed. Engl.* **1993**, *32*, 1340.
[26] J. M. Hunter, J. L. Fye, E. J. Rosecamp, M. F. Jarrold, *J. Phys. Chem.* **1994**, *98*, 1810.
[27] This is determined by the thermal conductivity and partial pressure of the quench gas, as well as by a steep temperature gradient in the gas chamber, which was achieved by placing a metal plate around the plasma chamber to provide efficient cooling of the quench gas.

Synthesis of Very Highly Ordered Liquid Crystalline Phases by Complex Formation of Polyacrylic Acid with Cationic Surfactants

Markus Antonietti* and J. Conrad

Ionic surfactants and oppositely charged polyelectrolytes spontaneously form addition complexes that precipitate from aqueous solution. Neighboring group effects, which begin to operate at very low concentrations, are important for the formation of such complexes. A highly cooperative zipper mechanism is observed, and the stoichiometry of the complexes (with respect to charge) is usually 1:1.[1-3]

The properties of such complexes in nonaqueous solvents and in the solid state have, however, only recently been investigated. The poly(*n*-alkyltrimethylammonium styrene sulfonate) system shows highly ordered lamellar structures, which clearly adopts different phase modifications when the chain length of the alkyl groups is varied.[4] The driving force for the formation of these phases is the incompatibility between the ionic backbone and alkyl side chains, otherwise known as the amphotropy of the system.

We now propose a system in which complex formation occurs at the polyacrylic acid backbone and in which steric effects prevent a parallel orientation of the *n*-alkyl chains and formation of the resulting layered structures. For the first time, yet more diverse phase structures can be achieved in this polymer system.

The polyelectrolyte–surfactant complex PAA–C_{12}, obtained by simple mixing of polyacrylic acid and dodecyltrimethylammonium chloride, is a highly elastic, deformable material. Even in an unextended cast film, strongly doubly refracting domains of only a few micrometers in size can be seen with a polarizing microscope. Extension results in necking and hardening of the material; at the same time, the size of the doubly refracting domains increases to the millimeter range. The observed effects are not temperature dependent; that is, the structure remains unchanged up to decomposition of the material. Figure 1 shows the photograph under a polarizing microscope of a slightly stretched sample; Figures 2 and 3 show the wide-angle and small-angle X-ray diffractograms of the unextended sample.



Fig. 1. Photograph under a polarizing microscope of PAA–C_{12} at an extension of $\lambda = 1.5$ nm.

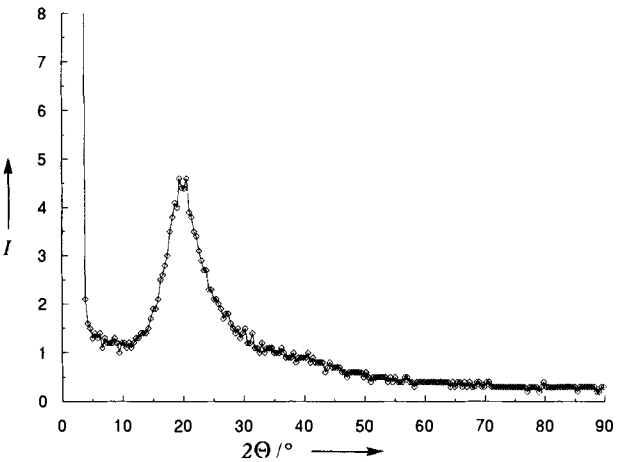


Fig. 2. Wide-angle diffractogram of PAA–C_{12}, $\lambda = 0.154$ nm, I = intensity (in counts per second).

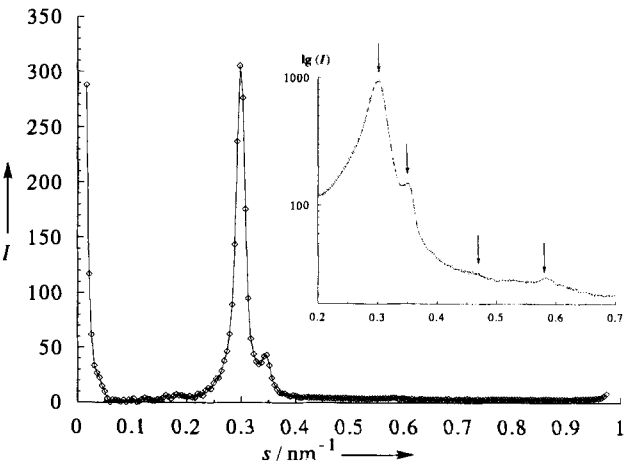


Fig. 3. Small-angle diffractogram of PAA–C_{12}, the scattering vector is defined as $s = 2\sin\theta/\lambda$. For clarity at higher orders of diffraction, the logarithmic plot of the filtered spectrum is included. I = intensity (in counts per second).

[*] Prof. Dr. M. Antonietti, J. Conrad
Max-Planck-Institut für Kolloid- und Grenzflächenforschung
Kantstrasse 55, D-14513 Teltow (FRG)
Telefax: Int. code + (3328)46-204

 © VCH Verlagsgesellschaft mbH, D-69451 Weinheim, 1994 0570-0833/94/1818-1869 $ 10.00+.25/0

The wide-angle X-ray data show that PAA–C_{12} is locally an amorphous unstructured material. The observed peak is clearly broader than for the analogous polystyrene sulfonate derivative; this indicates a higher disorder or a nonlamellar arrangement of the alkyl side chains.

The small-angle diffractogram shows a number of unusually narrow scattering peaks, which indicates the existence of a highly ordered liquid crystalline structure. A peak sequence of 1:1.16:1.63:2 can be identified from a logarithmic plot and the scattering at the extended sample. These results are indicative of a face-centered cubic lattice. A cell size of 5.80 nm can be deduced from the absolute position of the peak.

Clearly, the simple polyelectrolyte–surfactant complex poly(dodecyltrimethylammonium acrylate) PAA–C_{12} also spontaneously forms highly ordered, amphotropic liquid crystalline structures. In contrast to the analogous polystyrene sulfonate derivatives, which essentially exist in lamellar layers, PAA–C_{12} can be classified, based on its optical and mechanical behavior, as having a cylindrical morphology in which the ionic backbone chains are embedded in a continuous alkyl matrix. The symmetry type (face-centered cubic, FCC) determined by small-angle X-ray diffraction does not appear to agree with the cylindrical symmetry. This discrepancy might be explained by periodic fluctuations in thickness of the cylinder, which couple strongly because of the incompressibility; an FCC symmetry would thus result (Fig. 4). However, without extensive modeling of the electron density profile for this particular system, this remains speculation.

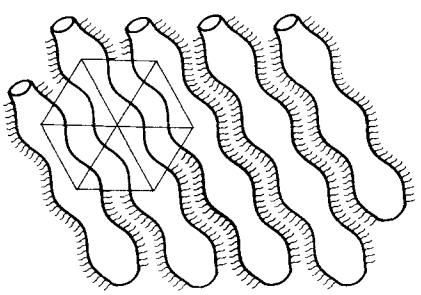


Fig. 4. Model for the structure of the amphotropic phase of PAA–C_{12}.

Such highly correlated fluctuations in thickness are not unusual, especially in lamellar structures, and are observed in lyotropic surfactant phases[5, 6] and, on a different scale, in block copolymers in the solid state.[7, 8] The phenomenon originates from the different packing of the alkyl chains and backbone and is also referred to as "frustration".[9]

In contrast to a simple FCC lattice, the structural model described above is also consistent with the polymeric nature of the backbone, which results from the presence of an extensive ionic phase. For PAA–C_{12}, the relative phase volumes of the disperse ionic phase and alkyl matrix range from about 0.3 to 0.7. These values are exactly in the region in which cylindrical morphology is also be observed for block copolymers. With this model, the size of the unit cell is 5.8 nm; the distance between the fluctuations along the chain is 4.10 nm.

In the complexes described, the average diameter of a cylinder can be estimated at about 2.1 nm from the lattice parameters and the relative phase volumes (obtained from the stoichiometry). From this value, the number of polymer chains per cylinder cross section can then be calculated. For an extended chain conformation, the maximum number is 5. Because of fluctuations in thickness and chain folding, a smaller number of around two or three is likely for steric reasons. Interestingly, this means that the chains would then act as a sort of "spun thread" of almost extended polymer chains (Fig. 5), a morphology which, until now, only had its parallel in nature,[10] but no synthetic analogues.



Fig. 5. Arrangement of the polymer chains in the cylindrical phase.

Electron microscopy and structure-sensitive solid-state NMR spectroscopy will now be used for further investigations into the structure of PAA–C_{12} to PAA–C_{18} complexes. It should be possible to extend the construction principle presented here to other polyelectrolyte complexes. Thus, by altering the polyelectrolyte (charge separation, molar volumes, hydrophobicity, glass-transition temperature) or the soap molecule (length, number of tails, functionality, platelet-like or disc-like structure), a wide spectrum of morphologies could be generated. Our simple approach to this system, based on self-organization, uses cheap starting materials which are available in large quantities. The further development of this class of materials may therefore be eagerly awaited.

Experimental Procedure

Polyacrylic acid (5.0 g, Aldrich, $M_w \approx 250000\ g\,mol^{-1}$) was dissolved in water (200 mL) and converted into the sodium salt with NaOH. Dodecyltrimethylammonium chloride (24 g, Aldrich) was added dropwise to water (200 mL) with stirring. The precipitated crude complex still contained large amounts of excess surfactant, salt, and water. The complex was purified by dissolving it in 2-butanol and carefully adding water until phase separation into a gelatinous phase rich in complex and a water phase occurred. The water phase was rich in salt and unconverted surfactant. The aqueous layer was discarded and the sol–gel separation repeated until no more chloride could be detected with silver nitrate. The solvent can be evaporated directly from thin layers of the gelatinous phase under vacuum. The elemental analysis of the complexes showed minimal residual quantities of sodium and chloride ions (<0.01%). The presence of salt and free surfactant (by Cl^- determination) and of unchanged acrylic acid units (by $Na^{\oplus}$ determination) in the product could thus be ruled out; the pure 1:1 complex was obtained. The film was dried under vacuum (24 h, 60 °C); high-resolution solid-state NMR spectroscopy was used to show that all butanol and water had been eliminated. Water is reabsorbed in low concentrations into the film under environmental conditions, this does not however influence the described effects.

Received: March 11, 1994
Revised: May 4, 1994 [Z 6749 IE]
German version: *Angew. Chem.* **1994**, *106*, 1927

[1] E. D. Goddard, *Colloids Surf.* **1986**, *19*, 301.
[2] K. Hayagawa, J. P. Santerre, J. C. T. Kwak, *Macromolecules* **1983**, *16*, 1642.
[3] K. Hayagawa, J. C. T. Kwak, *J. Phys. Chem.* **1982**, *86*, 3866; *ibid.* **1983**, *87*, 506.
[4] M. Antonietti, J. Conrad, A. Thünemann, *Macromolecules*, submitted.
[5] M. J. Rosen, *Surfactants and Interfacial Phenomena*, 2nd ed., Wiley, New York, **1989**.
[6] J. M. Seddon, *Biochim. Biophys. Acta* **1990**, *1*, 1031.
[7] F. S. Bates, G. H. Fredrickson, *Annu. Rev. Phys. Chem.* **1990**, *41*, 525.
[8] K. Almdal, K. A. Koppi, F. S. Bates, *Macromolecules* **1992**, *25*, 1743.
[9] P. G. de Gennes, *J. Phys. Lett.* **1983**, *44*, 1.
[10] E. Sackmann, *Macromol. Chem. (Oxford)* **1994**, *195*, 7.

 © VCH Verlagsgesellschaft mbH, D-69451 Weinheim, 1994 0570-0833/94/1818-1870 $ 10.00+.25/0

On the Nature of the Active Site in a CoAPO-18 Solid Acid Catalyst**

John Meurig Thomas,* G. Neville Greaves,* Gopinathan Sankar, Paul A. Wright, Jiesheng Chen, Andrew J. Dent, and Leonardo Marchese

Just as with crystalline enzymes, crystalline microporous inorganic catalysts, typified by zeolites, are amenable to direct, in situ X-ray (or neutron) study,[1, 2] a quantitative description of the local environment of the active site being obtainable from the diffraction pattern. The situation is not so straightforward with crystalline aluminophosphate-based catalysts, represented by MAPOs, where M is a divalent cation (Co, Ni, Zn, Mn, Mg etc) that isomorphously substitutes for some of the aluminum in the framework. Framework-substitution of trialent aluminum ions by divalent ones such as Co^{II} not only confers Brønsted acidity upon the resulting solid—a proton, loosely attached to one of the framework oxygen atoms, is required to maintain electroneutrality—it also introduces redox behavior.[3, 4] When the Co^{II} ion is oxidized to the Co^{III} state the Brønsted acidity necessarily disappears. Here, the concentration of M (in this case Co) is generally so low—seldom exceeding a few percent and often much less—that X-ray diffraction (XRD) cannot yield the desired (local) structural information. Under these circumstances, X-ray absorption spectroscopy (X-ray absorption near edge structure, XANES and extended X-ray absorption fine structure, EXAFS) is the preferred method of probing the environment of the active site, especially when it is used in combination[5] with X-ray diffraction, the principal purpose of the latter being to monitor the long-range integrity of the catalyst during the various processes of activation, deactivation and regeneration.

We recently described[6, 7] a family of molecular sieve catalysts in which minute amounts of cobalt ions are framework-substituted in place of aluminum ions in the open structure of a synthetic aluminum phosphate known as ALPO-18.[8] These solid acid catalysts $H_x(Co_xAl_{(1-x)}PO_4)$, $x \leq 0.04$, efficiently convert[7] methanol to light olefins (predominantly ethylene and propylene), a process well-known[9-11] to require more than modest Brønsted acidity. Typically, at 400 °C and a weight hourly space velocity (WHSV) of 1.5, methanol is completely converted to ethylene (22.4 percent), propylene (51.2), and C_4 olefins, chiefly butenes, (25.6) and a trace of methane.

The CoAPO-18 catalysts are synthesized hydrothermally in the presence of an organic template, *N,N*-diisopropylethylamine at 150 to 180 °C for three to ten days—full details are given elsewhere[6, 7]—the template-free samples being obtained by calcining the as-synthesized ones in gaseous oxygen at 550 °C for about one hour. Prior to use they were reduced in hydrogen at 400 °C.

ALPO-18 has a framework structure[12] closely related to that of the aluminosilicate (zeolitic) mineral chabazite. In the as-prepared, template-incarcerated state, samples of the CoAPO-18 catalyst (framework composition $Co_{0.04}Al_{0.96}PO_4$) are colored bright blue, consistent with Co^{II} in tetrahedral coordination. Upon calcination the color changes to green; IR and other spectroscopic measurements (to be reported fully elsewhere[13]) show that Co^{III} is then the predominant valence state. Idealized positions of cobalt in each valence state are shown in Figure 1. The spectroscopic changes shown in Figure 2 are consistent with local structures A and B of Scheme 1 for the redox Brønsted acid states exhibited by the catalyst.

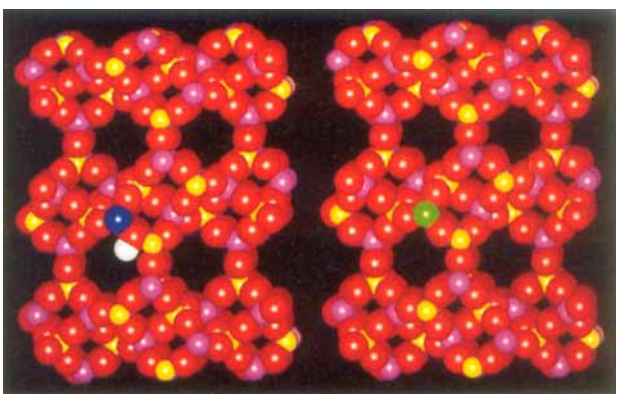


Fig. 1. Computer graphic representation of the cobalt-containing ALPO-18 structure. The framework is very similar to that of the aluminosilicate mineral chabazite. The actual colors of the calcined and reduced forms of the catalyst are green and blue, respectively. Color code: red, oxygen; blue, Co^{II}; green, Co^{III}; white, hydrogen; purple, phosphorus; yellow, aluminum.

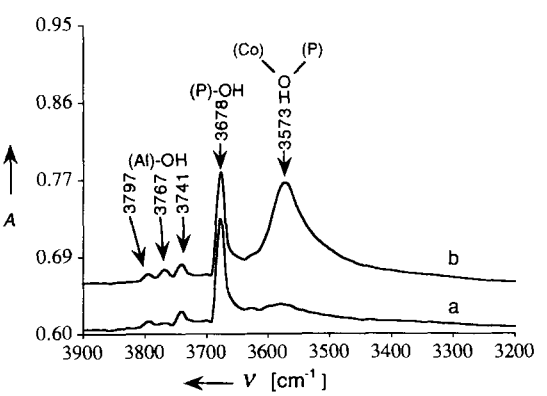
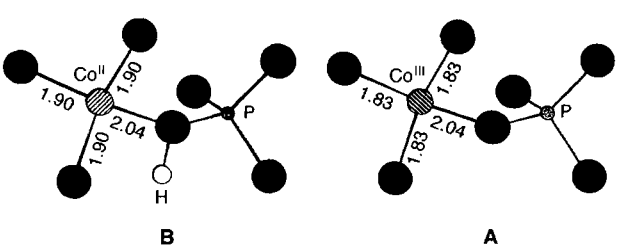


Fig. 2. IR spectra showing OH stretching vibration mode of CoAPO-18. a) Calcined in oxygen at 550 °C, b) reduced in hydrogen at 400 °C. *A* = absorption.



Scheme 1. Local structures of calcinated (A) and reduced CoAPO-18 (B).

[*] Prof. Sir John Meurig Thomas, Dr. G. Sankar, Dr. P. A. Wright, Dr J. Chen
Davy Faraday Research Laboratory
The Royal Institution of Great Britain
21 Albemarle Street, London W1X 4BS (UK)
Telefax: Int. code + (71)629-3569
Prof. G. N. Greaves, Dr. A. J. Dent
EPSRC, Daresbury Laboratory
Warrington, Cheshire WA4 4AD (UK)
Dr. L. Marchese
Dipartmento di Chimica I.F.M., Universita di Torino (Italy)

[**] We thank the Science and Engineering Research Council for the financial support and synchrotron beam time. We also thank Prof. C. R. A. Catlow, Dr. R. G. Bell, and P. A. Barrett for invaluable assistance.

 © VCH Verlagsgesellschaft mbH, D-69451 Weinheim, 1994 0570-0833/94/1818-1871 $ 10.00+.25/0

To make headway in the understanding of the catalytic behavior of CoAPO-18 it is important to define in quantitative terms the environment of the cobalt ion in the calcined and reduced states (the structures A and B of Scheme 1, respectively). This may be achieved from a series of in situ measurements using synchrotron radiation in which a combination of EXAFS spectra and XRD patterns are recorded. Details of two distinct kinds of combined EXAFS-XRD procedures that we have developed have been published previously.[14] In this study, because of the considerable dilution of the catalytically active transition metal ion, the EXAFS of cobalt was detected in fluorescence geometry, exploiting a multielement solid-state detector system.[15] By employing a rapidly scanning encoded monochromator[16] in QuEXAFS/XRD (QuEXAFS is the acronym for quick EXAFS mode[17, 18]), the recording of in situ cobalt EXAFS spectra were interpolated by those of XRD patterns, measured below the cobalt K-edge at 7430 eV ($\lambda = 1.6635(4)$ Å). Exposure times for EXAFS and XRD were 600 s and 258 s, respectively, so that with a deadtime of 42 s there is a total cycle time of 15 min. Specimens were mounted in a specially designed furnace with windows optimized for detecting X-ray fluorescent and transmitted beams, as well as a large range of diffraction angles.

Combined QuEXAFS/XRD results charting the in situ calcination and reduction of CoAPO-18 are given in Figure 3. In the course of these treatments there are no significant changes in the diffraction patterns demonstrating that the framework remains intact through the burn-out of the template and the subsequent activation of the catalyst. In contrast, the detailed environment of the Co ions, which amounts to a small fraction of the total structure, (by X-ray absorption) alters substantially, first through calcination and then on reduction. The oxidation of Co^{II} to Co^{III} that accompanies calcination results (Fig. 3 middle) in a 1.2 eV shift in the K-edge, in an increase in the pre-edge feature at 7710 eV, and in a decrease in frequency of the EXAFS oscillations. The latter reflects what amounts to a massive reduction in the oxygen nearest neighbor distance from 1.95 Å for Co^{II}–O to 1.83 Å for Co^{III}–O. Both these distances correspond to cobalt in high-spin states; the shorter bond length of Co^{III}–O lying comparatively close to the framework tetrahedral Al–O separations of 1.73 Å. Variations in the position of the absorption edge and of the cobalt–oxygen bond length with temperature are given in Figure 4. Note in particular that, in the temperature interval 300–500 °C, the Co^{II}–O distance falls prior to oxidation; this probably results from the collapse of the template. The final Co^{III}–O distance of 1.83 Å is reached by 500 °C and corresponds to state A in Scheme 1 and to the IR spectrum in Figure 2a.

The emergence of the new stretching bands at 3573 cm^{-1} (Fig. 2) on heating the calcinated CoAPO-18 in hydrogen, is attributable to Brønsted acid states.[7] This directly ties in with the structural changes upon reduction, in the cobalt EXAFS (Fig. 3 bottom and 4). We identify the restoration of the oxidation state from Co^{III} to Co^{II}, by the movement to lower energies in the K-edge position and diminution in the pre-edge feature (see Fig. 3 bottom). The EXAFS oscillation frequency is also enhanced corresponding to an increase in the primary cobalt–oxygen bond length from 1.83 Å to 1.90 Å—still significantly shorter than the 1.95 Å bond length of the starting material prior to calcination but now significantly longer than the 1.73 Å of the Al–O framework tetrahedral bonds. These changes are manifest between 300 °C and 400 °C, the working temperature of the CoAPO-18 catalyst.[7]

Detailed EXAFS analysis of CoAPO-18 in state B (Scheme 1) shows that the cobalt site in the activated material is not perfectly tetrahedral symmetrical, but that there is one longer cobalt–oxygen distance, close to 2.04 Å. This we tentatively ascribe to a protonated bridging oxygen between cobalt and a neighboring phosphorus.

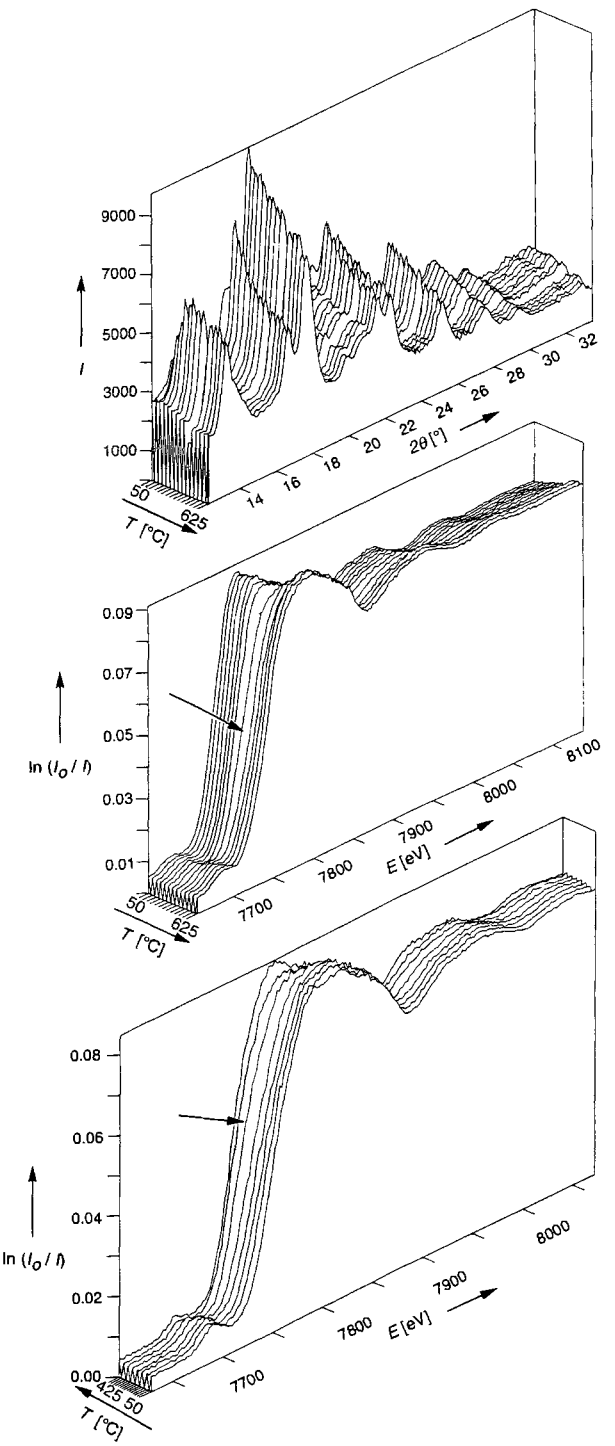


Fig. 3. Combined in situ XRD (top) and cobalt K-edge EXAFS (middle) recorded during the calcination of CoAPO-18. The shift in the K-edge on oxidation of Co^{II} to Co^{III} is indicated by the arrow. Bottom: In situ cobalt K-edge EXAFS measured during the course of the reduction of CoAPO-18, with the shift in the K-edge of Co indicated.

To our knowledge this is the first report describing the simultaneous changes in bond length and oxidation state of the active center of a solid inorganic catalyst, during calcination and reduction. All the redox changes that occur around cobalt in this

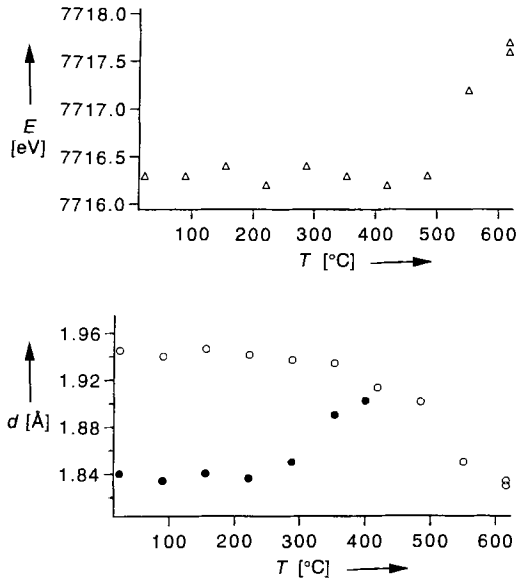


Fig. 4. Temperature variation of the position of Co K-edge, represented as E (top) and cobalt oxygen average bond lengths (d) measured from in situ EXAFS (bottom) during calcination (open circles) and reduction (filled circles) of CoAPO-18. Data were analyzed by using the EXCURVE suite of programs [19].

dilute metal catalyst CoAPO-18 when it is calcined in O_2 and then reduced in H_2 to generate Brønsted acidity take place around 350 °C, which is the temperature for the onset of catalysis. Quantum mechanical and other studies of the kind recently initiated[20, 21] are needed before the mechanistic details of the overall catalytic reaction can be elucidated.

Received: April 30, 1994 [Z 6887 IE]
German version: *Angew. Chem.* **1994**, *106*, 1922

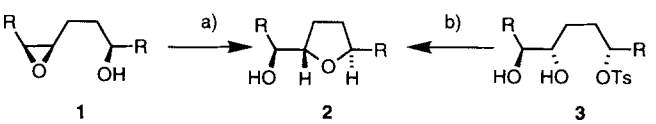
[1] J. M. Thomas, *Philos. Trans. R. Soc. London A* **1990**, *333*, 173; M. Czjek, H. Jobic, A. N. Fitch, T. Vogt, *J. Phys. Chem.* **1992**, *96*, 1535.
[2] D. H. Olson, E. Dempsey, *J. Catal.* **1969**, *13*, 221; A. K. Cheetham, M. M. Eddy, J. M. Thomas, *J. Chem. Soc. Chem. Commun.* **1983**, 23.
[3] C. Montes, M. E. Davis, B. Murray, M. Narayana, *J. Phys. Chem.* **1990**, *94*, 6425.
[4] B. Kraushaar-Czarnetszki, W. G. M. Hoogervorst, R. R. Andrea, C. A. Emeis, W. H. J. Stork, *J. Chem. Soc. Faraday Trans.* **1991**, *87*, 891.
[5] J. W. Couves, J. M. Thomas, D. Waller, R. H. Jones, A. J. Dent, G. E. Derbyshire, G. N. Greaves, *Nature* **1991**, *354*, 465.
[6] J. Chen, J. M. Thomas, R. P. Townsend, C. M. Lok, BR-B 93186443, **1993**.
[7] J. Chen, J. M. Thomas, *J. Chem. Soc. Chem. Commun.* **1994**, 603.
[8] S. T. Wilson, B. M. Lok, C. A. Messina, T. R. Cannan, E. M. Flanigen, *J. Am. Chem. Soc.* **1982**, *104*, 1146.
[9] W. O. Haag, R. M. Lago, P. B. Weisz, *Nature* **1984**, *309*, 589.
[10] E. G. Derouane in *Intercalation Chemistry* (Eds.: A. J. Jacobsen, M. S. Whittingham), Academic Press, New York, **1982**, p. 1.
[11] T. Inui, S. Phatanasari, H. Matsuda, *J. Chem. Soc. Chem. Commun.* **1990**, 205.
[12] A. Simmen, L. B. McCusker, C. Baerlocher, W. M. Meier, *Zeolites* **1991**, *11*, 654; W. M. Meier, D. H. Olson, *Atlas of Zeolite Structure Types*, Butterworths, **1992**, p. 72.
[13] L. Marchese, J. Chen, J. M. Thomas, S. Coluccia, A. Zecchina, *J. Phys. Chem.* in press.
[14] J. M. Thomas, G. N. Greaves, *Catal. Lett.* **1993**, *20*, 337, see also [18].
[15] G. E. Derbyshire, A. J. Dent, B. R. Dobson, R. C. Farrow, A. Felton, G. N. Greaves, C. Morrell, M. P. Wells, *Rev. Sci. Instrum.* **1992**, *63*, 814.
[16] B. R. Dobson, *Synchrotron Radiat. News*, **1994**, *7*, 21.
[17] G. Sankar, J. M. Thomas, P. A. Wright, S. Natarajan, A. J. Dent, B. R. Dobson, C. A. Ramsdale, G. N. Greaves, R. H. Jones, *J. Phys. Chem.* **1993**, *97*, 9550.
[18] B. S. Clausen, K. Grabaek, G. Steffensen, P. L. Hansen, H. Tøpsoe, *Catal. Lett.* **1993**, *20*, 23.
[19] S. J. Gurman, N. Binsted, I. Ross, *J. Phys. C: Solid State Phys.* **1984**, *17*, 143; P. Stephenson, G. N. Greaves, S. J. Gurman, *Synchrotron Radiat. News* **1991**, *4*, 29.
[20] G. J. Kramer, R. A. van Santen, C. A. Emeis, A. K. Nowak, *Nature* **1993**, *363*, 529.
[21] C. R. A. Catlow, J. D. Gale, *J. Phys. Chem.*, submitted; R. A. van Santen, personal communication to JMT.

A Multiple Five-Membered-Ring-Selective Williamson Reaction as a Key Step in the Stereoselective Construction of 2,5-Linked Oligo(tetrahydrofuran)s**

Holger Wagner and Ulrich Koert*

2,5-Linked oligo(tetrahydrofuran)s are important components of naturally and unnaturally occurring polyethers. Dimeric tetrahydrofurans of type **12** and **15** (see Scheme 3) form part of the structures of naturally occurring annonin compounds.[1] Unnatural oligo(tetrahydrofuran)s of type **8** (see Scheme 2) are of interest as potential elements of an ion channel active polyether helix.[2]

To date the acid-catalyzed, intramolecular ring opening of an epoxide **1** with the formation of the tetrahydrofuran **2** has been widely used (Scheme 1) for the stereoselective synthesis of 2,5-linked tetrahydrofurans.[3] A possible alternative is a five-membered-ring-selective intramolecular Williamson reaction of the dihydroxy-tosylate **3**.[4] The diol unit of **3** should be readily available with good stereocontrol by means of a Sharpless dihydroxylation.[5] We report here on the successful application of a multiple five-membered-ring-selective Williamson reaction for the synthesis of enantiomerically pure oligo(tetrahydrofuran)s.



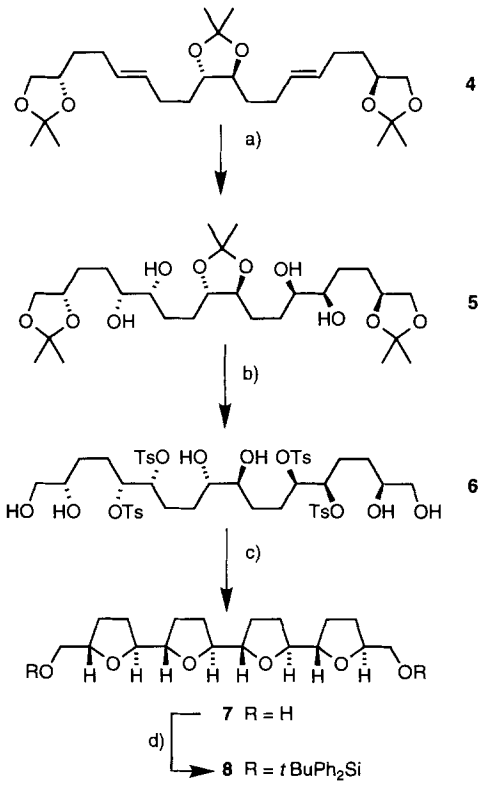
1 2 3

Scheme 1. Alternative synthetic routes to 2,5-disubstituted tetrahydrofurans; a) intramolecular epoxide opening; b) intramolecular five-membered-ring-selective Williamson reaction.

Sharpless dihydroxylation of the enantiomerically pure diene **4** yielded the tetraol **5** with a selectivity of 9:1 per double bond (determined by NMR spectroscopy) (Scheme 2). The quadruple tosylation and the subsequent triple, acidic acetonide cleavage led to the hexahydroxytetratosylate **6**. All four tetrahydrofuran rings were formed in a single step, in a stereocontrolled manner, by means of a quadruple Williamson reaction. The resulting water-soluble diol **7** could be converted to the di(*tert*-butyldiphenylsilyl) ether **8** which is soluble in organic solvents. The C_2 symmetry of the oligo(tetrahydrofuran) **8** was shown by the half set of signals in the ^1H and ^{13}C NMR spectra (Table 1).

[*] Dr. U. Koert, Dipl.-Chem. H. Wagner
Fachbereich Chemie der Universität
Hans-Meerwein-Strasse, D-35043 Marburg (FRG)
Telefax: Int. code + (6421)288-917

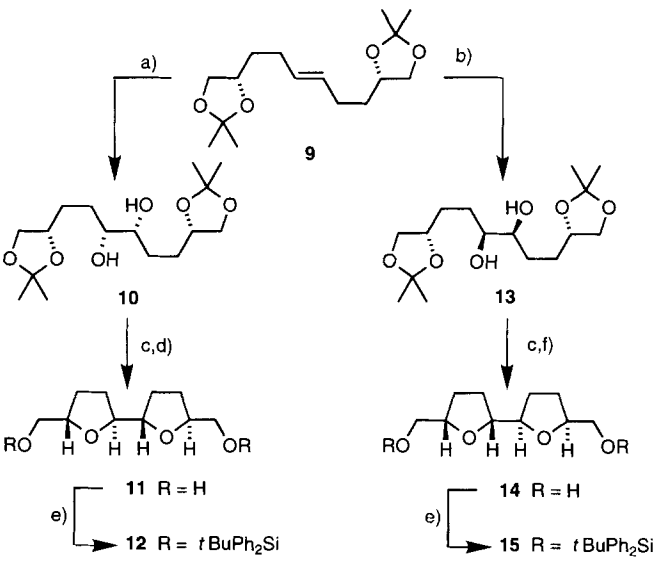
[**] This work was supported by the Deutsche Forschungsgemeinschaft and the Fonds der Chemischen Industrie. We thank Wacker AG and BASF AG for donatations of chemicals.



Scheme 2. Synthesis of the tetrameric tetrahydrofuran **8**; a) 1 equiv AD-mix-β, tBuOH/H_2O 1:1, 0 → 20 °C, 12 h (98%); b) 1. 16 equiv p-tosyl chloride, pyridine, 2. AcOH/H_2O 10:1, 40 °C, 8 h (89%, two steps); c) 12 equiv NaH, THF, 3 h, 40 °C (55%); d) tBuPh$_2$SiCl, imidazole, DMF (95%).

The strict five-membered-ring selectivity in the multiple Williamson reaction is remarkable. In terms of the extended Baldwin rules[6] the 5-*exo-tet* ring closure is clearly favored over the 6-*exo-tet* reaction and the reactions leading to other possible larger rings. No intermediates with only one, two, or three closed tetrahydrofuran rings were observed when the multiple reaction was followed by thin layer chromatography. This finding indicates a cooperative process and requires further study.

In order to investigate the extent of reagent control in the diastereoselective dihydroxylation step more closely we turned to compounds with only two tetrahydrofuran rings (Scheme 3) which are easier to analyze. Olefin **9** could be converted with the AD-mix-β[7] to diol **10** and, with the corresponding AD-mix-α, to diol **13**. The same stereoselectivity of 9:1 was observed for both reactions. In a control experiment compound **9** was dihy-



Scheme 3. Synthesis of the dimeric tetrahydrofurans **12** and **15**: a) 1 equiv AD-mix-β, tBuOH/H_2O 1:1, 0 → 20 °C, 12 h (98%); b) 1 equiv AD-mix-α, tBuOH/H_2O 1:1, 0 → 20 °C, 12 h (84%); c) 8 equiv p-tosyl chloride, pyridine (83%); d) 1. AcOH/H_2O 10:1, 40 °C, 8 h, 2. 8 equiv NaH, THF, 3 h, 40 °C, (89%, two steps); e) tBuPh$_2$SiCl, imidazole, DMF (90%); f) 1. AcOH/H_2O 10:1, 40 °C, 6 h, 2. 8 equiv NaH, THF, 3 h, 40 °C, (68%, two steps).

Table 1. Selected analytical and spectroscopic data for the compounds **4**, **8**, **11**, and **15**.

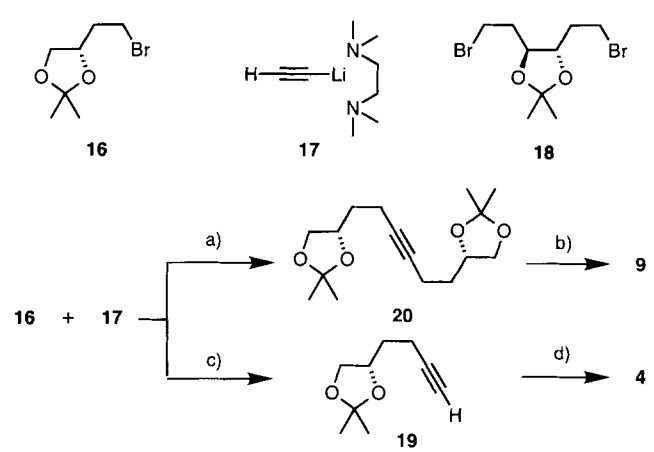
4: Colorless oil; $[\alpha]_D^{20} = -5.3$ ($c = 1.50$, $CHCl_3$); ^{1}H NMR [a]: $\delta = 1.28$, 1.30, 1.33 (each s, 3H), 1.42–1.53 (m, 3H), 1.59–1.71 (m, 1H), 1.93–2.20 (m, 4H), 3.43 (t, $J = 7.1$ Hz, 1H), 3.49–3.57 (m, 1H), 3.91–4.05 (m, 2H), 5.36–5.41 (m, 2H); ^{13}C NMR [b]: $\delta = 25.64$, 26.83, 27.20, 28.61, 28.87, 32.68, 33.34, 69.27, 75.46, 80.13, 107.79, 108.48, 129.69, 130.03; correct analysis for $C_{27}H_{46}O_6$.

8: Colorless oil; $[\alpha]_D^{20} = -5.2$ ($c = 4.05$, $CHCl_3$), ^{1}H NMR [a]: $\delta = 1.03$ (s, 9H), 1.60–2.09 (m, 8H), 3.59 (dd, $J = 10.3$, 5.7 Hz, 1H), 3.69 (dd, $J = 10.3$, 4.4 Hz, 1H), 3.85–3.93 (m, 2H), 3.94–4.00 (m, 1H), 4.08–4.16 (m, 1H), 7.31–7.39 (m, 6H), 7.64–7.69 (m, 4H); ^{13}C NMR [b]: $\delta = 19.25$, 26.85, 27.98, 28.23, 28.37, 28.44, 66.64, 79.67, 81.48, 81.78, 81.86, 127.57, 129.51, 133.81, 135.63; correct elemental analysis for $C_{50}H_{66}O_6Si_2$.

11: Colorless oil; $[\alpha]_D^{20} = +12.5$ ($c = 0.80$, $CHCl_3$), ^{1}H NMR [c]: $\delta = 1.53$–1.56 (m, 1H), 1.69–1.73 (m, 1H), 1.91–1.96 (m, 2H), 3.18 (br. s, 1H), 3.46 (dd, $J = 11.8$, 5.6 Hz, 1H), 3.65 (dd, $J = 11.8$, 3.1 Hz, 1H), 3.84–3.87 (m, 1H), 4.08–4.12 (m, 1H); ^{13}C NMR [d]: $\delta = 27.53$, 28.55, 64.57, 80.28, 82.22; correct elemental analysis for $C_{10}H_{18}O_4$.

15: Colorless oil; $[\alpha]_D^{20} = -8.5$ ($c = 2.00$, $CHCl_3$); ^{1}H NMR [a]: $\delta = 1.00$ (s, 9H), 1.46–1.99 (m, 4H), 3.51 (dd, $J = 10.2$, 6.6 Hz, 1H), 3.68 (dd, $J = 10.2$, 4.0 Hz, 1H), 3.68–3.76 (m, 1H), 3.99–4.07 (m, 1H), 7.28–7.36 (m, 6H), 7.59–7.65 (m, 4H); ^{13}C NMR [b]: $\delta = 19.19$, 26.82, 27.50, 28.06, 66.23, 79.64, 82.70, 127.53, 129.50, 133.67, 135.56; correct elemental analysis for $C_{42}H_{54}O_4Si_2$.

[a] 300 MHz ($CDCl_3$), 20 °C; [b] 75 MHz ($CDCl_3$), 20 °C; [c] 500 MHz ($CDCl_3$), 20 °C; [d] 126 MHz ($CDCl_3$), 20 °C.



Scheme 4. Synthesis of the olefins **9** and **4**; a) 1.2 equiv $LiNH_2$, NH_3, −33 °C, then 1.0 equiv **17**, then 2.0 equiv. **16**, −33 °C, 3 h (41%); b) 2.4 equiv Na, NH_3/THF 1:1, −33 °C, 2 h (90%); c) 1.3 equiv **17**, NH_3/THF 10:1, then 1.0 equiv **16**, −33 °C, 3 h (81%); d) 1. 4.3 equiv $LiNH_2$, NH_3; −33 °C, then 4.3 equiv **19**, 15 min, then 1.0 equiv **18**, −33 °C, 3 h (52%); 2. 4.4 equiv Na, NH_3/THF 1.5:1, −33 °C, 1.5 h (70%).

 © VCH Verlagsgesellschaft mbH, D-69451 Weinheim, 1994 0570-0833/94/1818-1874 $ 10.00+.25/0

droxylated with OsO_4/*N*-methylmorpholine-*N*-oxide which resulted in two diols **10** and **13** in a ratio of 1:1. The chiral centers of olefin **9**, therefore, have no controlling influence on the dihydroxylation. The observed stereocontrol is due solely to the Sharpless dihydroxylation reagent. Diols **10** and **13** can be converted by a multiple five-membered-ring-selective Williamson reaction analogous to the reaction in Scheme 2 into the dimeric tetrahydrofuranols **11** and **14**, respectively, and subsequently to the corresponding disilyl ethers **12** and **15**.

The enantiomerically pure alkenes **4** and **9** were prepared by standard methods (Scheme 4). The double alkylation of acetylene with bromide **16**[9] and the subsequent (*E*)-selective reduction to the olefin yielded compound **9**. Reaction of two equivalents of alkyne **19** with one equivalent of dibromide **18**[10] and subsequent (*E*)-selective reduction to the olefin yielded diene **4**.

The synthetic sequence of reagent-controlled, diastereoselective dihydroxylation and multiple five-membered-ring-selective Williamson reaction presented here opens up an efficient, bidirectional route to the enantiomerically pure oligo(tetrahydrofuran)s.

Received: April 28, 1994 [Z6877IE]
German version: *Angew. Chem.* **1994**, *106*, 1939

[1] a) J. K. Rupprecht, Y.-H. Hui, J. L. McLaughlin, *J. Nat. Prod.* **1990**, *53*, 237–278; b) U. Koert, *Tetrahedron Lett.* **1994**, *35*, 2517–2520; c) T. R. Hoye, P. R. Hanson, *ibid.* **1993**, *34*, 5043–5046.

[2] U. Koert, M. Stein, K. Harms, *Angew. Chem.* **1994**, *106*, 1238–1240; *Angew. Chem. Int. Ed. Engl.* **1994**, *33*, 1180–1182.

[3] a) J.-C. Harmange, B. Figadere, *Tetrahedron: Asymmetry* **1993**, *4*, 1711–1754; b) T. R. Hoye, J. Suhadolnik, *Tetrahedron* **1986**, *42*, 3309–3362; c) T. Nakata, G. Schmid, B. Vranesic, M. Okigawa, T. Smith-Palmer, Y. Kishi, *J. Am. Chem. Soc.* **1978**, *100*, 2933–2935.

[4] a) O. Mitsunobu in *Comprehensive Organic Synthesis, Vol 6* (Eds.: B. Trost, I. Fleming, E. Winterfeldt), Pergamon, Oxford, **1991**, p. 1–31; b) five-membered-ring-selective Williamson reaction: G. Fronza, C. Fuganti, P. Grasselini, G. Pedrocchi-Fantino, S. Servi, *Tetrahedron Lett.* **1993**, *34*, 2981-2984; c) five-membered-ring-selective THF formation with the use of allyl-Pd complexes: B. M. Trost, A. Tenaglia, *ibid.* **1988**, *29*, 2927-2930; d) five-membered-ring selectivity in the conversion of alkenediols to hydroxyiodotetrahydrofurans: P. A. Bartlett in *Selectivity - A Goal for Synthetic Efficiency* (Eds.: W. Bartmann, B. M. Trost), Verlag Chemie, Weinheim, **1984**, pp. 1-19.

[5] a) E. N. Jacobsen, I. Markó, W. S. Mungall, G. Schröder, K. B. Sharpless, *J. Am. Chem. Soc.* **1988**, *110*, 1968–1970; b) R. A. Johnson, K. B. Sharpless in *Catalytic Asymmetric Synthesis* (Ed.: I. Ojima), VCH, Weinheim, **1993**, pp. 227–272; c) S. C. Sinha, E. Keinan, *J. Org. Chem.* **1994**, *59*, 949–951.

[6] J. E. Baldwin, *J. Chem. Soc. Chem. Commun.* **1976**, 734–736.

[7] AD-mix-α (Aldrich No. 39275-8), AD-mix-β (Aldrich No. 39276-6).

[8] U. Koert, M. Stein, K. Harms, *Tetrahedron Lett.* **1993**, *34*, 2299–2302.

[9] B. Küchler, G. Voss, H. Gerlach, *Liebigs Ann. Chem.* **1991**, 545–552.

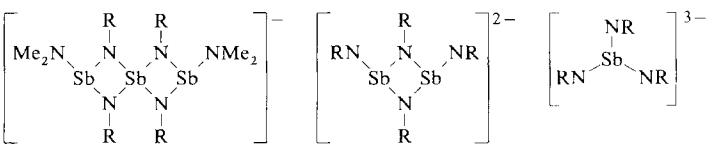
[10] Bromide **18** was synthesized from (3*S*,4*S*)-1,2,3,4-diepoxybutane [11] by a) reaction with CH_2=CH–MgCl (85%), b) acetonide protection (95%), c) ozonolysis with $NaBH_4$ workup, and d) conversion of the resulting diol to the dibromide [1. tosyl chloride, pyridine, 2. LiBr, THF (80%, two steps)].

[11] D. Seebach, H.-O. Kalinowski, B. Bastani, G. Crass, H. Daum, H. Dörr, N. P. DuPreez, V. Ehrig, W. Langer, C. Nüssler, H.-A. Oei, M. Schmidt, *Helv. Chim. Acta* **1977**, *60*, 301–325.

$[\{Sb_2(Ncy)_4\}_2Cu_4]$: A Mixed-Metal Antimony(III)/Copper(I) Complex Containing a Cu_4 Square Plane**

Donald Barr, Andrew J. Edwards, Samantha Pullen, Michael A. Paver, Paul R. Raithby, Moira-Ann Rennie, Christopher A. Russell, and Dominic S. Wright*

We recently demonstrated that stepwise metalation of primary amines (RNH_2) employing $[(Me_2N)_3Sb]$ as a reagent is an effective and versatile method of synthesizing Sb/Li heterometallic complexes which contain a range of polyamido Sb anions.[1–3] The "mixed-metalation" reaction of $[(Me_2N)_3Sb]$ with the anionic antimony complex $[(cyNH)_4Sb]^-Li^+$ produces $[(cyN)_4Sb_3(NMe_2)_2Li]$, containing the polynuclear amidoantimony anion $[(cyN)_4Sb_3(NMe_2)_2]^-$. The cage complex $[(PhCH_2CH_2NLi)_3Sb(thf)]_2$, containing the first structurally characterized $[Sb(NR)_3]^{3-}$ trianion, is the product of the reaction between $[(Me_2N)_3Sb]$ and the neutral amidolithium complex $[PhCH_2CH_2NHLi]_n$.[1] In addition to $[(Me_2N)_3Sb]$, the dimeric complexes $[(Me_2N)Sb(\mu\text{-}NR)]_2$, which have two reactive Me_2N groups,[2] can themselves be employed as metalating reagents. Thus, the reaction of $[(Me_2N)Sb(\mu\text{-}Ncy)]_2$ with $[cyNHLi]_n$ results in the rational assembly of $[\{Sb_2(Ncy)_4\}_2Li_4]$, which contains an $Sb_4N_8Li_4$ cage of two interlocked "broken" cubes and which is a potential source of the $[Sb_2(Ncy)_4]^{2-}$ dianion.[3] Currently, we are interested in using polyamidoantimony anions (Scheme 1) as novel ligands to a range of transition and main group metals. We report here the synthesis of **1** by the



Scheme 1. Polyamidoantimony anions.

transmetalation reaction between $[\{Sb_2(Ncy)_4\}_2Li_4]$ and CuCl (see Experimental Procedure) [Eq. (a)].

$$[\{Sb_2(Ncy)_4\}_2Li_4] + 4\,CuCl \xrightarrow{C_6H_5CH_3} \underset{\mathbf{1}}{[\{Sb_2(Ncy)_4\}_2Cu_4]} + 4\,LiCl \quad (a)$$

The X-ray crystallographic study of **1**[4] shows it to be a polyhedral cage complex, in which two terminal $[Sb_2(Ncy)_4]^{2-}$ ligands stabilize a central Cu_4 core (Fig. 1). The structure of **1** is very different to that of the analogous lithium compound

[*] Dr. D. S. Wright, Dr. A. J. Edwards, S. Pullen, M. A. Paver, Dr. P. R. Raithby, M.-A. Rennie, C. A. Russell
University Chemical Laboratory
Lensfield Road, Cambridge CB21EW (UK)
Telefax: Int. code + (223)336-362
Dr. D. Barr
Associated Octel Co., Ltd.
P.O. Box 17, Oil Sites Road
Ellesmere Port, South Wirral L654HF (UK)

[**] We gratefully acknowledge the Science and Engineering Research Council (UK) (A.J.E., M.A.P., P.R.R., C.A.R., D.S.W.), the Associated Octel Co., Ltd., Ellesmere Port (UK) (M.A.P., D.S.W.), the Royal Society (P.R.R., D.S.W.), the Nuffield Foundation (D.S.W.), and the Cambridge Crystallography Data Centre (M.-A.R.) for financial support. cy = cyclohexyl.

$[\{Sb_2(Ncy)_4\}_2Li_4]$ in which there is a tetrahedral arrangement of the four Li centers.[3] Although a number of mixed-metal Cu/Sb and Cu/As complexes has been structurally characterized,[5] the structure of **1** has a unique Cu/Sb framework. The structure illustrates for the first time that such polyamidoantimony anions can be employed as effective and robust ligands to other metals.

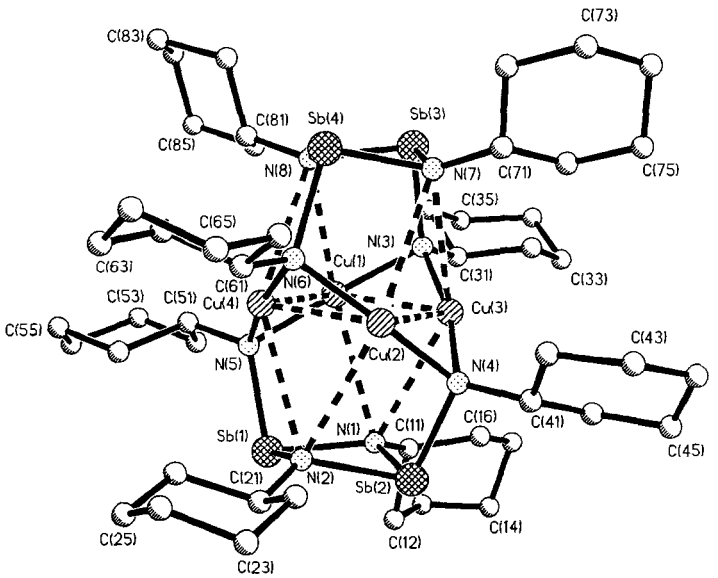


Fig. 1. The molecular structure of **1**. Hydrogen atoms have been omitted for clarity. Selected bond lengths [Å] and angles [°]: Sb(1)-N(1) 2.07(1), Sb(1)-N(2) 2.09(1), Sb(2)-N(1) 2.05(1), Sb(2)-N(2) 2.07(1), Sb(3)-N(7) 2.09(1), Sb(3)-N(8) 2.08(1), Sb(4)-N(7) 2.09(1), Sb(4)-N(8) 2.07(1), Sb(3)-N(3) 2.06(1), Sb(4)-N(6) 2.07(1), Sb(2)-N(4) 2.06(1), Sb(1)-N(5) 2.05(1), mean Cu···Cu 2.57, range (μ-cyN)···Cu 2.92–3.04, mean Cu-N to pendant Ncy 1.93; mean N-Sb-N 78.2, mean Sb-N-Sb 99.6; Cu···Cu···Cu 90.0, mean Cu-N-Cu 83.2.

The Cu_4 core of **1** is essentially square planar (range Cu···Cu···Cu 88.3(9)–91.1(9)°, sum of angles 360°) (Fig. 1). The pendant CyN arms of each terminal $[Sb(Ncy)_4]^{2-}$ ligand form Cu-(μ-N)-Cu bridges at opposite edges of the central Cu_4 unit (mean Cu–N 1.93 Å). Presumably, the Cu_4 fragment is largely held together by these Cu-(μ-N)-Cu bridges which result in a roughly linear coordination of the Cu centers of the core (mean N-Cu-N 168.7°). However, longer range Cu···(μ-N)···Cu interactions also occur with the Sb-bridging cyN centers of the $[Sb_2(Ncy)_4]^{2-}$ ligands (range 2.92–3.04 Å). As a result of these weak interactions, the $[Sb(\mu\text{-}Ncy)]_2$ rings are forced into a distinctly puckered conformation so as to bring the μ-N centers of each into closer contact with opposite Cu···Cu edges of the Cu_4 core. The possibility of Cu···Cu bonding in the Cu_4 unit of **1** cannot be discounted. The Cu···Cu distances in the core (mean 2.57 Å), although somewhat longer than those observed in $[CuCH_2SiMe_3]_4$ (2.42 Å),[6] are almost identical to those present in Cu metal (2.56 Å[7]). Within the $[Sb_2(Ncy)_4]^{2-}$ dianions the Sb–N distances are typical of those found in other amidoantimony complexes.[8]

A similar structural motif to that in **1** has been observed recently in $[\{(C_6H_4)_2O_2(Me_2SiNtBu)_2\}_2Cu_4]$,[9] in which two essentially organic dianions stabilize a Cu_4 square planar core (mean Cu···Cu 2.67 Å). However, whereas in **1** the four N donor centers of each $[Sb_2(Ncy)_4]^{2-}$ dianion (two pendant cyN, two μ-Ncy) bridge all four sides of the Cu_4 core, in $[\{(C_6H_4)_2O_2(Me_2SiNtBu)_2\}_2Cu_4]$ the four donor centers of each ligand (two pendant *t*BuN, two O) bridge only two adjacent sides of the Cu_4 fragment.

Experimental Procedure

A slurry of $[\{Sb_2(Ncy)_4\}_2Li_4]$ [3] (1.28 g, 1 mmol) in $C_6H_5CH_3$ (30 mL) was treated at 0 °C with CuCl (0.2 g, 4 mmol). Heating to reflux followed by stirring for 5 min yielded an intense yellow solution with precipitation of lithium chloride. Filtration through Celite with subsequent reduction to about 7 mL led to the precipitation of a yellow solid which redissolved by upon gentle warming. Storage at room temperature for 24 h yielded yellow crystalline blocks of **1**. First batch yield 0.55 g (36%). The relatively low yield is due to the high solubility of the complex; m.p. ca. 200 °C (decomp); ^{1}H NMR (C_6D_6, +25 °C, 250 MHz): δ = 3.8 (m), 2.5 (m), 1.5 (m) (cy groups). Satisfactory elemental analyses (C,H,N) were obtained.

Received: April 13, 1994 [Z 6844 IE]
German version: *Angew. Chem.* **1994**, *106*, 1960

[1] A. J. Edwards, M. A. Paver, M.-A. Rennie, P. R. Raithby, C. A. Russell, D. S. Wright, *J. Chem. Soc. Dalton Trans.*, in press.
[2] A. J. Edwards, M. A. Paver, P. R. Raithby, M.-A. Rennie, C. A. Russell, D. S. Wright, *Angew. Chem.* **1994**, *106*, 1334; *Angew. Chem. Int. Ed. Engl.* **1994**, *33*, 277.
[3] R. Alton, D. Barr, A. J. Edwards, M. A. Paver, M.-A. Rennie, P. R. Raithby, C. A. Russell, D. S. Wright, *J. Chem. Soc. Chem. Commun.* **1994**, 1481.
[4] Crystal data for **1**: $C_{48}H_{88}Cu_4N_8Sb_4$, M = 1518.42, triclinic, space group $P\bar{1}$, a = 10.690(2), b = 12.477(2), c = 23.137(5) Å, α = 86.62(3), β = 84.38(3), γ = 66.37(3)°, V = 2813.0(9) Å^3, Z = 2, ρ_{calcd} = 1.793 Mg m^{-3}, $F(000)$ = 1504, λ = 0.71073 Å, T = 153(2) K, $\mu(Mo_{K\alpha})$ = 3.410 mm^{-1}. Data were collected on a Siemens-Stoe AED diffractometer using an oil-coated rapidly cooled crystal mounted directly from solution (T. Kottke, D. Stalke, *J. Appl. Crystallogr.* **1993**, *26*, 615) of dimensions 0.37 × 0.33 × 0.32 mm by the θ/ω method ($7.02 \le 2\theta \le 45°$). Of a total of 7396 collected reflections, 7194 were unique. The structure was solved by direct methods (SHELXTL PLUS) and refined by full-matrix least squares on F^2 (SHELXL-93; G. M. Sheldrick, Göttingen, **1993**) to $R1$ = 0.0661 and $wR2$ = 0.1872 [$F > 4\sigma(F)$, for 3257 reflections] and $R1$ = 0.0868 and $wR2$ = 0.2352 (all data) [$R1 = \sum||F_o| - |F_c||/\sum|F_o|$, $wR2 = \{\sum w(F_o^2 - F_c^2)^2/\sum wF_o^4\}$, $w = 1/[\sigma^2(F_o^2) + (xP)^2 + yP]$, $P = (F_o^2 + 2F_c^2)/3$]. Largest difference between peak and hole in the final difference map, 2.226 and −1.925 e Å^{-3}. Further details of the crystal structure investigation are available on request from the Director of the Cambridge Crystallographic Data Centre, 12 Union Road, GB-Cambridge CB21EZ (UK), on quoting the full journal citation.
[5] See for example a) A. L. Rheingold, M. E. Fountain, *J. Crystallogr. Spectrosc. Res.* **1984**, *14*, 594; b) J. T. Gill, J. J. Mayerle, P. S. Welcker, D. F. Lewis, D. A. Ucko, D. J. Barton, D. Sowens, S. J. Lippard, *Inorg. Chem.* **1976**, *15*, 115; c) M. R. Churchill, W. J. Young, *ibid.* **1979**, *18*, 1133; d) A. H. Cowley, R. A. Jones, *Angew. Chem.* **1989**, *101*, 1089; *Angew. Chem. Int. Ed. Engl.* **1989**, *28*, 1018.
[6] J. A. J. Jarvis, B. T. Kilbourn, R. Pearce, M. F. Lappert, *J. Chem. Soc. Chem. Commun.* **1973**, 475.
[7] F. A. Cotton, G. Wilkinson, *Advanced Inorganic Chemistry*, 5th ed., Wiley, New York, **1988**; J. E. Huheey, *Inorganic Chemistry*, 3rd ed., Harper and Row, London, **1983**.
[8] a) W. Neubert, H. Pritzkow, H. P. Latscha, *Angew. Chem.* **1988**, *100*, 298; *Angew. Chem. Int. Ed. Engl.* **1988**, *27*, 287; b) H. W. Roesky, K. Hübner, M. Noltemeyer, M. Schäfer, *ibid.* **1991**, *103*, 856 and **1991**, *30*, 861; c) M. Björgvisson, H. W. Roesky, F. Pauer, G. M. Sheldrick, *Chem. Ber.* **1992**, *125*, 767–769; d) M. Rhiel, F. Weller, J. Pebler, K. Dehnicke, *Angew. Chem.* **1994**, *106*, 599; *Angew. Chem. Int. Ed. Engl.* **1994**, *33*, 569.
[9] M. Veith, K. L. Woll, *Chem. Ber.* **1993**, *126*, 2383.

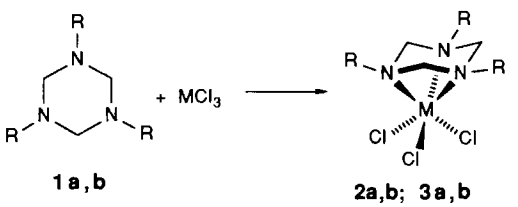
Cr^{III} and Fe^{III} Complexes with η^3-1,3,5-Triazacyclohexane Ligands**

Randolf D. Köhn* and Gabriele Kociok-Köhn

Many complexes having triazacyclononane and larger macrocyclic amines as ligands are known.[1] They are used as bioinorganic model systems and as catalysts for olefin polymerization.[2] Therefore, it is surprising that hardly any complexes with the smaller triazacyclohexane ligands **1** are known (see Scheme 1). Many N-alkylated triazacyclohexanes are commerically available, while the larger macrocyclic amines are much more expensive or can be obtained only by time-consuming syntheses.

Some poorly characterized Cr and Mo tricarbonyl complexes with **1**[3] are described. Only a few other complexes of this type have been characterized by X-ray crystallography,[4] and here the metal is mostly coordinated by only one nitrogen atom of **1**. The only case of η^3 coordination was found in a complex of **1b** with $InMe_3$;[4d] however, this structure could not be well refined owing to the highly disordered *i*Pr groups.

We have found that addition of **1** to solutions of $[CrCl_3(thf)_3]$ in THF or $FeCl_3$ in Et_2O results in the precipitation of the 1:1 complexes **2** and **3**, respectively (Scheme 1; for physical data of these and other new compounds see Table 1). These complexes



Scheme 1. Reactions of **1a** (R = Me) and **1b** (R = *i*Pr) with $[CrCl_3(thf)_3]$ in THF to give **2a** and **2b** (M = Cr), respectively, and with $FeCl_3$ in Et_2O to give **3a** and **3b** (M = Fe), respectively.

Table 1. Selected spectroscopic data of **2**–**4** [a].

2a: MS (450 °C): *m/z* 286 [M^+] [b]; IR (KBr) (< 600 cm^{-1}): $\tilde{\nu}$[cm^{-1}] = 509s, 419m, 390s, 373s, 313m, 293m.

2b: MS (390 °C): *m/z* 370 [M^+] [b]; IR (KBr) (< 600 cm^{-1}): $\tilde{\nu}$[cm^{-1}] = 555s, 372m, 377s, 370s, 340s, 331s

3a: MS (240 °C): *m/z* 254 [M^+ − HCl], [b]; ^{1}H-NMR (80 MHz, $CDCl_3$) ($\Delta\nu_{1/2}$): δ = 3.80 (3H, 12 Hz), 2.67 (3H, 6 Hz), 1.58 (9H, 11 Hz); IR (KBr) (< 600 cm^{-1}): $\tilde{\nu}$[cm^{-1}] = 507m, 330s, 300m

3b: ^{1}H NMR (270 MHz, $CDCl_3$) ($\Delta\nu_{1/2}$): δ = 3.89 (6H, 100 Hz), 2.69 (3H, 50 Hz), 1.58 (9H, 12 Hz); IR (KBr) (< 600 cm^{-1}): $\tilde{\nu}$[cm^{-1}] = 539m, 356m, 320s

4: MS (140 °C): *m/z* (%): 459 (0.6) [M^+ − Me], 387 (14.2) [$M^+ - CH_2SiMe_3$], 386 (1.3) [M^+ − $SiMe_4$], 372 (3.5) [$M^+ - Me - CH_2SiMe_3$], 300 (48) [$M^+ - 2(CH_2SiMe_3)$], 212 (10.2) [**1b**$^+$ − H], 72 (100) [*i*PrNH=CH_2^+]; ^{1}H NMR (270 MHz, C_6D_6), ($\Delta\nu_{1/2}$): δ = 5.8 (9H, 1000 Hz), −1.3 (18H, 700 Hz); IR (KBr) (< 600 cm^{-1}): $\tilde{\nu}$[cm^{-1}] = 543m, 525m, 498m, 471m, 467w, 464w, 444w, 441w, 437w, 370w, 312m

[a] MS: EI, 70 eV, correct isotope patterns. [b] Aditional signals for [M^+ − Cl], [$M^+ - (R-N{=}CH_2)$], [M^+ − Cl − $(R-N{=}CH_2)$], [$M^+ - 2(R-N{=}CH_2)$], [M^+ − Cl − $2(R-N{=}CH_2)$] (R = Me(**a**) or *i*Pr(**b**)).

[*] Dr. R. D. Köhn, Dr. G. Kociok-Köhn
Institut für Anorganische und Analytische Chemie
der Technischen Universität
Strasse des 17. Juni 135, D-10623 Berlin (FRG)
Telefax: Int. code + (30)314-22168

[**] This work was supported by the Deutsche Forschungsgemeinschaft, the Fonds der Chemischen Industrie, and the Graduierten Kolleg of the Bundesministerium für Bildung und Wissenschaft. R. D. K. thanks the Deutsche Forschungsgemeinschaft for a Habilitation fellowship and Prof. Dr. H. Schumann for the support of this work.

remain unchanged over several days when exposed to air, and the most inert complex **2b** was not even attacked by aqua regia. They are soluble in strongly polar solvents such as dimethylsulfoxide (DMSO); the iron complexes **3a**, **b** are also soluble in CH_2Cl_2 and $CHCl_3$.

Suitable crystals for X-ray crystallography were obtained by slow evaporation of a solution of **3a**[5] in CH_2Cl_2. Figure 1 shows the structure of **3a**. The triazacyclohexane ligand is coordinated through all three nitrogen atoms to the iron center. Although there is only one crystallographic mirror plane, the molecule has nearly C_{3v} symmetry. The Fe–N and Fe–Cl bond lengths are all 225 pm. These comparatively long Fe–N distances are similar to those in Fe^{III} trimethyltriazacyclononane complexes.[7] Since the bond lengths and angles in the ligand of **3a** show no unusual distortions, the nitrogen lone pair is assumed to form a 24° angle with the Fe–N axis (see Scheme 3). The resulting poor overlap can explain the long Fe–N bond length.

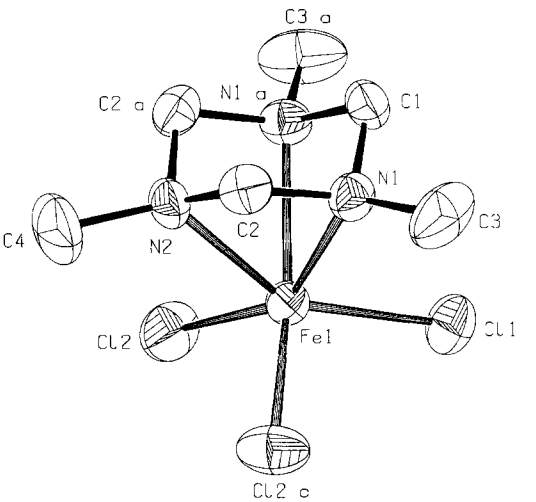


Fig. 1. Crystal structure of **3a** (ORTEP plot, ellipsoids for 50% probability, hydrogen atoms are omitted). Selected distances [pm] and angles [°]: Fe-Cl1 224.96(14), Fe-N1 225.3(2), N1-C1 146.0(3), N1-C3 147.0(4), Cl1-Fe-Cl2 103.37(4), Cl1-Fe-N1 94.36(7), Cl1-Fe-N2 150.79(9), N1-Fe-N2 60.98(9), Fe-N1-C3 129.8(2), C1-N1-C2 109.8(2), C1-N1-C3 114.4(3), N1-C2-N2 102.8(2).

Complex **2b** reacted slowly with $LiCH_2SiMe_3$ in toluene to form the brown dialkylated complex **4** (Scheme 2), a toluene soluble, but petroleum ether insoluble solid, in 42% yield. In the



Scheme 2.

workup the crude product soluble in petroleum ether includes a deep purple chromium-containing oil; the toluene-insoluble residue contains a brown chromium compound. No pure compounds were isolated from these fractions. No trialkylated com-

pound was isolated when **4** was treated with an excess of $LiCH_2SiMe_3$ or MeLi.

Complex **4** can be recrystallized from toluene; its crystal structure[6] shows a η^3-bound triazacyclohexane ligand. The Cr–N bonds *trans* to the alkyl groups are much longer (229.2 and 229.8 pm) than the bonds *trans* to the chloro ligand (218.1 pm). The average Cr–N bond length of 225.7 pm is nearly identical to the Fe–N distances in **3a**. The Cr–C distances (208.6 and 208.0 pm) and the Cr–Cl distance (231.6 pm) are in the normal range.

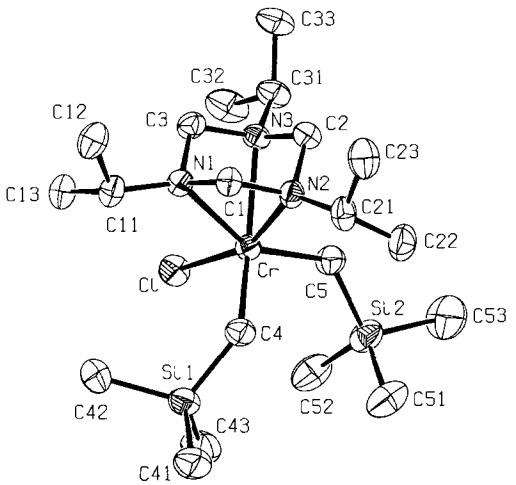
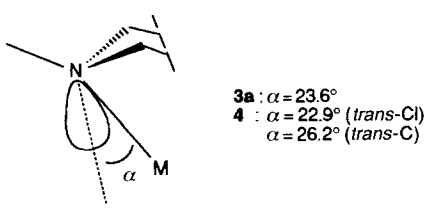


Fig. 2. Crystal structure of **4** (ORTEP plot, ellipsoids for 50% probability, hydrogen atoms are omitted). Selected distances [pm] and angles [°]: Cr-Cl 231.6(1), Cr-C4 208.6(5), Cr-N1 229.2(4), Cr-N2 218.1(4), N1-C1 147.7(6), N1-C11 149.3(6), Cl-Cr-C4 101.1(2), Cl-Cr-C5 94.4(2), C4-Cr-C5 105.7(2), Cl-Cr-N1 97.2(1), Cl-Cr-N2 157.8(1), C4-Cr-N3 151.5(1), N1-Cr-N2 62.7(1), Cr-N1-C11 133.0(3), Cr-N1-C1 90.0(3), Cr-N2-C21 130.6(3).

The bond lengths in **3a** and **4** are similar despite the sterically more demanding ligands in **4**. Elongated metal–N bonds were also found in the only other known complex with a η^3-triazacyclohexane ligand.[4d] As in **3a**, the C-N-C angles in **4** indicate that the nitrogen lone pair forms an angle of 23–26° with the Cr–N bond (Scheme 3).



Scheme 3. Angles between the N–M bonds and the position of the nitrogen lone pairs estimated from the C–N bonds.

Despite the ring strain in complexes with η^3-triazacyclohexane ligands, Cr^{III} and Fe^{III} complexes can be prepared easily and are stable in air and at temperatures well over 100 °C. Derivatization by reaction with $LiCH_2SiMe_3$ showed that the corresponding organometallic complexes can be obtained. Two crystal structures showed that the distances between the metal center and the cyclic amine are similar to those in complexes with *N,N',N''*-trimethyltriazacyclononane ligands despite the ring strain.

Experimental Procedure

All reactions were performed with standard Schlenk techniques, under dry argon, and in dry solvents when not stated otherwise. All compounds provided satisfactory elemental analyses (C,H,N,Cr,Fe).

2a: Triamine **1a** (0.10 mL, 0.71 mmol) (dried over 3 Å molecular sieves) was added to $[CrCl_3(thf)_3]$ (117 mg, 0.47 mmol) in 20 mL of THF at room temperature. After 30 min of stirring, the purple precipitate was isolated by filtration in the air and washed with Et_2O. After drying in vacuo, 122 mg of purple **2a** (90%) was obtained. M.p. 270 °C (decomp).

Complex **2b** was prepared analogously to **2a** from **1b** and $[CrCl_3(thf)_3]$ in THF, and was obtained as a purple powder (90% yield). M.p. 300 °C (decomp). **3a** (m.p. 170 °C (decomp)), and **3b** (m.p. 130 °C (decomp)) were prepared analogously to **2a** and **2b** from $FeCl_3$ in Et_2O, and were obtained as orange-yellow powders (90% yield).

4: Complex **2b** (543 mg, 1.46 mmol) and $LiCH_2SiMe_3$ (290 mg, 3.08 mmol) in 20 mL of toluene were stirred at room temperature for 4 d. The solvent was removed in vacuo and the purple residue washed with petroleum ether. The remaining brown solid was extracted with toluene. Concentration and drying in vacuo left 295 mg (42%) of brown **4**. The compound can be recrystallized from toluene at −20 °C, m.p. 150 °C (decomp).

Received: March 16, 1994
Revised version: April 26, 1994 [Z 6763 IE]
German version: *Angew. Chem.* **1994**, *106*, 1958

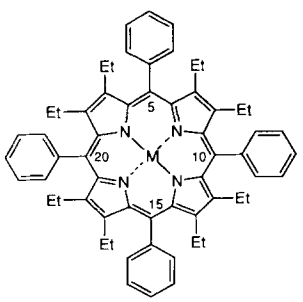
[1] P. Chaudhuri, K. Wieghardt, *Prog. Inorg. Chem.* **1987**, *35*, 329–436.
[2] L. Wang, T. C. Flood, *J. Am. Chem. Soc.* **1992**, *114*, 3169–3170.
[3] A. Lüttringhaus, W. Kullick, *Tetrahedron Lett.* **1959**, 13–15; H. Werner, *J. Organomet. Chem.* **1966**, *5*, 100–102.
[4] Literature survey: a) M. B. Hursthouse, M. Motevalli, P. O'Brien, J. R. Walsh, *Organometallics* **1991**, *10*, 3196–3200; b) R. Fuchs, P. Klüfers, *J. Organomet. Chem.* **1992**, *424*, 353–370; c) J. L. Atwood, F. R. Bennett, C. Jones, G. A. Koutsantonis, C. L. Raston, K. D. Robinson, *J. Chem. Soc. Chem. Commun.* **1992**, 541–543; d) D. C. Bradley, D. M. Frigo, I. S. Harding, M. B. Hursthouse, M. Motevalli, *ibid.* **1992**, 577–578.
[5] Crystal structure determination of **3a**: $C_6H_{15}N_3Cl_3Fe$, orthorhombic, space group *Pnma* (no. 62), $a = 13.516(2)$, $b = 11.815(3)$, $c = 7.962(3)$ Å, $V = 1271.4(6)$ Å^3, $Z = 4$, $\rho_{calcd} = 1.522$ Mg m^{-3}, $\mu(Mo_{K\alpha}) = 1.748$ mm^{-1}, $F(000) = 596$, $\lambda = 71.069$ pm, $T = 20$ °C, crystal dimensions: 0.55 × 0.35 × 0.35 mm, CAD-4 Enraf-Nonius diffractometer, ω-2θ scan, $6° \le 2\theta \le 50°$ ($0 \le h \le 16$, $0 \le k \le 14$, $0 \le l \le 9$); 1327 total reflections, 1071 unique and 1066 with $I > 4\sigma(I)$, which were used for refinement; empirical absorption correction DIFABS (min. 0.785, max. 1.296). The structure was solved with direct methods (SHELX-86) and refined anisotropically versus F^2 (SHELX-93). H atoms were refined isotropically. Residual electron density, min/max −0.58/0.43 eÅ^{-3}. Refinement of the 100 parameters by full-matrix least-squares resulted in $R_1 = 0.031$, $wR_2(F^2) = 0.085$, $GOF = 1.067$ [6].
[6] Crystal structure determination of **4** · 1.5 toluene: $(C_{20}H_{49}N_3ClSi_2Cr)$-$(C_7H_8)_{1.5}$, monoclinic, space group $P2_1/n$ (no. 14), $a = 12.830(3)$, $b = 14.675(5)$, $c = 19.287(11)$ Å, $\beta = 95.81(3)°$, $V = 3613(3)$ Å^3, $Z = 4$, $\rho_{calcd} = 1.1278(9)$ Mg m^{-3}, $\mu(Mo_{K\alpha}) = 0.47$ mm^{-1}, $F(000) = 1320$, $\lambda = 71.069$ pm, $T = -84$ °C, crystal dimensions: 0.18 × 0.35 × 0.55 mm, CAD-4 Enraf-Nonius diffractometer, ω-2θ scan, $2° \le 2\theta \le 50°$ ($0 \le h \le 15$, $0 \le k \le 17$, $-22 \le l \le 22$); 6894 total reflections, 4638 unique with $I > 4\sigma(I)$. 4600 reflections were used for refinement; empirical absorption correction DIFABS (min. 0.902, max. 1.141). The structure was solved with direct methods (SHELX-86) and refined anisotropically using difference Fourier syntheses (SHELX-76). H atoms were placed on calculated positions with d(CH) = 108 pm and $U_{iso} = 0.08$ Å^2. Residual electron density, min/max −0.57/0.81 eÅ^{-3}. Refinement of the 315 parameters by full-matrix least-squares resulted in $R = 0.066$, $R(int) = 0.016$. Every asymmetrical unit in the unit cell contains 1.5 molecules of toluene. The complete toluene molecule was placed on geometrically ideal positions and refined anisotropically. The other toluene molecule lies on an inversion center and is disordered. Atoms of this molecule were refined isotropically. No attempt was undertaken to calculate missing H atoms of this molecule. Further details of the crystal structure investigations may be obtained from the Fachinformationszentrum Karlsruhe, D-76344 Eggenstein-Leopoldshafen, on quoting the depository number CSD-58341.
[7] K. Wieghardt, S. Drücke, P. Chaudhuri, U. Flörke, H.-J. Haupt, B. Nuber, J. Weiss, *Z. Naturforsch. B* **1989**, *44*, 1093–1101.

 © VCH Verlagsgesellschaft mbH, D-69451 Weinheim, 1994 0570-0833/94/1818-1878 $ 10.00+.25/0

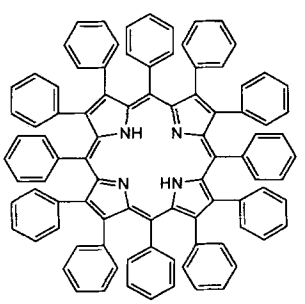
5,10,15,20-Tetra-*tert*-butylporphyrin and Its Remarkable Reactivity in the 5- and 15-Positions**

Tadashi Ema, Mathias O. Senge, Nora Y. Nelson, Hisanobu Ogoshi, and Kevin M. Smith*

Both 2,3,7,8,12,13,17,18-octaethylporphyrin H_2(OEP) and 5,10,15,20-tetraphenylporphyrin H_2(TPP) have been used extensively as models for natural porphyrin systems.[1] We recently showed that the hybrid of these two systems, 2,3,7,8,12,13,17,18-octaethyl-5,10,15,20-tetraphenylporphyrin (H_2(OETPP) **1**), displays quite remarkable physical and spectroscopic properties,[2] along with analogues such as dodecaphenylporphyrin (H_2(DPP) **2**),[3] 2,3,7,8,12,13,17,18-octaethyl-5,10,15,20-tetranitroporphyrin,[4] and various 2:3,7:8,12:13,17:18-tetraalkano-5,10,15,20-tetraphenylporphyrins.[2b, 5] In particular, for example, we showed that

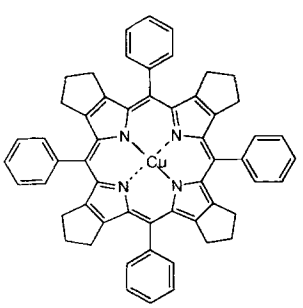


1 M = 2H
9 M = Zn

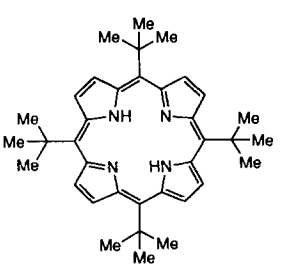


2

H_2(OETPP) and other highly congested dodecasubstituted porphyrins possess highly nonplanar conformations in the solid state and in solution,[2a, b] whereas the core macrocycle in the dodecasubstituted porphyrin copper(II) complex **3** is perfectly planar.[6] We suspected that nonplanar conformations approaching or similar to those in **1** and **2** might be achieved simply by attaching one or more *tert*-butyl groups to the porphyrin periphery. In the present paper we show that the prototype, 5,10,15,20-tetra-*tert*-butylporphyrin (H_2(TTBP) **4**), is so distorted that its fundamental reactivity no longer parallels that of regular porphyrins, or for that matter of any known nonplanar porphyrin.

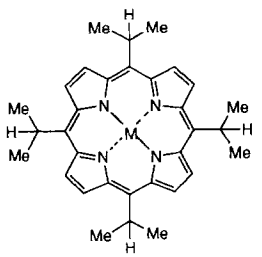


3



4

Treatment of equimolar amounts of pyrrole and pivalaldehyde at high dilution (26 mM) with BF_3 catalysis[7] provided minimal quantities of H_2(TTBP) detectable only by spectrophotometry. When the reaction was repeated with significantly higher concentrations of the reagents (150 mM), H_2(TTBP) (λ_{max} ($CHCl_3$) 446, 552, 596, 628, and 692 nm; Fig. 1) was isolated in 8.8% yield. Under similar conditions reaction of 2-methylpropanal with pyrrole gave a 5.1% yield of 5,10,15,20-tetraisopropylporphyrin (H_2(TIPP) **5**) (λ_{max} (CH_2Cl_2) 420, 524, 560, 602, and 656 nm; Fig. 1). Figure 1 shows the optical spectra of **4** and **5**. The significantly greater red shift of the bands of **4** indicate that it has presumably a greater deformation from planarity than **5**. A direct correlation between significant red shifts in the optical spectra with nonplanarity of the porphyrin core has been shown already.[2]



5 M = 2H
6 M = Ni
7 M = $4H^{2+}$

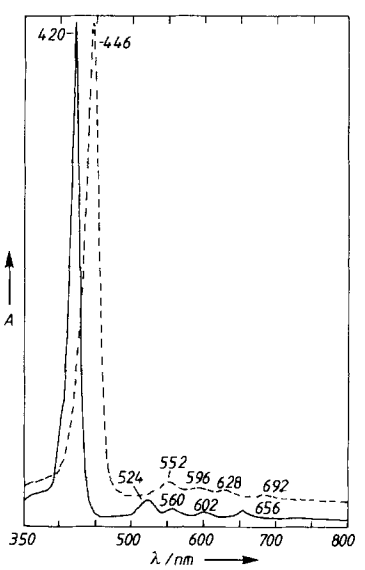


Fig. 1. Optical spectra of **4** (---) and **5** (—) in CH_2Cl_2.

Thus far we have been unable to obtain a satisfactory crystal structure for **4** or for any of its "normal" porphyrin derivatives. However, the single-crystal X-ray structure analysis of the nickel(II) complex of H_2(TIPP), [Ni(TIPP)] **6**, showed a nonplanar macrocycle conformation (λ_{max} (CH_2Cl_2) 422, 548, and 590 nm), indicated by an average deviation of the 24 macrocycle atoms from their least-squares plane by 0.36 Å; the largest out-of-plane displacements are observed for the *meso* carbon atoms (0.74 Å). These displacements are larger than those observed in, for example, [Ni(OEP)],[9] which proves that the steric interaction of the *meso*-isopropyl groups with neighboring β-pyrrole hydrogens leads to some distortion in the macrocycle (Fig. 2).[8a, 10] On the basis of the further bathochromic absorp-

[*] Prof. Dr. K. M. Smith, T. Ema,[+], Dr. M. O. Senge, N. Y. Nelson
Department of Chemistry, University of California
Davis, CA 95616 (USA)
Telefax: Int. code + (916)752-8995
Prof. Dr. H. Ogoshi
Department of Synthetic Chemistry, Kyoto University (Japan)
[+] Permanent address: Department of Synthetic Chemistry, Kyoto University
[**] This work was supported by a grant from the National Institutes of Health (HL-22252).

tion shifts observed for both the free base H_2(TTBP) and its nickel(II) complex (λ_{max} (CH_2Cl_2) 451, 582, 622 nm) relative to the corresponding TIPP derivatives, we conclude that TTBP has to be considerably more distorted than TIPP.

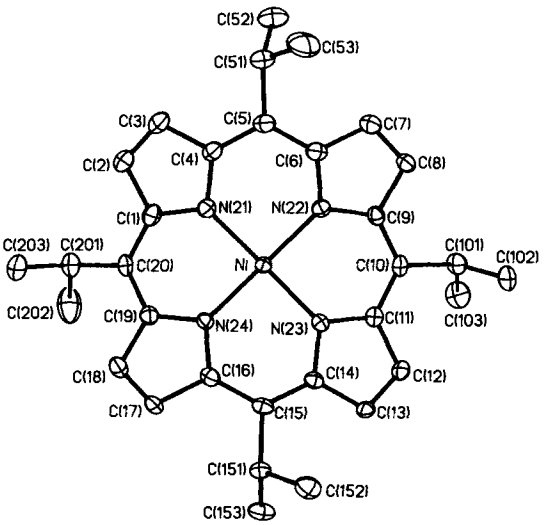
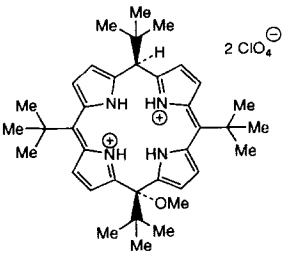


Fig. 2. Molecular structure of **6**. Ellipsoids are drawn at the 50% probability level; hydrogen atoms have been omitted for clarity. Selected structural features: Average Ni–N_p bond length: 1.896(3) Å; average angle of individual pyrrole rings with N_4 plane: 22.8°.

Although nonplanar porphyrins have significant atypical physical and electrochemical properties,[2–6] these substances (**3** and **4** as prototypes) have shown expected reactivity with regard to metal insertion and even protonation (though nonplanar porphyrins have been shown to be very strong bases compared with H_2(OEP) and H_2(TPP)). Treatment of H_2(OETPP), for example, with $HClO_4$/MeOH gave the corresponding dication diperchlorate (λ_{max} 464, 624, 678 nm). Similarly, treatment of H_2(TIPP) under the same conditions led to formation of **7** with absorption maxima at 424, 586, and 634 nm in CH_2Cl_2 (Fig. 3). However, when H_2(TTBP) **4** was treated under the same conditions, quite remarkably, protonation took place on a *meso* carbon atom (instead of on nitrogen) to yield **8** after nucleophilic addition of methanol. Figure 3 shows the optical spectrum of this diprotonated "porphodimethene" (5,15-dihydroporphyrin); Figure 4 shows its structure in the crystal.[8b] It is clear that protonation on carbon enables the eventual formation of the pophodimethene **8**, which dramatically relieves the steric congestion present in the nonplanar porphyrin **4**. Compound **8** has a roof-type structure, in which the two sp^3-hybridized *meso* carbon atoms facilitate significant out-of-plane rotations of the pyrrole rings to minimize steric interactions of the bulky *meso* substituents with β-pyrrole groups.



8

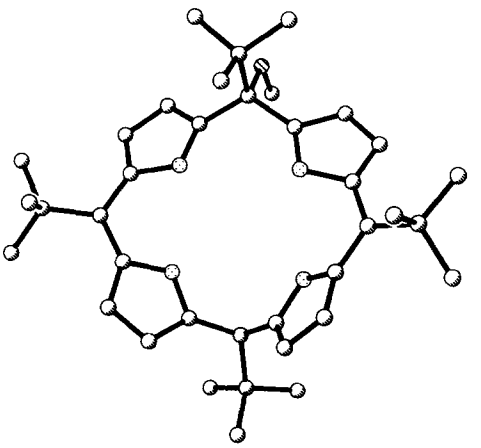


Fig. 4. Molecular structure of the porphyrin dication of **8**. Hydrogen atoms have been omitted for clarity. Selected structural features: Average C_a-N-C_a bond angle: 111.4(6)°; average C_m–C(*t*Bu) bond length: 1.547(10) Å; mean deviation of 24 core atoms from their least-squares plane: 0.47 Å.

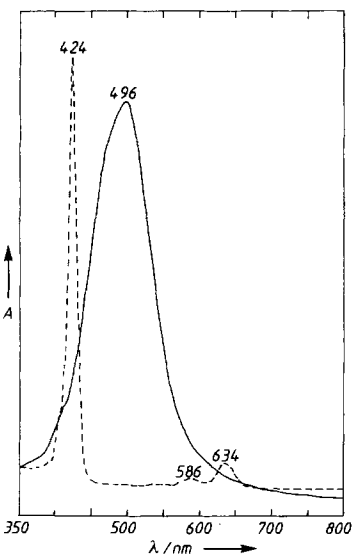
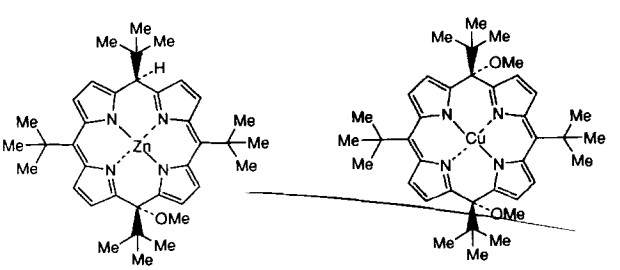


Fig. 3. Optical spectra of **7** (---) and **8** (—) in CH_2Cl_2 (containing $HClO_4$).

Treatment of H_2(OETPP) **1** with zinc(II) acetate in methanol/chloroform gave the "normal" zinc(II) chelate **9**, which exhibits absorption maxima in CH_2Cl_2 at 442, 574, and 630 nm, typical for a metalloporphyrin. In stark contrast, *prolonged* treatment of H_2(TTBP) **4** with the same reagents gave the zinc(II) porphodimethene **10**, in a reaction analogous with the formation of the dication **8**.[10] The reaction product has an absorption spectrum in CH_2Cl_2 with a single band at 456 cm and a shoulder at 570 nm. Figure 5 displays the molecular structure of **10**.[8c] Prolonged treatment of **4** with copper(II) acetate (an oxidant) in methanol/chloroform gave the copper(II) bismethoxypor-



10 **11**

 © VCH Verlagsgesellschaft mbH, D-69451 Weinheim, 1994 0570-0833/94/1818-1880 $ 10.00+.25/0

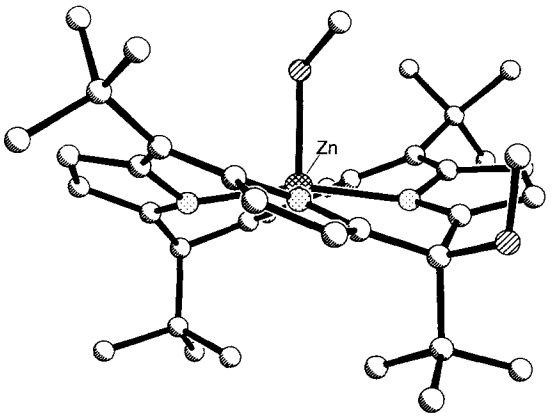


Fig. 5. Molecular structure of **10**. Hydrogen atoms have been omitted for clarity. Selected structural features: Average $Zn-N_p$ bond length: 2.023(4) Å; average $C_m-C(t\mathrm{Bu})$ bond length: 1.573(8) Å; average $C_m-O(CH_3)$ bond length: 1.446(7) Å; average deviations of the 24 core atoms from their least-squares plane: 0.414 Å.

phodimethene **11**. This is a product of metalation like the zinc(II) complex **10**, but here metalation is followed or preceded by oxidation to the π cation radical or π dication, followed by attack by methanol as a nucleophile.[10] The absorption spectrum of this compound in CH_2Cl_2 consists of two overlapping bands at 454 and 496 nm. Figure 6 shows the molecular structure of **11**.[8d] In the structures of both **10** and **11** the *tert*-butyl groups at the sp^3-hybridized *meso* carbons have a synaxial orientation. These compounds exhibit a roof-type macrocycle conformation, similar to the porphodimethenes prepared earlier by Buchler et al. through total synthesis.[11]

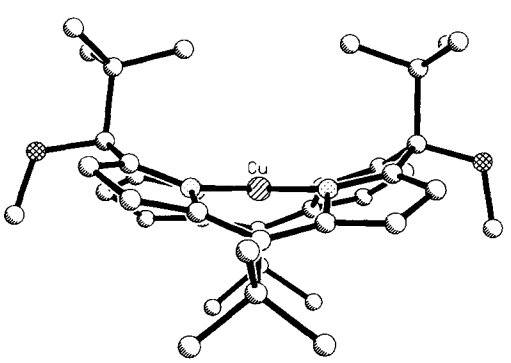


Fig. 6. Molecular structure of **11**. Hydrogen atoms have been omitted for clarity. Selected structural features: Average $Cu-N_p$ bond length: 1.950(8) Å; average $C_m-C(t\mathrm{Bu})$ bond length: 1.577(14) Å; average $C_m-O(CH_3)$ bond length: 1.426(12) Å; average deviations of the 24 core atoms from their least-squares plane: 0.437 Å.

It seems clear that H_2(TTBP) **4** must have an extremely distorted porphyrin macrocycle, possibly more distorted than any previously reported in our series on nonplanar porphyrins.[2-5] The degree of distortion appears to be so dramatic that normal protonation and metalation reactions are diverted to yield atypical products which no longer possess the pseudoplanar, fully conjugated porphyrin macrocycle.

Received: March 28, 1994 [Z 6804 IE]
German version: *Angew. Chem.* **1994**, *106*, 1951

[1] K. M. Smith, *Porphyrins and Metalloporphyrins*, Elsevier, Amsterdam, **1975**.
[2] a) K. M. Barkigia, M. D. Berber, J. Fajer, C. J. Medforth, M. W. Renner, K. M. Smith, *J. Am. Chem. Soc.* **1990**, *112*, 8851-8857; L. D. Sparks, C. J. Medforth, M.-S. Park, J. R. Chamberlain, M. R. Ondrias, M. O. Senge, K. M. Smith, J. A. Shelnutt, *ibid.* **1993**, *115*, 581-592; b) K. M. Barkigia, M. W. Renner, L. R. Furenlid, C. J. Medforth, K. M. Smith, J. Fajer, *ibid.* **1993**, *115*, 3627-3635.
[3] a) S. Tsuchiya, *Chem. Phys. Lett.* **1990**, *169*, 608-610; b) C. J. Medforth, K. M. Smith, *Tetrahedron Lett.* **1990**, *31*, 5583-5586; C. J. Medforth, M. O. Senge, K. M. Smith, L. D. Sparks, J. A. Shelnutt, *J. Am. Chem. Soc.* **1992**, *114*, 9859-9869.
[4] M. O. Senge, *J. Chem. Soc. Dalton Trans.* **1993**, 3539-3549; M. O. Senge, K. M. Smith, *J. Chem. Soc. Chem. Commun.* **1994**, 923-924.
[5] C. J. Medforth, M. D. Berber, K. M. Smith, J. A. Shelnutt, *Tetrahedron Lett.* **1990**, *31*, 3719-3722; J. A. Shelnutt, C. J. Medforth, M. D. Berber, K. M. Barkigia, K. M. Smith, *J. Am. Chem. Soc.* **1991**, *113*, 4077-4087.
[6] M. O. Senge, C. J. Medforth, L. D. Sparks, J. A. Shelnutt, K. M. Smith, *Inorg. Chem.* **1993**, *32*, 1716-1723.
[7] J. S. Lindsey, I. C. Schreiman, H. C. Hsu, P. C. Kearney, A. M. Margueretaz, *J. Org. Chem.* **1987**, *52*, 827.
[8] Crystal data. a) **5**: $C_{32}H_{36}N_4Ni$, $M_r = 535.4$, red plate from $CHCl_3/CH_3OH$, crystal size $0.5 \times 0.22 \times 0.08$ mm, monoclinic, space group $P2_1/c$, $a = 22.928(10)$, $b = 9.707(4)$, $c = 12.086(5)$ Å, $\beta = 92.86(4)°$, $V = 2687(2)$ Å^3, $Z = 4$, $\rho_{calcd} = 1.324$ Mg m^{-3}, Siemens R3m/V diffractometer, $2\theta_{max} = 55°$, $Mo_{K\alpha}$ radiation ($\lambda = 0.71069$ Å), ω-scan, $T = 130$ K, 6144 independent reflections, 3697 observed reflections with $F > 4.0\sigma(F)$, $\mu = 0.750$ mm^{-1}, structure solution with direct methods, 334 parameters refined, $R = 0.051$, $R_w = 0.045$, largest difference peak 0.74 e Å^{-3}. b) **8**: $[C_{37}H_{52}N_4O][ClO_4]_2$, $M_r = 767.7$, green plate from CH_2Cl_2/CH_3OH (containing 1% $HClO_4$), crystal size $0.16 \times 0.16 \times 0.14$ mm, monoclinic, space group $P2_1/c$, $a = 20.130(4)$, $b = 17.515(3)$, $c = 11.308(2)$ Å, $\beta = 105.19(2)°$, $V = 3848(1)$ Å^3, $Z = 4$, $\rho_{calcd} = 1.325$ Mg m^{-3}, Siemens P4 diffractometer with attached Siemens rotating anode, $2\theta_{max} = 112°$, $Cu_{K\alpha}$ radiation ($\lambda = 1.54178$ Å), $2\theta - \theta$, $T = 126$ K, 5025 independent reflections, 3329 observed reflections with $F > 3.0\sigma(F)$, $\mu = 2.003$ mm^{-1}, structure solution with direct methods, 470 parameters refined, $R = 0.088$, $R_w = 0.104$, largest difference peak 0.85 e Å^{-3}. c) **10**: $C_{38}H_{48}N_4O_2Zn \cdot CH_3OH$, $M_r = 690.2$, red parallelepiped from $CHCl_3/CH_3OH$, crystal size $1 \times 0.5 \times 0.25$ mm, triclinic, space group $P\bar{1}$, $a = 11.732(6)$, $b = 12.240(6)$, $c = 15.479(9)$ Å, $\alpha = 97.61(4)$, $\beta = 107.17(4)$, $\gamma = 114,25(4)°$, $V = 1852.4(15)$ Å^3, $Z = 2$, $\rho_{calcd} = 1.237$ Mg m^{-3}, Siemens R3m/V diffractometer, $2\theta_{max} = 55°$, $Mo_{K\alpha}$ radiation ($\lambda = 0.71069$ Å), ω-scan, $T = 130$ K, 8495 independent reflections, 6529 observed reflections with $F > 4.0\sigma(F)$, $\mu = 0.704$ mm^{-1}, structure solution with a Patterson Synthesis followed by structure expansion, 414 parameters refined, $R = 0.069$, $R_w = 0.078$, largest difference peak 1.15 e Å^{-3} (solvent region). d) **11**: $C_{38}H_{50}CuN_4O_2$, $M_r = 658.4$, red plate from $CHCl_3/CH_3OH$, crystal size $0.24 \times 0.14 \times 0.02$ mm, monoclinic, space group $P2_1/c$, $a = 12.309(7)$, $b = 21.402(13)$, $c = 12.773(8)$ Å, $\beta = 99.46(5)°$, $V = 3319(3)$ Å^3, $Z = 4$, $\rho_{calcd} = 1.317$ Mg m^{-3}, Siemens P4 diffractometer with attached Siemens rotating anode, $2\theta_{max} = 112°$, $Cu_{K\alpha}$ radiation ($\lambda = 1.54178$ Å) $2\theta - \theta$, $T = 126$ K, 4336 independent reflections, 2658 observed reflections with $F > 4.0\sigma(F)$, $\mu = 1.213$ mm^{-1}, structure solution with direct methods, 306 parameters refined, $R = 0.098$, $R_w = 0.104$, largest difference peak 1.57 e Å^{-3} (near Cu center). – In all cases the reflections were corrected for Lorentz, polarization, and absorption effects. All structures were solved and refined with the SHELXTL PLUS program system (G. M. Sheldrick, Universität Göttingen, **1989**). Refinements were carried out by full-matrix least-squares on $|F|$. Hydrogen atoms were included in calculated positions and refined with a riding model. Further details on the crystal structure determinations can be obtained from the Director of the Cambridge Crystallographic Data Centre, 12 Union Road, GB-Cambridge CB21EZ by quoting the full literature citation.
[9] E. F. Meyer, Jr., *Acta Crystallogr. Sect. B* **1972**, *28*, 2162-2167.
[10] Note that treatment of H_2(TIPP) or H_2(OETPP) with zinc(II) acetate or copper(II) acetate under these conditions gave the "normal" porphyrin-type chelates. Very brief treatment of H_2(TTBP) with nickel, copper, or zinc acetate gave metal chelates possessing optical spectra characteristic of normal nonplanar metalloporphrins; in the case of the zinc and copper chelates these were transformed with time into the porphodimethenes.
[11] A. Botulinski, J. W. Buchler, N. E. Abbes, W. R. Scheidt, *Liebigs Ann. Chem.* **1987**, *21*, 305-309 and references therein.

 © VCH Verlagsgesellschaft mbH, D-69451 Weinheim, 1994 0570-0833/94/1818-1881 $ 10.00+.25/0

$[\{Rh_2Cp^*_2(\mu\text{-}CH_2)_2\}_2(\mu\text{-}S_4)]^{2+}$: A Novel Tetranuclear Cationic Complex with a Rectangular S_4 Unit**

Kiyoshi Isobe,* Yoshiki Ozawa, Amelio Vázquez de Miguel,* Tian-Wei Zhu, Kui-Ming Zhao, Takanori Nishioka, Takashi Ogura, and Teizo Kitagawa

The oxidation of M–SH to M–S–S–M functionalities (M = metal) has been intensively studied in several metal complexes in connection with its significance in biological, mineralogical, and industrial processes.[1] There have, however, been few reports of the oxidation of the $M(\mu\text{-}SH)M$ functionality in metal complexes.[2] Since this functionality occurs commonly in many such processes, we felt that this chemistry warranted further investigation. Thus, we synthesized μ-methylene rhodium complexes **1** ($Cp^* = \eta\text{-}C_5Me_5$) containing the μ-SH ligand.[3] The oxidation of the μ-SH complexes afforded the novel tetranuclear complexes **2** by a unique intermolecular oxidative coupling. The D_{2h} symmetric S_4 unit in the complex has been of interest for both experimental and theoretical chemistry for a long time.[4]

Treatment of **1a** with O_2 in the presence of an excess of H_2S led to the formation of the tetranuclear rhodium complex **2a** · $3H_2O$ in 81% yield. This complex is amphiphilic, and is

$[Rh_2Cp^*_2(\mu\text{-}CH_2)_2(\mu\text{-}SH)]X$ **1**
1a: X = Cl; **1b**: X = BF_4; **1c**: X = BPh_4

$[\{Rh_2Cp^*_2(\mu\text{-}CH_2)_2\}_2(\mu\text{-}S_4)]XY$ **2**
2a: X = Cl, Y = OH; **2b**: X = Y = BF_4

soluble in water and in organic solvents such as CH_2Cl_2 and $(CH_3)_2CO$. The BF_4 complex **2b** was precipitated from an aqueous solution of **2a** · $3H_2O$ with $NaBF_4$. Both complexes **2** are diamagnetic and recrystallization from CH_2Cl_2/Et_2O yielded black crystals of **2a** · CH_2Cl_2 · $4H_2O$ and **2b**, respectively.

The structures of **2a** · CH_2Cl_2 · $4H_2O$ and **2b** (Fig. 1) were confirmed by single-crystal X-ray diffraction;[5] the structures of the cations of **2** are isostructural and have approximately $2/m$ symmetry. The complex cations consist of two $Cp^*_2Rh_2(\mu\text{-}CH_2)_2$ groups with a Rh–Rh single bond (2.6618(4) Å) and four S atoms lying in the same plane. The rectangular planar S_4 unit bridges two $Rh_2(\mu\text{-}CH_2)_2$ groups to form a Rh_4S_4 eight-membered ring with a new centrosymmetric chairlike core. Two of the four S–S distances (S1–S2* and S1*–S2 1.979(1) Å) in the S_4 unit are very short; their bond lengths lie between S–S distances observed for free S_2 (1.89 Å)[6] and H_2S_2 (2.055 Å).[7] Short S–S distances in S_2 ligands (1.962(1) Å), indicative of appreciable double-bond character,[8a] have also been found in many disulfido complexes,[8b] for example, $[\{CpRu(PMe_3)_2\}_2(\mu\text{-}S_2)](SbF_6)_2$. The other two distances in the S_4 unit (S1–S2 and S1*–S2*), however, are quite long (2.702(1) Å), but nonetheless are significantly shorter than the sum of the van der Waals radii of these atoms (3.60 Å). Similar S–S distances have been found in transannular S–S bonds in S_8^{2+} (2.86 Å)[9] and [1,5-{$(MeC_5H_4)Ru(PPh_3)$}$_2S_6$] (2.772(3) Å).[10]

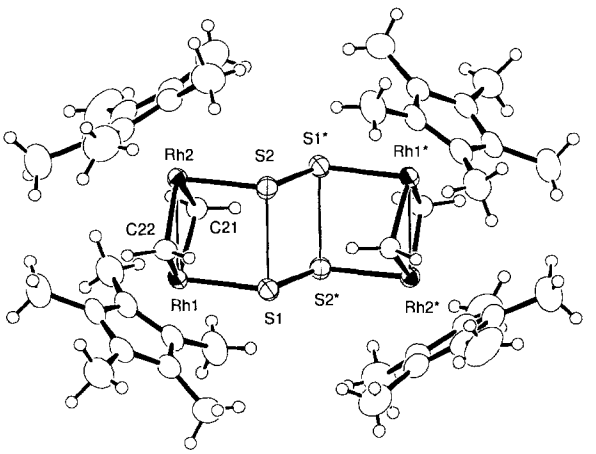


Fig. 1. Structure of the cation of **2b**. Selected bond lengths [Å] and angles [°]: Rh1–Rh2 2.6618(4), Rh1–S1 2.353(1), Rh2–S2 2.346(1), S1–S2* 1.979(1), S1–S2 2.702(1), Rh1–C21 2.034(3), Rh1–C22 2.054(3), Rh2–C21 2.038(3), Rh2–C22 2.062(3); Rh1-Rh2-S2 90.08(2), Rh2-Rh1-S1 90.90(2), Rh1-S1-S2* 112.15(4), Rh2-S2-S1* 111.16(4), Rh1-C21-Rh2 81.6(1), Rh1-C22-Rh2 80.6(1). The deviations of Rh1, Rh2, S1, and S2 from the least squares plane are 0.0009(5), −0.0008(5), −0.011(1), and 0.010(1) Å, respectively. (Atoms with * have equivalent coordinates $-x, -y, -z$.)

The Rh-Rh-S units form angles that are close to right angles (Rh1-Rh2-S2: 90.08(2), Rh2-Rh1-S1: 90.90(2)°). The Rh1, Rh2, S1, and S2 atoms form a plane: their deviations from the least squares plane are very small (Fig. 1). There is no torsional angle between the two Rh–Rh bonds; thus, the four S atoms lie in the same plane. This provides further evidence for bonding interactions within the S_4 unit. The Rh–S distances (2.353(1) and 2.346(1) Å) in **2** are in good agreement with the sum of the covalent radii, which can be taken to be 2.35 Å using $[Cp^*_2Rh_2(\mu\text{-}CH_2)_2(CH_3)_2]$ (1.32 Å for Rh)[11] and S_8 (1.03 Å for S) as reference compounds. The above data strongly support the proposed structure with an S_4 unit. The structure of the S_4 ligand in **2** resembles that of cyclobutadiene (Fig. 2). The different cyclobutadiene framework of Se_4 has been found in $[W_2(CO)_{10}Se_4]^{2+}$ in which the two $[W(CO)_5(\eta^2\text{-}Se_2)]^+$ groups are linked by long Se–Se bonds (3.015(2) Å); each set of two selenium atoms, which forms a short Se–Se bond (2.213(2) Å), is coordinated to a W atom.[12] Complexes **2** contain the first example of a D_{2h} symmetric S_4 unit which has been determined by X-ray analysis. Interestingly, the geometry of the S_4 unit in **2** is similar to those of the neutral S_4 molecule calculated by both Raghavachari et al.[4a] and Morokuma et al.[13]

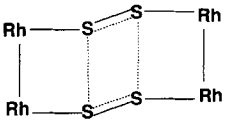


Fig. 2. The Rh_4S_4 framework of complexes **2**.

The character of the S–S bonds was further investigated by resonance Raman spectroscopy. The ν(S–S) and ν(Rh–S) stretching Raman bands were observed at 579 and 260 cm^{-1}, respectively, for an aqueous solution of **2a** · $3H_2O$. These modes are selectively resonance-enhanced with the excitations at 363.8 and 514.5 nm, respectively. Figure 3 shows resonance Raman spectra of **2a** · $3H_2O$ and of a sample enriched in ^{34}S in H_2O (excited at 363.8 nm). Since the band of [^{32}S] **2a** at

[*] Prof. K. Isobe, Dr. Y. Ozawa, Prof. T.-W. Zhu, Prof. K.-M. Zhao, T. Nishioka, Dr. T. Ogura, Prof. T. Kitagawa
Institute for Molecular Science
Myodaiji, Okazaki 444 (Japan)
Telefax: Int. code + (564)54-2254
Prof. A. Vázquez de Miguel
Departamento de Química Inorgánica, Universidad de Alcalá de Henares, E-28871 Alcalá de Henares, Madrid (Spain)
Telefax: Int. code + (1)885-4660

[**] We gladly acknowledge the award of a Japan Society for the Promotion of Science fellowship (A. V. de M.) and the World Bank for supporting this research.

579 cm^{-1} shows a down field shift of 15 cm^{-1} upon ^{34}S substitution (in close agreement with the expected shift ($\Delta\tilde{\nu}$ = 17 cm^{-1}) for the oscillator) we assign the band at 579 cm^{-1} to the ν(S–S) mode. Thus the $\tilde{\nu}$ value of **2a** is larger than those observed for disulfido complexes such as $[\{(CpRu(PMe_3)_2\}_2(\mu\text{-}S_2)](SbF_6)_2$, which has S–S double-bond character (530 cm^{-1}).[8a] The other ν(S–S) mode attributed to the weak S–S bond was not observed in the spectrum. This is in agreement with the calculations.[13] The band at 260 cm^{-1} of **2a** shows a slight ($\Delta\nu$ = 1–3 cm^{-1}) down field shift upon substitution with ^{34}S. This suggests the assignment of this band to the ν(Rh–S) stretch.

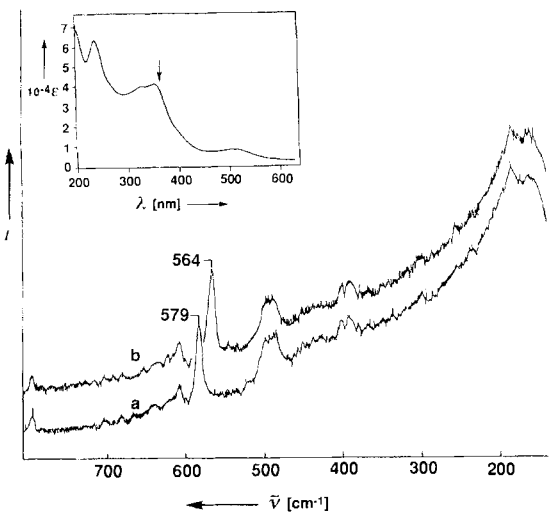


Fig. 3. Resonance Raman spectrum of **2a** · 3 H_2O at 25 °C in H_2O, excited at 363.8 nm: a) spectrum of $[^{32}S]$**2a** · 3 H_2O. b) spectrum of $[^{34}S]$**2a** · 3 H_2O. Inset: Electronic spectrum of **2a** · 3 H_2O at 25 °C in H_2O.

A simple formal charge comparison of **2** with that of the similar tetranuclear complex $[\{Rh_2Cp^*_2(\mu\text{-}CH_2)_2\}_2(\mu\text{-}CN)_2](PF_6)_2$[14] suggests that the S_4 unit has the charge of −2. Ab initio MO calculation, however, has revealed that the structure of the S_4 unit in **2** resembles that of the free neutral S_4 molecule.[13] This indicates that the rectangular isomer of neutral S_4 is stabilized in **2** by the appropriate arrangement of the Rh atoms. For instance, the length of the Rh–Rh bond (2.6618(4) Å) in the complex is almost as long as that of the long S–S bonds in the neutral S_4 rectangle.[4a, 13] Furthermore, the planar Rh_2S_2 framework and the lack of the torsional angle between two Rh–Rh bonds are requirements for the formation of the plane of the four S atoms.

Although the structure of the S_4 unit may change somewhat in the coordination sphere of a transition metal as compared to that of the free S_4 molecule,[13] our proposed structure should also be valid for other S_4 compounds[13] since our experimental results are consistent with calculations.

Compounds **1** are not oxidized in air in the absence of free H_2S. The use of excess H_2S may play an important role in formation of the $Rh(SH_2)$ species containing a framework such as $[Rh(SH)-Rh(SH_2)]^+$, in which the H_2S ligand attached to the cationic complex is most likely oxidized at first.[15] Although further experiments are needed to establish the mechanism for the oxidation, the reaction probably involves a three-electron process in which **1** is oxidized to **2**, and the oxygen is reduced to water [Eq. (a)].

$$2[Rh_2Cp^*_2(\mu\text{-}CH_2)_2(\mu\text{-}SH)]^+ + 2H_2S + 3/2\,O_2 \longrightarrow [\{Rh_2Cp^*_2(\mu\text{-}CH_2)_2\}_2(\mu\text{-}S_4)]^{2-} + 3H_2O \quad \text{(a)}$$

Experimental Procedure

Preparation of **2a** · 3 H_2O and **2b**: To a suspension of $[Rh_2Cp^*_2(\mu\text{-}CH_2)_2Cl_2]$ (0.50 g, 8.7×10^{-4} mol) in CH_3OH (40 cm^3) was bubbled H_2S for 30 min at 23 °C. The resulting red-brown solution of **1a** was exposed to O_2 gas with stirring for 48 h (the first 24 h at −47 °C and then at room temperature) using a balloon of O_2. The resulting deep brown mixture was filtered to remove the white solid of S_8 and evaporated to dryness in vacuo. The residue was extracted with H_2O/CH_2Cl_2 (150/30 cm^3). The product of **2a** · 3 H_2O was isolated from the water phase after removal of the water under a reduced pressure at 40 °C (0.44 g, 3.5×10^{-4} mol, 81%). The addition of $NaBF_4$ (1.0 g, 9.1×10^{-3} mol) in water (30 cm^3) to the water phase quickly gave a crystalline precipitate of **2b** (0.48 g, 3.9×10^{-4} mol, 89%). Recrystallization of **2a** · 3 H_2O and **2b** from CH_2Cl_2/Et_2O yielded black crystals of **2a** · CH_2Cl_2 · 4 H_2O and **2b**, respectively.

The preparation of a sample of **2a** · 3 H_2O enriched in ^{34}S was carried out similarly by use of $[^{34}S]H_2S$ (93.7 atom%, 50 cm^3) in a closed system. Satisfactory analyses have been obtained for **2a** · 3 H_2O, **2a** · CH_2Cl_2 · 4 H_2O, and **2b**. NMR data of **2a** · CH_2Cl_2 · 4 H_2O: ^1H NMR (400 MHz, CD_2Cl_2, 23 °C, TMS): δ = 9.80 (s, 2H; μ-CH_2), 9.05 (s, 2H; μ-CH_2), 8.87 (s, 2H; μ-CH_2), 7.65 (s, 2H; μ-CH_2), 1.71 (s, 60H; Cp*); ^{13}C NMR (100 MHz, CD_2Cl_2, 23 °C, TMS): δ = 185.90 (t, ^1J(Rh,C) = 27 Hz; μ-CH_2), 176.54 (t, ^1J(Rh,C) = 26 Hz; μ-CH_2), 104.45 (s; C_5Me_5), 10.26 (s; $C_5\mathit{Me}_5$); ^{103}Rh NMR (12.6 MHz, CD_2Cl_2, 23 °C, Rh metal): δ = +1345.

Received: March 29, 1994 [Z 6812 IE]
German version: *Angew. Chem.* **1994**, *106*, 1934

[1] A. Müller, B. Krebs, *Sulfur, Its Significance for Chemistry for the Geo-, Bio-, and Cosmosphere and Technology*, Elsevier, Amsterdam, **1984**.
[2] M. R. DuBois, *Chem. Rev.* **1989**, *89*, 1; C. Bianchini, C. Mealli, A. Meli, M. Sabat, *Inorg. Chem.* **1986**, *25*, 4617.
[3] Y. Ozawa, A. Vázquez de Miguel, K. Isobe, *J. Organomet. Chem.* **1992**, *433*, 183.
[4] a) K. Raghavachari, C. M. Rohlfing, J. S. Binkley, *J. Chem. Phys.* **1990**, *93*, 5862; b) G. D. Brabson, Z. Mielke, L. Andrews, *J. Phys. Chem.* **1991**, *95*, 79.
[5] The qualities of both crystal and structural data of **2b** are better than those of **2a** · CH_2Cl_2 · 4 H_2O. Crystal stucture analysis of **2b**: $(C_{44}H_{68}B_2F_8Rh_4S_4)$: black crystal, dimensions $0.38\times0.32\times0.18$ mm^3, monoclinic, space group $P2_1/a$ (no. 14), a = 21.536(3), b = 9.159(1), c = 12.916(2) Å, β = 100.46(1)°, V = 2505.3(7) $Å^3$, Z = 2, ρ_{calcd} = 1.737 $g\,cm^{-3}$. Rigaku AFC-5 diffractometer at 296 K with $Mo_{K\alpha}$ radiation (λ = 0.71073 Å) and θ-2θ scan (2θ < 55° range). A total of 6372 reflections were measured, of which 6116 reflections were independent, and the intensities were corrected for Lorentz-polarization factors. Absorption corrections were made by the Gauss numerical integration method ($\mu(Mo_{K\alpha})$: 1.495 mm^{-1}, T_{max} and T_{min}: 0.888 and 0.777). Structure solution: Patterson method with the SHELXS-86 program. Refinement for 416 parameters: all non-hydrogen and hydrogen atoms were found and refined anisotropically and isotropically, respectively, by a block-diagonal least-squares technique with UNICS III. Final $R(wR)$ value is 0.027 (0.041) against $|F|$ for 4798 reflections with $F > 3.0\sigma(F)$. Residual electron density: $(\Delta\rho)_{min}$ = −0.51 and $(\Delta\rho)_{max}$ = +0.75 e $Å^{-3}$. Details of the crystal structure investigations of **2a** · CH_2Cl_2 · 4 H_2O and **2b** may be obtained from the Fachinformationszentrum Karlsruhe, D-76344 Eggenstein-Leopoldshafen (FRG), on quoting the depository number CSD-58278.
[6] B. Meyer, *Chem. Rev.* **1976**, *76*, 367.
[7] G. Winnewisser, H. Winnewisser, W. Gordy, *J. Chem. Phys.* **1968**, *49*, 3465.
[8] a) J. Amarasekera, T. B. Rauchfuss, S. R. Wilson, *Inorg. Chem.* **1987**, *26*, 3328; b) A. Müller, W. Jaegermann, J. H. Enemark, *Coord. Chem. Rev.* **1982**, *46*, 245.
[9] C. G. Davies, R. J. Gillespie, J. J. Park, J. Passmore, *Inorg. Chem.* **1971**, *10*, 2781.
[10] J. Amarasekera, T. B. Rauchfuss, A. L. Rheingold, *Inorg. Chem.* **1987**, *26*, 2017.
[11] K. Isobe, A. Vázquez de Miguel, P. M. Bailey, S. Okeya, P. M. Maitlis, *J. Chem. Soc. Dalton Trans.* **1983**, 1441.
[12] a) C. Belin, T. Makani, J. Roziére, *J. Chem. Soc. Chem. Commun.* **1985**, 118; b) M. J. Collins, R. J. Gillespie, J. W. Kolis, J. F. Sawyer, *Inorg. Chem.* **1986**, *25*, 2057.
[13] A. M. Mebel, K. Morokuma, K. Isobe, *Inorg. Chem.*, submitted.
[14] J. Martinez, H. Adams, N. A. Bailey, P. M. Maitlis, *J. Organomet. Chem.* **1991**, *405*, 393.
[15] J. Amarasekera, T. B. Rauchfuss, *Inorg. Chem.* **1989**, *28*, 3875.

 © VCH Verlagsgesellschaft mbH, D-69451 Weinheim, 1994 0570-0833/94/1818-1883 $ 10.00+.25/0

Electron Delocalization in Ethynyl-Bridged Binuclear Ruthenium(II) Polypyridine Complexes**

Andrew C. Benniston, Vincent Grosshenny, Anthony Harriman,* and Raymond Ziessel*

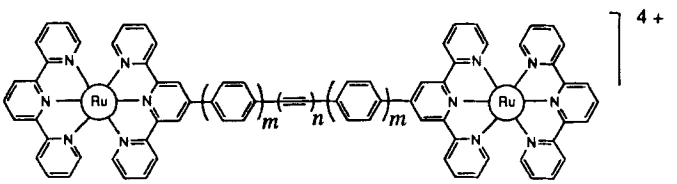
Photoactive transition metal chelate complexes figure prominently as chromophores in supramolecular systems where they are intended to promote long-range energy and/or electron transfers.[1] In order to ensure directionality it is necessary to construct rigid systems and, to increase the separation between components, it is desirable that the excited state is long lived.[2] The lifetimes of most luminescent metal chelates decrease with decreasing energy of the excited state.[3] However, for closely coupled binuclear complexes the triplet excited state lifetime may exceed the value expected simply on the basis of its energy level due to electron delocalization over an extended π^* system.[4-6] This can be a non-trivial effect and, for example, Meyer et al.[4] observed a 20-fold increase in triplet lifetime for a binuclear ruthenium(II) complex with respect to a corresponding mononuclear complex of comparable triplet energy. We have now observed even more pronounced temporal extension for certain ethynyl-substituted bis(terpy)-ruthenium(II) complexes (terpy = 2,2′:6′,2″-terpyridyl) in acetonitrile solution at 25 °C. Our strategy converts a poor sensitizer (i.e., the triplet lifetime is too short to facilitate long-range energy or electron transfer between weakly coupled reagents) into a potentially viable sensitizer. This finding is especially important because terpy is an ideal building block for construction of rigid supramolecular wires.

The ethynyl-bridged ruthenium(II) complexes (see Fig. 1) were synthesized by reacting, under mild conditions, the ditopic bis(terpy) ligands[7] with [Ru(terpy)(dmso)Cl_2] (dmso = dimethylsulfoxide).

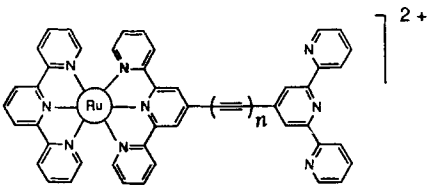
Complex **1** has a distorted octahedral structure[8] and, relative to tris(bpy)ruthenium(II) **2** (bpy = 2,2′-bipyridyl), a short-lived triplet state,[9] due to mixing between charge-transfer and

[Ru(terpy)$_2$] **1** [Ru(bpy)$_3$]$^{2+}$ **2**

(higher energy) metal-centered states. Thus, in deoxygenated acetonitrile solution at 25 °C, **1** exhibits extremely weak luminescence with a maximum (λ_p) at 650 nm for which the quantum yield (Φ_p) is <0.0002 and the lifetime (τ_p) is (565 ± 35) ps. In contrast, luminescence from **2** is centered at 621 nm and is characterized by $\Phi_p = 0.06$ and τ_p = (980 ± 20) ns. Both triplets are readily observed by laser flash photolysis techniques, with lifetimes (τ_t) of (610 ± 40) ps and (960 ± 30) ns, respectively, for **1** and **2**. Covalent attachment of two bis(terpy)ruthenium(II) complexes through one or two ethynyl groups attached to the 4′-position, giving **3a** and **3b**, respectively (Fig. 1), causes a



3a : $n = 1$ $m = 0$
3b : $n = 2$ $m = 0$
5a : $n = 1$ $m = 1$
5b : $n = 2$ $m = 1$



4a : $n = 1$
4b : $n = 2$

Fig. 1. Structures of the discussed ethynyl-substituted Ru^{II} complexes (counterion: PF_6^-)

dramatic increase in triplet lifetime, phosphorescence yield, and emission maximum (Table 1). There is an almost 1000-fold increase in triplet lifetime for a single ethynyl bridge, despite the decrease in triplet energy that occurs, and an additional increase in lifetime for a double ethynyl bridge. The corresponding mononuclear complexes, **4a** and **4b**, also show increased lifetimes and luminescence yields and decreased triplet energies but the changes are less pronounced than observed with the binuclear complexes (Table 1). Interestingly, insertion of a phenyl ring

Table 1. Photophysical properties measured for the discussed ruthenium(II) complexes in deoxygenated acetonitrile at 25 °C.

Compound	λ_p/nm [a]	Φ_p [b]	τ_p/ns [c]	τ_t/ns [d]
1	650	<0.0002	0.56	0.61
2	621	0.060	980	960
3a	722	0.0014	565	570
3b	735	0.0021	720	700
4a	690	0.0003	55	50
4b	710	0.0006	170	165
5a	670	<0.0001	3.2	3.6
5b	665	<0.0001	5.5	5.8

[a] Luminescence maximum, ±5 nm. [b] Luminescence quantum yield, ±20%. [c] Luminescence lifetime, ±8%. [d] Triplet lifetime measured by laser flash photolysis, ±10%.

between terpy and ethynyl groups, giving **5a** and **5b**, causes the triplet lifetimes and luminescence yields to approach those recorded for **1** but, in particular, the lifetimes still remain significantly longer than that of the unsubstituted compound (Table 1).

The decreased rates of nonradiative deactivation observed for **3** and **4** relative to **1** are attributed to selective population of ligands possessing extended π^* orbitals.[4-6] Thus, upon excitation the electron is promoted to the ethynyl-substituted terpy ligand where it is delocalized over the extended π-electron system that includes both terpy subunits. This hypothesis is sup-

[*] Prof. A. Harriman, Dr. A. C. Benniston
Center for Fast Kinetics Research
The University of Texas at Austin
Austin, TX 78712 (USA)
Telefax: Int. code + (512)471 6095
Dr. R. Ziessel, V. Grosshenny
Ecole Européenne des Hautes Etudes des Industries Chimiques de Strasbourg
IPCMS/GMI
1 rue Blaise Pascal, F-67008 Strasbourg (France)
Telefax: Int. code + 88 61 10 25

[**] This work was supported by the National Science Foundation (CHE 9102657) and the Centre National de la Recherche Scientifique.

ported by examination of the relevant absorption spectra: Thus, metal-to-ligand charge-transfer absorption maxima (λ_{max}) are apparent at 515 nm ($\varepsilon = 32800\ M^{-1}cm^{-1}$) and 457 nm ($\varepsilon = 15400\ M^{-1}cm^{-1}$) for **3a** and at 512 nm ($\varepsilon = 39300\ M^{-1}cm^{-1}$) and 453 nm ($\varepsilon = 20200\ M^{-1}cm^{-1}$) for **3b**, while a single maximum is observed for **1** at 470 nm ($\varepsilon = 16100\ M^{-1}cm^{-1}$). Comparison of the photophysical properties observed for **3** and **4**[10] suggests more pronounced electron delocalization in the binuclear complexes. Indeed, absorption and luminescence maxima are more red-shifted and triplet lifetimes are significantly longer for **3** than for **4**.

There is significant electronic coupling between terpy and ethynyl groups and among adjacent ethynyl groups. However, insertion of a phenyl ring into the π-electron system causes a substantial decrease in the magnitude of electronic coupling. This is evident from the less pronounced red-shifted absorption[11] and luminescence spectra, and from the shorter triplet lifetimes observed for **5** relative to **3**. Since it is known that electronic coupling between terpy and phenyl groups is significant in the ground state,[12] the decreased electronic communication found for **5** relative to **3** must arise from poor orbital overlap at the ethynyl–phenyl connection and not at the terpy–phenyl link. This may be due to poor spatial overlap of π* orbitals on the reactants or to an electronic factor.

Electron delocalization is also manifest in the triplet absorption spectra recorded after laser excitation at 532 nm. The triplet differential absorption spectrum recorded for **1** shows bleaching of the ground-state chromophore at 470 nm, a weak ligand-centered transition at higher energy, and very weak absorption stretching across the near infra-red region (Fig. 2a). In addition, **3a** and **3b** exhibit intense Gaussian-shaped absorption bands centered at 850 and 860 nm, respectively (Fig. 2b). These

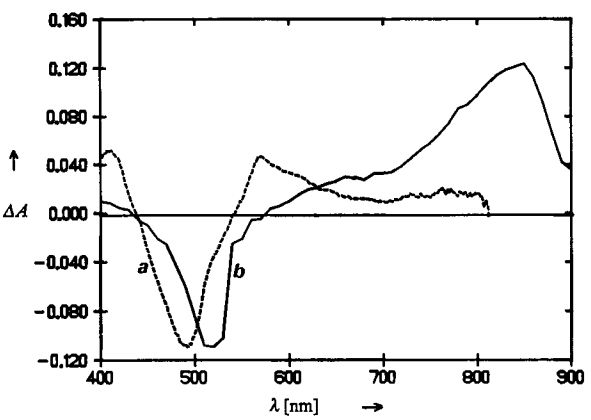


Fig. 2. Transient differential absorption spectra recorded (a) 50 ps after laser excitation of **1** and (b) 20 ns after laser excitation of **3a** in deoxygenated acetonitrile solution. Laser excitation was at 532 nm with a 30 ps pulse.

new bands arise from monophotonic excitation, and decay at a rate identical to that measured in the bleaching region or by emission. They are attributed to electron delocalization between the ethynyl-bridged terpy subunits. Comparable intervalence charge-transfer bands are observed for **4a** and **4b** at 595 and 630 nm, respectively, but not for the phenyl-bridged compounds **5a** and **5b**.

The enhanced triplet lifetimes observed for the ethynyl-substituted complexes can be attributed to selective population of the substituted ligand. Because of its lower energy, there will be less pronounced mixing of the charge-transfer state with the (higher energy) metal-centered state. Delocalization of the electron over an extended π*-orbital causes a reduction in the magnitude of electron–electron repulsion and a smaller nuclear displacement, which result in weakened overlap between vibronic levels in triplet and ground state manifolds.[13, 14] It is also noteworthy that addition of a second ethynyl group causes a further enhancement in triplet lifetime. This means that linear supramolecular systems might be constructed that could span a lipid bilayer but still retain a relatively long excited state lifetime.

Experimental Procedure

General procedure for preparation of the PF_6^- salts of **3a**, **3b**, **4a**, **4b**, **5a**, and **5b**. A stirred solution of $[Ru(terpy)(dmso)Cl_2]$ (2 equiv) and $AgBF_4$ (2.2 equiv) in Ar-purged CH_3OH (50 mL) was heated at 80 °C for 10 h. After cooling to room temperature, the deep red solution was filtered over cotton-wool and transferred via cannula to a CH_3OH (10 mL) suspension of the corresponding ditopic ligand [7] (100 mg scale, 1 equiv). During heating at 100 °C, complexation was evidenced by development of an orange coloration. After a few hours, the solution was filtered over Celite and NH_4PF_6 (10 equiv) in water (2 mL) was added. Slow evaporation of CH_3OH led to the precipitation of a deep red solid, which was filtered, washed with water and diethyl ether, and chromatographed (alumina, 3–10% CH_3OH/CH_2Cl_2). The resultant complexes were recrystallized from CH_3OH/toluene: **3a**, 25% yield, FAB-MS (*meta*-nitrobenzylalcohol (*m*-NBA)): *m/z* 1593 $[M^+ - PF_6]$. Analysis for $C_{62}H_{42}F_{24}N_{12}P_4Ru_2$ (M_r = 1737.10): calcd. C 42.87, H 2.44, N 9.68; found C 42.53, H 2.15, N 9.39; **3b**-$(PF_6)_4$: 28% yield, FAB-MS (*m*-NBA): *m/z* 1617 $[M^+ - PF_6]$. Analysis for $C_{64}H_{42}F_{24}N_{12}P_4Ru_2$ (M_r = 1761.12): calcd. C 43.65, H 2.40, N 9.54; found C 43.53, H 2.11, N 9.32; **4a**-$(PF_6)_2$: 68% yield, FAB-MS (*m*-NBA): *m/z* 968 $[M^+ - PF_6]$. Analysis for $C_{47}H_{31}F_{12}N_9P_2Ru$ (M_r = 1112.83): calcd. C 50.73, H 2.81, N 11.33; found C 50.49, H 2.62, N 11.06; **4b**-$(PF_6)_2$: 60% yield, FAB-MS (*m*-NBA): *m/z* 992 $[M^+ - PF_6]$. Analysis for $C_{49}H_{31}F_{12}N_9P_2Ru$ (M_r = 1136.85): calcd. C 51.77, H 2.75, N 11.09; found C 51.28, H 2.35, N 10.76; **5a**-$(PF_6)_4$: 18% yield, FAB-MS (*m*-NBA): *m/z* 1745 $[M^+ - PF_6]$. Analysis for $C_{74}H_{50}F_{24}N_{12}P_4Ru_2$ (M_r = 1889.30): calcd. C 47.05, H 2.67, N 8.90; found C 46.73, H 2.41, N 8.59; **5b**-$(PF_6)_4$: 22% yield, FAB-MS (*m*-NBA): *m/z* 1769 $[M^+ - PF_6]$. Analysis for $C_{76}H_{50}F_{24}N_{12}P_4Ru_2$ (M_r = 1913.32): calcd. C 47.71, H 2.63, N 8.78; found C 47.56, H 2.45, N 8.53.

All FAB-MS spectra showed the expected isotopic profile.

Received: February 21, 1994
Revised version: April 20, 1994 [Z 6702 IE]
German version: *Angew. Chem.* **1994**, *106*, 1956

[1] V. Balzani, F. Scandola, *Supramolecular Photochemistry*, Horwood, Chichester, **1991**.
[2] F. Vögtle, M. Frank, M. Nieger, P. Belser, A. von Zelewsky, V. Balzani, F. Barigelletti, L. De Cola, L. Flamigni, *Angew. Chem.* **1993**, *105*, 1706; *Angew. Chem. Int. Ed. Engl.* **1993**, *32*, 1643.
[3] T. J. Meyer, *Acc. Chem. Res.* **1989**, *22*, 163.
[4] S. Boyde, G. F. Strouse, W. E. Jones, T. J. Meyer, *J. Am. Chem. Soc.* **1990**, *112*, 7395.
[5] A. J. Downard, G. E. Honey, L. F. Phillips, P. J. Steel, *Inorg. Chem.* **1991**, *30*, 2259.
[6] J. R. Shaw, R. T. Webb, R. H. Schmehl, *J. Am. Chem. Soc.* **1990**, *112*, 1117.
[7] V. Grosshenny, R. Ziessel, *J. Organomet. Chem.* **1993**, *453*, C19; V. Grosshenny, R. Ziessel, *Tetrahedron Lett.* **1992**, *33*, 8075.
[8] R. P. Thummel, Y. Jahng, *Inorg. Chem.* **1986**, *25*, 2527.
[9] J. R. Winkler, T. L. Netzel, C. Creutz, N. Sutin, *J. Am. Chem. Soc.* **1987**, *109*, 2381.
[10] In acetonitrile, λ_{max} = 490 nm ($\varepsilon = 19200\ M^{-1}cm^{-1}$) and 459 nm ($\varepsilon = 12000\ M^{-1}cm^{-1}$) for **4a** and λ_{max} = 495 ($\varepsilon = 23000\ M^{-1}cm^{-1}$) and 461 nm ($\varepsilon = 14200\ M^{-1}cm^{-1}$) for **4b**.
[11] In acetonitrile, λ_{max} = 488 nm ($\varepsilon = 48500\ M^{-1}cm^{-1}$) for **5a** and λ_{max} = 490 nm ($\varepsilon = 62000\ M^{-1}cm^{-1}$) for **5b**.
[12] J.-P. Collin, P. Lainé, J.-P. Launay, J.-P. Sauvage, A. Sour, *J. Chem. Soc. Chem. Commun.* **1993**, 434.
[13] J. V. Caspar, T. J. Meyer, *J. Phys. Chem.* **1983**, *87*, 952.
[14] S. K. Doorn, R. L. Blackbourn, C. S. Johnson, J. T. Hupp, *Electrochim. Acta* **1991**, *36*, 1775.

 © VCH Verlagsgesellschaft mbH, D-69451 Weinheim, 1994 0570-0833/94/1818-1885 $ 10.00+.25/0

A Model for α-Keto Acid Dependent Nonheme Iron Enzymes: Structure and Reactivity of $[Fe^{II}_2(Me_2hdp)_2(bf)](ClO_4)$**

Yu-Min Chiou and Lawrence Que, Jr.*

α-Keto acid dependent nonheme iron enzymes[1] catalyze a variety of metabolic reactions involving the functionalization of an unactivated C–H bond, concomitant with the oxidative decarboxylation of the cofactor α-keto acid. A general reaction with substrate (A) proceeds according to Equation (a).

$$A + O_2 + RCOCOOH \longrightarrow AO + RCOOH + CO_2 \qquad (a)$$

Of the various enzymes in this category, only for the *Pseudo monas* 4-hydroxyphenylpyruvate (HPP) dioxygenase[2, 3] has an iron ligand been identified. The isolated enzyme is blue (λ_{max} = 595 nm, ε = 2600 $M^{-1}cm^{-1}$)[4] arising from a tyrosine-to-Fe^{III} charge-transfer transition on the basis of resonance Raman evidence;[5] the low energy of the transition further suggests that only *one* tyrosine is present in the iron coordination environment. Histidine residues are also proposed as ligands to the iron atom from the comparison of the amino acid sequences of enzymes in this class.[6]

In our first effort to model such enzymes, we have reported the properties of two benzoylformate complexes, **1** and **2**, which

$[Fe^{II}(6tla)(bf)](ClO_4)$ **1** $[Fe^{II}(tpa)(bf)](ClO_4)$ **2**

have pyridine-rich ligand environments.[7] These compounds react with dioxygen and undergo quantitative oxidative decarboxylation of the bound α-keto acid, but their reactions take place over a period of two days to a week. In light of the established coordination of the tyrosine residue in HPP dioxygenase, we have explored the effect of introducing a phenolato ligand on this chemistry and report our results in this communication.

The combination of the phenolate-containing tripodal ligand H-Me_2hdp,[8] NEt_3, Na(bf), and $Fe(ClO_4)_2 \cdot 6H_2O$ in MeOH affords complex **3**, from which orange prismatic crystals are obtained upon recrystallization from CH_3OH/Et_2O. Its X-ray structure[9] (Fig. 1) shows **3** to be $[Fe^{II}_2(Me_2hdp)_2(bf)](ClO_4)$, in which the two Fe^{II} centers are bridged by two phenolato ligands and the carboxylato group of the bf ligand. There is a pseudo twofold symmetry axis located at the center of the $[Fe_2(OR)_2]$ core. The Me_2hdp and bf ligands provide a six-coordinate, roughly octahedral ligand array about each iron atom. The Fe···Fe distance (3.049(2) Å) and Fe-O-Fe angles (93.2(2) and 91.6(2)°) are the *smallest* thus far reported for complexes with the generalized $[Fe^{II}_2(OR)_2]$ core,[10] most likely due to the presence of a third bridge, the bidentate carboxylato group of the bf ligand, between the iron(II) centers. This is the first example of such a triply bridged diiron(II) core, but related core structures are found among diiron(III)[11] and $Mn^{III}Mn^{(IV)}$[12] complexes.

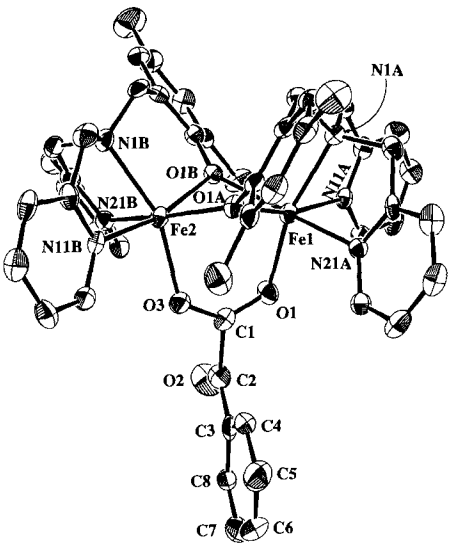


Fig. 1. ORTEP plot of the $[Fe^{II}_2(Me_2hdp)_2(bf)]^+$ ion of **3** (50% probability ellipsoids). Hydrogen atoms are omitted for clarity. Selected bond lengths [Å] and angles [°]: Fe1-O1 2.104(6), Fe1-O1A 2.055(5), Fe1-O1B 2.205(5), Fe1-N1A 2.208(7), Fe1-N11A 2.163(7), Fe1-N21A 2.189(7), Fe2-O3 2.098(6), Fe2-O1A 2.140(5), Fe2-O1B 2.045(5), Fe2-N1B 2.211(6), Fe2-N11B 2.174(7), Fe2-N21B 2.200(7), Fe1···Fe2 3.049(2); Fe1-O1A-Fe2 93.2(2), Fe1-O1B-Fe2 91.6(2), O1A-Fe1-O1B 76.3(2), O1A-Fe2-O1B 78.0(2), O1-C1-C2-O2 83(1).

Exposure of the yellow-orange solution of **3** to air in CH_3CN *immediately* turns it purple-blue (Fig. 2); the UV/VIS features are similar to those of the previously reported $[Fe^{III}_2O(hdp)_2(O_2CC_6H_5)](BPh_4)$.[13] The low-energy absorption band (562 nm) is associated with a Ph-O^--to-Fe^{III} charge-transfer transition, which is red-shifted from that of its hdp-analogue (522 nm) due to the electron-donating methyl substituents. The positive-ion FAB mass spectrum of the oxygenated products shows signals at *m/z* at 913 and 941, corresponding to parent ions of $[Fe^{III}_2(O)(Me_2hdp)_2(O_2CC_6H_5)]^+$ (**4**) and $[Fe^{III}_2(O)(Me_2hdp)_2(bf)]^+$ (**5**), respectively. The presence of two distinct complexes was also confirmed by HPLC analysis of the isolated organic products which shows approximately equimolar amounts of benzoic acid and benzoylformic acid. Thus, about half of **3** undergoes oxidative decarboxylation upon exposure to dioxygen, while the remaining half simply autoxidizes.

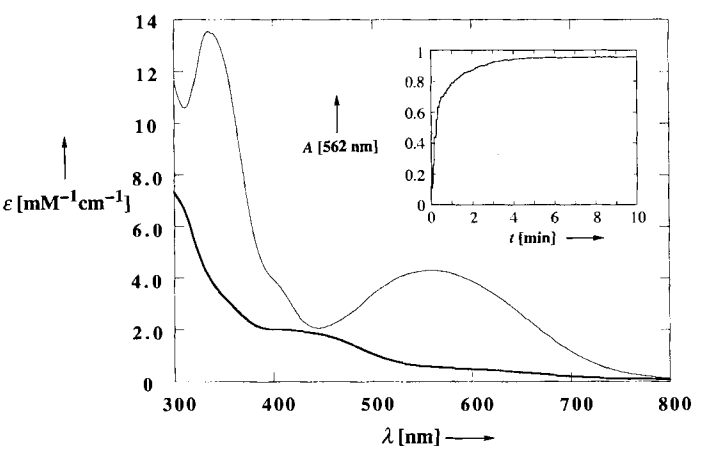


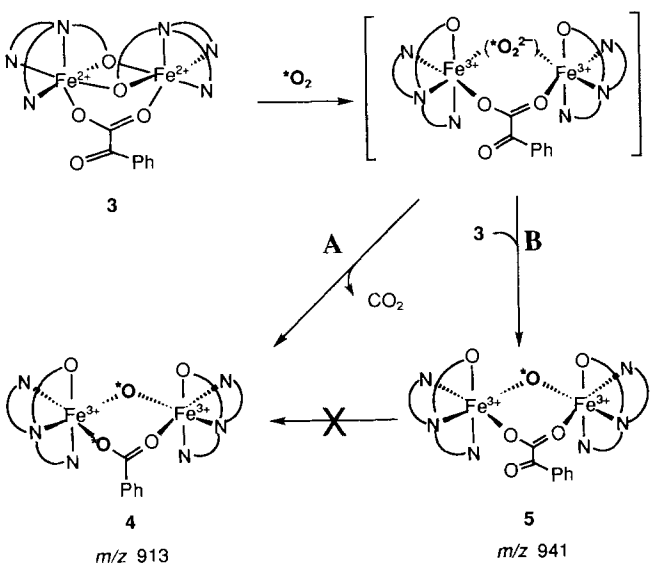
Fig. 2. UV/VIS spectra of **3** (bold line; λ_{max} = 450 nm (ε = 1800 $M^{-1}cm^{-1}$)) and its oxygenation products in CH_3CN (plain line) with features at 336 (ε = 13500), 410 (sh, ε = 3600), and 562 nm (ε = 4300 $M^{-1}cm^{-1}$). The inset shows the time-dependent change of the absorbance at λ = 562 nm at 20 °C upon exposure to O_2.

[*] Prof. L. Que, Jr., Y.-M. Chiou
Department of Chemistry, University of Minnesota
Minneapolis, MN 55455 (USA)
Telefax: Int. code + (612)626-7541

[**] This work was supported by the National Institutes of Health (GM-33162). We thank Professor Doyle Britton for his expertise in the X-ray diffraction experiments.—Abbreviations used: CI-MS = chemical ionization mass spectrometry; FAB-MS = fast atom bombardment mass spectrometry; bf = benzoylformate; hdp = 2-[(bis(2-pyridylmethyl)amino)methyl]phenolate; HPP = 4-hydroxyphenylpyruvate; Me_2hdp = 2-[(bis(2-pyridylmethyl)amino)methyl]-4,6-dimethylphenolate; 6tla = tris(6-methyl-2-pyridylmethyl)amine; tpa, tris(2-pyridylmethyl)amine.

To gain further insight into the mechanism, the reaction of **3** with dioxygen has also been carried out in $^{18}O_2$. FAB-MS results establish that both oxygen atoms from $^{18}O_2$ can be incorporated into **4**, as indicated in the isotope distribution of parent-ion envelope: *m/z* (%): 913 (2) $[[^{16}O_2]M^+]$; 915 (78) $[[^{16}O, ^{18}O]M^+]$; 917 (20) $[[^{18}O_2]M^+]$. The CI-MS of the isolated benzoic acid shows the incorporation of *one* ^{18}O atom in 84% yield, so the second ^{18}O is likely to be found on the μ-oxo bridge. The FAB mass spectrum shows only one ^{18}O atom is incorporated into complex **5**: *m/z* (%): 941 (68) $[[^{16}O]M^+]$; 943 (32) $[[^{18}O]M^+]$. Since the CI-MS data on the isolated benzoylformic acid shows no ^{18}O incorporation, the label incorporated in **5** must be on the μ-oxo bridge. The low level of isotope incorporation at the oxo bridges in **4** and **5** is probably due to the facile exchange with solvent water, as indicated in a parallel experiment carried out in $^{16}O_2$ with the addition of trace amounts of $H_2{}^{18}O$.[14]

Based on these results, we propose the mechanism shown in Scheme 1. Upon exposure to dioxygen, the iron(II) complex **3** is stoichiometrically converted to a (μ-peroxo)diiron(III) complex. Intramolecular nucleophilic attack of the bound peroxide at the α-carbon of the bf ligand results in the oxidative decarboxylation of this α-keto acid and the reduction of the peroxide to yield **4** (pathway A). In this pathway, complex **3** serves both as the reaction center and the substrate. Alternatively, this O_2 adduct can be reduced by a second molecule of **3** to afford the autoxidation product (**5**) (pathway B), as has been well documented for iron(II) porphyrins[15] and several nonheme iron(II) compounds.[16] The possibility that complex **5** converts to **4** upon exposure to O_2 can be excluded, since an acetonitrile solution of **5**, obtained by direct synthesis, remains unchanged in air for days (as monitored by ^{1}H NMR) without any formation of complex **4**. Therefore, iron(II) is required for the oxidative decarboxylation of the bf ligand.



Scheme 1. Proposed mechanism for the reaction of **3** with dioxygen in CH_3CN. The ligands are shown schematically. * = Isotopic labeling.

Complex **3** reacts with O_2 approximately three to four orders of magnitude faster than **1** and **2**. The inset in Figure 2 shows a pseudo-first-order increase of the absorbance at 562 nm at 20 °C, with k_{obs} of 2.8 min^{-1}. The facile oxygenation reaction of **3** may be due to two factors: the presence of the electron-rich phenolate which lowers the Fe^{III}/Fe^{II} redox potential and promotes the attack of dioxygen at the iron centers[17] and the presence of the dinuclear unit which facilitates reduction of O_2 to the peroxide state. However both factors also make the iron(II) centers much more susceptible to autoxidation, so the oxidizing equivalents generated in the reaction are used for the conversion of Fe^{II} to Fe^{III}, rather than substrate oxidation as in the cases of **1** and **2**. So the detailed mechanisms for the oxidative decarboxylation of the bound α-keto acid may differ for the mononuclear complexes **1** and **2** and the dinuclear complex **3**.

In HPP dioxygenase, the tyrosine ligand presumably facilitates the electrophilic attack of dioxygen as well, but the active site prevents formation of dinuclear complexes such as **4** and **5** to maintain its catalytic viability. Perhaps a sterically more hindered hdp-like ligand may prevent oxo-bridged dimer formation and form a mononuclear $[Fe^{II}(bf)]$ complex that reacts readily with O_2 to afford oxidative decarboxylation of α-keto acid and substrate oxidation. Further work in modeling α-keto acid dependent nonheme iron enzymes is in progress.

Experimental Procedure

Caution! Metal complexes with organic ligands and perchlorate ions are potentially explosive.

3: In an argon atmosphere, a solution of H-Me_2hdp (0.34 g, 1.0 mmol) and NEt_3 (0.10 g, 1.0 mmol) in MeOH was treated with $Fe(ClO_4)_2 \cdot 6H_2O$ (0.36 g, 1.0 mmol) to produce a light yellow solution. Addition of a solution of Na(bf) (0.09 g, 0.5 mmol) in MeOH afforded an orange solid upon stirring (75% yield). Recrystallization was accomplished by vapor diffusion of CH_3OH/Et_2O to yield diffraction quality crystals with the composition $3 \cdot CH_3OH$. Correct C,H,N analysis for $C_{51}H_{53}ClFe_2N_6O_{10}$.

5: H-Me_2hdp (0.34 g, 1.0 mmol) and NEt_3 (0.20 g, 2.0 mmol) were dissolved in MeOH (20 mL) and treated with $Fe(ClO_4)_3 \cdot 10H_2O$ (0.54 g, 1.0 mmol) in MeOH (1–2 mL) to afford a purple-blue solution. To this solution was added Na(bf) (0.09 g, 0.5 mmol). A purple-blue precipitate was obtained upon stirring (60% yield). Correct C,H,N analysis for $5 \cdot MeOH \cdot 3H_2O$: $C_{51}H_{59}ClFe_2N_6O_{14}$; positive-ion FAB-MS: *m/z*: 941 $[M^+]$.

Received: May 6, 1994 [Z 6904 IE]
German version: *Angew. Chem.* **1994**, *106*, 1969

[1] Reviews: a) M. T. Abbott, S. Udenfriend in *Molecular Mechanisms of Oxygen Activation* (Ed.: O. Hayaishi), Academic Press, New York, **1974**, pp. 167–214; b) H. M. Hanauske-Abel, V. Günzler, *J. Theor. Biol.* **1982**, *94*, 421–455; c) K. I. Kivirikko, R. Myllylä, T. Pihlajaniemi in *Post-Translation Modifications of Proteins* (Eds.: J. J. Harding, M. J. C. Crabbe), CRC, Boca Raton, FL, **1992**, pp. 1–51.

[2] a) J. Denum, S. Lindstedt, M. Rundgren, *Oxidases Relat. Redox Syst. Proc. Int. Symp. 3rd 1979*, **1982**, 519–542; b) R. A. Pascal, Jr., M. A. Oliver, Y.-C. J. Chen, *Biochemistry* **1985**, *24*, 3158–3165.

[3] U. Rüetschi, B. Odelhög, S. Lindstedt, J. Barros-Söderling, B. Persson, H. Jörnvall, *Eur. J. Biochem.* **1992**, *205*, 459–466.

[4] S. Lindstedt, M. Rundgren, *J. Biol. Chem.* **1982**, *257*, 11922–11931.

[5] F. C. Bradley, S. Lindstedt, J. D. Lipscomb, L. Que, Jr., A. L. Roe, M. Rundgren, *J. Biol. Chem.* **1986**, *261*, 11693–11696.

[6] a) R. Myllylä, V. Günzler, K. I. Kivirikko, D. D. Kaska, *Biochem. J.* **1992**, *286*, 923–927; b) U. Rüetschi, A. Dèllsen, P. Sahlin, G. Stenman, L. Rymo, S. Lindstedt, *Eur. J. Biochem.* **1993**, *213*, 1081–1089.

[7] a) Y.-M. Chiou, L. Que, Jr., *J. Am. Chem. Soc.* **1992**, *114*, 7567–7568; b) *J. Inorg. Biochem.* **1993**, *51*, 127.

[8] D. D. Cox, L. Que, Jr., *J. Am. Chem. Soc.* **1988**, *110*, 8085–8092.

[9] Complex **3** crystallizes in the monoclinic system, space group $P2_1/n$ (no. 14), with $a = 11.177(6)$, $b = 16.93(1)$, $c = 26.360(7)$ Å, $\beta = 95.22(3)°$, $V = 4968(8)$ Å^3, $Z = 4$. With the use of 4464 unique observed reflections for which $I(\text{obs}) > 2.00\,\sigma(I)$, collected at -101 °C with $Mo_{K\alpha}$ ($\lambda = 0.71073$ Å) radiation out to $2\theta_{max} = 48.0°$ on an Enraf-Nonius CAD-4 X-ray diffractometer, the structure was solved by direct methods and refined to $R = 0.070$ and $R_w = 0.065$. Further details of the crystal structure investigation are available on request from the Director of the Cambridge Crystallographic Data Centre, 12 Union Road, GB-Cambridge CB2 1EZ (UK), on quoting the full journal citation.

[10] a) B. S. Synder, G. S. Patterson, A. J. Abrahamson, R. H. Holm, *J. Am. Chem. Soc.* **1989**, *111*, 5214–5223; b) A. Stassinopoulos, G. Schulte, G. C. Papaefthymiou, J. P. Caradonna, *ibid.* **1991**, *113*, 8686–8697; c) A. Gerli, K. S. Hagen, L. G. Marzilli, *Inorg. Chem.* **1991**, *30*, 4673–4676; d) C. L. Spiro, S. L. Lambert, T. J. Smith, E. N. Duesler, R. R. Gagné, D. N. Hendrickson, *ibid.*

1981, *20*, 1229–1237; e) N. Kitajima, N. Tamura, M. Tanaka, Y. Morooka, *ibid.* **1992**, *31*, 3342–3343.

[11] a) K. L. Taft, C. D. Delfs, G. C. Papaefthymiou, S. Foner, D. Gatteschi, S. J. Lippard, *J. Am. Chem. Soc.* **1994**, *116*, 823–832; b) S. M. Gorun, G. C. Papaefthymiou, R. B. Frankel, S. J. Lippard, *ibid.* **1987**, *109*, 3337–3348; c) M. Mikuriya, Y. Kakuta, K. Kawano, T. Tokii, *Chem. Lett.* **1991**, 2031–2034; d) B. F. Anderson, J. Webb, D. A. Buckingham, G. B. Robertson, *J. Inorg. Biochem.* **1982**, *16*, 21–32.

[12] a) K. Wieghardt, *Angew. Chem.* **1989**, *101*, 1179–1198; *Angew. Chem. Int. Ed. Engl.* **1989**, *28*, 1153–1172, and references therein; b) J. S. Bashkin, A. R. Schake, J. B. Vincent, H.-R. Chang, Q. Li, J. C. Huffman, G. Christou, D. N. Hendrickson, *J. Chem. Soc. Chem. Commun.* **1988**, 700–702; c) U. Bossek, M. Saher, T. Weyhermüller, K. Wieghardt, *ibid.* **1992**, 1780–1782; d) S. Pal, J. W. Gohdes, W. C. A. Wilisch, W. H. Armstrong, *Inorg. Chem.* **1992**, *31*, 713–716.

[13] S. Yan, L. Que, Jr., L. F. Taylor, O. P. Anderson, *J. Am. Chem. Soc.* **1988**, *110*, 5222–5224.

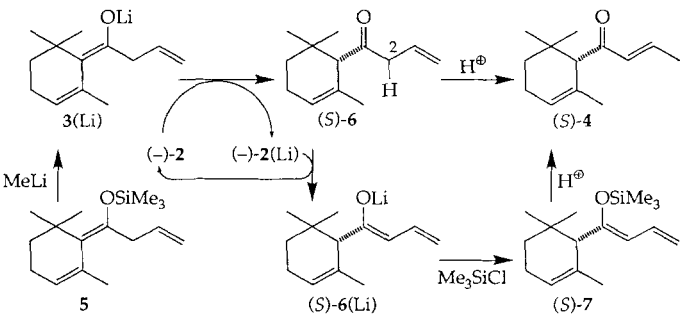
[14] **4**: FAB-MS: *m/z* (%): 913 (23) $[[^{16}O_2]M^+]$, 915 (77) $[^{16}O,^{18}O]M]$. **5**: FAB-MS: *m/z* (%): 941 (3) $[[^{16}O_2]M^+]$, 943 (28) $[[^{16}O,^{18}O]M]$, 945 (69) $[[^{18}O_2]M]$. The second ^{18}O atom found in **5** is likely due to the incorporation of $H_2{}^{18}O$ into the carbonyl oxygen of the bf ligand.

[15] L. Latos-Grazynski, R.-J. Cheng, G. N. La Mar, A. L. Balch, *J. Am. Chem. Soc.* **1982**, *104*, 5992–6000.

[16] a) W. B. Tolman, S. Liu, J. G. Bentsen, S. J. Lippard, *J. Am. Chem. Soc.* **1991**, *113*, 152–164; b) S. Ménage, Y. Zang, M. P. Hendrich, L. Que, Jr., *ibid.* **1992**, *114*, 7786–7792.

[17] J. W. Pyrz, A. L. Roe, L. J. Stern, L. Que, Jr., *J. Am. Chem. Soc.* **1985**, *107*, 614–620.

(and enolate-rich) at low conversion, as one equivalent of (−)-**2**(Li) is generated during this process. In order to test whether the enolate protonation is more enantioselective at low conversion, **3**(Li) was treated with 0.5 equivalents of (−)-**2** (−60 °C, 2 min) and the reaction mixture quenched with Me_3SiCl (2 equiv) (−60 → 20 °C, 30 min). Much to our surprise, no trace of **5** was detected; this indicated complete consumption of **3**(Li). Instead, approximately equal amounts of ketone (*S*)-**6** (94% *ee*) and the unexpected enol silyl ether (*S*)-**7** were formed.

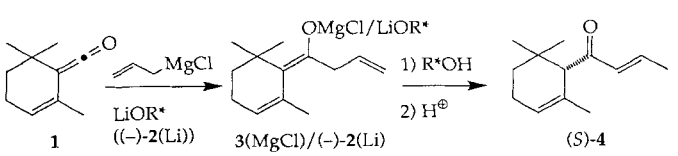


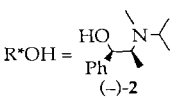
Scheme 1. "Autocatalytic" enantioselective protonation of **3**(Li).

Catalytic Enantioselective Protonation of Enolates

Charles Fehr* and José Galindo

In 1988, we reported the efficient synthesis of enantiomerically pure (*S*)-α-damascone ((*S*)-**4**) by the Grignard reaction with ketene **1** followed by enantioselective protonation[1–7] of the mixed Li/Mg enolate complex **3**(MgCl)/(−)-**2**(Li) ($E/Z \approx 9:1$[8a]) with (−)-*N*-isopropylephedrine ((−)-**2**) (80–84% *ee*, 84% yield; 99% *ee* after crystallization, 55% yield).[1] Conversely, the analogous magnesium-free lithium complex **3**(Li)/(−)-**2**(Li) showed lower enantiofacial discrimination (65% *ee*), and the lithium-free magnesium enolates **3**(MgCl) and **3**(MgCl)/(−)-**2**(MgCl) gave less than 20% *ee*.

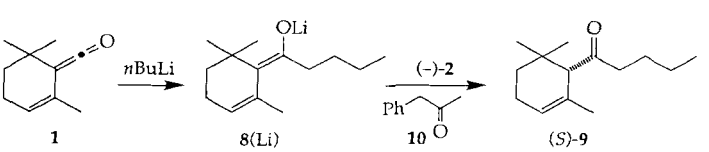




During further investigation of this reaction, we have found that protonation of the ligand-free enolate **3**(Li) ($E/Z \approx 98:2$[8a]), prepared from silyl enol ether **5**,[8b] with (−)-**2** affords (*S*)-**4** with excellent enantioselectivity (95% *ee*) (Scheme 1).[9, 10] Evidently, this protonation is only ligand-free

After purification by chromatography on silica (cyclohexane/ethyl acetate 99/1), (*S*)-**7** of high enantiomeric purity was isolated ($[\alpha]_D^{20} = -339$ ($c = 0.04$ in $CHCl_3$), 94% *ee*).[9] This enantioselective protonation is thus catalytic: the protonated intermediate (*S*)-**6** makes available an acidic proton (at C(2)) for the protonation of the chiral lithium alkoxide (−)-**2**(Li) ("autocatalytic system")[11] (Scheme 1). In a second experiment, **3**(Li) was protonated with 0.3 equivalents of (−)-**2** (−60 °C, 10 min), and the intermediate enolate (*S*)-**6**(Li) quenched with 5% aqueous HCl. Ketones (*S*)-**6** and (*S*)-**4** were obtained in 86% yield and 93% *ee* (from **5**).[12] This procedure certainly represents the most elegant access to the precious fragrance (*S*)-α-damascone ((*S*)-**4**).[13]

We then examined the enantioselective protonation of enolate **8**(Li), which was generated in situ from ketene **1** and *n*BuLi (1 equiv; THF, −100 → −70 °C) ($E/Z \geq 97.3$).[8a] With 1.1 equivalents of (−)-**2** (−70 °C, 2 min; −70 → −5 °C, 10 min), (*S*)-**9**[14] was obtained in 96% *ee* and 90% yield (Scheme 2).[10] However, with 0.5 equivalents of (−)-**2**, protonation was incomplete and afforded, after silylation and hydrolysis, (*S*)-**9** in 55% *ee*. The failure of "autocatalysis" is easily rationalized by the much weaker acidity of **9** (at C(2)) than that of **6**. To circumvent this problem, we then tested the combination of catalytic amounts of (−)-**2** with external achiral (or racemic) proton donors. Various CH-, OH-, and SH-acidic compounds, all of which are more acidic than **6** and **9** (at stereogenic center) by several orders of magnitude, were tested and shown to be effective.[15] For example, the catalytic enantioselective protonation of **8**(Li) with 0.2 equivalents of (−)-*N*-isopropylephedrine ((−)-**2**), followed by the addition of 0.85 equivalents of phenyl-2-

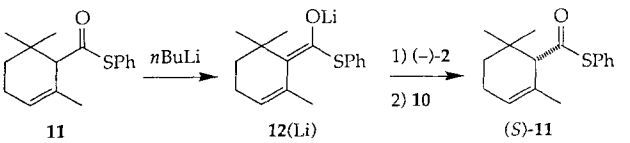


Scheme 2. Enantioselective protonation of **8**(Li) with stoichiometric or catalytic amounts of (−)-**2**.

[*] Dr. C. Fehr, J. Galindo
Firmenich SA, Research Laboratories
P.O. Box 239, CH-1211 Geneva 8 (Switzerland)
Telefax: Int. code + (22) 780-3436

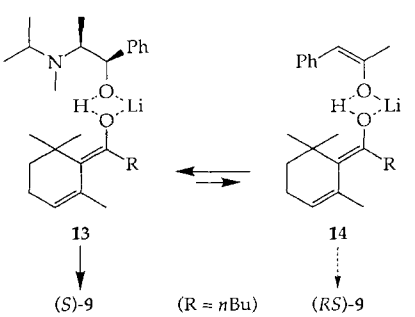
propanone (**10**), afforded (*S*)-**9** with 94% *ee* and 94% yield,[16] and use of 0.1 equivalent of (−)-**2** gave (*S*)-**9** with 85% *ee*.

The aforementioned concept was also successfully applied to the protonation of thiol ester enolate **12**(Li).[2, 3] The following example is described in a patent application from 1992,[3] and is the first published enantioselective enolate protonation with substoichiometric amounts of chiral proton donor. Racemic thiol ester **11** was deprotonated with 1.5 equivalents of *n*BuLi in THF/hexane at −100 °C. The resulting enolate **12**(Li) was protonated with (−)-**2** (0.5 equiv). Slow addition of **10** (1.55 equiv) in THF (40 min), stirring at −100 °C (75 min), and gradual warming to −10 °C (25 min) afforded (*S*)-**11** in greater than 98% *ee* and 81% yield. Thus, diminishing the amount of (−)-**2** from 2 equivalents[2a] to 0.5 equivalents results in less than 1% loss of enantioselectivity.[17]



11 **12**(Li) (*S*)-**11**

As proposed in previous publications,[2] we suggest that a tight transition state-like complex **13** is formed. This chiral enol/enolate "hybrid" (simplified representation)[18] undergoes an irreversible stereocontrolled C protonation. Complex **13** (R = *n*Bu) can be formed directly by proton transfer from **10** to a chiral enolate complex **8**(Li)/(−)-**2**(Li).[18] Alternatively, the enolate **8**(Li) may be O-protonated by **10** to give an achiral complex of type **14** (or the enol).[19] If the conversion of **14** to (*RS*)-**9** is much slower than that of **13** to (*S*)-**9**, rapid equilibration of achiral complex **14** (or the enol) and chiral complex **13** ensures successful enantioselective C protonation. Presumably, the nitrogen of (−)-**2** participates in and accelerates this proton transfer.



13 **14**

(*S*)-**9** (R = *n*Bu) (*RS*)-**9**

Experimental Procedure

(*S*)-**9**: A solution of **1** (1.0 g, 6.66 mmol) in THF (20 mL) was cooled to −100 °C (Et_2O, liquid N_2) and treated with 1.5 M *n*BuLi in hexane (4.60 mL, 6.66 mmol). The temperature was slowly raised to −70 °C (30 min). Then (−)-**2** (0.275 mg, 1.33 mmol) in THF (3 mL) was added in 1 min (−70 → −60 °C). This was followed by dropwise addition of **10** (0.76 g, 5.70 mmol) in THF (5 mL) over 8 min. The temperature was allowed to reach −5 °C over 30 min. The mixture was poured into stirred 5% aqueous HCl and extracted with Et_2O. The organic phase was washed successively with H_2O, saturated $NaHCO_3$, and saturated NaCl, dried (Na_2SO_4), evaporated, and twice distilled bulb-to-bulb (oven temperature 40–70 °C/0.05 Torr). A mixed fraction of (*S*)-**9** and **10** (1.41 g; 850 mg of (*S*)-**9**), and 450 mg of pure (*S*)-**9** ($[\alpha]_D^{20} = -449$ (*c* = 0.03 in $CHCl_3$), 94% *ee*) were obtained.[9] Yield: 94%. Basification of the acidic aqueous phase allowed quantitative recovery of (−)-**2**. [1–3]

Received: May 20, 1994 [Z 6959]
German version: *Angew. Chem.* **1994**, *106*, 1967

[1] C. Fehr, J. Galindo, *J. Am. Chem. Soc.* **1988**, *110*, 6909; C. Fehr, O. Guntern, *Helv. Chim. Acta* **1992**, *75*, 1023.
[2] a) C. Fehr, I. Stempf, J. Galindo, *Angew. Chem.* **1993**, *105*, 1091; *Angew. Chem. Int. Ed. Engl.* **1993**, *32*, 1042; b) *ibid.* **1993**, *105*, 1093 and **1993**, *32*, 1044; c) C. Fehr, *Chimia* **1991**, *45*, 253.
[3] C. Fehr, I. Stempf, J. Galindo (Firmenich), EP 593917 (prior October 13, 1992).
[4] E. Vedejs, N. Lee, S. T. Sakata, *J. Am. Chem. Soc.* **1994**, *116*, 2175; A. Yanagisawa, T. Kuribayashi, T. Kikuchi, H. Yamamoto, *Angew. Chem.* **1994**, *106*, 129; *Angew. Chem. Int. Ed. Engl.* **1994**, *33*, 107; K. Fuji, K. Tanaka, H. Miyamoto, *Tetrahedron: Asymmetry* **1993**, *4*, 247; T. Haubenreich, S. Hünig, H.-J. Schulz, *Angew. Chem.* **1993**, *105*, 443; *Angew. Chem. Int. Ed. Engl.* **1993**, *32*, 398; Y. Tatsuro, K. Koga, *Tetrahedron: Asymmetry* **1993**, *4*, 35; S. Takeuchi, N. Miyoshi, Y. Ohgo, *Chem. Lett.* **1992**, 551; S. Takeuchi, N. Miyoshi, H. Hirata, H. Hayashida, Y. Ohgo, *Bull. Chem. Soc. Jpn.* **1992**, *65*, 2001; E. Vedejs, N. Lee, *J. Am. Chem. Soc.* **1991**, *113*, 5483; K. Matsumoto, H. Ohta, *Tetrahedron Lett.* **1991**, *32*, 4729; A. Kumar, R. V. Salunkhe, R. A. Rane, S. Y. Dike, *J. Chem. Soc. Chem. Commun.* **1991**, 485; D. Potin, K. Williams, J. Rebek, Jr., *Angew. Chem.* **1990**, *102*, 1485; *Angew. Chem. Int. Ed. Engl.* **1990**, *29*, 1420; L. Duhamel, P. Duhamel, S. Fouquai, J. Eddine, O. Peschard, J.-C. Plaquevent, A. Ravard, R. Solliard, J.-Y. Valnot, H. Vincens, *Tetrahedron* **1988**, *44*, 5495; U. Gerlach, S. Hünig, *Angew. Chem.* **1987**, *99*, 1313; *Angew. Chem. Int. Ed. Engl.* **1987**, *26*, 1283; L. Duhamel, J.-C. Plaquevent, *J. Am. Chem. Soc.* **1978**, *100*, 7415; reviews: H. Waldmann, *Nachr. Chem. Tech. Lab.* **1991**, *39*, 413; L. Duhamel, P. Duhamel, J.-C. Launay, J.-C. Plaquevent, *Bull. Soc. Chim. Fr.* **1984**, II-421, and ref. [2c].
[5] For an enantioselective enol–ketone tautomerization, see: L. Duhamel, J.-C. Launay, *Tetrahedron Lett.* **1983**, *24*, 4209.
[6] For the catalytic, enantioselective tautomerization of photogenerated enols, see: F. Hénin, A. M'Boungou-M'Passi, J. Muzart, J.-P. Pète, *Tetrahedron* **1994**, *50*, 2849, and references therein.
[7] For enzyme or antibody catalyzed enantioselective C protonation of enols, see: J.-L. Reymond, K. D. Janda, R. A. Lerner, *J. Am. Chem. Soc.* **1992**, *114*, 2257; K. Matsumoto, S. Tsutsumi, T. Ihori, H. Ohta, *ibid.* **1990**, *112*, 9614.
[8] a) *E*/*Z* ratios determined by NOE experiments on the corresponding silyl ethers. b) **5** (*E*/*Z* ≈ 98:2) was obtained by fractional distillation (b.p. 80 °C/2 Torr).
[9] Determined by gas chromatography on either permethylated β-cyclodextrin in OV-1701 or a Megadex column (Megadex Capillary Columns Laboratory, Legnano, Italy).
[10] (*Z*)-free enolate is expected to give ≥98% *ee* (experiments underway).
[11] In a control experiment, (*S*)-**6** does not protonate **3**(Li) enantioselectively in the absence of (−)-**2**.
[12] Lower amounts of (−)-**2** gave a slower and less selective reaction.
[13] Other syntheses: K. Mori, M. Amaike, M. Itou, *Tetrahedron* **1993**, *49*, 1871, and ref. [1] and [2a].
[14] $[\alpha]_D^{20} = -454$ (*c* = 0.04 in $CHCl_3$). Determination of absolute configuration: (*S*)-α-cyclogeranic acid [2a] was converted into the acid chloride ($(COCl)_2$, CH_2Cl_2, 0 → 20 °C); alkylation by addition of *n*BuLi (THF, −78 °C).
[15] For the test experiments, **8**(Li) (prepared from **1** and *n*BuLi at −78 °C) was successively treated at −50 °C with (−)-**2** (0.5 equiv) and an achiral (or racemic) proton donor (0.5 equiv): (±)-**6** (94% *ee*), phenyl-2-propanone (**10**) (94% *ee*), (±)-ethyl 2-acetyl-4-methyl-4-pentenoate (93% *ee*), ethyl acetoacetate (90% *ee*), thiophenol (90% *ee*), 2,6-di-*tert*-butyl-4-methylphenol (90% *ee*), H_2O (90% *ee*), pivalic acid (90% *ee*), acetic acid (85% *ee*).
[16] Likewise, use of easily accessible (+)-**2** [1] afforded (*R*)-**9** (94% *ee*).
[17] With 0.2 equivalents of (−)-**2**, (*S*)-**11** was obtained with 81% *ee*.
[18] Possibly, these complexes are further aggregated with chiral or achiral ligands (see ref. [2c]).
[19] When an equimolar mixture of **10** and **8**(Li) was stirred at −50 °C for 15 min, and quenched with Me_3SiCl, the only silyl enol ether isolated was (*Z*)-1-phenyl-2-trimethylsilyloxy-1-propene. The catalytic, enantioselective protonation of **8**(Li), followed by silylation, affords the same (*Z*)-silyl enol ether. A mechanism invoking prior proton exchange between (−)-**2**(Li) and **10** is less likely, as preliminary experiments have shown that these proton transfers are slow and unselective (*E*/*Z* mixtures after silylation).

 © VCH Verlagsgesellschaft mbH, D-69451 Weinheim, 1994 0570-0833/94/1818-1889 $ 10.00+.25/0

Unchallenged Excellence in Inorganic Chemistry

Houben-Weyl. Methoden der Organischen Chemie. Band E 15, Teile 1–3. En-X- und In-X-Verbindungen. 4th Edition, supplementary volumes. Edited by *H. Kropf* and *E. Schaumann*. Thieme, Stuttgart, 1993. Part 1: pp. 1–1200, Part 2: pp. 1201–2530, Part 3: pp. 2531–3946, hardcover DM 6600.00, subscription price DM 5940.00.—ISBN 3-13-218504-3/3-13-797504-2/3-13-797604-9

The Houben-Weyl series of over 100 volumes has an unchallenged position at the peak of excellence in the secondary literature of chemistry. This high standard is based on a unique combination of comprehensiveness (practically every known compound class and reaction type is covered by a volume of Houben-Weyl), reliability (errors are rare), and consistency (the arrangement of the contents follows the same principles in all the volumes). It can be said at the outset that these supplementary volumes on ene-X and yne-X compounds entirely fulfill one's high expectations based on the earlier volumes.

Supplement E 15, which is in three parts and is the work of 26 authors, treats the full range of activated multiply-bonded systems that result from substitution by one or more oxygen- or nitrogen-containing groups. Part 1 begins with a lengthy chapter by H. Frauenrath on enol derivatives (enol esters, acetals, and ethers), followed by chapters on alkenyl hydroxyamines (K. Bott), boroenol ethers (A. Pelter), silylenol ethers (S. Pawlenko), and metal derivatives of enols (G. Klar, R. Kramolowski). The second half of Part 1 is devoted to alkene derivatives with one nitrogen-containing substituent, including detailed chapters on enamines (P. Rademacher), enehydrazines (A. J. Bittner, P. Rademacher), enazides (K. Banert), nitrosoalkenes (K. Bott), azoalkenes (J. G. Schantl), and nitroalkenes (E. Haslinger).

Part 2 is mainly concerned with 1,1- and 1,2-disubstituted alkenes with oxygen- and/or nitrogen-containing groups as substituents. There are chapters on derivatives of 1,2-enediols and 2-aminoenols (H. Kropf, F. Wöhrle), oxocarbones and semioxocarbones (H. Frauenrath), and ketene acetals and their derivatives (C. G. Bakker, J. W. Scheeren, H.-G. Heinen, W. Kantlehner et al.). Substantial contributions on ketenes (E. Schaumann, S. Scheiblich), ketene imines (H. Perst), and heteroketene acetals (H.-G. Heine, W. W. Mergen, W. Kantlehner) form the end of Part 2 and the beginning of Part 3. This continues with chapters on mono- and diheteroketenes (E. Schaumann, S. Scheiblich), tetraheterosubstituted alkenes (H.-G. Heine), and heterosubstituted allenes and butatrienes (R. W. Saalfrank, C.-J. Lurz, K. Banert). The volume ends with a detailed treatment of ynol ethers and ynamines by G. Himbert.

The arrangement of subject matter within the chapters follows the usual pattern. First the methods of preparation of a class of compounds are described in detail, with a distinction between methods based on synthesizing the carbon skeleton and those in which it is already available from elsewhere; in contrast conversion reactions are only described for representative examples. There are frequent cross-references to other Houben-Weyl volumes, and the work includes a comprehensive bibliography, a subject index arranged in the usual way, and (especially pleasing) an author index. The formula schemes are excellent, especially where stereochemical details have to be shown. The use of bold type to highlight the structural feature under discussion is very useful. Despite a thorough search I found scarcely any printing errors (an exception is Si instead of S on p. 598). The style of writing too is mostly above reproach; the few minor slips (such as that on p. 466: "Acidität der Enolform") are excusable. On the other hand, the terms regio- and stereoselectivity and regio- and stereospecificity have not always been used with the necessary care (pp. 176, 432, 461). From the standpoint of reaching an international readership it is, of course, a disadvantage that this supplement, like all its predecessors in the Houben-Weyl series, is in German. The editors' expressed intention to follow the example of Beilstein by publishing the fifth edition in English is therefore to be welcomed.

What other improvements could be made? In the view of this reviewer, the identification of sections by a mixture of Roman and Arabic numerals and of Latin and Greek letters is confusing and irritating; this is more of a hindrance than a help in finding one's way around the work, and should be replaced by a consistent decimal classification in future volumes. A more worrying problem is the use of the special Houben-Weyl nomenclature, which sometimes reveals serious deficiencies. For example, α,β-unsaturated ketones are described throughout the world as enones, but in Houben-Weyl they are called 3-oxo-alkenes. Consequently there is no entry in the index for 2-cyclohexenone. Another criticism is that the reader is subjected to a flood of unnecessary hyphens (e.g., "Chlor-trimethyl-silan"). However, these shortcomings do not detract from the very favorable overall verdict on Supplement E15: its perfection fully meets the high standard of Houben-Weyl, and no chemistry library that is to be taken seriously can afford to be without it.

Norbert Krause
Institut für Organische Chemie
der Technischen Hochschule
Darmstadt (FRG)

Asymmetric Synthesis of Natural Products. By *A. Koskinen*. Wiley, Chichester, 1993. 234 pp., paperback £ 16.95.—ISBN 0-471-93848-3

A wide choice of titles on asymmetric synthesis and stereochemistry by well-known authors has recently appeared in the books market. This seems to be a common phenomenon when an area of research reaches a certain stage in its devel-

This section contains book reviews and a list of new books received by the editor. Book reviews are written by invitation from the editor. Suggestions for books to be reviewed and for book reviewers are welcome. Publishers should send brochures or (better) books to Dr. Ralf Baumann, Redaktion Angewandte Chemie, Postfach 101161, D-69451 Weinheim, Federal Republic of Germany. The editor reserves the right of selecting which books will be reviewed. Uninvited books not chosen for review will not be returned.

opment at which it is worthwhile to review the overall picture and take stock. Such a situation applies in the case of this book by Ari Koskinen, in which he describes methods for asymmetric synthesis, illustrated by examples of successes in the field of natural products. The development of such methods has now reached a stage which is leading not just to individual applications but to progress in natural products syntheses on a broad front, and this in turn is contributing positively to advances in basic principles.

In his introduction the author is concerned to impress on the reader the importance of natural products chemistry, especially by describing examples in the field of pharmaceuticals. The enormous variety of natural products is well illustrated by dozens of structures which, like the schemes appearing later in the book, are excellently drawn and well set out. The examples range from very simple odor and flavor substances through pheromones and antibiotics to complex molecules such as cyclosporin, vitamin B_{12}, and palytoxin. The author offers his readers (or listeners, since the book is based on a lecture series) a highly original selection of examples with the aim of stimulating their interest in the subject. The brief sketch of the history of natural products in medicine (regrettably only four pages long) also contributes to that aim.

This is followed by a short (26-page) account of the basic principles of stereochemistry, explaining the concepts of chirality, topology, and asymmetric synthesis. The author evidently wished to ensure that the reader's understanding of the subsequent chapters should not be hindered by a lack of knowledge of the fundamentals of stereochemistry and nomenclature. In the limited available space he has been able to cover only the basic essentials of conformational analysis and the stereochemical descriptors. Nevertheless, the use of the terms *threo* and *erythro* is discussed, as well as examples of nonlinear effects. Thus the book is intended mainly for readers who already have some familiarity with the basic ideas of stereochemistry. It is pleasing to find that stereoelectronic effects are treated from a modern standpoint using clearly presented orbital models.

Chapter 3 (55 pp.) describes basic methods of asymmetric synthesis. Here again the treatment is limited to the essentials, covering reactions of carbonyl groups (nucleophilic addition, alkylation, enolate chemistry, Michael addition) and of olefins (epoxidation, hydroxylation, hydroboration, and the Diels–Alder reaction). The introduction to the effects of steric hindrance ("allylic strain") on the course of reactions and to the Cram and Felkin–Anh models could appropriately have been included in the first chapter. However, these topics have been very skillfully and effectively incorporated into the next section on reductions and alkylations of carbonyl compounds. The basic principles of the Felkin–Anh model are treated too briefly; experience has shown that students have difficulty in understanding the distinction between this and the Cram model. I also feel that the Sharpless epoxidation and enantioselective *cis*-hydroxylations should have been covered in more detail in view of their dominant role as reagent-controlled reactions. The Corey model to explain the high enantioselectivity of *cis*-hydroxylations should be well within the scope of advanced students, and also provides a good teaching opportunity for explaining the principles of catalysis in asymmetric reactions. The surveys giving formulas with the most important reagents, catalysts, and ligands, together with the names of the relevant authors, are very useful. In many cases typical *ee* values that can be obtained are also given. Here, however, it would have been helpful to include short tables showing the range of selectivities actually achieved.

The fourth and longest chapter (126 pp.) describes examples of syntheses of natural products in the areas of carbohydrates, amino acids and peptides, nucleosides and nucleotides, polyketides, isoprenoids, shikimic acid, and alkaloids. Here again, rather than assuming previous knowledge, the author explains the structure, biosynthesis, and pharmacological importance of each class of substances. Synthetic reaction schemes with detailed explanations of the individual steps are generally accorded an importance equal to that of descriptions of important compounds belonging to the class under discussion. A rigid and systematic connection with the earlier method-orientated chapters is not attempted; instead these are to be regarded as setting the scene and preparing the reader. In a book of this limited size the range of examples cannot, of course, be very comprehensive, but the author has skillfully presented a very good selection. This main part of the book can be regarded as a short introduction to modern natural products chemistry which is complete in itself.

Considering the wealth of information presented and the many structures shown, the incidence of errors has been kept reasonably low. Most of these are trivial; however the omission of the free radical dots in describing the mechanism of the endiin antibiotics (p. 13) makes this difficult to understand. This very reasonably priced book can be thoroughly recommended for all undergraduate and graduate students, as well as researchers and lecturers, who wish to learn about modern trends in natural products synthesis.

Karsten Krohn
Fachbereich Chemie und Chemietechnik
der Universität-Gesamthochschule
Paderborn (FRG)

Two Books on Solid Catalysts

Organic Chemistry Using Clays. By *M. Balogh* and *P. Laszlo*. Springer, Berlin, 1993. 184 pp., hardcover DM 188.00.—ISBN 3-540-55710-5

Catalysis over clays is an attractive alternative to the well established conventional chemical methods for many chemical transformations. The applications of clays in organic synthesis are summarized here in 17 chapters, each illustrated with formula schemes and supported by a comprehensive and up-to-date bibliography. The book is intended for organic as well as catalysis chemists.

Chapter 1 is concerned with electrophilic aromatic substitutions. The main emphasis is on alkylations, halogenations, and nitrations of arenes. Chapters 2 and 3 describe various types of addition and elimination reactions, respectively. Chapter 4 is devoted to oxidation of hydrocarbons and alkyl groups, ammoxidation reactions, dehydrogenation of aliphatic hydrocarbons, and oxidation of alcohols, thiols, sulfides, and amines. Chapter 5 deals with two types of aromatization reactions, including, for example, dehydrogenation of cycloalkanes. Chapter 6 deals with the hydrogenation of carbon–carbon multiple bonds, hydrogenation of aromatic rings, and reduction of carbonyl and other functional groups. Chapter 7 discusses the use of montmorillonite and bentonite clays in the synthesis of hydrocarbons and heterocyclic compounds. Diels–Alder reactions are known to be catalyzed by Lewis acids, and the use of clays as catalysts for these reactions is described in Chapter 8. The importance of clays in isomerization reactions is illustrated in Chapter 9. Chapter 10 deals with the dimerization of alkenes, reactions of heterocycles, and oxidative couplings of arenes. Montmorillonite, super-filtrol, and clayfen catalysts are used for these reactions. The next chapter is concerned with rearrangement reactions of arenes, illustrated by well chosen examples. Chapter 12 discusses the con-

 © VCH Verlagsgesellschaft mbH, D-69451 Weinheim, 1994 0570-0833/94/1818-1892 $ 10.00+.25/0

densation reactions of alcohols and thiols, coupling reactions of aromatic compounds, and aldol condensations. Chapter 13 deals with the thermal and hydrolytic decomposition of a wide variety of pesticides, which is very important from the viewpoint of protection of the environment; examples of the degradation of pesticides and decomposition of organic peroxides are discussed. Chapter 14 summarizes reactions of carbonyl compounds, the CO group being probably the most versatile functional group in organic chemistry. The reactions described include the formation of acetals and ketals, condensation reactions with amines and anilines, Knoevenagel condensations, and carbonyl group deprotection. Reactions of carboxylic acids and derivatives with alcohols, arenes, and ethylene are described in Chapter 15. Chapter 16 describes synthesis of amino acids, polymerization of amino acids, reactions of nucleotides, and formation of peptides from amino acid adenylates. Lastly, Chapter 17 contains the miscellaneous reactions which are not discussed in the previous chapters. The book ends with a glossary and subject index.

Balogh and Laszlo have produced a book that sets new standards. They inform the readers expertly, comprehensively, and without unnecessarily lengthy detail about the capabilities and range of applications of the various clay catalysts described. The book is nicely written and each chapter contains a separate list of references. It can be recommended unreservedly for the chemist working in academia or industry who wants detailed information about the applications of clay catalysts in organic synthesis.

Zeolite, Clay and Heteropoly Acid in Organic Reactions. By *Y. Izumi, K. Urabe* and *M. Onaka*. VCH Verlagsgesellschaft, Weinheim/VCH Publishers, New York, 1992. 166 pp., hardcover DM 128.00.—ISBN 3-527-29011-7/1-56081-700-3

This book by Y. Izumi, K. Urabe and M. Onaka describes the applications of solid catalysts in organic reactions. It contains three chapters with 350 references, giving a detailed survey of the state of research on this topic up to the end of 1991.

The first chapter comprises three sections giving a brief introduction to organic reactions on zeolites and montmorillonite clay. Each section (except the introduction) is divided into subsections discussing different reactions. The topics covered are the use of acid and base sites of zeolites in the *O*-alkylation of alcohols to ethers, *N*-monoalkylation of aniline derivatives, ring opening of epoxides, regioselective bromination with adsorbed bromine on zeolite, aldol reactions, Michael addition reactions, addition of ester enolates to ynoates, and carbon–carbon bond forming reactions.

Chapter 2 is devoted to clays which are potential catalysts in organic synthesis. After a short introduction to clays, this chapter discusses the structure and composition of clays, factors determining their catalytic efficiency, and new catalytic aspects of synthetic clays. Other topics covered are the selective hydroisomerization of n-hexane, selective dehydrogenation of cyclohexane, selective etherification of n-butyl alcohol, selective hydrolysis of chlorobenzene to phenol, and metathesis reaction of propene.

Chapter 3 discusses the usefulness of heteropoly acids in organic synthesis. This chapter describes the fundamental chemistry of heteropoly acids, and their uses in acid–base and redox molecular catalysis for various types of organic reactions.

The authors have succeeded in providing the reader with a lot of information regarding organic reactions over solid catalysts. The summary tables, reaction schemes, and literature references make it easier for the reader to get more deeply involved in this wide-ranging field of research and facilitate quick access to the original papers.

The book is a useful addition to the literature on zeolite, clay, and heteropoly acid in organic reactions. To those who are seriously interested in organic reactions using solid catalysts, I can recommend reading this neat and well written book.

Ganesh Pandey
Organic Chemistry (Synthesis) Division
National Chemical Laboratory
Pune (India)

Comprehensive Handbook on Hydrosilylation. Edited by *B. Marciniec*. Pergamon, Oxford, 1992. 754 pp., hardcover £ 150.00.—ISBN 0-08-040272-0

This book edited by Bogdan Marciniec is an extension of the Polish version of *Hydrosilylation*, published in 1981. The present monograph aims to provide a complete coverage of the literature from 1965 up to the beginning of 1990. Over 1360 literature references and 750 patents are included. The volume is divided into two parts. The first part is a critical survey of the scope and application of hydrosilylation reactions. The second part is a truly extensive tabulation of published hydrosilylation reactions from 1965 to 1990.

Part I consists of six chapters which deal with the systematic trends of the hydrosilylation reaction, focusing on catalyst, silane, and unsaturated substrate. Chapter 1 is a very brief introduction discussing the rationale and organization of the subject matter and its relation to other reviews in the field. Chapter 2 is a survey of mechanistic aspects of the hydrosilylation reaction including free radical, acid and base catalysis, and transition metal catalyzed reactions. Chapter 3 deals with the reactivity of the major classes of unsaturated organic compounds and their utility in the synthesis of organosilicon compounds. This chapter is organized by compound class with separate discussions of alkenes, dienes, alkynes, carbonyls, and other functional groups. The effects of substituents on the organosilane reagents with regard to reaction rate and regio- and stereoselectivity are described in Chapter 4. The chapter also includes practical applications to the synthesis of organosilicon monomers. Chapter 5 is a short discussion of the hydrosilylation reactions of unsaturated organosilicon compounds, which are important both as models for activated curing processes and as routes to the synthesis of carbosilane oligomers and polymers. Finally, Chapter 6 covers some practical applications of the hydrosilylation reaction including the role of organosilanes as coupling agents and as reducing agents for organic substrates. The use of hydrosilylation in polymer modification is also discussed. The topics covered in Part I are very generously illustrated by examples, but sometimes these get in the way of the guiding principles. Also numerous typographical errors, nomenclature lapses, and hard-to-read figures make this section of the book difficult for browsing or casual reading.

Part II of this volume is a nearly exhaustive compilation of hydrosilylation reactions from 1965 to 1990, and includes both literature and patent references. The 425 pages of data are organized into tables which list initial reagents, reaction conditions (catalyst, temperature, time, solvent, etc.), products with yields, and references. The primary division of the tables is according to trisubstituted silanes of increasing complexity (Si, C, and H numbers), followed by the type and complexity of unsaturated organic substrates (C and H numbers). The table is keyed to a separate bibliography giving the appropriate literature references. Patents are identified not only by the patent number

 © *VCH Verlagsgesellschaft mbH, D-69451 Weinheim, 1994* *0570-0833/94/1818-1893 $ 10.00+.25/0*

but also by an abstract number in *Chemical Abstracts* or *Ref. Zh. Khim.* Also included in this part of the volume is a key to abbreviations for solvents and functional groups and a glossary containing structural diagrams for some of the more complex organic substrates and products. Perhaps one of the greatest weaknesses of this type of tabular presentation is the constant need to move back and forth between the main table and the supporting glossaries. This is particularly relevant since many of the abbreviations are nonstandard (for example, *c* stands for chloroform), and for complex structures it is necessary to constantly refer to a glossary for structures which are identified only by numbers in the main table. However, this tabulation is a commendable feat and many will find this section of the book by far the most useful.

The treatment of hydrosilylation in the first six chapters is largely by detailed examples, and consequently it would not be a good introduction for the novice and should not be used as a textbook. However, the wealth of information which is presented in this volume should be of tremendous value to the practitioner of the hydrosilylation reaction, whether it be in an industrial or academic setting. As such, this book is an indispensable reference source.

Mark Fink
Department of Chemistry
Tulane University
New Orleans, LA (USA)

Iron–Carbene Complexes. (Series: Scripts in Inorganic and Organometallic Chemistry, Vol. 1.) Edited by *W. Petz*. Springer, Heidelberg, 1993. 202 pp., paperback DM 68.00. —ISBN 3-540-56258-3

The celebrations were premature! Anyone who hoped that this new series from the Gmelin-Institut für Anorganische Chemie would make it possible to build up a "home Gmelin" at a realistic and affordable cost will be bitterly disappointed. The initial concept, which is again stated in the preface to the first volume of this series, sounds very good: "...the new Gmelin series will review selected areas of inorganic and organometallic chemistry in textbook style. It will provide the lecturer, the advanced student, and the research chemist with a digest of the main features of each topic." As the first topic the publishers have chosen iron–carbene and iron–vinylidene complexes in which the iron atom also has a η^5 ligand (C_5H_5 or one of its derivatives). This is a sensible restriction when one considers that the systematic preparation and study of Fischer carbene complexes has now been going on for nearly thirty years, and it is no longer realistic to expect the whole of this extensive subject, with all the possibilities of central metal atom and substitution pattern, to be covered in a single monograph. The area treated here corresponds exactly to the volume of the original *Gmelin-Handbuch der Anorganischen und Metallorganischen Chemie* with the title "Organoiron Compounds B16a", containing about 260 pages.

To anyone familiar with the density of data in Gmelin, the task of producing a "digest of the main features" of this subject must seem rather like trying to write a short summary of the national postcode index. Practically all the shortening needed to compress the subject into 200 pages for the new publication *Iron–Carbene Complexes* has been achieved by taking out the formula index completely and eliminating all the literature references and the journal citations from the text of the original Gmelin (although, curiously, on the bottom line of p. 168 the last of the references has survived the massacre of its brothers).

However, this has severely reduced the book's potential readership. Specialists working on iron or other carbene complexes, after a first nibble at a topic, need to be given direct access to the original publications. One can perhaps envisage the book being used as a quick reference source for spectroscopic and X-ray structural data, but this use is greatly hindered by the incompleteness of the numerical data and the lack of a detailed overall index. Lecturers and students seeking a general overview of carbene complexes (or even one confined to iron as the central metal atom) will quickly abandon this book, since despite the declared aim of producing a work in "textbook style", this is clearly not that but a collection of data. The few general comments included at the beginnings of individual chapters are either too superficial or so brief that they cannot be understood without relevant previous knowledge.

In this connection one must also mention the many printing errors. In many cases parentheses are either missing or too many in number, and more seriously there are numerous spelling mistakes and incorrect formulas, sometimes altering the meaning. Examples are "$RHC{=}CNCH_3$" instead of $RHC{=}NCH_3$ (p. 32) and "Cp-(CO)(^{2}D)FeC=CH" instead of Cp(CO)-(^{2}D)FeC≡CH (p. 55), and on page 122 a rotational barrier is given as 7712 kJ/mol instead of 77 ± 2 kJ/mol. The "one-protein resonances" referred to on page 104 are presumably one-proton resonances.

There are also many errors in the figures. In Figures XII and XIII (p. 54) the cyclopentadienyl ligand is shown as "H_5C_6" instead of H_5C_5, and the Fp-containing sidechain of compound XXVIII on page 98 has an extra carbon atom. Although errors such as these only cause a shake of the head, the incorrect caption "(*S,S*)-chiraphos" under Figure IV (p. 184), which actually shows the *R,R* isomer, is inexcusable. Other errors that need no further comment are the description of the diastereomeric complexes VII and VIII (p. 27) as "enantiomeric cations", and the labeling of the abscissa in the figure on page 55 as "Wavenumber in nm".

Another source of annoyance is the lack of a glossary explaining the abbreviations used in the book, as also are the repeated explanations of familiar compound name abbreviations (e.g., dppe on pages 7, 10, 47, 178, 181, and 182), and the use of the same abbreviation for different groups (e.g., Fp* is used to represent $(C_5Me_5)(CO)_2Fe$ on pp. 104, 124, and 125, $(C_5H_4Me)(CO)_2Fe$ on pp. 117 and 123, and $(C_9H_7)(CO)_2Fe$ on pp. 123 and 124). The cross-references too show little sign of having been carefully checked. As well as references to the wrong chapters (pp. 114, 126, 158, 167), there are others mentioning chapters that do not even exist (pp. 152, 158, 197) and methods of preparation that are not given ("Method IV" on pp. 118, 121). These and many other errors are quite unacceptable, especially in a book of only 202 pages.

The verdict after looking through *Iron–Carbene Complexes*, which is also to be regarded as an initial sample for the new series *Scripts in Inorganic and Organometallic Chemistry*, is clear. By carrying out some intensive work on correcting the errors, providing a formula index for the whole work, and including all the references to original publications, the authors and the publishers would be performing a valuable service, not least to themselves.

Gerhard Roth
Fakultät für Chemie
der Universität Konstanz (FRG)

Prostacyclin and Thromboxane Synthase: New Aspects of Hemethiolate Catalysis

Volker Ullrich* and Roland Brugger

The arachidonic acid metabolites thromboxane A_2 and prostacyclin are highly potent regulators of cell physiology. They are both formed by enzymatic rearrangement of the 9,11-epidioxy prostaglandin H_2 catalyzed, however, by thromboxane and prostacyclin synthase, respectively. The two enzymes have been isolated, sequenced, and characterized as hemethiolate ("P450") enzymes. The different isomerization products can be explained on the same catalytic principle by a different ligation of the heme centers with the two epidioxy oxygens atoms. This requires different conformations for substrate binding at the active site, which is substantiated by the different inhibitors and amino acid sequences of the enzymes. In a hypothesis which has mechanistic principles in common with the P450-monooxygenases and the allene oxide synthases, oxy radicals are formed first and rearrange to carbon radicals. These could then rapidly be converted into carbocations by the ferrylthiolate or iron(III)thiyl structures formed as intermediates.

1. Introduction

The prostaglandins form a family of signalling molecules that communicate between cells of a given organ (autacoids). They mediate key events in inflammation, autoimmune diseases, or shock syndromes, but also in physiological regulation associated with growth, differentiation, parturition, or sleep (for reviews see [1–7]). Hence pharmacological research has focused on their pathways of biosynthesis and inhibition, and also on their mode of action. Like steroid hormones, prostaglandins are not stored and secreted but synthesized and released on demand. They are formed and degraded much more rapidly than steroids, and since they act exclusively within organs, only their degradation products rather than active prostaglandins can be found in blood or serum. Because of this and their low concentrations in tissues, the analysis, the structural evaluation and the chemical synthesis of prostaglandins have been a challenge (for reviews see [8–9]).

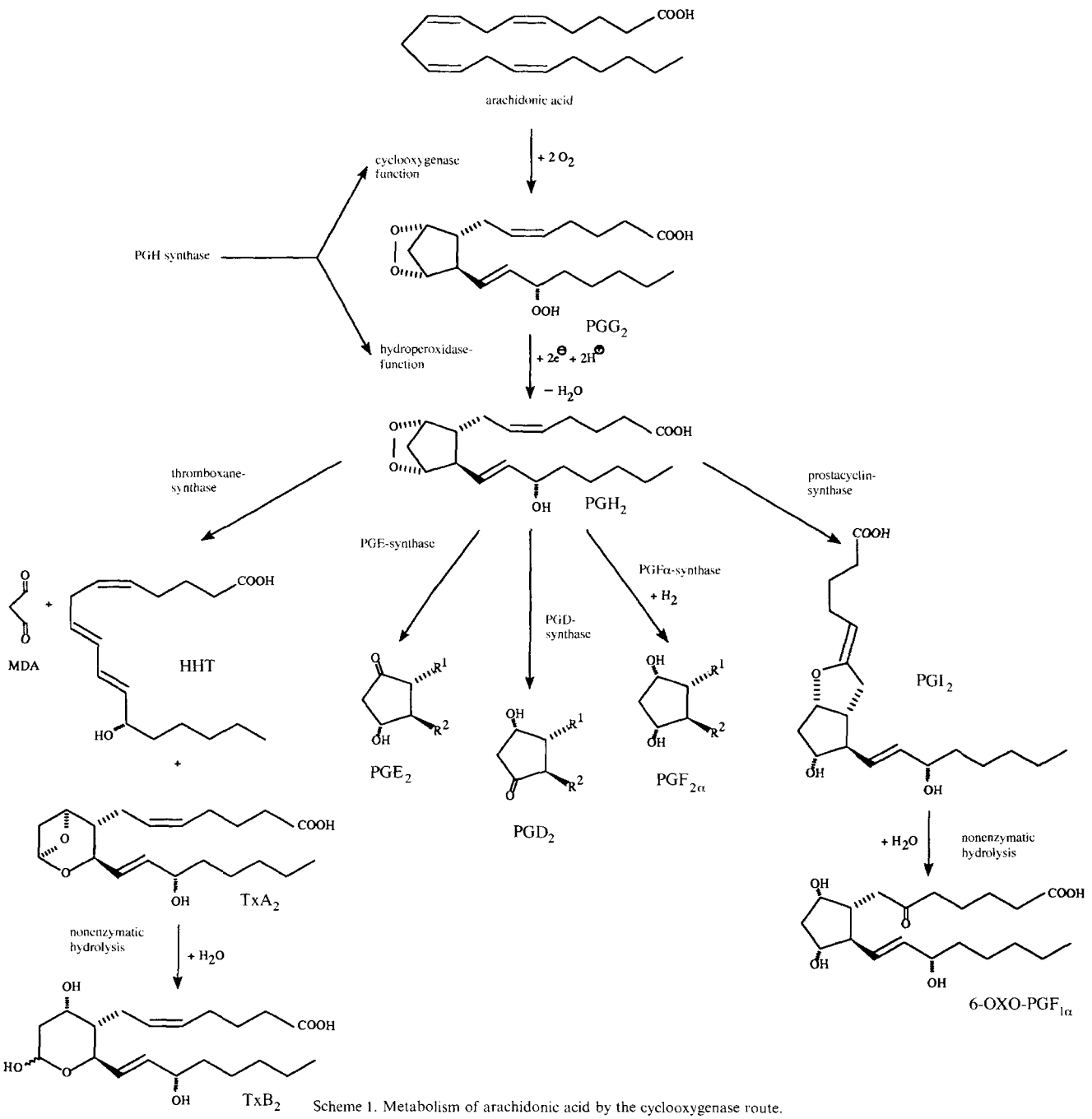
The biosynthetic pathways in higher organisms start out from arachidonic acid (5*Z*, 8*Z*, 11*Z*, 14*Z*)-icosatetraenoic acid), which on account of its four double bonds and abundance of allylic hydrogens offers a large biosynthetic potential.[10] Arachidonate is readily available from biological membranes after activation of phospholipases. The second step is then the conversion of arachidonate into 15-hydroxy-9α,11α-epidioxy-prosta-5,13-dienic acid (PGH_2).[11] This requires two enzymatic activities, that of cyclooxygenase and of a hydroperoxidase, which are colocated on PGH-synthase (see Scheme 1).

The detailed mechanism of PGH-synthase is still unknown, but the initial step of the cyclooxygenase reaction must involve hydrogen atom abstraction at C-13 of arachidonic acid, followed by isomerization with shift of the radical to C-11, dioxygenation, cyclization, and a second dioxygenation at C-15.[11] The resulting 15-hydroperoxyl radical is then reduced to the hydroperoxide (PGG_2) by the initially abstracted hydrogen atom. Thus, we are dealing with a radical reaction that is initiated, propagated, and terminated at the active site of cyclooxygenase. We shall meet this elegant principle of shielded radical catalysis at active sites of enzymes again with thromboxane and prostacyclin synthase.

The PGH_2 molecule contains the relatively weak epidioxy bond that can be opened for subsequent isomerization reactions leading to the five different prostaglandins (Scheme 1). It is obvious that prostaglandins D_2 and E_2 are formed after a heterolytic cleavage of the O–O bond by a nucleophilic mechanism. However, the biosynthesis of prostacyclin (PGI_2) and thromboxane (TxA_2) with the formation of the oxygen-containing heterocycles appears more complex. After labeling experiments with ^{18}O had established the isomerization character of both reactions,[12,13] mechanisms of heterolytic cleavage of the epidioxide and rearrangements to TxA_2[14] and PGI_2[15] have been proposed. Such chemistry requires an efficient stabilizing catalyst to prevent carbonyl formation from the positively charged oxygen atom. This led us to suggest an involvement of heme since heme containing thiolate ligands in the cytochrome P450 monooxygenases can transfer oxygen atoms from hydro-

[*] Prof. Dr. V. Ullrich, R. Brugger
Fakultät für Biologie Universität Konstanz
Postfach 5560, D-78434 Konstanz (FRG)
Telefax: Int. code + (7531)88-3099

 © *VCH Verlagsgesellschaft mbH, D-69451 Weinheim, 1994* *0570-0833/94/1919-1911 $ 10.00+.25/0*



Scheme 1. Metabolism of arachidonic acid by the cyclooxygenase route.



Volker Ullrich, born on September 5, 1939, in Wetzlar/Lahn, Germany, studied chemistry at the University of Giessen from 1958 to 1962 (Diplom under P. Ehrlich on nitride halides of barium) and obtained his doctorate in 1964 under Hj. Staudinger. He spent terms for research at the University of Philadelphia (R. W. Estabrook) and in Dallas before habilitating in the Faculty of Medicine at the University of Giessen in 1969 on the mechanism of monooxygenases. In 1971 he accepted the chair of Physiological Chemistry in the Faculty of Medicine at the University of the Saarland and in 1983 at the University of Constance, where he also was Prorektor from 1991 to 1993. He is active in the Deutsche Forschungsgemeinschaft and member of the Gesellschaft Deutscher Chemiker and the European Society of Biochemical Pharmacology among others. His main research interests are the chemistry and biochemistry of oxygen and their implications in the pharmacological field.

peroxides to organic substrates.[16, 17] This working hypothesis could be verified by making use of the characteristic P450 spectra which allowed us to isolate the two isomerases for converting PGH_2 into TxA_2 and PGI_2.[18]

In this review we briefly summarize our data and those of other groups, and focus on a comparison of the two enzymes that share a substrate and a catalytic site but form two different products with entirely different, and even antagonistic, pharmacological properties; PGI_2 is a potent vasodilatory and platelet-antiaggregatory prostanoid, whereas TxA_2 is vasoconstricting and strongly platelet-aggregating.[2] Our results have suggested biosynthetic mechanisms for the two compounds that have led to new insights on the principles of hemethiolate catalysis for other enzymes of this superfamily.

2. Isolation and Spectral Characterization

PGI_2 is primarily produced by the endothelium of blood vessels,[19] which therefore served as the starting material for purification.[20] In accordance with literature, the PGI_2-synthesizing enzymatic activity was associated with the endoplasmic reticulum obtained as the microsomal cell fraction.[21] Difference spectroscopy indeed revealed the presence of a P450 (= hemethiolate) protein with its characteristic carbon monoxide difference spectrum at 450 nm after treatment with sodium dithionite.[22] Enzymatic reduction by $NADPH_2$ could not be observed, which indicates that the P450 protein could not act as a monooxygenase. Solubilization of porcine aortic microsomes with detergents resulted in still active preparations, which could be further purified by affinity chromatography on a column packed with a stable CH_2–O analogue of PGH_2 (U46619),[23] by immunoaffinity chromatography,[24] or by classical methods (R. Brugger, unpublished). This purified fraction from the aorta yielded a homogeneous protein after SDS-polyacrylamide gel electrophoresis with a molecular weight of about 52 kDa and a PGI_2-synthase activity of about $3\ s^{-1}$.[25] Other enzyme parameters are listed in Table 1.

Thromboxane A_2 is released from blood platelets, which are thus a suitable starting material for the isolation of the isomerase. Hammarström and Falardeau[28] have already used it when they localized the synthesizing activity in the microsomal fraction. We identified a P450 protein in the same fraction, solubilized it with detergents, and further purified it to homogeneity.[29] On SDS gels it showed a band at 59 kDa and converted PGH_2 into TxB_2, the stable hydrolysis product of TxA_2. TxB_2 has a molecular activity of about $27\ s^{-1}$. Since the enzyme forms a second product, as will be discussed later, the molecular activity has at least to be doubled.

Table 1. Properties of PGI- and TxA-synthases.

	PGI synthase [23–25]	TxA synthase [25–28]
molecular weight, SDS gel [Da]	52000 (bovine), 49200 (porcine)	58800 (human), 53000 (porcine)
molecular weight from sequences	56600 (bovine) [a]	60500 (human), 58220 (murine)
$\lambda_{abs.}$ [nm] (ox.)	417, 532, 568	418, 537, 570
$\lambda_{abs.}$ [nm] (red. + CO)	424, 451, 545	424, 450, 545
g-tensors (EPR spectrum)	2.42, 2.25, 1.90	2.41, 2.25, 1.92
isoelectric points [pH] [b]	4.8–5.0 (bovine), 5.1 (porcine)	4.8 (human)
K_M [μM]	9 [b]	10–24
molecular activity [s^{-1}]	3.5–4.3	27 × 2 [c]
specific activity [μmol min^{-1} (mg protein^{-1})]	2–5	24.1 (human)

[a] T. Tanabe, S. Hara, A. Miyata, R. Brugger, V. Ullrich, unpublished. [b] R. Nüsing, R. Brugger, V. Ullrich, unpublished. [c] TxA_2 + HHT.

It is well established that the heme group in cytochrome P450 monooxygenases is linked to the thiolate group of a cysteine residue, which causes unusual spectral characteristics in the optical and the EPR spectra.[30–34] The spectral features in Figure 1 were redrawn from data published on the most thoroughly investigated camphor 5-monooxygenase from *Pseudomonas putida*.[35, 36]

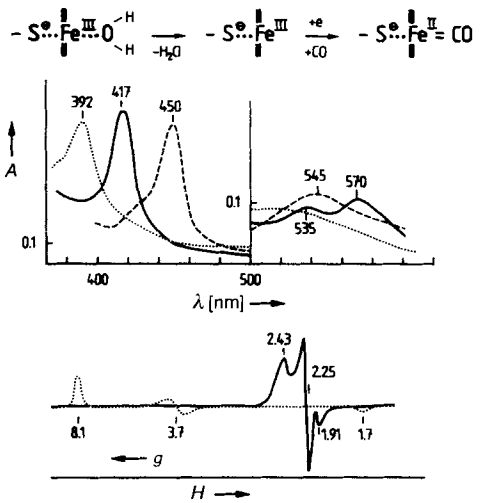


Fig. 1. Spectral characteristics of intermediates in reactions of cytochrome $P450_{CAM}$. Visible spectrum: —— Fe^{III}–H_2O complex, ····· five-coordinate high-spin Fe^{III}, ---- Fe^{II}–CO complex.

The oxidized iron(III) cytochrome P450 is low spin with an unusually narrow splitting of the g-tensor.[37] The Soret band of this species peaks at 417 nm, and by a comparison with heme models[38] as well as from the X-ray structure of $P450_{CAM}$,[39, 40] it contains water at the sixth coordination site. Upon addition of their substrates, which are generally lipophilic, the spectra of P450 monooxygenases change dramatically: EPR shows that the blue shift of about 26 nm in the Soret band is due to the generation of a high-spin five-coordinate iron center.[41] Upon reduction by sodium dithionite in the presence of carbon monoxide, the Soret band shifts to 450 nm. Denaturation of the protein or protonation of the thiolate ligand leads to inactive "P420" enzymes with Soret bands at 420 nm where they are located in most hemoproteins.[42]

Both PGI-synthase and TxA-synthase contain one heme molecule per polypeptide chain and show exactly the same optical and EPR properties as P450 monooxygenases, except that addition of the substrate PGH_2 does not cause the conversion into a high-spin complex, probably because the water ligand is replaced by the epidioxide ligand. In agreement with this assumption, only very subtle spectral changes are observed.[22] As shall be mentioned later, certain other substrate analogues are able to generate the complex containing a five-coordinate iron center.

Hence, all properties of a catalytic hemethiolate site are present in both isomerases. In agreement with the postulated role of the heme, it remains in the Fe^{III} state and need not be reduced enzymatically since no reduction of O_2 is required, in contrast to the P450 monooxygenases. Even the chemical reduction by dithionite in the presence of CO is slow and incomplete.

3. Amino Acid Sequences of the Enzymes

According to the spectral data, PGI- and TxA-synthases clearly belong to the hemethiolate superfamily of enzymes, which includes an ever-growing number of more than a hundred monooxygenases.[43] According to the proposed nomenclature, different families of hemethiolate proteins are defined when the amino acid sequence homology is less than 40%, an arbitrarily chosen value.

The sequences of these synthases were recently established in cooperation with the group of T. Tanabe in Osaka.[44] Human TxA-synthase has 533 amino acids, with homologies to several P450 enzymes but not exceeding 36% as established with human nifedipine monooxygenase (P450IIIA4). This was independently confirmed by Ohashi et al.[45] The recently published sequence of the murine enzyme showed 78% homology with that of the human protein.[26]

Interestingly, cysteine 479 could be identified by alignment as the ligand likely to coordinate to the heme group, and the 10 amino acids toward the N terminus from this cysteine were found to be identical with those of human steroid-17α monooxygenase from adrenals. Thus the P450 or hemethiolate nature could also be verified by the sequence data, and TxA-synthase can be considered as the first and so far only member of a new P450 family.

The sequence of PGI-synthase was expected to be highly interesting, since the use of the same substrate as TxA-synthase suggested a close relationship. The 500 amino acids exhibited a moderate homology of 31% with human cholesterol 7α-monooxygenase. Since only one cysteine was present close to the C terminus, the thiol group that binds heme must belong to this amino acid. The sequence around this heme binding site had some homology with several other P450 monooxygenases and with TxA-synthase. Very surprisingly however, the total homology between PGI- and TxA-synthase was only 16%, which is a statistical value. Therefore PGI-synthase also forms a new family within the hemethiolate proteins, and no phylogenetic relationship seems to exist between the synthases despite their close functional relationship. This was puzzling, but since the enzymes generate two different products from the same substrate, the clue to the unexpected differences could reside in a different folding of the active site. Indeed, inhibitor studies indicate large differences in the substrate binding site.

4. Substrates and Inhibitors

Since at present neither X-ray studies nor two-dimensional NMR spectroscopy are possible for either enzyme, conclusions with regard to substrate binding and the catalytic mechanisms must come from indirect evidence. Chemical modifications of the substrate PGH_2 and their spectral interactions with the heme chromophore, as well as inhibitor studies, provide sufficient information on the active site and the mechanisms involved.

In Table 2 substrates and products for the two enzymes are compared. The main physiological substrate is certainly PGH_2, which is fully converted into prostacyclin and detected as its hydrolysis product 6-oxo-$PGF_{1\alpha}$.[46] It has long been known that TxA-synthase forms not only TxA_2, but also (12*S*)-hydroxy-(5*Z*,8*E*,10*Z*)-heptadecatrienoic acid (HHT) plus malondialdehyde,[47] in fact to a similar or even greater extent (see Scheme 1). Since the latter products are also derived from a chemical fragmentation of the PGH_2 molecule with transition metal ions, they were not at first considered to be formed by the enzyme. However, the isolated enzyme as well as the enzyme expressed in the baculovirus system also generate 50–70% of fragmentation products.[48] Hence HHT is indeed an enzymatically generated product, and any proposed reaction mechanism must include its formation.

Table 2. Substrate specificity and metabolites of PGI- and TxA-synthases.

Substrates	TxA-synthase metabolites		PGI-synthase metabolites	
PGH_1	–	HHD	..	HHD
PGH_2	TxA_2	HHT	PGI_2	–
PGH_3	TxA_3	Δ^{14}-HHT	PGI_3	..
PGG_2	15-OOH-TxA_2	12-OOH-HHT	15-OOH-PGI_2	–
8-*iso*-PGH_2	–	8-*cis*-HHT	..	8-*cis*-HHT
(13*S*)-PGH_2	..	(10*S*)-HHT	–	..
15-oxo-PGH_2		KHT	15-oxo-PGI_2	KHT

A pharmacologically interesting substrate is PGH_3 (identical to PGH_2 except for an additional double bond between C-17 and C-18), which is the cyclooxygenase product of icosapentaenoic acid. Both isomerases can use PGH_3 as a substrate and convert it into PGI_3 or TxA_3. The latter acts as weaker agonist on the TxA_2-receptor for the contraction of smooth muscles and for platelet aggregation.[49] PGI_3 exhibits a similar potency to PGI_2. Therefore, a fish oil diet rich in icosapentaenoic acid has been claimed to have beneficial effects for patients susceptible to cardiac infarct.[50] Interesting results are observed with the corresponding PGH_1 (identical to PGH_2 except for the lack of the double bond between C-5 and C-6). A prostacyclin PGI_1 cannot be formed since the essential Δ^5 double bond is lacking. However, the fragmentation products (12*S*)-hydroxy-(8*E*,10*E*)-heptadecadienoic acid (HHD) and malondialdehyde are formed exclusively with a molecular activity of about 30 s^{-1}, that is, about ten times faster than PGI_2 from PGH_2. Surprisingly, as reported in the literature,[14, 51] TxA-synthase cannot convert PGH_1 to TxA_1 but again only to HHD and malondialdehyde. A chemical reason for the importance of the Δ^5 double bond is not evident in this case, but it is assumed that the carboxylate side chain would be a very sensitive determinant for substrate fixation at the active site. Interestingly, the molecular activity of thromboxane-synthase with PGH_1 is about the same as for TxA_2 plus HHT formation from PGH_2. This finding supports the view that HHT is derived from a common intermediate and suggests that for TxA-synthase the cleavage of the O-O bond is

rate-limiting, whereas for the slower reaction in the case of PGI-synthase, the kinetic limitation occurs at a later step. Further important information can be derived from use of the isomer 8-*iso*-PGH_2 as a substrate, which leads only to the fragmentation products and therefore documents how crucial the correct placement of the α side-chain is for the ring closure reaction of PGH_2 to give PGI_2.

Complementary information was obtained from inhibitor studies. Efforts to synthesize TxA-synthase inhibitors as highly specific platelet-antiaggregatory drugs has led to a variety of tightly (mostly stoichiometric) binding compounds. From the structure–activity relationships of these substances the orientation of the PGH_2 substrate at the active site of TxA-synthase could be deduced.[52, 53] Invariably, all tightly binding inhibitors contain a basic nitrogen atom that coordinates to the sixth ligand position of the iron center of the heme, and a lipophilic side chain containing a carboxylate group that extends about 10 Å at an angle of about 60° from the heme plane (Fig. 2).

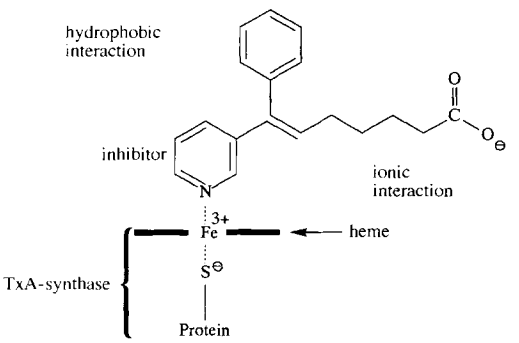


Fig. 2. Binding of inhibitors to the sixth coordination site of TxA-synthase.

From these studies developed the concept that the PGH_2 molecule binds with the epidioxy bridge at the iron atom, and that the side chain occupies the same position as the carboxylate side chain of the inhibitors. Among all compounds tested, the complex between the heme protein and a pyridine derivative with an appropriate carboxylate side chain in the *ortho* position did not display the typical N-ligand binding spectrum but a Soret band at 390 nm, indicative of a high-spin five-coordinate iron center. Such spectral behavior is in accord with weak binding to the active site but not to the heme iron because of steric hindrance of the *ortho*-substituted pyridine moiety. Since the spectrum indicates a free sixth ligand position, the endogenous ligand was obviously displaced. This ligand is probably a water molecule, which has been detected by X-ray analysis in the spectrally identical camphor monooxygenase.[39, 40]

According to spectra, none of the inhibitors of TxA-synthase, not even imidazole or simple pyridine derivatives, interact with PGI-synthase to inhibit this enzyme.[25, 53] This certainly is the prerequisite for their potential therapeutic application, since otherwise the beneficial effects of PGI-synthase would also be eliminated by TxA-synthase inhibition. Conclusions about the steric architecture of the active site of PGI-synthase are possible: low affinity for imidazole or pyridine ligation indicates a very limited space at the sixth coordination position of the iron center. A cyclopropylamine derivative (*trans*-2-phenylcyclopropylamine) was reported as an inhibitor of PGI-synthase, and, according to the spectral shifts, must coordinate through the nitrogen atom. Another nitrogen-containing compound, minoxidil (6-(1-piperidyl)-2,4-diaminopyrimidine-3-oxide), induces similar spectral changes and high binding affinity (K_S = 2.4 μM), but its inhibition of enzyme activity is weak (IC_{50} = 90 μM).[54] From these two examples of N-ligands it can be concluded that the sixth coordination site of iron in PGI-synthase is accessible only for nitrogen compounds with side chains extending almost perpendicular to the Fe–N coordination axis. Applied to the binding of PGH_2 to the active site, this conclusion implies an antiparallel orientation of the carboxylate and alkyl side chains; hence a completely different stereochemical conformation for PGI-synthase and TxA-synthase active sites would result (Fig. 3).

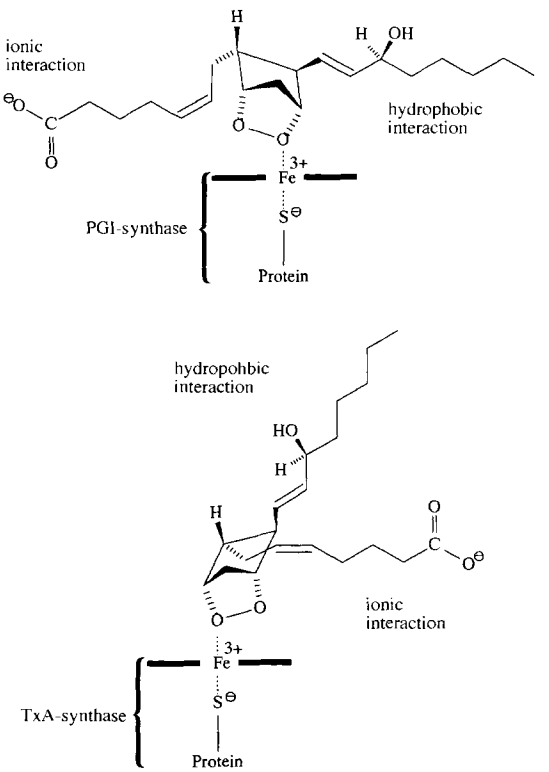


Fig. 3. Binding of the substrate to the active sites of PGI- and TxA-synthases.

5. Mechanistic Studies and Hypotheses

All attempts to explain the mechanisms of rearrangement from PGH_2 to PGI_2 or TxA_2 must start out with a cleavage of the O-O bond. A heterolytic cleavage leads to a positively charged oxygen atom either at C-9, which could easily form PGI_2,[15] or at C-11 to yield TxA_2.[14] No experimental evidence for a polar mechanism could, however, be obtained,[55] and indeed, the generation of a charged oxygen atom at the active site without immediate isomerization of PGH_2 to PGD_2 or PGE_2 would be highly unlikely.

The remaining mechanism of homolytic cleavage of the O-O bond was first postulated by Turner and Herz,[56] whose pro-

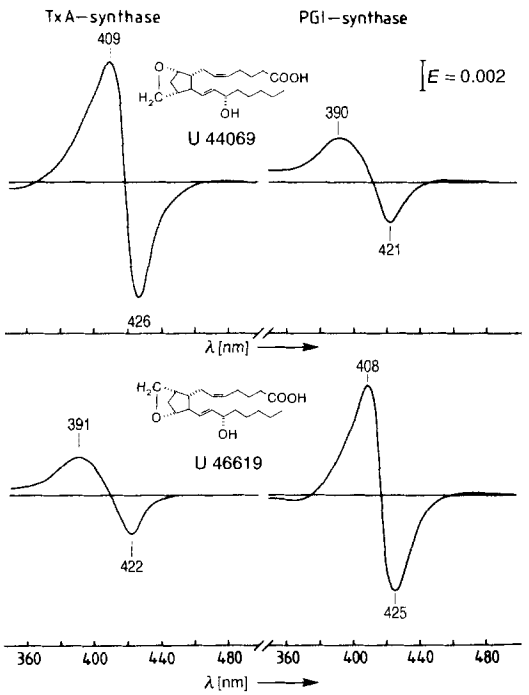
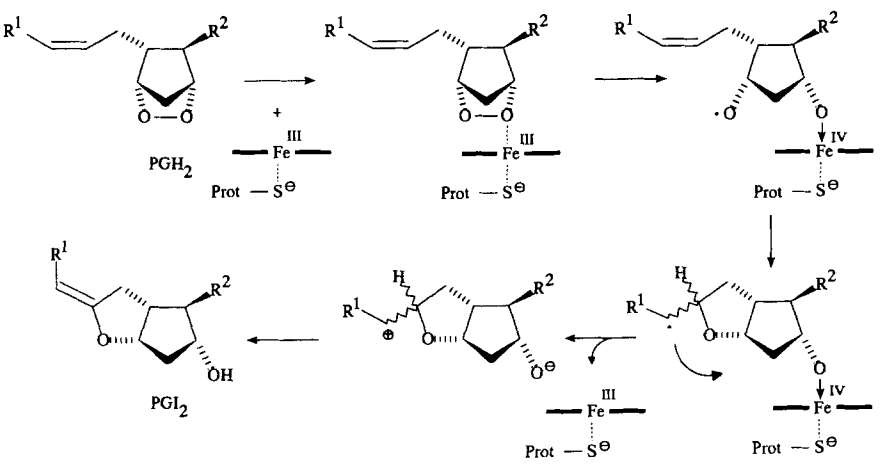


Fig. 4. Difference spectra (visible range) of complexes from solubilized TxA- and PGI-synthase and the PGH_2 analogues U44069 and U46619.



Scheme 2. Mechanism of PGI_2 biosynthesis. R^1: $(CH_2)_3-CO_2H$; R^2: $CH=CH-CHOH-(CH_2)_4-CH_3$.

posed splitting agent was Fe^{II}. The resulting Fe^{III} ion could serve as the oxidizing agent for the conversion of the intermediate radical at C-5. The assumption that iron is the catalyst for the epidioxy cleavage was compatible with our later discovery of a hemethiolate group at the active site, but a reduction of Fe^{III} in the heme can be excluded. Either the electron-donating properties of the Fe^{III}–hemethiolate group facilitated heterolytic splitting and the stabilization of a positive oxygen atom,[57] or the homolytic cleavage was assisted by the Fe^{III} form. Spectral investigations with stable PGH_2 analogues[25] demonstrated indirectly that homolytic cleavage was more likely.

The concept of stable substrate analogues as inhibitors of the PGH_2 isomerases seemed reasonable and had led to the early synthesis in pharmaceutical research of several analogues of PGH_2, including among others U46619 and U44069, in which the O–O group was substituted by a CH_2–O bridge.[58] These two isomers inhibited both PGI- and TxA-synthase, but influenced the spectra differently (Fig. 4).[25] Whereas U46619 produced a ligand-type difference spectrum with TxA-synthase, U44069 resulted in a typical "high-spin" spectrum with a peak at 390 nm. With PGI-synthase the situation was reversed. From this it could be concluded that the Fe^{III} ion coordinated to the 9-position in TxA-synthase but to the 11-position in PGI-synthase.[25]

If PGH_2 and its analogues bind tightly, the replacement of a coordinating oxygen atom by a methylene group would result in a five-coordinate iron center as in the enzyme–substrate complexes of P450 monooxygenase.[32]

Because of this unexpected discrimination of the two epidioxy oxygen atoms by both enzyme's catalytic sites, an interaction between Fe^{III} and the oxygen atom at C-11 was postulated in the complex between PGH_2 and PGI-synthase. This precluded a heterolytic cleavage with complexation by Fe^{III} of an oxygen cation and left only the homolytic scission facilitated by spin–spin coupling of the Fe^{III} ion to the 11-O radical; the free oxygen radical at C-9 is then the species that attacks the Δ^5 double bond[25] (Scheme 2).

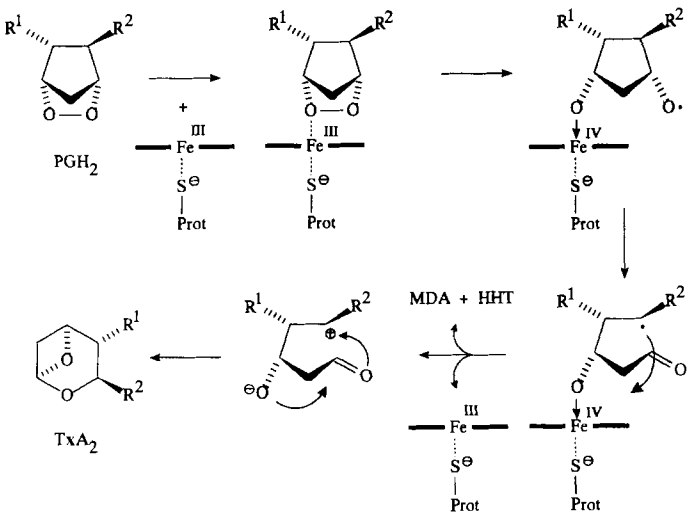
The resulting carbon radical at C4 is oxidized by the now formally Fe^{IV} species, and after migration of a proton from C-5 to 11-O, PGI_2 is formed. This mechanism agrees with the observed substrate specificity: ring closure occurs only when an *E*- or *Z*-configurated Δ^5 double bond in the α side chain between C-5 and C-6 has the same steric orientation as the epidioxy group at the cyclopentane ring.[25, 51] Any changes in the alkyl side chain seem to be irrelevant. Interestingly, PGH_1 (lacking the Δ^5 double bond) and 8-*iso*-PGH_2 are both converted into their respective fragmentation products HHD and 8-*cis*-HHT and malondialdehyde (Table 2). These products confirm that splitting of the epidioxy bridge is the initial step, which leads to fragmentation of the molecule if the appropriate steric orientation of the α-side chain is lacking.

According to the spectral data obtained with TxA-synthase, the heme iron coordinates to the oxygen atom 9-O of PGH_2, and the homolytic scission results in a free oxygen radical at C-11 (Scheme 3). This intermediate undergoes ring cleavage with formation of a radical at C-12 as already suggested by Turner and Herz.[56] As in PGI_2-synthase, the radical can be oxidized by the Fe^{IV} center to a carbocation, which then undergoes electrophilic rearrangement.[25]

The fact that 13,14-dihydro-PGH_2 fragments exclusively into HHD and malondialdehyde supports this mechanism, because the Δ^{13}-double bond would be required for an allylic stabilization of the radical at C-12. Fragmentation also occurs with PGH_1, 8-*iso*-PGH_2, and $\Delta^4(E)$-PGH_1,[51] which underlines the results of studies with inhibitors in which the binding of the α

side chain to the active site was an important factor. A characteristic feature of TxA-synthase is the formation of HHT and malondialdehyde as well as TxA_2 even with the physiological substrate PGH_2. At least 50% and up to 70% of PGH_2 is converted into these products for which no physiological role has yet been found. However, they are clearly formed enzymatically, and the intermediate from which they are derived is very likely the C-12 radical. Fragmentation would be unavoidable if the subsequent electron transfer (or a bonding orbital-overlap of the iron center and the carbon radical) is not fast. It remains to be seen whether the fragmentation products of TxA-synthase are just by-products of an imperfect enzyme or whether they fulfill a still unknown function in the signalling pathway.[59]

A comparison of the proposed mechanisms for PGI and TxA-synthase reveals the same basic principles of homolytic epidioxy cleavage assisted by spin coupling of Fe^{III}, rearrangement to a carbon radical, and, most importantly, the electronic interaction (oxidation or Fe–C bond formation) between the resulting carbon radical to the $[S-Fe-OR]^{3+}$ entity. Strict steric control of this step is essential, because as outlined in Figure 3, it requires two very different orientations of the PGH_2 molecule relative to the catalytic heme group.

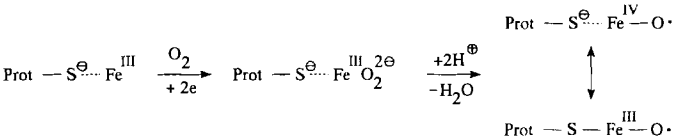


Scheme 3. Mechanism of TxA_2 biosynthesis. R^1: $CH_2-CH=CH-(CH_2)_3-CO_2H$; R^2: $CH=CH-CHOH-(CH_2)_4-CH_3$.

The very low homologies in the sequences of the enzymes would imply that folding of the polypeptide chains to form the active site must be very different. One explanation for this could be found in the concept of evolutionary mobile modules and motifs in proteins.[60] Presumably it was the phylogenetic need to develop entirely different foldings in the tertiary structures that led to the use of different polypeptides from preexisting steroid monooxygenases as building blocks for the protein domains of the two synthases.

6. Common Principles of Hemethiolate Catalysis

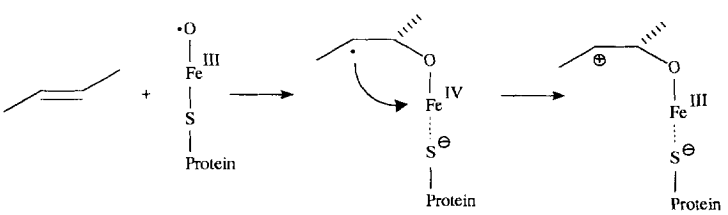
Spectroscopic properties and sequence analysis showed the close relationship of TxA- and PGI-synthase with the hemethiolate monooxygenases, in spite of their different enzymatic functions. A closer mechanistic investigation reveals that monooxygenases contain an additional function in the two-electron transfer to O_2 with the generation of an intermediate peroxo complex which eliminates water to give an oxenoid complex as the "active oxygen species"[61–63] (Scheme 4).



Scheme 4. Oxygen activation through formation of an oxenoid complex between cyctochrome P450 and oxygen.

In earlier work we mimicked all properties of the active oxygen intermediate by adding the oxygen atom donor, iodosylbenzene, to oxidized P450-monooxygenases.[64] This led to the development of model systems consisting of transition metals with iodosylbenzene.[65,66] Since the oxygen transfer with P450-monooxygenases involves the Fe^{III} state, it should also take place at the hemethiolate catalytic site of both synthases if an appropriate PGH_2 analogue is present as a substrate. With U46619 (see Fig. 4) and TxA-synthase in the presence of iodosylbenzene, two hydroxylated products could be detected by GC-MS, which, besides other products, were also formed in a hydroxylating system consisting of liver microsomal cytochrome P450's, $NADPH_2$, and oxygen.[67] Apparently the hemethiolate center of TxA-synthase exhibits the same oxygen transfer properties as that of monooxygenases.

This close analogy to the monooxygenases allows speculation about additional roles of the hemethiolate group in monooxygenase catalysis. Because of the radical attack of the active oxygen species at the monooxygenase substrates, a radical intermediate is expected, which, in case of an epoxidation at the double bond, would have to be oxidized either to a radical cation or to an intermediate iron–carbon bond (Scheme 5).



Scheme 5. Mechanism of epoxidation with heme-activated oxygen.

Unlike hydroxylations with OH radicals, no free radical intermediates have been detected in the enzymatic reaction. The electron transfer or the "rebound" process must thus be extremely fast, as only this would ensure enzymatic stereospecificity.

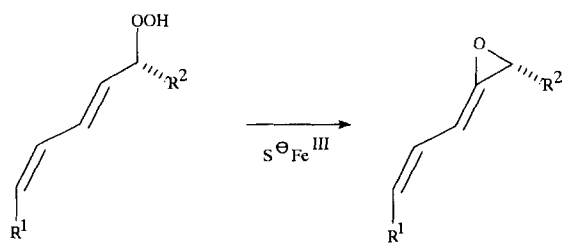
Comparison of this reaction sequence with the rearrangement process to PGI_2 or TxA_2 (Schemes 2 and 3) highlights the requirement for an immediate electron transfer step (Scheme 5). Accordingly, we propose that the unusual redox properties of

the hemethiolate site guarantee a very rapid uptake of an electron from a carbon-centered radical intermediate. That this occurs by a concerted pathway involving an iron–carbon bond is less likely because of the steric situation at the heme and the fragmentation seen with TxA-synthase. This fragmentation would be a typical consequence of a free radical pathway. Furthermore, some experiments with monooxygenases describe a partial racemization at the asymmetric carbon during hydroxylation, which again favors a free though short-lived carbon radical.[68]

7. Wider Implications of Hemethiolate Catalysis

The hemethiolate-catalyzed monooxygenations and the two rearrangement processes consist, in essence, of a primary step in which an oxygen radical is formed, which then attacks the substrate by a radical mechanism. In a third step a carbon-centered radical is oxidized either by electron transfer to the formal heme–Fe^{IV} center or through formation of an intermediate iron–carbon bond.

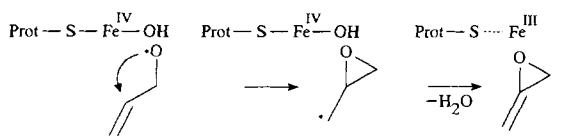
Recently a third type of P450-catalyzed reaction was described in which fatty acid hydroperoxides are converted into allene oxides by a hemethiolate enzyme from plants, corals, or starfish oocytes (Scheme 6).[69] According to the general path-



fatty acid hydroperoxide allene oxide

Scheme 6. The allene oxide synthase. R^1: C_7H_{14}–COOH; R^2: C_5H_{11}; ref. [69].

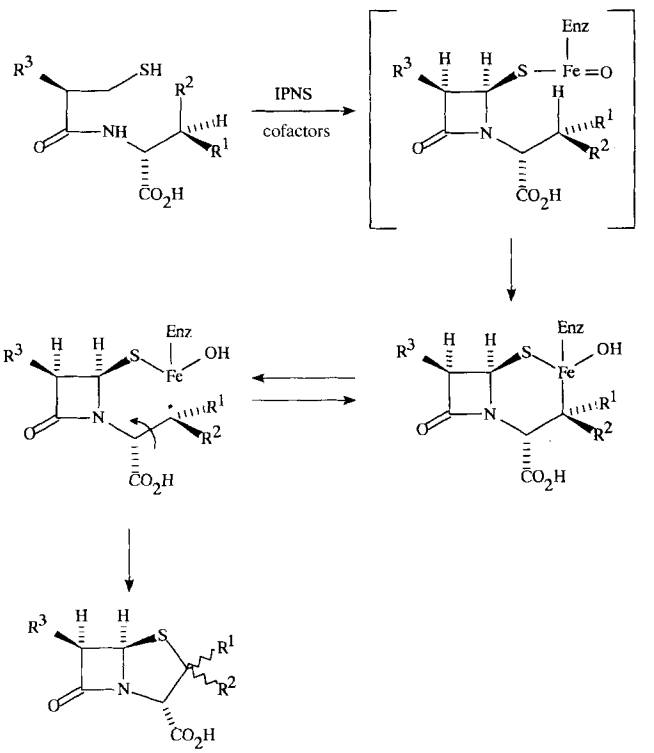
way postulated for hemethiolate catalysis, the rearrangement should proceed by a homolytic O-O bond cleavage, attack by the oxyradical at the adjacent double bond, and oxidation of the C radical (Scheme 7).



Scheme 7. Postulated mechanism of the hemethiolate-catalyzed rearrangement of fatty acid hydroperoxide to allene oxide.

The analogies between the epoxidations catalyzed by hemethiolate monooxygenases and the epidioxy rearrangements are apparent.

From the postulated sequence of events in hemethiolate mechanisms it is not implied that the iron is dependent on porphyrin as ligands. Many ironthiolate structures could exhibit similar properties. A good example may be the penicillin biosynthesis (Scheme 8), which has been thoroughly studied.[70] Here the nonheme $iron^{II}$ of isopenicillin N-synthase (IPNS) coordinates to the thiol group of the substrate and with molecular oxygen forms an oxenoid complex in which the oxygen has sufficient radical character to abstract the tertiary H atom of the valine residue. Spin–spin coupling between the resulting Fe^{IV}



Scheme 8. Mechanism of penicillin-N biosynthesis from ref. [71]; $R^1 = CH_3$, $R^2 = CH_3$, $R^3 = NH$–CO–$(CH_2)_3$–$CH(NH_2)$–COOH.

species and the carbon radical was postulated, but since the stereochemical integrity of the carbon center was lost (scrambling of R_1 and R_2),[71] the reaction is likely to proceed without iron–carbon bond formation. Again the final ring closure may result from a rebound process or an electron transfer to the Fe^{IV} species followed by an electrophilic rearrangement. The basic principles of postulated ironthiolate catalysis can thus be recognized in this desaturative cyclization.

No detailed studies are available on the mechanism for the chlorination of organic compounds with activated C-H bonds, catalyzed by chloroperoxidase, another hemethiolate enzyme.[72, 73] However, since H_2O_2 is the required cosubstrate and the chloride ion is bound at the active site,[74] the chlorination may also involve hydrogen atom abstraction from the substrate followed by electron transfer with subsequent addition of the chloride ion.

In summary, it appears that whenever an ironthiolate center combines with oxygen compounds that have an elevated oxidation potential, interesting S-Fe-O entities arise which initiate radical reactions followed by immediate electron transfer, with the result that radical chain reactions are avoided. This offers an excellent basis for enzyme catalysis. An application to homoge-

neous catalysis is hampered by the fact that thiolate ligands are by themselves candidates for oxygen or electron transfer, but appropriate shielding may open interesting possibilities in heterogeneous catalysis.

Our own contributions to this work have been supported over many years by the Deutsche Forschungsgemeinschaft and the Fonds der Chemischen Industrie. Our former colleagues M. Haurand, M. Hecker, and R. Nüsing are thanked for their contribution to this research. We also appreciate the cooperation with the research group of T. Tanake (Osaka, Japan).

Received: November 12, 1993 [A 35 IE]
German version: *Angew. Chem.* **1994**, *106*, 1987

[1] K. I. Williams, G. A. Higgs, *J. Pathol.* **1988**, *156*, 101–110.
[2] S. Moncada, J. R. Vane, *Pharmacol. Rev.* **1978**, *30*, 293–331.
[3] S. Bergström, L. A. Carlson, J. R. Weeks, *Pharmacol. Rev.* **1968**, *20*, 1–48.
[4] W. L. Smith, *Biochem. J.* **1989**, *259*, 315–324.
[5] O. Hayaishi, *J. Biol. Chem.* **1988**, *263*, 14593–14596.
[6] *Prostaglandins in Clinical Practice* (Eds.: W. D. Watkins, M. B. Peterson, J. R. Fletscher), Raven, New York, **1989**.
[7] K. Schrör, *Prostaglandine und verwandte Verbindungen*, Thieme, Stuttgart, **1984**.
[8] B. Samuelsson, *Angew. Chem.* **1983**, *95*, 854–864; *Angew. Chem. Int. Ed. Engl.* **1983**, *22*, 805–815.
[9] R. A. Johnson, *Adv. Prostaglandin Thromboxane Leukotriene Res.* **1985**, *14*, 131–154.
[10] P. Needleman, J. Turk, B. A. Jakschik, A. R. Morrison, J. B. Lefkowith, *Annu. Rev. Biochem.* **1986**, *55*, 69–102.
[11] W. L. Smith, L. J. Marnett, D. L. DeWitt, *Pharmacol. Ther.* **1991**, *49*, 153–179.
[12] M. Hamberg, J. Svensson, B. Samuelsson, *Proc. Natl. Acad. Sci. USA* **1975**, *72*, 2994–2998.
[13] R. A. Johnson, D. R. Morton, J. H. Kinner, R. R. Gorman, J. C. McGuire, F. F. Sun, N. Whittaker, S. Bunting, J. Salmon, S. Moncada, J. R. Vane, *Prostaglandins* **1976**, *12*, 915–928.
[14] U. Diczfalusy, P. Falardeau, S. Hammarström, *FEBS Lett.* **1977**, *84*, 271–274.
[15] J. Fried, J. Barton, *Proc. Natl. Acad. Sci. USA 1977*, *74*, 2199–2203.
[16] A. D. Rahimtula, P. J. O'Brien, *Biochem. Biophys. Res. Commun.* **1974**, *60*, 440–447.
[17] F. Lichtenberger, W. Nastainczyk, V. Ullrich, *Biochem. Biophys. Res. Commun.* **1976**, *70*, 939–946.
[18] V. Ullrich, H. Graf, *Trends Pharmacol. Sci.* **1984**, *5*, 352–355.
[19] S. Moncada, R. Gryglewski, S. Bunting, J. R. Vane, *Nature* **1976**, *263*, 663–665.
[20] P. Wlodawer, S. Hammarström, *FEBS Lett.* **1979**, *97*, 32–36.
[21] S. Bunting, R. Gryglewski, S. Moncada, J. R. Vane, *Prostaglandins* **1976**, *12*, 685–713.
[22] V. Ullrich, L. Castle, P. Weber, *Biochem. Pharmacol.* **1981**, *30*, 2033–2036.
[23] H. Graf, V. Ullrich in *Cytochrome P450, Biochemistry, Biophysics and Environmental Implications* (Eds.: E. Hietanen, M. Laitanen, O. Hanninen), Elsevier, New York, **1982**, pp. 103–106.
[24] D. L. DeWitt, W. L. Smith, *J. Biol. Chem.* **1983**, *258*, 3285–3293.
[25] M. Hecker, V. Ullrich, *J. Biol. Chem.* **1989**, *264*, 141–150.
[26] L. Zhang, M. B. Chase, R.-F. Shen, *Biochem. Biophys. Res. Commun.* **1993**, *194*, 741–748.
[27] R. F. Shen, H. H. Tai, *J. Biol. Chem.* **1986**, *261*, 11592–11599.
[28] S. Hammarström, P. Falardeau, *Proc. Natl. Acad. Sci. USA* **1977**, *74*, 3691–3695.
[29] M. Haurand, V. Ullrich, *J. Biol. Chem.* **1985**, *260*, 15059–15067.
[30] H. S. Mason, J. C. North, M. Vanneste, *Fed. Proc.* **1965**, *24*, 1172–1180.
[31] A. Röder, E. Bayer, *Eur. J. Biochem.* **1969**, *11*, 89–92.
[32] H. A. O. Hill, A. Röder, R. J. P. Williams, *Struct. Bonding (Berlin)* **1970**, *8*, 123.
[33] S. C. Tang, S. Koch, G. C. Papaefthymiou, S. Foner, R. B. Frankel, J. A. Ibers, R. H. Holm, *J. Am. Chem. Soc.* **1976**, *98*, 2424–2434.
[34] P. M. Champion, B. R. Stallard, G. C. Wagner, I. C. Gunsalus, *J. Am. Chem. Soc.* **1982**, *104*, 5469–5472.
[35] R. Tsai, C.-A. Yu, I. C. Gunsalus, J. Peisach, W. Blumberg, W. H. Orme-Johnson, H. Beinert, *Proc. Natl. Acad. Sci. USA 1970*, *66*, 1157–1163.
[36] J. A. Peterson, *Arch. Biochem. Biophys.* **1971**, *144*, 678–693.
[37] Y. Hashimoto, T. Yamano, H. S. Mason, *J. Biol. Chem.* **1962**, *237*, 3843–3844.
[38] V. Ullrich, H. H. Ruf, P. Wende, *Croat. Chem. Acta* **1977**, *49*, 213–222.
[39] T. L. Poulos, B. C. Finzel, A. J. Howard, *J. Mol. Biol.* **1987**, *195*, 687–700.
[40] T. L. Poulos, B. C. Finzel, I. C. Gunsalus, G. C. Wagner, J. Kraut, *J. Biol. Chem.* **1985**, *260*, 16122–16130.
[41] J. P. Collman, T. N. Sorrell, B. M. Hoffmann, *J. Am. Chem. Soc.* **1975**, *97*, 913–914.
[42] T. Omura, R. Sato, *J. Biol. Chem.* **1964**, *239*, 2370–2378.
[43] D. R. Nelson, T. Kamataki, D. J. Waxman, F. P. Guengerich, R. W. Estabrook, R. Feyereisen, F. J. Gonzalez, M. J. Coon, I. C. Gunsalus, O. Gotoh, K. Okuda, D. W. Nebert, *DNA Cell Biol.* **1993**, *12*, 1–51.
[44] C. Yokoyama, A. Miyata, H. Ihara, V. Ullrich, T. Tanabe, *Biochem. Biophys. Res. Commun.* **1991**, *178*, 1479–1484.
[45] K. Ohashi, K.-H. Ruan, R. J. Kulmacz, K. K. Wu, L.-H. Wang, *J. Biol. Chem.* **1992**, *267*, 789–793.
[46] J. A. Salmon, R. J. Flower, *Methods Enzymol.* **1982**, *86*, 93–99.
[47] M. Hecker, M. Haurand, V. Ullrich, U. Diczfalusy, S. Hammarström, *Arch. Biochem. Biophys.* **1987**, *254*, 124–135.
[48] C. Yokoyama, A. Miyata, K. Suzuki, Y. Nishikawa, T. Yoshimoto, S. Yamamoto, R. Nüsing, V. Ullrich, T. Tanabe, *FEBS Lett.* **1993**, *318*, 91–94.
[49] P. Needleman, A. Raz, M. S. Minkes, J. A. Ferrendelli, H. Sprecher, *Proc. Natl. Acad. Sci. USA 1979*, *76*, 944–948.
[50] S. Fischer, P. C. Weber, *Nature* **1984**, *307*, 165–158.
[51] S. Hammarström, U. Diczfalusy, *Adv. Prostaglandin Thromboxane Res.* **1980**, *6*, 267–274.
[52] K. Kato, S. Ohkawa, S. Terao, Z. Terashita, K. Nishikawa, *J. Med. Chem.* **1985**, *28*, 287–294.
[53] M. Hecker, M. Haurand, V. Ullrich, S. Terao, *Eur. J. Biochem.* **1986**, *157*, 217–223.
[54] M. Hecker, V. Ullrich, *Biochem. Pharmacol.* **1988**, *37*, 3363–3365.
[55] W. A. Pryor, J. P. Stanley, *J. Org. Chem.* **1975**, *40*, 3614–3615.
[56] J. A. Turner, W. Herz, *Experientia* **1977**, *33*, 1133–1134.
[57] H. Graf, H. H. Ruf, V. Ullrich, *Angew. Chem.* **1983**, *95*, 497–498; *Angew. Chem. Int. Ed. Engl.* **1983**, *22*, 487–488.
[58] G. L. Bundy, *Tetrahedron Lett.* **1975**, 1957–1960.
[59] M. Hecker, V. Ullrich, *Eicosanoids* **1988**, *1*, 19–25.
[60] R. F. Doolittle, P. Bork, *Sci. Am.* **1993**, *269*(4), 34–40.
[61] V. Ullrich, *J. Mol. Catal.* **1980**, *7*, 159–167.
[62] V. Ullrich, *Angew. Chem.* **1972**, *84*, 689–710; *Angew. Chem. Int. Ed. Engl.* **1972**, *11*, 701–712.
[63] R. E. White, M. J. Coon, *Annu. Rev. Biochem.* **1980**, *49*, 315–356.
[64] J.-A. Gustafsson, L. Rondahl, J. Bergman, *Biochemistry* **1979**, *18*, 865–870.
[65] J. T. Groves, W. J. Kruper, Jr., *J. Am. Chem. Soc.* **1979**, *101*, 7613–7615.
[66] J. T. Groves, W. J. Kruper, Jr., R. C. Haushalter, *J. Am. Chem. Soc.* **1980**, *102*, 6375–6377.
[67] M. Hecker, W. J. Baader, P. Weber, V. Ullrich, *Eur. J. Biochem.* **1987**, *169*, 563–569.
[68] J. T. Groves, G. A. McGlusky, R. E. White, M. J. Coon, *Biochem. Biophys. Res. Commun.* **1978**, *81*, 154–160.
[69] W.-C. Song, A. R. Brash, *Science* **1991**, *253*, 781–783.
[70] J. E. Baldwin, *J. Heterocycl. Chem.* **1990**, *27*, 71–78.
[71] J. E. Baldwin, R. M. Adlington, D. G. Marquess, A. R. Pitt, A. T. Russell, *J. Chem. Soc. Chem. Commun.* **1991**, 856–858.
[72] J. H. Dawson, M. Sono, *Chem. Rev.* **1987**, *87*, 1255–1276.
[73] J. H. Dawson, *Science* **1988**, *240*, 433–439.
[74] R. D. Libby, J. A. Thomas, L. W. Kaiser, L. P. Hager, *J. Biol. Chem.* **1982**, *257*, 5030–5037.

Toxicity of Chlorinated Organic Compounds: Effects of the Introduction of Chlorine in Organic Molecules

Dietrich Henschler*

Industrial "chlorine chemistry" is accused of polluting the environment with its products and having adverse effects on health. The accusation has been followed by the demand that this ill-defined branch of chemistry be simply abolished, a demand which has been repeated vigorously now for years. It grew out of misgivings such as those summarized here: 1. A number of polychlorinated cyclic compounds are very stable and highly lipophilic so that they accumulate in the environment and affect mankind through the food chain. Prominent examples are chlorinated pesticides, biphenyls, dibenzodioxins, and dibenzofurans. 2. Many chlorinated compounds are toxic for man and animals. Their genotoxicity (mutagenicity and carcinogenicity) plays a role in risk assessment; more and more chlorinated organic compounds are being shown to be carcinogenic and classified accordingly.

To date there are no comprehensive reviews of the toxicology of chlorinated organic compounds. The present treatise is the result of an attempt to analyze the situation systematically. It makes generalizations as to the kind and degree of toxicity of the most important classes of chlorinated organic compounds and elaborates recommendations for reduction and avoidance of risk during production, occupational handling, and general use.

1. Introduction

The present review is the condensed version of a detailed documentation,[1] which is to appear simultaneously as a monograph; wherever necessary in the text below, reference is made to this detailed account of the original data.

The study was based on the following questions:

1. What is the effect of the introduction of chlorine substituents on the toxicity of organic compounds?
2. Is there a defined relationship between the number of chlorine substituents introduced and the kind and degree of toxic effects in specific homologous groups of compounds?
3. Is it also possible to establish general rules for the effect of number and position of the chlorine substituents introduced on the toxicity of organic compounds of different classes?
4. Is it possible to identify "toxophoric" groups in chlorinated organic compounds and could such knowledge be used for purposes of risk reduction and avoidance when developing new chemical products?
5. What are the molecular mechanisms responsible for the toxicity or increases in toxicity of chlorinated organic compounds?

[*] Prof. Dr. D. Henschler
Institut für Toxikologie der Universität
Versbacher Strasse 9, D-97078 Würzburg (FRG)
Telefax: Int. code + (931)201-3446

Not all classes of chlorinated organic compounds were analyzed systematically in this study; a selection had to be made because of the differing and often inadequate amounts of data available. An initial overview of this extensive field revealed that relationships within classes are clearest in the series of chlorinated alkanes, alkenes, and alkynes. Data are also available—although not as plentiful—for chlorinated derivatives of benzene and phenol. The analysis concentrates on these five large classes of compounds.

Polychlorinated polycyclics such as the insecticides, DDT, lindane, aldrin, and dieldrin, polychlorinated biphenyls, polychlorinated fatty acids, and polychlorinated dibenzodioxins and dibenzofurans are not analyzed systematically in this review. These classes of compounds have been the subject of numerous systematic studies in recent years; the reader is referred to the relevant monographs and reviews. However, since these polychlorinated polycyclics share significant toxicological features which distinguish them, especially with respect to their carcinogenic potential, from the aliphatic and monocyclic compounds, their features are discussed separately in Section 14.

The analysis of toxicology and risk assessment is based on the following criteria: acute toxicity, subacute and subchronic toxicity, chronic toxicity, genotoxicity in the form of mutagenic and carcinogenic effects, and reproductive toxicity. Neurotoxicity and allergic effects could not be studied systematically because such data are available for only few compounds. The cases where such kinds of effect are known to be associated with the

 © VCH Verlagsgesellschaft mbH, D-69451 Weinheim, 1994 0570-0833/94/1919-1920 $ 10.00+.25/0 Angew. Chem. Int. Ed. Engl. 1994, 33, 1920–1935

introduction of chlorine into organic compounds are mentioned in the text.

2. C–Cl Bonds: Chemical Reactivity and Toxicological Properties

The presence of a chlorine–carbon bond affects the chemical properties of organic compounds and also has consequences on their toxicological behavior:

- The electron-withdrawing effect of chlorine, like that of other electron-withdrawing elements (e.g. F, O, N, P), increases the electrophilicity of the C atom to which it is attached. This facilitates or enables nucleophilic attack (with displacement of chlorine) on sp^3 carbon atoms; neighboring H atoms (α-position) and C–H bonds (β-position) are more highly polarized and H^+ elimination is facilitated.
- The relatively low binding energy of the C–Cl bond in alkanes (326 kJ mol^{-1}) results in relatively high chemical reactivity.
- The introduction of chlorine substituents makes organic compounds more lipophilic, facilitating interactions with hydrophobic sites, for example, in enzymes, and promoting enzymatic biotransformation in general.
- The inductive and/or mesomeric effects of a chlorine substituent influence the neighboring C–C sequences; the toxicological consequences depend on the class of compound involved:

  In alkanes the C–C bond becomes more labile so that oxidative attack can cleave bonds and result in radical formation.

  In alkenes the C=C bond is stabilized; this favors the insertion of oxygen to form reactive oxiranes during enzymatic oxidative attack because direct substitution is impeded or no longer possible. The situation is similar in arenes.

  In alkynes the reactivity of the C≡C bond is increased; this favors addition reactions.
- A chlorine substituent in allylic position is a good leaving group and facilitates the formation of resonance-stabilized carbocations which, by covalent binding to nucleophilic sites in biochemical structures, can produce primary toxic lesions and, in particular, genotoxic changes.

Thus it may be deduced that the introduction of chlorine substituents into organic compounds generally leads to increased chemical and biological reactivity and so to increased toxicity. In cases where enzymes activate chlorinated organic compounds to toxic intermediates, however, the situation is further complicated by the fact that the enzymes are not uniformly distributed, neither in the organism, nor in organs, nor in subcellular compartments. Because of the necessity to eliminate metabolic waste products, higher terrestrial organisms are equipped with enzyme systems which make lipophilic compounds more water-soluble and thus more readily eliminated in the urine. Thus lipophilicity is a prerequisite for this kind of enzymatic conversion; the enzyme apparatus is equipped with lipid membranes with appropriate solvent properties. The introduction of chlorine substituents into organic compounds generally makes them more lipophilic. Therefore it is to be expected that, in spite of their frequently increased chemical stability, chlorinated organic compounds are converted enzymatically more readily than their chlorine-free analogues.

The effects of all of these individual factors on chemical reactivity and toxicity have been studied in several series of homologous and analogous compounds, sometimes in detail. However, since, on the one hand, numerous other factors also influence the effects and, on the other, the enzyme systems involved have not yet been studied systematically, particularly, in warm-blooded organisms and their mechanisms of action are not fully understood, the effects of introducing chlorine into organic compounds may be predicted only to a very limited extent. Therefore, tests in appropriate biological systems are generally required to confirm or disprove such predictions.

3. Chlorinated Methane Derivatives

Methane is considered to be physiologically inert; toxic reactions are therefore not expected under the usual test conditions. Some of the few early inhalation studies have shown that methane first has effects on the organism when the concentrations in the inhaled air are above 50%. These effects are ascribed to lack of oxygen which can be prevented by increasing the partial pressure of oxygen in the inhaled test mixture. When sufficient oxygen is present, methane can be shown to have very weak central depressive (anesthetic) effects.



Dietrich Henschler, born 1924 in Glösa, studied medicine at the Universität Würzburg and obtained his doctorate in 1953 with a thesis on the laxative anthranol/anthraquinone glycosides. In 1953 he joined the Department of Pharmacology at the Universität Würzburg and obtained his "Habilitation" under W. Neumann with a thesis on structure-activity relationships and mechanisms of action of neurotoxic triaryl phosphates. In 1964 he became Associate Professor and in 1965 was appointed Professor of the new chair of Toxicology and Pharmacology at the Universität Würzburg. From 1969 onwards, he was chairman of the DFG Commission for the Investigation of Health Hazards of Chemical Compounds in the Work Area (MAK Commission). His work has centred on studies of the molecular toxicology of chlorinated organic compounds, especially chlorinated vinylic structures, and mechanisms of the organ specificity of cancerous manifestations. He is co-author of the leading text book in his field and of a series of toxicological monographs on hazardous substances at the workplace.

For all methane derivatives the introduction of chlorine results in toxic activity with various kinds of effect on the organism.[1]

The toxicology of a great number the chlorinated methanes has been studied intensively. Table 1 shows a synopsis of the results obtained in the various kinds of toxicity tests.

Acute toxicity: The LC_{50} and LD_{50} values obtained cannot generally be compared directly[1] because of non-uniform test conditions (different animal strains, exposure times, observation periods, etc.). The order of toxicity shown in the table was estimated taking these parameters into account. Differences in the order of toxicity for different administration routes (Table 1) may be explained in terms of the mechanisms of action involving different metabolic activation reactions (see below); the extent to which such reactions occur also depends on the administration route. The values given in Table 1 for the order of toxicity permit semiquantitative comparisons.

Chronic toxicity: Little data is available for a comparative evaluation. The MAK values (maximum workplace concentrations) shown as a guide demonstrate the influence of the number of chlorine substituents on the toxicity of the compounds. Dichloromethane appears not to fit into the series; this is illusory, resulting from the fact that only this MAK value is based on an acute effect (increase of the level of carboxyhemoglobin).

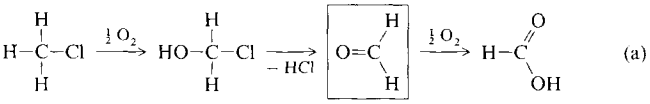
Mutagenicity: This is described in more than 80 publications; for all four compounds positive findings have been published. However, for trichloromethane and tetrachloromethane, negative results predominate numerically in bacterial tests (Ames test). Apart from chloromethane, all these compounds require metabolic activation to become mutagenic.

Carcinogenicity: All four chlorinated methane derivatives have yielded positive results in both mice and rats. There are also negative results but they can be ascribed to inadequate dose levels. The overall carcinogenic potency of the chlorinated methanes is relatively weak. At present, all these compounds are classified in Category IIIB[*] in the "List of MAK and BAT Values"[2] (see Table 6).

Reproductive toxicity: Tests revealed no evidence of prenatal toxicity except with chloromethane, which induced cardiac malformations.

Mechanisms of action: The toxicological mechanisms of action of the four chlorinated methane derivatives are fundamentally different. They account for both the kinds of toxicity and for the relative degrees of toxicity of these substances, especially for the differences in genotoxicity, in terms of the different chemical nature of the metabolically formed reactive intermediates.

Chloromethane is converted oxidatively by cytochrome P450 enzymes to formaldehyde[3] [Eq. (a)] which has been shown in in vitro test systems to be mutagenic. It is also conceivable that chloromethane itself has direct alkylating action; this could, however, not be distinguished unequivocally from the effects of formaldehyde.



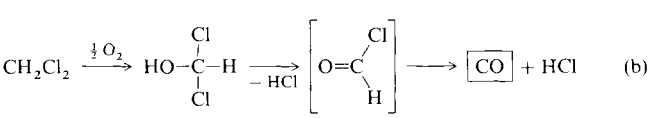
(a)

Table 1. Toxicity of chlorinated methanes: semiquantitative comparison on the basis of original data (given in detail in ref. [1]). Order of toxicity: 1 is the most toxic, 4 is the least toxic.

		CH_3Cl	CH_2Cl_2	$CHCl_3$	CCl_4	Comments
Acute toxicity	inhalation	1	4	3	2	order of toxicity, determined as LC_{50} or LD_{50} values
	ingestion	2	3	1	4	
	intraperitoneal	[a]	2	1	3	
	subcutaneous	[a]	1	2	3	
Chronic toxicity (critical toxicity)	MAK value/ $mL\,m^{-3}$	50 (kidney, male fertility)	100 (CO Hb level)	10 (kidney, liver)	10 (liver, kidney)	MAK value not comparable for CH_2Cl_2 because based on an acute effect
Mutagenicity						for $CHCl_3$ and CCl_4 mainly negative results
point mutations		+	+	(+)	(+)	
chromosomes aberrations		+	+	+	+	
cell transformations		+	+	+	+	
Carcinogenicity		+	+	+	+	results of carcinogenicity studies heterogeneous, positives all weak
Reproductive toxicity		+	(−)	(−)	(−)	(−) = only maternal toxicity + = cardiac malformations

[a] Not determined.

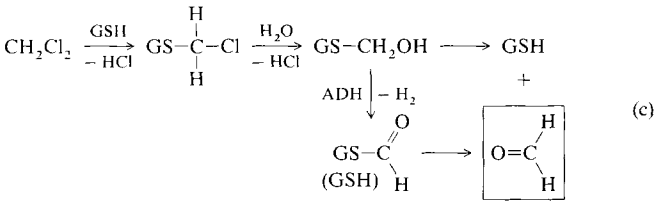
The situation is quite different for dichloromethane. This substance is also a substrate for P450 enzymes [Eq. (b)]. Formyl chloride which is the formal product of this reaction decomposes, however, to yield HCl and CO, and the latter determines



(b)

[*] Carcinogenic substances are summarized in Group III. This group is subdivided into A1, A2, and B (see Tables 4, 5, and 6).

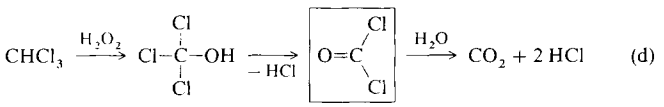
the toxicity by causing carboxyhemoglobin formation.[4] Genotoxicity is not associated with this metabolic pathway but, in addition to the oxidative (P450) metabolic pathway, there is also a reductive pathway[5] [Eq. (c)] involving coupling to glutathione (GSH).



(c)

The chloromethyl glutathione formed is considered to have alkylating activity and this would account for the genotoxic effects of dichloromethane.[6] However, this adduct is also converted to the mutagen, formaldehyde, by alcohol dehydrogenases (ADH). In any case, the demonstration of mutagenicity of dichloromethane in the Ames test requires the addition of glutathione and the enzyme glutathione transferase.[7] It has been suggested recently that the lung tumors observed in mice can be attributed to the presence of certain glutathione transferases which have a high specificity for dichloromethane coupling; these glutathione transferases are not found in other species.[8]

The oxidative action of cytochrome P450 on trichloromethane yields phosgene (carbonyl chloride)[9] [Eq. (d)] which,



(d)

being an acid chloride, is considered to have mutagenic properties; however, these have not yet been demonstrated for phosgene itself because of methodological problems.

The mechanism of the oxidative activation of carbon tetrachloride is again different since no C–H bond is available in this compound; activated oxygen formed by cytochrome P450-dependent monooxygenases (Mfo) cause the homolysis of a C–Cl bond [Eq. (e)] and formation of a trichloromethyl radical[10] which can produce genotoxic effects by binding to DNA.



(e)

Summary: All chlorinated methane derivatives have central anesthetic effects. This property, which is already present in methane although so weakly that it can be demonstrated only with difficulty, becomes marked with the introduction of chlorine, and increases with the number of chlorine substituents in the molecule. Trichloromethane (chloroform) was used as an anesthetic in surgery for almost one and a half centuries. The introduction of chlorine into the methane molecule, however, also opens the way for metabolic attack which results in toxic effects in other organs with all four chlorinated derivatives; the toxic effects are quite different in each case: chloromethane produces central nervous degeneration, dichloromethane carboxyhemoglobin formation, and trichloromethane and tetrachloromethane liver and kidney damage. Although the enzymatic activation yields different reactive metabolites from each of these compounds, all four have genotoxic properties, the prerequisite for their demonstrated carcinogenicity.

4. Chlorinated Ethane Derivatives

Ethane also has central anesthetic properties which, although somewhat more pronounced than those of methane, are still too weak for them to have been useful for medical purposes. The introduction of chlorine increases the anesthetic effects markedly;[11] chloroethane was used for a time as a mild anesthetic for short operations.

Acute toxicity: Studies in which the substance was administered by inhalation have been carried out with all the chlorinated ethanes apart from 1,1-dichloroethane and hexachloroethane, in most cases with rats. The acute toxicity of the derivatives, measured as LC_{50} values,[11] decreases in the order:

1,1,2,2-tetrachloroethane $\geqq$ 1,1,2-trichloroethane > pentachloroethane > 1,2-dichloroethane $\gg$ 1,1,1-trichloroethane $\gg$ chloroethane

In mice too, 1,1,2,2-tetrachloroethane is the most toxic derivative. The oral toxicity has been studied much less frequently than the inhalation toxicity but, where comparisons are possible, they confirm the order of toxicity seen in the inhalation studies. Similarly, the few LD_{50} values available for intraperitoneal, subcutaneous, and dermal administration are in accordance with the above order. The large difference between the toxicities of 1,1,2-trichloroethane and 1,1,1-trichloroethane is significant (four-hour LC_{50} values in the rat 2000 and 18000 $mL\,m^{-3}$, respectively, with similar differences for oral and intraperitoneal toxicity). This difference results from the fact that the metabolism of 1,1,2-trichloroethane yields the reactive intermediates chloroacetyl chloride and dichloroacetaldehyde, whereas 1,1,1-trichloroethane produces the much less toxic metabolites trichloroethanol, trichloroethanal (chloral), and trichloroacetic acid.

Chronic toxicity: Studies have been carried out for only a few chlorinated ethanes so that a systematic comparison of the long-term toxicity of all the members of this series is not possible. Here too, the MAK values[2] provide the best available measure of toxicity since long-term exposure to low concentrations of all of the compounds leads to toxic effects in parenchymatous organs, especially the liver. The data shown in Table 2 reveal a characteristic trend; the former MAK value of 1000 $mL\,m^{-3}$ for chloroethane was withdrawn recently because the substance has been shown to be carcinogenic.

The difference in the chronic toxicities of 1,1,1-trichloroethane and 1,1,2-trichloroethane, as for the acute toxicities, is a result of differences in metabolism. In addition, the data indicate that the chronic toxicity in this series of compounds increases drastically with the number of chlorine substituents.

Table 2. MAK values of chlorinated ethane derivatives [2].

Substance	MAK value/ mL m^{-3}	Target organs
chloroethane	[1000] [a]	lung, liver
1,1-dichloroethane	100	liver, kidney
1,1,1-trichloroethane	200	liver
1,1,2-trichloroethane	10	liver, kidney
1,1,2,2-tetrachloroethane	1	liver
pentachloroethane	5	liver
hexachloroethane	1	liver

[a] This value was withdrawn recently because the substance has been shown to be carcinogenic.

Mutagenicity: Tests on the mutagenic properties have been carried out with all the chlorinated ethanes. Positive results for mutagenicity were obtained with all the compounds except one, in every case after metabolic activation. This statement is not affected by the fact that for some of the compounds both positive and negative test results have been published; such inconsistent results are not unusual with substances which develop their mutagenic properties only after metabolic activation. The activation mechanism has been elucidated for 1,2-dichloroethane (see below). The only exception in this series of compounds is 1,1,1-trichloroethane which is converted metabolically via trichloroethanol and chloral to trichloroacetic acid; these metabolites are only weakly or not mutagenic; elimination of chlorine, which would yield reactive intermediates, does not occur.

Carcinogenicity: 1,2-dichloroethane has been shown to be unequivocally carcinogenic (A2 see also Table 5) in animal studies. Chloroethane (B, see Table 6), 1,1,2-trichloroethane (B), and 1,1,2,2-tetrachloroethane (B only in mice) are suspected carcinogens. Pentachloroethane and hexachloroethane have also proved to be carcinogenic. The mechanism of action for 1,2-dichloroethane has been shown[111] to involve coupling with glutathione (GSH) and formation of an episulfonium ion which has alkylating properties [Eq. (f)].

$$ClCH_2-CH_2Cl \xrightarrow[-HCl]{GSH} ClCH_2-CH_2-SG \longrightarrow \begin{matrix} H_2C \\ | \\ H_2C \end{matrix}\!\!>\!\!SG \qquad (f)$$

Summary: Like the chlorinated methanes, the chlorinated ethane derivatives have central anesthetic effects (anesthesia) which increase with the number of chlorine substituents. Accordingly, the acute toxicity also increases with the number of chlorine substituents up to four, and then decreases. The chronic toxicity is even more clearly dependent on the number of chlorine substituents, increasing up to six substituents; liver cell damage is the principle symptom of intoxication. In the series of chlorinated ethanes, as in the methanes, introduction of chlorine results in genotoxic activity. There are fewer positive mutagenicity results than with the chlorinated methane derivatives but this is most likely a matter of chance. Six of the chlorinated ethanes are carcinogenic; the mechanism demonstrated for 1,2-dichloroethane involves metabolic formation of an episulfonium ion after coupling with glutathione. The only non-genotoxic member of the series is 1,1,1-trichloroethane; this may be ascribed to the metabolic stability of the CCl_3 group.

5. Chlorinated Ethene Derivatives

Because of their industrial importance, chlorinated ethenes have been the subject of by far the most toxicity tests. Like methane and ethane, ethene has central anesthetic properties which are much more marked; ethene has been used as an anesthetic in clinical trials. Here too, chlorine substituents increase the anesthetic effects significantly;[1] trichloroethene was used for a long time as a mild anesthetic in obstetrics.

Ethene can be activated in oxidative metabolism to a genotoxic oxirane. The introduction of chlorine increases this kind of effect.[1]

Acute toxicity: All the chlorinated ethene derivatives, apart from 1,2-dichloroethene, have been studied in inhalation tests in both mice and rats and, in some cases, also in hamsters.[1] In this series of substances too, the LC_{50} values cannot be compared directly because of different exposure times and observation periods. However, the order of toxicity in both the mouse and rat is clear:

1,1-dichloroethene > tetrachloroethene > trichloroethene ≫ monochloroethene

The mouse is particularly sensitive to the renal and hepatic toxicity of 1,1-dichloroethene. The order of toxicity reflects the anesthetic effectiveness of the substances; that is, the cause of death in these studies was respiratory failure and/or circulatory collapse.

In acute oral toxicity tests, *trans*-1,2-dichloroethene was studied as well. The order of toxicity (LD_{50} values) found for the substances was different in mice and rats:

Mouse: 1,1-dichloroethene > *trans*-1,2-dichloroethene > trichloroethene ≫ tetrachloroethene

Rat: *trans*-1,2-dichloroethene ≧ 1,1-dichloroethene > tetrachloroethene > trichloroethene

Thus, the mouse is much more sensitive to trichloroethene than the rat to tetrachloroethene. These differences cannot yet be explained.

After intraperitoneal administration, the order of toxicity of these substances is largely the same in the mouse and rat:

trans-1,2-dichloroethene > trichloroethene > tetrachloroethene

Chronic toxicity: Chlorinated ethene derivatives have been studied intensively with regard to their chronic toxicity on inhalation because of the great practical importance of these substances. With all the compounds, the primary effects are liver and/or kidney damage which is most marked with 1,1-dichloroethene. This is reflected in the MAK values[2] (Table 3).

The dependence of chronic toxicity on the number of chlorine substituents is not as clear for the ethene derivatives as for chlorinated alkanes; this is a result of differences in the metabolic bioactivation reactions (see below).

Table 3. MAK values of chlorinated ethene derivatives [2].

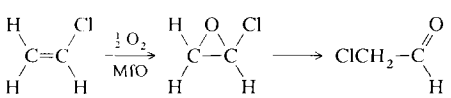
Substance	MAK value/ mL m^{-3}	Target organs
chloroethene (vinyl chloride)	[100] [a]	liver, kidney
1,1-dichloroethene	2	kidney
1,2-dichloroethene (*cis* and *trans*)	200	liver, kidney
trichloroethene	50	liver, kidney
tetrachloroethene	50	liver, kidney

[a] This value was withdrawn recently because the substance has been shown to be carcinogenic.

Mutagenicity: Numerous mutagenicity tests have been carried out on chlorinated ethene derivatives. None of the compounds is mutagenic as such; the activity develops after metabolic activation. Chloroethene, 1,1-dichloroethene, 1,2-dichloroethene, and trichloroethene are activated oxidatively and then yield positive results in mutagenicity tests. Trichloroethene and tetrachloroethene are activated by coupling with glutathione (the mechanism is described below). Thus indirect mutagenicity has been demonstrated for all the chlorinated ethene derivatives.

Carcinogenicity: The carcinogenicity of vinyl chloride has been demonstrated unequivocally in both man and experimental animals. In exposed workers, an otherwise very rare hemangiosarcoma of the liver was observed; it is not certain whether the substance is also a lung carcinogen. In experimental animals, tumors at several other locations were seen as well as the same kind of hepatic hemangiosarcomas. That vinyl chloride is carcinogenic suggested that all chlorinated ethenes could have carcinogenic potential. The suspicion has, however, not yet been confirmed in any other case as it has for vinyl chloride. 1,1-Dichloroethene, trichloroethene, and tetrachloroethene are classified in Category IIIB in the "List of MAK and BAT Values"[2] but the carcinogenicity of these substances is only weak. With trichloroethene and tetrachloroethene, a low incidence of kidney carcinomas was observed in rats. Recent observations suggest that trichloroethene also causes kidney tumors in man after long-term high-level exposure.[18] The mechanism may be explained in terms of a specific kind of metabolic transformation (see Scheme 1).

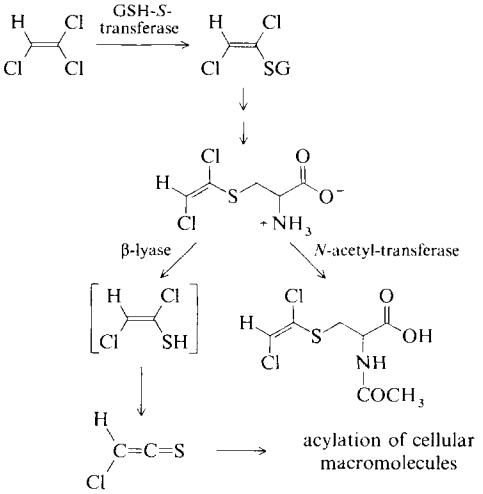
Mechanism of action: All chlorinated ethene derivatives are converted to reactive oxiranes by metabolism with cytochrome P450-dependent monooxygenases. The oxiranes can alkylate or acylate essential macromolecules, either directly or after intramolecular rearrangement to chlorinated aldehydes or acyl chlorides. The mechanism has been most intensively studied with vinyl chloride[12] [Eq. (g)].



(g)

In this manner, 1,1-dichloroethene is converted to chloroacetyl chloride, 1,2-dichloroethene to dichloroacetaldehyde, and tetrachloroethene to trichloroacetyl chloride.[13] With trichloroethene there are two possible rearrangement products, trichloroacetaldehyde and dichloroacetyl chloride; the formation of trichloroacetaldehyde (chloral) is thermodynamically favored.[13]

Trichloroethene and tetrachloroethene are not only metabolized by the oxidative pathway but also by a reductive pathway involving coupling to glutathione. This results in a complex sequence of additional activation steps which terminates in the formation of chlorinated thioketenes,[14] electrophilic species which have recently been shown to react with DNA[15] (Scheme 1).



Scheme 1. SG = glutathionyl.

The glutathione adduct formed in the primary step of this sequence is converted by cleavage of glutamic acid and glycine to the cysteine adduct which can either be *N*-acetylated to form the mercapturic acid, which is readily eliminated in the urine, or be enzymatically cleaved by β-lyase to yield a reactive thiol. Dehydrochlorination of the thiol yields the thioketene derivative.[16] The β-lyase is present in particularly high levels in the renal tubules and this accounts for the marked organ specificity associated with this class of compounds (renal carcinomas). The cysteine derivatives of trichloroethene, tetrachloroethene, dichloroacetylene, and hexachlorobutadiene are highly mutagenic.[17]

Summary: Ethene has central anesthetic activity which increases after the introduction of chlorine depending on the number of chlorine substituents. All chlorinated ethene derivatives have more or less severe toxic effects and some are genotoxic. In every case, these effects result from the action of metabolically formed reactive intermediates. The main metabolic pathway involves addition of oxygen to the olefinic bond to yield highly electrophilic oxiranes. These can rearrange to chlorinated aldehydes or acyl chlorides; acyl chloride formation is to be seen as a detoxication reaction. Chloroethene, 1,1-dichloroethene, and trichloroethene have clearly genotoxic and to different extents carcinogenic effects. In addition, trichloroethene and tetrachloroethene are metabolized by reductive processes which begin with the coupling to glutathione and end with the formation of electrophilic thioketenes. This metabolic pathway is responsible for the renal carcinogenicity of these substances. Recent

studies seem to confirm the renal carcinogenic activity of trichloroethene in man.[18]

6. Chlorinated Ethyne Derivatives

Acetylene (ethyne) has much more pronounced central anesthetic effects than ethene. The introduction of chlorine into the molecule, however, makes it so unstable that the expected (increase in) central anesthetic activity can no longer be demonstrated. Instead, dichloroacetylene has unique neurotoxic effects: it damages selectively the fifth cranial nerve (*N. trigeminus*). Dichloroacetylene is a frequent contaminant (degradation product) of trichloroethene or 1,1,2,2-tetrachloroethane; in such mixtures it is relatively stable.[19]

The acute inhalation toxicity of dichloroacetylene is extremely high: the six-hour LC_{50} value for the mouse is only 19 mL m^{-3}, the four-hour LC_{50} value for the rat is 55 mL m^{-3}.[20]

Dichloroacetylene is one of the most powerful known carcinogens. Exposure of mice and rats to a dichloroacetylene concentration of 9 or 14 mL m^{-3} for six hours, once or twice weekly, results in a high incidence of cystadenocarcinomas and cystadenomas of the kidney.[21] The mechanism of action involves enzymatic coupling with glutathione (GSH) to form 1,2-dichlorovinylglutathione, formation of the cysteine derivative, and its cleavage by β-lyase,[22] as has been described already for trichloroethene (see Section 5, Scheme 1).

7. Chlorinated Propane Derivatives

There is much less data available for this class of substances[1] than for the C_1 and C_2 compounds so that the general effects of introducing chlorine into the molecule are less clearly documented. However, propane itself has been tested for acute toxicity on inhalation; the 15-minute LC_{50} value is said to be more than 800 000 mL m^{-3}.

Acute toxicity: The four-hour LC_{50} values for the chlorinated propane derivatives tested in the rat can be compared directly and reveal the following order of toxicity:

1,2,3-trichloropropane (550 mL m^{-3}) > 1,1,2-trichloropropane (2000) > 1,2-dichloropropane (2900) > 1,1-dichloropropane (4000) > 1,1,1-trichloropropane (8000)

Once more, the 1,1,1-trichloro compound is the least toxic, a result of the stability of the trichloromethyl group to metabolic transformation. The chlorinated propane derivatives are more toxic than the corresponding ethane derivatives.

The relative acute oral toxicity of the chlorinated propane derivatives corresponds essentially with that seen after inhalation. However, 1,2,3-trichloropropane, tested in the rat in a comparative study with 1,2,2-trichloropropane, 1,1,2-trichloropropane, 1,1,1-trichloropropane, 1,2-dichloropropane, and 1,1-dichloropropane, is conspicuous for its very low oral LD_{50} value; it is only one third of the values found for 1,2,2-trichloropropane and 1,1,2-trichloropropane.

Subchronic and chronic toxicity: Very few studies of subchronic and chronic toxicity of chlorinated propanes have been carried out so that comparisons as for the other groups are not possible. There are MAK values[2] (now withdrawn) for 1,2-dichloropropane (75 mL m^{-3}) and 1,2,3-trichloropropane (50 mL m^{-3}). Neither value is adequately grounded but their dimension and order do confirm the general rule in the series of chlorinated alkanes that the toxicity increases with the number of chlorine substituents. The target organs identified in subchronic studies were liver and kidney.

Mutagenicity and carcinogenicity: 1,2-dichloropropane and 1,2,3-trichloropropane have, because of their industrial importance, been tested for mutagenicity and carcinogenicity. The theory of oxidative metabolism[12] with subsequent dehydrochlorination (formation of chlorinated acetones, aldehydes, or acyl chlorides) suggests that genotoxic activity is to be expected. The expectation has been fulfilled for 1,2-dichloropropane in individual tests and for 1,2,3-dichloropropane in most tests. In a long-term carcinogenicity study, 1,2-dichloropropane was not carcinogenic in the rat and weakly carcinogenic in the mouse (hepatocellular adenomas and carcinomas). 1,2,3-Trichloropropane, on the other hand, was clearly carcinogenic in both rat and mouse.

Summary: It may be concluded that in the group of propane derivatives as well, the introduction of chlorine into the molecule increases all toxic effects and produces genotoxicity.

8. Chlorinated Propene Derivatives

Some of the chlorinated propenes have been the subject of intensive toxicological study because of their use as pesticides (1,3-dichloropropene) or as starting materials for industrial syntheses (allyl chloride, 3-chloropropene).[1] The introduction of a chlorine substituent into an allylic position results in the formation of bifunctional agents in which not only the olefinic group plays a role, but also the chlorine as an active leaving group.[23] This has significant consequences for the toxicological behavior of the substances.

Acute toxicity: Several inhalation studies in the mouse and rat yielded LC_{50} values[1] in the following order of toxicity:

2,3-dichloropropene > 1,3-dichloropropene (*cis* and *trans*) > 3-chloropropene ≫ 2-chloropropene and 1-chloropropene

The situation for oral toxicity is a little different:

2,3-dichloropropene > 1,1,2,3-tetrachloropropene > 1,3-dichloropropene > 1,2,3-trichloropropene > 3-chloropropene ≫ 1-chloropropene

The few results available after intraperitoneal, subcutaneous, and dermal application are essentially consistent with the above order.

Chronic toxicity: There are only few comparable studies available. They indicate that 1,3-dichloropropene (technical mixtures and also the separated isomers) is about twenty times more toxic than allyl chloride. The mechanisms leading to the chronic toxicity have not been explained. It is not clear whether glutathione depletion, which plays an important role in the acute toxicity, is also significant for the chronic toxicity of these substances.

Mutagenicity: The mutagenicity of chlorinated propenes has been studied systematically.[24] All of the compounds in this

class which have a chlorine leaving group in allylic position are direct mutagens. The carbocation formed is resonance-stabilized and can alkylate nucleophilic reaction sites in essential macromolecules including DNA; some DNA adducts have been characterized.[25] Methyl substitution in any possible position increases the mutagenicity drastically.[24] Likewise, the introduction of a second chlorine substituent increases the mutagenicity to up to one hundred times that of allyl chloride.[23] The order of mutagenic potency found is as follows:

cis-1,3-dichloropropene > *trans*-1,3-dichloropropene ≫ 2,3-dichloropropene

Metabolic oxidation of the double bond to yield the oxirane, followed by intramolecular rearrangement, produces chloroacetone derivatives which are among the most powerful mutagens.[26]

Benzyl chloride ((chloromethyl)benzene) may also be seen as a chlorine-activated allyl compound; it is several times more mutagenic than allyl chloride.[24]

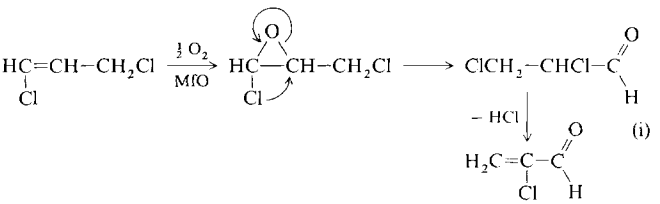
Carcinogenicity: A carcinogenic potential must be expected for the whole group of chlorinated propenes because they have all been shown to have genotoxic activity. To date, allyl chloride and 1,3-dichloropropenes of various grades of purity have been tested for carcinogenicity after oral administration. Allyl chloride was not carcinogenic in the rat and weakly carcinogenic in the mouse; it induced tumors in the forestomach, that is, at the site of contact with the biological material. This is as would be expected from the proposed mechanism of action (direct alkylation). 1-Chloropropene also produced forestomach tumors in mice. 1,3-Dichloropropene (technical mixture contaminated with 1% epichlorohydrin (1-chloro-2,3-epoxypropane)) yielded highly positive results in the rat and mouse and produced tumors in the stomach and the liver (rat) and also in the lung and urinary bladder (mouse). This marked carcinogenic activity has been ascribed to oxidation products in the technical mixture. The highly purified substance was no longer mutagenic and the addition of antioxidants to the technical mixtures largely prevented the formation of such oxidation products. Whether the carcinogenicity of the substance under practical conditions can be prevented by such measures is not known and does not seem very likely.

Mechanism of action: As already described in Section 4, the presence of the excellent leaving group (chlorine) in allylic position permits the formation of stable carbocations, as in the model case of allyl chloride [Eq. (h)]:

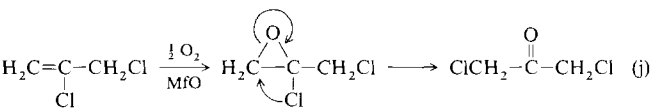
$$H_2C{=}CH{-}CH_2Cl \longrightarrow [H_2C{=}CH{=}CH_2]^+ + Cl^- \quad (h)$$

The stability of these cations has been calculated for a large number of homologous and analogous propene and butene derivatives;[23] it correlates well with the alkylating and mutagenic potency of the compounds.[24] DNA adducts have also been identified.[25]

In addition, the olefinic bond in chloropropene derivatives can be epoxidized by mixed function oxygenases (Mfo). The resulting oxiranes and the aldehydes and ketones formed by rearrangement are alkylating principles, for example, for 1,3-dichloropropene[26] [Eq. (i)] or for 2,3-dichloropropene [Eq. (j)].

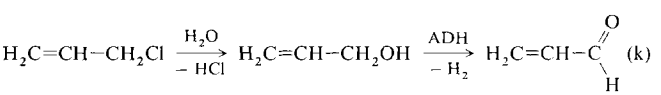


(i)



(j)

A third mechanism involves the hydrolysis of the allyl chlorine bond and subsequent oxidation of the alcohol to acrolein (2-propenal) [Eq. (k)]:



(k)

Acrolein, a bifunctional agent, attacks nucleophilic sites, for example, in DNA, by Michael addition[25] and so produces promutagenic DNA damage.

Thus there are three activation mechanisms which form highly alkylating and mutagenic intermediates from acrolein, chloroacrolein, and 1,3-dichloroacetone or the analogous compounds.[27] Which mechanisms are involved in specific cases is mainly determined by the simultaneously occurring enzymatic deactivation reactions; dominant is coupling to glutathione followed by formation of mercapturic acids which can be excreted in the urine.

Summary: The introduction of chlorine into propene, which itself is only weakly toxic, yields highly reactive compounds. As resonance-stabilized carbocations, these can alkylate essential biological macromolecules; alternatively, highly mutagenic products can be formed after enzymatic oxidation of the olefinic bond to yield oxiranes which rearrange to chlorinated aldehydes or ketones. Accordingly, all the chlorinated propene derivatives have been shown to be mutagenic and the few which have been tested to date in long-term animal studies have been found carcinogenic (1-chloropropene, 3-chloropropene, *cis*-1,3-dichloropropene, and *trans*-1,3-dichloropropene).

9. Chlorinated Butane Derivatives

Inhaled butane also has central depressive action; the effect is much more marked than that of propane. The four-hour LC_{50} value found for butane in the mouse was 282 $mL\,m^{-3}$ and in the rat 273 $mL\,m^{-3}$.[28] Introduction of chlorine into the molecule increases the toxicity in every respect.[1] The cytotoxicity of the chlorinated butanes is caused by metabolic activation products.

Acute toxicity: This has been investigated mainly after oral administration. The LD_{50} values[1] demonstrate that the toxicity increases with the number of chlorine substituents as follows:

2-chlorobutane > 1,1-dichlorobutane > 1-chlorobutane > pentachlorobutane ≫ hexachlorobutane > 1,2,3,4-tetrachlorobutane

Chronic toxicity: Insufficient data are available for this class of substances to make comparisons.

Genotoxicity: To date genotoxicity studies have been carried out with five chlorinated butane derivatives. Negative results were obtained with 1-chlorobutane and 1,4-dichlorobutane and weak positive results with *sec*-butyl chloride and *tert*-butyl chloride. 1,2,3,4-Tetrachlorobutane induced chromosomal aberrations in vivo. Thus a clear statement as to the mutagenic effects of the group as a whole is not possible.

Carcinogenicity: Studies have been carried out to date only with monochloro derivatives. Negative results were obtained with 1-chlorobutane after oral and intraperitoneal administration to mouse and rat; weak positive results were seen after intraperitoneal administration of *sec*-butyl chloride or *tert*-butyl chloride to the mouse.

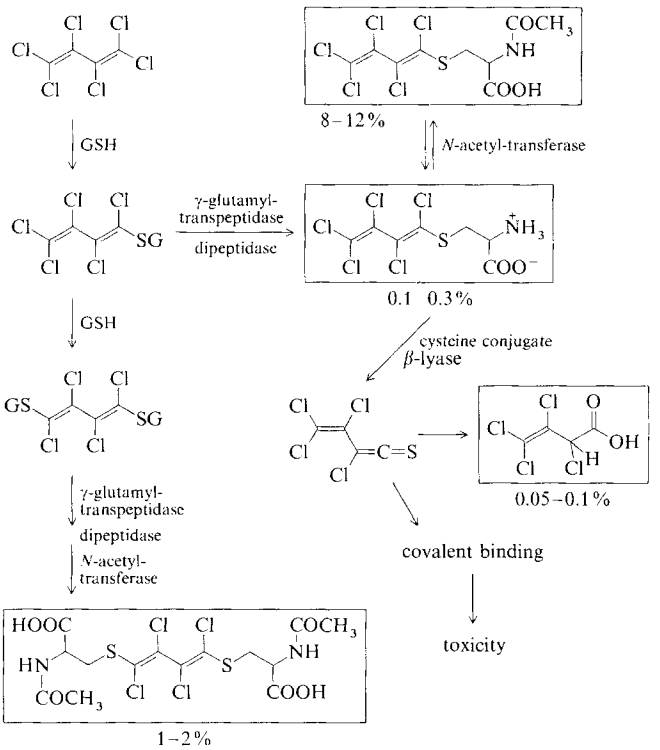
Summary: In spite of the paucity of data for the chlorinated butane derivatives, it may be concluded that the introduction of chlorine into the butane molecule increases the central depressive effects and the cytotoxicity; genotoxicity develops but apparently less markedly than in the propane, ethane, and ethene derivatives.

10. Chlorinated Butene Derivatives

The members of this class of compounds which are of particular interest are 1,3-butadiene, because of its use as the monomer, and hexachlorobutadiene, because of its great stability in the environment. In oxidative metabolism, 1,3-butadiene is converted to vinyl oxirane and then to 1,2:3,4-diepoxybutane (bioxirane);[29] both oxiranes are powerful mutagens.[30] Accordingly, in an inhalation study, 1,3-butadiene has been shown unequivocally to be a powerful carcinogen.[31]

Hexachlorobutadiene, however, is not subject to oxidative metabolism, unlike the analogous tetrachloroethene. On the other hand, a vigorous substitution reaction with glutathione (GSH) catalyzed by glutathione transferases takes place; both the monoadduct and diadduct with glutathione have been identified.[32] The subsequent peptidase-mediated cleavage of glycine and glutamic acid yields the cysteine adduct which is either converted by acetylation to the mercapturic acid, which is excreted in the urine, or by β-lyase-catalyzed cleavage to the reactive thiol. The thiol is converted—in analogy with the mechanism demonstrated for trichloroethene and tetrachloroethene (cf. Section 5, Scheme 1)—to the thioketene derivative, the ultimate mutagen (Scheme 2).

Since these processes take place largely in the renal tubules, when hexachlorobutadiene is fed to rats in long-term studies it induces highly organ-specific renal carcinomas.[33] Logically, hexachlorobutadiene has proved to be a powerful mutagen in bacterial tests, provided they were carried out in the presence of GSH and GSH transferase.[34]



Scheme 2. Urinary metabolites are in boxes.

11. Chlorinated Benzene Derivatives

Benzene is one of the toxicologically most intensively studied substances. It has three main kinds of action: a depressive effect on the central nervous system (anesthesia), liver damage, and depression of the hematopoietic systems which can lead to the development of various kinds of leukemia. Benzene is a relatively powerful human carcinogen. The introduction of chlorine into the benzene ring has very different effects on the three kinds of action of benzene: the (acute) central nervous depression is increased, the liver damage—at least with the derivatives with less chlorine substituents—is reduced, and the carcinogenicity is prevented.[1] Because of their considerable industrial importance, most chlorinated benzene derivatives and their isomers have been studied extensively.

Acute toxicity: The LC_{50} and LD_{50} values obtained in studies of the acute toxicity of benzene cannot be compared directly because of the very different conditions under which the studies were carried out. However, for all the administration routes used (inhalation, oral, other parenteral forms) the picture is similar: the toxicity increases with the number of chlorine substituents introduced into the molecule. Pentachlorobenzene and hexachlorobenzene exhibit a kind of toxicity not seen in the members of this series with less chlorine substituents: disturbance of porphyrin metabolism and a specific kind of liver damage.

Chronic toxicity: These substances have hardly been tested but all members of the series have been investigated in subchronic studies. Administered in the diet to rats and mice in three-month or six-month studies, the following order of toxicity was observed:

pentachlorobenzene > 1,2,4,5-tetrachlorobenzene >
1,2,3,5-tetrachlorobenzene > all trichlorobenzenes >
1,4-dichlorobenzene ≥ 1,2-dichlorobenzene ≥ monochlorobenzene

Thus the toxicity, measured here as the no observed effect level (NOEL), increases with the number of chlorine substituents.

Mutagenicity: The mutagenicity of all of the chlorinated benzene derivatives has been studied in a wide variety of different test systems. Apart from a few positive results which, on critical assessment, appear dubious or which are not acceptable because of inappropriate methods, the results obtained were all negative. Thus the chlorinated benzenes are neither direct nor indirect mutagens.

Carcinogenicity: In long-term carcinogenicity studies, negative results were obtained with chlorobenzene in mice and female rats, and questionably positive results in male rats. With 1,2-dichlorobenzene only negative results were obtained. 1,4-Dichlorobenzene induced a particular kind of renal carcinoma in male rats; this effect is said to be specific to this species and sex of animal and irrelevant for man;[35] the mechanism can be considered to involve effects on porphyrin metabolism on the one hand and hormone balance on the other. This applies in particular to hexachlorobenzene which is not mutagenic and may be classified as a non-genotoxic carcinogen.[36]

Summary: Substitution of the benzene ring with chlorine increases the acute and chronic toxicity in line with the number of chlorine substituents; the leukemogenic effects of benzene, however, are suppressed. This is probably a result of changes in the production of genotoxic metabolites which are considered to determine the leukemogenic activity of benzene: oxidative ring opening (with muconaldehyde as the genotoxic principle) and formation of 1,4-benzenediol (hydroquinone) derivatives.[37]

12. Chlorinated Phenol Derivatives

The literature on chlorinated phenols is very extensive and includes a wide variety of toxicological studies. The most important data have been assembled and evaluated in two monographs from IPCS (International Program of Chemical Safety, World Health Organization).[38] Because technical products containing unknown amounts of toxicity-determining impurities were tested in most of the studies, the conclusions cannot all be considered to be final. However, a clear picture does emerge from a review of the data available at present.

Toxicity: The introduction of chlorine susbstituents increases the toxicity of phenol enormously, not only the acute toxicity but also the subchronic and chronic toxicity. Here too, the increase in toxicity correlates with the number of chlorine substituents introduced into the molecule. As the number of chlorine substituents in the molecule increases, inhibition of oxidative phosphorylation becomes a predominant mechanism of toxic action; the other mechanisms are still largely unclear.

Mutagenicity: Tests of the mutagenicity have been carried out with practically all the chlorinated phenol derivatives and their isomers. The results are not consistent. However, negative findings predominate; some of the positive findings can be ascribed to the presence of impurities. It seems justified to conclude that there is no convincing evidence that the chlorinated phenols have genotoxic properties.

Carcinogenicity: Studies have been carried out with three chlorinated phenols, all with oral administration of high doses. 2,4-Dichlorophenol administered orally to mice and rats proved not to be carcinogenic. With 2,4,6-trichlorophenol[39] and pentachlorophenol,[40] however, positive results were obtained in both rodent species. Pentachlorophenol is clearly more effective than the trichloro compound. In addition, in the mouse skin test, monochlorophenol, dichlorophenols, and trichlorophenols have been shown to have tumor-promoting activity.[41] These results indicate that trichlorophenols could induce tumor formation by a non-genotoxic mechanism (see Section 14). The actual toxicological problem with the chlorophenols is contamination with polychlorinated dibenzodioxins and dibenzofurans.

13. The Significance of Chlorine Substituents in Organic Compounds on the Mutagenicity and Carcinogenicity

Of all the kinds of toxic effect (acute and chronic toxicity, neurotoxicity, reproductive toxicity, and genotoxicity), mutagenic and carcinogenic effects are clearly of most significance. This conclusion, which also reflects the more than proportional intensity of present-day toxicological testing and classification activities, is based on the following facts:

- The classical understanding of mutagenic and carcinogenic effects defines them as irreversible in principle. On the one hand, they are a result of covalent interaction of foreign substances with the genetic material (DNA bases); on the other, in spite of the ability of the organism to repair such chemically distinct DNA lesions, in practice some of them always remain unrepaired since repair mechanisms also operate according to high order kinetic functions. Thus accumulation of such primary lesions is observed after repeated and long-term exposure.
- Thresholds for mutagenic and typical carcinogenic effects cannot be determined either experimentally or from theoretical considerations. The usual kind of threshold concentrations considered to have no adverse effects on health (such as MAK and MIK values) can therefore not be established because every exposure concentration, however formulated, includes a certain residual risk which is rarely quantifiable.
- After transplacental distribution, systemic carcinogens can cause cancerous changes in the developing foetus which are first manifested after birth, during the juvenile stage, or even later.
- It is conceivable that genetic damage in the germ cells could result in transfer of damaged genetic material to later generations. Although such events have not yet been observed in man, they have been produced in animal studies, admittedly only under extreme conditions.
- Most cancers diagnosed today are resistant to therapy. In spite of enormous research efforts, significant progress in tumor therapy is not to be expected in the foreseeable future.

– Cancer is considered more important than other diseases as widespread in the population because of the great suffering it entails for the patient and the patient's family.

Chlorinated organic compounds make up a large proportion of the chemicals known to be germ cell mutagens and to cause cancer. The most important German list of carcinogenic substances[42] distinguishes between three categories, A1, A2, and B. If one includes in the assessment the substances suspected of causing cancer (category B in the "List of MAK and BAT Values"), which is justifiable for purposes of comparison, the compounds containing chlorine (about 50) currently make up more than one third of the substances classified in this list as carcinogens or suspected carcinogens.

The chlorinated organic compounds in the current "List of MAK and BAT Values" are shown in Table 4 (clearly carcinogenic in man (A1)), Table 5 (clearly carcinogenic in animal studies (A2)), and Table 6 (suspected carcinogens (B)). Review of the other large list of carcinogenic substances, the collection of monographs of the International Agency for Research on Cancer[43] in Lyon, adds another twelve chlorinated organic substances (partly mixtures) (Table 7).

Table 4. Chlorinated organic compounds shown to be carcinogenic in man (Category IIIA1).

bis(2-chloroethyl)sulfide	α-chlorinated toluenes: (mixture of
chloromethyl methylether	benzoyl chloride, (chloromethyl)benzene,
bis(chloromethyl)ether	(dichloromethyl)benzene,
4-chloro-*o*-toluidine	(trichloromethyl)benzene),
vinyl chloride	*N*-methyl-bis(2-chloroethyl)amine

Table 5. Chlorinated organic compounds shown to be carcinogenic in animal studies (Category IIIA2).

α-chlorinated toluenes (see Table 4)	1,3-dichloro-2-propanol
1-chloro-2,3-epoxypropane	1,3-dichloropropene (*cis* and *trans*)
chlorofluoromethane	dimethylcarbamoyl chloride
N-chloroformylmorpholine	epichlorohydrin (1-chloro-2,3-epoxypropane)
1,2-dibromo-3-chloropropane	4,4′-methylenebis(2-chloroanilin)
dichloroacetylene	pentachlorophenol
3,3′-dichlorobenzidine	2,3,7,8-tetrachlorodibenzo[*b*,*e*][1,4]dioxin
1,4-dichloro-2-butene	2,3,4-trichloro-1-butene
1,2-dichloroethane	1,2,3-trichloropropane

Table 6. Chlorinated organic compounds which are suspected carcinogens (Category IIIB).

allyl chloride	dichloromethane
chlordane	1,2-dichloro-1-methoxyethane
chlordecon	1,2-dichloropropane
chlorinated biphenyls	α,α-dichlorotoluene [a]
chloroethane	diethylcarbamoyl chloride
chloro-*N*-hydroxymethylacetamide	heptachlor
chloromethane	hexachlorobutadiene
3-chloro-2-methylpropene	1,1,2,2-tetrachloroethane
1-chloro-2-nitrobenzene	tetrachloroethene
1-chloro-4-nitrobenzene	tetrachloromethane
chloroparaffins	1,1,2-trichloroethane
chlorthalonil	trichloroethene
5-chloro-*o*-toluidine	trichloromethane
1,1-dichloroethene	α,α,α-trichlorotoluene [a]

[a] See Table 4 and 5.

Table 7. Additional chlorinated organic compounds which are listed as carcinogens by IARC (IARC = International Agency for Research on Cancer).

N,*N*′-bis(chloroethyl)nitrosourea
1-(2-chloroethyl)-3-cyclohexyl-1-nitrosourea
chlorinated phenols
chlorinated phenoxyacetic acids
4-chloro-*o*-phenylenediamine
3,3′-dichloro-4,4′-diaminodiphenylether
dichlorvos
hexachlorobenzene
hexachlorocyclohexane
melphalan
metronidazole
mirex
products of the chlorination of drinking water

When evaluating such lists it must be borne in mind that only a very small proportion of chlorinated organic compounds has been tested for carcinogenicity. In the past, interests and constraints have led to more or less randomly distributed testing of such compounds. An attempt at a systematic approach has been introduced with the German Chemicals Act but the effects of this act, especially for substances which have long been in use, are not to be expected in the immediate future.

Consideration of chlorinated organic compounds with mutagenic and carcinogenic properties reveals a number of molecular fragments which can be made responsible for the genotoxic effects. The mechanisms involved—when they are known—have been discussed already in the appropriate sections of this review. In every case, the mechanisms involve the reaction of electrophilic moieties with nucleophilic sites in biologically important macromolecules, more rarely with low molecular weight cell components (e.g., glutathione, see Schemes 1 and 2). Only few genotoxic chlorinated organic compounds are inherently electrophilic (direct genotoxicity); mostly the electrophilic forms are produced during metabolism in the organism (indirect genotoxicity).

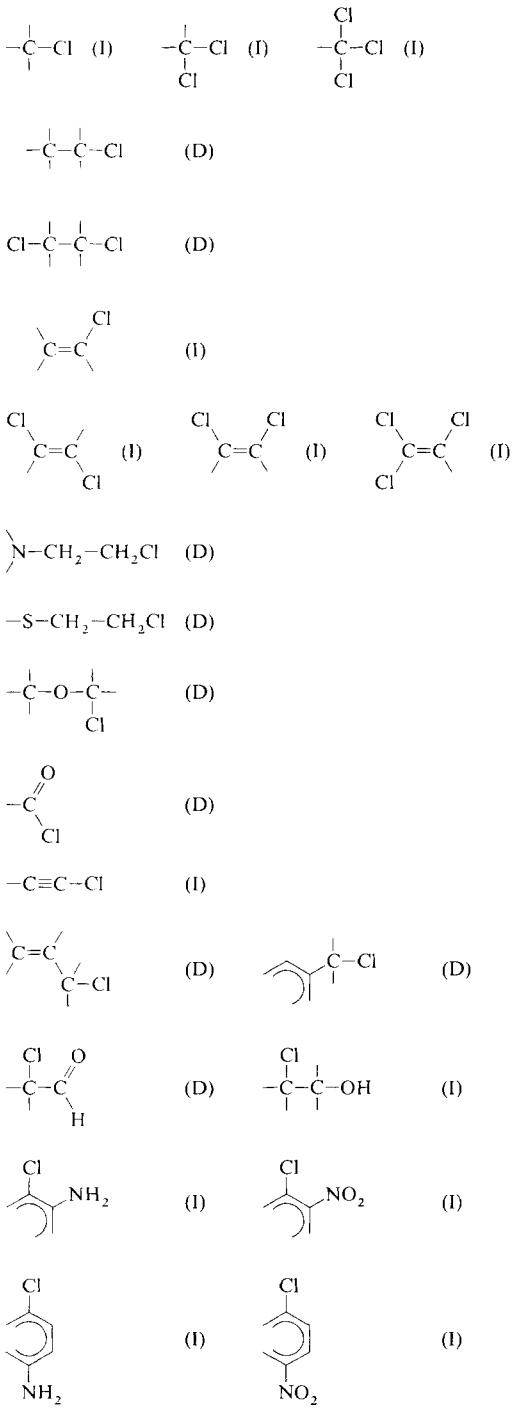
The molecular fragments which have been identified to date as having genotoxic activity are shown in Table 8. They are of particular importance in the conception of protective and avoidance strategies for regulatory measures and for the search for suitable alternative substances with less or no genotoxic activity.

A knowledge of which groups are toxophoric can be useful during product development. It forms a basis for prediction of whether or not genotoxic effects are to be expected. Such hypotheses, however, always require testing in biological systems since, as emphasized in Section 2 of this review, the numerous enzymes and conversion steps involved, especially during metabolic activation of substances in the organism, are highly complex and therefore poorly predictable. The hypothesis can, however, often be proved valid or invalid by a mutagenicity test in a simple model system.

14. Non-Genotoxic Carcinogenic Chlorinated Organic Compounds

Some of the chlorinated organic compounds found to be carcinogenic in animal studies stand out from the majority in that they do not have mutagenic effects. In the organism, they do not

Table 8. Chlorine-containing molecular fragments with genotoxic properties. (D = direct, I = indirect).



undergo metabolic transformation of relevance for their toxicity, unlike the genotoxic substances for which metabolic transformation involving cleavage of the C–Cl bond is a prerequisite for their activity. Although it is not always clear where an individual compound belongs, because the literature contains a few positive results of mutagenicity studies together with the numerous negative ones, mechanistic considerations make it possible to define this class of compounds clearly. It contains the polychlorinated cyclic hydrocarbons of the following types:

- polychlorinated dibenzodioxins and dibenzofurans
- polychlorinated biphenyls
- insecticides such as DDT and related compounds, hexachlorobenzene, hexachlorocyclohexane, heptachlor, chlordecone, chlordan
- pentachlorophenol
- longer chain chloroparaffins

The points which become apparent on consideration of the toxicology of these groups of compounds are detailed below.

- In the carcinogenicity studies with animals, very high doses, compared with the kinds of exposure found for man, were always necessary before carcinogenic effects were obtained at all.
- Severe inflammatory and degenerative symptoms were always seen in the experimental animals, especially in the organs in which cancer developed.
- The tumor incidence was never particularly high, and always lower than that found with the chlorinated organic compounds with genotoxic properties.
- The tumors developed on average much later than with other typical carcinogenic substances.
- The tumor locations were rather unspecific; tumor types characteristic for a particular substance, like liver hemangiosarcomas after chloroethene exposure, for example, did not develop in any case.
- Epidemiological studies have not been able to find clear correlations between exposure and cancer for any of these groups of substances, although carried out on a large scale and supported relatively well by exposure data. Recently, it has been claimed that tetrachlorodibenzodioxin (TCDD) causes a significant increase in tumor incidence, but it is only just a significant increase in the incidence of tumors of a kind which are anyway frequent and the increase is very small, at most marginal. The results of this one study[44] are in contrast with those of several others which did not find a statistically significant increase.[45–48]

The above features have led to the conclusion that the mechanisms of tumorigenesis operating with these substances must be fundamentally different from those found with genotoxic substances. Although the details of the mechanisms have not been elucidated for any of the substances, it seems justified to assume that the prerequisite for induction of cancer is severe organ or tissue damage, the massive cell death and subsequent cell replacement resulting in marked proliferative activity. Cell and tissue proliferation are accompanied by high rates of cell division. Cell division is indispensable for the transmission of genetic damage.[49] Since higher organisms experience constant very low levels of primary genetic damage resulting from all kinds of environmental factors,[50] the effect of increased proliferation is to increase the probability of the final manifestation of such damage in the form of tumors. Effects on hormone balance and immune status are considered to play an important role; such effects have been described in detail for DDT and related substances and for TCDD and polychlorobiphenyls (PCBs).

These mechanistic considerations result in the hypothesis that the carcinogenic effects of this type of substance cannot be expressed in the absence of cytotoxicity and increased cell proliferation, hormonal imbalance or disturbances of the immune system. There are threshold values for the induction of such changes and these can be determined with sensitive biological methods. On this basis it is possible to determine for these nongenotoxic chlorinated organic compounds threshold levels which do not cause impairment of health, cancer formation included.

15. Structure–Activity Relationships

In the present study, a series of representative homologous and analogous groups of chlorinated compounds has been evaluated because they are considered to throw light on structure–activity relationships. It was not intended to attempt to cover the whole field including uncommon substances or groups. Although the present investigation has not included some possibly important groups, conclusions which apply to chlorinated organic compounds in general may be drawn.

1. The introduction of chlorine into organic compounds is almost always associated with an increase in the toxic potential. Only rarely does chlorination produce no increase or even a decrease in effects. This observation applies for all kinds of toxic effect (acute, subchronic and chronic toxicity, reproductive toxicity, mutagenicity, and carcinogenicity).
2. There is also a tendency to an increase in toxicity with the number of chlorine substituents in a molecule; this can be seen as a general rule but a less stringent one than that for the effect of introducing chlorine in the first place.
3. The introduction of chlorine into the molecule frequently gives the substance new properties. New acute and subchronic effects are seen mainly in the parenchymatous organs (especially liver and kidneys, less often in the spleen), circulatory system, and central nervous system.
4. With the introduction of chlorine into the molecule, most of the organic substances discussed here become mutagenic and/or carcinogenic.
5. There is a wide variety of mechanisms of genotoxicity of chlorinated organic compounds. In most cases, the substance must be activated by metabolism in the organism to yield electrophilic intermediates which are able to bind covalently to essential macromolecules, especially DNA. Only relatively few kinds of compound can produce genotoxic effects directly, without metabolic activation (in particular, alkylating agents).
6. A considerable proportion of the chlorinated organic compounds which have been studied has carcinogenic activity. The proportion cannot be determined exactly because chlorinated organic compounds have not been tested systematically.
7. Carcinogenic chlorinated organic compounds can be divided into two fundamentally different groups: chlorinated aliphatic (and olefinic) hydrocarbons with short chain lengths (and, as a rule, high vapor pressures) are mostly carcinogenic because of their genotoxic activity, whereas polychlorinated cyclic compounds induce tumor formation by cytotoxic, never by genotoxic mechanisms. In the latter group, tumor induction always requires very high doses which also cause other kinds of damage.
8. Within groups of closely related chlorinated organic compounds (homologous and analogous series) where the toxicity is uniformly associated with a common chemically identifiable molecular fragment, it is possible to predict whether toxic effects (including genotoxic effects) will occur or not. With heterogeneous series of compounds (that is, with chemically different toxophoric groups), however, or in groups where several mechanisms of toxicity play a role, the predictability is much more restricted. This is mainly because a multitude of enzymatic activation and deactivation reactions can occur with the one molecule, often simultaneously, and can be dependent on or independent of each other.
9. There is one significant exception to the rules given in paragraphs 1. and 4. above: the introduction of chlorine into benzene suppresses its notorious and considerable leukemia-inducing effects. Presently available data indicate that this applies for all members of the extensive group of chlorinated benzene derivatives.

16. Conclusions: Strategies for Risk Assessment and Remedies for Toxicological Problems

For some time now, people have been demanding that "chlorine chemistry" be abolished totally and justifying this demand, on the one hand, with the high toxicity and carcinogenicity of some chlorine compounds together with their ability to accumulate in the environment, especially in food chains and, on the other, with the argument that chlorinated organic compounds are man-made, synthetic, foreign for the human organism and the rest of the biosphere; life processes have not been able to adapt to and develop defense mechanisms against these substances, as they have for numerous natural toxins.

The latter argument is not valid. To date, at least 1500 chlorine-containing compounds are known to be produced not only by plants, microbes, and other primitive organisms but also by higher animals.[51] Intensive research in this field extends the list constantly. The list of natural substances does not include highly chlorinated and perchlorinated hydrocarbons; these generally highly lipophilic and persistent substances which accumulate in certain environmental compartments are only known as synthetic chemicals at present. However, there are numerous genotoxic chlorinated and brominated organic compounds from natural sources with which a wide of variety of living organisms has always had to cope. Examples include tetrachloroacetone, polyhalogenated propenes, tetrabromo-2-propanol, dibromo-1-propanol, dichloroacetamide, polychlorinated terpenes, polychlorinated biphenyls, polychlorinated phenols.[51]

The risks associated with these toxic substances will continue to exist because it is practically impossible to regulate such natural processes—unlike the processes of synthetic chlorine chemistry. Some of these natural chlorine compounds function as hormones in certain living organisms.[52] When they are produced as defensive agents, for example, as antibiotics, they can

accumulate in very high concentrations in certain tissues of the producing organisms. Some prominent chlorine compounds, chloromethane, for example, are produced in much larger quantities in nature than synthetically, especially by primitive marine organisms[53] but also by higher plants.[54]

Chlorinated organic compounds are associated with two kinds of risk which are particularly important for the discussion of effects on health and the environment: the accumulation in certain environmental compartments as a result of high stability and lipophilicity, and the production of genotoxic effects resulting in cancer. There are solutions to the problems associated with both these kinds of risk.

- In spite of their high stability and persistence, polychlorinated cyclic compounds can be eliminated from the animate and inanimate world by means of a number of natural physical, chemical, and biological deactivation mechanisms. Of particular importance is UV irradiation;[55] microbial elimination of chlorine also plays an important role.[56, 57] Thus the remedy for the problem posed by this type of compound lies in the avoidance or large-scale reduction of deposition of the substances in the environment. One of the most sensitive criteria for the accumulation of polychlorinated compounds in the environment is seen in their transfer from a series of food chains into mother's milk. The most recent analyses carried out by the "Bundesgesundheitsamt" (German Federal Health Office) demonstrate that as a result of the now long-term reduction in the deposition of such substances in the environment, the levels of hexachlorobenzene, hexachlorocyclohexane, DDT and its metabolites, and polychlorinated biphenyls in mother's milk have decreased by up to half an order of magnitude during the last ten years.[58] There are other examples too. The effectiveness of such avoidance strategies can be monitored precisely these days with analytical chemical procedures and appropriate indicators. Here the situation could be improved further by appropriate research, and political support for such measures is necessary.
- Where genotoxic chlorinated organic compounds are handled, it is necessary to develop new avoidance strategies or improve existing ones. One kind of strategy involves the development of alternative substances without genotoxic activity or with much less activity. For certain classes of compounds, structure–activity relationships like those described in the specific sections of this review are already available; for other classes of compounds they could and should be developed further. Another kind of strategy involves the reduction of occupational and non-occupational exposure to the substances to harmless levels by improving respirators and personal protective clothing and by encapsulation of production processes. A classical example of the application of this kind of strategy is chloroethene (vinyl chloride). The first case of cancer (hemangiosarcoma of the liver) among PVC-polymerization workers was reported in 1974.[59] One year later the old plants in the Federal Republic of Germany had been exchanged for new ones, the exposure levels at the workplaces were reduced to comply with a hastily established TRK value (technical exposure limit)[60] and the vinyl chloride monomer levels in PVC products were reduced to safe concentrations. On these three levels, the PVC problem has been solved for synthesis, production, and use; partial solutions have been found for waste disposal.
- Effective recycling can reduce environmental damage or even avoid it completely in some areas. A systematic treatment of this field goes beyond the intentions of the present review and beyond the competence of toxicologists. None the less, it should be mentioned that modern cleaning systems, for example, for degreasing metals or dry-cleaning of clothing, are closed systems in which the volatile chlorinated hydrocarbons such as trichloroethene and tetrachloroethene are recovered completely without any significant loss of substances into the air.
- Particularly hazardous substances should no longer be produced or used. Careful quantitative risk assessment is required to determine which substances are particularly hazardous. At present, this is possible only for some chlorinated organic compounds. Toxicology and environmental chemistry, however, have produced the armory of methods required for such comparative risk assessment. They must just be used systematically in the various application areas. Here deficiencies remain and require the attention of scientific research, on the one hand, and of the political decision makers on the other.
- The most important aspect of avoidance strategies as they affect chlorinated organic compounds is the establishment and application of threshold values. Such thresholds are well-established for the workplace, the ambient air, for foods and drinking water. For non-genotoxic substances they may be based exclusively on health-determined criteria. For genotoxic substances it is also possible to justify the establishment and use of threshold values based on health effects. For mutagenic and carcinogenic substances, it is not possible to deduce non-effective threshold concentrations from the results of animal studies or from the theory of action of such substances. Finite doses always retain a finite effect which is generally not measurable in the low dose region and which at best can be estimated by means of more or less arbitrary arithmetic operations which are associated with errors of several orders of magnitude.[61] The application of a threshold value in such cases is thus always associated with a residual risk, albeit a small one. Such a threshold value can therefore not be established on the basis of scientific arguments alone. It requires political consensus as to the acceptable level of residual risk. There are two principles which may be applied when making such decisions: that of minimum risk (value as low as technically, analytically, and socio-economically feasible) and that of relative risk. The former, with its many compromises, is applied in the establishment of TRK values. The principle of relative risk compares the estimated residual risk with other risks; a political decision as to the acceptable increase in risk above the background of "unavoidable" risk will consider the increase in relation to the totality of risks and attempt to keep it in proportion. For chlorinated organic carcinogenic compounds it is self-evident that the acceptability be oriented on the exposure to naturally occurring compounds. Although in recent times the principle of establishing threshold levels has been subject to increasing criticism as an "end of pipe" approach, it is—compared with the others mentioned above—still the best established and most important instrument for

preventing adverse effects of exposure. It is also the instrument with the most readily comprehensible possibilities and limitations because it is based--in general and for the specific hazardous substance—on a great deal of knowledge and experience, on a data base which is generally not or only partially available for the alternative substances which would have to be introduced to replace any of those forbidden completely.

Thus, research into cause and effect has produced useful and tested instruments for risk recognition, evaluation, and reduction: exclusion of particularly persistent and dangerous substances, reduction of exposure of man and other living organisms, reduction of deposition in the environment, and the establishment of harmless threshold concentrations with monitoring procedures. These can be put to use for chlorinated organic compounds in the same way as for all kinds of potentially hazardous chemicals.

This review was suggested and promoted by the Verband der Chemischen Industrie, Frankfurt am Main, Germany, to whom I am indebted for valuable help with references.

Received: April 2, 1994 [A 59 IE]
German version: *Angew. Chem.* **1994**, *106*, 1997
Translated by Dr. A. E. Wild, Kulmbach, Germany

[1] D. Henschler, *Toxikologie chlororganischer Verbindungen. – Der Einfluß von Chlorsubstituenten auf die Toxizität organischer Moleküle*, VCH; Weinheim **1994**.

[2] List of MAK values. *Part 29, Senatskommission zur Prüfung gesundheitsschädlicher Arbeitsstoffe der Deutschen Forschungsgemeinschaft*. VCH Weinheim, **1993**.

[3] *Metabolism of methyl chloride to formate in rats:* D. J. Kornbrust, J. S. Bus, *Toxicol. Appl. Pharmacol.* **1982**, *65*, 135–143.

[4] *Metabolism of haloforms to carbon monoxide. I. In vitro studies:* A. E. Ahmed, V. L. Kubic, M. W. Anders, *Drug Metab. Dispos.* **1977**, *5*, 198–204.

[5] *Bioactivation of nephrotoxic haloalkenes by glutathione conjugation: formation of toxic and mutagenic intermediates by cysteine-conjugate β-lyase:* W. Dekant, S. Vamvakas, M. W. Anders, *Drug Metab. Rev.* **1989**, *20*, 43–83.

[6] *Expression of mammalian glutathione-S-transferase 5-5 in Salmonella typhimurium TA 1535 leads to base-pair mutations upon exposure to dihalomethanes:* R. Thier, J. B. Taylor, S. E. Pemble, W. G. Humphreys, M. Persmark, B. Ketterer, F. P. Guengerich, *Proc. Natl. Acad. Sci. USA* **1993**, *90*, 8576–8580.

[7] *The metabolic activation of dichloromethane and chlorofluoromethane in a bacterial mutation assay using Salmonella typhimurium:* T. Green, *Mutat. Res.* **1983**, *118*, 277–288.

[8] *Effect of varying exposure regimes on methylene chloride, induced lung and liver tumors in female B6C3F1 mice:* F. W. Kari, J. F. Foley, R. R. Maronpot, M. W. Anderson, *Carcinogenesis* **1993**, *14*, 819–826.

[9] *Phosgene: a metabolite of chloroform:* L. R. Pohl, B. Broosnan, N. F. Whittaker, G. Krishna, *Biochem. Biphys. Res. Commun.* **1977**, *79*, 684–691.

[10] *The reductive metabolism of halogenated alkanes by liver microsomal cytochrome P-450:* W. Nastainczyk, H. J. Ahr, V. Ullrich, *Biochem. Pharmacol.* **1982**, *31*, 391–396.

[11] *Stereochemistry of the glutathione-dependent biotransformation of vicinal-dihaloalkanes to alkenes:* J. C. Livesey, M. W. Anders, P. W. Langsvardt, C. L. Putzig, R. H. Reitz, *Drug Metab. Dispos.* **1982**, *10*, 201–204.

[12] *Halogenated alkanes, alkenes and alkynes:* D. Henschler in *Bioactivation mechanisms* (Ed.: M. W. Anders), Academic Press, New York, **1986**.

[13] *Chemical reactivity, biotransformation, and toxicity of polychlorinated aliphatic compounds:* G. Bonse, D. Henschler, *CRC Crit. Rev. Toxicol.* **1976**, *5*, 395–409.

[14] *Thioacylating agents as ultimate intermediates in the β-lyase catalyzed metabolism of S-(pentachlorobutadienyl)-L-cysteine:* W. Dekant, S. Vamvakas, D. Henschler, *Chem. Biol. Interact.* **1988**, *67*, 139–148.

[15] *Structures of DNA-adducts formed from haloketenes and halothioketenes: A study to identify possible adducts formed from trichloro- and perchloroethene through bioactivation by glutathione conjugation:* M. Müller, G. Birner, D. Henschler, W. Dekant, *IARC Sci. Publ. Ser.* **1994**, *125*, 423.

[16] *Thioketene formation from α-haloalkenyl 2-nitrophenyldisulfides: models for biological reactive intermediates of cytotoxic S-conjugates:* W. Dekant, G. Urban, C. Görsmann, M. W. Anders, *J. Am. Chem. Soc.* **1991**, *113*, 5120–5122.

[17] *Bacterial cysteine conjugate β-lyase and the metabolism of cysteine-S-conjugates: structural requirements for the cleavage of S-conjugates and the formation of reactive intermediates:* S. Vamvakas, K. Berthold, W. Dekant, D. Henschler, *Chem. Biol. Interact.* **1988**, *65*, 59–71.

[18] *Renal cell cancer in a population exposed to high concentrations of trichloroethene:* D. Henschler, K. Ulm, S. Lammert, S. Vamvakas, W. Dekant, unpublished.

[19] *"Polyneuritis cranialis" durch Vergiftung mit chlorierten Acetylenen beim Umgang mit Vinylidenchlorid-Copolymeren:* D. Henschler, F. Broser, H. C. Hopf, *Arch. Toxicol.* **1970**, *26*, 62–75; *Decomposition of the neuro- and nephrotoxic compound dichloroacetylene in the presence of oxygen: separation and identification of novel products:* D. Reichert, M. Metzler, D. Henschler, *J. Environ. Pathol. Toxicol.* **1980**, *4*, 525–532.

[20] *Generation and inhalation toxicity of dichloroacetylene:* D. Reichert, D. Ewald, D. Henschler *Food Cosmet. Toxicol.* **1975** *13*, 511–515.

[21] *Carcinogenicity of dichloroacetylene: an inhalation study:* D. Reichert, U. Spengler, W. Romen, D. Henschler, *Carcinogenesis* **1984**, *5*, 1411–1420.

[22] *Metabolism of ^{14}C-dichloroacetylene in rats:* W. Kanhai, M. Koob, W. Dekant, D. Henschler, *Xenobiotica* **1991**, *21*, 905–916.

[23] *Theoretical structure-activity study of mutagenic allyl chlorides:* D. W. Boerth, E. Eder, G. Rasul, J. Morais *Chem. Res. Toxicol.* **1991**, *4*, 368–372.

[24] *Mutagenic properties of allylic and α,β-unsaturated compounds: consideration of alkylating mechanisms:* E. Eder, D. Henschler, T. Neudecker, *Xenobiotica* **1982**, *12*, 831–848.

[25] *Allylic compounds bind directly to DNA: investigation of the binding mechanism in vitro:* E. Eder, D. Lutz, M. Jörns, *Chem. Biol. Interact.* **1987**, *61*, 97–108.

[26] *Mutagenicity of chloroolefins in the Salmonella/mammalian microsome test. III:* T. Neudecker, D. Henschler *Mutat. Res.* **1986**, *170*, 1–9.

[27] *The role of biotransformation in the genotoxicity of allylic compounds:* E. Eder, K. Dornbusch, G. Fischer, *Arch. Toxicol.* **1987**, *60*, 182–186.

[28] N. N., *Farmakol. Toksikol. (Moscow)* **1967**, *30*, 102; cited from the *Registry of Toxic Effects of Chemical Substances (Wash.)*, July **1992**.

[29] *Hepatic microsomal metabolism of 1,3-butadiene:* E. Malvoisin, M. Roberfroid, *Xenobiotica* **1982**, *12*, 137–144.

[30] *Mutagenicity of butadiene and butadiene monoxide:* C. De Meester, F. Poncelet, M. Roberfroid, M. Mercier, *Biochem. Biophys. Res. Commun.* **1978**, *80*, 298–305.

[31] Technical Report on the Toxicology and Carcinogenesis Studies of 1,3-Butadiene in B6C3F1-Mice: *Natl. Toxicol. Program*, **1984**; NTP-83-071.

[32] *Enzymatic conjugation of hexachloro-1,3-butadiene with glutathione: Formation of 1-(glutathion-S-yl) 1,2,3,4,4-1,2,3,4-tetrachlorobuta-1,3-diene:* W. Dekant, S. Vamvakas, D. Henschler, M. W. Anders, *Drug Metab. Dispos.* **1988**, *16*, 701–706.

[33] *Results of a two-year chronic toxicity study with hexachlorobutadiene in rats:* R. J. Kociba, D. G. Keyes, G. C. Jersey, J. J. Ballard, D. A. Dittenber, J. F. Quast, L. E. Wade, C. G. Hurniston, B. A. Schwetz, *Am. Ind. Hyg. Assoc. J.* **1977**, *38*, 589–602.

[34] *Mutagenicity of hexachloro-1,3-butadiene and its S-conjugates in the Ames-test: role of bioactivation by the mercapturic acid pathway in its nephrocarcinogenicity:* S. Vamvakas, S. J. Kordowich, W. Dekant, T. Neudecker, D. Henschler, *Carcinogenesis* **1988**, *9*, 907–910.

[35] *Gesundheitsschädliche Arbeitsstoffe. Toxikologisch-arbeitsmedizinische Begründung von MAK-Werten. 1,4-Dichlorbenzol.* (Ed.: D. Henschler), VCH, Weinheim, **1991**.

[36] *Hepatocarcinogenicity of hexachlorobenzene in rats and the sex difference in hepatic iron status and development of prophyria:* A. G. Smith, J. E. Francis, D. Dinsdale, M. M. Manson, J. R. P. Cabral, *Carcinogenesis* **1985**, *6*, 631–636.

[37] *Gesundheitsschädliche Arbeitsstoffe. Toxikologisch-arbeitsmedizinische Begründung von MAK-Werten. Benzol.* (Ed.: D. Henschler), VCH, Weinheim, **1992**.

[38] IPCS (International Program of Chemical Safety, World Health Organisation): *Vol. 71: Pentachlorophenol; Vol. 93: Chlorophenols other than pentachlorophenol!* Geneva, **1987**, and **1989**.

[39] *Bioassay of 2,4,6-Trichlorophenol: Natl. Toxicol. Program Tech. Rep. No. 155*, **1979**.

[40] *Toxicology and Carcinogenesis Study of Two Pentachlorophenol Technical Grade Mixtures: Natl. Toxicol. Program Tech. Rep. No. 349*, **1989**.

[41] *The tumor-promoting action of phenol and related compounds for mouse skin:* R. K. Boutwell, D. K. Bosch, *Cancer Res.* **1959**, *19*, 413–424.

[42] MAK-Werte-Liste, *Maximale Arbeitsplatzkonzentrationen. Deutsche Forschungsgemeinschaft*. Since Part 10 VCH, Weinheim, **1974**.

[43] IARC, International Agency for Research on Cancer, *Monograph Series on the Evaluation of Carcinogenic Risks to Humans*. Lyon/France Suppl. No. 7, **1987**.

[44] *Cancer mortality in workers exposed to 2,3,7,8-tetrachloro-dibenzo-p-dioxin:* M. A. Fingerhut, W. E. Halperin, D. A. Marlow, L. A. Piacitelli, P. A. Honchar, M. H. Sweeney, A. L. Griefe, P. A. Dill, K. Steenland, A. J. Suruda *N. Engl. J. Med.* **1991**, *324*, 212–218.

[45] *Phenoxy herbicides and cancer: Insufficient epidemiologic evidence for a causal relationship:* G. G. Bond, K. M. Bodner, R. R. Cook, *Fundam. Appl. Toxicol.* **1989**, *12*, 172–188.

[46] *How toxic is 2,3,7,8-tetrachlorodibenzo-p-dioxin to humans?* R. D. Kimbrough *J. Toxicol. Environ. Health* **1990**, *30*, 261–271.
[47] *Use of epidemiology data to assess the cancer risk of 2,3,7,8-tetrachlorodibenzo-p-dioxin:* L. Tollefson, *Regul. Toxicol. Pharmacol.* **1991**, *13*, 150–169.
[48] *Thirty-four-year mortality follow-up of BASF employees exposed to 2,3,7,8-TCDD after the 1953 accident:* A. Zober, P. Messerer, P. Huber, **1990**, *62*, 139–157.
[49] *Chemical and physical carcinogenesis: advances and perspectives for the 1990s.* C. C. Harris, *Cancer Res. (Suppl.)* **1991**, *51*, 5023s–5044s.
[50] *Spontaneous mutagensis: experimental, genetic and other factors.* K. C. Smith, *Mutat. Res.* **1992**, *277*, 139–162.
[51] *Naturally occurring organohalogen compounds – a survey:* G. W. Gribble, *J. Nat. Prod.* **1992**, *55*, 1353–95.
[52] *Punaglandins: halogenated antitumor eicosanoids from the octocoral Telesto riisei:* B. J. Baker, R. K. Okuda, P. T. K. Yu, P. J. Scheurer, *J. Am. Chem. Soc.* **1985**, *107*, 2976–2977; *Chlorovulones, new halogenated marine prostanoids with an antitumor activity from the stolonifer Clavularia viridis quoy and gaimard:* K. Iguchi, S. Kaneta, K. Mori, Y. Yamada, A. Honda, Y. Mori, *Tetrahedron Lett.* **1985**, *26*, 5787–5790.
[53] *Methyl chloride transferase: a carbocation route for biosynthesis of halometabolites:* A. M. Wuosmaa, L. P. Hager, *Science* **1990**, *249*, 160–162.
[54] V. A. Isidorow, *Organic Chemistry of the Atmosphere*, Springer, Berlin, **1990**.
[55] *Atmospheric life-times of dibenzo-p-dioxins and dibenzofuranes:* R. Atkinson, *Sci. Total Environ.* **1991**, *104*, 17–33.
[56] *Biodegradation of DDT by the white rot fungus Phanerochaete chrysosporiums:* J. A. Bumpus, S. D. Aust, *Appl. Environ. Microbiol.* **1987**, *53*, 2001-8.
[57] *Microbial degradation of halogenated hydrocarbons: a biological solution to pollution problems?* R. Müller, F. Lingens, *Angew. Chem.* **1986**, *98*, 778–787; *Angew. Chem. Int. Ed. Engl.* **1986**, *25*, 779–789.
[58] H. Beck, *Bundesgesundheitsblatt*, **1994**, in press.
[59] *Angiosarcoma of the liver in the manufacture of polyvinyl chloride:* J. L. Creech, M. N. Johnson, *J. Occup. Med.* **1974**, *16*, 150–151.
[60] DFG: *Maximale Arbeitsplatz-Konzentrationen, Part 18*, Verlag Chemie, Weinheim, **1982**, S. 611.
[61] *Carcinogenic Risk Assessment. A Toxicologist's View:* J. F. H. Purchase in *Risk Quantification and Regulatory Policy* (Eds. D. G. Hoel, R. A. Merrill, F. P. Perera), Banbury Report, Cold Spring Harbor Laboratory, **1985**.

A stop-gap solution?



If the latest library copy of Angewandte spends more time off the shelf than on, stop the gap with a personal subscription.

Just call or fax

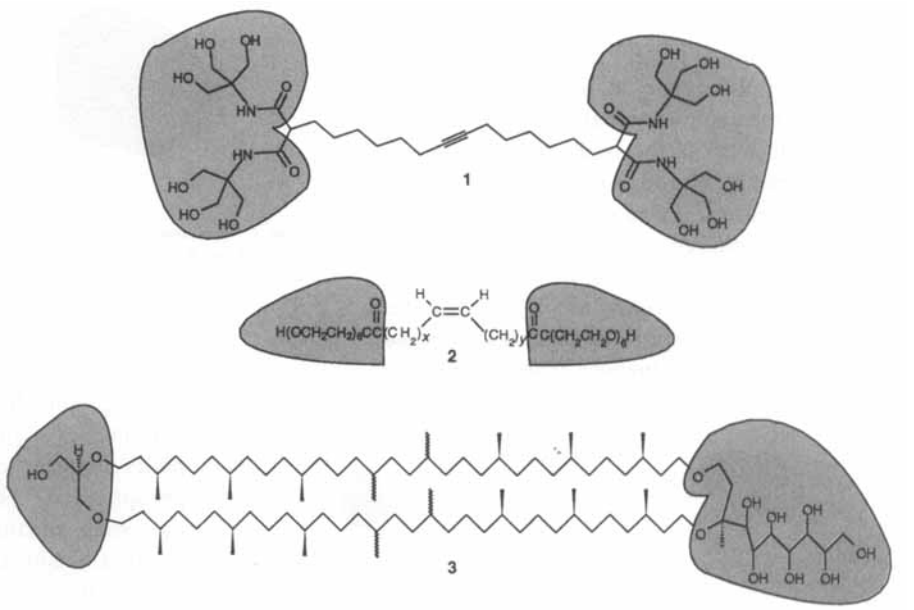
VCH

USA: Tel. 1-(800) 422-8824; Fax (305) 428-8201
UK: Tel. (0223) 321111, Fax (0223) 313221

Bolaamphiphiles: From Golf Balls to Fibers**

Gregory H. Escamilla and George R. Newkome*

A bolaamphiphile is simply defined as a molecule in which two or more hydrophilic groups are connected by hydrophobic functionalities (Scheme 1). Other terms such as bolaform amphiphile[1] or arborol[2] have been used to describe molecules possessing this architecture. Bolaform electrolytes or bolytes, a term introduced by Fuoss and Edelson in 1951,[1] are structurally similar, except the hydrophilic groups are ionic.[3] Since Fuhrhop and Mathieu[4] reported the synthesis and self-assembly of several bolaamphiphiles, other researchers have explored applications of this basic architecture. A search of current literature demonstrates the potential of bolaphiles, short for bolaamphiphiles, for the preparation of ultrathin monolayer membranes, the inclusion of functional groups into membranes, and the disruption of biological membranes, which could lead to therapeutic agents,[5,6] as well as their use as "antisense" agents,[7,8] as catalysts in reactions,[9-11] and as models for the membranes found in thermophilic archaebacteria.[12]



Scheme 1. Examples of bolaphiles; the basic elements are polar head groups (shaded) and lipophilic spacers (**1** from ref. [13], **2** from ref. [5], **3** from ref. [3]).

In natural membranes bolaform amphiphiles have chiral head groups, which are different in size and thus react stereoselectively with guest molecules.[3] In non-natural membranes binding sites can also be present,[9,22] or other functional groups can be incorporated such as redox- and/or photo-active moieties.[4] The repertoire of bolaamphiphiles is not limited to assemblies such as membranes and vesicles; specific "two-directional" arborols can form gels,[2,13-15] rods and tubules are formed by α-L-lysine-ω-aminobolaphiles.[16] When polymerizable functionalities are included either in the head groups or within the hydrophobic spacer, routes to extended covalently linked domains are opened up.[17,18]

Nontraditional structures (e.g., aqueous gels) result when noncovalent forces are coupled with a proper molecular architecture. The series of two-directional arborols synthesized by Newkome et al. demonstrates this variation on the theme of self-assembly.[13,14] In the proposed model of the aggregated structure one arborol is stacked upon the next; the hydrophobic chains

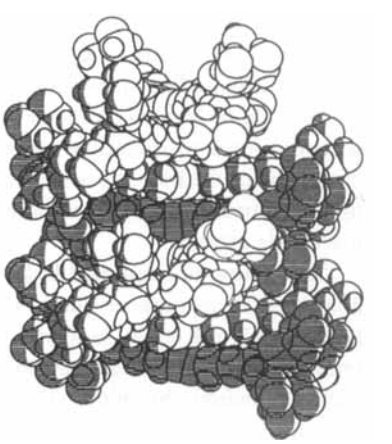
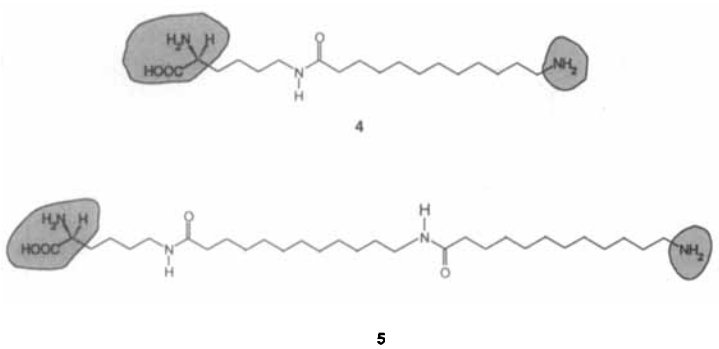


Fig. 1. Spatial representation of the stacking pattern calculated for **1**.

[*] Prof. G. R. Newkome, G. H. Escamilla
Center for Molecular Design and Recognition
Department of Chemistry
University of South Florida
Tampa, FL 33620-5250 (USA)
Telefax: Int. code + (813)974-4962

[**] This work was supported, in part, by the National Science Foundation (DMR-8906792 and DMR-9217331) and the Army Research Office (DAAHO4-93-G-0448).

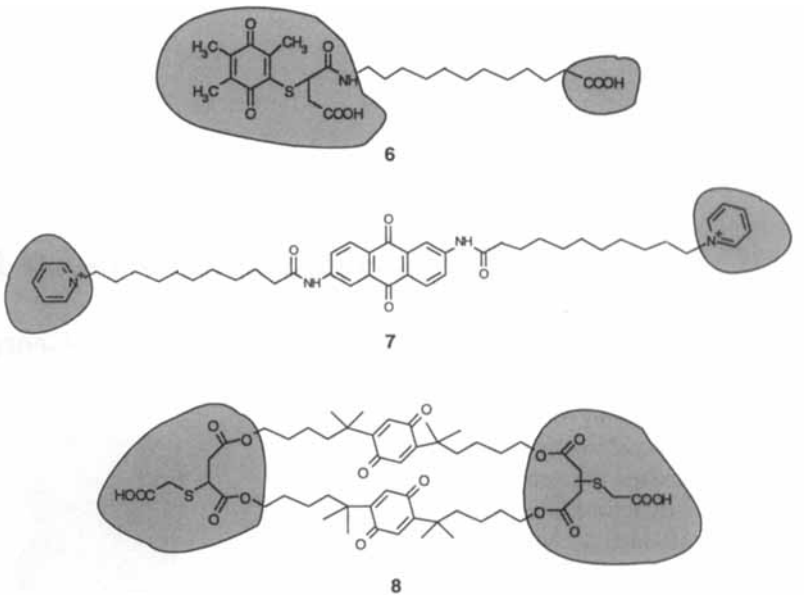
overlap and the hydrophilic hydroxyl groups are oriented out toward the aqueous solution (Fig. 1). Hydrogen bonding between the polar end groups and water results in a semisolid matrix. This proposed model is supported by the long fiberlike structures seen in electron micrographs of these assemblages.[13] As with micelle formation, there is a minimum spacer length needed for gelation to occur; for a saturated spacer this length is eight methylene units.[14] Aqueous mixtures of *N*,*N*′,*N*″,*N*‴-tetrakis[2-hydroxy-1,1-bis(hydroxymethyl)ethyl]hexadec-8-yne-1,1,16,16-tetracarboxamide and [18]crown-6 ether form particles rather than fibers, as evidenced by electron micrographs of resulting gels.[19] The rods and tubules described by Fuhrhop et al. follow an analogous pattern to the two-directional arborols.[16] When the racemic form of the lysine bolaphile **4** was used (Scheme 2), no rod or tubule formation was noted; in contrast, the racemate of the extended bolaphile **5** produced supramolecular assemblies identical to those formed by the pure enantiomers. The effect of configuration in molecular monolayers was shown to depend on membrane curvature in the same manner as in bilayers.[16]



Scheme 2. The unsymmetrical bolaphiles synthesized by Fuhrhop et al. for the generation of monolayer rods and tubules.

Fuhrhop et al. demonstrated[20] that placing quinone moieties in either the head groups or within the hydrophobic spacer resulted in redox-active membranes. The unsymmetrical bolaamphiphile **6** (Scheme 3) is a model of electron acceptors in photosynthesis and forms vesicles evident in electron micrographs. In the anticipated membrane organization all the quinone moieties should be located on the vesicle exterior. This assumption was confirmed by quantitative reduction of the quinone moieties with borohydride; since the reagent does not diffuse through lipid membranes, these "membrane quinones" must be part of the vesicle exterior.

The anthraquinone-based bolaphiles **7** or **8** could not form homogenous membranes due to steric interactions (Scheme 3). Bolaphiles **7** or **8** could, however, be integrated into host membranes formed by dihexadecylphosphate and dimethyldioctadecylammonium bromide. This bolaamphiphile fixed the quinone functionality at the center of the membrane and served as a model for pool quinones.[20] Electron transfer was further

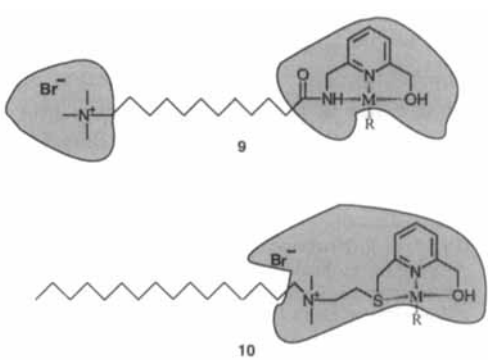


Scheme 3. The unsymmetrical bolaphile **6** was used to fix the quinone functionality at the surface of a micelle. **7** and **8** were used to position the quinone moiety within the membrane.

demonstrated by light-induced charge transfer between cationic porphyrins dissolved in water and membrane-bound anthraquinone bolaphiles.[21]

Bunton et al. proved that α,ω-bis(trimethylammonium) bolaphiles catalyze the spontaneous hydrolysis of 2,4-dinitrophenylphosphates.[11] The rate of hydrolysis was enhanced by micellar bolaphiles, and this rate enhancement followed the greater organization seen in vesicles formed by surfactants possessing longer spacers. Bolaphiles with hexadecane and dodecane spacers did not form micelles but small clusters instead, and the rate enhancement achieved was much lower than that with micelle-forming surfactants.[11]

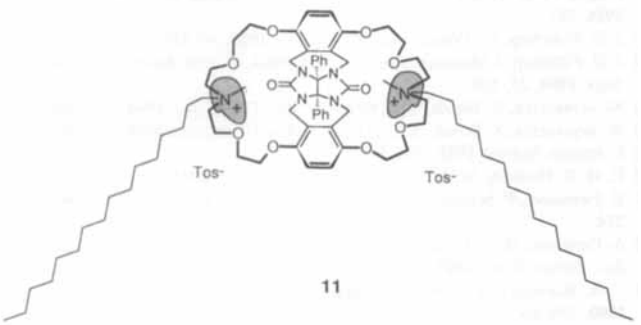
Fornasier et al. used metallomicelles formed from bolaphiles and surfactants with only one head group as catalysts for the cleavage of *para*-nitrophenyl picolinate.[9] Micelles generated from pyridine bolaphiles and Cu^{II} or Zn^{II} (Scheme 4) enhanced the rate of cleavage. As a comparison, the micelles generated from 6-{[2-(*n*-hexadecyldimethylamino)ethylthio]methyl}-2-(hydroxymethyl)pyridine bromide were not as effective catalysts. Increased electrostatic repulsion between the ammonium group



Scheme 4. The proximity of the charged head group to the binding site in **10** slows chelation of the metal relative to that with bolaphile **9**. M = Cu^{II}, Zn^{II}; R = *para*-nitrophenyl picolinate.

and the metal ion site explains the difference in effectiveness of the bolaform versus classical micelle. The crux of the catalytic process is formation of a ternary complex consisting of substrate, metal, and bolaform amphiphile as ligand.[9] These micelles demonstrate substrate discrimination, in other words, the correct substrate geometry is required for catalysis. Accordingly, no catalytic enhancement was found for the hydrolysis of the isomeric nicotinate and isonicotinate esters.

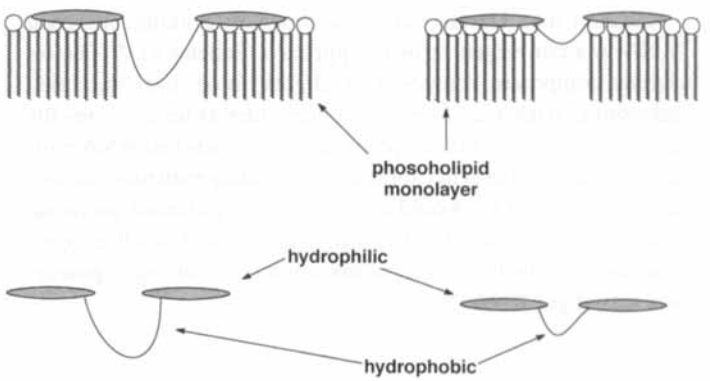
Nolte et al. recently reported[22] a functional vesicle formed by an assembly of hosts (Scheme 5) capable of binding guests such as resorcinol and 4-(4′-nitrophenylazo)resorcinol. In order



Scheme 5. Representation of bolaphile **11** used by Nolte et al. to prepare a functionalized vesicle.

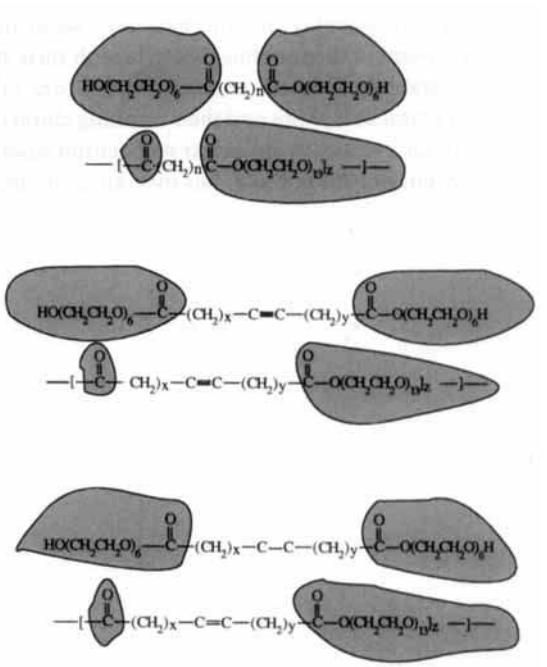
to maintain the hydrophobic binding site at the exterior of the vesicle, the authors used two quaternary nitrogen atoms each having a long alkyl chain. The rigidity of the binding site holds the charged nitrogen atoms apart and fixes the binding site near the plane of the nitrogen atoms and therefore the vesicle surface. Typical for lipids, the hydrophobic alkyl chains served to form the membrane interior. Interactions of solvent, binding sites, charged nitrogen atoms, and hydrophobic alkyl chains together govern the vesicular morphology, which was likened to a golf ball because of to its spherical shape and dimpled surface.[22] The golf ball analogy is completed by the concave shape of the binding site in the host. Examination of a cast film by X-ray diffraction yields a clear periodicity of 53 Å, which is approximately the length of two fully extended hexyldecylamine chains. Also, binding studies suggest that only half the total number of binding sites are able to interact with the guest. These data indicate a bilayer membrane with a thickness of approximately 53 Å.

Jayasuriya et al.[5] hypothesized that bolaform amphiphiles could be tailored to provide an optimal geometry for membrane disruption. Variation of either head groups or spacer could provide a "tunability" to target certain microorganisms. The bolaphiles[5] were proposed to disrupt membranes by insertion of their hydrophobic spacers into the lipid layer, which would cause a mismatch of the preferred geometries of the bolaphile and lipid. When more such interruptions occur, the membrane would become more destabilized (Scheme 6). Spacers with central triple or double bonds were made with the expectation that these functionalities would increase the disruptive capability of the bolaform amphiphiles. For alkane spacers ranging from decane to eicosane maximum activity was observed with pentadecane. In the olefinic analogues the geometry and position of the double bond were less important in determining membrane disruption than the overall length of the spacer. Similarly, the position of unsaturation was not important for the acetylenic bolaphiles.[5] A general trend was that maximum activity required an increase in spacer length when moving from saturated to olefinic to acetylenic spacers.



Scheme 6. Mechanism proposed by Jayasuriya et al. for the destabilization of a membrane by the insertion of the hydrophobic spacer of a bolaphile into the phospholipid layer and the resulting local defect.

The use of polymeric strings of bolaamphiphiles in membrane disruption was described by Jayasuriya et al. (Scheme 7).[6] The membrane disruptive activity of the polymeric bolaamphiphiles or "supramolecular surfactants" is up to 10^3 times greater than that of the monomeric analogues.[6] The precise origin of this amplification is not yet understood; however, several factors were proposed. Since the polymeric bolaamphiphiles have covalent linkages, the "bolaamphiphile defects" will be localized in the membrane and a high local concentration will be achieved. Domains of the supramolecular surfactant within the bilayer will be in equilibrium with nonaggregated membrane-bound



Scheme 7. Membrane-disruptive bolaphiles and their polymeric analogues.

 © VCH Verlagsgesellschaft mbH, D-69451 Weinheim, 1994 0570-0833/94/1919-1939 $ 10.00+.25/0

polymers. Repeat unit defects in the polymer are intrinsically more disruptive than the free monomer.[6] A polyester very similar to these "supramolecular surfactants" exhibited substantial protection for human CD4 + lymphocytes against HIV-1 during in vitro studies.[6] Thus a new route to nonionic membrane-disrupting agents is opened, in which activity and specificity can be tailored by molecular design.

Hudson and Damha have succeeded in making branched RNA in a convergent-growth approach (Scheme 8).[8] The resulting compound composed of oligothymine units, modified adenosine spacers, and terminal nucleotides as head groups fits the description of a bolaamphiphile. These branched RNA molecules could be useful in capturing and binding matching nucleotide sequences. This would allow access to potential antisense agents or ligands for affinity purification of the branch recognition factors, which catalyze the maturation or splicing of precursor messenger RNA.[8]



Scheme 8. An RNA-based bolaphile synthesized by Hudson and Damha.

Beyond these initial examples, basic questions remain concerning the conformation of bolaamphiphiles within micelles.[23] There is evidence that a bent conformation is adopted,[24] but micelles have been observed with very small hydrophobic cores and others are sometimes seen in electron micrographs with diameters that correspond to the length of the bolaphile.[23, 25] Among the many subjects for further exploration in the area of molecular self-assembly are the naturally occurring bolaamphiphiles found in thermophilic bacteria with their stereochemistry and stability in harsh environments. More robust membranes or chiral bolaphiles and their resulting chiral membranes could provide avenues to molecular recognition based on stereochemistry not only at one site, but over an entire membrane.[3]

Bolaamphiphiles, like cascade macromolecules,[26] have gained increasing attention recently, since they may offer insight into micellar systems that can mimic enzymes, act as therapeutic agents, or serve as tools in the investigation of molecular recognition and assemblages. Schenning's golf ball and the other examples described here illustrate the course Lehn set for supramolecular chemistry—structures alone are not the goal but rather the expression of a desired chemical, biological, or physical property.[27]

German version: *Angew. Chem.* **1994**, *106*, 2013

[1] R. M. Fuoss, D. J. Edelson, *J. Am. Chem. Soc.* **1951**, *73*, 269.
[2] G. R. Newkome, G. R. Baker, S. Arai, M. J. Saunders, P. S. Russo, V. K. Gupta, Z.-Q. Yao, J. E. Miller, K. Bouillon, *J. Chem. Soc. Chem. Commun.* **1986**, 752.
[3] J.-H. Fuhrhop, D. Fritsch, *Acc. Chem. Res.* **1986**, *19*, 130.
[4] J.-H. Fuhrhop, J. Matthieu, *Angew. Chem.* **1984**, *96*, 124; *Angew. Chem. Int. Ed. Engl.* **1984**, *23*, 100.
[5] N. Jayasuriya, S. Bosak, S. L. Regen, *J. Am. Chem. Soc.* **1990**, *112*, 5844.
[6] N. Jayasuriya, S. Bosak, S. L. Regen, *J. Am. Chem. Soc.* **1990**, *112*, 5851.
[7] I. Amato, *Science* **1993**, *260*, 491.
[8] R. H. E. Hudson, M. J. Damha, *J. Am. Chem. Soc.* **1993**, *115*, 2119.
[9] R. Fornasier, P. Scrimin, P. Tecilla, U. Tonellato, *J. Am. Chem. Soc.* **1989**, *111*, 224.
[10] A. Cipiciani, M. C. Fracassini, R. Germani, G. Savelli, C. A. Bunton, *J. Chem. Soc. Perkin Trans.* **1987**, 547.
[11] C. A. Bunton, E. L. Dorwin, G. Savelli, V. C. Si, *Recl. Trav. Chim. Pays-Bas* **1990**, *109*, 64.
[12] J.-M. Kim, D. H. Thompson, *Langmuir* **1992**, *8*, 637.
[13] G. R. Newkome, G. R. Baker, S. Arai, M. J. Saunders, P. S. Russo, K. J. Theriot, C. N. Moorefield, J. E. Miller, K. Bouillon, *J. Am. Chem. Chem. Soc.* **1990**, *112*, 8458.
[14] G. R. Newkome, X. Lin, C. Yaxiong, G. H. Escamilla, *J. Org. Chem.* **1993**, *58*, 3123.
[15] G. R. Newkome, C. N. Moorefield, G. R. Baker, R. K. Behera, G. H. Escamilla, M. J. Saunders, *Angew. Chem.* **1992**, *104*, 901; *Angew. Chem. Int. Ed. Engl.* **1992**, *31*, 917.
[16] J.-H. Fuhrhop, D. Spiroski, C. Boettcher, *J. Am. Chem. Soc.* **1993**, *115*, 1600.
[17] L. Gros, H. Ringsdorf, H. Schupp, *Angew. Chem.* **1981**, *93*, 311; *Angew. Chem. Int. Ed. Engl.* **1981**, *20*, 305.
[18] J.-H. Fendler, P. Tundo, *Acc. Chem. Res.* **1984**, *17*, 3.
[19] G. R. Newkome, G. H. Escamilla, M. J. Saunders, **1994**, unveröffentlichte Ergebnisse.
[20] J.-H. Fuhrhop, H. Hungerbuhler, U. Siggel, *Langmuir* **1990**, *6*, 1295.
[21] U. Siggel, H. Hungerbuhler, J.-H. Fuhrhop, *J. Chim. Phys.* **1987**, *84*, 1055.
[22] A. P. H. J. Schenning, B. de Bruin, M. C. Feiters, R. J. M. Nolte, *Angew. Chem.* **1994**, *106*, 1741; *Angew. Chem. Int. Ed. Engl.* **1994**, *33*, 1662.
[23] J.-H. Fuhrhop, R. Bach in *Advances in Supramolecular Chemistry, Vol. 2* (Ed.: G. W. Gokel), JAI Press, Greenwich, **1992**, p. 25.
[24] R. Zana, S. Yiv, K. M. Kale, *J. Colloid Interface Sci.* **1980**, *77*, 456.
[25] S. Yiv, R. Zana, *J. Colloid Interface Sci.* **1980**, *77*, 449.
[26] H.-B. Mekelburger, W. Jaworek, F. Vögtle, *Angew. Chem.* **1992**, *104*, 1609; *Angew. Chem. Int. Ed. Engl.* **1992**, *31*, 1571.
[27] J.-M. Lehn, *Angew. Chem.* **1990**, *102*, 1347; *Angew. Chem. Int. Ed. Engl.* **1990**, *29*, 1304.

 © VCH Verlagsgesellschaft mbH, D-69451 Weinheim, 1994 0570-0833/94/1919-1940 $ 10.00+.25/0

Molecules and Ions with Heptacoordinated Central Atoms

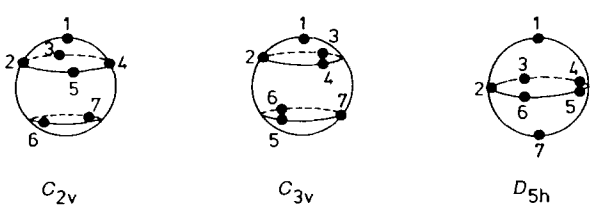
Rolf Minkwitz*

Since the valence-shell electron-pair-repulsion (VSEPR) model was developed to predict molecular structures, it has proved to be a strong stimulus for advances in structural chemistry. Key concepts to illustrate this are "stereochemical activity of lone pairs" or "steric demand of single and multiple bonds".

Heptacoordination is currently the focus of investigations by K. O. Christe et. al.,[1, 2] K. Seppelt et. al.,[3, 4] and J. K. Cockcroft et. al.[5, 6] So far it is only known for IF_7, ReF_7, and OsF_7, and the latter decomposes already at temperatures above 170 K.

Not until K. O. Christe et. al. characterized the "naked fluoride", the significance of which was previously highlighted[7] in this journal, could the anions $[XeF_5]^-$[8], $[OIF_6]^-$, $[TeF_7]^-$, $[OTeF_6]^{2-}$,[9] $[CH_3TeI]^{6-}$, and $[(CH_3)_2TeF_5]^-$[3] be prepared. Monomeric and/or unchelated complex cations with the coordination number (CN) 7 around the central atom are unknown.

For molecules and ions with coordination numbers 5 and 7 around their central atoms, we find many parallels with respect to their structural diversity and their intramolecular dynamics. For CN 5, calculations, which take into consideration that electrostatic repulsions occur between ligands, allow two polyhedra, the trigonal bipyramid and the square pyramid. Their difference in energy is small and they can be interconverted by a succession of angular shifts according to the Berry pseudorotation mechanism. For CN 7, three polyhedra with only small energy differences and minimum energies for the C_{2v} and C_{3v} structures[10] have been calculated under the same assumptions (Scheme 1).



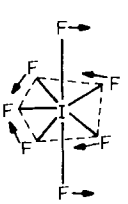
Scheme 1.

The results of earlier IR spectroscopic investigations[1] on IF_7 had been consistent with a pentagonal-bipyramidal stucture of the molecule. This assumption was confirmed by electron diffraction in the gas phase[11] in spite of much uncertainty in the structural data. Crystal structure analyses performed by K. Seppelt et. al. on salts with the $[TeF_7]^-$, $[CH_3OTeF_6]^-$, $[(CH_3O)_2TeF_5]^-$,[3] and $[OIF_6]^-$ anions give a more refined picture.[2] Without exception, these anions are distorted pentagonal bipyramids with slightly shortened bonds to the axial ligands. The large methoxy ligands and the oxygen atom in $[OIF_6]^-$ also occupy axial positions. The distortion relates to the fluorine atoms in close contact around the pentagonal base. They avoid steric crowding by arranging themselves above and below the theoretical plane of the pentagon.

Details of this puckering can be studied in the crystal structure of ReF_7, which has been determined at 1.5 K by T. Vogt, A. N. Fitch, and J. K. Cockcroft, by using high-resolution powder neutron diffraction.[6] The mean displacement of the equatorial F atoms from the ideal ring plane is 0.17 Å and the mean deviation from perpendicular of the angle between axial and equatorial Re–F bonds is 6.2°. The average $Re-F_{eq}$ and $Re-F_{ax}$ bonds are 1.851 and 1.823 Å, respectively, that is the axial bonds are 1.4% shorter. The F_{ax}-Re-F_{ax} angle is 174.6° in the crystal and 172.5° in the gas phase, as determined by electron diffraction analysis.[12] The crystallographic point symmetry of the molecule is C_1, but within experimental error it has a mirror plane, so that the molecular symmetry is C_s. Because of strong deviations of the distorted pentagonal bipyramid from ideal D_{5h} symmetry, the molecular structure at 1.5 K is interpreted as a frozen-in state of the pseudorotational motion.

In a remarkable paper by K. O. Christe, E. C. Curtis, and D. A. Dixon, problems of heptacoordination are discussed for IF_7 as the most-studied prototype. On steric grounds, there is no high-symmetry arrangement of five ligands with normal bond lengths in a plane. Therefore, dynamic ring puckering occurs with large vibrational amplitudes, comparable to the vibrational ring motion in cyclopentane. This "ring puckering", also termed "Bartell-type pseudorotation" by K. O. Christe, has an unexpectedly low vibrational frequency (59 cm^{-1} (0.17 kcal mol^{-1})), which means that there are thermally activated overtones even at very low temperatures. Unfortunately, these vibrations (E_2'' in D_{5h}) are neither IR nor Raman active and can be detected only indirectly in the form of very low-intensity combination bands.

All F atoms in neutral molecular fluorides and fluoro anions with CN 7 are equivalent by NMR spectroscopy. Aside from the very fast ring-puckering mechanism, this equivalence is attributed to a much slower fluxionality between the axial and the equatorial ligands according to the Berry mechanism. The lifetime of a single configuration for IF_7 is estimated to be 2.7×10^{-3} s. The exchange starts from a deformation mode at 265 cm^{-1}, and the activation energy corresponds to a multiple of this frequency. The ligand exchange motion as such is best described as a combination of the out-of-phase axial and equatorial deformation modes (described by the symmetry coordinates S_6 and S_7), accompanied by an out-of-plane twisting mode of the remaining three equatorial F atoms (Scheme 2).



Scheme 2.

In the $[OIF_6]^-$ ion, the O atom avoids the equatorial position because of a partial double bond and thus inhibits axial–equatorial fluxionality. Additionally, in crystalline $[(CH_3)_4N][OIF_6]$, the puckering of the equatorial F atom plane is static rather than fluxional, since interionic H ··· F contacts hinder the vibrations. Questions about the true structure of molecules with strong

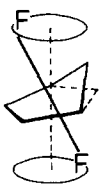
[*] Prof. Dr. R. Minkwitz
Fachbereich Chemie der Universität
D-44221 Dortmund (FRG)
Telefax: Int. code + (231)755-3771

fluxionality can only be answered with respect to the method of measurement and its corresponding time scale.

According to ab initio calculations at different theoretical levels, IF_7 in its minimum potential[1] has an undistorted D_{5h} symmetry. Indicative of this is the absence of microwave transitions and of a permanent dipole moment. Also, temperature-dependent crystal structure analyses of $[(CH_3)_4N][OIF_6]$ show that the ring puckering diminishes with falling temperature, that is the arrangement of the equatorial F atoms approaches the arrangement in a plane.

Normal coordinate analyses of IF_7, $[OIF_6]^-$, and $[XeF_5]^-$ give a picture of the vibrating molecule or ion. They are dynamically rather than statically distorted, and on average also have D_{5h} symmetry. According to force-field calculations, the equatorial (in-plane) deformation force constant is in good approximation a measure of the steric hindrance of the ligands in the pentagonal plane. Crowding increases with decreasing bond length and decreasing size of the central atom. It also increases with increasing size of the ligand and increasing temperature.

Because in electron diffraction in the gas phase the time scale is very short, such investigations register only average structures with an equilibrium symmetry between C_1 and C_s. Not only is the equatorial ring puckering evident, but also an inclination of the axial F atoms away from the ideal 180° angle towards approximately 171° for IF_7[1] and 172.5° for ReF_7.[12] Through the dynamic ring puckering in the pentagonal plane, these axial F atoms experience a non-uniform repulsion in such a way that they are each dynamically forced aside by the closest lying ligand (Scheme 3). In other words, the dynamic equatorial puckering gives rise to a coupled in-phase precession of the axial F atoms, which had earlier been interpreted by Bartell as a static inclination. We now know that it is a consequence of the dynamic ring puckering.



Scheme 3.

Molecules and ions with a heptacoordinated central atom do not adopt the minimum-energy structures of a capped prism (C_{3v} symmetry) or a capped octahedron (C_{2v} symmetry) as predicted by VSEPR theory. They rather reside on a slightly raised saddle point of the energy hypersurface, where they adopt a pentagonal-bipyramidal structure with D_{5h} symmetry. K. Seppelt has pointed out[3] that of the possible structures for compounds with coordination numbers 5, 8, and 7, the arrangement with the highest symmetry is also the most common one, and not the minimum-energy structure. This seems to be a general principle for the for the formation of such structures.

As regards chemical bonding, K. O. Christe et. al. have proposed a model,[11] in which the five pentagonal ligands are bound through $p_{x,y}$ hybrid orbitals from the central atom in a semiionic six-center, ten-electron bond. The axial ligands are mainly covalently bonded through two sp_z hybrid orbitals.

German version: *Angew. Chem.* **1994**, *106*, 2017

[1] K. O. Christe, E. C. Curtis, D. A. Dixon, *J. Am. Chem. Soc.* **1993**, *115*, 1520–1526.
[2] K. O. Christe, D. A. Dixon, A.-R. Mahjaub, H. P. A. Mercier, J. O. P. Sanders, K. Seppelt, G. J. Schrobilgen, W. W. Wilson, *J. Am. Chem. Soc.* **1993**, *115*, 2696–2706.
[3] A.-R. Mahjaub, R. Drews, K. Seppelt, *Angew. Chem.* **1992**, *104*, 1047–1050; *Angew. Chem. Int. Ed. Engl.* **1992**, *31*, 1036–1039.
[4] A.-R. Mahjaub, K. Seppelt, *J. Chem. Soc. Chem. Commun.* **1991**, 840–841.
[5] T. Vogt, A. N. Fitch, J. K. Cockcroft, *J. Solid State Chem.* **1993**, *103*, 275–279.
[6] T. Vogt, A. N. Fitch, J. K. Cockcroft, *Science*, **1994**, *263*, 1265–1267.
[7] K. Seppelt, *Angew. Chem.* **1992**, *104*, 299–300; *Angew. Chem. Int. Ed. Engl.* **1992**, *312*, 292–293.
[8] K. O. Christe, E. C. Curtis, D. A. Dixon, H. P. Mercier, J. C. P. Sanders, G. J. Schrobilgen, *J. Am.* Chem. *Soc.* **1991**, *113*, 3351–3361.
[9] K. O. Christe, J. C. P. Sanders, G. J. Schrobilgen, W. W. Wilson, *J. Chem. Soc. Chem. Commun.* **1991**, 837–840.
[10] *The VSPR Model of Molecular Geometry* (Eds.: R. Gillespie, I. Hargittai), Allyn and Bacon, Needham Heights, MA, USA **1991**, p. 58.
[11] W. J. Adams, B. H. Thomson, L. S. Bartell, *J. Chem. Phys.* **1970**, *53*, 4040–4046.
[12] E. J. Jakob, L. S. Bartell, *J. Chem. Phys.* **1970**, *53*, 2235–2242.

 © VCH Verlagsgesellschaft mbH, D-69451 Weinheim, 1994 0570-0833/94/1919-1942 $ 10.00+.25/0

$Rb_3[Nb_6SBr_{17}]$, the First Compound Containing an Isolated Trigonal-Prismatic Niobium Cluster**

Hermann Womelsdorf and H.-Jürgen Meyer*

The chemistry of reduced niobium halides is rich in clusters with differing structures. The niobium atoms form trigonal (Nb_3Br_8[1]), rhombic ($Cs[Nb_4Cl_{11}]$[2]), and tetrahedral (NbSeI[3]) clusters. The dominant structural motif, however, is that of the octahedral niobium cluster of the Nb_6X_{12} (X = F, Cl, Br) and of the Nb_6X_8 type (X = I[4]).[5] The binary halides Nb_6Cl_{14}[6] and Nb_6F_{15}[7] (analogous bromine compounds are not known), ternary compounds such as $In[Nb_6Cl_{15}]$[8] and $K_4[Nb_6Cl_{18}]$[9] as well as quaternary compounds such as $In_2Li_2[Nb_6Cl_{18}]$[10] and $CsEr[Nb_6Cl_{18}]$[11] all crystallize with Nb_6X_{12} type structures. The existence of an isolated trigonal-prismatic niobium cluster was suggested previously;[12] and with $Rb_3[Nb_6SBr_{17}]$, such a compound has now been synthesized and characterized for the first time.

In the crystal structure of $Rb_3[Nb_6SBr_{17}]$,[13] 18 bromine atoms are coordinated to the trigonal-prismatic, sulfur-centered Nb_6S unit (Fig. 1). Six of these bromine atoms lie above the six

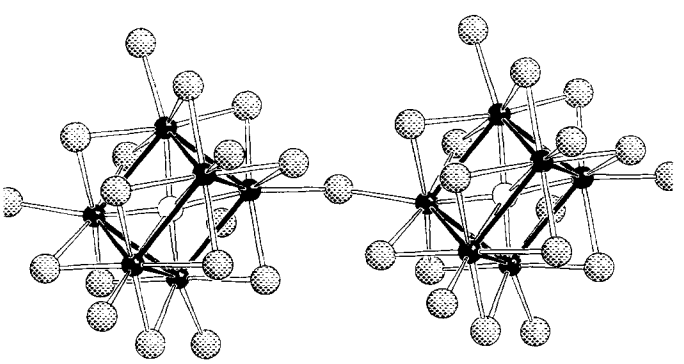


Fig. 1. Chains formed by linkage of the $[Nb_6SBr_{18}]^{4-}$ units through bromine atoms.

edges of the triangular faces of the prism at a distance (Nb–Br) of 257–261 pm, and a further six bromine atoms lie above the rectangular faces at a distance of 266–269 pm. The remaining six bromine atoms occupy terminal positions above the corners of the prism at a distance of 268–279 pm. The bromine atoms are nearly hexagonally close packed, and the niobium atoms occupy—analogous to the Nb_3Br_8 structure—the octahedral holes, from where they are slightly shifted towards one another. The $[Nb_6SBr_{18}]^{4-}$ units are linked through two terminal bromine atoms to form chains; the longest of the Nb–Br distances (279 pm) is found here. The Rb ions are situated between the chains of cluster molecules. Each Rb ion is surrounded in a nearly anticuboctahedral manner by twelve bromine atoms.

The Nb_6 cluster has a distorted trigonal-prismatic structure with Nb–Nb distances of 328 pm along the edges of the rectangles (here and in the following this term is assigned to those edges of the rectangles which are perpendicular to the planes of the triangular faces). The sulfur atom is located almost exactly in the center of the prism (the Nb–S distances are about 237 pm). The Nb–Nb distances along the edges of the triangle (295–298 pm, mean: 297 pm) are longer than those in Nb_3Br_8[1] by about 7–10 pm and correspond to the value usually found for octahedral niobium bromide clusters.[14] The Nb–Nb distances along the edges of the rectangles are rather long (328 pm) when compared to those in octahedral niobium clusters. Thus, the question arises whether Nb–Nb interactions occur along the edges of the rectangles of the prism.

MO calculations[15] on a $[Nb_6SBr_{18}]^{4-}$ unit show that the fourteen electrons available to the cluster for Nb–Nb bonds fill both the Nb–Nb bonding orbitals, which form the triangles, and those which are assigned to the edges of the rectangles. Indeed, small positive overlap populations (edges of the triangles: 0.25; edges of the rectangles: 0.05) are found between the niobium atoms of the edges of the rectangles. The energy level scheme of the $[Nb_6SBr_{18}]^{4-}$ unit can be constructed based of the MO analysis of a $Nb_3Br_{13}^{5-}$ unit[12] from the Nb_3Br_8 structure. This is illustrated in Figure 2, which shows the splitting of the niobium (d) energy states into—with respect to the interactions along the edges of the rectangles—bonding, nonbonding, and antibonding combinations in $Rb_3[Nb_6SBr_{17}]$. A relative measure for the bonding Nb–Nb interactions along the edges of the rectangles

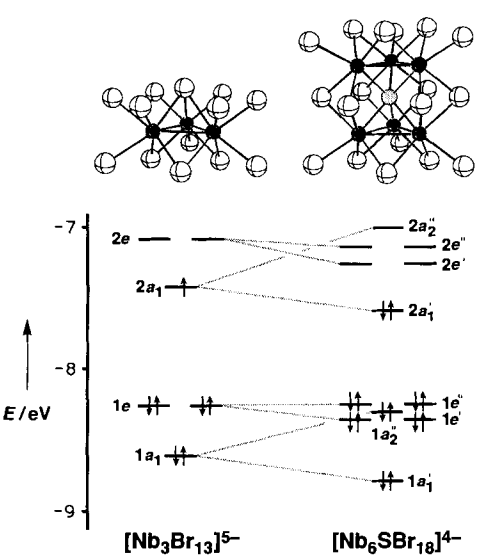
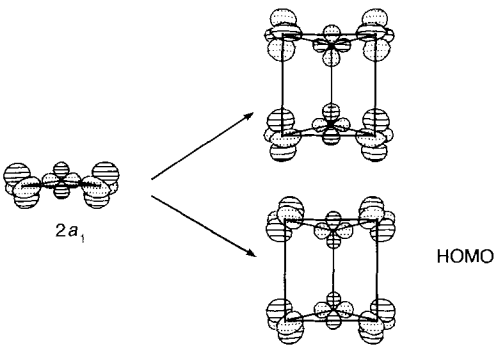


Fig. 2. Comparison of the filled d energy states of $Nb_3Br_{13}^{5-}$ [12] (left) with those of $[Nb_6SBr_{18}]^{4-}$ (right). The energy levels are labeled accoring to idealized C_{3v} and D_{3h} symmetry.

[*] Priv.-Doz. Dr. H.-J. Meyer, Dipl.-Chem. H. Womelsdorf
Institut für Anorganische Chemie der Universität
Callinstrasse 9, D-30167 Hannover (FRG)
Telefax: Int. code + (511)762-3006

[**] This work was supported by the Deutsche Forschungsgemeinschaft and the Fonds der Chemischen Industrie. We thank Prof. Dr. G. Meyer for providing funds from the Institute.

is the splitting of the a_1 states of two Nb_3 clusters (Fig. 2). The combinations of the $2a_1$ orbitals are shown in Scheme 1.



Scheme 1. The formation of a bonding (HOMO) and an antibonding combination (top) from $2a_1$ orbitals of two Nb_3 units.

The Nb_3 triangles of the trigonal-prismatic unit are held together by strong Nb–S bonds, whose states, like those of Nb–Br bonds, are lower in energy than those metal states shown in Figure 2. Weak Nb–Nb bonds strengthen this effect.

In centered clusters the interstitial atom is formally considered either as an electron donor or an electron acceptor. Zr_6CCl_{14}[16] serves as an example for the former. Here the electrons of the carbon atom are added to the cluster electrons: 6×4 (Zr) -14 (Cl) $+4$ (C) $=14$ electrons for metal–metal bonds. Centered clusters are rare for "electron-richer" metals; an example is the trigonal-antiprismatic Mo_6 unit in $Mo_6O(OEt)_{18}$ (16 electrons),[17] in which the oxygen center acts as an electron acceptor. In $Rb_3[Nb_6SBr_{17}]$ the number of electrons available to the cluster for metal–metal bonds is fourteen (6×5 (Nb) $+3\times1$ (Rb) -17×1 (Br) -2 (S) $=14$). Consideration of the MOs for $Rb_3[Nb_6SBr_{17}]$ confirms this, since the seven highest occupied energy states almost exclusively consist of Nb(d) states without noteworthy contributions from sulfur. Thus, the sulfur atom in the center of the cluster is an electron acceptor. Nevertheless, it can be assumed that without the interstitial sulfur atom, as for example in $K_4[Nb_6Br_{18}]$,[14] the Nb_6 prism is less stable than the competing octahedron.

$Rb_3[Nb_6SBr_{17}]$ is the first niobium cluster with an isolated trigonal-prismatic building block. The structural principle of a trigonal-prismatic, sulfur-centered niobium cluster was previously indicated in the structure of Nb_6I_9S,[18] where the sulfur atom resides in a distorted trigonal-prismatic environment formed by the triangular faces of two neighboring Nb_6 clusters.

Experimental Procedure

$Rb_3[Nb_6SBr_{17}]$ was obtained by the reaction of RbBr (124 mg), niobium (74 mg), $NbBr_5$ (345 mg), and sulfur (8 mg). The starting materials were weighed under an argon atmosphere in a glove box and placed into a niobium ampoule, which was sealed and afterwards melted in an evacuated quartz glass ampoule. The reaction mixture was allowed to react over a period of five days at 800 °C. $Rb_3[Nb_6SBr_{17}]$ was obtained as the main product (ca. 70%) in the form of black crystals. The remaining material consisted of fluffy crystals of the $Cs[Nb_3Br_7S]$ type.[19] $Rb_3[Nb_6SBr_{17}]$ is relatively stable in air and is also resistant against moisture for quite some time.

Received: February 23, 1994
Revised version: May 27, 1994 [Z67061E]
German version: *Angew. Chem.* **1994**, *106*, 2022

[1] A. Simon, H. G. von Schnering, *J. Less Common Met.* **1966**, *11*, 31.
[2] A. Broll, A. Simon, H. G. von Schnering, H. Schäfer, *Z. Anorg. Allg. Chem.* **1969**, *367*, 1.
[3] H. B. Yaich, J. C. Jegaden, M. Potel, M. Sergent, A. K. Rastogi, R. Tournier, *J. Less Common Met.* **1984**, *102*, 9.
[4] A. Simon, H. G. von Schnering, H. Schäfer, *Z. Anorg. Allg. Chem.* **1967**, *355*, 295.
[5] C. Perrin, M. Sergent, *Eur. J. Solid State Inorg. Chem.* **1991**, *28*, 933.
[6] A. Simon, H. G. von Schnering, H. Wöhrle, H. Schäfer, *Z. Anorg. Allg. Chem.* **1965**, *339*, 155.
[7] K.-J. Niehues, H. G. Nieder-Vahrenholz, H. G. von Schnering, H. Schäfer, *J. Less Common Met.* **1965**, *8*, 95.
[8] A. Lachgar, H.-J. Meyer, unpublished results.
[9] A. Simon, H. G. von Schnering, H. Schäfer, *Z. Anorg. Allg. Chem.* **1969**, *361*, 235.
[10] A. Lachgar, H.-J. Meyer, *J. Solid State Chem.* **1994**, *110*, 15.
[11] S. Ihmaïne, C. Perrin, M. Sergent, *Acta Crystallogr. Sect. C* **1989**, *45*, 705.
[12] H.-J. Meyer, *Z. Anorg. Allg. Chem.* **1994**, *620*, 81.
[13] Single-crystal X-ray structure data of $Rb_3[Nb_6SBr_{17}]$: monoclinic, space group $C2/c$ (no. 15), $a=1712(1)$, $b=1885.3(7)$, $c=939.7(5)$ pm, $\beta=90.77(4)°$, $V=3033.4$ Å^3, $Z=4$. Of 7976 measured reflections 4075 were symmetry independent, of which 1639 $F_0>4\sigma(F_0)$. $R_w(F^2)=0.13$, $R(F)$ with $F_0>4\sigma(F_0)=0.062$. Determination of the lattice parameters, of the Bravais type, and measurement of the intensities were carried out with a four-circle diffractometer Siemens-Stoe-AED 2 ($Mo_{K\alpha}$, $\mu=294$ cm^{-1}, $2\theta_{max}=58°$). Empirical absorption correction, structure determination with SHELXS-86, structure refinement with SHELXL-93. Further details of the crystal structure investigation may be obtained from the Fachinformationszentrum Karlsruhe, D-76344 Eggenstein-Leopoldshafen (FRG) on quoting the depository number CSD-400496.
[14] F. Ueno, A. Simon, *Acta Crystallogr. Sect. C* **1985**, *41*, 308.
[15] D. M. Proserpio, C. Mealli, *J. Chem. Educ.* **1990**, *67*, 399.
[16] J. D. Smith, J. D. Corbett, *J. Am. Chem. Soc.* **1986**, *108*, 1927.
[17] J. A. Hollingshead, R. E. McCarley, *J. Am. Chem. Soc.* **1990**, *112*, 7402.
[18] H.-J. Meyer, J. D. Corbett, *Inorg. Chem.* **1991**, *30*, 963.
[19] H.-J. Meyer, *Z. Anorg. Allg. Chem.* **1994**, *620*, 863.

O-Glycoside Syntheses under Neutral Conditions in Concentrated Solutions of $LiClO_4$ in Organic Solvents**

Herbert Waldmann,* Gerd Böhm, Uschi Schmid, and Herbert Röttele

Glycoconjugates have crucial functions in many important biological processes.[1] The development of efficient methods for the directed syntheses of tailored complex glycosides, which could, for example, be used to study these processes, is therefore of great importance, in particular in medicinal chemistry.[2]

Reliable routes for the syntheses of glycosides are the diverse variations of the Koenigs–Knorr reaction,[3] in which glycosyl halides must be activated by heavy metal salts. Furthermore, the transformations with glycosyl fluorides[4] and with trichloroacetimidates according to Schmidt et al.,[5] in which in both cases the glycosyl donor is activated by Lewis acids like $BF_3\cdot OEt_2$, and with thioglycosides, which are transformed into reactive glycosyl donors with alkylating agents,[4, 6] are particularly powerful methods for the chemical synthesis of oligosaccharides.

However, numerous polyfunctional glycoconjugates that are target compounds in complex oligosaccharide syntheses contain many reactive functionalities as well as acid- and base-labile glycosidic bonds. For example, the recently described total synthesis of the oligosaccharide part of calicheamycin γ_1^I[7] had to take into accout the high reactivity of nucleophilic amino and sulfide groups, and the synthesis of benzyl-protected fucosyl glycosides

[*] Prof. Dr. H. Waldmann, Dipl.-Chem. G. Böhm, Dipl.-Chem. U. Schmid, Dr. H. Röttele
Institut für Organische Chemie der Universität
Richard-Willstätter-Allee 2, D-76128 Karlsruhe (FRG)
Telefax: Int. code + (721)608-4825

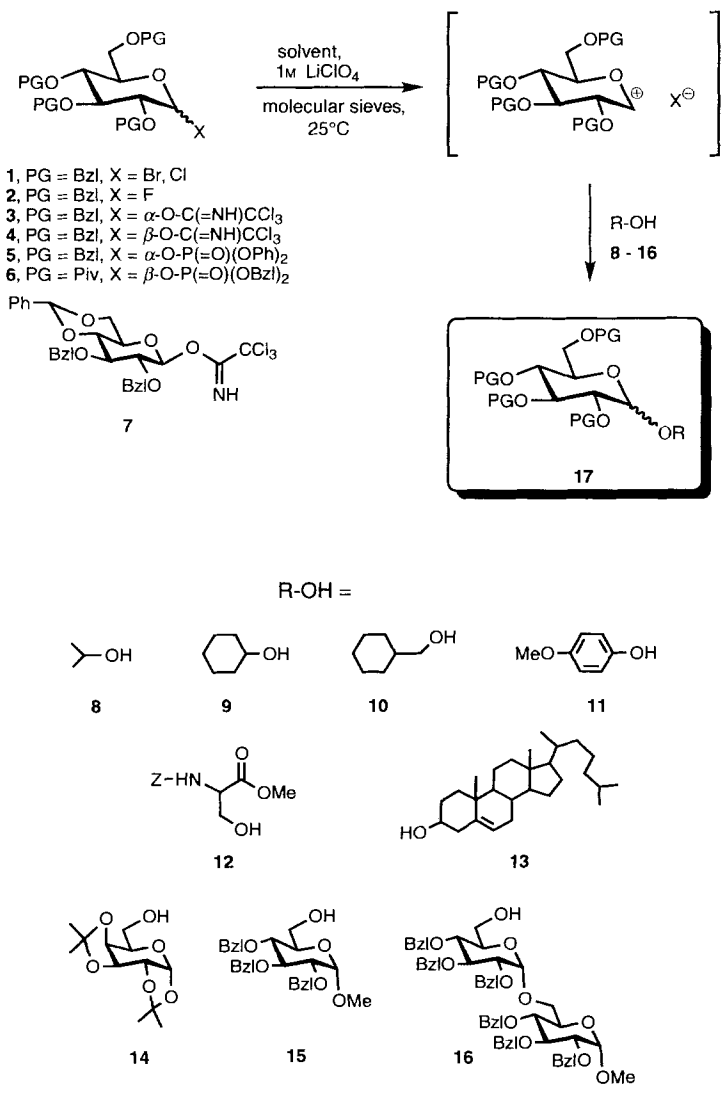
[**] This work was supported by the Deutsche Forschungsgemeinschaft and the Fonds der Chemischen Industrie.

was often substantially hampered by their high sensitivity to acid.[8] It is therefore desirable to develop methods for the chemical synthesis of O-glycosides that require very mild, and preferably neutral, conditions without the use of toxic and expensive heavy metal salts or other promoters like alkylating agents.

The concept behind our method was that the detachment of the leaving group X from glycosyl donors like **1**–**7** should be initiated by a solvent that could stabilize any potential glycosyl cation that might arise as intermediate (Scheme 1). The results of Grieco et al. and other research groups on the acceleration of cycloadditions and rearrangements[9] suggested that concentrated solutions of $LiClO_4$ in organic solvents might fulfill this criterion. We report now that these reaction media favor the formation of glycosyl cations from various glycosyl donors and thus are eminently suitable for O-glycoside syntheses under very mild conditions.

The model glycosyl donors **1**–**7** were used for the development of the method. Donors **1**–**5** have benzyl protecting groups that cannot influence the course of the synthesis through neighboring group effects. As leaving group X at the anomeric center, the halides Br^-, Cl^-, and F^-, trichloroacetimidate,[10] and diphenylphosphate[11] were employed. The stability of a benzylideneacetal group under the conditions of our synthesis method was studied with compound **7**.[12] The O-pivaloylated glucosyl phosphate **6**[12] was selected as acyl-proctected glycosyl donor in which the acyl protecting group at O-2 directs the steric course of the glycosylation. Model glucosyl acceptors were the simple aliphatic alcohols **8**–**10**, the aromatic alcohol **11**, the serine derivative **12**, the steroid **13**, the monosaccharides **14** and **15**, and the disaccharide **16**. The solvents were Et_2O, CH_2Cl_2, $CHCl_3$, and CH_3CN.

The glycosyl donors **1**–**7** react with the glycosyl acceptors **8**–**16** in concentrated solutions of $LiClO_4$ in the organic solvents without addition of promotors or reagents to form the O-glycosides **17** (Scheme 1, Table 1). According to preliminary experiments on the influence of the $LiClO_4$ concentration on the course of the reaction, the best results were achieved in 1 M solutions; all further investigations were performed at this concentration.



Scheme 1. Synthesis of O-glycosides in 1 M solutions of $LiClO_4$ in organic solvents.

Table 1. Results of the O-glycoside syntheses.

No.	Glycosyl donor	Glycosyl acceptor	Solvent	Yield [%] [a]	Anomeric ratio (α:β) [b]
1	**1** (X = Br)	**8**	Et_2O [c]	61	1:1
2	**2**	**10**	Et_2O [c]	63	2:1
3	**3**	**10**	Et_2O	79	1:1
4	**3**	**9**	Et_2O	63	1:1
5	**3**	**11**	Et_2O	56	1:1
6	**3**	**12**	Et_2O	50	1:1
7	**3**	**14**	Et_2O	45	1:1
8	**4**	**8**	CH_3CN	95	1:2
9	**4**	**8**	CH_2Cl_2	96	1:1
10	**4**	**11**	Et_2O	65	1:1
11	**4**	**12**	CH_2Cl_2	58	4:1
12	**4**	**14**	Et_2O	47	2:1
13	**4**	**16**	CH_2Cl_2	42	2.3:1
14	**7**	**15**	CH_2Cl_2	48	5:1
15	**5**	**8**	CH_2Cl_2	47	1:4
16	**5**	**10**	CH_2Cl_2	36	1:7
17	**5**	**13**	CH_2Cl_2	42	1:2
18	**6**	**8**	CH_2Cl_2	68	only β
19	**6**	**13**	$CHCl_3$	56	only β
20	**6**	**14**	$CHCl_3$	54	only β

[a] Based on chromatographically purified glycoside **17**. All glycosides **17** were identified in $CDCl_3$ solution by ^1H NMR spectroscopy (250 or 400 MHz). [b] Determined by integration of the relevant signals in the ^1H NMR spectra of the anomeric mixtures or by HPLC. [c] 1 equiv CsF was added as scavenger for acid.

Considering that under these mild conditions the glycosyl donors are not additionally activated, for example through the formation of better leaving groups at the anomeric center, and that the two reactants are always employed in equimolar amounts, the yields of **17** are satisfactory to high. The halogenoses **1** can for instance be employed as benzyl-protected donors (Table 1, no. 1), but higher yields are recorded if the trichloroacetimidates **3** and **4** are used. Particularly surprising is the finding that the glycosyl fluoride **2**, which usually can be activated only by strong Lewis acids like $BF_3 \cdot OEt_2$, and the alcohol **10** react to form the O-glycoside in high yield (Table 1, no. 2). With the α-configurated trichloroacetimidate **3**, the desired glycosides are obtained as 1:1 mixtures of the two anomers (Table 1, nos. 3–7), and with the β-imidate **4** as well as with the β-configurated glycosyl donor **7**, the α-glycosides are in general formed predominantly (Table 1, nos. 9–14). Distinct excesses of β-**17** were achieved with the benzyl-protected α-diphenyl-

phosphate **5** (Table 1, nos. 15–17). The solvents Et_2O, CH_2Cl_2, and $CHCl_3$ influence neither the magnitude nor the kind of the anomeric ratio. However, if the β-trichloroacetimidate **4** is treated with **8** in the solvent CH_3CN,[13] which stabilizes the glycosyl cation, the β anomer is in excess in contrast to the situation in CH_2Cl_2 (Table 1, nos. **8** and **9**). Thus with the trichloroacetimidate or diphenyl phosphate residue as leaving group at the anomeric center of the glycosyl donor and in the presence of benzyl protecting groups that are not capable of exerting neighboring group effects, the stereoselection in the synthesis of O-glycosides **17** can be deliberately steered to either direction. On the other hand, the pivalic acid ester in **6** participates anchimerically in the glycosylation, with the result that, as expected, the β-glycosides are formed with this glycosyl phosphate (Table 1, nos. 18–20).

The examples in Scheme 1 and Table 1 indicate that not only glycosides of simple aliphatic and aromatic alcohols can be formed under mild conditions and without additional promoters by our method reported here, but hydroxyamino acids and steroids can also be glycosylated and disaccharides synthesized successfully. Moreover the method is suitable for the construction of larger glycoconjugates, as the coupling of **4** with the disaccharide **16**, which yields the desired trisaccharide with satisfactory results, shows (Table 1, no. 13).

Received: May 11, 1994 [Z 6923 IE]
German version: *Angew. Chem.* **1994**, *106*, 2024

[1] Reviews: a) L. A. Lasky, *Science* **1992**, *258*, 964; b) S. Hakomori, *Adv. Cancer Res.* **1989**, *52*, 257; c) T. Feizi, *Nature* **1985**, *314*, 53; d) J. C. Paulson in *The Receptors, Vol. 2* (Eds.: M. Conn), Academic Press, New York, **1985**, p. 131.
[2] Review: J. H. Musser, *Annu. Rep. Med. Chem.* **1992**, *27*, 301.
[3] H. Paulsen, *Angew. Chem.* **1982**, *94*, 184; *Angew. Chem. Int. Ed. Engl.* **1982**, *21*, 155.
[4] Short Review: H. Waldmann, *Nachr. Chem. Tech. Lab.* **1991**, *39*, 675.
[5] Review: R. R. Schmidt, *Angew. Chem.* **1986**, *98*, 213; *Angew. Chem. Int. Ed. Engl.* **1986**, *25*, 212.
[6] a) P. Fügedi, P. J. Garegg, H. Lönn, T. Norberg, *Glycoconjugate J.* **1987**, *4*, 97; b) review on more recent methods of glycoside synthesis: K. Toshima, K. Tatsuta, *Chem. Rev.* **1993**, *93*, 1503.
[7] R. D. Groneberg, T. Miyazaki, N. A. Stylianides, T. J. Schulze, W. Stahl, E. P. Schreiner, T. Suzuki, Y. Iwabuchi, A. L. Smith, K. C. Nicolaou, *J. Am. Chem. Soc.* **1993**, *115*, 7593.
[8] See H. Kunz, C. Unverzagt, *Angew. Chem.* **1988**, *100*, 1763; *Angew. Chem. Int. Ed. Engl.* **1988**, *27*, 1697.
[9] Reviews: a) P. A. Grieco, *Aldrichimica Acta* **1991**, *24*, 59; b) H. Waldmann, *Angew. Chem.* **1991**, *103*, 1335; *Angew. Chem. Int. Ed. Engl.* **1991**, *30*, 1306.
[10] a) R. R. Schmidt, J. Michel, M. Roos, *Liebigs Ann. Chem.* **1984**, 1343; b) R. R. Schmidt, M. Stumpp, *ibid.* **1983**, 1249.
[11] R. R. Schmidt, M. Stumpp, *Liebigs Ann. Chem.* **1984**, 680.
[12] Compound **7** was synthesized analogously to **4** [10] by reaction of the appropriate carbohydrate deblocked in the 1-position with trichloroacetonitrile in the presence of K_2CO_3: colorless oil; $[\alpha]_D^{20} = -7$ ($c = 1.5$ in $CHCl_3$); ^1H NMR (250 MHz, $CDCl_3$, 25 °C, TMS): $\delta = 5.93$ (d, ^3J(1-H, 2-H) = 7.7 Hz, 1H; 1-H). Compound **6** was obtained analogously to the diphenylphosphate **5** [11] by reaction of the appropriate α-configurated trichloroacetimidate with dibenzylphosphate: m.p. 74 °C; $[\alpha]_D^{20} = -8.1$ ($c = 1$ in $CHCl_3$); ^1H NMR (250 MHz, $CDCl_3$, 25 °C, TMS): $\delta = 5.38$ (dd, ^3J(1-H, 2-H) = 7.9 Hz, ^2J(1H, P) = 6.7 Hz; 1H; 1-H).
[13] R. R. Schmidt, M. Behrend, A. Toepfer, *Synlett* **1990**, 694.

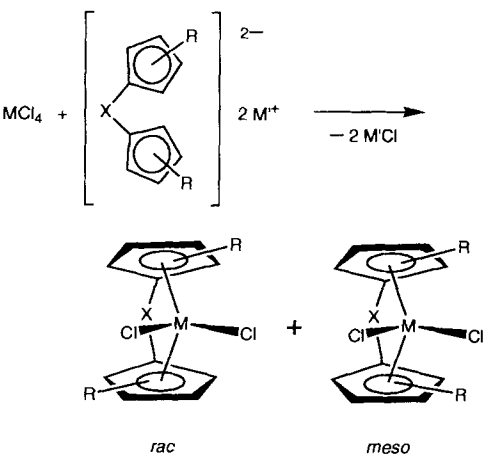
Doubly Bridged *rac*-Metallocenes of Zirconium and Hafnium**

Wolfgang A. Herrmann,* Marcus J. A. Morawietz, and Thomas Priermeier

Dedicated to Professor Wolfgang Hilger on the occasion of his 65th birthday

Since the discovery of stereospecific Ziegler–Natta polymerization with metallocene catalysts,[1] interest has concentrated on the optimization of the catalytic properties by variation of substituents.[2] Only recently was attention also turned to the *rac*/*meso* problem in the synthesis of *ansa*-metallocenes;[3] nevertheless, all concepts cling to the classical route [Eq. (a)].

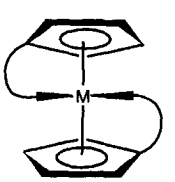
Disadvantages of this pathway are the required removal of the salt and the mostly moderate yields. Moreover, mixtures of *rac*/*meso* diastereomers are produced, which can often be separated only by several crystallization steps.



(a)

M = Ti, Zr, Hf
X = SiR'_2, $CR'_2CR'_2$
M' = Li, Na
R,R' = alkyl, aryl

In this communication we describe a salt-free synthesis in which the *rac*/*meso* isomer problem does not arise, and new metallocenes of the constitution of type **A** can be simply and universally prepared as potential catalysts. The concept is based on the treatment of homoleptic metal amides $[M(NR_2)_4]$ with functionalized cyclopentadienes.

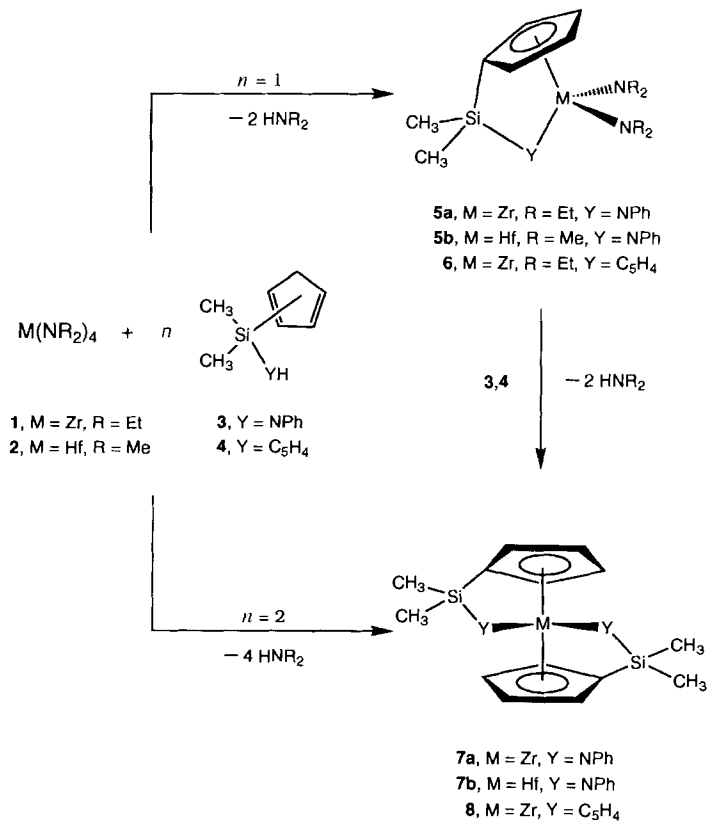


A

If zirconium and hafnium tetraamides **1** and **2** are treated with one equivalent of cyclopentadienyldimethyl(*N*-phenylamino)silane (**3**)[4] or bis(cyclopentadienyl)dimethylsilane (**4**)[5a] in toluene, two amide ligands are substituted (yields >98%, Scheme 1).

[*] Prof. Dr. W. A. Herrmann, M. J. A. Morawietz, T. Priermeier
Anorganisch-chemisches Institut der Technischen Universität München
Lichtenbergstrasse 4, D-85747 Garching (FRG)
Telefax: Int. code + (89)3209-3473

[**] This work was supported by the Fonds der Chemischen Industrie (scholarship for M. J. A. M.) and Hoechst AG (Zentralforschung).



Scheme 1. Synthesis of the metallocenes **5**–**8**.

The products **5** and **6** are susceptible to hydrolysis and very soluble in halogen-free organic solvents. The complexes **5** are oils, whereas **6** is a yellow solid crystallizable from *n*-hexane. As the ^{1}H, ^{13}C, and ^{29}Si NMR spectra show, **6** has a mirror plane.

The exhaustive exchange of the amide residues can be achieved either by treatment of **5** and **6** with the ligands **3** or **4**, respectively, or through quantitative substitution directly from the tetraamides **1** and **2** (Scheme 1).[6a] The *rac* configuration of the doubly bridged amido metallocenes **7** was proven by ^{1}H, ^{13}C, and ^{29}Si NMR spectroscopy. They are solids sensitive to hydrolysis and can be crystallized from apolar solvents. The crystal structure analysis confirms, in principle, the C_2 symmetry

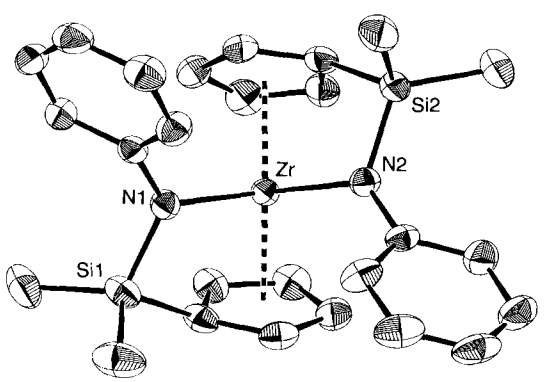


Fig. 1. Molecular structure of **7a** in the crystal (PLATON representation). Selected distances [pm] and angles [°]: Zr–Z1 220.7, Zr–Z2 221.7, Zr–N1 213.7(2), Zr–N2 212.7(2); Z1-Zr-Z2 133.0, N1-Zr-N2 106.48(8). Z1: Center of the cyclopentadienyl ring C11, C12, C13, C14, C15; Z2: Center of the cyclopentadienyl ring C31, C32, C33, C34, C35.

determined in solution, but the complex is slightly distorted in the crystal as a result of packing effects (Fig. 1).[6b, c]

It is striking that the twofold bridging and the steric bulk of the phenyl substituents cause no substantial distortion of the framework. Consequently the metallocenes **7** display the same characteristic features of common metallocenes like $[(C_5H_5)_2ZrCl_2]$ and $[Me_2Si(C_5H_4)_2ZrCl_2]$. The distances between the metal ion and the centers (Z) of the cyclopentadienyl rings in **7a** are 221 and 222 pm, in the typical range for a Zr–Z distance.[5b, c] The similarity is emphasized by the Z-Zr-Z′ angle of 133.0°, which may be compared with the usual value of between 125.4 and 128.3°.[5b, c]

The bis(cyclopentadienyl) ligand **4**, like **3**, can substitute either two or four amide ligands of **1**. Complete ligand exchange yields **8** almost quantitatively after sublimation. Like the complexes $[M(C_5H_5)_4]$[7] of titanium, zirconium, and hafnium, the *ansa* analogue **8** has a dynamic structure in solution. The ^{1}H and ^{13}C NMR spectra feign a fourfold η^5-coordination. The AA′BB′ splitting for monosubstituted cyclopentadienyl rings and the singlet for the CH_3 protons of the bridge remain unchanged to 163 K. In the crystal **8** is not $(\eta^5)_3$:(η^1)-coordinated like $[Zr(C_5H_5)_4]$,[7b] but $(\eta^5)_2$:$(\eta^1)_2$-coordinated like $[Ti(C_5H_5)_4]$[8a] and $[Hf(C_5H_5)_4]$[8b] (Fig. 2).[9]

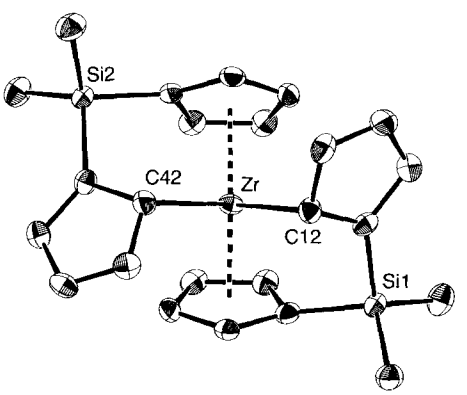


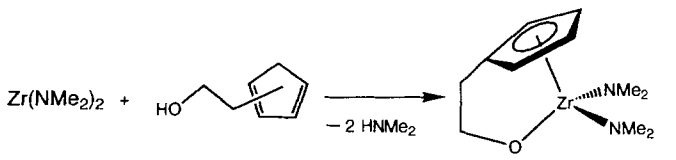
Fig. 2. Molecular structure of **8** in the crystal (PLATON representation). Selected distances [pm] and angles [°]: Zr–Z1 220.2, Zr–Z2 219.5, Zr–C12 245.5(3), Zr–C42 246.3(2); Z1-Zr-Z2 129.6, C12-Zr-C42 82.74(9). Z1: Center of the cyclopentadienyl ring C21, C22, C23, C24, C25; Z2: Center of the cyclopentadienyl ring C31, C32, C33, C34, C35.

This coordination behavior of a bridging bis(cyclopentadienyl) ligand is new in metallocene chemistry. Complex **8** is a model for an intermediate that is discussed in the formation and isomerization of metallocenes.[10] Like **7a**, compound **8** also does not have perfect C_2 symmetry as a result of packing effects. The Zr-η^1–C bonds are unusually long (245.5 and 246.3 pm). The characteristic Z-Zr-Z′ angle is 129.6°.

According to our results the treatment of homoleptic metal amides with nondeprotonated bidentate derivatives of cyclopentadiene is advantageous for the synthesis of metallocenes of type **A** and a promising alternative to classical transmetalation. Besides the easy access to *ansa*-metallocenes, new metallocenes with fixed C_2 symmetry are selectively accessible through this amide route and the principle of double bridging. This concept has substantial advantages over the former syntheses of *rac*-metallocene complexes: a) high stereoselectivity, that is, no *rac*/*meso* separation; b) quantitative yield; c) simple precursors and ligands accessible by common procedures in few steps; d) one step less, because deprotonation of the ligand is not required. The

complexes **7** are catalysts for ethylene and propylene polymerization if methyl aluminoxane (MAO) is used as activator.[11]

With this new method π ligands with alcoholate functions can also be introduced, as the example of **9** shows: this compound arises quantitatively from the complex $[Zr(NMe_2)_4]$ and the ligand $C_5H_5CH_2CH_2OH$ with loss of dimethylamine, which, as in the other cases, escapes as gas during the reaction [Eq. (b)];[12] this favors formation of the product.



(b)

9

Extension to other functionalized π-arene complexes of the early transition metals and rare earth metals, as well as to elements of the fourth main group, seem promising.[13]

Experimental Procedure

5a: Compounds **1** (569 mg, 1.5 mmol) and **3** (323 mg, 1.5 mmol) were each dissolved in toluene (10 mL), and the solutions were mixed at −78 °C. After the reaction mixture had warmed to 25 °C, it was heated at reflux for 3 h. The solvent was then removed under vacuum, and **5a** is obtained as dark red oil. Yield 665 mg (99%). ^{1}H NMR (400 MHz, C_6D_6, 25 °C, TMS): δ = 0.55 (s, 6H; $Si(CH_3)_2$), 0.87 (t, 12H, ^3J(H,H) = 6.7 Hz; $N(CH_2CH_3)_2$), 3.12 (dt, 4H, ^3J(H,H) = 6.7 Hz; $N(CH_2CH_3)_2$), 3.27 (dt, 4H, ^3J(H,H) = 6.7 Hz; $N(CH_2CH_3)_2$), 6.32 (t, 2H, ^3J(H,H) = 2.4 Hz; C_5H_4), 6.41 (t, 2H, ^3J(H,H) = 2.4 Hz; C_5H_4), 6.81 (t, 1H, ^3J(H,H) = 7.3 Hz; *p*-H), 7.02 (d, 2H, ^3J(H,H) = 7.3 Hz; *o*-H), 7.21 (t, 2H, ^3J(H,H) = 7.3 Hz; *m*-H); $^{13}C\{^1H\}$ NMR (100.4 MHz, C_6D_6, 25 °C, TMS): δ = 0.5 (s; $Si(CH_3)_2$), 15.6 (s; $N(CH_2CH_3)_2$), 43.5 (s; $N(CH_2CH_3)_2$), 108.9 (s; C_5H_4), 115.1 (s; C_5H_4), 118.9 (s; *o*-C), 121.5 (s; C_5H_4), 124.3 (s; *p*-C), 129.2 (s; *m*-C), 155.3 (s; C_6H_5); ^{29}Si NMR (DEPT, 79.5 MHz, C_6D_6, 25 °C, TMS): δ = −20.3 (s; $Si(CH_3)_2$); IR (neat): $\tilde{\nu}$ [cm^{-1}] = 3070 m (ν(=CH)), 3046 m sh (ν(=CH)), 2861 s (ν(C−H)), 997 s (ν_{sym}(N−C_2)), 575 m (ν(M−N)); MS (CI): *m/z* (%): 448 (100) [M^+], 432 (13) [M^+−CH_4], 376 (45) [M^+−NEt_2], 303 (6) [M^+−NEt_2−$HNEt_2$], 216 (4) [$(Me_2Si(C_5H_5)(NHC_6H_5)H)^+$].

6: Compounds **4** (376 mg, 2 mmol) and **1** (759 mg, 2 mmol) were each dissolved in 10 mL toluene and cooled to −78 °C. At this temperature the dissolved ligand was added dropwise. After the mixture had warmed to room temperature, it was stirred for 16 h. The solvent was removed under vacuum, and **6** was recovered as analytically pure yellow solid. Yield 840 mg (99%). ^{1}H NMR (400 MHz, C_6D_6, 30 °C, TMS): δ = 0.40 (s, 6H; $Si(CH_3)_2$), 0.96 (t, 12H, ^3J(H,H) = 6.7 Hz; $N(CH_2CH_3)_2$), 3.17 (q, 8H, ^3J(H,H) = 6.7 Hz; $N(CH_2CH_3)_2$), 5.77 (t, 4H, ^3J(H,H) = 2.4 Hz; C_5H_4), 6.51 (t, 4H, ^3J(H,H) = 1.8 Hz; C_5H_4); $^{13}C\{^1H\}$ NMR (100.4 MHz, C_6D_6, 30 °C, TMS): δ = −5.1 (s; $Si(CH_3)_2$), 14.7 (s; $N(CH_2CH_3)_2$), 47.7 (s; $N(CH_2CH_3)_2$), 109.8 (s; C_5H_4), 112.5 (s; C_5H_4), 117.3 (s; C_5H_4); ^{29}Si NMR (DEPT, 79.6 MHz, C_6D_6, 30 °C, TMS): δ = −15.9 (s; $Si(CH_3)_2$); MS (CI): *m/z* (%): 420 (48) [M^+], 405 (4) [M^+−CH_3], 347 (100) [M^+−$HNEt_2$], 276 (3) [M^+−$HNEt_2$−NEt_2]; IR (Nujol): $\tilde{\nu}$ [cm^{-1}] = 3010 w (ν(=CH)), 2960 vs (ν(C−H)), 1001 m (ν_{sym}(N-C_2)), 566 m (ν(M-N)).

7a: Compound **3** (430 mg, 2 mmol) dissolved in 10 mL toluene at −50 °C was added dropwise to a solution of **1** (379 mg, 1 mmol) in 10 mL toluene at −78 °C. The reaction mixture was allowed to warm to 25 °C and then heated at 120 °C for 12 h. The solvent was removed under vacuum, and **7a** remained as light yellow solid. Yield: 0.512 g (99%). ^{1}H NMR (400 MHz, C_6D_6, 25 °C, TMS): δ = 0.37, 0.45 (s, 6H; $Si(CH_3)_2$), 5.65 (q, 2H, J(H,H) = 2.4 Hz; C_5H_4), 5.89 (q, 2H, J(H,H) = 1.8, 3.0 Hz; C_5H_4), 5.95 (q, 2H, J(H,H) = 1.8, 2.4, 3.1 Hz; C_5H_4), 6.17 (q, 2H, J(H,H) = 1.8, 3.1 Hz; C_5H_4), 6.89 (t, 1H, ^3J(H,H) = 7.3 Hz; *p*-H), 6.96 (d, 2H, ^3J(H,H) = 7.9 Hz; *o*-H), 7.20 (t, 2H, ^3J(H,H) = 7.3 Hz; *m*-H); $^{13}C\{^1H\}$ NMR (100.4 MHz, C_6D_6, 25 °C, TMS): δ = −2.3, 1.0 (s; $Si(CH_3)_2$), 112.3 (s; C_5H_4), 113.5 (s; C_5H_4), 113.6 (s; C_5H_4), 117.0 (s; C_5H_4), 118.7 (s; *o*-C), 121.3 (s; C_5H_4), 124.3 (s; *p*-C), 128.9 (s; *m*-C), 157.1 (s; C_6H_5); ^{29}Si NMR (DEPT, 79.5 MHz, C_6D_6, 25 °C, TMS): δ = −20.5 (s; $Si(CH_3)_2$); MS (CI): *m/z* (%): 516 (100) [M^+], 501 (14) [M^+−CH_3]; IR (Nujol): $\tilde{\nu}$ [cm^{-1}] = 3062 w, 3023 m, 2948 s, 1585 s, 1477 s, 1260 vs, 1252 s sh, 920 s, 816 vs.

8: Compounds **4** (376 mg, 2 mmol) and **1** (379 mmol, 1 mmol) were each dissolved in 10 mL toluene and cooled to −78 °C. At this temperature the ligand was added dropwise. After warming to 25 °C the mixture was stirred for 16 h. The solvent was removed under vacuum, and the yellow-orange residue sublimed under high vacuum. Compound **8** was isolated as a yellow-orange solid at 70 °C and 2×10^{-4} Torr. Yield 440 mg (95%). ^{1}H NMR (400 MHz, C_6D_6, 30 °C, TMS): δ = 0.37 (s, 12H; $Si(CH_3)_2$), 5.70 (t, 4H, ^3J(H,H) = 1.8 Hz; C_5H_4), 5.86 (t, 4H, ^3J(H,H) = 2.4 Hz; C_5H_4); $^{13}C\{^1H\}$ NMR (100.4 MHz, C_6D_6, 30 °C, TMS): δ = −2.4 (s; $Si(CH_3)_2$), 111.8 (s; C_5H_4), 118.0 (s; C_5H_4), 124.5 (s; C_5H_4); ^{29}Si NMR (DEPT, 79.6 MHz, C_6D_6, 30 °C, TMS): δ = −17.6 (s; $Si(CH_3)_2$); MS (CI): *m/z* (%): 462 (100) [M^+], 186 (10) [$Me_2Si(C_5H_4)(C_5H_5)^+$].

Compounds **5b** and **7b** were prepared analogously.

Received: May 21, 1994 [Z 6962 IE]
German version: *Angew. Chem.* **1994**, *106*, 2025

[1] a) W. Kaminsky, K. Külper, H. H. Brintzinger, F. R. W. P. Wild, *Angew. Chem.* **1985**, *97*, 507–508; *Angew. Chem. Int. Ed. Engl.* **1985**, *24*, 507–508; b) J. A. Ewen, R. L. Jones, A. Razavi, J. D. Ferrara, *J. Am. Chem. Soc.* **1988**, *110*, 6255–6256.

[2] a) W. A. Herrmann, E. Herdtweck, J. Rohrmann, W. Spaleck, A. Winter, *Angew. Chem.* **1989**, *101*, 1536–1538; *Angew. Chem. Int. Ed. Engl.* **1989**, *28*, 1511–1512; b) W. A. Herrmann, W. Spaleck, J. Rohrmann, M. Antberg, A. Winter, P. Kiprof, J. Behm, *ibid.* **1992**, *104*, 1373–1376 and **1992**, *32*, 1347–1350; c) W. Spaleck, F. Küber, A. Winter, J. Rohrmann, B. Bachmann, M. Antberg, V. Dolle, E. F. Paulus, *Organometallics* **1994**, *13*, 954–963; d) H. H. Brintzinger, U. Stehling, J. Diebold, R. Kirsten, W. Röll, S. Jüngling, R. Mülhaupt, F. Langhauser, *ibid.* **1994**, *13*, 964–970.

[3] a) R. L. Halterman, M. J. Burk, S. L. Colleti, *Organometallics* **1991**, *10*, 2998–3000; b) H. H. Brintzinger, M. E. Huttenloch, J. Diebold, A. M. Gilbert, T. J. Katz, *ibid.* **1992**, *11*, 3600–3607; c) J. E. Bercaw, E. B. Coughlin, *J. Am. Chem. Soc.* **1992**, *114*, 7606–7607; d) B. Bosnich, W. W. Ellis, K. Hollis, W. Odenkirk, J. Whelan, R. Ostrander, A. L. Rheingold, *Organometallics* **1993**, *12*, 4391–4401.

[4] a) W. A. Herrmann, M. J. A. Morawietz, *J. Organomet. Chem.* **1994**, in press; b) J. H. Teuben, A. K. Hughes, A. Meetsma, *Organometallics* **1993**, *12*, 1936–1945.

[5] a) K. C. Frisch, *J. Am. Chem. Soc.* **1953**, *75*, 6050–6051; b) J. L. Petersen, C. S. Bajgur, W. R. Tikkanen, *Inorg. Chem.* **1985**, *24*, 2539–2546; c) T. S. Cameron, K. Prout, R. A. Forder, S. R. Critchley, B. Denton, G. V. Rees, *Acta Crystallogr. (Kopenhagen)* **1974**, *B30*, 2290–2304.

[6] a) K. H. Thiele, U. Böhme recently reported (*J. Organomet. Chem.* **1994**, *472*, 39–41) a similar zirconocene that was prepared by the common transmetalation route in only 27% yield (referred to the free ligand). b) **7a** crystallized from *n*-hexane at −30 °C in the orthorhombic space group $Pca2_1$ (no. 29) with a = 1350.4(2), b = 1096.6(1), c = 1695.5(2) pm, Z = 4, $V = 2511 \times 10^6$ pm^3, ρ_{calcd} = 1.370 g cm^{-3}, μ = 5.4 cm^{-1}, F(000) = 1072; $Mo_{K\alpha}$ radiation, −50 °C; Enraf-Nonius CAD4, ω scan, 5037 measured reflections, of which 4194 with $I > 0$ used in the refinement. Structure solution by Patterson methods, empirical absorption correction, no correction for decomposition. $R = \Sigma(||F_o| - |F_c||)/\Sigma|F_o| = 0.0261$, $R_w = [\Sigma w(|F_o| - |F_c|)^2/\Sigma w|F_o|^2]^{1/2} = 0.0241$, residual electron density + 0.52/−0.74 e Å^{-3}; PLATON: "The EUCLID package": A. L. Spek in *Computational Crystallography* (Ed.: D. Sayre), Clarendon, Oxford, **1982**, p. 528. c) Further details of the crystal structure investigation may be obtained from the Fachinformationszentrum Karlsruhe, Gesellschaft für wissenschaftlich-technische Information mbH, D-76344 Eggenstein-Leopoldshafen (FRG) on quoting the depository number CSD-58376 and the journal citation.

[7] a) F. A. Cotton, J. Takats, J. L. Calderon, *J. Am. Chem. Soc.* **1971**, *93*, 3587–3591; b) J. L. Atwood, R. D. Rogers, R. V. Bynum, *ibid.* **1978**, *100*, 5238–5239, and references therein.

[8] a) F. A. Cotton, J. L. Calderon, B. G. DeBoer, J. Takats, *J. Am. Chem. Soc.* **1971**, *93*, 3592–3597; b) V. I. Kulishov, E. M. Brainina, N. G. Bokiy, Y. T. Struchkov, *J. Organomet. Chem.* **1972**, *36*, 333–334.

[9] **8** crystallized from *n*-hexane at −35 °C in the monoclinic space group $P2_1/n$ (no. 14) with a = 1027.1(1), b = 1815.8(1), c = 1150.4(1) pm, β = 91.55(1)°, Z = 4, $V = 2145 \times 10^6$ pm^3, ρ_{calcd} = 1.437 g cm^{-3}, μ = 6.2 cm^{-1}, F(000) = 960; $Mo_{K\alpha}$ radiation, −80 °C; Enraf-Nonius CAD4, ω scan, 4139 measured reflections, of which 2919 with $I > 2.5\sigma(I)$ used for the refinement. Structure solution by Patterson methods, empirical absorption correction, no correction for decomposition. R = 0.0266, R_w = 0.0228, residual electron density +0.36/−0.27 e Å^{-3}. See ref. [6c].

[10] H. H. Brintzinger, A. Reinmuth, E. Barsties, K. Evertz, H. Wiesenfeldt, *J. Organomet. Chem.* **1989**, *369*, 359–370.

[11] On interaction of complexes **7** with MAO the C_2-symmetry need not necessarily be lost. According to present knowledge, it is more likely that the cleavage of the M–N bond affords an active, *rac*-species in which the amide function resides on the activator. Complex **7** is a good example with which to study such possibilities. Because of the reactive (protolyzable) M-N bond in **7**, the catalyst is possibly fixed to alumoxane surfaces. Experiments on this subject are under way.

[12] $C_5H_5CH_2CH_2OH$ was prepared by epoxide ring opening of ethylene oxide with $LiC_5H_5/BF_3 \cdot Et_2O$ in 58% yield. ^1H NMR (400 MHz, C_6D_6, 25 °C, TMS): $\delta = 2.54$ (t, 2H, $^3J(H,H) = 7.2$ Hz; CH_2CH_2OH), 2.80 (s, 2H, allyl. H), 3.60 (t, 2H, $^3J(H,H) = 7.2$ Hz; CH_2CH_2OH), 6.13, 6.18, 6.34 (m, 3H; vinyl. H); $^{13}C\{^1H\}$ NMR (100.4 MHz, C_6D_6, 25 °C, TMS): $\delta = 33.6$, 43.1, 61.8 (s; aliphat. C), 127.8, 130.8, 132.1, 145.4 (s, olefin. C); GC-MS: *m/z* (%): 110 (21) [M^+], 79 (100) [$M^+ - CH_2OH$], 66 (20) [$C_5H_6^+$]; IR (neat): $\tilde{\nu}$ [cm^{-1}] = 3345 vs (ν(O-H)), 3059 m (ν(= C-H)), 2926 s (ν(C-H)), 2892 s (ν(C-H)). **9** was obtained quantitatively by equimolar conversion of the starting materials. ^1H NMR (400 MHz, C_6D_6, 25 °C, TMS): $\delta = 2.27$ (t, 2H, $^3J(H,H) = 6.1$ Hz; CH_2CH_2O), 3.08 (s, 12H; $N(CH_3)_2$), 3.91 (t, 2H, $^3J(H,H) = 6.1$ Hz; CH_2CH_2O), 5.77 (t, 2H, $^3J(H,H) = 2.4$ Hz; C_5H_4), 6.13 (t, 2H, $^3J(H,H) = 3.1$ Hz; C_5H_4); $^{13}C\{^1H\}$ NMR (100.4 MHz, C_6D_6, 25 °C, TMS): $\delta = 31.8$ (s; CH_2CH_2O), 46.2 (s; $N(CH_3)_2$), 74.6 (s; CH_2CH_2O), 109.7 (s; C_5H_4), 110.8 (s; C_5H_4), 131.9 (s; C_5H_4); IR (Nujol): $\tilde{\nu}$ [cm^{-1}] = 3019 w, 2969 s, 2946 s sh, 2880 s, 2841 vs, 2835 s sh, 2759 s, 1041 s, 954 s, 938 s, 791 s.

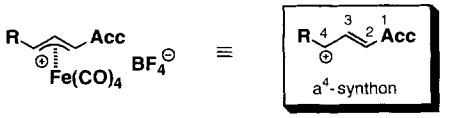
[13] W. A. Herrmann, M. J. A. Morawietz, F. Munck, W. Baratta, unpublished results.

Iron-Promoted, Regio- and Stereoselective Allylic Substitutions for the Synthesis of Alkenyl Sulfones Substituted at C-3**

Dieter Enders,* Bernd Jandeleit, and Gerhard Raabe

Catalytic and stoichiometric reactions of transition-metal π complexes containing unsaturated organic ligands are of growing significance in the development of countless preparative methods in organic synthesis.[1] Auxiliaries based on metal complexes are used in functionalization reactions primarily because of their ability to activate and to influence facial differentiation and stereoselection.[2] Complexes containing allyl ligands, which act as stabilized carbocation equivalents, have recently been of particular preparative interest owing to their enhanced reactivity towards nucleophiles. Alkyl-, aryl-, and acceptor-substituted (η^3-allyl)tetracarbonyliron(1 +) complexes undergo addition reactions with a multitude of soft carbon and heteroatom nucleophiles. Functionalization of the allyl unit proceeds with regio- and, above all, stereocontrol.[3] Demetalation ultimately yields complex and stereochemically well-defined target molecules. The scope of this type of reaction, in both its stoichiometric and catalytic variations, has now been extended by the use of other transition metals apart from iron, in particular, palladium,[4] molybdenum,[5] nickel,[6] and copper.[7]

Acceptor-substituted, cationic (π-allyl)carbonyliron complexes **A**[8] in their diastereo- and enantiomerically pure form are preparatively useful as intermediates in asymmetric synthesis. Here, **A** acts as an a^4-synthon **B** with planar chirality; an umpolung[9] of classical d^4-reactivity is observed.



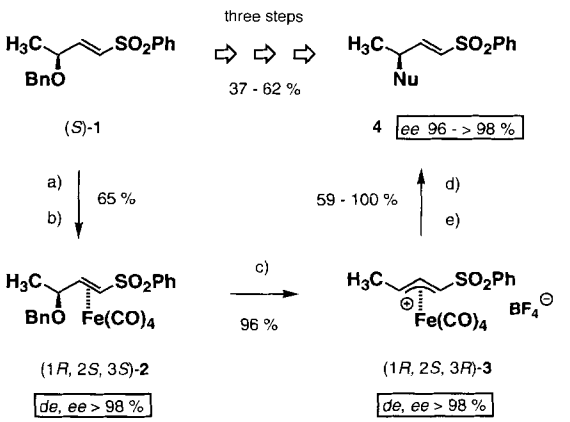
A **B**

Acc = CO_2R, SO_2Ph

[*] Prof. Dr. D. Enders, Dipl.-Chem. B. Jandeleit, Dr. G. Raabe
Institut für Organische Chemie der Technischen Hochschule
Professor-Pirlet-Strasse 1, D-52074 Aachen (FRG)
Telefax: Int. code + (241) 8888-127

[**] This work was supported by the Volkswagen-Stiftung and by the Fonds der Chemischen Industrie. We thank the companies Degussa AG, BASF AG, Bayer AG, and Hoechst AG for their donation of chemicals.

We now report on iron-promoted, regio- and stereoselective allylic substitution reactions of 1-phenylsulfonyl-substituted (η^3-allyl)tetracarbonyliron(1 +) tetrafluoroborate, which exhibits planar chirality. Sulfonyl-substituted allyl compounds of high enantiomeric purity are obtained by this method. Key steps in the synthesis are the diastereoselective complexation of $Fe(CO)_4$ with the easily accessible, enantiomerically pure sulfone (*S*)-**1**[10] to give the neutral η^2-olefin complex (1*R*, 2*S*, 3*S*)-**2** and the transformation of **2** into the enantiomerically pure, cationic iron complex with planar chirality (1*R*, 2*S*, 3*R*)-**3**. Regioselective addition of carbon and nitrogen nucleophiles to **3** followed by oxidative decomplexation provides access to highly enantiomerically enriched, alkenyl sulfones **4** substituted with a wide range of substituents at the allylic position (Scheme 1, Table 1).



Scheme 1. Synthesis of the (η^3-allyl)tetracarbonyliron(1 +) complex with planar chirality (1*R*, 2*S*, 3*R*)-**3**, and its reactions with C- and N-nucleophiles to give the 3-substituted sulfones **4**; a) $[Fe_2(CO)_9]$ (1.3 equiv), *n*-hexane, CO atmosphere, 3 d; b) fractional crystallization from ether/*n*-hexane; c) HBF_4 (1.2 equiv), ether, 30 °C; d) nucleophile (2.5–5 equiv), CH_2Cl_2 or THF, −78 °C to room temperature, 8 h or CH_3NO_2, room temperature, 24 h; e) $(NH_4)_2Ce(NO_3)_6/H_2O$ (4 equiv), 8 h or I_2/ether (4 equiv), 8 h.

Table 1. Iron-promoted allylic substitutions for the preparation of sulfones **4** substituted at C-3.

4 [a]	Nucleophile	Nucleophile/Complex	Reagents/Conditions	Yield [%] [b]	*ee* [%] [c] (Config.)
a	$LiCH(CO_2Me)_2$	2.5/1	[d]	99	>97(*R*) [e]
b	$Me_2C = CH(OSiMe_3)$	2.5/1	[f]	79	>97(*S*) [g]
c	$Me_2C = C(OMe)(OSiMe_3)$	2.5/1	[f]	quant.	>98(*S*)
d	$H_2C = C(tBu)(OSiMe_3)$	2.5/1	[f]	quant.	97(*R*)
e	$HNEt_2$	5/1	[f]	87	96(*S*)
f	Pyrrolidine	5/1	[f]	76	≥96(*S*)
g	Piperidine	5/1	[f]	98	>98(*S*)
h	1,3,5-$(MeO)_3C_6H_3$	3/1	[h]	99	≥97(*S*) [e]
i	$C_6H_5NMe_2$	5/1	[h]	59 [i]	>97(*S*)
j	*N*-Methylindole	5/1	[h]	99 [j]	>96(*S*)

[a] All new compounds gave correct elemental analyses or high-resolution mass spectra. [b] Yields of isolated substances after purification by flash chromatography. [c] Unless otherwise stated, *ee* determined by ^1H NMR spectroscopy (Varian Unity 500 MHz spectrometer) with the chiral cosolvent (−)-(*R*)-1-(9-anthryl)-2,2,2-trifluoroethanol. [d] THF, −78 °C to room temperature (RT), 8 h, $(NH_4)_2Ce(NO_3)_6$ (CAN), 8 h. [e] *ee* determined by ^1H NMR shift experiments with [Eu(hfc)$_3$] (500 MHz). [f] CH_2Cl_2, −78 °C to RT, 8 h, CAN, 8 h. [g] To determine *de* by ^1H NMR (500 MHz), **4b** was converted into the corresponding acetal with (−)-(2*R*, 3*R*)-2,3-butanediol. [h] CH_3NO_2, RT, 24 h, I_2, 8 h. [i] **4i** was isolated as the *para* isomer. [j] **4j** was obtained exclusively as the product substituted at C-3'.

Reaction of the Bn-protected (Bn = benzyl) alkenyl sulfone (*S*)-**1** with nonacarbonyldiiron in *n*-hexane under a carbon monoxide atmosphere and with exclusion of light[11] initially

yielded a mixture of the diastereomeric complexes (1*S*, 2*R*, 3*S*)-**2** and (1*R*, 2*S*, 3*S*)-**2** in a ratio of 15:85 (*de* = 70%). The diastereomers could not be separated by chromatography. However, fractional crystallization at −25 °C yielded the neutral, diastereo- and enantiomerically pure (η^2-olefin)tetracarbonyliron complex (1*R*, 2*S*, 3*S*)-**2** as pale yellow platelets in an average overall yield of 65% (*de* > 98%). The diastereomeric purity was easily determined from the doublets in the ^{1}H NMR spectrum corresponding to the methyl groups, which have clearly distinguishable chemical shifts [(1*R*, 2*S*, 3*S*)-**2**: $\delta = 0.90$; (1*S*, 2*R*, 3*S*)-**2**: $\delta = 0.85$, Table 2]. The iron complex **2** is remarkably

Table 2. Physical data for compounds (1*R*, 2*S*, 3*S*)-**2** and (1*R*, 2*S*, 3*R*)-**3**.

(1*R*, 2*S*, 3*S*)-**2**: M.p. 103 °C (decomp.); correct C,H analysis; $[\alpha]_D^{26} = +171.8$ ($c = 1.05$ in benzene); ^{1}H NMR (500 MHz, C_6D_6, 25 °C, TMS): $\delta = 0.90$ (d, $^3J = 6.1$ Hz, 3H; CH_3), 3.04 (qdd, $^3J_{vic} = 6.1$ Hz, $^3J_{H\gamma/H\beta} = 5.8$ Hz, $^4J_{H\gamma/Hx} = 0.3$ Hz, 1H; HC_γ), 3.29 (dd, $^3J_{trans} = 10.4$ Hz, $^3J = 5.8$ Hz, 1H; HC_β), 3.79 (d, $^2J_{gem} = 12.1$ Hz, 1H; OCH_2), 3.86 (dd, $^3J_{tans} = 10.4$ Hz, $^4J = 0.3$ Hz, 1H; HC_γ), 3.93 (d, $^2J_{gem} = 12.1$ Hz, 1H; OCH_2), 6.86–6.98 (m, 5H; C_6H_5), 7.03–7.11, 7.86–7.90 (2m, 5H; $SO_2C_6H_5$); ^{13}C NMR (125 MHz, C_6D_6, 25 °C, TMS): $\delta = 21.73$ (CH_3), 57.96 (C_β), 66.70 (C_α), 70.15 (OCH_2), 76.31 (C_γ), 127.83–132.53 ($C_{ortho, meta, para}$), 137.53 (CH_2C_{ipso}), 142.66 (SO_2C_{ipso}), 207.15 (CO); IR (*n*-hexane): $\tilde{\nu} = 2104$, 2035, 2026, 2002 cm^{-1} (Fe-CO); IR (KBr): $\tilde{\nu} = 1300$, 1144 (S = O), 1084 cm^{-1}; MS (70 eV): *m/z* (%) 414 (2.0) [$M^+ - 2$ CO], 386 (3.6) [$M^+ - 3$ CO], 358 (84) [$M^+ - 4$ CO], 267 (100) [$M^+ - 4$ CO, − OBn], 91 (55) [$C_7H_7^+$], 56 (48) [Fe^+].

(1*R*, 2*S*, 3*R*)-**3**: M.p. 153–155 °C (decomp.); correct C,H analysis; $[\alpha]_D^{21} = +158.3$ ($c = 0.96$ in acetone); ^{1}H NMR (500 MHz, CD_3NO_2, 25 °C, TMS): $\delta = 2.13$ (d, $^3J = 6.4$ Hz, 3H; CH_3), 4.64 (d, $^3J_{Hx,H\beta} = 10.1$ Hz, 1H; H_x), 4.93 (dqd, $^3J_{H\gamma/H\beta} = 12.4$ Hz, $^3J_{vic} = 6.4$ Hz, $^4J_{H\gamma,Hx} = 0.9$ Hz, 1H; $H\gamma$), 6.23 (dd, $^3J_{H\beta,H\gamma} = 12.4$ Hz, $^3J_{H\beta/Hx} = 10.1$ Hz, 1H; H_β), 7.70–7.92 (2m, 3H; HC_{meta}, HC_{para}), 8.07–8.15 (m, 2H; HC_{ortho}); ^{13}C NMR (125 MHz, CD_3NO_2, 25 °C, TMS): $\delta = 20.77$ (CH_3), 73.73 (Cα), 90.58 (C_γ), 97.65 (C_β), 129.46 (C_{ortho}), 131.54 (C_{meta}), 136.61 (C_{para}), 139.57 (C_{ipso}), 195.35, 196.10, 197.43, 197.67 (CO); IR (CH_2Cl_2): $\tilde{\nu} = 2102$, 2032, 2000 cm^{-1} (Fe-CO); IR (KBr): $\tilde{\nu} = 1448$, 1303/1147 (S = O), 1084 cm^{-1}; MS (70 eV): *m/z* (%) 195 (14) [$M^+ - Fe(CO)_4$, $- BF_4^-$], 77 (41) [$C_6H_5^+$], 56 (44) [Fe^+], 55 (100).

stable by comparison to similar sulfonyl- or sulfinyl-substituted olefin and diene complexes.[12] A particularly characteristic feature in the NMR spectra of **2** is the upfield shift of the signals of the atoms at the β position of the alkenyl system relative to

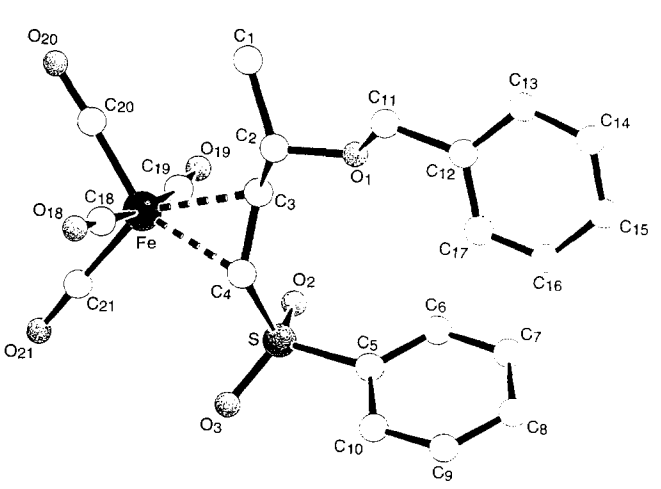


Fig. 1. Crystal structure of (1*R*, 2*S*, 3*S*)-**2** (SCHAKAL representation) [14].

those at the α position (^{1}H NMR: H_α: $\delta = 3.86$, H_β: $\delta = 3.29$; ^{13}C NMR: C_α: $\delta = 66.70$, C_β: $\delta = 57.96$). The crystal stucture of complex **2** is illustrated in Figure 1.[13]

Whilst the structural parameters of the equatorially substituted (η^2-olefin)Fe(CO)$_4$ fragment, which adopts a distorted trigonal bipyramidal geometry, are typical of this type of complex,[3m, 12, 16, 17] some structural aspects of the complexed ligand merit closer inspection. The SO_2Ph unit is twisted away from the Fe(CO)$_4$ moiety (C2-C3-C4-S −137(1)°); the terminal methyl group is, on the other hand, inclined slightly towards the Fe atom (C1-C2-C3-C4 −151(1)°). The "W-shaped" geometry adopted by the ligand fixes the *syn* arrangement of the methyl and sulfonyl groups with respect to β-hydrogen atom in the resulting cationic complex **3**. As a result of the single configuration at the 3-position, one side of the double bond unit is selectively blocked by the Fe(CO)$_4$ moiety, which lies *trans* to the OBn leaving group. This is of crucial importance to the course of reaction. In related cyclic systems, an "antisteric" *cis* complexation[3m, 17] seems to be kinetically favored; hence, the preference for the *trans* arrangement observed here can be explained by thermodynamic equilibration.

The cationic (η^3-allyl)tetracarbonyliron complex with planar chirality (**3**) was generated by precipitation of the (η^2-olefin)iron complex **2** from ether on addition of excess anhydrous tetrafluoroboric acid at 30 °C (Scheme 1).[11b] The OBn group was cleaved in this reaction. The complex was isolated in 96% yield and in virtually isomerically pure form (*de*, *ee* > 98%) as a moderately air-stable, pale yellow powder. The isomeric purity was determined from the signals in the ^{1}H NMR spectrum corresponding to the terminal methyl groups, which have clearly distinguishable chemical shifts (^{1}H NMR: (1*R*, 2*S*, 3*R*)-**3**: $\delta = 2.13$; (1*R*, 2*S*, 3*S*)-**3**: $\delta = 1.77$).[11b, 16] The ^{1}H NMR signal of the β-hydrogen atom shows coupling constants $^3J_{H\beta/H\gamma}$ and $^3J_{H\beta/Hx}$ of 12.4 and 10.1 Hz, respectively, which are characteristic for an *anti* arrangement; both the methyl and sulfonyl groups are thus *syn* to the β-hydrogen atom (Table 2). The transformation of (*S*)-**1** into (1*R*, 2*S*, 3*R*)-**3** therefore proceeds with inversion of the stereogenic center at the 3-position.

The nucleophilic additions were carried out by adding between 2.5 and 5 equivalents of nucleophile (lithium dimethylmalonate, silyl enol ether, secondary amine, electron-rich arene) in an appropriate solvent to a suspension (in CH_2Cl_2 or THF) or solution (in CH_3NO_2) of the cationic iron electrophile **3** at −78 °C and room temperature, respectively (Scheme 1, Table 1). The progress of reaction could be easily followed, since the suspended cationic iron complex gradually dissolved to give the soluble, neutral η^2-olefin complex. The nucleophilic arenes were added as solutions in CH_3NO_2; the reaction was complete after 24 h. Oxidative cleavage of the iron with aqueous ceric ammonium nitrate solution or, in the case of the arene-substituted compounds, with an iodine solution in ether affords, after workup and purification, 3-substituted alkenyl sulfones **4** of high enantiomeric purity (Table 1). The nucleophile added stereoselectively *anti* to the Fe(CO)$_4$ moiety[18] and regioselectively at the 3-position relative to the sulfonyl group. Thus, the overall reaction sequence proceeded with almost complete transfer of chirality (*ee* ≥ 96%) and retention (double inversion) with respect to the stereochemistry of the starting material. The absolute configurations indicated are based on the assumption of a uniform reaction mechanism and on an X-ray structure analysis of **4h**.[19] The coupling constants $^3J_{trans}$ between the olefinic protons in **4a–j** of 15.0–15.4 Hz confirm that neither olefinic nor allylic isomerization takes place under the reaction conditions in the sequence.

The strategy described above, namely, stereoselective chirality transfer (central → planar → central chirality) in (π-allyl)iron complexes synthesized from enantiomerically pure precursors that are readily available from natural products or enzymatic

reactions,[20] provides an efficient access to highly enantiomerically enriched alkenyl sulfones with a range of substitution patterns at the 3-position. This class of compound is of increasing importance.[21] By varying the starting material ((*S*)- or (*R*)-hydroxycarboxylic acids and aldehydes[20]), the double bond geometry of the ligand (*E* or *Z*), and the nucleophile, an extensive spectrum of products should become available.

Experimental Procedure

(1*R*, 2*S*, 3*S*)-**2**: A solution of $[Fe_2(CO)_9]$ (3.64 g, 13.0 mmol) and (*S*)-**1** (3.03 g, 10.0 mmol) in anhydrous *n*-hexane (150 mL) under argon was saturated with carbon monoxide. The suspension was stirred for 3 d at room temperature under carbon monoxide with exclusion of light. The mixture was diluted with anhydrous ether (100 mL) and filtered through Celite, which was then washed with ether. The clear yellow solution was concentrated under reduced pressure to between a third and a quarter of the original volume and was then fractionally crystallized at −25 °C. The pale yellow precipitate was washed with *n*-hexane (−20 °C) and dried under vacuum. A second crop was obtained from the mother liquor. Overall yield 3.24 g (69%).

(1*R*, 2*S*, 3*R*)-**3**: Complex **2** (4.70 g, 10.00 mmol) was dissolved in anhydrous ether (100 mL) under argon at 30 °C. A solution of HBF_4 in ether (54%, 1.64 mL, 12.0 mmol) was added dropwise with rapid stirring. After 2 h, the mixture was filtered, and the slightly yellowish solid was washed with anhydrous ether and dried under vacuum. Yield 4.32 g (96%). Analytically pure (1*R*, 2*S*, 3*R*)-**3** was obtained by fractional recrystallization from nitromethane solution with cold ether.

Procedure for the nucleophilic addition of lithium dimethylmalonate, silyl enol ethers, and secondary amines to (1*R*, 2*S*, 3*R*)-**3**: A suspension (10 mL per mmol of complex) of **3** (0.450 g, 1 mmol) in CH_2Cl_2 (silyl enol ethers, secondary amines) or THF (lithium dimethylmalonate) was treated at −78 °C with a solution of the nucleophile (2.5–5 equiv) in the appropriate solvent (1–2 mL). The reaction mixture was allowed to warm slowly to room temperature. A soluble neutral complex was obtained. For the oxidative decomplexation, the reaction mixture was treated with aqueous $(NH_4)_2Ce(NO_3)_6$ solution (4 equiv) and stirred for 8 h at room temperature. After extraction with CH_2Cl_2 and separation of the organic phase, Fe^{III} ions were removed from the latter by successive washing with saturated NH_4F solution (10 mL) and saturated NaCl solution (10 mL). The solution was then dried over $MgSO_4$, concentrated under reduced pressure, and purified by flash chromatography (silica gel, petroleum ether/ether mixture) to afford compounds **4a–g** in analytically pure form.

Procedure for the addition of electron-rich arenes to (1*R*, 2*S*, 3*R*)-**3**: A solution of **3** (0.450 g, 1 mmol) in CH_3NO_2 (10 mL per mmol of complex) was reacted at room temperature under carbon monoxide with a solution of the nucleophile (3–5 equiv in 1–2 mL). After 24 h, the mixture was diluted with an eightfold volume of ether, and the organic phase washed with saturated NaCl solution. Oxidative decomplexation was achieved by stirring at room temperature with I_2 (4 equiv) for 12 h. Excess I_2 was removed by shaking with $KHSO_3$ solution (10%, 10 mL). Additional workup as described above yielded compounds **4h–j** in analytically pure form.

Received: May 18, 1994 [Z6944IE]
German version: *Angew. Chem.* **1994**, *106*, 2033

[1] Overview: a) A. J. Pearson, *Tetrahedron* **1993**, *49*, 5415; b) *Comprehensive Organic Synthesis, Vol. 4* (Eds.: B. M. Trost, I. Fleming), Pergamon, Oxford, **1991**; c) M. F. Semmelhack in ref. [1b], p. 517; d) A. J. Pearson in ref. [1b], p. 663; e) R. D. Pike, D. A. Sweigart, *Synlett* **1990**, 565; f) S. C. Blystone, *Chem. Rev.* **1989**, *89*, 1663; g) G. Consiglio, R. W. Waymouth, *ibid.* **1989**, *89*, 257; h) A. J. Pearson in *The Chemistry of the Metal-Carbon Bond, Vol. 4* (Eds.: F. R. Hartley, S. Patai), Wiley, Chichester, **1987**, p. 889; i) L. A. P. Kane-Maguire, E. D. Honig, D. A. Sweigart, *Chem. Rev.* **1984**, *84*, 525.

[2] a) A. Rubio, L. S. Liebeskind, *J. Am. Chem. Soc.* **1993**, *115*, 891, and references therein; b) W.-Y. Zhang, D. J. Jakiela, A. Maul, C. Knors, J. W. Lauher, P. Helquist, D. Enders, *ibid.* **1988**, *110*, 4652, and references therein.

[3] Fe: a) T. H. Whitesides, R. W. Arhart, R. W. Slaven, *J. Am. Chem. Soc.* **1974**, *95*, 5792; b) A. J. Pearson, *Tetrahedron Lett.* **1975**, 3617; c) A. Salzer, A. Hafner, *Helv. Chim. Acta* **1983**, *66*, 1774; d) K. M. Nicholas, S. J. Landoulis, *J. Organomet. Chem.* **1985**, *285*, C13; e) A. Hafner, W. von Philipsborn, A. Salzer, *Helv. Chim. Acta* **1986**, *69*, 1757; f) G. S. Silverman, S. Strickland, K. M. Nicholas, *Organometallics* **1986**, *5*, 2117; g) J. W. Dieter, Z. Li, K. M. Nicholas, *Tetrahedron Lett.* **1987**, *28*, 5415; h) J. R. Green, M. K. Carroll, *ibid.* **1991**, *32*, 1141; i) Z. Li, K. M. Nicholas, *J. Organomet. Chem.* **1991**, *402*, 105; j) M.-C. P. Yeh, S.-I. Tau, *J. Chem. Soc. Chem. Commun.* **1992**, 13; k) C. Gajda, J. R. Green, *Synlett* **1992**, 973; l) T. Zhou, J. R. Green, *Tetrahedron Lett.* **1993**, *34*, 4497; m) W.-J. Koot, H. Hiemstra, W. N. Speckamp, *J. Chem. Soc. Chem. Commun.* **1993**, 156.

[4] Pd: a) O. Reiser, *Angew. Chem.* **1993**, *105*, 576; *Angew. Chem. Int. Ed. Engl.* **1993**, *32*, 547; b) C. G. Frost, J. Howart, J. M. J. Williams, *Tetrahedron: Asymmetry* **1992**, *3*, 1089.

[5] Mo: a) B. M. Trost, C. A. Merlic, *J. Am. Chem. Soc.* **1990**, *112*, 9590; b) J. W. Faller, D. Linebarrier, *Organometallics* **1988**, *7*, 1670.

[6] Ni: a) G. Consiglio, A. Indolese, *Organometallics* **1991**, *10*, 3425; b) E. Alvarez, T. Cuvigny, M. Julia, *J. Organomet. Chem.* **1988**, *339*, 199.

[7] Cu: a) T. Ibuka, K. Nakai, H. Habashita, Y. Hotta, N. Fujii, N. Nimura, Y. Miwa, T. Taga, Y. Yamamoto, *Angew. Chem.* **1994**, *106*, 693; *Angew. Chem. Int. Ed. Engl.* **1994**, *33*, 652; b) T. Ibuka, K. Nakai, H. Habashita, K. Bessho, N. Fujii, Y. Chounan, Y. Yamamoto, *Tetrahedron* **1993**, *49*, 9479; c) T. Ibuka, T. Taga, H. Habashita, K. Nakai, H. Tamamura, N. Fujii, Y. Chounan, H. Nemoto, Y. Yamamoto, *J. Org. Chem.* **1993**, *58*, 1207; d) T. Ibuka, Y. Yamamoto, *Synlett* **1992**, 769.

[8] a) P. Fey, dissertation, Universität Bonn, **1985**; b) U. Frank, dissertation, Technische Hochschule Aachen, **1990**; c) T. Schmitz, dissertation, Technische Hochschule Aachen, **1990**; d) M. Finkam, dissertation, Technische Hochschule Aachen, **1993**, e) D. Enders, M. Finkam, *Synlett* **1993**, 401; f) D. Enders, P. Fey, U. Frank, B. B. Lohray, T. Schmitz, unpublished.

[9] D. Seebach, *Angew. Chem.* **1979**, *91*, 259; *Angew. Chem. Int. Ed. Engl.* **1979**, *18*, 239.

[10] Synthesis of (*S*)-**1**: (*S*)-Ethyl lactate was converted into the Bn-protected (*S*)-lactaldehyde according to ref. [10a] and then reacted with the appropriate phenylsulfonyl-substituted phosphonate [10b] in a modified Horner olefination; a) Y. Ito, Y. Kobayashi, T. Kawabata, M. Takase, S. Terashima, *Tetrahedron* **1989**, *45*, 5767; b) I. Shahak, J. Almog, *Synthesis* **1970**, 145; c) M. W. Rathke, M. Nowak, *J. Org. Chem.* **1985**, *50*, 2624.

[11] a) E. Weiss, K. Stark, J. E. Lancaster, H. D. Murdoch, *Helv. Chim. Acta* **1963**, *46*, 288; b) J. Dieter, K. M. Nicholas, *J. Organomet. Chem.* **1981**, *212*, 107.

[12] A. Ibbotson, A. C. Reduto dos Reis, S. P. Saberi, A. M. Z. Slawin, S. E. Thomas, G. J. Tustin, D. J. Williams, *J. Chem. Soc. Perkin Trans. 1* **1992**, 1251, and references therein.

[13] For the X-ray crystal structure analysis, suitable crystals were obtained from ether/petroleum ether at 4 °C. $C_{21}H_{18}O_7SFe$, crystal dimensions ca. 0.4 × 0.4 × 0.2 mm, monoclinic, space group $P2_1(4)$, $a = 6.503(2)$, $b = 7.209(3)$, $c = 23.091(6)$ Å, $\beta = 93.40(1)°$, $V = 1080.6$ Å^3, $Z = 2$, $M_{calcd} = 470.28$, $\rho_{calcd} = 1.445$ g cm^{-3}. Total number of electrons per unit cell $F(000) = 484$, $Mo_{K\alpha}$ radiation ($\lambda = 0.71073$ Å, graphite monochromator), $\mu = 8.26$ cm^{-1}, Enraf-Nonius four-circle diffractometer, $\Omega/2\theta$ scans, 20 °C. 2670 independent reflections ($\pm h + k + l$), of which 1279 observed ($I > 2\sigma(I)$), $R_m = 0.07$, $\sin\theta/\lambda_{max} = 0.649$. Structure solution according to Patterson methods (SHELXS-86) [15a], all other crystallographic calculations were carried out with the Xtal3.2 program package [15b]. Positions of hydrogen atoms calculated. 270 refined parameters, $R = 0.068$, ($R_w = 0.073$), residual electron density $-1.3/+1.3$ e Å^{-3}. Further details of the crystal structure investigation may be obtained from the Fachinformationszentrum Karlsruhe, D-76344 Eggenstein-Leopoldshafen (FRG), on quoting the depository number CSD-58339.

[14] SCHAKAL 86, E. Keller, Universität Freiburg, **1986**.

[15] a) SHELXS-86, G. M. Sheldrick, Universität Göttingen, **1986**; b) *Xtal3.2 Reference Manual* (Eds.: S. R. Hall, H. D. Flack, J. M. Stewart), Universities of West Australia, Genf, Maryland, **1992**, Lamb, Perth.

[16] a) Y. Hsiou, Y. Wang, L.-K. Liu, *Acta Crystallogr. Sect. C* **1989**, *45*, 721; b) R. Guilard, Y. Dusausoy, *J. Organomet. Chem.* **1974**, *77*, 393; c) A. R. Luxmoore, M. R. Truter, *Acta. Crystallogr.* **1962**, *15*, 1117.

[17] a) D. Enders, T. Schmitz, G. Raabe, C. Krüger, *Acta Crystallogr. Sect. C* **1991**, *47*, 37; b) T. H. Whitesides, R. W. Slaven, J. C. Calabrese, *Inorg. Chem.* **1974**, *13*, 1895.

[18] D. Enders, M. Finkam, *Liebigs Ann. Chem.* **1993**, 551.

[19] D. Enders, B. Jandeleit, G. Raabe, Technische Hochschule Aachen, **1994**.

[20] D. Enders, D. Lauscher, M.-R. Kula, unpublished.

[21] a) N. S. Simpkins in *Sulphones in Organic Synthesis, Tetrahedron Organic Chemistry Series, Vol. 10* (Eds.: J. E. Baldwin, P. D. Magnus), 1. ed., Pergamon, Oxford, **1993**; b) N. S. Simpkins, *Tetrahedron*, **1990**, *46*, 6951; c) *The Chemistry of Sulphones and Sulfoxides* (Eds.: S. Patai, Z. Rappoport, C. J. Stirling), Wiley, Chichester, **1988**, d) P. L. Fuchs, T. F. Braish, *Chem. Rev.* **1986**, *86*, 903.

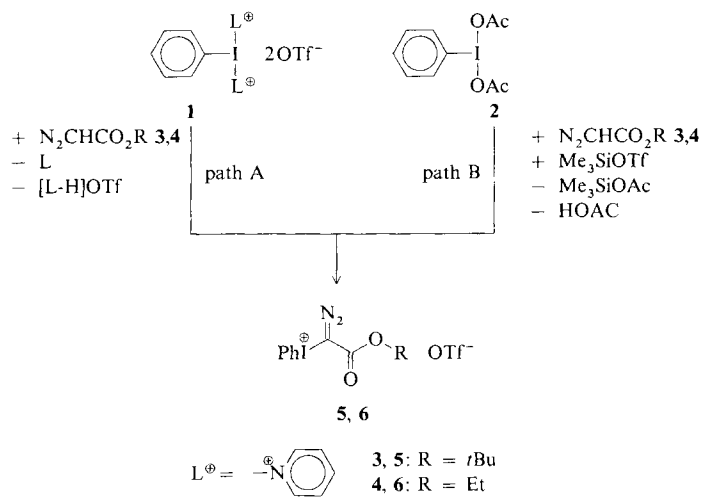
 © VCH Verlagsgesellschaft mbH, D-69451 Weinheim, 1994 0570-0833/94/1919-1951 $ 10.00+.25/0

α-Aryliodonio Diazo Compounds: S_N Reactions at the α-C Atom as a Novel Reaction Type for Diazo Compounds

Robert Weiss,* Jörg Seubert, and Frank Hampel

Three fundamental reaction types account for the versatility of diazo compounds as reagents in organic chemistry: S_E reactions at the α-C atom, carbene generation, and cycloadditions. Although this class of compounds and their reactions have been known for well over 100 years,[1] no examples of an S_N reaction at the α-C atom with retention of the diazo function have been reported.[2] This type of reaction would require functionalization of the α-C atom of the diazo compound with a potent nucleofuge. Since the aryliodonio function is such a nucleofuge,[3] we thought that the previously unknown α-aryliodonio diazo compounds would be suitable for the realization of this type of reaction. As we report here, this proposed type of reaction succeeded.

The title compounds, the first α-aryliodonio diazo compounds, are easily accessible via bis(onio)-substituted aryliodine(III) salts such as **1**, which we described recently.[4] Compound **1** reacted rapidly at room temperature with *tert*-butyl diazoacetate (**3**) and ethyl diazoacetate (**4**) to give the corresponding α-aryliodonio diazo compounds **5** and **6**, respectively (path A, Scheme 1).



Scheme 1. $OTf^- = CF_3SO_3^-$.

Both compounds were obtained along with protonated pyridine after precipitation with Et_2O. Subsequent fractional recrystallization provided both compounds in analytically pure form.

The same compounds were also prepared directly according to path B (Scheme 1) by the Lewis acid mediated (Me_3SiOTf) reactions of (diacetoxyiodo)benzene **2** with **3** and **4**. Salts **5** and **6** were obtained in good yields and without interfering impurities;[6] however, one additional mole equivalent of the diazo compound was consumed.[7]

The crystal structure of **5**[8] (Fig. 1) shows the typical T-shaped structure of iodine(III) compounds; the electronic requirements of the iodine center are met by the weakly coordinating anion (OTf^-; I1–O5: 2.705 Å) as a third ligand.[9] The C1–N1 distance (1.309 Å) and the N1–N2 distance (1.125 Å) are within the range expected for diazo compounds.[10] The C1-N1-N2 axis is almost linear (179.7°), which is also typical. The I1–C41 and I1–C1 bonds (2.112 and 2.050 Å, respectively) and the C1-I1-C41 angle (95.0°) are within the standard range for iodonio ylides, for example.[11]

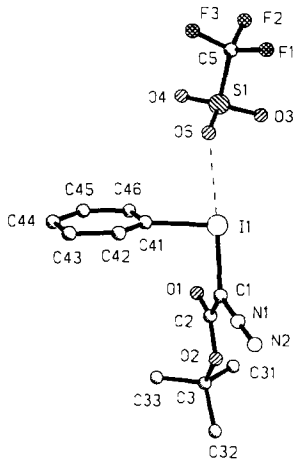
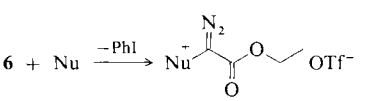


Fig. 1. Crystal structure of **5**. Important bond lengths [Å] and angles [°]: I1-C1 2.050(5), I1-C41 2.112(5), I1-O5 2.705(4), C1-N1 1.309(8), N1-N2 1.125(7), C41-I1-O5 82.4(2), C1-I1-C41 95.0(2), C1-I1-O5 177.0(2), N2-N1-C1 179.7(5).

This novel substitution pattern in a diazo compound causes an umpolung of the reactivity of the α-C atom. Thus nucleophilic substitutions can be carried out at the α-C atom for the first time. The reaction of **6** with a series of neutral nucleophiles under mild conditions (room temperature) led to the α-onio-substituted diazo compounds **7**–**11** [Eq. (a)].



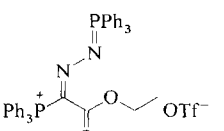
(a)

7 **11**

$-Nu^- =$ **7**: $-\overset{+}{N}$ **8**: $-\overset{+}{S}Me_2$ **9**: $-\overset{+}{A}sPh_3$ **10**: $-\overset{+}{S}bPh_3$ **11**: $-\overset{+}{N}Et_3$

The reaction with triphenylphosphane as the nucleophile proceeded further; phosphonio phosphazine **12**, which was previously prepared by Regitz et al. in a different approach,[12] formed regardless of stoichiometry and reaction conditions.

All new compounds can be stored at room temperature with exclusion of moisture and are easy to handle. The yields and spectroscopic data are given in Table 1.



12

If one considers the tendency of diazo compounds to eliminate N_2 and convert into carbenes, then this new class of compounds is in principle the synthetic equivalent of carbyne cations $RC:^+$. This aspect is under current investigation.

[*] Prof. Dr. R. Weiss, Dipl.-Chem. J. Seubert, Dr. F. Hampel
Institut für Organische Chemie
der Universität Erlangen-Nürnberg
Henkestrasse 42, D-91054 Erlangen (FRG)
Telefax: Int. code + (9131) 85-9132

Experimental Procedure

All reactions were conducted under nitrogen and in anhydrous solvents.

Synthesis of **5** and **6** from **1**: A suspension of 2 mmol of **1** in 20 mL of CH_2Cl_2 was treated with 2.1 mmol of **3** or **4**. After 10 min Et_2O was added to the clear yellow

 © VCH Verlagsgesellschaft mbH, D-69451 Weinheim, 1994 0570-0833/94/1919-1952 $ 10.00+.25/0

solution and a mixture of **5** or **6** and protonated pyridine precipitated. The latter was removed by fractional recrystallization from CH_2Cl_2/Et_2O.

Synthesis of **5** and **6** from **2**: A solution of 2.5 mmol of **2** in 20 mL of CH_2Cl_2 was treated with 2.5 mmol of Me_3SiOTf. Then 6 mmol of diazo ester **3** or **4** was added dropwise, which was accompanied by release of N_2. 30 min after N_2 release had stopped, Et_2O was added and **5** or **6** precipitated. Both compounds were removed by filtration, washed, and dried at 0.01 Torr.

Synthesis of **7**–**12**: A solution of 2 mmol of **6** in 20 mL of CH_2Cl_2 was treated with 2.5 mmol of the appropriate nucleophile. After 1 h the corresponding products were precipitated by addition of Et_2O, removed by filtration, washed with Et_2O, and dried at 0.01 Torr.

Table 1. Yields and spectroscopic data of compounds **5**–**12** [a]. Correct C,H,N analyses were also obtained.

5: Yellow powder; yield: 84% [b]; ^{1}H NMR (CD_3CN): $\delta = 1.46$ (s, 9H; CH_3), 7.58 (t, 2H; H-3/H-5 Ph), 7.75 (t, 1H; H-4 Ph), 8.10 (d, 2H; H-2/H-6 Ph); ^{13}C NMR (CD_3CN) [c]: $\delta = 28.14$ (CH_3), 87.00 ($C(CH_3)_3$), 117.63 (C-1 Ph), 121.70 (q, ^1J(C,F) = 320 Hz; CF_3), 133.05 (C-3/C-5 Ph), 134.25 (C-4 Ph), 136.24 (C-2/C-6 Ph), 160.86 (CO); IR: $\tilde{\nu}$[cm^{-1}] = 2100 (N_2), 1700 (CO).

6: Yellow powder; yield: 81% [b]; ^{1}H NMR (CD_3CN): $\delta = 1.25$ (t, 3H; CH_3), 4.28 (q, 2H; CH_2), 7.58 (t, 2H; H-3/H-5 Ph), 7.74 (t, 1H; H-4 Ph), 8.13 (d, 2H; H-2/H-6 Ph); ^{13}C NMR (CD_3CN) [c]: $\delta = 14.49$ (CH_3), 65.14 (CH_2), 117.71 (C-1 Ph), 121.65 (q, ^1J(C,F) = 320 Hz; CF_3), 133.04 (C-3/C-5 Ph), 134.33 (C-4 Ph), 136.47 (C-2/C-6 Ph), 162.12 (CO); IR: $\tilde{\nu}$[cm^{-1}] = 2100 (N_2), 1710 (CO).

7: Yellow powder; yield: 74%; ^{1}H NMR (CD_3CN): $\delta = 1.30$ (t, 3H; CH_3), 4.35 (q, 2H; CH_2), 8.20 (t, 2H; H-3/H-5 pyridine), 8.72 (t, 1H; H-4 pyridine), 8.90 (d, 2H; H-2/H-6 pyridine); ^{13}C NMR (CD_3CN) [c]: $\delta = 14.57$ (CH_3), 64.13 (CH_2), 122.00 (q, ^1J(C,F) = 320 Hz; CF_3), 130.00 (C-3/C-5 pyridine), 149.54 (C-4 pyridine), 150.25 (C-2/C-6 pyridine), 161.35 (CO), $\tilde{\nu}$[cm^{-1}] = 2115 (N_2), 1710 (CO).

8: Colorless powder; yield: 90%; ^{1}H NMR ($CDCl_3$): $\delta = 1.35$ (t, 3H; OCH_2CH_3), 3.33 (s, 6H; $S(CH_3)_2$), 4.35 (q, 2H; OCH_2CH_3); ^{13}C NMR ($CDCl_3$): $\delta = 14.08$ (OCH_2CH_3), 27.53 ($S(CH_3)_2$), 55.10 (CN_2), 63.40 (OCH_2CH_3), 120.46 (q, ^1J(C,F) = 320 Hz; CF_3), 160.29 (CO); IR: $\tilde{\nu}$[cm^{-1}] = 2140 (N_2), 1695 (CO).

9: Light yellow powder; yield: 95%; ^{1}H NMR ($CDCl_3$): $\delta = 1.20$ (t, 3H; CH_3), 4.27 (q, 4H; CH_2), 7.78 (mc, 15H; $AsPh_3$); ^{13}C NMR ($CDCl_3$): $\delta = 13.99$ (CH_3), 50.71 (CN_2), 63.65 (CH_2), 119.74 (C-1 $AsPh_3$), 121.00 (q, ^1J(C,F) = 320 Hz; CF_3), 131.38 (C-3/C-5 $AsPh_3$), 132.80 (C-2/C-6 $AsPh_3$), 135.14 (C-4 $AsPh_3$), 162.66 (CO); IR: $\tilde{\nu}$[cm^{-1}] = 2140 (N_2), 1705 (CO).

10: Light yellow powder; yield: 86%; ^{1}H NMR ($CDCl_3$): $\delta = 1.27$ (t, 3H; CH_3), 4.01 (q, 4H; CH_2), 7.64 (mc, 15H; $SbPh_3$); ^{13}C NMR ($CDCl_3$): $\delta = 13.81$ (CH_3), 48.16 (CN_2), 62.25 (CH_2), 121.00 (q, ^1J(C,F) = 320 Hz; CF_3), 127.62 (C-1 $SbPh_3$), 130.60 (C-3/C-5 $SbPh_3$), 133.04 (C-4 $SbPh_3$), 134.44 (C-2/C-6 $SbPh_3$), 166.13 (CO); IR: $\tilde{\nu}$[cm^{-1}] = 2110 (N_2), 1680 (CO).

11: Light yellow powder; yield: 53%; ^{1}H NMR ($CDCl_3$): $\delta = 1.33$ (t, 3H; OCH_2CH_3), 1.42 (t, 9H; $N(CH_2CH_3)_3$), 3.85 (q, 6H; $N(CH_2CH_3)_3$), 4.35 (q, 2H; OCH_2CH_3); ^{13}C NMR ($CDCl_3$): $\delta = 8.49$ ($N(CH_2CH_3)_3$), 14.40 (OCH_2CH_3), 56.42 ($N(CH_2CH_3)_3$), 63.54 (OCH_2CH_3), 79.02 (CN_2), 121.11 (q, ^1J(C,F) = 320 Hz, CF_3), 160.10 (CO); IR: $\tilde{\nu}$[cm^{-1}] = 2110 (N_2), 1700 (CO).

12: Colorless powder; yield: 72%; ^{1}H NMR (CD_3CN): $\delta = 0.92$ (t, 3H; CH_3), 3.96 (q, 2H; CH_2), 7.42 (mc, 30H; PPh_3); ^{13}C NMR (CD_3CN) [c]: $\delta = 14.16$ (CH_3), 62.04 (CH_2), 121.44 (d, ^1J(C,P) = 88.2 Hz; C-1 PPh_3), 122.00 (q, ^1J(C,F) = 320 Hz, CF_3), 124.23 (d, ^1J(C,P) = 95.6 Hz; C-1 PPh_3), 130.36 (d, ^3J(C,P) = 12.9 Hz; C-3/C-5 PPh_3), 130.56 (d, ^3J(C,P) = 12.9 Hz; C-3/C-5 PPh_3), 134.16 (d, ^2J(C,P) = 9.2 Hz; C-2/C-6 PPh_3), 134.42 (d, ^2J(C,P) = 11.0 Hz; C-2/C-6 PPh_3), 134.69 (d, ^4J(C,P) = 2.9 Hz; C-4 PPh_3), 135.03 (d, ^4J(C,P) = 3.7 Hz; C-4 PPh_3), 164.12 (d, ^2J(C,P) = 29.4 Hz; CO); ^{31}P NMR (CD_3CN): $\delta = 6.49$ (PPh_3^+), 27.17 (N = PPh_3).

[a] ^{1}H NMR (400 MHz, 25 °C, TMS), ^{13}C NMR (100 MHz, 25 °C, TMS), ^{31}P NMR (100 MHz, 25 °C, H_3PO_4), IR spectra measured in nujol. [b] Yield based on the synthesis from **2**. [c] The signal of the quaternary diazo carbon atom was not evident in any of these ^{13}C NMR spectra.

Received: May 25, 1994 [Z 6967 IE]
German version: *Angew. Chem.* **1994**, *106*, 2038

[1] T. Curtius, *Ber. Dtsch. Chem. Ges.* **1883**, *16*, 2230–2231.
[2] Reviews: a) M. Regitz, G. Maas, *Diazo Compounds*, 1st ed., Academic Press, Orlando, **1986**; b) M. Böhshar, J. Fink, H. Heydt, O. Wagner, M. Regitz, *Methoden Org. Chem. (Houben-Weyl) 4th ed. 1952–, Vol. E14b*, **1990**, p. 961–1371.
[3] Reviews: a) C. Willgerodt, *Die Organischen Verbindungen with Mehrwertigem Iod*, Enke, Stuttgart, **1914**; b) R. M. Moriarty, O. Prakash, *Acc. Chem. Res.* **1986**, *19*, 244–250; c) A. Varvoglis, *Synthesis* **1984**, 709–726; d) G. F. Koser in *The Chemistry of Functional Groups, Supplement D* (Eds.: S. Patai, Z. Rappoport), Wiley, Chichester, **1983**, pp. 1265–1351; e) A. Varvoglis, *Chem. Soc. Rev.* **1982**, *10*, 377–407; f) R. M. Moriarty, R. K. Vaid, *Synthesis* **1990**, 431–447; g) D. F. Banks, *Chem. Rev.* **1966**, *66*, 243–266; h) R. M. Moriarty, R. K. Vaid, G. F. Koser, *Synlett* **1990**, 365–383; i) P. J. Stang, *Angew. Chem.* **1992**, *104*, 281–292; *Angew. Chem. Int. Ed. Engl.* **1992**, *31*, 274–285; j) A. Varvoglis, *The Organic Chemistry of Polycoordinated Iodine*, 1st ed., VCH, Weinheim, **1992**.
[4] R. Weiss, J. Seubert, *Angew. Chem.* **1994**, *106*, 900–901; *Angew. Chem. Int. Ed. Engl.* **1994**, *33*, 891–893.
[5] When **4** was allowed to react for more than 1 h, **7**, the product of nucleophilic substitution, was obtained directly. Under analogous conditions **5** did not react.
[6] By structural variation of the diazo compound this alternative synthetic route provided a broad spectrum of these compounds.
[7] The initial step is most likely silylation of the diazo compound, during which one equivalent of the diazo compound is consumed as an auxiliary base. Cf.: M. Martin, *Synth. Commun.* **1983**, *13*, 809–811; H. Emde, G. Simchen, *Liebigs Ann. Chem.* **1983**, 816–834; c) T. Allspach, H. Gümpel, M. Regitz, *J. Organomet. Chem.* **1985**, *290*, 33–39.
[8] Crystal structure analysis of **5** ($C_{13}H_{14}F_3IN_2O_5S$); $M = 494.22$, monoclinic, space group $P2(1)/c$, $a = 15.066(3)$, $b = 10.769(2)$, $c = 12.500(2)$ Å, $\alpha = 90$, $\beta = 113.75(3)$, $\gamma = 90°$, $V = 1856.3(6)$ Å^3, $Z = 4$, $\rho_{calcd} = 1.768$ Mgm^{-3}, 12224 reflections ($4.0° > 2\theta > 54.0°$), of which 4098 were independent. $R1 = 0.0495$ for 2945 reflections with $F > 4\sigma(F)$; $wR2 = 0.1465$ for all data ($wR2 = [\Sigma w(F_o^2 - F_c^2)^2/[\Sigma w(F_o^2)]^{1/2}$); the measurement was conducted with an automatic four-circle diffractometer Nicolet R3m/V with $Mo_{K\alpha}$ radiation ($\lambda = 0.71073$) at 200 K. The structure was solved by direct methods (SHEXTL Plus 4.11 (Siemens)). All non-hydrogen atoms were refined anisotropicically versus F^2; the hydrogen atoms were refined isotropically in idealized, fixed positions according to a riding model (SHELXL93, G. M. Sheldrick, Universität Göttingen, **1993**). Further details of the crystal structure investigation may be obtained from the Fachinformationszentrum Karlsruhe, D-76344 Eggenstein-Leopoldshafen (FRG) on quoting the depository number CSD-58387.
[9] This value indicates that the coordination of the anion is weaker here than that in an iodonioacetylene described by Stang et al: P. J. Stang, A. M. Arif, C. M. Crittell, *Angew. Chem.* **1990**, *102*, 307–308; *Angew. Chem. Int. Ed. Engl.* **1990**, *29*, 287.
[10] S. Sorriso in *The Chemistry of the Diazonium and Diazo Groups, Vol. 1* (Ed.: S. Patai), Wiley, Chichester, **1978**, pp. 95–135.
[11] A. Varvoglis, *The Organic Chemistry of Polycoordinated Iodine*, 1st ed., VCH, Weinheim, **1992**, p. 209–211, 315–317, and references therein.
[12] M. Regitz, A. E. M. Tawfik, H. Heydt, *Liebigs Ann. Chem.* **1981**, 1865–1873.

Diastereoselective Reaction of a 1-Phosphaallyl Anion with an Alkyne: Structure of an Isolated Dihydrophospholyl Anion and Stereospecific Protonation to Give 2,3-Dihydrophosphole**

Edgar Niecke,* Martin Nieger, and Peter Wenderoth

Dedicated to Professor Reinhard Schmutzler on the occasion of his 60th birthday

Polar cycloaddition reactions are well documented for 2-aza- and 1,2-diazaallyl "anions" and have proved to be successful for the construction of heterocycles.[1] This reaction sequence is used particularly for the synthesis of 3,4-dihydro-2*H*-pyrroles, pyrrolidines, and pyridene derivatives.[2] In contrast, corresponding cycloaddition reactions of allyl anions are rare and are limited to compounds whose substituents are capable of stabilizing the negative charge in the 2-position.[1, 3]

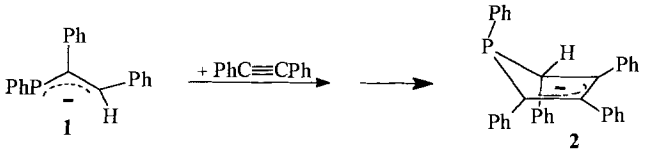
In the context of work on phosphaallyl anions[4] we recently reported on a surprisingly simple synthesis of the phosphindolyl system.[5] We have now extended our investigations on 1-phos-

[*] Prof. Dr. E. Niecke, Dr. M. Nieger, Dipl.-Chem. P. Wenderoth
Anorganisch-Chemisches Institut der Universität
Gerhard-Domagk-Strasse 1, D-53121 Bonn (FRG)
Telefax: Int. code + (228)73-5327

[**] This work was supported by the Deutsche Forschungsgemeinschaft and the Fonds der Chemischen Industrie.

phaallyl systems to cycloaddition reactions and have successfully synthesized and structurally characterized a heterocyclic system with a noncomplexed allyl anion as the central building block. The existence of separate ion pairs for allyl anionic systems has to our knowledge only been demonstrated by NMR spectroscopic investigations.[6]

The equimolar reaction of the 1-phosphaallyl anion **1** with tolane, which is accompanied by a change in color from purple to deep red, leads to the formation of an anion **2**. This can be isolated as **2**·Li(dme)$_3$ in the form of extremely air-sensitive crystals.[7]



The lithium salt of the dihydrophospholide **2** crystallizes in the chiral space group $P2_12_12_1$.[8] The lithium ion resides in an octahedral environment coordinated by three solvent molecules (DME). The shortest distances to the anion lie in the range of van der Waals contacts and thus confirm the presence of separate ions in the crystal. The anion has the absolute configuration P1: *S*, C4: *S* in the single crystal chosen for the structure analysis. The five-membered ring has a slightly twisted envelope conformation with the phosphorus atom at the vertex (Fig. 1).

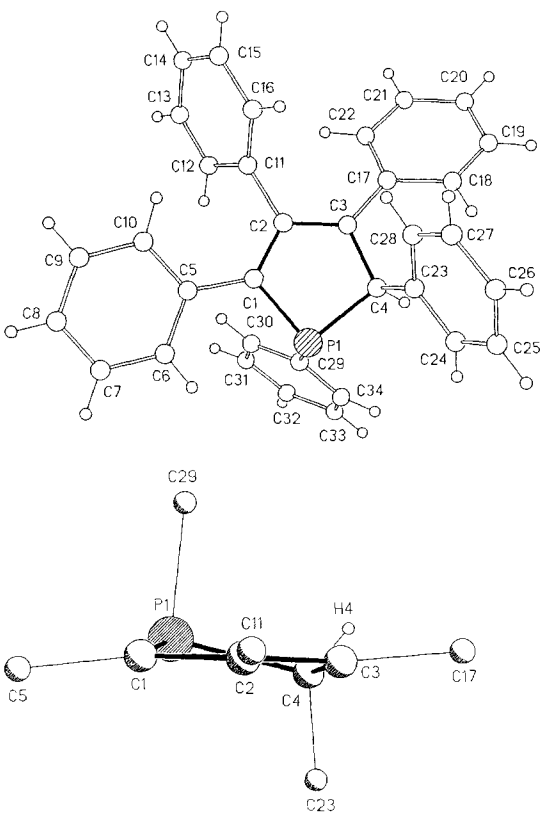
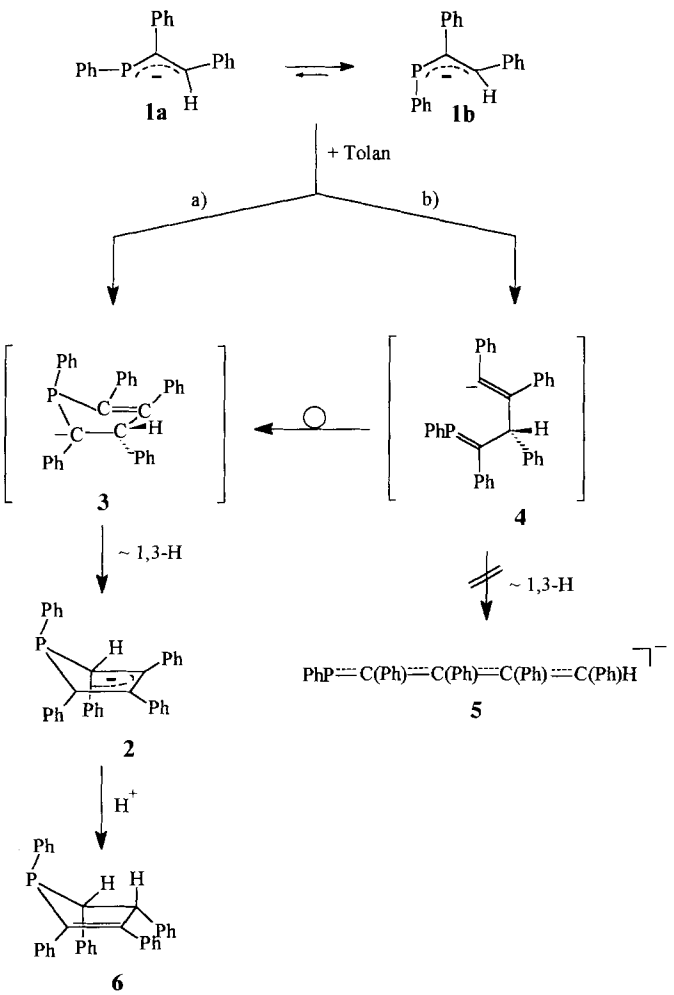


Fig. 1. Crystal structure of the anion of **2**·Li(dme)$_3$. Selected bond lengths [pm] and angles [°]: P1-C1 177.4(6), P1-C29 184.7(6), P1-C4 187.1(6), C1-C2 141.2(8), C2-C3 139.5(8), C3-C4 154.2(8); C1-P1-C29 102.0(3), C1-P1-C4 92.0(3), C4-P1-C29 99.2(3), C2-C1-C5 130.5(6), C2-C1-P1 110.4(5), C5-C1-P1 119.0(5), C3-C2-C1 117.0(5), C3-C2-C11 120.5(6), C1-C2-C11 122.4(6), C2-C3-C17 130.2(6), C2-C3-C4 111.9(6), C17-C3-C4 117.8(5).

Three of the five phenyl substituents (on C1–C3) are arranged propellerlike about the framework of the ring. The phenyl group at the phosphorus atom adopts a "flag pole" position and is orientated *trans* with respect to the substituent on C4. The allylic structure C1–C3 results from the short distances (C1–C2 141.2(8); C2–C3 139.5(8) pm), which, like the innercyclic angle at C2 (117.0(5)°), lie in the range of values typical for allyllithium complexes.[11] The bonds from these atoms to the *ipso* carbon atoms of the phenyl groups (C5, C11, and C17) correspond to single bond lengths (146–148 pm) between sp^2-hybridized carbon centers. As expected the distances of C4 to C3 and to C23 (154–155 pm) are longer. The bond lengths P1–C4 and P1–C29 (187.1(6) and 184.7(6) pm, respectively) correspond with the expected values for this combination of elements, in contrast, the P1–C1 bond is significantly shorter than expected (177.4(6) pm). This indicates a stabilization of the negative charge with the participation of the phosphorus atom.[12]

No evidence for the formation of an intermediate is obtained by following the reaction **1** → **2** by ^{31}P NMR spectroscopy in the temperature range $-60 < T < 25$ °C. The exclusive formation of one product (^{31}P NMR: $\delta = 36.8$) indicates a reaction path,[13] in which following the cycloaddition the anion **3** containing a localized double bond is stabilized by a *suprafacial* [1,3]-H shift to give the allylic system **2**. Investigations on the mechanism of the cycloaddition of allyl anions to (*E*)-stilbene[13b] lead to the belief that also for **1** the thermodynamically more unfavorable (*Z*,*Z*) isomer[4] **1a** takes part in the reaction.



 © VCH Verlagsgesellschaft mbH, D-69451 Weinheim, 1994 0570-0833/94/1919-1954 $ 10.00+.25/0

For a multistep reaction[14] it must be assumed that the acyclic "anion" **4** generated in the first step of the reaction rapidly cyclizes and thereby prevents the formation of a 1-phosphapentadienyl anion **5**.[15]

Regardless of the course of the reaction by path (a) or (b) the formation of only one product implies the highly stereoselective course of the reaction, and the occurrence of pairs of enantiomers is to be expected. The presence of a racemic mixture is supported by the protonation of **2** to give the corresponding 2,3-dihydrophosphole **6**,[16] which occurs strictly regio- and stereospecifically with the formation of one product, in which both enantiomers are present in the equal amounts.[17]

The composition and constitution of **6** can be derived from the high resolution mass spectrum (molecular peak) and the results of multinuclear NMR measurements. The double bond in the 4-position is confirmed by the two resonances in the olefinic region ($\delta = 142.2$, $J_{C,P} = 8.8$ Hz, and 147.4, 13.7 Hz), whose chemical shifts, like the size of the couplings to the phosphorus nucleus, correspond to known values for 2,3-dihydrophospholes.[18] The geometry of the two ring hydrogen atoms cannot be derived unambiguously from the ^{1}H NMR data ($\delta = 4.9$, $J_{H,P} = 6.9$ Hz, and 4.5, 8.3 Hz; $J_{H,H} = 8.3$ Hz), however, in a kinetically controlled reaction the protonation should lead to a *cis* arrangement of the hydrogen atoms.

Investigations into the dipolar cycloaddition of 1-phosphaallyl anions with heteropolar multiple bonding systems are currently in progress.

Received: April 30, 1994
Revised version: June 15, 1994 [Z68851E]
German version: *Angew. Chem.* **1994**, *106*, 2045

[1] R. R. Schmidt, *Angew. Chem.* **1973**, *85*, 235–270; *Angew. Chem. Int. Ed. Engl.* **1973**, *12*, 212–247; T. Kauffmann, *ibid.* **1974**, *86*, 715–750 and **1974**, *13*, 627–662.

[2] A. Dehnel, J. M. Kanabus-Kaminska, G. Lavielle, *Can. J. Chem.* **1988**, *66*, 310–318; T. Konakahara, N. Sugama, K. Sato, *Heterocycles* **1992**, *33*, 157–160.

[3] G. Boche, P. Martens, *Angew. Chem.* **1972**, *84*, 768–769; *Angew. Chem. Int. Ed. Engl.* **1972**, *11*, 724–725.

[4] E. Niecke, M. Nieger, P. Wenderoth, *J. Am. Chem. Soc.* **1993**, *115*, 6989–6990.

[5] E. Niecke, M. Nieger, P. Wenderoth, *Angew. Chem.* **1994**, *106*, 362–363; *Angew. Chem. Int. Ed. Engl.* **1994**, *33*, 353–354.

[6] D. H. O'Brien, C. R. Russel, A. J. Hart, *J. Am. Chem. Soc.* **1976**, *98*, 7427-7429. Structures of allyl anions as contact ion pairs are known: H. Bock, K. Ruppert, Z. Havlas, D. Fenske, *Angew. Chem.* **1990**, *102*, 1095-1097; *Angew. Chem. Int. Ed. Engl.* **1990**, *29*, 1042-1044; G. Boche, G. Fraenkel, J. Gabral, K. Harms, N. J. R. van Eikema Hommes, J. Lohrenz, M. Marsch, P. von R. Schleyer, *J. Am. Chem. Soc.* **1992**, *114*, 1562-1565.

[7] **2**·Li(dme)$_3$: The lithium salt of **1** (1.6 mmol) in DME (5 mL) was allowed to react at room temperature with tolan (1.6 mmol), dissolved in DME (7 mL), and stirred for 2 h at 25 °C. Crystallization at 4 °C afforded **2**·Li(dme)$_3$ as red orthorhombic crystals in 53% yield. ^{31}P NMR (DME, external H_3PO_4): $\delta = 36.8$. ^{13}C{^{1}H} NMR (DME, external TMS; ring and *ipso* C atoms): $\delta =$ 153.1 (d, J(P,C) = 11.8 Hz), 153.0 (d, J(P,C) = 8.0), 150.0 (d, J(P,C) = 12.1 Hz), 146.7 (d, J(P,C) = 4.2 Hz), 144.3, 144.1 (d, J(P,C) = 17.6 Hz), 71.2 (d, J(P,C) = 3.0 Hz, CH), 68.4 (d, J(P,C) = 14.9 Hz). The doublet structure of an additional resonance (δ ca. 61) is obscured by one of the DME signals.

[8] X-ray structure analysis of **2**·Li(dme)$_3$ ([$C_{34}H_{26}P$]$^-$[Li($C_4H_{10}O_2$)$_3$]$^+$): red crystals, crystal dimensions 0.20 × 0.25 × 0.40 mm^3; $M = 742.8$; orthorhombic, space group $P2_12_12_1$ (no. 19), $a = 11.587(1)$, $b = 16.981(4)$, $c = 22.089(4)$ Å, $V = 4.346(1)$ nm^3, $Z = 4$, $\mu(Cu_{K\alpha}) = 0.91$ mm^{-1}, $T = 208$ K, F(000) = 1592. 9604 reflections up to $2\theta_{max} = 120°$ were measured on an Enraf-Nonius CAD4 diffractometer with the $Cu_{K\alpha}$ radiation, 5985 of which were independent and were used for all calculations. The structure was solved by direct methods and refined to F^2 anisotropically, the H atoms were refined with a riding model (program: SHELXL-93 [9]). The final quality coefficient $wR2(F^2)$ was 0.202, with a conventional $R(F) = 0.072$ for 488 parameters and 255 restraints. An extinction correction was carried out. The absolute structure was determined by x-refinement [10]. Further details of the crystal structure investigation may be obtained from the Fachinformationszentrum Karlsruhe, D-76344 Eggenstein-Leopoldshafen (FRG) on quoting the depository number CSD-58316.

[9] G. M. Sheldrick, SHELXL-93, Universität Göttingen, **1993**.

[10] H. D. Flack, *Acta Crystallogr. Sect. A* **1983**, *39*, 876-881.

[11] G. Boche, H. Etzrodt, M. Marsch, W. Massa, G. Baum, H. Dietrich, W. Mahdi, *Angew. Chem.* **1986**, *98*, 84-85; *Angew. Chem. Int. Ed. Engl.* **1986**, *25*, 104–105; see likewise: T. Clark, E. Jemmis, P. von R. Schleyer, S. Binkley, J. Pople, *J. Organomet. Chem.* **1978**, *150*, 1-6.

[12] The lithium salt of a phosphinomethanide, $Me_2PC(H)SiMe_3$·Li(pmdta) also shows a comparably short P–C distance of 177.6 pm: H. K. Karsch, K. Zellner, P. Mikulcik, J. Lachmann, G. Müller, *Organometallics* **1990**, *9*, 190-194.

[13] See also: a) T. Kauffmann, K. Habersaat, E. Köppelmann, *Angew. Chem.* **1972**, *84*, 262-263; *Angew. Chem. Int. Ed. Engl.* **1972**, *11*, 291-292; b) W. T. Ford, G. F. Luteri, *J. Am. Chem. Soc.* **1977**, *99*, 5330-5333.

[14] W. Bannwarth, R. Eidenschink, T. Kauffmann, *Angew. Chem.* **1974**, *86*, 476–477; *Angew. Chem. Int. Ed. Engl.* **1974**, *13*, 468-469.

[15] Such a reaction course is observed for the reaction of the silylated 1,2-diphosphaallyl anion [$Me_3SiPPC(SiMe_3)_2$]$^-$ with a phosphaalkyne: G. Becker, personal communication.

[16] **6**: A solution of **2** (1.6 mmol) in DME (5 mL) was allowed to react with an equimolar amount phenylacetylene at room temperature. On stirring **6** began to precipitate after 5 h. To complete the reaction the mixture was left overnight and the white product was subsequently filtered through a frit. Repeated washing with DME and subsequent drying under high vacuum afforded **6** (619 mg, 83%). ^{31}P NMR (C_6D_6, external H_3PO_4): $\delta = 27.3$ (pseudo-q, J(P,H) = 7.6 Hz). ^{13}C{^{1}H} and ^{13}C{^{1}H, ^{31}P} NMR ($CDCl_3$, external TMS, ring and *ipso* C atoms): $\delta = 147.4$ (d, J(P,C) = 13.7 Hz), 142.2 (d, J(P,C) = 8.8 Hz), 138.9, 138.7 (d, J(P,C) = 14.5 Hz), 138.2 (d, J(P,C) = 0.9 Hz), 137.9 (d, J(P,C) = 24.4 Hz), 137.8 (d, J(P,C) = 13.8 Hz), 64.2 (d, J(P,C) = 5.0 Hz, CH), 58.3 (d, J(P,C) = 7.2 Hz, CH). ^{1}H NMR ($CDCl_3$, internal TMS; ring protons): $\delta = 4.9$ (dd, J(P,H) = 6.9 Hz, J(H,H) = 8.3 Hz), 4.5 (dd, J(P,H) = 8.3 Hz, J(H,H) = 8.3 Hz); MS (characteristic fragments): 466 (70%) [M^+], 389 (8%) [M^+–Ph], 288 (12%) [M^+–Ph_2C_2], 178 (94%) [$Ph_2C_2^+$], 91 (59%) [$C_7H_7^+$], 77 (80%) [Ph^+], 51 (57%) [$C_4H_3^+$].

[17] The enantiomeric ratio of **6** was determined to be 1:1 in (+)-(*R*)-1-phenylethylamine as solvent (^{31}P NMR: $\delta = 25.8$, 25.9). Rotation: $\alpha = 1.5(10)°$.

[18] L. D. Quin, S. G. Borleske, R. C. Stocks, *Org. Magn. Reson.* **1973**, *5*, 161-162.

Cyclopropanation by Methylene Transfer from (η^2-Formaldehyde)zirconocene Complexes**

Gerhard Erker,* Stefanie Schmuck, and Maximilian Bendix

Dedicated to Professor Thomas Kauffmann on the occasion of his 70th birthday

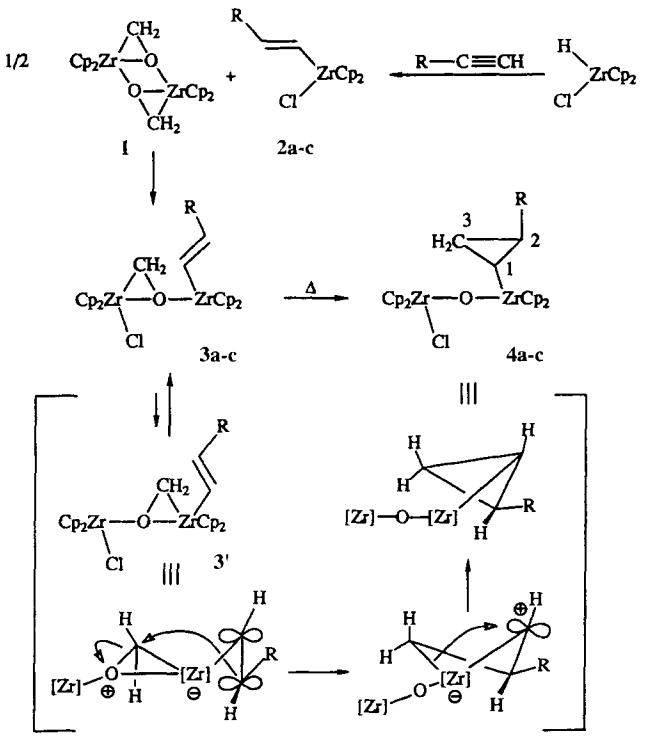
Multinuclear (η^2-formaldehyde)zirconocene complexes have some properties that are reminiscent of the chemistry of methylene on metal oxide surfaces.[1] Thus, [{(η^2-CH_2O)$ZrCp_2$}$_2$] (**1**)[2] reacts similarly to diazomethane[3] with catalytic amounts of triethylborane to give a smooth CH_2 transfer and methylene oligomerization. After oxidative workup of the resulting product mixture of alkylborane compounds, a Poisson distribution of 1-alkanols $HO(CH_2)_nC_2H_5$ with a degree of oligomerization n of up to 15 is obtained.[4] A natural extension of this work was to test whether the CH_2 groups of **1** could also be transferred to simple alkenes with cleavage of the good zirconocene oxide leaving group and thus produce cyclopropanes. Although with complex **1** such a direct transformation was not possible, this cyclopropane formation took place at a binuclear μ-oxozirconocene complex that bears a Zr–O bridging CH_2 group and a σ-bound alkenyl ligand simultaneously at the metal oxide matrix.

We have shown that **1** reacts with the metallocene chlorides [Cp_2MCl_2] of zirconium and hafnium to yield the dinu-

[*] Prof. Dr. G. Erker, Dr. S. Schmuck, Dr. M. Bendix
Organisch-chemisches Institut der Universität
Corrensstrasse 40, D-48149 Münster (FRG)
Telefax: Int. code + (251)83-9772

[**] This work was supported by the Fonds der Chemischen Industrie, the Deutsche Forschungsgemeinschaft, and the Alfried-Krupp-von Bohlen-und-Halbach-Stiftung.

clear [μ-(O-η^1:C,O-η^2-formaldehyde)]metallocene complexes [$Cp_2Zr(Cl)(CH_2O)MCp_2(Cl)$].[5] We have now used this reaction type to prepare the corresponding dinuclear metallocene complexes **3** from **1** and the (σ-alkenyl)zirconocene chlorides **2** (Scheme 1). The alkenyl complexes **2** were synthesized by hydrozirconation of the alkynes.[6]



Scheme 1. **a**: R = n-C_4H_9; **b**: R = n-C_3H_7; **c**: R = H.

The reaction of dimer **1** with (*E*)-1-hexenylzirconocene chloride **2a** was conducted in [D_8]tetrahydrofuran and monitored by ^{1}H and ^{13}C NMR spectroscopy. At room temperature the new compound **3a** is formed rapidly, and 30% is present together with the starting materials after 17 h.

The existence of a three-membered $ZrCH_2O$ ring in **3a** is deduced unambiguously from the typical ^{13}C NMR spectrum[7] (CH_2: δ = 68.6, ^1J(C,H) = 153 Hz). The complex **3a** could not be obtained in higher yields, because it undergoes a subsequent reaction at longer reaction duration or higher temperature. In this reaction the methylene group adds to the adjacent alkenyl unit to form a zirconium-substituted cyclopropane. We prepared the product **4a** directly in about 60% yield by reaction of **1** with **2a** in toluene at 90 °C (4 days) (see Table 1). According to the ^{1}H NMR spectrum of **4a**, the two substituents are *trans* at the cyclopropane ring, that is, the reaction proceeds with retention of the configuration of the starting compound **2a**.

The corresponding (σ-cyclopropyl)zirconium complexes **4b, c** arise on treatment of **1** with (*E*)-1-pentenylzirconocene chloride (**2b**) or vinylzirconocene chloride **2c**, respectively. In both cases monitoring the course of reaction by NMR spectroscopy makes direct detection of the intermediates **3a** and **3b** possible. The reaction of **1** with the acetylene–hydrozirconation product **2c** is, relative to the other two reactions (with **2a, b**), substantially less selective, and apart from the cyclopropylmetallocene complex **4c**, [$Cp_2Zr(Cl)$–O–$ZrCp_2(Cl)$] is also obtained in about 30% yield.

Table 1. Experimental details for the reaction of **1** with the alkenyl(chloro)zirconocenes **2a–c** as well as NMR data of complexes **3** and **4**.

3a (obtained from a 55:15:30-mixture of **1**, **2a** and **3a**, prepared from **1** and **2a** at 80 °C after 8 h, spectroscopic characterization): ^{1}H NMR ([D_8]THF): δ = 7.12 (dt, ^3J = 18.0, ^4J = 1.3 Hz, 1H, Zr-CH=), 6.23 (s, 10H, Cp), 5.87 (s, 10H, Cp), 5.80 (dt, ^3J = 18.0, ^3J = 6.3 Hz, 1H, Zr-CH=C*H*-), 2.42 (s, 2H, $ZrOCH_2$), 2.05 (m, 2H, =CH-CH_2-), 1.46–1.39 (m, 4H, -CH_2CH_2-), 0.97 (br. t, 3H, CH_3); ^{13}C NMR (C_6D_6): δ = 175.3 (^1J(C,H) = 123 Hz, Zr-CH=), 144.2 (^1J(C,H) = 147 Hz, Zr-CH=*C*H), 112.5 (^1J(C,H) = 174 Hz, Cp), 108.9 (^1J(C,H) = 174 Hz, Cp), 68.6 (^1J(C,H) = 153 Hz, $ZrOCH_2$), 39.0, 32.2, 22.9 (CH_2), 14.4 (CH_3).

4a: Synthesis from 400 mg (0.80 mmol) **1** and 540 mg (1.60 mmol) **2a** in 15 mL toluene (4 d, 90 °C). Recrystallized from toluene at −18 °C, yield: 550 mg (58%) **4a**, M.p.: 138 °C, $C_{23}H_{33}ClOZr_2$ (591.5): calcd. C 54.83, H 5.62; found C 54.34, H 5.53; IR (KBr): $\tilde{\nu}$ = 3102, 3087, 2959, 2919, 2868, 1723, 1637, 1441, 1262, 1098, 1016, 800, 735, 609 cm^{-1}; ^{1}H NMR (C_6D_6): δ = 5.98, 5.97, 5.90, 5.86 (s, each 5H, Cp), 1.72, 1.26 (m, each 1H, 4-H, 4-H'), 1.57 (m, 2H, CH_2), 1.44 (m, 2H, CH_2), 1.02 (br. t, 3H, CH_3), cyclopropyl: 1.02 (m, 1H, 2-H, hidden by CH_3 signal, identified by COSY), 0.87 (m, 1H, 3-H'), 0.66 (m, 1H, 3-H), −0.19 (m, 1H, 1-H); coupling constants: ^2J(3-H, 3-H') = 3.0, ^3J(1-H, 2-H) = 7.6 Hz, ^3J(1-H, 3-H') = 6.7 (*trans* coupling), ^3J(1-H, 3-H) = 10.0 (*cis* coupling), ^3J(2-H, 3-H) = 3.0 (*trans* coupling), ^3J(2-H, 3-H') = 7.5 Hz (*cis* coupling); ^{13}C NMR (C_6D_6): δ = 113.7 (^1J(C,H) = 172 Hz, Cp), 111.4 (^1J(C,H) = 172 Hz, Cp), 111.3 (^1J(C,H) = 172 Hz, Cp), 38.6 (^1J(C,H) = 122 Hz, CH_2), 36.5 (^1J(C,H) = 132 Hz, Zr-cyclopropyl-*C*H), 33.5 (^1J(C,H) = 127 Hz, CH_2), 25.6 (^1J(C,H) = 157 Hz, cyclopropyl-C-2), 23.4 (^1J(C,H) = 124 Hz, CH_2), 19.3 (^1J(C,H) = 158 Hz, cyclopropyl-C-3), 14.5 (^1J(C,H) = 121 Hz, CH_3).

3b (from a 29:28:43-mixture of **1**, **2b** and **3b**, prepared from **1** and **2b** at 80 °C after 8 h, spectroscopic characterization): ^{1}H NMR (C_6D_6): δ = 7.19 (dt, ^3J = 18.0, ^4J = 1.3 Hz, 1H, Zr-CH=), 5.98 (s, 10H, Cp), 5.72 (s, 10H, Cp), 2.40 (s, 2H, $ZrOCH_2$), 2.23 (m, 2H, =CHCH_2), 1.55 (m, 2H, CH_2), 1.06 (br. t, 3H, CH_3). ZrCH=C*H* resonance not observed; ^{13}C NMR (C_6D_6): δ = 175.5 (^1J(C,H) = 118 Hz, Zr-CH=), 143.9 (^1J(C,H) = 148 Hz, Zr-CH=CH), 112.5 (Cp), 108.9 (Cp), 68.6 (^1J(C,H) = 153 Hz, $ZrOCH_2$), 41.4 (=CH-CH_2), 23.1 (CH_2), 14.3 (CH_3).

4b: Synthesis from 250 mg (0.50 mmol) **1** and 340 mg (1.00 mmol) **2b** in 20 ml toluene (4 d, 90 °C), product precipitated from toluene at −18 °C, yield 340 mg (59%) **4b**, contains about ca. 10% nonidentified impurity, m.p. 121 °C, $C_{26}H_{31}ClOZr_2$ (577.4): calcd. C 54.08, H 5.41; found C 52.02, H 5.49; IR (KBr; $\tilde{\nu}$ = 3086, 2969, 2926, 2869, 1716, 1625, 1440, 1352, 1262, 1101, 1017, 802, 738, 610 cm^{-1}; ^{1}H NMR (C_6D_6): δ = 5.98(s, 5H, Cp), 5.97(s, 5H, Cp), 5.85 (s, 10H, 2Cp), 1.68, 1.22 (m, each 1H, 4-H, 4-H'), 1.53 (m, 2H, CH_2), 1.05 (br. t, 3H, CH_3), cyclopropyl: 1.05 (m, 1H, 2-H, hidden by CH_3 signal, identified by COSY), 0.86 (m, 1H, 3-H'), 0.65 (m, 1H, 3-H), −0.21 (m, 1H, 1-H); coupling constants: ^2J(3-H, 3-H') = 3.7, ^3J(1-H, 2-H) = 7.0 (*trans* coupling), ^3J(1-H, 3-H') = 7.6 (*trans* coupling), ^3J(1-H, 3-H) = 10.0 (*cis* coupling), ^3J(2-H, 3-H) = 3.7 (*trans* coupling), ^3J(2-H, 3-H') = 7.5 Hz (*cis* coupling); ^{13}C NMR (C_6D_6): δ = 113.7(2 Cp), 111.4 (Cp), 111.3 (Cp), 41.1 (CH_2), 36.5 (^1J(C,H) = 133 Hz, Zr-cyclopropyl-CH), 25.4 (^1J(C,H) = 155 Hz, cyclopropyl-C-2), 23.9 (CH_2), 19.3 (^1J(C,H) = 155 Hz, cyclopropyl-C-3), 14.7 (CH_3).

3c (from a 20:20:60-mixture of **1**, **2c** and **3c**, prepared from **1** and **2c** at room temperature in THF, spectroscopic characterization): ^{1}H NMR ([D_8]THF): δ = 7.52, 6.14, 5.54 (ABX, $^3J_{trans}$ = 19.5, $^3J_{cis}$ = 14.5, ^2J = 3.9 Hz, each 1H, Zr-CH=CH_2), 6.22 (s, 20H, Cp), 2.37 (s, 2H, $ZrOCH_2$); ^{13}C NMR ([D_8]THF): δ = 185.6 (^1J(C,H) = 120 Hz, Zr-CH=), 127.3 (^1J(C,H) = 153 Hz, ^2J(C,H) = 6 Hz, Zr-CH=*C*$_2$), 113.2 (Cp), 109.3 (Cp), 64.8 (^1J(C,H) = 153 Hz, $ZrOCH_2$).

4c: Synthesis from 300 mg (0.60 mmol) **1** and 338 mg (1.20 mmol) **2c** in 40 mL toluene (6 d, 90 °C), product isolated from toluene at −20 °C, yield 400 mg (44%) **4c**, contains ca. 30% [$(Cp_2ZrCl)_2O$]. ^{1}H NMR (C_6D_6): δ = 5.96 (s, 10H, Cp), 5.82 (s, 10H, Cp), cyclopropyl: 1.01 (m, 2H), 0.64 (m, 2H), −0.20 (m, 1H); coupling constants: ^2J = 3.0, ^3J(1-H, 2-H) = 7.6 (*trans* coupling, ^3J(1-H, 2-H') = 9.8 (*cis* coupling), ^3J(2-H, 3-H) = 4.3 (*trans* coupling), ^3J(2-H, 3-H') = 9.7 Hz (*cis* coupling); ^{13}C NMR (C_6D_6): δ = 113.7 (Cp), 108.0 (Cp), 26.5 (^1J(C,H) = 129 Hz, Zr-cyclopropyl-CH), 11.1 (^1J(C,H) = 155 Hz, cyclopropyl-CH_2).

Detailed studies to elucidate the mechanism of this cyclopropanation at the metallocene oxide framework have yet to be performed. However, we assume that the primarily formed compound **3** is in equilibrium with the isomer **3'** through a dyotropic rearrangement.[7, 8] In **3'** the methylene group to be transferred approaches very close to the alkenyl acceptor at the Zr–O–Zr template. Moreover the μ-oxobis(zirconocene) unit is a good leaving group, and the CH_2 group bridging the Zr and O atoms is activated for nucleophilic attack by the adjacent oxonium-type oxygen atom. Formation of a C–C bond between the alkene and the CH_2 group with cleavage of the C–O bond of the

three-membered Zr, O, C ring, followed by a 1,2-alkyl shift from the zirconium atom to the neighboring former alkene carbon atom (see Scheme 1) readily explains the formation of the cyclopropanation product **4** with the observed stereochemistry.

These reactions add to the examples of small organic units which approach each other and react at the molecular Zr–O–Zr metal oxide template stabilized by cyclopentadienyl ligands.[3, 9] Perhaps the chemistry of such molecular compounds can indeed shed some light on the possible individual steps of reactions at metal oxide phases in heterogeneous catalysis.[10]

Received: May 19, 1994 [Z 6948 IE]
German version: *Angew. Chem.* **1994**, *106*, 2043

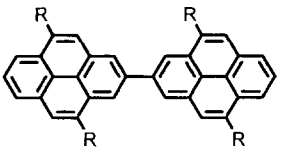
[1] Fischer–Tropsch chemistry parallels the chemistry of methylene on the metal/metal oxide catalyst surface in significant aspects: F. Fischer, H. Tropsch, *Brennst. Chem.* **1926**, *7*, 97; *Chem. Ber.* **1926**, *59*, 830; R. C. Brady III, R. Pettit, *J. Am. Chem. Soc.* **1980**, *102*, 6181; *ibid.* **1981**, *103*, 1287; E. L. Muetterties, J. Stein, *Chem. Rev.* **1979**, *79*, 479; C. K. Rofer-De Porter, *ibid.* **1981**, *81*, 447; W. A. Herrmann, *Angew. Chem.* **1982**, *94*, 118; *Angew. Chem. Int. Ed. Engl.* **1982**, *21*, 117, and references therein.
[2] G. Erker, U. Hoffmann, R. Zwettler, P. Betz, C. Krüger, *Angew. Chem.* **1989**, *101*, 644; *Angew. Chem. Int. Ed. Engl.* **1989**, *28*, 630.
[3] C. E. H. Bawn, A. Ledwith, *Prog. Boron Chem.* **1964**, *1*, 345, and references therein; see also: J. J. Tufariello, L. T. C. Lee, *J. Am. Chem. Soc.* **1966**, *88*, 4757; R. Köster, B. Rickborn, *ibid.* **1967**, *89*, 2782.
[4] G. Erker, S. Schmuck, U. Hoffmann, *J. Am. Chem. Soc.* **1991**, *113*, 2330; see also: K. Kropp, V. Skibbe, G. Erker, C. Krüger, *ibid.* **1983**, *105*, 3353; R. Köster, M. Yalpani, *Angew. Chem.* **1985**, *95*, 600; *Angew. Chem. Int. Ed. Engl.* **1985**, *24*, 572.
[5] G. Erker, M. Mena, M. Bendix, *J. Organomet. Chem.* **1991**, *410*, C5.
[6] J. Schwartz, J. A. Labinger, *Angew. Chem.* **1976**, *88*, 402; *Angew. Chem. Int. Ed. Engl.* **1976**, *15*, 333; G. Erker, R. Schlund, C. Krüger, *Organometallics* **1989**, *8*, 2349; I. Hyla-Kryspin, R. Gleiter, C. Krüger, R. Zwettler, G. Erker, *ibid.* **1990**, *9*, 517, and references therein.
[7] G. Erker, M. Bendix, R. Petrenz, *Organometallics* **1994**, *13*, 456.
[8] M. T. Reetz, *Adv. Organomet. Chem.* **1977**, *16*, 33; G. Erker, K. Kropp, *Chem. Ber.* **1982**, *115*, 2437.
[9] G. Erker, *Acc. Chem. Res.* **1984**, *17*, 103; *Angew. Chem.* **1989**, *101*, 411; *Angew. Chem. Int. Ed. Engl.* **1989**, *28*, 397, and references therein.
[10] For the description of remotely related molecular Fischer–Tropsch model compounds see: M. L. Turner, P. K. Byers, H. C. Long, P. M. Maitlis, *J. Am. Chem. Soc.* **1993**, *115*, 4417, and references therein.

2,2′-Bipyrenyl and *para*-Terpyrenyl—A New Type of Electronically Decoupled Oligoarylene

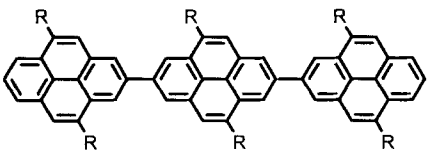
Martin Kreyenschmidt, Martin Baumgarten, Nikolay Tyutyulkov, and Klaus Müllen*

Preparative,[1] stereochemical,[2] and physical aspects[3] of biphenyls and oligophenylenes have received much attention. The frontier orbitals at the bridgehead centers have large atomic orbital coefficients, characteristic of biphenyl[4] and of related biaryls.[4–7] This causes a pronounced electronic interaction through the formal single bond, which decreases with increasing twisting around the bond. However, a stereoelectronic situation that is fundamentally new exists if the molecular orbital coefficients of the bridgehead centers are almost zero, and consequently the rings are electronically decoupled to a first approximation. The 2,2′-bipyrenyls **1** and the analogous *para*-terpyrenyls **2** fulfill this requirement.

Here we describe the synthesis of compounds **1** and **2**, which were unknown until now, and prove that the electronic interaction of the pyrene subunits differs substantially from that in other biaryls and oligoaryls. An important experiment is the charging of the aryl units with one electron each, which, in the case of the title compounds, gives oligoradicals.



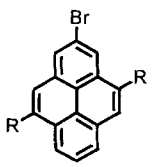
1

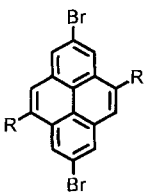


a: R = H
b: R = *n*-octyl
c: R = *n*-pentyl

2

2-Bromopyrenes **3** and 2,7-dibromopyrenes **4** are possible starting compounds for pyrene–pyrene coupling. However, such halogen compounds cannot be prepared by simple substitution at the pyrene. A further difficulty of the targeted syntheses of **1** and **2** from **3** and **4**, respectively, is the expected low solubility of the extended benzenoid systems; the inclusion of alkyl chains is thus necessary to increase the solubility, as in **3b**, **c** and **4b**, **c**, respectively.





a: R = H
b: R = *n*-octyl
c: R = *n*-pentyl

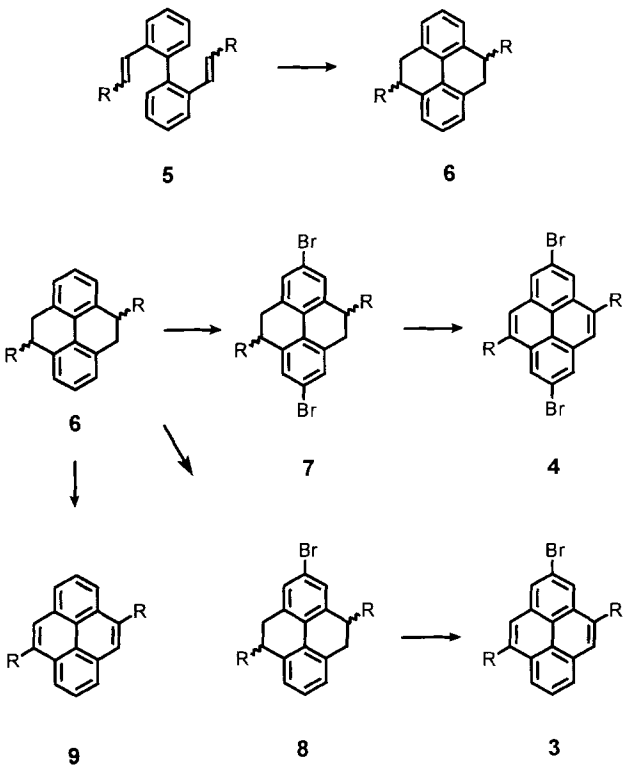
3 **4**

The highly soluble pyrene derivatives **3b**, **c** and **4b**, **c** were synthesized by the route outlined in Scheme 1.

2,2′-(Bis-1-dec-1-enyl)biphenyl (**5b**) is synthesized from either *n*-nonal and 2,2′-bis(triphenylphosphoniomethyl)biphenyl dibromide[8] (EtOH, EtONa, 70 °C, 4 h, 70%) or from diphenaldehyde[9] and nonyltriphenylphosphonium bromide (THF, *n*BuLi, −60 °C, 52%) by the Wittig reaction. The photochemical cyclization of **5b**, which exists as an isomeric *cis*–*trans* mixture, in hexane at 254 nm by irradiation with an 80 Watt Hg low-pressure lamp leads to 4,9-di-*n*-octyl-4,5,9,10-tetrahydropyrene (**6b**)[10] in 80% yield after purification by chromatography. Pyrene **6b** is converted to 2,7-dibromo-4,9-di-*n*-octyl-4,5,9,10-tetrahydropyrene (**7b**) by a new method of catalytic bromination with 5% Pd or Pt on activated carbon, each with two equivalents of Br_2 in *N*,*N*-dimethylformamide (DMF), at room

[*] Prof. Dr K. Müllen, Dipl.-Chem. M. Kreyenschmidt, Dr. M. Baumgarten
Max-Planck-Institut für Polymerforschung
Ackermannweg 10, D-55128 Mainz (FRG)
Telefax: Int. code + (6131)379-350
Prof. Dr. N. Tyutyulkov
University of Sofia, Faculty of Chemistry (Bulgaria)

temperature and a reaction time of 12 h. After bromination at the benzyl positions with *N*-bromosuccinimide, **7b** is aromatized to form **4b** in 60% yield (after column filtration and recrystallization twice from benzene) by addition of 1,8-diazabicyclo[5.4.0]-7-undecene in CCl_4. The di-*n*-pentyl compound **4c** and the 2-bromo derivatives **3b, c** are prepared in a similar way. The model compound 4,9-di-*n*-octylpyrene (**9b**) is obtained in 82% yield on aromatization of **6b**.

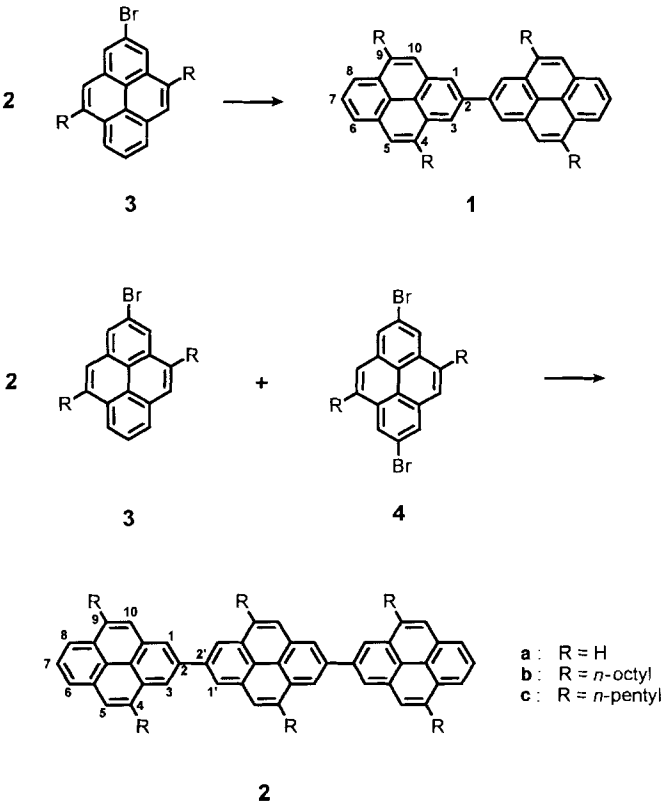


Scheme 1.

The bipyrenyl **1b** was obtained in 95% yield by coupling **3b** with $[Ni(cod)_2]$ according to Yamamoto (Scheme 2).[11] The *para*-terpyrenyl **2b** was synthesized analogously by reaction of two equivalents of **3b** and one equivalent of **4b** (53%). Compounds **1b** and **2b** were purified by size exclusion chromatography.

The interruption of the conjugation by bridging at positions at which atomic orbital coefficients are almost zero in **1** and **2** is shown in the electronic absorption spectra. The λ_{max} values of compounds **1b** and **2b** and of the monomeric model compound **9b** are shifted relative to one another by only a few wavelengths (0–9 nm, Table 1). Thus the oligopyrenyls differ significantly from oligoarylenes with a similar steric arrangement (biphenyl: $\lambda_{max} = 249$ nm and *para*-terphenyl: $\lambda_{max} = 279$ nm) and resemble to 9,9′-bianthryl (**10**) and higher oligo-9,10-anthrylenes in which a conjugation barrier is achieved by positioning the subunits orthogonally (**10**: $\lambda_{max} = 391$ nm; 2′,3′-dihexyl-9,10-trisanthrylene (**11**): $\lambda_{max} = 403$ nm[12]).

To investigate the "electronic decoupling" for the charged states too, compounds **1b** and **2b** were reduced chemically (potassium/THF) and electrochemically (tetrabutylammonium hexafluorophosphate/THF) and then characterized by ESR



Scheme 2.

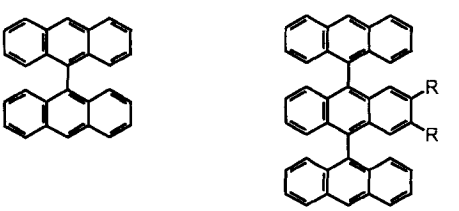
spectroscopy and by cyclic voltammetry. The cyclic voltammetry investigations, do indeed show that the first reduction potentials E_1 are virtually independent of the number of pyrene units (**1b**: $E_1 = -2.24$ eV, **2b**: $E_1 = -2.27$ eV). Furthermore, the

Table 1. Selected physical and spectroscopic data of **1b**, **2b**, and **9b**.

1b: MS (FD, 8 kV) *m/z* 850.5 [M^+]; ^{1}H NMR (500 MHz, $CDCl_3$ 30 °C): δ = 8.77–8.6 (d, ^4J(H,H) = 1.3 Hz, 4H; H1, H3), 8.34–8.16 (2 d, ^3J(H,H) = 7.85 Hz, ^3J(H,H) = 7.45 Hz, 4H; H6, H8), 8.05–7.98 (2 s, 4H; H5, H10), 8.02 (t, ^3J(H,H) = 7.7 Hz, 2H; H7), 3.41 (dt, ^3J(H,H) = 7.75 Hz, 8H; CH_2), 1.94–2.05 (m, 8H; CH_2), 1.55–1.61 (m, 8H; CH_2), 1.25–1.47 (m, 32H; CH_2), 0.83–0.9 (m, 12H; CH_3); UV/VIS (CH_2Cl_2): λ_{max} (ε) = 350 nm (100957), 333 nm (48615), 294 nm (112920), 251 nm (28850).

2b: MS (FS, 8 kV) *m/z* 1274.5 [M^+]; ^{1}H NMR (500 MHz, $CDCl_3$ 30 °C): δ = 8.64–8.83 (4 d, ^4J(H,H) = 1.4 Hz, 8H; H1,1′, H3,3′), 8.18–8.37 (4 d, ^3J(H,H) = 7.45 Hz and 7.95 Hz, 4H; H6, H8), 8.15, 8.08, 8.00 (3 s, 6H; H5,5′, H10), 8.05 (t, ^3J(H,H) = 7.7 Hz, (2H; H7), 3.34–3.49 (m, 12H; CH_2), 1.94–2.15 (m, 12H; CH_2), 1.29–1.65 (m, 60H; CH_2), 0.87–1.01 (m, 18H; CH_3); UV/VIS (CH_2Cl_2): λ_{max} (ε) = 353 nm (86075), 333 nm (64630), 301 nm (77370), 247 nm (40621).

9b: UV/VIS (CH_2Cl_2): λ_{max} (ε) = 344 nm.



charging of each pyrene subunit with one electron leads to only low Coulomb repulsions, which is deduced from the potential differences for dianion formation in **1b** ($E_1-E_2 = 0.16$ eV) and trianion formation in **2b** ($E_2-E_3 = 0.07$ eV). The first reduction potentials of 9,9'-bianthryl (**10**, $E_1 = -2.15$ eV) and of the corresponding trisanthrylene **11** ($E_1 = -2.16$ eV) also hardly differ. In the case of oligo(*para*-phenylenes), however, the first reduction potentials decrease with increasing number of phenylene rings because of the pronounced interaction between rings,[14-15] and a significant Coulomb interaction occurs on increasing the charge.

Remarkably, the formation of the dianion $\mathbf{1b}^{2-}$ does not lead to a diamagnetic state as in the dianions of biphenyl, 1,1'-binaphthyl and 3,3'-biperylenyl,[16] but to a diradical that shows a typical axially symmetric zero field splitting D = 7.90 mT = 73.78×10^{-4} cm^{-1} in frozen solution (T = 130 K). For $\mathbf{2b}^{2-}$, a zero field splitting of D = 7.83 mT = 73.24×10^{-4} cm^{-1} is measured that is almost equal to that of $\mathbf{1b}^{2-}$. The Coulomb interaction between the singly charged pyrene units in the dianion of **2b** is therefore so weak that the adjacent and not the two terminal pyrene units are charged (Fig. 1).

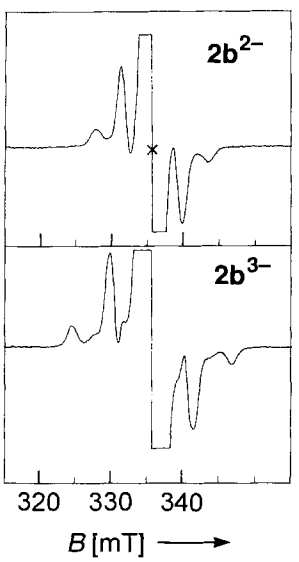


Fig. 1. ESR spectra for the bi- and triradicals $\mathbf{2b}^{2-}$ and $\mathbf{2b}^{3-}$ (THF/K; T = 150 K). The central signal (×) originates from contributions of the monoradical in the biradical.

Further reduction finally leads to the trianion with a quartet state $\mathbf{2b}^{3-}$ in which the zero field coupling D ($S = 3/2$) = 5.53 mT = 51.68×10^{-4} cm^{-1}. Also characteristic of the higher spin multiplicity are the considerably less intense signals of the forbidden $\Delta m_s = 2$ transitions. Therefore, the oligopyrenyls are converted into oligoradicals by charging, but the dipole interaction between the pyrene units is only about half as large as between the anthracene units in bis- and trisanthrylene (**10** and **11**, respectively) with $D(S=1) = 15$ mT and $D(S = 3/2)$ = 11.2 mT.[13]

For the di- ($\mathbf{1b}^{2-}$) and triradicals ($\mathbf{2b}^{3-}$), it is uncertain whether a ferromagnetic or antiferromagnetic exchange interaction is present. The spin multiplicity of the ground state in the dianion of $\mathbf{1b}^{2-}$ cannot be directly determined by Hund's rule, because the half-occupied HOMOs in the anions are localized on nonoverlapping lobes of atomic orbitals, and consequently the direct exchange interaction J_{dir} disappears as part of the effective exchange interaction to a first approximation. For the indirect exchange interaction J_{ind}, an antiferromagnetic interaction with a singlet-triplet energy difference of $E_T - E_S$ = 0.032 eV has been determined while taking the configuration interaction into account.[17-18] Also for the polyanion radical of the corresponding polymer[19] calculations suggest that J_{ind} (= −0.01 eV) provides the main contribution to the effective antiferromagnetic exchange interaction.

The temperature dependence of the intensity of the ESR signals from 4–100 K was therefore investigated for experimental proof of the nature of the interaction in the di- and triradicals $\mathbf{1b}^{2-}$, $\mathbf{2b}^{2-}$, and $\mathbf{2b}^{3-}$. An antiferromagnetic coupling for the intramolecular interaction between the charged pyrene subunits was proven since only monoradical contributions are detected at 4.5 K and components of the zero field splitting only become visible after further thermal excitation from 20 K for diradicals and 40 K for triradicals.

The linkage of pyrene units in the 2- and the 2- and 7-positions leads to an electronic decoupling and offers the possibility for oligoradical formation. However, it does not make a ferromagnetic interaction possible, unlike in *meta*-phenylene-bonded oligo- and polydiradicals.[20] The compounds in the title **1**, **2**, and **9** stimulate further studies in various ways: In physical studies, further criteria for the electronic decoupling of the pyrene units in **1** and **2** will be investigated; for instance, the possibility of a light-induced separation of charge in 1,1'- and 2,2'-bipyrenyl.[3b] In the preparative field, the transition from **1** and **2** into the analogous polymers is an obvious research goal.

Received: May 9, 1994 [Z 6908 IE]
German version: *Angew. Chem.* **1994**, *106*, 2062

[1] a) G. Bringmann, R. Walter, R. Weirich, *Angew. Chem.* **1990**, *102*, 1006; *Angew. Chem. Int. Ed. Engl.* **1990**, *29*, 977; b) T. Hayahi, K. Hayashizaki, Y. Itoh, *Tetrahedron Lett.* **1989**, *30*, 215; c) P. Kovacic, M. Jones, *Chem. Rev.* **1987**, *87*, 357.
[2] a) K. Mislow, M. A. W. Glas, H. B. Hopps, E. Simon, G. H. Wahl, *J. Am. Chem. Soc.* **1964**, *101*, 1710; b) K. E. Wilson, P. E. Pincock, *Can. J. Chem.* **1977**, *55*, 889; c) A. I. Meyers, R. J. Himmelsbach, *J. Am. Chem. Soc.* **1985**, *107*, 682; d) H. Brunner, J. Goldbrunner, *Chem. Ber.* **1989**, *122*, 2005.
[3] a) N. Mataga, H. Yao, T. Okada, W. Rettig, *J. Phys. Chem.* **1989**, *93*, 3383; b) M. Zander, W. Rettig, *Chem. Phys. Lett.* **1984**, *110*, 602; c) D. M. Ivory, G. G. Miller, J. M. Sowa, L. W. Shacklette, R. R. Chance, R. H. Baugham, *J. Chem. Phys.* **1979**, *71*, 1506.
[4] E. Heilbronner, H. Bock, *Das HMO-Modell und seine Anwendungen*, 2nd ed., Verlag Chemie, Weinheim, **1978**.
[5] M. Baumgarten, U. Anton, L. Gherghel, K. Müllen, *Synth. Met.* **1993**, *55-57*, 4801.
[6] U. Anton, A. Bohnen, K. H. Koch, H. Naarmann, H. J. Räder, K. Müllen, *Adv. Mater.* **1992**, *4*, 91.
[7] a) M. Dietrich, J. Mortensen, J. Heinze, *Angew. Chem.* **1985**, *97*, 502; *Angew. Chem. Int. Ed. Engl.* **1985**, *24*, 508; b) H. Hoshiro, K. Kimamura, M. Imamura, *Chem. Phys. Lett.* **1973**, *20*, 193; c) K. Müllen, M. Baumgarten, N. Tyutyulkov, S. Karabunarliev, *Synth. Met.* **1991**, *40*, 127.
[8] D. M. Hall, M. Leslie, E. Turner, *J. Chem. Soc.* **1950**, 711.
[9] J. Falbe, *Methoden Org. Chem. (Houben-Weyl) 4th ed. 1952*, Vol. E3U, **1983**.
[10] As the position of the alkyl chains in tetrahydropyrene 6 varies, a diastereomeric mixture results. However, this can only be separated by column chromatography after forming derivative 7.
[11] T. Yamamoto, A. Morita, Y. Miyazaki, T. Maruyama, H. Wakayama, Z. Zhou, Y. Nakamura, T. Kanbara, *Macromolecules* **1992**, *25*, 1214.
[12] U. Müller, A. Adam, K. Müllen, *Chem. Ber.* **1994**, *127*, 437.
[13] M. Baumgarten, U. Müller, A. Bohnen, K. Müllen, *Angew. Chem.* **1992**, *104*, 482; *Angew. Chem. Int. Ed. Engl.* **1992**, *31*, 448.
[14] R. H. Young, *J. Appl. Phys.* **1986**, *60*, 272.
[15] A. Bohnen, W. Heitz, K. Müllen, H. J. Räder, R. Schenk, *Macromol. Chem.* **1991**, *192*, 1679.
[16] K. H. Koch, K. Müllen, *Chem. Ber.* **1992**, *124*, 2091.
[17] P. W. Andersen, *Phys. Rev.* **1950**, *79*, 350; *ibid.* **1959**, *115*, 2.
[18] Calculations were carried out on all singly and doubly excited configurations between the four highest doubly occupied, the two singly occupied and the four lowest unoccupied MOs.
[19] N. Tyutyulkov, F. Dietz, K. Müllen, M. Baumgarten, S. Karabunarliev, *Theor. Chim. Acta* **1993**, *86*, 353.
[20] J. A. Berson, *Pure Appl. Chem.* **1987**, *59*, 1571.

 © VCH Verlagsgesellschaft mbH, D-69451 Weinheim, 1994 0570-0833/94/1919-1959 $ 10.00+.25/0

Ring Closures on Polymeric Supports—Formation of Extremely Large Macrocycles by Intrapolymeric Cyclooligomerizations**

Manfred Rothe,* Manfred Lohmüller, Ulrich Breuksch, and Günter Schmidtberg

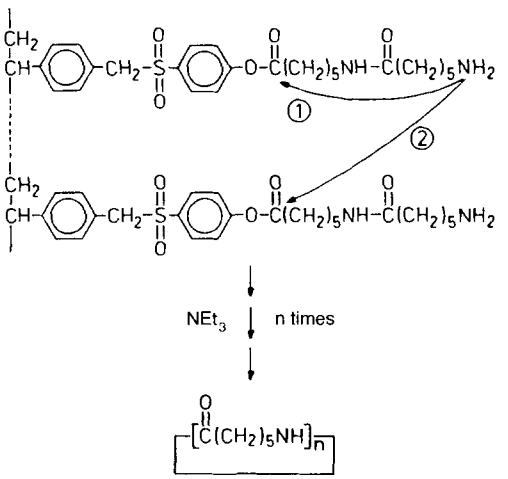
Dedicated to Professor Theodor Wieland on the occasion of his 80th birthday

The question of the spatial separation of functional groups within polymers is one of the most important current topics in chemistry on polymeric supports. Ideally, in insoluble, cross-linked polymers with low loading the reactive groups within the support, which has considerably reduced flexibility, are sterically isolated so that they can no longer interact. Under these conditions reactive, support-bound compounds should behave like those at high dilution.[1] In contrast, we report here on polycondensations and subsequent cyclizations within cross-linked polymeric supports, which for the first time led to the formation of polymeric rings.

The problem of the spatial separation of functional groups has been investigated in the last few years in various areas of organic chemistry. Steric isolation was detected in the case of the immobilization of resin-bound transition metal catalysts[2] and short-lived species (arynes),[3] as well as in the monofunctionalization of bifunctional molecules.[4] In other cases mainly intrapolymeric interactions between the functional groups occur, especially in ring closures on polymeric supports, which should avoid the large amounts of solvent required for reactions under high-dilution conditions. Thus, the cyclization of tri-, tetra-, and pentapeptides covalently bound to cross-linked polystyrene gave—in contrast to literature results[5, 6]—at best only low yields of cyclic monomers, which should have been formed owing to steric isolation of the individual peptide chains on the support. Instead, cyclic di-, tri-, and tetramers were the predominant products;[7] in other cases only cyclic dimers were found.[8]

In order to investigate the extent of the cyclooligomerization of support-bound linear compounds and test the new approach for the synthesis of very large rings, we used the polymer-bound oligoamide ε-aminohexanoyl-ε-aminohexanoic acid. We found that intrapolymeric reactions occur to an unexpected extent with formation of macrocycles consisting of at least 300 atoms.

Polystyrenes with a low degree of cross-linking (1% divinylbenzene; Bio-Beads S-X1, Bio-Rad, Munich (FRG)) served as the polymeric support, which was converted to the polymeric sulfide derivative by chloromethylation and reaction with *p*-mercaptophenol.[6] The support was subsequently esterified by treatment with the *tert*-butyloxycarbonyl(Boc)-protected dimer of ε-aminohexanoic acid in the presence of carbodiimide and 4-dimethylaminopyridine (loading 0.9 mmol g^{-1}). Oxidation of the sulfur atom with *m*-chloroperbenzoic acid[6] provided the corresponding sulfone and thus an oligoamide active ester of *p*-sulfonylphenol (Scheme 1). The Boc protecting group was removed with trifluoroacetic acid, and the protonated amino group was neutralized with an excess of triethylamine. At the same time, the suspended, polymer-bound, active ester cyclized in dimethylformamide, a good swelling solvent, at room temperature. The cyclic caprolactam oligomers[9, 10] that formed spontaneously are cleaved from the support upon ring closure and go into solution; in contrast, linear oligocondensation products remain bound to the support and thus cannot interfere in the isolation even of macrocycles with polyamide-like properties. Small amounts of ninhydrine-positive, linear oligoamides were removed by ion exchange in trifluoroethanol (TFE); these oligoamides go into solution in the workup by base-catalyzed solvolysis of unreacted active ester groups.



Scheme 1. $n = 2,4,6,\ldots 38,40$.

The mixture of cyclic oligoamides (69% yield) was separated by gel permeation chromatography (GPC) on Sephadex LH 20 in TFE, as well as on the mg scale by semipreparative HPLC on RP 18 phases (LiChrospher 100, 5 μm, Merck, Darmstadt) with a TFE/water gradient. All polymer-homologous rings were shown to be pure by analytical HPLC (Superspher 100, 4 μm, Merck, Darmstadt). The monodisperse cyclo(oligoamide)s with the structure *c*-$[NH(CH_2)_5CO]_{2n}$ with $n = 1-20$ were characterized by FD and electrospray (ESI) mass spectrometry. The largest monodisperse ring isolated was the cyclo(tetracosamer) of caprolactam composed of 40 monomer units (280 ring atoms, $M_{calcd} = 4526.4$, ESI-MS: $m/z = 4527$ $[MH^+]$). Even higher cyclic oligomers were detected by HPLC. Previously, monodisperse, HPLC-pure cyclic oligoamides of nylon-6 up to the hexamer were obtained only by ring closure in solution under high-dilution conditions.[9, 10] This demonstrates the importance of cyclization on polymeric supports in synthesis. Since the low solubility of caprolactam oligomers composed of ten and more units is similar to that of the corresponding linear polyamide (nylon-6), they can be separated considerably better from the noncyclized chains with the new method than by ring closure in solution; thus these compounds could be isolated for the first time.

The melting points of most of the cyclic oligomers (Table 1) are considerably higher than that of the corresponding linear polyamide (225 °C), but decrease with increasing ring size; the melting points of oligomers with more than 280 ring atoms reach the value of the polymer. These findings are significant with regard to the use of macrocycles as monodisperse models for chain folding in polymers.

Intrapolymeric reactions with formation of cyclic oligomers occur as soon as the reaction starts. Very large rings are formed

[*] Prof. Dr. M. Rothe, Dipl.-Chem. M. Lohmüller, Dr. U. Breuksch, Dr. G. Schmidtberg
Lehrstuhl Organische Chemie II
und Sektion Massenspektrometrie der Universität
D-89069 Ulm (FRG)
Telefax: Int. code + (731) 502-2038

[**] Linear and Cyclic Oligomers, Part 29. This work was supported by the Deutsche Forschungsgemeinschaft (SFB 239) and the Fonds der Chemischen Industrie. We thank Dr. F. Eisenbeiss, E. Merck, Darmstadt, for providing us with HPLC material. Part 28: M. Rothe in *Chemistry and Physics of Macrocycles* (Eds.: W. Fischer, R. C. Schulz, H. Sillescu). VCH, Weinheim, **1991**, p. 39.

mainly on long reaction times (ca. 48 h). As expected, first attempts at cyclization on cross-linked polystyrenes with very low loading (0.024 mmol g^{-1} Boc-di-ε-aminohexanoyl polymer), that is with a dilution 40 times higher, did not provide the extremely large rings. However, a remarkably high degree of intrapolymeric reactions was still found with formation of cyclic oligomers consisting of up to ten monomer units corresponding to a fourfold oligomerization.[11] In all cyclizations on the support a markedly higher degree of oligomerization was achieved than in the reactions with the same concentration in solution. Apparently, the grafted oligoamides are present in higher local concentrations on the support than in homogeneous solution.

Table 1. Cyclic oligoamides of ε-aminohexanoic acid with 1–40 monomer units (n).

n	Ring size	M	FD-MS $[M^+]$	FD-MS $[M^+ + Na]$	M.p. [°C]
1	7	113.2			69.5
2	14	226.3	226	249	348
4	28	452.6	452	475	256–257
6	42	679.0	678	701	260
8	56	905.3	904	927	253
10	70	1131.6	1130	1153	258
12	84	1357.9	1356	1379	261–262
14	98	1584.2		1606	261–263
16	112	1810.6	1808	1831	260–261
18	126	2036.9	2036	2060	258–260
20	140	2263.2	2261	2284	257
22	154	2489.5	[a]		248–250
24	168	2715.9	[a]		254
26	182	2942.2	[a]		248–250
28	196	3168.5	[a]		249–250
30	210	3394.8	3392	3315	246
32	224	3621.1	[a]		234
34	238	3847.4	[a]		228–230
36	252	4073.8	[a]		229–231
38	266	4300.1	[a]		229–231
40	280	4526.4	4527	4552	229

[a] The extremely large rings with $n > 20$ were also identified by plotting the elution volume from the HPLC analysis versus lg M; as expected, the values of all the rings form a line. The line formed by the values of the corresponding linear oligoamides has a markedly different slope. The IR spectra are in accord with the assigned structure. They become more and more similar with increasing ring size and are identical for rings from $n = 12$ on.

Our results thus show that cyclizations on polymeric supports are better suited for the preparation of very large rings with more than 100 ring atoms than for the synthesis of small cyclic monomers. Rings of this large size could be obtained previously only in the cycloalkane series by hydrogenation of macrocyclic oligoalkynes.[12] Their ready formation by the oligomerization of α,ω-dialkynes according to Sondheimer et al. [13] is based on the principle of "rigid groups": the drastic restriction of the conformational flexibility of the oligomer chains formed favors ring closure for suitable conformations. Our method for the synthesis of very large rings with several hundred ring atoms by cyclization of polymer-bound chains on highly loaded supports with a low degree of cross-linking can also be applied, however, to chains with high conformational flexibility, for example long oligoamides, for the formation of still larger rings.

In conclusion, the polymeric supports previously used with a low degree of cross-linking are apparently not rigid enough to force the steric isolation of functional groups, provided that the reactions are not faster than the movement of the polymer chains. On the contrary, the occurrence of extensive intrapolymer reactions proves that synthesis on supports is not synthesis simply on a solid phase but rather on highly solvated, flexible polymer chains.

Received: January 14, 1994
Revised version: May 30, 1994 [Z6619IE]
German version: *Angew. Chem.* **1994**, *106*, 2047

[1] J. I. Crowley, H. Rapoport, *Acc. Chem. Res.* **1976**, *9*, 135.
[2] W. D. Bonds, C. H. Brubaker, E. Chandrasekaran, C. Gibbons, R. H. Grubbs, L. C. Kroll, *J. Am. Chem. Soc.* **1975**, *97*, 2128.
[3] S. Mazur, P. Jayalekshmy, *J. Am. Chem. Soc.* **1979**, *101*, 677.
[4] C. C. Leznoff, *Acc. Chem. Res.* **1978**, *11*, 327.
[5] M. Fridkin, A. Patchornik, E. Katchalski, *J. Am. Chem. Soc.* **1965**, *87*, 4646.
[6] E. Flanigan, G. R. Marshall, *Tetrahedron Lett.* **1970**, 2403.
[7] M. Rothe, A. Sander, W. Fischer, W. Mästle, B. Nelson, *Proc. Am. Pept. Symp. 5th, 1977* **1977**, 506.
[8] A. R. Mitchell, R. B. Merrifield, *Proc. Am. Pept. Symp. 9th 1985* **1985**, 289.
[9] M. Rothe, F. W. Kunitz, *Liebigs Ann. Chem.* **1957**, *609*, 88.
[10] H. Zahn, H. Determann, *Chem. Ber.* **1957**, *90*, 2176.
[11] N. Huppmann, Diplomarbeit, Universität Ulm, **1992**.
[12] K. S. Lee, G. Wegner, *Makromol. Chem. Rapid Commun.* **1985**, *6*, 203.
[13] F. Sondheimer, Y. Amiel, R. Wolovsky, *J. Am. Chem. Soc.* **1959**, *81*, 4600.

The First Spectroscopic Identification of an Enol Radical Cation in Solution: The Anisyldimesitylethenol Radical Cation**

Michael Schmittel,* Georg Gescheidt,* and Maik Röck

Dedicated to Professor Christoph Rüchardt on the occasion of his 65th birthday

Although the conversions of ketones and their tautomeric enols in many useful reactions have, for a long time, played an important role in preparative organic chemistry, the first reports about the reactions of the corresponding keto[1] and enol radical cations in solution[2] have only recently appeared. Thus, enol radical cations probably play an important role in reactions of the ribonucleotide reductase[3] and diol dehydratase,[4] and it is highly likely that they are also involved in the α-umpolung of ketones induced by electron transfer[5] and in the synthesis of benzofurans[6] by the oxidation of stable enols. However, these reactive species could, up until now, only be directly detected in the matrix[7] or in the gas phase.[8]

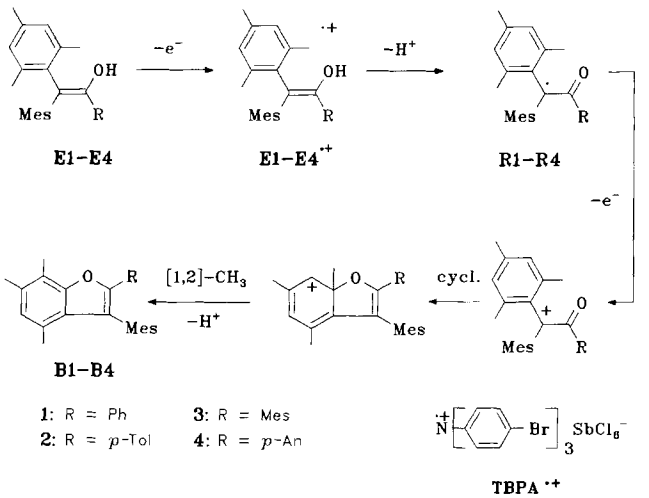
The results of mechanistic investigations[6] on the reactivity of enol radical cations indicate that, in accordance with the high acidity and analogous to phenol radical cations, the main reaction path is a fast deprotonation. Since it can be inferred from thermochemical cycles[9] that the tendency towards deprotonation of enol radical cations should decrease with decreasing oxidation potential of the enol, we have synthesized electron-rich enols of the Fuson type, which have been investigated ex-

[*] Prof. Dr. M. Schmittel,[+] Dipl.-Chem. M. Röck
Institut für Organische Chemie und Biochemie der Universität
Albertstrasse 21, D-79104 Freiburg (FRG)
[+] New address:
Institut für Organische Chemie der Universität
Am Hubland, D-97074 Würzburg (FRG)
Telefax: Int. code + (931)888-4606
Dr. G. Gescheidt
Institut für Physikalische Chemie der Universität Basel
Klingelbergstrasse 80, CH-4056 Basel (Switzerland)

[**] Enol Cation Radicals in Solution, Part 6. This work was supported by the Volkswagen Stiftung, the Fonds der Chemischen Industrie (grant awarded to M. R.), and the Freiwilligen Akademischen Gesellschaft, Basel (Treubel grant awarded to G. G.). - Part 5:[2].

 © VCH Verlagsgesellschaft mbH, D-69451 Weinheim, 1994 0570-0833/94/1919-1961 $ 10.00+.25/0

tensively by Rappoport et al.[10] These systems can be converted to the corresponding benzofurans[6] under one-electron oxidation conditions, however, up until now, the mechanism shown in Scheme 1 could only be confirmed indirectly.



Scheme 1. Mes = 2,4,6-trimethylphenyl, *p*-An = 4-methoxyphenyl.

While the cyclic voltammograms for enols **E1**–**E4** in acetonitrile show irreversible oxidation waves at low scan rates,[11] above 1000 Vs^{-1} they exhibit an increasingly stronger partial reduction wave which we assign to the reduction of the enol radical cation (Fig. 1). The enol radical cation **E4**$^{\cdot+}$ with a lifetime τ (at room temperature) of 4×10^{-4} s in acetonitrile (Table 1) and 1.9×10^{-2} s in dichloromethane proved to be the longest lived system and therefore we have concentrated on the investigation of **E4** in dichloromethane.

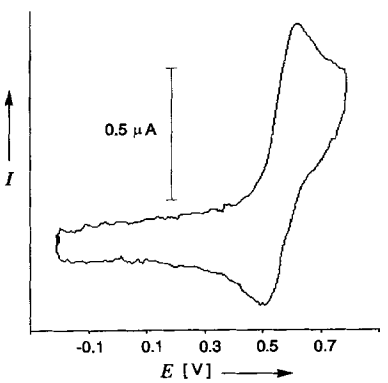


Fig. 1. Cyclic voltammogram (room temperature, versus ferrocene/ferrocenium) for the oxidation of enol **E4** at 2000 Vs^{-1} in acetonitrile.

Cyclic voltammetric investigations on **E4** and [D_1]**E4** in dichloromethane confirmed, for the first time, that an enol radical cation in solution was being detected. First of all the cyclic voltammograms of **E4** in the presence of 0–10 equivalents of trifluoroacetic acid were investigated. Within the detection limits neither the oxidation nor the reduction current was influenced at the applied scan rates. This is in accordance with the high acidity of **E4**$^{\cdot+}$ so that protonation of radical **R4** with formation of **E4**$^{\cdot+}$ cannot occur. When, however, the experiment was carried out in the presence of 7.5 equivalents[12] of deuterated trifluoroacetic acid the reduction current rose markedly. This finding can only be explained by the formation of [D_1]**E4** which is more slowly dedeuterated after one-electron oxidation because of a primary kinetic isotope effect. Through a simulation of the cyclic voltammograms[13] at scan rates of 14–500 Vs^{-1}, k_H/k_D could be determined to be 2.7 ± 0.5 (Fig. 2). Moreover, the primary isotope effect convincingly explains the effect of the solvent on τ, since acetonitrile is more basic than dichloromethane.

Table 1. Results of the fast-scan cyclic voltammetric investigations of enols **E1**–**E4** in acetonitrile or dichloromethane at room temperature. The potentials are related to the ferrocene/ferrocenium system.

Enol	$E_{1/2}$ [V]	pK_a [a]	ΔE_p [V]	v [Vs^{-1}]	i_{pc}/i_{pa} [b]	τ [b, c] [s]	τ [c, d] [s]
E1	0.67	7.4	0.20	14000	0.20	6×10^{-5}	
E2	0.64	7.9	0.21	10000	0.21	8×10^{-5}	
E3	0.76	5.9	0.19	8000	0.25	6×10^{-5}	
E4	0.57	9.1	0.12	4000	0.47	4×10^{-4}	1.9×10^{-2} [e]

[a] pK_a values of the enol radical cations in acetonitrile determined by a thermochemical cycle [9]. [b] In acetonitrile. [c] Lifetime. [d] In dichloromethane. [e] $i_{pc}/i_{pa} = 0.5$ at $v = 200\ Vs^{-1}$.

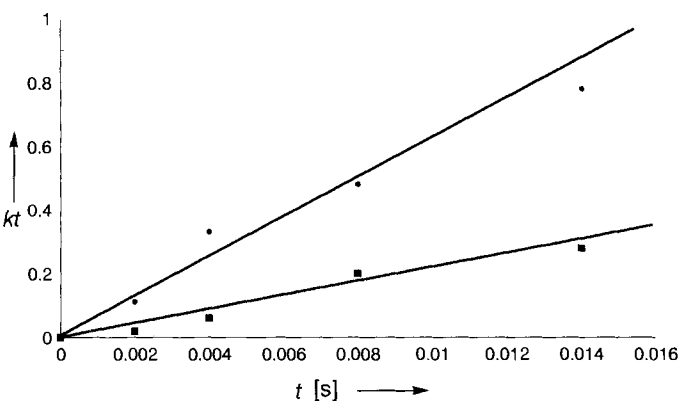


Fig. 2. Plot of the kinetic parameter kt [13] against t for **E4** (● k_H) and [D_1]**E4** (■ k_D) at room temperature.

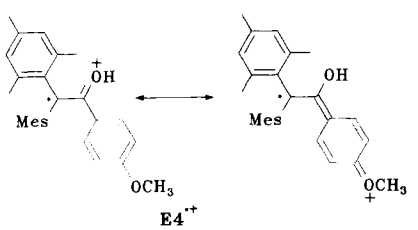
The detection of the enol radical cation **E4**$^{\cdot+}$ by ESR and ENDOR spectroscopy (ENDOR = Electron Nuclear DOuble Resonance) became possible by the one-electron oxidation of **E4** with tris(*p*-bromophenyl)aminium hexachloroantimonate in dichloromethane at −78 °C (persistence ca. 20 min); advantageously, neither of the subsequent products of the enol oxidation, that is the radical **R4** and the benzofuran radical cation **B4**$^{\cdot+}$, were present in detectable concentrations. Whereas the ESR spectrum consisted of a single unresolved signal the hyperfine coupling constants a_H of the protons could be determined by ENDOR spectroscopy. Although the multiplicities of the a_H cannot be established due to the unresolved ESR signals,[14] it is nevertheless possible to obtain structural information about **E4**$^{\cdot+}$. The highest a_H values agree very well with those of the dimesitylmethyl radical **R5**[14, 15] (Table 2). Thus, the a_H values 0.306 and 0.226 mT can be assigned to the *para*- and *ortho*-methyl groups of a mesityl substituent, while the next two a_H values[14] can be assigned to the corresponding positions of the other mesityl substituent. This reflects a marked "diphenylmethyl radical character" of **E4**$^{\cdot+}$. A much smaller spin popula-

Table 2. ENDOR and VIS spectroscopic data for the radical cations **E4**$^{\bullet+}$ and [D_1]**E4**$^{\bullet+}$ compared with that for **R4** and the dimesitylmethyl radical **R5**. The a_H values are arranged in order of size.

Radical	a_H [mT]						λ [nm]
E4$^{\bullet+}$	0.307	0.226	0.151	0.109	0.080	0.052	520, 404
[D_1]**E4**$^{\bullet+}$	0.308	0.229	0.150	0.107	0.076	-	520, 404
R5 [a]	0.338	0.215	0.145	-	-	-	
R4	0.227	0.203	0.170	0.111	0.088	-	572 (sh), 427

[a] See ref. [15], p. 636; a_H for the single proton is 1.157 mT.

tion in the remainder of the molecule is indicated by the ESR/ENDOR investigation of the deuterated derivative [D_1]**E4**$^{\bullet+}$. All the a_H values remain virtually unchanged, and the smallest coupling constant of 0.052 mT vanishes; it can, therefore, be assigned to the enol proton.[16] These findings corroborate a twisted geometry for **E4**$^{\bullet+}$ along the C(1)–C(2) double bond, which is also consistent with the results of AM1 geometry optimizations.[17] In addition the angle between the dimesitylmethyl and the hydroxy(*p*-methoxybenzyl) units is about 30°, and the C(1)–C(2) distance is 1.45 Å. The positive charge is stabilized in the latter segment of the molecule, while the spin population predominates in the dimesitylmethyl moiety. This finding is consistent with the considerably longer lifetime of **E4**$^{\bullet+}$ compared to **E1**$^{\bullet+}$ to **E3**$^{\bullet+}$, since the anisyl substituent is able to stabilize the positive charge very effectively (Scheme 2).



Scheme 2.

Such a structure is additionally supported by comparison with radical **R4** which is available from one-electron oxidation of the enolate.[18] The a_H values assigned to the dimesitylmethyl unit of **R4** (Table 2) are considerably smaller than those of **E4**$^{\bullet+}$ and mirror a more efficient spin delocalization in the α-carbonyl radical **R4**.[19] The clear distinction between radicals **E4**$^{\bullet+}$ and **R4** is also evident from the absorption spectra[20] measured simultaneously with the ESR spectra (Table 2). In this respect the spin density corresponds to that in enol ether[21] and ketene silyl acetal radical cations.[22]

The data presented here allow the existence of enol radical cations in solution to be definitively established for the first time. In addition the high acidity and the primary kinetic isotope effect confirm that these species react preferentially by deprotonation. In view of the widely accepted mechanism of action for ribonucleotide reductase[3] it will be interesting to see whether deprotonation is also the main reaction path for enol radical cations in aqueous solutions.

Received: May 10, 1994 [Z6917IE]
German Version: *Angew. Chem.* **1994**, *106*, 2056

[1] a) M. M. Green, G. J. Mayotte, L. Meites, D. Forsyth, *J. Am. Chem. Soc.* **1980**, *102*, 1464; b) J. Y. Becker, L. R. Byrd, L. L. Miller, Y. H. So, *ibid.* **1975**, *97*, 853; c) J. Y. Becker, L. L. Miller, T. M. Siegel, *ibid.* **1975**, *97*, 849; d) B. Danieli, G. Palmisano, *Chem. Ind. (London)* **1976**, 565.
[2] Enol Cation Radicals in Solution, 6. For part 5 see: M. Röck, M. Schmittel, *J. Chem. Soc. Chem. Commun.* **1993**, 1739.
[3] J. A. Stubbe, *Annu. Rev. Biochem.* **1989**, *58*, 257.
[4] G. Zubay, *Biochemistry*, Macmillan, New York, **1988**, p. 381.
[5] a) M. Schmittel, A. Abufarag, O. Luche, M. Levis, *Angew. Chem.* **1990**, *102*, 1174; *Angew. Chem. Int. Ed. Engl.* **1990**, *29*, 1144; b) M. Schmittel, *Top. Curr. Chem.* **1994**, *169*, 183.
[6] a) M. Schmittel, U. Baumann, *Angew. Chem.* **1990**, *102*, 571; *Angew. Chem. Int. Ed. Engl.* **1990**, *29*, 541; b) M. Schmittel, M. Röck, *Chem. Ber.* **1992**, *125*, 1611; c) M. Röck, M. Schmittel, *J. Prakt. Chem.* **1994**, *336*, 325.
[7] a) J. Gebicki, A. Marcinek, J. Michalak, J. Rogowski, T. Bally, W. Tang, *J. Mol. Struct.* **1992**, *275*, 249; b) A. Marcinek, J. Michalak, J. Rogowski, W. Tang, T. Bally, J. Gebicki, *J. Chem. Soc. Perkin Trans. 2* **1992**, 1353.
[8] G. Bouchoux, *Mass Spectrom. Rev.* **1988**, *7*, 1, 203.
[9] A. M. de P. Nicolas, D. R. Arnold, *Can. J. Chem.* **1982**, *60*, 2165.
[10] H. Hart, Z. Rappoport, S. E. Biali in *The Chemistry of Enols* (Ed.: Z. Rappoport), Wiley, New York, **1990**, p. 481.
[11] Cyclic voltammetry: function generator HP 3314A, storage oscilloscope HP 54510A, potentiostat according to C. Amatore, see C. Amatore, C. Lefrou, F. Pflüger, *J. Electroanal. Chem. Interfacial Chem.* **1989**, *270*, 43–59, gold microelectrodes with diameters of 5, 10, and 25 μm, electrolyte: 0.1 M tetra-*n*-butylammonium hexafluorophosphate, enol: 7 mM.
[12] Addition of more than 7.5 equivalents of deuterated trifluoroacetic acid did not increase the reduction current, which indicated that **E4** was completely converted to [D_1]**E4**. ^{1}H NMR investigations independently confirmed the facile H/D exchange of the hydroxy protons of **E4** in the presence of CF_3COOD.
[13] For the simulation with D. Gosser's program an $E_{qr}C_{irr}$ mechanism with $k_{het} = 0.1$ cm s^{-1} was assumed: D. K. Gosser, Jr. *Cyclic Voltammetry*, VCH, New York, **1993**. A working curve (i_{pc}/i_{pa} versus kt) was prepared from the peak current ratio of the simulated curves (determined according to Bellamy's method: A. J. Bellamy, *J. Electroanal. Chem. Interfacial Electrochem.* **1983**, *151*, 263) from which by plotting kt versus the time t (t: time required to scan from $E_{1/2}$ to E_i the rate constants k_H or k_D were obtained (R. S. Nicholson, I. Shain, *Anal. Chem.* **1964**, *36*, 706).
[14] The determination of the multiplicities of a_H by comparison of the spectral width of simulated and experimental ESR spectra did not give an unambiguous result largely because the expected high multiplicities (e.g. two or four almost equivalent *ortho*-methyl groups on the mesityl substituents) led to very flat edges of the ESR signal. A satisfactory agreement between the experimental and the simulated spectrum is obtained when the following mutiplicities are used (**E4**$^{\bullet+}$, a_H[mT]): 0.307 (3H), 0.226 (6H), 0.151 (3H), 0.108 (6H), 0.080 (2H), 0.052 (1H). This indicates an unequal distribution of the spin population in the two mesityl groups as well as a very small spin population in the OH and the anisyl groups. This finding is in agreement with the spin distribution calculated by INDO based on AM1 optimized geometry (cf. ref. [17]).
[15] A. Berndt, Carbon Radicals with Conjugated π systems in *Landolt-Börnstein, Magnetische Eigenschaften freier Radikale*, Springer, Berlin, **1977**, Chapter 4.
[16] Detection of the ^{2}H-ENDOR signal is not possible because of the small a_D value of about 0.007 mT.
[17] According to UHF-AM1 calculations (M. J. S. Dewar, E. G. Zoebisch, E. F. Healy, J. J. P. Stewart, *J. Am. Chem. Soc.* **1985**, *107*, 3902-3909) the energy potential of **E4**$^{\bullet+}$ is very flat, which is not surprising given the almost unhindered rotation of the MeO and OH groups and the many rotamers of the mesityl groups. Independent of these conformations we always found the deviation of the ethene fragment from planarity described in the text and the markedly elongated double C(1)=C(2) bond. The INDO calculations based on these geometries confirm a large proportion of the spin density in the dimesitylmethyl part: on average, the a_H of the *o*-methyl groups in one mesityl part are, for example, predicted as 0.32 mT, in the other as 0.15 mT. For the *p*-mesityl groups the results for a_H are 0.32 and 0.17 mT, respectively. According to INDO, the a_H in the anisyl group and in the OH groups are < 0.12 mT, whereas the a_H of the OH proton is between about 0.04 and 0.12 mT depending on the conformation of the freely rotating hydroxyl group. Considering the size and low symmetry of **E4**$^{\bullet+}$ the agreement between theoretical and experimental values is very satisfactory.
[18] M. Schmittel, M. Röck, G. Gescheidt, unpublished.
[19] The spin delocalization of similar α-carbonyl radicals has been reported in: B. Kubiak, M. Lehnig, W. P. Neumann, U. Pentling, A. K. Zarkadis, *J. Chem. Soc. Perkin Trans. 2* **1992**, 1443; further examples: see ref. [15].
[20] G. Gescheidt, *Rev. Sci. Instrum.* **1994**, *65*, 2145.
[21] a) L. Lopez, L. Troisi, *Tetrahedron* **1992**, *48*, 7321; b) M. C. R. Symons, B. W. Wren, *J. Chem. Soc. Perkin Trans. 2* **1984**, 511; c) G. Behrens, E. Bothe, G. Koltzenburg, D. Schulte-Frohlinde, *ibid.* **1980**, 883; d) G. Behrens, E. Bothe, J. Eibenberger, G. Koltzenburg, D. Schulte-Frohlinde, *Angew. Chem.* **1978**, *90*, 639; *Angew. Chem. Int. Ed. Engl.* **1978**, *17*, 604.
[22] S. Fukuzumi, M. Fujita, J. Otera, Y. Fujita, *J. Am. Chem. Soc.* **1993**, *114*, 10271.

 © VCH Verlagsgesellschaft mbH, D-69451 Weinheim, 1994 0570-0833/94/1919-1963 $ 10.00+.25/0

Matrix Spectroscopy of 2-Adamantylidene, a Dialkylcarbene with Singlet Ground State**

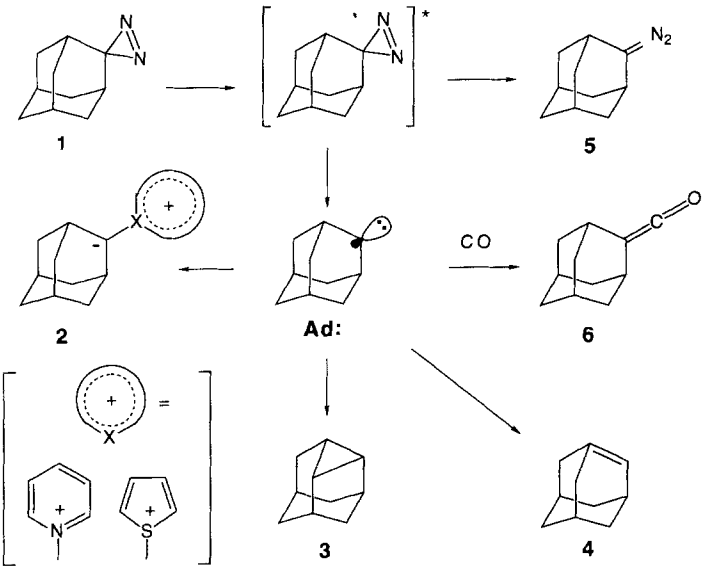
Thomas Bally*, Stephan Matzinger, Leo Truttmann, Matthew S. Platz,* and Scott Morgan

Identification of the ground state multiplicity (singlet S or triplet T) of carbene intermediates is of fundamental interest to synthetic, mechanistic, and theoretical chemistry. The issue is straightforward to resolve for triplet carbenes, which are persistent at cryogenic temperatures. In this case detection of the triplet state and assessment whether this is the ground state of the carbene or if it is thermally accessible from a singlet ground state species at the temperature of the experiment is unambiguous with EPR spectroscopy.[1] Unfortunately, failure to observe a triplet EPR spectrum does not constitute proof that a certain carbene has a singlet ground state, because the triplet may not be formed at all or be short-lived, even at cryogenic temperatures.

Dialkylcarbenes present a particular challenge in that they may rapidly decay by 1,2- or 1,3-insertion reactions to form olefins and cyclopropanes, respectively, even at cryogenic temperatures.[2, 3] Therefore, until recently only di-*tert*-alkylcarbenes could be observed directly in matrices (that is, not as trapping products), and these were found to possess triplet ground states.[4] In 1992 Sheridan et al. reported the spectroscopic identification of the first directly observed singlet dialkylcarbene, dicyclopropylcarbene,[5] where migration of the β-H atoms is prevented by keeping the corresponding C–H bonds perpendicular to the empty p-orbital through strong hyperconjugation of the latter with the Walsh MO's of the cyclopropyl moieties.[6] This hyperconjugation also favors the singlet state and may kinetically stabilize the carbene.

A similar geometrical constraint is realized in 2-adamantylidene (**Ad:**), which should therefore also be reasonably resistent to [1,2] H shift at cryogenic temperatures. Photolysis of adamantane-2-spiro-3′diazirine (**1**) under several low-temperature conditions failed to produce a triplet EPR spectrum, but **Ad:** can be intercepted by olefins and by pyridine or thiophene to form the ylides **2** (Scheme 1).[7] As the kinetics of this ylide formation are not influenced at room temperature by oxygen, an excellent trap of triplet carbenes, it was concluded that **Ad:** has a singlet ground state and that the triplet must lie at least 4.8 kcal mol^{-1} higher in energy.[7, 8] Finally, **Ad:** isolated in β-cyclodextrin was recently found to rearrange spontaneously to 2,4-dehydroadamantane (**3**) at room temperature.[9]

Herein we report the spectroscopy of **Ad:** in an argon matrix. Our results confirm that **Ad:** has a singlet ground state. In particular, we have found a characteristic absorption band of **Ad:**, which may be of general use in identifying other hydrocarbon carbenes with singlet ground states.



Scheme 1.

The difference spectrum in Figure 1 shows how a broad band with $\lambda_{max} \approx 620$ nm appears at the expense of the sharp diazirine peaks at 330–370 nm upon 30 minutes irradiation at 365 nm of **1** isolated at 10 K in an argon matrix. At the same time the IR

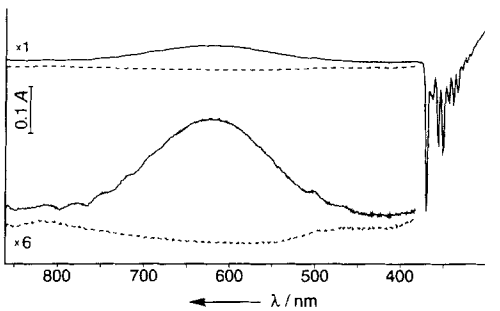


Fig. 1. UV/Vis difference spectra illustrating the formation of **Ad:** by 365 nm photolysis of **1** (solid lines) and the subsequent bleaching of **Ad:** by irradiation at $\lambda > 540$ nm (dashed lines). A = absorbance.

spectrum shows an increase of a group of intense peaks around 2050 cm^{-1}, which are indicative of a diazo moiety. Upon photolysis of this sample through a 540 nm cutoff filter for another 30 minutes, the broad visible band and some of the new bands in the IR spectrum disappear in concert (Fig. 2), while a new group of peaks arise which are identical to those of authentic **3** in argon; the diazo peaks remain unaffected.

If CO is added to the matrix containing **1**, formation of the 620 nm band after 365 nm photolysis is partially suppressed (Fig. 3), while the IR spectra show new features at 2110 cm^{-1}, the region typical of ketene groups, in addition to those of the diazo compound.

As in the experiments without CO, the 620 nm band could be bleached, and **3** was formed, albeit in smaller overall yield. In contrast, annealing of the CO-doped matrices led to an increase of the ketene absorptions (rather than those of **3**) at the expense of those of the primary photoproduct. Annealing the sample at 35 K after complete photolysis of **1** has no effect on the spectra.

[*] Prof. T. Bally, Dipl.-Chem. S. Matzinger, L. Truttmann
Institut de Chimie Physique de l'Université de Fribourg
Pérolles, CH-1700 Fribourg (Switzerland)
Fax: Int. code + (37)826-488; e-mail: Thomas.Bally@unifr.ch
Prof. M. S. Platz
Department of Chemistry
The Ohio State University
120 West 18th Avenue, Columbus, OH 43210-1173 (USA)
Fax: Int. code + (614)292-1685; e-mail: mplatz@magnus.acs.ohio-state.edu
Dr. S. Morgan
Department of Chemistry
Dana College, Blair, NE 68008 (USA)

[**] This work was supported through grants No. 20.34071-92 of the Swiss National Science Foundation and No. CHE-8814950 of the US National Science Foundation.

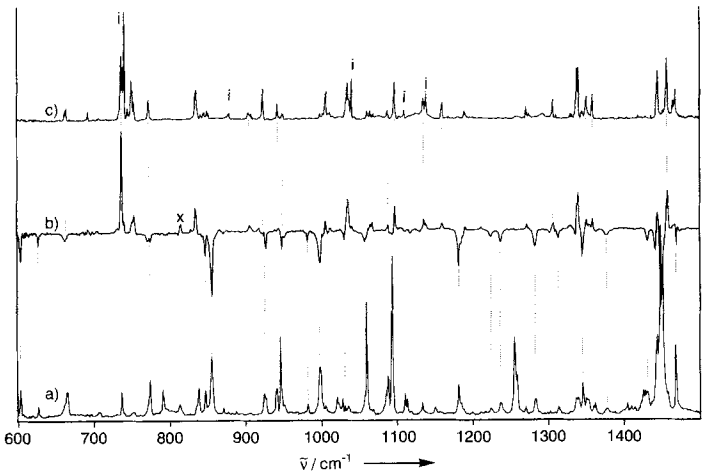


Fig. 2. a) IR spectrum after complete photolysis of **1** at 365 nm; b) difference spectrum after photolysis of sample of spectrum a at $\lambda > 540$ nm. Peaks pointing down are assigned to bleached **Ad:**, those pointing up (except for the band marked x) to newly formed **3**; c) IR spectrum of authentic **3** (bands marked "i" denote a small impurity).

These results provide strong evidence that the photoinduced rearrangement of **1** to diazoadamantane **5** is accompanied by the formation of **Ad:**. Both the appearance of ketene **6** in matrices containing CO (in part upon annealing) and the photochemical transformation to **3**, a known thermal rearrangement product of **Ad:** at room temperature,[9] can most readily be explained if **Ad:** is the carrier of the broad 620 nm absorption and the associated IR bands.

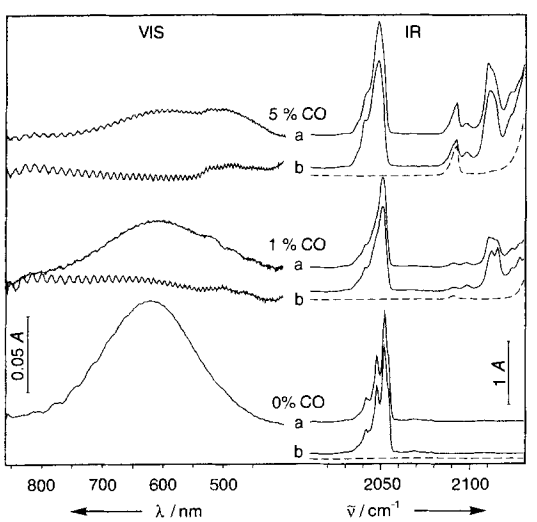


Fig. 3. EA and IR difference spectra illustrating the effect of CO concentration on the yield of **Ad:** and ketene **6**. Also seen in this spectrum is the formation of diazo compound **5**. Spectra **a** are obtained after 365 nm photolysis of **1**, and **b** after annealing at 25 K for 6 minutes. The dashed spectra are before 365 nm photolysis.

With regard to the question of the ground state multiplicity of **Ad:** we note that singlet dicyclopropylcarbene shows a similarly broad band with $\lambda_{max} = 490$ nm,[5] and that $^1CH_2$ has a weak transition with a long vibrational progression whose vertical component lies at about 1.5 eV (820 nm),[10] which corresponds to excitation of an electron from the sp hybrid lone pair to the empty p orbital. Conversely, $^3CH_2$ as well as triplet dialkylcarbenes do not absorb above 300 nm.[4, 11]

We have carried out ab initio CASSCF quantum chemical calculations[12] on the $^1A_1$ and $^3B_1$ states of **Ad:** as well as on tautomers **3** and **4**. The results are summarized in Figure 4. According to these calculations, the triplet state of **Ad:** is 3.1 kcal mol^{-1} more favorable. However, the stability of triplet states of alkylcarbenes is overestimated (or that of singlet states underestimated) by about 6 kcal mol^{-1} at this level of theory, and large basis sets and methods for efficient recovery of dynamic correlation effects are needed to remedy this.[14, 15] Therefore we see no contradiction between this result and the experimental energy difference of at least 4.8 kcal mol^{-1} in favor of ^{1}**Ad:**.[8] More importantly, both **3** and **4** are distinctly more stable than **Ad:**, but the reaction that gives **3** is much more exothermic, which may explain its exclusive formation from **Ad:** isolated in β-cyclodextrin.[9] The [1,2] hydrogen shift leading to **4** appears to be effectively prevented by keeping the empty p orbital on the carbene perpendicular to the migrating C–H bond.

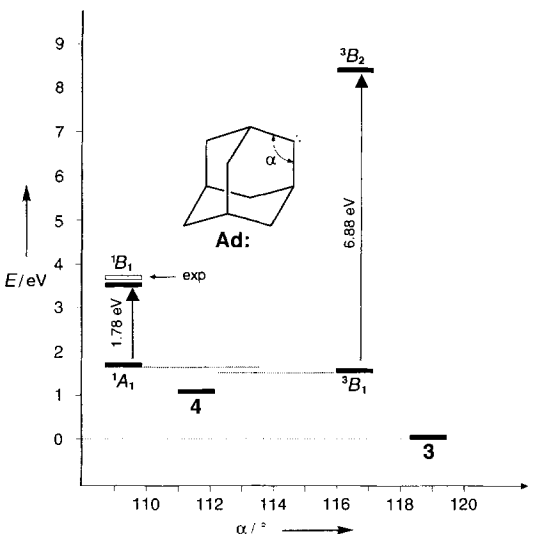


Fig. 4. Energy level diagram for **Ad:**, **3**, and **4** from 6-31G* CASSCF calculations [12]. The first excited states of singlet and triplet **Ad:** were calculated by the CIS procedure [16].

With the CASSCF-optimized geometries, CIS calculations[16] yielded a vertical excitation energy for ^{1}**Ad:** of 1.78 eV (695 nm), whereas the first excited state of ^{3}**Ad:** was predicted to be 6.88 eV (180 nm). Although the former energy is about 0.2 eV too low, the calculations clearly support the assignment of the 620 nm band to ^{1}**Ad:** (rather than ^{3}**Ad:**).[11] Apparently, alkyl substitution does not induce a major shift in this transition, and hence other singlet dialkylcarbenes should show similar bands which may facilitate their identification.

Experimental

1 was prepared according to literature procedures [18]. A sample of **3** was kindly provided by Prof. Udo Brinker (State University of New York at Binghamton) who also shared his recent data with us prior to their publication. The apparatus and procedure for matrix isolation experiments has been previously described [19]. 0.1 Torr (approximately the equilibrium vapor pressure at room temperature) of **1** were mixed with 100 Torr of argon in a 2.2 L bulb from which 80 Torr (approximately 10 mM Ar) were deposited on a CsI window held at 20 K for 2 h. Compound **1** was photolyzed with a 500 W medium-presssure mercury lamp fitted with a 365 nm interference filter; conversion of **Ad:** to **3** was achieved with a 1 kW argon resonance lamp and a 540 nm cutoff filter. Calculations were carried out with the 6-31G* basis

set using the GAUSSIAN92 [17] and GAMESS (US) programs [20] on SGI and IBM workstations.

Received: April 19, 1994
Revised: July 22, 1994 [Z6861IE]
German version: *Angew. Chem.* **1994**, *106*, 2048

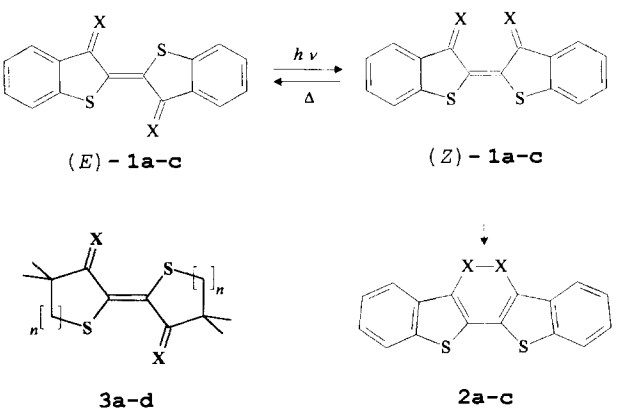
[1] A. M. Trozzolo, E. Wasserman in *Carbenes, Vol II* (Eds.: R. A. Moss, M. Jones), Wiley, New York, **1975**, p. 185.
[2] a) S. Wierlacher, W. Wander, M. T. H. Liu, *J. Am. Chem. Soc.* **1993**, *115*, 8943; b) E. J. Dix, M. S. Herman, J. L. Goodman *ibid.* **1993**, *115*, 10424; c) Private communication from Prof. R. Sheridan, University of Nevada, Reno.
[3] J. W. Storer, K. N. Houk, *J. Am. Chem. Soc.* **1993**, *115*, 10426.
[4] a) Di-*tert*-butylcarbene: J. E. Gano, R. H. Wettach, M. S. Platz, V. P. Senthilnathan, *J. Am. Chem. Soc.* **1982**, *104*, 2326; b) Diadamantylcarbene: D. R. Myers, V. P. Senthilnathan, M. S. Platz, M. Jones, Jr., *ibid.* **1986**, *108*, 4232.
[5] J. R. Ammann, R. Subramanian, R. S. Sheridan, *J. Am. Chem. Soc.* **1992**, *114*, 7592.
[6] P. B. Shevlin, M. L. McKee, *J. Am. Chem. Soc.* **1989**, *111*, 519, and references therein.
[7] a) R. A. Moss, M. J. Chang, *Tetrahedron Lett.* **1981**, *22*, 3749; b) S. Morgan, J. E. Jackson, M. Platz, *J. Am. Chem. Soc.* **1991**, *113*, 2728.
[8] In ref. [7] it was stated that the equilibrium concentration of ^{3}**Ad:** must be less than 10^{-3}; assuming that $T\cdot\Delta S_{el} = 0.62$ kcal mol^{-1} is the only entropy component that changes, the lower limit for the S/T enthalpy gap in **Ad:** is 4.77 kcal mol^{-1}.
[9] U. H. Brinker, R. Buchkremer, M. Kolodziejczyk, R. Kupfer, M. Rosenberg, M. D. Poliks, M. Orlando, M. Gross, *Angew. Chem.* **1993**, *105*, 1427; *Angew. Chem. Int. Ed. Engl.* **1993**, *32*, 1344.
[10] W. H. Green, N. C. Handy, P. J. Knowles, S. Carter, *J. Chem. Phys.* **1991**, *94*, 118, and references therein.
[11] We have also carried out INDO/S calculations (using geometries optimized with ab initio methods) on **3** and **4** which indicate that neither compound should show visible absorptions and hence cannot be the carriers of the 620 nm band.
[12] Complete active space multireference SCF including the sp hybrid orbitals and the p atomic orbital at the carbene center in the active space. The closed-shell singlet states of carbenes require a [2,2] multireference wavefunction for a correct description. For the $^3B_1$ states of **Ad:**, this amounts to a single-determinant ROHF calculation. For **4** ("adamantene") that has biradicaloid character due to its twisted double bond [13], the active space included the π and π^* MO's, whereas **3** was treated at the single-determinant ROHF level. Unconstrained geometry optimizations were carried out for all species and states considered. The $^3B_1$ state of **Ad:** converged in this procedure to a structure of C_2, symmetry, and the closed-shell $^1A_1$ state to a distorted C_s geometry that, however, lies only 0.03 kcal mol^{-1} below the C_{2v}-constrained minimum. As expected, **3** has C_s symmetry and **4** is unsymmetrical.
[13] J. Michl, G. J. Radziszewski, J. W. Downing, K. B. Wiberg, F. H. Walkerm R. D. Miller, P. Kovacic, M. Jawdosiuk, V. Bonačić-Koutecký, *Pure Appl. Chem.* **1983**, *55*, 315.
[14] a) M. M. Gallo, H. F. Schaefer III, *J. Phys. Chem.* **1992**, *96*, 1515; b) an excellent discussion of the factors influencing the S/T gap in methylcarbene has recently been provided by S. Khodabandeh, E. Carter, *ibid.* **1993**, *97*, 4360.
[15] We have calculated the S/T gap in methyl- and dimethylcarbene at the same level of theory used for our calculations on **Ad:**, both at their equilibrium geometries (where the angle α at the carbene carbon center is 105 and 110° for the singlets, respectively, and 129° for the triplets of both compounds) and also by fixing the angle α at the value it adopts in optimized ^{1}**Ad:** (109.5°) and ^{3}**Ad:** (116.5°), respectively. Thus, the calculated S/T gap in methylcarbene is 10.2 kcal mol^{-1}, that is, some 6 kcal mol^{-1} too high [14], and it reduces to 8.4 kcal mol^{-1} at the **Ad:** valence angles. For dimethylcarbene the S/T gap is 6.1 and 3.6 kcal mol^{-1}, respectively. Subtracting the approximately 6 kcal mol^{-1} error (from methylcarbene) yields a preference for the triplet ground state in dimethylcarbene (at the **Ad:** valence angles) of 2–3 kcal mol^{-1}, which should be similar in **Ad:**, in agreement with experiment.
[16] CI with all singly excited configurations as implemented in GAUSSIAN92 [17]: J. B. Foresman, M. Head-Gordon, J. A. Pople, M. J. Frisch, *J. Phys. Chem.* **1992**, *96*, 135.
[17] SGI-G92 Rev. E.2 and IBM-RS6000-G92 Rev. C). M. J. Frisch, G. W. Trucks, M. Head-Gordon, P. M. W. Gill, M. W. Wong, J. B. Foresman, B. G. Johnson, H. B. Schlegel, M. A. Robbs, E. S. Replogle, R. Gomperts, J. L. Andres, K. Raghavachari, J. S. Binkley, C. Gonzales, R. L. Martin, D. J. Fox, D. J. Defrees, J. Baker, J. J. P. Stewart, J. A. Pople, Gaussian Inc., Pittsburgh, PA, **1992**.
[18] a) A. C. G. Adding, J. Strating, H. Wynberg, J. L. M. A. Schlatmann, *Chem. Commun.* **1966**, 657; b) S. D. Isaev, A. G. Yurchenko, F. N. Stepanov, G. C. Kolyada, S. Novikov, *J. Org. Chem. (Engl. Transl.)* **1973**, *9*, 724; c) H. Bayley, J. R. Knowles, *Biochemistry*, **1978**, *17*, 2420; *ibid.* **1980**, *19*, 3883.
[19] T. Bally in *Radical Ionic Systems* (Eds.: A. Lund, M. Shiotani), Kluwer, Doordrecht, **1991**, p.3.
[20] M. W. Schmidt, K. K. Baldridge, J. A. Boatz, J. H. Jensen, S. Koseki, M. S. Gordon, K. A. Nguyen, T. L. Windus, S. T. Elbert, *QCPE Bull.* **1990**, *10*, 52.

3,3′-Bis(dicyanomethylene)-4,4,4′,4′-tetramethyl-2,2′-bithiolanylidene, a Compound Containing the Fundamental Chromophore of Thioindigo: (*E*/*Z*) and Valence Isomers, Thermo- and Photochromism**

Andreas Pawlik, Walter Grahn,* Axel Reisner, Peter G. Jones, and Ludger Ernst

Dedicated to Professor Christian Reichardt on the occasion of his 60th birthday

The reversible interconversion of the *E*/*Z* isomers of thioindigo **1a** (X = oxygen, Scheme 1) has been thoroughly investigated in solution and in the adsorbed state.[1, 2] Possible applications of the photochromism of **1a**, particularly for optical data storage and the conversion of solar energy, have stimulated considerable work.[2] The valence isomer pair (*Z*)-**1**/**2** should show a stronger photochromism than the (*E*/*Z*) isomers **1**. However, *cis*-thioindigo (*Z*)-**1a** cannot be transformed into the corresponding heteroanalogous cyclohexadiene **2a**. In contrast, the indigoid dyes **1b** (X = sulfur)[3] and **1c** (X = dicyanomethylene)[4] cannot be isolated and occur exclusively in the form of the 1,2-dithiine **2b** and cyclohexadiene **2c**, respectively.



Scheme 1. Thioindigo dyes **1** [**1a**: X = O; **1b** [3]: X = S; **1c** [4]: X = $C(CN)_2$], their valence isomers **2** [**2a**: X = O; **2b** [3]: X = S; **2c** [4]: X = $C(CN)_2$], and corresponding systems **3** with the fundamental chromophore of indigo [**3a** [6]: X = O, *n* = 1; **3b**: X = S, *n* = 1; **3c** [8]: $C(CN)_2$, *n* = 1; **3d** [9]: X = O, *n* = 2].

This is certainly due in part to the gain in π stabilization energy through the benzothiophene unit. This kind of stabilization is impossible for the dicyanomethylene analogue **3c**[5] of 2,2′-bithiolanylidene **3a**,[6] a compound having the fundamental chromophore of thioindigo. Quantum mechanical calculations (PM3[7]) underline this: the heats of formation for (*E*)-**3c** and (*Z*)-**3c**, 202.1 and 202.2 kcal mol^{-1} respectively, are approxi-

[*] Priv.-Doz. Dr. W. Grahn, Dipl.-Chem. A. Pawlik, Dipl.-Chem. A. Reisner
Institut für Organische Chemie der Technischen Universität
Hagenring 30, D-38106 Braunschweig (FRG)
Telefax: Int. code + (531) 391-5388
Prof. Dr. P. G. Jones
Institut für Anorganische und Analytische Chemie
der Technischen Universität Braunschweig
Prof. Dr. L. Ernst
NMR-Laboratorium der Chemischen Institute
Technische Universität Braunschweig

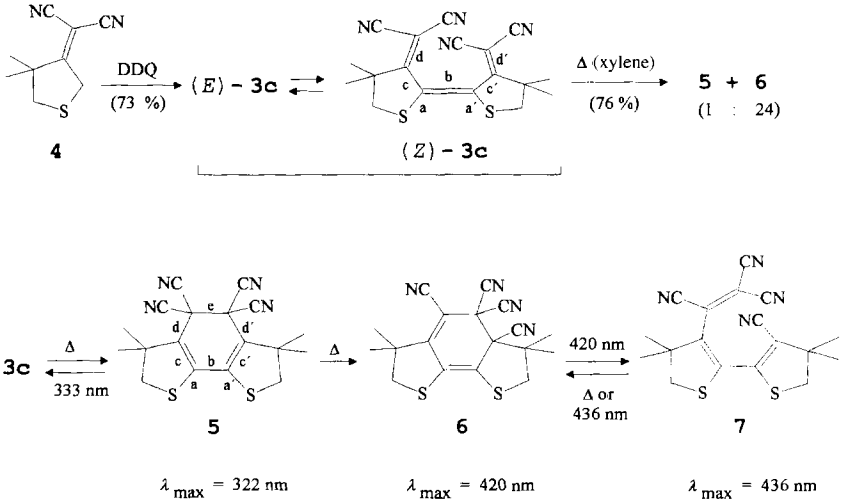
[**] This work was supported by the Fonds der Chemischen Industrie. A. P. thanks the state of Lower Saxony for a fellowship. We thank Prof. W. Lüttke, Universität Göttingen, for helpful discussions.

mately equal and only a little greater than that of valence isomer **5** (185.5 kcal mol^{-1}; see Scheme 2).

We report here on our synthesis of **3c**, its characterization by spectroscopy and X-ray crystallography, and its isomerization into *E*/*Z* and valence isomers.

The starting material for the synthesis of **3c** (Scheme 2) was the unknown 3-(dicyanomethylene)-4,4-dimethylthiolane (**4**),[8] which was prepared from 4,4-dimethylthiolan-3-one[6] and malonitrile in 38% yield. Oxidation of **4** with 2,3-dichloro-5,6-dicyano-*para*-benzoquinone (DDQ) gave **3c** as metallic black-green crystals in 73% yield.

According to X-ray analysis, **3c** occurs as a 1:1 mixture of the racemic *E*/*Z* isomers (*E*)-**3c** and (*Z*)-**3c** (Fig. 1).[10] In contrast to (*E*)-**3a**,[11] which has a planar chromophore, (*E*)-**3c** is quite twisted in order to reduce the strong steric interactions between the dicyanomethylene and *gem* dimethyl groups. As in **3a**, the thiolane rings in **3c** are considerably folded: (*Z*)-**3c** has almost an ideal envelope conformation—atoms C4 and C4′ lie outside the plane of the other atoms; in (*E*)-**3c** this is the case for atoms C3a and C3b. The central double bond b (Scheme 2) in (*Z*)-**3c** is twisted by 13°; in (*E*)-**3c** it is *syn* pyramidalized; C2a and C2b lie outside of the best plane through S1a, S1b, C3a, and C3b by 16 and 18 pm, respectively. The d,d′ bonds are only slightly twisted. The helicity of the chromophores is indicated by the large torsion angles about c,c′ (with b and d,d′, 46.5 and 55.4° for (*E*)-**3c**, and 32.6 and 28.2° for (*Z*)-**3c**).[10]



Scheme 2. Synthesis and consecutive rearrangement of **3c**. Photochromism of the pairs **5**/**3c** and **6**/**7**.

What is the ratio of isomers in solution? According to the ^{1}H NMR spectrum, (*E*)-**3c** and (*Z*)-**3c** are no longer present in equimolar amounts in solution (ratio major isomer/minor isomer about 4:1, assignment was not possible). Both show nonequivalent methyl and methylene groups, indicating that they are not planar. By using two-dimensional exchange spectroscopy (EXSY)[12] it is possible to observe the conversion of the *E* into the *Z* isomer (via the transition state structure with orthogonal molecular halves), as well as the interconversion of the enantiomers of the nonplanar *E* and *Z* forms (via the planar transition state structure).[13]

After two hours in refluxing xylene, **3c** gave a mixture of **5** as pale yellow crystals (3%) and **6** as yellow crystals (73%). The remainder is unreacted **3c**. Refluxing in toluene produced **5** and **6** in almost equal amounts, but the conversion of **3c** was only 30%. **5** can be reconverted into **3c** by irradiation with 333 nm light. Irradiating **6** with 420 nm light gave the orange valence isomer **7**, which can be reconverted into **6** thermally (20 h at 150 °C in 1,1,2,2-tetrachloro[D_2]ethane) in 37% yield and also photochemically (436 nm) in roughly 17% yield; the isosbestic points lie at 282, 300, 346, and 428 nm (see Scheme 2).[14]

The structures of **5** and **6** were confirmed by X-ray crystallography (Fig. 2).[10] The bonds involved in the isomerizations are listed in Table 1. Of interest is the long C–C single bond e in **5**, which reduces the steric interactions of the geminal cyano groups.[15] As expected, **6** is present as a racemate (chiral center at C3).[10]

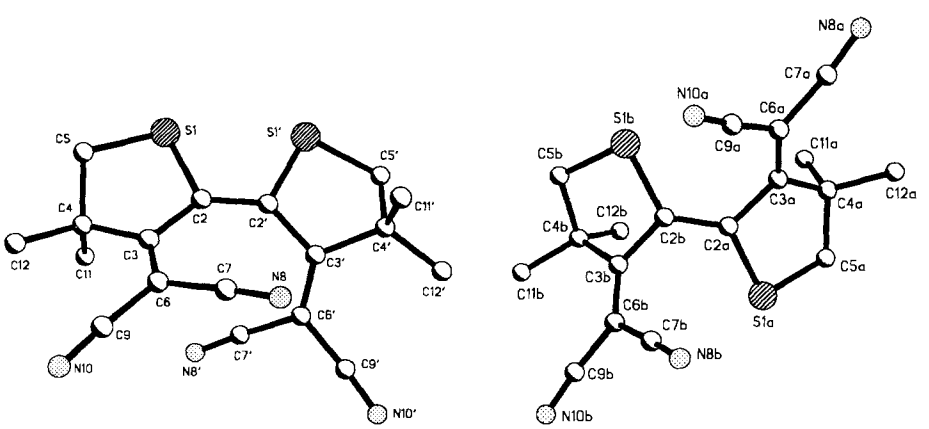


Fig. 1. Structures of one enantiomer of (*E*)-**3c** (right) and of (*Z*)-**3c** (left) in the crystal of **3c** [10].

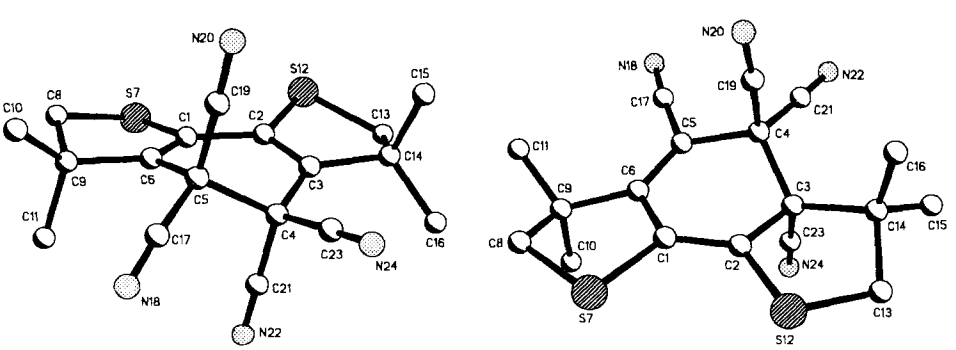


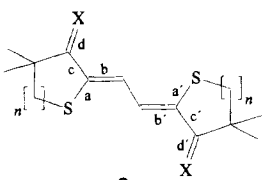
Fig. 2. Crystal structure of **5** [10] (left) and **6** [10] (right).

Table 1. Compounds **3a**, (*E*)-**3c**, (*Z*)-**3c**, **5**, and **6**: Lengths of the bonds involved in the isomerization [pm] (for a–e see Scheme 2).

Cmpd.	Bond				
	a a′	b	c c′	d d′	e
(*E*)-**3a** [11]	173.5(4)	137.2(7)	148.4(5)	121.6(5)	
(*E*)-**3c** [10]	175.6(3)	135.6(4)	145.8(4)	135.5(4)	
	176.0(3)		147.2(4)	134.7(4)	
(*Z*)-**3c** [10]	176.5(3)	137.1(4)	146.0(4)	135.9(4)	
	175.5(3)		146.2(4)	135.0(4)	
5 [10]	174.3(2)	145.5(2)	133.4(3)	151.9(2)	159.5(2)
	174.9(2)		133.5(3)	152.5(2)	
6 [10]	175.2(5)	132.3(7)	145.3(7)	134.6(7)	155.3(7)
	172.7(5)		152.0(7)	156.0(7)	

The NMR spectra of **5** are indicative of high symmetry, which is lost on conversion into **6**. The ^{1}H NMR spectrum of the valence isomer **7** shows two singlets for the *gem* dimethyl groups and also for the methylene groups. All the carbon nuclei, with the exception of the *gem* dimethyl groups in each ring, show different chemical shifts. In addition the characteristic signal of the nitrile-substituted C3 in **6** is missing. The unsymmetrical ring-opened structure of **7** is in accord with these results.

The vinylogous compound **8c** is important for the characterization of the chromophore of **3c** and was therefore synthesized[8] by condensation of thiolane **4** with *N*,*N*′-(1,2-ethandiylidene)bis(cyclohexylamine) (Scheme 3).[16]



8

Scheme 3. The next highest homologues of **3**, the vinylogous systems **8** [**8a** [6]: X = O, *n* = 1; **8c** [8]: X = C(CN)$_2$, *n* = 1; **8d** [9]: X = O, *n* = 2].

In contrast to **3c**, **8c** is present in the crystal solely in the (*Z*,*Z*) form shown, which corresponds to the *E* configuration of **3c** (Scheme 3). The dye **8c** has inversion symmetry with a planar central butadiene unit. The bonds d and d′ are slightly twisted by 13°. In comparison to (*E*)-**3c** the torsion angles in the chromophore about c and c′ (22°) are less than half as large in **8c**.[10]

The vinylogous dye **8c** shows typical indigo properties: low solubility in organic solvents and high thermal stability (m.p. 268–272 °C).

Comparison of the longest measured UV/VIS bands of (*E*)-**3a** and **8a** with the corresponding new dyes **3c** and **8c** shows that replacement of the carbonyl oxygen atom by a dicyanomethylene group produces a strong bathochromic effect (Table 2).[17] On going from **3c** to the next highest homologue **8c** there is drastic batho- and hyperchromism, while the change from (*E*)-**3a** to **8a** is accompanied by the low hypsochromism typical of indigoids.[18] How can this difference be explained?

Table 2. Experimental UV/VIS data for **3a**/**c**/**d** and **8a**/**c**/**d** and calculated UV/VIS data (PPP [20]) for **3c**/**8c**.

Cmpd. [8]	λ_{max} [nm] (ε_{max}) Ethanol	λ_{max} [nm] (ε_{max}) PPP	Cmpd. [6]	λ_{max} [nm] (ε_{max}) Ethanol	Cmpd. [9]	λ_{max} [nm] (ε_{max}) Methanol
(*E*)-**3c** / (*Z*)-**3c**	516 (6900)	447 (6500) 473 (8900)	(*E*)-**3a**	453 (12300)	(*E*)-**3d**	409 (4900)
			(*Z*)-**3a**	407 (12300)	(*Z*)-**3d**	363 (5900)
8c	564 (18100)	550 (27500)	**8a**	451 (26200)	**8d**	426 (15500) [a]

[a] In ethanol.

Unlike (*E*)-**3a** and **8a**, (*E*)-**3c**, (*Z*)-**3c**, and **8c** do not have a planar chromophore. The dihedral angles about the thiolane bond c,c′ calculated by PM3,[7] 53° [(*E*)-**3c**] and 39° [(*Z*)-**3c**], are in good agreement with the values determined by X-ray crystallography. Similar torsion is produced in indigo chromophores when the thiolane ring in **3a** is changed to a six-membered ring, as in **3d** (Table 2).[9] The result is hypsochromism, in agreement with the results from HMO calculations.[19] The measured bathochromism in going from **3d** to **8d** is a result of the smaller twist of the chromophores, as is also the case in going from **3c** to **8c**, and not an atypical indigo property.

In order to determine which isomer, (*E*)- or (*Z*)-**3c**, predominates in solution, we calculated the UV/VIS absorption maxima using the PPP method (Table 2).[20] The measured and calculated values for the **3c** mixture in solution are in satisfactory agreement, if the (*Z*)-**3c** isomer predominates. This is less twisted and should therefore absorb at a longer wavelength than the corresponding *E* isomer.

Of note is the large photochromism of 176 nm of the valence isomers **3c**/**5** in cyclohexane. As expected the longest wavelength maximum of **5** (λ = 324 nm) is blue-shifted by 62 nm relative to the corresponding thioindigo valence isomer **2c**.[4] Owing to the donor/acceptor substitution of the butadiene unit in **6**, its longest wavelength absorption maximum is shifted bathochromically by 98 nm in comparison to **5**. Ring opening of **6** to form **7** results in an increase in the acceptor strength and thus a further bathochromic shift of 16 nm.

The formation of valence isomers **5**, **6**, and **7** from **3c** can be regarded as a sequence of pericyclic reactions. (*Z*)-**3c** is converted by an electrocyclic reaction to cyclohexadiene **5**, which can be reconverted to (*Z*)-**3c** by electrocyclic ring opening. The appreciable steric interference in **5** is then reduced by the [1,5]-sigmatropic shift of a nitrile group resulting in **6**. This type of nitrile group migration in cyclohexadienes has been thoroughly studied.[21] Photochemical ring opening of **6** leads to the valence isomer **7**, which is in equilibrium with **6** by a thermal or photochemical ring closure. The valence isomer pairs **5**/(*Z*)-**3c** and **6**/**7** represent new structure types for the photochromic system that relies on the electrocyclic conversion of 1,3,5-hexatriene into 1,3-cyclohexadiene.[22] Important compounds containing this system include the dimethylenesuccinic anhydrides (fulgides)[23] and 1,2-bis(hetero)arylethenes,[24] which are the subjects of continuing studies and optimization for practical uses in optical information technology.

Experimental Procedure

To a solution of **4** (3.57 g, 20.0 mmol) [8] in 250 mL of dry CH_2Cl_2 containing 1 mL of dry pyridine was added DDQ (4.77 g, 21.0 mmol) in portions over 10 min at 0 °C. The reaction mixture was stirred for 1 h, then warmed to room temperature. A further 5 mL of dry pyridine was added, and the reaction mixture was stirred for another 3 h. After addition of 250 mL of CH_2Cl_2, the mixture was extracted with 10% NaOH (aq) (3 × 150 mL). Finally the organic phase was washed with water until neutral and dried over Na_2SO_4. After removal of solvent the residue was chromatographed on silica (200 g silica gel "60", 63–200 μm, Merck, Darmstadt; CH_2Cl_2). Recrystallization from cyclohexane/$CHCl_3$ 3:1 gave **3c** (2.56 g, 73%) [25].

3c: M.p. 184–186 °C; ^{1}H NMR (–60 °C): major isomer: δ = 3.23, 2.96 (both 1 d, J = 11.3 Hz, CH_2), 1.68, 1.39 (both 1 s, CH_3); minor isomer: δ = 3.25, 2.93 (both 1 d, J = 11.1 Hz, CH_2), 1.68, 1.29 (both 1 s, CH_3); IR: $\tilde{\nu}$ = 2225 cm^{-1} (CN); UV/VIS: λ_{max} (ε) = 498 nm (7300), 342 (17000) [cyclohexane]; 514 (6700), 346 (14900) [chloroform]; 512 (6200), 342 (12600) [acetonitrile]; 516 (6900), 346 (14700) [ethanol]; 508 (6800), 342 (14300) [acetic acid]; 534, 350 [KBr]; EI-MS: *m*/*z* (%): 352 (100) [M^+].

4: Fine, colorless needles, m.p. 23–24 °C; ^{1}H NMR: δ = 3.97 (s, 2H; 2-H), 2.90 (s, 2H; 5-H), 1.56 (s, 6H; CH_3); ^{13}C NMR: δ = 190.5 (C3), 112.0 (CN), 110.6 (CN), 82.2 [*C*(CN)$_2$], 50.0 (C4), 47.8 (C2), 40.8 (C5), 25.7 (CH_3); IR: $\tilde{\nu}$ = 2233 cm^{-1} (CN); UV/VIS: λ_{max} (ε) = 308 nm (500), 240 (12800) [acetonitrile]; EI-MS: *m*/*z* (%): 178 (100) [M^+].

5: Pale yellow rods, m.p. 154–155 °C; ^{1}H NMR: $\delta = 3.31$ (s, 4H; CH_2), 1.56 (s, 12H; CH_3); ^{13}C NMR: $\delta = 138.5$ (s), 119.8 (s), 109.3 (s), 50.3 (s), 48.3 (t), 43.2 (s), 24.3 (q); IR: $\tilde{\nu} = 2242\ cm^{-1}$ w (CN); UV/VIS: λ_{max} (ε) = 352 nm (1400, sh), 332 (3900, sh), 322 (4900), 316 (4600, sh), 276 (2000), 234 (9400) [cyclohexane]; 356 (1500, sh), 324 (4800), 276 (2600), 232 (9700) [acetonitrile]; EI-MS: *m/z* (%): 352 (74) [M^+], 337 (100) [$M^+ - CH_3$].

6: Yellow crystals, m.p. 198–201 °C; ^{1}H NMR: $\delta = 3.45$ and 3.09 (both a d, $^2J = 11.5$ Hz, both 1H; CH_2), 3.24 and 3.13 (both a d, $^2J = 11.2$ Hz, both 1H; CH_2), 1.77 (s, 3H; CH_3), 1.67 (s, 3H; CH_3), 1.65 (s, 3H; CH_3), 1.52 (s, 3H; CH_3); ^{13}C NMR: $\delta = 165.1$ (s), 134.4 (s), 130.4 (s), 112.8 (CN), 112.3 (CN), 110.8 (CN), 109.4 (CN), 93.2 (s), 59.7 (s), 52.8 (s), 48.9 (s), 47.4 (CH_2), 46.8 (CH_2), 39.9 (s), 25.9 (CH_3), 25.0 (CH_3), 24.8 (CH_3), 23.1 (CH_3); IR: $\tilde{\nu} = 2205\ cm^{-1}$ (CN); UV/VIS: λ_{max} (ε) = 420 nm (10500), 292 (7400), 240 (7700) [cyclohexane]; 426 (9900), 294 (7600), 242 (8200) [acetonitrile]; EI-MS: *m/z* (%): 352 (64) [M^+], 337 (100) [$M^+ - CH_3$].

7: Thick orange oil; irradiation of **6** in $CDCl_3$ with a Hg high-pressure lamp (photostationary equilibrium **6**/**7** = 1:1) and subsequent preparative thin-layer chromatography (silica gel "60 PF", Merck, 1.5 mm thick layer; toluene) provided **7** in 36% yield. ^{1}H NMR: $\delta = 3.271$ (s, 2H; CH_2), 3.267 (s, 2H; CH_2), 1.52 (s, 6H; CH_3), 1.40 (s, 6H; CH_3); ^{13}C NMR: $\delta = 150.3$ (s), 148.8 (s), 136.4 (s), 132.6 (s), 116.5 (s), 114.1 (s), 112.0 (s), 110.765 (s), 110.762 (s), 95.2 (s), 54.2 (s), 51.3 (s), 48.2 (CH_2), 46.2 (CH_2), 25.3 (CH_3), 24.3 (CH_3); IR: $\tilde{\nu} = 2231$, 2205 cm^{-1} (CN); UV/VIS: λ_{max} (ε) = 460 nm (6700, sh), 436 (8000), 312 (6000), 260 (8200) [cyclohexane]; 454 (6600), 312 (5900), 258 (7700) [acetonitrile]; EI-MS: *m/z* (%): 352 (48) [M^+], 337 (100) [$M^+ - CH_3$].

8c: Copper-colored crystals, m.p. 268–272 °C (decomp.); ^{1}H NMR: $\delta = 7.90$ (s, 2H; CH), 3.05 (s, 4H; CH_2), 1.61 (s, 12H; CH_3); IR: $\nu = 2222$, 2210 cm^{-1} (CN); UV/VS: λ_{max} (ε) = 568 nm, 552 (sh), 336 [cyclohexane, saturated]; 580 (20500), 340 (11000) [chloroform]; 560 (21300), 334 (10700) [acetonitrile]; 564 (18100), 336 (10000) [ethanol]; 650, 578, 344 [KBr]; EI-MS: *m/z* (%): 378 (100) [M^+].

Received: May 2, 1994 [Z6892IE]
German version: *Angew. Chem.* **1994**, *106*, 2058

[1] a) D. A. Rogers, J. D. Margerum, G. M. Wyman, *J. Am. Chem. Soc.* **1957**, *79*, 2464–2468; b) H. Zollinger, *Color Chemistry*, 2nd ed., VCH, Weinheim, **1991**, p. 193, and references therein.
[2] M. A. Mostoslavskii in *Organic Photochromes* (Ed.: A. V. El'tsov), Consultants Bureau, New York, **1990**, Chap. 2.
[3] a) W. Schroth, E. Hintzsche, H. Viola, R. Winkler, H. Klose, R. Boese, R. Kempe, J. Sieler, *Chem. Ber.* **1994**, *127*, 401–408; b) W. Schroth, E. Hintzsche, M. Felicetti, R. Spitzner, J. Sieler, R. Kempe, *Angew. Chem.* **1994**, *106*, 808–810; *Angew. Chem. Int. Ed. Engl.* **1994**, *33*, 739–741.
[4] a) R. Gompper, V. Figala, R. Kellner, A. Lederle, S. Lensky, W. Lipp, Lecture at the 11th Int. Colour Symposium in Montreux, Switzerland, Sept. 23–25, **1991**; b) R. Kellner, Dissertation, Universität München, **1991**.
[5] For the oxygen-analogous character of the dicyanomethylene group see: K. Wallenfels, K. Friedrich, J. Rieser, W. Ertel, H. K. Thieme, *Angew. Chem.* **1976**, *88*, 311–346; *Angew. Chem. Int. Ed. Engl.* **1976**, *15*, 261–270
[6] H. Hermann, W. Lüttke, *Chem. Ber.* **1968**, *101*, 1708–1714, 1715–1728.
[7] T. Clark, Universität Erlangen-Nürnberg, VAMPC MO Package, PC Version 4.45 von B. Wiedel, **1992**.
[8] A. Pawlik, planned dissertation, Technische Universität Braunschweig, **1994**.
[9] a) U. Luhmann, W. Lüttke, *Chem. Ber.* **1978**, *111*, 3246–3261; b) R. Hasenkamp, U. Luhmann, W. Lüttke, *ibid.* **1980**, *113*, 1708–1722.
[10] Crystal data for **3c**: $C_{18}H_{16}N_4S_2$, triclinic, $P\bar{1}$, $a = 1154.3(4)$, $b = 1167.7(4)$, $c = 1387.8(4)$ pm, $\alpha = 80.85(2)$, $\beta = 82.90(2)$, $\gamma = 72.53(2)°$, $V = 1.7559(10)$ nm^3, $Z = 4$, $T = -130$ °C. A red prism (0.7 × 0.35 × 0.15 mm) was mounted in inert oil (type RS3000, Riedel de Haën). Intensity data for 6534 reflections ($Mo_{K\alpha}$ radiation, $2\theta_{max} = 50°$) were collected on a Stoe STADI-4 diffractometer, of which 6250 were independent and 6225 were used for calculations. The structure was determined by direct methods and refined anisotropicically on F^2 (program SHELXL-93, H atoms included with a riding model) to $wR(F^2) = 0.126$, $R(F) = 0.053$ for 442 parameters. Crystal data for **5**: monoclinic, space group $P2_1/n$, $a = 858.3(2)$, $b = 2038.2(5)$, $c = 1029.7(2)$ pm, $\beta = 99.41(3)°$, $V = 1.7771(7)$ nm^3, $Z = 4$. Pale yellow prism (0.8 × 0.45 × 0.25 mm), 3641 intensities, 3139 independent ($R_{int} = 0.020$), 3126 used, $wR(F^2) = 0.092$, $R(F) = 0.036$, 221 parameters (otherwise as for **3c**). Crystal data for **6**: monoclinic, $P2_1/n$, $a = 1002.4(2)$, $b = 1546.2(3)$, $c = 1110.1(3)$ pm, $\beta = 91.84(3)°$, $V = 1.7197(7)$ nm^3, $Z = 4$, $T = -100$ °C. Yellow prism (0.8 × 0.7 × 0.3 mm), 3407 intensities, 3004 independent ($R_{int} = 0.060$), 2975 used, $wR(F^2) = 0.262$, $R(F) = 0.074$, 221 parameters (otherwise as for **3c**). Crystal data for **8c**: monoclinic, $P2_1/c$, $a = 874.2(2)$, $b = 956.6(2)$, $c = 1176.1(2)$ pm, $\beta = 107.98(2)°$, $V = 0.9355(3)$ nm^3, $Z = 2$, $T = -130$ °C. Blue plate (0.85 × 0.75 × 0.4 mm), 2661 intensities, 1646 independent ($R_{int} = 0.014$), 1643 used, $wR(F^2) = 0.077$, $R(F) = 0.029$, 120 parameters (otherwise as for **3c**). Further details of the crystal structures can be obtained from the Fachinformationszentrum Karlsruhe, D-76344 Eggenstein-Leopoldshafen (FRG), on quoting the depository numbers CSD-400957 (**3c**), CSD-400958 (**5**), CSD-400959 (**6**), CSD-400960 (**8c**).
[11] H. L. Ammon, H. Hermann, *J. Org. Chem.* **1978**, *43*, 4581–4586.
[12] J. Jeener, B. H. Meier, P. Bachmann, R. R. Ernst, *J. Chem. Phys.* **1979**, *71*, 4546–4553.
[13] The $\Delta G^\ddagger$ values for the transformations are estimated as 15–16 kcal mol^{-1} from the one-dimensional NMR spectra.
[14] For the irradiation in cyclohexane solution a fluorescence spectrophotometer MPF 44 from Perkin-Elmer was used, starting with a slit width of 2 nm and increasing to a maximum of 20 nm.
[15] According to Kellner [4b] bond e in **2c** is 161 pm long.
[16] L. Horner, E. Jürgens, *Chem. Ber.* **1957**, *90*, 2184–2189.
[17] A. R. Katritzky, W.-Q. Fan, D.-S. Liang, Q.-L. Li, *J. Heterocycl. Chem.* **1989**, *26*, 1541–1545.
[18] a) M. Klessinger, W. Lüttke, *Tetrahedron Suppl.* **1963**, *2*, 315–335; b) *Tetrahedron* **1966**, *22*, 3355–3365.
[19] H. Hermann, W. Lüttke, *Chem. Ber.* **1971**, *104*, 492–512.
[20] PPP Program PCSCF3D from U. Wild, Zürich, Version 4/1993 from B. Knieriem, Universität Göttingen. The parameters from R. Zahradnik and R. Gleiter, Universität Heidelberg were used (private communication); all CN and C(sp^2)–C(sp) bonds were parametrized externally with $\beta = -3.25$ and -2.318 eV, respectively; the twisting of the molecule was accounted for with $\beta = \beta_0 (\cos\tau)^2$. The geometries determined from X-ray analyses were used as the basis for the PPP calculations.
[21] D. J. Field, D. W. Jones, G. Kneen, *J. Chem. Soc. Perkin Trans. 1* **1978**, 1050–1058, and references therein.
[22] a) *Photochromism – Molecules and systems* (Eds.: H. Dürr, H. Bouas-Laurent), Elsevier, Amsterdam, **1990**; see also b) H. Noerenberg, H. Kratzin, P. Boldt, W. S. Sheldrick, *Chem. Ber.* **1977**, *110*, 1284–1293.
[23] a) J. Whittal in ref. [22a], Chapter 9; b) I. Willner, S. Rubin, J. Wonner, F. Effenberger, P. Bäuerle, *J. Am. Chem. Soc.* **1992**, *114*, 3150–3151.
[24] W. H. Laarhoven in [22a], Chapter 7; b) S. L. Gilat, S. H. Kawai, J.-M. Lehn, *J. Chem. Soc. Chem. Commun.* **1993**, 1439–1442.
[25] Spectroscopic data and elemental analyses are in accord with the structures assigned to compounds **3c**, **4**, **5**, **6**, **7**, and **8c**. [IR (KBr: **3c**, **5**, **6**, **8c**; neat: **4**, **7**), UV/VIS, ^{1}H NMR (400 MHz, $CDCl_3$, TMS; **3c** in CD_2Cl_2, δ ($CHDCl_2$) = 5.31), ^{13}C NMR (101 MHz, $CDCl_3$, $\delta = 77.05$), EI-MS(70 eV)].

A Thermally Stable Peroxocopper(II) Complex with Unusual μ_4-Coordination of the Peroxo Ligand**

Jörg Reim and Bernt Krebs*

Dedicated to Professor Philipp Gütlich on the occasion of his 60th birthday

Dioxygen transition metal complexes[1] have not only interesting spectroscopic and structural properties;[2] they also play a significant role in the catalytic oxidation of organic compounds[3] and in biological systems.[4] Most contain copper or iron centers that are responsible for the transport of oxygen and its subsequent reactions. Typical examples from the field of copper proteins are catechol oxidase[5] (which catalyzes the oxidation of *o*-diphenols to the corresponding *o*-quinones), tyrosinase (the longest known monooxygenase),[6] and hemocyanin[7] (the O_2 transport protein in arthropods and molluscs). They belong to the type III copper proteins, which are characterized by an antiferromagnetically coupled dicopper(II) site (EPR-silent). To understand the mechanistic, structural, and electronic aspects of oxygen binding to the copper(I) centers of the deoxy forms of these proteins model complexes for Cu^I/O_2 systems have been investigated in solution at low temperatures, in particular by Karlin et al.[8] In 1988 they crystallized the first cop-

[*] Prof. Dr. B. Krebs, Dipl.-Chem. J. Reim
Anorganisch-chemisches Institut der Universität
Wilhelm-Klemm-Strasse 8, D-48149 Münster (FRG)
Telefax: Int. code + (251)83-8366

[**] This work was supported by the Deutsche Forschungsgemeinschaft and the Fonds der Chemischen Industrie.

per-dioxygen complex and characterized it by X-ray crystallography.[9] The structure consists of two mononuclear copper(II) units bridged by a *trans*-μ-1,2-peroxo ligand. A dinuclear copper(II) model complex synthesized by Kitajima et al.,[10] which contains a planar μ-η^2:η^2-peroxo group and is likewise stable only at low temperatures, simulates the spectroscopic, magnetic, and structural properties of oxyhemocyanin. A recently reported crystal structure of the protein[11] also shows this type of coordination for the peroxo ligand.

We now present the first report on the synthesis and crystal structure of a peroxocopper(II) complex with unusual μ_4 coordination of the peroxo ligand, which is stable at room temperature. On treatment of $Cu(ClO_4)_2 \cdot 6H_2O$ with the new tridentate ligand 4-methyl-2,6-bis(pyrrolidinomethyl)phenol (HL), dark green crystals of the salt of **1** precipitate in the presence of air from a methanolic solution to which triethylamine and 3,5-di-*tert*-butylcatechol (3,5-DTBC) had been added.

$[Cu_4L_2(O_2)(OMe)_2(ClO_4)]ClO_4 \cdot MeOH$ **1**

The structure of the cation of **1** is depicted in Figure 1.[12] Figure 2 shows its central coordination unit for greater clarity.

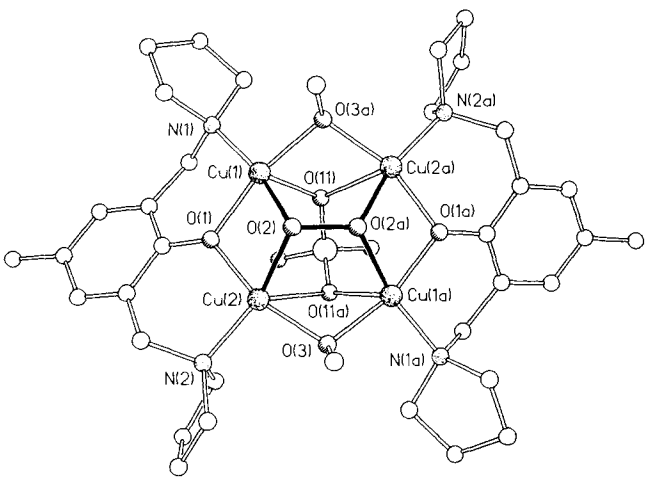


Fig. 1. Crystal structure of the cation of **1**.

In the center of the molecular cation, which lies on the twofold crystallographic axis, are four copper(II) ions forming an almost planar rectangle (dihedral angle 7.5(1)°). The longer sides [Cu(1)···Cu(2a) of 3.030(2) Å] are bridged by a methanolato ligand and the shorter sides [(Cu(1)···Cu(2) of 2.994(2) Å] by the μ-phenoxo unit of the deprotonated ligand L^-. The pyrrolidine groups of the L^- ligand are bound as terminal ligands to each of the copper atoms. Above the rectangle a peroxo group is bound end-on in a fourfold bridging μ_4-$(\eta^1)_4$ coordination at a distance of 1.008(2) [O(2)] and 1.078(2) Å [O(2a)] from the best Cu_4 plane. A perchlorate ligand situated below the Cu_4 rectangle is similarly bound to all four metal centers through O(11) [to Cu(1) and Cu(2a)] and O(11a) [to Cu(1a) and Cu(2)]. The copper atoms are thereby coordinated with typical Jahn-Teller distortion in a square-pyramidal environment; the perchlorate oxygen atoms occupy the apexes of the pyramid. The perchlorate ligand is bound unsymmetrically to the Cu_4 center; the axial bond lengths differ widely [2.411(3) Å for Cu(1)-O(11) and 2.693(3) Å for Cu(2)-O(11a)]. In contrast to these relatively long distances, the other Cu-O and Cu-N bond lengths vary between 1.920(3) for Cu(2)-O(3) and 2.006(3) Å for Cu(1)-N(1), thus lying in the usual range for copper(II) coordination compounds. The coordinated dioxygen unit has a characteristic O-O length for a peroxide O_2^{2-} of 1.453(4) Å.[2, 9, 10] The remarkable μ_4-coordination of the peroxo ligand described here was previously only observed in a tetranuclear Mo complex[13a] and in a hexanuclear Fe complex.[13b] Whereas in the first example the peroxo ligand also lies above the M_4 plane, the O_2^{2-} in the second example is bound in such a way that the O atoms are in a planar environment. This O_2^{2-} structural unit is also under discussion for tetranuclear Mn complexes in photosystem II[14a] as intermediate in the oxidation of water.[14b]

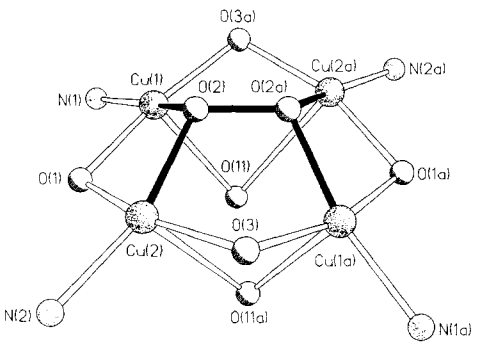


Fig. 2. Central coordination unit of the cation of **1**. Selected distances [Å] and angles [°]: Cu(1)-O(1) 1.939(2), Cu(1)-O(2) 1.961(2), Cu(1)-O(3a) 1.932(2), Cu(1)-N(1) 2.006(3), Cu(1)-O(11) 2.411(3), Cu(2)-O(11a) 2.693(3), Cu(2)-O(1) 1.941(3), Cu(2)-O(2) 1.939(2), Cu(2)-O(3) 1.920(3), Cu(2)-N(2) 1.986(3), Cu(1)···Cu(2) 2.994(2), Cu(1)···Cu(2a) 3.030(2), O(2)-O(2a) 1.453(4); Cu(1)-O(1)-Cu(2) 101.0(1), Cu(1a)-O(3)-Cu(2) 103.8(1), Cu(1)-O(11)-Cu(2a) 72.6(1), Cu(1)-O(2)-Cu(2) 100.3(1), Cu(1)-O(2)-O(2a) 113.7(2), Cu(2)-O(2)-O(2a) 113.8(2).

Another interesting structural feature is the μ-ClO_4^- unit. The perchlorate ion acts as bridging ligand in only relatively few complexes. In most of these cases it coordinates to two metal centers; up to now it has been characterized as tridentate ligand by X-ray crystallography in only two cases.[15] As far as we know, **1** is the first complex in which the perchlorate occurs as a fourfold coordinating ligand.

The synthesis of **1** forms part of our studies on the preparation of new functional models for the active site of catechol oxidase. They have previously led to some dinuclear copper(II) complexes with new tridentate ligands, the catecholase activity of which in solution is under investigation.[16] Under the basic reaction conditions described here, a Cu_2L^{3+} unit dimerizes with coordination of methanolate, peroxide, and perchlorate ions to form **1**. In the presence of coordinating anions an aggregation of complexes of this type is a favored reaction and leads, for example with halide or carboxylate groups, to similarly tetranuclear μ_4-oxo complexes.[17] For the formation of the peroxo complex **1**, a reduction of O_2 to O_2^{2-} is necessary. 3,5-DTBC acts as electron donor and is oxidized to quinone. If this electron transfer is mediated by copper(II) complexes, a copper(I) complex will be formed initially on oxidation of the catechol, and subsequently reoxidized by O_2 to the copper(II) form.[18] Detailed studies in solution are under way to elucidate the exact course of the reaction leading to **1**.

Experimental Procedure

HL: *p*-Cresol (5.41 g, 50 mmol) and pyrrolidine (7.82 g, 9.1 mL, 110 mmol) were dissolved in ethanol (60 mL). The solution was treated with 36% formaldehyde

 © VCH Verlagsgesellschaft mbH, D-69451 Weinheim, 1994 0570-0833/94/1919-1970 $ 10.00+.25/0

solution (8.9 mL, 115 mmol), stirred for 24 h under reflux, and then evaporated to dryness under vacuum. The residue was washed with 10% sodium carbonate solution (40 mL). This solution was extracted three times with ether, which was subsequently dried over sodium sulfate. The ether was removed under vacuum. Yield: 11.4 g (83%); yellow oil; ^{1}H NMR (300 MHz, $CDCl_3$): $\delta = 1.80$ (m, 8H), 2.23 (s, 3H), 2.59 (m, 8H), 3.70 (s, 4H), 6.85 (s, 2H); MS (70 eV): $m/z = 274$ [M^+], 257, 203, 188, 175, 160, 134, 105, 91, 84, 79, 70, 56, 43; correct elemental analysis.

1: $Cu(ClO_4)_2 \cdot 6H_2O$ (186 mg, 0.5 mmol) was dissolved in methanol (30 mL), and HL (69 mg, 0.25 mmol) was added. After addition of triethylamine (300 mg, 3 mmol) and 3,5-DTBC (56 mg, 0.25 mmol), dark green crystals of **1** precipitate. Decomposition above 330 °C; UV/Vis (dichloromethane): $\lambda_{max}(\varepsilon\ [M^{-1}cm^{-1}/Cu_4]) =$ 285 nm (11 680), 387 nm (6850), 420 nm (shoulder), 587 nm (370); determination of ν(O-O) has not been possible as **1** decomposes in the Raman laser; magnetic measurement: antiferromagnetic coupling, $\mu_{eff} \approx 0.9\ \mu_B$ (300 K); correct elemental analysis.

Received: May 26, 1994 [Z 6970IE]
German version: *Angew. Chem.* **1994**, *106*, 2040

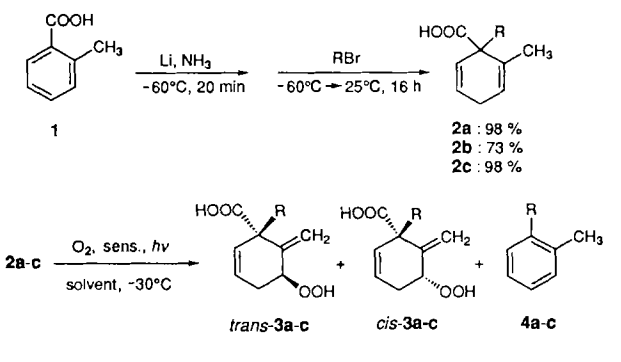
[1] A series of reviews have recently been published on this theme: *Chem. Rev.* **1994**, *94*, 567–856: Thematic Issue on "Metal-Dioxygen Complexes".
[2] a) M. H. Gubelmann, A. F. Williams, *Struct. Bonding (Berlin)* **1983**, *55*, 1–65; b) L. Vaska, *Acc. Chem. Res.* **1976**, *9*, 175–183.
[3] See for example a) K. A. Jørgensen, *Chem. Rev.* **1989**, *89*, 431–458; b) W. A. Herrmann, R. W. Fischer, W. Scherer, M. U. Rauch, *Angew. Chem.* **1993**, *105*, 1209–1212; *Angew. Chem. Int. Ed. Engl.* **1993**, *32*, 1157–1160; c) R. A. Sheldon, J. K. Kochi, *Metal-Catalyzed Oxidations of Organic Compounds*, Academic Press, New York, **1981**.
[4] See for example a) N. Kitajima, Y. Moro-oka, *Chem. Rev.* **1994**, *94*, 737–757; b) L. Que, Jr. in *Bioinorganic Catalysis* (Ed.: J. Reedijk), Dekker, New York, **1993**, pp. 347–393; c) R. D. Jones, D. A. Sommerville, F. Basolo, *Chem. Rev.* **1979**, *79*, 139–179.
[5] M. Trémolière, J. B. Bieth, *Phytochemistry* **1983**, *23*, 501–505.
[6] H. S. Mason, W. L. Folks, E. Peterson, *J. Am. Chem. Soc.* **1955**, *77*, 2914–2915.
[7] a) T. B. Freedman, J. S. Loehr, T. M. Loehr, *J. Am. Chem. Soc.* **1976**, *98*, 2809–2815; b) K. A. Magnus, H. Ton-That, J. E. Carpenter, *Chem. Rev.* **1994**, *94*, 727–735, and references therein.
[8] K. D. Karlin, M. S. Nasir, B. I. Cohen, R. W. Cruse, S. Kaderli, A. D. Zuberbühler, *J. Am. Chem. Soc.* **1994**, *116*, 1324–1336, and references therein.
[9] R. R. Jacobsen, Z. Tyeklár, A. Farooq, K. D. Karlin, S. Liu, J. Zubieta, *J. Am. Chem. Soc.* **1988**, *110*, 3690–3692.
[10] N. Kitajima, K. Fujisawa, Y. Moro-oka, F. Toriumi, *J. Am. Chem. Soc.* **1989**, *111*, 8975–8976.
[11] H. Ton-That, K. A. Magnus, *J. Inorg. Biochem.* **1993**, *51*, 65.
[12] Crystal structure data of **1**: crystal size $0.12 \times 0.20 \times 0.10$ mm, monoclinic, $P2_1/n$, $a = 14.797(8)$, $b = 11.007(7)$, $c = 15.434(10)$ Å, $\beta = 118.29(4)°$, $V = 2214$ Å^3, $Z = 2$, $\rho_{calcd} = 1.689$ gcm^{-3}, $2\theta_{max} = 54°$, $Mo_{K\alpha}$ radiation, ($\lambda = 0.71073$ Å), ω scan, temperature 150 K, 4857 symmetry independent reflections of which 2924 had $I > 2\sigma(I)$, 4856 reflections used in the refinement, no absorption correction ($\mu = 2.09$ mm^{-1}; max., min. transmission: 0.678, 0.280), structure solved with the Patterson method (SHELXL-86, G. Sheldrick, 1990), refinement on $|F^2|$ (SHELXL-93, G. Sheldrick 1993), 290 independent parameters, calculation of the H atoms in ideal positions, $R1 = 0.0357$ [$I > 2\sigma(I)$], $wR2 = 0.0760$ (all data), max. residual electron density 0.52 eÅ^{-3}. Further details of the crystal structure investigation may be obtained from the Fachinformationszentrum Karlsruhe, D-76344 Eggenstein-Leopoldshafen (FRG) on quoting the depository number CSD-400918 and the journal citation.
[13] a) R. Stomberg, L. Trysberg, I. Larking, *Acta Chem. Scand.* **1970**, *24*, 2678–2679; b) W. Micklitz, S. G. Bott, J. G. Bentsen, S. J. Lippard, *J. Am. Chem. Soc.* **1989**, *111*, 372–374.
[14] a) K. Wieghardt, *Angew. Chem.* **1994**, *106*, 765–768, and references therein.; *Angew. Chem. Int. Ed. Engl.* **1994**, *33*, 725–728, and references therein; b) J. G. Bentsen, W. Micklitz, S. Bott, S. J. Lippard, *J. Inorg. Biochem.* **1989**, *36*, 226.
[15] a) V. McKee, S. S. Tandon, *J. Chem. Soc. Dalton Trans.* **1991**, 221–230; b) Y. Agnus, R. Louis, B. Metz, C. Boudon, J. P. Gisselbrecht, M. Gross, *Inorg. Chem.* **1991**, *30*, 3155–3161.
[16] S. Teipel, B. Krebs, *J. Inorg. Biochem.* **1992**, *47*, 60.
[17] S. Teipel, K. Griesar, W. Haase, B. Krebs, *Inorg. Chem.* **1994**, *33*, 456–464.
[18] K. D. Karlin, Y. Gultneh, *Prog. Inorg. Chem.* **1987**, *25*, 219–327, and references therein.

Regio- and Diastereoselective Photooxygenation of Chiral 2,5-Cyclohexadiene-1-carboxylic Acids**

Torsten Linker* and Lothar Fröhlich

Highly functionalized chiral cyclohexanol derivatives are widespread substructures of natural products.[1] Previous synthetic approaches proceeded by stereoselective reductions or alkylations of cyclohexanones,[2] cycloadditions,[3] and enzymatic methods.[4] In the course of our investigations on the synthesis of dihydroxyvitamin D_3 (calcitriol),[5] we developed a new regio- and stereoselective entry to functionalized cyclohexenol derivatives, which constitute valuable building blocks for natural products.

Although the singlet oxygen ene reaction (Schenck reaction)[6] has been shown to be a powerful method for allylic oxyfunctionalization of cyclic[7] and acyclic[8] olefins, to date no example exists for chiral carboxylic acids. Therefore, we examined the triplet-sensitized photooxygenation of the racemic 2,5-cyclohexadiene-1-carboxylic acids **2a–c**. The substrates **2a–c** were prepared from 2-methylbenzoic acid (**1**) by Birch reduction[9] and subsequent alkylation in high yield. Photooxygenation afforded the hydroperoxides **3** in surprisingly high regio- and diastereomeric ratios (Scheme 1, Table 1). This is remarkable since



Scheme 1. Synthesis and photooxygenation of chiral 2,5-cyclohexadiene-1-carboxylic acids *rac*-**2a–c**. For clarity only one enantiomer of **3** is shown.

Table 1. Photooxygenation of 2,5-cyclohexadiene-1-carboxylic acids rac-**2** [a].

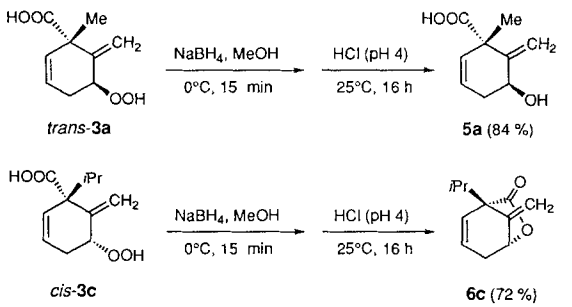
Entry	Carboxylic acid	R	Method [a]	*dr* [b] *trans*-**3**:*cis*-**3**	Yield [%] [c] *trans*-**3**	*cis*-**3**	**4**
1	**2a**	Me	A	87:13	68	10	19
2	**2a**	Me	B	92:8	90	8	–
3	**2a**	Me	C	>96:4	84	–	–
4	**2b**	Et	A	30:70	22	50	25
5	**2b**	Et	B	43:57	40	53	
6	**2b**	Et	C	75:25	51	17	
7	**2c**	*i*Pr	A	<4:96		68	28
8	**2c**	*i*Pr	B	<4:96	–	97	–
9	**2c**	*i*Pr	C	8:92	7	82	–

[a] Reaction conditions: O_2, 5×10^{-5} mol L^{-1} sensitizer, *hv* (2×250 W sodium lamp), solvent, −30 °C, 1 d; method A: tetraphenylporphine (TPP), chloroform; method B: TPP, chloroform + 2 equiv pyridine; method C: rose bengal, methanol, **2** as sodium salt. [b] Diastereomeric ratios (*dr*), determined by ^{1}H NMR spectroscopy of the crude product (400 MHz). [c] Isolated yields after column chromatography (all compounds gave correct elemental analyses).

[*] Dr. T. Linker, L. Fröhlich
Institut für Organische Chemie der Universität
Am Hubland, D-97074 Würzburg (FRG)
Telefax: Int. code + (931)888-4606

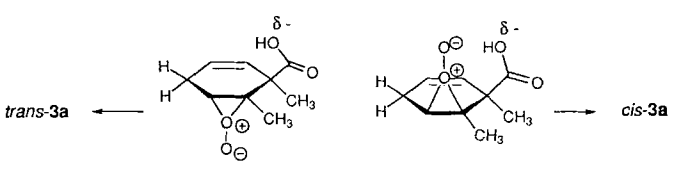
[**] This work was generously supported by the Fonds der Chemischen Industrie. We thank Prof. Dr. W. Adam, Würzburg, for his constant support.

singlet oxygen ene reactions of cyclic alkenes usually proceed with low selectivities.[10] Furthermore, the products *trans*-**3** and *cis*-**3** were obtained diastereomerically pure by column chromatography. The stereochemical assignment of the hydroperoxides **3** is based on NOE experiments (NOE = nuclear Overhauser enhancement). Additionally, the relative configuration was established unequivocally by chemical transformations, which simultaneously demonstrate the synthetic potential of the hydroperoxides (Scheme 2). Thus, sodium borohydride reduction of *trans*-**3a** and treatment with diluted hydrochloric acid afforded the 3-hydroxycarboxylic acid **5a**, whereas, *cis*-**3c** yielded smoothly the lactone **6c** under identical reaction conditions.



Scheme 2. Transformations of hydroperoxides *trans*-**3a** and *cis*-**3c**.

The high diastereoselectivities in the photooxygenation of chiral 2,5-cyclohexadiene-1-carboxylic acids are due to both steric and electronic factors. In all examined cases, the *cis* selectivity increased drastically by changing the substituents from methyl to ethyl and to isopropyl, which can only be rationalized by steric interactions. On the other hand, the methyl-substituted carboxylic acid **2a** (entries 1–3), shows a strong preference for *trans* attack of singlet oxygen, which must be due to electronic factors. If only steric interactions were encountered, a 1:1 mixture of diastereomeric hydroperoxides **3** should result since methyl and carboxyl groups possess nearly the same steric demand.[11] Evidently, unfavorable electronic repulsions in the perepoxide *cis*-**7a**,[12] are responsible for the high *trans* selectivity (Scheme 3). Therefore, increasing the negative charge of the carboxyl group (e.g. by deprotonation) should afford *trans* configurated products to an even higher extent.



Scheme 3. Electronic interactions in the perepoxide intermediate **7** which favor the *trans* selectivity in the photooxygenations.

To prove this hypothesis, we conducted the photooxygenations in the presence of two equivalents of pyridine (method B, entries 2, 5, and 8) or with the corresponding sodium salts (method C, entries 3, 6, and 9). In fact, the *trans* selectivities were increased significantly in all examples. Furthermore, the slightly basic reaction conditions suppressed completely the undesired formation of arenes **4** (entries 1, 4, and 7). Apparently, acid-catalyzed Grob fragmentation[13] affords arenes **4**, in accordance with known aromatizations of 2,5-cyclohexadiene-1-carboxylic acids.[14]

The 1-ethyl-substituted carboxylic acid **2b** (entries 4–6) is a particularly interesting substrate for photooxygenations. Since steric and electronic interactions are counterbalanced in this acid, it is possible to invert the diastereoselectivity simply by changing from chloroform as solvent (entry 4) to the sodium salt in methanol (entry 6).

In summary, the above results show that the singlet oxygen ene reaction of chiral carboxylic acids is a useful method for the regio- and stereoselective synthesis of functionalized cyclohexenol derivatives. Further investigations are currently underway in which we are attempting to influence the diastereoselectivity of this reaction by using different functional groups, and to extend the synthetic potential of the reaction sequence Birch reduction/photooxygenation. Since enantioselective Birch reductions are known,[15] the present methodology should provide a valuable route to natural products.

Experimental Procedure

cis-**3c**: A solution of **2c** (900 mg, 5 mmol), pyridine (790 mg, 10 mmol), and tetraphenylporphine (TPP) (ca. 2 mg) in chloroform (70 mL) was irradiated for 24 h with two external Philips G/98/2 SON 250-W sodium lamps at −30 °C, while a stream of dry oxygen gas was passed continously through the reaction mixture. Removal of the solvent under reduced pressure (30 °C) followed by column chromatography on silica gel (CH_2Cl_2/MeOH/HOAc 98/2/0.1) yielded 1.03 g (97%) of crystalline *cis*-**3c** (m.p. 101–102 °C). Characteristic ^{1}H NMR data (250 MHz, $CDCl_3$): δ = 0.88, 1.03 (2 d, J = 6.7 Hz, 3H; $CH(CH_3)_2$), 2.52 (sep, J = 6.7 Hz, 1H; $CH(CH_3)_2$), 4.57 (dd, J = 3.0, 3.7 Hz, 1H; CHOOH), 5.44, 5.52 (2 s, 1H, $C=CH_2$); ^{13}C NMR (63 MHz, $CDCl_3$): δ = 17.92, 17.97 (2 q; $CH(CH_3)_2$), 32.80 (d; $CH(CH_3)_2$), 85.29 (d; CHOOH), 119.70 (t; $C=CH_2$), 141.02 (s; $C=CH_2$).

Received: May 17, 1994 [Z.6942IE]
German version: *Angew. Chem.* **1994**, *106*, 2064

[1] K. C. Nicolaou, W.-M. Dai, R. K. Guy, *Angew. Chem.* **1994**, *106*, 38–69; *Angew. Chem. Int. Ed. Engl.* **1994**, *33*, 15–44; M. M. Campbell, M. Sainsbury, P. A. Searle, *Synthesis* **1993**, 179–193; G. H. Posner, H. Dai, K. Afarinkia, N. N. Murty, K. Z. Guyton, T. W. Kensler, *J. Org. Chem.* **1993**, *58*, 7209–7215.
[2] B. Hartmann, A. M. Kanazawa, J.-P. Deprés, A. E. Greene, *Tetrahedron Lett.* **1993**, *34*, 3875–3876; A. K. Singh, R. K. Bakshi, E. J. Corey, *J. Am. Chem. Soc.* **1987**, *109*, 6187–6189.
[3] S. P. Maddaford, J. L. Charlton, *J. Org. Chem.* **1993**, *58*, 4132–4138; K. C. Nicolaou, C.-K. Hwang, E. J. Sorensen, C. F. Clairborne, *J. Chem. Soc. Chem. Commun.* **1992**, 1117–1118.
[4] A. J. Carnell, G. Iacazio, S. M. Roberts, A. J. Willetts, *Tetrahedron Lett.* **1994**, *35*, 331–334; D. Seebach, S. Roggo, T. Maetzke, H. Braunschweiger, J. Cereus, M. Krieger, *Helv. Chim. Acta* **1987**, *70*, 1605-1615.
[5] Selected examples of calcitriol synthesis: C. Chen, D. Crich, *Tetrahedron* **1993**, *49*, 7943–7954; G. H. Posner, J.-C. Carry, T. E. N. Anjeh, A. N. French, *J. Org. Chem.* **1992**, *57*, 7012–7014; K. Nagasawa, Y. Zako, H. Ishihara, I. Shimizu, *Tetrahedron Lett.* **1991**, *32*, 4937-4940.
[6] H. H. Wasserman, J. L. Ives, *Tetrahedron* **1981**, *37*, 1825–1852; K. Gollnick, G. O. Schenck, *Pure Appl. Chem.* **1964**, *9*, 507–525.
[7] H.-S. Lin, L. A. Paquette, *Synth. Commun.* **1986**, *16*, 1275–1283; K. H. Schulte-Elte, V. Rautenstrauch, *J. Am. Chem. Soc.* **1980**, *102*, 1738–1740; J. A. Marshall, N. Cohen, A. R. Hochstetler, *ibid.* **1966**, *88*, 3408–3417.
[8] W. Adam, M. J. Richter, *Synthesis* **1994**, 176–180; W. Adam, B. Nestler, *J. Am. Chem. Soc.* **1993**, *115*, 5041–5049; W. Adam, H.-G. Brünker, *ibid.* **1993**, *115*, 3008–3009.
[9] H. van Bekkum, C. B. van den Bosch, G. van Minnen-Pathuis, J. C. de Mos, A. M. van Wijk, *Recl. Trav. Chim. Pays-Bas* **1971**, *90*, 137–149; R. M. Acheson, R. F. Flowerday, *J. Chem. Soc. Perkin Trans. 1* **1974**, 2339–2342.
[10] L. M. Stephenson, *Acc. Chem. Res.* **1980**, *13*, 419–425; J. S. Dutcher, J. G. Macmillan, C. H. Heathcock, *J. Org. Chem.* **1976**, *41*, 2663-2669;
[11] H. Förster, F. Vögtle, *Angew. Chem.* **1977**, *89*, 443–455; *Angew. Chem. Int. Ed. Engl.* **1977**, *16*, 429–448.
[12] For perepoxides as intermediates in singlet oxygen ene reactions see: M. Orfanopoulos, I. Smonou, C. S. Foote, *J. Am. Chem. Soc.* **1990**, *112*, 3607–3614; J. R. Hurst, S. L. Wilson, G. B. Schuster, *Tetrahedron* **1985**, *41*, 2191–2197.
[13] C. A. Grob, *Angew. Chem.* **1969**, *81*, 543–554; *Angew. Chem. Int. Ed. Engl.* **1969**, *8*, 535–546; C. A. Grob, P. W. Schiess, *ibid.* **1967**, *79*, 1–14 and **1967**, *6*, 1–15.
[14] I. K. Zhurkovich, D. V. Ioffe, *J. Org. Chem. USSR (Engl. Trans.)* **1974**, *10*, 216–218; A. J. Baker, A. C. Goudie, *J. Chem. Soc. Chem. Commun.* **1972**, 951.
[15] A. G. Schultz, *Acc. Chem. Res.* **1990**, *23*, 207–213; A. G. Schultz, M. Macielag, P. Sundararaman, A. G. Taveras, M. Welch, *J. Am. Chem. Soc.* **1988**, *110*, 7828–7841.

Tris(η^4-naphthalene)zirconate(2−)

Meehae Jang and John E. Ellis*

Dedicated to Professor Ernst Otto Fischer on the occasion of his 75th birthday

Naphthalene radical anion reductions of a variety of transition metal precursors including MCl_3 (M = V, Cr[1]), MCl_5 (M = Nb, Ta[2]), $TiCl_4$,[3] and $Co(C_5H_5)_2$[4] have been suggested or claimed to provide *anionic* homoleptic naphthalene complexes, but only one has been isolated, that is $[Ti(C_{10}H_8)_2]^{2-}$,[5] and none have been structurally characterized. Since naphthalene ligands can often be readily substituted by other Lewis bases,[6] compounds of the general formula $[M(C_{10}H_8)_x]^{z-}$ are potentially valuable synthetic equivalents for corresponding "naked" transition metal anions, M^{z-}, and are thereby related to Jonas's homoleptic ethylene complexes, $[Co(C_2H_4)_4]^-$ and $[Fe(C_2H_4)_4]^{2-}$.[7] For these reasons, we felt that it was important to determine the nature of an especially robust product obtained from the reaction of potassium naphthalenide and $ZrCl_4 \cdot 2THF$ (Scheme 1). To our surprise, salts **1** containing the anion $[Zr(\eta^4\text{-}C_{10}H_8)_3]^{2-}$ were obtained, instead of the expected and still unknown $[Zr(\eta^6\text{-}C_{10}H_8)_2]^{2-}$, which is isoelectronic with $[Mo(\eta^6\text{-}C_{10}H_8)_2]$.[6a, 8] The anion of **1** may be regarded as the first tris(arene)metal complex to contain only independent or unlinked arene ligands.[9, 10] It has also been identified in this study as the intermediate in the original synthesis of $[Zr(CO)_6]^{2-}$.[11]

$$ZrCl_4 \cdot 2THF + 6KC_{10}H_8 + 2nL \xrightarrow[-60 \rightarrow 0\,^\circ C]{DME} \underset{\mathbf{1}}{[KL_n]_2[Zr(C_{10}H_8)_3]} + 3C_{10}H_8 + 4KCl + 2THF$$

Scheme 1. **1a**: $n = 1$, L = [2.2.2]cryptand; **1b**: $n = 2$, L = [15]crown-5; DME = 1,2-dimethoxyethane.

Microcrystalline, deep red to nearly black **1a** and **1b** were isolated in 46 and 55% yields, respectively, as satisfactorily pure substances. Although highly reactive and air sensitive, they are thermally robust as dry solids and have survived for months at room temperature under an argon atmosphere without apparent deterioration. The ^1H and ^{13}C NMR spectra in solution and the CP/MAS ^{13}C NMR spectra of these salts showed that **1** was the only naphthalene complex present and established that its structure in solution and the solid state was identical. Also, the pattern of signals in the NMR spectra of **1** were independent of temperature (25 °C to −60 °C), solvent, concentration, counterion, and the presence of free naphthalene; this shows that the naphthalene ligands in **1** do not undergo facile exchange with free naphthalene at room temperature. The ^1H NMR spectra of **1** revealed that identical naphthalene groups were bound to zirconium through one ring each (i.e., four multiplets of equal intensity due to two AA'BB' systems of hydrogens were observed). Corresponding ^{13}C NMR spectra of solutions of **1** and the solid showed the presence of η^4-naphthalene ligands. The ^{13}C chemical shift value of the quaternary carbon in **1** ($\delta = +154$) is shifted downfield from that of free naphthalene and lies in the quaternary carbon region characteristic of previously reported η^4-naphthalene transition metal complexes.[12]

A single-crystal X-ray study on **1a** provided proof for the tris(η^4-naphthalene)zirconate(2−) formulation[13] and revealed a coordination environment about the zirconium of approximate C_{3v} local symmetry and trigonal-prismatic geometry as defined by midpoints of the long C–C vectors of the coordinated diene units (Fig. 1), similar to those previously observed for tris(η^4-butadiene)molybdenum(0)[14] and tris(cyclooctatetraene)niobate(1−).[15] The noncoordinating, planar six-membered ring and coordinated diene units of the naphthalene ring have corresponding dihedral angles of 37.1, 32.4, and 38.4°, which are within the range of values previously observed for other η^4-naphthalene complexes.[16, 17] The C–C distances in the η^4-diene units in **1** are similar to analogous ones in $[Ti(\eta^4\text{-}C_{10}H_8)_2(SnMe_3)_2]^{2-}$,[5] (s-*cis*-$\eta^4$-2,3-dimethylbutadiene)-zirconocene (**2**),[18] and $[Lu(\eta^4\text{-}C_{10}H_8)(\eta^5\text{-}C_5H_5)(dme)]$ (**3**).[17] In particular, these compounds exhibit a very similar long, short, long pattern in the C–C distances of the coordinated diene units, a feature characteristic of many early transition metal η^4-diene complexes[18, 19] and indicative of coordinated dienes which have some degree of anionic character.

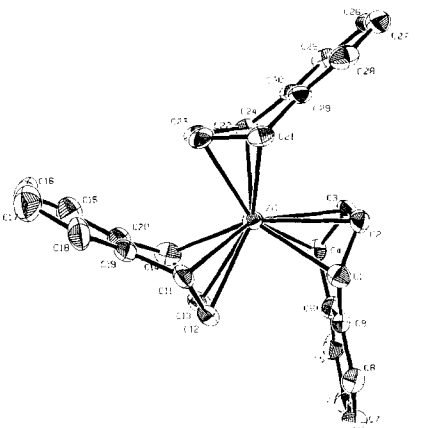


Fig. 1. Molecular structure of $[Zr(\eta^4\text{-}C_{10}H_8)_3]^{2-}$, 50% probability thermal ellipsoids. Important bond lengths [Å]: Zr-C1 2.482(6), Zr-C2 2.480(6), Zr-C3 2.474(6), Zr-C4 2.486(5), Zr-C11 2.480(6), Zr-C12 2.485(6), Zr-C13 2.471(6), Zr-C14 2.471(6), Zr-C21 2.496(5), Zr-C22 2.466(5), Zr-C23 2.470(6), Zr-C24 2.489(6), C1-C2 1.448(8), C2-C3 1.369(8), C3-C4 1.447(7), C1-C9 1.462(7), C4-C10 1.469(8), C11-C12 1.436(7), C12-C13 1.357(8), C13-C14 1.448(8), C11-C19 1.472(8), C14-C20 1.479(8), C21-C22 1.442(8), C22-C23 1.355(8), C23-C24 1.448(8), C21-C29 1.452(7), C24-C30 1.464(7). Mean C–C distance in the noncoordinating C_6 rings is 1.39(2) Å.

Structural and ^{13}C NMR data for the η^4-diene units bound to the metal atom in **1** and **2** are collected in Table 1 and indicate that the zirconium–diene interactions are remarkably similar in these otherwise very different compounds. For example, the ^{13}C chemical shift value for the atoms C2 and C3 in **1** is much closer to that of **2** than corresponding values previously reported for η^4-naphthalene complexes, (δ(C2,C3) = 84.0 for $[(\eta^4\text{-}C_{10}H_8)Cr(CO)_3]^{2-}$[12a]). Notably, however, the distinctive short, long, long, short patterns of the M–C(diene) bond

[*] Prof. Dr. J. E. Ellis, Dr. M. Jang
Department of Chemistry, University of Minnesota
Minneapolis, MN 55455 (USA)
Telefax: Int. code + (612)626-7541

[**] Highly Reduced Organometallics, Part 36. This work was supported by the U. S. National Science Foundation and the Petroleum Research Fund administered by the American Chemical Society. We thank Prof. Doyle Britton and Mr. John Campbell, University of Minnesota for carrying out the X-ray study. Part 35: J. E. Ellis, D. W. Blackburn, P. Yuen and M. Jang, *J. Am. Chem. Soc.* **1993**, *115*, 11616.

lengths in **2** and **3**, which are characteristic of metallocyclic σ^2,π complexes,[18] are not obviously present in **1**. These data show that individual naphthalene ligands in **1** are undoubtedly good acceptor groups, but not as effective as the corresponding single diene units in **2** or **3** (compound **3** has been formulated as a $(C_{10}H_8)^{2-}$-Lu^{3+} complex[17]).

Table 1. ^{13}C NMR data and average C–C and Zr–C distances of η^4-diene units in **1** and **2** [a].

Compd.	C Atoms	$\delta(^{13}C)/J$ [b]	C–C [Å] [d]	Zr–C [Å] [d]
1	C1, C4	64.2/151	C1–C2 1.442(8)	Zr–C1 2.486(9)
	C2, C3	112.6/161	C3–C4 1.448(8)	Zr–C4 2.482(10)
			C2–C3 1.360(8)	Zr–C2 2.477(10)
				Zr–C3 2.472(6)
2	C1, C4	55.4/140 [c]	C1–C2 } 1.451(4)	Zr–C1 } 2.300(3)
	C2, C3	119.9/– [c]	C3–C4 }	Zr–C4 }
			C2–C3 1.398(4)	Zr–C2 } 2.597(3)
				Zr–C3 }

[a] See ref. [12a] for the numbering system of the naphthalene rings in **1**, counterion is $[K[2.2.2]cryptand]^+$. Data for **2** are from ref. [18]. [b] Chemical shifts are relative to Me_4Si, $^1J(C,H)$ in Hz. [c] $\delta(^1J(C,H))$ values for C1,C4 and C2,C3 of (*s-cis*-η^4-butadiene)zirconocene are 49.6 (144) and 112.0 (165), respectively [18]. [d] The average C–C and Zr–C distances in **1** are for corresponding carbon atoms of the three η^4-$C_{10}H_8$ groups.

On this basis, an unambiguous formal oxidation state assignment for the zirconium center in **1** cannot be made at this time, but the value is most likely to lie somewhere between the extremes of -2 and $+4$. The Zr–C bond lengths in **1** are within the range of average values (2.40–2.60 Å) previously observed for unsaturated hydrocarbon–zirconium complexes.[20] Also the [K([2.2.2]cryptand)] cations are well separated from the anions in the crystalline lattice and have structures which are essentially identical to those previously observed in the iodide salt.[21]

The chemical properties of **1** will be reported on separately, but its reaction with CO is described here to establish its role as an intermediate in the naphthalenide-promoted reductive carbonylation synthesis of $[Zr(CO)_6]^{2-}$.[11] For example, when 1.50 g of pure **1b** was treated with CO at atmospheric pressure in DME (50 mL) at $-55\,^\circ C$, the deep red brown reactant slowly changed to an insoluble purple product. Under the same conditions as originally described,[11] except the filtration step was conducted at $-30\,^\circ C$, 1.17 g (92%) of satisfactorily pure **4** was isolated. A ^1H NMR spectrum ($CDCl_3$, 20 °C) of the pentane-soluble component of this reaction showed only free naphthalene and small amounts of [15]crown-5, thus confirming that coordinated naphthalene was liberated during the carbonylation step [Eq. (a)].

$$\mathbf{1b} + 6\,CO \xrightarrow[DME]{-55\,^\circ C} \underset{\mathbf{4}}{[K([15]crown\text{-}5)_2]_2[Zr(CO)_6]} + 3\,C_{10}H_8 \qquad (a)$$

In summary, we have established that the reduction of $ZrCl_4 \cdot 2THF$ by naphthalene radical anion provides good yields of the first tris(naphthalene)metal complex, $[Zr(\eta^4\text{-}C_{10}H_8)_3]^{2-}$, which bears an obvious resemblance to the previously known neutral tris(butadiene) complexes of molybdenum and tungsten.[14, 22] Whether analogous or related anionic tris(arene) or tris(diene) complexes of the early transition metals are generally accessible by the methods described in this report is currently under examination in this laboratory.

Experimental Procedure

All operations were carried out under an atmosphere of argon.

1a: A cold ($-50\,^\circ C$) solution of $ZrCl_4 \cdot 2THF$ (1.00 g, 2.65 mmol) in DME (120 mL) was added to a stirred, cold ($-60\,^\circ C$) solution of $KC_{10}H_8$ (16.1 mmol, prepared in the usual way [23] from K (0.63 g, 16.1 mmol) and $C_{10}H_8$ (2.72 g, 21.2 mmol)) in DME (55 mL). The reaction mixture became orange-red within minutes and was stirred at $-60\,^\circ C$ for 12 h and then allowed to warm to $-10\,^\circ C$ over a period of about 3 h with constant stirring. It was then filtered into a stirred solution of [2.2.2]cryptand (2.00 g, 5.31 mmol) in DME (10 mL) at 0 °C, whereupon product began to precipitate. The mixture was cooled to $-60\,^\circ C$ with stirring and filtered at this temperature to collect a dark red microcrystalline powder, which was carefully washed with cold ($-60\,^\circ C$) DME (3 × 20 mL), pentane (2 × 20 mL), and dried in vacuo. By this procedure 1.58 g (46%) of **1a** was obtained, based on $ZrCl_4 \cdot 2THF$, m.p. 171–173 °C (decomp.), correct elemental analyses, IR (mineral oil mull in C=C region): 1560, 1541 cm^{-1}; UV/VIS (THF): 470 nm, $\varepsilon = 2400$; 275 nm, $\varepsilon = 9700\ L\,mol^{-1}\,cm^{-1}$; ^1H NMR: (500 MHz, $[(CD_3)_2N]_3PO$ or $[D_{18}]HMPA$, 20 °C), only resonances due to anion shown: $\delta = 2.64$ (*m*, H1,H4), 3.92 (m, H2,H3), 5.42 (m, H6,H7 or H5,H8), 5.69 (m, H5,H8 or H6,H7); ^{13}C NMR: (125.7 MHz, $[D_{18}]HMPA$, 20 °C): $\delta = 64.2$ (d, C1,C4, $^1J(C,H) = 151$ Hz), 112.0 (d, C6,C7 or C5,C8, $^1J(C,H = 146$ Hz), 112.6 (d, C2,C3, $^1J(C,H) = 161$ Hz), 117.2 (d, C5,C8 or C6,C7, $^1J(C,H) = 150$ Hz), 154.6 (s, C9,C10). Assignment of the C2,C3 resonance is based on its high $^1J(C,H)$ value and trends previously established for (*s-cis*-η^4-butadiene)zirconocene [18] and η^4-naphthalene complexes [12]. Based on this assigment, ^1H,^{13}C correlation NMR spectra were used to assign carbon and hydrogen resonances of the coordinated portion of the naphthalene, but no unique assignment of C5,C8, C6,C7 or corresponding hydrogen atoms was possible. CP/MAS $^{13}C\{^1H\}$NMR (25.1 MHz, 20 °C): $\delta = 63$ (s, C1,C4), 111 (s, br, C6,C7 or C5,C8, and C2,C3), 116 (s, C5, C8 or C6,C7), 153 (s, C9, C10), also resonances at 54 (br) and 70 (s) due to [2.2.2]cryptand. Single crystals of **1a** were prepared by dissolving 0.50 g of pure **1a** in HMPA (15 mL), in which the anion was shown to be stable for weeks at room temperature. The intensely red solution was filtered, and diethyl ether was carefully layered on it. After two days at room temperature well-shaped crystals had deposited. A red-black prism was selected for this X-ray study. Red-black needles were also present and were shown to contain **1a** in the same space group but different unit cell by an independent X-ray study. NMR spectra of the crystals grown for the X-ray study were identical to those of the bulk microcrystalline sample of **1a**.

1b: By the same procedure as described for **1a**, $ZrCl_4 \cdot 2THF$ (2.00 g, 5.30 mmol) was treated with $KC_{10}H_8$ (32.0 mmol) in DME (250 mL) at $-60\,^\circ C$. The reaction mixture was stirred over a period of 6 h while slowly warming to 0 °C, and then filtered into a solution of [15]crown-5 (5.5 g, 25 mmol) in DME (20 mL). After stirring the resulting deep red filtrate for 0.5 h at 0 °C, it was cooled to $-55\,^\circ C$ and stirred at this temperature for 12 h. The sparingly soluble product was separated by filtration at $-50\,^\circ C$, thoroughly washed with cold DME and methylbutane at $-50\,^\circ C$, and then dried in vacuo at room temperature. By this procedure deep red brown microcrystalline **1b** was obtained (4.2 g, 55% yield) based on $ZrCl_4 \cdot 2THF$, darkens above 135 °C, m.p. 179–181 °C (decomp.). Correct elemental analyses. IR, UV/VIS, and NMR spectra properties of **1b** were identical to those of **1a** except for absorptions due to the cations. When the above procedures were carried out in DME alone or with [18]crown-6 in DME, thermally stable red microcrystalline powders having the composition (by ^1H NMR spectroscopy) $K_2[Zr(C_{10}H_8)_3] \cdot DME$ or $[K([18]crown\text{-}6)]_2[Zr(C_{10}H_8)_3] \cdot 2THF$ (following crystallization from THF/pentane) were obtained in about the same yields. NMR spectra established that **1** was the only naphthalene complex present in these products.

Received: May 19, 1994 [Z 6953 IE]
German version: *Angew. Chem.* **1994**, *106*, 2036

[1] a) G. Henrici-Olivé, S. Olivé, *J. Am. Chem. Soc.* **1970**, *92*, 4831; b) P. N Hawker, P. L. Timms, *J. Chem. Soc. Dalton Trans.* **1983**, 1123.
[2] C. G. Dewey, J. E. Ellis, K. L. Fjare, K. M. Pfahl, G. F. Warnock, *Organometallics* **1983**, *2*, 388.
[3] a) J. E. Ellis, *Polyhedron* **1989**, *8*, 1611; b) D. W. Blackburn, D. Britton, J. E. Ellis, *Angew. Chem.* **1992**, *104*, 1520; *Angew. Chem. Int. Ed. Engl.* **1992**, *31*, 1495.
[4] P. A. Leach, S. J. Geib, J. A. Corella, G. F. Warnock, N. J. Cooper, *J. Am. Chem. Soc.* submitted.
[5] J. E. Ellis, D. W. Blackburn, P. Yuen, M. Jang, *J. Am. Chem. Soc.* **1993**, *115*, 11616.
[6] a) E. P. Kündig, P. L. Timms, *J. Chem. Soc. Chem. Commun.* **1977**, 912; b) C. Elschenbroich, R. Möckel, *Angew. Chem.* **1977**, *89*, 908; *Angew. Chem. Int. Ed. Engl.* **1977**, *16*, 870; c) E. P. Kündig, C. Perret, S. Spichiger, G. Bernardinelli, *J. Organomet. Chem.* **1985**, *286*, 183.
[7] K. Jonas, *Angew. Chem.* **1985**, *97*, 292; *Angew. Chem. Int. Ed. Engl.* **1985**, *24*, 295.
[8] N. P. Do Thi, S. Spichiger, P. Paglia, G. Bernardinelli, P. Kündig, P. L. Timms, *Helv. Chim. Acta* **1992**, *75*, 2593.
[9] Compound **1** may also be called a tris(diene)metal complex, but since free naphthalene is generally regarded to be an arene, rather than a substituted diene, we prefer the tris(arene)metal classification.

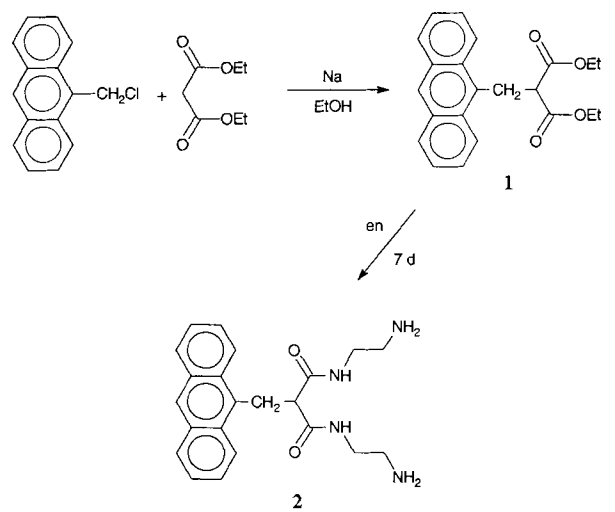
[10] The only previous examples of tris(arene)metal complexes appear to be the [2.2.2]paracyclophane derivatives, $[(p\text{-}C_6H_4CH_2CH_2)_3M]^+$ (M = Ag, Ga), where the metal ions are located at the edge of or within the cyclophane cavity, respectively. See: H. Schmidbaur, R. Hager, B. Huber, G. Müller, *Angew. Chem.* **1987**, *99*, 354; *Angew. Chem. Int. Ed. Engl.* **1987**, *26*, 338.
[11] K. M. Chi, S. R. Frerichs, S. B. Philson, J. E. Ellis, *Angew. Chem.* **1987**, *99*, 1203; *Angew. Chem. Int. Ed. Engl.* **1987**, *26*, 1190.
[12] a) R. D. Rieke, W. P. Henry, I. S. Arney, *Inorg. Chem.* **1987**, *26*, 420; b) H. Schäufele, D. Hu, H. Pritzkow, U. Zenneck, *Organometallics* **1989**, *8*, 396; c) R. L. Thompson, S. Lee, A. L. Rheingold, N. J. Cooper, *ibid.* **1991**, *10*, 1657; d) K. Jonas, C.-C. Häselhoff, R. Goddard, C. Krüger, *Inorg. Chim. Acta* **1992**, *198–200*, 533; e) C. Brodt, S. Niu, H. Pritzkow, M. Stephan, U. Zenneck, *J. Organomet. Chem.* **1993**, *459*, 283.
[13] Crystal data for **1a**: $C_{66}H_{96}K_2N_4O_{12}Zr$, monoclinic, $P2_1/n$ (no. 14), $a = 21.78(1)$; $b = 12.331(6)$, $c = 26.55(1)$, $\beta = 110.11(5)^\circ$, $V = 6695(12)$ Å^3, $Z = 4$, $\rho_{calcd} = 1.296$ g cm^{-3}, $\mu(Mo_{K\alpha}) = 3.43$ cm^{-1}, crystal dimensions = 0.60 × 0.50 × 0.35 mm^3. The intensities of 9933 reflections were measured at −96 °C ($0 < \theta < 23^\circ$) on an Enraf-Nonius CAD 4 diffractometer using $Mo_{K\alpha}$ radiation. The structure was solved by direct methods and all non-hydrogen atoms were refined anisotropically (full-matrix least-squares). For 5997 unique observed reflections [$(I) \geq 2.0\sigma(I)$], $R = 0.053$ and $R_w = 0.046$, GOF = 1.285. Further details of the crystal structure determination are available on request from the Director of Cambridge Crystallographic Data Centre, 12 Union Road, GB-Cambridge CB2 1EZ (UK), on quoting the full journal citation.
[14] P. S. Skell, M. J. McGlinchey, *Angew. Chem.* **1975**, *87*, 215; *Angew. Chem. Int. Ed. Engl.* **1975**, *14*, 195.
[15] L. L. Guggenberger, R. R. Schrock, *J. Am. Chem. Soc.* **1975**, *97*, 6693.
[16] Analogous dihedral angles ranging from 31° to 43° have been reported for other η^4-naphthalene metal complexes. See refs. [5, 12, 17] and references cited therein.
[17] A. V. Protchenko, L. N. Zakharov, M. N. Bochkarev, Y. T. Struchkov, *J. Organomet. Chem.* **1993**, *447*, 209.
[18] C. Krüger, G. Müller, G. Erker, U. Dorf, K. Engel, *Organometallics* **1985**, *4*, 215.
[19] a) G. Erker, C. Krüger, G. Müller, *Adv. Organomet. Chem.* **1985**, *24*, 1; b) G. Erker, J. Wicher, K. Engel, F. Rosenfeldt, W. Dietrich, C. Krüger, *J. Am. Chem. Soc.* **1980**, *102*, 6344; c) S. S. Wreford, J. F. Whitney, *Inorg. Chem.* **1981**, *20*, 3918; d) H. Yasuda, K. Tatsumi, A. Nakamura, *Acc. Chem. Res.* **1985**, *18*, 120; e) J. Blenkers, B. Hessen, F. van Bolhuis, A. J. Wagner, J. H. Teuben, *Organometallics* **1987**, *6*, 459.
[20] a) D. J. Cardin, M. F. Lappert, C. L. Raston, *Chemistry of Organozirconium and -hafnium Compounds*, Wiley, New York, **1986**, and references therein. b) G. M. Diamond, M. L. H. Green, N. M. Walker, *J. Organomet. Chem.* **1991**, *413*, C1; c) D. M. Rogers, S. R. Wilson, G. S. Girolami, *Organometallics* **1991**, *10*, 2419; d) J. C. Green, M. L. H. Green, N. M. Walker, *J. Chem. Soc. Dalton Trans.* **1991**, 173.
[21] B. Metz, D. Moras, R. Weiss, *Chem. Commun.* **1971**, 444.
[22] P. S. Skell, E. M. Van Dam, M. P. Silvon, *J. Am. Chem. Soc.* **1974**, *96*, 626.
[23] J. E. Ellis, S. R. Frerichs, B. K. Stein, *Organometallics* **1993**, *12*, 1048.

An Anthracene-Based Fluorescent Sensor for Transition Metal Ions**

Luigi Fabbrizzi,* Maurizio Licchelli, Piersandro Pallavicini, Angelo Perotti, and Donatella Sacchi

Fluorescence quenching and enhancement can be used effectively for the identification of ions in solution. Fluorescent sensors have been and are currently being designed for various cations and anions.[1] A fluorescent sensor is essentially a two-component compound, in which a light-emitting group is covalently linked to a receptor specific for a particular ion. Sensor efficiency requires that the ion–receptor interaction modifies the fluorescence of the light-emitting unit. Changes of fluorescence intensity of two orders of magnitude and more are often observed, in other words the fluorescence can be switched on and off.[2] By virtue of its strong luminescence and chemical stability, the anthracene unit has been widely used in the design of fluorescent sensors. In the classical approach, a tertiary amino group is attached to the aromatic framework, and the thermodynamically favored amine-to-anthracene electron transfer quenches fluorescence.[3] Binding of H^+ [4] or a metal ion (e.g., Na^+,[5] Zn^{2+})[6] substantially increases the oxidation potential of the amine, thus preventing the photoinduced electron transfer and allowing fluorescence. Incorporation of the tertiary amino group in a crown ether type framework has paved the way to fluorescent sensors for alkali and alkaline-earth metal cations.[5]

We wished to extend this concept to the recognition of transition metal cations. To this end we attached a chelating dioxotetraaza unit to the 9-position of anthracene, according to the synthetic route outlined in Scheme 1.



Scheme 1. Synthesis of fluorescent sensor **2**. en = ethylenediamine.

Compound **2** (H_2L) displays the typical emission spectrum of anthracene in acetonitrile/water (4:1); the intensity does not change over the pH range 2–12. Its pK_{a1} and pK_{a2} values are 8.3 and 9.6, respectively. This indicates that the following three species are present in solution: H_4L^{2+}, in which the two terminal amino groups are protonated, the predominant species at pH < 8, H_3L^+ at pH values from 8 to 10, and H_2L at pH > 10. The protonation state of the dioxotetraaza unit does not alter the fluorescence of the adjacent anthracene unit. However, if one equivalent of Cu^{II} is added to an acidic solution of **2**, the fluorescence intensity I_F steadily decreases on titration with NaOH. Complete fluorescence quenching is observed when the excess strong acid has been neutralized and two further equivalents of OH^- have been added. The plot of I_F vs. pH (Fig. 1) displays a sigmoidal curve typical of a switching effect. Insights on the quenching mechanism are provided by an analogous titration experiment performed inside a spectrophotometric cuvette. On addition of base, the solution becomes pink-violet, and an absorption band at 520 nm develops. The absorbance A reaches its limiting value after neutralization of the excess strong acid and addition of two further equivalents of base. The plot of A vs. pH (Fig. 1) shows a sigmoidal curve, which is symmetrical

[*] Prof. Dr. L. Fabbrizzi, Dr. M. Licchelli, Dr. P. Pallavicini, Prof. Dr. A. Perotti, Dr. D. Sacchi
Dipartimento di Chimica Generale, Università di Pavia
Via Taramelli 12, I-27100 Pavia (Italy)
Telefax: Int. code +(382) 528544

[**] This work was supported by the Ministero dell'Università e Ricerca Scientifica e Tecnologica, the Consiglio Nazionale delle Ricerche, and the Fondazione Lombardia Ambiente (fellowship for D. S.).

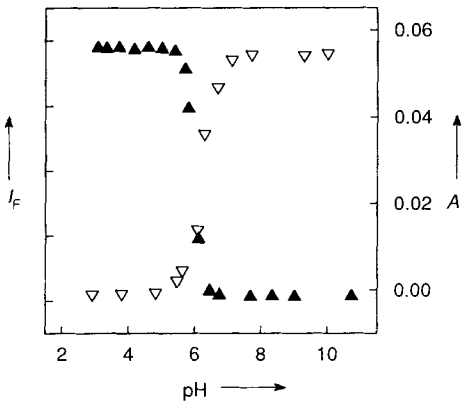


Fig. 1. Dependence of the fluorescence intensity (I_F, ▲) on pH and the absorbance of the band at 520 nm (A, ▽) for a solution of equimolar amounts of **2** and of Cu^{II} in $MeCN/H_2O$ (4:1).

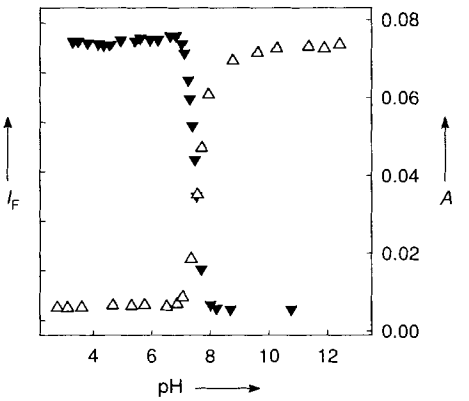
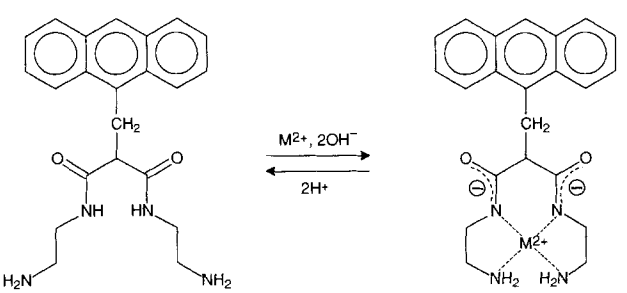


Fig. 2. Dependence of the fluorescence intensity (I_F, ▼) on pH and the absorbance of the band at 450 nm (A, Δ) for a solution of equimolar amounts of **2** and of Ni^{II} in $MeCN/H_2O$ (4:1).

to the I_F/pH profile and centered at the same pH (≈6). The pink-violet color arises from a d-d band of the square-planar complex **3** (M = Cu). Deprotonation of the two amide groups yields the tetradentate ligand L^{2-}, which chelates the metal atom. Copper(II)-promoted deprotonation of amide[7] and peptide[8] groups is a well-documented process in coordination chemistry and bioinorganic chemistry. Our findings demonstrate that the quenching of the anthracene fluorescence is associated with the coordination of the Cu^{II} ion by the dioxotetraaza unit of **2**. The radiationless deactivation of the excited state of the fluorophore can take place by means of either an energy transfer mechanism[9] (which should occur by electron exchange with an empty d orbital of the metal center[10]) or a Cu^{II}-to-anthracene electron transfer process (the oxidation of Cu^{II} to Cu^{III} is typically favored by the coordination of the deprotonated amide group).[11]



2 **3**

When one equivalent of Ni^{II} is added to a solution of **2** in aqueous acetonitrile, I_F decreases with increasing pH (Fig. 2). The plot of the absorbance at 450 nm (d-d transition) versus pH yields a symmetrical sigmoidal curve centered at pH ≈ 8. The absorption band at 450 nm corresponds to the yellow, low-spin, square-planar complex **3** (M = Ni).

It should be noted that if an acidic solution of **2** containing equimolar amounts of the 3d ions Mn^{II}, Co^{II}, and Zn^{II} (solution A) is titrated with base, I_F remains constant over the pH range 2–12. If one equivalent of Ni^{II} is added to solution A (to give solution B) titration with NaOH is accompanied by fluorescence quenching at pH ≈ 8 (sigmoidal curve similar to that in Fig. 2). Finally, if one equivalent of Cu^{II} is added to solution B and titration with base is performed, fluorescence is quenched at pH 6, as expected based on the results shown in Figure 1.

The absence of fluorescence quenching by Mn^{II} and Co^{II} ions is explained by the fact that these ions are not coordinated by the dioxotetraaza unit of **2**. The deprotonation of the amide group is very endothermic and can take place only if it is compensated energetically by the formation of a strong bond between the metal and the deprotonated amide group.[12] This is the case for the Cu^{II} and Ni^{II} ions, which profit greatly from ligand field stabilization effects. But it is not the case for divalent metal ions earlier in the first transition series such as Mn^{II} and Co^{II}. Spectrophotometric titration experiments confirm that Mn^{II} and Co^{II} ions are not coordinated by the dioxotetraaza unit of **2**: d-d bands are not observed even in strongly basic solutions. The shift of the I_F/pH sigmoidal curve to higher pH values upon transition from Cu^{II} to Ni^{II} reflects the stronger metal–ligand interactions and the greater stability of the Cu^{II} complex in solution in comparison to the Ni^{II} complex. The Zn^{II} ion (d^{10}) does not profit from ligand field effects and can thus neither promote deprotonation of amide groups nor be chelated by the dioxotetraaza unit in **2**. Zn^{II} is not redox active and does not possess any empty low-energy orbitals, which are essential for energy transfer and the radiationless decay of the anthracene excited state.

We have found that compound **2** is an efficient fluorescent sensor able to discriminate Cu^{II} and Ni^{II} ions from other divalent 3d metal ions. But can Cu^{II} and Ni^{II} be distinguished? It can be seen in Figures 1 and 2 that at pH ≈7, Cu^{II} promotes fluorescence quenching, while Ni^{II} does not. Thus, when a solution of

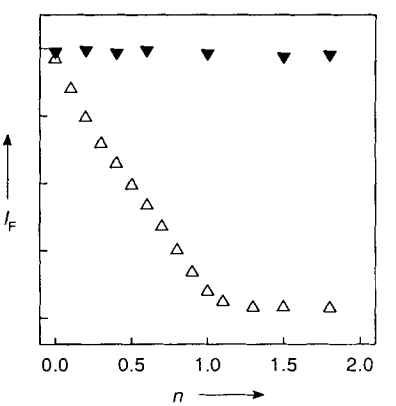


Fig. 3. Discrimination of Cu^{II} and Ni^{II} ions by the fluorescent sensor **2**. Ni^{II} is added to solution of **2** in $MeCN/H_2O$, which was adjusted to pH 7.1 with the 2,6-lutidine (▼). Then Cu^{II} is added (Δ). n = number of equivalents of the added metal ion.

2 was adjusted to pH 7.1 with 2,6-lutidine and Ni^{II} is added, no substantial decrease in I_F was observed, even after the addition of one or more equivalents of metal ion (Fig. 3). When Cu^{II} was added to the same solution, I_F decreased linearly and reached zero on addition of one equivalent of the metal ion (Fig. 3).

Until now anthracene-based fluorescent sensors for metal ions have been known primarily for alkali and alkaline-earth metal ions. Typically the uncomplexed sensor does not fluoresce and the binding of the metal to the receptor results in fluoresce; this switching mechanism is triggered by photoinduced electron transfer.[1] Compound **2** is the prototype of a new family of pH-sensitive anthracene-based fluorescent sensors for transition metal ions. Here the uncomplexed sensor fluoresces, and the interaction with the 3d metal ion leads to fluorescence quenching; this switching mechanism is triggered by energy transfer. Sensor selectivity towards transition metal ions can be modified by changing the structural features of the chelating unit: this unit can be cyclic or noncyclic, the number and arrangement of amide groups can be changed, and other heteroatoms can be included. We are currently designing and testing these types of sensors.

Experimental Procedure

1: Diethyl malonate (0.75 g, 4.72 mmol) and 9-chloromethylanthracene (0.91 g, 4.03 mmol) were added to a solution of sodium ethoxide in anhydrous ethanol (0.11 g, 4.72 mmol of Na in 20 mL of EtOH). The solution was heated at reflux for 18 h. The NaCl precipitate formed during the reaction was filtered off and the solvent evaporated in vacuo. The residue was redissolved in diethyl ether, and yellow crystals were obtained by slow evaporation. Yield: 68%. Correct C,H,N analysis for $C_{22}H_{22}O_4$.

2: Ethylenediamine (30 mL, freshly distilled over CaO) and **1** (0.5 g, 1.43 mmol) were stirred at room temperature under nitrogen for 7 d. Excess ethylenediamine was distilled off under reduced pressure. Treatment of the yellow residue with diethyl ether gave a pale yellow precipitate, which was filtered off and recrystallized from ethanol. Yield 74%, M.P. 205–208 °C. MS (70 eV): *m/z* 378 (M^+, 73%), 349 ($[M-CHNH_2]^+$, 52%), 191 ($C_{14}H_9CH_2^+$, 100%). Correct C,H,N analysis for $C_{22}H_{26}N_4O_2$.

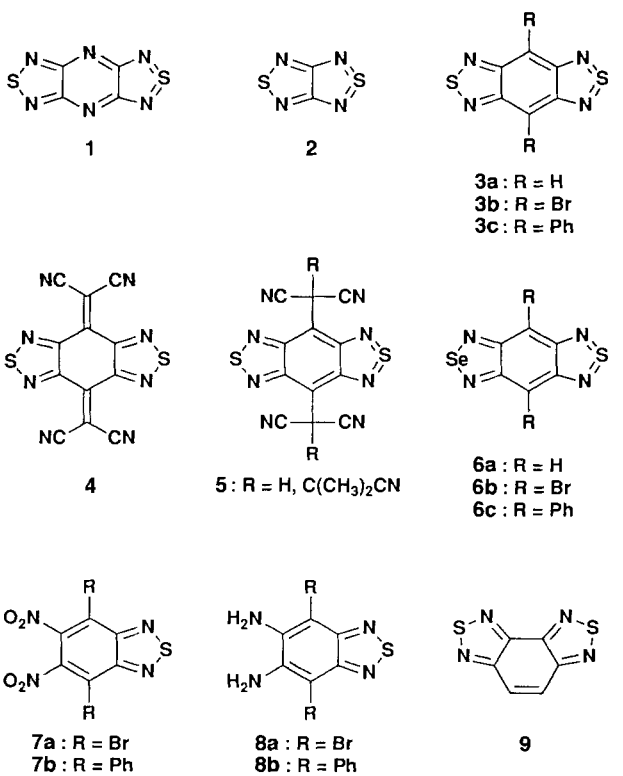
Received: May 13, 1994 [Z 6932 IE]
German version: *Angew. Chem.* **1994**, *106*, 2051

[1] R. A. Bissell, A. P. de Silva, H. Q. N. Gunaratne, P. L. M. Lynch, G. E. M. Maguire, C. P. McCoy, K. R. A. S. Sandanayake, *Top. Curr. Chem.* **1993**, *168*, 223.
[2] V. Goulle, A. Harriman, J.-M. Lehn, *J. Chem. Soc. Chem. Commun.* **1993**, 1034.
[3] R. A. Bissell, A. P. de Silva, H. Q. N. Gunaratne, P. L. M. Lynch, G. E. M. Maguire, K. R. A. S. Sandanayake, *Chem. Soc. Rev.* **1992**, 187.
[4] A. P. de Silva, R. A. D. D. Rupasinghe, *J. Chem. Soc. Chem. Commun.* **1986**, 1709.
[5] A. P. de Silva, S. A. de Silva, *J. Chem. Soc. Chem. Commun.* **1986**, 1709.
[6] E. U. Akkaya, M. E. Huston, A. W. Czarnik, *J. Am. Chem. Soc.* **1990**, *112*, 3590.
[7] M. Kodama, E. Kimura, *J. Chem. Soc. Dalton Trans.* **1979**, 325.
[8] D. W. Margerum, G. R. Dukes in *Metal Ions in Biological Systems, Vol. 1* (Ed. H. Sigel), Dekker, New York, **1974**, p. 157, an references therein.
[9] P. Suppan, *Chemistry and Light*, The Royal Society of Chemistry, Cambridge, **1994**, p. 66.
[10] V. Balzani, F. Scandola, *Supramolecular Photochemistry*, Horwood, London, **1991**, p. 71.
[11] L. Fabbrizzi, A. Perotti, A. Poggi, *Inorg. Chem.* **1983**, *22*, 1411.
[12] L. Fabbrizzi, T. A. Kaden, A. Perotti, B. Seghi, L. Siegfried, *Inorg. Chem.* **1986**, *25*, 321.

Benzobis(thiadiazole)s Containing Hypervalent Sulfur Atoms: Novel Heterocycles with High Electron Affinity and Short Intermolecular Contacts between Heteroatoms**

Katsuhiko Ono, Shoji Tanaka, and Yoshiro Yamashita*

Heterocycles containing hypervalent sulfur atoms have attracted considerable attention owing to their unique electronic structures and reactivities.[1] 1,2,5-Thiadiazole rings containing a tetravalent sulfur atom are more stable than the related thiophene rings found in the stable pyrazine derivative **1**[2] and the stable bicyclic compound **2**.[3] Compound **1** is a strong electron acceptor[4] and forms a ribbonlike structure by short intermolecular contacts between the hypervalent S atoms and the N atoms. In this context heterocycle **3a** is expected to have a high electron affinity and form a unique molecular network. This compound resembles the framework of bis([1,2,5]thiadiazolo)-tetracyanoquinodimethane (BTDA-TCNQ **4**), which is an electron acceptor in organic metals and forms a sheetlike network through short S···N≡C contacts.[5] However, **5**, which was prepared from **4**, is its only reported derivative.[6] We have now synthesized the λ^2,λ^4-benzobis(thiadiazole) derivatives **3b** and



[*] Prof. Dr. Y. Yamashita, K. Ono, Dr. S. Tanaka
Department of Structural Molecular Science
The Graduate University for Advanced Studies
and Institute for Molecular Science
Myodaiji, Okazaki 444 (Japan)
Telefax: Int. code + (564)54-2254

[**] This work was supported by research fellowships from the Japan Society for the Promotion of Science for Young Scientists. We thank Prof. Dr. K. Tanaka, Institute for Molecular Science, for conducting the X-ray crystallographic study, and Prof. Dr. S. Hirayama, Kyoto Institute of Technology, for the measurement of the fluorescence spectrum of **3c**.

3c and the analogous selenadiazoles **6b** and **6c**.[*] We report here their preparation and characterization, and the crystal structure of **3b**.

Reduction of dinitrobenzothiadiazole **7a**[7] with iron dust in acetic acid gave diamine **8a**.[8] Heterocycle **3b** was prepared in 74% yield by reaction of diamine **8a** with thionyl chloride in pyridine at room temperature. The analogous heterocycle **6b** was obtained in 40% yield from diamine **8a** and selenium dioxide. The palladium-catalyzed coupling ($[PdCl_2(PPh_3)_2]$) of bromide **7a** with phenyltributyl stannane[9] in tetrahydrofuran afforded **7b**, which was reduced with iron dust to give diamine **8b**. Heterocycle **3c** was prepared in 95% yield by reaction of diamine **8b** with *N*-thionylaniline and trimethylsilyl chloride in pyridine at 80 °C. The selenium compound **6c** was obtained in 82% yield from the diamine **8b** and selenium dioxide. These heterocycles were purified by sublimation under reduced pressure and isolated as deep red crystals for **3b** (decomp > 280 °C), purple prisms for **3c** (decomp 310–311 °C), purple crystals for **6b** (decomp > 280 °C), and blue crystals for **6c** (decomp 367–371 °C). The absorption maxima of **3b, c** and **6b, c** are listed in Table 1 and compared with that of benzobis(thiadiazole) **9**, whose thiadiazole ring can be represented by a standard Kekulé structure. The red shifts of **6b, c** from **3b, c** are regarded as a polar effect caused by the selenium atom. We thought that introduction of substituents in the 4- and 8-positions in **3** and **6** (**3a**/**6a** → **3b**, **c**/**6b**, **c**) would underscore this effect, since these positions have larger atomic orbital coefficients in the HOMO and the LUMO (Fig. 1).[10]

Table 1. Absorption maxima and fluorescence emission maxima of heterocycles **3**, **6**, and **9** [a].

Heterocycle	λ_{abs} [nm] (lg ε)	λ_{em} [nm]
3b	524 (3.64)	557
3c	558 (3.99)	642
6b	609 ([b])	643
6c	625 (4.01)	689
9	283 (4.57)	367

[a] In CH_2Cl_2. [b] Not obtained because of its low solubility.

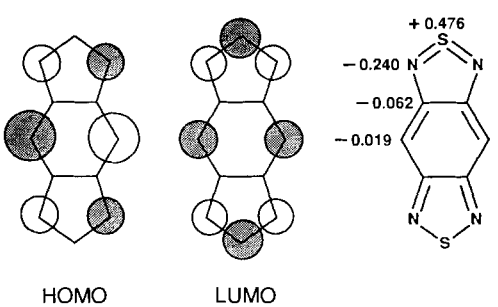


Fig. 1. HOMO, LUMO, and charge distribution of **3a** calculated by the MNDO-PM3 method.

The cyclic voltammograms (CV) of **3b, c** and **6c** in dichloromethane showed two reversible one-electron redox waves.[11] The half-wave reduction potentials are given in Table 2. The first reduction potentials of these heterocycles are comparable to that of *p*-benzoquinone ($E = -0.46$ V). The electron-withdrawing bromo groups at 4- and 8-positions further increase the reduction potentials (cf. **3b** and **3c**). The fact that the Kekulé-type isomer **9** is a weaker acceptor (Table 2) shows that the high electron affinity of **3** and **6** is attributable to the 14 π electron system containing a tetravalent sulfur atom, which generates more stable Kekulé-type thiadiazole moieties upon accepting an electron.

Table 2. Reduction potentials (in V) of heterocycles **3**, **6c**, and **9** [a].

Heterocycle	E_1	E_2	ΔE
3b	−0.35	−1.10	0.75
3c	−0.61	−1.30	0.69
6c	−0.53	−1.21	0.68
9	−1.45	–	–

[a] 0.1 M nBu_4NClO_4 in CH_2Cl_2, Pt electrode, scan rate 100 mVs^{-1}, potentials vs. standard calomel electrode (SCE).

A single crystal of **3b** obtained by recrystallization from benzonitrile was selected for X-ray structural analysis.[12] In the crystal the molecule is planar and has C_i symmetry (Fig. 2). The S–N bond lengths (given in Fig. 2) are shorter than those of **9** (1.615 and 1.620 Å),[13] and the N–C bond lengths longer (for **9**, 1.325 and 1.337 Å). The bond lengths in the thiadiazole rings are similar to those in the pyrazine derivative **1** (S–N 1.597 and 1.609 Å, N–C 1.347 and 1.370 Å).[2] Although the molecule is uniformly stacked along the *c* axis, the stacking shown in Figure 3a indicates less effective interactions between the HOMO and the LUMO (Fig. 1).

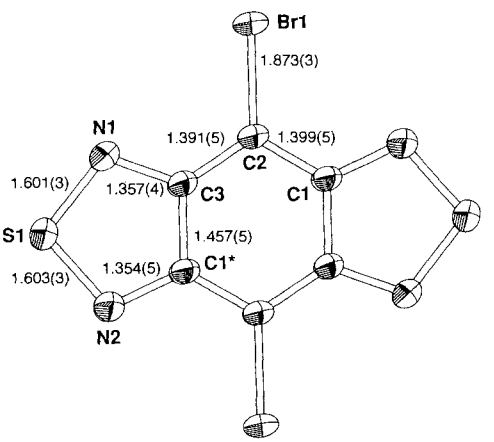


Fig. 2. Molecular structure of **3b** with bond lengths [Å] (ORTEP).

The crystal structure is composed of a set of two ribbon-type columns which extend in the [0 1 1] and [0 1 −1] directions and are characterized by short intermolecular S···N and N···N contacts (Fig. 3b). These columns interact with each other through short Br···N contacts to form a network. The distances of the relevant contacts, S···N, N···N, and Br···N, are significantly smaller than the sum of the van der Waals radii (3.35, 3.10, and 3.40 Å). According to the net atomic charges of **3a** calculated by the MNDO-PM3 method, the hypervalent S atoms have significant positive charge and the N atoms significant negative charge (Fig. 1). Thus, the S···N interactions are attributed to an electrostatic effect, which seems to induce dense packing in the crystal ($\rho_{calcd} = 2.58$ gcm^{-3}).

[*] Only one of the possible resonance forms is shown for each compound. For **6** the contribution of the structure containing a tetravalent Se atom is small.

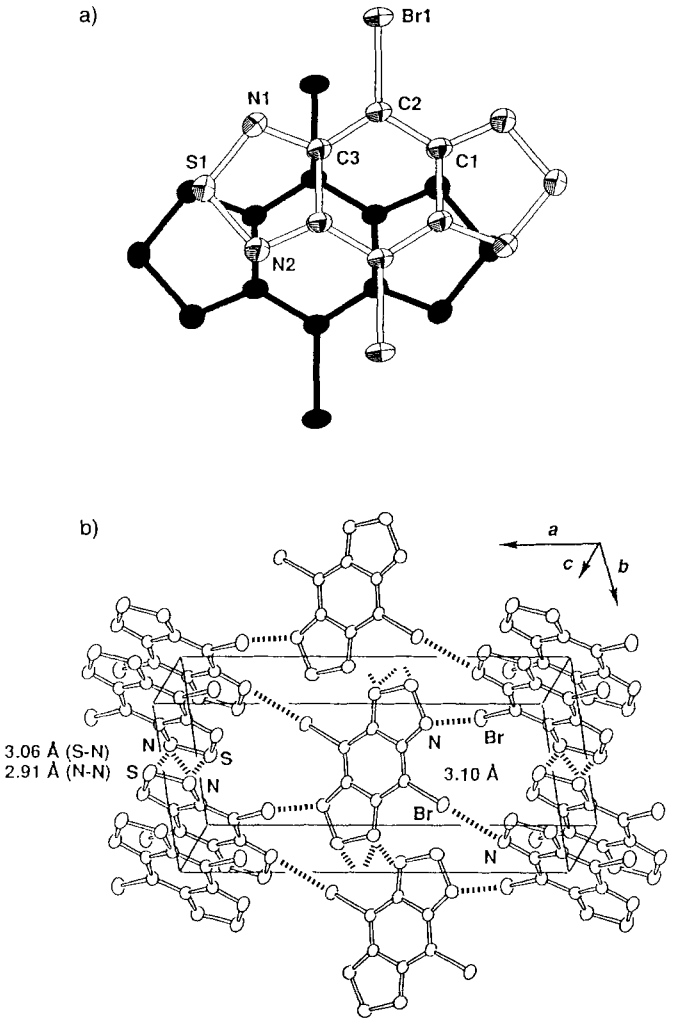


Fig. 3. Crystal structure of **3b**: a) stacking, b) ribbonlike network.

MNDO-PM3 calculations[10] for **3a** and **6a** also show that the energy levels of the HOMOs (− 8.73 eV for **3a** and **6a**) are higher than that of **9** (− 9.94 eV), and that the energy levels of the LUMOs (− 3.21 eV for **3a** and −3.30 eV for **6a**) are lower than that of **9** (−1.95 eV). These results are supported by the longer absorption maxima and the higher electron affinities of **3** and **6**. Thus, the electron properties of the heterocycles containing the hypervalent sulfur atoms are fairly different from those of the Kekulé-type isomer. On the other hand, substitution of a sulfur atom by a selenium atom little affects the HOMO and the LUMO of the 14π electron system.

Heterocycles **3** and **6** display fluorescence emission spectra, which have broad maxima (Table 1), upon photoexcitation in dichloromethane at room temperature.[14] Since **3** and **6** have high electron affinities, their photochemical behavior is of interest and currently under study.

Received: April 29, 1994 [Z 6880 IE]
German version: *Angew. Chem.* **1994**, *106*, 2030

[1] a) M. P. Cava, M. V. Lakshmikantham in *Comprehensive Heterocyclic Chemistry, Vol. 4* (Eds.: C. W. Bird, G. W. H. Cheeseman), Pergamon, New York, **1984**, p. 1037; b) C. A. Ramsden in *Comprehensive Heterocyclic Chemistry, Vol. 6* (Ed.: K. T. Potts), Pergamon, New York, **1984**, p. 1027; c) A. Ishii, J. Nakayama, J. Kazami, Y. Ida, T. Nakamura, M. Hoshino, *J. Org. Chem.* **1991**, *56*, 78; d) A. Tsubouchi, N. Matsumura, H. Inoue, *J. Chem. Soc. Chem. Commun.* **1991**, 520.

[2] Y. Yamashita, K. Saito, T. Suzuki, C. Kabuto, T. Mukai, T. Miyashi, *Angew. Chem.* **1988**, *100*, 428. *Angew. Chem. Int. Ed. Engl.* **1988**, *27*, 434.

[3] a) A. P. Komin, R. W. Street, M. Carmack, *J. Org. Chem.* **1975**, *40*, 2749; b) J. Kane, R. Schaeffer, *Cryst. Struct. Commun.* **1981**, *10*, 1403.

[4] Half-wave reduction potentials of **1**: $E_1 = +0.10$ V, $E_2 = -0.82$ V vs. SCE; measured with a Pt electrode in acetonitrile with 0.1 M Et_4NClO_4, scan rate 100 mVs^{-1} [2].

[5] T. Suzuki, H. Fujii, Y. Yamashita, C. Kabuto, S. Tanaka, M. Harasawa, T. Mukai, T. Miyashi, *J. Am. Chem. Soc.* **1992**, *114*, 3034.

[6] Y. Yamashita, T. Suzuki, T. Mukai, *J. Chem. Soc. Chem. Commun.* **1987**, 1184.

[7] T. Uno, K. Takagi, M. Tomoeda, *Chem. Pharm. Bull.* **1980**, *28*, 1909.

[8] Y. Tsubata, T. Suzuki, Y. Yamashita, T. Mukai, T. Miyashi, *Heterocycles* **1992**, *33*, 337.

[9] J. L. Wardell, S. Ahmed, *J. Organomet. Chem.* **1974**, *78*, 395.

[10] Calculated by the MNDO-PM3 method, MOPAC program, J. J. P. Stewart, *J. Comput. Chem.* **1989**, *10*, 209, 221.

[11] The CV of **6b** was not obtained because of its low solubility.

[12] X-ray structure data for **3b**: $C_6Br_2N_4S_2$, $M = 352.04$, monoclinic, space group $P2_1/n$, $a = 15.569(1)$, $b = 7.3990(4)$, $c = 3.9405(3)$ Å, $\beta = 90.192(4)°$, $V = 453.92(5)$ Å^3, $Z = 2$, $\rho_{calcd} = 2.58$ g cm^{-3}, $F(000) = 332$, $\mu(Cu_{K\alpha}) = 153.25$ cm^{-1}. A total of 1015 unique data for $2\theta_{max} = 140°$ was collected on an Enraf–Nonius CAD4 diffractometer ($Cu_{K\alpha}$ radiation, $\lambda = 1.5418$ Å, graphite monochromator, ω-2θ-scan) at 296 K. The structure was solved by Patterson methods and refined by full-matrix least-squares analysis giving values of $R = 0.024$, $R_w = 0.030$, max./min. residual electron density 0.37/−0.39 e Å^{-3} for 859 reflections with $F_o > 3\sigma F_o$. All calculations were performed using the teXsan programs. Further details of the crystal structure investigation may be obtained from the Fachinformationszentrum Karlsruhe, D-76344 Eggenstein-Leopoldshafen (FRG), on quoting the depository number CSD-58394.

[13] A. Gieren, H. Betz, T. Hübner, V. Lamm, R. Neidlein, D. Droste, *Z. Naturforsch. B* **1984**, *39*, 485.

[14] Details will be reported elsewhere.

Stereoselective Intramolecular Alkylation of Glycosylimides to Highly Functionalized Bicyclic 2,5-Azepanediones and Heterotricyclic [5.3.1.0^{2,6}]undecanamides**

Carsten Endres Sowa and Joachim Thiem*

N-Iodosuccinimide (NIS) is an effective and established reagent for the stereoselective glycosylation of glycals.[1] With secondary alcohols like, for example, cholesterol, the corresponding *N*-glycosylated succinimides could frequently be isolated as a by-product in substantial yields.[2, 3] In such cases, the succinimide anion apparently competes with weak nucleophiles to attack the intermediate iodonium ion. When no other nucleophiles or moisture is present and light is excluded, the stereoselective addition of NIS to the enol ether function of several glycals occurs with excellent yields.[4] The iodine substituent can always be quantitatively removed with Bu_3SnH/AIBN to give α-*N*-(2-deoxyglycosyl)succinimides.[4] This very simple preparative procedure and the high total yield is the motive for investigating the use of such glycosylimides in synthesis.

Kanaoka et al. photochemically converted *N*-alkylsuccinimides in a Norrish type II reaction to simple alkylated ε-lactams.[5, 6] In this way, *N*-cyclohexylsuccinimide, for example, was transformed in mg amounts into the enantiomeric mixture of 5,6-(perhydrobenzo)-4-oxo-ε-lactam, a bicyclic 2,5-azepanedione. In this reaction the α-position to the imide in the alkyl

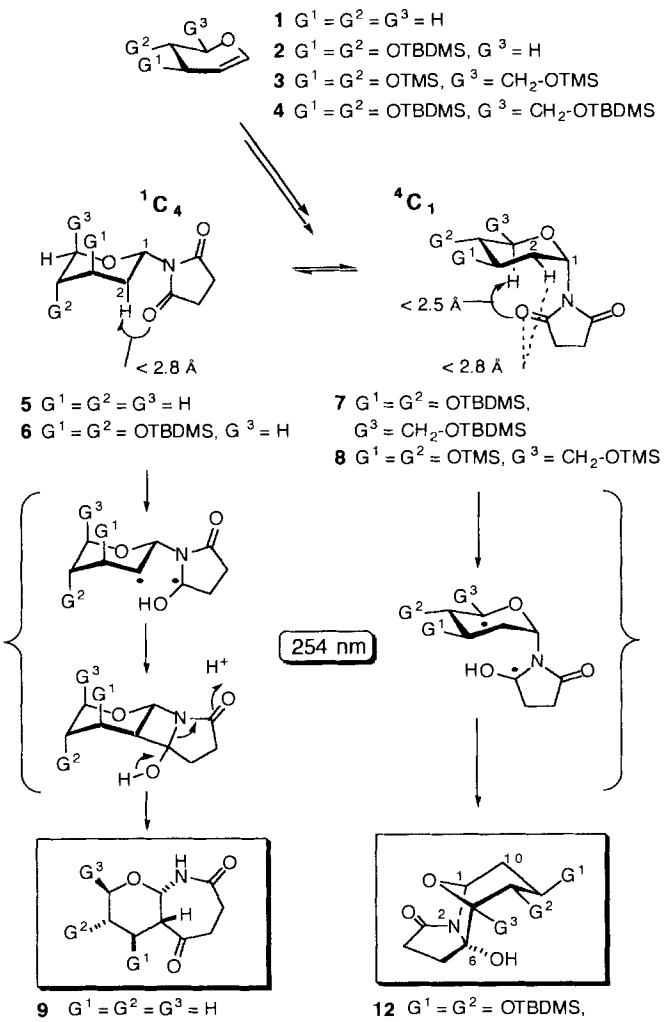
[*] Prof. Dr. J. Thiem, Dipl.-Chem. C. E. Sowa
Institute für Organische Chemie der Universität
Martin-Luther-King-Platz 6, D-20146 Hamburg (FRG)
Telefax: Int. code +(40) 4123-4325

[**] This work was supported by the Fonds der Chemischen Industrie.

residue undergoes *cis* radical alkylation, and the imide ring is expanded to the 4-oxo-ε-lactam. Griesbeck and Mauder applied this reaction to enantiomerically pure phthalimide derivatives of several simple amino acids.[7] As well as the predominantly β,γ-unsaturated amino acids, substituted dihydrobenzazepine-2,5-diones and a benzoannelated pyrrolizidinone were also isolated with remarkable diastereoselectivities.

It seemed of interest to investigate the corresponding reaction on highly functionalized monosaccharides. The model compound 3,4-dihydropyran (**1**) was treated with NIS and subsequently reduced to *N*-(tetrahydro-2-pyranyl)succinimide (**5**) with Bu_3SnH/AIBN. With this heterocyclic system, conformational aspects and also influences of protective groups in the saccharides could be excluded. The irradiation of **5** with UV light (254 nm) in acetonitrile proceeded regioselectively, as expected, to give the enantiomeric mixture of the bicyclic 2,5-azepanedione **9**. In this reaction the conditions, particularly the conversion, reaction time, and temperature, were optimized and then applied to the glycosylsuccinimides **6**, **7**, and **8** (Scheme 1).

The wavelength used precludes carbonyl, alkenyl, and phenyl groups as hydroxy protective groups, and silyl ethers proved to be advantageous. The 2-deoxyxylo derivative (**6**) produced the expected bicyclic 2,5-azepanedione **10** in a diastereoselective alkylation at C-2 with 52% yield. In contrast, the glycosylimides **7** and **8** react differently under the same conditions. The *tert*-butyldimethylsilyl-protected glycosylimide **7** forms the azepanedione **11** only as a by-product (21%) (Table 1). The main fraction results from a 1,7 hydrogen abstraction and subsequent C–C coupling at C-5 of the sugar to give the heterotricyclic compound **12** (62%). Changing the protective group to trimethylsilyl as in **8** gives a completely stereoselective alkylation of the monosaccharide to the tricyclic compound **13** with a yield of 83% (Table 1). The *exo* structure can be proven by a clear NOE effect of the alcoholic proton with the ring protons H-9 (5%) and H-10_{eq} (3%).



Scheme 1. Reaction mechanism of the photochemical cyclization of *N*-glycosylsuccinimides. TBDMS = *tert*-butyldimethylsilyl, TMS = trimethylsilyl.

Table 1. Typical experimental and physical data for **11** and **13** [a].

11: (1*S*, 7*R*, 8*R*, 9*R*, 10*R*)-8,9-Bis(*tert*-butyldimethylsiloxy)-10-(*tert*-butyldimethylsiloxymethyl)-11-oxa-2-aza-bicyclo[5.4.0]undecane-3,6-dione; M.p. 67 °C; ^{1}H NMR (400 MHz, $CDCl_3$, 25 °C, TMS): δ = 0.0–0.15 (18H, m, $SiMe_3$), 0.80–0.95 (27H, m, *t*Bu), 2.37 (ddd, H-4), 2.49 (ddd, H-4'), 2.54 (dd, H-7), 2.93 (ddd, H-5), 3.66 (d, H-9), 3.79 (ddd, H-5), 3.90–4.05 (3H, m, H-10, $CH_2OSitBuMe_2$), 4.40 (dd, H-8), 4.91 (dd, H-1), 6.62 (d, N-H); $J_{1,NH}$ = 7.6, $J_{4',4}$ = 13.2, $J_{4,5}$ = 6.6, 3.6, 4.0, 4.1, $J_{5,5}$ = 17.0, $J_{1,7}$ = 2.5, $J_{7,8}$ = 3.1, $J_{8,9}$ = 3.6; ^{13}C NMR (100 MHz): −5.3 bis −4.6 (6C, SiMe), 17.9–18.5 (3C, Si-*tert*-C), 25.7–26.6 (9C, SiCC), 31.2, 37.7 (C-4, C-5), 55.6 (C-7), 60.7 ($CH_2OSitBuMe_2$), 67.1, 71.9, 75.1 (C-8, C-9, C-10), 82.8 (C-1), 175.3 (C-3, NC=O), 206.3 (C-6, C=O)

13: M.p. 122 °C; ^{1}H NMR (400 MHz, $CDCl_3$, 25 °C, TMS): δ = 0.14, 0.19 (27H, s, Me), 1.78 (1H, ddd, $H\text{-}10_{ax}$), 2.04–2.10 (2H, m, H-5), 2.17–2.33 (2H, m, $H\text{-}10_{eq}$, H-4), 2.93 (1H, ddd, H-4), 3.65 (1H, d, H-CH_2OSiMe_3), 3.98 (1H, d, H-8), 4.25 (1H, ddd, H-9), 5.45 (1H, dd, H-1), 6.24 (1H, s, OH), $J_{1,10eq}$ = 1.5, $J_{1,10ax}$ = 2.0, $J_{10ax,10eq}$ = 13.2, $J_{9,10ax}$ = 10.2, $J_{9,10eq}$ = 6.5, $J_{8,9}$ = 8.2, $J_{4',4}$ = 15.2, $J_{4,5}$ = 8.2, 12.2 Hz; ^{13}C NMR (100 MHz): δ = −0.37, 0.34, 0.65 (9C, Me), 31.35 (C-10), 35.21 (C-5), 38.93 (C-4), 60.52 (CH_2OSiMe_3), 71.08, 75.42, (2C, C-8, C-9), 83.15 (C-7), 85.32 (C-1), 99.53 (C-6), 182.53 (C-3)

[a] Correct elementary analyses have been obtained for all new compounds.

By selecting the monosaccharide and protective groups, both sets of products are possible. The different conformations and the type of substitution at C-5 have crucial influences.[8] The abstraction of the hydrogen H-5 creates in the case of hexopyranoses an axial, tertiary radical, which is additionally stabilized by the ring oxygen. The short distance between the carbonyl group and H-5 results in the selective alkylation at C-5 of derivative **8**, as the conformation is sufficiently flexible ($^1C_4$: $^4C_1$ ≈ 1:1 according to ^{1}H NMR spectroscopy). Surprisingly, the TBDMS derivative **7** is almost exclusively in the $^1C_4$ chair conformation (*trans*-$J_{1,2}$ = 11.2, $J_{4,5}$ = 2.0 Hz). Though the flexibility is low, it is apparently enough for the synthesis of the tricyclic compound **12**, not the azepanedione **11**, as the main product. This assumption is supported by the temperature dependence of the product distribution. The proportion of the azepandione derivative **11** increases from 21% (**12**: 62%) at room temperature to 31% (**12**: 45%) at −5 °C. The conversion, however, decreases considerably, and further cooling eventually stops the reaction totally. At the moment, bridged and thus 3,6-anhydro sugars fixed in the $^1C_4$ chair form are being investigated, from which the exclusive formation of azepanedione derivatives are expected.

An intramolecular, stereoselective alkylation underlies both sets of products, which leads to highly functionalized enantiomerically pure heterocyclic compounds. The azepanediones **9**–**11** are [5.4.0]bicyclic α-oxo-aminals and therefore contain a novel substructure. The biological properties of this new class of substance are presently being screened. It is emphasized that, in one step, two adjacent quaternary and functionalized bridge

heads result from the synthesis of the heteroundecanamides **12** and **13**.

In this intramolecular carbon chain elongation of the monosaccharide, a cyclic derivative of a nonose is formed.[9] We are attempting to synthesize higher functionalized components by varying the glycal and by using other imides.

Experimental Procedure

(1*S*,6*S*,7*R*,8*S*,9*R*)-6-hydroxy-8,9-bis(trimethylsiloxy)-7-(trimethylsiloxymethyl)-11-oxa-2-aza-tricyclo[5.3.1.$0^{2,6}$]undecane-3-one **13**: 250 mg **8** (0.62 mmol) were dissolved in degassed, anhydrous acetonitrile or *n*-hexane and irradiated for 4 h at 18 °C with UV light (λ = 254 nm, 60 W low-pressure mercury lamp). The solvent was removed, and the raw product purified on silica gel. From a conversion of 76%, 157 mg (83%) remain.

Received: April 19, 1994 [Z 6863 IE]
German version: *Angew. Chem.* **1994**, *106*, 2041

[1] J. Thiem, W. Klaffke, *Top. Curr. Chem.* **1990**, *154*, 285–332.
[2] J. Thiem, P. Ossowski, *Liebigs Ann. Chem.* **1983**, 2215–2226.
[3] J. Thiem, S. Köpper, J. Schwentner, *Liebigs Ann. Chem.* **1985**, 2135–2150.
[4] L. Laupichler, C. E. Sowa, J. Thiem, *Bioorg. Med. Chem.*, in press.
[5] Y. Kanaoka, Y. Hatanaka, *J. Org. Chem.* **1976**, *41*, 400–401.
[6] Y. Kanaoka, *Acc. Chem. Res.* **1978**, *11*, 407–413.
[7] A. G. Griesbeck, H. Mauder, *Angew. Chem.* **1992**, *104*, 97–99; *Angew. Chem. Int. Ed. Engl.* **1992**, *31*, 73–75.
[8] An excellent summary can be found in: B. Giese, *Radicals in Organic Synthesis: Formation of Carbon-Carbon Bonds*, 1st edition, Pergamon, Oxford, **1986**; H. G. Viehe, Z. Janousek in *Substituent Effects in Radical Chemistry* (Ed.: R. Merenyi), Reidel, Dordrecht, **1986**; J. M. Tedder, *Angew. Chem.* **1982**, *94*, 433–442; *Angew. Chem. Int. Ed. Engl.* **1982**, *21*, 401–410.
[9] Syntheses of other nonose derivatives, particularly neuraminic acid derivatives: a) R. Julina, I. Müller, A. Vasella, R. Wyler, *Carbohydr. Res.* **1987**, *164*, 415–432; b) S. J. Danishefsky, M. P. De Ninno, S. H. Chen, *J. Am. Chem. Soc.* **1988**, *110*, 3929–3940; c) C. Augé, C. Gautheron, S. David, A. Malleron, B. Gavagé, B. Bouxon, *Tetrahedron* **1990**, *46*, 201–214; d) K. Okamoto, T. Goto, *ibid.* **1990**, *46*, 5835; e) M. P. DeNinno, *Synthesis* **1991**, 583.

Homoleptic Thiolato Complexes: Di- and Trinuclear Ti^{IV} Complexes with Unexpected Metal–Sulfur Cores, $[NMe_2H_2][Ti_2(SMe)_9]$ and $[Ti_3(SMe)_{12}]$**

Wolfram Stüer, Kristin Kirschbaum, and Dean M. Giolando*

Normally six-coordinate metal centers have approximate octahedral symmetry (O_h).[1] Notable exceptions are transition-metal complexes of the type $[M(1,2\text{-}S_2C_2R_2)_3]^-$ and $[M(1,2\text{-}S_2C_6H_4)_3]^-$, the majority of which adopt approximate trigonal-prismatic symmetry (D_{3h}).[2] Only recently, $[ZrMe_6]^{2-}$ was reported to be the first homoleptic complex with unidentate ligands which exhibits non-O_h symmetry.[3] In the course of our interest in complexes with six-coordinate metal centers[4] we have recently reported an unusual C_2-distortion from O_h geometry in $[Ti(S_2C_6H_4)_3]^{2-}$; the coordination about Ti can be described as *skew*-trapezoidal bipyramidal or, alternatively, the S_6 polyhedron can be considered pentagonal-bipyramidal, lacking an equatorial vertex.[5] To gain insights into the factors governing this coordination geometry we have prepared six-coordinate Ti^{IV} complexes containing unidentate thiolato ligands. X-ray structural analysis has revealed a trigonal distortion of the octahedral coordination about the Ti center in $[Ti_2(SMe)_9]^-$, and a novel trigonal-prismatic coordination geometry about the central Ti atom with two face-sharing O_h-symmetric TiS_6 cores in $[Ti_3(SMe)_{12}]$. In addition titanium thiolato complexes are of current interest due to their suitability as precursors for the formation of titanium sulfide thin films by chemical vapor deposition techniques. Success in this area of research has been demonstrated with $[Ti(StBu)_4]$ and $[TiCl_4(HSR)_2]$, where R = *cyclo*-pentyl and *cyclo*-hexyl.[6, 7]

Titanium thiolato complexes have been studied to a limited extent, and general routes to homoleptic complexes have been particularly elusive.[8, 9] Early work employed the reaction of $[Ti(NR'_2)_4]$ (R' = Me or Et) and RSH (R = Me, Et, or *i*Pr) which afforded complexes of general formula $[Ti(SR)_4(HSR)_x(NHR'_2)_y]$, where $(x + y)$ varied from 0.8 to 1.33.[10] Attempts to prepare $[Ti(SR)_4]$ from the reaction of $TiCl_4$ and RSH/NH_3 were not entirely successful because a mixture of compounds $[TiCl_{4-x}(SR)_x]$, where x varies from 1 to 4, was obtained.[10]

When we treated $[Ti(NMe_2)_4]$ with seven molar equivalents of MeSH, a dark red microcrystalline product, $[NMe_2H_2]$-**1**, was obtained in good yield.[11] Almost black single crystals crystal-

$[NMe_2H_2][Ti_2(SMe)_9]$ $[NMe_2H_2]$-**1**

lize from CH_2Cl_2/hexane mixtures; Figure 1 shows the solid-state structure of the $[Ti_2(SMe)_9]^-$ ion.[12] Bond lengths and

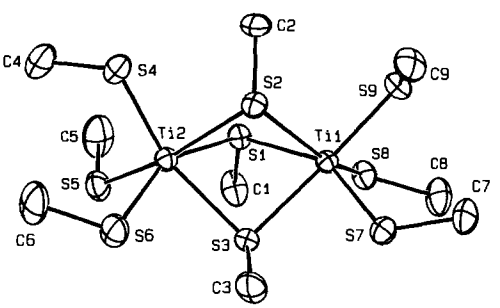


Fig. 1. Structure of **1**. Important distances [Å] and angles [°]: Ti-S (bridging) 2.511(1)–2.575(1) Å, Ti-S (terminal) 2.3211(9)–2.362(1) Å, *trans*-S-Ti-S 148.04(3) 162.42(4), *cis*-S-Ti-S 73.11(3)–115.63(3).

angles about the Ti centers compare well to those found for other Ti^{IV} complexes with MeS ligands.[13] The anion **1** contains two Ti atoms each coordinated by three terminal and three bridging MeS ligands. To a first approximation, the Ti_2S_9 framework may be described as a face-sharing bioctahedron which is unique for sulfur donor ligands; the closest structural analogue[14] is $[Ti_2Cl_9]^-$. While the $TiCl_6$ cores in $[Ti_2Cl_9]^-$ are close to the O_h limit, the TiS_6 cores in $[NMe_2H_2]$-**1** are significantly distorted with no major structural differences between the two TiS_6 cores. Both TiS_6 cores are trigonally distorted from O_h to the midpoint of the O_h-to-D_{3h} reaction coordinate: Ti1, twist angle of 31.10(4)° with dihedral angles between adjacent S_3 faces (δ) at b_1 of 40.37(4)° and b_2 of 92.50(3)°; Ti2, twist angle of 33.30(5)° with δ at b_1 of 42.83(5)° and b_2 of 92.13(3)°.[15] Interestingly, these MS_6 cores are similar to those observed for several $[M(1,2\text{-dithiolato})_3]^{2-}$ complexes, where M = Ti or Zr.[16]

[*] Dr. D. M. Giolando, W. Stüer, Dr. K. Kirschbaum
Department of Chemistry, University of Toledo
Toledo, OH 43606 (USA)
Telefax: Int. code +(419) 537-4033

[**] This work was supported by the petroleum Research Fund, administered by the American Chemistry Society.

The reaction of four equivalents of MeSH with $[Ti(NMe_2)_4]$ results in the isolation of red-brown single crystals of $[Ti_3(SMe)_{12}]$ (**2**).[17] Figure 2 shows the solid-state structure of the compound.[11] The bond lengths are similar to those observed in $[NMe_2H_2]$-**1**. Complex **2** lies on a crystallographic C_3 axis and has a linear chain of three Ti atoms, the two outer Ti atoms are coordinated by three terminal and three bridging MeS ligands, while the central Ti atom is coordinated by six bridging MeS ligands. Overall, the geometry of the Ti_3S_{12} framework may be described as a trigonal-prismatic center with a face-sharing octahedron on both trigonal faces. This novel arrangement has as its closest structural analogue in the metal thiolato-bridged "double cubane" complexes.[18] The arrangement of ligands in the two outer TiS_6 polyhedra is similar; both polyhedra are trigonally distorted from O_h: Ti2, twist angle of 49.22(3)° with δ at b_1 of 60.57(2)° and b_2 of 78.44(2)°; Ti3, twist angle of 44.50(3)° with δ at b_1 of 55.69(2)° and b_2 of 81.77(2)°.[15] A distortion is evidenced by the two Ti atoms being about 0.4 Å from the center of the S_6 core, shifted towards the external S_3 faces. For the central Ti atom the TiS_6 core is unusually close to the D_{3h} limit: Ti1, twist angle of 10.69(2)° with δ at b_1 of 14.44(7)° and b_2 of 109.60(2)°.

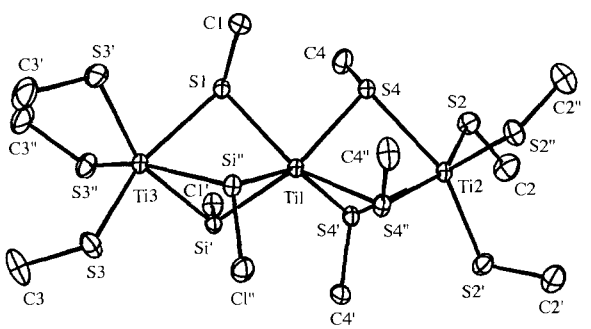


Fig. 2. Structure of **2**. Important distances [Å] and angles [°]: Ti2 and Ti3: Ti-S (bridging) 2.5580(8)-2.5732(9), Ti-S (terminal) 2.3134(7)-2.3177(7), *trans*-S-Ti-S 158.03(4)-159.62(4), *cis*-S-Ti-S 75.12(3)-101.88(4); Ti1: Ti-S 2.4319(8)-2.4355(8), *trans*-S-Ti-S 128.89(3)-143.74(3), *cis*-S-Ti-S 79.62(3)-84.14(2).

All of the trigonally distorted TiS_6 coordination geometries observed in $[NMe_2H_2]$-**1** and **2** are unexpected. Sterically, an O_h coordination, with a displacement of the Ti center towards the terminal MeS ligands, is anticipated. Computational studies[19] on d^0-ML_6 complexes suggest a tendency for a twofold distortion from O_h towards a bicapped tetrahedral (BCT) geometry, as observed[5] in $[Ti(S_2C_6H_4)_3]^{2-}$ which is midway along the O_h-to-BCT reaction coordinate. It is not readily apparent why the structural features of $[NMe_2H_2]$-**1** and **2** are observed. However, as discussed[3] for the D_{3h} structure of $[ZrMe_6]^{2-}$, a reduction of symmetry induced by a second-order Jahn-Teller effect may stabilize the trigonally twisted O_h coordination polyhedra. Noteworthy, non-O_h coordination geometries are favored by insignificant, or the absence of, M-L π-bonding.

The behavior of these compounds in solution is complicated and warrants further investigation. Our preliminary studies by NMR spectroscopy suggest that $[NMe_2H_2]$-**1** dissolves to afford **2** and at least one other compound. In dilute solutions (ca. 10^{-3} M, CD_2Cl_2, 21 °C) the ^1H NMR spectrum of $[NMe_2H_2]$-**1** contains two resonances at $\delta = 3.59$ and 3.13 (1:1 ratio), assigned to **2**, and single resonances assigned to coordinated Me_2NH ($\delta = 8.00$ and 2.42) and MeSH ($\delta = 2.05$ and 1.26). As the temperature decreases (−25, −60, and then to −85 °C) the NMR spectra undergo a series of changes: the resonances at $\delta = 8.00$, 3.59, and 3.13 are slightly broadened and shifted; a new feature at $\delta = 3.31$ appears as a sharp singlet at −25 °C, which is severely broadened at −85 °C; the resonance at $\delta = 2.42$ produces two broad singlets at $\delta = 2.77$ and 2.70 at −25 °C, which merge to a singlet at $\delta = 2.75$ at −60 °C and then reappear at −85 °C; and, those at $\delta = 2.05$ and 1.26 sharpen to a well-resolved doublet and quartet, respectively. For saturated solutions of $[NMe_2H_2]$-**1** at 21 °C a new, very broad feature at $\delta \approx 3.4$, is observed, while the resonance at $\delta = 3.13$ broadens and the remaining resonances are unchanged. Tentatively, these results indicate that on dissolution $[NMe_2H_2]$-**1** affords **2** and, possibly the mixed complex $[Ti(SMe)_4(SHMe)_x(NHMe_2)_y]$ identified in the earlier literature.[6]

Synthetic and structural studies on this class of compounds should have an impact on determining new aspects of six-coordinate complexes as well as providing advances to the development of titanium sulfide cathodes for battery technology. We are continuing our efforts to prepare homoleptic monotitanium complexes containing unidentate RS ligands and to elucidate the solution chemistry of this class of compounds.

Experimental Procedure

All reagents were purchased and used without further purification except where noted. All solvents were freshly distilled: hexanes and THF from Na/benzophenone; CH_2Cl_2 from P_2O_5. All experimental work was conducted under an inert atmosphere.

$[NMe_2H_2]$-**1**: A reaction flask containing $[Ti(NMe_2)_4]$ (0.450 g, 2 mmol) in THF (30 cm³) was immersed in liquid nitrogen, and MeSH (0.78 cm³, 14 mmol) was added in one portion. On warming the mixture to 21 °C the color changed from pale yellow to dark red-brown. Stirring was continued at 21 °C for 20 h. The solvent was evaporated under vacuum without warming and the resultant dark red microcrystalline solid was dried in vacuo for 2 h, correct C,H,N analysis. Single crystals suitable for X-ray crystallography were obtained after storage of a saturated hexane/CH_2Cl_2 solution at −10 °C for 1 week.

2: A reaction flask containing $[Ti(NMe_2)_4]$ (0.450 g, 2 mmol) in THF (30 cm³) was immersed in a dry-ice/acetone bath. MeSH (0.45 cm³, 8 mmol) was added in one portion. On warming the mixture to 21 °C the color changed from pale yellow to dark red-brown. Stirring was continued at 21 °C for 20 h. The solvent was evaporated under vacuum with the aid of a water bath. After removal of volatiles in vacuo the initially oily residue solidified. The dark red-brown solid was dissolved in a mixture of hexane (50 cm³) and CH_2Cl_2 (100 cm³) and stored at −10 °C. Dark red-brown single crystals suitable for X-ray crystallography were obtained, correct C,H,N analysis.

Received: March 22, 1994 [Z 6786 IE]
German version: *Angew. Chem.* **1994**, *106*, 2028

[1] J. E. Huheey, *Inorganic Chemistry*, 3rd ed. Harper & Row, New York, **1983**, Chap. 10.
[2] J. L. Martin, J. Takats, *Can. J. Chem.* **1989**, *67*, 1914-1923, and references therein D. L. Kepert, *Prog. Inorg. Chem.* **1977**, *23*, 1-65.
[3] P. M. Morse, G. S. Girolami, *J. Am. Chem. Soc.* **1989**, *111*, 4114-4116.
[4] J. Wegener, K. Kirschbaum, D. M. Giolando, *J. Chem. Soc. Dalton Trans.* **1994**, 1213-1218.
[5] M. Könemann, W. Stüer, K. Kirschbaum, D. M. Giolando, *Polyhedron* **1994**, *13*, 1415-1425.
[6] M. Bochmann, I. Hawkins, L. M. Wilson, *J. Chem. Soc. Chem. Commun.* **1988**, 344-345.
[7] C. H. Winter, T. S. Lewkebandara, J. W. Proscia, A. L. Rheingold, *Inorg. Chem.* **1993**, *32*, 3807-3808.
[8] P. J. Blower, J. R. Dilworth, *Coord. Chem. Rev.* **1987**, *76*, 121-185; C. A. McAuliffe, D. S. Barratt in *Comprehensive Coordination Chemistry, Vol. III* (Eds.: G. Wilkinson, R. D. Gillard, J. A. McCleverty), Pergamon, Oxford, **1987**, Chap. 31, pp. 323-361.
[9] a) C. P. Rao, J. R. Dorfman, R. H. Holm, *Inorg. Chem.* **1986**, *25*, 428-439; b) G. A. Sigel, P. P. Power, *ibid.* **1987**, *26*, 2819-2822.
[10] D. C. Bradley, P. A. Hammersley, *J. Chem. Soc. A* **1967**, 1894-1896.
[11] NMR data of $[NMe_2H_2]$ **1**: ^1H NMR (400 MHz, $CDCl_3$, 21 °C): $\delta = 3.59$ (s, Ti-SMe), 3.13 (s, Ti-SMe), 2.42 (s, NMe), 2.04 (br d, SMe), 1.22 (br q, SH); ^{13}C NMR ($CDCl_3$, 21 °C, APT): $\delta = 29.6$ (primary, Ti-SMe), 28.0 (primary, Ti-SMe).
[12] Crystal structure of $[NMe_2H_2]$-**1** and **2**: $[NMe_2H_2]$-**1**: $C_{11}H_{35}Ti_2NS_9$; $M = 565.78$; monoclinic, $P2_1/a$; $a = 16.366(4)$, $b = 8.789(1)$, $c = 19.187(2)$ Å.

$\beta = 111.20(1)$; $V = 2573(1)$ Å^3; $Z = 4$; $\rho_{calcd} = 1.46$ g cm^{-3}; $\lambda(Mo_{K\alpha}) = 0.71073$ Å; $\mu = 13.2$ cm^{-1}; $T = 253 \pm 1$ K; $R = 0.032$ for 3173 unique observed reflections ($F_o^2 > 3.0\sigma(F_o^2)$) of 5570 total data, 348 refined parameters. **2**: $C_{12}H_{36}Ti_3S_{12}$; $M = 708.89$; hexagonal, $R\bar{3}$; $a = 13.059(3)$, $c = 29.470(4)$ Å; $V = 4352(3)$ Å^3; $Z = 6$; $\rho_{calcd} = 1.62$ g cm^{-3}; $\rho_{obs} = 1.59$ g cm^{-3}; $\lambda(Mo_{K\alpha}) = 0.71073$ Å; $\mu = 16.3$ cm^{-1}; $T = 173 \pm 1$ K; $R = 0.031$ for 1580 unique observed reflections ($F_o^2 > 3.0\sigma(F_o^2)$) of 2160 total data. Structure solution for [NMe_2H_2]-**1** (**2**): Measurement on an Enraf-Nonius CAD4 diffractometer, graphite monochromator, $\omega - 2\theta$ scan technique, $2\theta_{max} = 52.0°$; correction of the anisotropic decay on I from 0.983 to 1.043 (from 0.943 to 1.010), empirical absorption correction on I from 0.844 to 0.998 (from 0.973 to 0.999), solution by direct methods of MULTAN (SIR), refinement by full-matrix least-squares, function minimized was $\sum w(|F_o| - |F_c|)^2$, weight w is defined as $4F_o^2/\sigma^2(F_o^2)$, hydrogen atoms located and refined isotropically (hydrogen atoms calculated on idealized positions and included in the refinement with $B_{iso} = 5.0$ Å^2 as riding atoms), $S = 1.06$ (1.76), largest shift $\leq 0.01\sigma$, high peak in final difference map 0.34(7) e Å^{-3} (0.43(9) e Å^{-3}), low peak $-0.12(7)$ e Å^{-3} ($-0.27(9)$ e Å^{-3}). Further details of the crystal structure determination are available on request from the Director of the Cambridge Crystallographic Data Centre, 12 Union Road, GB-Cambridge CB2 1EZ (UK), on quoting the full journal citation.

[13] T. A. Wark, D. W. Stephan, *Organometallics* **1989**, *8*, 2836–2843.

[14] T. J. Kistenmacher, G. D. Stucky, *Inorg. Chem.* **1971**, *10*, 122–132.

[15] E. L. Muetterties, L. J. Guggenberger, *J. Am. Chem. Soc.* **1974**, *96*, 1748–1756.

[16] $[Ti(S_2C_2H_4)_3]^{2-}$: see ref. [9a]; anion **1** of $[Ti(S_4C_4H_4)_3]^{2-}$: J. H. Welch, R. D. Bereman, P. Singh, *Inorg. Chem.* **1990**, *29*, 68–73; $[Zr(S_2C_6H_4)_3]^{2-}$: M. Cowie, M. J. Bennett, *ibid.* **1976**, *15*, 1595–1603.

[17] NMR spectroscopic data of **2**: ^{1}H NMR (CD_2Cl_2, 21 °C): $\delta = 3.56$ (s, Ti-SMe), 3.12 (s, Ti-SMe); ^{13}C-NMR (CD_2Cl_2, 21 °C, APT): $\delta = 29.55$ (primary, Ti-SMe), 28.35 (primary, Ti-SMe).

[18] S. Ciurli, M. Carrié, R. H. Holm, *Inorg. Chem.* **1990**, *29*, 3493–3501, and references therein.

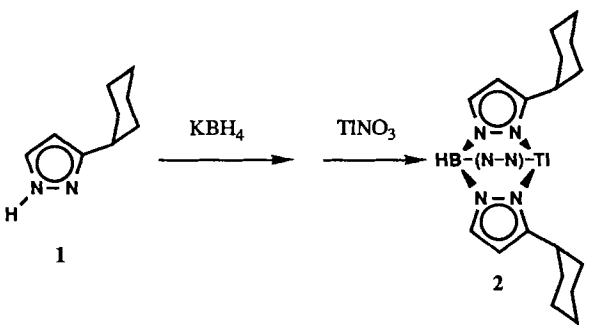
[19] A. Demolliens, Y. Jean, O. Eisenstein, *Organometallics* **1986**, *5*, 1457–1464; K. Tatsumi, I. Matsubara, Y. Inoue, A. Nakamura, K. Miki, N. Kasai, *J. Am. Chem. Soc.* **1989**, *111*, 7766–7777.

The First Structurally Characterized Metal Complex Involving the Free Acid of a New Tris(pyrazolyl)borate as Ligand

Arnold L. Rheingold,* Brian S. Haggerty, and Swiatoslaw Trofimenko*

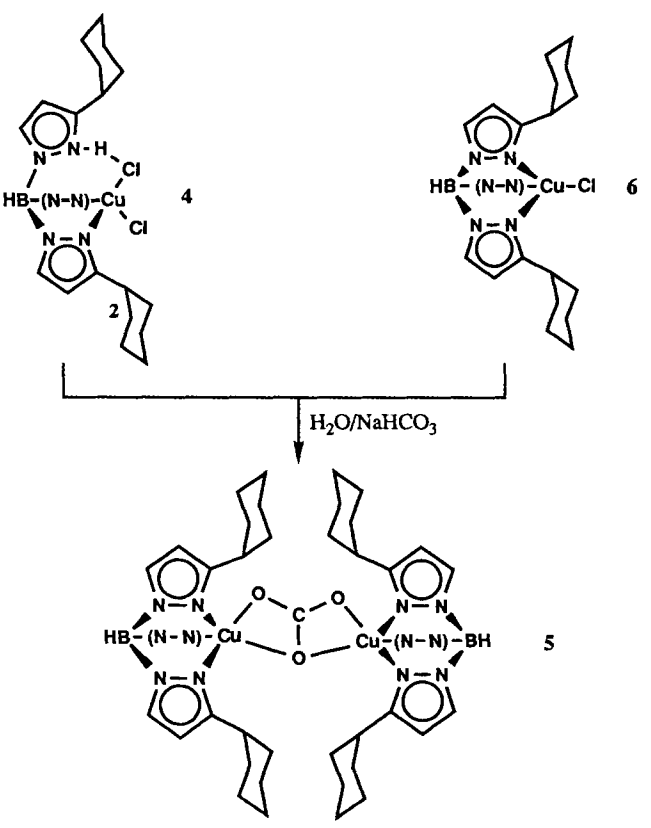
In this communication we report the first example of an isolated and structurally characterized metal complex involving the free acid of a new tris(pyrazolyl)borate as ligand. The scorpionato (polypyrazolylborato) ligands,[1] which have been known for almost 30 years,[2] have been used in the form of their alkali metal or thallium salts to synthesize a plethora of metal complexes. By contrast, their free acids $[R_nB(pz^*)_{4-n}]H$ (pz^* = 1-pyrazolyl or 1-pyrazolyl derivative; pz = pyrazolyl), obtained on acidification of the anions $[R_nB(pz^*)_{4-n}]^-$, received scant attention, although they have been known as long as the ligands themselves.[3] Such protonated species are often the intermediate stage for ligand hydrolysis to boric acid and the corresponding pyrazole. It was noted quite early that the scorpionate free acids can, in some cases, be used to obtain the same metal complexes as those derived from the anions.[3] The use of free acids was at times even necessary if the metal coreactant was stable predominantly at low pH, as for instance in the preparation of complexes $[TpTcCl_2O]$[4] and $[TpReO_3]$ (Tp = $HB(pz)_3$).[5] The uncoordinated pyrazolyl groups in the pzTp-($B(pz)_4$) and Tp ligands retain their donor ability and can be protonated, as in $[(pzTp)_2M]$[3] or $[Tp^*Rh(CO)_2]$ (Tp^* = $HB(3,5\text{-}Me_2pz)$).[6] When two pyrazolyl groups are available, bis chelates can be formed as in $[(\eta^3\text{-}CH_2CRCH_2)\text{-}Pd(pz)_2B(pz)_2Pd(\eta^3\text{-}CH_2CRCH_2)]^+$.[7] A complex involving a homoscorpionate free acid with all pyrazolyl groups participating in coordination has, however, never been obtained.

We have now synthesized and studied a new homoscorpionate ligand, hydrotris(3-cyclohexylpyrazol-1-yl)borate (= Tp^{Cy}),[8] prepared from 3-cyclohexylpyrazole (**1**) and KBH_4. This ligand was expected to provide a larger hydrophobic pocket around the metal than the related 3-isopropyl analogue Tp^{iPr}[9] and its variants $Tp^{iPr,4Br}$,[9] $Tp^{iPr,Me}$,[10] and Tp^{iPr2},[11] it is of special interest because ligands of this type are used to construct model compounds mimicking a variety of enzymes (Scheme 1).[12]



Scheme 1. -(N-N)- denotes the third, hidden 3-cyclohexylpyrazol-1-yl group.

As part of our investigations into complexes of type $Tp^{Cy}MX$, we tried to prepare $[Tp^{Cy}CuCl]$ (**6**) by adding a solution of



[*] Prof. Dr. A. L. Rheingold, B. S. Haggerty
Department of Chemistry, University of Delaware
Newark, DE 19716 (USA)
Dr. S. Trofimenko
Du Pont Company, Experimental Station 302/216
Wilmington, DE 19880-0302 (USA)
Telefax: Int. code +(302) 695-3817

 © VCH Verlagsgesellschaft mbH, D-69451 Weinheim, 1994 0570-0833/94/1919-1983 $ 10.00+.25/0

[$Tp^{Cy}Tl$] (**2**) in dichloromethane to a solution of $CuCl_2 \cdot 2H_2O$ in THF. Much to our surprise, we obtained a bright orange compound **4** instead of the expected chestnut-red crystals. The IR spectrum of **4** is quite different from that typical of the tetrahedral complexes [$Tp^{Cy}MCl$] (M = Co, Ni, Zn) isolated under the same conditions, and also from that of an authentic sample of **6** produced as the only product in the reaction of **2** with anhydrous $CuCl_2$ in dichloromethane. A BH stretch at 2538 cm^{-1} is observed in the IR spectrum of **4** (cf., 2488 cm^{-1} for **6**, and 2490 $\pm$ 3 cm^{-1} for $TpH^{Cy}MCl$, where M = Co, Ni, Zn). Although **4** is paramagnetic, its ^1H NMR spectrum shows the presence of a protonated nitrogen atom and two types of pyrazolyl groups in 2:1 ratio. Complex **4** was identified as [{(Tp^{Cy})H}$CuCl_2$]. This is the first instance of a scorpionate free acid, namely [(Tp^{Cy})H] (**3**), acting as ligand; its structure was established by X-ray crystallography.[13]

A plane of symmetry in the plane of the protonated pyrazolyl group is observed in the crystal structure of **4** (Fig. 1). The copper atom is coordinated to two 3-cyclohexylpyrazolyl groups and two chlorine atoms in a distorted tetrahedral configuration. The hydrogen atom of the protonated pyrazolyl group forms a hydrogen bond with the nearest chlorine atom (Cl2). The Cl2–H distance is short (2.18 Å), while the Cu–Cl2 bond (2.29 Å) is 0.1 Å longer than the Cu–Cl1 bond.

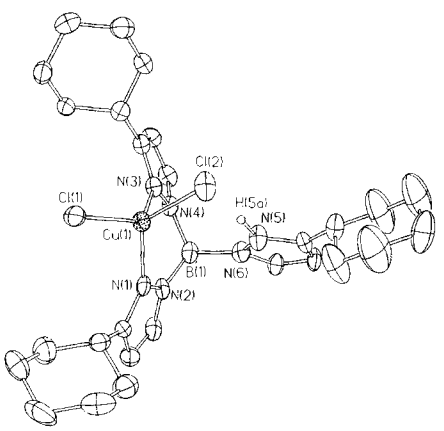


Fig. 1. ORTEP plot of the structure of **4** (ellipsoids at the 30% probability level). The hydrogen atoms, except H(5a), are omitted for clarity. Selected bond lengths [Å] and angles [°]: Cu(1)-Cl(1) 2.198(3), Cu(1)-Cl(2) 2.289(3), Cu(1)-N(1) 1.998(7), Cu(1)-N(3) 1.945(7), Cl(2)···H(5a) 2.184(9), N(5)-H(5a) 0.978(4); Cl(1)-Cu(1)-Cl(2) 104.4(1), Cl(1)-Cu(1)-N(1) 109.7(2), Cl(1)-Cu(1)-N(3) 127.7(2), Cl(2)-Cu(1)-N(1) 125.4(2), Cl(2)-Cu(1)-N(3) 95.6(2), N(1)-Cu(1)-N(3) 95.8(3), Cu(1)-Cl(2)···H(5a) 78.4(5), Cl(2)···H(5a)-N(5) 170.4(5).

Although **4** decomposes when chromatographed, it reacts cleanly with aqueous sodium hydrogencarbonate solution to yield the binuclear, deep emerald-green complex [($Tp^{Cy}Cu$)$_2$(μ-CO_3)]; the IR spectrum of **5** contains bands assigned to BH and CO at 2487 and 1584 cm^{-1}, respectively. The same binuclear complex is formed in the reaction of **6** with aqueous hydrogencarbonate solution; its structure was determined by X-ray crystallography.[14] In **5**, each Cu atom is bound to two oxygen atoms of the carbonato ligand and to three nitrogen atoms from the Tp^{Cy} ligand (Fig. 2). Two Cu–N bonds are marginally shorter than 2.0 Å and one is longer (2.25 Å). The structure is similar to that reported for [($Tp^{iPr2}Cu$)$_2$(CO_3)],[15] which was formed by reaction of [$Tp^{iPr2}Cu(OH)$] with CO_2; the Cu···Cu distance is slightly longer in **5** (4.058 versus 4.017 Å) because the steric bulk of the cyclohexyl group is somewhat greater than that of the isopropyl group. Incorporation of the cyclohexyl group thus causes a subtle change in the complex; this technique may assist in fine-tuning the various enzyme analogues that contain 3-isopropyl groups.

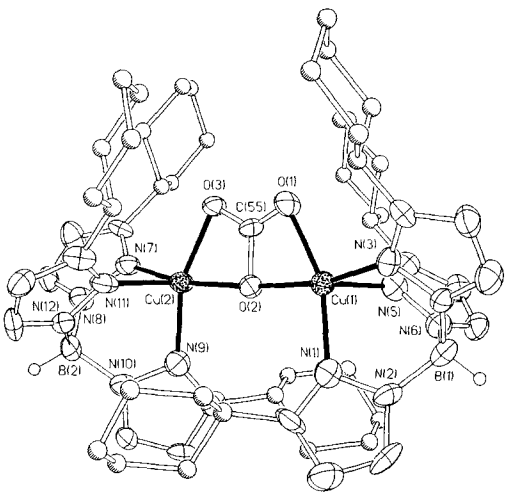


Fig. 2. ORTEP plot of the structure of **5** (ellipsoids at the 30% probability level). Only the atoms refined with anisotropic thermal parameters are shown as thermal ellipsoids. The hydrogen atoms, except those at B(1) and B(2), are omitted for clarity. Selected bond lengths [Å] and angles [°]: Cu(1)-O(1) 1.992, Cu(1)-O(2) 2.022, Cu(1)-N(1) 1.995, Cu(1)-N(3) 1.987, Cu(1)-N(5) 2.243, Cu(1)-C(55) 2.380, Cu(2)-O(2) 2.039, Cu(2)-O(3) 2.002, Cu(2)-N(7) 1.978, Cu(2)-N(9) 1.961, Cu(2)-N(11) 2.248, Cu(2)-C(55) 2.395, Cu(1)···Cu(2) 4.058; Cu(1)-N(1)-N(3) 92.0, Cu(1)-N(1)-N(5) 94.0, Cu(1)-N(5)-N(3) 85.7, Cu(1)-O(1)-N(1) 159.8, Cu(1)-O(1)-N(3) 102.3, Cu(1)-O(1)-N(5) 101.1, Cu(1)-O(2)-N(1) 98.1, Cu(1)-O(2)-N(3) 166.4, Cu(1)-O(2)-N(5) 102.5, Cu(1)-O(2)-O(1) 65.7, Cu(1)-O(1)-C(55) 31.7, Cu(1)-O(2)-C(55) 34.3, Cu(2)-N(9)-N(7) 91.0, Cu(2)-N(11)-N(7) 86.6, Cu(2)-N(9)-N(11) 95.4, Cu(2)-O(2)-N(7) 167.3, Cu(2)-O(2)-N(9) 97.7, Cu(2)-O(2)-N(11) 101.7, Cu(2)-O(3)-N(7) 103.9, Cu(2)-O(3)-N(9) 160.3, Cu(2)-O(3)-N(11) 98.3, Cu(2)-O(3)-O(2) 65.7, Cu(2)-C(55)-N(7) 135.4, Cu(2)-C(55)-N(9) 131.2, Cu(2)-C(55)-N(11) 100.6, Cu(2)-C855)-O(2) 34.0, Cu(2)-C(55)-O(3) 31.7.

We are unsure of the exact mechanism for the formation of **4** in this nonstoichiometric reaction and of the source of the proton, although it is likely to come from the water of hydration of $CuCl_2$. So far, the reaction of **2** with $CuCl_2$ in THF appears to be unique, since Co^{II}, Ni^{II}, and Zn^{II} chlorides produce only the expected [$Tp^{Cy}MCl$] complexes, as does anhydrous $CuCl_2$ in the absence of THF. Furthermore, the related ligand [$Tp^{iPr}Tl$] yielded, under the same conditions, only the expected $Tp^{iPr}CuCl$ complex, which can similarly be converted to the dinuclear complex [($Tp^{iPr}Cu$)$_2$(μ-CO_3)] with a CO band in the IR spectrum at 1600 cm^{-1}.

Experimental Procedure

1: Formylation of cyclohexyl methyl ketone with ethyl formate followed by reaction with hydrazine in a procedure similar to that used for preparing 3-isopropylpyrazole [9] yielded **1** as a viscous liquid in 64% yield: B.p. 150 °C/2.6 Torr; ^1H NMR: δ = 7.48 (d), 6.05 (d), 2.74 (tt), 2.03 (d), 1.80 (dt), 1.72 (d), 1.41 (sextet), 1.25 (m), signals in a ratio of 1:1:1:2:2:1:4:1; ^{13}C NMR: δ = 25.9 (4′-C), 26.1 (3′-C, 5′-C), 33.0 (2′-C, 6′-C), 36.0 (1′-C), 101.1 (4C), 134.9 (5C), 152.2 (3C).

2: A mixture of 3-cyclohexylpyrazole and KBH_4 (5:1) was heated until the theoretical amount of H_2 was given off. Excess 3-cyclohexylpyrazole was removed in vacuo. The crude product [$Tp^{Cy}K$] was then dissolved in dimethylformamide and converted to **2**: M.p. 142–143 °C; ^1H NMR: δ = 7.71 (d, broadened), 5.97 (d, even broader), 2.77 (m, very broad), 1.93 (s, broad), 1.81 (m), 1.74 (d), 1.40 (quin), 1.25 (tt), signals in a ratio of 1:1:1:2:2:1:4:1; ^{13}C NMR: δ = 26.1 (4′-C), 26.6 (3′-C, 5′-C), 34.2 (d, J = 51.4 Hz, 2′-C, 6′-C), 37.6 (d, J = 27 Hz, 1′-C), 100.9 (s, broad, 4C), 135.7 (s, somewhat broadened, 5C), 159.1 (d, J = 47 Hz, 3C).

4: A solution of **2** in CH_2Cl_2 was added to a rapidly stirred mixture of $CuCl_2 \cdot 2H_2O$ (in excess) in THF. After 30 min, the slurry was filtered through Celite, and the filtrate was evaporated. The dark brown residue was stirred with isopropyl alcohol, filtered, and washed with isopropyl alcohol. The bright orange solid [m.p. 156–158 °C (decomp.)] was recrystallized from CH_2Cl_2 (52% yield). IR: $\tilde{\nu}$(BH) = 2538 cm^{-1}; ^1H NMR: all peaks are broad, yet discernible: δ = 15.2 (NH), 8.30, 7.90 (pyrazolyl 5-H), 6.38, 6.28 (pyrazolyl 4-H), overlapping 2:1 patterns, 2.96 (H atom at the tertiary cyclohexyl C atom), 2.02, 1.84, 1.50, and 1.10 (4 × m, rest of the cyclohexyl protons).

5: A solution of **4** (or **6**) in CH_2Cl_2 was stirred with an aqueous solution of $NaHCO_3$. This resulted in a color change within seconds from orange to emerald green. The organic layer was separated and the solvent removed in vacuo. Green crystals of **5** were obtained in 76% yield: M.p. 200–202 °C (decomp.); IR: $\tilde{\nu}$(BH) = 2487, $\tilde{\nu}$(CO) = 1584 cm^{-1}.

6: A solution of **2** in CH_2Cl_2 was stirred with a large excess of anhydrous $CuCl_2$. After 20 min, the slurry was filtered through Celite, and the solvent was evaporated. A chestnut-red solid **6** was obtained in 82% yield: M.p. 156–158 °C; IR: $\tilde{\nu}$(BH) = 2488 cm^{-1}.

All the above compounds gave satisfactory elemental analyses.

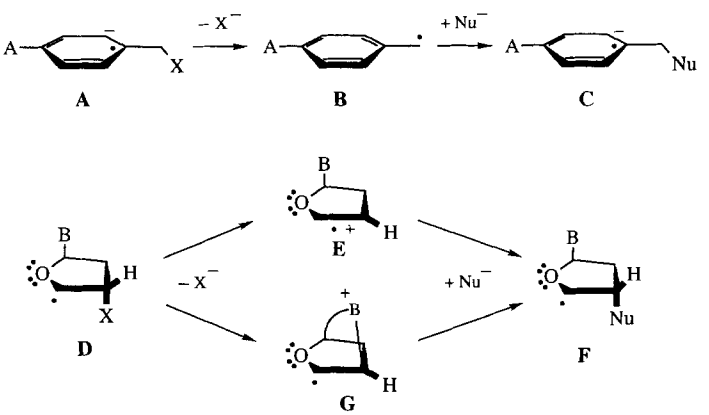
Received: April 19, 1994
Revised: June 15, 1994 [Z 6859 IE]
German version: *Angew. Chem.* **1994**, *106*, 2053

[1] S. Trofimenko, *Chem. Rev.* **1993**, *93*, 943–980.
[2] S. Trofimenko, *J. Am. Chem. Soc.* **1966**, *88*, 1842–1844.
[3] S. Trofimenko, *J. Am. Chem. Soc.* **1967**, *89*, 3170–3176.
[4] R. W. Thomas, G. W. Estes, R. C. Elder, E. Deutsch, *J. Am. Chem. Soc.* **1979**, *101*, 4581.
[5] J. A. Thomas, A. Davison, *Inorg. Chim. Acta* **1991**, *190*, 231–235.
[6] R. B. Ball, C. K. Ghosh, J. K. Hoyano, A. D. McMaster, W. A. G. Graham, *J. Chem. Soc. Chem. Commun.* **1989**, 341.
[7] a) S. Trofimenko, *J. Coord. Chem.* **1972**, *2*, 75–77; b) J. Bielawski, T. G. Hodges, W. J. Layton, K. Niedenzu, P. M. Niedenzu, S. Trofimenko, *Inorg. Chem.* **1986**, *25*, 87–90.
[8] The abbreviations for homoscorpionate ligands follow the system introduced in ref. [1].
[9] S. Trofimenko, J. C. Calabrese, P. J. Domaille, J. S. Thompson, *Inorg. Chem.* **1989**, *28*, 1091–1101.
[10] M. Cano, J. V. Heras, S. Trofimenko, A. Monge, E. Gutierrez, C. J. Jones, J. A. McCleverty, *J. Chem. Soc. Dalton Trans.* **1990**, 3577–3582.
[11] N. Kitajima, K. Fujisawa, C. Fujimoto, Y. Moro-oka, *Chem. Lett.* **1989**, 421–424.
[12] a) N. Kitajima, H. Fukui, Y. Moro-oka, Y. Mizutani, T. Kitagawa, *J. Am. Chem. Soc.* **1990**, *112*, 6402–6403; b) N. Kitajima, M. Osawa, M. Tanaka, Y. Moro-oka, *ibid.* **1991**, *113*, 8952–8953; c) N. Kitajima, K. Fujisawa, C. Fujimoto, Y. Moro-oka, S. Hashimoto, T. Kitagawa, K. Toriumi, K. Tatsumi, A. Nakamura, *ibid.* **1992**, *114*, 1277–1291, references therein; d) N. Kitajima, Y. Moro-oka, *Chem. Rev.* **1994**, *94*, 737–757.
[13] Crystallographic data for **4**: $(C_{27}H_{41}BCl_2CuN_6$, M_r = 594.9): monoclinic, space group Cc, a = 14.089(2), b = 18.574(3), c = 12.296(2) Å, β = 105.35(1)°, V = 3103.0(9) Å^3, Z = 4, ρ_{calcd} = 1.273 Mg/m^3, $\mu(Mo_{K\alpha})$ = 0.902 mm^{-1}. Data collected at 255 K with a Siemens P4 diffractometer ($Mo_{K\alpha}$ radiation, λ = 0.71073 Å, graphite monochromator, $2\theta_{max}$ = 48°); 2565 measured independent reflections, semi-empirical absorption correction applied to data set, T_{max}/T_{min} = 1.133, solution by direct methods with the Siemens SHELXTL-Plus (PC Version) program package [16]; E-statistics suggested the noncentrosymmetric alternative Cc, and the chemically sensible results of refinement indicated that this choice was correct; refinement of F^2 with all data with SHELXL-93 [17], $wR2$ = 0.1349 for all data ($w = 1/[\sigma^2(F_o^2) + (0.1000\,P)^2 + 0.0000\,P]$) with $P = (F_o^2 + 2F_c^2)/3$; the conventional R value for 2082 reflections with $I \geq 2\sigma(I)$ was 0.0471; all non-hydrogen atoms were refined with anisotropic thermal parameters, H atoms were included as idealized isotropic contributions (d(CH) = 0.960 Å, fixed U at 0.0800 Å^2) except for H(1) and H(5a) which were found and refined isotropically; refinement of a multiplicative term (η) for $\Delta f''$ indicates that the enantiomorph reported is correct [18].
[14] Crystallographic data for **5**: $(C_{58}H_{86}B_2Cu_2Cl_6N_{12}O_3$, M_r = 1360.8): monoclinic, space group $P2_1/n$, a = 16.619(8), b = 23.404(13), c = 17.605(6) Å, β = 90.43(3)°, V = 6861(7) Å^3, Z = 4, ρ_{calcd} = 1.317 Mg/m^3, $\mu(Mo_{K\alpha})$ = 0.903 mm^{-1}. Data collected at 254 K with a Siemens P4 diffractometer ($Mo_{K\alpha}$ radiation, λ = 0.71073 Å, graphite monochromator, $2\theta_{max}$ = 45°); 8939 measured independent reflections, no absorption correction applied to data set, solution by direct methods with the Siemens SHELXTL-Plus (PC Version) program package [16]; preliminary photographic characterization showed $2/m$ Laue symmetry, systematic absences in the diffraction data uniquely established the space group as $P2_1/n$; refinement of data with the SHELXTL-Plus program library; all non-hydrogen atoms except the cyclohexyl rings refined with anisotropic thermal parameters, H atoms were included as idealized isotropic contributions (d(CH) = 0.960 Å, fixed U at 0.0800 Å^2). Final R = 7.88% and wR = 8.31%. There are three molecules of dichloromethane in the unit cell [18].
[15] a) N. Kitajima, K. Fujisawa, T. Koda, S. Hikichi, Y. Moro-oka, *J. Chem. Soc. Chem. Commun.* **1990**, 1357–1358; b) N. Kitajima, S. Hikichi, M. Tanaka, Y. Moro-oka, *J. Am. Chem. Soc.* **1993**, *115*, 5496–5508.
[16] Siemens SHELXTL-Plus (PC Version) 4.21, Siemens Analytical X-ray Instruments, Madison, WI, **1990**.
[17] G. M. Sheldrick, SHELXTL-93, Program for Refinement of Crystal Structures, Göttingen, **1993**.
[18] Further details of the crystal structure investigation are available on request from the Director of the Cambridge Crystallographic Data Centre, 12 Union Road, GB-Cambridge CB2 1EZ (UK), on quoting the full journal citation.

The $S_{RN}2$ Pathway—A Mechanistic Alternative for Radicals in Polar Media?**

Hendrik Zipse*

The $S_{RN}1$ mechanism has been shown to provide an alternative pathway in reactions of benzylic and aromatic halides in which the direct S_N2 route is hindered by inefficient leaving groups.[1] The critical stages of the mechanism (Scheme 1, top) involve the formation of radical anion **A** by single electron transfer, heterolytic cleavage of the β C–X bond to yield the benzylic radical **B**, and subsequent addition of the nucleophile to form a new radical anion **C**. Electron transfer to another substrate molecule perpetuates the chain reaction. An isoelectronic variant of the $S_{RN}1$ mechanisms has been invoked recently to explain the product distribution found in reactions of DNA radicals.[2, 3] These can be formed under radiolytic conditions or in the presence of radical-forming reagents by hydrogen atom abstraction from the carbohydrate backbone. Ribofuranosyl radicals **D** have then been suggested to undergo β C–X bond cleavage to yield the radical cation **E**, which can be trapped by external nucleophiles to yield the product radicals **F** (Scheme 1, bottom). In both these cases a mechanistic alternative exists in the $S_{RN}2$ mechanism in which C–X bond cleavage occurs simul-



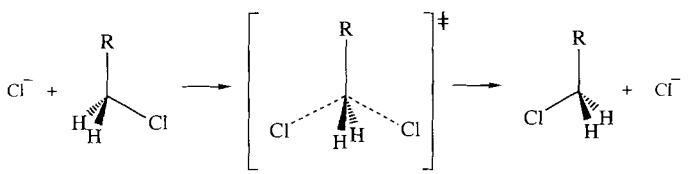
Scheme 1. Two examples of an $S_{RN}1$ mechanism. In the second case, alternative transition states are depicted. B = nucleotide base.

[*] Dr. H. Zipse
Institut für Organische Chemie der Technischen Universität
Strasse des 17. Juni 135, D-10623 Berlin (FRG)
Telefax: Int. code +(30)3142-1102

[**] This work was supported by the Fonds der Chemischen Industrie and the Zentraleinrichtung Rechenzentrum TU Berlin (computer time). Thanks are also due to Prof. B. Giese for detailed discussion and to Prof. H. Schwarz for generous support.

taneously with C–Nu bond formation. This bimolecular pathway has been ruled out for the classic benzyl halide system through experiments utilizing optically active substrates. However, an analogous strategy can not be used to elucidate the fate of radicals **D**, since the relative positions of reaction centers are fixed by the ribofuranosyl ring structure. Still, the $S_{RN}2$ mechanism is not unlikely for these systems because of the presence of internal nucleophiles (nucleotide bases) and high observed stereochemistry in trapping experiments.[3] These observations can well be rationalized by assuming initial C–X bond cleavage with nucleophilic assistance through the nucleotide base leading to a bridged radical cation **G**. Attack of external nucleophiles can reopen the ring structure to give product **F** with net retention of configuration at C3 of the ribofuranosyl ring system. Since DNA appears to be stable under nonradiolytic conditions, this mechanism requires the barrier for the open-shell system to be significantly lower than for the closed-shell system. This hypothesis, however, is not supported by what is known about α-substituent effects on S_N2 processes in closed-shell systems,[4, 5] in which cyano or benzyl substituents hardly affect the intrinsic activation barrier, and differences in observed rates can be traced back to differences in complexation energies between reactants. The question of intrinsic barrier heights for substitution reactions in open- and closed-shell systems is therefore also relevant from a fundamental point of view.

We have chosen the $Cl^- + RCH_2Cl$ system with $R = CH_3$ and $CH_2^\bullet$ as a model to investigate the variation of S_N2 barrier on formation of a radical in an adjacent position (Scheme 2).



a, $R = CH_3$; **b**, $R = CH_2^\bullet$

Scheme 2. The model system for the study of the $S_{RN}2$ mechanism.

The identity reaction offers the important benefit of not perturbing the variations in activation barriers by different exothermicities. Gas-phase reaction paths for the open- and closed-shell systems have been calculated at the ab initio MP2(FC)/6-31G* level (Fig. 1).[6, 7] The reaction coordinate r is defined as the difference in lengths of the forming and the breaking C–Cl bonds. This choice ensures a truly symmetrical reaction profile. It also facilitates comparison with the results obtained by Jorgensen et al. in their classic study of solvent effects on the nucleophilic substitution of methyl chloride with chloride anions.[8] The open- and closed-shell systems both form the expected ion–dipole complexes known from methyl transfer reactions (Fig. 2). This has also been found in a recent theoretical exam-

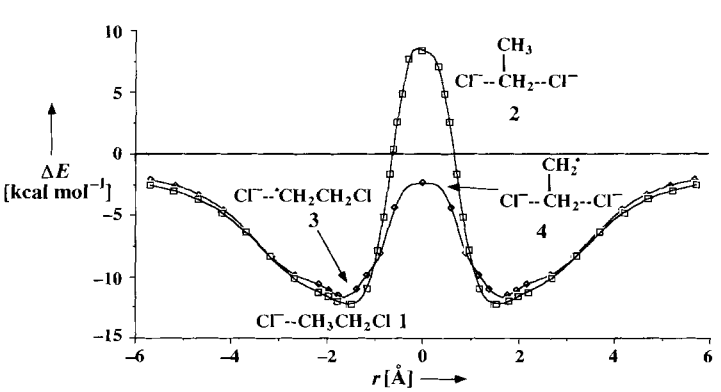


Fig. 1. Reaction paths for the S_N2 reaction of Cl^- + ethyl chloride (□) and the β-chloroethyl radical (○). Energies are given relative to separated reactants at the R/UMP2(FC)/6-31G* level of theory.

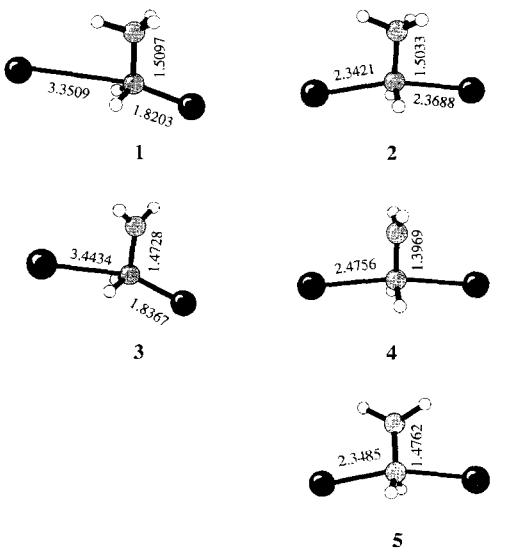


Fig. 2. Ion–dipole complexes and transition structures for the substitution reaction at ethyl chloride (**1**, **2**) and at the β-chloroethyl radical (**3**, **4**). (P)MP2(FC)/6-31G* optimized geometries are shown.

ination by Jensen.[9] The energy data for both systems have been collated in Table 1.[10] The complexation energy ΔE_c(MP2/6-31G*) is slightly larger for the closed-shell complex **1** (-12.3 kcal mol^{-1}) than for the open-shell analog **3** (-11.7 kcal mol^{-1}) or for the complex of methyl chloride and chloride anion (-10.3 kcal mol^{-1}).[8] This is probably due to favorable electrostatic attraction between the chloride ion and the CH_3 hydrogen atoms in **1**. Proceeding further along the reaction coordinate, the differences between the open- and closed-shell systems become much more drastic. The transition state for the closed-shell system **2** is located $+20.6$ kcal mol^{-1} above complex **1** and $+8.4$ kcal mol^{-1} above the separated reactants (ΔE_i and ΔE_a in Table 1). Transition structure **2** does not share the C_S symmetry of complex **1** since the methyl group rotation is not perfectly synchronized with the C–Cl bond breaking and making process.[9] A much smaller barrier is

Table 1. Complexation energies ΔE_c and activation barriers from separate reactants (ΔE_a) and from ion–dipole complexes (ΔE_i) in substitution reactions of between CH_3CH_2Cl or $^\bullet CH_2CH_2Cl$ and Cl^- [kcal mol^{-1}].

System and method	ΔE_c	ΔE_a	ΔE_i
$Cl^- + CH_3CH_2Cl$			
MP2(FC)/6-31G*//MP2(FC)/6-31G*	−12.3	+8.4	+20.6
ΔZPE(MP2(FC)/6-31G*)	+0.24	−0.53	−0.27
MP4(FC)/6-311 + G**//MP2(FC)/6-31G*	−11.6	+8.9	+20.5
$Cl^- + {}^\bullet CH_2CH_2Cl$			
PMP2(FC)/6-31G*//UMP2(FC)/6-31G*	−11.7	−2.4	+9.4
ΔZPE(UMP2(FC)/6-31G*)	+0.04	−0.26	−0.30
PMP4(FC)/6-311 + G**//UMP2(FC)/6-31G*	−10.8	−1.8	+9.0

 © VCH Verlagsgesellschaft mbH, D-69451 Weinheim, 1994 0570-0833/94/1919-1986 $ 10.00+.25/0

found in the open-shell system. Here, transition structure **4** is separated by $+9.4\ kcal\,mol^{-1}$ from complex **3** and by $-2.4\ kcal\,mol^{-1}$ from the separated reactants. The results are surprisingly insensitive to the level of theory; single point calculations at very modest (UHF/STO-3G) or much higher level (PMP4(SDTQ)/6-311 + G**) predict essentially the same picture. At the best theoretical level, the intrinsic barrier in the closed-shell system is higher by $\Delta\Delta E_i = +11.5\ kcal\,mol^{-1}$ than that of the open-shell system. The inclusion of differences in zero point vibrational energies (ΔZPE) has no influence on this result. Analysis of the MP2/6-31G* charges (CHELPG) shows that the presence of the radical center hardly affects the charge of the chloride ion. The chloride carries a negative charge of $-0.94e$ in closed-shell complex **1** and $-0.95e$ in open-shell complex **3**. These values are significantly reduced to -0.74 and -0.73 in the closed- and open-shell transition states **2** and **4**, respectively.

A theoretical investigation of ionic substitution reactions is necessarily incomplete without consideration of solvent effects.[8] This is especially true since it has been shown that the energy required to desolvate the reactants far exceeds the intrinsic gas-phase barrier. We have therefore used Monte Carlo (MC) fluid simulations to estimate the free energy of solvation changes along the reaction coordinate by the free energy perturbation method.[11, 12] On addition of the free energy of solvation and gas-phase potential energy contributions, the potential of mean force (pmf) curves for the closed- and open-shell system are obtained (Fig. 3). In the early stages of the reaction, desolvation of the approaching chloride anion appears to be slightly more advanced in the closed-shell system. The pmf curves for both systems almost coincide again, but around $|r| = 2.0$ where the gas-phase complexes are located. The pmf curves for both systems show no sign of complex formation. This is because the energy gained by attractive electrostatic interactions between the reactants is completely offset by the desolvation free energy. For $|r|$ values less than 1.0, the closed-shell pmf curve deviates increasingly from the open-shell curve. Both curves peak around $|r| = 0.0$: $\Delta E(\text{pmf}) = +22.4$ (open shell) and $+37.2\ kcal\,mol^{-1}$ (closed shell), relative to the value at $|r| = 5.7$. The barrier differences in solution would therefore be approximately $\Delta\Delta E(\text{pmf}) = +14.8\ kcal\,mol^{-1}$, which is 3.3 $kcal\,mol^{-1}$ more than in the gas-phase. Given the root mean square deviation for the free energy of solvation calculations of around $\pm 0.6\ kcal\,mol^{-1}$ for both curves, solvation clearly dominates the absolute barriers for substitution in solution, but hardly affects the relative barrier heights for the open- and closed-shell systems. Considering the similar chloride ion charges for both systems, this result had to be expected if chloride ion solvation/desolvation is the determining factor for the solution barrier.

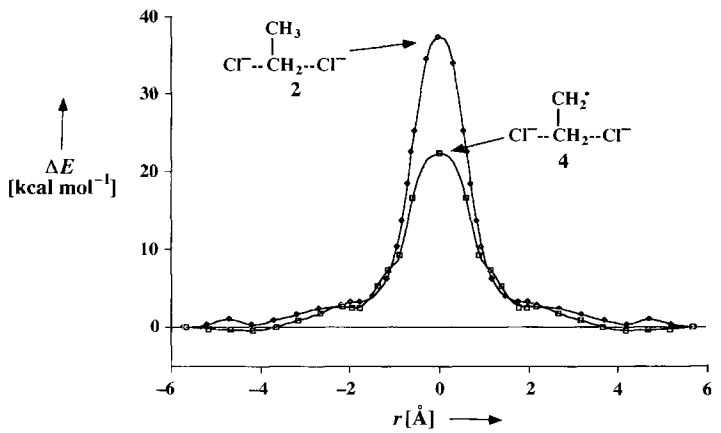


Fig. 3. Potential of mean force (pmf) in aqueous solution for the open- (□) and closed-shell (○) systems as a function of the reaction coordinate r.

The small differences in complexation energies ΔE_c in partial charge development and in solvation free energies convincingly rule out electrostatic effects as the source of differences in overall activation barriers between the open- and closed-shell systems. Steric effects can also be excluded, since open- and closed-shell species form ion–dipole complexes of similar strength. Also, the C–C bond connecting the reaction center with the substituent becomes shorter on going from the complex to the transition structure (Fig. 2), quite contrary to what would be expected if steric effects were a factor. This change is small for the closed-shell system ($\Delta R = -0.6$ pm), but large for the open-shell system ($\Delta R = 7.6$ pm). This bond length reduction indicates a stronger interaction between the CH_2 and Cl-C-Cl fragments in transition state **4** than in complex **3**. The magnitude of this increase can be estimated by the isodesmic reaction (a), in which the open- and closed-shell transition states are compared to methane and the methyl radical.

$$\text{TS (2)} + CH_3^{\cdot} \longrightarrow \text{TS (4)} + CH_4 \qquad \text{(a)}$$

With PMP2(FC)/6-31G*//UMP2(FC/6-31G* energies an energy difference ΔE of $-13.50\ kcal\,mol^{-1}$ is calculated. The Cl-C-Cl fragment in transition state **4** therefore stabilizes the radical center to a similar extent as benzyl or vinyl groups.[15] In complex **3**, the spin density is localized with coefficient 1.14 almost exclusively at the CH_2 carbon atom not involved in the reaction coordinate. All other centers have coefficients less than 0.1 (UHF/6-31G* values). In transition structure **4** the spin density is 0.85 at the methylene carbon atom and 0.18 at both chlorine atoms. Inspection of the molecular orbitals of transition structures **2** and **4** shows that the delocalization of spin density arises through mixing of the former radical SOMO (singly occupied molecular orbital) with the *lowest* of the three molecular orbitals building up the Cl-C-Cl fragment. Mixing of the SOMO with the second highest Cl-C-Cl molecular orbital is limited through the nodal characteristics of this MO. This finding also provides a rationale for the small effects α-nitrile substitution has on the S_N2 barrier, since stabilizing interactions with the lowest lying Cl-C-Cl fragment MO would then involve the π^*_{CN} orbitals, which have much higher orbital energies than the SOMO in the current case. The transition state stabilization by SOMO/NHOMO (NHOMO = next highest molecular orbital) interactions can also be estimated by calculation of the barrier for methylene group rotation in structure **4**. This strategy has been used before to estimate substituent effects for S_N2 reactions in model systems for closed-shell substitution reactions.[16] In the rotational transition structure **5** (see Fig. 2), no SOMO/NHOMO interactions are possible for geometric reasons. At the PMP2/6-31G*//UMP2/6-31G* level, the barrier for methylene group rotation in **4** is $+11.0\ kcal\,mol^{-1}$. This value is smaller than that derived from the isodesmic equation (a), but rather close to the difference in intrinsic barriers for the open- and closed-shell systems (PMP2/6-31G*: $+11.2\ kcal\,mol^{-1}$).

Since the barrier lowering for substitution reactions in open-shell systems has been predicted by theory, it is interesting to ask what further experimental evidence hints at $S_{RN}2$ reactions? The oligonucleotide radical studies by Giese et al. are closely related to DNA model studies by Murphy et al.[17] The authors noted

that, for the model system under study, only products from radical reactions are formed in systems lacking internal nucleophiles and only products from ionic reactions in otherwise similar systems that contain internal nucleophiles. In both cases the reactions were initiated by thermolysis of azobis(isobutylnitride) (AIBN). $S_{RN}1$ and $S_{RN}2$ reactions should also differ in their activation entropies. Because $S_{RN}2$ transition states are more ordered than the $S_{RN}1$ analogues, much more negative $\Delta S^{\neq}$ values (or smaller Arrhenius A factors) are expected for transition states with strong neighboring group participation. This has indeed been noted by Beckwith et al. for the acyloxy shift when highly substituted carbohydrate radicals are compared to smaller model systems lacking most of the sugar functionalities.[18] It thus appears that some experimental evidence justifies the assumption of $S_{RN}2$ pathways. The results of this theoretical study certainly encourage further exploration of the chemistry of radicals in polar media. This is, of course, most relevant to the study of radicals in biological environments.

Received: April 29, 1994 [Z 6882 IE]
German version: *Angew. Chem.* **1994**, *106*, 2019

[1] N. Kornblum, *Angew. Chem.* **1975**, *87*, 797; *Angew. Chem. Int. Ed. Engl.* **1975**, *14*, 734.
[2] a) C. von Sonntag, U. Hagen, A. Schön-Bopp, D. Schulte-Frohlinde, *Adv. Radiat. Biol.* **1981**, *9*, 109; b) B. Giese, J. Burger, T. W. Kang, C. Kesselbeim, T. Wittmer, *J. Am. Chem. Soc.* **1992**, *114*, 7322; c) K. C. Nicolaou, W.-M. Dai, *Angew. Chem.* **1991**, *103*, 1453; *Angew. Chem. Int. Ed. Engl.* **1991**, *30*, 1387.
[3] B. Giese, X. Beyrich-Graf, J. Burger, C. Kesselheim, M. Senn, T. Schäfer, *Angew. Chem.* **1993**, *105*, 1850; *Angew. Chem. Int. Ed. Engl.* **1993**, *32*, 1742.
[4] B. D. Wladkowski, J. L. Wilbur, J. I. Brauman, *J. Am. Chem. Soc.* **1994**, *116*, 2471.
[5] B. D. Wladkowski, K. L. Lim, W. D. Allen, J. I. Brauman, *J. Am. Chem. Soc.* **1992**, *114*, 9136.
[6] M. J. Frisch, M. Head-Gordon, G. W. Trucks, J. B. Foresman, H. B. Schlegel, K. Raghavachari, M. A. Robb, J. S. Binkley, C. Gonzalez, D. J. DeFrees, D. J. Fox, R. A. Whiteside, R. Seeger, C. F. Melius, J. Baker, R. L. Martin, L. R. Kahn, J. J. P. Stewart, S. Topiol, J. A. Pople, GAUSSIAN 92, Gaussian Inc., Pittsburgh, PA, **1992**.
[7] Geometry optimizations were performed at the RMP2(FC)/6-31G* level for the closed-shell system and at the UMP2(FC)/6-31G* level for the open-shell system (R = restricted, U = unrestricted, MP_n = *n*th order Møller-Plesset perturbation theory). MP2 energies given for the open-shell system are those obtained after spin projection of the lowest spin contaminant (PMP2). The $\langle S^2 \rangle$ values obtained after spin projection did not exceed 0.751. Single point energies have been calculated at the PMP4/6-311 + G** level of theory. The frozen core (FC) approximation has been used in all post-Hartree–Fock calculations.
[8] C. Jayaraman, S. F. Smith, W. L. Jorgensen, *J. Am. Chem. Soc.* **1985**, *107*, 154.
[9] F. Jensen, *Chem. Phys. Lett.* **1992**, *196*, 368.
[10] Absolute energies [Hartree] for stationary points at the (P)MP2(FC)/6-31G*//R/UMP2(FC)/6-31G*-Niveau: Cl^- −459.652104, CH_3CH_2Cl −538.524022, **1** −998.195648, **2** −998.162752, $^{\bullet}CH_2CH_2Cl$ −537.866621, **3** −997.537396, **4** −997.522474, **5** −997.504979, $CH_3^{\bullet}$ −39.670748, CH_4 −40.332553; at the (P)MP4(SDTQ,FC)/6-311 + G**//R/UMP2(FC)/6-31G* level: Cl^- −459.718163, CH_3CH_2Cl −538.683307, **1** −998.419914, **2** −998.387281, $^{\bullet}CH_2CH_2Cl$ −538.015310, **3** −997.750710, **4** −997.736351; zero point vibrational energies (R/UMP2(FC)/6-31G*): CH_3CH_2Cl 43.25, **1** 43.49, **2** 42.72, $^{\bullet}CH_2CH_2Cl$ 33.86, **3** 33.90, **4** 33.60, **5** 32.70.
[11] a) W. L. Jorgensen, *Acc. Chem. Res.* **1989**, *22*, 184; b) P. Kollman, *Chem. Rev.* **1993**, *93*, 2395.
[12] MC simulations employed a periodic box containing 396 TIP4P water molecules (TIP4P = transferable intermolecular potential, 4 point model) and one solute molecule. The solute was described by an all-atom model. Lennard-Jones potential parameters are identical to those employed in the $Cl^- + CH_3Cl$ study [8]. Coulomb parameters have been obtained by fitting the MP2/6-31G* electrostatic potential to point charges located at the atomic positions for a series of points along the reaction coordinate [13]. The free energy change for perturbation of one structure on the reaction coordinate to the next one was calculated by first equilibrating for 1×10^6 MC steps and then averaging for another 4×10^6 steps. All calculations have been performed with the BOSS program version 3.4 [14]. To cover the reaction path from $|r| = 0.0$ to $|r| = 5.7$, 25 steps were necessary in the open-shell system and 33 steps in the closed-shell system.
[13] C. M. Breneman, K. B. Wiberg, *J. Comput. Chem.* **1990**, *11*, 431.
[14] W. L. Jorgensen, BOSS, Version 3.4, Yale University, New Haven, CT, **1992**.
[15] D. J. Pasto, R. Krasnansky, C. Zercher, *J. Org. Chem.* **1987**, *52*, 3062.
[16] D. Kost, K. Aviram, *J. Am. Chem. Soc.* **1986**, *108*, 2006.
[17] A. P. Breen, J. A. Murphy, *J. Chem. Soc. Perkin Trans. 1* **1993**, 2979.
[18] A. L. J. Beckwith, P. J. Duggan, *J. Chem. Soc. Perkin Trans. 2* **1993**, 1673.

Corrigendum

In the communication "The Structures of Two Lithium Hydrazides: Is There Electron-Deficient Bonding?" by N. Metzler, H. Nöth, and H. Sachdev (*Angew. Chem. Int. Ed. Engl.* **1994**, *33*, 1746), the question was raised whether the compound $[t\mathrm{BuMe_2Si(Li)N-N(Li)SiMe_2}t\mathrm{Bu}]_3$ could be looked at as an electron-deficient compound. Although electron counting for this example would be compatible with a compound of the *arachno* type cluster, new examples of structures of compounds $[\mathrm{R(Li)N-N(Li)R}]_n$ and $[\mathrm{R(H)N-N(Li)NR}]_m$ (H. Nöth, H. Sachdev, M. Schmidt, and H. Schwenk, *Chem. Ber.* submitted; U. Klingebiel et al., *Proceedings VII. IRIS Conference*, Banff, **1994**) show that this is obviously an exception, and the coordination number greater or equal to 5 for the N atoms and greater or equal to 4 for the Li centers are due to the strongly polar contributions of the Li–N interactions.

 © VCH Verlagsgesellschaft mbH, D-69451 Weinheim, 1994 0570-0833/94/1919-1988 $ 10.00+.25/0

Pleasure in Principles

Principles of Electrochemistry. By *J. Koryta, J. Dvorák* and *L. Kavan*. Wiley, Chichester, 1993. 486 pp., paperback £ 24.95.—ISBN 0-471-93838-6
Electrochemistry. Principles, Methods, and Applications. By *C. M. A. Brett* and *A. M. O. Brett*. Oxford University Press, Oxford, 1993. 427 pp., paperback £ 25.00.—ISBN 0-19-855388-9

Electrochemistry has been transformed into an interdisciplinary science during the last few decades. It encompasses such widely different fields as the characterization of complex electrode processes, applications in synthesis, energy technology, and sensors, and the extensive areas of materials research and the biosciences. Publishers are therefore aiming to reach a wide readership by offering up-to-date textbooks at affordable prices. Two recent examples are the books reviewed here, which stress different aspects of the subject. *Principles of Electrochemistry*, written by three well-known authors of the Czech school, is mainly a survey of the thermodynamics of electrolyte solutions and electrode equilibria and of electrode kinetics. In contrast the second book, *Electrochemistry*, belongs to the tradition of the English-speaking school of textbooks, and emphasizes electrochemical methodology and applications in sensor technology.

This difference in emphasis of the two textbooks is easily seen from a summary of their contents. The book by Koryta et al. begins with an introduction to the theory of electrolytes, dealing with ion–solvent interactions, acid–base equilibria, polyelectrolytes and ampholytes, and the classical Debye–Hückel theory of interactions between ions. The second chapter discusses transport processes, with the main emphasis on the conductivity phenomena associated with ion migration. Chapter 3 contains an introduction to the thermodynamics of electrode equilibria. As well as explaining basic concepts such as electromotive force and the voltaic (electrochemical) and electric potentials, this chapter describes practical applications, including the determination of pH values and measurements of activity coefficients and dissociation constants. Chapter 4 briefly discusses the properties of the electrical double layer, including the classical Gouy–Chapman–Stern theory and the more recently developed "jelly" model.

The last two chapters are mainly devoted to modern developments in electrochemistry. As well as an introduction to electrode kinetics these chapters include brief descriptions of some important electrochemical methods. The recently developed ultramicroelectrode is mentioned, as also are in-situ methods that allow simultaneous measurements of spectroscopic data and electrical quantities. Other aspects touched on include homogeneous processes, electrocatalysis, deposition and separation of metals, and the broad field of bioelectrochemistry. Due attention is also given to the electrochemistry of conducting polymers.

Despite the inclusion of recent results such as these, a detailed study of the book leaves one with the impression that the view of electrochemistry presented here is that of the older generation of electrochemists, with a strong emphasis on thermodynamic principles. The reader wishing to approach the subject by this conventional route will find that the new third edition of "Koryta" is a reliable guide and tutor.

The Bretts' textbook begins with a description of the thermodynamics of electrochemical cells. This is followed in Chapter 2 by a discussion of the electrode/electrolyte boundary, introducing the theory of the electrical double layer. The kinetics of heterogeneous and homogeneous charge transfer and transport processes are then treated in concisely written chapters. The second, more extensive, part of the book consists of six chapters devoted to methods for investigating electrochemical processes. Modern measurement techniques, ranging from the widely used method of cyclic voltammetry to the various impedance methods, are treated at considerable length. Further chapters describe the many in-situ and ex-situ methods that have considerably extended the electrochemist's armory of experimental capabilities in recent years, such as the quartz microbalance and spectroscopic techniques.

In the third and last part of the book the authors describe modern applications of electrochemistry in basic research and in industry. Important topics include sensors based on ion-selective electrodes or amperometric detectors, modified electrodes, and corrosion phenomena. Bioelectrochemical phenomena are also discussed, as well as industrial processes such as electrosynthesis and metals deposition, and processes involving the conversion and storage of energy. Lastly there is an appendix containing some important mathematical relationships used for solving partial differential equations, diagrams of equivalent circuits, and basic principles of digital simulation methods. As in Koryta's book, a comprehensive bibliography is provided to enable the reader to study topics in greater depth.

With its emphasis on modern techniques of electrochemistry, the Bretts' book is certainly well suited to meet the wide-ranging needs of readers wishing to apply such methods in chemistry, physics, bioscience, and materials science. Despite the mathematical complexity of the theoretical concepts, the presentation is clear and understandable, enabling both beginners and interdisciplinary scientists to quickly build up a knowledge of methods relevant to their needs. They will be greatly helped in this by the practical advice about electrode materials, cell construction, and instrumentation.

To summarize, both these new paperbacks on electrochemistry offer sound and reliable introductions to this well-established field of physical chemistry. Readers who are mainly interested in the thermodynamic fundamentals, including the properties of electrolyte solutions,

This section contains book reviews and a list of new books received by the editor. Book reviews are written by invitation from the editor. Suggestions for books to be reviewed and for book reviewers are welcome. Publishers should send brochures or (better) books to Dr. Ralf Baumann, Redaktion Angewandte Chemie, Postfach 101161, D-69451 Weinheim, Federal Republic of Germany. The editor reserves the right of selecting which books will be reviewed. Uninvited books not chosen for review will not be returned.

 © *VCH Verlagsgesellschaft mbH, D-69451 Weinheim, 1994* *0570-0833/94/1919-1989 $ 10.00+.25/0*

should use the book by Koryta et al. For all those readers who wish to learn about the methods of electrochemistry and how to apply them, the book by Brett and Brett will prove a reliable guide.

Jürgen Heinze
Institut für Physikalische Chemie
der Universität Freiburg (FRG)

Organic Photochemistry. Principles and Applications. By *J. Kagan*. Academic Press, London, 1993. 234 pp., hardcover £ 40.00.—ISBN 0-12-394320-5

Anyone hoping to find here an up-to-date textbook of organic photochemistry will be disappointed. In the first place, this is not a book oriented towards teaching, as is already evident from the statement in the preface that "the order of topics... is totally arbitrary". Secondly, many important principles and applications of photochemistry have either been simply left out or have received inadequate treatment with an underemphasis that is difficult to understand. The author's comment that "old and well-established reactions and processes are described without references" is not a justification for neglecting a number of fundamental points. This apparently very subjectively-based book consists of two main parts, dealing with photochemical and photobiological aspects, respectively.

The first chapter introduces principles and mechanistic models of photochemical and photophysical processes; with only 25 pages it is too short. Some important principles, such as the first law of photochemistry, the Kasha rule, and the Franck–Condon principle, are mentioned but are not explained in the usual way. The mechanisms involved in the decay of electronically excited states are described in more detail, with a surprisingly large amount of space devoted to the quenching of photooxidation reactions. Chapter 2 gives a brief outline of experimental methods; only four literature references are given, two of which are useless. Thus the reader may safely skip over the first two chapters, if necessary referring instead to other standard textbooks. Chapters 3 and 4 give a rough idea of the photochemistry of the CC and CO double bonds. A few synthetic applications are described (limited to intramolecular reactions), and the di-π-methane rearrangement is mentioned. The mechanism given for this is probably incorrect; in any case, the work of H. Zimmerman is not discussed or even cited. On the other hand the author cites Doering's synthesis of bullvalene—not very consistent. Ten pages are devoted to the chemistry of the photoexcited carbonyl group; however, the Paternò–Büchi reaction receives less than a page. What is the reader supposed to make of a statement such as "Fortunately, the reaction is usually rather selective"? Chapter 5 on fragmentations describes some interesting and topical applications. The author puts a much greater emphasis on oxidation processes, which are discussed in Chapter 6, "Photochemistry with Oxygen". Unfortunately though, the description of the electronic states of molecular oxygen is limited to only four lines; here the interested reader will need to refer to the up-to-date reviews by Frimer and Ando. An appropriate amount of space is devoted to the generation, detection, and reactivity of singlet oxygen. The author also discusses the properties of other reactive species that can be generated photochemically, such as superoxide anion, atomic oxygen, S_2, and SO. Reference is also made to the possible biological activity of singlet oxygen, anticipating a topic treated in the second part of the book. In Chapter 7, on photoelectron transfer (PET) processes, the author manages to treat this subject without mentioning any of the names Marcus, Rehm, or Weller. Some up-to-date applications of PET processes in organic synthesis are described, giving some indication of the potential of this important class of reactions. For readers who already have a good knowledge of the repertoire of organic photochemistry, Chapter 8 on "Synthetic Applications" offers a wealth of information about interesting applications, from which they will pick up lots of useful ideas. However, it was not necessary to mention the synthesis of a triquinane by Cossy, Belotti, and Pete twice, first under δ,ε-unsaturated carbonyl compounds (8.14) then again under photochemical reductions (8.20).

In contrast to the above highly critical comments on the first part of the book, the second part, beginning with Chapter 9, can be emphatically recommended for the interested photochemist. Here the author's own research interests become dominant, and this improves the quality and the thoroughness of the discussions. The ways in which photochemistry interacts with biochemistry, biology, and medicine are well illustrated in Chapters 9–11 respectively, which describe important and highly topical developments in these fields. After an introduction to the photochemistry of amino acids and nucleic acids, the ways in which light radiation interacts with DNA are described (photochemically induced chain breaking, production of photoadducts, photoaffinity labeling, etc.). The important role of photooxidation processes in biochemical reactions is also mentioned and clearly explained. Under the heading "Photochemistry and Biology" the phototoxic effects of compounds which act as sensitizing agents are described. Those processes that can be described as "photochemistry without light" are also included in the discussion. There is also a very competent and informative discussion on light-induced changes to the human skin and their harmful consequences. Chapter 11 describes the medical applications of photochemical reactions that are continuing to grow in importance (PUVA therapy, photodynamic therapy, photosensitized inactivation of viruses). This and the preceding two chapters undoubtedly form the main strength of the book. It ends, in Chapter 12, with a brief outline of some applications of photochemical processes (more or less arbitrarily chosen). This rather personal foray into photochemistry by Kagan has certainly not turned out to be a student textbook or a work of reference; instead it is a wide-ranging and not very orderly collection of various aspects of organic photochemistry. Many readers interested in the subject will find it a source of useful ideas.

Axel G. Griesbeck
Institut für Organische Chemie
der Universität Würzburg (FRG)

Life During a Golden Age of Peptide Chemistry: The Concept and Development of Solid-Phase Peptide Synthesis. (Series: Profiles, Pathways, and Dreams. Series editor: *J. I. Seeman.*) By *B. Merrifield.* American Chemical Society, Washington, DC, 1993. XXI, 297 pp., hardcover $ 24.95.—ISBN 0-8412-1842-9

Bruce Merrifield's 1984 Nobel chemistry prize "for his development of methodology for chemical synthesis on a solid matrix" is unusual in that it was awarded for work conceived and singlehandedly achieved within 44 months. On May 26, 1959, Merrifield recorded the basic concept in his laboratory notebook (reproduced on p. 56): "There is a need for a rapid, quantitative, automatic method for synthesis of long chain peptides. A possible approach may be the use of chromatographic columns where the peptide is attached to the polymeric packing and added to by an activated amino acid, followed by removal of the protecting group and with repetition of the process until the desired peptide is built up.

 © VCH Verlagsgesellschaft mbH, D-69451 Weinheim, 1994 0570-0833/94/1919-1990 $ 10.00+.25/0

Finally the peptide must be removed from the supporting medium."

On January 31, 1963, he submitted to the *Journal of the American Chemical Society* his classic paper, "The Synthesis of a Tetrapeptide," which revolutionized peptide chemistry with his discovery of how to synthesize peptides in a "simpler, faster, more efficient way". Yet this unassuming, self-critical, and modest scientist says of this whirlwind tour de force: "When I look back at my old notebooks, I am amazed at how inefficient the early developmental work was. I seemed always to choose the wrong reaction to do first and was not able to identify the most important parameters as the work was progressing. At the end of the first two years the results were so poor, I wonder what made me think that this approach would ever succeed." (pp. 89–90).

He then reveals the secret of his success in research and simultaneously expresses his appreciation to his mentor and the institution to which he remained loyal throughout his career: "But from the outset I had a strong conviction that this was a good idea, and I am glad that I stayed with it long enough. I have always been grateful to Dr. Woolley for giving me the freedom in his laboratory to pursue the problem to the end and to the Rockefeller University for supporting me through a long nonproductive period." (p. 90).

Robert Bruce Merrifield was born on July 15, 1921, in Fort Worth, Texas, the only child of George Evan Merrifield, a furniture salesman, and Mittie Lorene Merrifield (née Lucas). The Great Depression forced his family to move frequently in search of work (he lived in 25 houses or apartments and had attended 11 schools by the time he started high school) and taught him the value of "steady, hard work and conservative approaches to problems" (p. 7). Raised primarily in California, he attended high school in Montebello, a small town east of Los Angeles, where he chose chemistry as a career as a result of an essay assignment on careers. He attended Pasadena Junior College for two years, followed by two years at the University of California, Los Angeles, from which he received his B. A. degree in 1943. He carried out routine work for a year at the Philip R. Park Research Foundation in San Pedro, California, but returned to UCLA for graduate work in biochemistry so that he could design his own experiments. Professor Max Dunn, with whom he had worked as an undergraduate, offered him a fellowship sponsored by the Anheuser Busch Company to develop ways to measure the purine and pyrimidine content of brewer's and baker's yeasts. While a teaching assistant in biochemistry, he met Elizabeth (Libby) Furlong, a biochemistry student who was to become his wife.

On June 19, 1949, Merrifield received his doctorate with a dissertation on microbiological assays of nucleic acid components; on June 20 he and Libby were married; and on June 21 they left for New York City. He had accepted a one-year postdoctoral appointment as research assistant to Dr. Dilworth Wayne Woolley at the Rockefeller Institute for Medical Research (since 1955 Rockefeller University), where he still works today. He considers Woolley "surely the most brilliant man I have known" and devotes almost an entire chapter to him. Merrifield became Associate Professor in 1957, Professor in 1966, and John D. Rockefeller, Jr. Professor in 1983.

Libby, who has been a close personal and professional partner in Merrifield's life, had received her master's degree in endocrinology at UCLA in 1947 and had completed all her examinations and requirements and almost all her doctoral research. However, upon her marriage she interrupted her studies, intending to return to them soon. The death of her Ph.D. supervisor and the rearing of six children (five girls and a boy) intervened. In 1980 she returned to the laboratory, collaborating with her husband on the synthesis of the antiviral protein interferon.

Merrifield's book is the longest volume to date in the "Profiles, Pathways, and Dreams" series, largely because of the detail with which he describes his work. After recounting his first published work on protein chemistry, coauthored with Woolley, which dealt with oxytocin, Merrifield presents his classic work on solid-phase peptide synthesis step-by-step, with page after page of day-to-day excerpts from his laboratory notebooks, including negative as well as positive experiments. To the best of our knowledge, no other author in this series makes such extensive use of primary experimental data. In so doing Merrifield provides the reader with a unique insight into the creative process as exemplified by the sequential thoughts of a master experimentalist. He also demonstrates the validity of his earlier statement: "the incidents that I recall the best are the negative experiences and the lessons I learned from them" (p. 10).

Through painstaking, meticulous research Merrifield determined the best conditions for his solid-phase peptide synthesis, and since his 1963 article appeared, thousands of peptides and other biological polymers, including carbohydrates and nucleic acids, have been synthesized using his method both by him and by others. In 1965, together with John Stewart, he automated the process, and today commercial models with microcomputer controls are available. In 1985 Richard A. Houghten, Jr. introduced the technique of using fine-mesh plastic bags ("tea bags") so that 10 to 50 or more peptides can be produced simultaneously. As many as 20.5 million different peptides can now be produced in a single synthesis. In related work Merrifield synthesized bradykinin (1963) and ribonuclease (1968), the latter being the first total synthesis of an enzyme.

Until 1969 Merrifield continued to work regularly at the laboratory bench, an activity that he truly enjoys, but he admits that "in recent years it has been very difficult to find a block of time large enough to be at all effective" (p. 97). Seemingly unaffected by receiving that "ne plus ultra" of the scientific life, the Nobel Prize, he sums up his career as follows: "I have lived my life by trying to make the best of what I have. I'm not a brilliant scientist who dashes into an area, hits the highlights, then dashes off to another. Rather, I am a conservative plodder. I like to focus on a subject that not too many are working on and stay with it until it's done, even if it doesn't seem to be working." (p. xxi).

We heartily recommend this autobiography of an extremely productive, hard-working, down-to-earth, family-oriented, and truly humble scientist to everyone interested in contemporary chemistry and the creative process.

George B. Kauffman,
Laurie M. Kauffman
California State University
Fresno, CA (USA)

Reactivity in Molecular Crystals. Edited by *Y. Ohashi.* VCH Verlagsgesellschaft, Weinheim/VCH Publishers, New York/Kodansha, Tokyo, 1993. 348 pp., hardcover DM 198.00, $ 130.00.—ISBN 3-527-29098-2/1-56081-857-3/4-06-206228-3

This book reports the results of a priority research project which was supported by the Japanese Ministry of Education, Science, and Culture in the period 1988–1990, and involved 34 scientists from the disciplines of physics, theoretical chemistry, crystallography, and organic chemistry. The considerable amount of new knowledge gained in this wide-ranging and fruitful area of fundamental physicochemical research is consolidated together

 © VCH Verlagsgesellschaft mbH, D-69451 Weinheim, 1994 0570-0833/94/1919-1991 $ 10.00+.25/0

here by the 38 Japanese authors named in the list of contents. It provides the reader with an overview of the present high standard of Japanese research in organic solid-state chemistry. On the other hand it also reveals which areas of research had not yet become established there, such as hole-burning, scanning tunneling microscopy, atomic force microscopy, small angle X-ray scattering, and gas–solid reactions. The arrangement of the contents in six chapters makes it easy to find one's way around the book, despite the scanty index in which only a few of the acronyms are explained. There is a noticeably high incidence of printing errors, but these do not affect the meaning.

Chapter 1 gives a useful survey of energy calculations for crystals. A new molecular dynamics method for predicting crystal packing patterns is also described and tested using benzene as an example. Chapter 2 reports significant new developments in fast time-resolved X-ray analysis. By applying high resolution electron spectroscopy to systems with high stability against electron-induced damage it is possible to obtain molecular-scale resolution, and one can study damage caused by electron bombardment. Organic films on graphite can be analyzed by Penning ionization electron spectroscopy, and CO adsorbates by time-resolved IR spectroscopy, while solid-state NMR spectroscopy is used to study the orientations of guest molecules in inclusion compounds. Polarized X-ray absorption fine structure analysis is used to study local asymmetric structures, while luminescence measurements can be used to detect energy transfer processes. Chapter 3 deals with "Crystalline-State Reactions", meaning very rare chemical reactions in which the crystals are retained with only very slight structural changes. Racemizations of cobaloximes and reversible intercalations in cholic acid crystals have been studied in detail by X-ray diffraction. In the photolysis of crystalline diazoalkanes and aryl azides it appears that the conditions for single-crystal to single-crystal reactions are only satisfied when the amounts converted are very small. Carbenes and nitrenes have been prepared at low temperatures with a view to possibly obtaining organic ferromagnetic materials. However, polycarbenes and polynitrenes which have long been known are not included here.

Chapter 4 contains a very useful summary of solid–solid reactions that have been investigated since 1987. Such reactions occur directly between powders when contacted with each other, without a solvent and (in most cases) without intermediate melting. Reactions that can occur in this way include rearrangements of pinacol, benzilic acid, and propargyl alcohol, Baeyer–Villiger oxidations, reductions using sodium borohydride, Grignard and Wittig reactions, oxidative couplings, dehydrations, etherifications, and the formation of host–guest complexes (sometimes enantioselectively). Also discussed incidentally in this chapter, although not falling within its main subject area, are some reactions of crystals with liquids and gases. However, solvents are excluded throughout.

The title of Chapter 5, "Stereoselective Solid-State Photoreaction", is surprising, since stereoselectivity is already well recognized as a property of innumerable photoreactions in crystals, such as four-center polymerizations of distyryl compounds, which are again included in this survey. Enantioselective syntheses can be carried out using clathrate crystals with a chiral host. Interestingly, dimerizations can occur despite the centers being separated by a distance of 7 to 10 Å. In the formation of ylides from photochromic heterocycles of the dihydropyridine type the question of stereoselectivity does *not* arise, and photoracemizations are certainly *not* stereoselective reactions.

The last chapter is again concerned with the relationship between crystal structure and reactivity. The polymerization efficiency of diethynylbenzenes is interpreted on the basis of purely static crystal structure considerations. In tunneling reactions of hydrogen or deuterium atoms with solid HD at 4.2 K and 1.9 K or with (apparently) glassy alkenes at 77 K, very large isotope effects were found, with selective formation of free radicals. Bimolecular Langmuir–Blodgett films are described in greater detail elsewhere. The crystal structures of complex sulfur heterocycles and the absolute configurations of chiral sulfoxides provide a starting point for research on new materials. Double macrocyclic inclusion complexes (cyclodextrin/crown-ether/metal ion or cyclodextrin/ferrocene) further extend the possibilities for molecular recognition with interesting crystal structures.

Not all the results from the project led to immediate practical applications, but many will be used for practical purposes in the near future. The book contains impressive evidence of fields in which Japanese solid-state research is ahead of that in the USA and Europe, and in particular shows that Japanese work will soon overtake that in Germany (in those areas where it still continues) unless the science ministries and regional parliaments of all the federal states quickly remove the legal obstacles to promoting first-class research projects in the universities.

Appearing as it does at the beginning of 1994, the book is two years too late, and is already outdated in many respects. Nevertheless, materials scientists will buy it as a useful reference source. During the next few years synthetic chemists, stereochemists, and crystallographers will expect it to be made available in their departmental libraries and will use it alongside more up-to-date sources.

Gerd Kaupp
FB 9—Organische Chemie I
der Universität Oldenburg (FRG)

Modern NMR Spectroscopy. 2nd Edition. By *J. K. M. Sanders* and *B. K. Hunter*. Oxford University Press, Oxford, 1993. 314 pp., paperback £ 23.50.—ISBN 0-19-855567-9

This book, whose first edition appeared in 1988, is intended for those chemists or NMR spectrometer users who do not have nor wish to acquire a deep understanding of NMR spectroscopy at a physical level, but who nevertheless want to be able to extract the maximum information from NMR spectra, mainly of liquid samples, using a few dozen routinely feasible techniques.

It consists of nine chapters, each of which begins by explaining the principles of the spectroscopic methods concerned using the classical vector formalism for the macroscopic magnetization. These explanations are excellently presented from a learning standpoint. Nevertheless, one cannot of course escape the inherent limitations of the vector representation, which is unable to give a satisfactory explanation of such important methods as the determination of pulses in the decoupler channel, which is essential for successful heteronuclear measurements, or multiple quantum spectroscopy. In each chapter an explanation of the basic principles is followed by a wealth of examples of applications in organic and organometallic chemistry, e.g. to steroids, alkaloids, oligosaccharides, rhodium carbonyls, vanadates, tin compounds, alkyllithium compounds, etc.

Chapter 1 is concerned with the basic one-dimensional single pulse experiment. Continuous wave (CW) spectroscopy is not discussed since it is nowadays obsolete. Basic concepts such as the rotating frame, the free induction decay (FID), digitization and its relationship to resolu-

tion, zero-filling, and dynamic range are explained. Here the authors are to be commended for aiming at consistency in the language used, at least within this book. In particular they point out a few misleading terms that have been adopted into NMR jargon but could cause problems for novices. Chapter 2 explains the concept of difference spectroscopy, with the main emphasis on homonuclear decoupling experiments. This chapter is very brief in accordance with the now minor importance of this method. Chapter 3, headed "Multiple-pulse Experiments", introduces the effects obtained with pulses of 180° (echoes, inversion) and 90° (polarization transfer, INEPT). However, whereas the vector formalism gives a simple and clear description of the effects of 180° pulses in coupled spin systems, the application to 90° pulses is considerably more difficult. These discussions are followed by useful hints for the operator on such matters as the calibration of pulses. Chapter 4 introduces two-dimensional NMR spectroscopy. Basic pulse sequences for identifying correlations due to scalar coupling through bonds are described (COSY, HMQC, INADEQUATE, TOCSY, etc.). Several pages are devoted to practical advice on matters such as spectral width and resolution in the newly added frequency dimension, phase cycles, field homogeneity, and apodization. However, as the instrument manufacturers use so many different programming languages the authors have not included actual pulse programs. Chapter 5 discusses strategies for molecular structure determination by correlation spectroscopy (COSY, H,C-COSY, INADEQUATE). The information yielded by such spectra is illustrated for both organic and inorganic molecules, some of which are quite complex. Chapter 6 is devoted to the use of cross-relaxation spectroscopy for obtaining qualitative and quantitative information about the local environments of nuclei. Here the nuclear Overhauser effect (NOE) is introduced and the most important measurement techniques are described (saturation-NOE, truncated NOE, and NOESY). Multiple spin effects and heteronuclear NOE measurements are discussed with suitable examples. The practical advice that is given, especially regarding the choice of mixing time and delay time in the NOESY experiment, will be very useful for the novice spectroscopist. Chapter 7 addresses the third basic type of interaction encountered in high-resolution NMR spectroscopy, chemical exchange. The nature of the spectra obtained for the cases of fast, medium, and slow exchange on the NMR time scale is described in a clear didactic way. The examples discussed range from tautomerism in organic compounds to fluxional exchange in inorganic complexes and to biochemical problems concerned with the binding of ligands to macromolecules. Chapter 8 is entitled "Editing". Here the word is used with a much wider meaning than usual, to include all the special techniques associated with modern pulse sequences, such as saturation of the water signal, heteronuclear decoupling, selective excitation using shaped pulses, and multiplicity editing. The last chapter briefly surveys the NMR spectroscopy of solids, introducing those interactions that are averaged out in high-resolution NMR spectroscopy of liquids, such as the dipolar coupling and the chemical shift anisotropy. The magic angle spinning (MAS) technique for averaging out tensor interactions and the cross-polarization technique for signal enhancement are described with examples. The discussion of 2D spectroscopy is limited to chemical shift correlations. This part of the book covers only the bare essentials, omitting important highlights of recent years such as the use of 2D spectra for directly studying dynamics in solids, and exact measurements of internuclear distances, e.g. between ^{13}C nuclei in a ligand bound to a protein within a solid membrane. The appendix summarizes the types of information obtainable by the different spectroscopic techniques, taking sucrose octaacetate as an example. This summary is very useful.

The book is written in a very readable style. Most of the figures are placed in the margins so that they do not interrupt the flow of the text, but at the same time are in a prominent position. Color has been used where it adds to the information content, e.g. in showing COSY spectra. The book gives an excellent survey of the most important NMR techniques and makes them accessible to a broad readership. However, in some places the authors' evaluation of the relative importance of particular methods differs from mine. For example, I feel that the 2D*J* technique is treated too prominently by being given five pages. On the other hand the heteronuclear techniques with proton detection (HMQC, HMBC, HSQC) are treated rather too briefly. Thus the HMBC method, which is an indispensable source of information on connectivity, especially for organic molecules, appears only as "HMQC tuned for long-range couplings", whereas the INADEQUATE technique, which is useless in most cases owing to low sensitivity, is nevertheless given several pages and some examples. The authors' verdict on ROESY that "This technique is far from straightforward and is not recommended for general use" also conflicts with my view. ROESY pulse programs are now available which work routinely without problems, often giving spectra of much better quality than those from NOESY.

To summarize, I strongly recommend this book for advanced undergraduate students and for research chemists who wish to gain maximum benefit from NMR spectroscopy in their preparative work and, where they have the opportunity, to make the best possible hands-on use of the capabilities of an NMR spectrometer. The many practical hints on performing NMR experiments will enable them to achieve that.

Christian Griesinger
Institut für Organische Chemie
der Universität Frankfurt
am Main (FRG)

New Books

Enzymes in Synthetic Organic Chemistry. By **C. H. Wong, G. M. Whitesides.** Elsevier Science Ltd., Oxford, **1994.** 370 pp., paperback, £ 25.00.—ISBN 0-08-035941-8

Macro-ion Characterization. From Dilute Solutions to Complex Fluids. Edited by **K. S. Schmitz.** American Chemical Society, Washington, **1994.** 547 pp., hardcover, $ 129.95.– ISBN 0-8412-2770-5

PCR. Grundlagen und Anwendungen der Polymerase-Kettenreaktion. Edited by **H. G. Grassen, G. E. Sachse, A. Schulte.** Gustav Fischer Verlag, Stuttgart, **1994.** 123 pp., ring binder, DM 38.00.—ISBN 3-437-20509-9

Analytikum. Methoden der analytischen Chemie und ihre theoretischen Grundlagen. Edited by **K. Doerffel, R. Geyer, H. Müller.** Deutscher Verlag für Grundstoffindustrie, Leipzig, **1994.** 643 pp., hardcover, DM 98.00.—ISBN 3-342-00644-7

Scent and Fragrances. The Fascination of Odors and their Chemical Perspectives. By **G. Ohloff.** Springer, Berlin, **1994.** 238 pp., DM 128.00.—ISBN 3-540-57108-6

Algebraic Approach to Simple Quantum Systems. With Applications to Perturbation Theory. By **B. G. Adams.** Springer, Berlin, **1994.** 451 pp., paperback, DM 68.00.—ISBN 3-540-57801-3

Nachrichten aus dem Elfenbeinturm. By **J. Lindenmann.** GIT Verlag, Darmstadt, **1993.** 176 pp., hardcover, DM 68.00.—ISBN 3-928856-11-0

Catalytic Hydroprocessing of Petroleum and Distillates. Edited by **M. C. Oballa, S. S. Shih.** Marcel Dekker, New York, **1994.** 480 pp., hardcover, $ 165.00.—ISBN 0-8247-9255-6

Phytochemical Dictionary of the Leguminosae. By **ILDIS, CHCD.** Chapman & Hall, London, **1994.** 1800 pp., hardcover, £ 595.00.—ISBN 0-412-39770-6

Disorder Effects on Relaxational Processes. Glasses, Polymers, Proteins. Edited by **R. Richert, A. Blumen.** Springer, Berlin, **1994.** 754 pp., hardcover, DM 348.00.—ISBN 3-540-57327-5

Macromolecular Complexes in Chemistry and Biology. Edited by **P. Dubin, J. Bock, R. M. Davis.** Springer, Berlin, **1994.** 360 pp., hardcover, DM 148.00.—ISBN 3-540-57166-3

Solvent Extraction in Biotechnology. Recovery of Primary and Secondary Metabolites. By **K. Schügerl.** Springer, Berlin, **1994.** 213 pp., hardcover, DM 168.00.—ISBN 3-540-57694-0

Ordering in Macromolecular Systems. Edited by **A. Teramoto, M. Kobayashi, T. Norisuye.** Springer, Berlin, **1994.** 353 pp., hardcover, DM 198.00.—ISBN 3-540-57817-X

Electrochemistry. Edited by **E. Steckhan.** Springer, Berlin, **1994.** 237 pp., hardcover, DM 168.00.—ISBN 3-540-57729-7

Fractals in Science. Edited by **A. Bunde, S. Havlin.** Springer, Berlin, **1994.** 298 pp., hardcover, DM 94.00.—ISBN 3-540-56221-4 (Macintosh Version)/ ISBN 3-540-56220-6 (MS-DOS Version)

Electrochemistry in Organic Synthesis. By **J. Volke, F. Liska.** Springer, Berlin, **1994.** 153 pp., hardcover, DM 98.00.—ISBN 3-540-57533-2

Atoms in Molecules. A Quantum Theory. By **R. F. W. Bader.** Oxford University Press, Oxford, **1994.** 456 pp., paperback, £ 25.00.—ISBN 0-19-855865-1

Environmental Chemistry of Soils. By **M. B. McBride.** Oxford University Press, Oxford, **1994.** 352 pp., hardcover, £ 35.00.—ISBN 0-19-507011-9

TYPIX - Standardized Data and Crystal Chemical Characterization of Inorganic Structure Types, Vol. 1. By **E. Parthe, L. Gelato, B. Chabot, M. Penzo, K. Cenzual, R. Gladyshevskii.** Springer, Berlin, **1993.** 260 pp., hardcover, DM 1200.00.—ISBN 3-540-93682-3

TYPIX - Standardized Data and Crystal Chemical Characterization of Inorganic Structure Types, Vol. 2. By **E. Parthe, L. Gelato, B. Chabot, M. Penzo, K. Cenzual, R. Gladyshevskii.** Springer, Berlin, **1993.** 408 pp., hardcover, DM 1300.00.—ISBN 3-540-93683-1

TYPIX - Standardized Data and Crystal Chemical Characterization of Inorganic Structure Types, Vol. 3. By **E. Parthe, L. Gelato, B. Chabot, M. Penzo, K. Cenzual, R. Gladyshevskii.** Springer, Berlin, **1994.** 512 pp., hardcover, DM 1150.00.—ISBN 3-540-93684-X

TYPIX - Standardized Data and Crystal Chemical Characterization of Inorganic Structure Types, Vol. 4. By **E. Parthe, L. Gelato, B. Chabot, M. Penzo, K. Cenzual, R. Gladyshevskii.** Springer, Berlin, **1994.** 416 pp., hardcover, DM 1150.00.—ISBN 3-540-93685-8

Isoquinoline Alkaloids. By **A. U. Rahman.** Elsevier, Amsterdam, **1994.** 782 pp., hardcover, $ 428.50.—ISBN 0-444-81888-X

The Lipid Handbook. Second Edition. Edited by **F. D. Gunstone, J. L. Harwood, F. B. Padley.** Chapman & Hall, London, **1994.** 1200 pp., hardcover, £ 255.00. ISBN 0-412-43320-6

Firmenhandbuch Chemische Industrie 1994/95. Bundesrepublik Deutschland. Edited by **Verband der Chemischen Industrie.** ECON Verlag, Düsseldorf, **1994.** 552 pp., hardcover, DM 168.00.—ISBN 3-430-12767-X

Liquid Crystals. Topics in Physical Chemistry, Vol. 3. Edited by **H. Stegemeyer, H. Baumgärtel, E. U. Franck, W. Grünbein.** Steinkopff, Darmstadt, **1994.** 250 pp., hardcover, DM 64.00.—ISBN 3-7985-0924-7

Oligosaccharide, Proteine und Glykoproteine in Frauenmilch und im Urin von Frühgeborenen. Analytische, strukturelle und funktionelle Aspekte. By **C. Kunz.** Thieme, Stuttgart, **1994.** 172 pp., hardcover, DM 58.00.—ISBN 3-13-138401-8

C8-C14. 8th edition. Edited by **U. Nohl, G. Olbrich.** Springer, Berlin, **1993.** 270 pp., hardcover, DM 1410.00.—ISBN 3-540-93678-5

C15-C21.5. 8th edition. Edited by **U. Nohl, G. Olbrich.** Springer, Berlin, **1994.** 273 pp., hardcover, DM 1450.00.—ISBN 3-540-93687-4

C22-C36.7. 8th edition. Edited by **U. Nohl, G. Olbrich.** Springer, Berlin, **1994.** 264 pp., hardcover, DM 1400.00.—ISBN 3-540-93688-2

Organic Syntheses Based on Name Reactions and Unnamed Reactions. By **A. Hassner & C. Stumer.** Elsevier, Oxford, **1994.** 452 pp., paperback, £ 28.00.—ISBN 0-08-040279-8

Solution Calorimetry. Edited by **K. N. Marsh, P. A. G. O'Hare.** Blackwell Scientific Publications, Oxford, **1994.** 331 pp., hardcover, £ 69.50.—ISBN 0-86542-852-2

The Organic Chemistry of Aliphatic Nitrogen Compounds. (International Series of Monographs on Chemistry - 28). By **B. R. Brown.** Oxford University Press, Oxford, **1994.** 767 pp., hardcover, £ 145.00.—ISBN 0-19-855783-3

Anticancer Drugs from Animals, Plants, and Microorganisms. By **G. R. Pettit, F. H. Pierson, C. L. Herald.** Wiley, Chichester, Great Britain, **1994.** 670 pp., hardcover, £ 78.00.—ISBN 0471-03657-9

Oscillations, Waves, and Chaos in Chemical Kinetics. By **S. K. Scott.** Oxford University Press, Oxford, **1994.** 90 pp., paperback, £ 4.99.—ISBN 0-19-855844-9

Synthetic Diamond. Emerging CVD Science and Technology. Edited by **K. E. Spear, J. P. Dismukes.** Wiley, Chichester, Great Britain, **1994.** 663 pp., hardcover, £ 74.00.—ISBN 0-471-53589-3

Handbook of Cosmetic and Personal Care Additives. Edited by **M. Ash, I. Ash.** Gover, Hampshire, Great Britain, **1994.** 969 pp., hardcover, £ 125.00.—ISBN 0-566-07470-2

Correlations, Transformations, and Interactions in Organic Crystal Chemistry. Edited by **D. W. Jones, A. Katrusiak.** Oxford University Press, Oxford, **1994.** 325 pp., hardcover, £ 50.00.—ISBN 0-19-855826-0

Microscale Organic Laboratory, 3rd Ed. By **D. W. Mayo, R. M. Pike, P. K. Trumper.** Wiley, Chichester, Great Britain, **1994.** 764 pp., hardcover, £ 36.50.—ISBN 0-471-57505-4

Handbook of Electron Spin Resonance. Data Sources, Computer Technology, Relaxation, and ENDOR. Edited by **C. P. Poole, Jr., H. A. Farach.** Oxford University Press, Oxford, **1994.** 660 pp., hardcover, £ 75.00.—ISBN 1.56396-044-3

Thermal Hazards of Chemical Reactions. (Industrial Safety Series, Vol. 4). By **T. Grewer.** Elsevier, Amsterdam, **1994.** 407 pp., hardcover, Dfl 380.00.—ISBN 0-444-89722-4

Grundkurs Chemie I, 2nd Ed. By **A. Arni.** VCH, Weinheim, **1994.** 354 pp., hardcover, DM 48.00.—ISBN 3-527-29230-6

Two-Dimensional NMR-Spectroscopy. Edited by **W. R. Croasmun, R. M. Carlson.** VCH, New York, **1994.** 550 pp., hardcover, DM 199.00/$ 125.00.—ISBN 1-56081-664-3

Chemische Kabinettstücke. By **H. W. Roesky, K. Möckel.** VCH, Weinheim, **1994.** 314 pp., hardcover, DM 68.00.—ISBN 3-527-29220-9

Grenzflächen- und Kolloidchemie. By **H.-D. Dörfler.** VCH, Weinheim, **1994.** 600 pp., softcover, DM 68.00.—ISBN 3-527-29072-9

Encyclopedia of Applied Physics. (Inductors to Magnetic Devices, Vol. 8). Edited by **G. L. Trigg.** VCH, Weinheim/New York, **1994.** 611 pp., hardcover, DM 430.00/ $ 295.00 (subscription price: DM 350.00/$ 235.00).—ISBN 3-527-26841-3/1-56081-067-X

Spectroscopic Techniques for Food Analysis. Edited by **R. H. Wilson.** VCH, New York, **1994.** 246 pp., hardcover, DM 165.00/$ 95.00.—ISBN 1-56081-037-8

Theoretische Optik. By **H. Römer.** VCH, Weinheim, **1994.** 270 pp., paperback, DM 58.00.—ISBN 3-527-29066-4

Chemistry of Nonaqueous Solutions. Current Progress. Edited by **G. Mamantov, A. I. Popov.** VCH, New York, **1994.** 377 pp., hardcover, DM 215.00/$ 125.00.—ISBN 1-56081-546-9

The Adventure Playground of Mechanisms and Novel Reactions. (Profiles, Pathways, and Dreams). By **R. Huisgen.** American Chemical Society, Washington, **1994.** 279 pp., hardcover, $ 24.95.—ISBN 0-8412-1832-3

Toxikologie für Chemiker. Stoffe, Mechanismen, Prüfverfahren. By **G. Eisenbrand, M. Metzler.** Thieme, Stuttgart, **1994.** 320 pp., paperback, DM 49.80.—ISBN 3-13-127001-2

A New Dimension to Quantum Chemistry. Analytic Derivative Methods in Ab initio Molecular Electronic Structure Theory. By **Y. Yamaguchi, Y. Osamura, J. D. Goddard, H. F. Schaefer III.** Oxford University Press, Oxford, **1994.** 471 pp., hardcover, £ 60.00.—ISBN 0-19-507028-3

Designing the Molecular World. Chemistry at the Frontier. By **Philip Ball.** Princeton University Press, Princeton, **1994.** 376 pp., hardcover, $ 29.95.—ISBN 0-691-00058-1

The Photochemical Synthesis of Fine Chemicals with Sunlight

Peter Esser, Bettina Pohlmann, and Hans-Dieter Scharf*

Dedicated to the memory of Klaus Gollnick

The light of the sun can be used directly for changing chemical structures photochemically. Any industrial application must conform to the limitations imposed by the spectral distribution of the photons from the sun, the interruptions to the radiation due to the day/night rhythm, and the weather. In this review, we describe the photochemical potential of the sun, give a fundamental treatment of the concept of photoreactors driven by sunlight (abbreviated to solar photoreactors), and give an account of the realization of this concept in the first pilot plant on the "Plataforma Solar de Almeria" in southern Spain and in other activities in this field. Based on experimental data from photochemical investigations on the pilot plant scale, possibilities, limitations, and the potential growth of solar photochemistry are described. Solar photochemistry, in our opinion, is a technique which could make a contribution to the chemistry of the future because of its photochemical synthesis potential, the avoidance of waste products, and the direct utilization of the sun, not only as a primary energy source, but also as a reaction partner.

1. Introduction

In photoreactions, in which the electronic excitation of a starting material is followed by chemical reaction, light must be regarded as a chemical reagent. The light must not only fulfill a particular quality requirement, namely that its wavelength must be able to be absorbed by the starting material, but, for single quantum processes, it must also be available in molar quantities. The efficiency of a photochemical reaction, the quantum yield, is the ratio of the amount of product in moles to the amount of absorbed radiation, measured in photons (1 Einstein = 1 mol photons). In photocatalytic chain reactions, the quantum yield can be considerably greater than 1. In the following article, interest is centered on so-called single quantum processes, that is, reactions with quantum yields less than or equal to 1. For this, it is necessary to provide the reagent photons quantitatively. Light, as a reagent, is remarkably reactive and selective. It can produce structural changes that either cannot be achieved by using ground state reactions or would require multistage processes. Photochemistry is in a position to make economically and ecologically valuable contributions to the synthesis of highly specialized products.

The normal route to artificial light starts from chemical energy (usually from coal and oil) or nuclear energy, which is changed first into electrical energy and then into light. The overall efficiency for this is at best only 9%. The use of fossil fuels leads to high emissions of carbon dioxide, and with nuclear energy the disposal of the used nuclear fuel and redundant equipment poses problems.

The utilization of solar photons provides an alternative. Here, a "renewable primary energy" can be directly linked to a chemical production process. The supply of radiation from the sun is affected both by the day/night rhythm and the weather, and is thus discontinuous. This has a decisive effect on process design and the siting of the plant with respect to geographical and climatic factors. The production location should not only enable the solar photochemistry to take place but should also provide all the peripheral energy for other reaction and processing stages before and after the solar photochemistry. Methods of technically utilizing sunlight in continuous processes may be divided into thermal and photon-linked branches (Fig. 1). The thermal energy of sunlight can be used directly, for instance for water desalination and solar thermal chemistry[1] or for the production of electricity.[2] The production of solar hydrogen deserves special mention because of its importance in both research and industry.[3] Methods for its production investigated range from the simple thermal decomposition of water to solar electrochemical processes and photocatalytic methods.[4] Hydrogen can be used as an energy carrier and as a chemical raw material. Another important branch of the technical utilization of solar radiation is photovoltaics.[5] In the primary step, a charge separation is produced by photons (photoelectric effect), and this can be used as electrical energy. Solar photochemistry can be divided into two main areas: solar detoxification processes (including

[*] Prof. Dr. H.-D. Scharf, Dr. P. Esser, Dipl.-Chem. B. Pohlmann
Institut für Organische Chemie der Technischen Hochschule
Professor-Pirlet-Strasse 1, D-52056 Aachen (FRG)
Telefax: Int. code + (241)8888127

 © VCH Verlagsgesellschaft mbH, D-69451 Weinheim, 1994 0570-0833/94/2020-2009 $ 10.00+.25/0

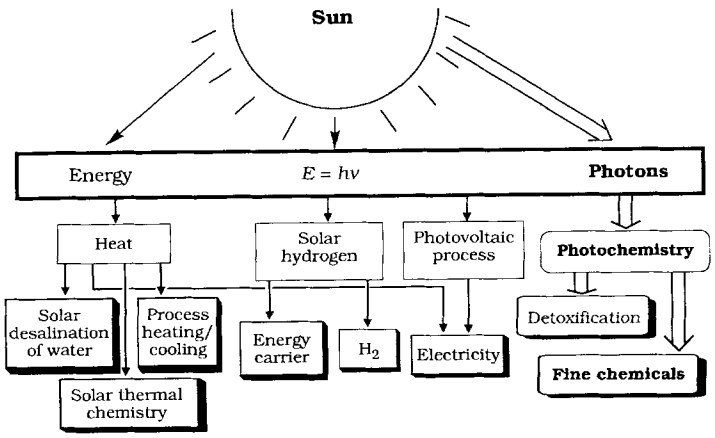


Fig. 1. The stream of photons from the sun can be used for energy production or can be directly coupled to a production process based on photochemistry. For a wide range of solar technologies, the concept of an energetically self-sufficient industrial unit can be realized.

the treatment of industrial waste water with a high concentration of halogenated hydrocarbons and the treatment of groundwater contaminated with pesticides to yield drinking water) and the solar photochemical synthesis of fine chemicals. This review deals only with the latter.

2. Earlier Work

The beginnings of organic photochemistry up to the first systematic research by Ciamician and Silber have been reviewed by Roth.[7] Early this century, photochemistry was closely linked to the use of the sun as the source of radiation, as in the investigations at Ciamician's laboratory on the roof of the chemical research buildings in Bologna.[7] It was also Ciamician who in 1912 in his New York lecture entitled "*The Photochemistry of the Future*"[8] presented a vision which is even more relevant today:

"*On arid lands there will spring up industrial colonies without smoke and without smokestacks, forests of glass tubes will extend over the plains, and glass buildings will rise everywhere; inside of these will take place the photochemical processes that hitherto have been the guarded secret of the plants, but that will have been mastered by human industry which will know how to make them bear even more abundant fruit than nature, for nature is not in a hurry and mankind is*".

In 1937, Alexander Schönberg, an emigrant from the National Socialist Republic of Germany, was appointed Professor at the Ain Shams University of Cairo. Here, he naturally found extremely favorable conditions for the investigation of photochemical reactions in sunlight. His work has led to his general recognition as a pioneer of preparative photochemistry.[9]

One of the first milestones in solar photochemistry was the synthesis of the anthelmintic ascaridol by Schenck et al. in 1943.[10] After the Second World War, Schenck erected the first solar chemical pilot plant for the synthesis of ascaridol in Ziegelhausen near Heidelberg, Germany, sponsored by the Marshall Plan (Fig. 2).[11] The plant was characterized by improvization

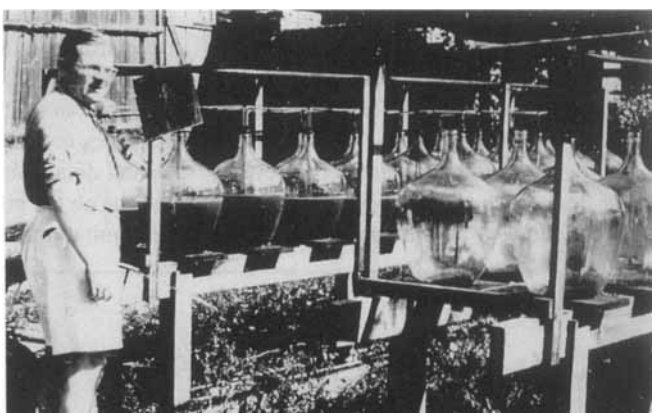
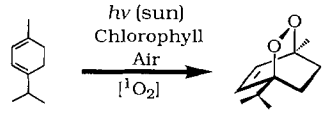


Fig. 2. Günther Otto Schenck and his pilot plant for the production of ascaridol in Ziegelhausen, near Heidelberg, Germany [11].

and simplicity. Air was passed into ordinary glass carboys containing α-terpinene in ethanol, with chlorophyll from the leaves of stinging nettles as the sensitizer. The sunlight and chlorophyll caused singlet oxygen to be produced from the oxygen of the air, and this caused the photooxidation of α-terpinene to ascaridol



Hans-Dieter Scharf, born 1930 in Leipzig, studied chemistry from 1949 to 1950 at the University of Leipzig and from 1954 to 1960 at the University of Bonn. After receiving his doctorate in 1960 for work on the Ipatiev reaction under the supervision of F. Korte he joined the staff of the Shell-Grundlagenforschungs GmbH in Birlinghoven near Bonn, where he carried out fundamental reseach, first as a research chemist, later as a section leader. From 1966 to 1968 he completed his habilitation at the University of Bonn on the theme "Photochemical [2 + 2] Cycloadditions" and shortly thereafter he accepted an appointment as Wissenschaftlicher Rat and as a Professor of Organic Chemistry at the Technische Hochschule Aachen. After rejecting several calls from other places, in 1972 he was appointed Full Professor and Director of the Institute for Organic Chemistry. His areas of reseach include photochemistry, chiral induction in photochemistry and energy storage, the synthesis of bicyclic acetal pheromones of pests and of deoxy sugars and their employment in the partial synthesis of antibiotics.



Scheme 1. Photooxidation of α-terpinene to ascaridol [10].

(Scheme 1). Discussion took place about the question of whether the oxidizing species was a sensitizer-oxygen complex, a view supported by Schenck et al.,[12] or was singlet oxygen, a theory originally proposed by Kautsky et al.[13] In 1964, Foote et al. showed that the latter theory was correct.[14]

Although the plant developed by Schenck was technically capable of improvement, this solar chemical production process was later abandoned because of the discontinuance of the pharmacological use of ascaridol due to its significant side effects.

The development of high-power lamps, especially low- and high-pressure mercury vapor lamps and subsequently lasers, enabled experimental photochemical plants to be moved from the roof to the laboratory. Photochemistry became a funded scientific area whose results have contributed greatly to the understanding of reaction mechanisms, stereochemistry, and the spectroscopic investigation of elementary steps and their kinetics. The outstanding work of Norrish and Porter on the photochemistry of free radicals in the gas phase led to the award of the Nobel Prize in 1967.[15] Furthermore, photochemistry has widened the range of available methods for preparative chemistry.

It is remarkable that in spite of scientific successes and insights in the area of photochemistry the technique has not been used on a large industrial scale for the production of chemical compounds. The reasons for this were and are first the high costs (electricity, limited lifetime of the lamps) of the molar quantities of photons necessary for single quantum processes where large amounts of product are desired (see Introduction). Second, standard chemical reactor technology cannot be applied to photochemical reactions. These reactions, which involve the interaction between light and matter, require new technological solutions (see Section 5).

Following the first oil crisis in the 1970s, research into the use of the sun as an energy source was revived and intensified. Photochemical reversible solar energy storage systems[16] and techniques for the production of solar hydrogen were investigated.[4, 17] Photochemical energy storage systems of quite acceptable capacities can be produced, although in general too few storage cycles are achievable for industrial applications.[18] These investigations therefore never went beyond the laboratory stage. However, more favorable conditions were found for inorganic reversible energy storage systems such as those based on magnesium hydride/magnesium, which are the subject of current research.[19] Intensive work is in progress on the solar production of hydrogen from water by photocatalytic decomposition as well as by electrolysis. A solar reactor with ruthenium complexes as photoredox catalysts has been described, but the long-term stability of this system is unacceptable for its use on an industrial scale.[20]

Since the end of the 1980s, intensive investigations into the solar detoxification of halogenated hydocarbons, especially using titanium dioxide catalysts, have taken place following the tightening of ecological standards. This has recently become the subject of solar field trials.[6] Experiments on the use of solar photons for the production of fine chemicals have been in progress since the beginning of the 1990s, following on from the earlier experiments in solar photochemistry.

3. Quality and Quantity of Solar Photon Streams

Sunlight strikes the earth's atmosphere with an intensity of 1367 Wm^{-2} (solar constant:[21] standard deviation ± 1.6 Wm^{-2}, maximum deviation ± 7 Wm^{-2}), but its intensity and spectral distribution is changed by its passage through the atmosphere (see ref. [21a] for a detailed discussion on solar radiation). Figure 3 gives a comparison between the extraterrestrial spectral distribution and the spectral distribution at the Plataforma Solar de Almeria (PSA, latitude 37.1° N, 500 m above sea level) on September 28, 1992 at 12:00 solar time (the sun at its zenith).

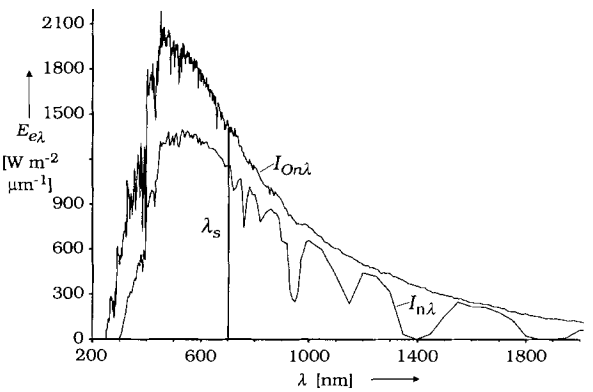


Fig. 3. Extraterrestrial spectral irradiance $I_{On\lambda}$ and direct normal spectral irradiance $I_{n\lambda}$ on the PSA on September 28, 1992 ($E_{e\lambda}$: spectral irradiance). The spectral distribution of the radiation on the PSA has been calculated, where l = 0.26 cm NTP, $\alpha = 0.7$, $\beta = 0.09$, and $w = 3$ cm (l: ozone layer thickness in cm NTP (normal temperature and pressure), α: wavelength exponent, β: Ångström's turbidity parameter, w: thickness of precipitable water vapor in a vertical column of air (cm)). The (fluid) limit of electronic excitation, 700 nm, is indicated in the diagram by a vertical line.

Of the extraterrestrial intensity, 1367 Wm^{-2}, the residual direct radiation intensity at the earth's surface is 892 Wm^{-2} in this example. At wavelengths less than 300 nm, almost no solar photons are detectable at the earth's surface. For photochemical purposes, only the region up to 700 nm is of interest, since photons of lower energy are in general not useful for photochemical reactions. Of the incident radiation (892 Wm^{-2}), 46% was in the photochemically interesting region (up to 700 nm) on the example day. In clear weather, as on the example day, the percentage distribution between visible and infrared radiation hardly changes on passage through the atmosphere. In cloudy weather, the ratio is shifted in favor of infrared radiation.

The attenuation of the extraterrestrial spectral irradiance $I_{On\lambda}$ by the atmosphere is described by Equation (a) in which $I_{b\lambda}$ is the

$$I_{b\lambda} = I_{On\lambda} \cos(\theta)\ \tau_\lambda \qquad \text{(a)}$$

direct spectral irradiance on a horizontal surface, θ is the zenith angle, and τ_λ is the spectral transmittance of the atmosphere. For surfaces tracking the sun in three dimensions, the expres-

sion simplifies to Equation (b), where $I_{n\lambda}$ is the direct spectral irradiance perpendicular (normal) to the irradiated surface.

$$I_{n\lambda} = I_{On\lambda}\,\tau_\lambda \qquad \text{(b)}$$

The spectral transmittance τ_λ of the atmosphere incorporates a number of transmittance coefficients [Eq. (c)], where $\tau_{r\lambda}$ is the

$$\tau_\lambda = \tau_{r\lambda}\,\tau_{a\lambda}\,\tau_{o\lambda}\,\tau_{g\lambda}\,\tau_{wa\lambda} \qquad \text{(c)}$$

spectral transmittance of the direct beam due to molecular (Rayleigh) scattering, $\tau_{a\lambda}$ is that for aerosols (scattering and absorption), $\tau_{o\lambda}$ is that of the ozone (absorption), $\tau_{g\lambda}$ is that of uniformly mixed gases (absorption by CO_2, O_2, N_2, N_2O, CO, CH_4...), and $\tau_{wa\lambda}$ is that of water vapor (absorption). For losses of light in the photochemically relevant region up to 700 nm, only the first three transmittances are significant. In particular, the transmittance due to molecular scattering $\tau_{r\lambda}$, decreases for short wavelengths. This leads to a higher proportion of short wave diffused radiation. Attenuation of wavelengths below 300 nm is caused by absorption by the ozone layer. This is shown in Figure 4 for the PSA on September 28, 1992. When

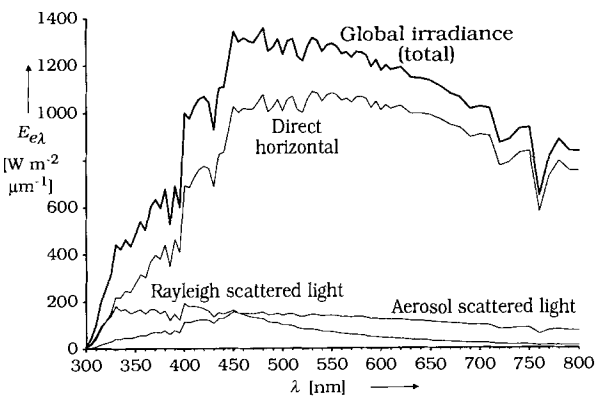


Fig. 4. The composition of the global spectral irradiance on a horizontal surface, which consists of direct spectral irradiance, Rayleigh scattered spectral irradiance, and aerosol scattered spectral diffuse irradiance is given for September 28, 1992 (a clear day) for the PSA. In clear weather other sources of diffuse radiation can be neglected.

direct normal and global horizontal radiation are compared, the result obtained with total spectral radiation is considerably different from that with UV (up to 385 nm) only (Fig. 5). Whereas for the total solar radiation and the range up to 700 nm (thick lines) the direct normal irradiance over the whole day is considerably more intense, the intensities of the direct and global radiation for the UV region (thin lines) are almost identical. The intensity of the direct UV radiation depends to a large extent on location. To illustrate the effect of location, Figure 5 also shows the calculated daily variation of direct normal irradiance for Aachen (51.8° N, 180 m above sea level) for both total spectral radiation and the UV range for identical weather data. The high quality of the weather data is in fact untypical for Aachen. The air normally is not as clear due to climatic and civilization effects.

Apart from the quality of the solar spectrum and its variations, the spectral distribution of the available photons is important for solar photochemistry. In Figure 6, the spectral photon irradiance $E_{p\lambda}$ is calculated from the spectral solar radiation in Figure 3. In Table 1, the available molar radiation figures up to certain wavelengths are given for the PSA location. Up to the photochemically useful wavelength of 700 nm at midday at the PSA on September 28, 1992 there was 6.65 mol($h\nu$)m^{-2}h^{-1} available.

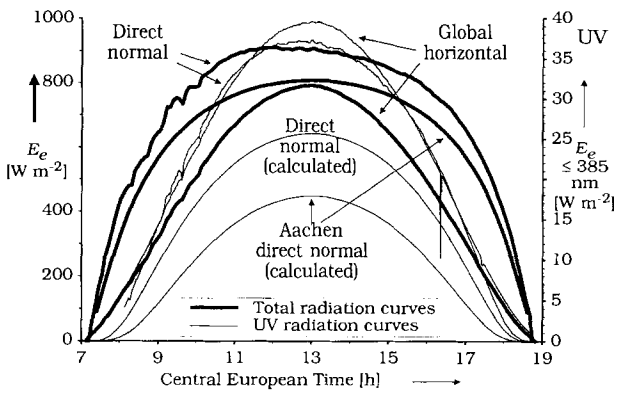


Fig. 5. Direct normal and global horizontal radiation on the PSA on September 28, 1992 during the course of the day (E_e: irradiation intensity). Direct and global total radiation is indicated by thick lines. UV radiation up to 385 nm is indicated by thin lines. With the aperture angle of the measuring equipment (ca. 5°, the sun being visible with an aperture angle of 0.52°) for the direct radiation and the high proportion of UV scattered light (see Fig. 4) which is deflected only minimally in clear weather (so-called circumsolar radiation), a high proportion of this scattered light is collected by the measuring equipment. Therefore, the calculated direct UV radiation is also shown by a thin line. To indicate the influence of location, based on the same weather conditions (l = 0.26 cm NTP, α = 0.7, β = 0.09, and w = 3 cm, see Legend for Fig. 3), a calculated plot of the direct UV and total radiation for Aachen is given. The UV part of the solar radiation is considerably more affected by weather and location.

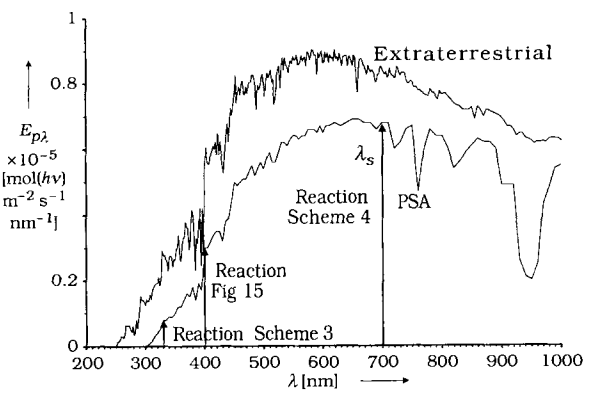


Fig. 6. Extraterrestrial and molar spectral direct solar irradiance on the PSA on September 28, 1992.

Table 1. Integration of the molar radiation from Figure 6 up to various wavelengths.

λ [nm]	Molar radiation [mol ($h\nu$) m^{-2} h^{-1}]
330	0.03
400	0.38
500	1.97
600	4.21
700	6.65

The measurement of direct normal solar radiation was carried out with pyroheliometers, and of global horizontal radiation with pyranometers.[21] The spectral range of the measurement can be restricted by the use of glass filters. It is necessary to make a calculation on the basis of the spectral transmittances from Equation (c) to derive the spectral photon distribution from these figures. The spectral distribution of the solar radiation can be calculated with good accuracy from the date, time, geographical location, and weather data,[21a] by adjustment of the measured values of the direct normal radiation.[22] (Note that in the Figures for which calculated radiation/time curves have been used, the weather data used are also given.)

4. The Photon Yields of the Solar Photochemical Synthesis of Fine Chemicals

The degree of conversion of the quantity of photons provided by a light source into a product by a photoreaction is affected by loss factors in the photoreactor and in the photochemical system. The photoreactor efficiency η_{PR} is the fraction of the amount of available photons that reaches the reaction space. The effect of the photochemical system used can be divided into the absorption yield η_{abs} and the product quantum yield Φ_R. The absorption yield η_{abs} is the fraction of those photons reaching the reaction space that are absorbed by the photochemical system. The product quantum yield Φ_R is defined as the fraction of the absorbed photons that lead to the desired reaction. The emission spectrum of the light source and the wavelength dependence of the various factors must be considered when determining the total photon yield η_g. In Equation (d), $n_{h\nu}(\lambda)$ is the

$$\eta_g = \frac{\int_0^{\lambda} n_{h\nu}(\lambda)\ \eta_{PR}(\lambda)\ \eta_{abs}(\lambda)\ \Phi_R(\lambda)\ d\lambda}{\int_0^{\lambda} n_{h\nu}(\lambda)\ d\lambda} = \frac{n_B}{\int_0^{\lambda} n_{h\nu}(\lambda)\ d\lambda} \quad \text{(d)}$$

quantity of spectral photons and n_B the quantity of product. For the product quantum yield, not only the effect of wavelength, but also the effect of the extent of the reaction (the conversion) must be considered.

In the calculation of the total photon yield, either the photochemical system with its individual threshold wavelength limit λ_{gr} can be the point of reference for the maximum wavelength of the photons to be considered, or the light source (in this case the sun) and its emission spectrum. The total photon yield then also includes a measure of the utilization of this emission spectrum.

When the sun is used as the light source, it is appropriate when calculating the total photon yield only to consider photons with a wavelength up to 700 nm, which is introduced as the solar chemical threshold wavelength: $\lambda_s \equiv$ solar chemical threshold wavelength $\equiv$ 700 nm. This is logical, as electronic excitation in general takes place up to this limit, as described above.

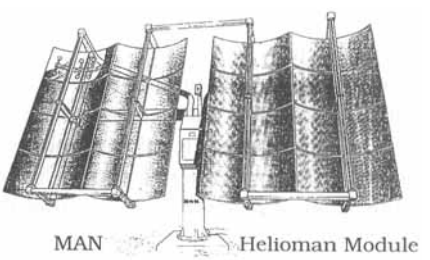
In the following discussion the concept of solar photon yield is based on the utilization of the solar photon spectrum up to 700 nm, limited by the efficiency factors of the solar reactor used and the photochemical system being investigated. In contrast to the definition in Equation (d), the degree of conversion is used as a measure of the molar production rather than the product formation. The chemoselectivity of the reactions described is almost complete.

5. Solar Reactors

When surface reactors are used, as in the Schenck pilot plant (see Fig. 2), the light is directly absorbed, without prior concentration, by the total sum of all the effective liquid surfaces. The Schenck pilot plant, with its glass construction and reactor design, represented only what was feasible in the post-war period, and was not optimized with respect to the light yield. The advantage of this kind of construction lies in the possibility of using both direct and diffuse radiation. However, the radiation intensity of the sun being limited, the space-time yield is low and the demand for "optical windows" is high.

On the other hand, reactors that concentrate the light enable a considerable reduction in the area of the optical windows and a higher space-time yield to be achieved. A disadvantage of light-concentrating reactors is that only the direct fraction of global radiation can be concentrated. A further loss of light results from the efficiency factor of the concentrator.

From the research projects for the utilization of the thermal properties of sunlight, a number of concentrator systems are available.[2a, 21b] The only system so far used commercially (in California) is for electricity production, and involves two-dimensional parabolic trough-shaped (parabolic trough collector) tracking mirrors with linear focusing (Fig. 7). Instead of heating



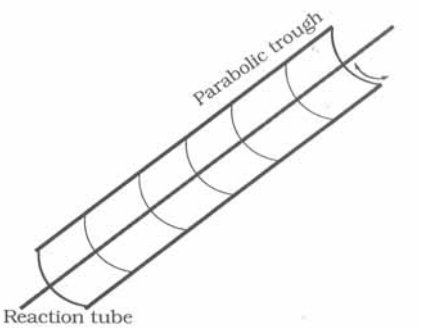


Fig. 7. Line-focusing parabolic trough collectors. Bottom: A two-dimensional trough that tracks the position of the sun. Top: A Helioman Module which can track in three dimensions, made by the company MAN [24]. It is fitted with a total of four parabolic troughs, and has a maximum height of 5.3 m and width of 8 m.

a temperature-stable oil at the line of focus of the parabolic mirrors, as is done when producing energy from the sun, photochemical reactions are carried out by irradiating the reaction solution in a glass tube located at the line of focus. This concentration system enables a degree of concentration corresponding to approximately 100 suns to be achieved in practice.[23] An advantage of this type of concentrator is its ease of manufacture.

A considerably higher degree of concentration of solar radiation can be produced by heliostat fields or parabolic mirrors (Fig. 8). Since the increased degree of concentration leads to an increase in the amount of heat entering the reaction solution, the degree of concentration of the solar radiation is limited by the temperature stresses in a given photoreaction and the extent to which these may be controlled by technical means. Eventually, most of the light absorbed by the reaction solution is converted into heat. The reaction enthalpy is usually small compared with the energy of the photochemical excitation. The heating can be limited by enabling the radiation not absorbed by the reaction solution to be transmitted through the reactor, or by preventing radiation with wavelengths above the wavelength limit of the photochemical reaction from entering the reaction solution at all by the use of a splitter mirror (short wave light passing through unhindered and long wave light being reflected). Reactors of this type (Fig. 8 bottom) are not yet used in practice.

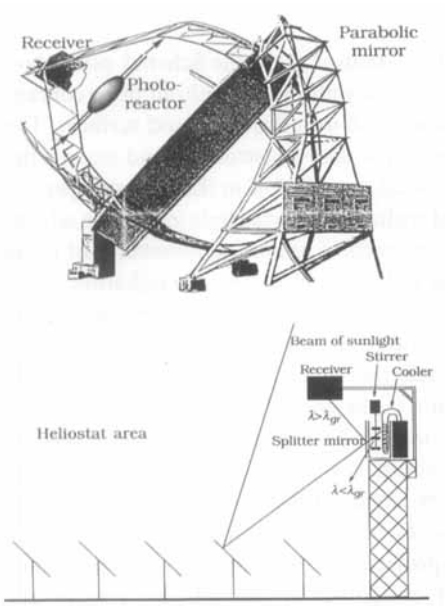


Fig. 8. Concentrating system: Top: A parabolic mirror (parabolic dish). A photoreactor is shown in front of the receiver for the utilization of thermal energy. For reactions that only use the UV part of solar radiation, there is enough energy remaining for its thermal properties to be utilized. Bottom: A heliostat area. The sunlight is concentrated on a tower by the mirror and heliostats. A solar photochemical reactor is shown on the tower. The long wave radiation is reflected by a selective mirror, increasing the total thermal efficiency of the equipment.

Special design problems are posed by reactions that need short wave solar light (ca. < 450 nm). Here, light concentration is frequently used to achieve high space-time yields. The choice of location is important. As short wave light is easily scattered, and, depending on the weather, is mostly deflected at small scattering angles, the use of a suitable design of the aperture angle of the light concentrating system can enable a large fraction of this circumsolar radiation to be collected (see also Fig. 5).

It could be objected that only a small part of solar UV light is used, and that it would be better to use the route: sun → electricity → UV artificial light. The production of UV light by this route is possible with an efficiency of about 3% (sun → electricity (e.g., photovoltaics) 10%; electricity → artificial light 30%). UV radiation (up to 400 nm) constitutes 8% of extraterrestrial solar radiation energy. At very good solar locations on the earth's surface (equatorial, high altitude, clear air), the figure becomes about 5% of the direct solar radiation. This approximate figure alone provides the justification for investigations into the utilization of solar UV radiation for photochemical purposes. If the solar UV radiation can also be concentrated, and the visible and IR radiation not used by the photochemical reactions can be utilized, for example by a thermal receiver (Fig. 8), attractive solar chemical systems present themselves.

The speed of photochemical reactions can be improved by high concentration of solar radiation as long as the starting materials do not undergo other types of excitation (such as excitation by two photons) which lead to side products or other types of products. Sizmann et al.[25] point out that a photon, which has the character of a particle, is a reactant subject to the thermodynamical law of mass action, indicating a photochemical reaction is reversible. That is, there can be a chemical equilibrium involving both the reactants and the radiation. Since photochemical reactions usually proceed at a point remote from equilibrium, and moreover the photochemical product formation is normally irreversible, the effect described by Sizmann et al. can be ruled out. The probability of two-photon processes is also improbable because of the need to observe thermal control in the reaction solution. It is therefore to be expected that the product formation will increase proportionally to the amount of radiation available.

For the more recent solar photochemical experiments in the field, parabolic trough collectors are used. At the present time, work commissioned by the AG Solar des Landes Nordrhein-Westfalen is being directed towards the development of experimental reactors in which the degree of solar concentration is high and variable. The first solar tests are planned for 1995 on the "Hochflussdichte-Sonnenofen", the construction of which has recently been completed, of the AG Solar in Köln Porz on land belonging to the Deutsche Forschungsanstalt für Luft- und Raumfahrt e. V. (DLR).

5.1. The Solar Reactors at the Max-Planck-Institut, Mülheim an der Ruhr, Germany

The solar reactors at the Max-Planck-Institut (MPI) for radiation chemistry in Mülheim an der Ruhr, Germany, are being operated on the roof of the Institute building (Fig. 9). Two types of reactor have been developed, with a single and double axis design, respectively.[26] At the heart of the solar reactors is a line focusing concentrator developed by the company HTC Solar (Lörrach) and included in the reactors built at the MPI.[27] The

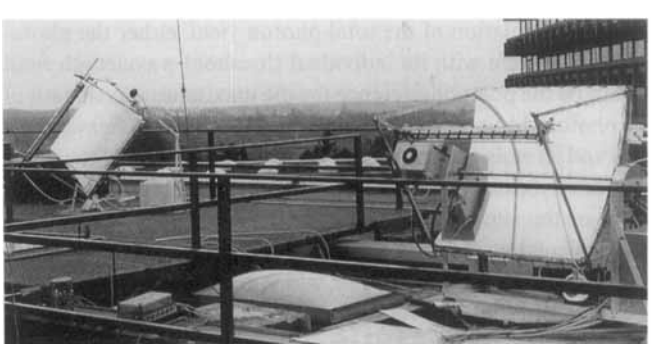
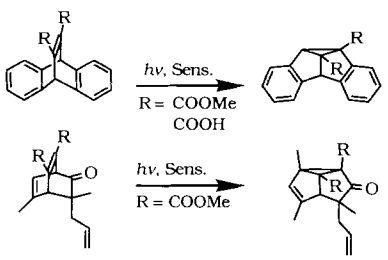


Fig. 9. Solar reactor equipment on the roof of the MPI in Mülheim.

reflector consists of a film of Hostaflon (100 cm × 100 cm) coated with aluminum by vacuum deposition and stretched over an aluminum chamber. A vacuum can be applied to the chamber, and a focus line can be produced by the film. Controlled defocusing can also be carried out to give control of the temperature of the reaction solution. At the focus line there is a silica tube 100 cm long and 1 cm in diameter. The theoretically possible concentration factor of 100 suns is reduced in practice to a maximum of 60 because of efficiency losses in the concentrating system. An automatic mechanism controlled by a photocell causes the mirror and reaction tube to track the sun. The solution is pumped at a rate of 90–100 $L\,h^{-1}$ through the irradiation tube. It then goes back into the storage vessel (2 L volume) through a cooling tower. Without cooling, this flow rate results in a maximum reaction temperature of 35 °C when water is the solvent.

This reactor has so far been used for photosensitized rearrangements of di-π-methane and oxadi-π-methane (Scheme 2)



Scheme 2. Di-π- and oxadi-π-methane rearrangement with sunlight [27]. Sens. = sensitizer.

in aqueous micellar solution.[28] The high heat capacity of the solvent water is an advantage. Moreover, no protective gas is required. In the micelles in which the photochemical reaction takes place, obviously only a very small oxygen concentration is present.

5.2. The SOLARIS Experiment

The SOLARIS experimental solar photochemical fine chemical syntheses were carried out at the Plataforma Solar de Almeria, Spain, by the Institut für Organische Chemie der Technischen Hochschule Aachen, Germany, in cooperation with the DLR, Köln, Germany. The conception and construction of the SOLARIS reactor was effectively carried out by G. Schneider (DLR). The solar experiments were performed between October 17, 1991 and February 15, 1992 and between September 18, 1992 and November 25, 1992. Three photochemical reactions with different threshold wavelengths were chosen as test reactions. The potential for solar irradiation in the different spectral regions with different threshold wavelengths had to be assessed experimentally. Other criteria, apart from the provision of the associated laboratory work, included a simple experimental procedure, availability of the starting materials, the use of solvents with the lowest possible toxic properties, a convenient method of following the reaction (by gas chromatography), and the suitability of the reaction products for synthesizing useful substances.

5.2.1. The SOLARIS Reactor

The SOLARIS reactor (loop) comprises the light concentration system, an absorber tube at the focal line of a parabolic trough collector, material feeding equipment, and a data collection system (Figs. 10–12). The feeding equipment (storage vessel, pump, heat exchanger, gas metering, etc.) of the loop is on a platform immediately next to the MAN Helioman Tracking

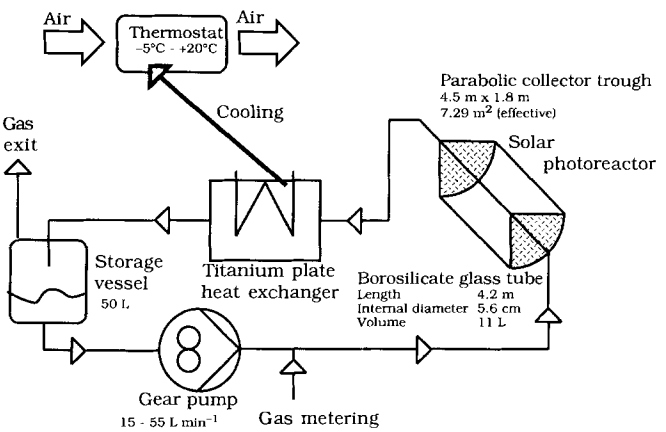


Fig. 10. Schematic diagram of the SOLARIS reactor.



Fig. 11. The MAN Helioman Module is shown on the right (east), and the feed platform is on the left (west). The latter is protected from the weather by a corrugated steel shed. The red color of the sensitizer Rose Bengal can be clearly seen in the absorber tube. In the background on the right, a MAN Helioman Module for the detoxification loop can be seen. The absorber tube shines white due to scattering by the titanium dioxide.



Fig. 12. View of the feed platform, which opens towards the north. The storage vessel can be seen in the left foreground. The process cooler is in the background. The control cabinet is on the wall on the right, and the gas fittings, with three gas bottles for nitrogen, oxygen, and ethene, are in the foreground.

Module but outside its range of movement. The reactor is of the tube reactor type with a closed recirculation system. The reaction solution is pumped out of the storage vessel and through the recirculating system. This contains a gas metering device and a static mixer, both at the point of highest pressure. The solution then leaves the platform and is fed through a flexible pipe to the inlet of the absorber tube. This inlet is situated underneath the parabolic trough collector. The absorber tube is at the focus of one of the parabolic trough collectors that track the sun. The tracking is performed by a Helioman Module to which the mirror and absorber tube are fixed.[24] This follows the sun by automatic three-dimensional tracking on two axes. The photochemical reaction takes place in the absorber tube, from the top end of which the reaction solution flows into a flexible pipe and then back to the feed section. Here, the heat that has been absorbed by the solution, mainly during its passage through the absorber tube (thermalized solar radiation), is removed. A process cooler supplies the heat exchanger with a cooling medium. The reaction solution leaving the heat exchanger flows back into the storage vessel. The reaction solution is pumped round the recirculating system until the desired degree of reaction (conversion) has been achieved. The loop had a minimum operating volume of 35 L and a maximum of 70 L. When working with oxygen and organic solvents (Section 5.2.4), sources of ignition had to be strictly excluded.

The efficiency of the light-concentrating system is affected by tracking defects of the Helioman Module, the reflectivity of the mirror surface, and the transparency of the glass tube. The equipment provided by the PSA (J. Blanco, S. Malato) for the solar photochemical experiments on the Helioman Module was similar to that for the 12 Helioman Modules used in a loop for the detoxification of impure water (detoxification loop).[29] The Helioman Module has a tracking accuracy of 95%. The mirror surface is made of aluminum foil. The reflectivity of this foil is not the optimum,[30] but represents a compromise between cost on the one hand and a reactor concept suitable for the investigation of the selected test reactions in the UV region on the other. The transparency of the absorber tube of borosilicate glass (Pyrex) in the focal line of the parabolic mirror has a value of 89% at 385 nm.

The reflectivity of the mirror and the transparency of the absorber tube are wavelength-dependent. The efficiency of the photoreactor $\eta_{PR}(\lambda)$, which is wavelength-dependent, is shown in Figure 13. The efficiency of the photoreactor over the entire spectral range up to the solar chemical threshold wavelength is 62%. The direct solar radiation is concentrated by a factor of about 20 suns in the absorber tube.

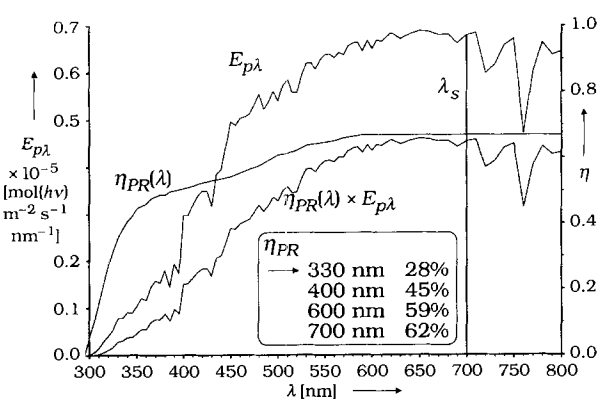
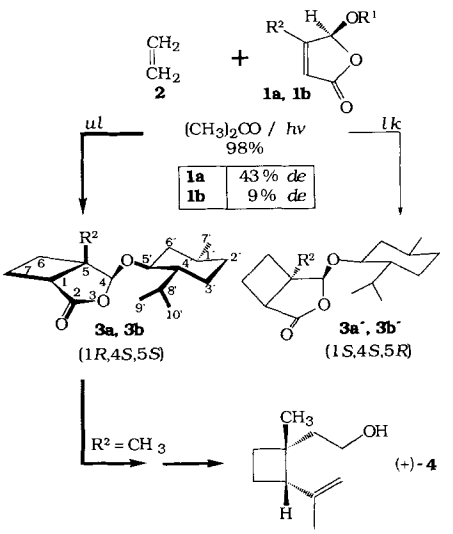


Fig. 13. The molar direct spectral irradiance ($E_{p\lambda} = n_{h\nu}(\lambda)$ per unit of surface and time) on the PSA on September 28, 1992, and the spectral radiation ($\eta_{PR}(\lambda) \times E_{p\lambda}$) (without reference to the concentration) influenced by the efficiency of the SOLARIS reactor ($\eta_{PR}(\lambda)$). The efficiency of the SOLARIS reactor for various spectral ranges is given in the box. Here, the spectral molar radiation shown is taken as the basis. The solar chemical threshold wavelength is also shown as a vertical line for orientation purposes.

5.2.2. *Photocycloaddition of Ethene to α,β-Unsaturated Carbonyl Compounds*

The acetone-sensitized [2 + 2] photocycloaddition[31] (Scheme 3) of ethene (**2**) to 5-alkoxy-[5*H*]-furan-2-one (**1**) has been investigated as a case of a photoreaction with sunlight with



Scheme 3. [2 + 2] Photocycloaddition reaction of **1** with **2**. R^1 = (+)-menthyl; **a**, R^2 = H; **b**, $R^2 = CH_3$.

a short wave limit. When acetone is used for sensitization, only light up to a threshold wavelength of 330 nm can be used for the photoreaction. The use of longer wavelength absorbing sensitizers was deliberately avoided. For the cyclobutanes **3b** and **3b'** from **2** and the 3-methylfuranone **1b**, or **3a** and **3a'** from **2** and the furanone **1a**, in the synthesis of grandisol **4** or its structural analogue demethylgrandisol[32] has been described. This reaction certainly shows no significant diastereoselectivity, but the diastereomers can be simply separated by chromatography.[33]

In the second SOLARIS phase, this type of reaction was carried out with the 5-ethoxyfuranone **1d** as the α,β-unsaturated ketone, which itself was a product of the first SOLARIS phase (see Section 5.2.4). The reaction is summarized in Figure 14. Using 2.1 mol of starting material, a conversion of 23% was obtained after two solar irradiation stages. After the first day, which was partly cloudy (Fig. 14), a partial conversion of only 6% was obtained, and, after a second day of clear, cloud-free weather, the figure was 16.4%. The radiation conditions on the second day can be regarded as the optimum for the location and time of year. In assessing the partial conversions, the unfavor-

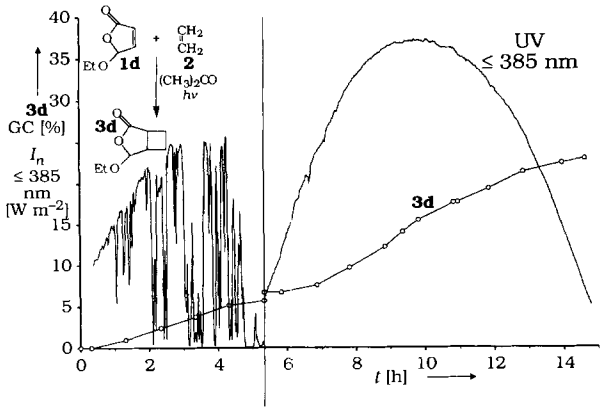


Fig. 14. The [2 + 2] photocycloaddition of **2** to **1d** was carried out on September 25 (left) and 28 (right), 1992 with 2.1 mol (270 g) starting material **1d** in acetone (36 L) at 10 °C). The progress of product **3d** formation (measured by GC analysis) is shown, and also the direct UV radiation up to 385 nm for the two days of the experiment, which are separated from each other by a vertical line. The radiation curve for the first day of the experiment shows a severely disturbed course, due to the passage of clouds. The smooth progress of the photoreaction leads to two product diastereomers in the ratio 2.6:1. The reaction solution, with a flow rate of 20 L min^{-1}, is heated 6 K between the inlet and outlet of the irradiation tube (September 28, maximum day temperature: 30 °C at midday). t = reaction time.

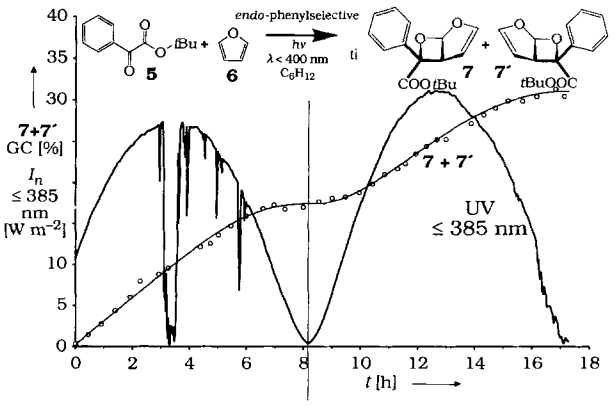


Fig. 15. **5** (1105 g, 5.2 mol) and **6** (2 L, 28 mol) in cyclohexane (33 L) were irradiated at 20 °C (temperature control) on two successive days (November 3, 4, 1992). The formation of **7** and **7′** was measured by GC analysis, and the direct solar UV irradiance was up to 385 nm for both days of the experiment. The two days are separated by a vertical line. The reaction solution, at a flow rate of 23 L min^{-1}, was heated 3 K between the inlet and exit of the irradiation tube (maximum day temperature: 26 °C).

able mirror area/reaction volume ratio for this reaction must be borne in mind, as well as the low molar solar radiation in the spectral range up to 330 nm, and the low photoreactor efficiency (28%) for this range. This results in a solar photon yield of just 0.1%. This reaction can be caused to give complete conversion with longer irradiation times, in a different part of the year, or with more irradiation stages. The solar photon yield can be further improved by reactor optimization by improving the glass and mirror materials.

5.2.3. *The Paternò–Büchi Reaction*

The photoinduced [2 + 2] photocycloaddition of carbonyl compounds to alkenes to form oxetanes offers an interesting possibility for synthesizing complex naturally-occurring and other substances.[34] Schreiber et al. have reported the synthesis of racemic asteltoxin,[35] avenaciolide,[36] a cadsurenone-ginkgolide hybrid,[37] and a seco-precursor of isolobophytolide.[38] Zamojski et al. was also able to synthesize a protected 3-deoxy-streptose derivative[39] from a furanooxetane precursor. Hambalek and Just used the method for synthesizing epioxetanocin.[40] Hoye and Richardson were able to achieve the shortest sarracenine synthesis so far using this key step.[41] A protected apiose,[42] a 3C-hydroxymethyl-branched pentose, was synthesized by photoaldolization of ((−)-8-phenylmenthyl)phenylglyoxylate with 2,2-dimethyl-1,3-dioxol, with complete asymmetric control.

The preparative use of the Paternò–Büchi reaction, especially of asymmetric compounds, is still in its infancy.

The reaction of (*tert*-butyl)phenylgloxylate (**5**) with furan (**6**) in cyclohexane was chosen as a model system to test the asymmetric Paternò–Büchi reaction under solar conditions. This reaction consistently proceeds regiochemically and stereochemically, as shown in Figure 15, to form **7** and **7′**. With a clean reaction, complete conversion based on the keto-component can be achieved. If the chiral phenylglyoxylate of 8-phenylmenthol or of *trans*-2-*tert*-butylcyclohexanol is used in the reaction,[43] the product oxetane is also diastereochemically uniform. The phenylgloxylates absorb light up to a wavelength of 400 nm from the molar spectral radiation of the sun (Fig. 16).



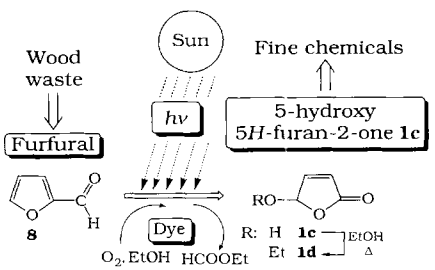
Fig. 16. Parabolic trough collector with absorptiopn tube. A Paternò–Büchi reaction takes place in the absorption tube (see Fig. 15). Since this reaction absorbs UV light, the reaction solution is colorless to pale yellow. A small flow of protective nitrogen gas is passed through, and some gas bubbles can be seen in the absorption tube.

The starting material shown as an example in Figure 15 was irradiated on two successive days. The radiation conditions on both days are certainly considerably worse than in the second day of the experiment described in Figure 14, but are classified as "good" for the time of year. On interrupting the reaction on the second day, a conversion of 32% was obtained. The size of the charge is so chosen that the UV light of the sun is almost completely absorbed within the cross-section (5.6 cm) of the absorber tube, up to a conversion of 95%. The photoreaction gives a quantum yield of about 0.1 at the chosen furan concentration (0.78 mol L^{-1}). The quantum yield is dependent on the concentration of the furan, and increases as its concentration increases.

The SOLARIS reactor does not have the optimum design for this reaction as far as the ratio of the reactor volume to the mirror surface is concerned. The photoreactor efficiency of 45% (see Fig. 13) for the spectral range up to 400 nm is capable of considerable improvement, especially with a better mirror surface. For the [2 + 2] photocycloaddition carried out, a solar photon yield of 0.3% is obtained. The overall photon yield for the utilization of solar radiation up to 400 nm is nevertheless in the region of 5% (photoreactor efficiency ca. 0.5 and product quantum yield ca. 0.1, see above).

5.2.4. *Singlet Oxygen Reactions*

The third test reaction was the dye-sensitized photooxidation of furfural (**8**) with oxygen to give the 5-hydroxyfuranone **1c** in alcoholic solution (Scheme 4). This reaction was first described



Scheme 4. Photooxidation of **8**, a renewable raw material, to **1c** (sometimes referred to as pseudoacid or maleic aldehyde acid).

by Schenck.[44] In it, the sensitizing light is absorbed from the visible spectral range. By an inter-system crossing step, the sensitization of the oxygen takes place from the triplet state of the sensitizer. Singlet oxygen is the result. Furfural (**8**), which is produced industrially by the action of mineral acids on materials such as oat husks, corn cobs, rice husks, groundnut shells, and reeds, can be replaced for the synthesis of **1c** by furfuryl alcohol[44b] or 2-furancarboxylic acid.[44b, 45] Both are produced from **8**. Because of the high temperatures during working up, Schenck could only isolate the 5-methoxy or 5-ethoxy analogues (**1d**), depending on the alcoholic solvent used. It was later shown that by operating below about 40 °C in the working up procedure, **1c** is the only reaction product.[46]

The use of **1c** as a C_4 building block in the synthesis of a large number of natural and synthetic substances has been described, and is summarized in Scheme 5. Because of the easy accessibility of the diastereomerically pure 5-menthyloxyfuranones **1a** and *ent*-**1a**,[47] these have recently been used for synthesizing C_4 building blocks or directly as chiral building blocks (Scheme 6).[48] The two furanones **1a** and *ent*-**1a** can be obtained in high yield by the condensation of the furanone **1c** with (+)- or (−)-menthol followed by crystallization from *n*-hexane[47] and thermal or proton-catalyzed epimerization.[63b, 64]

Rose Bengal (**10**) and methylene blue (**11**) are used as sensitizers for the solar dye-sensitized photooxidation of **8** (Fig. 17). Rose Bengal[71] has its absorption maximum at 555 nm. Only light up to a maximum wavelength of 600 nm is used. The absorption yield η_{abs} based on the quantity of irradiating photons of wavelength ≥ 700 nm is 0.63. Rose Bengal in ethanol as solvent has the highest singlet oxygen quantum yield (0.86) of all the sensitizers so far used for this purpose.[71a, 72] The combination of these two factors results in a solar sensitizing efficiency of 0.54 for Rose Bengal.

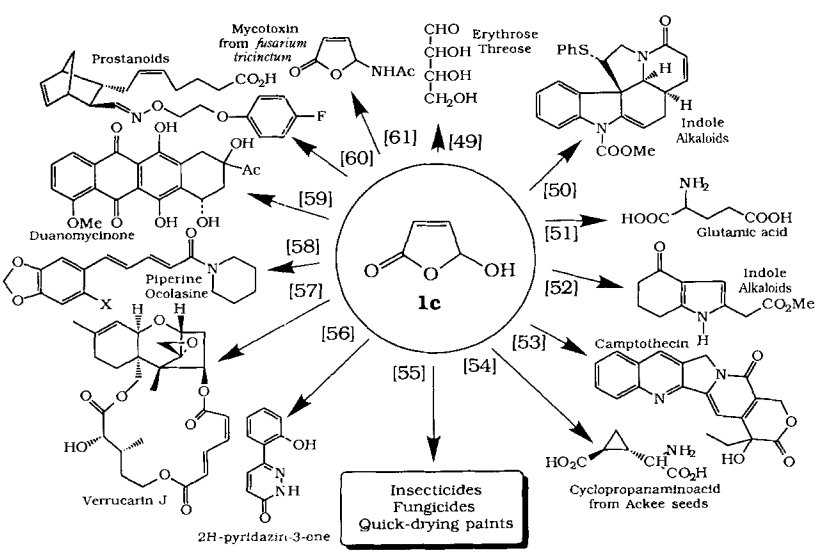
Methylene blue (**11**) has its absorption maximum at 685 nm. It can be electronically excited by light of wavelength up to 720 nm, so that, using the solar chemical threshold wavelength as the reference point, an absorption yield of 1.07 results. With methylene blue, the singlet oxygen quantum yield depends very much on the reaction conditions,[73] and has a value of about 0.35 for photooxidation in ethanol. This results in a solar sensitization efficiency of 0.37.

The photooxidative conversion of **8** into the 5-hydroxyfuranone **1c** proceeds to only a small extent directly. Under the reaction conditions, furfuraldiethylacetal (**12**) is formed, which reacts considerably more rapidly with singlet oxygen. Since the formation of **12** is catalyzed under the reaction conditions, the course of the reaction is autocatalytic. The kinetics of the photooxidation of **8** are summarized in Figure 18.

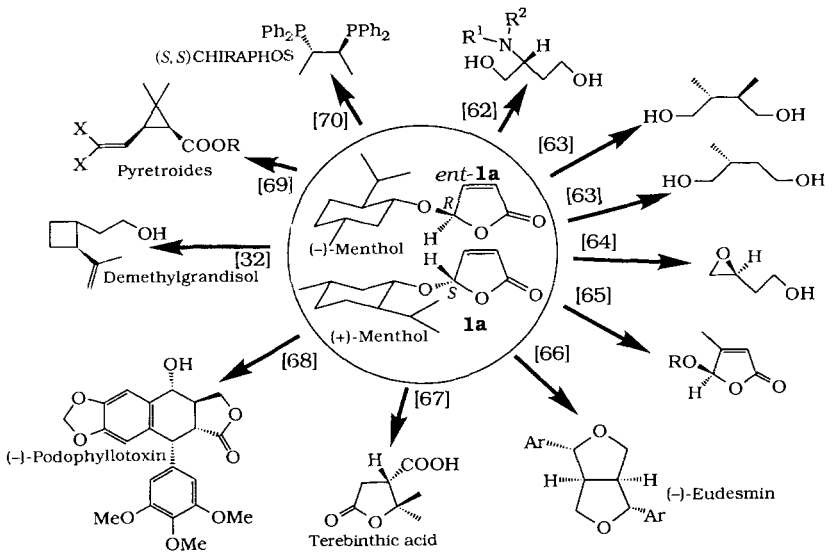
With a starting concentration of 1.1 mol L^{-1} **8** and a 97% conversion, a singlet oxygen utilization of 65% follows from the kinetics of the photooxidation. The reaction proceeds via the furfuraldiethylacetal intermediate to the extent of 80%.

In the two experimental phases on the PSA a total of 16 experiments were carried out, using just over 40 kg furfural **8**. The results of these experiments are illustrated by five examples, which are summarized in Table 2. The course of Experiment A is shown in Figure 19, and that of Experiment E in Figure 20.

Experiment A (Fig. 19) was carried out over 14 days. However, a period of bad weather meant that direct solar irradiation was only available for three days (Fig. 19). Even so, the radiation was interrupted on all these three



Scheme 5. Reaction "star" showing uses of **1c** in synthesis with literature references.



Scheme 6. Reaction "star" showing uses of **1a** and *ent*-**1a** in synthesis with literature references.

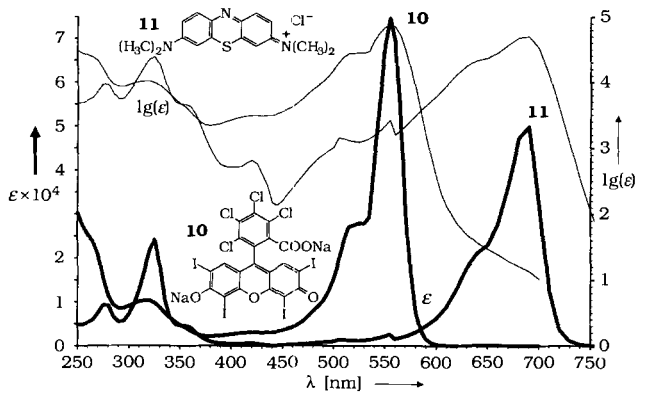


Fig. 17. UV/VIS absorption of Rose Bengal (**10**) and methylene blue (**11**).

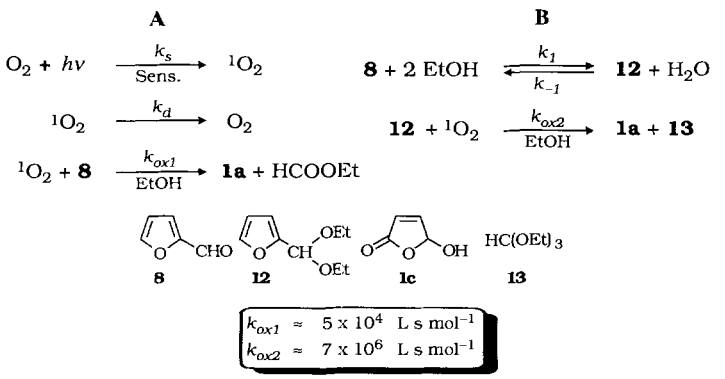


Fig. 18. Kinetics of the photooxidation of furfural (**8**). A) Direct reaction; B) via **12**.

days by the movement of clouds. Under these conditions, the reaction behaved remarkably robustly. The reaction starting materials can be left in the loop during bad weather without harm until direct solar radiation reappears.

An ideal experimental run is shown in the example of Experiment E in Figure 20. This indicates that with clear weather, and hence the best solar irradiation, the experiment can be completed shortly after midday after only five and a half hours irradiation.

Methylene blue (**11**) is clearly preferable to Rose Bengal (**10**) as a sensitizer for the photooxidation of **8**. This is at first surprising as the solar sensitization efficiency of **10** is 0.54, which compares with 0.37 for **11**. The weakly acidic reaction conditions, which also favor the formation of furfuralacetal, have a detrimental effect on the extinction values and singlet oxygen quantum yields of **10**, which is a dianion. This is convincingly demonstrated by comparing Experiments B and C in Table 2. In Experiment C, twice the amount of starting material is converted with an almost equal irradiation time and almost identical irradiation conditions. Furthermore, in Experiment B, the amount of sensitizer needed is extremely high, first because of the effect on the extinction properties of **10**, and second because of the

Table 2. Solar photooxidation of **8** in five examples.

Experiment		A	B	C	D	E
date		4, 12, 13 Dec. 1991	3–4 Feb. 1992	5–6 Feb. 1992	2 Nov. 1992	14 Nov. 1992
charge	[mol]	21.5	22.3	**45**	21.2 [a]	37.6 [b]
ethanol	[L]	35	35	30	35	35
sensitizer		**11**	**10**	**11**	**11**	**11**
(quantity in g)		(6.1)	(**11.2**)	(5.1)	(6.0)	(9.0)
T	[°C]	8	20	20	20	20
fluid flow	[L min^{-1}]	35	55	55	45	45
total radiation	[mol($h\nu$)]	140	413	436	114	226
total radiation	[kWh]	22.2	54.3	61.9	16.9	32.4
max. radiation	[W m^{-2}]	544	807	817	848	**873**
t	[h]	16	10.9	12.6	3.2	5.5
conversion	[%]	98.5	99.1	**99.7**	95.1	98.1
selectivity (**1c** + **1d**)	[%]	98.5	98.2	97.9	93.1	96.2
1c/**1d**		42/1	133/1	58/1	390/1	55/1
η_g	[%]	**15.4**	**5.4**	**10.3**	**17.7**	**16.3**

[a] furfuralacetal **12**. [b] Addition of 5 mL conc. HCl (furfural **8**/HCl = 625/1).

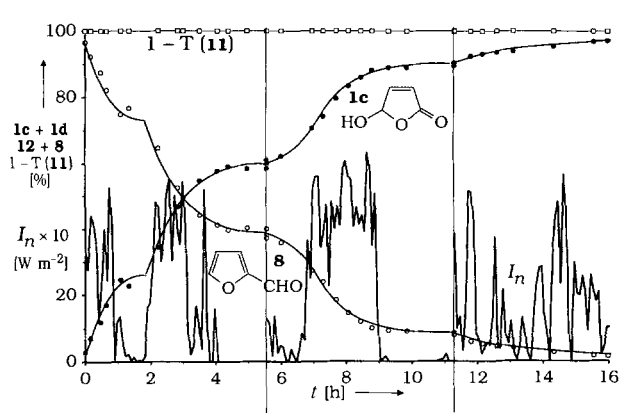


Fig. 19. In Experiment A, irradiation was carried out on three days (see Table 2). The following are given in percentages: starting materials (decreasing with time) (**8** + **12**, GC analysis), product (increasing with time) (**1c** + **1d**, GC analysis) and the absorbance (1 – T) by the sensitizer in the absorption tube (diameter of absorption tube: 5.6 cm, on the basis of an extinction measurement of 695 in a 1 cm cell). The direct solar radiation is also shown. The experimental days are separated by vertical lines.

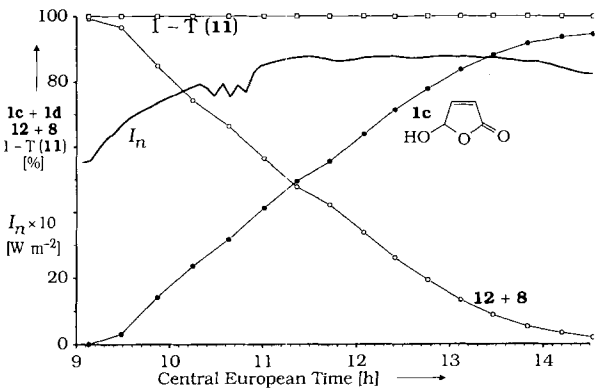


Fig. 20. In experiment E (see Table 2) the time (Central European Time) is shown on the x axis (see also legend to Fig. 19). At this time of the year, the sun is at its zenith at about 13:00 h. Between entering and leaving the irradiation tube, the reaction solution, flowing at 45 L min^{-1} was heated 3 K (maximum daily ambient temperature: 25 °C).

lower stability of **10** towards UV light compared with **11**. The sensitizer stability can be considerably improved by the exclusion of UV radiation by suitable choice of the mirror and the type of glass. Singlet oxygen sensitizers represent a considerable opportunity for optimization, not only from the point of view of stability, but more so because of the possibility for matching to the solar spectral radiation, while at the same time obtaining the highest possible quantum yields.

The photooxidation of **12**[74] proceeds with a higher rate constant k_{ox2} (see Fig. 18); thus the singlet oxygen utilization is higher. This substance was therefore used as the starting material in Experiment D. The reaction also shows the highest solar photon yield (17.7%) compared with the other reactions recorded in Table 2. A higher solar photon yield would be expected from the higher oxidation rate constant k_{ox2}. The appearance of clouds immediately after the start of the reaction led to extensive decomposition of **12** due the acetal formation equilibrium, leading to a reduction in the rate of the photooxidation reaction. A possible alternative to the use of **12** as the starting material to improve the efficiency is to accelerate attainment of the acetalization equilibrium by adding protons. This was investigated in Experiment E by adding a little hydrochloric acid. After only five and a half hours irradiation under the best irradiation conditions the experiment could be ended after the starting material (37.6 mol) had undergone 98.1% conversion. The overall solar photon yield was 16.3%. The selectivity is somewhat less than in the case of the photooxidation of **8** without acid addition, and the reaction is no longer so robust. A sufficiently high conversion, enabling the photoreaction to be ended, should be achieved after one day of irradiation.

Before making a conclusive comparison of the solar photon yields achieved, some further comments should be made about Experiments A and C. In Experiment A, because of the low maximum irradiation and the frequent cloud problems, the reaction mainly took place via **12**. Also, because of the extent of cloud cover, the molar solar irradiation could not be calculated with the same accuracy as would have been possible on a day of uninterrupted irradiation. Experiment C delivered the highest conversion figure (99.7%). The photon yields given in Table 2 are based on the conversions obtained in the respective reactions. In Experiment C, at a conversion of 98%, which is more interesting for comparison purposes, the solar photon yield was 11.6%. However, because of the high reaction rate in the absorber tube due to the high irradiation rate, there was an oxygen deficiency due to insufficient turbulence in the region of highest light absorption, although a more than sufficient total amount of oxygen was being passed through the absorber tube. After this experiment, in the second experimental phase, the problem of inadequate saturation by oxygen was solved by installing a mixing element in the middle of the absorber tube. The concentrated sunlight can lead to such high reaction rates that the demand for dissolved oxygen is a limiting parameter. The possibilities for solving the problem by the techniques used (increasing the pressure and the intensity of mixing the gas phase with the solution) have limits, imposed partly by the quenching properties of the singlet oxygen and partly by light scattering.

Comparisons of solar photon yields in Table 2 show that the increased cost of production of **12** is not justified, since the efficiency can also be much improved by adding protons to **8** in ethanol. It is prudent to limit the conversion to 97%. Higher conversions lead to a considerable reduction in the utilization of the solar photon stream.

The photon balance of the solar photooxidation of **8** is determined by the photoreactor efficiency (0.62), the solar sensitization efficiency (methylene blue **11**: 0.37), and the singlet oxygen utilization of the photooxidation (0.65). In practice, it was possible to obtain solar photon yields of 16%. This figure agrees with the separately determined values of the three efficiency factors mentioned. The photoreactor efficiency can be increased from 0.62 to 0.80 for the SOLARIS reactor by matching to the requirements of the singlet oxygen reaction. The need to optimize the sensitizer and the possibilities for influencing the kinetics of the photoreaction have already been discussed in some detail.

The photooxidation of **8** with artificial light from lamps gives an overall efficiency of 4.5%. In this calculation, the following efficiencies are assumed: electricity production: 30%, light production: 30%, photoreactor efficiency: 90%, singlet oxygen quantum yield: 86% (Rose Bengal **10** with artificial light optimally matched to the absorption of the sensitizer), and utilization of the singlet oxygen: 65% (as stated above). Caution must be used when comparing the figures, since a pure photon balance takes place with the sun, whereas with artificial light a mixture of energetic (including light production) and photon balances must be considered, but the advantage of the solar production route is still nevertheless apparent. This is even more the case if one considers that the optimum figures for the artificial light route have been used, whereas the solar reaction path is capable of further considerable improvement.

As well as the solar photon yield, the heat balance is also essential for the operation and design of solar photochemical reactors. Considerable amounts of energy are associated with the stream of photons. In the photochemical production of fine chemicals, the main aim is to produce complex chemical structures. The contribution of the reaction enthalpy to the heat balance can be neglected to a first approximation compared with the amount of energy absorbed for electronic excitation. The radiation absorbed by the photochemical system is completely thermalized, and must be removed from the system by cooling.

The relevant data obtained from the SOLARIS reactor is fundamentally of two different kinds. By the design of the SOLARIS reactor the light above the long wave absorption limit of the photochemical system and before the start of IR absorption (especially by the solvent) passes through the absorber tube essentially without absorption. The SOLARIS reactor is not completely thermally insulated. The experiments took place at a time of year with moderate outside temperatures, so that the convective thermal currents were mainly small.

The photooxidation of **8** is strongly exothermic, so that in this case the reaction enthalpy must be included in the heat balance. In the solar experiments, the extent of cooling required was 8 kWh kg^{-1} **1c**. If a solar reactor is insulated and the solar photon yield is optimized, the cooling can be reduced.

6. Conclusions

The sun provides a small but continuous photon radiation density. This must be concentrated to obtain high space-time yields in photochemical processes, enabling the photoreactor itself to be kept small. The choice of location, height above sea level, and geographical latitude is important. Photons with a wavelength of above 300 nm arrive at the earth's surface from the sun. For acetone-sensitized [2 + 2] photocycloaddition, which absorbs light only up to a wavelength of 330 nm, the basic feasibility has been indicated (Section 5.2.2). Improvements are both necessary and possible. On the other hand, the amount of solar radiation in the range below 330 nm is so small that artificial light sources are preferable in these cases even if the solar reactor is optimized. For photoreactions that absorb the complete solar UV radiation, as shown for the Paternò–Büchi reaction of phenyl glyoxylate **5** (Section 5.2.3., Fig. 15), improvements to the solar reactor by concentrating the light with line focusing parabolic troughs enable satisfactory space-time yields to be obtained. The attractiveness of concentrated sunlight of this wavelength range has also been demonstrated by the experiments in the solar reactor of the MPI in Mülheim (Section 5.1.). Here, the development of the more highly concentrating solar reactor concept (Section 5) is of particular interest.

Investigations of the singlet oxygen reaction in the SOLARIS reactor have demonstrated a realizable technology for the reactions which can utilize all visible sunlight. The solar photoreactors in which the sunlight is concentrated with parabolic trough collectors (described above) lend themselves to technically simple design. Unlike solar technology, which must inevitably be discontinuous because of the day/night rhythm, artificial lamps enable operation to be continuous. However, as well as the poor energy balance of artificial light exemplified by the photooxidation of furfural (**8**), there are other disadvantages. The intensity of photon flux from these lamps is limited, so that the scope for scaling up is limited compared with solar technology. Problems of cooling the lamps, the deposition of coatings on both sides of the glass window between the cooling water and the lamp, and the limited life span of lamps are avoided when the sun is used. Also, at least for singlet oxygen reactions, the proximity of the potentially explosive reaction mixture to the hot lamps means that high safety standards are required.

7. Industrial Photochemical Processes

The photochemical processes used in industry have been documented in a number of reviews,[20, 75] although it is noticeable that there has been a cessation of developments after over 20 years. These processes can be divided into free radical chain reactions (photochlorination, sulfochlorination, and sulfoxidation) with quantum yields considerably greater than 1 and photoreactions with quantum yields less than 1 (photonitrosylation, photooxidation, and photoelectrocyclic reactions). Following the decline in chlorine chemistry, a reduction in the industrial importance of photochlorination, sulfochlorination, and photonitrosylation is likely. The synthesis of vitamin D is a photoelectrocyclic reaction that is highly wavelength-selective and therefore unsuitable for the polychromatic solar spectrum. Of the photochemical processes currently in operation, the sensitized *cis/trans* isomerization included in the vitamin A acetate synthesis and the photooxidation processes are of interest. Photooxidation is at present mainly used in the synthesis of odoriferous substances (rose oxide, nerol oxide, desoxide, terpineol, myrtenol).[76] Dioxetanes (the disodium salt of spiro[adamanan-2,3′-(4-methoxy-4-(3-phosphonooxyphenyl)-1,2-dioxetane)] = AMPPD) are of increasing importance for chemiluminescence assays[77] in clinical chemical diagnostics, although the amounts required can be produced in laboratory irradiation apparatus.

To conclude, Figure 21 gives the available data for the singlet oxygen reaction in industrial processes together with the data from the experiments in the SOLARIS reactor.

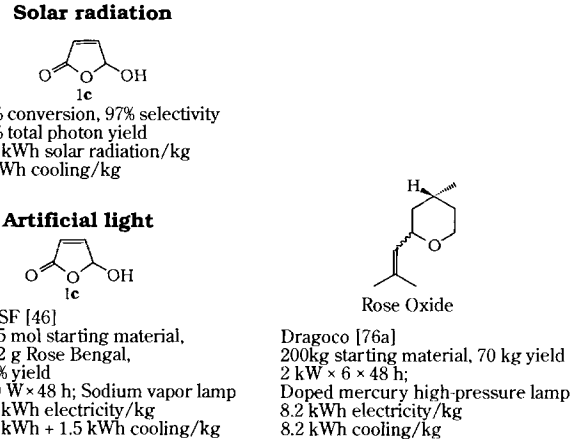


Fig. 21. Comparison of data for industrial and solar singlet oxygen reactions. The data for the production of rose oxide are applicable and are therefore listed. Cooling is performed either with a process cooler or by cooling water.

8. Future Outlook

The fundamental processes and techniques used to enable solar photochemical fine chemical synthesis to make a contribution to a "chemical technology of the future" have been described. In view of the generally low level of industrial interest in preparative photochemistry, there is still a long way to go. It is especially necessary to open up and adapt the photochemical synthesis potential for solar application in particular cases.

However, there is at the same time the option of going along this route in an economically and ecologically appropriate manner, closely matched to solar reaction conditions and local circumstances (see Fig. 1). For this, both "know-how" and especially "know-where" are required.

"Photochemical syntheses utilizing sunlight are not in general, and especially on an industrial scale, suitable for use in Europe or in the northern part of America, where sunlight is unreliable and often unavailable....." [9c]

An encouraging success for solar thermal chemistry was the very recent production of fullerene.[78] The high proportion of UV light in the electric arc processes used hitherto leads to partial decomposition of the fullerene.[78a] Highly concentrated solar radiation, up to 20000 suns and above,[78d] enables high temperatures to be achieved with a considerably lower proportion of UV, leading to a significant increase in the yield of fullerene and hopefully to an industrially attractive process.

A very important technical difference between thermal and photon solar chemistry is the degree of concentration of the solar radiation. In the first case, the extremely high concentration is the most significant advantage, but for photochemistry, which involves radiation concentration which is two orders of magnitude less, high space-time yields are obtained, and the limits of thermal control of the reaction system are reached. Here, photochemistry shows parallels to the photosynthesis model in which light energy is transferred from the chlorophyll-antenna complexes to the reaction center chlorophyll, thus using ultimately comparable degrees of energy concentration.

The SOLARIS reactor used here, together with the entire plant, was dismantled on November 18, 1992, by the DLR Köln on the PSA (Almeria) immediately after the final experiment. It is to be re-erected in Köln Porz.

Our thanks are due to Dipl.-Chem. P. Esser and Dipl.-Chem. I. Wöhrle for their support in the solar experiments, and also to Mr. Esser for contributions to the elucidation of the kinetics of the photooxygenation of furfural in the course of his work for his Diploma. We also thank Mrs. D. Gilliam for carrying out many experiments in preparation for the solar experiments, as well as Dr. N. Hoffmann (now at CNRS, VRA 459, Reims), Dr. H. Buschmann (now with Grünenthal GmbH, Aachen), and Dr. P. Jütten (now at the Hans Knöll Institut, Jena) for many discussions, and Dipl.-Ing. G. Schneider (now with EVT Stuttgart), Dr. M. Becker, and Dr. K. H. Funken, MD-ET DLR Köln for technical construction, and especially Mr. Schneider for the construction of the SOLARIS reactor. The SOLARIS experiment was cordially received by the PSA, Almeria, and was widely supported. We also thank the following, and the many other people whom they represent: W. Grasse and M. Sánchez (Directors of the PSA), J. A. Rodriguez and J. Hansen (Chief Engineers), and J. Blanco and S. Malato (detoxification loop—responsible engineer and chemist). Prof. Dr. H. Leismann (EHICS, Strasbourg) is thanked for determining the reflectivity of the aluminum foil and quantum yields. The construction of the SOLARIS loop and the first experimental phase (17 October 1991–15 February 1992) was financed by the DLR Köln through the Bundesministerium für Forschung und Technologie within the framework of the SOTA (SOLAR test center, Almeria) program. We also thank Dr. R. Hopp, Dr. W. Kuhn, and Dr. R. Pelzer (Haarmann & Reimer) for their support by supplying equipment and chemicals in the second experimental phase. Prof. Dr. G. O. Schenck is thanked for preparing Figure 2, and Prof. Dr. M. Demuth for information for Section 5.1. and for producing Figure 7. We are also obliged to the Fonds der Chemischen Industrie, to the Land Nordrhein-Westfalen (AG Solar NRW), as well as to Prof. Dr. K.-H. Büchel and Dr. W. Draber (Bayer AG). We also thank Mrs. I. Voss for her help in the preparation of the manuscript.

Received: September 30, 1993.
Revised version: January 4, 1994 [A 29 IE]
German version: *Angew. Chem.* **1994**, *106*, 2085
Translated by R. G. Leach, Basingstoke (UK)

[1] I. Dostrovsky, *Sci. Am.* **1991**, (12), 50.
[2] a) *Solar Power Plants* (Eds.: C.-J. Winter, R. Sizmann, L. L. Vant-Hull), Springer, Berlin, **1991**; b) W. Meinecke, M. Becker, H. Klaiß, *Brennst. Wärme Kraft* **1991**, *43*, 469.
[3] D. Wöhrle, *Nachr. Chem. Tech. Lab.* **1991**, *39*, 1256.
[4] V. N. Parmon, K. I. Zamaraev in *Photocatalysis Fundamentals and Applications* (Eds.: N. Serpone, E. Pelizzetti), Wiley, New York, **1989**, p. 565.
[5] W. Bloos, H. P. Hertlein, W. Knaupp, S. Nann, F. Pfisterer in ref. [2a], p. 283.
[6] a) D. F. Ollis, E. Pelizzetti, N. Serpone in *Photocatalysis Fundamentals and Applications* (Eds.: N. Serpone, E. Pelizzetti), Wiley, New York, **1989**, p. 603; b) O. Legrini, E. Oliveros, A. M. Braun, *Chem. Rev.* **1993**, *93*, 671; c) J. V. Anderson, H. Link, M. Bohn, B. P. Gupta, *Solar. Energy Mater.* **1991**, *24*, 538; d) D. Bahnemann, D. Bockelmann, R. Goslich, *ibid.* **1991**, *24*, 564; e) D. M. Blacke, J. Webb, C. Turchi, K. Margini, *ibid.* **1991**, *24*, 584; f) D. L. Alpert, J. L. Sprung, J. E. Pacheco, M. R. Prairie, H. E. Reilly, T. A. Milne, M. R. Nimlos, *ibid.* **1991**, *24*, 594; g) D. Bockelmann, R. Goslich, M. Hilgendorfff, D. Bahnemann in *Solar Thermal Energy Conversion, Vol. 7* (Eds.: M. Becker, K.-H. Funken, G. Schneider), Springer, Berlin, **1992**, p. 113; h) *Proc. 6th Symp. Sol. Therm. concentrating Technol.*, Editorial *CIEMAT* **1993**; i) D. Bahnemann, D. Bockelmann, M. Hilgendorff, G. Goslich, K. Wolff in *Solares Testzentrum Almeria* (Eds.: M. Becker, M. Böhmer, K.-H. Funken), C. F. Müller, Karlsruhe, **1993**, p. 309; j) C. Minero, E. Pelizzetti, S. Malato, J. Blanco, *Chemosphere* **1993**, *26*, 2103; k) J. Blanco, S. Malato, *Int. Sol. Energy Conf.*, San Francisco, **1994**; l) *Photocatalytic Purification and Treatment of Water and Air* (Eds.: D. F. Ollis, A. L-E Kabe), Elsevier, Amsterdam, **1993**; m) *Aquatic and Surface Photochemistry* (Eds.: G. R. Helz, R. G. Zepp, D. G. Crosby), Lewis Publishers, Boca Raton, FL, USA, **1994**.
[7] H. D. Roth, *Angew. Chem.* **1989**, *101*, 1220; *Angew. Chem. Int. Ed. Engl.* **1989**, *28*, 1193.
[8] G. Ciamician, *Science* **1912**, *36*, 385.
[9] a) A. Schönberg, *Präparative organische Photochemie*, Springer, Berlin, **1958**; b) A. Schönberg, G. O. Schenck, O.-A. Neumüller, *Preparative Organic Photochemistry*, Springer, Berlin, **1968**; c) A. Schönberg, A. Mustafa, *Chem. Rev.* **1947**, *40*, 181.
[10] G. O. Schenck, K. Ziegler, *Naturwissenschaften* **1944**, *32*, 157.
[11] a) G. O. Schenck, *Angew. Chem.* **1952**, *64*, 12; b) G. O. Schenck, *The Spectrum* **1990**, *3* (3), 1–8, 19. *ibid.* **1990**, *3* (4), 1–8.
[12] a) A. Schönberg, *Justus Liebigs Ann. Chem.* **1935**, *518*, 299; b) G. O. Schenck, *Angew. Chem.* **1957**, *69*, 579; c) K. Gollnick, G. O. Schenck in *1,4 Cycloaddition Reactions* (Ed.: J. Hamer), Academic Press, New York, **1967**, p. 255; d) K. Gollnick, G. O. Schenck, *Pure Appl. Chem.* **1964**, *9*, 507; e) E. J. Bowen, *Adv. Photochem.* **1963**, *1*, 23; f) R. Livingston, V. Subba Rao, *J. Phys. Chem.* **1959**, *63*, 794.
[13] a) H. Kautsky, H. de Bruijn, *Naturwissenschaften* **1931**, *19*, 1043; b) H. Kautsky, *Biochem. Z.* **1937**, *291*, 271.
[14] a) C. S. Foote, W. C. Wexler, *J. Am. Chem. Soc.* **1964**, *86*, 3879; b) C. S. Foote, *Acc. Chem. Res.* **1968**, *1*, 104.
[15] a) R. G. W. Norrish, *Angew. Chem.* **1968**, *80*, 868; b) G. Porter, *Angew. Chem.* **1968**, *80*, 882.
[16] a) E. Schumacher, *Chimia* **1978**, *32*, 193; b) G. Calzaferri, *ibid.* **1978**, *32*, 241; c) G. Jones, S.-H. Chiang, P.-T. Xuan, *J. Photochem.* **1979**, *10*, 1.
[17] a) M. Grätzel, *Acc. Chem. Res.* **1981**, *14*, 376; b) *Energy Resources through Photochemistry and Catalysis* (Ed.: M. Grätzel), Academic Press, New York, **1983**; c) J. Kiwi, K. Kalyanasundaram, M. Grätzel, *Sol. Energy Mater.* **1982**, *49*, 37.
[18] H.-D. Scharf, J. Fleischhauer, H. Leismann, I. Ressler, W. Schleker, R. Weitz, *Angew. Chem.* **1979**, *91*, 696; *Angew. Chem. Int. Ed. Engl.* **1979**, *18*, 652.
[19] B. Bogdanović, A. Ritter, B. Spliethoff, *Angew. Chem.* **1990**, *102*, 239; *Angew. Chem. Int. Ed. Engl.* **1990**, *29*, 223.
[20] a) A. M. Braun, M.-T. Maurette, E. Oliveros, *Photochemical Technology*, Wiley, Chichester, **1991**, p. 195; b) *Solar Energy Materials and Solar Cells*, Elsevier, Amsterdam, The Netherlands, **1994**, p. 32.
[21] a) M. Iqbal, *An Introduction to Solar Radiation*, Academic Press, New York, **1983**; for a more compact representation see b) A. Goetzberger, V. Wittwer, *Sonnenenergie Thermische Nutzung*, Teubner, Stuttgart, **1989**; c) G. von Bünau, T. Wolff, *Photochemie*, VCH, Weinheim, **1987**.

[22] P. Esser, Dissertation, Technische Hochschule Aachen, **1994**.

[23] The degree of concentration is defined as the increase in the energy flow density (here the direct radiation of the sun) passing through an aperture of given area (see ref. [2a]). For parabolic trough collectors, a good representation of the light concentration is given by the ratio of the width of the parabolic mirror to the inside diameter of the absorber tube multiplied by the photoreactor efficiency.

[24] *The IEA/SSPS Solar Thermal Power Plants* (Eds.: P. Kesselring, C. S. Selvage) Springer, Berlin, **1986**.

[25] R. Sizmann, P. Köpke, R. Busen in ref. [2a], p. 17.

[26] Very recent communication from M. Demuth of December 1993.

[27] a) A. Hülsdünker, A. Ritter, M. Demuth, *EPA Newsl.* **1992**, *45*, 23; b) A. Hülsdünker, A. Ritter, M. Demuth in *Solar Thermal Energy Conversion, Vol. 6* (Eds.: M. Becker, K.-H. Funken, G. Schneider), Springer, Berlin, **1992**; c) A. Hülsdünker, A. Ritter, M. Demuth in *Solar Thermal Energy Conversion, Vol. 7* (Eds.: M. Becker, K.-H. Funken, G. Schneider), Springer, Berlin, **1992**, p. 81; d) A. Hülsdünker, A. Ritter, M. Demuth in *Solares Testzentrum Almeria* (Eds.: M. Becker, M. Böhmer, K.-H. Funken), Müller, Karlsruhe, **1993**, p. 269.

[28] The following are recent review articles on di-π- and oxadi-π-methane rearrangements: a) *Comprehensive Organic Synthesis, Vol. 5* (Eds.: B. M. Trost, I. Fleming), Pergamon, Oxford, **1991**; b) O. De Lucchi, W. Adam in ref.[28a], p. 193; c) M. Demuth in ref.[28a], p. 215; d) M. Demuth in *Organic Photochemistry, Vol. 11* (Ed.: A. Padwa), Dekker, New York, **1991**, p.37.

[29] *Final Configuration of PSA Solar Detoxification Loop, Technical Report*, (Ed.: J. Blanco) 20. December **1991**.

[30] The reflective material was aluminum foil formed by vapor deposition on Hostaflon, the back surface of which was sealed to polyester film and fixed by adhesive to a carrier structure. The reflectivity of the the foil at a half aperture angle of 43.6 mrad and a wavelength of 600 nm was 79%. The half aperture angle is given by the geometry of the mirror and absorber tube. Scattered light within this half aperture angle still impinges on the inside diameter of the absorber tube and hence on the reaction solution.

[31] For more recent review articles on the [2 + 2] photoaddition of α,β-unsaturated carbonyl compounds see: a) D. I. Schuster in *The Chemistry of the Enones, Part 2* (Eds.: S. Patai, Z. Rappoport), Wiley, New York, **1989**, p. 623; b) D. Becker, N. Haddad, *Org. Photochem.* **1989**, *10*, 1; c) M. T. Crimmins in ref. [28a], p. 123; d) M. T. Crimmins, *Chem. Rev.* **1988**, *88*, 1435.

[32] a) N. Hoffmann, H.-D. Scharf, *Liebigs Ann. Chem.* **1991**, 1273; b) N. Hoffmann, Dissertation, Technische Hochschule Aachen, **1992**.

[33] N. Hoffmann, H.-D. Scharf, J. Runsink, *Tetrahedron Lett.* **1989**, *30*, 2639.

[34] a) J. A. Porco, S. L. Schreiber in ref. [28a], p. 151; b) H. Buschmann, Dissertation, Technische Hochschule Aachen, **1992**, p. 101.

[35] a) S. L. Schreiber, K. Satake, *J. Am. Chem. Soc.* **1983**, *105*, 6723; b) *ibid.* **1984**, *106*, 4186; c) *Tetrahedron Lett.* **1986**, *27*, 2575.

[36] S. L. Schreiber, A. H. Hoveyda, *J. Am. Chem. Soc.* **1984**, *106*, 7200.

[37] S. L. Schreiber, D. Desmaele, J. A. Porco, *Tetrahedron Lett.* **1988**, *29*, 6689.

[38] S. L. Schreiber, *Sience* **1985**, *227*, 857.

[39] T. Kozluk, A. Zamojski, *Collect. Czech. Chem. Commun.* **1983**, *48*, 1659.

[40] R. Hambalek, G. Just, *Tetrahedron Lett.* **1990**, *31*, 4693.

[41] T. R. Hoye, W. S. Richardson, *J. Org. Chem.* **1989**, *54*, 688.

[42] A. Nehrings, H.-D. Scharf, J. Runsink, *Angew. Chem.* **1985**, *97*, 882; *Angew. Chem. Int. Ed. Engl.* **1985**, *24*, 877.

[43] a) H. Buschmann, N. Hoffmann, H.-D. Scharf, *Tetrahedron: Asymmetry* **1991**, *2*, 1429; b) P. Esser, H. Buschmann, M. Meyer-Stork, H.-D. Scharf, *Angew. Chem.* **1992**, *104*, 1254; *Angew. Chem. Int. Ed. Engl.* **1992**, *31*, 1190.

[44] a) G. O. Schenck, DE-B 881193, **1953**; *Chem. Abstr.* **1956**, *50*, 5035; b) *Liebigs Ann. Chem.* **1953**, *584*, 156.

[45] F. Perez, F. Ramos, M. Victoria, ES-B 431794, **1972**; *Chem. Abstr.* **1972**, *87*, 22418.

[46] G. Bolz, W.-W. Wiersdorff (BASF), DE-B 2111119, **1972**; *Chem. Abstr.* **1972**, *77*, 151883.

[47] J. Martel, J. Tessier, J. P. Demoute (Roussel Uclaf), EP-B 23454, **1981**; for catalytic and kinetic separation of 5-alkoxy-5*H*-furan-2-ones see b) W. S. Faber, J. Kok, B. de Lange, B. L. Feringa, *Tetrahedron* **1994**, *50*, 4775.

[48] B. L. Feringa, J. C. de Jong, *Bull. Soc. Chim. Belg.* **1992**, *101*, 627.

[49] F. Fariña, M. D. Parellada, *An. Quim. Ser. C* **1983**, *79*, 165.

[50] a) P. Magnus, P. M. Cairns, C. S. Kim, *Tetrahedron Lett.* **1985**, *26*, 1963; b) *J. Am. Chem. Soc.* **1986**, *108*, 217.

[51] a) Y. Toyo, O. Iwao, JP-B 3218, **1955**; *Chem. Abstr.* **1957**, *51*, 16525; b) A. S. Marcus (du Pont), US-A 2859218, **1958**; *Chem. Abstr.* **1959**, *53*, 10061.

[52] F. Yuste, R. Sanchez-Obregon, *J. Org. Chem.* **1982**, *47*, 3665.

[53] a) A. I. Meyers, R. L. Nolen, E. W. Collongton, T. A. Narwid, *J. Org. Chem.* **1973**, *38*, 1974; b) H. G. M. Walraven, U. K. Pandit, *Tetrahedron* **1980**, *36*, 321.

[54] S. R. Landor, P. D. Landor, M. Kalli, *J. Chem. Soc. Perkin Trans 1* **1983**, 2921.

[55] a) H. U. Starcke, E. Schlenzka, G. Schenck (Henkel), DE-B 2538771, **1977**; *Chem. Abstr.* **1977**, *86*, 195234; b) H. Tomaschek, P. Berlinghof (Teroson), DE-B 3006017, **1981**; *Chem. Abstr.* **1982**, *95*, 134087; c) M. Kaeriyama, S. Takehiro, I. Kumita, K. Okuma, M. Ando, S. Hashimoto, H. Yoneda (Nippon Soda), JP-B 76146457, **1975**; *Chem. Abstr.* **1977**, *87*, 39528.

[56] A. J. Daggan, R. L. Webb, *US-A 4272440*, **1981**; *Chem. Abstr.* **1981**, *95*, 132936.

[57] a) W. R. Roush, T. Blizzard, *J. Org. Chem.* **1984**, *49*, 1772; b) W. C. Still, H. Ohmizu, *ibid.* **1981**, *46*, 5241.

[58] a) H.-D. Scharf, J. Janus, F. Dallacker, R. Moranek, *Liebigs Ann. Chem.* **1978**, 573; b) H.-D. Scharf, J. Janus, *Tetrahedron* **1979**, *35*, 385.

[59] a) F. M. Hauser, S. Prasanna, *J. Am. Chem. Soc.* **1981**, *103*, 6378; b) *J. Org. Chem.* **1979**, *44*, 2596.

[60] a) R. Jones, N. H. Wilson, EP-B 13608, **1980**; *Chem. Abstr.* **1981**, *94*, 46854; EP-B 43292, **1982**; *ibid.* **1982**, *96*, 217558; EP-B 13607, **1980**; *ibid.* **1981**, *94*, 191781.

[61] a) A. Fariña, M. V. Martin, M. C. Paredes, *Synthesis* **1973**, 167; b) J. A. Gratz, C. E. Cook, M. E. Wall, *Org. Prep. Proced.* **1970**, *2*, 51.

[62] a) B. L. Feringa, B. de Lange, *Tetrahedron Lett.* **1988**, *29*, 1303; b) B. de Lange, F. van Bolhuis, B. L. Feringa, *Tetrahedron* **1989**, *45*, 6799.

[63] a) J. F. G. A. Jansen, B. L. Feringa, *Tetrahedron Lett.* **1989**, *30*, 5481; b) B. L. Feringa, B. de Lange, J. C. de Jong, *J. Org. Chem.* **1989**, *54*, 2471; c) J. F. G. A. Jansen, Dissertation, Universität Groningen, **1991**; d) J. F. G. A. Jansen, B. L. Feringa, *Synth. Commun.* **1992**, *22*, 1367.

[64] B. L. Feringa, B. de Lange, *Tetrahedron* **1988**, *44*, 7213.

[65] a) B. de Lange, B. L. Feringa, *Tetrahedron Lett.* **1988**, *29*, 5317; b) ref. [63b].

[66] J. F. G. A. Jansen, B. L. Feringa, *Tetrahedron Lett.* **1991**, *32*, 3239.

[67] N. Hoffmann, *Tetrahedron: Asymmetry* **1994**, *5*, 879.

[68] a) R. van Speybroeck, H. Guo, J. van der Eycken, M. Vanderwalle, *Tetrahedron* **1991**, *47*, 4675; b) R. S. Ward, *Synthesis* **1991**, 719; c) E. J. Bush, D. W. Jones, *J. Chem. Soc. Chem. Commun.* **1993**, 1200; d) A. Pelter, R. S. Ward, L. Qianrong, J. Pis, *Tetrahedron: Asymmetry* **1994**, *5*, 909; e) A. Pelter, R. S. Ward, D. M. Jones, P. Madtocks, *J. Chem. Soc. Perkin Trans 1* **1993**, 2621; f) *ibid.* **1993**, 2631; g) A. Pelter, R. S. Ward, A. Abd-el-Ghani, *Tetrahedron: Asymmetry* **1994**, *5*, 329.

[69] A. Krief, P. Lecomoto, J. P. Demoute, W. Dumont, *Synthesis* **1990**, 275.

[70] J. F. G. A. Jansen, B. L. Feringa, *Tetrahedron: Asymmetry* **1990**, *1*, 719.

[71] a) G. O. Schenck, K. Gollnick, *Forschung des Landes Nordrhein-Westfalen No. 1256*, Westdeutscher Verlag, Köln and Opladen, **1963**; b) J. Paczkowski, J. J. M. Lamberts, B. Paczkowska, D. C. Neckers, *J. Free Radicals Biol. Med.* **1985**, 341; c) D. C. Neckers, *J. Photochem. Photobiol. A* **1989**, *47*, 1.

[72] K. Gollnick, G. O. Schenck, *Pure Appl. Chem.* **1964**, *9*, 507; E. Gandin, Y. Lion, A. Van de Vorst, *J. Photochem.* **1983**, *37*, 271; for a collection of singlet oxygen quantum yields of different sensitizers see F. Wilkinson, W. P. Helman, A. B. Ross, *J. Phys. Chem. Ref. Data* **1993**, *22*, 113.

[73] a) R. Bonneau, R. Pottier, O. Bagno, J. Joussot-Dubien, *J. Photochem.* **1975**, *21*, 159; b) R. W. Denny, A. Nickson, *Org. React.* **1973**, *20*, 177.

[74] a) I. Schopov, A. Obreschkov, I. M. Panayatov, *J. Prakt. Chem.* **1966**, *33*, 309; b) L. Cottier, G. Descotes, H. Nigay, J.-C. Parron, V. Gregoire, *Bull. Soc. Chim. Fr.* **1986**, *5*, 844.

[75] a) A. M. Braun, *Nachr. Chem. Tech. Lab.* **1991**, *39*, 515; b) H.-D. Scharf, H. Leismann, H. Koch, *Photochem. Convers. Symp.* **1983**, 133; c) K. H. Pfoertner, *J. Photochem.* **1984**, *25*, 91; d) *Photochem. Photobiol. A* **1990**, *51*, 81; e) M. Fischer, *Angew. Chem.* **1978**, *90*, 17; *Angew. Chem. Int. Ed. Engl.* **1978**, *17*, 16; f) A. Roloff, K. Meier, M. Riediker, *Pure Appl. Chem.* **1986**, *58*, 1267; g) H. Böttcher, J. Bendig, M. A. Fox, G. Hopf, H.-J. Timpe, *Technical Applications of Photochemistry*, Deutscher Verlag für Grundstoffindustrie, Leipzig, **1991**.

[76] a) K. Gollnick, *Chim. Ind. Milan* **1982**, *64*, 156; b) W. Rojahn, H. U. Warnecke, *Dragoco Rep. Engl. Ed.* **1980**, *6/7*, 158.

[77] For reviews on chemiluminescence assays see a) S. Albrecht, H. Brandl, W. Adam, *Chem. Unserer Zeit* **1990**, *24*, 227; b) S. Albrecht, H. Brandl, C. Schönfels, W. Adam, *ibid.* **1992**, *26*, 63; c) S. Albrecht, H. Brandl, W. Adam, *Nachr. Chem. Tech. Lab.* **1992**, *40*, 547, and references therein; d) A. Mayer, S. Neuenhofer, *Angew. Chem. 106*, **1994**, 1097; *Angew. Chem. Int. Ed. Engl.* **1994**, *33*, 1044.

[78] a) L. P. F. Chibante, A. Thess, J. M. Alford, M. D. Diener, R. E. Smalley, *J. Phys. Chem.* **1993**, *97*, 8696; b) the reactor is shown in R. Baum, *Chem. Eng. News* **1993**, *71* (35) 21; c) C. L. Fields, J. R. Pitts, M. J. Hale, C. Bingham, A. Lewandowski, D. E. King, *J. Phys. Chem.* **1993**, *97*, 8701; d) the "high flux density solar furance" in Colorado is the model for that built by AG Solar in Köln-Porz: A. Lewandowski, C. Bingham, J. O'Gallagher, R. Winston, D. Sagie, *Sol. Energy Mater.* **1991**, *24*, 550.

Thermal and Optical Switching of Iron(II) Complexes

Philipp Gütlich,* Andreas Hauser, and Hartmut Spiering

Dedicated to Professor Heinrich Nöth on the occasion of his 65th birthday

Transition metal chemistry contains a class of complex compounds for which the spin state of the central atom changes from high spin to low spin when the temperature is lowered. This is accompanied by changes of the magnetic and optical properties that make the thermally induced spin transition (also called spin crossover) easy to follow. The phenomenon is found in the solid state as well as in solution. Amongst this class, iron(II) spin crossover compounds are distinguished for their great variety of spin transition behavior; it can be anything from gradual to abrupt, stepwise, or with hysteresis effects. Many examples have been thoroughly studied by Mössbauer and optical spectroscopy, measurements of the magnetic susceptibilities and the heat capacities, as well as crystal structure analysis. Cooperative interactions between the complex molecules can be satisfactorily explained from changes in the elastic properties during the spin transition, that is, from changes in molecular structure and volume. Our investigations of iron(II) spin crossover compounds have shown that green light will switch the low spin state to the high spin state, which then can have a virtually unlimited lifetime at low temperatures (this phenomenom is termed light-induced excited spin state trapping—acronym: LIESST). Red light will switch the metastable high spin state back to the low spin state. We have elucidated the mechanism of the LIESST effect and studied the deactivation kinetics in detail. It is now well understood within the theoretical context of radiationless transitions. Applications of the LIESST effect in optical information technology can be envisaged.

1. Introduction

Thermally induced spin crossovers, that is, changes of the spin multiplicity within one and the same transition metal complex, are among the most fascinating "games" electrons play in the coordination chemistry of 3d elements with electron configuarations d^4 to d^7 (and d^8 when molecular symmetry is lower than O_h). This spin crossover phenomenon (less commonly called magnetic crossover, spin equilibrium, or spin isomerism) was discovered more than sixty years ago by Cambi et al. For iron(III) tris(dithiocarbamate)s,[1–4] they observed electronic states[5, 6] with occupations strongly dependent on temperature. It took more than thirty years for the first iron(II) complex with a temperature-dependent $^5T_{2g}(O_h) \rightleftharpoons {}^1A_{1g}(O_h)$ spin transition, $[Fe(phen)_2(NCS)_2]$ (phen = 1,10-phenanthroline), to be discovered.[7] This marked the start of very active research on the spin crossover phenomenon found in the solid state as well as in solution. Even at this early stage of spin crossover research it was apparent that the phenomenon is found very often in complexes of iron(II), iron(III), and cobalt(II), but also occasionally in those of nickel(II), cobalt(III), and manganese(III). The first thermal spin crossover in chromium(II) compounds was reported in 1989.[8] The unusual temperature dependence of the magnetic properties observed in cluster compounds such as Nb_6I_{11} and HNb_6I_{11} is also caused—so one assumes—by the spin crossover phenomenon.

The field has been covered in a series of review articles emphasizing different aspects. The first comprehensive articles[10–12] treated all spin crossover compounds known at the time and even then emphasized the distinct influence of the chemical environment, such as the particular ligand sphere. Towards the end of the sixties, a preference for investigations of the thermal high spin (HS) to low spin (LS) transition [(HS$\rightleftharpoons$LS] in octahedral iron(II) complexes developed,[13–23] probably because ^{57}Fe Mössbauer spectroscopy was such an extraordinary tool for following the spin transition as a function of temperature, pressure, time, concentration, and other variables of the system. Because the relaxation times of the Fe^{2+} (HS) and Fe^{2+} (LS) spin states are much longer (at least below 300 K) than the time resolution of the Mössbauer method (10^{-7} s), their resonance lines usually appear sharp and well resolved with characteristic Mössbauer parameters.[24] On the contrary, for the HS ($^6A_{1g}$) $\rightleftharpoons$ LS ($^2T_{2g}$) spin transition in iron(III) complexes, fluc-

[*] Prof. P. Gütlich, Dr. habil. H. Spiering
Institut für Anorganische Chemie und Analytische Chemie
der Universität
Staudinger Weg 9, D-55099 Mainz (FRG)
Telefax: Int. code + (6131)39-2990
Dr. habil. A. Hauser
Institut für Anorganische und Physikalische Chemie
der Universität Bern

 © VCH Verlagsgesellschaft mbH, D-69451 Weinheim, 1994 0570-0833/94/2020-2024 $ 10.00+.25/0 Angew. Chem. Int. Ed. Engl. 1994, 33, 2024–2054

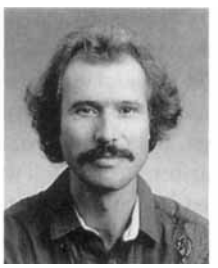
tuation rates are greater by several orders of magnitude . Thus, the relaxation times of the HS and LS states often approach the size of the Mössbauer time window, and consequently, we find strong broadening of the resonance lines, or even time-averaged spectra. This greatly complicates data evaluation and makes the pure HS and LS states hard to distinguish.

Apart from Mössbauer spectroscopy, at least half a dozen other methods are applied in spin crossover investigations. The magnetic susceptibilities ($\chi(T) = \gamma_{HS}\chi_{HS} + (1-\gamma_{HS})\chi_{LS}$) of solid spin crossover compounds (measured with a Faraday balance, a Foner type magnetometer, or a SQUID magnetometer), and of liquids (measured with Evans's NMR method) is a function of the temperature-dependent fractions of HS (γ_{HS}) and LS ($\gamma_{LS} = 1-\gamma_{HS}$) molecules. If χ_{HS} and χ_{LS} are known, $\gamma_{HS}(T)$ can be determined from these values and used as an ordering parameter for the spin transition as a function of temperature. The spin transition curve $\gamma_{HS}(T)$ obtained this way (and also from the integrals of the HS and LS absorption bands from optical spectra and, for solid spin crossover compounds, from those of the HS and LS Mössbauer resonance lines as well) can adopt very different forms. Cooperative interactions between the complex molecules have a crucial influence on the different spin transition functions $\gamma_{HS}(T)$ in the solid, whereas interactions between spin-changing molecules are virtually insignificant in the liquid phase. Therefore, the simple Boltzmann law always describes $\gamma_{HS}(T)$ in liquids. In the liquid phase, for instance in d^6 spin crossover compounds, the distribution over the different spin states contains the simple degeneracy of the $^1A_{1g}$ state as well as the 15-fold degeneracy of the $^5T_{2g}$ state. For solids, such a Boltzmann behavior of $\gamma_{HS}(T)$ is rather the exception.

Another valuable source of information are the temperature-dependent IR spectra. There is a clear increase in the central ion–ligand stretching frequency in the FIR range from approximately 250 cm^{-1} for the iron(II) HS state to approximately 400 cm^{-1} for the iron(II) LS state.[25, 26] The N–C stretching modes around 2000 cm^{-1} are a sensitive probe for many iron(II) spin crossover systems with NCS or NCSe ligands coordinating through nitrogen atoms, because going from the HS to the LS state shifts the band by about 40 cm^{-1} towards higher frequencies (see the review in ref. [18]). The IR spectroscopic data indicate a distinct increase in the metal–ligand bond strength on one hand, and of the N–C bond in the NCS or NCSe ligands on the other, upon transition from the HS to the LS state. The explanation becomes clear from the electronic rearrangement associated with the spin transition in an octahedral ligand field: $t_{2g}^4 e_g^2 (^5T_{2g}) \rightleftharpoons t_{2g}^6 (^1A_{1g})$. Looking at the MO scheme for octahedral complexes,[6, 27] we see that the e_g orbitals occupied in the HS state are antibonding in character. The increase in bond strength upon transition to the LS state is then jointly effected by their depopulation and the concomitant population of the t_{2g}



P. Gütlich



A. Hauser



H. Spiering

Philipp Gütlich studied Chemistry at the Technische Hochschule Darmstadt. After obtaining his doctorate (in Physical Chemistry/Nuclear Chemistry with K. H. Lieser) in 1963, he worked at the Nuclear Research Center Saclay/Paris and subsequently at Brookhaven National Laboratory/USA, where his research led him into the field of Mössbauer spectroscopy for the first time. After his return in 1966 he further diversified his experience into the field of theoretical chemistry at Uppsala and Oxford. In 1969 he completed his habilitation at the TH Darmstadt with a thesis on the application of Mössbauer spectroscopy in chemistry. He accepted the chair of Anorganische und Analytische Chemie at the University of Mainz in 1975. His main research interests are spectroscopy on transition metal compounds (problems of electronic structure, magnetism, phase change, and photochemistry) and application of Mössbauer and electronic spectroscopy (Auger, ESCA) to problems in technology. P. Gütlich received the Research Award of the Japanese Society for the Promotion of Science (JSPS) in 1989 and in 1993 together with O. Kahn (Paris) the Forschungspreis der Max-Planck-Gesellschaft.

Andreas Hauser, born in 1955 in Bern, Switzerland studied Chemistry at the University of Bern and obtained his doctorate under the supervision of H. U. Güdel in 1983. From 1984 to 1987 he worked as postdoctorate fellow at the Research School of the Australian National University in Canberra with J. Ferguson and thereafter as Wissenschaftlicher Mitarbeiter at the University of Mainz with P. Gütlich. There he completed his habilitation with a thesis on the photophysical properties of Fe^{II} coordination compounds. Since 1992 he has been Oberassistent at the Institut für Anorganische und Physikalische Chemie der Universität Bern. His research interests are photochemical and photophysical properties of transition metal compounds.

Hartmut Spiering, born in 1943 in Bad Wildungen, Germany, received his Doctorate in Physics at the University of Münster in 1978 under the supervision of H. Wegener and his habilitation at the University of Erlangen-Nürnberg for contributions to the methodology and application of Mössbauer spectroscopy. Since 1978 he has been Wissenschaftlicher Mitarbeiter at the University of Mainz in the research group of P. Gütlich.

orbitals. This in turn increases the $d_\pi - p_\pi$ backbonding towards the ligand. In complexes containing NCS and similar ligands together with arene ligands, backbonding to the aromatic ligand is dominant. This is accompanied by a partial depopulation of the antibonding π^*(N–C) orbitals to compensate the charge deficit at the central ion caused by the backbonding. As a consequence, the frequency of the N–C stretching mode increases.

Of course we have to expect that such striking changes in the metal–ligand bond strength will cause bond shortening. Indeed, temperature-dependent single crystal X-ray structure analyses of many iron(II) spin crossover compounds show that the Fe–N bond lengths shorten by about 20 pm when going from the HS to the LS state,[28] which corresponds to approximately 10% of the bond length or up to 5% of the unit cell volume. This must have its effect on the phonon system and the elastic properties of the lattice. This provides the driving force for the cooperative interactions which decisively influence the spin transition mechanism in the solid (see Section 3.4.1). Crystal structure analyses above and below the critical spin transition temperature $T_{1/2}(\gamma_{HS} = 0.5)$ also detect whether a change in the crystal structure (that is, in the space group) is associated with the spin transition, as well as the ever present changes in the bond lengths. Experience shows that gradual (continuous) spin transitions normally proceed without structural changes. Abrupt (discontinuous) spin transitions, however, are often associated with structural changes, which are frequently also accompanied by hysteresis effects of the $\gamma_{HS}(T)$ curve between falling and rising temperatures. Though the reverse reasoning is quite common in solid state research (namely that hysteresis effects during a phase change are indicative of an associated structural change), recent evidence proves it to be invalid (at least for spin transitions in the solid).[29–31] For those cases where a spin transition is associated with a structural change, the question about the original cause and the ensuing effect arises. From what we know today, both possibilities can be realized. A change of spins in the electronic ground state can be caused by a thermally induced lattice distortion, but a thermally induced spin transition can also deform the lattice. The possibility of observing lattice and molecular changes of the structure directly at the spin transition makes the various diffraction methods with X-rays, neutrons, and more recently also synchrotron radiation (including EXAFS[32, 33]) so eminently valuable for spin crossover research on solids, be they in the form of single crystals or powders (see refs. [28, 34–36]).

Amongst the plethora of physical methods for the investigation of spin crossover phenomena, calorimetric measurements are also well established. They show the spin transition and enable determination of the transition enthalpy and entropy, which, for the example of iron(II) spin crossover compounds, are $\Delta H = H_{HS} - H_{LS} \approx 6-15\ kJ\,mol^{-1}$ and $\Delta S = S_{HS} - S_{LS} \approx 40-65\ J\,K^{-1}\,mol^{-1}$ at spin transition temperatures around 130 K.[28] From C_p measurements on $[Fe(phen)_2(NCS)_2]$ and $[Fe(phen)_2(NCSe)_2]$, Sorai and Seki[37] concluded twenty years ago that the driving force behind the spin transition is the considerable entropy increase on going from the LS to the HS state. This is true for all spin crossover complexes, irrespective of the central ion. According to Sorai and Seki, the electronic (magnetic) contribution to the total measured gain in entropy of $\Delta S \approx 50\ J\,K^{-1}\,mol^{-1}$ is about 30%: $\Delta S_{mag} = R[\ln(2S+1)_{HS} - \ln(2S+1)_{LS}] = 13.4\ J\,K^{-1}\,mol^{-1}$. For complexes with a symmetry lower than O_h (such as C_{2v} in the case under discussion), the orbital contribution is insignificant. The major part of the remaining 70% of the entropy change stems roughly equally from contributions from intramolecular stretching modes and intramolecular deformation modes; only a comparatively small fraction is supposed to be attributable to changes in intermolecular vibrational modes. The authors conclude from the dominant share of the total entropy gain from the vibrational changes that long-range interactions from coupling between the electronic states and the phonon system must play an important role in the cooperative spin transition in the solid.

Over many years a good number of research groups[38–54] have worked on how the spin transition in the solid proceeds in detail, in particular on understanding the mechanism of the cooperative interactions and developing a theoretical model. Such a model should be formulated generally enough to include and account for all the experimental observations. In Section 3.4.1 the model of elastic interactions[40–44] developed in our group will be treated in depth.

Kinetic investigations of liquids and solids are especially enlightening. Relaxation rates have been measured for spin crossover systems which were perturbed from equilibrium by temperature jump, ultrasound, or irradiation with light, and for systems decaying from long-lived metastable states after thermal or optical excitation (see review articles in refs. [28] and [55]). ^{57}Fe Mössbauer spectroscopy adds to this variety of methods. Relaxation rates k around $10^7\ s^{-1}$ and related activation parameters can be determined from line shape analyses of relaxation-broadened Mössbauer absorption lines.[56–59] A special variant of Mössbauer spectroscopy is time-differential coincidence spectroscopy.[60] Here, the ^{57}Co(EC)^{57}Fe nuclear decay (EC = electron capture) in ^{57}Co-doped complexes is used as an "intrinsic clock" for a time scale from approximately 5–500 ns on one hand, and as an "intrinsic light source" for the creation of excited electron states on the other. These states then relax back to the ground state by intersystem crossing (ISC) processes along that very time scale.[61–63]

Contributions towards a better understanding of spin crossover processes have come from kinetic measurements supplying detailed data on lifetimes and activation parameters, from equilibrium measurements supplying thermodynamic data, and from spectroscopic investigations and quantum chemical calculations supplying molecular orbital and ligand field diagrams. Our own efforts serendipitously led us to the discovery of the LIESST effect in iron(II) spin crossover compounds in 1984.[64–66] Buhks et al.[67] have published a theoretical paper that led the way to understanding spin crossover dynamics. It was later applied to the interpretation of the HS → LS relaxation after light excitation (LIESST) in the solid by Hauser[68] (see Section 5.2).

Now that the essential aspects of spin crossover research have been sketched, we shall present the most important results and insights from our own spin crossover and LIESST research on solid iron(II) complexes. As our particular goal has for years been to apply a multitude of physical methods to a few suitable examples in order to gain an in-depth view and to learn as much as possible about the whys and wherefores of spin crossover and

LIESST, the emphasis will be on picolylamine and tetrazole complexes. We shall start the second section with some considerations on ligand field theory to clarify the conditions for thermally induced spin crossover. A discussion of the chemical and physical influences on spin crossover behavior in the solid follows. The section ends with a description of the structural changes associated with the spin transition. Model views based on elastic interactions developed from there will be the subject of Section 3, together with the thermodynamics of the spin transition. Sections 4 and 5 are dedicated to the LIESST effect and to kinetic investigations of the processes associated with it. The article ends with some concluding remarks on possible applications of spin crossover and the LIESST effect.

2. Thermal Spin Transitions in Iron(II) Complexes

2.1. Ligand Field Considerations—Theory

Iron(II) is a transition metal ion with six d electrons. In a complex where iron(II) is coordinated by six ligands, that is, in an octahedral ligand field (LF), the ^{2S+1}L terms of the free ion will be split according to the Tanabe–Sugano diagram,[69] as shown in Figure 1. The parameter along the x axis is the LF

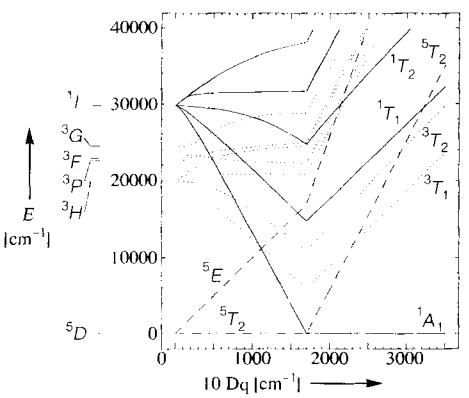


Fig. 1. Tanabe–Sugano diagram for an octahedral d^6 complex, calculated with the Racah parameters [6] of the free iron(II) ion according to Tanabe and Sugano [69].

strength expressed as 10 Dq, a measure for the influence of the ligands on the d electrons of the central ion.

Iron(II) complexes with ligands that exert only a weak influence on the d electrons of the central iron (for example, the paramagnetic $[Fe(H_2O)_6]^{2+}$ complex) have a HS $^5T_{2g}$ state as the ground state, stemming from the ^5D ground state of the free ion. With increasing ligand field strength, however, the LS $^1A_1$ state, based on the ^1I term of the free ion, is quickly lowered in energy; consequently, from a critical LF strength Δ_{crit} onward, it becomes the ground state of the complex. This is, for example, the case for the diamagnetic $[Fe(CN)_6]^{4-}$ complex.

For a proper appreciation of the importance of the crossover point at Δ_{crit} and the phenomenon of thermal spin transition, it is not sufficient to discuss the Tanabe–Sugano diagram alone, since it gives only the energies of the electronic excited states with respect to the energies of the corresponding ground state. The ligand field strength is not only determined by the properties of the ligand; it is also a strong function of the metal–ligand distance. For neutral ligands[6] Equation (1) holds in which μ

$$10\,Dq \approx \mu / r^6 \tag{1}$$

is the dipole moment of the ligand and r the metal–ligand distance. For a given ligand, 10 Dq(r) can be determined experimentally at the equilibrium distance r_0 of the corresponding ground state, that is, for the metal–ligand bond length. 10 Dq(r) can then be estimated for any r from the simple relation in Equation (2).

$$10\,Dq(r) = 10\,Dq(r_o)\left(\frac{r_o}{r}\right)^6 \tag{2}$$

For each ground state, LS or HS, we can apply a potential with the metal–ligand distance r (or the totally symmetric normal coordinate $Q = Q_{a_1}$) as the configuration coordinate. Now the electronic energies of the excited states can be calculated as a function of r, with 10 Dq(r) from Equation (2) and the Tanabe–Sugano diagram. One has to keep in mind that, contrary to 10 Dq, electron–electron interactions (that is, the Racah parameters B and C) depend only weakly on r. A natural consequence of this calculation is that for the other ligand field states the potential wells are shifted vertically as well as horizontally with respect to the reference state.

In the first place we are now interested in the $^5T_2$ potential well, which is always shifted towards a greater metal–ligand distance than that of the $^1A_1$ state, irrespective of the ligand (Fig. 2). This is understandable, since the $^5T_2$ state is based on

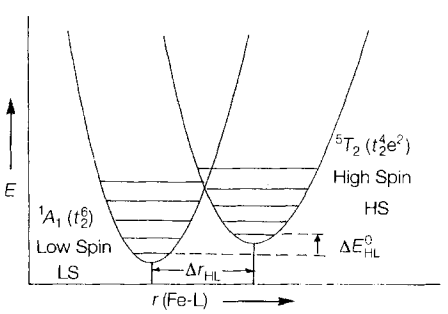


Fig. 2. Schematic representation of the potential wells for the $^1A_1$ and the $^5T_2$ states of an iron(II) spin crossover complex. The condition for a thermal spin transition is $\Delta E^0_{HL} \approx k_B T$. The nuclear coordinate is r(Fe–L).

the $(t_2^4e^2)$ configuration with two of the six d electrons in antibonding e orbitals, whereas the $^1A_1$ state of the (t_2^6) configuration has all six d electrons in the mainly nonbonding t_2 orbitals.

The relative vertical shift of the two potential wells, on the other hand, depends very much on the specific properties of the ligands. For complexes with suitable ligands, the difference in the zero point energies for the two states, $\Delta E^0_{HL} = E^0_{HS} - E^0_{LS}$, can fall within the range of thermal energies. In that case, only the $^1A_1$ state as the ground state is occupied at low temperatures. At higher temperatures, however, thermal occupation of the $^5T_2$ state occurs. Because the $^5T_2$ state is 15-fold degenerate and has a higher vibrational density of states, this entropy-driven thermal spin transition is almost quantitative.

What exactly does the energy term crossover point Δ_{crit} in the Tanabe–Sugano diagram signify? We can now safely identify it with the intercept of the two potentials in the configuration-coordinate diagram (Fig. 2). This point, however, can never correspond to an equilibrium configuration of the ground state, which means that iron(II) complexes at an equilibrium distance and LF strengths around Δ_{crit} are nonexistent in the ground state. Consequently, we always have $10\,Dq^{HS} < \Delta_{crit} < 10\,Dq^{LS}$ for spin crossover compounds, because there is the dependence of 10 Dq on r and the large difference $\Delta r_{HL} = r_{HS} - r_{LS}$ between the equilibrium distances.

Iron(II) spin crossover compounds mainly have sixfold nitrogen coordination. Typical values for r_{LS} range between about 1.96 and 2.00 Å; those for r_{HS} lie between about 2.16 and 2.20 Å and are typically longer by approximately 0.16–0.22 Å.[29, 70–72] From Equation (2) we derive Equation (3).

$$\frac{10\,Dq^{LS}}{10\,Dq^{HS}} = \left(\frac{r_{HS}}{r_{LS}}\right)^6 \approx 1.74 \qquad (3)$$

From the condition that ΔE_{HL} for a spin crossover complex must be of the order of thermal energies, we can define ranges for $10\,Dq^{LS}$ and $10\,Dq^{HS}$ where HS, LS, and spin crossover complexes can be expected. The range where we can expect spin

$10Dq^{HS} < 11\,000\ cm^{-1}$	HS complex
$10Dq^{HS} \approx 11\,500-12\,500\ cm^{-1}$ $10Dq^{LS} \approx 19\,00-21\,000\ cm^{-1}$	Spin crossover complex
$10Dq^{LS}$	$> 21\,500\ cm^{-1}$ LS complex

Scheme 1.

crossover complexes is very narrow. Minor changes in the ligands and also in the second coordination shell can shift the thermal spin transition to very different temperatures or even suppress it entirely.

In the foregoing considerations we have up to now (deliberately) not mentioned the "spin pairing energy" P, widely used in the literature, and its comparison with 10 Dq. The common argument that the difference between the average spin pairing energy P and 10 Dq must be of the same order as thermal energies for spin crossover complexes is too simple a notion to be correct, because the change in bond lengths during the spin transition is not taken into account. It is true that both quantities depend on r, but whereas the LF strength decreases from $10\,Dq^{LS}$ to $10\,Dq^{HS}$ by a factor of approximately 1.74 for the thermal spin transition, the average spin pairing energy changes only by about the same order as the nephelauxetic effect.[6]

2.2. Spin Transition Behavior in the Solid

While thermal spin transitions in liquids are always gradual (that is, the spin transition function $\gamma_{HS}(T)$ obeys a simple Boltzmann law), and spin transition curves of that type do exist in solids as well, the $\gamma_{HS}(T)$ curves generally look very different because of long-range cooperative interactions (Fig. 3). Accord-

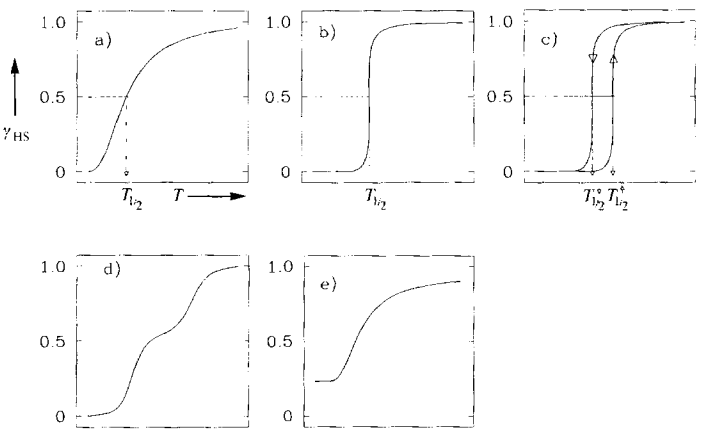


Fig. 3. Schematic representation of the spin transition types a–e (see text). $\gamma_{HS}(T)$ represents the fraction of complex molecules in the high spin state ($\gamma_{HS}(T_{1/2}) = 0.5$). In each case the temperature axis is plotted on the x axis and γ_{HS} on the y axis.

ing to the $\gamma_{HS}(T)$ curve shapes, spin transitions in solids can be classified as follows:

a) Spin transitions covering a wide temperature range (up to several hundred degrees Kelvin), called "gradual" (Fig. 3a).
b) Spin transitions changing from one "phase" to another within only a few ($\leq$10 K) Kelvin, called "steep" or "abrupt" (Fig. 3b).
c) Spin transitions showing hysteresis effects (Fig. 3c).
d) Spin transitions with two discernible steps (gradual or steep), and a step or a plateau along the $\gamma_{HS}(T)$ curve (Fig. 3d).

A distinction is quite often made between continuous and discontinuous spin transitions. From our point of view, types a), b), and d) would be continuous, and only type c) would have to be called discontinuous. In many cases, more so for continuous than for discontinuous transitions, an HS residual is observed at low temperatures ($\geq$4 K); that is, the $\gamma_{HS}(T)$ function does not approach zero, but rather a plateau (Fig. 3e). Dislocations and defects in the lattice are held responsible for this behavior (see Section 2.4.3).

Normally, continuous spin transitions in the solid are not accompanied by crystallographic changes, which means that the HS lattice above $T_{1/2}$ ($\gamma_{HS} = 0.5$) and the LS lattice below $T_{1/2}$ have the same space group.[34] Discontinuous spin transitions mostly entail crystallographic changes; refs. [21] and [34] contain many examples. Yet there are exceptions. Wiehl et al.[29] have, by variable-temperature single-crystal X-ray analyses, for the first time ascertained that a spin transition with hysteresis effects but without a change in the space group occurs in $[Fe(2\text{-pic})_3]Br_2 \cdot EtOH$ (2-pic = 2-(aminomethyl)pyridine). Gallois et al.[31] have described another example. These authors found the same space group for $[Fe(phen)_2(NCS)_2]$ (phen = 1,10-phenanthroline) above and below $T_{1/2} \approx 175$ K, even though the spin transition does exhibit hysteresis effects.[73]

For many years in spin crossover research there was a common notion that spin transitions in a solid were determined by the interplay of temperature-dependent lattice effects. Lattices contract with decreasing temperature. Metal–ligand distances thus shorten, which was associated with an increasing ligand field potential.[6] For cases where hysteresis effects in the $\gamma_{HS}(T)$

curve were observed, one expected an accompanying structural change of the lattice. Along these lines, the observation of spin transitions with hysteresis effects in the $\gamma_{HS}(T)$ curve, but without a change in the crystal structure as just described for two examples, was a great surprise. It demonstrated that spin transitions can have lives of their own. Today we know that the regular thermal lattice contraction with falling temperature does not play a decisive part in the spin transition phenomenon.

In light of Everett's theorems,[74–76] hysteresis effects during discontinuous spin transitions in some spin crossover systems have been thoroughly investigated.[21, 34, 77, 78] Everett assumes that domain formation among complex molecules with predominantly like spin plays an important role in the mechanism of discontinuous phase transitions. He has suggested that experimental verification of independent whole-domain conversion during a phase transition should be possible by scanning inner loops inside the primary hysteresis loop. The condition for this, according to his fourth theorem, is that the inner loops have the same form and area, no matter where the starting temperature on the boundary loop is chosen. For $[Fe(bt)_2(NCS)_2]$ (bt = 2,2′-bi-2-dihydrothiazole), whole-domain conversion could be confirmed.[78] The study has also established that for mechanically crushed (milled) material, the shapes and the areas of the inner loops are no longer the same. The conclusion is that long-range order in the unperturbed crystal is significantly damaged by the grinding procedure, and that the domain size is drastically reduced. The Everett model does not allow estimation of the actual size of the domains.

A spin transition in two steps, that is, with a plateau or a discontinuity near $T_{1/2}(\gamma_{HS} = 0.5)$, is a phenomenon first discovered in 1982 during investigations on $[Fe(2\text{-pic})_3]Cl_2 \cdot EtOH$.[79] Figure 4 shows $\gamma_{HS}(T)$ for this system. The transition is of the

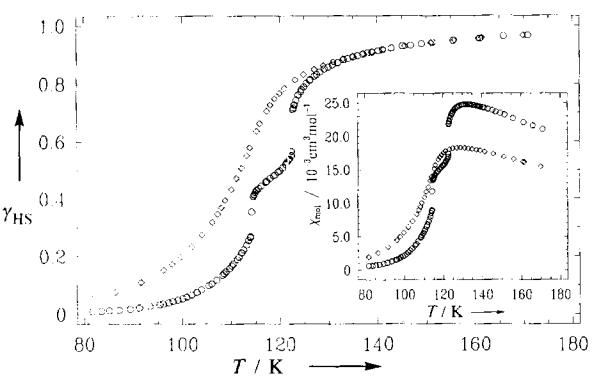


Fig. 4. Temperature dependence of the HS fraction $\gamma_{HS}(T)$ in $[Fe(2\text{-pic})_3]Cl_2 \cdot EtOH$ (○) and $[Fe_{0.73}Zn_{0.27}(2\text{-pic})_3]Cl_2 \cdot EtOH$ (◇) (from refs. [80, 81]).

continuous type; there is no change in the crystal structure with the spin transition. The Mössbauer spectra, however, show abrupt changes of the quadrupole splitting with temperature around the discontinuity, both for the HS and the LS state. This indicates that the discontinuity has to be regarded as somehow related to lattice changes, especially to changes in the close vicinity of the complexed central iron(II) ion. Incidently, the discontinuity is sensitive to chemical and physical changes (see also Sections 2.3 and 2.4). Our search for a sound explanation for this stepwise spin transition has only lately been rewarded with further insights.[80, 81] We have performed microcalorimetric measurements on a single crystal (approximately 20 mg) of $[Fe(2\text{-pic})_3]Cl_2 \cdot EtOH$. Earlier, Kaji and Sorai[83] had already measured the temperature dependence of the heat capacitiy of this compound with an adiabatic calorimeter (sample weight approximately 15 g); the discontinuous spin transition there was mirrored by two sharp peaks at 114 and 122 K (Fig. 5). Using a newly constructed microcalorimeter,[84] we have succeeded in reproducing the $C_p(T)$ curve of this compound with a single crystal of only about a thousandth of the weight (20 mg), with similar accuracy (Fig. 5). Included in Figure 5 are measure-

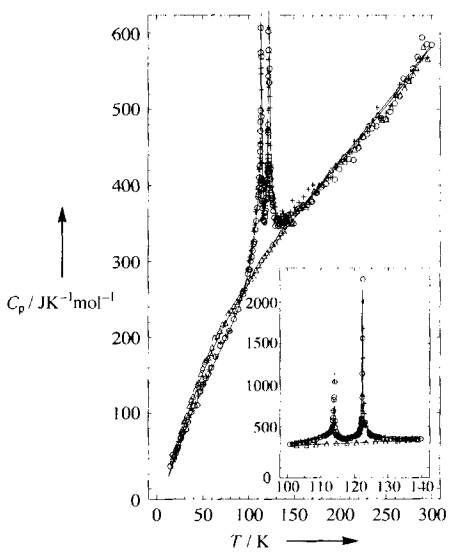


Fig. 5. Molar heat capacity C_p of $[Fe(2\text{-pic})_3]Cl_2 \cdot EtOH$ (○ and +) and $[Zn(2\text{-pic})_3]Cl_2 \cdot EtOH$ (△), measured on single crystals weighing approximately 20 mg in a newly constructed microcalorimeter [80]. The solid curve represents the measurements of Kaji and Sorai [83] performed with 15 g of polycrystalline material in a Nernst type calorimeter. The inset shows the enlarged area around the spin transition.

ments for the corresponding zinc complex, where a spin transition is not possible for the Zn^{2+} (d^{10}) ion, and no peak appears in the $C_p(T)$ curve. However, the lattice properties are very similar to those of the iron(II) HS complex, as the data show. For the iron complex, the mixing entropy, calculated from the $C_p(T)$ values near the discontinuity, is significantly lower than mixing entropy values calculated on the assumption of a statistical distribution between HS and LS molecules.[80, 81] An obvious explanation is that certain ordering phenomena must take place among the HS and LS molecules. The fact that cooperative interactions again play a special role in this spin crossover system is expressed in the disappearance[85] of the discontinuity in $\gamma_{HS}(T)$ on going from the pure $[Fe(2\text{-pic})_3]Cl_2 \cdot EtOH$ to the Fe_xZn_{1-x} mixed crystal (see Fig. 4). The measured $C_p(T)$ curve for this metal-diluted complex exhibits but one peak.[81]

Kambara[52] was the first to succeed in simulating a stepwise spin transition. Assumption of a sublattice structure for the HS and LS complexes leads to steplike behavior in $\gamma_{HS}(T)$. The sublattices originate from a quasi antiferromagnetic interaction between the complexes, where HS–LS pairs are preferred on the equipoints of a layered structure. Real et al.[53] also

explain the steplike transition they observed in the binuclear $[Fe(bt)(NCS)_2]_2bpym$ (bpym = 2,2'-bipyrimidine) complex by assuming an energetically favored mixed HS–LS or LS–HS state (that is, by antiferromagnetic interaction). These findings point to short-range quasi antiferromagnetic interactions as the source of steplike spin transitions.

2.3. Chemical Influences on the Spin Transition in a Solid

2.3.1. The Influence of Ligand Exchange and Substitution at a Coordinated Ligand in Iron(II)–Phenanthroline Complexes

The spin transition function $\gamma_{HS}(T)$ can be subjected to manifold chemical alterations of the spin crossover system. As representatives of the numerous iron(II) complexes, let us pick out the phenanthroline complexes. We shall see how, for example, the total exchange of a phen ligand for two NCS or NCSe groups on one hand, and substitution at the phen ligand on the other, influences the magnetic properties of the iron(II) central ion (see ref. [18] for a more comprehensive review of the field).

The LS character of the $[Fe(phen)_3]X_2$ complex (irrespective of the anion X^-) with a $^1A_1$ ground state down to very low temperatures ($\geq$4K) is well-known. If we now replace one of the three bidentate phen ligands by two *cis* NCS groups coordinating through N, the LF will be markedly weakened. The resulting $[Fe(phen)_2(NCS)_2]$ complex behaves purely HS at room temperature. The $\Delta E^0_{HL} \approx k_B T$ condition (see Fig. 2) for thermal spin crossover is met. Cooling to about 185 K produces a discontinuous spin transition into the LS($^1A_1$) state. The ^{57}Fe Mössbauer spectra in Figure 6 are an eye-catching demonstration of the abrupt crossover from the HS into the LS state within a narrow temperature interval of only some degrees Kelvin around 180 K. The transition has an associated hysteresis of $\Delta T = 0.2$ K,[73] but no associated change in the crystal structure.[31] The ligand exchange effect in the related bipyridyl complexes of iron(II) is very similar.[86]

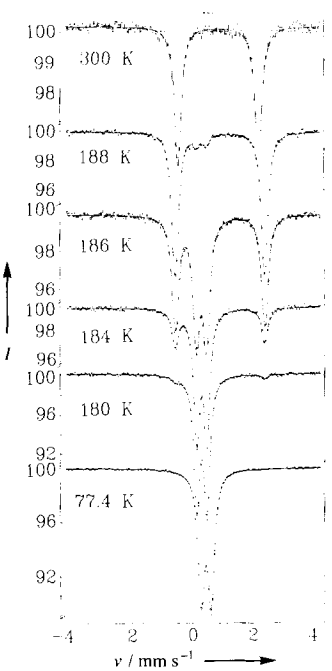


Fig. 6. ^{57}Fe Mössbauer spectra of $[Fe(phen)_2(NCS)_2]$ as a function of temperature (from ref. [18]). The ordinate in each case is the relative transmission I and the abscissa the relative velocity v between source and absorber.

A more subtle way to influence the LF strength at the central ion than changing the ligand entirely is substitution at the coordinated ligand. We shall illustrate this for the group of $[Fe(2\text{-}Y\text{-}phen)_3]X_2$ complexes.[18] On exchange of H for CH_3 groups at the 2-position (or 9-position) of the 1,10-phenanthroline ligand, the previously diamagnetic iron(II) complex becomes strongly paramagnetic ($^5T_2$ ground state).[87] This substitution overcompensates the stronger $\sigma(L \rightarrow M)$ donor effect of the methyl group (a consequence of its higher inductivity relative to that of the H atom) by increased steric hindrance. It causes an elongation of the neighboring Fe–N bond, and consequently a weakening of the ligand field strength.[6] Cooling the system brings about a spin transition to the $^1A_1$ ground state,[88–90] while the nature of the uncoordinated anion X determines whether the spin transition curve is shifted towards higher or lower temperatures. A thermal spin transition is still observed in the complex with $Y = CH_3O$ as a substituent.[91] Indeed, the transition temperature is notably higher than for the 2-CH_3-phen complex, which implies that the ligand field strength is somewhat greater for the CH_3O-phen complex than for the unsubstituted phen complex. Finally, the 2-Cl-phen complex is strictly HS across the entire temperature range. This compound no longer has a thermal spin transition and stays in the $^5T_2$ ground state down to 4K.[92, 93] The same is true for the iron(II) complex with 2,9-$(CH_3)_2$-phen as a ligand, apparently because the two methyl groups at the 2- and 9-positions are sterically more demanding. If we look at the $[Fe(2\text{-}Y\text{-}phen)_3]X_2$ complexes, the paramagnetic properties (for which γ_{HS} is a measure at a given temperature) increase along the $Y = H < CH_3O < CH_3 < Cl$ series. The series is not simply correlated with the bulkiness of the substituent, because the concurrent presence of the electronic effect with its influence on the basicity of the coordinating N atom superposes the steric effect. This reasoning could be corroborated from CNDO/2–MO calculations.[94]

A change of substituents at positions not adjacent to the N atom in the phen molecule does not alter the spin state of the corresponding $[FeL_3]X_2$ complexes relative to the unsubstituted $[Fe(phen)_3]X_2$ complexes. LS($^1A_1$) remains the stable ground state at all temperatures.[18, 95]

Many other examples of modifications of the magnetic properties of iron(II) in $[FeN_6]$ complexes after changing substituents have been reported.[16, 96–106] The effects of chemical changes in the ligand sphere extend from a more or less distinct $\gamma_{HS}(T)$ shift towards higher or lower temperatures (with the possibility of an additional change in the transition slope) to complete suppression of the spin transition (enabling only the HS state or the LS state to be observed at all temperatures). The widespread opinion that "custom-tuning" of the ligand field strength for thermal spin crossover is possible by taking advantage of steric and electronic effects combined with a suitable choice of ligands rather applies to spin crossover in solution. In the solid we have the additional influence of cooperative interactions, which make custom-tuning more difficult or even uncontrollable.

2.3.2. The Influence of Metal Dilution (Formation of Mixed Crystals)

Our scrutiny of $[Fe_xM_{1-x}(2\text{-pic})_3]X_2 \cdot sol$ systems corroborated the assumption that cooperative interactions play a key role in thermal spin crossover behavior. We have studied how the spin crossover behavior is influenced by metal dilution (M = Zn, Co, Mn), anion exchange (X = Cl, Br), exchange of the solvent molecule (sol = C_2H_5OH, CH_3OH, H_2O, $2H_2O$), and finally the H/D isotope effect.

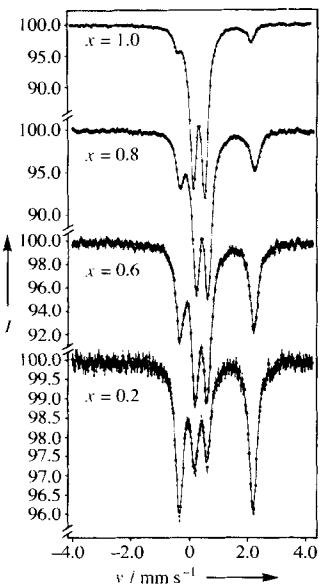


Fig. 7. ^{57}Fe Mössbauer spectra of $[Fe_xZn_{1-x}(2\text{-pic})_3]Cl_2 \cdot EtOH$ at $T = 101$ K.

Using ^{57}Fe Mössbauer spectroscopy we could show that for mixed crystals of $[Fe_xM_{1-x}(2\text{-pic})_3]Cl_2 \cdot EtOH$, with an unchanged crystal structure for all concentrations $0 \leq x \leq 1$, the $\gamma_{HS}(T)$ curve becomes more gradual as the iron concentration decreases. Concurrently, the spin transition temperature $T_{1/2}$ is shifted towards lower temperatures.[107-109] Decreasing iron content thus stabilizes the HS($^5T_2$) state, as can be clearly seen from the Mössbauer spectra in Figure 7 and the plot of $\gamma_{HS}(T)$ versus x in Figure 8. These experiments also revealed that spin crossover is a primary, entropy-driven, intramolecular phenomenon, not requiring interactions between neighboring iron complexes. Even in a highly diluted system ($x = 0.0009$), where the iron complexes are separated by as much as 50 Å and more, we find spin crossover behavior.

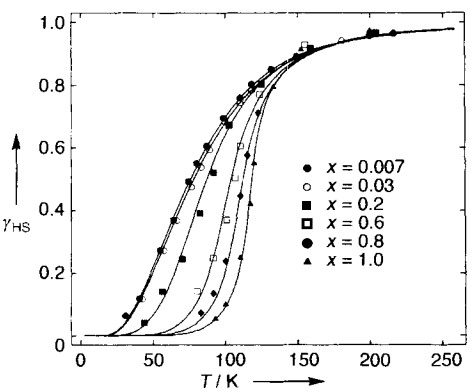


Fig. 8. Temperature dependence of the HS fraction $\gamma_{HS}(T)$, determined from the ^{57}Fe Mössbauer spectra of $[Fe_xZn_{1-x}(2\text{-pic})_3]Cl_2 \cdot EtOH$ for different concentrations x (from ref. [40]).

Figure 9 shows $\gamma_{HS}(T)$ curves of the highly diluted $[Fe(2\text{-pic})_3]^{2+}$ complex in different matrices and in liquid solutions. The similarity of the transition curves is striking; they seem only to be shifted with respect to the transition temperature—transitions in liquid solutions have the highest temperatures. The potential implication that only the energy gap ΔE^0_{HL} between the HS and LS states of the complex (see Fig. 2) is modified by the different matrices will lead to a more quantitative description in Section 3.1.

This conspicuous effect of metal dilution demonstrates that cooperative interactions must be involved in spin transitions in the solid. They are purely mechanical in nature. The key factor is a change in volume of the complexes, translated into a decrease of 3–5% of the crystal volume during the HS → LS transition. Our first efforts to use this concept as a basis for a better understanding of the thermal spin transition in solids led to a model which has "image pressure", lattice expansion and elastic interactions as characteristic features.[40, 41, 43, 44] In fact, it could satisfactorily reproduce experimental results from metal dilution experiments on $[Fe_xM_{1-x}(2\text{-pic})_3]Cl_2 \cdot EtOH$ (M = Zn, Co). More on this model will be reported in Section 3.

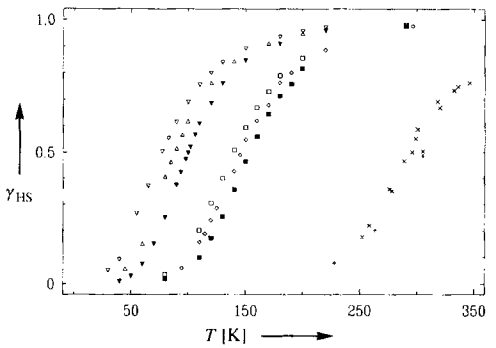


Fig. 9. Temperature dependence of the HS fraction $\gamma_{HS}(T)$ of the highly dilute $[Fe(2\text{-pic})_3]^{2+}$ complex in different lattices and in liquid solutions. ▽ $[Fe_{0.007}Zn_{0.993}(2\text{-pic})_3]Cl_2 \cdot EtOH$; △ $[Fe_{0.02}Co_{0.98}(2\text{-pic})_3]Cl_2 \cdot EtOH$; ▼ $[Fe_{0.03}Zn_{0.97}(2\text{-pic-}ND_2)_3]Cl_2 \cdot EtOD$; □ $[Fe_{0.02}Zn_{0.98}(2\text{-pic})_3]Cl_2 \cdot MeOH$; ◇ $[Fe_{0.01}Co_{0.99}(2\text{-pic})_3]Cl_2 \cdot MeOH$; ■ $[Fe_{0.01}Zn_{0.99}(2\text{-pic-}ND_2)_3]Cl_2 \cdot MeOD$; × $[Fe(2\text{-pic})_3]^{2+}$ complex in acetonitrile/water; + $[Fe(2\text{-pic})_3]^{2+}$ complex in methanol/water. (Solution data taken from ref. [110]).

Metal dilution experiments on other spin crossover systems such as $[Fe_xM_{1-x}(phen)_2(NCS)_2]$ (M = Mn, Co, Zn)[111] led to very similar insights as for the pic system: the $\gamma_{HS}(T)$ curve became more gradual as the iron concentration decreased, and the spin transition temperature $T_{1/2}$ was simultaneously shifted towards lower temperatures. Thus, decreasing iron content again stabilized the HS state.

2.3.3. *The Influence of Noncoordinating Anions*

Crystalline spin crossover compounds that are uncharged contain the anions necessary for electric neutrality coordinated directly at the metal center. An example is $[Fe(phen)_2(NCS)_2]$. It is obvious that in such a case the NCS^- ion is a direct codeterminant of the ligand field strength at the Fe^{2+} center. An exchange of NCS^- for anions exerting a much weaker (for example, halogens) or much stronger (for example, CN^-) LF would suppress the spin transition, and the resulting complexes would have temperature-independent HS or LS character, respectively.

In ionic lattices with cationic spin crossover complex components and uncoordinated counterions on lattice points remote from the metal center (for which we have many examples), the anion can nonetheless exercise a strong influence on spin crossover behavior. The reason is again cooperative interaction. Renovitch and Baker, Jr.[112] observed that the transition characteristics of the thermal spin transition in $[Fe(2\text{-pic})_3]Cl_2 \cdot EtOH$ depends strongly on the nature of the anion X (Cl^-, Br^-, or I^-). More detailed investigations on the chloride and the bromide[29, 79] have yielded the spin transition curves $\gamma_{HS}(T)$ shown in Figure 10. A discontinuous step is evident for the chloride and a weaker step with an additional hysteresis

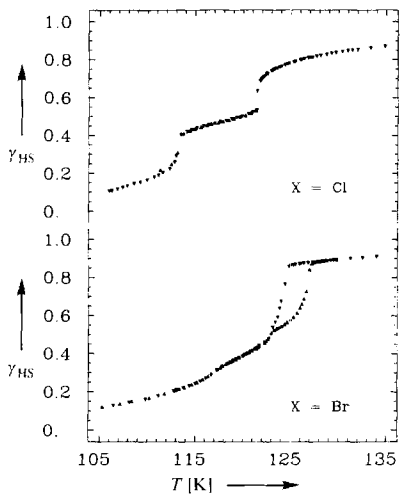


Fig. 10. Temperature dependence of the HS fraction $\gamma_{HS}(T)$ in the spin transition system $[Fe(2\text{-pic})_3]X_2 \cdot EtOH$ (X = Cl, Br) (from refs. [29, 79]).

effect for the bromide. The space group of the chloride is $P2_1/c$; that of the bromide is $P2_1/n$.[29] In both cases the space group remains unchanged during the spin transition.

2.3.4. The Influence of Uncoordinated Solvent Molecules

When a spin crossover compound is crystallized from certain solvents, solvent molecules are often incorporated into the lattice. They are located outside the ligand sphere, that is, not coordinated to the metal center. Just as uncoordinated anions can strongly influence spin crossover behavior as described in Section 3.3, one would expect an equally strong effect of uncoordinated solvent molecules on the spin transition.[16–18, 21, 22] We have investigated $[Fe(2\text{-pic})_3]Cl_2 \cdot sol$ complexes where sol = C_2H_5OH, CH_3OH, H_2O, and $2H_2O$ in detail and determined the $\gamma_{HS}(T)$ functions of the solvates using ^{57}Fe Mössbauer spectroscopy.[1–3, 114] The spin transition is continuous in the EtOH ($T_{1/2} = 121$ K) and the MeOH adduct ($T_{1/2} = 121$ K). For the monohydrate it is discontinuous with an unusually broad hysteresis loop ($\Delta T = T_{1/2}^{\uparrow} - T_{1/2}^{\downarrow} \approx 90$ K). For the dihydrate, finally, the spin transition is totally suppressed (the system adopts the $LS(^1A_1)$ state across the full temperature range). So the transition temperature (and likewise the energy gap ΔE_{HL}^0) increases along the solvent series $C_2H_5OH < CH_3OH < H_2O < 2H_2O$. The crystal structures of the solvates are different; the space groups are $P2_1/c$ (monoclinic, $Z = 4$) for the EtOH compound,[29, 82, 115] *Pbca* (orthorhombic, $Z = 8$) for the MeOH compound,[71, 116] and $P\bar{1}$ (triclinic, $Z = 2$) for the dihydrate.[116] For the monohydrate the structure is unknown. Both the EtOH and the MeOH adduct of the cationic $[Fe(2\text{-pic})_3]^{2+}$ complex have the same ligand arrangement (symmetry), which is meridional (C_{2v}), whereas the facial isomer (threefold symmetry) is adopted in the dihydrate. This difference is probably the reason why the thermal spin crossover behavior of the EtOH adduct resembles that of the MeOH adduct (the $\gamma_{HS}(T)$ curves are very similar), but deviates from that of the dihydrate, where the magnetic properties differ markedly. Here apparently, a stronger ligand field causes temperature-independent LS behavior. Distinct differences have also been found for the bridging hydrogen bonds in the EtOH and the MeOH compound on one hand, and for the dihydrate on the other. In the alcohol adducts, the $[Fe(2\text{-pic})_3]^{2+}$ complex ions are connected by $NH \cdots Cl \cdots NH$ contacts, and the alcohol molecule is joined to the Cl^- counterion through a $Cl \cdots HO$ hydrogen bond.[29, 71] In the dihydrate, however, the water molecules are bound directly to the $[Fe(2\text{-pic})_3]^{2+}$ complex. Apparently this leads to the facial isomer,[116] and we have to assume that the hydrogen bonds are actively involved in the spin crossover transition. To test this hypothesis at least qualitatively, we have carried out experiments with deuterated and ^{15}N isotope-substituted $[Fe(2\text{-pic})_3]Cl_2 \cdot sol$ complexes (see next section).

2.3.5. Isotope Effects

From Mössbauer experiments on the deuterated $[Fe(2\text{-pic})_3]Cl_2 \cdot sol$ (sol = C_2H_5OD, CH_3OD) systems, the LS state appeared to be stabilized by deuteration.[114] The spin transition curves $\gamma_{HS}(T)$ were of the same general shape as those for the nondeuterated solvates, but the transition temperatures $T_{1/2}$ were both shifted by about 15 K towards higher temperatures. This quite noticeable effect was first interpreted in terms of a widening of the energy gap ΔE_{HL}^0 between the lowest vibronic levels of the LS and the HS state, because deuteration had increased the reduced mass. Since this deuteration experiment uses C_2H_5OD and CH_3OD as solvents in the preparation of the complexes, the acidic amino group protons of the picolylamine ligand are also exchanged. Consequently the deuteration effect can have its origin in the $NH \cdots Cl$ as well as in the $Cl \cdots HOR$ hydrogen bonds. Presumably the influence of the NH hydrogen bond dominates, because the NH/OH ratio in the lattice is 3:1. Moreover, the NH positions form an integral part of the "path" between two neighboring complexes and can thus act as "communication links". They are likely to have a much stronger influence on elastic interactions than the solvent molecules have, which are just attached across OH groups much like pendulums. This view is supported by very thorough and precise H/D and $^{14}N/^{15}N$ isotope-exchange experiments on $[Fe(2\text{-pic})_3]Cl_2 \cdot EtOH$.[19, 117] In these experiments Köppen[117] observed the first steplike spin transition anomaly in nondeuterated $[Fe(2\text{-pic})_3]Cl_2 \cdot C_2H_5OH$ using very precise Mössbauer measurements. His measurements on the $[Fe(2\text{-pic})_3]Cl_2 \cdot C_2H_5OD$ com-

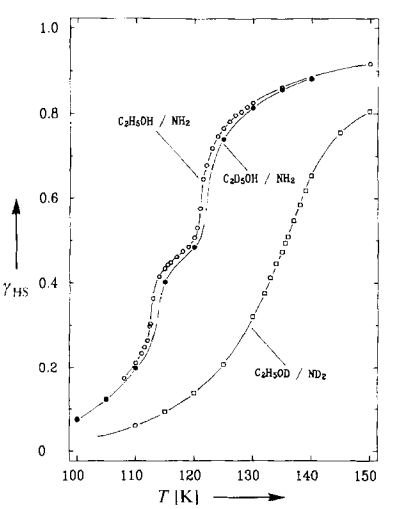


Fig. 11. Temperature dependence of the HS fraction to $\gamma_{HS}(T)$, determined from ^{57}Fe Mössbauer spectra for $[Fe(2\text{-pic})_3]Cl_2 \cdot C_2H_5OH$ in C_2H_5OH/NH_2 (not deuterated), C_2D_5OH/NH_2 (deuterated alkyl group of the ethane molecule), and C_2H_5OD/ND_2 (deuterated hydroxyl and amino groups) (from refs. [19, 117]).

pound in which exclusively the H atom of the alkyl group was exchanged yielded the same steplike $\gamma_{HS}(T)$ curve, but slightly shifted towards higher temperatures (Fig. 11). This H/D effect is clearly weaker than in the C_2H_5OD/ND_2 system, where the spin transition occurs at about 15 K higher without anomaly. This is probably also because the H/D exchange positions are direct links in the hydrogen bond chain for the C_2H_5OD/ND_2 system, whereas they are just dangling on the sides in the C_2D_5OH/NH_2 system. It also speaks for the importance of the H bonds involved in the cooperative interactions between the spin-changing metal centers. Studies of $^{14}N/^{15}N$ exchange in the NH_2 group of the picolyl ligand in $[Fe(2\text{-pic})_3]Cl_2 \cdot EtOH$ led to similar results. Here too, the steplike spin transition curve retains its shape and is just shifted slightly towards higher temperatures (Fig. 12). Again the $^{15}NH_2$ position is a direct link in the

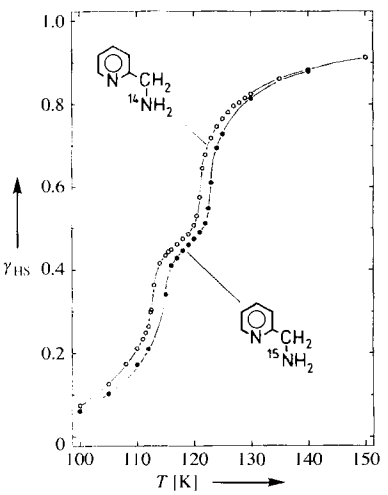


Fig. 12. Influence of $^{14}N/^{15}N$ exchange in the NH_2 group of the picolylamine ligand in $[Fe(2\text{-pic})_3]Cl_2 \cdot EtOH$ on the HS fraction $\gamma_{HS}(T)$, determined from the ^{57}Fe Mössbauer spectra, as a function of temperature (from refs. [19, 117]).

hydrogen bond and influences the spin crossover behavior. The fact that the effect is much smaller than the one in the C_2H_5OD/ND_2 system stems from a much smaller change in the reduced mass.

H/D exchanges at the 3,4,5-positions of the pyridyl ring in the $[Fe(2\text{-pic-py}D_3)_3]Cl_2 \cdot EtOH$ complex[117] have resulted in slight shifts towards higher temperatures, as expected for a mass increase from the above argument.[114] Here again the effects are minor because deuteration does not take place in the hydrogen bond. Upon deuteration of the CH_2 group in the 2-pic ligand of $[Fe(2\text{-pic-}CD_2)_3]Cl_2 \cdot EtOH$, Köppen[117] observed a similar, very minor shift of $\gamma_{HS}(T)$, but towards lower temperatures, which corresponds to a stabilization of the HS state (Fig. 13). Again deuteration took place outside the communication link; nevertheless this small shift of $\gamma_{HS}(T)$ towards lower temperatures is inconsistent with the expected effect from a mass increase.[114]

2.4. Physical Influences on the Spin Transition in Solids

From the very start, the aim of gaining a deeper insight into the spin crossover phenomenon and finally to understand its mechanism has stimulated research groups to look at the physical influences on thermal spin crossover in the solid. Experiments varying the pressure are obvious, but the influences of an external magnetic field and of changes in the crystal quality have been investigated as well. The attentive reader will have already noticed in our description of chemical influences on the spin crossover behavior (Section 2.3) that in one or other instance the true nature of this influence is a physical one, which is inherently associated with the chemical change on the system. Metal dilution, for example, creates the so-called image pressure, which can be positive or negative depending on the volume difference between the HS or LS iron(II) complex and the corresponding complex molecule in the host lattice. In Section 3.4 we shall demonstrate that the influence of this image pressure on neighboring HS or LS molecules is equivalent to an external pressure. In a way, the isotope effects treated in Section 2.3.5 should also be counted as physical influences, since these subtle changes on the system by a slight change of the reduced mass chiefly modify the phonon system and the elastic properties.

2.4.1. The Influence of Pressure

Because the complex molecules are bigger in the HS state than in the LS state (a general result from crystal structure analyses), we expect that increasing the pressure will favor the LS($^1A_1$) state; that is, at elevated pressure the spin transition will occur

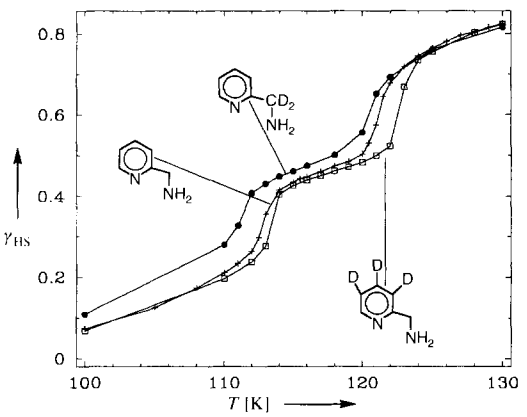


Fig. 13. Comparison of the HS fractions $\gamma_{HS}(T)$ for $[Fe(2\text{-pic})_3]Cl_2 \cdot EtOH$ (+), $[Fe(2\text{-pic-py}D_3)_3]Cl_2 \cdot EtOH$ (□), and $[Fe(2\text{-pic}CD_2)_3]Cl_2 \cdot EtOH$ (●) as a function of temperature (from ref. [117]).

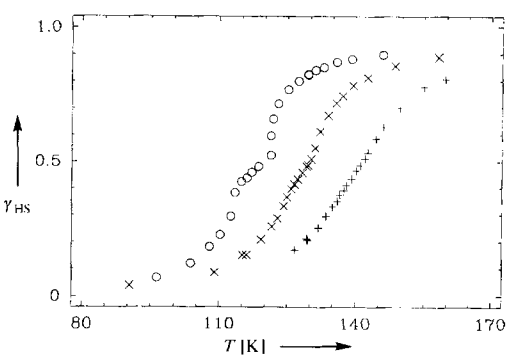


Fig. 14. The spin transition curve $\gamma_{HS}(T)$ for $[Fe(2\text{-pic})_3]Cl_2 \cdot EtOH$ at ambient pressure (○), 600 bar (×), and 1350 bar (+), determined from the area under the HS doublet in the Mössbauer spectra (from ref. [85]).

at higher temperatures than at ambient pressure. Experiments varying the pressure on iron(II) spin crossover complexes in the solid have always confirmed this.[118-126]

Our variable-pressure and variable-temperature Mössbauer experiments on $[Fe(2\text{-pic})_3]Cl_2 \cdot EtOH$ have shown that the $\gamma_{HS}(T)$ curve is shifted towards higher temperatures with increasing pressure, and that the step in it is progressively suppressed[85] (Fig. 14). In this study we have also determined the change in the unit cell volume associated with the spin transition, namely $\Delta V = V_{HS} - V_{LS} = 55.2$ Å^3, well in accord with the value of 62 Å^3 determined by X-ray analysis.[127] Metal dilution, as described in Section 2.3.2, has the same effect as applying external pressure. Incorporation of $[Fe(2\text{-pic})_3]^{2+}$ ions into a similar host lattice with bigger $[Zn(2\text{-pic})_3]^{2+}$ ions creates a negative image pressure, which stabilizes the HS state and shifts the $\gamma_{HS}(T)$ curve to lower temperatures with increasing Zn dilution (see Fig. 8). Simultaneously the step in $\gamma_{HS}(T)$ vanishes[85] (see Fig. 4). The influence of metal dilution on the spin transition behavior in the $[Fe_xMn_{1-x}(phen)_2(NCS)_2]$ system has been interpreted in the same way.[111] From ^{57}Fe Mössbauer spectra it was established that spin transition temperatures decrease with increasing metal dilution in mixed crystals in which the ionic radii $r(Mn^{2+}) > r(Fe^{2+}_{HS})$.

Pressures up to 1500 bar at temperatures around $T_{1/2}$ apparently changed the Lamb–Mössbauer factor f significantly.[123] The $f(p,T)$ behavior could be described by the Debye model.

Spin transition dynamics have been investigated as a function of pressure in liquids as well as in solids.[128] Adler et al.[57] have confirmed an increased HS → LS relaxation rate under pressure using line shape analysis of Mössbauer spectra and Blume's relaxation model.

2.4.2. The Influence of a Magnetic Field

Since different spin states have different magnetic properties, we expect magnetic fields to affect the spin transition curve. The magnitude of this effect is easily estimated.[129] In a first order approximation, $T_{1/2}$ changes as described by Equation (4),

$$\Delta T_{1/2} = \left[\frac{E^m_{HS} - E^m_{LS}}{S_{HS} - S_{LS}}\right]_{T_{1/2}} \quad \text{with} \quad E^m_j = -\chi_j B^2 \tag{4}$$

where S is the entropy at $T_{1/2}$. The temperature-independent susceptibility of the LS($^1A_1$) state ($\chi_{LS} \approx 10^{-4}$ cm^3 mol^{-1}) is approximately two orders of magnitude smaller than $\chi_{HS}(T) = \mu^2_{eff}/3k_BT = 5.2\ \mu_B$. Thus the change in the transition temperature is but the ratio between the differences in the magnetic energies ΔE^m_{HL} and the entropies ΔS_{HL} of the HS and LS states. For steep discontinuities, $\Delta S(T_{1/2})$ is obtained with good accuracy from the specific heat curve $C_p(T)$. For a typical value of $\Delta S(T_{1/2})$ of 50 J K^{-1} mol^{-1} in a field of 5 Tesla, the shift $\Delta T_{1/2}$ is -0.1 K. This is a very small value and difficult to verify experimentally. The only example where a very steep transition has been measured in different magnetic fields (1 and 5 Tesla) is $[Fe(phen)_2(NCS)_2]$.[129] For the stronger field the data yielded a shift of the spin transition curve of -0.11 ± 0.04 K, in good agreement with the estimate given above.

A theoretical study by Sasaki and Kambara[46] on spin transitions in magnetic fields is based on a model incorporating a cooperative Jahn–Teller interaction. Because only minor effects are to be expected for small fields (see above), these authors consider strong magnetic fields up to 100 Tesla. They present a comprehensive calculation of the HS state in a $^5T_2$ space ligand field approximation and predict a strong dependence of the spin transition on the magnetic field, due to stabilization of the high spin state. These calculations have so far eluded experimental verification.

2.4.3. The Influence of Sample Preparation

The spin transition behavior is considerably influenced by the quality of the crystalline material resulting from different preparative procedures. This observation suggested that additional post-preparative treatments, for example ball-milling or crushing in a mortar, should have a similar effect. Haddad et al.[132] were the first to observe significantly larger proportions of residual HS state (evident from a plateau in $\gamma_{HS}(T)$) and a less steep spin transition curve with increasing degree of milling. We have detected similar effects with the iron(II) complexes $[Fe(phen)_2(NCS)_2]$ and $[Fe(bipy)_2(NCS)_2]$ (bipy = 2,2′-bipyridyl):[73] with increasing grinding time in a ball mill, the very narrow hysteresis loop widens and flattens, and finally joins the low-temperature plateau at higher $\gamma_{HS}(T)$ values. Such grinding effects have also been observed for cobalt(II) spin crossover complexes.[133] From X-ray powder diffraction and electron microscopy studies we know that these effects are mainly caused by crystal defects introduced during sample preparation by milling or by rapid precipitation. They have less to do with particle size.

A particle size effect is, however, assumed by Wei and Jean[134] to explain their findings with Mössbauer spectroscopy on spin crossover compounds on supporting materials such as MgO, SiO_2, and activated charcoal. They observed a distinct (and in part also steep) increase of the HS fraction (at constant temperature) with increasing loads of spin crossover compound. The nature of the supporting material exerts less influence.

The application of spin crossover compounds in Langmuir–Blodgett (LB) films may be regarded as another special way of sample treatment. A French research group has introduced long-chain substituents (C_{17} and C_{18}) into the *o*-phenanthroline molecule, and after complexation with iron(II) (complex type $[FeL_2(NCS)_2]$), has obtained a Langmuir–Blodgett-compatible spin crossover system supported on CaF_2 or quartz.[135, 136] Thermal spin crossover was monitored with IR spectroscopy by following changes at the NCS^- ligand. $\gamma_{HS}(T)$ is much more gradual than for the initial complex $[Fe(phen)_2(NCS)_2]$: $T_{1/2}$ is about 260 K and the hysteresis width is approximately 4 K.

2.5. Structural Changes as a Consequence of Molecular Reorganization upon Spin Transition

Differences in the metal–ligand bond lengths between HS and LS state not only lead to a change in shape of the spin crossover molecule, but also cause lattice deformations, which in turn can entail crystallographic changes of the structure. The increase of the HS state population of the complexes with increasing temperature is more the cause than the effect of the

lattice deformation. This fact has for long been veiled by experimental observations that spin crossovers with hysteresis effects are accompanied by structural phase transitions. The variation of the lattice parameters with temperature seemed to adjust to the equilibrium between the smaller LS and the bigger HS complexes. This point of view was challenged until the discovery of a spin crossover with a temperature hysteresis but without a crystallographic change in structure.[29]

Lattice expansion with increasing fractions of HS molecules had been observed for many examples by variable-temperature X-ray studies of lattice parameters.[34] It finally emerged that the lattice volume is proportional to the fraction of HS molecules with a high degree of accuracy.[127] The total increase in volume $V(T)-V_{LS}(T_0)$ (relative to the unit cell volume in the LS state at a reference temperature T_0) is the sum of the linear volume increase due to lattice expansion, $V_{LS}\alpha_V(T-T_0)$ (α_V is the linear expansion coefficient), and the volume increase due to the spin transition, $\Delta V_{HL}\gamma_{HS}(T)$ [Equation (5)].

$$V(T) = V_{LS}(T_0) + V_{LS}\alpha_V(T-T_0) + \Delta V_{HL}\gamma_{HS}(T) \quad (5)$$

As the volume difference $\Delta V = V_{HS}-V_{LS}$ between the HS and LS unit cells is temperature independent, we can neglect the small differences between the expansion coefficients α_V of the pure HS and LS lattices. This first example of a spin crossover with a temperature hysteresis without a crystallographic change of structure[29] is especially convincing, because the anomalous spin transition in $[Fe(2\text{-pic})_3]Cl_2 \cdot EtOH$ with a step in the $\gamma_{HS}(T)$ curve is exactly mirrored (that is, with the same step) in the temperature dependence of the unit cell volume V and the lattice parameters a, b, and c themselves (Fig. 15). The influence of the spin transition on the lattice is also clearly demonstrated by crystal structure investigations on the $[Fe(ptz)_6](BF_4)_2$ (ptz = 1-propyltetrazole) spin crossover complex.[137] Irrespective of an overall volume decrease, certain distances in the lattice may well increase and thus cause a lattice deformation. This deformation can be adequately described by two tensors, an expansion tensor $\boldsymbol{\alpha}$ and a temperature-independent tensor $\boldsymbol{\varepsilon}$. An arbitrary lattice point with the vector $\boldsymbol{X}(T)$ at temperature T is related to the vector $\boldsymbol{X}(T_0)$ at temperature T_0 according to Equation (6).

$$\boldsymbol{X}(T) = [1 + \boldsymbol{X}(T-T_0) + \boldsymbol{\varepsilon}\gamma_{HS}(T)]\boldsymbol{X}(T_0) \quad (6)$$

Equation (5) is a special case of this equation with $\alpha_V = \text{trace}\,\boldsymbol{\alpha}$ and $\Delta V_{HL}/V_{LS} = \text{trace}\,\boldsymbol{\varepsilon}$. The curves in Figure 15 have been calculated with the experimental values for the HS fraction $\gamma_{HS}(T)$ from Figure 11. Table 1 lists the tensor components in the principal axes coordinate system and the orientation of the principal axes relative to the crystal axes for three similar compounds with different solvent molecules (EtOH and MeOH) and anions (Cl^- and Br^-). The deformation tensors $\boldsymbol{\varepsilon}$ and $\boldsymbol{\alpha}$ are very different; even their traces can differ by a factor of 2. The complex molecules might be pictured in the lattice as dilatation (LS → HS transition) centers which force a deformation onto the lattice. Evidently, different relative orientations of the anisotropic centers in the unit cell lead to different deformation tensors in the lattice, as a result of averaging. As the isotropic part of the dilatation centers (the volume increase δV_{HL} of a single complex molecule) is independent of the orientation, at first sight the traces of the tensors would be expected to be equal for all three examples. For the orthorhombic structure of $[Fe(2\text{-pic})_3]Cl_2 \cdot MeOH$ (space group *Pbca*) and the monoclinic structure of $[Fe(2\text{-pic})_3]Cl_2 \cdot EtOH$ (space group $P2_1/c$[115]) this is true. For the bromide, however, which has the same space group as the chloride/EtOH compound, the $\boldsymbol{\varepsilon}$ trace is more than twice as large. This seeming contradiction only resolves after the elastic properties of the compounds are also taken into account, for the elastic properties are the key factor for the macroscopic changes in volume.[138] We shall look at this in detail in Section 3.4.

Table 1. The components of the thermal expansion $\boldsymbol{\alpha}$ and the deformation tensor $\boldsymbol{\varepsilon}^{HL}$ as a result of the HS → LS transition referred to the principal axes system [a].

	$[Fe(2\text{-pic})_3]X_2 \cdot sol$		
$X_2 \cdot sol =$	$Cl_2 \cdot MeOH$	$Cl_2 \cdot EtOH$	$Br_2 \cdot EtOH$
α_1	0.85	1.86	1.54
α_2	0.33	0.31	0.53
α_3	0.64	−0.31	−0.30
Tr (α)	1.82	1.86	1.77
$\delta(\alpha)$	–	107	97
ε_1	0.18	2.93	4.45
ε_2	1.43	1.57	1.03
ε_3	0.83	−2.07	−0.19
Tr(ε)	2.44	2.43	5.29
$\delta(\varepsilon)$	–	14	−1

[a] The crystal systems for the similar compounds $[Fe(2\text{-pic})_3]Cl_2 \cdot EtOH$ and $[Fe(2\text{-pic})_3]Br_2 \cdot EtOH$ are monoclinic, and the crystallographic a axis forms an angle of δ with the x axis of the principal axes system (a anticlockwise with respect to x). In the orthorhombic system of $[Fe(2\text{-pic})_3]Cl_2 \cdot MeOH$ the principal axes (x,y,z) are parallel to the crystallographic axes (a,b,c). The units are: δ [ ], ε_i [10^{-2}], α_i [$10^{-4}K^{-1}$].

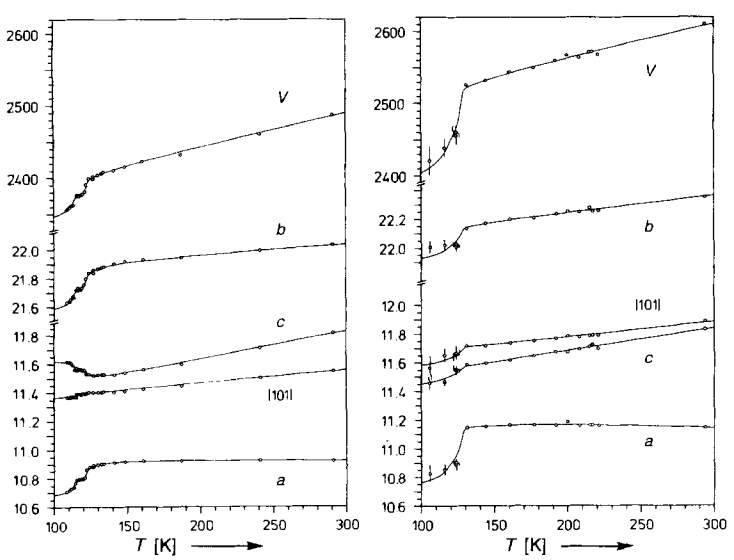


Fig. 15. Temperature dependence of the unit cell volume V [Å] and of the lengths of four vectors ($\boldsymbol{a}$, $\boldsymbol{b}$, $\boldsymbol{c}$, $|\boldsymbol{a}+\boldsymbol{c}|$) in the monoclinic crystal system (space group $P2_1/c$ with $Z = 4$) for $[Fe(2\text{-pic})_3]Cl_2 \cdot EtOH$ (left) and $[Fe(2\text{-pic})_3]Br_2 \cdot EtOH$ (right). The solid curves were calculated from the observed values for the HS fraction $\gamma_{HS}(T)$. For the hystersis effect in the Br^- system, $\gamma_{HS}(T^{\downarrow})$ was plotted from values obtained on decreasing the temperature (from ref. [29]).

3. Thermodynamics of Spin Transition Complexes

3.1. Dilute Mixed Crystal Systems

All highly dilute spin crossover complexes in which the concentration of Fe ions in lattice positions of Zn, Co, or Mn ions is 1–2% and less show very simple transition behavior. Their spin transitions are gradual and occur over a wider temperature range than the gradual spin transitions in undiluted Fe compounds. The difference can be attributed to a cooperative interaction between the HS and LS complexes, which is mostly suppressed in the very dilute systems. The population of the energy levels in the isolated complexes is then described by the Boltzmann law, which determines the thermodynamic spin equilibrium. If $Z_{HS}(T)$ and $Z_{LS}(T)$ are the densities of state of the HS and LS fractions, the HS fraction of the spin transition curve is given by Equation (7).

$$\gamma_{HS}(T) = Z_{HS}(T)/[Z_{HS}(T) + Z_{LS}(T)] \quad (7)$$

Because the volume of the complex has increased and its shape changed, part of the energy difference between the lowest HS and LS states of the complex is elastic energy. This fraction can be changed experimentally by incorporating the same complex into host lattices with different elasticity constants. Then the free energy per complex molecule $\Delta f_{HL} = f_{HS} - f_{LS}$ in two different host lattices should only differ by a constant energy contribution. The difference $\Delta f_{HL}(T)$ follows from the HS part with $f_i = -k_B T \ln Z_i$ [Eq. (8)].

$$\Delta f_{HL}(T) = -k_B T \cdot \ln[\gamma_{HS}(T)/(1-\gamma_{HS}(T))] \quad (8)$$

The simple shifting of the $\Delta f_{HL}(T)$ curves has been tested for the picolylamine complex $[Fe(2\text{-pic})_3]^{2+}$ (Fig. 16). The complex (with EtOH and MeOH as solvent molecules, in two cases also deuterated) was dissolved in solid Zn and Co compounds, and above 230 K in two liquid solvents. Figure 16 shows Δf_{HL} for all transitions. The shifts Δ' are relative to the transition of $[Fe(2\text{-pic})_3]Cl_2 \cdot EtOH$ with the lowest transition temperature. Clearly, the curves do not intersect, but are just shifted along the temperature axis. The solid lines, which are not fitted curves but freehand guides, all have identical shapes.

The interpretation of the shift Δ' is evident. If we disregard the influence of the polar solvent on the ligand field strength, we have free complexes that do not interact in the liquid solutions. There is no elastic energy to overcome on going from the HS to the LS state (work against ambient pressure is minimal and can be neglected). Upon incorporation into a crystal lattice, the complete set of energy levels of the HS state is shifted downward by $\Delta = \Delta'(\text{solution}) - \Delta'(\text{lattice})$, relative to the LS state. At ambient temperature the solution in this case[110] contains about the same number of HS and LS complex molecules. Because the HS complex molecules, along with the solvent molecules, fit best into the available structures, a HS crystal precipitates. So the lattice stabilizes the HS state by Δ (downward shift by Δ). Viewed from the LS state, the change in structure to convert into the LS ground state involves expenditure of elastic energy (of Δ), with the result that the HS state is already populated thermally at a lower temperature. It should be mentioned that the opposite case of a destabilization of the lattice HS state relative to the solution HS state has also been observed.[106]

Because a transition from the LS state to the HS state entails a volume increase, the LS state is stabilized by $\Delta = p\delta v_{HL}$ when an increasing external pressure p is applied. The term δv_{HL} is the volume change of the host crystal per complex molecule. Figure 17 shows Δf_{HL} at ambient pressure and at $p = 1350$ bar for

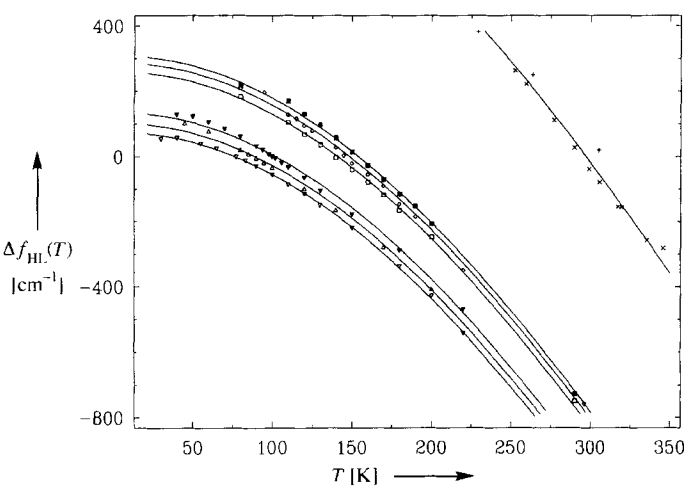


Fig. 16. The difference between the free energies $\Delta f_{HL}(T) = f_{HS}(T) - f_{LS}(T)$ of the highly dilute $[Fe(2\text{-pic})_3]^{2+}$ complexes in the HS and LS state in different lattices and in liquid solution. The values are derived from the spin equilibrium. ▽ $[Fe_{0.007}Zn_{0.993}(2\text{-pic})_3]Cl_2 \cdot EtOH$; △ $[Fe_{0.02}Co_{0.98}(2\text{-pic})_3]Cl_2 \cdot EtOH$ ($\Delta' = 20$ cm^{-1}); ▼ $[Fe_{0.03}Zn_{0.97}(2\text{-pic-ND}_2)_3]Cl_2 \cdot EtOD$ ($\Delta' = 86$ cm^{-1}); □ $[Fe_{0.02}Zn_{0.98}(2\text{-pic})_3]Cl_2 \cdot MeOH$ ($\Delta' = 225$ cm^{-1}); ◇ $[Fe_{0.01}Co_{0.99}(2\text{-pic})_3]Cl_2 \cdot MeOH$ ($\Delta' = 243$ cm^{-1}); ■ $[Fe_{0.01}Zn_{0.99}(2\text{-pic-ND}_2)_3]Cl_2 \cdot MeOD$ ($\Delta' = 282$ cm^{-1}); × $[Fe(2\text{-pic})_3]^{2+}$ complex in acetonitrile/water; + $[Fe(2\text{-pic})_3]^{2+}$ complex in methanol/water ($\Delta' \approx 800$ cm^{-1}). Observed values for the solutions are taken from ref.[110]. The curves (not fitted, just freehand viewing guides) are essentially parallel with a shift Δ' along the y axis.

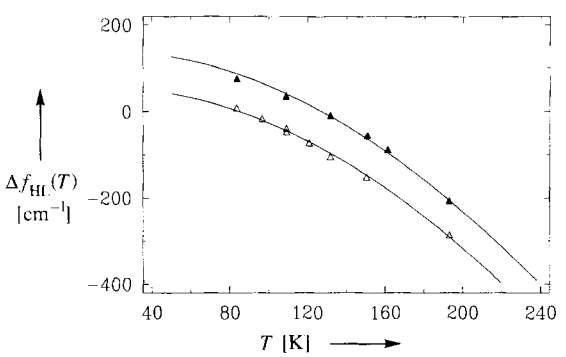


Fig. 17. The difference between the free energies $\Delta f_{HL}(T)$ of the highly dilute ($x = 0.03$) $[Fe(2\text{-pic})_3]^{2+}$ complex in the lattice of $[Zn(2\text{-pic-ND}_2)_3]Cl_2 \cdot EtOD$ at ambient pressure (△) and at $p = 1350$ bar (▲). Under an external pressure the free enthalpy is higher by $\Delta = 80$ cm^{-1} (from ref.[85]).

the compound $[Fe_{0.03}Zn_{0.97}(2\text{-pic-ND}_2)_3]Cl_2 \cdot EtOD$. The LS state stabilization of $\Delta = 80$ cm^{-1} corresponds to a volume increase of $\delta v_{HL} = 11.9$ Å^3, well within experimental error of a value of 12.3 Å^3 from variable-temperature X-ray measurements on the all-iron compound.[123]

Measurement of the spin equilibrium under pressure gives an impression of the internal pressure on the spin crossover complex molecule when the spin state changes in the crystal. A

simple consideration ($\Delta = -\frac{1}{2}p_{HL}\delta v_{HL}$) shows that a negative pressure of more than -25 kbar acts on the complex molecule to stabilize the HS state by $\Delta = 800\ cm^{-1}$. The assumption is that the essential deformation work is performed by the volume change, not by the change in shape. The latter would require a treatment of the full strain tensor instead of using merely the pressure (trace of the tensor). It will be shown in Section 3.4.1 that the isotropic part is 10–20%, so only pressures between -2.5 and -5 kbar actually act on the $[Fe(2\text{-pic})_3]^{2+}$ complexes, and the 80–90% of the elastic energy is due to the anisotropic strain in the crystal.

3.2. Concentrated Mixed Crystal Compounds

In concentrated systems (in particular, in mixed crystals with Fe concentrations of $0 \ll x \leq 1$), we have in any case an elastic interaction due to changes in shape and volume that is a function of the fraction $\gamma_{HS}(T)$ of the complexes in the HS state and entails a deviation from the Boltzmann type population. The simplest approach for the calculation of the free energy per complex molecule, f_x, is to consider a mixed crystal system of HS, LS, and M complexes (M = Zn, Co, etc.) [Eq. (9)].

$$f_x = x[\gamma_{HS}.f_{HS} + (1-\gamma_{HS})f_{LS} - Ts_{mix}(\gamma_{HS})] + (1-x)f_{Zn} + x\,w(\gamma_{HS}, x, T) + f_G \quad (9)$$

Here $w(\gamma_{HS}, x, T)$ is the interaction energy per Fe complex molecule and f_G is the free energy of the residual lattice, taken as independent of γ_{HS}. The mixing entropy between HS and LS molecules is $s_{mix} = -k_B[\gamma_{HS}\ln\gamma_{HS} + (1-\gamma_{HS})\ln(1-\gamma_{HS})]$, and contributions to the mixing entropy independent of γ_{HS} have been omitted. Because the interaction energy per complex molecule must vanish at infinite dilution ($w(\gamma_{HS}, x \to 0, T) \to 0$), the equilibrium condition $\partial f_x/\partial\gamma_{HS} = 0$ yields the Boltzmann type population given in Equation (7) for $x \to 0$.

From the temperature dependence of the spin equilibrium of a mixed crystal series (for example, the deuterated compounds $[Fe_xZn_{1-x}(2\text{-pic-}ND_2)_3]Cl_2\cdot EtOD$), we obtain an expression for w. Equation 10 follows from the equilibrium condition $\partial f_x/\partial\gamma_{HS} = 0$.

$$(\partial w/\partial\gamma_{HS})_T = -k_B T\cdot\ln[\gamma_{HS}(T)/(1-\gamma_{HS}(T)] - \Delta f_{HL} \quad (10)$$

The partial derivative $(\partial w/\partial\gamma_{HS})_T$ as a function of T and x can be calculated from the values of $\Delta f_{HL}(T)$ obtained from the transition curve for highly dilute lattices (see Fig. 16) and the experimental data for $\gamma_{HS}(T)$[139, 140] at concentration x. We have interpreted the temperature-independent energy difference of $\Delta f_{HL}(T)$ in the different lattices as an elastic energy difference. We now assume that the interaction between the complexes ($x > 0$) is chiefly elastic in nature as well, and their temperature dependence also negligible. We further assume that correlations between the HS excitations in the crystal are unimportant. Then w should be a function of γ_{HS} alone and should not explicitly depend on T. In Figure 18 we have therefore plotted the derivatives of w for several concentrations x over γ_{HS}. As a good approximation $\partial w/\partial\gamma_{HS}$ is a linear function: $\partial w/\partial\gamma_{HS} = \Delta - 2\Gamma\gamma_{HS}$. Figure 19 shows that both constants, Δ and Γ, are also proportional to the concentration: $\Delta(x)/x = 273\ cm^{-1}$ and $\Gamma(x)/x = 152\ cm^{-1}$.

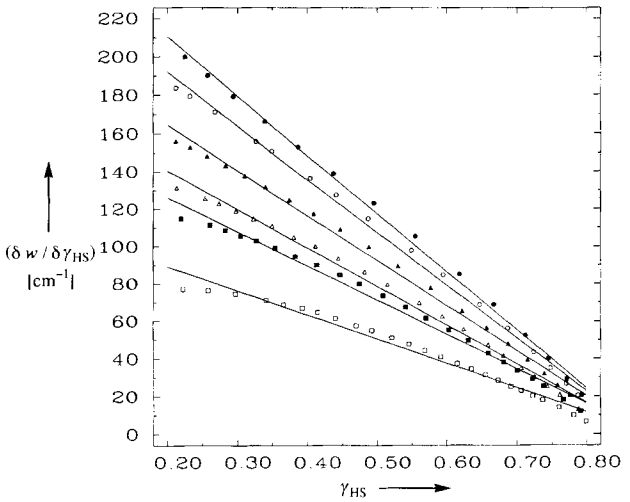


Fig. 18. The partial derivative $\delta w/\delta\gamma_{HS}$ as a function of γ_{HS} for different Fe concentrations x in $[Fe_xZn_{1-x}(2\text{-pic-}ND_2)_3]Cl_2\cdot EtOD$) with linear regression lines (from refs. [139, 140]). ●: $x = 1.00$; ○: $x = 0.91$; ▲: $x = 0.78$; △: $x = 0.68$; ■: $x = 0.60$; □: $x = 0.46$.

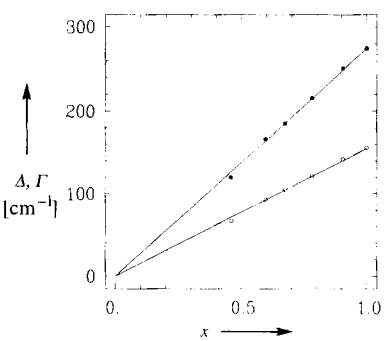


Fig. 19. $\Gamma(x) = 152\ cm^{-1}\cdot x$ (●) and $\Delta(x) = 273\ cm^{-1}\cdot x$ (○) as linear functions of the Fe concentration x. The linear regression lines were made to pass through the origin, so that the condition $w(x = 0) = 0$ is met (from ref. [140]).

This means that w fulfills the simplest possible phenomenological formulation, the Bragg–Williams approximation for a binary mixture with interaction between the components [Eq. 11]. The formal integration constant, which can only possibly be dependent on T and x, is included into the lattice contribution $f_G(x,T)$ or thought of as contained in this term from the start.

$$w(\gamma_{HS}, x) = \Delta(x)\gamma_{HS} - \Gamma(x)\gamma_{HS}^2 \quad (11)$$

The linear dependence of $\partial w/\partial\gamma_{HS}$ on x as well as on γ_{HS} was first discovered for the nondeuterated mixed crystal series[40] and later also verified for other mixed crystals.[41, 42, 81] However, a closer look reveals slight curvature in the line through the data points, especially towards large and small γ_{HS} values. At the end of Section 3 we shall present arguments to explain deviations from linearity. First we shall demonstrate that the free energy calculated from Equation (9) agrees well with observations from calorimetric results.

3.3. Specific Heat

The expression for free energy in Equation (9) was deduced solely from observations of the spin equilibrium $\gamma_{HS}(T)$. For an interacting system it is of the simplest imaginable form and was derived by different authors who used the expression in this or an equivalent formulation to parameterize the $\gamma_{HS}(T)$ curves.[28, 49] In Equation (9) one assumes that the different contributions (the HS/LS system and the corresponding lattice into which the Fe complex molecules are embedded) are additive. An interaction, also in the simplest approximation, is only considered in the HS/LS system.

This approach for the free energy was tested with calorimetric data. For these measurements we have chosen the $[Fe_xZn_{1-x}(2\text{-pic-}ND_2)_3]Cl_2 \cdot EtOD$ mixed crystal system, which has no structural (or other) order–disorder transition apart from the spin transition. In Figure 20 the specific molar heat is plotted for Fe

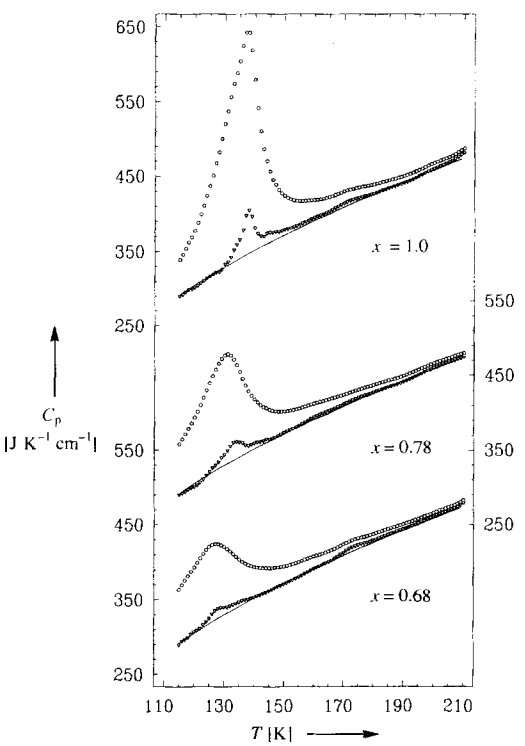


Fig. 20. The molar specific heats C_p of the mixed crystals $[Fe_xZn_{1-x}(2\text{-pic-}ND_2)_3]Cl_2 \cdot EtOD$ for three concentrations x as observed (○), and after subtraction of the specific heat due to the spin transition (▽). The subtracted fraction was calculated with the phenomenological approach for the free energy according to Equation (9). The solid smooth curves are extrapolations in the peak areas and averages of the data points beyond them. They are identified (see text) with the specific heats of a hypothetical, purely LS state lattice (from ref.[140]). The right hand axis refers to $x = 0.78$.

concentrations $x = 1.0$, 0.78, 0.68 for $T = 100$–200 K.[139, 140] As expected, the peak areas decrease with decreasing Fe concentrations and their maxima shift towards lower temperatures, equivalent to the transition curves $\gamma_{HS}(T)$ (see Fig. 8). As a consequence of the free energy expression we used, the specific heat C_p ($= -T\,\partial f_x/\partial_T{}^2$) is the sum of three terms [Eq. (12)].

$$C_p = x C_p^{HL} + x C_p^{LS} + (1-x) C_p^{Zn} \qquad (12)$$

$C_p^{LS}(T)$ and $C_p^{Zn}(T)$ is the specific heat of the pure LS and Zn lattices. $C_p^{LS}(T)$ is unknown in the transition area and at higher temperatures, and not accessible from direct measurements. Even though no suitable low-temperature calorimeter was available for measurements on the Fe complexes in the LS state, the free energy expression from Equation (9) could be tested by comparisons between members of the mixed crystal series. We subtract the measured $C_p^{Zn}(T)$ values (weighted by $(1-x/x)$) and the fraction $C_p^{HL}(T)$ (calculated from the $\gamma_{HS}(T)$-dependent terms of the free energy) from the observed values $C_p(T)/x$. This gives us the ▽ data points in Figure 20. Except for a small area around $T_{1/2}$, they are equal for all Fe concentrations and rise monotonously, as expected for $C_p^{LS}(T)$. The solid line is an extrapolation for $T = 125$–160 K, and the average of the ▽ data points outside this temperature interval. The small peak above this smoothed assumed function is only approximately 5% of the measured peak above the same $C_p^{LS}(T)$ curve. The thermodynamics of the gradual spin transition in question is thus very adequately described by the free energy expression from Equation (9), derived solely from the $\gamma_{HS}(T)$ curves.

3.4. Interpretation of the Interaction Term

3.4.1. Elastic Interaction

We have already stressed several times that the elastic interactions between the spin-changing complex molecules certainly play an important if not decisive role in the HS–LS transition. This section will show that the parameters $\Delta(x)$ and $\Gamma(x)$ in the interaction term for a mixed crystal series can be well understood if the elastic interaction is considered.

We use a simplified picture of the crystal, so that we can apply the theory of elasticity and derive quantitative expressions. The HS, LS, and M complex molecules are considered defects in their own crystal lattice into which they fit more or less well. The crystal lattice itself is seen as a homogeneous medium with certain elastic properties. Even for that simple model there is no adequate treatment in the literature. Therefore, as a further simplification, the elastic medium is assumed to be isotropic, so that it can be characterized by just two constants, the elastic (bulk) modulus K and the Poisson ratio σ.

Let us first look at the isotropic part of the defects only. A stress-free volume v_0 shall be reserved for a lattice site in the homogeneous medium. This volume can be occupied by volumes v_{HS}, v_{LS}, and v_M from a metal-diluted mixed crystal of the $[Fe_xZn_{1-x}(2\text{-pic})_3]X_2 \cdot sol$ type. They can be smaller or larger than v_0, and for the following simple consideration are assumed to be incompressible: When a volume v_α (α = HS, LS, M) is put into the medium (volume V), a stress field is built up, because the volumes v_{HS}, v_{LS}, and v_M are different from v_0. This stress field has an elastic energy [Eq. (13)].[138]

$$E = \tfrac{1}{2}K(\gamma_0-1)(v_\alpha-v_0)^2/v_0 - \tfrac{1}{2}K\gamma_0(\gamma_0-1)(v_\alpha-v_0)^2/V \qquad (13)$$

The Eshelby constant γ_0 is related to the Poisson ratio σ as follows: $0 \le \gamma_0 = 3(1-\sigma)/(1+\sigma) \le 3$. The second term in Equation (13) is very small since V/v_0 is of the order of Avogadro's number. It vanishes in an infinite medium, so the elastic energy

for an isolated complex in the lattice is given by the first term only. In a liquid solution, the inner degrees of freedom of the complex alone are active, and to these the difference in the elastic energies between the HS and the LS state during spin transition are added for the highly dilute mixed crystal. In this simple picture the energy difference between transitions in mixed crystals (see Fig. 16) is traced back to the differences in K, γ_0, and v_0. We shall not discuss this energy difference in the following.

In the finite crystal, an interaction between the defects gives rise to the second term. It is caused by the image pressure of the defect in a finite crystal. The crystal volume V changes upon incorporation of v_x on the v_0 site by more than just $v_x - v_0$, namely by δv_x [Eq. (14)].[138]

$$\delta v_x = \gamma_0(v_x - v_0) \tag{14}$$

This additional volume change $\delta v_x - (v_x - v_0) = (\gamma_0 - 1)(v_x - v_0)$ is formally attributed to a pressure $p_i = -K(\gamma_0 - 1)(v_x - v_0)/V$, and the second term in Equation (13) ($\frac{1}{2} p_i \delta v_x$) can be interpreted as volume work against that pressure.[138] Of course, the term "pressure" applies only for defects centered in a sphere, otherwise the stress field is no longer homogeneous. Eshelby, however, could show that δv_x remains valid irrespective of the form of V and the location of the defect. A homogeneous distribution of defects results in a homogeneous stress field, so again we can speak of a "pressure". The pressure is positive when ions with $v_x < v_0$ are incorporated and negative when bigger volumes are embedded. This effect can be used for the creation of positive or negative pressures by replacing atoms in the crystal with smaller or larger foreign atoms. The term "chemical pressure" is therefore also in use. Although small for a single defect, for one mole of defects it adds up to a finite entity which acts on all defects. For N defects in a crystal we obtain E_{total} according to Equation (15).

$$E_{\text{total}} = \tfrac{1}{2} K(\gamma_0 - 1) \sum_{i=1}^{N} (v_i - v_0)^2 / v_0 - \tfrac{1}{2} K \gamma_0 (\gamma_0 - 1) \left[\sum_{i=1}^{N} (v_i - v_0) \right]^2 / V \tag{15}$$

If we express the fraction x and γ_{HS} according to Equation (16) and consider the γ_{HS}-dependent terms in the elastic

$$\frac{1}{N} \sum_{i=1}^{N} (v_i - v_0) = x[\gamma_{\text{HS}}(v_{\text{HS}} - v_0) + (1 - \gamma_{\text{HS}})(v_{\text{LS}} - v_0)] + (1 - x)(v_{\text{M}} - v_0) \tag{16}$$

energy, we obtain an interpretation of $\Delta(x)$ and $\Gamma(x)$ within the phenomenological approach for the free energy [Eq. (17)].[140]

$$\Gamma(x) = x \tfrac{1}{2} K \gamma_0 (\gamma_0 - 1)(v_{\text{HS}} - v_{\text{LS}})^2 / v_c \tag{17a}$$

$$\Delta(x) = x K \gamma_0 (\gamma_0 - 1)(v_{\text{HS}} - v_{\text{LS}})(v_{\text{M}} - v_{\text{LS}}) / v_c \tag{17b}$$

The expression $v_c = V/\text{N}$ gives the volume per complex molecule. We see that Δ and Γ depend linearly on x, as is observed, and that all parameters can be experimentally determined. Note that v_0 is absent from the formulas. Thus, $\gamma_0(v_{\text{HS}} - v_{\text{LS}})/v_c$ is the relative volume increase on going from the LS to the HS state, that is, the trace of the ε tensor $\varepsilon_s^{\text{HL}}$ from a variable-temperature structure determination. We obtain $\varepsilon_s^{\text{ML}} = \gamma_0(v_{\text{M}} - v_{\text{LS}})/v_c$ from a comparison of the unit cell volumes of the metal compound and the Fe compound in the LS state. K and γ_0 are accessible as elasticity constants.

It should be stressed that for this type of interaction the Bragg–Williams approach is a very good approximation, since for the spherical part of the elastic interaction in an isotropic medium there is no direct, short-range interaction that could give rise to correlations between the HS and LS states. The image pressure is ubiquitous and effectively extends to infinity. The slowly changing anisotropic stress fields stemming from the location of the defects within V and its shape do not lead to short-range correlations.

If we use typical values (from X-ray structure analyses) for K ($= 10^{10}$ Pascal) and γ_0 ($= 1.5$; $\sigma = 1/3$) along with $\delta v_{\text{HL}} = 12\ \text{Å}^3$ and $v_c \approx 600\ \text{Å}^3$, we obtain $\Gamma = 20\ \text{cm}^{-1}$ for the interaction constant, which is merely 13% of the value of Γ in the free energy in the $[\text{Fe(2-pic-ND}_2)_3]\text{Cl}_2 \cdot \text{EtOD}$ system.[140] It is remarkable that the ratio $\Delta/\Gamma = 2\varepsilon_s^{\text{ML}}/\varepsilon_s^{\text{HL}}$ corresponds very well to the experimental value. The unit cell volumes of the M = Zn compound and the HS compound are almost equal. For example, at room temperature in the nondeuterated compound $[\text{M(2-pic)}_3]\text{Cl}_2 \cdot \text{EtOH}$, Mikami et al.[72] found 2485 Å^3 for the M = Fe(HS) compound and 2482 Å^3 for the Zn compound, whereas the difference between the HS and LS states is 57 Å^3. This predicts that $\Delta/\Gamma \approx 2$, in good agreement with the value of $273\ \text{cm}^{-1}/152\ \text{cm}^{-1} = 1.8$ obtained from the free energies. This correspondence apparently is the result of similar ionic radii for Zn^{2+} and Fe^{2+}(HS).

For both cases of mixed crystals $[\text{Fe}_x\text{Co}_{1-x}\text{(2-pic)}_3]\text{Cl}_2 \cdot \text{sol}$ (sol = EtOH and MeOH),[42] the ratio Δ/Γ is smaller than for the Zn compounds with the same solvent (Δ/Γ(EtOH) = 1.46[41] and Δ/Γ(MeOH) = 1.30 for Co and Δ/Γ(EtOH) = 1.58[44] and Δ/Γ(MeOH) = 1.60 for Zn), in accordance with the smaller Co^{2+} radius and the smaller unit cell volume, which was determined as 2467 Å^3 for $[\text{Co(2-pic)}_3]\text{Cl}_2 \cdot \text{EtOH}$ at room temperature. As we expected, the energy shift $\Delta(x)$ depends only on the chemical pressure of the substituted ions, whereas the interaction constant Γ is determined only by the density of the spin-changing Fe ions. Even though the ratio of the constants and the trends in size and concentration of the substituted ions are predicted quite well, the volume dilatation cannot explain the magnitude of the absolute values. It seemed reasonable to generalize the approach from the theory of elasticity for anisotropic defects, and thus, presumably, to keep these correct trends. This problem was treated in two articles,[43, 44] and the results are briefly summarized in the following.

The problem of anisotropic lattice deformation still has a relatively simple solution if the crystal (the homogeneous medium) has the shape of a sphere. An additional term, formed from the components of the trace-free tensor $\varepsilon_d^i = \varepsilon^i - \varepsilon_s^i/3 \cdot 1_3$ (i = HL, ML; 1_3 is the 3×3 unit matrix), is added to Δ and Γ. If $\varepsilon_{d,m}$ denotes the spherical components ($M = -2, -1, \ldots, 2$), Δ and Γ are defined by Equations (18).[43]

$$\Delta(x) = x K v_c (\gamma_0 - 1)/\gamma_0 \left[\varepsilon_S^{HL} \varepsilon_S^{ML} + \frac{3}{10}(2\gamma_0 + 1) \sum_m \varepsilon_{d,m}^{HL*} \varepsilon_{d,m}^{ML} \right] \quad (18a)$$

$$\Gamma(x) = x \frac{1}{2} K v_c (\gamma_0 - 1)/\gamma_0 \left[\left(\varepsilon_S^{HL} \right)^2 + \frac{3}{10}(2\gamma_0 + 1) \sum_m \varepsilon_{d,m}^{HL*} \varepsilon_{d,m}^{HL} \right] \quad (18b)$$

The proportionality to the concentration is, of course, retained. The extension of Equations (17a) and (17b) are contained in the second additive terms within the square brackets. The similar form of the expressions for Δ and Γ ensures that the ratio will still be close to 2. In Figure 21 the isotropic part (curve A) and the sum of the isotropic and anisotropic part (curve B) are plotted as a function of Γ/K versus γ_0 for the ε^{HL} tensors of two compounds.

As a new feature, the direct elastic interactions of the defects are treated in a third term, which vanishes for isotropic defects. This interaction energy can only be dealt with by numeric summation, since it depends on the relative positions and orientations of the defects in the single crystal. From X-ray crystal structure analysis we obtain the temperature-dependent average of the ε tensors belonging to the defects on the equipoints in the unit cell. For symmetrically equivalent lattice sites the corresponding ε tensors ε_i^{HL}(local) (the index i runs over all n positions in the unit cell) are distinguished only by their orientation. Under favorable conditions, namely if the average in crystals from different structures is formed in different ways, we can determine the local tensor ε_i^{HL} at the i-th equipoint. The necessary assumption is that the complex creates the same stress fields on transition from the HS to the LS state. This is true if their elastic properties are the same. The isotropic fraction $\delta v_{HL} = \gamma_0 (v_{HS} - v_{LS})$ is the same in different lattices (the complexes themselves are assumed to be incompressible, so $(v_{HS} - v_{LS})$ is independent of their environment) if γ_0 has the same value in both media. The data for the two spin crossover compounds in Figure 21 known so far do not contradict these requirements. They have exactly the same volume expansion δv_{HL}, so that at least an effective γ_0 must be the same for both compounds. They have different crystal structures with monoclinic (EtOH, $n = 4$) and orthorhombic (MeOH, $n = 8$) symmetry, well suited for the determination of all five ε tensor components belonging to the $[Fe(2\text{-pic})_3]^{2+}$ complex.[44] Whereas their isotropic components in the image pressure interaction are equal (ε_s is the same), the anisotropic contribution to the image pressure (curve B in Fig. 21) is much smaller for the MeOH system than for the EtOH system. This is a consequence of the different averaging over different equivalent orientations of the ε tensor in the two crystals.

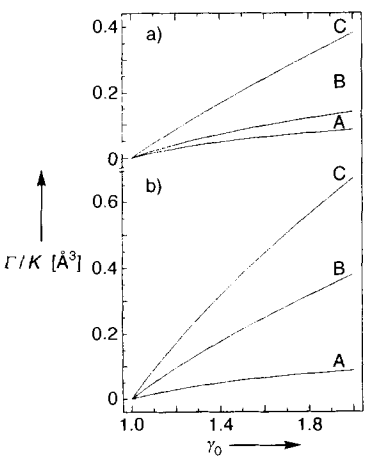


Fig. 21. The interaction constant Γ divided by the elastic (bulk) modulus K plotted versus the Eshelby constant γ_0 for two compounds $[Fe(2\text{-pic})_3]Cl_2 \cdot$sol: a) sol = MeOH and b) sol = EtOH. Γ/K was calculated from the deformation tensors ε^{HL} of the two compounds. The three curves for each compound show the different contributions included in the calculation. Curves A take into account only the isotropic part of the deformation tensor. Curves B include the interaction from the anisotropic image pressure. Curves C represent the total elastic interaction including the direct interaction between the HS complexes in a medium with a spherical shape (from ref. [44]).

A numerical summation of the direct interaction with the local tensor has been carried out over a sphere of radius 600 Å^3 (approximately). It can be shown analytically that further summation towards the edge of the macroscopic crystal will not yield any additional contribution as long as the microscopic sphere is contained in the macroscopic one. No special treatment was given to the interaction of the edge atoms in the crystal. In Figure 21 the C curves represent the sum over all elastic interactions. Especially for the MeOH compound (Fig. 21a), the direct interaction is the dominant part.

Applying the rigorous assumption of equal elastic constants K and γ_0 without any presupposition about the absolute values of the compressibility K, we now use the experimental values of $\Gamma^{MeOH} = 98\ cm^{-1}$ and $\Gamma^{EtOH} = 175\ cm^{-1}$ and their ratio ($\Gamma^{MeOH}/\Gamma^{EtOH} = 0.56$) to fix $\gamma_0 = 1.53$ at a point where the quotient of the theoretical curves in Figure 21 reaches the same ratio. At this point we have $\Gamma^{EtOH}/K = 0.43$ Å^3 and $K = 0.86 \times 10^{10}\ Nm^{-2}$, a value we can safely regard as typical for organometallic compounds of that kind.

In summary we conclude that a full description of the interaction term in the phenomenological approach for the free energy of a spin crossover compound can be derived from the microscopic elastic interaction between the HS and the LS complexes. Even though the simplified model of an isotropic elastic medium with a spherical shape does not allow exact quantitative comparisons with observed data, there is no question that the magnitude of the elastic contribution is of the same order as the experimental values. Any additional contribution is either small or a part of other contributions of which the sum must again be small.

3.4.2. Other Models

Two contributions to the interaction problem from the literature deserve some discussion. Zimmermann and König[141] have treated the phonon component in the interaction. They derive a phonon contribution of $bNk_B\theta(\Delta\theta/\theta)^2$, stemming from a change in the Debye temperature θ of the lattice upon transition from the LS to the HS state. It can be understood as follows. While the crystal volume increases as the HS fraction increases, the Debye temperature decreases because of the anharmonicity of the oscillator potentials. Consequently, the phonons acquire a higher density of states, and the free energy is lowered accordingly, not only as a result of the lower frequencies but, more crucially, of an increase in vibrational entropy. The nonlinear relationship between θ and γ_{HS} on one hand and the free energy of the Debye crystal on the other yields a $-bNk_B\theta(\Delta\theta/\theta)^2$ term as the coefficient of γ_{HS}^2 in a potential series

for γ_{HS}. This term is estimated at $-40\ cm^{-1}$ by the authors; this estimate is much too big for two reasons. The first is that the decrease in the vibrational frequencies on increasing the volume does not affect the intramolecular frequencies, with the result that only the Debye temperature θ for the long-wave acoustic branch related to the sonic speed and the elastic (bulk) modulus must be included. It is about 50 K. The change in the intramolecular frequencies is already accounted for in the difference of the free energies for the highly dilute systems. It contributes nothing to the interaction. By the same argument, N cannot be taken as the number of atoms in the complex, but rather is equal to 1, because the complex in the Debye model must be treated as a single entity. The high-temperature approximation for the constant $b \approx 3T/\theta$ holds in the transition range $T > 100$ K. The Grüneisen formula $\theta_{HS} = \theta_{LS}(V_{HS}/V_{LS})^{-\gamma_G}$ can be used to obtain an estimate for $\Delta\theta/\theta$ of 0.1 ($\gamma_G = 3$). The phonon contribution is therefore smaller than $3\ cm^{-1}$ and can still be neglected within the scope of the present discussion.

The theory of the second contribution was developed by Kambara,[38, 142, 143] who, within the framework of crystal field theory, regards the cooperative Jahn–Teller coupling of the 3d electrons to the molecular deformation as the cause for the HS → LS transition. In the first articles only the isotropic part (A_1 mode) was treated.[142, 143] Later the model was expanded to include the E_g mode. The change of vibrational modes, which proved to be significant, is not taken into account. Aside from the general shortcomings of crystal field theory, only direct elastic interactions are considered in this approach and the substantial part of the image pressure is entirely neglected. For the A_1 deformation (which in an isotropic medium entails no direct interaction) this means that only small corrections can play a role because of the anisotropy of the medium. The anisotropic Jahn–Teller interaction of the $^5T_{2g}$ HS state is certainly small, if significant at all. From its temperature-dependent quadrupole splitting we have proof that the T_{2g} triplet is already completely split in a highly dilute mixed crystal containing only a few Fe complexes.[144] The splitting, depending on the HS fraction γ_{HS}, barely changes for the pure Fe compound. This means that any deformation of the complex during the spin transition is independent of x and γ_{HS}, and that additional deformations due to the cooperative Jahn–Teller effect must be small. Even though, at first sight, the approach of Kambara seems to be an elegant one, because it contains the inner elasticity of the complexes, it obviously accounts only for rather small contributions. The parameters in his model cannot be translated into meaningful quantities which could be related to observed values of the deformation tensor and the changes in Fe–N bond lengths. Kambara himself has not tried such a verification.

4. Light-Induced Spin Transitions

Iron(II) coordination compounds have had a comparatively miserable standing compared to other transition metal complexes with respect to the investigation of their photophysical and photochemical properties. The primary reason was that they do not have optically excited states with long lifetimes as the latter do. Their low-energy LF states are generally associated with radiationless relaxations back to the ground state through a series of intersystem crossing (ISC) and internal conversion (IC) steps on a subnanosecond time scale.

After Decurtins et al.[64, 65] discovered the phenomenon of light-induced $^1A_1(LS) \rightarrow {}^5T_2(HS)$ transitions in iron(II) spin crossover compounds at temperatures far below the thermal spin transition temperature while investigating the spin transition in $[Fe(ptz)_6](BF_4)_2$ by optical spectroscopy, it became clear that iron(II) coordination compounds can also have photophysical properties worthy of attention. A two-step mechanism of ISC's with $\Delta S = 1$ each was postulated for the light-induced spin transition leading from the original $^1T_1$ excited LF state via a low-energy $^3T_1$ state to the final $^5T_2$ state. Because of the large difference in bond lengths associated with the transition from the LS to the HS state,[36, 72, 82] the energy barrier between the two states is big enough to "freeze" the system in the HS state at low temperatures. The phenomenon of the light-induced spin transition was therefore termed "light induced excited spin state trapping", in short LIESST.

Further work subsequently established the existence of the light-induced reverse transition (reverse-LIESST effect), and finally, evidence for the proposed mechanism with the $^3T_1$ state as an intermediate was discovered.[145, 146]

4.1. The $[Fe(ptz)_6](BF_4)_2$ Spin Crossover System

4.1.1. Thermal Spin Transition

The thermal spin transition in $[Fe(ptz)_6](BF_4)_2$ was first investigated by Franke et al.[100] and Müller et al.[78] by means of magnetic susceptibility measurements. In the concentrated solid the transition from the diamagnetic LS state to the strongly paramagnetic HS state involves a crystallographic first-order phase transition with a hysteresis effect of about 7 K ($T_c^{\uparrow} = 135$ K, $T_c^{\downarrow} = 128$ K) and a change in Fe–N bond lengths of $\Delta r_{HL} \approx 0.18$ Å.

Not only do the magnetic properties change with the spin transition, so does the color: $[Fe(ptz)_6](BF_4)_2$ in the LS state at 20 K is deep purple, whereas in the HS state at 293 K it is colorless. The corresponding single crystal absorption spectra with the direction of light propagation along the crystallographic c axis are shown in Figures 22a and 22b. The exctinction coefficients of the bands in the NIR and visible regions are within the range typical for spin-allowed LF transitions. According to the Tanabe–Sugano diagram in Figure 1, the one band in the room temperature spectrum at $\bar{\nu} = 11\,760\ cm^{-1}$ can be assigned without difficulty to the $^5T_2 \rightarrow {}^5E$ transition, and the two bands in the low-temperature spectrum at $\bar{\nu} = 18\,210$ and $26\,400\ cm^{-1}$ to the $^1A_1 \rightarrow {}^1T_1$ and $^1A_1 \rightarrow {}^1T_2$ transitions. The LF strengths for the HS and the LS state are given by Equations 19.[147]

$$10\,Dq^{HS} = E(^5E) - E(^5T_2) = 11\,760\ cm^{-1} \quad (19a)$$

$$10\,Dq^{LS} = E(^1T) - E(^1A_1) + (E(^1T_2) - E(^1T_1))/4 = 20\,550\ cm^{-1} \quad (19b)$$

Thus $10Dq^{LS}/10Dq^{HS} = 1.75$ and very close to the estimated value from Equation (3) (see Section 2.1).

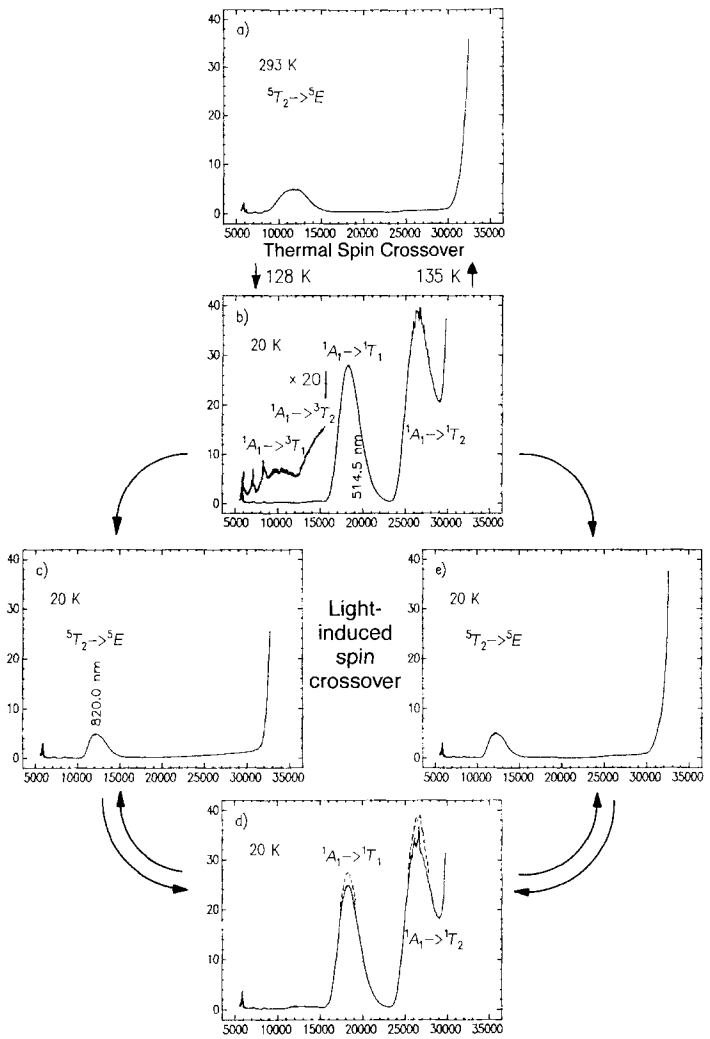


Fig. 22. Single crystal absorption spectra with the light propagating along the crystallographic c axis of $[Fe(ptz)_6](BF_4)_2$ in the range of the d–d transitions at a) 293 K and b) 20 K; c) after irradiation at 514.5 nm (20 K), d) after subsequent irradiation at 820 nm (20 K), e) after irradiation at 980 nm (20 K) (from ref.[146]). See text for an explanation of the overlay in b). In each case ε [L mol^{-1} cm^{-1}] is plotted along the y axis and $\tilde{\nu}$ [cm^{-1}] along the x axis.

The LS or HS fraction as a function of temperature can be determined from the explicit temperature dependence of the band intensity, for example for the $^1A_1 \rightarrow {}^1T_1$ band. The resulting transition curve for the thermal spin transition in $[Fe(ptz)_6](BF_4)_2$ with the well-known hysteresis is shown in Figure 23. It matches the curve obtained from susceptibility measurements well.[81, 100, 148]

The absorption spectra at 20 and 293 K of a mixed crystal $[Zn_{1-x}Fe_x(ptz)_6](BF_4)_2$ ($x \approx 0.1$) and those of the concentrated material are identical.[145] This implies that a complete thermal spin transition occurs also in the mixed crystal. The transition curve (see Fig. 23), however, is gradual with a transition temperature $T_{1/2} \approx 95$ K and without hysteresis because only minor elastic interactions are left at such a low Fe concentration.

By sufficiently rapid cooling, however, the first-order crystallographic phase transition in $[Fe(ptz)_6](BF_4)_2$ can be suppressed.[149] But also in the crystallographic high-temperature phase (space group $R\bar{3}$[100]) the thermal spin transition is complete. The corresponding transition curve with $T_{1/2} \approx 125$ K is

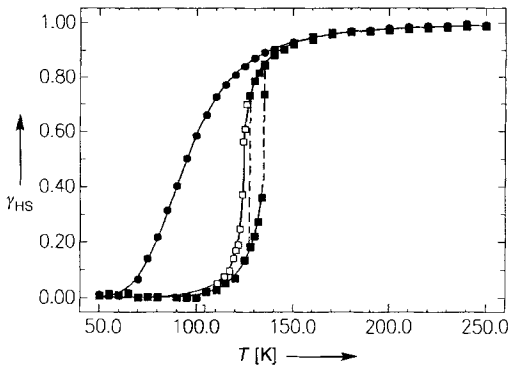


Fig. 23. The thermal spin transitions in $[Zn_{1-x}Fe_x(ptz)_6](BF_4)_2$ ($x \approx 0.1$, •) and $[Fe(ptz)_6](BF_4)_2$ (■) with a crystallographic phase transition and in the supercooled high-temperature phase (□), determined from the temperature dependence of the $^1A_1 \rightarrow {}^1T_1$ absorption band. The solid line for the dilute system (•) was calculated for the model of a unimolecular, temperature-dependent LS⇌HS equilibrium: $\Delta G_{HL} = \Delta H_{HL} - T\Delta S_{HL} = -k_B T \ln K$ with $\Delta H_{HL} = 462$ cm^{-1} and $\Delta S_{HL} = 4.9$ cm^{-1} K^{-1}. The critical temperatures for the concentrated system are $T_c^{\downarrow} = 135$ K and $T_c^{\downarrow} = 128$ K (from ref.[146]). The solid line connecting the points for the supercooled high-temperature phase was calculated with an interaction constant $\Gamma = 170$ cm^{-1}.

included in Figure 23. Still the transition is much steeper than for the isostructural mixed crystal $[Zn_{1-x}Fe_x(ptz)_6](BF_4)_2$. Following the thermodynamic considerations outlined in Section 3, it can be reproduced with an interaction constant Γ of about 170 cm^{-1}.[68, 80] Characteristically, the high-temperature spin transition curves of the concentrated and the dilute systems are parallel, because the volumes v_{Zn} of the Zn complex and v_{HS} of the Fe complex in the HS state are approximately equal.[137]

According to Figure 24 there are several triplet states additional to the higher excited quintet and singlet states. Spin for-

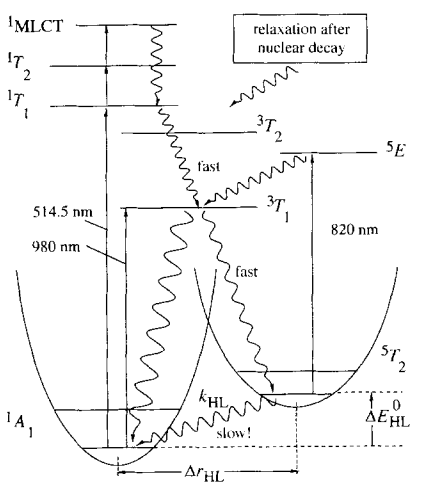


Fig. 24. Schematic representation of the excited higher LF states of a d^6 complex for LF strengths in the spin crossover range. Spin allowed d–d transitions are denoted by straight arrows. The scheme fully illustrates the complete mechanism of LIESST and reverse-LIESST.

bidden singlet → triplet transitions will not only be very weak but also as broad as the spin-allowed ones, since these triplet states are not based on the t_2^6 configuration like the $^1A_1$ ground state.

Indeed, a close inspection of the $[Fe(ptz)_6](BF_4)_2$ absorption spectrum at 20 K (see overlay in Fig. 22b) reveals two very weak and broad bands on the low energy side of the $^1A_1 \rightarrow {}^1T_1$ band. One is at $\tilde{\nu} = 10280\ cm^{-1}$ and the other (as a shoulder on the rising slope of the $^1A_1 \rightarrow {}^1T_1$ band) at $\tilde{\nu} \approx 14300\ cm^{-1}$, and they can be assigned to the spin forbidden $^1A_1 \rightarrow {}^3T_1$ and $^1A_1 \rightarrow {}^3T_2$ transitions.

4.1.2. Light-Induced Excited Spin State Trapping (LIESST)

Irradiation into the $^1A_1 \rightarrow {}^1T_1$ band of a $[Fe(ptz)_6](BF_4)_2$ crystal with the 514.5 nm line of an Ar^+ laser at temperatures below about 50 K completely bleaches the crystal within a short time. The absorption spectrum after irradiation again shows the $^5T_2 \rightarrow {}^5E$ band typical of the HS state in the NIR region, but the LS bands in the visible spectrum have disappeared (compare Figs. 22b and 22c). Consequently a complete light-induced LS → HS conversion has taken place. The absorption maximum of the $^5T_2 \rightarrow {}^5E$ band now is at $\tilde{\nu} = 12200\ cm^{-1}$, slightly blue-shifted from the 293 K value, exactly as expected for an LF transition upon cooling. At 20 K $10Dq^{HS}$ is thus $12000\ cm^{-1}$. At this temperature the HS state is a metastable one that virtually has an infinite lifetime. Only at temperatures above about 50 K does a noticeable thermal relaxation back to the LS state set in.

Figure 24 shows schematically the two-step ISC mechanism, postulated by Decurtins et al.,[65] with $\Delta S = 1$ for each step from the originally excited $^1T_1$ state via the $^3T_1$ state to the $^5T_2$ state. Because the energy level of the $^3T_1$ state is lower not only than the $^1T_1$ state but, for the spin crossover systems, also than the ^5E state, a light-induced reverse transition seems feasible. And indeed, if in a second step the colorless crystal is now irradiated in the band maximum of the $^5T_2 \rightarrow {}^5E$ transition at 820 nm with light from a Ti-sapphire laser while the temperature is kept at 20 K, its orginal red color soon returns. Figure 22d shows that effectively a light-induced reverse transition (reverse-LIESST) has occurred. However, the reverse transition is not quite complete. Even after repeated irradiation a saturation value for the LS fraction of only $\gamma_{LS} \approx 0.9$ is reached. The most straightforward explanation is that the LS species has a weak absorption band overlapping with the quintet band in such a way that this absorption in turn entails another light-induced LS → HS transition. Indeed the two spin-forbidden transitions of the LS species, the $^1A_1 \rightarrow {}^3T_1$ and the $^1A_1 \rightarrow {}^3T_2$ transitions, overlap with the $^5T_2 \rightarrow {}^5E$ transition (see Figs. 22a and 22b). Although the minimum between the two spin-forbidden transitions is just at 820 nm, the absorption does not quite return to zero.

The maximum of the $^1A_1 \rightarrow {}^3T_1$ band at $10280\ cm^{-1}$ (980 nm) is just to the low-energy side of the $^5T_2 \rightarrow {}^5E$ band. The crystal (with a normal LS spectrum at 20 K) can now be irradiated with a narrow band around 980 nm from a Ti-sapphire laser, and again a complete light-induced LS → HS conversion results (see Fig. 22e). This proves 1) that the two weak bands do not arise from impurities, and therefore their assignment to the spin-forbidden transitions is justified, and 2) that the mechanism for LIESST with the $^3T_1$ state as an intermediate state as shown in Figure 24 is correct.

LIESST and reverse-LIESST can also be followed quantitatively,[145] and the quantum yields of the ISC processes of the LIESST and reverse-LIESST mechanism can be determined.[146] Those for the first step, the $^1T_1 \rightarrow {}^3T_1$ transition for LIESST and the $^5E \rightarrow {}^3T_1$ transition for reverse-LIESST, are close to unity. The branching ratio from the $^3T_1$ state either into the $^1A_1$ ground state or the metastable $^5T_2$ state is about 1:4. The lower limit for the relaxation rate constants for the ISC processes (with the exception of the $^5T_2 \rightarrow {}^1A_1$ relaxation) is $10^9\ s^{-1}$, because up to now no transient populations of an intermediate state on the nanosecond time scale could be found with pulsed laser experiments.[150-152]

The $^5T_2 \rightarrow {}^1A_1$ relaxation, however, is very slow at low temperatures; in $[Fe(ptz)_6](BF_4)_2$ its metastable state at 10 K has a lifetime of roughly 40 days. Only above about 50 K does a noticeable thermal relaxation begin to set in. There, strong cooperative interactions are conspicuous in the concentrated solid (see Section 5).

4.2. The $[Fe(mtz)_6](BF_4)_2$ Spin Crossover System

In principle, by analogy with reverse-LIESST, it should also be possible to trigger a light-induced HS → LS conversion by irradiation in the NIR region for the case $\Delta E^0_{HL} < 0$ (that is, for stable HS complexes). For this, the minimum of the ^5E potential well must, at any rate, lie energetically above the well for the $^3T_1$ state, which is only the case for complexes whose LF strengths are not significantly below $10Dq^{HS}$ for a spin crossover compound.

Such a HS → LS conversion was first realised for the methyl-substituted compound $[Fe(mtz)_6](BF_4)_2$ (mtz = 1-methyltetrazole).[153] In this system the $[Fe(mtz)_6]^{2+}$ complexes are distributed over two nonequivalent lattice sites.[36] Complexes on the lattice site denoted as A show a thermal spin transition with a transition temperature $T_{1/2} \approx 75$ K. For those on the lattice site denoted as B, however, a doublet with a large quadrupole splitting characteristic of an HS state is observed in the Mössbauer spectrum even at low temperatures (see Fig. 25a). This means

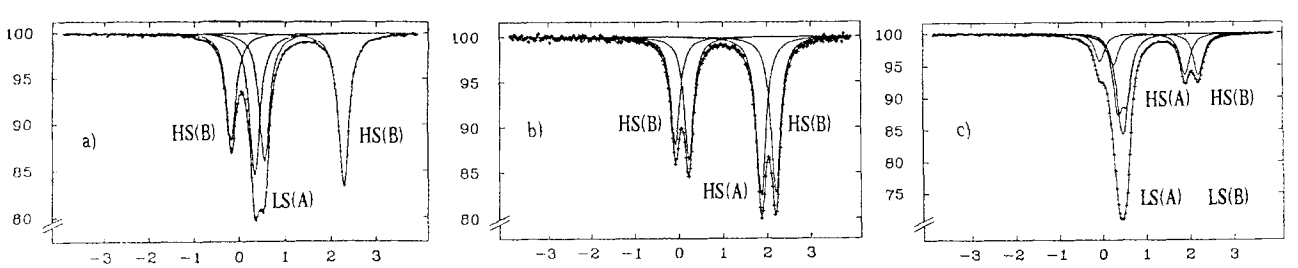


Fig. 25. Mössbauer spectra of $[Fe(mtz)_6](BF_4)_2$: a) at 20 K, b) at 20 K after irradiation in the visible range (300-600 nm), c) at 20 K after irradiation in the NIR region (700-1000 nm) (adapted from ref.[153]). The relative transmission is plotted along the ordinate and the relative velocity v [$mm\,s^{-1}$] between source and absorber along the abscissa.

that the HS state is the ground state on lattice site B and thus $\Delta E^0_{HL} < 0$.

The complex molecules on lattice site A show a LIESST behavior analogous to the one in $[Fe(ptz)_6](BF_4)_2$. Irradition in the visible region at 20 K causes a complete LS(A) → HS(A) conversion, whereas, as expected, the complexes on lattice site B remain unaffected (Fig. 25b). The light-induced HS state on lattice site A at 20 K has a lifetime similar to that in $[Fe(ptz)_6](BF_4)_2$, and likewise the HS(A) → LS(A) relaxation sets in at temperatures above about 50 K. Irradiation in the NIR region for the lattice site A as well as for the lattice site B results in a steady-state distribution with $\gamma_{LS}(A) \approx \gamma_{LS}(B) \approx 0.65$, just like in $[Fe(ptz)_6](BF_4)_2$ (Fig. 25c). However, for the lattice site B the light-induced HS(B) → (LS(B) conversion corresponds to the population of a metastable LS state. This state now has a very long lifetime at 20 K. Here the LS(B) → HS(B) relaxation does not set in until above about 50 K.

4.3. LIESST in Other Iron(II) Spin Crossover Systems

Since the discovery of LIESST in $[Fe(ptz)_6](BF_4)_2$, light-induced metastable HS states could be produced in a great number of Fe(II) spin crossover complexes. Not only in concentrated materials such as $[Fe(pic)_3]X_2 \cdot sol$ (X = Cl, Br; sol = MeOH, EtOH,[65] $[Fe(phen)_2(NCS)_2]$,[66] $[Fe(2\text{-mephen})_3](ClO_4)_2$ (mephen = methylphenanthroline),[154] and others,[155–157] but also in the dilute mixed-crystal systems $[Zn_{1-x}Fe_x(ptz)_6](BF_4)_2$,[146] $[M_{1-x}Fe_x(pic)_3]Cl_2 \cdot sol$ (M = Mn, Zn; sol = MeOH, EtOH,[152, 158] and $[Zn_{1-x}Fe_x(mepy)_3(tren)](PF_6)_2$ (mepy = methylpyridine, tren = tris(2-aminoethyl)amine),[152] and even in spin crossover complexes embedded in polymer foils,[159] among others in the $[Fe(2\text{-mephen})_3]^{2+}$ complex in polyvinylalcohol (PVA).[160] In the systems just mentioned the lifetimes of the metastable HS states at low temperatures range from 10^1 to 10^5 seconds.

In most of these systems, however, the d–d bands of the LS species are hidden by low-energy, intense metal–ligand charge-transfer (MLCT) bands. The MLCT bands for the LS state are much more intense than those for the HS state, because the shorter metal–ligand bond lengths in the LS state result in stronger overlap between metal and ligand orbitals.

4.3.1. The $[Fe\{(mepy)_3(tren)\}]^{2+}$ Complex

The thermal spin transition of iron(II) complexes with hexadentate ligands of the $\{(mepy)_y(py)_{3-y}(tren)\}$ ($y = 0$–3) type was first investigated by Hoselton et al.[70] by means of magnetic susceptibility measurements. In the $[Fe\{(mepy)_y(py)_{3-y}(tren)\}](PF_6)_2$ series, the thermal spin transition is gradual even in the concentrated solid. The transition temperature $T_{1/2}$ increases from about 215 K for $y = 3$ through about 290 K for $y = 2$ to about 380 K for $y = 1$. The complex with $y = 0$ remains in the LS state up to about 400 K. The increasing stabilization with the increasing number of methyl groups at the pyridyl rings is due to the associated mutual steric interaction of the Me groups, which favors the longer Fe–N distance in the HS state.

Optical spectroscopy with these complexes is only possible for highly dilute systems, because the MLCT band in the LS state is very intense. Figure 26a shows the single crystal absorption spectra of the dilute mixed crystal $[Zn_{1-x}Fe_x\{(mepy)_3(tren)\}](PF_6)_2$ ($x \approx 0.0003$) at temperatures between 15 and 325 K. The transition is gradual and the transition temperature $T_{1/2} \approx 210$ K is virtually equal to the one in the concentrated compound $[Fe\{(mepy)_3(tren)\}](PF_6)_2$.

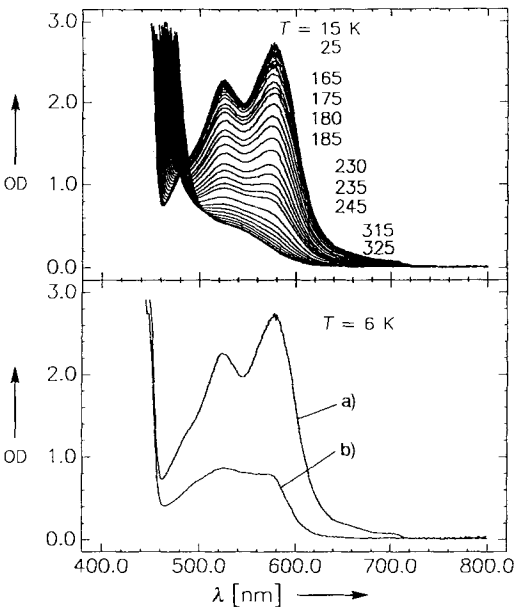


Fig. 26. Single-crystal absorption spectra of $[Zn_{1-x}Fe_x\{(mepy)_3(tren)\}](PF_6)_2$ ($x \approx 0.0003$). Top: at different temperatures in thermal equilibrium; bottom: at 6 K before and immediately after an irradiation with 514.5 nm (from ref.[152]). OD = optical density.

In Figure 26b, in addition to the normal low-temperature spectrum of $[Zn_{1-x}Fe_x\{(mepy)_3(tren)\}](PF_6)_2$, the spectrum immediately after irradiation with light at 514.5 nm is depicted. A comparison with Figure 26a shows that irradiating into the MLCT band causes a light-induced LS → HS conversion as well. The lifetime τ of the light-induced HS state is about 10 s at 6 K, much shorter than for $[Fe(ptz)_6](BF_4)_2$, and it decreases rapidly with increasing temperature.

4.3.2. The $[Fe(2\text{-mephen})_3]^{2+}$ and $[Fe(phen)_3]^{2+}$ Complexes

The $[Fe(2\text{-mephen})_3]^{2+}$ complex is a spin crossover complex in the solid (as $[Fe(2\text{-mephen})_3](ClO_4)_2$[88]) as well as embedded in polymer matrices.[160] The thermal spin transition is gradual in both cases, and the transition temperature $T_{1/2}$ is about 140 K. LIESST also occurs in this iron(II) spin crossover complex in both forms (in the concentrated solid for $[Fe(2\text{-mephen})_3]X_2$ (X = ClO_4, BPh_4)[154] and in various polymer matrices[160]) by irradiating into the MLCT band in the visible region.

The electronic structure of the $[Fe(2\text{-mephen})_3]^{2+}$ complex cannot be very different from that of the $[Fe(phen)_3]^{2+}$ or the $[Fe(bipy)_3]^{2+}$ complex. Although the latter two complexes are typical LS complexes, the HS state (longer Fe–N bond lengths) in the $[Fe(2\text{-mephen})_3]^{2+}$ complex is just stabilized enough with

respect to the LS state, by virtue of the steric interaction of the methyl groups, to turn the compound into a spin crossover complex. Conversely, the conditions in $[Fe(phen)_3]^{2+}$ and the $[Fe(bipy)_3]^{2+}$ complexes cannot be very different from those for spin crossover systems with $\Delta E^0 \approx 2500-3500\ cm^{-1}$.

Already several years before the LIESST effect was discovered, Ensling et al.[161] and Grimm et al.[162] had noted anomalous HS states additional to the LS state in the Mössbauer emission spectra of $[^{57}Co/Co(phen)_3](ClO_4)_2 \cdot 2H_2O$ at low temperatures. As possible explanations they considered either some radiation damage on one of the ligands, or a transient population of the $^5T_2$ state after nuclear decay of the ^{57}Co atom. Figure 27 depicts the time-integrated Mössbauer emission spectra of $[^{57}Co/Co(phen)_3](ClO_4)_2 \cdot 2H_2O$ at 40 (top) and at 172 K (bottom). The spectrum at 172 K with an only weakly split doublet shows an isomer shift and a quadrupole splitting characteristic for the LS state and also observable in the Mössbauer absorption spectrum of $[^{57}Co/Co(phen)_3](ClO_4)_2$. In the emission spectrum at 40 K beside the LS doublet and signals characteristic of iron(III), which is an "aliovalent" charge state as a consequence of nuclear decay, are two doublets with a large quadrupole splitting and isomer shifts characteristic for HS states. One of these doublets, denoted HS1 in the spectrum, has Mössbauer parameters very similar to those of the light-induced state in $[Fe(2\text{-mephen})_3](BPh_4)_2$.[154] The assignment of this HS1 state to the $^5T_2$ state in an otherwise unperturbed $[^{57}Fe(phen)_3]^{2+}$ complex seems appropriate. Grimm et al.[162] determined the lifetime of that state by time-differential Mössbauer emission spectroscopy (TDMS) to be about 390 ns at 10 K, about 205 ns at 47 K, and about 100 ns at 100 K.

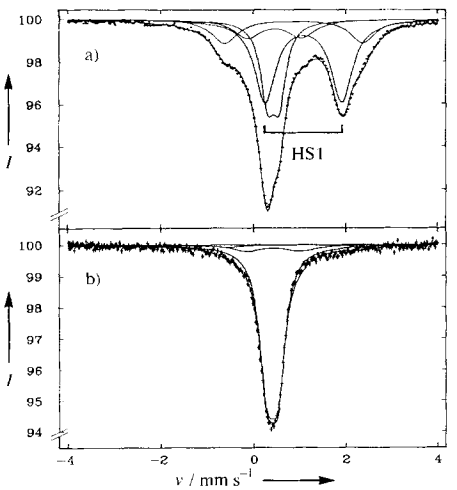


Fig. 27. Mössbauer emission spectra of $[^{57}Co/Co(phen)_3](ClO_4)_2 \cdot 2H_2O$ at a) 40 K and b) 172 K (adapted from ref.[62]). I [%] represents the relative transmission.

The question now is the following: is a light-induced transient population of a HS state also possible in a LS complex, and, if yes, is the nuclear decay-induced transient HS state the same as the light-induced HS state? It is true that Street et al.[163] and Creutz et al.[164] (in an experiment with a pulsed picosecond laser) found a transient state with a liftime $\tau \approx 0.71$ ns for $[Fe(phen)_3]^{2+}$ in solution. However, their assigments included a low-lying ^{3}MLCT state as well as $^1T_1$ and $^3T_1$ states, and they also did not exclude a $^5T_2$ state. For $[Fe(phen)_3]^{2+}$ embedded in a Nafion matrix on the other hand, the lifetime of the light-induced state is about 190 ns at an effective temperature of ≈ 50 K.[165] This lifetime is indeed in accord with the one determined from time-differential Mössbauer spectroscopy, and we can conclude that also in LS compounds the same HS state as in spin crossover compounds is populated after irradiation and after nuclear decay, but its lifetime τ is considerably shorter. Also, in complete agreement with the observations from LIESST experiments, much longer lifetimes of the HS state populated after nuclear decay were observed in the Mössbauer emission spectra of ^{57}Co-doped iron(II) spin crossover complexes.[166-170] By analogy, we call this effect NIESST, meaning nuclear decay-induced excited spin state trapping. The phenomenon has so far only been observed on the ^{57}Co-doped complexes just mentioned. Here the radioactive ^{57}Co atom functions as an intramolecular "quasi light source"—its decay supplies the excitation energy—and the ^{57}Fe daughter atom functions as an intrinsic clock in the time-differential Mössbauer emission spectroscopy experiments.[61, 62, 171]

5. The HS → LS Relaxation in Iron(II) Complexes

During the past years many studies have been performed on the dynamics of the HS → LS relaxation, especially for iron(II) spin crossover compounds in solution and at ambient temperatures.[128, 150, 172-178] Different experimental methods were used to determine the rate constants k_{HL} of the HS → LS relaxation. After the studies of McGarvey and Lawthers,[150] however, pulsed laser excitation has become the most common technique. In solution only a limited temperature range is accessible and $\ln[k_{HL}]$ versus $1/T$ plots (Arrhenius plots) usually resulted in straight lines. The results have accordingly been discussed in terms of semiclassical absolute rate theory. Experimental activation energies E^a for most of the iron(II) spin crossover complexes under study were found to be between $1000-1500\ cm^{-1}$ with preexponential factors A of $10^7-10^9\ s^{-1}$. Thus, values for k_{HL} in solution and at ambient temperatures are typically of the order of $10^6-10^8\ s^{-1}$.

For some iron(II) spin crossover complexes, the HS → LS relaxation rates and activation parameters determined with line shape analysis of Mössbauer spectra[42, 56-59] in the solid state around room temperature were similar to those in solution. This technique, however, is restricted to systems with transition temperatures $T_{1/2}$ around room temperature, because at temperatures where the rate constants k_{HL} fit into the Mössbauer time window of $10^6\ s^{-1} \leq k_{HL} \leq 10^8\ s^{-1}$, HS and LS species must be simultaneously present in sufficient concentrations.

With the discovery of LIESST and the elucidation of the mechanism of light-induced population of metastable HS states, new possibilites to study HS → LS relaxation in the solid and at low temperatures were opened.

The classical energy barrier E^c between the HS and LS potential wells is $2500-3000\ cm^{-1}$ for iron(II) spin crossover compounds with a small zero point energy difference ΔE^0_{HL}. Accordingly, for all iron(II) spin crossover compounds $k_{HL}(T \rightarrow 0)$ should approach zero at low temperatures. That this is not so

already became apparent from the low-temperature lifetimes τ mentioned in Section 4: the approximate value of τ is between 10^6 s ($k_{HL} \approx 10^{-6}$ s^{-1}) for the $[Fe(ptz)_6](BF_4)_2$ system and 10 s ($k_{HL} \approx 10^{-1}$ s^{-1}) for the $[Zn_{1-x}Fe_x\{(mepy)_3(tren)\}](PF_6)_2$ system. Xie and Hendrickson[151] have investigated the temperature dependence of the HS → LS relaxation rate constant $k_{HL}(T)$ in the $[Fe\{(mepy)_2(py)(tren)\}](PF_6)_2$ spin crossover system embedded in polystyrene sulfonate (PSS), using pulsed laser excitation. The value of approximately 10^4 s^{-1} they found for $k_{HL}(T \rightarrow 0)$ is somewhat larger than in the systems just mentioned, and also displayed a marked deviation from classical behavior: above about 100 K the HS → LS relaxation is thermally activated with activation parameters in the normal range, but below about 80 K k_{HL} is more or less temperature independent. This is typical for a tunneling process. Analogous behavior was found for the $[Fe(pic)_3]^{2+}$ complex in the metal-diluted mixed crystal $[Zn_{1-x}Fe_x(pic)_3]Cl_2 \cdot MeOH$ ($k_{HL}(T \rightarrow 0) \approx 10^{-1}$ s^{-1}) already mentioned,[58, 158] and even for the LS complex $[Fe(bipy)_3]^{2+}$ in the diluted mixed crystal $[Zn_{1-x}Fe_x(bipy)_3](PF_6)_2$ ($k_{HL}(T \rightarrow 0) \approx 10^{-6}$ s^{-1}).[165]

Thus the question arises which parameters govern the lifetime of the metastable HS state in such a way that in one extreme low-temperature tunneling rates $k_{HL}(T \rightarrow 0)$ of less than 10^{-6} s^{-1} and in the other more than 10^6 s^{-1} result. It is obvious that classical concepts for the understanding of the HS → LS relaxation process must fail. Already several years ago, Buhks et al.[67] pointed out that HS → LS relaxation is in all probability a highly nonadiabatic process.

5.1. The HS → LS Relaxation in Dilute Mixed-Crystal Systems

For a systematic determination of the HS → LS relaxation rate constants $k_{HL}(T)$ as a function of temperature, the Fe(II) spin crossover complexes $[Fe(ptz)_6]^{2+}$, $[Fe(pic)_3]^{2+}$, $[Fe\{(mepy)_y(py)_{3-y}(tren)\}]^{2+}$ ($y = 1-3$), and the LS complexes $[Fe\{(py)_3(tren)\}]^{2+}$ and $[Fe(bipy)_3]^{2+}$ from the diluted mixed-crystal systems $[Zn_{1-x}Fe_x(ptz)_6](BF_4)_2$ ($x \approx 0.1$), $[M_{1-x}Fe_x(pic)_3]Cl_2 \cdot sol$ (M = Mn, Zn; sol = MeOH, EtOH; $x \approx 0.0003$), $[Zn_{1-x}Fe_x\{(mepy)_y(py)_{3-y}(tren)\}](PF_6)_2$ ($y = 0-3$; $x \approx 0.0003$), and $[Zn_{1-x}Fe_x(bipy)_3](PF_6)_2$ ($x \approx 0.0001$) were considered.

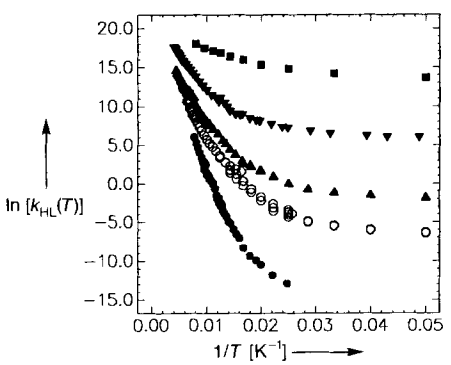


Fig. 28. Observed HS → LS relaxation rates as $\ln[k_{HL}(T)]$ versus $1/T$ plotted for $[Zn_{1-x}Fe_x(ptz)_6](BF_4)_2$ ●, $[Mn_{1-x}Fe_x(pic)_6]Cl_2 \cdot MeOH$ ○, $[Zn_{1-x}Fe_x\{(mepy)_3(tren)\}](PF_6)_2$ ▲, $[Zn_{1-x}Fe_x\{(py)_3(tren)\}](PF_6)_2$ ▼, and $[Zn_{1-x}Fe_x(bpy)_3](PF_6)_2$ ■ (from ref. [152]).

HS → LS relaxation curves after light-induced population of the metastable HS state were recorded on single crystals in transient transmission. Single exponential relaxation curves are found for these diluted systems for all cases.

Figure 28 shows the resulting HS → LS relaxation rate constants plotted as $\ln[k_{HL}(T)]$ versus $1/T$ for selected compounds. Though the relaxation process is thermally activated at elevated temperatures, there is a strong deviation from simple Arrhenius behavior towards a more or less temperature-independent relaxation rate for temperatures below about 100 K. Such a behavior is typical for a low-temperature tunneling process. In Table 2 the experimental low-temperature tunneling rate constants $k_{HL}(T \rightarrow 0)$ and the activation energy E^a with the preexponential factor A from the thermally activated region above about 100 K according to the Arrhenius law (20) are listed.

$$k_{HL}(T) = Ae^{-E^a/k_BT} \quad (20)$$

Also included in Table 2 are the transition temperatures $T_{1/2}$ for the thermal spin transition. The thermal transitions are all gradual and not accompanied by crystallographic phase transitions, since in this context we have only investigated dilute systems.

Table 2. Transition temperature $T_{1/2}$, activation energy E^a at high temperature, preexponential factor A, and low-temperature tunneling rate $k_{HL}(T \rightarrow 0)$ (determined at $T \approx 10$ K) for some iron(II) coordination compounds. The reduced energy gap p has been estimated from the exponential relation between $k_{HL}(T \rightarrow 0)$ and p (inverse energy gap law).

	$T_{1/2}$ [K]	E^a [cm^{-1}]	A [s^{-1}]	p	$k_{HL}(T \rightarrow 0)$ [s^{-1}]
$[Zn_{1-x}Fe_x(ptz)_6](BF_4)_2$	95	1100	5×10^7	< 1	ca. 5×10^{-7}
$[Mn_{1-x}Fe_x(pic)_3]Cl_2 \cdot EtOH$ [a]	76				6×10^{-6}
$[Zn_{1-x}Fe_x(pic)_3]Cl_2 \cdot EtOH$ [a]	95				2.5×10^{-5}
$[Mn_{1-x}Fe_x(pic)_3]Cl_2 \cdot MeOH$	118	907	2×10^8	ca. 1–2	2.5×10^{-3}
$[Zn_{1-x}Fe_x(pic)_3]Cl_2 \cdot MeOH$ [a]	140				9×10^{-3}
$[Zn_{1-x}Fe_x\{(mepy)_3(tren)\}](PF_6)_2$	210	837	5×10^8	ca. 3–4	1.4×10^{-1}
$[Fe\{(mepy)_2(py)(tren)\}]^{2+}$ [b]	270				ca. 5×10^1
$[Fe\{(mepy)(py)_2(tren)\}]^{2+}$ [b]	370				ca. 2×10^2
$[Zn_{1-x}Fe_x\{(py)_3(tren)\}](PF_6)_2$	> 400	640	1×10^9	ca. 7–8	4×10^2
$[Zn_{1-x}Fe_x(bpy)_3](PF_6)_2$	LS	364	2×10^9	ca. 11–13	6×10^5
$[Fe(phen)_3]^{2+}$ [c]	LS				ca. 5×10^6

[a] Ref. [158]. [b] Complex in poly(methylmethacrylate) (PMMA), $T_{eff} \approx 50$ K (compare comments in ref. [165]). [c] Complex in Nafion, $T_{eff} \approx 50$ K (compare comments in ref. [165]).

5.2. Nonadiabatic Multiphonon Relaxation

As already mentioned, classical concepts cannot explain the observed temperature dependence of the HS → LS relaxation rate constant. Several years ago Buhks et al.[67] suggested applying the theory of radiationless transitions based on Fermi's golden rule[179] to spin crossover dynamics. In this theory, HS → LS relaxation is described as a nonadiabatic process occurring between two distinct spin states in different nuclear configurations, where the electronic energy of the initial state is spontaneously transformed into vibrational energy of the final state. The simplest model for treating this problem is the "Single Configurational Coordinate" (SCC) model, in which the reac-

tion coordinate parallel to a certain nuclear coordinate is considered (Fig. 29). Since the nuclear configurations of the LS and

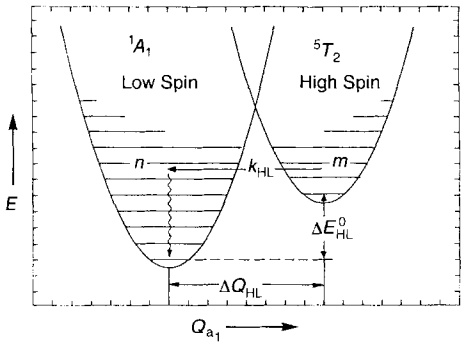


Fig. 29. Potential wells for the HS and LS states of Fe(II) in octahedral coordination along the totally symmetric normal coordinate Q with $\Delta Q_{HL} = \sqrt{6}\Delta r_{HL}$. In the simple SCC model, harmonic potentials with equal force constants are used.

the HS state differ predominantly in the metal–ligand distance $\Delta r_{HL} \approx 0.16-0.22$ Å, the reaction coordinate will be approximately equivalent to the totally symmetric normal coordinate with $\Delta Q_{HL} = \sqrt{6}\Delta r_{HL}$.[180]

If Fermi's golden rule and the Condon approximation are considered, the radiationless HS → LS relaxation rate constant in the SCC model is given by Equation (21),[179, 181] where β_{HL}

$$k_{HL}(T) = \frac{2\pi}{\hbar^2\omega}\beta_{HL}^2 F_p(T) \tag{21}$$

denotes the electronic matrix element, $\hbar\omega$ the oscillation frequency of the totally symmetric stretching mode, and $F_p(T)$ the thermally averaged Franck–Condon factor over the m vibrational levels of the initial state. The spin–orbit transition operator $\hat{H}_{SO}$[179] is the transition operator for ISC processes between distinct spin states that can be described by Born–Oppenheimer functions. For the HS → LS relaxation in iron(II) centers with $\Delta S = 2$, the $^5T_2$ and the $^1A_1$ states can only be mixed by higher order spin–orbit coupling. This gives an estimate for the electronic matrix element [Eq. (22)].[67]

$$\beta_{HL} = \langle\Phi_{LS}|\hat{H}_{so}|\Phi_{HS}\rangle \approx -150\,\mathrm{cm}^{-1} \tag{22}$$

If the potentials of the initial and the final states are approximated as harmonic potentials with equal force constants f and vibrational frequencies $\hbar\omega$, the thermally averaged Franck–Condon factor is given by Equation (23),[181] where the sum-

$$F_p(T) = \frac{\sum_m |\langle\chi_{m+p}|\chi_m\rangle|^2 e^{-m\hbar\omega/k_BT}}{\sum_m e^{-m\hbar\omega/k_BT}} \tag{23}$$

mation is over all vibrational levels m of the initial state, and the reduced energy gap p is defined by Equation (24).

$$p = \Delta E^0_{HL}/\hbar\omega \tag{24}$$

The energy gap p is a measure of the vertical displacement of the two potential wells relative to each other. From the point of view of energy conservation, only the transition from the m-th vibrational level of the initial state to the n-th vibrational level of the final state is allowed under the limiting condition (25).

$$n = m + p \tag{25}$$

In the SCC model the Franck–Condon factors $|\langle\chi_n|\chi_m\rangle|^2$ can be easily evaluated by using harmonic potentials and equal force constants.[182] For $T \to 0$, for example, F_p simplifies to Equation (26a) where S [Eq. (26b)] is the Huang–Rhys factor,

$$F_p(T \to 0) = |\langle\chi_p|\chi_o\rangle|^2 = \frac{S^p e^{-S}}{p!} \tag{26a}$$

$$S = \tfrac{1}{2} f\Delta Q_{HL}^2/\hbar\omega \tag{26b}$$

a measure for the horizontal displacement of the two potential wells relative to each other. With $\Delta Q_{HL} = \sqrt{6}\Delta r_{HL} \approx 0.5$ Å, a mean force constant f of 2×10^5 dyn cm^{-1}, and a typical vibrational energy $\hbar\omega$ of between 200 and 300 cm^{-1}, a value for S of between 40 and 50 can be estimated.[159]

For iron(II) complexes with a coordination sphere of six nitrogen atoms, the changes in bond length Δr_{HL}, the force constant f, and the vibrational energy $\hbar\omega$ (and therefore the Huang–Rhys factor S as well) will be restricted to a fairly narrow range. What can vary widely between two compounds, however, is ΔE^0_{HL} and thus the reduced energy gap p. Figure 30a shows a

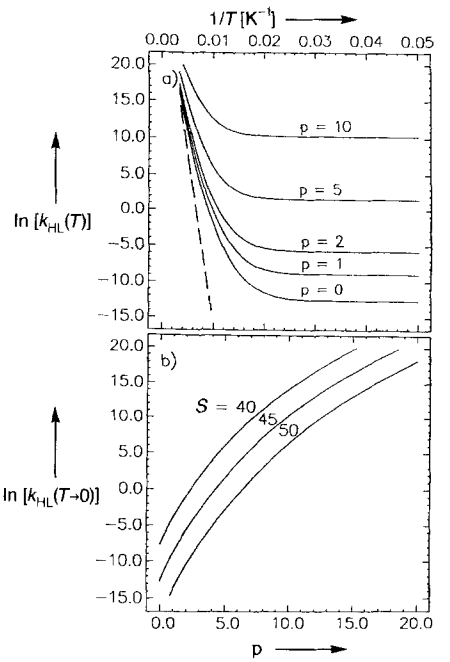


Fig. 30. a) Plots of $\ln[k_{HL}(T)]$ versus $1/T$ calculated from the simple SCC model with $S = 45$, $\hbar\omega = 250$ cm^{-1}, and the reduced energy gap p as a parameter. The dashed line represents the classical energy barrier $E^c = \hbar\omega S/4$ for small values of p. b) The low-temperature tunneling rate calculated with $\hbar\omega = 250$ cm^{-1} and $S = 40$, 45, 50, plotted as $\ln[k_{HL}(T \to 0)]$ versus p.

plot of $\ln[k_{HL}(T)]$ (calculated with $S = 45$ and $\hbar\omega = 250$ cm^{-1}) versus $1/T$, for different values of the reduced energy gap parameter p. The characteristic features of the curves reveal a temperature-independent tunneling rate at low temperatures

and a thermally activated relaxation process at higher temperatures. As can be seen from Figure 30b, the low-temperature tunneling rates $k_{HL}(T \rightarrow 0)$ thus calculated become very small for small reduced energy gaps p and increase exponentially with increasing p, which is termed the "inverse energy gap law" in the strong vibronic coupling limit $S \gg p$. The expected activation energies at elevated temperatures on the other hand decrease with increasing p. Even for $p = 0$ they are smaller than the classical energy barrier $E^c = S\hbar\omega/4$ (about 2500–3000 cm^{-1}). Consequently, the thermally activated relaxation is not triggered across the classical energy barrier either. It, too, must be interpreted as a nonadiabatic tunneling process from a thermally activated vibrational level of the HS state.

Clearly the $\ln[k_{HL}]$ versus $1/T$ curves calculated with the simple SCC model show the same general behavior as the experimental ones with an only weak temperature dependence for temperatures below about 80 K and a thermally activated regime above about 100 K. In the following, an increase of $k_{HL}(T \rightarrow 0)$ over as many as twelve orders of magnitude from approximately 5×10^{-7} s^{-1} for the $[Zn_{1-x}Fe_x(ptz)_6](BF_4)_2$ spin crossover system to 6×10^5 s^{-1} for the $[Zn_{1-x}Fe_x(bipy)_3](PF_6)_2$ LS system in the strong vibronic coupling limit $S \gg p$ of the SCC model is predicted as an inverse energy gap law.

Although $T_{1/2}$ of the thermal spin transition is but a crude measure of the energy gap ΔE^0_{HL} (and thus for p), the experimentally observed low-temperature tunneling rates do indeed increase dramatically with increasing $T_{1/2}$ (Fig. 31). For a more

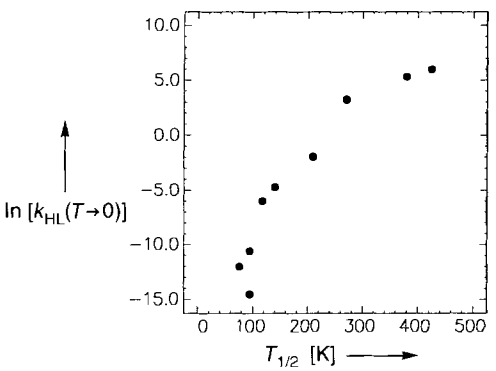


Fig. 31. Observed low-temperature tunneling rates plotted as $\ln[k_{HL}(T \rightarrow 0)]$ versus the transition temperature $T_{1/2}$ (from ref.[183]).

quantitative verification of the inverse energy gap law, the reduced energy gaps p of the investigated systems would have to be known. Unfortunately, ΔE^0_{HL} and therefore p are very difficult to determine experimentally.

For the three mixed-crystal compounds with a spin transition temperature $T_{1/2} < 100$ K in Table 2, $[Zn_{1-x}Fe_x(ptz)_6](BF_4)_2$, $[Mn_{1-x}Fe_x(pic)_3]Cl_2 \cdot EtOH$, and $[Zn_{1-x}Fe_x(pic)_3]Cl_2 \cdot EtOH$, a value of $p \leq 1$ is certainly reasonable, and for the $[Mn_{1-x}Fe_x(pic)_3]Cl_2 \cdot MeOH$ system with $T_{1/2} \approx 120$ K, $p \approx 1-2$ is appropriate. The observed low-temperature tunneling rates $k_{HL}(T \rightarrow 0)$ for the four compounds all lie within the range predicted by the simple SCC model around $S \approx 45$. For the $[Zn_{1-x}Fe_x(bipy)_3](PF_6)_2$ LS system, with a $\Delta E^0_{HL} \approx 2500-3500$ cm^{-1} not too far away from a spin crossover system, p is definitely greater than 10. For such a value of p we do indeed expect $k_{HL}(T \rightarrow 0)$ to be more than ten orders of magnitude larger than in the systems just mentioned. This leads us to the conclusion that the Huang–Rhys factor estimate of $S \approx 45$ is quite realistic, and we can assign the values of p listed in Table 2 for the reduced energy gap to the other compounds.

It would be presumptuous to expect a more quantitative agreement of the experimental $\ln[k_{HL}(T)]$ versus $1/T$ curves with the curves calculated on the basis of the SCC model with harmonic potentials and equal force constants, in view of the crude assumptions made. Although the model does predict a thermally activated HS → LS relaxation at elevated temperatures with an activation energy smaller than the classical energy barrier between the potential wells, the passage from the thermally activated process to the low-temperature tunneling process is much more gradual in the experimental curves than in the calculated ones. The symmetry of the investigated iron(II) complexes is in all cases lower than O_h, so that generally we must have more than just one totally symmetric normal coordinate. Especially for the $[Fe(pic)_3]^{2+}$ complex, where one half of the coordinating nitrogen atoms belong to NH_2 groups and the other half to pyridyl rings, at least two vibrational modes with rather different frequencies must be active. This may well be the cause of this much more gradual transition. Also, the observed activation energies in the high temperature regime are still lower than those calculated from the simple SCC model. Taking anharmonic terms in the potentials into account would correct the values in the right direction. The influence of anharmonic terms becomes noticeable only at higher temperatures in the strong coupling limit and does not entail a shift in the rates by several orders of magnitude, in contrast to the case of weak or intermediate vibronic coupling.[184]

In the SCC model, coupling to low-frequency phonons is generally neglected. The low-frequency phonons just provide a heat bath for energy dissipation and implicitly ensure energy conservation should there be an energy mismatch between the vibrational levels of the HS and the LS state. In reality this is certainly the case. At high temperatures, where the low-frequency phonons are mostly thermalized, the simplified approach of the SCC model is justified. At low temperatures, however, the coupling to the low-frequency phonons would have to be explicitly taken into account, for these phonons are the ones responsible for the fact that the experimental relaxation rates at low temperatures are not quite as temperature independent as the SCC model calculations predict.[158, 185]

What about other spin crossover systems, say for example those of iron(III) with a $^6A_1 \rightarrow {}^2T_2$ transition, or those of cobalt(II) with a $^2E \rightarrow {}^4T_1$ transition? At ambient temperatures, for iron(III) and cobalt(II) spin crossover complexes, HS → LS relaxation rates of around 10^7 to 10^{10} s^{-1} have been determined in solution.[55] Lawthers and McGarvey[186] were successful in using the pulsed laser excitation technique even for iron(III) systems. So at least for iron(III) systems a LIESST-like process does exist, and, in principle, the same type of temperature dependence of the HS → LS relaxation rates as with the iron(II) systems should be observed. The low-temperature tunneling rates for iron(III) and cobalt(II), however, are expected to be several orders of magnitude larger than for iron(II) spin crossover compounds, because Δr_{HL} and therefore S of the for-

mer are smaller. For iron(III) compounds, typical values for Δr_{HL} are 0.1 Å,[187] giving an S of about 17. Buhks et al.[67] have calculated an electronic matrix element of $\beta_{HL} \approx 50\ cm^{-1}$ for iron(III). From this a value for the low-temperature tunneling rate $k_{HL}(T \rightarrow 0)$ for small reduced energy gaps p of $10^5 - 10^7\ s^{-1}$ can be estimated. For iron(III) spin crossover compounds, a LIESST effect in the true sense can thus not be expected. For the cobalt(II) systems, the estimations are difficult to perform, since the ^2E state is generally susceptible to strong Jahn–Teller interactions and the SCC model here becomes a rather bad approximation. However, also for cobalt(II) no LIESST effect in the real sense can be expected.

5.3. Cooperative Effects on the HS → LS Relaxation in $[Fe(ptz)_6](BF_4)_2$

In Section 4.1 in the discussion on photophysical properties of the $[Fe(ptz)_6](BF_4)_2$ spin crossover compound, we pointed to the cooperative effects found also in this concentrated material, which, among other things, influence the thermal spin transition.

In the dilute mixed crystal $[Zn_{1-x}Fe_x(ptz)_6](BF_4)_2$ ($x \approx 0.1$), single exponential HS → LS relaxation curves, just like those of all mixed-crystal systems treated in Section 5.1, are observed.[188] The cooperative effects in concentrated materials, however, give rise to strong deviations from first-order kinetics.[66, 188] This will be the subject of the following discussion.

5.3.1. Experimental Results

Figure 32 shows the $^1A_1 \rightarrow {}^1T_1$ band of concentrated $[Fe(ptz)_6](BF_4)_2$ at 57.0 K, recorded at time intervals of 120 s following the light-induced LS → HS conversion. Figure 33

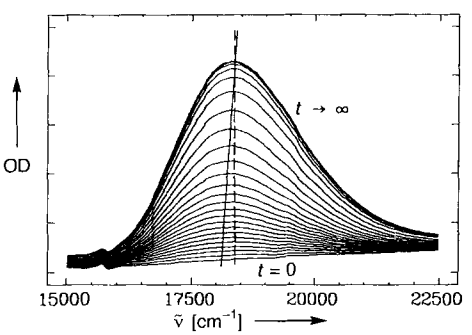


Fig. 32. Time dependence of the $^1A_1 \rightarrow {}^1T_1$ band in $[Fe(ptz)_6](BF_4)_2$ at 57.0 K after a complete light-induced LS → HS conversion. The spectra were recorded with time intervals of 120 s (from ref. [189]).

shows the HS → LS relaxation curves (as $\gamma_{LS}(t)$) in the supercooled crystallographic high-temperature phase at different temperatures between 50 and 60 K, obtained from the relative optical density at the band maximum as a function of time.

The deviation from single exponential behavior is obvious. The sigmoidal curve shape must be interpreted as a self-acceleration of the HS → LS relaxation with increasing proportions of LS γ_{LS}. The acceleration stems from the buildup of an internal

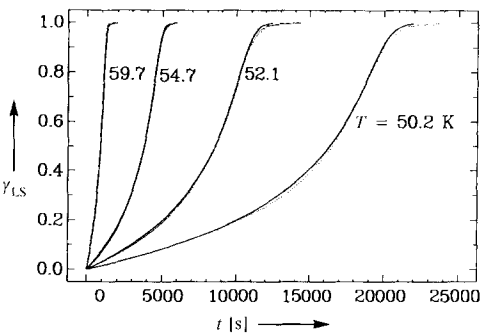


Fig. 33. Complete HS → LS relaxation curves for $[Fe(ptz)_6](BF_4)_2$ in the crystallographic high-temperature phase. (···) experimental values, (—) curve fits with Equation (28) for $k_{HL}(\gamma_{LS})$ (from ref. [189]).

pressure (image pressure) with increasing LS proportions, which in turn is caused by the volume change $\Delta V_{HL} = V_{HS} - V_{LS}$ of the complexes associated with the spin transition (see Sec-

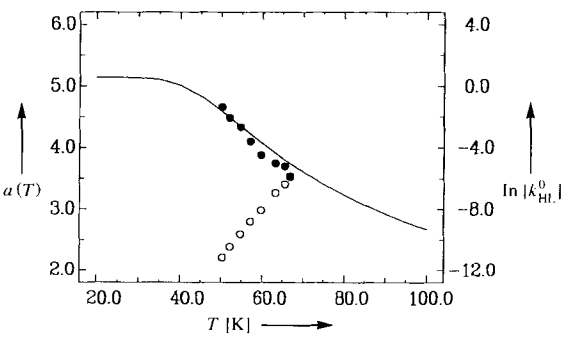


Fig. 34. $a(T)$ and $\ln[k^0_{HL}(T)]$ from the curve fit in Figure 33 for $[Fe(ptz)_6](BF_4)_2$. ●: observed $a(T)$; — —: calculated $a(T)$, see text; ○: $\ln[k^0_{HL}(T)]$ (from ref. [189]).

tion 3.4.1). The relaxation rate is a function of this pressure and therefore also a function of the LS proportion γ_{LS}. The differential equation (27) still holds, but now k_{HL} is no longer a constant,

$$\frac{d\gamma_{LS}}{dt} = k_{HL}(1 - \gamma_{LS}) \tag{27}$$

but itself a function of the LS proportion γ_{LS}. Nevertheless, the relaxation curves can be well described empirically on applying a phenomenological approach [Eq. (28)] for the $k_{HL}(\gamma_{LS})$ depen-

$$k_{HL}(\gamma_{LS}, T) = k^0_{HL}(T) \cdot e^{a(T)\gamma_{LS}} \tag{28}$$

dence. Included in Figure 33 are the HS → LS relaxation curves calculated with this phenomenological approach, and the agreement with the experimental curves is very good indeed. Figure 34 shows the values for $\Delta k^0_{HL}(T)$ and $a(T)$ obtained from a numerical curve fit. Within experimental error, $\Delta k^0_{HL}(T)$ is equal to the HS → LS relaxation rate $k_{HL}(T)$ of the exponential decay of the HS state in the dilute mixed crystal $[Zn_{1-x}Fe_x(ptz)_6](BF_4)_2$ with $x \approx 0.1$ (see Fig. 28). This is not surprising, since V_{Zn} and V_{HS}, as we have already mentioned, are about equal and therefore, at the beginning of the relaxation process, the internal pressure in pure $[Fe(ptz)_6](BF_4)_2$ is about the same size as that in the dilute mixed crystal.

A careful analysis of the position of the $^1A_1 \rightarrow {}^1T_1$ band reveals that the band maximum is shifted towards higher energy on relaxation.[189] Figure 35 shows this shift, which is linear in

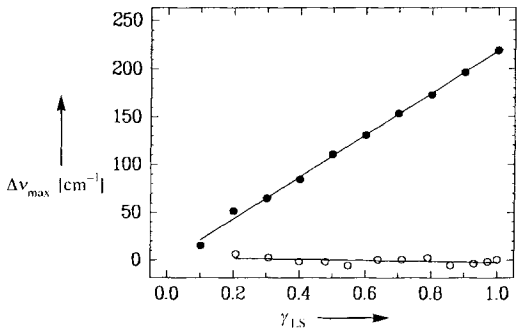


Fig. 35. Shift of the $^1A_1 \rightarrow {}^1T_1$ band maximum for $[Fe(ptz)_6](BF_4)_2$ at 57.0 K relative to the band maximum extrapolated to $\nu_{max}(\gamma_{LS} = 0) = 18000\ cm^{-1}$ as a function of the LS fraction γ_{LS}. •: observed; : linear regression with slope $\Delta\nu_0 = 219(4)\ cm^{-1}$. o: data for the dilute mixed crystal $[Zn_{1-x}Fe_x(ptz)_6](BF_4)_2$ ($x \approx 0.1$) for comparison (from. ref.[190]).

γ_{LS}, for the relaxation curve at 57.0 K. No such shift can be observed in the mixed crystal $[Zn_{1-x}Fe_x(ptz)_6](BF_4)_2$ ($x \approx 0.1$). According to the Tanabe–Sugano diagram (see Fig. 1), the shift for the concentrated system corresponds to an increase of the ligand field strength of the LS species by $\delta 10Dq^{LS}$ on relaxation [Eq. (29) where $\Delta\nu_{max} = 219(4)\ cm^{-1}$ is the slope of the linear

$$\delta 10Dq^{LS}(\gamma_{LS}) = 10Dq^{LS}(\gamma_{LS}) - 10Dq^{LS}(\gamma_{LS} = 0) = \Delta\nu_{max}\gamma_{LS} \quad (29)$$

regression in Figure 35]. Relative to average values for $10Dq^{LS}$ and $10Dq^{HS}$ of about 20550 and 12200 cm^{-1}, respectively (see Section 4), the value for $\Delta\nu_{max}$ is small.

5.3.2. Discussion Based on the SCC Model

As already mentioned, the increase of the relaxation rate at a given temperature ($a = 4.5$ at $T = 55$ K) is attributed to an increase of the internal pressure on relaxation. This increase effects a horizontal as well as a vertical displacement of the potential wells for the initial state and the final state relative to each other, as shown schematically in Figure 36. The zero point energy difference ΔE^0_{HL} and the change in bond length Δr_{HL} become a function of γ_{LS}. Naturally, therefore, the parameters in Equation (23) for the thermal average of the Franck–Condon factor $F_p(T)$ (the Huang–Rhys factor S and the reduced energy gap p) also become functions of γ_{LS} in the concentrated material.

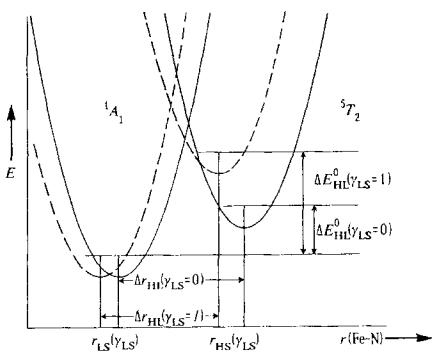


Fig. 36. Potential wells of HS and LS states, schematically illustrating relative horizontal and vertical shifts due to the build-up of an internal pressure during relaxation.

The change of the bond length differences $\delta\Delta r_{HL}(\gamma_{LS})$ on relaxation can be estimated from the $1/r^6$ dependence of the ligand field strength. $\delta\Delta r_{HL}$ between the start and the end of the relaxation process is approximately 2×10^{-3} Å, much smaller than $\Delta r_{HL} \approx 0.18$ Å. The resulting change of the Huang–Rhys factor on relaxation, $\delta S(\gamma_{LS})$, will also be much smaller than the average Huang–Rhys factor S itself. Thus, a linear dependence of $\delta S(\gamma_{LS})$ follows according to Equation (30).[189] An average value of $S \approx 45$ gives $a_s \approx -1$.

$$\delta S(\gamma_{LS}) := S(\gamma_{LS}) - S(\gamma_{LS} = 0) \approx 2\frac{\delta\Delta r_{HL}(\gamma_{LS})}{\Delta r_{HL}} S := a_s\gamma_{LS} \quad (30)$$

In principle, $10Dq^{LS}$ determines only the electronic energy of the excited states at the equilibrium distance of the LS state according to the Tanabe–Sugano diagram in Figure 1. Clack and Smith[191] used INDO-SCF-MO calculations to show the linear relationship with slope 1 between $10Dq^{LS}$ and the zero point energy difference ΔE^0_{HL} between the HS and the LS state. Consequently, Equation (31) is valid for the change of the zero point energy difference $\delta\Delta E^0_{HL}(\gamma_{LS})$ on relaxation. This corresponds to a total change of the zero point energy difference of $\Delta\nu_{max} = 219\ cm^{-1}$ on relaxation. Therefore, following the definition in Equation (24), the change of the reduced energy gap $\delta p(\gamma_{LS})$ is given in Equation (32). Since $\Delta\nu_{max}$ is of the order of $\hbar\omega$, a_p becomes approximately 1.

$$\delta\Delta E^0_{HL}(\gamma_{LS}) := \Delta E^0_{HL}(\gamma_{LS}) - \Delta E^0_{HL}(\gamma_{LS} = 0) \approx \delta 10Dq^{LS}(\gamma_{LS}) = \Delta\nu_{max}\gamma_{LS} \quad (31)$$

$$\delta p(\gamma_{LS}) := p(\gamma_{LS}) - p(\gamma_{LS} = 0) \approx \frac{\delta\Delta E^0_{HL}(\gamma_{LS})}{\hbar\omega} = \frac{\Delta\nu_{max}}{\hbar\omega} \cdot \gamma_{LS} := a_p\gamma_{LS} \quad (32)$$

Using $\delta p(\gamma_{LS})$ and $\delta S(\gamma_{LS})$, we can calculate the γ_{LS} dependence of the thermal Franck–Condon factor average $F_p(T)$ according to Equation (23). With some approximations Equation (33a) follows, in particular for the low-temperature tunneling rate in the strong vibronic coupling limit.[189] For S an average value

$$k_{HL}(\gamma_{LS}, T \rightarrow 0) \approx k_{HL}(\gamma_{LS} = 0,\ T \rightarrow 0) \cdot e^{a(T \rightarrow 0)\gamma_{LS}} \quad (33a)$$

$$a(T \rightarrow 0) = a_p \ln S - a_s \approx 5 \quad (33b)$$

of 45 was used and values of 1 and -1 as estimated above for a_p and a_s, respectively. The first term in Equation (33b), $a_p \ln S$, accounts for the increase of ΔE^0_{HL} on relaxation, in accord with the inverse energy gap law as treated in Section 5.2. The second term, a_s, results if the change in Δr_{HL} is taken into account as well.

One can now show numerically that this form is still valid for $T > 0$. The resulting curve for $a(T)$ is accordingly included in

Figure 34. Below about 50 K, in the low-temperature tunneling regime, $a(T)$ is temperature independent. Above this temperature, however, $a(T)$ decreases with $1/T$, well in accord even with the absolute values of the experimental observations. The cooperative effects of the HS → LS relaxation in $[Fe(ptz)_6](BF_4)_2$ can thus be explained in a way consistent with quantum mechanics by a simple SCC model of nonadiabatic multiphonon relaxation, which takes the spectroscopically observed displacements between the potential wells of the initial state and the final state into account.

Spiering et al.[40] (see Section 3) have treated the elastic interactions during spin transitions in solids as a continuous model, without stipulating in detail how the elastic energies are distributed. In the crystallographic high-temperature phase of $[Fe(ptz)_6](BF_4)_2$, a good part of this energy is apparently absorbed by the metal–ligand bonds. That this happens in a uniform way is quite understandable, since the inversion center of the high-symmetry space group must be retained in the complex.

5.3.3. Comparison with the Lattice Expansion Model

To finish our discussion, we shall now relate the thermodynamic treatment of the spin transition based on the lattice expansion model from Section 3 to the cooperative effects on HS → LS relaxation. Following the lines of thought of Adler et al.,[58, 59] we shall employ the semiclassical absolute rate theory. For $[Fe(ptz)_6](BF_4)_2$ with a low-temperature tunneling rate of $\Delta k^0_{HL}(T \rightarrow 0)$ of less than $10^{-6}\ s^{-1}$, the HS → LS relaxation in the temperature range under discussion is already a thermally activated process, as evidenced by rates of 10^{-4}–$10^{-2}\ s^{-1}$. According to absolute rate theory[174, 192] Equation (34) is applic-

$$k_{HL} = \frac{k_B T}{h} \kappa e^{-(\Delta H^{\ddagger}_{HL} - T\Delta S^{\ddagger}_{HL})/k_B T} \tag{34}$$

able, where $\Delta H^{\ddagger}_{HL}$ and $\Delta S^{\ddagger}_{HL}$ denote enthalpies and entropies of activation, and κ is a measure of the probability for an ISC process in the transitory state. We do not expect a strong dependence on the LS fraction for $\Delta S^{\ddagger}_{HL}$. It is rather $\Delta H^{\ddagger}_{HL}$ which shows a γ_{LS} dependence through the change in the elastic energy of the transition state $\Delta^{\ddagger}_E$ during the course of the relaxation [Eq. (35)].

$$\Delta H^{\ddagger}_{HL}(\gamma_{LS}) = H^{\ddagger}_{HL}(\gamma_{LS} = 0) + \Delta^{\ddagger}_E(\gamma_{LS}) \tag{35}$$

Here, $\Delta H^{\ddagger}_{HL}(\gamma_{LS} = 0)$ is the activation enthalpy at the beginning of the HS → LS relaxation. By analogy with the difference in the elastic energies between HS and LS state [see Equation (15)], the change $\Delta^{\ddagger}_E$ in the elastic energy of the transition state as a result of the changing internal pressure during relaxation, is given by Equation (36), where v_{HS} and v_{LS} are the

$$\Delta^{\ddagger}_E = -\frac{K(\gamma_0 - 1)\gamma_0}{v_c}(v_{HS} - v_{LS})(v_{HS} - v^{\ddagger})\gamma_{LS} = -2\Gamma q^{\ddagger}\gamma_{LS} \tag{36a}$$

$$q^{\ddagger} = \frac{v_{HS} - v^{\ddagger}}{v_{HS} - v_{LS}} \tag{36b}$$

volumes of the complex in the HS and LS states, and $v^{\ddagger}$ the volume of the activated complex. We neglect the concentration $\gamma^{\ddagger}$ of activated complex, since it is much smaller than 1. Having the linear γ_{LS} dependence of $\Delta^{\ddagger}_E$ in the thermally activated regime, we can now identify $a(T)$ with $\Delta^{\ddagger}_E$ by comparing Equations (34) and (28) according to Equation (37).

$$a(T) = 2\Gamma q^{\ddagger}/k_B T \tag{37}$$

As already mentioned and depicted in Figure 34, $a(T)$ obeys a $1/T$ dependence quite well, from which a value of about 164(6) cm^{-1} for $2\Gamma q^{\ddagger}$ results.

As the reaction coordinate is chiefly determined by the totally symmetric stretching mode, the volume $v^{\ddagger}$ of the activated complex must lie between the volumes v_{HS} and v_{LS}. Even though the force constants for the HS and LS states are not exactly equal, the classical intersection between the two potential wells is not too far from the median between r_{HS} and r_{LS}. Indeed, we obtain an approximate value of 0.5 for $q^{\ddagger}$ using the value of 170 cm^{-1} for Γ, the interaction constant, as it was determined from the thermal spin transition. We see that for the $[Fe(ptz)_6](BF_4)_2$ system in the crystallographic high-temperature phase with its high symmetry, the reaction coordinate is really well described by the totally symmetric stretching vibration.

6. Conclusion and Outlook

Though more than sixty years have passed since the discovery of thermal spin crossover for iron(III) complex compounds, it was not until the discovery of the phenomenon for iron(II) complexes during the sixties that a more exhaustive line of spin crossover research began to flourish. The reason is primarily that on one hand a large variety of different spin transition curves were observed in the solid, and on the other, solid state scientists had recourse to an excellent microscopic method for the investigation of the electronic structure of iron complexes after the Mössbauer effect was discovered. In addition, magnetic susceptibility studies, electron excitation and vibrational spectroscopy, crystal structure analysis, and calorimetry have yielded a host of data enabling us today to understand the essential aspects of thermal spin crossover and the relaxation of the metastable spin state created by irradiation (LIESST effect) in the solid as well as in the liquid state. Thus we have learned that the spin transition behavior can be drastically affected by changes in the ligand system, exchange of noncoordinating anions or solvent molecules in the solid, and by metal dilution. The same holds for changes in physical parameters such as pressure, magnetic environment, and crystal quality. All this allows us to change the ligand field strength at the metal center and to shift the spin transition curve along the temperature scale.

For more than two decades of spin crossover research, our interest has been almost exclusively directed towards the solid, because the spin transition types may vary so much in the solid, supplemented by the fact that spin transition behavior can be deliberately adjusted in solutions (by changing the steric and electronic influence of the ligand system), but such predictions in the solid were impossible. Already at an early stage of spin crossover research had it become clear that spin transitions in

the solid are accompanied by cooperative interactions which, additional to the immediate local (steric and electronic) influences on the complex, are responsible for the variety of spin transition types. Our main object was to clarify the nature of these interactions. The model we developed on the basis of elasticity theory, with the enormous volume changes and the associated changes in the elastic energies during the spin transitions under consideration, has significantly promoted our understanding of the interaction mechanism.

The discovery that iron(II) spin crossover compounds can also be switched between their different spin states by irradiation with light of different wavelengths (LIESST effect, where the metastable states can have extraordinarily long lifetimes) came as a surprise. Iron(II) coordination compounds had not been very prominent in photochemistry and had not attracted any special attention because they lack luminescent properties. From intensive studies of the kinetics of the radiationless decay of the LIESST state we have learned that the deviation of the decay curves from an exponential law can be well understood on the basis of the model of elastic interactions. The temperature dependence of the relaxation times (tunneling at lower temperatures and observance of the Arrhenius law at higher temperatures) is in accord with the theory of radiationless transitions.

The possibility of switching between two phases with very different optical and magnetic properties (as is the case with the LIESST effect) immediately suggests potential applications in optical information technology. Another objective of our studies was to sound out these possibilities. From our systematic investigation of the decay kinetics one must conclude that long-term storage using the LIESST effect is only possible at sufficiently low temperatures below 80 K. From our observations, optical switches using spin crossover/LIESST compounds with an LS state just still stable around room temperature seem conceivable, because the intersystem crossing processes involved in the decay mechanism are very fast (the reciprocals of the rate constants are in the subnanosecond range), they have high quantum yields ($LS \rightarrow HS \approx 1$), and the metastable HS states have lifetimes in the nanosecond range. The large differences between the refractive indices in the HS and the LS states of iron(II) complex compounds gives rise to their photodiffractive properties, which could be exploited especially with holographic methods.[190]

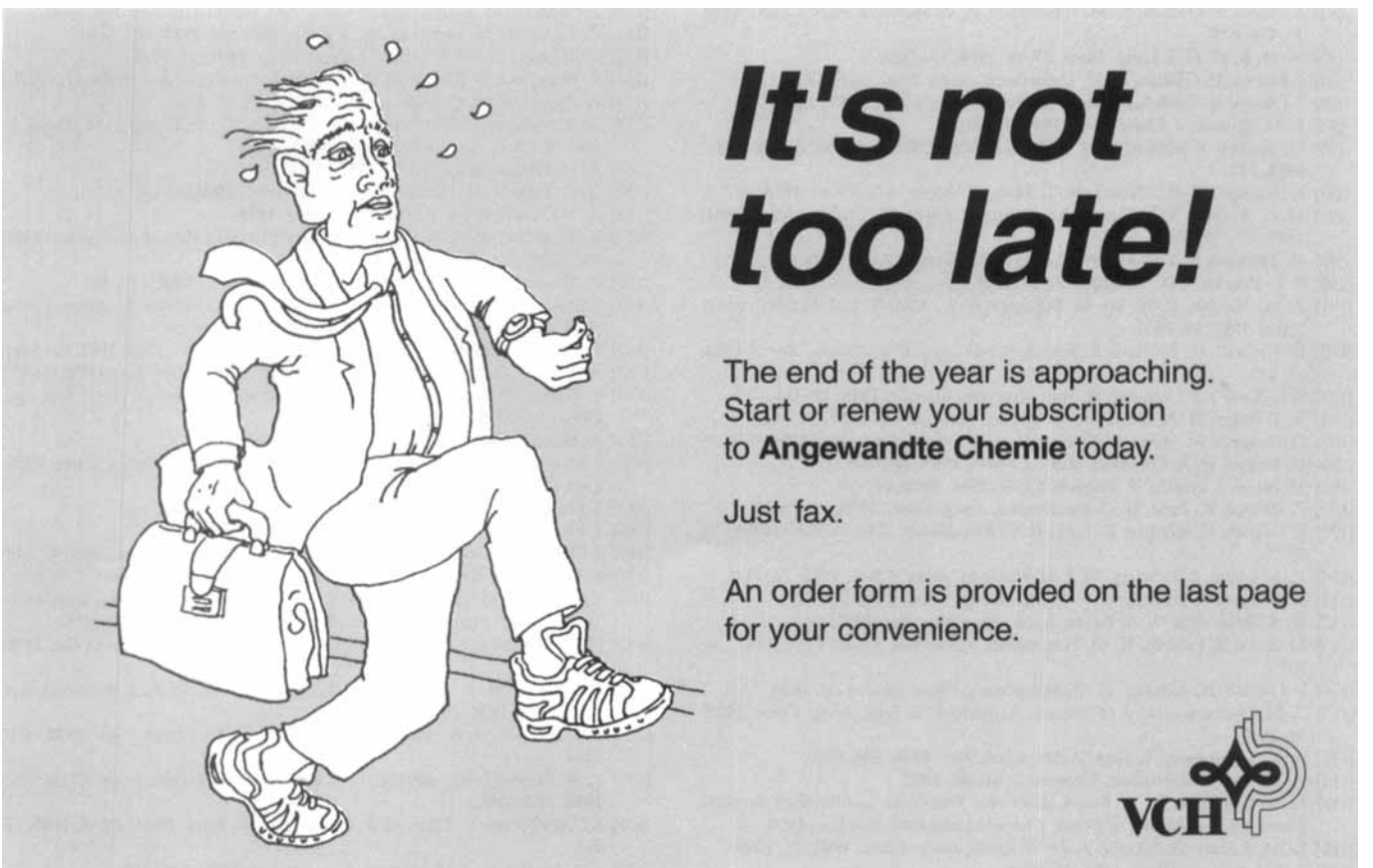
Special thanks are due to all collaborators (graduate and doctorate students, postdoctorate fellows) for their enthusiasm for the spin crossover and LIESST research presented in this article. Their names are cited in the references section. Thanks are also due to the Deutsche Forschungsgemeinschaft, the Bundesministerium für Forschung und Technologie, the Fonds der Chemischen Industrie, the Volkswagen Stiftung, and the Materialwissenschaftliches Forschungszentrum der Universität Mainz for financial support. A. Hauser is grateful to the Schweizerische Nationalfonds for scholarships and research funds.

Received: July 14, 1993 [A 81E]
German version: *Angew. Chem.* **1994**, *106*, 2109
Translated by Dr. U. Löchner, Heilbronn

[1] L. Cambi, A. Cagnasso, *Atti Accad. Naz. Lincei* **1931**, *13*, 809.
[2] L. Cambi, L. Szegö, *Ber. Dtsch. Chem. Ges.* **1931**, *64*, 259; *ibid.* **1933**, *66*, 656.
[3] L. Cambi, L. Szegö, A. Cagnasso, *Atti Accad. Naz. Lincei* **1932a**, *15*, 266; *ibid.* **1932b**, *15*, 329.
[4] L. Cambi, L. Malatesta, *Ber. Dtsch. Chem. Ges.* **1937**, *70*, 2067.
[5] The electronic LF states given here are those for ideal octahedral symmetry. In reality, spin crossover complexes almost always have a lower molecular symmetry.
[6] H. L. Schläfer, G. Gliemann, *Einführung in die Ligandenfeldtheorie*, Akademische Verlagsgesellschaft, Wiesbaden, **1980**, pp. 462.
[7] W. A. Baker, H. M. Bobonich, *Inorg. Chem.* **1964**, *3*, 1184.
[8] D. M. Halepoto, D. G. L. Holt, L. F. Larkworthy, G. J. Leigh, D. C. Povey, G. W. Smith, *J. Chem. Soc. Chem. Commun.* **1989**, 1322.
[9] H. Imoto, A. Simon, *Inorg. Chem.* **1982**, *21*, 308.
[10] L. F. Lindoy, S. E. Livingstone, *Coord. Chem. Rev.* **1967**, *2*, 173.
[11] E. K. Barefield, D. H. Busch, S. M. Nelson, *Q. Rev. Chem. Soc.* **1968**, *22*, 457.
[12] R. L. Martin, A. H. White, *Transition Met. Chem. Chem. Soc. NY* **1968**, *4*, 113.
[13] E. König, *Coord. Chem. Rev.* **1968**, *3*, 471.
[14] E. König, *Ber. Bunsenges. Phys. Chem.* **1972**, *76*, 975.
[15] E. König, G. Ritter in *Moessbauer Eff. Methodol.* (Eds: I. J. Gruverman, C. W. Seidel, D. K. Dieterly), Plenum, New York, **1974**, p. 9.
[16] H. A. Goodwin, *Coord. Chem. Rev.* **1976**, *18*, 293.
[17] P. Gütlich, *Adv. Chem. Ser.* **1981**, *194*, 405.
[18] P. Gütlich, *Struct. Bonding (Berlin)* **1981**, *44*, 83.
[19] P. Gütlich in *Chemical Mössbauer Spectroscopy* (Ed.: R. H. Herber), Plenum, New York, **1984**, pp. 27–64.
[20] P. Gütlich in *Mössbauer Spectroscopy Applied to Inorganic Chemistry, Vol 1* (Ed.: G. J. Long), Plenum, New York, **1984**, pp. 287–337.
[21] E. König, G. Ritter, S. K. Kulshreshta, *Chem. Rev.* **1985**, *85*, 219.
[22] H. Toftlund, *Coord. Chem. Rev.* **1989**, *94*, 67.
[23] P. Gütlich, A. Hauser, *Coord. Chem. Rev.* **1990**, *97*, 1.
[24] P. Gütlich, R. Link, A. X. Trautwein, *Mössbauer Spectroscopy and Transition Metal Chemistry*, Springer, Berlin **1978**.
[25] J. H. Takemoto, B. Hutchinson, *Inorg. Chem.* **1973**, *12*, 705.
[26] J. H. Takemoto, B. Streusand, B. Hutchinson, *Spectrochim. Acta Part A* **1974**, *30*, 827.
[27] C. J. Ballhausen, H. B. Gray, *Molecular Orbital Theory*, Benjamin, New York, **1965**.
[28] E. König, *Struct. Bonding* (Berlin) **1991**, *76*, 51.
[29] L. Wiehl, G. Kiel, C. P. Köhler, H. Spiering, P. Gütlich, *Inorg. Chem.* **1986**, *25*, 1565.
[30] V. Petrouleas, J.-P. Tuchagues, *Chem. Phys. Lett.* **1987**, *137*, 21.
[31] B. Gallois, J.-A. Real, C. Hauw, J. Zarembowitch, *Inorg. Chem.* **1990**, *29*, 1152.
[32] C. Cartier, P. Thuery, M. Verdaguer, J. Zarembowitch, A. Michalowicz, *J. Phys. Colloq. Suppl. No. 12*, **1986**, *47*, C8-563.
[33] H. Winkler, A. Sawaryn, A. X. Trautwein, A. S. Yousif, C. Hermes, H. Toftlund, R. H. Herber, *Hyperfine Interact.* **1988**, *42*, 921.
[34] E. König, *Prog. Inorg. Chem.* **1987**, *35*, 527.
[35] B. Gallois, T. Granier, F. Suez-Panama, J. A. Real, J. Zarembowitch, *Phase Transitions* **1991**, *32*, 193.
[36] L. Wiehl, *Acta Crystallogr. Sect. B* **1993**, *49*, 289.
[37] M. Sorai, S. Seki, *J. Phys. Chem. Solids* **1974**, *35*, 555.
[38] T. Kambara, *J. Phys. Soc. Jpn.* **1981**, *50*, 2257.
[39] S. Ohnishi, S. Sugano, *J. Phys. C: Solid State Phys.* **1981**, *14*, 39.
[40] H. Spiering, E. Meissner, H. Köppen, E. W. Müller, P. Gütlich, *Chem. Phys.* **1982**, *68*, 65.
[41] I. Sanner, E. Meißner, H. Köppen, H. Spiering, P. Gütlich, *Chem. Phys.* **1984**, *86*, 227.
[42] P. Adler, L. Wiehl, E. Meißner, C. P. Köhler, H. Spiering, P. Gütlich, *J. Phys. Chem. Solids* **1987**, *48*, 517.
[43] N. Willenbacher, H. Spiering, *J. Phys. C: Solid State Phys.* **1988**, *21*, 1423.
[44] H. Spiering, N. Willenbacher, *J. Phys.: Condens. Matter.* **1989**, *1*, 10089.
[45] T. Kambara, N. Sasaki, *J. Phys. Soc. Jpn.* **1982**, *51*, 1694.
[46] N. Sasaki, T. Kambara, *J. Phys. C: Solid State Phys.* **1982**, *15*, 1035.
[47] N. Sasaki, T. Kambara, *J. Phys. Soc. Jpn.* **1982**, *51*, 1571.
[48] F. Ogata, T. Kambara, N. Sasaki, K. I. Gondaira, *J. Phys. C: Solid State Phys.* **1983**, *16*, 1391.
[49] C. N. R. Rao, *Int. Rev. Phys. Chem.* **1985**, *4*, 19.
[50] M. Bacci, *Coord. Chem. Rev.* **1988**, *86*, 245.
[51] K. Takahashi, *Z. Phys. B: Condens. Matter* **1988**, *71*, 205.
[52] N. Sasaki, T. Kambara, *Phys. Rev. B: Condens. Matter* **1989**, *40*, 2442.
[53] J.-A. Real, H. Bolvin, A. Bousseksou, A. Dworkin, O. Kahn, F. Varret, J. Zarembowitch, *J. Am. Chem. Soc.* **1992**, *114*, 4650.
[54] A. Bousseksou, J. Nasser, J. Linares, K. Boukheddaden, F. Varret, *J. Phys. I* **1992**, *2*, 1381.
[55] J. K. Beattie, *Adv. Inorg. Chem.* **1988**, *32*, 1.
[56] P. Adler, H. Spiering, P. Gütlich, *Inorg. Chem.* **1987**, *26*, 3840.
[57] P. Adler, H. Spiering, P. Gütlich, *Hyperfine Interact.* **1988**, *42*, 1035.
[58] P. Adler, A. Hauser, A. Vef, H. Spiering, P. Gütlich, *Hyperfine Interact.* **1989**, *47*, 343.
[59] P. Adler, H. Spiering, P. Gütlich, *J. Phys. Chem. Solids* **1989**, *50*, 587.
[60] M. Alflen, C. Hennen, F. Tuczek, H. Spiering, P. Gütlich, Zs. Kajcsos, *Hyperfine Interact.* **1989**, *47*, 15.

[61] H. Spiering, M. Alflen, P. Gütlich, A. Hauser, C. Hennen, U. Manthe, F. Tuczek, *Hyperfine Interact.* **1990**, *56*, 1527.
[62] C. Hennen, M. Alflen, H. Spiering, P. Gütlich, *Hyperfine Interact.* **1990**, *56*, 1527.
[63] P. Gütlich, J. Ensling, F. Tuczek, *Hyperfine Interact.* **1994**, *84*, 447.
[64] S. Decurtins, P. Gütlich, C. P. Köhler, H. Spiering, A. Hauser, *Chem. Phys. Lett.* **1984**, *105*, 1.
[65] S. Decurtins, P. Gütlich, K. M. Hasselbach, H. Spiering, A. Hauser, *Inorg. Chem.* **1985**, *24*, 2174.
[66] S. Decurtins, P. Gütlich, C. P. Köhler, H. Spiering, *J. Chem. Soc. Chem. Commun.* **1985**, 430.
[67] E. Buhks, G. Navon, M. Bixon, J. Jortner, *J. Am. Chem. Soc.* **1980**, *102*, 2918.
[68] A. Hauser, Habilitation thesis, Universität Mainz. **1992**.
[69] S. Sugano, Y. Tanabe, H. Kamimura, *Multiplets of Transition Metal Ions (Pure Appl. Phys.* **1970**, *33*).
[70] M. A. Hoselton, L. J. Wilson, R. S. Drago, *J. Am. Chem. Soc.* **1975**, *97*, 1722.
[71] B. A. Katz, C. E. Strouse, *J. Am. Chem. Soc.* **1979**, *101*, 6214.
[72] M. Mikami-Kido, Y. Saito, *Acta Crystallogr. Sect. B* **1982**, *38*, 452.
[73] E. W. Müller, H. Spiering, P. Gütlich, *Chem. Phys. Lett.* **1982**, *93*, 567.
[74] D. H. Everett, W. I. Whitton, *Trans. Faraday Soc.* **1952**, *48*, 749.
[75] D. H. Everett, F. W. Smith, *Trans. Faraday Soc.* **1954**, *50*, 187.
[76] D. H. Everett, *Trans. Faraday Soc.* **1954**, *50*, 1077.
[77] E. König, G. Ritter, W. Irler, S. M. Nelson, *Inorg. Chim. Acta* **1979**, *37*, 169.
[78] E. W. Müller, H. Spiering, P. Gütlich, *J. Chem. Phys.* **1983**, *79*, 1439.
[79] H. Köppen, E. W. Müller, C. P. Köhler, H. Spiering, E. Meissner, P. Gütlich, *Chem. Phys. Lett.* **1982**, *91*, 348.
[80] R. Jakobi, *Dissertation*, Universität Mainz, **1991**.
[81] R. Jakobi, H. Spiering, P. Gütlich, *J. Phys. Chem. Solids* **1992**, *53*, 267.
[82] M. Mikami, M. Konno, Y. Saito, *Chem. Phys. Lett.* **1979**, *63*, 566.
[83] K. Kaji, M. Sorai, *Thermochim. Acta* **1985**, *88*, 185.
[84] Professor E. Gmelin, Max-Planck Institut für Festkörperforschung (Stuttgart) is thanked for sharing technical drawings and for his exceptional helpfulness.
[85] C. P. Köhler, R. Jakobi, E. Meissner, L. Wiehl, H. Spiering, P. Gütlich, *J. Phys. Chem. Solids* **1990**, *51*, 239.
[86] H. Inoue, H. Nakajima, T. Takahashi, H. Uchida, T. Shirai, E. Fluck, *Bull. Chem. Soc. Jpn.* **1986**, *59*, 3483.
[87] H. Irving, M. J. Mellor, *J. Chem. Soc.* **1962**, 5237.
[88] H. A. Goodwin, R. N. Sylva, *Aust. J. Chem.* **1968**, *21*, 83.
[89] J. Fleisch, Dissertation, D17, Technische Hochschule Darmstadt, **1976**.
[90] J. Fleisch, P. Gütlich, K. M. Hasselbach, E. W. Müller, *Inorg. Chem.* **1976**, *15*, 958.
[91] J. Fleisch, P. Gütlich, K. M. Hasselbach, E. W. Müller, *J. Phys. Colloq.* **1974**, *35*, C6-659.
[92] W. M. Reiff, G. J. Long, *Inorg. Chem.* **1974**, *13*, 2150.
[93] J. Fleisch, P. Gütlich, K. M. Hasselbach, *Inorg. Chim. Acta* **1976**, *17*, 51.
[94] J. Fleisch, P. Gütlich, K. M. Hasselbach, *Inorg. Chem.* **1977**, *16*, 1979.
[95] L. M. Epstein, *J. Chem. Phys.* **1964**, *40*, 435.
[96] G. Bradley, V. McKee, S. M. Nelson, J. Nelson, *J. Chem. Soc. Dalton Trans.* **1978**, 522.
[97] K. Madeja, W.-H. Böhmer, N.-T. Thuy, *Z. Anorg. Allg. Chem.* **1978**, *447*, 5.
[98] M. G. Burnett, V. McKee, S. M. Nelson, *J. Chem. Soc. Dalton Trans.* **1981**, 1492.
[99] H. Toftlund, S. Yde-Andersen, *Acta Chem. Scand. Ser. A* **1981**, *35*, 575.
[100] P. L. Franke, J. G. Haasnoot, A. P. Zuur, *Inorg. Chim. Acta* **1982**, *59*, 5.
[101] K. M. Kadish, C.-H. Su, D. Schaeper, C. L. Merrill, L. J. Wilson, *Inorg. Chem.* **1982**, *21*, 3433.
[102] D. Hojland, H. Toftlund, S. Yole-Andersen, *Acta Chem. Scand. Ser. A* **1983**, *37*, 251.
[103] S. P. Kao, Y. C. Jean, H. H. Wei, *Hyperfine Interact.* **1986**, *28*, 711.
[104] A. T. Baker, H. A. Goodwin, A. D. Rae, *Inorg. Chem.* **1987**, *26*, 3513.
[105] D. Onggo, J. M. Hook, A. D. Rae, H. A. Goodwin, *Inorg. Acta* **1990**, *173*, 19.
[106] D. Onggo, H. A. Goodwin, *Aust. J. Chem.* **1991**, *44*, 1539.
[107] M. Sorai, J. Ensling, P. Gütlich, *Chem. Phys.* **1976**, *18*, 199.
[108] P. Gütlich, R. Link, H. G. Steinhäuser, *Inorg. Chem.* **1978**, *17*, 2509.
[109] P. Gütlich, H. Köppen, R. Link, H. G. Steinhäuser, *J. Chem. Phys.* **1979**, *70*, 3977.
[110] H. L. Chum, J. A. Vanin, M. I. D. Holanda, *Inorg. Chem.* **1982**, *21*, 1146.
[111] P. Ganguli, P. Gütlich, E. W. Müller, *Inorg. Chem.* **1982**, *21*, 3429.
[112] G. A. Renovitch, W. A. Baker, Jr., *J. Am. Chem. Soc.* **1967**, *89*, 6377.
[113] M. Sorai, J. Ensling, K. M. Hasselbach, P. Gütlich, *Chem. Phys.* **1977**, *20*, 197.
[114] P. Gütlich, H. Köppen, H. G. Steinhäuser, *Chem. Phys. Lett.* **1980**, *74*, 3.
[115] A. M. Greenaway, C. J. O'Connor, A. Schrock, E. Sinn, *Inorg. Chem.* **1979**, *18*, 2692.
[116] A. M. Greenaway, E. Sinn, *J. Am. Chem. Soc.* **1978**, *100*, 8080.
[117] H. Köppen, Dissertation, Universität Mainz, **1985**.
[118] H. G. Drickamer, C. W. Frank, *Electronic Transitions and the High Pressure Chemistry and Physics of Solids*, Chapman and Hall, London, **1973**.
[119] D. M. Adams, G. J. Long, A. D. Williams, *Inorg. Chem.* **1982**, *21*, 1049.
[120] J. Pebler, *Inorg. Chem.* **1983**, *22*, 4125.
[121] E. König, G. Ritter, S. K. Kulshreshta, J. Waigel, H. A. Goodwin, *Inorg. Chem.* **1984**, *23*, 1896.
[122] S. Usha, R. Srinivasan, C. N. R. Rao, *Chem. Phys.* **1985**, *100*, 447.
[123] E. Meissner, H. Köppen, C. P. Köhler, H. Spiering, P. Gütlich, *Hyperfine Interact.* **1987**, *36*, 1.
[124] G. J. Long, B. B. Hutchinson, *Inorg. Chem.* **1987**, *26*, 608.
[125] J. K. McCusker, M. Zvagulis, H. H. Drickamer, D. N. Hendrickson, *Inorg. Chem.* **1989**, *28*, 1380.
[126] M. Konno, M. Mikami-Kido, *Bull. Chem. Soc. Jpn.* **1991**, *64*, 339.
[127] E. Meissner, H. Köppen, H. Spiering, P. Gütlich, *Chem. Phys. Lett.* **1983**, *95*, 163.
[128] R. A. Binstead, J. K. Beattie, E. V. Dose, M. F. Tweedle, L. J. Wilson, *J. Am. Chem. Soc.* **1978**, *100*, 5609.
[129] Y. Qi, E. W. Müller, H. Spiering, P. Gütlich, *Chem. Phys. Lett.* **1983**, *101*, 503.
[130] E. König, K. Madeja, *Inorg. Chem.* **1967**, *6*, 48.
[131] P. Ganguli, P. Gütlich, E. W. Müller, W. Irler, *J. Chem. Soc. Dalton Trans.* **1981**, 441.
[132] M. S. Haddad, W. D. Federer, M. W. Lynch, D. N. Hendrickson, *J. Am. Chem. Soc.* **1980**, *102*, 1468.
[133] E. W. Müller, H. Spiering, P. Gütlich, *Inorg. Chem.* **1984**, *23*, 119.
[134] H. H. Wei, Y. C. Jean, *Chem. Phys. Lett.* **1984**, *106*, 523.
[135] A. Ruaudel-Teixier, A. Barraud, P. Coronel, O. Kahn, *Thin Solid Films* **1988**, *160*, 107.
[136] P. Coronel, A. Barraud, R. Claude, O. Kahn, A. Ruaudel-Teixier, J. Zarembowitch, *J. Chem. Soc. Chem. Commun.* **1989**, 193.
[137] L. Wiehl, H. Spiering, P. Gütlich, K. Knorr, *J. Appl. Crystallogr.* **1990**, *23*, 151.
[138] J. D. Eshelby, *Solid State Phys.* **1956**, *3*, 79.
[139] R. Jakobi, Diplom thesis, Universität Mainz, **1985**.
[140] R. Jakobi, H. Spiering, L. Wiehl, E. Gmelin, P. Gütlich, *Inorg. Chem.* **1988**, *27*, 1823.
[141] R. Zimmermann, E. König, *J. Phys. Chem. Solids* **1977**, *38*, 779.
[142] T. Kambara, *J. Chem. Phys.* **1979**, *70*, 4199.
[143] T. Kambara, *J. Phys. Soc. Jpn.* **1980**, *49*, 1806.
[144] H. Köppen, E. Meissner, L. Wiehl, H. Spiering, P. Gütlich, *Hyperfine Interact.* **1989**, *52*, 29.
[145] A. Hauser, *Chem. Phys. Lett.* **1986**, *124*, 543.
[146] A. Hauser, *J. Chem. Phys.* **1991**, *94*, 2741.
[147] A. B. P. Lever, *Inorganic Electronic Spectroscopy* (*Stud. Phys. Theor. Chem.* **1984**, *33*).
[148] G. Schmitt, Diplom thesis, Universität Mainz, **1989**.
[149] A. Ozarowski, B. R. McGarvey, *Inorg. Chem.* **1989**, *28*, 2262.
[150] J. J. McGarvey, I. Lawthers, *J. Chem. Soc. Chem. Commun.* **1982**, 906.
[151] C.-L. Xie, D. N. Hendrickson, *J. Am. Chem. Soc.* **1987**, *109*, 6981.
[152] A. Hauser, A. Vef, P. Adler, *J. Chem. Phys.* **1991**, *95*, 8710.
[153] P. Poganiuch, S. Decurtins, P. Gütlich, *J. Am. Chem. Soc.* **1990**, *112*, 3270.
[154] P. Poganiuch, P. Gütlich, *Inorg. Chem.* **1987**, *26*, 455.
[155] A. W. Addison, S. Burman, C. G. Wahlgren, O. A. Rajan, T. M. Rowe, E. Sinn, *J. Chem. Soc. Dalton Trans.* **1987**, 2621.
[156] R. H. Herber, *Inorg. Chem.* **1987**, *26*, 173.
[157] D. C. Figg, R. H. Herber, *Hyperfine Interact.* **1990**, *62*, 99.
[158] A. Vef, Dissertation, Universität Mainz, **1993**.
[159] K.-U. Baldenius, A. K. Campen, H.-D. Hönk, A. J. Rest, *J. Mol. Struct.* **1987**, *157*, 295.
[160] A. Hauser, J. Adler, P. Gütlich, *Chem. Phys. Lett.* **1988**, *152*, 468.
[161] J. Ensling, B. W. Fitzsimmons, P. Gütlich, K. M. Hasselbach, *Angew. Chem.* **1970**, *82*, 638; *Angew. Chem. Int. Ed. Engl.* **1970**, *9*, 637.
[162] R. Grimm, P. Gütlich, E. Kankeleit, R. Link, *J. Chem. Phys.* **1977**, *67*, 5491.
[163] A. J. Street, D. M. Goodall, R. C. Greenhow, *Chem. Phys. Lett.* **1978**, *56*, 326.
[164] C. Creutz, M. Chou, T. L. Netzel, M. Okumura, N. Sutin, *J. Am. Chem. Soc.* **1980**, *102*, 1309.
[165] A. Hauser, *Chem. Phys. Lett.* **1990**, *173*, 507.
[166] J. Ensling, P. Gütlich, K. M. Hasselbach, B. W. Fitzsimmons, *Chem. Phys. Lett.* **1976**, *42*, 232.
[167] J. Fleisch, P. Gütlich, *Chem. Phys. Lett.* **1976**, *42*, 237.
[168] J. Fleisch, P. Gütlich, *Chem. Phys. Lett.* **1977**, *45*, 29.
[169] J. Fleisch, P. Gütlich, H. Köppen, *Radiochem. Radioanal. Lett.* **1980**, *42*, 279.
[170] P. Gütlich, H. Köppen, *J. Phys. Colloq. Suppl. No. 1* **1980**, *41*, C1-311.
[171] R. Albrecht, M. Alflen, P. Gütlich, Zs. Kajcsos, R. Schultze, H. Spiering, F. Tuczek, *Nucl. Instrum. Methods Phys. Res. Sect. A* **1987**, *A257*, 209.
[172] M. A. Hoselton, R. S. Drago, L. J. Wilson, N. Sutin, *J. Am. Chem. Soc.* **1976**, *98*, 6967.
[173] E. V. Dose, M. A. Hoselton, N. Sutin, M. F. Tweedle, L. J. Wilson, *J. Am. Chem. Soc.* **1978**, *100*, 1141.
[174] J. K. Beattie, R. A. Binstead, R. J. West, *J. Am. Chem. Soc.* **1978**, *100*, 3044.
[175] R. A. Binstead, J. K. Beattie, T. G. Dewey, D. H. Turner, *J. Am. Chem. Soc.* **1980**, *102*, 6442.
[176] J. DiBenedetto, V. Arkle, H. A. Goodwin, P. C. Ford, *Inorg. Chem.* **1985**, *24*, 456.
[177] J. K. Beattie, K. J. McMahon, *Aust. J. Chem.* **1989**, *41*, 1315.

[178] J. J. McGarvey, I. Lawthers, K. Heremans, H. Toftlund, *Inorg. Chem.* **1990**, *29*, 252.
[179] P. Avouris, W. M. Gelbart, M. A. El-Sayed, *Chem. Rev.* **1977**, *77*, 793.
[180] F. A. Cotton, *Chemical Applications of Group Theory*, Wiley, New York, **1991**.
[181] C. J. Donnelly, G. F. Imbush, *NATO ASI Ser. Ser. B* **1991**, *249*, 175.
[182] W. H. Fonger, C. W. Struck, *J. Chem. Phys.* **1974**, *60*, 1988.
[183] A. Hauser, *Coord. Chem. Rev.* **1991**, *111*, 275.
[184] M. D. Sturge, *Phys. Rev. B: Solid State* **1973**, *8*, 6.
[185] U. Manthe, Universität Mainz, personal communication, **1989**.
[186] I. Lawthers, J. J. McGarvey, *J. Am. Chem. Soc.* **1984**, *106*, 4280.
[187] J. G. Leipoldt, P. Coppens, *Inorg. Chem.* **1973**, *12*, 2269.
[188] A. Hauser, P. Gütlich, H. Spiering, *Inorg. Chem.* **1986**, *25*, 4245.
[189] A. Hauser, *Chem. Phys. Lett.* **1992**, *192*, 65.
[190] A. Hauser, *Coord. Chem. Rev.* **1991**, *111*, 275.
[191] D. W. Clack, W. Smith, *J. Chem. Soc. Dalton Trans.* **1974**, 2015.
[192] K. J. Laidler, *Chemical Kinetics*, McGraw-Hill, New York, **1965**.



Designer Proteins: On the Art of Synthesizing De Novo Metalloproteins**

Heinz-Bernhard Kraatz*

Dedicated to Professor P. Michael Boorman

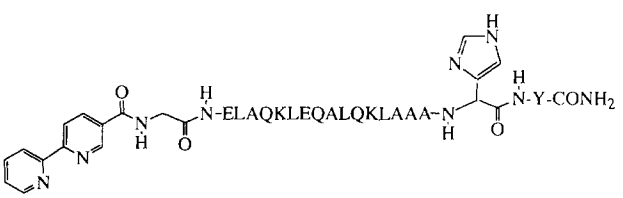
Contemporary research in chemistry often crosses the lines that previously divided the classical disciplines of chemistry and biology. Coordination chemistry has certainly been one of the areas of chemistry that has spanned the old boundaries. An inclusive definition of what constitutes coordination chemistry is emerging which requires "only that distinct molecular species be formed by the binding interaction."[1] The modeling of active sites of metalloenzymes has always been a great stimulus to coordination chemists. An excellent example for this is the "nitrogenase problem", which has played a pivotal role in the rapid development of the coordination chemistry of molybdenum and sulfur-based ligands. Recent advances in the de novo design of nonnatural proteins have allowed the combination of classical coordination chemistry and protein biochemistry. The main idea of the design is to reduce the highly complex naturally occurring proteins to the minimum structural features necessary for a certain function. The model protein is prepared by standard synthetic methodologies, and can be used to evaluate the structural assumptions that led to its design and thereby lead to an understanding of the intricate interplay between protein structure and function. Current research in this area following this approach has led to the successful design of a range of artificial proteins.[2]

Two major routes to the structural design of a de novo protein can be distinguished: a) the synthesis of a larger peptide with subdomains of known secondary structure, which will adopt a particular tertiary structure, and b) the design of smaller peptide subunits of known secondary structure and their assembly on a template to yield the final protein of a particular tertiary structure, such as desribed by Mutter et al.[3] The construction of specific and topologically predetermined protein structures from smaller amphiphilic peptide precursors by simple self-assembly is hampered by the tendency of peptides to establish an equilibrium between monomers and aggregates in aqueous solution. This makes controlling the number of participating peptides and their relative stereochemistry a formidable task indeed.

An important step forward in this area has been made by Ghadiri et al. with a metal ion mediated self-assembly process[4] in the spirit of the new inclusive definition of coordination chemistry. The coordination of chemically modified peptides to a metal center through a ligating group leads to the formation of a metal–peptide complex, thereby allowing control of the stereochemistry of the complex and the number of peptide subunits participating in the final de novo protein. To a large extent, the art of successfully applying this strategy lies in the choice of the metal center and the chemical modification of a specific peptide. This surprisingly simple approach has been applied to the synthesis of several helical metalloproteins with well-defined stereochemistry such as **1** (py = pyridine)[4a] and **2**.[4c]

trans-[$RuCl_2$(py-peptide)$_4$] **1**
cis-[$Ru(NH_3)_4$(His-peptide)$_2$]$^{3+}$ **2**

This idea has now been refined to such an extent that it has been possible to synthesize a Ru^{II} metalloprotein with a well-defined metal-binding site.[5] This was achieved with peptide **3**,



3

which has two potential metal-binding sites—an N-terminal bipyridine group (bpy) and an imidazole nitrogen atom of a histidine residue close to the C-terminus of **3**—and should favor a helical structure. Incorporation of the bpy functionality at the N-terminus of each peptide allowed direction of the self-assembly of three peptides with a Ru^{II} ion as a template to form a three-helix bundle protein. Kinetically inert **4** is produced exclusively. Since the three peptide subunits are in close proximity, short-range intramolecular hydrophobic interactions amongst

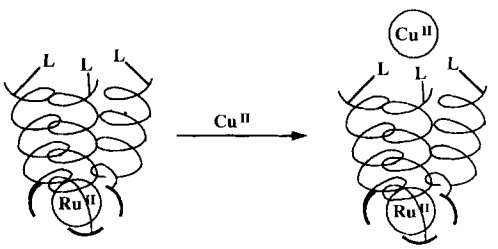
fac-[Ru^{II}(bpy-peptide)$_3$]$^{2+}$ **4**

the three metal-bound peptides exceed intermolecular interactions, which thereby facilitates the formation of the overall helical tertiary structure of **4** (circular dichroism) (CD) spectrum: $\theta_{222} = -23000\,^{\circ}cm^2dmol^{-1}$). UV/VIS spectroscopy ($\lambda_{max}$ = 289 and 475 nm), electrospray mass spectrometry (found: M = 6887 ± 2; calcd.: M = 6887), and gel permeation chromatogra-

[*] Dr. H.-B. Kraatz
Department of Organic Chemistry, The Weizmann Institute of Science
76100 Rehovot (Israel)
Telefax: Int. code + (8)34-4142

[**] This work was supported by the Minerva Gesellschaft, Munich (Germany). We thank Prof. D. Milstein for his encouragement and support.

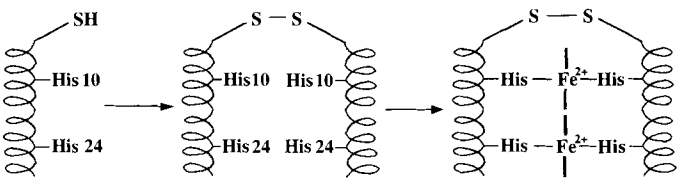
phy all provide unequivocal evidence for the identity of **4**. It is important to point out that because of this helical arrangement, the three His18-residues close to the C-termini of each of the three peptide subunits are close together, thereby forming an effective metal binding site. Coordination of Cu^{2+} to this binding site does not significantly alter the structure of the protein, which indicates the presence of this binding site after the self-assembly of **4** (CD spectrum: $\theta_{222} = -24000^\circ cm^2 dmol^{-1}$). Based on the marked decrease in the fluorescence emission of the adjacent tyrosine chromophore and analysis of the EPR ($g_{\|} = 2.27$ and $A_{\|} = 173\ cm^{-1} \times 10^4$) and UV/VIS ($\lambda_{max} = 375$ (charge transfer) and 495 nm) spectra, Ghadiri and Case[5] demonstrated that a Cu^{II} ion is able to bind to this metal-binding site and leads to the formation of the $Ru^{II}Cu^{II}$ protein **5** (Scheme 1).



4 **5**

Scheme 1.

Relevant in this context are the recent reports of the design and syntheses of cytochrome (cyt) models by Diederich et al.[6] based on polyether–amide dendrites encapsulating a central Zn porphyin core, and the approach by DeGrado et al. for the synthesis of artificial proteins.[7] In DeGrado's approach, several peptides have been synthesized consisting of two identical 31-residue helical subunits linked by a disulfide bridge. The peptides contain histidine residues which allow the coordination of Fe^{II} heme through two *trans* imidazole groups. The peptides accociate to dimeric four-helix bundle structures. Model protein **7** was designed from two identical subunits **6**, which each possess two histidine units (His10 and His24), to mimic the cyt b subunit of cyt bc_1. Compound **7** has two possible heme binding sites per peptide (based on two histidine residues) and an estimated separation between the Fe atoms of about 20 Å. Due to dimerization of the model protein **7**, addition of Fe^{II} heme leads to the incorporation of four redox centers at the four predetermined binding sites of the protein dimer. CD spectroscopy also confirms in this case that well-defined binding sites are present prior to heme coordination ($\theta_{222} = -26000^\circ cm^2 dmol^{-1}$). As expected the heme–protein complex exhibits a rhombic EPR spectrum ($g_z = 2.89$, $g_y = 2.24$, $g_x = 1.54$) confirming the coordination of low-spin Fe^{2+} through two *trans* imidazole groups.



6 **7** **8**

These are only two examples indicating the scope of this emerging area of research at the interface of protein chemistry and coordination chemistry. The synthesis of metal-binding metalloproteins and the introduction of redox-active metal centers into artificial proteins by self-assembly processes is surely only the beginning. One can certainly think of extending this approach to the incorporation of substrate-binding enzymatic functions, as already demonstrated by Sasaki and Kaiser,[8] and photosensitive metal centers in proteins which can then act as light-harvesting analogues of the photosystem of green plants.

German version: *Angew. Chem.* **1994**, *106*, 2143

[1] D. H. Busch, *Chem. Rev.* **1993**, *93*, 847–860.
[2] a) W. F. DeGrado, Z. R. Wasserman, J. D. Lear, *Science (Washington D.C. 1883-)* **1989**, *243*, 622–628; b) K. T. O'Neil, R. H. Hoess, W. F. DeGrado, *ibid.* **1989**, *243*, 774–778; c) K. T. O'Neil, W. F. DeGrado, *Trends Biochem. Sci.* **1990**, *15*, 59–64; d) K. S. Åkerfeldt, J. D. Lear, Z. R. Wasserman, L. A. Chung, W. F. DeGrado, *Acc. Chem. Res.* **1993**, *26*, 191–197; e) K. W. Hahn, W. A. Klis, J. M. Stewart, *Science (Washington D.C. 1883-)* **1990**, *248*, 1544–1547; f) A. Grove, M. Mutter, J. E. Rivier, M. Montal, *J. Am. Chem. Soc.* **1993**, *115*, 5919–5924; g) M. R. Ghadiri, J. R. Granja, L. K. Buehler, *Nature (London)* **1994**, *369*, 301–304.
[3] a) M. Mutter, S. Vuilleumier, *Angew. Chem.* **1989**, *101*, 551–571; *Angew. Chem. Int. Ed. Engl.* **1989**, *28*, 535–554; b) for a more recent example see: M. Mutter, G. G. Tuchscherer, C. Miller, K.-H. Altman, R. I. Carey, D. F. Wyss, A. M. Labhardt, J. E. Rivier, *J. Am. Chem. Soc.* **1992**, *114*, 1463–1470.
[4] a) M. R. Ghadiri, A. M. Fernholz, *J. Am. Chem. Soc.* **1990**, *112*, 9633–9635; b) M. R. Ghadiri, C. Soares, C. Choi, *ibid.* **1992**, *114*, 825–831; c) *ibid.* **1992**, *114*, 4000–4002.
[5] M. R. Ghadiri, M. A. Case, *Angew. Chem.* **1993**, *105*, 1663–1667; *Angew. Chem. Int. Ed. Engl.* **1993**, *32*, 1594–1597.
[6] P. J. Dandliker, F. Diederich, M. Gross, C. B. Knobler, A. Louati, E. M. Sanford, *Angew. Chem.* **1994**, *106*, 1821–1824; *Angew. Chem. Int. Ed. Engl.* **1994**, *33*, 1739–1742.
[7] D. E. Robertson, R. S. Farid, C. C. Moser, J. L. Urbauer, S. E. Mulholland, R. Pidikiti, J. D. Lear, A. J. Wand, W. F. DeGrado, P. L. Dutton, *Nature (London)* **1994**, *368*, 425–432.
[8] T. Sasaki, E. T. Kaiser, *J. Am. Chem. Soc.* **1989**, *111*, 380–381.

Novel Copper Nitrosyl Complexes: Contributions to the Understanding of Dissimilatory, Copper-Containing Nitrite Reductases

Bruce A. Averill*

Denitrification is the dissimilatory reduction of nitrogen-oxide species to gaseous products by bacteria, and occupies a central position in the global nitrogen cycle. As shown in Figure 1,

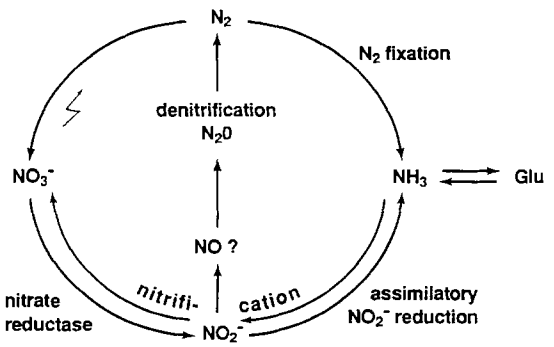


Fig. 1. A schematic of the reactions involved in inorganic nitrogen metabolism, showing the central position of the denitrification pathway.

denitrification provides the only route for recycling fixed nitrogen back into the atmosphere. In addition, denitrification is a major source of NO and N_2O, which play an significant role in ozone layer destruction and global warming. Denitrification is also important in bioremediation efforts and cycling of nutrients in aquifers and rock formations beneath the soil. Finally, NO, named the 1992 "Molecule of the Year" by *Science*, is a key chemical signal in a wide variety of processes. Consequently, microbial systems that evolve or consume NO are of substantial interest as potential models for the mammalian system, and the possible effects of NO generated by enteric or pathogenic bacteria remain an unexplored but potentially important area of research.

The pathway of denitrification has been the object of controversy for the past 10–15 years, with the focus of attention on the route from nitrite to nitrous oxide, and whether nitric oxide is an obligatory intermediate. As a result of recent contributions, it is now clear that, at least in most denitrifiers most of the time, reduction of NO_2 produces NO that is subsequently reduced to N_2O in a separate enzymatic step (Fig. 2).[1–3] The controversy was exacerbated by the existence of two distinct types of dissimilatory nitrite reductase, containing either two hemes or two copper per protein monomer, which exhibit significantly different chemistry.[4] These enzymes appear to operate on the same basic principles (one chromophore in the active site, either heme d_1 or Type 2 (non-blue) copper, plus one electron transfer site, either heme c or an unusual green variant of a Type 1 (blue) copper center, respectively).[5, 6] The heme enzymes produce almost exclusively NO from NO_2^-, but the copper enzymes are capable of producing significant amounts of N_2O from NO_2^- in the presence of NO.[7]

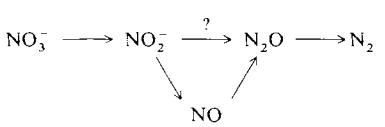


Fig. 2. The pathway of denitrification.

The existence and properties of well-defined model complexes have been central to an understanding of the structure and reactivity of many metalloenzymes and metalloproteins, including cytochrome P450, hemoglobin, hemerythrin, and iron-sulfur proteins.[8] In the case of the heme cd_1 nitrite reductases, ample synthetic precedents exist for interaction of NO with both Fe^{II}- and Fe^{III}-porphyrin complexes, and it seems clear that the enzymes operate by a mechanism involving protonation and dehydration of bound nitrite to give a Fe^{II}-heme-nitrosyl (Fe^{II}-NO^+) intermediate[9] that rapidly decomposes to NO and the Fe^{III}-heme by an internal electron transfer reaction. Until recently, however, model complexes for copper-containing nitrite reductases were notable solely by their absence; no structurally characterized copper-nitric oxide complexes were reported. Preliminary mechanistic studies on one copper nitrite reductase were interpreted as suggesting a mechanism similar to that utilized by the heme cd_1 enzymes, with a copper nitrosyl (possibly Cu^+-NO^+) species as an intermediate[10] (Fig. 3). In retrospect, the evidence originally reported for such a species is not particularly convincing, due largely to the lack of any model complexes for comparison.

The situation regarding models for copper enzymes has improved dramatically in the last three years, however, with reports by Karlin et al. and Tolman et al. of the synthesis of binuclear[11]

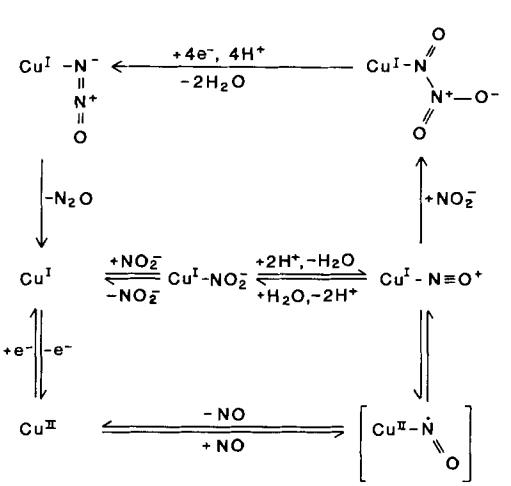


Fig. 3. Proposed mechanism for reactions of copper-containing nitrite reductases; (lower portion) reaction occurring at low levels of NO; (upper portion) possible reactions occurring in the presence of NO.

[*] Prof. B. A. Averill
E. C. Slater Instituut, Universiteit van Amsterdam
Plantage Muidergracht 12, NL-1018 TV Amsterdam (The Netherlands)
Telefax: Int. code + (20)525-5124

and mononuclear[12] copper–NO complexes, respectively; Tolman et al. also synthesized a series of Cu^{II}[13, 14] and Cu^{I}[15, 16] nitrite complexes. These complexes have provided structurally characterized benchmarks for comparison of corresponding properties with appropriate forms of the enzymes. The work by Tolman et al. is particularly significant due to the use of the biologically relevant hydrotris(pyrazolyl)borate and 1,4,7-triazacyclononane (tacn) ligands. These tridentate ligands provide nitrogen ligation that closely resembles that formed by three imidazole ligands in the pseudotetrahedral coordination sphere of the active site of the *Achromobacter cycloclastes* nitrite reductase determined in an elegant structural study by Adman et al.[17] As a result of the synthetic work, we now have available a variety of structurally characterized model complexes with biologically relevant ligands, including both monomeric Cu^{II}–NO_2^- and Cu^{I}–NO_2^- and dimeric Cu^{I}–Cu^{I} and Cu^{I}–Cu^{II} complexes with bridging NO_2^- ligands, as well as Cu–NO complexes[12] in which the electron distribution is not quite so readily assessed. The monomeric Cu^{I}–NO_2^- complex,[16] in which nitrite is N-coordinated, and the Cu–NO[12] complexes are of particular significance, since they are the first structurally defined model systems that approximate the structures of the enzyme–substrate or enzyme–product complexes in copper-containing nitrite reductases.

Perhaps most importantly, these synthetic complexes have now been utilized to provide the first *functional* models for the chemistry occurring on the copper nitrite reductases. The copper enzymes are unique in being able to incorporate nitrogen from nitric oxide into nitrous oxide, although whether the reaction involves coupling of nitric oxide with nitrite or with a second molecule of nitric oxide derived from nitrite remains unclear.[6] In the two lovely pieces of work that have appeared recently, Tolman et al. have synthesized complexes that are able to mimic certain aspects of the reactivity of the copper enzymes. Thus, the complex $[(i\mathrm{Pr}_3\mathrm{TACN})\mathrm{Cu}(\mathrm{NO}_2)]$, containing nitrite coordinated to Cu^{I} through nitrogen, reacts smoothly with two equivalents of acid to give NO quantitatively,[16] presumably via a Cu^{I}–NO^+ intermediate similar to that originally proposed for the copper nitrite reductases.[10] Further, Tolman et al. have shown that Cu^{I} complexes with appropriately functionalized hydrotris(pyrazolyl)borate ligands react with NO to produce N_2O and the Cu^{II}–NO_2^- complexes in a novel disproportionation reaction.[14] Initial kinetics studies clearly show that the reaction is first order in the Cu complex, ruling out a pathway involving a dimeric intermediate. Remaining possibilities include coupling of NOs in a dinitrosyl copper complex and direct coupling of coordinated NO with free NO to produce coordinated N_2O_2 as an intermediate (Fig. 4). The reaction evidently occurs at one metal center, making it highly relevant to the enzyme-mediated reactions, which almost certainly occur at a monocopper active site. In passing, the above reactions also provide the first well-characterized model system for disproportionation of NO in heterogeneous reactions catalyzed by copper-containing systems.

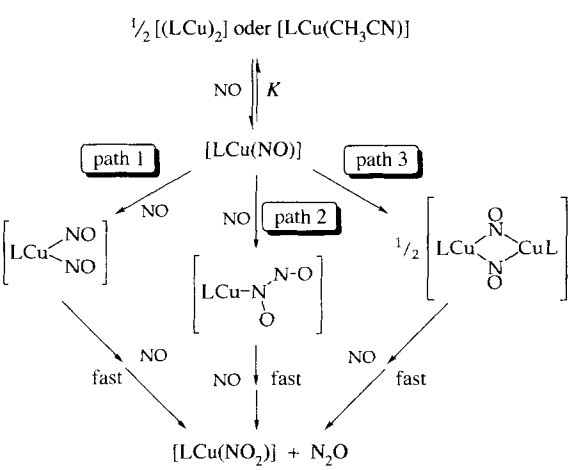


Fig. 4. Possible mechanisms for copper-mediated disproportionation of NO [14]. L = substituted tris(pyrazolyl)hydridoborate.

In only three years, we have thus come from an absence of any well-characterized copper nitrite or nitric oxide systems to having at our disposal a battery of structurally characterized compounds and a preliminary understanding of relevant reaction chemistry. By any standards, this constitutes remarkable progress.

German version: *Angew. Chem.* **1994**, *106*, 2145

[1] W. G. Zumft, *Arch. Microbiol.* **1993**, *160*, 253–264.
[2] R. W. Ye, B. A. Averill, J. M. Tiedje, *Appl. Environ. Microbiol.* **1994**, *60*, 1053–1058.
[3] P. M. H. Kroneck, J. Beuerle, W. Schumacher in *Metal Ions in Biological Systems, Vol. 28* (Eds.: H. Sigel, A. Sigel), Dekker, New York, **1992**, pp. 455–505.
[4] L. I. Hochstein, G. A. Tomlinson, *Annu. Rev. Microbiol.* **1988**, *42*, 231–261.
[5] E. Weeg-Aerssens, W. Wu, R. W. Ye, J. M. Tiedje, C. K. Chang, *J. Biol. Chem.* **1991**, *266*, 7496–7502.
[6] E. Libby, B. A. Averill, *Biochem. Biophys. Res. Commun.* **1992**, *187*, 1529–1535.
[7] M. A. Jackson, J. M. Tiedje, B. A. Averill, *FEBS Lett.* **1991**, *291*, 41–44.
[8] J. A. Ibers, R. H. Holm, *Science* **1980**, *209*, 223–235; K. D. Karlin, *ibid.* **1993**, *261*, 701–708.
[9] C.-H. Kim, T. C. Hollocher, *J. Biol. Chem.* **1984**, *259*, 2092–2099.
[10] C. L. Hulse, J. M. Tiedje, B. A. Averill, *J. Am. Chem. Soc.* **1989**, *111*, 2322–2323.
[11] P. P. Paul, K. D. Karlin, *J. Am. Chem. Soc.* **1991**, *113*, 6331–6332.
[12] S. M. Carrier, C. E. Ruggiero, W. B. Tolman, G. B. Jameson, *J. Am. Chem. Soc.* **1992**, *114*, 4407–4408; C. E. Ruggiero, S. M. Carrier, W. E. Antholine, J. W. Whittaker, C. J. Kramer, W. B. Tolman, *ibid.* **1993**, *115*, 11285–11298; W. B. Tolman, S. M. Carrier, C. E. Ruggiero, W. E. Antholine, J. W. Whittacker in *Bioinorganic Chemistry of Copper* (Eds.: K. D. Karlin, Z. Tyeklár), Chapman & Hall, New York, **1993**, pp. 406–418.
[13] W. B. Tolman, *Inorg. Chem.* **1991**, *30*, 4878–4880.
[14] C. E. Ruggiero, S. M. Carrier, W. B. Tolman, *Angew. Chem.* **1994**, *106*, 917–919; *Angew. Chem. Int. Ed. Engl.* **1994**, *33*, 895–897.
[15] J. A. Halfen, S. Mahapatra, M. M. Olmstead, W. B. Tolman, *J. Am. Chem. Soc.* **1994**, *116*, 2173–2174.
[16] J. A. Halfen, W. B. Tolman, *J. Am. Chem. Soc.* **1994**, *116*, 5475–5476.
[17] J. W. Godden, S. Turley, D. C. Teller, E. T. Adman, M. Y. Liu, W. J. Payne, J. LeGall, *Science* **1991**, *253*, 438–442.

A Novel Procedure for the Synthesis of Libraries Containing Small Organic Molecules**

Thomas Carell, Edward A. Wintner,
A. Bashir-Hashemi,* Julius Rebek, Jr.*

The traditional approach to finding an active pharmacological compound requires the synthesis of individual compounds and the evaluation of their biological activity. Hundreds of compounds are typically synthesized and screened before a substance with significant activity is identified which then serves as a lead structure for the development of potent drug candidates. The time-consuming process of finding a lead compound can be accelerated by synthesizing, instead of single compounds, mixtures (libraries) of potentially biologically active molecules. The libraries generated may each contain a vast number of different molecules. Modern screening and isolation procedures offer the means to identify and isolate compounds from a library which fulfill specific biological requirements.[1] To alleviate the difficulties in preparing and handling large mixtures of compounds, strategies have been developed in which libraries of linear peptides on a solid support are synthesized and screened for promising lead compounds.[2] While this method offers the possibility of preparing complex libraries, lead structures discovered from peptides linked to a support have certain disadvantages. Because of their intrinsic conformational flexibility, peptide lead compounds still require extensive modifications before a suitable drug candidate can be proposed. In addition, the conformation of the immobilized peptide may be significantly affected by its solid support, such that the measured biological response does not reflect the activity of the free compound in solution.

In order to overcome these problems, we investigated the synthesis and screening of chemical libraries of small, semirigid compounds free in solution. We explored the reaction between a rigid core molecule (Fig. 1) possessing multiple reactive functional groups and a mixture of small reactive organic molecules (building blocks). Each building block contains one complementary functional group able to form a covalent bond with the core molecule.

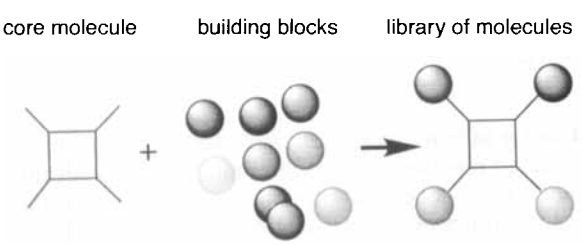
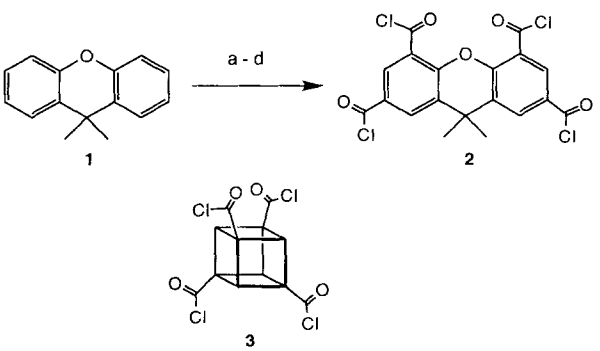


Fig. 1. Schematic representation of the generation of a library of small organic molecules.

In this approach, the spatial arrangement of the reactive groups on the core molecule defines the overall structure of the molecules in the library. By attaching the building blocks on the scaffold at random, every possible combination of building blocks can theoretically be generated. A variety of core molecules can be combined with a variety of building blocks in order to obtain nearly limitless libraries of conformationally restricted molecules. We chose as core molecules 9,9-dimethylxanthene-2,4,5,7-tetracarboxylic acid tetrachloride (**2**) and cubane-1,3,5,7-tetracarboxylic acid tetrachloride (**3**).[3] Attached building blocks are presented on the xanthene core molecule **2** in an overall disklike structure; on the cubane core molecule **3** the building blocks have a more spherical arrangement. The synthesis of the xanthene core molecule **2** was achieved in four steps starting from 9,9-dimethylxanthene (**1**) (Scheme 1).



Scheme 1. Cubane **3** and synthesis of xanthene derivative **2**. a) Br_2, cat. Fe powder, CH_2Cl_2, 2 h at 20 °C, 4 h at reflux, 93%; b) CuCN, *N*-methyl-2-pyrrolidine, 2 h, reflux, HNO_3 (20%), 10 h, reflux, 98%; c) NaOH, water, 14 h, reflux, 98%; d) PCl_5, benzene, 12 h, reflux, 68% [4].

Appropriate building blocks were selected after evaluation of numerous reactions between **2** and various individual amines. The products of these reactions were characterized and their HPLC properties examined for later experiments estimating library diversity (vide infra). Twenty-one amines, predominantly L-amino acid derivatives and small heterocycles (Scheme 2, Set 1), were chosen as building blocks for the generation of libraries; comparable reactivity towards the core molecule carboxylic acid chloride groups was the main criteria for tool selection. Additional functional groups on the amines were protected to define the regiochemistry between the building blocks and the core molecule, and to obtain initial libraries with good solubility in organic solvents.[5] The libraries were constructed by condensing one equivalent of a given tetracarboxylic acid tetrachloride core molecule in dichloromethane with four amine equivalents of a mixture of amines in dichloromethane. This approach minimizes competition effects between the amines for acid chloride groups and therefore should result in the synthesis of libraries with maximum diversity. The libraries thus generated

[*] Prof. J. Rebek, Jr., Dr. T. Carell, E. A. Wintner
Department of Chemistry, Massachusetts Institute of Technology
Cambridge, MA 02139 (USA)
Telefax: Int. code + (617)253-7929
Dr. A. Bashir-Hashemi
GEO-CENTERS
762 Rt. 15 South, Lake Hopatcong, NJ 07849 (USA)

[**] This research was supported by the National Institutes of Health, the Alexander-von-Humboldt Foundation (Feodor-Lynen fellowship to T. C.), and the National Science Foundation (predoctoral fellowship to E. W.). We thank Ken Shimizu for his synthesis of 9,9-dimethylxanthene-2,4,5,7-tetracarboxylic acid and Prof. K. Biemann for his advice regarding mass spectral analysis.

Set 1
L-alanine methyl ester, N^{ω}-4-methoxy-2,3,6-trimethylbenzene-sulfonyl-L-arginine-*p*-methoxybenzylamide* , O^4-*tert*-butyl-L-aspartic acid methyl ester, *S*-trityl-L-cysteinebenzylamide*, furfurylamine, O^5-*tert*-butyl-L-glutamic acid methyl ester, N^{im}-trityl-L-histidine-*n*-propylamide*, L-isoleucine *tert*-butyl ester, L-leucine methyl ester, N^{ε}-Boc-L-lysine methyl ester, L-methionine methyl ester, 4-methoxybenzylamine, *N*-methylpyrrol-2-ethylamine, L-phenylalanine methyl ester, L-proline methyl ester, O-*tert*-butyl-L-serine methyl ester, O-*tert*-butyl-L-threonine methyl ester, L-tryptophane methyl ester, O-*tert*-butyl-L-tyrosine methyl ester, L-valinecyclohexylamide*, L-valine methyl ester

Set 2
L-alanine *tert*-butyl ester, N^{ω}-4-methoxy-2,3,6-trimethylbenzenesulfonyl-L-arginine, L-asparagine *tert*-butyl ester, O^4-*tert*-butyl-L-aspartic acid *tert*-butyl ester, *S*-trityl-L-cysteine, O^5-*tert*-butyl-L-glutamic acid *tert*-butyl ester, glycine methyl ester, N^{im}-trityl-L-histidine, L-isoleucine *tert*-butyl ester, L-leucine *tert*-butyl ester, N^{ε}-Boc-L-lysine methyl ester, L-methionine methyl ester, L-phenylalanine *tert*-butyl ester, L-proline *tert*-butyl ester, O-*tert*-butyl-L-serine *tert*-butyl ester, O-*tert*-butyl-L-threonine methyl ester, L-tryptophane methyl ester, O-*tert*-butyl-L-tyrosine methyl ester, L-valine *tert*-butyl ester

Scheme 2. Amines (building blocks) used for the synthesis of libraries. Trityl = triphenylmethyl, Boc = *tert*-butoxycarbonyl. The amides marked with a star were synthesized by reaction of the fluorenylmethoxycarbonyl (FMOC) protected amino acid with *p*-methoxybenzylamine, benzylamine, *n*-propylamine, or cyclohexylamine and subsequent cleavage of the FMOC group [4.5].

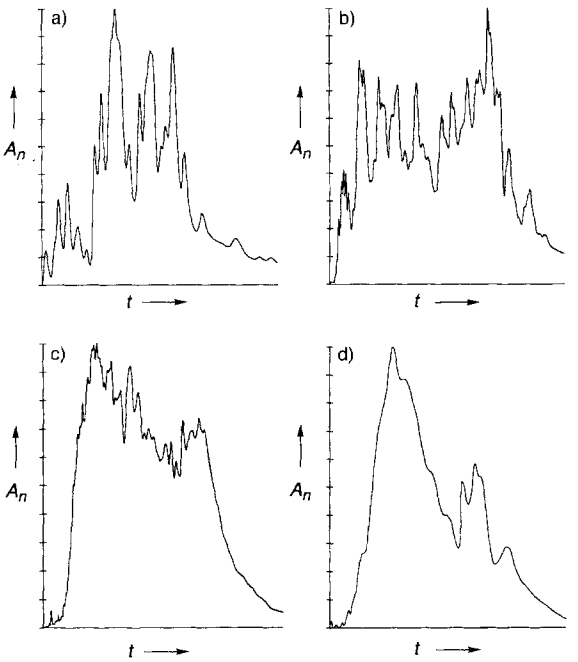


Fig. 2. Analytical HPLC traces (normalized) obtained from libraries of theoretically 136 (a), 1225 (b), 10440 (c), and 97461 compounds (d) [8]. The libraries were constructed with the **2** and 4, 7, 12, or all 21 of the amines listed in Scheme 2, Set 1.

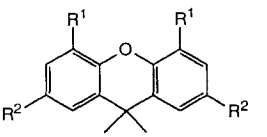
were purified by washing the dichloromethane solution with citric acid and sodium hydrogen carbonate solution to remove any unreacted starting material. By using the xanthene core molecule **2** and 4, 7, 12, or all 21 of the primary amines listed in Scheme 2, Set 1, libraries with increasing complexity were constructed containing theoretically 136, 1225, 10440, and 97461 different compounds, respectively.[6]

Corresponding reactions with the cubane core molecule **3** gave mixtures of fewer compounds (36, 245, 1860, and 16611, respectively), because the diversity of the libraries decreases with increasing symmetry of the core molecule. Even though the reaction products are complex mixtures of different compounds, the described procedure yielded powders which could be conveniently handled. More problematic was the clean conversion of these lipophilic libraries to their water-soluble forms; only the deprotected, water-soluble compounds were useful for later drug screening.

Hydrazinolysis or hydroxyl aminolysis of the methyl esters of the libraries gave the corresponding hydrazides and hydroxyl amides. Subsequent deprotection of the amino acid side chains with a mixture of trifluoroacetic acid, water, phenol, thioanisol, and ethanedithiol (82.5:5:5:5:2.5, reagent K)[7] yielded oils which were only slightly water-soluble. However, deprotection of the libraries constructed with 19 *tert*-butyl ester protected building blocks (Scheme 2, Set 2) with reagent K (4 h, room temperature) and subsequent treatment with diethyl ether/*n*-hexane afforded the libraries in the form of white powders with excellent solubility in water/dimethylsulfoxide (9:1).

We were not only interested in the synthesis of these libraries, but also in the determination of the variety of the compounds present in the libraries. In order to qualitatively determine library diversity, the mixtures containing theoretically 136, 1225, 10440, and 97461 compounds were evaluated by HPLC. The increasingly complex libraries featured increasingly complex HPLC traces (Fig. 2). In the chromatograms of lesser diversity (Fig. 2a, b) multiple peaks are readily observed in the spectra. The chromatogram of theoretically 97461 different compounds, however, contains no well-resolved peaks and tends towards a smooth curve. This is in agreement with the assumption of a much greater variety of compounds in the libraries constructed with 12 and 21 building blocks.

In order to investigate if our reactions between an acid chloride and a mixture of amine building blocks produce the statistical number of compounds expected, we synthesized and investigated smaller representative libraries. The readily accessible xanthenedicarboxylic acid dichloride **4** was used as a truncated core molecule for this purpose (Scheme 3).



2, $R^1 = R^2 = COCl$

a - c

4, $R^1 = COCl$, $R^2 = COOBz$

Scheme 3. Synthesis of **4**. a) Benzyl alcohol, pyridine, 2 h, 20 °C, 75%; b) HBr, CH_2Cl_2, 3 h, 0 °C, 72%; c) $(COCl)_2$, cat. DMF, CH_2Cl_2, 3 h, reflux, 97% [4].

With **4** and a mixture of ten selected building blocks from Scheme 2, Set 2, a representative library containing theoretically 55 compounds was synthesized such that each compound in the library had a distinct molecular weight.[6] This model library was then analyzed for the presence of all theoretically predicted molecules.

An HPLC trace of the library was similar to that obtained from the library with 136 compounds described above. The presence of roughly 40 peaks in the chromatogram hinted that indeed most of the desired compounds were present in the mixture. The model library was then subjected to plasma desorption or fast atom bombardment (FAB) mass spectrometry directly or after separation into various fractions by preparative HPLC.[8] The mass spectra contained nearly exclusively signals in the mass range expected for the molecules in the library, and little fragmentation was observed. In a detailed mass spectroscopic investigation of the 55-compound model library, 75% (42) of

the expected molecular ion peaks were observed, which confirms that a sizable fraction of the theoretically expected 55 compounds are present in the mixture. Further investigation of several representative water-soluble libraries with electrospray mass spectrometry and HPLC mass spectrometry are in progress to fully quantify the diversity of the model libraries.[9] However, the results presented here alone indicate that large and well-defined libraries of small organic molecules with a conformationally restricted, drug-related structure can be generated by condensing a core molecule with a set of primary amines.

In order to determine whether single compounds with interesting biological properties can be obtained from our libraries, we synthesized and screened several highly diverse mixtures using the cubanetetracarboxylic acid tetrachloride **3**, the xanthenetetracarboxylic acid tetrachloride **2**, and the 19 building blocks listed in Scheme 2, Set 2. After deprotection with reagent K and precipitation of the libraries from ether/*n*-hexane, the obtained white powders were screened in a modified trypsin assay for their ability to inhibit the trypsin-catalyzed cleavage of an amide bond.[10, 11] By employing a procedure described in the following communication,[11] we were able to extract from this mixture—in only four weeks of work—a molecule able to inhibit the trypsin-catalyzed reaction. The selection strategy enabled us to rapidly isolate from libraries of tens of thousands of compounds a single compound with the desired biological properties.[10, 11]

Experimental Procedure

General description of the synthesis of diverse libraries: Xanthene-2,4,5,7-tetracarboxylic acid tetrachloride **2** (100 mg, 0.217 mmol), a given mixture of amines (0.88 mmol total), and 5 mL of dichloromethane under argon were treated with 1 mL of triethylamine. The reaction mixture was stirred under argon for 3 h, then diluted with dichloromethane (50 mL) and washed with 1 M citric acid solution (2 × 75 mL) and with saturated sodium hydrogen carbonate solution (1 × 100 mL). The organic phase was dried over $MgSO_4$ and concentrated to afford a tan oil, which formed a tan foam in vacuo. The protecting groups were removed by stirring with reagent K [7] at room temperature for 4 h (reagent K: trifluoroacetic acid, water, phenol, thioanisol, and ethanedithiol 82.5:5:5:5:2.5). The solution was concentrated in vacuo and the libraries precipitated by adding cold diethyl ether and *n*-hexane. The white precipitate was filtered off, washed five times with cold diethyl ether, and dried in vacuo.

Received: February 15, 1994
Revised version: May 24, 1994 [Z6696IE]
German version: *Angew. Chem.* **1994**, *106*, 2159

[1] Different methodologies have been introduced for the parallel syntheses of peptides. For examples see: H. M. Geysen, R. M. Meloen, S. J. Barteling, *Proc. Natl. Acad. Sci. USA* **1984**, *81*, 3998–4002; R. A. Houghton *ibid.* **1985**, *82*, 5131–5135; S. P. A. Fodor, J. L. Read, M. C. Pirrung, L. Stryer, A. T. Lu, D. Solas, *Science* **1991**, *251*, 767–773. For reviews see: G. Jung, A. G. Beck-Sickinger, *Angew. Chem.* **1992**, *104*, 375–391.; *Angew. Chem. Int. Ed. Engl.* **1992**, *31*, 367–383; M. R. Pavia, T. K. Sawyer, W. H. Moos, *Bioorg. Med. Chem. Lett.* **1993**, *3*, 387–396.

[2] A. Furka, F. Sebestyén, M. Asgedom, G. Dibó, *Int. J. Pept. Protein Res.* **1991**, *37*, 487–493; K. S. Lam, S. E. Salmon, E. M. Hersh, V. J. Hruby, W. M. Kazmierski, R. J. Knapp, *Nature* **1991**, *354*, 82–84.

[3] A. Bashir-Hashemi, *Angew. Chem.* **1993**, *105*, 585–586; *Angew. Chem. Int. Ed. Engl.* **1993**, *32*, 612–613.

[4] All new compounds were fully characterized. A detailed description of the syntheses will be given elsewhere.

[5] For a general description of protection strategies in peptide synthesis see: M. Bodanszky, *Principles of Peptide Synthesis*, Springer, Berlin, **1984**.

[6] A computer program was developed to calculate the possible combinations of building blocks on a core molecule, the theoretical number of different compounds, their molecular weights, and the corresponding combinations of building blocks.

[7] D. King, C. Fields, G. Fields, *Int. J. Pept. Prot. Res.* **1990**, *36*, 255–266.

[8] Analytical HPLC chromatography was conducted on a Waters 600I system with a Waters 490I UV detector and an Ultrasphere SI column (4.6 mm × 25 cm, 80 Å, 5 μm) at a flow rate of 1.5 mL min^{-1}. The gradient used was twofold: 0% to 100% B in 30 min to 100% C in 15 min (A: hexane; B: ethyl acetate; C: ethyl acetate/methanol 94:6). For the preparative separations a NOVA PAK HR silica column (19 mm × 30 cm, 68 Å, 5 μm) and a flow rate of 3.0 mL min^{-1} were employed.

[9] For an investigation of an oligopeptide library with ion-spray mass spectrometry and HPLC mass spectrometry see: J. W. Metzger, K.-H. Wiesmüller, V. Gnau, J. Brünges, G. Jung, *Angew. Chem.* **1993**, *105*, 901–930; *Angew. Chem. Int. Ed. Engl.* **1993**, *32*, 894–896.

[10] For the isolation of a trypsin inhibitor through screening of a synthetic combinatorial library of peptides see: J. Eichler, R. A. Houghton, *Biochemistry*, **1993**, *32*, 11035–11041.

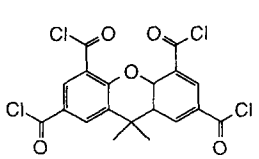
[11] T. Carell, E. A. Wintner, J. Rebek, Jr., *Angew. Chem.* **1994**, *106*, 2162; *Angew. Chem. Int. Ed. Engl.* **1994**, *33*, 2061–2064.

A Solution-Phase Screening Procedure for the Isolation of Active Compounds from a Library of Molecules**

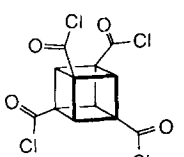
Thomas Carell, Edward A. Wintner, and Julius Rebek, Jr.*

In the preceding communication[1] we described an approach to molecular diversity that produces structurally biased libraries of small molecules in solution. As these libraries are synthesized as complex mixtures, this approach runs counter to the traditional teachings of synthetic organic chemistry in which single compounds of high purity are the goal. Because the new approach uses neither coding schemes[2] nor spatially isolated molecules,[3] conventional methods for screening and amplification are not applicable.[4] Accordingly, we have developed a solution-phase selection procedure for use with these mixtures, and we report here our initial findings.

All of the libraries were constructed by following a two-step procedure.[1] In the first step, a core molecule such as xanthene tetracarboxylic acid tetrachloride **1** or cubane tetracarboxylic acid tetrachloride **2** was condensed with a mixture of 19 protect-



1



2

ed L-amino acids designated as building blocks.[5] The diversity of compounds obtained in this reaction is determined by the number of building blocks used and by the symmetry of the core molecule. With 19 building blocks and xanthene **1**, 65 341 different variants are theoretically produced. By using cubane **2** with its higher symmetry, only 11 191 possible compounds are generated from the same set of building blocks. In the second step, the generated libraries were treated with a trifluoroacetic acid based reagent to remove acid-labile protection groups present on certain building blocks. After precipitation with diethyl ether/*n*-hexane, the mixtures were obtained in the form of white powders with sufficient solubility in a 9:1 mixture of water/dimethylsulfoxide (DMSO) for enzymatic studies.[1]

[*] Prof. J. Rebek, Jr., Dr. T. Carell, E. A. Wintner, Dr. A. J. Sutherland
Department of Chemistry, Massachusetts Institute of Technology
Cambridge, MA 02139 (USA)
Telefax: Int code + (617)253-7929

[**] This work was supported by the National Institutes of Health, the Alexander von Humboldt Foundation (Feodor-Lynen fellowship to T. C.), and the National Science Foundation (predoctoral fellowship to E. A. W.). We thank Prof. J. Stubbe for advice regarding the enzyme assay and Dr. A. J. Sutherland for corroborating several assay experiments.

The screening procedure was based on a trypsin assay as performed by Houghten et al. on peptide mixtures.[6] Our goal was to identify a compound within the library able to inhibit the trypsin-catalyzed hydrolysis of the amide bond in N^{α}-benzoyl-D,L-arginine-*p*-nitroanilide (BAPA). In the assays, the activity of the inhibitor was correlated inversely to the rate of *p*-nitroaniline released by the enzyme. The results of adding various libraries to the trypsin assay are shown in Figure 1.

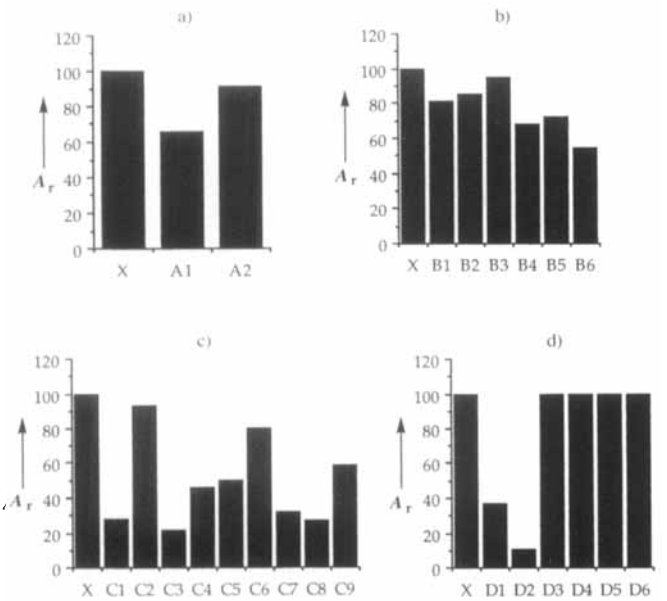


Fig. 1. Trypsin activity A_r in the presence of added libraries relative to that of a blank (X, $A_r = 100\%$) containing no added library material. Each bar represents average trypsin activity for four measurements. a) Trypsin activity [%] with the initial libraries A1 and A2 (in each case 2.5 mg in 50 mL of DMSO) constructed from the core molecules **1** and **2**, respectively, and 19 amino acid building blocks [1,5]. b) Trypsin activity [%] with the six sublibraries B1–B6 (in each case 2.5 mg in 50 mL of DMSO) constructed from core molecule **1** and 15 of the 19 amino acid building blocks (without *S*-Trt-Cys). B1: group G1 omitted; B2: group G2 omitted; B3: group G3 omitted; B4: group G4 omitted. B5: group G5 omitted. B6: Group G6 omitted. Groups G1–G6 are listed in Table 1. c) Trypsin activity [%] with the nine sublibraries C1–C9 (in each case 1.5 mg in 50 mL of DMSO) constructed from the core molecule **1** and eight of the nine building blocks from the amino acids in groups G1–G3 (Table 1). C1: Arg omitted; C2: Lys omitted; C3: His omitted; C4: Leu omitted; C5: Ile omitted; C6: Pro omitted; C7: Gly omitted; C8: Ala omitted; C9: Val omitted. d) Trypsin activity [%] with the six sublibraries D1–D6 (in each case 0.5 mg in 50 mL of DMSO). For a description of their compositions see text and Table 2.

Plot a in Figure 1 depicts the screening results obtained from the initial libraries (A1 and A2) generated from the core molecules **1** and **2** and the 19 protected amino acids.[5] Even though both libraries were constructed with the same set of building blocks, only library A1 caused a significant reduction of trypsin activity (approximately 30%). The fact that library A2, based on the cubane core molecule **2**, does not interfere substantially with enzyme reaction (activity 91%) suggests that merely the presence of certain functional groups is not enough to produce a trypsin inhibitor. Rather, the orientation and arrangement of these functional groups with respect to each other and the (relatively rigid) core molecule are also important.

In order to determine which of the 19 building blocks are essential for an active xanthene library, three further screening procedures were carried out.

The first experiment was developed to reduce the number of potentially active building blocks from 19 to 9. We divided the building blocks (without *S*-Trt-Cys) into six groups, G1–G6 (Table 1). Each group contained three building blocks with related side chains. Six sublibraries B1–B6 were then synthesized by using the xanthene core molecule **1** and five of the six building block groups G1–G6. The screening results from each sublibrary (plot b, Fig. 1) indicate that when certain amino acid groups were omitted from the set of 19, the ability of the library to inhibit the trypsin reaction was reduced. By ranking the activity of each sublibrary, the importance of the omitted group of amino acids could be ascertained. Sublibraries B1–B3, which do not contain the amino acids in groups G1–G3, showed highest trypsin activity. Therefore the nine amino acids in groups G1–G3 showed the greatest inhibitory activity in the context of the xanthene skeleton. Only these nine amino acids were examined in the second screening step.

Table 1. The building blocks in groups G1–G6; see [5] for protecting groups used.

G1	G2	G3	G4	G5	G6
Gly	Leu	Arg	Ser	Phe	Glu
Ala	Ile	Lys	Thr	Tyr	Asp
Val	Pro	His	Met	Trp	Asn

The second experiment reduced the number of potentially active building blocks from nine to five. Nine sublibraries (C1–C9) of eight building blocks each were synthesized with sequential omission of one of the nine protected amino acids. The screening results obtained from these nine sublibraries (plot c, Fig. 1) indicate that the sublibraries created without the building blocks N^{ε}-Boc-Lys-OMe, Leu-O*t*Bu, Ile-O*t*Bu, Pro-O*t*Bu, or Val-O*t*Bu (C2, C4, C5, C6, and C9, respectively) resulted in very high trypsin activities; they did not contain potent trypsin inhibitors. These five building blocks were therefore deduced to be the substituents predominantly responsible for the generation of inhibitors.

In the third round of screening, sublibraries were generated from the xanthene core molecule and mixtures of three or four of the five building blocks N^{ε}-Boc-Lys-OMe, Leu-O*t*Bu, Ile-O*t*Bu, Pro-O*t*Bu, and Val-O*t*Bu. Trypsin assays with these sublibraries confirmed the results of plot c, and showed that the highest inhibitory activity resulted from a library constructed of **1** and N^{ε}-Boc-Lys-OMe, Ile-O*t*Bu, Pro-O*t*Bu, and Val-O*t*Bu. Omission of any one of these four building blocks gave libraries with significantly reduced inhibitory activity.[7]

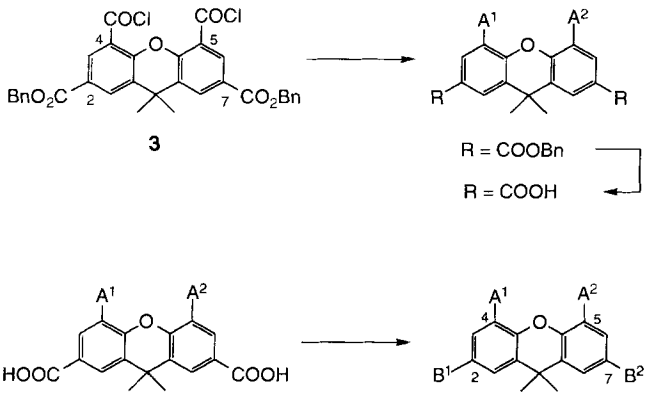
We were aided by the fact that with each round of screening, the sublibraries became less complex. The relative concentration of each compound increases as sublibraries become smaller, and since only active sublibraries are selected, the net effect is an "amplification" of the concentration of active compound(s) relative to inactive compounds. As activities of successive screening rounds become more pronounced, the sublibraries become ever easier to assay.

Thus, after only three rounds of screening, we were left with the 12 structural isomers of the Lys-Ile-Pro-Val-xanthene derivative. To determine the structure of the most potent molecule among the isomers, six more sublibraries (D1–D6, Table 2) were generated following the two-step synthetic procedure outlined schematically in Scheme 1.

For each sublibrary, the dibenzyl ester protected xanthene dicarboxylic acid dichloride **3**[1] was first reacted with only two of the four building blocks N^{ε}-Boc-Lys-OMe, Ile-O*t*Bu, Pro-O*t*Bu, Val-O*t*Bu. Debenzylation by hydrogenation of the resulting three-compound mixtures (H_2; 10% Pd/C; ethyl acetate/ethanol 9:1) followed by reaction with the other two building

Table 2. List of the amino acids attached to xanthene positions 4 and 5 (A^1, A^2), and positions 2 and 7 (B^1, B^2) in the generation of sub-libraries D1–D6.

Sublibrary	A^1,A^2	B^1,B^2
D1	Lys, Val	Ile, Pro
D2	Lys, Ile	Val, Pro
D3	Lys, Pro	Ile, Val
D4	Val, Ile	Lys, Pro
D5	Val, Pro	Lys, Ile
D6	Ile, Pro	Lys, Pro



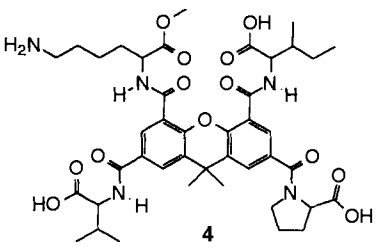
Scheme 1. Synthesis of the sublibraries D1–D6 (see Table 2 for A^1, A^2, B^1, B^2).

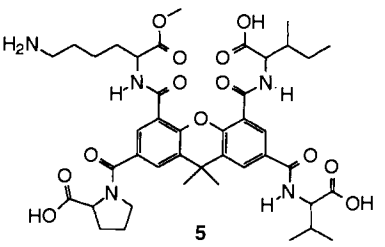
blocks (1*H*-benzotriazol-1-olato-*O*)tris(*N*-methylmethanaminato)phosphorus hexafluorophosphate (BOP), dimethylformamide (DMF), triethylamine (TEA) gave in each case a mixture of ten compounds. After cleavage of the acid-labile protection groups, the six sublibraries D1–D6 were obtained, each with a unique distribution of products. The amino acids and their positions on the core molecule are listed in Table 2.

The screening results obtained from these sublibraries (plot d, Fig. 1) indicate that only those mixtures in which the 4- and 5-positions were substituted with Lys/Val or Lys/Ile combinations contained inhibitory compounds (sublibraries D1 and D2, respectively). The most active mixture was D2; D1 was slightly less active. In contrast, sublibrary D3, which contained only compounds in which the 4- and 5-positions were substituted with Lys/Pro, showed no inhibitory activity. All three sublibraries in which the Lys building block was attached at positions 2 or 7 were inactive as well (sublibraries D4–D6). These results narrowed down the most potent inhibitor to **4** and **5**.

Compounds **4** and **5** were synthesized, and their activities were determined.[9] Despite their structural similarities, compound **4** is significantly more active than its structural isomer **5**. Compound **4** is a competitive inhibitor for trypsin ($K_i = 9 \pm 2 \times 10^{-6}$ M). Further investigations are underway to clarify the interaction of **4** with trypsin.

It must be noted that compound **4** is clearly not the only inhibitory compound present in the original library A1. The described screening procedure guided us to a set of structurally related molecules of which **4** was the most potent inhibitor. But this set may or may not include the most effective inhibitor from the given library with 19 building blocks. We are currently examining libraries in which certain substituents of **4** remain constant while others are "randomized" with various sets of the original 19 building blocks. This should allow us to jump from one set of active compounds to the next. By using this strategy we hope to determine the effectiveness of our present screening procedure in selecting the most potent inhibitor from the 65341 compounds in library A1.





Nevertheless, by applying our simple iterative screening procedure, we were able to isolate the single compound **4**, a nonlinear peptide inhibitor with a micromolar inhibition of trypsin, from a complex library of small organic molecules in solution in a few weeks. This result suggests that the synthesis and screening of molecular libraries from a core molecule and a variety of building blocks[1] is a useful means of exploring the structural landscape of small molecules and can complement the existing repertoire of methodologies for finding suitable lead compounds for pharmaceuticals. Furthermore, while this study used readily available protected L-amino acids and only two types of core molecules, any nucleophile leading to products of reasonable hydrolytic stability can be used with these or other core molecules. The potential variety of new libraries offered by this method is clearly limitless.

Received: June 16, 1994 [Z 7041 IE]
German version: *Angew. Chem.* **1994**, *106*, 2162

[1] T. Carell, E. A. Wintner, A. Bashir-Hashemi, J. Rebek, Jr., *Angew. Chem.* **1994**, *106*, 2159–2161; *Angew. Chem. Int. Ed. Engl.* **1994**, *33*, 2059–2061

[2] S. Brenner, R. A. Lerner, *Proc. Natl. Acad. Sci. USA* **1992**, *89*, 5381–5383; A. Borchardt, W. C. Still, *J. Am. Chem. Soc.* **1994**, *116*, 373–374; J. Nielsen, S. Brenner, K. D. Janda, *ibid.* **1993**, *115*, 9812–9813; J. M. Kerr, S. C. Banville, R. N. Zuckermann, *ibid.* **1993**, *115*, 2529–2530; M. H. J. Ohlmeyer, R. N. Swanson, L. W. Dillard, J. C. Reader, G. Asouline, R. Kobayashi, M. Wigler, C. Still, *Proc. Natl. Acad. Sci. USA* **1993**, *90*, 10922.

[3] H. M. Geysen, R. H. Meloen, S. J. Barteling, *Proc. Natl. Acad. Sci. USA* **1984**, *81*, 3998–4002; R. A. Houghten, *ibid.* **1985**, *82*, 5131–5135; S. P. A. Fodor, J. L. Read, M. C. Pirrung, L. Stryer, A. T. Lu, D. Solas, *Science* **1991**, *251*, 767–773; A. Furka, F. Sebastyen, M. Asgedom, G. Dibo, *Int. J. Pept. Protein Res.* **1991**, *37*, 487–493. For reviews see: G. Jung, A. Beck-Sickinger, *Angew. Chem.* **1992**, *104*, 375–391; *Angew. Chem. Int. Ed Engl.* **1992**, *31*, 367–383; M. R. Pavia, T. K. Sawyer, W. H. Moos, *Bioorg. Med. Chem. Lett.* **1993**, *3*, 387–386.

[4] For some solution-phase screening procedures for peptide libraries generated on a solid support with methods described above, see: A. M. Bray, N. J. Maeji, H. M. Geysen, *Tetrahedron Lett.* **1990**, *31*, 5811–5814; R. A. Houghten, C. Pinilla, S. E. Blondelle, J. R. Appel, C. T. Dooley, J. H. Cuervo, *Nature* **1991**, *354*, 84–86. C. Pinilla, J. R. Appel, P. Blanc, R. A. Houghten, *BioTechniques* **1992**, *13*, 901–905.

[5] Building blocks employed: L-alanine *tert*-butyl ester, N^{ω}-(4-methoxy-2,3,6-trimethylbenzenesulfonyl)-L-arginine, L-asparagine *tert*-butyl ester, O^4-β-*tert*-butyl-L-aspartic acid *tert*-butyl ester, *S*-trityl-L-cysteine, O^5-*tert*-butyl-L-glutamic acid *tert*-butyl ester, glycine methyl ester, N^{im}-trityl-L-histidine, L-isoleucine *tert*-butyl ester, L-leucine *tert*-butyl ester, N^{ε}-Boc-L-lysine methyl ester, L-methionine methyl ester, L-phenylalanine *tert*-butyl ester, L-proline *tert*-butyl ester, *O*-*tert*-butyl-L-serine *tert*-butyl ester, *O*-*tert*-butyl-L-threonine methyl ester, L-tryptophane methyl ester, *O*-*tert*-butyl-L-tyrosine methyl ester, L-valine *tert*-butyl ester. Trityl (Trt) = triphenylmethyl, Boc = *tert*-butoxycarbonyl. For a general desccription of pretection strategies in peptide chemistry see: M. Bodansky, *Principles of Peptide Synthesis*, Springer Verlag, New York, **1984**.

[6] J. Eichler, R. A. Houghten, *Biochemistry* **1993**, *32*, 11035–11041; C. Pinilla, J. R. Appel, P. Blanc, R. A. Houghten, *BioTechniques* **1992**, *13*, 901–905;

R. A. Houghten, C. Pinilla, S. E. Blondelle, J. R. Appel, C. T. Dooley, J. H. Cuervo *Nature*, **1991**, *354*, 84–86. For other trypsin assays, see: B. F. Erlanger, N. Kokowsky, W. Cohen, *Arch. Biochem. Biophys.* **1961**, *95*, 271–278. H. F. Gaertner, A. J. Puigserver, *Enzyme Microb. Technol.* **1992**, *14*, 150–155.

[7] T. Carell, J. Rebek, Jr., unpublished results.

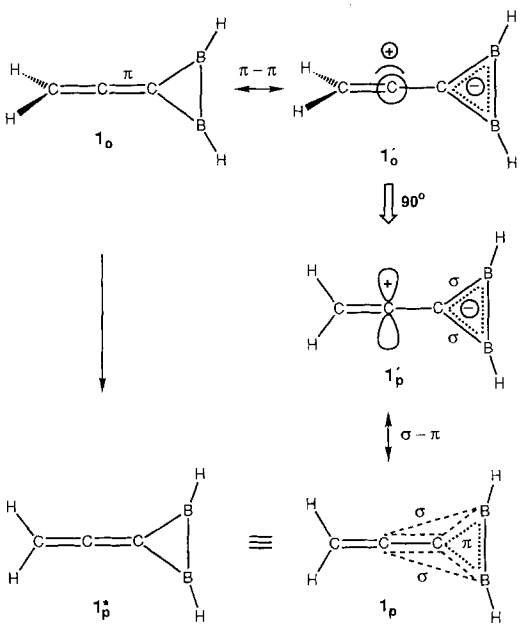
[8] M. Laskowski, Jr., I. Kato, *Ann. Rev. Biochem.* **1980**, *49*, 593–626.

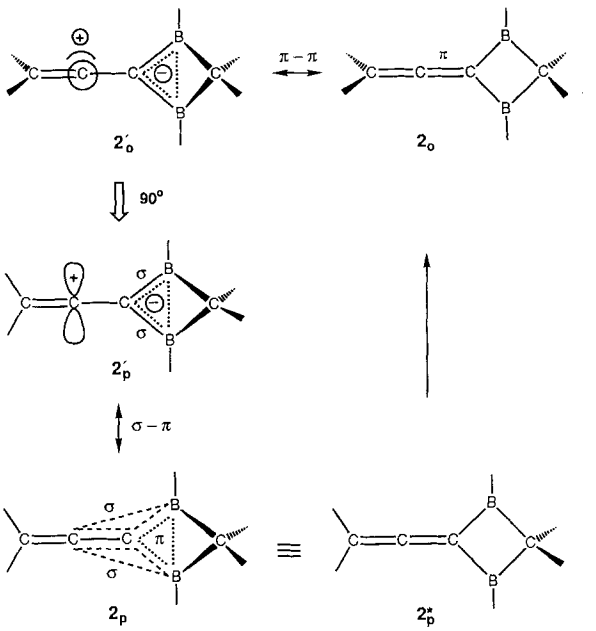
[9] Both compounds were fully characterized. A detailed description of their synthesis and characterization will be described elsewhere. Compound **3** was reacted first with N^{ε}-Boc-Lys-OMe and Ile-O*t*Bu (at positions 4 and 5), and the compound in which A^1 = Lys and A^2 = Ile was isolated through chromatography. Subsequent debenzylation and reaction of the resulting dicarboxylic acid with Pro-O*t*Bu and Val-O*t*Bu (at positions 2 and 7) gave four compounds from which the two isomers (A^1 = Lys, A^2 = Ile, B^1 = Val, B^2 = Pro and A^1 = Lys, A^2 = Ile, B^1 = Pro, B^2 = Val) were obtained individually by chromatography. Deprotection with trifluoroacetic acid and purification by reversed-phase preparative HPLC gave **4** and **5** as white powders. All analytical data (NMR, COSY, NOE, MS) are in agreement with the proposed structures. Initial experiments indicate that **4** is a specific trypsin inhibitor; **4** does not inhibit the activity of thrombin, a related serine protease, to any noticeable extent.

Nonclassical Stabilization of Planar Allenes: Low Rotational Barriers for Allene Double Bonds**

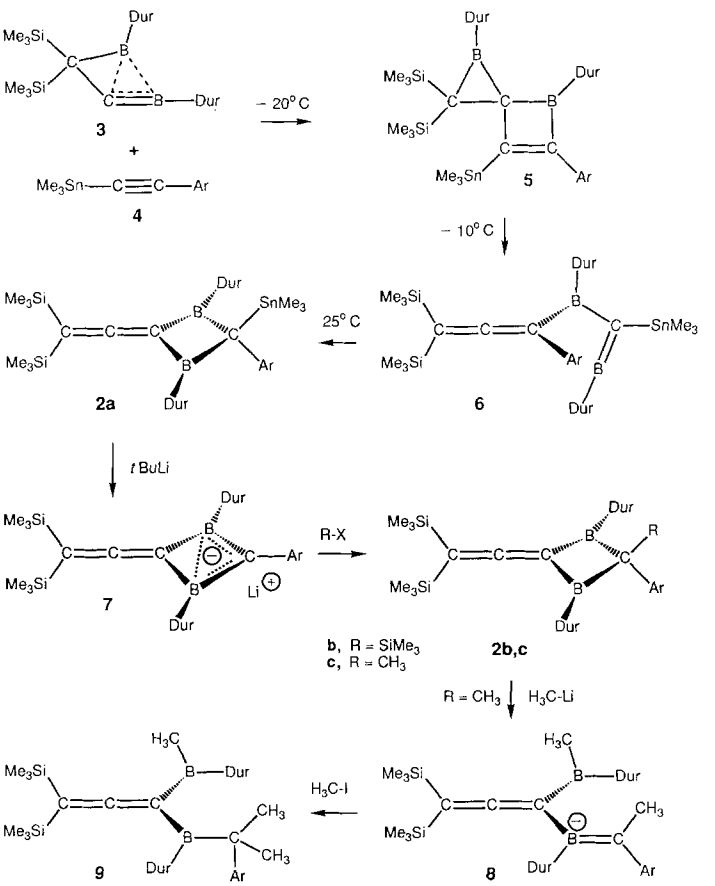
Dirk Steiner, Heinz-Jürgen Winkler, Sigrid Wočadlo, Stefan Fau, Werner Massa, Gernot Frenking, and Armin Berndt*

According to MP2/4-31G calculations of Schleyer et al.,[1] the orthogonal allene $\mathbf{1}_o$ is 11.6 kcal mol^{-1} higher in energy than the planar allene $\mathbf{1}_p$, which is misleadingly described by the classical formula $\mathbf{1}_p^*$. Polarization of the C–C double bonds adjacent to the boron atoms leads to the stabilization of the negative charge in the 2π-electron arene diboriranide[2] (resonance structure $\mathbf{1}_o'$). The positive charge of the formal vinyl cation can, however, only be stabilized through C–B hyperconjugation with the strained C–B σ bonds[2, 3] of the three-membered ring after





rotation around the polarized double bond. Optimum stabilization is achieved in planar $\mathbf{1}_p'$. These nonclassical interactions in $\mathbf{1}_p$ are adequately described by 3c–2e bonds.[2] We report here on the classical orthogonal allenes $\mathbf{2}_o$, which are related to **1** and have remarkably low barriers to rotation around C–C double bonds. This can be explained by the formation of planar, nonclassical allenes $\mathbf{2}_p$ in the transition state, which are stabilized as described above; the 2π-electron arene diboriranide in **1** has now been replaced by the 2π-electron arene homodiboriranide[4] in **2**.



[*] Prof. Dr. A. Berndt, Dipl.-Chem. D. Steiner, Dipl.-Chem. H.-J. Winkler, S. Wočadlo, S. Fau, Prof. Dr. W. Massa, Prof. Dr. G. Frenking
Fachbereich Chemie der Universität
D-35032 Marburg (FRG)
Telefax: Int. code +(6421) 28 89 17

[**] This work was supported by the Deutsche Forschungsgemeinschaft and the Fonds der Chemischen Industrie.

The methyleneborane **3** (Dur = 2,3,5,6-tetramethylphenyl, Ar = 3,5-di-*tert*-butylphenyl)[2] added to alkyne **4** at −20 °C to form **5**, which isomerized at −10 °C to **6**.[5] Rearrangement of **6** at 25 °C gave the allene **2a**. The aryl group, which was linked to an allene C atom in **6**, is now bound to the C atom between both B atoms in **2a**. The allene **2a** could be transformed by tin/lithium exchange with *t*BuLi to the lithium compound **7**, which gave the allenes **2b** and **2c** on treatment with chlorotrimethylsilane (X = Cl) and methyl iodide (X = I), respectively. The 1,1-diborylallene **9** was prepared for the purpose of comparison from **2c** via **8** by treatment with methyllithium and then methyl iodide. The structures of **2a**–**c**, **5**, **6**, and **9** were deduced from their NMR spectra (Table 1); those of **2a** and **2c** were confirmed by crystal structure analysis (Fig. 1, Table 2).[6]

The signal at $\delta = 85$ in the ^{11}B NMR spectrum of **9** lies in the region associated with boron atoms that are not in conjugation with π donors: due to mutual steric hindrance, the boryl substituents are twisted in such a way that the empty p orbitals of the boron atoms cannot interact with the π electrons of the allene. The signal at $\delta = 74$ in the ^{11}B NMR spectrum of **2c** indicates π delocalization as shown in **2′$_o$**; this is also reflected in the relatively long C2–C3 bond and in the shortened C2–B1 and C2–B2 bonds with respect to **2a** (see Table 2). The π delocalization corresponding to **2′$_o$** is less important in **2a** because C–Sn hyperconjugation reduces the electron deficiency at the boron atoms. This results in a long C1–Sn bond (224 compared with 212–214 pm for the Sn–CH_3 bonds), small B-C-Sn and Sn-C-C(aryl) angles, short C1–B1 and C1–B2 bonds, and shielding of the boron atoms ($\delta(^{11}B) = 63$). The geminal trimethylsilyl groups in **2a**–**c** give rise to two signals in the ^{1}H NMR spectrum only below 300, 263, and 173 K, respectively. These signals broaden at higher temperatures and coalesce at

Table 1. Selected physical data for compounds **2a**–**c**, **5**, **6**, and **9**.

2a: yellow crystals, m.p. 128 °C, yield 60%. – ^{1}H NMR (500 MHz, [D$_8$]toluene, −40 °C): δ = 0.15, 0.34 (2× br.s, 2× 9H, Si(CH$_3$)$_3$), 0.35 (br.s, 9H, Sn(CH$_3$)$_3$), 1.14 (s, 18H, C(CH$_3$)$_3$), 2.06, 2.18, 2.26, 2.52 (4× s, 4× 6H, *o*- and *m*-CH$_3$), 6.83 (s, 2H, *p*-H(Dur)), 7.16 (d, 2H, *o*-H(Ar)), 7.19 (t, 1H, *p*-H(Ar)); ^{13}C NMR (75 MHz, CDCl$_3$, 25 °C): δ = −3.5 (q, 3C, Sn(CH$_3$)$_3$), 0.7, 1.4 (2× br.q, 2× 3C, Si(CH$_3$)$_3$), 19.4, 19.5, 19.6, 20.4 (4× q, 4× 2C, *o*- and *m*-CH$_3$), 31.1 (q, 6C, C(CH$_3$)$_3$), 34.3 (s, 2C, *C*(CH$_3$)$_3$), 70.1 (s, 1C, CSi$_2$), 81.1 (s, 1C, sp^3-CB$_2$), 92.2 (s, 1C, sp^2-CB$_2$), 117.3 (d, 1C, *p*-C(Ar)), 122.9 (d, 2C, *o*-C(Ar)), 130.7 (d, 2C, *p*-C(Dur)), 132.6, 132.8, 133.6, 133.8 (4× s, 4× 2C, *o*- and *m*-C(Dur)), 141.6 (s, 1C, *i*-C(Ar)), 142.7 (br.s, 2C, *i*-C(Dur)), 149.1 (s, 2C, *m*-C(Ar)), 199.7 (s, 1C, C=*C*=C); ^{11}B NMR (96 MHz, CDCl$_3$, 25 °C): δ = 63.

2b: yellow crystals, m.p. 137 °C, yield 81%. – ^{1}H NMR (500 MHz, CDCl$_3$, −40 °C): δ = −0.23, 0.18 (2× s, 2× 9H, sp^2-CSi(CH$_3$)$_3$), 0.06 (s, 9H, sp^3-CSi(CH$_3$)$_3$), 1.04 (s, 18H, C(CH$_3$)$_3$), 1.74, 2.06, 2.25, 2.41 (4× s, 4× 6H, *o*- and *m*-CH$_3$), 6.75 (d, 2H, *o*-H(Ar)), 6.89 (m, 3H, *p*-H(Ar) and *p*-H(Dur)); ^{13}C NMR (100 MHz, CDCl$_3$, −30 °C): δ = 0.6, 1.5 (2× q, 2× 3C, sp^2-CSi(*C*H$_3$)$_3$), 2.4 (q, 3C, sp^3-CSi(*C*H$_3$)$_3$), 19.8, 20.0, 21.2 (3× q, total 8C, *o*- and *m*-CH$_3$), 31.0 (q, 6C, C(*C*H$_3$)$_3$), 34.3 (s, 2C, *C*(CH$_3$)$_3$), 70.2 (s, 1C, CSi$_2$), 77.6 (s, 1C, sp^3-CB$_2$), 96.5 (br.s, 1C, sp^2-CB$_2$), 116.6 (d, 1C, *p*-C(Ar)), 124.3 (d, 2C, *o*-C(Ar)), 130.5 (d, 2C, *p*-C(Dur)), 132.7, 132.9, 133.6, 133.8 (4× s, 4× 2C, *o*- and *m*-C(Dur)), 142.4 (s, 1C, *i*-C(Ar)), 142.9 (s, 2C, *i*-C(Dur)), 148.0 (s, 2C, *m*-C(Ar)), 198.4 (s, 1C, C=*C*=C); ^{11}B NMR (96 MHz, CDCl$_3$, 25 °C): δ = 67.

2c: yellow crystals, m.p. 157 °C, yield 63%. – ^{1}H NMR (400 MHz, CD$_2$Cl$_2$, −100 °C): δ = 0.04, 0.26 (2× s, 2× 9H, Si(CH$_3$)$_3$), 1.04 (s, 18H, C(CH$_3$)$_3$), 1.29 (s, 3H, B$_2$CCH$_3$), 1.75, 2.11, 2.25, 2.40 (4× s, 4× 6H, *o*- and *m*-CH$_3$), 6.84 (s, 2H, *p*-H(Dur)), 6.91 (d, 2H, *o*-H(Ar)), 7.03 (t, 1H, *p*-H(Ar)); ^{13}C NMR (75 MHz, CDCl$_3$, 25 °C): δ = 1.1 (6C, Si(CH$_3$)$_3$), 19.5, 19.9 (8C, *o*- and *m*-CH$_3$), 31.2 (6C, C(*C*H$_3$)$_3$), 31.7 (1C, B$_2$*C*CH$_3$), 34.5 (2C, *C*(CH$_3$)$_3$), 52.9 (1C, sp^3-CB$_2$), 70.7 (1C, CSi$_2$), 97.4 (1C, sp^2-CB$_2$), 117.7 (1C, *p*-C(Ar)), 122.6 (2C, *o*-C(Ar)), 130.7 (2C, *p*-C(Dur)), 132.8, 133.4 (2× 4C, *o*- and *m*-C(Dur)), 143.4 (2C, *i*-C(Dur)), 147.3 (1C, *i*-C(Ar)), 149.8 (2C, *m*-C(Ar)), 200.0 (1C, C=*C*=C); ^{11}B NMR (96 MHz, CDCl$_3$, 25 °C): δ = 74.

5: ^{13}C NMR (125 MHz, CDCl$_3$, −40 °C): δ = −9.9 (3C, Sn(CH$_3$)$_3$), 2.6, 2.3 (je 3C, Si(CH$_3$)$_3$), 28.7 (1C, CSi$_2$), 55.7 (^2J(Sn,^{13}C) = 62.8 Hz, 1C, CB$_2$), 167.8 (^1J(Sn,^{13}C) = 383.6 Hz, 1C, C=*C*Sn(CH$_3$)$_3$), 179.6 (1C, *C*=CSn(CH$_3$)$_3$); the other signals could not be assigned due to the overlap with signals from the starting material and product **6**.

6: ^{13}C NMR (100 MHz, CDCl$_3$, −20 °C): δ = −6.1 (q, 3C, Sn(CH$_3$)$_3$), 0.4 (q, 6C, Si(CH$_3$)$_3$), 19.5, 19.7, 20.7, 21.0 (4× q, 4× 2C, *o*- and *m*-CH$_3$), 31.1 (q, 6C, C(*C*H$_3$)$_3$), 34.4 (s, 2C, *C*(CH$_3$)$_3$), 78.0 (br.s, ^1J(Sn,^{13}C = 46.5 Hz, 1C, CB$_2$), 78.9 (s, 1C, CSi$_2$), 99.1 (s, 1C, C=*C*B), 119.4 (d, 1C, *p*-C(Ar)), 123.4 (d, 2C, *o*-C(Ar)), 128.9 (br.s, 1C, *i*-C(Dur)), 128.8 (d, 1C, *p*-C(Dur)), 132.1, 132.3, 133.0 (3× s, total of 8C, *o*- and *m*-C(Dur)), 135.8 (d, 1C, *p*-C(Dur)), 141.6 (s, 1C, *i*-C(Ar)), 142.9 (d, 2C, *o*-C(Dur)), 148.3 (br.s, 1C, *i*-C(Dur)), 149.1 (s, 2C, *m*-C(Ar)), 211.5 (s, 1C, C=*C*=C).

9: yellow crystals, m.p. 179 °C, yield 73%. – ^{1}H NMR (300 MHz, CDCl$_3$, 25 °C): δ = 0.25 (s, 18H, Si(CH$_3$)$_3$), 0.91 (s, 3H, H$_3$CB), 1.12 (s, 18H, C(CH$_3$)$_3$), 1.55, 1.77, 1.79, 1.97 (4× s, total 30H, CH$_3$(Dur) and ArC(CH$_3$)$_2$), 6.38, 6.55 (2× s, 2× 1H, *p*-H(Dur)), 6.82 (d, 2H, *o*-H(Ar)), 6.94 (t, 1H, *p*-H(Ar)); ^{13}C NMR (75 MHz, CDCl$_3$, 25 °C): δ = 1.2 (q, 6C, Si(CH$_3$)$_3$), 13.9 (q, 1C, H$_3$CB), 18.8, 18.9, 19.6, 21.1 (4× q, 4× 2C, *o*- and *m*-CH$_3$), 28.1 (q, 2C, ArC(CH$_3$)$_2$), 31.3 (q, 6C, C(CH$_3$)$_3$), 34.6 (s, 2C, *C*(CH$_3$)$_3$), 40.1 (s, 1C, Ar*C*(CH$_3$)$_2$), 72.6 (s, 1C, CSi$_2$), 91.2 (br.s, 1C, CB$_2$), 118.1 (d, 1C, *p*-C(Ar)), 121.5 (d, 2C, *o*-C(Ar)), 129.3, 129.4 (2× d, 2× 1C, *p*-C(Dur)), 130.3, 130.8, 131.7, 132.0 (4× s, 4× 2C, *o*- and *m*-C(Dur)), 147.7 (s, 2C, *m*-C(Ar)), 147.8, 149.3 (2× br.s, 2× 1C, *i*-C(Dur)), 149.8 (s, 1C, *i*-C(Ar)), 212.6 (s, 1C, C=*C*=C); ^{11}B NMR (96 MHz, CDCl$_3$, 25 °C): δ = 85.

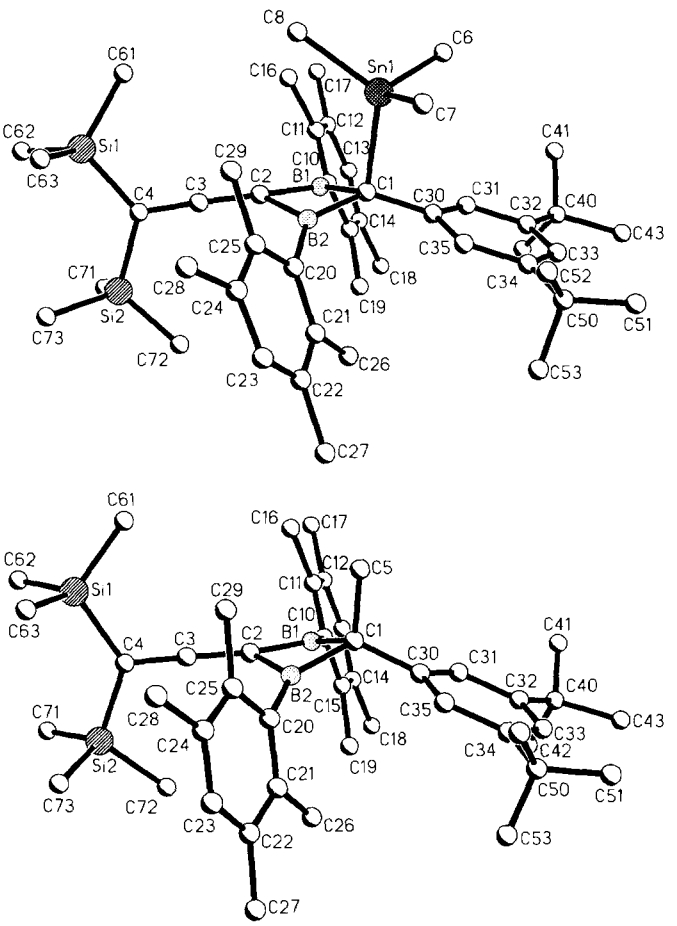


Fig. 1. Crystal structures of **2a** (top) and **2c** (bottom).

Table 2. Important distances [pm] and angles [°] in the crystal structures of **2a** and **2c**.

	2a	**2c**		**2a**	**2c** [a]
C1-B1	156.3(10)	160.2(12)	B1-C1-Sn	105.3(4)	107.2(7)
C1-B2	156.9(10)	162.8(12)	B2-C1-Sn	104.5(4)	110.3(7)
C2-B1	157.8(10)	151.7(12)	Sn-C1-C30	100.4(4)	108.8(7)
C2-B2	155.9(10)	153.1(12)	C1-B1-B2-C2	159.7(4)	157.2(9)
B1-B2	208.5(12)	211.1(14)			
C2-C3	131.6(10)	136.3(11)			
C3-C4	131.3(10)	131.8(11)			

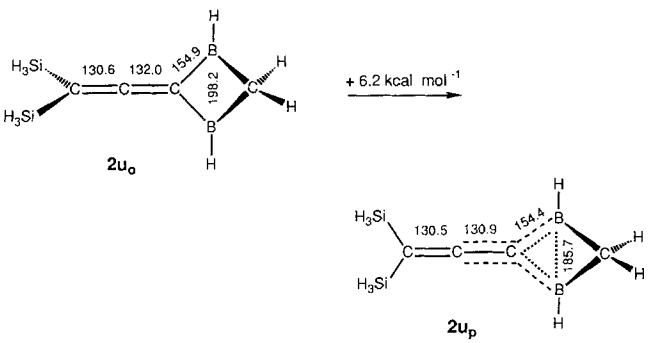
[a] C5 instead of Sn.

 © VCH Verlagsgesellschaft mbH, D-69451 Weinheim, 1994 0570-0833/94/2020-2065 $ 10.00+.25/0

315, 273, and 183 K, respectively. The activation energies for exchange were calculated to be 14.5 (**2a**), 12.6 (**2b**), and 8.6 (**2c**) kcal mol^{-1}, as determined by the temperature of coalescence and the difference in the chemical shifts at slow exchange.

The low barriers (rotation around the C–C double bond of an allene usually requires 46–47 kcal mol^{-1}[7]) and their dependence on the substituent at C1 can be explained when one assumes that exchange takes place by rotation around the C–CB_2 bond. The transition-state conformations are therefore planar allenes $\mathbf{2}_p$. Their negative charge is stabilized by $\pi-\pi$ delocalization towards homodiboriranides $\mathbf{2}'_p$, and their positive charge through $\sigma-\pi$ delocalization of the C(sp^2)–B σ bonds of the homodiboriranide rings as shown in $\mathbf{2}_p$. The Me_3Sn and Me_3Si substituents in **2a** and **2b** lower the electron deficiency of the boron atoms through C–Sn and C–Si hyperconjugation. The π delocalization as shown in $\mathbf{2}'_p$ as well as the subsequent σ delocalization as shown in $\mathbf{2}_p$ are therefore less important. The energies of the transition-state conformations of **2a** and **2b** are thus higher than that of **2c**.

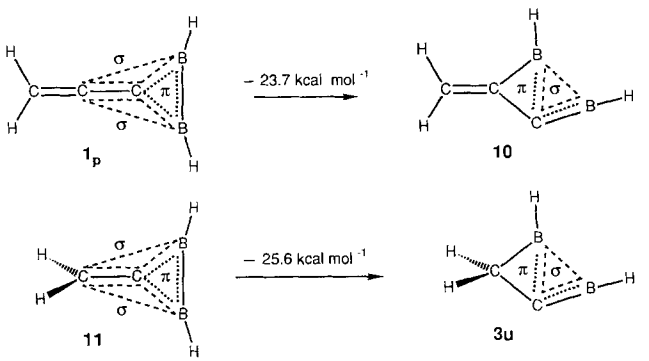
Our explanation for the low exchange barriers is supported by MP2/6-31G* calculations[8] for the model allene **2u**: The nonclassical planar allene $\mathbf{2u}_p$ is only 6.2 kcal mol^{-1} (MP2/6-31G* + ZPE[8]) higher in energy than the classical orthogonal



$\mathbf{2u}_o$. This difference in energy is consistent with the exchange barrier of 8.6 kcal mol^{-1} determined for **2c**. The strong homoaromatic π delocalization in the transition state $\mathbf{2u}_p$ is reflected in a short calculated B···B distance of 185.7 pm ($\mathbf{2u}_o$: 198.2 pm);[10] the strong C–B hyperconjugation results in a short bond length for the polarized C–CB_2 bond (130.9 pm), which is even shorter than the weakly polarized C–CB_2 bond of $\mathbf{2u}_o$ (132.0 pm). Similarly, a very short B–B bond (147.2 pm; 158.7 pm in $\mathbf{1}_o$) and a slightly shorter C–CB_2 bond (129.7 pm; 130.9 pm in $\mathbf{1}_o$) have been calculated for $\mathbf{1}_p$.[1] The influence of the silyl substituents on the rotational barrier is low: the energy difference between the orthogonal and planar forms of allene **2u** without silyl groups is 9.1 kcal mol^{-1} (MP2/6-31G* + ZPE[8]).

The energy difference between the orthogonal and planar allenes is approximately 37 kcal mol^{-1} less for **2c** than for alkyl-substituted allenes (46–47 kcal mol^{-1}[7]). Replacement of the homoaromaticity in **2** by the aromaticity in the diboriranide **1** should further stabilize the planar form and give rise to allenes with planar ground states. However, calculations at the MP2/6-31G* level show that the structure $\mathbf{1}_p$ is not a minimum on the potential hypersurface. The Hesse matrix has a negative eigenvalue, which indicates that $\mathbf{1}_p$ is a transition state. A geometrical optimization without symmetry constraints gives the minimum energy structure **10**, which is 23.7 kcal mol^{-1} more stable than $\mathbf{1}_p$ at the MP2/6-31G* level.

Thus, planar allenes are just as unlikely to be prepared by this route as the analogous orthogonal alkenes with the basic unit



11. The latter is 25.6 kcal mol^{-1} (MP2/6-31G*) higher in energy than the corresponding methyleneborane **3u**.[2, 11]

Received: May 27, 1994 [Z 6975 IE]
German version: *Angew. Chem.* **1994**, *106*, 2172

[1] K. Krogh-Jespersen, D. Cremer, D. Poppinger, J. A. Pople, P. von R. Schleyer, J. Chandrasekhar, *J. Am. Chem. Soc.* **1979**, *101*, 4843–4851. According to MP2/6-31G* calculations, $\mathbf{1}_p$ is 16.1 kcal mol^{-1} more stable than $\mathbf{1}_o$, which is a transition state (i = 1) at the MP2/6-31G* level.

[2] A. Berndt, *Angew. Chem.* **1993**, *105*, 1034–1058; *Angew. Chem. Int. Ed. Engl.* **1993**, *32*, 985–1009; R. Wehrmann, H. Meyer, A. Berndt, *ibid.* **1985**, *97*, 779–781 and **1985**, *25*, 788–790.

[3] A. Höfner, B. Ziegler, W. Massa, A. Berndt, *Angew. Chem.* **1989**, *101*, 188–190; *Angew. Chem. Int. Ed. Engl.* **1989**, *28*, 186–187.

[4] P. Willershausen, C. Kybart, N. Stamatis, W. Massa, M. Bühl, P. von R. Schleyer, A. Berndt, *Angew. Chem.* **1992**, *104*, 1278–1280; *Angew. Chem. Int. Ed. Engl.* **1992**, *31*, 1238–1240.

[5] The structure of **6** (Me_3Sn group linked to the carbon atom adjacent to the dicoordinated boron atom) follows clearly from the small ^{13}C, ^{119}Sn coupling constant of 46.5 Hz and the shielding of the C atom in the C–B double bond ($\delta(^{13}C) = 78$), which is characteristic of stannylmethyleneboranes (the corresponding compound with Me_3Sn instead of the aryl group shows values of $\delta(^{13}C) = 75.3$ and $^1J(^{13}C, ^{119}Sn) = 66$ Hz [2].

[6] Crystal structure analysis: yellow crystals of **2a** · 0.5 *n*-C_6H_{14} and **2c** were measured on a four-circle diffractometer (CAD4 Enraf-Nonius) at –80 °C and at room temperature (**2c**) with $Cu_{K\alpha}$ radiation ($\lambda = 154.178$ pm). **2a**: $C_{47}H_{74}B_2Si_2Sn \cdot 0.5\,C_6H_{14}$, crystal dimensions $0.3 \times 0.25 \times 0.2$ mm^3, monoclinic, space group $P2_1/n$, $Z = 4$, $a = 1326.5(1)$, $b = 947.4(1)$, $c = 4207.0(4)$ pm, $\beta = 91.99(1)°$, $V = 5283.9 \times 10^{-30}$ m^3, $\rho_{calcd} = 1.104$ g cm^{-3}; 7220 measured reflections up to $2\theta = 110°$ (ω scans), of which 6609 were independent. 4877 reflections with $F_o > 3\sigma(F_o)$, after Lorentz and polarization correction, were used for further calculations, no absorption correction ($\mu = 4.479$ mm^{-1}). The structure was solved with direct methods and refined with full matrix against the F_o data. The H atoms were included in the calculation riding on their bonding partners, partially on calculated positions and with common isotropic temperature factors refined in groups. For the rest of the atoms, anisotropic temperature factors were used. $R = 0.062$, $wR = 0.040$ ($w = 1/\sigma^2(F_o)$), maximum residual electron density 0.66 e Å^{-3}. – **2c**: $C_{45}H_{68}B_2Si_2$, crystal dimensions $0.4 \times 0.3 \times 0.15$ mm, monoclinic, space group $P2_1/n$, $Z = 4$, $a = 1399.3(3)$, $b = 2001.6(4)$, $c = 1666.7(3)$ pm, $\beta = 95.80(3)°$, $V = 4644.0 \times 10^{-30}$ m^3, $\rho_{calcd} = 0.982$ g cm^{-3}; 4353 measured reflections up to $2\theta = 94°$ (ω scans), of which 4166 were independent. 4165 reflections, after Lorentz and polarization correction, were used for further calculations; the structure was solved and refined as for **2a**. The refinement against the F_o^2 data (SHELXL-93) was complicated by disorder in the *tert*-butyl groups at C32 and C34; a "split atom model" description led to a $wR_2 = 0.225$, corresponding to a conventional $R = 0.076$ for 1759 reflections with $I > 2\sigma(I)$, and a maximum residual electron density of 0.27 e Å^3. Further details of the crystal structure investigation may be obtained from the Fachinformationszentrum Karlsruhe, D-76344 Eggenstein-Leopoldshafen, on quoting the depository number CSD-58377.

[7] The rotational barrier for the C–C double bond in 1,3-dimethyl- and 1,3-di-*tert*-butylallene were determined to be 46.17 and 46.91 kcal mol^{-1}, respectively: W. R. Roth, G. Ruf, P. W. Ford, *Chem. Ber.* **1974**, *107*, 48–52.

[8] The calculations were performed with the programs Gaussian 92 [9a] and TURBOMOLE [9b]. The geometries were optimized at the HF/6-31G* and MP2/6-31G* levels. The equillibrium structures were calculated as minima ($i = 0$) or transition states ($i = 1$) at the HF/6-31G* level. The zero-point vibration corrections (ZPE) were scaled with a factor of 0.89 at the HF/6-31G* level.

[9] a) Gaussian 92, Revision A: M. J. Frisch, G. W. Trucks, M. Head-Gordon, P. M. W. Gill, M. W. Wong, J. B. Foresman, H. B. Schlegel, K. Raghavachari, M. A. Robb, J. S. Binkley, C. Gonzalez, R. Martin, D. J. Fox, D. J. DeFrees, J. Baker, J. J. P. Stewart, J. A. Pople, Gaussian Inc., Pittsburgh, PA, **1992**; b) TURBOMOLE: R. Ahlrichs, M. Bär, M. Häser, H. Horn, C. Kölmel, *Chem. Phys. Lett.* **1989**, *162*, 165–169.

[10] The ring folding angle at the B–B diagonal is 32.3° in $2u_p$ and 31.3° in $2u_o$; the barriers to ring inversion of the folded four-membered ring are calculated as 4.5 kcal mol^{-1} for $2u_o$ and 5.5 kcal mol^{-1} for $2u_p$ and thus are significantly smaller than for a homodiboriranide without strong C–B hyperconjugation (7.9 kcal mol^{-1} [4]).

[11] P. H. M. Budzelaar, K. Krogh-Jespersen, T. Clark, P. von R. Schleyer, *J. Am. Chem. Soc.* **1985**, *107*, 2773–2779.

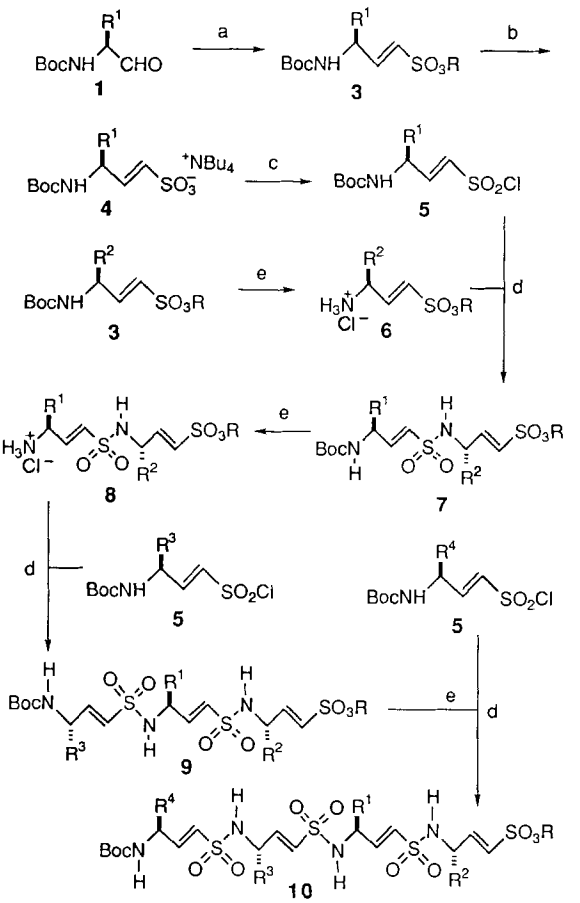
Synthesis of Sulfonamido-Pseudopeptides: New Chiral Unnatural Oligomers

Cesare Gennari,* Barbara Salom, Donatella Potenza, and Anthony Williams

Although many research groups have devoted their efforts during the past two decades to the replacement of the scissile peptide bond with mimetic groups,[1] relatively little is known about pseudopeptides characterized by the presence of the sulfonamide bond.[2] This modification creates a peptide bond surrogate with significant changes in polarity, H-bonding capability, and acid–base character (RSO_2NHR', $pK_a = 10–11$). Furthermore, the sulfonamide bond should show enhanced metabolic stability and structural similarity to the tetrahedral transition state involved in the amide bond enzymatic hydrolysis.[2a–c] This makes sulfonamidopeptides promising candidates in the development of protease inhibitors and new drugs.[3] The oligomers and the polymers should also be interesting molecular scaffolds, with specific pseudopeptide backbone conformations based on the hydrogen-bonding network.

Unfortunately α-aminosulfonamides are known to be unstable and to immediately decompose by fragmentation.[4] We have synthesized chiral vinylogous aminosulfonic acids (γ-amino-α,β-unsaturated) from natural α-amino acids, developed a straightforward protection–deprotection–coupling chemistry for the sulfonamide bond, and synthesized sulfonamido-pseudopeptides by an iterative process (Scheme 1).

N-Boc α-aminoaldehydes **1** (Boc = *tert*-butoxycarbonyl) were obtained from naturally occurring α-amino acids.[5] Wittig–Horner reaction with methyl- or ethyldiethylphosphoryl methanesulfonate **2** (R = Me, Et[6, 7a]) and *n*BuLi at −78 °C gave the corresponding α,β-unsaturated sulfonates **3** in good yield (75–85%) and complete *E* stereoselectivity.[6c] Cleavage of the methyl (ethyl) ester was effected by treatment of sulfonates **3** with nBu_4NI in refluxing acetone (100%).[7a, 8] This deprotection offers several advantages over related reactions leading to different sulfonate salts (e.g., Na^+, NH_4^+, $NHEt_3^+$)[7b–d]: a) the nBu_4N^+ salts **4** are easily handleable and soluble in organic solvents; b) they are the most suitable starting material for the next step. The activation step required an extensive search for appropriate reagents and conditions. After screening several different methods, we found that SO_2Cl_2/PPh_3 in dichloromethane[8] gives the corresponding sulfonyl chlorides **5** cleanly and in high yield (85–90%) as stable compounds which can be purified by chromatography, while other protocols (e.g., triphosgene/cat. dimethylformamide (DMF)/CH_2Cl_2,[9] $PCl_5/CHCl_3$[10]) were less efficient. The sulfonyl chlorides **5** were coupled with the amine salts **6** (CH_2Cl_2/1,8-diazabicyclo[5.4.0]undec-7-ene (DBU)/cat. 4-dimethylaminopyridine (DMAP)) to give the dimers **7**. Although the coupling step is unoptimized and needs further improvement, the dimers **7** were obtained in a reasonable yield (55–65%). Amine hydrochlorides **6** were prepared from *N*-Boc derivatives **3** by treatment with 3 M HCl in MeOH (room temperature, 3 h) followed by solvent removal (100%). The process can be further iterated to give trimers (e.g., **9**, 60%) and tetramers (e.g., **10**, 60%; R = Et, R^1 = Me, R^2 = *i*Pr, $R^3 = CH_2Ph$, $R^4 = CH_2CHMe_2$).



Scheme 1. Synthesis of sulfonamido-pseudopeptides from *N*-Boc α-aminoaldehydes. a) $(EtO)_2PO-CH_2SO_3R$ **2**, *n*BuLi, THF, −78 °C, 30 min, 75–85%. b) Bu_4NI, acetone, reflux, 10–16 h, 100%. c) SO_2Cl_2, Ph_3P, CH_2Cl_2, 3 Å molecular sieves, 0 → 25 °C, 3 h, 85–90%. d) CH_2Cl_2, DBU, cat. DMAP, 25 °C, 18 h, 55–65%. e) 3 M HCl in MeOH, 0 → 25 °C, 3 h, 100%.

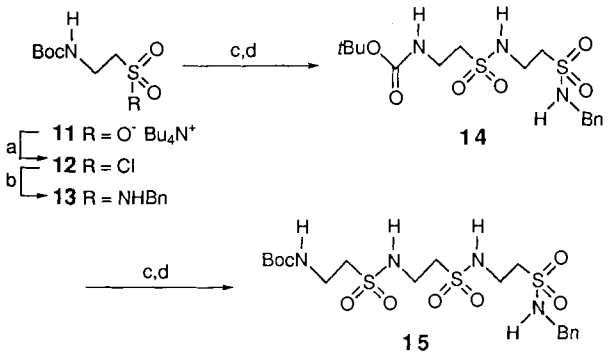
The stereochemical integrity was checked a) by α-methoxy-α-trifluoromethyl(phenyl)acetic acid (MTPA) derivatization[11] of hydrochlorides **6** and NMR analysis (^1H, ^{13}C, ^{19}F),[12] and b) by ^{13}C NMR analysis of dimers **7**.[13] The sulfonamide bond is formed from the sulfonyl chloride and the amine by a nucleophilic substitution at the four-coordinate sulfur.[14a] The alternative sequence involving an elimination–addition reaction via an achiral unsaturated sulfene,[14b] is not likely to occur as it would lead to a mixture of two diastereomeric dimers.[13]

Similar activation and coupling chemistry proved effective also for the synthesis of sulfonamido-pseudopeptides based on β-aminosulfonamides, which, unlike α-aminosulfonamides, are

[*] Prof. Dr. C. Gennari, B. Salom, Dr. D. Potenza, Dr. A. Williams
Dipartimento di Chimica Organica e Industriale
Università di Milano
Centro CNR per lo Studio delle Sostanze Organiche Naturali
via G. Venezian 21, 20133 Milano (Italy)
Telefax: Int. code + (2) 236-4369

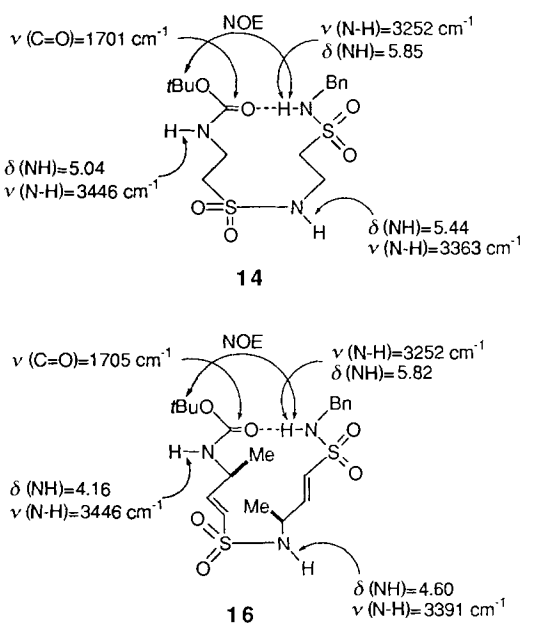
 © VCH Verlagsgesellschaft mbH, D-69451 Weinheim, 1994 0570-0833/94/2020-2067 $ 10.00+.25/0

known to be stable[2a-e, 4a] (Scheme 2). Saturated γ-aminosulfonic acids are also available, by the conjugate reduction of unsaturated sulfonate esters **3** with $Li(sBu)_3BH$ in THF (70–80%).[15]



Scheme 2. Sulfonamido-pseudopeptides derived from taurine. a) CH_2Cl_2, cat. DMF, triphosgene, 25 °C, 30 min. b) CH_2Cl_2, $PhCH_2NH_2$, DBU, 0 → 25 °C, 15 h (a + b = 82%). c) TFA/CH_2Cl_2 (1:1), 0 °C, 20 min, 100%. d) **12**, CH_2Cl_2, DBU, 0 → 25 °C, 15 h, 55–65%.

We have investigated the conformational preferences of the oligomers in chloroform by variable-temperature ^1H NMR spectroscopy,[16] FTIR spectroscopy,[16] and NOE experiments (NOE = nuclear Overhauser effect). The experimental results were complemented by computer modeling studies,[17] and show a strong preference for β-aminosulfonic derivatives (e.g., **14**) to form a twelve-membered ring and for γ-aminosulfonic derivatives (e.g., **9** and **16**) to form a fourteen-membered ring by intramolecular hydrogen bonding (dashed line, Scheme 3).[18] The folding ability deserves some comments: 1. The N–H–O angles are more linear in twelve- and fourteen-membered rings, thus strengthening the hydrogen bonds; 2. intramolecular hydrogen bonds between the nearest neighbor amide-type groups in the oligomer backbone (i.e., leading to smaller rings) are unfavorable.[16e] This is clearly inferred by the analysis of **14**-type monomers which show little six- or eight-membered ring hydrogen bonding, and of **16**-type monomers which show practically no seven- or nine-membered ring hydrogen bonding.



Scheme 3. ^1H NMR ($CDCl_3$, 10^{-3} M, room temperature) and FTIR ($CHCl_3$, 10^{-3} M, room temperature) spectroscopic studies of sulfonamido-pseudopeptides.

A few particularly relevant data regarding **9** and **16** are worth mentioning: *strong* NOE at the SO_2N-*H* involved in the hydrogen bonding upon irradiation of the *t*Bu of the Boc group (room temperature, 5×10^{-3} M solution in $CDCl_3$), shift to lower frequencies of both the $\nu_{C=O}$ (−30 and −25 cm^{-1}, respectively) and the ν_{N-H} (−138 cm^{-1}, for both) involved in the hydrogen bonding (room temperature, 1×10^{-3} M solution in $CHCl_3$), shift to lower field ($\Delta\delta$ = 1.2–1.5) for signal of the hydrogen involved in the hydrogen bonding (room temperature, 1×10^{-3} M solution in $CDCl_3$).

In summary, we have developed a straightforward approach for the iterative synthesis of sulfonamido-pseudopeptides based on chiral vinylogous aminosulfonic acids (γ-amino-α,β-unsaturated). The functionalization of the α,β-double bond and the extension of this chemistry to solid–phase synthesis are currently under investigation as well as the biological properties and folding patterns of this new array of chiral unnatural polymers.

Experimental Procedure

Coupling Procedure: Sulfonyl chloride **5** (0.525 mmol) was dissolved in CH_2Cl_2 (4.0 mL), and a solution of hydrochloride salt **6** or **8** (0.35 mmol) in CH_2Cl_2 (2.0 mL) containing DBU (0.052 mL, 0.35 mmol) and DMAP (8.4 mg, 0.070 mmol) was added in one portion. After the addition, more DBU (0.078 mL, 0.525 mmol) in CH_2Cl_2 (1.0 mL) was slowly added during 3 h. More sulfonyl chloride (0.175 mmol) was added, and the mixture was stirred overnight at room temperature, then diluted with CH_2Cl_2 and treated with pH7 phosphate buffer (2.0 mL). The aqueous phase was extracted with CH_2Cl_2, and the combined organic extracts were dried (Na_2SO_4) and evaporated. The crude product was purified by flash chromatography (*n*-hexane/EtOAc, ca. 1:1) to give the desired oligomer **7**, **9**, **10** in 55–65% yield. All compounds had correct C,H,N,S-analyses.

Tetramer **10** (R = Et, R^1 = Me, R^2 = *i*Pr, R^3 = CH_2Ph, R^4 = CH_2CHMe_2): The crude product was purified by flash chromatography (*n*-hexane/EtOAc, 60:40) to give the desired tetramer (60%). ^1H NMR (500 MHz, $CDCl_3$, 25 °C): δ = 0.92 (6H, t, Me_2CHCH_2, J = 6.9 Hz), 0.96 (3H, d, CH_3CHC, J = 6.5 Hz), 0.97 (3H, d, CH_3CHC, J = 6.8 Hz), 1.32 (2H, m, $CHCH_2C$), 1.35 (3H, d, CH_3CHN, J = 6.9 Hz), 1.39 (3H, t, $CH_3CH_2OSO_2$, J = 7.0 Hz), 1.43 (9H, s, $[CH_3]_3C$), 1.65 (1H, m, Me_2CHCH_2), 1.90 (1H, m, Me_2CHC), 2.77 (1H, dd, CHHPh, J = 13.9, J = 8.4 Hz), 3.03 (1H, dd, CHHPh, J = 13.9, J = 5.3 Hz), 3.90 (1H, m, Me_2CHCHN), 4.15–4.32 (5H, m, CH_3CHN, $PhCH_2CHN$, *i*BuC*H*N, $CH_3CH_2OSO_2$, J = 7.0 Hz), 4.39 (1H, d, *i*BuCHN*H*, J = 7.7 Hz), 4.52 (1H, d, $PhCH_2CHNH$, J = 5.5 Hz), 4.96 (1H, d, *i*PrCHN*H*, J = 8.2 Hz), 5.39 (1H, d, MeCHN*H*, J = 7.0 Hz), 5.91 (1H, d, BnCHCH=C*H*, J = 15.0 Hz), 6.35 (1H, d, CH=C*H*, J = 14.6 Hz), 6.42 (1H, d, CH=C*H*, J = 14.0 Hz), 6.44 (1H, d, *i*PrCHCH=C*H*, J = 14.8 Hz), 6.53 (1H, dd, MeCHC*H*=CH, J = 14.7, J = 5.9 Hz), 6.59 (1H, dd, BnCHC*H*=CH, J = 15.0, J = 5.1 Hz), 6.63 (1H, dd, CHC*H*=CH, J = 15.1, J = 6.4 Hz), 6.74 (1H, dd, *i*PrCHC*H*=CH, J = 14.8, J = 6.8 Hz), 7.18 (2H, d, Ar-H), 7.30 (1H, t, Ar-H), 7.35 (2H, t, Ar-H); ^{13}C NMR (DEPT, $CDCl_3$, 25 °C): δ = 14.85 (CH_3), 18.20 (CH_3), 18.63 (CH_3), 21.21 (CH_3), 21.66 (CH_3), 22.83 (CH_3), 24.58 (CH), 28.24 ($[CH_3]_3$), 32.39 (CH), 40.37 (CH_2), 43.14 (CH_2), 49.03 (CHN), 49.57 (CHN), 55.21 (CHN), 59.56 (CHN), 67.27 (OCH_2), 126.62 (CH=), 127.24 (CH=), 128.31 (CH=), 128.55 (CH=), 128.81 (CH=), 129.71 (CH=), 129.77 (CH=), 130.33 (CH=), 131.90 (CH=), 132.10 (CH=), 143.48 (CH=), 144.26 (CH=), 146.36 (CH=).

Received: June 17, 1994 [Z 7042]
German version: *Angew. Chem.* **1994**, *106*, 2181

[1] A. Giannis, T. Kolter, *Angew. Chem.* **1993**, *105*, 1303–1326; *Angew. Chem. Int. Ed. Engl.* **1993**, *32*, 1244–1267; J. Gante, *ibid.* **1994**, *106*, 1780–1802 and **1994**, *33*, 1699–1720.

[2] a) W. J. Moree, G. A. van der Marel, R. M. J. Liskamp, *Tetrahedron Lett.* **1992**, *33*, 6389–6392; b) *ibid.* **1991**, *32*, 409–412; c) W. J. Moree, L. C. van Gent, G. A. van der Marel, R. M. J. Liskamp, *Tetrahedron* **1993**, *49*, 1133–1150; d) A. Calcagni, E. Gavuzzo, F. Mazza, F. Pinnen, G. Pochetti, D. Rossi, *Gazz. Chim. Ital.* **1992**, *122*, 17–23; e) H. R. Kricheldorf, E. Leppert, *Synthesis* **1976**, 43–45; f) G. Pagani Zecchini, M. Paghalunga Paradisi, I. Torrini, G. Lucente, E. Gavuzzo, F. Mazza, G. Pochetti, *Tetrahedron Lett.* **1991**, *32*, 6779–6782; g) G. Luisi, A. Calcagni, F. Pinnen, *ibid.* **1993**, *34*, 2391–2392.

[3] a) M. J. Liskamp, *Angew. Chem.* **1994**, *106*, 661–664; *Angew. Chem. Int. Ed. Engl.* **1994**, *33*, 633–636; b) C. H. Levenson, R. B. Meyer, Jr., *J. Med. Chem.* **1984**, *27*, 228–232; c) R. Guégan, J. Diaz, C. Cazaubon, M. Beaumont, C.

Carlet, J. Clément, H. Demarne, M. Mellet, J.-P. Richaud, D. Segondy, M. Vedel, J.-P. Gagnol, R. Roncucci, B. Castro, P. Corvol, G. Evin, B. P. Roques, *ibid.* **1986**, *29*, 1152–1159; d) H. Mazdiyasni, D. B. Konopacki, D. A. Dickman, T. M. Zydowsky, *Tetrahedron Lett.* **1993**, *34*, 435–438.

[4] a) M. Frankel, P. Moses, *Tetrahedron* **1960**, *9*, 289–294; b) W. F. Gilmore, H.-J. Lin, *J. Org. Chem.* **1978**, *43*, 4535–4537; c) G. R. Moe, L. M. Sayre, P. S. Portoghese, *Tetrahedron Lett.* **1981**, *22*, 537–540; d) B. Garrigues, M. Mulliez, *Synthesis* **1988**, 810–813; e) D. Merricks, P. G. Sammes, E. R. H. Walker, K. Henrick, M. M. McPartlin, *J. Chem. Soc. Perkin Trans. 1* **1991**, 2169–2176.

[5] a) P. Garner, J. M. Park, *J. Org. Chem.* **1987**, *52*, 2361–2364; b) W. D. Lubell, H. Rapoport, *J. Am. Chem. Soc.* **1987**, *109*, 236–239; c) N. J. Miles, P. G. Sammes, P. D. Kennewell, R. Westwood, *J. Chem. Soc. Perkin Trans. 1* **1985**, 2299–2305; d) J. Jurczak, A. Golebiowski, *Chem. Rev.* **1989**, *89*, 149–164; e) M. T. Reetz, *Angew. Chem.* **1991**, *103*, 1559–1573; *Angew. Chem. Int. Ed. Engl.* **1991**, *30*, 1531–1546; f) M. T. Reetz, J. Kanand, N. Griebenow, K. Harms, *ibid.* **1992**, *104*, 1638 and **1992**, *31*, 1626–1629; g) M. R. Leanna, T. J. Sowin, H. E. Morton, *Tetrahedron Lett.* **1992**, *33*, 5029–5032.

[6] a) J. C. Carretero, L. Ghosez, *Tetrahedron Lett.* **1987**, *28*, 1101–1104; b) J. C. Carretero, M. Demillequand, L. Ghosez, *Tetrahedron* **1987**, *43*, 5125–5134; c) J. C. Carretero, J. Davies, J. Marchand-Brynaert, L. Ghosez, *Bull. Soc. Chim. Fr.* **1990**, *127*, 835–842.

[7] a) B. Musicki, T. S. Widlanski, *Tetrahedron Lett.* **1991**, *32*, 1267–1270; b) B. Musicki, T. S. Widlanski, *J. Org. Chem.* **1990**, *55*, 4231–4233; c) R. G. Henriques, T. S. Widlanski, T. Xu, J. D. Lambeth, *J. Am. Chem. Soc.* **1992**, *114*, 7311–7313; d) M. Kovacevic, Z. Brkic, Z. Mandic, M. Tomic, M. Luic, B. K. Prodic, *Croat. Chem. Acta* **1992**, *65*, 817–833.

[8] J. Huang, T. S. Widlanski, *Tetrahedron Lett.* **1992**, *33*, 2657–2660.

[9] R. C. Reynolds, P. A. Crooks, J. A. Maddry, M. S. Akhtar, J. A. Montgomery, J. A. Secrist III, *J. Org. Chem.* **1992**, *57*, 2983–2985.

[10] H. McIlwain, *J. Chem. Soc.* **1941**, 75–77.

[11] J. A. Dale, H. S. Mosher, *J. Am. Chem. Soc.* **1973**, *95*, 512–519.

[12] Starting from noncrystallized **3**, NMR analysis of the Mosher's amides revealed a ≥98:2 ratio of diastereoisomers, while starting from recrystallized **3**, the Mosher's amides were obtained as single compounds within the limits of NMR detection (>99:1).

[13] ^{13}C NMR analysis of dimers **7** revealed them to be single diastereomers.

[14] a) I. M. Gordon, H. Maskill, M. F. Ruasse, *Chem. Soc. Rev.* **1989**, *18*, 123–151; b) J. F. King, R. Rathore in *The Chemistry of Sulphonic Acids, Esters and their Derivatives* (Eds.: S. Patai, Z. Rappoport), Wiley, Chichester, **1991**, pp. 697–766.

[15] K. Hori, H. Kazuno, K. Nomura, E. Yoshii, *Tetrahedron Lett.* **1993**, *34*, 2183–2186.

[16] a) S. H. Gellman, G. P. Dado, G.-B. Liang, B. R. Adams, *J. Am. Chem. Soc.* **1991**, *113*, 1164–1173; b) G. P. Dado, S. H. Gellman, *ibid.* **1993**, *115*, 4228–4245; c) V. Dupont, A. Lecoq, J.-P. Mangeot, A. Aubry, G. Boussard, M. Marraud, *ibid.* **1993**, *115*, 8898–8906, and references therein.; d) E. A. Gallo, S. H. Gellman, *ibid.* **1993**, *115*, 9774–9788; e) G. P. Dado, S. H. Gellman, *ibid.* **1994**, *116*, 1054–1062.

[17] Usage-directed Still–Chang–Guida torsional Monte Carlo method [19a], as a part of BATCHMIN-MacroModel 3.1 molecular mechanics program [19b], was used for the conformational search on a Silicon Graphics Iris workstation. The conformers were minimized in chloroform using the GB/SA model included in BATCHMIN [19c]. MM2* parameters were used as implemented in MacroModel [19b], with the addition of suitable parameters for the sulfonamide group [19d].

[18] For a conformational analysis of vinylogous polypeptides, see: M. Hagihara, N. J. Anthony, T. J. Stout, J. Clardy, S. L. Schreiber, *J. Am. Chem. Soc.* **1992**, *114*, 6568–6570.

[19] a) G. Chang, W. C. Guida, W. C. Still, *J. Am. Chem. Soc.* **1989**, *111*, 4379–4386; b) F. Mohamadi, N. G. J. Richards, W. C. Guida, R. Liskamp, M. Lipton, C. Caufield, G. Chang, T. Hendrickson, W. C. Still, *J. Comput. Chem.* **1990**, *11*, 440–467; c) W. C. Still, A. Tempczyk, R. C. Hawley, T. Hendrickson, *J. Am. Chem. Soc.* **1990**, *112*, 6127–6129; d) L. Belvisi, O. Carugo, G. Poli, *J. Mol. Struct.* **1994**, *318*, 189–202.

Localization of Electrons in Intermetallic Phases Containing Aluminum**

Ulrich Häussermann, Steffen Wengert, Patrick Hofmann, Andreas Savin, Ove Jepsen, and Reinhard Nesper*

Dedicated to Professor Ewald Wicke on the occasion of his 80th birthday

Intermetallic phases and Zintl phases are important classes of compounds in inorganic chemistry which were for a long time considered as unusual. These compounds formed from metals, or from metals and semi-metals, possess a very large combinatorial potential, only a very small part of which has been investigated to date. Both classes demonstrate enormously varied, yet differing, aspects of structural chemistry, which are to some extent very complex. Unfortunately, the understanding of most of these structures causes great difficulties, in particular with regard to a description of their chemical bonding. These difficulties have already been reported in detail in this journal.[1]

The electron localization function (ELF) has developed into a useful tool for the interpretation of the chemical bond.[2] The ELF is particularly attractive for crystalline materials, because it is not wave vector dependent and, like electron density, is only a function of the three positional coordinates (x,y,z). Originally derived from the Hartree–Fock pair density for electrons with the same spin by Becke and Edgecombe,[3] it is a measure of the probability of finding an electron in the surroundings of another electron with the same spin. The ELF is normalized so that its dimensionless values lie between zero and one. Large values correspond to a high localization and mean that for an electron with a particular spin, located at (x,y,z), no other electron with the same spin is to be found in the vicinity. Such a situation may also be interpreted as meaning that an electron pair with α,β spin is localized in the region around (x,y,z).[4] This interesting result, that the probability of finding an electron pair is dependent on the location, is based entirely on the Fermi correlation. The Coulomb correlation, which opposes the formation of an electron pair, is not taken into consideration in the calculation of the ELF. High ELF values have indeed been found for those regions which correspond to bonds, lone pairs of electrons, and electron shells.

The term localization, in the sense of the ELF, describes thus the tendency of formation of electron pairs at a position (x,y,z), whereas the electron density $\rho(x,y,z)$ is the probability density for an electron in an arbitrary spin state at this position. The value ELF = 0.5 represents the situation in an homogeneous electron gas, a model system without atomic cores, which serves as a reference. The deviations from this value are caused by the presence of the atomic cores, that is, by the formation of a structure. As a result of these, domains of high localization are

[*] Prof. Dr. R. Nesper, Dipl.-Chem. U. Häussermann, Dipl.-Chem. S. Wengert, Dipl.-Chem. P. Hofmann
Laboratorium für Anorganische Chemie der Eidgenössischen Technischen Hochschule
Universitätstrasse 6, CH-8092 Zürich (Switzerland)
Telefax: Int. code + (1)632-1149

Priv.-Doz. Dr. A. Savin
CNRS, Laboratoire Dynamique des Interactions Moleculaires
Université Pierre et Marie Curie, Paris (France)

Dr. O. Jepsen
Max-Planck-Institut für Festkörperforschung, Stuttgart (FRG)

[**] This work was supported by the Schweizerische Nationalfonds zur Förderung der wissenschaftlichen Forschung.

formed, for example, in bonds, and domains of low localization, for example, between the electron shells in atoms.

In the meantime, the ELF has also been calculated by using density matrices from density functional methods[5] and even by using those from semiempirical calculations.[6] Strictly speaking, the interpretation given above does not hold for these procedures. In spite of this, the results correspond to a great extent, and we would like therefore to use our interpretation, independent of the method of calculation employed.[7]

Both the electron density and the ELF values are shown in the two-dimensional graphical representation. The electron densities are displayed as point densities and the corresponding ELF values coded in the form of a color scale, similar to that used in a map. High ELF values (ca. 0.8–1.0) are colored white; the series descends through brown and yellow to green for middle ELF values (ca. 0.5); blue and violet then indicating the lower end of the scale.[8]

The abrupt transition within the third period from the metallic bond in aluminum to the covalent bond in silicon can take place in a stepwise manner in intermetallic compounds and Zintl phases containing aluminum. This will be demonstrated using the series $Al \rightarrow CaAl_2 \rightarrow SrAl_2 \rightarrow BaAl_4 \rightarrow CaAl_2Si_2 \rightarrow Si$ as an example.[9]

The structure of elemental aluminum is a cubic close packed arrangement (fcc, Fig. 1a). Each Al atom has twelve nearest

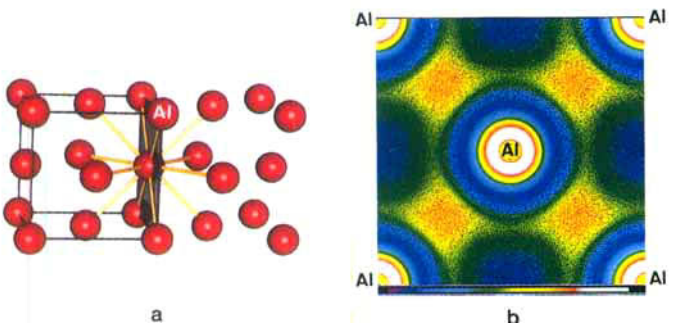


Fig. 1. a) Section from the fcc structure of aluminum showing the (100) plane and connecting lines to the twelve nearest neighbors (yellow). The edges of the unit cell are indicated by black lines in all structure diagrams. b) Electron density ρ (density of points) and ELF (color) for the (100) plane in Al. The ELF color scale is shown at the lower edge of the picture (see text). The electron shells of the cores cannot be entirely resolved in these diagrams, especially those of the heavier elements.

neighbors at a distance of 286.3 pm which form a cuboctahedral coordination. The ELF was calculated for the (100) plane (Fig. 1b). Clearly, the brown areas of highest localization can be recognized between nearest neighboring nuclei and the blue regions of lowest localization in the empty octahedral holes of the structure. The difference between the electron densities at these positions is approximately 100%, the ELF values, however, vary between 0.21 and 0.62, and clearly show that an electron-gas-like localization, which may perhaps have been expected, does not exist in elemental aluminum.

$CaAl_2$ crystallizes in the $MgCu_2$ structure (Fig. 2a) and thus belongs to the cubic Laves phases. All the Al atoms are symmetry-equivalent and connected to give a three-dimensional network of corner-sharing tetrahedra. Thus, each Al atom has six equivalent nearest neighbors at a distance of 284.2 pm. The Ca partial structure is diamond-like. If the twelve Al atoms at a distance of 333.2 pm are taken into consideration, the coordination polyhedron for Ca is a Friauf polyhedron (coordination number 16). The (110) plane contains zigzag chains of Ca atoms and bisects the Al_4 tetrahedra (cf. Fig. 2a). Regions with high ELF values are not only to be found between Al cores, but also extend between Al and Ca cores. The maximum ELF values are 0.74 (Fig. 2b). All tetrahedral faces lie in the (111) planes and

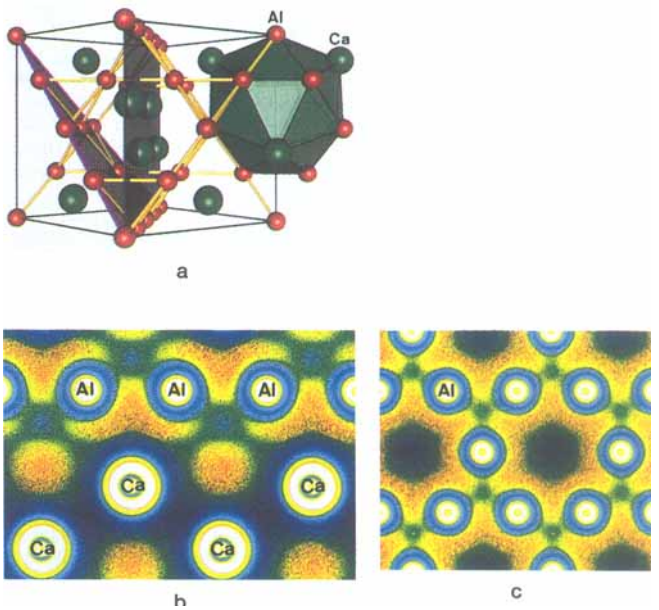


Fig. 2. a) Section from the cubic $CaAl_2$ structure (Ca: green; Al: red; edges of the Al_4 tetrahedra: yellow; coordination polyhedra of Ca: green) showing the (111) (violet border) and (110) planes (black border). b) ρ and ELF for the (110) plane in $CaAl_2$. c) ρ and ELF for the (111) plane in $CaAl_2$.

the corresponding Al atoms form the Kagomé net, a connection pattern comprising equal numbers of triangles and hexagons (3636 net, Fig. 2c). In the tetrahedral faces, green regions of electron-gas-like behavior is found. The localization in the middle of the hexagons is the lowest for the valence region (ELF = 0.115). The ELF values in $CaAl_2$ are admittedly higher than in metallic Al, they are, however, too small for usual covalent bonds. The structure of the localization pattern resembles that of banana bonds.

Figure 3a shows the $SrAl_2$ structure ($CeCu_2$ type) in which the Al atoms form slightly puckered nets of hexagonal rings stacked in the [100] direction. The Al–Al distances in the net are 278.6 and 279.9 pm. Longer bonds (293.0 pm) connect these nets through chains of four-membered rings which follow the [010] direction. All in all, the Al coordination polyhedron is a slightly distorted trigonal pyramid. The Sr atoms are located between the nets of six-membered rings and are coordinated by twelve Al atoms. The (040) plane cuts perpendicularly through the stacked nets of hexagonal rings. The Sr atoms, one sort of Al–Al bond in the nets (279.9 pm), and the long bonds connecting the nets all lie in this plane. The electron density distribution and the ELF for this plane are shown in Figure 3b. White regions can be distinguished between the Al cores, that is, regions of high ELF, which indicate a bonding electron pair. Figure 3c shows the localization behavior in one of the four-membered Al rings. In contrast to $CaAl_2$ (Fig. 2), the areas of highest localization in $SrAl_2$, with maximum ELF values of around 0.88, are entirely due to the Al partial structure, which can be described as a covalent network.

In the $BaAl_4$ structure, one sort of Al atom, which may be described as basal, forms a quadratic net with large Al–Al

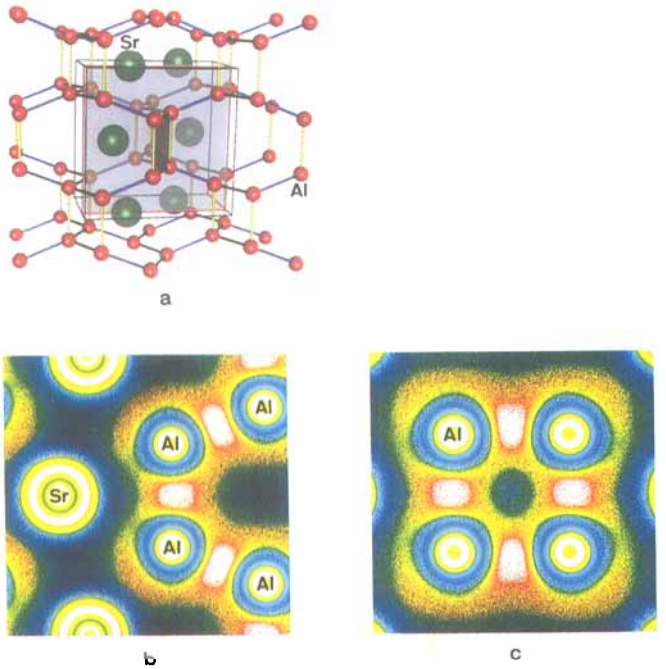


Fig. 3. a) Section from the $SrAl_2$ structure (Sr: green; Al: red). The Al–Al bonds forming the nets of hexagonal rings are colored blue and those connecting the nets yellow. The (040) plane is colored violet. Additionally, a four-membered Al ring from one of the chains of four-membered rings in the [010] direction is shaded for emphasis. b) ρ and ELF for the (040) plane in $SrAl_2$. c) ρ and ELF for a four-membered Al ring in $SrAl_2$.

distances of 321.0 pm (Fig. 4a). The squares are alternately capped from above and below by the second sort of Al atom, the apical ones, to form pyramids. In addition, these apical Al atoms connect the pyramid layers so that the tips of neighboring

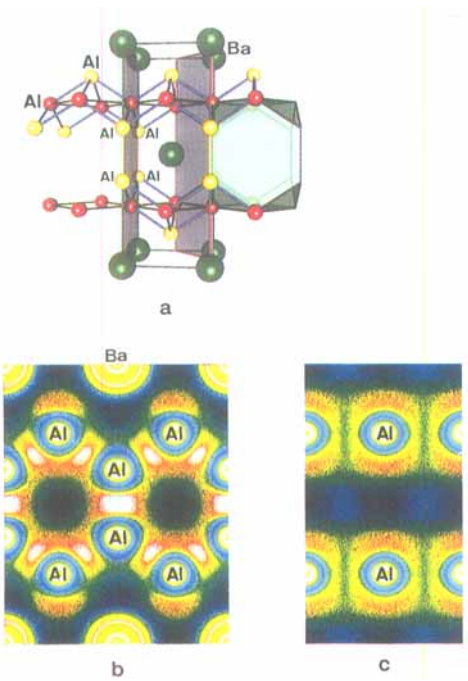


Fig. 4. a) Section from the $BaAl_4$ structure (Ba: green; apical Al: yellow; basal Al: red; coordination polyhedron of Ba: green). The (220) plane (red-violet border) contains the distances between the basal Al atoms (black rods), the (110) plane contains the bonds between the basal and the apical Al atoms (blue rods), and those between the apical Al atoms (yellow rods). b) ρ and ELF for the (100) plane in $BaAl_4$ (2 unit cells). c) ρ and ELF for the (220) plane in $BaAl_4$ (2 unit cells).

layers lie directly above one another. Each of the Ba atoms is situated in one of the large cavities between the layers and is coordinated by 16 Al atoms. The bonding in the Al framework was interpreted as follows:[10] The distance of 278.4 pm between the apical Al atoms represents a two-electron, two-center (2e–2c) bond; 6e–5c bonds are found between the apical and the basal Al atoms, although the distance is somewhat shorter (272.5 pm). The two types of bonds lie in the (100) plane, for which the electron density distribution and ELF are shown in Figure 4b and can be distinctly differentiated in this case. The larger white regions, with a maximum ELF value of 0.93 between the apical Al atoms, correspond to the electron pairs of the 2e–2c bonds. The smaller white regions between the apical and the basal Al atoms are attributed to multicenter bonds (highest localization value ca. = 0.85). The long Al–Al distances of the quadratic net lie in the (220) plane. The ELF runs through a minimum between these atoms, which can clearly be recognized by the green areas between the basal Al atoms, and which excludes the possibility of a bonding interaction (Fig. 4c). It is this conclusion which allows for the formulation of the 6e–5c bond as such.

Figure 5a shows the structure of $CaAl_2Si_2$. Al atoms and Si atoms form puckered double layers of hexagonal rings. Al and Si atoms are alternately arranged in a net of hexagonal rings at distances of 248.9 pm. The longer Al–Si bonds of 257.2 pm

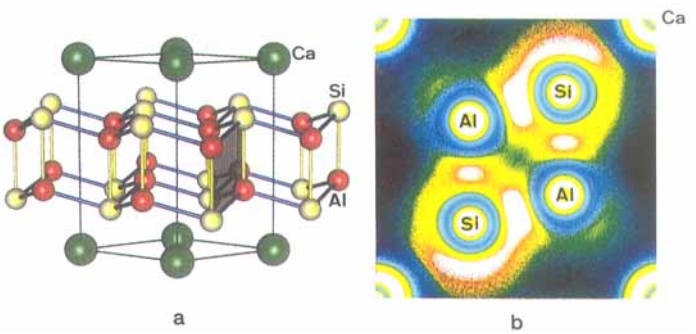


Fig. 5. a) Section from the hexagonal $CaAl_2Si_2$ structure (Ca: green; Al: red; Si: yellow). The short Al–Si distances in a layer of hexagonal rings are colored blue-violet, the long distances connecting the layers colored yellow. The central building block of the double layer, the oblique Al_2Si_2 four-membered ring, is shaded for emphasis. b) ρ and ELF for the (120) plane in $CaAl_2Si_2$. The section shows the Ca nuclei in the corners and an Al_2Si_2 four-membered ring.

connect to form a double layer. The Si atoms in a double layer always occupy the peripheral positions and are rather strangely coordinated by four Al atoms, somewhat resembling an umbrella, whereas the Al atoms are surrounded tetrahedrally by four Si atoms. The Ca atoms are located between the double layers in the middle of two six-membered rings. The (120) plane contains the central building unit of the double layer, an Al_2Si_2 four-membered ring with one long and three short Al–Si bonds. The ELF permits the recognition of a lone electron pair on the Si atom (maximum ELF value = 0.86 for this region). The highest localization values in the valence area of this compound (ca. 0.91), however, are found along the short Si–Al bond (Fig. 5b). This bond, like the longer Si–Al bond connecting the layers, is clearly polarized in the direction of the somewhat more electronegative Si atoms, the maximum ELF value lying at 0.84. The semi shell-shaped distribution of the high ELF values around Si indicates an intermediate state between the purely covalent and ionic situations represented by the formulas

 © VCH Verlagsgesellschaft mbH, D-69451 Weinheim, 1994 0570-0833/94/2020-2071 $ 10.00+.25/0

$Ca^{2+}(Al^{3+})_2(Si^{4-})_2$ and $Ca^{2+}(4b)[AlSi]^{2-}$.[*] A bonding interaction between Al atoms, as had been assumed in the literature,[11] cannot be recognized.

Silicon in the diamond structure (Fig. 6a) does of course have extended regions of high localization between the nuclei, where the bonding electron pairs are situated. Figure 6b shows the (110) plane. The large differences in the electron densities in the valence region are quite remarkable. Very little electron density (black areas) is found between the zigzag chains in comparison to that located in the regions between the cores, where the highest localization values (ELF = 0.95) are found.

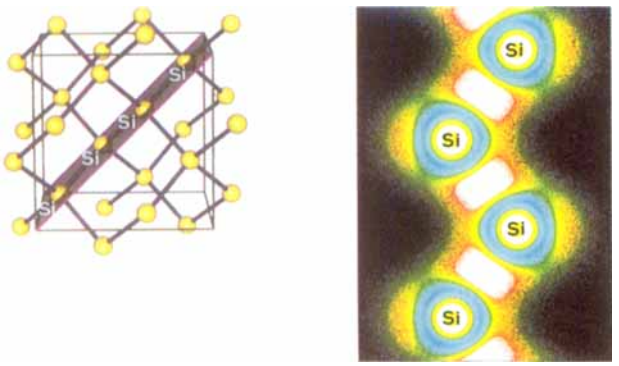


Fig. 6. a) Diamond structure showing the (110) plane. b) ρ and ELF for the (110) plane in α-Si.

Structures with large differences in electron density in the valence regions are normally divided into covalent and ionic structures. In contrast, intermetallic phases have a more uniform density distribution. In spite of this, our ELF results demonstrate that both bonding electron pairs and lone pairs do occur in these compounds, just as in the covalent and ionic structures which are understood in terms of the valence rules. For those compounds in which the chemical bond is described as a metallic bond (fcc Al and $CaAl_2$), the occurrence of numerous ELF maxima (with respect to the number of valence electrons in the unit cell) is characteristic; however, the absolute value of these does not usually exceed 0.75. The number and the position of these maxima can vary to a great extent within a simple structural type.[14] In structures with localized multicentered bonds (6e–5c bond within Al_5 pyramids in $BaAl_4$), the maximum ELF values lie above 0.8 in the regions of these bonds. For bonding electron pairs, maximum ELF values of about 0.9 are to be expected, whereas for lone pairs somewhat smaller values are found.

This relationship is further clarified in the Figures 7a–7d, in which the electron density (dotted line) and the ELF (full line) along symmetrical bonds are plotted in a one-dimensional representation. The shell structure of the cores is easily discernible. Figure 7a shows the Al–Al bond in fcc aluminum and Figure 7b the 2e–2c bond between the apical Al atoms in $BaAl_4$. The electron density difference in the middle of the bond amounts to only about 20%, but the ELF shows impressively the difference between the chemical bonds for the two Al pairs. The course of the ELF along the 2e–2c Al–Al bond is the same as that for the Si–Si bond in α-Si (Fig. 7c). The electron density in the middle of the Si–Si bond, however, is more than twice as

[*] $(4b)[AlSi]^{2-}$ refers to a four-bonded framework made of Si and Al in which each atom is assigned four valence electrons.

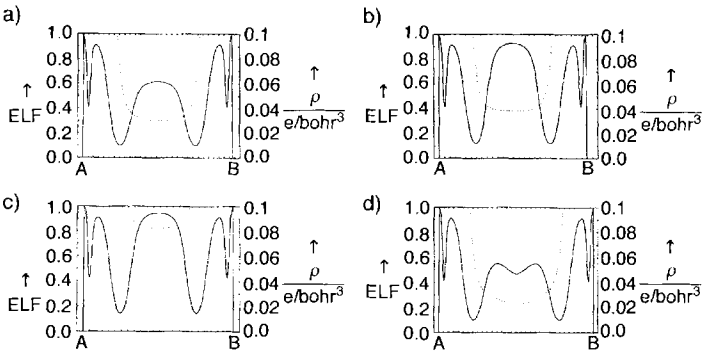


Fig. 7. ρ (dotted line) and ELF (full line) a) along the Al–Al bond in fcc aluminum, b) along the 2e-2c bond between the apical Al atoms in $BaAl_4$, c) along the Si–Si bond in α-Si, d) along the distance between basal atoms in $BaAl_4$. The atoms involved in a particular bond are labeled A and B accordingly.

large as that in the Al–Al bond. Finally, the situation for the large distance between the basal Al atoms in the $BaAl_4$ structure is shown in Figure 7d. The ELF minimum observed between these cores clearly shows the nonbonding character.

This discussion sheds new light on the problem of the interpretation of bond lengths in intermetallic phases: In $BaAl_4$, for example, the Al–Al distance, which is attributed to the 6e–5c bond, is about 6 pm shorter than the 2e–2c bond—contrary to expectations when bond lengths and bond orders are correlated with one another! Similarly, a bond order of around one has to be attributed to the Al–Al distance of 293 pm in $SrAl_2$, although this distance is considerably larger than the Al–Al distance in the metal (286.3 pm) with a bond order of 0.25. In our opinion, a simple relationship between bond length and bond strength[12] or bond order[13] does not exist in the compounds discussed here. In contrast, the ELF can be of decisive assistance in the classification of the diverse interatomic vectors in intermetallic compounds.

New approaches for a more quantitative interpretation of ELF results are being made by using a topological analysis of the ELF (x,y,z) scalar field. The unequivocal attribution of the numbers of electrons to the ELF maxima, described as localization attractors,[15] as well as the possibility of defining a scale of ionic character[16] must be mentioned at this point.

Received: March 19, 1994 [Z6778IE]
German version: *Angew. Chem.* **1994**, *106*, 2147

[1] R. Nesper, *Angew. Chem.* **1991**, *103*, 805; *Angew. Chem. Int. Ed. Engl.* **1991**, *30*, 789.
[2] A. Savin, A. D. Becke, J. Flad, R. Nesper, H. Preuß, H. G. von Schnering, *Angew. Chem.* **1991**, *103*, 421; *Angew. Chem. Int. Ed. Engl.* **1991**, *30*, 409.
[3] A. D. Becke, K. E. Edgecombe, *J. Chem. Phys.* **1990**, *92*, 5397.
[4] R. F. W. Bader, *Atoms in Molecules: A Quantum Theory*, Clarendon, Oxford, **1990**.
[5] A. Savin, O. Jepsen, J. Flad, O. K. Andersen, H. Preuß, H. G. von Schnering, *Angew. Chem.* **1992**, *104*, 186; *Angew. Chem. Int. Ed. Engl.* **1992**, *31*, 187.
[6] A. Burkhard, U. Wedig, H. G. von Schnering, A. Savin, *Z. Anorg. Allg. Chem.* **1993**, *619*, 437.
[7] A different interpretation of ELF is given by A. Savin et al. in [5].
[8] J. Flad, F.-X. Fraschio, B. Miehlich, Programm GRAPA, Institut für Theoretische Chemie der Universität Stuttgart, **1989**.
[9] All structural data taken from P. Villars, L. D. Calvert, *Pearson's Handbook of Crystallographic Data for Intermetallic Phases*, 2nd ed., ASM International, OH, USA, **1991**. Electron density distribution and ELF values calculated using the LMTO method (LMTO = linear muffin tin orbital): M. van Schilfgaarde, T. A. Paxton, O. Jepsen, O. K. Andersen, Program TB-LMTO. Empty spheres at the position $(0,0,\frac{1}{2})$ in the $CaAl_2Si_2$ structure (in the middle of the double layer, Ca at (0,0,0)) and at the site $(\frac{1}{2},\frac{1}{2},\frac{1}{2})$ in the Si–diamond structure (Si at (0,0,0)). The sizes of the muffin-tin spheres were chosen so that the best possible compromise between space-filling and overlap was achieved.

[10] C. Zheng, R. Hoffmann, *Z. Naturforsch. B* **1986**, *41*, 292.
[11] C. Zheng, R. Hoffmann, R. Nesper, H. G. von Schnering, *J. Am. Chem. Soc.* **1986**, *108*, 1876.
[12] L. Pauling, *The Nature of the Chemical Bond*, Cornell University Press, Ithaca, NY, **1960**; *Die Natur der chemischen Bindung*, Verlag Chemie, Weinheim, **1976**.
[13] M. O'Keefe in *Modern Aspects in Inorganic Crystal Chemistry* (*NATO ASI Ser. C* **1992**, *382*, S. 163.
[14] In fcc Ca, the maximum ELF values lie close to the octahedral holes.
[15] U. Häußermann, S. Wengert, R. Nesper, *Angew. Chem.* **1994**, *106*, 2150; *Angew. Chem. Int. Ed. Engl.* **1994**, *33*, 2073.
[16] B. Silvi, A. Savin, unpublished results.

Unequivocal Partitioning of Crystal Structures, Exemplified by Intermetallic Phases Containing Aluminum**

Ulrich Häussermann, Steffen Wengert, and Reinhard Nesper*

Dedicated to Professor Ewald Wicke on the occasion of his 80th birthday

Crystal chemical parameters, such as partial volumes,[1] partial charges,[2] bond strengths,[3] and coordination numbers[4] have long been successfully employed in crystal structure analysis to understand and to interpret structures. There have always been attempts to define such incremental parameters as unequivocally as possible. In this context, the partitioning of space in a crystal structure into domains of its building blocks[***][5] is a useful approach and delivers important information about the parameters mentioned above.

Using the ordering of spheres of equal size as an example, Niggli introduced the concept of the "Wirkungsbereich" as far back as 1927.[5] According to his definition, the Wirkungsbereich of a sphere comprises all points in space whose distances from the sphere are smaller than those to all other spheres. The simplest polyhedron marking this domain is constructed with perpendicular planes at the midpoints of the lines connecting neighboring spheres. When the hypothetical spheres, that is, the atoms or ions, have different radii, the connecting lines can be divided according to the ratio of the radii. In many cases this procedure does, however, lead to polyhedra that are not totally space-filling. The construction procedure developed by Fischer, Koch, and Hellner yields better results.[6] Here, the division of the connecting lines between neighboring spheres by means of the exponential plane construction guarantees that no gaps occur in the partitioning of space and always leads to a convex polyhedron for every occupied point position of the crystal structure. However, this method too is still dependent on the choice of radii for the spheres, that is, on the definition of atomic or ionic radii.[7]

According to Bader,[8] a clear partitioning of the three-dimensional space into atomic domains can be achieved by the analysis of the scalar field, the electron density $\rho(x,y,z)$, and the gradient $\Delta\rho(x,y,z)$. The (3,−1) saddle points[9] of the electron density play an important role here. The sum of all the trajectories[10] that end on these saddle points form surfaces in three-dimensional space, which define the atomic boundary. In crystalline structures, these surfaces form closed polyhedra around the atomic nuclei. The polyhedra fill the volume of the unit cell completely[*] and thus provide the best definition for atomic domains. In addition, the faces of the polyhedra fulfill the conditions for a vanishing density flow, that is, $\Delta\rho(x,y,z)\vec{n}(x,y,z) = 0$ for all points (x,y,z) on these faces, where $\vec{n}(x,y,z)$ is the unit vector perpendicular to the face.

The use of the scalar field, electron localization function (ELF),[11] also leads to an unequivocal partitioning of three-dimensional space. We will designate the resulting fragments as domains of electrons and atomic cores. The regions of space occupied by bonding electrons or lone pairs are examples of domains of valence electrons. Their centers correspond to the local ELF maxima ((3,−3) points) in the valence region. The positions of the nuclei also correspond to local maxima defined by the first electron shell. The other electron shells of the core are, however, not resolved, and the ELF minimum of the outermost filled shell is thus used to specify the domain of an atomic core. The sum of these domains once again fills the unit cell completely.

The boundaries of the domains can be used as limits of integration for the following volume integrals:

a) Volume of domain A: $V_A = \int_{V_A} dV$

b) Number of electrons in this domain A: $N_A = \int_{V_A} \rho(x,y,z)dV$

The volume and the corresponding number of electrons are important characteristic parameters of such a domain or Wirkungsbereich. In addition, the net charge of an atom can be calculated from the corresponding number of electrons of an atomic domain.[12]

There is of course a close relationship between the volume of an atomic domain and the number of electrons. This was recognized by Biltz as far back as 1934.[1] The analysis of the empirically determined domain volumes (volume increments) in a large number of compounds showed that these volumes depend to a large extent on the environment, that is, on the bonding character of the atoms in the structure. In addition to such local influences, Biltz was also able to confirm relationships between the core potentials and the volume requirement of the corresponding valence electrons. This allowed him to define volume increments for three main classes of compounds.

Based on Bader's definition of the domain of an atom, interesting relationships between chemical bonding, volume, and number of electrons can be clearly quantified. This is especially true for changes in these quantities with the formation of a compound. The domain of electrons based on the ELF can be used for the analysis of chemical bonding. Moreover, the volumes and the shapes of both types of domains contain important chemical information relevant to the structure. Based on the example of the series Al, $CaAl_2$, $SrAl_2$, $BaAl_4$, $CaAl_2Si_2$, and Si in which a transition from metallic to covalent bonding occurs,[13] these distinct possibilities of spatial partitioning will be described.[14]

Figure 1a (top) shows the contour diagram of the electron density for face-centerd cubic (fcc) aluminum in the (100) plane. The (3,−1) saddle points lie exactly at the midpoint between neighboring nuclei. The trajectories defining the atomic domains begin at the local density minima of the octahedral holes (edges of the unit cell) and end at the (3,−1) saddle points. In

[*] Prof. Dr. R. Nesper, Dipl.-Chem. U. Häussermann, Dipl.-Chem. S. Wengert
Laboratorium für Anorganische Chemie der Eidgenössischen Technischen Hochschule
Universitätstrasse 6, CH-8092 Zurich (Switzerland)
Telefax: Int. code + (1)632-1149

[**] This work was supported by the Schweizerische Nationalfonds zur Förderung der wissenschaftlichen Forschung.

[***] Also known as Wirkungsbereiche or Dirichlet domain.

[*] A requirement is that the nuclear positions are the sole electron density maxima. This is usually the case [8].

 © VCH Verlagsgesellschaft mbH, D-69451 Weinheim, 1994 0570-0833/94/2020-2073 $ 10.00+.25/0

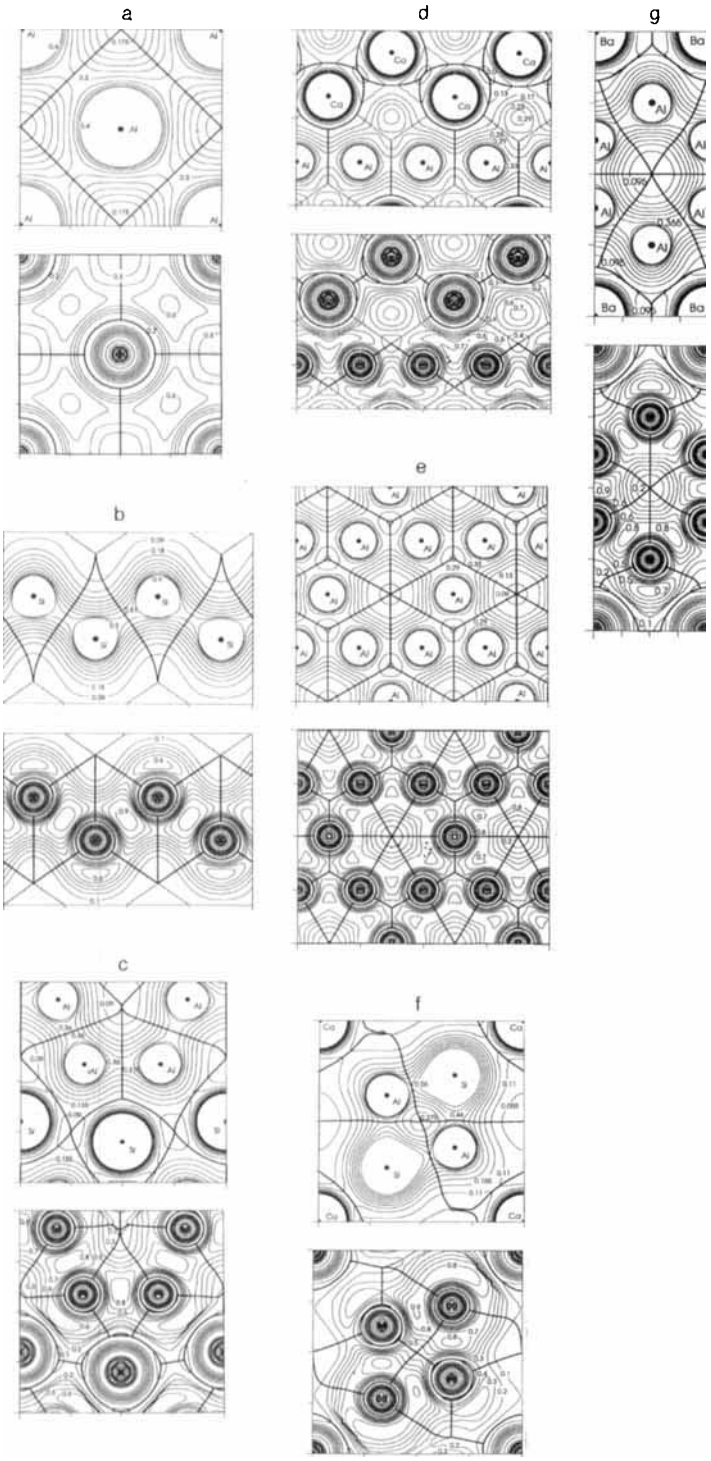


Fig. 1. Electron density distribution ρ (top; in units of 0.1 e bohr^{-3}) and ELF values (bottom; the interval between neighboring ELF lines is 0.1). The trajectories defining domains are shown as thicker lines. The analyzed crystallographic plane is given; this is followed by the range of contour lines for the electron density and the interval between neighboring contour lines (in e bohr^{-3}). a) (100) plane in fcc Al, 0.015 0.040, 0.0025. b) (110) plane in α-Si, 0–0.09, 0.009. Trajectories common to ρ and ELF are colored gray. c) (040) plane in $SrAl_2$, 0–0.045, 0.0045. d) (110) plane in $CaAl_2$, 0.005–0.045, 0.004. e) (111) plane in $CaAl_2$, 0.005–0.045, 0.004. f) (120) plane in $CaAl_2Si_2$, 0–0.055, 0.0055. g) (100) plane in $BaAl_4$, 0.005–0.05, 0.0045. The sectional planes of all the contour diagrams are shown in the drawings of the structures in ref. [13].

this simple case, they correspond exactly to the boundaries of the geometrical domain. In the three-dimensional picture, a cubooctahedron is formed as a convex polyhedron enclosing the atomic domain. Its vertices are the octahedral and tetrahedral holes of this structure (cf. Fig. 2a).

The ELF for the (100) plane is shown in Figure 1a, bottom. The maxima of this function occur between the atomic cores and, of course, in the region of the electron shells. Three critical points lie on every line connecting an octahedral hole and an atomic nucleus: the octahedral hole itself is a local ELF minimum; a (3,−1) saddle point follows, and finally, a further local minimum occurs at the boundary between the core and valence regions. Three trajectories emanate from these minima. One ends at the above-mentioned (3,−1) saddle point and forms, together with the trajectory starting from the octahedral hole, the boundary between the domains of the metallic bond in fcc aluminum. The other two trajectories end at (3,−1) saddle points on the line connecting two neighboring Al atoms. They virtually form a quarter circle and, together with symmetry-

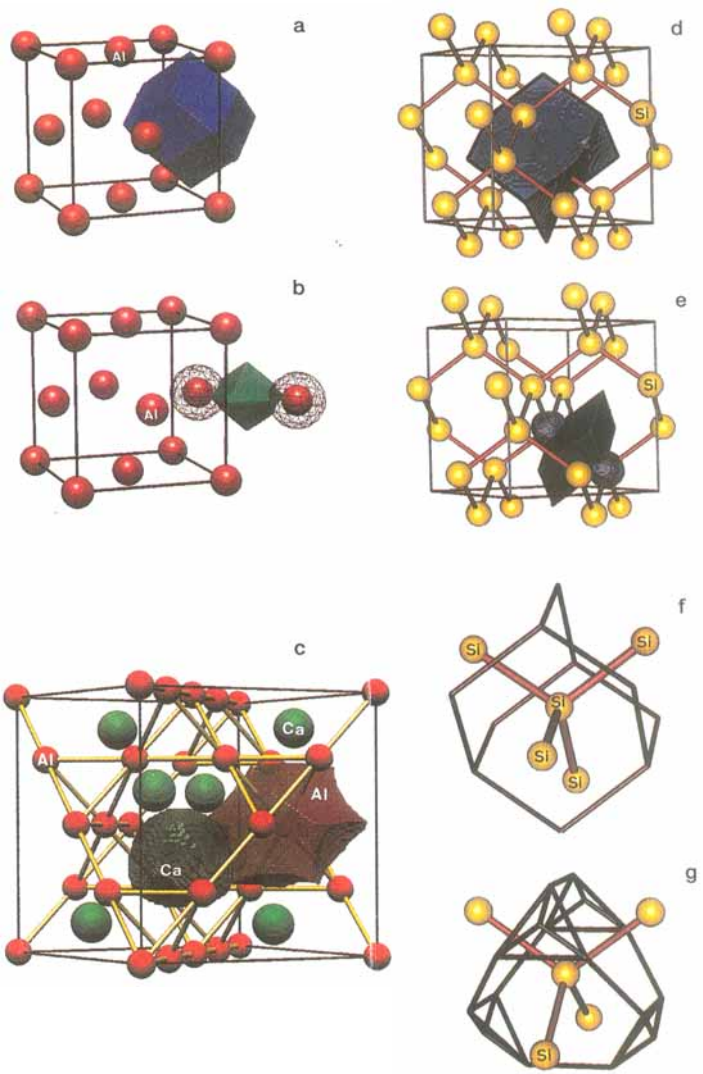


Fig. 2.a) Domain of an Al atom (blue) in fcc Al [20]. b) Domain of the metallic bond (green) in fcc Al. The adjacent atomic core domains shown as wire frames. c) Domain of a Ca atom (green) and of an Al atom (red) in $CaAl_2$. d) Domain of a Si atom (blue) in α-Si. e) Domains of a Si–Si single bond (black-green) and of two Si cores (blue). f) and g) Edges of different polyhedra enclosing atomic domains in α-Si: the saddle polyhedron from the Bader partitioning (f) and of the geometrically constructed convex polyhedron (g).

 © VCH Verlagsgesellschaft mbH, D-69451 Weinheim, 1994 0570-0833/94/2020-2074 $ 10.00+.25/0

equivalent trajectories, the boundary of the domain of the atomic core. A domain of the metallic bond is shown in Figure 2b. It can be seen that the complete ensemble of polyhedra representing the electronic domains also contains all the edges of the atomic domains.

α-Si in the diamond structure is also a simple, yet interesting example. The contour diagrams of the electron density and ELF (Fig. 1b) were calculated for the (110) plane. The domains of the Si atoms are defined by curved trajectories. The three-dimensional picture (Fig. 2d) shows a so-called saddle polyhedron. Its straight edges form an adamantane-like cage. However, the polyhedron faces are curved and correspond to the D^* minimal surface.[16] This saddle polyhedron was described by P. Pearce as the diamond saddle polyhedron (Fig. 2f).[15] The result of a simple geometrical domain construction is of course a convex polyhedron with flat faces. Its edges can be seen in Figure 2g. The domains of the Si–Si bonding electron pairs are defined exclusively by flat surfaces in this case (Fig. 2e). As in fcc Al, these polyhedra also contain the edges of the atomic domains. In both cases the common edges form the labyrinth network of a periodic minimal surface: the D^* surface in Si and the FF^*_{2x}-FP_2 surface in Al.[16] Labyrinth nets describe the tunnel system of a periodic minimal surface.[17] Whether or not the common trajectories generally have this relationship to periodic minimum surfaces has yet to be investigated in detail. In the binary compound $CaAl_2$ (Fig. 1d, 1e, and 2c), which like α-Si crystallizes in the space group $Fd\bar{3}m$, the Ca atoms lie on nodes of the labyrinth net of the D^* surface formed from these special trajectories.[*]

In Figures 1c, 1g, and 1f, the contour diagrams of the electron density distribution and ELF values are shown for high-symmetry planes of the compounds $SrAl_2$, $BaAl_4$, and $CaAl_2Si_2$, respectively. The domains of the electrons in $BaAl_4$ and $SrAl_2$ correspond to the different Al–Al bonds. In addition to the domains for the Al–Si bonds in $CaAl_2Si_2$, another one for the Si lone pair is observed, which is symmetrically coordinated by three Ca atoms (cf. Fig. 5 in ref. [13]).

The results of the volume integrations are summarized in Tables 1 and 2.[18] In the compounds $CaAl_2$ (Fig. 2a in ref. [13]) and $SrAl_2$ (Fig. 3a in ref. [13]), the extent of the charge transfer from the atoms of the alkaline earth metal to the more electronegative Al atoms is approximately the same; Ca and Sr have a positive net charge of $q \approx 1$. This means that a conclusion regarding the electron localization in the Al partial structure, as described in the simple Zintl–Klemm concept for semiconductors, may not necessarily be drawn from the effective charge transfer. Three electronic domains occur in $SrAl_2$ corresponding to the three different Al–Al bonds (Table 2). Electron numbers greater than 2 ($N_{val} = 2.13$) were assigned to the bonds with a length of 279.9 pm in the slightly puckered net of six-membered rings. This indicates the presence of a π-bonding component. In contrast, the domain of the long Al–Al bonds connecting the layers contains only 1.6 electrons. On the whole, relatively high localization values are observed (ELF_{max} is larger than 0.88 in all three cases; cf. Fig. 1c, bottom). In contrast, the localization in the electronic domains in $CaAl_2$ is distinctly weaker ($ELF_{max} = 0.739$; cf. Fig. 1d and 1e, bottom) in spite of the equally large charge transfer M → Al.

From a purely stoichiometric point of view, one would expect the larger charge transfer for MAl_4 in the series MAl_2, MAl_4. This is, however, not the case: in $BaAl_4$ (Fig. 4a in ref. [13]) the positive net charge on Ba is only 0.67 (Table 1). The Al atoms form a net of square pyramids. In the ternary variants of this structure type, the more electronegative atoms are usually found at the apical positions. In the binary $BaAl_4$, however, the apical Al atoms have a positive net charge of 0.43, while the basal Al

[*] The labyrinth net of the D^* surface in $CaAl_2$ is shifted by 1/8,1/8,1/8 relative to the position in α-Si.

Table 1. Classification of the atomic domains.

Compound	Domain	n [a]	V [b]	V_{elem} [c]	N_{val} [b]	q [d]
fcc-Al	Al atom	4	16.70	16.59	3.01	
	Σ		66.8 (66.4)		12.0 (12.0)	
$CaAl_2$	Ca atom	8	16.33	43.63	0.99	1.01
	Al atom	16	24.18	16.59	3.50	−0.50
	Σ		517.5 (519.3)		63.9 (64.0)	
$SrAl_2$	Sr atom	4	22.51	53.30	1.01	0.99
	Al atom	8	27.13	16.59	3.51	−0.51
	Σ		307.1 (306.3)		32.1 (32.0)	
$BaAl_4$	Ba atom	2	31.82	62.99	1.33	0.67
	Al_{apical} atom	4	18.50	16.59	2.57	0.43
	Al_{basal} atom	4	25.44	16.59	3.75	−0.75
	Σ		239.4 (239.0)		27.9 (28.0)	
$CaAl_2Si_2$	Ca atom	1	15.11	43.63	0.77	1.23
	Al atom	2	10.56	16.59	1.46	1.54
	Si atom	2	34.87	20.00	6.18	−2.18
	Σ		106.0 (105.5)		16.1 (16.0)	
α-Si	Si atom	8	20.05	20.00	4.03	
	Σ		160.4 (160.0)		32.2 (32.0)	

[a] n is the frequency of a domain in the unit cell. [b] V is the corresponding volume (in 10^6 pm^3) and N_{val} the corresponding number of valence electrons. The sums of the volumes for the domains and the numbers of electrons (Σ lines) are compared with the volumes and the total numbers of valence electrons in the unit cells (in parentheses). The deviations are less than 1% [18]. [c] V_{elem} is the atomic volume (in 10^6 pm^3) taken from the elemntal structure. [d] q is the net charge of a particular atom [12].

Table 2. Classification of the electronic domains.

Compound	Domain	n	ELF_{max} [a]	V [b]	N_{val} [b]	N_{val}/V [c]
fcc-Al	Al-Al (286.3 pm)	24	0.620	2.51	0.50	0.20
	Al core	4		1.53		
	Σ			66.5 (66.4)	11.9 (12.0)	
$CaAl_2$	Al-Al (284.2 pm)	48	0.739	8.82	1.30	0.15
	Ca core	8		8.99		
	Al core	16		1.51		
	Σ			519.4 (519.3)	62.2 (64.0)	
$SrAl_2$	Al-Al (278.6 pm)	4	0.889	15.54	2.01	0.13
	Al-Al (279.9 pm)	8	0.885	16.69	2.13	0.13
	Al-Al (293.0 pm)	4	0.884	11.37	1.60	0.14
	Sr core	4		13.39		
	Al core	8		1.51		
	Σ			306.4 (306.3)	31.5 (32.0)	
$BaAl_4$	Al_a-Al_a (278.4 pm)	2	0.928	16.97	2.05	0.12
	Al_b-Al_b (272.5 pm)	16	0.854	9.54	1.45	0.15
	Ba core	2		20.04		
	Al_{apical} core	4		1.52		
	Al_{basal} core	4		1.49		
	Σ			238.7 (239.0)	27.3 (28.0)	
$CaAl_2Si_2$	lone pair	2	0.858	13.88	1.96	0.14
	Al-Si (248.9 pm)	6	0.911	9.03	1.67	0.19
	Al-Si (257.2 pm)	2	0.842	4.92	1.00	0.20
	Ca core	1		9.12		
	Al core	2		1.55		
	Si core	2		0.91		
	Σ			105.8 (105.5)	15.9 (16.0)	
α-Si	Si-Si (235.1 pm)	16	0.947	9.61	2.02	0.21
	Si core	8		0.91		
	Σ			161.0 (160.0)	32.2 (32.0)	

[a] ELF_{max} is the largest ELF value in a domain. [b] V is the volume of a domain (in 10^6 pm^3) and N_{val} the corresponding number of valence electrons. Here, the sum of the numbers of electrons in the domains is always smaller than the total number of electrons in the unit cells. The deviation can be as large as 3% [18]. [c] N_{val}/V is the average electronic density (in e10^{-6} pm^{-3}) in a particular domain.

 © VCH Verlagsgesellschaft mbH, D-69451 Weinheim, 1994 0570-0833/94/2020-2075 $ 10.00+.25/0

atoms have a clear negative polarization ($q = -0.75$). This admittedly contradicts the net charge calculated from the population analysis in ref. [19] (but, see [12]); however, the number of electrons for the two electronic domains agree excellently with the results of the analysis of chemical bonding in ref. [19]: a two-electron, two-center (2e2c) bond connects the apical Al atoms (bond length 278.4 pm), whereas apical and basal Al atoms (Al–Al distance 272.5 pm) are bound through a 6e5c bond (this corresponds to 1.5 electrons per domain). The electron numbers attributed to the two electronic domains are 2.05 and 1.45, respectively.

In $CaAl_2Si_2$ (Fig. 5a in ref. [13]), the atoms of the alkaline earth metal have a higher oxidation state than in the binary aluminides ($q = 1.23$, Table 1). The polarization of the Al atoms is also distinctly positive ($q = 1.54$), although the difference in the electronegativity between Al and Si is small. A high net charge of -2.18 is observed for Si. The domain of the Si lone pair contains almost exactly two electrons ($N_{val} = 1.96$) and has, in agreement with the Gillespie–Nyholm rules, the largest volume of all electronic domains in this structure (Table 2). The short Al–Si distance of 248.9 pm within the puckered layer of six-membered rings and the longer distance between layers are not consistent with a 2e2c bond ($N_{val} = 1.67$ and 1.00, respectively). A total of six electrons are found distributed among four topological contacts.

For the positively polarized atoms of the alkaline earth metal, the volumes of the domains are between 2 and 2.5 times smaller than the atomic volumes in the elemental structures (cf. V and V_{elem} in Table 1). This reflects the well-known volume contraction observed in the formation of these compounds from their elements, since the increase in volume for the domain of the negatively polarized components only lies between 46% (Al in $CaAl_2$) and 74% (Si in $CaAl_2Si_2$). It would be interesting to determine just how far the electronegative component in intermetallic phases and Zintl phases can be reduced and what domain volumes result from this process. It seems important to us that well-defined effective charge transfer can also be considerable in intermetallic phases. The atomic domains of the alkaline earth metals basically resemble polarized spheres, and their shape is therefore still similar to that typical of ions.

Received: April 13, 1994 [Z6846IE]
German version: *Angew. Chem.* **1994**, *106*, 2150

[1] W. Biltz, *Raumchemie der festen Stoffe*, L. Voss Verlag, Leipzig, **1934**.
[2] R. S. Mulliken, *J. Chem. Phys.* **1955**, *23*, 1833.
[3] L. Pauling, *The Nature of Chemical Bond*, Cornell University Press, Ithaca, New York, **1960**; *Die Natur der chemischen Bindung*, Verlag Chemie, Weinheim, **1976**.
[4] R. Hoppe, *Angew. Chem.* **1970**, *82*, 7; *Angew. Chem. Int. Ed. Engl.* **1970**, *9*, 25.
[5] P. Niggli, *Z. Kristallogr.* **1927**, *65*, 391; *ibid.* **1928**, *68*, 404.
[6] W. Fischer, E. Koch, E. Hellner, *Neues Jahrb. Mineral. Monatsh.* **1971**, 227.
[7] W. Fischer, E. Koch, *Neues Jahrb. Mineral. Monatsh.* **1973**, 361.
[8] R. F. W. Bader, *Atoms in Molecules: A Quantum Theory*, Clarendon Press, Oxford, **1990** (this book contains a detailed overview of the literature); R. F. W. Bader, P. L. A. Popelier, T. A. Keith, *Angew. Chem.* **1994**, *106*, 647; *Angew. Chem. Int. Ed. Engl.* **1994**, *33*, 620 (this very good recent review gives a clear introduction to the quantum mechanical definition of an atom and of a functional group in a molecule; this definition is also the basis for the calculation of expectation values for such subsystems.)
[9] Saddle points are among the critical points for which $\nabla\rho(x,y,z) = 0$. Four types of critical points can occur. They are classified by the eigenvalues of the matrix of the second derivative. A (3,−3) point is a local maximum. Although, strictly speaking, $\nabla\rho(x,y,z)$ is not defined at the nuclear positions, the nuclear positions behave topologically like (3,−3) points. (3, +1) and (3,−1) points are saddle points. A (3,−1) point often occurs between neighboring nuclei and is therefore also described as a bond critical point. (3, + 3) points are local minima.
[10] Trajectories are lines along the gradient vector that indicate the direction from one point in space to another. Here, they run orthogonally to the lines of equal density. In crystalline structures they begin and end at critical points. All points in space, with the exception of the critical points, can only be traversed by a single trajectory.
[11] A. D. Becke, K. E. Edgecombe, *J. Chem. Phys.* **1990**, *92*, 5397.
[12] The net charge q_A of an atom A is the difference between the nuclear charge Z_A and the number of electrons N_A. The use of N_A as defined in the text for the determination of the net charge has the advantage that this definition is unambiguous. In contrast, the calculation of the net charge from quantum mechanical population analyses is dependent on the choice of definition for the parameter N_A, on the one hand, and of the basis set on the other. These factors can have a significant effect on the resulting net charge.
[13] U. Häussermann, S. Wengert, P. Hofmann, A. Savin, O. Jepsen, R. Nesper, *Angew. Chem.* **1994**, *106*, 2147; *Angew. Chem. Int. Ed. Engl.* **1994**, *33*, 2069. Here, all structures are depicted and discussed in detail.
[14] See ref. [9] in ref. [13].
[15] P. Pearce, *Structure in Nature is a Strategy for Design*, MIT Press, Cambridge, MA, USA, **1978**, p. 90.
[16] H. G. von Schnering, R. Nesper, *Z. Phys. B* **1991**, *83*, 407.
[17] S. T. Hyde, S. Andersson, *Z. Kristallogr.* **1984**, *168*, 221.
[18] The volume integrals were only calculated approximately: The volume of the domain A: $V_A \approx \sum_{i \in V_A} \Delta V_i$; corresponding number of electrons: $N_A \approx \sum_{i \in V_A} \rho_i \Delta V_i$. The index i refers to a grid point (x,y,z) at which ρ and ELF were calculated. The chosen grid-point density usually gave a ΔV_i of about 5×10^{-4} Å^3. The grid points i were subsequently attributed to a domain A by means of a simple algorithm. If a grid point happened to fall on the border between two domains, its volumes were divided among these according to the trajectory course. The sum of the volumes of the domains should give the volume of the unit cell. The deviations lie below 1% (see Table 1 and 2). Only the valence electron density was used in the calculation of the number of electrons in a particular atomic domain. This is because the contribution from the core functions cannot be determined by means of this simple method due to the large change near the nucleus. The sum of the number of electrons obtained by this method gives, to a good approximation, the total number of valence electrons in the unit cell (Table 1). Whether or not the numbers of electrons for the electronic domains also add up to the total number of valence electrons in the unit cell still has to be investigated in more detail. This seems to be the case for the structures of elemental Al and Si, whereas distinct deviations occur for the other compounds. One reason for this is probably the strong dependence of the core volumes of the alkaline earth metals on the size of the muffin-tin spheres. These volumes are possibly incorrect, in which case the adjacent electronic domains will also be affected.
[19] C. Zheng, R. Hoffmann, *Z. Naturforsch. B* **1986**, *41*, 292.
[20] P. Hofmann, R. Nesper, *Programm COLTURE*, Laboratorium für Anorganische Chemie der ETH Zürich, **1993**.

Totally Enantioselective Inversion of Configuration of (*S*)-(+)-Carnitine Derivatives

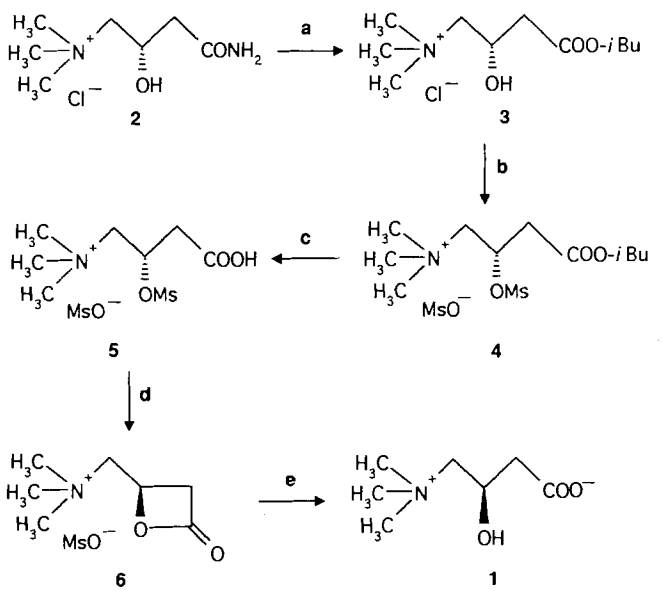
Ida Bernabei, Roberto Castagnani, Francesco De Angelis, Paolo De Witt Scalfaro, Fabio Giannessi,* Domenico Misiti, Sandra Muck, Nazareno Scafetta, and Maria Ornella Tinti

The importance of configuration in biologically active compounds,[1] which is emphasized by the strict rules governing the use of chiral compounds in medicinal applications, forces pharmaceutical companies to develop chiral drugs as single enantiomers.[2] In the case of carnitine, the "chirotechnological" problem has always been of concern, since only the (*R*)-(−) enantiomer **1** is biologically active[3] and is involved in fatty acid metabolism,[4] while the (*S*) isomer is a competitive inhibitor of the (*R*) isomer.[5]

[*] Dr. F. Giannessi, Dipl.-Chem. I. Bernabei, Dr. R. Castagnani, Dr. P. De Witt Scalfaro, Dr. S. Muck, Dipl.-Chem. N. Scafetta, Dr. M. O. Tinti
Dipartimento Ricerca Chimica, Sigma-Tau
Via Pontina Km 30.400, I-00040 Pomezia/Roma (Italy)
Telefax: Int. code + (6)9139-3638
Prof. Dr. F. De Angelis
Dipartimento di Chimica, Ingegneria Chimica e Materiali,
Università di L'Aquila (Italy)
Prof. Dr. D. Misiti
Dipartimento di Studi di Chimica e Tecnologia delle Sostanze Biologicamente Attive
Universitá "La Sapienza", Roma (Italy)

Industrially, the (*R*) isomer is produced economically and on a multiton scale by traditional fractional crystallization of the diastereoisomeric salt of racemic carnitinamide with D-canforic acid.[6] The obvious drawbacks of this procedure are the cost of production, storage or disposal costs for half the starting material, and the resulting chemical pollution. Chemical racemization of the undesired isomer, which would have allowed recrystallization of the resulting racemate, was not successful.[7] Dehydration followed by microbiological stereospecific rehydration of the double bond[8] is not feasible on an industrial scale. Also, asymmetric synthetic processes require large amounts of relatively costly starting materials, reagents, or catalysts.[9]

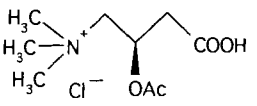
We report here on a straightforward and high-yielding route to (*R*)-(−)-carnitine (**1**) starting from the enantiomerically pure (*S*)-(+)-carnitinamide (**2**) (Scheme 1), which is formed as the undesired by-product during the production of the active enantiomer.[6]



Scheme 1. Asymmetric synthesis of (*R*)-(−)carnitine (**1**) from enantiomerically pure (*S*)-(+)-carnitinamide (**2**). a) *i*BuOH, HCl gas, reflux (90%); b) methanesulfonic anhydride (3 equiv), 80 °C, 24 h (99%); c) 2 M HCl, 55 °C, 20 h (90%); d) $NaHCO_3$ (1 equiv), RT, 20 h; e) $NaHCO_3$ (1 equiv), RT, 20 h, (99% over two steps; >99% *ee*). Ms = methanesulfonyl.

The key step is the totally enantioselective inversion of the stereogenic center, which is accomplished through the intermediacy of the (*R*) β-lactone **6**. We devised this β-lactone route after the classical Mitsunobu reaction[10] failed. We tentatively propose that this failure is caused by the intrinsic instability of the reaction intermediate owing to the high concentration of charge at the trimethylammonium moiety. Our strategy exploits the merits of the methanesulfonate **5**, namely, the electrophilicity of the β carbon atom and the nucleophilicity of the carboxylic function: this permits a strict stereochemical control of the reaction, which proceeds with hydroxyl group activation.[11]

The methanesulfonate **5** was obtained from the (*S*)-(+)-carnitinamide chloride **2** by standard reactions: sulfonylation was achieved by treatment of **3** with an excess of methanesulfonic anhydride in acetonitrile or, preferentially, by fusion of the reagent mixture at 80 °C.[12] Ester hydrolysis under acidic conditions yielded **5**. Treatment of **5** with one equivalent of $NaHCO_3$ in water at room temperature for 20 h gave the carnitine lactone **6** ($[\alpha]_D = -24.7$ ($c = 1$, MeOH)), which could not be crystallized.[13] Saponification with a second equivalent of $NaHCO_3$ gave the expected (*R*)-(−)-carnitine (**1**) (>99% *ee*) in quantitative yield.[14] The sign of the specific rotation of **6** suggests the (*R*) configuration for the β carbon atom—by analogy with the well-established configuration of acetyl-(*R*)-carnitine **7** ($[\alpha]_D = -27.3$ ($c = 1$, MeOH)). The total yield of the reaction sequence was 80%.



7

The stereochemical course of the reaction clearly indicates that the two key steps, formation of lactone **6** and its hydrolysis, must be totally stereoselective. Since the starting material **5** has an (*S*) and the lactone **6** an (*R*) configuration, the latter must have been formed with inversion of configuration at the stereogenic center. The trimethylammonium moiety probably favors the intramolecular approach of the carboxylate group, which leads to ring closure. Nucleophilic attack of the hydroxide ion at the acyl carbon atom results in totally regioselective ring opening of the β-lactone ring to give optically pure (*R*)-(−)-carnitine,[15] as expected for oxygen–acyl bond fission in a slightly basic medium.[11]

The β-lactone **6** and its enantiomer appear to open a general route to stereochemically controlled preparations of carnitine analogues and derivatives. Also, replacement of the mesylation reagents with other reagents might yield synthetically useful compounds with different active functional groups.

Experimental Procedure

3: A stirred suspension of **2** (10 g, 0.05 mol) in isobutyl alcohol (50 mL) was cooled at 4 °C and saturated with HCl gas. The reaction mixture was refluxed for 1 h and then filtered whilst still hot to remove NH_4Cl. The filtrate was concentrated under vacuum, and the residue was taken up twice into isobutyl alcohol (2 × 50 mL) and concentrated to dryness. The residue was triturated with acetone to give, after filtration, **3** (11.6 g, 90%). M.p. 150 °C (decomp.); $[\alpha]_D = +15.0$ ($c = 1$ in H_2O); ^1H NMR (300 MHz, D_2O, 25 °C): $\delta = 4.7$ (m, 1H), 4.0–3.9 (m, 2H), 3.5 (m, 2H), 3.2 (s, 9H), 2.7 (m, 2H), 2.0–1.9 (m, 1H), 0.9 (d, $^3J = 7$ Hz, 6H); IR (KBr): $\tilde{\nu}$[cm^{-1}] = 1730 (C=O); MS (FAB): *m/z*: 218 [*M*$^+$]; correct C, H, N, Cl analysis for $C_{11}H_{24}ClNO_3$

4: A mixture of **3** (2.5 g, 0.01 mol) and methanesulfonic anhydride (5.2 g, 0.03 mol) was heated at 80 °C for 24 h. The mixture was taken up into CH_2Cl_2 (20 mL), and the product was precipitated with Et_2O. This procedure was repeated three times in order to thoroughly eliminate the residual anhydride to give **4** (3.9 g, 99%). M.p. 137–140 °C (decomp.); $[\alpha]_D = +24.7$ ($c = 1$ in H_2O); ^1H NMR (300 MHz, D_2O, 25 °C): $\delta = 5.5$ (m, 1H), 3.9–3.8 (m, 3H), 3.6 (dd, $^2J = 16$ Hz, $^3J = 1.3$ Hz, 1H), 3.2 (s, 3H), 3.1 (s, 9H), 3.0 (m, 2H), 2.7 (s, 3H), 1.8 (m, 1H), 0.8 (d, $^3J = 7$ Hz, 6H); IR (KBr): $\tilde{\nu}$[cm^{-1}] = 1731 (C=O), 1341, 1200 (CH_3SO_3); MS (FAB): *m/z*: 296 [*M*$^+$]; correct C, H, N, S analysis for $C_{13}H_{29}NO_6S_2$

5: A solution of **4** (3.9 g, 0.01 mol) in HCl (2 N, 65 mL) was heated at 50 °C for 20 h. The solution was then concentrated to dryness under vacuum, and the residue was triturated with acetone to give, after filtration, pure **5** (3.3 g, 90%). M.p. 148–150 °C (decomp.); $[\alpha]_D = +22.0$ ($c = 1$ in H_2O); ^1H NMR (300 MHz, D_2O, 25 °C): $\delta = 5.5$ (m, 1H), 3.9 (dd, $^2J = 16$ Hz, $^3J = 10.6$ Hz, 1H), 3.6 (dd, $^2J = 16$ Hz, $^3J = 1.3$ Hz, 1H), 3.2 (s, 3H), 3.1 (s, 9H), 2.9 (m, 2H), 2.7 (s, 3H); IR (KBr): $\tilde{\nu}$[cm^{-1}] = 1713 (C=O), 1332, 1200 (CH_3SO_3); MS (FAB): *m/z*: 240 [*M*$^+$]; correct C, H, N analysis for $C_9H_{21}NO_8S_2$

1: $NaHCO_3$ (375.5 mg, 4.47 mmol) was added to a solution of **5** (1.5 g, 4.47 mmol) in H_2O (25 mL), and the solution was allowed to stand at room temperature for 20 h with stirring. Additional $NaHCO_3$ (375.5 mg, 4.47 mmol) was added and the solution was stirred at room temperature for 24 h. The solution was then transferred into Amberlite IRA-402 (20 g, OH-form), and eluted with deionized water till pH = 7. The collected eluate was concentrated (10 mL) and transferred onto Amberlite IRC-50 (20 g), and **1** was eluted completely. Evaporation under vacuum gave **1** in practically quantitative yield (720 mg, >99%).

6: A solution of **5** (1.5 g, 4.47 mmol) in H_2O was transferred onto Amberlite IRA-402 (30 g, activated as HCO_3^-) at 5 °C and eluted with cold water (5 °C). The eluate was allowed to stand for 4 h at room temperature to give, after water evaporation under vacuum, a crude product, which was taken up into CH_3CN and filtered. The filtrate was evaporated to dryness to give **6** (0.855 g, 80%) as a white solid. M.p. 160 °C (decomp.); $[\alpha]_D = -24.7$ ($c = 1$ in MeOH); ^1H NMR (300 MHz, D_2O, 25 °C): $\delta = 5.35–5.25$ (m, 1H), 3.98–3.89 (m, 3H), 3.54–3.46 (dd, $^2J = 16.8$ Hz,

 © VCH Verlagsgesellschaft mbH, D-69451 Weinheim, 1994 0570-0833/94/2020-2077 $ 10.00+.25/0

^3J = 4.8 Hz, 1 H), 3.26 (s, 9 H), 2.81 (s, 3 H); IR (KBr): $\tilde{\nu}$[cm^{-1}] = 1835 (C=O); MS (FAB): m/z: 144 [M^+]; correct C, H, N analysis for $C_8H_{17}NO_5S$.

Received: May 19, 1994 [Z 6952 IE]
German version: *Angew. Chem.* **1994**, *106*, 2202

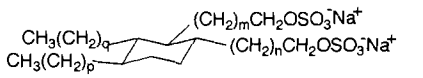
[1] R. Crossley, *Tetrahedron* **1992**, *48*, 8155–8178.
[2] S. C. Stinson, *Chem. Eng. News* **1992**, *70(39)*, 46–79; *ibid.* **1993**, *71(39)*, 38–65.
[3] Natural L-carnitine has the (*R*) configuration: T. Kaneko, R. Yoshida, *Bull. Chem. Soc. Jpn.* **1962**, *35*, 1153–1155.
[4] I. B. Fritz in *Current Concepts in Carnitine Research* (Ed.: A. L. Carter), CRC Press **1992**, pp. 107–119; K. L. Goa, R. N. Brogden, *Drugs* **1987**, *34*, 1–24; S. Di Donato, B. Garavaglia, M. Rimoldi, F. Carrara in *L-Carnitine and its Role in Medicine: from Function to Therapy* (Eds.: R. Ferrari, S. Di Mauro, G. Sherwood), Academic Press, **1992**, pp. 85–98.
[5] T. C. Vary, J. R. Neely, *Am. J. Physiol.* **1982**, *242*, H585–H592; R. Bressler, K. Brendel, *J. Biol. Chem.* **1966**, *241*, 4092–4097.
[6] C. Cavazza (Sigma-Tau), BE-B 877609, **1979** [*Chem. Abstr.* **1980**, *93*, 114973 v].
[7] Unpublished results.
[8] S. Shapiro, M. Bernardini, C. Sih (Sigma-Tau), EP-A1 457735, **1991** [*Chem. Abstr.* **1992**, *116*, 150142a].
[9] H. C. Kolb, Y. L. Bennani, K. B. Sharpless, *Tetrahedron: Asymmetry* **1993**, *4*, 133–141; M. Bols, I. Lundt, C. Pedersen, *Tetrahedron* **1992**, *48*, 319–324; F. D. Bellamy, M. Bondoux, P. Dodey, *Tetrahedron Lett.* **1990**, *31*, 7323–7326; H. Takeda, S. Hosokava, M. Aburatani, K. Achiva, *Synlett* **1991**, *3*, 193–194; P. Renaud, D. Seebach, *Synthesis* **1986**, *3*, 424–426; K. Bock, I. Lundt, C. Pedersen, *Acta Chem. Scand.* **1983**, *B37*, 341–344.
[10] O. Mitsunobu, *Synthesis* **1981**, *1*, 1–28; S. E. Ramer, R. N. Moore, J. C. Vederas, *Can. J. Chem.* **1986**, *64*, 706.
[11] A. Pommier, J. M. Pons, *Synthesis* **1993**, *5*, 441–459.
[12] a) F. Giannessi, N. Scafetta, I. Bernabei, M. O. Tinti, F. De Angelis, P. De Witt Scalfaro, D. Misiti (Sigma-Tau) RM93A00027, **1993**. b) An alternative route to the methanesulfonate derivative **5** could be conversion of (*S*)-(+)-carnitine perchlorate into its benzyl ester, followed by mesylation with methanesulfonyl chloride in pyridine, and final cleavage of the benzyl group by hydrogenation over Pd/C: F. Giannessi, M. L. Bolognesi, M. O. Tinti, F. De Angelis, P. De Witt Scalfaro, D. Misiti (Sigma-Tau) RM92A000915, **1992**. c) Alternatively, methanesulfonyl chloride in pyridine could be used in the mesylation of isobutyl ester **3**.
[13] The structure of lactone **6** was determined on an analytically pure sample (see *Experimental Procedure* for isolation, purification, and characterization) by ^{1}H NMR spectroscopy: the chemical shift of the proton linked to the β carbon atom is typical of acylcarnitines (cf., δ (**7**) = 5.6 (β-H) in D_2O).
[14] Lactone **6** need not be isolated [12a].
[15] $[\alpha]_D$ (**1**) = −31 (c = 10 in H_2O); for comparison, the specific rotation of (*S*)-(+)-carnitine obtained by hydrolysis of (*S*)-(+)-carnitinamide (**2**) is $[\alpha]_D$ = +31 (c = 10 in H_2O). We could not detect traces of the enantiomer of **1**; the enantiomeric purity (>99% *ee*) was established by treating the final product with (+)-1-(9-fluorenyl)ethylchloroformate [(+)-FLEC] and examining the resulting ester by HPLC [16].
[16] P. De Witt Scalfaro, R. Dejas, S. Muck, B. Galletti, D. Meloni, P. Celletti, A. Marzo, *J. Chrom. Biomed. Appl.*, **1994**, *657*, 67–73.

Assembly Properties of Bolaamphiphiles from Dimeric Acids**

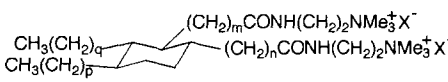
Pilar Bosch,* José L. Parra, and Alfonso de la Maza

Self-organization is an important feature of many biologically relevant molecules.[1] One of the most interesting questions which arises is whether it is possible to develop new materials that simulate natural supramolecular systems whose function is determined by their three-dimensional self-assembly.[2] Newkome et al. have described the synthesis of some compounds called arborols or dendrimers which form automorphogenic suprastructures possessing helical or ribbonlike morphologies.[3] We sought to demonstrate that the concept of supramolecular self-assembly can be extended to other organic compounds having a cyclohexane structure substituted with different ionic side groups and counterions.

Several bolaamphiphiles were prepared from an inexpensive mixture of α,ω-dicarboxylic acids (dimeric acid, versadyme),[4] which were obtained by thermal Diels–Alder cyclization of methyl-(10*E*,12*E*)-linoleate (from tall oil). Tetrasubstituted cyclohexane derivatives were obtained. The dianionic bolaamphiphile DAS **1** was synthesized by reduction of the dimeric acids with $LiAlH_4$ followed by reaction with chlorosulfonic acid and addition of Na_2CO_3. The resulting disulfate was obtained with an overall yield of 65%. Activation of the acid groups of the dimeric acids with thionyl chloride and reaction with *N*,*N*-dimethylethylenediamine followed by quaternization yielded DAC-I **2** (81%). Ion exchange on Dowex resin gave the cationic acid amides, DAC-Cl **3** and DAC-CO_3 **4** with yields of 88 and 86%, respectively. All the bolaamphiphiles gave satisfactory spectra (IR, ^{1}H NMR, FAB-MS) and elemental analysis.[5]



DAS **1**



DAC-I **2**, X=I; DAC-Cl **3**, X=Cl; DAC-CO_3 **4**, X=HCO_3

m + n + p + q = 26
m, n = 7–10
p, q = 3–6

The aggregation behavior was studied directly by transmission electron microscopy (TEM) and image analysis.[6] A buffer solution containing the bolaamphiphiles 0.5% (weight per volume) was sonicated for 15 min at 55 °C. When the internal volume of the sonicated samples was measured by dye encapsulation (carboxyfluorescein and pyranine) no closed vesicles formed. Sonicated samples were stained (1% uranyl acetate) for TEM imaging and then digitalized for image analysis. Depending on the TEM magnification, 1 pixel corresponds to 0.123, 0.246, 0.328, and 0.579 nm (DAC-Cl, DAS, DAC-CO_3, and DAC-I, respectively; Fig. 1).

Some rodlike structures with internal organization may be recognized for the anionic species DAS **1** in Figure 1. Cationic species form multilamellar arrangements whose specific features depend on the counterion. Thus, with the bicarbonate counterion (DAC-CO_3) a complex multilayer structure resembling a fingerprint is seen. In the case of chloride counterion the arrangement is less well defined. The presence of iodide counterion leads to the formation of more complex multilamellar aggregates (Fig. 1).

It seems that both the ionic character of the synthesized bolaamphiphiles and the counterions of the cationic compounds rule out the three-dimensional arrangement of such molecules. However, as described by Okahata et al.[6] the aggregate morphology of ionic dialkyl amphiphiles is relatively insensitive to the chemical structure, and vesicles and lamellae are the most common morphologies. In sharp contrast, the morphology of the aggregates formed by polyoxyethylene glyceryl α,α'-diethers

[*] Dr. P. Bosch, Prof. Dr. J. L. Parra, Dr. A. de la Maza
Departamento de Tensioactivos, CID-CSIC
C/Jorge Girona Salgado 18–26, E-08034 Barcelona (Spain)
Telefax: Int. code +(3) 204-5904

[**] This work was supported by the Generalitat Catalunya (Cirit postdoctoral fellowship grant EE92/1-111) for research at the Freie Universität Berlin (Prof. Dr. J. H. Fuhrhop). We thank J. Blavia and A. del Giorgio for the TEM measurements and image analysis, respectively, and G. von Knorring for his expert technical assistance.

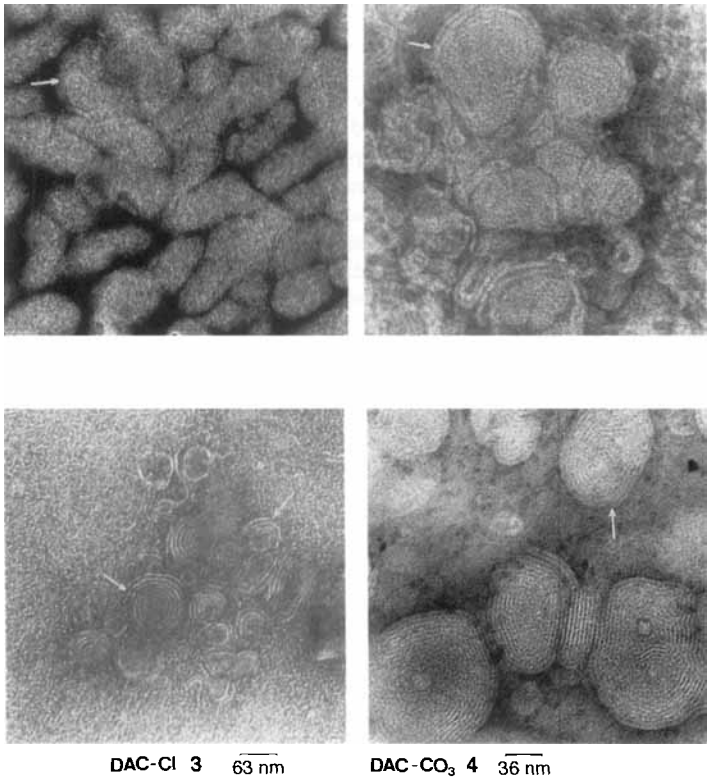


Fig. 1. TEM microphotographs of **1**–**4**. The white arrows point to the beginning of the three-dimensional open multilamellar structure.

($2C_n$-gl-xG) varies remarkably with their chemical structures.[7]

To obtain further information on some characteristics of self-assembly we determined the periods or the average distance of the pattern ordering in each lamellar structure by analysis of the TEM images. Two approaches were used: a) Fourier transformation (FT) and b) profile of direct measurements from digitalized TEM pictures (Fig. 2). The good correlation of the results obtained by the two methods is shown in Table 1. The largest period was found for DAC-I.

From physico-chemical studies we know that critical micelle concentrations (CMC) for DAS, DAC-I, DAC-Cl, and DAC-CO_3 are 1420, 20, 2600, and 300 ppm, respectively.[5] The areas for these bolaamphiphiles measured with a Langmuir film balance are 100, 116, 62, and 78 Å^2, respectively.[5] The most striking results are the lowest CMC value (20 ppm) and the highest area per molecule (116 Å) obtained for DAC-I. The peculiar three-dimensional arrangement of **2** and its lamellar period of 10 nm, the largest in the series, cannot be explained by the small difference between the van der Waals diameters of chloride (4.2 Å) and iodide (4.6 Å). An alternative explanation could be that a macrocycle of approximately 18 atoms is formed by hydrogen bonding between the two amide groups of both chains containing ionic head groups (Fig. 3). Thus, the chaotropic character[8] of the iodide anion closely bound to the trimethylammonium head group may prevent the formation of such a macrocycle. As a consequence, a more extended arrangement of the molecule with a greater surface area at the liquid–air interface would result. In addition, a more hydrophobic bolaamphiphile would have a lower CMC value. With the other counterions not having chaotropic characteristics the macrocyclic molecular arrangement could be maintained, and consequently a smaller surface area would be occupied by the bolaamphiphile molecule. Moreover, the macrocycle formation could account for the periods measured for the lamellae of the bolaamphiphiles (Table 1).

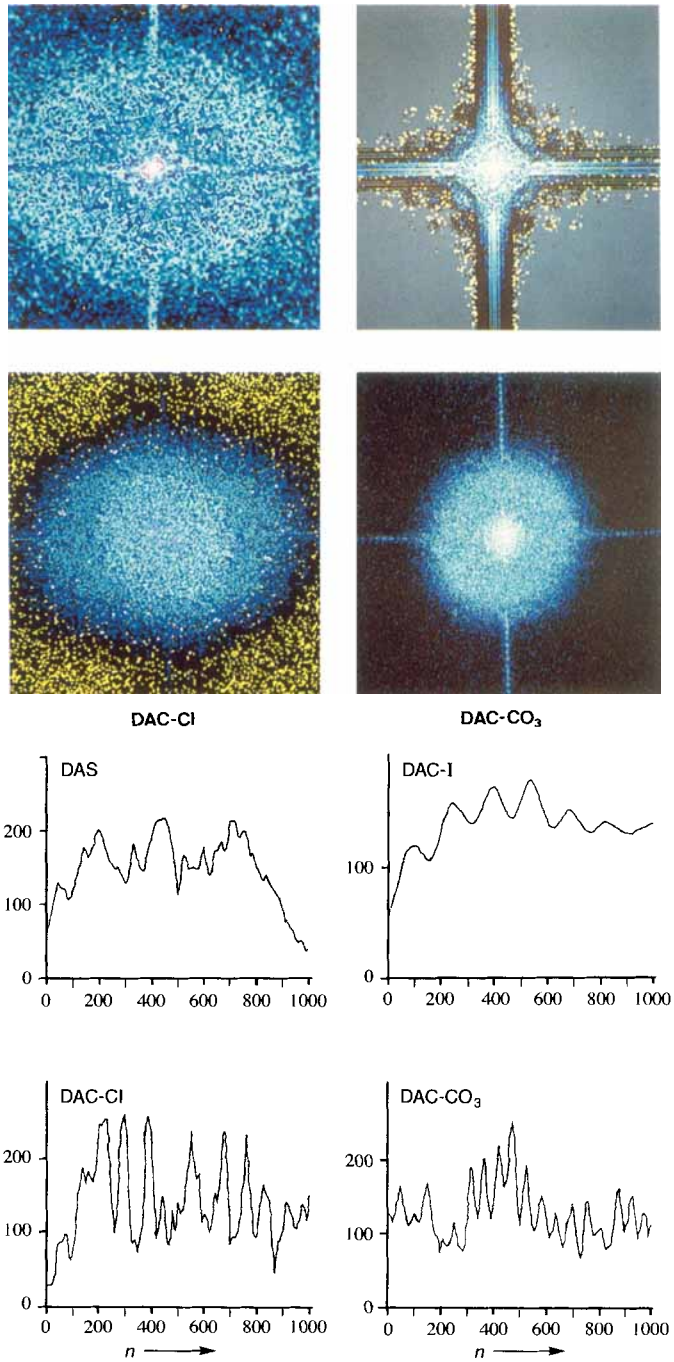


Fig. 2. Color pictures: Fourier transformations of TEM microphotographs for the bolaamphiphiles. Plots: Profiles of the digitalized TEM pictures. I = intensity, n = points. Ten points correspond to 1 pixel.

Table 1. Lamellar periods [nm] for **1**–**4** obtained experimentally by two methods.

Compound	TEM	FT
DAS **1**	0.63–1.25	0.7
DAC-Cl **3**	0.86–1.13	1
DAC-CO_3 **4**	1.6–1.92	1.7
DAC-I **2**	8–12	10

 © VCH Verlagsgesellschaft mbH, D-69451 Weinheim, 1994 0570-0833/94/2020-2079 $ 10.00+.25/0

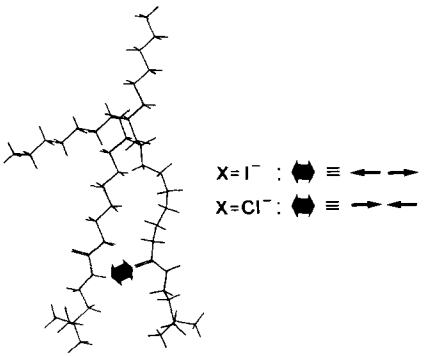


Fig. 3. Energy-minimized structure shows the formation of a macrocycle from the cationic bolaamphiphiles **2**–**4** through hydrogen bonds between the carbonyl O atom and the amide NH group. When X = I, the counterion disturbs the binding interaction by increasing the N–O distance.

It is noteworthy that bolaamphiphiles form multilamellar aggregates at low concentrations. The morphology of these stable aggregates depends on the bolaamphiphile's ionic groups and nature of the counterion.

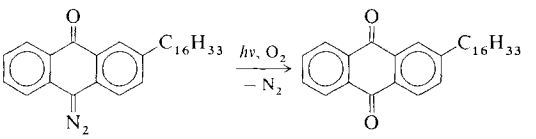
Received: March 8, 1994
Revised version: April 23, 1994 [Z 6738 IE]
German version: *Angew. Chem.* **1994**, *106*, 2157

[1] J. H. Fendler, *Membrane Mimetic Chemistry*, Wiley, New York, **1982**.
[2] J.-M. Lehn, *Angew. Chem.* **1990**, *102*, 1347; *Angew. Chem. Int. Ed. Engl.* **1990**, *29*, 1304.
[3] G. R. Newkome, C. N. Moorefield, G. R. Baker, R. K. Behera, G. H. Escamillia, M. J. Saunders, *Angew. Chem.* **1992**, *104*, 901; *Angew. Chem. Int. Ed. Engl.* **1992**, *31*, 917.
[4] J. H. Fuhrhop, W. Kaufmann, F. Schambil, *Langmuir* **1985**, *1*, 387.
[5] P. Bosch, F. J. Sánchez-Baeza, J. L. Parra, *Can. J. Chem.* **1993**, *71*, 2095.
[6] Y. Okahata, S. Tanamachi, M. Nagai, T. Kunitake, *J. Colloid Interface Sci.* **1981**, *82*, 401.
[7] J. Köning, C. Boettcher, H. Winkler, E. Zeitler, Y. Talmon, J. H. Fuhrhop, *J. Am. Chem. Soc.* **1993**, *115*, 693.
[8] T. Pigor, R. Lawaczek, *Z. Naturforsch. C* **1983**, *83*, 307.

Photodecomposition of 10-Diazo-2-hexadecylanthrone on Graphite Studied by Scanning Tunneling Microscopy

Roland Heinz, Andreas Stabel, Jürgen P. Rabe,*
Gerhard Wegner, Frans C. De Schryver,*
David Corens, Wim Dehaen, and Carsten Süling

Diazoanthrone has long been used in photoresists,[1] and the structure and spectroscopic properties of some *p*-benzoquinonediazides including 10-diazoanthrone have been discussed recently.[2] The excited state properties of this compound and the nature of the reaction products generated upon irradiation in solution have been studied in detail.[3] Other researchers have shown that a wide variety of organic compounds can be deposited from solution as two-dimensional (2D) crystals on the basal plane of highly oriented pyrolytic graphite (HOPG) and imaged in situ by scanning tunneling microscopy (STM) at the solid–fluid interface.[4] Until now photochemically unreactive organic molecules have been studied by STM; light-induced transformations in a thin liquid film have previously not been examined by this high-resolution technique. We report here on the first such STM study of the phototransformation of 10-diazo-2-hexadecylanthrone (**1**) to 2-hexadecyl-9,10-anthraquinone (**2**) [Eq. (a)].



1 **2** (a)

An oxygen-saturated 0.05 M solution (3 mL) of diazoanthrone **1** in 1,2,4-trichlorobenzene (Aldrich 99.9 + %) was irradiated for 24 h in a 1 cm quartz tube with a cold light source (Schott, KL 1500, light power 1.3 W). Since the solvent chosen has no easily abstractable hydrogen atoms, undesirable side reactions such as insertion into a C–H bond should be eliminated. The solution was saturated with oxygen to optimize the conversion of **1** into **2**. UV spectra were recorded before and after irradiation to confirm the transformation of **1** (starting material, $\lambda_{max} = 418$ nm) to anthraquinone **2** (photoproduct, $\lambda_{max} = 340$ nm). Compound **2** was also synthesized independently and characterized by UV spectroscopy.

Two-dimensional crystals precipitated from the above-mentioned solutions of **1** and of **2** and were analyzed with a scanning tunneling microscope constructed in our institute which allows imaging in situ at solid–liquid interfaces.[5] A droplet of a solution of **1** or **2** in 1,2,4-trichlorobenzene was applied to a vertically oriented piece of HOPG to form a thin liquid film (Fig. 1 top). The thickness of the liquid film in the vicinity of the STM tip is less than 20 μm (Fig. 1 bottom). The photoreaction was then studied in situ at the graphite–solution interface. An optical multimode PMMA fiber (diameter 1 mm) was used for irradiation (Fig. 1 top). The light intensity was approximately 5 $mWcm^{-2}$ at the graphite surface. The temperature of the graphite was measured in situ with a Pt 100 thermoresistor fixed at one side (Fig. 1 top). The temperature was simultaneously measured at the surface and at the side of the piece of graphite in a control experiment to exclude a nonnegligible temperature gradient. In another control experiment photochemically unreactive monolayers were imaged with and without illumination, and no difference was observed.

The STM images were obtained in constant height mode under ambient conditions (scan rate 0.3 Hz per image, positive tip bias). They were recorded on a videotape in real time and digitized later. Data as recorded without digital image processing are displayed in the figures. The tunneling tips were electrochemically etched (2 N KOH + 6 N NaCN) from a 0.25 mm Pt/Ir (80:20) wire. Every tip was then calibrated in situ by imaging the hexagonal graphite lattice ($a = 246$ pm).

Physisorption of diazoanthrone **1** and of anthraquinone **2** from 1,2,4-trichlorobenzene on HOPG leads to well-ordered 2D

[*] Prof. Dr. J. P. Rabe,[+] Dipl.-Chem. R. Heinz, Dipl.-Chem. A. Stabel, Prof. Dr. G. Wegner
Max-Planck-Institut für Polymerforschung
Postfach 3148, D-55021 Mainz (FRG)
Telefax: Int. code + (6131)379-100

[+] New address: Institut für Physikalische Chemie der Universität Mainz
Jakob-Welder-Weg 11, D-55099 Mainz (FRG)
Telefax: Int. code + (6131)39-3768

Prof. Dr. F. C. De Schryver, D. Corens, Dr. W. Dehaen, Dr. C. Süling
KU Leuven, Department of Chemistry
Celestijnenlaan 200F, B-3001 Heverlee (Belgium)

[**] The Belgian authors thank the Ministry of Wetenschapsbeleid for support (IUAP-II-16 and IUAP-III-040). The German authors acknowledge support through ESPRIT Basic Research Projects 7282 (TOPFIT) and 8523 (PRONANO). R.H. and A.S. thank the Fonds der Chemischen Industrie for Kekulé scholarships. F. C. De Schryver thanks the Alexander-von-Humboldt-Stiftung for support during his stay in Mainz.

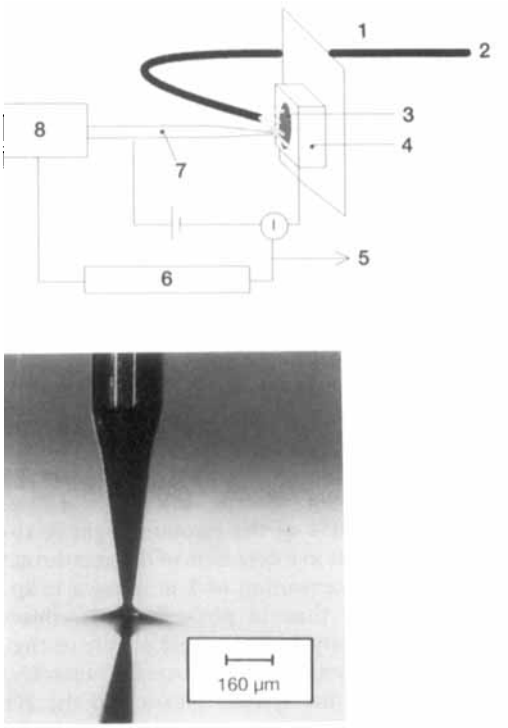


Fig. 1. Top: Schematic representation of the experimental setup. 1: Optical fiber, 2: light source, 3: thin film of solution, 4: HOPG, 5: image recording, 6: feedback, 7: STM tip, 8: piezo tube, x,y,z system. Bottom: Photograph of the STM tip in the film of solution.



Fig. 3. STM image of a 2D crystal of anthraquinone **2** on HOPG at submolecular resolution ($V_{tip} = 0.5$ V; $I = 1$ nA).

Table 1. Structural data of the two-dimensional crystals of **1** and **2**.

Parameters of the unit cell	**1**	**2**
a	1370 ± 50 pm	930 ± 50 pm
b	2750 ± 100 pm	3800 ± 100 pm
γ	120 ± 5°	85 ± 2°
No. of molecules	2	2
∢ (Alkyl chain, graphite axis)	0 ± 2°	0 ± 2
∢ (Lamella axis, graphite axis)	15 ± 2°	15 ± 2°
Distance between alkyl chains	473 ± 2 pm	450 ± 2 pm
Interlamellar distances (ΔL)	2450 ± 100 pm	3600 ± 100 pm

crystallites. As shown in Figures 2 and 3 the lamellar spacing of these crystallites differs by approximately 50%. The larger interlamellar distances (Fig. 3) can be observed only in case of the anthraquinone. This has been verified by imaging the independently synthesized anthraquinone **2**. Therefore the observation of the large structure can be regarded as a direct proof for the presence of the photoproduct. Table 1 summarizes the structural data of the 2D crystals of **1** and **2**. The respective models presented in Figures 4 and 5 are compatible with the STM images. However, the experimental images are only averaged images of systems that exhibit fast molecular dynamics on timescales not accessible to STM.

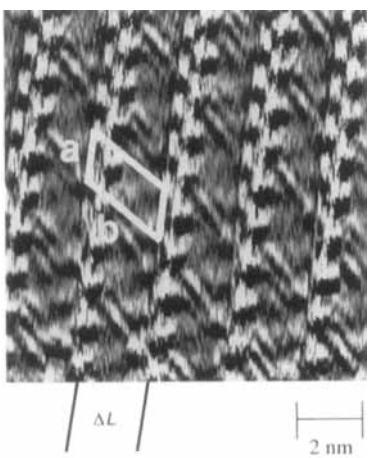


Fig. 2. STM image of a 2D crystal of diazoanthrone **1** on HOPG at submolecular resolution ($V_{tip} = 0.5$ V; $I = 3$ nA).

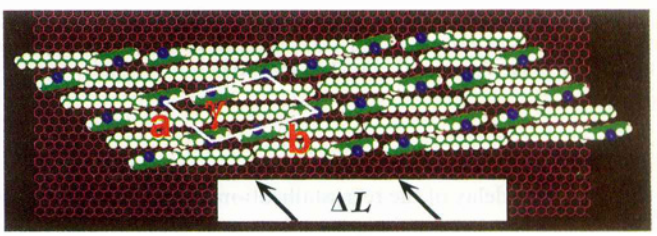


Fig. 4. Molecular model of diazoanthrone **1** on HOPG.

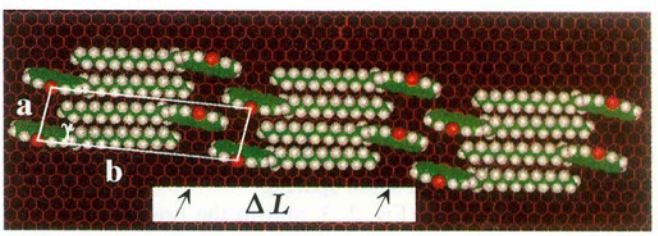


Fig. 5. Molecular model of anthraquinone **2** on HOPG.

The light-induced transformation of diazoanthrone **1** to anthraquinone **2** in trichlorobenzene can be followed in situ by STM. At the beginning a stable 2D crystal of **1** was observed. When one of its domain boundaries (Fig. 6a) was irradiated, the dissolution of the highly ordered molecular pattern was observed, starting at the domain boundary (Fig. 6b–d). When the irradiation was stopped, the highly ordered pattern reappeared and recrystallization of the molecules occurred (Fig. 6e, f). The dissolution–recrystallization cycle shown in Figure 6 was repeated several times within one hour. The time delay of the dissolution after irradiation had started *decreased*

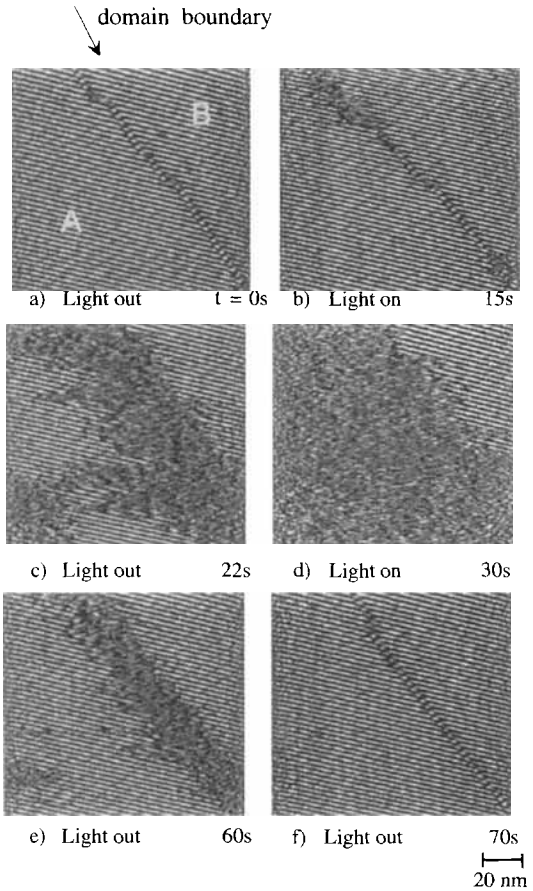


Fig. 6. Light-induced dissolution–recrystallisation cycle of diazoanthrone crystals on the basal plane of graphite ($V_{tip} = 0.3$ V; $I = 1$ nA).

from 30 s initially to approximately 5 s after six cycles. In contrast, the time delay of the recrystallization after irradiation had been halted *increased* in the same experiment from less than 30 s to several minutes. The irradiation had no influence on the temperature of the surface to within 0.1 °C. The starting material and the photoproduct could not be imaged simultaneously on the graphite surface. After complete conversion of **1** (irradiation for several hours) only the product **2** was observed. For the absorption of the 2D crystals with the large lamellar spacing (product) to take place, a large excess of the product with respect to the starting material is necessary. Even imaging of a solution of a 90/10 mixture of **2** and **1** resulted only in the lamellar structures with small spacing.

In the STM images (Fig. 2, 3, and 6) the bright rows (high tunneling current) are attributed to the aromatic moiety of the molecules and the darker rows (low tunneling current) to the alkyl chains. The use of STM as a tool to monitor the ex situ photoreaction was simplified by the large structural differences in the 2D crystals of the diazoanthrone and the anthraquinone. From in situ calibration with the help of the underlying graphite lattice and analysis of the Moiré pattern in the lamellae,[6] the structural parameters of the 2D crystals were evaluated with a high degree of accuracy. From these data we conclude that the alkyl chains are oriented parallel to one of the three main axes of the graphite. Domain boundaries as shown in Figure 6 are common in highly ordered 2D crystals and can be regarded as one of their intrinsic properties.[7]

In our in situ experiments no change of the surface temperature was observed. Therefore the dissolution and recrystallization process at the domain boundaries of the crystals of **1** (Fig. 6) can only be photoinduced. Physisorbed 2D crystallites at a liquid–solid interface are in equilibrium with the supernatant solution.[8] In our experiments the dynamics of molecular processes are too fast to be recorded by STM. Therefore the observed dynamics must be the result of a shift in the overall equilibrium between the solution and the 2D crystals. When the system is irradiated, the equilibrium is disturbed and the 2D crystals on the graphite surface dissolve. The domain boundaries represent thermodynamically favored sites for the dissolution process (Fig. 6b–d). These observations suggest the following explanation for the dissolution–recrystallizaton cycles: The system consists of two different phases. At the onset of the process phase a is represented by the 2D crystallite of **1**, which is covered by several less-ordered layers of **1**[9] with a total thickness of several nanometers. Phase b is the supernatant solution. Provided that the thickness of phase b is less than 20 μm (see Fig. 1b) and based on Beer's law ($c_0 = 0.05$ M, $\varepsilon = 10^{-4}$ mol cm^{-1} at λ_{max}), 90% of the incoming light is absorbed by phase b, which results in a depletion of diazoanthrone in phase b. However, the concentration of **1** in phase a is approximately 100 times higher than in phase b. As a consequence, the residual light intensity depletes phase a more strongly than phase b, and the 2D crystal in phase a starts to dissolve. When irradiation is stopped, the system relaxes and the 2D crystal is reformed. Phase b serves as a reservoir to provide the starting material **1**. During every dissolution–recrystallization cycle the absolute concentration in phase b decreases. This leads to a decrease in the time delay of the dissolution and an increase in the time delay of the relaxation process.

Experimental Procedure

1: Tosyl azide (0.523 g, 2.7 mmol) and piperidine (0.226 g, 22.7 mmol) were added to a suspension of 2-hexadecylanthrone (1 g, 2.4 mmol) in ethanol (30 mL). The mixture was stirred ca. 12 h at room temperature, concentrated, and chromatographed on silica gel with chloroform/hexane (1:1) as the eluent. Compound **1** was obtained in 47% (500 mg) yield; m.p. 64–65 °C (methanol); IR (KBr): $\tilde{\nu} = 2055$ (C=N$_2$), 1636 (C=O); ^{1}H NMR (400 MHz, $CDCl_3$): $\delta = 0.90$ (t, 3H), 1.25 (m, 26H), 1.65 (m, 2H), 2.70 (t, 2H), 7.27 (d, $J_o = 8$ Hz, 1H), 7.34 (d, $J_o = 8$ Hz, 1H), 7.40 (td, $J_o = 8$ Hz, $J_m = 2$ Hz, 1H), 7.53 (dd, $J_o = 8$ Hz, $J_m = 2$ Hz, 1H), 7.69 (td, $J_o = 8$ Hz, $J_m = 2$ Hz, 1H), 8.37 (d, $J_m = 2$ Hz, 1H), 8.55 (dt, $J_o = 8$ Hz, $J_m = 2$ Hz, $J_p = 1$ Hz, 1H); ^{13}C NMR ($CDCl_3$): $\delta = 14.1$, 22.7, 29.2, 29.3, 29.5, 29.6, 29.7, 30.9, 31.4, 31.9, 35.6, 64.5 (C=N$_2$), 120.6, 125.1, 127.0, 127.7, 128.3, 128.3, 128.4, 129.0, 129.9, 132.7, 133.7, 140.4, 180.1 (C=O); MS (CI): *m/z* (%): 445 (1, MH^+), 417 (16, $MH^+ - N_2$).

2: A suspension of 2-hexadecylanthrone (0.5 g, 1.2 mmol) in glacial acetic acid (20 mL) was added to a stirred suspension of chromium trioxide (0.5 g, 5 mmol) in glacial acetic acid (20 mL) at 10 °C. After 30 min of stirring at 0 °C and 2 h at room temperature, the mixture was poured into ice water (200 mL), extracted with CH_2Cl_2 (3 × 100 mL) and washed with water (2 × 100 mL). The combined extracts were dried ($MgSO_4$), the solvent was evaporated, and the crude product was chromatographed on silica gel with $CHCl_3$/hexane (3:1) as the eluent. Compound **2** was obtained in 75% yield (400 mg), m.p. 102–103 °C (hexane; ref. [10]: 100–103 °C); IR (KBr): $\tilde{\nu} = 1673$ (C = O); ^{1}H NMR (400 MHz): $\delta = 0.9$ (t, 3H), 1.25 (m, 26H), 1.65 (m, 2H), 2.75 (t, 2H), 7.60 (dd, 1H), 8 (m, 2H), 8.11 (d, 1H), 8.22 (d, 1H), 8.30 (m, 2H); MS (CI): *m/z* (%): 432 (29%, $M^{\cdot+}$), 222 (18, $M^{\cdot+}$-$C_{15}H_{31}$) 43 (100, $C_3H_7^+$).

Received: April 7, 1994 [Z 6832 IE]
German version: *Angew. Chem.* **1994**, *106*, 2154

[1] V. V. Ershov, G. A. Nikiforov, C. R. I. de Jonge, *Quinone Diazides*, Elsevier, Amsterdam, **1981**.
[2] W. Sander, G. Bucher, P. Komnick, J. Morawietz, P. Bubenischek, P. G. Jones, A. Chrapkowski, *Chem. Ber.* **1993**, *126*, 2101–2109.
[3] K. W. Field, G. B. Schuster, *J. Org. Chem.* **1988**, *53*, 4000–4006; M. W. Shaffer, E. Leyva, N. Soundararajan, E. Chang, D. H. S. Chang, V. Capuano, M. S. Platz, *J. Phys. Chem.* **1991**, *95*, 7273–7277; M. Regitz, *Methoden Org. Chem. (Houben-Weyl) 4th ed. 1952, Vol. 19b*, **1989**; W. Sander, *Angew. Chem.* **1990**, *102*, 362–372; *Angew. Chem. Int. Ed. Engl.* **1990**, *29*, 344–354; W. Sander, G. Zucher, S. Wierlacher, *Chem. Rev.* **1993**, *93*, 1583–1621.

[4] H.-J. Butt, R. Guckenberger, J. P. Rabe, *Ultramicroscopy* **1992**, *46*, 375–393; J. Frommer, *Angew. Chem.* **1992**, *104*, 1325–1357; *Angew. Chem. Int. Ed. Engl.* **1992**, *31*, 1298–1328; H. Fuchs, *J. Mol. Struct.* **1993**, *292*, 29–47; J. P. Rabe, S. Buchholz, L. Askadskaya, *Phys. Scr. I* **1993**, *T49*, 260–263; *Synth. Met.* **1993**, *54*, 339–349; J. P. Rabe in *Atomic and Nanoscale Modification of Materials: Fundamentals and Applications* (Ed.: P. Avouris) *NATO ASI Ser. E*, **1993**, *239*, 263–274.
[5] J. P. Rabe, M. Sano, D. Batchelder, A. A. Kalatchev, *J. Microsc. (Oxford)* **1988**, *152*, 573–583.
[6] J. P. Rabe, S. Buchholz, *Science* **1991**, *253*, 424–427.
[7] J. P. Rabe, S. Buchholz, *Phys. Rev. Lett.* **1991**, *66*, 2096–2099.
[8] G. H. Findenegg, M. Liphard, *Carbon* **1987**, *25*, 119–128.
[9] R. Hentschke, B. L. Schürmann, J. P. Rabe, *J. Chem. Phys.* **1992**, *96*, 6213–6221.
[10] S. B. Bowlus, *Synth. Commun.* **1984**, *14*, 391–395.

$[Cp_2Ti(C{\equiv}CtBu)_2]$ as an Alkynyl Transfer Reagent: Synthesis and Characterization of the Asymmetrically Bridged Heterodimetallic Complex $[Cp_2Ti(C{\equiv}CtBu)_2Pt(PPh_3)]\cdot 0.5\,THF$**

Jesús R. Berenguer, Juan Forniés,* Elena Lalinde,* and Antonio Martín

Since the report that $[Ni(CO)_4]$ reacts with $[Cp_2Ti(C{\equiv}CPh)_2]$ to give the side-on bridged chelate complex $[\{Cp_2Ti(C{\equiv}CPh)_2\}Ni(CO)]$,[1] a series of titanocene derivatives have been described in which a further metal ion is coordinated by alkynyl ligands:

$[\{Cp_2Ti(C{\equiv}CPh)_2\}Pt(PR_3)]$[2] $[\{Cp'_2Ti(C{\equiv}CSiMe_3)_2\}FeCl_2]$[3]

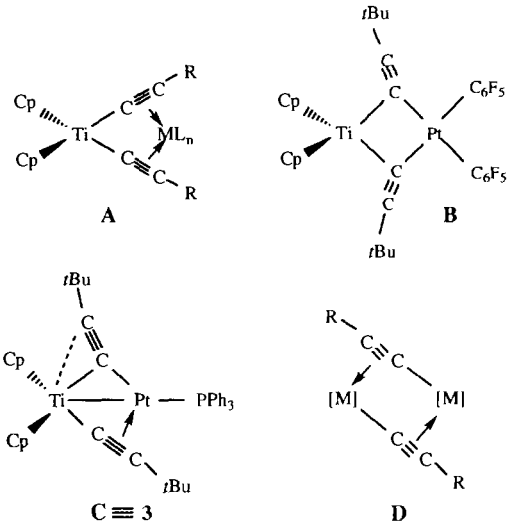
$[\{Cp'_2Ti(C{\equiv}CSiMe_3)_2\}CuCl]$[3]

$[Cp'_2Ti(C{\equiv}CSiMe_3)_2AgX]$ (X = Cl, CN, SCN, NO_2, ClO_4)[4]

$[\{Cp'_2Ti(C{\equiv}CPh)_2\}M(CO)]$ (M = Co,[5] Ni;[6] Cp′ = $C_5H_4SiMe_3$)

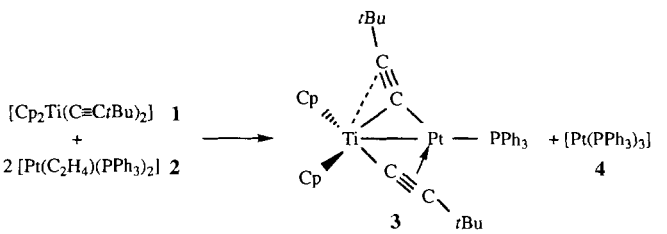
$[\{\eta^5\text{-}C_5HMe_4)Ti(C{\equiv}CSiMe_3)_2\}Mg(thf)Cl)]$[7]

All of these complexes display a "tweezer" structure (Scheme 1, **A**) in which the alkynyl groups act as two-electron ligands. Recently we reported on the synthesis of $[Cp_2Ti(\mu\text{-}\eta^1\text{-}C{\equiv}CtBu)_2Pt(C_6F_5)_2]$, an unusual complex in which the two $\mu\text{-}\eta^1\text{-}C{\equiv}CtBu$ ligands bridge both metal centers[8] (Scheme 1, **B**). Usually, only complexes of type **A** or **B** are obtained from reactions of $[Cp_2Ti(C{\equiv}CR)_2]$ with transition metal compounds; in no case has an alkynyl transfer been observed. In this paper we report on the synthesis of $[Cp_2Ti(C{\equiv}CtBu)_2Pt(PPh_3)]$ (**3**), a complex having an unusual asymmetric structure of type **C** (Scheme 1), the formation of which necessarily implies an alkynyl transfer from titanium to platinum.



Scheme 1.

The reaction of the alkynyl complex $[Cp_2Ti(C{\equiv}CtBu)_2]$ (**1**) with $[Pt(C_2H_4)(PPh_3)_2]$ (**2**) in tetrahydrofuran (THF) afforded a deep orange-red solution, from which moderately air-stable, red crystals of **3** were isolated. In addition, $[Pt(PPh_3)_3]$ (**4**) was obtained, which indicates that the PPh_3 liberated when **3** forms is in competition with titanium complex **1** for reaction with **2**. For that reason, **3** was obtained in better yield (55%) when the reaction was carried out with a Ti/Pt molar ratio of 1:2.



The elemental analysis and mass spectrum of **3** are in accord with this formulation. The well-resolved ^{31}P NMR spectrum of **3** indicates that it is a diamagnetic compound. It exhibits a single resonance (δ = 42.0) with a ^{195}Pt satellite pattern corresponding to the presence of a $PtPPh_3$ group. The IR spectrum of **3** exhibits a single, medium-intensity $\nu(C{\equiv}C)$ band (2003 cm^{-1}) at lower wavenumbers than the corresponding vibration in **1** (2061 cm^{-1}), which is consistent with the π coordination of the alkynyl group with an adjacent metal atom.[9] However, this band is much higher in energy than those observed for complexes of type **A**. For instance, $\nu(C{\equiv}C)$ for complexes $[\{Cp_2Ti(C{\equiv}CPh)_2\}PtL]$ (L = tertiary phosphane) with stoichiometries similar to that of **3** occurs at about 1800 cm^{-1}.[2] This suggests that the alkyne ligands in **3** have a different coordination mode.

A single-crystal X-ray diffraction study of **3** (Fig. 1)[10] clearly reveals that it is not a titanocene "tweezer" compound of type **A** but has an unsymmetrical structure (type **C**). The core of the molecule (Pt, Ti, C1, C2, C7, and C8) is planar (mean deviation 0.025 Å), and the phosphorus atom is also located in this plane (deviation 0.029 Å). Although each alkynyl group is π-bonded to a metal center, the strength of this interaction is very different in each case. The coordination of the platinum

[*] Prof. Dr. J. Forniés, Dipl.-Chem. J. R. Berenguer, Dr. A. Martín
Departamento de Química Inorgánica
Instituto de Ciencias Materiales de Aragón
Universidad de Zaragoza – C.S.I.C.
E-50009 Zaragoza (Spain)
Telefax: Int. code +(76) 567-920
Dr. E. Lalinde
Departamento de Química
Universidad de La Rioja
Obispo Bustamante 3, E-26001 Logroño (Spain)

[**] This work was supported by the Spanish Dirección General de Investigación Científica y Técnica (project PB92-0364 and a grant to J. R. B.). We thank Dr. B. Menjón for helpful discussions.

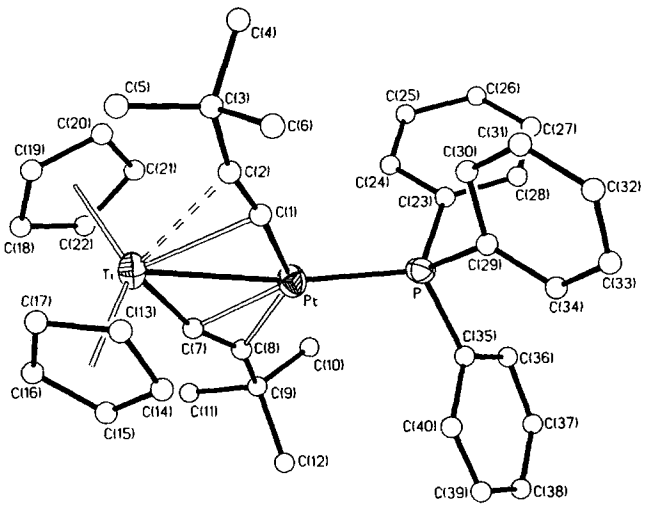


Fig. 1. Crystal structure of **3**·0.5THF. Selected bond lengths [Å] and angles [°]: Ti-C1 2.435(14), Ti-C2 2.795(14), Ti-C7 2.102(14), Pt-C1 1.990(13), Pt-C7 2.054(13), Pt-C8 2.191(15), C1-C2 1.197(19), C7-C8 1.236(19), Pt-P 2.247(3), Pt-Ti 2.789(3); Pt-C1-C2 171.4(13), Ti-C7-C8 163.8(12), C1-C2-C3 165.7(16), C7-C8-C9 147.8(15), Ti-C1-Pt 77.4(5), Ti-C7-Pt 84.3(5), C1-Ti-C7 91.3(5), C1-Pt-C7 107.0(6), C1-Pt-P 108.6(4), C1-Pt-C8 140.6(5), C8-Pt-P 110.7(4).

atom to the alkynyl moiety is almost symmetrical with very short Pt–C bond lengths (Pt–C7 = 2.054(13) Å and Pt–C8 = 2.191(15) Å), which suggests a very strong interaction of the platinum center with C7 and C8. As a result the alkyne skeleton is very distorted [Ti-C7-C8 163.8(12)°, C7-C8-C9 147.8(15)°]. The Ti–alkynyl side-on interaction is much weaker, as reflected by the Ti–C bond lengths (Ti–C1 = 2.435(14) Å and Ti–C2 = 2.795(14) Å) which are longer than the Pt–C distances and very different from each other. This suggests that this bond has predominately σ character. However, the Ti–C1 distance is longer than that in **B** (2.240(10), 2.257(10) Å).[8] In **B** the alkyne skeleton displays a very small distortion [Pt-C1-C2 171.4(13)° and C1-C2-C3 165.7(16)°]. It is noteworthy that although alkynyl ligands interact differently with the metal centers, the C≡C bonds have practically the same lengths. The Ti–Pt distance in **3** (2.789(3) Å) is shorter than that found in **B** (2.831(2) Å)[8] and compares well with the distances found in other Pt–Ti complexes for which dative Pt → Ti interactions have been suggested.[12] This short Pt–Ti distance and the diamagnetism of **3** suggest the existence of a Pt–Ti bond. The narrow Ti-C-Pt angles (77.4(5), 84.3(5)°) could be taken as further evidence of this Pt–Ti bond. However, in this kind of complex neither the magnetic properties, nor the intermetallic distances provide, per se, enough evidence to conclude whether a metal–metal bond actually exists.[13] Diamagnetism could be due to spin pairing through the bridging ligands, and short metal–metal distances can be enforced by the bridging ligands.

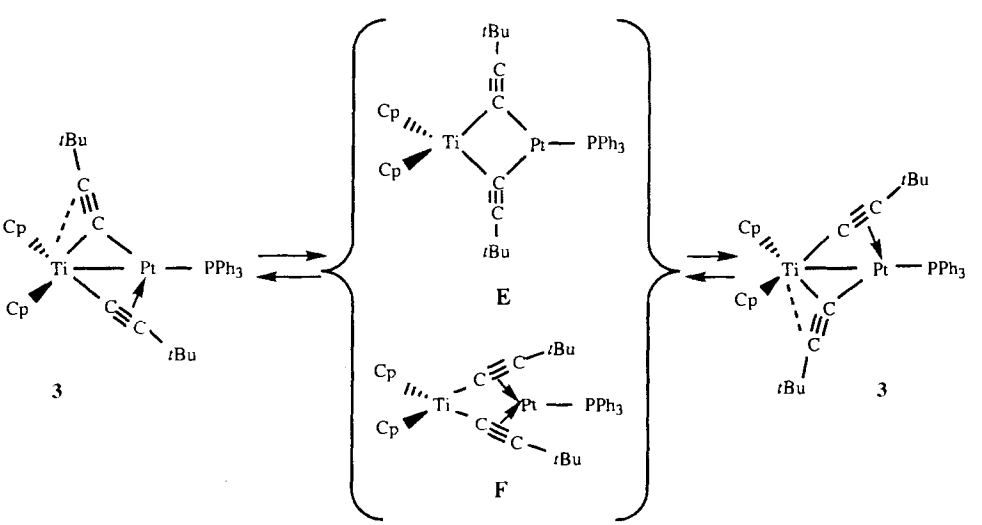
The structure of complex **3** in the solid state is not reflected in solution. The ^{1}H NMR spectrum of **3** shows that the two *tert*-butyl groups are equivalent at room temperature. This could be the result of a dynamic process involving a fast intramolecular σ migration of the C≡C*t*Bu ligands between the metal centers (Scheme 2). Such dynamic processes have been invoked for other polynuclear complexes with bridging alkyne ligands.[9, 14] Unfortunately, the dynamic process cannot be stopped even at the lowest temperature attainable (CD_2Cl_2, −92 °C). Under these conditions the signal due to the *t*Bu groups is very broad. The ^{13}C NMR spectrum is even less informative since the signals due to *t*Bu groups appear as narrow singlets through the entire temperature range. In addition, the only observed low-field signal (δ = 178.4), which was assigned to one of the alkyne C atoms, disappears at low temperatures.

The unusual behavior of $[Cp_2Ti(C{\equiv}C\,tBu)_2]$ (**1**) towards $[Pt(C_2H_4)(PPh_3)_2]$ (**2**) in acting as an alkynyl transfer reagent is especially surprising since $[Cp_2Ti(C{\equiv}CPh)_2]$ acts only as a chelating ligand in reactions with $[Pt(C_2H_4)_2(PPh_3)]$[2] and **2**.[15] Although in a few cases other bis(alkynyl) complexes have proved to be alkynyl transfer reagents (e.g., $[Cp'_2Zr(C{\equiv}CR)_2]$ in its reaction with $[Cp_2Zr(C_4H_6)]$[14] and *cis*-$[Pt(C_6F_5)_2(C{\equiv}CR)_2]^{2-}$ in its reaction with *cis*-$[Pt(C_6F_5)_2(thf)_2]$[9]), the resulting dinuclear complexes display a symmetrical doubly bridging μ-$\eta^{1:2}$-alkynyl system (Scheme 1, **D**). The formation of **3** can be formally considered as the result of the oxidative addition of a Ti^{IV}–C bond to a Pt^0 substrate to give a dinuclear Ti^{III}–Pt^I compound. Finally, the very different nature of the metal centers and their oxidation states can be the reason for the very different kinds of alkynyl–metal π interactions in **3**.

Our results clearly suggest that the electronic effects and/or steric demands of the alkynyl substituents affect the bonding features of the alkynyl ligands in these doubly bridged alkyne complexes.

Experimental Procedure

3: To a yellow solution of **1** [16] (32.5 mg, 0.10 mmol) in 6 mL of dry THF (distilled under N_2 from Na/benzophenone) under N_2 was added **2** [17] (143 mg, 0.20 mmol). The resulting red solution was concentrated to dryness, and the residue was treated with Et_2O (2 mL) and *n*-hexane (4 mL). The insoluble $[Pt(PPh_3)_3]$ (identified by its elemental analysis and IR spectrum, 60 mg, 64% yield) was removed by filtration, and the dark-red solution was concentrated and kept in the refrigerator for roughly 15 h. The dark-red solid obtained (**3**, 42 mg, 55% yield) was filtered and washed with cold *n*-hexane. IR (Nujol, polyethylene plates): ν = 2003 (m) cm^{-1}, ν(C≡C); ^{1}H NMR (300 MHz, CD_2Cl_2, 25 °C, $SiMe_4$): δ = 7.51 (m, Ph), 7.29 (m, Ph), 5.57 (s, Cp), 3.74 (m, THF), 1.84 (m, THF), 1.04 (s, *t*Bu); (−92 °C): δ = 7.46 (m, Ph),



Scheme 2.

7.3 (m, Ph), 5.6 (s, Cp), 3.62 (m, THF), 1.78 (m, THF), 1.05 (br.s, *t*Bu); ^{13}C NMR (25 °C): $\delta = 138.6$ (d, C_{ipso}, Ph; $^1J(P,^{13}C) = 44.3$ Hz, $^2J(^{195}Pt,^{13}C) = 30.2$ Hz), 134.8 (d, C_{ortho}, Ph, $^2J(P,^{13}C) = 13.4$ Hz, $^3J(^{195}Pt,^{13}C) = 25.5$ Hz), 129.6 (d, C_{para}, Ph, $^4J(P,^{13}C) = 2$ Hz), 128.1 (d, C_{meta}, Ph, $^3J(P,^{13}C) = 10.1$ Hz), 105.1 (s, Cp), 77.8 (s, $C(CH_3)_3$), 68.1 (s, THF), 32.6 (s, $C(CH_3)_3$), 26 (s, THF); (−92 °C): $\delta = 136.3$ (d, C_{ipso}, Ph, $^1J(P,^{13}C) = 45$ Hz), 133.7 (d, C_{ortho}, Ph, $^2J(P,^{13}C) = 13.4$ Hz), 129.1 (s, C_{para}, Ph), 127.4 (d, C_{meta}, Ph, $^3J(P,^{13}C) = 9.4$ Hz), 104 (s, Cp), 77.5 (s, $C(CH_3)_3$), 67.4 (s, THF), 31.4 (s, $C(CH_3)_3$), 25.1 (s, THF); $^{31}P\{^1H\}$ NMR ($CDCl_3$, 85% H_3PO_4, 25 °C): $\delta = 42.0$ ($^1J(^{195}Pt, P) = 4577$ Hz); EIMS: m/z (%) = 799 (47) [$M^+ + H$], 535 (46) [$M^+ - PPh_3$], 453 (100) [$PtPPh_3$]$^+$.

Received: April 8, 1994
Revised version: June 28, 1994 [Z 6833 IE]
German version: *Angew. Chem.* **1994**, *106*, 2196

[1] K. Yasufuku, H. Yamazaki, *Bull. Chem. Soc. Jpn.* **1972**, *45*, 2664.
[2] M. Ciriano, J. A. K. Howard, J. L. Spencer, F. G. A. Stone, H. Wadepohl, *J. Chem. Soc. Dalton Trans.* **1979**, 1749.
[3] H. Lang, M. Herres, L. Zsolnai, W. Imhof, *J. Organomet. Chem.* **1991**, *409*, C7.
[4] H. Lang, M. Herres, L. Zsolnai, *Organometallics* **1993**, *12*, 5008.
[5] H. Lang, L. Zsolnai, *J. Organomet. Chem.* **1991**, *406*, C5.
[6] H. Lang, W. Imhof, *Chem. Ber.* **1992**, *125*, 1307.
[7] S. I. Troyanov, V. Varga, K. Mach, *Organometallics* **1993**, *12*, 2820.
[8] J. R. Berenguer, L. R. Falvello, J. Forniés, E. Lalinde, M. Tomás, *Organometallics* **1993**, *12*, 6.
[9] J. Forniés, M. A. Gómez-Saso, E. Lalinde, F. Martínez, M. T. Moreno, *Organometallics* **1992**, *11*, 2873.
[10] Crystal data for **3**: $C_{42}H_{47}O_{0.5}PPtTi$, $M_r = 833.8$, monoclinic, space group $C2/c$, $a = 21.674(4)$, $b = 9.343(2)$, $c = 36.425(7)$ Å, $\beta = 92.23(3)°$, $V = 7370(3)$ Å^3, $Z = 8$, $\rho_{calc.} = 1.50$ g cm^{-3}, $\lambda(Mo_{K\alpha}) = 0.71073$ Å, $\mu = 40.8$ cm^{-1}, $F(000) = 3344$, $T = 293$ K, crystal dimensions $0.13 \times 0.38 \times 0.63$ mm. Crystallographic data were collected by Crystallytics Co. (Lincoln, Nebraska) on a Nicolet (Siemens) Autodiffractometer, $3 < 2\theta < 46°$ (ω scan); 5081 independent reflections, 2741 with $F > 4\sigma(F)$ were observed and used for structure refinement (program system SHELXTL-PLUS [11]). Cell constants were refined from 30 reflections (including Friedel pairs) with $15 < 2\theta < 30°$. An absorption correction based on Ψ scans was applied. Six standard reflections were measured every 300 reflections but showed no decay. The structure was solved by direct methods and refined on $|F_0|$ to $R = R' = 0.043$ for 397 variables (weighting scheme $\omega^{-1} = \sigma^2(F_0) + 0.0004F_0^2$), highest shift/error 0.001. Goodness of fit 1.13. All non-hydrogen atoms, except those of the solvent molecule were refined anisotropically. All hydrogen atoms were included in calculated positions and refined as riding atoms (C–H 0.96 Å and $U = 0.1065$ Å^3). A difference map following convergence showed no peaks higher than 1 e Å^{-3} (maximum/minimum difference density 0.76/−1.12 e Å^{-3}). Further details of the crystal structure investigation are available on request from the Director of Cambridge Crystallographic Data Centre, 12 Union Road, GB-Cambridge CB2 1EZ (UK), on quoting the full journal citation.
[11] *SHELXTL-PLUS Software Package for the Determination of Crystal Structures*, Release 4.0; Siemens Analytical X-ray Instruments, Inc., Madison, WI, USA, **1990**.
[12] F. Ozawa, J. W. Park, P. B. Mackenzie, P. W. Schaefer, L. M. Henling, R. H. Grubbs, *J. Am. Chem. Soc* **1989**, *111*, 1319.
[13] M. C. Baird, *Prog. Inorg. Chem.* **1968**, *9*, 1.
[14] a) G. Erker, W. Frömberg, R. Mynott, B. Gabor, C. Krüger, *Angew. Chem.* **1986**, *98*, 458; *Angew. Chem. Int. Ed. Engl.* **1986**, *25*, 463; b) G. Erker, W. Frömberg, R. Benn, R. Mynott, K. Angermund, C. Krüger, *Organometallics* **1989**, *8*, 911.
[15] The reaction of **2** (0.216 g, 0.29 mmol) and $[Cp_2Ti(C{\equiv}CPh)_2]$ (0.11 g, 0.29 mmol) in THF gave a mixture of products. The first fraction obtained by crystallization from THF/hexane was a yellow solid (0.045 g). The ^{31}P NMR spectrum indicates this to be a mixture of complexes. The second fraction, an orange microcrystalline product (0.1 g, 41% yield) was identified by elemental analysis, mass spectrum, and IR and NMR spectra as the previously reported $[Cp_2Ti(C{\equiv}CPh)_2Pt(PPh_3)]$ [2].
[16] H. Lang, D. Seyferth, *Z. Naturforsch. B* **1990**, *45*, 212.
[17] R. A. Head, *Inorg. Synth.* **1990**, *28*, 134.

Optically Active Reference Compounds for Environmental Analysis Obtained by Preparative Enantioselective Gas Chromatography**

Wilfried A. König,* Ingo H. Hardt, Bärbel Gehrcke, Detlev H. Hochmuth, Heinrich Hühnerfuss, Bernd Pfaffenberger, and Gerhard Rimkus

Dedicated to Professor Hansjörg Sinn on the occasion of his 65th birthday

The distribution and behavior of toxicologically relevant xenobiotics in the environment is of increasing scientific interest. Chiral, biologically active compounds whose enantiomers produce fundamentally different effects and whose *biological* degradation is, as a rule, enantioselective are of particular importance in this context. These properties have been observed in "cyclodiene" insecticides[1] and, more recently, in chiral α-1,2,3,4,5,6-hexachlorocyclohexane (α-HCH),[2] the enantiomers of which are selectively accumulated in living organisms. Using gas chromatography on modified cyclodextrins (CDs), we have been able to separate a number of polychlorinated hydrocarbons (PCHs) into their enantiomers: heptachlor and *cis*- and *trans*-chlordane, which were used as insecticides for decades; their metabolites *cis*-heptachlor epoxide and oxychlordane;[3] the atropisomeric polychlorinated biphenyls (PCBs);[4] and bromocyclen[5] (Fig. 1). Other groups have also used enantiose-

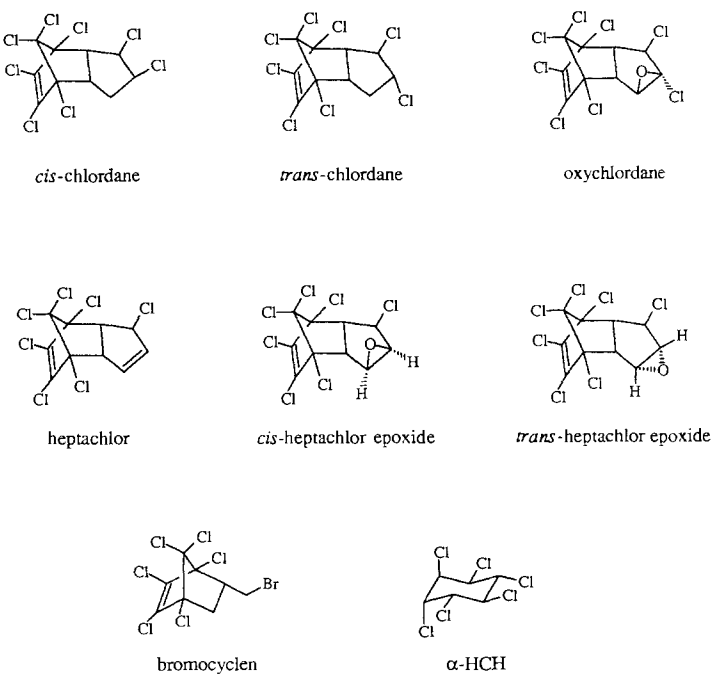


Fig. 1. Structural formulae of chiral xenobiotics.

[*] Prof. Dr. W. A. König, Dipl.-Chem. I. H. Hardt, Dipl.-Chem. B. Gehrcke, Dipl.-Chem. D. H. Hochmuth, Priv.-Doz. Dr. H. Hühnerfuss, Dipl.-Chem. B. Pfaffenberger
Institut für Organische Chemie der Universität
Martin-Luther-King-Platz 6, D-20146 Hamburg (FRG)
Telefax: Int. code + (40)4123-2893
Dr. G. Rimkus
Lebensmittel- und Veterinäruntersuchungsamt des Landes
Schleswig-Holstein, D-24537 Neumünster

[**] This research was sponsored by the Deutsche Forschungsgemeinschaft, the Fonds der Chemischen Industrie, and the Bundesministerium für Forschung und Technologie.

lective gas chromatography in the analysis of PCHs isolated from different compartments of the environment, and, in several cases, they have shown that these compounds are metabolized enantioselectively.[6]

Optically active samples of these compounds have already been obtained by enantioselective dehydrochlorination, separation of the enantiomers by liquid chromatography (α-HCH[7, 8]), and enantioselective synthesis (heptachlor, heptachlor epoxide, *cis*- and *trans*-chlordane[1, 9]); however, enantiomerically pure (or enriched) reference substances, which can be used in gas chromatography to determine the sequence of elution of enantiomers, are not commercially available. Using preparative gas chromatography columns with modified CDs as the chiral stationary phase, we have now succeeded in separating the enantiomers of a selection of PCHs on a milligram scale and with enantiomeric excesses of between 42 and over 99% (Fig. 2, Table 1).[12]

So far, preparative separations on columns packed with CDs have only been described for the highly volatile inhalation anesthetics enflurane[13] and isoflurane,[14] which have separation factors $\alpha > 2$ on capillary columns.[15] In the examples reported here, the separation factors are between 1.02 (e.g., heptachlor, *trans*-heptachlor epoxide, bromocyclen) and 1.10 (α-HCH). Although the quantity of sample injected in each *individual* run ranged from 2 to 7 mg, satisfactory to very high enantiomeric purity (with yields of 20–90% for each enantiomer) was obtained by fractionation. In each case, the enantiomers were characterized by measurement of optical rotation; the order of elution of the enantiomers can thus be determined for any CD derivative.[16]

Table 1. Isolated yield and enantiomeric excess (*ee*) obtained in the preparative resolution of the enantiomers of chiral xenobiotics by gas chromatography on cyclodextrin (CD) derivatives. In each case, the racemate (ca. 2 mg) in acetone (ca. 20 mL) was injected at an injector temperature of 200 °C; the total weight of sample was ca. 20 mg.

Compound	Yield [mg]	*ee* [%]	CD derivative
(+)-Heptachlor [a]	2.3	51.2	2,6-di-*O*-methyl-3-*O*-pentyl-β-CD [10]
(−)-Heptachlor	1.3	65.2	2,6-di-*O*-methyl-3-*O*-pentyl-β-CD
(+)-*cis*-Heptachlor epoxide	1.4	94.6	2,6-di-*O*-methyl-3-*O*-pentyl-γ-CD [10]
(−)-*cis*-Heptachlor epoxide [a]	1.1	98.8	2,6-di-*O*-methyl-3-*O*-pentyl-γ-CD
(+)-*trans*-Hepatachlor epoxide [a]	3.5	61.0	2,6-di-*O*-methyl-3-*O*-pentyl-β-CD
(−)-*trans*-Heptachlor epoxide	2.0	83.2	2,6-di-*O*-methyl-3-*O*-pentyl-β-CD
(+)-*cis*-Chlordane [a]	2.6	50.5	2,6-di*O*-methyl-3-*O*-pentyl-β-CD
(−)-*cis*-Chlordane	1.3	70.5	2,6-di-*O*-methyl-3-*O*-pentyl-β-CD
(+)-*trans*-Chlordane [a]	1.5	92.6	2,6-di-*O*-methyl-3-*O*-pentyl-β-CD
(−)*trans*-Chlordane	1.1	98.3	2,6-di-*O*-methyl-3-*O*-pentyl-β-CD
(+)-Oxychlordane	2.7	50.1	6-*O*-tex-2,3-dimethyl-β-CD [b] [11]
(−)-Oxychlordane [a]	3.5	42.8	6-*O*-tex-2,3-dimethyl-β-CD [b]
(+)-Bromocyclen	1.8	53.8	6-*O*-tex-2,3-dimethyl-β-CD [b]
(−)-Bromocyclen [a]	1.6	49.3	6-*O*-tex-2,3-dimethyl-β-CD [b]
(+)-α-HCH [c]	8.7	>99	2,6-di-*O*-methyl-3-*O*-pentyl-γ-CD
(−)-α-HCH [a]	7.0	>99	2,6-di-*O*-methyl-3-*O*-pentyl-γ-CD

[a] Enantiomer eluted first. [b] tex = dimethylthexylsilyl. [c] $[\alpha]_D^{20} = 127.6$ ($c = 2$, acetone).

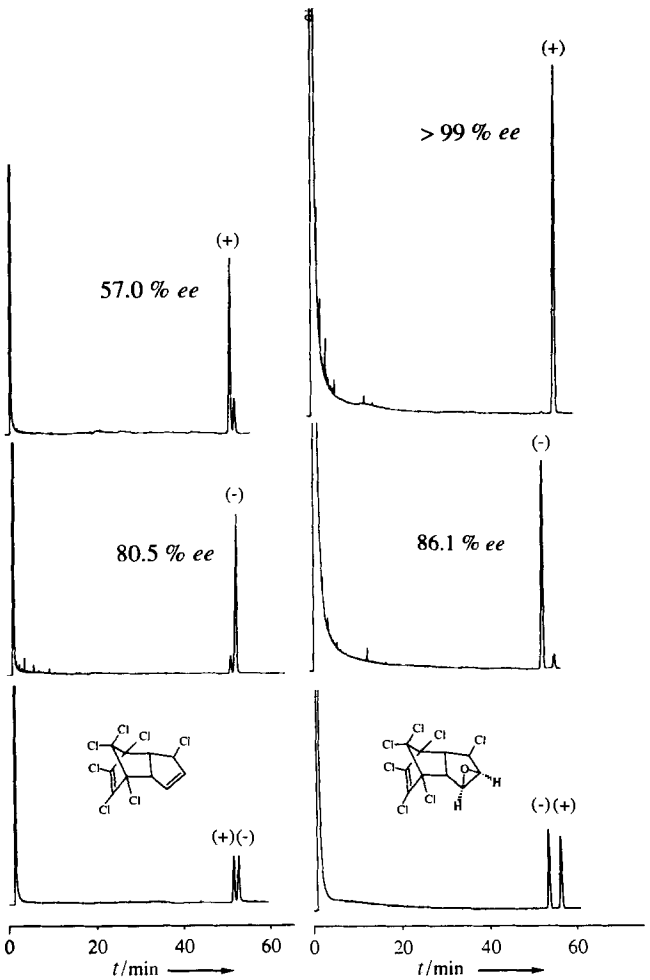


Fig. 2. Determination of the enantiomeric purity of heptachlor (left) by enantioselective gas chromatography on a "fused silica" capillary column (25 m) containing heptakis(2,6-di-*O*-methyl-3-*O*-pentyl)-β-cyclodextrin in polysiloxane OV 1701 (20%) at 130 °C and of *cis*-heptachlor epoxide (right) on a "fused silica" capillary column (25 m) containing heptakis(2,6-di-*O*-methyl-3-*O*-pentyl)-γ-cyclodextrin in polysiloxane OV 1701 (20%) at 160 °C; injector temperature 200 °C, detector temperature 250 °C; carrier gas, hydrogen.

The toxic compounds mentioned above are ubiquitous and are highly persistent contaminants in the environment; they are accumulated in the adipose tissue of higher organisms. Sea gull eggs, liver of roe deer and hare, and different seal organs were examined; the ratio of enantiomers for the metabolites *cis*-heptachlor epoxide and oxychlordane deviated significantly from 1.0 in all cases (Table 2). It is not only noticeable that the selectivity of metabolism differs greatly from one organism to the next, but also that the (+)-enantiomers are enriched in sea gull eggs and

Table 2. Enantiomer ratio (+/−, determined by gas chromatography) of *cis*-heptachlor epoxide and oxychlordane in various samples of sea gull eggs, hare liver, roe-deer liver (from Schleswig-Holstein), and adipose tissue from seals (from Iceland).

Sample	*cis*-Heptachlor epoxide	Oxychlordane
Sea gull egg, 1	-	2.3
Sea gull egg, 2	-	2.1
Sea gull egg, 3	-	1.8
Sea gull egg, 4	2.7	1.5
Sea gull egg, 5	1.6	1.5
Hare liver, 1	3.3	1.1
Hare liver, 2	2.5	1.0
Hare liver, 3	3.7	1.3
Hare liver, 4	2.6	1.3
Hare liver, 5	3.2	1.5
Roe-deer liver, 1	1	9
Roe-deer liver, 2	2	12
Roe-deer liver, 3	6	14
Roe-deer liver, 4	7	17
Roe-deer liver, 5	9	12
Seal, 1 (adipose tissue)	0.14	0.66
Seal, 2 (adipose tissue)	0.18	0.54
Seal, 1 (liver)	0.06	0.57
Seal, 2 (liver)	0.05	0.45
Seal, 1 (brain)	0.11	0.57
Seal, 2 (brain)	-	0.48

in the liver of roe deer and hare, whereas the (−)-enantiomers predominate in the adipose tissue of seals. Bromocyclen, which is used in Europe to counter parasitic infestations of pets and has been found in fresh water fish, in some cases, in surprisingly high concentrations of $>1\ mg\,kg^{-1}$, is also metabolized enantioselectively.[5] The ratio of enantiomers (peak area ratio of (+)-enantiomer/(−)-enantiomer) lies between 1.25 and 1.06.

The toxicological implications of these findings are not yet clear; however, the results show that the enzymatic degradation of the xenobiotics dicussed here is possible for at least one enantiomer. Degradation of both enantiomers may also be occurring at different rates. Enantioselective gas chromatography has not only proven to be a sensitive and selective analytical method for distinguishing between enzymatic and non-enzymatic degradation of chiral toxic compounds, but can also be used for the virtually complete preparative-scale resolution of enantiomers with low separation factors.

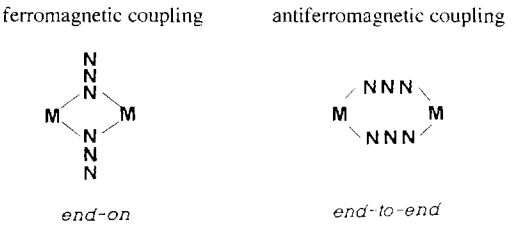
Received: April 2, 1994 [Z 6819 IE]
German version: *Angew. Chem.* **1994**, *106*, 2175

[1] A. Miyazaki, T. Hotta, S. Marumo, M. Sakai, *J. Agric. Food Chem.* **1978**, *26*, 975–977; A. Miyazaki, M. Sakai, S. Marumo, *ibid.* **1979**, *27*, 1403–1405; *ibid.* **1980**, *28*, 1310–1311.
[2] R. Kallenborn, H. Hühnerfuss, W. A. König, *Angew. Chem.* **1991**, *103*, 328–329; *Angew. Chem. Int. Ed. Engl.* **1991**, *30*, 320–321; H. Hühnerfuss, J. Faller, R. Kallenborn, W. A. König, P. Ludwig, B. Pfaffenberger, M. Oehme, G. Rimkus, *Chirality* **1993**, *5*, 393–399.
[3] W. A. König, D. Icheln, T. Runge, B. Pfaffenberger, P. Ludwig, H. Hühnerfuss, *J. High Res. Chromatogr.* **1991**, *14*, 530–536.
[4] W. A. König, B. Gehrcke, T. Runge, C. Wolf, *J. High Res. Chromatogr.* **1993**, *16*, 376–378.
[5] B. Pfaffenberger, H. Hühnerfuss, B. Gehrcke, I. H. Hardt, W. A. König, G. Rimkus, *Chemosphere*, in press.
[6] H.-R. Buser, M. D. Müller, *Anal. Chem.* **1992**, *64*, 3168–3175; H.-R. Buser, M. D. Müller, C. Rappe *Environ. Sci. Technol.* **1992**, *26*, 1533–1540; H.-R. Buser, M. D. Müller, *ibid.* **1993**, *27*, 1211–1220; M. D. Müller, M. Schlabach, M. Oehme, *ibid.* **1992**, *26*, 566; S. Mössner, T. R. Spraker, P. R. Becker, K. Ballschmiter, *Chemosphere* **1992**, *24*, 1171–1180; R. Kallenborn, M. Oehme, W. Vetter, H. Parlar, *ibid.* **1994**, *28*, 89–98.
[7] S. J. Cristol, *J. Am. Chem. Soc.* **1949**, *71*, 1894.
[8] K. Möller, C. Bretzke, H. Hühnerfuss, R. Kallenborn, J. N. Kinkel, J. Kopf, G. Rimkus, *Angew. Chem.* **1994**, *106*, 911–912; *Angew. Chem. Int. Ed. Engl.* **1994**, *33*, 882–884.
[9] H. Kleemeyer, W. Thiemann, *Chemosphere* **1986**, *15*, 687–692.
[10] W. A. König, B. Gehrcke, D. Icheln, P. Evers, J. Dönnecke, W. Wang, *J. High Res. Chromatogr.* **1992**, *15*, 367–372.
[11] W. A. König, B. Gehrcke, D. H. Hochmuth, C. Mlynek, H. Hopf, *Tetrahedron Asymm.* **1994**, *5*, 347–350.
[12] Steel columns (2 m × 5.3 mm) packed with equal proportions by weight of cyclodextrin derivative and polysiloxane OV 1701 (2.5%) on chromosorb G-HP (100–120 mesh) were used at temperatures between 110 and 160 °C with helium as the carrier gas at a pressure of between 310 and 600 kPa (corresponds to a flow rate of 240 and 620 mL min^{-1}, respectively); see also I. H. Hardt, W. A. König, *J. Chromatogr. A.* **1994**, *666*, 611–615.
[13] V. Schurig, H. Grosenick, B. S. Green, *Angew. Chem.* **1993**, *105*, 1690–1691; *Angew. Chem. Int. Ed. Engl.* **1993**, *32*, 1662–1663.
[14] D. U. Staerk, A. Shitangkoon, G. Vigh, *J. Chromatogr. A.* **1994**, *663*, 79–85.
[15] J. Meinwald, R. Thompson, D. L. Pearson, W. A. König, T. Runge, W. Francke, *Science* **1991**, *251*, 560–561.
[16] Reference samples can be obtained from Dr. Ehrenstorfer GmbH, Bgm.-Schlosser-Str. 6a, D-86199 Augsburg (FRG).

The Versatility of the Azido Ligand: Linkage of Ni^{II} Centers to Form a Chain with One End-to-End and Three End-On Bridges in Alternation**

Joan Ribas,* Montserrat Monfort, Barindra Kumar Ghosh, and Xavier Solans

In recent years several groups have investigated the correlation between magnetic and structural properties of μ-azido-nickel(II) complexes.[1, 2] We are now working systematically in this field[3–5] and have prepared two types of systems whose structures depend on the amino ligand employed (Scheme 1).



Scheme 1. Possible coordination modes for azido ligands.

The bridging ligand with its end-to-end (EE) coordination mode affords antiferromagnetic (AF) dinuclear[3a] and one-dimensional (1D) systems.[3b–e] End-on (EO) coordination is observed in some dinuclear,[4a, b] one tetranuclear,[4c] and several one-dimensional polymeric ferromagnetic (F) compounds.[4b] A new unexpected two-dimensional (2D) complex (Fig. 1) with both EE and EO bridges has also been characterized[5] and displays overall AF behavior with canting phenomenon at low temperatures. This variation in coordination modes, EE and EO, causes different magnetic couplings which appear to be general for the metal ions Cu^{II},[6] Mn^{II},[7] Mn^{III},[8] and Co^{II}.[9]

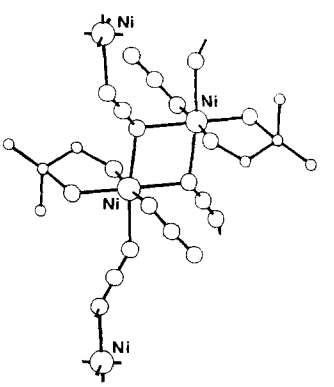


Fig. 1. Schematic representation of the structure of the 2D complex $[Ni(N_3)_2(dmpd)]_n$ (dmpd = 2,2-dimethylpropane-1,3-diamine), showing the different kinds of azido coordination: EO, EE, and terminal [5].

In continuation of our investigations we considered that the 2D system presents one terminal azido ligand on each Ni^{II} atom (Fig. 1), and it should thus be possible to have three EO bridges. We report here on the synthesis and characterization of $[Ni(N_3)_2(tmeda)]_n$ (tmeda = *N,N,N′,N′*-tetramethylethylenediamine), a novel compound in which the Ni^{II} centers are linked alternately by one EE and three EO bridges to form a chain (Fig. 2).[10] Each Ni^{II} center completes its distorted octahedral coordination by binding to one bidentate tmeda lig-

[*] Prof. J. Ribas, Dr. M. Monfort, Dr. B. K. Ghosh
Departament de Química Inorgànica, Universitat de Barcelona
Diagonal, 647, E-08028-Barcelona (Spain)
Telefax: Int. code + (343) 411-1492
Prof. X. Solans
Universitat de Barcelona (Spain)

[**] This work was supported by the Spanish Dirección General de Investigación Científica y Técnica (project PB91-0241).

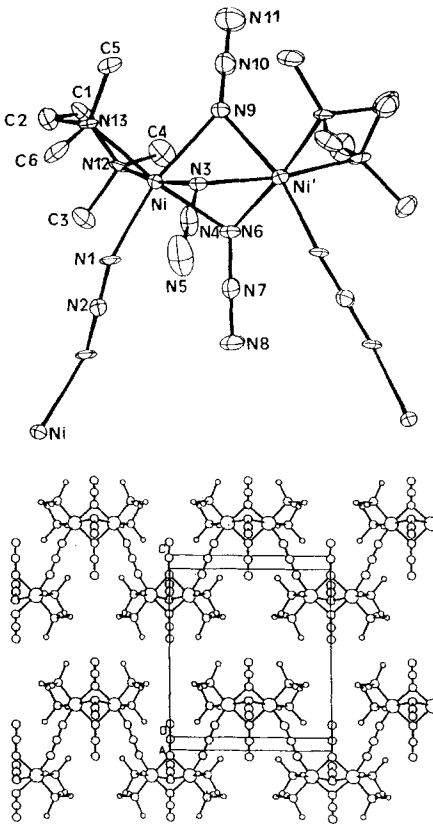


Fig. 2. Top: Crystal structure of $[Ni(N_3)_2(tmeda)]_n$. Selected bond lengths [Å] and angles [°] (standard deviation in parentheses): Ni-N1 2.062(4), Ni-N3 2.120(3), Ni-N6 2.139(5), Ni-N9 2.160(6), Ni-Ni' 2.8692(7), Ni-N12 2.132(3), Ni-N13 2.150(3); N1-Ni-N3 91.9(2), N1-Ni-N6 92.8(2), N3-Ni-N6 83.79(14), N1-Ni-N9 166.6(2), N3-Ni-N9 77.3(2), N6-Ni-N9 78.3(3), N2-N1-Ni 138.0(2), N1-N2-N1(ii) 180.0, Ni-N3-Ni' 85.16(13), Ni-N6-Ni' 84.3(2), Ni-N9-Ni' 83.2(3). Bottom: Arrangement in the crystal.

and. The most important features are the Ni-N-Ni angles. The average value in the EO bridge is 84.2°, which is the lowest value for any metal atom;[2-9] in the EE bridge the Ni-N-N angle is 138° with a Ni-N_3-Ni dihedral angle of 0°. These angles are relevant to the discussion of magnetic properties.

Variable-temperature solid-state magnetic susceptibility studies have been performed on a powder sample from 290 to 4 K. Overall antiferromagnetic interaction is evident from the magnetic behavior (Fig. 3). The χ_M value increases when the temperature decreases; reaches a maximum near 47 K, and then decreases as the temperature approaches 4 K. To explain the magnetic behavior we must assume two J values (alternating chain): J_1 for EE coordination and J_2 for EO coordination, where J_1 must be negative[3] (AF) and J_2 could be negative (AF) or positive (F) because of the low Ni-N-Ni angle. We have fitted the data with the Borrás formula[11a] for an antiferromagnetic, alternating $S = 1$ chain and with the standard formula[12] for a dinuclear Ni^{II} unit (i.e., assuming $J_2 = 0$). The parameters of the best fit and their reliability factors (R) are $J_1 = -31.8 \pm 0.3\ cm^{-1}$, $J_2 = -6.9 \pm 0.2\ cm^{-1}$, $g = 2.35$, and $R = 1.5 \times 10^{-4}$ for the alternating chain, and $J_1 = -29.3 \pm 0.5\ cm^{-1}$, $g = 2.26$, and $R = 6.6 \times 10^{-3}$ for a dinuclear unit (Fig. 3). The following values were obtained for the maximum susceptibility: 0.01141 (experimental), 0.01160 (alternating chain), and 0.01192 $cm^3\ mol^{-1}$ (dinuclear unit). In both cases the experimental value in this zone is lower than the theoretical, and the difference is even greater for the dinuclear model. This clearly indicates antiferromagnetic coupling in both parts of the chain

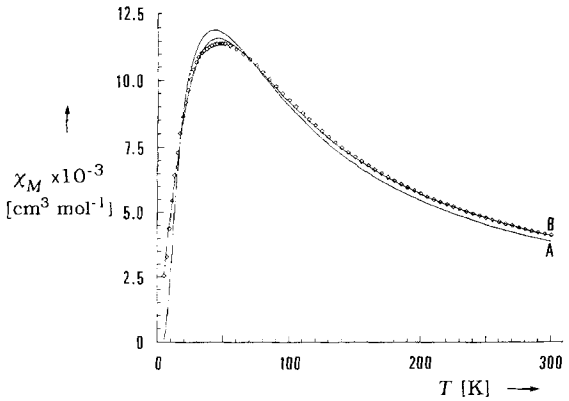


Fig. 3. Plots of χ_M (◇) versus T for $[Ni(N_3)_2(tmeda)]_n$. Solid lines correspond to the best fitting curves for dinuclear Ni^{II} complexes (A) and for an AF alternating chain (B).

(both J_1 and J_2 are negative). There is no formula in the literature for an $S = 1$, ferromagnetic-antiferromagnetic alternating chain, but according to the reported formula for an $S = 1/2$ system,[11b] the maximum should be higher than that for the dinuclear unit.

Our previous studies on 1D Ni^{II} complexes with EE coordination show that for a Ni-N-N angle of 138° and a Ni-N_3-Ni dihedral angle of 0° the J_1 value should be close to $-40\ cm^{-1}$.[3d,e] However, the behavior of the $Ni(N_3)_3Ni$ core is very difficult to predict. Indeed, all Ni^{II} complexes reported so far with EO bridge(s) are ferromagnetically coupled[2,4] with Ni-N-Ni angle(s) close to 103°. For similar Cu^{II} complexes Kahn et al. explained the ferromagnetic behavior by accidental orthogonality[13] and with the results of ab initio calculations on model systems,[14] which led to the theory of spin polarization. Accidental orthogonality appears for Cu-N-Cu angles close to 103°.[13] For the analogous Ni^{II} complexes the Ni-N-Ni angle ranges from 100 to 105°. Consequently, it is not surprising that all of these complexes are ferromagnetically coupled. In our case, the angle is 84° (average), the smallest yet reported for an azidometal complex.[15] This is also most likely the main reason for the net negative value of J_2 (AF) found in the experimental fitting.

In conclusion we state that the Ni^{II} complex described here is a further example in which the change of the nonbridging ligand (dmpd → tmeda) dramatically affects the coordination mode of the μ-azido ligand and, of course, the nature of magnetic interaction propagated through the bridge. We are currently attempting to elucidate the nature and magnitude of the interactions between two types of nickel centers of this novel system where the Ni-N-Ni angle of EO bridge ranges from 105° to 80°.

Experimental Procedure

A solution of tmeda (0.3 g 2 mmol) in MeCN (10 mL) was added dropwise to a stirred aqueous solution (25 mL) of $Ni(ClO_4)_2 \cdot 6\ H_2O$ (0.74 g, 2 mmol). After filtration, a solution of NaN_3 (0.26 g, 4 mmol) in water (10 mL) was added slowly. Within a few minutes a bit of greenish-white solid precipitated which was filtered off and discarded. Slow evaporation of the clear dark green solution for one week at room temperature provided X-ray quality green monocrystals (yield 0.42 g, 80%).

Received: May 4, 1994
Revised version: June 16, 1994 [Z 6894 IE]
German version: *Angew. Chem.* **1994**, *106*, 2177

[1] a) F. Wagner, M. T. Mocella, M. J. D'Aniello, Jr., A. H. J. Wang, E. K. Barefield, *J. Am. Chem. Soc.* **1974**, *96*, 2625; b) C. G. Pierpont, D. N. Hendrickson, D. M. Duggan, F. Wagner, E. K. Barefield, *Inorg. Chem.* **1975**, *14*, 604; c) P. Chaudhuri, M. Guttmann, D. Ventur, K. Wieghardt, B. Nuber, J. Weiss, *J. Chem. Soc. Chem. Commun.* **1985**, 1618.

[2] a) M. I. Arriortua, R. Cortés, L. Lezama, T. Rojo, X. Solans, M. Font-Bardía, *Inorg. Chim. Acta* **1990**, *174*, 263; b) R. Cortés, J. I. Ruiz de Larramendi, L. Lezama, T. Rojo, K. Urtiaga, M. I. Arriortua, *J. Chem. Soc. Dalton Trans.* **1992**, 2723.

[3] a) J. Ribas, M. Monfort, C. Diaz, C. Bastos, X. Solans, *Inorg. Chem.* **1993**, *32*, 3557; b) A. Escuer, R. Vicente, M. S. El Fallah, J. Ribas, X. Solans, M. Font-Bardía, *J. Chem. Soc. Dalton Trans.* **1993**, 2975; c) A. Escuer, R. Vicente, J. Ribas, M. S. El Fallah, X. Solans, *Inorg. Chem.* **1993**, *32*, 1033; d) A. Escuer, R. Vicente, J. Ribas, M. S. El Fallah, X. Solans, M. Font-Bardía, *ibid.* **1993**, *32*, 3727; e) *ibid.* **1994**, *33*, 1842.

[4] a) R. Vicente, A. Escuer, J. Ribas, M. S. El Fallah, X. Solans, M. Font-Bardía, *Inorg. Chem.* **1993**, *32*, 1920; b) J. Ribas, M. Monfort, C. Diaz, C. Bastos, X. Solans, *Inorg. Chem.* **1994**, *33*, 484; c) J. Ribas, M. Monfort, R. Costa, X. Solans, *ibid.* **1993**, *32*, 695.

[5] a) M. Monfort, J. Ribas, X. Solans, *J. Chem. Soc. Chem. Commun.* **1993**, 350; b) J. Ribas, M. Monfort, X. Solans, M. Drillon, *Inorg. Chem.* **1994**, *33*, 742.

[6] R. Cortés, M. K. Urtiaga, L. Lezama, J. I. Ruiz de Larramendi, M. I. Arriortua, T. Rojo, *J. Chem. Soc. Dalton Trans.* **1993**, 3685, and references therein.

[7] R. Cortés, J. L. Pizarro, L. Lezama, M. I. Arriortua, T. Rojo, *Inorg. Chem.* **1994**, *33*, 2697. The Mn-N-Mn-angle is 104.6° and J/k is +3.5 K.

[8] a) B. R. Stults, R. S. Marianelli, V. W. Day, *Inorg. Chem.* **1975**, *14*, 722; b) A. K. Gregson, N. T. Moxon, *ibid.* **1982**, *21*, 586.

[9] A. Bencini, C. A. Ghilardi, S. Midollini, A. Orlandini, *Inorg. Chem.* **1989**, *28*, 1958.

[10] X-ray structure analyses: Enraf-Nonius CAD4 diffractometer, $Mo_{K\alpha}$ irradiation, 0.71069 Å, graphite monochromator, 298 K. Lorentz polarization but no absorption corrections. Data collection, solution and refinement: $\omega/2\theta$, standard Patterson methods with SHELXS computer program, refinement: SHELXS93 computer program. The positions of the twelve methyl H atoms were determined by difference synthesis, while the position of the remaining four were computed and refined with an overall isotropic temperature factor and a riding model. $C_{12}H_{32}N_{16}Ni_2$ ($M = 517.92$), monoclinic, space group $C2/m$, $a = 16.366(3)$, $b = 11.3944(12)$, $c = 13.485(2)$ Å, $\beta = 113.34(1)°$, $V = 2309.9(6)$ Å^3, $Z = 4$, $\rho_{calcd} = 1.489$ g cm^{-3}, $\mu = 16.61$ cm^{-1}, crystal size $0.1 \times 0.2 \times 0.1$ mm^3, $F(000) = 1088.0$, 1843 unique reflections and 1793 assumed as observed with $I > 2\sigma(I)$, 189 parameters, $R(F_o) = 0.031$, $R_w(F_o) = 0.0766$, and $S = 0.982$. Further details of the crystal structure investigation are available on request from the Director of the Cambridge Crystallographic Data Centre, 12 Union Road, GB-Cambridge CB2 1EZ (UK), on quoting the full journal citation.

[11] a) J. J. Borrás-Almenar, Dissertation, Universitat de Valencia, **1992** (Address: Departament de Química Inorgànica – Universitat de Valencia – Doctor Moliner, 50, E-46100 Burjassot (Valencia, Spain); J. J. Borrás-Almenar, E. Coronado, J. Curely, R. Georges, *Inorg. Chem.*, in press; b) G. de Munno, M. Julve, F. Lloret, J. Faus, M. Verdaguer, A. Caneschi, *Angew. Chem.* **1993**, *105*, 1122; *Angew. Chem. Int. Ed. Engl.* **1993**, *32*, 1046.

[12] C. J. O'Connor, *Prog. Inorg. Chem.* **1982**, *29*, 239.

[13] J. Comarmond, P. Plumeré, J.-M. Lehn, Y. Agnus, R. Louis, R. Weiss, O. Kahn, I. Morgenstern-Badarau, *J. Am. Chem. Soc.* **1982**, *104*, 6330.

[14] M. F. Charlot, O. Kahn, M. Chaillet, C. Larrieu, *J. Am. Chem. Soc.* **1986**, *108*, 2574.

[15] P. Mason, G. A. Rusholme, *Chem. Commun.* **1971**, 496. The authors reported a diamagnetic dinuclear Mn^I complex with one CO and three EO azido ligands, but the crystal structure determination was not good.

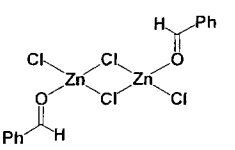
On the Nature of Zinc Chloride–Aldehyde Interactions**

Bodo Müller, Michael Ruf, and Heinrich Vahrenkamp*

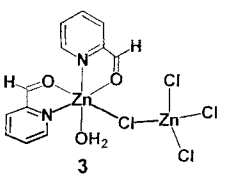
Among the large number of organic reactions that involve aldehydes as starting compounds or products, many are catalyzed by simple metal salts, $ZnCl_2$ being the most prominent co-reagent for carbonyl conversions.[1] This should imply that the coordination chemistry of aldehydes or the reactivity of aldehydes in the ligand sphere of complexes are attractive objects of study. However, the inherently low donor strength of aldehydes has limited the types of well-characterized metal–aldehyde complexes to some organometallic species of the inert heavy transition metals[2] and to classical chelate complexes like those of salicylic aldehyde.[3] The number of known adducts of metal halides with simple aldehydes[4] or aldehyde solvates of metal salts[5] is surprisingly small, and to our knowledge only one such complex[6] has been structurally characterized.[7]

We became interested in this type of compound through our work on the bioinorganic chemistry of zinc, specifically by attempts to model the active site of the zinc enzyme alcohol dehydrogenase. The immediate coordination sphere of the metal in this enzyme is S_2NZn-substrate,[9] and the closest approach to its static nature was achieved by Bochmann et al., who isolated complexes $[Zn(SeR)_2 \cdot R'CHO]_2$ ($R = C_6H_2tBu_3$, $R' =$ aromatic group) and determined the structure for $R' = p\text{-}C_6H_4OMe$.[10] In addition to working on this problem by preparing cysteine–zinc–(O donor) complexes we carried out a general screening of the donor/acceptor relations between simple zinc salts and monofunctional aldehydes. Here we report our findings for the zinc chloride system.

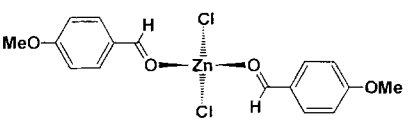
For aliphatic aldehydes, condensations and polymerizations seem to be preferred over coordination in the presence of $ZnCl_2$. But by dissolving anhydrous zinc chloride in a 100-fold excess of benzaldehyde and crystallizing by diffusion of petroleum ether into the solution, the compound [$ZnCl_2$ · benzaldehyde] (**1**) is obtained as colorless crystals.[11] Similarly, from *p*-methoxybenzaldehyde (anisaldehyde) the colorless 1:2 complex [$ZnCl_2$ · 2 anisaldehyde] (**2**) is formed. Reacting the potentially chelating aldehyde pyridine-2-carbaldehyde (L) in stoichiometric amounts with zinc chloride and one half equivalent of water in ether, a product with yet another stoichiometry, $[L_2Zn_2Cl_4 \cdot H_2O]$ (**3**), is precpitated as colorless crystals.



1



3



2

In **1**, **2**, and **3** the aldehyde ν(CO) bands in the IR spectrum at 1682, 1677, and 1663 cm^{-1}, respectively, are shifted by 20–50 cm^{-1} to lower wavenumbers, indicating coordination of the aldehydes through their oxygen atoms.[4, 5] Similarly the ^{1}H NMR signals in acetone of the aldehyde protons for **1** ($\delta = 10.02$), **2** ($\delta = 9.91$), and **3** ($\delta = 10.27$) respond to the complexation by low-field shifts of $\Delta\delta = 0.1–0.2$.

The crystals of **1** were not suitable for a structure detemination. The solubility of **1**, however, indicates the presence of a molecular species which, in accordance with Bochmann's selenolate complex,[10] may be formulated as a chloride-bridged dimer. The structure of **2** was obtained crystallographically.[12] Figure 1 shows one molecule of **2**, which to our knowledge is the first structurally characterized transition metal halide complex of a simple aldehyde. Complex **2** is a quite normal tetrahedral zinc complex with all bond lengths and angles at zinc within the

[*] Prof. Dr. H. Vahrenkamp, Dipl.-Chem. B. Müller, Dipl.-Chem. M. Ruf
Institut für Anorganische und Analytische Chemie der Universität
Albertstrasse 21, D-79104 Freiburg (FRG)
Telefax: Int. code + (761)203-6001

[**] This work was supported by the Deutsche Forschungsgemeinschaft.

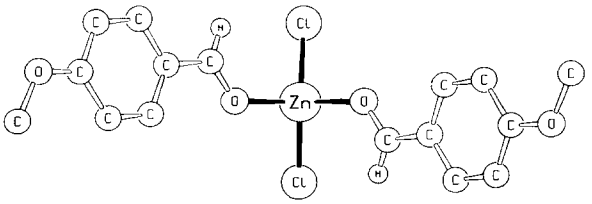


Fig. 1. Molecular structure of **2**. Selected bond lengths [pm] and angles [°]: Zn-Cl 219.8(1), Zn-O 202.0(4); O-Zn-O 100.2(2), Cl-Zn-Cl 130.0(1), Cl-Zn-O 105.0(1) and 106.5(1), Zn-O-C 127.3(4).

standard range, except for a slight increase of the Cl-Zn-Cl angle. Thus, there are no bonding features supporting the argument that such complexes should be difficult to obtain. This in turn means that unusual steric hindrance or the presence of special chalcogenolate ligands[10] are not prerequisites for their isolability. However, care must be taken in handling the compounds, since they are extremely hygroscopic. The structure (also obtained crystallographically) of **3**, which initially resulted from accidental access of water, underlines this.

The comparison of **1**, **2**, and **3** points to the subtleties governing the coordination behavior of the three aldehydes. In solid **1** the aldehyde donor seems to be unable to compete with a Zn–Cl unit for a coordination position on zinc despite the large excess of the aldehyde in solution. In **2** the *p*-methoxy substituent on the phenyl ring has sufficiently increased the donor capacity of the aldehyde to enable this. Complex **3** shows yet another way of balancing the donor abilities of the aldehyde and chloro ligands: one zinc ion binds both chelating aldehydes, the second one is only coordinated by chloro ligands.

These findings underline the ambiguity about the mode of coordination of the aldehydes, which is due to their low donor capacity. This in turn means that mechanistic implications about metal salt mediated organic reactions of aldehydes[1, 13] may have an equally high degree of ambiguity.

Received: May 9, 1994 [Z 6911 IE]
German version: *Angew. Chem.* **1994**, *106*, 2164

[1] a) *Comprehensive Organic Chemistry, Vol. 1* (Eds.: D. Barton, W. D. Ollis, J. F. Stoddart), Pergamon, Oxford, **1979**; b) R. Brettle in ref. [1a], pp. 943–1016; c) T. Laird in ref. [1a], pp. 1105–1160.
[2] Y. H. Huang, J. A. Gladysz, *J. Chem. Educ.* **1988**, *65*, 298–303.
[3] Papers that contain structural data: D. Hall, A. J. McKinnon, T. N. Waters, *J. Chem. Soc.* **1965**, 425–430; M. R. Truter, R. C. Watling, *J. Chem. Soc. A* **1967**, 1955–1963; R. J. Hill, C. E. F. Rickard, *J. Inorg. Nucl. Chem.* **1977**, *39*, 1593–1596; J. B. Hodgson, G. C. Percy, *Spectrochim. Acta Part A* **1978**, *34*, 777–780.
[4] F. Filippini, B. P. Susz, *Helv. Chim. Acta* **1971**, *54*, 1175–1178, and references therein.
[5] P. L. Verheijdt, P. H. van der Voort, W. L. Groeneveld, W. L. Driessen, *Recl. Trav. Chim. Pays-Bas* **1972**, *91*, 1201–1204, and references therein.
[6] S. E. Denmark, B. R. Henke, E. Weber, *J. Am. Chem. Soc.* **1987**, *109*, 2512–2514.
[7] Further structural studies involve a BF_3 adduct of anisaldehyde [8a] and a $MeAl(OR)_2$ adduct of *t*BuCHO [8b].
[8] a) T. M. Reetz, M. Hüllmann, W. Massa, S. Berger, P. Rademacher, P. Heymanns, *J. Am. Chem. Soc.* **1986**, *108*, 2405–2408; b) M. B. Power, S. G. Bott, D. L. Clark, J. L. Atwood, A. R. Barron, *Organometallics* **1990**, *9*, 3086–3097.
[9] H. Eklund, A. Jones, G. Schneider in *Zinc Enzymes* (Eds.: I. Bertini, C. Luchinat, W. Maret, M. Zeppezauer), Birkhäuser, Basel, **1986**, pp. 377–392.
[10] M. Bochmann, K. J. Webb, M. B. Hursthouse, M. Mazid, *J. Chem. Soc. Chem. Commun.* **1991**, 1735–1737.
[11] Previously described as a yellow powder: F. Filippini, B. P. Susz, *Helv. Chim. Acta* **1971**, *54*, 835–845.
[12] Crystal data for **2**: space group $P2_12_12$, $a = 896.4(1)$, $b = 1991.8(6)$, $c = 477.6(1)$ pm, 1689 reflections, 105 parameters, $R = 0.053$. The molecule of **2** is bisected by a twofold symmetriy axis. Further details of the crystal structure investigation may be obtained from the Fachinformationszentrum Karlsruhe, D-76344 Eggenstein-Leopoldshafen (FRG), on quoting the depository number CSD-380052.
[13] *Comprehensive Organic Synthesis, Vol. 2* (Eds.: B. M. Trost, I. Fleming), Pergamon, Oxford, **1991**.

Cyanide–Isocyanide Isomerism in CN-Bridged Organometallic Complexes**

Nianyong Zhu and Heinrich Vahrenkamp*

Bridged dinuclear complexes are a prime object of studies for mixed valence and electron transfer.[1] Among these complexes those with cyanide bridges have often been mentioned because of their obvious relation with Prussian Blue.[2] The actual number of studies of their redox and mixed-valence behavior, however, is still rather small.[3]

We have started a systematic preparative, structural, and electrochemical investigation of cyanide-bridged complexes, in search of "organometallic Prussian Blue".[4] Such complexes are amazingly easy to prepare, since almost any organometallic complex with cyanide ligands (neutral or anionic) can be used as a ligand itself for another organometallic unit, thereby establishing the CN links. Furthermore the oligonuclear species obtained this way seem to be highly inert towards M–CN–M′ → M–NC–M′ isomerizations, which are a common fate of classical complexes with CN links, leading to the thermodynamically preferred isomers.[2, 5] This behavior has allowed us to prepare and characterize for the first time stable pairs of organometallic species with cyanide/isocyanide isomerism, that is species which exist in the M(μ-CN)M′ as well as in the M(μ-NC)M′ forms.[6]

Here we report on two such pairs which relate to complexes that we have described before. The first pair, **1a** and **1b**, can be

$[Cp(CO)_2Fe(\mu\text{-}CN)Mn(CO)_2Cp]$ **1a** $[Cp(CO)_2Fe(\mu\text{-}NC)Mn(CO)_2Cp]$ **1b**

derived from the pseudosymmetrical anion $[Cp(CO)_2Mn(\mu\text{-}CN)Mn(CO)_2Cp]^-$.[4] Replacing one neutral $Cp(CO)_2Mn$ fragment on the left- or right-hand side of this complex by an isoelectronic cationic $Cp(CO)_2Fe$ fragment results in the pair of isomers **1**. Chemically this is achieved by either reacting $[Cp(CO)_2FeCN]$ in THF with $[(thf)Mn(CO)_2Cp]$ to give **1a** or $[Cp(CO)_2Fe(thf)]BF_4$ in CH_2Cl_2 with $Na[Cp(CO)_2Mn\text{-}CN]$ to give **1b**. Recrystallization from CH_2Cl_2/petroleum ether provides **1a** and **1b** in 25 and 45% yield, respectively.

Complexes **1a** (orange-red) and **1b** (red) can be distinguished by their colors, as evidenced by their absorptions in the visible range showing a broad featureless band extending from the UV for **1a** and one exhibiting a weak maximum at 495 nm for **1b**. The differences in their ν_{CO} bands and ^1H NMR spectra are very small.[9] However, the CN stretching frequency for **1b** (2100 cm^{-1}) is 50 cm^{-1} lower than that for **1a**, which means that for this pair of isomers the different electronic situations are not accommodated by the M–CO units but by the bridging CN ligand. The redox behavior of **1a** and **1b**[9] reflects the orientation of the bridging CN by a difference of 0.24 V in the $E_{1/2}$(ox) values.

The second pair of isomers completes a series of compounds starting with **2a** and $[\mathbf{2a}]^+$.[10] While **2a** was obtained from $Na[Cr(CO)_5CN]$ and [BrFe(dppe)Cp] (dppe = 1,2-bis(diphenylphosphano)ethane),[10] **2b** was prepared from $[(CO)_5Cr(thf)]$

$[(CO)_5Cr(\mu\text{-}CN)Fe(dppe)Cp]$ **2a** $[(CO)_5Cr(\mu\text{-}NC)Fe(dppe)Cp]$ **2b**

[*] Prof. Dr. H. Vahrenkamp, N. Zhu
Institut für Anorganische und Analytische Chemie der Universität
Albertstrasse 21, D-79104 Freiburg (FRG)
Telefax: Int. code + (761)203-6001

[**] This work was supported by the Graduiertenkolleg "Systeme mit ungepaarten Elektronen" and by the Landes-Schwerpunktprogramm "Elektroaktive Systeme für die Sensorik".

and [Cp(dppe)FeCN] in THF and recrystallized from CH_2Cl_2/petroleum ether in 62% yield. Both isomers of **2**, just like those of **1**, cannot be interconverted thermally up to their decomposition points around 150 °C. **2a** (red) and **2b** (yellow) differ clearly in their colors and in their optical absorption maxima (472 nm for **2a** and 402 nm for **2b**). This time the δ(Cp) and ν(CN) values[9] are quite similar, and the electronic difference is mostly reflected in the CO vibrations.[9] Specifically the A_1^1 band of the $Cr(CO)_5$ group which corresponds to the CO vibration *trans* to CN is about 30 cm^{-1} higher for **2a** (1898 cm^{-1}) than for **2b**. This might be expected because N-bonded CN is a weaker π acceptor than C-bonded CN. A comparison of **2b** with $[(CO)_5CrNCMe]$ (A_1^1 bands at 1869 and 1930 cm^{-1}, respectively) reveals clearly that the "ligand" [Cp(dppe)FeCN] in **2b** is extremely electron-rich. Irrespective of this, the HOMOs of **2a** and **2b** seem to be lower in energy than those of **1a** and **1b**, since both complexes **2** are about 0.2 V more difficult to oxidize than their counterparts **1**.[9]

The structure determinations of **2a** and **2b**[11, 12] reveal that it is almost impossible to distinguish the compounds in the solid state. The crystals are isomorphous (but clearly distinguished by their colors), and both structures can be presented by one drawing (Fig. 1). The bonding parameters are all normal. The differences between **2a** and **2b** are almost insignificant, but the trends in the Cr-CN-Fe backbones are as expected. Thus, the M–N distances are longer than the corresponding M–C distances because of weaker M–N vs. M–C backbonding, and the Fe–C bond in **2b** is the shortest of the M–(CN) bonds because the electron-rich iron unit has the most backbonding to offer, while the C–N bond length shows very little variation. The largest difference between **2a** and **2b** lies in the deviations from linearity at the bridging C and N atoms. We consider this bending of the molecules to result from packing forces. Isomorphism, a similar bending, and the near-to-identity of all bonding parameters were also observed for the pair of complexes $[(NH_3)_5Co(\mu\text{-}L)Co(CN)_5]$ (L = CN, NC).[8]

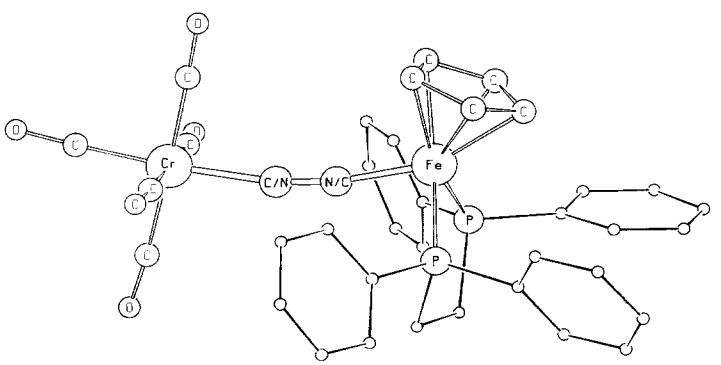


Fig. 1. Molecular geometry of **2a** and **2b**. Pertinent distances [pm] and angles [°] (values for **2b** in square brackets): Cr-C/Cr-N 206.4(5) [208.6(3)], C-N 115.8(7) [115.1(5)], Fe-N/Fe-C 193.5(4) [189.7(4)], Cr-C(CO *trans*) 183.8(6) [184.4(5)], Cr-C(CO *cis*, average) 188.6(6) [189.5(5)], Fe-P (average) 220.2(1) [218.5(1)]; Cr-C(N)-N(C) 170.7(4) [165.1(3)], Fe-N(C)-C(N) 169.8(4) [174.3(4)].

The spectroscopic and structural similarity within the pair of isomers **2a** and **2b**, which may be explained by their delocalized nature, extends itself to their cationic species. The molecular structure of the cation in [**2b**] $[BF_4]$[10] is again most similar to that of **2a** and **2b**, and a detailed investigation has revealed that the radical ion $\mathbf{2b}^+$ possesses a high degree of charge delocalization.[10]

The physical properties of the isomers and their tolerance of a change in the electron count underline the ability of the cyanide ligand to act as a mediator and transducer of electronic effects. The position of the ν(CN) vibration in the IR spectrum[9] and preliminary extended-Hückel MO calculations[13] indicate that the bridging cyanide ligand can respond to the donor/acceptor properties of both organometallic units by variation of its electronic situation without altering its bond length, just as has been observed for many solid-state metal-cyanide compounds.[14] Thus, it does not seem to be utterly unrealistic to search for "organometallic Prussian Blue".

Received: May 9, 1994 [Z 6912 IE]
German version: *Angew. Chem.* **1994**, *106*, 2166

[1] C. Creutz, *Prog. Inorg. Chem.* **1983**, *30*, 1–73.
[2] W. P. Fehlhammer, M. Fritz, *Chem. Rev.* **1993**, *93*, 1243–1280.
[3] F. L. Atkinson, A. Christofides, N. G. Connelly, H. J. Lawson, A. C. Loyns, A. G. Orpen, G. M. Rosair, G. H. Worth, *J. Chem. Soc. Dalton Trans.* **1993**, 1441–1450, and references therein; F. Scandola, R. Argazzi, C. A. Bignozzi, C. Chiorboli, M. T. Indelli, N. A. Rampi, *Coord. Chem. Rev.* **1993**, *125*, 283–292, and references therein.
[4] First communication: B. Oswald, A. K. Powell, F. Rashwan, J. Heinze, H. Vahrenkamp, *Chem. Ber.* **1990**, *123*, 243–250.
[5] For a case of terminal M–NC → M–CN isomerization cf. S. Alvarez, C. Lopez, *Inorg. Chim. Acta* **1982**, *64*, L99–L100.
[6] Among the inert classical complexes two such pairs have been reported: $[(H_2O)_5Cr(\mu\text{-}CN)Co(CN)_5]$ (spectroscopic characterization) [7] and $[(NH_3)_5Co(\mu\text{-}CN)Co(CN)_5]$ (structure determinations) [8].
[7] D. Gaswick, A. Haim, *J. Inorg. Nucl. Chem.* **1978**, *40*, 437–439.
[8] F. R. Fronczek, W. P. Schaefer, *Inorg. Chem.* **1974**, *13*, 727–732.
[9] IR (CH_2Cl_2): ν(CO): **1a**: $\tilde{\nu}$[cm^{-1}] = 2062s, 2017s, 1920s, 1843s; **1b**: 2063s, 2018s, 1922s, 1854s; **2a**: 2056w, 1930vs, 1898m; **2b**: 2064w, 1928vs, 1869m. ν(CN): **1a**: 2147vw; **1b**: 2099m; **2a**: 2115w; **2b**: 2103w. ^{1}H NMR (δ(Cp) TMS int., $CDCl_3$): **1a**: 5.07, 4.41; **1b**: 5.08, 4.40; **2a**: 4.15; **2b**: 4.22. Cyclovoltammetric data (first oxidation, E vs. Ag/AgCl, CH_3CN): **1a**: 0.11 V (quasi-rev.); **1b**: 0.35 V (rev.); **2a**: 0.32 V (rev.); **2b**: 0.53 V (irrev.).
[10] N. Zhu, H. Vahrenkamp, *J. Organomet. Chem.* **1994**, *472*, C5–C7.
[11] Crystal data: **2a**: space group $P2_1/c$, a = 1501.4(1), b = 1299.5(1), c = 1718.2(1) pm, β = 95.49(1)°, 5034 reflections, 424 parameters, R = 0.068. **2b**: space group $P2_1/c$, a = 1500.7(1), b = 1297.6(1), c = 1716.4(2) pm, β = 95.60(1)°, 5314 reflections, 424 parameters, R = 0.045 [12].
[12] Further details of the crystal structure investigation may be obtained upon request from the Fachinformationszentrum Karlsruhe, D-76344 Eggenstein-Leopoldshafen (FRG), on quoting the depository numbers CSD-380055 (for **2a**) and CSD-380056 (for **2b**).
[13] C. Marchand, H. Grützmacher, private communication.
[14] A. M. Golub, H. Köhler, V. V. Skopenko, *Chemistry of Pseudohalides* (*Topics in Inorganic and General Chemistry, Vol. 21* (Ed.: R. J. H. Clark)), Elsevier, Amsterdam, **1986**, pp. 77–185.

Calixarene-Based Macrocyclic Nonet ($S = 4$) Octaradical and its Acyclic Sextet ($S = 5/2$) Pentaradical Analogue**

Andrzej Rajca,* Suchada Rajca, and Raghavakaimal Padmakumar

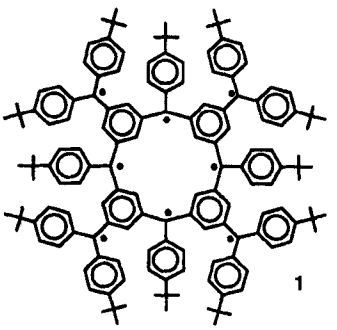
Very high-spin organic molecules are of current interest in relation to fundamental aspects of bonding and novel approaches to materials.[1] Synthesis of mesoscopic-size and well-defined high-spin organic molecules is one of the ultimate goals in the area of organic magnetism.[2, 3] The organic molecule with the

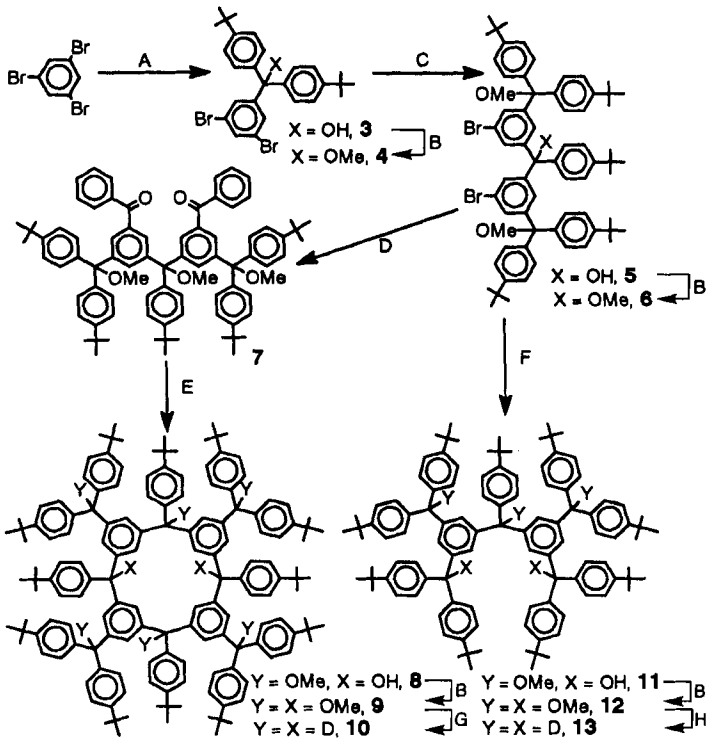
[*] Prof. A. Rajca, Dr. S. Rajca, Dr. R. Padmakumar
Department of Chemistry, University of Nebraska
Lincoln, NE 68588-0304 (USA)
Telefax: Int. code +(402) 472-9402

[**] This research was supported by the National Science Foundation (CHE-9203918). Mass spectral determinations were performed by the Midwest Center for Mass Spectrometry with partial support by the National Science Foundation (DIR-9017262). We thank Professor S. H. Liou for access to a SQUID magnetometer.

highest spin quantum number S is the nonacarbene ($S = 9$) prepared by Iwamura et al.[4] So far, strong ferromagnetic coupling could be maintained in molecules with up to around ten carbene or radical sites.[4, 5] Dendritic polyradicals with up to 31 radical sites were reported to possess lower than expected spin values. It was suggested that one of the possible reasons for the interruption of the spin coupling was the presence of defects, which were defined as failure to generate a radical site.[2] In acyclic spin-coupled structures, such as typical organic high-spin molecules, even a single defect may interrupt or weaken the only available pathway for spin coupling.[6, 7] This is in contrast to inorganic clusters or extended networks,[8] where an alternative pathway (to that containing the defect) is possible, as long as the number of defects is moderate.

We now report on two macrocyclic high-spin organic molecules, the calix[4]arene-based nonet ($S = 4$) octaradical **1** and its acyclic analogue **2**.[9] Both polyradicals are designed to minimize the potential impact of defects on spin coupling (conjugation): in **1** cyclic connectivity and in **2** the number of terminal sites was maximized. Spin coupling in the above polyradicals is interrupted when a defect divides the spin system into at least two uncoupled spin systems with lower spin. Because the minimum requirements for such interruptions (namely, *more than one* defect at the four-site calix[4]arene ring in **1** and one defect at the solitary central site in **2**) are quite stringent, we expect to obtain high-spin polyradicals with negligible amounts of low spin ($S = 1/2$, 1, etc.) contaminants.





Scheme 1. Synthesis of the polyethers: A: 1) *n*BuLi/ether, 2) 4,4'-di-*tert*-butylbenzophenone; B: NaH/THF, MeI; C: 1) *t*BuLi/ether, 2) methyl 4-*tert*-butylbenzoate; D: 1) *t*BuLi/THF, 2) 1-(4-*tert*-butylbenzoyl)pyrrolidine; E: 1) **6**/*t*BuLi/THF, 2) **7**; F: 1) *n*BuLi/THF, 2) 4,4'-di-*tert*-butylbenzophenone; G: 1) **9**/Na/K in THF or ether, 2) MeOD; H: 1) **12**/Li in THF, 2) MeOD.

First, polyethers **9** and **12** were synthesized (Scheme 1). In the key step, the assembly of calix[4]arene ring, a single isomer of **8** was isolated in approximately 20% yield.[10] The characteristic features of the ^{1}H NMR spectrum of **8** are: one signal for the hydroxyl groups, four for the methoxy groups (2/2/1/1), and seven for the *t*Bu groups (2/2/2/2/2/1/1); the symmetry in **8** is corroborated by the ^{13}C NMR spectrum. NMR spectroscopic investigations confirmed the fact that the two equivalent hydroxyl groups were replaced with two equivalent methoxy groups in the conversion of **8** to **9**.[10]

Treatment of octaether **9** with Na/K alloy in THF or diethyl ether and of pentaether **12** with Li metal in THF for 2–4 days gave solutions of the corresponding carbopolyanions. This was confirmed by the quenching products **10** and **13** obtained with deuterated methanol. Addition of one equivalent (or a small excess) of iodine to the carbopolyanions in THF at 180 K gave polyradicals **1** and **2**, respectively.[5] When a solution of **1** in THF/2-MeTHF was allowed to react with an excess of Na/K alloy at low temperature and then quenched with methanol, nondeuterated isotopomers of **10** were obtained; this suggests that the macrocyclic ring is intact in **1**.

The $\Delta m_s = 1$ regions of the electron spin resonance (ESR) spectra for **1** and **2** in THF or THF/2-MeTHF (10^{-4}–10^{-3} M) at 77 K are not sufficiently resolved to permit a meaningful spectral fit for these sterically congested polyradicals.[12a] A weak $\Delta m_s = 2$ signal is observed for **1** but not for **2** at 77 K; this is what one would qualitatively expect for such polyradicals with integral ($S = 4$) and half-integral ($S = 5/2$) spin quantum numbers.[12b] The product of the intensity I of the $\Delta m_s = 2$ signal for **1** and temperature T is constant in the range $T = 20$–80 K.

The bulk magnetization (M) of solutions of **1** and **2** in THF (8×10^{-4}–1×10^{-2} M) were measured as a function of magnetic field H (0–5.5 Tesla) at $T = 2$, 3, 5, and 10 K and as a function of temperature ($T = 2$–35 K) at $H = 1.0$ and 0.5 Tesla. The sample consisted of a band of a frozen polyradical solution (ca. 4 mm high) wedged between two bands of pure frozen solvent (ca. 60 mm high) in a 4 mm OD flame-sealed quartz tube. Such a sample does not allow for measurement of the amount of thermally unstable polyradical, but gives an adequate signal in the Quantum Design SQUID magnetometer and guarantees almost complete cancellation of the diamagnetic contribution to M.[2, 5] An adequate correction for diamagnetism was made for **1**. This was verified by comparing the plot of MT vs T ($T = 2$–35 K) with that of IT vs T ($T = 20$–80 K), where I is the $\Delta m_s = 2$ ESR-signal intensity for **1**. For the most dilute solutions, the data for M vs H/T were fitted to a Brillouin function with variable S and magnetization at saturation M_{sat}.[13] The coincidence of the plots for $T = 2$, 3, 5, and 10 K is consistent with the absence of intermolecular magnetic interactions in the dilute solution. In the concentrated solutions, the curves for M vs H/T at different temperatures do not overlap, and intermolecular antiferromagnetic interactions are accounted for with a mean-field parameter θ ($\theta < 0$, $|\theta| \leq 0.1$), that is, H/T is replaced with $H/(T - \theta)$.[14] The standard errors of the parame-

ters for the fits at each temperature are $<1\%$; discrepancies between the parameters for different temperatures and samples are $<5\%$, and the parameter dependence for S and M_{sat} ranges from around 0.3 at $T = 2$ K to around 0.8 at $T = 5$ K.[15] The values for S obtained from fitting are 3.8 and 2.3 for **1** and **2**, respectively (Fig. 1). In the absence of defects, high-spin polyradicals **1** and **2** with all unpaired electrons coupled ferromagnetically would be expected to have $S = 4.0$ and 2.5, respectively.[16]

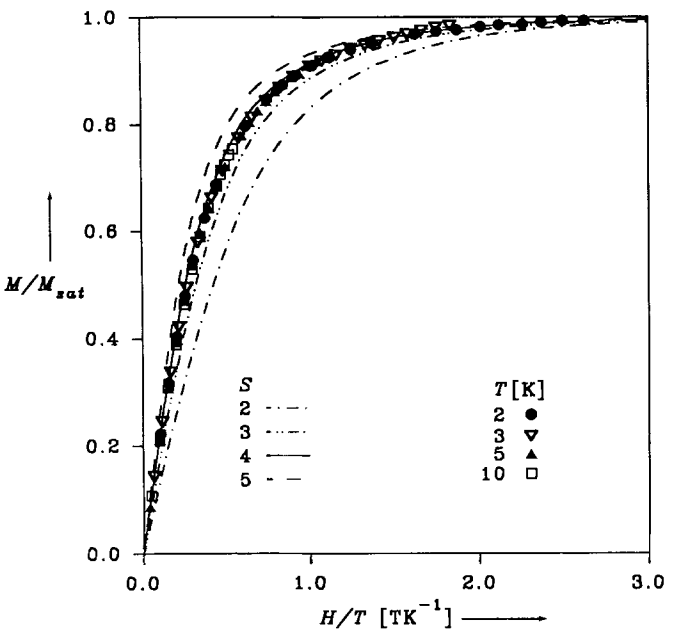


Fig. 1. Magnetization studies of **1** (8.5×10^{-4} M in THF) performed with a SQUID magnetometer. The plots of M/M_{sat} vs H/T are shown. The fit to a Brillouin function with variable S gives $S = 3.8$. The solid line corresponds to the Brillouin function with $S = 4$.

The magnetization data establishes that **1** and **2** have nonet ($S = 4$) and sextet ($S = 5/2$) ground states, respectively. The strength of the ferromagnetic coupling in **1** may be judged by the lack of a detectable thermal population of the low-spin excited states up to $T = 35$ K (or 80 K), as determined by either SQUID magnetometry or ESR spectroscopy. The magnetization data for **1** are drastically different from those for polyradicals with a comparable or larger number of sites, such as star-branched hepta- and decaradicals and their dendritic homologues.[2] For the latter, magnetization data could not be fitted to a single Brillouin function and the average values for S (between the low and high field values) were well below the theoretical values expected for high-spin systems without defects.

In summary, macrocyclic polyradical **1** with nonet ($S = 4$) ground state was prepared. This compound may provide a first step towards addressing the problem of defects in molecules with large numbers of interacting radical sites.

Received: May 11, 1994 [Z 6921 IE]
German version: *Angew. Chem.* **1994**, *106*, 2193

[1] a) H. Iwamura, *Adv. Phys. Org. Chem.* **1990**, *26*, 179; b) D. A. Dougherty, *Acc. Chem. Res.* **1991**, *24*, 88; c) H. Iwamura, N. Koga, *ibid.* **1993**, *26*, 346; d) W. T. Borden, H. Iwamura, J. A. Berson, *ibid.* **1994**, *27*, 109; e) A. Rajca, *Chem. Rev.* **1994**, *94*, 871.

[2] A. Rajca, S. Utamapanya, *J. Am. Chem. Soc.* **1993**, *115*, 10688.

[3] D. D. Awshalom, D. P. DiVincenzo, J. F. Smyth, *Science* **1992**, *258*, 414.

[4] N. Nakamura, K. Inoue, H. Iwamura, *Angew. Chem.* **1993**, *105*, 900; *Angew. Chem. Int. Ed. Engl.* **1993**, *32*, 872.

[5] A. Rajca, S. Utamapanya, S. Thayumanavan, *J. Am. Chem. Soc.* **1992**, *114*, 1884.

[6] N. Mataga, *Theor. Chim. Acta* **1968**, *10*, 372; for acyclic triradicals with $S = 3/2$ that are based upon 1,3,5-connected benzene, see J. Veciana, C. Rovira, N. Ventosa, M. I. Crespo, F. Palacio, *J. Am. Chem. Soc.* **1993**, *115*, 57, and references therein; a tetracarbene based upon the calix[4]arene ring is mentioned in ref. [1a].

[7] S. Sasaki, H. Iwamura, *Chem. Lett.* **1992**, 1759.

[8] D. P. Goldberg, A. Caneschi, S. J. Lippard, *J. Am. Chem. Soc.* **1993**, *115*, 9299.

[9] *Calixarenes: A Versatile Class of Macrocyclic Compounds* (Eds.: J. Vicens, V. Böhmer), Kluwer, Dordrecht, **1991**.

[10] a) Compounds **3**–**9**, **11** and **12**, have adequate ^{1}H NMR, ^{13}C NMR, and FABMS data. The IR spectra for compounds **3**–**9** confirm the presence of the OH and C–O groups. C/H analyses (**3**, **5**, **6**, and **9**) or high resolution FABMS (**4**) are satisfactory. b) Calix[4]arene **8**: M.p. 132–133 °C, FAB-MS (*ortho*-nitrophenyl octyl ether matrix), cluster: *m/z* (peak height) for $(M - OH)^+$: 2196.3(3.5), 2197.3(5), 2198.3(4.5), 2199.3(2.5); for $(M - OCH_3)^+$: 2182.3(7), 2183.3(10), 2184.3(8.5), 2185.3(5); calcd for $(M - OCH_3)^+$, $C_{159}H_{185}O_7$: 2182.41(5.5), 2183.42(10), 2184.42(9), 2185.42(5). ^{1}H NMR (300 MHz, $CDCl_3$, 20 °C): $\delta = 7.45$–6.50 (m, 60H), 2.821 (s, 2H, exchange with D_2O), 2.654 (s, 6H), 2.629 (s, 6H), 2.519 (s, 3H), 2.225 (s, 3H), 1.258 (s, 18H), 1.239 (s, 9H), 1.203 (s, 9H), 1.185 (s, 18H), 1.175 (s, 18H), 1.163 (s, 18H), 1.127 (s, 18H). ^{13}C{^{1}H} NMR (75 MHz, $CDCl_3$, 20 °C): $\delta = 150.0$–138.0 (20 signals), 130.0–124.0 (14 overlapping signals), 87.39, 86.97, 86.77, 86.62, 82.43, 52.40, 52.11, 51.87, 51.78, 35.0–31.0 (8 overlapping signals). IR (ZnSe): $\tilde{\nu} = 3500\ cm^{-1}$ (OH). – Calix[4]arene **9**: M.p. 166–167 °C, calcd for $C_{160}H_{192}O_8$: C 85.67, H 8.63%; found: C 86.05, H 8.88%. FAB-MS (ON-POE), cluster: *m/z* (peak height) for $(M - OCH_3)^+$: 2209.6(4), 2210.5(7), 2211.4(10), 2212.4(8), 2213.4(5); calcd for $(M - OCH_3)^+$, $C_{159}H_{189}O_7$: 2210.44(5.5), 2211.45(10), 2212.45(9), 2213.45(5). ^{1}H NMR: $\delta = 7.30$ 6.80 (m, 60H), 2.654 (s, 6H), 2.641 (s, 6H), 2.601 (s, 6H), 2.560 (s, 3H), 2.445 (s, 3H), 1.208, 1.181, 1.165 (s, 108H). ^{13}C{^{1}H} NMR: $\delta = 150.0$ 140.0 (19 overlapping signals), 129.0–124.0 (16 overlapping signals), 87.24, 87.15, 87.13, 86.84, 86.78, 52.18, 52.03, 52.00, 51.98, 51.93, 35.0–31.0 (5 overlapping signals). IR: OH not detected.

[11] Compounds **10** and **13** have adequate ^{1}H NMR and FABMS spectra; one of the isomers of **10** was separated. Reaction of **9** with Li in THF gave complex reaction mixtures; the FAB mass spectrum suggests incorporation of THF-like fragments.

[12] a) With the exception of one heptaradical ($S = 7/2$, ref. [5]), all polyarylmethyl polyradicals with $S > 2$ have unresolved dipolar couplings in their ESR spectra. b) One of the differences between the integral and half-integral spin systems is the presence in the former of an intense center peak in the $\Delta m_S = 2$ region: A. Rajca, S. Utamapanya, *J. Am. Chem. Soc.* **1993**, *115*, 2396.

[13] R. L. Carlin, *Magnetochemistry*, Springer, Berlin, **1986**, p. 14–18.

[14] A. Bino, D. C. Johnston, D. P. Goshorn, T. R. Halbert, E. I. Stiefel, *Science* **1988**, *241*, 1479.

[15] The reliability of the M vs H/T fits is indicated by low parameter dependence [dependence = 1 – (variance of the parameter, other parameters constant)/(variance of the parameter, other parameters changing)]. For example, application of a standard technique (ESR signal intensity vs temperature in the 15–90 K range) to a favorable case of diradical with $J/k = -20$ K gives a two-parameter fit with dependence of 0.6.

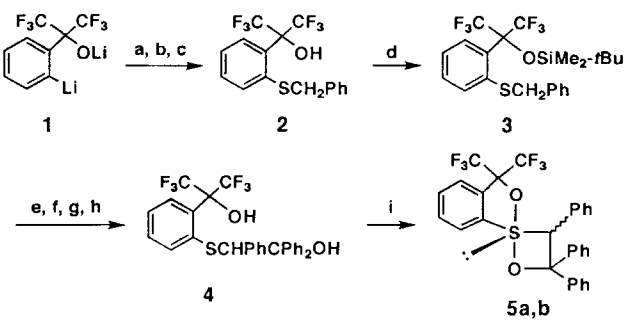
[16] One of the referees suggested fitting the magnetization data for **1** to a mixture of the polyradicals with $S = 4$ (defect-free **1**) and $S = 3.5$ (**1** with one defect), which would correspond to a simplified version of the procedure in ref. [2]. For a sample with $S = 3.83 \pm 0.03$, such fitting gives 66% ±10% octaradical with $S = 4$.

Synthesis, Structure, and Thermolysis of a Tetracoordinate 1,2λ⁴-Oxathietane**

Takayuki Kawashima,* Fumihiko Ohno, and Renji Okazaki*

The reaction of sulfur ylides with carbonyl compounds, known as the Corey–Chaykovsky reaction,[1] gives oxiranes. In sharp contrast, phosphorus ylides afford olefins regioselectively in the Wittig reaction.[2] In our research on oxetanes bearing high-coordinate main group elements at the position adjacent to the O atom, we have synthesized pentacoordinate 1,2-oxaphosphetanes, 1,2-oxasiletanides, and 1,2-oxastannetanides, in other words intermediates of the Wittig, Peterson, and tin-Peterson reactions, respectively.[3] We recently found that in contrast to other oxetanes 1,2-oxaselenetanes yield neither olefins nor oxiranes on heating.[4] This unique result prompted us to examine the reactivity of a tetracoordinate 1,2λ⁴-oxathietane,[5] a novel type of sulfurane.[6] We now report on the synthesis, crystal structure, and thermolysis of **5a**, the first tetracoordinate 1,2λ⁴-oxathietane.

Sequential treatment of dilithio derivative **1**[7] with elemental sulfur, benzyl bromide, and aqueous NH_4Cl gave benzyl sulfide **2** (86%) (Scheme 1). Protection of the hydroxyl group of **2**



Scheme 1. a) S_8, THF, 0 °C; room temperature (RT), ca. 15 h; b) $PhCH_2Br$, 0 °C; RT, 3 h; c) aq NH_4Cl; d) tBuMe$_2$SiOTf, Et_3N, CH_2Cl_2, 0 °C; RT, 20 h; e) 2 equiv LDA, THF, −78 °C, 5 min; f) $Ph_2C{=}O$, THF, −78 °C, 15 min; g) aq NH_4Cl; h) 2 equiv nBu$_4$NF, THF, 0 °C, 30 min; i) 1.2 equiv Br_2, 2.4 equiv Et_3N, CCl_4, 0 °C; RT, ca. 15 h.

with a *tert*-butyldimethylsilyl group (88%), deprotonation with lithium diisopropylamide (LDA) followed by reaction with benzophenone (95%), and desilylation with nBu$_4$NF (95%) gave the β-hydroxyalkyl sulfide **4**. Oxidative cyclization of **4** with Br_2 afforded **5a** (37%) with recovery of **4** (26%). Interestingly, the phenyl group at the 3-position is important for the isolation of 1,2-oxathietane;[8] in contrast, phenyl groups typically destabilize oxetanes having Group 14 and 15 elements and accelerate olefin formation.

In the ^{1}H NMR spectrum of **5a** a downfield shift ($\delta = 8.50$–8.53) for the *ortho* proton of the "Martin ligand" was observed, which is one of the features of compounds with a trigonal-bipyramidal (TBP) structure.[3a, b, d, 6b, c, e] In the ^{19}F NMR spectrum of **5a** two quartets were observed at $\delta_F = -76.0$ and -76.7 (^4J(F,F) = 8.1 Hz) owing to the chirality of the S atom.

The X-ray crystallographic analysis of **5a** indicates that it has a structure very similar to that of oxaselenetane **6** and that the phenyl group at the 3-position is *cis* to the lone pair of sulfur atom (Fig. 1).[9] The two oxygen atoms occupy apical positions,

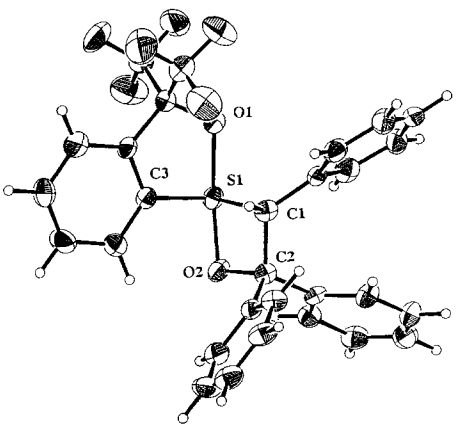
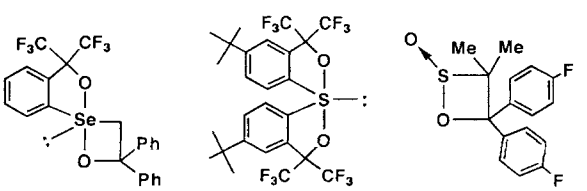


Fig. 1. Crystal structure of **5a** (ORTEP). Selected bond lengths [Å], bond angles [°], and torsion angles [°]: S1-O1 1.863(5), S1-O2 1.764(5), S1-C1 1.837(8), S1-C3 1.801(7), C1-C2 1.574(9), C2-O2 1.448(8); O1-S1-O2 167.4(3), O1-S1-C3 86.1(3), C1-S1-O2 77.2(3), S1-C1-C2 89.4(4), C1-C2-O2 96.0(5), S1-O2-C2 96.6(4); O2-S1-C1-C2 6.2(4), S1-C1-C2-O2 −7.5(5).

while two carbon atoms and a lone pair occupy equatorial positions. The bond angle O1-S1-O2 deviates from 180° by 12.6(3)°. The S1–O1 bond (1.863(5) Å) is as long as the S–O bond of sulfurane **7** (1.832(5) Å),[6b] but the S1–O2 bond (1.764(5) Å) is significantly shorter, a characteristic feature of TBP structures with electronically different apical groups.[3a, 4, 6c, e] However, both bonds are much longer than the S–O bond of β-sultine **8** (1.667(4) Å).[5a] The torsion angle S1-C1-C2-O2 (−7.5(5)°) is

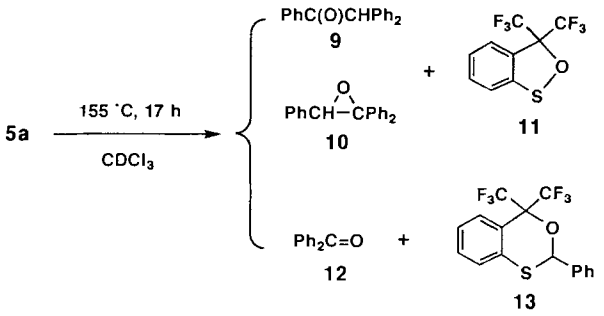


smaller than that of **8** (S-C-C-O 14.7°), indicating that the four-membered ring is almost planar; this is another a common structural feature of such oxetanes.[3, 4]

Thermolysis of **5a** was monitored by ^{19}F NMR spectroscopy (Scheme 2). The signals due to **5b** appeared soon after the reaction started, and the ratio (**5a**:**5b**) was constant (95:5) after 1 h. Finally cyclic sulfenate **11** (52%) and cyclic thioacetal **13** (31%) were formed as fluorine-containing compounds. The formation of a trace of oxirane **10** was confirmed by ^{1}H NMR spectroscopy. HPLC separation (column: JAIGEL 1H + 2H, Japan Analytical Industry) gave phenyl-migrated ketone **9** (47%) and benzophenone (**12**) (33%) along with **13** (31%), but **11** could not be isolated. As in the case of the oxaselenetane, thermolysis of oxathietane **5a** did not give an olefin. This indi-

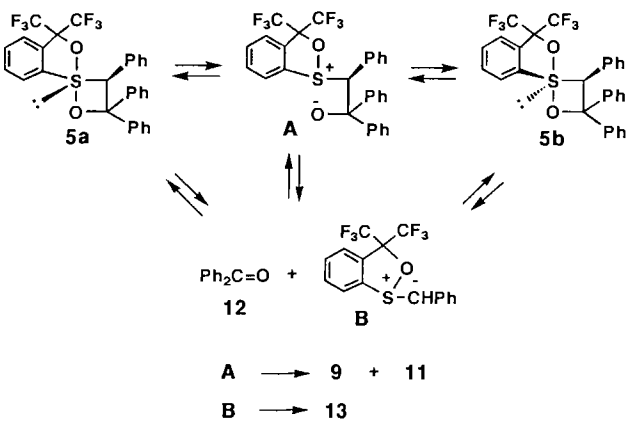
[*] Prof. Dr. T. Kawashima, Prof. Dr. R. Okazaki, F. Ohno
Department of Chemistry, Graduate School of Science
The University of Tokyo
7-3-1 Hongo, Bunkyo-ku, Tokyo 113 (Japan)
Telefax: Int. code + (3)5800-6899

[**] This work was supported in part by a Kurata Research Grant (T. K.) and a Grant-in-Aid for Scientific Research (B) (No. 04553062, T.K.) from the Ministry of Education, Science and Culture (Japan). We thank Dr. N. Tokitoh of the University of Tokyo for the determination of the X-ray structure of **5a**. We also thank Shin-Etsu Chemical, Central Glass, and Tosoh Akzo Co. Ltd. for gifts of silyl chlorides, hexafluorocumyl alcohol, and alkyllithium compounds, respectively.



Scheme 2.

cates that the bond energy of a chalcogen–oxygen double bond, even a sulfur–oxygen bond, is not sufficient for a Wittig-type reaction. Betaine **A** formed by heterolysis of the S–O bond leads to reactions such as C–S bond cleavage with phenyl migration (**9**[10] and **11**) and elimination of a ketone (**12** and **B**) (Scheme 3).



Scheme 3. Proposed mechanism for the thermolysis of **5a**.

Epimerization and fragmentation back to the starting ketone have never been observed for such hypervalent oxetanes.[11] It can be interpreted that **5** and/or betaine **A** is in equilibrium with ketone **12** and sulfonium ylide **B**, the latter of which undergoes Pummerer-type rearrangement to give **13** (Scheme 3). The presence of an oxirane in the reaction mixture suggests that a 1,2λ⁴-oxathietane may be an intermediate in the Corey–Chaykovsky reaction.

Experimental Procedure

A stock solution of bromine in CCl_4 (0.17 M, 3.1 mL, 1.2 equiv) was added to a solution of **4** [12] (238 mg, 0.43 mmol) and Et_3N (0.15 mL, 1.04 mmol) in CCl_4 (15 mL) at 0 °C. The mixture was allowed to warm to room temperature and stirred for about 15 h. The precipitate was filtered off with a glass filter, and the filtrate was concentrated in vacuo. The ^{19}F NMR spectrum of the residue showed two sets of two quartets due to diastereomers **5a** and **5b** (4:1). Purification by flash chromatography (SiO_2, hexane/CH_2Cl_2 (2:1)) gave **5a** (88 mg, 37%) and recovered **4** (62 mg, 26%), but **5b** could not be isolated. An analytically pure sample was obtained as colorless plates by recrystallization from ether–hexane, and single crystals for X-ray analysis were grown in the same solvent. **5a**: M.p. = 151.0–154.0 °C (decomp); Correct elemental analysis; high-resolution MS (70 eV): calcd. for $C_{23}H_{15}F_6O_2S$ (M^+ − Ph): *m/z* 469.0697, found: 469.0688; ^1H NMR (500.1 MHz, $CDCl_3$, 27 °C, TMS): δ = 6.73 (s, 1H), 7.04 (d, ^3J(H,H) = 7.4 Hz, 2H), 7.12–7.25 (m, 9H), 7.30 (t, ^3J(H,H) = 7.8 Hz, 2H), 7.40–7.42 (m, 2H), 7.56–7.60 (m, 2H), 7.62 (br, 1H), 8.50–8.53 (m, 1H); $^{13}C\{^1H\}$ NMR (125.8 MHz, $CDCl_3$, 27 °C, TMS): δ = 80.41 (s), 83.93 (sept, ^2J(C,F) = 31 Hz), 94.21 (s), 122.12 (q, ^1J(C,F) = 288 Hz), 122.49 (q, ^1J(C,F) = 288 Hz), 125.07 (s), 126.03 (br s), 127.06 (s), 127.09 (s), 127.10 (s), 127.67 (s), 127.87 (s), 128.35 (s), 128.81 (s), 130.54 (s), 130.83 (s), 131.57 (s), 131.59 (s), 132.33 (s), 132.49 (s), 138.54 (s), 142.73 (s), 148.19 (s); ^{19}F NMR (253.8 MHz, $CDCl_3$, 27 °C, $FCCl_3$): δ = −76.0 (q, ^4J(C,F) = 8.1 Hz), −76.7 (q, ^4J(C,F) = 8.1 Hz).

Received: May 16, 1994 [Z 6939 IE]
German version: *Angew. Chem.* **1994**, *106*, 2188

[1] A. W. Johnson, R. B. LaCount, *J. Am. Chem. Soc.* **1961**, *83*, 417–423; E. J. Corey, M. Chaykovsky, *ibid.* **1962**, *84*, 3782–3783; J. Aubé in *Comprehensive Organic Synthesis: Selectivity, Strategy, and Efficiency in Modern Synthetic Chemistry, Vol. 1* (Eds.: B. M. Trost, I. Fleming), Pergamon, Oxford, **1991**, Chap. 3.2, p. 822–825.

[2] Reviews: I. Gosney, A. G. Rowley in *Organophosphorus Reagents in Organic Synthesis* (Eds.: J. I. G. Cadogan), Academic Press, New York, **1979**, p. 17–153; B. E. Maryanoff, A. B. Reitz, *Chem. Rev.* **1989**, *89*, 863–927.

[3] a) T. Kawashima, K. Kato, R. Okazaki, *J. Am. Chem. Soc.* **1992**, *114*, 4008–4010; b) T. Kawashima, N. Iwama, R. Okazaki, *ibid.* **1992**, *114*, 7598–7599; c) *ibid.* **1993**, *115*, 2507–2508; d) T. Kawashima, K. Kato, R. Okazaki, *Angew. Chem.* **1993**, *105*, 941–942; *Angew. Chem. Int. Ed. Engl.* **1993**, *32*, 869–870.

[4] T. Kawashima, F. Ohno, R. Okazaki, *J. Am. Chem. Soc.* **1993**, *115*, 10434–10435.

[5] β-Sultines: a) M. D. M. Gray, D. R. Russell, D. J. H. Smith, T. Durst, B. P. Gimbarzevsky, *J. Chem. Soc. Perkin Trans. 1* **1981**, 1826–1830, and references therein.; β-Sultones: b) I. L. Knunyants, G. A. Sokolski, *Angew. Chem.* **1972**, *84*, 623; *Angew. Chem. Int. Ed. Engl.* **1972**, *11*, 583–595; c) M. Nagayama, O. Okumura, S. Noda, H. Mandai, A. Mori, *Bull. Chem. Soc. Jpn.* **1974**, *47*, 2158–2161, and references therein.

[6] Recent reviews: a) R. A. Hayes, J. C. Martin, *Sulfurane Chemistry* in *Organic Sulfur Chemistry, Theoretical and Experimental Advances*, (Eds.: F. Bernardi, I. G. Csizimadia, A. Mangini), Elsevier, Amsterdam, **1985**, Chap. 8; For some examples see: b) E. F. Perozzi, J. C. Martin, I. C. Paul, *J. Am. Chem. Soc.* **1974**, *96*, 6735–6744; c) L. J. Adzima, E. N. Duesler, J. C. Martin, *J. Org. Chem.* **1977**, *42*, 4001–4005; d) S. Ogawa, Y. Matsunaga, S. Sato, I. Iida, N. Furukawa, *J. Chem. Soc. Chem. Commun.* **1992**, 1141–1142; e) I. Kapovits, J. Rábai, D. Szabó, K. Czakó, Á. Kucsman, G. Argay, V. Fülöp, A. Kálmán, T. Koritsánszky, L. Párkányi, *J. Chem. Soc. Perkin Trans. 2* **1993**, 847–853.

[7] E. F. Perozzi, R. S. Michalak, G. D. Figuly, W. H. Stevenson III, D. B. Dess, M. R. Ross, J. C. Martin, *J. Org. Chem.* **1981**, *46*, 1049–1053.

[8] 3-Unsubstituted tetracoordinate 1,2-oxathietanes are very sensitive to moisture in air and are readily hydrolyzed to the corresponding dihydroxy sulfoxides [4].

[9] $C_{29}H_{20}F_6O_2S$, M_r = 546.53, crystal dimensions 0.950 × 0.600 × 0.150 mm, monoclinic, space group $P2_1/n$, a = 9.439(4), b = 9.092(3), c = 29.111(2) Å, β = 91.85(1)°, V = 2497(1) Å^3, Z = 4, ρ_{calcd} = 1.454 g cm^{-3}, R = 0.069 (R_w = 0.076). Further details of the crystal structure investigation are available on request from the Director of the Cambridge Crystallographic Data Centre, 12 Union Road, GB-Cambridge CB21EZ (UK), on quoting the full journal citation.

[10] Although product **9** seems to be produced in part by rearrangement of oxirane **10**, we believe that most of **9** was formed as shown in Scheme 3, taking into consideration the results of thermolysis of 1,2-oxaselenetanes [4].

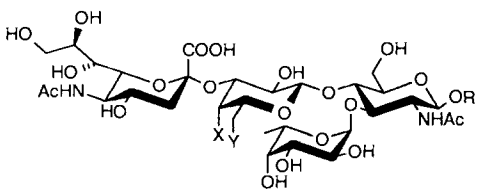
[11] For a similar epimerization promoted by an alcohol, see: F. Ramirez, I. Ugi, S. Pfohl, E. A. Tsolis, J. E. Pilot, C. P. Smith, D. Marquarding, P. Gillespie, P. Hoffmann, *Phosphorus* **1971**, *1*, 1–16.

[12] Colorless viscous oil: satisfactory ^1H, ^{13}C and ^{19}F NMR spectra.

Synthesis of Deoxy Sialyl Lewis^x Analogues, Potential Selectin Antagonists**

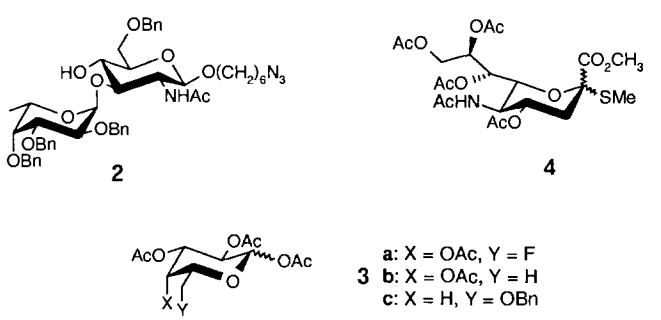
Wilhelm Stahl,* Ulrich Sprengard, Gerhard Kretzschmar, and Horst Kunz

The cell surface receptors E-, P-, and L-selectins[1] play a key role in the adhesion of leukocytes to endothelial cells and their subsequent invasion into tissue, a critical process at the onset of inflammatory diseases. The ligands of these receptors are sialyl Lewis^x (α-Neu5Ac-(2-3)-β-D-Gal-(1-4)-[α-L-Fuc-(1-3)]-β-Glc-NAc **1**) and related structures,[2] which are found on the cell surface as terminal carbohydrate sections of the glycoproteins and glycolipids. The controlled blocking of the carbohydrate–selectin binding is a new therapeutic approach[3] to battling inflammatory diseases.



1: X = Y = OH

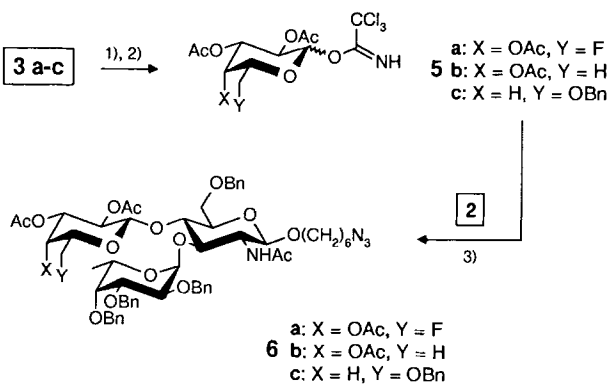
Sialyl Lewis^x derivatives with modified fucose,[4] neuraminic acid,[4, 5] and glucosamine residues[6] were synthesized both chemically and enzymatically for investigations of the structure–activity relationship. Based on the biological properties of these derivatives, conclusions were drawn on which structural elements are essential for the binding to selectins. In this context we describe the synthesis of deoxy analogues of sialyl Lewis^x with modified galactose units starting from intermediates **2**,[7] **3a–c**, and **4**[8] (Scheme 1).



Scheme 1.

Various strategies have been employed for the chemical preparation of sialyl Lewis^x.[9] The linear saccharide synthesis has several advantages over the convergent route: two reaction steps (blocking and deblocking of the anomeric center of galactose) are side-stepped, and the difficult purification of the *O*-acetyl-protected intermediates containing neuraminic acid, which are formed in the convergent synthesis,[7] is avoided.

The trichloroacetimidate method was applied for the construction of the stereoselective linkage of disaccharide **2** with the galactose derivative(s) (Scheme 2).[10] The acetyl protecting



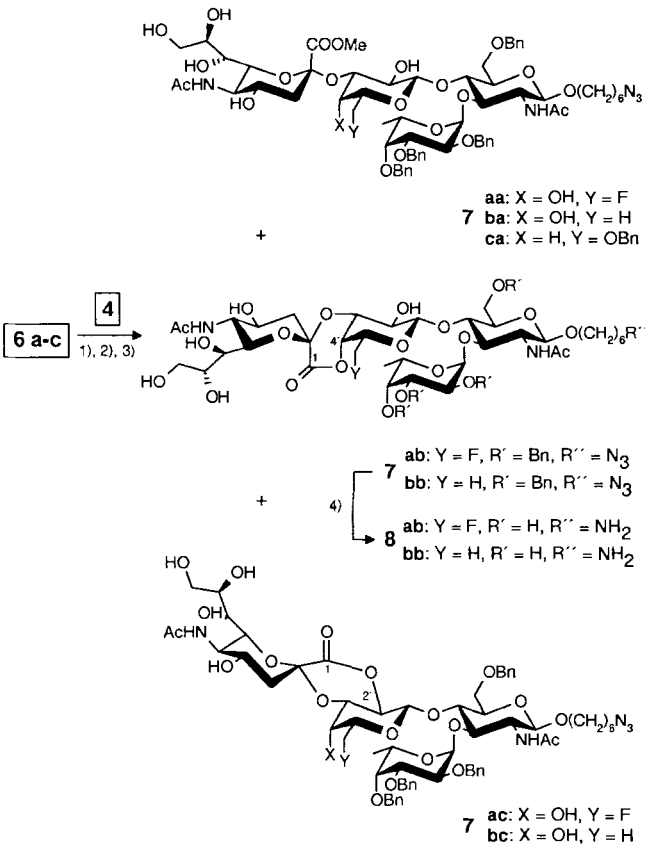
Scheme 2. 1) 1.5 equiv hydrazine acetate, DMF, 0 °C → room temperature, **a**: 68%, **b**: 71%, **c**: 82%; 2) trichloroacetonitrile, 1,8-diazabicyclo[5.4.0]undec-7-ene (DBU), CH_2Cl_2, **5a**: 99%, **5b**: 83%, **5c**: 93%; 3) **2**, $BF_3 \cdot OEt_2$, 3 Å molecular sieves, CH_2Cl_2, **6a**: 73% (3 equiv **5a**), **6b**: 45% (1.7 equiv **5b**), **6c** 74% (2.2 equiv **5d**).

group at the anomeric center of **3a–c** was cleaved with hydrazine acetate, and subsequent reaction with trichloroacetonitrile provided the corresponding trichloroacetimidates. Derivatives **5a**, **5b**, and **5c** were obtained in yields of 67, 59, and 76% for the two steps. Glycosidic linkage of the disaccharide acceptor **2** with donors **5a–c** in the presence of the promotor boron trifluoride–ether furnished trisaccharide **6a**[11] (3 equiv **5a**) in 73%, **6b** (1.7 equiv **5b**) in 45%, and **6c** (2.2 equiv **5c**) in 74% yield.[12] In each case the β-glycoside was obtained as the exclusive linkage product. The donor reactivity of imidates **5a** and **5c** toward the disaccharide receptor is comparable to that of the corresponding galactosylimidate;[7] the yields obtained under the same reaction conditions were similar.

Thioglycoside **4** served as the neuraminic acid donor in the sialylation. The *O*-acetyl groups of trisaccharides **6a–c** were cleaved to yield the appropriate acceptors.[13] These trisaccharides reacted with **4** in dichloromethane/acetonitrile in the presence of the promotors methylsulfenyl bromide (MST) and silver trifluoromethanesulfonate[14] between −70 and −40 °C to give the corresponding tetrasaccharides (Scheme 3). The laborious chromatographic purifiction of the reaction products can be simplified by first removing the acetyl protecting groups of the crude product of the sialylation reaction. Then unreacted **4** and related side products can be separated easily, and unreacted trisaccharide is recovered. In this way the reaction of **6a** afforded equal amounts of the methyl ester **7aa** and the 1-4′-lactone **7ab**[15] with a combined yield of 53% (over three steps). Only traces of the 1-2′-lactone **7ac** were isolated. **6b** was converted into **7bb**[15] with a yield of 48% over three steps, and only minimal amounts of **7ba** and **7bc** were isolated. Under the conditions described **6c** was converted into **7ca** exclusively in 9% overall yield (over three steps). This sialylation provided solely α-glycosides.

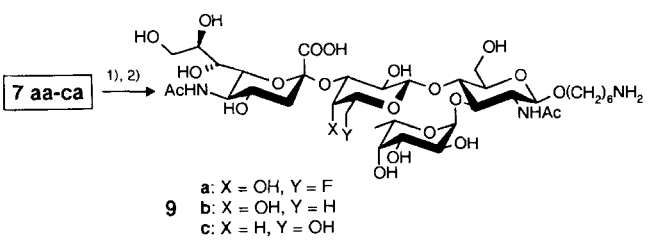
[*] Dr. W. Stahl
Hoechst AG, Allgemeine Pharma-Forschung, G 838
D-65926 Frankfurt am Main (FRG)
Telefax: Int. code + (69)331-399
Dipl.-Chem. U. Sprengard
Institut für Organische Chemie der Universität Mainz
and Zentralforschung der Hoechst AG
Dr. G. Kretzschmar, Zentralforschung der Hoechst AG
Prof. Dr. H. Kunz, Institut für Organische Chemie
der Universität Mainz

[**] The authors thank Prof. Dr. A. Lipták, Institute for Biochemistry, Debrecen, Hungary, for the galactose derivatives **3a–c**.



Scheme 3. 1) MeOH/NaOMe, **a**: 99%, **b**: 97%, **c**: 91%; 2) 2 equiv. **4**, MSB/AgOTf (1 equiv./2 equiv.), 3 Å molecular sieves, CH_2Cl_2/CH_3CN, $-70 \rightarrow -40\,^{\circ}C$; 3) MeOH/NaOMe, **7aa** 27%, **7ab**: 26%, **7ba**: 49%, **7ca**: 9%; 4) Pd, HCOOH, MeOH, **8ab** 43%, **8bb** 56%.

The benzyl ethers were cleaved by hydrogenolysis (Pd, methanol/formic acid); subsequent saponification of the ester or lactone with NaOH led to acids **9a**, **9b**, and **9c** in overall yields of 43, 56, and 58% (over two steps) (Scheme 4).



Scheme 4. 1) Pd, HCOOH, MeOH; 2) H_2O, NaOH; H_3O^+, **9a** 43%, **9b** 56%, **9c** 58%.

The efficient synthesis of sialyl Lewis^x described here has fewer steps than previously reported syntheses. In addition, the combination of thioglycoside **4** and the promotors methylsulfenylbromide and silver trifluoromethanesulfonate, which was used for the first time, proved to be an effective sialylation reagent.[9, 16] The reaction of two equivalents of donor **4** with one equivalent of acceptors **6a,b** gave exclusively the corresponding α-sialoglycosides in yields of 50–55%. The unreacted acceptor was recovered almost completely. Comparison with the corresponding Lewis^x derivative[7] as the acceptor shows that the modification in the galactose 6-position hardly affects the reactivity relative to that of **4**, since reaction under the same conditions gave almost the same yields. In contrast, the acceptor reactivity of the 4-deoxy derivative **6c** is permanently altered and can be attributed in part to the change in the electron density on the 3-hydroxyl group. The significantly reduced yield can be explained by the mismatched reactivity of the donor and acceptor. Remarkably, the 2′-lactone also does not form when the 4′-hydroxyl group is not present.

The O-glycosidically linked aminohexanol in **9a–c** allows attachment to a support.[17] Alternatively, this may be achieved by N-glycosidic linkage to the reducing end of the *N*-acetylglucosamine, for example, with the side-chain carboxyl group of aspartic acid.[18] Such compounds could be used to test the recently postulated multivalence theory for the interaction of E-selectin and sialyl Lewis^x.[19]

Preliminary investigations on the binding of **9a–c** to E-selectin[20] indicate that the native sialyl Lewis^x binds more strongly than analogues **9a–c**.[21] These results are a further contribution to the understanding of the interaction of sialyl Lewis^x with selectin receptors and to the development of therapeutically useful antagonists.

Received: May 5, 1994 [Z 6902 IE]
German version: *Angew. Chem.* **1994**, *106*, 2186

[1] a) J. C. Paulson in *Adhesion: Its Role in Inflammatory Disease* (Ed.: J. M. Harlan, D. Y. Liu), Freeman, New York, **1992**, p. 19; b) M. P. Bevilaqua, R. M. Nelson, *J. Clin. Invest.* **1993**, *91*, 379; c) T. A. Springer, *Cell* **1994**, *76*, 301, and references therein.

[2] a) T. Feizi, *Curr. Opin. Struct. Biol.* **1993**, *3*, 701; b) R. M. Nelson, S. Dolich, A. Aruffo, O. Cecconi, M. P. Bevilacqua, *J. Clin. Invest.* **1993**, *91*, 1157; c) C.-T. Yuen, K. Bezouska, J. O'Brien, M. Stoll, R. Lemoine, A. Lubineau, M. Kiso, A. Hasegawa, N. J. Bockovich, K. C. Nicolaou, T. Feizi, *J. Biol. Chem.* **1994**, *269*, 1595.

[3] Preliminary in vivo studies showed a marked therapeutic effect for the administration of sialyl Lewis^x against P-selectin-dependent, induced lung injuries (M. S. Mulligan, J. C. Paulson, S. DeFrees, Z.-L. Zheng, J. B. Lowe, P. A. Ward, *Nature* **1993**, *364*, 149) and against selectin-dependent myocardial reperfusion injuries (M. Buerke, A. S. Weyrich, Z. Zheng, F. C. A. Gaeta, M. J. Forest, A. M. Lefer, *J. Clin. Invest.* **1994**, *93*, 1140).

[4] B. K. Brandley, M. Kiso, S. Abbas, P. Nikrad, O. Srivasatava, C. Foxall, Y. Oda, A. Hasegawa, *Glycobiology* **1993**, *3*, 633.

[5] M. Yoshida, A. Uchimura, M. Kiso, A. Hasegawa, *Glycoconjugate J.* **1993**, *10*, 3.

[6] a) D. Tyrrell, P. James, N. Rao, C. Foxall, S. Abbas, F. Dasgupta, M. Nashed, A. Hasegawa, M. Kiso, D. Asa, J. Kidd, B. K. Bradley, *Proc. Natl. Acad. Sci. USA* **1991**, *88*, 10372; b) P. V. Nikrad, M. A. Kashem, K. B. Wlasichuk, G. Alton, A. P. Venot, *Carbohydr. Res.* **1993**, *250*, 145.

[7] U. Sprengard, H. Kunz, G. Kretzschmar, W. Stahl, unpublished.

[8] A. Hasegawa, H. Ohki, T. Nagahama, H. Ishida, M. Kiso, *Carbohydr. Res.* **1991**, *212*, 277.

[9] a) A. Kameyama, H. Ishida, M. Kiso, A. Hasegawa, *Carbohydr. Res.* **1991**, *209*, C1; b) K. C. Nicolaou, C. W. Hummel, N. J. Bockovich, C.-H. Wong, *J. Chem. Soc. Chem. Comm.* **1991**, 870; c) K. C. Nicolaou, C. W. Hummel, Y. Iwabuchi, *J. Am. Chem. Soc.* **1992**, *114*, 3126; d) H. Kondo, Y. Ichikawa, C.-H. Wong, *J. Am. Chem. Soc.* **1992**, *114*, 8748; e) A. Hasegawa, T. Ando, A. Kameyama, M. Kiso, *J. Carbohydr. Chem.* **1992**, *11*, 645; f) S. J. Danishefsky, J. Gervay, J. M. Peterson, F. E. McDonald, K. Koseki, T. Oriyama, D. A. Griffith, C.-H. Wong, D. P. Dumas, *J. Am. Chem. Soc.* **1992**, *114*, 8329; g) S. J. Danishefsky, K. Koseki, D. A. Griffith, J. Gervay, J. M. Peterson, F. E. McDonald, T. Oriyama, *ibid.* **1992**, *114*, 8331; h) A. Hasegawa, K. Fushimi, H. Ishida, M. Kiso, *J. Carbohydr. Chem.* **1993**, *12*, 1203.

[10] R. R. Schmidt, *Angew. Chem.* **1986**, *98*, 213; *Angew. Chem. Int. Ed. Engl.* **1986**, *25*, 212; *Pure Appl. Chem.* **1989**, *61*, 1257; in *Comprehensive Organic Chemistry*, *Vol. 6* (Eds.: B. M. Trost, I. Fleming), Pergamon, New York, **1991**, p. 33.

[11] Alternatively, the corresponding methylthioglycoside was prepared from **3a** ($MeSSiMe_3$, Me_3SiOTf; 89%) and used for glycosylation. Side reactions dominated when either methylsulfenyl bromide/silver trifluoromethanesulfonate (MSB/AgOTf) or dimethyl(methylthio)sulfonium trifluormethanesulfonate (DMTST) were used as the promotor. Trisaccharide **6a** can be prepared in 22% yield with *N*-iodosuccinimide/trifluoromethanesulfonic acid (NIS/TfOH).

[12] For glycosylation with modified galactoses see also: H. Paulsen, V. Rutz, I. Brockhausen, *Liebigs Ann. Chem.* **1992**, 747.

[13] See ref. [9] as well as K. Okamoto, T. Goto, *Tetrahedron* **1990**, *46*, 5835.

[14] With DMTST as the promotor **6a** was converted into **7aa**/**7ab** in 33% yield, with NIS/TfOH in 18% yield.

 © VCH Verlagsgesellschaft mbH, D-69451 Weinheim, 1994 0570-0833/94/2020-2097 $ 10.00+.25/0

[15] In order to characterize lactone formation **7ab** and **7bb** were converted into **8ab** and **8bb** by hydrogenolytic cleavage of the benzyl ether and reduction of the azide. The chemical shift of the 4' proton of the galactose provided structural proof for the 1-4'-lactone. For comparable lactones see: a) M. Numata, M. Sugimoto, K. Koike, T. Ogawa, *Carbohydr. Res.* **1987**, *163*, 209; b) J. Gervay, J. M. Peterson, T. Oriyama, S. J. Danishevsky, *J. Org. Chem.* **1993**, *58*, 5465. The formation of related 1-2'-lactones was previously reported [7a,g]: a) Y. Ito, T. Ogawa, *Tetrahedron* **1990**, *46*, 89; b) A. K. Ray, U. Nielsson, G. Magnusson, *J. Am. Chem. Soc.* **1992**, *114*, 2256. – ^{1}H NMR data: **8ab**: (300 MHz, $CDCl_3/CD_3OD$, 1/1), $\delta = 1.14$ (d, $J_{6,5} = 6.5$ Hz, 3H, 6-H, Fuc); 1.36–1.46 (m, 4H, CH_2); 1.54–1.71 (m, 4H, CH_2); 1.80 (dd, $J_{3ax,3eq} = 13$ Hz, $J_{3ax,4} = 11.1$ Hz, 1H, 3-H_{ax}, NeuNAc); 1.98, 2.00 (2 s, 6H, NHAc); 2.48 (dd, $J_{3eq,3ax} = 13$ Hz, $J_{3eq,4} = 5.2$ Hz, 1H, 3-H_{eq}, NeuNAc); 2.89 (t, $J_{H',H} = 7.4$ Hz, 2H, CH_2NH_2); 3.33 (m, 1H, 2-H, Gal); 3.62 (m, 1H, 2-H, Fuc); 3.77 (m, 1H, 5-H, NeuNAc); 4.17 (dd, $J_{3,2} = 9.4$ Hz, $J_{3,4} = 4.1$ Hz, 1H, 3-H, Gal); 4.31 (ddd, $J_{4,3eq} = 11.3$ Hz, $J_{4,3ax} = 5.2$ Hz, $J_{4,5} = 10.2$ Hz, 1H, 4-H, NeuNAc); 4.46 (d, $J_{1,2} = 7.9$ Hz, 1H, 1-H, GlucNAc); 4.61 (d, $J_{1,2} = 7.8$ Hz, 1H, 1-H, Gal); 5.01 (d, $J_{1,2} = 3.8$ Hz, 1H, 1-H, Fuc); 5.37 (d, $J_{4,3} = 4$ Hz, 1H, 4-H, Gal). **8bb**: (300 MHz, $CDCl_3/CD_3OD$, 1/1), $\delta = 1.13$ (d, $J_{6,5} = 6.5$ Hz, 3H, 6-H, Fuc); 1.37 (d, $J_{6,5} = 6.4$ Hz, 3H, 6-H, Gal); 1.38–1.46 (m, 4H, CH_2); 1.52–1.63 (m, 4H, CH_2); 1.79 (dd, $J_{3ax,3eq} = 12.7$ Hz, $J_{3ax,4} = 11.3$ Hz, 1H, 3-H_{ax}, NeuNAc); 1.98, 2.04 (2 s, 6H, NHAc); 2.47 (dd, $J_{3eq,3ax} = 13.1$ Hz, $J_{3eq,4} = 5.3$ Hz, 1H, 3-H_{eq}, NeuNAc); 2.91 (t, $J_{H',H} = 7$ Hz, 2H, CH_2NH_2); 4.12 (dd, $J_{3,4} = 4.1$ Hz, $J_{3,2} = 9.4$ Hz, 1H, 3-H, Gal); 4.34 (ddd, $J_{4,3eq} = 5.3$ Hz, 1H, 4-H, NeuNAc); 4.44, 4.52 (d, $J_{1,2} = 7.9$ Hz, 2H, 1-H, Gal, GlucNAc); 5.01, 5.12 (2 d, $J_{1,2} = 3.8$ Hz, $J_{4,5} = 3.8$ Hz, 2H, 1-H, Fuc, 4-H, Gal).

[16] T. J. Martin, R. R. Schmidt, *Tetrahedron Lett.* **1992**, *33*, 6123, and references therein.

[17] W. Stahl, M. Ahlers, A. Walch, E. Bartnik, G. Kretzschmar, S. Grabley, R. Schleyerbach, *Eur. Pat.* No. 9319098.7 (Hoechst AG).

[18] The synthesis of a corresponding sialyl Lewis^x derivative and its incorporation in glycopeptides are almost complete. For an analogous reaction with Lewis^x see: K. von dem Bruch, H. Kunz, *Angew. Chem.* **1994**, *106*, 87; *Angew. Chem. Int. Ed. Engl.* **1994**, *33*, 101.

[19] S. A. DeFrees, F. C. A. Gaeta, Y.-C. Lin, Y. Ichikawa, C.-H. Wong *J. Am. Chem. Soc.* **1993**, *115*, 7549, and references therein.

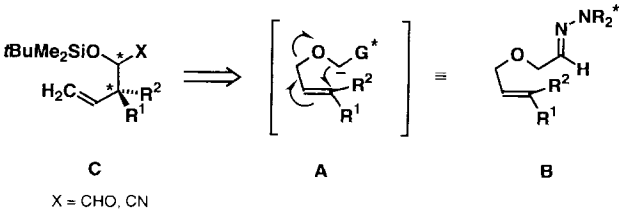
[20] For a detailed description of the HL60 cell assay with recombinant E-selectin see ref. [17].

[21] E. Bartnik, Hoechst AG, unpublished.

[2,3] Sigmatropic Wittig Rearrangement of Chiral Allyloxyacetaldehyde Hydrazones in the Diastereo- and Enantioselective Synthesis of Protected, γ,δ-Unsaturated α-Hydroxyaldehydes and Cyanohydrins**

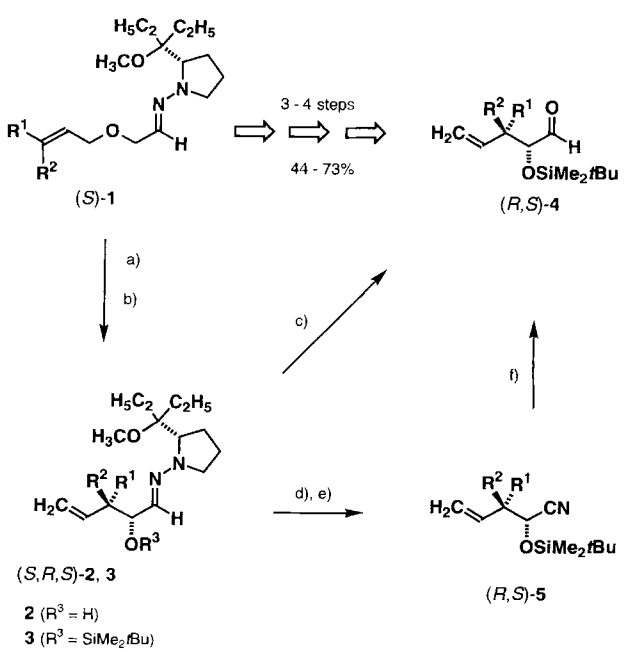
Dieter Enders,* Dirk Backhaus, and Jan Runsink

In the last twenty years the [2,3] sigmatropic Wittig rearrangement has become an important tool for the stereoselective formation of C–C bonds.[1, 2] The asymmetric version of the [2,3] sigmatropic Wittig rearrangement of chiral allyl ethers **A**-H, proceeding with chirality transfer, has found many applications in the field of natural product synthesis.[3] Asymmetric inductions with retention of the directing center have been achieved not only with substituents in the allyl part of the molecule,[4] but also with chiral auxiliaries G* in the anionic moiety **A** such as esters,[5] amides,[6] oxazolines,[7] and a η^6-arene-Cr(CO)$_3$ complex.[8] By appropriate variation of the group G* in **A** (in the form of a chiral hydrazone **B**), it should be possible to prepare protected α-hydroxyaldehydes (X = CHO) and cyanohydrins (X = CN) **C** stereoselectively. Both classes of compounds are of great interest due to their synthetic potential: Protected chiral α-hydroxyaldehydes are commonly used in the synthesis of natural products and pharmaceuticals,[9] and cyanohydrins can be easily converted to α-hydroxycarboxylic acids,[10] esters,[11] ketones,[12] aldehydes,[13] β-hydroxyamines[10b, 10c, 12] as well as α-amino acids[14] without racemization.[14c]



We report now the *syn* diastereo- and enantioselective synthesis of protected γ,δ-unsaturated α-hydroxyaldehydes (X = CHO) and cyanohydrins (X = CN) **C** from allyloxyacetaldehyde hydrazones **B**. The [2,3] sigmatropic Wittig rearrangement of the metalated hydrazone is the key step in the synthesis. After protection of the hydroxy function and oxidative cleavage of the auxiliary, either the aldehyde or the nitrile group can be formed selectively.

The metalation of the (*E*)-configurated (*S*)-1-amino-2-(1-ethyl-1-methoxypropyl)pyrrolidine (SAEP) hydrazones[15, 16] (*S*)-**1** with lithium diisopropylamide (LDA) in tetrahydrofuran/hexamethylphosphoric triamide (THF/HMPA) at −78 °C delivers the α-hydroxyhydrazones (*S,R,S*)-**2** with good *syn*/*anti* diastereoselectivity (87–95% *syn*) and with high asymmetric induction (81–92% *de*) (Scheme 1).[17] After purification by



Scheme 1. Asymmetric [2,3] sigmatropic Wittig rearrangement of SAEP hydrazones to aldehydes and cyanohydrins. a) 2.5 equiv LDA, THF/HMPA (5/1) −78 °C, 22 h, NH_4Cl, column chromatography; b) 2.4 equiv TBDMSCl, 3 equiv imidazole, DMF, room temperature, 5–20 h, column chromatography; c) ozone, petroleum ether, −78 °C, 120–180 s mmol^{-1}, column chromatography; d) HPLC separation of the minor isomer; e) 2.5 equiv MMPP·6H_2O, MeOH, 0 °C, 30–90 min, column chromatography; f) 2 equiv DIBAH, toluene, −78 °C, 2 h, MeOH, 0 °C, 2 h, H_2SO_4, 0 °C, 1 h, column chromatography. R^1, R^2 see Table 1.

[*] Prof. Dr. D. Enders, Dipl.-Chem. D. Backhaus, Dr. J. Runsink
Institut für Organische Chemie der Technischen Hochschule
Professor-Pirlet-Strasse 1, D-52074 Aachen (FRG)
Telefax: Int. code + (241)8888127

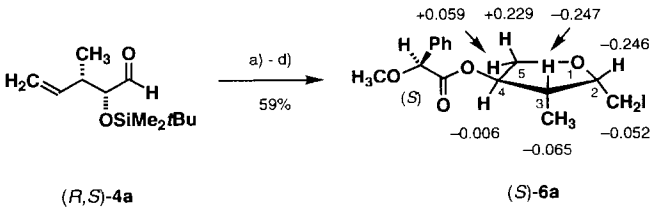
[**] This work was supported by the Deutsche Forschungsgemeinschaft (Leibniz-Program) and by the Fonds der Chemischen Industrie. We thank Degussa AG, BASF AG, Bayer AG, and Hoechst AG for donations of chemicals.

column chromatography the products of the rearrangement (*S,R,S*)-**2** are obtained in good yields (72–91%) as pale yellow liquids. Silylation of the hydroxy function with *tert*-butyldimethylsilyl chloride (TBDMSCl) in dimethylformamide (DMF)[18] leads, after chromatographic purification on deactivated silica gel, to the hydrazones (*S,R,S*)-**3** in unchanged isomer ratios and almost quantitative yields. The diastereomeric excess can be increased to >98% by using high-pressure liquid chromatography (HPLC), and for the hydrazone **3a** the *anti* isomer can also be separated in this way. The proportion of the predominant isomer can also be increased at the α-hydroxyhydrazone (*S,R,S*)-**2** stage by column chromatography or by HPLC. Ozonolysis of the protected rearrangement products (*S,R,S*)-**3** at −78 °C yields, after flash chromatography on Florisil, the silylated α-hydroxyaldehydes (*R,S*)-**4** in moderate to high yields (55–84%). With smaller R^1 groups the yield is lower (Table 1) because in these cases the double bond is also ozonolyzed. Additionally, a partial epimerization occurs during the hydrazone cleavage with ozone, such that the *ee* values of aldehydes **4** are 4–12% lower than the *de* values of the starting hydrazones **3**.

The protected cyanohydrins (*R,S*)-**5** are accessible in good yield (86–95%) by cleavage of the auxiliary with magnesium monoperoxyphthalate (MMPP).[19] As an alternative to ozonolysis, reduction with diisobutylaluminum hydride (DIBAH) yields the aldehydes (*R,S*)-**4**. This two-step method of cleaving the hydrazones leads to better overall yields of aldehydes than the direct ozonolysis (Table 1). Furthermore, since this method causes minimal racemization, the aldehydes **4** can be obtained with enantiomeric excesses of 94–97%.

The diastereomeric excesses of the hydrazones **2** and **3** were measured by ^{13}C NMR spectroscopy, while the enantiomeric excesses of the aldehydes **4** were determined by ^1H NMR spectroscopy, using the chiral cosolvent (−)-(*R*)-1-(9-anthryl)-2,2,2-trifluoroethanol, by comparison with the spectra of the corresponding racemate. The racemates were prepared analogously by [2,3] sigmatropic Wittig rearrangement of the corresponding *N,N*-dimethylhydrazones.

The absolute configurations of the aldehydes **4** were determined by derivatization and comparison of optical rotation. The α-methoxyphenylacetate esters (*R*)-**6a** and (*S*)-**6a** were prepared from the aldehyde **4a** in a four-step synthesis (Scheme 2). Measurement of the nuclear Overhauser effect showed that the relative configuration within the tetrahydrofuran ring of the major isomer[20] is 2,3-*cis*, 3,4-*trans*. The absolute configuration[21] follows from the ^1H NMR signals which are shifted to high field by the diamagnetic effect of the phenyl groups. As indicated in the structure (*S*)-**6a**, the aldehyde **4a** can be assigned the configuration *syn*-(2*R*,3*S*). The *syn* selectivity of the [2,3] Wittig rearrangement of the azaenolate of hydrazone (*S*)-**1**



Scheme 2. Derivatization of the aldehyde **4a** for the determination of the absolute configuration. The differences in the ^1H NMR shifts of (*S*)-**6a** and (*R*)-**6a** ($\Delta\delta = \delta(S) - \delta(R)$) at 500 MHz are given: a) $NaBH_4$, MeOH, 0 °C, 1 h; b) I_2, $NaHCO_3$, Et_2O/H_2O (5/2), room temperature, H_2O, 18 h; c) MeOH, HCl, 0 °C, 1 h; d) (*S*)- or (*R*)-α-methoxyphenylacetic acid, 4-dimethyaminopyridine (DMAP), dicyclohexylcarbodiimide (DCC), CH_2Cl_2, room temperature, 18 h, column chromatography (silica gel, ether/petroleum ether 1/4).

corresponds to selectivities found for other enolates,[1,4–6] for which several transition state models have been suggested.[22] The derivatization of the aldehyde **4a** (57% *de*)[17] (Scheme 2, a)–c)) by esterification with (*R*)-(−)-α-methoxy-α-(trifluoromethyl)phenylacetyl chloride (MTPACl) leads to the corresponding Mosher ester. The absolute configuration of the major isomer was confirmed by NMR spectroscopic investigations (modified Mosher method[23]). A comparison of the optical rotation of the 3-methylpent-4-ene-1,2-diol ($[\alpha_D^{20} = -40.4$ ($c = 0.85$ in $CHCl_3$))—prepared by reduction of aldehyde **4a** (*de* = 96%) with sodium borohydride and subsequent cleavage of the silyl protecting group with methanol/HCl—with the literature value[24] confirms the configuration as (2*R*,3*S*).

The configuration of the aldehyde **4b** was determined as (2*R*) by transformation to the (*R*)- and (*S*)-α-methoxyphenylacetate ester. The absolute configurations of aldehydes **4c**–**4e** were assigned based on the assumption of the same reaction pathway.

The asymmetric [2,3] sigmatropic Wittig rearrangement of SAEP hydrazones described here provides access to protected γ,δ-unsaturated α-hydroxyaldehydes and cyanohydrins with variable substitution in the β-position. The double bond, aldehyde, cyano, hydroxy, and cyanohydrin functionalities in these products should allow their use in the preparation of optically active building blocks in the synthesis of natural products and pharmaceuticals.

Experimental Procedure

α-Hydroxyhydrazones **2**: *n*-butyllithium (1.6 mL of a 1.6 M solution in *n*-hexane) was added dropwise to diisopropylamine (2.7 mmol) in anhydrous THF (2 mL) at 0 °C under argon. After 15 min the solvents were removed under vacuum and the residue taken up in THF (5 mL). After addition of HMPA (1 mL) the solution was cooled to −78 °C and the hydrazone (*S*)-**1** (1 mmol), dissolved in THF (1 mL), was added dropwise. After 22 h at −78 °C (for **2b** 6 h at −78 °C, then 15 min at 0 °C) the solution was hydrolyzed by addition of saturated NH_4Cl solution (20 mL). The organic phase was washed twice with water, and the aqueous phase washed several times with ether. The combined organic phases were dried over $MgSO_4$ and the

Table 1. Protected α-hydroxyaldehydes **4** and cyanohydrins **5** prepared by [2,3] sigmatropic Wittig rearrangement via the hydrazones **2** and **3**.

	R^1	R^2	Yield **2**/**3** [%]	*syn* [a] [%]	*de* [b] [%]	Yield **5** [%]	$[\alpha]_D^{20}$ (**5**) (*c*, $CHCl_3$)	Yield **4** [c] [%]	$[\alpha]_D^{20}$ (**4**) (*c*, $CHCl_3$)	*ee* [d] [%]
a	Me	H	86/93	95 [e]	91	96	+44.4 (1.0)	55 (82)	+15.1 (1.1)	96 (*R,S*)
b	Me	Me	72/94	-	81	86	+49.1 (1.0)	74 (73)	+7.5 (1.0)	95 (*R*)
c	Et	H	81/92	92	92	91	+68.9 (1.1)	79 (77)	+26.3 (1.0)	97 (*R,S*)
d	*n*Pr	H	91/93	92	92	88	+63.8 (1.1)	82 (81)	+28.9 (1.0)	94 (*R,S*)
e	*i*Pr	H	91/96	87	91	95	+66.5 (1.0)	84 (82)	+26.1 (1.1)	95 (*R,S*)

[a] Determined by ^{13}C NMR spectroscopy of **2**. [b] *de* value determined by ^{13}C NMR spectroscopy, which relates to both *syn* isomers; >98% *de* after purification of **3** by HPLC; in the ^{13}C NMR spectrum (300 MHz, 2 h) the minor isomer is not detectable. [c] By ozonolysis of **3**; the yields in brackets refer to the yields over two steps from the oxidation of **3** to **5** with MMPP and then reduction to **4** with DIBAH (85–92%). [d] From ^1H NMR experiments on aldehydes **4** obtained in two steps from **3** using (−)-(*R*)-1-(9-anthryl)-2,2,2-trifluoroethanol as cosolvent (Varian 500 MHz spectrometer). [e] >98% *syn* after separation of the minor isomer **3a** by HPLC; in the ^{13}C NMR (300 MHz, 2 h) the minor isomer can no longer be detected.

 © VCH Verlagsgesellschaft mbH, D-69451 Weinheim, 1994 0570-0833/94/2020-2099 $ 10.00+.25/0

solvents removed. The residue was purified by flash chromatography (silica gel, ether/petroleum ether 1/2).

Silylation of the hydroxy function: The hydrazone **2** (1 mmol) was dissolved in DMF (5 mL), treated with TBDMSCl (2.4 mmol) and imidazole (3 mmol), and stirred at room temperature for 5–20 h. At the end of the reaction (monitored by thin-layer chromatography) petroleum ether was added, the reaction mixture washed with water and dried over $MgSO_4$. After removal of the solvent the residue was purified by column chromatography (silica gel, ether/petroleum ether 1/40, 2.5% triethylamine). The major isomer can be enriched by HPLC (preprepared column silica gel 7 μ, length 250 mm, ether/petroleum ether 3/97 to 5/95).

Ozonolysis of the hydrazone **3** to the aldehyde **4**: The hydrazone (1 mmol) was dissolved in petroleum ether (ca. 40 mL) and cooled to −78 °C. Ozone was passed through the reaction solution. During the reaction the ozonolysis was interrupted by passing argon through the solution to allow the reacton to be followed by TLC. At the end of the reaction (120–180 s) the reaction mixture was allowed to warm to 0 °C under an argon stream. The solution was concentrated and the crude product purified by flash chromatography (Florisil, ether/petroleum ether 1/40 to 1/60).

Cleavage of the hydrazone **3** to give the nitrile **5**: The hydrazone (2 mmol) was dissolved in methanol (40 mL), cooled to 0 °C and MMPP·$6H_2O$ (5 mmol) added. After the end of the reaction (monitored by thin-layer chromatography, 30–90 min) ether and saturated $NaHCO_3$ were added, and the aqueous phase extracted with ether three times. The combined organic phases were washed several times with saturated NaCl solution, dried over $MgSO_4$, and the solvent removed on a rotary evaporator. The crude product was purified by column chromatography (silica gel, ether/petroleum ether 1/40).

Reduction of the nitrile **5** to the aldehyde **4**: The reaction was carried out as described in reference [13], and the crude product purified by column chromatography (Florisil, ether/petroleum ether 1/40) [25].

Received: May 21, 1994 [Z 6957 IE]
German version: *Angew. Chem.* **1994**, *106*, 2167

[1] Reviews: a) K. Mikami, T. Nakai, *Chem. Rev.* **1986**, *86*, 885; b) R. Brückner, *Nachr. Chem. Tech. Lab.* **1990**, *38*, 1506; c) K. Mikami, T. Nakai, *Synthesis* **1991**, 594; d) R. Brückner, *Kontakte (Darmstadt)* **1991**, (2) 3; *ibid* (3) 3; e) J. A. Marshall in *Comprehensive Organic Synthesis, Vol. 3* (Eds.: B. M. Trost, I. Fleming), Pergamon Press, London, **1991**, p. 975; more recent examples: f) E. J. Verner, T. Cohen, *J. Am. Chem. Soc.* **1992**, *114*, 375; g) R. Hoffmann, R. Brückner, *Chem. Ber.* **1992**, *125*, 1471; h) *Angew. Chem.* **1992**, *104*, 646; *Angew. Chem. Int. Ed. Engl.* **1992**, *31*, 647; i) K. Tomooka, T. Iyurashi, W. Watanabe, T. Nakai, *Tetrahedron Lett.* **1992**, *33*, 5795; j) H. Sakai, K. Fujimoto, T. Nakai, *Chem. Lett.* **1993**, 1397; k) K. Brickmann, R. Brückner, *Chem. Ber.* **1993**, *126*, 1227; l) D. Goeppel, I. Münster, R. Brückner, *Tetrahedron* **1994**, *50*, 3687; m) H. Audrian, T. Skydstrup, G. Ulibarri, C. Riche, A. Chiarone, D. S. Grierson, *ibid.* **1994**, *50*, 1462.

[2] For the stereoselective [2,3] Wittig rearrangements of racemic keto-*N*,*N*-dimethylhydrazones see a) M. Koreeda, J. I. Luengo, *J. Am. Chem. Soc.* **1985**, *107*, 5572; b) *J. Org. Chem.* **1989**, *54*, 5419.

[3] Literature up to 1991 see reference [1a–e]; more recent literature: a) D. S. Keegan, M. M. Midland, R. T. Werley, J. I. McLoughlin, *J. Org. Chem.* **1991**, *56*, 1185; b) C. L. Gwin, F. X. Webster, J. Kallmerten, *ibid.* **1991**, *56*, 2953; c) J. A. Marshall, X.-Y. Wang, *ibid.* **1991**, *56*, 4913; d) N. Sin, J. Kallmerten, *Tetrahedron Lett.* **1993**, *34*, 753; e) M. H. Kress, B. F. Kuller, Y. Kishi, *ibid.* **1993**, *34*, 8047; f) S. Y. Wei, K. Tomooka, T. Nakai, *Tetrahedron* **1993**, *49*, 1025; g) Z.-Q. You, M. Koreeda, *Tetrahedron Lett.* **1993**, *34*, 2597; h) H. Okamura, S. Kuroda, S. Ikegami, K. Tomika, Y. Sujimoto, S. Sakaguchi, Y. Ho, T. Katsuki, M. Yamaguchi, *Tetrahedron* **1993**, *49*, 10531; i) J. A. Marshall, Y. Tang, *J. Org. Chem.* **1993**, *58*, 3233.

[4] a) H. Priepke, R. Brückner, *Angew. Chem.* **1988**, *100*, 285; *Angew. Chem. Int. Ed. Engl.* **1988**, *27*, 278; b) E. Nakai, T. Nakai, *Tetrahedron Lett.* **1988**, *29*, 4587; c) R. Brückner, *Chem. Ber.* **1989**, *122*, 703; d) H. Priepke, R. Brückner, *ibid.* **1990**, *123*, 153; e) K. Tomooka, M. Watanabe, T. Nakai, *Tetrahedron Lett.* **1990**, *31*, 7353; f) S. W. Scheuplein, A. Kusche, K. Harms, R. Brückner, *Chem. Ber.* **1990**, *123*, 917; g) K. Tomooka, K. Ishikawa, T. Nakai, *Synlett* **1993**, 527.

[5] O. Takahashi, K. Mikami, T. Nakai, *Chem. Lett.* **1987**, 69.

[6] a) K. Mikami, O. Takahashi, T. Kasuga, T. Nakai, *Chem. Lett.* **1985**, 1729; b) M. Uchikawa, T. Hanamoto, T. Katsuki, M. Yamaguchi, *Tetrahedron Lett.* **1986**, *27*, 4577.

[7] a) K. Mikami, F. Fujimoto, T. Nakai, *Tetrahedron Lett.* **1984**, *25*, 6011; b) K. Mikami, T. Kasuga, K. Fujimoto, T. Nakai, *Tetrahedron* **1986**, *27*, 4185.

[8] a) J. Brocard, M. Mahmoudi, L. Perlinski, L. Maciejewski, *Tetrahedron Lett.* **1989**, *30*, 2549; b) M. Uemura, H. Nishimura, Y. Hayashi, *J. Organomet. Chem.* **1989**, *376*, C3.

[9] a) T. Mukaiyama, Y. Sakito, *Chem. Lett.* **1979**, 1027; b) T. Mukaiyama, Y. Sakito, S. Tamaka, M. Asami, *ibid.* **1980**, 1223; c) D. C. Baker, L. D. Hawkins, *J. Org. Chem.* **1982**, *47*, 2179; d) J.-C. Depezay, Y. LeMerrer, C. Gravier-Pelletier, D. Micas-Languin, F. Mestre, A. Duréault, *ibid.* **1989**, *54*, 2409; e) C. J. Sih, C.-Q. Han, D. DiTullio, Y.-F. Wang, *ibid.* **1986**, *51*, 1253; f) M. Hirami, H. Hioki, S. Ho, *Tetrahedron Lett.* **1988**, *29*, 3125; g) C. H. Heathcock, K. Takai, *J. Org. Chem.* **1985**, 50, 3247; h) K. Mikami, T.-P. Loh, T. Naka, *Tetrahedron: Asymmetry* **1990**, *1*, 13.

[10] a) B. R. Mathews, H. Gountzos, W. R. Jackson, K. G. Watson, *Tetrahedron Lett.* **1989**, *30*, 5157; b) T. Ziegler, B. Horsch, F. Effenberger, *Synthesis* **1990**, 575; c) F. Effenberger, *Microbial Reagents in Organic Synthesis* **1992**, *381*, 25.

[11] a) H. Gudeon, R. Hill, E. Isaacs, *J. Chem. Soc.* **1951**, 1926; b) D. Lauscher, D. Enders, unpublished results.

[12] a) W. R. Jackson, H. A. Jacobs, G. S. Jayatilake, B. R. Mathews, K. G. Watson, *Aust. J. Chem.* **1990**, *43*, 2045; b) W. R. Jackson, H. A. Jacobs, B. R. Mathews, G. S. Jayatilake, K. G. Watson, *Tetrahedron Lett.* **1990**, *31*, 1447.

[13] M. Hayashi, T. Toshiga, K. Nakatani, K. Ono, N. Oguni, *Tetrahedron* **1994**, *50*, 2821, and references therein.

[14] a) F. Effenberger, U. Stelzer, *Angew. Chem.* **1991**, *103*, 866; *Angew. Chem. Int. Ed. Engl.* **1991**, *30*, 873; b) P. Zandbergen, J. Brusse, A. van der Gen, C. G. Kruse, *Tetrahedron: Asymmetry* **1992**, *3*, 769; c) For enzymatic reactions of optically active cyanohydrins see: F. Effenberger, *Angew. Chem.* **1994**, *106*, 1609; *Angew. Chem. Int. Ed. Engl.* **1994**, *33*, 1555.

[15] D. Enders, H. Kipphardt, P. Gerdes, L. J. Breña-Valle, V. Bushan, *Bull. Soc. Chim. Belg.* **1988**, *97*, 691.

[16] a) Synthesis of the hydrazones (*S*)-**1**: The aldehydes, obtained by reaction of the allyl alcohols with ethyl bromoacetate, bromoacetaldehyde diethyl acetal, or 3-chloro-1,2-propanediol follwed by reduction with DIBAH, acidic cleavage of the acetal or sodium periodate cleavage of the diol, were transformed to hydrazone (*S*)-**1** with SAEP; b) sodium periodate cleavage: H. Dumas, Y. Vo-Quang, F. Le Goffic, *J. Chem Soc. Chem. Commun.* **1989**, 34.

[17] By the rearrangement of the sterically less demanding (*S*)-1-amino-2-methoxymethylpyrrolidine (SAMP) hydrazone, analogous to (*S*)-**1a**, significantly lower asymmetric induction was achieved (93% *syn*, 57% *de*).

[18] E. J. Corey, A. Venkateswarlu, *J. Am. Chem. Soc.* **1972**, *94*, 6190.

[19] A. Plant, D. Enders, unpublished results. For oxidative MMPP cleavage of ketohydrazones see D. Enders, A. Plant, *Synlett* **1990**, 725.

[20] The *cis* selectivity of the iodocyclization amounted to 75%.

[21] a) B. M. Trost, J. L. Belletire, S. Godleski, P. G. McDougal, J. M. Balkovec, *J. Org. Chem.* **1986**, *51*, 2370; b) L. A. Paquette, C. L. Lau, *ibid.* **1987**, *52*, 1635; M. Adamczieski, E. Quiñoà, P. Crews, *ibid.* **1990**, *55*, 240; c) D. Parker, *Chem. Rev.* **1991**, *91*, 1441; d) T. Pekh, E. Lippmaa, M. Lopp, A. Paju, B. C. Borer, R. J. K. Taylor, *Tetrahedron: Asymmetry* **1993**, *4*, 1527.

[22] a) K. Mikami, Y. Kimura, N. Kishi, T. Nakai, *J. Org. Chem.* **1983**, *48*, 279; b) K. Mikami, T. Nakai in *Physical Organic Chemistry 1986* (Ed.: M. Kobayashi), Elsevier, Amsterdam, **1987**, p. 153; c) Y.-D. Wu, K. N. Houk, J. A. Marshall, *J. Org. Chem.* **1990**, *55*, 1421.

[23] a) J. A. Dale, H. S. Mosher, *J. Am. Chem. Soc.* **1973**, *95*, 512; b) I. Ohtani, T. Kusumi, Y. Kashman, H. Kakisawa, *ibid.* **1991**, *113*, 4092; c) *J. Org. Chem.* **1991**, *56*, 1296; d) T. Hamada, T. Kusumi, M. O. Ishitsuka, H. Kakisawa, *Chem. Lett.* **1992**, 33; e) M. Mori, F. Saitoh, N. Uesaka, M. Shibasaki, *ibid.* **1993**, 213; f) Y. Inouye, Y. Sugo, T. Kusumi, N. Fusetani, *ibid.* **1994**, 419.

[24] R. E. Ireland, T. K. Highsmith, L. D. Gegnas, J. L. Gleason, *J. Org. Chem.* **1992**, *57*, 5071: $[\alpha]_D = -30.6$ ($c = 1.21$ in $CHCl_3$).

[25] All new compounds gave correct elemental analysis and consistent spectroscopic data (IR, NMR, MS).

Wacker Oxidation of 1-Decene to 2-Decanone in the Presence of a Chemically Modified Cyclodextrin System: A Happy Union of Host–Guest Chemistry and Homogeneous Catalysis**

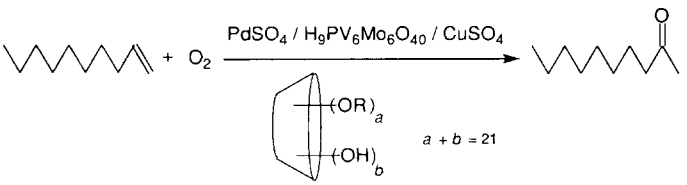
Eric Monflier, Emilie Blouet, Yolande Barbaux, and André Mortreux*

The oxidation of olefins to ketones catalyzed by palladium/copper or palladium/heteropolyacid systems, which is generally known as the Wacker process, has been the subject of several studies.[1] Because of their insolubility in water, higher α-olefins require the presence of polar organic solvent to be oxidized

[*] Prof. Dr. A. Mortreux
Laboratoire de Catalyse Hétérogène et Homogène
Groupe de Chimie Organique Appliquée, URA CNRS 402
BP 108, F-59652 Villeneuve d'Ascq Cedex (France)
Telefax: Int. code + (20)43-6585
Dr. E. Monflier, Dr. E. Blouet, Prof. Dr. Y. Barbaux
Université d'Artois, Faculté des Sciences Jean Perrin
Sac Postal 18, F-62307 Lens Cedex (France)

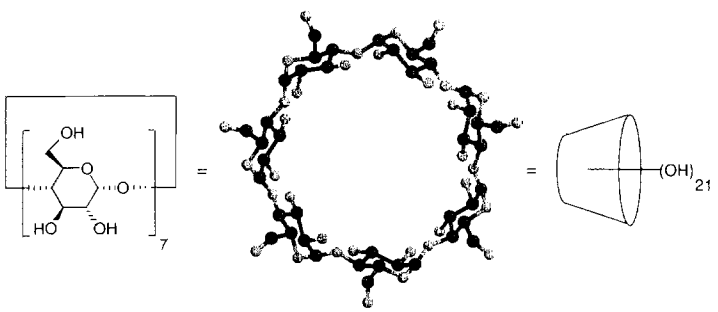
[**] This work was supported by the CNRS.

efficiently.[2] Recently, Alper et al. reported the oxidation of higher olefins in a two phase system in the presence of cyclodextrins.[3] Nevertheless, even in the presence of cyclodextrins or polar organic solvents, the oxidations proceeded at moderate rates and with poor yields and selectivities. We report here on the high-yield oxidation (up to 98%) of 1-decene to 2-decanone with $PdSO_4/H_9PV_6Mo_6O_{40}/CuSO_4/O_2$ and chemically modified cyclodextrins in a two-phase system (Scheme 1).



Scheme 1. Catalytic oxidation of 1-decene to 2-decanone. A schematic representation of the β-cyclodextrin is shown; R = CH_3, $CH_2CH(OH)CH_3$.

The results obtained with various catalytic systems are shown in Table 1. β-Cyclodextrin (β-CD), a cyclic oligosaccharide composed of seven glucopyranose units (Scheme 2),[4] was used

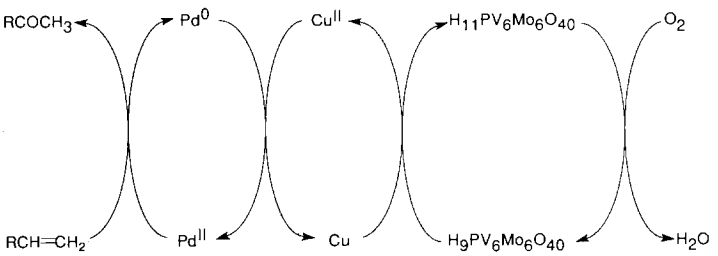


Scheme 2. Schematic representations of β-cyclodextrin.

as the inverse-phase transfer catalyst.[5] The palladium(II)/copper(II)/β-cyclodextrin system gave 2-decanone, but the yields (38%) and selectivities (49%) were low (Table 1, entry 1). However, in the presence of catalytic amounts of the heteropolyacid $H_9PV_6Mo_6O_{40}$, 2-decanone was obtained in a good yield (58%) and selectivity (80%) (Table 1, entry 6). In this case, the isomerization of 1-decene to give 2-, 3-, 4-, and 5-decenes was considerably reduced. It is noteworthy that addition of copper sulfate to the palladium/heteropolyacid system increased the selectivity (Table 1, entries 4 and 6).

These results can be rationalized if one considers that copper sulfate or the heteropolyacid alone reoxidize palladium(0) to palladium(II) species less efficiently than the copper sulfate/heteropolyacid couple. Indeed, faster reoxidation reduces the concentration of the palladium(0) and palladium hydride species, which are responsible for isomerization,[6] and isomerization is thus suppressed. The oxidation of such palladium species has already been described.[2c, 7a, 8]

The efficiency of our binary system can be explained by the stabilization of the heteropolyacid by copper(II) and/or the replacement of the two-step reversible electron transfer with three steps of lower activation energy (Scheme 3). This system shows similarities with biochemical processes in which oxidation becomes very mild when redox couples with progressively lower redox potentials interact. Similar systems have been described by Bäckvall[7] and Vasilevskis.[2c]



Scheme 3. Redox cycles involved in the oxidation of Pd^0.

In our two-phase system, the $PdSO_4/H_9PV_6Mo_6O_{40}/CuSO_4$ combination was the most efficient. The transfer of material between organic and aqueous phases is brought about by the cyclodextrin (CD).[5] The CD, which has a hydrophobic host cavity, can form an inclusion complex with an organic molecule and transport it into the aqueous phase. The efficiency of transfer depends on the solubility of the CD in water; this can be modified by functionalization with hydrophilic or lipophilic groups.[4] To our knowledge, the use such chemically modified CDs in biphasic reactions catalyzed by transition-metal complexes has not yet been studied. We were therefore interested in investigating the influence of such functionalized CDs on the transfer of material.

The yields and selectivities obtained in the oxidation of 1-decene to 2-decanone in the presence of various modified CDs are shown in Table 2. The extent of conversion of 1-decene strongly depended on the magnitude of the angular aperture in the CD (Table 2, entries 1–3). The optimal size for the cavity is reached in β-CD (entry 3). A larger aperture, such as in γ-CD,[4] resulted in a drastic decrease in the extent of 1-decene conver-

Table 1. Catalytic oxidation of 1-decene.

No.	Catalytic system [a] Pd^{II}	HPA [g]	Cu^{II}	β-CD	Gas phase [b]	t [h]	Conversion [c] (1-decene) [mol %]	Yield [c] (2-decanone) [mol %]	Yield [c] (isomeric decenes) [d] [mol %]	Selectivity (2-decanone formation) [e] [mol %]	Selectivity (2-decanone oxodecenes) [f] [mol %]
1	$PdCl_2$	–	$CuCl_2$	+	O_2	16	77	38	38	49	97
2	$PdSO_4$	–	$CuSO_4$	+	O_2	16	30	18	12	60	98
3	$PdSO_4$	+	–	+	O_2/N_2	6	74	41	33	55	99
4	$PdSO_4$	+	–	+	O_2	6	75	53	21	70	98
5	$PdSO_4$	+	$CuSO_4$	–	O_2	6	25	5	20	20	>99
6	$PdSO_4$	+	$CuSO_4$	+	O_2	6	72	58	14	80	99

[a] For quantities used, see *Experimental Procedure*. [b] $p = 1$ bar; O_2/N_2 1/5 (v/v). [c] Determined by gas chromatography. [d] 2-, 3-, 4-, and 5-decene. [e] Yield (2-decanone) / conversion (1-decene). [f] Yield (2-decanone) / yield (decanal + 2-, 3-, 4-, 5-decanone). [g] Heteropolyacid $H_9PV_6Mo_6O_{40}$.

 © VCH Verlagsgesellschaft mbH, D-69451 Weinheim, 1994 0570-0833/94/2020-2101 $ 10.00+.25/0

Table 2. Oxidation of 1-decene with $PdSO_4/H_9PV_6Mo_6O_{40}/CuSO_4/O_2$ in the presence of cyclodextrins (see Scheme 1) [a].

No.	Type	R	Cyclodextrin a	b	$\bar{M}_r$	Conversion [b] (1-decene) [mol %]	Yield [b] (2-decanone) [mol %]	Yield [b] (isomeric decenes) [c] [mol %]	Selectivity (2-decanone formation) [d] [mol %]	TN [e]
1	α	H	18	0		55	44	11	80	20
2	γ	H	24	0		27	16	11	61	7
3	β	H	21	0		72	58	14	80	27
4	β	CH_3	12.6	8.4	1310	100	98	1	98	46
5	β	$COCH_3$	21	0	2017.79	34	17	17	50	8
6	β	$CH_2CHOHCH_3$	4.2	16.8	1380	81	74	6	92	34
7	β	$CH_2CHOHCH_3$	6.3	14.7	1500	90	83	6	92	39

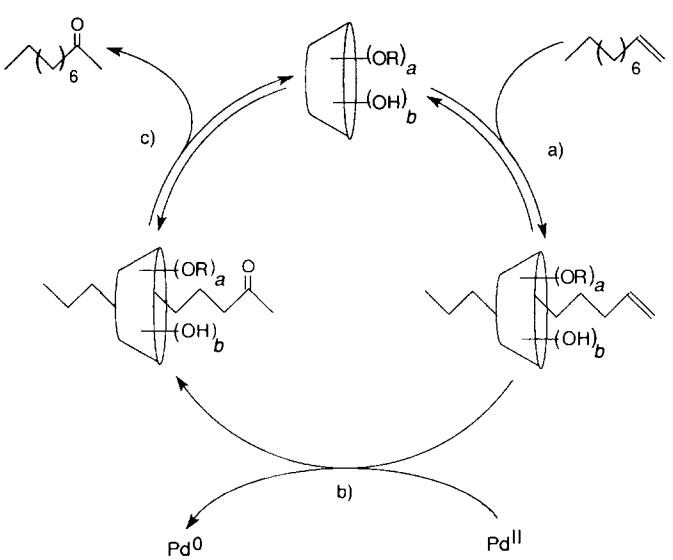
[a] For quantities used and reaction conditions, see *Experimental Procedure*. [b] Determined by gas chromatography. [c] 2-, 3-, 4-, and 5-decene. [d] Yield (2-decanone) / conversion (1-decene). [e] TN (turnover number), here: mole equivalents (2-decanone) / mole equivalents ($PdSO_4$).

sion; however, a smaller aperture, such as in α-CD,[4] gave only a small decrease. These results indicate molecular recognition based on reversible interactions between the CD host cavity and 1-decene.[4]

The yields obtained with CDs modified by polar or nonpolar groups are given in entries 3 to 7 (Table 2). Unexpectedly, 2-decanone was obtained in very high yield (98%) with methylated β-CD (Table 2, entry 4). The 2-hydroxypropyl-β-CDs with different degrees of substitution also gave 2-decanone in high yields (Table 2, entries 6 and 7).

We believe that the most important factor influencing these results is the degree of solubility of the CDs in water. The acylated β-CD is totally insoluble in water and cannot transfer 1-decene into the aqueous phase; the 2-hydroxypropyl-β-CD is more soluble and can therefore transfer 1-decene more readily. The fact that the highest conversion was obtained with methylated β-CD could be explained by its high solubility both in water and the organic layer. Another possible explanation is the lower stability of the host–guest complexes; this would facilitate the dissociation–association reactions between the organic compounds and CD (Scheme 4, steps a) and c)).[9] These properties of the methylated β-CD probably increase exchange at the phase boundary. The surprising selectivity could be due to the ability of β-CD to cause preorientation of 1-decene in the host cavity. The interactions between CD, 1-decene, palladium, and heteropolyacid will not be discussed here. Inclusion complexes between CD and transition-metal complexes have already been reported.[10]

At the present time, we are investigating the formation of inclusion complexes and the use of these modified CDs in other reactions. This preliminary study suggests that modified CDs will become important for reactions catalyzed by transition-metal complexes in aqueous–organic two-phase systems.



Scheme 4. Formation and dissociation of the inclusion complexes of a modified β-cyclodextrin with 1-decene (a) and 2-decanone (c), and the oxidation of 1-decene with Pd^{II} (b).

Experimental Procedure

In a typical experiment, $PdSO_4 \cdot 2H_2O$ (0.206 g, 0.86 mmol), $CuSO_4$ (1.64 g, 10 mmol), $H_9PV_6Mo_6O_{40}$ (8 mmol, synthesized according to ref. [11]), and 2,6-dimethyl-β-CD (1.3 g, 1 mmol) were introduced with water (30 mL, 1.66 mol) and 1-decene (7.6 mL, 40 mmol) into a 250 mL flask. Oxygen was bubbled through the solution ($p = 1$ bar), which was vigorously stirred at 80 °C for 6 h. The solution was then cooled, and the organic layer was analyzed by GLC with undecane as internal standard. Products were identified by comparing the retention times and spectral properties with those of authentic samples.

Received: April 20, 1994 [Z6865IE]
German version: *Angew. Chem.* **1994**, *106*, 2183

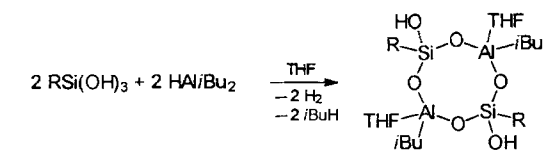
[1] a) G. W. Parshall, S. D. Ittel, *Homogeneous Catalysis. The Applications and Chemistry of Catalysis by Soluble Transition Metal Complexes*, 2nd ed., Wiley-Interscience, New York, **1992**, pp. 138–142; b) K. I. Matveev, *Kinet. Catal. Engl. Transl.* **1977**, *18*, 716–728.
[2] a) J. E. Bäckvall, R. E. Bruce, *Tetrahedron Lett.* **1988**, *29*, 2885–2888; b) J. Tsuji, H. Nagashima, H. Nemoto, *Org. Synth.* **1984**, *62*, 9–13; c) J. Vasilevskis, J. C. De Deken, R. J. Saxton, J. D. Fellmann, L. S. Kipnis (Catalytica Associates), USA 4723041, **1988**, CA: **1987**, *107*, 17 860 201, and references therein.
[3] a) H. A. Zahalka, K. Januszkiewicz, H. Alper, *J. Mol. Catal.* **1986**, *35*, 249–253; b) A. Harada, Y. Hu and S. Takahashi, *Chem. Lett.* **1986**, 2083–2084.
[4] a) G. Wenz, *Angew. Chem.* **1994**, *106*, 851; *Angew. Chem. Int. Ed. Engl.* **1994**, *33*, 803–822; b) W. Saenger, *ibid.* **1980**, *92*, 343 and **1980**, *19*, 344–362.
[5] Y. Goldberg, *Phase Transfer Catalysis, Selected Problems and Applications*, Gordon and Breach Science Publishers, **1992**, p. 364–366; E. V. Dehmlow, S. S. Dehmlow, *Phase Transfer Catalysis*, 3rd ed., VCH, Weinheim, **1993**.
[6] R. F. Heck, *Palladium Reagents in Organic Syntheses*, Academic Press, London, **1985**, S. 19–21, and references therein.
[7] a) J. E. Bäckvall, R. B. Hopkins, H. Grennberg, M. M. Mader, A. K. Awasthi, *J. Am. Chem. Soc.* **1990**, *112*, 5160–5166; b) J. E. Bäckvall, A. K. Awasthi, Z. D. Renko, *ibid.* **1987**, *109*, 4750–4752.
[8] E. G. Zhizhina, N. B. Shitovo, K. I. Matveev, *Kinet. Catal. Engl. Transl.* **1981**, *22*, 1153–1157.
[9] H. Ikeda, R. Kojin, C. J. Yoon, T. Ikeda, *J. Incl. Phenom. Mol. Recognit. Chem.* **1989**, *7*, 117–124.
[10] a) H. M. Colquhoun, J. F. Stoddart, D. J. Williams, *Angew. Chem.* **1986**, *98*, 483; *Angew. Chem. Int. Ed. Engl.* **1986**, *25*, 487–507; b) L. N. Lewis (General Electric Company), *Eur. Pat. Appl.* 447622 A2, **1991**, CA: **1992**, *116*, 107486d.
[11] S. F. Davison, B. E. Mann, P. M. Maitlis, *J. Chem. Soc. Dalton Trans.* **1984**, 1223–1228.

Soluble Organic Derivatives of Aluminosilicates with $Al_2Si_2O_4$ and $Al_4Si_2O_6$ Frameworks**

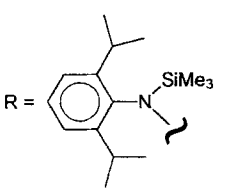
Mavis L. Montero, Isabel Usón, and Herbert W. Roesky*

Dedicated to Professor Klaus Möckel on the occasion of his 65th birthday

Although aluminosilicates are widely found in nature and have achieved great practical and commercial significance as zeolites, there are few soluble organic derivatives of these compounds.[1] Feher et al.[2] have described an $AlSi_7$ aluminosilasesquioxane; however, this is not very suitable for the construction of zeolites by the sol-gel process, because the Si–C bonds are almost inert towards hydrolysis. The aim of our investigations was therefore the synthesis of soluble organic derivatives of aluminosilicates, containing good leaving groups on the silicon and aluminum atoms. In an attempt to achieve this goal we treated the silanetriol **1**[3] with $HAliBu_2$ (**2**). Depending on the stoichiometry and the temperature of the reaction the organic derivatives **3** and **4** were obtained.



1 **2** **3**



Compound **3** was formed by the addition of **1** to a solution of **2** in THF at −78 °C. In this way the starting material **1** does not condense. Isobutane and hydrogen are formed in the reaction. Compound **3** is very soluble in common organic solvents, and single crystals can be obtained from *n*-hexane. The structure of **3** (Fig. 1) contains an eight-membered $Al_2Si_2O_4$ ring with bridging oxygen atoms. The ring has a chair conformation; the O(2) and O(2A) atoms lie 0.38 Å above the plane formed by the other six atoms (deviation 0.03 Å). The same structural unit is found in the mineral gismondine[4] $(CaAl_2Si_2O_8(H_2O)_4)_n$ in which, however, the condensed eight-membered $Al_2Si_2O_4$ rings exist in both the chair and boat conformations. The coordination at the aluminum atoms in **3** is distorted tetrahedral with bond angles of 99.4(2) to 116.2(2)°. The Al–O bond lengths within the ring (average 1.72 Å) are in very good agreement with the corresponding lengths in gismondine (1.75 Å). As expected the Al–O bonds to the coordinating THF molecules are longer (1.879(5) Å). The silicon atoms have likewise a distorted tetrahedral environment with bond angles of 106.2(2) to 113.6(2)°.

[*] Prof. Dr. H. W. Roesky, Dipl.-Chem. M. L. Montero, Dr. I. Usón
Institut für Anorganische Chemie der Universität
Tammannstrasse 4, D-37077 Göttingen (FRG)
Telefax: Int. code + (551)39 33 73

[**] This work was supported by the Deutsche Forschungsgemeinschaft, the Fonds der Chemischen Industrie, the Bundesministerium für Forschung und Technologie, and the Hoechst AG. I. U. thanks the European Community for a post-doctoral grant (ERB CHBG 93 0338).

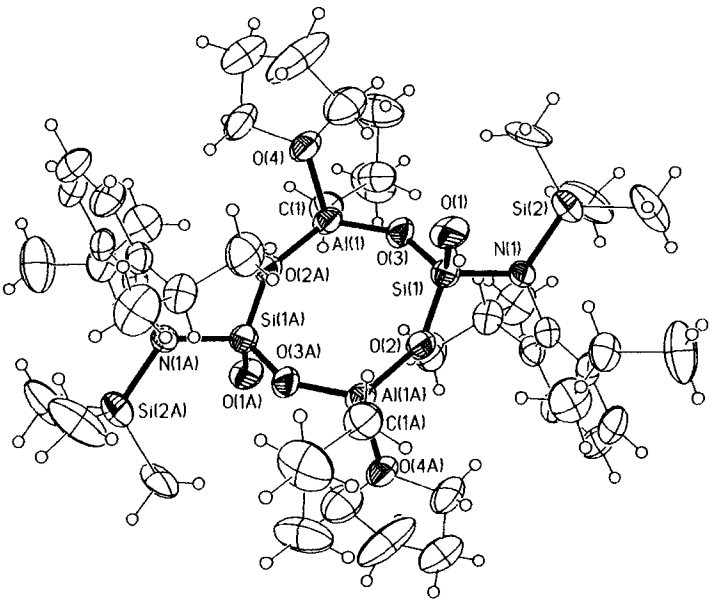
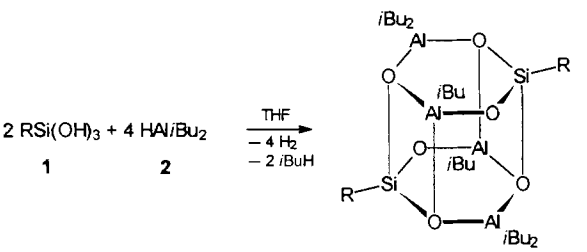


Fig. 1. Crystal structure of **3**. Selected bond lengths [Å] and angles [°]: Al(1)-O(2) 1.717(4), Al(1)-O(3) 1.718(4), Al(1)-O(4) 1.879(5), Al(1)-C(1) 1.945(7), Si(1)-O(2) 1.598(4), Si(1)-O(3) 1.590(4), Si(1)-O(1) 1.813(5), Si(1)-N(1) 1.735(5); O(2)-Al(1)-O(3) 116.1(2), O(3)-Al(1)-O(4) 99.4(2), O(3)-Al(1)-C(1) 116.2(3), O(2)-Al(1)-O(4) 100.2(2), O(2)-Al(1)-C(1) 113.1(3), O(4)-Al(1)-C(1) 109.3(3), O(2)-Si(1)-O(3) 113.6(2); O(2)-Si(1)-N(1) 108.9(2), O(3)-Si(1)-N(1) 111.1(2), O(2)-Si(1)-O(1) 109.8(2), O(3)-Si(1)-O(1) 106.2(2), O(1)-Si(1)-N(1) 107.0(2).

The average length of the endocyclic Si–O bonds (1.59 Å) is in good agreement with that in gismondine, whereas the exocyclic Si–O bonds are significantly longer (Si–OH 1.813(5) Å).[5] The OH stretch at 3413 cm^{-1} in the IR spectrum is characteristic for **3**.



1 **2** **4**

The reaction of **1** with **2** in the molar ratio 1:2 yields compound **4** as a colorless crystalline solid. The results of the crystal structure analysis of **4** (Fig. 2) show that the $Al_4Si_2O_6$ framework is built up of two four-membered $AlSiO_2$ and four six-membered Al_2SiO_3 rings, and can be described as a bitruncated distorted octahedron.[5]

The $Al_4Si_2O_6$ framework in **4** can be derived from the $Al_2Si_2O_4$ ring in **3** by the additional coordination of two aluminum atoms (Al(1), Al(1A)), which are bound to the hydroxy group at one silicon atom and to the two oxido bridging ligands at the other silicon atom in **3**. In order to make this coordination possible the eight-membered ring must be folded. In the resulting cage the coordination geometry of the six metal atoms deviates more strongly from tetrahedral geometry than in **3** (bond angles of 80.0–125.2° at the aluminum atoms and of 91.4–115.3° at the silicon atoms). The distances to the μ_2-oxygen atoms are almost as large as those in **3** and gismondine[4] (Al(1)–O(3)) 1.745(2), Si(1)–O(3) 1.598(2) Å), whereas the

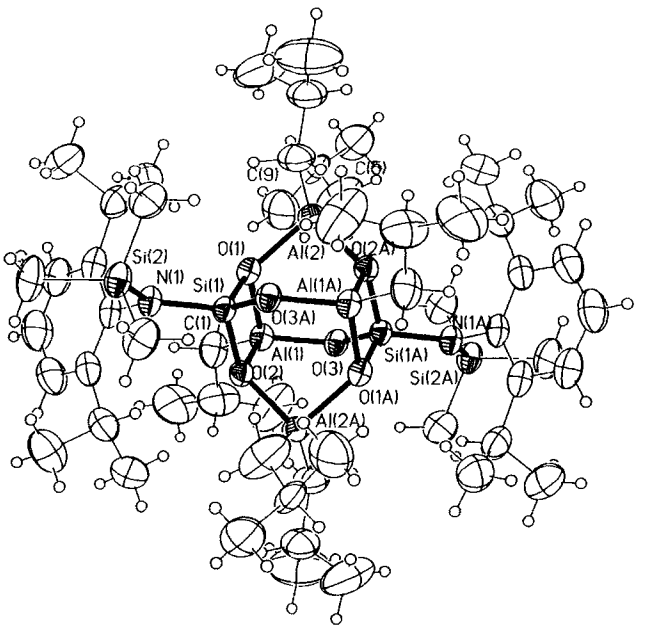


Fig. 2. Crystal structure of **4**. Selected bond lengths [Å] and angles [°]: Al(1)-O(2) 1.869(2), Al(1)-O(3) 1.745(2), Al(1)-O(1) 1.878(2), Al(1)-C(1) 1.933(3), Al(2)-O(1) 1.879(2), Al(2)-O(2) 1.882(2), Al(2)-C(5) 1.938(4), Al(2)-C(9) 1.976(3), Si(1)-O(3) 1.598(2), Si(1)-O(2) 1.680(2), Si(1)-O(1) 1.685(2), Si(1)-N(1) 1.688(2); O(3)-Al(1)-O(2) 103.54(9), O(3)-Al(1)-O(1) 104.09(9), O(2)-Al(1)-O(1) 79.98(9), O(3)-Al(1)-C(1) 123.4(1), O(2)-Al(1)-C(1) 118.5(1), O(1)-Al(1)-C(1) 118.4(1), O(1)-Al(2)-O(2) 95.33(9), O(1)-Al(2)-C(5) 111.1(2), O(2)-Al(2)-C(5) 106.5(2), O(1)-Al(2)-C(9) 110.1(1), O(2)-Al(2)-C(9) 103.9(1), C(5)-Al(2)-C(9) 125.2(2), O(3)-Si(1)-O(2) 110.3(1), O(2)-Si(1)-O(1) 91.4(1), O(3)-Si(1)-O(1) 110.5(1), O(3)-Si(1)-N(1) 112.8(1), O(2)-Si(1)-N(1) 114.7(1), O(1)-Si(1)-N(1) 115.3(1).

bonds to the μ_3-oxygen atoms are significantly longer (average Al–O 1.87, Si–O 1.69 Å).

The four silicon, the two nitrogen, two aluminum (Al(1), Al(1A)) and two oxygen atoms (O(3), O(3A)) lie in a plane (deviation 0.006 Å), which is perpendicular (89.8°) to the plane (deviation 0.006 Å) of the atoms Al(2), Al(2A), O(1), O(1A), O(2), and O(2A).

The compounds **3** and **4** should be particularly promising starting materials for the synthesis of new zeolites under mild conditions by sol-gel processes, because both the Si–N and the Al–C bonds can be readily cleaved hydrolytically.

Experimental Procedure

3: A solution of **1** (1.63 g, 5.00 mmol) in THF (30 mL) was added dropwise at −78 °C to a solution of $HAliBu_2$ (0.71 g, 5.00 mmol) in *n*-hexane/THF (5 mL, 20 mL) and stirred. The mixture was then allowed to warm to room temperature and volatiles were removed under vacuum. The residue was crystallized from *n*-hexane (30 mL) and **3** (3.85 g, 80%) was obtained. M.p. 178 °C; ^{1}H NMR (250 MHz, [D$_6$]DMSO, TMS): $\delta = -0.27$ (d, 2H, ^3J(H,H) = 6.5 Hz, $CH_2CH(CH_3)_2$), 0.03 (s, 9H, $Si(CH_3)_3$), 0.70 (m, 1H, $CH_2CH(CH_3)_2$), 0.81 (d, 6H, ^3J(H,H) = 6.5 Hz, $CH_2CH(CH_3)_2$), 1.06 (d, 6H, ^3J(H,H) = 6.9 Hz, $CH(CH_3)_2$), 1.13 (d, 6H, ^3J(H,H) = 6.9 Hz, $CH(CH_3)_2$), 1.77 (m, 4H, THF), 3.60 (m, 4H, THF), 3.85 (m, 2H, $CH(CH_3)_2$), 4.56 (s, 1H, OH), 6.80 (m, 3H, H_{arom}); ^{29}Si NMR (50 MHz, [D$_6$]DMSO, TMS): $\delta = -77.0$ ($SiO_2(OH)$), 1.27 ($Si(CH_3)_3$); IR (KBr, Nujol): $\tilde{\nu}$[cm^{-1}] = 3413, 1438, 1363, 1248, 1063, 963, 803, 685, 417; MS (EI): *m/z* (%): 234(20) [$Al_2Si_2O_6N_2^+$], 161 (100) [$C_{12}H_{17}^+$]; correct elemental analysis.

4: A solution of **2** (0.95 g, 6.70 mmol) was placed in *n*-hexane (35 mL) and THF (25 mL). A solution of **1** (1.10 g, 3.35 mmol) in THF (25 mL) was added dropwise to this at −78 °C over an hour. The mixture was allowed to warm to room temperature and subsequently heated to reflux for 3 h. Thereafter it was cooled to room temperature and the volatile components as well as the solvent were removed under vacuum. A white solid remained, which was dissolved in *n*-hexane (20 mL). On cooling this solution (−21 °C) **4** (1.12 g, 61%) was obtained as a white, microcrystalline solid. M.p. > 200 °C (decomp.); ^{1}H NMR (250 MHz, C_6D_6, TMS): $\delta = -0.43$ (d, 2H, ^3J(H,H) = 6.6 Hz, $CH_2CH(CH_3)_2$), 0.30 (s, 9H, $Si(CH_3)_3$), 0.50 (d, 4H, ^3J(H,H) = 6.6 Hz, $CH_2CH(CH_3)_2$), 0.87 (m, 3H, $CH_2CH(CH_3)_2$), 1.05 (d, 6H, ^3J(H,H) = 6.5 Hz, $(CH(CH_3)_2)$), 1.19–1.27 (m, 3H, $CH_2CH(CH_3)_2$), 1.42 (d, 6H, ^3J(H,H) = 6.5 Hz, $(CH(CH_3)_2)$), 3.61 (m, 2H, $CH(CH_3)_2$), 7.03 (m, 3H, H_{arom}); ^{29}Si NMR (79 MHz, C_6D_6, TMS): $\delta = -65.3(SiO_3)$, 12.5 ($Si(CH_3)_3$); IR (KBr, Nujol): $\tilde{\nu}$[cm^{-1}] = 1246, 1186, 1053, 915, 801, 684, 599, 483; MS(EI): *m/z* (%): 1041 (100) [$M^+ - CH_2CH(CH_3)_2$]; correct elemental analysis.

Received: May 11, 1994 [Z69251E]
German version: *Angew. Chem.* **1994**, *106*, 2198

[1] A. F. Wells, *Structural Inorganic Chemistry*, 5th ed., Clarendon, Oxford **1984**; S. Engels, *Anorganische Festkörperreaktionen*, Akademie, Berlin **1981**; A. Zecchina, G. Spoto, S. Bordiga, A. Ferrero, G. Petrini, G. Leofanti, M. Padovan, *Zeolite Chemistry and Catalysis* (Ed.: P. A. Jacobs), Elsevier, Amsterdam **1991**; F. Schwochow, L. Puppe, *Angew. Chem.* **1975**, *87*, 659; *Angew. Chem. Int. Ed. Engl.* **1975**, *14*, 620.

[2] a) F. J. Feher, T. A. Budzichowski, K. J. Weller, *J. Am. Chem. Soc.* **1989**, *111*, 7288; b) F. J. Feher, K. J. Weller *Organometallics*, **1990**, *9*, 2638.

[3] N. Winkhofer, A. Voigt, H. Dorn, H. W. Roesky, A. Steiner, D. Stalke, A. Reller, *Angew. Chem.* **1994**, *106*, 1414; *Angew. Chem. Int. Ed. Engl.* **1994**, *33*, 1352.

[4] K. Fischer, *Am. Mineral.* **1963**, *48*, 664.

[5] Crystal structure data of **3**: $C_{46}H_{88}Al_2N_2O_8Si_4$, $M_r = 963.50$, monoclinic, space group $P2_1/n$, $a = 10.333(2)$, $b = 20.258(3)$, $c = 14.059(3)$ Å, $\beta = 107.08(1)°$, $V = 2812.9(5)$ Å^3, $Z = 2$, $\rho_{calcd} = 1.138$ g cm^{-3}, $F(000) = 1048$, $\lambda = 0.71073$ Å, $T = 150$ K, $\mu(Mo_{K\alpha}) = 0.184$ mm^{-1}. The intensities were measured on a Stoe-Siemens AED four-circle diffractometer on a crystal with the dimensions $0.60 \times 0.15 \times 0.15$ mm in the range from $7° \leq 2\theta \leq 45°$ according to the Learnt-profile-method [6]. Of the 3793 reflections collected 3668 were independent and 3638 were used for the refinement of the structure. $R1 = \Sigma|F_o - F_c|/\Sigma F_o = 0.0718$ ($F > 4\sigma F$), $wR2 = [\Sigma w(F_o^2 - F_c^2)^2/\Sigma wF_o^4]^{1/2} = 0.2019$ (all data) for $w^{-1} = \sigma^2(F_o^2) + (g_1 \cdot P)^2 + g_2 \cdot P$ with $P = (F_o^2 + 2F_c^2)/3$ and $g_1 = 0.0399$ and $g_2 = 7.1139$; min./max. residual electron density: 0.487/−0.287 eÅ^{-3}. Crystal structure data of **4**: $C_{58}H_{106}Al_4N_2O_6Si_4 \cdot C_6H_{14}$, $M_r = 1185.86$, monoclinic, space group $P2_1/n$, $a = 13.115(2)$, $b = 18.531(3)$, $c = 15.395(3)$ Å, $\beta = 92.82(2)°$, $V = 3737.1(9)$ Å^3, $Z = 2$, $\rho_{calcd} = 1.054$ g cm^{-3}, $F(000) = 1300$, $\lambda = 0.71073$ Å, $T = 213$ K, $\mu(Mo_{K\alpha}) = 0.169$ mm^{-1}. The intensities were measured on a Stoe-Siemens AED four-circle diffractometer on a crystal with the dimensions $0.5 \times 0.5 \times 0.5$ mm in the range from $7° \leq 2\theta \leq 50°$ according to the Learnt-profile-method [6]. Of the 8925 reflections collected 6555 were independent and 6544 were used for the refinement of the structure. $R1 = \Sigma|F_o - F_c|/\Sigma F_o = 0.0531$ ($F > 4\sigma F$), $wR2 = [\Sigma w(F_o^2 - F_c^2)^2/\Sigma wF_o^4]^{1/2} = 0.1587$ (all data) for $w^{-1} = \sigma^2(F_o^2) + (g_1 \cdot P)^2 + g_2 \cdot P$ with $P = (F_o^2 + 2F_c^2)/3$ and $g_1 = 0.0826$ and $g_2 = 2.812$; min./max. residual electron density: 0.437/−0.420 eÅ^{-3}. Both structures were solved by direct methods (SHELXS-90) [7] and refined versus F^2 by the least squares method with all data (SHELXL-93) [8]. All non-hydrogen atoms were refined anisotropically. The hydrogen atoms were included in the refinement in ideal positions. Further details of the crystal structure investigations are available on request from The Director of the Cambridge Crystallographic Data Centre, 12 Union Road, GB-Cambridge CB2 1EZ (UK), on quoting the full journal citation.

[6] W. Clegg, *Acta Crystallogr. Sect. A* **1983**, *39*, 158.

[7] G. M. Sheldrick, *Acta Crystallogr. Sect. A* **1990**, *46*, 467.

[8] G. M. Sheldrick, SHELXL-93, Göttingen, **1993**.

NiO/CaO-Catalyzed Formation of Syngas by Coupled Exothermic Oxidative Conversion and Endothermic CO_2 and Steam Reforming of Methane

Vasant R. Choudhary,* Amarjeet M. Rajput, and Bathula Prabhakar

The safe, energy-efficient conversion of methane to syngas (with a H_2/CO ratio close to 2.0 for methanol and Fischer–Tropsch synthesis) with high conversion, selectivity, and yield is of great practical importance. In this way natural gas can be used effectively by its conversion to more valuable and/or easily transportable products.[1] Presently, syngas is produced from methane mostly by catalytic steam reforming,[2, 3] which suffers

[*] Dr. V. R. Choudhary, A. M. Rajput, Dr. B. Prabhakar
Chemical Engineering Division, National Chemical Laboratory
Pune 411008 (India)
Telefax: Int. code +(212)330233/334761

from several limitations such as a very high energy requirement, a high H_2/CO product ratio not suitable for methanol and Fischer–Tropsch synthesis, and poor selectivity for CO. Many research groups have attempted to convert methane to syngas without external energy by the catalytic partial oxidation of methane.[4–10] Although this conversion is mildly exothermic, a small decrease in CO selectivity (due to the total combustion of methane, which is highly exothermic) results in a large increase in the reaction temperature. In addition, a high methane conversion coupled with high space velocity (reaction rate per unit volume) leads to production of a large amount of heat in a small catalyst zone. Since it is very difficult to remove the reaction heat from the reactor, particularly for a large-scale operation, the process becomes very hazardous and/or difficult to control. We have overcome the limitations of the endo- and exothermic methane-to-syngas conversion processes and report here on the coupling of the two reactions, which are carried out simultaneously over the same catalyst (NiO/CaO) to produce syngas with a H_2/CO ratio close to 2.0. A very high conversion of methane is achieved at high space velocities and hence, with high productivity, energy efficiency, and safety. Our results show that by manipulating the process conditions (particularly the reaction temperature and CH_4/O_2, CH_4/CO_2, and CH_4/H_2O ratios in feed) the coupled process can be made mildly exothermic, nearly thermoneutral, or mildly endothermic. Thus little or no external energy is required, and this coupled process may be adapted for operation in a simple adiabatic reactor, which has several added advantages.

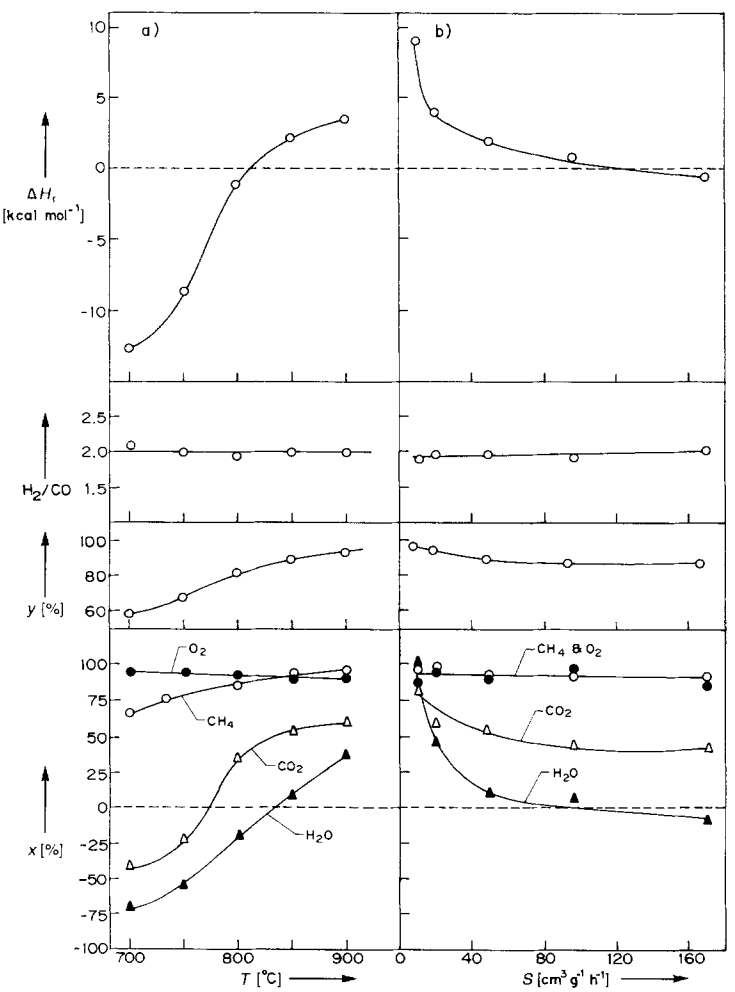


Fig. 1. Influence of a) reaction temperature T and b) space velocity S on the coupled process. x = conversion, y = CO yield or conversion of CH_4 and CO_2 to CO, ΔH_r = heat of reaction. a) $S = 48300\ cm^3 g^{-1} h^{-1}$, $CH_4/O_2 = 2.1$, $CH_4/CO_2 = 10$, $CH_4/H_2O = 10$; b) $T = 850\ ^\circ C$, $CH_4/O_2 = 2.1$, $CH_4/CO_2 = 10$, $CH_4/H_2O = 10$.

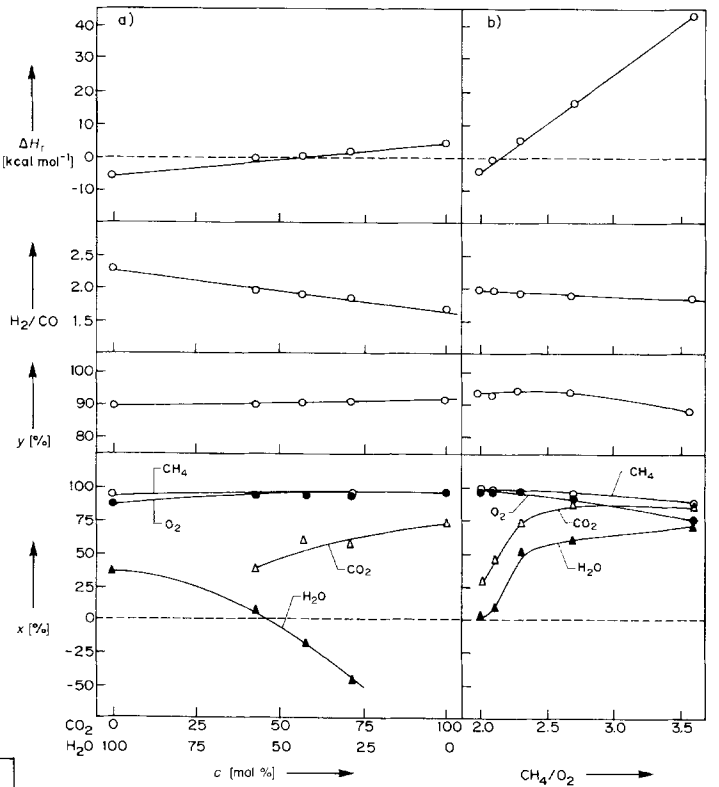


Fig. 2. Influence of a) relative concentration c of CO_2 and H_2O and b) CH_4/O_2 ratio in feed on the coupled process. x = conversion, y = CO yield or conversion of CH_4 and CO_2 to CO, ΔH_r = heat of reaction, S = space velocity. a) $T = 850\ ^\circ C$, $CH_4/O_2 = 2.1$, $CH_4/[O_2 + \frac{1}{2}(CO_2 + H_2O)] = 1.77$, $S = 47500\ cm^3 g^{-1} h^{-1}$; b) $T = 850\ ^\circ C$, $CO_2/H_2O = 1.0$, $CH_4/[O_2 + \frac{1}{2}(CO_2 + H_2O)] = 1.83$, $S = 48200\ cm^3 g^{-1} h^{-1}$.

Our results on the coupling of the two reactions under different process conditions are summarized in Figures 1 and 2. The negative conversions of CO_2 and H_2O indicate that these reactants are formed in the coupled process. The net heat of the reaction (ΔH_r) is estimated by subtracting the heat of formation (at the reaction temperature) of the components in feed from that of the components present in the product stream.

High methane conversions (above 90%) and a H_2/CO ratio close to 2.0 at high space velocities (hence with high CO productivity) are possible by adjusting the process conditions, particularly the reaction temperature and the CH_4/O_2 and $CH_4/(H_2O + CO_2)$ ratios in the feed. The H_2/CO ratio can be decreased or increased by increasing or decreasing, respectively, the CO_2/H_2O ratio in the feed. The coupled process occurs in a most energy-efficient and safe manner with the requirement of little or no external energy because the heat produced in the exothermic reactions is used for the endothermic reactions occurring simultaneously. The following exothermic and endothermic reactions occur in the coupled process (at 700–900 °C).

Exothermic Reactions

$$CH_4 + \tfrac{1}{2}O_2 \longrightarrow CO + 2H_2 + 5.2\ kcal\,mol^{-1} \quad (1)$$

$$CH_4 + 2O_2 \longrightarrow CO_2 + 2H_2O + 191.5\ kcal\,mol^{-1} \quad (2)$$

$$CO + H_2O \longrightarrow CO_2 + H_2 + 8.0\ kcal\,mol^{-1} \quad (3)$$

(water–gas shift reaction)

Endothermic Reactions

$$CH_4 + CO_2 \longrightarrow 2CO + 2H_2 - 62.2\ kcal\,mol^{-1} \quad (4)$$

$$CH_4 + H_2O \longrightarrow CO + 3H_2 - 54.2\ kcal\,mol^{-1} \quad (5)$$

The influence of various process parameters on the conversion of methane, O_2, CO_2, and H_2O, and on the H_2/CO ratio and the net heat of reaction (ΔH_r) in the coupled process is as follows:

1. When the temperature is increased the conversion of methane, CO_2, and H_2O increases but that of O_2 decreases (Fig. 1a); the H_2/CO product ratio is not changed, and the heat of reaction increases (i.e. exothermicity or endothermicity of the process decreases or increases, respectively).

2. Owing to the increase in the space velocity (Fig. 1b), the conversion of CO_2 and H_2O decreases but that of methane and O_2 is affected only to a very small extent. The H_2/CO ratio is not affected. However, the net heat of reactions is decreased.

3. With the increase in the concentration of CO_2 relative to that of H_2O in the feed (Fig. 2a), the conversion of CO_2 increases but that of H_2O decreases. The conversion of CH_4 and O_2 is almost unaffected. The H_2/CO ratio decreases and the heat of reaction increases. The desired H_2/CO ratio can be obtained by manipulating the relative concentrations of CO_2 and H_2O in the feed.

4. When the CH_4/O_2 ratio in the feed is increased (Fig. 2b), the conversion of CH_4 and O_2 decreases but that of CO_2 and H_2O increases; the H_2/CO ratio decreases and the net heat of reaction increases.

In general, when the reaction temperature and the CH_4/O_2 ratio are increased, the exothermicity of the process decreases (or the endothermicity of the process increases). When the space velocity is increased, the exothermicity increases because of the occurance of exothermic and endothermic reactions to different extents. Owing to the very low net heat of the reaction and consequently a low adiabatic temperature change, it may be possible to operate the coupled process adiabatically. A simple packed-bed reactor could be used which has much lower capital and process operation costs. However, for the adiabatic operation, the catalyst bed would probably no longer be isothermal.

Experimental Procedure

The NiO/CaO catalyst (Ni/Ca = 3.0) was prepared from a thick paste of thoroughly mixed, finely ground nickel nitrate, calcium hydroxide, and deionized water. The paste was dried and heated in air at 600 °C for 4 h. The solid was powdered, pressed without a binding agent, crushed to particles of 22–30 mesh, and calcined in air at 930 °C for 4 h. The catalytic oxidative conversion and CO_2 and steam reforming reactions were carried out at atmospheric pressure by continuously passing a mixture of pure methane, O_2, CO_2, and steam at different temperatures, feed ratios, and gas hourly space velocities (GHSV, measured at 0 °C and 1 atm) in a quartz microreactor (i.d.: 10 mm) containing about 0.2–1.0 g catalyst (pretreated at 930 °C for 1 h in a flow of moisture-free N_2). The reaction temperature was measured with a Chromel-Alumel thermocouple located in the catalyst bed. The water from the product stream was condensed at 0 °C. The feed and products were analyzed by an on-line gas chromatography. The C, H and O balances were within 4% error.

Received: March 24, 1994
Revised version: June 9, 1994 [Z 6794 IE]
German version: *Angew. Chem.* **1994**, *106*, 2179

[1] J. R. Anderson, *Appl. Catal.* **1989**, *47*, 177–196.
[2] *Encyclopedia of Chemical Technology*, *Vol. 12* (Eds.: R. E. Kirk, D. F. Othmer), 3rd ed., Wiley Interscience, New York, **1980**, p. 938.
[3] *Ullmann's Encyclopedia of Industrial Chemistry*, *Vol. A12*, 5th ed., VCH, Weinheim, **1989**, p. 169.
[4] A. T. Ashcroft, A. K. Cheetham, J. S. Foord, M. L. H. Green, C. P. Grey, A. G. Murrell, P. D. F. Vernon, *Nature* **1990**, *344*, 319–321.
[5] D. Dissanayake, M. P. Rosynek, K. C. C. Kharas, J. H. Lunsford, *J. Catal.* **1991**, *132*, 117–127.
[6] V. R. Choudhary, A. M. Rajput, B. Prabhakar, *Catal. Lett.* **1992**, *15*, 363–370; *J. Catal.* **1993**, *139*, 326–328.
[7] V. R. Choudhary, A. S. Mamman, S. D. Sansare, *Angew. Chem.* **1992**, *104*, 1273–1274; *Angew. Chem. Int. Ed. Engl.* **1992**, *31*, 1189–1190.
[8] J. A. Lapszewicz, X.-Z. Jiang, *Prepr. Am. Chem. Soc. Div. Petr. Chem.* **1992**, *37*(1), 252; **1993**, *38*(4), 815–818.
[9] D. A. Hickman, L. D. Schmidt, *Science* **1993**, *259*, 343–346; *J. Catal.* **1992**, *138*, 267–282.
[10] V.R. Choudhary, V. H. Rane, A. M. Rajput, *J. Phys. Chem.* **1992**, *96*, 8686–8688; *Catal. Lett.* **1993**, *22*, 289–295.

Purely Organic Mixed-Valence Molecules with Nanometric Dimensions Showing Long-Range Electron Transfer. Synthesis, and Optical and EPR Studies of a Radical Anion Derived from a Bis(triarylmethyl)Diradical**

Jacques Bonvoisin,* Jean-Pierre Launay, Concepció Rovira, and Jaume Veciana*

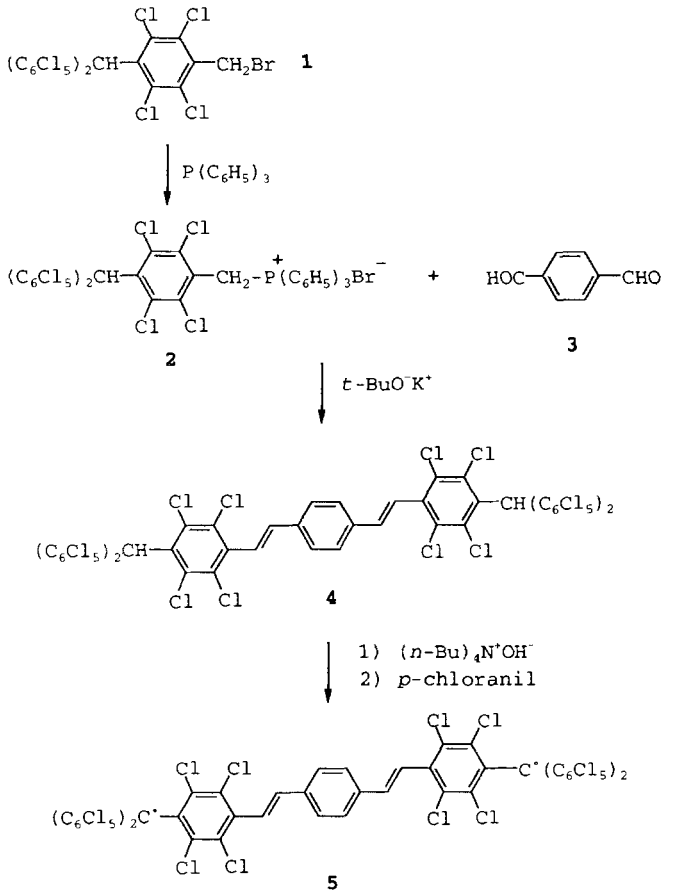
In the area of molecular electronics one of the big challenges is to design and produce molecular wires at least 100 Å long. So far these types of structures have been obtained only by lithography.[1] A molecular wire is composed of at least two redox sites linked by a bridge. One of the major purposes of this bridge is to mediate the transfer of electrons from one site to the other. Rules for the prediction and control of the electron propagation in these compounds would be particularly important. Although many organometallic compounds of this type are known, only few purely organic, mixed-valence compounds have been synthesized and studied up to now[2] owing to their high instability.

Polychlorinated triphenylmethyl radicals typically have high thermal and chemical stability. These electroactive species give, either chemically or electrochemically, the corresponding anions and cations, which are also quite stable species.[3] Thus it seemed interesting to prepare and study symmetrical molecules consisting of two of these radicals linked with different types of bridges. These diradicals could be converted by partial reduction or oxidation to the corresponding radical anions or radical cations. The resulting mixed valence species could therefore display interesting long-range electron transfer phenomena. At the same time this kind of symmetrical diradical could permit the study of the influence of the oxidation state of each redox site in the molecule on the electron transfer.

We report here on our study of the radical anion derived from **5**. This diradical contains two perchlorotriphenylmethyl radical units linked by an all-*trans* *p*-divinylbenzene bridge, which produces a nominal separation between redox centers of about 18.9 Å. This distance between the two methyl carbon atoms was determined with a CPK model and is practically independent of

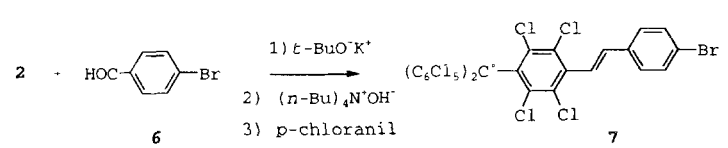
[*] Dr. J. Bonvoisin, Dr. J.-P. Launay
Molecular Electronics Group, CEMES-LOE/CNRS
29 rue Jeanne Marvig, F-31055 Toulouse Cedex (France)
Telefax: Int. code + 6225-7999
Dr. J. Veciana, Dr. C. Rovira
Institut de Ciència de Materials de Barcelona
Campus de la U.A.B., E-08193-Bellaterra (Spain)
Telefax: Int. code + (3)580-5729

[**] This work was supported by the Programa Nacional de Nuevos Materiales, (CICYT, grant no. MAT 91/0553), the Programa Nacional de Química Fina (CIRIT-CICYT, grant no. QFN91-4220-C01). J.-P. L. and J. B. thank the CNRS for financial support.



rotations about the single bonds of the divinylbenzene bridge. The related monoradical **7** was also prepared for comparison purposes.

The diradical **5** was synthesized from **1**[4] via **2** and **4**. **5** is a brown, microcrystalline, air-stable solid. The related monoradical **7** was prepared analogously from **2** and **6**, and shows physicochemical properties similar to those of **5**.[5]



The anions of **5** and **7** were prepared electrochemically in solution. The most important spectroscopic and electrochemical data for the compounds examined are listed in Table 1.

In a detailed magnetic study of diradical **5** based on EPR and magnetic susceptibility measurements in the temperature range of 4–300 K[6] a very weak magnetic interaction on the EPR timescale was observed between the two unpaired electrons over the entire temperature range. The estimated limits for the *intramolecular exchange coupling constant*, J^{intra}, of diradical **5** are $15\ cm^{-1} \gg J^{intra}/hc \gg 10^{-3}\ cm^{-1}$, as ascertained from EPR and magnetic susceptibility measurements.[7] Furthermore, the EPR spectrum of diradical **5** in a frozen rigid medium at 100 K shows that the average interspin separation is about 14 Å. This distance is somewhat smaller than the nominal separation of 18.9 Å between the two methyl carbon atoms where most of the spin density is localized. This result is in agreement with a certain degree of electronic conjugation in the π system of the molecule, owing to the *para* connectivity of the divinylbenzene bridge. Thus the effective separation of the redox sites in **5** is less than that determined with the CPK model.

Table 1. Spectroscopic and electrochemical data of the radical and anionic compounds [a].

Cmpd.	$\Delta H_{1/2}$	EPR [b] a^1H	$a^{13}C_x$	$a^{13}C_{arom}$	UV-VIS [c] $\lambda(10^3\ \varepsilon)$	Electrochemistry [d] $E_{1/2}$
5	0.95	0.95 (2H)	14.0	5.9, 6.4	339(33.1), 386(57.4), 440(20.7), 600(3.2)	−0.23
5$^{\bullet}$	0.85	1.90 (1H)	[e]	[e]	–	–
5^{2}	–	–	–	–	339(32.3), 522(49.3), 606(46.4)	
7	1.00	1.80 (1H)	29.5	10.7, 13	295(22.4), 386(28.2), 430(15.9), 567(1.5)	−0.32 [f]
7^{-}	–	–	–	–	301(18.3), 525(22.6) 570(22.9)	–

[a] In dichloromethane at room temperature, except for **5**$^{\bullet-}$ which was measured at 200 K. [b] Linewidths and hyperfine coupling constants (in Gauss) are computer-simulated values; *g*-values are 2.0027 ± 0.0003. [c] λ_{max} in nm, and ε in $M^{-1}cm^{-1}$. [d] nBu_4NPF_6 (0.1 M) as supporting electrolyte (vs SCE) Pt wire working electrode, 0.1 Vs^{-1} scan rate. [e] Not observed. [f] Irreversible process.

The electrochemical properties of **5** are in accord with the weak electronic interaction present in this diradical. The cyclic voltammogram of this diradical shows a unique and reversible two-electron reduction wave (Table 1), which was unambiguously confirmed by coulometry to occur at a constant potential of −0.4 V (versus the standard calomel electrode (SCE)). The reduction of **5** was also followed by UV/VIS-NIR spectroscopy. During the reduction the sharp band at 386 nm characteristic of **5** decreases and disappears completely, while the band at 339 nm does not change at all (Fig. 1). At the same time two new broad, intense bands at 522 and 606 nm grow in, which correspond to the continuous formation of the dianion **5**$^{2-}$. Finally, a weak, broad band centered at 1400 nm increases and then decreases during the reduction. This behavior corresponds to

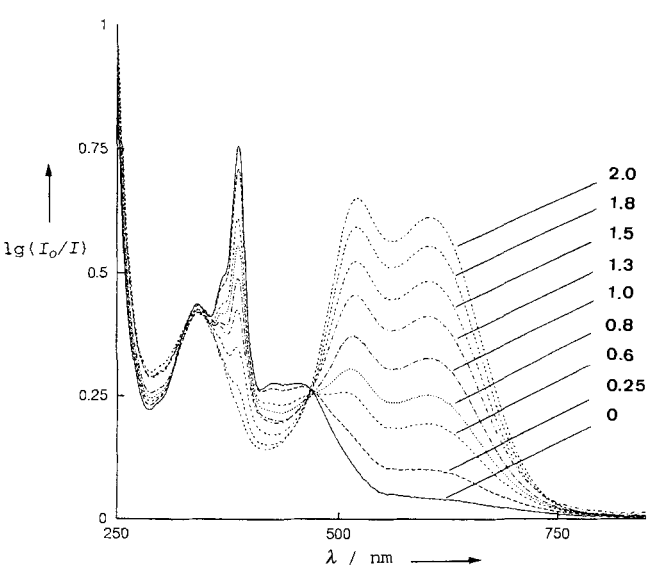


Fig. 1. Evolution of the electronic spectrum in the UV/VIS region in the course of the reduction of **5**. The number of added electrons is given on each spectrum.

that expected for an intermediate species showing intramolecular electron transfer (intervalence transition).[8]

This assignment was confirmed by theoretical calculations following the method employed by Nelsen et al.[9] The energy of an intervalence transition comes from two contributions, λ_{in} and λ_{out}, which correspond to the rearrangements of the internal medium (the molecule) and the outside medium, respectively. The internal Marcus term (λ_{in}) can be obtained by a suitable quantum chemical calculation.[9] Applying this method to $(C_6Cl_5)_3C^{\cdot}$ and using Dewar's semiempirical AM1 method,[10] provides a value of 4.93 kcal mol^{-1} for λ_{in}.[11] The outer shell term (λ_{out}) can be estimated with Equation (a).

$$\lambda_{out} = 332.4\ g(r,d)\ \gamma\ [\text{kcal mol}^{-1}] \qquad \text{(a)}$$

Equation (a) uses a dielectric continuum model with the geometrical parameter $g(r,d)$. The latter is calculated from r, the effective radius of the localized charge, which is represented as a sphere centered at the carbon atom in our case, and R, the distance between the centers of the carbon atoms [Eq. (b)]. γ is

$$g(r,d) = 1/r - 1/R \qquad \text{(b)}$$

the Marcus solvent parameter, which is 0.380 for CH_2Cl_2. With r = 5.4 Å, from the X-ray structure of the perchlorotriphenylmethyl radical,[12] and R = 14 Å (or 18.9 Å) as the distance between the redox sites, one obtains λ_{out} = 14.37 kcal mol^{-1} (or 16.70 kcal mol^{-1}) and finally λ = 19.30 kcal mol^{-1} (or 21.63 kcal mol^{-1}), that is, 0.837 eV (or 0.938 eV), in fairly good agreement with the experimental value of 0.787 eV (see below). Interestingly, λ_{in} provides a noteworthy contribution here, whereas in the related case of partly oxidized tertiary aromatic amines[13] this term was almost negligible relative to λ_{out}.

In order to experimentally determine the effective electronic coupling V_{ab} (in cm^{-1}) between the redox sites of **5** we can use the Hush equation (c). Here R is the effective separation of

$$V_{ab} = [2.05 \times 10^{-2} \sqrt{\varepsilon_{max}\, \bar{\nu}_{max}\, \Delta\bar{\nu}_{1/2}}]\, R^{-1} \qquad \text{(c)}$$

the redox sites (in Å), ε_{max} is the maximum extinction coefficient (in M^{-1} cm^{-1}), $\bar{\nu}_{max}$ is the transition energy, and $\Delta\bar{\nu}_{1/2}$ is the full width at half height (both in cm^{-1}) of the intervalence absorption band. The variation of this absorption band versus the average reduction state can be used to determine the comproportionation constants K_c according to Equation (d).[8]

$$K_C = [\mathbf{5}^{\cdot -}]^2/[\mathbf{5}][\mathbf{5}^{2-}] \qquad \text{(d)}$$

In the present case, K_c is 7. This value is employed in Equation (e) for the calculation of the corrected spectra (Fig. 2).

$$\varepsilon_{\cdot -} = [(2 + \sqrt{K_c})/\sqrt{K_c}]\varepsilon_{\cdot -\,(app)} - (\varepsilon_{\cdot\cdot} + \varepsilon_{2-})/\sqrt{K_c} \qquad \text{(e)}$$

$\varepsilon_{\cdot -}$ and $\varepsilon_{\cdot -\,(app)}$ are the true and the apparent extinction coefficients of the radical anion $\mathbf{5}^{\cdot -}$, and $\varepsilon_{\cdot\cdot}$ and ε_{2-} are the extinction coefficients of diradical **5** and dianion $\mathbf{5}^{2-}$, respectively.

Band deconvolution of the corrected spectrum of $\mathbf{5}^{\cdot -}$ was performed, assuming Gaussian profiles, in order to separate the intervalence band from bands of the nearby radical and/or anion chromophore. This deconvolution procedure has already been described elsewhere,[8] and has the advantage of giving a better estimate of the Marcus λ value. The following parameters for the intervalence absorption band gave satisfactory agreement with the experimental data: $\bar{\nu}_{max}$ = 6349 cm^{-1}

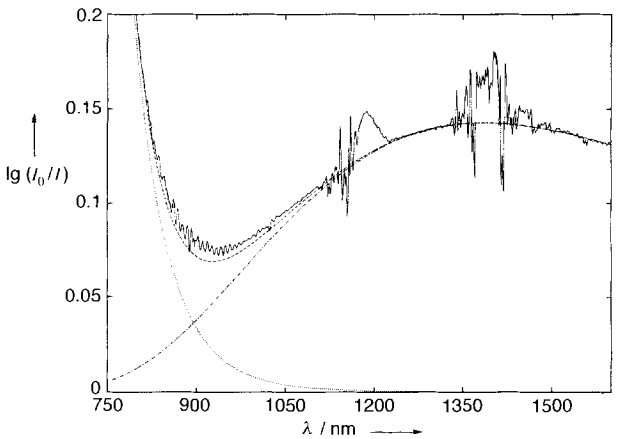


Fig. 2. Corrected electronic spectra for $\mathbf{5}^{\cdot -}$: — experimental spectrum; ---- simulated spectrum (sum of the intervalence transition band - - - - - - and the radical and/or anion chromophore transition band · · · ·). The two bands at 1200 and 1350 nm are artifacts due to solvent absorption.

(i.e. $\lambda = E_{opt}$ = 0.787 eV), $\Delta\bar{\nu}_{1/2}$ = 2940 cm^{-1}, and ε_{max} = 677 M^{-1} cm^{-1}. Finally, application of these parameters to Equation (c) provides the effective electronic coupling for $\mathbf{5}^{\cdot -}$. When 14 Å is used as the effective separation of the redox sites, V_{ab} is 167 cm^{-1} (0.021 eV). For R = 18.9 Å, V_{ab} = 122 cm^{-1} (0.015 eV) is obtained. This method has already been successfully employed to determine the V_{ab} parameter for several mixed-valence dinuclear ruthenium compounds.[8]

The electron transfer in $\mathbf{5}^{\cdot -}$ was also studied by EPR spectroscopy. The EPR spectrum of $\mathbf{5}^{\cdot -}$ at 200 K displays two symmetrical lines (Fig. 3a) with an ^{1}H hyperfine coupling constant very close to that of monoradical $\mathbf{7}^{\cdot}$ (Table 1). This result clearly demonstrates that at this temperature the unpaired electron of radical anion $\mathbf{5}^{\cdot -}$ is localized on the EPR timescale on one stilbene-like moiety only. When the temperature is increased, a new central line gradually emerges between the two initial ones. This evolution is consistent with the increase of the electron jump rate on going from 200 K (the slow-exchange limit) to 300 K (the fast-exchange limit) due to a thermally activated electron transfer between the two equivalent redox sites. The EPR spectra of $\mathbf{5}^{\cdot -}$ at various temperatures were fairly well simulated by using the parameters given in the Table 1 and the program of Heinzer.[14] The best fit was made by varying the rate constant k_{th} for the thermally activated electron transfer between the two equivalent sites. The experimental and simulated EPR spectra are compared in Figure 3; the simulation parameters are also included. The resulting k_{th} values give a linear Eyring plot [$\ln(k_{th}/T)$ vs $1/T$] with a correlation coefficient of 0.998. From the slope of this plot we have calculated a value for the barrier to the thermal electron transfer, $\Delta H^{\ddagger}$, of 2.69 kcal mol^{-1} K^{-1} (0.117 eV).

According to Hush theory, the energy of the intervalence transfer absorption band, E_{opt}, corresponds to the energy for the vertical electron transfer between the sites. In the limit of a vanishingly small electronic interaction, the barrier to the thermal electron transfer is then predicted to be one-quarter of E_{opt}, because of the usual parabolic shape of energy wells [Eq. (f)].

$$E_{opt} = 4\Delta H^{\ddagger} \qquad \text{(f)}$$

The difference between one-quarter of the experimental optical electron transfer energy (0.787 eV/4 = 0.197 eV) and the thermal electron transfer energy (0.117 eV) should be the effective electronic coupling, which in this case is 0.08 eV, a markedly higher value than that found experimentally with Equation (c)

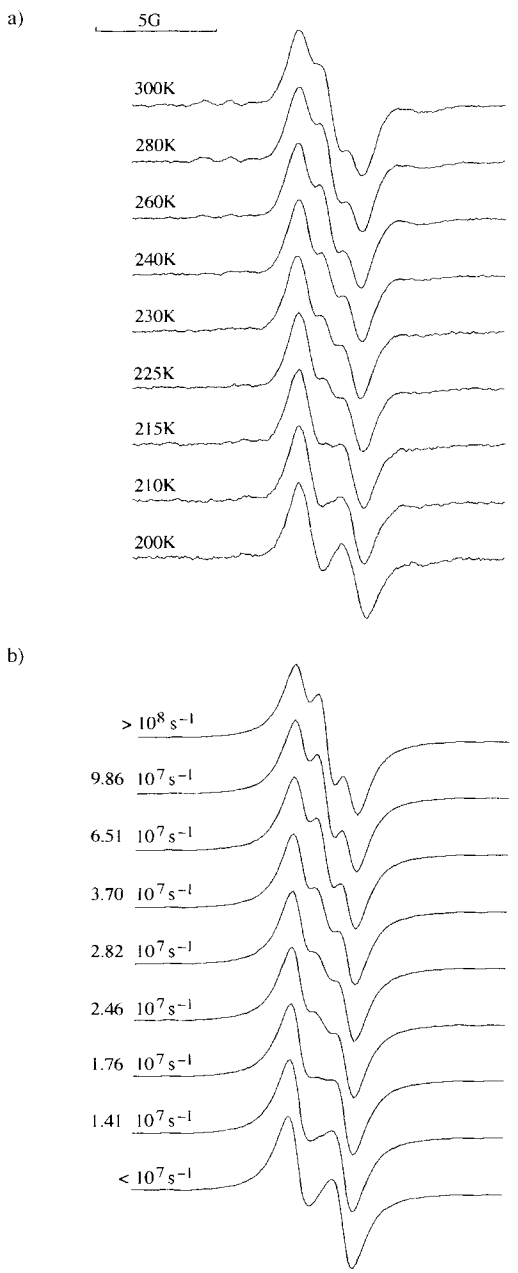


Fig. 3. Experimental (a) and simulated (b) EPR spectra of $5^{\bullet-}$ at different temperatures in CH_2Cl_2 with 0.1 M of nBu_4NPF_6. Spectra recorded at the very end of the reduction process. At this stage, the major species present in the solution is the EPR-silent dianion 5^{2-}. Most of the observed EPR signal is due to radical anion $5^{\bullet-}$, since for statistical reasons diradical **5** must have a negligible concentration. The simulated spectra were performed using a^1H (1 H) = 1.90 G, $\Delta H_{1/2}$ = 0.85 G, and the electron exchange rate constant given on each spectrum.

(0.015 to 0.02 eV). This discrepancy could come from the use of Equation (c) to calculate V_{ab}, which may not be correct for organic compounds. The separation R between the redox sites, which is employed in Equation (c), is not perfectly defined, because in the ground state the wavefunction of the electron is not fully localized on the radical carbon atom, but has important extensions on the adjacent phenyl rings. This has already been pointed out by Nelsen et al.[2a] and also by two of us[13] for organic nitrogen compounds. Alternatively, the discrepancy may result from nuclear tunneling effects, which may lead to an apparent lowering of the thermal activation barrier in organic compounds.[15a]

We have proved that $5^{\bullet-}$ displays an intervalence transition and have determined the thermal electron transfer energy. The radical anion is one of the rare examples for which optical and thermal electron transfer can be observed and correlated. The only other system for which such studies have been reported appeared very recently.[15b]

Received: May 3, 1994 [Z 6893 IE]
German version: *Angew. Chem.* **1994**, *106*, 2190

[1] P. B. Fischer, S. Y. Chou, *Appl. Phys. Lett.* **1993**, *62*, 2989; W. Chen, H. Ahmed, *J. Vac. Sci. Technol. B* **1993**, *11* (6), 2519; S. Itoua, C. Joachim, B. Rousset, N. Fabre, *Nanotechnology* **1994**, *5*, 1.

[2] a) S. F. Nelsen, J. A. Thomson-Colon, M. Katfory, *J. Am. Chem. Soc.* **1989**, *111*, 2809; b) T. H. Jozefiak, J. E. Almlöf, M. W. Feyereisen, L. L. Miller, *ibid.* **1989**, *111*, 4105; S. F. Rak, L. L. Miller, *ibid.* **1992**, *114*, 1388; c) A. H. Schroeder, S. Mazur, *ibid.* **1978**, *100*, 7339; S. Mazur, C. Streekumar, A. H. Schroeder, *ibid.* **1976**, *98*, 6713; d) S. Utamapanya, A. Rajca, *ibid.* **1991**, *113*, 9242; e) J. P. Telo, C. B. L. Shohoji, B. Herold, G. Grampp, *J. Chem. Soc. Faraday Trans.* **1992**, *88*, 47; G. Grampp, W. Harrer, W. Jaenicke, *ibid.* **1987**, *83*, 161, and references therein.; f) F. Gerson, T. Wellauer, A. M. Oliver, M. N. Paddon-Row, *Helv. Chim. Acta* **1990**, *73*, 1586, and references therein; g) M. Ballester, I. Pascual, J. Riera, J. Castañer, *J. Org. Chem.* **1991**, *56*, 217.

[3] M. Ballester, J. Riera, J. Castañer, A. Rodriguez, *Tetrahedron Lett.* **1971**, 2079; M. Ballester, J. Riera, J. Castañer, J. Veciana, C. Rovira, *J. Org. Chem.* **1982**, *47*, 4498; M. Ballester, *Acc. Chem. Res.* **1985**, *18*, 380; J. Veciana, J. Riera, J. Castañer, N. Ferrer, *J. Organomet. Chem.* **1985**, *297*, 131; O. Armet, J. Veciana, C. Rovira, J. Riera, J. Castañer, E. Molins, J. Rius, C. Miravitlles, S. Olivella, J. Brichfeus, *J. Phys. Chem.* **1987**, *91*, 5608, and references therein.

[4] M. Ballester, J. Veciana, J. Riera, J. Castañer, C. Rovira, O. Armet, *J. Org. Chem.* **1986**, *51*, 2472.

[5] Diradical **5**: dark brown microcrystals (85%); m.p. 268–269 °C. IR (KBr): $\tilde{\nu}$ [cm^{-1}] = 3025(w), 1624(w), 1510(m), 1330(vs), 1255(s), 960(w), 810(m), 800(m); VIS (THF): λ_{max} (log ε) = 338 (4.49), 384 (4.77), 422 (4.25), 458 (4.27), 605 (3.61) nm; magnetic suszeptibility (4–300 K): $\theta = -11$ K, $\mu_{eff} = 2.41\ \mu_B$. Radical **7**: dark green microcristals (90%); m.p. 244–245 °C. IR (KBr): $\tilde{\nu}$ [cm^{-1}] = 3024(w), 1630(w), 1585(w), 1505(m), 1485(m), 1400(m), 1330(vs), 815(m), 805(m), 735(m); UV-VIS ($_6H_{12}$). λ_{max} (log ε) = 295 (4.37), 383 (4.45), 425 (4.23), 567 (3.17) nm; magnetic susceptibility (80–300 K) $\theta = -2$ K, $\mu_{eff} = 1.78\ \mu_B$.

[6] C. Rovira, J. Veciana, O. Armet, J. Castañer, J. Riera, E. Vincent, P. Radhakrishna, *Mol. Cryst. Liq. Cryst.* **1988**, *156*, 301.

[7] The upper limit of J^{intra} was determined from the experimental Weiss constant and the Bleaney–Bowers expression for a dimer using the approximation for the high-temperature limit. See R. L. Carlin, *Magnetochemistry*, Springer, Berlin, **1986**, p. 76. The lower limit of J^{intra} was deduced from the value of the ^1H hypefine coupling constant showed by **5**. See L. Salem, C. Rowland, *Angew. Chem.* **1972**, *84*, 86, *Angew. Chem. Int. Ed. Engl.* **1972**, *11*, 92.

[8] A. C. Ribou, J. P. Launay, K. Takahashi, T. Nihira, S. Tarutani, C. W. Spangler, *Inorg. Chem.*, **1994**, *33*, 1325.

[9] S. F. Nelsen, S. C. Blackstock, Y. Kim, *J. Am. Chem. Soc.* **1987**, *109*, 677.

[10] MOPAC 93.00, J. J. P. Stewart; M. J. S. Dewar, E. G. Zoebish, E. F. Healy, J. P. Stewart, *J. Am. Chem. Soc.* **1985**, *107*, 3902; M. J. S. Dewar, E. G. Zoebish, *J. Mol. Struct. (Theochem)* **1988**, *180*, 1.

[11] In the AM1 calculations the geometry was optimized and UHF option was used for the open-shell neutral radical.

[12] J. Rius, C. Miravitlles, E. Molins, M. Crespo, J. Veciana, *Mol. Cryst. Liq. Cryst.* **1990**, *187*, 155.

[13] J. Bonvoisin, J.-P. Launay, M. van der Auweraer, F. C. de Schryver, *J. Phys. Chem.* **1994**, *98*, 5052.

[14] J. Heinzer, *Mol. Phys.* **1971**, *22*, 167; *Quantum Chemistry Program Exchange* **1972**, No. 209.

[15] a) S. Nelsen, H. Chang, J. J. Wolff, J. Adamus, *J. Am. Chem. Soc.* **1993**, *115*, 12276; b) S. Nelsen, J. Adamus, J. J. Wolff, *ibid.* **1994**, *116*, 1589.

Polynuclear Lanthanide Complexes: Formation of a Selenium-Centered Sm_6 Complex, $[\{(C_5Me_5)Sm\}_6Se_{11}]$**

William J. Evans,* Gerd W. Rabe, Mohammad A. Ansari, and Joseph W. Ziller

We have been exploring the utility of the organosamarium complexes $[(C_5Me_5)_2Sm(thf)_2]$[1] and $[(C_5Me_5)_2Sm]$[2] in the assembly of unusual polyelement anions involving the main group elements. $[(C_5Me_5)_2Sm]$ complexes containing $(Bi_2)^{2-}$, $(Sb_3)^{3-}$, and $(Se_3)^{2-}$ ions have been obtained from $BiPh_3$,[3] $SbnBu_3$,[4] and elemental selenium.[5] The chemistry of Group 16 elements has proven to be complicated, since several series of compounds can form depending upon reaction conditions and the stoichiometries of the reagents. For example, for E = S, Se, Te two classes of complexes, $[\{(C_5Me_5)_2Sm(thf)\}_2(\mu\text{-}E)]$ and $[\{(C_5Me_5)_2Sm\}_2(\mu\text{-}\eta^1\text{:}\eta^3\text{-}Se_3)(thf)]$ have been fully identified and can be interconverted.[5, 6] $(E_2)^{2-}$ complexes are also accessible in this system, as exemplified by the synthesis of $[\{(C_5Me_5)_2Sm\}_2(\mu\text{-}\eta^2\text{:}\eta^2\text{-}Te_2)]$.[5, 7] Other complexes were observed in the $(C_5Me_5)_2Sm/E$ system, but until now were not identifiable.

We report here a new product from this reaction system, $[\{(C_5Me_5)Sm\}_6Se_{11}]$ (**1**), the first representative of a new class of polynuclear lanthanide complexes. Since complex **1** contains seventeen samarium and selenium atoms, it may be of interest for preparation of dilute semiconducting materials containing lanthanide metals and chalcogenides, an area which has recently seen considerable activity.[8–12] Complex **1** also appears to be unique among chalcogen compounds. Although numerous transition metal/chalcogenide clusters stabilized with substituted phosphanes, thiols, or organic ligands are known,[13] none have the structure found in **1**.

Complex **1** is reproducibly obtained from NMR samples of $[\{(C_5Me_5)_2Sm\}_2(\mu\text{-}\eta^1\text{:}\eta^3\text{-}Se_3)(thf)]$ (**2**)[5] in toluene at ambient temperature over three to seven days in a nitrogen-containing glovebox. Single crystals with the same unit cell parameters were obtained from three different samples of **2** in toluene, but crystals were not obtained from benzene. Attempts to synthesize S and Te analogues by this method have been so far unsuccessful. The low solubility of **1** in solvents with which it does not react has hampered characterization by NMR spectroscopy, but **1** could be definitively identified by X-ray crystallography (Fig. 1).[14]

The six $(C_5Me_5)Sm$ units in **1** describe an octahedron distorted in one plane such that the only Sm-Se-Sm angles which are not close to the expected 90° and 180° values are the 74.6(1)° Sm(1)-Se(6)-Sm(3) and 105.4(1)° Sm(1′)-Se(6)-Sm(3) angles (and their inversion-symmetry equivalents). The $Sm-C(C_5Me_5)$ distances (2.679 Å average) clearly indicate the presence of Sm^{III}, since no $Sm^{II}-C(C_5Me_5)$ distance less than 2.79(1) Å has been reported.[15, 16]

The eleven Se atoms in **1** can be divided into three sets. There are four pairs of selenium atoms, Se(1)–Se(2), Se(4)–Se(5), and their inversion equivalents, which have Se–Se distances of 2.376(2) and 2.361(2) Å. These distances are similar to those found in other structures containing $(Se_2)^{2-}$ ions.[17] In each of these pairs, one selenium atom, Se(1) and Se(5), is 2.869(2) to 2.880(2) Å from two samarium atoms. These distances are longer than the 2.782(1) and 2.779(1) Å Sm–Se distances in $[\{(C_5Me_5)_2Sm(thf)\}_2(\mu\text{-}Se)]$,[5] but shorter than the 2.917(1) to 3.007(1) Å distances in $[\{(C_5Me_5)_2Sm\}_2(\mu\text{-}\eta^1\text{:}\eta^3\text{-}Se_3)(thf)]$.[5] The other selenium atoms in each pair Se(2) and Se(4), are oriented toward three samarium atoms at longer distances, 2.989(2) to 3.308(2) Å.

The second type of selenium in **1** is the unique central Se(6) which is located 3.123(1) to 3.186(1) Å from the six samarium atoms. The third type of selenium in **1**, Se(3) (and its inversion equivalent), is located 2.859(2) to 2.951(2) Å from three samarium atoms. Se(6), Se(3), and Se(3′) must bear a −4 charge to make up the difference between the four $(Se_2)^{2-}$ ions and the six $[(C_5Me_5)Sm]^{2+}$ units. A $(Se_3)^{4-}$ ion has never been identified in the past to our knowledge, but it is isoelectronic with the known $(I_3)^-$ ion.[18, 19] The 2.749(2) Å Se(3)–Se(6) distance is consis-

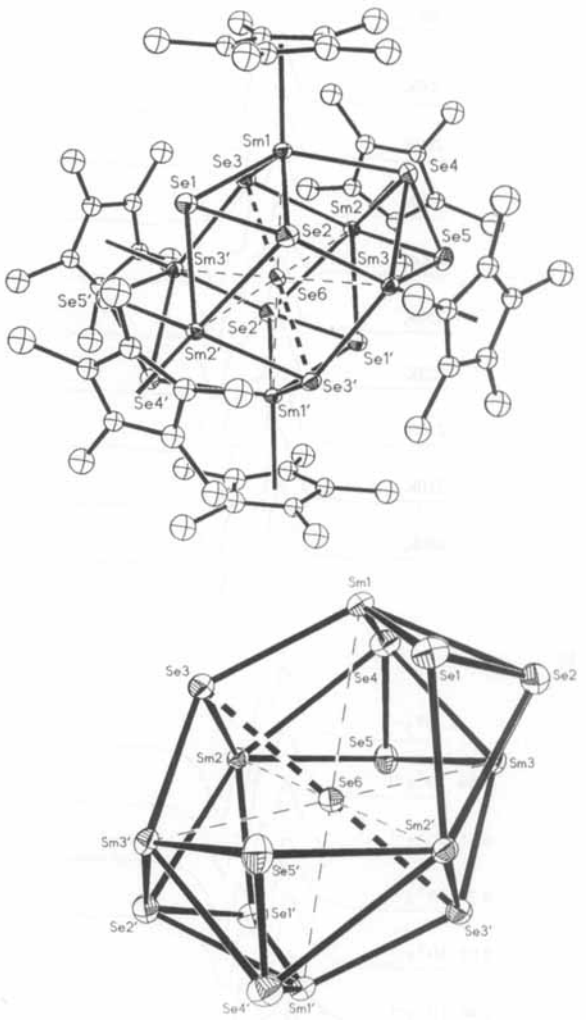


Fig. 1. Top: Molecular structure of **1**. Bottom: Structure of the central Sm_6Se_{11} core of **1**. Important distances [Å] and angles [°]: Sm(1)-Se(1) 2.869(2), Sm(1)-Se(2) 3.036(2), Sm(1)-Se(3) 2.859(2), Sm(1)-Se(4) 2.989(2), Sm(1)-Se(6) 3.182(2), Sm(2)-Se(1′) 2.880(2), Sm(2)-Se(3) 2.951(2), Sm(2)-Se(4) 3.308(2), Sm(2)-Se(6) 3.123(1), Sm(2)-Se(2′) 3.237(2), Sm(3)-Se(2) 3.026(2), Sm(3)-Se(4) 2.994(2), Sm(3)-Se(5) 2.878(2), Sm(3)-Se(6) 3.186(1), Se(1)-Se(2) 2.376(2), Se(3)-Se(6) 2.749(2), Se(4)-Se(5) 2.361(2); Sm(1)-Se(1)-Sm(2′) 104.0(1), Sm(1)-Se(2)-Sm(3) 79.0(1), Sm(1)-Se(2)-Sm(2′) 92.4(1), Sm(1)-Se(3)-Sm(2) 98.1(1), Sm(1)-Se(4)-Sm(2) 88.2(1), Sm(3)-Se(4)-Sm(2) 92.6(1), Sm(1)-Se(4)-Sm(3) 80.3(1), Sm(3)-Se(5)-Sm(2) 105.0(1), Sm(1)-Se(6)-Sm(1′) 180.0(1), Sm(1)-Se(6)-Sm(2) 88.2(1), Sm(1)-Se(6)-Sm(3) 74.6(1), Sm(3)-Se(6)-Sm(2) 92.6(1), Se(3)-Se(6)-Se(3′) 180.0(1).

[*] Prof. W. J. Evans, Dr. G. W. Rabe,[+] Dr. M. A. Ansari, Dr. J. W. Ziller
Department of Chemistry, University of California
Irvine, CA 92717 (USA)

[+] New address: Anorganisch-chemisches Institut
der Technischen Universität München

[**] This work was supported by the National Science Foundation (USA). G. W. R. thanks the Stiftung Stipendien-Fonds des Verbandes der Chemischen Industrie (FRG) for a Liebig fellowship.

tent with a $(Se_3)^{4-}$ ion: it is longer than the 2.37 Å average single bond length in $(Se_2)^{2-}$ species, just as the 2.901(1) and 2.904(1) Å I–I distances[19] in symmetrical $(I_3)^-$ are longer than the 2.70 Å single bond length in I_2.[20] Precedence for chalcogen–chalcogen distances longer than typical single bonds is found in the $(Te_7)^{4-}$ ion.[21, 22]

It is unlikely that hexanuclear **1** is unique in lanthanide chemistry. The closest organolanthanide complexes in the literature are the oxo-centered square-pyramidal systems $[(C_5H_5)_5Ln_5(OMe)_8O]$ (Ln = Y[23], Gd[24]) and the capped butterfly fluoride complex $[(C_5Me_5)_6Yb_5F_9]$.[25] The mechanism of formation of **1** and related species is under investigation.

Received: April 13, 1994 [Z 6843 IE]
German version: *Angew. Chem.* **1994**, *106*, 2200

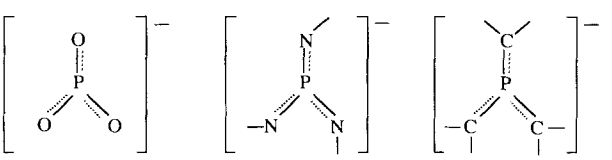
[1] W. J. Evans. *Polyhedron* **1987**, *6*, 803.
[2] W. J. Evans, L. A. Hughes, T. P. Hanusa, *J. Am. Chem. Soc.* **1984**, *106*, 4270.
[3] W. J. Evans, S. L. Gonzales, J. W. Ziller, *J. Am. Chem. Soc.* **1991**, *113*, 9880.
[4] W. J. Evans, S. L. Gonzales, J. W. Ziller, R. J. Doedens, *J. Chem. Soc. Chem. Commun.* **1992**, 1138.
[5] W. J. Evans, G. W. Rabe, J. W. Ziller, *Inorg. Chem.* **1994**, *33*, 2719.
[6] D. J. Berg, C. J. Burns, R. A. Andersen, A. Zalkin, *Organometallics* **1989**, *8*, 1865.
[7] A. Zalkin, D. J. Berg, *Acta Crystallogr. Sect. C* **1988**, *44*, 1488.
[8] A. G. Strzelecki, P. A. Timinski, B. A. Helsel, P. A. Bianconi, *J. Am. Chem. Soc.* **1992**, *114*, 3159.
[9] D. R. Cary, J. Arnold, *J. Am. Chem. Soc.* **1993**, *115*, 2520.
[10] a) M. Berardini, T. J. Emge, J. G. Brennan, *J. Am. Chem. Soc.* **1993**, *115*, 8501; b) M. Berardini, T. J. Emge, J. G. Brennan, *J. Chem. Soc. Chem. Commun.* **1993**, 1537.
[11] a) I. P. Parkin, J. C. Fitzmaurice, *Polyhedron* **1993**, *12*, 1569; b) W. E. Piers, L. R. MacGillivray, M. Zaworotko, *Organometallics* **1993**, *12*, 4723.
[12] A. Recknagel, M. Noltemeyer, D. Stalke, U. Pieper, H.-G. Schmidt, F. T. Edelmann, *J. Organomet. Chem.* **1991**, *411*, 347.
[13] a) D. Fenske, J. Ohmer, J. Hachgenei, K. Merzweiler, *Angew. Chem.* **1988**, *100*, 1300; *Angew. Chem. Int. Ed. Engl.* **1988**, *27*, 1277; b) I. G. Dance, *Polyhedron* **1986**, *5*, 1037.
[14] Crystal data for **1** · 2 toluene: $C_{74}H_{106}Se_{11}Sm_6$, monoclinic $P2_1/n$, a = 13.715(2), b = 14.427(4), c = 21.486(4) Å, β = 103.626(15)°, V = 4131.9(16) Å^3, at 163 K. $R(F) = 0.055$ for 4505 reflections having ($|F_o| > 3.0\sigma|F_o|$). The structure was solved by direct methods (SHELXTL) and refined by least-squares techniques. Hydrogen atoms were included using a riding model with d(C-H) = 0.96 Å. All the heavy atoms were refined anisotropically, and carbon atoms were refined isotropically. Further details of the crystal structure investigation may be obtained from the Fachinformationszentrum Karlsruhe, D-76344 Eggenstein-Leopoldshafen (FRG), on quoting the depository number CSD-58274.
[15] W. J. Evans, S. E. Foster, *J. Organomet. Chem.* **1992**, *433*, 79.
[16] W. J. Evans, J. W. Grate, H. W. Choi, I. Bloom, W. E. Hunter, J. L. Atwood, *J. Am. Chem. Soc.* **1985**, *107*, 941.
[17] M. A. Ansari, J. A. Ibers, *Coord. Chem. Rev.* **1990**, *100*, 223.
[18] a) M. B. Cingi, A. M. M. Lanfredi, A. Tiripichio, G. Bandoli, D. A. Clemente, *Inorg. Chim. Acta* **1981**, *52*, 237; b) K.-F. Tebbe, B. Freckmann, M. Hörner, J. Strähle, *Acta Crystallogr. Sect. C* **1985**, *41*, 660.
[19] G. V. Gridunova, V. E. Shklover, Y. T. Struchkov, V. D. Vil'chevskaya, N. L. Podobedova, A. I. Krylova, *J. Organomet. Chem.* **1982**, *238*, 297.
[20] R. W. G. Wyckoff, *Crystal Structures, Vol. 1*, 2nd ed., Interscience, New York, **1963**, p. 53.
[21] J. M. McConnachie, M. A. Ansari, J. C. Bollinger, R. J. Salm, J. A. Ibers, *Inorg. Chem.* **1993**, *32*, 3201.
[22] U. Müller, C. Grebe, B. Neumüller, B. Schreiner, K. Z. Dehnicke, *Z. Anorg. Allg. Chem.* **1993**, *619*, 500.
[23] W. J. Evans, M. S. Sollberger, *J. Am. Chem. Soc.* **1986**, *108*, 6095.
[24] H. Schumann, G. Kociok-Köhn, J. Loebel, *Z. Anorg. Allg. Chem.* **1990**, *581*, 69.
[25] P. L. Watson, T. H. Tulip, I. Williams, *Organometallics* **1990**, *9*, 1999.

Monomeric Tris(imino)metaphosphates**

Edgar Niecke,* Matthias Frost, Martin Nieger, Volker von der Gönna, Alexander Ruban, and Wolfgang W. Schoeller

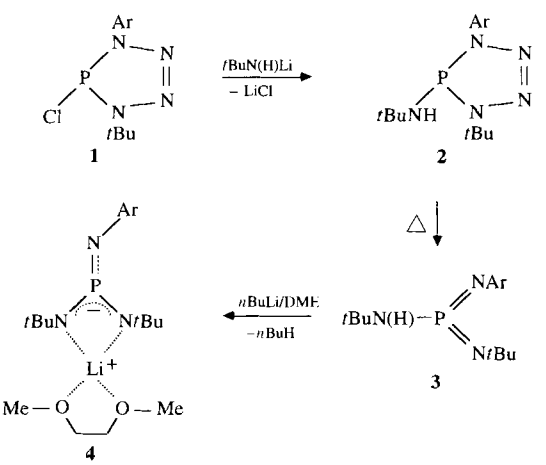
Dedicated to Professor Nils Wiberg on the occasion of his 60th birthday

The existence of monomeric metaphophosphate (**I**) in the gas phase[1] and in the matrix[2] is well-documented. Furthermore, **I** is discussed as a component of mechanistic processes in a series of phosphorylation reactions in solution.[3] Theoretical studies on **I** as well as on anions of the general type $[PXYZ]^-$ (X,Y,Z = O, S, CH_2) reveal the unusual electronic behavior of such species;[4] to date only one representative of the type **III** has been isolated and structurally characterized in the form of its lithium salt.[5, 6] We report here on the synthesis and structure of the lithium salts of tris(imino)metaphosphates (**II**), which exist either as lithium complexes[7] or as "separated ions" depending on their substituents.



I II III

The reaction of the chlorodihydrotetrazaphosphole **1**[8] (Ar = 2,4,6-tri-*tert*-butylphenyl) with lithium *tert*-butyl amide affords the amine **2**, which can be converted thermally with elimination of N_2 into the aminobis(imino)phosphorane **3**. Subsequent metalation with *n*-butyllithium in 1,2-dimethoxyethane (DME) leads to the lithium complex **4** of the

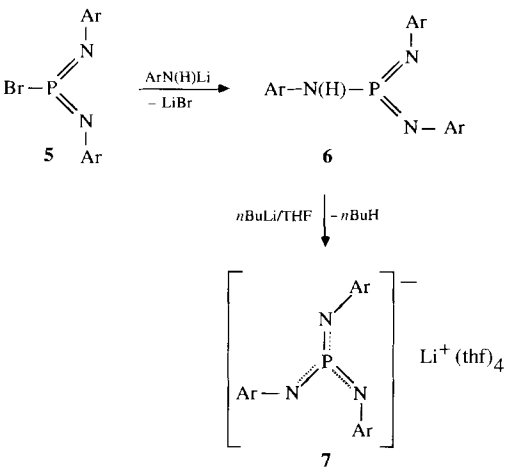


1 2 3 4

[*] Prof. Dr. E. Niecke, Dr. M. Frost, Dr. M. Nieger, Dr. V. von der Gönna, Dr. A. Ruban
Anorganisch-chemisches Institut der Universität
Gerhard-Domagk-Stasse 1, D-53121 Bonn (FRG)
Telefax: Int. code + (228) 735327
Prof. Dr. W. Schoeller
Fakultät für Chemie der Universität Bielefeld (FRG)

[**] This work was supported by the Deutsche Forschungsgemeinschaft (SFB 334) and the Fonds der Chemischen Industrie.

tris(imino)metaphosphate. The free anion in **7** can be obtained from the bromobis(imino)phosphorane **5**[9] by Br/NHAr exchange to give **6** followed by metalation in THF.



The composition and constitution of the precursors **2**, **3**, and **6** can be obtained from the high-resolution mass spectrum (molecular ion) and the results of multinuclear NMR measurements. The structures of the lithium tris(imino)metaphosphates **4** and **7** were elucidated by X-ray crystal structure analyses.[10] Figure 1 shows the structure of the lithium complex **4**. The

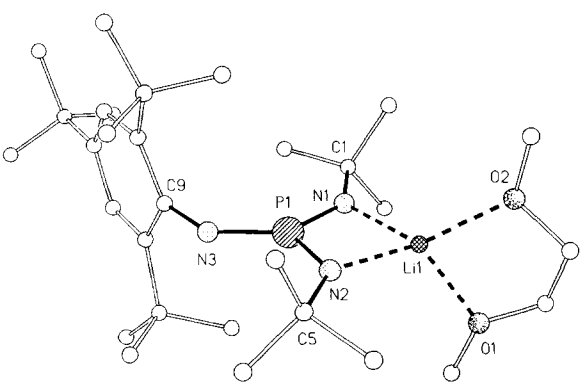


Fig. 1. Crystal structure of **4**. Selected bond lengths [pm] and angles [°]: P1-N1 155.4(2), P1-N2 156.7(2), P1-N3 154.3(2), N1-Li1 202.1(5), N2-Li1 197.9(5); N1-P1-N2 105.3(1), N2-P1-N3 121.1(1), N1-P1-N3 133.6(1), P1-N1-Li1 88.4(2), P1-N2-Li1 89.6(2), N1-Li1-N2 76.6(2), P1-N1-C1 139.7(2), P1-N2-C5 131.1(2), P1-N3-C9 131.9(2).

phosphorus atom resides in a trigonal-planar environment. The carbon atoms of the substituents linked with the nitrogen atoms also lie in this plane; of these the two *tert*-butyl groups at N1 and N2 have an *exo*/*exo* arrangement. The formation of two N–Li bonds (197.9 and 202.1 pm) as well as a relatively small N1-P1-N2 angle at phosphorus (105.3°) is associated with this conformation. A similar bonding situation is shown by 1,3-diaza-2-phosphaallyllithium complexes.[14] The P–N distances (154.3–156.7 pm) in **4** are significantly longer than those in the corresponding substituted bis(imino)phosphoranes.[15]

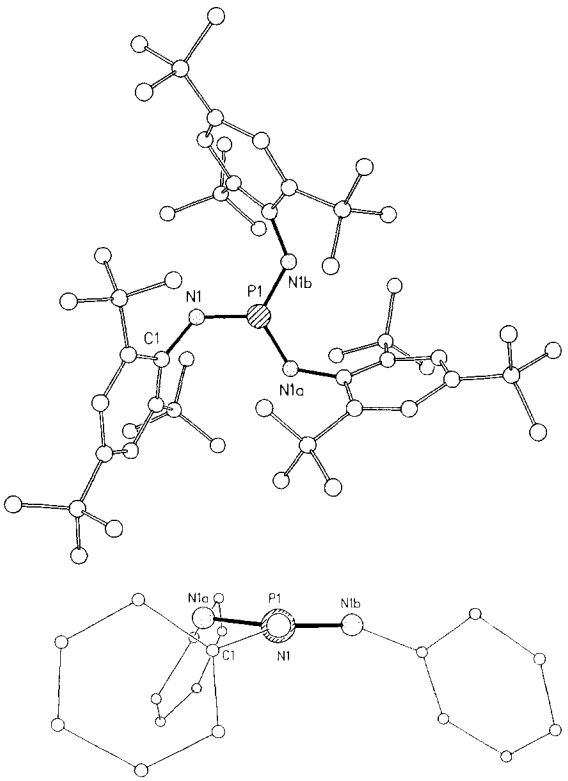


Fig. 2. Top: Crystal structure of the anion of **7**. Selected bond lengths [pm] and angles [°]: P1–N1 156.5(5), N1–C1 140.9(10); N1-P1-N1 119.9(1), C1-N1-P1 126.7(5). Bottom: Simplified representation showing the pyramidalization of the imine nitrogen atom.

In contrast to the metaphosphate unit in **4**, that in **7** is uncoordinated (Fig. 2). The shortest distance between the lithium atom tetrahedrally coordinated by four solvent molecules (THF) and the nitrogen atom N1 is 722 pm. The anion has C_3 symmetry; that is, the three imino groups are equivalent. The aryl substituents are arranged propellor-like around the central PN_3 framework (angle between the PN_3 and the aryl plane is 66°). The twist about the P–N bond is remarkable when compared to that in **4** and that in the sulfur triimide isoelectronic to **7**;[16] the *ipso* carbon atoms of the aryl groups each project 41 pm below the PN_3 plane (angle between the N–C vector and the PN_3 plane is 17.5°).

In order to establish whether the reduction in symmetry of **7** is an inherent property of the tris(imino)metaphosphate ion or is attributed to the steric effects in the crystal, quantum chemical calculations were carried out on the parent compound $[P(=NH)_3]^-$.[17] The most stable structure has C_{3h} symmetry (RHF/6-31 + G(d,p) optimized, P–N 156.2 pm, ∢ N 111.6°). A structural isomer with two hydrogen atoms in an *exo*/*exo* conformation (C_s symmetry), as occurs in the lithium complex **4**, is 3.4 kcal mol^{-1} higher in energy (HP + SD (tq) 6-31G(d,p) + zero-point vibration correction). Furthermore, the quantum chemical calculations showed that in metaphosphates of the type PX_3^- (X = SiH_2, PH, CH_2, S, NH, O) the tendency toward a reduction of symmetry (pyramidalization at phosphorus and/or twist of the π system) decreases with increasing electronegativity of the ligands X.[18] Since the geometry at the imine nitrogen atom in **7** deviates from that predicted by theory, it is assumed that van der Waals interactions between the solvent ligands of the cation and the sterically demanding substituents on the nitrogen atoms of the anion lead to the twisting about the P–N bond.

Experimental Procedure

2: A solution of **1** (4.25 g, 10 mmol) in diethyl ether (30 mL) was treated with the equimolar quantity of lithium *tert*-butyl amide at −30 °C. After the mixture had been warmed to 20 °C, the solvent was removed under vacuum, the resulting lithium chloride filtered, and the yellow residue taken up in *n*-hexane (10 mL). Compound **2** crystallized as fine needles at −30 °C. Yield: 3.45 g (72%), m.p. 83–85 °C (decomp.); ^{31}P NMR ($CDCl_3$): $\delta = 32.1$; ^{1}H NMR ($CDCl_3$): $\delta = 7.39$ (s, *m*-CH), 2.85 (d, $J = 4.7$ Hz, NH), 1.54 (s), 1.42 (s), 1.28 (s), 1.21 (s), 0.93 (d, $J = 0.9$ Hz, each *t*Bu); MS (40 eV): *m/z* (%): 433 (12) [$M^+ - N_2$], 418 (41) [$M^+ - N_2 - CH_3$], 362 (100) [(*t*BuN(H)P=NAr)$^+$]

3: **2** (3 g, 6.5 mmol) was dissolved in absolute DME (20 mL) and stirred for 2 h under reflux. At the beginning of the reaction a violent evolution of nitrogen was observed. After the solution had been concentrated and cooled to −30 °C, the aminobis(imino)phosphorane **3** was isolated as a fine crystalline white solid. Yield: 2.3 g (81%), m.p. 95–98 °C; ^{31}P NMR ($CDCl_3$): $\delta = 39.5$; ^{1}H NMR ($CDCl_3$): $\delta = 7.30$ (s, *m*-CH), 1.82 (d, $J = 3.8$ Hz, NH), 1.50 (s, *o*-C(CH_3)$_3$), 1.36 (d, $J = 7.2$ Hz, N(H)C(CH_3)$_3$), 1.27 (s, *p*-C(CH_3)$_3$), 1.15 (s, NC(CH_3)$_3$); MS (40 eV): *m/z* (%): 433 (21) [M^+], 362 (100) [(*t*BuN(H)P=NAr)$^+$].

4: *n*BuLi (2.9 mL, 1.6 M in *n*-hexane) was slowly added dropwise to a solution of the bis(imino)phosphorane **3** (2.0 g, 4.6 mmol) in DME (20 mL) at −60 °C. After complete addition the mixture was stirred for 1 h. The solution was then concentrated to half the volume. Compound **4** precipitated at −30 °C within two weeks in the form of yellow, prismatic crystals. Yield 0.9 g (37%).

6: **5** (2.0 g, 3.8 mmol) was dissolved in THF (50 mL) and treated with lithium 2,4,6-tri-*tert*-butylphenyl amide (1.1 g, 3.8 mmol). The solution was stirred overnight, subsequently all volatile components were removed under vacuum. The residue was taken up in toluene (30 mL), and the lithium amide which had been formed was removed by filtration. The product **6** precipitated from the concentrated solution in the form of pale yellow needlelike crystals. Yield: 2.4 g (84%), m.p. 167–169 °C (decomp.); ^{31}P NMR (C_6D_6/THF, 25 °C): $\delta = 22.1$.

7: **6** (1.00 g, 1.2 mmol) was dissolved in THF (70 mL) and treated with *n*-butyllithium (0.76 mL, 1.6 M in *n*-hexane). This resulted in the spontaneous precipitation of **7** as an amorphous solid. The product was obtained in crystalline form by redissolving the precipitate at 60 °C, followed by slow cooling (10 °C per h) to room temperature. Yield: 0.9 g (90%), m.p. 92–93 °C (decomp.); ^{31}P NMR (C_6D_6/THF): $\delta = 41.3$; ^{1}H NMR (C_6D_6/DME): $\delta = 7.44$ (s, 6H), 1.68 (s, 54 H), 1.40 (s, 27 H).

Received: May 28, 1994 [Z 6980IE]
German version: *Angew. Chem.* **1994**, *106*, 2170

[1] a) D. J. Harvan, J. R. Hass, K. L. Bush, M. M. Bursey, F. Ramirez, S. Meyerson, *J. Am. Chem. Soc.* **1979**, *101*, 7409–7410; b) S. Meyerson, D. J. Harvan, J. R. Hass, F. Ramirez, J. F. Marecek, *ibid.* **1984**, *106*, 6877–6883.

[2] a) S. N. Jenny, J. S. Ogden, *J. Chem. Soc. Dalton Trans.* **1979**, 1465–1467; b) L. Bencivenni, K. A. Gingerich, *J. Mol. Struct.* **1983**, *98*, 195.

[3] a) J. M. Friedman, J. R. Knowles, *J. Am. Chem. Soc.* **1985**, *107*, 6126–6127; b) S. Freeman, J. M. Friedman, J. R. Knowles, *ibid.* **1987**, *109*, 3166–3168; c) J. M. Friedman, S. Freeman, J. R. Knowles, *ibid.* **1988**, *110*, 1268–1275, and references therein.

[4] a) C. Lerch, J. Niemann, W. W. Schoeller, *Phosphorus Sulfur* **1987**, *30*, 503; b) A. Streitwieser, A. Rajca, R. S. McDowell, R. Glaser, *J. Am. Chem. Soc.* **1987**, *109*, 4184–4188; c) M. W. Schmidt, R. N. Truong, M. S. Gordon, *ibid.* **1987**, *109*, 5217–5227; d) H. Sun, D. A. Hrovat, T. W. Borden, *ibid.* **1987**, *109*, 5275–5276.

[5] R. Appel, E. Gaitzsch, F. Knoch, *Angew. Chem.* **1985**, *97*, 574–575; *Angew. Chem. Int. Ed. Engl.* **1985**, *24*, 589–590.

[6] A monomeric structure was also assumed for the tetraphenylarsonium salt of trithiometaphosphate based on the results of field desorption MS studies: H. W. Roesky, R. Ahlrichs, S. Brode, *Angew. Chem.* **1986**, *98*, 91-93; *Angew. Chem. Int. Ed. Engl.* **1986**, *25*, 82-83.

[7] A lithium complex of a iminobis(methylene)metaphosphate is known: R. Appel, P. Schulte, F. Knoch, *Phosphorus, Sulfur* **1988**, *37*, 195-198.

[8] E. Niecke, M. Nieger, V. von der Gönna, *Chem. Ber.* **1990**, *123*, 2329-2333.

[9] A. Ruban, M. Nieger, E. Niecke, *Angew. Chem.* **1993**, *105*, 1544-1545; *Angew. Chem. Int. Ed. Engl.* **1993**, *32*, 1419-1420.

[10] Crystal structures of **4** and {**7**}: [Li($C_4H_{10}O_2$)][$C_{26}H_{47}N_3P$] {[Li(C_4H_8O)$_4$][$C_{54}H_{87}N_3P$]}: yellow crystals {yellow crystals}, crystal dimensions 0.15 × 0.40 × 0.45 {0.35 × 0.35 × 0.50} mm: $M = 529.7$ {1104.6}; triclinic {hexagonal}, space group $P\bar{1}$ (no. 2) {$P6_3$ (no. 173)}, $a = 8.908(5)$ {15.116(3)}, $b = 11.888(3)$, $c = 16.994(4)$ {18.735(7)} Å, $\alpha = 89.65(2)$, $\beta = 80.68(3)$, $\gamma = 77.47(3)°$, $V = 1.733(1)$ {3.707(2)} nm^3, $Z = 2$ {2}, $\mu(Cu_{K\alpha}) = 0.89$ {0.65} mm^{-1}, $T = 200$ {193} K, $F(000) = 584$ {1220}, 7839 {2124} reflections up to $2\theta_{max} = 130°$ {120°} were measured with $Cu_{K\alpha}$ radiation on an Enraf-Nonius CAD4 diffractometer, of these 5891 {1884} were independent and were used for all calculations. The structure was solved by direct methods and refined anisotropically against F^2, the H atoms were refined with a riding model (SHELXL-93 [11]), $wR2(F^2) = 0.199$ {0.291}, $R(F) = 0.067$ {0.101} for 375 {268} parameters and 24 {201} restraints. An empirical absorption correction with the program DIFABS [12] was carried out for **4**. One imino-*t*Bu group is disordered. A semiempirical absorption correction based on Ψ scans was carried out for **7** and the absolute structure was determined by *x* refinement [13]. The relatively high *R* value is attributed to the disorder of the *p*-*t*Bu group and the THF molecules. Further details of the crystal structure investigations may be obtained from the Fachinformationszentrum Karlsruhe, D-76344 Eggenstein-Leopoldshafen (FRG), on quoting the depository number CSD-58351.

[11] G. M. Sheldrick, SHELXL-93, Universität Göttingen, **1993**.

[12] N. Walker, D. Stuart, *Acta Crystallogr. Sect. A* **1983**, *39*, 158–166.

[13] H. D. Flack, *Acta Crystallogr. Sect. A* **1983**, *39*, 876–881.

[14] a) R. Detsch, E. Niecke, M. Nieger, W. W. Schoeller, *Chem. Ber.* **1992**, *125*, 1119–1124; b) M. Frost, Dissertation, Universität Bonn, **1994**.

[15] E. Nicke, D. Gudat in *Multiple Bonding and Low Coordination in Phosphorus Chemistry* (Eds.: M. Regitz, O. J. Scherer), Thieme, Stuttgart, **1990**, pp. 392 404.

[16] O. Glemser, S. Pohl, F. M. Tesky, R. Mews, *Angew. Chem.* **1977**, *89*, 829–830; *Angew. Chem. Int. Ed. Engl.* **1977**, *16*, 789–790.

[17] The calculations were carried out wiht the Gaussian 92 program, Gaussian 92, Revision A: M. J. Frisch, G. W. Trucks, M. Head-Gordon, P. M. W. Gill, M. W. Wong, J. B. Foresman, B. G. Johnson, J. B. Schlegel, M. A. Robb, E. S. Replongle, R. Comperts, J. L. Andres, K. Raghavachari, J. S. Binkley, C. Gonzalez, R. L. Martin, D. J. Fox, D. J. De Frees, J. Baker, J. J. P. Stewart, J. A. Pople, Gaussian Inc., Pittsburgh, PA, **1992**. All structures were characterized by vibrational analysis (harmonic aprroximation).

[18] W. W. Schoeller, J. Strutwolf, E. Niecke, *THEOCHEM*, submitted.

Intramolecular Photocyclization of ω,ω-Diphenyl-(ω − 1)-alken-1-ols by an Exciplex Quenching Mechanism**

Kazuhiko Mizuno,* Toshiyuki Tamai, Toshinori Nishiyama, Kyoko Tani, Mayumi Sawasaki, and Yoshio Otsuji

Photochemical polar addition of nucleophiles to alkenes can be achieved by photoinduced electron transfer.[1–6] This photoreaction often proceeds via radical cations of alkenes, which are generated by photoinduced electron transfer from the alkene to an electron acceptor; this reaction is generally very efficient in polar media such as acetonitrile. Recently, we found that the efficiency of the photoaddition of alcohols to arylalkenes sensitized by 9,10-anthracenedicarbonitrile **A** depends markedly on the structure of the alkenes and the nature of the solvents.[5] The photoaddition of methanol to 1,1-diphenylpropene occurs more efficiently in less polar aromatic solvents such as benzene and toluene than in acetonitrile. We now report the regio- and stereoselective intramolecular photoaddition of ω,ω-diphenyl-(ω-1)-alkenols in the presence of **A**.[7] One step in this photoreaction is the quenching of the **A**–arylalkene exciplex by the terminal OH group present in the alkenol.

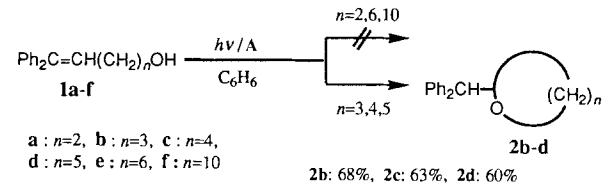
Irradiation of a solution of 6,6-diphenyl-5-hexenol (**1c**, 0.2 mmol) and a catalytic amount of **A** (0.04 mmol) in benzene through an aqueous $CuSO_4$–NH_3 filter solution ($\lambda > 400$ nm) gave 2-(diphenylmethyl)tetrahydropyran (**2c**) in 63% yield (isolated product).[8] The intramolecular photocyclization of **1c** occurred efficiently in aromatic solvents such as benzene and

[*] Dr. K. Mizuno, T. Nishiyama, K. Tani, M. Sawasaki, Prof. Dr. Y. Otsuji
Department of Applied Chemistry, College of Engineering
University of Osaka Prefecture, Sakai, Osaka 593 (Japan)
Dr. T. Tamai
Osaka Municipal Technical Research Institute, 1-6-50
Morinomiya, Joto-ku, Osaka 536 (Japan)

[**] This work was supported in part by a Grant-in-Aid for Scientific Research from the Ministry of Education, Science and Culture of Japan. We thank Dr. Y. Masaki, Dr. C. Pac, and Prof. S. Yanagida, Osaka University, for measurements of fluorescence lifetimes of 9,10-anthracenedicarbonitrile.

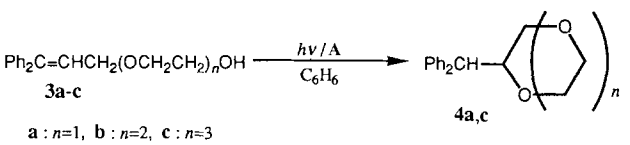
toluene and in halogenated solvents such as dichloromethane but less efficiently in acetonitrile, propionitrile, and ethyl acetate.[9]

The photoreactions of **1b** and **1d** under similar conditions gave the corresponding cyclized products **2b** and **2d** in good yields. In contrast **1a** and **1e–f**, which have shorter or longer methylene chains between the carbon–carbon double bond and the OH group, did not give any cyclized products. In the photoreactions of more flexible alkenes **3a–c**, only **3a** afforded the 1,4-dioxane **4a** in low yield.[10] The photocyclization of 3-substituted 6,6-diphenyl-5-hexenols **5a–c**[11] in benzene was



a : n=2, **b** : n=3, **c** : n=4, **d** : n=5, **e** : n=6, **f** : n=10

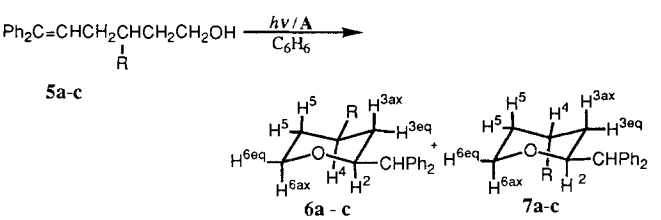
2b: 68%, **2c**: 63%, **2d**: 60%



a : n=1, **b** : n=2, **c** : n=3

4a: 22%, **4b**: trace, **4c**: 1%

stereoselective and gave the *cis* and *trans* 4-substituted 2-(diphenylmethyl)tetrahydropyrans **6a–c** and **7a–c**, respectively, in about a 4:1 ratio.[8] The *cis*/*trans* isomer ratios were little affected by the reaction temperature, solvent, and substituents.[12] The quantum yields for the formation of the cyclized products **2**, **6**, and **7** in benzene were five to ten times higher than those in acetonitrile.



a : R=CH_3, **b** : R=*t* Bu, **c** : R=Ph

6a+7a: 65%, **6b+7b**: 41%, **6c+7c**: 49%

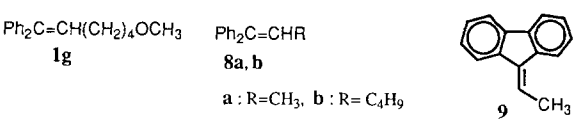
The fluorescence of 9,10-anthracenedicarbonitrile **A** in acetonitrile was efficiently quenched by all the arylalkenes at nearly diffusion-controlled rates; the rate constants for the fluorescence quenching were in the range of 3.3×10^8–1.3×10^{10} $M^{-1} s^{-1}$ ($\tau_{A,air} = 16.1$ ns in acetonitrile and 15.2 ns in benzene). However, the Stern–Volmer constants K_{sv} in benzene were much smaller than those in acetonitrile (Table 1). For **1a**, **1f**, and 1,1-diphenylpropene (**8a**), the K_{sv} values were much smaller than that of 9-ethylidenefluorene (**9**),[5, 13] although the oxidation potentials of these alkenes are almost the same. The fluorescence lifetime of **A** in benzene in the presence of methanol (1 M) was almost the same as that in the absence of methanol ($\tau_{air,C_6H_6} = 15.2$ ns, $\tau_{air,C_6H_6/CH_3OH} = 14.9$ ns). However, the K_{sv} value for **1f** in the presence of methanol was four times greater than that in neat benzene and almost the same as those for **1b**, **c**

Table 1. Stern–Volmer constants for the fluorescence quenching of **A** in various solvents and oxidation potentials of arylalkenes and other compounds.

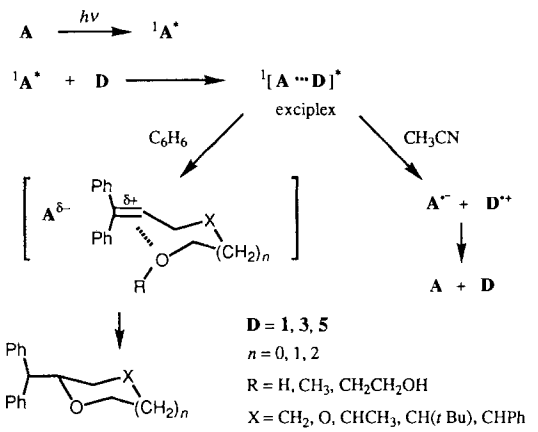
Alkene	$E^{ox}_{p/2}$ [a] [V]	K_{sv} [b] [M^{-1}] C_6H_6	C_6H_6/MeOH [c]	MeCN
1a	1.14	6		110
1b	0.97	43		156
1c	1.18	24		122
1d	1.06	15		153
1e	1.01	17		177
1f	1.07	8	34	161
1g		30		
3a	1.16	6		83
3b	1.15	27		148
3c	1.16	96		206
8a	1.13	5	27	134
8b		6		168
9	1.06	47	49	106

[a] Oxidation potentials (V vs. $Ag/AgClO_4$) were determined by cyclic voltammetry: Pt electrode, Bu_4NClO_4 (0.1 M) in CH_3CN. [b] Stern–Volmer constants for the fluorescence quenching of **A** in three solvents: [A] = 1×10^{-4} M. [c] In C_6H_6 in the presence of CH_3OH (1 M).

and the ether **1g**. Furthermore, weak emissions from the **A**/**8a**, **b** exciplexes and the **A**/**1g** exciplex were observed in benzene at longer wavelengths than the emission from $^1A^*$.[14]



We propose the exciplex quenching mechanism shown in Scheme 1 for the 9,10-anthracenedicarbonitrile (**A**) sensitized intramolecular photoaddition of **1a–f**. In benzene, a reversible



Scheme 1. Exciplex quenching mechanism for the **A**-sensitized intramolecular photocyclization of ω,ω-diphenyl-($\omega-1$)-alkenols.

exciplex[15] is formed between the **A** in the excited singlet state and the diphenylalkene moiety of the ω-hydroxyalkene. This exciplex is quenched by the OH group within the molecule.[16, 17] For **1b–d**, exciplex quenching leads to the five- to seven-membered transition state structures that are favorable for the formation of cyclized products. Exciplexes of the hydroxy ethers **3b**, **c** are not quenched by the OH group, but by the oxygen atom of the oxyethylene group. Therefore, **3b**, **c** have relatively large K_{sv} values, although the photoreaction of **3b**, **c**

gives hardly any cyclized products.[18] The intramolecular photoreaction is extremely efficient compared to the intermolecular photoaddition. In fact, the intramolecular photoaddition occurs smoothly even at high concentrations of the alkenes ([**1b**] = 0.001 - 0.1 M).

Photoinduced electron transfer in acetonitrile is known to occur rapidly to produce radical ions. However, in our system, the radical cations, probably solvent-separated radical cations, are less reactive toward alcohols. Solvent-separated radical ions will be inactivated by rapid back electron-transfer.[19] In fact, the addition of $Mg(ClO_4)_2$ to the reaction systems suppresses the formation of cyclized products.[19]

Received: May 5, 1994 [Z 6898 IE]
German version: *Angew. Chem.* **1994**, *106*, 2203

[1] Reviews: S. L. Mattes, S. Farid, *Org. Photochem.* **1983**, *6*, 233; G. J. Kavarnos, N. J. Turro, *Chem. Rev.* **1986**, *86*, 401; J. Mattay, *Angew. Chem.* **1987**, *99*, 825; *Angew. Chem. Int. Ed. Engl.* **1987**, *26*, 825; F. D. Lewis in *Photoinduced Electron Transfer, Part C* (Eds.: M. A. Fox, M. Chanon), Elsevier, Amsterdam, **1988**, p. 1; J. Mattay, *Synthesis*, **1989**, 233; K. Mizuno, Y. Otsuji, *Top. Curr. Chem.* **1994**, *169*, 301.

[2] R. A. Neunteufel, D. R. Arnold, *J. Am. Chem. Soc.* **1973**, *95*, 4080; Y. Shigemitsu, D. R. Arnold, *J. Chem. Soc. Chem. Commun.* **1975**, 407; A. J. Maroulis, Y. Shigemitsu, D. R. Arnold, *J. Am. Chem. Soc.* **1978**, *100*, 535; A. J. Maroulis, D. R. Arnold, *Synthesis* **1979**, 819; D. R. Arnold, X. Du, *J. Am. Chem. Soc.* **1989**, *111*, 7666; D. R. Arnold, X. Du, K. M. Henseleit, *Can. J. Chem.* **1991**, *69*, 839; K. Mcmahon, D. R. Arnold, *ibid.* **1993**, *71*, 450.

[3] T. Majima, C. Pac, H. Sakurai, *J. Am. Chem. Soc.* **1981**, *103*, 4499.

[4] F. D. Lewis, R. J. DeVoe, D. B. MacBlane, *J. Org. Chem.* **1982**, *47*, 1392; P. G. Gassman, K. D. Olson, *Tetrahedron Lett.* **1983**, *24*, 19; P. G. Gassman, K. J. Bottorff, *ibid.* **1987**, *28*, 5449; S. L. Mattes, S. Farid, *J. Am. Chem. Soc.* **1986**, *107*, 1426; T. Hirano, S. Shiina, M. Ohashi, *J. Chem. Soc. Chem. Commun.* **1992**, 1544; Y. Inoue, T. Okano, N. Yamasaki, A. Tai, *ibid.* **1993**, 718.

[5] K. Mizuno, I. Nakanishi, N. Ichinose, Y. Otsuji, *Chem. Lett.* **1989**, 1095.

[6] F. D. Lewis, G. D. Reddy, S. Schneider, M. Gahr, *J. Am. Chem. Soc.* **1989**, *111*, 6465; *ibid.* **1991**, *113*, 3498; F. D. Lewis, G. D. Reddy, *Tetrahedron Lett.* **1992**, *33*, 4249; A. Sugimoto, R. Hiraoka, H. Inoue, T. Adachi, *J. Chem. Soc. Perkin. Trans. 1*, **1992**, 1559; A. Sugimoto, R. Hiraoka, N. Fukuda, H. Kosaka, H. Inoue, *ibid.* **1992**, 2871.

[7] This work was presented in part at the United States/Japan seminar, "New Aspects of Molecular Photochemistry in Photoconversion", Tsukuba, Japan, April 13–17, 1992.

[8] The cyclized products were characterized by their ^{1}H NMR, ^{13}C NMR, and two-dimensional COSY and NOESY spectra. **2c**: ^{1}H NMR (270 MHz, $CDCl_3$): δ = 1.24–1.33 (m, 1H; 3eq-H), 1.40–1.58 (m, 4H; 4-H, 5-H), 1.76–1.79 (m, 1H; 3ax-H), 3.38–3.47 (m, 1H; 6ax-H), 3.88 (d, J = 9.26 Hz, 1H; 7-H), 3.95–3.96 (m, 1H; 6eq-H), 4.00–4.02 (m, 1H; 2-H), 7.13–7.35 (m, 10H); IR (KBr): ν = 1091 cm^{-1}; MS (70 eV): m/z: 252 (M^+). – **6c**: ^{1}H NMR (270 MHz, $CDCl_3$): δ = 1.39–1.53 (m, 1H; 3eq-H), 1.67–1.84 (m, 3H; 3ax-H, 5-H), 2.70–2.82 (m, 1H; 4-H), 3.51–3.73 (m, 1H; 6eq-H), 3.95 (d, J = 9.40 Hz, 1H; 7-H), 4.09–4.16 (m, 2H; 2-H, 6ax-H), 7.13–7.35 (m, 15H); IR (KBr): ν = 1100, 1042 cm^{-1}; MS (70 eV); High-resolution MS of M^+: 328.1936 (calcd $C_{24}H_{24}O$: 328.1827). – **7c**: ^{1}H NMR (270 MHz, $CDCl_3$): δ = 1.68–1.78 (m, 1H; 3eq-H), 1.87–1.98 (m, 3H; 3ax-H, 5-H), 3.13–3.25 (m, 1H; 4-H), 3.63–3.71 (m, 1H; 6eq-H), 3.78–3.88 (m, 1H; 6ax-H), 4.38 (d, J = 9.40 Hz, 1H; 7-H), 4.55–4.63 (m, 1H; 2-H), 7.14–7.36 (m, 15H); IR (KBr): ν = 1125, 1084 cm^{-1}; MS (70 eV): High-resolution MS of M^+: 328.1817 (calcd $C_{24}H_{24}O$: 328.1827).

[9] Relative quantum yields for the formation of **2c** in various solvents: 0.70 (C_6H_6), 0.72 (PhMe), 0.22 ($MeCO_2Et$), 1.0 (CH_2Cl_2), 0.07 (EtCN), 0.06 (MeCN).

[10] The phenanthrene–1,4-benzenedicarbonitrile sensitized photoreaction of **3a–c** in acetonitrile gave **4a–c** (yields: 13% for **4a**, 6% for **4b**, 9% for **4c**). These reactions probably proceed via the radical cations of **3a–c** [3].

[11] **5c**: ^{1}H NMR (270 MHz, $CDCl_3$): δ = 1.76–1.98(m, 2H), 2.39–2.47 (m, 2H), 2.80–2.90 (m, 1H), 3.37–3.52 (m, 2H), 5.96 (t, J = 7.45 Hz, 1H), 7.01–7.37 (m, 15H); IR (film): ν = 3400 cm^{-1}; MS (70 eV): high-resolution MS of M^+: 328.1842 (calcd $C_{24}H_{24}O$: 328.1827).

[12] Product ratios of **6a–c**/**7a–c** in different solvents: **6a**/**7a** = 83:17 (CCl_4), 82:18 (C_6H_6), 80:20 (CH_2Cl_2), 80:20 (C_2H_5Br), 84:26 (MeCN); **6b**/**7b** = 72:28 (CCl_4), 71:29 (C_6H_6), 75:25 (CH_2Cl_2), 81:19 (EtBr), 79:21 (MeCN); **6c**/**7c** = >98:>2 (CCl_4), 83:17 (C_6H_6), 80:20 (CH_2Cl_2), 78:22 (EtBr), 83:17 (MeCN). Ratios at different temperatures: **6a**/**7a** = 79:21 (–20 °C, CH_2Cl_2), 73:27 (50 °C, CH_2Cl_2), 72:28 (70 °C, CH_2Cl_2), 85:15 (–60 °C, C_6H_5Me), 78:22 (10 °C, C_6H_5Me), 73:27 (80 °C, C_6H_5Me), 72:28 (150 °C, C_6H_5Me).

[13] The fluorescence of ^{1}**A*** was efficiently quenched by **9**, probably as a result of the sandwich-type π-π interaction.

[14] The exciplex emissions were quenched by adding methanol to the benzene solutions.

[15] Although **1a**, **1f**, and **8a** have oxidation potentials similar to those of **1b–e** and **9**, their K_{sv} values are relatively small (Table 1). The formation of reversible exciplexes is postulated based on these results. See D. A. Labianca, G. N. Taylor, G. S. Hammond, *J. Am. Chem. Soc.* **1972**, *94*, 3679.

[16] R. A. Caldwell, L. Smith, *J. Am. Chem. Soc.* **1974**, *96*, 2994; D. Creed, R. A. Caldwell, *ibid.* **1974**, *96*, 7369; D. Creed, R. A. Caldwell, H. Ohta, D. C. DeMacro, *ibid.* **1977**, *99*, 277; C. Pac, H. Sakurai, *Chem. Lett.* **1976**, 1067; T. Majima, C. Pac, H. Sakurai, *Bull Chem. Soc. Jpn.* **1978**, *51*, 1811.

[17] The **A**-sensitized photoaddition of methanol to 1,1-diphenylethene (DPE) in acetonitrile is inefficient [5]; the phenanthrene–1,4-benzenedicarbonitrile sensitized photoaddition in acetonitrile is efficient [3]. The π complex [(phenanthrene–DPE)$^{\cdot+}$], which has a longer lifetime than the solvent-separated radical cation of DPE, has been proposed as a key intermediate by Pac et al. [3]. In the **A**-sensitized intramolecular photocyclization in benzene, the solvent may act as a π donor to stabilize the radical cation of ω-hydroxyalkenes. K. Mizuno, K. Nakanishi, Y. Otsuji, *Chem. Lett.* **1988**, 1833. See also ref. [19].

[18] It is notable here that the large K_{sv} values do not necessarily lead to the efficient formation of the cyclized products. For **3a**, an intramolecular hydrogen bond may be formed between the OH groups and the oxygen atom of the oxyethylene group, and hence the exciplex is quenched less efficiently.

[19] K. Mizuno, N. Ichinose, Y. Otsuji, *J. Org. Chem.* **1992**, *57*, 1855 and references cited therein.

Electrifying Reading!

Structure of Electrified Interfaces. Edited by *J. Lipkowski* and *P. N. Ross*. VCH Verlagsgesellschaft, Weinheim/VCH Publishers, New York, 1993. 406 pp., hardcover DM 196.00, $ 125.00.—ISBN 3-527-28787-6/0-89573-787-6

This book, edited by two well recognized electrochemists, is the second volume in a new series appearing in the specialist electrochemical literature. Compared with the many other series in this field, some of which have continued for many years, this new one aims to win the reader over by setting out different objectives. Instead of collecting together in one volume a rather haphazard collection of reviews on mostly unrelated electrochemical topics, here the editors aim to offer articles by experts on a single general theme of special importance. Aspects specific to particular methods or to the authors' own research are to be relegated to the background. In the first volume of this new series, which dealt with the adsorption of molecules on metal electrodes, these aims were not fully achieved. In contrast the impression from the chapter titles in this second volume is of a treatment that is not dominated by methods. As the title of the volume indicates, the emphasis is on a general consideration of all types of phase boundaries under the influence of electric fields, which of course includes both solid–liquid and solid–gas interfaces. The fact that in nearly every case the solid phase is a metal, despite the growing interest in semiconductor electrodes, is an indication of the large difference that still exists with regard to the state of knowledge and development of general models. On the other hand, numerous studies in the area of vacuum physics are mentioned.

In the first chapter M. van Hove gives a thoroughly systematic description of the surface crystallography at metal–gas interfaces. After a lucid introduction to the standard nomenclature and a brief description of some important methods of investigation, the author discusses typical examples of surface reconstruction and adsorption. In Chapter 2, P. N. Ross extends the above treatment to solid–liquid interfaces. Here there is slightly more emphasis on experimental aspects, as in this case the surface crystallography is often studied by ex-situ methods. The critical process of transfering the sample is discussed in detail. The examples are confined to systems that are thoroughly understood, namely metallic and ionic adsorbates and surface structural changes that depend on the electrode potential. In Chapter 3 surface reconstruction is discussed very methodically for many different electrochemical systems by D. M. Kolb. However, the experimental results described are so many and varied and are covered in such detail that this sometimes threatens to obscure the essentials. The surface crystallography existing in vacuum becomes modified on contact with a condensed phase, and then depends on many other parameters and is by no means always stable. However, any expectations that this might open up new methods in electrocatalysis are dampened by sober considerations. The interaction with the reactands, which are usually strongly adsorbed, destroys the reconstruction and with it any catalytically active surface properties that it conferred. In the fourth chapter M. P. Soriaga discusses molecular adsorption at single crystal surfaces. At first glance it might seem that this contribution rightfully belongs instead to the first volume of the series, but its presence here is fully justified by the emphasis on structural aspects of the adsorbate, with only a brief treatment of the experimental procedure and of the relationship to results obtained for metal–gas interfaces. The author concludes by correctly pointing out that the theoretical treatment and modeling of interactions between electrodes and adsorbed molecules has up to now received insufficient attention in relation to its practical importance. In Chapter 5, G. Pirug and H. P. Bonzel discuss the influence of coadsorbed alkali metals on the interactions at a metal–water interface, on the basis of intensive experimental studies of the metal–vapor boundary. Whereas most previous interpretations by electrochemists have been based on the strong adsorption of various anions, this article emphasizes the special role of cations in the double layer. The authors rightly point out that on this topic there is still insufficient interaction between vacuum physics and electrochemistry.

In the sixth chapter W. Schmickler considers the metal–electrolyte phase boundary from the standpoint of theoretical physics. The author discusses all the main aspects of developing models and illustrates these by examples involving the specific adsorption of simple ions. Continuing this topic in the following chapter, K. Heinziger reports on molecular dynamics studies of water molecules at phase boundaries. Experiments on solid–vapor interfaces have confirmed these calculations, encouraging the author to believe (hopefully correctly) that the method can soon be applied successfully to phase boundaries of importance in electrochemistry. In Chapter 8, Z. Borkowska and U. Stimming discuss the effects of anions in forming structures within the electrochemical double layer, based on studies of electrochemical phase boundaries in a hydrated perchloric acid over a wide range of temperatures. Regrettably, however, it is not clear how these studies can contribute to a better understanding of structured electrochemical double layers. In the last (very long) chapter, F. T. Wagner discusses methods and results in the simulation of electrochemical double layers in ultra-high vacuum (UHV), a technique introduced by J. K. Sass. This article goes far beyond the ground covered in Chapter 5 (Pirug and Bonzel); the critical reader may feel that it might have better to leave out the shorter of these two chapters, or to relate it more appropriately to Chapter 9. After briefly introducing some important physical concepts for discussing phase boundaries, Wagner takes a

This section contains book reviews and a list of new books received by the editor. Book reviews are written by invitation from the editor. Suggestions for books to be reviewed and for book reviewers are welcome. Publishers should send brochures or (better) books to Dr. Ralf Baumann, Redaktion Angewandte Chemie, Postfach 101161, D-69451 Weinheim, Federal Republic of Germany. The editor reserves the right of selecting which books will be reviewed. Uninvited books not chosen for review will not be returned.

critical look at some common prejudices about the validity of carrying over results from UHV studies into electrochemistry and refutes them. Although a comprehensive theoretical model of the double layer in UHV is still only a dream, the extensive knowledge gained from UHV studies has proved very useful in the interpretation of spectroelectrochemical results. The growing importance of spectroscopic methods in electrochemistry makes it certain that modeling of the double layer in UHV will continue to play an important role in the future.

The visual quality of the text and figures comes up to one's highest expectations. Each article is followed by a bibliography, though these vary considerably in comprehensiveness. Even many very recent papers that appeared only shortly before the manuscript deadline are included, but happily there are few references to unpublished work, making it easy for the interested reader to explore further. The short index is a useful aid to finding specific topics in the articles. The book will be of great value to the readership envisaged by the editors, namely advanced students and scientists with interests in the chemistry and physics of phase boundaries involving electric fields. The book is an essential addition to every relevant departmental library, but owing to the high price, understandable in view of the high standard of production and the limited potential readership, it is less likely to find its way onto readers' private bookshelves.

Rudolf Holze
Fachbereich Chemie
der Technischen Universität
Chemnitz-Zwickau (FRG)

Nobel Laureates in Chemistry, 1901–1992. Edited by *L. K. James*. American Chemical Society, Washington, DC, 1993. 814 pp., hardcover $ 69.95/paperback $ 34.95.—ISBN 0-8412-2459-5/0-8412-2690-3

Nobel prizes have a special fascination like that of Oscars or Olympic medals, with a public appeal which is widely promoted, despite the pretence to scorn hero worship as a relic of feudalism. We need our role models. It is the personalities rather than the circumstances that seem to be important in making things happen. The fuss and the jostling for the limelight in the competition for Nobel prizes may appear unseemly, but probably only to those who have no real prospect of success in that game. For the observer of current events, Nobel prize awards represent the ultimate in top-class research. The public looks on spellbound, enjoys the spectacle of the rather comical eggheads in their remote world winning the lottery, and returns to everyday business. But an emotional response of this kind encourages the public to open its purse to fund research, as people then feel that they have been involved and have shared in the results, especially when the laurel wreaths indirectly enhance the standing of their own region.

This latest volume in the American Chemical Society's *History of Modern Chemical Sciences* series also aims to harness that response and thereby reach a wider and younger audience, and by revealing the roots of the towering and ever more exciting tree of chemical knowledge to inform and encourage readers to emulate these models. What could be better for that purpose than brief portraits of the Nobel prizewinners, describing their origins, education, and achievements, and finally their rewards of recognition? These are inspiring success stories with a dash of anecdote, rarely a progress from Cinderella to queen, but often from stable-lad to winner of races.

Why have the Nobel prizes come to be so highly esteemed? It is because the choice of winners from the large range of candidates has, on the whole, been based on decisions that were generally accepted. Right from the start this was a difficult task calling for many compromises, because although the possibilities to be considered were initially few and manageable, a great many suggestions and arguments were received. The Nobel Committee has taken great care in laying down standards, in justifying these, and in keeping to them—a fact which must always be acknowledged despite the fashionable trend to criticize. Its decisions command a level of trust resting on a quality that has now been maintained for nearly a hundred years.

At the turn of the century when Alfred Nobel, to ease his conscience which was weighed down by dynamite, donated his wealth to set up the foundation, most people were convinced that there was light at the end of the tunnel of progress (although he himself may already have had doubts). The attitude of innocent dilettantist euphoria had given way to a serious, science-driven industrialization, and the successes of the chemical and physics-based industries and of medicine, in both therapy and theory, had given people still unused to such ideas an appreciation of the possibilities of applied research. The association of names of individual scientists with results of research in fields such as dyes, medicines, vaccines, X-rays, and atomic and cosmic forces was just at the limit of understanding of lay people. Information and emotion were supplied by the press, and competition by the spirit of empire—the best performances of the year and of a lifetime were rewarded. There was a widespread feeling of satisfaction that we had evidently come quite a long way.

Since then the Nobel prizes have been awarded on almost ninety occasions (the sequence was not completely stopped even during wars, despite the fact that these did not leave even the Swedish peacefulness entirely undisturbed). The list of over a hundred prizewinners is impressive enough in itself—the first recipients: J. H. van't Hoff, E. Fischer, S. Arrhenius, and the youngest ones at the time: E. J. Corey, R. R. Ernst, R. A. Marcus—it is also interesting that both the beginning and the end of the current list illustrate the close interaction that has always existed between the molecular and biological sciences. But even these few names are enough to show how, since the beginning around 1900, the emphasis in research of Nobel prize quality has moved from Europe to North America, catalyzed by the large forced exodus of talent during the 1930s, now seen with hindsight by those not involved as a blessing. The shift of interest from organic and physical chemistry to biochemistry and from single molecules to the clusters and macromolecules of interacting aggregates also reflects the prevailing trend. As well as rewarding individual achievements, in other cases a lifetime's work was honored. To reinforce this point, one's sense of justice is reassured by the recognition not only of a timely piece of research but also of a breakthrough in concepts or in the introduction of new (perhaps easier) methods, often involving systems several orders of magnitude smaller. The fact that the self-made man has become rarer, while success depends more on origins and background, illustrates the increasing trend to professionalization. It also follows from this that the Nobel prizes will remain the preserve of the highly industrialized nations unless special help is given. Thus it is a pointless exercise to identify "family pedigrees" in which Nobel prizes breed more Nobel prizes. Although that is true (sometimes even with regard to multiplication of families), it is not the Nobel prizes and their aura but the research group and its ambience that generate a tradition of success and eventually gain recognition in Stockholm.

 © VCH Verlagsgesellschaft mbH, D-69451 Weinheim, 1994 0570-0833/94/2020-2118 $ 10.00+.25/0

The way in which the Nobel prize system was set up under the old guard, who had so many irons in the fire, seems to have been rather haphazard. The specialization of modern times may make it easier to identify a particular achievement with one, or perhaps two, names, but there are so many! This too is a result of overall trends.

These biographies, with a mixture of broad perspectives and sidelong glances, of facts and traditions, written with expert knowledge but regrettably often in a rather colorless style, together paint a picture that is full of valuable information. Using small brush-strokes it shows how each Nobel laureate became involved in his or her field of work, how the environment and the thirst for knowledge interacted and formed each other, and how the route to the Nobel prize often seems in retrospect to have been laid down in advance in a unique and direct way—at least in these accounts, which undoubtedly have as one of their aims to motivate students, in the hope that they will not only learn about science and history but will themselves generate more.

Most of the laureates' biographies in this well produced and stoutly bound book are compressed into about ten pages and accompanied by a contemporary photograph from the archives of the Nobel foundation. A clear and consistent structure is used throughout, in which upbringing and education are followed by scientific achievements and honors, and in many cases by a short "moral of the story" which can be distilled from that particular life. It is a book for relaxation and bedtime reading—but certainly not for the evening of life, rather for the young, even though the style is a little dull. But anyway, young people are very sensible nowadays.

Lothar Jaenicke
Institut für Biochemie
der Universität Köln (FRG)

Leaving No Stone Unturned: Pathways in Organometallic Chemistry. (Series: Profiles, Pathways, and Dreams. Series editor: *J. I. Seeman.*) By *F. G. A. Stone.* American Chemical Society, Washington, DC, 1993. XXIV, 240 pp., hardcover $ 24.95.—ISBN 0-8412-1826-9

"Research in chemistry has enabled me and my wife to establish an extensive but nevertheless tightly knit network of human relations with other chemists, and in many cases with their families also. This network, the excitement of discovery, and the game of making new compounds, are probably the main factors for the word 'retirement' not being found in my vocabulary. One is singularly fortunate if one is able to focus for most of one's waking hours on a type of work that grows into a hobby, while at the same time opportunities occur for social contact with colleagues of many different nationalities and ethnic backgrounds, all having in common an interest in investigating new fields." (p. 202).

This statement by Gordon Stone, a universally well-liked "chemist's chemist" and "experimentalist's experimenter" with a "green thumb" for synthesis, summarizes his multiple loves—for chemistry, research, teaching, family, students, and colleagues. In the words of a former student, "He cares for the whole of the individual, just as he cares for the whole of chemistry." (p. xxi). Stone's dedication is evident: "My students never need to make an appointment. I am like a pastor who looks after his parishioners." (p. xxi). Another characteristic trait is his modesty. He sums up his achievements with the disarming pronouncement: "I have been lucky to do what I liked" (p. xix). He begins his volume in Jeff Seeman's popular series with a paean to the rapidly expanding field of organometallic chemistry and then explains: "a collection of autobiographies by active practitioners of organic chemistry would be incomplete without a contribution from an organometallic chemist, and this is my main justification for writing this book." (p. 4).

Francis Gordon Albert Stone (he never uses his full name) was born in Exeter, southwest England in 1925, the only child of Sidney Charles Stone, a British civil servant, and his wife Florence. His parents wanted him to become an accountant, but he decided on a career in chemistry, his best subject at the Exeter school. However, he was rejected by London University because the grades on his final examinations at Exeter were unsatisfactory (the letter of rejection is reproduced on p. 10). Undeterred, he spent a year at Medway Technical College at Gillingham to improve his knowledge of chemistry and applied to three colleges at Cambridge University on the basis of these same "unsatisfactory" examination grades. Accepted by all three, in 1945 he entered Christ's College, Cambridge, the first in his family to attend a university. He graduated in 1948 with first class honors. Always one to see the positive side of any event in his life and never one to rationalize his shortcomings, Stone remarks: "The lesson I learned from my rejection by London University was to have faith in one's own ability and not to be easily rebuffed by the actions of others." (p. 11).

Stone received his Ph.D. degree for his research on boron hydrides supervised by Harry Emeléus in 1951, whereupon he spent two years as a Fulbright postdoctoral scholar at the University of Southern California with Anton B. Burg, from whom he learned that "success in chemistry is most likely to result from careful experimentation and especially hard work." (p. 17). He also received "superb training in the manipulation of compounds in the absence of air..., which ...proved invaluable when [he] took up research in organometallic chemistry." (p. 18).

In 1954 Stone met Judith Hislop of Sydney, Australia, whom he subsequently married and to whom his book is dedicated. The couple later had three sons—James, Peter, and Derek. That same year he joined Eugene G. Rochow's group at Harvard University as a postdoctoral assistant. Several months later he became an instructor and began his first independent research (on boron compounds) with William A. G. Graham and Herbert D. Kaesz, the first of a long series of graduate students, who figure prominently on almost every page of the book. When future (1973) Nobel chemistry laureate Geoffrey Wilkinson left Harvard for Imperial College, London in 1956, Stone was appointed to the vacant assistant professorship, which included the teaching of a graduate course in advanced inorganic chemistry. In preparing his lectures from the original literature he found that the most exciting articles involved the synthesis of transition metal compounds with organic ligands, the field in which Wilkinson had specialized. In 1958 R. Bruce King and Tom A. Manuel became the first of his numerous graduate students to work on organometallic compounds.

In 1962 Stone returned to Great Britain to join the staff of Queen Mary College of the University of London, where he remained for only ten months. In 1963 he moved to Bristol University to become the first occupant of a newly established chair of inorganic chemistry. During his 27 years at Bristol he never took a sabbatical leave because he is "a firm believer in the need for research supervisors to be on hand to remove as far as possible any real or imagined impediments placed in the way of the work being done by their young colleagues." (p. 117). Here, as well as continuing his research on synthetic organometallic chemistry with undiminished interest, he served on a number of important but time-consuming govern-

ment committees, work to which he devotes an entire chapter. The British University Grants Committee appointed him chairman of its chemistry review panel. The results of his review of teaching and research in chemistry and their funding at British universities, published as *University Chemistry: The Way Forward* (1988), became known as "the Stone Report" (he modestly neglects to mention this fact).

In 1990 Stone reached the mandatory retirement age of 65 and moved to Baylor University to continue his research under the auspices of the Robert A. Welch Foundation. Typically concerned with his students, he now accepts only postdoctoral fellows because he thinks that he might become too old to supervise graduate students during what he considers an excessively long time required to complete the doctoral program in the United States. By retaining their home in England as well as maintaining one in Waco, the Stones are able to avoid both the British winter and the Texas summer.

Stone began his research on organometallic compounds at a time when the subject was just beginning to attract wide interest. Consequently, he and his students are responsible for many of the fundamental discoveries in the field, including cyclooctatetraenyl, cycloheptatrienyl, allyl, and fluorocarbon complexes of transition metals, species with silicon–ruthenium bonds, iron–tin compounds, many metal cluster compounds, including those with bridging alkylidyne ligands, pentalene complexes, metallacarboranes, low-valent platinum compounds such as $[Pt(C_2H_4)_3]$, complexes with heteronuclear metal–metal bonds, including bonds bridged by alkylidene or alkylidyne groups, and most recently (in Texas), alkylidyne(carborane)-metal species. He also pioneered the use of instruments in characterizing these new compounds.

The consummate synthetic chemist, Stone devotes his penultimate chapter to answering the question "Why Make New Compounds?" He maintains not only that "in the domain of organometallic chemistry those engaged in synthesis have usually been far ahead of predictions made by theoretical chemists" (p. 107) but also that "predictions from theoretical chemists can sometimes impede preparative work." (p. 107). He further believes that "research projects at the undergraduate level serve the useful purpose of stressing that chemistry is an intensely practical subject and that theory is driven by experiment and not, as often presented, the other way around." (p. 198). Yet he pays tribute to theory in his acknowledgement of his use of 1981 Nobel chemistry laureate Roald Hoffmann's "isolobal model". In a holograph letter of July 17, 1992 (p. xxiii) congratulating Stone on receiving an honorary degree from his home university, Exeter, Hoffmann writes: "What has always impressed me is how you could know ahead of time what the theoreticians would later come up with! So while I benefitted from your popularization of the isolobal analogy as a synthetic tool, I know full well that *you* didn't need that analogy at all, that you know deeply and surely, what it took me and others, in our round about way, years to find."

Synthetic organometallic chemistry is an intensely competitive field, a fact of which Stone is well aware: "Just as an actor is judged by his most recent performance, so organometallic chemists are judged by their most recent work." (p. 105). However, he is supremely sensitive to the feelings of his students and coworkers, which remain his primary concern. For example, whenever a breakthrough occurred in his laboratory, he would encourage other members of his group to place their own projects on hold and help with the new experimental work, but he would "leave no doubt in the mind of any member of the group that each individual's contribution will not be forgotten." (p. 139). He also states that "it's very hard to work in my group and not get a publication as a result" (p. xxi)..." in order to make the coauthor's curriculum vitae look reasonable for the next job application." (p. 182). But his concern with his students extends long after they have worked with him. He details their achievements and awards and follows their careers as conscientiously as his own. Most of the book's 61 illustrations are informal snapshots of Stone with students or colleagues taken at home or during his extensive travels. Scrupulous in assigning credit, he admits: "My co-workers have suggested many original projects for research that I would not have conceived myself." (p. 197).

This engaging autobiography of a warm, personable human being, one of the giants of organometallic chemistry, should interest not only researchers in the field but also chemists and historians of chemistry in general.

George B. Kauffman,
Laurie M. Kauffman
California State University
Fresno, CA (USA)

The Kinetics of Heterogeneous Electron Transfer Reactions in Polar Solvents

William Ronald Fawcett* and Marcin Opallo

Data for heterogeneous electron transfer reactions obtained in the last ten years have been examined within the context of contemporary theory. Special attention is focused on systems for which rate constants and activation parameters are available as functions of solvent and of temperature. The role of reactant structure in determining the kinetic parameters is also considered. Double layer effects both at unmodified and modified electrodes are discussed in detail. Experimental techniques, especially those suited to measuring fast reactions, are also outlined.

1. Introduction

Since the early 1980s there has been a great increase in interest in medium effects for electron transfer (ET) reactions. This revival was spurred by the appearance of several theoretical papers[1-4] that predicted the existence of dynamic solvent effects in the kinetics of ET. The first experimental evidence for such a dynamic effect in a heterogeneous ET reaction, presented by Kapturkiewicz and Behr,[5] was quickly followed by a report describing similar effects for a homogeneous ET reaction.[6] Since then a significant body of experimental evidence for solvent and other medium effects has been gathered in the literature. These experiments have focused on three areas, namely, homogeneous self-exchange ET, heterogeneous ET, and time-resolved fluorescence spectroscopy involving intramolecular ET. At the same time, significant advances have been made in the theoretical description of ET processes.

Several recent reviews have focused on the development of the theory of this elementary reaction and its application to experimental results.[7-9] Heitele[9] has examined in a particularly lucid and useful manner the theory of dynamic solvent effects in ET. On the experimental side, Barbara and Jarzeba[10] have reviewed experimental results in time-resolved fluorescence spectroscopy. Weaver[11] has discussed data for homogeneous ET reactions, especially those obtained in his laboratory.

The subject of the present review is heterogeneous ET. The discussion is limited to simple reactions, that is, those in which both oxidized and reduced forms remain in solution, only one electron is transferred, and no chemical bonds are broken or formed. Since the original work of Kapturkiewicz and Behr[5] on dynamic solvent effects, a large number of related studies have appeared in the literature. Our goal is to examine these results within the context of contemporary theoretical development and to show their relationship to other experiments describing medium effects in ET. No attempt is made here to discuss theory in detail since this has already been done.[7-9] However, a few aspects of theory that were not considered in previous reviews and that are particularly relevant to the analysis of experimental data are considered. As well as presenting the important results obtained, we also discuss advances in experimental techniques. It is important to emphasize that the improved understanding of the role of the medium in ET has been due in great part to the fact that faster processes in condensed media can now be followed experimentally with precision. Finally, it should be pointed out that heterogeneous ET is usually studied in the presence of an inert electrolyte to improve solution conductivity and maintain diffusion as a means of mass transfer. As a result, the medium for the ET reaction involves not only the solvent, but also the ions of the electrolyte that form the double layer at the electrode. Double layer effects play an important role in heterogeneous ET and are also considered in this review.

[*] Professor W. R. Fawcett
Department of Chemistry
University of California
Davis, CA 95616 (USA)
Telefax: Int. code +916/752-8995
Dr. M. Opallo
Institute of Physical Chemistry
Polish Academy of Sciences
PL-01-224 Warsaw (Poland)

2. Theory

2.1. Estimation of the Activation Parameters

One of the important problems considered in recent years is improvement of the estimation of the Gibbs energy of activation ΔG^* and related kinetic parameters. ΔG^* is traditionally regarded as composed of two parts, the inner sphere contribution ΔG^*_{is} and the outer sphere contribution ΔG^*_{os}.[12] Estimation of the former requires a description of the changes in bond lengths and

 © VCH Verlagsgesellschaft mbH, D-69451 Weinheim, 1994 0570-0833/94/2121-2131 $ 10.00+.25/0

angles that accompany the activation process, and is often based on the appropriate spectroscopic data.[13] The outer sphere component, which accounts for the work done to reorganize the solvent environment around the reactant has usually been calculated by using a model based on the Born theory of ionic solvation.[12, 13] In the case of the simple heterogeneous ET reaction [Eq. (1)] this contribution is given by Equation (2),

$$A + e \rightarrow B \tag{1}$$

$$\Delta G_{os}^{*} = \frac{N_0 e_0^2}{32\pi\varepsilon_0}\left(\frac{1}{r_A} - \frac{1}{r_c}\right)\left(\frac{1}{\varepsilon_{op}} - \frac{1}{\varepsilon_s}\right) \tag{2}$$

where N_0 is the Avogadro constant, e_0 the fundamental electronic charge, r_A the radius of the reactant A represented as a sphere, r_c the distance from its image in the electrode, ε_{op} the optical relative permittivity of the solvent and ε_s the corresponding static value (measured at very low frequencies at which the molecules are able to reorient to the changing electric field), and ε_0 the permittivity of free space. An important point in application of this relationship is the value of r_A, since most reactants are not spherical. This aspect is considered in more detail in Section 6. In determining ΔG_{os}^{*} in recent work, the distance r_c has usually been assumed to be effectively infinity, the stabilizing effect of any image formed in the electrode being neglected. Certainly, in cases where in the ET reaction the reactant and product do not interact with the electrode itself, r_c is equal to $2r_A + 2d_i$ where d_i is the thickness of the layer of solvent molecules and closest approaching counterions, that is, between the reactant and the geometrical electrode/solution interface. Thus, r_c corresponds at least to three molecular diameters; that is, it is of the order of six times r_A. Moreover, the efficiency with which the image is formed in the electrode can be questioned in the light of the spatial dispersion of the solvent dielectric permittivity and electric field penetration into the metal electrode.[14, 15] Kornyshev et al.[14, 15] applied the nonlocal electrostatic treatment to the estimation of ΔG_{os}^{*} for both heterogeneous and homogeneous ET reactions, and concluded that this quantity actually increases as the reaction site moves closer to the electrode, instead of decreasing as predicted by Equation (2). However, the sharp boundary model used in these calculations[15] can be criticized, because it is not applicable in regions where the dielectric properties of the system are changing markedly over short distances, such as near a reactant at the reaction site in the double layer. Nevertheless, a comparison of activation enthalpies for the same reaction under homogeneous and heterogeneous conditions (see Section 5, Table 3) suggests the r_c is sufficiently large that $1/r_c$ can be neglected in the calculation of ΔG_{os}^{*} for the heterogeneous process. This assumption is made in the following discussion.

The estimation of ΔG_{os}^{*} has been further improved by the use of nonprimitive models for ionic solvation, especially the mean spherical approximation (MSA).[16, 17] On the basis of the hypothetical two-step charging process associated with thermal electron transfer described by Marcus,[18] ΔG_{os}^{*} can be regarded as the difference between the Gibbs solvation energies of the reacting system at optical frequencies and at static frequency. This can be seen when Equation (2) is rewritten as Equation (3),

$$\Delta G_{os}^{*} = -\frac{N_0 e_0^2}{32\pi\varepsilon_0 r_A}\left(1 - \frac{1}{\varepsilon_{op}}\right) + \frac{N_0 e_0^2}{32\pi\varepsilon_0 r_A}\left(1 - \frac{1}{\varepsilon_s}\right) \tag{3}$$

a form that clearly shows the relationship of the Marcus model to the Born continuum model for ionic solvation. Following earlier work of Wolynes,[19] McManis and Weaver[20] wrote expression (4) for ΔG_{os}^{*} in the MSA, where r_s is the radius of a solvent molecule represented as a sphere, and λ_{op} and λ_s are polarization parameters calculated from ε_{op} and ε_s [Eq. (5), (6)].

$$\Delta G_{os}^{*} = -\frac{N_0 e_0^2}{32\pi\varepsilon_0}\left[\left(1 - \frac{1}{\varepsilon_{op}}\right)\frac{1}{(r_A + r_s/\lambda_{op})} - \left(1 - \frac{1}{\varepsilon_s}\right)\frac{1}{(r_A + r_s/\lambda_s)}\right] \tag{4}$$

$$16\varepsilon_{op} = \lambda_{op}^2(1 + \lambda_{op})^4 \tag{5}$$

$$16\varepsilon_s = \lambda_s^2(1 + \lambda_s)^4 \tag{6}$$

When applied to ion solvation at static frequencies,[21] the parameter λ_s accounts for the polarizability, softness, and nonsphericity of the solvent molecule, which is otherwise represented as a hard sphere with a central point dipole. For polar solvents, the value of λ_s is in the range of 2.0 to 2.9,[22] so the MSA estimate of the static contribution to ΔG_{os}^{*} is considerably smaller than the Born estimate. In the case of the high frequency solvation, λ_{op} is close to unity; the optical contribution to ΔG_{os}^{*} is thus also greatly reduced from the continuum value. However, it is doubtful whether the MSA model developed for a system of hard spheres with point charges and point dipoles at static frequencies[19–22] can be applied at optical frequencies



W. Ronald Fawcett was born in Chatham, Ontario, Canada in 1939. He studied physics and chemistry at the University of Toronto, obtaining a Ph.D. in physical chemistry in 1964 under the direction of Professor M. J. Dignam. He then spent two years in the laboratory of Professor Roger Parsons at the University of Bristol as a NATO post-doctoral fellow. In 1966 he returned to Canada to join the faculty of the Chemistry Department at the University of Guelph, obtaining the rank of Professor in 1977. In 1984, he moved to the University of California at Davis. His research interests include theoretical and experimental studies of double layer structure and its role in the kinetics of interfacial reactions. Much of his experimental work is associated with the electrochemistry of nonaqueous solvents and has included the use of these systems in high energy density batteries and the production of semiconductors based on metal chalcogenides.

where there is no orientational contribution to dipolar polarization.[23] Thus, the McManis–Weaver (MW) model[20] can be questioned within the context of the MSA.

A quite different approach to applying the MSA to estimation of ΔG^{*}_{os} was taken by Fawcett and Blum (FB).[23] Firstly, they assumed that the optical contribution is given to a good approximation by the Born estimate. Secondly, the polarization parameter at static frequencies was obtained from the Gibbs solvation energies of simple monoatomic, monovalent ions rather than from Equation (6). As a result, Equation (7) gives the expression

$$\Delta G^{*}_{os} = -\frac{N_0 e_0^2}{32\pi\varepsilon_0}\left[\left(1-\frac{1}{\varepsilon_{op}}\right)\frac{1}{r_A}-\left(1-\frac{1}{\varepsilon_s}\right)\frac{1}{(r_A+r_s/\lambda_i)}\right] \quad (7)$$

for ΔG^{*}_{os}, where the parameter λ_i depends on whether the ion is a cation or an anion, but not on its size. Stated otherwise, the FB model predicts that the Gibbs activation energy to form a monovalent cation from a neutral molecule by electrooxidation is different from that to form a monovalent anion from the same reactant by electroreduction, all other system parameters remaining the same. This follows from the experimental observation that the extent of solvation of cations and anions of the same radius in a given solvent is not the same.[24]

Two other activation parameters, the enthalpy ΔH^{*}_{os} and entropy of activation ΔS^{*}_{os}, may be determined from the temperature coefficient of the Gibbs energy. From Equation (3), estimation of ΔS^{*}_{os} on the basis of the Born model requires knowledge of the temperature coefficients $d\varepsilon_s/dT$ and $d\varepsilon_{op}/dT$, which are available for all polar solvents used in electrochemical studies.[24, 25] In the case of the MW model the temperature coefficients $d\lambda_s/dT$ and $d\lambda_{op}/dT$ are also needed. These may be obtained from the experimental coefficients $d\varepsilon_s/dT$ and $d\varepsilon_{op}/dT$ after differentiating Equations (5) and (6) with respect to temperature.[22] Finally, the temperature coefficient $d\lambda_i/dT$ is required in the FB model. These quantities were extracted from experimental solvation entropy data for the alkali metal cations and halide anions.[22] Once ΔS^{*}_{os} has been obtained, the activation enthalpy ΔH^{*}_{os} can be found by adding $T\Delta S^{*}_{os}$ to ΔG^{*}_{os}.

Values of ΔG^{*}_{os} and ΔH^{*}_{os} determined from the models described here in twelve polar solvents are collated in Table 1. The reactant size parameter r_A was set equal to 0.37 nm, a value appropriate for the metallocenes,[26] whose ET kinetics have been studied extensively both homogeneously and heterogeneously.[11] ΔG^{*}_{os} and ΔH^{*}_{os} differ by only a few kJ mol^{-1} at the most, and in the MSA model the difference is negligible for most solvents. However, the assumption made regarding the high frequency contribution and the method of estimating the polarization parameter at low frequencies affect the values based on the MSA considerably. ΔG^{*}_{os} estimated from the MW model is about 90% of that obtained by the continuum Marcus model, but the FB model provides estimates of ΔG^{*}_{os} only 62% of the Marcus estimate for a reaction involving cations, and 80% for a reaction involving anions. These differences are significant, and the quality of the models should be able to be verified experimentally.

The major problem with the MSA approach is that a proper estimate of ion–dipole interactions at high frequencies has yet to be made. Some support for the FB assumption comes from the finding that the MSA estimates of the dielectric properties of a polar solvent at optical frequencies agree well with those based on classical models.[27] However, the separate problem of ion–dipole interactions at high frequencies needs to be addressed as well.

2.2. Estimation of the Pre-Exponential Factor

Much has been written already about the pre-exponential factor in the rate constant for ET especially with respect to dynamic solvent effects.[1–4, 7, 9, 11] The discussion here is limited to aspects that relate to heterogeneous ET and to appropriate expressions for the rate constant. In the transition state theory formalism,[13] the standard heterogeneous rate constant is usually written as in Equation (8), where κ is the electronic trans-

$$k_s = \kappa K_p \nu_n \exp(-\Delta G^{*}/RT) \quad (8)$$

mission coefficient, K_p the encounter pre-equilibrium constant, and ν_n the nuclear barrier-crossing frequency. κ is unity for an adiabatic reaction and falls below unity as the extent of diabaticity increases. The extent of diabaticity is connected with the degree of interaction between the free energy surfaces for the reactant and product, and is determined by the electronic matrix coupling element H_{ab}.[13] The value of H_{ab} can also affect the

Table 1. Gibbs energy and enthalpy of activation for a simple heterogeneous electron transfer reaction in selected polar solvents according to the Marcus [12], McManis–Weaver (MW) [20], and Fawcett-Blum (FB) models [23]. The reactant radius is assumed to be 0.37 nm and the imaging distance, ∞. The units for ΔG^{*}_{os} and ΔH^{*}_{os} are kJ mol^{-1}. Oxidations to cations are indicated by (+/0) and reduction to anions by (0/−).

Solvent	Marcus model		MSA (MW)		MSA (FB)			
	ΔG^{*}_{os}	ΔH^{*}_{os}	ΔG^{*}_{os}	ΔH^{*}_{os}	$\Delta G^{*}_{os}(+/0)$	$\Delta H^{*}_{os}(+/0)$	$\Delta G^{*}_{os}(0/-)$	$\Delta H^{*}_{os}(0/-)$
acetone (AC)	23.3	20.8	20.1	20.8	15.3	14.0	18.4	18.2
acetonitrile (AN)	24.8	21.2	22.5	21.8	16.1	14.4	20.3	19.3
butyronitrile (BuN)	22.5	20.3	19.3	19.8	14.3	13.9	17.6	18.0
benzonitrile (BzN)	18.3	16.5	16.5	17.1	9.5	9.0	13.6	14.0
dimethylacetamide (DMA)	21.5	18.3	19.6	20.2	13.9	11.9	16.1	15.3
dimethylformamide (DMF)	21.7	19.2	19.8	20.4	14.0	12.9	16.8	17.6
dimethylsulfoxide (DMSO)	20.5	18.1	19.5	18.7	12.7	12.3	16.1	16.7
hexamethylphosphoramide (HMPA)	20.5	19.5	17.7	20.5	13.1	13.4	14.9	16.4
methanol (MeOH)	25.2	23.2	23.0	24.1	16.9	16.3	22.4	20.9
nitrobenzene (NB)	18.2	16.8	17.0	18.7	8.9	8.8	13.9	14.8
nitromethane (NM)	23.3	20.3	21.4	21.2	14.1	12.8	19.0	18.4
propylenecarbonate (PC)	22.5	19.7	21.3	21.0	13.7	12.9	17.8	17.3

nuclear barrier-crossing frequency ν_n: when H_{ab} is large and the barrier rounded, ν_n falls below its value for small values of H_{ab}.[4, 28] Simple relationships connecting these quantities are given by the Landau–Zener model[13] according to which the electron tunneling frequency ν_e is given by Equation (9), where N_0 is Avogadro's constant and h Planck's constant. The electronic transmission coefficient is then given by Equation (10).

$$\nu_e = \frac{2H_{ab}^2}{N_0 h}\left(\frac{4\pi^3}{\Delta G^*/RT}\right)^{1/2} \tag{9}$$

$$\kappa = \frac{2[1 - \exp(-\nu_e/2\nu_n)]}{2 - \exp(-\nu_e/2\nu_n)} \tag{10}$$

When $\nu_e \gg \nu_n$, $\kappa = 1$, and the reaction is adiabatic. However, when $\nu_e \ll \nu_n$, the expression for κ is given by Equation (11), and

$$\kappa = \nu_e/\nu_n \tag{11}$$

electron tunneling controls the magnitude of the pre-exponential factor. This diabatic limit occurs in cases where the extent of interaction between the reactant and electrode is minimized, for instance, in the presence of a blocking film on the electrode. In this case both H_{ab} and ν_e are small, and κ is given by Equation (11). Obviously, the structure of the electrode/solution interface plays an important role in determining these quantities.

The encounter pre-equilibrium constant K_p has been defined within the context of the encounter pre-equilibrium model for heterogeneous ET reactions[29] and contains the terms describing double layer and steric effects. In the absence of steric interactions, K_p is approximately 60 pm for a spherical reactant.[29] Thus, after correction for double layer effects, the upper limit for the product κK_p is about 60 pm. Lower values can be due to steric effects or departure from reaction adiabaticity. Because of the very approximate nature of the models used to estimate κ and K_p individually, it is preferable to cite only the product κK_p obtained from an analysis of experimental data.[30]

The component ν_n of the pre-exponential factor depends on vibrational modes within the reactant and the solvent to an extent which is contingent upon the relative importance of the inner and outer sphere contributions to the activation barrier. When the reaction is adiabatic and the inner sphere contribution to ΔG^* is small, this frequency is given by Equation (12),[1–4] where τ_L is the longitudinal solvent relaxation time. For Debye solvents in the continuum approximation, τ_L is given by Equation (13),[31] where ε_∞ is the high-frequency relative solvent permittivity and τ_D the Debye relaxation time. Values of τ_L have been collected for a large number of polar solvents[32] whose behavior is well approximated by the Debye model. The pre-exponential factor is thus predicted to depend on the solvent's dielectric relaxation properties, parameters which are quite different in origin to those which determine the Gibbs activation energy barrier.

$$\nu_n = \tau_L^{-1}\left(\frac{\Delta G^*}{4\pi RT}\right)^{1/2} \tag{12}$$

$$\tau_L = \frac{\varepsilon_\infty \tau_D}{\varepsilon_s} \tag{13}$$

When the inner sphere activation barrier is large, or the reaction adiabaticity is weak, the dependence of the pre-exponential factor on solvent is weakened. A convenient, approximate way of writing ν_n is then Equation (14),[33] where ν_{is} is the frequency

$$\nu_n = \nu_{is}^{1-\theta}\tau_L^{-\theta} \tag{14}$$

associated with an intramolecular vibration. Combining Equations (8) and (14), the standard rate constant may be expressed as in Equation (15). The factor A contains all the contributions

$$k_s = A\tau_L^{-\theta}\exp(-\Delta G^*/RT) \tag{15}$$

to the pre-exponential factor that to a first approximation do not depend on the solvent, and θ is a fraction between 0 and 1. This way of expressing the solvent dependence was first given by McGuire and McLendon[34] and is especially convenient for discussing the experimentally observed solvent dependence. It is also suggested by the theoretical analysis presented by Nadler and Marcus.[35] An unattractive feature of Equation (15) is that the factor A has fractional dimensions of time when θ is a fraction.[33]

The nuclear barrier-crossing frequency determined from known values of ν_{is} and τ_L is of the order of 10^{12} to 10^{14} s^{-1}. As a result, the upper limit for the pre-exponential factor for heterogeneous ET is approximately 6000 $cm\,s^{-1}$. For a reaction with a Gibbs energy barrier of 20 $kJ\,mol^{-1}$, this corresponds to a standard rate constant of 2 $cm\,s^{-1}$ at 25 °C, which is shown to be of the correct order of magnitude by kinetic data collected to date.

Some mention should be made of solvents that do not follow the simple Debye model. Most solvents exhibit multiple relaxation when the frequency dependence of the dielectric permittivity is examined over a sufficiently wide range.[36] Estimation of τ_L is more complex for these systems,[37] but can be made on the basis of the work of Hynes.[28] Solvents for which non-Debye behavior is important are the alcohols and protic amides.[36] In these systems in which τ_L is a function of time,[37] the value observed at very short times (high-frequency limit) are relevant to the type of reaction considered here. Thus, when the relaxation modes at higher frequencies are considered in the estimation of τ_L for alcohols, the kinetic data obtained in these solvents fall into line with those obtained in simpler solvents.[33]

As a note of caution, it should be remembered that the Debye model on which the estimation of τ_L is based is a continuum model and therefore does not recognize the unique properties of the solvent in the vicinity of the reactant. Thus, the local value of τ_L may be quite different from that obtained from the Debye parameters [Eq. (13)]. However, since the majority of systems studied to date display clear correlations between $\ln k_s$ and $\ln \tau_L$, a simple relation apparently exists between the actual local relaxation time and that estimated by the Debye model. This problem can be elucidated by using ultrafast spectroscopic relaxation techniques, and work in that direction has been initiated.[10]

Finally, it should be noted that the above discussion has been made within the context of Marcus theory, which, strictly speaking, was developed for adiabatic reactions.[12] Electronic effects are included in this model heuristically by way of the electronic transmission coefficient κ. An alternative approach is that of

Dogonadze,[38] which is based on a quantum mechanical description of a manifold of potential energy surfaces. The quantum mechanical approach was recently extended by Schmickler,[39] and its relationship to relevant experimental observations discussed in detail.

3. New Developments In Experimental Methods

To test the predictions made by contemporary theory, the standard rate constants for fast heterogeneous ET reactions must be determined. Efforts in this direction have most often involved ultramicroelectrodes.[40-42] The current flowing in the electrochemical cell when microelectrodes are the working electrode is typically 100 to 1000 times smaller than that at a conventional dropping mercury electrode, so problems due to iR drop and capacitative current are greatly reduced. Ultramicroelectrodes are often metal wires with diameters of the order of microns which are sealed in glass so that a disc is exposed to the electrolyte solution. Electrode materials include platinum, gold, and carbon, and must be carefully polished before each experiment. The gold disc electrode may be modified to a mercury hemisphere by electrodeposition of mercury,[43, 44] or by exposing the gold disc to a pool of highly purified mercury for a short time.[45] Attempts have also been made to fabricate electrodes of nanometer dimensions, called nanodes.[46] However, the area of the conducting material exposed to the solution is extremely difficult to define due to problems in sealing glass to metal rods of such small diameter.[47] As a result interpretation of current–voltage data with a view to obtaining kinetic information is impossible.[47, 48]

The most popular technique for determining kinetic parameters using ultramicroelectrodes has been cyclic voltammetry with fast scan rates.[42, 49, 50] However, extraction of the kinetic information is not straightforward and requires careful analysis of the effects of any uncompensated iR drop.[51]

Another technique introduced recently by Baranski[43, 44, 52-54] is high-frequency a.c. admittance voltammetry at ultramicroelectrodes. By working at higher frequencies, linear mass-transfer conditions are maintained at the working electrode. Moreover, the resistance of the system, and interfacial capacitance are monitored directly in the experiment, which enables any problems with the state of the electrode/solution interface to be easily recognized. Baranski[54] has carried out a detailed analysis of the possible errors in these experiments and shown how the frequency range may be optimized for a kinetic study given the electrode area, solution resistance, and double layer capacity. These experiments involve a fairly simple extension of well-known admittance methods[55, 56] and are easily performed at frequencies up to 100 kHz. As a result, rate constants can be measured up to 10 $cm\,s^{-1}$ with reasonable precision.[44, 45, 53, 57] Bard et al.[58-61] demonstrated that scanning electrochemical microscopy can determine fast ET kinetics precisely. In such an experiment, a ultramicroelectrode of micrometer dimensions, which is normally used to probe the surface of a substrate very close to it, acts as a working electrode, and the reactant is dissolved in the small volume of solution between the ultramicroelectrode and the closely positioned substrate. They have shown that mass transfer conditions are such that fast ET kinetics can be measured in both aqueous[58, 59] and highly resistive nonaqueous media.[60, 61] Results from these experiments for the electrooxidation of ferrocene in acetonitrile[59] and the electroreduction of buckminsterfullerene in benzonitrile[61] agree well with data obtained earlier using high-frequency admittance methods.[53, 57]

Osteryoung et al.[62, 63] described a short time pulse voltammetric technique for studying fast heterogeneous reactions at ultramicroelectrodes. In the normal pulse mode, the electrode potential is stepped to a potential where a faradaic process occurs and held at the final potential for a fixed time of the order of microseconds while the resulting current transient is recorded.[62] The kinetic information is obtained from the faradaic current measured towards the end of the pulse. The electrode is held at each potential for some milliseconds, so that the effects of mass transfer near the electrode are obliterated by diffusion before the next pulse is applied. This technique was recently applied to determining standard rate constants for ferrocene and anthracene in acetonitrile and dichloromethane.[63]

Mahlendorf and Heinze[64] recently used impedance spectroscopy to study fast electron transfer reactions at a Pt electrode of conventional size in highly resistive non-aqueous media. Their method of data analysis differs significantly from that of Baranski[44, 54] and requires the extraction of five parameters by nonlinear regression. They obtained a standard rate constant for the oxidation of ferrocene in dichloromethane slightly smaller than that found by admittance techniques at ultramicroelectrodes[53] when one corrects for a higher experimental temperature (293 K). These authors[64] were unsuccessful in obtaining kinetic data in acetonitrile.

Some feeling for the experimental problems in determining rate constants for fast heterogeneous reactions can be obtained by comparing data reported recently by various laboratories for the kinetics of electrooxidation of ferrocene in acetonitrile (Table 2). Acetonitrile is a solvent of low viscosity with a short longitudinal relaxation time (about 0.2 ps), and ferrocene is a reactant with a low inner sphere reorganization energy. These factors combine to make ET rapid in this system. Examination of the data summarized in Table 2 reveals an unacceptably large range for rate constants reported during the last seven years from 2×10^{-2} to 220 s^{-1}, that is, by four orders of magnitude!

Table 2. Standard rate constants k_s for the electrooxidation of ferrocene at a platinum electrode in acetonitrile from recent experimental studies.

Method	k_s [$cm\,s^{-1}$]	Electrolyte [a]	T [K]	Ref.
fast-scan cyclic voltammetry	1.1	0.5 M $TBABF_4$	[b]	[65]
slow linear sweep voltammetry	0.09	0.1 M TBAP	298	[66]
fast-scan cyclic voltammetry	0.95 ± 0.44	0.6 M TBAP	[b]	[49]
fast-scan cyclic voltammetry	2.2 ± 0.8	0.5 M TEAP	294	[50]
slow linear sweep voltammetry	220 ± 120	0.3 M TBAP	[b]	[46]
high-frequency admittance	2.6 ± 0.3	0.1 M TBAP	285	[53]
cyclic voltammetry	0.0194	0.1 M $LiClO_4$	298	[67]
short time pulse voltammetry	1.2 ± 0.3	0.5 M $TBAPF_6$	298	[63]
scanning electrochemical microscopy	3.8 ± 0.8	0.52 M $TBABF_4$	[b]	[60]

[a] TEAP = tetraethylammonium perchlorate, TBAP = tetrabutylammonium perchlorate, $TBABF_4$ = tetrabutylammonium tetrafluoroborate, $TBAPF_4$ = tetrabutylammonium hexafluorophosphate. [b] Room temperature.

If the two low results[66, 67] and the high result[46] are removed, a much more acceptable range, from 1 to 4 $cm\,s^{-1}$, is found. Differences in electrolyte nature and concentration, and in temperature cause some of the observed scatter in the remaining data. The very high result by Penner et al.[46] is almost certainly due to problems in defining the area of the electrode exposed to the solution when electrodes of diameters significantly less than 1 μm are used.[47, 48, 60] The same comment can be applied to the low result of Russell et al.,[66] who used a ring microelectrode. The low result reported by Abbott et al.[67] at an electrode of conventional dimensions is attributed to uncompensated iR drop. The results obtained by fast-scan cyclic voltammetry at ultramicroelectrodes[49, 50, 65] fall somewhat below the most recent result by Mirkin et al.,[60] probably as a result of some uncompensated iR drop[51] and effects due to nonlinear diffusion.[60, 68] The rate constant estimated from the data of Baranski et al.[53] on the basis of available temperature coefficient data[53, 69, 70] is 3.8 $cm\,s^{-1}$ at 298 K. Thus, the standard rate constants determined for this reaction by scanning electrochemical microscopy and high frequency admittance agree within experimental error. The recent result of Karpinski and Osteryoung[63] is somewhat smaller for reasons that are difficult to assess, but that also may be related to uncompensated iR drop.

The above results demonstrate that one must exercise great care in the measurement of fast ET kinetics. However, experimental techniques are now available which can provide precise data for rapid reactions. This means that important theoretical questions can be examined on the light of reliable experimental data.

4. Effects of the Solvent

The major focus of experimental work during the last ten years has been to understand the role of the solvent.[71, 72] The clear dynamic solvent effect, which is especially pronounced when the inner sphere reorganizational energy is small, is most easily demonstrated by a double logarithmic plot of the standard rate constant measured in various solvents against the solvent's longitudinal relaxation time. Data for the electrooxidation of ferrocene[53] and 1,4-diaminobenzene[73] are shown in Figure 1. Quite good linear relationships are obtained; the slope for the 1,4-diaminobenzene system is less than that for the ferrocene system. The scatter observed is attributed to the fact that the variation in ΔG_{os}^{*} with solvent is ignored in making such a plot. The exact relationship between $\ln k_s$ and $\ln \tau_L$ [Eq. (16)] is derived from Equation (15). The variation in $\ln \tau_L$ obtained

$$\ln k_s = \ln A - \theta \ln \tau_L - \Delta G_{is}^{*}/RT - \Delta G_{os}^{*}/RT \qquad (16)$$

from many systems[5, 45, 53, 69, 73–79] is significantly greater than variation in $\Delta G_{os}^{*}/RT$ for a typical selection of polar solvents. In early work[5] it was also pointed out that a correlation exists with the logarithm of the solvent's viscosity.

Considerable discussion has centered on the separation of the solvent effect due to the pre-exponential factor from that due to the Gibbs energy barrier.[11, 31, 33, 40] If both τ_L and ΔG_{os}^{*} are known, the parameters A and θ are easily determined by using linear regression techniques. In most cases ΔG_{os}^{*} is either unknown or difficult to estimate. However, the Marcus model[12] predicts that it is proportional to the solvent's Pekar factor $\gamma = 1/\varepsilon_{op} - 1/\varepsilon_s$. An approximate linear relationship between ΔG_{os}^{*} and γ is also found when the former quantity is estimated with the FB model.[22] Thus, Equation (16) can be written in an approximate form [Eq. (17)], where K is a solvent independent

$$\ln k_s \approx K - \theta \ln \tau_L - g\gamma \qquad (17)$$

constant and g the proportionality constant relating ΔG_{os}^{*} to γ. The parameters θ, g, and K can be determined from a two-parameter regression with $\ln \tau_L$ and the Pekar factor γ as independent variables.[30] Such an analysis requires that $\ln \tau_L$ and γ are not correlated to one another, and that data are available in at least four of solvents. This analysis has been applied successfully to kinetic data for several heterogeneous ET reactions[30, 45, 77] and is especially useful in obtaining an estimate of θ. Weaver[11] has strongly criticized this method of analysis, pointing out that there is a weak correlation between $\ln \tau_L$ and γ. As illustration, a very weak correlation is present for the group of 15 polar solvents considered in Figure 2 ($r = 0.733$): γ becomes smaller as the value of $\ln \tau_L$ increases. Obviously, any rigorous statistical analysis must take this into consideration,

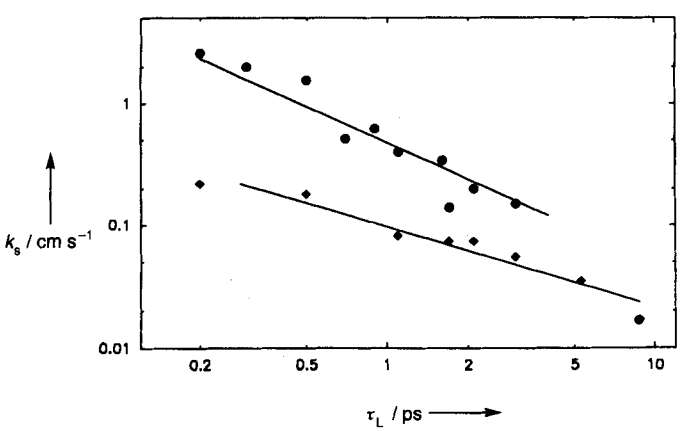


Fig. 1. Double logarithmic plots of the standard rate constant for the electrooxidation of ferrocene (●) [53] and 1,4-diaminobenzene (♦) [73] obtained in aprotic solvents against the longitudinal relaxation time of the solvent.

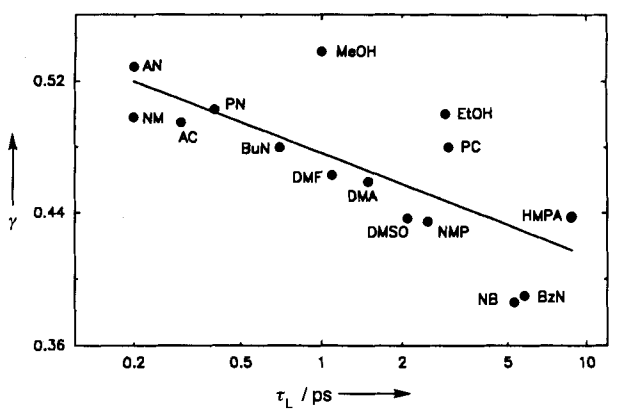


Fig. 2. Plot of the Pekar factor γ for a polar solvent against the logarithm of its longitudinal relaxation time τ_L. The abbreviations for the solvents are given in Table 1 except for ethanol (EtOH), *N*-methylpyrrolidone (NMP) and propionitrile (PN).

but the degree of correlation seen for the 15 solvents chosen would not preclude an analysis of kinetic data obtained, provided the level of experimental error in the standard heterogeneous ET rate constant is low. Therefore, experimental studies of solvent effects must be designed with careful consideration of the degree of correlation between $\ln \tau_L$ and the Pekar factor γ. For example, Phelps et al.[80] recently reported a study of solvent effects on the electrooxidation of several sesquibicyclic hydrazines in the seven polar solvents acetone, acetonitrile, nitromethane, dimethylformamide, dimethylsulfoxide, nitrobenzene, and methanol. The correlation between $\ln \tau_L$ and γ is more important for this group of solvents ($r = 0.895$); consequently, since there is no hope of separating the contributions from the pre-exponential factor and the activation barrier on the basis of Equation (17), less objective methods must be used to assess these data. A more careful selection of solvents used would have allowed firmer conclusions to be made about the role of the solvent for these systems.

In other techniques for analyzing the solvent effect, one of the solvent-dependent terms is assumed to be known, the observed rate constant is corrected for it, and then the other solvent effect is examined with respect to the corrected rate constant.[11] For instance, if one assumes values for ΔG^*_{os}, Equation (16) may be rearranged [Eq. (18)], so that a plot of the left hand side against

$$\ln k_s + \Delta G^*_{os}/RT = \ln A - \Delta G^*_{is}/RT - \theta \ln \tau_L \qquad (18)$$

$\ln \tau_L$ should yield θ. This procedure was followed in two recent studies[80, 81] with the continuum estimates of ΔG^*_{os} [Eq. (2)] and $r_c \rightarrow \infty$. As these values of ΔG^*_{os} are almost certainly high by at least RT and perhaps by as much as 4 RT (depending on the nature of the reaction), the analyses are of doubtful value. A more interesting method of estimating ΔG^*_{os} uses the optical energies for intramolecular ET in the bis(ferrocenyl)acetylene cation and related compounds.[11, 82, 83] The energy associated with transfer of one electron from one ferrocene group to the other across the acetylene bridge is assumed to be directly related to ΔG^*_{os} for homogeneous ET between ferrocene and the ferrocenium cation in a given solvent. The estimates of ΔG^*_{os} from these data are approximately 85% of those obtained by the continuum model and therefore closer to results from the MSA (Table 1). They have mainly been employed in the analysis of data for homogeneous ET with metallocenes.[11] This method of estimating ΔG^*_{os} is considered in more detail in Section 6.

A method applied to perfectly adiabatic reactions ($\theta = 1$) made use of Equations (2) and (12), so that the standard rate constant was corrected for solvent dependence of the pre-exponential factor.[84, 85] (In ref. [85] the method was incorrectly applied to some reactions that are not perfectly adiabatic ($\theta < 1$).) This method is not of great interest now, because a large body of evidence indicates that Equation (2) overestimates the value of ΔG^*_{os} (see Section 2.1).

Some mention should be made of the model for solvent effects on rate constants for heterogeneous ET reactions proposed by Abbott et al.[67] on the basis of data for the oxidation of ferrocene in 16 nonaqueous solvents. These authors ignored the possible dependence of the pre-exponential factor of the rate constant on solvent relaxation, and attributed solvent dependence to variation in ΔG^* with solvent basicity, acidity, polarity, and polarizability. Indeed, the thermodynamic properties in ion solvation can be related to solvent basicity for cations and solvent acidity for anions,[134] but ion solvation at optical frequencies was not considered in the models that they discuss. Considering the poor quality of most correlations reported by Abbott et al.[67] and the probability that their kinetic data are strongly influenced by iR drop, the conclusions reached in their study are difficult to accept.

The general picture that has emerged recently is that the solvent contribution to the pre-exponential factor can vary over a wide range of values of θ. On examination of the available data,[33] we showed that the magnitude of θ was connected to the magnitude of the rate constant observed in a given solvent: as the reaction becomes slower, θ decreases (see Fig. 1). This is attributed to a larger contribution to the activation barrier from internal vibrational modes, and/or weak reaction adiabaticity. When θ is sufficiently small a linear correlation can be observed between the logarithm of the standard rate constant and the Pekar factor γ, as noted by Weaver et al.[86] for the tri(hexafluoroacetylacetonato)ruthenium(III) system.

In conclusion, although many studies of solvent effects have now been carried out, and the presence of a dynamic effect has been clearly established, the role of the solvent cannot be assessed on the basis of these data alone. This is chiefly because no good method of estimating the activation barrier exists except for the simplest systems. One way around this problem is to determine the activation enthalpy for the reaction by studying the temperature dependence of the heterogeneous rate constant. These experiments are considered in the following section.

5. The Experimental Activation Enthalpy

The temperature dependence of the standard rate constant for heterogeneous ET is particularly useful if available in different polar solvents, and also for both the homogeneous and heterogeneous reaction. The expression for the experimental activation enthalpy [Eq. (19)] is derived from Equation (15). ΔH^*_{is} is

$$\Delta H^*_{ex} = -R \frac{\partial \ln k_s}{\partial (1/T)} = \Delta H^*_{is} + \Delta H^*_{os} + \theta \Delta H_L \qquad (19)$$

the inner sphere activation enthalpy, and ΔH_L the enthalpy arising from the temperature dependence of the longitudinal relaxation time. ΔH_L is related to the temperature dependence of the Debye relaxation time τ_D, and the high-frequency and static dielectric constants ε_∞ and ε_s [Eq. (13)]. Values of the temperature coefficients of τ_D and ε_s are available for most polar solvents,[87] and that for ε_∞ can be estimated from the temperature coefficient of the refractive index of the solvent.[88] ΔH_L is not insignificant and varies from about 4 kJ mol^{-1} for solvents in which ET is fast to $\sim$13 kJ mol^{-1} for solvents in which ET is slow.

Solvent-dependent ΔH^*_{ex} data have been collected for a number of heterogeneous ET reactions including the electroreduction of the cobaltacenium cation,[69] cobaltocene,[88] the acetylacetonato complexes of Mn^{III} and Fe^{III},[77] benzophenone,[45] and a manganese(III) porphyrin.[79] Data are also available for

the electrooxidation of ferrocene[53, 70] and tetrathiofulvalene.[78] In general, ΔH_{ex}^{*} increases with increasing solvent viscosity, as predicted by the ΔH_L term in Equation (19). The most interesting system from the point of view of heterogeneous ET is cobaltacene, because this molecule may be both oxidized to a cation and reduced to an anion. On the basis of the FB model the activation parameters for these reactions should not be the same, in contradiction to the predictions of the Marcus model. As activation enthalpy data are additionally available for the homogeneous ET between the cobaltacenium cation and the cobaltocene molecule,[89] this system is chosen here for more detailed examination.

The available data for the redox reactions of cobaltocene are summarized in Table 3. Where comparisons can be made, ΔH_{ex}^{*}

Table 3. Experimental activation enthalpy ΔH_{ex}^{*} for various redox reactions of cobaltacene in several aprotic solvents and the longitudinal relaxation enthalpy ΔH_L for the solvent. Oxidations to cations are indicated by (+/0) and reduction to anions by (0/−).

Solvent	ΔH_L [kJ mol^{-1}]	ΔH_{ex}^{*} [kJ mol^{-1}]		
		homogeneous (+/0) [89]	heterogeneous (+/0) [69]	heterogeneous (0/−) [88]
AC	3.7	18.4	20.9	-
AN	5.6	18.0	18.8	24.4
BuN	6.5	-		24.6
BzN	11.9	19.7	-	-
DMA	8.0	-	-	24.6
DMF	6.9	-	20.9	-
DMSO	10.7	20.1	23.0	25.1
HMPA	11.5	23.4	-	-
PC	13.4	-	-	28.0

for the homogeneous oxidation reaction is smaller than that for the corresponding heterogeneous reaction. Furthermore, ΔH_{ex}^{*} for the heterogeneous reduction reaction is larger than that for the oxidation reaction.[88] The experimental results are often smaller than the continuum estimates of ΔH_{os}^{*} (see Table 1). Since both the inner sphere activation enthalpy and the longitudinal relaxation enthalpy contribute to ΔH_{ex}^{*}, these data strongly confirm that the continuum estimates of ΔH_{os}^{*} are too large. One method of testing the models considered here is to plot $\Delta H_{ex}^{*} - \Delta H_{os}^{*}$ against ΔH_L and to obtain θ from the slope and ΔH_{is}^{*} from the intercept.[88] These plots using the FB estimates of ΔH_{os}^{*} are shown in Figure 3 for both the homogeneous and heterogeneous data. Reasonable linear plots are obtained for both cases, the slope being larger for the homogeneous data. The FB model seems to overestimate the activation parameters for the homogeneous case, perhaps because the two reactants are close to one another in the transition state. This conclusion is supported by the observation that the intercept which gives ΔH_{is}^{*} is significantly smaller than independent estimates of this quantity (2.1 kJ mol^{-1} [89]). When the same analysis is applied to the heterogeneous data, very striking results are obtained with the FB model: the data for the electroreduction of cobaltacene lie on the same line as those for the electrooxidation of the same molecule. These results support the proposition that differences in the solvation of cations and anions at static frequencies must be considered in estimating the activation parameters for ET reactions.[23]

Comparison of ΔH_{ex}^{*} for homogeneous and heterogeneous reactions of other systems demonstrates different features. In

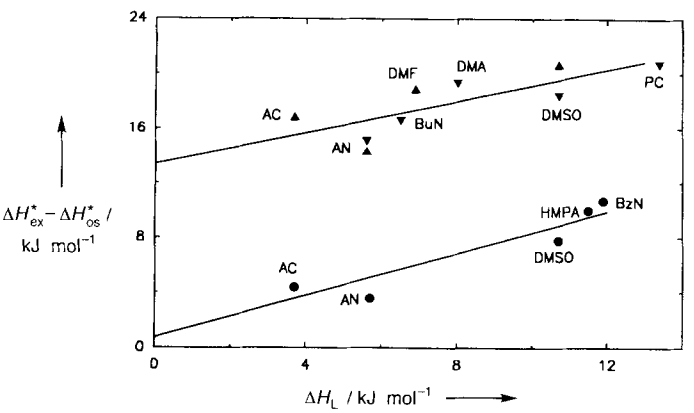


Fig. 3. Plot of the difference between the experimental activation enthalpy (ΔH_{ex}^{*}) and the outer sphere contribution according to the FB model (ΔH_{os}^{*}) for redox reactions with cobaltacene against the activation enthalpy for longitudinal relaxation ΔH_L. The homogeneous reaction is the oxidation of cobaltacene (●) and the heterogeneous reaction both oxidation (▲) and reduction (▼). The solid lines were obtained by linear regression using all the homogeneous or heterogeneous data (▲ and ▼). The ordinate for the heterogeneous data has been shifted vertically by 10 kJ mol^{-1} for clarity. The abbreviations for the solvents are given in Table 1.

the case of 1,4-diaminobenzene, the values of ΔH_{ex}^{*} determined for the heterogeneous reaction in acetonitrile and dimethylformamide[90] are much larger than the corresponding quantities for the homogeneous reaction.[91] This is certainly partly due to the dynamic solvent effect in the heterogeneous reaction,[73] which is absent from the homogeneous system.[30, 92] A more detailed analysis is not possible because data are available for only two solvents. Similar comments apply to the tetrathiafulvalene system.[78]

Particularly interesting results were described recently by Mu and Schultz,[79] who demonstrated both by means of rate constants and activation enthalpies for the reduction of a Mn^{III} porphyrin complex in six aprotic solvents that a dynamic solvent effect operates in a system with a quite large inner reorganization energy ($\Delta G_{is}^{*} = \Delta H_{is}^{*} \approx 16$ kJ mol^{-1}). These results suggest that factors other than those usually considered[1-4, 9, 11, 28] are important in determining the degree of reaction adiabaticity and hence the magnitude of the dynamic solvent effect. The reactant in this study is clearly nonspherical, and the authors estimated the effective radius from diffusion coefficient data. However, their values for ΔG_{os}^{*} and ΔH_{os}^{*} were based on the continuum model and therefore are probably too large. As a result, θ calculated from the solvent effect at 25 °C was different from that obtained from the activation enthalpy data.[79] When these quantities are deduced from the FB model, the values of θ (approximately 0.7) from the two analyses agree.

The temperature dependence of the standard rate constant in a series of polar solvents gives an additional powerful tool for examining the nature of the ET step. Under these circumstances the degree of reaction adiabaticity can be assessed provided an estimate of the effective radius of the reactant can be made. This subject is discussed in the following section.

6. Effects of the Reactant

The data available in the literature demonstrates that the standard rate constant in a given solvent varies by four orders of magnitude with the nature of the reactant.[33] Much of this

change is usually associated with variation in ΔG_{is}^{*} within the group of reactants considered, but some is also due to changes in ΔG_{os}^{*}. To gauge the ΔG_{os}^{*} contribution, an estimate of the effective radius of the reactant is needed. For this reason, much experimental effort has been directed at the metallocenes, which are simple from the point of view that they can be represented to a good approximation as spheres,[26] and buckminsterfullerene, whose heterogeneous ET kinetics have been studied more recently.[57, 61, 93] Quite good values of ΔG_{os}^{*} and ΔH_{os}^{*} were derived for buckminsterfullerene from the FB model when the effective reactant radius was assumed to be equal to the crystallographic radius (360 pm) plus the van der Waals radius of carbon (70 pm).[93]

However, most reactants are not spherical, and other methods must be used to deal with the shape of the molecule and the charge distribution within it. In early work Peover and Powell[94] studied the kinetics of electroreduction of nitrocompounds. As the charge on the anion radical formed became more delocalized, say on a benzene ring, the rate of reaction increased. A similar effect was observed in the electroreduction of a series of quinones in which the standard rate constant increased with the increasing number of benzene rings in the series benzoquinone < naphthoquinone < anthraquinone.[95]

Fawcett and Kharkats[96] extended the model proposed by Peover and Powell[94] to take into account volume correction terms when the reactant is represented as two contiguous conducting spheres. The expression for the effective radius r_e (neglecting the effect of images) is then given in Equation (20) where $F(r_x, r_i)$ is defined according to Equation (21). Here f_1

$$r_e = \left[\frac{f_1^2}{a} + \frac{f_2^2}{b} + 2\frac{f_1 f_2}{c} - f_1^2 F(c, b) - f_2^2 F(c, a)\right]^{-1} \quad (20)$$

$$F(r_x, r_i) = \frac{r_x}{2(r_x^2 - r_i^2)}\left[\frac{r_i}{r_x} - \left(1 - \frac{r_i^2}{r_x^2}\right)\ln\frac{r_x + r_i}{(r_x^2 - r_i^2)^{1/2}}\right] \quad (21)$$

and f_2 are the fractions of the total charge on spheres 1 and 2, a is the radius of sphere 1, b the radius of sphere 2, and c the distance between the centers of the spheres. For contiguous spheres, $c = a + b$. The first three terms represent the effect of the charges on the spheres irrespective of the fact that part of the solvation sheath of a given sphere is excluded by the proximity of the other sphere. The fourth and fifth terms account for the effects of the finite volume of each sphere. The excluded volume terms result in an increase in the effective radius of the reactant, and consequently in a decrease in ΔG_{os}^{*}. The effect is small if the radii of the two spheres are equal, but increases in importance as the relative sizes of the spheres change.[96] The effective radius can be used in the MSA model to obtain an improved estimate of ΔG_{os}^{*}, for example, by replacing r_A in Equation (7) by r_e.

Fawcett and Fedurco[45] recently extended the above model to the benzophenone system, which was represented as three contiguous spheres each in contact with two others. Two equally large spheres enclosed each of the phenyl rings and a smaller sphere surrounded the carbonyl group. In this case the excluded volume effect is more important. When the diameters of the contiguous spheres are defined by the structure of the molecule, such a model probably underestimates the extent of the solvation because of the chosen spherical shape for each part of the molecule. A better representation would involve contiguous ellipsoids, each extending somewhat further beyond the extreme parts of the molecule. However, a model with ellipsoids would involve more adjustable parameters and therefore would be less easily justifiable by experiment.

The excluded volume effect can also be used to explain the fact that the activation enthalpy for the homogeneous ET of the cobaltacenium (+/0) system is slightly smaller than that for it heterogeneous ET (see Table 3). According to Kharkats,[97] ΔG_{os}^{*} for homogeneous transfer of one electron between a spherical reactant of radius a to another of radius b is given within the context of Marcus continuum theory by Equation (22), in which r_e is defined by Equation (23) and the quantities c and $F(r_x, r_i)$

$$\Delta G_{os}^{*} = \frac{N_0 e_0^2}{16\pi\varepsilon_0 r_e}\left(\frac{1}{\varepsilon_{op}} - \frac{1}{\varepsilon_s}\right) \quad (22)$$

$$r_e = \left[\frac{1}{a} + \frac{1}{b} - \frac{2}{c} - F(c, a) - F(c, b)\right]^{-1} \quad (23)$$

have the same meaning as in Equation (20). When the spheres have equal radii and are in contact, ΔG_{os}^{*} is 6% smaller than when the excluded volume terms are ignored. This correction can also be made to yield the corresponding relationship for the MSA [Eq. (24)].

$$\Delta G_{os}^{*} = -\frac{N_0 e_0^2}{16\pi\varepsilon_0}\left[\left(1 - \frac{1}{\varepsilon_{op}}\right)\frac{1}{r_e} - \left(1 - \frac{1}{\varepsilon_s}\right)\frac{1}{(r_e + r_i/\lambda_i)}\right] \quad (24)$$

A different approach to dealing with the effects of molecular shape has been used by Grampp et al.[78, 91, 92, 98] In their work, the molecule is represented as an ellipsoid with semiaxes a, b, and c. This approach has been applied especially to data for homogeneous self-exchange reactions of organic molecules such as 1,4-diaminobenzene and its derivatives, tetracyanoethylene, tetracyano-*p*-quinonedimethane, and tetrathiofulvalene,[98] but also to heterogeneous ET reactions.[78] Such a description of the system requires more parameters than a model based on two continguous spheres. When applied to a diabatic system with data available both as a function of solvent and temperature,[91, 92] a detailed assessment of the mutual orientation of the reactants in the transition state is possible.[98] To date this approach has been limited to the Marcus continuum model for ΔG_{os}^{*}, but it could be easily extended to a nonprimitive model such as the MSA.

It should be emphasized that the above models have treated the reacting system as a conductor. There may be circumstances when such an assumption is not appropriate as discussed by German and Kuznetsov.[99, 100] These authors have considered the effects of polarizability on the estimation of ΔG_{os}^{*}, and developed models in which the reactant is represented as a dielectric cavity of given shape with embedded point charges. Hupp et al.[101] have shown that a dielectric cavity model is successful in accounting for the solvent dependence of optical intervalence charge-transfer absorption bands for symmetrical mixed-valence compounds. Charge transfer within the species $[(NH_3)_5Ru^{III}(4,4'\text{-bipyridine})\text{-}Ru^{II}(NH_3)_5]^{5+}$ was treated as dipole inversion within a low dielectric cavity; the length of the dipole (0.51 nm) was calculated from intervalence Stark effect measurements.[102] In contrast, a model based on conducting

spheres separated by a fixed distance [Eq. (22)] did not give a reasonable description of the same data. These authors obtained their spectroscopic data in very dilute solutions, thereby avoiding the effects of ion pairing on the spectral features. If the model based on two conducting spheres is valid, the absorption frequency observed in various solvents should be linear in the solvents' Pekar factor γ, and its slope will be determined by the geometrical parameters for the system [Eq. (23)]. Although this plot is linear,[101] the slope is much less than expected on the basis of reasonable values for the size parameters. A similar result is obtained for the bis(ferrocenyl)acetylene cation.[11, 82, 83] The analysis carried out by Hupp et al.[101] is quite important, because it suggests that a redox couple connected through a nonconducting bridge is not a good model for estimating the Gibbs activation energy for the homogeneous ET of the same redox couple.

Other compounds for which interesting structural effects on ET are seen are metalloporphyrins[79, 134–137] and oligodecker sandwich compounds.[138] An important question in metalloporphyrin redox chemistry is whether ET takes place at the metal ion or the porphyrin ring. Mu and Schultz[135] showed that the porphyrin-centered oxidation of Mn^{III} tetraphenylporphyrin chloride is much faster than the metal-centered reduction of the same compound. This observation was attributed to the much larger effective radius of the reactant and correspondingly smaller ΔG_{os}^{*} in the oxidation reaction in which the charge density is distributed over the porphyrin ring. Anxolabéhère et al.[136] concluded from kinetic data for the reduction of some tetraphenylporphyrin complexes and related compounds of more complex structure in DMF that solvent reorganization plays an important role in these fast heterogeneous ET reactions. Fawcett et al.[137] examined the redox chemistry of a stable (isoporphyrinato)zinc complex. The kinetic parameters they measured and their comparison with those for (octaethylporphyrinato)zinc suggest that ET takes place at the ring rather than the central metal ion. Interpretation of these data is greatly facilitated when activation parameters are measured.[79, 137]

Michels and Schmickler[138] have reported a study of heterogeneous ET with oligodecker sandwich compounds. These molecules are derived from metallocenes with 2,3-dihydro-1,3-diborol as a bridging ligand, for example 1,3,4,5-tetraethyl-2-methyl-1,3-diborolylbis(cyclopentadienyl)iron (BlFc). Many of these molecules can be both oxidized and reduced, and undergo some degree of inner sphere reorganization.[138] In the case of the BlFc, the rate constant for the oxidation process was 20 times larger than that for reduction at an Au electrode in dichloromethane. The activation enthalpies were 13.5 and 18.3 kJ mol^{-1} for the oxidation and reduction steps, respectively. These results suggest that inner sphere reorganization is not important for BlFc and support the general conclusion of the FB model that ΔG_{os}^{*} should be smaller for the formation of a cation by oxidation of a molecule than for the formation of an anion. Further studies of these systems would be interesting in the light of this question and others discussed in this review.

In summary, considerable progress has been made in recent years to develop reliable methods of estimating the effective size of the reactant in heterogeneous ET. As the theory of ion solvation progresses to develop nonprimitive models of nonspherical ions our understanding of the role of reactant shape in determining ET parameters will improve.

7. Double Layer Effects

Most recent studies of heterogeneous ET have involved redox couples in which the most highly charged species is a monovalent cation or anion. Often, an organic or organometallic molecule is selected to minimize double layer effects and effects due to ion pairing in the bulk of the electrolyte solution. Consequently, much less attention has been paid to redox couples of transition metal complexes with higher charge, although the structural effects in such systems are much easier to describe.

The choice of electrolyte is also important in establishing electrostatic conditions at the electrode/solution interface. In organic solutions, the electrolyte is most often a tetraalkylammonium (TAA^+) salt with a hard anion such as perchlorate, tetrafluoroborate or hexafluorophosphate. These salts are chosen to avoid ion pairing, which occurs with smaller ions, or problems with ionic adsorption on the electrode. For example, the anion radicals formed from nitro compounds strongly associate with alkali metal cations.[103, 104]

In addition, the presence of halide ions in the electrolyte makes it very difficult to interpret kinetic data obtained positive of the potential of zero charge, because these ions are strongly adsorbed on polarizable metals from all known polar solvents.[105] TAA^+ ions also adsorb on the electrode, but the nature of the adsorption appears to be more electrostatic rather than chemical, and solvophobicity plays a role. These ions also form aggregates with some anion radicals; notable examples are the strong ion associates found between C_{60}^{-} and C_{60}^{2-} anions and TAA^+ cations.[57]

When heterogeneous ET occurs at potentials negative of the point of zero charge in the presence of TAA^+ ions, the standard rate constant decreases with increasing size of the alkyl group,[106–113] though the activation enthalpy is relatively independent of cation size.[45, 106, 108, 112, 113] Moreover, the relative magnitudes of the inhibitory effect increases as the electrode potential is made more negative.[111] These observations can be rationalized if it is assumed that the TAA^+ ions are adsorbed on the electrode to form a monolayer whose thickness and extent depend on the size of the ion and electrode potential.[111–113] On the basis of capacity data we proposed[113] that the alkyl arms of these ions are bent when the chain contains more than three carbon atoms with the result that the distance of closest approach of the central nitrogen atom is approximately constant for the larger ions. This model can explain the decrease in standard rate constant as electron tunneling through a layer of TAA^+ ions.[114–116] Since the activation enthalpy depends only on the solvent and not on the size of the TAA^+ ion, ET must take place outside the adsorbed ionic layer in a region where reactant and product are still interacting chiefly with surrounding solvent molecules.[111, 113]

Other recent work on electron tunneling through barrier films has involved self-assembled monolayers. Miller et al.[117, 118] used ω-hydroxythiols to form a self-assembled monolayer on a gold electrode. The thiol functionality at one end of the hydrocarbon chain reacts with gold to form a mercaptide, thereby anchoring the molecule to the surface. Interactions between water and the hydroxy groups at the other end of the molecule make the monolayer compact. These authors[117, 118] showed that electron tunneling is the main mechanism for ET to a redox

system outside the monolayer in solution. By varying the chain length of the molecule forming the self-assembled monolayer they demonstrated that the tunneling current depends exponentially on film thickness. This corresponds to an exponential decrease in the electronic transmission coefficient κ in Equation (8).[115, 116]

Chidsey[119] used a self-assembled monolayer on gold with an electroactive terminal group on a fraction of the anchored groups to study ET through films of varying thickness. The electroactive terminal group was ferrocene, which is oxidized to the ferrocenium cation by fast ET. The monolayer consisting of hydrocarbon chains with 15 CH_2 groups slowed the reaction down sufficiently for collection of ET kinetic data over a voltage range of almost 2 V. Analysis of the dependence of the rate constant on potential provided evidence that the Gibbs activation energy is indeed a quadratic function of potential as predicted by Marcus theory.[12] Chidsey estimated the experimental value of ΔG^* for the ferrocene/ferrocenium system in water to be 20.5 kJ mol^{-1}. This result is significantly lower than the estimate of ΔG^*_{os} in water by continuum theory (25.8 kJ mol^{-1}). The FB model yields 17.4 kJ mol^{-1} for the same quantity. As a small contribution from inner sphere reorganization must be added (about 1 kJ mol^{-1}), the experimental result is very close to the value predicted by the MSA.

In a similar study by Finklea and Hanshew,[120] the redox group was pentaammine(pyridine)ruthenium$^{3+/2+}$. The experimental value for ΔG^* varied somewhat with the length of the hydrocarbon chain and presence or absence of spacer chains in the self-assembled monolayer. The role of the low dielectric monolayer in determining ΔG^*_{os} thus seems to change in the systems studied. Their results also support the conclusion that ΔG^*_{os} is overestimated by the continuum model [Eq. (2)].

Smith and White[121] have discussed double layer effects on both the thermodynamic and kinetic properties of a self-assembled monolayer modified with a redox couple. Since the redox couple is not present in the bulk of the solution, the equilibrium potential for the surface-attached redox couple depends on the local (micro) potentials at their oxidized and reduced forms when these are significantly different from the average potential in the bulk of the solution. These authors[121] determined an average potential ϕ^p in the plane through the centers of the redox species from measurable thermodynamic quantities, and showed that when this potential is used to approximate the local potential, a reasonable description of the variation in equilibrium potential of the redox couple with dielectric properties of the interface is possible. Furthermore, the effect of the charge associated with the redox couple on the shape of the current-voltage curve in linear sweep voltammetry depends on the dielectric properties of the interfacial region, their potential dependence, and the potential of zero charge. The calculations were performed according to the classical Frumkin theory[122, 123] for double layer effects in electrode kinetics. Creager and Weber[124] extended this work by considering double layer effects on the current–time transients in potential step experiments involving a self-assembled monolayer modified with a redox couple.

The Frumkin equation for the logarithm of the forward rate constant of the redox couple [see Eq. (1)], corrected for the double layer is usually written as Equation (25) where k_f is the

$$\ln k_f + z_A f\phi^d = \ln k_s + \alpha_a f(\phi^d - E - E_s) \quad (25)$$

forward rate constant, ϕ^d the average potential drop across the diffuse layer, z_A the charge on the reactant, E the electrode potential, E_s the standard electrode potential, α_a the apparent transfer coefficient, and $f = F/RT$. The transfer coefficient is termed apparent, because the actual potential experienced by the reactant may differ from ϕ^d for a variety of reasons, which are generally termed discreteness-of-charge effects.[125–127] These effects are most noticeable when discrete charges are fixed at a dielectric discontinuity in the system[128] such as the electrode/solution interface for an unmodified electrode, or the hydrocarbon/solution interface in the systems studied by Chidsey[119] and Finklea and Hanshew.[120] The local potential at an anchored redox system Ψ^p may differ significantly from the average value in the plane through their centers (ϕ^p). When this is true, the potential drop ϕ^d in Equation (25) should be replaced by the local potential Ψ^p.[127]

Becka and Miller[129] studied double layer effects at uncharged self-assembled monolayers and showed that the kinetics of heterogeneous ET at the monolayer/solution interface depends both on the charge on the reactant and the composition of the monolayer. The reduction of $[Fe(CN)_6]^{3-}$ at a ω-hydroxyldodecanethiol monolayer was considerably faster than at a dodecanethiol monolayer at potentials negative of the potential of zero charge. The authors attributed the difference to the fact that the self-assembled monolayer terminated with the hydroxy group is less hydrophobic, and the reactant can approach closer to the insulating film. In the case of $[Fe(bipyridine)CN_4]^-$, the opposite effect, namely, a faster reaction at the methyl-terminated monolayer, is observed. This reactant is more hydrophobic and bears a smaller charge. These results can also be partly attributed to discreteness-of-charge effects. Because of the large change in dielectric constant from a low value in the oil-like monolayer (about 2) to a high value in the aqueous solution (about 78), the reactant experiences strong repulsion at the monolayer/solution boundary. The electrostatic effect[128] is much more important for the polyvalent $[Fe(CN)_6]^{3-}$ ion.

Discreteness-of-charge effects have also been discussed for heterogeneous ET reactions at mercury electrodes in the presence of specifically adsorbed nonreacting ions.[130–133] Three of the systems studied[131–133] involved transition metal complexes in which the metal ion is reduced from the +3 to +2 oxidation state in the presence of specifically adsorbed anions. By carrying out these experiments at constant ionic strength, and examining the changes in the corrected logarithm of the rate constant ($y = \ln k_f + z_A f\phi^d$) with adsorbed charge density σ_a at constant potential drop across the inner layer ($E - E_s - \phi^d$), the electrostatic effects of the adsorbed ions with a minimum in change in other double layer properties can be examined [see Eq. (25)]. Because the adsorbed ions are located at the metal/solution interface, their electrostatic accelerating effect is significantly reduced by the shielding effect of the metal. If the simple Frumkin equation were correct, the kinetic parameter y would be independent of ($E - E_s - \phi^d$) for changes in the surface coverage by adsorbed anions. In the case of $[Co(NH_3)F]^{2+}$, y decreases with increasing σ_a as qualitatively expected on the basis of the discreteness-of-charge effect.[133] However, when an anion such as tetrathionate is reduced in the presence of adsorbed

iodide anions, the decelerating effect of the adsorbed charge is overestimated when discreteness-of-charge effects are ignored, and the value of y increases with increasing σ_a.[130] Further analysis of these data[130–133] led to a more detailed description of the double layer effect including the location of the reaction site with respect to adsorbed ions and counterions.

Double layer effects can be quite important in heterogeneous ET reactions especially when the reactants are highly charged. Analysis of these effects requires interfacial thermodynamic data for the electrolyte system under investigation. The lack of these data has often prevented attempts to examine the double layer effect in more detail. However, modern experimental techniques, especially those based on impedance, provide these data relatively easily. Double layer effects at self-assembled monolayers, which are excellent systems for testing in more detail the theories which have been in the literature for some time, are just beginning to be investigated.

8. Conclusions

Studies of solvent effects for heterogeneous ET reactions have done much to increase the understanding of fundamental aspects of this elementary chemical reaction. This is especially true when kinetic data are obtained both as a function of solvent and of temperature so that the variation in activation enthalpy may also be examined. Studies of the redox reactions of the metallocenes[44, 53, 69, 70, 74, 88, 89, 110] have been especially important because the reactants are relatively spherical in shape and undergo very small internal reorganization on ET.

There is strong evidence from recent experimental work that the activation parameters for outer sphere reorganization are overestimated by the original Marcus formulation.[12] This is not at all surprising, since it is well-known from equilibrium solvation data for simple ions that the Born model gives unrealistically high values of the Gibbs energy and enthalpy of solvation. The most important feature of any improvement on the Born model is that it recognizes the differences in the solvation of cations and anions. The rate constant for formation of a cation from a molecule is expected to be faster than that for formation of an anion, all other factors remaining the same, as in the case of cobaltacene[88, 110] and related compounds.[138] This prediction should be examined for other molecules for which these reactions can be carried out.

Heterogeneous ET can be understood in at least as much detail as homogeneous ET. Although double layer effects must be considered, their importance can be reduced by careful choice of the electrolyte. Homogeneous ET kinetics has the additional complication that the reactants may assume a particular configuration with respect to one another in the transition state.[98] Such steric effects need to be examined in more detail, but they should be simpler in the heterogeneous ET reaction where the electrical field due to the charge on the electrode plays an important role.[106] Changes in the nature of the steric effect with the type of ET reaction may be the cause of the differences in the relative ordering of rate constants for various metallocenes seen in the homogeneous and heterogeneous regimes.[11]

Self-assembled monolayers with anchored redox groups[119, 120] have provided an interesting new way of studying heterogeneous ET. In these systems, the environment of the redox reaction is entirely different from that at the electrode/solution interface. Thus, the comparison of data obtained in the two systems will provide valuable information on the role of environmental effects in heterogeneous ET.

In conclusion, the understanding of ET has advanced considerably during the last decade. Though it has provided a fruitful area for both theoretical and experimental work, many problems remain to be solved, and research in this field will continue to present a challenge.

Recent work from this laboratory discussed in this review was supported by the Office of Naval Research, Washington, and by the National Science Foundation, Washington (Grant No. CHE 9008171).

Received: September 17, 1993 [A 26]
German version: *Angew. Chem.* **1994**, *106*, 2239

[1] L. D. Zusman, *Chem. Phys.* **1980**, *49*, 295; *ibid.* **1983**, *80*, 29.
[2] I. V. Alexandrov, *Chem. Phys.* **1980**, *51*, 449.
[3] M. Y. Ovchinnikova, *Theor. Exp. Chem. Engl. Transl.* **1981**, *17*, 651.
[4] D. F. Calef, P. G. Wolynes, *J. Phys. Chem.* **1983**, *87*, 3387.
[5] A. Kapturkiewicz, B. Behr, *J. Electroanal. Chem. Interfacial Electrochem.* **1984**, *179*, 187.
[6] W. Harrer, G. Grampp, W. Jaenicke, *Chem. Phys. Lett.* **1984**, *112*, 263.
[7] B. Bagchi, *Annu. Rev. Phys. Chem.* **1989**, *40*, 115.
[8] M. Newton, *Chem. Rev.* **1991**, *91*, 767.
[9] H. Heitele, *Angew. Chem.* **1993**, *105*, 378; *Angew. Chem. Int. Ed. Engl.* **1993**, *32*, 359.
[10] P. Barbara, W. Jarzeba, *Adv. Photochem.* **1990**, *15*, 1.
[11] M. J. Weaver, *Chem. Rev.* **1992**, *92*, 463; see also M. J. Weaver, G. E. McManis, *Acc. Chem. Res.* **1990**, *23*, 294.
[12] R. A. Marcus, *J. Chem. Phys.* **1965**, *43*, 679.
[13] N. Sutin, *Prog. Inorg. Chem.* **1983**, *30*, 441.
[14] P. G. Dzhavakhidze, A. A. Kornyshev, L. I. Krishtalik, *J. Electroanal. Chem. Interfacial Electrochem.* **1987**, *228*, 329.
[15] D. K. Phelps, A. A. Kornyshev, M. J. Weaver, *J. Phys. Chem.* **1990**, *94*, 1454.
[16] L. Blum, *Chem. Phys. Lett.* **1974**, *26*, 200; *J. Chem. Phys.* **1974**, *61*, 1556.
[17] S. A. Adelman, J. M. Deutch, *J. Chem. Phys.* **1974**, *60*, 3935.
[18] R. A. Marcus in *Special Topics in Electrochemistry* (Ed.: P. A. Rock), Elsevier, Amsterdam, **1977**.
[19] P. G. Wolynes, *J. Chem. Phys.* **1987**, *86*, 5133.
[20] G. E. McManis, M. J. Weaver, *J. Chem. Phys.* **1989**, *90*, 1720.
[21] L. Blum, W. R. Fawcett, *J. Phys. Chem.* **1992**, *96*, 408.
[22] W. R. Fawcett, L. Blum, *J. Chem. Soc. Faraday Trans.* **1992**, *88*, 3339.
[23] W. R. Fawcett, L. Blum, *Chem. Phys. Lett.* **1991**, *187*, 173.
[24] Y. Marcus, *Ion Solvation*, Wiley-Interscience, New York, **1985**.
[25] J. A. Riddick, W. B. Bunger, T. K. Sakano, *Organic Solvents*, 4th edition, Wiley-Interscience, New York, **1986**.
[26] L. I. Krishtalik, N. M. Alpatova, E. V. Ovsyannikova, *Electrochim. Acta* **1991**, *36*, 435.
[27] L. Blum, W. R. Fawcett, *J. Phys. Chem.* **1993**, *97*, 7185.
[28] J. T. Hynes, *J. Phys. Chem.* **1986**, *90*, 3701.
[29] J. T. Hupp, M. J. Weaver, *J. Electroanal. Chem. Interfacial Electrochem.* **1983**, *152*, 1; J. T. Hupp, M. J. Weaver, *J. Phys. Chem.* **1984**, *88*, 1463.
[30] W. R. Fawcett, C. A. Foss, Jr., *J. Electroanal. Chem. Interfacial Electrochem.* **1989**, *270*, 103.
[31] H. L. Friedman, *J. Chem. Soc. Faraday Trans. 2* **1983**, *79*, 1465.
[32] W. R. Fawcett, C. A. Foss, Jr., *Electrochim. Acta* **1991**, *36*, 1767; *J. Electroanal. Chem. Interfacial Electrochem.* **1991**, *306*, 71.
[33] W. R. Fawcett, M. Opallo, *J. Electroanal. Chem. Interfacial Electrochem.* **1993**, *349*, 273.
[34] M. McGuire, G. McLendon, *J. Phys. Chem.* **1986**, *90*, 1549.
[35] W. Nadler, R. A. Marcus, *J. Chem. Phys.* **1987**, *86*, 3906.
[36] J. Barthel, K. Bachhuber, R. Buchner, H. Hetzenauer, *Chem. Phys. Lett.* **1990**, *165*, 369; J. Barthel, K. Bachhuber, R. Buchner, J. B. Gill, M. Kleebauer, *ibid.* **1990**, *167*, 62.
[37] W. R. Fawcett, *Chem. Phys. Lett.* **1992**, *199*, 153.
[38] R. R. Dogonadze in *Reactions of Molecules at Electrodes* (Ed.: N. S. Hush) Wiley-Interscience, New York, **1971**, Chap. 3.
[39] W. Schmickler, *J. Electroanal. Chem. Interfacial Electrochem.* **1986**, *204*, 31.
[40] M. Fleischmann, S. Pons, D. R. Rolison, P. P. Schmidt, *Ultramicroelectrodes*, Datatech Systems, Morgantown, NC, USA, **1987**.
[41] C. P. Andrieux, P. Hapiot, J. M. Saveant, *Chem. Rev.* **1990**, *90*, 723.

[42] J. Heinze, *Angew. Chem.* **1993**, *105*, 1327; *Angew. Chem. Int. Ed. Engl.* **1993**, *32*, 1268; *ibid.* **1991**, *103*, 175 and **1991**, *31*, 170.
[43] W. Lu, A. S. Baranski, *J. Electroanal. Chem. Interfacial Electrochem.* **1992**, *335*, 105.
[44] K. Winkler, A. S. Baranski, *J. Electroanal. Chem. Interfacial Electrochem.* **1993**, *346*, 197.
[45] W. R. Fawcett, M. Fedurco, *J. Phys. Chem.* **1993**, *97*, 7075.
[46] R. M. Penner, M. J. Heben, T. L. Longin, N. S. Lewis, *Science* **1990**, *250*, 1118.
[47] A. S. Baranski, *J. Electroanal. Chem. Interfacial Electrochem.* **1991**, *307*, 287.
[48] K. B. Oldham, *Anal. Chem.* **1992**, *64*, 646.
[49] D. O. Wipf, E. W. Kristensen, D. R. Deakin, R. M. Wightman, *Anal. Chem.* **1988**, *60*, 306.
[50] A. M. Bond, T. L. E. Henderson, D. R. Mann, T. F. Mann, W. Thormann, C. G. Zoski, *Anal. Chem.* **1988**, *60*, 1878.
[51] L. K. Safford, M. J. Weaver, *J. Electroanal. Chem. Interfacial Electrochem.* **1991**, *312*, 69.
[52] A. S. Baranski, *J. Electrochem. Soc.* **1986**, *133*, 93.
[53] A. S. Baranski, K. Winkler, W. R. Fawcett, *J. Electroanal. Chem. Interfacial Electrochem.* **1991**, *313*, 367.
[54] A. S. Baranski, *J. Electroanal. Chem. Interfacial Electrochem.* **1991**, *300*, 309.
[55] M. Sluyters-Rehbach, J. Sluyters, *Compr. Treatise Electrochem. 1980–1985* **1984**, *9*, Chap. 4.
[56] D. D. Macdonald, *Transient Techniques in Electrochemistry*, Plenum, New York, **1977**, Chap. 7.
[57] W. R. Fawcett, M. Opallo, M. Fedurco, J. W. Lee, *J. Am. Chem. Soc.* **1993**, *115*, 196.
[58] A. J. Bard, M. V. Mirkin, P. R. Univin, D. O. Wipf, *J. Phys. Chem.* **1992**, *96*, 1861.
[59] M. V. Mirkin, A. J. Bard, *J. Electrochem. Soc.* **1992**, *139*, 3535.
[60] M. V. Mirkin, T. C. Richards, A. J. Bard, *J. Phys. Chem.* **1993**, *97*, 7672.
[61] M. V. Mirkin, L. O. S. Bulhoes, A. J. Bard, *J. Am. Chem. Soc.* **1993**, *115*, 201.
[62] M. A. M. Noel, J. J. O'Dea, R. A. Osteryoung, *J. Electrochem. Soc.* **1992**, *139*, 1231.
[63] Z. J. Karpinski, R. A. Osteryoung, *J. Electroanal. Chem. Interfacial Electrochem.* **1993**, *349*, 285.
[64] F. Mahlendorf, J. Heinze, *J. Electroanal. Chem. Interfacial Electrochem.* **1993**, *352*, 119.
[65] M. I. Montenegro, D. Pletcher, *J. Electroanal. Chem. Interfacial Electrochem.* **1986**, *200*, 371.
[66] A. Russell, K. Repka, T. Dibble, J. Ghoroghchian, J. J. Smith, M. Fleischmann, C. H. Pitt, S. Pons, *Anal. Chem.* **1986**, *58*, 2961.
[67] A. P. Abbott, C. L. Miaw, J. F. Rusling, *J. Electroanal. Chem. Interfacial Electrochem.* **1992**, *327*, 31.
[68] J. Labagnini, P. Pastore, F. Magno, *J. Electroanal. Chem. Interfacial Electrochem.* **1992**, *333*, 1.
[69] T. Gennett, D. F. Milner, M. J. Weaver, *J. Phys. Chem.* **1985**, *89*, 2787.
[70] L. K. Safford, M. J. Weaver, *J. Electroanal. Chem. Interfacial Electrochem.* **1992**, *331*, 857.
[71] W. R. Fawcett, *Langmuir* **1989**, *5*, 661.
[72] Z. Galus, *Pure Appl. Chem.* **1991**, *63*, 1705.
[73] M. Opallo, *J. Chem. Soc. Faraday Trans 1* **1986**, *89*, 2287.
[74] G. E. McManis, M. N. Golovin, M. J. Weaver, *J. Phys. Chem.* **1986**, *90*, 6563.
[75] M. Opallo, A. Kapturkiewicz, *Electrochim Acta* **1985**, *30*, 1301.
[76] D. A. Corrigan, D. H. Evans, *J. Electroanal. Chem. Interfacial Electrochem.* **1987**, *233*, 161.
[77] W. R. Fawcett, M. Opallo, *J. Electroanal. Chem. Interfacial Electrochem.* **1992**, *331*, 815.
[78] G. Grampp, A. Kapturkiewicz, W. Jaenicke, *Ber. Bunsenges. Phys. Chem.* **1990**, *94*, 439.
[79] X. H. Mu, F. A. Schultz, *J. Electroanal. Chem. Interfacial Electrochem.* **1993**, *353*, 349.
[80] D. K. Phelps, M. T. Ramm, Y. Wang, S. F. Nelson, M. J. Weaver, *J. Phys. Chem.* **1993**, *97*, 181.
[81] R. M. Nielson, M. J. Weaver, *J. Electroanal. Chem. Interfacial Electrochem.* **1989**, *260*, 15.
[82] G. E. McManis, A. Gochev, R. M. Nielson, M. J. Weaver, *J. Phys. Chem.* **1989**, *93*, 7733.
[83] M. J. Powers, T. J. Meyer, *J. Am. Chem. Soc.* **1978**, *100*, 4393.
[84] W. Harrer, G. Grampp, W. Jaenicke, *J. Electroanal. Chem. Interfacial Electrochem.* **1986**, *209*, 23.
[85] W. R. Fawcett, C. A. Foss, Jr., *J. Electroanal. Chem. Interfacial Electrochem.* **1988**, *252*, 221.
[86] M. J. Weaver, D. K. Phelps, R. M. Nielson, M. N. Golovin, G. E. McManis, *J. Phys. Chem.* **1990**, *94*, 2949.
[87] W. R. Fawcett, *Chem. Phys. Lett.* **1990**, *174*, 167.
[88] W. R. Fawcett, M. Opallo, *J. Phys. Chem.* **1992**, *96*, 2920.
[89] R. M. Nielson, G. E. McManis, M. N. Golovin, M. J. Weaver, *J. Phys. Chem.* **1988**, *92*, 3441.
[90] A. Kapturkiewicz, W. Jaenicke, *J. Chem. Soc. Faraday Trans. 1* **1987**, *83*, 2727.
[91] G. Grampp, W. Jaenicke, *Ber. Bunsenges. Phys. Chem.* **1984**, *88*, 335.
[92] G. Crampp, W. Jaenicke, *Ber. Bunsenges. Phys. Chem.* **1984**, *88*, 325.
[93] W. R. Fawcett, M. Opallo, M. Fedurco, J. W. Lee, *J. Electroanal. Chem. Interfacial Electrochem.* **1993**, *344*, 375.
[94] M. E. Peover, J. S. Powell, *J. Electroanal. Chem. Interfacial Electrochem.* **1969**, *20*, 427.
[95] J. O. Howell, R. M. Wightman, *Anal. Chem.* **1984**, *56*, 524.
[96] W. R. Fawcett, Y. I. Kharkats, *J. Electroanal. Chem. Interfacial Electrochem.* **1973**, *47*, 413.
[97] Y. I. Kharkats, *Electrokhimiya* **1973**, *9*, 881.
[98] G. Grampp, W. Jaenicke, *Ber. Bunsenges. Phys. Chem.* **1991**, *95*, 904.
[99] E. D. German, A. M. Kuznetsov, *Electrochim. Acta* **1981**, *26*, 1595.
[100] E. D. German, A. M. Kuznetsov, *Elektrokhimiya* **1990**, *26*, 931.
[101] J. T. Hupp, Y. Dong, R. L. Blackbourn, H. Lee, *J. Phys. Chem.* **1993**, *97*, 3278.
[102] D. H. Oh, S. G. Boxer, *J. Am. Chem. Soc.* **1990**, *112*, 8161.
[103] B. G. Chauhan, W. R. Fawcett, A. Lasia, *J. Phys. Chem.* **1977**, *81*, 1476.
[104] W. R. Fawcett, A. Lasia, *J. Phys. Chem.* **1978**, *82*, 1114.
[105] M. D. Levi, A. V. Shlepakov, B. B. Damaskin, I. A. Bagotskaya, *J. Electroanal. Chem. Interfacial Electrochem.* **1982**, *138*, 1.
[106] A. S. Baranski, W. R. Fawcett, *J. Electroanal. Chem. Interfacial Electrochem.* **1979**, *100*, 287.
[107] D. A. Corrigan, D. C. Evans, *J. Electroanal. Chem. Interfacial Electrochem.* **1980**, *106*, 287.
[108] C. Russel, W. Jaenicke, *J. Electroanal. Chem. Interfacial Electrochem.* **1984**, *180*, 205.
[109] A. Kapturkiewicz, M. Opallo, *J. Electroanal. Chem. Interfacial Electrochem.* **1985**, *185*, 15.
[110] T. Gennett, M. J. Weaver, *J. Electroanal. Chem. Interfacial Electrochem.* **1985**, *186*, 179.
[111] R. A. Petersen, D. H. Evans, *J. Electroanal. Chem. Interfacial Electrochem.* **1987**, *222*, 129.
[112] D. H. Evans, A. G. Gilicinski, *J. Phys. Chem.* **1992**, *96*, 2528.
[113] W. R. Fawcett, M. Fedurco, M. Opallo, *J. Phys. Chem.* **1992**, *96*, 9959.
[114] J. W. Schultze, K. J. Vetter, *Electrochim. Acta* **1973**, *18*, 889.
[115] W. Schmickler, *J. Electroanal. Chem. Interfacial Electrochem.* **1977**, *82*, 65.
[116] J. Lipkowski, C. Buess-Hermann, J. P. Lambert, L. Gierst, *J. Electroanal. Chem. Interfacial Electrochem.* **1986**, *202*, 169.
[117] C. Miller, P. Cuendet, M. Grätzel, *J. Phys. Chem.* **1991**, *95*, 877.
[118] C. Miller, M. Grätzel, *J. Phys. Chem.* **1991**, *95*, 5225.
[119] C. E. D. Chidsey, *Science* **1991**, *251*, 919.
[120] H. O. Finklea, D. D. Hanshew, *J. Am. Chem. Soc.* **1992**, *114*, 3173.
[121] C. P. Smith, H. S. White, *Anal. Chem.* **1992**, *64*, 2396.
[122] A. N. Frumkin, *Potensialy Nulevogo Zariada*, Izdatel'stovo Nauka, Moscow, **1979**, Chap. 9.
[123] P. Delahay, *Double Layer and Electrode Kinetics*, Wiley-Interscience, New York, **1965**, Chap. 9.
[124] S. E. Creager, K. Weber, *Langmuir* **1993**, *9*, 844.
[125] W. R. Fawcett, S. Levine, *J. Electroanal. Chem. Interfacial Electrochem.* **1973**, *43*, 175.
[126] W. R. Fawcett, *J. Chem. Phys.* **1974**, *61*, 3842.
[127] W. R. Fawcett, *Can. J. Chem.* **1981**, *59*, 1844.
[128] S. Levine, J. Mingins, G. M. Bell, *J. Electroanal. Chem. Interfacial Electrochem.* **1967**, *13*, 280.
[129] A. M. Becka, C. J. Miller, *J. Phys. Chem.* **1993**, *97*, 6233.
[130] W. R. Fawcett, K. Markušova, *Can. J. Chem.* **1982**, *60*, 2038.
[131] W. R. Fawcett, K. Markušova, *Can. J. Chem.* **1983**, *61*, 2821.
[132] W. R. Fawcett, K. Markušova, *Can. J. Chem.* **1984**, *62*, 1497.
[133] W. R. Fawcett, P. H. Solomon, *J. Electroanal. Chem. Interfacial Electrochem.* **1988**, *251*, 183.
[134] W. R. Fawcett, *J. Phys. Chem.* **1993**, *97*, 9540.
[135] X. H. Mu, F. A. Schultz, *Inorg. Chem.* **1990**, *29*, 2877.
[136] E. Anxolabéhère, D. Lexa, J.-M. Savéant, *J. Phys. Chem.* **1992**, *96*, 1266.
[137] W. R. Fawcett, M. Feduro, K. M. Smith, H. Xie, *J. Electroanal. Chem. Interfacial Electrochem.* **1993**, *354*, 281.
[138] L. Michels, W. Schmickler, *J. Electroanal. Chem. Interfacial Electrochem.* **1990**, *295*, 139.

Otto Roelen, Pioneer in Industrial Homogeneous Catalysis

Boy Cornils,* Wolfgang A. Herrmann, and Manfred Rasch

Dedicated to Wolfgang Hilger on the occasion of his 65th birthday

Otto Roelen discovered the oxo synthesis (hydroformylation) in 1938, and despite all the problems created by the war years he was able to explore successfully the fundamental aspects related to its application up to the point of building the first plant. At the same time he laid the groundwork for industrial utilization of homogeneous organometallic catalysts. Almost simultaneously, his contemporary, Walter Hieber, was investigating the basic chemistry of the same catalysts, but with no knowledge whatsoever of their potential application. Hydroformylation today constitutes one of the most important industrial examples of a homogeneous catalytic process.

A unique opportunity for academic and industrial chemists to engage in a goal-oriented collaborative effort with respect to an important new synthetic method was missed in this case, however—missed less as a consequence of events of the day than because of the differing mentalities of two difficult personalities. In less turbulent times these two unpredictable individuals might well have collaborated. A number of contemporary documents published here for the first time, supplemented by Allied reports related to "hidden reparations," provide interesting insights into the nature of this particular discovery and its subsequent course of development.

1. The Researcher and the Man: University, Research Institute, and Industry

"...that Herr dipl. Ing. Roelen has been educated both theoretically and practically to such an extent that he would represent no obstacle to further progress in the work being conducted there. To all intents and purposes, R. carried out his thesis work completely independently, indeed very reliably, and with an equivalent amount of diligence. The only thing I might criticize is his tendency to theorize, but this is probably only a result of the fact that R. did an unbelievable amount of both work and reading. With respect to his knowledge, R. is far above the average for other doctoral candidates."[**]

This brief report accurately describing the distinguishing characteristics of its subject was written by Prof. Alexander Gutbier of the Laboratory for Inorganic Chemistry and Inorganic Chemical Technology at the Technische Hochschule Stuttgart and accompanied Otto Roelen on June 26, 1922 when he arrived at the Kaiser-Wilhelm-Institut für Kohlenforschung (KWI) in Mülheim an der Ruhr, where he would begin work under the supervision of Prof. Franz Fischer, Director of the Institute, and Fischer's Section Leader, Dr. Hans Tropsch, in the general area of hydrocarbon synthesis.[1]

Although Otto Roelen was himself born in Mülheim on March 22, 1897, and as a high school student witnessed the official dedication of the KWI on July 27, 1914, his future career was in no sense as predestined as it might appear in retrospect. Roelen attended the Königliche Realgymnasium (Royal High School) in his hometown, where he was awarded a wartime diploma on August 4, 1914. He did not immediately volunteer for military service, however, choosing instead to serve a six-month internship at the nearby blast furnace and foundry works of the Friedrich Wilhelms-Hütte before registering as a chemistry student at the Technische Hochschule München. He was one of only 21 students there between 1914 and 1918, and must have taken the introductory chemistry course taught by Wilhelm Manchot (cf. Section 3.1). Roelen was finally drafted in July of 1915, and participated as an artillerist in the battles in Flanders, where he was wounded in 1917. At that time he held the rank of artillery mate with the 2nd Marine Artillery Division of the 2nd Heavy Corps Artillery Regiment.[2] Subsequent to his injury he was no longer considered fit for active duty, and was employed as a "chemical technician" at the Royal Submarine Shipyard in Wilhelmshaven, where he was stationed when the war ended. By his own report he had joined a local Workers' and Soldiers'

[*] Prof. Dr. B. Cornils
Hoechst AG, D-65926 Frankfurt am Main (FRG)
Telefax: Int. code + (69) 305-301954
Prof. Dr. W. A. Herrmann
Anorganisch-chemisches Institut
der Technischen Universität München
Lichtenbergstrasse 4, D-85747 Garching (FRG)
Dr. M. Rasch
Thyssen AG, Archiv
D-47161 Duisburg (FRG)

[**] The original German quotations may be found in the German issue, *Angew. Chemie* **1994**, *106*, 2219–2238

Council ("Arbeiter- und Soldatenrat"),[3] but nothing is known regarding the reasons for his apparent participation in the Council Movement, and there is in fact no independent documentation of this involvement. Indeed, it seems quite inconsistent with his later attitudes, and he was never again active in politics. His alleged membership in the Wilhelmshaven Workers' and Soldiers' Council may simply have served as a protective shield during the British "denazification" process, in which Roelen was classified as presenting "no objection," and he never mentioned the matter again.

By the winter semester of 1918/19 Roelen had already resumed his chemical studies at the Technische Hochschule Stuttgart, where after six semesters, in March 1922, he was awarded a degree.[4] This was followed by an internship in the iron and steel industry, spent in the research laboratories of Hoesch in Dortmund. He was apparently unable there to find a suitable topic for a doctoral dissertation, however, and for this reason omitted all reference to the experience in his later résumés. On the other hand, Hoesch did make explicit mention of Roelen's work in the context of the 50th anniversary of its research division.[5] It was evidently during the course of this internship in Dortmund that Roelen contacted the director of the KWI regarding the possibility of pursuing doctoral work at the Institute. In response to the positive evaluation from Prof. Gutbier cited above, Franz Fischer sent the following note to Otto Roelen:[6]

> "Herr Professor Gutbier has written to me and expressed the opinion that you would be in a position to carry out scientifically worthwhile doctoral studies in one of our areas of research. I am therefore prepared to accept you as a doctoral candidate, and I request that you meet with me so I can discuss with you both the topic and the literature that will be an essential part of your preparation."

Since 1921 the KWI had been engaged in intensive investigations in the area of gas synthesis, with the goal of producing liquid hydrocarbons. One of the reasons for this activity was the fact that Rhineland-Westphalian heavy industries, a source of financial support for the Institute, were interested in finding ways of utilizing their excess coke-oven off-gases.[7b] Fischer and Tropsch were studying as one possible starting point the catalytic preparation of "Synthol," a mixture of liquid hydrocarbon- and oxygen-containing oils described in prewar patents issued to BASF,[8] and derived from the reaction of carbon monoxide with hydrogen under high pressure. Much of the ini-



B. Cornils



M. Rasch



W. A. Herrmann

Boy Cornils was born in Bremen in 1938. His chemical studies led to a doctoral degree in industrial chemistry (Technische Universität Hannover, 1964). He started his career at the Ruhrchemie AG (Oberhausen) and became head of research and development (including development of biphasic hydroformylation), before moving to Hoechst AG (Frankfurt) in 1984. His responsibilites have ranged from research to management. He is the author of several publications on such topics as homogeneous and heterogeneous catalysis, fluorine chemistry, syntheses involving carbon monoxide, organometallic compounds, aspects of chemical engineering, specialty chemicals, and coal gasification, and holds a number of patents.

Wolfgang A. Herrmann was born in 1948 in Kelheim/Donau (Bavaria). After studying chemistry (Diplom at the Technische Universität München) and completing a research thesis with E. O. Fischer in 1971, he obtained his doctorate in 1973 on a topic dealing with organometallic stereochemistry under H. Brunner at the Universität Regensburg. From 1975–1976 he carried out research with P. S. Skell at the Pennsylvania State University, and in 1978 completed his habilitation with a thesis entitled "Organometallic Syntheses with Diazoalkanes." He was appointed professor at the Universität Regensburg (1979), and full professor at the Universität Frankfurt (1982). In 1985 he accepted a chair at the Technische Universität München as the successor to E. O. Fischer. His area of research is synthetic and catalytic chemistry, primarily in organometallic chemistry. He is the author of 350 publications, and holds 30 patents. His work has frequently been the subject of special recognition, including the German–French Alexander-von-Humboldt Prize (1988), the Otto-Bayer Prize (1990), and the Max-Planck Research Prize (1991). He is a member of the Akademie der Wissenschaften und der Literatur zu Mainz (1990), and received an honorary doctorate from the University of Lyon (1990).

Manfred Rasch was born in 1955 in Dortmund and studied history and mathematics at the Ruhr-Universität Bochum with the goal of teaching in a "Gymnasium." He spent the years 1984–86 as a teaching intern and was subsequently appointed to the academic staff at the Max-Planck-Institut für Kohlenforschung at Mülheim an der Ruhr where the Director, Prof. Wilke, charged him until 1992 with the responsibility of conducting research on the history of the Institute. He received his doctorate at Bochum in 1989, and a teaching position at the same institution in 1990. Since 1992 he has been head of the archives at the Thyssen AG in Duisburg. In addition to four monographs he is credited with fifty other publications related to the history of chemistry, science, and technology as well as the application of computer techniques to archival work.

tial work was directed toward mechanistic aspects of the process (the "formate theory"). Nevertheless, Fischer and his co-workers failed to develop a satisfactory scientific explanation of the synthesis, remarking simply in their first publication:[9]

> "We wish therefore to conclude this section regarding the theory of Synthol formation by noting that for the time being we are giving first priority, relative to other possible explanations, to the notion of synthesis through carbon monoxide addition to alcohols, albeit without claiming that we have definitely proven this to be the mechanism."

In their explanation of the course of the reaction leading to Synthol, Fischer and Tropsch assumed that methane and formaldehyde arose as intermediates, which is the reason why Fischer et al. (including the young doctoral candidate Otto Roelen; cf. Fig. 1) carried out an extensive series of experiments related to



Fig. 1. Otto Roelen (third from left) at the Technische Hochschule in Stuttgart, Inorganic Laboratory, 1922.

methane combustion and the formation and decomposition of formaldehyde.[10] Despite these efforts, Fischer and his coworkers never succeeded in detecting more than traces of the presumed intermediates.[7]

Roelen had completed the experimental part of his work before the institute's summer holidays began, and even though his doctorate had not yet been officially granted he decided to move on immediately to the Technische Hochschule Berlin-Charlottenburg, where in August 1923 he joined the research group of Prof. Hans T. Bucherer. He remained in Berlin until March 1924, transcribing during this period his dissertation entitled "I: Über die katalytische Zersetzung des Formaldehyds bei höheren Temperaturen. II: Über die teilweise Verbrennung von Methan zu Formaldehyd mit Luft" (I: Concerning the Catalytic Decomposition of Formaldehyde at Higher Temperatures. II: Concerning the Partial Combustion of Methane to Formaldehyde with Air), which was evaluated very favorably by Bucherer:[11]

> "The efforts of Dr. Roelen merit special recognition; he has tried to extract the greatest possible measure of scientific benefit from the investigations he initiated, based on his own reflection and careful observations. I have no doubt that he will develop into a successful and exceptionally able scientific colleague, and wish him from my heart all the best for his long-term future."

Bucherer was not the only one who regarded Otto Roelen as an "exceptionally able" chemist; the same was true of the chemistry faculty at the TH Stuttgart, which on the basis of his work and especially his performance in the oral examination rewarded him with the grade "very good." Prof. W. Küster, Roelen's adviser in Stuttgart, thereby exceeded Franz Fischer's recommendation, which attested to work that had been conducted "with diligence, care, and understanding," and Roelen's "full engagement in the theoretical aspects as well, in the course of which he developed his own independent views. On the basis of the results, which represent a considerable advance over prior knowledge, as well as the way in which Herr Roelen mastered the problems that developed," Fischer nevertheless proposed only a grade of "good."[12] This may have been one reason why Roelen did not apply for a position at the KWI immediately upon receiving his doctorate, although the letter of appreciation he sent to Fischer provides no evidence of ill will between them. Another possible reason could be that Roelen was interested in seeking independent appraisal of his research results. Thus, his dissertation concluded with the following paragraph, appended quite self-confidently to the bibliography:[13]

> "The partial combustion of methane to formaldehyde represents a special case in the broad context of gas-phase reactions, one which holds out promise for extensive development and rich reward from the standpoint of both science and industry. It is my intention to occupy myself further with these matters, especially the combustion of methane."

Otto Roelen's thoughts even as he worked on his doctorate apparently were not simply those of a chemist, but of a businessman as well. On June 10, 1924, he applied for a patent on a "Verfahren zur Durchführung der teilweisen Verbrennung von Methan zu Formaldehyd" (Process for Accomplishing the Partial Combustion of Methane to Formaldehyde).[14] Objections were raised to this patent, however, and it was not actually issued until April 2, 1930. Since it did not even then produce any financial benefits for Roelen, he abandoned his patent rights in the very same year.[15] On October 15, 1924, he again took up research at the KWI for Kohlenforschung, this time as a regular member of the scientific staff.

Although Otto Roelen was often described as having a "tendency to theorize," he lacked the publication record that even in those days was essential to a successful scientist. Thus, during the period 1924/25 he was a co-author with Tropsch of three articles, all based on his dissertation, but the only independent publication he was permitted to release was a literature summary under the title "Über die Verbrennung von Methan zur Formaldehyd" (Concerning the Combustion of Methane to Formaldehyde).[16] This lack of publications cannot be attributed exclusively to the hierarchical structure of the Institute, which reserved the right of first publication to the Director, because after 1927 Roelen served as head of the Institute's pilot-plant facilities, with the rank of group leader. In comparison with other group leaders

his publication record continued to be meager, and was confined almost exclusively to lectures. Roelen was much more interested in technical issues, of which there were many, because the Director of the Institute envisioned in-house development of the KWI-discovered Fischer–Tropsch (FT) process all the way to technical maturity. In the years that followed, and even during his time as an industrial chemist, Roelen's list of publications included considerably more patents than other forms of communication.

Otto Roelen was one of those involved in the initial discovery of the FT synthesis. During his lifetime he regarded his personal role in this discovery as having been quite significant, although the chemical world generally was more inclined to recognize his contributions to industrial applications of the process.[17] One of his contributions, according to his own testimony, was preparation of the technically relevant catalysts. But in the second published report on the FT process by Fischer and Tropsch, Roelen is accorded only a note of appreciation—and even that in conjunction with references to the work of others as well.[18]

There is no doubt that Otto Roelen played an important part in the technical development of the FT synthesis. In 1927 he assumed responsibility for the pilot plant, which was especially appropriate, since a love for theorizing was accompanied throughout his life by an interest in practical and technical questions viewed from the perspective of an industrial chemist. Many important innovations associated with industrial implementation of the FT synthesis are attributable to Roelen, including his "independent temperature controller for a gas-fired oven" and a "sulfur determination apparatus" that he developed jointly with his assistant Walter Feißt, a device which was subsequently produced under license by a glassblower in Essen.[19] Tropsch left the institute in the summer of 1928, and in 1929 Fischer–Tropsch activities at the pilot-plant facility were merged with those in the laboratory and placed under Otto Roelen's direct supervision. Thereafter his role in the further development of the FT process was second only to that of Franz Fischer, who expressed his confidence in Roelen to the outside world in the following communication dated March 10, 1931:[20]

> "With the departure of Dr. Fuchs, our oldest and most senior chemist, Dr. Roelen, head of the development department, assumes the duties of proxy for the Director with respect to general management of the Institute."

Meanwhile, Roelen and his co-workers in the previously mentioned FT pilot facility (built in 1926) had been working on gas purification (a constant and virulent problem throughout the development of the FT process). Other important issues they addressed included the arrangement of the reactors ("catalyst ovens," "Kontaktofen" in German; by 1934, 38 different modifications had been tested), reactor cooling, and temperature measurement. These experiments are exceptionally well documented, since all the scientific personnel of the Institute were required to submit weekly reports to the Director. Many of the often hand-written reports have in the meantime disappeared, as have Roelen's originals. But in this context he was quite cautious: all Roelen's reports were typed, which permitted him to retain a carbon copy for his personal records. The latter have since become a part of the archives of the Max-Planck-Institut für Kohlenforschung, where they constitute an interesting source of information on technical refinement of the FT synthesis.[21]

Although activities at the KWI pilot plant were centered most directly on industrial development of the FT synthesis, interesting scientific results were acquired as well. Thus, Roelen discovered in July 1930 that the optimal stoichiometric ratio for $CO:H_2$ was 1:2.[22] The pilot-plant staff also attempted for the first time in November 1930 to run the FT reaction in the liquid phase as an elegant approach to solving the problem of adequate cooling. Temperature control was indeed achieved, but the typical catalysts of that period resulted in a rate of reaction too low to be practical.[23]

It was not until the National Socialists seized political power that industrial-scale implementation of the FT reaction promised to become a reality. A general license for the process was assigned to Ruhrchemie AG in Oberhausen-Holten on October 27, 1934. Quite independently of ongoing licensing negotiations with Franz Fischer, Ruhrchemie began construction of its own pilot plant, and acquired from the Institute the services of Otto Roelen to supervise the work. Roelen was apparently glad to leave the institute, which had been unable to offer him a permanent position. He had also frequently come into conflict with the authoritarian director as a result of his own unorthodox interpretation of his responsibility for keeping fixed hours—a situation that eventually caused problems at Ruhrchemie as well. The agreement Roelen reached with Ruhrchemie on October 23, 1934, read as follows:[24]

> "In the pilot plant we have constructed for the preparation of gasoline according to the Fischer–Tropsch process, you [Otto Roelen] will assume responsibility for managing the fine purification as well as the actual synthesis itself, including preparation of the purifying material and the catalysts, and for managing the laboratory... You also have the right and the responsibility to examine the rest of the pilot plant and offer suggestions regarding its operation in the interest of efficient organization."

In order to adapt existing FT technology to industrial practice, Roelen found himself engaged in problems of gas desulfurization, catalyst preparation and formulation, and the economically important issue of catalyst regeneration. Without the innovations introduced by Roelen and his co-workers Feißt and Heckel it would have been necessary soon to abandon the host of FT facilities so quickly set up during the mid-1930s, because at first no method could be found for regenerating the cobalt catalysts. Roelen and Walter Feißt ultimately succeeded in developing a catalyst preparation method in which the interfering impurities were removed by prior precipitation. This process[25] and Roelen's basic patent for the standard magnesium-containing FT catalyst[26] were implemented at all the FT plants prior to 1945, and even after 1945 at the Chemische Werke Bergkamen. Many of Roelen's other discoveries were incorporated after World War II into the South African Sasol facilities, constructed under license from Lurgi/Ruhrchemie.

Otto Roelen thus served as "chief chemist" for the general licenser, and as a result of the contractually assured exchange of expertise among the various FT plants he was also among the best-informed practitioners in the field. Nevertheless, neither he

nor Helmut Pichler, his successor in the Mülheim research group, was assigned responsibility for the "Reichsamtsversuche" (Official Government Investigations), a set of comparative evaluations of various FT catalysts conducted at the Fischer–Tropsch plant in Schwarzheide. This function was instead assumed by Herbert Kölbel from the FT producer Gewerkschaft Rheinpreußen. Roelen was apparently overburdened with other work, and also considered an interested party because of his own catalyst-development activities. Moreover, in 1941 he began developing a process for the methanization of carbon monoxide, on the basis of which a first "gas station" (in the literal sense) was erected in Essen, to be followed by similar facilities at the Opel works in Rüsselsheim and, after World War II, in Bochum at the Carolinenglück mine, in Düsseldorf, and at Röhm & Haas in Darmstadt.[27]

When the war ended, Roelen was in Gebhardshagen near Salzgitter, and at first he managed to avoid questioning by Allied specialists (cf. Section 2.2) by moving out to the farm of some friends, where he recuperated from an illness. When he finally returned to Oberhausen in 1945, British military authorities had already learned of his importance and the information he possessed. On November 4, 1945, the British Ministry of Fuel and Power ordered his transfer to Wimbledon:[28]

> "From the Investigations of the Field Teams in Germany and from examinations of captured documents it seemed probable that Dr. Otto Roelen had a more complete knowledge of the research side of the Fischer–Tropsch process than any other person in Germany... Among his own achievements were the development of the fine-purification process and the discovery of the 'Oxo' reaction."

Upon returning from England Roelen engaged initially in literature work for Ruhrchemie AG and the military government, pursuing no chemical research whatsoever. Roelen described the FT synthesis from a historical point of view in the first postwar edition of *Ullmanns Enzyklopädie der Technischen Chemie*. This led to a quarrel with his former colleague at the KWI, Helmut Pichler, because Roelen's contribution covered only the "medium-pressure fixed-bed synthesis" as one variant on the FT process, not the "Fischer–Pichler medium-pressure synthesis" (an expression occasionally utilized by Franz Fischer), which Pichler wished to see treated.[31] After 1949 Roelen became Assistant Head, and on October 1, 1955, once again Head of the Ruhrchemie Research Laboratories and Executive Secretary of the company. He officially retired on March 31, 1962.[29]

In the years after his retirement Otto Roelen not only enjoyed the respect of the scientific community but was also honored with a number of awards, including the 1963 Adolf-von-Baeyer Medal from the Gesellschaft Deutscher Chemiker (GDCh) and the Normann Medal of the Deutsche Gesellschaft für Fettwissenschaft (DGF) (cf. Fig. 2).[29] In 1983 on the occasion of his 86th birthday, and in recognition of his accomplishments in fundamental processes of coal and petroleum chemistry, he was awarded an honorary doctorate from the Technische Hochschule Aachen. As early as the end of 1944 he was nominated by the Ruhrchemie AG for the Dr.-Fritz-Todt prize. However, since at that time the oxo synthesis had not yet achieved any industrial significance, the responsible authorities declined to present him with the award, an outcome for which he had every reason to be grateful in the postwar years.[30]



Fig. 2. Otto Roelen (left) in 1963 at the presentation of the Normann Medal by the DGF.

Apart from this, Roelen's retirement years were devoted to his numerous hobbies. Many of these he had taken up earlier, as is evident from a close scrutiny of his publications and his personal papers from his years at the KWI and Ruhrchemie. He eventually found the leisure necessary to prepare comprehensive articles describing his contributions to the oxo[32] and Fischer–Tropsch[17, 22] syntheses, in which he laid considerable stress on those aspects relevant to the history of chemistry. All three papers are exceedingly informative, because he was able to write them not only as one of the direct participants, but also with perspective acquired after four decades, analogous to G. Schiemann's situation as he looked back over the field of fluorine chemistry (cf. Fig. 3).



Fig. 3. Friendly exchange between two chemists for whom reactions were named: G. Schiemann (1899–1967, the Schiemann reaction for fluorination of arenes) and O. Roelen (1897–1993) in conversation at the bowling alley ("Kegelbahn") of the Ruhrchemie AG; photo taken July 23, 1964.

Another important issue for Roelen was his personal health, with which he conducted systematic experiments. It was this period of experimentation that led to an article entitled "Behandlung der Luftwege mit angereicherten Meersalz-Aerosolen" (Treatment of the Respiratory Tract with Enriched Sea-Salt

Aerosols),[33] in which he provided experimental details regarding what was apparently a very positive set of experiences, extending even to the question of the most appropriate materials for constructing an inhaler. Roelen was particularly intensively engaged with questions of the relationship between nourishment and one's state of health, occasionally displaying the zeal of a true missionary. This led to a number of short manuscripts[34, 35] as well as papers and personal experiments on the subject of allergens.[36]

Roelen shared with the great chemist William Crookes (1832–1919), inventor of the crookes tube for investigating cathode rays, an inclination toward questions that would typically be regarded as the exclusive domain of parapsychology.[37] Whereas Crookes pursued the occult and nurtured a "familiar relationship with 'materialized personalities'," Otto Roelen spent his time in the "shadow world between the known and the unknown,"[37] searching for quantifiable experimental verification of oscillation phenomena, whose "objectification" he felt always on the verge of achieving until a stroke in 1981 prevented him from pursuing further experimental work and applying his recently acquired extensive knowledge of electronics and semiconductors. His typewritten manuscript on questions relevant to oscillation[38] describes his experiments in detail, with photographic documentation of his experimental setup and an account of results he acquired in the 3.18-cm wavelength range. But it also conveys his singular conviction that "oscillatory perception," like color blindness, is confined to only a minority of sensitized individuals. In sharp contrast to his attitudes in many other respects, he concluded the 1980 typescript with the resigned observation: "Much that is observed for the first time remains inexplicable..."

But his greatest academic obsession during retirement was a lively interest in historical and didactic problems related to research, probably stimulated in part by his excellent insight into his own discovery of the oxo synthesis and his deep disappointment for having failed to recognize the true nature of the catalysis involved (Section 3.2). A study by Roelen dated as early as 1968 and entitled "Emotik—Von den Überzeugungen und ihren heimlichen Herrschern"[39] ("Emotik"—Convictions and Their Secret Masters) explores the contrasts between opinions and convictions, considering their rational and emotional content as well as their treatment by natural scientists in light of the methodological skepticism expressed by Descartes. The motif of "semantic deception" on the part of nonscientists appears at a very early date as well; indeed, it is little wonder that in his circle of friends he came to be known as an evangelist on behalf of C. P. Snow,[40] who began in 1959 to call attention to fundamental incompatibilities between the pronouncements and worldviews of scientists and those of humanists ("The Two Cultures,"[41] still referred to euphemistically as "literate circles"). Roelen concluded in 1968 that

> "this cultural dilemma... exposed by Snow is so alarming precisely because those with a humanistic education—who persist in their denial, ignorance, and misunderstanding of the achievements of science—are the very ones occupying the seats of power."

The symptoms and consequences of this cultural dilemma can be formulated earnestly,[42, 43] satirically,[44] or in a martial spirit, the latter illustrated by Roelen's 1983 response to the question of how scientific discoveries come about:[45]

> "A further example of the way research is hampered by the spirit of the times is presented by the attack on science and technology... The demand is made that scientific research... should assume a set of moral obligations, and subject itself to social planning. This has been very clearly expressed, for example, in concepts developed at the former Max-Planck-Institut in Starnberg for the culmination of the sciences.
>
> "Such demands are advanced by people who have never engaged in experimental research, and who are able to maintain their positions only by semantic blurring and factual errors...."

2. His Greatest Achievement: The Oxo Synthesis

2.1. History of the Discovery

It was in 1934 that Roelen moved to the Ruhrchemie AG, and it marked a turning point in his life. Adolf Hitler's Third Reich was aiming its sights quite openly and single-mindedly toward military conflict with Germany's neighbors. Military preparations quickly involved the chemical industry, including Ruhrchemie, whose fertilizer business had become increasingly unprofitable following collapse of the international cartel negotiations coupled with the compulsory cartel and international trade restrictions imposed by the German nitrogen syndicate and aggressive quota politics on the part of the I. G. Farbenindustrie (I. G.) conglomerate.[46] All of this had affected Ruhrchemie in one way or another.

One possibility for escaping the desolate economic situation called for broadening the company's product spectrum, which led to efforts directed toward coal chemistry (methanization, methane cracking to yield benzene or acetylene), as well as an increase in activity at the Chemische Fabrik Holten GmbH, which had been established in 1929. The latter originated as a joint venture operated by Ruhrchemie AG and the Th. Goldschmidt AG in Essen for preparing glycol from ethylene isolated from coke-oven gas. Even as the plant was being built, the market leader in this sector, I. G. Farben, insisted on becoming involved financially in the new operation and playing a significant role in marketing, demands that were in fact met. This serves as yet another example of the way I. G. insinuated itself into the plans of outside concerns, just as it had in the disputes related to fertilizers. Persistent interference of this type was one of the constant factors over a period of many years that marked the tense relationship linking Ruhrchemie and Otto Roelen himself with I. G. Farben and its chemists. Attempts are still being made to this day by I. G. apologists to rewrite history in such a way as to gloss over the picture of this domineering, no-holds-barred monopolizer.[46]

One potentially promising foothold for Ruhrchemie was the Fischer–Tropsch synthesis (cf. Section 1). Following preliminary negotiations and attempts by I. G. to limit competition with its own fuel production based on coal hydrogenation, Ruhrchemie acquired the rights to the FT process as general licensee, which entailed the obligation to pursue development of the tech-

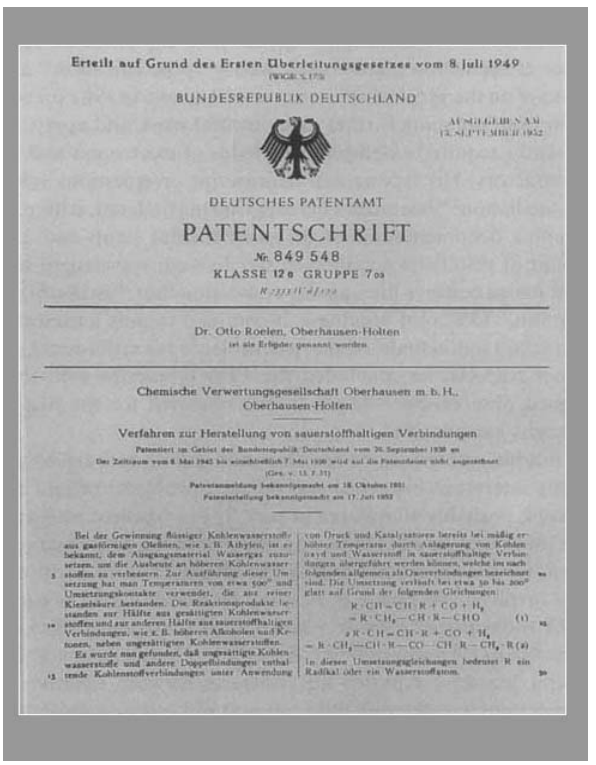
nology to the point of constructing a demonstration facility and a pilot plant capable of producing 5000 t/a.[47]

Otto Roelen was thus fully aware of what awaited him as he, his colleague Dr. Feißt, and his chief technician Hanisch made the move in 1934 from the KWI in Mülheim to the Ruhrchemie works in nearby Holten, a suburb of the city of Oberhausen. And he was also well prepared. As head of the FT demonstration facility at the KWI he was effectively predestined to undertake this assignment and assume the responsibility for Fischer–Tropsch development efforts at Ruhrchemie. The Ruhrchemie organizational plan during the period 1934–1945 as presented in BIOS Report 447[28] indicates that Roelen's FT research activities were initially transferred from Ruhrchemie itself to the sister corporation Ruhrbenzin,[47] and then back again to Ruhrchemie. This plan also documents a deliberate policy (for reasons of secrecy) of mutual isolation of all the various research facilities, a policy basically consistent with Roelen's own temperament, but which nonetheless hindered the constructive exchange of ideas. Even BIOS Report 447 contains disparaging remarks with regard to this organizational structure.[28]

The emphasis in Roelen's work with Ruhrchemie was still on the continued development of the FT synthesis in 1938, when seven FT plants were either already in operation or on the verge of starting production. The general licenser was compelled to deal with a great many questions during the construction and early operational phases of these new facilities, most of which became the responsibility of Roelen's department—often without preliminary screening or prioritization. This work load was augmented by the obligation to certify all FT catalyst charges and the additional burden of a laborious and time-consuming search for a substitute for cobalt, a strategically important and exceedingly costly metal that served as the basis for FT catalysts. The latter problem was made all the more troublesome by the fact that it necessarily entailed very prolonged test cycles. One particularly urgent aspect of FT studies at that time concerned attempts to recycle "gasol" hydrocarbons (C_2–C_4 compounds, including olefins and especially ethylene)[48] as a way of incorporating them into higher hydrocarbons. In contrast to later research on "selective FT synthesis,"[49] ethylene was completely useless for gasoline synthesis. Based on agreements between the licensees, and as part of an official exchange of information, attempts were to be made to ascertain whether and to what extent it was feasible to incorporate lower olefins into the product through recycling, and whether NH_3 might also be suitable for inclusion in a "growing FT chain."

At the end of 1937 in the course of these investigations Roelen discovered the aldehyde synthesis that was later to bear his name (the Roelen reaction, hydroformylation, oxo synthesis). The actual discovery was a direct consequence of problems encountered with two atmospheric-pressure FT ovens, one of which had been charged with ethylene and the other with ammonia, ovens that were connected for waste-disposal purposes by a common off-gas pipe (for complete details see ref. [32]). In the course of this particular experiment a white residue accumulated in the piping, the odor of which was reminiscent of aldehyde–ammonia compounds (specifically the aldimine derived from ammonia and propionaldehyde, where the latter had arisen from the reaction of ethylene with synthesis gas). This observation set Roelen on the trail of the oxo synthesis. Experiments designed to establish optimal reactions conditions and the overall potential of the reaction were resumed on July 26, 1938, as soon as the appropriate pressure equipment had been acquired. Intensive investigations followed, and by September 20, 1938, the first patent application on the oxo synthesis was filed. Finally on June 17, 1952, a patent was issued with the number 849 548[50] (Fig. 4) covering the following claims:

"Procedure for the preparation of oxygen-containing compounds in which unsaturated hydrocarbons (e.g., olefinic hydrocarbons) are treated at elevated pressure and temperatures up to approximately 200 °C with water gas or other gas mixtures containing carbon monoxide and hydrogen."


Erteilt auf Grund des Ersten Überleitungsgesetzes vom 8. Juli 1949

BUNDESREPUBLIK DEUTSCHLAND

DEUTSCHES PATENTAMT

PATENTSCHRIFT

Nr. 849 548

KLASSE 12 o GRUPPE 7 02

Dr. Otto Roelen, Oberhausen-Holten

Chemische Verwertungsgesellschaft Oberhausen m. b. H., Oberhausen-Holten

Verfahren zur Herstellung von sauerstoffhaltigen Verbindungen

Fig. 4. Facsimile of the first oxo patent from 1938/1952 [50].

In a retrospective paper describing the discovery of the oxo synthesis, prepared in 1977 and entitled "Beitrag zur Psychologie der naturwissenschaftlichen Forschung" (Contribution to the Psychology of Scientific Research), Roelen provided a lengthy case history of this exceptional chapter "in the larger context of the catalytic reduction of carbon monoxide."[32] (Incidentally, the description he furnished in 1946 for BIOS Report 447[28] is identical in content.) Roelen includes in this case history experiments undertaken at BASF in 1913, in which higher hydrocarbons and oxygen-containing compounds were first formed catalytically from CO and H_2 at elevated pressures.[8] Fischer and Tropsch (later Roelen as well) used these experiments as their starting point in 1922 and thereafter at what was then the KWI

(today the Max-Planck-Institut) in Mülheim when they utilized iron catalysts to prepare "Synthol," a mixture of oxygen-containing compounds. These later experiments were conducted at quite high pressures. The more active the catalyst, the lower the required pressure, and the more the nature of the product shifted in the direction of hydrocarbons, an observation that led ultimately to discovery of the atmospheric-pressure Fischer–Tropsch synthesis (cf. Section 1).[51, 52]

Quite independently of Fischer's experiments, Smith, Hawk, and Golden[53] at the United States Bureau of Mines had also attempted to introduce ethylene into the reactant stream in an atmospheric-pressure FT reaction over a cobalt catalyst. With the exception of high pressure, all the essential conditions were thus established for the subsequently discovered oxo synthesis. (FIAT Report No. 1000 actually describes parenthetically —and quite incorrectly— the paper by Smith et al. as the "first publication of the basic Oxo reaction,"[54] presumably in reaction to claims of success arising out of the Third Reich.) Smith, Hawk, and Golden did indeed obtain some aldehydes and alcohols, but they interpreted them explicitly to be intermediates produced in the course of the FT reaction. Roelen formulated the matter rather more logically when he asserted that[32]

> "the cited Americans did indeed carry out the aldehyde synthesis in 1930, but they did not discover it. Their presuppositions with respect to the reaction mechanism prevented them from recognizing that a second, independent reaction was involved. This intellectual inhibition was confirmed for the author orally in the course of a later visit."

Intellectual inhibitions and presuppositions regarding the nature of the catalysis played a role in the later history of the oxo synthesis as well (cf. Section 3.2). Thus, because of the "general impression of the experts that oxygen-containing by-products of the FT synthesis were inevitably and inseparably related to the mechanism of hydrocarbon synthesis,"[32] an independent synthesis of oxygen-containing products was never even considered. This is confirmed by widespread acceptance of the Synthol (I. G. Farbenindustrie[55]) and Oxyl (Ruhrchemie AG[48, 56, 57]) syntheses as variants of the FT synthesis.

Thus, in 1937/38 Roelen's real intellectual accomplishment in analyzing the operational disruption described above was freeing himself from any preconception about oxygen-containing compounds and their inevitable appearance as intermediates in a normal FT hydrocarbon synthesis. Perhaps most important, the absence of a typical series of compounds with increasing molecular mass led him to suspect the existence of an independent synthesis of propionaldehyde [Eq. (a)] and diethyl ketone based on ethylene that had been introduced into the

$$H_2C{=}CH_2 + CO + H_2 \xrightarrow{cat.} H_3C{-}CH_2{-}CHO \qquad (a)$$

reaction mixture.[32] He concluded that such a reaction, if it occurred, must be dependent on pressure, and that propionaldehyde formation would be favored by an increase in pressure. The first high-pressure oxo reaction (243 °C/100 bar) was conducted on July 26, 1938, and it confirmed Roelen's suspicions. Subsequent process optimization for the oxo reaction involved parameters clearly outside the range appropriate for an FT reaction, including relatively low temperature and high CO/H_2 pressure. Shortly thereafter studies were initiated on possible applications of the new synthesis, and patent protection was sought as outlined previously.

The term "oxo" as applied to this reaction was coined by the Ruhrchemie patent department, and was intended to suggest a general reaction for the synthesis of both aldehydes *and* ketones (i.e., oxo compounds), although it was later established that this flexibility is limited to ethylene. The "invention" itself was noteworthy from one additional standpoint: a German patent was never actually issued until July 1952, and then on the basis of the Patent Transition Law ("Patentüberleitungsgesetz") of the Federal Republic of Germany, whereas French, Italian, and American versions appeared (but attracted little notice) during World War II.[58, 59] The war itself had the effect of depriving Roelen of the international monetary fruits of his discovery, because all foreign patent rights assigned to Germans were confiscated after the war. As a result Roelen and Ruhrchemie received royalty payments only from the German oxo facilities operated by BASF and Hüls, not from the much larger foreign producers.

It should be noted in passing that the discovery of the oxo synthesis is still controversial; experience has shown that successful children are frequently claimed by multiple fathers. In discussing the matter, Roelen always emphasized the fact, underscored in his retrospective description of the discovery, that the definitive experiments were carried out at his own risk, and that their further pursuit was against the express wishes of company management:[32]

> "Thereafter experiments on the effect of synthesis-gas supplements were abandoned at the instruction of the management."

That was in December 1937; based on the considerations described above, Roelen modified the experimental protocol between January and June of 1938 in such a way that it was possible for a first successful high-pressure experiment to be carried out on July 26, 1938.

As usual, management saw things in a somewhat different light. In the "Minutes of a Presidial and Executive Board Meeting of the Ruhrchemie and Ruhrbenzin Aktiengesellschaft on February 6, 1940"[60] remarks on the subject of fatty alcohols by F. Martin, at that time Chairman of the Board of both Ruhrchemie and Ruhrbenzin,[61] are recorded as follows:

> "Martin sketched out the history of the development of the process for preparing aldehydes and fatty alcohols. Concerns related to the disposal of relatively large quantities of gasols derived from fuel synthesis, materials with only a limited potential for exploitation, had induced him to direct Dr. Roelen to undertake experiments into the possibility of utilizing these gases for further reaction with water gas. It was found that the olefins could in fact be converted into straight-chain and isoaldehydes ... ."

Martin told the same story during the first round of questioning by C. C. Hall's CIOS team, who reported as follows: "In the gasol fraction, they had large amounts of propene and butene for which they had no use, so Martin instructed his chemists to find some more use for these compounds."[124]

In other words, the Executive Board had its own interpretation, at least with respect to causation in the history of the discovery. It is safe to assume that Otto Roelen was not aware of the corresponding minutes, which during the war were declared to be "confidential" (and that he never saw them after the war since he was not a member of the Executive Board). Thus, it is all the more noteworthy that he continued to insist on the role played by successful insubordination—not the last time, incidentally, that insubordination was to have a place in Ruhrchemie's history of the oxo synthesis.

2.2. The Industrial Oxo Synthesis during the Early Years

The oxo synthesis was an excellent match for the raw materials accessible to the Ruhrchemie AG, which had Fischer–Tropsch facilities as a source of olefins, experience in catalyst preparation, and water-gas generators (cf. Figs. 5 and 6[124]). The oxo synthesis was also well suited to the war-oriented economic politics of the National Socialists, so much so that it quickly attracted the greedy attention of others. The first entry dealing with Roelen's discoveries in the minutes of the Executive Board of Ruhrchemie is the above-cited account by Martin regarding the history of the matter.[60] The record continues as follows:

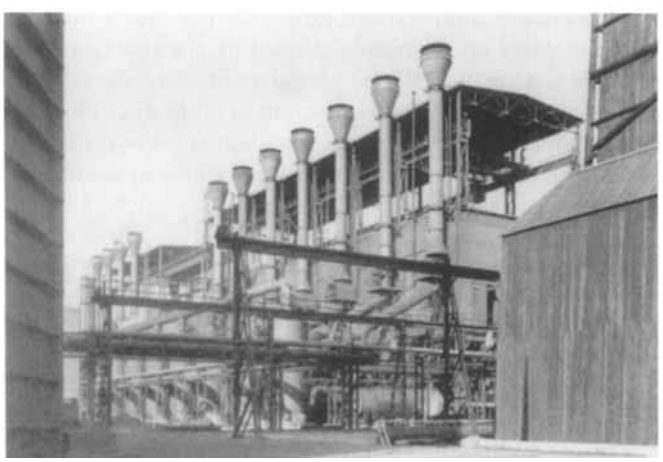


Fig. 5. The eleven water-gas generators used to supply the Fischer–Tropsch facilities at Ruhrchemie (1941).



Fig. 6. Atmospheric-pressure Fischer–Tropsch reactor at the Ruhrchemie plant (left), with the vessel used for introducing a catalyst charge (1942).

> "At the instigation of the government it is now likely that together with I. G. and Henkel we will construct a synthesis facility with a capacity of 120000 t/a in Upper Silesia ... It is further anticipated that Ruhrchemie's share of the investment will somehow take the form of a licensing agreement ... Martin noted in addition that prior to approaching Henkel and I. G. it would also be advisable to confer with Goldschmidt ... ."

Ruhrchemie and I. G. then jointly established the Chemische Verwertungsgesellschaft Oberhausen mbH, a corporation that assumed all rights related to the oxo process and was prepared to grant licenses. The nature of further interaction with Henkel and I. G. was spelled out in detail in a meeting of the Executive Board on July 4, 1940.[62] Another company, the Oxogesellschaft mbH, controlled equally by Ruhrchemie, Henkel, and I. G.,[63] was expected to erect a 15000 t/a facility for the production of synthetic fatty alcohols, whereby

> "further processing of crude intermediates to finished products by the company itself [i.e., Ruhrchemie; clarification by the authors] is out of the question, since in accordance with the government's wishes facilities belonging to Henkel and I. G. have been set aside for this purpose."

The extent to which "the government's wishes" were actually a reflection of influential guidance of I. G. can only be a matter of speculation today. Interestingly, this joint venture between Ruhrchemie and I. G. was later interpreted as Ruhrchemie's admission of parallel discovery of the oxo synthesis by I. G.:[64]

> "Comme, d'autre part, l'I. G. Farbenindustrie de Ludwigshafen avait elle aussi trouvé indépendamment cette réaction, un accord est intervenu entre la Ruhr-Chemie et l'I. G."[*]

This interpretation, which is contradicted by the facts, is presumably related to a similarly incorrect report issued by the U.S. Naval Technical Mission in Europe;[138] there is no proof to substantiate it, and it has found no backers despite efforts in that direction. For example, the oxo synthesis as defined above has sometimes (not surprisingly) been attributed to Reppe, as a special case of the "... general group of reactions between olefins, carbon monoxide and additional compounds such as ... and H_2 ..."[54] investigated and claimed by him, and it has occasionally been peddled as such by Reppe and his disciples.[65] Interestingly, BIOS Reports 273 and 355, which are dedicated more directly to Reppe, do make mention of the oxo synthesis (indeed, with $[Ni(CO)_4]$ as catalyst!) but without naming Otto Roelen.[119]

[*] "Since I. G. Farbenindustrie also discovered this reaction independently, an agreement was arranged between Ruhrchemie and I. G."

Although Board Member Kost (General Director of the Ruhrchemie Shareholders, Gewerkschaft Rheinpreussen) correctly noted during the meeting of the Executive Board that the planned venture "was not consistent with the concept that led to the formation of Ruhrchemie and Ruhrbenzin"—namely the production of chemicals independently of I. G.[47]—his opposition proved futile. Kost nevertheless ensured that his reservations would be expressed very clearly in the minutes:[62]

> "Today's events are another example of I. G.'s efforts to buy up the primary products of the Fischer synthesis and thereby prevent the companies [e.g., Ruhrchemie; clarification by the authors] from participating in the profits derived from finishing."

In this way Ruhrchemie AG was once again prevented from gaining direct access to the market.

On November 13, 1940, the Executive Board of Ruhrchemie resolved to construct a facility for producing 7000 t/a of fatty alcohols; Henkel was to assume Ruhrchemie's portion of the construction costs.[66] A year later the oxo facility was under construction,[67] after Oxogesellschaft mbH[63] on February 28, 1941, issued a construction order to Ruhrchemie on behalf of its three partners (Ruhrchemie, BASF, and Henkel) to establish a "facility in which ca. 10000 t/a of olefins with a chain length of C_{11}–C_{17} are to be converted by the oxo process into fatty alcohols or fatty acids"[68]—and thus into detergents. Because the relevant minutes of the meeting of the Executive Board are no longer available (presumably as a consequence of the war), it is impossible to reconstruct a complete chronology of this first commercial application of the oxo synthesis (cf. Figs. 7 and 8). It is

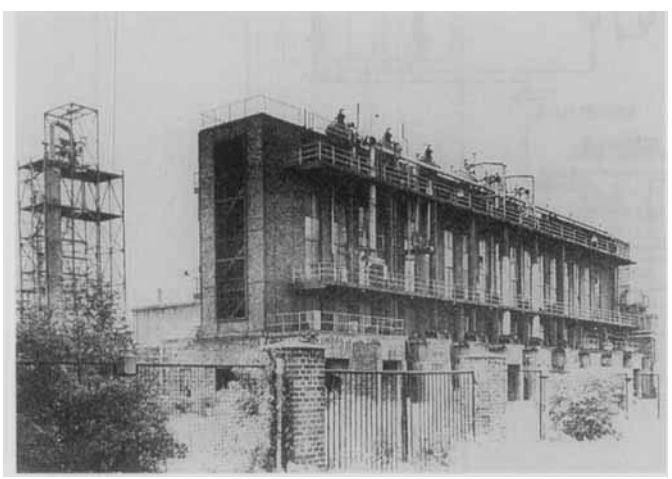


Fig. 7. Ruhrchemie oxo facility, shown under construction (1943).

clear, however, that with the exception of tests related to some of the components, the facility itself was never in operation during the war years,[124] perhaps in part because I. G. was able, upon payment of licensing fees, to test the available Ruhrchemie know-how directly in its own pilot facilities. With up to 100 tons per month of its own oxoalcohols produced in this way, I. G. had little further interest in a plant not under its direct control.[54] The Chemische Verwertungsgesellschaft Oberhausen mbH, charged with "the exploitation of chemical processes [and] the projection of facilities for licensees . . .",[69] was not dissolved until 1973,[70] serving into the 1950s as patent applicant on behalf of both Ruhrchemie and BASF with respect to inventions relevant to the oxo process.

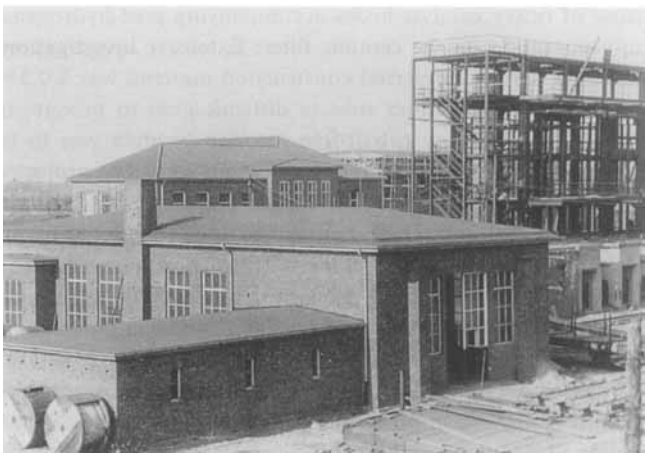


Fig. 8. Distillation facilities and administration building of the Oxo GmbH.

FIAT Report 1000[54] provides a wealth of interesting information (which would otherwise have been lost) regarding the development of the oxo process during the war. Otto Roelen's attention in Oberhausen-Holten was concentrated on the preparation of higher fatty alcohols intended for conversion into detergents and soaps.[124] I. G. had no access to FT olefins, and therefore devoted its efforts exclusively to the utilization of lower olefins (C_5–C_{10}) and the production of plasticizers of the palatinol type, as well as the further utilization of lower aldehydes (e.g., in perfumes; cf. references to Reppe in ref. [28]).

Ruhrchemie's first oxo facility consisted of a "prefractionator" for the starting olefins, oxo and hydrogenation stages, a filtration system, and final distillation towers (cf. also refs. [54, 71]). The FIAT report actually contains the first use of the English expression "to oxonate," intended as a counterpart to the German "oxieren";[72] the latter was an unfortunate piece of terminology invented by the Ruhrchemie patent department, which only later replaced it by the more correct "Hydroformylierung"[73] (hydroformylation) and the alternatives "Roelen Synthesis" (proposed by Hall in 1946[74]) and "Roelen Reaction (Adkins, 1948[75]). Nevertheless, the term "oxieren" continues to be part of the technical vocabulary at oxo facilities operated by BASF and Ruhrchemie; even semiotic heresy can prove to be surprisingly persistent!

The flow sheet reproduced in Figure 9 provides details concerning the first oxo facility constructed by Ruhrchemie in Holten. The reaction was to be carried out in batch mode at 135 °C and a pressure of 200 bar. Plans called for using a standard FT catalyst consisting of cobalt, thorium oxide, magnesium oxide, and kieselguhr in a 100:5:8:200 ratio, to be introduced as a suspension (slurry) that would subsequently be ground together with the olefin. After transfer to a second reactor and purging of the gas, crude oxo product was to be hydrogenated in a single phase over the same catalyst, leading to the desired fatty alcohols. Preliminary experiments indicated a probable catalyst consumption of roughly 300 kg per day, primarily be-

cause of heavy catalyst losses accompanying post-hydrogenation separation on the ceramic filter. Extensive investigations indicated that the preferred construction material was 3/0.5% chromium–molybdenum steel, a difficult item to procure in those days. The now cobalt-free reaction product was to be fractionally distilled in a final purification step. The projected average yield was 80%; 20% of the starting olefin was expected to be converted into a high-boiling fraction (referred to by the CIOS team as "thick oils," a literal translation of the German "Dicköle"[124]), consisting primarily of aldols. It was thought that these could be largely hydrogenated to the corresponding alcohols (including 2-ethylhexanol[124]).

In keeping with the "oxo agreement" that had been concluded with Ruhrchemie, other oxo pilot plants were to be established at I. G. plants in Leuna, Ludwigshafen, and Oppau. Instead of Roelen's batch procedure these plants were designed for continuous fixed-bed and slurry processes; carrier-free cobalt catalysts (e.g., cobalt naphthenate or acetate) were added subsequently to make up for cobalt losses (for details on the equipment and the corresponding engineering see ref. [54]). A remarkable number of the engineering and equipment features found in the Oberhausen and I. G. facilities were incorporated into later industrial oxo plants, including the cooling systems (liquid or gas), gas circulation schemes, grinding and introduction of suspended catalysts, pressure filtration of the pyrophoric catalysts, pumped transport of suspended catalysts, and carbonyl generators.

The first oxo facility constructed under license was destined for the explosives manufacturer Bombrini–Parodi–Delfino in Colleferro/Rome. Plans called for the conversion of ethylene into 25–30 tons per month of propionaldehyde, which was then to be reacted with formaldehyde to give trimethylolethane (TME, 2-hydroxymethyl-2-methyl-1,3-propanediol), a potential substitute for the important explosives intermediate pentaerythritol. This facility was designed for continuous production with a suspended catalyst (FT catalyst, suspended in diesel oil), but by the time the war ended only the corresponding reactor had been sent from Holten to Italy.[54] Experiments related to the conversion of propionaldehyde to TME had been entrusted to G. Natta, among others,[76] which explains Natta's early familiarity with the oxo synthesis (and his acquaintance with the Chairman of the Board of Ruhrchemie, F. Martin[77]).

The work in Holten and at the I. G. plants led not only to valuable engineering data, it also shed light on a number of fundamental chemical principles,[28, 48, 54, 57, 71] some of which were later "rediscovered" by others. This is the case, for example,

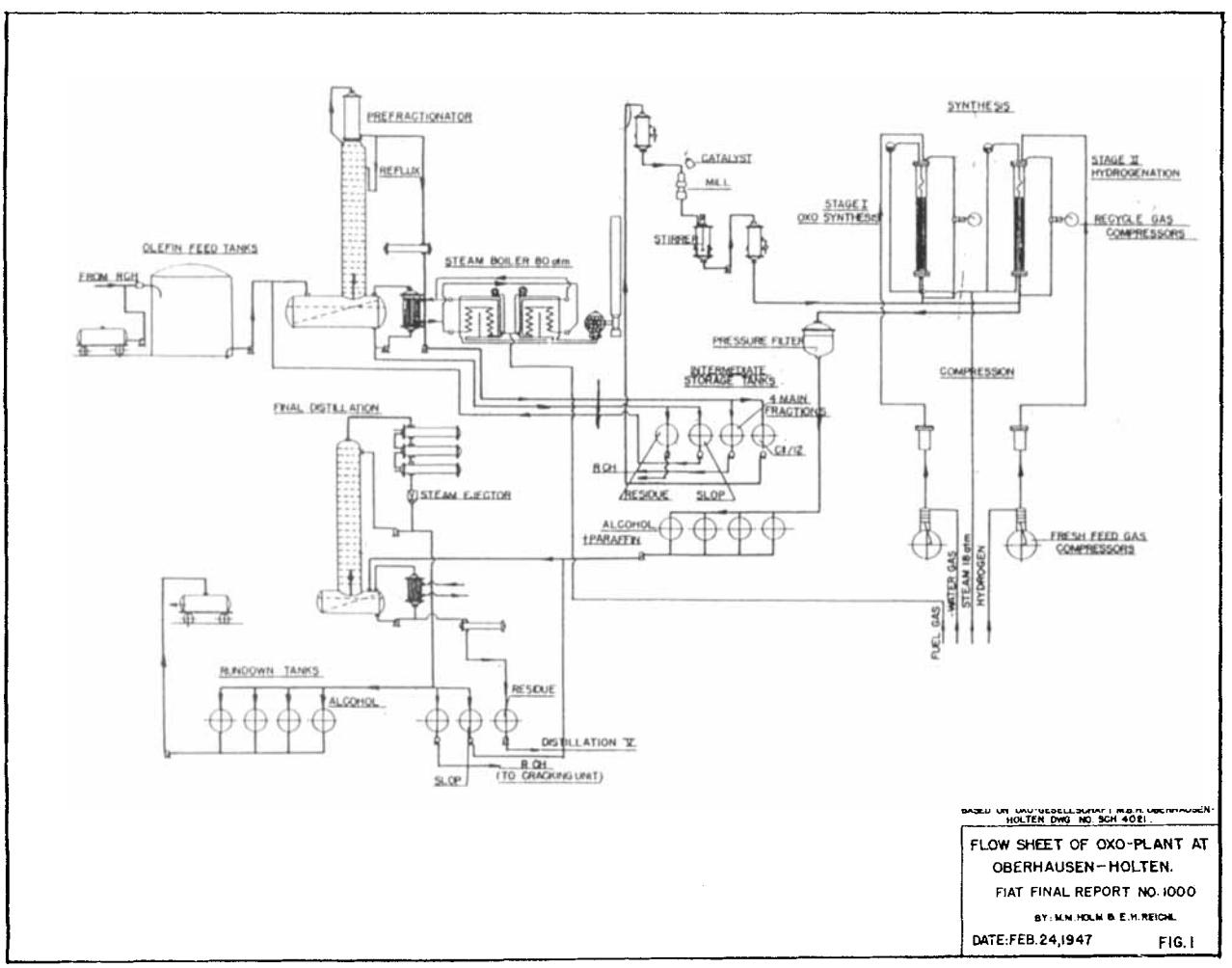


Fig. 9. Schematic diagram (flow sheet) of the oxo facility at Holten (Fig. 1 in ref. [54]).

with what has come to be known as "Keuleman's rule,"[78] according to which steric and electronic factors ensure that hydroformylation of isobutene will produce almost exclusively 3-methylbutanal, a phenomenon already observed by both I. G. and BASF[79] as well as Roelen himself,[80, 81] and communicated in the FIAT report[54] (cf. also ref. [64]).

The reports of the Allied commissions of inquiry (e.g., BIOS, CIOS, and FIAT) make unusually fascinating reading even today.[82] These special units consisting of outstanding specialists from science and industry followed on the heels of the troops. Their assignment was to provide the respective countries (and, less explicitly, individual firms) with information on German scientific and technological progress during the war years, as well as insight into the current level of German know-how. It is also important to recognize in this context that at least the American FIAT teams—consisting of 6000 experts assigned exclusively to an investigation of the German chemical industry—were granted extraordinarily comprehensive powers, including the right (in the true spirit of the late James Bond) "to remove, arrest, and intern individual Germans."[82, 122, 123]

The discrepancy between official instructions from the government and personal obligations to individual firms made it easier for many of those questioned to limit the amount of information they provided, and in some cases even to introduce obstacles. A striking example is Otto Roelen's behavior with respect to the Farragher Report on Fischer–Tropsch research at Ruhrchemie, prepared in 1947 by Warren F. Farragher (who had already served as co-author of the CIOS report covering the entire Oberhausen facility[57]). Farragher was employed by the Houdry Process Corp. in Philadelphia. His report was to be based on testimony from various German experts, and was allegedly for the United States Government.[122] Otto Roelen had given the impression that he was quite willing to provide information during his questioning from November 1945 to September 1946 as a civil intern in Wimbledon, although he himself always regarded this period as one of defamatory "imprisonment" (cf. Fig. 10).[48] With respect to Farragher's demands, however, he was utterly intractable. The events leading up to the report were described by Roelen in the preface to his own account as follows:[83]

> "As former head of the research laboratory I was assigned the task of preparing a report on Ruhrchemie. Owing to my imprisonment in London, I was a very familiar figure at the relevant British office in Düsseldorf. There I learned that the Farragher operation was in no sense being conducted under orders from the occupation forces, but amounted instead to a private effort on behalf of American industry. In view of this situation I did indeed undertake and in fact complete the requested Ruhrchemie report, but in spite of an anticipated and delivered scolding, I did not submit it punctually. As a result, Mr. Farragher returned to the United States with eight Fischer–Tropsch reports..., but not with one from Ruhrchemie... For this reason the contents of the Ruhrchemie report have remained largely unknown."

Moreover, Ruhrchemie refused even at a later date to permit *cost-free* distribution of the report, and after the currency reform (1948) it enlisted the Economics Ministry of the State of North Rhine-Westphalia in support of its position relative to Farragher when the latter returned to Europe in 1950/51.[47] Only through Roelen's preface, cited above, did the whole process—described with revealing openness by Gimbel[82] as well—become fully understandable (cf. Fig. 11).



Fig. 10. Otto Roelen as a civil intern at the Beltane School, Wimbledon, 1945/46.



Fig. 11. Otto Roelen in Oberhausen at the time the Farragher Report was prepared (1947), shown here with his legendary briefcase.

The opinions reflected in the Allied reports with respect to new and, from their perspective, previously unknown developments such as the oxo synthesis were somewhat mixed. The reports remain a fundamentally sound source of insight into the state of technology in 1945 (albeit with occasional ambiguities as a result of misunderstandings). The quality of the information is of course a function of the competence of the particular investigators involved. Thus, reports on the oxo synthesis are quite varied, depending on whether they were prepared by the two-man teams Hasche/Boundy[71] and Withers/West,[48] or one of the groups associated with Farragher,[57] Hall,[28] or Holm[54] (cf. Fig. 12). Some of the inquisitors made liberal use



Fig. 12. Discussion of the FIAT Reports at the Martin family's garden house in Mülheim-Uhlenhorst, April 1947 [from the left: Rosendahl, Weinrotter (KWI Mülheim), Gehrke, Martin, Roelen (all three from the Ruhrchemie AG), Koch (KWI)]; photo taken by Mr. Atwell, FIAT].

of information from the interviews in their own publications, adding critical commentary on the historical development of the oxo reaction—from the British perspective, for example—and showing no hesitancy when it came to value judgments (cf. Hall,[74, 124] for example, who published a somewhat embellished version of his CIOS reports[57]). All the reports are tainted with at least a whiff of industrial espionage—quite understandably, given the history of the Third Reich; this was regarded by the British, for example, as a form of "hidden reparations" and compensation "... not only in direct damage, but in loss of time for research and re-equipment ... ."[123] The expropriation of all foreign patent rights, which was very painful and also financially devastating for the victims (including Otto Roelen), had deprived both the discoverers and their companies of the fruits of their labor. The following opening comment from the reports is thus especially moving to read:[71]

> "This report is issued with the warning that, if the subject matter should be protected by British Patents or Patent applications, this publication cannot be held to give any protection against action for infringement."

This statement was rarely extended by "and/or US Patents,"[84] and never adapted to cover patent rights of the other victorious powers—clear indication in whose interest the interrogations were actually conducted. It is therefore not surprising that oxo facilities in the United States benefited.[85] Contemporary press reports announcing the opening of new plants often ignored the country of origin for the process, and almost never mentioned the name Roelen. France was in this respect an exception. Oxo developments there were greatly influenced by a former Ruhrchemie employee, Lemke, who had worked in Oberhausen from 1941 until 1945.[86]

Economic data in the Allied reports is also interesting. During his interrogation Otto Roelen expressed himself in very vague terms:[87]

> "Finally Roelen said that he did not know if the oxo-process would be an economic proposition in peace time, but it was possible that it would, since Germany had to import large quantities of natural oils for production of soap and detergents."

Economic calculations, presumably based on a merger of the National Socialist wartime and self-sustaining economic projections with those drawn up by the Military High Command (and therefore not very reliable), estimated for the preparation of 100 kg of fatty alcohols a cost of 78 Reichsmark (RM) (for the Oberhausen facility, with a capacity of 12000 t/a[57, 124]); the cost under continuous operation was expected to fall to ca. 60 RM per 100 kg, assuming an olefin price of 45 RM per 100 kg. For comparison, the cost of primary FT product was estimated at roughly 24 RM per 100 kg (Bergkamen facility, 1944[74]).

A few additional comments are in order with respect to the subsequent history of the first oxo plant, that at Oberhausen-Holten. Activity here during the war was limited to the testing of a few of the individual components, and orderly production was never achieved. The facility was damaged during the final months of the war, but not so severely that its resurrection would have been impossible, or possible only at unreasonable cost.[124] Thus, the struggle to retain the oxo plant, along with an attempt to prevent demolition of the largely destroyed FT facility, was a life-and-death matter for Ruhrchemie in the immediate postwar years. It was argued for example, that the oxo plant was needed to guarantee the hygiene and health of an undernourished population, which was living under a threat of epidemics and hence in need of a reliable source of soap and cleansing agents based on synthetic fatty alcohols. In other attempts to stall demolition of the oxo facility Ruhrchemie accepted a foreign partner (the Sunlicht subsidiary of Unilever) in the Oxo GmbH, and worked on negotiation of a contract with the British concern Balduin, which (because it belonged to the Allies) might have offered some protection in the interest of acquiring detergent alcohols for its own purposes from the oxo facility.[47]

Nothing helped, however. By 1950, one of the two production lines of the oxo plant had been dismantled (Fig. 13)—only to be reconstructed at considerable expense starting in 1951. Never



Fig. 13. Dismantling of the Ruhrchemie facilities under the protection of the British Occupation Forces; the banner reads "Dismantlers, now begin your work!" [120].

theless, it soon became apparent that regular supply of starting olefins from the kogasin fraction of FT products or pyrolysis of FT waxes could not be assured, owing to the uncertain future of German FT facilities. As a result, a total of only about 3000 t of C_{10}–C_{18} oxo product was produced during the period 1953–1955.

The situation was further complicated by the fact that the original facility had become technically obsolete, and scientific information and technical experience gained in the meantime at the license-free production plants in the United States made it apparent that an oxo process based on the technical specifications of the original Ruhrchemie facility was unlikely to be successful. Synthetic detergent alcohols at that time were also not in a position to compete qualitatively with the natural alternatives. Moreover, an excellent supply of short- and medium-chain olefins was available (from cracking plants, or polymer olefins, C_6 to C_{12}), and interest had grown in producing the corresponding aldehydes resulting from the first step of the oxo synthesis (whereas the original oxo facility had been designed to produce higher detergent alcohols in a single step). Perhaps most important, so much had been learned about the mechanism of the oxo reaction that promising development potential was not apparent for the Ruhrchemie technology, based as it was on batch-slurry operation with a Fischer–Tropsch catalyst (cf. Section 3.2). Given a loss of interest on the part of Henkel, BASF (which in the early postwar years, like Ruhrchemie, continued to file patent applications on the oxo process through the Chemische Verwertungsgesellschaft mbH) drew the appropriate consequences as well, and abandoned its joint partnership with Ruhrchemie AG[88] in order to pursue its own interests—with payment of appropriate license fees. As matters developed, work began in 1958 on the perfection of a second "Ruhrchemie oxo process," culminating in a production capacity of roughly 335000 t/a. The new process attracted the interest of many licensees, and at its peak constituted the basis for over 20% of the newly erected oxo plants throughout the world. This success story was due in large measure to efforts of the Ruhrchemie engineering department, but Otto Roelen's research again played an important role.[89]

Several observations dating back to the war years were clearly suggestive of the true nature of the catalysis (homogeneous), the catalytically active species (tetracarbonylhydridocobalt), and at least parts of the reaction mechanism. The initially inexplicable and troublesome loss of cobalt through soluble cobalt compounds,[28] the pyrophoric nature of the catalyst,[54] and the elegant utilization of cobalt carbonyl for catalytic purposes[28, 54] might all have served as starting points for early speculation on the reaction mechanism, had such speculation not been hampered by specific mental blocks (cf. Section 3.2).

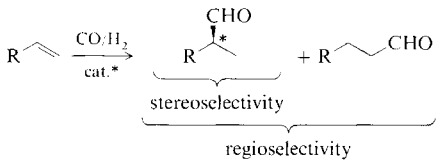
2.3. The Significance and Status of the Oxo Synthesis Today

The oxo synthesis has long been, and remains even now, an important industrial process; indeed, from a quantitative standpoint among catalytic organometallic processes it is second only to the Ziegler process for the manufacture of polyethylene and polypropylene. World capacity is currently ca. 6×10^6 t/a. Without going into detail on the present state of development with respect to the major oxo producers, we can still predict that three developments will determine the future significance of the oxo synthesis:

- As the literature indicates, continuing intense research and development in the area of hydroformylation is directed toward innovative applications of homogeneous catalysis, including regio- and stereoselective transformations of suitable starting materials.
- Oxo facilities in the highly industrialized countries will in the future be characterized largely by "highly sophisticated" applications involving regioselective hydroformylation, to be followed in due course by stereoselective reactions leading to unique and valuable products (i.e., special intermediates, formed perhaps enantioselectively), all in conjunction with tailored catalysts.
- World demand for "classical" oxo products (plasticizer and detergent alcohols) will increasingly be met by oxo facilities in less developed countries with access to the necessary resources (raw materials and labor). Many years of free-wheeling licensing politics, coupled with a high degree of automation that has reduced the demand for skilled personnel, now makes it possible for third-world countries (counter to Biblical prophecy) to harvest the fruits of development from fields they did not themselves sow, contributing "only" the essential inexpensive raw materials. Moreover, as the standard of living rises in these countries, so too will demand for certain oxo products that have increasingly become subjects of concern in countries with a higher level of "ecological awareness" (e.g., phthalate plasticizers).

In this respect the oxo synthesis will follow a trend already apparent in chemistry generally: highly industrialized countries will devote their oxo facilities to Roelen reactions and follow-up steps leading to such highly specialized, "ecologically accept-

able" oxo compounds as pharmaceuticals and crop-protection agents. Consistent with this classical scenario, research and development will prepare the way by perfecting an improved line of catalysts. The improvements themselves will be fundamental in nature, encompassing both regioselectivity and stereoselective control over the course of the reaction [Eq. (b)].



(b)

3. Lost Opportunities

3.1. Hieber's Pioneering Work in the Area of Metal Carbonyls

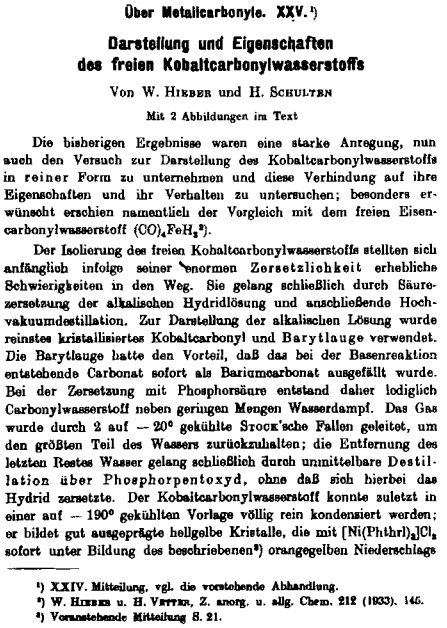
Our current vantage point makes it clear that in the very year the oxo synthesis was discovered the time was ripe for a synergism to develop between the brilliant research efforts of Otto Roelen and Walter Hieber (1895–1976). Had this come to pass, both mechanistic understanding and industrial development of the hydroformylation reaction would have benefited enormously.

Walter Hieber, born on December 18, 1895, in Waldhausen (Württemberg) a son of the pastor and later Minister of Education Johannes Hieber, earned his doctorate in 1919 at the University of Tübingen under the supervision of the coordination chemist Rudolf F. Weinland. Habilitation followed at the University of Würzburg in July 1924. The first theme Hieber addressed in his habilitation thesis blazed the trail for his later work on the chemistry of carbon monoxide complexes: "It is not permissible to regard secondary valence simply as a residual valence or a fragmented main valence." Following a brief guest appearance in Jena, Hieber held professorships at the Universities of Heidelberg (until 1932) and Stuttgart before moving in 1935 at the age of 39 to the Technische Hochschule München as the successor to Geheimrat (Privy Councilor) Wilhelm Manchot (1869–1945). Hieber served in Munich as Professor and Director of the Inorganic Chemical Institute until his retirement in 1964. His predecessor, Manchot, was himself active and quite successful in the field of metal carbonyls (e.g., $[Au(CO)Cl]$, $[Os(CO)_3Cl_2]$), which was then still in its infancy, and it was for this reason that the young Hieber's brilliant work on reactions of this class of compounds came to Manchot's attention.[125, 126] Since 1927 Hieber had been trying to establish the extent to which carbon monoxide in metal complexes could be replaced by amines as a way of characterizing the metal carbonyls $[M(CO)_x]$ in the form of "elemental complexes." During the course of a set of experiments with pentacarbonyliron, suggested to him by Alwin Mittasch of BASF,[103, 125, 127] Hieber quickly recognized the principle that came to be known as valence disproportionation.[128] Nonoxidizing acids were used to protonate the readily accessible carbonylmetalates—anions with the formula $[M(CO)_n]^{m-}$ containing metal atoms in negative (!) oxidation states—to give a completely new class of "carbonyl hydrides" of the transition metals. The first spectacular example was "iron carbonyl hydride" with the formula $[H_2Fe(CO)_4]$, a colorless, clear, light- and temperature-sensitive, volatile substance, the isolation and manipulation of which required the experimental skills of a master.[129] Whereas its discoverers immediately assigned the correct structural formula to the compound, including bonding between the metal and atomic hydrogen, other authors were still ruminating many years later over the isomeric "hydrocarbonyls," with structures involving -COH ligands.[54]

In his continuing search for meaningful bonding interpretations Hieber formulated the H_2Fe group in $[H_2Fe(CO)_4]$ as a "pseudonickel atom" (essentially an isoelectronic substitution). This simple idea led him to the conclusion that a "cobalt carbonyl hydride" with the formula $[HCo(CO)_4]$ should also be possible; this compound would effectively complete the series $[Fe(CO)_5]$, $[H_2Fe(CO)_4]$, **$[HCo(CO)_4]$**, and $[Ni(CO)_4]$. While still in Heidelberg (1932) he in fact succeeded in demonstrating the existence of this highly volatile compound by the acid decomposition of amine-containing cobalt carbonyls.[130] The substance proved to be much less stable and even more reactive than the analogous iron compound. At this point Hieber was suddenly confronted with competition from America: Coleman and Blanchard of the Massachusetts Institute of Technology, completely unaware of Hieber's publications (all of which had been in German), reported in a paper submitted July 28, 1935, the reaction of $K[Co(CO)_4]$ with HCl, from which they isolated "a light yellow crystalline solid which melts at $-33\,^{\circ}C$ to a sulfur yellow liquid."[131] Although these authors had clearly recognized the acidic character of $[HCo(CO)_4]$, "the other experiments related to cobalt carbonyl hydride reported by the cited authors were conducted so inexactly, and the results were so imprecise, that one can dispense with discussing them further, especially since they have for some time been largely superseded by our own investigations."[132] Nevertheless, Hieber received from the American authors "a letter expressly acknowledging our priority in the discovery of the metal carbonyl hydrides."[132] Indeed, manuscripts received by journal editors from Hieber in 1932[130] and on February 9, 1936,[99] clearly do establish this priority.

The synthesis and properties of $[HCo(CO)_4]$ are described very precisely in two masterpieces of experimental work carried out in collaboration with H. Schulten (Fig. 14).[132, 133] The compound was prepared by means of the recently discovered "base reaction" (now commonly referred to in textbooks as the "Hieber base reaction") of the cobalt carbonyl $[Co_2(CO)_8]$ with barium hydroxide in a high-vacuum apparatus.[132] The melting point was determined "with a pentane thermometer calibrated by the Imperial Physical-Technical Facility, Berlin" and reported as $-26.2\,^{\circ}C$:[132] Swabian precision in every detail!

Although Walter Hieber published 200 additional experimental papers on metal carbonyls, those dealing with the carbonyl hydrides are regarded as the most original. They are also the most important if one includes in this category the "high-pressure direct syntheses" of metal carbonyls, developed for this category of substances. Hieber together with H. Schulten and R. Marin achieved a total synthesis of $[HCo(CO)_4]$ starting with cobalt powder and synthesis gas in 1938.[101, 102] Depending on the pressure and temperature, the major product of the reaction was either $[Co_2(CO)_8]$ or $[HCo(CO)_4]$. This particular piece of work—fundamentally important with respect to hydroformyla-



Über Metallcarbonyle. XXV.[1]

Darstellung und Eigenschaften des freien Kobaltcarbonylwasserstoffs

Von W. Hieber und H. Schulten

Mit 2 Abbildungen im Text

Die bisherigen Ergebnisse waren eine starke Anregung, nun auch den Versuch zur Darstellung des Kobaltcarbonylwasserstoffs in reiner Form zu unternehmen und diese Verbindung auf ihre Eigenschaften und ihr Verhalten zu untersuchen; besonders erwünscht erschien namentlich der Vergleich mit dem freien Eisencarbonylwasserstoff $(CO)_4FeH_2$[2]).

Der Isolierung des freien Kobaltcarbonylwasserstoffs stellten sich anfänglich infolge seiner enormen Zersetzlichkeit erhebliche Schwierigkeiten in den Weg. Sie gelang schließlich durch Säurezersetzung der alkalischen Hydridlösung und anschließende Hochvakuumdestillation. Zur Darstellung der alkalischen Lösung wurde reinstes kristallisiertes Kobaltcarbonyl und Barytlauge verwendet. Die Barytlauge hatte den Vorteil, daß das bei der Basenreaktion entstehende Carbonat sofort als Bariumcarbonat ausgefällt wurde. Bei der Zersetzung mit Phosphorsäure entstand daher lediglich Carbonylwasserstoff neben geringen Mengen Wasserdampf. Das Gas wurde durch 2 auf −20° gekühlte Stock'sche Fallen geleitet, um den größten Teil des Wassers zurückzuhalten; die Entfernung des letzten Restes Wasser gelang schließlich durch unmittelbare Destillation über Phosphorpentoxyd, ohne daß sich hierbei das Hydrid zersetzte. Der Kobaltcarbonylwasserstoff konnte zuletzt in einer auf −190° gekühlten Vorlage völlig rein kondensiert werden; er bildet gut ausgeprägte hellgelbe Kristalle, die mit $[Ni(Phthrl)_2]Cl_2$ sofort unter Bildung des beschriebenen[2]) orangegelben Niederschlags

[1]) XXIV. Mitteilung, vgl. die vorstehende Abhandlung.
[2]) W. Hieber u. H. Vetter, Z. anorg. u. allg. Chem. 212 (1933). 145.
[3]) Vorangehende Mitteilung S. 21.

Fig. 14. Facsimile of the title page of Hieber and Schulten's first paper on $[HCo(CO)_4]$ [132,133].

tion as well—was submitted for publication on November 24, 1938,[101] very soon after Otto Roelen filed the first oxo patent application.[50] The relevance of Hieber's pioneering work to the reaction mechanism of hydroformylation thus becomes obvious. An article in an American journal first alluded to the possible connection ("We suggest that a hydride is the reagent effective in the synthesis"[75]), and FIAT Report 1000 also speaks of "hydrocarbonyl $Co(CO)_x(H)_y$" as the reactive species,[54] referring to information provided by Otto Roelen of Ruhrchemie and Kurt Schuster of BASF (cf. Section 3.2).

It remains one of the ironies in the history of science that Walter Hieber (Fig. 15) never met Otto Roelen, who was almost exactly his age. Hieber's students maintained that he never even sought such a contact. Moreover, the name Roelen is nowhere cited in any of Hieber's publications, although he frequently mentioned the "Reppe chemistry" that was also strongly influenced by his work. By contrast, Otto Roelen kept himself well informed of results from the laboratory in Munich, and shortly after the war he proved to be a friendly and interested host in Oberhausen for field-trip groups from Munich. Helmut Behrens, at that time a young instructor under Hieber[134] and later a professor in Erlangen, recalls: "In the course of a field trip to Oberhausen in the early 1950s Dr. Roelen asked me to remain an extra half day so I could discuss with him recent progress in the Munich metal carbonyl chemistry. His interest was so keen that he offered to provide me with the company car to catch up with the rest of the group."[135]

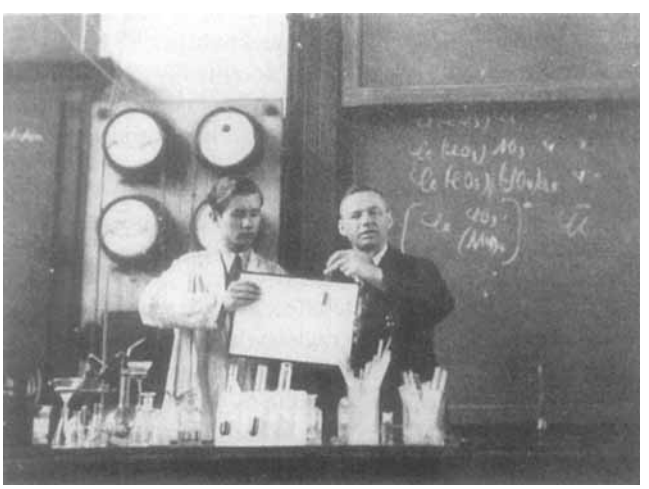


Fig. 15. Walter Hieber during one of his lectures on experimental inorganic chemistry (on the left, his assistant H. Behrens).

We have no way of knowing why Hieber never became involved in questions regarding the mechanism of hydroformylation. It is a matter he appears predestined to have tackled, given his knowledge of the catalytic substance $[HCo(CO)_4]$. Was he marked too strongly by the classical attitude of coordination chemists like Weinland? Was his interest in new complexes and an understanding of the underlying bonding theory more compelling than any effects such materials might have on organic compounds and any possible industrial applications? Was he too preoccupied with the metal carbonyl class of compounds per se? In any event, posterity is keenly aware of this loss of a unique opportunity for synergism between academic and industrial laboratories with mutually complementary expertise. It is also interesting to speculate whether such a symbiosis might have significantly hastened the next major advance: the shift from organocobalt to organorhodium catalysts for hydroformylation, which in fact began only in the 1970s.[89]

Germany remained the world leader in metal carbonyl chemistry until the end of the 1950s thanks to the tremendous success of the school surrounding Walter Hieber. As part of one of the "four-year-plan institutes" designated by the Reich Economics Ministry, Hieber's research group could depend on the requisite continuity in its research even during the period 1939–1945. Given these circumstances, three factors must be taken into account if one wishes to understand why Roelen's and Hieber's paths never intersected. First, scientific research was much more compartmentalized in those days than it is now. Research areas were "marked out" by specific individuals, and "claims"—once established (usually in the form of concluding sentences in the relevant groundbreaking papers)—were generally respected. Hieber defended his research interests in an especially dedicated way against every potential encroacher, and was thus all the more annoyed in 1954 when E. O. Brimm et al. of the Ethyl Corporation presented a report describing the preparation of $[Mn_2(CO)_{10}]$, the target of a decades-long search.[139] Hieber himself always respected the territorial claims of others. We are aware of only a single exception: the isocyanide complexes, which Friedrich Klages could legitimately have claimed for himself.[140] Second, until the groundbreaking discoveries of Ziegler and Natta, practical applications were essentially ignored by all organometallic chemists, who restricted their attention to preparative developments and an understanding of reactivity. In the academic world, catalysis was regarded as an erratic field steeped in empiricism and lacking intellectual pretensions.

Third, mechanistic thinking was not yet well established in metal complex chemistry in the days of Hieber and Roelen, and neither scientist was particularly fond of the type of speculative excursion that would have been required to formulate what we

would today regard as the relatively simple set of steps constituting the Roelen reaction [olefin–metal complexation, which Roelen already suspected, followed by transformation of the alkyl group into an acyl group, and subsequent hydride transfer; Eqs. (c) through (e)]:[89, 114]

$$RCH{=}CH_2 + [HCo(CO)_4] \longrightarrow \underset{\displaystyle HCo(CO)_4}{RCH{=}CH_2} \longrightarrow [RCH_2{-}CH_2{-}Co(CO)_4] \quad (c)$$

$$[RCH_2{-}CH_2{-}Co(CO)_4] + CO \longrightarrow [RCH_2CH_2{-}CO{-}Co(CO)_4] \quad (d)$$

$$[RCH_2CH_2{-}CO{-}Co(CO)_4] + H_2 \longrightarrow RCH_2CH_2{-}CHO + [HCo(CO)_4] \quad (e)$$

In fact, it was not until 1960 that these three homogeneous-phase reactions were sufficiently well known and understood for Heck and Breslow to derive the complete mechanism.[114] One might with a bit of restraint surmise that in today's internationally cross-linked scientific community, potential relationships between apparently independent research areas would have been recognized much more quickly. On the other hand, even now, every innovative field of research requires a certain amount of time to mature, and we must not forget that in 1938, the year hydroformylation was discovered, metal carbonyl chemistry was scarcely a decade old.

3.2. The Long Road to Understanding the Oxo Synthesis as a Case of Homogeneous Catalysis

It may seem strange that Otto Roelen, a reflective and observant investigator, did not see the nature of the catalysis involved in hydroformylation for so long—indeed, into the postwar era. However, given the circumstances of the times and Roelen's own particular way of thinking, it all becomes quite understandable. On one hand, working and living conditions during the Third Reich were hardly normal, despite an appearance of orderliness and the regime's brutally rigorous attitude toward "law and order." Researchers at that time, occupied as they were with a surplus of militarily vital projects, were a privileged lot, but they were still restricted in their movements, and subject to the same limitations and threats as other citizens living in that absolute war economy. The Ruhrchemie premises experienced a total of 1020 alarms and 27 bombings during the course of the war,[47] and this affected Otto Roelen (who lived in the immediate vicinity of the plant) just as much as it did his contemporaries. A constant sensation of not having slept enough, together with persistent threats to his very existence, were hardly conducive to pondering over mechanistic aspects of the oxo synthesis or questions related to the nature of the catalysis in the new reaction. Holm et al. expressed the matter directly in similar tones in FIAT Report 1000:[54]

> "This deficiency stems from the wartime necessity of placing the emphasis upon industrial application and development rather than on fundamental studies."

The collective harassment of "comrades" by the Nazi regime by constant warnings and threats was bound to take a toll on a loner like Otto Roelen. It prevented him from working properly, and it denied him the leisure necessary for conducting proper literature searches, as he himself later acknowledged. Symptomatic of the pressures is a Ruhrchemie in-house newsletter from that period, the content of which ranges from instructions from the "Head of the Works Committee" to threats from the "Workforce Combat Patrol Leader," culminating in "knitting for the final victory":[90]

> "Our participation in the wool collection for the army on the Eastern Front. Dr. Roelen's research laboratory is deserving of special mention. Through his initiatives it was possible to accomplish the astonishing feat of assembling 167 individual items for the army, including a large number of lined vests... ."

Moreover, notwithstanding all the apparent efficiency of the Nazis there was still a shocking level of disorganization in many employment and research activities,[91] and Roelen's involvement in too many research projects unrelated to the oxo synthesis had exceeded his capacity (cf. the report of Otto Roelen's interrogation in December 1945 at Wimbledon[28, 48]). Keeping up with the technical literature also became increasingly difficult under the weight of external factors. In the last years of the war the literature was hardly accessible at all (several of the German journals quit publishing altogether after about 1942, including *Chemische Berichte*, *Chemische Industrie*, and *Öl und Kohle*). The way research was organized generally, especially at Ruhrchemie (see above[28]), coupled with the Nazi mania with respect to secrecy, also prevented the fruitful exchange of ideas with colleagues. Moreover, in the early phases of his discovery Otto Roelen had been inclined to undertake personally as much as possible of the fundamental work of development and refinement, as well as the preparation and filing of patent applications.

Nevertheless, the most important factor, as Roelen himself later complained and elaborated in numerous conversations and several lectures on the subject of "Research Psychology,"[39, 45, 92] was a distinct mental block during the war years—probably due in part to strong preconceptions—against accepting the notion of a *new* type of catalysis. Like many of his contemporaries, Otto Roelen was fascinated by catalysis as a spectacular, modern (albeit empirical) science, but he took it for granted that catalysis generally was equivalent to "chemistry at a catalyst surface" (Kontakt), in other words that it was a *heterogeneous* phenomenon. The idea of homogeneous catalysis was admittedly not completely unknown (Mittasch and Sabatier[93] both mentioned it briefly), but it was limited conceptually to simpler and technically unspectacular reactions, and did not yet encompass the present definition[94] of a transformation in which there is

> "a molecular distribution of the catalytically active species, which is therefore highly dispersed and consequently might be present at very low concentration (into the ppm range)."

Mittasch's views had an aftereffect as well, such that homogeneous catalysis was viewed exclusively in the context of "a material 'invention of nature'," and the "material 'substrate' of all natural phenomena" (i.e., biocatalysis, according to present-day terminology). This lingering reflection of Berzelius, for whom "the concept of a catalyst was useful primarily for purposes of physiology,"[95] was acknowledged as such by Mittasch in his own writings.

For chemists in Otto Roelen's generation, catalysis in the everyday use of the term referred to *heterogeneously* catalyzed transformations associated with a series of empirical investigations: the ammonia synthesis, coal hydrogenation, hardening of fats, the Fischer–Tropsch synthesis, and other industrial-scale and forward-looking technologies. Organometallic catalysts and reactants were essentially unknown except in the case of a few special and exotic applications (e.g., the Grignard reaction, Mond process).

An additional obstacle was the firm assumption that the oxo synthesis depended on heterogeneous catalysis, which meant that any observations to the contrary tended to be dismissed. Thus, the discovery that the reaction products always contained significant amounts of cobalt was not taken as evidence suggestive of the *nonheterogeneous* nature of the reaction. Ostwald's definition of a catalyst as a "substance that alters the rate of a reaction without appearing in the final product"[96] implies that a substance that does appear in the final product might be almost anything, but certainly not a catalyst. In this sense Berzelius' simpler definition of catalysts as "substances the mere presence of which confers chemical activity not found in their absence"[95] was more useful and less misleading.

Experimental findings should at the least have led Roelen and his contemporaries to be somewhat suspicious, because the assumption of an unchanged catalyst was incompatible with the observed facts, which were also not explained by the secondary hypothesis that the reaction conditions simply resulted in partial physical dissolution of certain catalyst components. Moreover, experiments initiated during the war in an attempt to convert the oxo synthesis from a reaction based on suspension techniques to some other alternative were motivated less by a mechanistic way of looking at the reaction than by a desire to increase the effective utilization of the catalyst. Even developments like the Leuna variant, the BASF continuous process in a fixed-bed reactor,[54] and the "diaden" approach (alternate utilization of the oxo and hydrogenation chambers)[117] had their origin not in the possibility that this might be a homogeneously catalyzed reaction, but rather (as nearly as can be established today) in a desire to achieve optimal reaction or temperature control and at the same time increase productivity (cf. ref. [28]).

This is all in the face of the fact that Hieber's most crucial papers had already been published, and the important observations of the early oxo researchers had already been made. Thus, even though it seemed self-evident that a commercial (large-scale) oxo synthesis should be based on the usual catalysts from the heterogeneous FT process, it very soon became common practice to compensate for massive losses of cobalt by the introduction of additional soluble cobalt compounds.[28, 54] The effect of this material could only have been homogeneous, not heterogeneous, and it did not in any way take the place of other components of the FT catalyst; indeed, the additives were deemed responsible for an observed instability of the FT catalyst itself. Especially revealing in this context were experiments conducted by Reppe in Ludwigshafen for a continuous process in a fixed-bed reactor, which presupposed subsequent cobalt removal and separate hydrogenation of the resulting oxo aldehydes over copper–chromite catalysts.[54, 79] One other curiosity is worth noting: a "miraculous" hydroformylation achieved with metals that do not form carbonyl complexes such as calcium, magnesium, and zinc, ingredients that among other things were partially responsible for the structural composition of the classical FT catalysts.[97] The person who dreamed up this particular patent application, an American by the name of Whitman (related to the famous American poet?) mentions in the general section of his application in a very pointed and convincing way that the use of volatile carbonyl complexes actually does nothing but cause problems, and it might therefore be better to add elements of atomic number 12–30, which do not form carbonyl complexes. At least Otto Roelen's own patent[59] was properly cited in this case; the same could not always be said for other authors.[98]

Given the ubiquitous presence of cobalt carbonyls in all the various streams of the oxo reaction– reactants, off-gas, and gas and liquid recycle systems –and in the product itself, Roelen was led to postulate quite early that volatile "cobalt hydrocarbonyls," described by Hieber in 1934,[99] were the truly active oxo catalysts. This conclusion was influenced by the fact that active oxo catalyst could be prepared starting with a wide range of cobalt compounds,[28] as well as by the experimental observation that cobalt,[99–102] but not the oxo-inactive nickel,[54] formed a hydridocarbonyl (hydride shift rule[103]). The hydroformylation of ethylene in particular was carried out at a very early date with dissolved cobalt carbonyls. The lack of consistency in Roelen's ideas regarding the mechanism of the oxo synthesis is underscored by the view he expressed as late as 1945 that the threshold temperature for carbonyl formation must lie below that for formation of cobalt carbide.[54] The possibility of stoichiometric hydroformylation[80] may also have contributed to the confusion.

Interestingly, while possible roles for dissolved carbonyls or hydridocarbonyls[64, 80, 81, 104, 105] in the oxo synthesis were subsequently discussed, Adkins and Krsek[75] were the first to describe the reaction explicitly as "nonheterogeneous," and it was Storch et al.,[121] Berty and Markó,[106] and Natta[107] who first explicitly used the descriptive term "homogeneous." A 1951 patent application by Kuhlmann, describing the catalytic application of gas-phase carbonylhydridocobalt,[108] refers to a "lack of homogeneity," but more in the sense of a lack of experimental homogeneity. A parting shot in the battle to formulate hydroformylation as a heterogeneous process ("... an assumption that even now has scattered adherents ... ," as Falbe[78] cautiously expressed it in 1967) was fired as late as 1963 by Aldridge et al.,[109] but vigorously criticized by Macho et al.[110] The generation of tetracarbonylhydridocobalt, first suspected by Otto Roelen[54] and later proposed by numerous authors,[65, 75, 81, 105, 111, 112] was finally proven by the work of I. Wender et al.[113]

Complete unanimity regarding the mechanism of hydroformylation was achieved with the appearance of a persuasive paper by Heck and Breslow.[114] Apart from early kinetic investigations by Natta et al.[76] and their subsequent conclusions regarding the kinetic order of the reaction,[77] several very divergent interpretations were proposed along the way to an unambiguous formulation of the mechanism, including addition of $[HCo(CO)_x]$ to the C–C double bond of the starting olefin followed by a transformation to a more stable hydridocarbonyl containing less CO (foreshadowing the later dualism of hydridotri- and hydridotetracarbonylcobalt), and a cyclopropyl (more precisely: cyclopropenone) structure[124] with preferen-

tial anti-Markovnikov attack of the formyl group (based on Reppe and Asinger; a summary is provided in refs. [54,65,115]). The term "π complex" for the product resulting from the addition of $[HCo(CO)_4]$ to a double bond was first suggested by Klopfer,[105] and then discussed by Roelen in connection with "crypto ions,"[111] although until 1947 he had clung to the possibility of intermediate formation of a carbide in the "genetic sequence" leading from CO to aldehydes.[104] In 1957 Asinger provided a valuable overview of current ideas on the mechanism of the oxo reaction.[115]

3.3. Pioneer of Industrial Homogeneous Catalysis

Although there has been general consensus regarding the nature of the incorporation of "cobalthydridocarbonyl" since 1949 and publication of the work of Adkins and Krsek (e.g., refs. [73, 75, 105, 111] with mechanisms based on findings by Martin[112] and Natta et al.[107, 118]), it took many years and several duels between adherents of Reppe[65] and Dupont et al.[116] before the currently accepted mechanism of the oxo reaction was firmly established. This occurred 22 years after hydroformylation was discovered, and then not as a result of efforts by the discoverer or other protagonists of the oxo synthesis, but by Heck and Breslow.[114] Nevertheless, Otto Roelen can rightfully be identified as the pioneer of modern industrial homogeneous catalysis. His discovery of hydroformylation sensitized the chemists of his day to the potential for industrial application of organometallic catalysts (ten years prior to the equally history-making work of Ziegler and Natta), and smoothed the way for an understanding of the homogeneous version of catalysis as an independent, versatile, and commercially successful method for preparing important basic chemicals and specialty products. More than that, recognition of the catalytic potential of metal coordination compounds – coupled with further stimulus from the exciting discoveries of ferrocene[136] and dibenzenechromium[137] – gave an unprecedented impetus to organometallic chemistry in the 1950s. Carbon monoxide chemistry in particular cast a bright light on this ascendancy that began with the groundbreaking work of Otto Roelen and Walter Hieber.

One is compelled to agree with Otto Roelen's later formulation of the quintessence of his personal experience, set against a background of personal prejudice:[45]

> "... fantasy and the powers of imagination can fulfill their appointed role as intellectual 'sources of raw material' only if they are allowed to develop fully and without restriction, and if nothing stands in the way of one's intellectual processing of a research field in any direction whatsoever, neither habitual patterns of thought nor preconceptions."

In his reflections on his personal failure to recognize the nature of the homogeneous catalysis underlying the oxo reaction,[45] Roelen thus paid tribute to the true meaning of his favorite author Descartes' "methodological skepticism." He was indeed the discoverer of the oxo synthesis, but not – as he had hoped – the one who unraveled its mechanism. Otto Roelen's special significance, extending into the present, is to be sought rather in the fact that as the pioneer in the first industrially successful synthesis involving organometallic catalysts he raised the level of consciousness regarding the technical relevance and broad applicability of homogeneous catalysis – in spite of every attack from aggressive "heterogenophiles."

Received: March 21, 1994 [A 56 IE]
German version: *Angew. Chem.* **1994**, *106*, 2219
Translated by Dr. W. E. Russey, Huntingdon, PA (USA)

[1] Letter from Gutbier to Fischer, June 26, 1922, in: Max-Planck-Institut for Kohlenforschung (Archiv MPI), Personnel Records (PA) Otto Roelen (OR).
[2] KWI questionnaire and "proof of Aryan status" dated May 4, 1933; Archiv MPI, PA OR.
[3] Typewritten curriculum vitae for Otto Roelen from ca. 1947, in: private estate of OR, Königswinter.
[4] Handwritten curriculum vitae for Otto Roelen dated October 8, 1924; Archiv MPI, PA OR.
[5] F. Petzold, *Zum 50jährigen Bestehen des Hauptlaboratoriums der Hoesch-Köln Neuessen Aktiengesellschaft in Dortmund*, Düsseldorf, **1937**, p. 18.
[6] Letter from Fischer to Otto Roelen dated June 28, 1922; Archiv MPI, PA OR.
[7] a) M. Rasch, *Geschichte des Kaiser-Wilhelm-Instituts für Kohlenforschung 1913–1943*, VCH, Weinheim, **1989**; b) in ref. [7a], p. 159 ff.
[8] BASF (no inventor; Schuster [65] later identified Mittasch and Schmidt as the inventors), DRP 293787, **1913**; DRP 295202 and 295203, **1914**; A. Mittasch, M. Pier, K. Winkler (BASF), DRP 660619, **1924**.
[9] F. Fischer, H. Tropsch, *Brennst. Chem.* **1923**, *4*, 276, in particular p. 284.
[10] H. Tropsch, O. Roelen, *Gesammelte Abh. Kennt. Kohle* **1925**, *7*, 15.
[11] Recommendation from Prof. Bucherer dated October 7, 1924, Archiv MPI, PA OR.
[12] Evaluation of Otto Roelen's dissertation, February 21, 1924, Archiv MPI, PA OR.
[13] Copy of Otto Roelen's 1924 dissertation in the library of the MPI.
[14] O. Roelen, DE 497694, **1924/1930**.
[15] Deutsches Patentamt, Außenstelle Berlin, entry in the patent register.
[16] H. Tropsch, O. Roelen, *Brennst. Chem.* **1924**, *5*, 37; *Gesammelte Abh. Kennt. Kohle* **1925**, *7*, 15, 175; O. Roelen, *ibid.* **1925**, *7*, 111.
[17] O. Roelen, *Erdöl Kohle Erdgas Petrochem.* **1978**, *31*, 524.
[18] F. Fischer, H. Tropsch, *Chem. Ber.* **1926**, *59*, 836.
[19] Information from the Archiv MPI, PA OR.
[20] Letter from Fischer to the Administrator of the Institute, Mr. Lindemann, dated March 10, 1931, Archiv MPI No. 01-023.
[21] Archiv MPI, 99.
[22] O. Roelen, *Erdöl Kohle Erdgas Petrochem.* **1977**, *30*, 456.
[23] See ref. [7a], p. 233 ff.
[24] Hoechst AG, Werk Ruhrchemie, PA OR.
[25] O. Roelen (Ruhrchemie AG), DRP 718509, **1937/1942**; DRP 763967, **1936/1952**; O. Roelen, W. Feißt (Ruhrchemie AG), DRP 764888, **1938**.
[26] H. Heckel, O. Roelen (Ruhrchemie AG, DRP 764643, **1937/1952**.
[27] Combined Intelligence Objectives Sub-Committee (CIOS), Report No. XXXIII-5, Item No. 30; British Intelligence Objectives Sub-Committee (BIOS), Final Report No. 1094, Item No. 30; *Ullmanns Encykl. Tech. Chem. 3rd ed.* **1957**, *9*, 744 ff.
[28] BIOS, Final Report No. 447, Item No. 30, **1946**.
[29] B. Cornils, W. A. Herrmann, C. W. Kohlpaintner, *Nachr. Chem. Tech. Lab.* **1993**, *41*, 544.
[30] Letter from the Dr.-Fritz-Todt Prize, Essen branch, to Ruhrchemie AG dated January 16, 1945, in Hoechst AG, Werk Ruhrchemie, PA OR.
[31] Correspondence Archiv MPI, PA Helmut Pichler.
[32] O. Roelen, *Chem. Exp. Didakt.* **1977**, *3*, 119.
[33] O. Roelen, *Zentralbl. Biol. Aerosol Forsch.* **1962**, *10*, 532.
[34] O. Roelen, unpublished manuscripts "Eiweißarme Kost gegen Eiweiß-Mast" (1975), "Trinkwasser in Flaschen" (1972), "Zuckerverzehr als Krankheitsursache", "Über die sogenannte Butter- and Margarine-Frage" (1965), and "Verunreinigungen in Rheinuferfiltraten" (1973).
[35] O. Roelen, *Vitalst. Zivilisationskrankh.* **1963** (5).
[36] O. Roelen, unpublished manuscripts "Über alimentäre Allergene" (1974) and "Getreidekeime als Allergene" (1976).
[37] K. Przibram in *Das Buch der großen Chemiker, Vol. II* (Ed.: G. Bugge), Verlag Chemie, Berlin, **1929/1930**, p. 288 f., 297; G. Stein, *The Sorcerer of Kings: The Case of Daniel Dunglas Home and William Crookes*, Prometheus, **1993**.
[38] O. Roelen, unpublished manuscripts "Schichtenbildung im luftelektrischen Raum" (1969), "Wohnungsentstörung" (1970), "Raumorientierte polarisierte Mikrowellen und ihre physiologische Bedeutung" (1971/1972), and "Pendelkunde" (1980).
[39] O. Roelen, "Emotik", unpublished manuscript (1968).
[40] C. P. Snow, *Die zwei Kulturen*, Klett, Stuttgart, **1959**; *The Two Cultures and The Scientific Revolution*, Cambridge University Press, Cambridge, England, **1959**.
[41] H. Kreuzer, W. Klein, *Über Snows "Die zwei Kulturen" C. P. Snows These in der Diskussion"*, Klett-Cotta im Deutschen Taschenbuch-Verlag, München, **1987**.
[42] K. Steinbuch, *Falsch programmiert*, Deutsche Verlags-Anstalt, Stuttgart, **1968**.

[43] K. Reumann, "Frankfurter Allgemeine Zeitung", August 15, 1987.
[44] E. Wolf, "Die Zeit", March 13, 1964.
[45] O. Roelen, honorary doctorate acceptance address at the Technische Hochschule, Aachen, January 21, 1983.
[46] G. Plumpe, *Die I.G. Farbenindustrie AG*, Duncker & Humblot, Berlin, **1990**.
[47] M. Rasch, *Geschichte der Ruhrchemie AG*, Privatdruck, unpublished manuscripts (1993).
[48] BIOS, Final Report No. 511, Item No. 30.
[49] C. D. Frohning, B. Cornils, *Hydrocarbon Process.* **1974** (11); 143; B. Büssemeier, C. D. Frohning, B. Cornils, *ibid.* **1976** (11), 105.
[50] O. Roelen (Chemische Verwertungsgesellschaft mbH), DE 849548, **1938/1952**.
[51] Ref. [9], in particular p. 281 ff.
[52] F. Fischer, H. Tropsch, *Gesammelte Abh. Kennt. Kohle* **1929**, *8*, 495; F. Fischer, H. Küster, *Brennst. Chem.* **1933**, *14*, 3.
[53] D. F. Smith, C. O. Hawk, P. L. Golden, *J. Am. Chem. Soc.* **1930**, *52*, 3221.
[54] BIOS and Field Information Agency, Technical (FIAT), FIAT Final Report No. *1000*, **1945**.
[55] B. Cornils, W. Rottig in *Chemierohstoffe aus Kohle* (Ed.: J. Falbe), Thieme, Stuttgart, **1977**, p. 323f.
[56] W. Rottig, F. Duftschmid, *Ullmanns Encykl. Tech. Chem., 3rd ed.* **1957**, *9*, 742.
[57] CIOS, File No. XXXII-96, Item No. 30.
[58] Ruhrchemie AG, FR 860289, **1939**; IT 376283, **1939** and 382427, **1940**.
[59] Ruhrchemie AG, US 2327066, **1943**.
[60] Minutes of the Ruhrchemie Aktiengesellschaft Executive Board meeting of February 6, 1940, VS-Akten Hoechst AG, Werk Ruhrchemie (Ablage Rechtsabteilung).
[61] H. Tramm, *Chem. Ing. Tech.* **1952**, *24*, 181.
[62] Minutes of the Ruhrchemie Aktiengesellschaft Executive Board meeting of July 4, 1940, VS-Akten Hoechst AG, Werk Ruhrchemie (Ablage Rechtsabteilung).
[63] Notarized document No. 220/1940, Dr. Karl Lohmar, notary, Oberhausen (Ablage Rechtsabteilung, Hoechst AG, Werk Ruhrchemie).
[64] A. Willemart, *Bull. Soc. Chim. Fr.* **1947**, *14*(5), 152.
[65] C. Schuster, *Fortschr. Chem. Forsch.* **1951/1953**, *2*(2), 311.
[66] Analogous to ref. [62], meeting of November 13, 1940.
[67] Analogous to ref. [62], meeting of November 19, 1941.
[68] Letter from the Oxogesellschaft mbH to Ruhrchemie AG dated February 28, 1941 (Ablage Rechtsabteilung, Hoechst AG, Werk Ruhrchemie).
[69] Articles of association for the Chemische Verwertungsgesellschaft Oberhausen GmbH, entered into by the Ruhrchemie AG and the I. G. Farbenindustrie AG on December 11, 1940 (Ablage Rechtsabteilung, Hoechst AG, Werk Ruhrchemie).
[70] Amtsgericht Oberhausen-Rhld., Handelsregister Abteilung B, No. 83 from December 10, 1973.
[71] CIOS, Report No. XXVII-18, Item No. 22, **1945**.
[72] P. Lino, L. Paleari, *Ullmanns Encykl. Tech. Chem. 3rd ed.* **1962**, *13*, 60–72.
[73] H. Adkins, G. Krsek, *J. Am. Chem. Soc.* **1949**, *71*, 3051.
[74] C. C. Hall, *Chem. Ind. (London)* **1947** (2), 67.
[75] H. Adkins, G. Krsek, *J. Am. Chem. Soc.* **1948**, *70*, 383.
[76] G. Natta, *Chim. Ind. (Milan)* **1942**, *24*, 389; G. Natta, E. Beati, *ibid.* **1945**, *27*, 84.
[77] G. Natta, P. Pino, *Chim. Ind. (Milan)* **1949**, *31*, 109, 111.
[78] J. Falbe, *Synthesen with Kohlenmonoxid*, Springer, Berlin, **1967**, p. 4.
[79] Work carried out by Nienburg (Oppau plant of I. G, later BASF), discussed in explicit terms in ref. [54], p. 15; (H. J. Nienburg, A. Gemassmer, Chemische Verwertungsgesellschaft Oberhausen mbH), DE 888687, **1953** (patented, and thus registered from September 19, 1942).
[80] O. Roelen, *Angew. Chem.* **1948**, *60*, 62.
[81] O. Roelen in *Naturforschung and Medizin in Deutschland 1939–1946* (German edition of the FIAT Review of German Science), *Vol. 36* (Präperative organische Chemie), *Part I* (Ed.: K. Ziegler), Dieterichsche Verlagsbuchhandlung, Wiesbaden, **1948**, p. 155.
[82] J. Gimbel, *Science, Technology and Reparations*, Stanford University Press, Stanford, **1990**.
[83] O. Roelen, Die Entwicklung der Fischer-Tropsch-Synthese bei der Ruhrchemie Aktiengesellschaft, manuscript, Oberhausen, **1948**.
[84] BIOS, Final Report No. 1038, Item No. 30.
[85] *Chem. Eng. (N.Y.)* **1948**, *55*, (11), 328; *Chem. Eng. News* **1948**, *26*, Part II, 3694; *ibid.* **1949**, *27*, Part I, 245; *Pet. Refin.* **1952** (3), 149; *Chem. Eng. (N.Y.)* **1953**, *60*, (8), 346; *Pet. Refin.* **1954** (12), 141; *Chem. Eng. News*, **1955**, *33*, Part 1, 594; I. Wender, *Pet. Refin.* **1956** (12), 197; *Chem. Ind. (Maclean-Hunter)* **1948** (8), 211.
[86] H. Lemke (Etablissm. Kuhlmann), FR 1108983, **1953**, and subsequent patents.
[87] See ref. [28], p. 44.
[88] For example, the sale of the BASF share in the Chemische Verwertungsgesellschaft Oberhausen to the Ruhrchemie AG, document register 424/1959 of Dr. K. Lohmar, notary, Oberhausen, and 5626/1959 of Dr. K. Ackermann, notary, Ludwigshafen (Ablage Rechtsabteilung, Hoechst AG, Werk Ruhrchemie).
[89] B. Cornils, "Hydroformylation" in *New Syntheses with Carbon Monoxide* (Ed.: J. Falbe), Springer, Berlin, **1980**, p. 162.
[90] Company newsletter of Ruhrchemie AG "Mitteilungen for die Betriebs(Werks)gemeinschaft Ruhrchemie," Issues 1–9, **1941–1943**; here: No. 2/February 1942.
[91] K.-H. Ludwig, *Technik and Ingenieure im Dritten Reich*, Droste, Düsseldorf, **1974**.
[92] O. Roelen, "Wissenschaftsgläubigkeit and Wissenschaftsfeindlichkeit" in *Blinklichter*, Schulzeitung der Otto-Pankok-Schule, Mülheim, **1979**.
[93] a) P. Sabatier, *Die Katalyse in der organischen Chemie*, Akademische Verlagsgesellschaft, Leipzig, **1927**; b) A. Mittasch, *Kurze Geschichte der Katalyse in Praxis und Theorie*, Springer, Berlin, **1939**; c) A. Mittasch, *Über Katalyse und Katalysatoren*, Springer, Berlin, **1936**.
[94] J. Falbe, C. D. Frohning, "Homogene Katalyse" in *Katalysatoren, Tenside und Mineralöladditive* (Eds.: J. Falbe, U. Hasserodt), Thieme, Stuttgart, **1978**, p. 5.
[95] Cited in ref. [93c].
[96] W. Ostwald, *Über Katalyse*, Akademische Verlagsgesellschaft, Leipzig, **1923**; W. Ostwald, *Grundriß der allgemeinen Chemie*, 4th ed., Steinkopff, Dresden, **1909**.
[97] G. M. Whitman (E. I. du Pont de Nemours Co.), US 2462448, **1946**.
[98] W. F. Gresham, R. E. Brook (E. I. du Pont de Nemours Co.), US 2497303, **1945/1950**.
[99] W. Hieber, *Z. Elektrochem. Angew. Phys. Chem.* **1934**, *40*, 158.
[100] W. Hieber, *Angew. Chem.* **1936**, *49*, 463.
[101] W. Hieber, H. Schulten, R. Marin, *Z. Anorg. Allg. Chem.* **1939**, *240*, 261.
[102] W. Hieber, *Angew. Chem.* **1942**, *55*, 7.
[103] W. Hieber, *Adv. Organomet. Chem.* **1970**, *8*, 1.
[104] O. Roelen, *Angew. Chem.* **1948**, *60*, 62, 213.
[105] O. Klopfer, *Angew. Chem.* **1949**, *61*, 266.
[106] J. Berty, L. Markó, *Acta Chim. Acad. Sci. Hung.* **1953**, *3*, 177.
[107] G. Natta, *Brennst. Chem.* **1955**, *36*(11/12), 176.
[108] Etabl. Kuhlmann, GB 705300, **1951**.
[109] C. L. Aldridge, H. B. Jonassen, *J. Phys. Chem.* **1958**, *62*, 869; C. L. Aldridge, H. B. Jonassen, *J. Am. Chem. Soc.* **1963**, *85*, 886; H. B. Jonassen, *Nature* **1960**, *188*, 404.
[110] V. Macho, E. J. Mistrik, M. Ciha, *Collect. Czech. Chem. Commun.* **1964**, *29*, 826.
[111] O. Roelen, *Angew. Chem.* **1951**, *63*, 482.
[112] A. R. Martin, *Chem. Ind. (London)* **1954**, 1536.
[113] I. Wender, H. W. Sternberg, M. Orchin, *J. Am. Chem. Soc.* **1953**, *75*, 3041; *Catalysis, Vol. II* (Ed.: P. H. Emmet), Reinhold, New York, **1957**.
[114] R. F. Heck, D. S. Breslow, *Chem. Ind. (London)* **1960**, 467; *J. Am. Chem. Soc.* **1961**, *83*, 4023.
[115] F. Asinger, *Chemie und Technologie der Monoolefine*, Akademie-Verlag, Berlin, **1957**, p. 650.
[116] G. Dupont, P. Piganiol, I. Vialle, *Bull. Soc. Chim. Fr.* **1948**, *15*, 529.
[117] A. Elbel, A. Gemassmer, W. Wenzel (Chemische Verwertungsgesellschaft Oberhausen mbH), DE 896341, **1943/1953**.
[118] G. Natta, R. Ercoli, S. Catellano, *Chim. Ind. (Milan)* **1955**, *37*, 6.
[119] BIOS, FIAT Final Reports No. 273, **1945** and 355, **1946**.
[120] M. Rasch, *Technikgeschichte* **1987**, *54*(2), 101.
[121] H. H. Storch, N. Golumbic, R. B. Anderson, *The Fischer-Tropsch and Related Syntheses*, Wiley, Chapman & Hall, New York, London, **1951**, p. 441.
[122] W. F. Farragher, *Chem. Eng. News* **1948**, *26*(51), 3816.
[123] *Chem. Ind. (London)* **1947**, 587.
[124] CIOS, Report No. XXVII-69, Item No. 30/5.01, **1945**.
[125] Summaries in: W. A. Herrmann, *Chem. Unserer Zeit* **1988**, *22*, 113; *J. Organomet. Chem.* **1990**, *383*, 21; *Kontakte (Darmstadt)* **1991** (1), 22; *Erzmetall* **1990**, *43*, 69.
[126] a) H. Werner, *Angew. Chem.* **1990**, *102*, 1109; *Angew. Chem. Int. Ed. Engl.* **1990**, *29*, 1077; b) F. G. A. Stone, *Leaving No Stone Unturned, Pathways in Organometallic Chemistry* (Ed.: J. J. Seeman), American Chemical Society, **1993**.
[127] Obituary: E. O. Fischer, *Chem. Ber.* **1979**, *112*, XXI.
[128] First reports: W. Hieber, F. Sonnenkalb, *Ber. Dtsch. Chem. Ges.* **1928**, *61*, 558, 2421.
[129] W. Hieber, F. Leutert, *Z. Anorg. Allg. Chem.* **1932**, *204*, 145; *Naturwissenschaften* **1931**, *19*, 360; *Ber. Dtsch. Chem. Ges.* **1931**, *64*, 2832; W. Hieber, H. Vetter, *Z. Anorg. Allg. Chem.* **1933**, *212*, 145.
[130] W. Hieber, F. Mühlbauer, E. A. Ehmann, *Ber. Dtsch. Chem. Ges.* **1932**, *65*, 1090.
[131] G. W. Coleman, A. A. Blanchard, *J. Am. Chem. Soc.* **1936**, *58*, 2160.
[132] W. Hieber, H. Schulten, *Z. Anorg. Allg. Chem.* **1937**, *232*, 29.
[133] W. Hieber, H. Schulten, *Z. Anorg. Allg. Chem.* **1937**, *232*, 17.
[134] Summary: H. Behrens, *J. Organomet. Chem.* **1975**, *94*, 139.
[135] H. Behrens, personal communication to W. A. H. on January 18, 1994.
[136] T. J. Kealy, P. L. Pauson, *Nature* **1951**, *168*, 1039; S. A. Miller, J. A. Tebboth, J. F. Tremaine, *J. Chem. Soc.* **1952**, 632.
[137] E. O. Fischer, W. Hafner, *Z. Naturforsch.* **1955**, *10*, 665.
[138] BIOS, US Naval Technical Mission in Europe, BIOS Miscellaneous Report No. 60 (September 1945).
[139] E. O. Brimm, M. A. Lynch, W. J. Sesny, *J. Am. Chem. Soc.* **1954**, *76*, 3831.
[140] F. Klages, K. Mönckemeyer, *Chem. Ber.* **1950**, *83*, 501.

New Upswing of Organolanthanoid Research: A Very Promising Revival of Organocerium(IV) Chemistry and the First Stable Lanthanoid(II/III)–Carbene Complexes

R. Dieter Fischer*

What chance of survival has the cyclooctatetraene dianion $C_8H_8^{2-}$ in the presence of a cerium(IV) compound? Well-documented redox potentials[1] clearly suggest rapid oxidation [Eq. (a)].

$$C_8H_8^{2-} + 2Ce^{4+} \longrightarrow C_8H_8 + 2Ce^{3+} \quad (a)$$

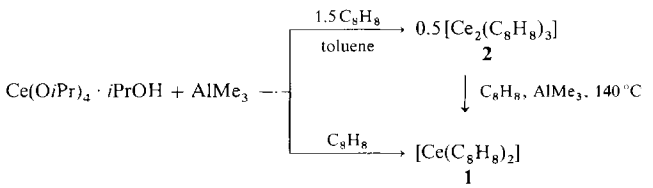
Even UCl_4 is reduced by 1,3,5,7-(*tert*-$C_4H_9)_4C_8H_4^{2-}$ to elemental(!) uranium,[2] and in the classical synthesis of "uranocene"[3] (bis([8]annulene)uranium(IV)) [Eq. (b)] at least one

$$U^{IV}Cl_4 + 2K_2(C_8H_8) \xrightarrow[-4KCl]{THF} [U^{IV}(\eta^8\text{-}C_8H_8)_2] \quad (b)$$

intermediate uranium(III) species[4] occurs. A "targeted" synthesis of reportedly air-stable green "cerocene" (bis([8]annulene)cerium(IV)) in 1972 [Eq. (c)][5] has proved not to be

$$(C_5H_5NH)_2[Ce^{IV}Cl_6] + 2K_2(C_8H_8) \xrightarrow[-4KCl]{THF} \underset{\mathbf{1}}{[Ce^{IV}(C_8H_8)_2]} + 2(C_5H_5NH)Cl \quad (c)$$

reproducible.[6] Nevertheless, in 1976, authentic, brown-black $[Ce(C_8H_8)_2]$ (**1**)[7] was isolated in addition to the then expected[8] compound $[Ce_2(C_8H_8)_3]$ (**2**) (Scheme 1).



Scheme 1. Synthesis and reactivity of $[Ce(C_8H_8)_2]$ **1** [7].

However, the existence of bis([8]annulene)cerium(IV) could only be reliably confirmed later,[6, 9] and the first crystal structure analysis was not achieved until 1991 on the 1,1′-dimethyl derivative **6**,[10] obtained according to Equation (d).

$$\underset{\mathbf{5}\text{ (green)}}{K[Ce^{III}(CH_3C_8H_7)_2]} \xrightarrow[-Ag, KI]{AgI} \underset{\mathbf{6}\text{ (dark red)}}{[Ce^{IV}(\eta^8\text{-}CH_3C_8H_7)_2]} \quad (d)$$

Many other, very desirable investigations, however, have still not been possible chiefly because of the extreme chemical sensitivity and the poor solubility of the few so far known bis([8]annulene)cerium(IV) complexes. An unusual challenge for the experimentalist results, moreover, from detailed quantum chemical studies,[11] according to which the singlet ground state of the $[Ce(C_8H_8)_2]$ molecule mainly derives from the (valence) electron configuration $4f^1e_{2u}^3$ (and not $4f^0e_{2u}^4$). If this interesting postulate could be confirmed experimentally, it would be shown that the cerium ion in bis([8]annulene)cerium exists in the oxidation state +III and that—from a more physical point of view—there would be a close analogy between the unusual ground state of the sandwich molecule and a Kondo ion in a metal lattice.[11] Since cyclooctatetraene may form a planar dianion $C_8H_8^{2-}$ or radical anion $C_8H_8^{\cdot-}$,[12] it could belong to that category of ligands, such as 2,2′-bipyridine in particular, for which the oxidation state of the metal atom they complex cannot be clearly assigned.[13]

A fresh point of departure has now been signalized by experimental results by Edelmann et al.:[14a–c] These authors synthesized for the first time the extremely sensitive, green cerium(III) sandwich complexes **7** and **8**, which contain two- and threefold trimethylsilylated cyclooctatetraenes, respectively, and subsequently converted them in situ into the corresponding uncharged bis([8]annulene)cerium(IV) complexes **9** (deep purple oil) and **10** (deep purple crystals, m.p. 38 °C) [Eqs. (e) and (f)].

$$\underset{\mathbf{7}}{Li[Ce^{III}\{1,4\text{-}(SiMe_3)_2C_8H_6\}_2]} \xrightarrow[-Ag, LiI]{AgI} \underset{\mathbf{9}}{[Ce^{IV}\{1,4\text{-}(SiMe_3)_2C_8H_6\}_2]} \quad (e)$$

$$\underset{\mathbf{8}}{K[Ce^{III}\{1,3,6\text{-}(SiMe_3)_3C_8H_5\}_2]} \xrightarrow[-Ag, KI]{AgI} \underset{\mathbf{10}}{[Ce^{IV}\{\eta^8\text{-}1,3,6\text{-}(SiMe_3)_3C_8H_5\}_2]} \quad (f)$$

The lithium salt **7** had been described by Cloke et al. shortly before,[14d] while only Edelmann et al. succeeded in preparing

[*] Prof. Dr. R. D. Fischer
Institut für Anorganische und Angewandte Chemie der Universität
Martin-Luther-King-Platz 6, D-20146 Hamburg (FRG)
Telefax: Int. code + (40)4123-2893

 © VCH Verlagsgesellschaft mbH, D-69451 Weinheim, 1994 0570-0833/94/2121-2165 $ 10.00+.25/0

the 1,3,6-$(SiMe_3)_3C_8H_5^{2-}$ anion extending corresponding attempts by Cloke et al.

The multiply silylated sandwich complexes **9** and **10** are diamagnetic as expected and not only very soluble in nonpolar solvents such as hexane and pentane, but also briefly stable in air. The crystal structure analysis of the well-crystallizing complex **10** (Fig. 1) confirms the expected[10] sandwich structure with two almost parallel, η^8-coordinate eight-membered rings and Me_3Si substituents positioned slightly *exo*, which contribute to a notable degree of shielding of the cerium(IV) ion. The average Ce–C distance (270.4 pm) is only slightly shorter than in the bis([8]annulene)cerate(III) anion of **13** (275.3 pm; see below). The corresponding values for **6** (269.2 pm[10]) and [K(diglyme)][$Ce^{III}(C_8H_8)_2$] (273.9 pm[16]; diglyme = diethylenegylcol dimethyl ether) also lie very close to one another.

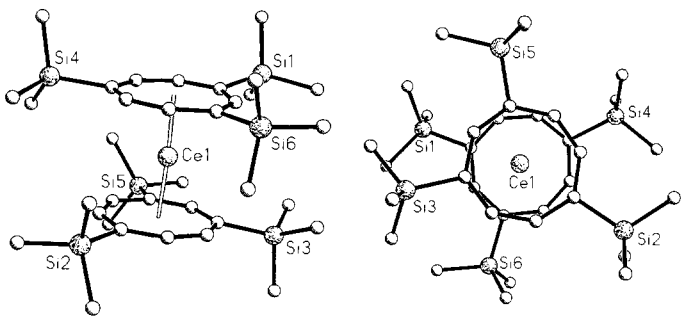


Fig. 1. Crystal structure of the complex **10** [14a]. Side view (left) and top view (right).

It should now also be possible to finally decide whether the anion $[Ce^{III}(cot')_2]^-$ (cot' = $(Me_3Si)_nC_8H_{8-n}^{2-}$ with $n = 0-3$) can in fact be reduced to the dianion $[Ce^{II}(cot')_2]^{2-}$ (cf. **4** in Scheme 1), and whether the solvent-free $[Ce_2(cot')_3]$ (cf. **2** in Scheme 1) may even be a true lanthanoid triple-decker complex. In a reaction analogous to that in Equation (b), Edelmann et al. also treated UCl_4 with $K_2[1,3,6\text{-}(SiMe_3)_3C_8H_5]$ and obtained dark green $[U^{IV}\{1,3,6\text{-}(SiMe_3)_3C_8H_5\}_2]$ (**11**), which was again stable in air for a short time.[14a–c] Perhaps even cerium(IV) compounds and $K_2[(SiMe_3)_nC_8H_{8-n}]$ ($n = 2,3$) react after all to give bis([8]annulene)cerium complexes (cf. Eq. (c))? And why couldn't the multistep mechanism for the formation of $[U^{IV}(C_8H_8)_2]$[4] (see Eq. (b)) be elucidated further with the aid of silylated ligands? The new bis([8]annulene)cerium and -uranium derivatives, which are relatively easy to handle, should also be well suited for systematic electrochemical investigations; to date only the potential of the redox pair $[Ce^{IV}(C_8H_8)_2]$/$[Ce^{III}(C_8H_8)]^-$ has been determined by cyclic voltammetry. The E^0 value is -1.28 V[4, 6] and differs significantly from that for the likewise organometallic redox pair $[Ce^{IV}(C_5H_5)_3(OiPr)]$/$[Ce^{III}(C_5H_5)_3(OiPr)]^-$ ($+0.32$ V)[15b] and especially from representative E^0 values of purely inorganic redox pairs in H_2O (pH < 7); for example $+1.61$ V.[1a]

Edelmann et al. have already carried out several reactions with **9**, **10**, and **11**, which reflect a promising and also preparatively interesting redox chemistry of their new bis([8]annulene)-metal(IV) compounds. Thus, despite the very negative E^0 value of **1**, complex **9** is readily reduced by cobaltocene (E^0 for $([Co^{II}(C_5H_5)_2]/[Co^{III}(C_5H_5)_2]^+) = -0.86$ V[17]) to give the new compound **12**,[14a] which has initially been formulated as a salt [Eq. (g)].

$$[Ce^{IV}\{1,4\text{-}(SiMe_3)_2C_8H_6\}_2] \xrightarrow[THF]{[Co^{II}(C_5H_5)_2]} [Co^{III}(C_5H_5)_2][Ce^{III}\{1,4\text{-}(SiMe_3)_2C_8H_6\}_2] \quad \text{(g)}$$

9 (purple) → **12** (green, pyrophoric)

The occurrence of two signals for the two C_5H_5 ligands in the ^1H NMR spectrum ([D_8]THF) of **12** at higher field than usual for the diamagnetic $[Co^{III}(C_5H_5)_2]^+$ ion ($\delta = 1.30$, 0.90[14a]) does, however, not rule out possible surprises with regard to the true structure of solid **12**. The genuine salt **13**,[18] which has already been characterized by crystal structure analysis, is formed from **10** [Eq. (h)] when elemental ytterbium is used as the reducing agent.

$$2[Ce^{IV}\{1,3,6\text{-}(SiMe_3)_3C_8H_5\}_2] \xrightarrow[THF]{Yb^0} [Yb^{II}(thf)_6][Ce^{III}\{1,3,6\text{-}(SiMe_3)_3C_8H_5\}_2]_2 \quad \text{(h)}$$

10 (purple) → **13** (green)

The cation of **13** loses all of its six thf ligands surprisingly easily. Interestingly, for several contact ion pairs of the type $[M^IL_x\{Ln^{III}(cot)_2\}]$ (L = ligand, Ln = lanthanoid, cot = $C_8H_8^{2-}$), an η^8 coordination of an otherwise coordinatively unsaturated alkali metal ion by one of the ring ligands[10, 19] (Fig. 2 left) has been established by X-ray crystallography; hence, an ideal tetra-decker arrangement is conceivable for the THF-free, purple product **13a**. (Fig. 2 right)[14b, c] Indeed, the

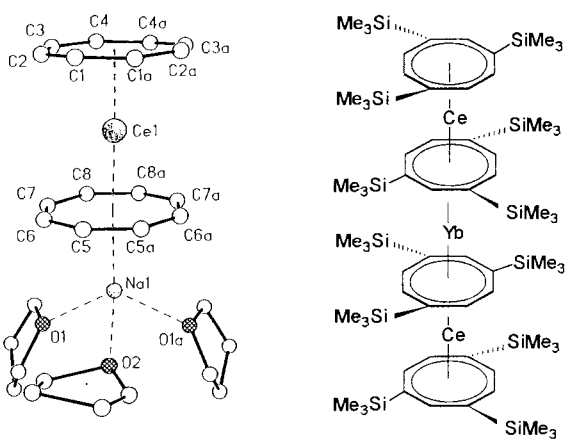


Fig. 2. Left: Crystal structure of the complex $[Na(thf)_3(\mu\text{-}C_8H_8)Ce(C_8H_8)]$ [19]. Right: Possible structure of **13a**.

mass spectrum of **13a** shows a molecular peak with an appropriate isotopic pattern.[18] In an analogous way, reactions according to Equation (i) with Ln = Eu, Sm, Yb could, in the absence of any coordinating solvents, possibly lead to heterodimetal triple-decker compounds.

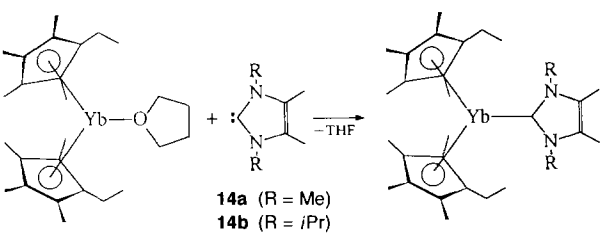
$$[Ce^{IV}(cot)_2] + [Ln^{II}(cot')] \longrightarrow [(cot')Ln^{III}(\mu\text{-}cot)Ce^{III}(cot)] \quad \text{(i)}$$

Recently, Evans et al. impressively demonstrated that organolanthanoid(II) compounds, particularly those of the type $Cp^*_2Ln^{II}L_n$ ($Cp^* = C_5Me_5$; Ln = Sm, Yb; L = ligand), offer an almost unlimited synthesis potential. This is exemplified by the reactions of $[Cp^*_2Sm]$ with some unsaturated reaction partners such as CO,[20] N_2,[21] N_2H_2,[22] alkyne,[23] mono-,[24] and polyolefins.[25] The essential driving force for these reactions is the strong reduction potential of the samarium(II) complex. Hereby, as in the case of the unexpected course of the reaction with the cycloolefin C_8H_8 [Eq. (j)],[26] samarium(III) com-

$$2[Sm^{II}Cp^*_2(thf)_2] + C_8H_8 \longrightarrow [Sm^{III}Cp^*(C_8H_8)] + [Sm^{III}Cp^*_3] \qquad (j)$$

pounds are always formed. On this background, it will be interesting to see the results of corresponding reactions with Edelmann's new bis([8]annulene)cerium/uranium compounds instead of neat C_8H_8.

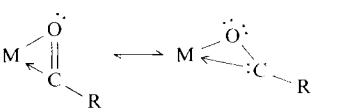
The reduction potential of the homologous $[Cp^*_2Yb^{II}]$ is not quite as strong as that of $[Cp^*_2Sm^{II}]$. Thus, several conventional adducts $[Cp^*_2Yb^{II}L_n]$ ($n = 1,2$) with an unsaturated nucleophile L (e.g. alkene,[27] alkyne,[28] and even pyridine[29]) could be isolated. Several homologous imidazol-2-ylidenes **14** (Scheme 2) have now turned out to be reducible neither with $[(C_5Me_4Et)_2Yb^{II}(thf)]$ nor with $[Cp^*_2Sm^{II}(thf)]$.



Scheme 2. Synthesis of the carbene complexes **15** (R = Me) and **16** (R = *i*Pr) [32a]. The π-electron pair of each nitrogen atom is not shown.

In 1991 Arduengo et al. first reported on imidazol-2-ylidenes with particularly voluminous groups R; these were the first carbenes that could be isolated and crystallized.[30] This result catalyzed fervent activity with regard to the development of numerous complexes with Arduengo-carbenes.[31] The first stable ytterbium(II)-carbene complexes **15** and **16**, which form surprisingly readily by the replacement of a THF ligand with a carbene (Scheme 2), were characterized by Schumann et al. as Fischer-type carbene complexes without detectable metal → ligand backbonding.[32a] The black compounds are thermally very stable and diamagnetic; the crystal structure analysis of **15** reveals an apparently strong Yb → C σ-donor bond (Yb–C distance 255.2 pm, comparable to the mean Yb–N distance of 256.5 pm in $[Cp^*_2Yb^{II}(NC_5H_5)_2]$[29]), as well as coplanarity of the ylide five-membered ring with its five substituent atoms, suggesting sp^2-hybridized ring atoms. Simultaneously with Schumann et al., Arduengo and co-workers have described the corresponding Sm(II) complexes $[Cp^*_2Sm^{II}L_n]$ (L = **14a**; $n = 1$, **17**; $n = 2$, **18**).[32b] Both **18** and the so far unique lanthanoid(III)-carbene complex $[Eu^{III}(thd)_3L]$ **19** (thd = 2,2,6,6-tetramethylheptane-3,5-dionate) have already been subjected to crystal structure analyses.[32b] Considering that isocyanides have so far been the only uncharged ligands in organolanthanoid chemistry that coordinate through just one carbon atom,[33] the entry of Arduengo's carbenes into this field will clearly have a significant impact. In some contrast to the present excitement of most coordination chemists there is still controversy surrounding whether all compounds with very nucleophilic two-coordinate carbon atoms, which, however, lack the intrinsic reactivity of "classic" carbenes, should still be correctly classed as carbenes.[34] In the meantime the synthesis of homologous imidazol-2-germylenes[35] and imidazol-2-silylenes[36] has already been successfully completed, providing also a basis for the access of novel lanthanoid compounds with unusual metal-to-germanium and -silicon bonds.

Finally it should be recalled that 15 years ago Marks et al. characterized organoactinoid and lanthanoid complexes with a η^2-acyl ligand as complexes containing a Fischer-carbene ligand (Scheme 3), directly anchored through its heteroatom to the metal ion.[37] This description was based on the distinct carbene-like reactivity of the relatively loosely coordinated acyl carbon atom (the M–O distance is shorter than the M–C distance).



Scheme 3. η^2-acyl ligand with carbene-like properties [37].

German version: *Angew. Chem.* **1994**, *106*, 2253

[1] a) J. E. Huheey, *Anorganische Chemie*, de Gruyter, Berlin, **1988**, p. 1079 ff.; $E^0(Ce^{III}/Ce^{IV}) = +1.61$ V; b) H. Lehmkuhl, S. Kintopf, E. Janssen, *J. Organomet. Chem.* **1973**, *56*, 41: $E^0(C_8H_8/C_8H_8^{2-}) = -1.75$ to -1.99 V.

[2] A. Streitwieser, Jr. in *Organometallics of the f-Elements* (Eds.: T. J. Marks, R. D. Fischer), Reidel, Dordrecht, **1979**, p. 164.

[3] A. Streitwieser, Jr., U. Müller-Westerhoff, *J. Am. Chem. Soc.* **1968**, *90*, 7364.

[4] a) *Fundamental and Technological Aspects of Organo-f-Element Chemistry* (Eds.: T. J. Marks, I. L. Fragalà), Reidel, Dordrecht, **1985**; b) A. Streitwieser, Jr., S. A. Kinsley in ref. [4a], p. 81.

[5] B. L. Kalsotra, R. K. Multani, B. D. Jain, *Chem. Ind. (London)* **1972**, 339.

[6] A. Streitwieser, Jr., S. A. Kinsley, J. T. Ringsbee, I. L. Fragalà, E. Ciliberto, N. Rösch, *J. Am. Chem. Soc.* **1985**, *107*, 7786.

[7] A. Greco, S. Cesca, G. Bertolini, *J. Organomet. Chem.* **1976**, *113*, 321; G. Deganello, *Transition Metal Complexes of Cyclic Olefins*, Academic Press, London, **1979**, p. 295.

[8] In analogy to the formally homologous titanium complex; cf. H. Breil, G. Wilke, *Angew. Chem.* **1966**, *78*, 942; *Angew. Chem. Int. Ed. Engl.* **1966**, *5*, 898.

[9] See ref. [4], p. 77ff

[10] T. R. Boussie, D. C. Eisenberg, J. Rigsbee, A. Streitwieser, Jr., A. Zalkin, *Organometallics* **1991**, *10*, 1922.

[11] M. Dolg, P. Fulde, W. Küchle, C.-S. Neumann, H. Stoll, *J. Chem. Phys.* **1991**, *94*, 3011; M. Dolg, P. Fulde, H. Stoll, H. Preuss, A. Chang, R. M. Pitzer, *Chem. Phys.* in press.

[12] G. I. Fray, R. G. Saxton, *The Chemistry of Cyclooctatetraene and its Derivatives*, Cambridge University Press, Cambridge, **1978**, p. 28.

[13] C. K. Jørgensen, *Oxidation Numbers and Oxidation States*, Springer, Berlin, 1969, p. 141ff.

[14] a) U. Kilimann, R. Herbst-Irmer, D. Stalke, F. T. Edelmann, *Angew. Chem.* **1994**, *106*, 1684; *Angew. Chem. Int. Ed. Engl.* **1994**, *33*, 1618; b) U. Kilimann, lecture at the "Tag der Seltenen Erden '93", Göttingen, Dezember 8, 1993; c) U. Kilimann, Dissertation, Universität Göttingen, **1993**; d) N. C. Burton, F. G. N. Cloke, S. C. P. Joseph, H. Karamallakis, A. A. Sameh, *J. Organomet. Chem.* **1993**, *462*, 39.

[15] Corresponding results are also known for $[Ce^{IV}(C_5H_5)_3X]^+$ and $[Ce^{III}(C_5H_5)_3]$: a) W. J. Evans, T. J. Deming, J. W. Ziller, *Organometallics* **1989**, *8*, 1581; b) A. Gulino, M. Casarin, V. P. Conticello, J. G. Gaudiello, H. Mauermann, I. Fragalà, T. J. Marks, *ibid.* **1988**, *7*, 2360.

[16] K. O. Hodgson, K. N. Raymond, *Inorg. Chem.* **1972**, *11*, 3030.

[17] U. Kölle, F. Khouzami, *Angew. Chem.* **1980**, *92*, 658; *Angew. Chem. Int. Ed. Engl.* **1980**, *19*, 640.

[18] U. Kilimann, D. Stalke, F. T. Edelmann, personal communication.
[19] U. Kilimann, M. Schäfer, R. Herbst-Irmer, F. T. Edelmann, *J. Organomet. Chem.* **1994**, *469*, C15.
[20] W. J. Evans, J. W. Grate, L. A. Hughes, H. Zhang, J. L. Atwood, *J. Am. Chem. Soc.* **1985**, *107*, 3728.
[21] W. J. Evans, T. A. Ulibarri, J. W. Ziller, *J. Am. Chem. Soc.* **1988**, *110*, 6877.
[22] W. J. Evans, G. Kociok-Köhn, V. S. Leong, J. W. Ziller, *Inorg. Chem.* **1992**, *31*, 3592.
[23] W. J. Evans, I. Bloom, W. E. Hunter, J. L. Atwood, *J. Am. Chem. Soc.* **1983**, *105*, 1401.
[24] W. J. Evans, T. A. Ulibarri, J. W. Ziller, *J. Am. Chem. Soc.* **1990**, *112*, 219.
[25] W. J. Evans, T. A. Ulibarri, J. W. Ziller, *J. Am. Chem. Soc.* **1990**, *112*, 2314; *Organometallics*, **1991**, *10*, 134.
[26] W. J. Evans, S. L. Gonzales, J. W. Ziller, *J. Am. Chem. Soc.* **1991**, *113*, 7423.
[27] Alkene = $[(C_2H_4)Pt(PPh_3)_2]$: C. J. Burns, R. A. Andersen, *J. Am. Chem. Soc.* **1987**, *109*, 915.
[28] 2-Butyne: C. J. Burns, R. A. Andersen, *J. Am. Chem. Soc.* **1987**, *109*, 941.
[29] T. D. Tilley, R. A. Andersen, B. Spencer, A. Zalkin, *Inorg. Chem.* **1982**, *21*, 2647.
[30] A. J. Arduengo, III, R. L. Harlow, M. Kline, *J. Am. Che. Soc.* **1991**, *113*, 361.
[31] Cf. literature cited in refs. [32] and [34].
[32] a) H. Schumann, M. Glanz, J. Winterfeld, H. Hemling, N. Kuhn, T. Kratz, *Angew. Chem.* **1994**, *106*, 1829; *Angew. Chem. Int. Ed. Engl.* **1994**, *33*, 1733; b) A. J. Arduengo, III, M. Tamm, S. J. McLain, J. C. Calabrese, F. Davidson, W. J. Marshall, *J. Am. Chem. Soc.* **1994**, *116*, 7927.
[33] J. H. Burns, W. H. Baldwin, *J. Organomet. Chem.* **1976**, *120*, 361.
[34] R. Dagani, *Chem. Eng. News* **1994**, *72* (May 5), 20.
[35] W. A. Herrmann, M. Denk, J. Behm, W. Scherer, F.-R. Klingan, H. Bock, B. Solouki, M. Wagner, *Angew. Chem.* **1992**, *104*, 1489; *Angew. Chem. Int. Ed. Engl.* **1992**, *31*, 1485.
[36] M. Denk, R. Lennon, R. Hayashi, R. West, A. V. Belyakov, H. P. Verne, A. Haaland, M. Wagner, N. Metzler, *J. Am. Chem. Soc.* **1994**, *116*, 2691.
[37] T. J. Marks, V. W. Day in ref. [4a], p. 115; J. M. Manriquez, P. J. Fagan, T. J. Marks, *J. Am. Chem. Soc.* **1979**, *101*, 5075; E. A. Maatta, T. J. Marks, *ibid.* **1981**, *103*, 3576; K. G. Moloy, T. J. Marks, V. W. Day, *ibid.* **1983**, *105*, 5696; see also: B. E. Bursten, R. J. Strittmatter, *Angew. Chem.* **1991**, *103*, 1085; *Angew. Int. Ed. Engl.* **1991**, *30*, 1069.

The Lithocene Anion and "Open" Calcocene—New Impulses in the Chemistry of Alkali and Alkaline Earth Metallocenes

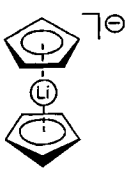
Dietmar Stalke*

The impetus given to the field of organometallic chemistry by the discovery of bis(cyclopentadienyl)iron(II), ferrocene, is quite unique. The cyclopentadienyl anion $C_5H_5^-$ (Cp) and its substituted derivatives ($C_5H_{5-n}R_n^-$), especially the pentamethylcyclopentadienyl anion $C_5Me_5^-$ (Cp*), are the most frequently used substituents when the steric shielding of a metal center is required. While in the mid 1950s a rapid development in the synthesis of bis(cyclopentadienyl) complexes of main group and transition metal elements took place, the corresponding compounds of the alkaline earth metals have until very recently been one of the sleeping beauties of organometallic chemistry.

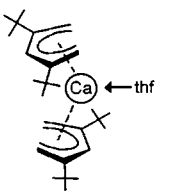
The s-block metals are highly electropositive, thus their complexes are mainly ionic. The highly polar nature of alkyllithium compounds and Grignard reagents forms the basis of their preparative use. Up to now compounds containing the heavier alkaline and alkaline earth metals have been almost neglected. Only recently has interest focused on, for instance, alkaline earth metal compounds as precursors to metal oxides for chemical vapour deposition (CVD) and sol-gel processes. Ideally, CVD precursors for thin films should be easy to synthesize, volatile, and free of halide or silyl groups. The sol-gel process requires starting materials that can be specifically hydrolyzed in a reproducible way. This is why the investigation of alkali and alkaline earth metallocenes is an important and advantageous goal.

[*] Priv.-Doz. Dr. D. Stalke
Institut für Anorganische Chemie der Universität
Tammannstrasse 4, D-37077 Göttingen (FRG)
Telefax: Int. code + (551)39-2582

Two very recent results, the synthesis and structure determination of the simplest metallocene $[Cp_2Li]^-$ **1** and of the "open" calcocene **2** are taken to highlight a flourishing field of research.



1

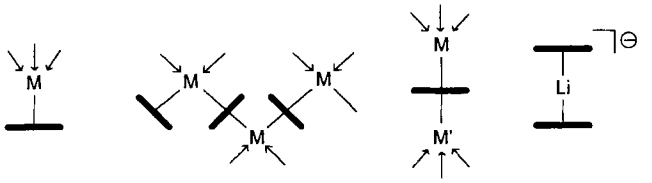


2

Cyclopentadienyl Alkali Metal Complexes

The physical properties of CpLi are those of a typical salt.[1] It is almost insoluble in hydrocarbons, has a high melting point, and a low volatility. These facts had hampered the structure determination of donor-free, CpLi until now. It is mainly because of the pioneering work of Jutzi et al. that we nevertheless possess structural information on CpLi derivatives. They introduced three trimethylsilyl groups to the C_5 skeleton, and the solubility of the corresponding compound increased drastically. These silylated cyclopentadienyllithium derivatives can be crystallized with nitrogen donor bases. These derivatives are all monomeric in the solid state. The lithium atom is more or less ideally η^5-coordinated to the C_5 framework. The coordination sphere of the lithium atom is completed by mono-, bi-, or tridentate nitrogen donor bases (structure type **A**, Table 1). Examina-

Table 1. Cyclopentadienyl alkali metal complexes.



Compound [a]	Coordination type	M-$Cp_{centroid}$ [pm]	Ref.
$[(Me_3Si)_3C_5H_2Li(pmdeta)]$	**A**	198	[3a]
$[Me_3SiC_5H_4Li(tmeda)]$	**A**	193	[3b]
$[(Me_3Si)_3C_5H_2Li(quin)]$	**A**	179	[3c]
$[(Me_3Si)_3C_5H_2Li(tmeda)]$	**A**	199	[3c]
$[MeC_5H_4Li(tmeda)]$	**A**	191	[3d]
[CpLi([12]-Krone-4)]	**A**	206	[3e]
$[Cp^*Na(py)_3]$	**A**	240	[3f]
$[(C_6H_5CH_2)_5C_5K(thf)_3]$	**A**	279	[3g]
$[Me_3SiC_5H_4Li]_\infty$	**B**	197	[4a]
$[CpNa(tmeda)]_\infty$	**B**	265	[4b]
$[(MeCO)C_5H_4Na(thf)]_\infty$	**B**	253	[4c]
$[Cp^*K(py)_2]_\infty$	**B**	279	[3d]
$[Me_3SiC_5H_4K]_\infty$	**B**	278	[4d]
$[MeC_5H_4Li_2(tmeda)_2]^+$	**C**	200	[5a]
$[Li(pmdeta)][Cp_2Tl]$	**C**	225	[5b]
$[Li(pmdeta)][Cp_2SnN(SiMe_3)_2]$	**C**	225	[5c]
$[Na(pmdeta)][Cp_3Sn]$	**C**	255	[5d]
$[(isodiCp)_2Li]^-$	**D**	200	[6]
$[Cp_2Li]$	**D**	201	[7]

[a] pmdeta = $MeN(CH_2CH_2NMe_2)_2$; tmeda = $Me_2NCH_2CH_2NMe_2$; quin = $C_9H_{13}N$; thf = tetrahydrofuran; py = pyridine; isodiCp = isodicyclopentadienyl anion (= 4,5,6,7-tetrahydro-4,7-methano-1*H*-inden-1-ide).

tion of the metal ring centroid ($Cp_{centroid}$) distances is very instructive. With this experimental feature it is possible to elucidate the contribution of single structural determining parameters like charge distribution, steric requirement, radius or electronegativity of metal centers, or influence of donor bases in these polar organometallic compounds,[2] and makes it easier to understand coordination patterns.

The Li–$Cp_{centroid}$ distance in substituted cyclopentadienyllithium derivatives ranges from 179[3c] to 206 pm.[3e] The more donor centers that are coordinated to the lithium atom, the less important (hence the longer) becomes the Li–Cp contact. The three silyl groups in $[(Me_3Si)_3C_5H_2Li(quin)]$[3c] increase the electron density within the ring to such an extent that the anion is particularly attractive to the lithium cation (Li–$Cp_{centroid}$ 179 pm). In this complex the lithium cation coordinates only one nitrogen donor base. In the [CpLi([12]crown-4)] complex the lithium cation is supplied electron density by four donor oxygen atoms, hence the Li–$Cp_{centroid}$ distance (206 pm) is relatively long. $[Cp^*Na(py)_3]$[3f] and $[(C_6H_5CH_2)_5C_5K(thf)_3]$[3g] are also monomers.

In the coordination type **B** two- or three-dimensional polymeric nets are built. In $[Me_3SiC_5H_4Li]_\infty$[4a] and $[Me_3SiC_5H_4K]_\infty$[4a] no further solvation of the metal is observed. It is worthy to note that the Na–$Cp_{centroid}$ distance changes from 240 pm in $[Cp^*Na(py)_3]$[3f] to 265 pm in $[CpNa(tmeda)]_\infty$.[4b] The shortest Na–$Cp_{centroid}$ contact is found in the monomer, because the sodium atom is coordinated to only one Cp* anion, rather than to two Cp anions as in the polymer. Apart from steric crowding, the fact that one positive charge has to be distributed between two negative centers certainly results in increasing distances. The K–$Cp_{centroid}$ distance, however, seems to be almost invariant against the degree of oligomerization or the presence of donor bases. In monomeric $[(C_6H_5CH_2)_5C_5K(thf)_3]$[3g] this distance is 279 pm, like that in the two-dimensional polymeric $[Cp^*K(py)_2]_\infty$,[3f] and almost unchanged from the 278 pm in unsolvated $[Me_3SiC_5H_4K]_\infty$.[4d] In the monomer the distance is probably elongated because the steric requirement of the bulky $C_5(CH_2C_6H_5)_5$ anion prevents closer contact between the metal and the C_5 framework.

The opposite case in which two positive charges have to share one negative charge has been structurally characterized as well (structure type **C**). In the cation $[MeC_5H_4Li_2(tmeda)_2]^+$, the two lithium atoms are η^5-coordinated to the single MeC_5H_4 anion. The average Li–$Cp_{centroid}$ distance of 200 pm is quite long but falls in the normal range. Only when the lithium atom competes with a significantly more electronegative element like tin or thallium for a single Cp anion (EN of Li: 1.0, of Sn and Tl: 1.8), does the Li–$Cp_{centroid}$ distance increase considerably. In $[(\eta^5\text{-Cp})Tl(\mu_2\text{-}\eta^2\text{-Cp})Li(pmdeta)]$[5b] and in $[(\eta^5\text{-Cp})(Me_3Si)_2NSn(\mu_2\text{-}\eta^5Cp)Li(pmdeta)]$[5c] the Li–$Cp_{centroid}$ distance is 225 pm. The tin and thallium atoms both claim more electron density from the Cp anion, which makes them less attractive to the lithium atom. The Na–$Cp_{centroid}$ distance to the μ_2-bridging Cp anion in $[(\eta^5\text{-Cp})_2Sn(\mu_2\text{-}\eta^5\text{-Cp})Na(pmdeta)]$[5d] of 255 pm is almost the same as the one in polymeric $[(MeCOC_5H_4Na(thf)]_\infty$.[4c]

Recently Gautheron and Paquette et al. published the synthesis and crystal structure of the $[(isodiCp)_2Li]^-$ ion in which the lithium atom lies on a center of inversion between the two Cp ligands.[6] With the structure determination and the synthesis of $[Ph_4P][Cp_2Li]$ according to Equation (a), Harder et al. achieved

$$Ph_4PCl + 2\,CpLi \longrightarrow \underset{[Ph_4P]\text{-}\mathbf{1}}{[Ph_4P][Cp_2Li]} + LiCl \qquad (a)$$

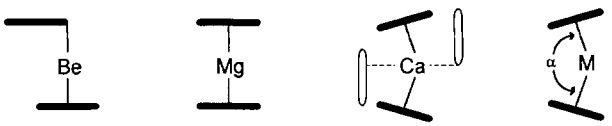
the characterization of the simplest metallocene, the lithocene anion **1**.[7] The sandwich complex **1** has almost D_{5d} symmetry; the lithium atom is found on the inversion center (coordination type **D**). The Li–$Cp_{centroid}$ distance of 201 pm is almost identical with that in the $[MeC_5H_4Li_2(tmeda)_2]^+$ ion and in the $[(isodiCp)_2Li]^-$ ion (Table 1). Apparently the competition between two Cp anions for one lithium cation (**D**) results in the same distance as the competition between two lithium cations for one Cp anion (**C**), because the absolute value of the sum of charges is the same. The distance between the rings of 402 pm is considerably longer than the interlayer distance in graphite of 335 pm; thus steric hindrance of the two five-membered rings with respect to each other can be excluded. The controversial question of whether hydrogen-out-of-plane bending occurs towards or away from the metal[8] could not be answered unequivocally for the $[Cp_2Li]$ anion from this experiment, because even at $-40\,^\circ C$ libration of the Cp rings is quite high. This is indicative of a fairly low rotational barrier of the Cp ligand about the metal. Good low-temperature neutron data would certainly be beneficial.

Harder et al. confirmed the existence of lithocene, deduced previously from conductivity measurements,[9a] NMR spectroscopic,[8d, 9b] and cryoscopic[9c] experiments, in the solid state. This success should be used as a basis for the study of the bis(cyclopentadienyl) compounds of the heavier alkali metals as well.

Alkaline Earth Metallocenes

The comparison of the lithocene anion with the isoelectronic alkaline earth metallocenes is very interesting. The isotype $[Cp_2Mg]$ has almost the same structural parameters as the $[Cp_2Li]$ anion. The $Mg-Cp_{centroid}$ distance is 198 pm.[11a] Apparently the Cp ligands (staggered) in the solid state can come closer together than in the gas phase (eclipsed) ($Mg-Cp_{centroid}$ 201 pm[11b]). This shows once again the close relationship between the elements lithium and magnesium (among other criteria the almost identical radius of Li^+ and Mg^{2+} is decisive). $[Cp_2Li]^-$ and $[Cp_2Mg]$ adopt the same coordination type in the solid state, schematically depicted as **D** (Table 1) and **F** (Table 2), which can be rationalized as a pentagonal antiprism.

Table 2. Alkaline earth metallocenes.



E F G H

M = Ca, Sr, Ba

Compound	Coordination type	M^{2+}-radius [pm] [c]	M–C [pm] [d]		α [°] [d]		Ref.
$[Cp_2Be]$	**E**	35	193	–	180	–	[10a, b]
$[Cp_2Mg]$	**F**	66	230	234	180	180	[11a, b]
$[Cp_2Ca]$	**G** [a]	99	280	–	119	–	[12]
$[Cp_2^*Ca]$	**H**	99	264	261	147	154	[13a, b]
$[(tBu_2C_5H_5)_2Ca(thf)]$	**H** [b]	99	276	–	147	–	[18]
$[Cp_2^*Sr]$	**H**	112	–	275	–	149	[15]
$[Cp_2^*Ba]$	**H**	134	299	290	131	148	[15, 16]

[a] Average values of the two η^5-coordinated rings. [b] In the complex a thf molecule is coordinated to the calcium atom at the open side. [c] Values taken from: *CRC Handbook of Chemistry and Physics*, CRC Press, Cleveland, **1973**. [d] The first value refers to a single-crystal X-ray structure determination, the second to the gas phase electron diffraction experiment.

In $[Cp_2Be]$, however, the coordination polyhedron formed is quite different. The Be^{2+} ion, which is almost half the size of the Mg^{2+} ion, is η^1/η^5-coordinated between two Cp rings (**E**). Furthermore, in the solid state,[10a] it is disordered with regard to the η^1/η^5 and η^5/η^1 position. The distance between the two Cp rings is only 331 pm, and hence falls below the interlayer distance in graphite (335 pm). The assumed increase in M–C bond length of about 33 pm because of the increase of ionic radii going from $[Cp_2Mg]$ (230 pm) to $[Cp_2Ca]$ (280 pm) is significantly exceeded[12] (Table 2). Compared to $[Cp_2Mg]$, $[Cp_2Ca]$ exhibits a completely different coordination type (**G** instead of **F**), emphasizing a well-known argument from the cyclpentadienyl alkali metal complexes: In $[Cp_2Ca]$ the posititve charge of the Ca^{2+} ion is not only shared by two η^5-bound Cp rings, but is distributed between four substituents. Apart from the two η^5-coordinated ligands there are significant Ca–C contacts to a η^3- and η^1-coordinated ring. That the M–C bond is lengthened when several Cp ligands compete for one metal is also true for the alkaline earth metallocenes. This effect is certainly not exclusively due to steric requirements. Bond lengthening is also found in the $[CpMg(pmdeta)]^+$ ion of the solvent-separated ion pair $[CpMg(pmdeta)][Cp_2Tl]$.[5b] The $Mg-Cp_{centroid}$ distance in this cation is 208 pm; in neutral $[Cp_2Mg]$ it is 198 pm.

The expected Ca–C distances of 264 pm in the solid state[13a] and 261 pm in the gas phase[13b] are only found in monomeric $[Cp_2^*Ca]$. The structure of this calcocene derivative shows a different, a priori unexpected phenomenon: the two rings are not aligned coplanar like in **F** but are bent with respect to each other ascribing a $Cp_{centroid}$-M-$Cp_{centroid}$ angle (α in Table 2) of 147 and 154° (solid state and gas phase, respectively) (**H**). On first sight this bent structure, despite the missing lone pair, is as puzzling as the coplanar rings in $[(Ph_5C_5)_2Sn:]$[14a] or in $[Cp_2^*Si:]$,[14b] in which the lone pair is assigned exclusively s character.

$[Cp_2^*Sr]$[15] and $[Cp_2^*Ba]$,[15, 16] bis(cyclopentadienyl) compounds of the heavier alkaline earth metals, also adopt bent monomeric structures of type **H**. Long-range intermolecular interactions causing packing effects, and the f-orbital bonding contribution, which might be responsible for bent structures, are to date almost ruled out. It is now assumed that ligands polarize a large positive charge (bent structures have been found, for example, in $[Cp_2^*Sm]$ and $[Cp_2^*Eu]$) and induce a dipole. This dipole can interact with negatively charged ligands more effectively.[17] Apparently holistic features like radii, charges, polarities, etc. seem to be most fruitful in structural interpretation in this area of organometallic chemistry. The estimated energy required to bend an alkaline earth metallocene by 20° is only 2–3.5 kJ mol^{-1}.[15]

The first open calcocene **2**,[18] was recently synthesized by Hanusa et al. according to Equation (b). This complex is

$$2[K(tBu_2C_5H_5)] + CaI_2 \xrightarrow{THF} \underset{\mathbf{2}}{[(tBu_2C_5H_5)_2Ca(thf)]} + 2KI \qquad (b)$$

also a bent monomer of type **H**. Because of the coordination of thf the question of whether this bend is intrinsic or induced by base coordination remains open. However, it is certain that the pentadienyl ligand is planar and π-bonded to the calcium atom. The average Ca–C distance of 276 pm is relatively long.

This is even more remarkable since transition metal pentadienyl complexes normally exhibit equally long or even shorter M–C distances than those in the related cyclopentadienyl complexes. Certainly the elongation of the Ca–C bonds in **2** is neither caused by the frequently referenced steric requirement nor by coordination by donor bases, since the distance in the sterically more crowded $[(iPr_5C_5)_2Ca]$[19a] is 264 pm and in $[(MeC_5H_4)_2Ca(dme)]$[19b] 268 pm. The acyclic pentadienyl ligand offers a wide range of bonding modes (σ, η^3, η^5) that are in principle easily interconvertible.[20] Here the Ca^{2+} center behaves like a d- or f-block metal to which acyclic penta-

 © VCH Verlagsgesellschaft mbH, D-69451 Weinheim, 1994 0570-0833/94/2121-2170 $ 10.00+.25/0

dienyl ligands normally bond in an η^5 coordination. In $[(Me_2C_5H_5)_2Mg(tmeda)]$, however, both pentadienyl ligands are terminally σ-bonded.[21] The Mg–C distance in this complex is 218 pm, hence significantly shorter than the corresponding distance in $[Cp_2Mg]$ of 230 pm.

The work of Hanusa et al.[22] in particular has contributed to a better understanding of the bonding in alkaline earth metallocenes. Further success in this flourishing area of research of alkali and alkaline earth metallocenes will most certainly be achieved in the near future. For instance, it is quite evident that one should also investigate the corresponding heterocyclopentadienyl complexes. The replacement of a CH group with an isoelectronic ER group (E = Si, Ge, Sn, Pb) or with E′ = N, P, As, Sb, Bi should give rise to further types of coordination. Other potent π donors like the cyclooctatetraene ligand, which has proved to be very useful especially in f-block element chemistry,[23] may be employed as well.

These opportunities indicate that there is still a lot to be discovered. This becomes more exciting and necessary, the more it becomes apparent that our knowledge for describing and predicting the coordination behavior in this class of substances is not by any means sufficient. To extend our understanding, a great deal of experimental work is still required.

German version: *Angew. Chem.* **1994**, *106*, 2256

[1] Reviews: a) P. Jutzi, *Adv. Organomet. Chem.* **1986**, *26*, 217; b) *Pure Appl. Chem.* **1989**, *61*, 1731; c) *ibid* **1990**, *62*, 1035; d) *J. Organomet. Chem.* **1990**, *400*, 1; e) E. Weiss, *Angew. Chem.* **1993**, *105*, 1565; *Angew. Chem. Int. Ed. Engl.* **1993**, *32*, 1501.

[2] C. Lambert, P. von R. Schleyer, *Angew. Chem.* **1994**, *106*, 1187; *Angew. Chem. Int. Ed. Engl.* **1994**, *33*, 1129.

[3] a) P. Jutzi, E. Schlüter, C. Krüger, S. Pohl, *Angew. Chem.* **1983**, *95*, 1015; *Angew. Chem. Int. Ed. Engl.* **1983**, *22*, 994; b) M. F. Lappert, A. Singh, L. M. Engelhardt, A. H. White, *J. Organomet. Chem.* **1984**, *262*, 271; c) P. Jutzi, E. Schlüter, S. Pohl, W. Saak, *Chem. Ber.* **1985**, *118*, 1959; d) A. Hammel, W. Schwarz, J. Weidlein *Acta Crystallogr. Sect. C* **1990**, *46*, 2337; e) H. Chen, P. Jutzi, W. Leffers, M. M. Olmstead, P. P. Power, *Organometallics* **1991**, *10*, 1282; f) G. Rabe, H. W. Roesky, D. Stalke, F. Pauer, G. M. Sheldrick, *J. Organomet. Chem.* **1991**, *403*, 11; g) J. Lorberth, S.-H. Shin, S. Wocadlo, W. Massa, *Angew. Chem.* **1989**, *101*, 793; *Angew. Chem. Int. Ed. Engl.* **1989**, *28*, 735.

[4] a) W. J. Evans, T. J. Boyle, J. W. Ziller, *Organometallics* **1992**, *11*, 3903; b) T. Aoyagi, H. M. M. Shearer, K. Wade, G. Whitehead, *J. Organomet. Chem.* **1979**, *175*, 21; c) R. D. Rogers, J. L. Atwood, M. D. Rausch, D. W. Macomber, W. P. Hart, *ibid.* **1982**, *238*, 79; d) P. Jutzi, W. Leffers, B. Hampel, S. Pohl, W. Saak, *Angew. Chem.* **1987**, *99*, 563; *Angew. Chem. Int. Ed. Engl.* **1987**, *26*, 583.

[5] a) S. D. Stults, R. A. Andersen, A. Zalkin, *J. Am. Chem. Soc.* **1989**, *111*, 4507; b) D. R. Armstrong, R. Herbst-Irmer, A. Kuhn, D. Moncrieff, M. A. Paver, C. A. Russell, D. Stalke, A. Steiner, D. S. Wright, *Angew. Chem.* **1993**, *105*, 1807; *Angew. Chem. Int. Ed. Engl.* **1993**, *32*, 1774; c) M. A. Paver, C. A. Russell, D. Stalke, D. S. Wright, *J. Chem. Soc. Chem. Commun.* **1993**, 1349; d) M. G. Davidson, D. Stalke, D. S. Wright, *Angew. Chem.* **1992**, *104*, 1265; *Angew. Chem. Int. Ed. Engl.* **1992**, *31*, 1226.

[6] F. Zaegel, J. C. Gallucci, P. Meunier, B. Gautheron, M. R. Sivik, L. A. Paquette, *J. Am. Chem. Soc.* **1994**, *116*, 6466.

[7] S. Harder, M. H. Prosenc, *Angew. Chem.* **1994**, *106*, 1830; *Angew. Chem. Int. Ed. Engl.* **1994**, *33*, 1744.

[8] a) S. Alexandratos, A. Streitwieser Jr., H. F. Schaefer III, *J. Am. Chem. Soc.* **1976**, *98*, 7959; b) E. D. Jemmis, S. Alexandratos, P. von R. Schleyer, A. Streitwieser Jr., H. F. Schaefer III, *ibid.* **1978**, *100*, 5695; c) E. D. Jemmis, P. von R. Schleyer, *ibid.* **1982**, *104*, 4781; d) A. Paquette, W. Bauer, M. R. Sivik, M. Bühl, M. Feigel, P. von R. Schleyer, *ibid.* **1990**, *112*, 8776.

[9] a) W. Strohmeier, H. Lansfeld, F. Gernert, *Z. Elektrochem.* **1962**, *66*, 823; b) M. Eiermann, K. Hafner, *J. Am. Chem. Soc.* **1992**, *114*, 135; c) R. den Besten, S. Harder, L. Brandsma, *J. Organomet. Chem.* **1990**, *385*, 153.

[10] a) C. H. Wong, T. Y. Lee, K. J. Chao, S. Lee, *Acta Crystallogr. Sect. B* **1972**, *28*, 1662; K. W. Nugent, J. K. Beattie, T. W. Hambley, M. R. Snow, *Aust. J. Chem.* **1984**, *37*, 1601; b) A. Almenningen, A. Haaland, J. Lusztyk, *J. Organomet. Chem.* **1979**, *170*, 271.

[11] a) W. Bünder, E. Weiss, *J. Organomet. Chem.* **1975**, *92*, 1; b) A. Haaland, J. Lusztyk, J. Brunvoll, K. B. Starowieyski, *ibid.* **1975**, *85*, 279.

[12] R. Zerger, G. Stucky, *J. Organomet. Chem.* **1974**, *80*, 7.

[13] a) R. A. Williams, T. P. Hanusa, J. C. Huffman, *Organometallics* **1990**, *9*, 1128; b) R. A. Andersen, J. M. Boncella, C. J. Burns, R. Blom, A. Haaland, H. V. Volden, *J. Organomet. Chem.* **1986**, *312*, C49.

[14] a) M. J. Heeg, C. Janiak, J. J. Zuckerman, *J. Am. Chem. Soc.* **1984**, *106*, 4259; b) P. Jutzi, U. Holtmann, D. Kanne, C. Krüger, R. Blom, R. Gleiter, I. Hyla-Kryspin, *Chem. Ber.* **1989**, *122*, 1629.

[15] R. A. Andersen, R. Blom, C. J. Burns, H. V. Volden, *J. Chem. Soc. Chem. Commun.* **1987**, 768.

[16] R. A. Williams, T. P. Hanusa, J. C. Huffman, *J. Chem. Soc. Chem. Commun.* **1988**, 1045.

[17] M. Guido, G. Gigli, *J. Chem. Phys.* **1976**, *65*, 1397.

[18] J. S. Overby, T. P. Hanusa, *Angew. Chem.* **1994**, *106*, 2300; *Angew. Chem. Int. Ed. Engl.* **1994**, *33*, 2191.

[19] a) R. A. Williams, K. F. Tesh, T. P. Hanusa, *J. Am. Chem. Soc.* **1991**, *113*, 4843; b) A. Hammel, W. Schwarz, J. Weidlein *J. Organomet Chem.* **1989**, *378*, 347.

[20] a) P. Powell, *Adv. Organomet. Chem.* **1986**, *26*, 125; b) R. D. Ernst, *Chem. Rev.* **1988**, *88*, 1255; c) R. D. Ernst, J. W. Freeman, P. N. Swepston, D. R. Wilson, *J. Organomet. Chem.* **1991**, *402*, 17.

[21] H. Yasuda, M. Yamauchi, A. Nakamura, T. Sei, Y. Kai, N. Yasuoka, N. Kasai, *Bull. Chem. Soc. Jpn.* **1980**, *53*, 1089.

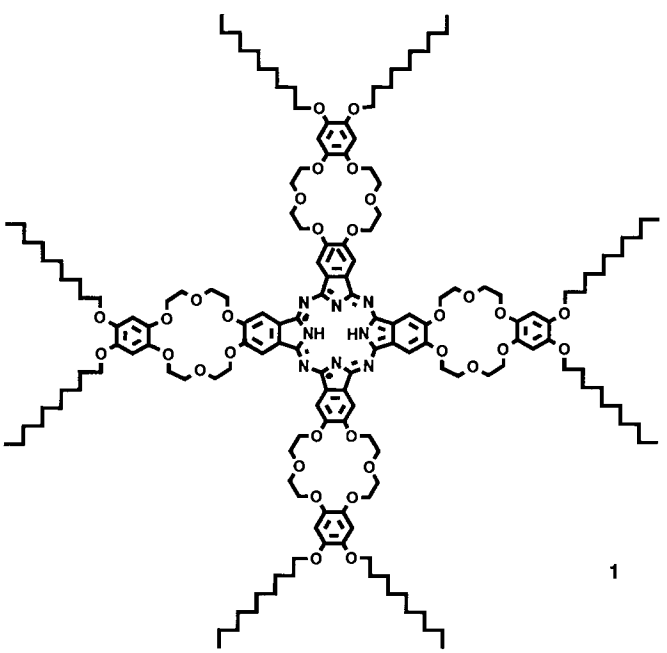
[22] a) T. P. Hanusa, *Polyhedron* **1990**, *9*, 1345; b) *Chem. Rev.* **1993**, *93*, 1023.

[23] D. Stalke, *Angew. Chem.* **1994**, *106*, 2253; *Angew. Chem. Int. Ed. Engl.* **1994**, *33*, 2165.

Construction of a Multiwired Molecular Cable of Micrometer Length by a Self-Assembly Process**

Cornelus F. van Nostrum, Stephen J. Picken, and Roeland J. M. Nolte*

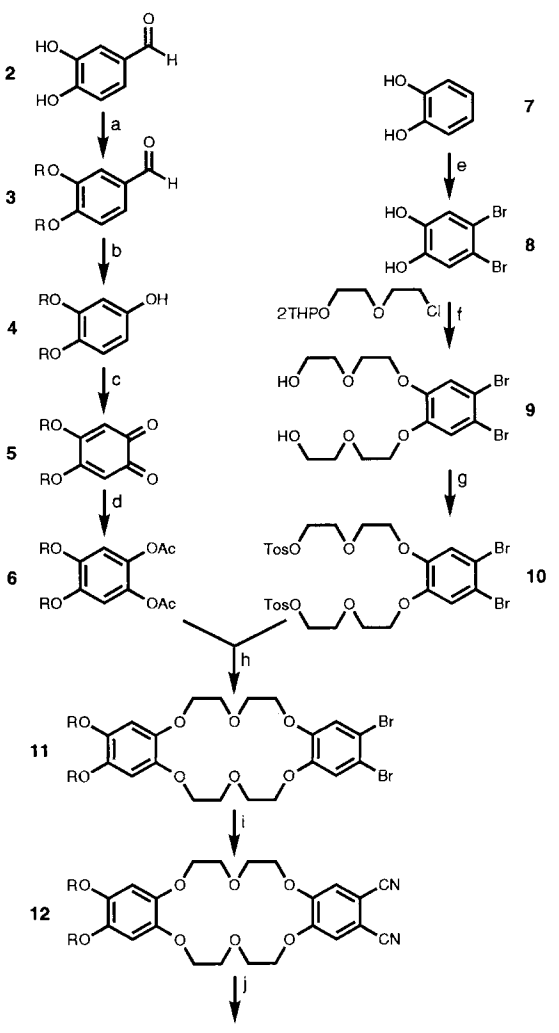
The engineering of molecules and molecular systems that can form nanometer-sized structures is currently receiving a great deal of attention.[1-3] An interesting challenge is the construction of molecular wires and molecular channels capable of transporting electrons and ions. For example, phthalocyanines substituted with long hydrocarbon side chains have been reported to form conducting mesophases in which the molecules are stacked in columns. Electron conduction within the columns is fast, whereas it is slow between the columns.[4, 5] In previous papers we have shown that crown ether molecules can be stacked to create ion conducting channels.[6, 7] Here we describe a novel liquid-crystalline molecule (**1**) that self-assembles in



1

chloroform solution to form a molecular cable. This cable contains a central wire of stacked phthalocyanines, four molecular channels built up from stacked crown ether rings and a surrounding hydrocarbon mantle. Isolated cables with molecular thickness and a length of several micrometers can be recognized in electron microscopy images.

Phthalocyanine **1** was prepared from crown ether **12** by a cyclization reaction (see Scheme 1). The crown ether was synthesized from **11**, which in turn was assembled from the building blocks **6** and **10**. The starting compound for **6** was 3,4-dihydroxybenzaldehyde (**2**). This compound was alkylated with decyl



Scheme 1. R = $C_{10}H_{21}$; a) DMF, $nC_{10}H_{21}Br$ (2.1 equiv), K_2CO_3 (2.2 equiv), N_2, 16 h (84%); b) $CHCl_3$/MeOH (1/1, v/v), H_2O_2 (0.75 equiv), H_2SO_4 (0.2 equiv), 5 h (65%); c) THF/H_2O (2.7:1, v/v), $K(SO_3)_2NO$ (2.5 equiv), KH_2PO_4 (0.6 equiv), $Bu_4N^+Cl^-$ (0.4 equiv), 2 h (80%); d) AcOH/Ac_2O (1/1, v/v), reflux, Zn (4 equiv), reflux, 30 min, (88%); e) CCl_4, Br_2 (2 equiv), 0 °C → room temperature (RT), 16 h (91%); f) *n*BuOH, NaOH (2 equiv), $ClCH_2CH_2OCH_2CH_2OTHP$ (2 equiv), N_2, reflux, 16 h, HCl (2.1 equiv), RT, 1 h (49%); g) pyridine, *p*TosCl (2.4 equiv), −10 °C, 2 h, RT, 16 h (93%); h) **6**, *n*BuOH, NaOH (2.5 equiv), N_2, reflux, **10** (1 equiv), reflux, 16 h (58%); i) DMF/pyridine (200:1, v/v), CuCN (3 equiv), N_2, reflux, 40 h; subsequently, NH_4OH/H_2O, O_2, 2 h (75%); j) $(CH_3)_2NCH_2CH_2OH$, reflux, 40 h (30%).

[*] Prof. Dr. R. J. M. Nolte, C. F. van Nostrum
Department of Organic Chemistry, NSR Center
University of Nijmegen
NL-6525 ED Nijmegen (The Netherlands)
Telefax: Int. code + (80)553450
Dr. S. J. Picken
AKZO Research Laboratories, Arnhem (The Netherlands).

[**] This research was financially supported by the Dutch Innovatie-gericht Onderzoekprogramma (IOP) of the Ministry of Economic Affairs. We thank R. van Puijenbroek (AKZO) for carrying out the SAXS measurements.

bromide ($\rightarrow$ **3**) and subsequently converted into 3,4-bis(decoxy)phenol (**4**) by a Baeyer–Villiger type of oxidation.[8] Treatment of the phenol with Fremy's radical[9] under phase transfer conditions yielded 4,5-bis(decoxy)-1,2-benzoquinone (**5**), which was converted into 1,2-bis(acetoxy)-4,5-bis(decoxy)benzene (**6**; for characterization see Table 1) by reduction with zinc/acetic acid/acetic anhydride. The overall yield of **6** from **2** was 38%. The synthesis of the second building block **10** was performed using more standard reactions. Catechol (**7**) was brominated and subsequently alkylated with tetrahydropyranyl-(THP)-protected diethyleneglycol monochloride to give, after in situ deprotection, compound **9**. Reaction of **9** with *p*-toluenesulfonyl chloride gave compound **10** as a highly viscous oil in 42% overall yield (Table 1). The coupling of the two fragments was carried out by first hydrolyzing **6** and subsequently treating the resulting catecholate in situ with **10**. The two bromine atoms of **11** were substituted by nitrile groups with copper cyanide in *N*,*N*-dimethylformamide (DMF). Finally, the resulting crown ether **12** was converted into phthalocyanine **1** by refluxing in *N*,*N*-dimethylaminoethanol (overall yield from **6** and **10** 13%). Compound **1** was purified by repeated recrystallization from chloroform. Spectroscopic and elemental analysis were consistent with the proposed structure (Table 1).

Table 1. Characteristic physical data of **1**, **6**, and **10**.

1: IR ($CHCl_3$): $\tilde{\nu}$ = 3294 (NH), 2925, 2853 (CH_2), 1603, 1529, 1413 (Ar), 1490, 1391, 1369, 1101 (phthalocyanine), 1280 (ArO), 1134 (COC), 1022 (NH), 863 cm^{-1} (ArH); ^1H NMR (400 MHz, $CDCl_3$, 53 °C): δ = 6.64 (s, 8H, ArH), 3.6–4.9 (m, 80H, CH_2O), 1.2–1.8 (m, 128H, CH_2), 0.89 (s, 24H, CH_3); elemental analysis: $C_{168}H_{250}N_8O_{32}.CHCl_3$: calcd C 67.36, H 8.40, N 3.72, found C 67.18, H 8.28, N 3.74%

6: IR (KBr): $\tilde{\nu}$ = 2800–3100 (CH_2, CH_3, ArH), 1760 (C = O), 1605, 1510 (Ar), 1230, 1180 cm^{-1} ($C_{Ar}O$); ^1H NMR (100 MHz, $CDCl_3$): δ = 6.68 (s, 2H, ArH), 3.94 (t, 4H, CH_2O), 2.26 (s, 6H, CH_3C = O), 1.2–1.9 (m, 32H, CH_2), 0.88 (t, 6H, CH_3); MS (CI): *m/z*: 506 [M^+]; elemental analysis: $C_{30}H_{50}O_6$: calcd C 71.11, H 9.95, found C 71.42, H 9.82%

10: IR ($CHCl_3$): $\tilde{\nu}$ = 2800–3100 (CH_2, ArH), 1350, 1170 (SO_3), 1245, 1190 ($C_{Ar}O$), 655 cm^{-1} (ArBr); ^1H NMR (100 MHz, $CDCl_3$): δ = 7.13–7.85 (m, 8H, ArH), 7.03 (s, 2H, ArH), 3.6–4.25 (m, 16H, CH_2), 2.38 (s, 6H, CH_3); MS (FAB): *m/z*: 752 [$M^+ + 1$]

Crown ether phthalocyanine **1** showed thermotropic liquid crystalline behavior as was evident from differential scanning calorimetry (DSC), polarizing microscopy, and small angle X-ray scattering (SAXS) measurements. A transition to a highly viscous, birefringent mesophase was observed at 148 °C on heating (ΔH = 130 kJ mol^{-1}). Large hysteresis was observed on cooling: the transition to the crystalline phase occurred at 105 °C. No transition to the isotropic phase was observed below the decomposition temperature of the compound (320 °C). The large number of peaks in the SAXS measurements at room temperature indicated a crystalline phase. In the mesophase at 170 °C an intense peak, corresponding to a spacing of 35.10 Å, and a very broad peak, corresponding to 4.5 Å, were visible. The former peak probably is the (100) reflection of a hexagonal columnar phase with an intercolumnar distance of 40.5 Å.

Generally, alkoxy- and crown-ether-substituted phthalocyanines are highly soluble in organic solvents. Surprisingly, **1** was only soluble in boiling chloroform and in boiling toluene. A solution of **1** (at a concentration of 7 mg mL^{-1} or more) in chloroform formed a gel on cooling. A UV/Vis spectrum of a dilute solution (11 μM) of **1** in chloroform at 50 °C showed a split Q-band at 660 and 700 nm that is typical for nonaggregated metal-free phthalocyanines. However, when this solution was cooled to room temperature a blue shift of the bands and a broadening of the signals was observed, which is characteristic of aggregated phthalocyanine species (Fig. 1).

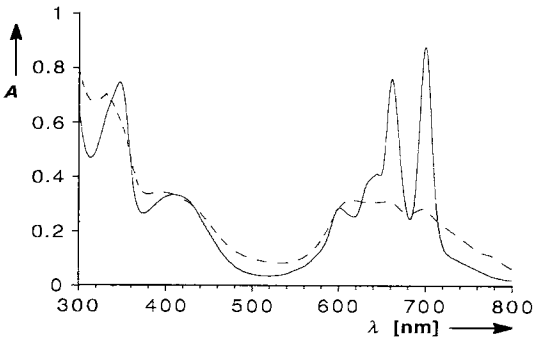


Fig. 1. UV/Vis spectra of **1** in chloroform (11 μM) at 25 °C (– – –) and 50 °C (——).

The structure of the aggregates was elucidated with the help of transmission electron microscopy (TEM). Compound **1** (7 mg) was boiled in chloroform (1 mL), and after the solution had cooled, a drop of the resulting gel was placed on a carbon-coated copper grid. After one minute the grid was blotted dry and shadowed with platinum at an angle of approximately 45°. Two representative TEM pictures are shown in Figure 2. At low magnifications fibers with a length in the order of micrometers, which form a network structure, are observed. At higher magnifications these fibers are seen to consist of bundles of single parallel strands. The thickness of these strands equals the diameter of a molecule of **1** as estimated from CPK space-filling molecular models, that is, 50–60 Å. Several isolated strands can be observed with the same diameter. At lower concentrations of **1** in chloroform, that is, below the gel-forming point, fibers are still present, but they are smaller, and no network is formed.

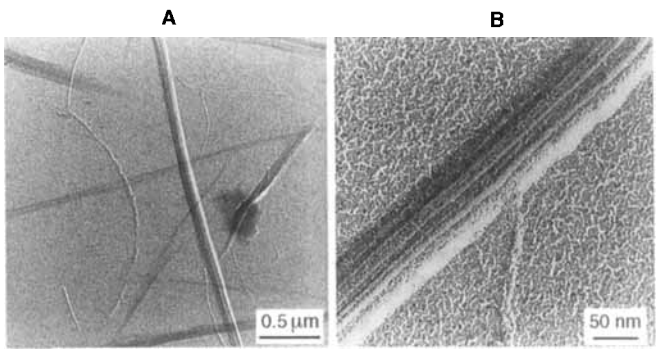


Fig. 2. Transmission electron micrographs of a gel of **1** in chloroform. A): Isolated single strands and bundles of parallel strands of **1**. B): Magnification showing individual strands of molecules **1**, which have diameters of 60 Å.

The conclusion from these experiments is that crown ether phthalocyanine **1** self-assembles into extremely long stacks of molecular thickness, which consist of more than 10^4 molecules. To the best of our knowledge, evidence for the formation of such large phthalocyanine aggregates has not been reported before. Apparently, the attractive forces between the molecules are so strong that complete solvation is prevented at room tempera-



Fig. 3. Schematic representation of the multiwired molecular cable formed by self-assembly of crown ether phthalocyanine **1**. In the mesophase the individual molecules probably rotate around their stacking axis (see ref. [10]).

ture. As shown schematically in Figure 3 a stack of molecules **1** can be considered to be a multiwired molecular cable. In view of its structural resemblance to the crown-ether-substituted phthalocyanine polymers previously studied by us,[7] it is reasonable to postulate that the molecular cable is capable of conducting ions and electrons. Apart from that, the transition of **1** from the solid state to the mesophase is probably accompanied by a change in electronic and ionic conductive properties. We are currently investigating this in detail, as well as the polymerization of the dihydroxysilicon derivative of **1** to give a polymerized molecular cable.

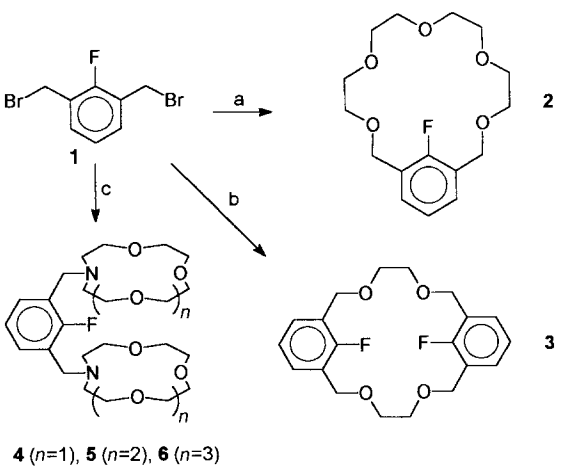
Received: March 26, 1994
Revised version: June 21, 1994 [Z 6799 IE]
German version: *Angew. Chem.* **1994**, *106*, 2298

[1] G. M. Whitesides, J. P. Mathias, C. T. Seto, *Science* **1991**, *254*, 1312.
[2] J.-M. Lehn, *Angew. Chem.* **1990**, *102*, 1347; *Angew. Chem. Int. Ed. Engl.* **1990**, *29*, 1304.
[3] A. Harada, J. Li, M. Kamachi, *Nature* **1993**, *364*, 516.
[4] J. Simon, P. Bassoul in *Phthalocyanines, Properties and Applications, Vol. 2* (Eds.: C. C. Leznoff, A. B. P. Lever), VCH, New York, **1993**, pp. 223-299.
[5] P. G. Schouten, J. M. Warman, M. P. de Haas, J. F. van der Pol, J. W. Zwikker, *J. Am. Chem. Soc.* **1992**, *114*, 9028.
[6] M. F. M. Roks, R. J. M. Nolte, *Macromolecules* **1992**, *25*, 5398.
[7] O. E. Sielcken, L. A. van de Kuil, W. Drenth, J. Schoonman, R. J. M. Nolte, *J. Am. Chem. Soc.* **1990**, *112*, 3086.
[8] M. Matsumoto, H. Kobayashi, Y. Hotta, *J. Org. Chem.* **1984**, *49*, 4740.
[9] H. Zimmer, D. C. Lankin, S. W. Horgan, *Chem. Rev.* **1971**, *71*, 229.
[10] A. P. M. Kentgens, B. A. Markies, J. F. van der Pol, R. J. M. Nolte, *J. Am. Chem. Soc.* **1990**, *112*, 8800.

cannot form stable metal complexes. The goal of our research work is the synthesis of macrocycles that have only a few fluorine atoms incorporated into the cyclic structure. Upon complexation of metal ions, the fluorine should act as a "detector", since the ^{19}F NMR signals shift upon complexation.[3] The high sensitivity, combined with a large signal dispersion and the absence of a natural background make ^{19}F NMR spectroscopy an ideal tool for investigation.[4]

Recently we reported the synthesis of a partially fluorinated [2.2.2]cryptand.[5] This compound forms complexes with metal ions; however, the ^{19}F NMR signals shift only slightly upon complexation, since no direct metal–fluorine contacts are formed. Such an interaction becomes more likely if a carbon–fluorine bond is directed towards the center of the crown ether. The relatively small steric demand of the fluorine atom is not expected to interfere with the binding of metal ions; on the contrary it is hoped that formation of a σ-donor bond between fluorine and the metal ion will increase the stability of the metal complexes.

The building block used for the synthesis of the fluorine-containing macrocycles was 1,3-bis(bromomethyl)-2-fluorobenzene (**1**), which was treated with tetraethyleneglycol, ethyleneglycol, or azacrown ethers to yield fluorocrown ethers (Scheme 1).[6]



Scheme 1. a) KO*t*Bu, tetraethyleneglycol, b) KO*t*Bu, ethyleneglycol, c) Na_2CO_3, aza[9 + 3*n*]crown-(*n* + 3).

Complexes of Partially Fluorinated Macrocycles with a Metal–Fluorine σ-Donor Bond and Their Suitability as Metal Ion Indicators**

Herbert Plenio* and Ralph Diodone

Even though a rather large number of macrocyclic polyethers is known,[1] only few fluorine-containing crown ethers[2] have been reported, and in most of these all of the hydrogen atoms are substituted by fluorine. As a result of the electron-withdrawing nature of the CF_2 units, the oxygen or nitrogen atoms in these polyethers no longer exhibit Lewis basicity and therefore

[*] Dr. H. Plenio, Dipl.-Chem. R. Diodone
Institut für Anorganische und Analytische Chemie der Universität
Albertstrasse 21, D-79104 Freiburg (FRG)
Telefax: Int. code + (761)203-5987

[**] This work was supported by the Fonds der Chemischen Industrie. The authors thank Prof. Dr. H. Vahrenkamp for his support and Dr. E. Keller for hints in determining the crystal structure.

The macrocyclic ligands **2**–**6** were obtained in yields of 30 to 80%. In these compounds the carbon–fluorine bond is directed towards the region that is expected to be the binding site for metal ions.

The reaction of compounds **2**, **4**, **5**, and **6** with metal salts leads to the complexation of a metal ion, while at the same time the ^1H, ^{13}C, and ^{19}F NMR resonances of the ligands are shifted; in contrast, no such effects were observed for **3**. The ^{19}F NMR resonances (300 K) reported for the various metal complexes represent the averaged ^{19}F NMR signals for the metal-free and metal-containing ligands (fast exchange). The absolute values of these signal shifts are, however, only large in the ^{19}F NMR spectra, in which values up to $\Delta\delta = 8.8$ have been observed.

Figure 1 shows the differences in chemical shift ($\Delta\delta$) obtained by adding an approximately tenfold molar excess of metal salt to the fluoroxylene bis(crown ethers) **4**–**6**; however, in most cases addition of metal salt beyond a twofold excess does not markedly change the position of the signals. It was

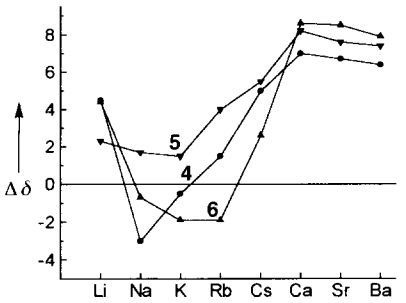


Fig. 1. Observed differences in the chemical shift for the ^{19}F NMR resonances upon complexation of the free bis(crown ethers) **4**–**6**, with Li^+, Na^+, K^+, Rb^+, Cs^+, Ca^{2+}, Sr^{2+}, and Ba^{2+}. In case of **5**-Rb^+ two signals are observed: a very broad one and one whose position is concentration-dependent.

found that alkaline earth metal ions give rise to a larger difference in chemical shift than alkali metal ions; this behavior is most likely a result of the higher charge density of the former. However, no conclusion about the relative or absolute stabilities of the complexes can be drawn from the final values given. Selective complexation is observed when metal ions with largely differing radii compete for binding to the macrocycle. For example, addition of Li^+ or Mg^{2+} has a negligible effect on the ^{19}F NMR titration curves of **2** with Na^+ or K^+. Figure 2 depicts the results for the ^{19}F NMR titrations of fluorocrown ether **2** with solutions of various metal salts. The experimentally determined curves show that close to the equivalence point, the steep curve in the stoichiometric region becomes a straight line which asymptotically approaches the limiting value and indicates that formation of a stoichiometric 1:1 metal:ligand complex has taken place. This graph can be regarded as a calibration curve that allows the determination of the metal ion concentration if either the ligand concentration or the formation constant of the complex is known.

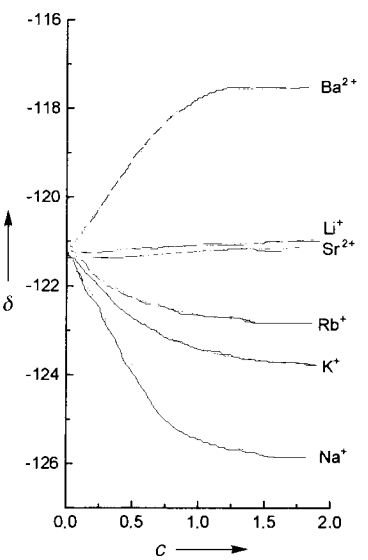


Fig. 2 Plot of the ^{19}F NMR chemical shifts of **2** as a function of added equivalents c of metal ion. The titration was carried out with solutions of the perchlorates of Li^+, Na^+, K^+, Rb^+, Sr^{2+}, and Ba^{2+} in CH_3CN.

From Figures 1 and 2 it becomes apparent that some ^{19}F NMR signals are shifted to higher field while others are shifted to lower field. Reinhoudt et al. have reported a similar phenomenon in the ^1H NMR spectra of the non-fluorinated analogues of **2**. They proposed an explanation based on the complementarity of the size of the cavity and ion.[7] Although this hypothesis succeeded in explaining the observed differences in chemical shift for the ^1H NMR resonances of the non-fluorinated analogues, such a simple explanation is not forthcoming for the compounds described herein. For the alkali metals, the "size-match" and the observed shift of the signals in the NMR spectra seem to correlate, since the absolute differences in the NMR chemical shift are largest when the metal ion fits well in the macrocycle or, alternatively, when a crown ether-sandwich complex can be formed. However, this simple model does not hold for the divalent alkaline earth metal ions.

Whereas NMR spectroscopy can provide information on the formation of metal complexes of partially fluorinated macrocycles, it is not possible to draw a more definitive conclusion regarding the nature and strength of the metal–fluorine interactions. This is also due to the fact that no scalar coupling to the fluorine was detected in the ^{19}F NMR.

In order to make more accurate statements about possible metal–fluorine contacts in the solid state, an X-ray structure analysis was performed for one of the metal complexes.[8, 9] Single crystals of **2**·$Ba(ClO_4)_2$ were obtained by diffusion of diethyl ether into a solution of the metal complex in acetonitrile. In the crystal, barium is ten-coordinate (Fig. 3) with seven short

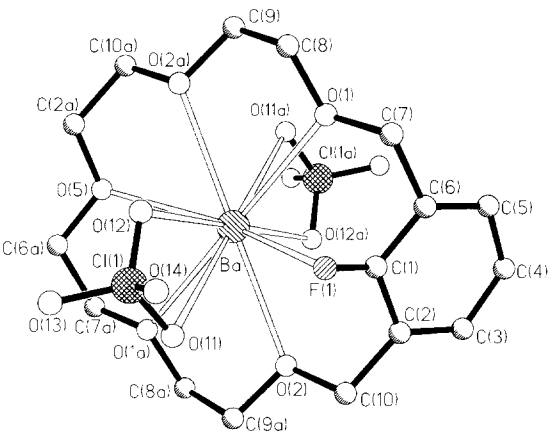


Fig. 3 Structure of **2**·$Ba(ClO_4)_2$ in the crystal. For clarity the hydrogen atoms have been omitted. Selected bond lengths [pm] and angles [°]: Ba–F(1) 279.9(8), Ba–O(1) 279.4(5), Ba–O(2) 279.5(5), Ba–O(12) 281.0(7), Ba–O(11) 301.0(6), F(1)–C(1) 134.8(10); Ba–F(1)–C(1) 80.5(5), Ba–C(1)–F(1) 72.2(5).

(279.4–281.0 pm), one medium (289.9 pm), and two long distances (301.0 pm) to the coordinating atoms. The Ba–F distance is 279.9(8) pm and is therefore in the same range as the short Ba–O distances. Short metal–fluorine distances have been reported for several metal alkoxides[10] and aryl metal compounds;[11] they are regarded to be similar to the interactions of ethers and amines with metal ions.[12] Ba–O distances of approximately 280 pm have also been observed in the structure of benzo[18]crown-6·$Ba(ClO_4)_2$ and can therefore be considered as typical.[13] The C(1)–Ba distance (289.9(8) pm) is significantly shorter than the two long Ba–O distances. This raises the question of whether the interaction of Ba^{2+} with the C(1)–F(1) bond can be classified as η^2 bonding—a similar trend towards polyhapticity has also been observed in the solid-state structures of some benzylmetal compounds.[14]

To decide whether metal–fluorine contacts make a positive contribution towards the stability of metal complexes in solution or if on the other hand steric hindrance dominates, we have carried out a simple competition experiment. In this experiment, the ^1H, ^{13}C, and ^{19}F NMR spectra of a 1:1:1 mixture of **2**, its non-fluorinated analogue, and Na^+ were recorded. We found that the complex of **2** with Na^+ is more stable by a factor of 1.5. The same trend is also reflected in the heterogeneous stability constants determined by picrate extraction.[15, 16] For the metal ions Na^+, K^+, and Cs^+ the stability constant is always larger for the fluorine-containing compound **2** than for the non-fluorinated analogue.

The short Ba–F(1) distances in **2**·$Ba(ClO_4)_2$ are indicative of a direct σ donor bond from F(1) to the metal ion. From the large chemical shifts of the ^{19}F NMR resonance it can be deduced that bonding of F(1) to cations of the alkali and alkaline earth metal ions also exists in solution.

Experimental Procedure

2: KO*t*Bu (920 mg, 8.2 mmol) and tetraethyleneglycol (688 mg, 3.6 mmol) were dissolved in toluene (100 mL) and the resulting solution was heated under reflux for 1 h. A solution of 1,3-bis(bromomethyl)-2-fluorobenzene (1000 mg, 3.6 mmol) in toluene (40 mL) was then slowly added at room temperature while vigorously stirring. Stirring at room temperature was continued for 12 h, and the solution was then heated under reflux for 2.5 h. The reaction mixture was allowed to cool to room temperature, the precipitate was filtered off, and the solvent was removed from the filtrate under vacuum. Distillation of the residue at 0.1 Torr/200 °C afforded compound **2** as a colorless oil (R_f = 0.35). Yield: 656 mg (58%). ^1H NMR (CD_3CN): δ = 3.46 (s, 8H, OCH_2), 3.50–3.59 (m, 8H, OCH_2), 4.51 (d, J = 1.1 Hz, 4H, $ArCH_2$), 7.07 (t, J = 7.5 Hz, 1H, ArH), 7.32 (t, J = 7.2 Hz, 2H, ArH). ^{13}C NMR ($CDCl_3$): δ = 67.38 (d, ^3J(C,F) = 3.5 Hz, $ArCH_2$), 69.24 (OCH_2), 70.42 (OCH_2), 70.46 (OCH_2), 70.63 (OCH_2), 123.34 (d, J(C, F) = 4.7 Hz, Ar), 125.36 (d, ^2J(C, F) = 15.1 Hz, Ar), 131.00 (d, J(C, F) = 4.8 Hz, Ar), 160.23 (^2J(C, F) = 15.1 Hz, Ar), 160.23 (d, ^1J(C, F) = 250.2 Hz, Ar). ^{19}F NMR ($CDCl_3$, $CFCl_3$): δ = −122.20 (t, J = 7.1 Hz). ^{19}F NMR (CD_3CN, $CFCl_3$): δ = −126.81 (t, J = 7.1 Hz). $C_{16}H_{23}FO_5$ (314.35) calcd (found): C 61.12 (60.43), H 7.38 (7.29).

^{19}F NMR titrations: A solution of **2** (0.95 mg, 3 μmol) in CD_3CN (0.5 mL) was titrated with the corresponding metal perchlorates (3 μmol per 0.1 mL CD_3CN). The ^{19}F NMR shifts were referenced internally to $CFCl_3$ and determined on a Bruker 200 ACF (^{19}F: 188 MHz) at 300 K. In a control experiment, the ^{19}F NMR resonance for 1,3-bis(bromomethyl)-2-fluorobenzene did not change upon addition of metal perchlorates; hence, interactions between the metal ions and $CFCl_3$ which might affect the standard can be ruled out. Differences in NMR chemical shifts when employing CD_3CN as solvent are reproducible to at least ±0.02 ppm when NMR data is collected at the same temperature and using similar concentrations of reactants. The maximum sensitivity of the measurement technique described herein (5 mm NMR tube, data collection time: 30 min, 188 MHz) allows for the detection of 0.01 μmol metal ions in 0.5 mL sample volume. This is equivalent to a metal ion concentration of 2×10^{-5} mol L^{-1}.

Received: June 7, 1994 [Z 7008 IE]
German version: *Angew. Chem.* **1994**, *106*, 2267

[1] a) J. S. Bradshaw, K. E. Krakowiak, R. M. Izatt, *Aza-Crown Macrocycles* (Series: *The Chemistry of Macrocyclic Compounds*), Wiley, New York, **1993**; b) B. Dietrich, P. Viout, J. M. Lehn, *Macrocyclic Chemistry*, VCH, Weinheim, **1993**; c) G. W. Gokel, *Crown Ethers & Cryptands*, The Royal Society of Chemistry, Letchworth, **1991**; d) F. Vögtle, *Supramolekulare Chemie*, Teubner, Stuttgart, **1992**.

[2] a) T. Y. Lin, W. I. Bailey, R. J. Lagow, *J. Chem. Soc. Chem. Commun.* **1985**, 1350; b) *Pure Appl. Chem.* **1988**, *60*, 473; c) W. D. Clark, T. Y. Lin, S. D. Maleknia, R. J. Lagow, *J. Org. Chem.* **1990**, *55*, 5933; d) T. Y. Lin, R. J. Lagow, *J. Chem. Soc. Chem. Commun.* **1991**, 12; e) W. B. Farnham, D. C. Roe, D. D. Dixon, J. C. Calabrese, R. L. Harlow, *J. Am. Chem. Soc.* **1990**, *112*, 7707; f) M. H. Hung, W. B. Farnham, A. E. Feiring, S. Rozen, *ibid.* **1993**, *115*, 8954; g) M. Shionoya, E. Kimura, Y. Iitaka, *ibid.* **1990**, *112*, 9237.

[3] a) M. J. W. Prior, R. J. Maxwell, J. R. Griffiths, *NMR Basic Princ. Prog.* **1992**, *28*, 102; b) G. A. Smith, H. L. Kirschenlohr, J. C. Metcalfe, S. D. Clarke, *J. Chem. Soc. Perkin Trans. 2* **1993**, 1205; c) G. A. Smith, P. G. Morris, T. R. Hesketh, J. C. Metcalfe, *Biochim. Biophys. Acta* **1986**, *889*, 72.

[4] *Multinuclear NMR Spectroscopy* (Ed.: J. Mason), Plenum, New York, **1987**.

[5] H. Plenio, *Inorg. Chem.*, in press.

[6] E. Weber, F. Vögtle, *Chem. Ber.* **1976**, *109*, 1803.

[7] a) D. N. Reinhoudt, R. T. Gray, F. DeJong, C. J. Smit, *Tetrahedron* **1977**, *33*, 563; b) R. T. Gray, D. N. Reinhoudt, C. J. Smit, Ms. I. Veenstra *Recueil* **1976**, *95*, 258.

[8] X-ray structure analysis of **2**·$Ba(ClO_4)_2$($C_{16}H_{23}BaCl_2FO_{13}$): crystal dimensions 0.5 × 0.4 × 0.3 mm^3, monoclinic, space group $P2_1/n$, Z = 2, a = 9.631(2), b = 9.298(2), c = 13.518(3) Å, α = 99.28(3)°, V = 1194.7(4) $Å^3$, ρ_{calcd} = 1.81 $g cm^{-3}$, θ = 2.4 26°, T = 293 K, reflections (collected, independent): 2510, 2365, empirical absorption correction, $\mu(Mo_{K\alpha})$ = 1.966 mm^{-1}, data/parameters = 2000/169, full-matrix, least-squares on F^2, H atoms "riding-model", R values [$I > 4\sigma(I)$]: $R1$ = 0.0464, $wR2$ = 0.1297, GOOF = 1.07, residual electron density: + 0.71/−0.49 e $Å^{-3}$. In the crystal, the molecules are disordered along the b axis and rotated by 180° relative to each other; in both orientations forbidden van der Waals contacts are not observed. Atoms C(3), C(4), C(5), and F(1) are not part of this structural superposition and were refined with an occupancy factor of 0.5. The apparent centrosymmetric space group $P2_1/n$ is a result of this disorder. Further details of the crystal structure investigation may be obtained from the Fachinformationszentrum Karlsruhe, D-76344 Eggenstein-Leopoldshafen (FRG), on quoting the depository number CSD-400937.

[9] G. M. Sheldrick, *SHELXS-86*, *SHELXL-93*, Universität Göttingen, **1986**, **1993**.

[10] J. A. Samuels, E. B. Lobkovsky, W. E. Streib, K. Folting, J. C. Huffman, J. W. Zwanziger, K. G. Caulton, *J. Am. Chem. Soc.* **1993**, *115*, 5093.

[11] a) X. Yang, C. L. Stern, T. J. Marks, *Organometallics* **1991**, *10*, 840; b) A. D. Horton, A. G. Orpen, *ibid.* **1991**, *10*, 3910; c) S. Brooker, N. Bertel, D. Stalke, M. Noltemeyer, H. W. Roesky, G. M. Sheldrick, F. T. Edelmann, *ibid.* **1992**, *11*, 192; d) F. T. Edelmann, *Comments Inorg. Chem.* **1992**, *12*, 259.

[12] P. Murray-Rust, W. C. Stallings, C. T. Monti, R. K. Preston, J. P. Gluster, *J. Am. Chem. Soc.* **1983**, *105*, 3206, and references therein.

[13] D. L. Hughes, C. L. Mortimer, M. R. Truter, *Inorg. Chim. Acta* **1978**, *29*, 43.

[14] D. Hoffmann, W. Bauer, F. Hampel, N. J. R. van Eikema Hommes, P. von R. Schleyer, P. Otto, U. Pieper, D. Stalke, D. S. Wright, R. Snaith, *J. Am. Chem. Soc.* **1994**, *116*, 528.

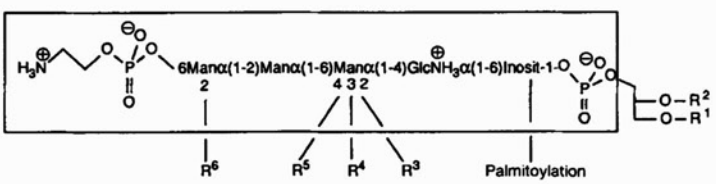
[15] S. S. Moore, T. L. Tarnowski, M. Newcomb, D. J. Cram, *J. Am. Chem. Soc.* **1977**, *99*, 6398.

[16] Even though these heterogeneous stability constants are not precisely correlated with the Gibbs energy of complexation, they allow for a good prediction of the relative stabilities of metal complexes for structurally related systems.

Synthesis of a GPI Anchor of Yeast (*Saccharomyces cerevisiae*)**

Thomas G. Mayer, Bernd Kratzer, and Richard R. Schmidt*

Glycosylphosphatidylinositols (GPIs) are a class of naturally-occurring glycophospholipids, discovered about ten years ago, that anchor the C-termini of proteins and glycoproteins to the membrane of eukaryotic cells.[1] Analysis of the GPI anchors of *Trypanosoma brucei* variant surface glycoprotein (VSG),[1,2] murine brain Thy-1,[3] *Leishmania major* promastigate surface protease,[4] *Trypanosoma cruzi* 1G7 antigen,[5] and human erythrocyte acetylcholinesterase[6] gave the general structure shown in Scheme 1 (framed).

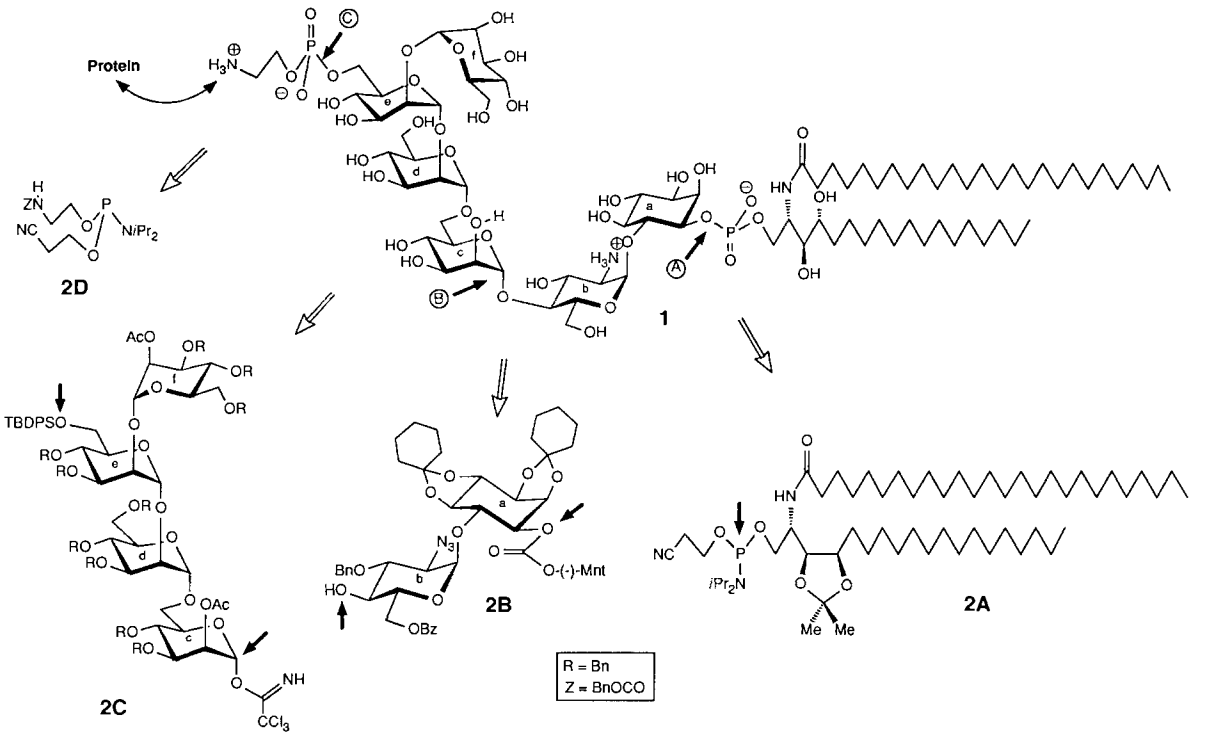


Scheme 1. Structure of GPI anchors.

The occurrence of additional carbohydrate (R^4–R^6) or ethanolamine phosphate (R^3) side chains is species-specific,[7] and there is a noticeable difference in membrane-anchoring lipid structures depending on species and cell type. In the case of glycerolipids (variation of R^1 and R^2), the lipids are made up of *sn*-1,2-dimyristoylglycerin in *T. brucei* VSGs,[8] *sn*-1-stearoyl-2-lysoglycerin in *T. brucei* procyclic acidic repetitive protein,[9] *sn*-1-alkyl-2-acylglycerin in bovine and human erythrocyte acetylcholinesterase[10] and human folate binding protein,[11] and *sn*-1,2-diacylglycerin in torpedo acetylcholinesterase.[12] In addition, the inositol residue can be palmitoylated. In GPI anchors of yeast (*Saccharomyces cerevisiae*), ceramides containing

[*] Prof. Dr. R. R. Schmidt, Dipl.-Chem. T. G. Mayer, Dipl.-Chem. B. Kratzer
Fakultät Chemie der Universität
Postfach 5560 M 725, D-78434 Konstanz (FRG)
Telefax: Int. code + (7531)88-3135

[**] This work was supported by the Deutsche Forschungsgemeinschaft and the Fonds der Chemischen Industrie.



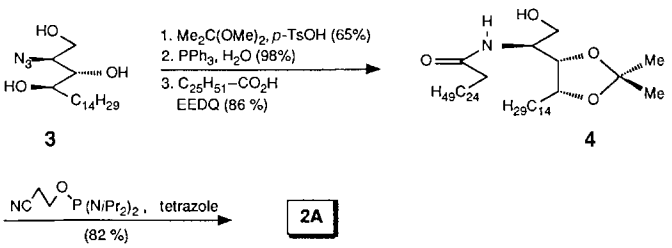
Scheme 2. Retrosynthesis of GPI anchor **1**.

phytosphingosine were also found as a membrane anchors instead of glycerolipids.[13,14] The typical structure of such a GPI anchor is shown in Scheme 2 (**1**).

The role of GPI-anchored proteins in cell–cell recognition, in interactions with bioactive factors, and as enzymes have been discussed.[1] Moreover, there are increasing indications that intracellular signal transfer triggered by insulin is caused by compounds that are structurally related to glycosylphosphatidylinositols.[15] The GPI anchor itself and its partial structures are thus gaining in significance as mediators of regulatory processes, and the chemical synthesis of structurally homogeneous GPI anchors and their derivatives is an important objective for biological investigations. The appropriate combination of lipid, phosphate, carbohydrate, and, when necessary, peptide chemistry has been successfully employed for the synthesis of partial structures[16–23] and the diacylglycerin-based GPI anchor of *Trypanosoma crucei*.[24] We report here on a versatile strategy for the first total synthesis (Scheme 2) of the ceramide-containing GPI anchor **1** of yeast (*Saccharomyces cerevisiae*).

The strategy we followed for the synthesis of **1** is convergent and versatile. The target molecule was cleaved at positions Ⓐ–Ⓒ into the fragments **2A**–**2D** (Scheme 2), which should have many applications, either directly or after structural modification (especially at O-3 or O-4 of the mannose building block c), in the synthesis of a great variety of GPI anchors. Our aim is to demonstrate the efficiency of this strategy with respect to the synthesis of the individual components and the coupling to form the target molecule. Here, the formation of the crucial glycosidic bonds is based on highly anomer-selective reactions with O-glycosyltrichloroacetimidates as glycosyl donors,[25] and phosphorylation by the phosphite amide method.[22,26] Appropriate selection of protecting groups enables their final cleavage in two simple, high-yielding reaction steps.

The ceramide component **2A**, which contains phytosphingosine as nitrogen base, was prepared starting from the readily available azide derivative **3** (Scheme 3).[27] Reaction with dimethoxypropane in the presence of *p*-toluenesulfonic acid (*p*-TsOH) as catalyst afforded the 3,4-O-protected derivative regioselectively; azide reduction according to the method used by Staudinger et al.[28] and N-acylation with cerotic acid (hexacosanic acid) in the presence of 2-ethoxy-1-ethoxycarbonyl-1,2-dihydroquinoline (EEDQ) as condensation agent produced the 1-O-unprotected ceramide **4** in high yield. The desired component **2A** (Table 1) was obtained by reaction with the bifunctional phosphitylation reagent cyanoethoxybis(diisopropylamino)phosphane in the presence of tetrazole as activator.



Scheme 3. Synthesis of **2A**.

For the synthesis of the α-glucosaminyl(1-4)inositol compound **2B**, the readily available trichloroacetimidate **5**[29] and the D-*myo*-inositol derivative **6**,[22] for which a high yield synthesis has been developed,[30] were employed as starting materials (Scheme 4). The 6-O-glycosylation of the acceptor **6** with the glycosyl donor **5** in diethyl ether at room temperature with trimethylsilyl trifluoromethanesulfonate (TMSOTf) as catalyst led exclusively to formation of the α-linked product **7** in high yield. Earlier unsatisfactory α-selectivities and/or yields in the synthesis of **7**[16–21, 24] were overcome by the judicious choice of protecting groups for the starting materials and by optimizing

Table 1. Selected physical data for compounds **2A**, **7**, **2B**, **13**, **14**, **2C**, **16**, **17**, **18**, **20**, and **1** [a].

2A: δ_H (250 MHz) = 0.82–0.87 (t, J = 6.3 Hz, 6H, 2 CH_3), 1.12–1.66 (m, 90H, 2 $CH(CH_3)_2$, $C(CH_3)_2$, 36 CH_2), 2.07–2.16 (m, 2H, CH_2–CO), 2.58–2.64 (t, J = 6.3 Hz, 2H, CH_2CN), 3.50–4.18 (m, 9H, CH_2CH_2CN, 2 × 1-H, 2-H, 3-H, 4-H, 2 × $CH(CH_3)_2$), 5.84–5.88 (d, J(2-H,NH) = 9.0 Hz, 1H, NH); δ_P (161.7 MHz) = 148.57, 148.67 (10:7)

7: δ_H (250 MHz) = 3.37 (dd, J = 3.6, 10.6 Hz, 2b-H), 4.93 (dd, J = 3.9 Hz, 1a-H), 5.38 (d, J = 3.6 Hz, 1b-H)

2B: δ_H (400 MHz) = 3.27 (dd, J = 3.7, 10.3 Hz, 2b-H), 4.51 (dd, J = 4.2, 6.6 Hz, 2a-H), 4.91 (dd, J = 2.9 Hz, 1a-H), 5.24 (d, J = 3.7 Hz, 1b-H)

13: δ_H (250 MHz) = 4.86 (d, J = 1.8 Hz, 1c-H), 4.95 (d, J = 1.7 Hz, 1d-H), 5.47 (dd, J = 1.9, 2.9 Hz, 2d-H)

14: δ_H (250 MHz) = 4.78 (d, J = 1.2 Hz, 1c-H), 4.86 (d, J < 1 Hz, 1d-H), 5.22 (d, J < 1 Hz, 1e-H), 5.53 (dd, J < 1 Hz, 2e-H)

2C: δ_H (250 MHz) = 4.85 (d, J < 1 Hz, 1d-H), 5.09 (d, J < 1 Hz, 1f-H), 5.37 (d, J < 1 Hz, 1e-H), 5.48 (dd, J = 2.9 Hz, 2c-H), 5.58 (dd, J < 1 Hz, 2f-H), 6.14 (d, J = 1.4 Hz, 1c-H), 8.63 (s, NH)

16: δ_H (250 MHz, $CDCl_3/CD_3OD/D_2O$ (9/7/1), $CHCl_3$ as internal standard (δ = 7.23)) = 2.86 (dd, J = 4.0, 9.2 Hz, 2b-H), 5.19 (d, J = 3.9 Hz, 1b-H); δ_P (161.7 MHz, $CDCl_3/CD_3OD/D_2O$ (9/7/1)) = 0.989; FAB-MS (matrix: glycerin/3-nitrobenzyl alcohol (1/1), positive-ion mode): m/z (%): 1100 (42) [M^+ + H], 678 (100), 422 (64)

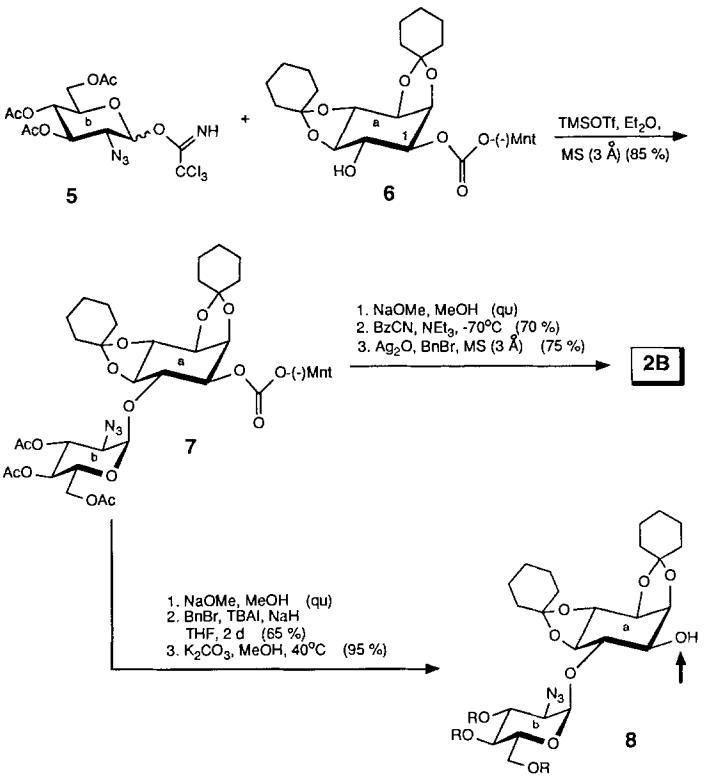
17: δ_H (400 MHz) = 4.58(s, 1d-H), 4.96 (s, 1a-H), 5.09 (s, 1f-H), 5.30 (d, J = 2.9 Hz, 1b-H), 5.36 (s, 1e-H), 5.41 (d, J < 1 Hz, 1c-H), 5.53 (br. s, 2c-H), 5.58 (br. s., 2f-H); δ_C (100.4 MHz) = 96.55 (J(C,H) = 177.30 Hz, C-1b), 99.22 (J(C,H) = 170.86 Hz, C-1d), 99.60 (J(C,H) = 175.69 Hz, C-1c), 100.12 (J(C,H) = 172.74 Hz, C-1f), 100.24 (J(C,H) = 169.51 Hz, C-1e)

18: δ_H (250 MHz) = 3.31 (dd, J = 3.5, 9.5 Hz, 2b-H), 4.92, 5.10, 5.21, 5.29 (alle br. s, 1c, d, e, f-H), 5.14 (dd, J = 3.6 Hz, 1a-H), 5.26 (d, J = 3.5 Hz, 1b-H)

20: δ_H (400 MHz, $CDCl_3/CD_3OD$ (3/1)) = 4.71, 4.93, 5.02, 5.13 (s, br. s, br. s, s, 1c, d, e, f-H), 5.48 (d, $J \approx 3$ Hz, 1b-H); δ_P (161.7 MHz, $CDCl_3/CD_3OD$ (3/1)) = −0.356, −3.895 (8:10). FAB-MS (matrix: 3-nitrobenzyl alcohol with NaI, negative-ion mode): m/z (%): 3664 (46) [M^{2-} + Na^+ + NaI], 3514 (100) [M^{2-} + Na^+], 1137 (90)

1: δ_H (250 MHz, [D_6]DMSO/D_2O (40/1), T = 60 °C) = 4.86, 4.91, 5.02, 5.16 (d, J < 1 Hz, s.s, d, J < 1 Hz, 1c, d, e, f-H), 5.42 (d, $J \approx 3$ Hz, 1b-H); δ_P (161.7 MHz, [D_6]DMSO/D_2O (40/1, T = 60 °C) = 0.788, 1.407 (84:100); FAB-MS (matrix: glycerin/3-nitrobenzyl alcohol (1/1), positive-ion mode): m/z: 1872 [M + H^+]; Negativ-Ionen-Modus: m/z: 1868 [M^{2-} + H^+]

[a] ^{1}H-, ^{13}C- and ^{31}P-NMR spectra in $CDCl_3$, unless otherwise indicated.



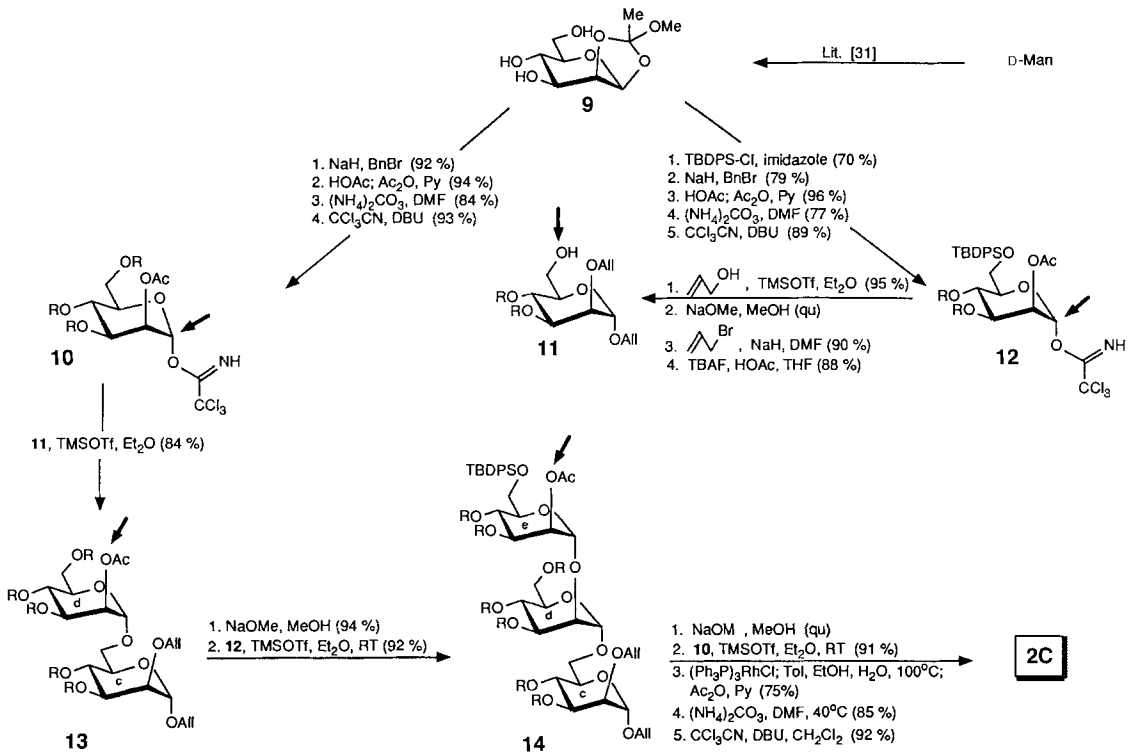
Scheme 4. Synthesis of **2B** and **8**. MS = molecular sieve, qu = quantitative, R = Ac, Mnt = menthyl.

reaction conditions. The 1a-O-unprotected compound **8** was obtained by selective cleavage of the acetyl protecting groups with NaOMe/MeOH, O-benzylation with NaH/benzyl bromide in the presence of tetra-*n*-butylammonium iodide (TBAI), and cleavage of the carbonate residue with K_2CO_3/MeOH at 40 °C. The synthesis of unit **2B** was performed by selective deacetylation of **7**. Regioselective 6b-O-benzoylation with benzoyl cyanide at −70 °C was then followed by regioselective 3b-O-benzylation with benzyl bromide in the presence of Ag_2O. The 4b-O-unprotected acceptor **2B** could thus be obtained directly from **7** in good overall yield without having to resort to complex manipulations of protecting groups. The structure of **2B** was confirmed by ^{1}H NMR data (Table 1).

The synthesis of tetramannose unit **2C** started from the orthoester **9** (Scheme 5), which is readily available from D-mannose.[31] The synthon **10** was obtained by the following reaction sequence: benzylation with benzyl bromide/NaH, opening of the orthoester with glacial acetic acid, acetylation, selective 1-O-deacetylation with ammonium carbonate in dimethylformamide (DMF), and conversion into the trichloroacetimidate with trichloroacetonitrile, in the presence of diazabicycloundecene (DBU) as base. The 2-O-acetyl group in **10** promotes α-selective glycosylations; the pattern of protecting groups in **10** also corresponds to that required for the monomer units d and f of **2C** (see Scheme 2). The e-monomer component **12** was obtained by regioselective 6-O-silylation of **9** with *tert*-butyldiphenylsilyl chloride (TBDPS-Cl) in the presence of imidazole, benzylation, opening of the orthoester, acetylation, selective 1-O-deacetylation, and conversion into the trichloroacetimidate. The c-monomer unit of the tetrasaccharide **2C** was also prepared from **12** in a straightforward reaction sequence: the allyl-α-glycoside was generated from **12** in almost quantitative yield by reaction with allyl alcohol under standard conditions; deblocking of the 2-O-acetyl group, 2-O-allylation with allyl bromide/NaH in DMF, and removal of the 6-O-silyl group with TBAF in glacial acetic acid/THF yielded the 6-O-unprotected derivative **11**.

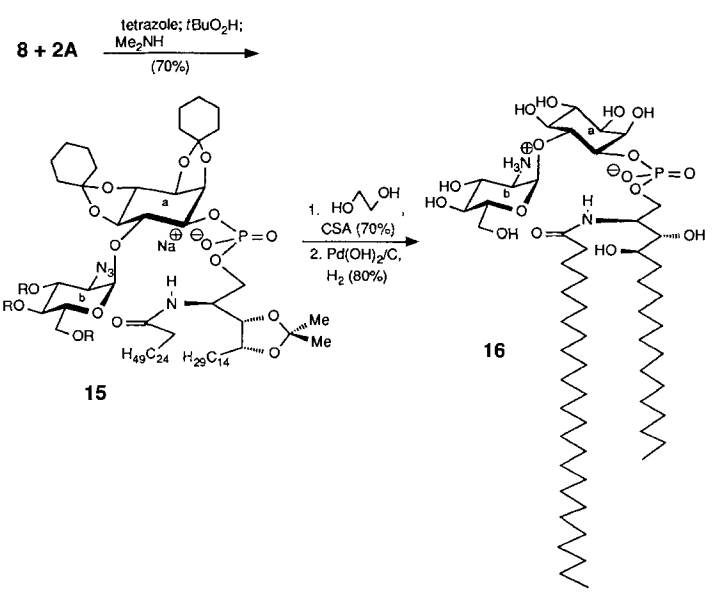
Reaction of the mannosyl donor **10** with acceptor **11** in diethyl ether at room temperature with TMSOTf as catalyst gave the α(1-6)-linked disaccharide **13** in good yield. Cleavage of the 2d-O-acetyl group with NaOMe/MeOH and glycosylation with the mannosyl donor **12** under the same conditions afforded the α(1-2)-α(1-6)-linked trisaccharide **14**, again in high yield. The desired α(1-2)-α(1-2)-α(1-6)-linked tetrasaccharide was obtained almost quantitatively by cleavage of the 2e-O-acetyl group and glycosylation with the mannosyl donor **10** under the conditions previously described. The 1c- and 2c-O-allyl groups were subsequently removed by treatment with the Wilkinson catalyst and hydrolysis, and the free hydroxyl groups were acetylated with acetic anhydride/pyridine. The building block **2C** was obtained by regioselective cleavage of the 1c-O-acetyl group and conversion to the trichloroacetimidate. Thus, starting from the mannose units **10**–**12**, **2C** was obtained α-specifically in high yield. The structure of **2C** was confirmed by its ^{1}H NMR spectrum (Table 1).

The N-benzyloxycarbonyl(Z)-protected aminoethylphosphite component **2D** was prepared according to published procedures.[24]



Scheme 5. Synthesis of **2C**. RT = room tempertaure, All = allyl, R = Ac.

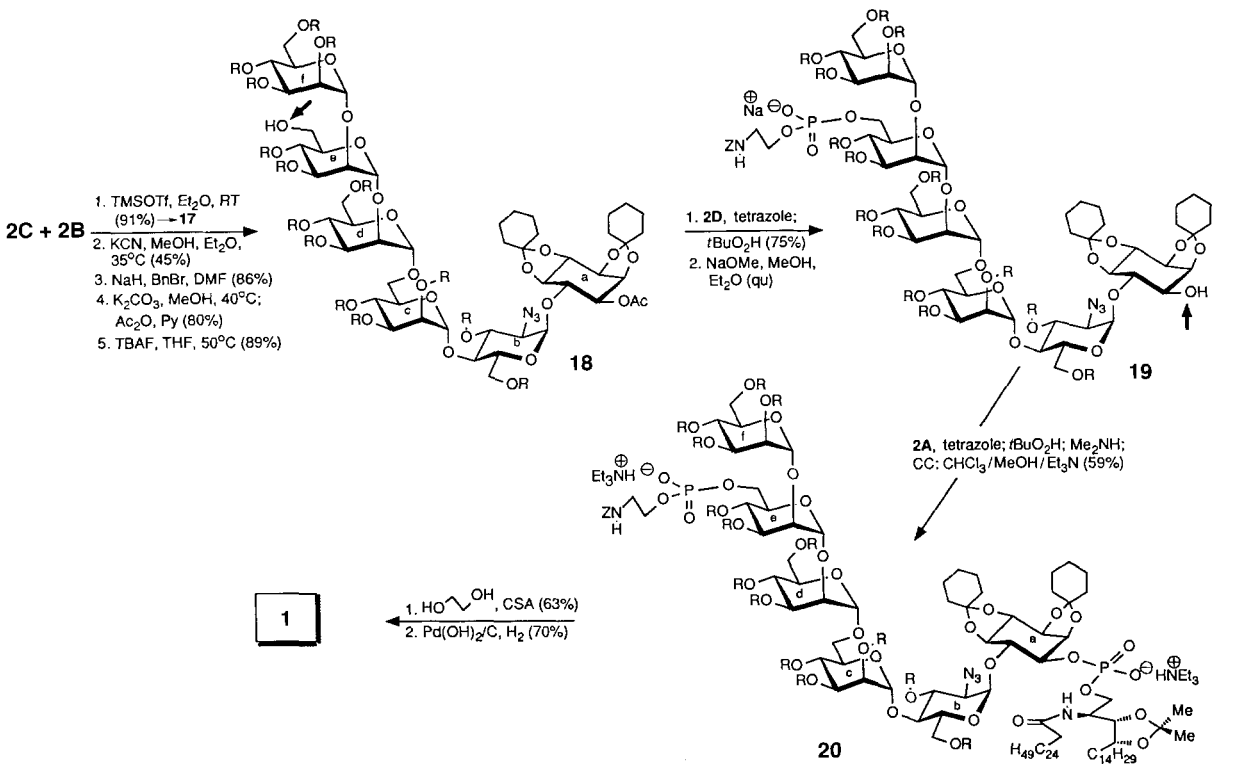
To test the overall synthetic strategy, in which the coupling of the **2DBC** moiety with the **2A** moiety was planned as the last step, component **8** was combined with the ceramide phosphite **2A** (Scheme 6). The required phosphite diester formation was achieved by activation with tetrazole; subsequent oxidation to the phosphate with *tert*-butylhydroperoxide and cleavage of the cyanoethyl group by treatment with dimethylamine afforded the ceramide-1-phosphate derivative **15** with 70% overall yield. Camphorsulfonic acid (CSA) catalyzed the cleavage of the O-cyclohexylidene and O-isopropylidene groups in the presence of glycol. The simultaneous hydrogenolysis of the benzyl and azide groups readily yielded the GPI derivative **16**, which was characterized by NMR and mass spectroscopy (Table 1).



Scheme 6. Coupling of **8** with **2A**. R = Ac.

Encouraged by this result, we started on the synthesis of **1** (Scheme 7). The glycosyl donor **2C** was first reacted with the acceptor **2B** in ether at room temperature, in the presence of TMSOTf as catalyst (→**17**); the (1-4) linkage between these two components was thus formed α-selectively in good yield. Formation of the α-linkage was corroborated by the C,H coupling constants (INEPT): $169.51 > J_{C,H} > 177.30$ Hz. All acyl groups were subsequently removed with KCN as base, and the free hydroxyl groups were benzylated with benzyl bromide and NaH. This step was followed by cleavage of the 1a-carbonate group and by acetylation of the 1a-OH group. Only then was the 6e-OH group deprotected with TBAF in THF to yield fragment **18**, which was used for the coupling with **2D**. By activation of **2D** with tetrazole and oxidation of the condensation product with *tert*-butylhydroperoxide, the Z-protected aminoethyl phosphate residue was introduced at the 6e-O position of **18** in 75% yield. Cleavage of the cyanoethyl group and the 1a-O-acetyl group gave component **19**, which was now converted into **1** as described for the synthesis of **16**. The coupling of **19** with **2A** was performed by activation with tetrazole, oxidation, and cleavage of the cyanoethyl group with dimethylamine. The product was purified by column chromatography (CC) with $CHCl_3$/MeOH/Et_3N (100/3/1). The bis(triethylammonium) salt was isolated, and the structure confirmed by NMR (^1H, ^{31}P) and MS data (Table 1). Simultaneous cleavage of the O-isopropylidene and O-cyclohexylidene groups with glycol in the presence of CSA as catalyst followed by hydrogenolysis of the Z-group, the O-benzyl protecting groups, and the azide group yielded the target GPI anchor **1** (10 mg), which was characterized by NMR and MS data (Table 1).

The ready accessibility of all starting materials, the high regio- and diastereoselectivities, and the high yields obtained in all reaction steps as well as the facile cleavage of the protecting



Scheme 7. Total synthesis of **1**. R = Ac.

groups form an excellent basis for further successful chemical syntheses in this field.

Received: June 28, 1994 [Z 7079 IE]
German version: *Angew. Chem.* **1994**, *106*, 2289

[1] M. A. J. Ferguson, A. F. Williams, *Annu. Rev. Biochem.* **1988**, *57*, 285–320; G. A. M. Cross, *Annu. Rev. Cell Biol.* **1990**, *6*, 1–39; R. Thomas, R. A. Dwek, T. W. Rademacher, *Biochemistry* **1990**, *29*, 5413–5422; M. C. Field, *Glycoconjugate J.* **1992**, *9*, 155–159; A. M. Tartakoff, N. Singh, *Trends Biochem. Sci.* **1992**, *17*, 470–473.

[2] M. A. J. Ferguson, K. Haldar, G. M. A. Cross, *J. Biol. Chem.* **1985**, *260*, 4963–4968.

[3] S. W. Homans, M. A. J. Ferguson, A. F. Williams, *Nature* **1988**, *333*, 269–272.

[4] P. Schneider, M. A. J. Ferguson, S. W. Homans, *J. Biol. Chem.* **1990**, *265*, 16955–16964.

[5] M. L. Günther, M. A. J. Ferguson, *J. Biol. Chem.* **1992**, *267*, 6820–6828.

[6] M. A. Deeg, D. R. Humphrey, S. M. Yang, *J. Biol. Chem.* **1992**, *267*, 18573–18580.

[7] M. A. J. Ferguson, *Curr. Opin. Struct. Biol.* **1991**, *1*, 522–529.

[8] M. A. J. Ferguson, G. A. M. Cross, *J. Biol. Chem.* **1985**, *260*, 14547–14555.

[9] M. C. Field, G. A. M. Cross, *J. Biol. Chem.* **1991**, *266*, 8392–8400.

[10] W. L. Roberts, T. L. Rosenberry, *J. Biol. Chem.* **1988**, *263*, 18776–18784.

[11] C. A. Luhrs, B. C. Slomiany, *J. Biol. Chem.* **1989**, *264*, 21446–21449.

[12] P. Butikofer, F. A. Knypers, C. Shackleton, *J. Biol. Chem.* **1990**, *265*, 18983–18987.

[13] A. Conzelmann, A. Puoti, R. L. Lester, C. Desponds, *EMBO J.* **1992**, *11*, 457–466; C. Fankhauser, S. W. Homans, J. E. Thomas-Oates, M. J. McConville, C. Desponds, A. Conzelmann, M. A. J. Ferguson, *J. Biol. Chem.* **1993**, *268*, 26365–26374.

[14] A ceramide anchor was also found in the *D. discoideum* contact-side A-protein: J. Stadler, G. Bauer, *EMBO J.* **1989**, *8*, 371–377.

[15] A. R. Saltiel, J. A. Fox, P. Sherline, P. Cuatrecasas, *Science* **1986**, *233*, 967–972; G. Romero, L. Luttrell, A. Rogol, K. Zeller, E. Hewlett, J. Larner, *ibid.* **1988**, *240*, 509–511; H.-N. Caro, M. Martin-Lomas, M. Bernabé, *Carbohydr. Res.* **1993**, *240*, 119–131.

[16] C. Murakata, T. Ogawa, *Carbohydr. Res.* **1992**, *234*, 75–91.

[17] D. R. Mootoo, P. Konradsson, B. Fraser-Reid, *J. Am. Chem. Soc.* **1989**, *111*, 8540–8542; U. E. Udodong, R. Madsen, C. Roberts, B. Fraser-Reid, *ibid.* **1993**, *115*, 7886–7887.

[18] R. Verduyn, C. J. J. Elie, C. E. Dreef, G. A. van der Marel, J. H. van Boom, *Recl. Trav. Chim. Pays-Bas* **1990**, *109*, 591–593.

[19] R. Plourde, M. d'Alarcao, A. R. Saltiel, *J. Org. Chem.* **1992**, *57*, 2606–2610.

[20] A. Zapata, M. Martin-Lomas, *Carbohydr. Res.* **1992**, *234*, 93–106.

[21] S. V. Ley, L. L. Young, *Synlett* **1992**, 997–998; G. J. Boons, P. Grice, R. Leslie, S. V. Ley, L. L. Young, *Tetrahedron Lett.* **1993**, *34*, 8523–8526.

[22] B. Kratzer, T. G. Mayer, R. R. Schmidt, *Tetrahedron Lett.* **1993**, *34*, 6881–6884.

[23] A. Y. Frantova, A. E. Stepanov, A. S. Bushnev, E. N. Zvonkova, V. I. Slwets, *Tetrahedron Lett.* **1992**, *33*, 3539–3542.

[24] C. Murakata, T. Ogawa, *Carbohydr. Res.* **1992**, *235*, 95–114.

[25] R. R. Schmidt, *Angew. Chem.* **1986**, *98*, 213–236; *Angew. Chem. Int. Ed. Engl.* **1986**, *25*, 212–235; R. R. Schmidt, W. Kinzy, *Adv. Carbohydr. Chem. Biochem.* **1994**, *50*, in press.

[26] W. Bannwarth, V. Trzeciak, *Helv. Chim. Acta* **1987**, *70*, 175–186, and references therein.

[27] R. R. Schmidt, T. Maier, *Carbohydr. Res.* **1988**, *174*, 169–179.

[28] H. Staudinger, J. Meyer, *Helv. Chim. Acta* **1919**, *2*, 635–646; H. Staudinger, E. Hauser, *ibid.* **1921**, *4*, 861–886.

[29] G. Grundler, R. R. Schmidt, *Lieibigs Ann. Chem.* **1984**, 1826–1847; R. U. Lemieux, R. M. Ratcliffe, DOS 2816340 (October 19, 1975); *Chem. Abstr.* **1979**, *90*, 87846k.

[30] The resolution of enantiomers was achieved by crystallization from petroleum ether (b.p. 65 °C).

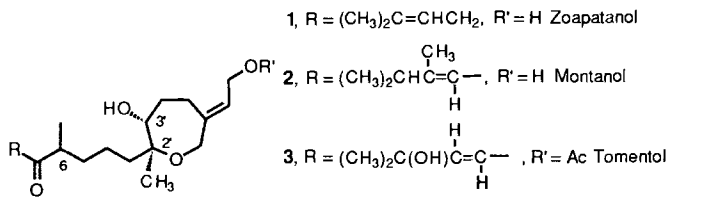
[31] T. G. Mayer, Diplomarbeit, Universität Konstanz, **1993**.

 © VCH Verlagsgesellschaft mbH, D-69451 Weinheim, 1994 0570-0833/94/2121-2181 $ 10.00+.25/0

A Total Synthesis of (+)-2′*S*, 3′*R*-Zoapatanol**

Barry M. Trost,* Paul D. Greenspan, Holger Geissler, Jung H. Kim, and Nicholas Greeves

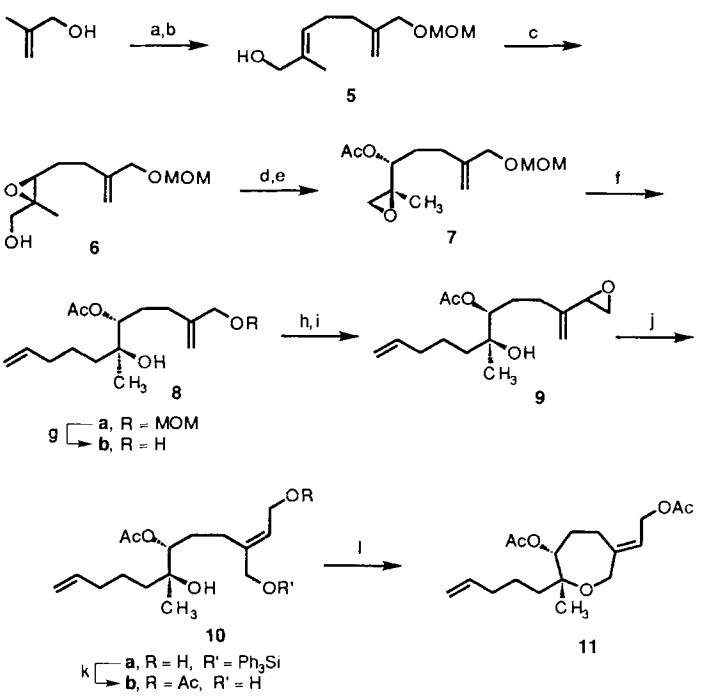
Extraction of the leaves of the Mexican zoapatle plant *Montanoa tomentosa*, which have been used as a contraceptive in folk medicine, led to isolation of a series of oxepanes **1**–**4**.[1] The



extraordinary biological activity that prompted recent speculations on the contribution of further metabolites to this activity[2] and the unusual structural motif of these diterpenoids stimulated a number of total syntheses,[3] none of which have culminated in an asymmetric synthesis. In addition to the stereocontrolled synthesis of the oxepane core, the correct introduction of the exocyclic double bond represents a significant challenge. We wish to report the first asymmetric synthesis of zoapatanol, which addresses both of these stereochemical issues.

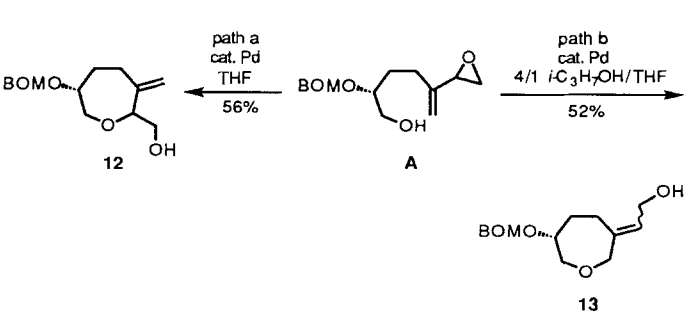
The asymmetric synthesis of the oxepane core depends upon Sharpless epoxidation[4] of the allyl alcohol **5**, which is readily available from the dianion of methallyl alcohol as shown in Scheme 1.[5] Use of L-(+)-diethyl tartrate (DET) as chiral ligand at −40° for 12–24 h gave the epoxide **6** in 90% yield and greater than 95% *ee* (typically 96–98% *ee*) as determined by NMR spectroscopy of the Mosher esters.[6] Attempts to introduce a side chain in **6** through alkylation by Payne rearrangement[7] failed. However, a sequential protocol initiated by a titanium-promoted regioselective opening of the epoxide[8] with acetate as the nucleophile, which sets the two key stereocenters of the subsequent oxepane in 2′*S*,3′*R* configuration, followed by conversion of the diol into the epoxide **7**, successfully primed the system for introduction of the side chain.

Several attempts to bring in a side chain bearing the carbonyl group in various protected forms using cuprate chemistry gave no opening of the epoxide **7** in spite of the excellent reactivity of this epoxide towards an *n*-butylcuprate reagent. Seizing upon this dramatic difference, we examined a cuprate bearing an olefin as a carbonyl surrogate (convertible to a carbonyl function by Wacker oxidation).[9] Not surprisingly, the cuprate from 3-butenylmagnesium bromide reacted well to give the tertiary alcohol **8a**. The corresponding diol **8b**, obtained by acid hydrolysis, underwent a straightforward conversion to the requisite epoxide **9**.



Scheme 1. Synthesis of the oxepane core. a) 2.2 equiv *n*-C_4H_9Li, tetramethylethylenediamine (TMEDA), ether, $(CH_3)_2C{=}CHCH_2Br$, then methoxymethyl chloride (MOM-Cl), $(i\text{-}C_3H_7)_2NC_2H_5$, CH_2Cl_2, 92%. b) 4 mol% SeO_2, *t*-C_4H_9OOH, 10 mol% salicylic acid, CH_2Cl_2, room temperature (RT), 53%. c) *t*-C_4H_9OOH, 6 mol% L-(+)-DET, 5 mol% $Ti(OC_3H_7\text{-}i)_4$, 4 Å molecular sieve, CH_2Cl_2, −40 °C, 90%. d) HOAc, $Ti(OC_3H_7\text{-}i)_4$, CH_2Cl_2, −10 °C, then TsCl, 4-dimethylaminopyridine (DMAP), CH_2Cl_2, 0 °C, 95%. e) Amberlite IRA-400 (OH) resin, THF, 78%. f) $H_2C{=}CHCH_2CH_2MgBr$, CuI, THF, −40 °C, 91%. g) 6N HCl, CH_3OH, 50 °C, 62%. h) Dess-Martin periodinane, CH_2Cl_2, 0 °C, 84%. i) $(CH_3)_3S^+ {}^-O_3SCH_3$, NaOH, H_2O, CH_2Cl_2, RT, 85%. j) 2.5 mol% $[(dba)_3Pd_2]\cdot CHCl_3$ (dba = dibenzylidene acetone), 25 mol% $(i\text{-}C_3H_7O)_3P$, Ph_3SiOH, THF, RT, 67%. k) Ac_2O, DMAP, CH_2Cl_2, RT then CH_3CN, H_2O, KF, 70 °C, 79%. l) $(CF_3SO_2)_2O$, 2,6-lutidine, CH_2Cl_2, 74%.

Cyclization of vinyl epoxide **9** was envisioned to create the proper olefin geometry, since palladium has a bias to ionize such systems preferentially to the *syn* π-allylpalladium complex. Studies on the model compound **A** revealed an interesting dichotomy in terms of regioselectivity [Eq. (1)]. Palladium-catalyzed cyclization of **A** in THF led exclusively to **12** by proximal attack of the hydroxy nucleophile, presumably as a result of hydrogen bonding between the hydroxyl group of the nucleophile and the departing oxygen of the epoxide.[10] Interrupting such hydrogen bonding by employing an exogeneous alcohol as solvent indeed appears to reorient the reaction partners to give the desired product **13**, formed by distal attack, as the major regioisomer, in a 3:1 mixture of (*E*/*Z*) isomers. No attempt was made to optimize olefin geometry in this model. However, all attempts to effect either palladium-catalyzed, or any acid-



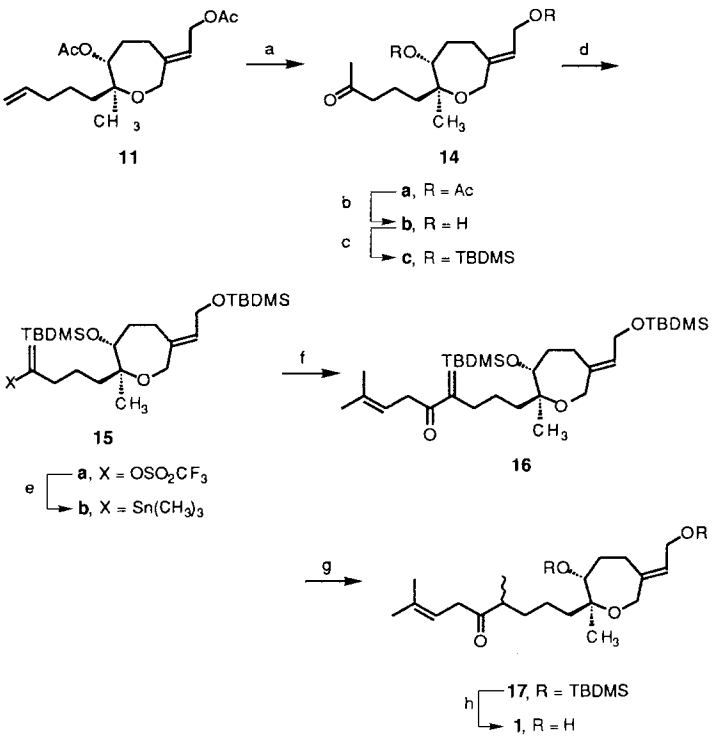
[*] Prof. Dr. B. M. Trost, Dr. P. D. Greenspan, Dr. H. Geissler, Dr. J. H. Kim, Dr. N. Greeves
Department of Chemistry, Stanford University
Stanford, CA 94305-5080 (USA)
Telefax: Int. code + (415)725-0259

[**] This research was supported by fellowships for P. D. G. (NIH), H. G. (Humboldt-Stiftung), J. H. K. (Pfizer), and N. G. (Harkness Foundation). We thank the General Medical Sciences Institute of the National Institutes of Health (NIH) for generous financial aid and especially Dr. Stefan Scheiblich who performed some of our early studies. The mass spectra were recorded at the Mass Spectrometry Facility of the University of California at San Francisco, which is sponsored by the Division of Research Resources.

(including Lewis acid) or base-catalyzed cyclization of **9** to an oxepane failed, presumably as a result of the diminished nucleophilicity of a tertiary alcohol.

Intermolecular reactions with common oxygen nucleophiles and palladium catalysis also failed to give satisfactory selectivity for the S_N2' type attack. However, exposing a 1.4:1 mixture of triphenylsilanol and epoxide **9** to 2.5 mol% of $[(dba)_3Pd_2]\cdot CHCl_3$ in THF at ambient temperature gave the distal product **10a**, exclusively in the ***E*** configuration as desired.[11] On differentiation of the two primary hydroxy groups as in **10b**, this compound was converted into the triflate,[12] which spontaneously cyclized under the reaction conditions to **11**.

After the absolute and relative stereochemistry of the core had been established, elaboration of the side chain was required to complete the synthesis. As outlined in Scheme 2, Wacker oxidation proceeded well to generate the methyl ketone **14a**. At this point, exchange of the protecting groups from acetyl to *tert*-butyldimethylsilyl was performed to minimize problems of chemoselectivity. Many attempts to achieve carbonylative cross-coupling[13, 14] at low CO pressures with the vinyl triflate **15a** (formed with 2-bis(trifluorosulfonyl)amino-5-chloropyridine[15]) and a prenylstannane failed, as did similar attempts at the electronic inverse, namely, with vinylstannane (**15b**)[16] and prenyl halide. However, on increasing the CO pressure to 34 atm and adding molecular sieves to reduce protodestannylation, prenyl chloride underwent carbonylative alkylation of the vinylstannane **15b** to give a 76% yield at 80% conversion (based on recovered starting material) of the bis(silyl ether) of (+)-dehydrozoapatanol (**16**). Chemoselective conjugate reduction occurred smoothly with the Stryker reagent[17] to give (+)-zoapatanol, after desilylation[18] of **17**. The spectroscopic properties were identical to those recorded for the natural product.



Scheme 2. Introduction of the side chain. a) LiCl, $PdCl_2$, CuCl, dimethylformamide (DMF), H_2O, O_2, RT, 90%. b) K_2CO_3, CH_3OH, H_2O, 93%. c) *tert*-Butyldimethylsilyl chloride (TBDMS-Cl), imidazole, DMF, 55 °C, 85%. d) Potassium bis(trimethylsilyl)amide, 2-N(SO_2CF_3)$_2$-5-ClC_5H_3N), THF, −78 °C, 82%. e) $[(CH_3)_3Sn]_2$, 3% $[(Ph_3P)_4Pd]$, LiCl, THF, 60 °C, 82%. f) $(CH_3)_2C=CHCH_2Cl$, 34 atm CO, 10% $[(dba)_3Pd_2]\cdot CHCl_3$, 20 mol% Ph_3P, 3 Å molecular sieve, PhH, 60 °C, 76%. g) $[Ph_3PCuH]_6$, H_2O, PhH, 94%. h) HF, H_2O, CH_3CN, RT, 90%.

Besides providing the first asymmetric synthesis of this biologically fascinating system, there are several noteworthy features of this synthesis. The strategy employs three palladium-catalyzed processes: allylic alkylation, Wacker oxidation, and carbonylative cross-coupling. The regio- and diastereoselectivity of the allylic alkylation is particularly interesting. Whereas a role for the nucleophile in controlling regioselectivity is anticipated, its influence on olefin geometry is not. The fact that only the *E* product **10a** is obtained, in contrast to what happens with other oxygen nucleophiles in this systems,[19] suggests that the silanol may coordinate with the epoxide oxygen to help promote formation of the sterically and thermodynamically preferred *syn* complex. The use of the carbonylative cross-coupling at a late stage of the synthesis provides an opportunity to diverge

Table 1. Spectroscopic characterization of selected intermediates.

6: IR($CDCl_3$): $\tilde{\nu}$ = 3601, 1150, 1103, 1053 cm^{-1}; ^1H NMR ($CDCl_3$, 400 MHz): δ = 5.09 (s, 1H), 4.97 (s, 1H), 4.64 (s, 2H), 4.02 (s, 2H), 3.67 (dd, J = 12.2, 4.2, 1H), 3.57 (dd, J = 12.2, 8.6, 1H), 3.38 (s, 3H), 3.06 (t, J = 6.2 Hz, 1H), 2.15–2.32 (m, 2H), 1.75 (q, J = 7.6 Hz, 2H), 1.72–1.85 (m, 1H), 1.29 (s, 3H); ^{13}C NMR ($CDCl_3$, 100 MHz): δ = 144.6, 112.4, 95.6, 70.0, 65.3, 60.9, 59.7, 55.3, 29.9, 26.4, 14.2; $[\alpha]_D^{25}$ −18.7 (c = 1.27, $CHCl_3$).

8a: IR($CDCl_3$): $\tilde{\nu}$ = 3605, 1731, 1373, 1242, 1150, 1105, 1049 cm^{-1}; ^1H NMR ($CDCl_3$, 400 MHz): δ = 5.78 (ddt, J = 17.0, 10.3, 6.7 Hz, 1H), 5.06 (s, 1H), 5.00 (dd, J = 17.1, 1.8 Hz, 1H), 4.97 (dd, J = 10.0, 2.1 Hz, 1H), 4.91 (s, 1H), 4.86 (dd, J = 9.9, 3.0 Hz, 1H), 4.62 (s, 2H), 3.98 (s, 2H), 3.37 (s, 3H), 2.10 (s, 3H), 1.98–2.10 (m, 4H), 1.70–1.87 (m, 3H), 1.36–1.67 (m, 4H), 1.15 (s, 3H); ^{13}C NMR ($CDCl_3$, 100 MHz): δ = 171.0, 144.8, 138.4, 114.8, 112.1, 95.5, 78.9, 74.0, 70.0, 55.3, 37.1, 34.1, 29.7, 27.0, 23.7, 22.5, 21.0; $[\alpha]_D^{25}$ + 6.5° (c = 1.65, $CDCl_3$)

10b: IR($CDCl_3$): $\tilde{\nu}$ = 3608, 1731, 1374, 1242, 1026 cm^{-1}; ^1H NMR ($CDCl_3$, 400 MHz): δ = 5.79 (ddt, J = 17.0, 6.7 Hz, 1H), 5.41 (t, J = 7.4 Hz, 1H), 5.01 (dq, J = 17.1, 1.7 Hz, 1H), 4.96 (d, J = 9.4 Hz, 1H), 4.84 (dd, J = 10.2, 7.8 Hz, 1H), 4.67 (ABX, $\Delta\nu$ = 27.6 Hz, J = 12.4, 7.5 Hz, 2H), 4.14–4.22 (m, 2H), 2.45–2.52 (m, 1H), 2.10 (s, 3H), 2.06 (s, 3H), 2.02–2.25 (m, 2 H), 1.60–1.91 (m, 4H), 1.38–1.54 (m, 4H), 1.15 (s, 3H); ^{13}C NMR ($CDCl_3$, 100 MHz): δ = 171.5, 171.1, 143.9, 138.5, 122.0, 114.8, 78.5, 74.0, 60.7, 60.0, 37.3, 34.1, 32.0, 27.1, 23.3 (2), 22.4, 21.1

11: IR($CDCl_3$): $\tilde{\nu}$ = 1731, 1602, 1374, 1252, 1240, 1027 cm^{-1}; ^1H NMR ($CDCl_3$, 400 MHz): δ = 5.80 (ddt, J = 17.0, 10.3, 6.7 Hz, 1H), 5.38 (t, J = 7.0 Hz, 1H), 5.00 (dq, J = 17.3, 1.8 Hz, 1H), 4.95 (dd, J = 10.3, 1.0 Hz, 1H), 4.75 (dd, J = 9.6, 3.9 Hz, 1H), 4.50 (ABX, $\Delta\nu$ = 18.4 Hz, J = 12.8, 7.2 Hz, 2H), 4.31 (AB, $\Delta\nu$ = 51.7 Hz, J = 16.4 Hz, 2H), 2.26–2.36 (m, 2H), 2.06 (s, 3H), 2.05 (s, 3H), 1.98–2.11 (m, 2H), 1.87–1.96 (m, 1H), 1.60–1.70 (m, 1H), 1.40–1.51 (m, 4H), 1.16 (s, 3H); ^{13}C NMR ($CDCl_3$, 75 MHz): δ = 171.2, 170.6, 146.9, 138.9, 117.7, 114.8, 79.0, 77.2, 62.8, 59.8, 38.2, 33.9, 30.7, 29.4, 22.1, 21.1, 20.7, 17.2

14b: IR(neat): $\tilde{\nu}$ = 3445, 1708, 1438, 1375, 1364, 1100, 1058 cm^{-1}; ^1H NMR ($CDCl_3$, 300 MHz): δ 5.44 (t, J = 6.9 Hz, 1H), 4.35 (d, J = 17.4 Hz, 1H), 4.28 (d, J = 17.4 Hz, 1H), 4.15 (dd, J = 12.9, 7.2 Hz, 1H), 4.05 (dd, J = 12.9, 6.4 Hz, 1H), 3.55 (m, 1H), 2.45–2.50 (m, 2H), 2.19–2.39 (m, 2H), 2.15 (s, 3H), 2.05 (b, 1H), 1.47–1.90 (m, 7H), 1.17 (s, 3H); ^{13}C NMR ($CDCl_3$, 75 MHz): δ = 209.7, 143.6, 122.8, 80.0, 75.7, 63.0, 57.8, 43.7, 37.6, 32.9, 30.7, 29.9, 17.4, 17.3; $[\alpha]_D^{25}$ +10.6° (c = 1.26, CH_2Cl_2)

16: IR(neat): $\tilde{\nu}$ = 1683, 1473, 1463, 1384, 1379, 1361, 1257, 1111, 1078 cm^{-1}; ^1H NMR ($CDCl_3$, 300 MHz): δ = 5.97 (s, 1H), 5.72 (s, 1H), 5.24–5.30 (m, 2H), 4.24 (d, J = 15.9 Hz, 1H), 3.98–4.12 (m, 3H), 3.40–3.50 (m, 1H), 3.37 (d, J = 6.9 Hz, 2H), 2.15–2.25 (m, 4H), 1.72–1.83 (m, 1H), 1.72 (s, 3H), 1.61 (s, 3H), 1.29–1.61 (m, 5H), 1.03 (s, 3H), 0.87 (s, 9H), 0.83 (s, 9H), 0.03 (s, 6H), 0.01 (s, 3H), 0.00 (s, 3H); ^{13}C NMR ($CDCl_3$, 75 MHz): δ = 200.3, 148.7, 142.6, 134.8, 123.8, 122.8, 116.8, 80.6, 77.7, 63.0, 59.0, 39.9, 37.8, 33.7, 31.4, 31.1, 26.0 (3), 25.8 (3), 25.7, 21.7, 18.4, 18.1, 17.9, 15.1, −3.9, −4.8, −5.2 (2); $[\alpha]_D^{20}$ + 9.6° (c = 1.42, $CHCl_3$)

1: IR(neat): $\tilde{\nu}$ = 3332–3483, 1707, 1459, 1453, 1439, 1102, 1059, 1031 cm^{-1}; ^1H NMR ($CDCl_3$, 300 MHz): δ = 5.40–5.48 (m, 1H), 5.26–5.34 (m, 1H), 4.26 (s, 2H), 4.07–4.15 (m, 2H), 3.51 (dt, J = 7.7, 3.7 Hz, 1H), 3.15 (d, J = 7.1 Hz, 2H), 2.55–2.63 (m, 1H), 2.19–2.39 (m, 2H), 1.77–1.89 (m, 1H), 1.76 (s, 3H), 1.65–1.75 (m, 2H), 1.64 (s, 3H), 1.51–1.63 (m, 2H), 1.24–1.44 (m, 5H), 1.15 (s) and 1.14 (s) (total 3H), 1.089 (d, J = 8.0 Hz) and 1.088 (d, J = 7.0 Hz) (total 3H); ^{13}C NMR ($CDCl_3$, 100 MHz): δ = 213.3, 144.5/144.4, 135.5, 122.8/122.7, 116.0, 80.1, 76.0/75.8, 63.3/63.2, 58.3/58.2, 45.9, 41.1/41.0, 38.1/37.8, 33.5/33.4, 33.2/33.1, 30.6/30.4, 25.8, 21.3/21.1, 18.6, 18.1/17.9, 16.9/16.7; $[\alpha]_D^{20}$ +12.0 ± 1.2° (c = 0.31, $CHCl_3$)

into other members of the class. Finally, dehydrozoapatanol **16** enables selective modification at an important site of the molecule.

Received: May 26, 1994 [Z 6969 IE]
German version: *Angew. Chem.* **1994**, *106*, 2296

[1] S. D. Levine, R. E. Adams, R. Chen, M. L. Cotter, A. F. Hirsch, V. V. Kane, R. M. Kanojia, C. Shaw, M. P. Wachter, E. Chin, R. Huettemann, P. Ostrowski, J. L. Mateos, L. Noriega, A. Guzmán, A. Mijarez, L. Tovar, *J. Am. Chem. Soc.* **1979**, *101*, 3404; R. M. Kanojia, M. P. Wachter, S. D. Levine, R. E. Adams, R. Chen, E. Chin, M. L. Cotter, A. F. Hirsch, R. Heuttemann, V. V. Kane, P. Ostrowski, C. J. Shaw, J. L. Mateos, L. Noriega, A. Guzmán, A. Mijarez, L. Tovar, E. Shefter, *J. Org. Chem.* **1982**, *47*, 1310; F. C. Seaman, A. J. Malsom, N. K. Fischer, *Phytochemistry* **1984**, *23*, 464; L. Quijano, J. S. Calderon, G. F. Gomez, M. V. Rosario, T. Rios, *ibid* **1985**, *24*, 2337; Y. Oshima, G. A. Cordell, H. S. Fong, *ibid.* **1986**, *25*, 2567.

[2] G. B. Marcelle, N. Bunyapraphatsara, G. A. Cordell, H. S. Fong, K. C. Nicolaou, R. E. Zipkin, *J. Nat. Prod.* **1985**, *48*, 739; R. M. Kanojia, E. Chin, C. Smith, R. Chen, D. Rowand, S. D. Levine, M. P. Wachter, R. E. Adams, D. W. Hahn, *J. Med. Chem.* **1985**, *28*, 796.

[3] K. C. Nicolaou, D. A. Claremon, W. E. Barnette, *J. Am. Chem. Soc.* **1980**, *102*, 6611; R. Chen, D. S. Rowand, *ibid.* **1980**, *102*, 6609; V. V. Kane, D. L. Doyle, *Tetrahedron Lett.* **1981**, *22*, 3031; R. C. Cookson, N. J. Liverton, *J. Chem. Soc. Perkin Trans. 1* **1985**, 1589; P. Kocienski, C. Love, R. Whitby, *Tetrahedron Lett.* **1988**, *29*, 2867. For an attempt at an asymmetric total synthesis that appeared after completion of this work, see G. Pain, D. Desmaële, J. d'Angelo, *Tetrahedron Lett.* **1994**, *35*, 3085.

[4] Y. Gao, R. M. Hanson, J. M. Klunder, S. Y. Ko, H. Masamune, K. B. Sharpless, *J. Am. Chem. Soc.* **1987**, *109*, 5765.

[5] B. M. Trost, D. M. T. Chan, T. N. Nanninga, *Org. Synth.* **1984**, *62*, 58. Availability of 10 M n-C_4H_9Li makes concentration the more dilute solutions normally used unnecessary.

[6] J. A. Dale, H. S. Mosher, *J. Am. Chem. Soc.* **1973**, *95*, 512.

[7] G. B. Payne, *J. Org. Chem.* **1962**, *27*, 3819.

[8] M. Caron, K. B. Sharpless, *J. Org. Chem.* **1985**, *50*, 1557.

[9] J. Tsuji in *Comprehensive Organic Synthesis* (Eds.: B. M. Trost, I. Fleming, S. V. Ley), Pergamon, Oxford, **1991**, pp. 449–468.

[10] See B. M. Trost, A. Tenaglia, *Tetrahedron Lett.* **1988**, *29*, 2931.

[11] B. M. Trost, N. Ito, P. D. Greenspan, *Tetrahedron Lett.* **1993**, *34*, 1421.

[12] P. J. Stang, M. Hanack, L. R. Subramanian, *Synthesis* **1982**, 85.

[13] F. K. Sheffy, J. P. Godschalx, J. K. Stille, *J. Am. Chem. Soc.* **1984**, *106*, 4833; S. Katsumura, S. Fujiwara, S. Isoe, *Tetrahedron Lett.* **1988**, *29*, 1173; see also J. H. Merrifield, J. P. Godschalx, J. K. Stille, *Organometallics* **1984**, *3*, 1108.

[14] Review: J. K. Stille, *Angew. Chem.* **1986**, *98*, 504; *Angew. Chem. Int. Ed. Engl.* **1986**, *25*, 508.

[15] D. L. Comins, A. Dehghani, *Tetrahedron Lett.* **1992**, *33*, 6299.

[16] W. D. Wulff, G. A. Peterson, W. E. Bauta, K.-S. Chan, K. L. Faron, S. R. Gilbertson, R. W. Kaesler, D. C. Yang, C. K. Murray, *J. Org. Chem.* **1986**, *51*, 277.

[17] W. S. Mahoney, D. M. Brestensky, J. M. Stryker, *J. Am. Chem. Soc.* **1988**, *110*, 291.

[18] As in all previous syntheses, zoapatanol is obtained as a mixture epimeric at C-6. The stereochemistry has not been rigorously established for the natural product. The diastereomers were inseparable. At 300 MHz, the ^{1}H NMR spectrum shows evidence for the presence of two diastereomers in the doubling of the signals for the protons of the C-2 and C-6 methyl groups. According to the NMR spectrum the diastereomeric ratio is 1:1.

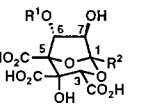
[19] Carboxylic acids reacted as nucleophiles, but were only moderately regioselective; the *E*/*Z* ratio was approximately 4.5:1.

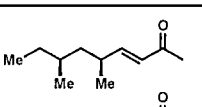
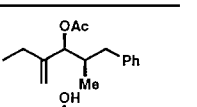
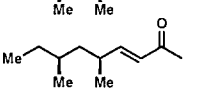
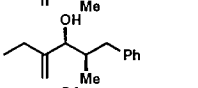
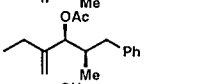
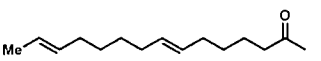
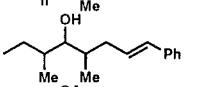
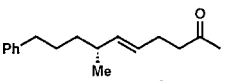
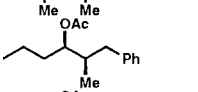
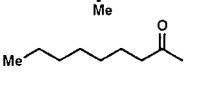
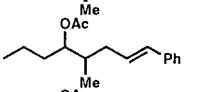
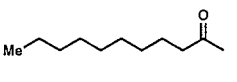
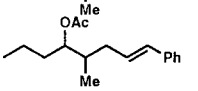
Zaragozic Acid A/Squalestatin S1: Synthetic and Retrosynthetic Studies**

Kyriacos C. Nicolaou,* Eddy W. Yue, Yoshimitsu Naniwa, Francesco De Riccardis, Alan Nadin, James E. Leresche, Susan La Greca, and Zhen Yang

In 1992, researchers at Glaxo[1] and Merck[2] independently reported the isolation and characterization of a family of structurally related natural products, which they respectively named the squalestatins and the zaragozic acids. The three squalestatins (S1, S2, and H1, **1a–c**, Table 1) and five zaragozic acids (A, B, C, D, and D_2, **1a**, **2a–d**, Table 1)[3,4] isolated so far have been shown to be potent and selective inhibitors of mammalian and fungal squalene synthase both in vivo and in vitro.[5] Consequently, they may act as therapeutically useful serum cholesterol-lowering agents, and a number of analogs have been prepared for structure–activity relationship studies.[6,7] Zaragozic acid A/squalestatin S1 also displays activity against a wide spectrum of important yeast and fungal pathogens,[1a] and is a potent inhibitor of *ras*-farnesyltransferase.[8] It has recently

Table 1. The squalestatins S1, S2, and H1 (**1a–1c**) and the zaragozic acids A–D_2 (**1a**, **2a–d**).



Compound	R^1	R^2
zaragozic acid A/squalestatin S1 **1a**		
squalestatin S2 **1b**		
squalestatin H1 **1c**	H	
zaragozic acid B **2a**		
zaragozic acid C **2b**		
zaragozic acid D **2c**		
zaragozic acid D_2 **2d**		

[*] Prof. K. C. Nicolaou, E. W. Yue, Y. Naniwa, F. De Riccardis, A. Nadin, J. E. Leresche, S. La Greca, Z. Yang
Department of Chemistry, The Scripps Research Institute
10666 North Torrey Pines Road, La Jolla, CA 92037
and
Department of Chemistry and Biochemistry, University of California
San Diego, 9500 Gilman Drive, La Jolla, CA 92093 (USA)
Telefax: Int. code + (619)554-6738

[**] We thank Dr. Kenneth E. Wilson (Merck & Co. Inc., Rahway) for a generous gift of zaragozic acid A. The work was financially supported by the National Institutes of Health, fellowships from Glaxo (E. W. Y.), Teijin Corporation, Japan (Y. N.), the Swiss National Science Foundation (J. E. L.), and by a grant from Merck, Sharp and Dohme. We thank Drs. Dee H. Huang and Gary Siuzdak of The Scripps Research Institute for NMR and mass spectroscopic assistance, respectively.

 © VCH Verlagsgesellschaft mbH, D-69451 Weinheim, 1994 0570-0833/94/2121-2184 $ 10.00+.25/0

been demonstrated that zaragozic acid A/squalestatin S1 has a moderately high affinity for Ca^{2+} ions, a property speculated to be the cause of its observed biological activity.[9] As a prelude to a total synthesis of zaragozic acid A/squalestatin S1, its minor congeners, and designed synthetic analogs, we initiated preliminary retrosynthetic and synthetic studies in this area.

Our strategy is shown in Figure 1. Disconnection of the C_6 ester side chain (step 1), unraveling of the C1 acetal (step 2) and cleavage of the C1–C7 bond (step 3) led to aldehyde **5**[10] and acyl anion equivalent **6**. In principle, this approach would enable the synthesis of all the zaragozic acids/squalestatins from a single key intermediate. In order to define clearly the protecting groups and the final synthetic stages, we targeted **3** as a specific late stage key intermediate and embarked on degradative studies on the natural product.

The degradation and reassembly of zaragozic acid A (**1a**) is outlined in Scheme 1.[11] Zaragozic acid A tribenzyl ester **7** was formed in almost quantitative yield by refluxing the natural product with a slight excess of *N,N*-dicyclohexyl-*O*-benzylisourea[12] in toluene. Deacetylation using the Merck[2b] conditions (3% HCl/MeOH) provided the triol **8** in good yield (51% plus 37% recovered starting material). Longer reaction times led to significant methanolysis of the C3 benzyl ester. The allylic alcohol **8** was selectively protected to give the *para*-methoxybenzyl (PMB) ether **9** (68% plus 26% recovered starting material). Hydrolysis of the α,β-unsaturated ester followed

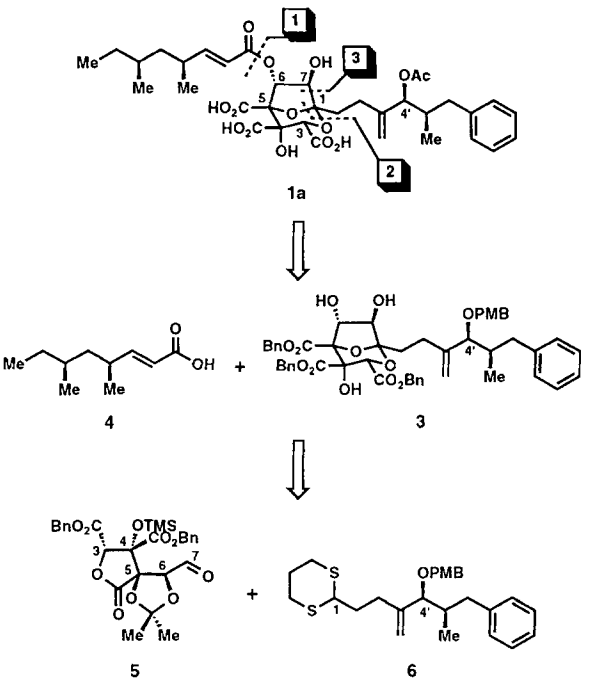
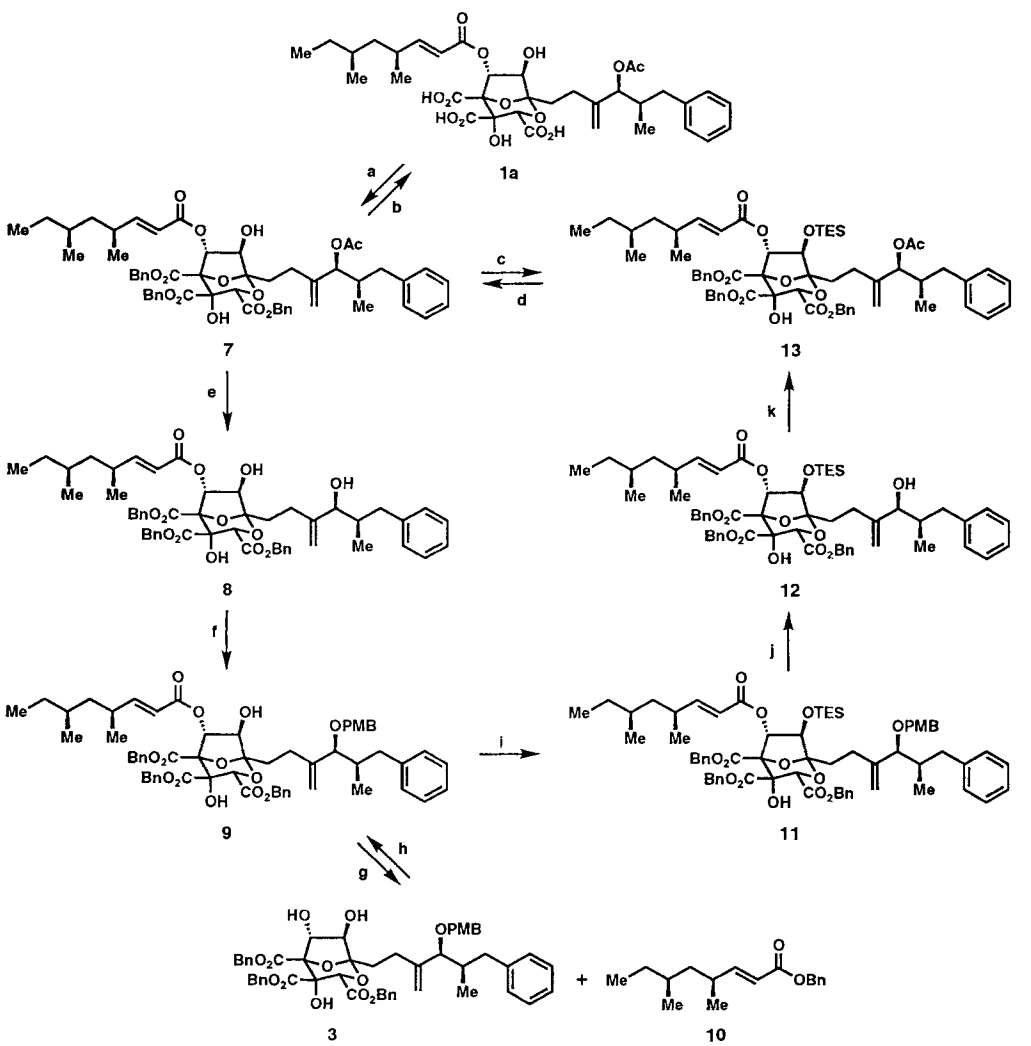


Fig. 1. Retrosynthetic analysis of zaragozic acid A/squalestatin S1 (**1a**).



Scheme 1. Retrosynthetic and synthetic studies with **1a**. a) *N,N'*-dicyclohexyl-*O*-benzylisourea (4.2 equiv), toluene, reflux, 2 h, 99%; b) 10% Pd/C (1.0 wt.equiv), 1,4-cyclohexadiene, 1,4-dioxane, 110 °C, 2 h, >70% crude, 50% after HPLC (reverse phase C18, MeOH/0.1% aqueous AcOH (4/1), flow rate 9 mL min^{-1}, retention time 13.8 min); c) TESOTf (1.1 equiv), pyridine (1.5 equiv), CH_2Cl_2, 22 °C, 10 min, 95%; d) TBAF (1.2 equiv), THF, 0 °C, 15 min, 85%; e) 3% HCl/MeOH, 0 °C, 1.5 h, 51% (plus 37% **7**); f) $Cl_3CC(OPMB)=NH$ (2.0 equiv), CSA (0.1 equiv), 22 °C, 3 h, 68% (plus 26% **8**), g) 1. LiOH (10 equiv), THF/H_2O (2/1), 22 °C, 12 h; 2. *N,N'*-dicyclohexyl-*O*-benzylisourea (4.5 equiv), toluene, reflux, 2 h, 42% **3**, 62% **10**; h) 1. **10** (1.0 equiv), LiOH (15 equiv), THF/MeOH/H_2O (2/1/1), 22 °C, 4 h; 2. **3** (1.0 equiv), EDC (1.25 equiv), DMAP (0.6 equiv), CH_2Cl_2, 22 °C, 10.5 h, 47% (3:2 mixture of the C6-acyl- (**9**) and the C7-acyl compound; plus 20% **3**); i) TESOTf (1.1 equiv), pyridine (1.5 equiv), CH_2Cl_2, 22 °C, 20 min, 79%; j) DDQ (1.2 equiv), CH_2Cl_2/H_2O (20/1), 22 °C, 1 h, 98%; k) Ac_2O (2.5 equiv), pyridine (3.0 equiv), DMAP (0.1 equiv), CH_2Cl_2, 22 °C, 4 h, 99%.
TESOTf = triethylsilyl trifluoromethanesulfonate, TBAF = tetrabutylammonium fluoride, THF = tetrahydrofuran, PMB = *para*-methoxybenzyl, CSA = (±)-10-camphorsulfonic acid, EDC = 1-(3-dimethylaminopropyl)-3-ethylcarbodiimide hydrochloride, DMAP = 4-dimethylaminopyridine, DDQ = 2,3-dichloro-5,6-dicyano-1,4-benzoquinone.

 © VCH Verlagsgesellschaft mbH, D-69451 Weinheim, 1994 0570-0833/94/2121-2185 $ 10.00+.25/0

by workup with excess *N,N*-dicyclohexyl-*O*-benzylisourea (toluene, reflux, 2 h) cleanly gave the triol **3** (Table 2) in 42% yield and benzyl ester **10** in 62% yield.

Reconstitution of the natural product began with selective acylation of the C6 hydroxyl group of **3** with (*E*)-(4*S*,6*S*)-4,6-dimethyl-2-octenoic acid **4** to give a 3:2 mixture of C6- and C7-acylated products. However, on subsequent removal of the allylic PMB group, selective acetylation of the C4′ hydroxyl group could not be achieved, which led us to consider temporary protection of the C7 hydroxyl group with a TES ether (**9** → **11**, 79%). Removal of the PMB group from **11** with DDQ afforded **12** in 98% yield, which upon C4′ acetylation and desilylation gave the allylic acetate **7** (85% yield overall) via the intermediate **13**. Removal of the three benzyl esters by transfer hydrogenolysis[13] gave the triacid **1a** (>70% crude, 50% after HPLC), identical in all respects to an authentic sample of zaragozic acid A (**1a**).[11]

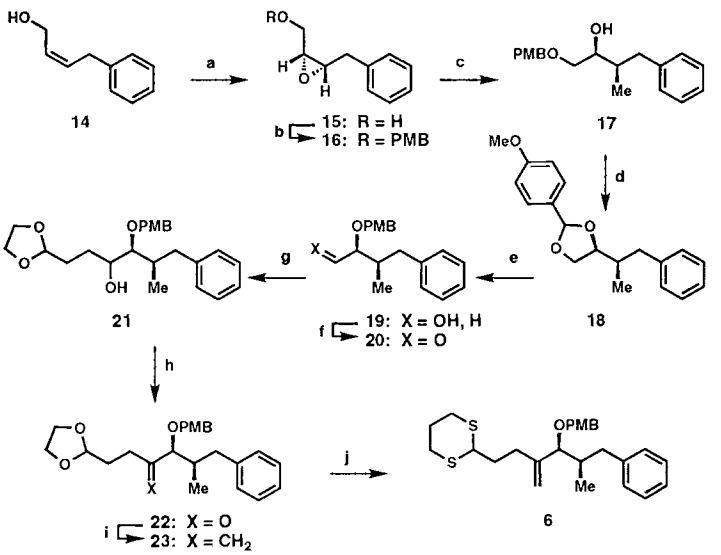
Table 2. Selected physical data for **3**, **4**, and **6**.

3: $[\alpha]_D^{22} = -20.9$ ($c = 0.55$ in $CHCl_3$); $R_f = 0.29$ (silica, ethyl acetate/petroleum ether 2/3); IR (film): $\tilde{\nu}$ = 3487, 3330, 3027, 2929, 2853, 1746, 1617, 1512, 1454, 1246, 1034 cm^{-1}; ^1H NMR (500 MHz, $CDCl_3$): δ = 7.30–7.13 (m, 20H, arom. H), 7.07 (d, J = 7.1 Hz, 2H, $MeOC_6H_4$), 6.86 (d, J = 8.6 Hz, 2H, $MeOC_6H_4$), 5.28 (d, J = 12.2 Hz, 1H, $PhCH_2O$), 5.17 (s, 1H, H3), 5.14 (d, J = 12.1 Hz, 1H, $PhCH_2O$), 5.08 (s, 2H, $C=CH_2$), 5.06 (s, 1H, H6), 4.99 (d, J = 12.1 Hz, 1H, $PhCH_2O$), 4.97 (d, J = 12.1 Hz, 1H, $PhCH_2O$), 4.85 (d, J = 12.1 Hz, 1H, $PhCH_2O$), 4.82 (d, J = 12.1 Hz, 1H, $PhCH_2O$), 4.45 (d, J = 11.4 Hz, 1H, $MeOC_6H_4CH_2$), 4.14 (d, J = 11.4 Hz, 1H, $MeOC_6H_4CH_2$), 4.05 (s, 1H, H7), 3.79 (s, 3H, OCH_3), 3.78 (s, 1H, 4-OH), 3.50 (d, J = 6.1 Hz, 1H, $CHOCH_2Ar$), 3.46 (br. s, 1H, 6-OH), 2.65 (dd, J = 13.5, 5.7 Hz, 2H, $CH(CH_3)CH_2Ph$), 2.46 (br. s, 1H, 7-OH), 2.39–2.29 (m, 1H, $CH_2C=CH_2$), 2.29 (dd, J = 13.5, 9.0 Hz, 1H, $CH_2C=CH_2$), 2.20–2.09 (m, 3H, $CH_2CH_2C(=CH_2)$, $CHCH_3$), 0.85 (d, J = 6.6 Hz, 3H, CH_3); ^{13}C NMR (125 MHz, $CDCl_3$): δ = 168.9, 166.1, 159.0, 146.1, 141.2, 134.8, 134.7, 134.5, 130.9, 129.4, 129.2, 128.6, 128.5, 128.4, 128.2, 125.6, 113.7, 112.8, 105.8, 91.3, 85.4, 82.3, 78.6, 75.2, 74.7, 70.1, 68.4, 67.7, 67.4, 55.3, 49.2, 40.0, 37.6, 33.9, 33.7, 29.7, 25.5, 24.9, 24.3, 14.8; HR-MS ($C_{52}H_{54}O_{13}Cs$ [$(M + Cs)^+$]): calcd 1019.2619; found 1019.2640.

4: $[\alpha]_D^{22} = +46.4$ ($c = 0.06$ in $CHCl_3$); $R_f = 0.62$ (silica, ethyl acetate/petroleum ether 2/3); IR (film): $\tilde{\nu}$ = 2962, 2919, 2681, 1696, 1649, 1459, 1418, 1288, 986, 939 cm^{-1}; ^1H NMR (500 MHz, $CDCl_3$): δ = 6.93 (dd, J = 15.6, 8.5 Hz, 1H, $CH=CHCO_2H$), 5.79 (d, J = 15.6 Hz, 1H, $CH=CHCO_2H$), 2.46–2.42 (m, 1H, $CH(CH_3)CH=CH$), 1.43–1.27 (m, 3H, $CH_3CH_2CH(CH_3)CH_2$), 1.16–1.10 (m, 2H, $CH_3CH_2CH(CH_3)CH_2$), 1.05 (d, J = 6.7 Hz, 3H, $CH(CH_3)CH=CH$), 0.87–0.84 (m, 6H, $CH_3CH_2CHCH_3$); ^{13}C NMR (125 MHz, $CDCl_3$): δ = 171.2, 157.6, 118.6, 43.1, 34.3, 31.8, 29.7, 20.1, 18.7, 11.1; HR-MS ($C_{10}H_{19}O_2$ [$(M + H)^+$]): calcd 171.1385; found 171.1391.

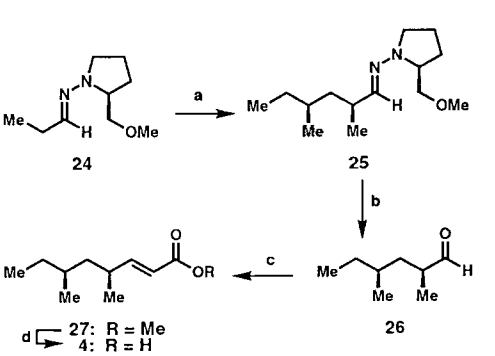
6: $[\alpha]_D^{22} = -33.6$ ($c = 0.17$ in $CHCl_3$); $R_f = 0.64$ (silica, ethyl acetate/petroleum ether 1/4); IR (film): $\tilde{\nu}$ = 2904, 1611, 1512, 1454, 1247 cm^{-1}; ^1H NMR (500 MHz, $CDCl_3$): δ = 7.28–7.23 (m, 4H, arom. H), 7.18–7.15 (m, 1H, arom. H), 7.10 (d, J = 7.3 Hz, 2H, arom. H), 6.88 (d, J = 8.4 Hz, 2H, arom. H), 5.09 (d, J = 6.4 Hz, 2H, $C=CH_2$), 4.47 (d, J = 11.4 Hz, 1H, OCH_2Ar), 4.14 (d, J = 11.3 Hz, 1H, OCH_2Ar), 4.06 (t, J = 6.8 Hz, 1H, SCHS), 3.81 (s, 3H, OCH_3), 3.48 (d, J = 6.5 Hz, 1H, $CHOCH_2Ar$), 2.87–2.84 (m, 4H, $SCH_2CH_2CH_2S$), 2.68 (dd, J = 13.4, 5.3 Hz, 1H, CH_2Ph), 2.30–2.15 (m, 4H, $CHHPh$, $CH_2C=CH_2$, SCH_2CHHCH_2S), 1.98–1.86 (m, 4H, $CHCH_3$, $CH_2CH_2C=CH_2$, SCH_2CHHCH_2S), 0.85 (d, J = 6.5 Hz, 3H, $CHCH_3$); ^{13}C NMR (125 MHz, $CDCl_3$): δ = 158.9, 146.0, 141.1, 130.9, 129.3, 129.1, 128.1, 125.7, 113.6, 113.0, 85.8, 70.0, 55.2, 47.1, 40.0, 37.6, 33.5, 30.5, 27.8, 26.0, 14.8; HR-MS ($C_{26}H_{34}O_2S_2Cs$ [$(M + Cs)^+$]): calcd 575.1055; found 575.1061.

Our retrosynthetic scheme also required a synthesis of the C1 alkyl side chain **6** and the C6 acyl side chain **4**.[14] The synthesis of **6** is outlined in Scheme 2. Sharpless asymmetric epoxidation[15] of the allylic alcohol **14** gave the epoxide in good yield and in approximately 81% *ee*.[16] Protection of the primary alcohol and regioselective opening of the epoxide ($AlMe_3$, *n*-BuLi)[17] gave the alcohol **17** as a single regioisomer (by 500 MHz ^1H NMR analysis) in 65% yield overall. Transfer of the PMB protecting group to the secondary alcohol via the PMB acetal[18] **18** followed by Swern oxidation[19] of the resulting alcohol **19** gave the aldehyde **20** in 42% overall yield. Three-carbon homologation of the aldehyde with 2-(1,3-dioxolan-2-yl)ethylmagnesium bromide gave the acetal **21** as a mixture of diastereoisomers (ratio 1:1 determined by 500 MHz ^1H NMR analysis). Oxidation with the Dess–Martin periodinane,[20] and Tebbe methylenation[21] gave the olefin **23** in 78% yield (two steps). Olefin **23** was crystalline, and a single recrystallization from cyclohexane increased the enantiomeric excess to 98% (according to ^1H NMR and ^{19}F NMR analysis of the Mosher's ester following C4′ PMB deprotection). Completion of the synthesis was achieved by transthioacetalization[22] to give the dithiane **6** (61% yield) (Table 2).



Scheme 2. Synthesis of the side chain at C1 (**6**). a) *t*BuOOH (2.0 equiv), $Ti(OiPr)_4$ (0.1 equiv), diisopropyl-D-tartrate (0.14 equiv), 4 Å molecular sieves (0.5 wt. equiv), CH_2Cl_2, −20 °C, 24 h, 84%; b) PMBCl (1.25 equiv), NaH (1.2 equiv), nBu_4NI (0.04 equiv), THF, reflux, 30 min, 73%; c) $Al(CH_3)_3$ (2.0 equiv), *n*BuLi (0.3 equiv), toluene, −20 °C, 24 h, 89%; d) DDQ (1.1 equiv), CH_2Cl_2, 4 Å molecular sieves (0.25 wt. equiv), 22 °C, 4 h, 53%; e) DIBAl-H (1.2 equiv), CH_2Cl_2, −78 °C, 2 h, 81%; f) $(COCl)_2$ (1.5 equiv), DMSO (2.0 equiv), Et_3N (4.0 equiv), CH_2Cl_2, −78 °C, 2 h, 98%; g) Mg (3.3 equiv), 2-(2-bromoethyl)-1,3-dioxolane (3.0 equiv), THF, 22 °C, 6 h, 73%; h) Dess-Martin periodinane (1.2 equiv), CH_2Cl_2, 22 °C, 20 min, 92%; i) Tebbe reagent (1.2 equiv), THF, 22 °C, 1 h, 85%; j) $iBu_2AlSCH_2CH_2CH_2SAliBu_2$ (2.0 equiv), benzene, 22 °C, 12 h, 61%. DIBAl-H = diisobutylaluminum hydride, DMSO = dimethylsulfoxide.

The C6 acyl side chain was synthesized in four steps as shown in Scheme 3. Alkylation of the hydrazone **24**[23] with commercially available (*S*)-1-iodo-2-methylbutane gave the hydrazone



Scheme 3. Synthesis of the side chain at C6 (**4**). a) 1. iPr_2NH (1.1 equiv), *n*BuLi (1.05 equiv), THF, 0 °C, 15 min; 2. **24** (1.0 equiv), 0 °C, 4 h; 3. *n*BuLi (1.05 equiv), −20 °C, 2 h; 4. (*S*)-$CH_3CH_2CH(CH_3)CH_2I$ (1.2 equiv), −100 °C → −50 °C, 1.5 h; b) O_3, CH_2Cl_2, −78 °C, 30 s; c) $Ph_3P=CHCO_2CH_3$ (1.2 equiv), CH_2Cl_2, 22 °C, 5 h, 30% overall yield from **24**; d) LiOH (3.0 equiv), $MeOH/H_2O$ (3/1), 22 °C, 3 h, 90%.

 © VCH Verlagsgesellschaft mbH, D-69451 Weinheim, 1994 0570-0833/94/2121-2186 $ 10.00+.25/0

25 as a 96:4 mixture of diastereoisomers. Ozonolysis of the crude reaction mixture provided the aldehyde **26**,[24] and Wittig olefination gave the ester **27** (30% yield overall). Hydrolysis of the ester afforded, in 90% yield, acid **4** (Table 2), identical in all respects with an authentic sample.[25]

The chemistry described outlines potential final steps from a projected synthetic intermediate, details efficient and stereoselective routes to the C1 and C6 side chains, and should facilitate the total synthesis of zaragozic acid A/squalestatin S1 (**1a**), and related compounds. In the following communication,[10] we report the synthesis of the first fully functionalized core of the zaragozic acids/squalestatins.

Received: August 8, 1994 [Z 7221 IE]
German version: *Angew. Chem.* **1994**, *106*, 2306

[1] Squalestatins S1, S2 and H1: a) M. J. Dawson, J. E. Farthing, P. S. Marshall, R. F. Middleton, M. J. O'Neill, A. Shuttleworth, C. Stylli, R. M. Tait, P. M. Taylor, H. G. Wildman, A. D. Buss, D. Langley, M. V. Hayes, *J. Antibiot.* **1992**, *45*, 639; b) P. J. Sidebottom, R. M. Highcock, S. J. Lane, P. A. Procopiou, N. S. Watson, *ibid.* **1992**, *45*, 648.

[2] Zaragozic acids A, B, and C: a) J. D. Bergstrom, M. M. Kurtz, D. J. Rew, A. M. Amend, J. D. Karkas, R. G. Bostedor, V. S. Bansal, C. Dufresne, F. L. VanMiddlesworth, O. D. Hensens, J. M. Liesch, D. L. Zink, K. E. Wilson, J. Onishi, J. A. Milligan, G. Bills, L. Kaplan, M. Nallin Omstead, R. G. Jenkins, L. Huang, M. S. Meinz, L. Quinn, R. W. Burg, Y. L. Kong, S. Mochales, M. Mojena, I. Martin, F. Pelaez, M. T. Diez, A. W. Alberts, *Proc. Natl. Acad. Sci. USA* **1993**, *90*, 80; b) K. E. Wilson, R. M. Burk, T. Biftu, R. G. Ball, K. Hoogsteen, *J. Org. Chem.* **1992**, *57*, 7151; c) C. Dufresne, K. E. Wilson, D. Zink, J. Smith, J. D. Bergstrom, M. Kurtz, D. Rew, M. Nallin, R. Jenkins, K. Bartizal, C. Trainor, G. Bills, M. Meinz, L. Huang, J. Onishi, J. Milligan, M. Mojena, F. Pelaez, *Tetrahedron* **1992**, *47*, 10221; d) C. Santini, R. G. Ball, G. D. Berger, *J. Org. Chem.* **1994**, *59*, 2261; e) O. D. Hensens, C. Dufresne, J. M. Liesch, D. L. Zink, R. A. Reamer, F. VanMiddlesworth, *Tetrahedron Lett.* **1993**, *34*, 399. Zaragozic acids D and D_2: C. Dufresne, K. E. Wilson, S. B. Singh, D. L. Zink, J. D. Bergstrom, D. Rew, J. D. Polishook, M. Meinz, L. Huang, K. C. Silverman, R. B. Lingham, M. Mojena, C. Cascales, F. Pelaez, J. B. Gibbs, *J. Nat. Prod.* **1993**, *56*, 1923.

[3] Zaragozic acid A is identical with squalestatin S1.

[4] Recently, nineteen additional squalestatins containing different alkyl and ester side chains and the first description of five minor relatives containing the novel 6-deoxy-, 7-deoxy-, or 6,7-dideoxy- "core" have been reported; their biological profile is currently unknown: W. M. Blows, G. Foster, S. J. Lane, D. Noble, J. E. Piercey, P. J. Sidebottom, G. Webb, *J. Antibiot.* **1994**, *47*, 740.

[5] a) A. Baxter, B. J. Fitzgerald, J. L. Hutson, A. D. McCarthy, J. M. Motteram, B. C. Ross, M. Sapra, M. A. Snowden, N. S. Watson, R. J. Williams, C. Wright, *J. Biol. Chem.* **1992**, *267*, 11705; b) Ref. [1a]; c) I. Abe, J. C. Tomesch, S. Wattanasin, G. D. Prestwich, *Nat. Prod. Rep.* **1994**, 279.

[6] a) M. G. Lester, G. M. P. Giblin, G. G. A. Inglis, P. A. Procopiou, B. C. Ross, N. S. Watson, *Tetrahedron Lett.* **1993**, *34*, 4357; b) G. M. P. Giblin, R. Bell, A. P. Hancock, C. D. Hartley, G. G. A. Inglis, J. J. Payne, P. A. Procopiou, A. H. Shingler, C. Smith, S. J. Spooner, *Bioorg. Med. Chem. Lett.* **1993**, *3*, 2605; c) P. A. Procopiou, E. J. Bailey, J. L. Hutson, B. E. Kirk, P. J. Sharratt, S. J. Spooner, N. S. Watson, *ibid.* **1993**, *3*, 2527; d) N. S. Watson, R. Bell, C. Chan, B. Cox, J. L. Hutson, S. E. Keeling, B. E. Kirk, P. A. Procopiou, I. P. Steeples, J. Widdowson, *ibid.* **1993**, *3*, 2541; e) R. J. P. Cannell, M. J. Dawson, R. S. Hale, R. M. Hall, D. Noble, S. Lynn, N. L. Taylor, *J. Antibiot.* **1994**, *47*, 247; f) D. Andreotti, P. A. Procopiou, N. S. Watson, *Tetrahedron Lett.* **1994**, *35*, 1789; g) P. J. Sharratt, J. L. Hutson, G. G. A. Inglis, M. G. Lester, P. A. Procopiou, N. S. Watson, *Bioorg. Med. Chem. Lett.* **1994**, *4*, 661.

[7] a) Y. P. Chiang, T. Biftu, G. A. Doss, S. P. Plevyak, R. W. Marquis, J. D. Bergstrom, M. M. Kurtz, D. J. Rew, G. D. Berger, *Bioorg. Med. Chem. Lett.* **1993**, *3*, 2029; b) C. H. Kuo, S. P. Plevyak, T. Biftu, W. H. Parsons, G. D. Berger, *Tetrahedron Lett.* **1993**, *34*, 6863; c) T. Biftu, J. J. Acton, G. D. Berger, J. D. Bergstrom, C. Dufresne, M. M. Kurtz, R. W. Marquis, W. H. Parsons, D. R. Rew, K. E. Wilson, *J. Med. Chem.* **1994**, *37*, 421.

[8] F. Tamanoi, *Trends Biol. Sci.* **1993**, *18*, 349.

[9] W. Bal, A. F. Drake, M. Jezowska-Bojczuk, H. Kozlowski, L. D. Pettit, P. J. Sadler, *J. Chem. Soc. Chem. Commun.* **1994**, 555.

[10] K. C. Nicolaou, A. Nadin, J. E. Leresche, S. La Greca, T. Tsuri, E. W. Yue, Z. Yang, *Angew. Chem.* **1994**, *106*, 2309; *Angew. Chem. Int. Ed. Engl.* **1994**, *33*, 2187.

[11] We thank Dr. Kenneth E. Wilson (Merck & Co., Inc., Rahway) for a generous gift of zaragozic acid A.

[12] For a discussion of this undeservedly neglected method of esterification, see L. J. Mathias, *Synthesis* **1979**, *11*, 561.

[13] For hydrogenolysis of the C3 benzyl ester of a zaragozic acid derivative under similar conditions, see ref. [7c].

[14] For a previous synthesis of a C1 side chain equivalent of zaragozic acid A, see A. J. Robichaud, G. D. Berger, D. A. Evans, *Tetrahedron Lett.* **1993**, *34*, 8403.

[15] a) T. Katsuki, K. B. Sharpless, *J. Am. Chem. Soc.* **1980**, *102*, 5974; b) Y. Gao, R. M. Hanson, J. M. Klunder, S. Y. Ko, H. Masamune, K. B. Sharpless, *ibid.* **1987**, *109*, 5765.

[16] Measured by 500 MHz ^{1}H NMR and ^{19}F NMR analysis of the Mosher's esters: J. A. Dale, D. L. Dull, H. S. Mosher, *J. Org. Chem.* **1969**, *34*, 2543.

[17] A. Pfaltz, A. Mattenberger, *Angew. Chem. Suppl.* **1982**, 161.

[18] M. Nakatsuka, J. A. Ragan, T. Sammakia, D. B. Smith, D. E. Uehling, S. L. Schreiber, *J. Am. Chem. Soc.* **1990**, *112*, 5583.

[19] A. J. Mancuso, S.-L. Huang, D. Swern, *J. Org. Chem.* **1978**, *43*, 2480.

[20] a) D. B. Dess, J. C. Martin, *J. Org. Chem.* **1983**, *48*, 4155; b) *J. Am. Chem. Soc.* **1991**, *113*, 7277; c) R. E. Ireland, L. Liu, *J. Org. Chem.* **1993**, *58*, 2899.

[21] F. N. Tebbe, G. W. Parshall, G. S. Reddy, *J. Am. Chem. Soc.* **1978**, *100*, 3611.

[22] T. Satoh, S. Uwaya, K. Yamakawa, *Chem. Lett.* **1983**, 667.

[23] a) D. Enders in *Asymmetric Synthesis, Vol. 3* (Ed.: J. D. Morrison), Academic, Orlando, **1984**, p. 275; b) D. Enders, J. Tiebes, N. DeKimpe, M. Keppens, C. Stevens, G. Smagghe, O. Betz, *J. Org. Chem.* **1993**, *58*, 4881.

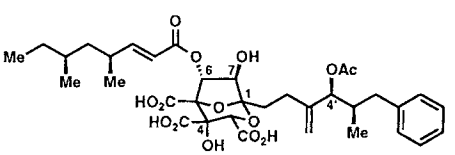
[24] *Ent*-**26** has recently been used in a synthesis of (+)-bourgeanic acid: J. D. White, A. T. Johnson, *J. Org. Chem.* **1994**, *59*, 3347.

[25] Authentic sample obtained by hydrolysis of **10** [LiOH (3 equiv), MeOH/H_2O (3:1), 25 °C, 4 h, 87%].

Synthesis of the First Fully Functionalized Core of the Zaragozic Acids/Squalestatins**

Kyriacos C. Nicolaou,* Alan Nadin, James E. Leresche, Susan La Greca, Tatsuo Tsuri, Eddy W. Yue, and Zhen Yang

The zaragozic acids/squalestatins (e.g. zaragozic acid A[1]/squalestatin S1,[2] **1**) are a novel class of natural products, recently isolated from various fungal cultures by researchers at



1

Merck and Glaxo. In addition to remarkable biological activity, the majority of the zaragozic acids/squalestatins possess a novel, highly oxygenated 4,6,7-trihydroxy-2,8-dioxobicyclo-[3.2.1]-octane-3,4,5-tricarboxylic acid "core" and differ only in the nature of the alkyl side chain at C1 and the ester side chain at C6. There have recently been several reports describing the successful synthesis of models of the bicyclic core,[3] but these all lack the characteristic tricarboxylate functionality and suitable devices or strategies for synthetic elaboration to the natural

[*] Prof. K. C. Nicolaou, A. Nadin, J. E. Leresche, S. La Greca, T. Tsuri, E. W. Yue, Z. Yang
Department of Chemistry, The Scripps Research Institute
10666 North Torrey Pines Road, La Jolla, CA 92037
and
Department of Chemistry and Biochemistry, University of California
San Diego, 9500 Gilman Drive, La Jolla, CA 92093 (USA)
Telefax: Int. code + (619)554-6738

[**] The work was financially supported by the National Institutes of Health, fellowships from the Swiss National Science Foundation (J. E. L.), Shionogi & Co., Ltd. (T. T.), Glaxo, Inc. (E. W. Y.), and by a grant from Merck, Sharp and Dohme. We thank Drs. Dee H. Huang, Raj Chadha and Gary Siuzdak of The Scripps Research Institute for NMR, X-ray crystallographic and mass spectroscopic assistance, respectively.

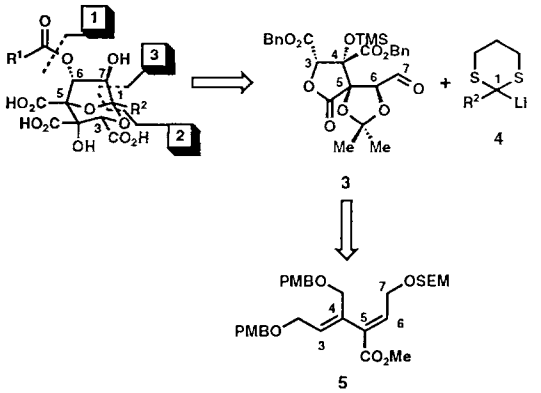
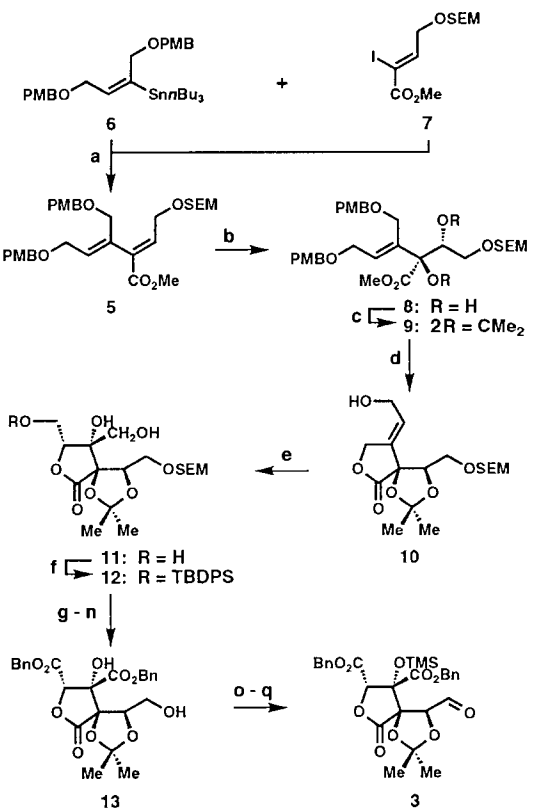


Fig. 1. Retrosynthetic analysis of the zaragozic acids/squalestatins. For abbreviations see Schemes 1 and 2.



Scheme 1. Synthesis of key intermediate **3**. a) **6** (1.1 equiv), **7** (1.0 equiv), $Pd(CH_3CN)_2Cl_2$ (0.1 equiv), DMF, 3 d, 25 °C, 70%; b) $K_3Fe(CN)_6$ (3 equiv), $K_2OsO_2(OH)_4$ (0.01 equiv), $(DHQD)_2PHAL$ (0.05 equiv), K_2CO_3 (3 equiv), $CH_3SO_2NH_2$ (1.5 equiv), tBuOH/H_2O (1/1), 36 h, 0 °C, 20% (plus 50% **5**); c) 2-methoxypropene (5 equiv), PPTS (0.2 equiv), CH_2Cl_2, 12 h, 0 °C, 88%; d) DDQ (3 equiv), $CHCl_3$/H_2O (20/1), 12 h, 25 °C, 86%; e) OsO_4 (0.05 equiv), NMO (3 equiv), THF/tBuOH/H_2O (1/1/1), 18 h, 0 °C, 83%; f) TBDPSCl (1.3 equiv), imidazole (2 equiv), DMAP (0.05 equiv), DMF, 40 h, 25 °C, 89%; g) Dess–Martin periodinane (1.1 equiv), CH_2Cl_2, 24 h, 25 °C, 89%; h) $NaClO_2$ (3 equiv), NaH_2PO_4 (1.05 equiv), 2-methyl-2-butene (4.2 equiv), tBuOH/H_2O (4/1), 5 h, 25 °C; i) *N*,*N*′-dicyclohexyl-*O*-benzylisourea (1.5 equiv), toluene, 1 h, 100 °C, 96% (2 steps); j) TBAF (1.2 equiv), AcOH (2 equiv), THF, 2 h, 0 °C, 96%; k) Dess–Martin periodinane (1.5 equiv), CH_2Cl_2, 12 h, 15 °C; l) $NaClO_2$ (3 equiv), NaH_2PO_4 (1.05 equiv), 2-methyl-2-butene (4.2 equiv), tBuOH/H_2O (4/1), 4 h, 25 °C; m) *N*,*N*′-dicyclohexyl-*O*-benzylisourea (1.5 equiv), toluene, 1 h, 100 °C, 68% (3 steps); n) TFA (50 equiv), CH_2Cl_2, 2 h, 0 → 25 °C, 88%; o) $CH_3N(TMS)$-$COCF_3$, 1 h, 90 °C; p) PPTS (0.01 equiv), CH_2Cl_2/CH_3OH (10/1), 5 min, 25 °C; q) Dess–Martin periodinane (3 equiv), CH_2Cl_2, 1 h, 25 °C, 88% (3 steps). DMF = *N*,*N*-dimethylformamide, Bu = butyl, PPTS = pyridinium *para*-toluenesulfonate, DDQ = 2,3-dichloro-5,6-dicyano-1,4-benzoquinone, NMO = 4-methylmorpholine *N*-oxide, THF = tetrahydrofuran, TBDPS = *tert*-butyldiphenylsilyl, DMAP = 4-dimethylaminopyridine, TBAF = tetrabutylammonium fluoride, TFA = trifluoroacetic acid, TMS = trimethylsilyl, PMB = *para*-methoxybenzyl, SEM = 2-(trimethylsilyl)ethoxymethyl.

products. In the preceeding communication,[4] we disclosed a general strategy for the synthesis of the zaragozic acids/squalestatins and now wish to report a synthesis of the first fully oxidized core of the zaragozic acids/squalestatins, compounds **16a**–**18a** and their C7 epimers **16b**–**18b**. Our retrosynthetic analysis is shown in Figure 1. The key intermediate aldehyde **3** was expected to arise by a series of functional group manipulations from diene **5**, asymmetry being introduced by a Sharpless dihydroxylation.[5]

The synthesis is summarized in Scheme 1. Diene **5** was synthesized in 70% yield by a Stille coupling[6] between vinylstannane **6**[7] and vinyl iodide **7**.[8] The dihydroxylation of diene **5** was best effected by using an enriched version of AD-mix β, containing 1% $K_2OsO_2(OH)_4$ and 5% of the chiral ligand $(DHQD)_2PHAL$. Although the yield is moderate (40% based on recovered starting material), the reaction is extremely reliable and can be run conveniently on a large scale.[9] The absolute and relative configurations depicted were confirmed by X-ray crystallography of compound **12a**, esterified at C3 with 3,5-dinitrobenzoic acid, and at C4 with (−)-camphanic acid (Fig. 2).[10] Protection of the diol **8** as an acetonide and deprotection of the PMB protecting group gave the allylic alcohol **10** via intermediate **9** on spontaneous lactonization. Dihydroxylation of the allylic alcohol with OsO_4/NMO and concomitant translactonization furnished the crystalline triol **11** as a single diastereoisomer. A series of functional group interconversions as outlined in Scheme 1 gave the diester **13** in 52% overall yield from diol **12**. Completion of the synthesis of the key aldehyde **3** (Table 1) was achieved by protection of the alcohol at C4 as a TMS ether and oxidation of the alcohol at C7 with the Dess–Martin periodinane.[11] By this route, multi-gram quantities of aldehyde **3** can be synthesized in 22 steps (longest linear sequence 19 steps) from readily available starting materials.

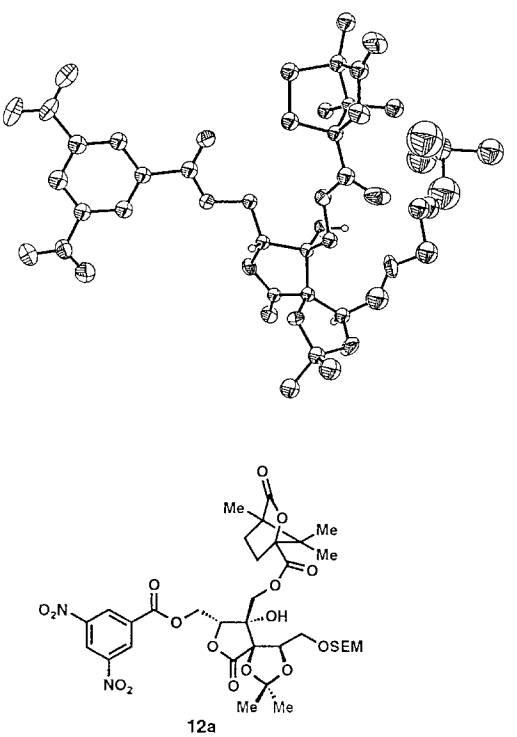
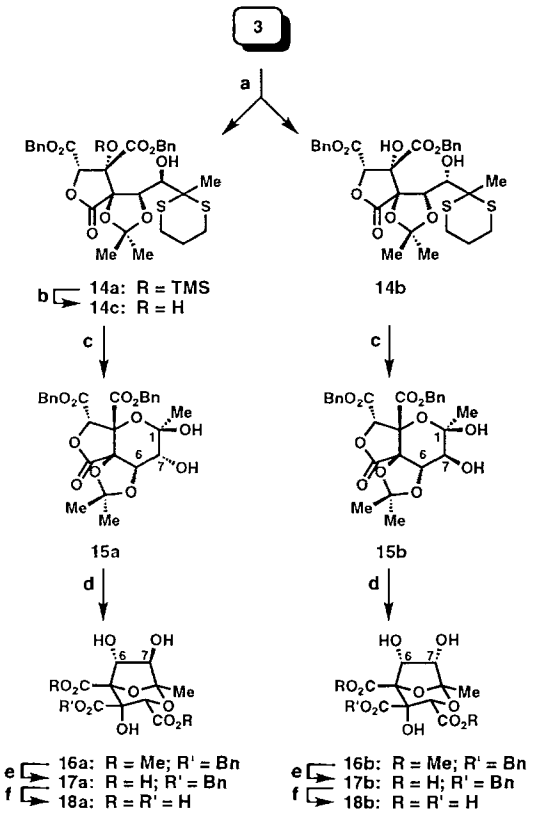


Fig. 2. ORTEP representation (top) of **12a** (bottom).

Addition of aldehyde **3** to 2-methyl-2-lithio-1,3-dithiane[12] (Scheme 2) gave the two epimeric dithianes **14a** and **14b** as major products (ratio approximately 1:1.3). Since the minor epimer **14a** retained the TMS group, chromatographic separation was facilitated.[13] Separate hydrolysis of the dithiane moiety with $Hg(ClO_4)_2/CaCO_3$ gave the lactols **15a** and **15b** as



Scheme 2. Synthesis of the zaragozic acid/squalestatin core: compounds **16a**–**18a** and their C7 epimers **16b**–**18b**. a) 1. 2-Methyl-1,3-dithiane (3.0 equiv), *n*BuLi (3.0 equiv), THF, −23 °C, 1.5 h; 2. −78 °C, 1 h, **14a** (28%) and **14b** (35%); b) 2% HCl in CH_3OH, 10 min, 25 °C, 76%; c) $Hg(ClO_4)_2$, (1.2 equiv), $CaCO_3$ (1.3 equiv), THF/H_2O (5/1), 2 h, 25 °C, **15a** (73%) and **15b** (76%); d) 2% HCl/CH_3OH, 10 h, 60 °C, **16a** (56%) and **16b** (54%); e) $LiOH \cdot H_2O$ (20 equiv), THF/H_2O (1/1), 25 °C, 19 h, >90%; f) H_2, Pd/C, CH_3OH, 25 °C, 5 h, 100%; Bn = benzyl.

single anomers in good yield. A ROESY experiment ($CDCl_3$, 298 K, mixing time 400 ms) on the major lactol diastereoisomer **15b** revealed large NOEs between (C1-Me) and H6, between H6 and H7, and between (C7-OH) and the acetonide methyl, suggesting that the stereochemistry is 1*R*,7*S* (the (1*R*,7*R*) configuration of **15a** was similarly determined). Lactols **15a** and **15b** possess the complete, fully oxygenated carbon skeleton of the zaragozic acid/squalestatin core, and it was gratifying to observe that rearrangement to the bicyclic cores, **16a** and **16b**, respectively, (a multistep process involving methanolysis of the lactol, the lactone, the acetonide, and the C3 benzyl ester, and ketalization) could be readily achieved in a single operation by warming with 2% HCl in MeOH (60 °C, 10 h).[14] The suspected 6*R*,7*S* stereochemistry of **16b** was confirmed by the coupling constant ($J_{H6,H7} = 6.3$ Hz),[15] and by NOE measurements.[16] Similarly, the 6*R*,7*R* configuration of **16a** was demonstrated by the small coupling constant ($J_{H6,H7} = 2.3$ Hz)[1, 2] and NOE measurements. Selective hydrolysis of the methyl esters of **16a** at C3 and C5 could be readily achieved with lithium hydroxide to yield the diacid **17a** in greater than 90% yield. Finally, hydrogenolysis of the benzyl ester of **17a** gave the triacid **18a** in essentially quantitative yield. A similar set of reactions converted the triester **16b** into triacid **18b**, epimeric at C7, via diacid **17b**.

Table 1. Selected data for compounds **3**, **16a** and **16b**.

3: $R_f = 0.20$ (silica, ethyl acetate/petroleum ether 1/6); IR (film): $\tilde{\nu}$ = 2936, 2857, 1806, 1764, 1738, 1456, 1384, 1351, 1254, 1222, 1191, 1144, 1085 cm^{-1}; ^{1}H-NMR (500 MHz, $CDCl_3$): δ = 9.53 (d, J = 0.7 Hz, 1H, CHO), 5.34 (d, J = 12.1 Hz, 1H, PhC*H*H), 5.23 (s, 2H, $PhCH_2$), 5.21 (s, 3H, H3), 5.15 (d, J = 12.1 Hz, 1H, PhCH*H*), 4.80 (d, J = 0.7 Hz, 1H, H6), 1.51 (s, 3H, Me), 1.37 (s, 3H, Me), 0.14 (s, 9H, Me); ^{13}C-NMR (125 MHz, $CDCl_3$): δ = 192.0, 171.6, 168.5, 166.4, 133.9, 128.9, 128.8, 128.7, 128.6, 128.5, 114.1, 88.4, 85.3, 84.0, 79.5, 68.7, 68.5, 26.7, 25.8, 1.6; HR-MS ($C_{28}H_{32}O_{10}SiNa$ [(M + Na)$^+$]): calcd: 579.1662; found: 579.1669.

16a: $R_f = 0.25$ (silica, ethyl acetate); IR (film): $\tilde{\nu}$ = 3466, 2919, 2851, 1748, 1444, 1266, 1169, 1045 cm^{-1}; ^{1}H-NMR (500 MHz, $CDCl_3$): δ = 7.48–7.35 (m, 5H, Ph), 5.39 (d, J = 12.0 Hz, 1H, PhC*H*H), 5.28 (d, J = 12.0 Hz, 1H, PhCH*H*), 5.16 (d, J = 2.3 Hz, 1H, H6), 5.15 (s, 1H, H3), 4.16 (d, J = 2.3 Hz, 1H, H7), 3.72 (s, 3H, CO_2Me), 3.59 (s, 3H, CO_2Me), 1.72 (s, 3H, C1-Me); ^{13}C-NMR (125 MHz, $CDCl_3$): δ = 169.1, 166.9, 166.7, 134.6, 129.0, 128.7, 128.5, 105.1, 91.5, 83.4, 78.2, 75.2, 74.4, 68.6, 52.9, 52.4, 22.0; HR-MS ($C_{19}H_{22}O_{11}Na$ [(M + Na)$^+$]): calcd: 449.1060; found: 449.1072.

16b: $R_f = 0.25$ (silica, ethyl acetate/petroleum ether 5/1); IR (Film): $\tilde{\nu}$ = 3429, 2924, 2854, 1749, 1445, 1382, 1270, 1234, 1171, 1107 cm^{-1}; ^{1}H-NMR (500 MHz, $CDCl_3$): δ = 7.47–7.38 (m, 5H, Ph), 5.39 (d, J = 11.9 Hz, 1H, PhC*H*H), 5.32 (dd, J = 6.3, 6.3 Hz, 1H, H6), 5.28 (d, J = 11.9 Hz, 1H, PhCH*H*), 4.69 (s, 1H, H3), 4.32 (dd, J = 6.3, 6.3 Hz, 1H, H7), 3.75 (s, 1H, C4-OH), 3.72 (s, 3H, C5-CO_2Me), 3.57 (s, 3H, C3-CO_2Me), 3.08 (d, J = 6.3 Hz, 1H, C6-OH), 3.03 (d, J = 6.3 Hz, 1H, C7-OH), 1.72 (s, 3H, C1-Me); ^{13}C-NMR (125 MHz, $CDCl_3$): δ = 169.1, 166.5, 166.4, 134.5, 129.1, 128.7, 128.6, 109.0, 92.4, 74.6, 73.9, 71.0, 68.7, 52.8, 52.5, 19.3; HR-MS ($C_{19}H_{22}O_{11}Na$ [(M + Na)$^+$]): calcd: 449.1060; found: 449.1065.

The described chemistry opens a flexible, efficient and enantioselective route to the fully oxidized core of the zaragozic acids/squalestatins and paves the way for a total synthesis of these novel natural products.

Received: August 3, 1994 [Z 7210 IE]
German version: *Angew. Chem.* **1994**, *106*, 2309

[1] a) J. D. Bergstrom, M. M. Kurtz, D. J. Rew, A. M. Amend, J. D. Karkas, R. G. Bostedor, V. S. Bansal, C. Dufresne, F. L. VanMiddlesworth, O. D. Hensens, J. M. Liesch, D. L. Zink, K. E. Wilson, J. Onishi, J. A. Milligan, G. Bills, L. Kaplan, M. Nallin Omstead, R. G. Jenkins, L. Huang, M. S. Meinz, L. Quinn, R. W. Burg, Y. L. Kong, S. Mochales, M. Mojena, I. Martin, F. Pelaez, M. T. Diez, A. W. Alberts, *Proc. Natl. Acad. Sci. USA* **1993**, *90*, 80
[2] a) M. J. Dawson, J. E. Farthing, P. S. Marshall, R. F. Middleton, M. J. O'Neill, A. Shuttleworth, C. Stylli, R. M. Tait, P. M. Taylor, H. G. Wildman, A. D. Buss, D. Langley, M. V. Hayes, *J. Antibiot.* **1992**, *45*, 639; b) P. J. Sidebottom, R. M. Highcock, S. J. Lane, P. A. Procopiou, N. S. Watson, *ibid.* **1992**, *45*, 648.
[3] a) H. Abdel-Rahman, J. P. Adams, A. L. Boyes, M. J. Kelly, D. J. Mansfield, P. A. Procopiou, S. M. Roberts, D. H. Slee, N. S. Watson, *J. Chem. Soc. Chem. Commun.* **1993**, 1839; b) H. Abdel-Rahman, J. P. Adams, A. L. Boyes, M. J. Kelly, D. J. Mansfield, P. A. Procopiou, S. M. Roberts, D. H. Slee, P. J. Sidebottom, V. Sik, N. S. Watson, *ibid.* **1993**, 1841; c) H. Abdel-Rahman, J. P. Adams, A. L. Boyes, M. J. Kelly, R. B. Lamont, D. J. Mansfield, P. A. Procopiou, S. M. Roberts, D. H. Slee, N. S. Watson, *J. Chem. Soc. Perkin Trans. 1* **1994**, 1259; d) V. K. Aggarwal, M. F. Wang, A. Zaparucha, *J. Chem. Soc. Chem. Commun.* **1994**, 87; e) M. K. Gurjar, S. K. Das, U. K. Saha, *Tetrahedron Lett.* **1994**, *35*, 2241; f) L. M. McVinish, M. A. Rizzacasa, *Tetrahedron Lett.* 1994, *35*, 923; g) L. J. Brzezinski, D. D. Levy, J. W. Leahy, *207th National Meeting of the American Chemical Society*, San Diego, **1994**, ORGN 368; h) S. Caron, C. H. Heathcock, *208th National Meeting of the American Chemical Society*, Washington DC, **1994**, ORGN 299.
[4] K. C. Nicolaou, E. W. Yue, Y. Naniwa, F. De Riccardis, A. Nadin, J. E. Leresche, S. La Greca, Z. Yang, *Angew. Chem.* **1994**, *106*, 2306; *Angew. Chem. Int. Ed. Engl.* **1994**, *33*, 2184.
[5] K. B. Sharpless, W. Amberg, Y. L. Bennani, G. A. Crispino, J. Hartung, K. S. Jeong, H. L. Kwong, K. Morikawa, Z. M. Wang, D. Xu, X. L. Zhang, *J. Org. Chem.* **1992**, *57*, 2768.
[6] J. K. Stille, B. L. Groh, *J. Am. Chem. Soc.* **1987**, *109*, 813.

 © VCH Verlagsgesellschaft mbH, D-69451 Weinheim, 1994 0570-0833/94/2121-2189 $ 10.00+.25/0

[7] Prepared from 2-butyne-1,4-diol by the following sequence: a) NaH (2.5 equiv), PMBCl (2.5 equiv), nBu$_4$NI (0.04 equiv), DMF, 25 °C, 8 h, 94%; b) Bu$_3$SnH (1.1 equiv), Pd(PPh$_3$)$_2$Cl$_2$ (0.015 equiv), THF, 25 °C, 17 h, 94%.

[8] Prepared by a Wittig reaction between 2-(trimethylsilyl)ethoxymethyloxyethanal and methyl iodo(triphenylphosphoranylidene)acetate (benzene, 25 °C, 24 h, 78%; the Z/E ratio is 30/1 according to the 300 MHz ^{1}H NMR analysis).

[9] The enantiomeric excess of the dihydroxylation step was determined to be approximately 78% by ^{19}F and ^{1}H NMR analysis of the Mosher's ester of allylic alcohol **10** (J. A. Dale, D. L. Dull, H. S. Mosher, *J. Org. Chem.* **1969**, *34*, 2543).

[10] Compound **12a** (m.p. 146–147 °C, heptane/ethyl acetate) was prepared from **12** by the following sequence of reactions: 1) (−)-camphanic acid chloride (3 equiv), pyridine, DMAP (0.1 equiv), 25 °C, 6 h, 73%; 2) TBAF (1.2 equiv), AcOH (2.0 equiv), THF, 0 °C, 1 h, 84%; 3) 3,5-dinitrobenzoyl chloride (3.0 equiv), pyridine, DMAP (0.1 equiv), 25 °C, 1 h, 75%. The mixture of diastereoisomers was recrystallized until only the major diastereoisomer was present (500 MHz ^{1}H NMR analysis). Crystals were then grown by slow evaporation of the solvent from a solution in hot heptane/ethyl acetate. Complete details will be reported in a full account of this work.

[11] a) D. B. Dess, J. C. Martin, *J. Org. Chem.* **1983**, *48*, 4155; b) *J. Am. Chem. Soc.* **1991**, *113*, 7277; c) R. E. Ireland, L. Liu, *J. Org. Chem.* **1993**, *58*, 2899.

[12] a) D. Seebach, E. J. Corey, *J. Org. Chem.* **1975**, *40*, 231. b) b) For a recent review on the synthetic uses of 1,3-dithianes see: P. C. Bulman Page, M. B. van Niel, J. C. Prodger, *Tetrahedron* **1989**, *45*, 7643.

[13] This reaction is currently somewhat capricious; variable amounts of products sometimes arise from attack at the C3 ester.

[14] The choice of these conditions was prompted by the rearrangement of a compound with a similar pattern of functional groups: E. Campbell, B. J. Newhouse, J. Bordner, E. F. Kleinman, *Tetrahedron* **1993**, *49*, 7437.

[15] A coupling constant of J(H6,H7) = 6.5 Hz for a 6*R*,7*S* core (M. G. Lester, G. M. P. Giblin, G. G. A. Inglis, P. A. Procopiou, B. C. Ross, N. S. Watson, *Tetrahedron Lett.* **1993**, *34*, 4357) and J(H6,H7) = 9.5 Hz for a (6*S*,7*R*) core (ref. [3b]) have been reported. A typical coupling constant J(H6,H7) for the naturally occurring 6*R*,7*R* core is 2 Hz (ref. [2b]).

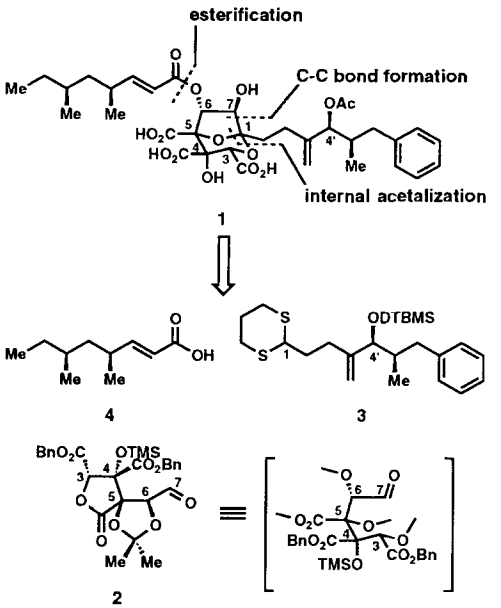
[16] A ROESY experiment ($CDCl_3$, 298 K, mixing time 400 ms) aided assignment of all the proton resonances. Large reciprocal NOEs were observed between H3, H7, and H6. In a 1D NOE difference spectrum ($CDCl_3$, 298 K), the NOE between H3 and H7 was about 8%, and between H3 and H6 about 6%.

Total Synthesis of Zaragozic Acid A/ Squalestatin S1**

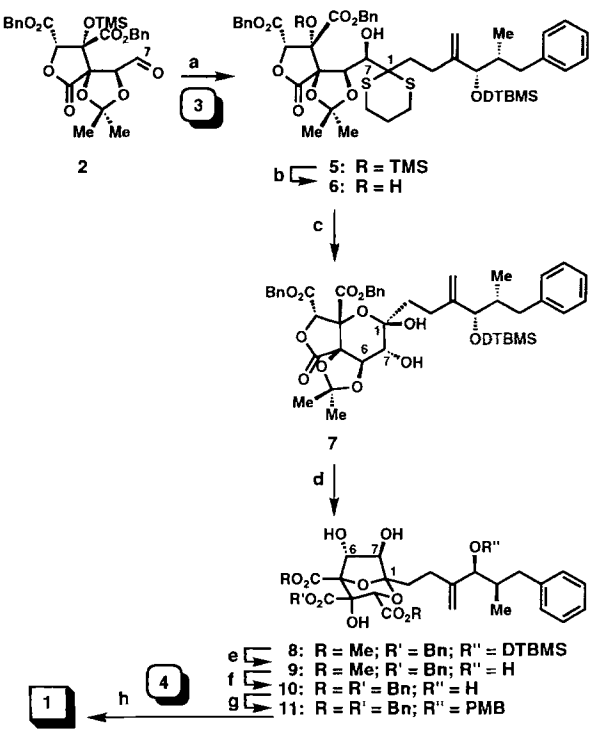
Kyriacos C. Nicolaou*, Alan Nadin, James E. Leresche, Eddy W. Yue, and Susan La Greca

In the previous two papers,[1, 2] we described our model studies directed towards a total synthesis of zaragozic acid A/squalestatin S1 (**1**). Herein we record the first total synthesis of this compound in its naturally occurring enantiomeric form by a convergent and flexible strategy applicable to the construction of all members of the class.

Our retrosynthetic strategy for the total synthesis of **1** required building blocks **2**–**4** (Scheme 1). Relying on this plan, and assured by the zaragozic acid skeletal rearrangement described in the preceding paper,[2] we embarked on the total synthesis as outlined in Scheme 2. Thus, aldehyde **2**[2] was treated with the lithio derivative of dithiane **3**[1] to afford two



Scheme 1. Retrosynthetic analysis of zaragozic acid A/squalestatin S1 (**1**).



Scheme 2. Reagents and conditions. a) **3** (1.5 equiv), nBuLi, THF, −30 °C, 1.5 h, then **2**, THF, −78 °C, 5 min, 75%; b) 2% HCl in MeOH/CH_2Cl_2 (1/1), 25 °C, 5 min, 100%; c) Hg(ClO$_4$)$_2$ (1.2 equiv), $CaCO_3$ (1.3 equiv), THF/H_2O (5/1), 25 °C, 2 h, 83%; d) 1.8% HCl in MeOH, 78 °C, 21 h, 50%; e) 49% aqueous HF/MeNO$_2$ (1/10), 0 °C, 24 h, 30%; f) LiOH·H_2O (10 equiv), THF/H_2O (2/1), 25 °C, 1 h, then *O*-benzyl-*N*,*N*′-dicyclohexylisourea (4.5 equiv), THF, 55 °C, 1.5 h, 74% (2 steps); g) CSA (0.1 equiv), $Cl_3CC(OPMB)=NH$ (1.0 equiv), CH_2Cl_2, 25 °C, 45 min, **11** (21%), **10** (37%); h) see Ref. [1]. Bn = Benzyl, CSA = (±)-10-camphorsulfonic acid, DTBMS = di-*tert*-butylmethylsilyl, PMB = *para*-methoxybenzyl, TMS = trimethylsilyl. All new compounds exhibited satisfactory spectral data (Table 1). Yields were based on spectroscopically and chromatographically homogeneous materials.

[*] Prof. Dr. K. C. Nicolaou, A. Nadin, J. E. Leresche, E. W. Yue, S. La Greca
Department of Chemistry, The Scripps Research Institute
10666 North Torrey Pines Road, La Jolla, CA 92037
and
Department of Chemistry and Biochemistry, University of California
San Diego, 9500 Gilman Drive, La Jolla, CA 92093 (USA)
Telefax: Int. code + (619)554-6738

[**] We thank Dr. Kenneth E. Wilson (Merck, Rahway) for a generous gift of zaragozic acid A. This work was financially supported by the National Institutes of Health, fellowships from Glaxo (E. W. Y.), the Swiss National Science Foundation (J. E. L.), and by a grant from Merck, Sharp and Dohme, and Pfizer Inc. We thank Dr. Dee H. Huang and Dr. Gary Siuzdak of The Scripps Research Institute for the NMR spectra and mass spectrometry measurements, respectively.

Table 1. Selected physical data of compounds **5**, **8** and **10**.

5: $[\alpha]_D^{22} = +30.9$ ($c = 0.89$ in $CHCl_3$); $R_f = 0.37$ (silica gel, ethyl acetate/petroleum ether 1:4); IR (film): $\tilde{\nu} = 3396, 2931, 2856, 1799, 1752, 1456, 1374, 1253, 1069\,cm^{-1}$; ^1H NMR (500 MHz, $CDCl_3$): 7.36–7.16 (m, 15H, arom. H), 5.56 (d, $J = 2.0$ Hz, 1H, C*H*OH), 5.49 (s, 1H, C*H*CO_2Bn), 5.24 (d, $J = 12.5$ Hz, 1H, OC*H*HPh), 5.22 (s, 2H, OCH_2Ph), 5.14 (d, $J = 12.5$ Hz, 1H, OCH*H*Ph), 5.08 (br. s, 1H, C=C*H*H), 5.00 (d, $J = 2.0$ Hz, 1H, C*H*CHOH), 4.96 (br. s, 1H, O*H*), 4.88 (br. s, 1H, C=CH*H*), 4.14 (d, $J = 5.5$ Hz, 1H, C*H*C=CH_2), 3.18–3.10 (m, 1H, CH_2), 3.02–2.96 (m, 1H, CH_2), 2.84 (dd, $J = 13.0$, 3.4 Hz, 1H, CH_2), 2.64–2.61 (m, 2H, CH_2), 2.53–2.17 (m, 4H, CH_2), 2.06–2.02 (m, 1H, CH_2), 1.91–1.87 (m, 3H, CH_2 and C*H*Me), 1.40 (s, 3H, C(CH_3)$_2$), 1.24 (s, 3H, C(CH_3)$_2$), 1.05 (s, 9H, *t*Bu), 0.98 (s, 9H, *t*Bu), 0.78 (d, $J = 6.5$ Hz, 3H, *Me*CH), 0.26 (s, 9H, $SiMe_3$), 0.07 (s, 3H, SiMe); ^{13}C NMR (125 MHz, $CDCl_3$): 171.7, 168.8, 165.9, 149.9, 141.6, 134.5, 134.1, 129.1, 128.5, 128.4, 128.4, 128.3, 128.0, 125.5, 111.0, 110.7, 84.8, 81.7, 81.5, 80.3, 79.5, 71.1, 68.4, 67.6, 58.7, 40.1, 40.0, 28.2, 27.9, 26.3, 26.2, 25.5, 24.9, 23.6, 21.0, 13.9, 2.3, −7.7; HR-MS ($C_{55}H_{78}Si_2S_2O_{11}Cs$ [$(M + Cs)^+$]): calcd: 1167.3578; found: 1167.3502.

8: $[\alpha]_D^{22} = -6.9$ ($c = 0.29$ in $CHCl_3$); $R_f = 0.42$ (silica gel, ether); IR (film): $\tilde{\nu} = 3449, 2931, 2856, 1747, 1455, 1253, 1118, 1081\,cm^{-1}$; ^1H NMR (500 MHz, $CDCl_3$): 7.46–7.15 (m, 10H, arom. H), 5.38 (d, $J = 12.0$ Hz, 1H, PhC*H*HO), 5.29 (d, $J = 12.0$ Hz, 1H, PhCH*H*O), 5.19 (s, 1H, C*H*CO_2CH_3), 5.15 (d, $J = 2.5$ Hz, 1H, H6), 5.11 (s, 1H, C=C*H*H), 4.96 (s, 1H, C=CH*H*), 4.18 (d, $J = 2.5$ Hz, 1H, H7), 4.15 (d, $J = 5.0$ Hz, 1H, H4'), 3.71 (s, 3H, CO_2Me), 3.58 (s, 3H, CO_2Me), 2.83 (dd, $J = 14.0$, 4.0 Hz, 1H, CH_2), 2.51–2.42 (m, 1H, CH_2), 2.30–2.19 (m, 3H, CH_2), 2.15–2.10 (m, 1H, CH_2), 1.93–1.87 (m, 1H, C*H*Me), 1.04 (s, 9H, *t*Bu), 0.96 (s, 9H, *t*Bu), 0.79 (d, $J = 6.5$ Hz, 3H, Me), 0.07 (s, 3H, SiMe); ^{13}C NMR (125 MHz, $CDCl_3$): 169.0, 166.8, 148.8, 141.5, 134.6, 129.0, 128.9, 128.6, 128.5, 128.0, 125.5, 111.1, 105.8, 91.4, 82.4, 81.2, 78.6, 75.3, 74.5, 68.6, 52.9, 52.3, 40.0, 39.8, 33.4, 28.1, 27.8, 24.0, 21.0, 20.9, 14.1, −7.8; HR-MS ($C_{41}H_{58}SiO_{12}Cs$ [$(M + Cs)^+$]): calcd: 903.2752; found: 903.2775.

10: $[\alpha]_D^{22} = -8.8$ ($c = 0.80$ in $CHCl_3$); $R_f = 0.43$ (silica gel, petroleum ether/ethyl acetate 1:3); IR (film): $\tilde{\nu} = 3477, 3063, 3031, 2961, 2931, 2854, 1747, 1632, 1556, 1497, 1454, 1384, 1352, 1276, 1187, 1155, 1122, 1028\,cm^{-1}$; ^1H NMR (500 MHz, $CDCl_3$): 7.29–7.09 (m, 20H, arom. H), 5.23 (d, $J = 12.1$ Hz, 1H, PhC*H*O), 5.18 (s, 1H, C*H*CO_2CH_3), 5.10 (d, $J = 12.1$ Hz, 1H, PhC*H*O), 5.06 (br. s, 1H, C=C*H*H), 5.05 (1H, d, $J = 2.3$ Hz, 1H, H6), 5.02 (br. s, 1H, C=CH*H*), 4.95 (d, $J = 12.1$ Hz, 1H, PhC*H*O), 4.92 (d, $J = 12.1$ Hz, 1H, PhC*H*O), 4.72 (d, $J = 12.2$ Hz, 1H, PhC*H*O), 4.68 (d, $J = 12.2$ Hz, 1H, PhC*H*O), 4.13 (d, $J = 2.3$ Hz, 1H, H7), 3.95 (br. d, $J = 6.5$ Hz, 1H, H4'), 3.93 (br. s, 1H, OH), 2.70 (dd, $J = 13.5$, 4.9 Hz, 1H, CH_2), 2.51–2.45 (m, 1H, CH_2), 2.32–2.27 (m, 1H, CH_2), 2.24 (dd, $J = 13.5$, 9.7 Hz, 1H, CH_2), 2.15–2.11 (m, 2H, CH_2), 1.90–1.88 (m, 1H, C*H*Me), 0.82 (d, $J = 6.6$ Hz, 3H, Me); ^{13}C NMR (125 MHz, $CDCl_3$): 168.6, 166.5, 166.0, 150.5, 141.0, 134.6, 129.2, 128.6, 128.5, 128.4, 128.2, 125.7, 112.6, 106.1, 91.3, 83.0, 78.8, 78.6, 75.3, 74.8, 68.1, 67.9, 67.7, 39.9, 38.2, 33.5, 25.4, 14.2; HR-MS ($C_{44}H_{46}O_{12}Cs$ [$(M + Cs)^+$]): calcd: 899.2044; found: 899.2065.

diastereoisomers, compound **5** (Table 1) and the corresponding C7 epimer (75% total yield in an approximate 1:1 ratio), which had been desilylated under the reaction conditions. Product **5** was separated from its C7 diastereoisomer by flash column chromatography, and the TMS and dithiane protecting groups were removed sequentially by standard methods to afford lactol **7** via intermediate **6** (80% overall yield).

Exposure of **7** to the rearrangement conditions (1.8% HCl in methanol at 78 °C, 24 h) led smoothly to the desired product **8** in 50% yield (Table 1). During the course of this reaction several new compounds appeared but were converted slowly into **8**, which apparently represents the thermodynamically most stable skeleton of the central region of the molecule. It should be noted that before choosing the previously reported,[3] but very rarely used, di-*tert*-butylmethylsilyl (DTBMS) protecting group for the allylic alcohol, two other groups [*para*-methoxybenzyl (PMB) and *tert*-butyldiphenylsilyl (TBDPS)] were utilized but failed to withstand the rearrangement conditions. The PMB ether suffered displacement by methanol even at ambient temperatures, and the TBDPS group was removed under the rearrangement conditions which led to the formation of spiroacetals.[4]

Proceeding with the synthesis, desilylation of **8** [49% aqueous HF/nitromethane (1/10), 0 °C, 24 h] gave the tetraol **9** in 30% yield.[5, 6] Selective alkaline hydrolysis of the two methyl esters of **9** followed by esterification with *O*-benzyl-*N*,*N*′-dicyclohexylisourea[7] (4.5 equiv, THF, 55 °C) furnished the tribenzyl ester **10** (Table 1) in 74% overall yield.

Selective protection of the allylic alcohol **10** as a PMB ether with one equivalent of *p*-methoxybenzyl trichloroacetimidate with a catalytic amount of (±)-10-camphorsulfonic acid afforded compound **11**, identical (^1H and ^{13}C NMR, IR, TLC, $[\alpha]_D$), to an authentic sample obtained by degradation from the natural product.[1] Compound **11** was converted into zaragozic acid A (**1**) by the sequence:[1] a) esterification of the C6 hydroxyl group with (*E*)-(4*S*, 6*S*)-4,6-dimethyl-2-octenoic acid (**4**); b) silylation of the C7 hydroxyl group with triethylsilyl trifluoromethanesulfonate (TESOTf); c) replacement of the PMB with an acetate group by using 2,3-dichloro-5,6-dicyano-1,4-benzoquinone (DDQ) followed by acetic anhydride treatment; and d) desilylation with fluoride ion and debenzylation of the esters by transfer hydrogenolysis.

The described chemistry demonstrates the usefulness of the asymmetric dihydroxylation reaction[2, 8] and of several substrate-controlled reactions in the synthesis of complex molecules, and shows the power of a newly discovered cascade rearrangement in the synthesis of the zaragozic acids. The convergent and flexible nature of the opened route to zaragozic acid A (**1**) makes the entire class of these natural products and their designed analogs now accessible by total synthesis.

Received: September 23, 1994 [Z 7348 IE]
German version: Angew. Chem. **1994**, *106*, 2312

[1] K. C. Nicolaou, E. W. Yue, Y. Naniwa, F. De Riccardis, A. Nadin, J. E. Leresche, S. La Greca, Z. Yang, *Angew. Chem.* **1994**, *106*, 2306; *Angew. Chem. Int. Ed. Engl.* **1994**, *33*, 2184

[2] K. C. Nicolaou, A. Nadin, J. E. Leresche, S. La Greca, T. Tsuri, E. W. Yue, Z. Yang, *Angew. Chem.* **1994**, *106*, 2309; *Angew. Chem. Int. Ed. Engl.* **1994**, *33*, 2187.

[3] a) R. S. Bhide, B. S. Levison, R. B. Sharma, S. Ghosh, R. G. Salomon, *Tetrahedron Lett.* **1986**, *27*, 671; b) T. J. Barton, C. R. Tully, *J. Org. Chem.* **1978**, *43*, 3649.

[4] This experiment was carried out on the (7*S*) stereoisomer and the exact structures of the spiroacetals formed are still under investigation.

[5] a) R. F. Newton, D. P. Reynolds, M. A. W. Finch, D. R. Kelly, S. M. Roberts, *Tetrahedron Lett.* **1979**, *20*, 3981; b) R. F. Newton, D. P. Reynolds, C. F. Webb, S. M. Roberts, *J. Chem. Soc. Perkin Trans. 1* **1981**, 2055; c) Y. Ogawa, M. Nunomoto, M. Shibasaki, *J. Org. Chem.* **1986**, *51*, 1625.

[6] Accompanying **9** were several by-products, including the 4′-epimeric alcohol and two rearranged, primary allylic alcohols. Numerous other desilylation conditions resulted in either no reaction, ester hydrolysis, or complete destruction of **8**.

[7] L. J. Mathias, *Synthesis* **1979**, *11*, 561.

[8] K. B. Sharpless, W. Amberg, Y. L. Bennani, G. A. Crispino, J. Hartung, K. S. Jeong, H. L. Kwong, K. Morikawa, Z. M. Wang, D. Xu, X. L. Zhang, *J. Org. Chem.* **1992**, *57*, 2768.

Synthesis and Crystal Structure of the "Open" Calcocene $[(t\mathrm{Bu}_2\mathrm{C}_5\mathrm{H}_5)_2\mathrm{Ca} \cdot \mathrm{thf}]$**

Jason S. Overby and Timothy P. Hanusa*

The recent surge of activity with organometallic compounds of the heavy alkaline earth metals calcium, strontium, and barium has focused on complexes containing alkyl-substituted cyclopentadienyl ligands.[1] Much less work has been done on compounds with other anionic unsaturated ligands,[2, 3] and none of these has been structurally characterized. As an alterna-

[*] Prof. T. P. Hanusa, J. S. Overby
Department of Chemistry, Vanderbilt University
Nashville, TN 37235 (USA)
Telefax: Int. code +(615) 322-4936

[**] This work was supported by the Donors of the Petroleum Research Fund, administered by the American Chemical Society.

tive to the cyclopentadienyl group, the acyclic pentadienyl ligand would be among the most interesting, since this ligand exhibits a variety of bonding modes to metals (η^1, η^3, η^5) that are in principle interconvertible.[4, 5] Largely through the work of Ernst et al. pentadienyl complexes have been described for many transition elements and some f- and p-block metals.[6] We now report the synthesis and X-ray crystal structure of the first bis(pentadienyl)complex of calcium, which displays both surprising similarities to, and differences from, its transition metal analogues.

Reaction of two equivalents of K[2,4-tBu$_2$C$_5$H$_5$] with CaI$_2$ in THF at low temperature produces the yellow complex [(2,4-tBu$_2$C$_5$H$_5$)$_2$Ca · thf]. It has limited solubility in THF and only slight to trace solubility in hydrocarbons. A substantial amount (ca. 20%) of the coupled ligand (2,4,7,9-tetra-*tert*-butyl-1,3,7,9-decatetraene) is also formed in the reaction, evidence that a radical reaction competes with halide metathesis in this system.[7] The ^{1}H NMR spectrum of the calcium complex in [D$_8$]THF displays a slightly split tBu resonance and broadened resonances for the pentadienyl protons; this could be evidence for a fluxional process in solution, although solubility constraints limit the information available from the NMR spectrum.

The solid-state structure of the calcium complex was obtained by X-ray analysis on a yellow crystal slowly grown from a saturated solution of the compound in hexane.[8] The compound exists as a monomeric species with two planar η^5-pentadienyl ligands (as evidenced by the narrow range of Ca–C distances from 2.74(1)–2.81(2) Å) and a single coordinated thf molecule (Fig. 1). As such, it is the first "open metallocene" of a Group 2

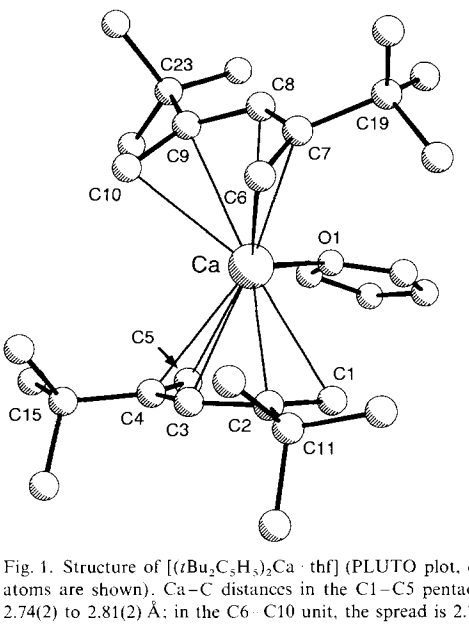


Fig. 1. Structure of [(tBu$_2$C$_5$H$_5$)$_2$Ca · thf] (PLUTO plot, only the non-hydrogen atoms are shown). Ca–C distances in the C1–C5 pentadienyl unit range from 2.74(2) to 2.81(2) Å; in the C6–C10 unit, the spread is 2.74(1) to 2.77(2) Å. The mean deviations of the pentadienyl carbon atoms from the least square planes are 0.015 Å and 0.0098 Å for C1–C5 and C6–C10, respectively. Selected distances [Å] and angles [°]: C1-C2 1.38(1), C2-C3 1.37(2), C2-C11 1.57(2), C3-C4 1.44(2), C4-C5 1.37(1), C4-C15 1.52(2), C6-C7 1.37(2), C7-C8 1.46(2), C7-C19 1.58(3), C8-C9 1.42(2), C9-C10 1.38(2), C9-C23 1.55(2); C1-C2-C3 127(1), C2-C3-C4 133(1), C3-C4-C5 125(1), C(6)-C(7)-C(8), 126(2), C7-C8-C9 128(2), C8-C9-C10 128(2).

metal, comparable to the open metallocenes of the transition metals.[5] The only other structurally characterized main-group pentadienyl complex, [(C$_7$H$_{11}$)$_2$Mg(tmeda)],[9] like the zinc pentadienyl complexes [(C$_5$H$_7$)ZnCl · tmeda] (tmeda = *N,N,N′,N′*-tetramethylethylenediamine)[10] and [(2,4-tBu$_2$C$_5$H$_5$)$_2$Zn],[6] has sigma-bonded, monohapto ligands. In this respect, the Ca^{II} center is acting like a d- or f-block metal, whose structurally characterized pentadienyl compounds usually contain pentahapto ligands.

Apart from the pentadienyl binding mode, the calcium complex displays several structural features that are distinctly untypical of transition metal pentadienyl complexes. The average Ca–C bond length of 2.76(2) Å is somewhat longer than the value observed in other formally seven-coordinate organocalcium complexes (e.g., 2.678(9) Å in [{1,3-(SiMe$_3$)$_2$C$_5$H$_3$}$_2$Ca · thf],[11, 12] and 2.67(1) Å in [{Cp*CaI · (thf)$_2$}$_2$] (Cp* = C$_5$Me$_5$)[13]). In contrast, transition metal pentadienyl complexes usually display M–C distances that are equal to, or slightly shorter than, related M–Cp distances (e.g., 2.211(2) Å in [{2,4-(CH$_3$)$_2$C$_5$H$_5$}$_2$V][14] vs. 2.280(5) Å in [Cp$_2$V][15]). The Ca–O(thf) distance of 2.439(9) Å is also moderately long for a seven-coordinate calcium center; the analogous Ca–O distances in [{1,3-(SiMe$_3$)$_2$C$_5$H$_3$}$_2$Ca · thf][11] and [{Cp*CaI · (thf)$_2$}$_2$][13] are 2.329(3) and 2.40(1) Å, respectively.

The two pentadienyl ligands adopt an almost perfect "*anti*-eclipsed" conformation: the plane containing Ca, C3, and the midpoint between C1 and C5 forms an angle of 174.4° with the plane containing Ca, C8, and the midpoint between C6 and C10. This is the first time such a wide angle has been observed in an open metallocene: typical values are near the angle of 60° for the "*gauche*-eclipsed" conformation, although twist angles up to 89.8° have been found (Fig. 2).[14] The presence of the thf ligand

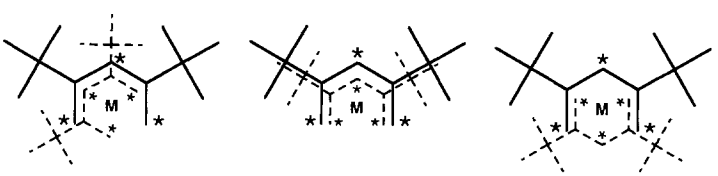


Fig. 2. Possible *gauche*-eclipsed (left), *syn*-eclipsed, and *anti*-eclipsed (right) conformations of the calcocene; the negatively charged atoms are marked with asterisks. The *anti*-eclipsed form is observed in the title complex.

complicates a straightforward analysis of the factors that may be involved, but the *anti*-eclipsed arrangement may partially reflect an attempt by the tBu$_2$C$_5$H$_5$ units to avoid unfavorable steric interactions; the closest contact between tBu groups is at 4.28 Å, which puts them outside van der Waals contact.

Although undoubtedly important, steric effects are probably not the only determinant of the pentadienyl orientation. In the calcocene [{1,3-(SiMe$_3$)$_2$C$_5$H$_3$}$_2$Ca · thf], the cyclopentadienyl ligands are twisted by only 29.2°,[11, 12] despite having two bulky trimethylsilyl groups on each ring. By virtue of a relatively small interplanar angle of 133.2°, the closest contact between SiMe$_3$ groups is 4.3 Å. The angle between the planes in the pentadienyl complex, however, is markedly larger at 146.5°. Thus it appears that the pentadienyl complex could have adopted a nearly "*syn*-eclipsed" conformation that would avoid severe steric repulsions. The *anti*-eclipsed conformation, however, places the formally charged carbon atoms of the pentadienyl ligands (1, 3, 5, 6, 8, 10) in an octahedral arrangement around the metal center; this would serve to maximize electrostatic bonding. A *gauche*-eclipsed conformation also generates an octahedral charge distribution, but the potential steric repulsions between the ligands would be much more severe.

The limited solubility provided by the tBu$_2$C$_5$H$_5$ ligand precludes its use with the larger strontium and barium centers. For

these metals, pentadienyl ligands that provide better solubility (such as $(Me_3Si)_2C_5H_5$[16]) will be needed to make their study feasible.

Experimental Procedure

$K[tBu_2C_5H_5]$ [6] (0.250 g, 1.16 mmol) and CaI_2 (0.170 g, 0.58 mmol) were mixed in THF (30 mL) under nitrogen at −78 °C. After stirring overnight at room temperature, a white precipitate and a yellow solution remained. The precipitate was removed by filtration, and the filtrate evaporated to dryness. The tan residue was washed twice with hexane to remove the tetraene by-product (ca. 20%), and then dried under vacuum, leaving $[(tBu_2C_5H_5)_2Ca \cdot thf]$ as an air-sensitive pale yellow solid (0.111 g, 41%). Anal. calcd. for $C_{30}H_{54}CaO$: C, 76.53; H, 11.56. Found: C, 67.66; H, 10.10. Although the C, H values from elemental analysis are low, the molar C:H ratio is 0.56, in agreement with the predicted value. ^1H NMR (300 MHz, [D$_8$]THF, 20 °C): $\delta = 0.11$ (s), 1.04 (s, *t*Bu), 1.09 (s, *t*Bu), 1.74 (β-C_4H_8O), 3.58 (α-C_4H_8O), 5.3–5.7 (br). The compound is insufficiently soluble in [D$_8$]THF to obtain useful ^{13}C NMR data. Attempts to sublime the compound (80–120 °C, 10^{-6} Torr) caused it to decompose. Small amounts of crystalline material were obtained by allowing a saturated hexane solution of the complex to evaporate slowly at room temperature.

Received: May 13, 1994 [Z 6930 IE]
German version: *Angew. Chem.* **1994**, *106*, 2300

[1] T. P. Hanusa, *Polyhedron* **1990**, *9*, 1345–1362.
[2] D. S. Hutchings, P. C. Junk, W. C. Patalinghug, C. L. Raston, A. H. White, *J. Chem. Soc. Chem. Commun.* **1989**, *15*, 973–974.
[3] A. Yanagisawa, S. Habaue, H. Yamamoto, *J. Am. Chem. Soc.* **1991**, *113*, 8955–8956.
[4] P. Powell, *Adv. Organomet. Chem.* **1986**, *26*, 125–164.
[5] R. D. Ernst, *Chem. Rev.* **1988**, *88*, 1255–1291.
[6] R. D. Ernst, J. W. Freeman, P. N. Swepston, D. R. Wilson, *J. Organomet. Chem.* **1991**, *402*, 17–25.
[7] Structure of the tetraene: J. S. Overby, T. P. Hanusa, *Acta Crystallogr. Sect C*, in press.
[8] Crystal data: $C_{30}H_{54}CaO$, $M = 470.84$, monoclinic, space group $P2_1/n$, $a = 10.005(5)$, $b = 22.254(8)$, $c = 14.434(6)$ Å, $\beta = 104.97(3)°$, $V = 3105(4)$ Å^3, $Z = 4$, $\rho_{calcd} = 1.007$ g cm^{-3}, $F(000) = 1048$, $\lambda = 0.71069$ Å, $T = 20$ °C, $\mu(Mo_{K\alpha}) = 2.1$ cm^{-1}, crystal size: $0.20 \times 0.41 \times 1.08$, $6° \le 2\theta \le 45°$; of 6870 reflections collected, 3316 were unique, and the 1856 with $F > 2.00\sigma(F)$ were used for refinement. No decay or absorption correction; solution was with SHELXS-86 and Fourier techniques. All non-hydrogen atoms were refined anisotropically; hydrogen atoms were inserted in calculated positions and not refined. $R = 0.079$; $R_w = 0.086$. 91% of the observed data were $\le 35°$ in 2θ; this led to a less satisfactory refinement and larger errors than normal; a second crystal displayed the same problem. A final difference map was featureless (0.28/−0.24 e Å^{-3}). Further details of the crystal structure investigation are available on request from the Director of the Cambridge Crystallographic Data Centre, 12 Union Road, GB-Cambridge CB2 1EZ (UK), on quoting the full journal citation.
[9] H. Yasuda, M. Yamauchi, A. Nakamura, T. Sei, Y. Kai, N. Yasuoka, N. Kasai, *Bull. Chem. Soc. Jpn.* **1980**, *53*, 1089–1100.
[10] H. Yasuda, Y. Ohnuma, A. Nakamura, Y. Kai, N. Yasuoka, N. Kasai, *Bull. Chem. Soc. Jpn.* **1980**, *53*, 1101–1111.
[11] P. Jutzi, W. Leffers, G. Müller, B. Huber, *Chem. Ber.* **1989**, *122*, 879–884.
[12] L. M. Engelhardt, P. C. Junk, C. L. Raston, A. H. White, *J. Chem. Soc. Chem. Commun.* **1988**, 1500–1501.
[13] M. J. McCormick, S. C. Sockwell, C. E. H. Davies, T. P. Hanusa, J. C. Huffman, *Organometallics* **1989**, *8*, 2044–2049.
[14] R. D. Ernst, C. F. Campana, D. R. Wilson, J. Z. Liu, *Inorg. Chem.* **1984**, *23*, 2732–2734.
[15] A. Haaland, *Acc. Chem. Res.* **1979**, *12*, 415–422.
[16] K. Kunze, A. M. Arif, R. D. Ernst, *Bull. Soc. Chim. Fr.* **1993**, *130*, 708–711.

$[Ru_3(CO)_6(\eta^5:\eta^1\text{-}C_5H_4)_3]$: The First Six-Membered Ru_3C_3 Ring Formed by Insertion of C_5H_4 Units into Metal–Metal Bonds of $[Ru_3(CO)_{12}]$**

Alejandro J. Arce,* Ysaura De Sanctis, Jorge Manzur, and Mario V. Capparelli

The cyclopentadienyl ligand has played a key role in the development of organometallic chemistry,[1] and cyclopentadienyl complexes (π- or σ-bonded to a central metal atom or to two metal atoms) of many transition metals are known.[2] Many syntheses and studies of mononuclear cyclopentadienyl derivatives of group VIII transition metals have been reported, but only few polynuclear cyclopentadienyl complexes are known, and new types of interesting compounds have been recently synthesized.[3]

Mononuclear cyclopentadienyl derivatives have been of more practical value: a variety of cyclopentadienyl-containing complexes are used in a broad range of catalytic reactions,[4] though their full potential has yet not been realised. Cyclopentadienyl (C_5H_5) and cyclopentadienylidene (C_5H_4) bridges in polynuclear compounds have attracted little attention so far.[5] The use of the diazocyclopentadiene ($C_5H_4N_2$) has made the synthesis of monohalocyclopentadienyl and multiply substituted cyclopentadienyl complexes readily accessible.[6] Diazocyclopentadiene reacts with metal–metal triple bonds, as in the reaction with $[Mo_2(CO)_4Cp_2]$,[7] to afford a cyclopentadienylidene derivative $[Mo_2(CO)_3(\eta^5\text{-}Cp)_2(\mu\text{-}\eta^5:\eta^1\text{-}C_5H_4)]$ (N_2 and CO elimination). In this compound the organic ligand acts both as a terminal σ-alkyl ligand to the $[(\eta^5\text{-}Cp)Mo(CO)_2]$ fragment and as an aromatic η^5-system to the $[(\eta^5\text{-}Cp)Mo(CO)]$ unit. The overall result is a metal-bridging, six-electron-donating ligand.

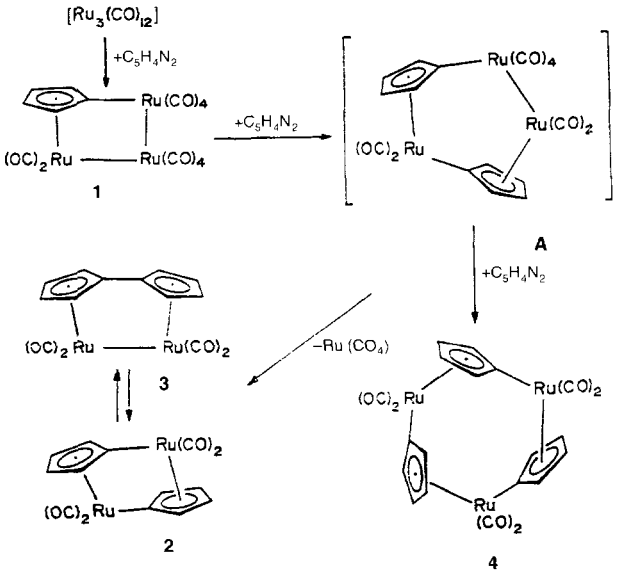
When ketene ($H_2C{=}C{=}O$) reacts with $[Os_3(CO)_{10}(CH_3CN)_2]$, the C=C bond of ketene is broken to afford the compound $[Os_3(CO)_{11}(\mu\text{-}CH_2)]$.[8] The same compound can also be obtained by treating $[Os_3(CO)_{11}(CH_3CN)]$ with CH_2N_2.[9] In view of these results we tried to synthesize C_5H_4-bridged clusters from triruthenium clusters and $C_5H_4N_2$ in order to obtain μ,η^1-cyclopentadienylidene complexes such as $[Ru_3(CO)_{11}(C_5H_4)]$, which might contain the dimetallacyclopropane unit, like the product from the reaction between diazomethane and triosmium clusters. The outcome was products with a different type of bonding.

The reaction of $[Ru_3(CO)_{12}]$ with $C_5H_4N_2$ in THF under reflux gave complexes **1**, **3**, and **4** in 46, 20, and 25% yield, respectively (Scheme 1). Compounds **1** and **4** are formed with concomitant elimination of N_2 and CO and are thermally stable. All the products were characterized by ^1H NMR and IR spectroscopy, and the X-ray structures of **1** and **4** were determined.[10]

Compound **3** has been synthesized[11] by the reaction of $[Ru_3(CO)_{12}]$ and dihydrofulvalene and can be converted into compound **2** by photocleavage (sunlight) of the Ru–Ru bond in THF. Under our reaction conditions **2** also reverts thermally to **3** as described in the earlier synthesis. Compounds **2** and **4** can also

[*] Dr. A. J. Arce, M. Sc. Y. De Sanctis, Dr. M. V. Capparelli
Centro de Química, Instituto Venezolano de Investigaciones Científicas, IVIC
Apartado 21827, Caracas 1020-A (Venezuela)
Telefax: Int. code +(2) 501-1350
Prof. J. Manzur
Universidad de Chile, Facultad de Ciencias Físicas y Matemáticas
Casilla 2777, Santiago (Chile)

[**] The authors want to thank the Venezuelan National Research Council (CONICIT) for providing funds for the purchase of the Rigaku AFC7S diffractometer and auxiliary equipment (Project PI-092) and the Chilean National Research Council (CONICYT) for financial support of this work.



Scheme 1.

be obtained by direct reaction of **1** and diazocyclopentadiene in THF under reflux. After 20 min complete conversion was achieved. We postulate that the species formed in the early stages of the reaction is **A** (Scheme 1), an open Ru_3 compound which in the presence of diazocyclopentadiene converts readily into the new cyclotrimer **4**. To account for the formation of **3** the intermediate species **A** loses a $Ru(CO)_4$ unit to afford the cyclodimer **2**, which was confirmed by comparison of the IR and ^1H NMR spectroscopic data with those reported earlier (see *Experimental*).[11] Recently Vahrenkamp reported the insertion of a C_5H_4 unit[12] into a metal–metal bond by the reaction of $Ph_3P{=}C(CH)_4$ and $[Ru_3(CO)_{12}]$ and gave spectroscopic evidence for compound **1**.

The crystal structure analysis of compound **1**[10a] (Fig. 1) showed that it is an open Ru_3 cluster, with two metal–metal bonds, bridged by an $\eta^5{:}\eta^1$-C_5H_4 moiety, which makes **1** a

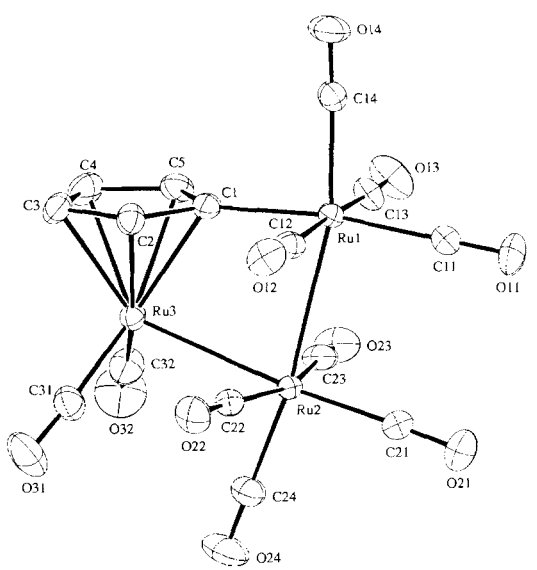


Fig. 1. Molecular structure of **1** (ORTEP plot; thermal ellipsoids represent 30% probability). Selected bond lengths [Å] and angles [°]: Ru1–Ru2, 2.9486(6), Ru2–Ru3, 2.8256(7), Ru1–C1, 2.105(6), Ru3–C1, 2.270(6), Ru3–C*n* (mean for $n = 2$–5) 2.231(7); C1–Ru1–Ru2, 76.4(2), Ru1–Ru2–Ru3, 83.56(2), Ru2–Ru3–C1, 76.8(2), Ru1–C1–Ru3, 123.1(3).

50-electron cluster. The molecule has a plane of symmetry defined by the three Ru atoms, four CO groups, and C1. (The metal atoms are within 0.003 Å of the plane, while the mean deviation for all 12 atoms defining the plane is 0.061 Å.[13]) Therefore, this crystal structure is an example of an achiral molecule crystallizing in a chiral space group.

An X-ray structure determination for **4** was needed to establish the mode of bonding. The crystallographic study[10b] (Fig. 2) revealed that this compound is a novel cyclic trimer with no metal–metal bonds, derived from the insertion of C_5H_4 units into Ru–Ru metal bonds. The $Ru(CO)_2$ units are held together by $\eta^5{:}\eta^1$-C_5H_4 ligands. The resulting Ru_3C_3 metallacycle has a twist-boat conformation, with Ru1 and C1c at 0.79 and 0.53 Å from the mean plane through Ru2, Ru3, C1a and C1b.

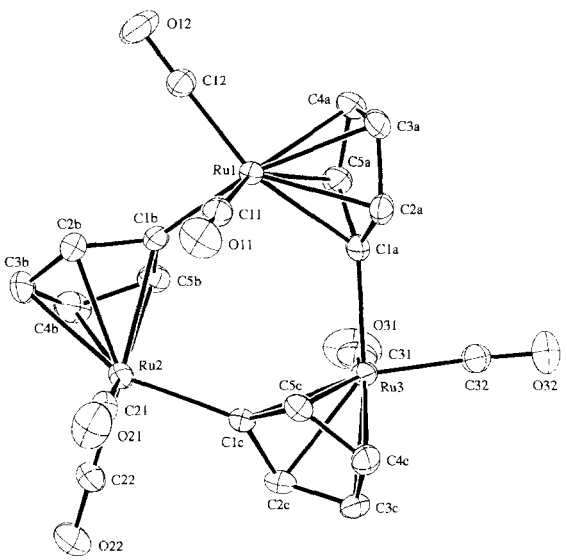


Fig. 2. Molecular structure of **4** (ORTEP plot; thermal ellipsoids represent 30% probability). Selected bond lengths [Å] and angles [°]: Ru1–C1b, 2.084(4), Ru2–C1c, 2.104(4), Ru3–C1a, 2.095(5), Ru1–C1a, 2.293(4), Ru2–C1b, 2.308(4), Ru3–C1c, 2.300(4), Ru1–C*n*a (mean for $n = 2$–5) 2.238(5), Ru2–C*n*b (mean for $n = 2$–5) 2.241(5), Ru3–C*n*c (mean for $n = 2$–5) 2.247(5); C1a–Ru1–C1b, 97.9(2), C1b–Ru2–C1c, 96.7(2), C1c–Ru3–C1a, 102.0(2), Ru1–C1a–Ru3, 129.5(2), Ru2–C1b–Ru1, 130.0(2), Ru2–C1c–Ru2, 132.1(2).

In **1** and **4** the C_5H_4 moiety is bonded to two metal atoms as a metallocyclopentadienyl, six-electron-donor ligand, rather than as a cyclopentadienylidene ligand. In both compounds the $Ru_2(\eta^5{:}\eta^1$-$C_5H_4)$ units display similar structural features: a) within each $Ru(\eta^5$-$C_5H_4)$ moiety, the Ru–C1 distance is significantly longer than the other four metal-carbon distances (0.039 Å in **1**, average of 0.058 Å in **4**); b) of the two Ru–C bonds formed by each C1 atom, the π bond involved in the η^5 coordination is significantly longer than the σ bond involved in η^1 coordination (0.165 Å in **1**, average of 0.206 Å in **4**). All the Ru–C(Cp) bond lengths are similar to those found in $[Ru_3(CO)_9(PPh_3)(C_5H_4)]$[12] and in **2**;[11] the averages of the four shorter Ru–C(Cp) distances (2.231 Å in **1**, 2.242 Å in **4**) are close to the mean of 2.236 Å compiled in ref. [14]. All the compounds described here show an $\eta^5{:}\eta^1$ coordination of the cyclopentadienyl bridge. The tendency of the cyclic ring to aromatize seems to be responsible for the preference of $\eta^5{:}\eta^1$ complexation in trinuclear clusters rather than carbene–diolefin coordination.

In conclusion we found that **4** $[Ru_3(CO)_6(\eta^5{:}\eta^1$-$C_5H_4)_3]$ is the first six-membered Ru_3C_3 ring system formed by a facile insertion of C_5H_4 units into metal–metal bonds of $[Ru_3(CO)_{12}]$. This pro-

 © VCH Verlagsgesellschaft mbH, D-69451 Weinheim, 1994 0570-0833/94/2121-2194 $ 10.00+.25/0

cedure opens up the possibility for a suitable access to new ruthenium complexes with μ-η^5:η^1-C_5H_4 units as bridging ligands.

Experimental Procedure

A solution of $[Ru_3(CO)_{12}]$ (200 mg, 0.32 mmol) and freshly distilled diazocyclopentadiene [15] (40 μL, 0.5 mmol) in dried THF (40 mL) was heated at reflux under nitrogen for one hour. After evaporation of the solvent, thin-layer chromatography (SiO_2) of the orange-red residue, eluting with pentane:dichloromethane 4:1 (v:v) gave three bands. Compound **1** was recovered as pale yellow crystals from hexane in 46% yield, compound **2** as a pale yellow solid in 20% yield, and compound **4** as colorless crystals (cyclohexane) in 25% yield. On exposing a solution of compound **3** in THF to sunlight for 4 h, complete conversion to **2** was achieved (IR monitoring). **1**: IR(C_6H_{12}) $\tilde{\nu}$(CO) [cm^{-1}]: 2113w, 2066s, 2047w, 2031vs, 2001s, 1987sh, 1949w. ^1H NMR ($CDCl_3$, 300 MHz, 296 K, J in Hz): δ = 5.29 (dd, 2H, J = 1.8, 1.8), 4.39 (dd, 2H, J = 1.8, 1.8). **2**: IR(CH_2Cl_2) $\tilde{\nu}$(CO) [cm^{-1}]: 2012vs, 1960vs. ^1H NMR ($CDCl_3$, 300 MHz, 296 K, J in Hz): δ = 5.39 (dd, 4H, J = 2.0, 2.0), 4.68 (dd, 4H, J = 2.0, 2.0). **3**: IR(CH_2Cl_2) $\tilde{\nu}$(CO) [cm^{-1}]: 2019vs, 1952vs. ^1H NMR ($CDCl_3$, 300 MHz, 296 K, J in Hz): δ = 5.69 (dd, 4H, J = 1.9, 1.9), 3.95 (dd, 4H, J = 1.9, 1.9). **4**: IR(C_6H_{12}) $\tilde{\nu}$(CO) [cm^{-1}] 2017vs, 1970vs. ^1H NMR ($CDCl_3$, 300 MHz, 296 K, J in Hz): δ = 5.29 (dd, 6H, J = 2.1, 2.1), 4.95 (dd, 6H, J = 2.1, 2.1).

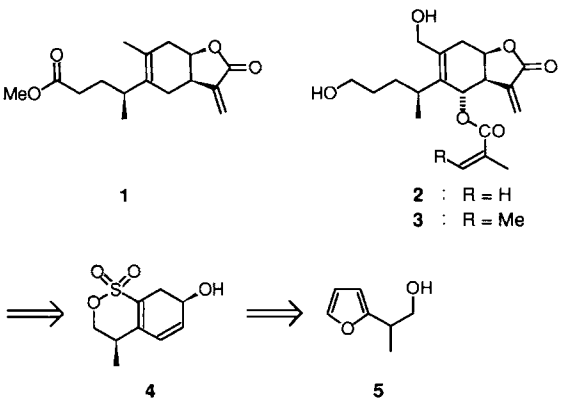
Received: June 3, 1994 [Z 6989 IE]
German version: *Angew. Chem.* **1994**, *106*, 2277

[1] a) *Comprehensive Organometallic Chemistry, Vol. 3–7* (Eds.: G. Wilkinson, F. G. A. Stone, W. Abel), Pergamon, Oxford, **1982**; b) *Adv. Organomet. Chem.* **1964**, *1*; *ibid.* **1989**, *29*.
[2] C. Janiak, H. Schumann, *Adv. Organomet. Chem.* **1991**, *33*, 291.
[3] J. L. Kersten, A. L. Rheingold, K. H. Theopold, C. P. Casey, R. A. Wiedenhoefer, C. E. C. A. Hop, *Angew. Chem.* **1992**, *104*, 1364; *Angew. Chem. Int. Ed. Engl.* **1992**, *31*, 1341; b) J. J. Schneider, *ibid.* **1992**, *104*, 1422 and **1992**, *31*, 1392.
[4] I. E. Ninfant'ev, M. V. Borzov, A. V. Churakov, S. G. Mkoyan, L. O. Atovmyan, *Organometallics* **1992**, *11*, 3942.
[5] N. J. Coville, K. E. du Plooy, W. Pickl, *Coord. Chem. Rev.* **1992**, *116*, 1.
[6] W. A. Herrmann, M. Huber, *Chem. Ber.* **1978**, *111*, 3124.
[7] W. A. Herrmann, G. Kriechbaum, C. Bauer, E. Guggolz, M. L. Ziegler, *Angew. Chem.* **1981**, *93*, 838; *Angew. Chem. Int. Ed. Engl.* **1981**, *20*, 815.
[8] A. J. Arce, A. J. Deeming, *J. Chem. Soc. Chem. Commun.* **1982**, 364.
[9] a) J. R. Shapley, A. C. Sievert, M. R. Churchill, H. J. Wasserman, *J. Am. Chem. Soc.* **1981**, *103*, 6975; b) B. F. G. Johnson, J. Lewis, P. Raithby, J. Sankey, *J. Organomet. Chem.* **1982**, *231*, C65.
[10] a) Crystal structure of **1**: $C_{15}H_4O_{10}Ru_3$, M = 647.40, orthorhombic, $P2_12_12_1$ (No. 19), a = 13.368(2), b = 17.531(2), c = 7.867(2) Å, V = 1843.6(6) Å^3, Z = 4, ρ_{calcd} = 2.33 g cm^{-3}, $\mu(Mo_{K\alpha})$ = 24.8 cm^{-1}, $F(000)$ = 1224. Rigaku AFC7S diffractometer, graphite-monochromated $Mo_{K\alpha}$ radiation (λ = 0.71069 Å). Solution by direct methods [16]. Refinement on F by full-matrix least-squares with $w = \sigma(F)^{-2}$ [17], non-H atoms anisotropically, H-atoms in calculated positions (C-H 0.96 Å, B_{iso} refined). Corrections for Lorentz polarization, absorption [18], and extinction (isotropic). Last cycle: 2188 unique data [$I > 3\sigma(I)$], 258 parameters, R = 0.0237, R_w = 0.0313, S = 1.445, max. shift/e.s.d. = 0.001, residual electron density = −0.74/0.49 e Å^{-3}. b) Crystal structure of **4**: $C_{21}H_{12}O_6Ru_3$, M = 663.53, monoclinic, $C2/c$ (No. 15), a = 17.759(2), b = 8.769(3), c = 27.588(2) Å, V = 4085(1) Å^3, Z = 8, ρ_{calcd} = 2.16 g cm^{-3}, $\mu(Mo_{K\alpha})$ = 22.3 cm^{-1}, $F(000)$ = 2544. Rigaku AFC7S diffractometer, graphite-monochromated $Mo_{K\alpha}$ radiation (λ = 0.71069 Å). Solution by direct methods [19]. Refinement on F by full-matrix least-squares with $w = \sigma(F)^{-2}$ [17], non-H atoms anisotropically, H-atoms in calculated positions (C-H 0.96 Å, B_{iso} refined). Corrections for Lorentz polarization, absorption [20], and extinction (isotropic). Last cycle: 4015 unique data [$I > 3\sigma(I)$], 283 parameters, R = 0.0282, R_w = 0.0329, S = 2.816, max. shift/e.s.d. = 0.001, residual electron density = −0.74/0.61 e Å^{-3}. Further details of the crystal structure investigations are available on request from the Director of the Cambridge Crystallographic Data Centre, 12 Union Road, GB-Cambridge CB2 1EZ (UK), on quoting the full journal citation.
[11] K. P. C. Vollhardt, T. W. Weidman, *J. Am. Chem. Soc.* **1983**, *105*, 1676.
[12] D. Heineke, H. Vahrenkamp, *Angew. Chem.* **1993**, *105*, 1142; *Angew. Chem. Int. Ed. Engl.* **1993**, *32*, 1048.
[13] For the eight pairs of out-of-plane non-hydrogen atoms, the mean deviation of their middle points is $-\sum|d - d'|/2n$ = 0.044 Å (n = 8).
[14] A. G. Orpen, L. Brammer, F. H. Allen, O. Kennard, D. G. Watson, R. Taylor, *J. Chem. Soc. Dalton Trans.* **1989**, S1.
[15] W. von E. Doering, C. H. DePuy, *J. Am. Chem. Soc.* **1953**, *75*, 5955.
[16] G. M. Sheldrick, *Acta Crystallogr. Sect. A* **1990**, *45*, 467.
[17] *teXsan. Single Crystal Structure Analysis Software, Version 1.6*, Molecular Structure, The Woodlands, TX, USA, **1993**.
[18] A. C. T. North, D. C. Phillips, F. S. Mathews, *Acta Crystallogr. Sect. A* **1968**, *24*, 351.
[19] H. F. Fan, *SAPI-91. Structure Analysis Programs with Intelligent Control*, Rigaku, Tokyo, Japan, **1991**.
[20] N. Walker, D. Stuart, *Acta Crystallogr. Sect. A* **1983**, *39*, 158.

A Short and Highly Stereoselective Synthesis of the 1,10-*seco*-Eudesmanolide Ivangulin**

Peter Metz,* Jörn Stölting, Mechtild Läge, and Bernt Krebs

The bicyclic sesquiterpene lactones ivangulin (**1**),[1] eriolanin (**2**),[2] and eriolangin (**3**)[2] (Scheme 1) belong to the class of the 1,10-*seco*-eudesmanolides, the more highly oxygenated members of which, **2** and **3**, display significant antileukemic activity



Scheme 1. Retrosynthetic analysis of **1**–**3**.

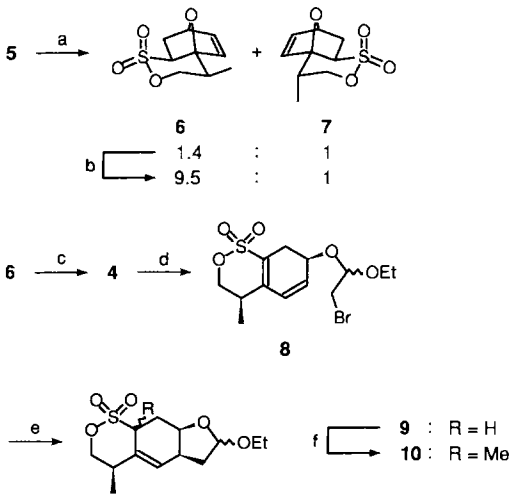
in vivo. A central problem associated with the diastereoselective synthesis of **1**,[3] **2**,[4, 5] and **3**[4] is control of the relative configuration of the exocyclic stereogenic center. Based upon our studies on intramolecular Diels–Alder reactions of vinylsulfonates[6–8] and the synthetic elaboration of the resultant sultones,[7, 9, 10] we can retrosynthetically convert all three natural products to sultone **4** (Scheme 1). In **4** two of the stereogenic centers of the target molecules in a 1,5-relationship are already present with correct relative configuration; moreover, the latent primary alcohol offers the possibility of chain extension, and the endocyclic 1,3-diene activates all further positions which are substituted in the cyclohexene moiety of **1**–**3**. Sultone **4** in turn is rapidly available from furan **5**[11] using a methodology[6, 9] developed by us. Here we report an efficient synthesis of **1** by a thermodynamically controlled intramolecular Diels–Alder reaction of the vinylsulfonate of **5**, a radical cyclization of a derivative of **4**, as well as a reductive sultone cleavage.

When **5** is treated with vinylsulfonyl chloride,[13] the primarily formed, spectroscopically characterized (^1H, ^{13}C NMR) vinylsulfonate undergoes an intramolecular cycloaddition[6–8] at 0 °C (12 h) to give a 1.4:1 mixture of the two *exo*-sultones **6** and **7** (Scheme 2). An equilibration through retro-Diels–Alder reaction only takes place in refluxing toluene and eventually leads to a ratio of 9.5:1 in favor of the thermodynamically more stable diastereomer **6** with equatorial methyl group.[14] To avoid side reactions of the vinylsulfonate of **5** regenerated in the equi-

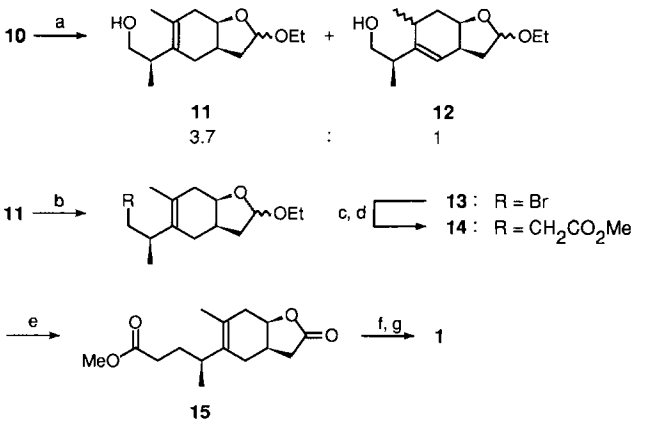
[*] Priv.-Doz. Dr. P. Metz, Dipl.-Chem. J. Stölting
Organisch-chemisches Institut der Universität
Corrensstrasse 40, D-48149 Münster (FRG)
Telefax: Int. code +(251)83-9772
M. Läge,[+] Prof. Dr. B. Krebs[+]
Anorganisch-chemisches Institut der Universität Münster (FRG)

[+] X-ray diffraction analysis.

[**] This work was supported by the Deutsche Forschungsgemeinschaft, the Fonds der Chemischen Industrie, and the Ministerium für Wissenschaft und Forschung des Landes Nordrhein-Westfalen. We thank BASF AG for a PhD fellowship to J. Stölting.



Scheme 2. a) $H_2C{=}CHSO_2Cl$, Et_3N, THF, 0 °C. b) Toluene, BHT, reflux (86% from **5**). c) LDA, TMEDA, THF, −78 °C (85%). d) $BrCH(OEt)CH_2Br$, $PhNEt_2$ [18], CH_2Cl_2, 25 °C (98%). e) $[Cr_3(OAc)_4(H_2O)_2]$, $H_2NCH_2CH_2NH_2$, THF, H_2O, 25 °C (83%). f) MeLi, THF, −78 °C; MeI, 0 °C (93%).



Scheme 3. a) Li, NH_3(l), THF, −60 °C (73%). b) CBr_4, Ph_3P, pyridine, 25 °C (83%). c) $NaCH(CO_2Me)_2$, dimethylformamide, hexamethylphosphoric acid triamide, 100 °C. d) PhSH, K_2CO_3, DMF, 90 °C (38% **14** from **13**). e) $Na_2Cr_2O_7$, H_2SO_4, acetone, 0 °C (83%). f) $MeOCO_2MgOMe$, DMF, 130 °C. g) CH_2O, PhNHMe, NaOAc, HOAc, H_2O, 25 °C (67% **1** from **15**, 78% **1** based on converted **15**).

librium at elevated temperature, a small amount of the radical scavenger BHT (2,6-di-*tert*-butyl-4-methylphenol) is added. After separation of the cycloadducts by chromatography[15] or recrystallization (ethyl acetate), the desired major isomer **6** is isolated in pure form. Moreover, the separated diastereomer **7**, too, is subjected to the equilibration during the next run, so that a continuous conversion into the major isomer **6** ensues. The relative configurations of **6** and **7** follow from diagnostic coupling constants in the ^{1}H NMR,[16] if a chair conformation of the δ-sultone is assumed. An X-ray diffraction analysis[17] of the minor product **7**, which yielded suitable crystals, served as unambiguous proof of the spatial orientation of the methyl group.

In the presence of tetramethylethylenediamine (TMEDA), basic ring opening[9, 10] of **6** to dienol **4** with lithium diisopropylamide (LDA) proceeds almost without disturbing dehydration to the corresponding benzene derivative. For construction of the γ-lactone of **1** in masked form, **4** is first coupled with the adduct from ethyl vinyl ether and bromine prepared in situ to give the mixed acetal **8**.[18] When **8** is cyclized with tri-*n*-butylstannane (azobis*iso*butyronitrile, toluene, reflux),[19, 20] **9** and its double bond isomer with S–C=C unit are formed in a ratio of 2:1 (84%). Complete regioselectivity in favor of **9** is achieved by a chromium(II)-induced cyclization[21] of **8**. Methylation of the allyllithium species generated from **9** with methyllithium[22] occurs only in α-position to sulfur with formation of the diastereomeric alkylation products **10**.

Due to faster protonation at the less substituted terminus of the allyllithium intermediate,[9, 10, 23] a reductive desulfurization of **10** with lithium in liquid ammonia leads with good selectivity to the tetrasubstituted olefin **11** which, after chromatographic separation[15] from **12**, is converted[24] to bromide **13** (Scheme 3). The side chain of **1** is completed by reaction of **13** with sodium dimethylmalonate followed by demethoxycarbonylation[25] of the resultant substituted malonate, and Jones oxidation[19, 21] of acetal **14** unmasks the γ-lactone **15**. For α-methylenation to ivangulin (**1**),[26] we use a two-step sequence consisting of carboxylation of **15** with methyl methoxymagnesium carbonate[27] and subsequent Mannich reaction with decarboxylation[28] which succeeds with complete chemoselectivity.[29]

Starting from 2-acetylfuran, our sultone route featuring excellent control of the relative configuration of the stereogenic center located on the side chain requires only 15 steps to the 1,10-*seco*-eudesmanolide **1**, and thus halves the number of steps needed in the previously published synthesis of this natural product.[3] Utilization of **9** for the synthesis of eriolanin (**2**) and eriolangin (**3**) is currently under investigation.

Received: June 24, 1994 [Z 7074 IE]
German version: *Angew. Chem.* **1994**, *106*, 2275

[1] W. Herz, Y. Sumi, V. Sudarsanam, D. Raulais, *J. Org. Chem.* **1967**, *32*, 3658–3662.
[2] S. M. Kupchan, R. L. Baxter, C.-K. Chiang, C. J. Gilmore, R. F. Bryan, *J. Chem. Soc. Chem. Commun.* **1973**, 842–843.
[3] P. A. Grieco, T. Oguri, C.-L. J. Wang, E. Williams, *J. Org. Chem.* **1977**, *42*, 4113–4118.
[4] P. A. Grieco, T. Oguri, S. Gilman, *J. Am. Chem. Soc.* **1980**, *102*, 5886–5891.
[5] M. R. Roberts, R. H. Schlessinger, *J. Am. Chem. Soc.* **1981**, *103*, 724–725; R. H. Schlessinger in *Organic Synthesis Today and Tomorrow* (Eds.: B. M. Trost, C. R. Hutchinson), Pergamon, Oxford, **1981**, p. 251–258; T. Wakamatsu, N. Miyachi, F. Ozaki, M. Shibasaki, Y. Ban, *Tetrahedron Lett.* **1988**, *29*, 3829–3832.
[6] E. Bovenschulte, P. Metz, G. Henkel, *Angew. Chem.* **1989**, *101*, 204–206; *Angew. Chem. Int. Ed. Engl.* **1989**, *28*, 202–203.
[7] P. Metz, M. Fleischer, R. Fröhlich, *Synlett* **1992**, 985–987.
[8] P. Metz, M. Fleischer, *Synlett* **1993**, 399–400.
[9] P. Metz, E. Cramer, *Tetrahedron Lett.* **1993**, *34*, 6371–6374.
[10] P. Metz, U. Meiners, R. Fröhlich, M. Grehl, *J. Org. Chem.* **1994**, *59*, 3687–3689.
[11] G. Schmid, T. Fukuyama, K. Akasaka, Y. Kishi, *J. Am. Chem. Soc.* **1979**, *101*, 259–260; B. Alcaide, P. Areces, E. Borredon, C. Biurrun, J. P. Castells, J. Plumet, *Heterocycles* **1990**, *31*, 1997–2002. We prepare **5** by a Wittig reaction [12] ($Ph_3P{=}CH_2$, ether, 25–35 °C) followed by hydroboration/oxidation (BH_3, THF, petroleum ether, THF, 0–25 °C; NaOH, H_2O_2, 40–50 °C) from commercially available 2-acetylfuran (64% total yield).
[12] Cf. W. J. Davidson, J. A. Elix, *Aust. J. Chem.* **1973**, *26*, 1059–1067.
[13] C. S. Rondestvedt, Jr., *J. Am. Chem. Soc.* **1954**, *76*, 1926–1929.
[14] For synthetic elaboration of **5** in practice, the solvent is removed after esterification with vinylsulfonyl chloride (1.5 h at 0 °C), and the crude vinylsulfonate is heated directly in refluxing toluene (10 min; yield **6** + **7** and diastereomeric ratio **6**:**7** as in Scheme 2).
[15] Preparative HPLC (Waters Delta Prep 3000; steel column Waters Porasil 125 Å, 15–20 μm, 300 mm length, 50 mm ∅; ether/ethyl acetate/petroleum ether 1/2/2).
[16] Selected ^{1}H NMR data (300 MHz, $CDCl_3$) of (1*S**,2*S**,4*R**,1′*S**)- and (1*R**,2*R**,4*S**,1′*S**)-1-(1-methylethyl)-7-oxa-5-norbornene-2,2′-sultone (**6** and **7**, respectively). **6**: δ = 3.16 (dd, ^3J(2-H, 3-H_{exo}) = 3.5, ^3J(2-H, 3-H_{endo}) = 7.9 Hz, 1H; 2-H), 4.31 (dd, ^2J(2′-H_a, 2′-H_b) = 11.8, ^3J(2′-H_a,1′-H) = 5.2 Hz, 1H; 2′-H_a), 4.50 (dd, ^2J(2′-H_b, 2′-H_a) = 11.8, ^3J(2′-H_b,1′-

H) = 11.9 Hz, 1H; 2'-H_b); 7: δ = 3.26 (dd, ^3J(2-H, 3-H_{exo}) = 3.2, ^3J(2-H, 3-H_{endo}) = 7.9 Hz, 1H; 2-H), 4.23 (dd, ^2J(2'-H_a, 2'-H_b) = 11.6, ^3J(2'-H_a,1'-H) = 1.4 Hz, 1H; 2'-H_a), 4.92 (dd, ^2J(2'-H_b, 2'-H_a) = 11.6, ^3J(2'-H_b, 1'-H) = 2.3 Hz, 1H; 2'-H_b).

[17] X-ray diffraction analysis of 7: crystal dimensions 0.15 × 0.22 × 0.2 mm, space group *Pbca*, a = 13.818(3), b = 10.098(2), c = 14.086(4) Å, V = 1965.6 Å^3, Z = 8, $\rho_{calcd.}$ = 1.46 g cm^{-3}, Siemens-P3 diffractometer, $Mo_{K\alpha}$ radiation, 2θ-range 4–54°, measuring method $\omega/2\theta$-scan, scan rate 3.5–29.3° min^{-1}, T = 293 K, 2161 independent reflections measured, 1100 of which observed ($I > 1.96\,\sigma(I)$), 131 variables refined, direct methods (SHELXTL-plus), least-square fit, R = 0.0682, R_w = 0.0536. Further details of the crystal structure investigation are available on request from the Fachinformationszentrum Karlsruhe, D-76344 Eggenstein-Leopoldshafen, on quoting the depository number CSD-58430.

[18] If triethylamine is used instead of *N,N*-diethylaniline, aromatization predominates.

[19] G. Stork, R. Mook, Jr., S. A. Biller, S. D. Rychnovsky, *J. Am. Chem. Soc.* **1983**, *105*, 3741–3742.

[20] For intramolecular radical addition to cyclic 1,3-dienes, see: C. E. Schwartz, D. P. Curran, *J. Am. Chem. Soc.* **1990**, *112*, 9272–9284.

[21] For corresponding reductive cyclization reaction of α-bromoacetals and a monoolefin unit, see: C. Hackmann, H. J. Schäfer, *Tetrahedron* **1993**, *49*, 4559–4574.

[22] The use of methyllithium is essential here. For deprotonation of other sulfones (see e. g. **6**) successfully applied bases such as LDA or *n*BuLi [7, 9] do not cause conversion of **9**.

[23] A ratio **11**:**12** of 3.7:1 is reproducibly obtained if all resultant diastereomers of **10** are used. Preliminary mechanistic studies show that the regioselectivity of this reductive sultone cleavage is highly dependant upon the relative configuration of diastereomers **10** at the acetal carbon atom.

[24] A. K. M. Anisuzzaman, R. L. Whistler, *Carbohydr. Res.* **1978**, *61*, 511–518.

[25] E. Keinan, D. Eren, *J. Org. Chem.* **1986**, *51*, 3165–3169.

[26] We thank Priv.-Doz. Dr. M. Göbel, Universität Frankfurt, for sending us a sample of authentic (+)-ivangulin.

[27] M. Stiles, H. Finkbeiner, *J. Am. Chem. Soc.* **1959**, *81*, 505–507.

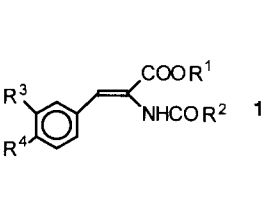
[28] M. M. Murta, M. B. M. de Azevedo, A. E. Greene, *J. Org. Chem.* **1993**, *58*, 7537–7541.

[29] A thorough GC/MS analysis of the crude product confirms that no additional methylenation products are formed apart from **1**.

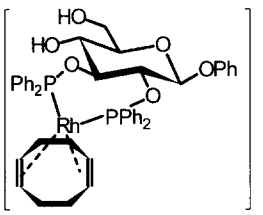
Increase in the Enantioselectivity of Asymmetric Hydrogenation in Water Influenced by Surfactants or Polymerized Micelles**

Arvind Kumar, Günther Oehme,* Jean Pierre Roque, Manuela Schwarze, and Rüdiger Selke*

The hydrogenation of sparingly soluble compounds using slightly soluble complexes of rhodium(I) biphosphanes or biphosphinic acid esters as catalysts in water can be considerably accelerated by the addition of solubilizing agents that form micelles.[1] In the asymmetric hydrogenation of methyl (*Z*)-2-*N*-acetylaminocinnamate (**1f**), the substrate exclusively used up to now, the enantioselectivity is lower in water than in other solvents (particularly alcohols) for all of the catalysts investigated in the absence of surfactants and is increased relative to the blank by the addition of amphiphilic compounds. Thus it seems important to determine whether this is only an apparent increase in enantioselectivity, caused, for example, by suppressing the influence of unspecific catalyst impurities (perhaps metallic rhodium) that reduce the selectivity, as a consequence of the considerably shorter reaction times relative to the blanks.



1



2

Our investigations into the hydrogenation of a large number of substrates (**1a**–**n**) with the catalyst **2** conclusively favor a real increase in selectivity, presumably by optimizing the conformation of the catalyst, which is concentrated on the micelle surface, in the transition state. By adding sodium dodecylsulfate (SDS) in substoichiometric amounts, the enantioselectivity of the hydrogenation of the esters **1a**–**h** increases to 96–98% *ee* (*S*)-*N*-acyl-α-amino acid ester, almost independent of the wide-ranging solubility of the substrates (Table 1). It corresponds to a sevenfold increase of the average relative enantioselectivity Q[2] over the blank in water without surfactant:

$$Q = \frac{q(\mathrm{SDS_{H_2O}})}{q(\mathrm{blank_{H_2O}})} = 7.4 \pm 1.3$$

The doubled relative enantioselectivity

$$Q' = \frac{q(\mathrm{SDS_{H_2O}})}{q(\mathrm{blank_{MeOH}})} = 2.1 \pm 0.6$$

shows that the reported enantiomeric excess in methanol (see ref. [3]) is also clearly exceeded, although the reaction rate is generally higher in methanol. The experimentally determined enantiomeric ratio—here *S*/*R*—is used as the value q.

The lower enantioselectivities of hydrogenations in methanol without surfactants also supports a real increase in selectivity caused by micelle-forming compounds in water, because, due to the high reaction rate in methanol, the explanation of an influence of less active, unspecific catalyst impurities cannot be applicable.

Strongly in favor of our postulate of a real increase in selectivity influenced by surfactants is the high Q value of 5.2 for the completely water-soluble **1n**, as here the reaction rate is also high in the blank. The increase in activity of about one order of magnitude can be explained by the solubilizing influence of the surfactant on the catalyst. For the acids **1i**–**m** and ester **1n**, no clearcut increase in the enantioselectivity over the corresponding blanks in methanol by SDS addition can be detected ($Q' = 1.2 \pm 0.3$).

[*] Prof. Dr. P. Selke, Dr. A. Kumar,[+] M. Schwarze
Max-Planck-Gesellschaft
Arbeitsgruppe "Asymmetrische Katalyse" an der Universität
Buchbinderstrasse 5–6, D-18055 Rostock (FRG)
Telefax: Int. code + (381)46693-24
Prof. Dr. G. Oehme
Institut für Organische Katalyseforschung an der Universität Rostock, e. V.
Prof. Dr. J. P. Roque
Université Montpellier II, Laboratoire de Chimie Organique Physique
Montpellier (France)

[+] Permanent address: Central Drug Research Institute, Lucknow (India)

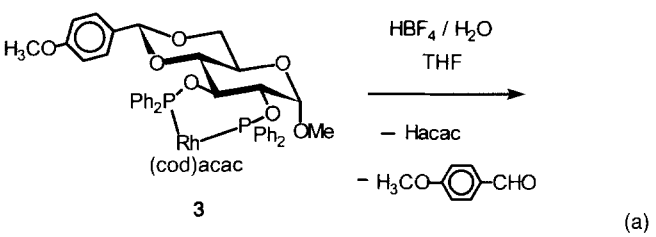
[**] Carbohydrate Phosphinites as Chiral Ligands for Asymmetric Syntheses Catalyzed by Complexes, Part 11. This work was supported by the Fonds der Chemischen Industrie. We thank H. Burneleit and P. Barthelemy for preparative work, and Dr. C. Fischer and K. Kortus for the chromatographic determination of the enantioselectivity. Part 10: [7]

Table 1. Hydrogenation of the ester substrates **1a–h** and **1n** and the acid substrates **1i–m** with and without the addition of surfactant.

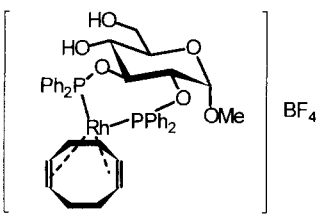
Substrate					L [%] [a]	Hydrogenation [b] $t_{1/2}$ [min]		% *ee* (*S*)			
	R^1	R^2	R^3	R^4		blank in H_2O	+50 mg SDS	blank in H_2O	+50 mg SDS	Q	Q' [c]
1a	C_2H_4OH	Ph	MeO	MeO	0.7	1170	58	–	95.6	–	2.4
1b	Me	Me	MeO	MeO	1.6	2250	151	77.2	96.5	7.2	1.2
1c	Et	Me	MeO	MeO	1.9	2600	58	82.0	97.2	6.9	1.7
1d	Me	Me	MeO	AcO	2.0	1500	49	83.0	98.1	9.7	2.4
1e	C_2H_4OH	Ph	MeO	HO	3.7		20		96.7	–	3.1
1f	Me	Me	H	H	21.5	390	6	83.4	97.2	6.4	2.0
1g	Me	Me	MeO	HO	23.0	415	14	82.8	97.3	6.9	1.9
1h	C_2H_4OH	Me	MeO	HO	31.0	429	21	–	–	–	–
										$\bar{Q}$: 7.4 ± 1.3	$\bar{Q}'$: 2.1 ± 0.6
1i	H	Ph	MeO	HO	7.4	–	67	–	96.3		1.6
1j	H	Me	H	H	11.0	–	13		96.3	–	1.3
1k	H	Me	MeO	AcO	24.0	–	29	–	95.7		1.1
1l	H	Me	MeO	MeO	40.0	–	18	–	95.6		1.2
1m	H	Me	H instead of aryl		40.0	87	4	78.6	95.9	5.7	0.9
											$\bar{Q}'$: 1.2 ± 0.3
1n	Me	Me	H instead of aryl		100.0	32	3	76.8	95.1	5.2	1.0

[a] Solubility of **1** as the percentage of 1 mmol which dissolves in 15 mL water at 25 °C. [b] Hydrogenation conditions: 1 mmol substrate, 0.01 mmol catalyst **2**, 15 mL solvent, 25 °C, 0.1 MPa H_2. [c] Calculated using the values for % *ee* in methanol from ref. [3].

Particularly interesting was the introduction of the new precatalyst **4**, recently synthesized by our group [Eq. (a)].[4] Essential for the synthesis was the support of the hydrolysis by the electronic influence of the methoxy function of the anisylidene protective group. Only products that clearly showed lower activities in water (with similar enantioselectivity) were obtained from the analogous benzylidene compounds as a consequence of contamination by the initial chelate.[5] In contrast, due to its good solubility, the hydrogenation times in the aqueous blanks are surprisingly short with **4**, obtained from the anisylidene compound **3**. The complete conversion of the substrate **1** to the methyl ester of *N*-acetylphenylalanine in 1.5 h with a half-life $t_{1/2}$ of 33 min warranted the assumption that unspecific hydrogenations do not falsify the blank result of the enantioselectivity of 61.1 % *ee* (*S*) (Table 2). The addition of SDS also with **4** raises the selectivity considerably (94 % *ee* (*S*), $Q = 7.8$).



3 (a)



4

The reason for the influence of the amphiphile on the stereoselectivity is not easy to explain, as an influence on the conformation of the catalyst in the transition state cannot be identified spectroscopically. A change in the mechanism of the catalyst at the micelle surface is not expected. The Eyring plot obtained by varying the temperature does not display any point of inflection. Very probably the surface-active substances are effective in their micellar form, as the critical micelle concentration must be approached for the maximal increase in the activity and enantioselectivity. However, the effect can be achieved with less modifier when polymerized micelles are used. These are formed by irradiating ω-undecenyl sulfate as depicted in Equation (b) and are effective at considerably lower concentrations

$$n\ CH_2{=}CH(CH_2)_9{-}OSO_3Na \xrightarrow{\gamma\text{-irradiation}} (CH_2{-}CH(CH_2)_9{-}OSO_3Na)_n \quad (b)$$

$n = 40-60$

Table 2. Comparison of the sensitivity of the catalysts derived from **2** and **4** to the addition of surfactants; 1 mmol substrate **1f**.

Surfactants	Solvents [a]	[Rh(**Ph-β**-glup-OH)(cod)]$^+$ **2** $t_{1/2}$ [min]	% *ee* (*S*)	$q = S/R$	Q [b] H_2O [c]	MeOH [c]	[Rh(**Me-α**-glup-OH)(cod)]$^+$ **4** $t_{1/2}$ [min]	% *ee* (*S*)	$q = S/R$	Q [b] H_2O [c]	MeOH [c]
–	MeOH	3	94.8	37	–	–	3	73.9	6.7	–	–
	H_2O	390	83.4	11		–	33	61.1	4.1	–	–
0.13 mmol SDS	H_2O	6	97.1	68	6.1	1.8	2	94.0	32	7.8	4.9
0.13 mol equiv SO_3Na groups in polymerized micelles	H_2O	6	95.7	46	4.1	1.2	4	93.5	30	7.2	4.5

[a] For conditions see Table 1. [b] $Q = q(\text{mic}_{H_2O})/q(\text{blank}_{sol.})$. [c] Solvent for blank experiments.

due to their stability. To utilize the polymer to its full effect (Fig. 1) the precatalyst is first dissolved in methanol, which is subsequently completely removed. This preformation in methanol also has a positive effect on the monomeric SDS due to the better solubility. The polymer effect here, however, does not increase the reactivity as much as in the case of acetal hydrolysis.[6]

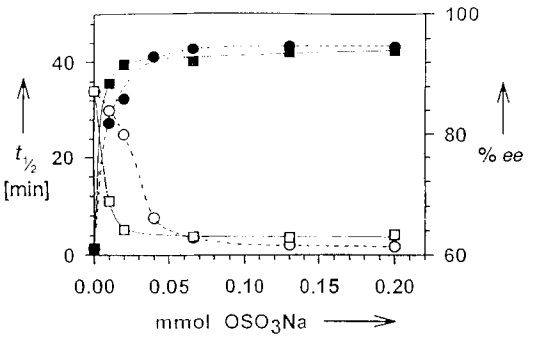


Fig. 1. Hydrogenation of 1 mmol **1f** in 15 mL H_2O in the presence of micelle-forming substances with 0.01 mmol precatalyst **4** (for conditions see Table 1). Open symbols: $t_{1/2}$; filled symbols: % *ee* (*S*); circles: SDS as micelle-forming substance; squares: polymerized micelles with OSO_3Na groups.

The function of the precatalyst **4** is determined by the axial aglycone. As we were recently able to demonstrate, induction of chirality in hydrogenation reactions decreases with an increasing number of axial substituents on the pyranose ring in analagous rhodium(I) chelate complexes of type **3**, which are protected by a benzylidene group in the 4,6-position of the carbohydrate residue.[7] Thus we have now also demonstrated this decrease in optical induction for the first of the conformatively less rigid analogues carrying an axially oriented substituent without the inflexibility imposed by the dioxane ring (Table 2). The enantioselectivity of such conformatively labile seven-membered chelates was shown to be very sensitive to the influences of a modifier.[8, 9] We conjecture that this is a key to direct optical induction over a wide range.

Experimental Procedure

The experimental procedures for the hydrogenation, the synthesis of the precatalyst **2** and the substrates, the derivatization of the hydrogenated products, and the determination of the enantioselectivity are described or referred to in ref. [3], and the synthesis of polymerized micelles in ref. [6]. With polymerized micelles the formation of the catalyst was performed in methanol. For all experiments of Figure 1 and Table 2—but not for those of Table 1—a homogenous solution was made from the precatalyst and the micelle-forming compounds under argon in methanol (5 mL) by stirring for 1 h. The solvent was then removed under vacuum, the dry residue dispersed in water (15 mL) under argon by stirring for 1 h, the substrate added, stirred for 10 min, the argon atmosphere replaced with hydrogen, and the hydrogenation started by stirring. The hydrogenated products were isolated by exhaustive extraction with dichloromethane. For the acid hydrogenation products and the ester from **1f**, the results of the determination of selectivity were additionally checked in double experiments by conversion in methanol to exclude the possibility of enantiomer enrichment during isolation. For this, the hydrogenation suspension was quantitatively evaporated to dryness, and the residue dissolved in methanol. This procedure was also applied to all experiments with the precatalyst **4**. For the enantiomeric excesses determined by gas chromatography, the standard deviation was less than ± 1 % *ee*; similar results were also obtained for the derivatized hydrogenation products of **1a**, **e**, **h**, and **i**, which were separated by HPLC. To determine the substrate solubility, a small excess of substrate was stirred in water (100 mL) at 25 °C for 1 h, the filtrate evaporated on a watch glass, dried under vacuum, and the residue weighed.

Synthesis of **5**, the glucopyranoside ligand of **3**: A solution of methyl-4,6-*O*-anisylidene-α-D-glucopyranoside (21.78 g, 32 mmol) in pyridine (20 mL) was added to Ph_2PCl (15.53 g, 70.4 mmol) in THF (100 mL) within 5 min with vigorous stirring. Pyridine hydrochloride precipitated out. The next day the solid residue was extracted four times with boiling THF until only the pyridine hydrochloride remained. The pooled solutions were subsequently reduced under vacuum to 50 mL. The target compound crystallized out at 0 °C and was obtained in a very pure form in low yield after recrystallization in anhydrous, oxygen-free toluene/triethylamine (70/30): 10.8 g (33.3%), m.p. 175–178 °C; $[\alpha]_D^{25} = +86.9$ ($c = 2$ in $CHCl_3$); ^{31}P NMR (101.2 MHz, [D_5]pyridine, 25 °C): $\delta = 113.6$ (d, $^3J(P,P) = 2.5$ Hz), 116.5 (d, $^3J(P,P) = 2.5$ Hz); ^{13}C NMR (62.8 MHz, [D_5]pyridine, 25 °C): $\delta = 54.5$, 54.8 (CH_3/α-CH_3), 62.7 (C6), 68.7 (C2,3,4,5), 99.5 (d, $^3J(C,P) = 6$ Hz; C1), 101.3 (C7) and arene-C signals; correct elemental analysis (C,H,P); MS (70 eV): *m/z* 680 ([M^+]).

Synthesis of **4**: [Rh^I(cod)(acac)] (1.55 g, 5 mmol) and **5** (3.4 g, 5 mmol) were dissolved in THF (5 mL) to afford the chelate, and 40% aqueous HBF_4 (10 mmol) added. The yellow solution turned red. After 28 h, of which 10 h were at 65 °C, the solution was filtered to remove impurities. Oxygen-free diethyl ether (40 mL) were stirred into the filtrate, and the complex separated out as an orange syrup. The remaining yellow solution was decanted, and diethyl ether (40 mL) was again added to the oil. The product **4** crystallized out: 4.3 g (89.7%); ^{31}P NMR (101.2 MHz, $CDCl_3$, 25 °C): $\delta = 132.7$ (dd, $^1J(P,Rh) = 178$, $^2J(P,P) = 27$ Hz), 137.3 (dd, $^1J(P,Rh) = 181$, $^2J(P,P) = 27$ Hz); ^{13}C NMR (62.8 MHz, $CDCl_3$, 25 °C): $\delta = 27.9$, 28.9, 30.7, 30.9 (CH_2 of cod), 55.1 (CH_3), 60.9 (C6), 68.7, 70.7, 76.2 ($^3J(C,P) = 8$ Hz), 80.8 ($^3J(C,P) = 9$ Hz) (C2,3,4,5), 98.3 (d, $^3J(C,P) = 4$ Hz; C1), 101.5, 102.2 (CH of cod), 128.5–134.6 (C-phenyl); LSI-MS (positive, matrix: sulfolane): *m/z* 773 [$M^+ - BF_4$], 665 [773 − cod].

Received: May 24, 1994 [Z6965IE]
German version: *Angew. Chem.* **1994**, *106*, 2272

[1] G. Oehme, E. Paetzold, R. Selke, *J. Mol. Catal.* **1992**, *71*, L1; I. Grassert, E. Paetzold, G. Oehme, *Tetrahedron* **1993**, *49*, 6605.
[2] To substantiate the usefulness of the value *Q* for comparison of the selectivity see ref. [3].
[3] R. Selke, C. Facklam, H. Foken, D. Heller, *Tetrahedron: Asymmetry* **1993**, *4*, 369.
[4] In ref. [3] the formulas are erroneously given for the complex derived from methyl-α-D-glucopyranoside, which at that time was not known.
[5] R. Selke, P. Barthelemy, J. P. Roque, „*Chiral Reactions in Heterogeneous Catalysis*", ChiCat-Symposium, Brüssel, Oktober 1993.
[6] B. André, B. Boyer, G. Lamaty, J. P. Roque, *Tetrahedron Lett.* **1991**, *32*, 1881.
[7] R. Selke, M. Schwarze, H. Baudisch, I. Grassert, M. Michalik, G. Oehme, N. Stoll, B. Costisella, *J. Mol. Catal.* **1993**, *84*, 223.
[8] D. Seebach et al. have a fascinating example from (taddol)titanium coordination chemistry, in which the induction range extends from 90% *ee* (*R*) to over 90% *ee* (*S*) product: D. Seebach, D. A. Plattner, A. K. Beck, Y. M. Wang, D. Hunzicker, *Helv. Chim. Acta* **1992**, *75*, 2171. Results, deductions, and literature about the dependence of the enantioselectivity on the ligand conformation in analogous catalyst chelate complexes can also be found here.
[9] Investigations have, for example, produced an inversion of the route of induction for a precatalyst analogous to **3** with a 4,6-*O*-benzylidene protective group upon changing to apolar solvents: R. Selke, *J. Prakt. Chem.* **1987**, *329*, 717.

Towards One-Dimensional Carbon Wires Connecting Single Metal Centers: A Cumulenic C_5 Chain that Mediates Charge Transfer between Rhenium and Manganese Termini**

Weiging Weng, Tamás Bartik, and John A. Gladysz*

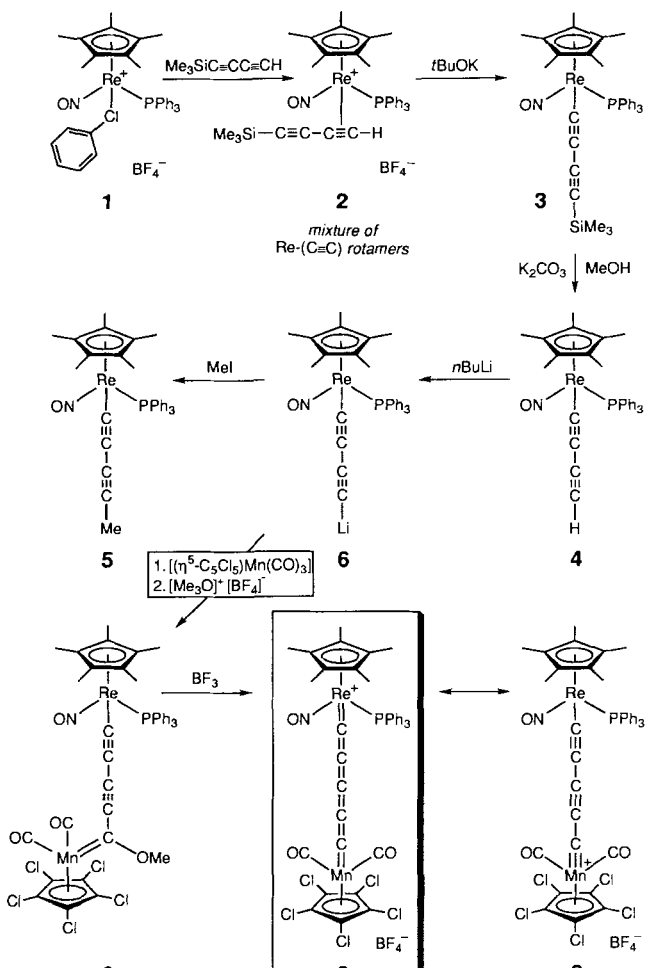
Compounds in which linear elemental carbon chains span two transition metals, [$L_nMC_xM'L'_n$], exhibit a variety of unusual physical and chemical properties.[1] However, only complexes with $x = 1-4$ have been isolated to date. We have been particularly interested in charge transfer and electron delocalization across the wire-like C_x moieties[2–4] and have sought to study such phenomena in longer-chain compounds. We reported earlier that C_3 complexes can be prepared by methoxide group ab-

[*] Prof. Dr. J. A. Gladysz, Dr. W. Weng, Dr. T. Bartik
Department of Chemistry, University of Utah
Salt Lake City, UT 84112 (USA)
Telefax: Int. code +(801)581-8433

[**] We thank the National Science Foundation for support of this research.

straction from bimetallic Fischer carbene complexes of the formula $[L_nMC{\equiv}CC(OMe){=}M'L'_{n'}]$.[2] These are in turn accessed from $[L_nMC{\equiv}CLi]$ species, metal carbonyl complexes, and $[Me_3O]^+[BF_4]^-$. In this communication, we describe the extension of this methodology to a C_5 complex,[5] which shows several remarkable properties relative to its C_3 counterpart.

The substitution-labile chlorobenzene complex **1**[16] was treated in situ with the 1,3-diyne $HC{\equiv}C{-}C{\equiv}CSiMe_3$. Workup gave the terminal alkyne complex **2** in 95% yield (Scheme 1). Reaction of **2** and *t*BuOK gave the σ complex **3** (96% yield). Protodesilylation (K_2CO_3/CH_3OH) gave the air-stable butadiynyl complex **4** (84% yield), which melted with decomposition at 105–108 °C. Complexes **2**–**4** and other new compounds below were characterized by microanalysis, IR and NMR (^1H, ^{13}C, ^{31}P) spectroscopy (Table 1). Most features were similar to those of the monoalkynyl analogues;[7] however, the $\tilde{\nu}$(NO) values in the IR spectrum were 7–20 cm^{-1} higher, and additional bands assigned to C≡C were observed (2139–1975 cm^{-1}).



Scheme 1. Synthesis of the C_5-bridged bimetallic complex **9**.

Complex **4** was treated with 1.0 equiv of *n*BuLi in THF at −80 °C. When the reaction was monitored by ^{31}P NMR, resonances were observed at δ = 21.3 and 21.0 (70:30; **4**, δ = 21.0). One sharp resonance was obtained when the sample was warmed to 10–20 °C (δ = 21.0). Addition of MeI, either at −80 °C or room temperature, gave the 1,3-pentadiynyl complex **5** (δ = 20.9) in 95% yield, as determined by NMR and IR spectroscopy.[8] These data were taken as evidence for the formation of C_4Li complex **6**, which is possibly present as a mixture of aggregates. The deprotonation of a butadiynyl iron complex and subsequent reactions with metal halides to give $[L_nMC{\equiv}C{-}C{\equiv}CM'L'_n]$ complexes has been previously reported by Wong.[9]

We sought to elaborate **6** to a bimetallic Fischer carbene complex. Thus, $[(\eta^5\text{-}C_5H_5)Mn(CO)_3]$ and $[Me_3O]^+[BF_4]^-$ were added to **6** under various conditions; however, no evidence was found for an adduct with a $ReC{\equiv}C{-}C{\equiv}CC(OMe){=}Mn$ linkage, although the corresponding reaction of the lower homologue **7** worked well.[2] The major product was **5**. Hence, an analogous

$[\{Re^*\}(C{\equiv}CLi)]$ **7**, $\{Re^*\} = (\eta^5\text{-}C_5Me_5)Re(NO)(PPh_3)$

Table 1. Selected data for the new compounds:

2: Tan solid, m.p. 118–121 °C (decomp.); ^1H NMR (300 MHz, CD_2Cl_2, 25 °C, CD_2Cl_2 int.): δ = 7.79–7.50 (m, 6H; $3C_6H_5$), 7.48–7.31 (m, 9H; $3C_6H_5$), 7.09/8.24 (major/minor rotamer) (d, J(H, P) = 19.7/4.7 Hz, 1H; ≡CH *syn*/*anti* to PPh_3), 1.85/1.77 (s, 15H; $C_5(CH_3)_5$), 0.34/−0.37 (s, 9H; $Si(CH_3)_3$); $^{13}C\{^1H\}$ NMR (75 MHz, CD_2Cl_2, 25 °C, CD_2Cl_2 int.): δ = 134.0 (d, J(C, P) = 10.7 Hz; *o*-Ph), 133.3 (br s; *p*-Ph), 129.9 (br d, J(C, P) = 3.7 Hz; *m*-Ph), 114.9/113.2 (s; C≡CSi), 110.3/109.9 (s; $C_5(CH_3)_5$), 92.1/92.9 (d, J(C, P) = 3.6/7.0 Hz, HC≡*C*), 96.6/108.0 (d, J(C, P) = 18.0/2.4 Hz; HC≡C), 95.2/110.4 (s; C≡*C*Si), 9.65 (s; $C_5(CH_3)_5$), −0.51/−0.98 (s; $Si(CH_3)_3$); $^{31}P\{^1H\}$ NMR (121 MHz, C_6D_6, 25 °C, 85% H_3PO_4 ext.): δ = 21.1/17.6 (s, 21:79); IR (CH_2Cl_2/KBr): $\tilde{\nu}$ = 2139/2138 (m) (C≡C), 1706/1694(s) cm^{-1} (NO); MS (positive ions FAB (Cs^+), 3-nitrobenzyl alcohol (3-NBA)/CH_2Cl_2 matrix): *m*/*z* (%) 736 (100) [M^+]. Correct elemental analysis.

3: Orange solid, m.p. 105–108 °C (decomp.); ^1H NMR (300 MHz, C_6D_6, 25 °C, TMS): δ = 7.75–7.63 (m, 6H; $3C_6H_5$), 7.04–6.95 (m, 9H; $3C_6H_5$), 1.55 (s, 15H; $C_5(CH_3)_5$), 0.17 (s, 9H; $Si(CH_3)_3$); $^{13}C\{^1H\}$ NMR (75 MHz, C_6D_6, 25 °C, C_6D_6 int.): δ = 135.3 (d, J(C, P) = 51.6 Hz; *i*-Ph), 134.3 (d, J(C, P) = 10.7 Hz; *o*-Ph), 130.1 (d, J(C, P) = 2.3 Hz; *p*-Ph), 128.4 (d, J(C, P) = 10.1 Hz; *m*-Ph), 112.3 (s; ReC≡*C*), 105.8 (d, J(C, P) = 15.9 Hz; Re*C*≡C), 100.6 (s; $C_5(CH_3)_5$), 93.5 (d, J(C, P) = 2.7 Hz; *C*≡CSi), 80.6 (s; C≡*C*Si), 10.0 (s; $C_5(CH_3)_5$), 0.91 (s; $Si(CH_3)_3$); $^{31}P\{^1H\}$ NMR (121 MHz, C_6D_6, 25 °C, 85% H_3PO_4 ext.): δ = 21.1 (s); IR (CH_2Cl_2/KBr): $\tilde{\nu}$ = 2118/2119(m), 2098/2097(m) (C≡C), 1653/1648(s) cm^{-1} (NO); MS (EI, 30 eV): *m*/*z* (%) 735 (100) [M^+]. Correct elemental analysis.

4: Orange solid; m.p. 84–86 °C (decomp.); ^1H NMR (300 MHz, C_6D_6, 25 °C, TMS): δ = 7.75–7.65 (m, 6H, $3C_6H_5$), 7.07–6.94 (m, 9H; $3C_6H_5$), 1.95 (d, J(H, P) = 1.0 Hz, 1H; ≡CH) 1.57 (s, 15H; $C_5(CH_3)_5$); $^{13}C\{^1H\}$ NMR (75 MHz, C_6D_6, 25 °C, C_6D_6 int.): δ = 135.4 (d, J(C, P) = 51.4 Hz; *i*-Ph), 134.3 (d, J(C, P) = 10.9 Hz; *o*-Ph), 130.2 (s; *p*-Ph), 128.3 (d, J(C, P) = 10.0 Hz; *m*-Ph), 110.8 (s; ReC≡C), 102.1 (d, J(C, P) = 15.9 Hz; ReC≡C), 100.5 (s; $C_5(CH_3)_5$), 72.4 (s; *C*≡CH), 65.2 (s; C≡*C*H), 10.0 (s; $C_5(CH_3)_5$); $^{31}P\{^1H\}$ NMR (121 MHz, C_6D_6, 25 °C, 85% H_3PO_4 ext.): δ = 20.9 (s); IR (CH_2Cl_2/KBr): $\tilde{\nu}$ = 3305/3287(m) (≡C-H), 2115/2113(s), 1975/1975(w) (C≡C), 1644/1645(s) cm^{-1} (NO); MS (EI, 70 eV): *m*/*z*(%) 663(4) [M^+]. Correct elemental analysis.

5: Yellow-orange solid, m.p. 61–65 °C (decomp.); ^1H NMR (300 MHz, C_6D_6, 25 °C, TMS): δ = 7.80–7.72 (m, 6H; $3C_6H_5$), 7.07–6.92 (m, 9H; $3C_6H_5$), 1.81 (s, 3H; ≡CCH_3), 1.61 (s, 15H; $C_5(CH_3)_5$); $^{13}C\{^1H\}$ NMR (75 MHz, C_6D_6, 25 °C, C_6D_6 int.): δ = 135.7 (d, J(C, P) = 50.6 Hz; *i*-Ph), 134.4 (d, J(C, P) = 10.2 Hz; *o*-Ph), 130.1 (s; *p*-Ph), 128.3 (d, J(C, P) = 9.8 Hz; *m*-Ph), 111.6 (s, ReC≡*C*), 100.3 (s; $C_5(CH_3)_5$), 96.8 (d, J(C, P) = 17.3 Hz; ReC≡C), 71.9 (s; C≡*C*CH_3), 69.1 (d, J(C, P) = 3.1 Hz; *C*≡CCH_3), 10.0 (s; $C_5(CH_3)_5$), 4.5 (s; ≡*C*CH_3); $^{31}P\{^1H\}$ NMR (121 MHz, C_6D_6, 25 °C, 85% H_3PO_4 ext.): δ = 21.0 (s); IR (CH_2Cl_2/KBr): $\tilde{\nu}$ = 2193/2194(m), 2027/2029(m) (C≡C), 1644/1644(s) cm^{-1} (NO); MS (EI, 70 eV): *m*/*z* (%) 677 (100) [M^+].

8 and **9**: see Experimental Procedure.

10: Yellow-brown solid, m.p. 101–106 °C (decomp.); ^1H NMR (300 MHz, CD_2Cl_2, 25 °C, CD_2Cl_2 int.): δ = 7.57–7.46 (m, 15H; $3C_6H_5$), 1.93 (s, 15H; $C_5(CH_3)_5$); $^{13}C\{^1H\}$ NMR (75 MHz, C_6D_6, 25 °C, C_6D_6 int.): δ = 287.8 (s; Mn≡C), 221.1 (d, J(C, P) = 11.8 Hz; ReCC), 218.2 (s; CO), 218.0 (s; CO), 168.9 (s; ReC*C*), 133.5 (d, J(C, P) = 11.3 Hz; *o*-Ph), 132.6 (s; *p*-Ph), 129.7 (d, J(C, P) = 11.1 Hz; *m*-Ph), 108.0 (s; $C_5(CH_3)_5$) 100.1 (s; C_5Cl_5), 10.1 (s; $C_5(CH_3)_5$); $^{31}P\{^1H\}$ NMR (121 MHz, CD_2Cl_2, 25 °C, 85% H_3PO_4 ext.): δ = 19.7 (s); IR (CH_2Cl_2): $\tilde{\nu}$ = 1899(vs) (C=C=C), 2047(m), 2007(w) (C≡O), 1717(s) cm^{-1} (NO); UV/VIS (CH_2Cl_2): λ_{max} (ε) = 266 sh (17000), 334 sh (16000), 414 (49000), 554 sh nm (2700); MS (positive ions FAB (Cs^+), 3-NBA/benzene matrix): *m*/*z* (%) 998(30) [M^+], 615 (100) [$\{Re^*\}^+ + 1$]. Correct elemental analysis.

reaction was conducted with $(\eta^5\text{-}C_5Cl_5)Mn(CO)_3$,[10] which should be more conducive to nucleophile addition from the standpoints of both reaction rate and equilibrium. Workup gave the dark purple C_5OMe complex **8** (77% yield).[11] Thus, the ReC≡C–C≡CLi moiety in **6** is less basic and/or nucleophilic than the ReC≡CLi moiety in **7**, a trend often observed for organic analogues.

Toluene/hexane solutions of **8** were treated with excess BF_3 gas (Scheme 1). The C_5 complex **9** precipitated as a dark brown solid. Workup gave **9** (52% yield) that was approximately 94% pure by NMR spectroscopy. Several unusual properties of **9** became immediately apparent and have so far precluded further purification or crystallization. First, **9** is extremely light-sensitive, both in solution and the solid state. Second, **9** decomposes on the time scale of hours in the dark at room temperature; the rate apparently depends upon the concentration of **9**. In all cases, a black decomposition product formed that gave ESR signals and broad NMR signals.[12] Elemental analyses gave values for the carbon, hydrogen, and chlorine content that were within 1–5% of those calculated for **9**.

Complex **9** was characterized spectroscopically. The ^{13}C NMR spectrum showed a downfield ReC signal ($\delta = 218.4$) with a $^2J(C, P)$ value (12.5 Hz) near the range typical of $^+Re{=}C$ linkages (10.0–12.3 Hz) and smaller than that characteristic of Re–C≡ linkages (15.8–17.3 Hz).[13] Other signals assigned to the C_5 chain were observed at $\delta = 296.2$ (MnC), 119.1, 110.6, and 107.0. The $\tilde{\nu}$(NO) value (1718 cm^{-1}) in the IR spectrum was in a range diagnostic of cationic $^+Re{=}C$ compounds (1719–1698 cm^{-1}) and much higher than that characteristic of neutral Re–C≡C compounds (1653–1630 cm^{-1}). Thus, the cumulene resonance form $^+Re{=}C{=}C{=}C{=}C{=}C{=}Mn$ dominates over the alternative $Re{-}C{\equiv}C{-}C{\equiv}C{-}C{\equiv}Mn^+$ (Scheme 1).[15] A very strong IR band at 1953 cm^{-1} was presumed to be associated with the cumulene fragment.

We sought to characterize the optical properties of **9**. As a prelude, the new C_3 complex **10** was prepared similarly to **9** from ReC≡CLi complex **7**. Complex **10**, and the previously reported chlorine-free analogue **11**, did not exhibit any unusual photo-

$[\{Re^*\}(CCC)Mn(CO)_2(\eta^5\text{-}C_5Cl_5)]^+\ [BF_4]^-$ **10**

$[\{Re^*\}(CCC)Mn(CO)_2(\eta^5\text{-}C_5H_5)]^+\ [BF_4]^-$ **11**

chemical or thermal reactivity.[2] Thus, the cyclopentadienyl chlorines in **9** are not an intrinsic source of instability. This implicates the carbon chain length in **11** as the key labilizing feature. Complex **10** exhibited signals in the IR ($\tilde{\nu} = 1717$(s) (NO), 1899(vs) cm^{-1} (C=C=C)) and ^{13}C NMR ($\delta = 221.1$ (d, $^2J(C, P) = 11.8$ Hz; ReC), 287.8 (s; MnC), 168.9 (s; CCC)) spectra indicative of a dominant "cumulenic" resonance form, $^+Re{=}C{=}C{=}C{=}Mn$. These results parallel those for **11**, which was also crystallographically characterized.[2]

The UV/visible spectra of **9**–**11** are compared in Figure 1. The yellow-brown solutions show very intense absorptions at 480 (**9**), 414 (**10**), and 392 (**11**) nm ($\varepsilon = 60\,500$, 49000, and 56000 $M^{-1}cm^{-1}$, respectively). Weaker bands occur at longer wavelengths (634, 554 sh, and 484 nm; $\varepsilon = 4800$, 2700, and 3700 $M^{-1}cm^{-1}$). Thus, either increased carbon chain lengths (**9** vs **10**) or electronegative chlorine substituents on the manganese cyclopentadienyl ligand (**10** vs **11**) result in absorptions at longer wavelengths. The latter trend suggests that the transitions have appreciable rhenium-to-manganese charge transfer character.

Attempts to trap **9** as a stable adduct have to date been unsuccessful. No reaction occurs with TCNE, ethylene, or SMe_2 at ambient temperature, and PMe_3 gives a complex mixture of unusual products. Nonetheless, we anticipate an array of unusual properties for this series of compounds. Further examples of complexes with C_5 and longer chains will be reported in the near future.

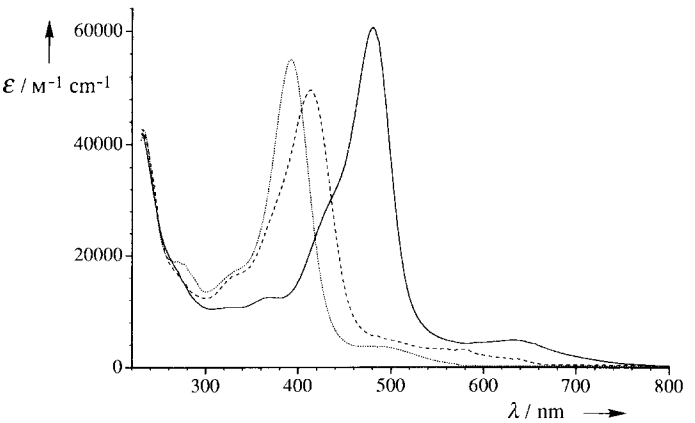


Fig. 1. UV/visible spectra of compounds **9**–**11**. (CH_2Cl_2, ambient temperature, $c = 2.3\text{-}3.9 \times 10^{-5}$ M). — **9**, ---- **10**, · · · · **11**.

Experimental Procedure

8: A Schlenk tube was charged with **4** (0.048 g, 0.072 mmol) in THF (5 mL). The mixture was cooled to −80 °C. Then *n*BuLi (36 μL, 2.3 M in hexane) was added with stirring. After 1 h, a solution of $[(\eta^5\text{-}C_5Cl_5)Mn(CO)_3]$ [10] (0.028 g, 0.075 mmol) in THF (3 mL) was added via a cannula. After 1 h, the cold bath was removed. After a further hour, the red-orange solution was transferred via a cannula to a Schlenk flask that had been charged with $[Me_3O]^+[BF_4]^-$ (0.050 g, 0.32 mmol). The mixture was cooled to −80 °C and stirred for 0.5 h. The cold bath was then removed. After 0.5 h, the sample was concentrated to ca. 2 mL, and hexane (10 mL) was added. Chromatography (N_2, Florisil; hexane → hexane/THF 1/1 (v/v)) gave a deep purple fraction. The solvent was removed under oil pump vacuum to give **8** as a dark purple powder (0.059 g, 0.056 mmol, 77%). M.p. 114–116 °C; ^1H NMR (300 MHz, C_6D_6, 25 °C, TMS): $\delta = 7.65\text{-}7.55$ (m, 6H; $3C_6H_5$), 7.12–6.95 (m, 9H; $3C_6H_5$), 3.53 (s, 3H; OCH_3), 1.55 (s, 15H; $C_5(CH_3)_5$); $^{13}C\{^1H\}$ NMR (75 MHz, C_6D_6, 25 °C, C_6D_6 int.): $\delta = 288.9$ (s; Mn=C), 228.2 (s; CO), 228.1 (s; CO), 167.1 (d, $J(C, P) = 14.8$ Hz; Re*C*≡C), 134.2 (d, $J(C, P) = 52.4$ Hz; *i*-Ph), 134.0 (d, $J(C, P) = 10.8$ Hz; *o*-Ph), 130.7 (s; *p*-Ph), 128.6 (d, $J(C, P) = 10.3$ Hz; *m*-Ph), 127.4, 116.3, 82.4 (3s; C≡*CC*≡*CC*=), 102.1 (s; $C_5(CH_3)_5$), 97.0 (s; C_5Cl_5), 63.3 (s; OCH_3), 9.9 (s; $C_5(CH_3)_5$); $^{31}P\{^1H\}$ NMR (121 MHz, C_6D_6, 25 °C, 85% H_3PO_4 ext.): $\delta = 20.6$ (s); IR (CH_2Cl_2/KBr): $\tilde{\nu} = 2057/2054$(m), 2046/2044(m) sh (C≡C), 1965/1962(s), 1925/1922(s) (C≡O), 1655/1657(s) cm^{-1} (NO); UV/VIS (CH_2Cl_2): λ_{max} (ε) = 264 sh (29000), 318 (19000), 376 sh (13000), 502 sh (14500.) 562 nm (21000); MS (positive ions FAB (Cs^+), 3-NBA/benzene matrix): *m/z* (%) 1053 (3) [*M*$^+$], 614 (100) [{Re}$^+$]. Correct elemental analysis.

9: This procedure was carried out in the dark. A Schlenk tube was charged with **8** (0.094 g, 0.089 mmol), toluene (10 mL), and hexane (8 mL). The mixture was cooled to −60 °C. Then BF_3 gas was bubbled through the solution for 1 min. A dark solid precipitated. The supernatant was removed with a syringe, and the solid was washed with hexane (3 × 5 mL) and dried under oil pump vacuum. The solid was extracted with CH_2Cl_2 (2 × 2 mL). The extracts were filtered through a Celite pad (1 cm). Hexane (10 mL) was added, and the dark brown precipitate was collected by filtration, washed with hexane (2 × 2 mL), and dried under oil pump vacuum to give **9** (0.051 g, 0.046 mmol, 52%). ^1H NMR (300 MHz, CD_2Cl_2, 25 °C, CD_2Cl_2 int): $\delta = 7.64\text{-}7.49$ (m, 9H; $3C_6H_5$), 7.48–7.36 (m, 6H; $3C_6H_5$), 1.95 (s, 15H; $C_5(CH_3)_5$); $^{13}C\{^1H\}$ NMR (75 MHz, CD_2Cl_2, −20 °C, CD_2Cl_2 int.): $\delta = 296.2$ (s; MnC), 220.8 (s; CO), 220.2 (s; CO), 218.4 (d, $J(C, P) = 12.5$ Hz; ReC), 133.2 (d, $J(C, P) = 10.9$ Hz; *o*-Ph), 132.4 (s; *p*-Ph), 129.5 (d, $J(C, P) = 10.6$ Hz; *m*-Ph), 119.1, 110.6, 107.0 (3s; *CCCCC*), 108.5 (s; $C_5(CH_3)_5$), 100.4 (s; C_5Cl_5), 10.0 (s; $C_5(CH_3)_5$); $^{31}P\{^1H\}$ NMR (121 MHz, CD_2Cl_2, 85% H_3PO_4 ext.): $\delta = 20.5$ (s); IR (CH_2Cl_2/KBr): $\tilde{\nu} = 2045/2042$(s), 2008/1996(s) (C≡O), 1953/1948(vs) (C=C=C=C=C), 1718/1705(s) cm^{-1} (NO); UV/VIS (CH_2Cl_2): λ_{max} (ε) = 262 (19000), 370 (12500), 442 sh (33000), 480 (60000), 634 nm (4800); MS (positive ions FAB (Cs^+), 3-NBA/CH_2Cl_2 matrix): *m/z* (%): 1022 (4) [*M*$^+$], 614 (100) [{Re}$^+$].

Received: May 31, 1994 [Z 6986]
German version: *Angew. Chem.* **1994**, *106*, 2272

[1] a) H. Lang, *Angew. Chem.* **1994**, *106*, 569–572; *Angew. Chem. Int. Ed. Engl.* **1994**, *33*, 547–550; b) W. Beck, B. Niemer, M. Wieser, *ibid.* **1993**, *105*, 969–996 and **1993**, *32*, 923–949; c) main group analogues: H. J. Bestmann, D. Hadawi, H. Behl, M. Bremer, F. Hampel, *ibid.* **1993**, *105*, 1198–1200 and **1993**, *32*, 1205–1208.

[2] W. Weng, J. A. Ramsden, A. M. Arif, J. A. Gladysz, *J. Am. Chem. Soc.* **1993**, *115*, 3824–3825.
[3] N. Le Narvor, C. Lapinte, *J. Chem. Soc. Chem. Commun.* **1993**, 357–359.
[4] a) Y. Zhou, J. W. Seyler, W. Weng, A. M. Arif, J. A. Gladysz, *J. Am. Chem. Soc.* **1993**, *115*, 8509–8510; b) J. W. Seyler, W. Weng, Y. Zhou, J. A. Gladysz, *Organometallics* **1993**, *12*, 3802–3804.
[5] For an unusual complex in which the carbons of a bent C_5 linkage are coordinated to three, two, zero, zero, and three cobalts, respectively, see G. H. Worth, B. H. Robinson, J. Simpson, *Organometallics* **1992**, *11*, 501–513.
[6] T.-S. Peng, C. H. Winter, J. A. Gladysz, *Inorg. Chem.* **1994**, *33*, 2534–2542.
[7] J. A. Ramsden, W. Weng, J. A. Gladysz, *Organometallics* **1992**, *11*, 3635–3645.
[8] The ^{31}P NMR shifts of $\{Re^*\}(C\equiv C-C\equiv CX)$ complexes are much less sensitive to the nature of X than those of $ReC\equiv CX$ analogues.
[9] A. Wong, P. C. W. Kang, C. D. Tagge, D. R. Leon, *Organometallics* **1990**, *9*, 1992–1994.
[10] a) S. A. Kur, M. J. Heeg, C. H. Winter, *Organometallics* **1994**, *13*, 1865–1869; b) W. A. Hermann, M. Huber, *J. Organomet. Chem.* **1977**, *140*, 55–61.
[11] Analogous reactions with the monochlorocyclopentadienyl complex $[(\eta^5\text{-}C_5H_4Cl)Mn(CO)_3]$ gave mixtures of **5** and a C_5OMe adduct that we could not easily purify.
[12] Isolated by precipitation with hexane or ether. Found (two independently prepared samples): C, 44.77–42.64; H, 3.54–3.17; Cl, 12.51–12.41. Calcd for precursor **9**: C, 43.33; H, 2.73; Cl, 15.99. A UV/visible spectrum showed no features at > 300 nm other than intense tailing. A FAB mass spectrum showed no peaks with m/z higher than 614 ($[\{Re^*\}^+]$). IR (CH_2Cl_2): $\tilde{\nu}$ = 1726(s) br, 2043(s), 1974(s), and weaker unresolved bands at 1850–2000 cm^{-1}; ^1H NMR (300 MHz, CD_2Cl_2, 25 °C, CD_2Cl_2 int.): δ = 7.75 (br m; C_6H_5), 1.95 (s; $C_5(CH_3)_5$); ^{31}P NMR (121 MHz, CD_2Cl_2, 25 °C, 85% H_3PO_4 ext.): δ = 22 (br s); ESR (CH_2Cl_2) (g) 2.02 (sextet, A_{iso} 97 G).
[13] Limiting values are taken from **3**–**5** and pentamethylcyclopentadienyl complexes in ref. [4a] and [8].
[14] The ^{13}C NMR chemical shifts of the ReC and CMn units are also consistent with this conclusion, although the former is intermediate between limiting model compounds, and the latter must be compared with neutral carbene and cationic carbyne complexes of the $[(\eta^5\text{-}C_5H_5)Mn(CO)_2]$ fragment [2].

A Novel Hexamer of But$C\equiv P$: Synthesis, Structure, and Theoretical Studies**

Vinicius Caliman, Peter B. Hitchcock, John F. Nixon,* Matthias Hofmann, and Paul von Ragué Schleyer*

The organic and organometallic chemistry of phosphaalkynes ($RC\equiv P$) is developing rapidly.[1–4] The very recent report[5] by de Meijere and co-workers of the "cage" hydrocarbon $C_{12}H_{12}$ (**1**), with D_{3d} symmetry, prompts us to describe the synthesis and structure of the novel isostructural $P_6C_6tBu_6$ cage compound (**2**) that represents the largest known oligomer of the phosphaalkyne tBuC≡P.

A landmark in the chemistry of phosphaalkynes was Regitz et al.'s synthesis and structural characterization of the very stable tetraphosphacubane $P_4C_4tBu_4$ (**3**), made either thermally from tBuC≡P or more efficiently by use of the precursor complex $[Zr(\eta^5\text{-}C_5H_5)_2(P_2C_2tBu_2)]$.[6, 7] Previously[8] the related pentameric cage compound $P_5C_5tBu_5$ (**4**) was obtained readily by oxidative coupling of the 1,3-di- and 1,2,4-triphosphacyclopentadienyl ring systems **5** and **6**. The structure of pentamer **4** is closely related to that of the tetraphosphacubane, **3** as one corner C atom of the "cube" can be considered to be replaced by a triangle of CCP atoms (Fig. 1).

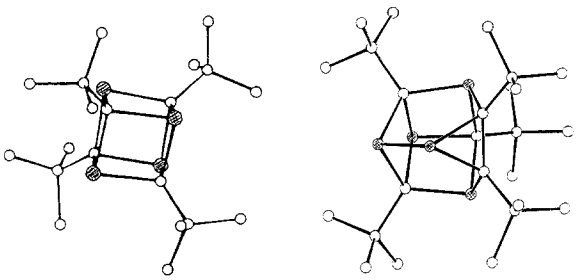


Fig. 1. Structure of **3** (left) and **4** (right) in the crystal. (○ carbon, ● phosphorus) [6–8].

Whereas the $P_3C_2tBu_2^-$ ring ion exhibits η^1- and η^5-ligating behavior towards transition metals, the corresponding $P_2C_3tBu_3^-$ ion only exhibited η^5- or η^3-ligation.[1, 9, 10] Since the structurally well characterized η^1-$P_3C_2tBu_2$ complexes typified by $[M(\eta^1\text{-}P_3C_2tBu_2)_x(PR_3)_yX_z]$ (M = Pd, Pt; X = halide; $x = 2, y = 2, z = 0$; $x = 1, y = 2, z = 1$) all contained stabilizing phosphane ligands,[11] we have now carried out a reaction of the more labile complex $[PtCl_2(cod)]$ (cod = 1,5-cyclooctadiene) with a mixture of the $P_3C_2tBu_3^-$ and $P_2C_3tBu_3^-$ ring ions in dimethoxyethane and obtained nonmetal-containing organophosphorus compounds, presumably via unstable organometallic intermediates.

The reaction product mixture was chromatographed and the known $P_5C_5tBu_5$ (**4**), $P_5C_5tBu_5H_2$ (**7**), and the new compound $P_4C_6tBu_6H_2$ (**8**), whose structure is similar to **7**, were separated and characterized by their $^{31}P\{^1H\}$ NMR spectra.[8, 12, 13] Of special interest was a fraction which yielded a colorless compound (**2**), which exhibited a parent ion in the mass spectrum at m/e = 600, indicative of a hexamer of tBuCP. The $^{31}P\{^1H\}$ NMR spectrum of **2** is very simple, consisting of two singlets of relative intensity 2:1 whose chemical shifts are characteristic of $\lambda^3\sigma^3$ P atoms (δ = 4.8 (P^A), 184.0 (P^B); relative to H_3PO_4). The simplicity of the ^1H NMR spectrum (singlets at δ = 1.64 and 1.25 of relative intensity 1:2) strongly suggests a highly symmetric cage structure.

The molecular structure of $P_6C_6tBu_6$ (**2**), which was established subsequently by a single crystal X-ray structural determination,[14] consists of a lanternlike hexameric cage containing two 3-membered CCP rings (Fig. 2). There is a close similarity between the C_{2h} symmetry exhibited by **2** and the D_{3d} symmetry of the $C_{12}H_{12}$ hydrocarbon p-[$3^2.5^6$]-octahedrane (**1**, Fig. 3, left),[5] as well as the obvious structural relationship of **2** to the D_{3d} structure computed recently for the hypothetical P_{12} molecule **9**[15] (Fig. 3, right). These results provide further strong support for previous contentions about the similarity in chemical behavior of P and CR fragments in both organic and organometallic chemistry.[1, 2, 3]

Ab initio calculations on oligomers of HCP as a model for tBuCP oligomers were performed with the Gaussian 92 program.[19] The MP2(fu)/6-21G* (fu = full, all electrons correlated) geometry of the model hexamer is in good accord with that determined for **2**. Experimental bond lengths and bond angles for $P_6C_6tBu_6$ and corresponding theoretical values for $P_6C_6H_6$ are summarized in Figure 4. Reaction energies computed at different levels for the HCP → 1/n(HCP)n (n = 2–6) reac-

[*] Prof. Dr. J. F. Nixon, V. Caliman, Dr. P. B. Hitchcock
School of Chemistry and Molecular Sciences, University of Sussex
GB-Brighton BN1 9QJ (UK)
Telefax: Int. code +(273)67-7196
Prof. P. von R. Schleyer, Dipl.-Chem. M. Hofmann
Computer-Chemie-Centrum des Instituts für Organische Chemie
der Universität Erlangen-Nürnberg
Nägelsbachstrasse 25, D-91052 Erlangen (FRG)
Telefax: Int. code +(9131)85-9132

[**] We thank the Science and Engineering Research Council (SERC), the Brazilian Government (CNPq) (fellowship for V.C.), and the Deutsche Forschungsgemeinschaft (Graduierten Kolleg für Phosphor Chemie) for financial support.

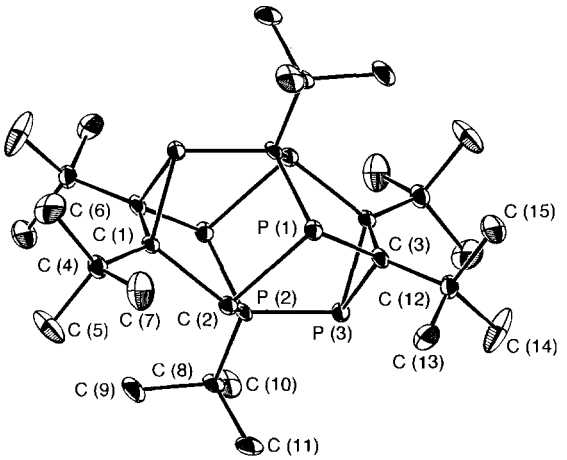


Fig. 2. Molecular structure of **2**. Selected bond lengths [Å] and bond angles [°]: P(1)-P(2) 2.208(2), P(1)-C(2') 1.856(3), P(1)-C(3) 1.894(5), P(2)-C(1) 1.886(4), P(2)-C(2) 1.859(5), P(3)-C(1') 1.859(4), P(3)-C(2) 1.857(5), P(3)-C(3) 1.853(6), C(1)-C(3') 1.562(6), C(1)-C(4) 1.575(6), P(2)-P(1)-C(2) 99.3(2), P(2)-P(1)-C(3) 97.8(2), C(2')-P(1)-C(3) 102.1(2), P(1)-P(2)-C(1) 97.7(1), P(1)-P(2)-C(2) 99.0(1), C(1)-P(2)-C(2) 102.3(2), C(1')-P(3)-C(2) 104.7(2), C(1')-P(3)-C(3) 49.8(2), C(2)-P(3)-C(3) 104.9, P(2)-C(1)-P(3') 114.0(2), P(3)-C(1)-C(3') 64.9(2), P(3')-C(1)-C(4) 116.0(3), C(3)-C(1)-C(4) 131.6(4), P(1')-C(2)-P(2) 106.3(2), P(1')-C(2)-P(3) 108.9(2).

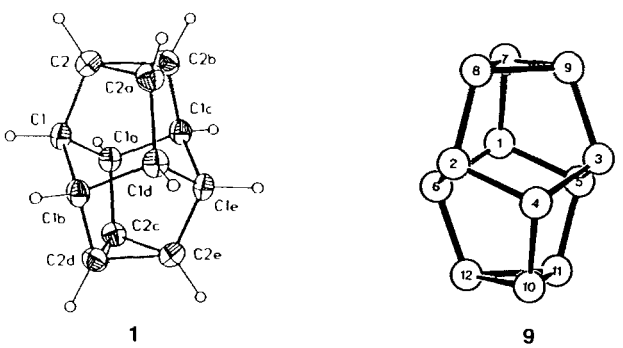


Fig. 3. Molecular structure of $C_{12}H_{12}$ **1** [5] in the crystal (left) and predicted structure of P_{12} **9** [15] (right).

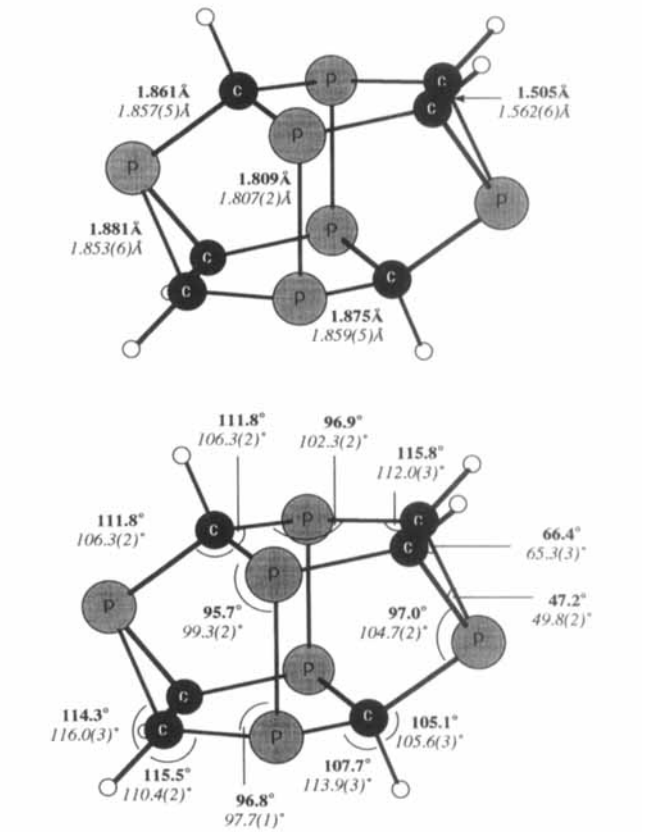


Fig. 4. Comparison of the calculated (RMP2(fu)/6-31G*-level, boldface) and the experimentally determined bond lengths and bond angles (italics) of **2**.

tions are listed in Table 1. The following molecules were chosen: $n = 2$, diphosphatetrahedrane;[20] $n = 3$, 1,2,3-triphosphabenzene;[21] $n = 4$, bishomoprismane;[22] $n = 5$, model compound similar to **4**; $n = 6$, $(HCP)_6$ model compound similar to **2**. The energies differ somewhat with the level of theory employed but interesting trends are obvious. For example, dimerization is less favorable than higher oligomerizations. Tetramers, which are well-known experimentally, are nevertheless calculated to be thermodynamically somewhat less stable than trimers. Despite this, trimers are so far only known as ligands complexed by metal fragments.[1-3, 18] Perhaps free trimers are not easily formed but react easily to give higher oligomers, whereas tetramers are formed by condensation of two dimers rather than through a trimeric stage. For $n = 2$–6, the extent of stabilization of each HCP unit by oligomerization increases with n, with the exception of $n = 3$, which suggests an extraordinary stabilization of trimers.

Just as the pentameric structure **4** can be built by replacing one edge of the tetrameric cube by a three-membered ring, the hexamer structure **2** corresponds to a cube in which two opposite edges are replaced by three-membered rings. However, while the substitution pattern of the pentamer **5** is directly analogous to the cube, this pattern is different in the hexamer **4**.

Table 1. Oligomerization energies per HCP unit for the reaction $HCP \rightarrow 1/n(HCP)_n$ in kcal mol^{-1}.

Method	ΔH(0 K) [a]				
			n		
	2 [b]	3 [c]	4 [d]	5 [e]	6 [f]
MP2	−9.7	−29.4	−28.4	−31.1	−36.0
MP3	−11.4	−31.7	−30.6	−32.8	−37.4
MP4DQ	−10.1	−29.6	−29.2	−31.6	−36.1
MP4SDQ	−8.5	−28.2	−27.9	−30.3	−34.8
Becke3LYP	−13.6	−35.1	−31.1	−32.1	−35.9
Becke3LYP/6-311G**	−11.4	−31.7	−28.6	−29.6	−33.5
			ΔG(298 K) [g]		
Becke3LYP/6-311G**	−6.6	−24.9	−20.5	−20.7	−24.0

[a] Energies were derived from single point calculations employing the 6-31G** basis set and MP2(fu)/6-31G* geometries, and are corrected for scaled zero-point vibrational energies obtained at HF/6-31G*. [b] See ref. [20]. [c] See ref. [21]. [d] See ref. [22]. [e] $(HCP)_5$ model for **4**. [f] $(HCP)_6$ model for **2**. [g] Enthalpy and entropy corrections are derived from scaled frequencies computed at HF/6-31G*.

A hypothetical hexamer with a structure like **2**, but like that of the known cube and pentamer, is computed to lie somewhat lower in energy (2.7 kcal mol^{-1} at Becke3LYP/6-31G**//MP2(fc)/6-31G**, see C_s in Table 2). A hexagonal prism (D_{3d}) not containing any P–P or C–C bonds (D_{3d}) was found to be disfavored by about 58 kcal mol^{-1} relative to the C_{2h} model for **2**.

Interestingly Alrichs et al.,[15] on the basis of theoretical calculations, have proposed that P_{12} (**9**) and P_{16} clusters may be new forms of phosphorus. However, because both species are thermodynamically unfavorable with respect to elemental P_4, they may need additional stabilization by ligation to suitable

 © VCH Verlagsgesellschaft mbH, D-69451 Weinheim, 1994 0570-0833/94/2121-2203 $ 10.00+.25/0

Table 2. Relative energies for hypothetical hexamers $(HCP)_6$ in kcal mol^{-1} [a].

Method	Relative energy for symmetry		
	C_{2h}	C_s	D_{3d}
MP2(fc)/6-31G* [b]	0.0	−4.7	+71.5
Becke3LYP/6-31G**	0.0	−2.7	+58.2

[a] Computed at MP2(fc)/6-31G* geometries and corrected for zero-point vibrational energies at HF/6-31G*. [b] fc = frozen core, only valence electrons correlated.

transition metal–ligand fragments. On the other hand, the synthesis of the organophosphorus hexamer **2** suggests that higher oligomers of *t*BuCP may also be stable. Further studies on these types of compound, including cages, containing phosphorus (and/or arsenic), carbon, and also transition metals such as Co and Rh will be topics of future papers.

Experimental Procedure

Phosphaalkene $(Me_3Si)P{=}C(OSiMe_3)tBu$ [16,17] (10 mmol) was stirred overnight with an excess of sodium metal in 10 mL of dimethoxyethane (dme) to afford a red solution of a mixture of the anions $P_3C_2tBu_2^-$ and $P_2C_3tBu_3^-$. The solution was cooled to −30 °C, and a suspension of $[PtCl_2(cod)]$ (0.75 g, 2 mmol) in dme (15 mL) was added, and the mixture stirred for 4 h before being warmed to room temperature. After removal of solvent under vacuum, the product mixture was extracted with petroleum ether (60–80 °C), concentrated, and chromatography (silica gel petroleum ether) gave **4** (0.012 g), **7** (0.040 g), and **8** (0.057 g) (identified by their characteristic $^{31}P\{^1H\}$ NMR spectra and a single crystal X-ray diffraction study on the latter [12]), and a fraction (0.032 g) containing **2** and an as yet unidentified compound containing 4 P atoms as evidenced by its $^{31}P\{^1H\}$ NMR spectrum. Crystals of **2** (ca. 2% yield) suitable for the single crystal X-ray study were obtained by cooling the mixture of **2** and **8**. The characterization by mass spectroscopy and NMR spectroscopy were also performed on these crystals.

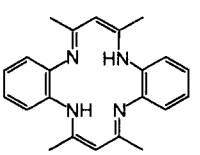
Received: May 13, 1994 [Z 6931 IE]
German version: *Angew. Chem.* **1994**, *106*, 2284

[1] J. F. Nixon, *Chem. Rev.* **1988**, *88*, 1327.
[2] J. F. Nixon, *Chem. Ind. (London)* **1993**, 404.
[3] M. Regitz, *Chem. Rev.* **1990**, *90*, 191.
[4] *Multiple Bonds and Low Coordination in Phosphorus Chemistry* (Eds: M. Regitz, O. J. Scherer), Thieme, Stuttgart, **1990**, p. 58ff.
[5] C.-H. Lee, S. Liang, T. Haumann, R. Boese, A. de Meijere, *Angew. Chem.* **1993**, *105*, 611; *Angew. Chem. Int. Ed. Engl.* **1993**, *32*, 559.
[6] T. Wettling, J. Schneider, O. Wagner, C. G. Kreiter, M. Regitz, *Angew. Chem.* **1989**, *101*, 1035; *Angew. Chem. Int. Ed. Engl.* **1989**, *28*, 1013.
[7] T. Wettling, B. Geissler, R. Schneider, S. Barth, P. Binger, M. Regitz, *Angew. Chem.* **1992**, *104*, 761; *Angew. Chem. Int. Ed. Engl.* **1992**, *31*, 758.
[8] R. Bartsch, P. B. Hitchcock, J. F. Nixon, *J. Organomet. Chem.* **1989**, *375*, C31.
[9] P. B. Hitchcock, J. F. Nixon, G. J. D. Sillett, *New J. Chem.* **1989**, *13*, 353.
[10] R. Bartsch, P. B. Hitchcock, J. F. Nixon, *J. Organomet. Chem.* **1989**, *373*, C17; *J. Chem. Soc. Chem. Commun.* **1990**, 472.
[11] J. F. Nixon, G. J. D. Sillett, *J. Organomet. Chem.* **1993**, *461*, 237.
[12] **8**: MS: parent ion: *m/e* 540. ^{31}P NMR: $\delta = 15.1$ P(3), 92.7 P(1), 97.9 P(2), 321.8 P(4); $J(P1)(P2) = 30.5$; $J(P1)(P3) = 273.5$; $J(P2)(P4) = 126.0$; $J(P3)(P4) = 7.6$ Hz. The structure of **8** was also confirmed by a single-crystal X-ray diffraction study. (V. Caliman, P. B. Hitchcock, J. F. Nixon, unpublished).
[13] R. Bartsch, P. B. Hitchcock, J. F. Nixon, *J. Chem. Soc. Chem. Commun.* **1990**, 1307; *ibid.* **1989**, 1046.
[14] Crystal data on **2**: $C_{30}H_{54}P_6$, $M = 600.6$, monoclinic, space group $C2/c$ (no. 15), $a = 17.025(8)$, $b = 12.496(3)$, $c = 17.469(5)$ Å, $\beta = 120.03(3)$, $V = 3217.6$ Å^3, $Z = 4$, $\rho_{calcd.} = 1.24$ g cm^{-3}. The structure was solved with direct methods and refined to $R = 0.068$ ($R' = 0.074$) using 2009 reflections with $|F^2| > 2\sigma(F^2)$, measured on an Enraf-Nonius-CAD4-diffractometer. Further details of the crystal structure investigation are available on request from the Director of the Cambridge Crystallographic Centre, 12 Union Road, GB-Cambridge CB2 1EZ, on quoting the full journal citation.
[15] M. Häser, U. Schneider, R. Ahlrichs, *J. Am. Chem. Soc.* **1992**, *114*, 9551.
[16] G. Becker, *Z. Anorg. Allg. Chem.* **1977**, *430*, 66.
[17] G. Becker, H. Schmidt, G. Uhl, W. Uhl, M. Regitz, W. Rösch, U. J. Vogelbacher, *Inorg. Synth.* **1990**, *27*, 243.
[18] P. B. Hitchcock, C. Jones, J. F. Nixon, *Angew. Chem.* **1994**, *106*, 478; *Angew. Chem. Int. Ed. Engl.* **1994**, *33*, 463.
[19] Gaussian 92/DFT, Revision R.2, M. J. Frisch, G. W. Trucks, H. B. Schlegel, P. M. W. Gill, B. G. Johnson, M. W. Wong, J. B. Foresman, M. A. Robb, M. Head-Gordon, E. S. Replogle, R. Gomperts, J. L. Andres, K. Raghavachari, J. S. Binkley, C. Gonzalez, R. L. Martin, D. J. Fox, D. J. Defrees, J. Baker, J. J. P. Stewart, J. A. Pople, Gaussian, Inc., Pittsburgh PA, **1993**.
[20] Diphosphatetrahedrane was reported to he the most stahle dimer: a) W. W. Schoeller, T. Busch, *Angew. Chem.* **1993**, *105*, 635; *Angew. Chem. Int. Ed. Engl.* **1993**, *32*, 617; b) M. T. Nguyen, L. Landuyt, L. G. Vanquickenhorne, *J. Org. Chem.* **1993**, *58*, 2817.
[21] Investigation of 25 $(HCP)_3$ trimers of benzene, dewar benzene, prismane, henzvalene, and biscyclopropenyl type structures revealed 1,2,3-triphosphabenzene as the most stahle. (MP4/6-31 + G**//MP2(fu)/6-31G* + 0.89 ZPE(HF/6-31G*): M. Hofmann, unpublished).
[22] The bishomoprismane (1.2,4.6-tetraphosphatetracyclo-[3.3.0.0$^{(2,4)}$.0$^{(3,6)}$]-oct-7-ene) is the thermodynamically most stable molecule of a set of $(HCP)_4$ models for experimentally known tetrainers of phosphaalkynes. (MP4/6-31G**//MP2(fu)/6-31G* + 0.89 ZPE(HF/6-31G*) unpuhlished).
[23] J. B. Foresman, Æ. Frisch, *Exploring Chemistry with Electronic Structure Methods: A Guide to Using Gaussian*, Gaussian Inc., Pittsburgh, PA, **1993**.

Tetraaza[14]annulenezirconium(IV) Complexes with Butadiene Ligands and their Relationship with Bis(cyclopentadienyl)zirconium(IV) Complexes**

Luca Giannini, Euro Solari, Carlo Floriani,* Angiola Chiesi-Villa, and Corrado Rizzoli

In recent years zirconocenes with diene ligands have become some of the most versatile organometallic building blocks. This development dates back to pioneering work by Erker et al. and Nakamura et al.[1] A significant advance in this field would arise from the use of a metal complex fragment with different steric and electronic properties from those of zirconocene. Some years ago we suggested the use of tetramethyltetraazadibenzo[14]annulene metal(IV) complex ([tmtaaM], metal = Ti, Zr, Hf, Nb) as a $[Cp_2M]$ equivalent,[2, 3] which should show some significant differences in terms of a) the number and arrangement of available coordination sites, b) the size of the cavity formed by the ligand, and hence the reactivity of the metal center toward incoming substrates, and c) the Lewis acidity at the metal center and at the ligand.



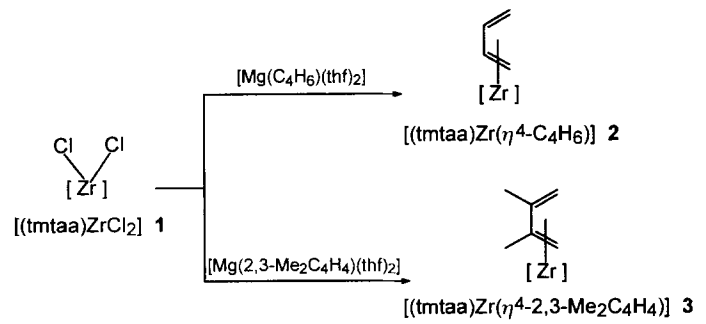
H_2tmtaa

We report here on a novel class of (butadiene)zirconium complexes. For the synthesis we employed starting materials which we recently reported in detail.[2e] *cis*-[(tmtaa)$ZrCl_2$] (**1**)[2e] was treated with $[Mg(C_4H_6)(thf)_2]$ and $[Mg(2,3\text{-}Me_2C_4H_4)(thf)_2]$ to give the corresponding butadiene complexes **2** and **3**, respectively (Scheme 1).[4]

The two complexes **2** and **3** have been isolated and characterized, and in the case of **2** an X-ray structure analysis has been carried out.[5] There are two crystallographically independent molecules (A and B) of **2** in the asymmetric unit, and four

[*] Prof. Dr. C. Floriani, L. Giannini, Dr. E. Solari
Institut de Chimie Minérale et Analytique
Université de Lausanne
BCH 3307, CH-1015 Lausanne (Switzerland)
Telefax: Int. code + (21) 692 39 05
Prof. Dr. A. Chiesi-Villa, Dr. C. Rizzoli
Dipartimento di Chimica, Università di Parma (Italy)

[**] This work was supported by the Fonds National Suisse de la Recherche Scientifique (Grant no. 20-33420-92) and Ciba-Geigy SA (Basel, Switzerland).



Scheme 1.

four independent solvent molecules (toluene). Figure 1 shows a Schakal view of molecule A. The [(tmtaa)Zr] moiety has the usual saddle-shape conformation, and structural parameters (values in square brackets refer to molecule B) are similar to

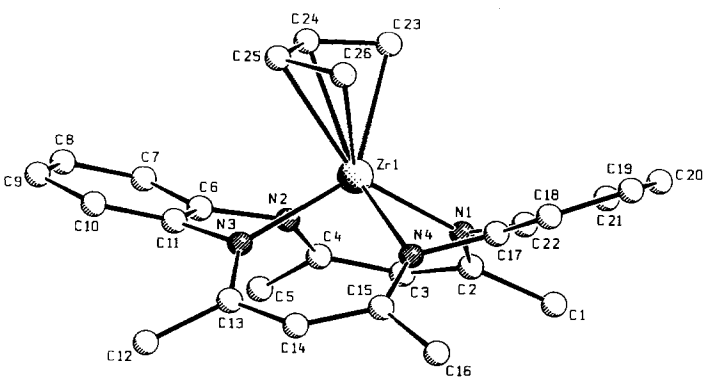
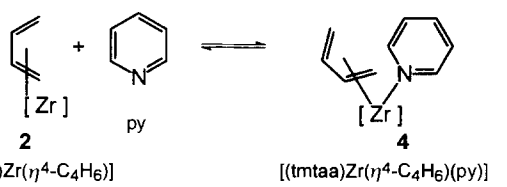


Fig. 1. Crystal structure of **2** (Schakal view of molecule A; values in square brackets refer to molecule B). Bond lengths [Å]: Zr1–N1 2.187(6) [2.185(5)], Zr1–N2 2.252(7) [2.252(6)], Zr1–N3 2.250(6) [2.248(5)], Zr1–N4 2.180(6) [2.214(6)], Zr1–C23 2.387(8) [2.407(10)], Zr1–C24 2.428(7) [2.440(11)], Zr1–C25, 2.434(8) [2.433(9)], Zr1–C26 2.399(9) [2.396(9)], C23–C24, 1.366(12) [1.394(12)], C24–C25 1.436(13) [1.397(12)], C25–C26 1.431(16) [1.418(11)]. Bond angles [°]: C25-Zr1-C26 34.4(3) [34.1(3)], C24-Zr1-C25, 34.4(3) [33.3(3)], C23-Zr1-C24, 32.9(3) [33.4(3)], N2-Zr1-N3 71.2(2) [71.4(2)], N3-Zr1-N4 80.8(2) [81.9(2)], N1-Zr1-N2 81.9(2) [81.8(2)], N1-Zr1-N4 74.6(2) [74.1(2)].

those of **1**.[2e] The zirconium atom projects above the N_4 plane by 1.046(1) Å. [1.040(1) Å]. The plane of the butadiene carbon atoms is nearly parallel to the N_4 plane; the dihedral angle is 4.4(4)° [5.7(3)°]. The η^4 coordination of the butadiene is supported by the Zr–C distances, which all fall in a very small range (Fig. 1). Such distances are, however, longer than those usually observed for Zr–C σ bonds.[6] The three C–C bond lengths within the butadiene ligand, averaged for both A and B molecules and taking the rather large standard deviations into consideration, are nearly identical. Thus, the bonding mode of the butadiene ligand in **2** can be described as π^2,η^4. The structural and spectroscopic characteristics of the $[(C_4H_6)Zr]$ moiety in **2** should be compared to those in $[Cp_2Zr]$ derivatives,[1] both in solution and in the solid state. In this context it should be noted that: a) The *cis* form is the only butadiene conformer detected in the solid state following isolation both at room temperature and at −25 °C. b) We did not observe any *cis–trans* isomerization upon heating or photolyzing either **2** or **3**. c) The assignment of the ^{1}H NMR signals for **3** is trivial, while for **2** a computer-generated simulation was necessary; the latter is in agreement with a butadiene ligand with a *cis* conformation.[7] d) The pattern of splittings of the butadiene protons in the ^{1}H NMR spectrum of **2** is temperature independent, while, in contrast, the chemical shifts depend on the temperature. The above-mentioned data emphasize the difference between the butadiene complexes **2** and **3** (π^2,η^4) and the cyclopentene (σ^2,π,η^4) complexes in the $[Cp_2Zr]$ series.[1] A variety of the bonding modes of butadiene to zirconium ranging from the π^2,η^4 to the σ^2,π,η^4 mode can be found in complexes with a set of ligands different from the bis(cyclopentadienyl) moiety.[8]

Such a major difference should be reflected in the reactivity and depends chiefly upon the number and geometry of the frontier orbitals available on the [(tmtaa)Zr] fragment[9] as opposed to those on the $[Cp_2Zr]$ one. This is revealed by the reversible binding of pyridine by **2**, which leads to complex **4** (Scheme 2).[10]



Scheme 2.

Complex **4**[11] (Fig. 2) may be isolated in the solid state with a further molecule of crystallization (pyridine). The presence of pyridine does not drastically affect the structural parameters of the $[(\eta^4\text{-}C_4H_6)Zr]$ moiety, but causes a rearrangement of the

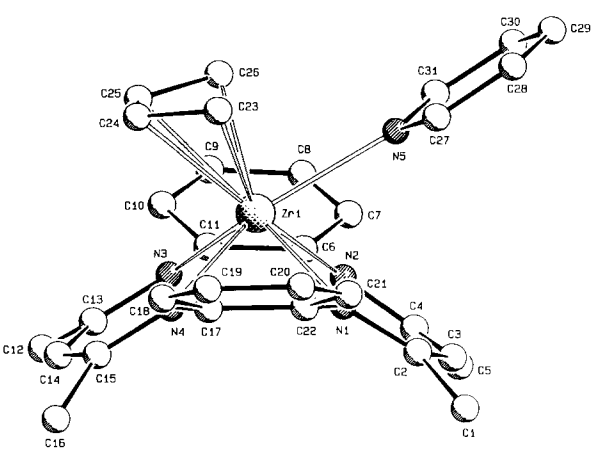


Fig. 2. Crystal structure of **4** (Schakal view). Bond lengths [Å]: Zr1–N1 2.286(3), Zr1–N2 2.301(3), Zr1–N3 2.254(3), Zr1–N4 2.270(3), Zr1–N5 2.435(3), Zr1–C23 2.383(4), Zr1–C24 2.476(4), Zr1–C25 2.491(4), Zr1–C26 2.414(3), C23–C24 1.444(5), C24–C25 1.391(6), C25–C26 1.422(5). Bond angles [°]: C25-Zr1-C26 33.6(1), C24-Zr1-C25 32.5(1), C23-Zr1-C24 34.5(1), N2-Zr1-N3 69.52(1), N3-Zr1-N4 79.2(1), N1-Zr1-N2 78.8(1), N1-Zr1-N4 68.7(1).

butadiene moiety: in comparison with complex **2**, this is rotated by about 90° with respect to the N_4 core. This is best demonstrated by the dihedral angles that the C24–C25 bond forms with the N···N lines (C24–C25 ∢ N2···N3, 91.1(3)° in complex **4** vs 1.1(5)° [0.3(5)°] in complex **2**, and C24–C25 ∢ N1···N4, 90.6(3)° in complex **4** vs 1.9(5)° [1.3(6)°] in complex **2**). The η^4 bonding mode of the butadiene ligand is slightly affected by the coordinated pyridine molecule. The Zr–C24 and Zr–C25 bond lengths are significantly longer, as

a consequence of a small shift of the butadiene ligand that allows the pyridine ligand to approach the zirconium center. Other small, but significant, differences are: a) the out-of-plane distance of the Zr center from the N_4 core [1.191(1) Å], and b) the bending of the butadiene ligand with respect to the N_4 plane [dihedral angle 11.2(2)°]. The three C–C bond lengths within the butadiene ligand range from 1.391(6)–1.444(5) Å. Such a small variation fully supports the η^4 bonding mode of the butadiene ligand as observed in complex **2**. The reaction shown in Scheme 2 can be viewed as a model for the approach of a reactive substrate to the metal center close to the butadiene ligand in the coordination sphere.

Experimental Procedure

2: **1** (11.80 g, 18.2 mmol) and $[Mg(C_4H_6)(thf)_2]$ (4.78 g, 21.5 mmol) were suspended in hexane (350 mL) at −35 °C. The mixture was allowed to warm to room temperature and stirred overnight. Volatiles were removed by evaporation in vacuo to leave an orange powder, to which toluene (450 mL) and hexane (200 mL) were added, and the mixture was stirred at room temperature for 2 h. This gave a suspension of a dark microcrystalline solid and a very fine solid in a dark brown supernatant. The mixture was heated to boiling and filtered while hot. The resulting brown solution was kept at −20 °C for 4 d to yield deep red prismatic crystals of **2**, which were collected at −20 °C. Washing this product with hexane (2 × 50 mL) at room temperature afforded solvent-free **2** as a brown microcrystalline powder (4.62 g, 52%). Anal. calcd for $C_{26}H_{28}N_4Zr$: C 64.03, H 5.79, N 11.49. Found: C 64.28, H 6.00, N 11.44. ^{1}H NMR ([D$_8$]toluene, 25 °C): δ = 7.19–7.10 (m, 8H, Ph), 5.31 (s, 2H, CH), 5.17 (m, 2H, $H_{5,6}$), 2.60 (m, 2H, $H_{3,4}$), 2.26 (s, 12H, CH_3), 0.94 (m, 2H, $H_{1,2}$). ^{1}H NMR (C_6D_6, 25 °C): δ = 7.00–6.89 (m, 8H, Ph), 5.14 (s, 2H, CH), 5.10 (m, 2H, H(5,6)), 2.54 (m, 2H, H(3,4)), 2.05 (s, 12H, CH_3), 0.91 (m, 2H, H(1,2)). ^{1}H NMR ([D$_5$]pyridine): δ = 7.30–7.03 (m, 8H, Ph), 5.56 (m, 2H, H(5,6)), 5.04 (bs, 2H, CH), 2.23 (s, 12H, CH_3), 1.20 (m, 2H, H(1,2)), 1.05 (m, 2H, H(3,4)). ^{1}H NMR ([D$_8$]THF, 25 °C): δ 7.47–7.25 (m, 8H, Ph), 5.50 (s, 2H, CH), 4.56 (m, 2H, H(5,6)), 2.53 (s, 12H, CH_3), 1.78 (m, 2H, H(3,4)), 0.21 (m, 2H, H(1,2)).

3: This complex was prepared by using a procedure analogous to that for **2** (61% yield). Anal. Calcd for $C_{28}H_{32}N_4Zr$: C 65.20, H 6.25; N 10.86. Found: C 65.01, H 6.52; N 11.00. ^{1}H NMR (C_6D_6, 25 °C): δ = 7.09–6.86 (m, 8H, Ph), 5.13 (s, 2H, CH), 2.20 (d, 2H, H(3,4)), 2.06 (s, 12H, CH_3), 1.51 (s, 6H, CH_3-butadiene), 0.77 (bd, 2H, $H_{1,2}$). ^{1}H NMR ([D$_5$]pyridine), 25 °C): δ = 7.34–7.10 (m, 8H, Ph), 4.95 (bs, 2H, CH), 2.21 (s, 12H, CH_3), 1.99 (s, 6H, CH_3-butadiene), 1.14 (d, 2H), 0.98 (d, 2H).

4: **2** (1.32 g, 2.7 mmol) was almost completely dissolved in pyridine (200 mL), the dark solution was filtered, and hexane (550 mL) was added. The resulting solution was kept at 8 °C for 24 h. This afforded large crystals of **4**·(C_5H_5N), which were collected and briefly dried in vacuo (1.13 g, 1.75 mmol, 64.8%). Anal. Calcd for $C_{36}H_{38}N_6Zr$: C 66.94, H 5.93, N 13.01. Found: C 66.91, H 5.91, N 12.95. ^{1}H NMR (C_6D_6, 25 °C): δ = 8.52 (m, 4H, pyridine), 7.00–6.87 (m, 10H, Ph + py), 6.63 (m, 4H, pyridine), 5.17 (m, 2H, H(5,6)), 5.11 (s, 2H, CH), 2.38 (m, 2H, H(3,4)), 2.05 (s, 12H, CH_3), 0.95 (m, 2H, H(1,2)). The spectrum is similar to that of pure **2** in C_6D_6; only the protons of the butadiene system and the CH group of the tmtaa ligand manifest a shift in the direction of the values observed in [D$_5$]pyridine. When complex **4** was dissolved in THF, followed by removal of volatiles in vacuo, and this procedure was repeated three times, complex **2** was obtained free of pyridine.

Received: May 26, 1994 [Z 6971 IE]
German version: *Angew. Chem.* **1994**, *106*, 2279

[1] G. Erker, C. Krüger, G. Müller, *Adv. Organomet. Chem.* **1985**, *24*, 1–39, and references therein; H. Yasuda, K. Tatsumi, A. Nakamura, *Acc. Chem. Res.* **1985**, *18*, 120–126 and references therein; H. Yasuda, Y. Kajihara, K. Mashima, K. Nagasuna, K. Lee, A. Nakamura, *Organometallics* **1982**, *1*, 388–396; G. Erker, U. Dorf, R. Benn, R.-D. Reinhardt, *J. Am. Chem. Soc.* **1984**, *106*, 7649–7650; G. Erker, K. Engel, U. Korek, P. Czisch, H. Berke, P. Caubère, R. Vanderesse, *Organometallics* **1985**, *4*, 1531–1536; G. Erker, T. Mühlenbernd, R. Benn, A. Rufinska, *ibid.* **1986**, *5*, 402–404; G. Erker, R. Lecht, J. L. Petersen, H. Bönnemann, *ibid.* **1987**, *6*, 1962–1967; M. Akita, K. Matsuoka, K. Asami, H. Yasuda, A. Nakamura, *J. Organomet. Chem.* **1987**, *327*, 193–209; H. B. Bürgi, K. C. Dubler-Steude, *J. Am. Chem. Soc.* **1988**, *110*, 4953–4957; G. Erker, R. Aul, *Organometallics* **1988**, *7*, 2070–2072; G. Erker, F. Sosna, R. Zwettler, C. Krüger, *ibid.* **1989**, *8*, 450–454; H. Yasuda, T. Okamoto, Y. Matsuoka, A. Nakamura, Y. Kai, N. Kanehisa, N. Kasai, *ibid.* **1989**, *8*, 1139–1152; G. Erker, S. Friedrich, N. Ralf, *Chem. Ber.* **1990**, *123*, 821–827; G. Erker, M. Babil, *ibid.* **1990**, *123*, 1327–1329; D. R. Swanson, E. Negishi, *Organometallics* **1991**, *10*, 825–826; R. Beckhaus, D. Wilbrandt, S. Flatau, H. Böhmer, *J. Organomet. Chem.* **1992**, *423*, 211–222; G. Erker, R. Pfaff, C. Krüger, S. Werner, *Organometallics* **1993**, *12*, 3559–3568; G. Erker, R. Noe, C. Krüger, S. Werner, *ibid.* **1992**, *11*, 4174–4177; G. Erker, R. Pfaff, *ibid.* **1993**, *12*, 1921–1926.

[2] a) S. Ciurli, C. Floriani, A. Chiesi-Villa, C. Guastini, *J. Chem. Soc. Chem. Commun.* **1986**, 1401–1403; b) C. Floriani, S. Ciurli, A. Chiesi-Villa, C. Guastini, *Angew. Chem.* **1987**, *99*, 86–88; *Angew. Chem. Int. Ed. Engl.* **1987**, *26*, 70–72; c) C. Floriani, M. Mazzanti, S. Ciurli, A. Chiesi-Villa, C. Guastini, *J. Chem. Soc., Dalton Trans.* **1988**, 1361–1365; d) E. Solari, S. De Angelis, C. Floriani, A. Chiesi-Villa, C. Rizzoli, *Inorg. Chem.* **1992**, *31*, 96–101; e) S. De Angelis, E. Solari, E. Gallo, C. Floriani, A. Chiesi-Villa, C. Rizzoli, *ibid.* **1992**, *31*, 2520–2527; f) R. Uhrhammer, D. G. Black, T. G. Gardner, J. D. Olsen, R. F. Jordan, *J. Am. Chem. Soc.* **1993**, *115*, 8493–8494; g) C. H. Yang, J. A. Ladd, V. L. Goedken, *J. Coord. Chem.* **1988**, *18*, 317–323 and references therein.

[3] For systems related to the [Cp_2M] or [M(tmtaa)] fragments see: a) C. Floriani, E. Solari, F. Corazza, A. Chiesi-Villa, C. Guastini, *Angew. Chem.* **1989**, *101*, 91–93; *Angew. Chem. Int. Ed. Engl.* **1989**, *28*, 64–66; b) C. Floriani, *Polyhedron* **1989**, *8*, 1717–1722; c) F. Corazza, E. Solari, C. Floriani, A. Chiesi-Villa, C. Guastini, *J. Chem. Soc., Dalton Trans.* **1990**, 1335–1344; d) J. M. Rosset, C. Floriani, M. Mazzanti, A. Chiesi-Villa, C. Guastini, *Inorg. Chem.* **1990**, *29*, 3991–3996; e) E. Solari, C. Floriani, A. Chiesi-Villa, C. Rizzoli, *J. Chem. Soc. Dalton Trans.* **1992**, 367–373; f) H. Brand, J. Arnold, *Organometallics* **1993**, *12*, 3655–3665.

[4] S. S. Wreford, J. F. Whitney, *Inorg. Chem.* **1981**, *20*, 3918–3924.

[5] Crystal structure analysis of **2**: $C_{26}H_{28}N_4Zr \cdot 2C_5H_8$, M = 672.0, triclinic, space group $P\bar{1}$, a = 16.319(3), b = 18.426(5), c = 12.084(3) Å, α = 104.93(2), β = 95.17(2), γ = 77.06(2)°, V = 3419.7(15) Å^3, Z = 4, ρ_{calcd} = 1.305 g cm^{-3}, $F(000)$ = 1408, $Mo_{K\alpha}$ radiation (λ = 0.71069 Å), $\mu(Mo_{K\alpha})$ = 3.47 cm^{-1}, crystal dimensions 0.16 × 0.18 × 0.24 mm. The structure was solved by the heavy atom method and anisotropically refined for all non-hydrogen atoms. One of the four independent toluene molecules of crystallization (C61–C66) was found to be statistically distributed over two positions (A and B) isotropically refined with site occupation factors of 0.5 by applying a rigid body constraint to the rings. The hydrogen atoms, except those attached to the methyl carbon atoms C37, C47, and C57, which were placed in calculated positions, were located from a difference map and introduced as fixed contributors in the last stage of refinement (U_{iso} = 0.05 and 0.10 Å^2 for those related to the complex and to three toluene molecules, respectively). The hydrogen atoms of the disordered C61–C67 toluene molecule were ignored. For 6073 unique observed reflections [$I > 2\sigma(I)$] collected at T = 123 K ($5 < 2\theta < 50°$) on a Rigaku AFC6S diffractometer and corrected for absorption the final R value was 0.056 (unit weights). All calculations were carried out with the use of SHELX-76 on an IBM AT personal computer equipped with an INMOS T800 transputer [12].

[6] D. J. Cardin, M. F. Lappert, C. L. Raston, *Chemistry of Organo-Zirconium and -Hafnium Compounds*, Horwood, Chichester, **1986**.

[7] ^{1}H NMR data were recorded on a Bruker ARX-400 NMR spectrometer and analyzed with the PC software package PERCH (PEak reseaRCH).

[8] J. Blenkers, B. Hessen, F. van Bolhuis, A. J. Wagner, J. H. Teuben, *Organometallics* **1987**, *6*, 459–469; M. D. Fryzuk, T. S. Haddad, S. J. Rettig, *ibid.* **1989**, *8*, 1723–1732; B. Hessen, J. Blenkers, J. H. Teuben, G. Helgesson, S. Jagner, *ibid.* **1989**, *8*, 2809–2812; P. J. Vance, T. J. Prins, B. E. Hauger, M. E. Silver, M. E. Wemple, L. M. Pederson, D. A. Kort, M. R. Kannisto, S. J. Geerligs, R. S. Kelly, J. J. McCandless, J. C. Huffman, D. G. Peters, *ibid.* **1991**, *10*, 917–924; G. M. Diamond, M. H. Green, N. M. Walker, J. A. K. Howard, S. A. Mason, *J. Chem. Soc., Dalton Trans.* **1992**, 2641–2646.

[9] T. R. Ward, C. Floriani, unpublished results.

[10] The reversible binding of CO by a [$Zr(C_6H_4)_2$(dmpe)] has been reported: R. P. Beatty, S. Datta, S. S. Wreford, *Inorg. Chem.* **1979**, *18*, 3139.

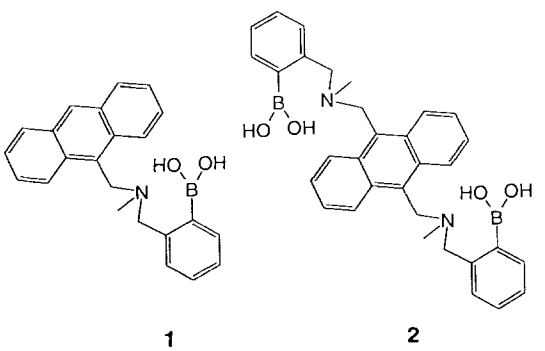
[11] Crystal structure analysis of **4**: $C_{31}H_{33}N_5Zr \cdot C_5H_5N$, M = 646.0, monoclinic, space group $P2_1/c$, a = 13.922(6), b = 12.145(5), c = 18.275(8) Å, β = 96.05(4), V = 3073(2) Å^3, Z = 4, ρ_{calcd} = 1.396 g cm^{-3}, $F(000)$ = 1344, $Cu_{K\alpha}$ radiation (λ = 1.54178 Å), $\mu(Cu_{K\alpha})$ = 32.23 cm^{-1}, crystal dimensions 0.11 × 0.21 × 0.28 mm. The structure was solved by the heavy atom method and anisotropically refined for all non-hydrogen atoms. The hydrogen atoms were located from a difference Fourier map and introduced as fixed contributors in the last stage of refinement (U_{iso} = 0.04 and 0.06 Å^2 for the complex and pyridine solvent molecule, respectively). For 5090 unique observed reflections [$I > 2\sigma(I)$] collected at T = 123 K ($6 < 2\theta < 140°$) on a Rigaku AFC6S diffractometer and corrected for absorption the current R value is 0.055 (R_w = 0.070). All calculations were carried out with the use of SHELX-76 on an IBM AT personal computer equipped with an INMOS T800 transputer [12].

[12] Further details of the crystal structure investigations are available on request from the Director of the Cambridge Crystallographic Data Centre, 12 Union Road, GB-Cambridge CB2 1EZ (UK), on quoting the full journal citation.

A Glucose-Selective Molecular Fluorescence Sensor**

Tony D. James, K. R. A. Samankumara Sandanayake, and Seiji Shinkai*

Photoinduced electron transfer (PET) has been employed in the design of fluorescent molecular sensors for protons and metal ions;[1] however, there are relatively few fluorescent molecular sensors for small neutral molecules. Our group[2-11] as well as others[12-17] have started to exploit the interactions of boronic acids with saccharides[18] for the development of receptor sites for saccharide detectors. Selective detection of saccharides is our aim, but to achieve this goal we must manipulate the characteristics of the boronic acid. We have found that two-point interrogation by a diboronic acid is the most expeditious approach towards the selective detection of saccharides.[4-7] The spatial disposition of the two boronic acid moieties determines which saccharide is bound preferentially. With PET sensor **1** in mind[11] and by reference to molecular models we discovered that the 9,10-diaminomethylanthracene skeleton **2** provides a perfect cleft for glucose.[19] The two inwardly facing boronic acid moieties are perfectly spaced and aligned for the 1,2- and 4,6-hydroxyl groups of glucose.



1 **2**

Synthesis of the desired boronic acid as the protected boronate ester was readily achieved (Scheme 1).[11, 20] Figure 1 shows the fluorescence intensity of **2** as a function of the concentration of the saccharides (titration curves) at pH 7.77 (33.3% methanol buffer). The stability constants are: D-glucose (log $K_a = 3.6$); D-allose (log $K_a = 2.8$); D-fructose (log $K_a = 2.5$); D-galactose (log $K_a = 2.2$) and ethyleneglycol (log $K_a = -0.20$).

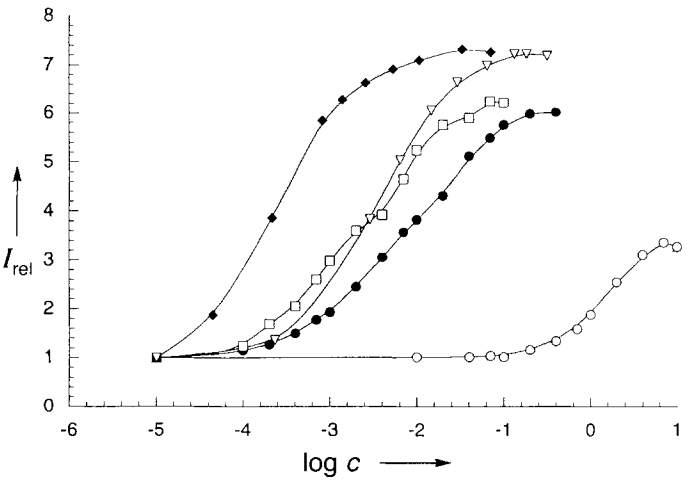
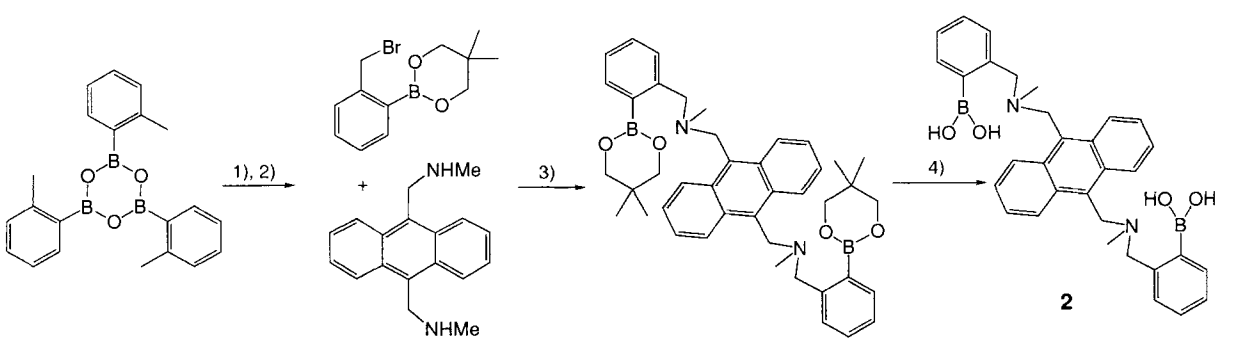


Fig. 1. Relative fluorescence intensity I_{rel} of **2** as a function of the saccharide and ethyleneglycol concentrations log c at 25 °C; 1.0×10^{-5} M of **2** in 33.3% MeOH/H_2O buffer at pH 7.77, $\lambda_{ex} = 370$ nm, $\lambda_{em} = 423$ nm. ♦ D-glucose, □ D-allose, ▽ D-fructose, ● D-galactose, ○ ethyleneglycol.

The main species involved are presented in Scheme 2. With **2** four main species exist under the experimental conditions. The fluorescent species are: **2a** (a noncyclic 2:1 complex) and **2b** (a cyclic 1:1 complex). With ethyleneglycol the fluorescent species can only be the 2:1 complex **2a**. With D-glucose the large stability is indicative of a shift in the equilibrium towards the intramolecular 1:1 complex **2b**.

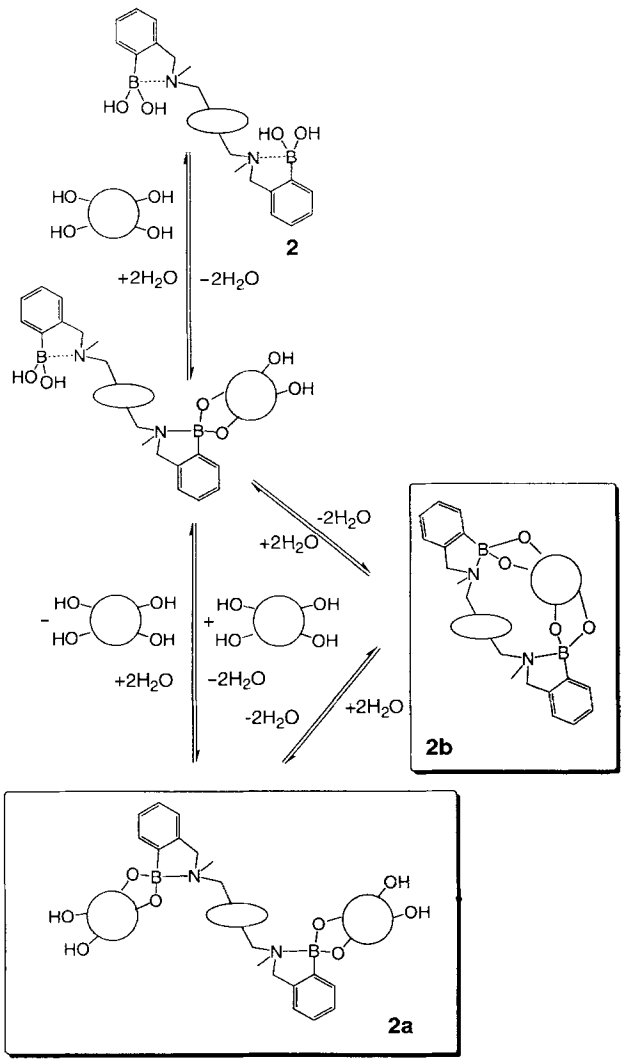
The existence of the 1:1 complex **2b** with D-glucose was substantiated by ^{1}H and 2D COSY90 NMR measurements. Figure 2 shows the ^{1}H NMR spectrum of the D-glucose 1:1 complex **2b** (see Table 1). The large up-field shift of the signal of H3 ($\delta = -0.3$) is indicative of a proton pointing directly at the π electrons of anthracene. The splitting of the anthrylic and benzylic protons is also characteristic of structural rigidification in a 1:1 complex. With D-allose, D-fructose, and D-galactose no 1:1 complex could be detected in the ^{1}H NMR spectra. The secondary ion mass spectra (positive ion) of a 1:1 mixture of **2** with D-glucose, D-allose, D-fructose, and D-galactose each contained the M^+ ion of **2b**; with D-fructose this signal was weak



Scheme 1. Synthesis of boronic acid derivative **2**. Reagents (yields): 1) *N*-bromosuccinimide, azobisisobutyronitrile, CCl_4, reflux (60%); 2) 1.1 equiv 2,2-dimethyl-1,3-propanediol, $PhCH_3$, Dean–Stark (quant); 3) 0.4 equiv diamine, 1.1 equiv K_2CO_3, THF (5%); 4) 33.3% MeOH/H_2O, pH 7.77 (quant).

[*] Prof. S. Shinkai, Dr. T. D. James, Dr. K. R. A. S. Sandanayake
Shinkai Chemirecognics Project, ERATO, Aikawa 2432-3
Kurume, Fukuoka 830 (Japan)
Telefax: Int. code +(942) 37-6125

[**] T. D. J. and K. R. A. S. S. wish to thank Dr. F. Ohseto and Dr. M. Mikami (Research Development Corporation of Japan Chemirecognics Project) for helpful advice and discussions. We would also like to thank Miss R. Iguchi for technical assistance.



Scheme 2. The anthracene framework is symbolized by an ellipse, the sugar molecules by circles with four OH groups.

Table 1. ^{1}H NMR assignment of D-glucose complex **2b** (see also Fig. 2).

Assignment	δ value
Complex	
H1	5.18
H2	3.01
H3	−0.30
H4	2.68 (masked)
H5	3.43
H6 and H6′	3.73
Ha1 and Ha2 or Ha3 and Ha4	3.93 and 4.85 (masked)
Ha1 and Ha2 or Ha3 and Ha4	4.10 and 4.60
Hb1 and Hb2 or Hb3 and Hb4	5.66 and 6.80
Hb1 and Hb2 or Hb3 and Hb4	6.13 and 6.78
NCH_3 or H_3CN	2.42
NCH_3 or H_3CN	2.68
Solvent	
CH_3OH	3.30
CH_3OH	4.89
Protecting group [a]	
$(CH_3)_2C(CH_2OH)_2$	0.85
$(CH_3)_2C(CH_2OH)_2$	3.40
$(CH_3)_2C(CH_2OH)_2$	4.89

[a] The protecting group is removed under the conditions of the NMR experiment.

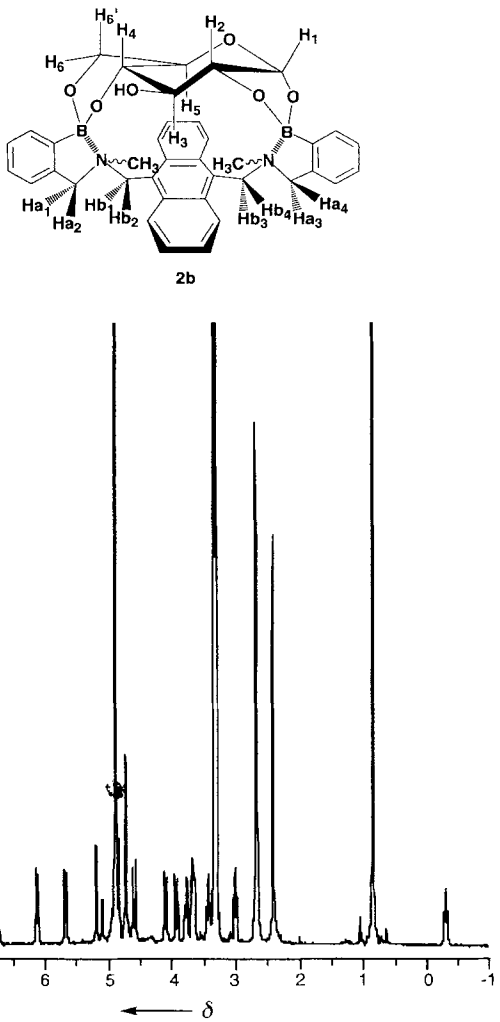


Fig. 2. ^{1}H NMR spectrum of the 1:1 complex of D-glucose and **2**. The pyranose form is depicted but the furanose form has not been ruled out.

and the spectrum also contained a signal for the M^+ ion of **2a**.

From CPK models the predicted order of stability of the 1:1 complexes **2b** are: D-glucose ≈ D-allose > D-galactose > D-fructose. D-glucose and D-allose have different configurations at C3 (H3). From the ^{1}H NMR studies of the D-glucose 1:1 complex **2b**, the C3 proton points towards the π electrons of the anthracene moiety. In the corresponding D-allose complex the C3 hydroxyl group must also be directed towards the anthracene π electrons. Since the D-allose complex (log K_a) is significantly less stable than the D-glucose complex, the π electron/hydroxyl interaction must therefore be unfavorable. The lack of correlation between the predicted and observed order for D-galactose and D-fructose is likely caused by a difference in the stability of the 2:1 complex **2a** rather than of the 1:1 complex **2b**. The mass spectral data confirms this assumption, since with D-fructose the M^+ ion of the 2:1 complex **2a** is detected, but with D-galactose only the M^+ ion of the 1:1 complex **2b** is observed.

Interestingly, the maximum fluorescence changes observed with **2** are over a concentration range suitable for the detection of physiological glucose levels. In blood three main monosaccharides are present: D-glucose (0.3–1.0 mM), D-fructose (≤0.1 mM), and D-galactose (≤0.1 mM). When D-glucose is titrated in the presence of 0.1 mM D-fructose or D-galactose, the

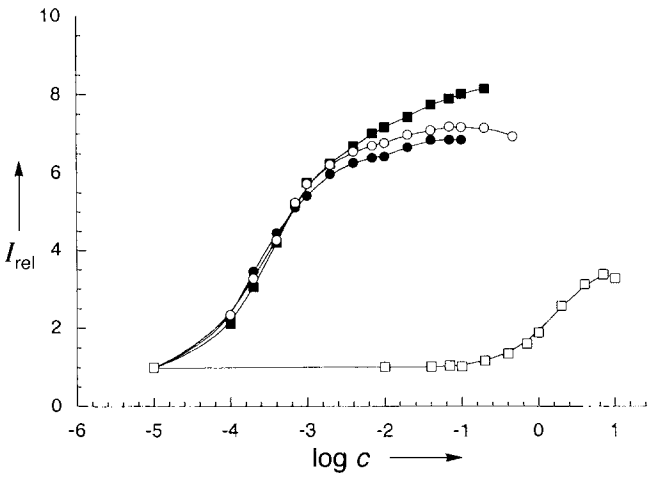


Fig. 3. Relative fluorescence intensity I_{rel} of **2** as a function of the glucose concentration log c with and without 0.1 mM D-galactose or D-fructose at 25 °C; 1.0×10^{-5} M of **2** in 33.3% MeOH/H_2O buffer at pH 7.77, $\lambda_{ex} = 370$ nm, $\lambda_{em} = 423$ nm. ● D-galactose/D-glucose, ■ D-fructose/D-glucose, ○ D-glucose, □ ethyleneglycol.

observed stability (log K_a) is the same as that obtained with D-glucose alone (Fig. 3).

In conclusion, a PET sensor has been designed that is selective for glucose. We believe that it will be possible to construct other saccharide-selective sensors if particular attention is paid to the spatial disposition of the two boronic acid moieties with respect to the hydroxyl groups of the target saccharides.

Received: April 5, 1994
Revised version: July 2, 1994 [Z 6823 IE]
German version: *Angew. Chem.* **1994**, *106*, 2287

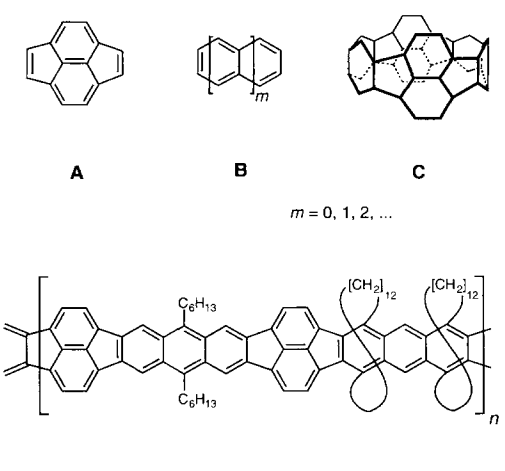
[1] Reviews: A. J. Bryan, A. P. de Silva, S. A. de Silva, R. A. D. Rupasingha, K. R. A. S. Sandanayake, *Biosensors* **1989**, *4*, 169; R. Bissel, A. P. de Silva, H. Q. N. Gunaratna, P. L. M. Lynch, G. E. M. Maguire, K. R. A. S. Sandanayake, *Chem. Soc. Rev.*, **1992**, *21*, 187.
[2] S. Shinkai, K. Tsukagoshi, Y. Ishikawa, T. Kunitake, *J. Chem. Soc. Chem. Commun.* **1991**, 1039.
[3] K. Tsukagoshi, S. Shinkai; *J. Org. Chem.* **1991**, *56*, 4089.
[4] K. Kondo, Y. Shiomi, M. Saisho, T. Harada, S. Shinkai, *Tetrahedron* **1992**, *48*, 8239.
[5] Y. Shiomi, K. Kondo, M. Saisho, T. Harada, K. Tsukagoshi, S. Shinkai, *Supramol.* **1993**, *2*, 11.
[6] Y. Shiomi, M. Saisho, K. Tsukagoshi, S. Shinkai, *J. Chem. Soc. Perkin Trans. 1* **1993**, 2111.
[7] G. Deng, T. D. James, S. Shinkai, *J. Am. Chem. Soc.* **1994**, *116*, 4567–4572.
[8] T. D. James, T. Harada, S. Shinkai, *J. Chem. Soc. Chem. Commun.* **1993**, 857, 1176 (corrigendum).
[9] T. D. James, K. Murata, T. Harada, K. Ueda, S. Shinkai, *Chem. Lett.* **1994**, 273.
[10] R. Ludwig, T. Harada, K. Ueda, T. D. James, S. Shinkai, *J. Chem. Soc. Perkin Trans. 2* **1994**, *4*, 697.
[11] T. D. James, K. R. A. S. Sandanayake, S. Shinkai, *J. Chem. Soc. Chem. Commun.* **1994**, 477.
[12] J. Yoon, A. W. Czarnik, *J. Am. Chem. Soc. Chem. Commun.* **1994**, 477.
[13] L. K. Mohler, A. W. Czarnik, *J. Am. Chem. Soc.* **1993**, *115*, 7037.
[14] L. K. Mohler, A. W. Czarnik, *J. Am. Chem. Soc.* **1993**, *115*, 2998.
[15] G. Wulff, B. Heide, G. Helfmeier, *J. Am. Chem. Soc.* **1987**, *108*, 1089.
[16] G. Wulff, H.-G. Poll, *Makromol. Chem.* **1987**, *188*, 741.
[17] Review: G. Wulff, *Pure Appl. Chem.* **1982**, *54*, 2093.
[18] From our work and that of others [2–17] it is known that the boronate ester is rapidly and reversibly formed under basic conditions. The same rapid equilibrium condition also exists in *ortho* aminoboronic acids at neutral pH [11, 16]. Non-covalent interactions are described with such terms as "recognition", "complex", and "binding constants". These terms will be used to describe the equilibrium between covalent boronate ester and free boronic acid under these conditions.
[19] "Cleft" type receptors have been extensively studied by J. Rebek Jr., et al. J. Rebek, Jr., *Acc. Chem. Res.* **1990**, *23*, 399 and references therein.
[20] R. T. Hawkins, H. R. Snyder, *J. Am. Chem. Soc.* **1960**, *82*, 3863; H. R. Snyder, R. T. Hawkins, W. J. Lennarz, *ibid.* **1960**, 82, 3053; H. R. Snyder, M. S. Konecky, W. J. Lennarz, *ibid.* **1958**, *80*, 3611.

Synthesis of a Fully Unsaturated "Molecular Board"**

Matthias Löffler, Arnulf-Dieter Schlüter,* Katrin Gessler, Wolfram Saenger, Jean-Marc Toussaint, and Jean-Luc Brédas

Dedicated to Professor Henry Hall, Jr., on the occasion of his 70th birthday

Our current research is focused on the synthesis of structurally perfect, fully unsaturated double-stranded polymers.[1] These are potentially interesting as materials for application in areas such as electrical conductivity, optical nonlinearity, electroluminescence, and photovoltaics.[2–5] Unsaturated polymers of this kind should have a planar, boardlike structure, a feature which inevitably renders them insoluble. For the synthesis of insoluble and yet well-defined polymers, precursor concepts have proved very successful for those cases in which the first step is the preparation of a characterizable and processable polymer which then, in a second step, is converted into the desired polymer. Here we report the synthesis of a double-stranded Diels–Alder (DA) polymer and its polymer-analogous conversion into the unsaturated, all-carbon polymer **1** (Scheme 1). The backbone of **1** consists of a regular sequence of typical substructures of fullerenes, like the pyracylene **A** and the oligoacene **B** ($m = 2$). Polymer **1** is the second member of a new class of



1

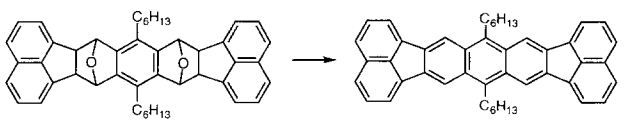
Scheme 1. Some fullerene substructures A, B, and C and the structure of the fully unsaturated, double-stranded polymer **1**.

[*] Prof. Dr. A.-D. Schlüter, M. Löffler
Institut für Organische Chemie der Freien Universität
Takustrasse 3, D-14195 Berlin (FRG)
Telefax: Int. code +(30) 8383357
K. Gessler, Prof. Dr. W. Saenger
Institut für Kristallographie der Freien Universität Berlin (FRG)
Dr. J.-M. Toussaint, Prof. Dr. J.-L. Brédas
Université de Mons-Hainaut
Service de Chimie des Materiaux Nouveaux, Mons (Belgium)

[**] This work was supported by the Bundesministerium für Forschung und Technologie, the Fonds der Chemischen Industrie, and the Deutsche Forschungsgemeinschaft. We also thank W. Lamer for the SEC measurements, O. Klein and G. Buntkowski for recording ^{13}C CP/MAS spectra, and C. Bartel for help with some of the experiments. The work in Mons was partially supported by the Belgian Government "Pole d'Attraction Interuniversitaire en Chimie Supramoléculaire at Catalyse" and the Belgian "Programme d'Impulsion en Technologie de l'Information" (contract 1T/SC/22), FNRS-FRFC, an IBM Academic Joint Study, and the Commission of European Community through the ESPRIT Basic Research Action TOPFIT Project 7282.

polymers composed of substructures of fullerenes.[6] It closely resembles the open-chain analogue **C** of the belt-region of C_{60}. We also discuss the results of calculations on the electronic structure of the parent compound of **1**, which bears no hexyl substituents. These calculations are aimed at providing a description of the interactions between these substructures.

The selection of the precursor polymer and the kind of chemistry needed for its conversion into the target structure resulted from the key observation that compound **2**, regardless of its actual stereochemistry (six diastereomers) can be dehydrated with *p*-toluenesulfonic acid (*p*-TsOH) to benzodifluoranthene **3** in yields of virtually 100% (Scheme 2).[7] To our knowledge,

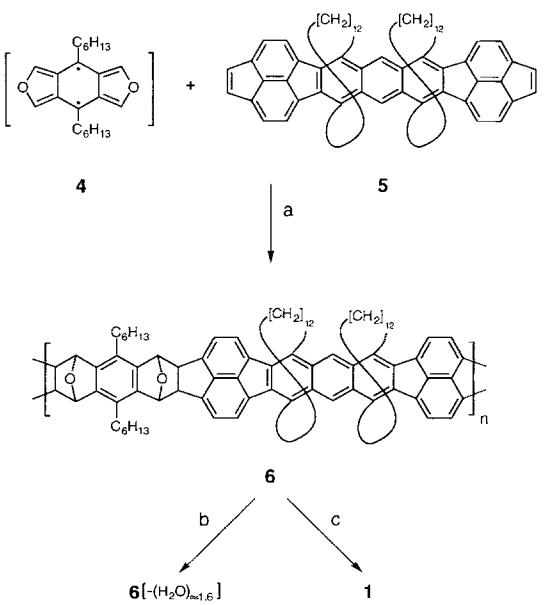


2 **3**

Scheme 2. Dehydration of the model compound **2**.

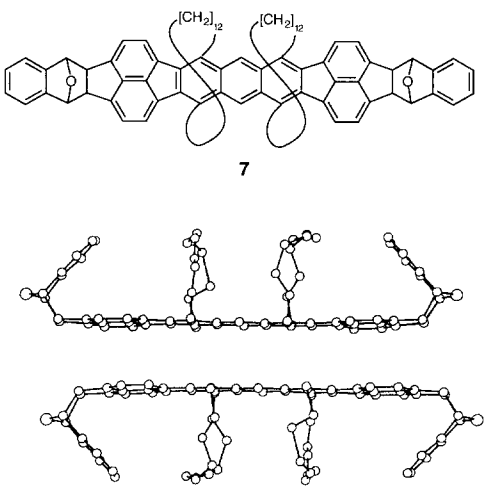
this is the first and to date only successful way of converting precursor molecules by dehydration into polycyclic aromatic compounds, which proceeds reproducibly and cleanly. The dehydration does not seem to be catalyzed by *p*-TsOH; thus, it should be possible to control the number of water molecules removed by stoichiometry (see below). These features make a polymer with the structural subunits of **2** an ideal candidate for a polymer analogous application. We, therefore, synthesized polymer **6** and subsequently dehydrated it with *p*-TsOH.

The synthetic route to **6** involves the DA-polyaddition of the in situ prepared bisdiene **4** with the bisdienophile **5** (Scheme 3).



Scheme 3. Synthesis of the precursor polymer **6** and its conversion into polymer **1**: a) **4** (583 mg, 0.51 mmol), **5** (410 mg; 0.51 mmol), 110 °C, toluene (50 mL), 24 h, precipitation into methanol/hexane; b) **6** (24.3 mg), *p*-TsOH (5.4 mg, 1.3 equiv/repeat unit), 110 °C, toluene (15 mL), 24 h, precipitation into methanol; c) **6** (48.6 mg), *p*-TsOH (25 mg, 4.0 equiv/repeat unit), 110 °C, toluene (20 mL), 24 h, precipitation into methanol.

"Monomer" **4** has proved very versatile in countless poly-DA-additions;[11] monomer **5** deserves some comments.[8] First, **5** is bridged by flexible alkyl chains ("loops"). This should help to increase the solubility of the precursor and the target polymer. The loops, like straight alkyl chains,[9] are effective solubilizers for entropic reasons, but are also good for enthalpic reasons because they disturb the packing of "flat boards". Second, this allows one to obtain a polymer with repeating units, which already contain extended aromatic regions. Therefore only a few dehydration steps are necessary to generate large conjugated areas. As to the question of solubility, the crystal structure[10, 11] of a diastereomer of model compound **7**[8] provides an insight into how the "molecular boards" would most probably pack if alkyl loops were not present (Fig. 1). The



7

Fig. 1. Model compound **7** and its crystal structure (ORTEP).

diastereomer of **7** shown forms sandwichlike structures in which the planar regions are arranged almost on top of each other at van der Waals distance. This situation cannot occur in the polymer because of the randomness of the relative orientations of the loops.

Polymer **6** was obtained as a yellow-orange material in 85–95% yield. The molecular weight of **6**, in contrast to other DA-ladder polymers, has a pronounced effect on its solubility in common organic solvents at room temperature. The ratio of soluble, yet relatively low-molecular-weight material to insoluble but high-molecular-weight material can be adjusted by changing the conditions. For example, heating a 0.005 M mixture of the monomers **4** and **5** to 110 °C for 24 h in toluene gave a material which was completely soluble in benzene [size exclusion chromatography in THF versus polystyrene: $M_n = 5000$ ($p_n = 4-5$); $M_w = 11100$ ($P_w = 10$); $D = 2.2$]. If the same experiment was carried out at higher monomer concentration (0.135 M), the amount of soluble material was reduced to 25–30% [$M_n = 7200$ ($P_n = 6-7$); $M_w = 30200$ ($P_w = 26$); $D = 4.2$]. In this context it is important to note: a) A sample of the soluble polymer remained completely soluble if it was heated in toluene under reflux for 3 d. Cross-linking does, therefore, not seem to play a role. b) The formation of insoluble material can be prevented if dodecyl instead of hexyl chains are used as solubilizers. The determination of the structure of polymer **6** is based chiefly upon the ^1H and ^{13}C NMR spectra for the soluble and the ^{13}C CP/MAS solid-state NMR spectrum for the insol-

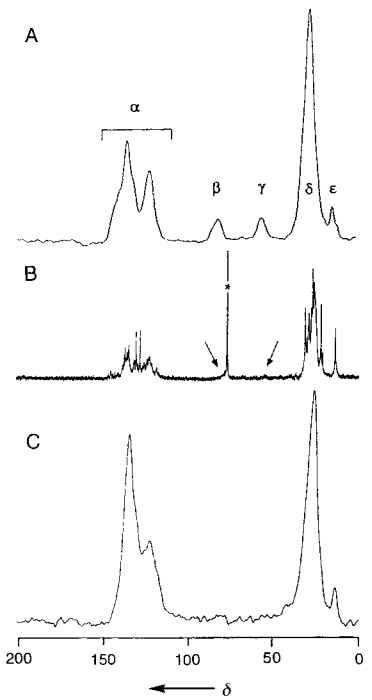


Fig. 2. ^{13}C CP/MAS NMR spectra (300 MHz) of polymers **6** (A) (α = C-arom., β = C–O, γ = H-C-C-O, $\delta = CH_2$, $\varepsilon = CH_3$) and **1** (C), and ^{13}C NMR spectrum (270 MHz, $CDCl_3$) of partially dehydrated polymer **6** (B). Signals due to residual β- and γ-C atoms and the solvent are marked with arrows and an asterisk.

uble part. The latter is shown in Figure 2 together with a signal assignment which is based on the chemical shifts of four diastereomers of model compound **2**. The ^1H NMR signals of **6** are relatively broad; therefore a detailed stereochemical (sequence) analysis was not undertaken. The C,H values from elemental analysis match the theoretical values within 0.5%. The excellent match between the UV spectra of **3** and **6** (Fig. 3) is also in accordance with the proposed structure.

In order to establish the point at which the polymer becomes insoluble, the initial dehydration studies were aimed at a partial dehydration. Preliminary experiments were done on a low-molecular-weight fraction (M_n = 5000, M_w = 10500) of **6** by heating in toluene under reflux for 24 h in the presence of 1.3 equivalents of *p*-TsOH per mole repeat unit. The dehydration was accompanied by a color change from intense orange to red. The reaction mixture remained homogeneous. A representative UV spectrum of the material obtained shows that the λ_{max} value is shifted bathochromically from 500 to 600 nm. The degree of dehydration has not yet been determined quantitatively. A comparison of the ^{13}C NMR spectrum (Fig. 2B) with that of the starting material, however, suggests that more than 80% of the oxygen bridges as well as the adjacent hydrogen atoms have been removed. Only low intensities for the signals assigned to the ether (β) and bridgehead (γ) carbon atoms are observed. The fact that the partially dehydrated materials are still soluble in common organic solvents, even though a large proportion of the kinks have been removed, underlines the effectiveness of the alkyl substituents as solubilizers. The second step involved the attempt to drive the dehydration to completion. For this the same experiments were carried out with an excess of *p*-TsOH. The material obtained in this way was only sparingly soluble. Its UV spectrum (Fig. 3) shows no further bathochromic shift, but instead a significant increase in the intensity of the long wavelength absorption bands. This is a clear indication that more water molecules have been removed from the backbone of the polymer. Furthermore, the ^{13}C CP/MAS NMR spectrum of this material (Fig. 2C), does not indicate the presence of any "residual water" in the structure. The data from elemental analysis match the calculated values within 1.0%. The soluble high-molecular-weight fractions of **6** gave comparable results.

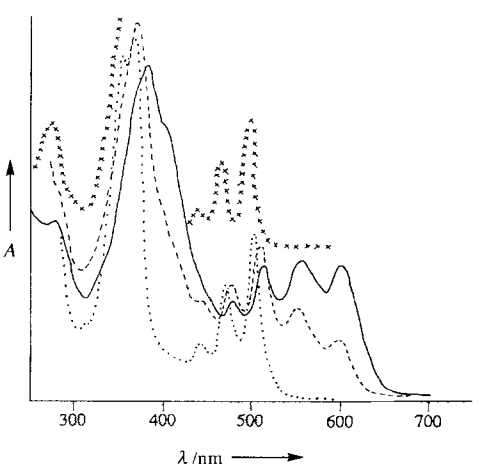


Fig. 3. UV/VIS spectra of model compound **7** in chloroform (λ_{max}(lg ε) = 497 (4700)) (crossed line) and of polymer **6** (dotted line), partially dehydrated **6** (dashed line), and fully dehydrated **1** (solid line). A = absorption (arbitrary units).

Parallel to the synthetic work, theoretical investigations were undertaken on the unsubstituted form of **1** to determine the electronic structure and to outline the origin of the band gap[4] in this polymer. The structure of the trimer was first optimized by the semiempirical AM1 technique, a method well-known for its reliable determinations of geometries on conjugated compounds.[12] Then, in a second step, the central part of the optimized trimer was used as input for band-structure calculations with the valence effective Hamiltonian (VEH) technique;[13] this method provides accurate determinations of essential electronic parameters in organic compounds, such as ionization potential, electron affinity, and band-gap values. From the optimized geometric structure of **1**, it appears that the polymer backbone can be simply envisioned as a regular succession of naphthalene and anthracene units that are linked to each other by single carbon–carbon bonds. The bond lengths and angles along the conjugated backbone obtained from the calculations are indeed almost identical to the ones optimized in discrete naphthalene and anthracene molecules. The most important electronic parameters calculated for the unsubstituted form of polymer **1** are given in Table 1 together with those obtained for naphthalene and anthracene. The calculated band gap for the polymer is 2.1 eV, a value in excellent agreement with the long wavelength absorption in the UV spectrum of the substituted polymer (Fig. 3). The bonding–antibonding electronic patterns appearing on the polymer electronic bands have been analyzed and compared to those obtained for the electronic levels of naphthalene and anthracene. It appears that the HOMO of the polymer arises from an antibonding interaction between the HOMOs of naphthalene and anthracene while the LUMO of the polymer comes from the bonding interaction between the LUMO of naphthalene and LUMO +1 of anthracene.

Table 1. VEH-calculated values of solid-state ionization potential (IP), electron affinity (EA), and energy gap (Eg) for the unsubstituted polymer **1**, naphthalene, and anthracene. Values in eV.

Compound	IP	EA	Eg
Polymer **1** [a]	4.96	−2.81	2.15
Naphthalene	6.20	−1.60	4.60
Anthracene	5.65	−2.17	3.48

[a] Parent compound without hexyl substituents.

The properties of the polymer are currently under investigation with a view to its application in the areas mentioned in the introduction.

Received: June 1, 1994 [Z 6987 IE]
German version: *Angew. Chem.* **1994**, *106*, 2281

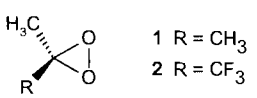
[1] A.-D. Schlüter, *Adv. Mater.* **1991**, *3*, 282–291.
[2] S. Kivelson, O. L. Chapman, *Phys. Rev. B* **1983**, *28*, 7236–7243.
[3] L. Yu, M. Chen, L. R. Dalton, *Chem. Mater.* **1990**, *2*, 649–659.
[4] J. J. Brédas, R. Silbey, *Conjugated Polymers, The Novel Science and Technology of Highly Conducting and Nonlinear Optically Active Materials*, Kluwer, Dordrecht, **1991**.
[5] M. Schwoerer, *Phys. Bl.* **1994**, *50*, 52–55.
[6] First example: A.-D. Schlüter, M. Löffler, V. Enkelmann, *Nature* **1994**, *368*, 831–834.
[7] H. Schirmer, A.-D. Schlüter, V. Enkelmann, *Chem. Ber.* **1993**, *126*, 2543–2546.
[8] M. Löffler, A.-D. Schlüter, *Synlett* **1994**, 75–78.
[9] See for example M. Ballauff, *Angew. Chem.* **1989**, *101*, 261–276; *Angew. Chem. Int. Ed. Engl.* **1989**, *28*, 253–267.
[10] Single crystals of **7** were grown from toluene. 6565 unique reflections were collected on an Enraf-Nonius Turbo-CAD4 diffractometer with Ni-filtered $Cu_{K\alpha}$ radiation from a rotating-anode generator. ($\lambda = 1.542$, $\omega/2\theta$ scan mode, $2\theta_{max} = 120°$, nominal resolution $\lambda/2 \sin\theta_{max} = 0.89$ Å. Ψ scan absorption correction, $T = 260$ K). The data were corrected for radiation damage (12% reduction in intensity of three reference reflections). Space group triclinic, $P\bar{1}$, $Z = 2$ with two toluene per formula unit in the asymmetric unit, $a = 12.390(4)$, $b = 16.164(6)$, $c = 18.96(2)$ Å, $\alpha = 87.67(5)$, $\beta = 83.30(5)$, $\gamma = 68.66(3)°$, $V = 3514(4)$ Å^3. The structure was determined by direct methods using program SIR92 and refined with SHELX76 and SHELX93 on the basis of 3643 reflections with $|F_o| \geq 3\sigma(|F_o|)$. H atoms bonded to the aromatic C atoms were placed in their calculated positions. Two atoms in one of the aliphatic chains, C45 and C49 are twofold disordered with 0.5 occupancy. The cocrystallized toluene molecules are fully ordered. The relatively high crystallographic R factor (0.15) is associated with radiation damage of the crystal, with only 55% of the data above $3\sigma(|F_o|)$, and with the atom disorder. The extended aromatic system is virtually planar; with no atom deviating more than 0.105 Å from the weighted least-squares plane [11].
[11] Further details of the crystal structure investigation may be obtained from the Fachinformationszentrum Karlsruhe, D-76344 Eggenstein-Leopoldshafen on quoting the depository number CSD-58461.
[12] M. J. S. Dewar, E. G. Zoebisch, E. F. Healy, J. J. P. Stewart, *J. Am. Chem. Soc.* **1985**, *107*, 3902–3909.
[13] G. Nicolas, P. Durand, *J. Chem. Phys.* **1979**, *70*, 2020–2021; J. M. André, L. A. Burke, G. Delhalle, G. Nicolas, P. Durand, *Int. J. Quantum Chem.* **1979**, *13*, 283–287; J.-L. Brédas, R. R. Chance, R. Silbey, G. Nicolas, P. Durand, *J. Chem. Phys.* **1981**, *75*, 255–267.

Dimesityldioxirane—A Dioxirane Stable in the Solid State**

Andreas Kirschfeld, Sengodagounder Muthusamy, and Wolfram Sander*

Dedicated to Professor Christoph Rüchardt on the occasion of his 65th birthday

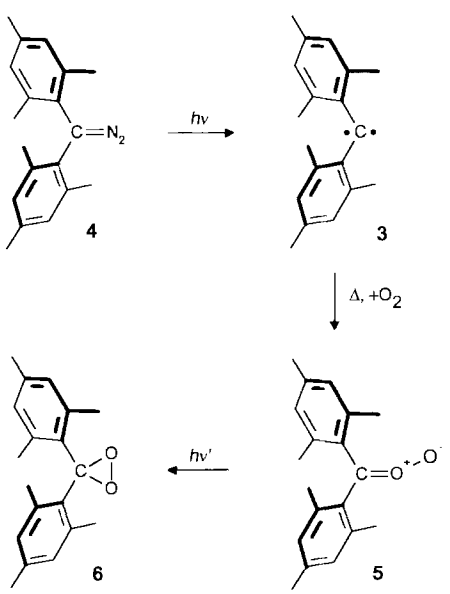
Since the discovery by Murray and Jeyaraman[1] in 1985 that dimethyldioxirane (**1**) can be synthesized and is stable in acetone, **1** has become an important and powerful oxidant in organic chemistry.[2–5] The only other dioxirane that has found synthetic application is methyl (trifluoromethyl)dioxirane (**2**), introduced by Curci et al.[6] Dioxiranes **1**, **2**, and a few other alkyl-substituted derivatives were synthesized by the oxidation of the corresponding ketones with Caroate,[7] a method originally developed by Edwards and Curci.[8, 9] These dioxiranes are moderately stable in solution at room temperature, but cannot be isolated as pure compounds. Two stable perfluorinated dioxiranes seem to have been synthesized by Talbott and Thompson by fluorination of the lithium salts of ketone hydrates.[10] Recently Russo and DesMarteau[11] reported the synthesis of difluorodioxirane from FCOOF and CsF/ClF. This gaseous dioxirane is stable at room temperature for several days.



1 R = CH_3
2 R = CF_3

The most general route to dioxiranes is the oxidation of diazo compounds either directly with singlet oxygen[12] or by first photochemically generating the carbenes followed by a thermal reaction with triplet oxygen.[13] Both routes lead to the highly labile carbonyl *O*-oxides as primary products, which upon irradiation into their strong UV/Vis absorptions (370–550 nm) rearrange to dioxiranes. These intense absorptions enable the identification of the carbonyl oxides by time resolved spectroscopy (laser flash photolysis, LFP) in solution at room temperature if the lifetime is of the order of μs to ms,[12, 14–17] or by matrix isolation spectroscopy at cryogenic temperatures.[13] Although carbene oxidation has been used to generate a variety of dioxiranes, this method has not yet been applied to synthesis on a preparative scale, because the solvent, the conditions of photolysis, and the temperature have to be carefully controlled to avoid carbene reactions (such as dimerization and insertion into the solvent) or secondary reactions of the dioxiranes (rearrangement to esters or reduction to ketones).

Dimesitylcarbene **3** exhibits a lifetime in solution at room temperature which is two orders of magnitude larger than that of diphenylcarbene (200 vs. 1.7 µs),[18] but the reactivity of these two carbenes towards O_2 is roughly equal.[19] Thus, although the sterically demanding substituents prevent most bimolecular chemistry, the small O_2 molecule is able to approach the carbene center almost unhindered. In an LFP study Scaiano et al. were able to generate carbonyl oxide **5** as a transient species by laser photolysis of oxygen-containing solutions of diazomethane **4**. In acetonitrile **5** shows an intense absorption band at 390 nm and a first-order decay of its intensity several orders of magnitude slower than other carbonyl oxides.[19] This makes **3** an ideal candidate for the study of the oxidation of carbenes in solution.



Here we describe the first synthesis of a dioxirane isolable at room temperature—both in solution and in pure form—by the

[*] Prof. Dr. W. Sander, Dipl.-Chem. A. Kirschfeld, Dr. S. Muthusamy
Lehrstuhl für Organische Chemie II der Ruhr-Universität
Universitätsstrasse 150, D-44780 Bochum (FRG)
Telefax: Int. code +(234)7094-353

[**] This work was financially supported by the Deutsche Forschungsgemeinschaft, the Bundesministerium für Forschung und Technologie (EUROTRAC 07EU761 6), and the Fonds der Chemischen Industrie. S. M. thanks the Alexander von Humboldt Foundation for a postdoctoral fellowship and A. K. the Land Niedersachsen for a postgraduate fellowship.

oxidation of a diazo compound. Dimesityldiazomethane **4** was dissolved in an oxygen-saturated mixture of $CFCl_3$ and $(CF_2Br)_2$, which formed a transparent glass[20] upon cooling to 77 K. Irradiation of this glass at 77 K into the absorption maximum of **4** (λ_{max} = 498 nm, irradiation at $\lambda > 515$ nm) produced a new species with an intense, broad absorption at 398 nm, very similar in band position and shape to that of **5**[19] (Fig. 1). After

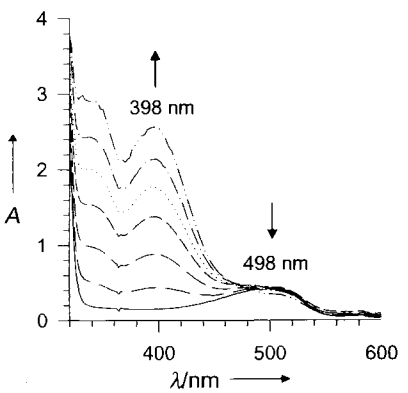


Fig. 1. UV/Vis absorption spectra obtained after irradiation of diazo compound **4** ($\lambda > 515$ nm, 77 K). Solid line: absorption spectrum of **4** before photolysis. The other spectra were recorded at 30 min intervals during photolysis.

the glass was melted at 160 K and the solution warmed to 195 K (−78 °C), the yellow compound persisted for several hours, while at 243 K (−30 °C) it disappeared within several minutes. The yellow species is extremely photolabile, and rapidly disappears upon irradiation at $\lambda > 475$ nm. The absorption spectrum, the observed photochemistry, and the product analysis after warming indicate that the yellow intermediate is carbonyl oxide **5**. After warming the final reaction mixture to room temperature, the solvent was evaporated and the products were separated by reversed-phase HPLC (Fig. 2). Two of the prod-

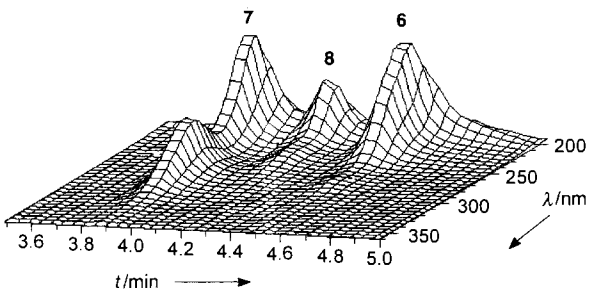
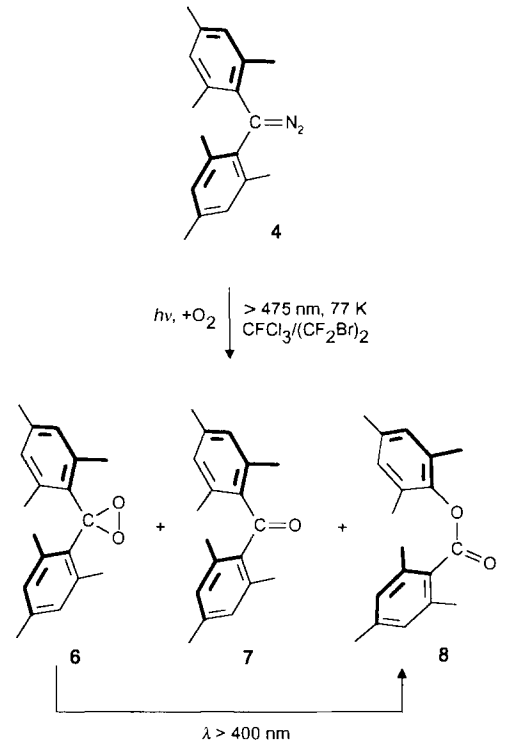


Fig. 2. HPLC separation of the reaction mixture after photolysis of **4** ($\lambda > 475$ nm, 77 K).

ucts were identified as dimesityl ketone **7** (9% yield by ^{1}H NMR) and mesityl mesitoate **8** (23% yield) by comparison with authentic material. Several minor products have not yet been identified.

The main product, which was obtained in up to 55% yield, was characterized by ^{1}H and ^{13}C NMR spectroscopy and mass spectrometry as dimesityldioxirane (**6**). The ^{13}C NMR chemical shift of the quaternary carbon atom of the dioxirane ring was observed at $\delta = 103$, close to the value reported for **1** ($\delta = 102$).[2a, b] In solution at room temperature or as crystalline solid, dioxirane **6** slowly rearranges to yield ester **8** as the only product (in $CDCl_3$ less than 10% conversion per day). Upon irradiation with $\lambda > 400$ nm, **6** rearranges quantitatively to **8** within several minutes.



To synthesize larger quantities of **6**, the irradiation of **4** was performed in $CFCl_3$ at 183 K. The yield of dioxirane **6** was still 50% on irradiation with $\lambda > 495$ nm (30% with $\lambda > 475$ nm irradiation), and up to 10 mg of the dioxirane could be obtained in a single run. There was no significant dependence of the yield on the ratio of $CFCl_3$ and $(CF_2Br)_2$ in the solvent mixture.

In summary, we have shown that the diazo route is suitable for the synthesis of a dioxirane on a preparative scale. The mesityl groups not only stabilize **6**, but also allow observation of an intermediate, which is most likely carbonyl oxide **5**. This would be the first carbonyl oxide to be stable in solution at low temperature. We are currently exploring the chemistry of **5** and **6** and the scope of this new synthesis of dioxiranes.

Experimental Procedure

Photolyses were carried out with a Hg high-pressure arc lamp (Osram HBO 500 W in an Oriel Lamp housing with quartz optics) and suitable cut-off or interference filters. Compounds **4** [21], dimesitylketone **7** [22], and mesityl mesitoate **8** [23] were prepared and purified according to literature procedures.

Preparation of **6** in an organic glass: A solution of 2.9×10^{-3} mmol of **4** in 2 mL of a mixture of $CFCl_3$ and $(CF_2Br)_2$ (1:1 v/v) was saturated with oxygen at −20 °C for 20 min and then cooled to 77 K to form a transparent glass. After irradiation with $\lambda > 475$ nm for 3 h the mixture was warmed to room temperature, and the solvent removed under reduced pressure. The residue was dissolved in methanol and purified by HPLC (RP-18 phase with methanol as eluent).

Preparation of **6** in solution: A solution of 20 mg (0.07 mmol) of **4** in $CFCl_3$ (25 mL) was purged with oxygen at 183 K for 15 min. The mixture was irradiated with $\lambda > 495$ nm with continued oxygen purging at the same temperature. The reaction was monitored by HPLC, and **4** completely disappeared after 4 h irradiation. The solvent was removed under reduced pressure, and the dioxirane (colorless crystals) purified as described above.

M.p. 62–64 °C (dec); ^{1}H NMR (400 MHz, $CDCl_3$): δ = 2.21 (s, 12H), 2.26 (s, 6H), 6.82 (s, 4H); ^{13}C NMR ($CDCl_3$): δ = 20.77 (CH_3), 21.46 (CH_3), 103.06 (C), 130.75 (CH), 131.10 (CH), 137.70 (C), 138.94 (C); MS: *m/z* (%): 300 (59, $[M + NH_4]^+$), 283 (100, $[M + H]^+$), 267 (20, $[M + H - O]^+$); IR (CCl_4): $\tilde{\nu}$ = 2923

(m), 1612 (m), 1571 (w), 1456 (m), 1295 (w), 1242 (m), 881 (m), 852 (s) cm^{-1}; UV/VIS (CH_3OH): $\lambda_{max}(\varepsilon)$ = 206 (41000), 278 nm (1700).

Received: May 18, 1994 [Z 6946 IE]
German version: *Angew. Chem.* **1994**, *106*, 2261

[1] R. W. Murray, R. Jeyaraman, *J. Org. Chem.* **1985**, *50*, 2847–2853.
[2] a) W. Adam, Y. Y. Chan, D. Cremer, J. Gauss, D. Schenkow, M. Schindler, *ibid.* **1987**, *52*, 2800–2803; b) L. Cassidei, M. Fiorentino, R. Mello, O. Sciacovelli, R. Curci, *ibid.* **1987**, *52*, 699–700; c) R. W. Murray, *Chem. Rev.* **1989**, *89*, 1187–1201.
[3] R. W. Murray, *Mol. Struct. Energ.* **1988**, *6*, 311–351.
[4] S. A. Kafafi, R. I. Martinez, J. T. Herron, *Mol. Struct. Energ.* **1988**, *6*, 283–310.
[5] W. Adam, R. Curci, J. O. Edwards, *Acc. Chem. Res.* **1989**, *22*, 205–211.
[6] R. Mello, M. Fiorentino, C. Fusco, R. Curci, *J. Am. Chem. Soc.* **1989**, *111*, 6749–6757.
[7] R. W. Murray, M. Singh, R. Jeyaraman, *J. Am. Chem. Soc.* **1992**, *114*, 1346–1351.
[8] J. O. Edwards, R. H. Pater, R. Curci, F. Di Furia, *Photochem. Photobiol.* **1979**, *30*, 63–70.
[9] R. Curci, M. Fiorentino, L. Troisi, J. O. Edwards, R. H. Pater, *J. Org. Chem.* **1980**, *45*, 4758–4760.
[10] R. L. Talbott, P. G. Thompson (Minnesota Mining and Manufg. Co.), US-A 3632606, **1972**; [*Chem. Abstr.* **1972**, *76*, 99638t].
[11] A. Russo, D. D. DesMarteau, *Angew. Chem.* **1993**, *105*, 956–958; *Angew. Chem. Int. Ed. Engl.* **1993**, *32*, 905–907.
[12] H. L. Casal, S. E. Sugamori, J. C. Scaiano, *J. Am. Chem. Soc.* **1984**, *106*, 7623–7624.
[13] W. Sander, *Angew. Chem.* **1990**, *102*, 362–372; *Angew. Chem. Int. Ed. Engl.* **1990**, *29*, 344–354.
[14] N. H. Werstiuk, H. L. Casal, J. C. Scaiano, *Can. J. Chem.* **1984**, *62*, 2391–2392.
[15] H. L. Casal, M. Tanner, N. H. Werstiuk, J. C. Scaiano, *J. Am. Chem. Soc.* **1985**, *107*, 4616–4620.
[16] T. Sugawara, H. Iwamura, H. Hayashi, A. Sekiguchi, W. Ando, M. T. H. Liu, *Chem. Lett.* **1983**, 1261–1262.
[17] B. R. Arnold, J. C. Scaiano, G. F. Bucher, W. W. Sander, *J. Org. Chem.* **1992**, *57*, 6469–6474.
[18] a) B. C. Gilbert, D. Griller, A. S. Nazran, *J. Org. Chem.* **1985**, *50*, 4738–4742; b) A. S. Nazran, D. Griller, *J. Am. Chem. Soc.* **1984**, *106*, 543–547.
[19] J. C. Scaiano, W. G. McGimpsey, H. L. Casal, *J. Org. Chem.* **1989**, *54*, 1612–1616.
[20] A. Grimison, G. A. Simpson, *J. Phys. Chem.* **1968**, *72*, 1776–1779.
[21] H. E. Zimmerman, D. H. Paskovich, *J. Am. Chem. Soc.* **1964**, *86*, 2149–2160.
[22] a) E. P. Kohler, R. Baltzly, *J. Am. Chem. Soc.* **1932**, *54*, 4015–4026; b) D. J. Thoennes, C. L. Wilkins, W. S. Trahanovsky, *J. Magn. Reson.* **1974**, *13*, 18–26.
[23] G. W. Thiessen, W. N. Farr, *J. Org. Chem.* **1959**, *24*, 559–560.

Platinum(II) Complexes with Porphyrin Ligands—Additive Cytotoxic and Photodynamic Effect**

Henri Brunner* and Herbert Obermeier

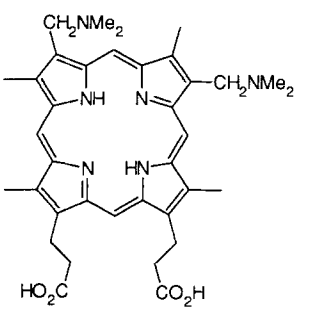
Porphyrins are used in photodynamic therapy for the treatment of tumors.[1, 2] When irradiated with light of a wavelength of about 630 nm, the porphyrins act as photosensitizers. The singlet oxygen that is formed kills the cell.[1, 3]

Porphyrins are accumulated in the tumor tissue. There are two explanations: According to the older theory the uptake occurs through low density lipoproteins (LDL), which play an important role in cholesterol metabolism. Since tumor cells show a higher LDL receptor activity than normal cells, a specific enrichment in malignant tissue results.[4] The newer theory ascribes the selectivity to the lower pH value of tumor tissue relative to normal tissue, which implies a larger proportion of neutral particles that penetrate the cell membrane in the tumor.[5, 6]

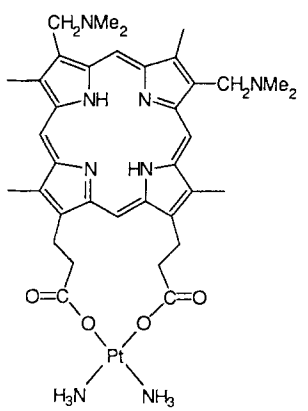
The cytostatic drugs diammine(dichloro)platinum(II) (cisplatin) and diammine(cyclobutanedicarboxylato)platinum(II) (carboplatin) have become the most important cancer chemotherapeutics during the last years.[7, 8] However, they act unspecifically and damage all rapidly growing body tissues as well as the tumor.

Making use of the enrichment of porphyrins in malignant tissue we are now trying to accumulate cytostatic platinum complexes specifically in the tumor tissue. We bind the $(NH_3)_2Pt$ moiety to the carboxylato groups of the two propionic acid side chains of porphyrins,[9] thereby obtaining systems similar to carboplatin.

Because of the carrier properties of porphyrins a specific enrichment of the cytostatic platinum complex in the tumor tissue should be achieved (drug targeting). In addition, on irradiation the porphyrins should be tumor-destructive. With the ligand/complex pair **1**/**2** as example we now prove the additivity of the two effects in cell culture experiments.



1



2

The synthesis of ligand **1** started from deuteroporphyrin dimethyl ester.[10] The two dimethylamino functions in 3- and 8-position were introduced by substitution with the "Eschenmoser salt" *N,N*-dimethylmethyleneammonium iodide.[11] After acidic ester hydrolysis ligand **1** was obtained.[12] To activate cisplatin for complexation, it was hydrolyzed with silver nitrate and chromatographed on a basic ion exchanger.[13] Diammine(diaqua)platinum(II) hydroxide was formed, which reacted with **1** in ethanol/water to give the porphyrin platinum(II) complex **2**[14].

The additivity of the cytotoxic effect of platinum and the photodynamic activity of the porphyrin in **1** and **2** were tested in vitro with the MDA-MB-231 mammatumor cell line. The seeding of the cells, the addition of the compounds, and the workup were carried out as previously described.[13, 15] During the three days of incubation of the compounds in the dark, the cell proliferation was inhibited by the platinum effect of the complex. Afterwards the cell cultures were irradiated for 20 minutes with an IR lamp that emits incoherent, red light within the wavelength range 600–800 nm. To determine the vitality of the cells the cell cultures were colored with 3-(4,5-dimethylthiazol-2-yl)-2,5-diphenyltetrazolium bromide (MTT), and the concentration of cells was obtained by measuring the optical

[*] Prof. Dr. H. Brunner, Dr. H. Obermeier
Institut für Anorganische Chemie der Universität
D-93040 Regensburg (FRG)
Telefax: Int. code +(941) 943-4439

[**] The work was supported by the Deutsche Forschungsgemeinschaft and the Fonds der Chemischen Industrie. We thank Dr. R.-M. Szeimies of the Klinik und Poliklinik für Dermatologie of the Universität Regensburg for help with the cell culture experiments.

density in a photometer. The concentrations of ligand **1**, complex **2**, a **1**/cisplatin mixture, cisplatin, and photofrin were 10^{-5} mol L^{-1}. Photofrin, an oligomer fraction of hematoporphyrin derivative enriched to 80–90%, is at present the only phorphyrin used in clinical tests.[2]

The data of Table 1 correspond to the vitality of the cells with respect to untreated control groups, which define 100%. Ligand

Table 1. Comparison of the antitumor activity of ligand **1**, complex **2**, **1**/cisplatin mixture, cisplatin, and Photofrin in a concentration of 10^{-5} mol L^{-1} in vitro towards the MDA-MB-231 mammatumor cell line in water. The values are the average of 16 measurements, which varied by about 10–20%.

	without irradiation	with irradiation
1	>100	81
2	63	38
1/cisplatin	53	14
cisplatin	49	44
Photofrin (10 μg mL^{-1})	100	20

1 was not active without irradiation; it became tumor-destructive only on irradiation, reducing the cell proliferation to about 81%. By complexation with platinum the activity was improved. Complex **2** had cytostatic potential even without irradiation and reduced the vitality of the cells to values of approximately 63%. On irradiation the activity of the complex increased, and the cell proliferation was reduced to 38%. This demonstrates the additivity of the phototoxic effect of the porphyrin and the cytostatic effect of the platinum in the complex. Cisplatin alone and together with **1** reduced the cell proliferation to about 50%. On irradiation of the combination **1**/cisplatin the additional photodynamic effect of ligand **1** operated (reduction to 14%). Photofrin attained vitality values of 20% in a concentration of 10 μg mL^{-1}. If a molecular weight of 1000 is assumed for Photofrin, the concentration is 10^{-5} mol L^{-1}.

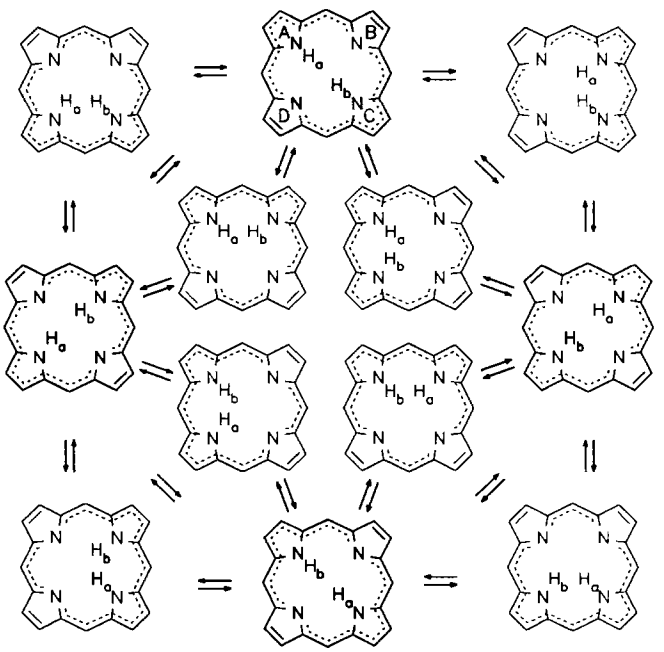
Received: June 30, 1994 [Z 7085 IE]
German version: *Angew. Chem.* **1994**, *106*, 2305

[1] R. Pottier, *Photosensitisation: Molecular, Cellular and Medical Aspects*, Springer, Berlin, **1988**, p. 2.
[2] T. J. Dougherty, *Adv. Photochem.* **1992**, *17*, 275.
[3] M. Landthaler, A. Rück, R.-M. Szeimies, *Hautarzt* **1993**, *44*, 69.
[4] T. J. Dougherty, *Photochem. Photobiol.* **1987**, *46*, 569.
[5] R. Pottier, J. C. Kennedy, *J. Photochem. Photobiol. B* **1990**, *8*, 1.
[6] A. J. Bonnett, J. C. Kennedy, R. A. Jones, P. Nadeau, R. Pottier, *J. Photochem. Photobiol B* **1990**, *6*, 309.
[7] B. K. Keppler, *Metal Complexes in Cancer Therapy*, VCH, Weinheim, **1993**.
[8] B. K. Keppler, *Nachr. Chem. Tech. Lab.* **1987**, *35*, 1029.
[9] H. Obermeier, Ph.D. Thesis, Universität Regensburg, **1994**.
[10] W. S. Caughey, J. D. Alben, W. Y. Fujimoto, J. L. York, *J. Org. Chem.* **1966**, *31*, 2631.
[11] K. M. Smith, R. K. Pandey, F.-Y. Shian, N. W. Smith, P. Iakovides, T. J. Dougherty, *Proc. SPIE Int. Soc. Opt. Eng.* **1992**, *1654*, 274.
[12] **1**: Violet powder, m.p. >250 °C, yield 89%. IR (KBr): $\tilde{\nu}$ = 1720 cm^{-1} (CO); ^{1}H NMR (250 MHz, [D$_6$]DMSO): δ = 11.20 (s, 2H; COOH), 10.41, 10.36, 10.23, 10.16 (4s, 4H; =CH), 5.86, 5.81 (2s, 4H; CH_2NMe_2), 4.33 (m, 4H; $=CCH_2$), 3.92, 3.81, 3.71, 3.63 (4s, 12H; $=CCH_3$), 3.16 (s, 12H; NMe_2), ca. −4 (br., =NH).
[13] H. Brunner, F. Maiterth, B. Treittinger, *Chem. Ber.*, in press.
[14] **2**: Brown powder, m.p. >250 °C, yield 50%. IR (KBr): $\tilde{\nu}$ = 1560 cm^{-1} (CO) cm^{-1}; PI LISIMS: (glycerol/DMSO): *m/z*: 625 $[1 + H]^+$; ^{1}H NMR (250 MHz, [D$_6$]DMSO): δ = 10.46, 10.41, 10.32, 10.29 (4s, 4H; =CH), 5.30 (m, 3H; CH_2NMe_2), 4.36 (m, 4H; $=CCH_2$), 3.94 (m, 6H; NH_3), 3.74, 3.65 (2s, 12H; $=CCH_3$), 3.18 (m, 4H; O_2CCH_2), 2.81 (2s, 12H; NMe_2), −3.88 (s, 2H; =NH). Correct CHN analysis.
[15] H. Brunner, F. Maiterth, B. Treittinger, *Z. Naturforsch. B* **1992**, *47*, 942.
[16] Waldmann Lichttechnik, Type PDT 1200; distance of lamp 1.0 m; intensity 50 mW cm^{-2}; power 60 J cm^{-2}; R.-M. Szeimies, R. Hein, W. Bäumler, A. Heine, M. Landthaler, *Acta Derm. Venereol.* **1988**, *74*, 315.

Free Acid Porphyrin and Its Conjugated Monoanion**

Jürgen Braun, Christian Hasenfratz, Reinhard Schwesinger, and Hans-Heinrich Limbach*

Porphyrin ($PorH_2$) and its derivatives are amphoteric, and the two inner protons are highly mobile between the four nitrogen atom sites (Scheme 1). This tautomerism takes place both in the

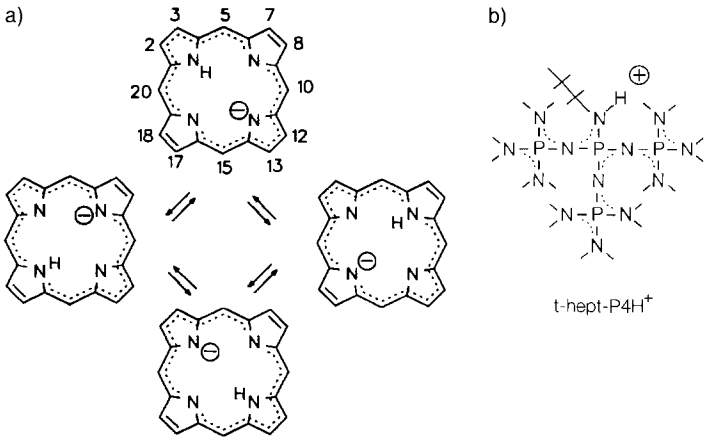


Scheme 1. The tautomerism of porphyrin $PorH_2$ according to ref. [3c,i,j].

liquid[1, 2] and in the solid state[3, 4] and has been studied from a theoretical standpoint as a model reaction for double proton transfer in polyatomic molecules.[5] The basicity of $PorH_2$, which led to the frequently used name "metal-free base porphyrin", enables a protonation by acids generating the stable dication $PorH_4^{2+}$,[1c, d] probably via a monoprotonated intermediate $PorH_3^+$. The acidity of porphyrin is manifested in the release of two protons during the formation of metalloporphyrins. However, so far the term "free acid porphyrin" has not been justified because the conjugated metal-free monoanion $PorH^-$ (Scheme 2)—judged as unstable[6]—has never been observed experimentally. This paper shows that $PorH^-$ is a stable species which can easily be generated from $PorH_2$ by reaction with very strong organic bases in aprotic medium, and can be characterized by NMR and UV/VIS spectroscopy. Moreover, it is shown that $PorH^-$ is also subject to a degenerate intramolecular tautomerism of the remaining single proton (Scheme 2a). The dynamics observed for this process shed new light on the mechanism of the porphyrin tautomerism.

[*] Prof. Dr. H.-H. Limbach, Dr. J. Braun
Institut für Organische Chemie der Freien Universität
Takusstrasse 3, D-14195 Berlin (FRG)
Telefax: Int. code +(30) 838-5320
Priv.-Doz. Dr. R. Schwesinger, Dipl.-Chem. C. Hasenfratz
Institut für Organische Chemie der Universität Freiburg

[**] This work was supported by the Deutsche Forschungsgemeinschaft and the Fonds der Chemischen Industrie.



Scheme 2. a) The tautomerism of the conjugated porphyrin monoanion $PorH^-$. b) Structure of the protonated phosphazene base t-hept-P4H$^+$ [9].

To avoid complications in the NMR experiments arising from ^{14}N quadrupole relaxation, ^{15}N-labeled porphyrin[7] was employed as a precursor of $PorH^-$. The choice of the base was critical. Conventional inorganic bases immediately form metalloporphyrins such as $PorM^-M^+$ or PorM;[8] neutral organic bases B are required which, on one hand, must be strong enough to remove an inner proton of $PorH_2$. On the other hand, the structure of the base should be such that fast intermolecular proton transfer between BH^+ and $PorH^-$ is slow on the NMR time scale. Higher phosphazene bases, for example, "t-hept-P4"≡1,1,1,5,5,5-hexakis(dimethylamino)-3-(1,1,2,2-tetramethylpropyl)imino-3-[tris(dimethylamino)phosphoranylidene]amino-1λ^5,3λ^5,5λ^5,-1,4-triphosphazadiene (shown in its protonated form in Scheme 2b) were suitable. The syntheses and properties of phosphazene bases have been described recently.[9]

Figure 1a depicts the superposed experimental and calculated NMR signals of the inner protons of ^{15}N-labeled porphyrin in [D$_8$]THF.[3j, 10] Because of the low solubility of $PorH_2$, the concentration was only 1 mM. As established previously,[3j] the signal of the inner protons of $PorH_2$ appears at $\delta = -3.5$ and exhibits a doublet at low temperature, arising from scalar coupling with the attached ^{15}N nucleus and indicating localized inner protons. The coupling constant is $^1J_{^1H,^{15}N} \approx 98$ Hz and decreases slightly with increasing temperature. A differential line broadening of the $^1H-^{15}N$ doublet, observed at low temperature, arises from reduced molecular mobility and interference between the $^1H-^1H$ and the $^1H-^{15}N$ dipolar interaction, as well as the chemical shift anisotropy.[11] As the temperature is increased, rotational diffusion becomes faster, and the asymmetry disappears. At the same time, a doublet–pentet transition is observed at about 250 K, arising from a fast intramolecular proton transfer between all four nitrogen atoms. The line-shape changes were calculated[10, 3h] by varying the rate constant $2k^{HH}$, which corresponds to the inverse average lifetime of a given tautomer in Scheme 1.

In the presence of phosphazene bases, the solubility of porphyrin is drastically increased. The superposed experimental and calculated high field signals of a 15 mM solution of $PorH_2$ in [D$_8$]THF in the presence of a twofold excess of t-hept-P4 are depicted in Figure 1b. Signs of $PorH_2$ can no longer be detected, but a new species is observed. At 152 K again a $^1H-^{15}N$ doublet is observed at $\delta = -2.7$ typical for an inner porphyrin proton (Fig. 1b). The scalar coupling constants $^1J_{^1H,^{15}N}$ are similar to those of the parent compound. The differential line broadening is more pronounced as the spectra were taken at lower temperatures. As the temperature is raised, the doublet–pentet transition proving a fast intramolecular tautomerism of a central porphyrin proton could be observed as in the parent compound; however, the transition occurs already around 200 K instead of 250 K, which indicates that the tautomerism of the new porphyrin species is much faster than in the parent compound. This observation can only be explained by the formation of a stable conjugated monoanion $PorH^-$. Its structure is confirmed by analyzing the signals of protons attached to the peripheral carbon atoms. At 152 K, two exchange-broadened lines arising from the methine protons 5H/20H and 10H/15H appear at $\delta = 9.79$ and 9.73 ($PorH_2$: $\delta = 10.5$[1h]). Furthermore, as expected, four exchange-broadened singlets appear at $\delta = 9.04$, 8.90, 9.15, and 8.93 for the β-pyrrole protons, which are tentatively assigned to the 7H/18H, 8H/17H, 2H/3H, and 12H/13H positions. These signals broaden and coalesce into a single line at about 200 K. In contrast, at low temperatures $PorH_2$ contributes only two β-pyrrole signals to the ^1H spectra.[1h] The NMR signals of t-hept-P4 and t-hept-P4H$^+$ were not analyzed. Subsequent NMR experiments showed that the formation of conjugated porphyrin monoanion is not restricted to the parent compound but is a common feature of substituted porphyrins, for example, tetraphenylporphyrin (TPP) and octaethylporphyrin (OEP).

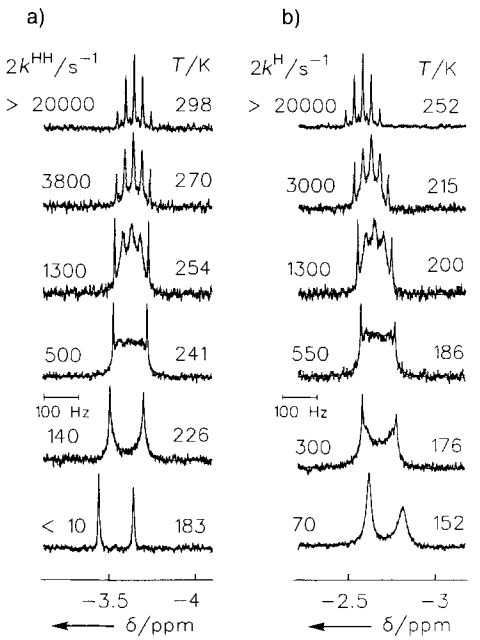


Fig. 1. Superposed experimental and calculated variable-temperature 500 MHz ^1H NMR signals of the inner protons of ^{15}N-labeled $PorH_2$ dissolved in [D$_8$]THF (a) (adapted from ref. [3j]) and $PorH^-$ (15 mM) generated by dissolving the parent compound together with a twofold excess of t-hept-P4 (b). The sample contained approximatively 34% $PorD^-$ which does not contribute to the signals. 6.5 μs 60° pulses, 9 kHz spectral width, 3.5 s repetition time, up to 3000 scans for (a) and 600 for (b) [10].

The changes in the UV/VIS and fluorescence spectra upon deprotonation of $PorH_2$ are illustrated in Figure 2. The spectra of $PorH_2$ (Figs. 2a and 2b) were previously recorded and discussed.[6, 12] The transition of lowest energy (Q_x band, $S_0 \rightarrow S_1^x$) appearing for $PorH_2$ at 615 nm is shifted in $PorH^-$ to 600 nm (Fig. 2c). The assignment to the 0-0 transition is confirmed by the fluorescence data (Fig. 2d). No evidence of a band calculated to appear at 700 nm[6] could be found, but the Soret band of $PorH_2$ at 390 nm is shifted to 420 nm in the monoanion and is more intense. In addition, major spectral changes are observed in the region between 480 and 580 nm.

 © VCH Verlagsgesellschaft mbH, D-69451 Weinheim, 1994 0570-0833/94/2121-2216 $ 10.00+.25/0 Angew. Chem. Int. Ed. Engl. 1994, 33, No. 21

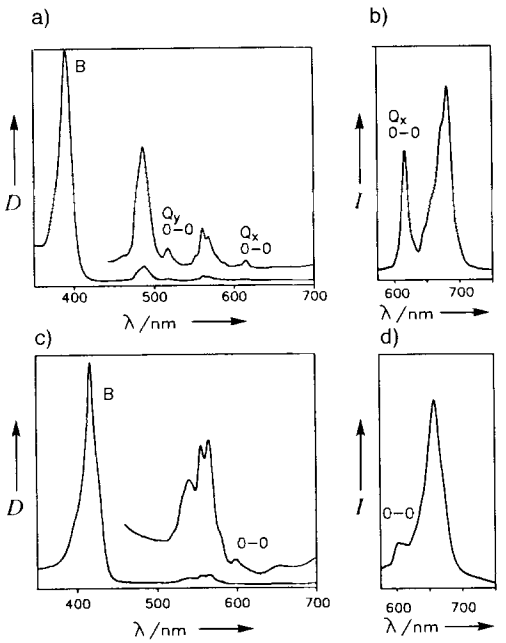


Fig. 2. a) Room temperature UV/VIS and b) fluorescence spectra of $PorH_2$ dissolved in THF, excitation wave length 570 nm. c) and d) Corresponding spectra of $PorH^-$/t-Hept-P4H$^+$ in THF. *D*: optical density; *I*: Intensity.

To estimate the pK_a of free acid porphyrin, a titration experiment of the more soluble OEP with the base t-bu-P4≡3-*tert*-butylimino-1,1,1,5,5,5-hexakis(dimethylamino)-3-[tris(dimethylamino)phosphoranylidene]amino)-1λ^5,3λ^5,5λ^5-1,4-triphosphazadiene[13] was performed. The deprotonation of OEP was followed by monitoring the Soret band shift. At concentrations of 0.01 M of t-bu-P4 in dry THF, OEP was deprotonated to approximately 85% at room temperature. From this result we extrapolate using a procedure described previously[13] an absolute pK_a value for OEP of 37 to 38 in acetonitrile. For the parent compound $PorH_2$ we expect a slightly lower value of about 35 to 36.

In conclusion, we have shown that the conjugated monoanion $PorH^-$ of porphyrin is a stable species in aprotic solvents and can easily be generated by dissolving the parent compound with an appropriate strong metal-free base. The labels "free acid porphyrin" and "free base porphyrin" are, therefore, equally justified. The tautomerism of $PorH^-$ is much faster than that of $PorH_2$. This observation can be explained by the fact that the single proton transfer in $PorH^-$ is degenerate (Scheme 2a) but leads to *cis* intermediates of higher energies in the case of $PorH_2$ (Scheme 1).[3j] The tunneling probabilities at low temperatures are, therefore, much higher for $PorH^-$ than for $PorH_2$, at comparable barrier heights. Studies of the kinetic H/D and solid state isotope effects of $PorH^-$ tautomerism, which could confirm this interpretation, are under way.

Received: May 11, 1994 [Z 6928 IE]
German version: *Angew. Chem.* **1994**, *106*, 2302

[1] a) C. B. Storm, Y. Teklu, *J. Am. Chem. Soc.* **1972**, *94*, 1745; b) C. B. Storm, Y. Teklu, E. A. Sokoloski, *Ann. N. Y. Acad. Sci.* **1973**, *206*, 631; c) R. J. Abraham, G. E. Hawkes, K. M. Smith, *Tetrahedron Lett.* **1974**, 1483; d) *J. Chem. Soc. Perkin Trans 2* **1974**, 1483; e) H. J. C. Yeh, M. Sato, I. Morishima, *J. Magn. Reson.* **1977**, *26*, 365; f) D. Gust, J. D. Roberts, *J. Am. Chem. Soc.* **1977**, *99*, 3637; g) C. S. Irving, A. Lapidot, *J. Chem. Soc. Chem. Commun.* **1977**, 184; h) H.-H. Limbach, J. Hennig, *J. Chem. Soc. Faraday Trans. 2* **1979**, *75*, 752; i) J. Hennig, H.-H. Limbach, *J. Magn. Reson.* **1982**, *49*, 322; j) S. S. Eaton, G. R. Eaton, *J. Am. Chem. Soc.* **1977**, *99*, 1601; k) H.-H. Limbach, J. Hennig, D. Gerritzen, H. Rumpel, *Faraday Discuss. Chem. Soc.* **1982**, *74*, 822; l) P. Stilbs, M. E. Moseley, *J. Chem. Soc. Faraday Trans. 2* **1980**, *76*, 729; m) P. Stilbs, *J. Magn. Reson.* **1984**, *58*, 152; n) J. Hennig, H.-H. Limbach, *J. Am. Chem. Soc.* **1984**, *106*, 869; o) H.-H. Limbach, *Dynamic NMR Spectrocopy in the Presence of Kinetic Isotope Effects* (*NMR Basic Princ. Prog.* **1990**, *26*, Chap. 2).

[2] a) M. Schlabach, B. Wehrle, H.-H. Limbach, E. Bunnenberg, A. Knierzinger, A. Y. L. Shu, B. R. Tolf, C. Djerassi, *J. Am. Chem. Soc.* **1986**, *108*, 3856; b) M. Schlabach, H. Rumpel, H.-H. Limbach, *Angew. Chem.* **1989**, *101*, 84; *Angew. Chem. Int. Ed. Engl.* **1989**, *28*, 78; c) M. Schlabach, H.-H. Limbach, E. Bunnenberg, A. Y. L. Shu, B. R. Tolf, C. Djerassi, *J. Am. Chem. Soc.* **1993**, *115*, 4554; d) M. J. Crosswell, M. M. Harding, S. Sternhell, *ibid.* **1986**, *108*, 3608; e) M. J. Crosswell, L. D. Field, M. M. Harding, S. Sternhell, *ibid.* **1987**, *109*, 2335.

[3] a) H.-H. Limbach, J. Hennig, R. D. Kendrick, C. S. Yannoni, *J. Am. Chem. Soc.* **1984**, *106*, 4059; b) H.-H. Limbach, B. Wehrle, H. Zimmermann, R. D. Kendrick, C. S. Yannoni, *ibid.* **1987**, *109*, 929; c) *Angew. Chem.* **1987**, *99*, 241; *Angew. Chem. Int. Ed. Engl.* **1987**, *26*, 247; d) B. Wehrle, H.-H. Limbach, M. Köcher, O. Ermer, E. Vogel, *ibid.* **1987**, *99*, 914 and **1987**, *26*, 934; e) B. Wehrle, H. Zimmermann, H.-H. Limbach, *Ber. Bunsenges. Phys. Chem.* **1987**, *91*, 941; f) H.-H. Limbach, B. Wehrle, M. Schlabach, R. D. Kendrick, C. S. Yannoni, *J. Magn. Reson.* **1988**, *77*, 84; g) L. Frydman, A. C. Olivieri, L. E. Diaz, B. Frydman, F. G. Morin, C. L. Mayne, D. M. Grant, A. D. Adler, *J. Am. Chem. Soc.* **1988**, *110*, 336; h) L. Frydman, A. C. Olivieri, L. E. Diaz, B. A. Valasinas, B. Frydman, *ibid.* **1988**, *110*, 5651; i) M. Schlabach, B. Wehrle, J. Braun, G. Scherer, H.-H. Limbach, *Ber. Bunsenges. Phys. Chem.* **1992**, *96*, 821; j) J. Braun, M. Schlabach, B. Wehrle, M. Köcher, E. Vogel, H.-H. Limbach, *J. Am. Chem. Soc.* **1994**, *116*, 6593.

[4] a) S. Völker, J. H. van der Waals, *Mol. Phys.* **1976**, *32*, 1703; b) S. Völker, R. Macfarlane, *IBM J. Res. Dev.* **1979**, *23*, 547.

[5] a) J. Almlöf, *Int. J. Quantum Chem.* **1974**, *8*, 915; b) H.-H. Limbach, J. Hennig, *J. Chem. Phys.* **1979**, *71*, 3120; c) H.-H. Limbach, J. Hennig, J. Stulz, *ibid.* **1983**, *78*, 5432; d) H.-H. Limbach, *ibid.* **1984**, *80*, 5343; e) V. A. Kusmitsky, K. N. Solovyov, *J. Mol. Struct.* **1980**, *65*, 219; f) A. Sarai, *J. Chem. Phys.* **1982**, *76*, 5554; g) *ibid.* **1984**, *80*, 5431; h) G. I. Bersuker, V. Z. Polinger, *Chem. Phys.* **1984**, *86*, 57; i) K. M. Merz, C. H. Reynolds, *J. Chem. Soc. Chem. Commun.* **1988**, *90*; j) Z. Smedarchina, W. Siebrand, T. A. Wildman, *Chem. Phys. Lett.* **1988**, *143*, 395; k) D. C. Rawlings, E. R. Davidson, M. Gouterman, *Theor. Chim. Acta* **1982**, *61*, 227.

[6] J. V. Knop, A. Knop, *Z. Naturforsch. A* **1970**, *25*, 1720, 1726.

[7] ^{15}N-labeled porphyrin was synthesized from $^{15}NH_4Cl$ (95% enrichment, Chemotrade, Leipzig) with slightly modified versions of the procedures described for the unlabeled compounds. See also R. M. Silverstein, E. E. Ryskiewicz, S. W. Chaikin, *J. Am. Chem. Soc.* **1954**, *76*, 4485; F. R. Longo, E. J. Thorne, A. D. Adler, S. Dym, *J. Heterocycl. Chem.* **1975**, *12*, 1305.

[8] J. Arnold, D. Y. Dawson, C. G. Hoffman, *J. Am. Chem. Soc.* **1993**, *115*, 2707.

[9] R. Schwesinger, C. Hasenfratz, H. Schlemper, L. Walz, E.-M. Peters, K. Peters, H. G. von Schnering, *Angew. Chem.* **1993**, *105*, 1420; *Angew. Chem. Int. Ed. Engl.* **1993**, *32*, 1361.

[10] The NMR samples were prepared on a vacuum line as described in Ref. [1o]. [D_8]THF was dried over potassium–sodium/anthracene.

[11] a) H. Shimidzu, *J. Chem. Phys.* **1964**, *40*, 3357; b) H. Rüterjans, E. Kaun, W. E. Hull, H.-H. Limbach, *Nucleic Acids Res.* **1982**, *10*, 7027; c) R. H. Griffey, C. D. Poulter, Z. Yamaizumi, S. Nishimura, R. E. Hurd, *J. Am. Chem. Soc.* **1982**, *104*, 5811; d) M. Guéron, J. L. Leroy, R. H. Griffey, *ibid.* **1983**, *105*, 7262.

[12] a) A. Gamgee, *Z. Biol. (Munich)* **1897**, *34*, 505; b) M. Gouterman, *J. Chem. Phys.* **1959**, *30*, 1139; c) *ibid.* **1960**, *33*, 1523; d) *J. Mol. Spectrosc.* **1961**, *6*, 138; e) R. J. Abraham, *Mol. Phys.* **1961**, *4*, 145; f) H. Kuhn, W. Huber, *Helv. Chim. Acta* **1959**, *42*, 363; g) H. C. Longuet-Higgins, C. W. Rector, J. R. Platt, *J. Chem. Phys.* **1950**, *18*, 1174; h) G. R. Seely, *ibid.* **1957**, *27*, 125; i) J. E. Falk, *Porphyrins and Metalloporphyrins*, Elsevier, Amsterdam, **1964**; j) M. Gouterman, G. E. Khalil, *J. Mol. Spectrosc.* **1974**, *53*, 88.

[13] R. Schwesinger, H. Schlemper, *Angew. Chem.* **1987**, *99*, 1212; *Angew. Chem. Int. Ed. Engl.* **1987**, *26*, 1167.

 © VCH Verlagsgesellschaft mbH, D-69451 Weinheim, 1994 0570-0833/94/2121-2217 $ 10.00+.25/0

A Carbene–Iron Chelate Complex as a Source of a Ferraborane Derivative**

Sylvain Nlate, Pierre Guénot, Sourisak Sinbandhit, Loic Toupet, Claude Lapinte, and Véronique Guerchais*

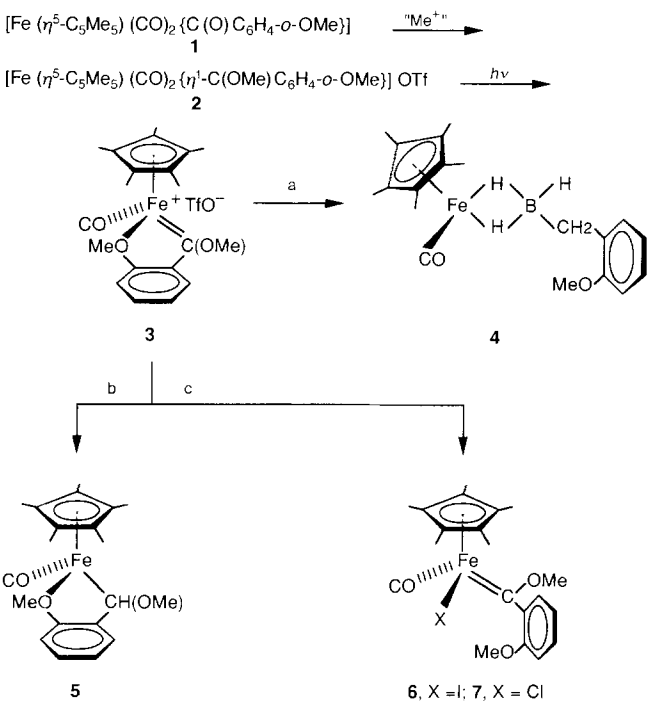
Carbene complexes supplemented by a labile ligand are of interest because such ligands protect potentially vacant coordination sites for subsequent reactions.[1, 2] Moreover, migration of the incoming substrate to the carbene fragment should be promoted, since the resulting 16-electron intermediate can be stabilized by further chelation.[1] Although intramolecular reactions of carbene complexes of Group 6 transition metals have been widely developed,[1, 3] examples involving iron complexes are still scarce.[4] This led us to investigate the properties of the readily available anisyl carbene complex **3** (Tf = trifluoromethanesulfonyl), in order to examine the impact of the labile *ortho* methoxy group on the reactivity. We now report the synthesis and X-ray crystal structure of the organoborato complex **4** with an η^2-coordinated borato ligand.[5, 6]

The C,O-chelated carbene complex **3** was prepared in 76% yield by O-methylation of the corresponding acyl derivative **1**, followed by photochemically induced loss of CO and intramolecular coordination of the *ortho* methoxy group of the carbene complex **2**. Treatment of a THF solution of complex **3** at −80 °C with two equivalents of $NaBH_4$ resulted in almost quantitative formation of **4**, which was isolated as brown crystals (Scheme 1). The new compound **4** was identified on the basis of high-resolution mass spectrometry, IR and multinuclear NMR spectroscopy, elemental analysis, and crystal structure analysis.

In the ^{1}H NMR spectrum (C_6D_6), the bridging hydrogen atoms give rise to a broad pseudo-quartet at $\delta = -17.87$ (2H, $^1J(B,H) \approx 43$ Hz, whereas the terminal B–H resonates at $\delta = 6.35$ (pseudo-q, 1H); the magnitude of $^1J(B,H)$ (ca. 108 Hz) is characteristic of a B–H terminal hydrogen. The methylene group appears as a broad signal at $\delta(^1H) = 2.60$, which is transformed into a doublet of triplets ($^3J(H,BH) = 5$, $^3J(H,BH_2) = 2.5$ Hz) upon ^{11}B decoupling (55 ppm). Although positioned downfield, the boron chemical shift compares well with those reported for the η^2-hydroborato Ta complexes.[7] The nondecoupled ^{13}C NMR spectrum (C_6D_6) of **4** exhibits a triplet for the carbonyl ligand ($^2J(C,H) = 7$ Hz), which confirms the presence of two Fe–H bonding interactions. The Mössbauer spectrum shows the characteristic parameters (IS = 0.104 mm s^{-1} vs Fe, QS = 1.898 mm s^{-1}) of a diamagnetic iron(II) species;[8] the borane ligand is a three-electron donor, as required for an 18-electron count at iron(II). In agreement with the proposed structure, the mass spectrum shows ions at $m/z = 133$ (100%) for $[BH_2CHC_6H_4$-*o*-OMe$]^+$ and 232 (11%) for $[Fe(C_5Me_5)(CO)(BH_2)]^+$.

[*] Dr. V. Guerchais, Dr. S. Nlate, Dr. C. Lapinte
Laboratoire de Chimie des Complexes de Métaux de Transition et Synthèse Organique
URA CNRS 415, Université de Rennes 1
Campus de Beaulieu, F-35042 Rennes Cedex (France)
Telefax: Int. code +99 28 16 46
Dr. P. Guénot, Dr. S. Sinbandhit
Centre Régional de Mesures Physiques de l'Ouest
Université de Rennes 1
Dr. L. Toupet
Groupe Matière Condensée et Matériaux, URA CNRS 815
Université de Rennes 1

[**] This work was supported by the Centre National de la Recherche Scientifique (CNRS) and the University of Rennes. We thank T. B. Marder (University of Waterloo, Canada) for insightful discussions. We also thank F. Varret and J. Linarès (University of Paris 6) for assistance with the Mössbauer spectra.



Scheme 1. Reactions of nucleophiles with complex **3**. a) $NaBH_4$ (2 equiv) in THF; −80 °C; b) $NaBH_4$ in THF/MeOH (9/1) or $LiBEt_3H$ (1 equiv) in THF; −80 °C; c) nBu_4NI or $(PPh_3)NCl$ in CH_2Cl_2.

The X-ray structure analysis of **4** reveals the presence of two molecules in two slightly different conformations in the asymmetric unit. The carbonyl ligand of the first molecule is disordered between two positions, and in the second molecule (Fig. 1) the carbon atoms of the C_5Me_5 ligand show a particularly large thermal coefficient. Of the atoms coordinated to the boron center, only the carbon and the bridging hydrogen atoms are located with normal B–H and B–C bond lengths.[6, 10] The terminal hydrogen atom was not found with a Fourier difference, but set in the theoretical position before the last refinements.

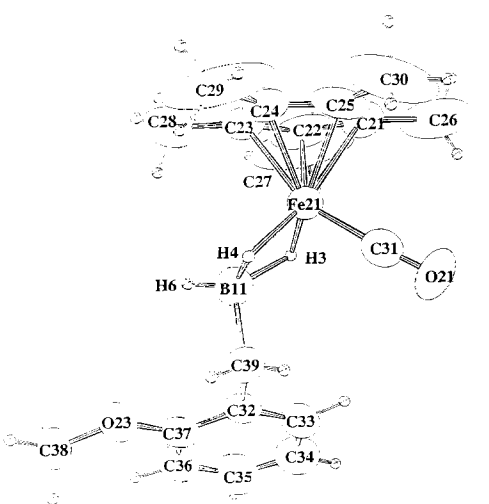


Fig. 1. Crystal structure of **4** (ORTEP diagram of the molecule with the ordered CO ligand, thermal ellipsoids at the 50% probability level). Selected distances [Å] and angles [°]: C39–B11 1.57(2), C32–C39 1.50(2), Fe21–C31 1.76(1), O21–C31 1.13(2), O23–C37 1.36(1), O23–C38 1.38(1); Fe21–C31–O21 175.(1), O23–C37–C32 118.(1), C37–O23–C38 121.(1).

Treatment of **3** with one equivalent of $LiBEt_3H$ in THF afforded the complex **5** (Scheme 1) as the single product (93% yield). According to the ^1H and ^{13}C NMR spectra, the reaction gave exclusively one diastereoisomer. Similarly, reaction of complex **3** with $NaBH_4$ in THF/MeOH (9/1) afforded **5**; under these reaction conditions, the formation of a $MeOH-BH_3$ adduct inhibits any further reduction to **4** (Scheme 1). We have found that other nucleophiles, such as halides, displace the coordinated methoxy group in **3**. Thus, reaction of **3** with nBu_4NI or $(PPh_3)_2NCl$ selectively afforded the carbene halide complexes **6** (X = I) and **7** (X = Cl), respectively, in 85% yield. This result demonstrates the high lability of the chelated *ortho* methoxy group – generally, O-demethylation is observed in the methoxycarbene, which regenerates the starting acyl complexes.[11]

Reduction of alkoxycarbene complexes $[\{Fe\}=C(OR')R]^+$ to give alkyl derivatives $[\{Fe\}-CH_2R]$ has been observed under certain reaction conditions.[4, 12] This process probably involves an alkylidene complex $[\{Fe\}=CHR]^+$ derived from acid-catalyzed elimination of the α-alkoxy group;[13] however, there is no precedence for the formation of such a complex in reductions with boranes. Reaction of the dicarbonyl complex **2** with $NaBH_4$ in pure THF afforded the η^1-benzyl derivative $[Fe(\eta^5\text{-}C_5Me_5)(CO)_2\{\eta^1\text{-}CH_2C_6H_4\text{-}o\text{-}OMe\}]$. The methylene group was formed under the same reaction conditions as those used in the synthesis of complex **4**. Formation of the borohydride complex **4** may, therefore, proceed with formal insertion of a molecule of BH_3 into an iron–carbon bond.

Related insertion reactions of boranes have been reported only for coordinatively unsaturated complexes (Rh,[14] Ta,[7] Zr[15]). The formation of **4** is probably promoted by the facile dissociation of the *ortho* methoxy group as demonstrated above. This is supported by the fact that the acetonitrile carbene complex $[Fe(\eta^5\text{-}C_5Me_5)(CO)(CH_3CN)\{C(OMe)Me\}]OTf$[16] exhibits the same behavior; the related complex $[Fe(\eta^5\text{-}C_5Me_5)(CO)\{\eta^2\text{-}H_2BH(CH_2CH_3)\}]$ is similarly obtained by $NaBH_4$ reduction.[17] Moreover, the boron ligand is readily displaced by addition of PMe_3 to compound **4**, which results in the formation of the adduct $[Me_3P-BH_2(CH_2C_6H_4\text{-}o\text{-}OMe)]$ and the hydrido complex $[Fe(\eta^5\text{-}C_5Me_5)(CO)(PMe_3)(H)]$.

Experimental Procedure

3: A CH_2Cl_2 solution (10 mL) of **2** (0.547 g, 1 mmol) was irradiated for 3 h. After removal of the solvent under vacuum, the solid was washed with ether. Crystallization from CH_2Cl_2/Et_2O gave 0.498 g (96%) of **3** as brown crystals. ^1H NMR (300 MHz, $CDCl_3$): δ = 7.65 (m, Ar), 7.43 (m, Ar), 7.21 (m, Ar), 4.78 (s, 3H, OMe), 3.95 (s, 3H, OMe(Ar)), 1.61 (s, 15H, C_5Me_5); $^{13}C\{^1H\}$ NMR (75.47 MHz, $CDCl_3$): δ = 325.8 (=C), 213.1 (CO), 167.7, 137.2, 134.8, 125.0, 118.9, 115.9 (Ar), 95.0 (C_5Me_5), 71.4 (OMe), 69.9 (OMe(Ar)), 9.5 (C_5Me_5); IR (Nujol): $\tilde{\nu}$[cm^{-1}] = 1977s (ν(CO)); elemental analysis for $C_{21}H_{23}O_6FeSF_3$: calcd C 48.66, H 4.86; found C 48.70, H 4.80%.

4: In a typical reaction, **3** (0.518 g, 1 mmol) was treated with $NaBH_4$ (0.076 g, 2 mmol) in THF (15 mL) at −80 °C. The initial brown color turned into yellow-orange at −30 °C. After evaporation of THF to dryness, the residue was extracted with pentane (2 × 10 mL). Cooling the resulting solution to −20 °C gave 0.301 g (85%) of **4** as brown microcrystals. ^1H NMR (300 MHz, C_6D_6): δ = 7.29 (dd, ^3J(H,H) = 7, ^4J(H,H) = 1.7 Hz, 1H, Ar), 7.06 (td, ^3J(H,H) = 8, ^4J(H,H) = 1.8 Hz, 1H, Ar), 6.93 (td, ^3J(H,H) = 7, ^4J(H,H) = 1 Hz, 1H, Ar), 6.65 (d, ^3J(H,H) = 8 Hz, 1H, Ar), 6.35 (br. pseudo-q, 1H, ^1J(B,H) ≈ 108 Hz, $BH_{terminal}$), 3.46 (s, 3H, OMe(Ar)), 2.60 (br.m, 2H, CH_2), 1.39 (s, 15H, C_5Me_5), −17.87 (br. pseudo-q, 2H, ^1J(B,H) ≈ 43 Hz, $B\text{-}H_{bridging}$); $^1H\{^{11}B$ (55 ppm)$\}$ NMR (C_6D_6): δ = 6.35 (br.s, $BH_{terminal}$), 2.60 (dt, ^3J(H,BH) = 5, ^3J(H,BH_3) = 2.5 Hz, CH_2) −17.87 (br.s, $BH_{bridging}$); $^{13}C\{^1H\}$ NMR (75.47 MHz, $CDCl_3$): δ = 218.8 (CO), 157.4, 134.8, 130.3, 125.3, 120.9, 110.8 (Ar), 90.8 (C_5Me_5), 55.0 (OMe(Ar)), 33.3 (br.m, BCH_2), 10.1 (C_5Me_5); $^{11}B\{^1H\}$ NMR (96.295 MHz, C_6D_6/C_6H_6, Et_2OBF_3 as external standard): δ = 55.33 (br.s); IR (Nujol): $\tilde{\nu}$[cm^{-1}] = 1962s (ν(CO)); zero field Mössbauer data (298 K): IS = 0.104 mms^{-1} vs Fe, QS = 1.898 mms^{-1}; high resolution MS (70 eV): *m/z* calcd for $[M-2H]^+$ ($C_{19}H_{25}O_2{}^{11}B^{56}Fe$) 352.1297 (found 352.130), $[M-2H-CO]^+$ 324.1348 (found 324.134), $[M-3H-CO]^+$ 323.1269 (found 323.127); elemental analysis for $C_{19}H_{27}O_2BFe$: calcd C 64.45, H 7.69; found C 64.55, H 7.62%.

5: ^1H NMR (300 MHz, C_6D_6): δ = 6.85 (m, Ar), 6.48 (m, Ar), 6.43 (m, Ar), 5.99 (m, Ar), 4.35 (s, 1H, CH), 3.25 (s, 6H, OMe and OMe(Ar)), 1.37 (s, 15H, C_5Me_5); $^{13}C\{^1H\}$ NMR (75.47 MHz, C_6D_6): δ = 224.3 (CO), 158.5 (one (Ar) is obscured by C_6D_6), 125.6, 123.2, 102.4, 93.6 (Ar), 87.7 (C_5Me_5), 69.6 (CH), 58.1 (OMe), 54.2 (OMe), 8.8 (C_5Me_5); IR (Nujol): $\tilde{\nu}$[cm^{-1}] = 1925s (ν(CO)); elemental analysis for $C_{20}H_{26}O_3Fe$: calcd C 64.88, H 7.08; found C 64.33, H 7.05%.

6: ^1H NMR (300 MHz, C_6D_6): δ = 7.89 (d, ^3J(H,H) = 7 Hz, 1H, *o*-H), 6.93 (t, ^3J(H,H) = 7 Hz, 1H, *p*-H), 6.72 (t, ^3J(H,H) = 7 Hz, 1H, *m*-H), 6.36 (d, ^3J(H,H) = 8 Hz, 1H, *m*-H), 3.48 (s, 3H, OMe), 3.17 (s, 3H, OMe(Ar)), 1.72 (s, 15H, C_5Me_5); $^{13}C\{^1H\}$ NMR (75.47 MHz, C_6D_6): δ = 334.9 (=C), 221.6 (CO), 149.9, 141.8, 129.4, (one (Ar) is obscured by C_6D_6), 121.4, 110.3 (Ar) 97.3 (C_5Me_5), 63.5 (OMe), 54.6 (OMe(Ar)), 10.5 (C_5Me_5); IR (Nujol): $\tilde{\nu}$[cm^{-1}] = 1930s (ν(CO)); elemental analysis for $C_{20}H_{25}O_3FeI$: C 48.42, H 5.08; found C 48.80, H 5.04%.

Received: March 21, 1994
Revised: June 22, 1994 [Z 6781 IE]
German version: *Angew. Chem.* **1994**, *106*, 2294

[1] a) K. H. Dötz, *Metal Carbenes in Cycloaddition Reactions (Organometallics in Organic Synthesis)* (Eds.: A. de Meijere, H. tom Dieck), Springer, Berlin, **1987**, p. 93); b) D. B. Grotjhan, K. H. Dötz, *Synlett* **1991**, 381, and references therein; c) K. H. Dötz, A. Rau, K. Harms, *Chem. Ber.* **1992**, *125*, 2137; d) K. H. Dötz, H. Larbig, K. Harms, *ibid.* **1992**, *125*, 2143.

[2] For semilabile bimetallic complexes, see P. Braunstein, M. Knorr, E. Villarroya, A. Decian, J. Fischer, *Organometallics* **1991**, *10*, 3714, and references therein.

[3] See, for example, C. P. Casey, A. J. Shusterman, *Organometallics* **1985**, *4*, 736; B. C. Söderberg, L. S. Hegedus, *ibid.* **1990**, *9*, 3113, and references therein; H. Adams, N. A. Bailey, C. E. Tattershall, M. J. Winter, *J. Chem. Soc. Chem. Commun.* **1991**, 912.

[4] a) M. Brookhart, W. B. Studabaker, *Chem. Rev.* **1987**, *87*, 411; b) W. Petz, *Iron Carbene Complexes (Inorganic and Organometallic Chemistry)* Springer, Berlin, **1993**, p. 142; *Gmelin Handbook of Inorganic and Organometallic Chemistry*, Springer, Berlin, **1994**, part B16a.

[5] T. J. Marks, J. R. Kolb, *Chem. Rev.* **1977**, *77*, 263.

[6] a) An iron complex containing a monodentate tetrahydroborato ligand (η^1-BH_4) has been reported: M. V. Baker, L. D. Field, *J. Chem. Soc. Chem. Commun.* **1984**, 996; R. Bau, H. S. H. Yuan, M. V. Baker, L. D. Field, *Inorg. Chim. Acta* **1986**, *114*, L27. b) For an example of an Fe complex with a tetrahydroborato ligand (η^2-H_2BH_2), see C. A. Ghilardi, P. Innocenti, S. Midollini, A. Orlandini, *J. Organomet. Chem.* **1982**, *231*, C78; *J. Chem. Soc. Dalton Trans.* **1985**, 605. c) For a Fe–H–B three-center interaction, see G. E. Herberich, T. Carstensen, D. P. J. Köffer, N. Klaff, R. Boese, I. Hyla-Kryspin, R. Gleiter, M. Stephan, H. Meth, U. Zenneck, *Organometallics* **1994**, *13*, 619.

[7] Q. Jiang, P. J. Carroll, D. H. Berry, *Organometallics* **1993**, *12*, 177.

[8] C. Roger, P. Hamon, L. Toupet, H. Rabaâ, J.-Y. Saillard, J.-R. Hamon, C. Lapinte, *Organometallics* **1991**, *10*, 1045.

[9] Crystal structure analysis of **4**: Enraf-Nonius CAD4 diffractometer, $Mo_{K\alpha}$ radiation, μ = 7.93 cm^{-1}, T = 294 K. Orthorhombic, $Pna2_1$, a = 30.674(9), b = 8.028(5), c = 15.518(7) Å, V = 3821(2) Å^3, ρ_{calcd} = 1.231 gcm^{-3}, Z = 8.3850 unique reflections, 2093 observed with $I > 1.5\sigma(I)$ (scan: $\omega/2\theta$ = 1, *hkl*: 0.36, 0.9, 0.18). Lp correction, correction for isotropic decay and empirical absorption correction, solution by direct methods (DELFT-1990), R = 0.049, R_w = 0.047, $w = 1/\sigma(F_0)^2 = [\sigma^2(I) + (0.04F_0^2)^2]^{-1/2}$, residual electron density (min./max.) = +0.23/1.25 eÅ^{-3}. Further details of the crystal structure investigation may be obtained on request from the Cambridge Crystallographic Data Centre, 12 Union Road, GB-Cambridge CB2 1EZ (UK), on quoting the full journal citation.

[10] a) X. Meng, N. P. Rath, T. P. Fehlner, A. L. Rheingold, *Organometallics* **1991**, *10*, 1986; b) R. T. Baker, R. L. Harlow, S. A. Westrott, T. B. Marder, Waterloo, personal communication; c) G. Jia, A. J. Lough, R. H. Morris, *J. Organomet. Chem.* **1993**, *461*, 147.

[11] a) A. Davison, D. L. Reger, *J. Am. Chem. Soc.* **1972**, *94*, 9237; b) T. Bodnar, A. R. Cutler, *J. Organomet. Chem.* **1981**, *213*, C31; c) M. Brookhart, J. R. Tucker, *J. Am. Chem. Soc.* **1981**, *103*, 979; d) M. Brookhart, J. R. Tucker, G. R. Husk, *ibid.* **1983**, *105*, 258; e) G. J. Baird, S. G. Davies, T. R. Marbely, *Organometallics* **1984**, *3*, 1764; f) T. Forschner, K. Menard, A. Cutler, *J. Chem. Soc. Chem. Commun.* **1984**, 121.

[12] M. Brookhart, R. C. Buck, *J. Am. Chem. Soc.* **1989**, *111*, 559.

[13] Brookhart et al. found that a basic medium ($NaBH_4$/MeOH/MeO^-) avoids the further reduction of (α-alkoxy)alkyl complexes, see ref. [4a].

[14] R. T. Baker, D. W. Ovenall, R. L. Harlow, S. A. Westcott, N. J. Taylor, T. B. Marder, *Organometallics* **1990**, *9*, 3028.

[15] J. A. Marsella, K. G. Caulton, *J. Am. Chem. Soc.* **1982**, *104*, 2361.

[16] S. Nlate, C. Lapinte, V. Guerchais, *Organometallics* **1993**, *12*, 4657.

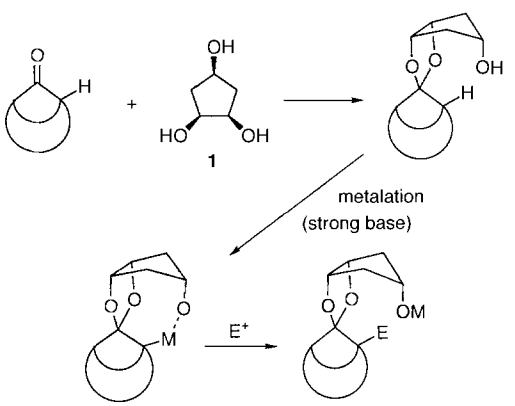
[17] S. Nlate, *Dissertation*, Universität Rennes, **1993**, and unpublished results.

Bridgehead Functionalization of Non-Enolizable Ketones: The First Preparatively Useful Methods**

Urs P. Spitz and Philip E. Eaton*

A bridgehead hydrogen α to a carbonyl group in a small polycyclic system is not enolizable, but its acidity is enhanced inductively by the adjacent carbonyl group. Investigations here and elsewhere[1] have shown that norbornanone and other such ketones undergo efficient aldol dimerization when treated with powerful bases like lithium tetramethylpiperidide (LiTMP). However, despite intense efforts, we have been unable to trap the putative intermediate pseudo-enolates with electrophiles other than the ketone itself. Even reagents containing in situ electrophiles such as LiTMP/Me_3SiCl[2] or LiTMP/$HgCl_2$[3] fail. The inability to achieve bridgehead substitution by these or other methods presents a serious obstacle to achieving concise syntheses of cage compounds and other polycyclics.[4]

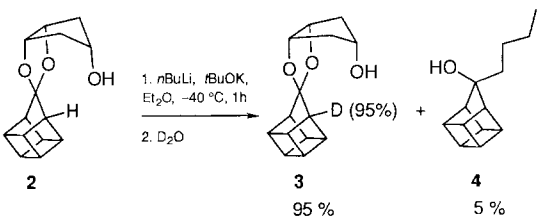
Directed metalation is well-established and of great synthetic importance for substituting aromatics,[5] cubanes,[3, 6] and cyclopropanes.[7, 8] To apply this approach to the problem of bridgehead substitution we developed the idea of using the auxiliary *cis,cis*-1,2,4-cyclopentanetriol (**1**).[9] Acetalization of bridgehead ketones with **1** would place a hydroxyl group in close proximity to one of the bridgehead hydrogen atoms (see Scheme 1), and this offers the possibility of its participation in deprotonation of this bridgehead position.



Scheme 1.

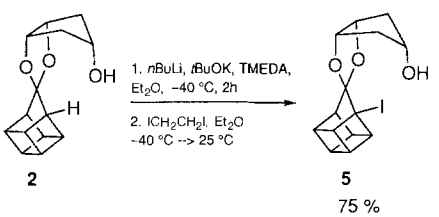
In our initial experiments we employed the homocubanone acetal **2** as the test substrate. Many attempts to metalate it failed. Usually 9-alkylhomocuban-9-ols (e.g. **4**), arising from base-induced cleavage of the acetal, were predominant products. However, reaction of **2** with *n*-butyllithium in the presence of *N,N,N',N'*-tetramethylethylenediamine (TMEDA) in ether at room temperature followed by quenching with D_2O did lead, as desired, to significant mono α-deuteriation.[10]

In the next experiments, potassium *tert*-butoxide was added to the reaction mixture: this was based on the idea that the potassium alkoxide of the auxiliary along with added alkyllithium would generate a local superbase.[11] Indeed, these conditions greatly accelerated the reaction, increased the degree of metalation (deuteriation), and reduced the interfering acetal cleavage. For example, treatment of **2** with a mixture of *n*-butyllithium (5 equiv) and potassium *tert*-butoxide (5 equiv) in ether at $-40\,^{\circ}C$ for 1 hour followed by addition of D_2O gave **3** in 95% yield with greater than 95% α-deuteriation (MS and NMR) and only about 5% cleavage [Eq. (a)].



(a)

The homocubane bridgehead metalation was turned into a useful synthetic procedure by substituting iodination for deuteriation. Transfer of the metalated reaction mixture into excess diiodoethane in ether at $-40\,^{\circ}C$ gave the iodinated acetal **5**, which could be isolated cleanly in 75% overall yield [Eq. (b)]. Hydrolysis of **5** can be expected to give 1-iodo-9-homocubanone, a cubane carboxylic acid precursor (by way of Favorskii contraction).[12]



(b)

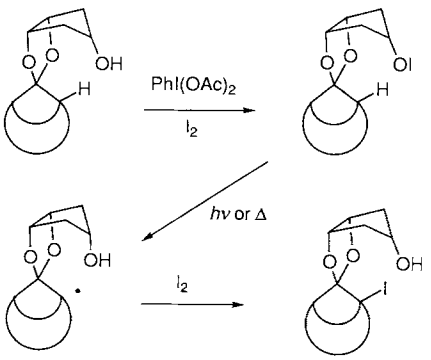
The idea behind the design of auxiliary **1** was to position a hydroxyl group so that it might "participate" in the formation/stabilization of the desired carbanion.[13] This reasoning proved to be simplistic, which is not surprising considering the probable complexity of the carbanion superstructure.[8a] Indeed, when the hydroxyl group in acetal **2** was epimerized,[14] thus moving it further from the reaction site, metalation could still be achieved with comparable efficiency. Furthermore, some metalation (about 10% after 1 hour) occurred even when the hydroxyl group was absent, provided that TMEDA was present in the reaction mixture. Confusing the matter further, we found that the homologous acetal derived from *cis,cis*-1,2,4-cyclohexanetriol did not undergo metalation at all. Clearly, there is much yet to be learned about the real role of the auxiliary.

As useful (if puzzling) as the metalation described above will prove, it has obvious limitations: base-induced cleavage of the acetal, necessity for enhanced C-H acidity, fragility of other functionality to powerful bases, etc. Fortunately, we have found that the auxiliary approach to bridgehead functionalization can be applied in a much less limited way.

Radical reactions have been used frequently for remote C-H activation.[15] The most popular versions are the Barton and hypohalite reactions.[15, 16] As bridgehead iodo compounds are of particular utility, we focused on hypoiodites. These are readily generated in situ from alcohols[17] and decompose to oxo-radicals upon photolysis or thermolysis. Our system (Scheme 2)

[*] Prof. P. E. Eaton, Dr. U. P. Spitz
Department of Chemistry
The University of Chicago
5735 S. Ellis Ave., Chicago, IL 60637 (USA)
Telefax: Int. code + (312) 702-0805

[**] This work was supported by the National Science Foundation (USA). We are grateful to Dr. H. Higuchi and Dr. Y. Tobe for their early contributions to this project.



Scheme 2.

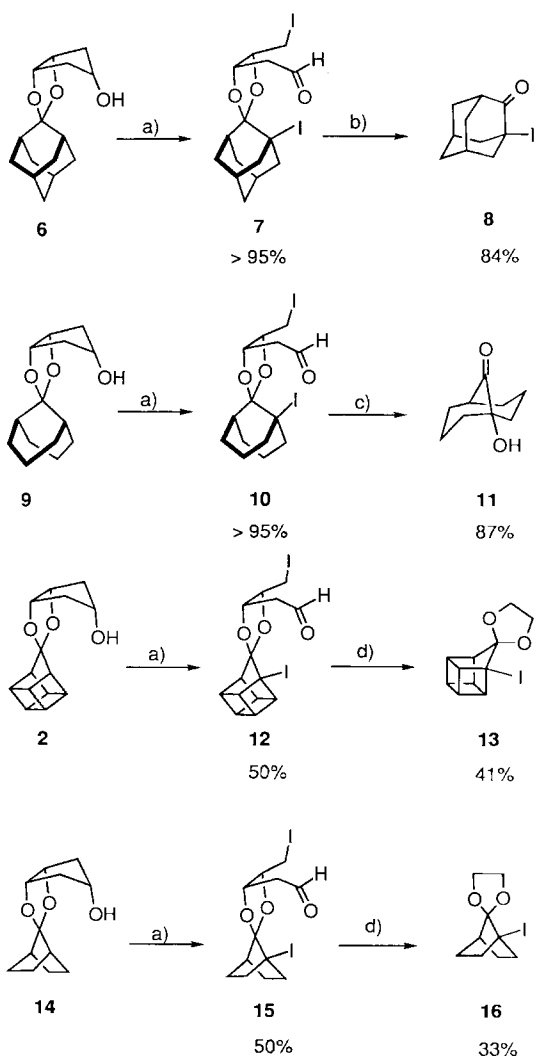
is set up to direct the oxoradical to abstract a bridgehead hydrogen.[18]

In a typical experiment, a cyclohexane solution (0.01 M) of an acetal (**2**, **6**, **9**, or **14**), iodobenzene diacetate (3 equiv), and iodine (2.5 equiv) was irradiated for 45 min with a 250 W tungsten lamp.[17] Substantial iodination at the bridgehead was observed (Scheme 3). Incidental to the desired process, cleavage of the cyclopentane ring occurred.[19] The ratio of functionalized to unfunctionalized substrates was estimated by integration of the corresponding aldehyde hydrogen NMR signals. Afterwards, the remains of the auxiliary could be removed or transformed in various ways, as illustrated.[20] Complete α-functionalization (>95%) of adamantanone and of 9-bicyclononanone was achieved. Even in the norbornanone and homocubanone systems about 50% bridgehead iodination was obtained; these are astonishingly high yields considering the notorious lack of reactivity at these sites.

In these radical reactions the mechanism of activation (direction) is much clearer than in the earlier metalations. Control experiments showed that functionalization does not occur if the 4-hydroxyl group of the auxiliary is epimerized or absent.[21]

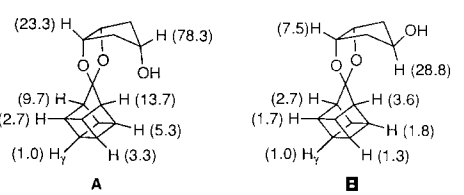
Although much improvement is still needed, these pioneering examples open new doors in the chemistry of polycyclic compounds. We note, for example, that once bishomohexaprismandione is made, the methodology introduced here provides a way to set it up for Favorskii contraction to the long-sought hexaprismane.[22]

Received: May 9, 1994 [Z 6909 IE]
German version: *Angew. Chem.* **1994**, *106*, 2263



Scheme 3. a) Iodobenzene diacetate, iodine, *hν*, cyclohexane, reflux, 45 min; b) triphenylmethyl tetrafluoroborate, CH_2Cl_2, 12 h, 25 °C; c) 5% H_2SO_4, dioxane, 16 h, 100 °C; d) 5% H_2SO_4, ethylene glycol, 16 h, 105 °C, sealed flask.

[1] A) P. G. Gassman, F. V. Zalar, *J. Am. Chem. Soc.* **1966**, *88*, 3070; b) A. Nickon, J. L. Lambert, J. E. Oliver, D. F. Covey, J. Morgan, *ibid.* **1976**, *98*, 2593; c) C. S. Shiner, A. H. Berks, A. M. Fisher *ibid.* **1988**, *110*, 957; d) N. H. Werstiuk, *Tetrahedron* **1983**, *39*, 205, and references therein.
[2] T. D. Krizan, J. C. Martin, *J. Am. Chem. Soc.* **1983**, *105*, 6155.
[3] a) P. E. Eaton, G. T. Cunkle, G. Marchioro, R. M. Martin, *J. Am. Chem. Soc.* **1987**, *109*, 948; b) P. E. Eaton, G. Castaldi, *ibid.* **1985**, *107*, 724.
[4] P. E. Eaton, Y. S. Or, S. J. Branca, B. K. R. Shankar, *Tetrahedron* **1986**, *42*, 1621.
[5] For a review see: V. Snieckus, *Chem. Rev.* **1990**, *90*, 879.
[6] a) P. E. Eaton, C. H. Lee, Y. Xiong, *J. Am. Chem. Soc.* **1989**, *111*, 8016; b) P. E. Eaton, Y. Xiong, J. P. Zhou, *J. Org. Chem.* **1992**, *57*, 4277; c) P. E. Eaton, Y. Xiong, C.-H. Lee, *J. Chin. Chem. Soc.* **1991**, *38*, 303.
[7] a) P. E. Eaton, R. G. Daniels, D. Casucci, G. T. Cunkle, P. Engel, *J. Org. Chem.* **1987**, *52*, 2100; b) D. J. Gallagher, C. G. Garrett, R. P. Lemieux, P. Beak, *ibid.* **1991**, *56*, 853; c) P. E. Eaton, K. A. Lukin, *J. Am. Chem. Soc.* **1993**, *115*, 11370.
[8] a) For a review on metalation of non-aromatic compounds: G. W. Klumpp, *Recl. Trav. Chim. Pays-Bas* **1986**, *105*, 1. b) Directed metalation generally fails with simple cyclobutanes as they are insufficiently acidic[3b].
[9] The original procedure (F. G. Cocu, T. Posternack, *Helv. Chim. Acta* **1971**, *54*, 1676) was improved substantially, as will be reported later.
[10] The ^{1}H NMR signals in acetal **2** and its epimer[14] were assigned based on Eu(hfc)$_3$-induced chemical shifts. The shifts (see **A** and **B**) were measured relative to the *γ-anti* proton, that most removed from the hydroxyl group. As expected, the shift reagent coordinated primarily to the free hydroxyl group; the resonance of the geminal hydrogen was shifted much more than any other. The two homocubyl resonances that experienced the most downfield shift were assigned to the two bridgehead protons. Each of these appeared as a triplet integrating for 1 hydrogen. Of the two, the one with the greater downfield shift was assigned to the proton *syn* to the 5-carbon ring of the auxiliary. As expected, the shift difference was less in the epimer. After metalation/deuteriation (**2** → **3**) the signal for the homocubyl proton with the greatest downfield shift was almost completely absent; this establishes that deuteriation (and thus metalation) had occurred at the homocubyl bridgehead carbon on the same side as the hydroxyl group of the activating auxiliary.



[11] Mixtures of potassium alkoxides and alkyllithiums form superbases (LiCKOR). For a review see: M. P. Schlosser, *Pure Appl. Chem.* **1988**, *60*, 1627.
[12] P. J. Chenier, *J. Chem. Educ.* **1978**, *55*, 286.
[13] S. M. Bachrach, J. P. Ritchie, *J. Am. Chem. Soc.* **1989**, *111*, 3134.
[14] E. J. Corey, M. C. Desai, T. A. Engler, *J. Am. Chem. Soc.* **1985**, *107*, 4339.

[15] For a review see: W. Carruthers, *Some Modern Methods of Organic Chemistry*, 3rd ed., Cambridge University Press, New York, **1986**, chap. 4.
[16] D. H. R. Barton, J. M. Beaton, L. E. Geller, M. M. Pechet, *J. Am. Chem. Soc.* **1961**, *83*, 4076.
[17] a) K. Heusler, J. Kalvoda, P. Wieland, G. Anner, A. Wettstein, *Helv. Chim. Acta* **1962**, *45*, 2575; b) J. I. Concepción, C. G. Francisco, R. Hernández, J. A. Salazar, E. Suaréz, *Tetrahedron Lett.* **1984**, *25*, 1953; c) J. Lusztyk, D. Pagé, *ibid.* **1994**, *35*, 1003, and references therein.
[18] Not much is understood about the structural requirements for successful hydrogen atom abstraction from a C–H bond. Empirically, the ideal distance between the oxo radical and the C–H carbon atom is 2.5–2.7 Å [15]. In the cases at hand, this arrangement is easily achieved in the adamantane and bicyclononane systems, but is more difficult to obtain in the norbornane and homocubane systems.
[19] a) When $PhI(OAc)_2$ was the limiting reagent, some of the bridgehead-iodinated product had the auxiliary acetal intact. b) For information relevant to the acetal cleavage see: J. L. Courtneidge, J. Lusztyk, D. Pagé, *Tetrahedron Lett.* **1992**, *33*, 3053.
[20] For cleavage of acetals with trityl tetrafluoroborate see: D. H. R. Barton, P. H. Magnus, L. E. Geller, G. Smith, D. Zurr, *Chem. Com.* **1971**, *83*, 861.
[21] The homologous auxiliary *cis,cis*-1,2,4-cyclohexanetriol is not effective.
[22] Bishomohexaprismanedione might be accessible by oxidation of bishomohexaprismane [23]: a) O. Reiser, *Angew. Chem.* **1994**, *106*, 73; *Angew. Chem. Int. Ed. Engl.* **1994**, *33*, 69; b) D. H. R. Barton, P. E. Eaton, W.-G. Liu, *Tetrahedron Lett.* **1991**, *32*, 6263.
[23] G. Metha, S. Padwa, *Tetrahedron* **1991**, *47*, 7807.

Toward Unified Enantioselective Chromatography with a Single Capillary Column Coated with Chirasil-Dex**

Volker Schurig,* Martin Jung, Sabine Mayer, Simona Negura, Markus Fluck, and Hansjörg Jakubetz

The simplified Golay equation (a) describes the chromatographic process in an open tubular column the walls of which

$$H = \frac{B}{u} + Cu = \frac{2D_m}{u} + f(k)\frac{d_c^2}{D_m}u \qquad \text{(a)}$$

are coated with a stationary phase.[1] It predicts that at a given inner diameter d_c the optimum efficiency (that is, the minimum plate height H_{min}) is independent of the nature of the mobile phase and that the optimum mobile phase velocity (u_{opt}) depends only on the diffusion coefficient D_m at a defined retention factor k [Eq. (b) and (c)][2] (Fig. 1). Thus, it should be possible to

$$H_{min} = 2\sqrt{BC} = d_c f_1(k) \qquad \text{(b)}$$

$$u_{opt} = \sqrt{\frac{B}{C}} = \frac{D_m}{d_c} f_2(k) \qquad \text{(c)}$$

analyze competing substrates, for example, enantiomers, on a single column with different chromatographic modes by employing a gas, a supercritical fluid, or a liquid (of different polarity, pH, or composition) as mobile phase. Here we verify this prediction for enantiomer separation on a chiral stationary phase.

[*] Prof. Dr. V. Schurig, Dr. M. Jung, Dr. S. Mayer, Dipl.-Ing. S. Negura, Dipl.-Chem. M. Fluck, Dipl.-Chem. H. Jakubetz
Institut für Organische Chemie der Universität
Auf der Morgenstelle 18, D-72076 Tübingen (FRG)

[**] This work was supported by Deutsche Forschungsgemeinschaft and Fonds der Chemischen Industrie. We are grateful to Professor Knabe, Saarbrücken, for supplying a specimen of (*R*)-(−)-hexobarbital. LC = liquid chromatography, CEC = capillary electrochromatography, SFC = chromatography with supercritical fluids, GC = gas chromatography.

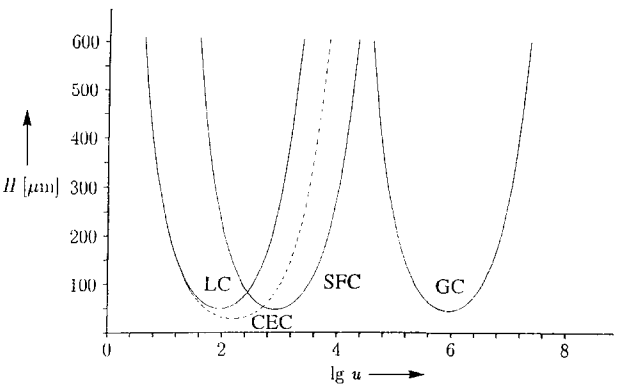
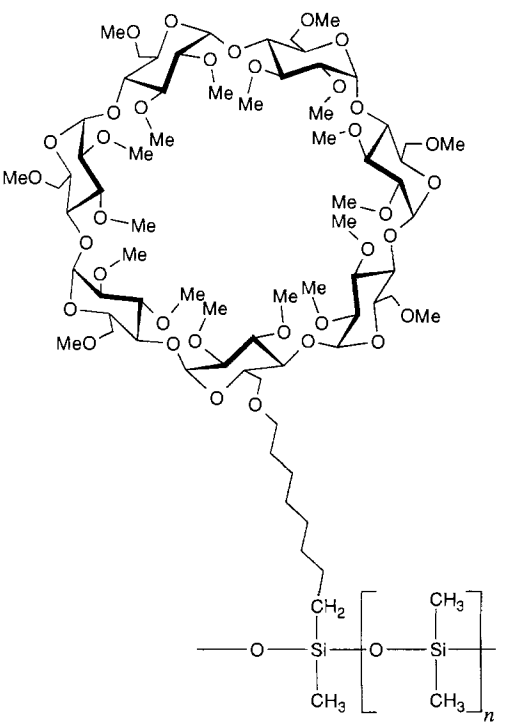


Fig. 1. Height of a theoretical plate H versus the logarithm of the velocity u [$\mu m\,s^{-1}$] of the mobile phase, according to Equation (a) for a capillary column with 50 μm i.d. $k = 5$, D_m[$\mu m^2 s^{-1}$] = 10^7 (GC), 10^4 (SFC), 10^3 (LC, CEC), $f(k)_{parabol} = (1 + 6k + 11k^2)/(96(1 + k)^2)$ [note that in CEC, H_{min} and u_{opt} are different from those of the other chromatographic techniques due to the nearly flat flow profile (dotted curve), $f(k)_{flat} = k^2/(16(1 + k)^2)$.

We previously demonstrated that Chirasil-Dex (Scheme 1)[3] can be employed as an immobilizable chiral stationary phase for enantiomer separation both in capillary GC and SFC.[4] Subsequently we found that Chirasil-Dex is even compatible with buffers in CEC. Thus, enantiomer separation on the chiral surface Chirasil-Dex has been achieved by CEC.[5]


MeO
OMe
Me
Me
Me

The feasibility of this approach is demonstrated in Figure 2.[6] Racemic hexobarbital can be separated on the same fused silica capillary column coated with Chirasil-Dex by all four current chromatographic methods irrespective of the nature of the mobile phase. As the result of the different diffusion coefficients D_m in gases and liquids (cf. caption of Fig. 1), the optimal velocity u_{opt} of the mobile phase is four orders of magnitude lower in capillary LC and CEC than that in GC (cf. Fig. 1). However, H_{min} and u_{opt} also depend on the retention factor k [Eq. (b) and (c)]. Fortunately, while k is quite large in GC and intermediate in SFC, very small values ($k < 1$) are encountered in CEC and LC notably for the first eluted enantiomer. Consequently, analysis times are not too long, and the elution bands are especially narrow for the first eluted enantiomer. However, as seen in Figure 2 (left), GC turns out to be the fastest method, in agreement with Equation (c).

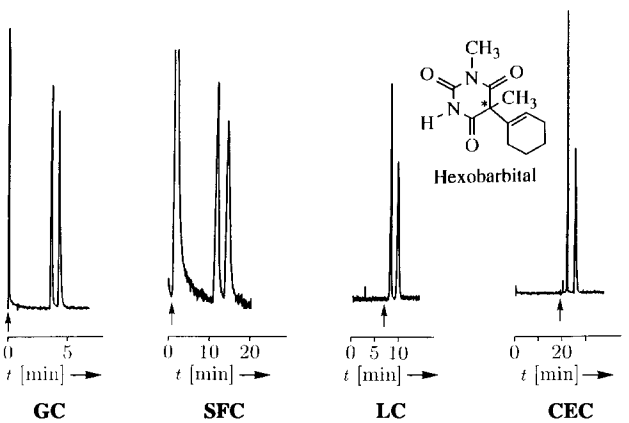


Fig. 2. Separation of hexobarbital enantiomers on a 80 cm × 50 μm (i.d.) fused silica capillary column coated with Chirasil-Dex (film thickness ≈ 0.15 μm) by GC, SFC, LC, and CEC. Conditions: GC: $T = 145\,^{\circ}C$, $p = 1.0$ bar (H_2); SFC: $\rho = 0.25\ g\,mL^{-1}$ (CO_2), $T = 60\,^{\circ}C$; LC: $p = 0.15$ bar, $T = 20\,^{\circ}C$, buffer (borate/phosphate; pH 7)/acetonitrile (90/10, v/v); CEC: $U = 30$ kV, buffer (borate/phosphate; pH 7)/acetonitrile (90/10, v/v), $T = 20\,^{\circ}C$. The arrows in the chromatograms indicate the dead time.

To the best of our knowledge LC in an open tubular column has been used here for enantiomer separation on chiral stationary phases for the first time. Significantly, a CE instrument equipped with a pressure-driven injection system can be employed for open tubular LC. Important advantages over HPLC with packed columns are low flow rates facilitating coupling techniques (LC-MS), high column permeability leading to small pressure drops, and low heat capacity. The amounts of chiral stationary phase and solvent required are minimized in open tubular CEC and LC. According to Equation (b) efficiency is further improved with smaller inner diameters d_c. One disadvantage of using short narrow-bore capillary columns is the limited sample capacity. The continuous improvement of injection techniques and (on-column) detection devices, notably in CEC and LC instrumentation, may eventually overcome these problems. Moreover, the important merit of miniaturization, namely short analysis times, leads to large, narrow peaks and thus enhances detectability.

Hitherto, the unified approach demonstrated here employed a single capillary column coated with a chiral stationary phase in different chromatographic modes. Further investigations into the use of a unified instrument design to carry out GC, SFC, and LC are in progress,[7] also in enantiomer analysis. Enantioselective open tubular LC and CEC has already been performed on the same instrument employing a pressure-driven injection system. The loss of efficiency for the first eluted enantiomer can clearly be recognized (cf. the narrow CEC peak in Fig. 2) when passing from the flat flow profile characteristic for CEC to the parabolic profile inherent to LC.

Chirasil-Dex coated on silica can also be employed for the preparative enantiomer separation of hexobarbital by HPLC. Collection of the first fraction, identified as (*R*)-(−)-hexobarbital by comparison with an authentic sample,[8] allowed the determination of the elution order of hexobarbital enantiomers on Chirasil-Dex with different mobile phases. For all five methods (capillary GC, SFC, LC, CEC, and packed HPLC) the configuration of the first eluted enantiomer is *R*-(−).

Experimental

Chirasil-Dex was synthesized and coated onto fused silica capillaries as previously described in detail [9]. The column length was 1 m and the inner diameter 50 μm. For UV detection an optical window, located at a distance of 80 cm from the injection port, was prepared by burning off about 3 mm of the polyimide outer coating. After performing CE and LC, the column was shortened to the position of the optical window (at 80 cm).

A Carlo-Erba gas chromatograph Fractovap (Fisons, Mainz, Germany) equipped with FID was used. The carrier gas was hydrogen (99.999%), and the split ratio 1:200. SFC was performed on a Carlo-Erba SFC 3000 system (Fisons, Mainz, Germany) as previously described [10]. CEC and open tubular LC were performed with the capillary electrophoresis system "PRINCE" (Bischoff, Leonberg, Germany) equipped with an on-column UV detector. The sample was injected by the pressure-driven method (40 mbar, 5 s) and detected at 220 nm. The coated column was conditioned with buffer overnight (30 kV) and was rinsed between each chromatographic run with water and methanol.

The order of measurements was CEC, LC, SFC, GC. The sequence was repeated two months later in reverse order to determine the elution order of hexobarbital enantiomers.

Received: May 21, 1994 [Z 6961 IE]
German version: *Angew. Chem.* **1994**, *106*, 2265

[1] M. J. E. Golay in *Gas Chromatography* (Ed.: D. H. Desty), Butterworth, London, **1958**, p. 36.
[2] G. Guiochon, C. L. Guillemin, *J. Chromatogr. Libr.* **1988**, *42*, 105.
[3] Chirasil-Dex employed in this work contains 16% (w/w) permethylated β-cyclodextrin. Statistically, out of 90 silicon atoms, one carries a cyclodextrin moiety.
[4] V. Schurig, D. Schmalzing, M. Schleimer, *Angew. Chem.* **1991**, *103*, 994–996; *Angew. Chem. Int. Ed. Engl.* **1991**, *30*, 987–989.
[5] S. Mayer, V. Schurig, *J. High Resolut. Chromatogr.* **1992**, *15*, 129–131; *J. Liq. Chromatogr.* **1993**, *16*, 915–931; V. Schurig, S. Mayer (Universität Tübingen), DE-A 4136462.7, **1991**.
[6] V. Schurig, M. Jung, S. Mayer, S. Negura, H. Grosenick, M. Fluck, A. Glausch, presented Analytica '94 in München, Abstracts p. 52.
[7] D. Ishii, T. Niwa, K. Ohta, T. Takeuchi, *HRC & CC J. High Resolut. Chromatogr. Chromatogr. Commun.* **1988**, *11*, 800–801.
[8] J. Knabe, D. Strauß, *Angew. Chem.* **1968**, *80*, 483–484; *Angew. Chem. Int. Ed. Engl.* **1968**, *7*, 463–464; J. Knabe, *Pharmazie* **1993**, *48*, 883–889.
[9] D. Schmalzing, Dissertation, Universität Tübingen, **1991**; V. Schurig, D. Schmalzing, U. Mühleck, M. Jung, M. Schleimer, P. Mussche, C. Duvekot, J. Buyten, *J. High Resolut. Chromatogr.* **1990**, *13*, 713–717; M. Jung, V. Schurig, *J. Microcolumn Sep.* **1993**, *5*, 11–22.
[10] M. Jung, V. Schurig, *J. High Resolut. Chromatogr.* **1993**, *16*, 215–223.

 © VCH Verlagsgesellschaft mbH, D-69451 Weinheim, 1994 0570-0833/94/2121-2223 $ 10.00+.25/0

Primed for Success

Handbook of Enantioselective Catalysis with Transition Metal Compounds. Vol. I: Products and Catalysts, Vol. II: Ligands–References. By *H. Brunner* and *W. Zettlmeier*. VCH Verlagsgesellschaft, Weinheim/VCH Publishers, New York, 1993. 917 pp., hardcover DM 598.00.—ISBN 3-527-29068-0/1-56081-811-5

Of the many new specialist books on chemistry that continue to appear, it is rare to find one that gives an immediate impression of being an indispensable addition to the chemical literature. This two-volume handbook on enantioselective catalysis by Brunner and Zettlmeier is undoubtedly one of these exceptions, in which the authors have succeeded well in their aim of bringing some order to the jungle of chiral metal catalysts and their reactions. The work excels through being very up-to-date, through the careful collecting together of the vast amount of data (covering about 13000 reactions and 2000 ligands) and the comprehensiveness thereby achieved, and through the wealth of information that one can extract from the concisely arranged collection.

The two volumes make up an inseparable whole. Volume I covers reactions with chiral metal catalysts, while Volume II contains a comprehensive list of all the chiral ligands known up to about 1992. Each ligand has been assigned a number, so that in Volume I each catalyst can be described concisely by a combination of the metal with the ligand number.

The reactions in Volume I are arranged according to the molecular formula of the product. This is followed by the full reaction equation, in which as much information as possible has been given within a small space. The product formulas highlight the chiral centers at which chirality has been introduced through the action of the catalyst. This is especially useful in cases where the educt already contains one or more chiral centers which are not configurationally stable under the reaction conditions. Alongside the reaction arrow are shown the absolute configuration of the product and the maximum optical yield achieved with the first-named catalyst in the next column. Other catalysts that have been used for the same reaction but gave lower yields are also listed. For each reaction and each ligand all the relevant literature references are listed in Volume II in order of the year of publication, an unusual and helpful arrangement which allows one to quickly find the most recent publications.

The only criticism of this excellent handbook is that one could propose improvements that would allow even more efficient ways of retrieving the information. Firstly, in Volume II the list of ligands does not tell one where to look in Volume I to find reactions in which particular ligands are used. Secondly, since the reactions in Volume I are arranged according to the molecular formula of the product rather than according to reaction type, it would be useful to have an additional index listing the reactions contained in Volume I according to reaction types (e.g. hydrogenations, cyclopropanations, etc.). However, to have included these improvements would certainly have increased the size of the handbook beyond that which was intended, and although they would provide extra convenience for the user they would add nothing to the information content of the work.

Nevertheless, in view of the continuing exponential growth in the numbers of metal catalysts and of their reactions, the authors should be encouraged to eventually produce a version in the form of a computerized data bank with all the searching algorithms that might conceivably be useful.

To sum up, this data collection will be indispensable for every chemist who is concerned with chiral molecules. Since it is reasonably priced I feel justified in recommending not only that every departmental library should buy the book, but also that individual research laboratories should have their own copies.

Oliver Reiser
Institut für Organische Chemie
der Universität Göttingen (FRG)

Chemical Bonding. By *M. J. Winter*. 90 pp., ISBN 0-19-855694-2.—**Organometallics 1. Complexes with Transition Metal–Carbon σ-Bonds.** By *M. Bochmann*. 91 pp., ISBN 0-19-855751-5.—**Organometallics 2. Complexes with Transition Metal–Carbon π-Bonds.** By *M. Bochmann*. 89 pp., ISBN 0-19-855813-9.—**Bifunctional Compounds.** By *R. S. Ward*. 90 pp., ISBN 0-19-855808-2.—All in the series Oxford Chemistry Primers, Oxford University Press, Oxford, 1994. Paperbacks, £ 4.99 each.

The *Oxford Chemistry Primers* series, in which 24 titles have appeared up to now, aims to provide chemistry students with simple and quick introductions to specific areas of organic and inorganic chemistry. Each volume of about 90 pages contains material that would be covered in eight to ten course lectures. The emphasis on explanations and reasoning rather than on learning facts is intended to equip the student with the basic principles for understanding an area of study.

Chemical Bonding is intended for those just starting their studies. It begins with a brief historical outline in which the atomic orbital model and the Periodic System are developed very lucidly and with little mathematics. This is followed by chapters dealing with the bonding between two atoms. In Chapters 2, after a short section on the Lewis concepts of the nature of bonding, the author introduces the principle of a linear combination of atomic orbitals, with the help of molecular orbital energy level schemes and orbital diagrams. Chapter 3 is concerned with the VSEPR model, then in the final chapter the extension of the molecular orbital approach to polyatomic molecules is discussed. The excellent illustrations provid-

This section contains book reviews and a list of new books received by the editor. Book reviews are written by invitation from the editor. Suggestions for books to be reviewed and for book reviewers are welcome. Publishers should send brochures or (better) books to Dr. Ralf Baumann, Redaktion Angewandte Chemie, Postfach 101161, D-69451 Weinheim, Federal Republic of Germany. The editor reserves the right of selecting which books will be reviewed. Uninvited books not chosen for review will not be returned.

 © VCH Verlagsgesellschaft mbH, D-69451 Weinheim, 1994 0570-0833/94/2121-2225 $ 10.00+.25/0

ed throughout the volume enable the reader to gain a good appreciation of the spatial distribution of the electrons in atoms and chemical bonds. The representation of orbitals and bonds by electron density dot diagrams succeeds especially well. On the other hand it is regrettable that answers are not provided for the exercise problems included at the end of each chapter, since this means that they are not suitable for individual private study by beginners. Only a few literature references for more advanced reading are given, but these are sufficient.

Organometallics 1 and *Organometallics 2* deal with compounds containing metal–carbon σ-bonds and π-bonds respectively. The first of these volumes begins by explaining some basic concepts, then describes the chemistry of metal carbonyl, metal alkyl, and metal carbene complexes in turn. *Organometallics 2* begins by briefly repeating and extending the fundamental principles, then discusses the most important organometallic π-complexes. Basic methods of synthesis, bonding concepts, and chemical reactivities are described for each class of compounds, illustrated by appropriate examples. In each chapter the most important statements are summarized in display boxes. Where particular complexes have applications as catalysts for organic syntheses or polymerizations, or as biosensors, these are highlighted in indented paragraphs. Thus, by clearly emphasizing the essential points, the reader is given a feel for the relative importance of the material. In these two volumes also the illustrations are excellent and contribute to the clarity of presentation. The ground covered in these volumes is quite adequate for a first introduction. On the other hand the indexes (50 and 72 entries respectively) are rather scanty.

The volume *Bifunctional Compounds* offers an interesting collection of material of a kind that is unlikely to be found in conventional textbooks. It deals with the chemistry of organic compounds whose special reactive properties arise from the presence of two interacting functional groups. In addition to descriptions of the synthesis and reactions of dienes, enamines, dicarbonyl compounds, and other bifunctional compounds, there are chapters on the selective introduction of protecting groups and on cyclizations. The volume includes exercise problems (with answers), and is intended for advanced students and research chemists.

The concept underlying the *Oxford Chemistry Primers* series, whereby the teaching material is divided into small subject areas and presented individually, has the important advantage that the material is more topical and up-to-date than in conventional textbooks. New developments can be quickly incorporated, and space can also be given to aspects that are on the borders of the discipline (e.g. Volume 22: *Fractals in Chemistry*). The volumes offer a good basis for small seminars in which the work could be extended to suit individual needs. However, compared with a comprehensive textbook this teaching concept cannot give such a good overview of the whole field of organic and inorganic chemistry. Consequently the overall perspective and interconnection of the individual topics must be provided from some other source. If the volumes of this series are used as supporting reading to accompany a teaching course, the lecturers will need to link the separate topics together by providing greater depth and additional material. If this can be done effectively, the concept of a textbook of chemistry made up of units that can be combined and extended to suit individual needs could be very successful.

Burkhard König
Institut für Organische Chemie
der Technischen Universität
Braunschweig (FRG)

Scanning Tunneling Microscopy and Spectroscopy. Theory, Techniques, and Applications. Edited by *D. A. Bonnell*. VCH Verlagsgesellschaft, Weinheim/VCH Publishers, New York, 1993. 436 pp., hardcover DM 196.00, $ 125.00.—ISBN 3-527-27920-2/0-89573-786-X

It can be said straight away that this book is a must for everyone concerned with surface physics studies using high resolution microscopy and microanalysis. Although it is scarcely a decade since the invention of the scanning tunneling microscope, it has now been widely adopted in fields ranging from materials science to the biological sciences, thanks to the simplicity of the underlying concept and its remarkable ability to give direct imaging of atoms and molecules. However, apart from the short monograph by Hamann and Heitschold (Akademie Verlag, Berlin, 1992), there has hitherto been no comprehensive treatment of the subject which is also suitable for newcomers, and gives an introduction to the principles and main areas of application. Therefore this book, by a team of authors who are all actively engaged in the field, has been compiled with the needs of advanced students in the area of surface physics in mind. It will also be useful to university lecturers in physics, chemistry, and biology as a source for preparing courses. However, it is not intended to be a textbook in the conventional sense; there are many aspects that cannot yet be presented conclusively, as rapid developments are still taking place. Instead it is more of a snapshot of the knowledge that experiments have so far yielded, the theoretical understanding of which is still at a tentative stage; one such topic is the role of the conductivity of organic molecules in the generation of scanning tunneling images. According to the preface the book sets out to bridge the gap between existing monographs and specialist review articles, for the benefit of the reader who wishes to make a start in the field and is interested in the basic principles, the design of instruments, and the potential applications.

It is to the credit of the editor, Dawn Bonnell, that the individual contributions have not been simply strung together in a haphazard way; instead there is a logical structure and relationship between the chapters, which makes the work suitable as a course book. It is divided into three parts. The first part begins with a brief historical survey of the developments leading up to the invention of the scanning tunneling microscope, followed by an exposition of the basic principles: the construction of the microscope and its use, the theory of scanning tunneling microscopy, and the methods of spectroscopy. Part 2 deals with the structure of the specimen and the probe tip, the two basic elements involved in image formation. The discussion is mainly concerned with the surfaces of crystalline solids, their thermodynamic properties, and the defects of real surfaces. The preparation of the tip for scanning tunneling microscopy is then described, along with general aspects of specimen preparation. Part 3, with the title "Related Techniques and Applications", includes an introduction to scanning atomic force microscopy, probably the most important of the further developments based on the scanning probe microscopy principle. This part is completed by accounts of applications of scanning tunneling microscopy in electrochemistry and biology.

The book gives a good overview of the subject, and treats the most important experimental and theoretical aspects with appropriate thoroughness. However, the choice of applications strikes me as being rather arbitrarily restricted. Instead of the chapter on ballistic electron emission microscopy (BEEM), which should be classified as a "related technique", I would have preferred to see more space devoted

to techniques based on frictional or magnetic interactions between the probe tip and the specimen, such as nanometer-scale manipulation, optical near-field microscopy, or new developments in scanning atomic force microscopy. It is, of course, unavoidable that some restrictions must be applied in choosing the examples of applications, and how this is done must certainly depend on the preferences of the authors of the individual sections. Here the examples are in general well chosen and are representative of the whole field. It is only in the final chapter, "Biological Applications of the Scanning Probe Microscope", that I would have preferred more caution to be exercised by citing only results that are established with reasonable certainty, especially with regard to the imaging of DNA molecules, since here there is a very high risk of artefacts.

The quality of production contributes greatly to the book's readability. In a few places, however, I would have liked the figure legends to be more precise and to contain more explanation, and not all the quantities that occur in the mathematical formulas are fully explained. The extensive lists of literature references at the ends of the chapters are excellent, as also are the index and the definitions of variables and explanations of acronyms in the appendix. There are inevitably some printing errors, especially in names (Röhrer instead of Rohrer, Fostes instead of Foster, Henkl instead of Heckl, etc.), and these need to be corrected in a future edition. A German translation would help the book to reach the very wide readership that it deserves. However, the price of the present edition is too high for a student textbook.

Wolfgang M. Heckl
Fakultät für Physik
der Universität München (FRG)

Four Books on Fullerenes

Fullerenes, a novel soluble form of carbon, have now been available in preparative quantities for about three years. The fascination aroused by these hollow spherical molecules has captivated scientists from a number of different disciplines, and many have become involved in intensive research on this class of compounds. The soccerball-shaped (or football-shaped) molecule buckminsterfullerene (C_{60}) has rapidly become one of the most thoroughly studied in all parts of the world, as is evident from the large numbers of original papers, review articles, and conference reports that have appeared since September 1990. This field of study has now developed to a stage where monographs are in order, as is shown by the recent publication of four books.

Buckminsterfullerenes. Edited by *W. E. Billups* and *M. A. Ciufolini*. VCH Verlagsgesellschaft, Weinheim/VCH Publishers, New York, 1993. 339 pp., hardcover DM 96.00.—ISBN 3-527-89608-2/1-56081-608-2

In this book of 13 chapters some of the physicists, chemists, and theoreticians who have been involved in work on fullerenes from its beginnings summarize their own research. This multiauthor approach has the advantage that the individual contributions are of a very high quality, but it does mean that some overlapping of subject matter is unavoidable. The "fullerenes era" began with the mass spectrometric investigations of the C_{60} cluster, as is very nicely described by R. F. Curl in Chapter 1. He also includes a brief account of the discovery of the "empty" fullerenes and of endohedral metallofullerenes. In Chapter 2 H. W. Kroto, one of the discoverers of the fullerenes, and his coworkers describe their research, ranging from radioastronomical and chemical studies of the cyanopolyynes, through the discovery of the spherical cluster, up to the current work on chemical modifications of the fullerenes. They also briefly discuss the preparation of fullerenes in an arc discharge and their separation, isolation, and physical properties. The impressive results obtained by the Sussex group on the halogenation of C_{60}, on the solid state properties, on the alkali metal superconductors, and on the "bucky tubes" and giant fullerenes complete this chapter, which is a miniature "fullerene story" in its own right within the book. In Chapter 3 F. Diederich and coworkers describe the methods used to isolate the various fullerenes, in a lucid presentation similar to a laboratory procedure for separation of analytical samples. The interplay between theory and experiment has proved to be especially fruitful in research on fullerenes, and in the next chapter this is well illustrated by studies to determine the structures of the higher fullerenes such as the chiral form C_{76} or on the isomerization of fullerenes. Next come two purely theoretical chapters, one by Scuseria on ab initio calculations leading to structures for C_{60}, its hydrogenated and fluorinated derivatives, giant fullerenes, and dwarf fullerenes, and the second by White and coworkers on theoretical predictions of the properties of fullerene derivatives. These chapters are also of considerable interest to preparative chemists, since the observed reactivities of the fullerenes correlate very well with the calculated geometrical and electronic structures. The next three chapters are concerned, mainly from a theoretical standpoint, with the important topic of the electronic properties of C_{60}, which leads up to the superconductivity of the alkali-metal doped fullerenes. The last four chapters are experimentally orientated; the aspects of fullerenes treated here are their endohedral gas phase chemistry, their electrochemistry, and preparative organic chemistry. After reading in this book such items as H. Schwarz's impressive results on helium inclusion complexes, or F. Wudl's very lively account of the historical development of fullerene chemistry, the newcomer to the field will already have acquired a good knowledge of the chemical properties of C_{60}.

The Fullerenes. Edited by *H. W. Kroto, J. E. Fischer* and *D. E. Cox*. Pergamon, Oxford, 1993. 314 pp., hardcover £ 29.95.—ISBN 0-08-042152-0

This monograph too has been put together on the multiauthor principle. It contains two introductory articles by the editors and 23 individual contributions by well-known researchers in the fullerenes area, which are grouped in two sections. Many of the names represented in the book reviewed above occur again here. Not surprisingly, therefore, a good many of the articles in the two books are quite similar; this is the case, for example, in the contribution by Olah's group, although the treatment here is considerably more detailed. The contents of the first part of the book are arranged in exactly the same form as has appeared in special issues of the journal *Carbon*, also published by Pergamon. The arrangement is in fact very good, as exemplified in the article "Some Well Characterized Reactivities of Buckminsterfullerene (C_{60})", by Fagan and coworkers (DuPont), which provides impressive evidence of the capabilities of this group. Like the previous one, this book covers the entire field of fullerenes research, but here the treatment is more detailed. It is therefore intended not so much for the reader seeking a general overview of fullerenes but rather for the specialist wanting more specific information. However, this does not apply to every article. For example, readers wishing to know about the discovery of the fullerene synthesis will find it well described in the first article, by Krätschmer and Huffman

 © VCH Verlagsgesellschaft mbH, D-69451 Weinheim, 1994 0570-0833/94/2121-2227 $ 10.00+.25/0

who made that discovery, and for those interested in the superconductivity of fullerenes the two articles by Holczer et al. and by Schlüter et al. offer a good introduction. However, on the whole the book is mainly a collection of specialist contributions. These have been put together in a way that is to some extent structured, starting with descriptions of the fullerenes then going on to deal more specifically with the chemistry and physics of fullerenes in the solid state. In a rational sequence (though one that is not always strictly followed), the articles deal in turn with the discovery of the fullerenes, mass spectrometric studies, isolation and characterization, the chemistry of fullerenes, superconductivity, and solid state properties. Despite the fact that research on fullerenes continues to progress very rapidly, with the risk that any book is already out-of-date as soon as it is published, this compilation represents the most important current knowledge covering a wide variety of topics, especially in the articles on physical and theoretical aspects.

Fullerene C_{60}. History, Physics, Nanobiology, Nanotechnology. By *D. Koruga, S. Hamerloff, J. Withers, R. Loutfy* and *M. Sundareshan*. Elsevier, Amsterdam, 1993. 380 pp., hardcover HFl 200.00.—ISBN 0-444-89833-6

This book contains poems, cartoons, and a good deal of Egyptian and Greek mythology. D. Koruga, the principal author, does not always succeed in establishing a clear connection between this material and the fivefold symmetry elements of C_{60} or the "biofullerenes". Serious research on fullerenes is at best only touched on briefly. In some cases published work that is mentioned in the text along with its authors does not appear at all in the bibliography. In one of the collages a cover picture from the journal *Science* showing C_{60} as the Molecule of the Year is needlessly combined with one of the authors' own scanning transmission micrographs. Sometimes Koruga has illustrated the text with photographs on which he appears superimposed, and a dream that he once had is classed as one of the most important events in the history of the fullerenes. The book is divided into three parts entitled "Science of Fullerenes", "From Nanobiology to Nanotechnology", and "Fullerene C_{60}: Production, Technology and Applications". The first part begins with a historical survey from the viewpoint of the authors. This is followed by a discussion of icosahedral symmetry which begins with ancient China, then sets out some general symmetry rules which are normally covered in a first-year course. Next the physical properties of C_{60} are discussed, with a strong emphasis on STM studies. The second part has scarcely anything to do with fullerenes; the topics discussed include biological molecules and slipper animalcules (Paramecium). This part ends by discussing a number of topics including the "Herz model" and the "C_{60} light machine", in which the authors establish a "pentagonal" connection between C_{60}, the birth of Christ, and the beginning of civilization. In the third part we at last learn a little about fullerene and potential applications. This book will certainly seem very strange to the non-specialist reader; for the specialist it has no value other than as a talking point.

The Fullerenes. New Horizons for the Chemistry, Physics and Astrophysics of Carbon. Edited by *H. W. Kroto* and *D. R. M. Walton*. Cambridge University Press, Cambridge, 1993. 154 pp., paperback £ 17.95.—ISBN 0-521-45917-6

In October 1992 the Royal Society held a seminar, of which H. W. Kroto was one of the organizers, entitled "A Post-Buckminsterfullerene View of the Chemistry, Physics and Astrophysics of Carbon". This little book contains reprints of 14 papers by the participants, all of whom are well known in the field, together with the main contributions to the discussion sessions following each paper. The book begins with an excellent contribution by Osawa on the relationship between the C_{60} structure and two-dimensional aromatic systems. This is of particular interest in view of the fact that the C_{60} structure was first envisaged by Osawa, as a three-dimensional "superaromatic molecule", as long ago as 1970. Since then not only Osawa's predictions, but also many of those described in the second paper by D. E. H. Jones (better known under the pseudonym Daedalus), have since been confirmed. The giant fullerenes and tubes that were postulated have since been observed experimentally. Another very exciting prediction by Daedalus that very large giant fullerenes, because of their low density at ambient temperature and pressure, should be supercritical liquids, has still to be put to the test. In the next article R. F. Curl (see the review of the first book) again reports on mass spectrometric investigations into the formation of fullerenes. The following contribution on the synthesis of fullerenes is again written by the discoverers of the method, Krätschmer and Huffman. Next there are articles on the structural systematology of the fullerenes (Fowler), the electronic properties of C_{60} (Haddon), studies of interstellar matter (Jura and Pillinger), and the reactivity of C_{60} (Taylor). Kroto and Walton then contribute a review of their classic investigations on polyynes and fullerenes, and Mackay and Terrones discuss theoretical aspects of fullerenes with negative curvatures. The book ends with a look at the common structural features of the fullerenes and geodesic domes. The compact form of this little book, the good choice of topics, and the high quality of the individual articles, which never wander off into unnecessary detail, make it well worth reading, both for interested non-specialists and for those closely involved with fullerenes.

Andreas Hirsch
Institut für Organische Chemie
der Universität Tübingen (FRG)

 © VCH Verlagsgesellschaft mbH, D-69451 Weinheim, 1994 0570-0833/94/2121-2228 $ 10.00+.25/0

From an Insecticide to Plato's Universe—The Pagodane Route to Dodecahedranes: New Pathways and New Perspectives

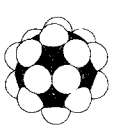
Horst Prinzbach* and Klaus Weber

Dedicated to Professor Christoph Rüchardt on the occasion of his 65th birthday

The original concept for the synthesis of pentagonal dodecahedranes by the conversion of structurally similar, high-energy [1.1.1.1]pagodanes relied on catalytic dehydrocyclizations. As a consequence, preparative limitations were preprogrammed. With multiple functionalization of these pagodanes, alternative cyclization methods became viable. These efficient processes allowed access to a multitude of pentagonal and nonpentagonal, carba- and heterocyclic dodecahedral skeletons with widely variable substitution patterns. Such a roundabout route provided the $(CH)_{20}$ basic framework with high efficiency, and long-lacking thermochemical data could be ascertained calorimetrically. In spite of the unusually pronounced pyramidalization of their olefinic centers, singly and doubly unsaturated dodecahedranes with isolated C=C bonds proved to be kinetically quite stable, but underwent dimerization on thermal activation. Dodecahedranes with a higher degree of unsaturation (trienes–decaenes, C_{20} fullerene?) have been found so far only in the gas phase. Higher fullerenes, including C_{60}, have been identified by mass spectrometry after exposure of halogenated dodecahedranes and pagodanes to a 248-nm excimer laser. Transannular electron delocalization has been verified for the "slender" pagodane/isopagodane and even for the "spherical" dodecahedrane cages.

Prologue

For many years the $(CH)_{20}$ hydrocarbon dodecahedrane **1**, organic chemists' transliteration of the platonic dodecahedron[1] with its historical and cultural background, which has more recently been recognized as the perhydrogenated C_{20} fullerene **2**, had the aura of a utopian object. In fact, worldwide efforts to synthesize this hydrocarbon, which is intriguing for a number of reasons, had remained unsuccessful.[2] Confronted with the task of interconnecting 20 methine units with stereochemical control through 30 C–C bonds to form twelve five-membered rings, even the Almighty apparently had given up—neither **1** nor derivatives better accessible through isoprene metabolism have ever been found in Nature. However, the "Mount Everest of alicyclic chemistry" was finally conquered, and the ascent mastered by the Paquette team at Ohio State University stands out as a landmark in organic synthesis.[3] Yet for all its elegance, this route has the intrinsic disadvantage of low flexibility. Functionalization or modification of the skeleton is only possible on the finished structure[4]—a fundamental problem given the molecular symmetry.



1



2

In the parallel[2] and subsequently conducted search[5] for an alternative, if possible more direct and more versatile route only our group in Freiburg has been successful thus far.[6] We have already published reviews on the concept of this "pagodane route" to dodecahedranes and on its utilization particularly for the preparation of the parent compound **1**.[7, 8] In the meantime the conceptual advantages of this route, its variability and effi-



Artist: Myriam Thyes, Master of Fine Arts at the Kunstakademie Düsseldorf, 1993.

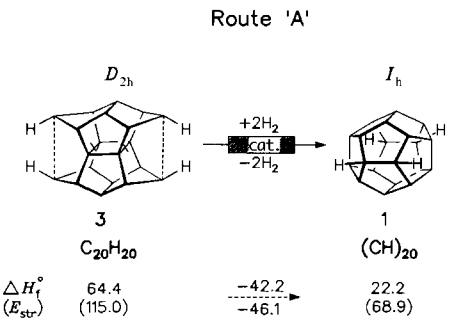
[*] Prof. Dr. H. Prinzbach, Dr. K. Weber
Chemisches Laboratorium
Institut für Organische Chemie und Biochemie
Albertstrasse 21, D-79104 Freiburg (FRG)
Telefax: Int. code +(761)203-5987

 © *VCH Verlagsgesellschaft mbH, D-69451 Weinheim, 1994* *0570-0833/94/2222-2239 $ 10.00+.25/0*

ciency, have been confirmed numerous times, and new aspects of the chemistry of these cage compounds have arisen. In order to facilitate evaluation of the type and extent of the progress we will briefly recapitulate the basic concept and previous status of the project. The reader will hopefully share in the "ups and downs" and the surroundings of a venture full of surprises, and the unceasing confrontation inevitable in a journey of this length with the necessarily high demands concerning the efficiency of each individual synthetic step.

1. The Concept

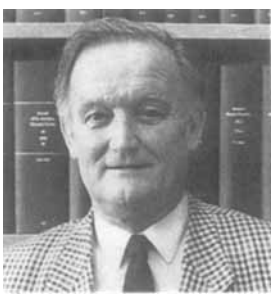
Two prominent properties of the undecacycle **1** are its high symmetry (I_h) and low energy content. The symmetry directed every synthetic approach that relied on construction of this C_{20} unit from two subunits ($C_{10} + C_{10}$, $C_{15} + C_5$).[2] The fact that **1** is the energy sink, the stabilomer,[9, 10] of the $(CH)_{20}$ family, provided incentive for Schleyer's group and others[2, 11] to attempt to rearrange energy-rich and suitably structured $C_{20}H_{20}$ isomers into **1**—as exercised with great success in "adamantane land". Even though this strategy had met with failure in various versions (or just for that reason?), such a procedure with the $C_{20}H_{20}$ pagodane **3**[12] as precursor (Route 'A', Scheme 1) was fascinating:[13] The high structural similarity of **3** to **1** is reflected in the symmetry, D_{2d} versus I_h (and also in the IUPAC names). After all, with twelve cyclopentane rings already present in **3** only two of the strained cyclobutane bonds have to be hydrogenolytically cleaved and two transannular bonds formed by dehydrogenation. Moreover, the gain in enthalpy of formation and strain energy, 40–50 kcal mol^{-1} (according to MM2 calculations), is considerable. Admittedly, one could only speculate on the course of the one-pot transformation **3** → **1** (Route 'A'), which in the end was a sequence of numerous individual steps, and on the potential intervention of kinetically "dead" intermediates. Still, it was undisputed that for steric reasons the formation of a transannular bond between the methylene groups could only be brought about after opening of the respective lateral cyclobutane bond. The controlled stepwise sequence **3** → **4** → **5** → **6** → **7** → **1** (Route 'B', Scheme 2) was the preferred alternative in the event that the "black box" variant 'A' would not be realizable. Route 'B' merged with the Paquette synthesis at the stage of secododecahedrane **7**. It should be noted that at each step in the sequence consisting of the $2\sigma \rightarrow 2\pi$ cleavage (**4**), hydrogenation (**5**, **6**), and dehydrogenation (**7**, **1**), the convexity of the molecular skeleton (d_1 in Å) increases and the lateral distance (d_2) decreases, thereby favoring lateral C–C connection. The listed enthalpies (from MM2 calculations)[14] differ markedly in absolute terms from those measured calorimetrically (see Table 1), but as with the strain energies, the trend is reliable, except with regard to the ring opening **3** → **4**. This latter step has been shown unequivocally to be endothermic;[15] the MM2 calculations underestimate in known fashion the destabilization of the diene by the transannular π,π repulsion.[13, 16] Yet, complications had to be anticipated with these "hyperstable" olefins[17] given the low exothermicity of the two hydrogenation steps—at roughly 15 kcal mol^{-1} only about half of the standard value of 30 kcal mol^{-1}—and the parallel increase in strain energy. In the original concept for Route 'B',[7, 8] cyclizations *before* the hydrogenations **4** → **8** and **5** → **9** were not formulated. Because of the considerable positive changes in enthalpy and strain under the conditions of the dehydrogenating cyclization (**7** → **1**), isolation of unsaturated dodecahedranes, predicted to be extremely reactive,[3] was not expected to be possible. Route 'C' (Scheme 3), the alternating sequence of hydrogenolysis (**10**, **7**) and formation of C–C bonds (**11**, **1**) by dehydrogenation was, a priori, only a third choice. Particularly the endothermic cyclization **10** → **11** was judged as highly



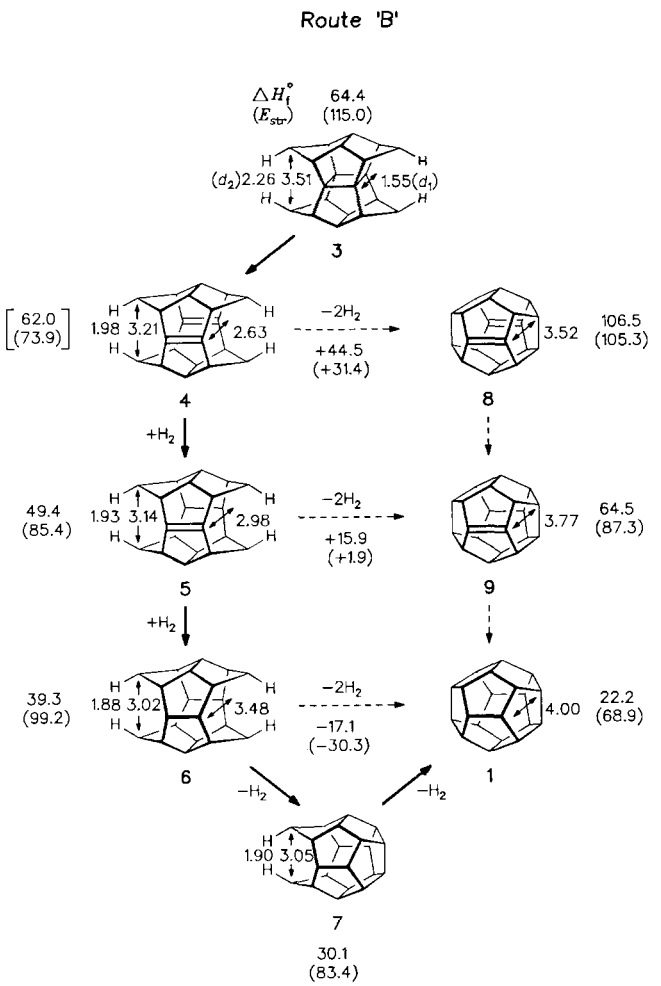
3 : undecacyclo[9.9.0.0^{1,5}.0^{2,12}.0^{2,18}.0^{3,7}.0^{6,10}.0^{8,12}.0^{11,15}.0^{13,17}.0^{16,20}]icosane

1 : undecacyclo[9.9.0.0^{2,9}.0^{3,7}.0^{4,20}.0^{5,18}.0^{6,16}.0^{8,15}.0^{10,14}.0^{12,19}.0^{13,17}]icosane

Scheme 1. Here and in all following schemes the ΔH_f° and E_{str} values (MM2) are given in kcal mol^{-1}.



Horst Prinzbach was born in 1931 in Haslach im Kinzigtal (Black Forest, Germany). After studying chemistry in Freiburg, he obtained his doctorate there (1955, A. Lüttringhaus) and spent two years (1957–1959) as a post-doctoral fellow at Yale University, working with W. von E. Doering. He obtained his "Habilitation" at Freiburg in 1962 ("Sesquifulvalenes—A Contribution to the Chemistry of 'Nonbenzenoid Aromatics'"). In 1965 he accepted a chair of organic chemistry at the University of Lausanne (Switzerland), and in 1969 he returned to the University of Freiburg. Besides a number of other awards, Horst Prinzbach received the Adolf-von-Bayer Denkmünze of the German Chemical Society (1989). His scientific activities are centered around chemistry of "nonbenzenoid aromatics", preparative organic photochemistry, polyelectron pericyclic processes, total syntheses of aminoglycoside antibiotics, and in particular the syntheses and properties of unusual structures (including homobenzenes, pagodanes, dodecahedranes).

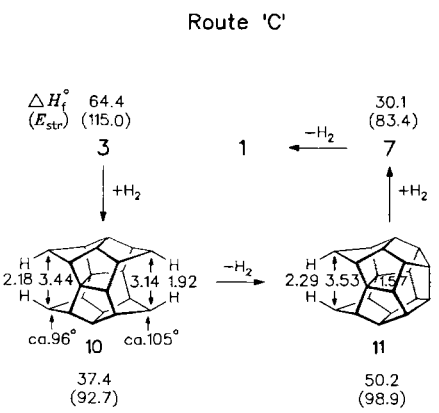


Scheme 2.

Table 1. Calculated (MM2, top line) and experimentally determined (bottom line) values for ΔH_f° and E_{str} (the latter in brackets) [kcal mol^{-1}] for pagodanes **3** and **17**, and for dodecahedranes **1** and **68**.

3	17	1	68
64.4 (115.0)	−91.7 (130.8)	22.2 (68.9)	−183.4 (64.7)
47.88 ±0.91 (95.57)	−107.33 ±0.85 (110.03)	(22.4 ±1 (61.4 ±1))	−151.80 ±0.82 (61.36)

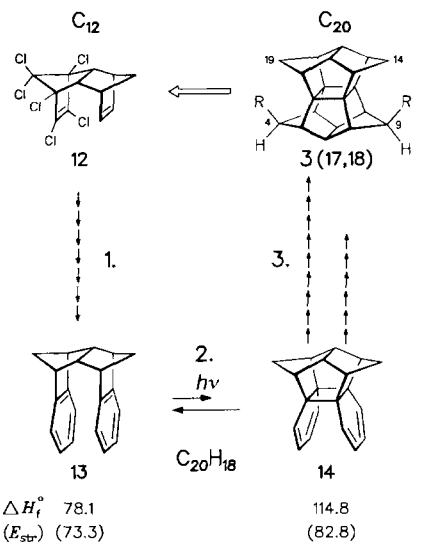
problematic. In reality, this route was accomplished only along other methodical approaches (see Scheme 14).



Scheme 3.

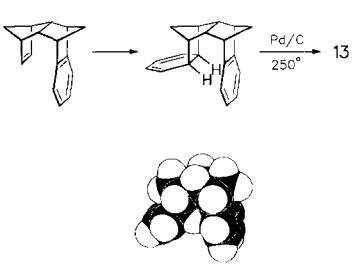
2. The Basis—From Isodrin to Pagodanes

The value of our concept for the ascent to dodecahedrane **1** starting from [1.1.1.1]pagodane **3** was dependent on an acceptable "price" for **3**. This prerequisite could be fulfilled with the optimized reaction sequence subdivided in Scheme 4 into three stages. The starting material was (at the time of planning) the cheap, industrially produced C_{12} chlorohydrocarbon isodrin **12**. (In the meantime this product, permitted only for limited use as an insecticide, has become considerably more expensive.) If one considers the grand total of about 60 (or 45) changes in bonding on the way from **12** to **3** (or to the diesters **17**/**18** of primary interest), which are compressed into 14 (11) reaction steps with consequent exploitation of the given symmetry situations, the overall yield of 22–24% achieved implies a yield of over 95% for each individual functional change.[18] This route leaves no room for further optimization; it constitutes the basis of all our pertinent activities during the last few years.



Scheme 4.

In the first stage two benzenoid rings were annulated onto **12**. The single annulation was achieved following a reliable method by Mackenzie.[19] For the second annulation, conducted analogously, an apparently trivial dehydrogenation leading to aromatization became an early stumbling block—still not completely overcome. In this reaction the hydrogen atoms deep in the opposite π electron cloud are rather inaccessible for the catalyst.



An extensive study into optimization of this dehydrogenation concluded with a protocol that prescribed heating the dihydro precursor to 250 °C with an almost tenfold amount of Pd/C. The costs, nevertheless, could be held within limits, as the catalyst remained active over several

cycles and could be reprocessed subsequently. Yields of 80% were obtained reproducibly for 16-g runs. There are good reasons to assume that the transannular π,π repulsion enforced under these extreme conditions—an indication is the pyramidalization, if only weak, of the *o,o'*-C centers—is instrumental for the subsequent photoreaction. According to X-ray structural analysis (cf. Fig. 1) the almost perfectly synperiplanar ("face-to-face") benzenoid chromophores in the annulation positions are only 3.04 Å apart.[20]

The benzo/benzo photocycloaddition **13** → **14**, the second stage, is essentially the key reaction of the concept[21]—the discovery of the formation of a four-membered ring between nonfunctionalized benzenoid rings, previously unknown in arene photochemistry, became the initial spark of the pagodane/dodecahedrane project. Neither direct irradiation of **13** with light of wavelength $\lambda > 280$ nm nor sensitized excitation produced any visible effect. However, when a dilute degassed solution of **14** was irradiated with monochromatic light at 254 nm, an equilibrium mixture of **13** and **14** (7:3) resulted. For a photoreaction of this type the lack of any competing reaction is remarkable. The explanation: The cyclohexadiene chromophores,[22] which in **14** are σ-coupled through the cyclobutane ring, call for a much more intense long-wavelength absorption which is in the range of the charge transfer (CT) absorption of **13**. At 254 nm the extinction coefficients are roughly inversely proportional to the measured equilibrium ratio. As an additional surprise, unexpected in degree and significant for the continuation of the synthesis, photoproduct **14**, a "*syn* dimeric benzene" (Fig. 1), is thermally quite stable; its half-life at 120 °C amounts to a substantial 130 min.

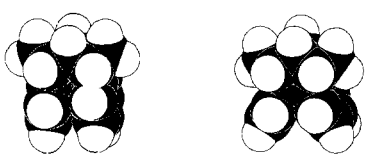
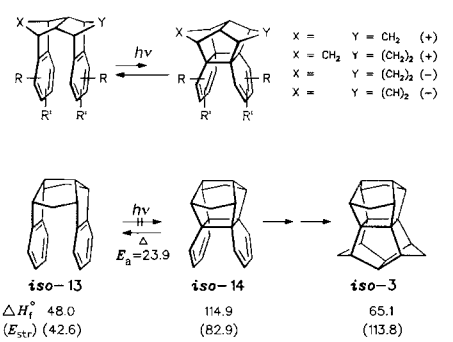
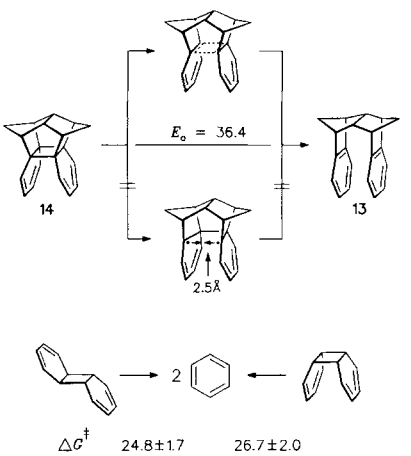


Fig. 1. Schakal plots of **13** (left) and **14** (right).

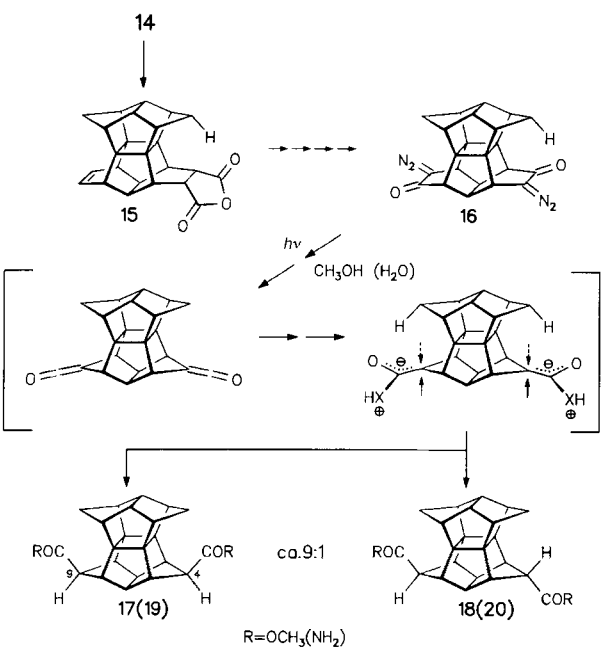
Benzo/benzo cycloadditions of the type **13** → **14** possess considerable synthetic potential. Subsequent studies including photomechanistic investigations[23] with the aim of defining the limiting conditions of this photoreaction have underlined the exceptionally favorable situation in **13** in particular with regard to transannular distance, π,π interaction, and rigidity of the skeleton.[24] The rather narrow scope of the reaction became obvious: cycloaddition occurs with various functionalizations of **13** (R,R')[25] and after homologation of one bridge (X,Y) but not after homologation of both bridges.[26] The cycloaddition *iso*-**13** → *iso*-**14** on the way to [1.1.1.1]isopagodane (*iso*-**3**) was also unrealized.[27]



The degree of kinetic stabilization conferred on **14** by its molecular corset, and quantified by kinetic data, was helpful, if not essential, for the project. For comparison, according to the work of Schröder, Oth et al.,[28] Grimme et al.,[29] Berson et al.,[30] and Yang et al.,[31] noncorseted *anti*/*syn* dimeric benzenes fragment even at room temperature. *iso*-**14**, Prepared in a roundabout way from *iso*-**13**, is also relatively labile, as the skeleton of *iso*-**14** cannot deliver comparable "kinetic protection".[33] The cleavage **14** → **13** is a special case mechanistically. Roth, Doering, et al.[33] argue that the rigidity prohibits the separation of the radical centers to the extent necessary for bond cleavage to occur by a radical pathway. Instead a concerted symmetry-forbidden [2 + 2] cycloreversion pathway via an antiaromatic four-centered transition state is followed.



The third stage consists of converting the tricyclododecatetraene part of **14** into the lower pagodane "half" (Scheme 5) by the domino Diels–Alder addition to **14** giving **15**,[34] and ring

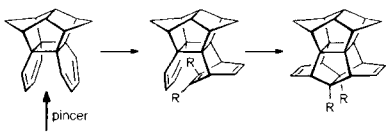


Scheme 5.

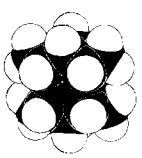
contraction on both sides of the [2.2.1.1]pagodane through the bis(diazoketone) intermediates (C_s- and C_2-**16**). The persistance of **14** was once again fortunate for the almost quantitative regio- and stereospecific addition yielding **15** (80 °C). A cage effect, irrelevant for the preparation of **3** but essential for the subsequent developments, dictated the stereochemical outcome of the photo-Wolff rearrangement. A roughly 9:1 mixture of

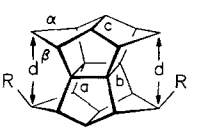
syn,syn and *syn,anti* diesters **17**/**18** (or the corresponding dicarboxylic acids) was obtained from anhydrous methanol (or moist tetrahydrofuran). The addition of methanol (water) to the ketene intermediates proceeds with obviously high (unfortunately not complete) steric control; *anti* protonation enforces the less favorable *syn* placement of the ester (acid) functions, which is energetically more "expensive" by about 7 kcal mol^{-1} (see Table 1). The base-catalyzed conversion of **17**/**18** into the thermodynamically more stable *anti,anti* diesters proceeded correspondingly slowly. The dicarboxamides **19**/**20** were produced directly by photolysis in liquid ammonia, again in a ratio of approximately 9:1.

The "pincer" addition to **14**, also of interest with regard to the directed multiple functionalization of **1**, requires "slim", rodlike dienophiles. This particular pathway dominates, for example, in the high-pressure addition of dicyanoacetylene. The cooperative [4 + 2 + 2 + 4] mechanism plausible given the spatial relationships in **14** is, however, no longer considered.[35]



In spite of their high strain pagodanes are thermally unusually stable. The waxy hydrocarbon **3** melts without decomposition at 243 °C (260 °C, high-pressure differential thermal analysis[36]) and remains unchanged up to at least 600 °C (gas phase). A defined fragmentation pattern is not evident in the electron impact mass spectrum; generally the M^+ signals are by far the most intense. The $^{13}C,H$ coupling constants for the tertiary hydrogen atoms reflect the relatively high s character caused by the strained structure. X-ray structural analyses, for example for **3**[37] and **17**[12] (Fig. 2), provide evidence for some of the trends





R = H (CO_2CH_3)

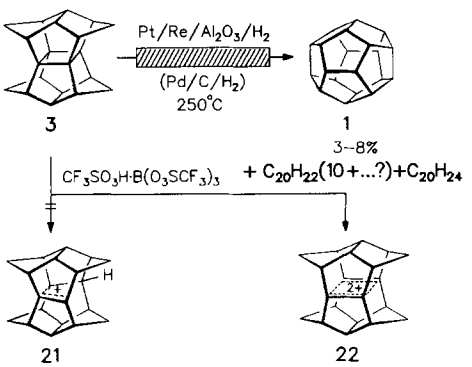
a: 1.549 (1.552) α: 96.1 (95.0)
b: 1.573 (1.589) β: 99.4 (99.5)
c: 1.589 (1.625)
d: 3.530 (3.611)

Fig. 2. Selected structural data (a–d in Å, α,β in °) for pagodanes **3** and **17**.

considered important for the chemical behavior (see Scheme 1). The "lateral" bonds in the four-membered rings (b) are significantly longer than the "frontal" ones (a); the α and β angles in the norbornane subunits deviate only slightly from those of the parent norbornane. The anticipated increase in transannular strain (Table 1) caused by the *syn* ester group is reflected by the lengthening particularly of the "ridge" bonds (c). The Schakal plot of **3** (Fig. 2, left) shows the van der Waals contact of the *syn* methylene hydrogen atoms in the half-cages as well as the shielding of the central four-membered ring from all sides by the surrounding hydrogen atoms.

3. The First Dodecahedranes—Limitations of the Dehydrocyclization Strategy

With the availability of pagodanes in decigram quantities the race appeared to be over. The catalyzed conversion **3** → **1** (Route 'A'),[11] which relied on the expertise of the Schleyer and Maier groups, ended with brilliant success and bitter disappointment simultaneously (Scheme 6). The catalysts optimized

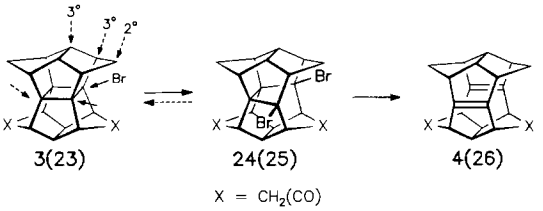


Scheme 6.

for such purposes actually did provide **1**, but the reproducible yields remained at 3–8% (besides 19–46% secopagodane **10** and additional $C_{20}H_{22}$ and $C_{20}H_{24}$ components), far below that expected and thus ruling out further preparative utilization. It could only be said that **10** was a "dead end" in this "black box" reaction (Route 'C') and not a precursor to **1**, and that **5** (**6**) was not among the by-products.[6]

According to the findings of Olah et al. pagodane **3** reacted with high selectivity in super acids,[38] successful reagents for catalytic isomerizations in "adamantane land", although **1** was not obtained as hoped. Instead two electrons were removed from the central four-membered ring of **3** to give the surprisingly persistent D_{2h}-symmetrical dication **22**,[37, 39] the unusual properties of which will be referred to later (Section 10). Even with super acids of relatively low oxidizing power, protonation of **3** as a potential entry into the isomerization cascade was outweighed by oxidation. Stabilization by homoconjugation as in the independently generated 2-secopagodyl cation **21**[39] is apparently of no help.

When secopagodane **10** was excluded as a precursor to **1** in the above "black box" reaction, bissecodiene **4** became a viable alternative. The directed preparation of **4** from **3** evolved as a serious challenge for Route 'B'. The expectation, based on the MM2 calculations (see Scheme 2), of isomerizing **3** thermally to **4**, turned out to be naive. Naphthalene was not exactly the desired goal of the gas-phase thermolysis, but its formation pointed to a mechanistically and thermochemically informative fragmentation pathway. Unfavorable oxidation potentials prohibited the isomerization via the corresponding radical cations, which would have been especially attractive as a catalytic process. The two-step procedure of bromine addition and fragmenting bromine elimination established for other small-ring propellanes (Scheme 7)[40] was the solution. Given the potential for competing processes, the sequence proceeded with surprising selectivity. The reaction of **3** with bromine, thermally slow



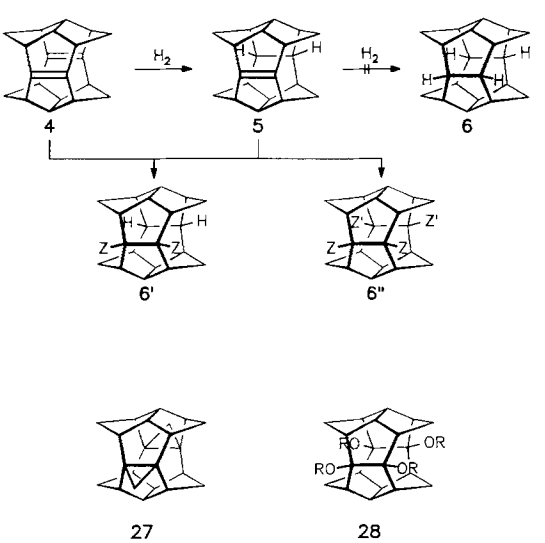
Scheme 7.

but fast under irradiation, yielded exclusively the addition product **24** (extremely prone to hydrolysis, cf. **21**!) within the short time (minutes) necessary for total conversion. Reversion back to **3** during the subsequent elimination, which is significant at lower temperature, remained minimal (< 5%) above 150 °C. It should be noted that the carbonyl groups in pagodanedione **23** reduce both the rate of conversion and the rate of hydrolysis of the intermediate **25**, but not the uniformity of the reaction leading to the dienedione **26**.

The absence of radical substitution in the course of the conversions **3(23)** → **24(25)** must be regarded as fortuitous, in view of the structural similarities of **3** to norbornane and the known radical substitution pattern of the latter.[41] In the [2.2.1.1]pagodane skeleton, as in bicyclo[2.2.2]octane, radical attack takes place preferentially at the [2.2]bridgeheads.

Because of its unusually close, nearly perfectly synperiplanar C=C bonds, bissecododecahedradiene **4** is the prototype of a per se interesting class of cage olefins (see Section 10). The through-space (TS) homoconjugation, which approaches classical π,π conjugation and is evident by UV and photoelectron spectroscopy,[42] causes **4** to be highly reactive vis-a-vis electrophilic or radical partners. The π bonds are formally part of *cis,cis*- and *trans,trans*-1,6-cyclodecadiene rings;[43] because of the C_3 spacers, the TS component of the π,π splitting of the PE bands is not adversely affected by a through-bond contribution.[44] As a consequence of the increase in strain associated with the sp^2 to sp^3 rehybridization (hyperstability), these olefins can act at best only to a limited extent as alkene components in reversible cycloadditions (potential "protective measures").

The difficulties predicted for the olefins **4** and **5** in the catalytic hydrogenation indeed dealt a fatal blow to Route 'B'. Compound **4** could still be hydrogenated to **5**—with reduction of the π,π repulsion as driving force—but the latter was a dead end. Under forcing conditions dehydrogenation (**3**, **4**) and isomerization (**10**) were detractions. Irreversible methods for saturation including cyclopropanation (e.g. **27**), epoxidation, and *cis* hydroxylation (e.g. **28**) are not subject to this limitation (Scheme 8). Multiply modified (Z,Z') derivatives (**6'**,**6"**) with shortened C,C and H,H distances across the cavity, favorable for the dehydrocyclization, became accessible. The X-ray structures of **27** and **28** (Fig. 3), as representatives of the bisseco series, underline the relation between the hybridization of the formerly olefinic centers, the convexity of the cage, and the lateral distances. With a C1–C11 distance of 3.69 Å, compound **28** is already similar to the dodecahedrane; the H ··· H distances across the cavity of 1.70–1.83 Å reveal considerable compression.[45]



Scheme 8.

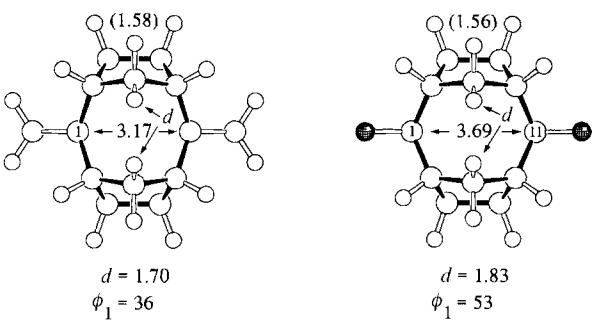
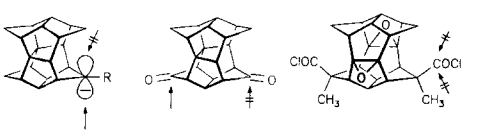


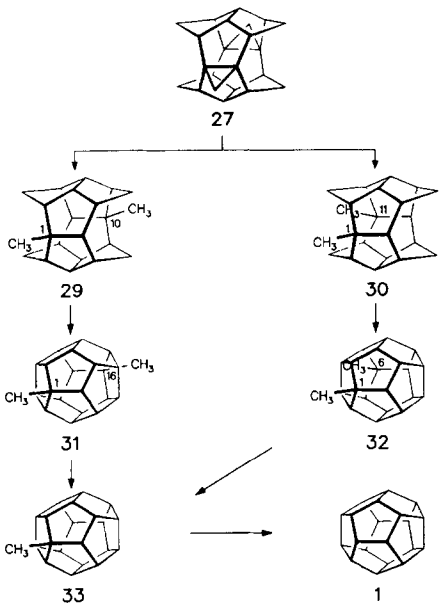
Fig. 3. Selected structural data (*d* in Å, φ in °) for bissecododecahedranes **27** (left) and **28**. R = $CH_2C_6H_5$ (right).

Three examples demonstrate to what extent increasing contraction of the half-cage affects the "lateral chemistry" when going from pagodanes to seco structures. Protonation (alkylation) on the open side takes place exclusively from the *anti* direction; hydrazone formation with "open" ketones is ruled out, and α-methylated *syn* acid chlorides are stable toward hydrolysis.



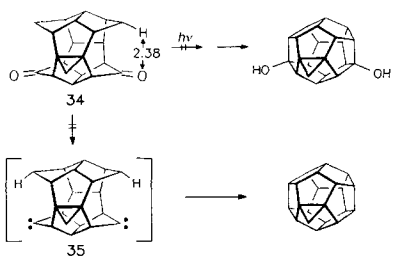
For the final dehydrocyclizations (cf. **6** → **7** → **1** in Scheme 2), mixtures of the substrate with as much as a 100-fold excess of catalyst (Pd/C) are heated up to 250 °C. It was no surprise that the cleavage of the C-Z/Z' bonds in the precursors **6'** (**6"**) and dehydrogenative olefin formation (cf. **5** → **4**) became unavoidable. One of the prominent exceptions is presented in Scheme 9. In the dehydrocyclization of the dimethyl derivatives **29**/**30**, generated by hydrogenolysis from the dicyclopropa precursor **27**, competing dehydrogenation is excluded. With 75–80% dodecahedranes **1** and **31**–**33** the overall result was excellent; however, total dealkylation to give pure **1** or separation into the individual components was only possible with considerable loss of material.[46]

As prelude to the next section a supplement: The lateral C–C bond formations implied in the strategy of Route 'B' (Scheme 2) are, in principle, variants of the widely used 1,5-cyclization in conformationally more or less fixed cyclooctanes.[47] What could be more straightforward



Scheme 9.

than to apply those proven methods to difunctionalized bissecododecahedranes such as the 4,9-diketone **26** and its derivatives, or to "dicarbenes" derived therefrom? To make a long story short, all activities in this direction ultimately came to nothing. The problems involved are exemplified with the two alternative methods given in Scheme 10. Under

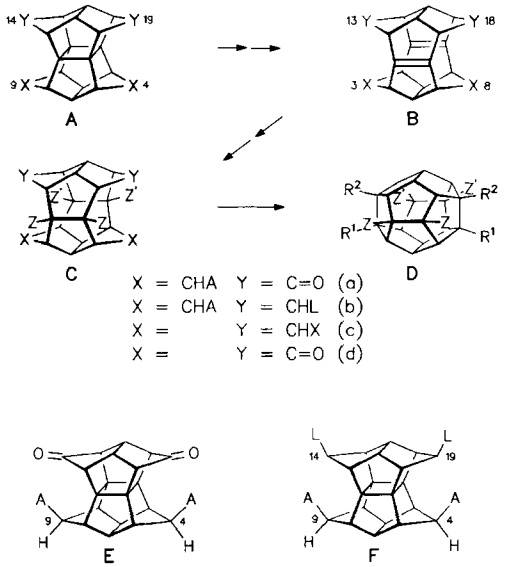


Scheme 10.

the usual excitation conditions for Norrish type II reactions the bissecocyclopropadione **34** remained unchanged; hydrogen transfer could not be induced even with the frequently more favorable solid-state irradiation, although the O–H distances were clearly below the critical limit. The Achilles' heel: the relative position of the partners in the rigid half-cage deviates significantly from that of the ideal transition state ("in-plane orbital mechanism"). In this context it should be pointed out that the homo-Norrish type photoreaction played a central role in the Paquette synthesis.[3] Carbene insertion (**35**), frequently successful especially in the polyquinane area,[48] was not applicable in these half-cages; either the carbene precursor could not be prepared or the carbene could not be liberated.

4. The Breakthrough—Dodecahedranes from 4,9,14,19-Tetrafunctionalized Pagodanes

The limitation with regard to the method of cyclization inherent to the original concept of Route 'B' should be overcome with suitably 4,9,14,19-tetrafunctionalized pagodanes (**A** in Scheme 11). "Suitable" functional groups (X, Y) are compatible with the method of opening the four-membered rings (→ **B**)

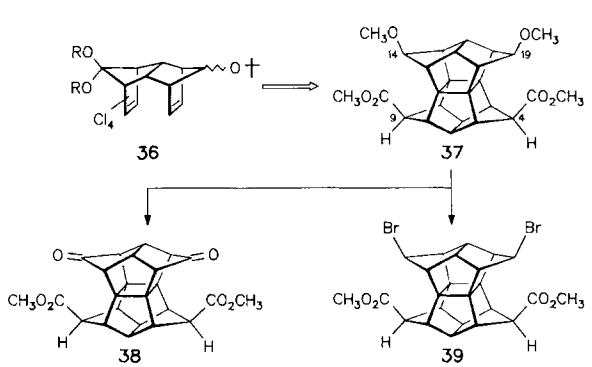


Scheme 11.

and with the saturation of the olefin (→ **C**), and permit cyclization (→ **D**) without endangering the existing substitution patterns. When these prerequisites are fulfilled, even previously blocked direct routes from unsaturated bisseco compounds leading to unsaturated dodecahedranes (**4** → **8**, **5** → **9**, Scheme 2) should become viable. Two of the alternative methods used hitherto [(a)–(d)], the aldol (Claisen) addition (a) and S_N2 substitution (b) applied to substrates of type **E** and **F**, respectively, will be dealt with here. At this point, the postulate for the activating groups A to be in the *syn* position and the leaving groups L to be in the *anti* position must be emphasized.

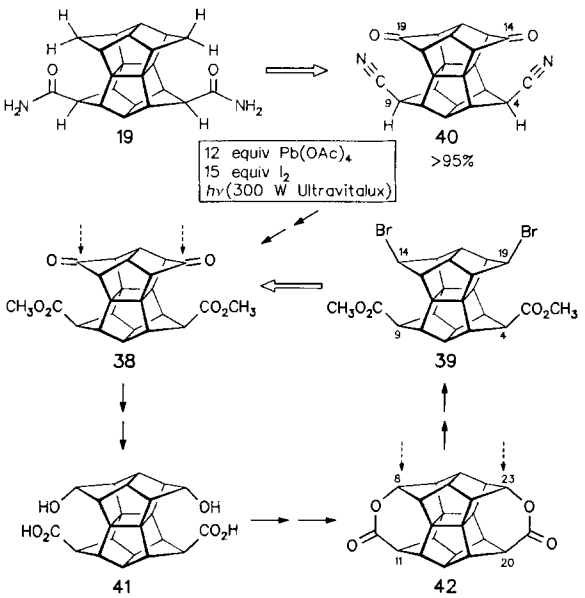
How good were the chances of functionalizing the 14(19)-methylene positions in the 4,9-disubstituted pagodanes (**17**/**19**, **23**), possibly with anchimeric assistance by the 4-*syn*,9-*syn* substituents, by using classical chemistry or biocatalysis? Or would it be better to duplicate the pagodane synthesis with a suitably modified isodrin analogue ("de novo synthesis")?

In parallel attempts the biocatalytic route was ruled out first. The expectation was, based on literature reports, that enzymatic hydroxylation could be achieved selectively for the 14(19)-positions with the directing assistance of *syn*-oriented groups such as CH_2OH, CO_2H, and $CONH_2$, which would also possibly improve the water solubility, but these hopes did not materialize.[49] Success came first with the de novo synthesis (Scheme 12).[50] The 14-*anti*,19-*anti*-dimethoxypagodane-4-



Scheme 12.

syn,9-*syn*-diester **37** (together with ca. 10% *syn,anti* isomer) was obtained from the 11,11,12-trisalkoxy-substituted isodrin analogue **36** (not exactly cheap) with roughly comparable effort but considerably lower overall yield (6.5%; ca. 84% for each of the 16 operations) along a reaction sequence that was closely patterned after the original (cf. Scheme 4). Thus, **37** provided access to ideal candidates (**E**, **F**) for the aldol (a) and the S_N2 variants (b) in Scheme 11, diketodiester **38** and 14-*anti*-19-*anti*-dibromodiester **39**, respectively. Prior to the decision whether to continue the program on this basis, the breakthrough came with the third approach (Scheme 13).[51] The

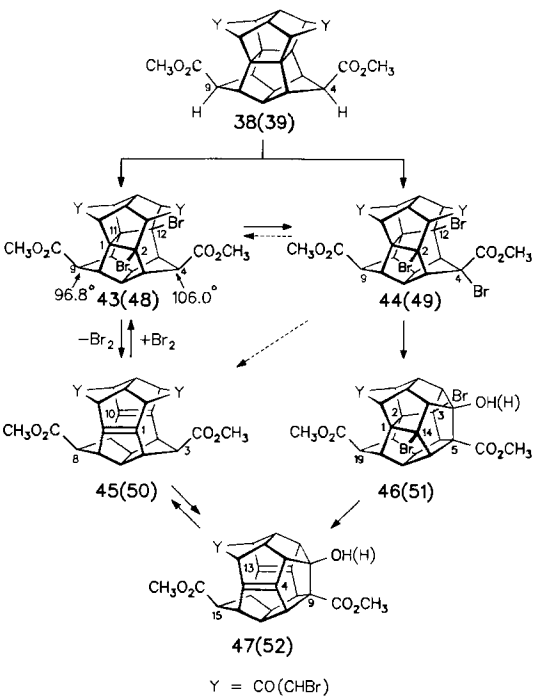


Scheme 13.

syn,syn-dicarboxamide **19** was converted into the diketodinitrile **40** by a Barton-type method in a one-pot operation. The "recipe" formulated after time-consuming optimization is detailed in Scheme 13; an almost quantitative yield was reproducible in 10-g runs. The complexity of the ketonitrile formation, the mechanistic details of which are still not clarified, was not so remarkable since oxidations ("double substitutions") by the combination of $Pb(OAc)_4$ and I_2, and photochemical conversion of iodoamides into nitriles were known from the literature.[52] The supposedly unprecedented uniformity was more amazing. After all, each of the at least 14 steps proceeding through radicals—seven for each side of the molecule—had to proceed practically quantitatively. In these half-cages steric and stereoelectronic effects cooperate apparently in an optimal fashion.

In **40** the acid-labile pagodane skeleton is deactivated to such an extent that it survived the sterically strongly retarded saponification to the dicarboxylic acid without too much damage (24 h reflux in conc. HCl/acetic acid)—as will be seen an essential measure and only possible under acid catalysis. With a total yield of 15–18% for the diketodiester **38** based on isodrin **12** (compared with 6.5% for the de novo synthesis), the aldol route had an acceptable start.[53] Obviously **38** could also serve as basis for **39** and hence for the S_N2 route. An elegant solution, which was judged to be adequate at the time, was provided by the sequence of regiospecific reduction (**41**), lactonization (**42**), and regiospecific substitution (75% yield of **39** based on **40**).[54]

The next step intended in the concept (Scheme 11) was the conversion of the tetrafunctionalized pagodanes **A** into the bissecodienes **B**, following the procedure successful with the basic skeleton and simple derivatives (Scheme 14). The accumu-



Scheme 14.

lation of functionalities in pagodanes such as **38**–**40** was not, however, without consequences, both for the photoaddition and for the fragmenting elimination of bromine; the latter was favored only above 150 °C. In fact, the addition was either completely prevented (**40**) or slowed down so much that substitution primarily at the ester-bearing positions (C-4(9)) became competitive or comparably fast. Still, the aldol intermediate **38** could be selectively photobrominated to give the tribromide **44** (92%), if only at incomplete conversion. The subsequent substitution of C-9 is markedly slower, in agreement with the smaller valence angle. The fatal blow for the use of **44** in the sequential reductive substitution and elimination (**44** → **43** → **45**) was the yield of bissecodiene **45** with at best 60%. A competing reaction partly responsible for the low yield indicated the solution, once more in the form of efficient "cage control". Under hydrogenolysis conditions (Pt, 1 atm H_2) **44** underwent quantitative transannular cyclization to yield the "isododecahedrane" **46** rather than reductive substitution to give the dibromide **43**. When in addition the 1,4-bromoelimination in **46** could be directed with high selectivity to afford the more stable and less strained secodiene **47** (90%), and when the latter opened smoothly to give **45** under alkaline work-up conditions, the problem for the aldol route was solved in a nearly perfect, though somewhat lengthy fashion.

For the "S_N2 intermediate" **39** (Y = CHBr) again the shortest pathway to the bissecodiene **52** was barred. The challenge was once more the control of the photobromination—arrest at the stage of the pentabromide **49** (>90%), after addition (**48**) and substitution on one side. The most economical exploitation of **49**, a one-pot reaction (Zn/DMF) furnishing the secododecahedradiene **52** directly by 1,4- and 1,5-bromoelimination (**49** → **50** → **52**), was only moderately efficient (close to 60% yield). As partial compensation the hydrogenolysis **49** → **48** could be accomplished completely uniformly, unlike the analogous reaction of **44**, and without affecting the other bromine substituents. As the elimination **48** → **50** proceeded without complications after the exchange of zinc by iron, the S_N2 route, too, was well served with an overall yield of at least 80% for the three-step sequence **39** → **49** → **48** → **50**.

The fragmentation patterns in the mass spectra of the secopagodanes **48**/**49**, the (bis)secododecahedradienes **50**/**52**, and the isododecahedrane **51** deserve attention with regard to the (radical) cyclization methodology listed under (c) in Scheme 11. Intensive signals for the $C_{20}H_{14}$, $C_{20}H_{12}$, and $C_{20}H_{10}$ ions, resulting from the elimination of (H)Br and $CH_3CO_2(H)$ units, are assigned to multiply unsaturated dodecahedranes originating from lateral radical recombination (cf. also Scheme 27).

Typical for the nonpentagonal isododecahedranes **46**(**51**) is that they are hybrids of pagodane and dodecahedrane "halves". In the X-ray structure of **51** (Fig. 4)[55] a correspondingly large

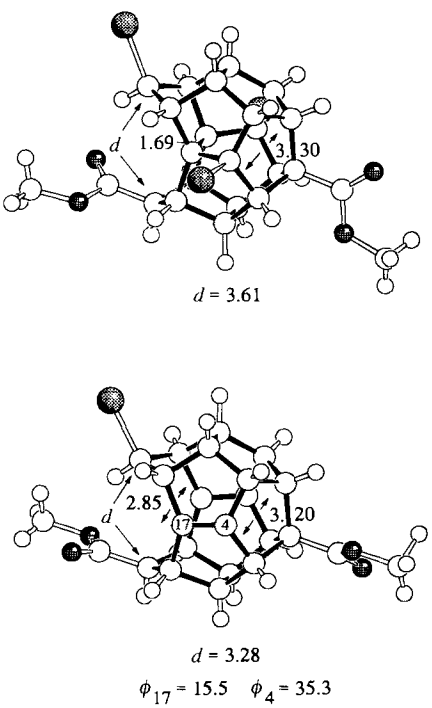
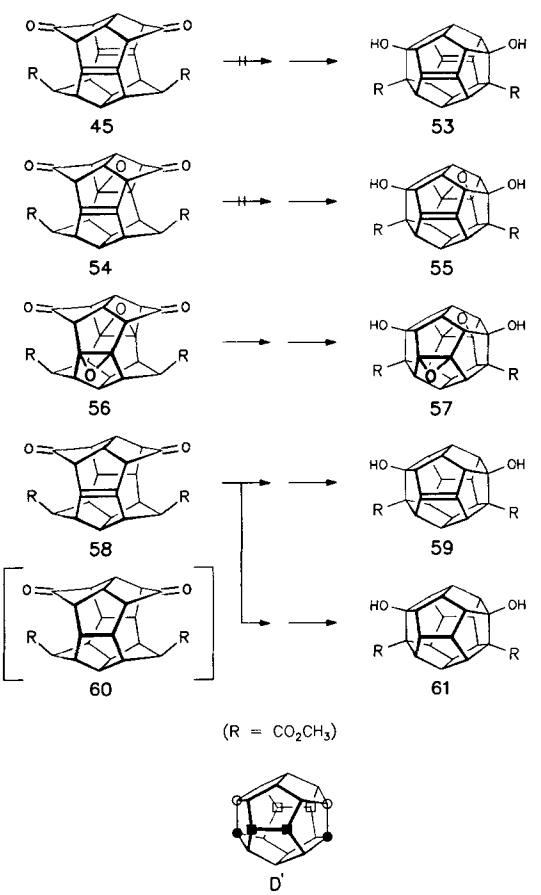


Fig. 4. Selected structural data (*d* in Å, ϕ in °) for isododecahedrane **51** (above) and secododecahedradiene **52** (below).

C10–C19 distance of 3.61 Å is observed (cf. 3.530 Å (3.611 Å) for **3** (**17**) in Fig. 2). The C1–C2 bond broken en route to **52** is, at 1.69 Å, one of the longest C–C single bonds measured.[56] The secododecahedradienes **47** (**52**) are hybrids of the nearly flat bissecodiene (cf. **27** in Fig. 3, **45** in Fig. 6) and the already significantly bulged 1,16-dodecahedradiene (cf. diepoxide **57** in Fig. 5 as the best model subjected hitherto to X-ray structural analysis). Correspondingly, the distances across the cavity on the "open" side of the molecule are short; the π,π distance and the pyramidalization of 35.3° on the "closed" side are large. According to "π orbital axis vector" analysis, the $(\theta_{\sigma\pi}-90)°$ value, a measure of the pyramidalization of C4(12) in the bissecodiene parent structure, surpasses that of the icosahedral C_{60} fullerene.[57]

Under the influence of their strongly electron-withdrawing functional groups (quantified inter alia by the oxidation and ionization potentials[58]) the bissecodienes **45** and **50** are easier to handle—less sensitive to oxygen and ionic or radical species. The hyperstability of the monoenes (**58**, **65**) is not affected, which provided the chance of varying the substitution pattern nearly at will en route from **B** to **C** (Z,Z'), an option not possible at the stage of the dodecahedradienes (e.g. **62**), which are no longer hyperstable. The drawback was already stated above: reversible cycloadditions, valued as potential protective measures for the highly sensitive C=C bonds of the unsaturated dodecahedranes, are not possible at this stage.

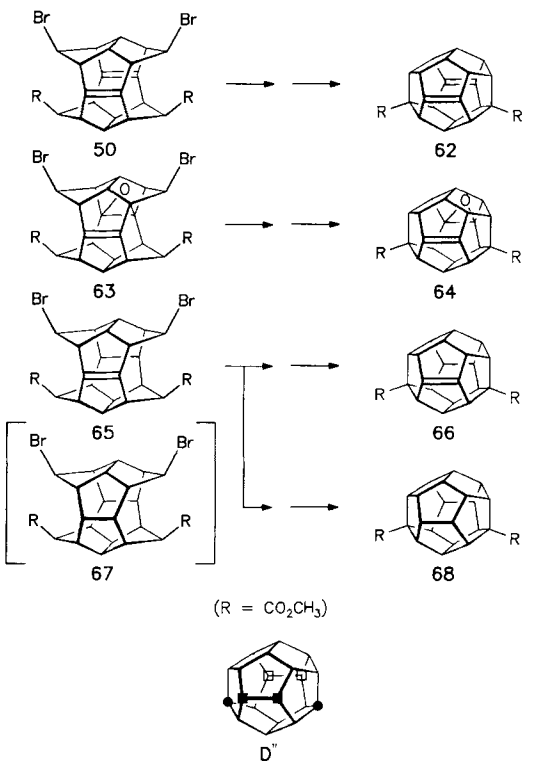
The scope and limitations of the cyclizations **C** → **D** following the aldol variant[53] are illustrated with the five examples in Scheme 15. In agreement with predictions based on calculations, only the endothermic cyclizations leading to diene **53** and eneepoxide **55** are not realized. (Attempts to conduct the reactions irreversibly had no success, probably for steric reasons.) Dodecahedranes with four (**61**), six (**59**), and eight (**57**) pairwise



Scheme 15.

symmetrically functionalized positions (**D'**) were obtained almost quantitatively under controlled basic conditions.

The irreversible S_N2 variant (Scheme 16), as expected, allowed access to the diene **62** and to the eneepoxide **64**. Indeed the reactions were quite clean (over 90% yield), when the particular reactivity of both starting material and product was taken



Scheme 16.

into account with a phosphazene base and careful exclusion of oxygen. The saturated diester **68**, which was an important intermediate in later work (vide infra), was prepared in analogy to **61** by "hydrogenating cyclization" of the ene precursor **65**. In toto, the set of dodecahedranes (**D'**) prepared by the aldol reaction is complemented by those obtained by the S_N2 reaction (**D''**) with two (**68**), four (**66**), and six (**62**, **64**) functionalized positions.[54]

The X-ray structures of the dimethyl ethers of **57** and **61** (Fig. 5) disclose how the vicinal substituent pairs are accommodated in the crystal lattice and how strongly the dodecahedral skeleton is flattened as a result of epoxide annulation.[59]

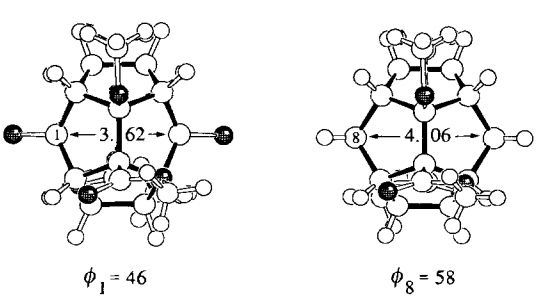
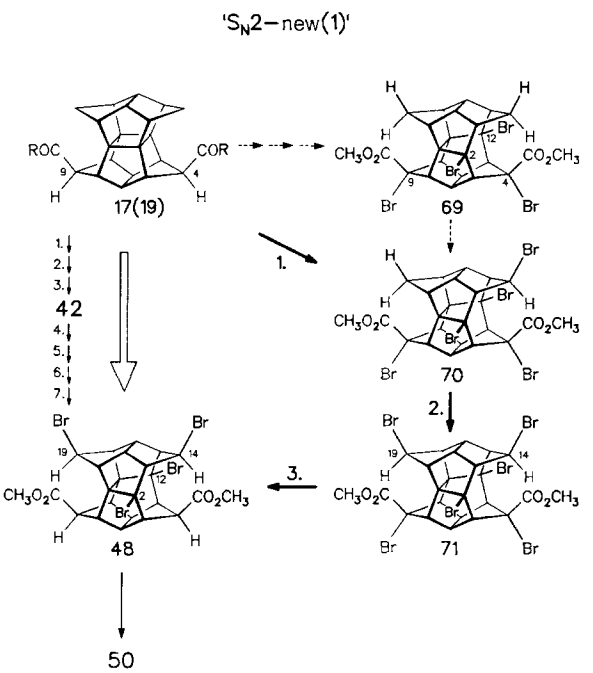


Fig. 5. Selected structural data (distance in Å, ϕ in °) for dodecahedranes **57** (left) and **61** (right) as dimethyl ethers.

5. More Economy—The Breakthrough after the Breakthrough

For all the enthusiasm about the preparative potential of the aldol and S_N2 routes, and implicitly about the ways and means for converting the directly introduced 4,9-disubstitution (Scheme 5) into the 4,9,14,19-tetrasubstitution of the pagodane intermediates (Scheme 13), the S_N2 version in particular was very labor-intensive, and for some of the projects based thereon almost prohibitive. Impressive improvements are presented in this section.

As a shorter alternative to the S_N2 version, the route from the pagodane diester **17** to the central bissecododecahedradiene **50**, outlined in Scheme 17, by means of a straightforward sequence

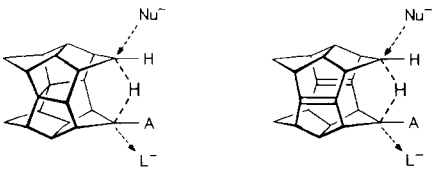


Scheme 17.

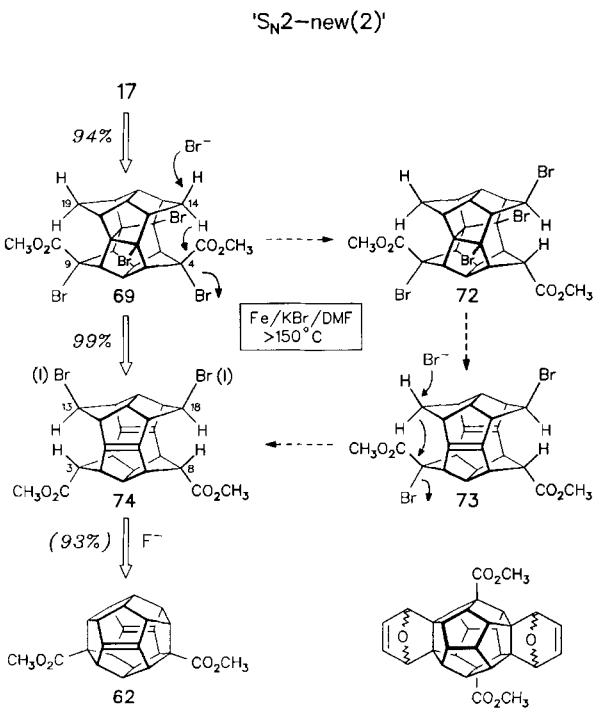
of additive/substitutive brominations and reductive/fragmentative debrominations (tetrabromide **69**, pentabromide **70**, hexabromide **71**, tetrabromide **48**) had been considered and tested very early on. For a long time, however, this approach yielded no practical results, as no satisfactory solutions could be achieved for two of the manipulations, the photobromination **70** → **71** and the second reduction of **71** (C-9)—explainably slow processes. Recently, these deficiences could be remedied by changing the light source and the medium. And since the multistep sequence from **17** to **48** was compressed into three operations (**17** → **70** → **71** → **48**)—compared with seven steps in the previous route via bislactone **42**—the time required for the preparation of the "S_N2 dodecahedranes" (Scheme 16) was reduced by two-thirds, and in addition the overall yield increased by more than one-half.[60]

"Appetite comes with eating." Isn't there an even shorter, quicker, more efficient way? Why not use hydride transfer across the cavity in the half-cages of the secopagodanes (cf. the

C4–C14 distance of 3.14 Å in **10**, Scheme 3) and the bissecododecahedranes (cf. the C3–C13 distances of 3.21–3.02 Å in **4**–**6**, Scheme 2), which are predestined for this purpose, for a directed functionalization of the methylene positions? One is reminded of the numerous literature examples of such transannular processes in eight-membered rings, in particular in those that are conformationally restricted.[47, 61] In fact, this strategy did open up new perspectives (Scheme 18).

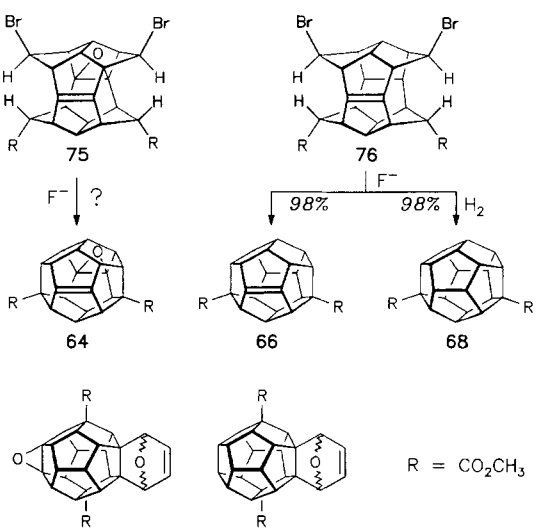


The tetrabromide **69**, which was not isolated on the way from the pagodane diester **17** to the secopentabromide **70**, but secured almost homogeneously under controlled bromination conditions, fulfilled the requirements for the combination of hydrogen transfer and *anti* substitution on both sides along with 1,4-bromine elimination. Finally optimized as a one-pot process, the reaction of **69** with Fe/KBr in boiling dimethylformamide (DMF) gave an almost quantitative yield of the bissecodibromodiene diester **74**, the all-*anti* isomer of **50**. Control experiments confirmed the sequence of events (**72** before **73**).[60]



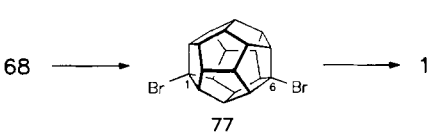
Scheme 18.

Thus, the pagodane → bissecodiene opening was condensed into two operations, and the time required for the preparation of gram quantities of **74** with an overall yield of more than 90% was reduced to a few days. Yet, this achievement had its drawbacks: the kinetic acidity of the 3-*syn*,8-*syn* hydrogen atoms in **74** is considerably less than that in **50**, since the effective steric pressure on the ester groups operative in **50** is absent (ca. 10 kcal mol^{-1} each; ca. 7 kcal mol^{-1} each in **17**, Table 1). In addition, the *syn* hydrogen atoms are rather inaccessible (cf. the problem with the dehydrogenation leading to **13**). None of the bases successful with **50** could be used for deprotonation and cyclization of **74** to give the dodecahedradiene **62**. Once again the steric situation in the seco half-cages almost led to failure. The small "naked" fluoride base recently introduced by Schwesinger[62] was the remedy. With this base, **62** could be isolated in roughly 50% yield as such or as the double furan adduct (mixture of isomers); with better leaving groups than those in **74** (13,18-diiodide) the yield could be raised to better than 90%. After epoxidation or hydrogenation of **74** to **75** and **76**, respectively, the 3(8)-*anti* analogues of **63** and **65**, the steric situation in the half-cage was even worse. The F$^-$-catalyzed cyclization (in the presence of furan) of either **75** or the diepoxide gave no uniform result (opening of epoxides through the ester enolate?); however, reaction of **76** provided a very high yield (98%) of dodecahedrene **66** in pure or protected form (Scheme 19). Note: the saturated diester **68** was obtained via **76** (**66**) with an almost quantitative yield in a one-pot operation.



Scheme 19.

At the close of this chapter it must be emphasized that with the now much more readily available diester **68** a much more efficient access to dodecahedrane **1** was achieved. Of several alternatives explored, the sequence of Barton-type degradation to the 1,6-dibromide **77** and reduction with an overall yield of 90% fulfilled even the highest expectations (Scheme 20). The

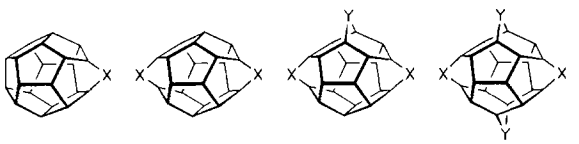


Scheme 20.

problem to be solved was the efficient trapping of the intermediate dodecahedryl radicals in spite of strong frontal shielding.[63] Now that dodecahedrane was available by a highly efficient approach, the barrier was lowered for burning at least 0.5 g of a still most valuable material ("who wants to burn diamonds?") for a combustion calorimetric determination of the thermochemical data. The enthalpy of formation deduced for parent **1** from the corresponding values for the pagodanes **3**/**17** and dodecahedrane diester **68** in collaboration with Rüchardt/Beckhaus and Paquette confirmed the reliability of the trends derived from the force field calculations claimed at the outset (Table 1).[64] In absolute terms the MM2 values are better than the ones from ab initio calculations.[65]

6. Nonpentagonal (Hetero)Homologous Dodecahedranes

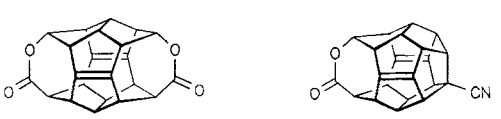
A preparative extension of the dodecahedrane synthetic scheme was aimed at the modification of the C_{20} perimeter by the insertion of functionalized carba- or heteroelements, as outlined by formulae **G**–**K**. First examples of simply expanded structures (**G**, X = CHR, C=O, N, CH^+) have been described by Paquette's group.[3]



G H I K

We can only convey here some examples of a multitude of nonpentagonal, (hetero)homologous dodecahedranes that have been developed from 4,9,14,19-tetrafunctionalized pagodanes. It is understood that the increasing strain associated with exchange of [3.3.0] with [3.3.X] elements in the C_{20} perimeter is a limiting factor.

Lactone-bridged pagodanes can be converted into the homologous, nonpentagonal dodecahedradienes **78** (**H**, X = OCO) and **79** (**G**, X = OCO) by standard procedures.[66]



78 79

The X-ray structure (Fig. 6) of **78** gives a clear idea of the "flattening" of the molecular skeleton enforced by the bridges and the much greater similarity to bissecodienes (e.g. **45** as an example analyzed by X-ray structural analysis) than to pentagonal dodecahedradienes (e.g. **62**).[67] Accordingly, the behavior of compound **78** more closely resembles that of the bissecodiene. Monolactone **79** is a typical hybrid of **78** and **62** as judged

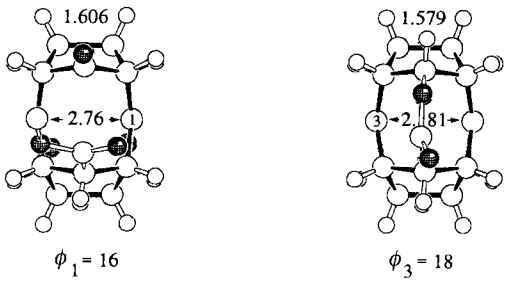
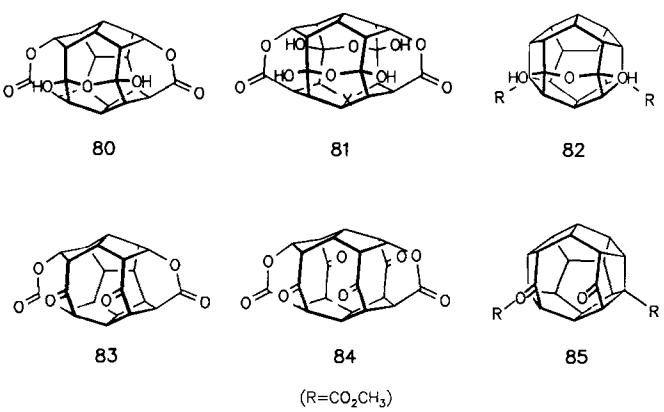


Fig. 6. Selected structural data (distance in Å, ϕ in °) for the bissecodiene **45** (left) and the nonpentagonal dodecahedradiene **78** (right).

by the criteria of olefin strain, pyramidalization, and π,π interaction.

The ether bridges in homologues **80** (**I**, X = OCO, Y = O) and **81** (**K**, X = OCO, Y = O) were installed by ozonation of the corresponding olefins (inter alia **78**). The rapid thermal loss of oxygen from the primary peroxides (Y = O–O) is also evidence for high strain in these skeletons. The same is true for the oxa-homo structure **82** (**G**, X = O) gained in analogous fashion from the dodecahedrene **66**. The α,α'-dihydroxyethers **80**–**82** are valuable precursors of the caged di- and tetraketones **83**–**85**, which have an almost parallel, unusually close alignment of carbonyl groups.[68]



80 81 82

83 84 85

(R=CO_2CH_3)

7. Variations on the Periphery

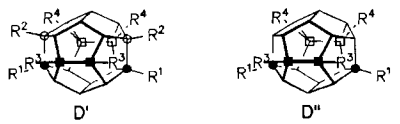
Structure **1** is nearly free of angle strain;[69] the measured strain energy of roughly 61 kcal mol^{-1} (Table 1) stems almost exclusively from interactions between the strictly eclipsed C–H bonds. How does the strain change when two (vicinal or in 1,3-positions), three, or more hydrogen atoms in **1** are replaced by OH groups or halogens?[70] Is it possible to replace all 20 hydrogen atoms?

A glance at Tables 2 and 3 is helpful for better understanding the problems and opportunities connected with positioning or changing one or more functionalities on this rigid periphery.[71] A second, vicinal OH group "costs" practically nothing, whereas the "price" for a second vicinal F, Cl, or Br substituent is about 3, 4, or 7.5 kcal mol^{-1}, respectively. The difference of 3.4 kcal mol^{-1} between 1,2- and 1,3-dibromides will be addressed below as a directing effect for selective substitution.

Table 2. Increase in strain energy [kcal mol^{-1}] predicted by MM2 calculations upon mono-, di-, and trisubstitution of **1** (E_{str} = 68.9 kcal mol^{-1}).

X	1	1, 2	1, 3	1, 2, 3
OH	0.07	0.12	0.10	0.17
F	3.80	6.82	7.60	9.84
Cl	1.91	5.95	3.81	10.34
Br	4.32	11.96	8.58	20.21

The substitution patterns (**D'**, **D''**) introduced directly in the aldol and S_N2 routes (Schemes 15 and 16) can be varied extensively: R^1 (R^2) by modification or degradation of the original CO_2CH_3 (OH) groups, and R^3 (R^4) via the monoenes/monoepoxides (**59**, **66**, **55**, **64**) and dienes/diepoxides (**62**, **57**), respectively.[54] Ansa derivatives should have allowed attack at hitherto inaccessible positions ("remote functionalization"), but the outcome was preparatively of no use.

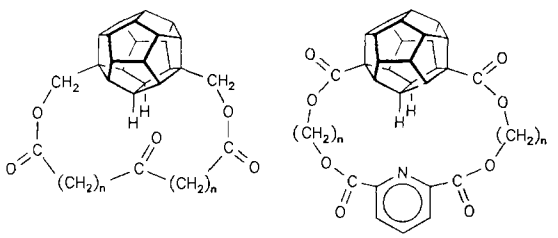


D' D''

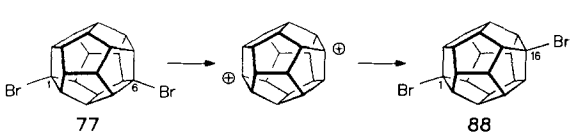
R^1 = CO_2CH_3, CO_2H, COCl, $CONH_2$, $COCH_3$, CHO, CH_2OH, $CH_2NH_3^{\oplus}$ CH_2Cl, CH_2Br, CN, NHCOO*t*Bu, $NHCOCH_3$, $NH_3^{\oplus}$, $OCOCF_3$, F, Cl, Br, I

R^2 = OH, OCH_3, OAc, $OCOCF_3$, O–CO–CO–Cl, O–CO–CO–OCH_3, Cl

R^3, R^4 = H, Cl, Br, OH, $OCOCF_3$, O, NR, S, N_3R



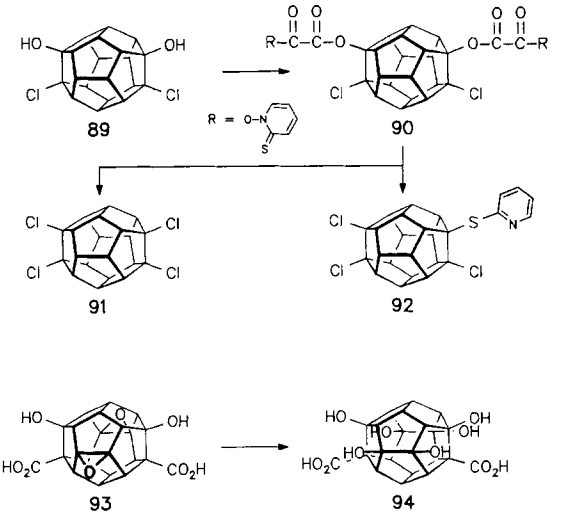
Here are some examples of the preparation of polyhalogenated (hydroxylated) dodecahedranes wanted inter alia as precursors of polyunsaturated dodecahedranes.[72] The 1,6-diester **68** was a valuable intermediate for the preparation of 1,6-dihalides by a radical or cationic route, as already shown above for the dibromide **77** (Scheme 21). Frontal hindrance in dodecahedryl radicals became only seriously detrimental in the case of the diiodide. With the known, thermodynamically controlled isomerization (**88**) in super acid media, the 1,6-dibromide **77** leads to the series of 1,16-difunctionalized derivatives.



77 88

Scheme 21.

High vicinal strain controlled the radical conversion of the dichlorodiol **89** into the tetrachloride **91** (Scheme 22). Preparation of the Barton intermediate **90** was extremely slow, and the

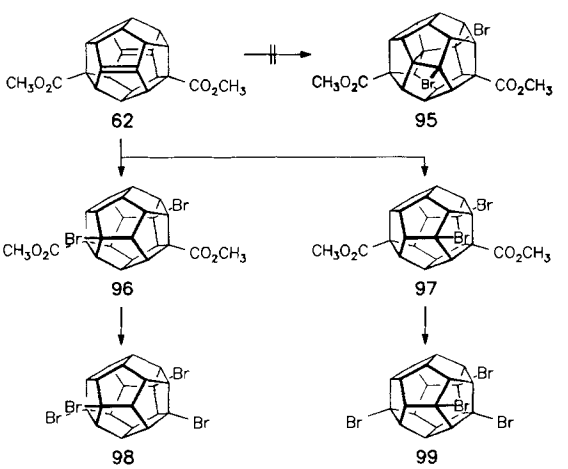


89 90 91 92 93 94

Scheme 22.

intermolecular radical recombination faced competition by the "intramolecular" recombination (**92**).[73] During ionic processes hydrogen atom migration on the molecular surface did not compete.[3, 4] Thus the vicinal diols were formed almost homogeneously by acid-catalyzed opening of the epoxides; for example **93** yielded the readily water-soluble hexahydroxydicarboxylic acid **94**.

The unsaturated dodecahedranes are markedly different in their behavior toward electrophiles compared with the bisseco olefins. For example, in the double *cis*-addition of HBr to **62**, homoconjugate addition here to give the didehydrododecahedrane **95**, generally dominant for the bissecodienes (e.g. **4**, **45**, **50**), had no chance (Scheme 23). The double Barton degradation of the isolated nonvicinally substituted dibromodiesters **96**/**97** to the C_2/C_s-tetrabromides **98**/**99** was efficient.

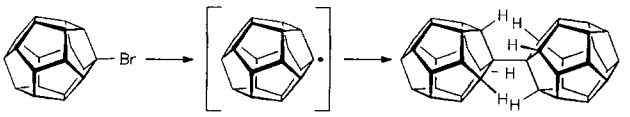


62 95 96 97 98 99

Scheme 23.

It should be stressed that the sterically demanding dimerization of two dodecahedryl radicals has not been observed in any of the numerous radical processes. When bromide **100** was subjected to suitable Wurtz coupling conditions, the presumably rigidly eclipsed didodecahedryl **102** (E_{rot} = 34.2 kcal mol^{-1},

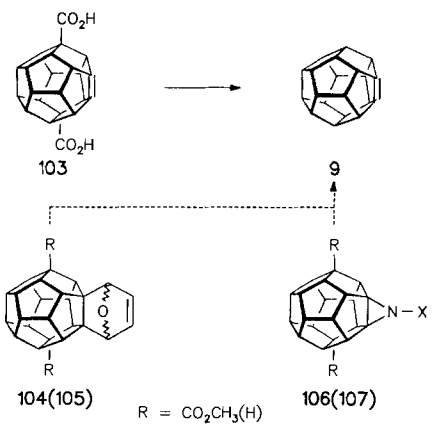
MM2) could be generated in low yield besides **1** as major component (Scheme 24).[74] Direct characterization of the dodecahedryl radical **101** has not yet been achieved.[75]



100 101 102

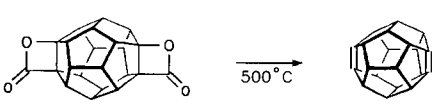
Scheme 24.

The unsaturated dodecahedranes, as π_2 components with a relatively low-lying LUMO,[76] participate readily in [4 + 2]-cycloadditions, for example with 1,3-butadiene and furan even at room temperature.[77] The perspectives in the area of annulated carba- and heterocycles have been documented on numerous occasions. Aziridines and furan adducts also act as "protected olefins" in substituent manipulations. Thus, conversion of the sensitive enedicarboxylic acid **103** into the even more sensitive parent ene **9** could be effected by double decarboxylation of the adducts with furan or tosylazide and gas-phase thermolysis of **105** or low-temperature nitrosation of **107** (X = NO) (Scheme 25).



Scheme 25.

The bis-β-lactone **108**, a doubly hetero-annulated derivative (and hence the aldol product **61**) emerged as precursor of choice for the 1,16-dodecahedradiene **8**, which is even more oxygen-sensitive than the monene **9**[78] and much desired as a model for transannular interactions (Scheme 32). The special nature of the C=C bonds to be formed (Ψ ca. 45°!) once again[79] necessitated very drastic conditions (gas-phase thermolysis, 500 °C) for the decarboxylation, which was first observed in the mass spectrum, without **8** suffering detectable damage (Scheme 26).



108 8

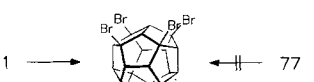
Scheme 26.

With the availability of **1** in gram quantities the possibilities for polyfunctionalization could be explored experimentally on a wider basis. Polya's group theoretical approach provided the insight, as shown by the data in Table 3, that this venture only made sense statistically for the $C_{20}H_{19}X$, $C_{20}H_1X_{19}$, and $C_{20}X_{20}$ compounds, even for identical functionalities (X).[71]

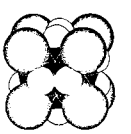
Table 3. Numbers of structural isomers (Polya).

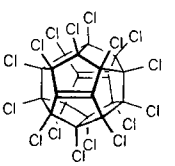
Formula	Isomers	Formula	Isomers
$C_{20}H_{19}X$	1	$C_{20}H_{14}X_6$	371
$C_{20}H_{18}X_2$	5	$C_{20}H_{13}X_7$	693
$C_{20}H_{17}X_3$	15	$C_{20}H_{12}X_8$	1135
$C_{20}H_{16}X_4$	58	$C_{20}H_{11}X_9$	1466
$C_{20}H_{15}X_5$	149	$C_{20}H_{10}X_{10}$	1648

Electrophilic monosubstitution ($C_{20}H_{19}X$) and, under thermodynamic control via the 1,16-dication, selective 1,16-disubstitution ($C_{20}H_{18}X_2$) was practiced by the groups of Paquette and Olah in many cases.[4] Our investigations into the polybromination of **1** under kinetic control support a directing effect that is too weak, however, to be exploited preparatively. Under relatively mild conditions the T_d-symmetrical octabromide **109**, the only $C_{20}H_{12}Br_8$ isomer without vicinal Br substituents, was identified in admixture with lower bromides. In control experiments with the 1,6-dibromide **77**, the only one of the five $C_{20}H_{18}Br_2$ isomers that cannot proceed to **109**, no octabromide was found. The surprise: under "brutal" conditions all of the hydrogen atoms in **1** could be replaced, but "halogen balls" like **110** and **111** have extremely low solubility and can be manipulated only to a very limited extent.[63] Fluorination experiments under "brutal" conditions cause cleavage of the skeleton. Experiments in a NaF matrix (70 °C) led to $C_{20}H_2F_{18}$ (selectively) and even to $C_{20}F_{20}$.[74, 80]

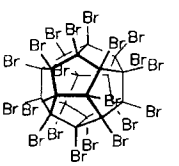


109





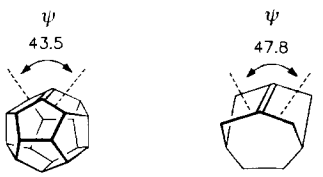
110



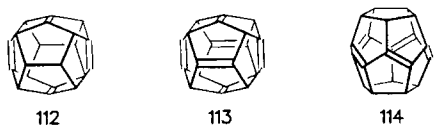
111

8. Polyunsaturated Dodecahedranes—C_{20} Fullerene?

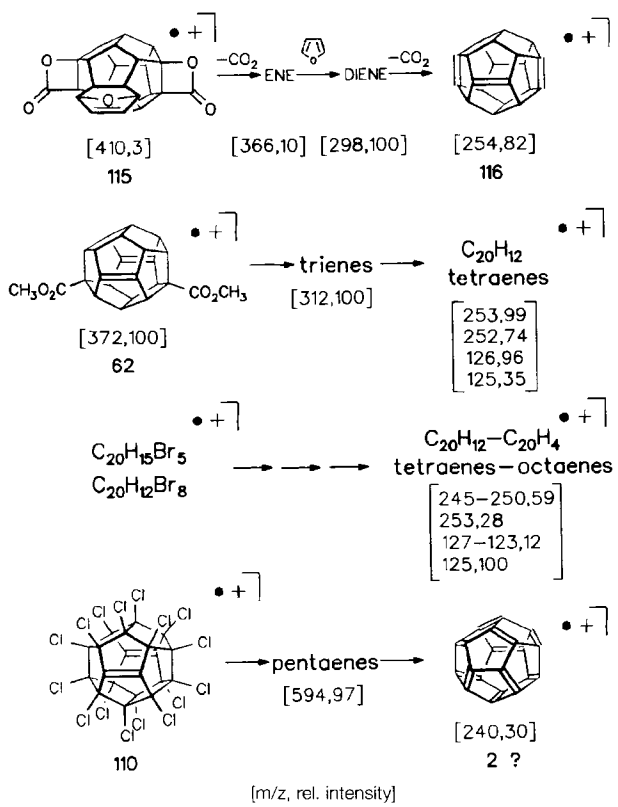
The isolation of the unsaturated dodecahedranes (**8**, **9**, **59**, **62**, **64**, **66**) with their highly bent "diradicaloid" C=C bonds (Ψ) was quite surprising. Such a degree of kinetic stabilization as a consequence of steric shielding through four allylic hydrogen atoms was unexpected; the similarly pyramidalized bicyclo-[3.3.2.$0^{3,7}$]dec-3(7)-ene dimerized upon warming of the argon



matrix (ca. 40 K).[81] One could speculate that even polyunsaturated dodecahedranes would be isolable as long as the C=C bonds are not conjugated, for example tbe D_{2h} tetraene **112** and the T_h hexaene **113**. An exciting "inner life" is anticipated for these compounds as well as their radical cations and dications (see Section 10).[82] Conjugation of double bonds, as in [4*n* + 2]-pentaene **114**[83] or even in decaene **2**, in any case signals a considerably reduced or extremely low persistence.



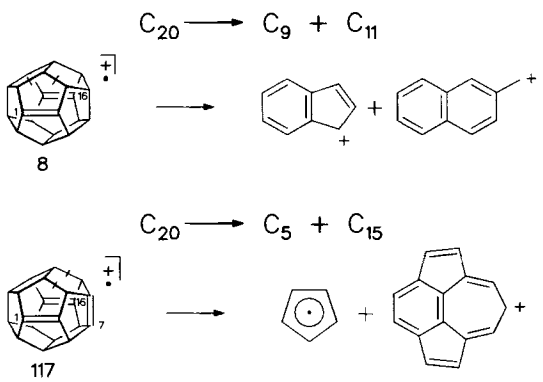
For the existence of polyunsaturated dodecahedranes in the gas phase there is in fact quite convincing MS evidence (Scheme 27).[66] The mass spectrum of **115** shows the fragmentation pattern of the functional groups and indicates that the



Scheme 27. The *m/z* values and the relative intensities of the signals are given in square brackets.

triene ion **116** is a relatively stable entity. In the spectrum of the diene diester **62**, (protonated) tetraene ions ($C_{20}H_{13}$, $C_{20}H_{12}$) are the dominant fragments; the intense $C_{20}H_{12}^{2+}$ signal could well be an indication of π conjugation. In the MS analysis of the bromide mixture ($C_{20}H_{15}Br_5$ to $C_{20}H_{12}Br_8$), which was prepared to find evidence of the T_d-symmetric octabromide **109**, pentaene ions prevail (*m/z* 250, *m/2z* 125, *m/3z* 83.3) besides (protonated) octaene to tetraene ions; the high intensity of the signals for the multiply charged ions is again taken as evidence for π conjugation. In the spectrum of the $C_{20}Cl_{16}$ product the assignment of the signal at *m/z* 240 to the radical cation of the C_{20} fullerene **2** is still speculative; $C_{20}Cl_{10}$ pentaenes have been substantiated by a signal at *m/z* 594.[63] The possible existence of the smallest, extremely strained fullerene has become a subject of debate following recent ab initio calculations.[84]

The fragmentation of the pagodane framework into two C_{10} halves (above 700 °C) was a thermochemically informative and mechanistically intriguing reaction.[8] Depending on the number and the positions of C=C bonds on the dodecahedrane periphery, various reaction channels for thermal fragmentation should be possible. First hints do indeed exist (Scheme 28).

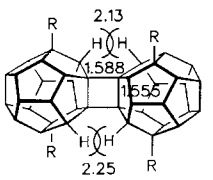


Scheme 28.

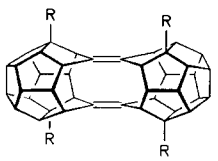
MS fragmentations of type $C_{20} \rightarrow C_9 + C_{11}$ and $C_{20} \rightarrow C_5 + C_{15}$ have been proposed for the 1,16-diene **8** and for the 1,7,16-triene **117**, respectively (but not for the 1,5,16-isomer **116**).[54]

9. From C_{20} via C_{40} to C_{60}

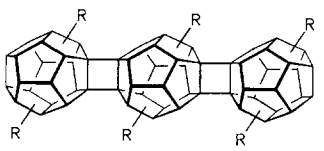
First examples show that the reluctance of unsaturated dodecahedranes to undergo [$\pi_2 + \pi_2$] or ene cycloadditions[85] could be overcome. On heating the ene diester **66** in the solid (exclusion of O_2) the sample melted at roughly 180 °C. Increasing the temperature to about 300 °C caused resolidification as a consequence of a selective [2 + 2] dimerization. For one of the two dimers (C_{2h}, C_{2v}), which was separated chromatographically (**118**, R = CO_2CH_3), X-ray structural analysis indicated that primarily lengthening of the intercage cyclobutane bonds limits the nonbonding H,H interactions.[86] The diene "tubes" **119** resulting from metathetical cyclobutane ring opening promise deeper insight into electron delocalization in organic cages (see Section 10). The one-electron oxidation wave of the octaalkylated cyclobutane **118**, measured by cyclic voltammetry (CV) (E_p = 1.60 V, **119**$^{\bullet+}$?), is irreversible and only a little higher than that of the pagodane diester **17** (1.52 V). For analogous "trimers" (**120**, **121**) diene diester **62** and ene diester **66** are the starting materials.



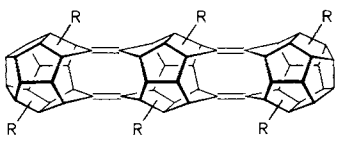
118



119

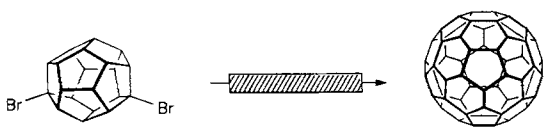


120



121

Related to these "oligomers" are the findings of a laser desorption time-of-flight mass spectroscopic study with dodecahedranes and pagodanes.[87] The prominent discovery: C_{40} "dimers" to C_{100} "pentamers" are formed from the 1,6-dibromododecahedrane **77** after desorption with a 248-nm excimer laser (Scheme 29). At higher ion velocities oligomers appear



77 122

$v \approx 650\,m\,s^{-1}$: $C_{20}H_{18} \rightarrow C_{20}H_{18}Br \rightarrow C_{40}H_{28}Br \rightarrow C_{60}H_{43} \rightarrow C_{80}H_{55} \rightarrow C_{100}H_{65}$
$v \approx 750\,m\,s^{-1}$: $C_{20}H_{18} \rightarrow C_{20}H_{18}Br \rightarrow C_{40}H_{30} \rightarrow C_{40}H_{30}Br \rightarrow C_{60}H_{45}$

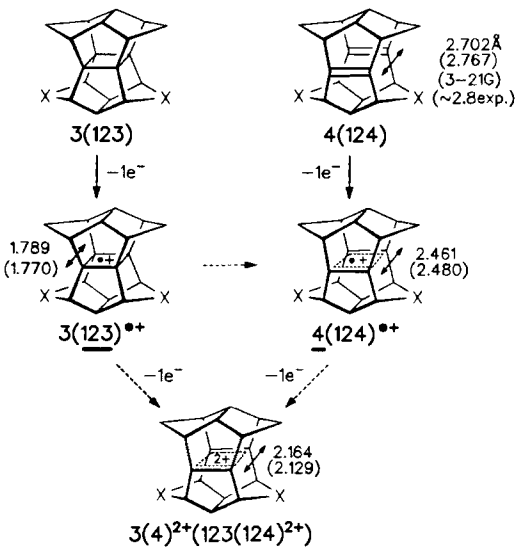
Scheme 29.

which, upon release of all hydrogen atoms and uptake of considerable kinetic energy, rearrange into pure fullerenes, preferably C_{60} (**122**). Nonbrominated substrates such as **68** and **118** give rise to practically no oligomers or fullerenes. This "mechanism" for formation of C_{60} extends the spectrum of the routes so far discussed only for non-three-dimensional sources.

10. The "Inner Life"—Electron Delocalization in Pagodane and Dodecahedrane Cages

The inclusion of guest molecules in (hydro)carbon cages, in particular **1**, was already a popular area of research before the fullerenes opened new dimensions.[88] Since the diagonal distance in **1** is 4.5 Å, a cavity about 1.5 Å across remains after subtraction of the carbon van der Waals radii. Early calculations indicated that this is sufficient for the accommodation of small ions (H^+, Li^+, Be^{2+}, Mg^{2+}) without use of excessive force.[89] Would it be possible to include even a helium atom? Experiments such as those by Saunders et al. should provide an answer.[90] What about smaller guests, for example electrons as participants in transannularly delocalized π systems?

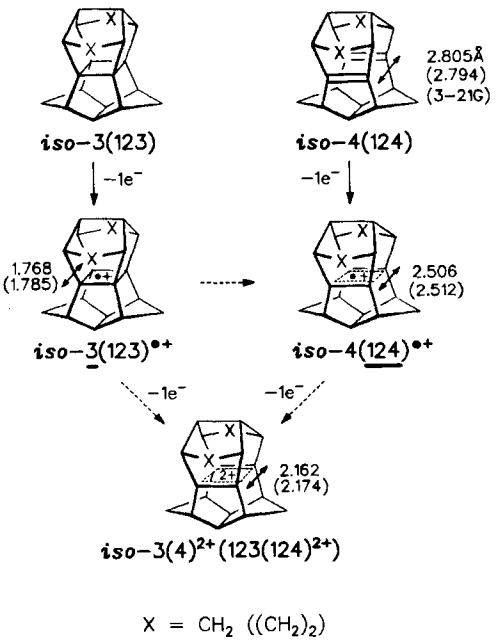
As a reminder: the deeply colored four-center, three-electron (4c/3e) [1.1.1.1] radical cation $\mathbf{4}^{\bullet+}$,[91] which is stable for days at room temperature, and the σ-bishomoaromatic 4c/2e [1.1.1.1] dication $\mathbf{3(4)}^{2+}$ (Scheme 30) are two of the spectacular "spin-offs" of pagodane chemistry.[37, 38] Both ions can be produced



Scheme 30.

from **3** as well as from **4**. The "extended" $\mathbf{4}^{\bullet+}$ is differentiated from the "tight" $\mathbf{3}^{\bullet+}$ inter alia by the $a_{H\beta}$ coupling constants in the ESR spectrum (Fig. 7). The latter, the true [1.1.1.1] pagodane radical cation $\mathbf{3}^{\bullet+}$, is of interest as a potentially "frozen" cyclobutane radical cation[92] and could not be detected even under special ESR (20 K) and MS conditions.[93] In the very fast isomerization $\mathbf{3}^{\bullet+} \rightarrow \mathbf{4}^{\bullet+}$ the symmetry-forbidden concerted pathway is presumably avoided. Electronic and geometric factors cooperate in $\mathbf{4}^{\bullet+}$ and $\mathbf{3(4)}^{2+}$ in almost ideal fashion. The four participating "sp^2" centers are favorably oriented in a rectangular fashion, but the structure is nevertheless flexible enough to allow the shortening of the transannular distances that promote the electron delocalization; elimination of hydrogen is considerably impeded ("anti-Bredt stabilization").[94] A thermodynamically meaningful quantification of the homoconjugative stabilization in $\mathbf{4}^{\bullet+}$ is reflected in the difference $\Delta E = 0.91$ V of the (reversible) oxidation potentials for **4** (0.66 V) and the monoene **5** (1.57 V) determined by cyclic voltammetry (CV). In this context, it should be recalled that analysis of the neutral diene **4** by photoelectron spectroscopy had furnished an unusually high value of 1.90 eV for the through-space homoconjugation, quite close to classical conjugation in 1,3-butadiene (2.46 eV).[42] The [2.2.1.1] ions, the "tight" $\mathbf{123}^{\bullet+}$ (?) and $\mathbf{123(124)}^{2+}$, are considerably less persistent; hydrogen elimination is facilitated in the homologous parts of the molecules.

The relationship between the structure and the stability of these unusual ions has become clearer with the recently re-



Scheme 31.

ported [1.1.1.1]- and [2.2.1.1]isopagodanes (*iso*-**3**, *iso*-**123**, Scheme 31).[32, 95] The fixation of the four-center core of the ions of *iso*-**3** (D_{2d}) in the square geometry is a priori unlikely,[96] but opening to "extended" geometries was made difficult by the skeleton. First experimental findings are in line with these predictions.[97] In contrast to results with **3**, the radical cation of *iso*-**3** is only observed by γ-irradiation in a Freon matrix; between 20 and 140 K it has been characterized as the symmetry-reduced (C_{2v}), "tight" (cyclobutanoid) *iso*-$\mathbf{3}^{\bullet+}$ (Fig. 7). Accordingly, the CV oxidation wave of *iso*-**3** was not reversible. The situation with *iso*-**123** is totally different. The resulting radical cation is the "extended" *iso*-$\mathbf{124}^{\bullet+}$, which is about as persistent as $\mathbf{4}^{\bullet+}$; even the second CV oxidation *iso*-$\mathbf{124}^{\bullet+} \rightarrow$ *iso*-$\mathbf{123(124)}^{2+}$ is reversible. The extent that the altered geometries of the isodications affect the σ homoaromaticity was probed very recently by Olah, Prakash, and Herges. The dications generated from *iso*-**3** and *iso*-**123(124)** in SbF_5/SO_2ClF at $-78\,^{\circ}C$ are both "aromatic" (*iso*-$\mathbf{3(4)}^{2+}$ and *iso*-$\mathbf{123(124)}^{2+}$, respectively; IGLO calculations). The resulting gain in energy is probably instrumental for the lengthening of the transannular distance (ca. 1.8 Å in *iso*-$\mathbf{4}^{\bullet+}$) to about 2.2 Å as postulated for *iso*-$\mathbf{3(4)}^{2+}$.

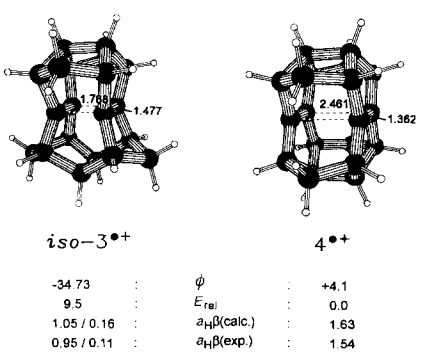
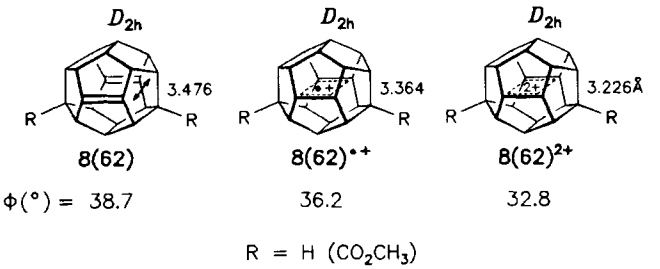


Fig. 7. Ab initio (3-21G) structures (distance in Å, ϕ in °), relative energies [kcal mol^{-1}], and coupling constants [mT] of the 4c/3e radical cations *iso*-$\mathbf{3}^{\bullet+}$ and $\mathbf{4}^{\bullet+}$.

Do through-space interactions in dodecahedrane cages have a chance? In the 1,16-diene **8**, as in bissecodiene **4**, the C=C bonds have an ideal synperiplanar alignment, yet the shortest transannular π,π distance is roughly 3.5 Å (Scheme 2). In addition, as a consequence of the high pyramidalization of the olefinic centers, radial extension of the π orbitals into the cage is reduced. According to most recent calculations[98] and ESR,[99] PE,[100] and CV studies,[58] the transannular relationships in **8** and its derivatives (**62**) as well as in their ions are in principle of the same type, but they have divergent intensities (Scheme 32). In **8** the through-space homoconjugation is cut to

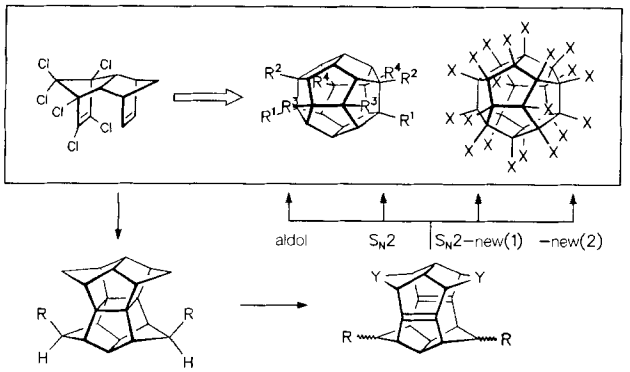


Scheme 32.

almost one-fifth of that in **4**, the first CV oxidation wave is no longer reversible, and the radical cation can no longer be observed in solution. Thus there was great excitement when a moss green radical cation persisted for hours after γ-irradiation of **8** in a Freon matrix (77 K) and was identified as the 4c/3e ion $\mathbf{8}^{\bullet+}$ having D_{2h} symmetry within the hyperfine timescale—in contrast to *iso*-$\mathbf{3}^{\bullet+}$ and $\mathbf{4}^{\bullet+}$ an early point on the reaction coordinate (D_{2h}) for the ethylene/ethylene$^{\bullet+}$ cycloaddition. With a π,π distance only slightly (3-21G) differing from that of the neutral molecule (on account of the higher structural rigidity) this radical cation is truly a borderline situation for homoconjugation! This would be even more true for the dication $\mathbf{8}^{2+}$, which is a no-longer-utopian shortterm target; however, ab initio calculations predict it to be more like a bis(radical cation).[37]

Epilogue

"From Isodrin to Plato's Universe"—the expectations of flexibility and efficiency for the pagodane route to dodecahedrane[4, 5] have been more than met. En route to dodecahedranes (Scheme 33) the highly optimized first section, construction of the pagodanes from isodrin (Scheme 4), could be complemented by a comparably expeditious second one, transformation of the 4,9-disubstituted pagodanes via 3,8,13,18-tetrafunctionalized bissecododecahedradienes. The productive interplay of planning, intuition, and serendipity in reactions of fascinating, if not unprecedented selectivities as a consequence of the entropic support from special cage situations has made the parent skeleton **1** as well as a vast array of multiply and even totally functionalized (unsaturated) dodecahedranes accessible with high efficiency. In the most recent version (Scheme 18) only days are required for the three-step preparation of dodecahe-



Scheme 33.

dranes from pagodanes. With increasing economy of the synthetic processes new targets can be envisaged.

To be free over years to work on projects that more than ever provoke the questions "why? for what reason? for what purpose?" is a privilege—motivation for all the people involved to seek solutions even for seemingly hopeless situations, to optimize processes, and to substitute the good with something even better. And for that there was regular occasion; the struggle for higher yields and efficiency was permanent. Were the synthetic routes per se rewarding goals of the project, unusual properties connected with the unusual structures have satisfied more extensive demands. The cage ions with their unusual bonding situations suffice as attestation. The unexpected persistence of the unsaturated dodecahedranes came as a real bonus. Have "new horizons" been revealed? This depends on the point of view of the observer.[1101] For us, dealing with these polycyclic molecular structures remains full of surprises.

Finally, reference should be made to the "Acknowledgements" of the last progress report with W.-D. Fessner.[8] *The work of the co-workers named therein (Dr. G. Lutz, Dr. H.-P. Melder, Dr. R. Pinkos, Dr. B. A. R. C. Murty, Dr. P. R. Spurr) laid the foundation for their successors (Dr. K. Scheumann, Dr. F. Wahl, Dr. K. Weber, the graduate students T. Voss, A. Weiler, M. Bertau, E. Sackers). Our work has been supported by a competent spectroscopy service (Dr. D. Hunkler, Dr. M. Keller, Dr. J. Wörth, and their co-workers), and a skillful technical staff (J. Leonhardt, M. Lutterbeck, G. Leonhardt-Lutterbeck, S. Ruf). In proven fashion Dr. L. Knothe and G. Fehrenbach helped with the manuscript. The cooperation with the colleagues C. Rüchardt/H.-D. Beckhaus (Freiburg), G. Olah/G. K. Surya Prakash (Los Angeles), H. Fritz (Basel), R. Herges (Erlangen), H.-D. Martin/B. Mayer (Düsseldorf), J. Heinze (Freiburg), G. Rihs (Basel), H. Irngartinger (Heidelberg), C. Krüger (Mülheim an der Ruhr), A. Haas/M. Lieb (Bochum) was a source of constant stimulation. This project was generously supported by the Deutsche Forschungsgemeinschaft, the Fonds der Chemischen Industrie, and BASF AG. Ciba-Geigy, Basel provided decisive help with the repeated production of a precursor material on the kg scale.*

Received: May 13, 1994 [A 67 IE]
German version: *Angew. Chem.* **1994**, *106*, 2329

[1] Whilst four of the regular ("most beautiful") platonic solids were assigned to the four elements, the fifth (dodecahedron) was attributed to a particular element ("quinta essentia"), which would also encompass the entire Universe: Plato, *Timaios* (*Sämtliche Werke, Bd. 5* (Ed.: E. Grassi), Rowohlt, Hamburg, **1959** (reprint **1985**)); E. Heilbronner, J. D. Dunitz, *Reflections on Symmetry*, VCH Verlag Helvetica Chimica Acta, Basel, **1993**, p. 12; W. Grahn, *Chem. Unserer Zeit* **1981**, *15*, 52, and references therein; F. Vögtle, *Reizvolle Moleküle in der Organischen Chemie*, Teubner, Stuttgart, **1987**.

[2] For a historic summary see refs. [3, 8].
[3] a) L. A. Paquette, *Chem. Rev.* **1989**, *89*, 1051; b) *Cage Hydrocarbons* (Ed.: G. A. Olah), Wiley, New York, **1990**, c) "The [n]Peristylane-Polyhedrane Connection": L. A. Paquette in ref. [3b], p. 313.
[4] G. A. Olah, G. K. S. Prakash, T. Kobayashi, L. A. Paquette, *J. Am. Chem. Soc.* **1988**, *110*, 1304; L. A. Paquette, J. C. Weber, T. Kobayashi, Y. Miyahara, *ibid.* **1988**, *110*, 8591; G. A. Olah, G. K. S. Prakash, W.-D. Fessner, T. Kobayashi, L. A. Paquette, *ibid.* **1988**, *110*, 8599.
[5] S. H. Bertz, G. A. Kourouklis, A. Jayaraman, G. Lannoye, J. M. Cook, *Can. J. Chem.* **1993**, *71*, 352; X. Fu, J. M. Cook, *J. Org. Chem.* **1992**, *57*, 5121; G. Mehta, R. K. Reddy, *Tetrahedron Lett.* **1988**, *29*, 3607; S. Lalitha, J. Chandrasekhar, G. Mehta, *ibid.* **1990**, *31*, 4219.
[6] W.-D. Fessner, B. A. R. C. Murty, J. Wörth, D. Hunkler, H. Fritz, H. Prinzbach, W. R. Roth, P. von R. Schleyer, A. B. McEwen, W. F. Maier, *Angew. Chem.* **1987**, *99*, 484; *Angew. Chem. Int. Ed. Engl.* **1987**, *26*, 452.
[7] H. Prinzbach, W.-D. Fessner in *Organic Syntheses: Modern Trends* (Ed.: O. Chizhov), Blackwell, Oxford, **1987**, p. 103.
[8] "The Pagodane Route to Dodecahedranes": W.-D. Fessner, H. Prinzbach in ref. [3b], p. 353.
[9] S. A. Godleski, P. von R. Schleyer, E. Osawa, W. T. Wipke, *Prog. Phys. Org. Chem.* **1981**, *13*, 63; S. A. Godleski, P. von R. Schleyer, E. Osawa, Y. Inamoto, Y. Fujikura, *J. Org. Chem.* **1976**, *41*, 2596.
[10] T. Iizuka, M. Imai, N. Tanaka, T. Kan, E. Osawa, *Shizen Kagaku Hen* **1981**, *30*, 5; [*Chem. Abstr.* **1982**, *97*, 126567m]; A. T. Balaban, M. Banciu, U. Ciorba, *Annulenes, Benzo-, Hetero-, Homo-Derivatives and their Valence Isomers, Vol. 2*, CRC, Boca Raton, FL, **1987**, p. 92.
[11] "My Thirty Years in Hydrocarbon Cages: From Adamantane to Dodecahedrane": P. von R. Schleyer in ref. [3b], p. 1; "Catalytic Routes to Adamantane and its Homologues": M. A. McKervey, J. J. Rooney in ref. [3b], p. 39.
[12] W.-D. Fessner, H. Prinzbach, G. Rihs, *Tetrahedron Lett.* **1983**, *24*, 5857.
[13] W.-D. Fessner, Dissertation, Universität Freiburg, **1986**.
[14] N. L. Allinger, *J. Am. Chem. Soc.* **1977**, *99*, 8127; N. L. Allinger, H. L. Flanagan, *J. Comput. Chem.* **1983**, *4*, 399.
[15] W.-D. Fessner, B. A. R. C. Murty, P. R. Spurr, R. Pinkos, J.-P. Melder, H. Fritz, H. Prinzbach, *Chem. Ber.* **1992**, *125*, 1697.
[16] K. B. Lipkowitz, M. A. Peterson, *Chem. Rev.* **1993**, *93*, 4263, and references therein; O. Ermer, *Aspekte von Kraftfeldrechnungen*, Baur, München, **1981**.
[17] W. F. Maier, P. von R. Schleyer, *J. Am. Chem. Soc.* **1981**, *103*, 1891.
[18] W.-D. Fessuer, G. Sedelmeier, P. R. Spurr, G. Rihs, H. Prinzbach, *J. Am. Chem. Soc.* **1987**, *109*, 4626.
[19] K. Mackenzie, *J. Chem. Soc.* **1965**, 4646.
[20] G. Sedelmeier, W.-D. Fessner, R. Pinkos, C. Grund, B. A. R. C. Murty, D. Hunkler, G. Rihs, H. Fritz, C. Krüger, H. Prinzbach, *Chem. Ber.* **1986**, *119*, 3442.
[21] H. Prinzbach, G. Sedelmeier, C. Krüger, R. Goddard, H.-D. Martin, R. Gleiter, *Angew. Chem.* **1978**, *90*, 297; *Angew. Chem. Int. Ed. Engl.* **1978**, *17*, 271.
[22] R. Gleiter, H. Zimmermann, W.-D. Fessner, H. Prinzbach, *Chem. Ber.* **1985**, *118*, 3856.
[23] Together with K. Schaffner, S. A. Braslavski, J. Michl; M. Schottelius, Diplomarbeit, Universität Freiburg, **1994**.
[24] R. Thiergardt, M. Keller, M. Wollenweber, H. Prinzbach, *Tetrahedron Lett.* **1993**, *34*, 3397; M. Wollenweber, D. Hunkler, M. Keller, L. Knothe, H. Prinzbach, *Bull. Soc. Chim. Fr.* **1993**, *130*, 32.
[25] G. Sedelmeier, W.-D. Fessner, C. Grund, P. R. Spurr, H. Fritz, H. Prinzbach, *Tetrahedron Lett.* **1986**, *27*, 1277.
[26] W. Grimme, private communication.
[27] B. A. R. C. Murty, P. R. Spurr, R. Pinkos, C. Grund, W.-D. Fessner, D. Hunkler, H. Fritz, W. R. Roth, H. Prinzbach, *Chimia* **1987**, *41*, 32; R. Pinkos, Diplomarbeit, Universität Freiburg, **1986**; K. Weber, Diplomarbeit, Universität Freiburg, **1989**.
[28] H. Röttele, W. Martin, J. F. M. Oth, G. Schröder, *Chem. Ber.* **1969**, *102*, 3985.
[29] A. Bertsch, W. Grimme, G. Reinhardt, H. Rose, P. M. Warner, *J. Am. Chem. Soc.* **1988**, *110*, 5112; W. Grimme, H. G. Köser, *Angew. Chem.* **1980**, *92*, 307; *Angew. Chem. Int. Ed. Engl.* **1980**, *19*, 307.
[30] J. A. Berson, R. F. Davis, *J. Am. Chem. Soc.* **1972**, *94*, 3658.
[31] N. C. Yang, B. J. Hrnjez, M. G. Horner, *J. Am. Chem. Soc.* **1987**, *109*, 3158; N. C. Yang, T. Noh, H. Gan, S. Halfon, B. J. Hrnjez, *ibid.* **1988**, *110*, 5919.
[32] M. Wollenweber, Dissertation, Universität Freiburg, **1993**; M. Wollenweber, R. Pinkos, H. Prinzbach, *Angew. Chem.* **1994**, *106*, 84; *Angew. Chem. Int. Ed. Engl.* **1994**, *33*, 117.
[33] W. von E. Doering, W. R. Roth, R. Breuckmann, L. Figge, H. W. Lennartz, W.-D. Fessner, H. Prinzbach, *Chem. Ber.* **1988**, *121*, 1.
[34] T. L. Ho, *Tandem Organic Reactions*, Wiley, New York, **1992**, pp. 131, 202; L. F. Tietze, U. Beifuss, *Angew. Chem.* **1993**, *105*, 137; *Angew. Chem. Int. Ed. Engl.* **1993**, *32*, 131; T.-C. Chou, M.-S. Yang, C.-T. Lin, *J. Org. Chem.* **1994**, *59*, 661.

[35] F. G. Klärner, U. Artschwager-Perl, W.-D. Fessner, C. Grund, R. Pinkos, J.-P. Melder, H. Prinzbach, *Tetrahedron Lett.* **1989**, *30*, 3137.
[36] R. Krombach, J. Ellert, G. M. Schneider, H. Prinzbach, *Thermochim. Acta* **1993**, *216*, 335.
[37] G. K. S. Prakash, V. V. Krishnamurthy, R. Herges, R. Bau, H. Yuan, G. A. Olah, W.-D. Fessner, H. Prinzbach, *J. Am. Chem. Soc.* **1988**, *110*, 7764; R. Herges, P. von R. Schleyer, M. Schindler, W.-D. Fessner, *ibid.* **1991**, *113*, 3649.
[38] "Carbocations and Electrophilic Reactions of Cage Hydrocarbons": G. A. Olah in ref. [3b], p. 103.
[39] G. K. S. Prakash, W.-D. Fessner, G. A. Olah, G. Lutz, H. Prinzbach, *J. Am. Chem. Soc.* **1989**, *111*, 746.
[40] P. E. Eaton, G. H. Temme, *J. Am. Chem. Soc.* **1973**, *95*, 7508; W. T. Borden, I. L. Reich, L. A. Sharpe, R. B. Weinberg, H. J. Reich, *J. Org. Chem.* **1975**, *40*, 2438.
[41] E. C. Kooyman, G. C. Vegter, *Tetrahedron* **1958**, *4*, 382.
[42] D. Elsässer, K. Hassenrück, H.-D. Martin, B. Mayer, G. Lutz, H. Prinzbach, *Chem. Ber.* **1991**, *124*, 2863.
[43] P. Bischof, E. Heilbronner, *Helv. Chim. Acta* **1970**, *53*, 1677.
[44] R. Gleiter, D. Kratz, W. Schäfer, V. Schehlmann, *J. Am. Chem. Soc.* **1991**, *113*, 9258; K. B. Wiberg, R. D. Adams, P. J. Okarma, M. G. Matturo, B. Segmuller, *J. Am. Chem. Soc.* **1984**, *106*, 2200; E. Honegger, E. Heilbronner, K. B. Wiberg, *J. Electron Spectrosc. Relat. Phenom.* **1983**, *31*, 369.
[45] B. A. R. C. Murty, R. Pinkos, P. R. Spurr, W.-D. Fessner, G. Lutz, H. Fritz, D. Hunkler, H. Prinzbach, *Chem. Ber.* **1992**, *125*, 1719; G. Lutz, Dissertation, Universität Freiburg, **1990**.
[46] G. Lutz, R. Pinkos, B. A. R. C. Murty, P. R. Spurr, W.-D. Fessner, J. Wörth, H. Fritz, L. Knothe, H. Prinzbach, *Chem. Ber.* **1992**, *125*, 1741.
[47] G. Haufe, G. Mann, *Chemistry of Alicyclic Compounds*, Elsevier, Amsterdam, **1989**, p. 373; C. J. Lancelot, J. J. Harper, P. von R. Schleyer, *J. Am. Chem. Soc.* **1969**, *91*, 4294; P. G. Gassman, J. M. Hornback, *ibid.* **1969**, *91*, 4282.
[48] I. T. Jacobson, *Acta Chem. Scand.* **1967**, *21*, 2235; L. A. Paquette, *Top. Curr. Chem.* **1984**, *119*, 1.
[49] T. Pracht, Diplomarbeit, Universität Freiburg, **1988**.
[50] J.-P. Melder, H. Prinzbach, *Chem. Ber.* **1991**, *124*, 1271.
[51] R. Pinkos, G. Rihs, H. Prinzbach, *Angew. Chem.* **1989**, *101*, 312; *Angew. Chem. Int. Ed. Engl.* **1989**, *28*, 303.
[52] D. H. R. Barton, A. L. J. Beckwith, A. Goosen, *J. Chem. Soc.* **1965**, 181; J. E. Baldwin, D. H. R. Barton, I. Dainis, J. L. C. Pereira, *J. Chem. Soc. C* **1968**, 2283; W. Carruthers, *Some Modern Methods of Organic Synthesis*, 3rd ed., Cambridge University Press, Cambridge, **1986**, p. 263.
[53] J.-P. Melder, R. Pinkos, H. Fritz, J. Wörth, H. Prinzbach, *J. Am. Chem. Soc.* **1992**, *114*, 10213.
[54] R. Pinkos, J.-P. Melder, K. Weber, D. Hunkler, H. Prinzbach, *J. Am. Chem. Soc.* **1993**, *115*, 7173.
[55] H. Prinzbach, R. Pinkos, K. Weber, H. Irngartinger, U. Reifenstahl, *Tetrahedron Lett.* **1990**, *31*, 5459.
[56] E. Ogawa, K. Kanematsu in *Molecular Structure and Energetics, Vol. 3* (Eds.: J. F. Liebman, A. Greenberg), VCH, Weinheim, **1986**, Chapter 7.
[57] R. C. Haddon, *Science* **1993**, *261*, 1545; *J. Am. Chem. Soc.* **1990**, *112*, 3385; private communication.
[58] K. Weber, G. Lutz, L. Knothe, J. Mortensen, J. Heinze, H. Prinzbach, *J. Chem. Soc. Perkin Trans. 2*, submitted.
[59] J.-P. Melder, H. Prinzbach, G. Rihs, *Tetrahedron Lett.* **1990**, *31*, 1129.
[60] M. Bertau, R. Pinkos, K. Weber, J. Leonhardt, H. Prinzbach, unpublished.
[61] L. Stéhelin, L. Kanellias, G. Ourisson, *J. Org. Chem.* **1973**, *38*, 851.
[62] R. Schwesinger, R. Link, G. Thiele, H. Rotter, D. Honert, H.-H. Limbach, F. Männle, *Angew. Chem.* **1991**, *103*, 1376; *Angew. Chem. Int. Ed. Engl.* **1991**, *30*, 1372.
[63] F. Wahl, J. Wörth, H. Prinzbach, *Angew. Chem.* **1993**, *105*, 1788; *Angew. Chem. Int. Ed. Engl.* **1993**, *32*, 1722.
[64] H. D. Beckhaus, C. Rüchardt, D. R. Lagerwall, L. A. Paquette, F. Wahl, H. Prinzbach, *J. Am. Chem. Soc.*, in press.
[65] R. L. Disch, J. M. Schulman, *J. Am. Chem. Soc.* **1988**, *110*, 2102; J. M. Schulman, private communication.
[66] R. Pinkos, J.-P. Melder, H. Fritz, H. Prinzbach, *Angew. Chem.* **1989**, *101*, 319; *Angew. Chem. Int. Ed. Engl.* **1989**, *28*, 310.
[67] M. Keller, K. Scheumann, K. Weber, T. Voss, H. Prinzbach, H. Irngartinger, U. Reifenstahl, *Tetrahedron Lett.* **1994**, *35*, 1531.
[68] T. Voss, H. Prinzbach, *Tetrahedron Lett.* **1994**, *35*, 1535; T. J. Chow, T. K. Wu, *ibid.* **1989**, *30*, 1279.
[69] L. A. Paquette, R. J. Ternansky, D. W. Balough, G. Kentgen, *J. Am. Chem. Soc.* **1983**, *105*, 5446; L. A. Paquette, J. C. Weber, T. Kobayashi, *ibid.* **1988**, *110*, 103.
[70] J. M. Schulman, T. Venanzi, R. L. Disch, *J. Am. Chem. Soc.* **1975**, *97*, 5335; K. Balasubramanian, *Chem. Rev.* **1985**, *85*, 599.
[71] F. Wahl, Dissertation, Universität Freiburg, **1993**.
[72] K. Scheumann, Dissertation, Universität Freiburg, **1993**; K. Scheumann, F. Wahl, H. Prinzbach, *Tetrahedron Lett.* **1992**, *33*, 615.
[73] W. B. Motherwell, D. Crich, *Free Radical Chain Reactions* in *Organic Synthesis*, Academic Press, New York, **1992**.
[74] A. Weiler, Diplomarbeit, Universität Freiburg, **1994**.
[75] L. A. Paquette, D. R. Lagerwall, H.-G. Korth, *J. Org. Chem.* **1992**, *57*, 5413.
[76] D. A. Hrovat, W. T. Borden, *J. Am. Chem. Soc.* **1988**, *110*, 4710.
[77] K. Weber, Dissertation, Universität Freiburg, **1993**; K. Weber, H. Fritz, H. Prinzbach, *Tetrahedron Lett.* **1992**, *33*, 619.
[78] J.-P. Melder, R. Pinkos, H. Fritz, H. Prinzbach, *Angew. Chem.* **1990**, *102*, 105; *Angew. Chem. Int. Ed. Engl.* **1990**, *29*, 95.
[79] G. E. Renzoni, T.-K. Yin, W. T. Borden, *J. Am. Chem. Soc.* **1986**, *108*, 7121.
[80] Experiments conducted with A. Haas, M. Lieb (Universität Bochum).
[81] J. G. Radszizewski, T.-K. Yin, F. Miyake, G. E. Renzoni, W. T. Borden, J. Michl, *J. Am. Chem. Soc.* **1986**, *108*, 3544.
[82] R. Herges, private communication.
[83] The crown conformation of the [10] annulene with axial C–H bonds is energetically extremely unfavorable: Y. Xie, H. F. Schaefer III, G. Liang, J. P. Bowen, *J. Am. Chem. Soc.* **1994**, *116*, 1442.
[84] D. Bakowies, W. Thiel, *J. Am. Chem. Soc.* **1991**, *113*, 3704; V. Parasuk, I. Almof, *Chem. Phys. Lett.* **1991**, *184*, 187; C. J. Brabec, E. Anderson, B. N. Davidson, S. A. Kajihara, Q. M. Zhang, J. Bernholc, D. Tomanec, *Phys. Rev. B* **1992**, *46*, 7326; G. v. Helden, M. T. Hsu, N. G. Gotts, P. R. Kemper, M. T. Bowers, *Chem. Phys. Lett.* **1993**, *204*, 15.
[85] W. T. Borden, *Chem. Rev.* **1989**, *89*, 1097; W. Luef, R. Keese, *Top. Stereochem.* **1991**, *20*, 231; R. Haag, B. Ohlhorst, M. Noltemeyer, A. Schuster, D. Kuck, A. de Meijere, *J. Chem. Soc. Chem. Commun.* **1993**, 1727.
[86] K. Weber, T. Voss, M. Keller, H. Prinzbach, unpublished.
[87] E. E. B. Campbell, R. Tellgmann, F. Wahl, H. Prinzbach, *Int. J. Mass Spectrom. Ion Processes* **1994**, *136*, 209.
[88] W. E. Billups, M. A. Ciufolini, *Buckminsterfullerenes*, VCH, Weinheim, **1993**; F. Diederich, Y. Rubin, *Angew. Chem.* **1992**, *104*, 1123; *Angew. Chem. Int. Ed. Engl.* **1992**, *31*, 1101.
[89] V. I. Minkin, R. M. Minayev, Y. A. Zhdanov, *Nonclassical Structures of Organic Compounds*, MIR, Moscow, **1987**, p. 238.
[90] M. Saunders, H. A. Jiménez-Vázquez, R. J. Cross, R. J. Poreda, *Science* **1993**, *259*, 1428; M. Saunders, H. A. Jiménez-Vázquez, R. J. Cross, S. Mroczkowski, M. L. Gross, D. E. Giblin, R. J. Poreda, *J. Am. Chem. Soc.* **1994**, *116*, 2193.
[91] H. Prinzbach, B. A. R. C. Murty, W.-D. Fessner, J. Mortensen, J. Heinze, G. Gescheidt, F. Gerson, *Angew. Chem.* **1987**, *99*, 488; *Angew. Chem. Int. Ed. Engl.* **1987**, *26*, 457.
[92] H. D. Roth, *Top. Curr. Chem.* **1992**, *163*, 131; K. Ishiguro, I. V. Khudyakov, P. F. McGarry, N. J. Turro, H.-D. Roth, *J. Am. Chem. Soc.* **1994**, *116*, 6933.
[93] T. Drewello, W.-D. Fessner, A. J. Kos, C. B. Lebrilla, H. Prinzbach, P. von R. Schleyer, H. Schwarz, *Chem. Ber.* **1988**, *121*, 187.
[94] F. Gerson, G. Gescheidt, S. F. Nelsen, L. A. Paquette, M. F. Teasley, L. Waykole, *J. Am. Chem. Soc.* **1989**, *111*, 5518.
[95] Cf. with the effort directed towards [0.0.0.0]pagodanes: T. Pracht, K. Weber, H. Fritz, L. Knothe, H. Prinzbach, *J. Chin. Chem. Soc. (Taipei)* **1994**, *41*, 1.
[96] R. Herges, H. Neumann, H. Prinzbach, unpublished.
[97] H. Prinzbach, M. Wollenweber, R. Herges, H. Neumann, G. Gescheidt, R. Schmidlin, unpublished; see also T. Bally, *Chimia* **1994**, *48*, 378.
[98] R. Herges, unpublished.
[99] K. Weber, H. Prinzbach, R. Schmidlin, F. Gerson, G. Gescheidt, *Angew. Chem.* **1993**, *105*, 907; *Angew. Chem. Int. Ed. Engl.* **1993**, *32*, 875.
[100] H.-D. Martin, B. Mayer, K. Weber, H. Prinzbach, *Chem. Ber.*, submitted.
[101] "How should Chemists think?": R. Hoffmann, *Sci. Am.* **1993**, *268*(2), 40.

Technetium Radiopharmaceuticals— Fundamentals, Synthesis, Structure, and Development

Klaus Schwochau*

Technetium-99m radiopharmaceuticals are increasingly finding application in nuclear medicine for scintigraphic and emission tomographic imaging, morphologic description and functional testing of organs. Over 80% of the radiopharmaceuticals currently clinically used are labeled with the short-lived, metastable nuclide ^{99m}Tc, whose nuclear properties are almost optimal with regard to a low radiation exposure of the patient and an effective detection of the emitted γ quanta. $^{99m}TcO_4^-$ can be easily prepared without the use of accelerator systems through generator columns. Most of the ^{99m}Tc radiopharmaceuticals are complexes which are synthesized by reduction of $^{99m}TcO_4^-$ in the presence of suitable ligands. To achieve a high organ specificity, some understanding of the relationship between the structure of the diagnostic agent and its organ distribution is necessary. Structure analyses can be carried out on analogous compounds of the long-lived nuclide technetium-99g; these compounds are obtainable in weighable quantities. The development of new ^{99m}Tc radiopharmaceuticals is a challenge to coordination chemists. The syntheses, molecular structures, and applications of the most important ^{99m}Tc radiopharmaceuticals will be described in this review, and current directions and tendencies of the development will be shown.

1. Introduction

Radiopharmaceuticals mostly are organic or inorganic compounds with definite composition that contain a short-lived radionuclide as stoichiometric component. But also macromolecular biomolecules that are not stoichiometrically labeled with a radionuclide can be used as radiopharmaceuticals, as can chemically unbound radionuclides such as the noble gases ^{81m}Kr, ^{85}Kr, ^{27}Xe, and ^{133}Xe. Radiopharmaceuticals are used in very low concentrations and have no intentional pharmacologic effect. The aim of the diagnostic application is the detailed description of the morphologic structure of organs and, in particular, the testing of their physiological function through the accumulation of a radionuclide, whose emitted γ radiation permits the tomographic in vivo imaging of the organs. Suitable radionuclides include, for positron-emission tomography (PET) ^{11}C ($t_{1/2}$ = 20 min), ^{13}N ($t_{1/2}$ = 10 min), and ^{18}F ($t_{1/2}$ = 110 min), for single photon emission tomography (SPET) ^{99m}Tc ($t_{1/2}$ = 6 h), ^{123}I ($t_{1/2}$ = 13 h), and ^{201}Tl ($t_{1/2}$ = 73.5 h).

On average over 80% of the radiopharmaceuticals used in clinics are labeled with ^{99m}Tc, the metastable nuclear isomer of the long-lived technetium-99g in the ground state, which is obtained in weighable amounts from the fission of uranium-235 in nuclear reactors.[1, 2] ^{99m}Tc radiopharmaceuticals are used preferably because of the almost optimal nuclear properties of ^{99m}Tc as well as its convenient availability by using commercial generator columns.[3] The physical half-life of ^{99m}Tc of only 6 h and the absence of tissue-damaging corpuscular radiation[4] allow the injection of activities of more than 30 mCi (1110 MBq) with low radiation exposure of the patient.[5] The half-life is, however, long enough to carry out the labeling syntheses and the scintigraphic measurements without significant losses in activity. On the one hand, the energy of the emitted photons of 140 keV is sufficient to also study organs lying deep in the body. On the other hand, photons of this energy can be collimated with lead collimators with relatively low wall thickness and be detected effectively with NaI(Tl) scintillation counters.[6] ^{99g}Tc, the decay product of ^{99m}Tc, is a pure β-emitter with a half-life of 2.1×10^5 a and does not contribute noticeably to the radiation exposure.

For the synthesis of specific radiopharmaceuticals, the versatile chemistry of this transition element, apparent from the existence of compounds in a large number of technetium oxidation states, is an advantage. However, the labeling requires the complexing of ^{99m}Tc with suitable functional groups. Metabolizable biomolecules must always be functionalized as complexing ligands, and as a result suffer a change in their biochemical properties, especially through coordination to the central technetium atom. Consequently, the use of ^{99m}Tc complexes with ligands without biomolecular character or the use of non-complex compounds such as tetraoxotechnetate(VII) $^{99m}TcO_4^-$ was more successful to date. The development of new ^{99m}Tc radiopharmaceuticals is currently focused more on complexes whose

[*] Prof. Dr. K. Schwochau
Institut für Chemie und Dynamik der Geosphäre
Forschungszentrum Jülich GmbH (KFA)
D-52425 Jülich (FRG)
Telefax: Int. code + (2461)61-2484

ligands are chosen under consideration of the expected stability, lipophilicity, charge, and structure of the radiopharmaceuticals. For specific syntheses, knowledge of the relationship between molecular structure and organ distribution is necessary. Molecular structures are, however, only analyzable on weighable technetium compounds, which are obtained by synthesis of a model radiopharmaceutical with the long-lived nuclide technetium-99g. Its structure can then determined with the standard methods used in complex chemistry. After transferring the synthesis process from the ^{99g}Tc to the ^{99m}Tc compounds, the analogous structure of the product can be confirmed by radiochromatographic techniques (HPLC, TLC) or electrophoresis.

2. Preparation of ^{99m}Tc

^{99m}Tc is available through the decay of ^{99}Mo (Fig. 1),[4] and ^{99}Mo can be obtained by irradiation of natural molybdenum or of enriched molybdenum-98 with thermal neutrons in a nuclear

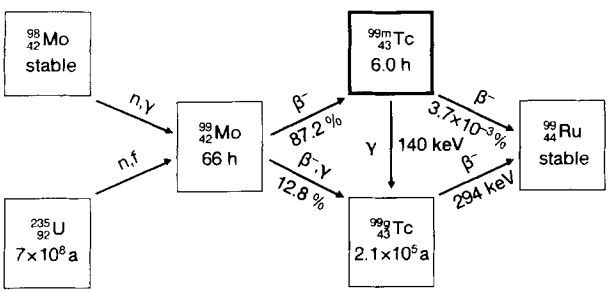


Fig. 1. Formation and decay of ^{99m}Tc and ^{99g}Tc [4].

reactor. The cross section of the reaction ^{98}Mo(n_{th},γ)^{99}Mo amounts to 0.13 barn.[7] Molybdenum trioxide, ammonium molybdate, or molybdenum metal are used as target compounds. This so-called (n,γ)-molybdenum-99 is obtained in high nuclidic purity; the specific activity, however, amounts to only a few Ci per g. In contrast, molybdenum-99 with a specific activity of more than 10^4 Ci (3.7×10^8 MBq) g^{-1} is obtainable by fission of ^{235}U with thermal neutrons in a fission yield of 6.1 atom%.[8] Natural or ^{235}U-enriched uranium in the form of metal, uranium-aluminum alloys or uranium dioxide, is used for the fission. The isolation requires many separation steps, particularly for the separation of other fission products and transuranium elements which are also formed.

The nuclide ^{99}Mo decays with a 87% probability to ^{99m}Tc, which almost quantitatively converts, by isomeric transition with a half-life of 6 h under emission of photons of the energy 140 keV, to the ground state ^{99g}Tc; the loss of photons due to internal conversion is about 10%.[9] Only 4×10^{-3}% of the decay products of ^{99m}Tc leads, under β^--emission, directly to stable ^{99}Ru.

The nuclide ^{99m}Tc is separated from ^{99}Mo mainly by column chromatography, and only for special cases by sublimation processes or solvent extraction. The development of the first chromatographically functioning ^{99m}Tc generator succeeded, as early as at the end of the 1950s, at the Brookhaven National Laboratory, USA.[10, 11] Currently acidic aluminum oxide with anion exchange properties is used as column packing material. ^{99}Mo is bound as MoO_4^{2-} at the top end of the column, whilst ^{99m}Tc can simply be eluted as negatively charged $^{99m}TcO_4^-$ with a physiological (0.15 M) sodium chloride solution. $^{99m}TcO_4^-$ is regenerated on the generator column by ^{99}Mo decay (Fig. 2).[9]

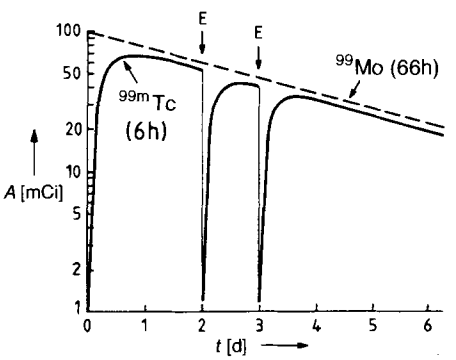


Fig. 2. Production of the ^{99m}Tc activity (A) in the system ^{99}Mo/^{99m}Tc after elution E from the generator column [9].

The ^{99m}Tc activity A_T formed after time t as a percentage of the activity A_M of the parent nuclide ^{99}Mo can be calculated according to Equation (a), where $\delta = 87.2\%$ is the branching

$$\frac{A_T}{A_M} = \delta \frac{\lambda_T}{\lambda_T - \lambda_M}(1 - e^{-(\lambda_T - \lambda_M)t}) \quad \text{(a)}$$



Klaus Schwochau is a chemist and researcher at the Institut für Chemie und Dynamik der Geosphäre of the Forschungszentrum Jülich GmbH (KFA). He obtained his doctorate in 1961 at the Universität zu Köln, habilitated in 1971 at the Technische Hochschule in Aachen, and became Professor for Inorganic Chemistry at the Technischen Hochschule in Aachen in 1977. His research activities have concentrated on the chemistry of the radioactive elements, particularly on the coordination chemistry of technetium, and for several years also on the development of new technetium radiopharmaceuticals. In addition, at the Institut für Erdöl und Organische Geochemie of the KFA, he works on problems of petroleum formation and the behavior of pollutants in the soil.

ratio, that is, the probability of the decay of ^{99}Mo into ^{99m}Tc, and $\lambda_T = 0.1155\ h^{-1}$ is the radioactive decay constant of the daughter nuclide (^{99m}Tc), and $\lambda_M = 0.0105\ h^{-1}$ is that of the mother nuclide. As an example, 24 h after elution of the generator column, the activity of ^{99m}Tc is already 88.2% of that of ^{99}Mo. The total concentration of TcO_4^- ($^{99m}Tc + {}^{99}Tc$) in the eluate is about 10^{-6}–10^{-8} M.[12] For imaging and functional testing of organs in human bodies, about 0.5–30 mCi (18.5–1110 MBq) ^{99m}Tc are needed, which corresponds to a maximum of 6 ng.

The generator eluates must be sterile and pyrogen free, and their nuclidic purity must conform to the demands of the European Pharmacopoeia. Under the assumption that ^{99m}Tc is applied within 12 h of the elution, the upper limits for ^{99m}Tc per mCi ^{99m}Tc obtained from molybdenum-99 by fission are: 1 μCi (3.7×10^4 Bq) ^{99}Mo, 50 nCi (1850 Bq) ^{103}Ru, 50 nCi (1850 Bq) ^{131}I, 100 nCi (3700 Bq) for all other γ-emitters together, 0.6 nCi (22.2 Bq) ^{89}Sr, 0.06 nCi (2.22 Bq) ^{90}Sr, and 1 pCi (3.7×10^{-2} Bq) for each α-emitter.[13]

3. Organ Imaging

The ^{99m}Tc injected into the body, depending on its chemical form and its molecular structure, concentrates in the organ to be investigated, and emits 140 keV γ-quanta which permits the imaging of the organ using planar scintigraphic or emission tomographic processes. The imaging of the spatial distribution of the radionuclide in the organ proceeds through the focusing of the gamma camera on sections or planes. The camera head moves circularly or elliptically around the patient; the rotation axis coincides with longitudinal axis of the body. Within the reconstructed layers the obtainable resolution, under favorable measurement conditions, amounts to about 7 mm. The resolution is particularly dependent on the collimator and the distance between collimator and object.[14]

The lead collimator has many, mostly parallel holes. It shields the detector from background radiation. The image resolution of the collimator improves with decreasing hole diameter and increasing length of the bore. Collimators in gamma cameras for the detection of the 140 keV γ-quanta of ^{99m}Tc have up to 40000 bores, hole diameters from 1–2 mm, and lead septa with a wall thickness of 0.25 mm.[15, 16]

The detector is a Tl-activated NaI single crystal of about 0.6 cm thickness and over 25 cm diameter.[9] Thicker crystals have, on the one hand, the disadvantage that multiple absorptions can occur, which reduce the image resolution; on the other hand, the detector sensitivity increases with growing thickness of the crystal.

4. Synthesis Procedures

For the development of ^{99m}Tc radiopharmaceuticals of definite composition and structure, the synthesis and characterization of the concipated compounds with long-lived technetium-99g which is available in weighable amounts, is indispensible. Microgram or even milligram quantities of ^{99m}Tc could hardly be handled experimentally due to the short half-life of 6 h and the enormous radioactivity; for example, 100 μg $Na^{99m}TcO_4$ already have an activity of 270 Ci (10^7 MBq). In contrast, 50 mg $Na^{99g}TcO_4$, a β^--emitter with 0.45 mCi (160 MBq), can be handled relatively easily in a well-ventilated fume cupboard, without any special radiation protection, but applying the generally accepted rules regarding radiation protection. The weak β^- radiation ($E_{max} = 0.29$ MeV) is largely shielded by the glass walls of standard laboratory vessels.[17]

Technetium occurs as a transition element of the seventh subgroup of the periodic table in the oxidation states of +7 to −1 and tends towards complex formation. Its chemical behavior is closely related to that of the homologous element rhenium because of the small differences in atomic and ionic radii.[18] Tetraoxotechnetate(VII) and tetraoxorhenate(VII) belong to the thermodynamically most stable compounds of technetium and rhenium, in contrast to tetraoxomanganate(VII). The standard electrode potential in acidic aqueous solutions amounts to only + 0.738 V for TcO_4^-/TcO_2, but +1.695 V for MnO_4^-/MnO_2. If TcO_4^- is reduced in the absence of sufficiently strong complexing ligands, the oxidation state + 4 often manifests itself through the formation of the sparingly soluble TcO_2 hydrate.[2]

The starting material for the synthesis of technetium radiopharmaceuticals is $Na^{99m}TcO_4$, which is available after elution of the generator column with physiological saline as 0.15 M aqueous NaCl solution. The concentration of $^{99m}TcO_4^-$ in the eluate is about 50–500 mCi (1.85×10^3–1.85×10^4 MBq) per 5 mL, corresponding to 2×10^{-8}–2×10^{-7} M. $^{99m}TcO_4^-$ can be used as such for thyroid and brain imaging; however, for brain imaging only then, when the blood-brain barrier (BBB) is not intact.[19] The synthesis of other ^{99m}Tc radiopharmaceuticals requires the reduction of TcO_4^- in the presence of suitable complexing ligands throughout.

A variety of reducing agents can be used for the reduction of $^{99m}TcO_4^-$. Transition metal ions such as Ti^{III}, Cr^{II}, Cu^{I}, and Fe^{II} that tend toward complex formation should be avoided, since they could compete with ^{99m}Tc for ligands. Equally unsuitable are oxalates, formates, hydroxylamine, and hydrazine, which form undesired complexes with ^{99m}Tc. One must remember that even when using the common reducing agent Sn^{II}, technetium can form heteronuclear complexes, such as the Tc-Sn-dimethylglyoxime complex $[Tc(DMG)_3(\mu\text{-}OH)SnCl_3]$ on reduction of TcO_4^- with Sn^{II} in the presence of dimethylglyoxime.[20, 21] The potentials vs. the standard hydrogen electrode of several suitable redox systems for the reduction of TcO_4^- are given in Table 1.[22]

The controlled-potential electrolytic reduction of $^{99m}TcO_4^-$ at chemically inert electrodes, for example at Hg or Pt cathodes, is also applicable. It often permits the reduction to defined oxidation states in 5–10 min and avoids the addition of reducing agents which cause impurities in the radiopharmaceutical solution.[23] The electrolytic reduction has found little application in clinical practice, since it requires more equipment.

The synthesis of the radiopharmaceutical from $^{99m}TcO_4^-$, reducing agent, and complexing ligand should preferably proceed in one step directly after elution of $^{99m}TcO_4^-$ from the generator column and must be carried out in a solvent which is suitable for intravenous injections, such as physiological sodium chloride solution. The use of ethanol additives in concentrations up to

Table 1. Standard electrode potentials of redox systems [22] for the reduction of tetraoxotechnetate(VII).

Medium	Redox system				E_0 [V]
	$S_2O_3^{2-}$	$+ 3H_2O \rightleftharpoons 2H_2SO_3$	$+ 2H^+$	$+ 4e^-$	0.40
	Sn^{2+}	$\rightleftharpoons Sn^{4+}$	+	$2e^-$	0.15
acidic	$S_2O_6^{2-}$	$+ 2H_2O \rightleftharpoons 2SO_4^{2-}$	$+ 4H^+$	$+ 2e^-$	− 0.22
	H_3PO_3	$+ H_2O \rightleftharpoons H_3PO_4$	$+ 2H^+$	$+ 2e^-$	− 0.276
	H_3PO_2	$+ H_2O \rightleftharpoons H_3PO_3$	$+ 2H^+$	$+ 2e^-$	− 0.50
	$[Sn(OH)_3]^-$	$+ 3OH^- \rightleftharpoons [Sn(OH)_6]^{2-}$	+	$2e^-$	− 0.90
	SO_3^{2-}	$+ 2OH^- \rightleftharpoons SO_4^{2-}$	$+ H_2O$	$+ 2e^-$	− 0.936
basic	HPO_3^{2-}	$+ 3OH^- \rightleftharpoons PO_4^{3-}$	$+ 2H_2O$	$+ 2e^-$	− 1.12
	$S_2O_4^{2-}$	$+ 4OH^- \rightleftharpoons 2SO_3^{2-}$	$+ 2H_2O$	$+ 2e^-$	− 1.12
	BH_4^-	$+ 8OH^- \rightleftharpoons H_2BO_3^-$	$+ 5H_2O$	$+ 8e^-$	− 1.24
	$H_2PO_2^-$	$+ 3OH^- \rightleftharpoons HPO_3^{2-}$	$+ 2H_2O$	$+ 2e^-$	− 1.570

5 vol. % is permissible. The reagents used should not be toxic and the injected solutions must be sterile and pyrogen free. ^{99m}Tc should occur predominantly in the expected complex form and molecular structure, that is the so-called radiochemical purity should exceed 90% to ensure a high organ specificity.

5. Kits

Kits are sterile and pyrogen-free reagent mixtures, which are dried by lyophilization and stored under nitrogen in ampules. These contain the substance to be labeled (complexing ligand) and generally a reducing agent, usually Sn^{II}. The kits can be purchased and stored for long periods of time. The labeling with ^{99m}Tc proceeds shortly before use of the radiopharmaceutical by addition of the ^{99m}Tc generator eluate. Table 2 shows ^{99m}Tc radiopharmaceuticals, prepared from purchasable kits, which are currently used for the scintigraphic imaging of organs.

Amongst ^{99m}Tc radiopharmaceuticals for brain imaging, TcO-d,l-hexamethyl-propylene-amine oxime (TcO-d,l-HM-PAO),[25-27] TcO-*N*,*N*'-1,2-ethanediyl-bis(L-cysteine-diethyl ester(TcO-L,L-ECD),[28,29] and a boric acid adduct of technetium dimethylglyoxime TcCl(dimethylglyoxime)-(2-methyl-1-propyl)boron ($TcCl(DMG)_3$2MP)[26,30,31] (see Scheme 1) are capable of penetrating the intact blood-brain barrier due to their neutral and lipophilic character. The blood-brain barrier controls the exchange of material between blood and brain, and ensures the necessary stable environment in the brain.[32,33] Tc-diethylenetriaminepentaacetic acid,[34,35] whose molecular structure is not yet unambiguously known, Tc-glucoheptonate[36] (see Scheme 2), and sodium tetraoxotechnetate(VII)[9] can usually not pass through the blood-brain barrier, but can be used when the blood-brain barrier has been damaged, for example by tumors.

TcO-d,l-HM-PAO is formed by reduction of $^{99m}TcO_4^-$ with Sn^{II} in the presence of the ligand d,l-HM-PAO. The human brain accumulates for example 3.4–5.7% of the injected activity up to 8 h after the injection.[37] Figure 3 shows as example an emission tomogram, obtained by using ^{99m}TcO-d,l-HM-PAO, of the brain of a patient with focal blood hypoperfusion. According to structural investigations on ^{99g}Tc-d,l-HM-PAO the molecular structure of the complex is a square pyramid with the oxygen atom at the apex (Scheme 1a). Technetium in the oxidation state + 5 is located 0.68 Å above the basal plane defined by the four nitrogen atoms. The oxime-oxygen atoms form a strong intramolecular hydrogen bond. The complex carries no charge.[25]

TcO-L,L-ECD can also be prepared by reduction of $^{99m}TcO_4^-$ with Sn^{II} and subsequent complexing with the ligand. The brain takes up almost 5% of the injected activity dose within a few minutes; after an hour this falls to 4%.[29] The ^{99g}Tc complex, with a distorted square-pyramidal geometry of the donor atoms

Table 2. ^{99m}Tc Radiopharmaceuticals in kits for scintigraphic imaging of human organs [6,9,24].

Organ	^{99m}Tc-labeled substance	*A* mCi (MBq)	Application
brain	TcO-d,l-HM-PAO	7–15 (259–555)	regional blood perfusion, cerebral stroke, ischemia, dementia, epilepsy, tumors
	TcO-L,L-ECD	25–30 (925–1110)	regional blood perfusion, trauma, cerebral stroke, focal epilepsy
	$TcCl(DMG)_3$2MP		regional perfusion
	Tc-DTPA	5–20 (185–740)	blood perfusion, tumor localization
	Tc-glucoheptonate	15–20 (555–740)	blood perfusion
	sodium tetraoxotechnetate(VII)	10–20 (370–740)	blood perfusion, regional accumulation, cerebral lesions
thyroid	sodium tetraoxotechnetate(VII)	0.5–2 (18.5–74)	morphology, vascularity, function
lungs	Tc-MAA, particle size 10–40 μm	1–16 (37–600)	blood perfusion, shunt diagnosis, vessel scintigraphy
	Tc-DTPA aerosol	5.4 (200)	ventilation
heart	Tc-HEXAMIBI	10–30 (370–1110)	blood perfusion, ischemia, myocardial infarction, coronary arteries
	Tc-CDO-MeB	15 (555)	blood perfusion, coronary arteries, myocardial infarction
liver, gall	Tc-HIDA and derivatives	5–15 (185–555)	liver and gall bladder function, gall bladder infection
	Tc-sulfur colloid	1–3 (37–111)	liver morphology, tumors, abscesses
kidneys	$TcO\text{-}MAG_3$	1–20 (37–740)	nephrological and urological complaints, kidney tubuli function
	Tc-DMSA	1–5 (37–185)	function diagnosis, morphology
skeleton	Tc-MDP and derivatives	10–20 (370–740)	skeleton-scintigraphy, bone metastases, sarcoma, osteomyelitis, arthritis.

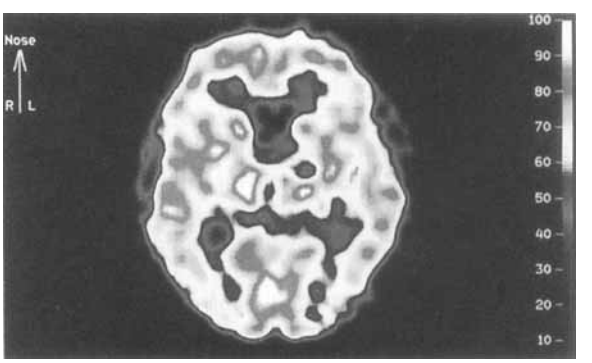
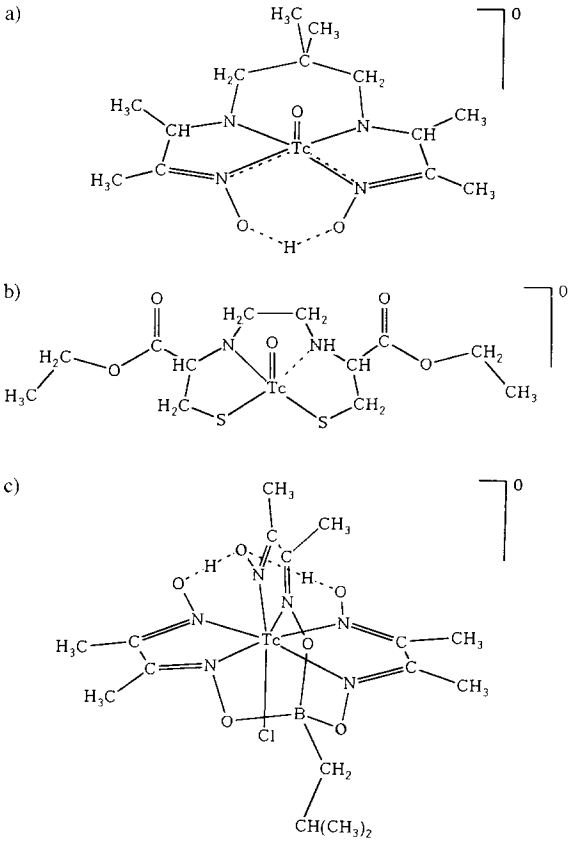


Fig. 3. Emission tomogram of the brain of a patient suffering from focal blood hypoperfusion; taken after injection of ^{99m}TcO-d,l-HM-PAO. The scale on the right-hand edge of the picture gives the count rate per 10 mm^2 [%].

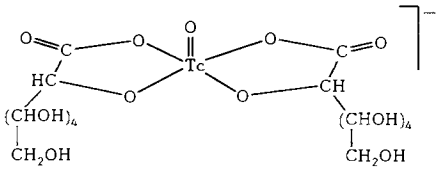
(Scheme 1 b) with the oxygen atom at the apex, and an oxidation state of + 5, has a similar structure to that of ^{99g}Tc-d,l-HM-PAO. Also the distance of the central atom from the N_2S_2 plane is similar with 0.73 Å. Since one nitrogen atom is protonated, this complex is again uncharged.[28]



Scheme 1. Structural formulas of ^{99m}Tc radiopharmaceuticals that can pass through the blood-brain barrier: a) TcO-d,l-HM-PAO, b) TcO-L,L-ECD, c) TcCl-(DMG)$_3$2MP.

TcCl(DMG)$_3$2MP forms by reduction of $^{99m}TcO_4^-$ with $SnCl_2$ in the presence of dimethylglyoxime and 2-methylpropylboric acid. The testing of this complex for clinical applications in brain imaging does not appear to be completed yet. In the brain of baboons, the uptake 5 min after injection amounted to 2.8 % of the injected dose; the biological half-life of the decrease in activity in the brain was determined to be 86 min.[30] As shown in Scheme 1c, technetium in TcCl(DMG)$_3$2MP has the relatively rare coordination number 7, the oxidation state + 3, and is surrounded by the nitrogen atoms of three dioxime ligands and a covalently bonded chlorine atom. The boron atom resides in a tetrahedral environment, bound to three dioxime oxygen atoms and the 2-methylpropyl group. The remaining three oxygen atoms of the dioxime ligands are bound to each other through two strong hydrogen bonds. The complex is also neutral.[38]

For the synthesis of ^{99m}Tc-diethylenetriaminepentaacetic acid (Tc-DTPA), $^{99m}TcO_4^-$, after reduction with tin(II) chloride, is treated with calcium-sodium-diethylenetriaminepentaacetate. Experimental investigations indicate the anionic character of the complex and the oxidation state of + 4 for the technetium atom.[34, 35, 39, 40] Tc-glucoheptonate is obtained by reaction of a mixture of calcium glucoheptonate and $SnCl_2$ with $^{99m}TcO_4^-$. The molecular structure[36] reproduced in Scheme 2 follows from NMR and IR spectra and shows a Tc^V=O core and two five-membered glucoheptonate rings, which are bidentately bound through oxygen atoms to the technetium center. Finally, $Na^{99m}TcO_4$ is injected as generator eluate for brain imaging. It accumulates particularly in the choroid plexus (vascular plexus in the region of the brain ventricles).



Scheme 2. Structural formula of Tc-glucoheptonate, a radiopharmaceutical, which can normally not pass through the blood-brain barrier.

Sodium tetraoxotechnetate(VII) is used predominantly for thyroid imaging.[9] Similarly to iodide, perhaps due to similar ion size and charge, $^{99m}TcO_4^-$ is taken up by the thyroid, but unlike iodine it is not incorporated by thyroglobulin. The uptake of TcO_4^- amounts to about 3–4% of the injected activity 30 min after injection and decreases to 1–2% after 6 h.[41] Figure 4 shows the scintiphotograph of a normal thyroid 1 h after injection of $Na^{99m}TcO_4$.

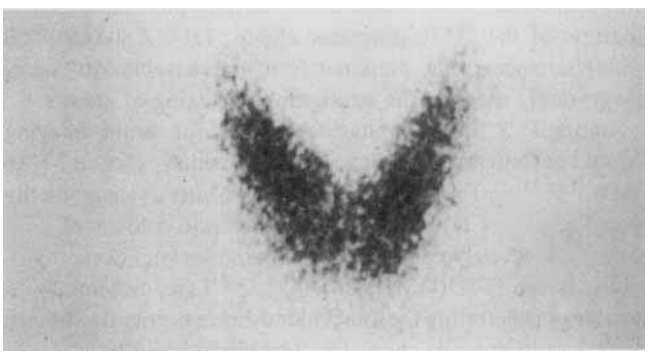
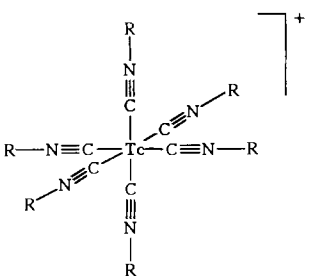


Fig. 4. Scintiphotograph of a normal thyroid; from the front, taken after injection of $Na^{99m}TcO_4$ [9], that is the thyroid lobe shown on the left-hand side of the picture corresponds to the one on the right-hand side of the body.

^{99m}Tc-labeled macroaggregated human serum albumin (Tc-MAA) for lung imaging is prepared by reduction of $^{99m}TcO_4^-$ with $SnCl_2$ in the presence of a human serum albumin solution. The labeling proceeds at pH 5.5, the isoelectric point of the albumin, in a yield of over 95%. It does not yet appear to be known in which oxidation state and how ^{99m}Tc is bound. The accumulation of Tc-MAA in the lung occurs because particles with a size exceeding 10 μm are held in the capillaries of the lungs. About 10^6 Tc-MAA particles per injection are applied, but the number of capillaries occluded by this, relative to the total number of lung capillaries of 2.8×10^{11}, is negligible. The biological half-life of the Tc-MAA particles in the lung amounts to 2–3 h.[9] For lung ventilation examinations, Tc-DTPA is recommended as aerosol, which is exhaled again after 8 h.

Currently, two ^{99m}Tc radiopharmaceuticals are mainly used for heart imaging (see Table 2), the cation hexakis(2-methoxy-2-methylpropyl-isonitrile)technetium(I) (Tc-HEXAMIBI) in the form of the tetrafluoroborate salt, and the neutral complex chloro{tris(cyclohexanedione dioxime)}-methylboratotechnetium(III) (Tc-CDO-MeB).

Tc-HEXAMIBI is synthesized by reduction of $^{99m}TcO_4^-$ with $Na_2S_2O_4$ in the presence of the isonitrile ligand[42] or in a kit by reaction of tetrakis(2-methoxy-2-methylpropyl-1-isonitrile)-copper(I) tetrafluoroborate with $SnCl_2$ and $^{99m}TcO_4^-$.[43] The uptake in the human heart amounts to about 1.5% of the injected activity and only decreases to 1% after 4 h. The background activity in the blood, lungs, liver, and spleen are sufficiently low.[44] The expected molecular structure for the cationic complex is given in Scheme 3. The structure of the precursor of Tc-HEXAMIBI, hexakis-(*tert*-butylisonitrile)technetium(I), has been determined by X-ray analysis.[45] Here, the Tc center is surrounded octahedrally by the isonitrile ligands; the Tc–C distance is 2.029 Å.

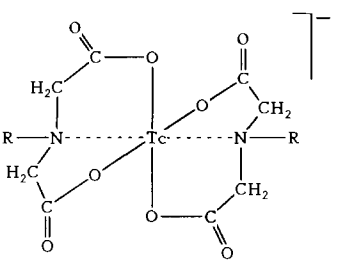


Scheme 3. Structural formula of Tc-HEXAMIBI. R = CH_2–$C(CH_3)_2$–OCH_3.

Tc-CDO-MeB is prepared by reaction of $^{99m}TcO_4^-$ with a mixture of 1,2-cyclohexanedione dioxime, methylboric acid, and $SnCl_2$ as reducing agent.[46] Five minutes after injection, 2.2% of the injected activity are measured in the human heart muscle, which is, however, washed out noticeably more quickly than Tc-HEXAMIBI. But, the uptake of Tc-CDO-MeB proceeds more rapidly.[47] The blood activity 15 min after the injection still amounts to 9.5% of the injected dose.[48] The molecular structure corresponds to the structure of the complex $TcCl(DMG)_3 2MP$ described in Scheme 1c.[38]

Labeled iminodiacetic acid derivatives, particularly ^{99m}Tc-*N*-(2,6-dimethylphenylcarbamoylmethyl)iminodiacetic acid (Tc-HIDA) as well as ^{99m}Tc-sulfur colloid with a particle size of about 0.1 μm, are commonly used ^{99m}Tc radiopharmaceuticals for liver and gall bladder imaging.

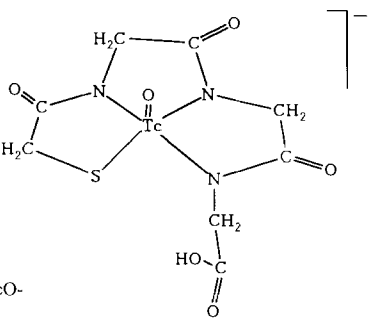
Tc-HIDA is obtained by reduction of $^{99m}TcO_4^-$ with $SnCl_2$ in the presence of the iminodiacetic acid derivative. Over 95% of the ^{99m}Tc is bound in the complex. The scintiphotograph can already be recorded a few minutes after injection. Scheme 4 shows the coordination of the technetium center in the HIDA complex. Two tridentate ligands chelate technetium in the oxidation state + 3 through the carboxyl-oxygen atoms and the imino-nitrogen atoms in an octahedral arrangement. The complex is uninegatively charged.[49, 50]



Scheme 4. Structural formula of Tc-HIDA.

^{99m}Tc-sulfur colloid is used for liver as well as spleen imaging. The preparation proceeds by reaction of $^{99m}TcO_4^-$ with $S_2O_3^{2-}$ in acidic solution; $^{99m}TcO_4^-$ is almost completely converted. The reaction product is mainly a mixture of $^{99m}Tc_2S_7$ and colloidal sulfur.[51] 80–85% of the colloid is accumulated in the liver, 5–10% in the spleen, and the rest in the bone marrow. Scintiphotographs can already be recorded 5–10 min after injection. The effective half-life of the colloid in the liver is almost equal to the physical half-life of ^{99m}Tc.[9]

^{99m}TcO-mercaptoacetyltriglycine (TcO-MAG_3) was developed a few years ago[52] for renal scintigraphy, particularly for testing the functioning of the renal tubuli. A kit for its preparation is now available.[53] $^{99m}TcO_4^-$ and benzoyl mercaptoacetyltriglycine are reduced in aqueous solution by $SnCl_2$, with concomitant elimination of the benzoyl protecting group. The labeling proceeds with a yield of more than 95%. A few minutes after injection, about 50% of the injected activity is taken up by the kidneys. After 30 min, more than 70% of the injected dose is found in the urine.[54, 55] In Tc-MAG_3, technetium occurs in the + 5 oxidation state and resides in a distorted square-pyramidal environment, surrounded by three nitrogen atoms and one sulfur atom in the basal plane and one oxygen atom at the apex (Scheme 5). The structure agrees with that found for ReO-mercaptoacetyltriglycerine.[56, 57]



Scheme 5. Structural formula of TcO-MAG_3.

Tc-dimercaptosuccinic acid (Tc-DMSA) has been used for kidney imaging for quite a while (Fig. 5). $^{99m}TcO_4^-$ is reduced with $SnCl_2$ for complex formation in the presence of DMSA. The binding of ^{99m}Tc is almost complete. Three hours after injection, about 50% of the activity has been taken up by the

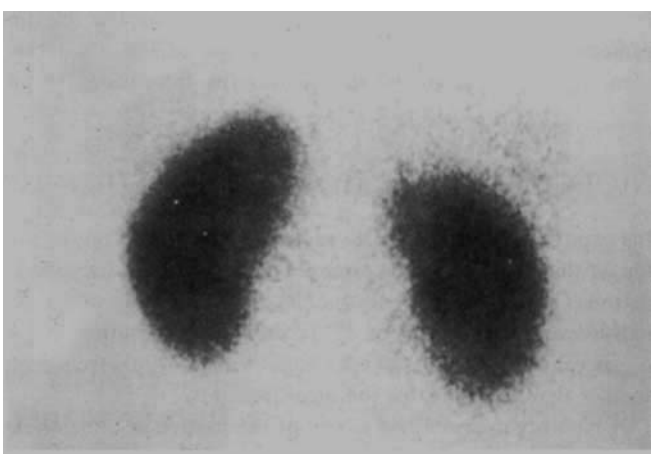


Fig. 5. Scintiphotograph of normal kidneys; from behind, taken after injection of Tc-DMSA [9], that is, the kidney shown on left-hand side of the picture corresponds to one on the left-hand side of the body.



Fig. 6. Scintiphotograph of a normal skeleton, taken after injection of Tc-MDP [9]. The injection site is labeled with an arrow.

kidneys, and 10–20% is excreted in the urine during the first 2 h. ^{99m}Tc-DMSA specifically localizes in the proximal convoluted tubule.[55] The structure of the Tc-DMSA complex has not yet been unambiguously determined.[58]

^{99m}Tc-methylene diphosphonate (Tc-MDP) has proved effective for bone imaging (Fig 6). It is formed by reduction of $^{99m}TcO_4^-$ with tin(II) chloride in the presence of sodium methylene diphosphonate. Again the conversion is almost complete. The bone scanning is performed 2–3 h after injection to reduce the background activity in the body. In 24 h 75–85% of the activity is excreted in the urine.[9] Evidently, several Tc-MDP complexes, whose compositions and structures have not been established to date, are produced under the given conditions for the preparation.[59] Derivatives of methylene diphosphonate, such as hydroxyethylidene, hydroxymethylene, and dicarboxypropane diphosphonate are also used for bone imaging after complex formation with ^{99m}Tc.

6. Development

The ^{99m}Tc radiopharmaceuticals listed in Table 2 are the result of systematic developments and accidental discoveries. None of the complexes meets the conditions of ideal radiopharmaceuticals without limitations.

In addition to the physical half-life $t_{1/2} = t_{phys}$, the biological half-life t_{bio} is of importance; the latter indicates the time after which, regardless of radioactive decay, the activity of the radiopharmaceutical in the body has decreased to one-half by biological elimination. Naturally, t_{bio} is dependent on the relevant radiopharmaceutical. The so-called effective half-life t_{eff} follows from t_{phys} and t_{bio} according to Equation (b). In consideration of

$$t_{eff} = \frac{t_{phys} \cdot t_{bio}}{t_{phys} + t_{bio}} \qquad \text{(b)}$$

the exposure of the patient to radiation, t_{eff} should not be any longer than it takes to carry out the required diagnostic investigation. The value of t_{eff} is always less than the shorter of the two half-lives t_{phys} and t_{bio}. For ^{99m}Tc radiopharmaceuticals $t_{bio} < t_{phys}$ is valid throughout, and the biological half-life is frequently smaller than desirable for the measurements.

A high organ specificity is one of the particular aims of the development of radiopharmaceuticals. The injected activity should preferably accumulate in the organ to be investigated, that is a high activity ratio of target organ to the nontarget areas of the body is desired. High activity in adjacent organs and specifically in the blood can severely obscure the target organ image, the reproduction of structural details, and the function testing quite considerably. In addition, a high organ specificity permits the reduction of the injected activity dose and consequently the exposure of the patient to radiation.

A radiopharmaceutical should not change chemically in vivo during its transport to the target organ, in other words, it should be kinetically inert. However, the metabolization of the labeled complex in the target organ can be of advantage, particularly if the functioning of the organ should be tested. The in vivo stability prior to the accumulation in the organ is a necessary precondition if information concerning the relationships between molecular structure and organ distribution is to be gained.

In the forefront of efforts to develop ^{99m}Tc radiopharmaceuticals are brain and heart agents.

6.1. Brain Radiopharmaceuticals

Brain radiopharmaceuticals should be capable of penetrating the intact blood-brain barrier. The barrier arises from epithelial-like tight junctions that virtually cement adjoining capillary endothelium together in the brain microvasculature.[32, 33] Lipid-soluble, uncharged molecules can pass through the blood-brain barrier by simple diffusion, as long as a concentration difference exists on both sides of the capillary wall. The lipophilicity of complexes is often quantified by the logarithm of the octanol/water partition coefficient P_{oct}. Compounds with values of log P_{oct} between 0.9 and 2.5 appear to penetrate the blood-brain barrier rather easily, whilst more strongly lipophilic substances are increasingly bound to blood components.[60] Such relations are, however, dependent on the character of the complex.[61] The permeability of the blood-brain barrier also increases, as expected, with decreasing molar mass.[62]

^{99m}Tc brain radiopharmaceuticals developed to date appear to penetrate the blood-brain barrier by simple diffusion. However, nonlipid-soluble substances, such as glucose as the most important energy source of the brain cells and essential amino acids, which can not be synthesized by the brain, must also be able to pass through the membrane of the endothelial cells. Systems in the endothelial cells are available for this special transport which make the normal osmotic diffusion of glucose and for example large neutral amino acids much easier. At least ten of these amino acids, amongst others also L-phenylalanine, penetrate the membranes of the endothelial cells by the same transport system.[32] The binding of an uncharged ^{99m}Tc complex to a large neutral amino acid could, by using this transport system of the endothelial cells, accelerate the passage of ^{99m}Tc into the brain.[63]

Apart from the diffusion of radiopharmaceuticals into the brain, the retention in the brain is of great importance for scintigraphic investigations. In particular, their rediffusion from the brain should be limited, either by binding to (in) the brain cells or through metabolization (metabolic trapping). The development of new ^{99m}Tc brain radiopharmaceuticals is concentrated on complex compounds, which not only can penetrate the blood-brain barrier in the direction of the brain, but also lose their neutral or/and lipophilic character by metabolization in

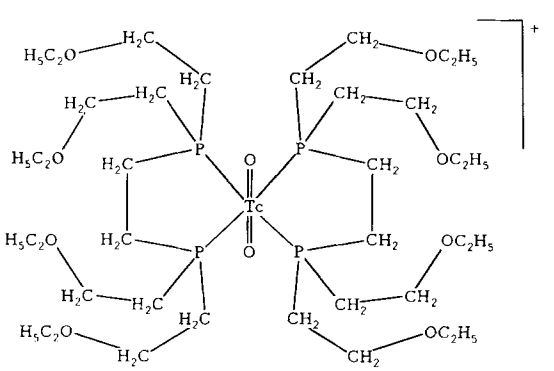
the brain, so that the diffusion out of the brain is hindered.[19, 31] For example, the relatively long retention time of TcO-L,L-ECD in the brain was explained by an increase in the polarity of this complex by hydrolysis of an ester group in the brain,[28] even though some doubt now exists about this interpretation.[31]

6.2. Heart Radiopharmaceuticals

A working hypothesis for the development of ^{99m}Tc myocardial perfusion imaging agents is the assumption that unipositively charged complexes preferably concentrate in the heart muscle tissue (myocardium).[64] The hypothesis is based on the known concentration of alkali metal ions, such as K^+, Rb^+, and Cs^+ as well as particularly Tl^+, which still used as $^{201}Tl^+$ in competition with the ^{99m}Tc radiopharmaceuticals described in Section 5 for heart imaging. However, the nuclear properties of ^{201}Tl (decay by electron capture with $t_{1/2} = 73.5$ h, maximum γ energy 167 keV for only 8.8% decay probability) and its necessary production in accelerators are disadvantageous when compared to ^{99m}Tc. It is also known that several NH_4^+ derivatives accumulate in the heart muscle.[65] Whether, in addition to K^+ ions, other simple cations such as Tl^+ concentrate in the heart muscle cells via Na^+/K^+-adenosinetriphosphatase (Na^+/K^+-ATPase) has yet to be proven. Probably, the Na^+/K^+-ATPase does not participate in the uptake of the Tc-HEXAMIBI cation.[66] Finally, it must be emphasized that the cationic character of ^{99m}Tc myocardial perfusion imaging agents is not an essential precondition with regard to the use of neutral Tc-CDO-MeB. However, it is washed out of the heart muscle tissue more rapidly than Tc-HEXAMIBI.

The lipophilicity of the diagnostic agent is also of importance for its uptake in the heart. Agent-dependent parabola-like functions between the accumulation in the myocardium and log P_{oct} were observed.[66] A reason for the decrease in the accumulation at high lipophilicity values (log $P_{oct} > 5$) will again be the binding of the agent to blood protein.

A further cationic ^{99m}Tc myocardial perfusion imaging agent was developed only recently, $^{99m}TcO_2$-bis[1,2-bis{bis(2-ethoxyethyl)phosphino}ethane]$^+$.[67, 68] Scheme 6 shows the molecular structure of this Tc^V complex. According to a crystal structure analysis of the ^{99g}Tc complex both bidentate diphosphane ligands lie in a plane; perpendicular to this plane is the linear



Scheme 6. Structural formula of the unipositively charged cation TcO_2-bis[1,2-bis{bis(2-ethoxyethyl)phosphino}ethane]$^+$.

trans-TcO_2 unit.[68] Noticeable are the eight ethoxyethyl groups of the ligands, which apparently contribute to reduce the disadvantageous background activity in the blood and in the liver, which is known from other ^{99m}Tc phosphane complexes. The uptake of the cationic complex in the heart amounts to 1.2% of the injected activity, which only decreases to 1% 2 h after injection. The synthesis proceeds by reduction of $^{99m}TcO_4^-$ with $SnCl_2$ in the presence of 1,2-bis[bis(2-ethoxyethyl)phosphino]-ethane, which is also called tetrofosmine.[68]

7. Summary and Future Prospects

^{99m}Tc radiopharmaceuticals are widely applied in nuclear medicine for planar scintigraphic and tomographic (SPET) imaging and for testing the functioning of organs such as the brain, thyroid, lungs, heart, liver, gall bladder, kidneys, and skeleton. In particular, this is due to the excellent nuclear properties of ^{99m}Tc and its easy preparation in generator columns. Composition and structure of the radiopharmaceuticals can be determined with the analogous compounds of the long-lived nuclide ^{99g}Tc which can be prepared in weighable quantities. The efforts to develop defined diagnostic agents have given new impulses to the coordination chemistry of technetium[69] and contributed significantly to the understanding of the chemistry of this radioelement. The synthesis of specially designed radiopharmaceuticals with higher organ specificity requires deeper insights into the relationship between the structure of the agent, its associated physicochemical properties, and the organ distribution. Misleading differences of distribution between the bodies of animals and man are not uncommon. Stereoselective uptake and retention of technetium radiopharmaceuticals are well known.[28, 70] The structures of several technetium radiopharmaceuticals that have been in use for several decades, such as Tc-DTPA, Tc-DMSA, and Tc-MDP, have still not been characterized.

^{99m}Tc is no physiological nuclide such as ^{11}C, which is accepted by the body and metabolized in biomolecules.[71] But, still it cannot be excluded that specially designed ^{99m}Tc labeled biomolecules are taken up by the body as analogue tracers.[63] Since long-chain fatty acids are the major energy source for the heart muscle, many attempts were made to improve the uptake and retention of ^{99m}Tc in the myocardium by binding to functionalized fatty acids. The expected accumulation was, however, not observed, not even for cationic complexes containing fatty acids.[72] Recently the complexing of ^{99}Tc/^{99m}Tc by a functionalized D-glucose, 2-amino-2-deoxy-D-glucosoxime, was successful. High accumulations in the myocardium or in the brain were not observed.[73]

In a wider sense ^{99m}Tc-labeled monoclonal antibodies, which are used in immunoscintigraphy mainly for tumor localization,[74] can also be classed as technetium radiopharmaceuticals. ^{99m}Tc can, after reduction of $^{99m}TcO_4^-$ and partial cleavage of the disulfide bridges in the antibody, be bound by the thiol groups. The indirect labeling through bifunctional ligands, such as diethylenetriaminepentaacetic acid or diaminodithiol derivatives,[75] which complex the radionuclide and concomitantly bond to the antibody, has to date been less successful and is still under development. After labeling with a radionuclide, mono-

clonal antibodies accumulate specifically in tumor tissue by binding to so-called tumor markers, such as proteins, glycoproteins, glycolipids, or polysaccharides, which are formed by tumor cells. However, unspecific binding to normal tissue can not be completely excluded. With ^{99m}Tc-labeled monoclonal antibodies it was possible to gain high contrast images 2–24 h after injection of an activity of about 27 mCi (1000 MBq). The smallest imaged lesion had a diameter of 0.6 cm.[74]

Long incubations of the labeled monoclonal antibodies in the blood can possibly be avoided by the pretargeting method, for example with the avidin-biotin system. The glycoprotein avidin disposes of four binding sites that are highly specific and have a high affinity for biotin. Very recently, by pretargeting, an image of a brain tumor was successfully obtained only 30 min after the injection of ^{99m}Tc-labeled biotin, which was bound to propylene-amine-oxime (PnAO) (cf. Scheme 1a) for complexing the ^{99m}Tc.[76] The tumor-specific monoclonal antibody bonded to avidin was injected three days earlier to localize the tumor. The affinity of avidin and biotin for each other is 5–7 orders of magnitude higher than those of antibodies for tumors.[74]

The physiological function of organs, the testing of which is the predominant aim of the application of radiopharmaceuticals, is often controlled by receptors. They are found as glycoproteins on the cell surface or as soluble proteins inside a cell and bind the associated ligands through complementary structures. Receptors exhibit high ligand affinity, specificity, stereoselectivity, and saturability. Radiopharmaceuticals bound to receptors permit insights into special physiological processes, in particular, changes in receptor concentration are thought to be related to certain disease states of an organ.[77] Many receptor-specific radiopharmaceuticals with radionuclides such as ^{11}C, ^{18}F, ^{75}Br, ^{77}Br, or ^{123}I are known. However, apparently only one receptor-binding ^{99m}Tc radiopharmaceutical is known, ^{99m}Tc-galactosyl-neoglycoalbumin (Tc-NGA),[78] which binds to the hepatocyte-specific membrane receptor (HBP) for at least 4 h.[79] Clinical tests after injection of about 5 mCi (185 MBq) Tc-NGA per patient indicate that with liver diseases such as hepatoma, cirrhosis, and liver metastases the logarithm of the HBP concentration is directly related to the reduced functional hepatocyte mass.[80]

Very recently, attempts were made to develop radiopharmaceuticals for the detection of hypoxic tissue in tumors, in the heart as well as in the brain by binding ^{99m}Tc complexes to nitroimidazole derivatives. It is known that nitroimidazole can be selectively trapped with reactive metabolites in hypoxic cells by enzymatic reduction of the nitro group in the absence of oxygen. The redox potential of the nitroimidazole derivative appears to be a measure of the intensity of the reduction and the trapping. In preliminary investigations a 2-nitroimidazole derivative was bonded through a methylene group to the neutral brain agent ^{99m}TcO-propylene-amine-oxime.[81] Animal experiments show that the labeled compound was selectively retained in hypoxic brain and heart tissue.[82, 83]

I thank Univ.-Doz. Dr. F. Fazekas, Neurologische Universitätsklinik Graz, for the gift of a copy of the tomogram shown in Figure 3. I would further like to thank Prof. Dr. Gopal B. Saha, Department of Nuclear Medicine, Clinical Foundation Cleveland, Ohio, and the Springer Verlag, Heidelberg, for permission to reproduce the Figures 4, 5, and 6. My thanks are also due to the referees of this manuscript for some stimulating comments and to Susan and Harald Poelchau for reviewing the English version.

Received: September 21, 1993 [A 281E]
German version: *Angew. Chem.* **1994**, *106*, 2349
Translated by Dr. H. B. Friedrich, Munich, FRG

[1] *Gmelin Handbook of Inorganic Chemistry, Technetium, Suppl. Vol. 1, 2*, 8th ed., Springer, Berlin, **1982/83**.
[2] K. Schwochau, *Radiochim. Acta* **1983**, *32*, 139–152.
[3] M. Molter, *Chem.-Ztg.* **1979**, *103*, 41–52.
[4] E. Browne, R. B. Firestone in *Table of Radioactive Isotopes* (Ed.: V. S. Shirley), Wiley, New York, **1986**.
[5] E. Deutsch, K. Libson, *Comments Inorg. Chem.* **1984**, *3*, 83–103.
[6] M. J. Clarke, L. Podbielski, *Coord. Chem. Rev.* **1987**, *78*, 253–342.
[7] Nuclear Data Center, Brookhaven, **1973**, BNL 325.
[8] *Gmelin Handbook of Inorganic Chemistry, Technetium, Suppl. Vol. 2*, 8th ed., Springer, Berlin, **1983**, p. 145.
[9] G. B. Saha, *Fundamentals of Nuclear Pharmacy*, 2nd ed., Springer, Berlin **1984**.
[10] W. D. Tucker, M. W. Greene, A. J. Weiss, A. P. Murrenhoff (BNL 3746), *Trans. Am. Nucl. Soc.* **1958**, *1*, 160.
[11] P. Richards, W. D. Tucker, S. C. Srivastava, *Int. J. Appl. Radiat. Isot.* **1982**, *33*, 793–799.
[12] E. Deutsch, W. R. Heineman, J. P. Zodda, C. C. Williams, *Int. J. Appl. Radiat. Isot.* **1982**, *33*, 843–848.
[13] Monograph of the European Pharmacopoeia commission PA, PH, Exp. 14, T (76) 1, Com. 9.1.1977.
[14] K. Jordan, *Meßtechnik in der Emissions-Computertomographie* (*Handbuch der Medizinischen Radiologie Bd. XV, Teil 1B* (Ed.: L. Diethelm, F. Heuck, O. Olsson, F. Strnad, H. Vieten, A. Zuppinger), Springer, Berlin, **1983**).
[15] D. Lange, *Nuklearmedizinische bildgebende Verfahren* (*Physik der bildgebenden Verfahren in der Medizin* (Eds.: H.-J. Maurer, E. Zieler), Springer, Berlin, **1984**).
[16] H. J. Hermann, *Nuklearmedizin*, 2nd ed., Urban und Schwarzenberg, München, **1989**.
[17] K. Schwochau, *Chem.-Ztg.* **1978**, *102*, 329–337.
[18] K. Schwochau in *Technetium in Chemistry and Nuclear Medicine 2* (Eds.: M. Nicolini, G. Bandoli, U. Mazzi), Cortina International, Verona/Raven, New York, **1986**, pp. 12–23.
[19] H. F. Kung, *Brain Radiopharmaceuticals* (*Radiopharmaceuticals: Progress and clinical Perspectives, Vol. 1* (Ed.: A. R. Fritzberg), CRC, Boca Raton, FL, **1986**, pp. 21–39).
[20] E. Deutsch, R. C. Elder, B. A. Lange, M. J. Vaal, D. G. Lay, *Proc. Natl. Acad. Sci. USA* **1976**, *73*, 4287–4289.
[21] K. E. Linder, J. Gougoutas, M. Malley, A. D. Nunn, S. Unger, *J. Labelled Compd. Radiopharm.* **1989**, *26*, 266–268.
[22] M. C. Day, Jr., J. Selbin, *Theoretical Inorganic Chemistry*, 2nd ed., Reinhold Book, New York, **1969**.
[23] C. D. Russel, J. Majerik, *Int. J. Appl. Radiat. Isot.* **1978**, *29*, 109–114.
[24] S. C. Srivastava, P. Richards in *Radiotracers for Medical Applications, Vol. 1* (Ed.: G. V. S. Raysudu), CRC, Boca Raton, FL, **1983**, Chapter 4, pp. 107–185.
[25] S. Jurisson, E. O. Schlemper, D. E. Troutner, L. R. Canning, D. P. Nowotnik, R. D. Neirinckx, *Inorg. Chem.* **1986**, *25*, 543–549.
[26] H. F. Kung, *Semin. Nucl. Med.* **1990**, *20*, 150–158.
[27] R. C. Walovitch, S. J. Williams, N. D. Lafrance, *Nucl. Med. Biol.* **1990**, *17*, 77–83.
[28] D. S. Edwards, E. H. Cheesman, M. W. Watson, L. J. Maheu, S. A. Nguyen, L. Dimitre, T. Nason, A. D. Watson, R. Walovitch in *Technetium and Rhenium in Chemistry and Nuclear Medicine 3* (Eds.: M. Nicolini, G. Bandoli, U. Mazzi), Cortina International/Verona und Raven/New York, **1990**, pp. 433–444.
[29] J. Léveillé, G. Demonceau, M. De Roo, P. Rigo, R. Taillefer, R. A. Morgan, D. Kupranick, R. C. Walovitch, *J. Nucl. Med.* **1989**, *30*, 1902–1910.
[30] R. K. Narra, A. D. Nunn, B. L. Kuczynski, R. J. DiRocco, T. Feld, D. A. Silva, W. C. Eckelman, *J. Nucl. Med.* **1990**, *31*, 1370–1377.
[31] D. P. Nowotnik, *Technetium-based Brain Perfusion Agents* (*Radiopharmaceuticals, Chemistry and Pharmacology* (Ed.: A. D. Nunn), Dekker, New York, **1992**, pp. 37–95).
[32] G. W. Goldstein, A. L. Betz, *Spektrum der Wissenschaft*, November **1986**, 82–91.
[33] W. M. Pardridge, *Annu. Rev. Pharmacol. Toxicol.* **1988**, *28*, 25–39.
[34] P. Bläuenstein, K. Girgenrath, H. Hügli, G. Anderegg, P. Jordan, K. May, *J. Labelled Compd. Radiopharm.* **1981**, *18*, 194–195.
[35] S. Seifert, B. Noll, R. Münze, *Int. J. Appl. Radiat. Isot.* **1982**, *33*, 1393–1398.
[36] W. de Kieviet, *J. Nucl. Med.* **1981**, *22*, 703–709.
[37] P. F. Sharp, F. W. Smith, H. G. Gemmell, D. Lyall, N. T. S. Evans, D. Gvozdanovic, J. Davidson, D. A. Tyrrell, R. D. Pickett, R. D. Neirinckx, *J. Nucl. Med.* **1986**, *27*, 171–177.

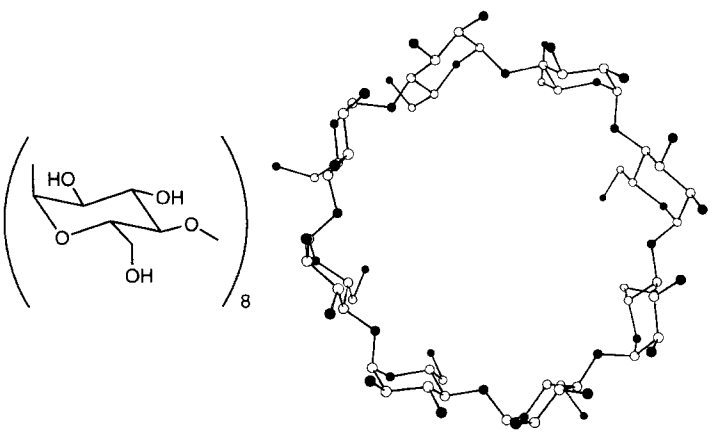
[38] E. Linder, M. F. Malley, J. Z. Gougoutas, S. E. Unger, A. D. Nunn, *Inorg. Chem.* **1990**, *29*, 2428–2434.
[39] C. D. Russel, R. C. Crittenden, A. G. Cash, *J. Nucl. Med.* **1980**, *21*, 354–360.
[40] E. Janovici, M. Kosinski, P. Lerch, A. G. Maddock, *Dev. Nucl. Med.* **1986**, *10*, 161–172.
[41] M. T. Hays, B. Wesselwosky, *J. Nucl. Med.* **1973**, *14*, 785–792.
[42] D. Piwnica-Worms, J. F. Kronauge, B. L. Holman, A. Davison, A. G. Jones, *Invest. Radiol.* **1989**, *24*, 25–29.
[43] Du Pont Radiopharmaceutical Division, Billerica, Massachusetts, USA 01862, *J. Nucl. Med.* **1993**, *34*, Nr. 6.
[44] F. J. T. Wackers, D. S. Berman, J. Maddahi, D. D. Watson, G. A. Beller, H. W. Strauss, C. A. Boucher, M. Picard, B. L. Holman, R. Fridrich, E. Inglese, B. Delaloye, A. Bischof-Delaloye, L. Camin, K. McKusick, *J. Nucl. Med.* **1989**, *30*, 301–311.
[45] T. H. Tulip, J. Calabrese, J. F. Kronauge, A. Davison, A. G. Jones in *Technetium in Chemistry and Nuclear Medicine 2* (Eds.: M. Nicolini, G. Bandoli, U. Mazzi), Cortina International, Verona/Raven, New York, **1986**, pp. 119–121.
[46] R. K. Narra, A. D. Nunn, B. L. Kuczynski, T. Feld, P. Wedeking, W. C. Eckelmann, *J. Nucl. Med.* **1989**, *30*, 1830–1837.
[47] A. D. Nunn, *Semin. Nucl. Med.* **1990**, *20*, 111–118.
[48] D. W. Seldin, L. L. Johnson, D. K. Blood, M. J. Muschel, K. F. Smith, R. M. Wall, P. J. Cannon, *J. Nucl. Med.* **1989**, *30*, 312–319.
[49] M. D. Loberg, A. T. Fields, *Int. J. Appl. Radiat. Isot.* **1978**, *29*, 167–173.
[50] C. E. Costello, J. W. Brodack, A. G. Jones, A. Davison, D. L. Johnson, S. Kasina, A. R. Fritzberg, *J. Nucl. Med.* **1983**, *24*, 353–355.
[51] J. Steigman, N. A. Solomon, L. L-Y. Hwang, *Appl. Radiat. Isot.* **1986**, *37*, 223–229.
[52] A. R. Fritzberg, S. Kasina, D. Eshima, D. L. Johnson, *J. Nucl. Med.* **1986**, *27*, 111–116.
[53] A. M. Verbruggen, M. J. K. De Roo, *Renal Radiopharmaceuticals* (*Radiopharmaceuticals, Chemistry and Pharmacology* (Ed.: A.4D. Nunn), Dekker, New York, **1992**, pp. 365–430).
[54] A. Taylor, Jr., D. Eshima, P. E. Christian, W. W. Wooten, L. Hansen, K. McElvany, *J. Nucl. Med.* **1988**, *29*, 616–622.
[55] A. Taylor, Jr., D. Eshima, A. R. Fritzberg, P. E. Christian, S. Kasina, *J. Nucl. Med.* **1986**, *27*, 795–803.
[56] T. N. Rao, D. Adhikesavalu, A. Camerman, A. R. Fritzberg, *Inorg. Chim. Acta* **1991**, *180*, 63–67.
[57] D. L. Nosco, R. G. Manning, A. Fritzberg, *J. Nucl. Med.* **1986**, *27*, 939.
[58] J. L. Moretti, J. R. Rapin, J. C. Saccavini, A. Lageron, M. Le Poncin, A. Bardy, *Int. J. Nucl. Med. Biol.* **1984**, *11*, 270–274.
[59] C. L. De Ligny, W. J. Gelsema, T. G. Tji, Y. M. Huigen, H. A. Vink, *Nucl. Med. Biol.* **1990**, *17*, 161–179.
[60] D. D. Dischino, M. J. Welch, M. R. Kilbourn, M. E. Raichle, *J. Nucl. Med.* **1983**, *24*, 1030–1038.
[61] K. Leesmeister, K. Schwochau, *Nucl. Med. Biol.* **1992**, *19*, 73–78.
[62] V. A. Levin, *J. Med. Chem.* **1980**, *23*, 682–684.
[63] U. Pleger, K. Schwochau (Forschungszentrum Jülich), DE-B4128183C1, **1993**, 1–7.
[64] E. Deutsch, W. Bushong, K. A. Glavan, R. C. Elder, V. J. Sodd, K. L. Scholz, D. L. Fortman, S. J. Lukes, *Science* **1981**, *214*, 85–86.
[65] D. M. Wieland, E. A. Deutsch, *Cationic Radiotracers as myocardial Radiopharmaceuticals* (*Radiopharmaceuticals: Progress and Clinical Perspectives, Vol. I* (Ed.: A. R. Fritzberg), CRC, Boca Raton, FL, **1986**, pp. 1–20).
[66] A. D. Nunn, *Single Photon Radiopharmaceuticals for Imaging Myocardial perfusion* (*Radiopharmaceuticals, Chemistry and Pharmacology* (Ed.: A. D. Nunn), Dekker, New York, **1992**, pp. 97–140).
[67] B. Higley, F. W. Smith, T. Smith, H. G. Gemmell, P. D. Gupta, D. V. Gvozdanovic, D. Graham, D. Hinge, J. Davidson, A. Lahiri, *J. Nucl. Med.* **1993**, *34*, 30–38.
[68] J. D. Kelly, A. M. Forster, B. Higley, C. M. Archer, F. S. Booker, L. R. Canning, K. W. Chiu, B. Edwards, H. K. Gill, M. McPartlin, K. R. Nagle, I. A. Latham, R. D. Pickett, A. E. Storey, P. M. Webbon, *J. Nucl. Med.* **1993**, *34*, 222–227.
[69] K. Schwochau, *Radiochim. Acta* **1993**, *G3*, 103–110.
[70] D. P. Nowotnik, L. R. Canning, S. A. Cumming, R. C. Harrison, B. Higley, G. Nechvatal, R. D. Pickett, I. M. Piper, V. J. Bayne, A. M. Forster, P. S. Weisner, R. D. Neirinckx, W. A. Volkert, D. E. Troutner, R. A. Holmes, *Nucl. Med. Commun.* **1985**, *6*, 499–506.
[71] G. Stöcklin, *Eur. J. Nucl. Med.* **1992**, *19*, 527–551.
[72] L. Astheimer, K. H. Linse, N. Ramamoorthy, K. Schwochau, *Nucl. Med. Biol.* **1987**, *14*, 545–553.
[73] H. J. Steinmetz, Dissertation, Technische Hochschule Aachen, **1993**.
[74] M. Magerstädt, H. J. Hachmann, L. Kuhlmann, L. Seidel, *Chem.-Ztg.* **1990**, *114*, 123–128.
[75] R. M. Reilly, *Nucl. Med. Commun.* **1993**, *14*, 347–359.
[76] P. Koch, H. R. Mäcke, *Angew. Chem.* **1992**, *104*, 1492–1494; *Angew. Chem. Int. Ed. Engl.* **1992**, *31*, 1507–1509.
[77] W. C. Eckelmann, *Clinical potential of receptor based radiopharmaceuticals* (*Radiopharmaceuticals: Progress and clinical Perspectives, Vol. II* (Ed.: A. R. Fritzberg), CRC, Boca Raton, FL, **1986**, pp. 89–113).
[78] D. R. Vera, K. A. Krohn, R. C. Stadalnik, P. O. Scheibe, *Radiology* **1984**, *151*, 191–196.
[79] D. R. Vera, R. C. Stadalnik, K. A. Krohn, *J. Nucl. Med.* **1985**, *26*, 1157–1167.
[80] R. C. Stadalnik, D. R. Vera, E. S. Woodle, W. L. Trudeau, B. A. Porter, R. E. Ward, K. A. Krohn, L. F. O'Grady, *J. Nucl. Med.* **1985**, *26*, 1233–1242.
[81] K. E. Linder, J. Cyr, Y. W. Chan, N. Raju, K. Ramalingam, D. P. Nowotnik, A. D. Nunn, *J. Nucl. Med.* **1992**, *33*, 319.
[82] R. DiRocco, B. Kuczynski, J. Pirro, *J. Nucl. Med.* **1993**, *34*, 92P.
[83] W. L. Rumsey, B. Patel, B. Kuczynski, A. Bauer, R. DiRocco, J. Pirro, A. D. Nunn, H. W. Strauss, R. K. Narra, *J. Nucl. Med.* **1993**, *34*, 15P.

Taking Fullerenes from Large Molecules to Supramolecules

Edwin C. Constable*

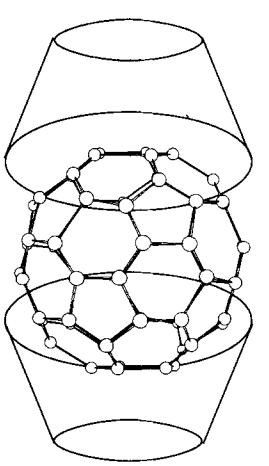
As in all forms of human endeavor, chemistry has, from time to time, especially favored topics. The early to mid-1980s were characterized by the study of high-temperature superconductors, whilst the twin themes of supramolecular chemistry and the chemistry of the new allotropes of carbon, the fullerenes, ran through the late 1980s and the 1990s. By the strict definition of Jean-Marie Lehn[1] the fullerenes and their derivatives are merely large molecules—they do not possess the intermolecular bonding interactions that characterize supramolecules. Isolated examples of fullerene-containing supramolecules have been reported,[2] but recently, a series of independent reports have appeared which have as the common theme the placement of a fullerene guest into a suitably designed host molecule. Apart from the obvious elegance of these systems, application of this supramolecular chemistry offers a facile purification method for specific fullerenes from the usual mixture present in carbon soot.

The key observation is that certain cyclic host molecules possess cavities having the correct dimensions for the inclusion of a fullerene guest. The critical observations date back to 1992 when Wennerström and co-workers described the solubilization of C_{60} in water by complexation with the host molecule γ-cyclodextrin.[3] The cyclodextrins (CDs) constitute a family of cyclic oligosaccharides prepared from starch. The commonest forms are α-CD with six glucopyranose units and a cavity diameter of 500 pm, β-CD with seven units and a cavity diameter of 650 pm, and γ-CD (**1**, Scheme 1), which contains eight sugar subunits and has a cavity 850 pm in diameter. Wennerström recognized that the cavities of α- and β-CD are too small to encapsulate a C_{60} molecule, but that γ-CD might just be large enough. Although γ-CD is a little too small to completely encapsulate C_{60}, it could form a 2:1 complex as depicted by structure **2**. Wennerström et al. then showed that when an aqueous solution of γ-CD was boiled with a solid mixture of C_{60} and C_{70}, an aqueous solution containing only a CD–C_{60} complex (> 99%) was obtained. C_{60} was not extracted when β-CD was used. Spectrophotometric and molecular modeling studies indicated the likely formation of a 2:1 CD–C_{60} complex. Extraction of the aqueous solution of the adduct with toluene yielded a pure solution of C_{60} in the organic phase. The purification of significant quantities of C_{60} by this method is probably not practical, as the limiting concentration of the γ-CD–C_{60} complex in the aqueous phase is of the order of 10^{-4} mol dm^{-3}.



Scheme 1. Two views of γ-CD **1**. In the structure on the right the oxygen atoms are shaded and the hydrogen atoms have been omitted.

Although the studies of Wennerström et al. provided the basic idea, they had not achieved the extraction of fullerenes from a liquid phase, nor had they demonstrated that it was possible to develop a preparative-scale method for the purification of C_{60} using the CD complex. The first problem was addressed by Williams and Verhoeven, who recognized that the cavity in the related host system calix[8]arene (**3**) was the correct size for a C_{60} guest (Scheme 2).[4] These authors then demonstrated that an aqueous solution of the sulfonate derivative **4** extracted only C_{60} from toluene solutions of C_{60} and C_{70} to give a yellow aqueous solution of a **4**–C_{60} complex. We will return to the structures of calix[8]arene–C_{60} adducts shortly.

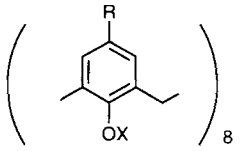


2

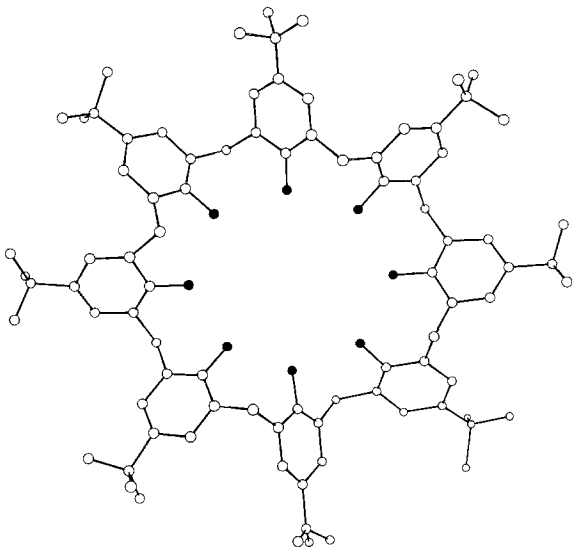
In a paper in this journal, Yoshida and co-workers have returned to the constitution of the CD–C_{60} complex.[5] They have used the liquid-phase extraction of fullerenes from toluene to aqueous solution to confirm the selective formation of complexes of C_{60} with γ-CD. Neither the inclusion of C_{70} was observed, nor complexation with α- or β-CD was detected. When the

[*] Prof. E. C. Constable
Institut für Anorganische Chemie der Universität Basel
Spitalstrasse 51, CH-4056 Basel (Switzerland)
Telefax: Int. code + (61)322-1554

 © VCH Verlagsgesellschaft mbH, D-69451 Weinheim, 1994 0570-0833/94/2222-2269 $ 10.00+.25/0



3 X = H R = H
4 X = $(CH_2)_3SO_3Na$ R = H
5 X = H R = *t*Bu



Scheme 2. Top: General formula for calix[8]arenes **3**–**5**. Bottom: Structure of **5**; the oxygen atoms are shaded and the hydrogen atoms have been omitted.

authors refluxed a (purple) solution of C_{60} in toluene with aqueous γ-CD, all of the C_{60} was transferred to the aqueous phase. Subsequent purification by precipitation, freeze-drying, and recrystallization gave purple crystals of a pure 2:1 γ-CD–C_{60} complex. Detailed NMR and CD spectroscopic studies have led the authors to propose the bicapped structure **2** for the 2:1 complex. Molecular modeling studies support this formulation.

The first successful *purifications* of fullerenes by host–guest chemistry were published concurrently by the groups of Atwood[6] and Shinkai[7] earlier this year. Both relied on the specificity exhibited by calix[8]arene for C_{60} to develop preparatively useful methods for the purification of fullerenes. Atwood et al. demonstrated that a one-phase reaction of toluene solutions of C_{60} with a toluene solution of calix[8]arene **5** gave a precipitate of a 1:1 **5**–C_{60} complex. When carbon soot was used, the crude product consisted of 89% C_{60} and 11% C_{70} complex. This corresponds to a 90% extraction of the C_{60} content of the soot! Two recrystallizations of the mixture of C_{60} and C_{70} complexes gave the 1:1 complex of C_{60} with a purity of >99.5%. Treatment of the residues and the mother liquors provided C_{70} fractions of 87% purity. Both groups then addressed the question of release of the fullerenes from the calix[8]arene complexes. This proved to be simplicity itself. Treatment of the 1:1 complex with chloroform (presumably in the course of attempts to obtain NMR spectra) led to the precipitation of the fullerene; the host went into solution. The efficiency of this method for the isolation of C_{60} is impressive. Atwood et al. report that they can obtain 0.28 g of pure C_{60} from 7.5 g of carbon soot, and also present preliminary findings regarding the use of calix[6]arenes for the enrichment of C_{70} fractions. Shinkai and his co-workers also describe the selectivity of calix[8]arene derivatives over calix[6]arene and calix[4]arene for the extraction of C_{60}. In their hands, 0.200 g of carbon soot containing 72 wt% of C_{60} yielded 0.102 g of 99.8% pure C_{60}. Very recently, Verhoeven et al. have described further studies on the **5**–C_{60} system.[8] The 1:1 complex was isolated as a metallic green solid from the reaction of C_{60} with **5** in carbon disulfide. The green solid decomposed to its constituents upon dissolution in chloroform. Verhoeven et al. also confirm the selective binding of C_{60} over C_{70}.

What is the nature of the bonding between the host and the fullerene guest? The primary interaction appears to be related to the π-bonding properties of the aromatic surface of the guest. However, there are conflicting interpretations with the different host systems. It is thought that C_{60} may act as a π-acid,[9] and that its binding to the γ-CD may arise from a charge transfer type of interaction involving the lone pairs on the oxygen atoms of the sugar, ether, and hydroxyl groups. This is supported by the electronic spectrum of the adduct, which is typical of a charge transfer complex. A secondary stabilizing feature is thought to be the formation of hydrogen bonds between the two γ-CD hosts.

In the case of the calix[8]arene host **5**, the primary interactions are thought to be between the CH_3 groups of the *tert*-butyl substituents and the π-cloud of the fullerene. In other words, the fullerene is acting as a π-donor! This type of CH–π interaction is well established for calixarenes[10] and might explain why the C_{60} forms a complex with a host that is a little too small for it. The guest is not deep in the cavity, but lies above it and has primary interactions with the *tert*-butyl surface. This also explains why the binding of C_{60} to calix[8]arenes lacking these *tert*-butyl substituents is very weak. Decomposition of the complex by chloroform may now be interpreted in terms of competitive hydrogen bonding between the acidic CH group of the solvent and both the fullerene and the aromatic surfaces of the calix[8]arene.[11] These aspects of the 1:1 complex of **5** and C_{60} might be relevant for the situation in solution, but it does not appear to be correct for the solid-state species. Shinkai and Atwood assume that the calix[8]arene is in a bucket-shaped conformation, although both are aware that there is a mismatch between the sizes of the host and the guest. However, calix[8]arenes are conformationally mobile and can adopt conformations in which aromatic rings point "up" or "down". In the conformation assumed by Shinkai and Atwood all of the aromatic rings point in the same direction. In detailed ^{13}C NMR studies of the 1:1 **5**:C_{60} complex, Verhoeven et al. presents compelling evidence that **5** adopts a conformation in which two of the aromatic rings are oriented in the opposite direction to the rest—the alternate-cone conformation.[8] This conformer should have a slightly larger cavity more appropriate to the C_{60} guest. We must, perhaps, await detailed crystallographic studies of these complexes to clarify the nature of the host–guest interactions in the solid state.

Why are these results exciting? There are two answers to this question. The first is transparent, and relates to the preparation of fullerenes. Host–guest chemistry offers the promise of cheap and convenient methods for the rapid isolation of highly pure fullerenes. Shinkai et al. comment that their method allows them "to obtain the gram-order of high-purity C_{60} without us-

ing any precious apparatus".[7] In these cost-conscious days, perhaps we should note Atwood's financial argument that the approach "will lead to a 50-fold reduction in the cost of production of high-purity C_{60}, noting the current Aldrich price of \$2800 per gram".[6] Perhaps a note of caution is required here. The *commercial* cost of fullerenes is probably as much dictated by limited demand and novelty as by the actual production costs. The price would undoubtedly drop if a market existed for 100 kg quantities of C_{60}! Conventional separations of fullerenes rely upon chromatography, and although the original methods based upon silica or alumina stationary phases[12] were time-consuming and inefficient, the use of activated charcoal columns allows the relatively facile separation of gram quantities of pure C_{60}.[13] For the state-of-the-art isolation of C_{60} there is probably little difference between chromatographic or extraction methods in terms of time or cost. The real question relates to the specific purification of the higher fullerenes. The Atwood extraction technique gives a hint of a future methodology, but a recent paper by Tour et al. reveals that chromatography over a silica gel/charcoal stationary phase is presently the most efficient way of isolating tangible quantities (> 1 g) of C_{70}.[14] However, the large volumes of solvents used and the relatively long separation times mean that the "extractors" may improve on this in the near future!

The second reason why this area is so thought provoking is more general. Personally, I am interested in the ramifications of these separation methods for inorganic chemistry. The fullerenes C_{60} and C_{70} are allotropes of the element carbon. Many other elements have allotropes possessing different molecular structures. One must speculate upon the possibility of using such size-based methods for the separation and purification of such homoelemental compounds. Is the rapidly developing chemistry of the fullerenes the dawn of a whole new era in the chemistry of the main group elements? For this, we will have to wait future results.

German version: *Angew. Chem.* **1994**, *106*, 2359

[1] J.-M. Lehn, *Angew. Chem.* **1988**, *100*, 92; *Angew. Chem. Int. Ed. Engl.* **1988**, *27*, 89.

[2] O. Ermer, *Helv. Chim. Acta* **1991**, *74*, 1339; O. Ermer, C. Robke, *J. Am. Chem. Soc.* **1993**, *115*, 10077; F. Diederich, J. Effing, U. Jonas, L. Jullien, T. Plesnivy, H. Ringsdorf, C. Thilgen, D. Weinstein, *Angew. Chem.* **1992**, *104*, 1683; *Angew. Chem. Int. Ed. Engl.* **1992**, *31*, 1599; A. L. Balch, V. J. Catalona, J. W. Lee, M. M. Olmstead, *J. Am. Chem. Soc.* **1992**, *114*, 5455; S. H. Friedman, D. L. DeCamp, R. P. Sijbesma, G. Srdanov, F. Wudl, G. L. Kenyon, *ibid.* **1993**, *115*, 6506.

[3] T. Andersson, K. Nilsson, M. Sundahl, G. Westman, O. Wennerström, *J. Chem. Soc. Chem. Commun.* **1992**, 604.

[4] R. M. Williams, J. W. Verhoeven, *Recl. Trav. Chim. Pays-Bas* **1992**, *111*, 531.

[5] Z. Yoshida, H. Takekuma, S. Takekuma, Y. Matsubara, *Angew. Chem.* **1994**, *106*, 1658; *Angew. Chem. Int. Ed. Engl.* **1994**, *33*, 1597.

[6] J. L. Atwood, G. A. Koutsantonis, C. L. Raston, *Nature* **1994**, *368*, 229.

[7] T. Suzuki, K. Nakashima, S. Shinkai, *Chem. Lett.* **1994**, 699.

[8] R. M. Williams, J. M. Zwier, J. W. Verhoeven, G. H. Nachtegaal, A. P. M. Kentgens, *J. Am. Chem. Soc.* **1994**, *116*, 6965.

[9] Z. Yoshida, I. Dogane, H. Ikehira, T. Endo, *Chem. Phys. Lett.* **1992**, *201*, 4816.

[10] C. D. Gutsche, *Calixarenes*, Royal Society of Chemistry, Cambridge, **1989**.

[11] W. L. Jorgenson, D. L. Severence, *J. Am. Chem. Soc.* **1990**, *112*, 4768; J. L. Atwood, F. Hamada, K. D. Robinson, G. W. Orr, R. L. Vincent, *Nature* **1991**, *349*, 685; J. L. Atwood, S. G. Bott, G. Jones, C. L. Raston, *J. Chem. Soc. Chem. Commun.* **1992**, 1349.

[12] A. S. Koch, K. C. Khemani, F. Wudl, *J. Org. Chem.* **1991**, *56*, 4543; P. Bhyrappa, A. Penicaud, M. Kawamoto, C. A. Reed, *J. Chem. Soc. Chem. Commun.* **1992**, 936; K. Chatterjee, D. H. Parker, P. Wurz, K. R. Lykke, D. M. Gruen, L. M. Stock, *J. Org. Chem.* **1992**, *57*, 3253; K. C. Khemani, M. Prato, F. Wudl, *ibid.* **1992**, *57*, 3254.

[13] W. A. Scrivens, P. V. Bedworth, J. M. Tour, *J. Am. Chem. Soc.* **1992**, *114*, 7917.

[14] W. A. Scrivens, A. M. Cassell, B. L. North, J. M. Tour, *J. Am. Chem. Soc.* **1994**, *116*, 6939.

 © *VCH Verlagsgesellschaft mbH, D-69451 Weinheim, 1994* *0570-0833/94/2222-2271 $ 10.00+.25/0*

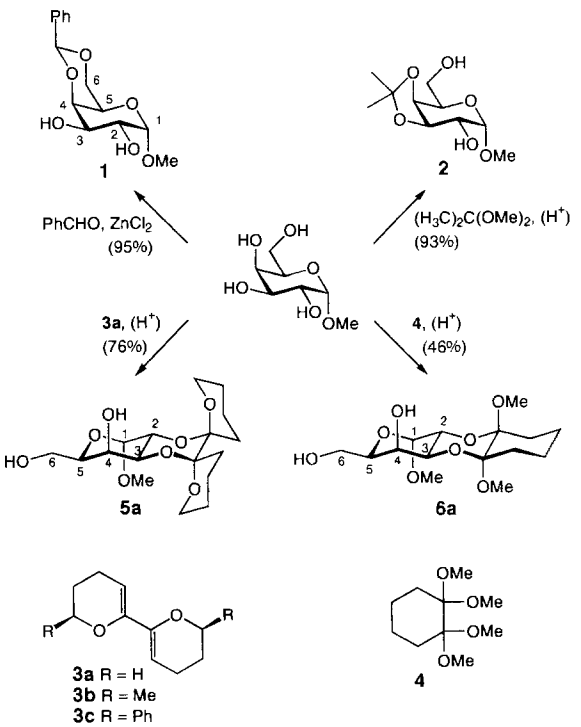
The Selective Blocking of *trans*-Diequatorial, Vicinal Diols; Applications in the Synthesis of Chiral Building Blocks and Complex Sugars

Thomas Ziegler*

For efficient chemical synthesis of complex oligosaccharides, protecting group strategies and blocking techniques are of overriding significance. It is usually unavoidable first to prepare protected smaller saccharide units that enable a directed selective formation of the glycosidic bond and sequential construction of larger saccharides. To this end all functional groups with the exception of the projected reaction center in the saccharide building block to be glycosylated (the glycosyl acceptor) must, as a rule, be protected, and only in particularly favorable cases can partially protected glycosyl acceptors be used for regioselective glycosylation. In the glycosyl donor, the saccharide building block that must be linked to the glycosyl acceptor, the protecting groups must be very precisely tuned to the planned glycosylation method. Both the reactivity of glycosyl donor and glycosyl acceptor and the anomeric selectivity of the glycosylation step is dominated by the protecting groups. The search for novel protecting group strategies is therefore as urgent for the carbohydrate chemist as the need for useful glycosylation methods.

Of the classical protecting groups of esters, ethers, and acetals that are favored in saccharide synthesis, the benzylidene and isopropylidene protecting groups have particular significance, because both open the possibility of blocking two hydroxyl functions in a monosaccharide simultaneously and selectively. As the example of methyl-α-D-galactopyranoside in Scheme 1 illustrates, benzylidene acetals can be the major product from 1,3-diols, so that in the protected galactose derivative **1** the hydroxyl functions of positions 2 and 3 are available for further reaction. In contrast, isopropylidene acetals can be selectively prepared from vicinal *cis*-diols, with the result that in the example **2** chosen here the hydroxyl functions of positions 2 and 6 remain free.[1] Although isopropylidene acetals can also be synthesized from monosaccharides with vicinal *trans*-diequatorial diols, these acetals are usually so acid-labile that they are difficult to handle and are therefore less suitable for glycosylation reactions.

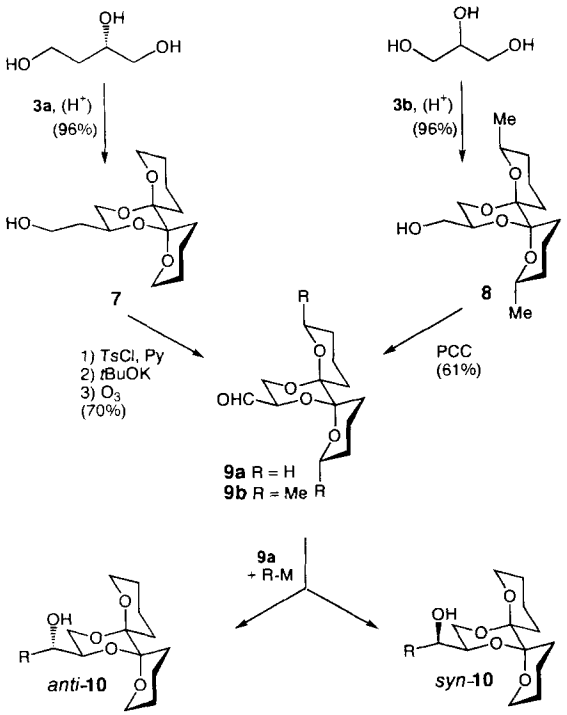
In the search for acetal protecting groups for vicinal *trans*-diequatorial diols that can be selectively introduced, the research group of S. V. Ley in Cambridge, England, recently developed the dispiroketal (Dispoke)[2] and cyclohexane-1,2-diacetal (CDA) protecting groups.[3] The former can be introducted by acetalization of a diol with the readily accessible 3,3′,4,4′-tetrahydro-6,6′-bis-2*H*-pyran[4, 5] (bis-DHP, **3a**), the latter by acetalization with the just as easily obtainable 1,1,2,2,-tetramethoxycyclohexane **4**.[3] In the case of the methyl-α-D-galactopyranoside (Scheme 1), the *trans*-diequatorial hydroxyl functions of positions 2 and 3 can be highly selectively blocked as the Dispoke-protected galactoside **5a** (76%)[5] or the CDA-protected galactoside **6a** (46%)[3] in this way. Dispoke and CDA derivatives of monosaccharides are therefore useful complements to benzylidene and isopropylidene derivatives. Like the classical acetal protecting groups, the Dispoke group can be removed hydrolytically under acidic conditions, preferably by transacetalization with ethylene glycol.[5]



Scheme 1.

The exceptionally high selectivity of the Dispoke and CDA groups can be explained by a steric interaction of the neighboring spiro centers and the equatorial arrangement of the alkyl residue as well as a strong anomeric effect of the two acetal functions.[2, 3] This high selectivity is particularly impressively reflected in the reaction of (*S*)-1,2,4-butanetriol with bis-DHP (**3a**) and a catalytic amount of camphorsulphonic acid (CSA), in which the dispiroketal **7** (96%) is obtained as exclusive stereoisomer[2] (Scheme 2). In the case of the symmetric glycerine, a "desymmetrization" of glycerine can even be achieved during the Dispoke formation by the use of chiral C_2-symmetric bis-DHP derivative **3b**. Here the only product is the enantiomerically pure compound **8** (96%). The compounds **7** and **8** can be transformed into the corresponding Dispoke-protected glycerinaldehydes **9**, which not only are thermally more stable than the isopropylidene glycerinaldehyde,[2, 6] but also have a distinctly higher *anti*-selectivity in the 1,2-addition of carbon nucleophiles to the aldehyde function[2] (Table 1).

[*] Dr. T. Ziegler
Institut für Organische Chemie und Isotopenforschung der Universität
Pfaffenwaldring 55, D-70569 Stuttgart (FRG)
Telefax: Int. code + (711)685-4269



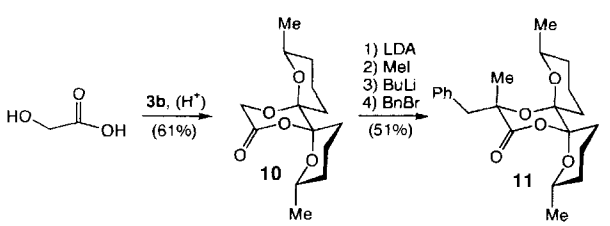
Scheme 2. R see Table 1.

Table 1. Reaction of **9a** with organometallic compounds RM [2].

RM	Conditions [a]	Yield [%]	**10** *anti*:*syn*	Ref. [b]
MeLi	Et_2O/THF, −78 °C, 22 h	82	82:18	60:40
MeMgCl	THF, −78 °C, 24 h	92	81:19	–
$Me_2CuLiMe_2S$	Et_2O, −78 °C, 20 h	69	12:88	18:82
EtMgBr	THF, −78 °C, 6 h	62	73:27	–
$H_2C{=}CHMgBr$	THF, −78 °C, 4 h	56	91:9	60:40
$(H_2C{=}CH)_2Zn$	THF, 25 °C, 48 h	84	67:33	–
$HC{\equiv}CMgBr$	THF, −78 °C, 5 h	65	89:11	44:56
$CH_2{=}CHCH_2MgBr$	THF, −78 °C, 18 h	89	68:32	60:40

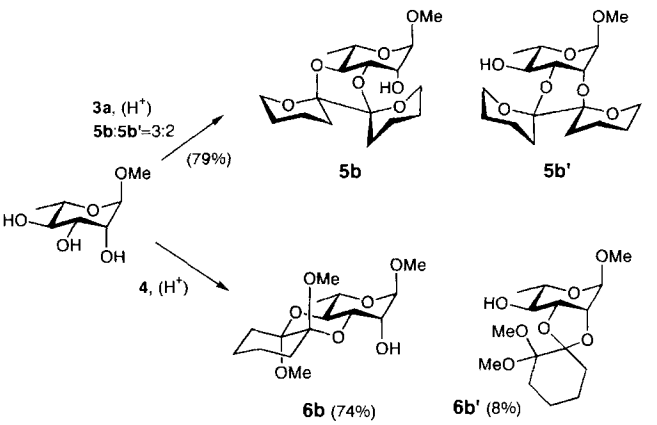
[a] THF = tetrahydrofuran. [b] Reaction of isopropylidene glycerinaldehyde with the corresponding organometallic compound.

In the same way glycolic acid can be stereoselectively transformed into the Dispoke derivative **10** (61%) with enantiomerically pure **3b**.[7] Formation of the ester enolate, alkylation with methyl iodide, renewed enolate formation and treatment with benzyl bromide then give highly diastereoselectively in 51% yield the protected α-hydroxycarbonic acid derivative **11** (Scheme 3).[7] It can be predicted that the C_2-symmetric Dispoke group will rapidly become popular as auxilliary in the stereoselective synthesis of small building blocks.



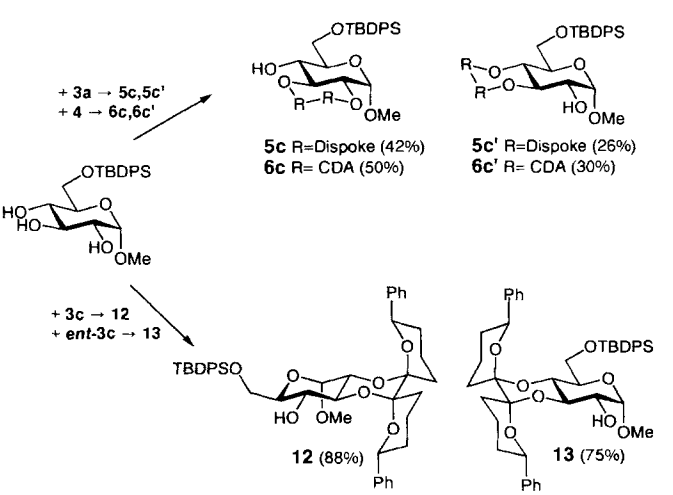
Scheme 3. LDA = lithium diisopropylamide.

Besides the 2,3-protected galactosides **5a** and **6a** (Scheme 1), other monosaccharides from the *gluco*, *manno*, *rhamno*, *fuco*, *xylo*, *lyxo*, and *arabino* series can be converted into the corresponding Dispoke- and CDA-blocked derivatives **5** and **6**.[3, 8] However, the regioselectivity of the acetal formation of Dispoke derivatives can in some cases (for instance, methyl-α-L-rhamnopyranoside) lead to mixtures of the 3,4- and 2,3-derivatives **5b** and **5b'**, respectively.[8] For the CDA analogues **6**, the ratio is most often shifted so far to the side of the *trans*-diequatorially blocked compounds **6b** that a preparative application seems meaningful[3] (Scheme 4).



Scheme 4.

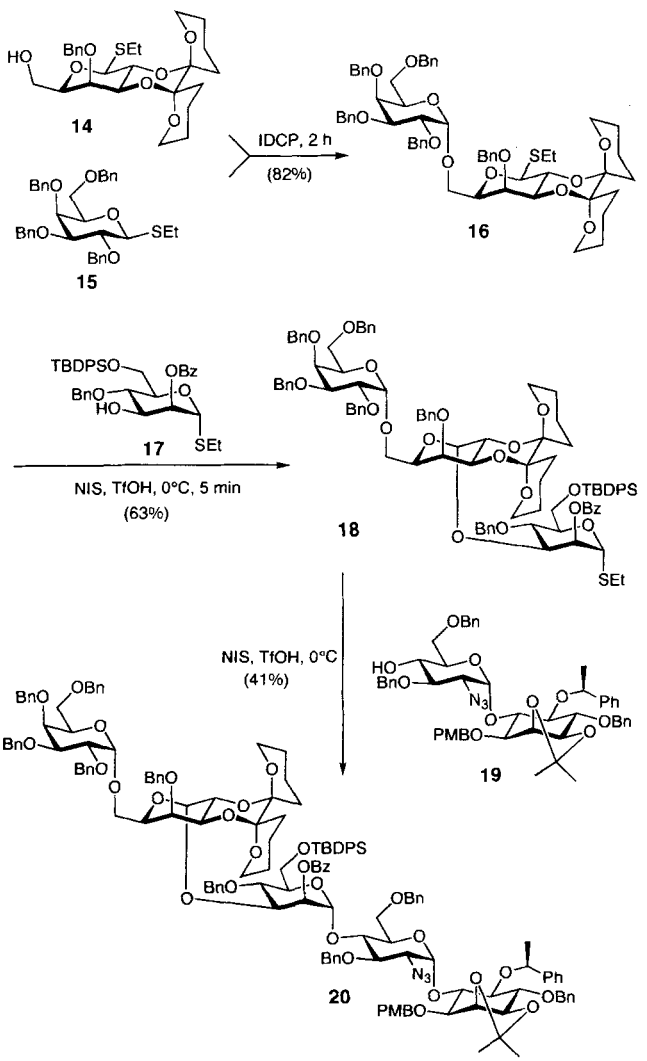
On the other hand the Dispoke and CDA protection for D-glucopyranosides presents problems, because here all secondary OH groups are *trans*-diequatorially arranged. Both with bis-DHP **3a** and with 1,1,2,2-tetramethoxycyclohexane **4**, mixtures of the 2,3- and 3,4-protected glucosides **5c**,**6c** and **5c'**,**6c'**, respectively, are obtained.[3, 8, 9] If, however, analogous to the "desymmetrization" of glycerine, phenyl-substituted, chiral bis-DHP **3c** is used, for glucose derivatives the two regioisomers **12** and **13** can be prepared in a highly selective synthesis through double diastereoselection[10] (Scheme 5).[11]



Scheme 5. TBDPS = *tert*-butyldiphenylsilyl.

 © VCH Verlagsgesellschaft mbH, D-69451 Weinheim, 1994 0570-0833/94/2222-2273 $ 10.00+.25/0

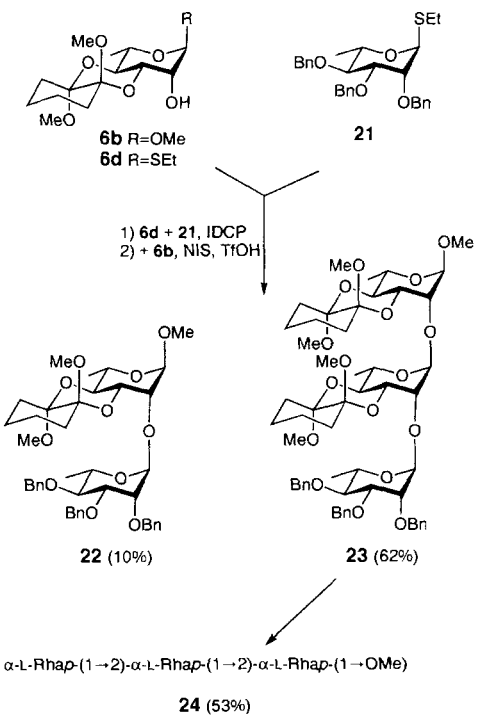
For strategies with the Dispoke or CDA protecting groups in oligosaccharide synthesis the concept of armed and disarmed glycosyl donors[1,2] is especially fruitful. According to this principle the reactivity of a glycosyl donor is diminished by deactivating protecting groups (e.g. acyl groups) or by restricting the flexibility of the pyranose ring by bridging two hydroxyl functions (e.g. acetal protecting groups). Such a disarmed donor can then function as a glycosyl acceptor and participate in a selective reaction with a reactive armed (most often benzyl-protected) glycosyl donor. The conformation-stabilizing Dispoke and CDA groups are plainly predestined to disarm a glycosyl donor. For example, the ethyl-1-thio-β-D-galactoside **14**, conformationally fixed by a Dispoke group and thus disarmed, undergoes a smooth reaction with thiogalactoside **15**—reactive as a result of benzyl protection—and the mild activator iodonium dicollidine perchlorate (IDCP) to form disaccharide **16**[13] (Scheme 6). Through the subsequent use of the more reactive activator *N*-iodosuccinimide (NIS), disaccharide **16** is armed and reacts with the 2-*O*-benzoyl-protected and thus disarmed thiomannoside **17** as glycosyl acceptor in attractive yield to afford trisaccharide **18**.



Scheme 6. TfOH = trifluoromethansulfonic acid, PMB = *para*-methoxybenzenyl.

The transformation of **18** as trisaccharide donor without further protecting group manipulation is achieved with the pseudo disaccharide acceptor **19** and NIS after prolonged reaction times. The pentasaccharide **20**, a fragment of the GPI anchor of *Trypanosoma brucei*, is thus obtained in 41% yield.[13]

Based on the concept of armed and disarmed glycosyl donors, the trisaccharide **23** can be constructed very elegantly from the two CDA-protected rhamnosides **6b** and **6d** in a one-pot reaction similar to the ciclamycin trisaccharide synthesis[14] in two steps as follows:[15] The IDCP-catalyzed condensation of armed thiorhamnoside **21** and disarmed glycosyl acceptor **6d** yields as intermediate a disaccharide that reacts immediately without further purification with the CDA derivative **6b** under NIS activation to form **23** (62%). The disaccharide **22** is also found as by-product (10%), which arises in the second glycosylation step from unconverted **21** and added **6b**. The final deblocking of saccharide **23** furnishes the *Streptococcus* antigen trisaccharide **24** (Scheme 7).



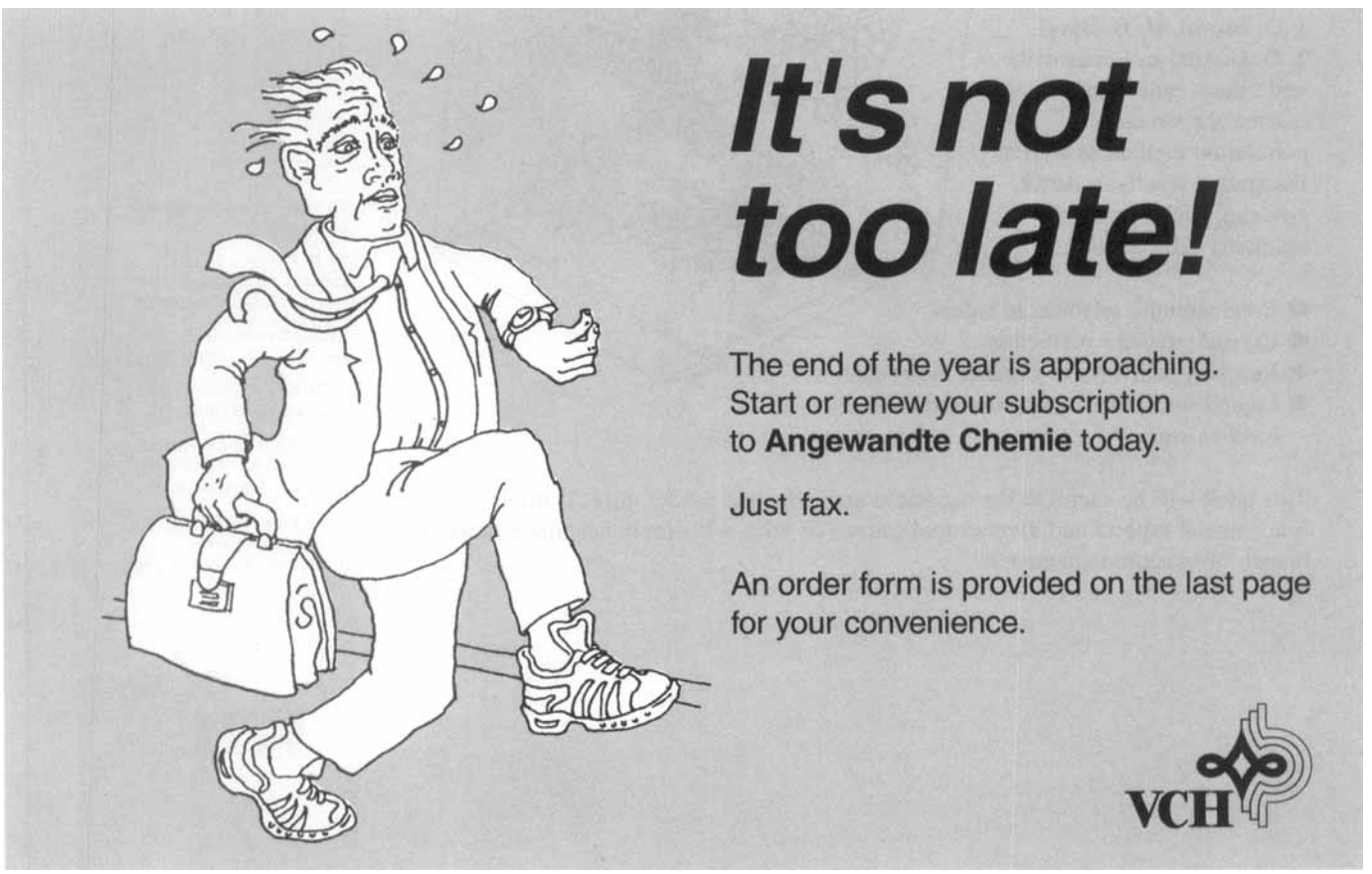
Scheme 7. Rha*p* = rhamnopyranose.

In particular, the examples given in Schemes 6 and 7 for the application of Dispoke and CDA groups in oligosaccharide synthesis demonstrate magnificently that with these novel protecting groups complex sugars can be synthesized very efficiently. The Dispoke and CDA acetals should therefore rapidly become standard practice in carbohydrate chemistry.

German version: *Angew. Chem.* **1994**, *106*, 2362

[1] T. W. Greene, P. G. M. Wuts, *Protective Groups in Organic Chemistry*, 2nd ed., Wiley, New York, **1991**; P. J. Kocienski, *Protecting Groups*, Thieme, Stuttgart, **1994**.
[2] S. V. Ley, M. Woods, A. Zanotti-Gerosa, *Synthesis* **1992**, 52–54.
[3] S. V. Ley, H. W. M. Priepke, S. L. Warriner, *Angew. Chem.* **1994**, *106*, 2410–2412; *Angew. Chem. Int. Ed. Engl.* **1994**, *33*, 2290–2292.

[4] S. Gohsal, G. P. Luke, K. S. Kyler, *J. Org. Chem.* **1987**, 52, 4296–4298.
[5] S. V. Ley, R. Leslie, P. D. Tiffin, M. Woods, *Tetrahedron Lett.* **1992**, *33*, 4767–4770.
[6] G.-J. Boons, D. A. Entwistle, S. V. Ley, M. Woods, *Tetrahedron Lett.* **1993**, *34*, 5649–5652.
[7] R. Downham, K. S. Kim, S. V. Ley, M. Woods, *Tetrahedron Lett.* **1994**, *35*, 769–772.
[8] S. V. Ley, G.-J. Boons, R. Leslie, M. Woods, D. M. Hollinshead, *Synthesis* **1993**, 689–692.
[9] A. B. Hughes, S. V. Ley, H. W. M. Priepke, M. Woods, *Tetrahedron Lett.* **1994**, *35*, 773–776.
[10] S. Masamune, W. Choy, J. S. Petersen, L. R. Sita, *Angew. Chem.* **1985**, *97*, 1–31; *Angew. Chem. Int. Ed. Engl.* **1985**, *24*, 1–30.
[11] D. A. Entwistle, A. B. Hughes, S. V. Ley, G. Visentin, *Tetrahedron Lett.* **1994**, *35*, 777–780.
[12] B. Fraser-Reid, U. E. Udodong, Z. Wu, H. Ottoson, R. Merritt, C. S. Rao, C. Roberts, *Synlett* **1992**, 927–942; G. H. Veeneman, J. H. van Boom, *Tetrahedron Lett.* **1990**, *31*, 275–278.
[13] G.-J. Boons, P. Grice, R. Leslie, S. V. Ley, L. L. Yeung, *Tetrahedron Lett.* **1993**, *34*, 8523–8526.
[14] S. Raghavan, D. Kahne, *J. Am. Chem. Soc.* **1993**, *115*, 1580–1581.
[15] S. V. Ley, H. W. M. Priepke, *Angew. Chem.* **1994**, *106*, 2412; *Angew. Chem. Int. Ed. Engl.* **1994**, *33*, 2292.



 © *VCH Verlagsgesellschaft mbH, D-69451 Weinheim, 1994* *0570-0833/94/2222-2275 $ 10.00+.25/0*

Synthesis and Structure of the First Hybrid Borazine–Phosphazene Ring**

Derek P. Gates, Ralf Ziembinski, Arnold L. Rheingold, Brian S. Haggerty, and Ian Manners*

Inorganic heterocycles have attracted considerable attention because of the interesting questions they pose with respect to structure and bonding and their function as precursors to inorganic polymers by ring-opening polymerization, and to ceramics by pyrolysis.[1–3] Borazines and cyclic phosphazenes (1,3,5,2λ^5, 4λ^5, 6λ-triazatriphosphinines) represent two of the most well-studied classes of these compounds.[4, 5] In contrast, very few examples of rings constructed from boron, nitrogen, and phosphorus atoms have been reported and none of these can be regarded as an authentic borazine–phosphazene hybrid.[6, 7]

One of the best characterized boron–nitrogen–phosphorus rings is **1**. This compound has been prepared by several routes, of which one is the reaction of $[Cl_3P{=}N{=}PCl_3][BCl_4]$ with $[MeNH_3]Cl$.[6] The boratophosphazene **1** was previously characterized spectroscopically, and a zwitterionic structure was proposed in the solid state. However, electrical conductivity measurements have provided evidence for the formation of an ion pair through chloride loss from boron in polar solvents such as nitrobenzene.[8] To clarify the nature of **1** and in view of the complete absence of any crystallographic studies of six-membered rings of this type, a single-crystal X-ray diffraction study of this species was undertaken.

Colorless crystals of **1** were obtained by cooling a solution of the compound in CH_2Cl_2 to $-30\,^{\circ}C$ over several days. Two views of the molecular structure of **1** are shown in Figure 1.[9] The BP_2N_3 ring deviates significantly from planarity and the sum of the internal angles for the ring is 711.6(6)° (expected value 720°). In particular, the boron atom in **1** is 0.39(1) Å removed from the best plane of the other five ring atoms as is clearly apparent in the side-on view of **1** in Figure 1 bottom. The P–N bonds flanking N(3) [P(1)–N(3) and P(2)–N(3)] are shorter (average, 1.547(4) Å) than those involving the methyl-substituted nitrogen atoms N(1) and N(2) [P(1)–N(1) and P(2)–N(2)] (average, 1.593(4) Å). This suggests a greater degree of π bonding in the case of the former bonds which is consistent with the presence of a positive charge on N(3). For comparison, the phosphorus–nitrogen bonds in $[Cl_3P{=}N{=}PCl_3]^+$ are 1.51–1.56 Å long.[10] Significantly, however, the P(1)–N(1) and P(2)–N(2) bonds (average, 1.593(4) Å) are similar in length to the P–N bonds in $(NPCl_2)_3$ (1.58 Å)[11] and are far shorter than a typical P–N single bond (ca. 1.78 Å).[12] This indicates that the lone pairs on N(1) and N(2) are involved in the π-bonding to the phosphorus atoms of the P(1)-N(3)-P(2) fragment. Further evidence for π-bonding is provided by the trigonal-planar rather than pyramidal environments of N(1) and N(2). In contrast to the P–N bonds, the B–N bonds have lengths (average, 1.533(5) Å) which are indicative of predominantly single bond character. For example, the accepted bond length range for a B–N single bond is about 1.58–1.59 Å, whereas B=N double bonds are generally about 1.41 Å, and in borazines, the bond length is slightly longer at about 1.43 Å.[13] Nevertheless, the skeletal B–N bonds are still significantly shorter than a typical single bond, suggesting the possibility of some degree of π character in the skeletal N-B-N moiety. This postulate is supported by a careful consideration of the environment about the boron atom B(1). Remarkably, the two boron–chlorine bonds differ significantly. The B(1)–Cl(5) bond lies approximately in the best plane of the BP_2N_3 ring and is 1.847(5) Å long which is

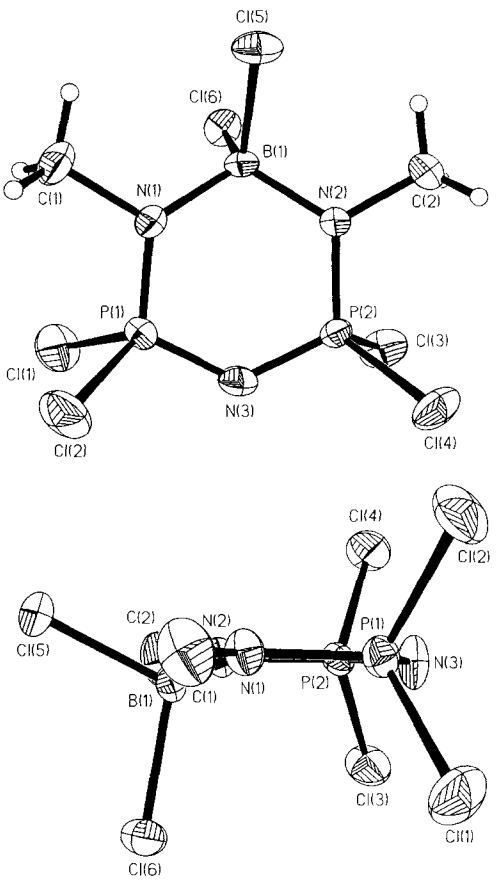


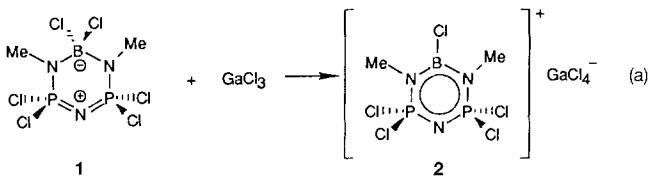
Fig. 1. Crystal structure of **1**. Selected bond lengths [Å] and angles [°]: P(1)-N(3) 1.551(4), P(2)-N(3) 1.544(4), P(1)-N(1) 1.583(4), P(2)-N(2) 1.602(4), N(1)-B(1) 1.536(6), N(2)-B(1) 1.531(5), Cl(5)-B(1) 1.847(5), Cl(6)-B(1) 1.903(4); P(1)-N(3)-P(2) 125.7(3), N(1)-P(1)-N(3) 113.9(2), N(2)-P(2)-N(3) 113.7(2), P(1)-N(1)-B(1) 122.2(3), P(2)-N(2)-B(1) 122.2(3), N(1)-B(1)-N(2) 113.9(3).

[*] Prof. I. Manners, D. P. Gates, Dr. R. Ziembinski,
Department of Chemistry, University of Toronto
80 St. George Street, Toronto, Ontario, M5S 1A1 (Canada)
Telefax: Int. code +(416)978-8775
Prof. A. L. Rheingold, B. S. Haggerty
Department of Chemistry and Biochemistry
University of Delaware, Newark, DE 19716 (USA)

[**] This work was supported by the Natural Science and Engineering Research Council of Canada (NSERC). D. P. G. also thanks NSERC for a Graduate Fellowship, R. Z. acknowledges the Deutscher Akademischer Austauschdienst (DAAD) for a Postdoctoral Fellowship, and I. M. is grateful to the Alfred P. Sloan Foundation for a Fellowship (1994–1996).

comparable to that found in cyclic chloroborane–amine adducts such as the dimeric species $(Cl_2BNMe_2)_2$ (1.830(10) Å).[14] In contrast, the B(1)–Cl(6) bond is approximately perpendicular to the best plane of the six-membered ring (Fig. 1 bottom) and is significantly elongated to 1.903(4) Å. Together with the significant shortening of the skeletal B–N bonds, this elongation suggests that Cl(6) is close to heterolytic dissociation which would generate a "borazine-like" planar environment at B(1). In view of this possibility, halide abstraction from **1** was attempted by using $GaCl_3$.

Addition of $GaCl_3$ in CH_2Cl_2 to **1** in the same solvent [Eq. (a)] gave no obvious color change. However, analysis of the



1 **2**

reaction mixture by ^{11}B NMR spectroscopy showed that **1** (δ = 5.38 (triplet)) was completely consumed and that a new product **2** with a singlet resonance at δ = 31.7 had formed. The ^{11}B NMR resonance for **2** is substantially broader than that for **1** which is consistent with the presence of a planar rather than tetrahedral environment at boron. In addition, the ^{11}B NMR chemical shift for **2** is similar to that for the borazine $(ClBNMe)_3$ (δ = 31.2).[15] The ^{31}P NMR resonance of **2** at δ = 35.5 is shifted downfield compared to the corresponding singlet resonance of **1** at δ = 28.2. The ^1H NMR spectrum of **2** shows a methyl proton resonance centered at δ = 3.36 which is shifted slightly downfield from that of **1** at δ = 3.23. Although the NMR spectroscopic data for **2** was clearly consistent with the successful abstraction of the chloride from **1** using $GaCl_3$, conclusive proof is provided by a single-crystal X-ray diffraction study.

Two alternative views of the molecular structure of **2**[16] are shown in Figure 2. The structure confirmed that a chlorine atom attached to boron in **1** had been abstracted to yield a boron–nitrogen–phosphorus cation with $[GaCl_4]^-$ as counterion. In contrast to the structure of **1**, the BNP ring in **2** is virtually planar (Fig. 2 bottom); the N(1) atom exhibits the largest deviation from the best plane (0.11(1) Å), and the sum of the internal angles for the ring is 718(1)°. There are no significant interactions between the cation and the anion; the shortest B···Cl(6) distance is 3.223(3) Å, and the shortest N(1)···Cl(9) distance is 3.980(3) Å. A clear difference between the structures of **1** and **2** is apparent in the N(2)-B-N(3) bond angle. This angle shows a substantial increase from 113.9(3)° in **1** to a value of 124.2(6)° in **2** which is consistent with a decrease in the coordination number at boron from 4 to 3. In addition, the B–N bond lengths in **2** (1.429(10) Å) are much shorter than in **1** (1.533(5) Å). This indicates a degree of π-bond character in **2** similar to that found in borazines (B–N bond length ca. 1.43 Å).[13] In contrast to the environment at boron, the bond lengths and angles in the phosphazene portion of the ring are virtually identical to those in **1**. However, the P(1)–N(2) and P(2)–N(3) bonds are longer in **2** (average, 1.624(6) Å) than the analogous bonds in **1** (average, 1.593(5) Å) which can be attributed to the greater degree of π-bonding between nitrogen and boron in the former species.

Further work is underway, aimed at gaining greater understanding of the reactivity of **1** and **2** and at investigating the potential use of these compounds as precursors to BN–PN based polymers and ceramics.

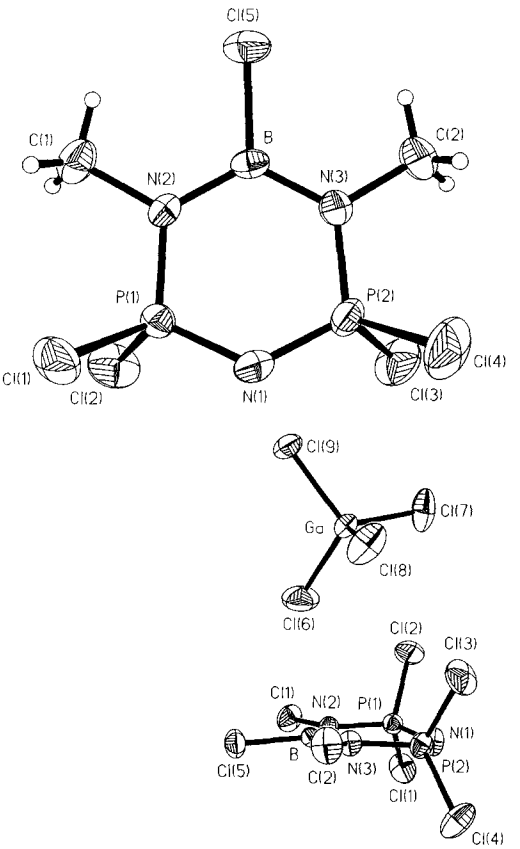


Fig. 2. Crystal structure of **2**. Selected bond lengths [Å] and angles [°]: P(1)-N(1) 1.551(7), P(2)-N(1) 1.551(6), P(1)-N(2) 1.623(6), P(2)-N(3) 1.625(7), N(2)-B 1.436(9), N(3)-B 1.422(10); P(1)-N(1)-P(2) 125.4(4), N(1)-P(1)-N(2) 112.2(3), N(1)-P(2)-N(3) 112.0(4), P(1)-N(2)-B 121.5(5), P(2)-N(3)-B 122.2(4), N(2)-B-N(3) 124.2(6).

Experimental Procedure

2: A solution of $GaCl_3$ (0.26 g, 1.5 mmol) in CH_2Cl_2 (20 mL) was added to a pale yellow solution of **1** (0.47 g, 1.4 mmol) in CH_2Cl_2 (20 mL) in an flame-dried evacuated chamber [17] at room temperature. No color change was observed in the reaction mixture after it had been stirred, but the reaction was shown to be quantitative by ^{31}P NMR. The solvent was removed in vacuo over approximately four hours by slow condensation into a flask held about 10 cm above liquid nitrogen. This yielded beige fibrous needles, which were recrystallized from CH_2Cl_2 by slow removal of solvent in vacuo. The colorless crystals obtained were washed three times with cold hexanes. Yield: 0.33 g (47%). ^{31}P NMR ($CDCl_3$; H_3PO_4 ext.), δ = 35.0; ^{11}B NMR (CH_2Cl_2/D_2O; $BF_3 \cdot OEt_2$ ext.), δ = 31.7; ^1H NMR ($CDCl_3$; TMS ext.), δ = 3.36 (m). Elemental analysis: $C_2H_6BCl_9GaN_3P_2$: calcd. C 4.50, H 1.13, N 7.87, found C 4.50, H 1.12, N 7.72.

Received: June 6, 1994 [Z 7004 IE]
German version: *Angew. Chem.* **1994**, *106*, 2367

[1] See for example H. W. Roesky, K. V. Katti, U. Seseke, M. Witt, E. Egert, R. Herbst, G. Sheldrick, *Angew. Chem.* **1986**, *88*, 447; *Angew. Chem. Int. Ed. Engl.* **1986**, *25*, 477; R. Hasselbring, H. W. Roesky, A. Heine, D. Stalke, G. Sheldrick, *Z. Naturforsch. B* **1993**, *48*, 43; K. Waggoner, H. Hope, P. P. Power, *Angew. Chem.* **1988**, *100*, 1765; *Angew. Chem. Int. Ed. Engl.* **1988**, *12*, 1699; H. V. R. Dias, P. P. Power, *ibid.* **1987**, *99*, 1320 and **1987**, *26*, 1270; J. C. van de Grampel, *Coord. Chem. Rev.* **1992**, *112*, 247; N. Burford, T. Chivers, M. Hojo, W. G. Laidlaw, J. F. Richardson, M. Trsic, *Inorg. Chem.* **1985**, *24*, 709; T. Chivers, K. S. Dhathathreyan, S. W. Liblong, T. Parks, *ibid.* **1988**, *27*, 1305; N. Burford, T. M. Parks, B. W. Royan, B. Borecka, T. S. Cameron, J. F. Richardson, E. J. Gabe, R. Hynes, *J. Am. Chem. Soc.* **1992**, *114*, 8147; P. Paetzold, C. von Plotho, G. Schmid, R. Boese, *Z. Naturforsch. B* **1984**, *39*, 1069.

[2] See for example H. R. Allcock, *Adv. Mater.* **1994**, *6*, 106; I. Manners, H. R. Allcock, G. Renner, O. Nuyken, *J. Am. Chem. Soc.* **1989**, *111*, 5478; J. A. Dodge, I. Manners, H. R. Allcock, G. Renner, O. Nuyken, *ibid.* **1990**, *112*,

1268; H. W. Roesky, M. Lücke, *Angew. Chem.* **1989**, 101, 480; *Angew. Chem. Int. Ed. Engl.* **1989**, *28*, 493; F. Sauls, L. V. Interrante, *Coord. Chem. Rev.* **1993**, *128*, 193; W. Schnick, *Angew. Chem.* **1993**, *105*, 846; *Angew. Chem. Int. Ed. Engl.* **1993**, *32*, 806; A. H. Cowley, R. A. Jones, *ibid.* **1989**, *101*, 1235 and **1989**, *28*, 1208.

[3] I. Manners, *Adv. Mater.* **1994**, *6*, 68; M. Liang, I. Manners, *J. Am. Chem. Soc.* **1991**, *113*, 4044; D. A. Foucher, A. J. Lough, I. Manners, *Inorg. Chem.* **1992**, *31*, 3034.

[4] W. Maringgele in *The Chemistry of Inorganic Homo and Heterocycles, Vol. 1* (Eds.: I. Haiduc, D. B. Sowerby), Academic Press, London, **1987**, chapter 2.

[5] H. R. Allcock, *Phosphorus-Nitrogen Compounds*, Academic Press, New York, **1972**; C. W. Allen, *Coord. Chem. Rev.* **1994**, *130*, 137.

[6] H. Binder, *Z. Naturforsch. B* **1971**, *26*, 616; H. Binder, J. Palmtag, *ibid.* **1979**, *34*, 179; F. G. Sherif, C. D. Schmulbach, *Inorg. Chem.* **1966**, *5*, 322.

[7] P. Paetzold, C. von Plotho, E. Niecke, R. Rüger, *Chem. Ber.* **1983**, *116*, 1678.

[8] H. Becke-Goehring, H. J. Müller, *Z. Anorg. Allg. Chem.* **1968**, *362*, 51.

[9] Crystal data for $C_2H_6BCl_6N_3P_2$ **1**: $P2_1/c$, $a = 9.119(2)$, $b = 7.765(2)$, $c = 18.862(4)$ Å, $\beta = 103.50(3)^\circ$, $V = 1298.7(5)$ Å^3, $Z = 4$, $\mu = 15.34$ cm^{-1}, $Mo_{K\alpha}$ ($\lambda = 0.71073$ Å), $\varrho_{calcd} = 1.834$ g cm^{-3}, 298 K, Siemens P4 diffractometer with graphite monochromator, colorless crystal ($0.38 \times 0.40 \times 0.46$ mm) mounted in a capillary. Of 3246 reflections collected ($4 \le 2\theta \le 55^\circ$) 2946 were independent ($R_{merg} = 0.0252$) and 2242 were observed with $F_o \ge 4\sigma(F_o)$. Solution by direct methods which located the Cl atoms, non-hydrogen atoms were refined with anisotropic thermal parameters, hydrogen atoms fixed and idealized ($d_{CH} = 0.960$ Å, U fixed at 0.0800 Å^2), $R = 0.0482$, $wR = 0.0509$, GOF = 1.50, $N_o/N_v = 17.2$, and $\Delta\rho_{max} = 0.43$ eÅ^{-3} [18].

[10] R. Faggiani, R. J. Gillespie, J. F. Sawyer, J. D. Tyrer, *Acta Crystallogr. Sect. B* **1980**, *36*, 1014.

[11] G. J. Bullen, *J. Chem. Soc.* **1971**, 1450.

[12] D. E. C. Corbridge, *Phosphorus: An Outline of its Chemistry, Biochemistry and Technology*, Elsevier, Amsterdam, **1990**.

[13] P. Paetzold, *Adv. Inorg. Chem. Radiochem.* **1987**, *31*, 123, 137.

[14] H. Hess, *Acta Crystallogr.* **1963**, *16*, A74.

[15] B. Wrackmeyer, H. Nöth, *Chem. Ber.* **1976**, *109*, 3480.

[16] Crystal data for $C_2H_6BCl_9GaN_3P_2$ **2**: $P\bar{1}$, $a = 8.613(2)$, $b = 9.259(3)$, $c = 12.712(3)$ Å, $\alpha = 93.34(2)$, $\beta = 100.96(2)$, $\gamma = 112.71(2)^\circ$, $V = 908.3(4)$ Å^3, $Z = 2$, $\mu = 29.98$ cm^{-1}, $Mo_{K\alpha}$ ($\lambda = 0.71073$ Å), $\delta_{calcd} = 1.951$ g cm^{-3}, 297 K, Siemens P4 diffractometer with graphite monochromator, colorless crystal ($0.10 \times 0.36 \times 0.41$ mm) mounted in a capillary. Of 5504 reflections collected ($4 \le 2\theta \le 60^\circ$) 5285 were independent $R_{int.} = 0.0165$, and 2419 were observed with $F_o \ge 5\sigma(F_o)$. Solution by direct methods which located the Ga and Cl atoms, non-hydrogen atoms were refined with anisotropic thermal parameters, hydrogen atoms fixed and idealized ($d_{CH} = 0.960$ Å, U fixed at 0.0800 Å^2), $R = 0.0479$, $wR = 0.0597$, GOF = 1.23, $N_o/N_v = 14.8$, and $\Delta\rho_{max} = 0.69$ eÅ^{-3} [18].

[17] The vessel used was a modification of that described in: N. Burford, J. Müller, T. M. Parks, *J. Chem. Educ.* **1994**, *71*, 807.

[18] Further details of the crystal structure investigations may be obtained from the Fachinformationszentrum Karlsruhe D-76344 Eggenstein-Leopoldshafen (FRG) on quoting the depository number CSD-58352.

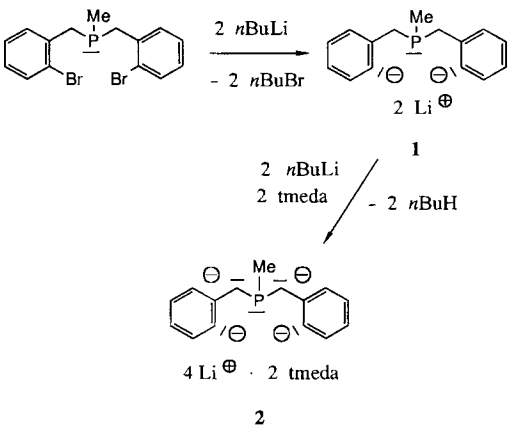
Tetralithiated Dibenzyl(methyl)phosphane**

Martin Winkler, Martin Lutz, and Gerhard Müller*

Polar di- and polymetalated organic compounds (polycarbanions)[1] have attracted widespread interest because of their synthetic potential and the intriguing problems associated with their structure and bonding.[2] For dimetalated organic compounds, in particular, a plethora of preparative, structural, spectroscopic, and theoretical information is available. Far less is known about polar organometallic compounds containing triply[3] or higher charged carbanions. Prominent examples of tetrametalated carbon compounds are tetralithiomethane[4] and other polylithium compounds obtained by perlithiation or lithiation of alkynes, for example C_3Li_4, C_5Li_4,[5] and tetrametalated 2,4-hexadiyne and 1,8-cyclotetradecadiyne.[6] Other highly metalated organometallic compounds are tetralithiated 1,2,3,4-tetraphenyl-1,3-butadiene[7] and 1,1-dimethyl-2,3,4,5-tetraphenyl-1-silacyclopentadiene,[8] 3,3′,5,5′-tetrakis(kaliomethyl)-biphenyl,[9] 2,3-bis(α-kaliobenzyl)-1,4-dikalio-1,4-diphenylbutane,[10] polylithiated aromatic rings[11] including ferrocene,[12] and multiply charged anions derived from molecules with extended π systems[13] including fullerenes.[14] Precise structural information on most of these systems is scarce, however, because polymetalated organic compounds tend to be highly associated in the solid state thereby often preventing structure elucidation in solution as well as the growing of single crystals.

In the course of studies of the ligand properties of *ortho*-metalated benzylphosphanes towards main group metals[15] we became interested in *o,o′*-dilithiated dibenzyl(methyl)phosphane (**1**), a valuable starting material for the preparation of metal complexes of this dianionic phosphane ligand.[16] The dilithium compound **1** is conveniently prepared from bis(2-bromobenzyl)methylphosphane[17] and *n*BuLi in pentane at −20 °C in 79% yield.[18] The almost exclusive *ortho*-dilithiation is proven by reactions of **1** with D_2O and dimethyldisulfide which yield the respective *ortho*-derivatives. Monolithiation amounts to only 10% of the total product yield under these conditions. Compound **1** is only sparingly soluble in pentane as well as in aromatic solvents which prevented further characterization especially by NMR spectroscopic methods.[19]

We now found that a suspension of **1** in pentane at room temperature may be further lithiated with excess *n*BuLi in the presence of *N,N,N′,N′*-tetramethylethylenediamine (tmeda) to give the pentane-soluble red tetralithium compound **2** in 50% yield. In addition to the *ortho*-carbon atoms, in **2** also the α-carbon atoms of dibenzyl(methyl)phosphane are deprotonated. Thus, the organolithium complex **2** contains a surprisingly small quadruply charged carbanion formally comprising not less than five lone pairs of electrons. The tetralithiation was again proven by hydrolysis of **2** with D_2O. In addition, **2** was also characterized by an X-ray structure determination,[20] which also yielded valuable insight into the origin of the stability of this highly charged carbanion.



2

In the solid state **2** is a dimer with crystallographically imposed centrosymmetry (Fig. 1). The deprotonation of the *ortho*-carbon atoms of the phenyl rings (C2, C9) clearly follows from their coordination to lithium atoms, while that of the α-carbon atoms C7 and C14 is evident from their planar geometry (H

[*] Prof. Dr. G. Müller, Dipl.-Chem. M. Winkler, Dipl.-Chem. M. Lutz
Fakultät für Chemie der Universität
Universitätsstrasse 10, D-78464 Konstanz (FRG)
Telefax: Int. code + (7531)88-3140

[**] This work was supported by the Fonds der Chemischen Industrie and the State of Baden-Württemberg (Forschungsschwerpunkt "Metallzentrierte Substrattransformationen").

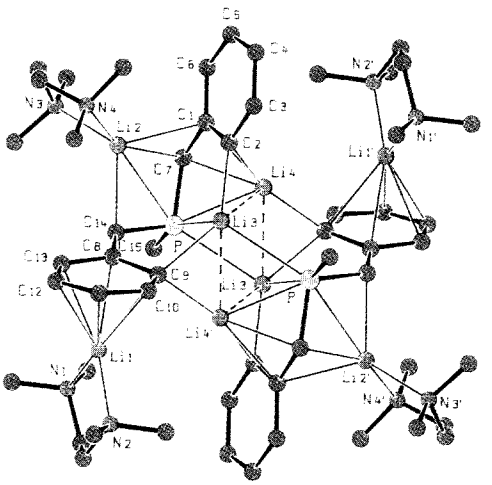


Fig. 1. Structure of the dimer of **2** in the crystal (SCHAKAL plot; atoms with arbitrary radii; H atoms omitted for clarity; primed atoms are related to those without a prime by a crystallographic center of inversion; the central rhombus of lithium atoms is indicated by the red dashed lines). Important distances [Å] and angles [°]: Li2-P 2.79(1), Li2-C1, 2.42(2), Li2-C7 2.35(1), Li2-C14 2.25(1), Li3-P 2.70(1), Li3-P' 2.73(1), Li3-C2 2.12(1), Li3-C9 2.19(2), Li4-P 2.50(2), Li4-C2 2.15(2), Li4-C1 2.26(2), Li4-C7 2.27(2), Li4-C9' 2.14(2), P-C7 1.796(7), P-C14 1.775(7), P-C15 1.821(8), C1-C7 1.45(1), C8-C14 1.42(1), Li3···Li4 2.62(2), Li3···Li4' 2.51(2); C7-P-C14 109.1(3), C7-P-C15 99.0(4), C14-P-C15 103.8(4), C1-C2-C3 115.1(6), C8-C9-C10 115.6(7), C2-C1-C7 120.1(6), C9-C8-C14 123.3(7), P-C7-C1 121.0(5), P-C14-C8 126.4(5), Li4-Li3-Li4' 102.7(5), Li3-Li4-Li3' 77.3(5). Torsion angles [°]: C2-C1-C7-P 9.9(9), C9-C8-C14-P 8(1).

atoms located). Dimer formation is brought about by four bridging lithium atoms (Li3, Li4, Li3', Li4') arranged in a planar, almost perfectly equilateral rhombus (Fig. 1). Due to the bridging nature of these four lithium atoms each of the carbanions forms close contacts to not less than six lithium cations. Five of them (Li2, Li3, Li4, Li3', Li4') are arranged in close proximity to the carbanionoid centers (α- and *ortho*-C atoms), the *ipso*-phenyl atoms, and the phosphorus atom. In particular, Li2 is bonded in η^4 fashion to the nonplanar fragment comprising C1, C7, P, C14. The bridging atom Li3 connects both *ortho*-carbon atoms and the phosphorus atom of one ligand with the phosphorus atom of the second, while Li4 is η^4 π bonded to the fragment comprising C2, C1, C7, P and in addition to the *ortho*-C atom C9'. As a clear consequence of the good steric shielding of most of the anion by these five lithium atoms, the Li1 atom is η^6 π bonded to the least shielded phenyl ring C8–C13 (Li–C 2.32(1)–2.54(1) Å).[21] Due to the coordinative unsaturation of the Li1 and Li2 centers by carbanion contacts, only these are further complexed by tmeda molecules. The bonding pattern of Li2 and particularly those of Li3 and Li4 are without precedent. They involve Li–C distances between 2.12(1) and 2.42(2) Å, while the Li–P distances are between 2.50(2) and 2.79(1) Å, a range commonly observed in many complexes of lithium with anionic phosphanes, however.[22] The latter deserves special mention since the (phosphane) P atom in addition to three covalently bonded C atoms is coordinated to not less than four Li atoms, which likewise has no precedent in the literature.

In addition to the electrostatic stabilization of the tetracarbanion in **2** by tight ion pairing with six Li^+ counterions, further stabilization of the anion is gained from extensive delocalization of the negative charges as well as from the at least partial onium character of the phosphorus center brought about by the large number of Li^+ contacts. The first effect is particularly evident from the almost perfect planarity of both benzylic fragments P-CH-C_6H_4 and the short bonds C1–C7 (1.45(1) Å) and C8–C14 (1.42(1) Å). The latter effect, which has long been known to be the dominating stabilizing factor for the carbanionoid centers in phosphorus ylides,[23] is reflected in the slightly shortened bonds between phosphorus and the benzylic carbon atoms (P–C7 1.796(7), P–C14 1.775(7) Å). Finally, the intraring bond angles at the metalated phenyl carbon atoms C2 and C9 deserve comment. From a variety of metal aryl structures they are well known to be characteristically smaller than the sp^2 standard.[24] This is believed to be due to the concentration of the negative charge at this carbon atom in an orbital with increased s-character, thus leaving more p-character for the bonds to the neighboring carbon atoms with consequent reduction in bond angle. With 115.1(6)° and 115.6(7)° at C2 and C9, respectively, the effect is noticeably smaller in **2** than in prototypal phenyllithium structures, where a range of 111.2–114.6° is usually encountered.[24, 25] We take this as a further indication of the superior charge delocalization in the tetracarbanion in **2**.

Synthesis and structure of **2** strongly indicate that benzylphosphanes and benzylphosphonium cations should be particularly well suited as starting materials for the formation of highly charged carbanions by multiple lithiation.

Experimental Procedure

All experiments were carried out under rigorous exclusion of atmospheric oxygen and moisture. Solvents were dried according to established procedures and redestilled immediately prior to use. NMR: Jeol JNM GX 400(^{13}C, ^{31}P, ^{7}Li), Bruker WM 250 (^{1}H).

1: Bis(2-bromobenzyl)methylphosphane (2.33 g, 6.0 mmol) was suspended in pentane (50 mL) to which diethyl ether (0.3 mL) was added. After the mixture had been cooled to −40 °C *n*BuLi (9 mL, 18 mmol, 2 M solution in pentane) was added dropwise. The reaction mixture was allowed to warm to −20 °C and stirred for 4 h. A slightly yellow precipitate formed which was filtered off, washed with pentane (50 mL) and dried in vacuo. Yield: 1.15 g (4.8 mmol, 79%) of **1**.

Reaction of **1** with D_2O: **1** (0.55 g, 2.4 mmol) was suspended in pentane (25 mL) and D_2O (1.5 mL) was added. After the mixture had been stirred for a short while both phases became colorless and clear. The phases were separated and the pentane phase washed twice with H_2O. The pentane was removed in vacuo and the residue dissolved in $CDCl_3$ for the NMR measurements. The ^{1}H and ^{31}P NMR spectra are virtually identical with those of $(C_6H_5CH_2)_2PCH_3$ [17b]. $^{13}C\{^{1}H\}$NMR (105.3 MHz, 25 °C, TMS ext.) of (*o*-D-$C_6H_4CH_2)_2PCH_3$: δ = 10.56 (d, ^{1}J(P,C) = 18.5 Hz, CH_3), 36.47 (d, ^{1}J(P,C) = 16 Hz, CH_2), 125.69 (s, C-4), 128.20/128.32 (s, C-3/5), 128.73 (dt, ^{1}J(D,C) = 24, ^{3}J(P,C) = 5.6 Hz, C-2), 129.05 (d, ^{3}J(P,C) = 4.9 Hz, C-6), 137.60 (d, ^{2}J(P,C) = 4.9 Hz, C-1).

Reaction of **1** with MeSSMe: **1** (0.55 g, 2.4 mmol) was suspended in pentane (25 mL) and MeSSMe (1 mL, 1.1 g, 11 mmol) was added dropwise whereupon the reaction mixture warmed up slightly. The pentane phase was washed three times with H_2O (1.5 mL), the pentane was removed in vacuo, and the residue characterized by NMR in $CDCl_3$. According to the PCH_3 to SCH_3 ratio in the ^{1}H NMR, the reaction product consists of a 9:1 mixture of di- and monosubstitution products. NMR data of (*o*-MeS-$C_6H_4CH_2)_2PCH_3$: ^{31}P NMR (161.83 MHz, 25 °C, 85% H_3PO_4 ext.): δ = −28.6, s. ^{1}H NMR (250 MHz, R.T., TMS ext.): δ = 1.03 (d, ^{2}J(P,H) = 3.6 Hz, PCH_3), 2.44 (s, SCH_3), 2.91 (d, $^{2}J(H_A,H_B)$ = 13.4 Hz, CH_2), 3.11 (d, CH_2), 7.05–7.26 (m, Ph). $^{13}C\{^{1}H\}$NMR (105.3 MHz, 25 °C, TMS ext.): δ = 11.33 (d, ^{1}J(P,C) = 18.5 Hz, PCH_3), 16.28 (s, SCH_3), 34.75 (d, ^{1}J(P,C) = 17.2 Hz, CH_2), 124.80 (s, C-4), 126.10 (s, C-3), 126.50 (s, C-5), 129.65 (d, ^{2}J(P,C) = 7.4 Hz, C-1), 136.46 (d, ^{3}J(P,C) = 6.1 Hz, C-6), 137.36 (d, ^{3}J(P,C) = 2.5 Hz, C-2).

Synthesis of **2** by dilithiation of **1**: As described above, bis(2-bromobenzyl)methylphoshane (2.1 g, 5.4 mmol) was treated at −10 °C in pentane (50 mL) to which diethyl ether (0.3 mL) was added with *n*BuLi (6 mL, 15 mmol, 2.5 M solution in hexane). The yellow precipitate formed after 2.5 h was filtered off, washed with pentane (15 mL), and resuspended in pentane (40 mL). At room temperature more *n*BuLi (6 mL, 15 mmol, 2.5 M solution in hexane) was added dropwise, followed by tmeda (1 mL, 0.77 g, 6.6 mmol). A clear red solution formed which was stirred for 1.5 h after which a red solid slowly precipitated. Further tmeda (1 mL, 0.77 g, 6.6 mmol) was added and the mixture was stored at −25 °C overnight. The precipitate was filtered off. Yield: 1.3 g (2.7 mmol, 49.7%) of **2**. ^{31}P NMR (161.83 MHz, 25 °C, 85% H_3PO_4 ext.): $\delta(C_6D_6)$ = −49.5, br. s. ^{7}Li NMR (155.37 MHz, 1 M LiCl/H_2O ext.): δ (52 °C, C_6D_6) = −0.30, s; δ (0 °C, [D_8]toluene) = −1.37, br. s; −0.66, br. s; 1.43, br. s; 1.99, br. s.

Reaction of **2** with D_2O: **2** (1.3 g, 2.7 mmol) was dissolved in pentane (25 mL) and D_2O (2.0 mL) was added. The phases were separated and the pentane phase washed twice with H_2O (5 mL). The pentane was removed in vacuo and the remaining oil dissolved in $CDCl_3$ for the NMR measurements. The ^{31}P NMR spectrum is virtually identical with that of $(C_6H_5CH_2)_2PCH_3$ [17b]. ^{1}H NMR (250 MHz, 25 °C, TMS ext.) of (*o*-D-$C_6H_4CHD)_2PCH_3$: δ = 0.87 (d, ^{2}J(P,H) = 3.4 Hz), 2.6 (br. s,

CHD), 2.8 (br. s, CHD), 7.10–7.16 (m, Ph), 7.20–7.27 (m, Ph). $^{13}C\{^1H\}$ NMR (105.3 MHz, R.T., TMS ext.): $\delta = 10.4$ (d, $^1J(P,C) = 18.3$ Hz, CH_3), 36.0 ("q" = dt, $^1J(P,C) \approx {}^1J(C,D) = 19$ Hz, CHD), 125.7 (s, C-4), 128.2/128.3 (s, C-3/5), 128.73 (dt, $^1J(D,C) = 27.0$, $^3J(P,C) = 6.0$ Hz, C-2), 129.0 (d, $^3J(P,C) = 5.5$ Hz, C-6), 137.6 (d, $^2J(P,C) = 4.9$ Hz, C-1).

Received: June 9, 1994 [Z 7021 IE]
German version: *Angew. Chem.* **1994**, *106*, 2372

[1] Highly polar organometallics, especially those of the alkaline metals, are commonly referred to as "carbanions". This oversimplified view has long been criticized as organometallic compounds never contain isolated carbanions neither in the solid state nor in solution. For a recent discussion of the subject see: C. Lambert, P. von R. Schleyer, *Angew. Chem.* **1994**, *106*, 1187; *Angew. Chem. Int. Ed. Engl.* **1994**, *33*, 1129.

[2] R. B. Bates in *Comprehensive Carbanion Chemistry*, Bd. A (Eds.: E. Buncel, T. Durst), Elsevier, Amsterdam, **1980**, p. 1; R. B. Bates, C. A. Ogle, *Carbanion Chemistry*, Springer, Berlin, **1983**; P. von R. Schleyer, *Pure Appl. Chem.* **1983**, *55*, 355; *ibid.* **1984**, *56*, 151; W. N. Setzer, P. von R. Schleyer, *Adv. Organomet. Chem.* **1985**, *24*, 353; C. Schade, P. von R. Schleyer, *ibid.* **1987**, *27*, 169; E. Grovenstein, Jr. in *Comprehensive Carbanion Chemistry, Bd. C* (Eds.: E. Buncel, T. Durst), Elsevier, Amsterdam, **1987**, p. 175; A. Maercker, M. Theis, *Top. Curr. Chem.* **1987**, *138*, 1; A. Maercker, *Methoden Org. Chem. Houben-Weyl 4th ed. 1952-*, Bd. E19d, **1993**, p. 448.

[3] D. Hellwinkel, W. Schenk, *Angew. Chem.* **1969**, *81*, 1049; *Angew. Chem. Int. Ed. Engl.* **1969**, *8*, 987; J. J. Bahl, R. B. Bates, W. A. Beavers, C. R. Launer, *J. Am. Chem. Soc.* **1977**, *99*, 6126; R. D. Howells, H. Gilman, *Tetrahedron Lett.* **1974**, 1319; V. S. Bleshinskii, S. V. Bleshinskii, *Izv. Akad. Nauk Kirg. SSR* **1982**, 47; J. Klein, A. Medlik, A. Y. Meyer, *Tetrahedron* **1976**, *32*, 51; J. Klein, *ibid.* **1983**, *39*, 2733; *ibid.* **1988**, *44*, 503; C. Rücker, *J. Organomet. Chem.* **1986**, *310*, 135; A. Rajca, L. M. Tolbert, *J. Am. Chem. Soc.* **1987**, *109*, 1782; J. Klein, L. Weiler, *Isr. J. Chem.* **1984**, *24*, 69.

[4] A. Maercker, M. Theis, *Angew. Chem.* **1984**, *96*, 990; *Angew. Chem. Int. Ed. Engl.* **1984**, *23*, 995; *Organomet. Synth.* **1986**, *3*, 398; A. Maercker, *Angew. Chem.* **1992**, *104*, 598; *Angew. Chem. Int. Ed. Engl.* **1992**, *31*, 584.

[5] R. West, *Adv. Chem. Ser.* **1974**, *179*, 563.

[6] J. Klein, J. Y. Becker, *J. Chem. Soc. Perkin Trans. 2* **1973**, 599; J. Y. Becker, *Tetrahedron Lett.* **1976**, 2159; J. Klein in *The Chemistry of the Carbon-Carbon Triple Bond* (Ed.: S. Patai), Wiley, New York, **1978**, p. 343.

[7] V. R. Sandel, B. Belinky, T. Stefaniak, D. Kreil, *J. Org. Chem.* **1975**, *40*, 2116.

[8] D. H. O'Brien, D. L. Breeden, *J. Am. Chem. Soc.* **1981**, *103*, 3237.

[9] D. Wilhelm, T. Clark, P. von R. Schleyer, *Tetrahedron Lett.* **1982**, *23*, 4077.

[10] G. Boche, K. Buckl, *Angew. Chem.* **1978**, *90*, 291; *Angew. Chem. Int. Ed. Engl.* **1978**, *17*, 284.

[11] E. Aharon-Shalom, J. Y. Becker, J. Bernstein, S. Bittner, S. Shaik, *Tetrahedron Lett.* **1985**, *26*, 2783; J. R. Baran, Jr., C. Hendrickson, D. A. Laude, Jr., R. J. Lagow, *J. Org. Chem.* **1992**, *57*, 3759.

[12] A. F. Halasa, D. P. Tate, *J. Organomet. Chem.* **1970**, *24*, 769.

[13] R. Schenk, K. Müllen, O. Wennerström, *Tetrahedron Lett.* **1990**, *31*, 7367; A. Rajca, *J. Am. Chem. Soc.* **1990**, *112*, 5889, 5890; *J. Org. Chem.* **1991**, *56*, 2557; A. Rajca, S. Utamapanya, J. Xu, *J. Am. Chem. Soc.* **1991**, *113*, 9235; S. Utamapanya, A. Rajca, *ibid.* **1991**, *113*, 9242; A. Rajca, S. Utamapanya, *J. Org. Chem.* **1992**, *57*, 1760.

[14] J. W. Bausch, G. K. Surya Prakash, G. A. Olah, D. S. Tse, D. C. Lorents, Y. K. Bae, R. Malhotra, *J. Am. Chem. Soc.* **1991**, *113*, 3205; D. Dubois, K. M. Kadish, S. Flanagan, R. E. Haufler, L. P. F. Chibante, L. J. Wilson, *ibid.* **1991**, *113*, 4364; D. Dubois, K. M. Kadish, S. Flanagan, L. J. Wilson, *ibid.* **1991**, *113*, 7773.

[15] G. Reber, J. Riede, G. Müller, *Z. Naturforsch. B.* **1988**, *43*, 915; G. Müller, J. Lachmann, J. Riede, *ibid.* **1992**, *47*, 823; G. Müller, J. Lachmann, *ibid.* **1993**, *48*, 1248; G. Müller, J. Lachmann, A. Rufinska, *Organometallics* **1992**, *11*, 2970; G. Müller, J. Lachmann, *Z. Naturforsch. B* **1993**, *48*, 1544.

[16] M. Winkler, Diplomarbeit, Universität Konstanz **1994**. See ref. [17a] for the respective di-Grignard reagent and a Mg complex.

[17] a) K. Jurkschat, H.-P. Abicht, *Z. Chem.* **1985**, *25*, 338; b) H.-P. Abicht, K. Jurkschat, *ibid.* **1988**, *28*, 371; c) G. Müller, M. Waldkircher, M. Winkler, *Z. Naturforsch. B*, in press.

[18] The kinetically controlled, exclusive *ortho*-lithiation of benzylphosphines by lithium–halogen exchange was first introduced by Abicht and Issleib: H.-P. Abicht, K. Issleib, *Z. Anorg. Allg. Chem.* **1976**, *422*, 237; *ibid.* **1978**, *447*, 53.

[19] Compound **1** is much better soluble in ethers but it cannot be excluded yet that in these solvents slow rearrangement to the thermodynamically more stable α-lithiated compound takes place. For the first time such a rearrangement has been observed recently for *o*-lithiobenzyl(dimethyl)phosphane in diethyl ether: M. Waldkircher, G. Müller, unpublished observations.

[20] Crystal structure data: Enraf-Nonius CAD4 diffractometer, $Mo_{K\alpha}$ radiation, $\lambda = 0.71069$ Å, graphite monochromator, $T = -75\,^{\circ}C$. $C_{27}H_{45}Li_4N_4P$, $M_r = 484.416$, monoclinic, space group $P2_1/n$ (No. 14), $a = 14.227(4)$, $b = 14.927(9)$, $c = 14.570(4)$ Å, $\beta = 99.98(1)^{\circ}$, $V = 3047(2)$ Å^3, $Z = 2$ dimers, $\varrho_{calcd} = 1.056$ g cm^{-3}, $\mu(Mo_{K\alpha}) = 1.1$ cm^{-1}, $F(000) = 1048$. 5938 measured reflections, 2825 of which were independent ($R_{int} = 0.153$, *hkl* range: ±13, +14, ±14, $((\sin\vartheta)/\lambda)_{max} = 0.481$ Å^{-1}, $\vartheta/2\vartheta$ scans, $\Delta\omega = 0.75 + 0.35 \tan\vartheta$). Lp but no absorption correction; solution by direct methods (SHELXS-86); H atoms at C7, C14, C15 located. Anisotropic refinement of the non-H atoms (H atoms constant) on all independent F^2; $R(F) = 0.188$, $wR(F^2) = 0.197$, GOF = 1.024, $w = 1/[\sigma^2(F_o^2) + (0.0733 \cdot P)^2 + 3.18 \cdot P]$, $P = [\max(F_o^2, 0) + 2F_c^2]/3$ ($R(F) = 0.062$, $wR(F^2) = 0.137$ for reflections with $I \geq 2.0\sigma(I)$. $\Delta\varrho_{fin}$(max/min) = 0.35/−0.37 e Å^{-3} (SHELXL-93). Further details of the crystal structure investigation may be obtained from the Fachinformationszentrum Karlsruhe, D-76344 Eggenstein-Leopoldshafen (FRG) on quoting the depository number CSD-58425.

[21] Halfsandwich-type η^6 π bonding of lithium to phenyl rings with Li–C distances similar to those in **2** has been known for a long time: see ref. [2].

[22] H. H. Karsch, G. Grauvogl, P. Mikulcik, P. Bissinger, G. Müller, *J. Organomet. Chem.* **1994**, *465*, 65; H. H. Karsch, G. Baumgartner, S. Gamper, J. Lachmann, G. Müller, *Chem. Ber.* **1992**, *125*, 1333; H. H. Karsch, K. Zellner, S. Gamper, G. Müller, *J. Organomet. Chem.* **1991**, *414*, C39; H. H. Karsch, K. Zellner, G. Müller, *J. Chem. Soc. Chem. Commun.* **1991**, *466*; S. Harder, L. Brandsma, J. A. Kanters, A. Duisenberg, J. H. van Lenthe, *J. Organomet. Chem.* **1991**, *420*, 143; H. H. Karsch, K. Zellner, P. Mikulcik, J. Lachmann, G. Müller, *Organometallics* **1990**, *9*, 190, and references therein; L. T. Byrne, L. M. Engelhardt, G. E. Jacobsen, W.-P. Leung, R. I. Papasergio, C. L. Raston, B. W. Skelton, P. Twiss, A. H. White, *J. Chem. Soc. Dalton Trans.* **1989**, 105; L. M. Engelhardt, J. MacB. Harrowfield, M. F. Lappert, I. A. MacKinnon, B. H. Newton, C. L. Raston, B. W. Skelton, A. H. White, *J. Chem. Soc. Chem. Commun.* **1986**, 846; A. M. Arif, A. H. Cowley, R. A. Jones, J. M. Power, *ibid.* **1986**, 1446.

[23] H. Schmidbaur, J. Jeong, A. Schier, W. Graf, D. L. Wilkinson, G. Müller, C. Krüger, *New J. Chem.* **1989**, *13*, 341.

[24] S. Harder, P. F. Ekhart, L. Brandsma, J. A. Kanters, A. J. M. Duisenberg, P. von R. Schleyer, *Organometallics* **1992**, *11*, 2623.

[25] D. Thoennes, E. Weiss, *Chem. Ber.* **1978**, *111*, 3157; H. Hope, P. P. Power, *J. Am. Chem. Soc.* **1983**, *105*, 5320; U. Schümann, J. Kopf, E. Weiss, *Angew. Chem.* **1985**, *97*, 222; *Angew. Chem. Int. Ed. Engl.* **1985**, *24*, 215; T. Maetzke, D. Seebach, *Helv. Chim. Acta* **1989**, *72*, 624; G. Girolami, M. E. Riehl, K. S. Suslick, S. R. Wilson, *Organometallics* **1992**, *11*, 3907.

Phosphane Coordination to Magnesium: Synthesis and Structure of Bis[*ortho,ortho'*-bis{(dimethylphosphino)-methyl}phenyl]magnesium**

Andreas Pape, Martin Lutz, and Gerhard Müller*

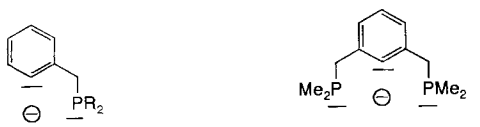
Coordination of phosphanes to organomagnesium species has only been demonstrated in solution as yet. As could be shown by ^{25}Mg NMR spectroscopy, $[Cp_2Mg]$ is complexed by PMe_3 and $Me_2PCH_2CH_2PMe_2$ in solution; however, isolation of definite adducts is ruled out by the ease of dissociation of the complexes.[1] In contrast to phosphanes, phosphides such as $PHPh^-$ are noticeably better complexing agents to magnesium, which permitted the isolation and structural characterization of [(tmeda)Mg(PHPh)$_2$] (tmeda = *N,N,N',N'*-tetramethylethylenediamine), a molecular complex with magnesium–phosphorus bonds.[2]

In previous work we showed that *ortho*-metalated benzylphosphanes **A** (R = Ph, Me)[3] are valuable bidentate (C, P) chelating ligands due to the intramolecular phosphorus complexation favored by the phosphane donor site held in close spacial proximity to the carbanionoid function.[4] This complexation potential is particularly evident from the ease of formation of stable complexes with a large number of main group metals

[*] Prof. Dr. G. Müller, Dipl.-Chem. A. Pape, Dipl.-Chem. M. Lutz
Fakultät für Chemie der Universität
Universitätsstrasse 10, D-78464 Konstanz (FRG)
Telefax: Int. code + (7531)88-3140

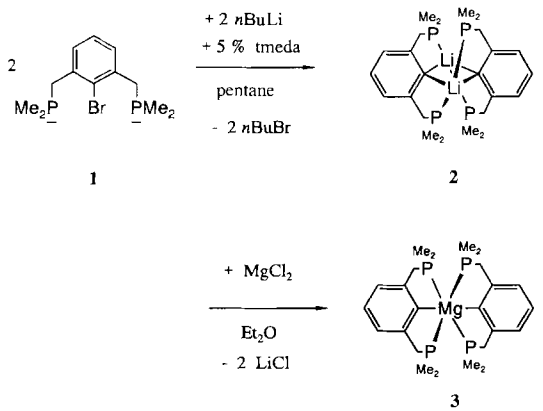
[**] This work was supported by the Fonds der Chemischen Industrie and the State of Baden-Württemberg (Forschungsschwerpunkt "Metallzentrierte Substrattransformationen"; fellowship to A.P.). We are grateful to Prof. Dr. L. M. Venanzi, ETH Zürich, for valuable suggestions concerning the synthesis of **1**.

known to be notoriously weak phosphorus acceptors.[5] In an effort to extend these studies to the potentially tridentate (P,C,P) ligand **B**, we were initially interested in its lithium complex as a convenient starting material for the preparation of other main group element complexes.[6] We report here on its synthesis and structure, as well as its use for the preparation of a stable diarylmagnesium complex containing magnesium-coordinated phosphano groups which could be fully characterized structurally both in solution and in the solid state.



A **B**

The organolithium compound $[\{Li[o,o'\text{-}(Me_2PCH_2)_2C_6H_3]\}_2]$ (**2**) was prepared in 77% yield from the corresponding bromide **1**[7] by metal–halogen exchange with *n*BuLi in pentane at



1 **2**

3

223 K in the presence of 5% tmeda. The structure of **2** in the solid state, as revealed by an X-ray structure determination,[8] shows the presence of two crystallographically independent dimers with approximate *222* (D_2) symmetry (Fig. 1). In both dimers the lithium atoms bridge the metalated carbon atoms of the two phenyl rings that are almost perpendicular to the central planar Li-C-Li-C four-membered ring.[9] In addition to the two carbanionoid carbon atoms, the strongly distorted tetrahedral coordination sphere of each lithium is completed by two phosphorus atoms of the *o*-CH_2PMe_2 substituents of the ligands. Each Li atom is coordinated to one phosphano function of each ligand; thus the ligand **B** in **2** acts in a tridentate (P,C,P) fashion to two different Li atoms. The organolithium compound **2** strongly resembles the structure proposed for the lithium complex of the corresponding nitrogen ligand[4b] which was verified for dimeric 2,3,5,6-tetrakis[(dimethylamino)methyl]phenyllithium.[10] However, the Li–N bonds (2.109(3) Å) in the latter are significantly shorter than the Li–P bonds in **2**.[11] The dimeric nature of **2** largely persists in toluene at least up to room temperature, as revealed by NMR spectroscopy.[12] At 193 K the structure is static and the ^{7}Li NMR (triplet, $^1J(^7Li,^{31}P)$ = 44 Hz) and ^{31}P NMR spectra (quartet) clearly indicate the coordination of the lithium centers by two phosphorus atoms. At room temperature the dimer is fluxional as indicated by the coupling of the ^{7}Li nucleus to all four ^{31}P nuclei (quintet,

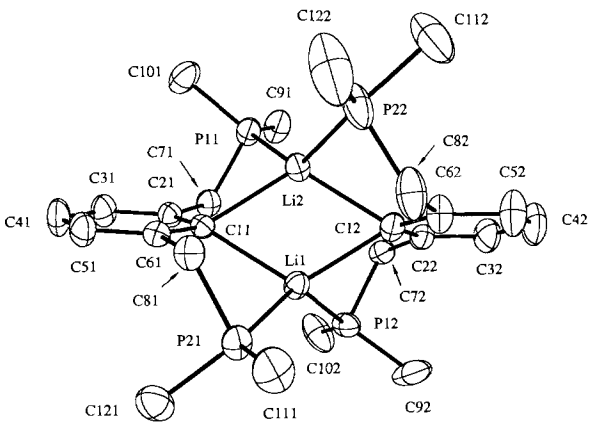


Fig. 1. Molecular structure of one of the two crystallographically independent dimers in the crystals of **2** and atomic numbering scheme adopted (ORTEP plot, displacement ellipsoides at the 50% probability level, H atoms omitted for clarity). Important bond lengths [Å] and angles [°] for both dimers: Li1-C11 2.252(4)/2.229(4), Li1-C12 2.257(4)/2.225(4), Li2-C11 2.249(4)/2.290(4), Li2-C12 2.258(4)/2.262(4), Li1-P21 2.668(3)/2.544(4), Li1-P12 2.667(3)/2.513(4), Li2-P11 2.668(4)/2.550(4), Li2-P22 2.627(4)/2.586(4); C11-Li1-C12 115.5(2)/117.4(2), C11-Li2-C12 115.6(2)/113.4(2), Li1-C11-Li2 64.6(1)/64.3(1), Li1-C12-Li2 64.3(1)/64.8(1). Dihedral angles [°]: C11, C21, C31, C41, C51, C61/Li1, C11, Li2, C12 79.9/69.3; C12, C22, C32, C42, C52, C62/Li1, C11, Li2, C12 79.6/71.5; C11, C21, C31, C41, C51, C61/C12, C22, C32, C42, C52, C62 21.2/39.3.

$^1J(^7Li,^{31}P)$ = 21 Hz), while each ^{31}P nucleus, on the other hand, couples to both ^{7}Li nuclei (septet). A $\Delta G^{\neq}$ of about 50 kJ mol^{-1} is estimated from the coalescence temperatures.

The reaction of **2** with anhydrous $MgCl_2$ in Et_2O/THF at 203 K affords the arylmagnesium compound **3** in 90% yield. The superior thermal stability of **3** follows from decomposition only at temperatures above 473 K. In the solid state[13] the central magnesium atom in **3** is six-coordinate with an approximately octahedral coordination geometry, consisting of two carbon atoms *trans* to each other (C1-Mg-C1′ 178.10(8)°) and all four phosphorus atoms of the two ligands occupying the remainder of the coordination sites (Fig. 2).[14] Thus, both lig-

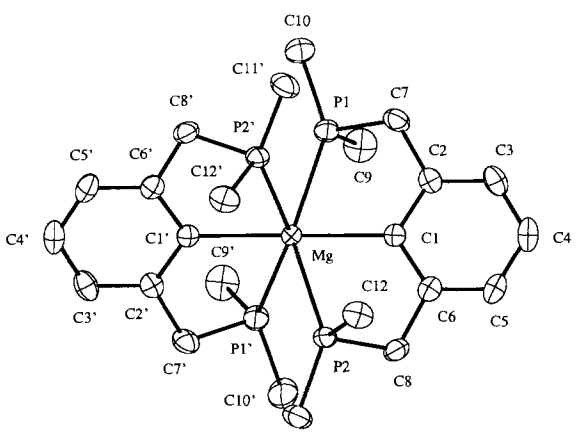


Fig. 2. Solid-state molecular structure of **3** and atomic numbering scheme adopted. (Primed atoms are related to those without a prime by a crystallographic twofold axis which is approximately perpendicular to the paper plane and passes through the Mg atom). Important bond lengths [Å] and angles [°]: Mg-C1 2.216(1), Mg-P1 2.770(1), Mg-P2 2.761(1), C1-C2 1.413(2), C1-C6 1.410(2), C2-C7 1.516(2), C6-C8 1.517(2), P1-C7 1.831(2), P2-C8 1.835(2); C1-Mg-C1′ 178.10(8), P1-Mg-P2 148.98(1) P1-Mg-P2′ 86.96(2) P1-Mg-P1′ 103.84(3), C1-Mg-P1 74.75(4), C1-Mg-P2 74.30(4), C1-Mg-P1′ 106.47(4), C1-Mg-P2′ 104.42(4), Mg-P1-C7 92.36(6), Mg-P2-C8 92.80(6), P1-C7-C2 111.5(1), P2-C8-C6 110.3(1), C7-C2-C1 119.2(1), C8-C6-C1 119.3(1), C2-C1-Mg 122.4(1), C6-C1-Mg 122.5(1), C2-C1-C6 115.1(1). Dihedral angles [°]: C1, C2, C3, C4, C5, C6/C1′, C2′, C4′, C5′, C6′ 38.6, Mg, C1, C2, C7/Mg, P1, C7 137.1, Mg, C1, C6, C8/Mg, P2, C8 135.8.

 © VCH Verlagsgesellschaft mbH, D-69451 Weinheim, 1994 0570-0833/94/2222-2282 $ 10.00+.25/0

ands act as tridentate (P,C,P) ligands to the same central Mg atom. The entire molecule has crystallographic *2* (C_2) symmetry. As imposed by the ligand shape, the two phosphorus atoms of one ligand likewise are arranged *trans* to each other at the magnesium center, but noticeable deviations from the ideal angles in an octahedron result from the formation of four chelating five-membered rings upon complexation of magnesium. In particular, the *trans* angles P1-Mg-P2 amount to only 148.98(1)°. The Mg–P bond lengths, for which there is no precedent in the literature, are 2.761(1) and 2.770(1) Å. They are at the upper limit of the range commonly observed for phosphorus dative bonds to the diagonally related lithium,[15] although it should be kept in mind that the coordination numbers of the metal atom in lithium phosphane complexes are generally smaller than in **3**, that is, shorter bonds result. The only molecular Mg–P bond lengths determined so far are those in [(tmeda)Mg(PHPh)$_2$] (2.587(5), 2.592(5) Å).[2, 16] The observed bond length shortening with respect to **3** is paralleled when going from lithium phoshane complexes[15] to lithium phosphide complexes.[17] The accomodation of the exceedingly long Mg–P bonds in the five-membered chelate rings is only made possible by pronounced envelope conformations of the latter (see Fig. 2) which, as a consequence, lead to a remarkably small dihedral angle of only 38.6° between the phenyl rings. The best comparison is probably the analogous Mg complex of the bis-methoxymethyl ligand [*o*,*o*′-(MeOCH$_2$)$_2$C$_6$H$_3$]$^-$ for which the dihedral angle (75.3°) is much closer to a perpendicular arrangement.[4e] The Mg–C bonds in **3** (2.216(1) Å) are at the upper end of Mg–C(phenyl) bond lengths in octahedral magnesium complexes.[4d, 18] In the complex of the bis(methoxymethyl)ligand they are 2.093(4) and 2.105(4) Å.[4e]

In toluene **3** apparently maintains its molecular structure. Apart from line broadening effects no significant change in the ^{1}H and ^{31}P NMR spectra is observed on cooling to 183 K. Particularly informative is the room temperature ^{13}C NMR signal of the *ipso*-C atom C1 at $\delta = 174.5$ (Fig. 3). Analysis of the complex multiplet (AX_2X_2' spin system) not only allows the extraction of the coupling constants (with relative signs) with the ^{31}P nuclei of both ligands (^2J(C,P) = +50, ^2J(C,P′) = +19 Hz) but also that between the ^{31}P nuclei of the different ligands (^2J(P,P′) = ±38 Hz), strongly indicating that also in solution all four phosphano groups are magnesium-coordinated.

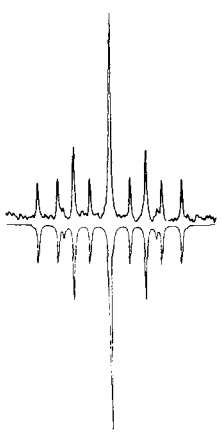


Fig. 3. ^{13}C NMR signal of the *ipso*-C atom C1 in **3** at room temperature. Upper trace: experimental spectrum; lower trace: simulated spectrum (LAOCN-5 [19]).

In summary, we could show that in spite of the inherent weakness of P–Mg dative bonds, magnesium complexation by phosphanes may be achieved if geometrically favorable anionic phosphanes are employed. The fact that in **3** the magnesium atom is complexed by all four phosphano groups of the two ligands is a direct consequence of the geometrically favorable five-membered chelate ring formation brought about by the ligand system **B**. For the synthesis of further main group element complexes of **B** the new organometallic compounds **2** and **3** should be ideal starting materials, a potential which we are currently exploring.

Experimental Procedure

All experiments were carried out under rigorous exclusion of atmospheric oxygen and moisture. Solvents were dried according to established procedures and redestilled immediately prior to use. NMR: Jeol JNM GX 400 (^{13}C: 100.53 MHz, ^{31}P: 161.83 MHz, ^{7}Li: 155.57 MHz), Bruker AC 250 (^{1}H).

2: To a suspension of **1** (8.9 g, 29 mmol) in *n*-pentane (50 mL), was added tmeda (1.4 mmol). At 223 K *n*BuLi (14.5 mL, 29 mmol, 2 M solution in pentane) was added dropwise under stirring. The phosphane dissolved and **2** started to precipitate. The mixture was stirred for 1 h and the temperature was allowed to warm to 258 K. The solid was filtered off at room temperature and washed twice with pentane (25 mL) and dried under reduced pressure. Single crystals suitable for X-ray diffraction were obtained from toluene/pentane. Yield: 5.2 g (11 mmol; 77%) of **2**. Slightly yellow, pyrophoric crystals, m.p. 403 K (decomp). Analysis for $C_{24}H_{38}Li_2P_4$ (464.344): calcd: C 62.08, H 8.25; found: C 60.64, H 8.26. ^{31}P{^{1}H}NMR ([D$_8$]toluene, 298 K, 85% H_3PO_4 ext.): $\delta = -41.8$ (sept., ^1J(P,Li) = 21 Hz), δ (193 K) = −40.5 (quart., ^1J(P,Li) = 44 Hz), $T_{coal.} = 253 \pm 5$ K, $\Delta G^{\neq} = 52$ kJ mol^{-1}. ^{7}Li NMR ([D$_8$]toluene, 293 K, 1 M LiBr/THF ext.): $\delta = 3.1$ (quint., ^1J(P,Li) = 21 Hz), δ (193 K) = 3.2 (t, ^1J(P,Li) = 44 Hz), $T_{coal.} = 233 \pm 5$ K, $\Delta G^{\neq} = 48$ kJ mol^{-1}. ^{1}H NMR (C_6D_6, 293 K, TMS int.): $\delta = 0.81$ (br. s, 12H; CH_3), 3.02 (br. s, 4H; CH_2), 6.99 (d, ^3J(H,H) = 7.3 Hz, 2H; H-3,5), 7.26 (t, ^3J(H,H) = 7.3 Hz, 1H; H-4), δ ([D$_8$]toluene, 213 K) = 0.73 (br. d, ^2J(P,H) = 3.8 Hz, 12H: CH_3), 2.34 (dd, ^2J(H$_A$,H$_B$) = 11.8, ^2J(P,H) = 9.6 Hz, 2H; CH_2), 3.39 (d, ^2J(H$_A$,H$_B$) = 11.8 Hz, 2H; CH_2), 7.01 7.35 (m, 3H; Ph), $T_{coal.} = 268 \pm 5$ K, $\Delta G^{\neq} = 51$ kJ mol^{-1}. ^{13}C{^{1}H}NMR ([D$_8$]toluene, 293 K, TMS int.): $\delta = 12.1$ (m, CH_3), 46.8 (m, CH_2), 123.9, m, 125.9 s, (C-3,4,5), 151.8 (m, C-2,6), 183.0 (m, C-1), δ (223 K) = 11.1 (s, C_AH_3), 12.8 (s, C_BH_3), 46.1 (s, CH_2).

3: To a solution of **2** (5.2 g, 11 mmol) in Et_2O (50 mL), a solution of anhydrous $MgCl_2$ (10 mmol) in THF (50 mL) was added dropwise under stirring at 203 K. The reaction mixture was allowed to warm to room temperature and the solvents were removed under reduced pressure. The remaining solid was dissolved at 313 K in toluene, the LiCl was filtered off, and the solution was cooled to 277 K whereupon large colorless crystals of **3** · toluene started to precipitate. Yield: 5.8 g (20 mmol; 90%) of **3**. Colorless, highly air-sensitive crystals, m.p. > 473 K (decomp). Analysis for $C_{24}H_{38}Mg_2P_4 \cdot C_7H_8$ (566.92): calcd: C 65.68, H 8.18; found: C 63.91, H 8.22. Crystals suitable for X-ray diffraction were grown in the same way from benzene and were found to be **3** · benzene. ^{31}P{^{1}H}NMR (C_6D_6/[D$_8$]toluene, 293/223 K, 85% H_3PO_4 ext.): $\delta = -51.3$, s. ^{1}H (C_6D_6/[D$_8$]toluene, 293/183 K, TMS int.): $\delta = 0.81$ (s, 12H; CH_3), 2.94 (br. s, 4H; CH_2), 7.00 7.27 (m, 3H; H-3,4,5). ^{13}C{^{1}H}NMR ([D$_8$]toluene, 293 K, TMS int.): $\delta = 11.4$ (s, CH_3), 43.4 (7 signals, 2:2:3:5:3:2:2, 1–3 Hz; CH_2), 125.1 (5 signals, 4:5:15:5:4, ca. 2 Hz; C-3,5), 125.4 (s, C-4), 146.6 (5 signals, 2:3:9:3:2, ca. 2 Hz; C-2,6), 174.5 (9 signals, 4:5:8:4:22:4:8:5:4, ca. 20 Hz; C-1, see text).

Received: June 23, 1994 [Z 7070 IE]
German version: *Angew. Chem.* **1994**, *106*, 2375

[1] R. Benn, H. Lehmkuhl, K. Mehler, A. Rufińska, *Angew. Chem.* **1984**, *96*, 521; *Angew. Chem. Int. Ed. Engl.* **1984**, *23*, 534; H. Lehmkuhl, K. Mehler, R. Benn, A. Rufińska, C. Krüger, *Chem. Ber.* **1986**, *119*, 1054; review: R. Benn, A. Rufińska, *Angew. Chem.* **1986**, *98*, 851; *Angew. Chem. Int. Ed. Engl.* **1986**, *25*, 861.

[2] E. Hey, L. M. Engelhardt, C. L. Raston, A. H. White, *Angew. Chem.* **1987**, *99*, 61; *Angew. Chem. Int. Ed. Engl.* **1987**, *26*, 81.

[3] H.-P. Abicht, K. Issleib, *Z. Anorg. Allg. Chem.* **1976**, *422*, 237; *ibid.* **1978**, *447*, 53.

[4] Internal complexation of various donor groups, in particular $-NMe_2$ and $-OMe$ incorporated into anionic ligands, has been known for a long time. *Some leading references for lithium and magnesium complexes: a) H. Dietrich,* D. Rewicki, *J. Organomet. Chem.* **1981**, *205*, 281; b) J. T. B. H. Jastrzebski, G. van Koten, M. Konijn, C. H. Stam, *J. Am. Chem. Soc.* **1982**, *104*, 5490; c) G. W. Klumpp, P. J. A. Geurink, A. J. Spek, A. J. M. Duisenberg, *J. Chem. Soc. Chem. Commun.* **1983**, 814; d) P. R. Markies, G. Schat, O. S. Akkerman, F. Bickelhaupt, W. J. J. Smeets, P. van der Sluis, A. L. Spek, *J. Organomet. Chem.* **1990**, *393*, 315; e) P. R. Markies, R. M. Altink, A. Villena, O. S. Akkerman, F. Bickelhaupt, W. J. J. Smeets, A. L. Spek, *ibid.* **1991**, *402*, 289; f) S. Harder, P. F. Ekhart, L. Brandsma, J. A. Kanters, A. J. M. Duisenberg, P. von R. Schleyer, *Organometallics* **1992**, *11*, 2623; g) F. Bickelhaupt, *J. Organomet. Chem.* **1994**, *475*, 1.

[5] G. Reber, J. Riede, G. Müller, *Z. Naturforsch. B* **1988**, *43*, 915; G. Müller, J. Lachmann, J. Riede, *ibid.* **1992**, *47*, 823; G. Müller, J. Lachmann, *ibid.* **1993**, *48*, 1248; G. Müller, J. Lachmann, A. Rufińska, *Organometallics* **1992**, *11*, 2970; G. Müller, J. Lachmann, *Z. Naturforsch. B* **1993**, *48*, 1544.

[6] To our knowledge, ligands of type **B** have been used exclusively in transition metal complexes which were prepared largely by cyclometalation reactions of the respective hydrogen or bromo derivatives: C. J. Moulton, B. L. Shaw, *J. Chem. Soc. Dalton Trans.* **1976**, 1020; C. S. Creaser, W. C. Kaska, *Inorg. Chim. Acta* **1978**, *30*, L325; S. Nemeh, C. Jensen, E. Binamira-Soriage, W. C. Kaska, *Organometallics* **1983**, *2*, 1442; H. Rimml, L. M. Venanzi, *J. Organomet. Chem.* **1983**, *259*, C6; *ibid.* **1984**, *260*, C52; *Phosphorus, Sulfur Relat. Elem.* **1987**, *30*,

 © VCH Verlagsgesellschaft mbH, D-69451 Weinheim, 1994 0570-0833/94/2222-2283 $ 10.00+.25/0

297; H. Rimml, Dissertation, Nr. 7562, ETH Zürich, **1984**; L. M. Venanzi, ETH Zürich, personal communication.

[7] A. Pape, Diplomarbeit, Universität Konstanz, **1992**, and unpublished work.

[8] Crystal structure data of **2**: Enraf-Nonius CAD4 diffractometer, $Mo_{K\alpha}$ radiation, $\lambda = 0.71069$ Å, graphite monochromator, $T = 183(2)$ K, $C_{24}H_{38}Li_2P_4$, $M_r = 464.344$, triclinic, space group $P\bar{1}$ (No. 2), $a = 9.648(2)$, $b = 15.316(4)$, $c = 20.081(6)$ Å, $\alpha = 103.22(2)$, $\beta = 99.19(2)$, $\gamma = 91.04(2)°$, $V = 2847(1)$ Å^3, $Z = 4$ dimers, $\rho_{calcd} = 1.083$ g cm^{-3}, $\mu(Mo_{K\alpha}) = 2.7$ cm^{-1}, $F(000) = 992$. The integrated intensities of a total of 13677 reflections were measured, 12908 of which were unique ($R_{int} = 0.023$, $((\sin\vartheta)/\lambda)_{max} = 0.647$ Å^{-1}, hkl range $+12$, ± 19, ± 25, $\vartheta/2\vartheta$ scans, $\Delta\omega = 0.9 + 0.35 \tan\vartheta$). Lorentz-polarization corrections were applied, those for intensity decay (-1.6%) and absorption were not considered necessary. The structure was solved by automated Patterson methods (SHELXS-86). All 75 H atoms except one were located in difference syntheses, the latter was calculated in idealized geometrical position. In the final refinement cycles they were included as fixed atom contributions ($U_{iso} = 0.05$ Å^2), while all other atoms were refined with anisotropic displacement parameters. Refinement was done on F_o^2 and all unique data were used except two structure factors which were excluded due to their abnormally negative value. Refinement of 541 parameters converged at $R(F)/wR(F^2) = 0.082/0.118$, GOOF = 1.012, $w = 1/[\sigma^2(F_o^2) + (0.0563 \cdot P)^2 + 1.19 \cdot P]$ with $P = [\max(F_o^2, 0) + 2F_c^2]/3$ (SHELXL-93). The final difference map was featureless with $\Delta\rho_{fin}(max/min) = +0.31/-0.35$ e Å^{-3}.

[9] It should be noted that deviations from a strictly perpendicular arrangement of the bridging phenyl rings with respect to the central M, C, M, C ring have also been observed to a varying degree in the classic dimeric structures of Al_2Ph_6 and $[(tmeda)LiPh]_2$: J. F. Malone, W. S. McDonald, *J. Chem. Soc. Chem. Commun.* **1967**, 444; D. Thoennes, E. Weiss, *Chem. Ber.* **1978**, *111*, 3157.

[10] A. A. H. van der Zeijden, G. van Koten, *Recl. Trav. Chemi. Pays-Bas* **1988**, *107*, 431; W. J. J. Smeets, A. L. Spek, A. A. H. van der Zeijden, G. van Koten, *Acta Crystallogr. Sect. C* **1987**, *43*, 1429.

[11] The Li–P bond lengths in **2** differ significantly in the two crystallographically independent dimers (see caption to Fig. 1). This is a consequence of a noticeably different dihedral angle between the two phenyl rings in each dimer (dimer 1: 21.2°; dimer 2: 39.3°). Given the known inherent weakness of P–Li dative bonds, conformational differences of this type should be easily feasible energetically even in **2**, where they are accompanied by bond length differences, and are almost certainly caused by the crystalline environment of the molecules. Drastic differences in bond lengths between chemically equivalent bonds clearly caused by the crystalline environment are rare and we are not aware of any other example with differences as large as those in **2**.

[12] Cryoscopic molecular weight determinations of **2** in benzene at 278 K (several concentrations) consistently indicated an average molecular weight of about 1.6 monomers. Apart from systematic errors resulting from the extreme air and moisture sensitivity of **2**, this may be caused be increasing amounts of monomers being present in solution at higher temperatures.

[13] Crystal structure data of **3**: $T = 183(2)$ K, $C_{24}H_{38}MgP_4 \cdot C_6H_6$, $M_r = 552.885$, monoclinic, space group $C2/c$ (No. 15), $a = 13.320(2)$, $b = 12.661(2)$, $c = 19.764(6)$ Å, $\beta = 106.86(1)°$, $V = 3190(1)$ Å^3, $Z = 4$, $\rho_{calcd} = 1.151$ g cm^{-3}, $\mu(Mo_{K\alpha}) = 2.7$ cm^{-1}, $F(000) = 1184$. 7553 measured reflections, 3617 of which were unique ($R_{int} = 0.028$, $((\sin\vartheta)/\lambda)_{max} = 0.647$ Å^{-1}, hkl range ± 17, $+16$, ± 25, $\vartheta/2\vartheta$ scans, $\Delta\omega = 0.9 + 0.35 \tan\vartheta$). Lorentz-polarization but no absorption correction. Direct methods (SHELXS-86), all H atoms located. Refinement of 247 parameters on all unique F_o^2 converged at $R(F)/wR(F^2) = 0.056/0.081$, GOOF = 0.993, $w = 1/[\sigma^2(F_o^2) + (0.0432 \cdot P)^2 + 1.16 \cdot P]$ with $P = [\max(F_o^2, 0) + 2F_c^2]/3$ (SHELXL-93). $\Delta\rho_{fin}$ (max/min) $= +0.25/-0.22$ e Å^{-3}. Further details of the crystal structure investigations may be obtained from the Fachinformationszentrum Karlsruhe, D-76344 Eggenstein-Leopoldshafen (FRG), on quoting the depository number CSD-58455.

[14] A similar structure has been proposed for the Mg complex of the analogous nitrogen ligand [4e].

[15] Li–P distances in the hitherto crystallographically examined cases generally range between 2.5 and 2.65 Å, but longer bonds have also been observed: H. H. Karsch, G. Grauvogl, P. Mikulcik, P. Bissinger, G. Müller, *J. Organomet. Chem.* **1994**, *465*, 65; H. H. Karsch, G. Baumgartner, S. Gamper, J. Lachmann, G. Müller, *Chem. Ber.* **1992**, *125*, 1333; H. H. Karsch, K. Zellner, S. Gamper, G. Müller, *J. Organomet. Chem.* **1991**, *414*, C 39; H. H. Karsch, K. Zellner, G. Müller, *J. Chem. Soc. Chem. Commun.* **1991**, 466; S. Harder, L. Brandsma, J. A. Kanters, A. Duisenberg, J. H. von Lenthe, *J. Organomet. Chem.* **1991**, *420*, 143; H. H. Karsch, K. Zellner, P. Mikulcik, J. Lachmann, G. Müller, *Organometallics* **1990**, 9, 190, and references therein; L. T. Byrne, L. M. Engelhardt, G. E. Jacobsen, W.-P. Leung, R. I. Papasergio, C. L. Raston, B. W. Skelton, P. Twiss, A. H. White, *J. Chem. Soc. Dalton Trans.* **1989**, 105; L. M. Engelhardt, J. MacB. Harrowfield, M. F. Lappert, I. A. MacKinnon, B. H. Newton, C. L. Raston, B. W. Skelton, A. H. White, *J. Chem. Soc. Chem. Commun.* **1986**, 846; A. M. Arif, A. H. Cowley, R. A. Jones, J. M. Power, *J. Chem. Soc. Chem. Commun.* **1986**, 1446.

[16] In the magnesium polyphosphide MgP_4 Mg–P distances of 2.608(3), 2.635(3), and 2.862(3) Å are observed: H. G. von Schnering, G. Menge, *Z. Anorg. Allg. Chem.* **1976**, *422*, 219.

[17] Leading references for lithium-phosphide structures: G. Becker, B. Eschbach, D. Käshammer, O. Mundt, *Z. Anorg. Allg. Chem.* **1994**, *620*, 29; E. Hey-Hawkins, E. Sattler, *J. Chem. Soc. Chem. Commun.* **1992**, 775; D. M. Anderson, P. B. Hitchcock, M. F. Lappert, W.-P. Leung, J. A. Zora, *J. Organomet. Chem.* **1987**, *333*, C13; P. Brooks, D. C. Craig, M. J. Gallagher, A. D. Rae, A. Sarroff, *ibid.* **1987**, *323*, C1; R. A. Bartlett, M. M. Olmstead, P. P. Power, *Inorg. Chem.* **1986**, *25*, 1243; P. B. Hitchcock, M. F. Lappert, P. P. Power, S. J. Smith, *J. Chem. Soc. Chem. Commun.* **1984**, 1669; R. A Jones, A. L. Stuart, T. C. Wright, *J. Am. Chem. Soc.* **1983**, *105*, 7459.

[18] Review on the structures of organomagnesium compounds: P. R. Markies, O. S. Akkerman, F. Bickelhaupt, W. J. J. Smeets, A. L. Spek, *Adv. Organomet. Chem.* **1991**, *32*, 147.

[19] LAOCN-5: Analysis of Isotropic NMR Spectra of Spin-1/2-Systems, L. Cassidei, O. Sciacovelli, University of Bari, Bari, Italy, (QCPE Program No. 458).

Self-Assembly and Structure of a 3 × 3 Inorganic Grid from Nine Silver Ions and Six Ligand Components**

Paul N. W. Baxter, Jean-Marie Lehn,* Jean Fischer, and Marie-Thérèse Youinou

Self-assembly of noncovalent architectures from "programmed" components has become a central theme of supramolecular chemistry in recent years.[1, 2] In particular, inorganic superstructures are spontaneously generated from suitably designed ligands and selected metal ions that "read" the binding sites according to their coordination algorithm. We have described the self-assembly of several types of entities, such as, double[1, 3, 4] and triple[5] helical complexes (termed helicates) as well as circular,[6] capped,[7] and cylindrical[6] multicomponent inorganic architectures.

Furthermore, the ordering of metal ions and organic partners into defined arrays presents intriguing prospects for the development of electroionic devices for information storage. To this end, the controlled generation of novel types of two- and three-dimensional arrays of metal ions is of direct interest.

Along these lines, rigid, linear polytopic ligands containing bidentate chelating sites might be able to self-assemble into square-matrix arrays of metal centers with ions of tetrahedral coordination geometry. Thus, an n-topic ligand would form an $n \times n$ inorganic grid ($[n \times n]$G) based on n^2 metal ions and $2n$ ligand components. This is illustrated schematically in Figure 1

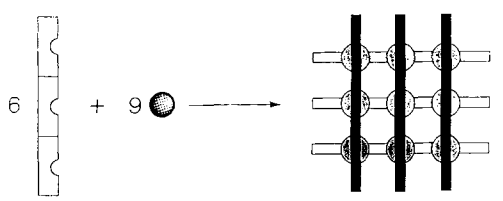
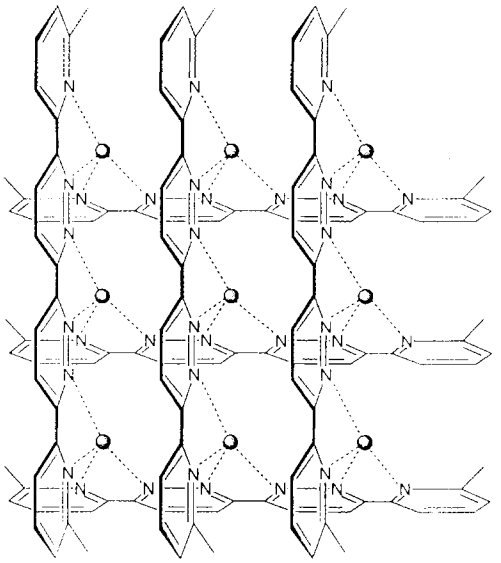


Fig. 1. Schematic representation of the formation of a 3 × 3 inorganic supramolecular grid from six tritopic linear ligands and nine metal ions.

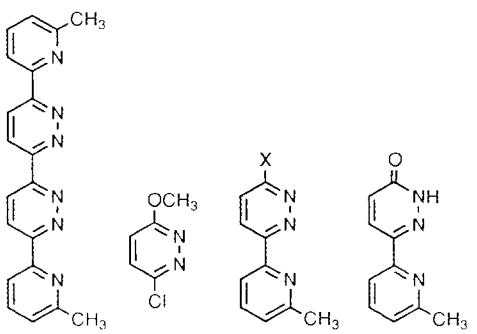
[*] Prof. Dr. J.-M. Lehn, Dr. P. N. W. Baxter
Laboratoire de Chimie Supramoléculaire
Institut Le Bel, Université Louis Pasteur
4, rue Blaise Pascal, 67000 Strasbourg (France)
Telefax: Int. code +(88) 41-1020
Prof. Dr. J. Fischer, Dr. M.-T. Youinou
Laboratoires de Cristallochimie et de Chimie Structurale,
et de Chimie des Métaux de Transition et de Catalyse
Institut Le Bel, Université Louis Pasteur, Strasbourg

[**] This work was supported by the CNRS (URA 422 and URA 424). We thank P. Maltèse for the ^{109}Ag NMR measurements.

for $n = 3$. We now describe the self-assembly of the inorganic 3×3 grid **1** consisting of an array of nine silver(I) metal ions and six tritopic ligands **2**. The corresponding ditopic ligand 3,6-bis(2-pyridyl)pyridazine has been found to assemble into a 2×2 square complex built from four ligands and four copper(I) ions[8a] and has also been introduced into macrobicyclic structures forming dinuclear cryptates.[8b]



1: $[Ag_9L_6]^{9+}$ (L = **2**)



2 **3** **4** X = OCH_3 **5**

6 X = Cl

The ligand 6,6′-bis[2-(6-methylpyridyl)]-3,3′-bipyridazine **2** was prepared in the following way: A toluene solution of 3-chloro-6-methoxypyridazine **3** (1 equiv) and 2-methyl-6-trimethylstannylpyridine (1.3 equiv) was refluxed in the presence of a catalytic amount of $Pd(PPh_3)_4$ for 20 h.[9a] Chromatographic workup of the reaction mixture gave **4** in 83–90% yield (m.p. = 61–62 °C). The latter was demethylated by gentle reflux in excess 33% HBr/CH_3COOH for 48 h to afford **5** in 92% yield (m.p. 228–229 °C). Subsequent chlorination of **5** upon heating with excess $POCl_3$ led to **6** in 98% yield (m.p. = 148–149 °C). Finally, coupling of **6** (1 equiv) in the presence of the reduced nickel catalyst (generated from a mixture nBu_4NI (1 equiv), zinc powder (1 equiv), and $[NiBr_2(PPh_3)_2]$ (0.3 equiv))[9b] in dimethylformamide at 55 °C gave compound **2** in 80% yield (m.p. = 307–308 °C). The overall yield of **2** from **3** was 63%.

The complex of ligand **2** with silver ions was prepared quantitatively from **2** and $AgCF_3SO_3$ in a ratio of 1:1.5 in the following manner: To 0.051 g (0.15 mmol) of **2** and 0.058 g (0.226 mmol) of silver triflate (Aldrich, 99%) was added nitromethane (5 mL). The mixture was sonicated for 1 min. The cloudy yellow suspension was then stirred for 12 h at room temperature. During the first hour of stirring, all suspended solid dissolved to give a clear yellow solution. The solvent was then removed under reduced pressure to yield a bright yellow powder. This was briefly sonicated in benzene, then isolated by filtration under vacuum, further washed with benzene, and pumped dry. Drying under high vacuum (25 °C/5×10^{-7} Torr) for 2 days gave the product in 99% yield.

The substance thus obtained was characterized by microanalysis,[10] ^1H, ^{13}C and ^{109}Ag NMR spectroscopy, and X-ray crystallography. The NMR spectral data, in particular, are consistent with a complex having the 3×3 gridlike structure **1**. The ^1H NMR spectrum shows two sets of signals in a 2:1 ratio corresponding to ligand **2** in two different environments. The ^{109}Ag NMR spectrum was especially informative. A structure such as **1** is expected to give three resonances in 4:4:1 ratios for the silver ions located at the corners, the midpoints of the edges, and the center of the 3×3 grid, respectively. This was indeed found to be the case (Fig. 2).

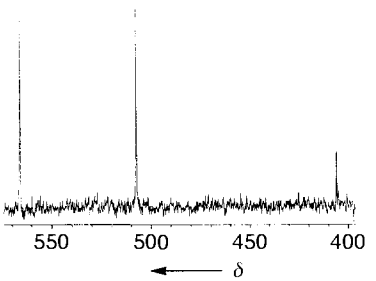
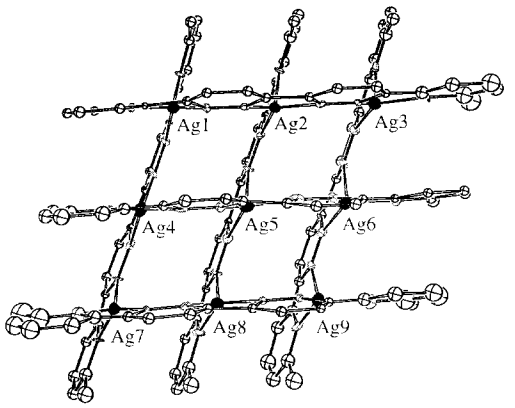


Fig. 2. ^{109}Ag NMR spectrum of complex $[Ag_9L_6](CF_3SO_3)_9$ (L = **2**) at 18.620 MHz in $[D_3]$nitromethane; chemical shifts (from left to right) = 566.06, 507.56, and 406.13 with respect to a 2 M solution of $AgNO_3$ in D_2O.

The complex was crystallized from nitromethane, and its structure was determined by X-ray crystallography.[11] This indicates that the complex contains $[Ag_9L_6]^{9+}$ ions **7** (L = **2**; Fig. 3, top), uncoordinated triflate anions, and solvent molecules. The overall arrangement in **7** is that of a 3×3 grid of nine Ag^I ions; the diamond-type shape results from deformation of the regular square represented in **1**. The grid consists of a distorted rhombus with a dihedral angle of about 72° between the mean planes of the ligands and an average Ag···Ag distance of approximately 3.72(3) Å. All silver ions are in a distorted tetrahedral environment with the same average dihedral angle of about 72(3)° between the N-Ag-N planes of the two chelating subunits at each Ag^I site. The Ag1, Ag3, Ag7, and Ag9 ions lie at the vertices and almost in a single plane (Ag1–Ag3 = 7.403(4), Ag1–Ag7 = 7.529(4), Ag3–Ag9 = 7.432(4), and Ag7–Ag9 = 7.418(4) Å; inner angles Ag3-Ag1-Ag7 = 107.04(5) and Ag1-Ag3-Ag9 = 72.81(4)°). A second set of four silver ions is inserted into the first rhombus; these form a twisted quasi-rectangle (Ag2–Ag4 = Ag6–Ag8 = 6.026(4), Ag4–Ag8 = 4.367(4), and Ag2–Ag6 = 4.444(4) Å; inner angles Ag4-Ag2-Ag6 = 90.58(6), Ag2-Ag4-Ag8 = 88.20(6), Ag2-Ag6-Ag8 = 87.54(6), and Ag4-Ag8-Ag6 = 91.37(6)°). The center is occupied by the ninth silver Ag5. The nine silver ions define a slightly warped saddle-type surface: Ag5 is located in the mean plane of the silver ions; the pairs Ag2/Ag8 and Ag4/Ag6 lie respectively about 0.25 Å above and below this plane, and Ag3/Ag7 and

 © VCH Verlagsgesellschaft mbH, D-69451 Weinheim, 1994 0570-0833/94/2222-2285 $ 10.00+.25/0



7

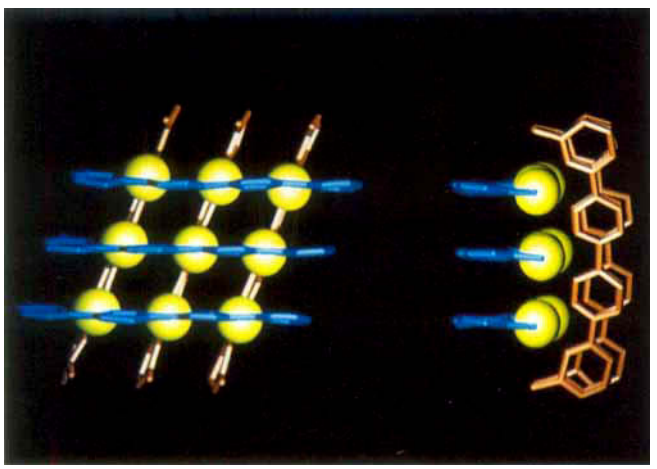


Fig. 3. Cystal structure of the self-assembled 3×3 inorganic grid **7** ($[Ag_9L_6]^{9+}$, L = **2**). Top: ORTEP representation. Bottom: computer representation showing the top view (left) and the side view (right).

Ag1/Ag9 are respectively about 0.06 Å above and below. The central Ag5 ion is coordinated to four pyridazine (pz) nitrogen atoms (mean Ag–N = 2.437 Å); the silver ions lying at the vertices of the rhombus (Ag1, Ag3, Ag7, and Ag9) are each bound to two pyridine (py) and two pyridazine nitrogen atoms (mean Ag–N = 2.323 Å); the median silver ions (Ag2, Ag4, Ag6, and Ag8) interact with one pyridine and three pyridazine nitrogen atoms (mean Ag–N = 2.342 Å).

The six ligands **2** are divided into two sets of three, one of which is above and the other below the mean plane formed by the nine silver ions. Although each bidentate chelate ring formed with a silver ion is planar, within each ligand there is a significant twisting from planarity, with a maximum deviation of 16.3(4)°. The average distance between the mean planes of two neighboring ligand units is about 3.74(8) Å, that is, somewhat larger than that expected for van der Waals contacts (ca. 3.4 Å). The slight bending seen for the ligand in the complex (Fig. 3, bottom right) may be, at least in part, a consequence of the geometry of the pyridazine ring, which is not a regular hexagon.

The chemical shifts of the ^{109}Ag NMR spectrum are expected to depend on both the nature of the nitrogen binding sites and the number of neighboring Ag^I ions. Thus, the signals from left to right in Figure 2 may be assigned as follows [Ag (position) (number of vicinal Ag atoms) (nitrogen sites)]: Ag (vertex) (2) (py_2pz_2), Ag (edge) (3) ($pypz_3$), and Ag (center) (4) (pz_4).

The generation of the $[3 \times 3]$G **7** represents the spontaneous and correct assembly of a closed inorganic superstructure from a total of fifteen components, six ligands, and nine metal ions. It displays the three basic levels of operation of a programed supramolecular system: recognition, orientation, and termination;[1, 6] geometric, thermodynamic, and entropic factors play a role. The analysis of the effects that influence the generation of **7** will benefit from the extension of the present work to other grid systems.

The self-assembly of complex **7** opens the way to a whole family of polynuclear inorganic $m \times n$ grids, which represent a new facet in the controlled arrangement of metal ions into specific arrays and patterns. Square- and rectangular-type arrangements would result from systems with ligands containing the same ($m = n$) or different ($m \neq n$) number of binding sites, respectively. Grids based on octahedral metal centers and on ligands containing binding subunits of terpyridine type may also be envisaged.[16]

Finally, one should note the analogy of such gridlike structures with grids based on quantum dots[17] that are of great interest in microelectronics. The grid structures discussed above consist of *ion dots* of yet smaller size than quantum dots and do not necessitate microfabrication, but rather form spontaneously by self-assembly. Such architectures may represent multistate, digital supramolecular chips for information storage in and retrieval from these inscribed patterns, which could be addressed by means of light or electrically. The different states could in principle result either from different local features at a given x, y coordinate, in an ion dot fashion, or from specific overall optical or oxidation levels. The extension into three dimensions, with stacks of grids leading to layered arrays, may be envisaged.

Received: July 9, 1994 [Z 7115 IE]
German version: *Angew. Chem.* **1994**, *106*, 2432

[1] J.-M. Lehn, *Angew. Chem.* **1990**, *102*, 1347; *Angew. Chem. Int. Ed. Engl.* **1990**, *29*, 1304.
[2] a) J. S. Lindsey, *New J. Chem.* **1991**, *15*, 153; b) G. M. Whitesides, J. P. Mathias, C. T. Seto, *Science* **1991**, *254*, 1312; c) D. Philp, J. F. Stoddart, *Synlett* **1991**, 445.
[3] J.-M. Lehn, A. Rigault, J. Siegel, J. Harrowfield, B. Chevrier, D. Moras, *Proc. Natl. Acad. Sci. USA* **1987**, *27*, 2565; J.-M. Lehn, A. Rigault, *Angew. Chem.* **1988**, *100*, 1121; *Angew. Chem. Int. Ed. Engl.* **1988**, *27*, 1095.
[4] For a review on related complexes, see: E. C. Constable, *Tetrahedron* **1992**, *48*, 10013.
[5] R. Krämer, J.-M. Lehn, A. DeCian, J. Fischer, *Angew. Chem.* **1993**, *105*, 764; *Angew. Chem. Int. Ed. Engl.* **1993**, *32*, 703.
[6] P. Baxter, J.-M. Lehn, A. DeCian, J. Fischer, *Angew. Chem.* **1993**, *105*, 92; *Angew. Chem. Int. Ed. Engl.* **1993**, *32*, 69.
[7] E. Leize, A. Van Dorsselaer, R. Krämer, J.-M. Lehn, *J. Chem. Soc. Chem. Commun.* **1993**, 990.
[8] a) M.-T. Youinou, N. Rahmouni, J. Fischer, J. A. Osborn, *Angew. Chem.* **1992**, *104*, 771; *Angew. Chem. Int. Ed. Engl.* **1992**, *31*, 733; b) K. Watson, J.-M. Lehn, unpublished results.
[9] For coupling procedures, see: a) Y. Yamamoto, Y. Azuma, H. Mitoh, *Synthesis* **1986**, 564; b) M. Iyoda, H. Otsuka, K. Sato, M. Oda, *Bull. Chem. Soc. Jpn.* **1990**, *63*, 80.
[10] Elemental analysis: found (calcd) for $1 \cdot (CF_3SO_3)_9 \cdot (H_2O)_3$: C 35.10 (35.14), H 2.52 (2.33), N 11.28 (11.44).
[11] X-ray structure analysis of $1 \cdot (CF_3SO_3)_9 \cdot (CH_3NO_2)_5 \cdot (CH_3OH) \cdot (H_2O)_7$ ($C_{135}H_{129}N_{41}O_{43}F_{27}S_9Ag_9$): $M = 4818.1$, yellow crystals, monoclinic, $a = 28.579(4)$, $b = 22.450(2)$, $c = 31.494(3)$ Å, $\beta = 116.35(2)°$, $V = 18107.4$ Å^3, $Z = 4$, $\rho_{calcd} = 1.767$, $F_{000} = 9584$, $\mu = 11.516$ cm^{-1}, space group $P2_1/n$. A suitable crystal of $1 \cdot (CF_3SO_3)_9 \cdot (CH_3NO_2)_5 \cdot (CH_3OH) \cdot (H_2O)_7$ ($500 \times 420 \times 400$ μm^3), obtained by slow evaporation of nitromethane, was selected in Paratone-N oil (Exxon) and mounted on the end of a glass fiber. 34284 reflexions were collected on a CAD4-F diffractometer at −100 °C with $Mo_{K\alpha}$ radiation ($\lambda = 0.7107$ Å, graphite monochromator), $\theta/2\theta$ scans, variable speed, scan width = 2.10 + 0.34 tg(θ)°, $2° < \theta < 25°$. Three standard reflections measured every hour during the data collection period showed a decay in intensity of 13%; corrected with a linear, time-dependent function. The raw data were converted to intensities and corrected for Lorentz and polarization factors. Absorption corrections calculated from the psi scans of 4 reflections were applied. Finally, 12897 reflections with $I > 3\sigma(I)$ were used to determine and refine the structure. The positions of the nine Ag atoms were found by direct methods. The rest of the nonhydrogen atoms were located in successive difference Fourier maps. Due to high thermal motion, the O and F atoms of 3 out of 9 triflate anions were not well resolved. Up to this stage, the Molen program

[12] on a Vax computer was used for all calculations. To take advantage of noncrystallographic symmetry introduced by chemically identical moities, the structure was refined with the SHELX-93 software package [13] (F^2 refinements). The 12 pyridazines, the 12 methylpyridines, the 9 triflate anions, and the 5 nitromethane molecules were refined as identical, rigid groups (σ of equivalent bond lengths: 0.03 Å); the geometries were taken from ref. [8], [8], [14], and [15], respectively. The pyridazine and methylpyridine groups were restrained to be planar within 0.2 Å. These restraints reduced the number of variables in the refinement to 624; this takes into account the poor observed data/measured data ratio and hence the low diffraction power of the crystals. All hydrogen atoms were omitted. Final $R(F) = 0.109$. Further details of the crystal structure investigation are available on request from the Director of the Cambridge Crystallographic Data Centre, 12 Union Road, GB-Cambridge CB2 1EW (UK), on quoting the full journal citation.

[12] Molen, *An Interactive Structure Solution Procedure*, Enraf-Nonius, Delft, Holland, **1990**.

[13] SHELXL-93, G. M. Sheldrick, Universität Göttingen, **1993**.

[14] A. Gimelseed, E. L. Bominaar, E. Bill, A. X. Trautwein, H. Winkler, H. Nasri, P. Doppelt, D. Mandon, J. Fischer, R. Weiss, *Inorg. Chem.* **1990**, *29*, 2741.

[15] J. M. Kessler, J. H. Nelson, J. Fischer, A. DeCian, W. H. Bearden, N. Fujii, unpublished results.

[16] G. Hanan, J.-M. Lehn, unpublished results.

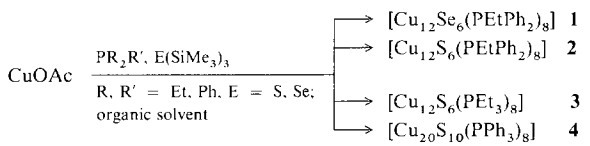
[17] M. A. Reed, *Sci. Am.* **1993**, *268*, 98; *Spektrum der Wissenschaft*, **March 1993**, p. 52.

$[Cu_{44}Se_{22}(PEt_2Ph)_{18}]$ and $[Cu_{44}Se_{22}(PnButBu_2)_{12}]$: Synthesis and Structure of Two Copper Clusters with Isomeric Cu–Se Frameworks**

Stefanie Dehnen and Dieter Fenske*

Dedicated to Professor Larry Dahl on the occasion of his 65th birthday

We recently reported on new sulfur- and selenium-bridged copper clusters, synthesized by the reaction of copper(I) acetate with tertiary phosphanes and $E(SiMe_3)_2$ (E = S, Se). The molecular structures of the resulting clusters **1**–**3**, and **4** (see Scheme 1) containing 12 and 20 copper atoms, respectively, were characterized by X-ray crystal structure analysis.

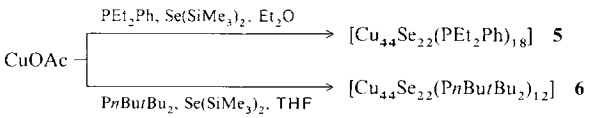


Scheme 1.

In analogous reactions of $E(SiMe_3)_2$ with CuCl instead of CuOAc as starting material, so far only selenium-bridged copper clusters could be synthesized,[2] which, however, exhibit considerably larger $[Cu_2Se]_n$ cluster frameworks. Examples include the compounds $[Cu_{30}Se_{15}(PiPr_3)_{12}]$, $[Cu_{70}Se_{35}(PEt_3)_{22}]$, and $[Cu_{146}Se_{73}(PPh_3)_{30}]$.[2]

Evidently, the anion of the copper(I) compound used influences the formation of the cluster; thus, it was possible to isolate previously unknown smaller clusters as well as sulfur-bridged copper clusters in a crystalline form. Compounds **1**–**4** may possibly be considered as intermediates in the formation of larger cluster compounds.[1, 2]

In a further attempt to prepare corresponding intermediates of larger copper clusters, we treated CuOAc with $Se(SiMe_3)_2$ in the presence of PEt_2Ph or $PnButBu_2$ in diethyl ether and THF, respectively (Scheme 2). In this way we isolated the compounds



Scheme 2.

5 and **6** in high yields (80–85%) (Scheme 2), and these were characterized by X-ray structure analysis.[3] There are no indications that other clusters are formed in the reactions.

The structure of **5** in the crystal is shown in Figure 1 top. Significant differences in the structure of **5** can be seen in comparison to those of other known selenium-bridged copper clusters with 36 and more copper atoms. Unlike in $[C_{70}Se_{35}(PEt_2Ph)_{23}]$ and $[Cu_{146}Se_{73}(PPh_3)_{30}]$,[2] whose structures can be derived from a hexagonal closest packing of Se atoms, and where the copper atoms fill the holes, a rather shell-like cluster framework is observed for **5**, similar to that found for smaller ligand-clad $[Cu_2Se]_n$ clusters.[2]

The core of the cluster has at most C_s symmetry even when the carbon atoms and slight distortions are neglected. The mirror plane passes through the atoms Se 9, Cu 7, and Cu 13. A possible threefoldness (D_{3h} symmetry) with a rotation axis through Se 1 and Se 22 is ruled out by a "defect" in the copper framework that occurs instead of an additional copper atom between the atoms Cu 17, Cu 30, Cu 31, and Cu 41. In this way, however, the composition $Cu_{44}Se_{22}$ corresponding to $[Cu_2E]_n$ (E = S, Se) is guaranteed, which applies for almost all known sulfur- or selenium-bridged copper clusters.

The selenium framework in **5** (Fig. 2 top) can be described as a deltohedron consisting of 20 selenium atoms (Se 1–Se 7, Se 9–Se 14, and Se 16–Se 22), which contains two additional selenium atoms in the center (Se 8 and Se 15). No bonding interactions exist between the selenium atoms (Se–Se distances 381.8–450.8 pm).

The polyhedron is formed by two hexagonal antiprisms (Se 2–Se 14 and Se 9–Se 21) linked through a hexagonal face; the free hexagonal faces are each capped by an additional Se atom (Se 1 and Se 22). If the corners of the polyhedron are joined, one obtains 36 almost equilateral triangles on the surface of the polyhedron.

Of the 44 copper atoms, 18 are situated just above and 18 just below the triangles of the selenium deltohedron.

The 18 copper atoms (Cu 1–Cu 18) that are arranged above the surface of the chalcogen polyhedron bear the 18 PEt_2Ph groups, which shield the Cu–Se core of the cluster of **5** with an almost closed ligand shell. These copper atoms—with the exception of Cu 6, Cu 10, and Cu 17, for which in each case one neighboring selenium atom is significantly further away from the metal atom than the other two—are coordinated tetrahedrally by three selenium atoms and one phosphorus atom. In contrast, the 18 Cu atoms, which are located just below the selenium triangles, form no Cu–P bonds and are—like Cu 6, Cu 10, and Cu 17—aproximately trigonal-planar coordinated. The remaining eight Cu atoms (Cu 37–Cu 44) are found inside the cluster, and form two trigonal prisms linked through a triangular face (Cu 40, Cu 41, Cu 42). In these prisms one corner remains unoc-

[*] Prof. Dr. D. Fenske, Dipl.-Chem. S. Dehnen
Institut für Anorganische Chemie der Universität
Engesserstrasse, Geb. Nr. 30.45, D-76131 Karlsruhe (FRG)
Telefax: Int. code + (721)661-921

[**] This work was supported by the Deutsche Forschungsgemeinschaft (SFB 195) and the State of Baden-Württemberg.

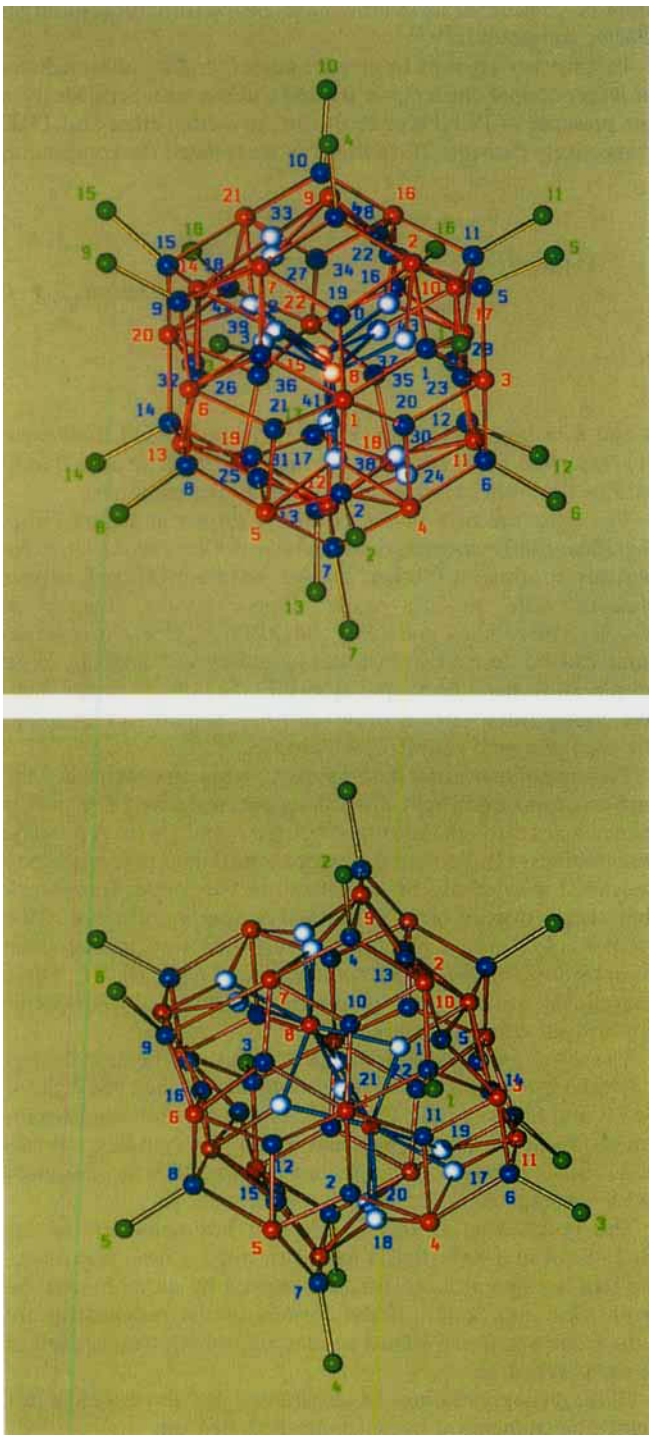


Fig. 1. Structures of **5** (top) and **6** (bottom) in the crystal (drawn without organic groups): Cu: blue, Se: red, P: green; for clarity all the atoms shown have been assigned color-coded numbers which correspond to the appropriate elements. Bond lengths and Cu–Cu distances [pm] (error ±0.8 pm): **5**: Cu–Se (tetrahedral environment) 244.3–293.7, Cu–Se (trigonal-planar environment) 235.1–273.8, Cu–P 220.3–223.9, Cu–Cu 251.1–293.9. **6**: Cu–Se (tetrahedral environment) 240.9–278.5, Cu–Se (trigonal-planar environment) 231.7–289.9, Cu–P 224–227.6, Cu–Cu 250.7–299.8.

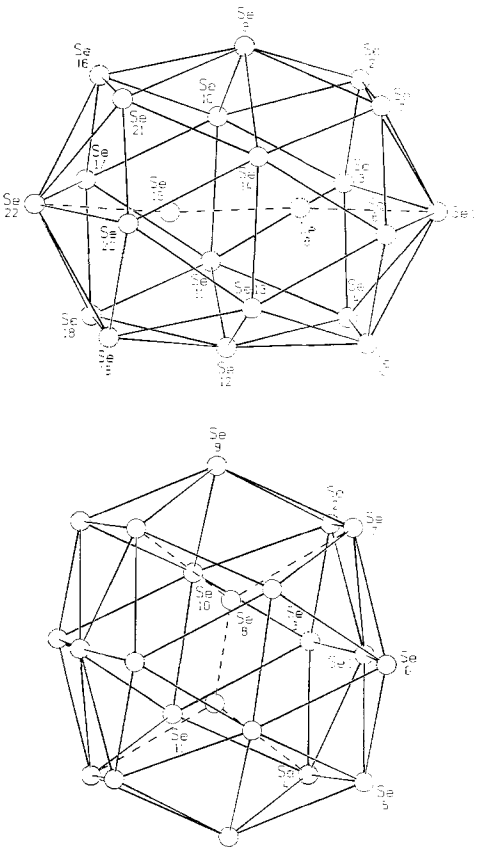


Fig. 2. The Se_{22} framework in **5** (top) and **6** (bottom); the lines drawn between the Se atoms do not represent bonds. For clarity only selected lines are shown between selenium atoms in the center of the cluster and selenium atoms on the surface of the polyhedron. Se–Se distances [pm] (error ±0.9 pm): **5**: 381.8–450.8, **6**: 341.2–462.4.

cupied – the previously mentioned "defect" in the cluster framework. The selenium atoms Se8 and Se15 sit in the center of the two prisms. Through bonding to these selenium atoms and to two further selenium atoms of the selenium polyhedron, the copper atoms Cu40, Cu41, and Cu42 likewise achieve near trigonal-planar coordination. The inner Cu_8Se_2 structural fragment is highlighted in Figure 1 top by lighter colored spheres, together with four additional copper atoms of the cluster periphery that belong to a $Cu_{12}Se_2$ unit that differs considerably from the corresponding one in **6**.

Despite the fact that the cluster core has the same composition with 44 copper and 22 selenium atoms, the structure of **6** in the crystal (Fig. 1 bottom) differs considerably from that of **5**; thus, the Cu–Se frameworks of both compounds may be considered isomeric. Unlike **5**, **6** has an inversion center. If the carbon atoms and the slight distortions of the Cu-Se-P framework are neglected, **6** has approximate C_{4h} symmetry; the fourfold axis runs through the atoms Se8 and Se8′.

Particularly apparent in this comparison is the different number and arrangement of the phosphane ligands in the cluster periphery, a fact which can be attributed to the differing spatial requirements of the various organic groups attached to the phosphorus atoms in **5** (PEt_2Ph) and **6** ($PnButBu_2$); Tolman's cone angles amount to 136.3° for PEt_2Ph and 165.3° for $PnButBu_2$.[4] Consequently, in **6** there is only room for 12 phosphane ligands on the cluster surface for the shielding of the Cu–Su core.

This difference in the ligand shell, and thus in the number of copper atoms that coordinate above the surface of the deltohedron to selenium atoms seems decisive for a structural change in the cluster core: the six additional copper atoms without Cu–P bonds in **6** (Cu2, Cu3, Cu5 and inverted positions) move into the Cu–Se core below the surface of the cluster. Furthermore, four of the eight copper atoms that form an inner Cu_8Se_2 unit in **5** (cf. Fig. 1 top) are forced outwards until they lie just below

the periphery; thus 12 Cu–P units are located just above and 28 copper atoms just below the surface of the Se deltohedron.

The copper structure in **6**, which could be considered as a reorganized version of that in **5**, is accompanied by a strong distortion of the selenium polyhedron shown in Figure 2 bottom. The nonbonding Se–Se distances are 341.2–462.4 pm.

As in **5**, the polyhedron is obtained by linking two hexagonal antiprisms together through a hexagonal face and by capping the two free hexagonal faces with an additional selenium atom (Se1 and Se1′) each. However, the hexagons are distorted to such an extent that they are no longer planar. The polyhedron can no longer be described as a deltohedron built up from 36 equilateral triangles, a circumstance which is already apparent by the fact that in **6** 40 copper atoms (instead of 36 in **5**) are arranged on the Se_{26} surface. Of these 40 metal atoms, 32 are μ_3-coordinated to 32 Se_3 triangles. The copper atoms bound to phosphorus —with the exception of Cu4 and Cu7—like those in **5** are almost tetrahedrally coordinated, whereas those without a Cu–P bond reside in a trigonal-planar environment, surrounded by three selenium atoms. Cu4 and Cu7, also located in a near trigonal-planar environment, are coordinated by two selenium atoms and one phosphorus atom. The remaining eight copper atoms (Cu17, Cu18, Cu19, Cu20, and inverted positions) have to share a Se_3 face as coordination site pairwise; thus, these four triangles are greatly extended and can be better described as two Se_4 rectangular faces (Se4, Se7, Se9, Se11, and inverted positions). The metal atoms last mentioned act as μ_2-bridges along the sides of the nearly square Se_4 rectangles. By bonding to Se8 or Se8′, they also achieve nearly trigonal-planar coordination.

As a result of this change, the structure of the central $Cu_{12}Se_2$ unit, whose atoms are highlighted by lighter colored spheres in Figure 1 bottom, is completely different from that of the corresponding Cu–Se fragment in **5**. This $Cu_{12}Se_2$ unit in **6**, which occurs along the fourfold axis of the molecule—perpendicular to the orientation of the analogous structure fragment in **5**, could be interpreted as a segment from a chain of *trans*-corner-sharing octahedra.

The structure-determining influence of tertiary phosphanes on $[Cu_2Se]_n$ clusters has previously been shown by ab initio calculations with PH_3 as model ligand.[1] This result is underlined by the experimental findings here. The noticeable similarities in the molecular structures of **5** and **6**, despite significant differences, suggest the possibility that in fact the number and the steric demand of the phosphane ligands can eventually lead to a reorganization of the cluster framework, after the energetically most favorable basic structure of the copper–selenium cluster of a certain composition favored under the reaction conditions has been formed.

How can the influence of the phosphane shell transfer its effect to the inside of the cluster? Whether, for example, electronic effects through the change in the total number of valence electrons (872 VE in **5** and 860 VE in **6**) or the desire of the copper and selenium atoms to achieve particular coordination numbers are decisive, is still not certain. It can also not be ruled out that the phosphane ligands control the arrangement of copper and selenium atoms from the beginning of the growth of the cluster, until their influence then gives way to other structure-determining influences at increasing cluster sizes.

The compositions of **5** and **6** suggest the presence of a Cu_{44}^{44+} framework and 22 Se^{2-} ligands in both cases. Consequently the oxidation state +1 (d^{10} configuration) can be assigned to all the copper atoms; thus, these compounds can be placed in the series containing most of the known sulfur- and selenium-bridged copper clusters,[1, 2] which is also in agreement with bond theory. Hence, bonding interactions between the copper atoms can be neglected. The distances between the copper atoms (Cu4–Cu37 251.1 pm to Cu5–Cu23 293.9 pm in **5**; Cu3–Cu12 250.7 pm to Cu2–Cu15 299.8 pm in **6**) also support this assumption; the Cu–Cu interactions are at best considered as dispersion interactions.[1] The coherence of the cluster framework is therefore essentially based on the bridging of the metal atoms by the selenido ligands.

If the structure of **5** is studied with regard to the question of whether this cluster might possibly be an intermediate in the formation of larger clusters such as $[Cu_{70}Se_{35}(PEt_2Ph)_{23}]$,[2] it becomes clear that the two molecular structures are not topologically related to each other. Instead of the arrangement of selenium atoms in hexagonal A-B-A layers between layers of copper atoms, an ellipsoid-shaped deltohedron of selenium atoms is formed in **5**. Also the fact that no crystals of the cluster $[Cu_{70}Se_{35}(PEt_2Ph)_{23}]$ were obtained in the reaction carried out for the synthesis of **5** indicates that the two compounds are formed independently from each other. Thus, it is clearly evident that the influence of the anion of the copper salt not only has an effect on the rate of cluster formation, but also on the actual formation mechanism.

It is conceivable that the copper–selenium clusters isolated so far[1, 2] constitute PR_3-stabilized (R = organic group) sections from structures in the formation of copper(I) selenide; finally, for the largest characterized clusters $[Cu_{70}Se_{35}(PEt_2Ph)_{23}]$ and $[Cu_{146}Se_{73}(PPh_3)_{30}]$ a relationship has been found to the known structure of β-Cu_2Se.[2]

Experimental Procedure

All steps for the preparations of **5** and **6** were carried out under a nitrogen atmosphere and in dry solvents.

5: $PEtPh_2$ (1.61 mL, 6 mmol) was added to a suspension of CuOAc (0.37 g, 3 mmol) in diethyl ether (25 mL), which resulted in the dissolution of the CuOAc. The reaction mixture was cooled to −78 °C and treated with $Se(SiMe_3)_2$ (0.37 mL, 1.5 mmol). The solution was allowed to warm to −20 °C over 8 d, during which time it turned red and dark red rhombuses of **5** crystallized out (yield 85%).

6: $PnBuiBu_2$ (0.75 mL, 3 mmol) was added to a suspension of CuOAc (0.37 g, 3 mmol) in diethyl ether (25 mL), which resulted in the dissolution of the CuOAc. The reaction mixture was cooled to −78 °C and treated with $Se(SiMe_3)_2$ (0.37 mL, 1.5 mmol). The solution was allowed to warm to −20 °C over 20 d, during which time it turned red brown and black rhombuses of **5** crystallized out (yield 80%).

Received: June 17, 1994 [Z 7043 IE]
German version: *Angew. Chem.* **1994**, *106*, 2369

[1] S. Dehnen, A. Schäfer, D. Fenske, R. Ahlrichs, *Angew. Chem.* **1994**, *106*, 786–790; *Angew. Chem. Int. Ed. Engl.* **1994**, *33*, 746–749.

[2] D. Fenske, H. Krautscheid, S. Balter, *Angew. Chem.* **1990**, *102*, 799–801; *Angew. Chem. Int. Ed. Engl.* **1990**, *29*, 796–799; D. Fenske, H. Krautscheid, *ibid.* **1990**, *102*, 1513–1515 and **1990**, *29*, 1452–1454; H. Krautscheid, D. Fenske, G. Baum, M. Semmelmann, *ibid.* **1993**, *105*, 1364–1367 and **1993**, *32*, 1303–1305.

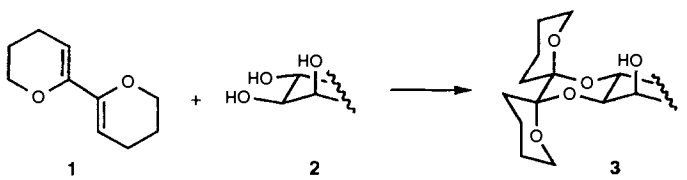
[3] X-ray structure analyses: STOE IPDS diffractometer; $Mo_{K\alpha}$, 213 K, data collection and refinement: **5**: $a = 1946.5(6)$, $b = 1937.5(6)$, $c = 3613.6(6)$ pm, $\alpha = 86.07(2)$, $\beta = 87.73(2)$, $\gamma = 60.63(2)°$, $V = 12078(6) \times 10^6$ pm^3, space group $P\bar{1}$ (no. 2), $Z = 2$, $\mu(Mo_{K\alpha}) = 7.09$ mm^{-1}, $2\theta_{max} = 51°$; 80138 reflections, of which 35842 are independent, 14582 with $(I > 4\sigma(I)$, 1322 parameters (Se, Cu, P refined anisotropically; the carbon atoms of the ethyl groups are partly double disordered, their atomic positions were refined isotropically; one carbon atom could not be determined from the data set; the phenyl rings were refined as rigid groups); $R = 0.067$. Half a molecule of solvent per formula unit was identified. **6**: $a = 1995.7(12)$, $b = 2069(2)$, $c = 2129(2)$ pm, $\alpha = 108.30(6)$, $\beta = 117.43(6)$, $\gamma = 97.47(6)°$, $V = 7003(12) \times 10^6$ pm^3; space group $P\bar{1}$ (no. 2), $Z = 1$, $\mu(Mo_{K\alpha}) = 6.07$ mm^{-1}, $2\theta_{max} = 52°$; 46692 reflections, of which 25142 are independent, 9315 with $I > 4\sigma(I)$, 734 parameters (Se, Cu, P refined anisotropically, C refined isotropically); the positions of the H atoms were calculated); $R = 0.081$. Three solvent molecules were identified per asymmetric unit. Further details of the crystal structure investigations may be obtained from the Fachinformationszentrum Karlsruhe, D-76344 Eggenstein-Leopoldshafen (FRG), on quoting the depository number CSD-58381.

[4] C. A. Tolman, *Chem. Rev.* **1977**, *77*, 131–348.

Cyclohexane-1,2-diacetals (CDA): A New Protecting Group for Vicinal Diols in Carbohydrates

Steven V. Ley,* Henning W. M. Priepke, and Stuart L. Warriner

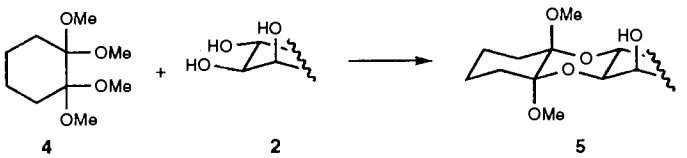
Recently we introduced the dispiroketal protecting group (Dispoke) as a selective protective group for diequatorial 1,2-diol units in carbohydrates (Scheme 1).[1, 2] The regio- and diastereoselectivity of the reaction of 3,3',4,4'-tetrahydro-6,6'-bi-2*H*-pyran (bis-DHP, **1**) with pyranosides such as **2** arises



Scheme 1. Only the relevant portion of the pyranoside is shown.

from the stabilizing influence of the four anomeric effects in the resulting dispiroketal **3** and the equatorial arrangement of all four alkyl substituents of the central 1,4-dioxane unit. Although we observed the exclusive formation of only one isomer with many carbohydrates, the results with important *manno*-type sugars were less satisfactory. The low yields and the lack of regioselectivity were attributed to the low solubility of these compounds in chloroform and the instability of **1** when heated over prolonged periods of time.[3]

To develop the general concept further, we considered the use of 1,1,2,2-tetramethoxycyclohexane (**4**) as a new alternative reagent for carbohydrate protection (Scheme 2). Reaction of **4**



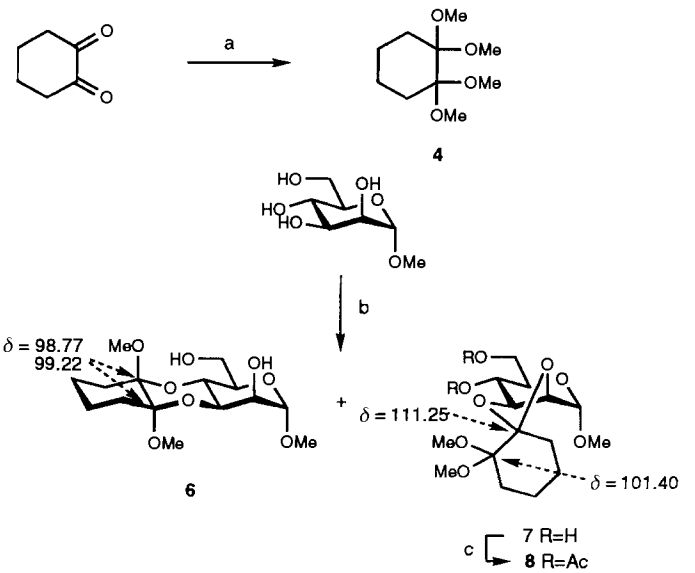
Scheme 2. Only the relevant portion of the pyranoside is shown.

with **2** should furnish selectively the cyclohexane-1,2-diacetal **5** where all the regulatory elements mentioned above should govern the outcome of the reaction. In the product **5** both methoxy groups should be oriented in the axial position to obtain the maximum anomeric stabilization, while all four sterically demanding alkyl substituents should be placed in the favored equatorial positions. To overcome the solubility problem we chose methanol, a solvent frequently used for acetalizations of carbohydrates.[4] With this solvent the diacetal **5** should be formed under thermodynamically controlled conditions.

[*] Prof. Dr. S. V. Ley, Dr. H. W. M. Priepke, S. L. Warriner
Department of Chemistry, University of Cambridge
Lensfield Road, Cambridge CB2 1EW (UK)
Telefax: Int. code + (223)336-442

[**] Cyclohexane-1,2-diacetals in Synthesis, Part 1. We are grateful to Dr. P. Raithby, Cambridge, for the X-ray structure determination and Dr. M. Thompson, SmithKline Beecham, for helpful discussions. This work was supported by Schering Agrochemicals Ltd (Schering Fellowship of Bio-Organic Chemistry for H.W.M.P.), SmithKline Beecham (Research Studentship for S.L.W.), Pfizer Central Research, and the BP Research Endowment.

The required 1,1,2,2-tetramethoxycyclohexane (**4**) was readily obtained in 75% yield from inexpensive 1,2-cyclohexanedione by reaction with trimethyl orthoformate in methanol containing a few drops of conc. H_2SO_4 (Scheme 3). In the initial



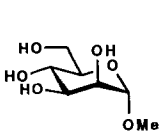
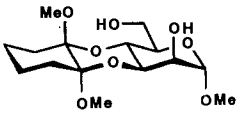
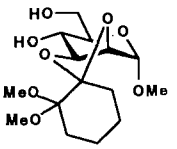
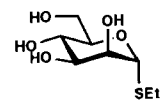
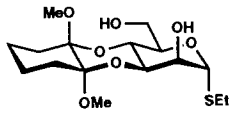
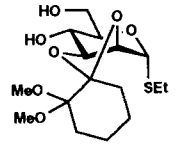
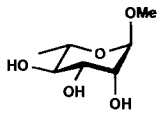
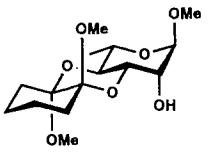
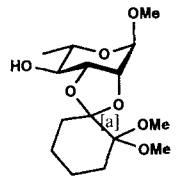
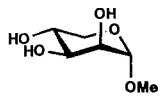
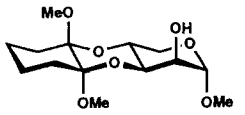
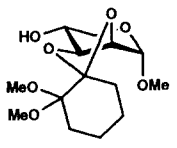
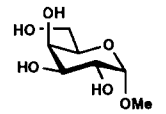
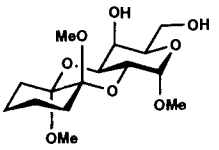
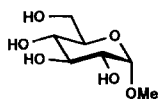
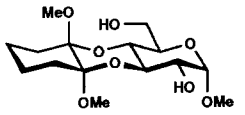
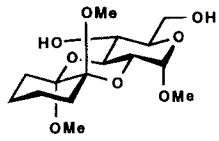
Scheme 3. Synthesis of **4** and protection of methyl α-D-mannoside: a) MeOH, $CH(OMe)_3$, cat. H_2SO_4, reflux, 75%; b) **4**, MeOH, $CH(OMe)_3$, reflux, cat. CSA, 48% **6** and 11% **7**; c) Ac_2O, pyridine, 97%.

experiment methyl α-D-mannoside was investigated, as this substrate failed to react under the standard dispoke reaction conditions (bis-DHP **1**, $CHCl_3$, (±)-camphorsulfonic acid (CSA)).[2] By using 1.4 equivalents of **4** in boiling methanol with a trace of trimethyl orthoformate and a catalytic amount of CSA, the acetalization reaction proceeded smoothly to give the 3,4-protected sugar **6** as the major reaction product in 48% yield. Purification of **6** was achieved by recrystallization from diethyl ether, and its structure was unambiguously assigned by X-ray crystallography.[5] Protection of the *cis*-2,3-diol unit occurred only to a minor extent. Interestingly the major side product[6] was the 1,3-dioxolane **7**. Its structure was deduced from the significant downfield shift of the signal of one of the acetal carbons in the ^{13}C NMR spectra ($\delta = 111.25$ and 101.40 in **7** vs. 98.77 and 99.22 in **6**).[7] To confirm the assigned structure, **7** was converted into the acetate **8**, which showed the expected downfield shift for the H-4 signal (H-4: $\delta = 4.41$ in **7**, $\delta = 5.02$ in **8**). Moreover its ^1H NMR spectra is very similar ($\Delta\delta < 0.03$, $\Delta J < 0.6$ Hz) to that of the isopropylidene analogue.[8]

To improve the yield of **6** the dioxolane **7** was treated in boiling methanol with a trace of CSA. After four days **6** was obtained in 35% yield and recovered **7** in 16% yield. This result suggests that the acetalization reaction is reversible and that the isomer ratio is governed by thermodynamic control under the prolonged reaction time.

Next, we converted other pyranosides into the corresponding diacetals. Table 1 summarizes these results and compares them with the related dispoke protection.[1, 2, 9, 10] We were able to transform ethyl 1-thio-α-D-mannopyranoside in good selectivity and yield into the crystalline 3,4-protected adduct **9** and small amounts of its isomer **10**. Methyl α-L-rhamnopyranoside, which gave a disappointing 3:2 mixture with dispoke protection,[1] was also converted in high yield into diacetal **11**. Again the 3,4-protected derivative **11** could be easily separated from re-

Table 1. Synthesis of simple CDA- and Dispoke-protected pyranosides.

Sugar	CDA Protection 3,4-protected		CDA Protection 2,3-protected		Dispoke Protection 3,4	Dispoke Protection 2,3
		48%		11%	0%	0%
D-*manno*-	**6**		**7**			
		53%		10% [a]	36%	[b]
D-*manno*-	**9**		**10**			
		74%		8%	47%	32%
L-*rhamno*-	**11**		**12**			
		45%		11% [a]	62%	0%
D-*lyxo*-	**13**		**14**			
	[c]			46%	0%	76%
D-*galacto*-			**15**			
		30% [d]		50% [d]	26%	42%
D-*gluco*-	**16**		**17**			

[a] Contaminated with minor amounts of other isomers. [b] Other minor products were formed but not readily identified. [c] A multitude of products were evident but were not isolated. [d] An inseparable mixture of **16** and **17** was obtained.

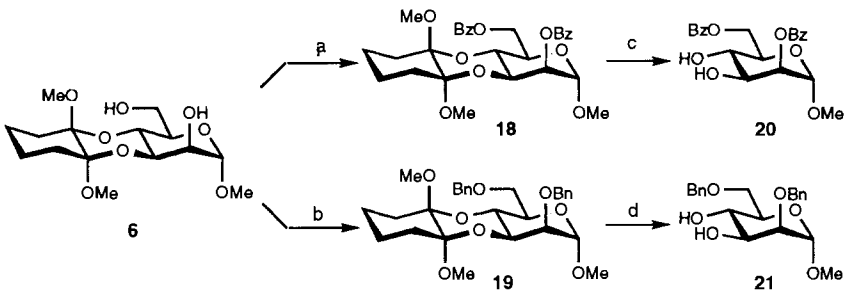
gioisomers by a combination of chromatography and crystallization. With methyl α-D-lyxopyranoside we obtained the 3,4-adduct **13** in 45% yield along with dioxolane **14** in 11% yield. This is the only case in the series of sugars with an axially oriented 2-hydroxyl group where bis-DHP **1** gives better selectivity and yield than diacetal **4**.[1]

Next, we tried to protect methyl α-D-galactopyranoside which could be converted regioselectively by the dispoke methodology.[2] Disappointingly, we could see many more side products by thin-layer chromatography than usual. This may have resulted from epimerization at the anomeric center. However, we were able to isolate the *trans*-protected adduct **15** in 46% yield, although here the separation from other isomers was rather difficult. The use of other solvents (acetonitrile, dimethylformamide, $CHCl_3$) neither improved the yield nor the selectivity of the reaction. We observed the same difficulties for the corresponding arabino- and fucopyranosides.[11] Apparently CDA protection is superior in the *manno*-configurated pyranosides, while dispoke protection is the method of choice for sugars having the *galacto* ring configuration. The methods are therefore complementary.

We also converted methyl α-D-glucopyranoside into an inseparable 3:5 mixture of the corresponding 3,4- and 2,3-protected sugars **16** and **17** in 80% yield. Although we could not improve the selectivity for either of the two *trans* diol units, the yield was higher compared to the dispoke protection.[9]

The usefulness of a protecting group is highly dependent on the ease with which it is removed at the end of a synthetic sequence. Therefore the compatibility of the CDA unit was investigated with some protection/deprotection conditions. We

could easily convert **6** in high yield into the corresponding dibenzoate **18** or the dibenzyl ether **19** using standard conditions (Scheme 4). Finally, removal of the CDA moiety was achieved by treatment with aqueous trifluoroacetic acid (TFA). A 19:1 TFA:H_2O mixture removed the cyclohexane diacetal group of **18** in 20 min to furnish **20** in 96% yield,[12] while a 4:6 TFA:H_2O mixture smoothly converted **19** into **21** in 16 h.



Scheme 4. Derivatization and deprotection of **6**. a) BzCl, pyridine, 94%; b) NaH, DMF, BnBr, nBu$_4$NI, 78%; c) TFA/H_2O 19:1, 20 min, 96%; d) TFA/H_2O 4:6, 16 h, 86%.

The new CDA methodology is a versatile procedure for the protection of diequatorial 1,2-diols especially in *manno*-type sugars where regioselective introduction of 3,4-protection is rather difficult. For rhamnosides this was, until now, only accessible by a four-step sequence.[13] Furthermore, the CDA unit induces a conformational rigidity into the sugar ring which, by analogy to our findings with dispoke derivatives,[14] should modify the reactivity of a potential glycosyl donor leaving group. The behavior of CDA-protected sugars in glycosylations is described in the following paper.[15]

Experimental Procedure

1,1,2,2-tetramethoxycyclohexane (**4**): Conc. sulfuric acid (8 drops) was added to a stirred solution of 1,2-cyclohexanedione (11.2 g, 0.10 mmol) in methanol (15 mL) and trimethyl orthoformate (30 mL). The resulting black solution was refluxed for 16 h and then neutralized with sodium bicarbonate (ca. 1 g). After evaporation of the solvent, the crude material was purified by column chromatography on silica gel (Merck 9385) to furnish **4** as colorless liquid (15.3 g, 75%). ^{1}H NMR ($CDCl_3$, 200 MHz): δ = 1.31–1.48 (m, 4H), 1.60–1.75 (m, 4H), 3.32 (s, 12H); ^{13}C NMR ($CDCl_3$, 50 MHz): δ = 21.67, 30.61, 49.25, 102.07.

Typical acetalization: Preparation of **6** and **7**: CSA (308 mg, 1.33 mmol) was added to a stirred solution of methyl α-D-mannopyranoside (3.46 g, 17.8 mmol), **4** (4.60 g, 24.4 mmol) and trimethyl orthoformate (2.0 mL) in dry methanol (25 mL), and the mixture was heated under reflux for 16 h. After neutralization with $NaHCO_3$ (ca. 0.5 g), the solvent was removed in vacuo, and the crude material was purified by column chromatography on silica gel (Merck 9385) to furnish **7** (666 mg, 11%) as an off-white foam and slightly impure **6**, which was further purified by slow crystallization from diethyl ether to give clean **6** (2.83 g, 48%). **6**: $[\alpha]_D^{25}$ = +191 (c = 0.94, $CHCl_3$); m.p. 168 °C (Et_2O); ^{1}H NMR ($CDCl_3$, 400 MHz): δ = 1.29–1.43 (m, 2H), 1.45–1.55 (m, 2H), 1.62–1.82 (m, 4H), 2.25 (br. t, J = 5.8 Hz, 1H), 2.89 (s, 1H), 3.20 (s, 3H), 3.21 (s, 3H), 3.35 (s, 3H), 3.72–3.86 (m, 3H), 3.92 (br. s, 1H), 4.14 (dd, J = 10.6, 2.9 Hz, 1H), 4.25 (dd, J = 2 × 10.0 Hz, 1H), 4.72 (d, J = 0.9 Hz, 1H); ^{13}C NMR ($CDCl_3$, 100 MHz): δ = 21.35 (2 ×), 27.00 (2 ×), 46.79, 46.93, 54.88, 61.41, 63.88, 65.84, 68.83, 70.05, 70.72, 98.77, 99.22, 101.21. **7**: $[\alpha]_D^{25}$ = +19.8 (c = 0.89, $CHCl_3$); ^{1}H NMR ($CDCl_3$, 400 MHz): δ = 1.37–1.87 (m, 8H), 2.17 (br t, J = 6.2 Hz, 1H), 2.74 (d, J = 5.0 Hz, 1H), 3.27 (s, 3H), 3.32 (s, 3H), 3.40 (s, 3H), 3.64 (ddd, J = 8.4, J = 2 × 4.2 Hz, 1H), 3.72 (ddd, J = 8.3, 6.5, 5.3 Hz, 1H), 3.80–3.86 (m, 2H), 4.30 (dd, J = 2 × 6.4 Hz, 1H), 4.41 (d, J = 6.3 Hz, 1H), 4.88 (s, 1H); ^{13}C NMR ($CDCl_3$, 100 MHz): δ = 21.59, 22.89, 30.71, 35.68, 49.13, 49.98, 55.23, 62.89, 69.56, 70.17, 78.37, 98.92, 101.40, 111.25.

Received: June 7, 1994 [Z 7006 IE]
German version: *Angew. Chem.* **1994**, *106*, 2410

[1] S. V. Ley, R. Leslie, P. D. Tiffin, M. Woods, *Tetrahedron Lett.* **1992**, *33*, 4767–4770.
[2] S. V. Ley, G.-J. Boons, R. Leslie, M. Woods, D. M. Hollinshead, *Synthesis* **1993**, 689–692.
[3] Improvements to our original procedure for these derivatives can be achieved by using ultrasound to enhance the solubility. R. Leslie, S. V. Ley, unpublished results.
[4] A. Klausener, *Methoden Org. Chem. (Houben-Weyl), 4th ed. 1952-*, Bd. E14a/1, **1991**, pp. 100–112 and 167.
[5] Further details of the crystal structure investigation are available on request from the Director of the Cambridge Crystallographic Data Centre, 12 Union Road, GB-Cambridge, CB2 1EZ (UK), on quoting the full journal citation.
[6] Other isomers were also isolated but only in very minor amounts. The spectral data of all isolated isomers will be published in due course.
[7] J. G. Buchanan, M. E. Chacón-Fuertes, A. R. Edgar, S. J. Moorhouse, D. I. Rawson, R. H. Wightman, *Tetrahedron Lett.* **1980**, *21*, 1793–1796.
[8] M. E. Evans, F. W. Parrish, *Carbohydr. Res.* **1977**, *54*, 105–114.
[9] A. B. Hughes, S. V. Ley, H. W. M. Priepke, M. Woods, *Tetrahedron Lett.* **1994**, *35*, 773–777.
[10] All new compounds gave satisfactory spectroscopic and analytical data.
[11] S. V. Ley, H. W. M. Priepke, S. L. Warriner, unpublished results.
[12] For a "one-pot" preparation of *n*-octyl 2,6-di-benzoyl-α-D-mannopyranoside in 32% yield, see S. Oscarson, A.-K. Tidén, *Carbohydr. Res.* **1993**, *247*, 323–328.
[13] V. Pozsgay, J.-R. Brisson, H. J. Jennings, *Can. J. Chem.* **1987**, *65*, 2764–2769.
[14] G.-J. Boons, P. Grice, R. Leslie, S. V. Ley, L. L. Yeung, *Tetrahedron Lett.* **1993**, *34*, 8523–8527.
[15] S. V. Ley, H. W. M. Priepke, *Angew. Chem.* **1994**, *106*, 2412; *Angew. Chem. Int. Ed. Engl.* **1994**, *33*, 2292.

A Facile One-Pot Synthesis of a Trisaccharide Unit from the Common Polysaccharide Antigen of Group B *Streptococci* Using Cyclohexane-1,2-diacetal (CDA) Protected Rhamnosides**

Steven V. Ley* and Henning W. M. Priepke

In the previous paper[1] we introduced the use of cyclohexane-1,2-diacetals (CDA) in a new one-step procedure for the regioselective protection of the 3,4-hydroxyl groups of rhamnosides and mannosides. We will show here that the CDA protecting group is also able to tune the reactivity of a glycosyl donor in glycosylation reactions.

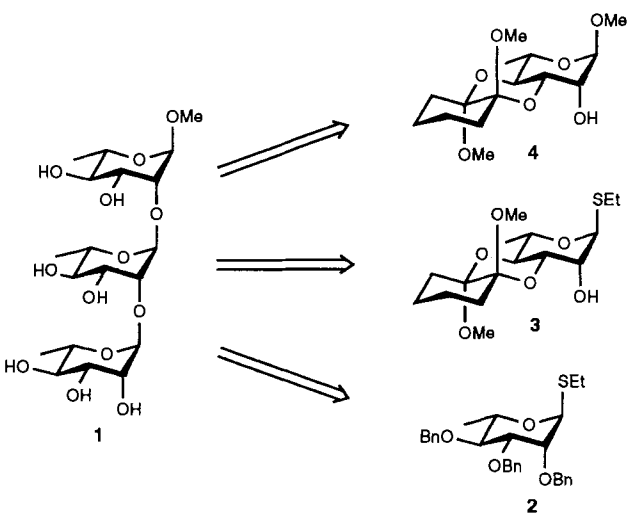
The important armed/disarmed concept introduced by Fraser-Reid et al. has proven to be a powerful tool in the concise preparation of complex oligosaccharides.[2] It relies upon the fact that the reactivity of a glycosyl donor can be regulated by the flanking protecting group at C-2 owing to stereoelectronic effects (e.g., ether = armed, ester = disarmed). According to Fraser-Reid et al.,[3] a sugar can be also considered to be disarmed in glycosylation reactions when a cyclic acetal group is attached to the pyranose ring. In this case, the formation of the intermediate cyclic oxocarbenium ion is more difficult because the required ring flattening in the pyranose ring is inhibited by the annulated acetal function.

[*] Prof. Dr. S. V. Ley, Dr. H. W. M. Priepke
Department of Chemistry, University of Cambridge
Lensfield Road, Cambridge CB2 1EW (UK)
Telefax: Int. code + (223)336-442

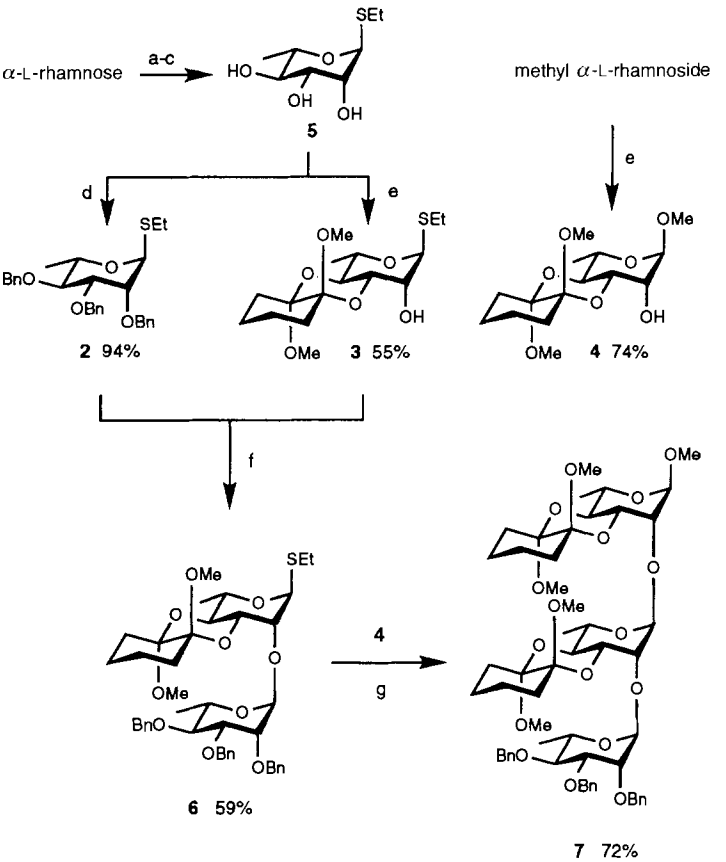
[**] Cyclohexane-1,2-diacetals in Synthesis, Part 2. This work was supported by Schering Agrochemicals Ltd (Schering Fellowship in Bio-Organic Chemistry for H.W.M.P.), Pfizer Central Research, and the BP Research Endowment. Part 1: [1].

Recently,[4] we demonstrated that dispiroketal (dispoke) protected sugars exhibit a third level of reactivity in glycosylation reactions which we called "semidisarmed", as their reactivity lies between fully armed and fully disarmed sugars. We therefore expected a similar tuning of reactivity with CDA-protected pyranosides. We report here on the synthesis of methyl α-L-(1 → 2)-trirhamnoside **1**, a common substructure and the immunodominant epitope of the group-specific polysaccharide of group B *Streptococci*.[5] As this organism is responsible for bacterial meningitis in newborn infants, the synthesis of **1** and various analogues has attracted the interest of several research groups.[6]

For the synthesis of **1** we would require monosaccharide building blocks **2**, **3** and **4** (Scheme 1). The terminal unit at the



Scheme 1.



Scheme 2. Synthesis of monosaccharides **2**–**4** and stepwise synthesis of trisaccharide **7**: a) Ac_2O, pyridine, 92%; b) EtSH, $BF_3 \cdot Et_2O$, 69% α + 7% β anomer; c) K_2CO_3, MeOH, 94%; d) BnBr, NaH, DMF, TBAI; e) 1,1,2,2-tetramethoxycyclohexane, CSA, MeOH, $HC(OMe)_3$; f) IDCP, 4 Å molecular sieves, 1,2-dichloroethane (DCE); Et_2O 1:4, 0 °C → room temperature; g) NIS, cat. TfOH, DCE:Et_2O 1:1, 4 Å molecular sieves, 0 °C.

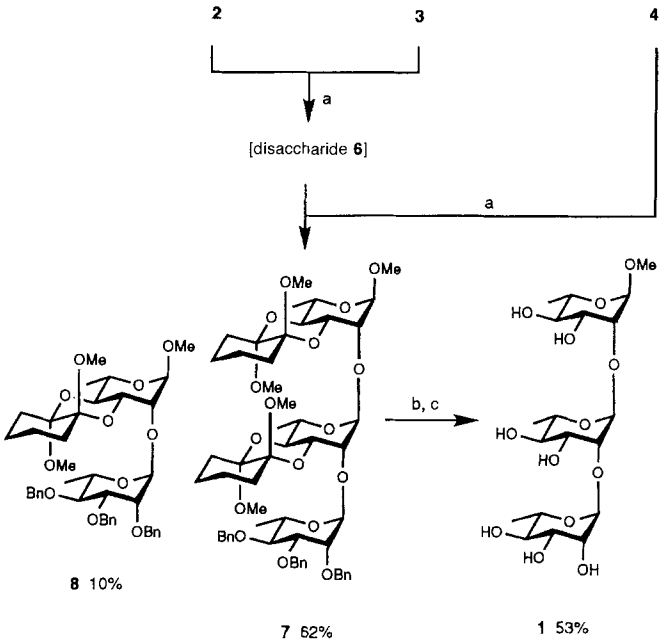
nonreducing end should be the fully armed glycosyl donor **2**. The central part, the diprotected ethyl 1-thio-α-L-rhamnopyranoside **3**, should ideally act either as acceptor or as donor under carefully selected reaction conditions without any functional group interconversion. It should be possible to selectively activate the S-ethyl group of fully armed **2** in presence of the disarmed sugar **3**, which should be easily reacted later with the methyl glycoside **4**.

The precursor for **2** and **3** was the ethyl 1-thio-α-L-rhamnopyranoside **5**, which was prepared from α-L-rhamnose by a known three-step procedure (Scheme 2).[7a, b] Perbenzylation of **5** furnished **2** in 94% yield.[7a, c] Conversion of **5** into **3** with 1,1,2,2-tetramethoxycyclohexane was achieved in 55% yield using our standard CDA protection conditions.[1, 8] The preparation of **4** has already been described.[1] The monosaccharides **3** and **4** were therefore each prepared from the corresponding glycosides in one-step procedures, shortening the usual four-step route to 3,4-diprotected rhamnose units dramatically.[6a, 7]

With all monosaccharides in hand, we first investigated a stepwise approach to the synthesis of **1**. The choice for the activation of the armed donor **2** was the mild thiosugar activator iodonium dicollidine perchlorate (IDCP)[9] to guarantee the selective reaction of the S-ethyl group of the fully armed donor **2** in presence of the semidisarmed acceptor **3**. Indeed, under these reaction conditions the only glycosidation product obtained was the disaccharide **6**, which was isolated exclusively as the α anomer. No homocoupling of **3** was detected. Obviously CDA protection efficiently deactivates the attached sugar moiety relative to a fully armed glycosyl donor. Further reaction of disaccharide **6** with acceptor **4** by use of the more potent activator trifluoromethanesulfonic acid/*N*-iodosuccinimide (TfOH/NIS)[10] yielded the trisaccharide **7** in 72% yield,[11] again exclusively as the α anomer.

As we could perform two successive glycosylations without any functional group interconversions, it was possible to develop a one-pot synthesis of **7**.[12] According to Fraser-Reid et al. the selective activation of a fully armed *O*-pentenyl glycosyl donor in the presence of a disarmed *O*-pentenyl acceptor is possible even if the potent promoter TfOH/NIS is used.[2a]

We therefore investigated a one-pot conversion to the trisaccharide **7** by using TfOH/NIS for both glycosylation steps (Scheme 3). After activation of a mixture of armed **2** and disarmed **3** with TfOH/NIS, analysis by thin-layer chromatography revealed that disaccharide **6** was the sole reaction product. Only traces of unreacted glycosyl donor **2** remained. After addition of the second acceptor **4** the disaccharide **6** could be activated by addition of NIS and small portions of TfOH to afford the trisaccharide **7** in an excellent overall yield of 62%. To our knowledge this is the first example where the armed/disarmed concept has been applied for a one-pot synthesis of a trisaccharide. It is also noteworthy that nearly stoichiometric amounts of the three monosaccharide units could be used. Disaccharide **8** was isolated as a side-product from addition of unreacted **2** to an excess of the second acceptor **4**. The target trisaccharide **1** was obtained in 53% overall yield by heating **7** with AcOH/



Scheme 3. One-pot synthesis of **7** and deprotection to **1**. a) NIS, cat. TfOH, DCE:Et_2O 1:1, 4 Å molecular sieves, 0 °C; b) AcOH:H_2O 2:1, 100 °C, 2 h; c) H_2, Pd/C, EtOH:AcOH 20:1.

H_2O 2:1 at 100 °C to remove the acetals, followed by debenzylation and chromatography on Sephadex G-15.[13]

The CDA protecting group has proved to be especially useful since it converts the attached sugars into disarmed bifunctional glycosyl donor/acceptor "hermaphrodites". Deprotection of CDA units is possible under mild conditions, and the number of steps for the synthesis of **1** is therefore considerably reduced.

Received: June 7, 1994 [Z 7007 IE]
German version: *Angew. Chem.* **1994**, *106*, 2412

[1] S. V. Ley, H. W. M. Priepke, S. L. Warriner, *Angew. Chem.* **1994**, *106*, 2410; *Angew. Chem. Int. Ed. Engl.* **1994**, *33*, 2290.
[2] a) B. Fraser-Reid, U. E. Udodong, Z. Wu, H. Ottosson, J. R. Merritt, C. S. Rao, C. Roberts, R. Madsen, *Synlett* **1992**, 927–942; b) D. R. Mootoo, P. Konradsson, U. Udodong, B. Fraser-Reid, *J. Am. Chem. Soc.* **1988**, *110*, 5583–5584.
[3] B. Fraser-Reid, Z. Wu, C. W. Andrews, E. Skowronski, J. P. Bowen, *J. Am. Chem. Soc.* **1991**, *113*, 1434–1435.
[4] G.-J. Boons, P. Grice, R. Leslie, S. V. Ley, L. L. Yeung, *Tetrahedron Lett.* **1993**, *34*, 8523–8526.
[5] a) F. Michon, J.-R. Brisson, A. Dell, D. L. Kasper, H. J. Jennings, *Biochemistry* **1988**, *27*, 5341–5351; b) F. Michon, R. Charlifour, R. Feldman, M. R. Wessels, D. L. Kasper, A. Gamian, V. Pozsgay, H. J. Jennings, *Infect. Immun.* **1991**, *59*, 1690–1696.
[6] a) V. Pozsgay, J.-R. Brisson, H. J. Jennings, *Can. J. Chem.* **1987**, *65*, 2764–2769; b) J. C. Castro-Palomino, M. Hernandez Rensoli, J. Sarracent Perez, M. Herrera Montes de Oca, V. Verez Bencomo, *VII. Eur. Carbohydr. Symp.*, Abstract A 166, Cracow, **1993**.
[7] a) **2** and **5** were prepared according to the procedure given for the corresponding methyl 1-thio-α-L-rhamnopyranoside: V. Pozsgay, H. J. Jennings, *J. Org. Chem.* **1988**, *53*, 4042–4052; for the preparation of **5** see also: b) G. H. Veeneman, L. J. F. Gomes, J. H. van Boom, *Tetrahedron* **1989**, *45*, 7433–7448; for the preparation of **2** see also: c) A. K. Ray, U. B. Maddali, A. Roy, N. Roy, *Carbohydr. Res.* **1990**, *197*, 93–100.
[8] We also isolated other isomers in a minor amounts. All new compounds gave satisfactory spectroscopical and analytical data.
[9] G. H. Veeneman, J. H. van Boom, *Tetrahedron Lett.* **1990**, *31*, 275–278.
[10] G. H. Veeneman, S. H. van Leeuwen, J. H. van Boom, *Tetrahedron Lett.* **1990**, *31*, 1331–1334.
[11] **7**: Amorphous solid, $[\alpha]_D^{29} = -106$ ($c = 0.97$, $CHCl_3$); FAB-MS: *m/z*: 1020.50 (M^+); ^1H NMR (500 MHz, $CDCl_3$): δ = 1.22 (d, J = 5.8, 3H), 1.23 (d, J = 6.0, 3H), 1.28–1.80 (m, 16H), 1.34 (d, J = 6.1, 3H), 3.09, 3.17, 3.18, 3.24, 3.32 (5 × s, 5 × 3H), 3.60 (dd, 2 × J = 9.4, 1H), 3.75 (dq, J = 9.7, J = 5.8, 1H), 3.75–3.85 (m, 1H), 3.80 (2 × t, 2 × J = 10.2, 2H), 3.86 (dq, J = 9.7, J = 6.0, 1H), 3.91 (dd, J = 2.4, J = 1.7, 1H), 3.97 (dd, J = 9.5, J = 3.2, 1H), 4.02 (dd, J = 3.0, J = 1.9, 1H), 4.07 (dd, J = 10.0, J = 2.7, 1H), 4.18 4.21 (m, 2H), 4.557 (d, J = 11.6, 1H), 4.560 (d, J = 1.3, 1H), 4.60 (d, J = 11.3, 1H), 4.63 (d, J = 11.0, 1H), 4.66 (d, J = 12.6, 1H), 4.80 (d, J = 12.6, 1H), 4.95 (d, J = 11.1, 1H), 5.12 (s, 1H), 5.45 (d, J = 1.6, 1H), 7.23–7.36 (m, 13H), 7.46 (brd, J = 6.9, 2H); ^{13}C NMR (100 MHz, $CDCl_3$): δ = 16.73, 16.80, 18.21, 21.25 (2 ×), 21.42 (2 ×), 26.93, 27.02 (2 ×), 27.26, 46.38, 46.53, 46.71, 46.89, 54.48, 67.01, 67.41, 68.14, 69.33, 69.47, 69.53, 69.67, 71.83, 72.00, 74.17, 74.55, 75.11, 75.37, 79.54, 80.85, 97.79, 98.44 (2 ×), 98.52 (2 ×), 100.26, 100.57, signals for aromatic carbon atoms at 127.31, 127.38, 127.68, 127.83, 128.18, 128.24, 138.86, 139.02.
[12] Recently two other one-pot syntheses of trisaccharides were published: a) S. Raghavan, D. Kahne, *J. Am. Chem. Soc.* **1993**, *115*, 1580–1581; b) H. Yamada, T. Harada, H. Miyazaki, T. Takahashi, *Tetrahedron Lett.* **1994**, *35*, 3979–3982.
[13] The physical data of **1** is in accord with the published data [6a].

1-Carba-*arachno*-pentaboranes(10) from Dimethyldi(1-propynyl)silane and Ethyldiboranes(6)**

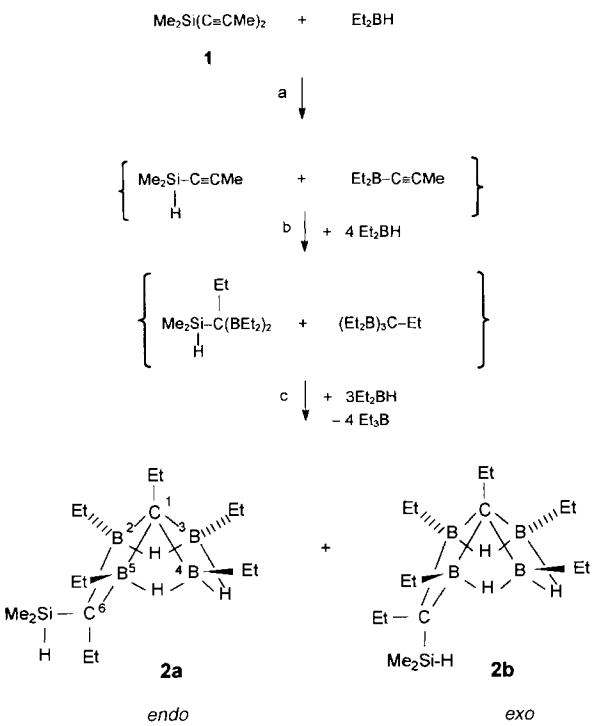
Roland Köster, Günter Seidel, and Bernd Wrackmeyer*

For 1-alkynyltrimethylsilanes $Si-C_{alkynyl}$ bond cleavage with the formation of Me_3SiH competes with C≡C hydroboration[1] if alkyldiboranes(6) [e.g. $(Et_2BH)_2$, but not, however, (9-H-9-BBN)$_2$] are present in excess during the reaction. Thus, the experimentally determined hydride number[2] for dimethyldi(1-propynyl)silane (**1**) is not 4, but rather 4.7; in other words additional hydride is consumed by $Si-C_{alkynyl}$ bond cleavage. We have now studied the reaction of **1** with ethyldiboranes(6) ("Et_2BH"[3, 4]), which proceeds by $Si-C_{alkynyl}$ bond cleavage and exhaustive C≡C hydroboration (Scheme 1). From this reaction we obtained the novel 1-carba-*arachno*-pentaboranes(10) **2** (molecular formula $C_{16}H_{40}B_4Si$, M = 304 g mol^{-1}) in 61% yield and 92% purity without optimization.

The requisite large excess of Et_2BH (undiluted and Lewis base free, in contrast to other normal hydroboration agents) has at least three different functions, and is therefore referred to as a "hydride bath" rather than the comparatively unspecific description of excess hydride. Initially, the $Si-C_{alkynyl}$ bond cleavage, necessary for the formation of **2**[1, 5] is predominant in the hydride bath. This leads to dimethyl(1-propynyl)silane and diethyl(1-propynyl)borane (Scheme 1, step a), which, after BEt/BH exchange, are presumably held together in the hydride bath by BHB bridges. The excess of Et_2BH thereby accounts also for the rapid and complete hydroboration of all the unsaturated C≡C bonds (step b). The third function of the excess Et_2BH present consists of the concluding B–H-catalyzed elimination of Et_3B[6] (step c). The ^{11}B NMR spectrum of the reaction solution proves that the two stereoisomers **2a** and **2b** form spontaneously under these conditions.

The structures proposed for the BHB-containing isomers **2a** and **2b**, formed in a ratio of 55:45, are supported experimentally

[*] Prof. Dr. B. Wrackmeyer
Laboratorium für Anorganische Chemie der Universität
D-95440 Bayreuth (FRG)
Telefax: Int. code + (921) 55-2535
Prof. Dr. R. Köster, Dipl.-Ing. G. Seidel
Max-Planck-Institut für Kohlenforschung
D-45466 Mülheim an der Ruhr (FRG)
[**] Boron Compounds, Part 118 (from R. K.). Part 117: R. Köster, W. Schüssler, G. Seidel, D. Bläser, R. Boese, *Chem. Ber.* **1994**, *127*, 1843–1849.

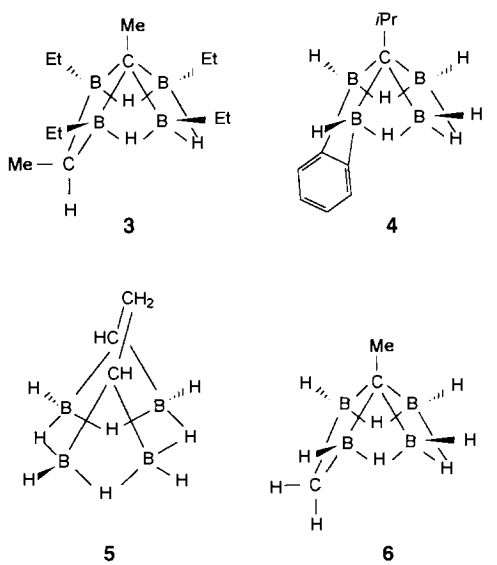


Scheme 1. Reaction of **1** with Et_2BH; *endo*/*exo* refers to the orientation of the silyl substituent relative to the carborane framework.

by the hydroboration of 1-decene, which converts **2a, b** completely into trialkylboranes only above 120 °C, followed by the oxidative determination of twelve B–C bonds with Me_3NO.[7] The low reactivity towards 1-decene distinguishes **2** from alkyldiboranes(6). The degradation of **2** through alcoholysis yields a hydride content which can be used to calculate the number of B–H–B and Si–H bonds present. Deuteration with Et_2BD leads to the D_3 derivative (according to MS data), and in the IR spectrum the strikingly high intensity of the (BHB, SiH) bands for **2a** and **2b** around 2100 cm^{-1} is sharply reduced. In the presence of γ-picoline, **2a** and **2b** remain unchanged, and hence do not form N–B addition compounds, in contrast to alkyldiboranes(6).

The structures of **2a** and **2b** are verified by their NMR data.[8] The $\delta(^{11}B)$ values (**2a,b**: 14.9, −12.1; 13.5, −12.1) alone rule out the possibility of "simple" alkyldiboranes(6) with BH_2B bridges.[9] The appearance of Me_2SiH signals in the ^1H and ^{29}Si NMR spectra is consistent only with Si–C bond cleavage (see Scheme 1, step a). Starting from each Me_2SiH group in **2a** and **2b**, the structures of the isomers may be "unraveled" by using numerous NMR techniques. The routine applications 2D $^1H/^1H$ COSY, 2D $^{13}C/^1H$ HETCOR, and 2D $^{29}Si/^1H$ HETCOR at room temperature were conducted to confirm the linkage of the respective nuclei through the coupling constants ($^3J(^1H,^1H)$, $^1J(^{13}C,^1H)$, $^2J(^{13}C,^1H)$, $^1J(^{29}Si,^1H)$, $^2J(^{29}Si,^1H)$, and $^3J(^{29}Si,^1H)$). In addition 2D $^{13}C/^1H$ HETCOR experiments, based on $^1J(^{13}C,^1H)$ and $^2J(^{13}C,^1H)$, were carried out at low temperature. This allowed the ^{13}C NMR signals of BCH_2, C^1, and C^6, which are broad at room temperature, to be assigned to their respective ^1H NMR signals. Of the 1D NMR techniques used, special mention should be given to $^{13}C/^{13}C$ INADEQUATE measurements [$^1J(^{13}C,^{13}C)$ coupling constants], selective $^1H\{^{11}B\}$ double resonance experiments (assignment of the ^1H and ^{11}B NMR signals), $^1H/^1H$ NOE difference spectra (determination of the spatial proximity of the B^2/B^5 Et and C(Et)$SiMe_2H$ groups), and the ^{13}C-*J*-modulated NMR spectra measured at −60 °C. The latter experiment permits the undisturbed observation of the resonance signals due to the quaternary carbon atoms C^1 and C^6, which at room temperature are very broad and of low intensity. The $^{13}C^6$ resonance signal may be clearly distinguished from that of $^{13}C^1$ owing to the ^{29}Si satellite signals, which can only be easily observed in this way. The results of these experiments leads conclusively to the number and sequence of the B–H, B–C, C–H, C–C, Si–H, and Si–C bonds. Of note is the low-frequency position of the $^{13}C^6$ NMR signals (**2a**: −6.8; **2b**: −13.2). The $^{13}C^1$ resonance signals are likewise at low frequency (**2a**: 10.3, **2b**: 6.2), which is characteristic for an apical carbon atom.[10] The comparatively large[11] coupling constant $^1J(^{13}C^1,^{13}C_{Et}) = 45.1$ Hz is in agreement with an increase in s-electron density in the C^1-C_{Et} hybrid orbital, which is expected owing to the formal sp hybridization of this carbon atom. For **2a** and **2b**, analysis of the 500 MHz ^1H NMR spectrum in the region of the B-ethyl and C-ethyl groups reveals an additional structural element, a mirror plane passing through C^1 and C^6. Thus, an A_2M_3 spin system is present for both the C^1 and C^6-ethyl groups, whereas an ABM_3 spin system results for each of the B-ethyl groups.

The 1-carba-*arachno*-pentaborane type, isoelectronic with *arachno*-pentaborane(11), has already been proposed for **3** as one of the numerous products of the lithium metal dehalogenation of Et_2O-BF_3/Et_3B mixtures in THF.[12] The existence of the parent species CB_4H_{10} was presumed based on mass spectrometric data and an incompletely described IR-spectrum.[13] The CB_4-carborane **4** with μ-C_2 bridges between the atoms B^2 and B^5 can now be prepared in a quite different manner.[14] NMR data[15, 16] and MO calculations[17] support the assumption that the repeatedly discussed $C_3B_4H_{12}$ product obtained from tetraborane(10) and propyne does not have the proposed structure **5**,[15] but rather the 1-carba-*arachno*-pentaborane(10) structure **6**. With their stability and obviously high ease of formation, 1-carba-*arachno*-pentaboranes(10) must therefore be taken into consideration upon future investigations of multiply C-borylated organic compounds. All derivatives to date contain a μ-C_1 or μ-C_2 bridge between B^2 and B^5. The multiply borylated carbon atom incorporated into a BH-rich system is forced into the highly coordinated apical position in **2**–**4** and **6**,



which would otherwise be avoided for *nido* or *arachno* clusters containing boron and carbon atoms.[18]

The results reported here indicate that the hydroboration of metal-substituted 1-alkynes holds a far greater synthetic potential than was previously assumed. This is based not only on the known regioselective directing effect of organometallic substituents,[19] but also on the lability of certain heteroatom-substituted carbon compounds.[1, 20]

Experimental Procedure

endo/exo-**2a,b**: **1** (6.04 g, 44.3 mmol) was added dropwise at room temperature over 4 h to Et_2BH [3.4] (35.9 g, 387.7 mmol hydride) [64.2 MHz-^{11}B NMR: δ = 87 (ca. 52% Et_3B), 28.5 (ca. 24% $Et_2BH_2BEt_2$), 14, −12 (1:1, ca. 24% **2a,b**)]. Ethene was introduced at 50–55 °C to convert excess hydride into Et_3B [$\delta(^{11}B)$ = 87.0 (ca. 78%), 14, −12 (ca. 22%)], after which most of the Et_3B was removed under vacuum (10^{-1}–0.001 Torr). Distillation (0.001 Torr; bath temperature ≤ 95 °C) of the clear, colorless liquid [$\delta(^{11}B)$ = 87 (ca. 13%), 14, −12 (ca. 87%)] gave, after an initial fraction (0.61 g), 0.93 g of a highly viscous residue, and a main fraction of 9.0 g of which 8.26 g was **2a,b** (61%) with b.p. 96–100 °C (0.001 Torr, bath temperature ≤ 130 °C). **2a,b**: IR ($CDCl_3$): $\tilde{\nu}$ = 2097 cm^{-1} (vs, BHB, SiH); EI-MS (70 eV): *m/z*: 304 (M^+, 11% rel. int.), 261 (18), 162 (50), 133 (B_3 fragment, 100), 93 (B_2 fragment), 47), 59 (17), 41 (22).

Reaction of **2a,b** with Me_3NO [7]: Reaction of **2a,b** (0.304 g, 1 mmol) with anhydrous Me_3NO (excess) in boiling toluene gave a mixture of $B(OR)_3$ and $[(RO)_2B]_2O$ ($\delta(^{11}B)$ = 18.2): found 11.4% B_C; calcd 14.22% B_C for $B(OR)_3$ (formed from **2a,b**); after prior treatment with 1-decene at 135 °C to prevent the formation of $[(RO)_2B]_2O$: found 13.68% B_C.

Reaction of **2a,b** with 2-ethylhexanol: At room temperature **2a,b** remained unchanged (^{11}B NMR). Slow elimination of H_2 began at ca. 50 °C with the formation of R_2BO ($\delta(^{11}B)$ = 55.0) and RBO_2 compounds ($\delta(^{11}B)$ = 31.0); above 140 °C **2a,b** was no longer detected by ^{11}B NMR spectroscopy; found 3.7 mmol H_2 (92.5%) per mmol **2a,b**.

Reaction of **2a,b** with $(Et_2BD)_2$: After warming with excess Et_2BD for 40 min at ca. 130 °C: IR: $\tilde{\nu}$ = 2490 (BH), 2100 (SiH), 1565 (BH_2B), 1465 cm^{-1} (BDB); MS: *m/z*: 304 (no D, ca. 17%), 305 (1D, ca. 26%), 306 (2D, ca. 31%), 307 (3D, ca. 26%).

Received: May 6, 1994
Revised version: July 27, 1994 [Z 6903 IE]
German version: *Angew. Chem.* **1994**, *106*, 2380

[1] R. Köster, G. Seidel, F. Lutz, C. Krüger, G. Kehr, B. Wrackmeyer, *Chem. Ber.* **1994**, *127*, 813–820.
[2] For a definition and determination of the hydride number see R. Köster, L. Synoradzki, *Chem. Ber.*, **1984**, *117*, 2850–2862, specifically p. 2862.
[3] For ethyldiboranes(6) "Et_2BH", cf. R. Köster, G. Bruno, P. Binger, *Justus Liebigs Ann. Chem.* **1961**, *644*, 1–22.
[4] Composition on the basis of ^{11}B NMR measurements: $\delta(^{11}B)$ = 87.0 (Et_3B), 28.5 ($Et_2BH_2BEt_2$), 35.2, 16.8 (Et_2BH_2BHEt), 41.5, 3.7 ($Et_2BH_2BH_2$) in the proportion 1 : 1.5 : 0.1 : 0.3; a ^{11}B NMR signal of observable intensity for $EtHBH_2BHEt$ ($\delta(^{11}B)$ = 23.0) occurred only with a higher hydride content.
[5] If Et_2BH is not present in excess, compounds **2** arise in significantly lower quantities; principal products are then compounds formed from the complete C≡C hydroboration of **1** and further reactions: R. Köster, G. Seidel, R. Boese, B. Wrackmeyer, *Z. Naturforsch.*, submitted.
[6] a) „Aliphatische Triorganoborane durch Austausch von Organoresten mittels Katalyse: R. Köster *Methoden Org. Chem. (Houben-Weyl) 4th ed. 1952–*, Bd. XIII, 3a, **1982**, pp. 18–24; b) R. Köster, H.-J. Horstschäfer, P. Binger, P. K. Mattschei, *Liebigs Ann. Chem.* **1975**, 1339–1356.
[7] R. Köster, Y. Morita, *Justus Liebigs Ann. Chem.* **1967**, *704*, 70–90.
[8] ^{1}H NMR (500 MHz, 25 °C, $CDCl_3$): **2a**: δ = 0.18 (d, $SiMe_2$), 4.02 (sept, $^1J(^{29}Si,^1H)$ = 175 Hz; SiH), 1.62 (q), 0.93 (t), (C^1-Et), 1.25 (q), 0.98 (t), (C^6-Et); **2b**: δ = 0.12 (d, $SiMe_2$), 3.58 (sept, $^1J(^{29}Si,^1H)$ = 178 Hz; SiH), 1.61 (q), 0.92 (t), (C^1-Et), 1.47 (q), 1.07 (t) (C^6-Et); **2a**, **2b** (not assigned): δ = 0.41 (br. s, B^3HB^4), −1.22 (br. s), −1.43 (br. s), (B^2HB^3 und B^4HB^5): 0.75 (m), 0.68 (m), 0.57 (m), 0.53 (m) (BCH_2), 1.07 (t), 1.03 (t), 1.02 (t), 1.00 (t), (BCH_2CH_3); ^{11}B NMR (160.5 MHz, 25 °C, $CDCl_3$): **2a**, **2b** (not assigned): δ = 14.9 (s), 13.5 (s) (B^2, B^5), −12.1, −12.1 (B^3,B^4); ^{13}C NMR (125.7 MHz, 25 °C, $CDCl_3$; $^{13}C_B$ signals at −50 °C, 62.6 MHz): **2a**: δ = −2.0 ($SiMe_2$), 10.3, 17.4, 14.6 ($^1J(^{13}C^1, ^{13}C_{Et})$ = 45.1, $^1J(^{13}C_{CH_2}, ^{13}C_{CH_3})$ = 34.9 Hz; C^1-Et), −6.8, 31.7, 15.2 ($^1J(^{29}Si, ^{13}C^6)$ = 50.7, $^1J(^{13}C^6, ^{13}C_{Et})$ = 33.0, $^1J(^{13}C_{CH_2}, ^{13}C_{CH_3})$ = 34.9 Hz; C^6-Et); **2b**: δ = −2.5 ($SiMe_2$), 6.2, 16.8, 14.7 ($^1J(^{13}C^1, ^{13}C_{Et})$ = 45.1, $^1J(^{13}C_{CH_2}, ^{13}C_{CH_3})$ = 34.9 Hz; C^1-Et), −13.2, 23.7, 15.9 ($^1J(^{29}Si, ^{13}C^6)$ = 60.7, $^1J(^{13}C^6, ^{13}C_{Et})$ = 29.1, $^1J(^{13}C_{CH_2}, ^{13}C_{CH_3})$ = 34.91 Hz; aC^6-Et); **2a**, **2b** (not assigned): δ = 10.9, 8.8, 3.5, 3.3 (BCH_2), 13.5, 13.4, 13.36, 13.3 (BCH_2CH_3); ^{29}Si NMR (49.7 MHz, 25 °C, $CDCl_3$): **2a**: δ = −14.3 ($^1J(^{29}Si, ^{13}C_{Me})$ = 49.6, $^1J(^{29}Si, ^{13}C^6)$ = 50.7 Hz); **2b**: δ = −3.5 ($^1J(^{29}Si, ^{13}C_{Me})$ = 48.5, $^1J(^{29}Si, ^{13}C^6)$ = 60.7 Hz).
[9] a) B. Wrackmeyer, R. Köster, *Methoden Org. Chem. (Houben-Weyl) 4th ed. 1952–*, Band XIII, 3c, **1984**, pp. 377–611; b) B. Wrackmeyer, *Annu. Rep. NMR Spectrosc.* **1988**, *20*, 61–203; c) A. R. Siedle, *ibid.* **1988**, *20*, 205–314.
[10] H. Hogeveen, P. W. Kwant, *Acc. Chem. Res.* **1975**, *8*, 413–420.
[11] L. B. Krivdin, G. A. Kalabin, *Russ. Chem. Rev. (Engl. Transl.)* **1988**, *57*, 1–16.
[12] R. Köster, G. Benedikt, M. A. Grassberger, *Justus Liebigs Ann. Chem.* **1968**, *719*, 187–209, specifically p. 196.
[13] D. S. Matteson, P. K. Mattschei, *Inorg. Chem.* **1973**, *12*, 2472–2475.
[14] B. Gangnus, H. Stock, W. Siebert, M. Hofmann, P. von R. Schleyer, *Angew. Chem.* **1994**, *106*, 2383; *Angew. Chem. Int. Ed. Engl.* **1994**, *33*, 2296.
[15] a) R. Greatrex, N. N. Greenwood, M. Kirk, *J. Chem. Soc. Chem. Commun.* **1991**, 1510–1511; b) M. A. Fox, R. Greatrex, N. N. Greenwood, M. Kirk, *Polyhedron* **1993**, *12*, 1849–1853.
[16] The ^{1}H and ^{13}C NMR data and $^1H/^1H$ NOE difference spectra given in ref. [15b], suggested for structure **5**, are likewise consistent with the proposed structure **6**.
[17] a) M. Hofmann, P. von R. Schleyer, personal communication; M. A. Fox, R. Greatrex, M. Hofmann, P. von R. Schleyer, *Angew. Chem.* **1994**, *106*, 2384; *Angew. Chem. Int. Ed. Engl.* **1994**, *33*, 2298; b) A. Korkin, personal communication.
[18] R. E. Williams in *Electron Deficient Boron and Carbon Clusters* (Eds.: G. A. Olah, K. Wade, R. E. Williams), Wiley, New York, **1991**, pp. 11–93.
[19] For the regioselective directing effect in the hydroboration of 1-alkynyl- and 1-alkenylboranes [6b], and 1-alkynyl- and 1-alkenylsilanes, see a) N. Hosmane, N. N. Sirmokadam, M. N. Ollenhauer, *J. Organomet. Chem.* **1985**, *279*, 359–371; b) B. Wrackmeyer, *Polyhedron* **1986**, *5*, 1709–1721; c) K. Uchida, K. Utimoto, H. Nozaki, *J. Org. Chem.* **1976**, *41*, 2941–2942; d) J. A. Soderquist, J. C. Colberg, L. Del Valle, *J. Am. Chem. Soc.* **1989**, *111*, 4873–4878.
[20] For hydroboration of 1-alkynylstannanes, $Sn-C_{alkynyl}$ bond cleavage is always observed: B. Wrackmeyer, C. Bihlmayer, M. Schilling, *Chem. Ber.* **1983**, *116*, 3182–3191.

1-Alkyl-2,5-(*ortho*-phenylene)-1-carbapentaborane(10)**

Bernd Gangnus, Harald Stock, Walter Siebert,* Matthias Hofmann, and Paul von Ragué Schleyer*

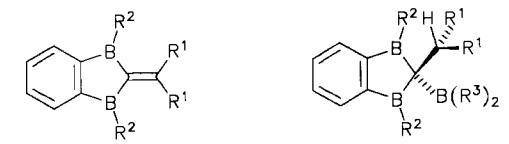
Dedicated to Professor Egon Uhlig on the occasion of his 65th birthday

We recently reported on the synthesis of 2,3,5-tricarba-*nido*-hexaboranes by double hydroboration of 1,4-dibora-1,4-dihydropentafulvenes and 4,5-bis(isopropylidene)-1,3-diborolanes with diethylborane under elimination of triethylborane.[1, 2] The analogous reaction of the benzoannelated pentafulvenes **1a** with $HBCl_2 \cdot Et_2O$ and that of **1b**[3] with $(Et_2BH)_2$ leads only to **2a** and **2b**, respectively, since the C=C bond of the benzene ring between the boron atoms in **2a,b** is not hydroborated. Cl/H exchange in **2a** by using LiH or by reaction of **1c**[4] with $BH_3 \cdot THF$ should lead to the formation of **2c** as an intermediate, which we expected to rearrange to the *nido*-carborane **3a**. We report here on the unexpected formation of the 1-carbapentaboranes **4**.

The reaction of **2a** with LiH does not afford a defined product;[4] however, **1a,d** surprisingly react with excess $LiBH_4$ to give deprotonated **4a,b**, whose protonation with $HBF_4 \cdot Et_2O$ yielded the carboranes **4a,b**. According to the results of GC-MS, **4** is formed in more than 80% yield; the isolated yield of

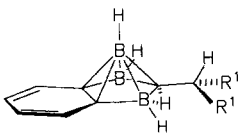
[*] Prof. Dr. W. Siebert, Dr. B. Gangnus, Dipl.-Chem. H. Stock
Anorganisch-chemisches Institut der Universität
Im Neuenheimer Feld 270, D-69120 Heidelberg (FRG)
Telefax: Int. code + (6221)56-4197
Prof. Dr. P. von R. Schleyer, Dipl.-Chem. M. Hofmann
Computer-Chemie-Centrum des Instituts I für Organische Chemie
der Universität Erlangen-Nürnberg
Nägelsbachstrasse 25, D-91052 Erlangen (FRG)
Telefax: Int. code + (9131)85-9132

[**] This work was supported by the Deutsche Forschungsgemeinschaft (SFB 247) and the Fonds der Chemischen Industrie.

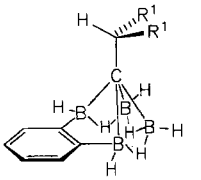


1	a	b	c	d	e
R^1	Me	Me	Me	$(CH_2)_2$	$(CH_2)_2$
R^2	Cl	Me	H	Cl	H

2	a	b	c	d
R^1	Me	Me	Me	$(CH_2)_2$
R^2	Cl	Me	H	H
R^3	Cl	Et	H	H



3	a	b
R^1	Me	$(CH_2)_2$



4	a	b
R^1	Me	$(CH_2)_2$

sublimed **4a** is 36%. The constitution of **4a** is deduced from the spectroscopic data, and it is supported by the results of combined ab initio/IGLO/NMR calculations.[5] The broad ^{13}C NMR signal of the apical C atom at $\delta = 12$ is characteristic; likewise the *ipso*-carbon atoms of the benzene ring give a broad signal, whose chemical shift (**4a,b**: $\delta = 145$, 147) rules out that these atoms take part in the framework of the cluster.

Two doublets with different coupling constants occur in the ^{11}B NMR spectrum of **4a**. The couplings with the bridging hydrogen atoms are not resolved. Two signals were also observed for the deprotonated 1-carbapentaborane, which was obtained by treatment of **4a** with NaH or BuLi. Noteworthy is the low-field shift of a signal by about 5 ppm ($-5.7 \rightarrow -0.5$). The ^1H NMR spectrum of **4a** shows an AA'BB' pattern in the aromatic region as well as a septet and a doublet for the isopropyl group. In the $^1H\{^{11}B\}$ NMR spectrum, four signals appear for hydrogen atoms attached to boron. The two low-field signals were assigned to terminal hydrogen atoms, the other two signals to bridging hydrogen atoms. The IR spectrum showed three broad bands in the region of terminal BH stretching frequencies (see Experimental Procedure).

The parent compound of **4**, 1-carba-*arachno*-pentaborane(10) CB_4H_{10}, was described as unstable and could not be fully characterized.[6] The formation of a CB_4 carborane was assumed in the mixture of reaction products from $Li/Et_2O \cdot BF_3/Et_3B$ in THF;[7] two 1-carba-*arachno*-pentaboranes(10) could be obtained in 61% yield by the reaction of $Me_2Si(C{\equiv}CMe)_2$ with $[Et_2BH]_2$.[8] Their spectroscopic data are in agreement with those for **4a**,**b**.

Table 1. Calculated and experimental chemical shifts for carbapentaboranes(10).

Bridge between B2 and B5	R at C1	$\delta(^{13}C1)$	$\delta(^{11}B2,5)$	$\delta(^{11}B3,4)$	Method
H^+	H	−15.9	−11.2	−11.2	IGLO(DZ)
H, H	H	−15.9	+21.3	+10.6	IGLO(DZ)
ethylene	H	−15.4	+9.1	−8.3	IGLO(DZ)
		−18.5	+12.9	−4.9	GIAO-SCF/tzpdz
		−10.1	+12.3	−8.1	GIAO-MP2/tzpdz
ethylene	Me	−13.5	+11.8	−6.8	IGLO(DZ)
ortho-phenylene	H	−9.3	+9.2	−7.9	IGLO(DZ)
ortho-phenylene	*i*Pr	+14.2	+14.2	−7.2	IGLO(DZ)/ BLYP/6-31G* [a]
ortho-phenylene	*i*Pr	+12	+10.0	−5.7	experiment [a]
ortho-phenylene	cyclopentyl	+14	+9.7	−5.1	experiment [b]

[a] Compound **4a**. [b] Compound **4b**.

The calculated chemical shifts for derivatives of carbapentaborane(10) are given in Table 1. In addition to IGLO(DZ)[9] calculations, GIAO/tzpdz calculations at SCF and MP2 level[5b,10] can also be performed on the simplest model for the title compounds (ethylene bridge and hydrogen as substituent at C1). In all cases the calculated $\delta^{11}B$ values are in good agreement with those obtained experimentally. In contrast, the calculations on the simpler model compounds for the apical C1 atom each yield a high-field shift. Only calculations on **4a** itself can reproduce the unusual NMR signal of the apical C atom satisfactorily, and thus support the structure shown in Figure 1.

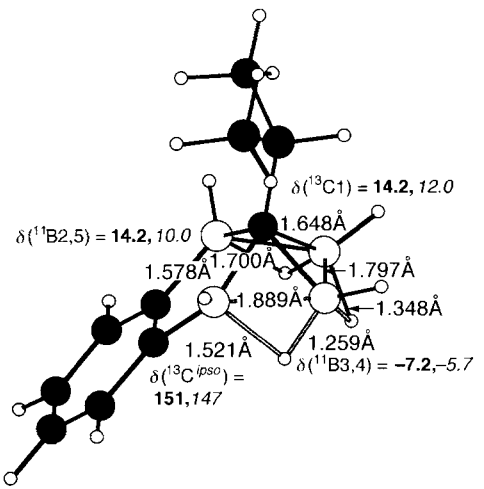


Fig. 1. The geometry (C_s) of **4a** optimized by BLYP/6-341G* calculations as well as its chemical shifts (printed in boldface) calculated with IGLO(DZ), and the measured data (printed in italics).

1-Carbapentaboranes **4** therefore show the peculiarity that the C atom occupies the most highly coordinated position in the *arachno* cluster.

Experimental Procedure

4a: THF (20 mL) was added to a suspension of **1a** (1.36 g, 6.1 mmol) [3] in pentane (10 mL) at −78 °C, the resulting suspension of **1a**·2THF was added in portions over a 30 min period to a solution of $LiBH_4$ (0.53 g, 24.3 mmol) in THF (20 mL) at −78 °C. Subsequently the mixture was stirred at 20 °C for 2 h, and then $HBF_4 \cdot Et_2O$ (1.98 g, 12.2 mmol) was added dropwise at −40 °C. After the evolution of H_2 had finished, the mixture was heated to 20 °C and the solvents were removed at 1 Torr. The oily yellow residue was treated with hexane (50 mL), filtered, and after removal of the solvent at 1 Torr, the residue was sublimed at 40 °C/10^{-3} Torr. Yield: 0.4 g (36%), m.p. 47 °C. ^1H NMR (200 MHz, $CDCl_3$): $\delta = -0.7$ (br, s, 1H), 0.98 (d, 6H, $^3J(H,H) = 6.9$ Hz), 1.97 (sept, 1H, $^3J(H,H) = 6.9$ Hz), 2.1 (br, s, 2H), 3.3 (br, q, 2H, $^1J(B,H) = 106$ Hz), 4.1 (br, q, 2H, $^1J(B,H) = 145$ Hz), 7.30 (m, 2H), 7.53 (m, 2H). ^{11}B NMR (64.2 MHz, $CDCl_3$): $\delta = -5.7$ (d, 2B, $^1J(B,H) = 145$ Hz), 10.0 (d, 2B, $^1J(B,H) = 106$ Hz). ^{13}C NMR (50.3 MHz, $CDCl_3$, 240 K): $\delta = 12$ (C1), 24.5 (CH_3), 30.9 (CH), 129.6 (C_{ar}), 131.5 (C_{ar}), 147 (*ipso*-C). IR (hexane): $\tilde{\nu}_{BH}$ [cm^{-1}] = 2502 s, 2576 m, 2594 m. EI MS: *m/z* (%): 182 (M^+, 88), 181 ($M^+ - H$, 100), 165 ($M^+ - CH_3 - 2H$, 10), 137 ($M^+ - C_3H_7 - 2H$, 33), 125 ($C_nH_4CB_3H_4^+$, 57).

4b: The synthesis was achieved analogously to that for **4a**, starting from **1d** [4], yield 45%, b.p. 55 °C/10^{-2} Torr. ^{11}B NMR ($CDCl_3$): $\delta = 9.7$ (d, 2B, $^1J(B,H) = 112$ Hz), −5.1 (d, 2B, $^1J(B,H) = 136$ Hz). ^{13}C NMR ($CDCl_3$): $\delta = 14$ (C1), 28.7 (CH_2), 37.0 (CH_2), 44.0 (CH), 129.2 (C_{ar}), 131.2 (C_{ar}), 147 (*ipso*-C).

Deprotonated **4a**: To a solution of **4a** (0.36 g, 2 mmol) in THF (15 mL) at −78 °C, was added a suspension of NaH (48 mg, 2 mmol) in THF (10 mL), or *n*BuLi (0.8 mL of a 2.5 M solution in *n*-hexane) was added by syringe. The mixture was stirred at −78 °C for 2 h, subsequently warmed to 20 °C, and the solvent was removed under vacuum. The resulting anion shows the following signals in the ^{11}B NMR spectrum ([D_8]THF): $\delta = 9.9$ (s, 2B), −0.5 (s, 2B).

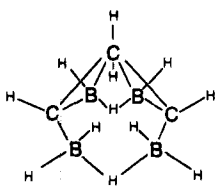
Received: May 19, 1994 [Z 69471E]
German version: *Angew. Chem.* **1994**, *106*, 2383

[1] A. Fessenbecker, A. Hergel, R. Hettrich, V. Schäfer, W. Siebert, *Chem. Ber.* **1993**, *126*, 2205–2210.
[2] W. Siebert, R. Hettrich, H. Pritzkow, *Angew. Chem.* **1994**, *106*, 215–216; *Angew. Chem. Int. Ed. Engl.* **1994**, *33*, 203–204.
[3] A. Fessenbecker, H. Schulz, H. Pritzkow, W. Siebert, *Chem. Ber.* **1990**, *123*, 2273–2278.
[4] B. Gangnus, Dissertation, Universität Heidelberg, **1993**.
[5] a) M. Bühl, P. von R. Schleyer, *J. Am. Chem. Soc.* **1992**, *114*, 477–491; b) M. Bühl, J. Gauss, M. Hofmann, P. von R. Schleyer, *ibid.* **1993**, *115*, 12385–12390.
[6] D. S. Matteson, P. K. Mattschei, *Inorg. Chem.* **1973**, *12*, 2472–2475.
[7] R. Köster, G. Benedikt, M. A. Grassberger, *Justus Liebigs Ann. Chem.* **1968**, *719*, 187–209; see there especially p. 196.
[8] R. Köster, G. Seidel, B. Wrackmeyer, *Angew. Chem.* **1994**, *106*, 2380; *Angew. Chem. Int. Ed. Engl.* **1994**, *33*, 2294; see also M. A. Fox, R. Greatrex, M. Hofmann, P. von R. Schleyer, *ibid.* **1994**, *106*, 2384 and **1994**, *33*, 2298.
[9] For the IGLO method see W. Kutzelnigg, M. Schindler, U. Fleischer, *NMR: Basic Princ. Prog.* **1990**, *23*, 165. DZ stands for Huzinaga basis sets of double zeta quality: S. Huzinaga, *Approximate Atomic Wavefunctions*, University of Alberta, Edmonton, **1971**.
[10] a) J. Gauss, *Chem. Phys. Lett.* **1992**, *191*, 614; b) *J. Chem. Phys.* **1993**, *99*, 3629-3643. The GIAO-MP2 procedure was implemented in ACESII. ACESII, An Ab initio program system: J. F. Stanton, J. Gauss, J. D. Watts, W. J. Lauderdale, R. J. Bartlett, *Quantum Theory Project*, University of Florida, **1991**.

The Structures of Alkyl Derivatives of *arachno*-1-CB_4H_{10} from Reactions of B_4H_{10} with Alkynes**

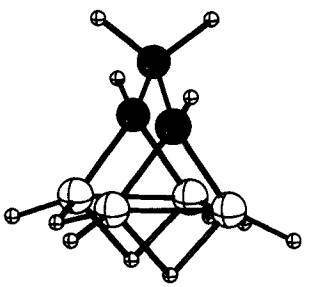
Mark A. Fox, Robert Greatrex,* Matthias Hofmann, and Paul von Ragué Schleyer*

This work was inspired by early investigations of Grimes et al. in the late 1960s,[1] in which derivatives of the *nido* carboranes CB_5H_9, $C_2B_4H_8$, and $C_3B_3H_7$ were synthesized by the reaction of B_4H_{10} with alkynes at temperatures in the range 25–50 °C. The formation of compounds such as 2,3- and 2,4-Me_2-2,3,4-$C_3B_3H_5$ and 4-Me-2-CB_5H_8 from the reaction of B_4H_{10} with HC≡CH was particularly noteworthy because it indicated that C–C bond cleavage was taking place under very mild conditions and in the absence of metal catalysts. As the mechanisms of these reactions are still not understood, we have been searching for intermediates that might lead to new insights. The "hot–cold" reaction of MeC≡CH with B_4H_{10}, which yielded an unstable species with the composition $C_3B_4H_{12}$ but with an unknown structure, exemplifies the complexities of such chemistry.[2]



1

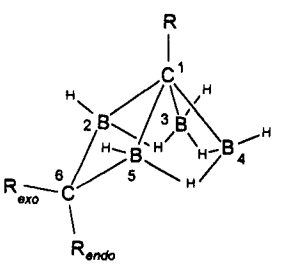
On the basis of NMR data and the relationship to the *closo*-$[B_{10}H_{10}]^{2-}$ structure, the $C_3B_4H_{12}$ product had been assigned the tricarba-*hypho*-heptaborane structure **1** with an intact (albeit H-rearranged) C_3H_4 moiety.[2] However, this proposal was not supported by subsequent ab initio computations. Optimization of starting geometries corresponding to **1** led to the quadruply bridged form of $CH_2(CH(BH_2)_2)_2$ **2** (Fig. 1), but this was excluded from consideration by both the high symmetry (C_{2v}) and the computed (IGLO) NMR chemical shifts.



2

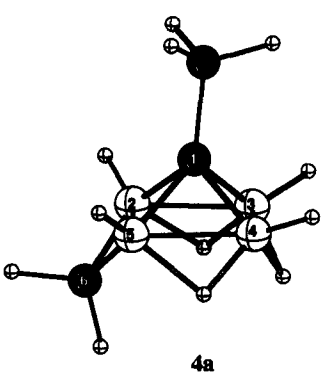
Fig. 1. Calculated structure of **2**. Selected distances [Å]: C-C 1.522, B-C 1.567, B-B with C bridge 1.830, B-B without C bridge 2.274.

We studied the gas-phase reaction at 70 °C of B_4H_{10} with the alkynes HC≡CH, MeC≡CH, EtC≡CH, and MeC≡CMe, and found that analogous compounds were formed in all except the first of these four systems. The unstable compound with a molecular ion at *m/z* 106 from the B_4H_{10}/EtC≡CH reaction gave a ^1H NMR spectrum which was similar to that of $C_3B_4H_{12}$,[2,3] except that an ethyl group was clearly indicated in the former. The evidence suggested strongly that this compound was *arachno*-$EtC_2B_4H_9$ and that $C_3B_4H_{12}$ was in fact the methyl analogue, despite the fact that no peak of relative intensity 3 had been observed in the $^1H\{^{11}B\}$ spectrum of the latter. We examined structures of *arachno*-$MeC_2B_4H_9$ with intact CH_3CCH_2 moieties generated by ab initio calculations, but these did not fit the experimental NMR data of $C_3B_4H_{12}$. We then considered structural alternatives with separated CH_3C and CH_2 units, in other words those which might have been formed by Grimes's C≡C bond cleavage reactions. The first trials employing the combined ab initio/IGLO/NMR method,[4] which we have found to give very good agreement with experimental data on known carboranes,[5] yielded highly gratifying results with the parent (but experimentally unknown) *arachno* $C_2B_4H_{10}$ system **3**. The



	R	R_{endo}	R_{exo}
3	H	H	H
4a	Me	H	H
4b	H	Me	H
5a	Et	H	H
5b	H	H	Et
6a	Me	Me	H
6b	Me	H	Me

MP2(fc)/6-31G* optimized structure of the $C_3B_4H_{12}$ candidate **4a** with a methyl group at the apical carbon (Fig. 2) gave com-



4a

Fig. 2. Calculated structure of *arachno*-carborane **4a**. Selected distances [Å] and angles [°]: B2-B3 1.849, B3-B4 1.812, B2-B5 2.052, B2-C1 1.680, B2-C6 1.588, B2-H (bridge to B3) 1.453, B3-H (bridge to B2) 1.266; C1-B2-C6 101.7, B2-C1-B3 68.9, B2-C1-B5 75.3, B2-C6-B5 80.5, B3-C1-B4 69.6.

[*] Dr. R. Greatrex, Dr. M. A. Fox
School of Chemistry, University of Leeds
Leeds LS2 9JT (UK)
Telefax: Int. code +(532) 336-565
Prof. Dr. P. von R. Schleyer, Dipl.-Chem. M. Hofmann
Computer-Chemie-Centrum des Instituts I für Organische Chemie
der Universität Erlangen-Nürnberg
Nägelsbachstrasse 25, D-91052 Erlangen (FRG)
Telefax: Int. code +(9131) 859132

[**] This work was supported by the Science and Engineering Research Council (Grant GR/H03667), the Deutsche Forschungsgemeinschaft, the Fonds der Chemischen Industrie, the Royal Society, and Borax Consolidated Ltd.

puted chemical shifts in remarkably good agreement with the experimental NMR data (Table 1). The MP2(fc)/6-31G* energy of **4a** is 150.6 kJ mol^{-1} lower than that of **2**. These data establish the structure as **4a** securely. This compound is the smallest known *arachno* carborane and the first carborane derivative related to *arachno*-B_5H_{11}.

Table 1. Experimental [a] and IGLO(DZ)-calculated [b] ^{11}B, ^{13}C, and ^1H NMR chemical shifts for *arachno*-2,5-μ-CH_2-1-CB_4H_8 derivatives [8].

	C(1)	B(2,5)	B(3,4)	C(6)
3	−/−22.8	−/−1.7	−/−18.5	−/−22.5
4a [c]	[d]/−21.0	+1.6/+0.5	− 20.1/−17.9	− 24.5/−21.0
4b [e]	−/−21.7	−/+2.9	− 21.8/−18.6	−/−22.1
5a [f]	−/−11.1	+0.3/−0.7	− 20.6/−19.9	−/−17.1
5b [g]	−/−18.8	−/−1.0	− 22.7/−18.2	−/−13.3
6a	−/−14.6	+4.3/+2.5	− 20.4/−18.1	−/−16.3
6b	−/−17.0	+2.8/+1.3	−19.7/−17.8	−/−17.0

[a] $T \approx 230$ K; standards $BF_3 \cdot OEt_2$ and TMS. [b] Standards $BF_3 \cdot OEt_2$ with primary reference B_2H_6 ($\delta = 18.2$) and TMS. [c] δ (^1H) for **4a** (exp./calcd.): H_t(2,5) 3.25/4.41, H_t(3,4) 2.33/3.51, H_μ(2,3 and 4,5) 0.68/−0.9, CH_3 1.61/0.71, CH_{exo} −0.91/−0.72, CH_{endo} −1.40/−1.78. [d] Resonance predicted to be coincident with that from C(6), but probably too broad to be observed. [e] Calculated shifts for *exo* form: δ (^{11}B) = − 2.7 (B(2/5)), −20.0 (B(3/4)); δ (^{13}C) = 20.0 (CH_3), −9.1 (C1), −18.7 ($CHCH_3$). [f] Methyl fragment of ethyl group *anti* to methylene bridge. Calculated shifts for *syn* isomer: −1.9 (B(2,5)), −15.3 (B(3,4)). [g] Ethyl group *exo* to cluster, and methyl fragment of ethyl group *anti* to CH vector.

The structures of the compounds from the B_4H_{10}/EtC≡CH and B_4H_{10}/MeC≡CMe reactions (**5a** and **6a**, respectively) were also established by the ab initio/IGLO/NMR method, and similar calculations were carried out for the three isomers (**4b**, **5b**, and **6b**) whose presence in minor amount was indicated in the NMR spectra of the derivatives **4a**, **5a**, and **6a**, respectively. The ratio of the two isomers (**a**:**b**) was found to be 6:1 for **4**, 30:1 for **5**, and 4:1 for **6**. Geometries were optimized at the MP2(fc)/6-31G* level,[6] and chemical shifts were computed with the IGLO method.[7] Relative MP2(fc)/6-31G* energies were corrected for zero vibrational energies at HF/6-31G* scaled by 0.89. These computational results helped to confirm the various products as 1-Me-carborane **4a**, *endo*-Me-carborane **4b**, 1-Et-carborane **5a**, *exo*-Et-carborane **5b**, 1-Me-*endo*-Me-carborane **6a**, and 1-Me-*exo*-Me-carborane **6b**. Consistent with experimental findings, **4a** was computed to be 8.0 kJ mol^{-1} lower in energy than isomer **4b**, which in turn was 2.9 kJ mol^{-1} more stable than the unobserved *exo* isomer (R_{exo} = Me). For **5a**, the two conformations of the ethyl group had nearly the same energy and both gave acceptable agreement with the experimental data. **6b** was found to be 1.6 kJ mol^{-1} higher in energy than **6a**. **5b** is likely to be the *exo* ethyl isomer of **5a**. Various conformers with an *endo* ethyl group were found to have an energy higher by about 5 kJ mol^{-1} and the computed B(3,4) chemical shifts showed poorer agreement with the experimental value. The B(2,5) resonance was obscured by peaks from the major isomer **5a**.[8]

Structures related to **3**–**6** were first proposed by Köster et al. in 1968 for products derived from dehalogenation reactions[9] and for derivatives of the unknown phosphorus-bridged parent borane 2,5-μ-$(PH_2)B_5H_8$,[10] which is isoelectronic with *arachno*-2,5-μ-CH_2-1-CB_4H_8. Very recently, Wrackmeyer et al. have prepared polysubstituted derivatives akin to **3**–**6** and Köster's proposals by reactions of dialkylboranes with dialkynylsilanes.[11] Siebert et al. describe an analogous system with an *ortho*-phenylene bridge instead of the $CHR_{exo/endo}$ moieties in **3**–**6**.[12]

It is now well established that B_4H_{10} decomposes at room temperature and above, initially to form the nonisolable intermediate $\{B_4H_8\}$ and dihydrogen.[13] In the formation of the *arachno* $C_2B_4H_{10}$ derivatives it appears that $\{B_4H_8\}$ fuses with the alkyne, cleaves the C–C triple bond, and transfers one of its hydrogen atoms to the carbon atom of the bridging methylene group. The result is an intriguing snapshot of the cleavage of a C–C triple bond by a borane.

Experimental Procedure

In a typical reaction, a mixture of 0.67 mmol of B_4H_{10} and 0.67 mmol of MeC≡CH was heated in a reaction vessel (1 L) at 70 °C. The reaction was monitored by bleeding the mixture continuously into a Kratos MS30 mass spectrometer coupled to an MSS data system. When the alkyne had disappeared (after ca. 0.4 h) the reaction was quenched by pumping the mixture into a U-trap surrounded by liquid nitrogen. This process was repeated twenty times, and the combined products were then separated on a high-vacuum low-temperature fractionation column [14]. The species leaving the column were monitored by mass spectrometry, and the desired product (in this case **4a**) was collected. A small amount of 2-Me-2,3-$C_2B_4H_7$, identified by its NMR spectra [15], was always present as a minor impurity [3] and could not be removed by repeated fractionation of **4a**. The analogous procedure with EtC≡CH and MeC≡CMe in place of MeC≡CH gave **5a** and **6a**, respectively; the compounds 2-Et-2,3-$C_2B_4H_7$ and 2,3-Me_2-2,3-$C_2B_4H_6$ [16], respectively, were present as minor impurities. NMR spectra were recorded at ca. 230 K. Experimental chemical shifts are given for the minor isomers only for peaks which are well resolved from those of the major isomer.

4a: Approximate yield: 2%; EI-MS: m/z (%) = 92 (M^+, 73), 76 ($M^+ - CH_4$, 79), 63 ($M^+ - C_2H_5$, 100); ^{11}B NMR (128 MHz, $CDCl_3$): δ = 1.6 (d, 2B, J(B,H_t) = 145 Hz; B2), −20.1 (ddd, 2B, J(B,H_t) = 165, J(B,H_μ(2,3/4,5)) = 63, J(B,H_μ(3,4)) = 37 Hz; B(3,4)); $^{13}C\{^1H\}$ NMR (100 MHz, $CDCl_3$): δ = 18.0 (CH_3), −24.5 (CH_2); $^1H\{^{11}B\}$ NMR (400 MHz, $CDCl_3$): δ = 3.25 (br.s, 2H; B(2,5)H), 2.23 (br.s, 2H; B(3,4)H), 1.61 (s, 3H; CH_3), 0.68 (br.s, 2H; H_μ(2,3/4,5)), −0.91 (m, 1H, ^2J(H,H) = 16, J(H,H) = 4; CH_{exo}), −1.40 (m, 1H, ^2J(H,H) = 16, J(H,H) = 6 Hz; CH_{endo}), −2.16 (br.s, 1H; H_μ(3,4)).

4b: ^{11}B NMR: δ = − 21.8 (ddd, J(B,H_t) = 169, J(B,H_μ(2,3)) = 64, J(B,H_μ(3,4)) = 37 Hz; B(3/4)); $^1H\{^{11}B\}$ NMR: δ = 0.68 (d, 3H, ^3J(H,H) = 8 Hz; *endo*-CH_3), −0.27 (br.s, 2H; H_μ(2,3/4,5)), −0.80 (m, 1H; CH_{exo}).

5a: Approximate yield: 1.5%; EI-MS: m/z (%) = 106 (M^+, 97), 77 ($M^+ - C_2H_5$, 84), 63 ($M^+ - C_3H_7$, 100); ^{11}B NMR: δ = 0.3 (d, 2B, J(B,H_t) = 149 Hz; B(2/5)), −20.6 (ddd, 2B, J(B,H_t) = 165, J(B,H_μ(2,3/4,5)) = 64, J(B,H_μ(3,4)) = 37 Hz; B(3/4)); $^1H\{^{11}B\}$ NMR: δ = 3.27 (br.s, 2H; B(2/5)H), 2.24 (br.s, 2H; B(3/4)H), 1.95 (q, 2H, ^3J(H,H) = 7 Hz; CH_2CH_3), 0.97 (t, 3H, ^3J(H,H) = 7 Hz; CH_2CH_3), 0.54 (br.s, 2H; H_μ(2,3/4,5)), −0.95 (m, 1H, ^2J(H,H) = 16, J(H,H) = 4 Hz; CH_{exo}), −1.41 (m, 1H, ^2J(H,H) = 16, J(H,H) = 6 Hz; CH_{endo}), −2.27 (br.s, 1H; H_μ(3,4)).

5b: ^{11}B NMR: δ = − 22.7 (ddd, 2B, J(B,H_t) = 169, J(B,H_μ(2,3/4,5)) = 64, J(B,H_μ(3,4)) = 37 Hz; B(3/4)).

6a: Approximate yield: 4%; EI-MS: m/z (%) = 106 (M^+, 96), 91 ($M^+ - CH_3$, 49), 77 ($M^+ - C_2H_5$, 89), 63 ($M^+ - C_3H_7$, 100); ^{11}B NMR: δ = 4.3 (d, 2B, J(B,H_t) = 145 Hz; B(2/5)), −20.4 (ddd, 2B, J(B,H_t) = 169, J(B,H_μ(2,3/4,5)) = 61, J(B,H_μ(3,4)) = 37 Hz; B(3/4)); $^1H\{^{11}B\}$ NMR: δ = 3.26 (br.s, 2H; B(2,5)H), 2.24 (br.s, 2H; B(3,4)H), 1.60 (s, 3H; C(1)CH_3), 0.63 (d, 3H, ^3J(H,H) = 6 Hz; *endo*-CH_3), 0.05 (br.s, 2H; H_μ(2,3/4,5)), −0.58 (br.m, 1H; CH_{exo}), −2.21 (br.s, 1H; H_μ(3,4)).

6b: ^{11}B NMR: δ = 2.8 (d, 2B, J(B,H_t) = 141 Hz; B(2/5)), −19.7 (ddd, 2B, J(B,H_t) ≈ 173, J(B,H_μ(2,3/4,5)) ≈ 64, J(B,H_μ(3,4)) = 37 Hz; B(3/4)); $^1H\{^{11}B\}$ NMR: δ = 3.03 (br.s, 2H; B(2,5)H), 2.17 (br.s, 2H; B(3,4)H), 1.66 (s, 3H; C(1)CH_3), 0.95 (d, 3H, ^3J(H,H) = 6 Hz, *exo*-CH_3), 0.78 (br.s, 2H; H_μ(2,3/4,5)), −1.10 (br.m, 1H; CH_{endo}), −2.13 (br.s, 1H; H_μ(3,4)).

2-Et-2,3-$C_2B_4H_7$: ^{11}B NMR: δ = − 0.48 (m, 1B, J(B,H_t) = 160 Hz, B(5)), −2.71 (dd, 1B, J(B,H_t) = 157, J(B,H_μ) = 46 Hz; B(4)), −3.48 (dd, 1B, J(B,H_t) = 155, J(B,H_μ) = 49 Hz; B(6)), −50.43 (m, 1B, J(B,H_t) = 182 Hz; B(1)); $^1H\{^{11}B\}$ NMR: δ = 6.12 (br.s, 1H; C(3)H), 3.51 (br.s, 1H; B(5)H), 3.33 (br.s, 1H; B(4)H), 3.27 (br.s, 1H; B(6)H), 2.47 (q, 2H, ^3J(H,H) = 7 Hz; CH_2), 1.16 (t, 3H, ^3J(H,H) = 7 Hz; CH_3), −0.99 (br.s, 1H; B(1)H), −2.15 (br.s, 1H; H_μ(5,6)), −2.18 (br.s, 1H; H_μ(4,5)).

Received: June 21, 1994 [Z 7055 IE]
German version: *Angew. Chem.* **1994**, *106*, 2384

[1] C. L. Bramlett, R. N. Grimes, *J. Am. Chem. Soc.* **1966**, *88*, 4269–4270; R. N. Grimes, C. L. Bramlett, *ibid.* **1967**, *89*, 2557—2560; R. N. Grimes, C. L. Bramlett, R. L. Vance, *Inorg. Chem.* **1968**, *7*, 1066–1070; D. A. Franz, J. W. Howard, R. N. Grimes, *J. Am. Chem. Soc.* **1969**, *91*, 4010–4011; D. A. Franz, R. N. Grimes, *ibid.* **1971**, *93*, 387–394.

[2] a) R. Greatrex, N. N. Greenwood, M. Kirk, *J. Chem. Soc. Chem. Commun.* **1991**, 1510–1511; b) M. A. Fox, R. Greatrex, N. N. Greenwood, M. Kirk, *Polyhedron* **1993**, *12*, 1849–1853.

 © VCH Verlagsgesellschaft mbH, D-69451 Weinheim, 1994 0570-0833/94/2222-2299 $ 10.00+.25/0

[3] Corrections to ref. [2b]: ^{1}H NMR: $\delta = 2.33$ should read 2.23, 1.61 (s, 3H; CH(e)$_3$, (the signal for the methyl group in **4a** was earlier mistakenly attributed to two CH groups, because the relative integrated intensity of the signal in the ^{1}H{^{11}B} spectrum was consistently observed to be 2 rather than 3)), −2.16 (s, 1H; BH(i)B); ^{13}C NMR: $\delta = 18.0$ (C(1)H$_3$). H(j) in ref. [2b] is from the impurity 2-Me-2,3-$C_2B_4H_7$.
[4] T. Onak, D. Tran, J. Tseng, M. Diaz, J. Arias, S. Herrera, *J. Am. Chem. Soc.* **1993**, *115*, 9210–9215, and references therein.
[5] M. Bühl, P. von R. Schleyer, *J. Am. Chem. Soc.* **1992**, *114*, 477–491; P. von R. Schleyer, J. Gauss, M. Bühl, R. Greatrex, M. A. Fox, *J. Chem. Soc. Chem. Commun.* **1993**, 1766–1768.
[6] GAUSSIAN 92: M. J. Frisch, G. W. Trucks, M. Head-Gordon, P. M. W. Gill, M. W. Wong, J. B. Foresman, B. G. Johnson, H. B. Schlegel, M. A. Robb, E. S. Replogle, R. Gomez, L. Andres, K. Raghavachari, J. S. Binkley, C. Gonzalez, R. L. Martin, D. J. Defrees, J. Baker, J. J. P. Stewart, J. A. Pople, Gaussian 92, Gaussian Inc., Pittsburgh, PA, USA, **1992**.
[7] IGLO: W. Kutzelnigg, *Isr. J. Chem.* **1980**, *19*, 193–200; W. Kutzelnigg, *J. Chem. Phys.* **1982**, *76*, 1919–1933; W. Kutzelnigg, M. Schindler, U. Fleischer, *NMR: Basic Princ. Prog.* **1990**, *23*, 165.
[8] The numbering system used is that recommended for *arachno*-B_5H_{11} by IUPAC in *Nomenclature of Inorganic Chemistry, Recommendations 1990* (Ed.: G. J. Leigh) Blackwell, Oxford, **1990**, p. 220.
[9] R. Köster, G. Benedikt, M. A. Grassberger, *Justus Liebigs Ann. Chem.* **1968**, *719*, 187–209.
[10] A. B. Burg, H. Heinen, *Inorg. Chem.* **1968**, *7*, 1021–1025; I. B. Mishra, A. B. Burg, *ibid.* **1972**, *11*, 664–666; D. E. Coons, D. F. Gaines, *ibid.* **1987**, *26*, 1985–1988; R. W. Miller, K. J. Donaghy, J. T. Spencer, *Organometallics* **1991**, *10*, 1161–1172.
[11] R. Köster, G. Seidel, B. Wrackmeyer, *Angew. Chem.* **1994**, *106*, 2380; *Angew. Chem. Int. Ed. Engl.* **1994**, *33*, 2294.
[12] B. Gangnus, H. Stock, W. Siebert, M. Hofmann, P. von R. Schleyer, *Angew. Chem.* **1994**, *106*, 2383; *Angew. Chem. Int. Ed. Engl.* **1994**, *33*, 2296.
[13] N. N. Greenwood, R. Greatrex, *Pure Appl. Chem.* **1987**, *59*, 857–868, and references therein.
[14] J. Dobson, R. Schaeffer, *Inorg. Chem.* **1970**, *9*, 2183; D. F. Shriver, M. A. Drezdzon, *The Manipulation of Air-sensitive Compounds*, 2nd ed., Wiley-Interscience, New York, **1986**, p. 193.
[15] T. Onak, R. P. Drake, G. B. Dunks, *Inorg. Chem.* **1964**, *3*, 1686–1690.
[16] T. Onak, F. J. Gerhart, R. E. Williams, *J. Am. Chem. Soc.* **1963**, *85*, 3378–3380.

Intramolecular [2 + 2] Cycloadditions of 2,2′-Bis(1-arylvinyl)-Substituted Biphenyls Induced by Photo Electron Transfer**

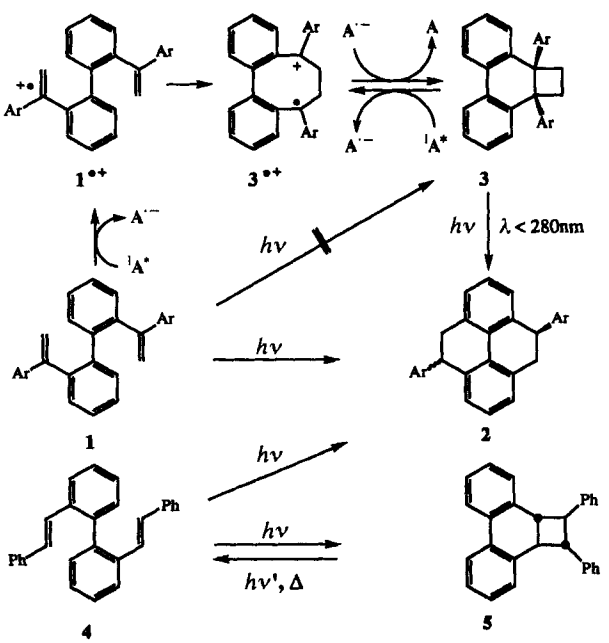
Oliver Sadlek, Klaus Gollnick, Kurt Polborn, and Axel G. Griesbeck*

The *intermolecular* [2 + 2] cyclodimerization of 1,1-diphenylethylene under photo electron transfer (PET) conditions[1] has already been studied in detail.[2] In the absence of oxygen it affords, after electron transfer to the electronically excited acceptor (mainly 9,10-anthracenedicarbonitrile **A**), a 1,2-radical cation that, after formation of the 1,1,4,4-tetraphenyl-substituted 1,4-radical cation and back electron transfer, reacts further to 1,1,2,2-tetraphenylcyclobutane and other products. The intermediate 1,4-radical cations are trapped by oxygen in a radical chain reaction to form 1,2-dioxanes in high yield.[3] We report here on corresponding *intramolecular* reactions.

[*] Prof. Dr. A. G. Griesbeck[+]
Institut für Organische Chemie der Universität
Am Hubland, D-97074 Würzburg (FRG)
Dipl.-Chem. O. Sadlek, Prof. Dr. K. Gollnick,[++] Dr. K. Polborn[+++]
Institut für Organische Chemie der Universität München
[+] New address: Institut für Organische Chemie der Universität
Greinstrasse 4, D-50939 Köln (FRG)
Telefax: Int. code + (221)470-5102
[++] Deceased 27.10.1993
[+++] Crystal structure analysis
[**] This work was supported by the Deutsche Forschungsgemeinschaft.

In order to use a substrate comparable to that studied in the intermolecular reaction, we chose the 2,2-bis(1-arylvinyl)-substituted biphenyls **1**.[4] They are particularly interesting, because their first excited singlet states react further to form the tetrahydropyrenes **2**; that is, they follow an independent reaction pathway. According to Padwa et al.,[5] no trace of the potentially photolabile [2 + 2] cyclization product **3a** can be observed even after short irradiation of **1a** (for direct excitation, $\lambda = 360$ nm). This is remarkable, because the direct irradiation of the positional isomer 2,2′-distyrylbiphenyl **4** primarily affords a strained, *trans*-fused cyclobutaphenanthrene (**5**), which on further irradiation (at shorter wavelengths of $\lambda = 300$ nm, or on thermolysis) reacts irreversibly to form the pyrene derivative **2a**. It is thus in a photochemically induced equilibrium with the starting material.[6] As a stilbene derivative, **4** behaves "reasonably", but in the long run the high ring strain of **5** takes its toll.

To achieve an intramolecular [2 + 2] cycloaddition with the coupled 1,1-diarylethylenes **1a–c** as well, the irradiation (excitation wavelength $\lambda_{exc} > 375$ nm) of **1** in acetonitrile (5×10^{-2} M) was performed in the presence of **A** (2×10^{-4} M). In all these cases, over 95% of the *cis*-1,2,2*a*,10*b*-tetrahydro-2*a*,10*b*-diarylcyclobuta[*l*]phenanthrene **3a–c** was formed (Scheme 1). These



Scheme 1. Photochemical transformation of 2,2′-bis(arylvinyl)-substituted biphenylene. **a**: Ar = Ph, **b**: Ar = *p*-MrPh, **c**: Ar = *p*-MeOPh; DCA = 9,10-dicyanoanthracene.

compounds were isolated analytically pure in good yields (Table 1). Surprisingly, this reaction was also possible with solutions containing higher concentrations of **1** and in the presence of lithium perchlorate. Under both these sets of conditions, the formation of *intermolecular* dimerization products should be favored, in one case because of simple concentration effects and in the other because of a special salt effect that leads to a prolonged lifetime for the radical cation.[7] This course is taken by, for instance, the photodimerization of stilbene to tetraphenylcyclobutane under comparable conditions with a quantum yield of $\Phi = 0.33$.[8] That nevertheless under the given conditions only **3** is obtained emphasizes the high tendency toward irreversible formation of the radical cation $\mathbf{3}^{\bullet+}$ from the precursor radical cation $\mathbf{1}^{\bullet+}$.

Table 1. Oxidation potentials, free energies of reaction, and calculated and experimentally determined electron transfer rate constants for **1a–c**.

Cmpd.	E_{ox} [a]	ΔG_{ET} [b]	k_{ET} [c]	k_q [d]	Yield of **3** [%] [e]
1a	1.28	−17.75	1.40	0.97	73
1b	1.23	−18.91	1.41	0.95	68
1c	1.18	−22.19	1.44	1.47	81

[a] In V, versus the saturated calomel electrode (SCE), irreversible, 10^{-1} M nBu$_4$ClO$_4$ in acetonitrile; sweep rate: 0.2 V min^{-1}. [b] In kcal mol^{-1} with $E_{red}(\mathbf{A}) = -0.91$ V, $E_s(\mathbf{A}) = 2.90$ eV [10]. [c] $M^{-1}s^{-1} \times 10^{10}$, calculated according to ref. [11]. [d] $M^{-1}s^{-1} \times 10^{10}$. Stern-Volmer kinetics with 10^{-5} M **A** in acetonitrile; substrate concentration: 10^{-3}–10^{-2} M, $R = 0.996 \pm 0.002$. [e] After crystallization from ethanol; samples for analytical studies were chromatograped (SiO_2, petroleum ether/ethyl acetate 10:1).

The high reactivity of the starting compounds in the presence of ^{1}**A*** is reflected in the oxidation potentials of **1a–c**. They are smaller by about 0.5 V (for **1a**) to 0.1 V (for **1c**) than those of the comparable 1,1-diarylethylenes;[9] the electron transfer should thus be almost diffusion-controlled in all cases (Table 1). The oxidation potential of **1a** is particularly strongly decreased and even approaches that of 1,1-dianisylethylene. The experimentally determined fluorescence quenching constants agree well with the rate constants calculated according to the Rehm–Weller equations.[11] Since the irradiation in the presence of typical triplet sensitizer like rose bengal ($E_T = 39.6$ kcal mol^{-1}, $\Phi_T = 0.76$[12]) does not cause a change in the starting compounds **1a–c**, an energy transfer mechanism both by ^{3}**A** ($E_T = 38.3$ kcal mol^{-1}, $\Phi_T > 0.02$[13]) and by ^{1}**A** (for which **2** must be formed) can be ruled out.

Under the reactions conditions radical cations with longer lifetimes should be trapped by triplet oxygen or by the superoxide anion.[3] On irradiation of **1a** under oxygen, however, only **3a** could be isolated, whereas analogous treatment of the substrates **1b,c** yielded a variety of nonidentifiable oxidation products. When the conversion was low, predominantly the [2 + 2] cyclization products **3b,c** were detected by spectroscopy, though with increasing duration of the irradiation the proportion of these compounds decreased. The same product composition was also found when the primary products of the electron transfer reaction (**3a–c**) were irradiated under oxygen in the presence of **A**. Apparently, as a result of the low oxidation potentials, an **A**-induced electron transfer with reformation of the intermediate **3**$^{\bullet+}$ is possible, in particular for the compounds **3b** and **c** ($E_{ox} = 1.58$ and 1.48 V respectively). Direct photochemical excitation ($\lambda_{exc} > 280$ nm) converts the PET products **3a,b** quantitatively into the pyrenes **2a,b**,[14] possibly via the biaryls **1**, though only **1b** could be detected. Addition of **A** to an irradiated solution of **3** suppresses the formation of **2**.

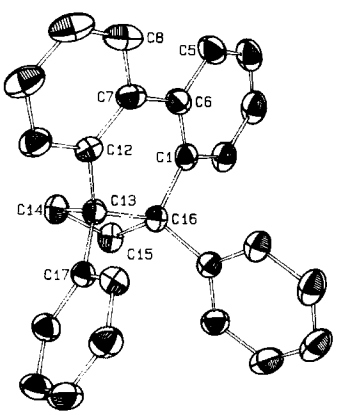


Fig. 1. Structure of **3a** in the crystal (ORTEP). Selected distances [pm] and angles [°]: C1-C6 139.5(2), C6-C7 (148.6(2), C13-C14 155.5(2), C13-C16 159.3(2), C13-C17 152.9(2); C5-C6-C7-C8 −5.56(8), C12-C13-C16-C1 −22.05 (6), C16-C13-C14-C15 19.07(8).

In the cyclization of **1** initiated by the photo electron transfer process described here, the products **3** are formed with high *cis* diastereoselectivity in all cases. For compound **3a** the structure was confirmed by a crystal structure analysis[15] (Fig. 1); from the similar NMR data[16] for **3b** and **3c**, we postulate a *cis* configuration for these substances, too. This high stereoselectivity for the (reversible) cyclization of the radical cation **3**$^{\bullet+}$ after reduction by the **A** radical anion can be explained in two ways: a) The configuration is already fixed by the one-electron two-center bond in the redical cation **3**$^{\bullet+}$, or b) the intermediate formed after electron back transfer, which has a dibenzocycloocta-1,3,5-triene structure, undergoes a (thermal) disrotatory ring closure. Because the latter reaction is expected to be very fast, the two alternatives cannot be distinguished at present.

We could thus show that for the 2,2′-bis(1-arylvinyl)-substituted biphenyls **1** the intramolecular PET-induced cycloisomerization is an efficient method for the highly stereoselective synthesis of cyclobutaphenanthrenes **3**, which are not accessible by the classical photochemical route.

Received: May 31, 1994 [Z6984IE]
German version: *Angew. Chem.* **1994**, *106*, 2399

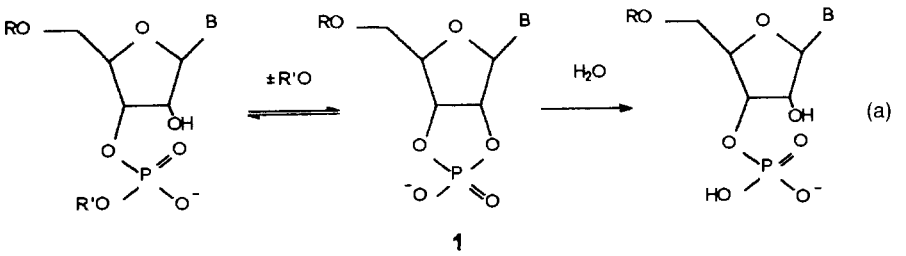
[1] a) J. Mattay, M. Vondenhof, *Top. Curr. Chem.* **1991**, *159*, 219; b) F. D. Lewis in *Photoinduced Electron Transfer. Part C: Photoinduced Electron Transfer Reactions: Organic Substrates* (Eds.: M. A. Fox, M. Chanon), Elsevier, New York, **1988**, p. 1; c) S. L. Mattes, S. Farid, *Org. Photochem.* **1983**, *6*, 233.
[2] S. L. Mattes, S. Farid, *J. Am. Chem. Soc.* **1986**, *108*, 7356–7361.
[3] K. Gollnick, A. Schnatterer, *Tetrahedron Lett.* **1984**, *25*, 185–188.
[4] **1a**: G. Wittig, W. Stilz, *Justus Liebigs Ann. Chem.* **1957**, *598*, 93–104; **1b** and **1c** analogously.
[5] A. Padwa, C. Doubleday, A. Mazzu, *J. Org. Chem.* **1977**, *42*, 3271–3279.
[6] A. J. W. Tol, W. H. Laarhoven, *J. Org. Chem.* **1986**, *51*, 1663–1668.
[7] K. Gollnick, G. Wellnhofer, *J. Photochem. Photobiol.* **1993**, *74*, 137–145.
[8] F. D. Lewis, D. E. Johnson, *J. Photochem.* **1977**, *7*, 422.
[9] G. Utschik, Dissertation, Universität München, **1988**.
[10] I. R. Gould, L. J. Mueller, S. Farid, *Z. Phys. Chem.* **1991**, *170*, 143–157.
[11] a) D. Rehm, A. Weller, *Isr. J. Chem.* **1970**, *8*, 259; b) A. Weller, *Z. Phys. Chem.* **1982**, *133*, 93–98.
[12] S. E. Braslavsky, K. Heihoff in *Handbook of Organic Photochemistry, Vol. 1* (Ed.: J. C. Scaiano), CRC, Boca Raton, FL, USA, **1989**, p. 327.
[13] L. E. Manring, C. I. Gu, C. S. Foote, *J. Phys. Chem.* **1983**, *87*, 40.
[14] Mixtures of *cis* and *trans* diastereomers (about 1:1). This transformation did not succeed for the anisyl derivative **3c**, presumably because of contamination by **A**.
[15] $C_{27}H_{22}$: $M_r = 358.49$, orthorhombic, $P2_12_12_1$ (no. 18) $a = 10.988(3)$, $b = 12.937(4)$, $c = 13.801(5)$ Å, $V = 1961.8$ Å^3, $Z = 4$, $\rho_{calcd} = 1.214$ g cm^{-3}, $\lambda(Mo_{K\alpha}) = 0.637$ cm^{-1}, 2999 reflections of which 2523 were observed ($I > 3\sigma(I)$, $R = 0.0272$, $R_w = 0.0369$) for 253 parameters. Further details are available on request from the Director of the Cambridge Crystallographic Data Centre, 12 Union Road, GB-Cambridge CB2 1EZ (UK), on quoting the full journal citation.
[16] At room temperature the rotation about the C(cyclobutane)–aryl bond is hindered: the signals of the *o,o′* and *m,m′* carbon atoms have different chemical shifts in the ^{13}C NMR spectrum ($\Delta\delta$ for the *m,m′* C atoms in **3a** is 5.5, in **3c** 4.4); the rotation about the biaryl axis (according to the crystal structure analysis the twist angle of **3a** is 5.6°) requires a lower activation energy (six signals for the phenanthrene C atoms). At + 60 °C the signals for the *o,o′* and *m,m′* carbon atoms of **3a** coalesce.

 © VCH Verlagsgesellschaft mbH, D-69451 Weinheim, 1994 0570-0833/94/2222-2301 $ 10.00+.25/0

Biomimetic Phosphonylation and Phosphorylation of Glycoses and Deoxynucleosides**

Svetomir B. Tzokov, Ivan T. Devedjiev, Emilia K. Bratovanova, and Dimiter D. Petkov*

While DNA is nearly inert, RNA is rapidly hydrolyzed in mildly basic solutions. Todd et al.[1] attributed the high reactivity of phosphodiester bonds in RNA to the "nucleophilic catalysis" by the neighboring 2'-hydroxyl group; the hydrolysis proceeds via the 2',3'-cyclic phosphate intermediate **1** [Eq. (a)].



(a)

1

Alkyl esters of glycerol phosphate react similarly.[2] The ribonuclease A catalyzed hydrolysis also takes advantage of this mechanism.[3] The reverse reaction of the first step of reaction (a) (transesterification) has also been observed, and by this process both simple alkyl phosphates of nucleosides and dinucleoside monophosphates have been obtained enzymically[4, 5] and chemically.[6] The importance of the vicinal hydroxyl group at the cleavage site in the Tetrahymena ribozyme reaction has been underlined recently.[7]

The growing interest in oligonucleotides and oligosaccharides and their use in antisense technology[8] and glycobiology[9] has stimulated the development of methods for the large-scale synthesis of chemically and chirally pure sugar phosphates.[10–12] Here we report a one-pot reaction for the efficient and specific phosphonylation and phosphorylation of glycoses and deoxynucleosides, which is analogous to the biochemical reactions.

Recently Devedjiev et al.[13, 14] showed that phosphinic acid **2** ($R^1 = R^2 = H$), epoxides, and aliphatic alcohols reacted via intermediates 2-hydroxyalkyl phosphinate **3** and probably alkyl phosphinate **4** to give alkyl phosphonic acids **5** in nearly quantitative yields [Eq. (b)]. As in the biochemical reaction (a), the presence of the vicinal hydroxyl group in **3** is crucial, since 2-deoxyalkyl phosphinates do not react.[14] We have tentatively assumed that if alkyl phosphinate **4** is an intermediate, the reaction of the other phosphorus oxo acids (phosphonic acid **2** ($R^1 = OH$, $R^2 = H$) and phosphoric acid **2** ($R^1 = R^2 = OH$)) must stop at **4**, since the rearrangement **4** ⇌ **5** is possible with alkyl phosphinate ($R^1 = R^2 = H$) only.[11, 12]

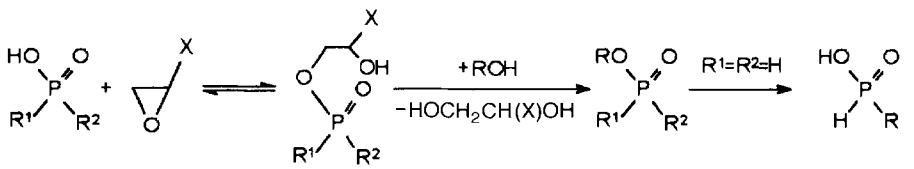
Actually, when phosphonic or phosphoric acid reacts with an alcohol (D-glucose or thymidine) and an epoxide (propylene oxide or epichlorohydrin) in anhydrous organic solvent (dioxane or pyridine), only alkyl phosphonates **4** ($R^1 = H$, $R^2 = OH$) or alkyl phosphates **4** ($R^1 = R^2 = OH$) are isolated (Table 1). The crude yields are nearly quantitative. Characteristically the reaction with D-glucose is regio- and stereospecific, affording one of the five possible constitutional isomers and the α-anomer only. This is not the case with thymidine, since protection of the 5'-hydroxyl group is required to obtain thymidine 3'-phosphonate or 3'-phosphate (Table 1).

The chemical process (b) is a condensation reaction, in which the easily available epoxides serve as the condensation agent. This esterification provides the phosphorus oxo acids with a structural feature (hydroxyl group adjacent to the esterified hydroxyl group) known from biochemical studies[1–5, 7] to make available a specific reaction pathway of low activation energy. Such reactions imitating the pathway and/or results of the biochemical reactions have been called biomimetic by Breslow.[15]

In contrast to the biochemical reaction (a), the β-hydroxyl group leaves as 1,2-diol in the biomimetic reaction (b). This suggests that the route via the cyclic phosphate is not the only mechanistic pathway for hydrolysis and aminolysis of β-hydroxyesters of phosphonic and phosphoric acids. Instead of acting as a nucleophilic catalyst, the vicinal hydroxyl group could function as a general acid catalyst, as in the case of ribozymic reactions.[16]

The regio- and stereospecificity in the reaction with D-glucose (only the α-anomer is isolated, Table 1) is not surprising when one considers the kinetic anomeric effect in the reaction of glycopyranoses.[17] A lack of regiospecificity is observed with thymidine; both the 5'- and 3'-hydroxyl groups are subject to reaction (b). This feature, however, makes it possible to use the reaction in oligonucleotide synthesis after selective hydroxyl group protection. Indeed, 5'-dimethoxytritylation afforded DMT-thymidine 3'-H-phosphonate (Table 1), a building block for the efficient and rapid preparation of oligonucleotides.[11] Protected derivatives of deoxyadenosine, deoxyguanosine, and deoxycytidine react similarly.

The biomimetic reaction described here is remarkably versatile and will benefit DNA and carbohydrate synthesis. It provides easy access to sugar phosphonates and phosphates under mild conditions and in good overall yields without elaborate protective group manipulations.



(b)

2 X = CH_3, CH_2Cl **3** **4** **5**

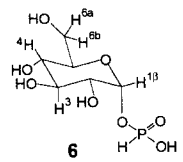
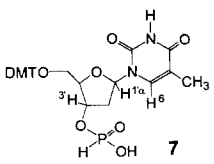
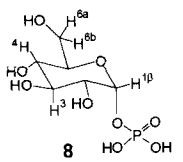
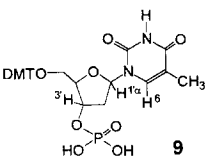
[*] Prof. Dr. D. D. Petkov, Dipl.-Bioeng. S. B. Tzokov, Dr. E. K. Bratovanova
Laboratory of BioCatalysis, Institute of Organic Chemistry
Bulgarian Academy of Sciences, 1113 Sofia (Bulgaria)
Telefax: Int. code + (2) 700-225
Doz. Dr. I. T. Devedjiev
Laboratory of Polycondensation Processes, Institute of Polymers
Bulgarian Academy of Sciences

[**] This work was supported by the Bulgarian National Research Fund.

Experimental Procedure

General procedure for phosphonylation/phosphorylation: Equimolar amounts (0.02 mol) of crystalline phosphonic or phosphoric acid, glucose or nucleoside, and propylene oxide or epichlorohydrin were dissolved in 20 mL of pyridine (dried over KOH). After an initial weakly exothermic period (30 min), the reaction mixture was stirred for 1 h at 40 C and then concentrated to dryness. In the case of the glycosyl

Table 1. Physical data and chemical yields of the products obtained from the reaction of phosphorus oxo acids, epoxides (propylene oxide or epichlorohydrin) and alcohols (D-Glucose or DMT[a]-thymidine). The products gave satisfactory phosphorus analyses.

Phosphorus oxo acid	Product	H	^{1}H NMR data [b] δ	J_{ij} [Hz]	Yield [c] [%]
	 **6**	H1β	4.99 (dd)	3.5 (1 2) 12.8 (1 P)	85
		H3	3.49 (t)	9.5 (3 4)	
		H4	3.40 (t)	9.5 (3 4)	
		H6a	3.89 (dd)	1.5 (5 6a) 12.0 (6a6b)	
		H6b	3.70 (dd)	10.8 (5 6b) 12.0 (6a6b)	
		H-P	6.89 (d)	673.1 (P H)	
	 **7**	H1'α	6.40 (dd)	7.2 (1'2') 6.6 (1'2'')	83
		H3'	5.00 (s)		
		H_3C	1.35 (m)		
		H_3CO	3.80 (s)		
		H-N	7.60 (m)		
		H-P	6.90 (d)	621.0 (P H)	
	 **8**	H1β	5.35 (d)	3.6 (1 2)	87
		H3	3.50 (t)	9.5 (3 4)	
		H4	3.40 (m)		
		H5	3.48 (m)		
		H6a	3.89 (dd)	1.5 (5 6a) 12.5 (6a6b)	
		H6b	3.64 (dd)	10.5 (5 6b)	
	 **9**	H1'α	6.40 (dd)	7.2 (1'2') 6.6 (1'2'')	85
		H3'	4.65 (s)		
		H_3C	1.76 (s)		
		H_3CO	3.80 (s)		
		H-N	7.80 (m)		
		H6	7.65 (m)		

[a] 5'-*p*,*p*'-Dimethoxytrityl. [b] Measured in D_2O at 250 MHz in FT mode on a Bruker WM-250 spectrometer. [c] Purified product.

derivatives the residue (crude product) was dissolved in water and chromatographed first on a column of Dowex 1W-8X(OH^-) (1 × 30 cm) with 0.02 M NaCl as eluent and then on a column of Dowex 50W-8X(H^+) (1 × 30 cm) with water as eluent. In the case of the DMT-thymidyl derivatives the crude product was dissolved in chloroform and chromatographed on a column of silica gel 60 (2.6 × 20 cm) with gradient elution with chloroform–methanol (0–20%).

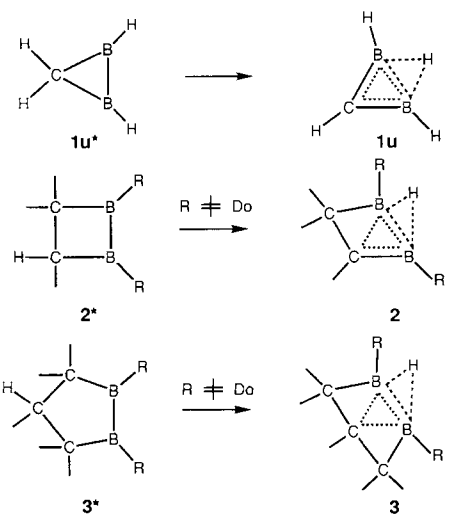
Received: May 16, 1994 [Z 6940 IE]
German version: *Angew. Chem.* **1994**, *106*, 2401

[1] D. M. Brown, D. I. Magrath, A. H. Nielson, A. R. Todd, *Nature* **1956**, *177*, 1124–1128.
[2] O. Bailly, J. Gaume, *Bull. Soc. Chim. Fr.* **1936**, *2*, 1396–1399.
[3] M. R. Eftink, R. L. Biltonen, *Biochemistry* **1983**, *22*, 5123–5134.
[4] L. A. Heppel, P. R. Whitefeld, R. Markham, *Biochem. J.* **1954**, *56*, 34–38.
[5] E. K. Bratovanova, V. Kasche, D. D. Petkov, *Biotechnol. Lett.* **1993**, *15*, 347–352.
[6] G. M. Tener, H. G. Khorana, *J. Am. Chem. Soc.* **1955**, *77*, 5349–5351.
[7] D. Herschlag, F. Eckstein, T. R. Cech, *Biochemistry* **1993**, *32*, 8312–8321, 8299–8311.
[8] E. P. Uhlmann, A. Peyman, *Chem. Rev.* **1990**, *90*, 544–584.
[9] A. Kobata, *Acc. Chem. Res.* **1993**, *26*, 319–405.
[10] J. E. Marugg, M. Tromp, E. Kuyl-Yeheskiely, G. E. van der Marel, J. H. van Boom, *Tetrahedron Lett.* **1986**, *27*, 2661–2664.
[11] O. Sakatsume, H. Yamane, H. Takaku, N. Yamamoto, *Tetrahedron Lett.* **1989**, *30*, 6375–6378.
[12] M. M. Sim, H. Kondo, C.-H. Wong, *J. Am. Chem. Soc.* **1993**, *115*, 2260–2267.
[13] I. Devedjiev, V. Ganev, G. Borisov, L. Zabski, Z. Jedlinski, *Phosphorus Sulfur Silicon Relat. Elem.* **1989**, *42*, 167–170.
[14] I. Devedjiev, G. Borisov, *Phosphorus Sulfur Silicon Relat. Elem.* **1990**, *53*, 37–42.
[15] R. Breslow, *Chem. Soc. Rev.* **1972**, *1*, 553–561.
[16] D. Herschlag, F. Eckstein, T. R. Cech, *Biochemistry* **1993**, *32*, 8312–8321.
[17] A. J. Kirby, *The Anomeric Effect and Related Stereoelectronic Effects at Oxygen*, Springer, Berlin, **1983**, p. 3.

Nonclassical 1,2-Diboretanes and 1,2-Diborolanes**

Dirk Steiner, Christian Balzereit, Heinz-Jürgen Winkler, Nicolaos Stamatis, Matthias Hofmann, Paul von Ragué Schleyer, Werner Massa, and Armin Berndt*

Diborirane is 50.8 kcal mol^{-1} [1b] more stable in the tautomeric H-bridged arrangement **1u**[***] (B–H–B diborirane)[1, 2] than in the classical structure **1u***.[3] Here we show that nonclassical structures, **2** (B–H–B homodiborirane) and **3** (B–H–B dihomodiborirane), are also favored for the homologous 1,2-diboretanes and 1,2-diborolanes when the boron atoms are electron-deficient. Known 1,2-diboretanes[4] and 1,2-diborolanes[5] have dialkylamino substituents (R = Do = donor) at the boron atoms; hence, the boron atoms are no longer electron-deficient and—as usual[6]—the classical structures **2*** and **3*** are favored.



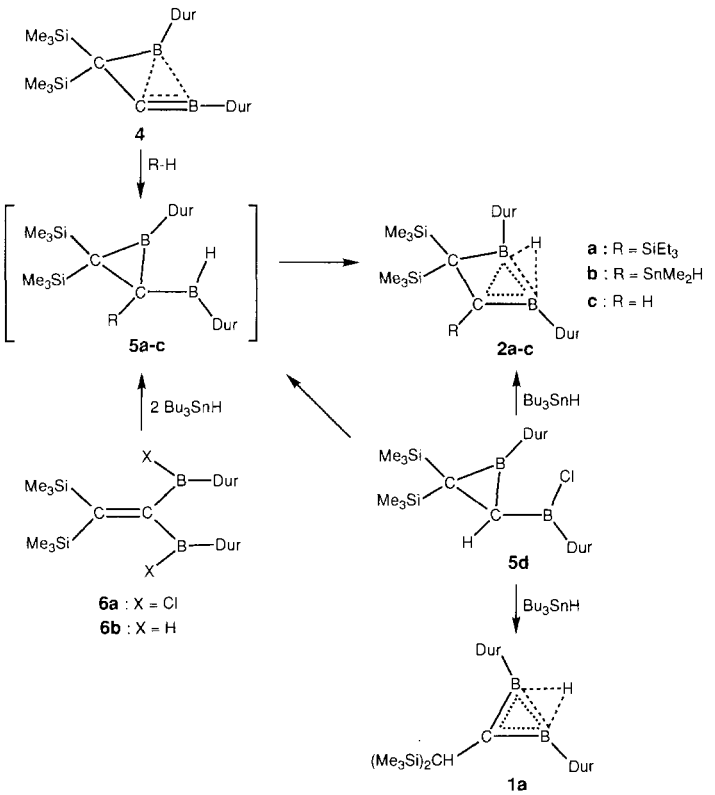
The nonclassical 1,2-diboretanes **2a,b** (Dur = 2,3,5,6-tetramethylphenyl) were obtained by addition of triethylsilane or dimethylstannane, respectively, to methyleneborane **4**.[2b] The borylboriranes **5a,b** are probable intermediates, but eluded detection by NMR spectroscopy even when a mixture of the reactants was kept below −40 °C. Compound **2c** as well as **1a**[2b] were formed in the reaction of borylborirane **5d**[7] and tributylstannane. However, **2c** could be obtained in quantitative yield by reaction of **6a**[2b] with tributylstannane. In this reaction, **6b** is probably formed as the initial product, which then undergoes intramolecular hydroboration to yield **5c**.

[*] Prof. Dr. A. Berndt, Dipl.-Chem. D. Steiner, Dipl.-Chem. C. Balzereit, Dipl.-Chem. H.-J. Winkler, Dr. N. Stamatis, Prof. Dr. W. Massa
Fachbereich Chemie der Universität
D-35032 Marburg (FRG)
Telefax: Int. code + (6421) 28-8917
Prof. Dr. P. von R. Schleyer, Dipl.-Chem. M. Hofmann
Computer-Chemie-Centrum des Instituts für Organische Chemie der Universität Erlangen-Nürnberg
Nägelsbachstrasse 25, D-91052 Erlangen (FRG)

[**] This work was supported by the Deutsche Forschungsgemeinschaft, the Volkswagen-Stiftung, the Convex Computer Cooperation, and the Fonds der Chemischen Industrie. The authors thank J. Gauss for a copy of the program GIAO-MP2.

[***] The letter "u" is used for the unsubstituted basic structure of a compound class, and an asterisk indicates the (nonexistent but more familiar) classical forms of the nonclassical compounds.

 © VCH Verlagsgesellschaft mbH, D-69451 Weinheim, 1994 0570-0833/94/2222-2303 $ 10.00+.25/0



The NMR data of **2a–c** (Table 1) suggested that these compounds are H-bridged 1,2-diboretanes. In order to test this hypothesis, chemical shifts for the parent compound **2u** were computed (GIAO-MP2/tzp[8, 9]). The impressive correlation between calculated and experimentally measured chemical shifts (Table 2) supported the presence of the nonclassical structure,

Table 1. Selected physical data for compounds **1a** and **2a–c**.

1a: colorless needles, m.p. 175 °C, yield 50–80%. – ^{1}H NMR (300 MHz, $CDCl_3$, 25 °C): $\delta = -0.01$ (s, 18H, $Si(CH_3)_3$), 1.85 (s, 1H, $CHSi_2$), 2.24, 2.29 (2 × s, each 6H, *o*- and *m*-CH_3), 6.97 (s, 2H, *p*-H)- 7.34 (br.s, 1H, BHB); ^{13}C NMR (125 MHz, $CDCl_3$, – 30 °C): $\delta = 0.1$ (q, 6C, $Si(CH_3)_3$), 20.1, 20.4, (2 × q, each 4C, *o*- and *m*-CH_3), 20.5 (d, 1C, $CHSi_2$), 131.7 (d, 2C, *p*-C), 133.3 (s, 4C, *m*-C), 133.6 (br. s, 2C, *i*-C), 136.9 (s, 4C, *o*-C), 140.3 (br. s, 1C, CB_2); ^{11}B NMR (96 MHz, $CDCl_3$, 25 °C): $\delta = 23$.

2a: colorless crystals, m.p. 168 °C (decomp.), yield 78%. – ^{1}H NMR (500 MHz, $CDCl_3$, – 30 °C): $\delta = -0.10, 0.16$ (2 × s, each 9H, $Si(CH_3)_3$), 0.73–0.96 (m, total of 15H, $Si(CH_2CH_3)_3$), 1.94 (br.), 2.13 (br.), 2.17, 2.25, 2.29, 2.46, 2.54 (br.) (7 × s, total of 24H, *o*- and *m*-CH_3), 4.30 (br. s, 1H, BHB), 6.96, 7.05 (2 × s, each 1H, *p*-H); ^{13}C NMR (125 MHz, $CDCl_3$, – 30 °C): $\delta = 2.7$, 3.2 (2 × q, each 3C, $Si(CH_3)_3$), 6.6 (t, 3C, $Si(CH_2CH_3)_3$), 8.9 (q, 3C, $Si(CH_2CH_3)_3$), 19.7 (br.), 20.4, 20.5, 20.6, 21.8 (br.), 22.9 (6 × q, total of 8C, *o*- and *m*-CH_3), 32.1 (s, 1C, CSi_2), 68.2 (s, 1C, CB_2), 130.8, 133.7 (2 × d, each 1C, *p*-C), 132.4, 132.7, 133.1 (br.), 133.6 (br.), 137.1, 138.6, 139.2 (br.), 139.8 (br.) (8 × s, each 1C, *o*- and *m*-C), 133.5, 137.0 (2 × br. s, each 1C, *i*-C); ^{11}B NMR (96 MHz, $CDCl_3$, 25 °C): $\delta = 3$, 48.

2b: colorless crystals, m.p. 143 °C (decomp.), yield 71%. – ^{1}H NMR (500 MHz, $CDCl_3$, – 30 °C): $\delta = -0.14$, 0.17 (2 × s, each 9H, $Si(CH_3)_3$), 0.44, 0.71 (2 × s, each 3H, $Sn(CH_3)_2$), 2.09, 2.15, 2.19, 2.25, 2.52 (5 × s, total of 24H, *o*- and *m*-CH_3), 4.41 (br. s, 1H, BHB), 5.29 (s, 1H, SnH), 6.95, 7.10 (2 × s, each 1H, *p*-H- Dur); ^{13}C NMR (125 MHz, $CDCl_3$, – 30 °C): $\delta = 1.2$, 4.5 (2 × q, each 1C, $Sn(CH_3)_2$, 1.5, 1.8 (2 × q, each 3C, $Si(CH_3)_3$), 20.4, 20.5, 20.7 (3 × q, total of 8C, *o*- and *m*-CH_3), 35.0 (s, 1C, CSi_2), 73.9 (s, 1C, CB_2), 130.7, 135.6 (2 × br. s, each 1C, *i*-C), 131.7, 134.8 (2 × d, each 1C, *p*-C), 132.9, 133.7, 136.9, 139.1, 140.9 (5 × s, total of 8C, *o*- and *m*-C); ^{11}B NMR (96 MHz, $CDCl_3$, 25 °C): $\delta = 2$, 48; ^{119}Sn NMR (149 MHz, $CDCl_3$, – 30 °C): $\delta = 57.3$ ($J(^{119}Sn,H) = 2216$ Hz).

2c: colorless crystals, m.p. 150–152 °C, yield quantitative by NMR spectroscopy. ^{1}H NMR (500 MHz, $CDCl_3$, – 30 °C): $\delta = -0.01, 0.27$ (2 × s, each 9H, $SiCH_3$), 2.02 (br.), 2.10, 2.32 (br.), 2.38, 2.67, 2.83 (br.) (6 × s, total of 24H, *o*- and *m*-CH_3), 3.34 (br., 1H, BHB), 3.98 (d, 1H, CHB, $^3J(H, H) = 13.5$ Hz), 7.07, 7.20 (2 × s, each 1H, *p*-H); ^{13}C NMR (125 MHz, $CDCl_3$, – 30 °C): $\delta = -0.3$, 0.5 (each 3C, $SiCH_3$), 18.0, 19.4 (br., each 1C, *o*- and *m*-CH_3), 18.8, 20.1, 20.2, 20.5, 20.6 (total of 6C, *o*- and *m*-CH_3), 30.6 (1C, CSi_2), 73.8 (1C, $J(^{13}C,H) = 166$ Hz, CHB), 131.2, 134.6 (each 1C, *i*-C), 131.6, 134.3 (each 1C, *p*-C), 132.0, 132.6, 132.9, 138.1, 139.0, 140.4, 141.2 (total of 8C, *o*- and *m*-C); ^{11}B NMR (96 MHz, $CDCl_3$, 25 °C): $\delta = 5$, 44.

Table 2. Comparison of experimental and calculated data for **2a–c**, **2u**, and **2d**.

	2a	**2b**	**2c**	**2u**	**2d**
$\delta(^{11}B1)$	3	2	5	– 2.6	–
$\delta(^{11}B2)$	48	48	44	+ 43.5	–
$\delta(^{13}C3)$	68.2	73.9	73.8	+ 71.2	
$\delta(^{13}C4)$	32.1	35.0	30.6	+ 24.2	–
B1 B2 [pm]	179.9(3)	–	–	172.0	174.9
B2–C3 [pm]	147.2(3)	–	–	146.7	147.2
C3–C4 [pm]	158.9(3)		–	150.2	149.9
C4–B1 [pm]	156.9(3)	–	–	157.2	156.9
B1 C3 [pm]	172.3(3)	–	–	170.9	170.1
B1–H1 [pm]	122.7	–		133.0	–
B2–H1 [pm]	136.9	–	–	134.0	–
B2-B1-C3-C4 [°]	133.7(2)	–	–	140.3	141.0

which was finally confirmed by a single-crystal X-ray structure analysis. Figure 1 shows the crystal structure of **2a**.[10]

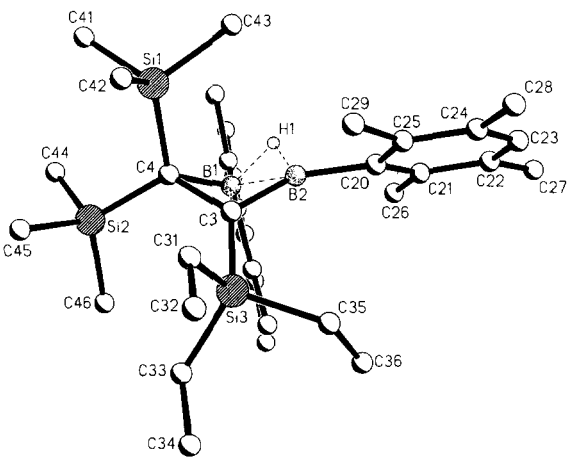
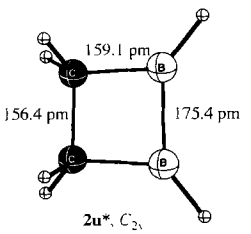


Fig. 1. Crystal structure of **2a**.

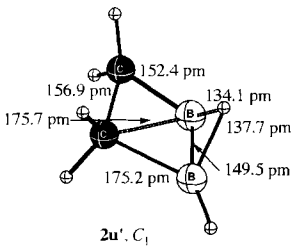
When the substituent effects are taken into account, the geometry of **2a** agrees well with that calculated for **2u** (Table 2): the duryl substituents decrease the electron-deficiency of the boron atoms and thus the nonclassical interactions; the sterically demanding trialkylsilyl groups at C3 and C4 are most likely responsible for the lengthening of the C3–C4 bond (158.9 vs. 150.0 pm in **2u**) and the increased folding along the B1–C3 bond (46.3 vs 39.7° in **2u**). An NBO analysis[11] (NBO = natural bond orbital) provided the following results regarding the electronic structure of **2u**: The methylene group is bonded in a classical fashion. The CB_2 framework is held together by a 2c–2e bond (between the C–B pair that is not C-bridged) and two 3c–2e bonds (BHB and BCB). In isomer **2u'**, which is less stable by 26.1 kcal mol^{-1} (MP2(fc)/6-31G*), the two boron atoms are joined by two 3-center bonds (BHB and BCB) and, in addition, by a classical 2-center bond. The carbon atom, now also as a CH_2 group, is bonded to the boron atoms only by a nonclassical 3c–2e bond. These bonding arrangements are reflected in the distances between atoms: The partial double bond character of B2–C3 manifests itself in the short bond lengths (**2a**: 147.2, **2u**: 146.7 pm), and the long B–B distance (**2a**: 179.9, **2u**: 172.0 pm) corresponds to that in diborane(6) **7** with

two bridging hydrogen atoms.[12, 13] The less stable isomer **2u'** has a large B2–C3 distance of 175.2 pm and a small B–B distance of 149.5 pm, reminiscent of the nonclassical diborane(4) **8**.[12, 14] The classical **2u*** is not an energy minimum, but rather a transition state.



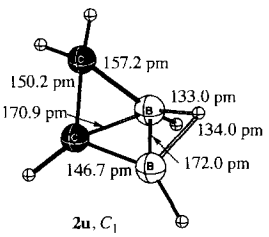
2u*, C_{2v}

E_{rel} = 34.5 kcal mol^{-1}



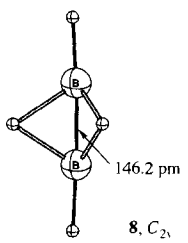
2u', C_1

E_{rel} = 26.1 kcal mol^{-1}

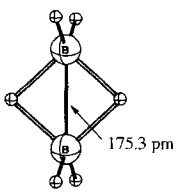


2u, C_1

E_{rel} = 0.0 kcal mol^{-1}

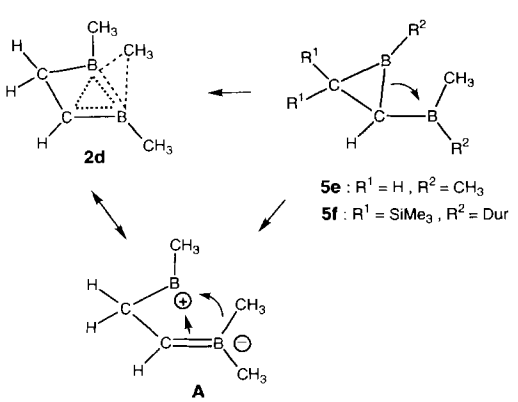


8, C_{2v}



7, D_{2h}

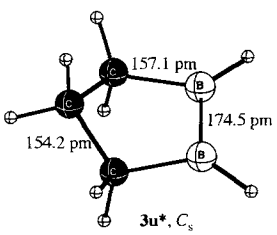
The geometry of the H-bridged 1,2-diboretanes differs only slightly from that of methyl-bridged **2d**. The latter geometry was obtained by performing calculations on borylborirane **5e**.[7] The electronic structure of the nonclassical 1,2-diboretane **2** can therefore be described in terms of a strong α-agostic type interaction[2b] between the electron-deficient boryl boron atom and the neighboring strained C–B bond of the three-membered ring in **5**. It is this interaction that gives rise to the 3c–2e bond between B1, B2, and C3. The boron atom of the three-membered ring thus has an increased positive charge (cf., resonance structure **A**) and participates in a β-agostic interaction[2b, 15]



with a σ bond of the boryl substituent (B–CH_3 for **5e**, B–H for **5a–c**) and thereby forms the second 3c–2e bond.

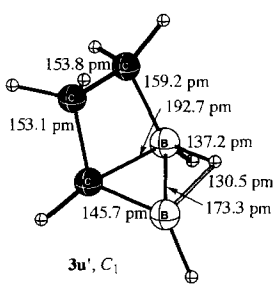
We were able to show the presence of a weak α-agostic interaction of the same type (C–B hyperconjugation) in the boryl borirane **5f**.[7] Due to the sterically demanding duryl substituents in **5f**, strong interactions of the type that transform **5e** to **2d** are obviously not possible here. However, when the methyl group at the boryl boron atom is replaced by an H atom, the duryl groups are no longer effective in preventing nonclassical interactions.

Calculations predict that for 1,2-diborolane the nonclassical structure **3u'** is stabilized by only 2.5 kcal mol^{-1} and the B-H-B dihomo structure **3u** by 18.9 kcal mol^{-1} relative to the classical structure **3u*** (MP2(fc)/6-31G* + 0.93ZPE).



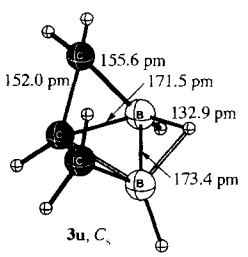
3u*, C_s

E_{rel} = 18.9 kcal mol^{-1}



3u', C_1

E_{rel} = 16.4 kcal mol^{-1}



3u, C_s

E_{rel} = 0.0 kcal mol^{-1}

Experimentally and theoretically derived data both show that a nonclassical, H-bridged homodiborirane structure is favored for those 1,2-diboretanes in which the boron atoms are not bonded to strongly electron-donating groups. Based on calculations, an analogous dihomodiborirane structure can be expected for 1,2-diborolanes.

Received: June 21, 1994 [Z 7058 IE]
German version: *Angew. Chem.* **1994**, *106*, 2391

[1] a) K. Krogh-Jespersen, D. Cremer, D. Poppinger, J. A. Pople, P. von R. Schleyer, J. Chandrasekhar, *J. Am. Chem. Soc.* **1979**, *101*, 4843–4851; b) E. D. Jemmis, G. Subramanian, G. N. Srinivas, *ibid.* **1992**, *114*, 7939–7941.

[2] a) R. Wehrmann, H. Meyer, A. Berndt, *Angew. Chem.* **1985**, *97*, 779–781; *Angew. Chem. Int. Ed. Engl.* **1985**, *24*, 788; b) A. Berndt, *ibid.* **1993**, *105*, 1034–1058 and **1993**, *32*, 985–1009, and references therein.

[3] The nonclassical diborirane with a planar tetracoordinated carbon atom is 17.5 kcal mol^{-1} lower in energy than **1u*** but 33.3 kcal mol^{-1} higher in energy than **1u** [1b].

[4] A. Krämer, J.-K. Uhm, S. E. Garner, H. Pritzkow, W. Siebert, *Z. Naturforsch. B* **1990**, *45*, 1019–1021; R. Littger, H. Nöth, M. Thomann, M. Wagner, *Angew. Chem.* **1993**, *105*, 275–277; *Angew. Chem. Int. Ed. Engl.* **1993**, *32*, 295–297; W. Maringgele, A. Heine, M. Noltemeyer, A. Meller, *J. Organomet. Chem.* **1994**, *468*, 25–35.

[5] G. E. Herberich, C. Ganter, L. Wesemann, R. Boese, *Angew. Chem.* **1990**, *102*, 914–915; *Angew. Chem. Int. Ed. Engl.* **1990**, *29*, 912–913; G. Knörzer, H. Seyffer, W. Siebert, *Z. Naturforsch. B* **1990**, *45*, 1136–1138; G. Gabbert, W. Weinmann, H. Pritzkow, W. Siebert, *Angew. Chem.* **1992**, *104*, 1670–1672; *Angew. Chem. Int. Ed. Engl.* **1992**, *31*, 1603–1605; G. Gabbert, H. Pritzkow, M. Kaschke, W. Siebert, *Chem. Ber.* **1994**, *127*, 1363–1368.

[6] G. E. Herberich, H. Ohst, H. Mayer, *Angew. Chem.* **1984**, *96*, 975–976; *Angew. Chem. Int. Ed. Engl.* **1984**, *23*, 969–970, and references therein; M. Bühl, P. von R. Schleyer, M. A. Ibrahim, T. Clark, *J. Am. Chem. Soc.* **1991**, *113*, 2466–2471.

 © VCH Verlagsgesellschaft mbH, D-69451 Weinheim, 1994 0570-0833/94/2222-2305 $ 10.00+.25/0

[7] P. Willershausen, G. Schmidt-Lukasch, C. Kybart, J. Allwohn, W. Massa, M. L. McKee, P. von R. Schleyer, A. Berndt, *Angew. Chem.* **1992**, *104*, 1417–1420; *Angew. Chem. Int. Ed. Engl.* **1992**, *31*, 1384–1386.

[8] GIAO-MP2: a) J. Gauss, *Chem. Phys. Lett.* **1992**, *191*, 614; b) J. Gauss, *J. Chem. Phys.* **1993**, *99*, 3629–3643. The algorithm was implemented in ACESII. (ACESII, an *ab-initio* program system: J. F. Stanton, J. Gauss, J. D. Watts, W. J. Lauderdale, R. J. Bartlett, Quantum Theory Project, University of Florida, FL, **1991**, **1992**); the abbreviation tzp stands for triple zeta plus polarization basis sets: A. Schäfer, H. Horn, R. Ahlrichs, *J. Chem. Phys.* **1992**, *97*, 2571–2577.

[9] MP2(fc)/6-31G* geometries (fc = frozen core, i.e. only valence electrons were correlated) calculated with Gaussian 92: M. J. Frisch, G. W. Trucks, M. Head-Gordon, P. M. W. Gill, M. W. Wong, J. B. Foresman, B. G. Johnson, H. B. Schlegel, M. A. Robb, E. S. Replogle, R. Gomperts, J. L. Andres, K. Raghavachari, J. S. Binkley, C. Gonzalez, R. L. Martin, D. J. Fox, D. J. Defress, J. Baker, J. J. P. Stewart, J. A. Pople, Gaussian Inc., Pittsburgh, PA, **1992**.

[10] X-ray structure analysis with a four-circle diffractometer (CAD4, Enraf-Nonius) with $Cu_{K\alpha}$ radiation ($\lambda = 154.178$ pm) at $-60\,^{\circ}C$: colorless crystals of **2a** ($C_{34}H_{60}B_2Si_3$), crystal dimensions $0.6 \times 0.5 \times 0.5$ mm^3, triclinic, space group $P\bar{1}$, $Z = 2$, $a = 1166.9(2)$, $b = 1240.4(2)$, $c = 1348.1(3)$ pm, $\alpha = 76.81(3)$, $\beta = 83.68(3)$, $\gamma = 72.54(3)^{\circ}$, $V_{EZ} = 1810.4 \times 10^{-30}$ m^3, $\rho_{calcd} = 1.054$ g cm^{-3}, total of 5665 reflections collected in ω-scan mode for $2\theta \leq 120^{\circ}$; Lorentz and polarization correction; all 5357 independent reflections used in subsequent calulations; no absorption correction ($\mu = 13.3$ cm^{-1}). The structure was solved by direct methods and refined with full matrix against the F_o^2 data. Several hydrogen atoms, including H1, could be localized by difference Fourier synthesis; all hydrogens were considered in the calculations "riding" on their bonding partners in groups with common isotropic temperature factors. Anisotropic temperature factors were used for all other atoms. $wR_2 = 0.1414$ and $R = 0.049$ for 5062 reflections with $I > 2\sigma(I)$. The maximum residual electon density was 0.36 e Å^{-3}. Further details of the crystal structure investigation may be obtained from the Fachinformationszentrum Karlsruhe, D-76344 Eggenstein-Leopoldshafen (FRG), on quoting the depository number CSD-58380.

[11] A. E. Reed, L. A. Curtiss, F. Weinhold, *Chem. Rev.* **1988**, *88*, 899–926.

[12] The B–B distances reported here for **7** and **8** were calculated at the same level as the geometries of **2u** and **2u'**.

[13] D. S. Jones, W. N. Lipscomb, *J. Chem. Phys.* **1969**, *51*, 3133–3134: d(B–B) = 176 pm.

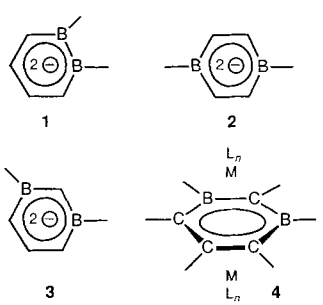
[14] L. A. Curtiss, J. A. Pople, *J. Chem. Phys.* **1989**, *90*, 4314–4319: d(B–B) = 145.9 pm.

[15] Starting from **A**, the interaction that gives rise to the methyl bridge in **2d** is a γ-agostic one.

A 1,3-Diboratabenzene**

Christian Balzereit, Heinz-Jürgen Winkler, Werner Massa, and Armin Berndt*

While derivatives of 1,2- and 1,4-diboratabenzenes **1** and **2** are known,[1, 2] those of 1,3-diboratabenzene **3** have only been obtained as π complexes **4** with transition metals (M = Co, Fe).[3, 4] We report here on the first dilithium compound **3a** of a 1,3-diboratabenzene dianion.



When the tetracarbahexaborane **5** was reduced by lithium in tetrahydrofuran (THF), **3a** was obtained as the only product. The oxidation back to **5** was achieved by heating **3a** in boiling 1,2-dibromoethane. Analogous direct redox transformations are not known for the two- and three-dimensional arenes[5] **6** and **7** (R = alkyl),[6] which are isoelectronic with **3a** and **5**, respectively.

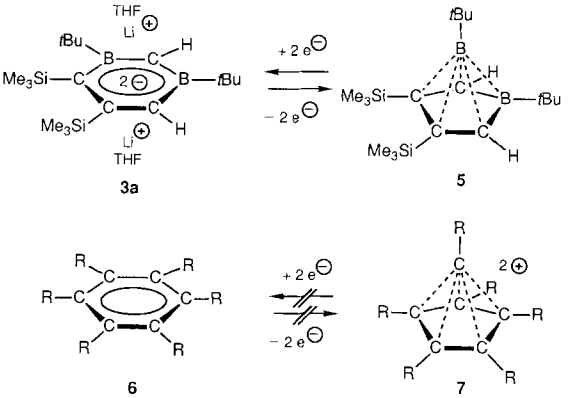


Figure 1 shows the crystal structure of **3a**.[7] The lithium ions, which are each coordinated to one molecule of THF, are positioned above and below the center of the almost planar six-membered ring (maximum deviation from best plane 6.1(4) pm; distances between plane and lithium cations 170.3 (Li1) and 166.6 pm (Li2)). A similar arrangement has been observed for the lithium ions coordinated to tetramethylethylenediamine (TMEDA) in the 1,2-diboratabenzene **1a**.[1] However, the structure of **3a** shows a disorder that can be described by an alternative arrangement of the molecule obtained by an exchange of the *t*Bu–B3 and Me$_3$Si–C5 units. Figure 1 and the geometric descriptions refer to the major conformation (59%). The steric strain between the trimethylsilyl and *tert*-butyl groups positioned *ortho* to one another is relieved by distorsion of the angles at B3 and C5 and by changes in the torsional angles around the bonds B3–C4 and C4–C5. The Li···B distances, which are not affected by the disorder, are distinctly shorter (227.7 and 232.9 pm) than those in **1a** (247.1 and 255.3 pm). The C–B1 bonds in the ring are comparable in length (151.5 and 152.5 pm) to those in **1a** (150.5 pm); the remaining bond lengths in the ring cannot be discussed because of the observed disorder.

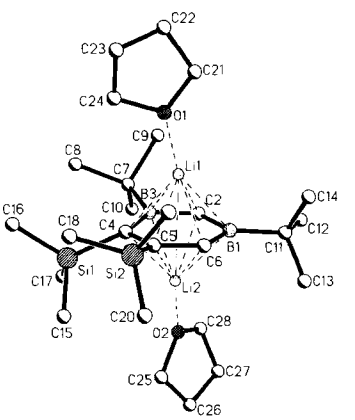


Fig. 1. Crystal structure of **3a**. Selected distances which that are not affected by the disorder of Si2 and C7 [pm] and angles [°]: B1–C2 152.5(6), B1–C6 151.5(6), Li1–B1 232.9(8), Li2–B1 227.7(8), Li1–C2 222.1(8), Li2–C2 223.7(8), Li1–C6 221.9(8), Li2–C6 221.9(8), Li1–C4 233.6(8), Li2–C4 218.6(8); C2-B3-C7 110.9(3), C7-B3-C4 125.3(3), C6-C5-Si2 109.9(3), Si2-C5-C4 127.0(3); C7-B3-C4-Si1 37.0(5), Si1-C4-C5-Si2 −38.9(5).

The signals in the ^{11}B NMR spectrum of **3a** (Table 1, $\delta = 40$ and 46) are in the range characteristic for tricoordinate boron atoms bearing negative π charge[8] (cf., $\delta = 37.5$ in **8**[9]). The

[*] Prof. Dr. A. Berndt, Prof. Dr. W. Massa,
Dipl.-Chem. C. Balzereit, Dipl.-Chem. H.-J. Winkler
Fachbereich Chemie der Universität
D-35032 Marburg (FRG)
Telefax: Int. code + (6421) 28-8917

[**] This work was supported by the Deutsche Forschungsgemeinschaft and the Fonds der Chemischen Industrie

Table 1. Selected physical data for **3a**, **5**, **12**, **13**, and **15**.

3a: colorless crystals, m.p. 179–183 °C, yield: quantitative by NMR spectroscopy, isolated 60%. ^{1}H NMR (300 MHz, C_6D_6, 25 °C): δ = 0.48, 0.57 (2 × s, each 9H, $SiMe_3$), 1.46, 1.58 (2 × s, each 9H, *t*Bu), 6.51, 6.95 (2 × s, each 1H, BCH); ^{1}H NMR (500 MHz, $CDCl_3$, −30 °C): δ = 0.20, 0.21 (2 × s, each 9H, $SiMe_3$), 0.95, 1.05 (2 × s, each 9H, *t*Bu), 5.88, 6.57 (2 × s, each 1H, BCH); ^{13}C NMR (75 MHz, C_6D_6, 25 °C): δ = 4.8, 8.3 (2 × q, each 3C, $SiMe_3$), 32.8, 35.1 (2 × q, each 3C, *t*Bu), 115.9 (br.d, 1C, B_2CH, ^1J(C,H) = 120 Hz), 118.0 (br.s, 1C, SiCB), 123.8 (br.d, 1C, BCH, ^1J(C,H) = 136 Hz), 160.9 (s, 1C, CSi); ^{13}C NMR (125 MHz, $CDCl_3$, −30 °C): δ = 4.0, 7.4 (each 3C, $SiMe_3$), 20.8, 24.4 (each 1C, CMe_3), 32.0, 34.2 (each 3C, *t*Bu), 114.1 (br., 1C, B_2CH), 117.0 (1C, SiCB), 122.8 (1C, BCH), 160.2 (1C, CSi); ^{11}B NMR (96 MHz, $CDCl_3$, 25 °C): δ = 40, 46.

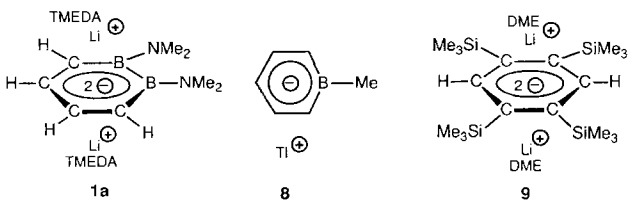
5: yellow crystals, m.p. 138 °C, quantitative yield. ^{1}H NMR (300 MHz, $CDCl_3$, 25 °C): δ = 0.35 (s, 18H, $SiMe_3$), 0.72, 1.11 (2 × s, each 9H, *t*Bu), 4.67 (s, 2H, CHB); ^{13}C NMR (75 MHz, $CDCl_3$, 25 °C): δ = 1.3 (q, 6C, $SiMe_3$), 31.1, 33.3 (2 × q, each 3C, *t*Bu), 95.3 (br.d, 2C, CHB, ^1J(C,H) = 159 Hz), 115.4 (s, 2C, CSi); ^{11}B NMR (96 MHz, $CDCl_3$, 25 °C): δ = −42, 28.

12: yellow oil, quantitative yield by NMR spectroscopy. ^{1}H NMR (400 MHz, $CDCl_3$, −40 °C): δ = 0.05, 0.07, 0.14 (3 × s, each 9H, $SiMe_3$), 0.94, 1.10 (2 × s, each 9H, *t*Bu), 7.42 (s, 1H, sp^2-CH); ^{13}C NMR (100 MHz, $CDCl_3$, −30 °C): δ = −0.2, 2.4, 3.7 (3 × q, each 3C, $SiMe_3$), 20.4, 23.5 (2 × br.s, each 1C, CMe_3), 27.8, 30.1 (2 × q, each 3C, *t*Bu), 29.4 (s, 1C, CSi_2), 53.6 (br.s, 1C, CB_2), 153.3 (d, 1C, CH of the four-membered ring, ^1J(C,H) = 168 Hz), 185.7 (s, 1C, CSi of the four-membered ring); ^{11}B NMR (96 MHz, $CDCl_3$, 25 °C): δ = 45, ca. 80.

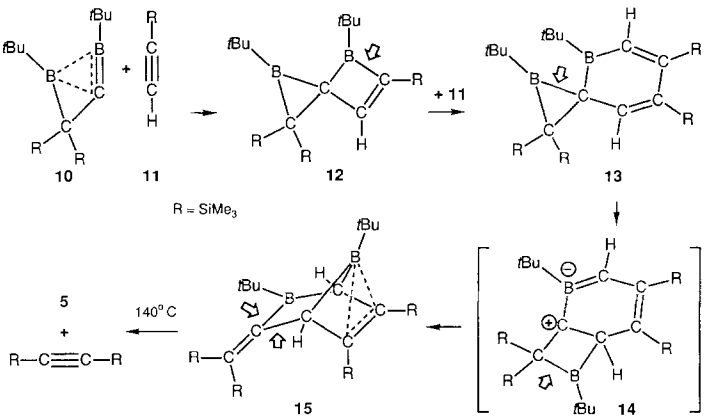
13: ^{1}H NMR (400 MHz, $CDCl_3$, 5 °C): δ = 0.09, 0.21, 0.31, 0.32 (4 × s, each 9H, $SiMe_3$), 0.92, 1.00 (2 × s, each 9H, *t*Bu), 6.40, 7.31 (2 × s, each 1H, sp^2-CH); ^{13}C NMR (100 MHz, $CDCl_3$, 0 °C): δ = 2.0, 2.2, 5.5, 5.8 (each 3C, $SiMe_3$), 30.3, 30.35 (each 3C, *t*Bu), 41.4 (1C, CSi_2), 65.7 (br., 1C, CB_2), 137.3, 155.3 (each 1C, sp^2-CSi), 145.6, 146.5 (each 1C, sp^2-CH); ^{11}B NMR (96 MHz, pentane, 25 °C): δ = 70, 79.

15: yellow crystals, m.p. 120 °C (transformation into **5**), 90% yield. ^{1}H NMR (300 MHz, $CDCl_3$, 25 °C): δ = 0.00, 0.26, 0.32, 0.36 (4 × s, each 9H, $SiMe_3$), 0.83, 1.12 (2 × s, each 9H, *t*Bu), 3.00, 3.56 (2 × s, each 1H, BCH); ^{13}C NMR (75 MHz, $CDCl_3$, 25 °C): δ = 1.4, 1.7, 2.7, 3.2 (4 × q, each 3C, $SiMe_3$), ca. 15, ca. 25 (2 × very br.s, each 1C, CMe_3), 30.4, 31.8 (2 × q, each 3C, *t*Bu), 53.7, 60.1 (2 × br.d, each 1C, CHB, ^1J(C,H) = 146 and 145 Hz, respectively); 135.2 (s, 1C, CSi_2), 145.8, 149.1 (2 × br.s, each 1C, sp^2-CSi), 181.4 (very br.s, 1C, sp^2-CB); ^{11}B NMR (96 MHz, $CDCl_3$, 25 °C): δ = −9, 67.

ring carbon atoms in **3a** (δ(^{13}C, 125 MHz, −30 °C) = 114.1 (C2), 117.0 (C6), 122.8 (C4), and 160.2 (C5)) are more strongly deshielded than in **1a** (δ(^{13}C) = 104.6 and 108.5); in the latter, less negative charge can be taken by the boron atoms because of the amino substituents. The position of the signal in the ^{7}Li NMR spectrum of **3a** (δ = −5.8) is comparable to that in the spectrum of the 6π arene cyclopentadienyllithium (δ(^{6}Li) = −6.3;[10] cf., however, δ(^{7}Li) = +10.7 for the 8π-electron system **9**[11], DME = 1,2-dimethoxyethane). Even after addition of [12]crown-4, the contact ion pair in **3a** is not disrupted (δ(^{7}Li) = −5.2).



The carborane **5** was obtained as follows: Reaction of the methyleneborane **10**[12] with trimethylsilylacetylene **11** yielded the bicyclic compound **15**. The diboraspiro compounds **12** and **13**[13] were unambiguously characterized as intermediates by NMR spectroscopy in solution (the bonds that are broken are designated with an arrow in each case). The spontaneous transformation of **13** into **15** probably occurs via the σ complex **14** resulting from an intramolecular electrophilic substitution of **13**.[14] After the opening of the Si_2C–B bond in **14**, attack of the



exocyclic boron atom at the sp^2 carbon atom bearing a hydrogen atom produces **15**.

The crystal structure (Fig. 2) shows **15** to have the rare[15, 16] dihomoborirene structure; this can also be deduced from the

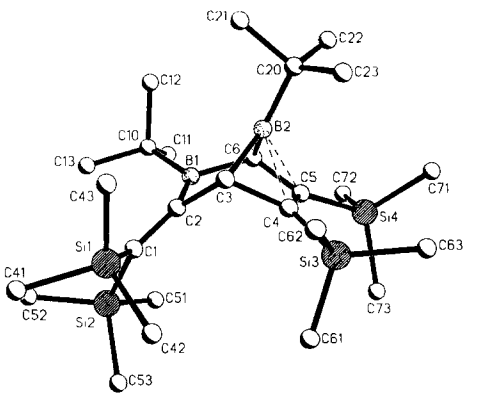


Fig. 2. Crystal structure of **15**. Selected distances [pm] and angles [°]: C1–C2 136.3(7), B1–C2 152.0(8), B1–C6 159.7(8), B2–C4 187.2(9), B2–C5 188.0(9), C4–C5 137.5(7); B1-C2-C1 134.0(6), C1-C2-C3 125.2(5), B1-C2-C3 100.7(5), C2-B1-C6 109.5(5), B2-C3-C4 72.8(4), B2-C6-C5 72.7(4), B2-C3-C2 112.4(5), B2-C6-B1 98.8(5), C4-C5-Si4 130.8(5), C5-C4-Si3 132.0(4); Si3-C4-C5-Si4 0.4(9), C3-C2-C1-Si1 19.5(8), C3-C2-C1-Si2 −150.1(5), B1-C2-C1-Si1 −157.3(5), B1-C2-C1-Si2 33.1(9)

shielding of the boron atom (δ(^{11}B) = −9) interacting with the SiC–CSi double bond. When heated to 140 °C, **15** was transformed quantitatively to **5** with elimination of bis(trimethylsilyl)acetylene. The structure of **5** follows from the positions of the signals in its ^{11}B NMR spectrum (δ = 28 and −42), which are characteristic for tetracarbahexaboranes.[17]

Received: June 22, 1994 [Z 7060 IE]
German version: *Angew. Chem.* **1994**, *106*, 2394

[1] G. E. Herberich, B. Heßner, M. Hostalek, *Angew. Chem.* **1986**, *98*, 637–638; *Angew. Chem. Int. Ed. Engl.* **1986**, *25*, 642–643.
[2] G. E. Herberich, B. Heßner, *Chem. Ber.* **1982**, *115*, 3115–3127.
[3] G. E. Herberich, B. Hessner, N. Klaff, H. Ohst, *J. Organomet. Chem.* **1989**, *375*, 161–166, and references therein.
[4] B. Deobald, J. Hauss, H. Pritzkow, D. Steiner, A. Berndt, W. Siebert, *J. Organomet. Chem.*, **1994**, *481*, 205–210.
[5] For competition between two- and three-dimensional arenes, see H. Michel, D. Steiner, S. Wočadlo, J. Allwohn, N. Stamatis, W. Massa, A. Berndt, *Angew. Chem.* **1992**, *104*, 629–632; *Angew. Chem. Int. Ed. Engl.* **1992**, *31*, 607–610.
[6] H. Hogeveen, P. W. Kwant, *Acc. Chem. Res.* **1975**, *8*, 413–420; H. Hogeveen, E. M. G. A. van Kruchten, *J. Org. Chem.* **1981**, *46*, 1350–1353, and references therein; H. Schwarz, *Angew. Chem.* **1981**, *93*, 1046–1059; *Angew. Chem. Int. Ed. Engl.* **1981**, *20*, 991–1003; K. Krogh-Jespersen, *J. Am. Chem. Soc.* **1991**, *113*, 417–423.

[7] Crystal structure analyses: colorless crystals of **3a** and **15** were investigated on a four-circle diffractometer (CAD4, Enraf-Nonius) at −80 °C with $Cu_{K\alpha}$ radiation ($\lambda = 154.178$ pm). **3a**: $C_{18}H_{38}B_2Li_2Si_2 \cdot 2THF$, crystal dimensions $0.6 \times 0.3 \times 0.2$ mm³, monoclinic, space group $P2_1/c$, $Z = 4$, $a = 972.2(2)$, $b = 1173.5(2)$, $c = 2890.7(6)$ pm, $\beta = 98.45(3)°$, $V_{EZ} = 3262.1 \times 10^{-30}$ m³, $\rho_{calcd} = 0.998$ g cm⁻³; 3994 measured reflections in the range up to $2\theta = 110°$ (ω scans), 3903 of which were independent and were used for the further calculations after Lorentz and polarization correction; no absorption correction ($\mu = 11.0$ cm⁻¹). The structure was solved by direct methods and refined against the F_o^2 data with full matrix. A disorder showing up in the difference Fourier syntheses was accounted for by a "split atom model" where a C5–$SiMe_3$ group superposes the B3–*t*Bu unit at B3 and, vice versa, a B3–*t*Bu group superposes the C5–$SiMe_3$ unit at C5. Due to these superpositions, geometric restraints of the B–C (160 pm) and Si–C (187 pm) bond length were used during refinement, and the temperature factors of atoms approaching each other were defined to be equal. In this way good convergence and a maximal residual electron density 0.35 e Å⁻³ were achieved. The distribution of the alternative arrangements of the molecules was determined to be 59.3(4) and 40.7%. The H atoms were localized in part by difference Fourier syntheses; the others were calculated; they were included in the calculation riding on their bonding partners and with isotropic temperature factors common by groups. Anisotropic temperature factors were used for all the remaining atoms except C7; $wR_2 = 0.2066$ (SHELX 93 program), corresponding to $R = 0.069$ for 2951 reflections with $F_o > 4\sigma(F_o)$, maximal residual electron density 0.33 e Å⁻³. - **15**: $C_{26}H_{56}B_2Si_4$, crystal dimensions $0.7 \times 0.3 \times 0.2$ mm³, monoclinic, space group $P2_1/n$, $Z = 4$, $a = 928.9(2)$, $b = 1655.2(3)$, $c = 2154.4(4)$ pm, $\beta = 92.80(3)°$, $V_{EZ} = 3308.5 \times 10^{-30}$ m³, $\rho_{calcd} = 1.009$ g cm⁻³; 4461 reflections in the range up to $2\theta = 110°$ (ω scans), 4157 of which were independent. 4154 reflections were used for further calculations after Lorentz and polarization correction; the structure solution and refinement as for **3a** led to $wR_2 = 0.1955$, corresponding to $R = 0.064$ for 2123 reflections with $F_o > 4\sigma(F_o)$, and a maximal residual electron density of 0.34 e Å⁻³. Further details of the crystal structure investigations may be obtained from the Fachinformationszentrum Karlsruhe, D-76344 Eggenstein-Leopoldshafen (FRG), on quoting the depository number CSD-58435.

[8] M. M. Olmstead, P. P. Power, K. J. Weese, *J. Am. Chem. Soc.* **1987**, *109*, 2541–2542; M. Pilz, J. Allwohn, P. Willershausen, W. Massa, A. Berndt, *Angew. Chem.* **1990**, *102*, 1085–1087; *Angew. Chem. Int. Ed. Engl.* **1990**, *29*, 1030–1032.

[9] G. E. Herberich, H. J. Becker, C. Engelke, *J. Organomet. Chem.* **1978**, *153*, 265–270; Crystal structure of a boratabenzene: G. Herberich, B. Schmidt, U. Englert, T. Wagner, *Organometallics* **1993**, *12*, 2891–2893.

[10] L. A. Paquette, W. Bauer, M. R. Sivik, M. Bühl, M. Feigel, P. von R. Schleyer, *J. Am. Chem. Soc.* **1990**, *112*, 8776–8789, and references therein.

[11] A. Sekiguchi, K. Ebata, C. Kabuto, H. Sakurai, *J. Am. Chem. Soc.* **1991**, *113*, 7081–7082.

[12] A. Berndt, *Angew. Chem.* **1993**, *105*, 1034–1088; *Angew. Chem. Int. Ed. Engl.* **1993**, *32*, 985–1009, and references therein

[13] In **13**, the trimethylsilyl groups are bound to neighboring carbon atoms as in **15**. This can be deduced from long range coupling constants $^3J(^{13}C,H)$ of 9 and 11 Hz for the sp^2-C atoms in **13** that bear no protons. The 1,3-arrangement of the $SiMe_3$ groups has been established by a crystal structure analysis for a derivative of **13** with duryl groups instead of *tert*-butyl groups [14].

[14] C. Balzereit, C. Kybart, H.-J. Winkler, W. Massa, A. Berndt, *Angew. Chem.* **1994**, *106*, 1579–1581; *Angew. Chem. Int. Ed. Engl.* **1994**, *33*, 1487–1489.

[15] P. J. Fagan, E. G. Burns, J. C. Calabrese, *J. Am. Chem. Soc.* **1988**, *110*, 2979–2980; P. J. Fagan, unpublished results, cited in [16].

[16] J. M. Schulman, R. L. Disch, P. von R. Schleyer, M. Bühl, M. Bremer, W. Koch, *J. Am. Chem. Soc.* **1992**, *114*, 7897–7901.

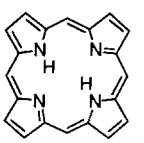
[17] B. Wrackmeyer, G. Kehr, *Polyhedron* **1991**, *10*, 1497–1506, and references therein.

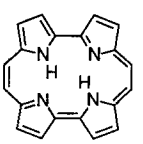
Corrphycene: A New Porphyrin Isomer**

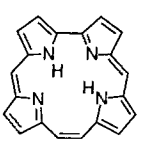
Jonathan L. Sessler,* Eric A. Brucker, Steven J. Weghorn, Michael Kisters, Martin Schäfer, Johann Lex, and Emanuel Vogel*

Dedicated to Sir Derek Barton on the occasion of his 75th birthday

The porphyrins, represented by the general structure **1**, [18]-porphyrin-(1.1.1.1),[1] have developed into a subject of interdisciplinary research par excellence, in part because of their importance in the fields of chemistry, biology, and medicine. Indeed, the perennial interest engendered by these tetrapyrrolic macrocycles had already, in the 1960s, inspired Woodward[2] and Johnson[3] to expand the scope of porphyrin chemistry through the design and synthesis of structural variants of porphyrins (e.g., sapphyrins and corroles). In pursuing this goal, they were guided by the [18]annulene model of the porphyrin electronic structure, a model which emphasizes the presence of an 18 π electron conjugation pathway in the molecule. During the last few years, thanks in large measure to progress in preparative methods—biomimetic cyclizations,[4] reductive couplings[5] (McMurry Reaction) etc.—the number of new porphyrinoid macrocycles, from which a variety of practical applications might be expected, has increased dramatically.


1


2


3

In spite of the above interest, the simple concept of reorganizing the basic building blocks of the porphyrins—four pyrrole moieties and four methine units—to form tetrapyrrolic structural isomers of porphyrin was first realized only in 1986 with the synthesis of the porphycene **2**[6]—[18]porphyrin-(2.0.2.0). Since **2** was shown by a wide range of spectroscopic, structural, and metal complexation studies to have a porphyrinoid nature,[7] the question inevitably arose as to whether other isomers of porphyrin might also exist. A theoretical analysis based on electronic structure of all conceivable isomers containing an N_4 coordination site and [18]annulene conjugation, carried out by Waluk and Michl in 1991,[8] gave credence to the supposition that porphyrin isomers other than **2** might also prove to be porphyrin-like. In fact, a close correspondence between many of these putative structures and the known isomers **1** and **2** was implied, particularly in the case of [18]porphyrin-(2.1.0.1)[9] (**3**) and [18]porphyrin-(2.1.1.0).[10–12] According to later semiempirical calculations (carried out with the MOPAC series of

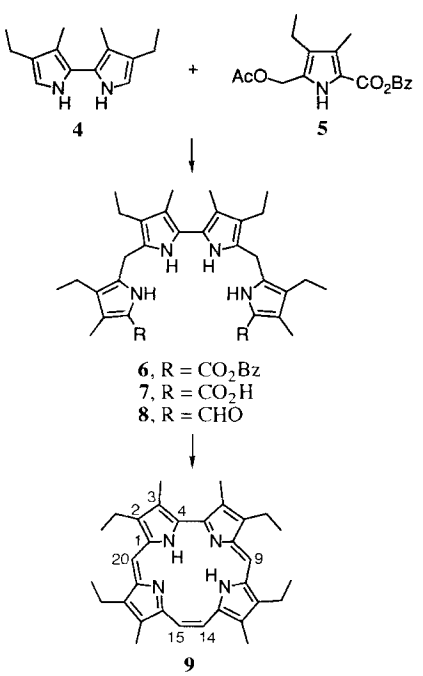
[*] Prof. Dr. J. L. Sessler, E. A. Brucker, S. J. Weghorn
Department of Chemistry and Biochemistry
The University of Texas at Austin
Austin, TX 78712 (SA)
Telefax: Int. code + (512)471-7550

Prof. Dr. E. Vogel, Dipl.-Chem. M. Kisters, Dipl.-Chem. M. Schäfer, Dr. J. Lex
Institut für Organische Chemie der Universität
Greinstrasse 4, D-50939 Köln (FRG)
Telefax: Int. code + (221)470-5102

[**] This work was supported by the National Science Foundation (Grant CHE 9122161), the Alexander von Humboldt Foundation (J. L. S.) and the Deutsche Forschungsgemeinschaft (E. V.). The authors thank Dr. N. Jux, Dr. L. Neumann, and Mr. R. Deponte for useful advice concerning some aspects of the corrphycene synthesis.

programs[13]), both of these isomers have a planar ring framework and are only slightly strained. In the case of isomer **3**, these theoretical predictions have been confirmed by experiment; this was done by the synthesis and subsequent study of its tetramethyl-tetraethyl ("etio") derivative **9**. Because compound **9** (and its parent system **3**) combines structural elements of both corrole (direct bipyrrolic linkage) and porphycene (acene fragment C···CH···CH=C) within the same overall framework, the trivial name corrphycene is suggested for this new class of porphyrin-like tetrapyrrolic macrocycles.

The choice of **9** as the target molecule instead of the presumably more soluble octaethyl derivative was prompted by a desire to minimize the steric interactions arising from the inner alkyl groups of the bipyrrole unit, since such interactions could, it was thought, lead to noticeable deformations of the ring framework.[6d] On a different level, in planning an approach to the synthesis of **9** (Scheme 1), it was helpful to realize that the decisive synthetic step, one analogous to the reductive coupling of the bipyrrole dialdehyde with titanium tetrachloride/zinc used in the synthesis of porphycene,[6a] might best proceed via an as yet unknown open-chain, diformyl tetrapyrrolic intermediate. Thus, in terms of strategy, the synthesis of **9** would consist of first preparing the α,ω-dialdehyde **8**, and then coupling it under reductive conditions to generate a tetrahydrocorrphycene intermediate. This latter species, in accord with what is observed in the case of the porphyrinogens, would be expected to undergo facile oxidation to give the corresponding aromatic species **9**.



Scheme 1. The reaction **4** + **5** → **6**: *p*-Toluenesulfonic acid monohydrate, isopropanol, reflux, 10 h (55%); **6** → **7**: H_2, Pd/C, THF, triethylamine, 3 h (dicarboxylic acid not isolated); **7** → **8**: $HC(OEt)_3$, trifluoroacetic acid, −20 °C, 30 min (**6** → **8**: 85%); **8** → **9**: a) Zn/CuCl, $TiCl_4$, THF, 0 °C, 30 min; b) $FeCl_3$, 2 h (3%).

The known tetrapyrrolic α,ω-dibenzyl ester **6**,[14] available from the *para*-toluenesulfonic acid catalyzed condensation of the α-unsubstituted bipyrrole **4** with the acetoxymethyl-activated pyrrole **5**, was used for the preparation of **8**. Debenzylation to the diacid **7** was achieved by treating **6** with hydrogen in the presence of 10% palladium on charcoal in tetrahydrofuran. After removal of the solvent, intermediate **7** was subjected to a Clezy formylation[15] (triethyl orthoformate and trifluoroacetic acid) at −20 °C. In this transformation the product (dialdehyde **8**) was isolated as an amorphous, blue solid (yield 85%) by the slow addition of a 2:1 mixture of water and acetone to the reaction medium. Since this compound was pure (as judged by ^{1}H NMR spectroscopy), a recrystallization step (which might have led to a reduction in yield, Table 1) was not employed. Rather, intermediate **8** was carried on directly to the final reductive coupling step. Here, the best results were achieved if the reaction was not conducted under the usual conditions for porphycene synthesis (THF at reflux), but rather at 0 °C in THF followed by treatment with aqueous $FeCl_3$ solution to complete the necessary tetrahydrocorrphycene-to-corrphycene oxidation process. After chromatographic purification on silica gel with a mixture of dichloromethane and toluene (1/1) saturated with NH_3 as the eluent and subsequent recrystallization from dichloromethane/hexanes (1/1), **9** was finally obtained as fine violet needles with a melting point of 270–272 °C (yield 3%).

Table 1. Selected physical data for the new compounds. ^{1}H NMR: 300 MHz, $CDCl_3$; ^{13}C NMR: 75.5 MHz, $CDCl_3$; IR: CsI; MS: EI, 70 eV.

8: M.p. 188–190 °C (crude product); ^{1}H NMR: δ = 11.19 (br. s; NH), 10.29 (br. s; NH), 8.49 (s; CHO), 3.80, 2.53, 2.46, 2.02, 1.99, 1.15, 1.05; ^{13}C NMR: δ = 175.56, 138.40, 132.79, 128.50, 124.41, 122.03, 121.69, 121.13, 113.98, 22.35, 18.05, 17.02, 16.02, 15.46, 10.75, 8.70; IR: $\tilde{\nu}$ = 3300, 2962, 2928, 1617, 1560, 1498, 1377, 1309, 1276, 1154, 1116, 1085, 1062 cm^{-1}; UV/Vis (CH_2Cl_2): λ_{max} (ε) = 272 (24400), 308 (32200), 589 nm (2200); MS: *m/z* (%): 514 (100) [M^+]; high-resolution MS (FAB): $C_{32}H_{42}N_4O_2$, calcd 514.330777, found 514.328389.

9: M.p. 270–272 °C (dichloromethane/hexanes); ^{1}H NMR: δ = 9.89 (s, 2H; H-9,20), 9.87 (s, 2H; H-14,15), 3.98 (q, 4H; H-11a,18a), 3.95 (q, 4H; H-2a,7a), 3.63 (s, 6H; H-3a,6a), 3.53 (s, 6H; H-12a,17a), 1.81 (t, 6H; H-2b,7b), 1.80 (t, 6H; H-11b,18b), −2.08 (br. s, 2H; NH); ^{13}C NMR: δ = 145.15, 144.62, 142.57, 142.11, 140.01, 139.19, 135.54, 129.26, 109.39, 102.68, 20.92, 20.60, 18.61, 18.48, 15.58, 12.80; IR: $\tilde{\nu}$ = 3274, 2961, 2929, 2867, 1594, 1467, 1448, 1207, 1057, 995, 847, 762 cm^{-1}; UV/Vis (benzene): λ_{max} (ε) = 415 (139400), 511 (13700), 540 (3800), 577 (5600), 584 (4300), 632 nm (1900); MS: *m/z* (%): 478 (100) [M^+], 239 (21) [M^{2+}]; high-resolution MS (FAB): $C_{32}H_{39}N_4$ [$(M+H)^+$], calcd 479.317473, found 479.319015; correct elemental analysis.

11: M.p. 283–285 °C (dichloromethane/hexanes); ^{1}H NMR: δ = 9.65 (s, 2H; H-9,20), 9.54 (s, 2H; H-14,15), 3.88 (q, 4H; H-11a,18a), 3.80 (q, 4H; H-2a,7a), 3.51 (s, 6H; H-3a,6a), 3.43 (s, 6H; H-12a,17a), 1.72 (t, 6H; H-11b,18b), 1.51 (t, 6H; H-2b,7b); ^{13}C NMR: δ = 150.27, 144.52 143.44, 143.24, 141.26, 137.43, 134.46, 129.19, 106.41, 100.06, 20.33, 19.52, 17.98, 17.78, 14.34, 12.61; IR: $\tilde{\nu}$ = 2959, 2927, 2866, 1734, 1465, 1445, 1282, 1258, 1154, 1132, 1121, 1057, 879, 797 cm^{-1}; UV/Vis (CH_2Cl_2): λ_{max} (ε) = 251 (15300), 277 (9700), 330 (8600), 396 (106400), 434 (31200), 455 (20100), 547 (6400), 619 nm (5200); MS: *m/z* (%): 534 (100) [M^+], 267 (23) [M^{2+}]; high-resolution MS (FAB): $C_{32}H_{36}N_4Ni$, calcd 534.229345, found 534.228709; correct elemental analysis.

The spectra provide strong evidence that the corrphycene **9** is in fact a bona fide aromatic porphyrinoid compound. The chemical shifts observed in the room temperature ^{1}H NMR spectrum (300 MHz, $CDCl_3$), for instance, correspond fully to those expected for a porphyrin-like system; the protons of the C_{20} perimeter resonate at relatively low field (two singlets, relative intensity 1:1 at δ = 9.89 and 9.87), while those of the interior (that is, N-bound pyrrolic) protons appear at relatively high field (broad singlet at δ = −2.08) (Fig. 1). Remarkably, the signals of the perimeter protons of **9**, etioporphyrin I (**1a**), and also etioporphycene (**2a**)[6d] resonate at almost the same frequency (δ = 10.08 and 9.52, for the latter two systems, respectively). Further, the simplicity of the ^{1}H NMR spectrum for **9** implies a formal equivalence of the two halves of the molecule (effective C_{2v}, C_s, or C_2 molecular symmetry; that is, frameworks that are planar, bowl-shaped, or twisted, respectively). This equivalence can be explained as follows: Either the molecule is a corrphycene tautomer with symmetrically arranged imino protons, or it is the actual species **9** with N-bound protons that undergo rapid tautomerization on the NMR time scale. The observation that the NH signal is split into two signals of equal intensity at lower temperatures leads us to favor the latter

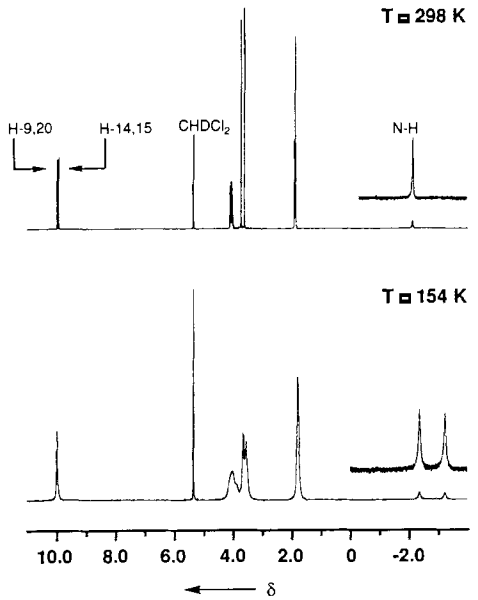


Fig. 1. ^{1}H NMR spectra (300 MHz; CD_2Cl_2/CF_2Br_2 with the addition of Al_2O_3 to guarantee anhydrous conditions) of **9** at 298 K (top) and 154 K (bottom).

assignment. From the coalescence temperature of the NH signals (185 K) a free energy of activation $\Delta G^{\neq}$ of 8.3 kcal mol^{-1} can be calculated (corresponding values for porphyrins are on the order of 10–15 kcal mol^{-1}[16b]). The ^{13}C NMR spectrum (75.5 MHz, $CDCl_3$) at room temperature is consistent with the ^{1}H NMR spectrum in terms of the symmetry of **9**. However, solubility problems and other dynamic processes involving the alkyl groups preclude a more detailed interpretation of the low-temperature ^{13}C NMR spectrum. Thus, the tentative conclusion of a planar or near-planar overall ring structure for **9** rests at present only on its ^{1}H NMR spectrum, specifically the chemical shift values recorded for the perimeter and N-bound protons.[17]

The UV/Vis spectrum (benzene) of **9** (Fig. 2) reveals a pronounced Soret-type band at $\lambda = 415$ nm ($\varepsilon = 139400$), that is slightly red-shifted relative to that of the corresponding etioporphyrin. It also reveals five Q-like transitions at $\lambda(\varepsilon) = 511$ (13700), 540 (3800), 577 (5600), 584 (4300), and 632 nm (1900).

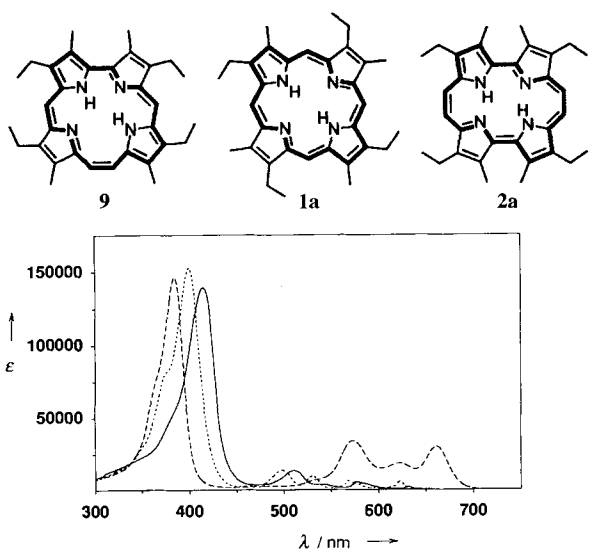
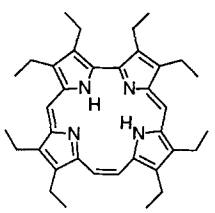


Fig. 2. UV/Vis spectra (benzene) of etiocorrphycene **9** (—), etioporphyrin I **1a** (·····) and etioporphycene **2a** (----) (in each case the 18π conjugation system appears in bold type).

In the IR spectrum of **9**, an N–H stretching vibration is found at 3274 cm^{-1}. The straightforward detection of this mode is in contrast to what is observed in the case of porphycenes; in these systems the relevant N–H strectching mode is IR-nonobservable due to the presence of strong internal N–H···N hydrogen bonds. However, the IR spectral behavior of corrphycene **9** is directly analogous to that of the porphyrins for which ν_{N-H} values on the order of 3300–3360 cm^{-1} are routinely recorded.[18]

The mass spectrum of **9** (EI, 70 eV) revealed the presence of the expected molecular ion (m/z 478) as the base peak, as well as a further prominent peak corresponding to the doubly charged molecular ion (m/z 239, 23%).

Crystal disorder precluded a direct X-ray structure analysis of **9**. Fortunately, however, these problems of crystal disorder were not observed in the case of the octaethylcorrphycene analogue **10**, a compound obtained by a synthesis similar to that described above[19] (Fig 3). In the solid state, octaethylcorrphycene[20] **10** has an approximate C_2 molecular symmetry, that stems, in part, from the conformations of the ethyl groups. The ring framework of **10** is nearly planar (the maximum deviation of the C and N atoms from the mean plane of the ring is ±0.082 Å), in line with the theoretical predictions for that of parent **3**. The planarity of the former compound was observed in spite of possible destabilizing van der Waals repulsions that might have arisen from the ethyl groups in the 3 and 6 positions. However, as is true for octaethylporphycene,[6d] these ethyl groups and the steric interactions they engender do cause a stretching of the C4–C5 bond (from 1.397 Å in porphycene[6a] to 1.423 Å in the present instance). They also induce a contraction of the N1-C4-C5 and C4-C5-N2 angles (to 114.0° compared to those in octaethylporphycene of 118.5°). As a consequence, the pyrrole rings affected are more precisely directed towards the center of the molecule in corrphycene than they are in porphycene. Actually, with regard to the C=CH–CH=C structural unit, there is a further noteworthy difference between **10** and the structurally characterized porphycenes. Specifically, relative to those of the porphycenes the C13-C14-C15 and C14-C15-C16 angles are widened by no less than 6–7° (to about 138°); nevertheless, compound **10**, like its porphycene analogues, exhibits equivalent bond lengths in this unit. Thus this bond equivalence feature may serve as a good criterion for judging aromaticity in these kinds of molecules.



10

The N-bound hydrogen atoms of **10** were localized unequivocally in the X-ray structure. These atoms were found together (that is, *cis* to one another) on the two pyrrole moieties of the bipyrrole unit. The X-ray diffraction analysis of **10** thus reveals a striking dichotomy between the NH tautomerism deduced in solution and the structure observed in the solid state (note: the room temperature and low temperature ^{1}H NMR spectra of **10** correspond to those of **9**). Nonetheless, the observed "*cis*"-like localization of the N-bound hydrogen atoms in the solid state agrees with the observed structural parameters for the pyrrole rings of the bipyrrole moiety as well as those of the other two pyrrolic entities in **10**, at least as compared to those of the corresponding subunits in porphyrins (pyrrole and pyrrolenine,

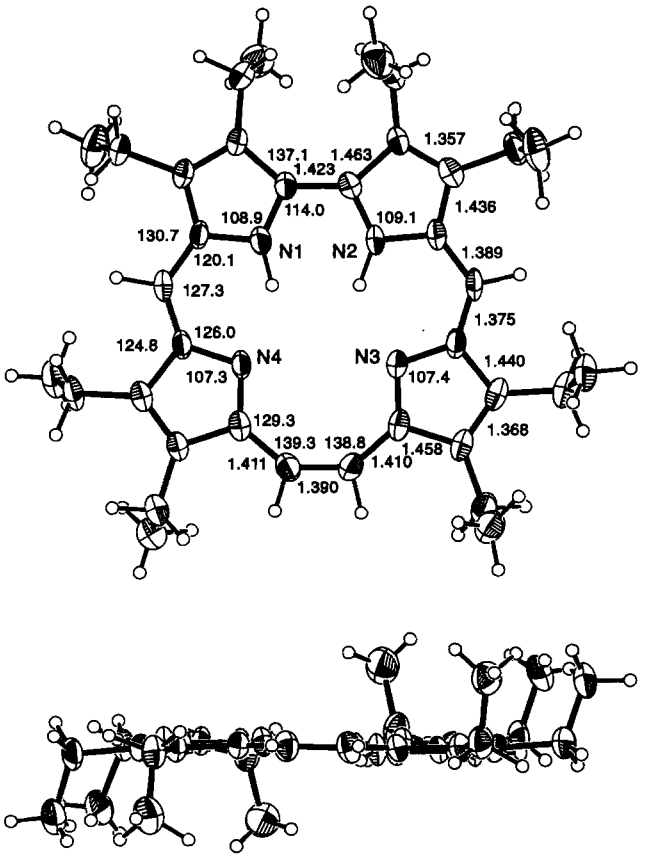


Fig. 3. Crystal structure of octaethylcorrphycene **10** (top: top view; bottom: side view). Ellipsoids are drawn at the 40% probability level. Selected bond lengths [Å] and angles [ ] (standard deviation approximately 0.006 Å and 0.3°): N1···N2 2.539 A, N1···N4 2.799 Å, N3···N4 3.447 Å.

respectively). Interestingly, while the four nitrogen atoms of the coordination core in porphyrin and porphycene form a square and a rectangle, respectively, their arrangement in **10** defines a well-characterized trapezoid. Thus, the strong internal N-H···N hydrogen bonds, typical for porphycenes, do not exist in **10**, because the N1–N4 and N2–N3 distances are relatively large.

In spite of seemingly unfavorable N_4 core geometry present in **10**, the corrphycenes act as astonishingly good porphyrin-like ligands. Indeed, corrphycenates of Ni^{II}, Cu^{II}, Zn^{II}, and Fe^{II} have already been isolated. For instance, heating **9** with nickel(II) acetate tetrahydrate in dimethylformamide produces the stable divalent nickel complex **11**, which, after conventional workup and recrystallization from dichloromethane/hexanes (1/1), is obtained as violet needles (m.p. 283–285 °C, yield 75%). The ^{1}H NMR and the UV/Vis spectra of **11** are modulated relative to those of the free ligand in ways that parallel the changes observed in the course of the same metalation process in porphyrins.

Currently work is focused on exploring further the coordination chemistry of corrphycene and on carrying out more detailed comparisons between this compound and its isomeric analogues, porphyrin, porphycene, and hemiporphycene.[10, 11] Research on the chemistry of porphyrin isomers has received an added stimulus from the recent papers of Furuta et al.[21] and Latos-Grażýnski et al.,[22] who described a new type of porphyrin isomer, the "inverted porphyrins", a class of molecules that is distinguished by its unusual metal coordination chemistry.[23] Indeed, this work, in conjunction with that reported here, leads us to suggest that the coordination chemistry of tetrapyrrolic aromatic macrocycles might well be richer than had been previously conceived.

Experimental Procedure

8: Owing to the photolability of intermediates, the reaction sequence **6** → **8** was carried out in light-protected glassware. Dibenzyl ester **6** [14] (7.25 g, 10 mmol) and 10% palladium on charcoal (3 g) were stirred in absolute tetrahydrofuran (750 mL) under a hydrogen atmosphere for 3 h. The catalyst was then filtered off, and the solvent removed under vacuum. The remaining solid, diacid **7**, was treated with triethyl orthoformate (33.5 mL, 0.2 mol), and the mixture cooled to −20 °C; to this stirred mixture was then added trifluoroacetic acid (50 mL, 0.65 mol) over a period of 15 min (here the reagent order could also be reversed). To complete the reaction, the mixture was stirred for a further 15 min at −20 °C and then 30 min at room temperature. All the operations described were carried out under an inert atmosphere (argon). Finally, the product was precipitated by addition over 30 min of a mixture of 300 mL water and 150 mL acetone. After filtration, washing with water, and drying, the dialdehyde **8** was obtained as an amorphous blue powder. M.p. 188–190 °C (crude product); yield 5.66 g (85%). Compound **8** so obtained is pure as judged by ^{1}H NMR spectroscopy, and was therefore used directly in the ensuing reductive coupling step.

9: Under argon, zinc dust (50.4 g, 0.8 mol) and copper(I) chloride (9.9 g, 0.1 mol) were added to 1.2 L of absolute tetrahydrofuran. Titanium tetrachloride (46.2 mL, 0.42 mol) was added dropwise, and the resulting mixture was heated at reflux for 1 h. Thereafter, it was cooled to 0 °C, and a solution, also at 0 °C, of **8** (3.08 g, 6 mmol) in tetrahydrofuran (1.5 L) was added over a period of 30 min. The solution was stirred for a further 5 min before being hydrolyzed by the addition of concentrated aqueous ammonia (0.5 L). The resulting organic phase was then washed with saturated sodium chloride solution until neutral. To complete the oxidation, this solution was then stirred for 2 h with a 5% aqueous iron(III) chloride solution (300 mL) and then worked up in the conventional manner. After chromatography on silica gel (column: 5 × 50 cm) with dichloromethane/toluene (1/1) as the eluent (the eluent was saturated with NH_3 gas to suppress the protonation of product on the column), **9** was obtained as a major mobile fraction. Recrystallization from dichloromethane/hexanes (1/1) provided etiocorrphycene as fine violet needles. M.p. 270–272 °C; yield 98.2 mg (3.0%).

11: Compound **9** (48 mg, 0.1 mmol) and nickel acetate tetrahydrate (90 mg, 0.5 mmol) were heated at reflux in dimethylformamide (10 mL) for 1 h. The solution was then treated with 100 mL dichloromethane, washed twice with water (2 × 100 mL), and worked up as usual. Chromatography on silica gel (column: 1 × 10 cm) with hexanes/dichloromethane (3/1) and recrystallization from dichloromethane/hexanes (1/1) yielded the nickel complex **11** as violet needles. M.p. 283–285 °C; yield 40 mg (75%). Stability (Buchler [24]). II.

Received: March 14, 1994 [Z 6761 IE]
Publication delayed at authors' request
German version: *Angew. Chem.* **1994**, *106*, 2402

[1] This nomenclature was suggested by M. Gosmann, B. Franck, *Angew. Chem.* **1986**, *98*, 1107; *Angew. Chem. Int. Ed. Engl.* **1986**, *25*, 1100; T. Wessel, B. Franck, M. Möller, U. Rotewald, M. Läge, *ibid.* **1993**, *105*, 1201 and **1993**, *32*, 1148.

[2] R. B. Woodward, *International Symposium on Aromaticity*, Sheffield, **1966**; see also M. J. Broadhurst, R. Grigg, A. W. Johnson, *J. Chem. Soc. Perkin Trans. 1* **1972**, 2111; V. J. Bauer, D. L. J. Clive, D. Dolphin, J. B. Paine III, F. L. Harris, M. M. King, J. Loder, S.-W. C. Wang, R. B. Woodward, *J. Am. Chem. Soc.* **1983**, *105*, 6429.

[3] A. W. Johnson in *The Porphyrins, Vol. 1* (Ed.: D. Dolphin), Academic Press, New York, **1978**, p. 235, and references therein.

[4] D. Mauzerall, *J. Am. Chem. Soc.* **1960**, *82*, 2601; A. R. Battersby, G. L. Hodgson, M. Ihara, E. McDonald, J. Saunders, *J. Chem. Soc. Perkin Trans. 1* **1973**, 2923; G. Bringmann, B. Franck, *Liebigs Ann. Chem.* **1982**, 1272.

[5] a) T. Mukaiyama, T. Sato, J. Hanna, *Chem. Lett.* **1973**, 1041; b) J. E. McMurry, M. P. Fleming, *J. Am. Chem. Soc.* **1974**, *96*, 4708; c) J. E. McMurry, *Acc. Chem. Res.* **1983**, *16*, 405; d) *Chem. Rev.* **1989**, *89*, 1513.

[6] a) E. Vogel, M. Köcher, H. Schmickler, J. Lex, *Angew. Chem.* **1986**, *98*, 262; *Angew. Chem. Int. Ed. Engl.* **1986**, *25*, 257; b) E. Vogel, *Pure Appl. Chem.* **1990**, *62*, 557; c) *ibid.* **1993**, *65*, 143; d) E. Vogel, P. Koch, X.-L. Hou, J. Lex, M. Lausmann, M. Kisters, M. A. Aukauloo, P. Richard, R. Guilard, *Angew. Chem.* **1993**, *105*, 1670; *Angew. Chem. Int. Ed. Engl.* **1993**, *32*, 1600.

[7] Photophysics: P. F. Aramendia, R. W. Redmond, S. Nonell, W. Schuster, S. E. Braslavsky, K. Schaffner, E. Vogel, *Photochem. Photobiol.* **1986**, *44*, 555; UV/Vis spectroscopy: J. Waluk, M. Müller, P. Swiderek, M. Köcher, E. Vogel, G. Hohlneicher, J. Michl, *J. Am. Chem. Soc.* **1991**, *113*, 5511; ^{15}N CPMAS NMR spectroscopy: B. Wehrle, H.-H. Limbach, M. Köcher, O. Ermer, E. Vogel, *Angew. Chem.* **1987**, *99*, 914; *Angew. Chem. Int. Ed. Engl.* **1987**, *26*, 934; ESR spectroscopy: A. Berman, A. Michaeli, J. Feitelson, M. K. Bowman, J. R. Norris, H. Levanon, E. Vogel, P. Koch, *J. Phys. Chem.* **1992**, *96*, 3041; J.

 © VCH Verlagsgesellschaft mbH, D-69451 Weinheim, 1994 0570-0833/94/2222-2311 $ 10.00+.25/0

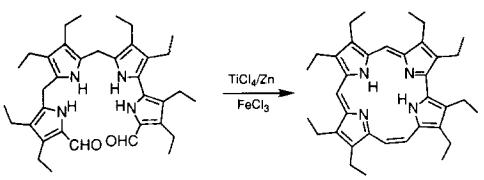
Schlüpmann, M. Huber, M. Toporowicz, M. Köcher, E. Vogel, H. Levanon, K. Möbius, *J. Am. Chem. Soc.* **1988**, *110*, 8566; cyclic voltammetry: J. P. Gisselbrecht, M. Gross, M. Köcher, M. Lausmann, E. Vogel, *ibid.* **1990**, *112*, 8618; C. Bernard, J. P. Gisselbrecht, M. Gross, E. Vogel, M. Lausmann, *Inorg. Chem.* **1994**, *33*, 2393.

[8] J. Waluk, J. Michl, *J. Org. Chem.* **1991**, *56*, 2729.

[9] The numbering of the systematic name of **3** deviates from that used in the text. Systematic name for the given structure of **3**: 21,22,23,24-tetraazapentacyclo-[16.2.1.1^{2,5}.1^{7,10}.1^{13,16}]tetracosa-1(20),2(21),3,5,7,9,11,13(23),14,16,18-undecene.

[10] [18]Porphyrins-(2.1.1.0), in the form of the nickel complexes of two regioisomeric triphenylcarboxyethyl derivatives, were first obtained by H. J. Callot et al. They were isolated as unexpected rearrangement products from a demetalation–metalation sequence involving homoporphyrins. A free-base porphyrin-(2.1.1.0), liberated from the corresponding nickel complex by the addition of concentrated sulfuric acid, proved to be a porphyrin-like aromatic compound. The structure of [18]porphyrin-(2.1.1.0) is midway between that of **1** and **2**. This prompted the authors to propose the name "hemiporphycene" for this new porphyrin isomer: H. J. Callot, B. Metz, T. Tschamber (unpublished). We are very grateful to Professor Callot for allowing us to view a draft of his manuscript.

[11] The synthetic principle involved in the preparation of the isocorroles (E. Vogel, Y. Hellwig, B. Binsack, J. Lex, unpublished) and corrphycenes—reductive carbonyl coupling of the corresponding α,ω-dialdehydes—was successfully applied to the preparation of hemiporphycenes. Thus, the α,ω-dialdehyde **12**, obtained in crude form, was converted into the octaethylhemiporphycene **13**



12 **13**

[violet crystals from dichloromethane/methanol (2/1), M.p. 219–220 °C; UV/Vis (dichloromethane): λ_{max} = 360 (ε = 40200), 405 (153700), 512 (7600), 552 (25900), 583 (9200), 632 nm (10800)], a species that can, in turn, be transformed into a wide range of metallohemiporphycenes: E. Vogel, M. Bröring, J. Lex, J. L. Sessler, unpublished results.

[12] Other novel porphyrinoid macrocycles have also been prepared recently by reductive carbonyl coupling: G. De Munno, F. Lucchesini, R. Neidlein, *Tetrahedron* **1993**, *49*, 6863; D. C. Miller, M. R. Johnson, J. J. Becker, J. A. Ibers, *J. Heterocycl. Chem.* **1993**, *30*, 1485; M. R. Johnson, D. C. Miller, K. Bush, J. J. Becker, J. A. Ibers, *J. Org. Chem.* **1992**, *57*, 4414; D. C. Miller, M. R. Johnson, J. A. Ibers, *ibid.* **1994**, *59*, 2877; Z. Hu, C. Scordilis-Kelley, M. P. Cava, *Tetrahedron Lett.* **1993**, *34*, 1879; Z. Hu, M. P. Cava, *ibid.* **1994**, *35*, 3493.

[13] PM3/UHF procedure implemented using the program MOPAC 6.0: J. J. P. Stewart, *J. Comput. Chem.* **1989**, *10*, 209. The authors thank Dipl.-Chem. M. Roeb, Institute of Physical Chemistry, University of Cologne, for the calculations.

[14] J. L. Sessler, T. Morishima, V. Lynch, *Angew. Chem.* **1991**, *103*, 1018; *Angew. Chem. Int. Ed. Engl.* **1991**, *30*, 977; J. L. Sessler, A. K. Burrell, *Top. Curr. Chem.* **1991**, *161*, 177.

[15] P. S. Clezy, C. J. R. Fookes, A. J. Liepa, *Aust. J. Chem.* **1972**, *25*, 1979.

[16] a) *Porphyrins and Metalloporphyrins* (Ed.: K. M. Smith), Elsevier, Amsterdam **1975**; b) H. Scheer, J. J. Katz in Ref.[16a], p. 399.

[17] No signals due to splitting of the possibly diastereotopic protons in the CH_2 groups were evident in the low-temperature ^{1}H NMR spectrum. Such splittings would imply an inversion process, and therefore also the existence of a nonplanar ring framework with C_s symmetry.

[18] H. Bürger in Ref.[16a], p. 528.

[19] Octaethylcorrphycene **10**: violet rhombic crystals from methanol/dichloromethane (2/1), m.p. 178–180 °C; UV/Vis (dichloromethane): λ_{max} (ε) = 414 (151900), 511 (15800), 541 (4000), 576 (6400), 585 sh (4400), 630 nm (2600); E. Vogel, J. L. Sessler, S. Pracht, M. Bröring, unpublished results. Compound **10** will be described fully in a planned publication on metallocorrphycenes.

[20] Crystal structure data of **10**: $C_{36}H_{46}N_4$, crystals from *tert*-butyl methyl ether; triclinic, space group $P\bar{1}$, a = 9.512(2), b = 12.773(3), c = 13.238(3) Å, α = 96.16(2), β = 93.68(2), γ = 106.36(2)°, Z = 2, ρ_{calcd} = 1.163 g cm^{-3}; μ_{Mo} = 4.70 cm^{-1}; 5359 independent reflections, 2411 observed reflections: θ_{max} = 25°; $R1$ = 0.0873, $wR2$ = 0.1906. Enraf-Nonius CAD4 diffractometer (room temperature, $Mo_{K\alpha}$ radiation, λ = 0.71069 Å). The structure was solved using direct methods, and refined (heavy atoms with anisotropic, H atoms with isotropic temperature factors) with F^2 for all observed reflections ($F_o^2 > 2\sigma F_o^2$); $wR2 = [\Sigma w(F_o^2 - F_c^2)^2/\Sigma w(F_o^2)^2]^{1/2}$. Program used: for the structure solution MolEN (Enraf–Nonius) and for refinement SHELXL-93 (G. M. Sheldrick, University of Göttingen); calculated on the DV facility of the regional calculation center of the University of Cologne. Further details of the crystal structure determination can be obtained from the Director of the Cambridge Crystallographic Data Centre, 12 Union Road, GB-Cambridge CB2 1EZ, on quoting the full journal citation.

[21] H. Furuta, T. Asano, T. Ogawa, *J. Am. Chem. Soc.* **1994**, *116*, 767.

[22] P. J. Chmielewski, L. Latos-Grażyński, K. Rachlewicz, T. Glowiak, *Angew. Chem.* **1994**, *106*, 805; *Angew. Chem. Int. Ed. Engl.* **1994**, *33*, 779.

[23] J. L. Sessler, *Angew. Chem.* **1994**, *106*, 1410; *Angew. Chem. Int. Ed. Engl.* **1994**, *33*, 1348.

[24] J. W. Buchler in Ref.[16a], p. 157.

Practical and Rapid Vicinal Hydroxylation of Alkenes by Catalytic Ruthenium Tetraoxide**

Tony K. M. Shing,* Vincent W.-F. Tai, and Eric K. W. Tam

The use of ruthenium tetraoxide as an oxidant for organic functional group transformations has been well recognized.[1] In 1981, the Sharpless group reported[2] an improved procedure for the cleavage of alkenes and oxidation of a range of functional groups with a catalytic amount of ruthenium tetraoxide and a stoichiometric amount (>2 equiv) of sodium metaperiodate in a two-phase solvent system (CCl_4, CH_3CN,[3] H_2O in a ratio of 2:2:3). This experimental protocol has since been employed for the oxidative fission of alkenes[2, 4] and diols,[5] and for the oxidation of primary alcohols,[6] and phenyl,[2, 7] furan,[8] and thiophene[8a] rings to carboxylic acids, of ethers to esters,[2, 9] of acetylenes to 1,2-diketones,[10] and of cyclic sulfites to cyclic sulfates.[11] However, the dihydroxylation[12] of olefins with RuO_4 has not been achieved in acceptable yields.[13] As an extension of Sharpless's work, we report here the first practical and rapid synthesis of vicinal *cis*-diols from alkenes with catalytic RuO_4.

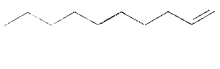
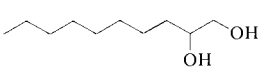
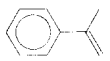
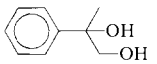
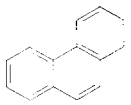
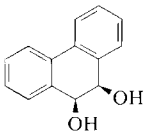
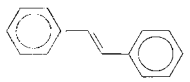
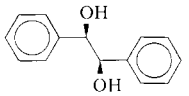
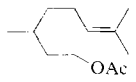
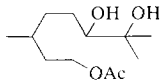
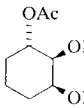
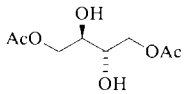
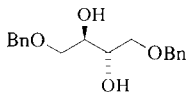
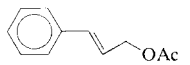
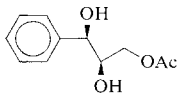
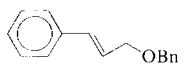
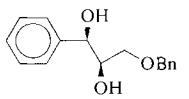
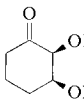
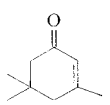
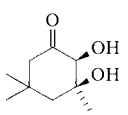
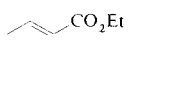
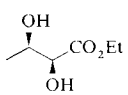
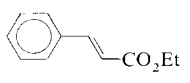
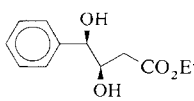
We found that when the reaction was conducted in a two-phase solvent system of ethyl acetate, acetonitrile, and water in a ratio of 3:3:1 in the presence of 0.07 molequiv of $RuCl_3 \cdot 3H_2O$ and 1.5 molequiv of $NaIO_4$ and at 0 °C, very rapid (within minutes) dihydroxylation of alkenes occurred in good yields. Our results shown in Table 1 indicate that this procedure works well with a wide range of alkenes. Simple olefins (entries 1–4) are particularly reactive, and the reactions were complete within 30 s. The C–C double bonds in allyl acetates and allyl benzyl ethers, as well as in α,β-unsaturated ketones and esters, all underwent facile *cis*-dihydroxylations within minutes. It appears that electron-withdrawing groups in conjugation with or adjacent to the C–C double bond tend to slow down the reaction a bit, but still these vicinal hydroxylations are very rapid and hence could be regarded as "flash dihydroxylations". It is noteworthy that the diastereoselectivity of the dihydroxylation of cyclohexenyl acetate (entry 8) was found to be roughly 10:1 in favor of the *anti* product. More examples of the diastereoselectivity of the flash dihydroxylation are being studied.

One limitation of this method is that if the resulting diol is highly soluble in water (entry 13), the yield of the reaction is poor, probably because of the concomitant oxidative cleavage

[*] Dr. T. K. M. Shing, V. W.-F. Tai, E. K. W. Tam
Department of Chemistry
The Chinese University of Hong Kong
Shatin, Hong Kong
Telefax: Int. code + (852) 603-5057

[**] This work was supported by the Croucher Foundation. We thank S. Y. Tong for technical assistance.

Table 1. Reaction times and yields of isolated products for the RuO_4-catalyzed *cis*-dihydroxylation of alkenes.

Entry	Alkene	Diol	*t* [min]	Yield [%]
1			0.5	67
2			0.5	58
3			0.5	58
4			0.5	70
5			3	65
6			3	60
7			3	67
8			3	72
9			3	68
10			3	76
11			3	69
12			3	68
13			0.5	36
14			3	81
15			3	55
16			3	77

of the diol in the aqueous layer by $NaIO_4$. This is also reflected in the results in entries 15 and 16; the lower yield of the former case is believed to be due to the higher solubility of the resultant diol in water. We are currently investigating an alternative co-oxidant to substitute for $NaIO_4$.

Since RuO_4 is both less toxic and less expensive than OsO_4, the present flash *cis*-dihydroxylation protocol should become an attractive alternative for the syntheses of vicinal diols.

Experimental Procedure

To a vigorously stirred solution of the alkene (1.0 mmol) in EtOAc/CH_3CN (6 mL each) at 0 °C (ice bath) was added a solution of $RuCl_3 \cdot 3H_2O$ (0.07 mmol) and $NaIO_4$ (1.5 mmol) in distilled water (2 mL). The two-phase mixture was stirred vigorously for 3 min and quenched with a saturated aqueous solution of $Na_2S_2O_3$ (10 mL). The aqueous phase was separated and extracted with EtOAc (3 × 15 mL). The combined extracts were dried ($MgSO_4$) and filtered. Concentration of the filtrate followed by flash chromatography afforded the diol.

Received: June 20, 1994 [Z70531E]
German version: *Angew. Chem.* **1994**, *106*, 2408

[1] Review: J. L. Courtney in *Organic Syntheses by Oxidation with Metal Compounds* (Eds.: W. J. Mijs, C. R. H. I. De Jonge), Plenum, New York, **1986**, Chapter 8, p. 445.
[2] P. H. J. Carlsen, T. Katsuki, V. S. Martîn, K. B. Sharpless, *J. Org. Chem.* **1981**, *46*, 3936.
[3] CH_3CN was added to prevent catalyst inactivation and was crucial for the increased effectiveness and reliability of the catalytic RuO_4 oxidations.
[4] a) F. X. Webster, J. Rivas-Enterrios, R. M. Silverstein, *J. Org. Chem.* **1987**, *52*, 689; b) B. E. Rossiter, T. Katsuki, K. B. Sharpless, *J. Am. Chem. Soc.* **1981**, *103*, 464.
[5] a) V. S. Martîn, M. T. Nuñez, C. E. Tonn, *Tetrahedron Lett.* **1988**, *29*, 2701; b) M. Caron, P. R. Carlier, K. B. Sharpless, *J. Org. Chem.* **1988**, *53*, 5185.
[6] a) J. M. Chong, K. B. Sharpless, *J. Org. Chem.* **1985**, *50*, 1560; b) S. J. Hecker, M. L. Minich, *ibid.* **1990**, *55*, 6051.
[7] a) M. T. Nuñez, V. S. Martîn, *J. Org. Chem.* **1990**, *55*, 1928; b) M. Kasai, H. Ziffer, *ibid.* **1983**, *48*, 712.
[8] a) M. Kasai, H. Ziffer, *J. Org. Chem.* **1983**, *48*, 2346; b) Y. Kobayashi, M. Kusakabe, Y. Kitano, F. Sato, *ibid.* **1988**, *53*, 1586.
[9] P. F. Schuda, M. B. Cichowicz, M. R. Heimann, *Tetrahedron Lett.* **1983**, *24*, 3829.
[10] a) R. Zibuck, D. Seebach, *Helv. Chim. Acta* **1988**, *71*, 237; b) G. Adam, R. Zibuck, D. Seebach, *J. Am. Chem. Soc.* **1987**, *109*, 6176.
[11] Y. Gao, K. B. Sharpless, *J. Am. Chem. Soc.* **1988**, *110*, 7538.
[12] At present, OsO_4 is the most reliable reagent for the *cis*-dihydroxylation of alkenes to give the corresponding *cis*-diols: M. Schröder, *Chem. Rev.* **1980**, *80*, 187.
[13] Sharpless and Akashi reported the first successful stereospecific *cis*-dihydroxylation of *E*- and *Z*-cyclododecenes with RuO_4 at −78 °C (ca. 20% yield in each case), but they commented that this was not a practical route to diols owing to the poor yields: K. B. Sharpless, K. Akashi, *J. Am. Chem. Soc.* **1976**, *98*, 1986.

Self-Assembly of a Dimeric Porphyrin Host**

Christopher A. Hunter* and Luke D. Sarson

Biological receptors are often composed of multicomponent assemblies of flexible molecules which organize themselves into well-defined three-dimensional structures. The binding sites thus generated can show a very high substrate complementary.[1] Viruses are one of the most spectacular examples, where a single nucleic acid strand is recognized by an assembly of thousands of proteins.[2] The underlying principle, self-assem-

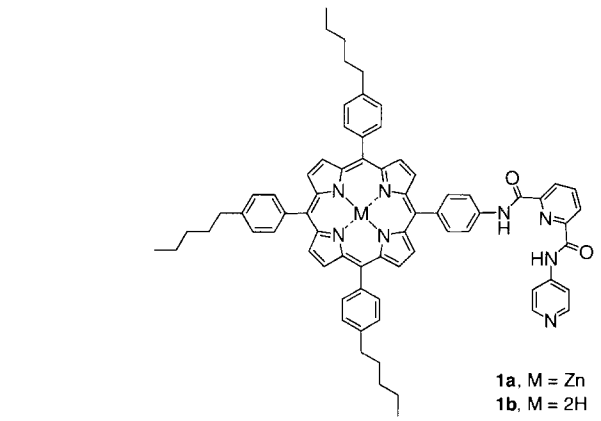
[*] Dr. C. A. Hunter, L. D. Sarson
Department of Chemistry
University of Sheffield
Sheffield S3 7HF (UK)
Telefax: Int. code +(742) 738673

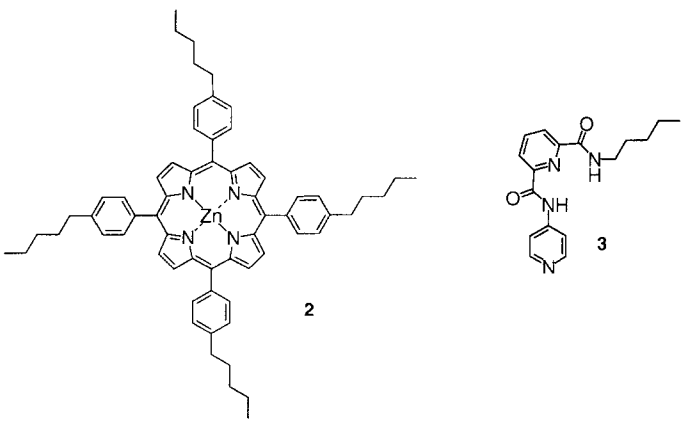
[**] This research was supported by the Overseas Research Council, Glaxo, and The University of Sheffield. We thank Sue Bradshaw for the molecular weight determination by vapor pressure osmometry.

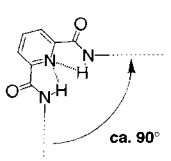
bly, has only recently begun to be exploited by chemists in the design of synthetic molecular receptors.[3] We describe here the use of metalloporphyrin coordination chemistry to direct the self-assembly of a very stable cyclic porphyrin dimer which recognizes derivatives of terephthalic acid through hydrogen-bonding interactions.

The coordination of a pyridine ligand to a zinc porphyrin is an ideal interaction for the study of noncovalent self-assembly.[4, 5] Since the association constant for the interaction is roughly $10^3\ M^{-1}$, the complexes are reasonably stable. Complexation can be detected by a range of spectroscopic techniques allowing self-assembly to be monitored across a wide range of concentrations. Finally, the properties of the assemblies can be readily tuned by chemical synthesis.[6]

The metal centers in zinc porphyrins such as **1a** and **2** are five-coordinate and can coordinate one pyridine ligand such as **3** perpendicular to the plane of the porphyrin. Therefore a self-assembled dimer can be generated if a pyridine ligand is covalently attached to a zinc porphyrin, oriented at 90° to the plane of the porphyrin. Molecular modeling suggested that this could be achieved by using a 2,6-pyridine-dicarboxamide to connect the porphyrin and the pyridine.[7] This linker has internal hydrogen bonds which reduce the 120° angle expected for *meta*-substituted arenes to approximately 96° (Scheme 1).[8]

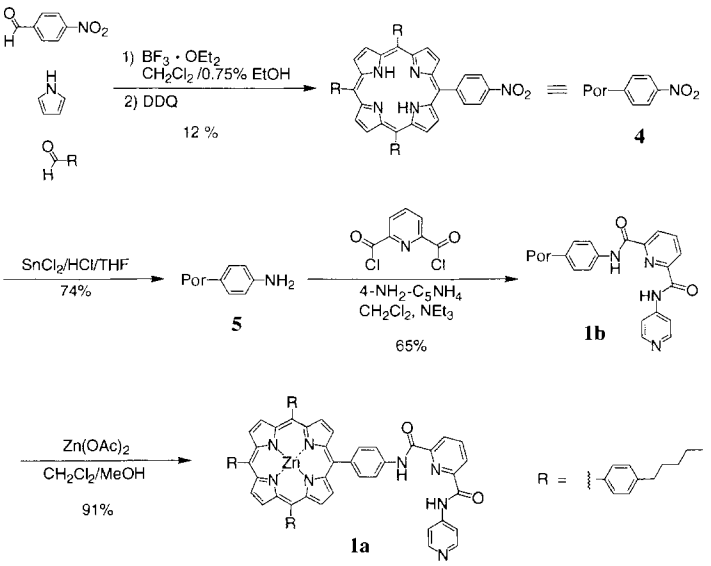




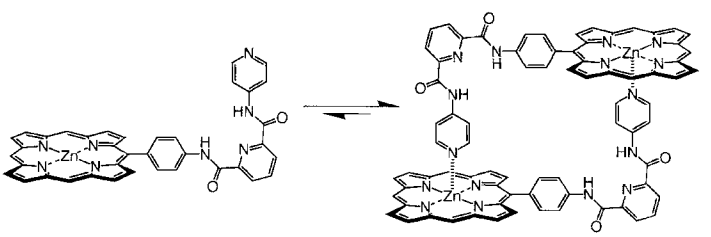


Scheme 1. The arms of a 2,6-pyridinedicarboxamide derivative are oriented approximately perpendicular to one another.

The synthesis of **1a** is outlined in Scheme 2. Results from a range of spectroscopic measurements all indicate that **1a** exists exclusively as a self-assembled dimer at concentrations between 10^{-7} and 10^{-2} M in chlorinated organic solvents at room temperature (Scheme 3). The ^{1}H NMR and UV/VIS absorption and emission spectra of **1a** are essentially concentration independent in this range and differ significantly from the corresponding spectra of **2** (see e.g. Fig. 1). The ^{1}H NMR signals due to the pyridine protons are shifted upfield, which suggests that they lie over the face of the porphyrin ring and are affected by the porphyrin ring current. The maxima in the UV/VIS absorption and emission maxima are both red-shifted. In fact, the spectra of **1a** closely resemble the spectra of the reference complex **2** · **3** (see e.g. Fig. 1), which implies that **1a** is fully bound across this concentration range. Vapor pressure osmometry gave an average molecular weight of 2233 ± 79 g mol^{-1} for **1a** in $CHCl_3$ solution at 37 °C. This corresponds to 1.98 ± 0.07 molecules of **1a** per assembly.[9]



Scheme 2. Synthesis of zinc porphyrin complex **1a**. DDQ = 2,3-dichloro-5,6-dicyano-1,4-benzoquinone.



Scheme 3. Self-assembly of the dimer of **1a**. The 4-pentylphenyl substituents on the *meso* positions of the porphyrin are omitted for clarity.

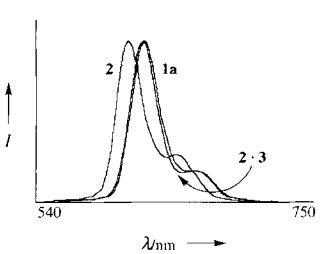
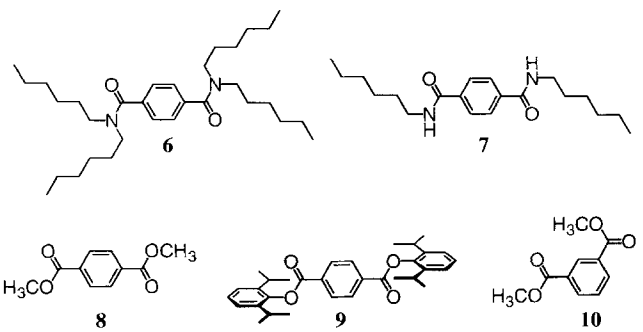


Fig. 1. UV/VIS emission spectra of **1a**, **2**, and the complex **2** · **3** (CH_2Cl_2, $c = 10^{-6}$ M).

At concentrations below 10^{-7} M, the UV/VIS emission spectra of **1a** becomes concentration dependent, but at low concentrations the signals become less intense and disappear into the noise. The association constant is therefore difficult to determine with any degree of accuracy but is at least $10^8\ M^{-1}$ in CH_2Cl_2. This indicates a remarkable degree of cooperativity in the self-assembly process, given that the corresponding association constant for the reference complex **2** · **3** is $5.6 \times 10^3\ M^{-1}$ in CH_2Cl_2. The orientation of the two recognition sites and the rigidity of the linking group ensure that **1a** is almost perfectly self-complementary and so self-assembles very efficiently.

Self-assembly of the dimer of **1a** generates a macrocyclic complex containing a spacious cavity with inwardly directed hydrogen-bond recognition sites. The recognition properties of the dimer were investigated by ^{1}H NMR titration with substrates **6**–**10** in $CDCl_3$ (Table 1). The dimer of **1a** selectively



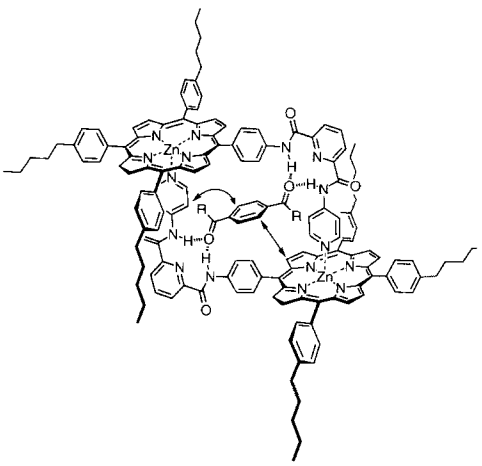
binds terephthalic acid derivatives that can form a hydrogen bond with each of the four amide groups directed into the cavity (Scheme 4). Amides **6** and **7** are bound more strongly than the ester **8**, possibly because of the greater basicity of the amide oxygens. Increasing steric bulk around the carbonyl group as in **9** inhibits complexation. Isophthalic acid derivatives such as **10** are bound only weakly, as the distance between the carbonyl groups is too short for the simultaneous formation of hydrogen bonds to the amide groups at both ends of the cavity. Complexation can be observed with the free base porphyrin **1b**, but the association constants are more than an order of magnitude less than those measured for **1a**.

Table 1. Association constants [M^{-1}] determined by titration in $CDCl_3$ followed by ^{1}H NMR spectroscopy. Errors are ±10%.

Guest	Host	
	1a	**1b**
6	1400	18
7	>1400 [a]	– [a]
8	40	2
9	<1	<1
10	<1	<1

[a] Owing to the low solubility of 7 these association constants cannot be determined accurately.

The structure in Scheme 4 is supported by the observed complexation-induced changes in chemical shifts in the ^{1}H NMR spectra. The signals due to the amide protons in **1a** are shifted downfield on complexation, indicating that they are involved in hydrogen-bonding interactions with the carbonyl groups of the



Scheme 4. The dimer of **1a** recognizes terephthalic acid derivatives by hydrogen-bonding to the carbonyl oxygens. Intermolecular NOEs observed for the complex $(\mathbf{1a})_2 \cdot \mathbf{8}$ are indicated with arrows. R = $NH(CH_2)_5CH_3$.

guest. The signals of the guest are shifted upfield on complexation, suggesting that the guest molecule is positioned over the porphyrin plane and is affected by the porphyrin ring current. NOEs observed in a two-dimensional ^{1}H NMR NOESY spectrum confirm that the guests are complexed inside the cavity rather than on the outside face of one of the porphyrins (Scheme 4).

We have demonstrated a powerful new approach to the construction of functionalized macrocycles with cavities suitable for selective molecular recognition. Since the self-assembly is under thermodynamic control, the macrocyclization is quantitative, which offers significant advantages over the formation of macrocycles through covalent bonds.[1] Owing to the high degree of cooperativity between the interaction sites, **1a** exists as the fully assembled dimer at all concentrations examined. In addition, the rich photochemistry of the porphyrin units may confer interesting photochemical properties on such assemblies.

Experimental Procedure

4: 4-Nitrobenzaldehyde (4.97 g, 32.85 mmol) and 4-pentylbenzaldehyde (10.1 g, 57.2 mmol) were dissolved in 9 L of dry CH_2Cl_2 containing 58.5 mL of dry ethanol and freshly distilled pyrrole (6.25 mL, 90 mmol). The solution was purged with N_2 for 10 min. Then $BF_3 \cdot OEt_2$ (5.1 mL, 40.6 mmol) was added, and the solution was stirred for 90 min. 2,3-Dichloro-5,6-dicyano-1,4-benzoquinone (DDQ) (20.5 g, 90 mmol) was added, and the solution was stirred for 90 min. NEt_3 (12.6 mL, 90 mmol) was added, and the solution was concentrated to dryness on a rotary evaporator. The resulting solid was placed on a glass sinter and washed with 20 L of CH_3OH. The porphyrin products were purified by repeated column chromatography (florisil then silica gel, $CHCl_3$/petroleum ether). Recrystallization from $CHCl_3/CH_3OH$ gave **4** as a purple solid. Yield 2.3 g (12%). ^{1}H NMR (400 MHz, $CDCl_3$): δ = 8.92 (2H, d), 8.88 (4H, s), 8.73 (2H, d), 8.63 (2H, d), 8.40 (2H, d), 8.12 (6H, d), 7.56 (6H, d), 2.96 (6H, t), 1.93 (6H, quint.), 1.54 (12H, m), 1.04 (9H, t), −2.75 (2H, s); FAB-MS: *m/z* 869 [M^+]. UV/VIS (CH_2Cl_2): λ_{max} [nm] = 421, 518, 554, 593, 649.

5: To a solution of **4** (0.63 g, 0.73 mmol) in 30 mL of THF was added $SnCl_2 \cdot 2H_2O$ (1.45 g, 6.5 mmol) in 25 mL of concd HCl. The mixture was vigorously stirred in a preheated oil bath (65–70 °C) and then cautiously made basic with concd NH_3. 100 mL of $CHCl_3$ was added, and the mixture was stirred for 30 min. The organic layer was put aside, and the aqueous layer was extracted into $CHCl_3$ three times. The combined organic phases were filtered, washed once with dilute NH_3, three times with H_2O, and concentrated to dryness (70 °C, 1 Torr). The residue was purified by column chromatography (silica gel, $CHCl_3$). Recrystallization from $CHCl_3/CH_3OH$ gave **5** as a purple solid. Yield 0.45 g (74%). ^{1}H NMR (400 MHz, $CDCl_3$): δ = 8.91 (2H, d), 8.87 (4H, s), 8.87 (2H, d), 8.11 (6H, d), 7.99 (2H, d), 7.53 (6H, d), 7.05 (2H, d), 2.95 (6H, t), 1.92 (6H, quint.), 1.53 (12H, m), 1.04 (9H, t), −2.75 (2H, s); FAB-MS: *m/z*: 840 [M^+]. UV/VIS (CH_2Cl_2): λ_{max} [nm] = 422, 519, 557, 594, 650.

1b: To a solution of **5** (94 mg, 0.112 mmol), 4-aminopyridine (242 mg, 2.58 mmol) and dry NEt_3 (0.38 mL, 2.73 mmol) in 100 mL of dry CH_2Cl_2 was added over

20 min a solution of pyridine-2,6-dicarbonyl dichloride (275 mg, 1.35 mmol) in 50 mL of dry CH_2Cl_2. After 20 h of stirring the mixture was washed with 1 M HCl twice, then 1 M KOH, and H_2O before it was dried over Na_2SO_4. Column chromatography (silica gel, CH_2Cl_2/CH_3OH) followed by recrystallization from $CHCl_3$/petroleum ether gave **1b** as a purple solid. Yield 77 mg (65%). ^1H NMR (400 MHz, $CDCl_3$): δ = 9.77 (1H, s), 9.70 (1H, s), 8.90 (2H, d), 8.88 (2H, d), 8.87 (4H, d), 8.69 (1H, d), 8.67 (2H, d), 8.60 (1H, d), 8.31 (2H, d), 8.28 (1H, t), 8.18 (2H, d), 8.12 (6H, d), 7.80 (2H, d), 7.56 (6H, d), 2.95 (6H, t), 1.93 (6H, quint.), 1.53 (12H, m), 1.02 (9H, t), −2.75 (2H, s). FAB-MS: *m/z* 1065.4 [M^+]. UV/VIS (CH_2Cl_2): λ_{max} [nm] = 421, 518, 554, 593, 649.

1a: A solution of **1b** (77 mg, 0.072 mmol) and $Zn(OAc)_2$ (135 mg, 0.616 mmol) in 10 mL of CH_2Cl_2/CH_3OH was stirred for 60 min. Column chromatography (basic alumina, CH_2Cl_2/CH_3OH) followed by recrystallization from CH_2Cl_2/petroleum ether gave **1a** as a purple solid. Yield 74 mg (91%). ^1H NMR (400 MHz, $CDCl_3$): δ = 9.28 (1H, s), 8.93 (2H, d), 8.88 (2H, d), 8.87 (2H, d), 8.78 (2H, d), 8.76 (1H, s), 8.45 (2H, d), 8.20 (2H, d), 8.19 (2H, br.), 8.18 (2H, d), 8.15 (1H, d), 8.05 (4H, d), 8.01 (1H, t), 7.57 (2H, d), 7.51 (4H, d), 5.97 (2H, d), 3.00 (2H, t), 2.93 (4H, t), 2.49 (2H, br.), 1.94 (2H, quint.), 1.92 (4H, quint.), 1.53 (12H, m), 1.04 (3H, t), 1.02 (6H, t). FAB-MS: *m/z* 1127 [M^+]. UV/VIS (CH_2Cl_2): λ_{max} [nm] = 431, 565, 606.

Received: June 24, 1994 [Z 7072 IE]
German version: *Angew. Chem.* **1994**, *106*, 2424

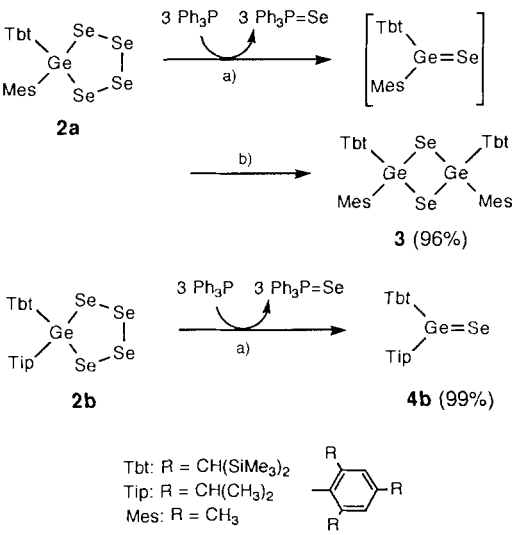
[1] J. S. Lindsey, *New J. Chem.* **1991**, *15*, 153.
[2] A. Klug, *Angew. Chem.* **1983**, *95*, 579; *Angew. Chem. Int. Ed. Engl.* **1983**, *22*, 565.
[3] M. Kim, G. W. Gokel, *J. Chem. Soc. Chem. Commun.* **1987**, 1686; A. Schepartz, J. P. McDevitt, *J. Am. Chem. Soc.* **1989**, *111*, 5976; M. Fujita, J. Yazaki, K. Ogura, *J. Am. Chem. Soc.* **1990**, *112*, 5645; O. F. Schall, K. Robinson, J. L. Atwood, G. W. Gokel, *ibid.* **1991**, *113*, 7434; A. W. Schwabacher, J. Lee, H. Lei, *ibid.* **1992**, *114*, 7597; C. M. Drain, R. Fischer, E. G. Nolen, J.-M. Lehn, *J. Chem. Soc. Chem. Commun.* **1993**, 243; N. Branda, R. Wyler, J. Rebek, *Science* **1994**, *263*, 1267.
[4] U. Rempel, B. von Maltzen, C. von Borczyskowski, *Pure Appl. Chem.* **1993**, *65*, 1681; H. L. Anderson, *Inorg. Chem.* **1994**, *33*, 972; Y. Kobuke, H. Miyaji, *J. Am. Chem. Soc.* **1994**, *116*, 4111.
[5] S. Anderson, H. L. Anderson, J. K. M. Sanders, *Acc. Chem. Res.* **1993**, *26*, 469.
[6] J. S. Lindsey, R. W. Wagner, *J. Org. Chem.* **1989**, *54*, 828.
[7] C. A. Hunter, D. H. Purvis, *Angew. Chem.* **1992**, *104*, 779; *Angew. Chem. Int. Ed. Engl.* **1992**, *31*, 792; Y. Hamuro, S. J. Geib, A. D. Hamilton, *ibid.* **1994**, *106*, 465 and **1994**, *33*, 446.
[8] Molecular modeling was performed on a Silicon Graphics Indigo 2 workstation using the Macromodel implementation of the MM3 force field.
[9] Data is at the 95% confidence level.

Synthesis and Structure of the First Stable Germaneselone**

Tsuyoshi Matsumoto, Norihiro Tokitoh, and Renji Okazaki*

Recently much attention has been paid to the chemistry of compounds containing multiple bonds with Group 14 elements.[1] Species with double bonds between germanium and Group 16 elements are congeners of carbonyl compounds and are of current interest because of their unusual structure and reactivity. We recently reported[2] the synthesis and crystal structure of the first germanethione Tbt(Tip)Ge=S (**1**), which is kinetically stabilized by virtue of the two sterically bulky protecting groups, namely, 2,4,6-tris[bis(trimethylsilyl)methyl]-phenyl (Tbt[3]) and 2,4,6-tris(isopropy)phenyl (Tip). In contrast to germanethiones, which have been reported in the literature,[4] very little is known about germaneselones (species containing a germanium–selenium double bond).[5] We report here on the synthesis, structure, and reactivity of the first stable diaryl germaneselone Tbt(Tip)Ge=Se (**4b**).

1,2,3,4,5-Tetraselenagermolanes (**2a**, Ar = Mes; **2b**, Ar = Tip)[6] were treated with 3 equiv of triphenylphosphine in hexane (Scheme 1). In the case of **2a**, only 1,3,2,4-diselenadigermetane **3**, a dimerization product of the intermediate Tbt(Mes)Ge=Se (**4a**), was obtained along with a quantitative amount of triphenylphosphine selenide. A similar dimerization reaction was also previously observed for mesityl-substituted germanethione Tbt(Mes)Ge=S.[7]



Scheme 1. a) hexane/Δ; b) dimerization.

By contrast, the reaction of **2b**, which bears bulkier groups on the germanium atom, gave a red solution. After filtration of precipitated triphenylphosphine selenide under argon, the red solution was concentrated to give almost pure germaneselone **4b** as red crystals. Germaneselone **4b** was extremely sensitive to oxygen and moisture, but it was thermally quite stable under inert atmosphere.

The X-ray structure analysis[8] of **4b** reveals that the two bulky groups effectively prevent the oligomerization of the germanium–selenium bond; **4b** is monomeric in the solid state (Fig. 1). The sum of the bond angles around the germanium atom is 359.3°; this indicates that a trigonal planar geometry is adopted by the Ge=Se unit. It is also notable that the Ge–Se bond length (2.180(2) Å) is approximately 10% less than that reported for typical Ge–Se single bonds;[6a, 9] this result agrees well with the calculated value.[10] There seems no significant conjugation between the two aryl groups and the Ge–Se double bond in the solid state: the dihedral angles between the aryl planes and the plane containing Ge(1), Se(1), C(1), and C(10) atoms are 38.85° for the Tbt group and 70.13° for the Tip group.

Germaneselone **4b** gave satisfactory spectral and analytical data. The ^{77}Se NMR spectrum shows one singlet (at δ = 940.6) at much lower field than is typical for compounds containing a Ge–Se single bond (e.g., the ^{77}Se NMR signal for $(H_3Ge)_2Se$ is observed at δ = −612 relative to $(H_3C)_2Se$).[11] On the other hand, most of dialkyl selenoketones give rise to signals in the range δ = 1600–2200.[12] Germaneselone **4b** shows a character-

[*] Prof. Dr. R. Okazaki, T. Matsumoto, Prof. Dr. N. Tokitoh
Department of Chemistry, Graduate School of Science
The University of Tokyo
7-3-1 Hongo, Bunkyo-ku, Tokyo 113 (Japan)
Telefax: Int. +(3)5800-6899

[**] This work was supported by the Ministry of Education, Science, and Culture, Japan (grant no. 05236102). We are grateful to Dr. Y. Furukawa, The University of Tokyo, and Mr. K. Kawauchi, JEOL, for the measurement of the FT Raman spectrum of **4b**. We also thank ASAI Germanium Research Institute, Shin-etsu, and Tosoh Akzo for the generous gifts of tetrachlorogermane, chlorosilanes, and alkyllithiums, respectively.

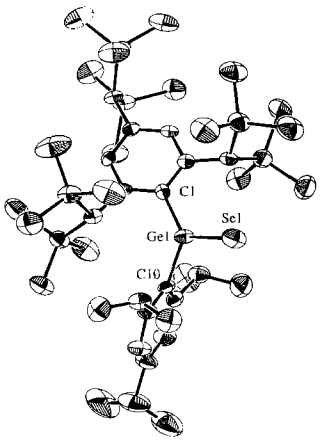
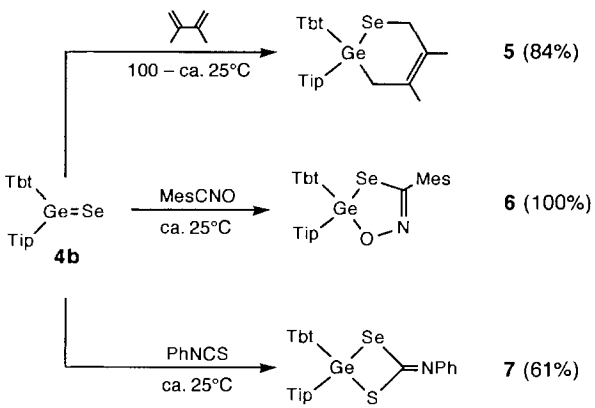


Fig. 1. ORTEP plot of the crystal structure of **4b** with thermal ellipsoids at the 30% probability level. Selected bond lengths [Å] and bond angles [°]: Ge1-Se1 2.180(2), Ge1-C1 1.932(9), Ge1-C10 1.945(9); Se1-Ge1-C1 126.4(3), Se1-Ge1-C10 113.8(3), C1-Ge1-C10 119.1(4).

istic strong Raman band at 382 cm^{-1} corresponding to the stretching frequency of the Ge=Se unit; the energy of this vibration is less than that for germanethione **1** (521 cm^{-1}). In the electronic spectrum, an absorption maximum attributed to the n–π* transition of the Ge=Se bond appears at 519 nm ($\varepsilon = 140$); this band is red-shifted compared to that in germanethione **1** (450 nm). A similar effect is observed in the corresponding carbon analogues (thioketone vs selenoketone).[13]

Reaction of **4b** with 2,3-dimethyl-1,3-butadiene in hexane in a sealed tube at 100 °C gave [4 + 2] cycloadduct **5** in 84% yield. Similarly, **4b** readily reacted with mesitonitrile oxide and phenyl isothiocyanate to produce [3 + 2] and [2 + 2] cycloadducts **6** and **7**, respectively. These results indicate that the germaneselone has double-bond character similar to that observed in its selenoketone carbon analogue.[13b, 14]



The thermal behavior of the [4 + 2] cycloadduct **5** should be noted: When a hexane solution of **5** was heated at 50 °C, the color of the solution changed from colorless to red. The fact that this change was reversible and that the thermally induced reaction (50 °C) of **5** in the presence of mesitonitrile oxide gave **6** (90%) shows that **5** undergoes facile retro-Diels–Alder reaction. Hence, **5** may be regarded as a useful, stable source of germaneselone **4b**.

Experimental Procedure

4b: An orange solution of **2b** (500 mg, 0.436 mmol) and triphenylphosphine (340 mg, 1.30 mmol) in hexane (3 mL) was refluxed for 2 h under an argon atmosphere. The solution turned red, and triphenylphosphine selenide was precipitated quantitatively with cooling to room temperature. After filtration of the selenide under argon, the residual red solution was concentrated in a glovebox filled with argon to give pure germaneselone **4b** (392 mg, 99% yield) as red crystals; m.p. 191–194 °C; ^{1}H NMR (500 MHz, C_6D_6, 27 °C, TMS): δ = 0.148 (s, 18H), 0.177 (s, 18H), 0.247 (s, 18H), 1.19 (d, ^3J(H,H) = 6.9 Hz, 6H), 1.34 (d, ^3J(H,H) = 6.9 Hz, 6H), 1.46 (d, ^3J(H,H) = 6.9 Hz, 6H), 1.49 (s, 1H), 2.73 (sept, ^3J(H,H) = 6.9 Hz, 1H), 3.40 (br.s, 1H), 3.41 (sept, ^3J(H,H) = 6.9 Hz, 2H), 3.79 (br.s, 1H), 6.51 (br.s, 1H), 6.68 (br.s, 1H), 7.05 (s, 2H); ^{13}C NMR (125 MHz, C_6D_6, 27 °C, TMS): δ = 1.11 (q), 1.37 (q), 1.67 (q), 22.28 (q), 24.09 (q × 2), 27.39 (d), 29.08 (br.d × 2), 31.83 (d), 34.83 (d), 36.52 (d), 122.64 (d × 2), 124.38 (d), 128.29 (d), 144.04 (s), 147.42 (s), 149.58 (s), 150.06 (s), 150.43 (s), 151.01 (s × 2), 152.08 (s); ^{77}Se NMR (51.5 MHz, C_6D_6, 27 °C, Me_2Se): δ = 940.6; FT Raman (solid, excitation with Nd-YAG laser, 1064 nm) 382 cm^{-1}. FAB-MS: *m/z* found: 908.3455; calcd: $C_{42}H_{83}{}^{74}GeSeSi_6$: 908.3409 ($[M + H]^+$).

Received: July 7, 1994 [Z 7106 IE]
German version: *Angew. Chem.* **1994**, *106*, 2418

[1] a) J. Barrau, J. Escudié, J. Satgé, *Chem. Rev.* **1990**, *90*, 283; b) J. Satgé, *Adv. Organomet. Chem.* **1982**, *21*, 241; c) P. Rivière, M. Rivière-Baudet, J. Satgé, *Comprehensive Organometallic Chemistry, Vol. 2*, Pergamon, New York, **1982**, p. 399, and references there in.

[2] N. Tokitoh, T. Matsumoto, K. Manmaru, R. Okazaki, *J. Am. Chem. Soc.* **1993**, *115*, 8855. The synthesis and some reactions of the corresponding stannanethione and stannaneselone have also been reported: N. Tokitoh, M. Saito, R. Okazaki, *ibid.* **1993**, *115*, 2065; Y. Matsuhashi, N. Tokitoh, R. Okazaki, M. Goto, *Organometallics* **1993**, *12*, 2573.

[3] Although 2,4,6-tris[bis(trimethylsilyl)methyl]phenyl group has been denoted as Tb in our previous papers, we will now use the abbreviation Tbt in order to avoid confusion with the chemical symbol for terbium.

[4] Germanethiones: a) J. Barrau, V. Balaji, J. Michl, *Organometallics* **1989**, *8*, 2034; b) V. N. Khagashesku, S. E. Boganov, P. S. Zuev, O. M. Nefedov, J. Tamás, A. Gömöry, I. Besenyei, *J. Organomet. Chem.* **1991**, *402*, 161; c) M. Veith, S. Becker, V. Huch, *Angew. Chem.* **1989**, *101*, 1287; *Angew. Chem. Int. Ed. Engl.* **1989**, *28*, 1237; d) M. Veith, A. Detemple, V. Huch, *Chem. Ber.* **1991**, *124*, 1135; See also ref. [1].

[5] Dimesityl germaneselone as intermediate: T. Tsumuraya, S. Sato, W. Ando, *Organometallics* **1988**, *7*, 2051.

[6] a) N. Tokitoh, T. Matsumoto, R. Okazaki, *Tetrahedron Lett.* **1992**, *33*, 2531; synthesis of Tbt(Ar)MX_4 (M = Si, Ge, Sn; X = S, Se): b) N. Tokitoh, H. Suzuki, T. Matsumoto, Y. Matsuhashi, R. Okazaki, M. Goto, *J. Am. Chem. Soc.* **1991**, *113*, 7047; c) N. Tokitoh, Y. Matsuhashi, R. Okazaki, *Tetrahedron Lett.* **1991**, *32*, 6151; d) Y. Matsuhashi, N. Tokitoh, R. Okazaki, M. Goto, S. Nagase, *Organometallics* **1993**, *12*, 1351.

[7] N. Tokitoh, T. Matsumoto, H. Ichida, R. Okazaki, *Tetrahedron Lett.* **1991**, *32*, 6877.

[8] Crystallographic data for **4b**: $C_{42}H_{82}GeSeSi_6$, M = 907.17, triclinic, a = 13.507(2), b = 20.662(5), c = 9.468(2) Å, α = 96.35(2), β = 89.49(2), γ = 98.49(2)°, V = 2597(1) Å^3, Z = 2, space group $P\bar{1}$, $\rho_{calcd.}$ = 1.160 g cm^{-3}, μ = 14.35 cm^{-1}. The crystal was mounted in a glass capillary. Data was collected on a Rigaku AFC5R diffractometer with $Mo_{K\alpha}$ radiation (λ = 0.71069 Å, graphite monochromator), and the structure solved by direct methods. All non-hydrogen atoms were refined anisotropically. The final cycle of full-matrix least-squares refinement was based upon 3395 observed reflections [$I > 3\sigma(I)$] and 451 variable parameters with R (R_w) = 0.058 (0.062). Intermolecular Ge···Se distance between neighboring molecules in the crystals was found to be 5.690(2) Å. Further details of the crystal structure investigation are available on request from the Director of the Cambridge Crystallographic Data Centre, 12 Union Road, GB-Cambridge CB2 1EZ (UK), on quoting the full journal citation.

[9] The Ge–Se single-bond length ranges from 2.337 to 2.421 Å: a) M. Weidenbruch, A. Ritschl, K. Peters, H. G. Schnering, *J. Orgamomet. Chem.* **1992**, *438*, 39; b) M. Dräger, K. Häberle, *ibid.* **1985**, *280*, 183; c) V. L. Ross, M. Dräger, *Z. Anorg. Allg. Chem.* **1981**, *472*, 109, and references therein.

[10] The Ge–Se bond length in H_2Ge=Se was calculated [HF/DZ(d, p)] to be 2.152 Å. S. Nagase, Yokohama National University, private communication.

[11] H. C. E. McFahrlane, W. McFarlane in *Multinuclear NMR* (Ed.: J. Mason), Plenum Press, New York, **1987**, p. 417, and references therein.

[12] a) T. C. Wong, F. S. Guziec, Jr., C. A. Moustakis, *J. Chem. Soc. Perkin Trans. 2* **1983**, 1471; b) E. R. Cullen, F. S. Guziec, Jr., C. J. Murphy, T. C. Wong, K. K. Andersen, *J. Am. Chem. Soc.* **1981**, *103*, 7055; c) R. Okazaki, A. Ishii, N. Inamoto, *J. Chem. Soc. Chem. Commun.* **1983**, 1429.

[13] a) Thioketones: F. Duus in *Comprehensive Organic Chemistry, Vol. 3* (Eds.: D. H. R. Barton, W. D. Ollis), Pergamon, Oxford, **1979**, p. 373; b) Selenoketones: F. S. Guziec, Jr., in *The Chemistry of Organic Selenium and Tellurium Compounds, Vol. 2* (Ed.: S. Patai), Wiley, New York, **1986**, p. 215, and references therein.

[14] a) G. Erker, R. Hock, C. Krüger, S. Werner, F.-G. Klärner, U. Artschwager-Perl, *Angew. Chem.* **1990**, *102*, 1082; *Angew. Chem. Int. Ed. Engl.* **1990**, *29*, 1067; b) R. Boese, A. Haas, M. Spehr, *Chem. Ber.* **1991**, *124*, 51; c) M. Segi, T. Takahashi, H. Ichinose, G. M. Li, T. Nakajima, *Tetrahedron Lett.* **1992**, *33*, 7865; d) K. Okuma, K. Kojima, I. Kaneko, H. Ohta, *Chem. Lett.* **1991**, 1053; e) K. Okuma, K. Kojima, H. Ohta, *Phosphorus Sulfur Silicon* **1993**, *80*, 259.

 © VCH Verlagsgesellschaft mbH, D-69451 Weinheim, 1994 0570-0833/94/2222-2317 $ 10.00+.25/0

Biomimetic Model for a Photosynthetic Reaction Center: A Porphyrin with a Covalently Linked, Redox-Active Crown Ether**

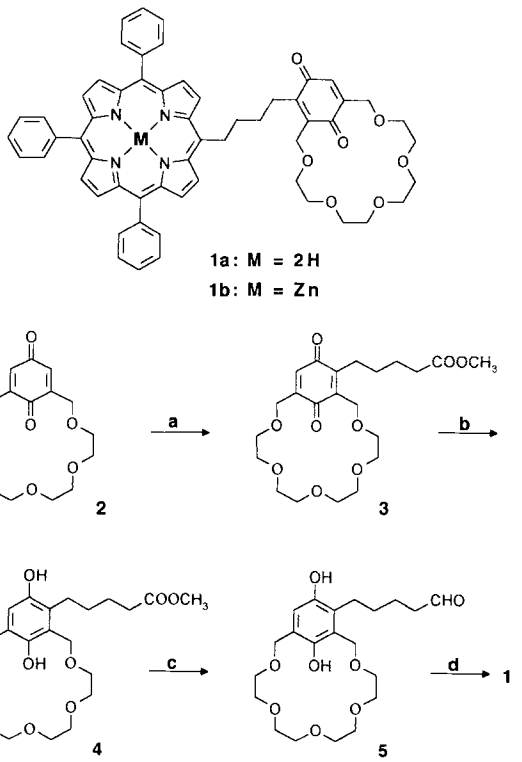
Licheng Sun, Jörg von Gersdorff, Dominique Niethammer, Peizhu Tian, and Harry Kurreck*

Dedicated to Professor Wolfgang Lüttke on the occasion of his 75th birthday

In the course of investigations into light-induced electron-transfer (ET) reactions occurring in the primary processes of photosynthesis, the fact that the high efficiency of charge separation depends on the structure and redox potential of the pigments and on their relative arrangement, with respect to each other and the surrounding protein matrix, has been intensively discussed.[1] Tailor-made porphyrins with covalently linked quinones (P-Q's) have been shown to be useful biomimetic models that allow a controlled variation in the parameters mentioned above.[1, 2] Attempts have recently been made to build noncovalent, supramolecular structures with stereochemically well-defined relationships between donor and acceptor, for example, by using the Watson/Crick base pairing concept.[3] Another approach employs crown ethers as photoactive macrocycles. J.-M. Lehn et al. demonstrated that irradiation of a Ag-ion-containing porphyrin–crown ether results in ET from the porphyrin to the Ag ion with subsequent ejection of elemental silver from the crown.[4] Dimerization and complexation of counterions in porphyrin–crown ethers have also been studied with optical and EPR spectroscopic methods.[5] The compounds in these studies were, however, not redox-active.

In order to be able to model two of the parameters that govern ET in P-Q's (the reduction potential of the quinone acceptor and the energy of reorganization[1]) on an otherwise unchanged substrate, we synthesized **1a**. Its acceptor fragment is similar to the recently published redox-active crown ether–quinone (CEQ).[6] The flexible $(CH_2)_4$ bridge in **1a** should allow the compound to adopt an energetically favorable and thus well-defined conformation in anisotropic media, such as, inverse micelles or liquid crystals. The role of the medium is to simulate the function of the protein matrix in the photosynthetic reaction center. The decisive steps in the synthesis are the C–C linkage of the tetramethylene fragment to the CEQ with oxidative decarboxylation (**2** → **3**),[7] the reduction of the hydroquinone ester to the aldehyde with diisobutyl aluminum hydride (DIBAL-H) (**4** → **5**),[8] and finally the formation of the porphyrin by the reaction of the aldehyde with benzaldehyde and pyrrole according to the reliable one-pot synthesis for *meso*-substituted porphyrins developed by Lindsey et al.[9] (**5** → **1a**, Scheme 1).[10]

From the literature data for the 2,6-dimethyl-substituted CEQ derivative of **2**, it was expected that the crown ethers of both the precursors and the target molecule **1a** would bind alkali metal ions such as Na^+. With EPR spectroscopy on the semiquinone derivative **1b**,[11] we were able to show that the coupling constants change relative to those in the uncomplexed crown ether after complexation with Na^+ ions. With the help of electron nuclear double resonance (ENDOR) spectroscopy, we were able to identify the Na ENDOR lines positioned around the free Na frequency as well as the proton ENDOR signals and the signs of the coupling constants (general TRIPLE resonance).[12] Figure 1 shows both ENDOR spectra.



Scheme 1. Synthesis of **1a**; reagents, conditions, and yields: a) HOOC-$(CH_2)_4COOCH_3$, $AgNO_3/(NH_4)_2S_2O_8$, CH_2Cl_2/H_2O, 25%. b) $Na_2S_2O_4$, $CHCl_3/H_2O$, room temperature, quantitative. c) 1. DIBAL-H, ether, −85 °C; 2. H_2O/SiO_2, 90%. d) 1. C_6H_5CHO, pyrrole, CH_2Cl_2, CF_3COOH, room temperature; 2. tetrachloro-*p*-benzoquinone, reflux, 2 h, 4%.

It is particularly interesting to compare the ^1H NMR spectra (500 MHz) of **1a** and **1b** (Fig. 2). Although there are almost no differences between the chemical shifts of the CEQ protons of, for example, **3** and **1a** (Fig. 2, top), the incorporation of Zn within **1a** (to form **1b**) gives rise to a significant upfield shift of the CEQ signals (Fig. 2, middle), despite the butylene spacer between the porphyrin and quinone moieties. This effect can only be explained by a folding of the CEQ towards the central Zn atom of the porphyrin, which brings the CEQ protons under the influence of the porphyrin ring current.[13] Molecular modeling calculations confirm a distinct energy minimum for the structure shown in Figure 3, bottom. The intramolecular character of this complexation is confirmed by the fact that the mixture of the free base **1a** and Zn–tetraphenylporphyrin (Zn–TPP) does not show an upfield shift of the CEQ protons (Fig. 2, bottom); therefore, an *intermolecular* complexation does not occur.

Further evidence for the CEQ folding was obtained by EPR investigation of the triplet excited state of the porphyrin. The following points should be noted:

1. The triplet state of the Zn–TPP fragment could be identified in the EPR spectrum at around 120 K in toluene with in situ irradiation; a good signal-to-noise ratio was obtained (cf. ref. [14]).
2. The triplet state of the porphyrin donor in a P-Q can only be reached photochemically if the singlet ET has been slowed down to such an extent (e.g., through cooling or use of a

[*] Prof. Dr. H. Kurreck, Dr. L. Sun, Dr. J. von Gersdorff, Dr. D. Niethammer, P. Tian
Institut für Organische Chemie der Freien Universität
Takustrasse 3, D-14195 Berlin (FRG)
Telefax: Int. code + (30)838-4248

[**] This work was supported by the Deutsche Forschungsgemeinschaft (SFB project 337 and normal funding) and the Fonds der Chemischen Industrie. L. Sun thanks the Alexander-von-Humboldt-Stiftung for a fellowship.

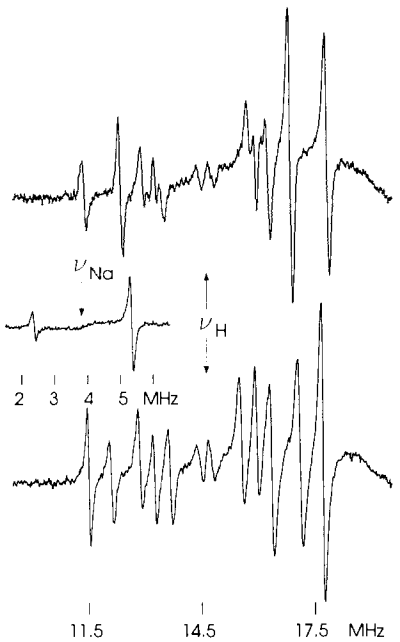


Fig. 1. ENDOR spectra of $\mathbf{1b}^{\bullet-}$ (230 K, top) and Na-$\mathbf{1b}^{\bullet-}$ (250 K, bottom) in methanol; radical formation with benzoin as reducing agent and tetrabutylammonium hydroxide as base. Formation of Na-$\mathbf{1b}^{\bullet-}$ by addition of a solution of sodium tosylate. MW power, RF power, hyperfine coupling constants (MHz $\pm$ 0.02) of $\mathbf{1b}^{\bullet-}$: 10 mW, 150 W, -6.45, $+4.52$, $+3.32$, $+2.68$, $+2.35$, $+0.34$; of Na-$\mathbf{1b}^{\bullet-}$: 15.9 mW, 300 W, -6.22, $+5.04$, $+3.51$, $+2.75$, $+1.94$, $+0.30$, 2.96 (Na). The signs were determined with general TRIPLE resonance spectroscopy for Na-$\mathbf{1b}^{\bullet-}$ and extended to the data for the radical $\mathbf{1b}^{\bullet-}$.

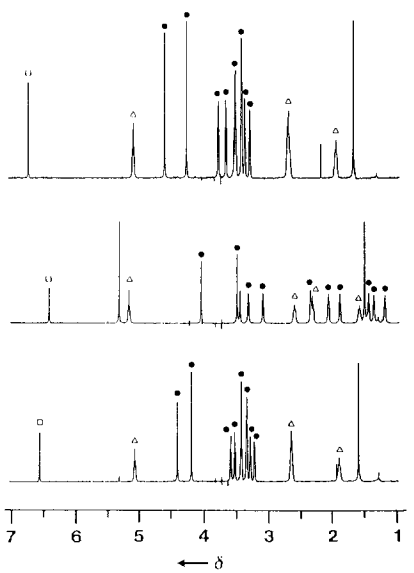


Fig. 2. High-field portion of the ^{1}H NMR spectra (500 MHz, $CDCl_3$, 25 °C, TMS) of **1a** (top), **1b** (middle), and a mixture of **1a** with Zn–TPP. Note the positions of the marked CEQ protons (□: quinone proton, △: butylene protons, ●: crown ether protons).

nonpolar solvent) that spin-orbit intersystem crossing (SOISC) can compete successfully.[15]

3. The corresponding hydroquinone derivatives of the P-Q's cannot undergo ET; the triplet state should therefore be accessible by ISC and be detectable.

For purposes of comparison, Figure 4 (top) shows the low-temperature EPR spectra in toluene of a P-Q with a butylene bridge[16] but lacking the crown ether substituent. In this case,

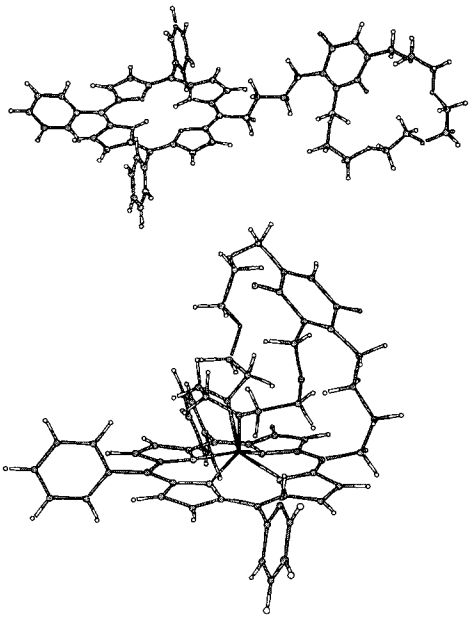


Fig. 3. Extended structure (top, **1a**) and the favored structure of **1b** after incorporation of Zn (according to the molecular modeling program Quanta 3.3). The folding of the CEQ towards the porphyrin can be seen clearly in **1b**.

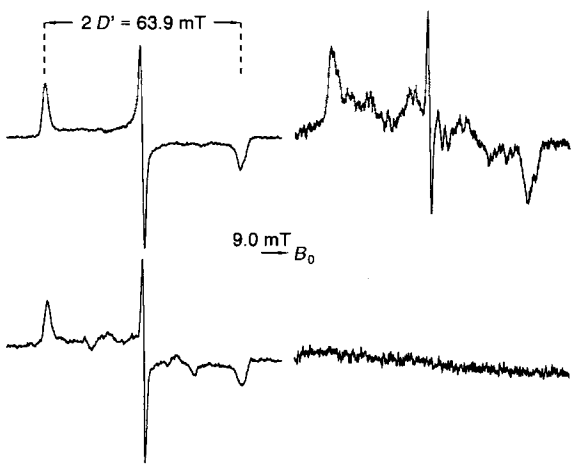


Fig. 4. Photoinduced EPR triplet spectra (measured in situ) of the porphyrin portion of porphyrin hydroquinones (left) and quinones (right). Top: analogue of **1b** lacking the crown ether substituent linked to the quinone; bottom: **1b**. Not shown here is the $\Delta m = 2$ transition ("half-field transition") characteristic of triplet systems, which was also detected. For the P-Q **1b**, a triplet excited state could not be detected under the measurement conditions used (see text).

the porphyrin triplet state can not only be identified unambiguously for the hydroquinone, but also for the P-Q itself. The signal-to-noise ratio is worse for the quinone derivative, because a certain amount of singlet ET occurs. In contrast, the crown ether shows a triplet state only for the hydroquinone; no triplet state of the porphyrin is detected for the quinone system **1b**. Presumably, in the case of **1b**, the folding of CEQ results in such spatial proximity of donor and acceptor that the singlet ET dominates even under the chosen reaction conditions; the singlet ET is, on the other hand, no longer effective at low temperatures for the P-Q without the crown ether because of the greater distance between donor and acceptor.

Finally, the UV/VIS spectrum of **1a** shows systems of bands characteristic of porphyrins, while the intramolecular complexation at the central atom of **1b** results in extensive shifts in the positions of the maxima of up to 10 nm.[17]

It may be assumed that the structural changes after incorporation of Zn have a profound influence on the ET properties of these P-Q's. Time-resolved optical and EPR measurements as well as studies of the redox potentials are underway, and compounds of type **1a** with rigid cyclohexylene bridges are under investigation.

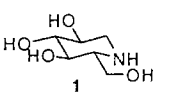
Received: June 9, 1994 [Z70191E]
German version: *Angew. Chem.* **1994**, *106*, 2396

[1] M. Bixon, J. Fajer, G. Feher, J. H. Freed, D. Gamliel, A. J. Hoff, H. Levanon, K. Möbius, R. Nechushtai, J. R. Norris, A. Scherz, J. L. Sessler, D. Stehlik, *Isr. J. Chem.* **1992**, *32*, 363, and references therein.
[2] D. Gust, T. A. Moore, *Adv. Photochem.* **1991**, *16*, 1; *Top. Curr. Chem.* **1991**, *159*, 103; M. R. Wasielewski, *Chem. Rev.* **1992**, *92*, 435; H. Kurreck, M. Huber, *Angew. Chem.*, in press; *Angew. Chem. Int. Ed. Engl.*, in press.
[3] J. L. Sessler, B. Wang, A. Harriman, *J. Am. Chem. Soc.* **1993**, *115*, 10418, and references therein.
[4] J.-M. Lehn, *Supramolecular Photochemistry* (Ed.: V. Balzani) (*NATO ASI Ser. Ser. C* **1987**, *214*, 29f).
[5] V. Thanabal, V. Krishnan, *J. Am. Chem. Soc.* **1982**, *104*, 3643; G. Bhaskar Maiya, V. Krishnan, *Inorg. Chem.* **1985**, *24*, 3253; T. K. Chandrashekar, H. van Willigen, M. H. Ebersole, *J. Phys. Chem.* **1985**, *89*, 3453; H. van Willigen, T. K. Chandrashekar, *J. Am. Chem. Soc.* **1986**, *108*, 709.
[6] M. Delgado, R. E. Wolf, Jr., J. R. Hartman, G. McCafferty, R. Yagbasan, S. C. Rawle, D. J. Watkin, S. R. Cooper, *J. Am. Chem. Soc.* **1992**, *114*, 8983.
[7] **3**: ^{1}H NMR (250 MHz, $CDCl_3$): $\delta = 1.46$ (quint, 2H; CH_2), 1.68 (quint, 2H; CH_2), 2.32 (t, 2H; CH_2), 2.56 (t, 2H; CH_2), 3.56 (m, 8H; CH_2 (crown ether)), 3.62 (m, 4H; CH_2 (crown ether)), 3.68 (s, 3H; CH_3), 3.76 (m, 4H; CH_2 (crown ether)), 4.44 (s, 2H; a-CH_2 (crown ether)), 4.63 (s, 2H; a-CH_2 (crown ether)), 6.74 (s, 1H (quinone)); MS (EI, 70 eV): *m/z* (%): 45 (100), 89 (85), 246 (96), 440 (14) [M^+].
[8] **5**: ^{1}H NMR (250 MHz, $CDCl_3$): $\delta = 1.53$ (quint, 2H; CH_2), 1.71 (quint, 2H; CH_2), 2.47 (t, 2H; CH_2), 2.68 (t, 2H; CH_2), 3.67 (m, 16H; CH_2 (crown ether)), 4.57 (s, 2H; a-CH_2 (crown ether)), 4.68 (s, 2H; a-CH_2 (crown ether)), 6.55 (s, 1H (quinone)), 9.76 (s, 1H; CHO); MS (EI, 70 eV): *m/z* (%): 45 (100), 89 (76), 218 (19), 328 (16), 412 (87) [M^+].
[9] J. S. Lindsey, I. C. Schreimann, H. C. Hsu, P. C. Kearney, A. M. Marguerettaz, *J. Org. Chem.* **1987**, *52*, 827.
[10] **1a**: ^{1}H NMR (500 MHz, $CDCl_3$): $\delta = -2.78$ (s, 2H; N-H), 1.89 (quint, 2H; CH_2), 2.65 (m, 4H; CH_2), 3.25 (t, 2H; CH_2 (crown ether)), 3.33 (t, 2H; CH_2 (crown ether)), 3.37 (m, 4H; CH_2 (crown ether)), 3.48 (m, 4H; CH_2 (crown ether)), 3.63 (t, 2H; CH_2 (crown ether)), 3.73 (t, 2H; CH_2 (crown ether)), 4.24 (s, 2H; a-CH_2 (crown ether)), 4.57 (d, 2H; a-CH_2 (crown ether)), 5.07 (t, 2H; CH_2); 6.72 (br. s, 1H (quinone)), 7.77 (m, 9H; *m*-, *p*-H (phenyl)), 8.20 (m, 6H; *o*-H (phenyl)), 8.79 (s, 4H; 12-, 13-, 17-, 18-H (porphyrin)), 8.92 (d, $J = 4.50$ Hz, 2H; 2-, 8-H (porphyrin)), 9.48 (d, $J = 4.71$ Hz, 2H; 3-, 7-H (porphyrin)); MS (FAB): *m/z* (%): 539 (39), 552 (100), 579 (43), 727 (13), 918 (10) [M^+], 920 (65) [$(M + 2H)^+$], 921 (87) [$(M + 3H)^+$]; **1b**: ^{1}H NMR (500 MHz, $CDCl_3$): $\delta = 1.15$ (br.s, 2H; CH_2 (crown ether)), 1.32 (br.s, 2H; CH_2 (crown ether)), 1.41 (br.s, 2H; CH_2 (crown ether)), 1.54 (quint, 2H; CH_2), 1.86 (br.s, 2H; CH_2 (crown ether)), 2.04 (br.s, 2H; CH_2 (crown ether)), 2.29 (t, 2H; CH_2), 2.32 (br.s, 2H; CH_2 (crown ether)), 2.57 (quint, 2H; CH_2), 3.07 (br.s, 2H; CH_2 (crown ether)), 3.30 (br.s, 2H; CH_2 (crown ether)), 3.47 (s, 2H; a-CH_2 (crown ether)), 4.03 (s, 2H; a-CH_2 (crown ether)), 5.16 (t, $J = 6.88$ Hz, 2H; CH_2), 6.41 (s, 1H (quinone)), 7.76 (m, 9H; *m*-, *p*-H (phenyl)), 8.18 (m, 6H; *o*-H (phenyl)), 8.85 (br.s, 4H; 12-, 13-, 17-, 18-H (porphyrin)), 8.97 (d, $J = 4.59$ Hz, 2H; 2-, 8-H (porphyrin)), 9.55 (d, $J = 4.71$ Hz, 2H; 3-, 7-H (porphyrin)); MS (FAB): *m/z* (%): 600 (41), 613 (100), 789 (20), 981 (25) [$(M + H)^+$], 983 (64) [$(M + 3H)^+$].
[11] EPR, ENDOR, and TRIPLE resonance spectra were measured on a Bruker EPR spectrometer (ER 220D, ER 200D); the ER 220D was equipped with a Bruker ENDOR resonator ER 200 ENB and with an NMR additional unit, which was built within the group. For details concerning the equipment see, for example, H. Kurreck, P. Tian, H. Dieks, J. von Gersdorff, H. Newman, H. Schubert, T. Stabingis, A. Wiehe, J. Sobek, *Appl. Magn. Reson.* **1994**, *6*, 17. The photoexcited states were generated by in situ irradiation through a slit in the EPR resonator with a 1000 W Hg–Xe lamp (Oriel) with a 570 nm cut-off filter (Schott) (EPR microwave power, 5 mW; field modulation, 5 μT).
[12] Whereas the nature of the nucleus can only be deduced indirectly from an EPR spectrum, for example, through the coupling pattern, ENDOR spectroscopy—and in this respect the close relationship to NMR spectroscopy is clear—allows the unambiguous identification of the magnetic nucleus by determination of the free nucleus frequency: cf., H. Kurreck, B. Kirste, W. Lubitz, *Angew. Chem.* **1984**, *96*, 171; *Angew. Chem. Int. Ed. Engl.* **1984**, *23*, 173; *Electron Nuclear Double Resonance Spectroscopy of Radicals in Solution*, VCH, New York, **1988**.
[13] Folding of this type in a pyropheophytine anthraquinone was also observed recently by NMR spectroscopy; the corresponding upfield shifts are smaller by several orders of magnitude than the ones for **1b**: cf., A. Y. Tauber, R. K. Kostiainen, P. H. Hynninen, *Tetrahedron* **1994**, *50*, 4723.
[14] A. Scherz, H. Levanon, *J. Phys. Chem.* **1980**, *84*, 324.
[15] F. Lendzian, J. Schlüpmann, J. von Gersdorff, K. Möbius, H. Kurreck, *Angew. Chem.* **1991**, *103*, 1536; *Angew. Chem. Int. Ed. Engl.* **1991**, *30*, 1461; F. Lendzian, B. von Maltzan, *Chem. Phys. Lett.* **1991**, *180*, 191, and references therein.
[16] For a description of these P-Q's, see J. von Gersdorff, B. Kirste, H. Kurreck, *Liebigs Ann. Chem.* **1993**, 897; the reduction of the P-Q's to the hydroquinone derivatives was performed with sodium dithionite immediately before the measurement.
[17] J. Sobek, L. Sun, P. Tian, J. von Gersdorff, H. Kurreck, unpublished results.

An Enantioselective Synthesis of Deoxynojirimycin**

Andrew J. Rudge, Ian Collins, Andrew B. Holmes,* and Raymond Baker

Deoxynojirimycin (**1**) and its derivatives have attracted much interest as synthetic targets owing to their potent glycosidase and related biological activity. The majority of syntheses of this molecule have utilized starting materials from the chiral pool, in particular, the carbohydrates glucose and sorbose.[1] Routes employing other chiral pool sources such as glutamic acid,[2] *myo*-inositol,[3] diethyl tartrate,[4] and serine[5] as building blocks to introduce at least one stereocenter have also been reported. To our knowledge, with the exception of the elegant use of aldolases,[6] and the intermolecular nitrone dipolar cycloaddition approach of Vasella et al.,[7] no asymmetric syntheses using induced diastereoselectivity from a chiral auxiliary have been published. We report a novel synthesis of this important azasugar in which the key step is an intramolecular nitrone cycloaddition[8] to assemble the piperidine ring. Other important features are the use of an enantioselective aldol reaction[9] to introduce two of the three ring oxygen substituents, a highly regio- and stereoselective dehydration of a secondary alcohol with the Martin sulfurane reagent,[10] and the stereoselective reduction of an ozonide with diisobutylaluminum hydride (DIBAL-H).

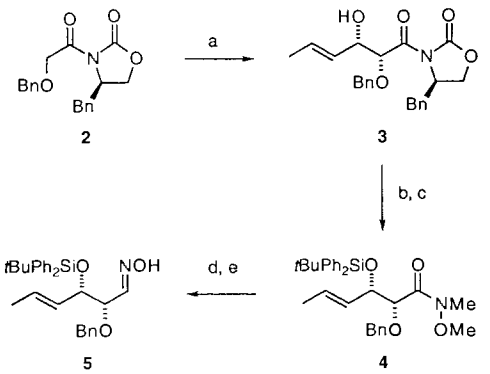


1

The imide **2**, prepared by acylation of the phenylalanine-derived oxazolidinone[11] with benzyloxyacetyl chloride,[12] underwent a diastereoselective aldol reaction[13a,b] with crotonaldehyde to give the *syn* product **3** in good yield (Scheme 1). The use of freshly distilled dibutylboron triflate (Bu_2BOTf) was found to be essential for the reproducibility of this reaction.[11] Formation of the Weinreb amide,[14] followed by silylation of the crude secondary alcohol gave the fully protected diol **4**. The oxazolidinone auxiliary was easily recovered under these condi-

[*] Dr. A. B. Holmes, A. J. Rudge, Dr. I. Collins[+]
University Chemical Laboratory
Lensfield Road, Cambridge CB2 1EW (UK)
Telefax: Int. code + (1223) 336-362
Dr. R. Baker
Neurosciences Research Centre
Merck Sharp and Dohme
[+] Present address: Merck, Sharp and Dohme
Harlow CM20 2QR (UK)

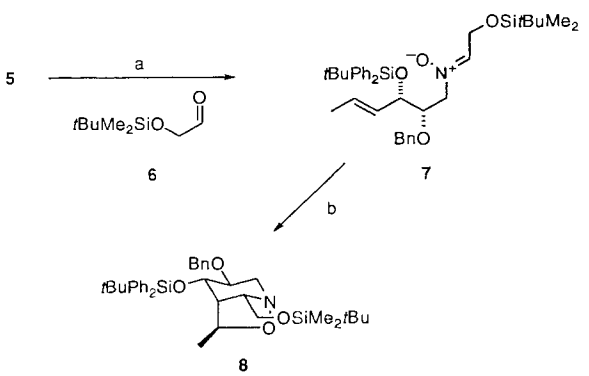
[**] This work was supported by the Engineering and Physical Sciences Research Council (UK) and Merck, Sharp and Dohme (Cooperative Awards in Science and Engineering). We thank Pfizer Central Research (Sandwich) for financial support and The Royal Society for the award of a Royal Society Leverhulme Senior Research Fellowship (to A. B. H.). We thank Prof. S. V. Ley for drawing our attention to the Martin sulfurane.



Scheme 1. Synthesis of the oxime **5** using an enantioselective aldol reaction. a) Bu_2BOTf, NEt_3, -78 °C, in toluene, then crotonaldehyde -78 °C to ca. 20 °C (90%); b) MeNH(OMe)·HCl, $AlMe_3$, CH_2Cl_2, ca. 20 °C; c) $tBuPh_2SiCl$, imidazole, *N*,*N*-dimethylformamide (DMF), ca. 20 °C (90% from **3**); d) DIBAL-H, toluene, -78 °C; e) NH_2OH·HCl, NaOAc, EtOH–H_2O, ca. 20 °C (93% from **4**).

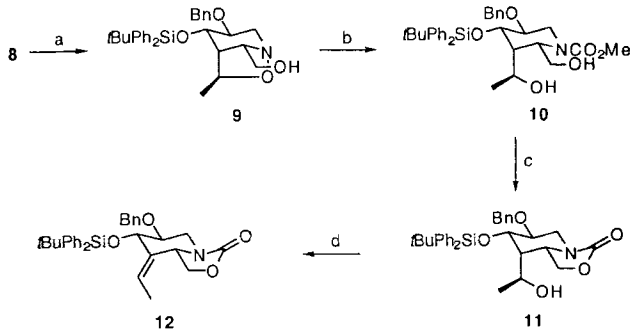
tions. Conversion to the oxime **5**, isolated as a 4:1 mixture of isomers, was then achieved by reduction with DIBAL-H and condensation with hydroxylamine hydrochloride.

Reduction of the oxime **5** with $NaCNBH_3$ under acidic conditions furnished a hydroxylamine intermediate, which upon reaction with the aldehyde **6**[15] afforded the nitrone **7** in good yield (Scheme 2). Cycloaddition in refluxing benzene yielded the isoxazolidine **8**. The predominance of this product results from the preferred all-equatorial disposition of both ether substituents on the developing six-membered ring, which folds in a chairlike transition state structure. This contrasts strongly with the marked preference for formation of the axial product in the cycloaddition of analogues of **7** carrying only a single allylic ether substituent.[17] The kinetic preference for a six-membered ring over a seven-membered ring during carbon–carbon bond formation, which is thought to precede carbon–oxygen bond formation in nitrone dipolar cycloadditions, secures the correct regioselectivity.[18]



Scheme 2. Intramolecular cycloaddition of the nitrone **7**. a) $NaCNBH_3$, MeOH, pH 4, ca. 20 °C, then aldehyde **6**, CH_2Cl_2, ca. 20 °C (80%); b) Benzene, reflux (72%).

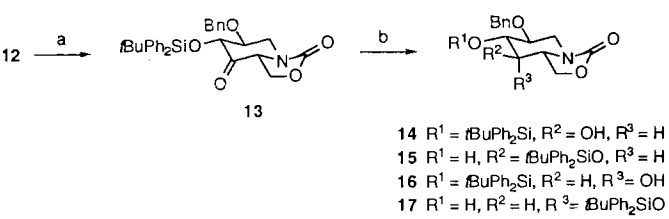
The primary silyl ether was deprotected by treatment of the cycloadduct **8** with hydrogen fluoride–pyridine (Scheme 3). Reprotection of the alcohol **9** as a methyl carbonate followed by reductive N–O bond scission led to the methyl carbamate **10** as a result of acyl migration. Formation of the crystalline cyclic carbamate **11** was promoted by stirring in toluene (bath temperature 120 °C) with sodium hydroxide and 4 Å molecular sieves. A variety of reagents was explored to effect elimination of the



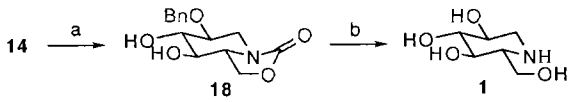
Scheme 3. Formation and dehydration of the alcohol **11**. a) HF–pyridine, THF, ca. 20 °C (90%); b) MeOCOCl, NaH, THF, ca. 20 °C, then Zn, AcOH–EtOH–H_2O, 60 °C (99%); c) NaOH, 4 Å molecular sieves, toluene, 120 °C (bath temperature) (77%); d) $Ph_2S[OC(CF_3)_2Ph]_2$ (Martin sulfurane), CH_2Cl_2, ca. 20 °C (96%).

secondary alcohol **11** to an exocyclic alkene. All the common reagents showed disappointing yields and selectivities. However, the Martin sulfurane[10] was found to exhibit an exceptionally regio- and stereocontrolled elimination to provide the more substituted alkene **12**. The reaction is believed to follow an E_2 pathway, and proceeds by way of a charged leaving group.[10] Consequently, it is presumed that the selectivity arises from the kinetic acidity of the equatorial proton that is antiperiplanar to the electron-deficient C–N(C=O) bond of the piperidine ring.[19]

Oxidative cleavage of the alkene **12** was best achieved by ozonolysis followed by a reductive workup employing triphenylphosphane (Scheme 4). Reduction of the resulting ketone **13** with a variety of hydride reagents was complicated by 1,2-silyl migration in the alkoxide intermediate. For instance, reduction with sodium borohydride furnished a mixture of four alcohols **14**–**17** (22%, 15%, 36%, and 10%, respectively). A more stereoselective reduction was observed with sterically demanding sources of hydride. With L-Selectride only the axial isomers **16** (37%) and **17** (7%) were observed. A satisfactory route from the ketone to the equatorial alcohol **14** (45% yield) was achieved with DIBAL-H. However, ozonolysis of the alkene **13** followed by direct treatment of the ozonide with DIBAL-H at -78 °C afforded the alcohol **14** in a single step (43%). To our knowledge this is the first example of the reduction of an ozonide directly to an alcohol with DIBAL-H. Clearly, chelation of DIBAL-H to the α-siloxy group plays an important part in controlling this selectivity. Deprotection of the alcohol **14** in a three-stage sequence (Scheme 5) involving desilylation (to **18**), hydrogenolysis, and aqueous hydrolysis gave deoxynojirimycin (**1**), which was identical in all respects to an authentic sample.[2b, 20, 21]



Scheme 4. Ozonolysis of alkene **12** and hydride reduction. a) Ozone, CH_2Cl_2, -78 °C, then PPh_3, ca. 20 °C (66%); b) Reduction (see text).



Scheme 5. Synthesis of deoxynojirimycin (**1**). a) Tetrabutylammonium fluoride, THF, ca. 20 °C (62%); b) H_2, Pd/C, HCl, MeOH, ca. 20 °C, then KOH, MeOH – H_2O, reflux (43%).

In summary, a concise enantioselective synthesis of deoxynojirimycin has been achieved in twelve steps from achiral starting materials in which a (*Z*)-boron enolate of an Evans oxazolidinone was used to control both simple and induced diastereoselectivity.[22] The method lends itself to the stereocontrolled syntheses of potentially important biologically active molecules. Work is now underway to extend this methodology to the synthesis of other biologically interesting polyhydroxylated piperidines and indolizidines.

Experimental Procedure

Conversion of **12** into **14**: Ozone was bubbled through a stirred solution of the alkene **12** (21.8 mg, 0.041 mmol) in CH_2Cl_2 (20 mL) at −78 °C for 5 min. At this point saturation was evident by the blue color of the reaction mixture and by the dark brown color of potassium iodide solution receiving the exhaust gases from the reaction. Nitrogen was bubbled through the reaction for 10 min to flush out the excess ozone before the addition of DIBAL-H (1 M in dichloromethane, 0.4 mL, 0.4 mmol). After being stirred for 1 h at −78 °C, the reaction was quenched with methanol (2 mL) and allowed to warm to ca. 20 °C. The reaction mixture was poured into a vigorously stirred emulsion of ethyl acetate (100 mL), saturated aqueous ammonium chloride (50 mL), and saturated aqueous sodium potassium tartrate (50 mL). Stirring was continued for 1 h, at which point the two phases were separated and the aqueous phase extracted with ethyl acetate (50 mL). The combined organic phases were dried over magnesium sulfate, filtered, and concentrated to dryness on a rotary evaporator. The residue was filtered through a short column of silica gel (eluting with 50% EtOAc/hexane) and purified by high-pressure liquid chromatography (eluting with 40% EtOAc/hexane) to give the alcohol **14** (9.2 mg, 43%) as a colorless gum; R_f 0.20 (30% EtOAc/hexane); (calcd for $C_{30}H_{35}NO_5Si$: C 69.6, H 6.8, N 2.7; found: C 69.3, H 7.0, N 2.6); $[\alpha]_D^{20} = -15.8$ ($c = 1.64$ in $CHCl_3$); IR (CCl_4): $\tilde{\nu}$ [cm^{-1}] = 3580 w (OH), 1775 s (C=O); ^1H NMR (400 MHz, $CDCl_3$, 20 °C, TMS): $\delta = 1.01$ (s, 9H; $(CH_3)_3C$), 2.20 (d, $^3J = 2.6$ Hz, 1H; OH), 2.58 (dd, $^3J = 10.2$, 13.3 Hz, 1H; NCH*H*), 3.38 (ddd, $^3J = 3.8$, 7.8, 9.4 Hz, 1H; NCH), 3.46–3.53 (m, 2H; BnOC*H* and HOCH), 3.63 (t, $^3J = 8.7$ Hz, 1H; SiOCH), 4.08 (dd, $^3J = 5.6$, 13.3 Hz, 1H; NC*H*H), 4.18 (dd, $^3J = 3.8$, 9.1 Hz, 1H; NCHCH*H*), 4.23 (d, $^3J = 11.2$ Hz, 1H; PhCH*H*), 4.32 (dd, $^3J = 7.9$, 8.9 Hz, 1H; NCHC*H*H), 4.40 (d, $^3J = 11.2$ Hz, 1H; C*H*HPh), 6.99–7.01 (m, 2H; 2 of 3 × Ph), 7.24–7.27 (m, 3H; 3 of 3 × Ph), 7.31–7.46 (m, 6H; 6 of 3 × Ph), 7.62–7.71 (m, 4H; 4 of 3 × Ph); ^{13}C NMR (100.6 MHz, $CDCl_3$, 20 °C, TMS): $\delta = 19.6$ (s), 27.1 (q), 42.7 (t), 57.5 (d), 66.5 (t), 71.8 (t), 74.4 (d), 76.9 (d), 79.0 (d), 127.65 (d), 127.69 (d), 127.81 (d), 127.97 (d), 128.19 (d), 129.85 (d), 130.00 (d), 132.9 (s), 133.5 (s), 135.7 (d), 135.9 (d), 137.6 (s), 156.8 (s); MS (Chemical Ionization): *m/z* (%) 535 (22) [($M^+ + NH_4$)], 518 (32) [($M^+ + H$], 440 (86), [($M^+ - Ph$)], 108 (100) [($PhCH_2OH^+$)], 91 (75) [($PhCH_2^+$)]; ($M^+ + H$) calculated for $C_{30}H_{36}NO_5Si$ 518.2363; found 518.2364.

Received: June 14, 1994 [Z 7034 IE]
German version: *Angew. Chem.* **1994**, *106*, 2416

[1] For a recent review of the synthesis and biological activity of deoxynojirimycin (**1**) see A. B. Hughes, A. J. Rudge, *Nat. Prod. Reports* **1994**, *11*, 135.
[2] N. Ikota, *Heterocycles* **1989**, *29*, 1469.
[3] a) N. Chida, Y. Furuno, S. Ogawa, *J. Chem. Soc. Chem. Commun.* **1989**, 1230; b) N. Chida, Y. Furuno, H. Ikemoto, S. Ogawa, *Carbohydr. Res.* **1992**, *237*, 185.
[4] H. Iida, N. Yamazaki, C. Kibayashi, *J. Org. Chem.* **1987**, *52*, 3337.
[5] A. Dondoni, P. Merino, D. Perrone, *Tetrahedron* **1993**, *49*, 2939.
[6] a) R. L. Pederson, M.-J. Kim, C.-H. Wong, *Tetrahedron Lett.* **1988**, *29*, 4645; b) R. L. Pederson, C.-H. Wong, *Heterocycles* **1989**, *28*, 477; c) T. Ziegler, A. Straub, F. Effenberger, *Angew. Chem.* **1988**, *100*, 717; *Angew. Chem. Int. Ed. Engl.* **1988**, *27*, 716; d) A. Straub, F. Effenberger, P. Fischer, *J. Org. Chem.* **1990**, *55*, 3926; e) K. K.-C. Liu, T. Kajimoto, L. Chen, Z. Zhong, Y. Ichikawa, C.-H. Wong, *ibid.* **1991**, *56*, 6280.
[7] A. Vasella, R. Voeffray, *Helv. Chim. Acta* **1982**, *65*, 1134.
[8] A. B. Holmes, C. Swithenbank, S. F. Williams, *J. Chem. Soc. Chem. Commun.* **1986**, 265; A. L. Smith, S. F. Williams, A. B. Holmes, L. R. Hughes, Z. Lidert, C. Swithenbank, *J. Am. Chem. Soc.* **1988**, *110*, 8696; A. B. Holmes, A. L. Smith, S. F. Williams, L. R. Hughes, Z. Lidert, C. Swithenbank, *J. Org. Chem.* **1991**, *56*, 1393; I. Collins, M. E. Fox, A. B. Holmes, S. F. Williams, R. Baker, I. T. Forbes, M. Thompson, *J. Chem. Soc. Perkin Trans. 1* **1991**, 175; A. B. Holmes, A. B. Hughes, A. L. Smith, S. F. Williams, *ibid.* **1992**, 1089; A. B. Holmes, A. B. Hughes, A. L. Smith, *ibid.* **1993**, 633.
[9] D. A. Evans, J. Bartroli, T. L. Shih, *J. Am. Chem. Soc.* **1981**, *103*, 2127.
[10] R. Arhart, J. C. Martin, *J. Am. Chem. Soc.* **1972**, *94*, 5003.
[11] J. R. Gage, D. A. Evans, *Org. Synth.* **1989**, *68*, 83.
[12] a) M. J. Kukla, J. M. Fortunato, *J. Org. Chem.* **1984**, *49*, 5003; b) S. A. Glover, S. L. Golding, A. Goosen, C. W. McCleland, *J. Chem. Soc. Perkin Trans. 1* **1983**, 2479.
[13] a) D. A. Evans, S. L. Bender, J. Morris, *J. Am. Chem. Soc.* **1988**, *110*, 2506; b) D. A. Evans, S. W. Kaldor, T. K. Jones, J. Clardy, T. J. Stout, *ibid.* **1990**, *112*, 7001.
[14] S. Nahm, S. M. Weinreb, *Tetrahedron Lett.* **1981**, *22*, 3815.
[15] The aldehyde **6** was prepared by silylation of ethane-1,2-diol followed by Swern oxidation [16]. The benzyloxy analogue has also been prepared [12b].
[16] A. Mancuso, S.-L. Huang, D. Swern, *J. Org. Chem.* **1978**, *43*, 2480.
[17] I. Collins, A. Nadin, A. B. Holmes, M. E. Long, J. Man, R. Baker, *J. Chem. Soc. Perkin Trans 1* **1994**, 2205.
[18] W. Oppolzer, S. Siles, R. L. Snowden, B. H. Bakker, M. Petrzilka, *Tetrahedron Lett.* **1979**, *20*, 4391; *Tetrahedron* **1985**, *41*, 3497; P. N. Confalone, E. M. Huie, *Org. React.* **1988**, *36*, 1.
[19] C. K. Ingold, *Proc. Chem. Soc. London* **1962**, 265.
[20] a) S. Inouye, T. Tsuruoka, T. Ito, N. Niida, *Tetrahedron* **1968**, *23*, 2125; b) H. J. G. Broxterman, G. A. van der Marel, J. J. Neefjes, H. L. Ploegh, J. H. van Boom, *Recl. Trav. Chim. Pays-Bas* **1987**, *106*, 571.
[21] Data for synthetic **1**: ^1H NMR (400 MHz, D_2O, TMS): $\delta = 2.55$ (dd, $J = 12.4$, 10.8 Hz, 1H), 2.66 (ddd, $J = 3.0$, 6.1, 9.3 Hz, 1H), 3.22 (dd, $J = 5.1$, 12.4 Hz, 1H), 3.29 (t, $J = 9.3$ Hz, 1H), 3.35 (t, $J = 8.9$ Hz, 1H), 3.53 (ddd, $J = 5.1$, 8.9, 10.9 Hz, 1H), 3.67 (dd, $J = 6.1$, 11.9 Hz, 1H), 3.85 (dd, $J = 2.9$, 11.9 Hz, 1H); ^{13}C NMR (100 MHz, D_2O, TMS): $\delta = 47.5$ (t), 59.7 (d), 60.0 (t), 69.5 (d), 70.2 (d), 77.3 (d). Specific optical rotation $[\alpha]_D^{20} = +36.9$ ($c = 0.16$ in water) [ref. [20b] $[\alpha]_D^{20} = +36$ ($c = 0.02$ in water)].
[22] All new compounds showed satisfactory analytical (microanalysis and/or high resolution mass spectrometry) and spectroscopic (IR and NMR) data.

$[Mn_4Te_4(SC_3H_7)_4]^{4-}$ and $[Mn_4Te_4(SeC_3H_7)_4]^{4-}$: Novel Heterocubane Clusters of Manganese**

Hans-Oscar Stephan and Gerald Henkel*

Dedicated to Professor Wilhelm Preetz on the occasion of his 60th birthday

Sulfido(thiolato) transition metal complexes are biologically relevant as models for the active sites of metalloproteins such as ferredoxins and nitrogenases, and for this reason they have been the subject of investigation for some time now.

To date, the following compounds have been isolated with divalent metal ions: compounds with adamantane-type structures, for example $[Zn_{10}S_4(SPh)_{16}]^{4-}$ and $[Cd_{17}S_4(SPh)_{28}]^{2-}$; complexes of the formula $[M_3S(SR)_6]^{2-}$ with an incomplete mixed metal–sulfur cubane structure (M = Fe, Co) or an incomplete sulfur cubane structure (M = Ni); and the cobalt–sulfur complex $[Co_8S_6(SPh)_8]^{n-}$ ($n = 4$, 5) with a complete metal cubane structure.[1] With the exception of the Ni complexes, the metal centers in all these compounds—just as in the mixed-cubane clusters $[Fe_4S_4(SR)_4]^{n-}$ ($n = 1-3$)[2, 3] and in the $[Fe_6S_6(SR)_6]^{3-}$[4] clusters with a metal-deficient cubane structure—are tetrahedrally coordinated; however, the metals listed here have fractional oxidation numbers that lie between two and three.

[*] Prof. Dr. G. Henkel, Dr. H.-O. Stephan
Fachgebiet Anorganische Chemie der Universität
Lotharstrasse 1, D-47048 Duisburg (FRG)
Telefax: Int. code + (203) 3792110

[**] This work was supported by the Deutsche Forschungsgemeinschaft, the Bundesministerium für Forschung und Technologie, and the Fonds der Chemischen Industrie.

In spite of intensive research, it was not possible until now to isolate heterocubane clusters of the composition $[M_4X_4(SR)_4]^{4-}$ (X = S, Se, Te), in which the metal atoms are exclusively divalent—not even by the attempted replacement of the sulfide ions by selenide or telluride ions. We were recently able to show with the synthesis of $[Mn_4Te_4(Te\mathit{i}C_3H_7)_4]^{4-}$,[5] however, that the oxidation state + 2 can be stabilized in heterocubane clusters by a complete tellurium ligand environment. With compounds **1** and **2**, we have now succeeded in synthesizing and characterizing the first sulfur- and selenium-containing heterocubane clusters with divalent metal ions, and at the same time also the first chalcogenido(thiolato) and chalcogenido(selenolato)manganese complexes.

$[Mn_4Te_4(S\mathit{i}C_3H_7)_4]^{4-}$ **1** $[Mn_4Te_4(Se\mathit{i}C_3H_7)_4]^{4-}$ **2**

The reaction of mixtures of $\mathit{i}C_3H_7XNa$ (X = S, Se) and $MnBr_2$ (molar ratio 3:1) with $(SiMe_3)_2Te$ in acetonitrile leads to the formation of **1** or **2**, which can be isolated as **3** and **4**, respectively, after the addition of $[Et_4N]Br$.

$(Et_4N)_4[Mn_4Te_4(S\mathit{i}C_3H_7)_4]\cdot 2\,MeCN$ **3**

$(Et_4N)_4[Mn_4Te_4(Se\mathit{i}C_3H_7)_4]\cdot 1.5\,MeCN$ **4**

According to the results of the crystal structure analyses,[6] **1** and **2**[7] are discrete complex ions (Fig. 1). Their Mn_4Te_4 frameworks are constructed from Mn_4 and Te_4 tetrahedra which are intertwined in such a way that the corners of one tetrahedron lie above the centers of the faces of the other. Since the edges of these tetrahedra differ in length, distorted Mn_4Te_4 cubes are formed with idealized T_d symmetry. The average Mn–Te distances are 2.783 Å (**1**) and 2.768 Å (**2**) with a difference of 0.015 Å. The differences in the Mn···Mn and Te···Te distances are of a similar magnitude: On going from **1** to **2**, they are shortened by 0.022 Å to 3.282 Å and by 0.019 Å to 4.387 Å, respectively. The terminally coordinated $\mathit{i}C_3H_7X^-$ ligands are bonded at distances of 2.413 Å (X = S; **1**) and 2.537 Å (X = Se; **2**) and are thus each 0.029 Å shorter than the corresponding distances in $[Mn(SPh)_4]^{2-}$[8] and $[Mn(SePh)_4]^{2-}$.[9]

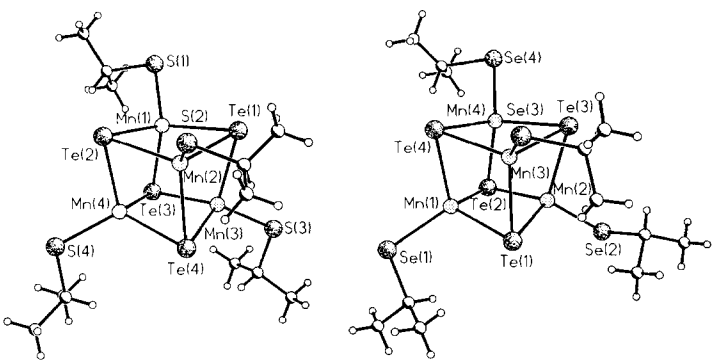


Fig. 1. Left: Structure of the complex anion **1** in crystals of **3**. Important distances [Å] and ranges of angles [°]: Mn···Mn 3.241(1)–3.422(1), Mn(1)-S(1) 2.412(2), Mn(2)-S(2) 2.397(2), Mn(3)-S(3) 2.441(2), Mn(4)-S(4) 2.403(2), Mn(1)-Te(1) 2.782(1), Mn(1)-Te(2) 2.773(1), Mn(1)-Te(3) 2.796(1), Mn(2)-Te(1) 2.773(1), Mn(2)-Te(2) 2.763(1), Mn(2)-Te(4) 2.805(1), Mn(3)-Te(1) 2.791(1), Mn(3)-Te(3) 2.785(1), Mn(3)-Te(4) 2.804(1), Mn(4)-Te(2) 2.755(1), Mn(4)-Te(3) 2.766(1), Mn(4)-Te(4) 2.799(1); Te-Mn-Te 100.5(1)–107.5(1), Te-Mn-S 103.3(1)–121.7(1), Mn-Te-Mn 70.7(1)–75.9(1). Right: Structure of the complex anion **2** in crystals of **4** [7]. Important distances [Å] and ranges of angles [°]: Mn···Mn 3.214(4)–3.358(4), Mn(1)-Se(1) 2.538(4), Mn(2)-Se(2) 2.538(4), Mn(3)-Se(3) 2.542(4), Mn(4)-Se(4) 2.532(4), Mn(1)-Te(1) 2.747(4), Mn(1)-Te(2) 2.802(4), Mn(1)-Te(4) 2.776(4), Mn(2)-Te(1) 2.755(4), Mn(2)-Te(2) 2.763(4), Mn(2)-Te(3) 2.777(4), Mn(3)-Te(1) 2.754(4), Mn(3)-Te(3) 2.758(4), Mn(3)-Te(4) 2.776(4), Mn(4)-Te(2) 2.778(4), Mn(4)-Te(3) 2.765(4), Mn(4)-Te(4) 2.778(4); Te-Mn-Te 102.1(1)–107.0(1), Te-Mn-Se 107.5(1)–120.0(1), Mn-Te-Mn 71.3(1)–74.4(1).

The Mn_4X_4 units in **1** and **2** are slightly distorted. Their symmetry does not deviate in a systematic manner from the point group T_d, unlike the cubane frameworks of many structurally related iron complexes. The values of the Mn–Te bond lengths are spread over typical ranges about common average values (2.755–2.805 Å in **1**; 2.747–2.802 Å in **2**).

The formation of mixed $M^{2+}/X^{2-}/YR^-$ complexes with $[M_4X_4]^0$ frameworks is unexpected due to the high overall charge of four electrons, since other spatial arrangements would permit a smaller formal charge per metal atom. Examples for this are the metal cubanes $[M_8S_6L_8]^{n-}$ (M = Co, L = SPh, n = 4, 5;[10] M = Fe, L = I, n = 4[11]) and the adamantane-type compounds $[M_{10}S_4(SPh)_{16}]^{4-}$ (M = Zn, Cd),[12] $[Cd_{17}S_4(SPh)_{28}]^{2-}$,[13] and $[Cd_{32}S_{14}(SPh)_{36}(dmf)_4]$.[14] The surprising stability of **1** and **2** presumably results from the specific electronic and steric properties of the tellurido ligands, and the circumstance that manganese in a tetrahedral chalcogenide environment can at most be divalent. Indeed, as yet we have been unable to replace the telluride ions by selenide or sulfide ions.

An important difference to the structurally analogous iron complexes lies in the unexpectedly long metal–metal distances in **1** and **2**, which are about 0.5 Å longer than the comparable distances in $[Fe_4Te_4(S\mathit{i}C_3H_7)_4]^{2-}$ (2.808 Å) and $[Fe_4Te_4(S\mathit{i}C_3H_7)_4]^{3-}$ (2.815 Å).[5] An expected value for the Mn···Mn distances can be estimated by extrapolating the Fe···Fe contacts in the hypothetical anion $[Fe_4Te_4(S\mathit{i}C_3H_7)_4]^{4-}$ (2.822 Å), and subsequently adding the difference of 0.242 Å which occurs in the metal–metal distance in simple thiolato complexes $[M_2(SEt)_6]^{2-}$ on going from Fe (2.978 Å) [15] to Mn (3.220 Å).[16] The value obtained in this way is 3.064 Å. The observed Mn···Mn distances are in fact 0.281 Å (**1**) and 0.240 Å (**2**) longer than this value and therefore rule out any significant Mn–Mn bonding. This finding contradicts the generally accepted MO models for complexes of the composition $[M_4S_4(SR)_4]^{n-}$. According to these models, when the number of cluster valence electrons lies between 45 and 60, all six of the bonding molecular orbitals (MO) of the M_4 cluster are fully occupied, and the valence electrons in excess of the number 45 are distributed among the eight nonbonding MOs.[17]

The cause of this change in the properties is possibly due to the energetic order of the bonding and nonbonding orbitals being swapped on going from iron to manganese. In this case, an average Mn–Mn bond order of 1/3 can be predicted, which is consistent with the observed conditions.

Cyclic voltammetric measurements on **3** and **4** show that the complex anions **1** and **2**, respectively, do not undergo reversible or quasi-reversible electronic transitions. The current–voltage curves are dominated by the redox behavior of the tellurido ligands, which are oxidized to ditelluride ions and subsequently to polytelluride ions.

Experimental Procedure

All manipulations were carried out in a glove box under an inert atmosphere (N_2). **3**, **4**: $MnBr_2$ (1.07 g, 5 mmol) was dissolved in MeCN (30 mL), and $NaS\mathit{i}C_3H_7$ (1.47 g, 15 mmol) or $NaSe\mathit{i}C_3H_7$ (2.17 g, 15 mmol) was added. $(Et_4N)Br$ (1.05 g, 5 mmol) was added and the mixture was then stirred for about 15 h. The reaction solution was filtered and $(SiMe_3)_2Te$ (5 mmol) in MeCN (20 mL) was added dropwise. The resulting deep red solution remained clear and was stirred 48 h before being evaporated under reduced pressure to about 7 mL. Subsequent layering with diethyl ether led to the desired products, after the solutions had been left to stand

for several days. Yields: **1**: 1.3 g (0.84 mmol, 67%); **2**: 580 mg (0.33 mmol, 27%); correct C, H, N, S analyses; UV/VIS (MeCN): λ_{max} [nm] (ε) = 504 (151) for **1**; 500 (256) for **2**.

Received: May 20, 1994 [Z 6960IE]
German version: *Angew. Chem.* **1994**, *106*, 2422

[1] B. Krebs, G. Henkel in *Rings, Clusters and Polymers of Main Group and Transition Elements* (Ed.: H. W. Roesky), Elsevier, Amsterdam, **1989**, p. 439, and references therein.
[2] T. O'Sullivan, M. M. Millar, *J. Am. Chem. Soc.* **1985**, *107*, 4096.
[3] a) J. M. Berg, R. H. Holm in *Iron-Sulfur Proteins* (Ed.: T. G. Spiro), Wiley, New York, **1982**, p. 1, and references therein; b) B. Krebs, G. Henkel, *Angew. Chem.* **1991**, *103*, 785; *Angew. Chem. Int. Ed. Engl.* **1991**, *30*, 769.
[4] D. Coucouvanis, *Acc. Chem. Res.* **1991**, *24*, 1, and references therein.
[5] H.-O. Stephan, C. Chen, G. Henkel, K. Griesar, W. Haase, *J. Chem. Soc. Chem. Commun.* **1993**, 886.
[6] Crystal structure analysis: Siemens P4RA four-circle diffractometer, $Mo_{K\alpha}$ radiation (λ = 0.71073 Å), graphite monochromator, rotating anode generator, scintillation counter. T = 150 K, empirical absorption corrections, SHELXTL-PLUS program, direct methods, full-matrix least-squares refinement: **3**: $C_{48}H_{114}Mn_4N_6S_4Te_4$, M = 1633.85, triclinic, space group $P\bar{1}$, a = 11.966(3), b = 12.648(4), c = 25.152(6) Å, α = 77.18(2), β = 78.14(2), γ = 75.68(2)°, V = 3551 Å^3, Z = 2, ρ_{calcd} = 1.528 g cm^{-3}, $\mu(Mo_{K\alpha})$ = 2.46 mm^{-1}, transmission range 0.957–0.298, crystal dimensions ca. 0.52 × 0.23 × 0.16 mm, ω scan, $2\theta_{max}$ = 54°, 15489 unique reflections, $R(R_w)$ = 0.0465 (0.0505) for 12325 observed reflections ($I > 2\sigma(I)$), 623 variables, all non-hydrogen atoms anisotropic, H atoms fixed at idealized positions, one common isotropic temperature factor for the H atoms of each organic residue, one scaling factor, one isotropic extinction parameter. **4**: $C_{47}H_{112.5}Mn_4N_{5.5}Se_4Te_4$, M = 1800.93, monoclinic, space group $C2/c$, a = 47.349(8), b = 15.452(2), c = 39.401(7) Å, β = 96.66(1)°, V = 28639 Å^3, Z = 16, ρ_{calcd} = 1.671 g cm^{-3}, $\mu(Mo_{K\alpha})$ = 4.35 mm^{-1}, transmission range 0.362–0.308, crystal dimensions ca. 0.62 × 0.24 × 0.22 mm, ω scan, $2\theta_{max}$ = 44°, 13375 unique reflections, $R(R_w)$ = 0.0653 (0.0636) for 8511 observed reflections ($I > 2\sigma(I)$), 754 variables, anions anisotropic, cations and solvent molecules isotropic, solvent molecules disordered and electron densities in part not completely resolved, H atoms not considered, one scaling factor, one isotropic extinction parameter. Further details of the crystal structure investigations may be obtained from the Fachinformationszentrum Karlsruhe, D-76344 Eggenstein-Leopoldshafen (FRG) on quoting the depository number CSD-58363.
[7] Compound **4** contains two symmetry-independent complex anions **2**, which display different orientations of the *iso*-propyl groups due to packing effects; however, they differ only slightly from one another with regard to their Mn_4Te_4 frameworks. For this reason, a depiction of the second entity was omitted in Fig. 1, right.
[8] D. Swenson, N. C. Baenziger, D. Coucouvanis, *J. Am. Chem. Soc.* **1978**, *100*, 1932.
[9] W. Tremel, B. Krebs, K. Greiwe, W. Simon, H.-O. Stephan, G. Henkel, *Z. Naturforsch. B* **1992**, *47*, 1580.
[10] a) G. Christou, K. S. Hagen, R. H. Holm, *J. Am. Chem. Soc.* **1982**, *104*, 1744; b) G. Christou, K. S. Hagen, J. K. Bashkin, R. H. Holm, *Inorg. Chem.* **1985**, *24*, 1010.
[11] S. Pohl, U. Opitz, *Angew. Chem.* **1993**, *103*, 869; *Angew. Chem. Int. Ed. Engl.* **1993**, *32*, 863.
[12] a) A. Choy, D. Craig, I. G. Dance, M. Scudder, *J. Chem. Soc. Chem. Commun.* **1982**, 1246; b) I. G. Dance, A. Choy, M. L. Scudder, *J. Am. Chem. Soc.* **1984**, *106*, 6285.
[13] G. S. H. Lee, D. C. Craig, I. Ma, M. L. Scudder, T. D. Bailey, I. G. Dance, *J. Am. Chem. Soc.* **1988**, *110*, 4863.
[14] N. Herron, J. C. Calabrese, W. E. Farneth, Y. Wang, *Science* **1993**, *259*, 1426.
[15] K. S. Hagen, R. H. Holm, *Inorg. Chem.* **1984**, *23*, 418.
[16] A. D. Watson, C. Pulla Rao, J. R. Dorfman, R. H. Holm, *Inorg. Chem.* **1985**, *24*, 2820.
[17] S. Harris, *Polyhedron* **1989**, *8*, 2843, and references therein.

Structure of a Mixed Phosphate/Phosphonate Layered Zirconium Compound from Synchrotron X-Ray Powder Diffraction Data**

Damodara M. Poojary, Baolong Zhang, and Abraham Clearfield*

Despite new developments in instrumentation and methods, structure determination from powder diffraction data is still not a routine procedure. Until now the most complex structures solved by this method include those of the β-Ba_3AlF_9,[1] the trivalent metal phosphites $(M_2HPO_3)_3 \cdot 4H_2O$ (M = Ga, Al, Fe),[2, 3] $(AlPO_4)_3 \cdot CH_3NOH$,[4] and $[\{HgRu(CO)_4\}_4]$.[5] β-Ba_3AlF_9 and gallium phosphite contain 29 atoms (including H atoms) in the asymmetric unit. The structure of the former compound was solved from conventional powder diffraction data while a combination of neutron and synchrotron data were used for the solution of the Ga compound. Here we report the X-ray powder structure analysis of a new layered compound (**1**) in which one of the phosphate groups contains a large organic complexant.

$$[Zr_2(PO_4)\{O_3PCH_2N(CH_2CO_2H)_2\}\{O_3PCH_2N(CH_2CO_2H)(CH_2CO_2)\}(H_2O)_2]$$
1

Layered zirconium phosphate compounds are of interest because of their practical application in areas such as ion exchange, catalysis, and intercalation chemistry. Most of the zirconium phosphate compounds studied thus far are structurally related to either $Zr(HPO_4)_2 \cdot H_2O$ (α-ZrP)[6] or to $Zr(PO_4)(H_2PO_4) \cdot 2H_2O$ (γ-ZrP).[7, 8] Since these Zr compounds are difficult to obtain as a single crystal, their structures can be determined only from their powder diffraction data. Using powder methods, we have determined the structures of a number of layered compounds and discovered some new phosphatozirconium layer types different from those of α- and γ-ZrP.[9, 10] Compound **1** is a mixed phosphate/phosphonate layered compound with an unusual Zr/P ratio of 2/3.

Preliminary X-ray powder data were collected on a Rigaku rotating anode automated diffractometer ($Cu_{K\alpha}$ radiation; 50 kV, 180 mA). The pattern was indexed by Ito methods.[11] The systematic absences were consistent with the space group $P2/c$ or Pc. Integrated intensities were extracted from the profile, and a Patterson map was computed using unambiguously indexed low angle reflections. The positions of the Zr atom and the P atoms located from this map were then entered into the program GSAS[12] for Rietveld refinement. A series of Fourier maps revealed the positions of the oxygen atoms that complete the coordination of the metal atom and the P atoms, but no atoms of the phosphonatomethyliminodiacetic acid group, $O_3PCH_2N(CH_2CO_2H)_2$ (PMIDA) could be located. To improve the quality of the data and to locate the light atoms, we collected Synchrotron powder diffraction data on beam line X7A at the National Synchrotron Light Source using a Ge(111) monochromator and Ge(220) analyzing crystal. The sample was

[*] Prof. Dr. A. Clearfield, Dr. D. M. Poojary, B. Zhang
Department of Chemistry, Texas A & M University
College Station, TX 77843 (USA)
Telefax: Int. code +(409) 845-4719

[**] We gratefully acknowledge financial support from the National Science Foundation (grant No. DMR-9107715) and from the National Synchrotron Light Source, Brookhaven National Laboratory, which is supported by the U.S. Department of Energy, Division of Materials Science and Division of Chemical Sciences (for the data collection). We thank Dr. David E. Cox for assistance in obtaining the synchrotron data.

contained in a capillary, and the data were collected on a rotating sample in steps of 0.008° for the range $4° \leq 2\theta \leq 60°$. Counting time per step varied from 1 to 10 s. Rietveld refinement and further structure solution was then started with this new data set, which allowed the location and refinement of all the nonhydrogen atoms in the structure. Crystallographic data are given in Tables 1 and 2, and the observed and calculated powder patterns in Figure 1.

Table 1. Crystallographic data for **1**.

Scan range (2θ) 4–60°, increment 0.008°, time for each measurement 1–10 s, synchrotron radiation; $\lambda = 1.1487$ Å.

$C_{10}H_{19}N_2O_{20}P_3Zr_2$, $M_r = 762.35$, space group $P2/c$ (13), $a = 14.9010(3)$, $b = 8.6541(1)$, $c = 9.1367(1)$ Å, $\beta = 97.960(2)°$, $V = 1666.9$ Å^3, $Z = 2$, $\rho_{calcd} = 2.19$ Mg m^{-3}, $T = 23$ °C. No. of contributing reflections $N_o = 850$, no. geometric observations $N_{var} = 50$; distances [Å]: P–O 1.53(2), Zr–O 2.03(3), O–O (PO_4) 2.55(2), O···O (ZrO_6, *cis*) 2.90(2); 60 structural parameters, 11 profile parameters. R_{wp}(statistical) = $R_{wp}/(\chi^2)^{1/2} = 0.07$, $\chi^2 = \sum w(I_o - I_c)^2/(N_o - N_{var})$, $R_{wp} = (\sum w(I_o - I_c)^2/\sum [wI_o^2])^{1/2} = 0.129$, $R_p = (\sum |I_o - c_c|/\sum I_c) = 0.101$, $R_F = \langle |F_o| - |F_c| \rangle \langle |F_o| \rangle = 0.067$.

Table 2. Positional [Å] and isotropic thermal parameters U_{iso} [Å^2] for **1**.

Atom	x [Å]	y [Å]	z [Å]	U_{iso} [Å^2]
Zr1	0.1026(2)	0.2558(4)	0.0582(3)	0.049(2)
P1	0.1227(4)	0.1117(6)	0.4197(6)	0.015(8)
P2	0	0.5429(9)	0.25	0.015
O1	0.1415(6)	0.150(1)	0.262(1)	0.014(9)
O2	0.1375(6)	0.939(1)	0.453(1)	0.014
O3	0.0239(4)	0.158(1)	0.440(1)	0.014
O4	0.0615(5)	0.443(1)	0.165(1)	0.014
O5	0.0596(6)	0.350(1)	0.859(1)	0.014
O(W)	0.2283(5)	0.341(1)	0.058(1)	0.014
O7	0.4567(11)	0.214(2)	0.424(2)	0.12(1)
O8	0.4153(5)	0.423(2)	0.257(2)	0.12
O9	0.3553(15)	0.157(2)	0.906(2)	0.12
O10	0.3838(20)	0.995(2)	0.702(3)	0.12
N1	0.2903(8)	0.226(2)	0.522(2)	0.10(1)
C1	0.1967(6)	0.222(1)	0.553(1)	0.08(1)
C2	0.3023(8)	0.336(2)	0.403(2)	0.08
C3	0.3956(12)	0.317(3)	0.360(3)	0.08
C4	0.3559(11)	0.267(3)	0.658(2)	0.08
C5	0.3523(22)	0.128(2)	0.759(2)	0.08

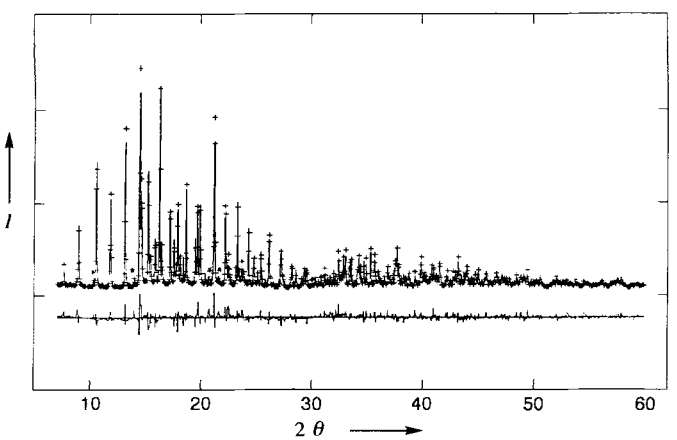


Fig. 1. Superimposed observed and calculated diffraction profiles (top, X-ray intensity versus 2θ) and their difference (bottom).

The metal coordination and the atom labeling are given in Figure 2, and the arrangement of the layers in the lattice in Figure 3. The structure contains both phosphate and phosphonate groups. The phosphorus atom of the phosphate is located on a twofold axis, while that of the phosphonate is in a general position thus giving a Zr/P ratio of 2:3. The phosphate group is situated nearly in a plane (atoms P2, O4, O5) at $x = 0$ and bridges four zirconium atoms which are arranged slightly above and below this plane. Also, all three oxygens (O1, O2, and O3) of the phosphonate group are involved in binding to metal atoms. The octahedral coordination of a single metal atom is completed by an oxygen atom from each of two phosphate groups, three oxygen atoms of phosphonate groups, and an oxygen of the water molecule.

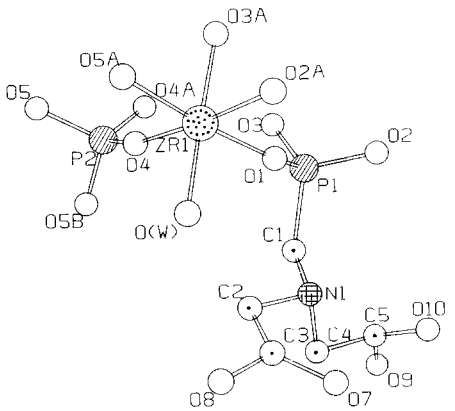


Fig. 2. Schematic representation of the structure of **1** showing the coordination about the zirconium atom and the numbering scheme. Selected bond lengths [Å] and angles [°]: Zr1-O1 2.083(5), Zr1-O2 2.042(6), Zr1-O3 2.070(5), Zr1-O4 2.029(5), Zr1-O5 2.015(6), Zr1-O(W) 2.012(6); average values for P-O 1.55(1), O-Zr-O 90 (*trans*: 177), O-P-O 110(1).

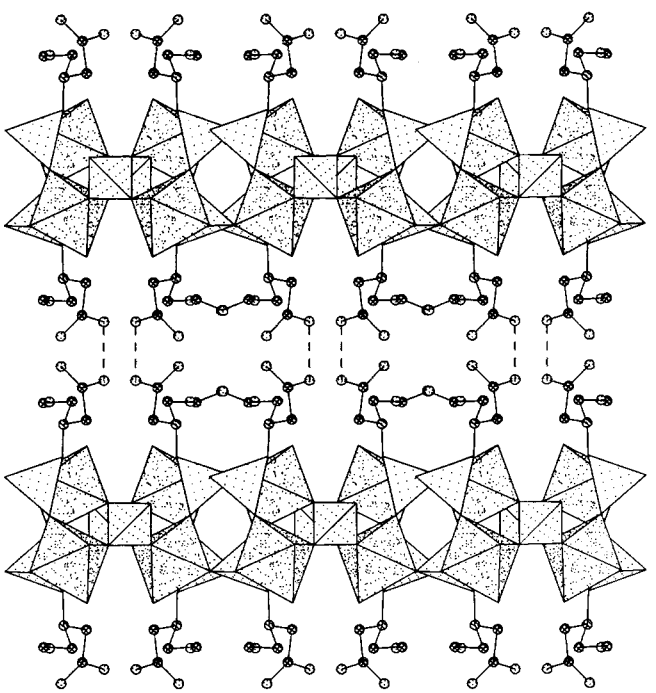


Fig. 3. Projection of the structure down the b axis showing the layer arrangement. The sketch depicts ZrO_6 as octahedra, PO_4 and PO_3C moieties as tetrahedra, and the $N(CH_2CO_2H)_2$ groups, and indicates the hydrogen bonding (- - -).

 © VCH Verlagsgesellschaft mbH, D-69451 Weinheim, 1994 0570-0833/94/2222-2325 $ 10.00+.25/0

The carboxylate oxygens of the PMIDA group are not involved in metal binding; instead they are positioned near the center of the metal phosphate layers. The carboxylate groups from the neighboring layers are linked to each other by hydrogen bonds. One such bond is between O7 of the C3-carboxylate and O10 of the C5-carboxylate group of the adjacent layer (O7 $\cdots$ O10 = 2.82(3) Å). The other hydrogen bond involves two O8 oxygen atoms (O8 $\cdots$ O8′ = 2.54(1) Å) related by a twofold axis at $\frac{1}{2}, y, \frac{1}{4}$. On the basis of this symmetry restriction and the charge requirement, we postulate that these two oxygens share a proton. In other words, there exists only one proton for two of the C3-carboxylate groups while the C5-carboxylate group is fully protonated. This feature may be better explained if we reduce the symmetry to the noncentric space group, *Pc*. In this space group, the structure contains two independent PMIDA groups, and the charge balance is achieved by deprotonation of a carboxylate group in one of the PMIDA groups. This explanation agrees well with the results from ^{31}P MAS NMR spectrum, which shows a doublet for the phosphonate groups rather than a single resonance. However, the refinement of the structure in *Pc* (37 atoms) did not converge, possibly due to the limited number of observed reflections. The PMIDA group also appears to interact with the coordinated water molecule through its oxygen atom, O9 (O9 $\cdots$ O(W) = 2.96(2) Å). The P1–C1 bond distance of 1.80(1) Å agrees well with that found for other phosphonate structures.[13–15] The carbon atoms C1, C2, and C4 are in a regular tetrahedral environment C2–C3 = 1.51(1), C4–C5 = 1.52(1) Å). The average C-N-C bond angle is 111(1)° and the N–C distance 1.48(1) Å. The carboxylate groups are nearly planar with an average bond angle of 119(1)°, and the average of the C–O bond distances in these groups is 1.36(1) Å.

To the best of our knowledge this is the first example of a mixed phosphate/phosphonate system that has been structurally characterized. Despite the unusual Zr/P ratio of 2:3 the title compound shows some similarities with the well-known α- and γ-zirconium phosphates. The bridging nature of the phosphate in this compound is similar to that observed for γ-ZrP, while the binding of the phosphonate resembles that in α-ZrP. The γ-structure contains an additional H_2PO_4 group, which links to only two metal atoms. Compound **1** is the first zirconium phosphate layer compound that has been observed to contain a metal-coordinating water molecule, although this frequently occurs with other metal atoms.[15, 16] Intercalation and ion exchange reactions of **1** are under investigation.

Experimental Procedure

H_2PMIDA (2.27 g, 10 mmol), [16]) was dissolved in 5N ammonium hydroxide (30 mL). The pH was adjusted to 1 by adding HCl, and this solution was then mixed with 85% phosphoric acid (0.68 mL, 10 mmol). A solution of $[ZrFA_6]^{2-}$ was prepared by dissolving $ZrOCl_2 \cdot 8H_2O$ (3.22 g, 10 mmol) in distilled water (20 mL) and HF (1 mL). The metal and the PMIDA solutions were mixed in a Teflon flask fitted with a Teflon condensor and heated in an oil bath at 60 °C for a week. The white crystalline powder was filtered hot, rinsed with distilled water, and dried at 60 °C in an oven for one day.

Received: May 28, 1994 [Z 6979 IE]
German version: *Angew. Chem.* **1994**, *106*, 2420

[1] A. Le Bail, *J. Solid State Chem.* **1993**, *103*, 287.
[2] R. E. Morris, W. T. A. Harrison, J. M. Nicol, A. P. Wilkinson, A. K. Cheetham, *Nature* **1992**, *359*, 519.
[3] D. M. Poojary, Y. Zhang, D. E. Cox, P. R. Rudolf, S. Cheng, A. Clearfield, *J. Chem. Crystallogr.* **1994**, *24*, 155.
[4] P. R. Rudolf, C. Saldarriaga-Molina, A. Clearfield, *J. Phys. Chem.* **1986**, *90*, 6122.
[5] N. Masciocchi, P. Cairati, F. Ragaini, A. Sironi, *Organometallics* **1993**, *12*, 4499.
[6] J. M. Troup, A. Clearfield, *Inorg. Chem.* **1977**, *16*, 3311.
[7] A. N. Christensen, E. K. Andersen, I. G. K. Andersen, G. Alberti, M. Nielsen, M. S. Lehman, *Acta Chem. Scand.* **1990**, *44*, 865.
[8] D. M. Poojary, B. Zhang, Y. Dong, G. Peng, A. Clearfield, *J. Phys. Chem.*, in press.
[9] D. M. Poojary, L. A. Vermeulen, E. Vicenzi, A. Clearfield, M. E. Thompson, *Chem. Mater.*, in press.
[10] D. M. Poojary, B. Zhang, A. Clearfield, *J. Chem. Soc. Dalton Trans.* **1994**, 2453.
[11] J. W. Visser, *J. Appl. Crystallogr.* **1969**, *2*, 89.
[12] A. Larson, R. B. Von Dreele, *GSAS. Generalized Structure Analysis System*, Los Alamos National Laboratory, **1988**.
[13] D. M. Poojary, H.-L. Hu, F. L. Campbell III, A. Clearfield, *Acta Crystallogr. Sect. B* **1993**, *49*, 996.
[14] Y. Zhang, A. Clearfield, *Inorg. Chem.* **1992**, *31*, 2821.
[15] C. Bhardwaj, H.-L. Hu, A. Clearfield, *Inorg. Chem.* **1993**, *32*, 4294.
[16] K. Moedritzer, R. R. Irani, *J. Org. Chem.* **1966**, *31*, 1603.

Unusually Large Isotope Effects on NMR Chemical Shifts of Paramagnetic Organometallic Compounds**

Robert A. Heintz, Thomas G. Neiss, and Klaus H. Theopold*

NMR spectroscopy applied to paramagnetic molecules typically suffers from so-called isotropic shifts and more or less severe line broadening.[1] The former invalidate the empirical correlation between resonance frequency and chemical environment, and the latter obscures internuclear coupling and sometimes even prevents detection of resonances. Despite these obvious drawbacks, paramagnetism may yet hold advantages even for NMR spectroscopy. We report here the observation of unusually large isotope effects on both ^{1}H and ^{13}C NMR chemical shifts of a paramagnetic organometallic complex (Paramagnetic Isotope Effect on Chemical Shift, PIECS). This phenomenon appears to be widespread[2] and may prove to be a useful tool for the investigation of structure and reactivity of molecules with unpaired electrons.

As part of our investigation of paramagnetic organometallic chromium complexes,[3] we have previously reported the synthesis and structural characterization of $[\{Cp''Cr(\mu_3\text{-}H)\}_4]$ (**1**; see Scheme 1, $Cp'' = \eta^5\text{-}C_5Me_4Et$).[4] Variable-temperature magnetic susceptibility measurements carried out with a Faraday balance showed **1** to have a temperature-dependent effective magnetic moment. At ambient temperature **1** exhibited $\mu_{eff} = 3.5\ \mu_B$, and cooling led to a decrease in the magnetic moment, as expected for antiferromagnetic coupling of the metal centers. Despite its sizable magnetic moment, **1** exhibits rather distinct ^{1}H and ^{13}C NMR spectra.

In an attempt to gauge its thermal stability, a C_6D_6 solution of **1** in a sealed NMR tube was heated to 50 °C and periodically monitored by NMR spectroscopy. After two days, the ^{1}H NMR spectrum displayed two new resonances (at $\delta = 7.5$ and 6.9), very similar in appearance to the resonances attributed

[*] Prof. Dr. K. H. Theopold, Dr. R. A. Heintz
Department of Chemistry and Biochemistry
Center for Catalytic Science and Technology
University of Delaware
Newark, DE 19716 (USA)
Telefax: Int. code +(302) 831-6335
Dr. T. G. Neiss
Hercules Inc., Wilmington, DE 19808 (USA)

[**] This research was supported by the U.S. National Science Foundation (CHE-9122580) and by the Alfred P. Sloan Foundation (Sloan Research Fellowship to K. H. T., 1992–1994).

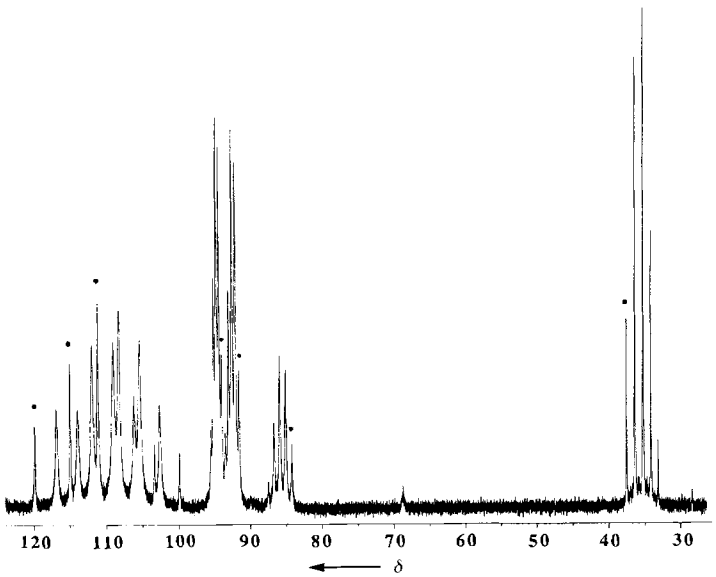
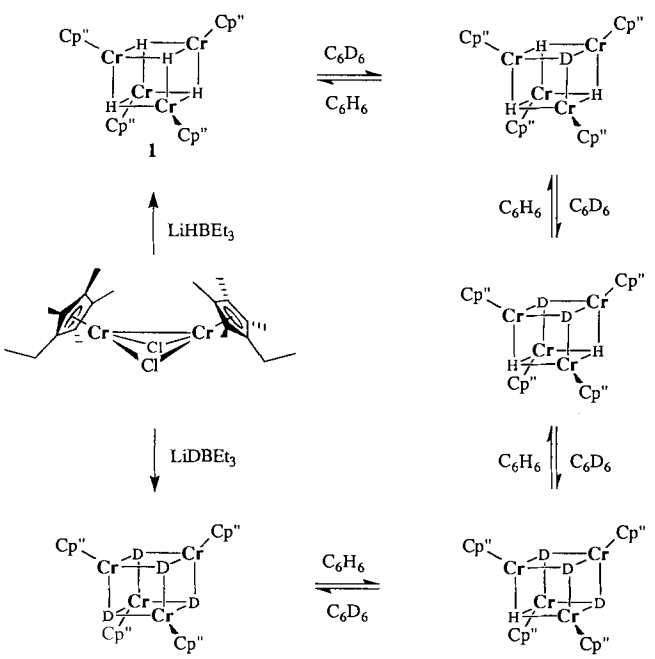


Fig. 1. ^{13}C NMR spectrum (125.8 MHz, 298 K, [D_8]toluene) of a statistical mixture of isotopomers of the general composition [$Cp''_4Cr_4(\mu_3\text{-}H)_{4-n}(\mu_3\text{-}D)_n$] ($n = 0$–4). Filled circles indicate the resonances of unlabeled [$Cp''_4Cr_4(\mu_3\text{-}H)_4$].

to the ring-bound methyl groups of **1**, and an upfield shoulder to the resonance caused by the methylene group. Further heating led to the appearance of additional resonances until, after four weeks, the low-field part of the spectrum ($\delta = 6$–8) exhibited at least seven broad and overlapping peaks of various intensities. The ^{13}C NMR spectra of the sample revealed a parallel evolution; each of the seven original resonances of **1** split up into a group of several peaks. Figure 1 shows such a



Scheme 1.

^{13}C NMR spectrum. Close examination revealed that each of the seven original singlets had been transformed into a set of five resonances in the approximate proportions 13:30:33:19:5. We propose that this spectrum results from a mixture of isotopomers of the constitution [$Cp''_4Cr_4(\mu_3\text{-}H)_{4-n}(\mu_3\text{-}D)_n$] (i.e. [$D_0$]-**1**, [$D_1$]-**1**, ... [$D_4$]-**1**) formed by H/D exchange with the deuteriated solvent (Scheme 1). The results of several experiments support this hypothesis. After prolonged heating of **1** in C_6H_6, followed by removal of the solvent, and addition of C_6D_6, NMR analysis showed only the seven original singlets of **1**. Reaction of [{Cp″Cr(μ-Cl}$_2$] with Li[DBEt$_3$] (95% D) yielded a sample of **1** featuring two sets of seven resonances in the ^{13}C NMR spectrum. The most intense set of resonances had the same chemical shifts as the lowest field signals in Figure 1; they presumably belong to the completely deuteriated [D_4]-**1**. The minor set of resonances had intermediate chemical shifts and was consistent with the spectrum expected of [D_3]-**1**, which results from residual hydride in the deuteride reagent. Exposure of this mixture to an excess of H_2 (1 atm, several days) restored the spectrum of [D_0]-**1**. Finally, treatment of **1** with a stoichiometric amount of D_2 yielded a sample with a ^{13}C NMR spectrum much like that shown in Figure 1. The H/D exchange is most facile with H_2 (D_2) gas; it proceeds more slowly with benzene or toluene, and apparently not at all with saturated hydrocarbons (e.g. cyclohexane).

The observed isotope effects on the ^{13}C chemical shifts of **1** range from $\Delta\delta = 0.37$ to 3.06 per H/D substitution (see Table 1)! The ring carbons, which are directly bonded to the

Table 1. ^{13}C NMR chemical shifts of [D_n]-**1** in [D_8]toluene at 298 K (δ values).

Cmpd.	C_{Et}	C_d [a]	C_u [a]	Me_d	Me_u	CH_2	CH_3
[D_0]-**1**	119.94	115.05	111.22	94.03	91.60	84.28	37.65
[D_1]-**1**	116.94	111.99	108.29	94.42	92.13	85.13	36.46
[D_2]-**1**	113.98	109.08	105.41	94.80	92.61	85.97	35.34
[D_3]-**1**	? [b]	106.18	102.66	95.17	93.07	86.75	34.26
[D_4]-**1**	? [b]	103.40	99.91	95.52	93.53	87.54	33.23

[a] d = downfield, u = upfield. [b] Resonance obscured by larger peak.

spin-carrying chromium atom, show the biggest effect; the corresponding resonances of [D_0]-**1** and [D_4]-**1** differ by up to $\Delta\delta = 11.7$. The signal for the methyl carbon of the ethyl substituent (four bonds from the nearest hydride ligand) shows the next biggest effect, while the signals for methyl groups directly attached to the ring are least shifted. Subsequent H/D substitutions consistently attenuate the shift; thus the incorporation of the fourth deuterium has only roughly 90% of the effect of the first one. The effect is slightly less pronounced in the ^1H NMR spectrum. While the signals for protons of the ethyl group show only modest shifts, those of the ring-bound methyl groups suffer upfield shifts of $\Delta\delta = 0.2$–0.45 per H/D substitution. These isotope effects are at least an order of magnitude larger than comparable shifts observed for diamagnetic molecules.[5] While we believe this to be the first observation of paramagnetically induced isotope shifts in ^{13}C NMR spectroscopy, a few reports exist about analogous effects in ^1H NMR spectroscopy.[2] It is likely that other NMR-active nuclei will show similar effects, and their discovery is limited only by the usual requirements for the detection of reasonably sharp NMR resonances of paramagnetic molecules (i.e. fast electron relaxation).

What causes these unusually large isotope shifts in **1**? In general, isotropic shifts consist of two contributions, namely the Fermi contact shift and the dipolar shift.[1] Without any independent measure of the magnetic anisotropy of **1**, the separation of these two effects is impossible. However, both depend on the magnitude of the magnetic susceptibility, and we believe that in this particular case the isotopic substitution may actually affect

the susceptibility of the complex. Due to the lower zero-point energy of Cr–D bonds, they are expected to be slightly shorter than Cr–H bonds. H/D substitution in **1** may therefore lead to small changes in the H(D) positions, and possibly even to contraction of the Cr–Cr distances. Such structural changes should affect the coupling constant J of the antiferromagnetic interaction (i.e. $|J_{[D_0]\text{-}\mathbf{1}}| < |J_{[D_4]\text{-}\mathbf{1}}|$), leading to a shift in the relative population of the various spin states and hence the average susceptibility. Some support for this proposal is provided by the observation that the direction of the isotope shifts induced by deuteriation in all cases parallels the effects of a decrease in temperature. While χ_m of solid **1** decreases upon cooling, the ^{13}C NMR resonances of the ring carbons and the methyl group of the ethyl substituent move upfield, and those of the methylene carbon and the ring-bound methyl groups shift downfield. Examination of Table 1 reveals shifts in the same directions brought about by progressive deuterium incorporation. According to our proposal, both cooling and deuteriation are expected to shift the spin equilibrium toward lower average spin multiplicity, and the parallel effects on the chemical shifts are consistent with this notion.

Whatever the mechanisms responsible for PIECS, they seem to occur with some regularity, and they can be very large. The following demonstrates how this phenomenon can be put to good use. Note, that the mixed isotopomers [D_1]-**1**, [D_2]-**1**, and [D_3]-**1** each feature two sets of chemically inequivalent Cp″ ligands. Thus, one might have expected a total of eight resonances in Figure 1 for each kind of carbon atom. One possible explanation for the observation of one resonance only for each isotopomer is the occurrence of a fluxional process. Such a process might be frozen out at lower temperature. Accordingly, Figure 2 shows the temperature dependence of one set of ^{13}C NMR resonances. Upon cooling, the three intermediate resonances broaden, collapse, and eventually reemerge to give a total of at least seven peaks. The estimated rate constant for the exchange process at the coalescence temperature is $k_{248\ K} = 120\ s^{-1}$, and substitution of this value into the Eyring equation yields $\Delta G^{\ddagger} = 12$ kcal mol^{-1}. Previously determined activation barriers for fluxional processes involving hydride migration in metal clusters range from 3 to 19 kcal mol^{-1}[6] and encompass the value found for **1**. This straightforward detection and kinetic characterization of the hydride migration in **1** would have been impossible for a diamagnetic analogue, in other words in the absence of PIECS.

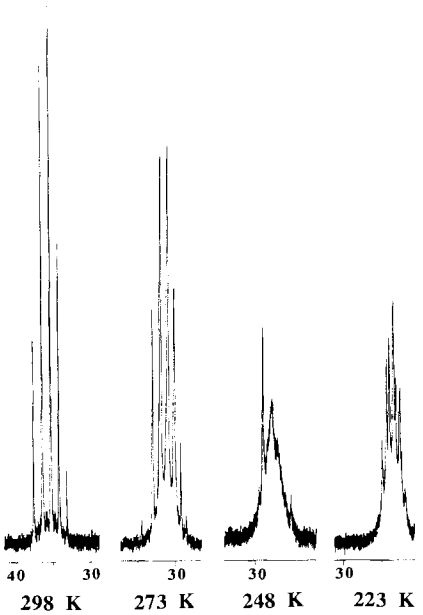


Fig. 2. Temperature dependence of the ^{13}C NMR resonances attributed to the methyl groups of the ethyl substituents of $[Cp''_4Cr_4(\mu_3\text{-}H)_{4-n}(\mu_3\text{-}D)_n]$ ($n = 0$–4).

A number of examples suggest that NMR spectra of paramagnetic compounds frequently exhibit unusually large isotope effects on chemical shifts. Under favorable circumstances, these isotope shifts may facilitate experiments on paramagnetic complexes (e.g. labeling studies, dynamic NMR studies, etc.), which cannot be done with diamagnetic molecules.

Experimental Procedure

1: To a stirred suspension of 1.004 g (8.17 mmol) of $CrCl_2$ in 60 mL of THF was added 1.271 g (8.14 mmol) of $EtMe_4C_5Li$. The reaction was allowed to stir for 2 h at room temperature. To this solution was slowly added 8.1 mL (8.1 mmol) of $LiHBEt_3$ (1.0 M in THF) by syringe. The mixture was stirred for another 30 min, and then the THF was removed under vacuum. The resulting sticky brown solid was extracted with pentane and the extract filtered. The pentane solution was concentrated and cooled to $-30\,^{\circ}C$ to yield 0.991 g (1.22 mmol, 60%) of **1**. ^1H NMR (C_6D_6): $\delta = 7.9$ (s, 6H), 7.3 (s, 6H), 3.4 (s, 2H), 1.1 (s, 3H); ^{13}C NMR (C_6D_6): $\delta = 119.9, 115.0, 111.2, 94.0, 91.6, 84.3, 37.6$; IR (KBr): $\tilde{\nu} = 2960$ (s), 2901 (s), 2868 (s), 2714 (w), 1448 (s), 1365 (s), 1303 (w), 1018 (m), 945 (w), 551 (s) cm^{-1}. Analysis calculated for $C_{44}H_{72}Cr_4$: C 65.65; H 8.97. Found: C 65.55; H 8.88. μ_{eff}(299 K) = 3.50 μ_B (1.75 μ_B/Cr).

[D_4]-**1**: The procedure was the same as described above, except $LiDBEt_3$ (95% D) was used. A mixture of $[Cp''_4Cr_4(\mu_3\text{-}D)_4]$ ([D_4]-**1**, ca. 80%) and $[Cp''_4Cr_4(\mu_3\text{-}D)_3(\mu_3\text{-}H)]$ ([D_3]-**1**, ca. 20%) was obtained. ^1H NMR (C_6D_6): [D_4]-**1**: $\delta = 6.8$ (s), 6.2 (s), 3.1 (s), 1.1 (s); [D_3]-**1**: $\delta = 7.0$ (s), 6.4 (s), 3.1 (s), 1.1 (s); ^{13}C NMR (C_6D_6): [D_4]-**1**: $\delta = 108.9, 103.7, 100.5, 95.4, 93.4, 87.6, 33.7$; [$D_3$]-**1**: $\delta = 111.7, 106.7, 103.2, 95.1, 93.0, 86.8, 34.8$ ppm.

Received: June 10, 1994 [Z 7025 IE]
German version: *Angew. Chem.* **1994**, *106*, 2389

[1] I. Bertini, C. Luchinat, *NMR of Paramagnetic Molecules in Biological Systems*, Benjamin/Cummings, Menlo Park, CA, USA, **1986**.
[2] a) R. R. Horn, G. W. Everett, Jr., *J. Am. Chem. Soc.* **1971**, *93*, 7173; b) B. Evans, K. M. Smith, G. N. La Mar, D. B. Viscio, *ibid.* **1977**, *99*, 7070; c) K. H. Theopold, J. Silvestre, E. K. Byrne, D. S. Richeson, *Organometallics* **1989**, *8*, 2001; d) N. Hebendanz, F. H. Köhler, F. Scherbaum, B. Schlesinger, *Magn. Reson. Chem.* **1989**, *27*, 798; e) C. J. Medforth, F.-Y. Shiau, G. N. La Mar, K. M. Smith, *J. Chem. Soc. Chem. Commun.* **1991**, 590.
[3] K. H. Theopold, *Acc. Chem. Res.* **1990**, *23*, 263.
[4] R. A. Heintz, B. S. Haggerty, H. Wan, A. L. Rheingold, K. H. Theopold, *Angew. Chem.* **1992**, *104*, 1100; *Angew. Chem. Int. Ed. Engl.* **1992**, *31*, 1077.
[5] P. E. Hansen, *Prog. Nucl. Magn. Reson. Spectrosc.* **1988**, *20*, 207.
[6] a) L. R. Nevinger, J. B. Keister, *Organometallics* **1990**, *9*, 2312; b) E. Band, E. L. Muetterties, *Chem. Rev.* **1978**, *78*, 639; c) J. Evans, *Adv. Organomet. Chem.* **1977**, *16*, 319.

Hf_3Te_2: A New and Remarkable Layered Compound**

Robert L. Abdon and Timothy Hughbanks*

Binary, early-transition-metal chalcogenides of surprisingly simple composition continue to be found. Recent attention to this chemistry and advances in synthetic methodology have produced Ta_3S_2,[1,2] Ta_6Te_5,[3] Ta_2Te_3,[4] and Ta_2Se.[5] Investigations of tantalum- and niobium-rich chalcogenides have yielded novel layered materials with structures related to the body-cen-

[*] Prof. T. Hughbanks, R. L. Abdon
Department of Chemistry
Texas A & M University, College Station, TX 77843 (USA)
Telefax: Int. code +(409)847-8860

[**] This work was generously supported by the National Science Foundation (Grant DMR-9215890) and by the Robert A. Welch Foundation (Grant A-1132).

tered cubic (bcc) metals. Ta_2Se can be regarded as an insertion phase containing four layers of bcc-like tantalum sandwiched between layers of selenium. An isostructural sulfide exists in the ternary compound $Ta_{1.60}Nb_{0.40}S$.[6, 7] At the composition $Ta_{1.64}Nb_{0.86}S$ (M_5S_2) five layers of bcc metal are found between the sulfide layers.[8] Mixed tantalum/niobium sulfides having higher niobium content have been prepared,[9, 10] but their structures are similar to the niobium-rich sulfides $Nb_{21}S_8$ and $Nb_{14}S_5$, which are less closely related to the bcc-metal structure.

Preparative investigations of hafnium-rich tellurides incorporating later 3d transition metals have produced Hf_8MnTe_6 and Hf_8FeTe_6.[11] These materials are structurally related to the condensed cluster Ta compounds $Ta_{11}M_2Se_8$, Ta_8MSe_8, and $Ta_9M_2S_6$.[12–14] In our attempts to prepare related, ternary compounds of hafnium and tellurium, the binary phase Hf_3Te_2 was discovered. This remarkable material is the only reduced, binary hafnium telluride, and like Ta_2Se, it has a simple structure and composition.

We prepared Hf_3Te_2 by direct reaction of stoichiometric amounts of the elements (Hf 96.9%, including 2.9% Zr, and Te 99.99%; Johnson Matthey) in sealed Nb capsules, which were in turn sealed in evacuated and flame-baked silica tubes. The temperature of the reaction vessel was increased uniformly to 1000 °C over 5 days, and the product was isolated in quantitative yield after 10 more days at this temperature. Attempts to grow single crystals by vapor phase transport with $TeCl_4$ repeatedly produced only microcrystalline powders. However, by employing KCl as a flux (molar ratio, 2 KCl: 1 Hf_3Te_2) and cycling the reaction temperature between 950 °C and 1000 °C repeatedly over a two-week period, black, square crystals suitable for single-crystal X-ray studies were obtained (Table 1).[15] No contamination by niobium was detected in elemental analysis of the product.

Table 1. Structural parameters for Hf_3Te_2: space group $I4/mmm$ (no. 139), $Z = 2$; $a = 3.6837(3)$ Å, $c = 17.901(2)$ Å.

Atom	x	y	z	U (equiv) [Å$^2 \times 10^3$]
Hf1	0	0	0	7 (1)
Hf2	1/2	1/2	0.0962	7 (1)
Te1	0	0	0.1690	7 (1)

As in Ta_2Se and the mixed Ta/Nb sulfides, Hf_3Te_2 is formally an insertion phase related to that of bulk body-centered cubic metal. After every three layers of hafnium, two layers of tellurium are inserted. The result is a layered structure in which slabs are made up from three square nets of hafnium sandwiched between two layers of tellurium (Fig. 1). These Te-Hf_3-Te sandwiches are stacked, with only weak interlayer interactions, to form the full three-dimensional structure. Within the slabs, the more oxidized metal centers (Hf2) are those bound to four tellurium atoms at the exterior of the layer. Each of these metal atoms forms four bonds to the hafnium atoms (Hf1) in the central net (3.1229(4) Å) and one longer bond through the slab (3.4454(12) Å) to a symmetry-equivalent atom. Each tellurium is five-coordinate with respect to hafnium atoms in the same slab (Te1–Hf2, $4 \times 2.9120(5)$; Te1-Hf1, $1 \times 3.0245(9)$ Å). Guinier powder films show two very weak lines, suggesting the possibility of a ($\sqrt{2}a \times \sqrt{2}b$) superlattice. The existence of this superlattice could not be detected in the single crystal study, and currently is under investigation.

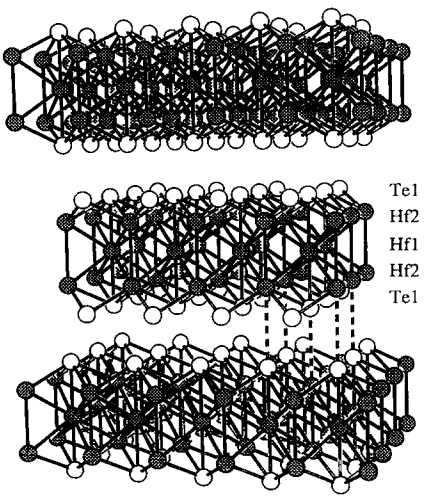


Fig. 1. The Hf_3Te_2 structure viewed approximately along the {110} direction. Hf atoms are shown as dotted circles and Te as open circles. Only interatomic distances less than 3.6 Å are shown as bonds.

The electronic band structure of Hf_3Te_2 was calculated with the extended Hückel method.[16] The Fermi level lies just below a pronounced minimum in the total density of states (DOS) diagram (Fig. 2a). Projected DOS diagrams show that the energy levels between -15.0 and -10.5 eV are primarily localized on Te (Fig. 2b), while the higher levels have mainly Hf d and s character (Fig. 2c). The mixing of Hf-based orbitals into the Te-based manifold gives evidence for significant Hf–Te covalency. Crystal orbital overlap populations (COOPs)[17] yielded a valence electron concentration (VEC) that indicates that all levels with strongly Hf–Hf bonding character are filled (Fig. 3). At the same time, these levels have only moderately antibonding Hf–Te character. Isoelectronic Zr_3Te_2 adopts a defect-WC structure, as do the other known Group IV chalcogenides of the same composition.[18–20] Although these calculations rationalize the structure of Hf_3Te_2, the underlying factors controlling the choice between structural types for isoelectronic compounds remain unclear.

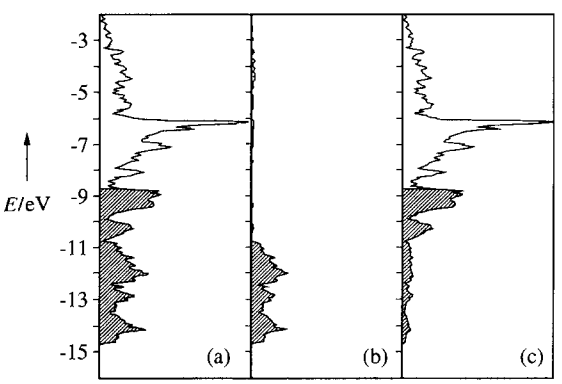


Fig. 2. a) Total density of states (DOS) diagram for Hf_3Te_2. The energy range includes the Te 5p bands and the Hf d and s bands. b) Tellurium contribution to the DOS. c) Hafnium contribution to the DOS. Filled levels are shaded.

The title compound belongs to a broader class of chalcogenides having a structure based on the stacking of 4^4 nets of atoms. The transition from three-dimensional to two-dimensional structures in these materials is determined by the lattice

 © VCH Verlagsgesellschaft mbH, D-69451 Weinheim, 1994 0570-0833/94/2222-2329 $ 10.00+.25/0

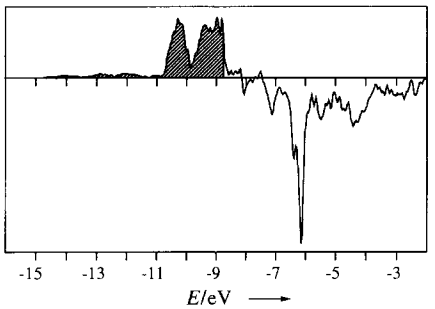


Fig. 3. Crystal orbital overlap population (COOP) curves showing averaged Hf Hf interactions in Hf_3Te_2. Levels above the energy axis are bonding while those below are antibonding. Filled levels are shaded.

constant *a* and the size of the chalcogenide. In ZrGeTe (PbFCl type), the stacking sequence of the nets is Te-Zr-Ge_2-Zr-Te. The larger *a* dimension of 3.866 Å reduces steric crowding in the Te nets and permits much shorter Zr–Te contacts between adjacent layers. On the other hand, isostructural ZrSiTe has a significantly shorter *a* axis (3.692 Å) that precludes such interlayer Zr–Te bonding.[21, 22] In Hf_3Te_2 the *a* dimension is only 3.6837(3) Å, slightly shorter than that of ZrSiTe. The Hf–Te contacts between adjacent layers in Hf_3Te_2 are 4.195 Å, too long for significant Hf–Te bonding. The Te–Te distances between adjacent layers of 3.785 Å suggest that the structure is highly two-dimensional, with van der Waals interactions between the slabs.

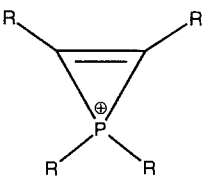
Received: May 19, 1994 [Z 6950IE]
German version: *Angew. Chem.* **1994**, *106*, 2414

[1] S.-J. Kim, K. S. Nanjundaswamy, T. Hughbanks, *Inorg. Chem.* **1991**, *30*, 159–164.
[2] H. Wada, M. Onoda, *Mater. Res. Bull.* **1989**, *24*, 191–196.
[3] M. Conrad, B. Harbrecht in *IVth Eur. Conf. Solid State Chem.*, Gesellschaft Deutscher Chemiker, Dresden, **1992**, p. 324.
[4] M. Conrad, B. Harbrecht, *J. Alloys Comp.* **1992**, *187*, 181–192.
[5] B. Harbrecht, *Angew. Chem.* **1989**, *101*, 1696–1698; *Angew. Chem. Int. Ed. Engl.* **1989**, *28*, 1660–1662.
[6] K. S. Nanjundaswamy, T. Hughbanks, *J. Solid State Chem.* **1992**, *98*, 278–290.
[7] X. Yao, G. J. Miller, H. F. Franzen, *J. Alloys Comp.* **1992**, *183*, 7–17.
[8] X. Yao, H. F. Franzen, *J. Am. Chem. Soc.* **1991**, *113*, 1426–1427.
[9] X. Yao, H. F. Franzen, *J. Solid State Chem.* **1990**, *86*, 88–93.
[10] X. Yao, H. F. Franzen, *J. Alloys Comp.* **1992**, *182*, 299–312.
[11] R. L. Abdon, T. Hughbanks, *Chem. Mater.* **1994**, *6*, 424–428.
[12] B. Harbrecht, *J. Less Common Met.* **1988**, *141*, 59–71.
[13] M. Conrad, B. Harbrecht, *J. Alloys Comp.* **1993**, *197*, 57–64.
[14] B. Harbrecht, H. F. Franzen, *J. Less Common Met.* **1985**, *113*, 349–360.
[15] Single-crystal X-ray analysis: intensity data were collected on a Siemens R3 diffractometer with $Mo_{K\alpha}$ radiation ($\mu = 75.518\ mm^{-1}$); crystal size $0.2 \times 0.2 \times 0.001$ mm; θ–2θ scan, $2\theta_{max} = 70°$; 1014 reflections ($\pm h$, $\pm k$, l), laminar empirical absorption correction based on psi-scans, 188 independent reflections $I > 2\sigma(I)$. $R(F_o)/R_w(F^2) = 0.0197/0.0512$. Further details of the crystal structure investigation are available on request from the Director of the Cambridge Crystallographic Data Centre, 12 Union Road, GB-Cambridge CB2 1EZ, on quoting the full journal citation.
[16] R. Hoffmann, *J. Chem. Phys.* **1963**, *39*, 1397–1398; M. Whangbo, R. Hoffmann, *J. Am. Chem. Soc.* **1978**, *100*, 6093–6098. Parameters for Hf were obtained from a charge-iterative calculation on Hf_2S. Parameters for Te were taken from ref. [11].
[17] T. Hughbanks, R. Hoffmann, *J. Am. Chem. Soc.* **1983**, *105*, 3528–3537.
[18] H. Hahn, B. Harder, U. Mutschke, P. Ness, *Monatsh. Chem.* **1957**, *292*, 82–96.
[19] H. Hahn, P. Ness, *Z. Anorg. Allg. Chem.* **1959**, *302*, 39–49.
[20] H. Sodeck, H. Mikler, K. Komarek, *Monatsh. Chem.* **1979**, *110*, 1–8.
[21] H. Onken, K. Vierheilig, H. Hahn, *Z. Anorg. Allg. Chem.* **1964**, *233*, 267–279.
[22] W. Bensch, P. Dürichen, *Acta Crystallogr. Sect. C* **1994**, *50*, 346–348.

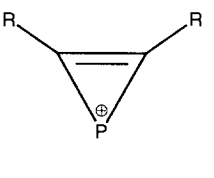
Synthesis and Characterization of the First Compounds Containing a Stable Phosphirenyl Cation: Crystal and Molecular Structure of $[Ni(\eta^3\text{-}PC_2tBu_2)(\eta^5\text{-}P_3C_2tBu_2)W(CO)_5]$**

Anthony G. Avent, F. Geoffrey N. Cloke, Kevin R. Flower, Peter B. Hitchcock, John F. Nixon,* and David M. Vickers

Phosphirenium salts **1**[1–3] do not exhibit aromatic behavior[4] presumably because the 3dπ-2pπ interaction between the phosphorus atom and the C=C double bond is weak as in the isoelectronic silirene.[5] On the other hand it has been proposed[6] that a strong 3pπ-2pπ interaction might be expected between the electron-deficient phosphorus atom and the double bond in the phosphirenyl cation **2** which represents the simplest



1

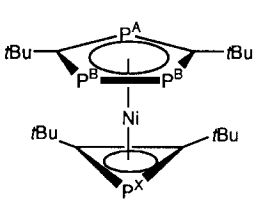


2

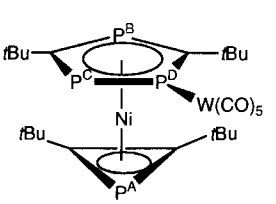
2π-aromatic species containing phosphorus. To date, however, all attempts to synthesize this type of compound have been unsuccessful,[7, 8] for example treatment of the chlorophosphirene ring ClPC(Ph)=CPh with metal salts containing the $[BF_4]^-$ or $[BPh_4]^-$ ions led only to the fluoro- or phenyl-substituted phosphirenes XPC(Ph)=CPh (X = F, Ph), respectively.

Theoretical calculations on silirenyl cations[9] suggest that, if synthesized, they would not be aromatic; on the other hand it has been proposed that phosphirenyl cations would receive some extra stabilization by cyclic delocalization if the destabilizing *n*-π interaction were suppressed by P complexation.[6, 10]

We describe herein the first synthesis of the phosphirenyl cation **2**, (R=*t*Bu) as a ligand in the red-orange nickel complex **3**, whose structure has been elucidated by mass spectrometric and multinuclear NMR studies and confirmed by a single-crystal X-ray structural study on its $[W(CO)_5]$ adduct **4**.



3



4

Recently[11] we described the first direct application of metal vapor synthesis using phosphaalkynes; cocondensation of

[*] Prof. Dr. J. F. Nixon, Dr. A. G. Avent, Prof. Dr. F. G. N. Cloke, Dr. K. R. Flower, Dr. P. B. Hitchcock, D. M. Vickers
School of Chemistry and Molecular Sciences
University of Sussex
GB-Brighton, BN1 9QJ, Sussex (UK)
Telefax: Int. code +(273)677196

[**] We thank the Engineering and Physcial Sciences Research Council for their continuing support of our work.

molybdenum vapor with the phosphaalkyne tBuC≡P afforded tris-(η^4-2,4-di-*tert*-butyl-1,3-diphosphacyclobutadiene)molybdenum(0), [Mo(η^4-P_2C_2tBu$_2$)$_3$]. Extension of this synthetic approach to other transition metals gives the known pentaphosphaferrocene [Fe(η^5-P_2C_3tBu$_3$)(η^5-P_3C_2tBu$_2$)][12] and the new paramagnetic chromium and vanadium analogues.[13]

The reaction of tBuC≡P with nickel atoms at 77 K, however, affords two red-orange products, **3** and **5**, both of molecular

[Ni(η^4-P_2C_2tBu$_2$)$_2$] **5**

formula NiP_4C_4tBu$_4$. Complex **5** was identified as bis(η^4-2,4-di-*tert*-butyl-1,3-diphosphacyclobutadiene)nickel(0), which was previously reported by Binger et al.[14] using a different synthetic route.

The structure of the isomeric nickel complex **3** was deduced to be [Ni(η^3-PC_2tBu)(η^5-P_3C_2tBu)], which contains the novel phosphirenyl cation $(PC_2t\text{Bu}_2)^+$ as ligand, from 1) its characteristic mass spectrum, which exhibits a parent ion at $m/z = 458$ showing the typical isotopic pattern, and peaks consistent with the expected fragmentation, the strongest peak at $m/z = 320$ corresponding to the loss of tBuC≡CtBu from the parent compound, and 2) from its ^{1}H, ^{31}P{^{1}H}, and ^{13}C{^{1}H} NMR spectra, in particular, the multiplet at $\delta = 178.9$ in the ^{13}C NMR spectrum which analyses as the A part of an AMXY spin system (Table 1) and is characteristic of the ring carbon of the P_3C_2 moiety. The ^{31}P{^{1}H} NMR spectrum analyses as an AB_2X spin system, the AB_2 part being assigned to the P_3C_2 ring. Since the ^{1}H and ^{13}C{^{1}H} NMR spectra establish two chemically equivalent CtBu fragments, the presence of the three-membered PC_2 ring is confirmed. Of special significance is the chemical shift of the P^X resonance in the three-membered ring, which lies very close to that observed for the fully characterized, structurally related complex [Ni(η^3-P_3)(η^5-C_5H_3tBu$_2$)].[15]

Table 1. Selected spectroscopic and analytical data for compounds **3** and **4** [a].

3: ^{1}H NMR: $\delta = 1.45$ (d, $^4J_{PXH} = 0.9$ Hz, 18H, C(CH$_3$)), 1.14 (s, 18H, C(CH$_3$)); ^{31}P{^{1}H}-NMR: AB_2X, $\delta = 155.4$ (P^A), 145.1 (P^B), −161.2 (P^X), $J_{PAPB} = 51.8$, $J_{PAPX} = 5.1$, $J_{PBPX} = 16.0$ Hz; ^{13}C{^{1}H}-NMR: $\delta = 32.4$ (s, C(*C*H$_3$)), 32.9 (d, $J_{CPX} = 4.3$ Hz, C(*C*H$_3$)), 36.8 (A part of AMXX′, $J_{AM} = 9.3$, $J_{AX} + J_{AX'} = 9.2$ Hz (A = C(CH$_3$), M = P^A, XX′ = P^B), 40.0 (A part of AMXX′, $J_{AM} = 18.5$, $J_{AX} + J_{AX'} = 12.4$ Hz, A = *C*(CH$_3$), M = P^A, XX′ = P^B), 94.6 (d, $J_{CPX} = 70.0$ Hz, ring-C), 178.9 (A part of AMXY, $J_{AM} = 78.7$, $J_{AX} + J_{AY} = 104.4$ Hz, $\Delta\delta_{XY} = 31.6$) [b]; MS (70 eV) m/z(%) 458 (14) [M^+], 358 (5) [$M^+ - C_5H_9P$].

4: ^{1}H NMR (318 K): $\delta = 1.12$ (s, 18H, C(CH$_3$)$_3$), 1.38 (s, 18H, C(CH$_3$)$_3$); (248 K): $\delta = 1.08$ (s, 18H, C(CH$_3$)$_3$), 1.26 (s, 9H, C(CH$_3$)$_3$), 1.47 (s, 9H, C(CH$_3$)$_3$); ^{31}P{^{1}H} NMR (253 K): $\delta = -144.7$ (d, $^2J_{PAPD} = 22.3$ Hz, P^A), 86.6 (ddd, $^1J_{PDW} = 226.5$, $^1J_{PDPC} = 439.3$, $^2J_{PDPB} = 52.7$, $^2J_{PDPA} = 22.3$ Hz, P^D), 129.9 (dd, $^1J_{PCPD} = 439.3$, $^2J_{PCPB} = 46.6$ Hz, P^C), 149.1 (dd, $^2J_{PBPD} = 52.7$ Hz, P^B); ^{13}C{^{1}H} NMR (253 K): $\delta = 31.4$ (s, C(*C*H$_3$)), 31.9 (s, C(*C*H$_3$)), 32.1 (s, C(*C*H$_3$)), 32.3 (s, C(*C*H$_3$)), 35.5 (dd, $^3J_{CP} = 5.4$, $^3J_{CP} = 11.0$ Hz, C(CH$_3$)), 35.9 (dd, $^3J_{CP} = 8.9$, $^3J_{CP} = 8.9$ Hz, C(CH$_3$)), 39.57 (dd, $^1J_{CP} = 15.9$ Hz, C(CH$_3$)), 39.61 (dd, $^1J_{CP} = 22.2$ Hz, C(CH$_3$)), 97.7 (d, $^1J_{CP} = 69.6$ Hz, ring-C), 100.9 (d, $^1J_{CP} = 71.1$ Hz, ring-C), 159.9 (ddd, $^1J_{CP} = 83.6$, $^1J_{CP} = 64.3$, $^2J_{CP} = 9.5$ Hz, ring-C), 176.4 (dd, $^1J_{CP} = 78.9$, $^1J_{CP} = 91.8$ Hz), 196.4 (d, $^2J_{CPD} = 2.5$, $^1J_{CW} = 126.6$ Hz, *cis*-CO), 198.8 (d, $^2J_{CPD} = 31.0$ Hz, *trans*-CO); MS (70 eV) m/z(%) 782(17) [M^+]; elemental analysis: found: C 38.72, H 4.71; calcd.: C 38.35, H 4.63.

[a] ^{1}H: 500 MHz, [D$_8$]toluene; ^{13}C{^{1}H}: 125.76 MHz, [D$_8$]toluene; ^{31}P{^{1}H}: 202.6 MHz, [D$_8$]toluene. [b] For all AMXX′ spin systems $J_{XX'}$ is assumed to be large.

Although it has not yet been possible to obtain single crystals of **3** suitable for an X-ray crystallographic study, treatment of **3** with [W(CO)$_5$(thf)] readily afforded dark red crystals of its [W(CO)$_5$] adduct **4**. Variable-temperature ^{31}P{^{1}H} and ^{1}H NMR studies on **4** established that the [W(CO)$_5$] fragment is η^1-ligated to one of the P atoms of the P–P unit in the P_3C_2 ring; this is similar to that previously established in the complexes [Fe(η^5-P_3C_2tBu$_2$)$_2$W(CO)$_5$] and [Fe(η^5-P_3C_2tBu$_2$)(η^5-P_2C_3tBu$_3$)W(CO)$_5$].[16]

The ^{31}P{^{1}H} NMR spectrum of **4** at room temperature is deceptively simple (Table 1) because the [W(CO)$_5$] moiety undergoes an *intra*molecular exchange between the adjacent P^C and P^D nuclei of the P_3C_2 ring, as previously observed in related systems.[17–19] On cooling the sample to −20 °C this dynamic process is suppressed, and the ^{31}P{^{1}H} NMR spectrum reveals the expected four different types of phosphorus environments with only the signal of the P^D atom exhibiting ^{183}W satellites ($J_{PW} = 226.5$ Hz). Interestingly there is a significant ^2J coupling between the P^A atom of the three-membered ring and the tungsten-substituted P^D atoms in the five-membered ring (vide infra).

Complexes **3** and **4** can thus be formally considered as Ni^0 compounds in which the triphosphacyclopentadienyl anion is η^5-ligated and the phosphirenyl cation is η^3-ligated to the metal center. The stabilizing effect of the electron-rich 3d^{10} Ni center on the phosphirenyl cation would be consistent with the results of INDO-SCF-MO calculations on [Ni(η^3-C_3H_5)(η^5-C_5H_5)] which indicate that there is a substantial transfer of charge from the metal center to the η^3-cyclopropenyl group.[20]

The molecular structure[21] of **4** (Fig. 1) confirms the presence of the three-membered phosphirenyl ring system and that the

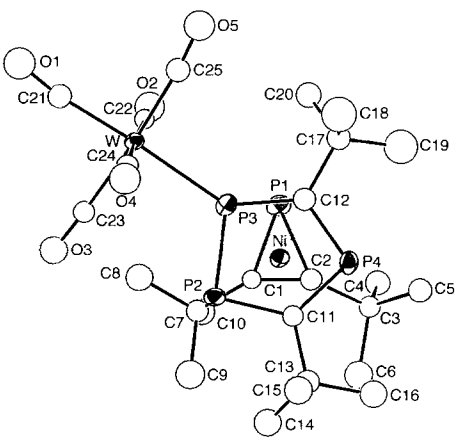


Fig. 1. Molecular structure of **4**. Selected bond lengths [Å] and bond angles [°]. M1 and M2 are the centroids of the three- and five-membered rings, respectively. Ni-P1 2.207(5), Ni-P2 2.397(5), Ni-P3 2.354(5), Ni-P4 2.354(5), Ni-C1 2.02(2), Ni-C2 2.04(2), Ni-C11 2.24(2), Ni-C12 2.12(2), Ni-M1 1.860, Ni-M2 1.692, W-P3 2.517(5), P1-C1 1.78(2), P1-C2 1.82(2), P2-P3 2.111(7), P2-C11 1.74(2), P4-C12 1.76(2), C1-C2 1.33(3); M1-Ni-M2 176.0, P3-W-C21 176.7(7), C1-P1-C2 43.3(8), P3-P2-C11 96.4(7), P2-P3-C12 101.6(7), C11-P4-C12 99.6(9), P1-C1-C2 70(1), P1-C2-C1 67(1).

two ring systems lie essentially parallel to each other (dihedral angle about 4°). The Ni–P and Ni–C bond lengths to the three-membered PC_2 ring are significantly shorter than the corresponding distances to the five-membered P_3C_2 ring, which parallels the behavior previously observed[22] for the complex [Ni(η^3-C_3Ph_3)(η^5-C_5H_5)]. The short C1–C2 bond (1.33(3) Å) in the $PC_2t\text{Bu}_2$ ring of **4** implies significant double bond character, as was found[23] in the unsymmetrically ligated η^3-cyclopropenyl cation in [Ni(η^3-C_3Ph_3)(PPh$_3$)$_2$] PF_6. Calculations by Maclagen on the the parent phosphirenyl cation $PC_2H_2^+$ show optimized geometries of C–C (1.340 Å) and P–C (1.703 Å) at the HF/6-31G* level, and C–C (1.350 Å) and P–C (1.728 Å) at the MP3/6-31G* level.[24] The aromatic character of the free phosphirenyl cation is corroborated by recent ab initio calculations by Laali et al, who have also obtained low-temperature

NMR evidence for a persistent phosphirenyl cation in a compound formulated as $(PhtBuC_2P)^+[B(OSO_2CF_3)_4]^-$.[25]

In **4**, the slightly shorter C–C bond length (1.33(3)Å) and the elongated P–C bonds (1.78(2)Å and 1.82(2)Å) would suggest incomplete delocalization when compared with the theoretical models of the free ligand, although the effect of a bound transition metal fragment on the latter is not clear. The Ni–P1 bond (2.207(5)Å) in **4** lies close to the average Ni–P bond length found by Scherer et al.[15] in $[Ni(\eta^3\text{-}P_3)(\eta^5\text{-}C_5H_3tBu_2)]$. It is noteworthy that in **4** the P1 atom in the three-membered ring lies closest to P3 in the five-membered ring, suggesting that the large $^2J_{PP}$ coupling constant between these nuclei may have a through space component similar to that previously observed for $[Fe(\eta^5\text{-}P_3C_2tBu_2)_2]$.[12]

Experimental Procedure

3: Electron beam (400 W) vaporized nickel (0.99 g) was cocondensed with an excess of *t*BuCP (20 g) at 77 K over a period of 2.5 h. The residue was washed from the belljar with petroleum ether (40–60°) and filtered through a celite pad to remove colloidal metal. Removal of solvent in vacuo afforded a dark oil. Extraction of the oil into petroleum ether (40–60°) followed by chromatographic workup on alumina (4% m/m H_2O) with petroleum ether (40–60°) as eluent afforded **3** as an oil (ca. 0.2 g, 3%) and **5** (0.2 g, 3%) analytically pure, after recrystallization from pentane. For spectroscopic data see Table 1.

4: To $[W(CO)_5(thf)]$ generated in situ from $[W(CO)_6]$ (0.10 g) in THF (25 mL) was added **3** (ca. 0.05 g) and the mixture stirred for 4h. The solvent was removed in vacuo to yield a dark oil. Extraction of the oil into petroleum ether (40–60°) followed by chromatographic workup on Kieselgel 60 GF_{254} with petroleum ether (40–60°) as eluent afforded **4** as a microcrystalline powder on removal of solvent. Recrystallization from pentane (223 K) afforded analytically pure **4** (0.05 g, 58%), see Table 1 for spectroscopic data.

Received: June 20, 1994 [Z 7052 IE]
German version: *Angew. Chem.* **1994**, *106*, 2406

[1] K. S. Forgers, H. Hogeveen, R. F. Kingma, *Tetrahedron Lett.* **1983**, *24*, 643.
[2] R. Breslow, L. A. Deuring, *Tetrahedron Lett.* **1984**, *25*, 1345.
[3] A. Marinetti, F. Mathey, *J. Am. Chem. Soc.* **1985**, *107*, 4700.
[4] F. Mathey, A. Marinetti, *Bull. Soc. Chim. Belg.* **1984**, *93*, 533.
[5] J. C. Barthelat, G. Tringuier, G. Bertrand, *J. Am. Chem. Soc.* **1979**, *101*, 3785.
[6] B. Deschamps, F. Mathey, *Tetrahedron Lett.* **1985**, *26*, 4595.
[7] O. Wagner, M. Ehle, M. Birkel, J. Hoffmann, M. Regitz, *Chem. Ber.* **1991**, *124*, 1207.
[8] M. Regitz, H. Memmesheimer, J. Hoffmann, M. Ehle, *Workshop on Actual Developments in Low Coordination Phosphorus Chemistry*, Palaiseau, France, March 1992.
[9] M. Gordon, P. Boudjouk, F. Anwain, *J. Am. Chem. Soc.* **1983**, *105*, 4972.
[10] F. Mathey, *Pure Appl. Chem.* **1987**, *59*, 993.
[11] F. G. N. Cloke, K. R. Flower, P. B. Hitchcock, J. F. Nixon, *J. Chem. Soc. Chem. Commun.* **1994**, 489.
[12] R. Bartsch, P. B. Hitchcock, J. F. Nixon, *J. Chem. Soc. Chem. Commun.* **1987**, 1946.
[13] F. G. N. Cloke, K. R. Flower, J. F. Nixon, D. M. Vickers, unpublished results.
[14] T. Wettling, G. Wolmershäuser, P. Binger, M. Regitz, *J. Chem. Soc. Chem. Commun.* **1990**, 1541.
[15] O. J. Scherer, T. Dave, J. Braun, G. Wolmershäuser, *J. Organomet. Chem.* **1988**, *350*, C20.
[16] R. Bartsch, A. Gelessus, P. B. Hitchcock, J. F. Nixon, *J. Organomet. Chem.* **1992**, *430*, C10.
[17] R. Bartsch, D. Carmichael, P. B. Hitchcock, M. F. Meidine, J. F. Nixon, G. J. D. Sillett, *J. Chem. Soc. Chem. Commun.* **1988**, 1615.
[18] P. B. Hitchcock, J. F. Nixon, G. J. D. Sillett, *Nouv. J. Chim.* **1989**, *13*, 353.
[19] J. F. Nixon, G. J. D. Sillett, *J. Organomet. Chem.* **1993**, *461*, 237.
[20] D. W. Clack, K. D. Warren, *J. Organomet. Chem.* **1978**, *149*, 401.
[21] a) Crystal data for **4**: $C_{25}H_{36}NiO_5P_4W$, $M = 783.0$, triclinic, space group $P\bar{1}$ (no. 2), $a = 9.415(4)$, $b = 12.021(9)$, $c = 13.964(4)$ Å, $\alpha = 78.31(4)$, $\beta = 81.66(3)$, $\gamma = 86.51(5)°$, $V = 1530(1)$ Å^3, $Z = 2$, $\varrho_{calcd} = 1.70$ g cm^{-3}, $(Mo_{K\alpha}) = 46.9$ cm^{-1}, CAD4; 4241 measured reflections, 3448 observed ($I > 2\sigma(I)$), $R = 0.072$, $R_w = 0.089$ ($w = 1/\sigma^2(F_o)$) for 175 parameters. b) Further details of the crystal structure investigation are available on request from the Director of the Cambridge Crystallographic Data Centre, 12 Union Road, GB-Cambridge CB2 1EW (UK), on quoting the full journal citation.
[22] R. M. Tuggle, D. L. Weaver, *Inorg. Chem.* **1971**, *10*, 1504.
[23] C. Mealli, S. Midolli, S. Moneti, L. Sacconi, *Angew. Chem.* **1980**, *92*, 967; *Angew. Chem. Int. Ed. Engl.* **1980**, *19*, 931.
[24] R. G. A. R. Maclagan, *Chem. Phys. Lett.* **1989**, *163*, 349.
[25] M. Regitz (Kaiserslautern), K. K. Laali (Kent State, Ohio), personal communication, **1994**.

Phase Transitions in Self-Assembled Monolayers Detected by Electrochemistry**

Antonella Badia, Roberta Back, and R. Bruce Lennox*

Self-assembled monolayers (SAMs) of *n*-alkanethiols (RSH) on metals have been used both as models for organic surfaces and as modulators of metal surface properties.[1] These SAMs are prepared under readily accessible laboratory conditions, and the strong interaction between the metal substrate (Au, Pt, Ag, Cu, Hg, etc.) and the sulfur atom provides a monolayer film that is sufficiently stable to desorption to allow spectroscopic, diffraction, and electrochemical experiments to be performed with a minimum of precautions.[1] Grazing-angle FT-IR studies and grazing incidence diffraction experiments of a typical $n\text{-}C_{18}H_{37}S$ monolayer on a Au(111) surface show that molecular ordering is present.[2, 3]

One key aspect of SAMs that has so far eluded detailed description concerns the question of film thermodynamics and, more specifically, the nature of film phases. A very recent X-ray diffraction study has shown that 2D structural phase transitions may be observable in SAMs.[4] This reveals that, like Langmuir and Langmuir-Blodgett films,[5] SAMs do indeed have a complex phase behavior. Contact angle/wetting studies hint at rearrangement processes in RS–Au monolayers,[6] while temperature dependent FT-IR studies reveal only gradual changes,[7] and not the discontinuities expected from first-order processes. We have addressed the important problem of phase properties of SAMs by using the electron transfer process between a water-soluble redox species and an RSH-modified Au electrode as a probe of the monolayer film structure. We have discovered that phase transitions do, in fact, occur and that film preparation protocols play a crucial role in their formation.

Electrochemical thermograms for RS–Au electrodes (R = $n\text{-}C_{16}H_{33}$ to $C_{20}H_{41}$) were obtained over an approximate temperature range of 10 to 65 °C. Electrodes which exhibit striking discontinuities in the electrochemical thermograms were prepared by a variation on the conventional preparation protocols.[1, 8] Specifically, polycrystalline Au electrodes were immersed in thiol solutions and kept at 23 ± 2 °C for prolonged periods (days to weeks). Conventional protocols usually employ much shorter times (minutes to hours), a variety of heating/annealing procedures, and reimmersion in thiol solution after each experiment, or cosurfactants in the thiol solution.[9]

One of the most interesting properties of RS monolayers is their ability to attenuate the rate of electron transfer between a water-soluble redox couple and the underlying metal electrode.[2e, 9a–c, 10] The transmonolayer electron transfer mechanism has been studied with several soluble or monolayer-bound redox couples and a variety of electrochemical techniques.[2c, 9–11] The electrodes discussed here were thoroughly blocked: the capacitance values were reduced, the $[Fe(CN)_6]^{3-}$ reduction currents greatly attenuated relative to bare Au electrodes, and the features in cyclic voltammograms that are diagnostic of pinholes or bare patches in the films were absent.

[*] Prof. R. B. Lennox, A. Badia
Department of Chemistry, McGill University
801 Sherbrooke Street West, Montreal, Quebec H3A 2K6 (Canada)
Telefax: Int. code +(514) 398-3797
Dr. R. Back
Max-Planck-Institut für Polymerforschung, Mainz (FRG)

[**] This work was supported by the Natural Sciences and Engineering Research Council of Canada (NSERC).

The temperature dependence of the iron(III) cyanide reduction current, observed at constant overpotential, for a representative $C_{18}H_{37}S$–Au electrode is shown in Figure 1. The reduction of $[Fe(CN)_6]^{3-}$ at a clean bare electrode increases montonically with increasing temperature (Fig. 1, dashed line),

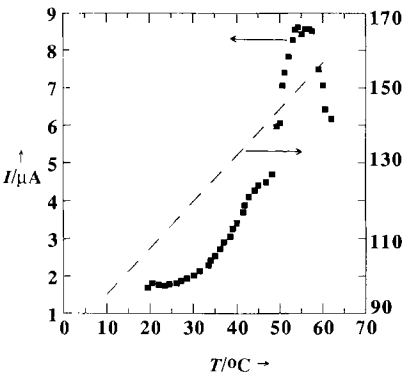
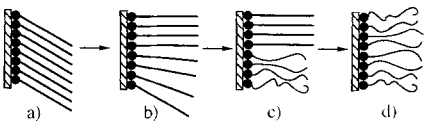


Fig. 1. Electrochemical thermograms (plot of current I vs. temperature T) for $[Fe(CN)_6]^{3-}$ reduction at bare Au (dashed line) and $C_{18}H_{37}S$–Au (■) electrodes obtained by cyclic voltammetry (0.020 M $K_3[Fe(CN)_6]$, 0.1 M KBr, scan rate $v = 20$ mVs^{-1}), temperature corrected overpotential $\eta = -250$ mV.

as is expected for an activated process.[12] For each chain length studied, the modified Au electrode, however, exhibits a pronounced current maximum. In all cases except the nineteen-carbon chain, a distinct shoulder on the low temperature side of the maximum is also observed. Clearly, these substantial current changes reflect temperature-induced modification of the SAM as a barrier to electron transfer. Previous studies suggest that the overall rate-limiting step in the case of well-blocked RS–Au electrodes is electron tunneling[1d, 9a, b, 10d, e, 11f] although some data is also consistent with a permeation mechanism.[9a, 10a, b, e, g, 13] Current derived exclusively from a through-bond tunneling mechanism, for example, should be either temperature-independent or should increase with increasing temperature, depending on whether there is an activation component to the electron transfer[12a] On the other hand, current derived from permeation of the redox couple into the monolayer would exhibit a complex temperature dependence, as it would depend on the relationship between film structure, the solvent–monolayer partition coefficient, the diffusion coefficient of the redox couple in the monolayer, and interfacial resistances. The data in Figure 1 is clearly inconsistent with tunneling, but is qualitatively consistent with a complex permeability-linked process.

Our experiments with SAMs prepared under prolonged immersion in the thiol solution exhibit striking parallels to the temperature-dependent permeability profiles of phosphatidylcholine lipid vesicles to Na^+, K^+, H_2O.[14] Bilayer lipid vesicles have been extensively characterized by calorimetric and spectroscopic techniques and are known to undergo a series of phase transitions, the two most prominent being a gel/liquid-crystal transition (at $T = T_m$) and an untilting/rippling transition (at $T = T_p$).[15] This untilting transition preceeds T_m by 3–6 °C, depending on the alkyl chain length. Large anomalous increases in transmembrane permeability are observed at $T_m \pm 5$ °C.[14] These large current fluxes are attributable to transient dislocations or grain boundaries found at the interface between domains of the coexisting gel and liquid-crystalline phases. These boundaries provide a low energy barrier to ion and solute diffusion across the membrane. Recent theoretical studies support



Scheme 1. Sketch of physical interpretation of the phase transitions in SAMs. a) Close-packed, b) coexistence of tilted and untilted chains, c) coexistence of melted and unmelted chains, d) melted chains.

this experimentally based description.[16] The current maxima described here are thus believed to arise from regions where diffusion is facilitated in the monolayer at coexistence boundaries between ordered and disordered alkyl chain domains (Scheme 1). It is interesting to note that evidence for electron tunneling in the well-studied lipid vesicle systems is decidedly lacking and that permeation processes are in fact responsible for current generation in these systems.[17]

The temperatures at which the current maxima (T_m^e) and shoulders (T_p^e) are observed in the electrochemical thermograms correlate (1:1) with T_m values (measured by calorimetry) of di-*n*-acylphosphatidylcholines of equivalent chain length (Fig. 2A, slope = 1.0).[15] This correlation arises because the underlying Au substrate dictates that the RSH chain packing

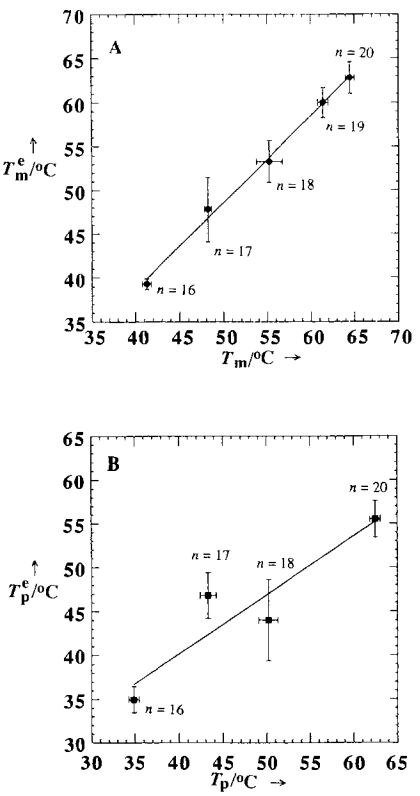


Fig. 2. A) Relationship between the electrochemically determined temperature T_m^e for $C_nH_{2n+1}S$/Au ($n = 16$–20) and T_m of the gel/liquid-crystal phase transitions of di-*n*-acylphosphatidylcholines measured by DSC. Error bars represent standard deviations reported here (T_m^e) and in the literature [15] (T_m). Slope = 1.0, correlation coefficient $r = 0.998$. B) Pretransition observed in the electrochemical thermograms of the modified electrode (T_p^e) vs. the pretransition of phosphatidylcholines (T_p). T_p^e has not been observed for $C_{19}H_{37}S$–Au, nor has T_p been reported for corresponding phospholipid [15]. Slope = 0.67, correlation coefficient $r = 0.920$.

configuration and density are very similar in the two cases. The underpotential deposition of Pb[10c] established the surface composition of our bulk Au electrodes to be 70% Au(110) and 30% Au(111); consequently the areas occupied by the chains

are 46.9 Å^2 and 43.5 Å^2,[3c] respectively. *n*-Dicylphosphatidylcholines, by comparison, occupy 43–48 Å^2 in their condensed phase.[15] Clearly, the phosphatidylcholine headgroup and the Au lattice serve the same purpose – to enforce a defined packing density on the alkyl chains. The surface packing of chains in a RS monolayer on a Au(100) surface is 18% more dense.[3c] Because phosphatidylethanolamine lipids are packed tighter and have higher T_m's than phosphatidylcholines, we expect an RS monolayer on Au(100) to exhibit higher T_m^e's than those shown in Figure 2.

The T_p^e for the monolayer also correlates with phosphatidylcholine data, but (given the scatter in the data) may be attenuated to about 70% of the lipid T_p value (Fig. 2B, slope = 0.67). This may arise because the position of the headgroup is fixed in the SAMs where the Au–S bond eliminates the possibility of vertical motion of the alkyl chains necessary for a periodic rippling of the surface. The current increase at T_p^e is caused by enhanced permeability along tilt/untilt boundaries in the monolayer.

The experimental observation of thermally induced changes in RS–Au monolayers depends upon two conditions. Firstly, only if contact times between electrode and monolayer-forming solutions are prolonged (from days to weeks) will the features shown in Figure 1 arise. Chain ordering is apparently a very slow process[1d, 18] and may also be accompanied by RSH-assisted Au reconstructions. Dissolution of Au surface features or reconstructions of the binding sites of the sulfur on the Au are also possible.[19, 20] Secondly, the thermal history of the electrode is important. The complex behavior does not arise for many as prepared electrodes and all annealed electrodes. These share another form of temperature dependence, to be described elsewhere in a detailed description of the electrochemistry.[21] Preliminary studies show that kinetics are important in these systems. Figure 3 shows the behavior of a $C_{16}H_{33}S$–Au electrode under a heat-cool-reheat cycle. These annealed electrodes do not re-exhibit a maximum (as in Fig. 1) unless subjected to prolonged cooling at about 5 °C.

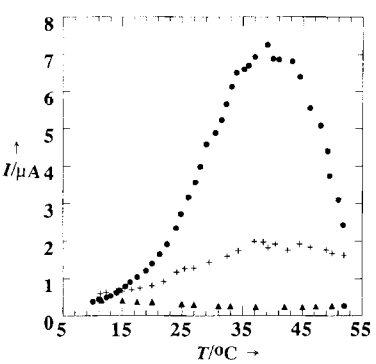


Fig. 3. Electrochemical thermogram (see Fig. 1 caption for experimental details) showing a heat-cool-reheat cycle for a $C_{16}H_{33}S$–Au electrode. The $C_{16}H_{33}S$–Au electrode was cycled as follows: • initial heating curve of the electrode modified at 23 ± 2 °C; ▲ the electrode was cooled to 15 °C, removed from the electrochemical cell, and held at about 5 °C in air for 18 h; + $C_{16}H_{33}S$–Au electrode was subjected to a second heating cycle.

We conclude that SAMs which have been prepared under conventional conditions or have been annealed may be viewed as assemblies of disordered chains with short range order (as reported by FT-IR). However, the order is insufficient to manifest phase transitions. Interestingly, order/disorder transitions are predicted by molecular dynamics simulations,[22] and a recent analysis shows that a domain must be a minimum size to manifest a phase co-existence region.[23, 24]

The film discontinuities responsible for the electrochemical thermogram features (Fig. 1) are intrinsic to SAMs that have been prepared under the experimental conditions described. The film discontinuities reported here are *not* the ill-defined pathological defects frequently invoked as disclaimers of film imperfection. These latter generic defects are synonomous with thin patches, defect regions commensurate with Au substrate defect structures, or regions where a coadsorbate is clustered. The sites of enhanced passive diffusion responsible for maxima as in Figures 1 and 2 are clearly thermodynamically controlled. This is apparent, because they exist at defined temperatures and are determined solely by the chain length of the alkane thiol adsorbate. Correlation with lipid thermotropic behavior suggests that the lattice spacing imposed by the Au substrate determines the chain packing density. Our studies suggest that order/disorder phase transitions are possible in SAMs. It is clearly more correct (and interesting) to consider RS–Au monolayers as structures with both rich phase properties and complex reorganization kinetics than to view them as "defect-free" hydrocarbon slabs.

Experimental Procedure

n-Octadecanethiol ($C_{18}H_{37}SH$; Aldrich, 98%) was recrystallized three times from ethanol. *n*-Hexadecanethiol ($C_{16}H_{33}SH$), heptadecanethiol ($C_{17}H_{35}SH$), nonadecanethiol ($C_{19}H_{39}SH$), and icosanethiol ($C_{20}H_{41}SH$) were synthesized by standard procedures. Their purity was monitored by ^1H and ^{13}C NMR spectroscopy, thin layer chromatography, mass spectrometry (NH_3, CI), and melting point determination by differential scanning calorimetry (DSC). The melting point measurements by DSC are particularly useful in detecting the presence of trace amounts of homologous hydrocarbons.

Bulk polycrystalline Au electrodes (0.020 cm^2 geometric area; BAS, West Lafayette, IN) were mechanically polished (Buehler, Ecomet II polisher) on microcloth pads with alumina (Buehler) slurries of decreasing particle size (1.0, 0.3, and 0.05 μm). The polished electrodes were sonicated in H_2O to remove any residual polishing alumina from the Au surface. The sonicated Au electrodes were then rinsed copiously with H_2O and subsequently with absolute ethanol, and were immediately immersed in RSH solutions. The Au substrates were immersed in 5 mL argon-saturated ethanol solutions (to prevent the formation of thiol multilayers) of the thiol in sealed glass vials (2–5 mM RSH) at 23 ± 2 °C for days to weeks [25]. The RSH-modified electrodes were rinsed copiously with ethanol, followed by H_2O, immediately prior to the electrochemical experiments.

The RS–Au working electrode was introduced into a degassed, thermostated (Haake G circulating bath) 150 mL cell containing 0.1 M KBr electrolyte (Anachemia) and 0.020 M $K_3[Fe(CN)_6]$ (BDH). Deionized H_2O (18 MΩcm^{-1}) was obtained from a Milli-Q water system (Millipore; 3 bed ion-exchange/1 bed organic removal cartridge unit) connected to distilled water. The counter electrode was a Pt wire (Aldrich), and all potentials are referred to a Ag/AgCl electrode (BAS; 3 M NaCl). Currents were obtained from cyclic voltammograms (BAS 100B electrochemical analyzer) at 20 mVs^{-1} between +500 mV and −150 mV. Typical heating rates of 0.2 to 0.3 °Cmin^{-1} were used for all experiments. The $[Fe(CN)_6]^{3-}$ reduction current reported at each temperature was measured from the cathodic segment of the cyclic voltammogram at $\eta = -250$ mV for $[Fe(CN)_6]^{3-/4-}$ at that temperature.

Received: March 1, 1994
Revised: June 20, 1994 [Z 6719 IE]
German version: *Angew. Chem.* **1994**, *106*, 2429

[1] a) A. Ulman, *An Introduction to Ultrathin Organic Films From Langmuir-Blodgett to Self-Assembly*, Academic Press, San Diego, CA, **1991**, pp. 237–304; b) C. D. Bain, G. M. Whitesides, *Angew. Chem. Adv. Mater.* **1989**, *101*, 522–528; *Angew. Chem. Int. Ed. Engl. Adv. Mater.* **1989**, *28*, 506–512; c) G. M. Whitesides, P. E. Laibinis, *Langmuir* **1990**, *6*, 87–96; d) L. H. Dubois, R. G. Nuzzo, *Annu. Rev. Phys. Chem.* **1992**, *43*, 437–463, and references therein.

[2] a) R. G. Nuzzo, L. H. Dubois, D. L. Allara, *J. Am. Chem. Soc.* **1990**, *112*, 558–569; b) P. E. Laibinis, G. M. Whitesides, D. L. Allara, Y.-T. Tao, A. N. Parikh, R. G. Nuzzo, *ibid.* **1991**, *113*, 7167–7177; c) M. D. Porter, T. B. Bright, D. L. Allara, C. E. D. Chidsey, *ibid.* **1987**, *109*, 3559–3568.

[3] a) L. Strong, G. M. Whitesides, *Langmuir* **1988**, *4*, 546–558; b) N. Camillone, C. E. D. Chidsey, G. Liu, T. M. Putvinski, G. Scoles, *J. Chem. Phys.* **1991**, *94*, 8493–8502; c) N. Camillone, C. E. D. Chidsey, G. Liu, G. Scoles, *ibid.* **1993**, *98*, 3503–3511, 4234–4245; d) C. E. D. Chidsey, G. Liu, P. Rowntree, G. Scoles, *ibid.* **1989**, *91*, 4421–4423.

[4] P. Fenter, P. Eisenberger, K. S. Liang, *Phys. Rev. Lett.* **1993**, *70*, 2447–2450.
[5] a) S. W. Barton, B. N. Thomas, E. B. Flom, S. A. Rice, B. Lin, J. B. Peng, J. B. Ketterson, P. Dutta, *J. Chem. Phys.* **1988**, *89*, 2257; b) K. Kjaer, J. Als-Nielsen, C. A. Helm, P. Tippmann-Krayer, H. Mohwald, *Thin Solid Films* **1988**, *159*, 17.
[6] a) A. Ulman, *Adv. Mater.* **1991**, *3*, 298–303; b) S. E. Evans, R. Sharma, A. Ulman, *Langmuir* **1991**, *7*, 156–161.
[7] a) R. G. Nuzzo, E. M. Korenic, L. H. Dubois, *J. Chem. Phys.* **1990**, *93*, 767–773; b) L. H. Dubois, B. R. Zegarski, R. G. Nuzzo, *J. Electron Spectrosc. Relat. Phenom.* **1990**, *54/55*, 1143.
[8] a) C. D. Bain, E. B. Troughton, Y.-T. Tao, J. Evall, G. M. Whitesides, R. G. Nuzzo, *J. Am. Chem. Soc.* **1989**, *111*, 321–335; b) R. G. Nuzzo, D. L. Allara, *ibid.* **1983**, *105*, 4481–4483.
[9] a) C. Miller, P. Cuendet, M. Gratzel, *J. Phys. Chem.* **1991**, *95*, 877–886; b) C. Miller, M. Gratzel, *ibid.* **1991**, *95*, 5225–5233; c) M. A. Fox, D. M. Collard, S. E. Creager, *Langmuir* **1990**, *6*, 1617–1620; d) H. O. Finklea, D. D. Hanshew, *J. Electroanal. Chem. Interfacial Electrochem.* **1993**, *347*, 327–340; e) H. O. Finklea, M. S. Ravenscroft, D. A. Snider, *Langmuir* **1993**, *9*, 223–227.
[10] a) H. O. Finklea, S. Avery, M. Lynch, T. Furtsch, *Langmuir* **1987**, *3*, 409–413; b) C. E. D. Chidsey, D. N. Loiacono, *ibid.* **1990**, *6*, 682–691; c) S. E. Creager, L. A. Hockett, G. K. Rowe, *ibid.* **1992**, *8*, 854–861; d) A. M. Becka, C. J. Miller, *J. Phys. Chem.* **1992**, *96*, 2657–2668; e) *ibid.* **1993**, *97*, 6233–6239; f) H. O. Finklea, D. A. Snider, J. Fedyk, E. Sabatini, Y. Gafni, I. Rubinstein, *Langmuir* **1993**, *9*, 3660–3667; g) K. Doblhofer, J. Figura, J.-H. Fuhrhop, *ibid.* **1992**, *8*, 1811–1816.
[11] a) C. E. D. Chidsey, *Science* **1991**, *251*, 919–922; b) C. E. D. Chidsey, C. R. Bertozzi, T. M. Putvinski, A. M. Mujsce, *J. Am. Chem. Soc.* **1990**, *112*, 4301–4306; c) D. M. Collard, M. A. Fox, *Langmuir* **1991**, *7*, 1192–1197; d) G. K. Rowe, S. E. Creager, *ibid.* **1991**, *7*, 2307–2312; e) J. J. Hickman, D. Ofer, C. Zou, M. S. Wrighton, P. E. Laibinis, G. M. Whitesides, *J. Am. Chem. Soc.* **1991**, *113*, 1128–1132; f) H. O. Finklea, D. D. Hanshew, *ibid.* **1992**, *114*, 3173–3181; g) E. Katz, N. Itzhak, I. Willner, *Langmuir* **1993**, *9*, 1392–1396; h) A. J. Black, T. T. Wooster, W. E. Geiger, M. N. Paddon-Row, *J. Am. Chem. Soc.* **1993**, *115*, 7924–7925.
[12] a) R. A. Marcus, N. Sutin, *Biochim. Biophys. Acta* **1985**, *811*, 265; b) F. Mollers, R. Memming, *Ber. Bunsenges. Phys. Chem.* **1972**, *76*, 475; c) V. Marecek, Z. Samec, J. Weber, *J. Electroanal. Chem. Interfacial Electrochem.* **1978**, *94*, 169.
[13] A. Swietlow, M. Skoog, G. Johannson, *Electroanalysis* **1992**, *4*, 921–928.
[14] a) D. Papahadjopoulous, K. Jacobson, S. Nir, T. Isac, *Biochim. Biophys. Acta* **1973**, *311*, 33; b) E. Corvera, O. G. Mouritsen, M. A. Singer, M. J. Zuckerman, *ibid.* **1992**, *1107*, 261.
[15] D. Marsh, *Handbook of Lipid Bilayer Membranes*, CRC, Boca Raton, FL, **1991**, pp. 135–150.
[16] L. Cruzeiro-Hansson, O. G. Mouritsen, *Biochim. Biophys. Acta* **1988**, *944*, 63.
[17] a) J. N. Robinson, P. J. Cole-Hamilton, *Chem. Soc. Rev.* **1991**, *20*, 49–94; b) S. V. Lymar, J. K. Hurst, *J. Phys. Chem.* **1994**, *98*, 989, and references therein; c) L. Hammarström, H. Berglund, M. Almgren, *ibid.* **1994**, *98*, 9588–9593.
[18] a) G. Hahner, C. Woll, M. Buck, M. Grunze, *Langmuir* **1993**, *9*, 1955–1958; b) C. D. Bain, E. B. Troughton, Y. T. Tao, J. Evall, G. M. Whitesides, R. G. Nuzzo, *J. Am. Chem. Soc.* **1989**, *111*, 321.
[19] K. Edinger, A. Golzhauser, K. Demota, C. Woll, M. Grunze, *Langmuir* **1993**, *9*, 4–8.
[20] H. Sellers, A. Ulman, Y. Shnidman, J. E. Eilers, *J. Am. Chem. Soc.* **1993**, *115*, 9389–9401.
[21] A. Badia, R. Back, R. B. Lennox, unpublished.
[22] a) J. Hautman, M. L. Klein, *J. Chem. Phys.* **1990**, *93*, 7483–7492; b) W. Mar, M. L. Klein, *Langmuir* **1994**, *10*, 188–196.
[23] J. I. Siepmann, I. R. McDonald, *Langmuir* **1993**, *9*, 2351–2355.
[24] We do not yet understand why ordering is apparently induced by annealing (ref. [4]). The observation conditions in that study and this paper (UHV vs. aqueous electrolyte) are, however, quite different.
[25] Y.-T. Kim, R. L. McCarley, A. J. Bard, *Langmuir* **1993**, *9*, 1941–1944.

Synthesis of the First Microporous Aluminum Phosphonate with Organic Groups Covalently Bonded to the Skeleton**

Kazuyuki Maeda,* Yoshimichi Kiyozumi, and Fujio Mizukami

Zeolites and similar microporous solids are important materials for adsorbents and catalyst systems and can be used as ion exchangers and for many other applications.[1] Therefore, great effort has been made to develop new microporous crystalline materials.[1, 2] Among them, compounds of the family of aluminophosphates (ALPO) adopt a great variety of structures depending on the synthesis conditions, in particular, on the organic additives used as the structure-directing agent.[3] In these microporous solids, however, the wall of the channel is generally composed of oxygen atoms, which are larger than aluminum and phosphorus atoms.[4] The character of the micropore, therefore, is fundamentally determined by the arrangement of the oxygen atoms, but also from the elements incorporated in the framework. In this study we wanted to develop a new family of microporous aluminophosphonates whose channel walls are modified by the introduction of organic groups directly attached to the phosphorus atoms.

A zirconium phosphite–diphosphonate, a microporous inorganic–organic polymer has been reported previously.[5] The proposed structural model of this compound is based on zirconium phosphite layers partly pillared by organic groups.[5] The structure of the novel microporous aluminum methylphosphonate AlMepO-β prepared by us differs from this structure: it is based on a three-dimensional inorganic framework, in which organic groups are covalently bonded to the skeleton.

AlMepO-β was obtained as needlelike crystals in a hydrothermal reaction in which no structure-directing agent was used; however, cationic or neutral amines are usually necessary for synthesis of ALPOs.[3] The elemental analyses of AlMepO-β synthesized in this way gave the following composition; C 10.5, H 3.2, Al 15.2, P 27.6%. The P/Al ratio calculated from the elemental analyses is 1.58 and the H_2O/Al ratio is estimated to be 0.5 from both the elemental analyses and thermogravimetry. The values obtained correspond fairly well with the ideal composition of the neutral salt of aluminum methylphosphonate, $Al_2(CH_3PO_3)_3 \cdot H_2O$ (C 10.2, H 3.1, Al 15.2, P 26.3%).

The powder X-ray diffractogram of AlMepO-β (Fig. 1, bottom) showed a characteristic pattern with a strong reflection at

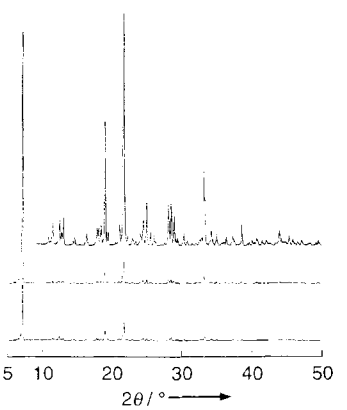


Fig. 1. X-ray powder diffraction pattern of AlMepO-β (bottom) and AlMepO-β dehydrated at 500 °C for 6 h (middle and top (× 10)).

[*] K. Maeda, Y. Kiyozumi, Dr. F. Mizukami
Surface Chemistry Division
National Institute of Materials and Chemical Research
1-1 Higashi, Tsukuba, Ibaraki 305 (Japan)
Telefax: Int. code +(298) 54-4709

[**] We thank Dr. J. Akimoto, National Institute of Materials and Chemical Research, Tsukuba, Japan, for the X-ray diffraction measurement of the single crystal.

7.2° ($d = 12.3$ Å). The reflections were indexed to a rhombohedral unit cell; a few lines were attributed to impurities. The cell dimensions were refined to give $a = b = 24.72(2)$, $c = 25.33(2)$ Å (hexagonal axes).[6] Since AlMepO-β degassed at 500 °C under vacuum for 6 h also gave an essentially identical diffraction pattern (Fig. 1, middle), it can be concluded that AlMepO-β is not a layered compound intercalating water, but a microporous solid with a three-dimensional framework which adsorbs water. From the above compositional formula and the density (1.65 g mL^{-1}) of a crystal, the number of $Al_2(CH_3PO_3)_3 \cdot H_2O$ units per unit cell, which should be crystallographically meaningful, is estimated at 36. The framework density, the number of tetrahedrally surrounded atoms (T) per 1000 Å^3, is generally used to discriminate microporous phases from densely packed phases. A microporous phase is present in most cases if the framework density is smaller than 20–21 T per 1000 Å^3.[7] The calculated framework density of AlMepO-β (13.5 T per 1000 Å^3),[8] which is as small as that for the known aluminophosphates VPI-5 (14.2) and MAPSO-46 (13.7),[7] supports a microporous structure, although there should be methyl groups in the cavities.

The ^{27}Al MAS-NMR spectrum of AlMepO-β (Fig. 2a) shows two sharp signals at $\delta = -17.6$ and 41.2, which are assigned to six- and four-coordinate aluminum centers, respectively (ratio of 1:3). The chemical shift of $\delta = 41.2$ lies in the range of signals reported for aluminophosphates[9, 10] whose (AlO_4) units are surrounded by four phosphate units. Also the position of the signal at $\delta = -17.6$ corresponds to those reported for six-coordinate aluminum atoms in ALPOs, which are coordinated to water molecules.[9] Because dehydration of AlMepO-β by evacuation at 400 °C did not change the intensity ratio of the two peaks, we can conclude that the observed six-coordinate aluminum centers are indeed present in the framework structure.

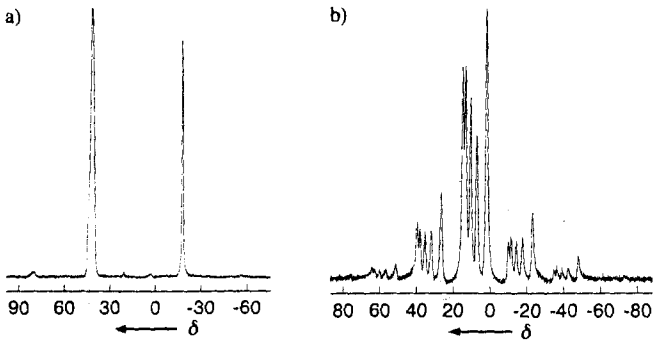
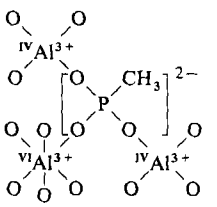


Fig. 2. ^{27}Al MAS-NMR spectrum (a) and ^{31}P MAS-NMR spectrum (b) of AlMepO-β.

The ^{31}P MAS-NMR of AlMepO-β showed five sharp signals at $\delta = 1.5, 6.9, 10.3, 13.1$, and 14.7 (intensity ratio ca. 2:1:1:1:1; Fig. 2b), while that of methylphosphonic acid gave a broad signal at $\delta = 37.6$. The number of the signals suggests that the number of the crystallographically independent atoms is at least five, probably six. In various microporous aluminophosphates, a phosphate group connected with four aluminate units generally gives rise to peaks in the range $-23 \geq \delta \geq -34$,[11] which is typical for tetrahedrally coordinated phosphorus oxide. The difference in chemical shifts of these phosphates ($-23 \geq \delta \geq -34$) and those of AlMepO-β ($1 \leq \delta \leq 15$) almost correspond to the shift of the signal to lower field ($\Delta\delta = 37.6$) caused by the substitution of a hydroxy group for a methyl group in phosphoric acid.

The ^{13}C CP/MAS NMR spectrum, which showed a cluster of incompletely resolved peaks ($11 \leq \delta \leq 14$) in the region of the chemical shift of methylphosphonic acid [$\delta = 11.3$ (d, ^1J(C,P) = 140 Hz)], also supports the proposal that the methyl groups in AlMepO-β remain bonded to the phosphorus atom. From the above NMR results and elemental analysis, it is reasonable to propose that two of the O atoms of the CH_3PO_3 unit are bound to two Al centers with coordination number four and that one O atom is bound to a six-coordinate Al center. All AlO_n groups are only surrounded by CH_3PO_3 units (Scheme 1). AlMepO-β is a new network, in which three AlO_n groups are coordinated to the P atoms, and formal AlO_4 and AlO_6 groups are included.



Scheme 1. Postulated repeat unit of the structure of AlMepO-β.

The nitrogen adsorption isotherm for AlMepO-β degassed at 400 °C for 6 h shown in Figure 3 is classified as Langmuir type (the type 1 of the IUPAC classification[12]) and is typical of microporous substances.[13] The micropore volume of the sample is estimated to be 0.117 cm^3 g^{-1} based on the DR plot,[14] and the BET specific surface area is calculated at 297 m^2 g^{-1}; for the latter the values of the low-pressure region of the isotherm ($p/p_0 < 0.04$) were used.[15]

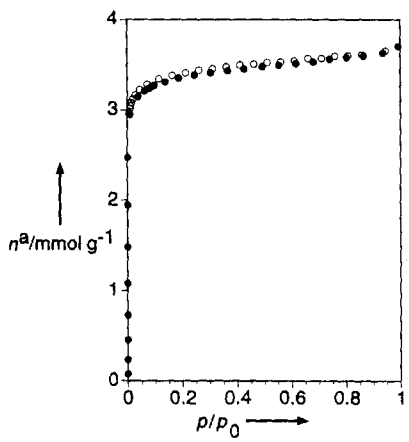


Fig. 3. Nitrogen adsorption isotherm of AlMepO-β degassed at 400 °C for 6 h; •: adsorption branch, o: desorption branch.

Recently Huo et al. revealed that micellar, cubic, and hexagonal phases of periodic surfactant/inorganic composites can be obtained for various combinations of inorganic species and surfactants.[16] They also suggested that a monoalkylphosphate used as a surfactant could be a part of the frameworks in compounds with Zn or Al. Among the three phases, the hexagonal one MCM-41[17] contains unidimensional channels stuffed with surfactants. Accordingly, we presume that AlMepO-β possesses channels lined by methyl groups, since the steric hindrance between the organic groups should be minimized in a larger pore. This assumption is supported by a water adsorption isotherm of AlMepO-β, which shows the hydrophobic character.[18] At present, further detailed structural analyses including crystallographic studies are in progress.

The sizes and shapes of micropores bordered by organic groups can be varied by changing the phosphonic acids and the synthesis conditions. Such porous materials with ordered structures of organic functional groups not only will serve as sorption media and separation materials, but also may find unique electric or optic applications.

 © VCH Verlagsgesellschaft mbH, D-69451 Weinheim, 1994 0570-0833/94/2222-2336 $ 10.00+.25/0

Experimental Procedure

Typical synthesis: Pseudo-boehmite powder (PURAL SCF from Condea Chemie; 74.4 wt.% Al_2O_3, 25.6 wt.% water) and methylphosphonic acid (Aldrich, 98 wt.%) were dispersed in water ($Al:P:H_2O = 1:1.5:40$) by stirring at ambient temperature for 1 h. Subsequently, the mixture was hydrothermally treated at 160 °C for 48 h under an autogenous pressure using an autoclave with a Teflon sleeve in a thermostated oven. The air-dried crystals were subjected to elemental analyses and ICP analyses (Al and P). The density of a single crystal was determined pycnometrically.

Received: June 8, 1994 [Z 7012 IE]
German version: *Angew. Chem.* **1994**, *106*, 2429

[1] R. Szostak, *Molecular Sieves*, Van Nostrand Reinhold, New York, **1989**.
[2] M. E. Davis, R. F. Lobo, *Chem. Mater.* **1992**, *4*, 756.
[3] S. T. Wilson, B. M. Lok, C. A. Messina, T. R. Cannan, E. M. Flanigen, *J. Am. Chem. Soc.* **1982**, *104*, 1146; E. M. Flanigen, B. M. Lok, R. L. Patton, S. T. Wilson in *New Developments in Zeolite Science and Technology* (Eds.: Y. Murakami, A. Iijima, J. W. Ward), Elsevier, Amsterdam, **1986**, pp. 103.
[4] J. V. Smith, *Chem. Rev.* **1988**, *88*, 149.
[5] G. Alberti, U. Costantino, F. Marmottini, R. Vivani, P. Zappelli, *Angew. Chem.* **1993**, *105*, 1396; *Angew. Chem. Int. Ed. Engl.* **1993**, *32*, 1357.
[6] The rhombohedral lattice was confirmed initially by a single-crystal X-ray diffraction, and the lattice parameters were approximately determined. The reflections from the small crystals were not strong enough to be used in the refinement of the lattice parameter. Accordingly, the refinement was based on the nine best resolved peaks ($2\theta = 18-30°$) in the powder X-ray diffractogram.
[7] W. M. Meier, D. H. Olson, *Atlas of Zeolite Structure Types*, 3rd ed., Butterworth-Heinemann, London, **1992**, pp. 3.
[8] In this case the framework density is calculated as the total of tetrahedrally and octahedrally coordinated atoms per 1000 Å^3, although normally only tetrahedrally coordinated atoms are taken into consideration.
[9] C. S. Blackwell, R. L. Patton, *J. Phys. Chem.* **1988**, *92*, 3965.
[10] D. Müller, I. Grunze, E. Hallas, G. Ladwig, *Z. Anorg. Allg. Chem.* **1983**, *500*, 80.
[11] D. Akporiaye, M. Stöcker, *Zeolites* **1992**, *12*, 351.
[12] K. S. W. Sing, D. H. Everett, R. A. W. Haul, L. Moscou, R. A. Pierotti, J. Rouquerol, T. Siemieniewska, *Pure Appl. Chem.* **1985**, *57*, 603.
[13] S. J. Gregg, K. S. W. Sing, *Adsorption, Surface Area and Porocity*, Academic Press, London, **1982**, pp. 195.
[14] M. M. Dubinin, L. V. Radushkevich, *Proc. Acad. Sci. USSR* **1947**, *55*, 331.
[15] K. Kaneko, C. Ishii, *Colloids Surf.* **1992**, *67*, 203.
[16] Q. Huo, D. I. Margolese, U. Ciesla, P. Feng, T. E. Gier, P. Sieger, R. Leon, P. M. Petroff, F. Schüth, G. D. Stucky, *Nature* **1994**, *368*, 317.
[17] C. T. Kresge, M. E. Leonowicz, W. J. Roth, J. C. Vartuli, J. S. Beck, *Nature* **1992**, *359*, 710.
[18] K. Maeda, unpublished results.

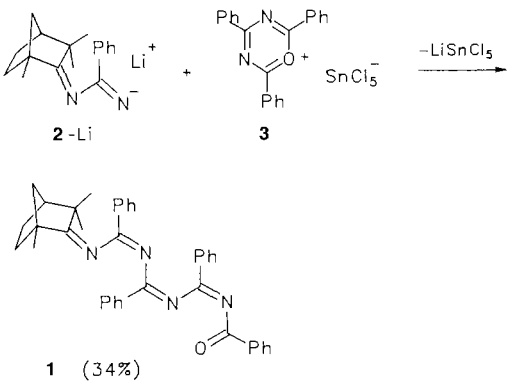
1-Oxa-3,5,7,9-tetraazadecapentaene, a Model Oligonitrile with a Helical Structure in the Crystalline State**

Martin Buhmann, Manfred H. Möller, Ute Rodewald, and Ernst-Ulrich Würthwein*

Dedicated to Professor C. Reichardt on his 60th birthday

Polyacetylenes (polyenes) have become important recently as advanced materials on account of their special electrical and optical properties. However, to our surprise, hardly any linear polynitriles have been investigated. Their defined unsaturated chains with carbon and nitrogen atoms in an alternating sequence[1] contain polar C=N bonds, together with the free electron pairs on the nitrogen atoms; both should lead to interesting physical and chemical properties not feasible in the polyacetylenes. Pursuing a systematic concept we have developed new routes in organic chemistry for the controlled synthesis of oligonitriles with defined chain lengths. In two recent publications we have reported on 1-oxa-3,5-diazahexatrienes[2] and 1-oxa-3,5,7-triazaocatetraene;[3] here we publish our results on the longest yet synthesized of this type of compound with ten chain atoms, a 1-oxa-3,5,7,9-tetraazadecapenta-1,3,5,7,9-ene. To enable further chain lengthening, all these molecules contain a terminal carbonyl group,[4] which should hardly influence the electronic system of the oligonitrile.

Target molecule **1** is easily synthesized by the reaction of the lithiated 1,3-diazabutadiene **2**-H[5] with the 1,3,5-oxoniadiazine salt **3**[6] at −78 °C, followed by purification by flash chro-



matography and recrystallization (in addition about 10% of 2,4,6-triphenyl-1,3,5-triazine is formed). The constitution of **1** was clearly established by means of IR and ^{13}C NMR spectroscopy (Table 1). In solution at room temperature **1** shows a single set of sharp NMR signals; the presence of several isomers or ring-chain tautomers like those we observed with the shorter homologues[2, 3] can therefore be excluded for the NMR time scale available to us.

Table 1. Selected spectroscopic and analytical properties of **1**[a].

IR (KBr): $\tilde{\nu} = 3050\ cm^{-1}$ (w, arom. CH), 2950 (m), 2860 (w, aliph. CH), 1685 (m, C=O), 1640 (s, C=N), 1600 (vs), 1580 (s), 1560 (vs), 1480 (w), 1440 (m), 1310 (s), 1260 (vs), 1165 (m), 1020 (m), 690 (vs); ^1H-NMR (300 MHz, $CDCl_3$): $\delta = 0.53$ (br. s, 3H, CH_3), 0.59 (s, 3H, CH_3), 0.75 (s, 3H, CH_3), 0.95–1.14 (m, 3H, trimethylnorbornylidene H), 1.32–1.58 (m, 3H, trimethylnorbornylidene H), 1.77 (d, 1H, trimethylnorbornylidene H), 7.11 (m, 2H, arom. H), 7.21–7.49 (m, 12H, arom. H), 7.90 (m, 2H, *o*-H), 8.11 (m, 2H, *o*-H), 8.18 (m, 2H; *o*-H); ^{13}C-NMR (75.47 MHz, $CDCl_3$): $\delta = 16.17$ (CH_3), 22.67 (CH_3), 24.62 (CH_2), 25.56 (CH_3), 32.83 (CH_2), 43.20 (CH_2), 45.64 (CH), 46.40 (C_{qu}), 53.63 (C_{qu}), 127.6, 127.7, 127.9, 128.0, 128.8, 129.1, 129.4 (*o*/*m*-C), 131.1, 131.1, 131.7 (*p*-C), 134.0, 134.1, 135.1, 136.4 (*i*-C), 160.2 (NC=N), 161.4 (NC=N), 162.2 (NC=N), 178.1 (C=O), 186.8 (C = N); UV (diethyl ether): λ_{max} (lg ε) = 210 (4.518), 251 nm (4.530); MS (70 eV): *m/z* (%): 564 (2) [M^+], 459 (6) [M^+−PhCO], 384 (3), 356 (7) [M^+ − PhCO − PhCN], 309 (28) [M^+ − PhCO − $C_{10}H_{16}N$], 239 (30), 105 (77) [$PhCO^+$], 103 (100) [$PhCN^+$], 77 (48) [Ph^+].

[a] Satisfactory C,H,N microanalysis obtained.

For the determination of the configuration and conformation of **1** in the crystalline state an X-ray structure analysis[7] was performed. In the following discussion the crystallographic numbering (Fig. 1) is used. There are two independent mole-

[*] Prof. Dr. E.-U. Würthwein, Dr. M. Buhmann
Organisch-chemisches Institut der Universität
Corrensstrasse 40, D-48149 Münster (FRG)
Telefax: Int. code + (251)83-9772
Dr. M. H. Möller, Dipl.-Ing. U. Rodewald
Anorganisch-chemisches Institut der Universität Münster

[**] Unsaturated Heterochains, Part 3. This work was supported by the Fonds der Chemischen Industrie and by BASF AG, Ludwigshafen. We would like to thank Prof. Dr. G. Henckel (University of Duisburg) for the low-temperature measurements. Part 2: [3a]

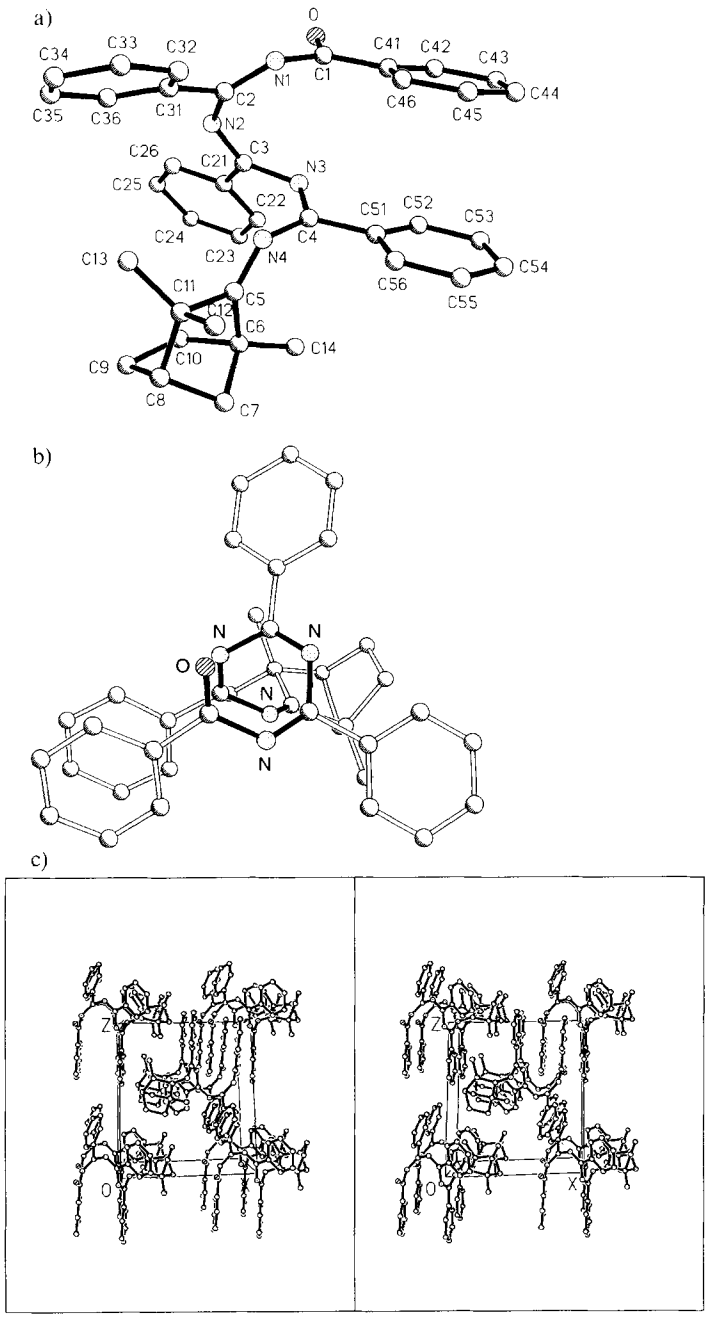


Fig. 1. XS plot [14] of the structures of isomers **1a** (a) and **1b** (viewed down the helix axis, b) in the crystalline phase. The stereoplot (c) shows the crystal packing of **1** (view onto the x,z plane).

cules of **1** in a unit cell, one of which is present uniquely as an (*P*)-helix with a (*Z*)-configurated N4=C5 bond (isomer **1a**) and the other is disordered: an (*M*)-helix with an (*E*)-N4=C5 bond (68%, isomer **1b**) is overlapped by 32% of an (*M*)-helix with a (*Z*) N4=C5 bond (isomer **1c**). The 3_1-helical structures in the oligonitrile part of all three isomers **1a–c** are formed by the all-(*Z*)-configurated C=N bonds with *gauche* C–N conformations of identical sense in which isomer **1a** has the opposite helical sense to isomers **1b** and **1c**. All the isomers contain an (*R*)-trimethylnorbornylidene group as a consequence of the synthetic method and are therefore diastereoisomeric. The isomerism and the disorder are an indication to us that the importance of the configuration of the trimethylnorbornylidene as an almost spherical end group should not be overemphasized. Apparently, different configurations find sufficient space in the crystal lattice. A dependence of the helical sense on the absolute configuration of the trimethylnorbornyl group does not, therefore, exist; rather, if the configuration of the trimethylnorbornylidene residue and the N4=C5 bond is neglected, the helices are present as mirror images. The pitch of the helices is 3.4–4.3 Å; the two phenyl groups on C1 and C4 are also about the same distance apart (3.5–3.8 Å); in graphite[8] there are corresponding separations between two layers, and similar electronic interactions may be expected here.

The preference for a three-dimensional structure over a planar all-*trans* configuration can be explained by looking at simple model compounds. 1,3-Diazabutadiene, according to experimental and quantum mechanical investigations[9, 10] is present in a preferred *gauche* conformation of the central C–N single bond; in this way a low dipole moment can be achieved by bond dipole compensation. The (*Z*) configuration of the C=N bonds is already favored in the shorter oligonitrile model compounds.[2, 3] The combination of these two structural elements leads inevitably to tertiary structures with helical elements.

By means of ab initio quantum mechanical calculations (MP3/6-31G*//6-31G*)[11] on isomers of 1-oxa-3,5,7,9-tetraazadecapenta-1,3,5,7,9-ene as a model compound (that is, without considering the phenyl groups), we searched for evidence of an energetic preference for the helical structure in isolated molecules in the gas phase (Fig. 2). No evidence was

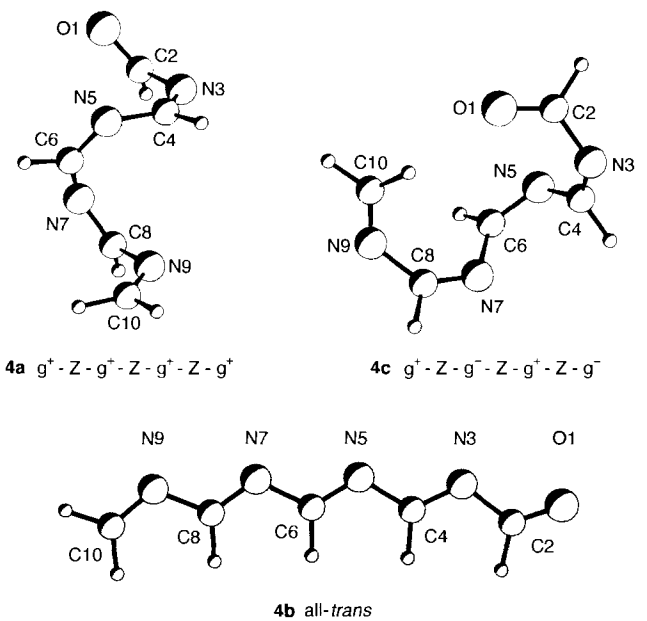


Fig. 2. Structures **4a–c** calculated by ab initio methods (6-31G*//6-31G*).

found; instead the helical structure **4a** is of relatively high energy (E_{rel}(**4a**) = 7.56 kcal mol^{-1}) and exhibits a high dipole moment (8.02 Debye) whose vector lies approximately in the direction of the axis of the helix. The calculated pitch (4 Å) corresponds with that determined for **1** by X-ray analysis. Even higher in energy, as expected, is the planar and—because of the unequal C-N-C and N-C-N bond angles—bow-shaped all-*trans* configurated isomer **4b** (E_{rel}(**4b**) = 10.1 kcal mol^{-1}, μ = 11.79 Debye).[12] The lowest energy isomer is calculated to be the all-(*Z*) configuration with alternating (+)-*gauche* and (−)-*gauche* conformations about the C–N bonds (E_{rel}(**4b**) = 0.00 kcal mol^{-1}; E_{tot}(MP3/6-31G*//6-

31G* = −486.86848 Hartree); the best dipole moment compensation is achieved through the short helical sections with opposed senses in this isomer ($\mu = 1.92$ Debye). According to these results the tertiary structure determined by X-ray crystallography is the result of intra- and intermolecular packing effects in which the bulkiness of the phenyl groups on C1 and C4 plays an important role. In the packing diagrams of **1** (Fig. 1c) these phenyl rings are arranged parallel to the *y*,*z* plane. Thus a particularly favorable packing of the helices (3_1-helices, Fig. 1b), which resemble three bladed propellers seen from the top, can be achieved. The crystal structures and model quantum mechanical calculations for the shorter homologues (similarly without taking the phenyl groups into account) agree very well.[12, 3]

From the diversity of the established structures a high intramolecular flexibility may be deduced. In our earlier studies we estimated low barriers for rotation around the C–N bonds (about 4–5 kcal mol^{-1});[10] also (*E*)/(*Z*) isomerization of the C=N bonds seems possible, during which transition states with a zwitterionic cumulene structure are traversed (about 20 kcal mol^{-1} activation energy for 1,3-diazabutadienes,[9] and 12 kcal mol^{-1} for *N*-acylimines[13]). This may also explain the discrepancy between the single set of signals found in the NMR spectra for a solution and the complex X-ray results.

The X-ray and quantum mechanical results also supply a convincing explanation for the electronic spectra of **1**; since there is clearly no extended π-electron system present ($\lambda_{max} < 270$ nm) but a sequence of strongly twisted amidine units and an amide unit, no long-wavelength π–π* absorption bands appear; the π–π* transitions are hidden by arene bands.

Experimental Procedure

1: *n*-Butyllithium solution (1.6 M, 2.7 mL, 4.4 mmol) was slowly added to a solution of *N*,*N*-(1,3,3-trimethylbicyclo[2.2.1]hept-2-ylidenebenzamidine [5] (2-H, 1.11 g, 4.4 mmol) in THF (15 mL) at −78 °C. After 5 min a suspension of 2,4,6-triphenyl-1,3,5-oxadiazinium pentachlorostannate (**3**, 2.65 g, 4.4 mmol) in THF (50 mL) was added dropwise, and the reaction mixture was stirred at −78 °C. The reaction mixture was allowed to warm to room temperature over approximately 12 h. After 27 h the mixture was cooled to 0 °C, and the cloudy, yellow solution was shaken with 40 mL of ice cold 1 N sodium hydroxide solution. The aqueous solution was extracted twice with dichloromethane (20 mL). The combined organic phases were dried over magnesium sulfate, and the solvent removed under vacuum. The residue was taken up in a little dichloromethane, filtered, and worked up by flash chromatography (petroleum ether/diethyl ether 2/1, **1**: $R_{f(DC)} = 0.24$). The yellow residue thus obtained was recrystallized from diethyl ether. Yield 0.84 g (34%) **1**, pale yellow crystals; m.p. 155 °C.

Received: June 8, 1994 [Z7014IE]
German Version: Angew. Chem. 1994, 106, 2386

[1] D. Wöhrle, *Makromol. Chem.* **1974**, *175*, 1751–1760; *Adv. Polymer Sci.* **1972**, *10*, 35–107.
[2] M. Buhmann, M. H. Möller, E.-U. Würthwein, *Chem. Ber.* **1993**, *126*, 957–967.
[3] a) M. Buhmann, M. H. Möller, U. Rodewald, E.-U. Würthwein, *Chem. Ber.* **1993**, *126*, 2467–2476; b) M. Buhmann, Dissertation, Universität Münster, **1993**; c) H. Naarmann, E.-U. Würthwein, M. Buhmann, DE-A 4 223 264, **1992** [*Chem. Abstr.* **1994**, *120*, 269854g].
[4] W. Funke, K. Hornig, M. H. Möller, E.-U. Würthwein, *Chem. Ber.* **1993**, *126*, 2069–2077.
[5] F. Bondavalli, O. Bruno, P. Schenone, W. Filipelli, S. Russo, E. Marmo, *Farmaco* **1987**, *42*, 335–340.
[6] R. R. Schmidt, *Chem. Ber.* **1965**, *98*, 334–345; see also R. Fuks, M. Strebelle, A. Wenders, *Synthesis* **1977**, 788–789.
[7] Crystallographic data for **1** ($C_{38}H_{36}N_4O$, $M_r = 564.7$: triclinic, space group $P\bar{1}$, $a = 1093.4(2)$, $b = 1195.7(2)$, $c = 1300.7(3)$ pm, $\alpha = 68.36(3)$, $\beta = 86.36(3)$, $\gamma = 80.45(3)$, $Z = 2$, $\rho_{calcd} = 1.201$ g cm^{-3}, $\mu = 0.7$ cm^{-1}. Measured at 293(2) K with an Enraf–Nonius CAD4 diffractometer, $Mo_{K\alpha}$ radiation, graphite monochromator; 18826 measured reflections, of which 18541 are independent ($R_{int} = 0.0326$). Solution by direct methods. SHELXTL-PLUS program [14]. $R = 0.0648$, $wR2 = 0.1745$. Confirmation of the structure solution by means of a smaller set data from a low temperature measurement (77 K) on the same crystal. All positions of the non-hydrogen atoms anisotropic; all hydrogen atoms were geometrically determined and their positional and temperature parameters coupled with the associated carbon atoms. Further details of the crystal structure investigation may be obtained from the Fachinformationszentrum Karlsruhe, D-76344 Eggenstein–Leopoldshafen (FRG) on quoting the depository number CSD–58228, the names of the authors, and the journal citation.
[8] N. N. Greenwood, A. Earnshaw, *Chemistry of the Elements*, Pergamon, Oxford **1985**, p. 303 ff.
[9] P. Luthardt, M. H. Möller, U. Rodewald, E.-U. Würthwein, *Chem. Ber.* **1989**, *122*, 1705–1710.
[10] K. B. Wiberg, P. R. Rablen, M. Marquez, *J. Am. Chem. Soc.* **1992**, *114*, 8654–8668.
[11] GAUSSIAN 92, Revision B: M. J. Frisch, G. W. Trucks, M. Head-Gordon, P. M. W. Gill, M. W. Wong, J. B. Foresman, B. G. Johnson, H. B. Schlegel, M. A. Robb, E. S. Replogle, R. Gomperts, J. L. Andres, K. Raghavachari, J. S. Binkley, C. Gonzales, R. L. Martin, D. J. Fox, D. J. DeFrees, J. Baker, J. J. P. Stewart, J. A. Pople, Gaussian Inc., Pittsburgh PA, **1992**. MP3: C. Møller, M. S. Plesset, *Phys. Rev.* **1934**, *46*, 618; M. J. Frisch, R. Krishnan, J. A. Pople, *Chem. Phys. Lett.* **1980**, *75*, 66. Details of the calculated structures (GAUSSIAN-92 Archive Entries) can be obtained from E.-U. W.
[12] Finite cluster calculations of polymers with all-*trans* configuration: J. Chandrasekhar, P. K. Das, *J. Phys. Chem.* **1992**, *96*, 679–685.
[13] R. Allmann, R. Kupfer, M. Nagel, E.-U. Würthwein, *Chem. Ber.* **1984**, *117*, 1597–1605.
[14] G. Sheldrick, SHELXTL-PLUS, Programmsystem zur Kristallstrukturbestimmung, Siemens AG, **1989**.

Tether-Directed Remote Functionalization of Buckminsterfullerene: Regiospecific Hexaadduct Formation**

Lyle Isaacs, Richard F. Haldimann, and François Diederich*

Following the development of a great variety of methods for monofunctionalization,[1] the regiospecific formation of covalent polyadducts has become the frontier in the chemistry of buckminsterfullerene C_{60}.[2] Reversible reactions with transition metal complexes[3] or halogens[4] yield the thermodynamically most stable isomer or an isomer that selectively crystallizes out of the reaction mixture. Alternatively, mixtures of many possible multiple adducts are produced by successive, irreversible reactions at the C_{60} sphere. Purification is then achieved by tedious, scale-limiting HPLC separation of the isomeric mixtures or by recrystallization, when possible.[2] In an attempt to develop a more rational approach to the production of one desired regioisomer in multiple functionalization reactions, we turned to the tether-directed remote functionalization of C_{60}, a concept that was introduced by Breslow for the regioselective functionalization of steroids and long-chain alkanes.[5] Here, we describe the application of remote functionalization to the regiospecific formation of bis- and trisadducts of C_{60}. With a trisadduct as the starting material, formation of a hexaadduct with the six functional groups aligned in pseudooctahedral positions on the C_{60} surface (positions *a*–*f* in Fig. 1) is readily achieved. This unique functionalization pattern has previously only been described for transition metal complexes.[3, 6] All compounds are isolated in pure form without the application of HPLC methods.

[*] Prof. F. Diederich, L. Isaacs, R. F. Haldimann
Laboratorium für Organische Chemie
ETH Zentrum, Universitätstrasse 16
CH-8092 Zürich (Switzerland)
Telefax: Int. code + (1) 632-1109

[**] This work was supported by the Schweizerischer Nationalfonds zur Förderung der wissenschaftlichen Forschung.

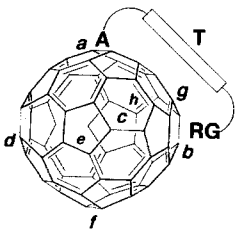


Fig. 1. Schematic depiction of the tether-directed remote functionalization of C_{60}. The bonds a–f (in red) represent the six pseudooctahedrally disposed double bonds on the C_{60} sphere; bonds g and h (in green) do not react with the reactive group for steric reasons. A = anchor, T = tether, RG = reactive group.

First, we targeted the regiospecific production of an equatorial bisadduct of C_{60} (Fig. 1) using a reactive group anchored by a tether to the fullerene. As the anchor, we chose the carboxylate of the methanofullerene carboxylic acid **7**[7] (Scheme 2) and as reactive group, a 2-substituted 1,3-butadiene known to undergo irreversible Diels–Alder reactions with C_{60} at 6-6 bonds (bonds between two fused six-membered rings).[8] The choice of the tether between anchor and reactive group was critical for the regioselective attack. Its size and shape were chosen to favor attack at the equatorial bond b (Fig. 1) over attack at the other possible reactive 6-6 bonds g and h located in the same hemisphere in somewhat closer proximity to the anchor bond a (Fig. 1). PM3 computational studies[9] show that the chosen 4-substituted benzyl alcohol tether in **1** (Scheme 1) would lead to a preference for the targeted bisadduct **2a** over regioisomer **2b**. The heat of formation of **2a** is calculated to be 6.5 kcal mol^{-1} lower than that of the lowest energy conformer of **2b** (Fig. 2). A close examination of the calculated geometry of **2b** shows that the tether is too short in the conformer shown and too long in the higher energy conformer in which the double bond of the cyclohexene boat is oriented towards the anchor. This mismatch of the tether length leads to distortions in the bridging benzene ring and also to skewing of the ester group, which both increase the heat of formation. The different symmetries of **2a** (C_s) and **2b** (C_1) should make it easy to identify by ^{13}C NMR spectroscopy the bisadduct formed.

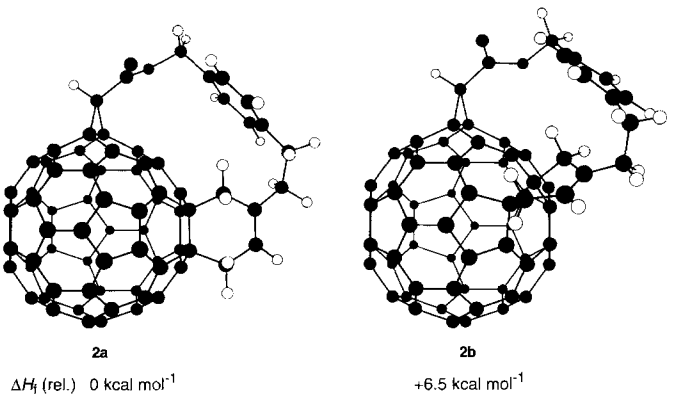
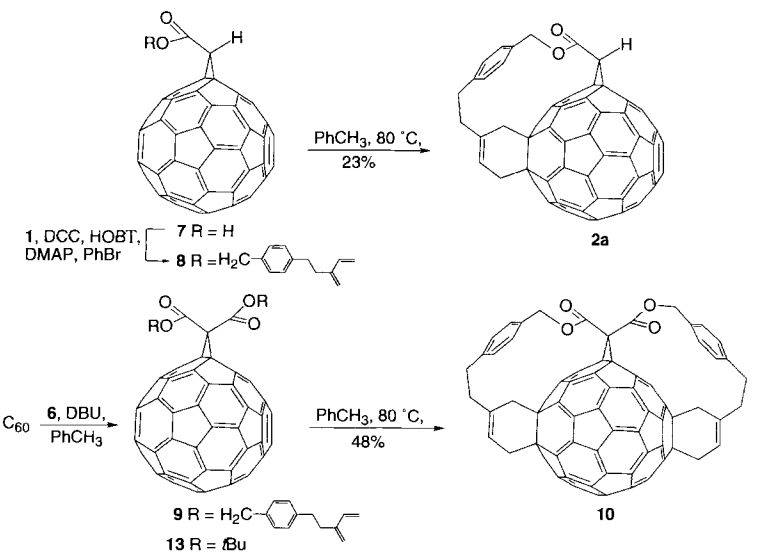
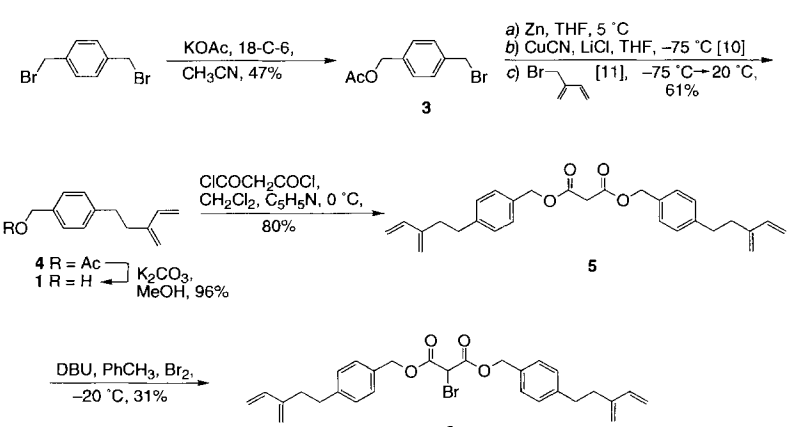


Fig. 2. PM3-calculated structures and heats of formation for the two possible regioisomeric bisadducts **2a** and **2b**.



Scheme 2. Synthesis of the bis- and trisadducts **2a** and **10**. DCC = dicyclohexylcarbodiimide, HOBT = 1-hydroxybenzotriazole, DMAP = 4-dimethylaminopyridine.

The synthesis of **1**, which contains both tether and reactive group, is shown in Scheme 1. Reaction of **1** with **7** (Scheme 2) under dicyclohexylcarbodiimide (DCC) coupling conditions[7] afforded the intermediate wine-red methanofullerene **8**, which was purified by flash chromatography (SiO_2, toluene/hexane 2/1) and identified in solution by the two diagnostic UV/VIS absorption bands of a monoadduct at λ_{max} = 429 and 692 nm. Further characterization was not attempted owing to the rapid polymerization of **8** upon evaporation to dryness. However, heating of a solution of **8** (ca. 0.1 mM) in toluene to 80 °C led to a color change from wine-red to yellow-orange. Flash chromatography (SiO_2, toluene/hexane, 2/1) followed by recrystallization (CS_2/hexane) afforded the isomerically pure bisadduct **2a** in 23% yield, which was fully characterized spectroscopically (Table 1). The presence of 32 signals for the fullerene C atoms in the ^{13}C NMR spectrum demonstrates conclusively that the Diels–Alder reaction occurred at the equatorial double bond b (Fig. 1) with formation of the C_s-symmetrical isomer. The bisadduct, like the other highly functionalized fullerenes described below, is air- and light-sensitive and must be stored under argon in the dark. One other fullerene product (ca. 5% yield) was also present in the reaction mixture, but matrix-assisted laser desorption–ionization time-of-flight mass spectrometry (MALDI-TOF MS)



Scheme 1. Synthesis of the "tether–reactive group" fragments **1** and **6**. 18-C-6 = [18]crown-6, DBU = 1,8-diazabicyclo[5.4.0]undec-7-ene.

Table 1. Selected physical data of compounds **2a**, **10**, **11**, and **12** [a,b].

2a: Black solid. $R_f = 0.51$ (SiO_2, toluene/hexane, 2:1). M.p. > 270 °C. ^{1}H NMR (CS_2/$(CD_3)_2CO$ in capillary, 300 MHz): δ = 7.06 (s, 4 H), 6.47 (t, J = 5.4, 1 H), 5.09 (s, 2 H), 4.47 (s, 1 H), 3.66 (d, J = 5.4, 2 H), 3.33 (s, 2 H), 3.06 (s, 4 H); ^{13}C NMR (CS_2/$(CD_3)_2CO$ in capillary, 125.8 MHz): δ = 163.46, 160.19, 156.41, 149.16, 148.35, 147.90, 147.42, 146.81, 146.53, 146.32, 146.29, 146.26, 145.99, 145.86, 145.33, 145.20, 145.09, 144.99, 144.69, 144.23, 144.11, 144.01, 143.20, 143.14, 142.59, 142.49, 142.22, 140.32, 139.09, 138.97, 138.58, 136.59, 132.72, 130.79, 128.51 (br), 125.98, 69.60, 68.00, 65.78, 64.99, 43.77, 41.71, 40.14, 35.67, 34.75; UV/VIS (CH_2Cl_2): λ_{max} [nm] = 508 sh (ε = 2180), 449 (3050), 427 (4030), 399 sh (4000), 397 sh (3250), 349 sh (15340), 309 sh (32040), 279 sh (51370), 248 (77100); MALDI-TOF MS: m/z 948 (100%, M^+).

10: Black solid. $R_f = 0.60$ (SiO_2, toluene). M.p. > 270 °C. ^{1}H NMR ($Cl_2DCCDCl_2$, 300 MHz): δ = 7.13 (br s, 8 H), 6.52 (t, J = 5.3, 2 H), 5.18 (s, 4 H), 3.80 (d, J = 5.3, 4 H), 3.42 (s, 4 H), 3.06 (s, 8 H). ^{13}C NMR ($Cl_2DCCDCl_2$, 125.8 MHz): δ = 162.88, 158.36, 153.58, 146.97, 146.50, 146.24, 145.70, 145.51, 145.19, 144.60, 143.09, 142.81, 142.27 (br), 140.17, 139.90, 139.72, 139.57, 132.02, 130.61, 128.62 (br), 125.93, 69.34, 69.13, 62.90, 62.85, 54.45, 43.53, 39.93, 35.49, 34.49; UV/VIS (CH_2Cl_2): λ_{max} [nm] = 498 (ε = 3120), 468 (1660), 368 sh (6320), 337 sh (13830), 308 sh (20970), 264 (41350); MALDI-TOF MS: m/z 1162 (100%, M^+).

11: Orange solid. $R_f = 0.13$ (SiO_2, toluene). M.p. > 270 °C. ^{1}H NMR ($CDCl_3$, 300 MHz): δ = 7.20 (br s, 4 H), 7.12 (br s, 4 H), 6.41 (t, J = 5.3, 2 H), 5.19 (s, 4 H), 4.40–4.20 (m, 4 H), 3.60 (dd, J = 5.3, 14.1, 2 H), 3.56 (dd, J = 5.3, 14.1, 2 H), 3.28 (d, J = 14.3, 2 H), 3.18 (d, J = 14.3, 2 H), 3.06 (br s, 8 H), 1.32 (t, J = 7.1, 3 H), 1.30 (t, J = 7.1, 3 H); ^{13}C NMR ($CDCl_3$, 75 MHz): δ = 163.42, 163.11, 162.42, 158.10, 156.70, 153.26, 152.16, 150.21, 148.14, 147.23, 147.14, 146.19, 146.11, 145.82, 145.36, 145.31, 145.08, 145.00, 144.45 (2 x), 142.65, 142.44 (2 x), 141.95, 141.93, 141.85, 141.16, 140.78, 139.83, 139.51, 139.47, 131.85, 130.37, 130.28, 128.25, 125.39, 71.82, 68.61, 67.49, 67.28, 62.74, 62.63, 62.47, 62.25, 53.60, 52.72, 42.82, 39.32, 35.02, 34.23, 14.13 (2 x); UV/VIS (CH_2Cl_2): λ_{max} [nm] = 578 (ε = 1040), 556 sh (1350), 533 sh (2370), 492 (3550), 459 (3880), 414 sh (5620), 386 (8740), 278 (71650); MALDI-TOF MS: m/z 1320 (100%, M^+).

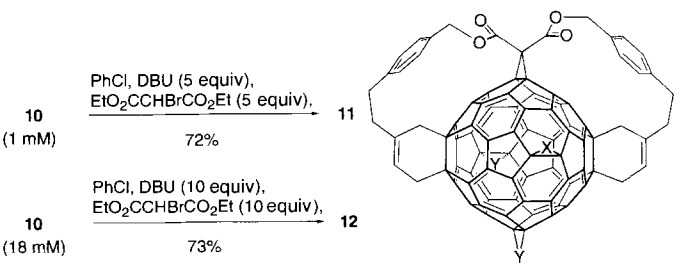
12: Yellow solid. $R_f = 0.41$ (SiO_2, CH_2Cl_2). M.p. > 270 °C. ^{1}H NMR ($CDCl_3$, 300 MHz): δ = 7.25–7.05 (br m, 8 H), 6.16 (t, J = 5.5, 2 H), 5.22 (s, 4 H), 4.34 (q, J = 7.1, 4 H), 4.28 (q, J = 7.1, 4 H), 4.24 (q, J = 7.1, 4 H), 3.21 (d, J = 5.5, 4 H), 3.05–2.85 (m, 12 H), 1.35 (t, J = 7.1, 6 H), 1.29 (t, J = 7.1, 6 H), 1.26 (t, J = 7.1, 6 H); ^{13}C NMR ($CDCl_3$, 125.8 MHz): δ = 164.14, 163.85, 163.67, 162.99, 155.27, 155.07, 145.77, 145.41, 145.29, 144.85, 143.65, 143.36, 143.14, 142.51, 139.98, 139.73, 139.34, 139.08, 131.75, 130.24, 128.26, 125.12, 70.66, 68.56, 65.88, 62.62, 62.53, 62.42, 61.70, 61.60, 45.84, 45.52, 44.54, 42.29, 39.61, 34.84, 34.23, 14.14, 14.03, 14.00; UV/VIS (CH_2Cl_2): λ_{max} [nm] = 353 sh (ε = 21790), 332 sh (35000), 308 sh (64390), 288 (73260); MALDI-TOF MS: m/z 1637 (100%, M^+), 1593 (41, $[M-EtO]^+$), 1481 (48, $[M-EtO_2CCCO_2Et]^+$).

[a] All new compounds in Scheme 1 were fully characterized by ^{1}H and ^{13}C NMR, FT-IR, and EI-MS data, as well as by elemental analysis or high-resolution MS. [b] MALDI-TOF MS spectra were measured with 2,5-dihydroxybenzoic acid or 2-(4-hydroxyphenylazo)benzoic acid as the matrix.

showed it to be a by-product due to oxidation[2d] of **2a** rather than a regioisomeric bisadduct. The rather low isolated yield of **2a** is a reflection of the difficulties encountered with its chromatographic separation from its oxidation product.

For the regiospecific formation of a trisadduct resulting from double Diels–Alder addition to the two equatorial double bonds *b* and *d* (Fig. 1), the doubly tethered system **6** was prepared (Scheme 1) and anchored to C_{60} by the versatile α-bromomalonate alkylation method introduced by Bingel.[12] Addition of **6** to C_{60} (2 equiv) in toluene with DBU as base gave methanofullerene **9**. Following flash chromatography (SiO_2, toluene/hexane, 1/1 then 2/1) to recover the excess C_{60}, the identity of **9** was established by ^{1}H NMR and UV/VIS spectroscopy. The ^{1}H NMR spectrum showed all expected resonances for tether and reactive groups, and the electronic absorption spectrum contained the two diagnostic monoadduct bands at λ_{max} = 429 and 690 nm. Heating of a solution of **9** in toluene (ca. 0.07 mM) at 80 °C for 83 h resulted in a color change from wine-red to yellow-orange. Flash chromatography (SiO_2, toluene) afforded a single trisadduct (48% yield based on **6**), which was assigned the C_{2v}-symmetrical structure **10** on the basis of its spectroscopic data (Table 1). The ^{1}H NMR spectrum of **10** is similar to that of **2a**, except that the signal corresponding to the methine resonance in the methano bridge is absent. The ^{13}C NMR spectrum shows the expected 17 resonances for the fullerene C atoms in a C_{2v}-symmetrical molecule.

The fact that we had access to relatively large quantities (ca. 100 mg batches) of trisadduct **10**, prompted us to test the regioselectivity of further reactions on the fullerene sphere. The regioselectivity observed by Hirsch et al.[2b] in the formation of a trisadduct (*a*,*b*,*c*-functionalized, Fig. 1) from an equatorial bisadduct (*a*,*b*-functionalized) made us optimistic that further functionalization of **10** would lead to regioisomerically pure tetra- through hexaadducts. When a 1 mM solution of **10** in chlorobenzene was reacted with five equivalents of diethyl α-bromomalonate and DBU at room temperature (Scheme 3), the



Scheme 3. Synthesis of the tetra- and hexaadducts **11** and **12**.

C_s-symmetrical bright red tetraadduct **11** functionalized at the *a*,*b*,*c*,*d* bonds was selectively obtained in 72% yield. The ^{1}H NMR spectrum of **11** shows two sets of ethyl ester resonances, and the presence of 32 fullerene-core resonances in the ^{13}C NMR spectrum supports the assigned molecular symmetry (Table 1). When an 18 mM solution of **10** was reacted with a tenfold excess of the reagents, flash chromatography (SiO_2, CH_2Cl_2) allowed the isolation of the bright yellow hexaadduct **12** in 73% yield. The overall yield of **12** was a remarkable 35% based on C_{60}.

In the MALDI-TOF mass spectrum of **12**, the expected molecular ion appears as the base peak at m/z = 1637, in addition to weaker peaks resulting from the fragmentation of the ethyl malonates. In accord with the proposed C_{2v}-symmetrical structure, the ^{1}H NMR spectrum contains three nonequivalent ethoxy groups, and the ^{13}C NMR spectrum shows 17 resonances for the fullerene core C atoms. Hexaadduct **12** is highly soluble and dissolves readily in chlorinated and aromatic solvents; more than 40 mg can be dissolved in 1 mL of $CHCl_3$.

The change in the extent of conjugation in the fullerene chromophore when passing from a mono- to a hexaadduct is readily apparent from the visual color changes. Accordingly, the electronic absorption spectra change dramatically (Fig. 3). Compared to C_{60}, compound **13** (Scheme 2), which is typical of methanofullerene monoadducts, shows much less fine structure in the 400 to 700 nm range, and a hypsochromic shift of λ_{max} for the broad, long-wavelength band to about 500 nm is observed. Two additional diagnostic bands appear at about λ_{max} = 430 and 700 nm. The characteristic peak at λ_{max} = 700 nm in the spectrum of **13** is no longer observed for the bisadduct **2a**, and the broad band in the visible region is further hypsochromically shifted to λ_{max} = 449 nm. Trisadduct **10** exhibits little fine structure in its electronic absorption spectrum, and the characteristic band at λ_{max} at about 430 nm, present in the mono- and bisadducts, is not observed. However, a new strong band appears at the surprisingly long wavelength of λ_{max} = 498 nm. The spec-

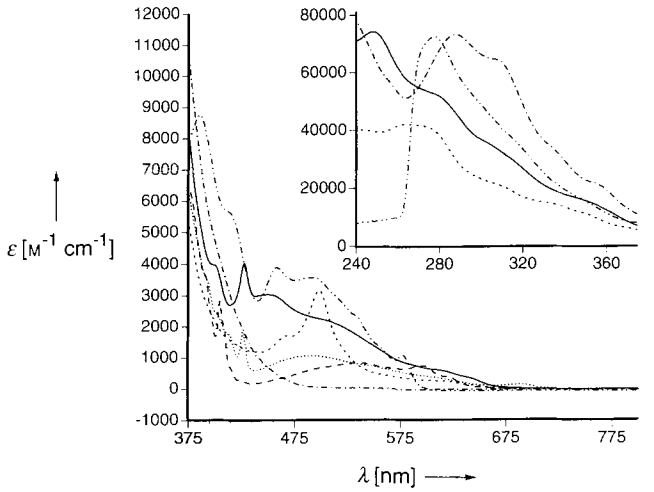


Fig. 3. Electronic absorption spectra of C_{60} (---), **2a** (—), **10** (-----), **11** (·····), **12** (-·-·-), and **13** (····) in CH_2Cl_2.

trum of the tetraadduct **11** is much more intense and structured than that of **10**; no absorption is observed beyond 600 nm in the spectrum of **11**. Hexaadduct **12** has a π system composed of eight benzene-type rings placed in the corners of a cube; each ring is connected to three neighboring rings by biphenyl-type *meta* bonds. Absorption above 475 nm is no longer observed; this is consistent with a drastic reduction in π conjugation as compared to the precursor molecules.

The described tether-directed remote functionalization methodology should provide a versatile entry into the unexplored area of multiply and differentially functionalized buckminsterfullerenes, which may prove to be useful in chemical, materials, and biomedical applications.

Experimental Procedure

Trisadduct **10**: To a solution of C_{60} (264 mg, 0.367 mmol) and **6** (96 mg, 0.183 mmol) in toluene (155 mL) was added DBU (29 mg, 0.187 mmol) in toluene (5 mL) over 5 min. After 2.75 h, the reaction mixture was concentrated to 100 mL, diluted with hexane (100 mL), and chromatographed (SiO_2). Unreacted C_{60} was recovered with a 1:1 mixture of toluene/hexane as eluent; the monoadduct **9** was eluted with a 2:1 mixture. The resulting solution was concentrated on a rotary evaporator to remove the hexane and then diluted to 1.5 L with toluene. The solution was thoroughly deoxygenated by bubbling Ar through the solution for 1.5 h and then heated at 80 °C for 83 h. The reaction mixture was concentrated and loaded onto a column (SiO_2), which was eluted with toluene. Recrystallization from $CHCl_3$/MeOH followed by drying at 25 °C/10^{-1} Torr gave **10** (102 mg, 48% yield) as a black solid.

Hexaadduct **12**: A solution of diethyl α-bromomalonate (42.1 mg, 0.176 mmol) in anhydrous chlorobenzene (0.45 mL) was added under argon to trisadduct **10** (20.5 mg, 0.0176 mmol), and DBU (26.8 mg, 0.176 mmol) in anhydrous chlorobenzene (0.55 mL) was subsequently added to the suspension. After 5 min, a bright red, homogeneous reaction mixture was obtained. After 2 h, the mixture was loaded onto a SiO_2 column and eluted with CH_2Cl_2. The bright yellow product was collected and concentrated to dryness. Recrystallization from CH_2Cl_2/pentane gave, after drying at 25 °C/10^{-1} Torr, **12** (21.1 mg, 73% yield) as a yellow solid.

Received: July 21, 1994 [Z 7150 IE]
German version: *Angew. Chem.* **1994**, *106*, 2434

[1] a) R. Taylor, D. R. M. Walton, *Nature* **1993**, *363*, 685–693; b) A. Hirsch, *Angew. Chem.* **1993**, *105*, 1189–1192; *Angew. Chem. Int. Ed. Engl.* **1993**, *32*, 1138–1141; c) F. Diederich, L. Isaacs, D. Philp, *Chem. Soc. Rev.* **1994**, *23*, 243–255.

[2] a) J. M. Hawkins, A. Meyer, T. A. Lewis, U. Bunz, R. Nunlist, G. E. Ball, T. W. Ebbesen, K. Tanigaki, *J. Am. Chem. Soc.* **1992**, *114*, 7954–7955; b) A. Hirsch, I. Lamparth, H. R. Karfunkel, *Angew. Chem.* **1994**, *106*, 453–455; *Angew. Chem. Int. Ed. Engl.* **1994**, *33*, 437–438; c) C. C. Henderson, C. M. Rohlfing, R. A. Assink, P. A. Cahill, *ibid.* **1994**, *106*, 803–805 and **1994**, *33*, 786–788; d) M. Tsuda, T. Ishida, T. Nogami, S. Kurono, M. Ohashi, *J. Chem. Soc. Chem. Commun.* **1993**, 1296–1298.

[3] a) P. J. Fagan, J. C. Calabrese, B. Malone, *J. Am. Chem. Soc.* **1991**, *113*, 9408–9409; b) F. N. Tebbe, R. L. Harlow, D. B. Chase, D. L. Thorn, G. C. Campbell, Jr., J. C. Calabrese, N. Herron, R. J. Young, Jr., E. Wasserman, *Science* **1992**, *256*, 822–825; c) P. J. Fagan, J. C. Calabrese, B. Malone, *Acc. Chem. Res.* **1992**, *25*, 134–142; d) A. L. Balch, D. A. Costa, J. W. Lee, B. C. Noll, M. M. Olmstead, *Inorg. Chem.* **1994**, *33*, 2071–2072.

[4] a) P. R. Birkett, P. B. Hitchcock, H. W. Kroto, R. Taylor, D. R. M. Walton, *Nature* **1992**, *357*, 479–481; b) P. R. Birkett, A. G. Avent, A. D. Darwish, H. W. Kroto, R. Taylor, D. R. M. Walton, *J. Chem. Soc. Chem. Commun.* **1993**, 1230–1232; c) A. G. Avent, P. R. Birkett, J. D. Crane, A. D. Darwish, G. J. Langley, H. W. Kroto, R. Taylor, D. R. M. Walton, *ibid.* **1994**, 1463–1464.

[5] R. Breslow, *Acc. Chem. Res.* **1980**, *13*, 170–177.

[6] A hexaadduct of C_{60} with di(ethoxycarbonyl)methylene has been reported by A. Hirsch and I. Lamparth at the International Winterschool "Electronic Properties of Novel Materials": Progress in Fullerene Research in Kirchberg, Austria, March 5–12, 1994. Book of Abstracts.

[7] L. Isaacs, F. Diederich, *Helv. Chim. Acta* **1993**, *76*, 2454–2464.

[8] B. Kräutler, M. Puchberger, *Helv. Chim. Acta* **1993**, *76*, 1626–1631.

[9] a) J. J. P. Stewart, *J. Comput. Chem.* **1989**, *10*, 209–220; 221–264; b) F. Diederich, L. Isaacs, D. Philp, *J. Chem. Soc. Perkin Trans 2* **1994**, 391–394.

[10] S. C. Berk, P. Knochel, M. C. P. Yeh, *J. Org. Chem.* **1988**, *53*, 5791–5793.

[11] a) E. J. Corey, N. H. Andersen, R. M. Carlson, J. Paust, E. Vedejs, I. Vlattas, R. E. K. Winter, *J. Am. Chem. Soc.* **1968**, *90*, 3245–3247; b) R. C. Krug, T. F. Yen, *J. Org. Chem.* **1956**, *21*, 1082–1086; c) R. L. Frank, R. P. Seven, *Org. Syn. Coll. Vol. 3*, **1955**, 499–500.

[12] C. Bingel, *Chem. Ber.* **1993**, *126*, 1957–1959.

Polar Superstructures Stabilized by Polymeric Oxometal Units: Columnar Liquid Crystals Based on Tapered Dioxomolybdenum Complexes**

André G. Serrette and Timothy M. Swager*

The design of molecule-based materials requires the controlled assembly of specific superstructures that effectively transform discrete molecular properties into collective material properties. Liquid crystalline (mesomorphic) materials are the best examples of designed supermolecular materials, and the cooperative physical properties of these materials have led to numerous technological applications. The continued development of liquid crystal based technologies requires new types of mesomorphic materials that integrate novel structural elements and physical properties. To this end, liquid crystals and transition metals have been combined to give metallomesogens, materials with new properties.[1] In this report we describe columnar mesomorphism in a new class of metallomesogen based upon dioxomolybdenum complexes with tapered structures. The polymeric $(\cdot\cdot Mo{=}O\cdots Mo{=}O\cdot\cdot)_n$ units in these materials provide a strong organization force that directs the assembly process and stabilizes the mesophase.

Thermotropic columnar liquid crystalline phases of disc-shaped molecules have been extensively studied. However, in recent years the structural diversity of materials displaying a columnar mesophase has grown to include hemi-disc,[2] phasmidic,[3] bowlic,[4] octahedral,[5] and tapered mesogens.[6] Of these columnar materials, the stabilization of mesophases based upon tapered materials is most demanding, requiring the simultaneous assembly of four molecular units to produce the

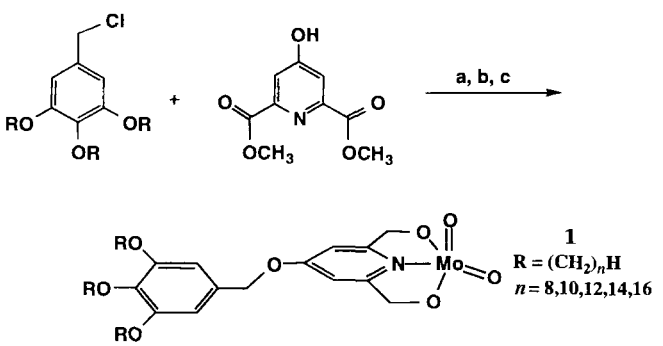
[*] Prof. T. M. Swager, A. G. Serrette
Department of Chemistry,
University of Pennsylvania
Philadelphia, PA 19104-6323 (USA)
Telefax: Int. code + (215) 573-2112

[**] This work was supported by the Office of Naval Research and the National Science Foundation.

disc-shaped units which combine to give columnar superstructures. The group of Percec has studied this assembly process and has pointed out the similarities with the association of proteins to form the tobacco mosaic virus.[6a-e] Previous investigations found that the organization of tapered units into columnar mesophases requires strong organizational forces such as the complexation of ions by crown ethers, the segregation of hydrophobic and hydrophilic groups, hydrogen bonding, charge transfer interactions, and the tethering of the mesogens to a polymer.[6]

In an effort to design new types of ferroelectric materials, we are investigating metallomesogen assemblies based upon polar polymeric $(\cdots M{=}O\cdots M{=}O\cdots)_n$ structures.[7] We are particularly interested in hexagonal columnar phases in which the polymeric structure manifests an axial supermolecular dipole along the column's axis. In such a material the hexagonal symmetry leads to dipolar frustration which prevents the antiparallel (antiferroelectric) dipolar order generally observed in achiral polar liquid crystals.[8] Hence, a hexagonal array of dipoles must exhibit either random (paraelectric) dipolar order or a polar (ferroelectric) organization.

We have synthesized the tapered complexes (pyridinediyl-2,6-dimethanolato)dioxomolybdenum **1**, which were designed to form polymeric structures (Scheme 1).[9] When the side chains



Scheme 1. a) 5.0 equiv Na_2CO_3, cat. NaI, acetone, reflux, 2 days, 84–86%. b) (1) 5.5 equiv $NaBH_4$, THF/MeOH (4/1), 0 °C 1 h, 25 °C 2 h, reflux 14 h; (2) 8.0 equiv Na_2CO_3, H_2O, reflux, 2 h, 66–73%. c) 1.0 equiv $[MoO_2(acac)_2]$, $CHCl_3$/MeOH (1/4), reflux, 3 h, 81–83%.

are sufficiently long ($n > 8$), **1** exhibits enantiotropic liquid crystalline behavior (Table 1). The optical textures viewed with a polarizing microscope (Fig. 1) are characteristic of hexagonal

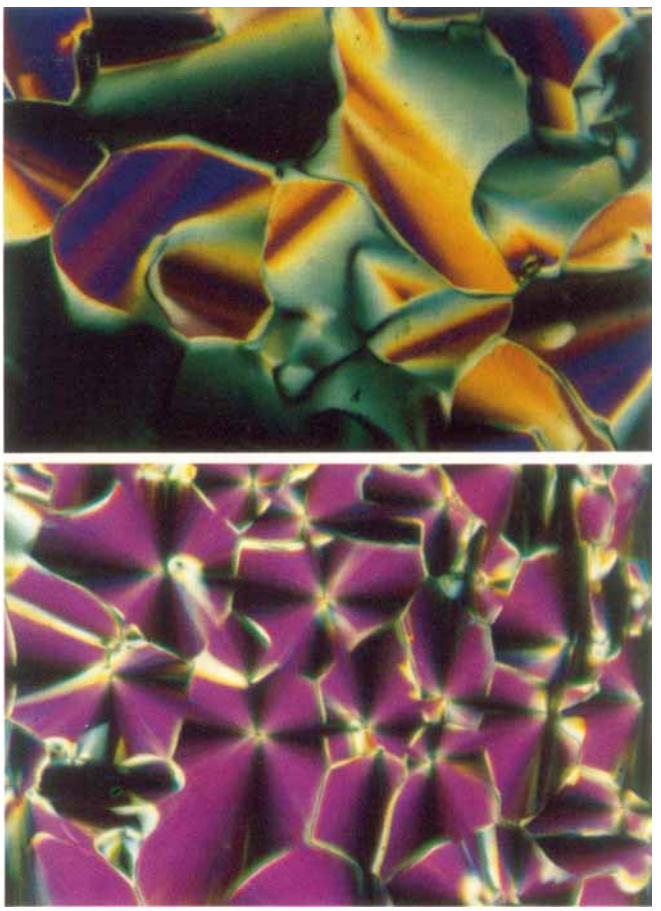


Fig. 1. Optical textures of **1**, $n = 10$, which are typical of hexagonal columnar phases. Top: A relatively thin sample at 121 °C which shows linear birefringent defects and areas of uniform extinction. Bottom: A thicker sample which displays a fan texture at 125 °C.

columnar phases (Φ_h)[10] and display linear birefringent defects, large areas of uniform extinction, and fan domains. Similar to classical discotic phases, the mesophase of **1** mesophase is optically negative. X-ray diffraction (XRD) from the mesophase (Table 2) reveals one strong low-angle peak, two weaker peaks at somewhat higher angle, and a broad halo at wide angle. The low-angle peaks are the (100), (110), and (200) reflections of a hexagonal lattice, and the d-spacing scales as $1:(1/3)^{1/2}:1/2$,

Table 1. Phase behavior of **1** [a]. The transition temperatures and the enthalpies (in parentheses) are given in °C and kcal mol^{-1}, respectively, and were determined by differential scanning calorimetry (10 K min^{-1}).

n	Phase transitions
8	K $\underset{122.4\ (7.5)}{\overset{135.1\ (7.3)}{\rightleftharpoons}}$ I
10	K $\underset{85.9\ (3.5)}{\overset{106.2\ (3.4)}{\rightleftharpoons}}$ Φ_h $\underset{131.0\ (0.3)}{\overset{131.4\ (0.3)}{\rightleftharpoons}}$ I
12	K $\underset{85.8\ (2.5)}{\overset{96.0\ (2.3)}{\rightleftharpoons}}$ Φ_h $\underset{137.0\ (0.4)}{\overset{140.8\ (0.4)}{\rightleftharpoons}}$ I
14	K $\underset{86.1\ (2.4)}{\overset{94.6\ (2.5)}{\rightleftharpoons}}$ Φ_h $\underset{131.9\ (0.3)}{\overset{135.5\ (0.3)}{\rightleftharpoons}}$ I
16	K $\underset{31.5\ (6.0)}{\overset{42.8\ (7.4)}{\rightleftharpoons}}$ K $\underset{75.6\ (1.7)}{\overset{96.0\ (1.8)}{\rightleftharpoons}}$ Φ_h $\underset{139.5\ (0.2)}{\overset{140.8\ (0.3)}{\rightleftharpoons}}$ I

[a] K = crystalline phase, I = isotropic phase, Φ_h = hexagonal columnar phase.

Table 2. XRD data of the Φ_h phase of **1** at 120 °C.

n	Lattice constant a [Å]	Peaks obsd. (calcd)	Miller indices
10	36.34	31.47 (31.47)	(100)
		18.21 (18.17)	(110)
		4.6	halo
12	38.57	33.35 (33.35)	(100)
		19.22 (19.25)	(110)
		16.63 (16.68)	(200)
		4.6	halo
14	40.45	35.03 (35.03)	(100)
		20.17 (20.22)	(110)
		17.46 (17.52)	(200)
		4.6	halo
16	42.61	37.89 (37.89)	(100)
		21.83 (21.87)	(110)
		18.83 (18.95)	(200)
		4.6	halo

 © VCH Verlagsgesellschaft mbH, D-69451 Weinheim, 1994 0570-0833/94/2222-2343 $ 10.00+.25/0

respectively. The presence of a single broad halo at wide angle indicates that there are only weak liquidlike interactions between the mesogens. Consistent with a highly disordered phase, the mesophase-to-isotropic transition enthalpies are small (0.2–0.4 kcal mol^{-1}, Table 1), and the mesophases have qualitatively high fluidity. The Φ_h phase was observed to supercool slightly (3.6–3.8 °C) for the $n = 12$ and 14 compounds. The stability range of the Φ_h phases is 25–45 K, and the phases at lower temperature are labeled as crystalline (K) since the Φ_h-to-K transition has a greater tendency to supercool. However, we do find that these crystal phases are still very disordered, and XRD shows them to have similar diffraction patterns and lattice constants within 1.3% of those exhibited by the Φ_h phase. These similarities between the K and Φ_h phases are also reflected in the fact that most of the Φ_h-to-K transition enthalpies are small.

As mentioned earlier, the organization of tapered mesogens into a columnar mesophase requires a greater thermodynamic driving force than the dipolar attractions that stabilize most liquid crystalline phases.[6] Alone, the pyridinediyl-2,6-dimethanol ligands do not display liquid crystalline behavior. Therefore the ability of **1** to exhibit a stable columnar mesophase arises from the dioxomolybdenum functionality and its tendency to form polymeric $(\cdots Mo{=}O\cdots Mo{=}O\cdots)_n$ structures. Because the dioxomolybdenum unit displays characteristic symmetric and asymmetric Mo=O stretching bands that shift to lower energy in a polymeric structure,[9, 11] the degree of polymeric association could be determined by variable-temperature infrared spectroscopy (VT-IR). As shown for **1**, $n = 14$, in Figure 2, the respective symmetric and asymmetric vibrational

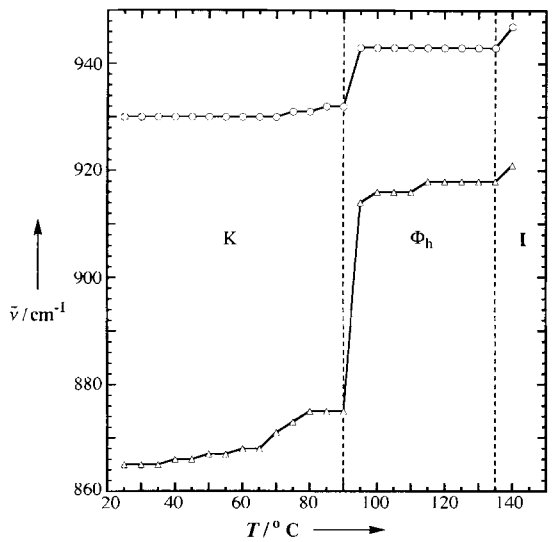
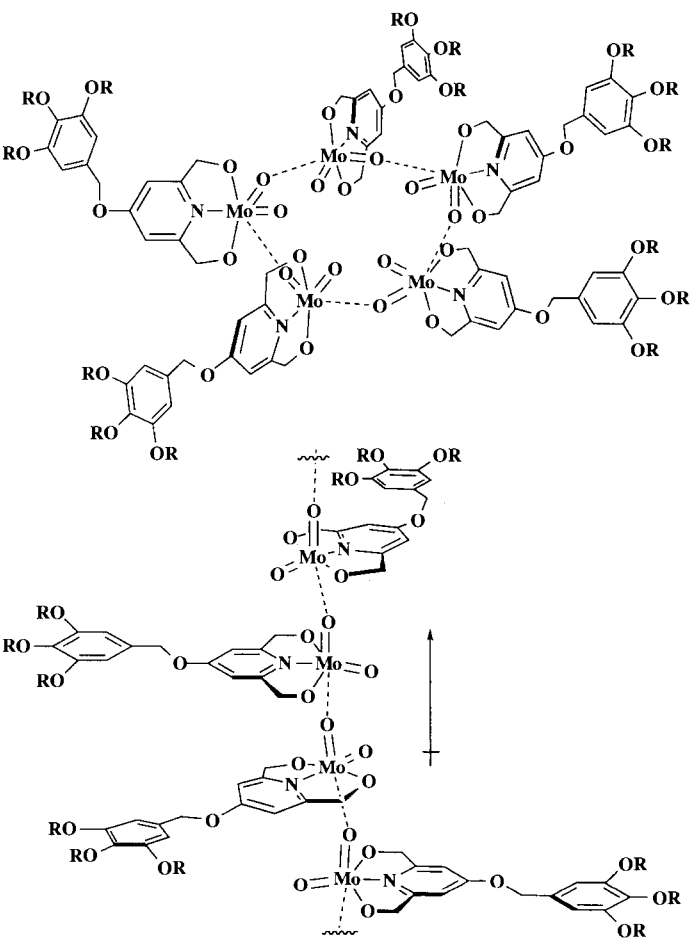


Fig. 2. Plot of the $Mo(O)_2$ stretching frequencies as a function of temperature for **1**. $n = 14$. The circles and triangles are assigned to the $Mo(O)_2$ symmetric and asymmetric stretching modes respectively. A small shift in the I → Φ_h transition indicates that a weakly polymeric structure is formed. The large shift in the Φ_h → K transitions indicates that a strong polymeric structure with strong interactions results.

modes of the $Mo(O)_2$ units in the isotropic phase are observed at 946 cm^{-1} (^{18}O: 893 cm^{-1}) and 921 cm^{-1} (^{18}O: 876 cm^{-1}), and are indicative of a monomeric structure. Upon entering the mesophase, both of these bands shift to slightly lower energy by 4 to 6 cm^{-1}, suggesting the formation of a polymeric structure held together by weak interactions. Further cooling into the crystal phase produces a dramatic shift of both infrared modes to lower energy. The shift of the asymmetric band is greatest at about 50 cm^{-1}, and the shift in the symmetric band is about 13 cm^{-1}. The greater shift of the asymmetric band in both phases is also suggestive of a polymeric structure.

The supermolecular structure of the mesophase of **1** may be deduced from the molecular shape, the lattice dimensions of relative to the molecule's size, and the previously described IR data, which suggest a polymeric or associated structure held together by weak forces. The most reasonable organization whereby a tapered mesogen can produce a columnar phase is one in which the molybdenum head groups are positioned near the center of the column. The effective size of the mesogenic core of **1** in the Φ_h phase can be determined from a plot of the intercolumnar spacing a vs. side-chain length n which yields a straight line. A linear regression of this plot ($R = 0.9995$) gives a slope of 1.03 Å per n and an intercept of 26.1 Å, which is about twice the size of the mesogenic core (i.e. **1**, $n = 0$).[12] This extrapolated value is consistent with a structure in which the molecules extend radially from the center of the column. The VT-IR spectra show only small shifts of the Mo=O bands in the liquid crystalline phase. However, the fact that the crystal phase exhibits a strong polymeric association with a similar structure supports the presence of a weakly associated polymer in the mesophase. On the basis of the IR data alone we cannot discount the possibility of oligomeric macrocyclic (rosette) assemblies (Scheme 2, top). A macrocyclic structure would most



Scheme 2. Possible structures of the Φ_h phase of **1**. The rosette structure (top) is unlikely considering the arguments given in the text. The more likely structure (bottom) has a polymeric $(\cdots Mo{=}O\cdots Mo{=}O\cdots)_n$ assembly which stabilizes the columnar superstructure and manifests a dipole (arrow) along the column's axis.

closely resemble the structures previously proposed for other tapered liquid crystalline materials.[6] However, in the present case, the macrocyclic structure is unreasonable since it would orient the polar oxo groups not assembled in the polymer inward, which generates strong repulsive forces at the column's core. Additionally, macrocyclic association would require the planes of all of the pyridine rings to be oriented along the column's axis. This organization would be highly unusual for a thermotropic liquid crystal since it does not allow for optimal dipolar interactions between neighboring aromatic rings. Thus, we propose that **1** displays the superstructure shown at the bottom of Scheme 2 with the $(\cdots Mo{=}O\cdots Mo{=}O\cdots)_n$ polymeric chain oriented along the column's axis. This organization gives rise to supermolecular dipoles along the columns axis which are frustrated by the hexagonal symmetry of the mesophase. The fluid nature should allow for a facile reorientation of these dipoles, and the electrical properties of these novel materials will be the subject of future reports.

Received: June 17, 1994 [Z7044IE]
German version: *Angew. Chem.* **1994**, *106*, 2378

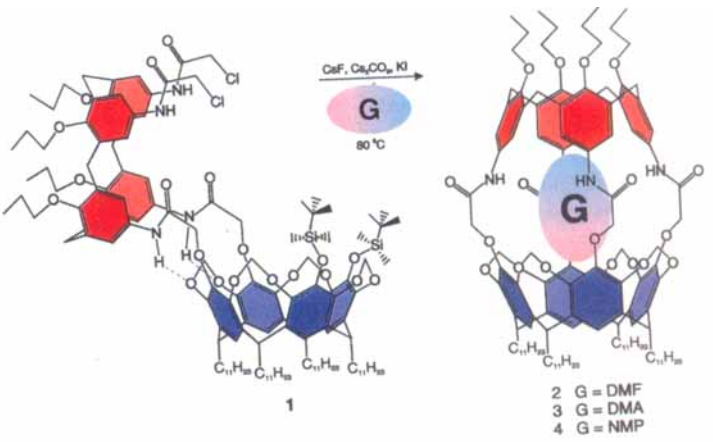
[1] For reviews on metallomesogens: a) A. M. Giroud-Godquin, P. M. Maitlis, *Angew. Chem.* **1991**, *103*, 370; *Angew. Chem. Int. Ed. Engl.* **1991**, *30*, 375; b) P. Espinet, M. A. Esteruelas, L. A. Oro, J. L. Serrano, E. Sola, *Coord. Chem. Rev.* **1992**, *117*, 215; c) S. A. Hudson, P. M. Maitlis, *Chem. Rev.* **1993**, *93*, 861.
[2] a) J. Barberá, C. Cativiela, J. L. Serrano, M. M. Zurbano, *Adv. Mater.* **1991**, *3*, 602; b) C. K. Lai, A. G. Serrette, T. M. Swager, *J. Am. Chem. Soc.* **1992**, *114*, 7949; c) H. Zheng, C. K. Lai, T. M. Swager, *Chem. Mater.* **1991**, *6*, 101.
[3] a) J. Malthête, A.-M. Levelut, N. H. Tinh, *J. Phys. Lett.* **1985**, *46*, L875; b) J. Malthête, N. H. Tinh, A.-M. Levelut, *J. Chem. Soc. Chem. Commun.* **1986**, *1*, 548; c) J. Malthête, A. Collet, A.-M. Levelut, *Liq. Cryst.* **1989**, *5*, 123.
[4] a) J. Malthête, A. Collet, *J. Am. Chem. Soc.* **1987**, *109*, 7544; b) *Nouv. J. Chim.* **1985**, *9*, 151; c) A.-M. Levelut, J. Malthête, A. Collet, *J. Phys. (Paris)* **1986**, *47*, 351; d) R. Poupko, Z. Luz, N. Spielberg, H. Zimmermann, *J. Am. Chem. Soc.* **1989**, *111*, 6094; e) H. Zimmermann, R. Poupko, Z. Luz, J. Billard, *Z. Naturforsch. A* **1985**, *40*, 149; f) *ibid.* **1986**, *41*, 1137; g) L. Lei, *Mol. Cryst. Liq. Cryst.* **1987**, *146*, 41, and references therein; h) W. Kranig, H. W. Spiess, H. Zimmermann, *Liq. Cryst.* **1990**, *7*, 123; i) G. Cometti, E. Dalcanale, A. Du vosel, A.-M. Levelut, *J. Chem. Soc. Chem. Commun.* **1990**, 163; j) L. Wang, Z. Sun, X. Pei, Y. Zhu, *Chem. Phys.* **1990**, *142*, 335; k) B. Xu, T. M. Swager, *J. Am. Chem. Soc.* **1993**, *115*, 1159.
[5] H. Zheng, T. M. Swager, *J. Am. Chem. Soc.* **1994**, *116*, 761.
[6] a) V. Percec, G. Johansson, J. Heck, G. Ungar, S. V. Batty, *J. Chem. Soc. Perkin Trans. 1* **1993**, 1411; b) D. Tomazos, G. Out, J. Heck, G. Johansson, V. Percec, M. Möller, *Liq. Cryst.* **1994**, *16*, 509; c) V. Percec, D. Tomazos, J. Heck, H. Blackwell, G. Ungar, *J. Chem. Soc. Perkin Trans. 2* **1994**, 31; d) V. Percec, J. Heck, D. Tomazos, F. Falkenberg, H. Blackwell, G. Ungar, *J. Chem. Soc. Perkin Trans. 1* **1993**, 2799; e) V. Percec, J. Heck, M. Lee, G. Ungar, A. Alvarez-Castillo, *J. Mater. Chem.* **1992**, *2*, 1033; f) M. Ebert, R. Kleppinger, M. Soliman, M. Wolf, J. H. Wendorff, G. Latterman, G. Staufer, *Liq. Cryst.* **1990**, *7*, 533; g) W. Paulus, H. Ringsdorf, S. Diele, G. Pelzl, *Liq. Cryst.* **1991**, *9*, 807.
[7] a) A. G. Serrette, T. M. Swager, *J. Am. Chem. Soc.* **1993**, *115*, 8879; b) H. Zheng, P. J. Carroll, T. M. Swager, *Liq. Cryst.* **1993**, *14*, 1421; c) A. Serrette, P. J. Carroll, T. M. Swager, *J. Am. Chem. Soc.* **1992**, *114*, 1887.
[8] For a discussion of polar frustration in bowlic liquid crystals see ref. [4e].
[9] (Pyridinediyl-2,6-dimethanolato)dioxomolybdenum has been shown to have a bent polymeric structure with a $Mo{=}O\cdots Mo$ angle of 157°: J. Berg, R. H. Holm, *Inorg. Chem.* **1983**, *22*, 1768.
[10] Since the mesogens are not disc-shaped, we follow the phase designation Φ_b.
[11] Other $[LMo(O)_2]$ systems show similar shifts. O. A. Rajan, A. Chakravorty *Inorg. Chem.* **1981**, *20*, 660.
[12] The size of the mesogenic core is defined as the distance from the molybdenum center to the 4′ oxygen attached to the phenyl ring. According to crystal structure data (ref. [9]) and computer modeling this distance is 13.0 Å.

A Novel Type of Stereoisomerism in Calix[4]arene-Based Carceplexes

Peter Timmerman, Willem Verboom, Frank C. J. M. van Veggel, John P. M. van Duynhoven, and David N. Reinhoudt*

Carcerands are well known for the ability to trap guest molecules in their interior.[1, 2] During synthesis they form carceplexes by capturing guest molecules from the medium that cannot leave the cavity without the rupture of at least one covalent bond of the host.[3–6]

All carcerands hitherto synthesized have D_{4h} symmetry. Different orientations of the guest molecule inside such cavities do not lead to diastereomeric structures due to the overall symmetry of the carceplex. In a previous paper we reported the first carceplex constructed from both a calix[4]arene and a resorcinol unit (**2**), which has C_{4v} symmetry.[7] This carceplex containing one molecule of *N*,*N*-dimethylformamide (DMF) inside the cavity[8] was isolated in 27% yield as a by-product in the synthesis of an organic molecule with a rigid cavity of nanometer dimensions.[7] Here we report two new carceplexes (**3** and **4**) and describe their synthesis, structure, and dynamic behavior. These carceplexes exhibit a novel type of stereoisomerism as a result of different orientations of the guest molecule inside the cavity.



When a solution of **1**, which was prepared as described previously,[7] in *N*,*N*-dimethylacetamide (DMA) was added over 8 hours to a solution of CsF, Cs_2CO_3, and KI in DMA at 80 °C, and the mixture stirred for a further 16 hours at this temperature, carceplex **3** was isolated without further purification in essentially quantitative yield. The ^{1}H NMR spectrum of **3** (Fig. 1) is consistent with C_{4v} symmetry, indicating that rotation of the guest DMA molecule about the molecular axis is fast on the ^{1}H NMR (chemical shift) time scale.[9] All guest proton signals exhibit dramatic upfield shifts as a result of the shielding effect of the aromatic rings. Similar upfield shifts of guest proton signals have been frequently observed for the "Cram" carcerands.[4, 5] The spectrum of **3** shows two broad singlets at $\delta = -1.0$ and -2.0, representing the *N*-methyl group *cis* to the carbonyl group that normally resonates at $\delta = 2.8$, and the methyl group of the acetyl unit, which resonates $\Delta\delta = 4.0$ up-

[*] Prof. Dr. Ir. D. N. Reinhoudt, Dr. P. Timmerman, Dr. W. Verboom, Dr. Ir. F. C. J. M. van Veggel, Dr. J. P. M. van Duynhoven
Laboratory of Organic Chemistry, University of Twente
P.O. Box 217, NL-7500 AE Enschede (The Netherlands)
Telefax: Int. code + (31)53312738

 © VCH Verlagsgesellschaft mbH, D-69451 Weinheim, 1994 0570-0833/94/2222-2345 $ 10.00+.25/0

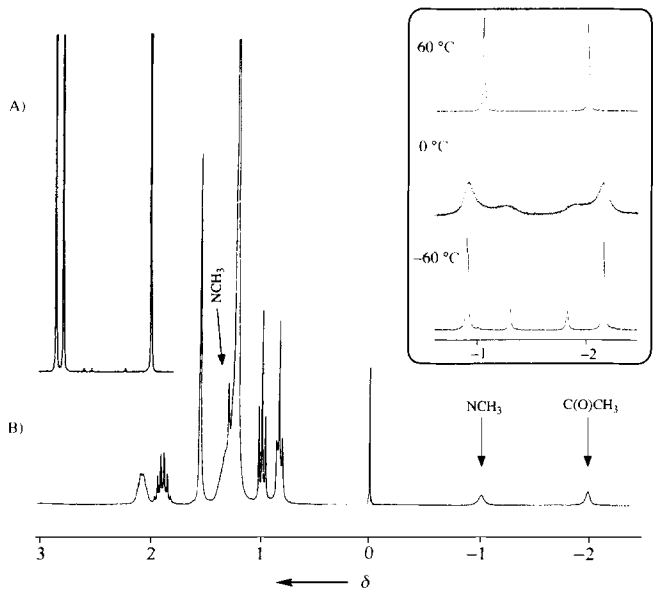
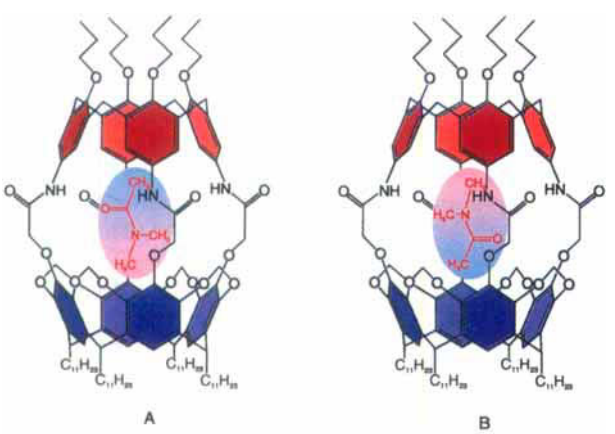


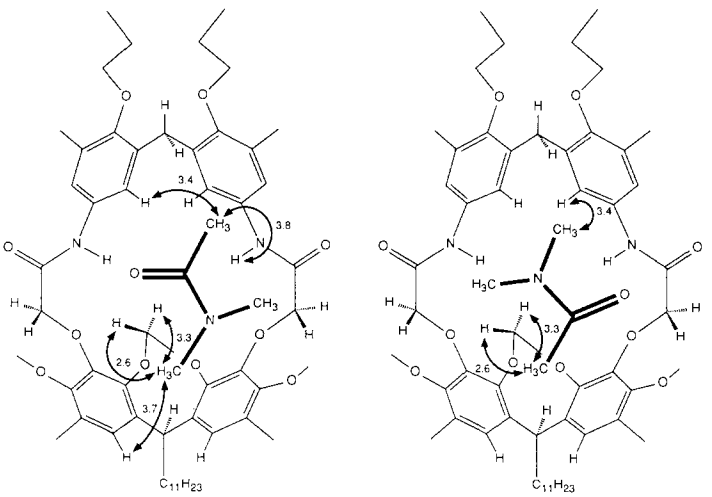
Fig. 1. ^{1}H NMR spectra (250 MHz) of DMA (A) and carceplex **3** (B) in $CDCl_3$ at room temperature; the framed inset shows sections of the ^{1}H NMR spectra (400 MHz) of **3** at different temperatures.

field from its normal position at $\delta = 2.0$, respectively.[10] The methyl group *trans* to the carbonyl resonates at $\delta \approx 1.3$ (obscured by the multiplet of the undecyl chains), which is only $\Delta\delta = 1.6$ upfield from its normal position. Apparently, it is not located close to the aromatic rings of the cavity.

Cooling the sample causes the ^{1}H NMR signals to decoalesce at 0 °C (Fig. 1). At temperatures below −30 °C the broad signals are split into two sets, one of two small, equally intense singlets at $\delta = -1.3$ and -1.8, flanked by the larger singlets of the other at $\delta = -0.9$ and -2.2 also with equal intensity. 2D EXSY experiments revealed that the large singlet at $\delta = -0.9$ shows exchange with the small singlet at $\delta = -1.3$, while the other large singlet at $\delta = -2.2$ exchanges with the small singlet at $\delta = -1.8$. Apparently, calix[4]arene-carceplex **3** switches between two isomeric states **A** and **B** in which the DMA molecule



occupies different orientations inside the cavity of **3**. The structures of **A** and **B** were determined by NOESY experiments (see Fig. 2). The acetyl group's methyl protons in isomer **A** (large singlet at $\delta = -2.2$) exclusively show NOE connectivities with protons that are located in the upper region of **3**, such as the NH protons and the aromatic protons of the calixarene *ortho* to these amide groups (Scheme 1, left), while the protons of the *N*-methyl *cis* to the carbonyl group (large singlet at $\delta = -0.9$) show NOEs with protons located in the lower region of **3**, like the protons of the methylenedioxy bridge pointing inwards or outwards and the aromatic protons of the resorcinol moiety close to the undecyl chains. The set of small singlets of **B** at $\delta = -1.3$ and -1.8 shows opposite NOEs (Scheme 1, right). The protons giving rise to the singlet at $\delta = -1.8$ exclusively show NOE connectivities with protons located at the lower regions of **3**, and those assigned to the singlet at $\delta = -1.3$ with protons located in the upper part of **3**. The relevant intermolecular distances in the two isomers were determined semiquantitatively[11, 12] by using the initial rate approximation.[13]



Scheme 1. Orientation of the guest DMA in the major isomer **A** (left) and in the minor isomer **B** (right) of **3**. The arrows link protons that give rise to NOEs; the numbers give the intermolecular distances.

The type of stereoisomerism observed here, which is very similar to that observed in certain rotaxanes,[14] is novel, because it is based on different orientations of two molecular components that are *not* covalently attached. Since no official nomenclature exists for this type of stereoisomerism, we tentatively propose the name *carceroisomerism* (referring to the hindered rotation of a molecule inside the cavity of a carcerand).

The two isomers (carceromers) **A** and **B**, which are not equally abundant ($\Delta G = 0.7$ kcal mol^{-1} at −60 °C in $CDCl_3$),[15a] show fast exchange on the ^{1}H NMR time scale above room temperature, but give rise to separate signals below −30 °C. The activation enthalpy ($\Delta H^{\neq}$) for isomerization was calculated to be 13 ± 1 kcal mol^{-1} from ^{1}H NMR line shape analysis.[16a]

Another important point is evident from the NOESY spectrum of carceplex **3**: protons belonging to the host give rise to distinctly different resonances in the two isomers. This is most clear for the protons of the methylenedioxy bridges that point into the cavity. These protons resonate at $\delta = 4.0$ in the major isomer **A** and have an NOE with the large singlet of the methyl group *cis* to the carbonyl group ($\delta = -0.9$). In the minor isomer the resonance for these methylene protons is slightly shifted downfield to $\delta = 4.1$. This signal gives an NOE exclusively with the small singlet of the acetyl's methyl group at $\delta = -1.8$, which unambiguously proves that this resonance belongs to the minor isomer **B**.

When the reaction of **1** with CsF, Cs_2CO_3, and KI was carried out in 1-methyl-2-pyrrolidinone (NMP) under the same conditions as used for DMA, carceplex **4** was isolated in 50% yield.

 © VCH Verlagsgesellschaft mbH, D-69451 Weinheim, 1994 0570-0833/94/2222-2346 $ 10.00+.25/0

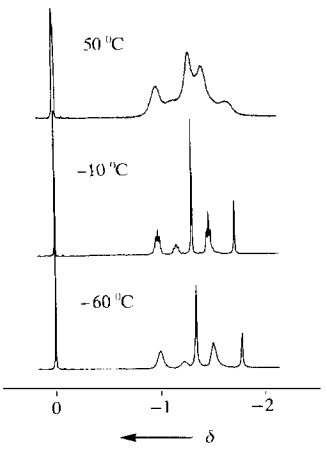
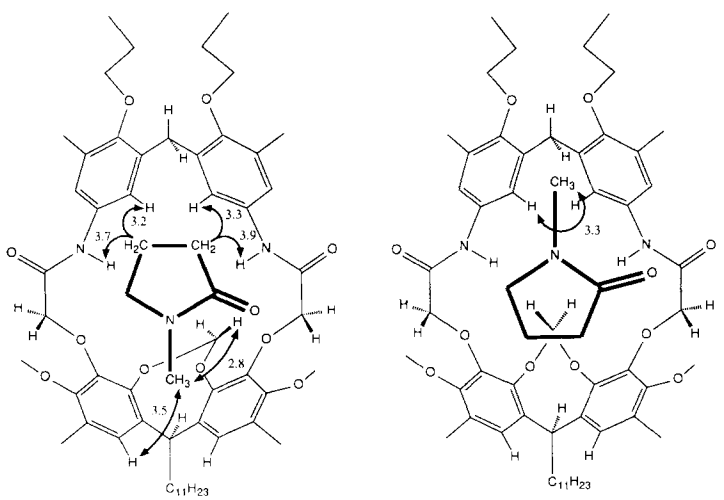


Fig. 2. Sections of the ^{1}H NMR spectra of carceplex **4** at different temperatures.

The presence of unequal amounts of two isomers can be most clearly observed at $-10\,^{\circ}C$ (see Fig. 2). The two singlets at $\delta = -1.3$ and -1.7 represent the methyl groups of incarcerated NMP in the major and minor isomer, respectively ($\Delta G = 0.4$ kcal mol^{-1} at $-60\,^{\circ}C$ in $CDCl_3$).[15b] DQ-COSY and NOESY experiments revealed that the multiplet at $\delta = -1.0$ arises from the 4-CH_2 group of NMP in the major isomer. The corresponding chemical shift for the minor isomer is -1.5 and is obscured by the triplet of the 3-CH_2 group of NMP in the major isomer. The small triplet at $\delta = -1.2$ is assigned to the 3-CH_2 group of NMP in the minor isomer. The 5-CH_2 groups of NMP in both isomers resonate at much lower field ($\delta \approx 1.4$ and 1.5), since they are not located close to the aromatic rings of the cavity.

From a systematic evaluation of the NOEs between host and guest protons, the structure of both isomers could be easily determined (Scheme 2).[17] The *N*-methyl group of NMP in the major isomer is located in the lower part of carceplex **4** as it shows strong NOE connectivities only with the protons of the methylenedioxy bridges and the aromatic protons of the resorcinol moiety close to the undecyl chains. In the minor isomer this methyl group is located in the upper part of the cavity, since it exclusively exhibits NOEs with NH and with the aromatic protons of the calixarene ortho to the amide groups. The 3- and 4-CH_2 groups both give strong NOEs with NH and the protons of the calixarene ortho to the amide groups in the major isomer, whereas these protons in the minor isomer give NOEs exclusively with the protons of the methylenedioxy bridges and with the aromatic protons of the resorcinol moiety close to the undecyl chains. All relevant intermolecular distances between host and guest protons in the two isomers were determined semiquantitatively[11, 17] with the initial rate approximation.[13]



Scheme 2. Orientation of the guest NMP in the major isomer (left) and in the minor isomer (right) of **4**. The arrows link protons that give rise to NOEs; the numbers give the intermolecular distances.

Warming a sample of **4** to 50 °C causes the NMP resonances to coalesce. This coalescence, which is related to isomerization of the two carceromers, takes place at a much higher temperature for **4** than for **3** (DMA carceplex). The activation enthalpy $\Delta H^{\ddagger}$ of 16 ± 1 kcal mol^{-1}[16b] for the rotation is 4 kcal mol^{-1} higher than for **3**.[18] This is primarily because NMP is one carbon atom larger, but the cyclic structure of NMP also renders this molecule much more rigid than DMA, which may also contribute to a higher energy barrier for carceromerization.

When the sample is cooled to $-60\,^{\circ}C$, the guest proton signals broaden markedly. This broadening is most probably related to rotation of the guest molecule about the C_4 axis of the carcerand, a process that becomes progressively slower with larger guest molecules.

The energy barriers for isomerization in carceplexes **3** and **4** is much higher than that for carceplex **2**. Even at $-60\,^{\circ}C$ an averaged ^{1}H NMR spectrum for the isomers of carceplex **2** is observed.

The type of stereoisomerism observed in carceplexes **3** and **4** constructed from calix[4]arene and resorcinol units provides a novel type of molecular switch, with potential applications in the fields of data storage and molecular electronics.[21]

Received: July 14, 1994 [Z 7126 IE]
German version: *Angew. Chem.* **1994**, *106*, 2437

[1] D. J. Cram, *Nature* **1992**, *356*, 29–36.
[2] For the use of hemicarcerands in stabilizing highly reactive species, like cyclobutadiene, see D. J. Cram, M. E. Tanner, R. Thomas, *Angew. Chem.* **1991**, *103*, 1048–1051; *Angew. Chem. Int. Ed. Engl.* **1991**, *30*, 1024–1027.
[3] D. J. Cram, S. Karbach, Y. Hwan Kim, L. Baczynskyj, K. Marti, R. M. Sampson, G. W. Kalleymeyn, *J. Am. Chem. Soc.* **1988**, *110*, 2554–2560.
[4] J. Bryant, M. T. Blanda, M. Vincenti, D. J. Cram, *J. Am. Chem. Soc.* **1991**, *113*, 2167–2172.
[5] J. C. Sherman, C. B. Knobler, D. J. Cram, *J. Am. Chem. Soc.* **1991**, *113*, 2194–2204.
[6] R. G. Chapman, N. Chopra, E. D. Cochien, J. C. Sherman, *J. Am. Chem. Soc.* **1994**, *116*, 369–370.
[7] P. Timmerman, W. Verboom, F. C. J. M. van Veggel, W. P. van Hoorn, D. N. Reinhoudt, *Angew. Chem.* **1994**, *106*, 1313–1315; *Angew. Chem. Int. Ed. Engl.* **1994**, *33*, 1292–1295.
[8] No exchange of the guest DMF for deuterated solvent DMF was observed after heating a solution of **2** in [D$_7$]DMF for 1 hour at 100 °C, which unambiguously proves that the guest molecule is trapped inside the cavity.
[9] The molecular axis is defined as the axis connecting the centers of the calix[4]arene and resorcinol moieties.
[10] Conclusive evidence for the identity of the methyl groups was found by heating a solution of **3** in [D$_5$]nitrobenzene. Above 100 °C the singlet at $\delta = -1.0$ coalesces as a result of the hindered rotation about the C–N bond, a process that is slow on the ^{1}H NMR time scale at room temperature, but fast at temperatures above 100 °C. In this way the singlet at $\delta = -2.0$ was assigned to the methyl group of the acetyl unit and the singlet at $\delta = -1.0$ to the *N*-methyl group *cis* to the carbonyl group.
[11] All intermolecular distances between protons of host and guest vary between a minimum and maximum value because of fast rotation of the guest molecule about the C_4 axis of the host. Since NOEs between two protons are inversely proportional to the sixth power of the intermolecular distance, short distances contribute much more to the NOE than large distances. For this reason the calculated distances between two protons should be interpreted as the upper limit for the minimum distance between those protons rather than an averaged distance.
[12] For the two isomers **A** and **B** of carceplex **3** the intermolecular distances in Å (± 0.2 Å) in Scheme 1 have been determined (only parts of the structures are shown for clarity).
[13] R. R. Ernst, G. Bodenhausen, A. Wokaun in *International Series of Monographs on Chemistry, Vol. 14* (Eds.: R. Breslow, J. B. Goodenough, J. Halpern, J. S. Rowlinson), Clarendon, Oxford, **1987**, Chapter 9.
[14] R. A. Bissell, E. Córdova, A. E. Kaifer, J. F. Stoddart, *Nature* **1994**, *369*, 133–137.
[15] A systematic search using Quanta/CHARMM Version 3.3 was carried out in order to find as many local minima as possible that correspond to different orientations of the guest molecule inside the cavity. The search was performed

by rotation of the guest about the x (0–60°), y (0–330°) and z axes (0–330°) in steps of 30° each, followed by energy minimization (conjugate gradient) until the root mean square (RMS) of the gradient was less than 0.01. Visual inspection of the minimized structures revealed that they correspond to several different orientations of the guest inside the host. The lowest energy structure of each orientation was minimized further with ABNR (ABNR = adopted basis set Newton–Raphson) until the RMS of the gradient was less than 0.001. a) For carceplex **3** seven energy minima with different orientations of DMA inside the cavity were found. Molecular Dynamics Simulations at 300 K revealed that all orientations isomerize to either of the two lowest energy orientations within 100 psec. The two lowest energy orientations are structurally identical (within the experimental error of the NOE measurements) with the two isomers **A** and **B** found experimentally. The internal energy (ΔE) of the major isomer was calculated to be 1.7 kcal mol^{-1} lower than that of **B**. This energy difference [E (isomer **B**) − E (isomer **A**)] is slightly higher than the experimentally determined Gibbs free energy difference (ΔG) of 0.7 kcal mol^{-1}. b) For carceplex **4** six minima with different orientations of NMP inside the cavity were found. Also here the two lowest energy orientations were structurally identical (within the experimental error of the NOE measurements) with **A** and **B** [17]. In this case the major isomer was calculated to be 1.3 kcal mol^{-1} lower in energy. Again ΔE is higher than the experimental determined ΔG of 0.4 kcal mol^{-1}.

[16] The isomerization of **3** and **4** was studied using the computer simulation program Conjugate Peak Refinement ("TRAVEL") [19]. For a given isomerization process this program finds saddle points on the adiabatic potential energy surface. CHARMM Version 22g3 was used for the TRAVEL studies. a) In case of **3**, an activation energy for interconversion between the two lowest energy structures of 9.8 kcal mol^{-1} was calculated [20], which is 3.2 kcal mol^{-1} lower than the experimentally determined activation enthalpy. b) In case of **4**, an activation energy for interconversion between the two lowest energy structures was calculated at 12.4 kcal mol^{-1} [20], which is 3.6 kcal mol^{-1} lower than the experimentally determined value.

[17] The intermolecular distances in Å (±0.2 Å) in Scheme 2 have been determined for the two isomers of **4** (only parts of the structures are shown for clarity).

[18] Attempts to determine the activation enthalpy for interconversion using ^{1}H NMR line shape analysis were hampered by the complexity of the spectrum. The activation enthalpy was therefore determined by measuring the exchange rate by EXSY (at five different temperatures).

[19] S. Fischer, M. Karplus, *Chem. Phys. Lett.* **1992**, *194*, 252–261.

[20] A physically realistic activation energy for interconversion was only found when one (in case of **3**) or two (in case of **4**) of the higher energy structures were used as intermediates.

[21] a) J. S. Miller, *Adv. Mater.* **1990**, *2*, 98–99; b) *ibid.* **1990**, *2*, 378–379.

Corrigenda

In the communication "Spectroscopic Studies of Anhydroretinol, an Endogenous Mammalian and Insect *retro*-Retinoid" by F. Derguini, K. Nakanishi, J. Buck, U. Hämmerling, and F. Grün (*Angew. Chem. Int. Ed. Engl.* **1994**, *33*, 1837–1839) an editorial error was made in the description of the UV/VIS spectrum of the all-*trans*-anhydroretinol **4**. A weak band at $\lambda = 262$ nm was incorrectly attributed to *cis* double bonds. This absorption actually arises from bending of the conjugated system induced by sterid hindrance. Because this bending is enhanced by the *cis* double bonds of sterically hindered *cis* isomers, it is called the "*cis*-band". This term does not necessarily imply the presence of a *cis* double bond.

In the review "Otto Roelen, Pioneer in Industrial Homogeneous Catalysis" by B. Cornils, W. A. Herrmann, and M. Rasch (*Angew. Chem. Int. Ed. Engl.* **1994**, *33*, 2144–2163), the names of two of the authors were assigned to the wrong photographs. The central picture is of W. A. Herrmann and the right-hand picture is of M. Rasch.

Observing and Applying Secrets of the Cell

Gene Regulation in Eukaryotes. By *E. Wingender*. VCH Verlagsgesellschaft, Weinheim/VCH Publishers, New York, 1993. 430 pp., hardcover DM 178.00, $ 120.00.—ISBN 3-527-28460-5/1-56081-706-2

Anyone who is concerned on an everyday basis with the subject of eukaryotic gene regulation will appreciate how demanding a task Edgar Wingender has set himself in writing a monograph on this highly topical theme. It is obviously very difficult to take into account all the new research results that are continually appearing. It is greatly to the credit of the author and publishers that this book covers even work that has been published very recently.

The material is arranged in a way that progresses from the general to the specific, skillfully introducing the reader to the secrets of cellular processes in eukaryotic organisms. The first chapter reveals the complexity of the regulation scenario in a eukaryotic cell. Chapters 2 to 4 describe in detail the 'principal characters' involved in gene regulation, the three RNA polymerases. As in most stage productions, the effectiveness of the main actor depends on his interaction with the supporting players. The author goes on to describe the indispensable transcription factors which play the supporting roles, pointing out also that the same actor can appear in several different productions. Thus, for example, zinc finger proteins have essential roles in gene regulation in molds, insects, and vertebrates. The author discusses widely varied but precisely chosen examples in which the zinc finger ribbon motif controls the regulation of cell processes. Here the RNA polymerases are cast in ever more exciting and important roles.

Another class of transcription factors has as its common feature a homeobox which is homologous to the 'helix–turn–helix' DNA ribbon motif of the regulatory proteins in prokaryotes. In the chapter on these the author shows that as well as homeobox proteins there are other types of transcription factors, such as the 'helix–loop–helix' and 'leucine zipper', which can, for example, interact cooperatively so as to enable a *Drosophila* embryo to undergo differentiation.

Virtually every aspect of gene regulation is mentioned, including such topics as signal transduction via a 'second messenger', and steroid receptors which come into direct contact with the promotors of the genes concerned. Not only the specialist but also the reader approaching the subject for the first time will benefit from the book. It is unlikely that one would want to read through the book from beginning to end, and probably that is not what the author intends. Instead he has put together a compendium on the subject of gene regulation in eukaryotes, so that each reader can satisfy his or her thirst for knowledge in the relevant areas of this currently very important field. For example, if one looks in the index under 'GCN4', one is directed to an informative account of the importance of this yeast transcription factor, including also a mention of transcription factors that function similarly in other eukaryotes (in this case the vertebrate proto-oncogene c-jun). At the end of of each section within a chapter there is a useful summary which enables the reader to consolidate the foregoing material. Another excellent idea is that of the gray 'boxes' which are placed at appropriate points in the text to give background information on, for example, c-Raf1, c-Mos, Ras, EGF, and thyroid hormones. The list of abbreviations, although not exhaustive, is also a useful aid. I found only a few shortcomings, such as inconsistencies between figures and legends (e.g., Figs. 9, 10), repetition of the information about Raf1 (cf. pp. 69, 249), and the inaccurate description of the uvrABC endonuclease as an enzyme rather than a multienzyme complex, but these do not detract significantly from the high standard of the book. The plain and straightforward style of the text does not rob the subject of eukaryotic gene regulation of any of its splendor. The book should be in every library where students of molecular genetics and related subjects occasionally spend time (or ought to do so).

As with every theatrical production, it is the audience who determine whether it is a success. The same will also apply to this book, and therefore I recommend you to buy it and visit the show!

Michael Schweizer
Institute of Food Research
Genetics and Microbiology Department
Norwich (UK)

Biotechnology. Vol. 2. Genetic Fundamentals and Genetic Engineering. Edited by *H.-J. Rehm* and *G. Reed*. VCH Verlagsgesellschaft, Weinheim, 1993. XIII, 880 pp., hardcover DM 490.00.—ISBN 3-527-28312-9

"This is, consequently, the first book which deals comprehensively with all aspects of genetics in biotechnology..." This sentence on the first page of the book reviewed here describes the ambitious goal that the 32 authors have set themselves; the claim to have achieved it is at least partly justified. The idea of collecting together in a single volume all the knowledge of microbial and molecular genetics that is relevant to biotechnology undoubtedly addresses a real gap in the literature. The very rapid growth of knowledge in the areas of genetic fundamentals and genetic engineering during the 1970s played a key role in the development of biotechnology, and these sciences continue to provide the main nucleus for innovation.

However, this aspect is only brought out to a limited extent in this volume, which instead follows the overall concept of the twelve-volume work, with a greater emphasis on 'classical' biotechnology than on its molecular genetic aspects.

The main subject matter of this volume is divided into three areas. First, classical

This section contains book reviews and a list of new books received by the editor. Book reviews are written by invitation from the editor. Suggestions for books to be reviewed and for book reviewers are welcome. Publishers should send brochures or (better) books to Dr. Ralf Baumann, Redaktion Angewandte Chemie, Postfach 101161, D-69451 Weinheim, Federal Republic of Germany. The editor reserves the right of selecting which books will be reviewed. Uninvited books not chosen for review will not be returned.

genetics (181 pp.) is treated in five chapters, covering mutagenesis, genetic exchange processes in prokaryotic and lower eukaryotic organisms, and cell fusion and gene-mapping in animals and plants. Molecular genetics (178 pp.) is treated in four chapters: structure and function of DNA, principles of gene expression, DNA sequencing, and DNA synthesis. The section on genetic engineering deals first with microorganisms (170 pp.), with five chapters covering gram-negative and gram-positive bacteria, yeast cells and yeast plants, and an introduction to practical methods based on *Escherichia coli* as an example. There are then two chapters on plant systems (122 pp.) and two on animal systems (170 pp.), each topic being divided into work with cells and with transgenic organisms. The volume ends with 19 pages on safety aspects of biotechnology.

The task of covering "all aspects of genetics in biotechnology", from the basic principles of classical microbiology and genetics to the latest methods of genetic engineering, is an enormous undertaking, and some compromises are unavoidable. One such compromise is the omission of borderline topics. Among those that have been sacrificed are the use of 'bioinformation technology' for projects on gene-mapping and sequencing, the use of PCR (polymerase chain reaction) and other analytical methods of genetic engineering to identify individuals, groups of organisms, and complex populations, and the in-vitro molecular genetics techniques of 'evolutionary biotechnology'. Biodiversity and the conservation of genetic resources, which constitute the genetic foundations of biotechnology, are also not discussed. The chapter on safety aspects of biotechnology is confined to a discussion of administrative measures, and contains no mention of the experimental findings accumulated over many years, e.g., from the 'worst case' experiments carried out in the 1980s, or from the many studies of releases into the environment.

The heterogeneity often found in multiauthor works has been avoided in an exemplary way in this volume, except for the figures, which vary greatly in quality. In contrast to the mainly black-and-white photographs and diagrams, many of which are good, there are a few partly colored figures whose information content is unconvincing. Compromises are also evident in the subject index, to the detriment of the book. The quality of the index is especially important in a reference work such as this. It is very annoying to find that, although the index lists general methods of gene transfer treated in the chapter on plant cells, other applications are not mentioned or are very difficult to find. Examples of this are the use of liposomes (only listed in the index under "DNA uptake by sperms"), electroporation (two incorrect entries in the index), biolistics (not in the index), and antisense-RNA and antisense-ribozymes (here "antisense" only occurs in the index as a subsidiary term under "ribozyme", and it is left to chance whether the reader finds the figure on page 637 in which this technique is explained).

However, shortcomings such as these do not greatly detract from the usefulness of this information-packed and otherwise cleverly assembled collection of review articles. Such diverse readers as biology students, laboratory administrators, and research specialists will all gain much from referring to this volume—provided that their library has not already lent it out! Those who might consider buying their own copy, despite its price, should note its particular advantage in being thoroughly readable and written in such a clearly understandable way that one could almost recommend it as a textbook. However, it could only be used for this purpose by advanced students, because it contains a great wealth of detailed information.

Owing to the increasingly wide use of the methods of biotechnology, its rapid pace of development, and not least the introduction of legislation to control genetic engineering, there is an urgent need for a readily understandable, applications-orientated, and up-to-date reference source on the subject. Although this volume has occasional shortcomings, it is certainly a very welcome contribution to meeting this need.

Dietmar Blohm
Fachbereich 2
Biotechnologie und Molekulare Genetik
Universität Bremen (FRG)

 © VCH Verlagsgesellschaft mbH, D-69451 Weinheim, 1994 0570-0833/94/2222-2350 $ 10.00+.25/0

One Hundred Years Lock-and-Key Principle**

Albert Eschenmoser*

When we look at modern organic chemistry and ask ourselves where we are going, then the spirit of no other organic chemist of the past appears to be nearer to our present-day thinking than that of Emil Fischer. In saying this, I refer, of course, to Fischer's legacy of the "lock-and-key" concept, an idea which – together with Pauling's later extension to transition states – constitutes the foundation on which all our modern structural modeling of the selectivity of intermolecular communication in chemistry and biology rests. Rightly, therefore, this symposium commemorates the concept's centenary, and the organizers are to be congratulated for their insight and initiative.

By the spirit of Emil Fischer, however, I also mean (and perhaps above all) Fischer's attitude as an organic chemist towards biology. It is the attitude that made and continues to make the biological world the major and deepest source of inspiration for research in organic chemistry, be it in a direct or an indirect way, or just as a reference for achievement. Organic chemistry has returned to this attitude only relatively recently after a period of splendid isolation in organo-chemical self-complacency for more than half a century after Emil Fischer's time.

Today, we marvel at Fischer's foresight in choosing the research fields in which he decided to spend his lifetime as a scientist, fields in which he created an oeuvre that makes him today the unique pioneering figure for organic chemistry, biochemistry, and molecular biology alike. His focus on the basic structural and synthetic chemistry of carbohydrates, nucleotides, and polypeptides, the three families of organic matter that later were recognized as the three pillars on which the living world is built, his interest in and practical use of enzymes as chemical catalysts, and his concern about their mode of action all differentiate him from the natural-products chemists of the self-complacency period, when the recurring pleasures of successful constitutional analyses and syntheses of nicely crystallizing low molecular weight objects, beautiful colors of pigments, fine odors of terpenes, and interesting biomedical properties of alkaloids lured the chemists away from proteins and nucleic acids, from those constitutionally repetitive and "nasty" materials that later revealed themselves as the most important part of the task originally assigned to the chemistry that was named organic, namely, the task of studying the substances produced by living organisms.

If Emil Fischer lived in our time, and if he happened not to be a biologist, he would quite probably be a practitioner of what today is called supramolecular chemistry, judging by the pronounced flair he had for structure and synthesis. In this field of chemical enterprise chemists set out to systematically conquer through synthesis new domains of the structure space of organic matter.

Let us call to mind that the portion of sequence space occupied by DNA and proteins during biological evolution is infinitesimally small compared to the overall size of these structure spaces; and the structure space of organic matter as a whole is infinitely greater than the space within which living matter is evolving. Clearly, moving within a structure space, be it by Nature herself or by synthetic chemists, demands the process of *selection*—selection of structures based on specific criteria. In this context we can distinguish two types of selection: post-synthesis and pre-synthesis selection. Darwinian selection is the prototypical example of the first, but also a chemist's discovery of an unexpected structure with an unexpected property that is put to good use is an example. The second type of selection represents—at least in traditional thinking—the molecular scientist's dream: it is the construction of a specific object based on theory; that is, the scientist selects the object to be synthesized in advance. Selection criteria are always utilitarian, be it fitness for survival, or for technological, scientific, or cultural application. In the supramolecular chemist's space walks, utility is connected with a given structure's specific properties; such properties manifest themselves in the transfer of information from the structure to a receiver, most often another molecular or supramolecular structure. And thus, mutual and strictly selective molecular recognition—Fischer's **lock and key**—is the central issue.

Therein lies that underlying dichotomy in structure space exploration in chemical research: post-synthesis selection (discovery) versus pre-synthesis selection (design). The recent sudden rise of encoded combinatorial synthesis within chemistry should make us reflect: we witness the transplant of a principle of synthesis from the heart of biology into the center of chemistry. An exciting period is ahead of us in which we shall be able to watch and compare the power of the two selection modes in chemical synthesis and their impact on the evolution of chemistry.

[*] Prof. Dr. A. Eschenmoser
Laboratorium für Organische Chemie
ETH-Zentrum
Universitätstrasse 16, CH-8092 Zürich (Switzerland)
Telefax: Int. code +(1) 632-1043

[**] Introductory remarks at the symposium "Supramolecular Chemistry: 100 Years Lock-and-Key Principle" in Mainz on August 12, 1994, organized by F. Diederich and H. Ringsdorf.

 © VCH Verlagsgesellschaft mbH, D-69451 Weinheim, 1994 0570-0833/94/2323-2363 $ 10.00+.25/0

100 Years "Schlüssel-Schloss-Prinzip": What Made Emil Fischer Use this Analogy?**

Frieder W. Lichtenthaler*

Emil Fischer's famous lock-and-key analogy (Schlüssel-Schloss-Prinzip) for the specifity of enzyme action has provided successive generations of scientists with a mental picture of molecular recognition processes, and thus has shaped to a marked degree the development not only of organic chemistry, but, through its extension to basic live processes, that of biology and medicine as well. The hundredth anniversary of the first use of this most fertile metaphor provides a welcome opportunity not only for highlighting its paramount importance, but for gaining an understanding and appreciation of the creative processes involved, of the constructive reasoning and the thought patterns underlying the fundamental insight. Accordingly, this account attempts to trace how Fischer was led to the lock-and-key analogy, based on the state of knowledge and the views prevailing at the time. It reveals that Fischer, who had a pronounced tendency against any sort of theoretical speculation, refrained from taking this metaphor any further, that is to the obvious extensions of what turns the key, and what kind of doors are then opened. Except for a small refinement -the differentiation of main key and special keys to account for the fact that some yeasts can ferment a larger number of hexoses than others—he rather expounded on the scope of the lock-and-key picture: "I am far from placing this hypothesis side by side to the established theories of our science, and readily admit, that it can only be thoroughly tested, when we are able to isolate the enzymes in a pure state and thus investigate their configuration." Others, most notably P. Ehrlich und F. Lillie, by introduction of the concept of stereocomplementarity into medicine and biology, induced the lock-and-key analogy to become something of a dogma for explaining principal life processes.

Ich halte Lehre und Studium der historischen Entwicklung der Wissenschaft für unentbehrlich.... Unsere Lehrbücher versagen darin.
Richard Willstätter[1]

Emil Fischer's famous lock-and-key analogy for the specifity of enzyme action has provided successive generations of scientists with their mental picture of molecular recognition processes, and, thus has shaped to a marked degree the development not only of organic chemistry, but, by extension to basic life processes, that of biology and medicine as well.

Fischer's seminal paper in which he first used the lock-and-key metaphor appeared in *Berichte der Deutschen Chemischen Gesellschaft* of 1894.[2] Thus, a century has passed away since and accordingly, this provides a unique opportunity to commemorate the 100th anniversary of this most fertile hypothesis—not only for historical purposes or for keeping pivotal facts from oblivion, but for gaining an understanding and appreciation of the creative processes involved, of the thought patterns underlying the fundamental insight, and the constructive reasoning that eventually led to it. A comprehension of these factors appears to be required to get a true measure of the magnitude and significance of Fischer's basic contribution.

Any attempt—after a 100 years—to trace what led Fischer to the lock-and-key analogy, must go back to the state of knowledge and the views pevailing at the time, that is around 1890, and to the scientific school from which Fischer emerged. In 1871, he had entered the University of Bonn, where he attended lectures by A. Kekulé and R. Clausius, yet, in the following year transferred to the University of Strassburg to study with Adolf Baeyer, earning his doctorate with him in 1874 at the age of 22. A year later, while working already independently in Baeyer's laboratory, he accidentally discovered phenylhydrazine[3] which was to become the key reagent for his exploration of the sugars, when, ten years later, he finally applied it to the then existing sugars.[4]

The research school of Adolf Baeyer (1835–1917[5]), from which Fischer emerged—first in Strassburg, and then for 40 years after 1875 at the University of Munich—was a major "forge" of talent. A group photograph[6] of 1878 (Fig. 1)

[*] Prof. Dr. F. W. Lichtenthaler
Institut für Organische Chemie der Technischen Hochschule
Petersenstrasse 22, D-64287 Darmstadt (FRG)
Telefax: Int. code + (6151)166674

[**] Based on a Commemorative Lecture presented at the European Research Conference "Supramolecular Chemistry: 100 Years Schloss-Schlüssel-Prinzip", Mainz, August 12, 1994.



Fig. 1. Photograph of the Baeyer group in early 1878 at the laboratory of the University of Munich (room for combustion analysis), with inscriptions from Fischer's hand [6].

attests to that almost literally: the unusually wide hood in the background is certainly more reminiscent of a forge than of a laboratory. In the center Adolf Baeyer, wearing a prominent hat; since several others also wear headgear, we may deduce that in the winter of 1878 the heating was deficient in that laboratory. To the right of Baeyer the 25-year-old Emil Fischer, in a peaked cap and strikingly self-confident three years after his Ph.D.; to the left Jacob Volhard (1834–1910), who was in charge of the analytical division in Baeyer's institute, and whose successor Fischer was to become in Munich a year later (1879), and at the University of Erlangen in 1882.

Fischer, at Munich, pursued several classical organic research topics: the phenylhydrazones of acetaldehyde, benzaldehyde, and furfural were unequivocally characterized and structurally



Frieder W. Lichtenthaler, born 1932 in Heidelberg, studied chemistry at the University of Heidelberg from 1952–1956 and received his doctorate there in 1959 under F. Cramer for research on enol phosphates. The following three years he spent as a postdoctoral fellow at the University of California, Berkeley, with Hermann O. L. Fischer—the only of Emil Fischer's sons who survived the first World War. He subsequently worked as an assistant at the Technische Hochschule Darmstadt, where he acquired his "Habilitation" in 1963, was appointed associate professor in 1968, and was promoted to full professor in 1972. His research activities center on the generation of enantiopure building blocks from sugars, their utilization in the synthesis of oligosaccharides and complex non-carbohydrate natural products, the computer simulation of chemical and biological properties of sugars, and studies towards the utilization of carbohydrates as organic raw materials.

secured;[7] over a number of years (1876–1880) he did extensive investigations on rosaniline dyes with his cousin Otto Fischer (Fig. 1, far left, sitting),[8] and in 1881 he started work on purines, investigating the structure of caffeine,[9] research that eventually led to his classification of the purines. In 1882 at the age of 30, he moved from Munich to Erlangen, accepting the chair of chemistry at that university, and there he was intensely occupied with the conversion of phenylhydrazine into N-heterocycles,[10] which led to the Fischer indole synthesis.[11] It was in Erlangen in 1884, that is after having left Baeyer's sphere of influence for over two years, that he began his studies on sugars, by reaction of those that were known at the time (glucose, fructose, galactose, maltose, sucrose, and lactose) with phenylhydrazine.[3, 12] The hydrazones and osazones obtained thereby have not only rendered invaluable service for the identification and isolation of the then existing sugars, but also have been instrumental in the preparation of new ones. In 1888 Fischer had moved to the University of Würzburg by then—he discovered a new hexose in this way:[13] gentle oxidation of mannitol with nitric acid gave a mixture which could not be characterized as such, but on exposure to phenylhydrazine afforded a crystalline phenylhydrazone, isomeric with the one generated from glucose (Fig. 2). By the acid hydrolysis of this product, an as yet unknown hexose was obtained, which he named mannose.

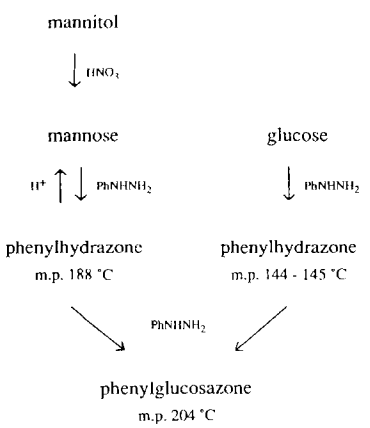


Fig. 2. Synthesis of mannose from mannitol in 1888 [13] soon thereafter to be discovered in nature [16].

It is in this stage of Fischer's purely chemical-synthetic studies of sugars, in the first of four papers with Hirschberger on mannose,[13–15] that we find, rather unpreparedly, the lapidary sentence:[13] "Mannose is avidly fermented by beer yeast at room temperature even in strongly diluted aqueous solution." For Fischer, however, it was not a peculiar, remote thing to incorporate yeast into his investigations, since he had developed a curiosity in yeast fermentation as a youth already – sparked by the entrepreneurship of his father. Laurens Fischer was a successful businessman, and in 1870—Emil was 18 by then—he invested a large amount of money in the foundation of a beer brewery in Dortmund, an enterprise that was later turned into a stock company, the "Dortmunder Aktienbrauerei" of today; Laurens Fischer was chairman of the board for several decades.

In the winter of 1876/1877, Emil Fischer spent three months at the University of Strassburg on Baeyer's suggestion obviously, since he held the position of an assistant at his Munich institute to acquire more expertise in quantitative analysis in the laboratory of Prof. Rose. A delightful passage of Fischer's autobiography elaborates on his encounter with yeast there:[17]

"During the winter semester of 1876/1877 I again was in Strassburg, and there, through Dr. Albert Fitz, a wealthy winegrower from the Palatinate, was introduced to the book of Pasteur "Etudes sur la bière", that had just appeared. Therein, this ingenious researcher had laid down his experiences on the contamination of beer-yeast by other microorganisms and their harmful effect on the quality of the beer. When I reported on this to my father, he urged me to study this subject very thoroughly, which I gladly did since it interested me scientifically. A fine microscope was immediately acquired, and with the help of Dr. Fitz and the botanist Prof. de Bary I made studies on moulds, sprouts, and yeasts, from which I later profited immensely in my investigations of the sugars. For the time being, however, I had to make practical use of this new knowledge.

Accordingly, I moved with my microscope to Dortmund for several weeks, to train the workers of the brewery in the new identification procedures. Presumably, I was the first chemist in Germany who attempted this, and have to admit, that I was met with substantial distrust by the men. They made every effort to lead me astray with false statements on the origin and the quality of the yeast under examination. They became more serious-minded though after I could find out, with the help of the microscope, those yeast types that were spoiled. Yet, I did not succeed in instructing any of the men in the correct use of the microscope."

Through these activities, Fischer obviously had developed a keen interest in the subject, because he remarks: "The chemistry of yeasts interested me so highly, that I certainly would have done own research in this field had I stayed longer in Strassburg."[17]

Seen in this context, it was a quite obvious move for Fischer (Fig. 3) to test whether the newly prepared hexose, of which the



Fig. 3. Emil Fischer (1852–1919) in 1889 [18].

set of reactions summarized in Figure 2 had shown it to be the 2-epimer of glucose, would also be fermented by yeast. Similarly, when racemic sugars became available by his investigations of the formose reaction, it became standard practice to expose them to "ordinary beer yeast" for evaluation of their fermentability. Thus, besides proving that D-mannose indeed formed ethanol on yeast fermentation (Fig. 4),[15] it was estab-

D-mannose	⟶	CO_2 + ethanol	[13,15]
D,L-fructose	⟶	L-fructose	[19,20]
D,L-mannose	⟶	L-mannose	[20]
D,L-glucose	⟶	L-glucose	[21]
D,L-galactose	⟶	L-galactose	[22]
D-gulose	—X⟶		[23]
L-gulose	—X⟶		[24]
D-*manno*-heptose	—X⟶		[25]
D-*gluco*-heptose	—X⟶		[26]

Fig. 4. Fischer's early observations (1888–1892) on the fermentation of sugars with beer yeast [27].

lished that in the case of racemic glucose, mannose, galactose, and fructose, only the D component was devored, allowing the isolation and characterization (as hydrazones and osazones) of the corresponding L-sugars.

The study of the fermentation of these sugars was a by-product of his synthetic work, until, at the end of 1891, he had proceeded so far as to have reached the goal: the relative configurations of the sugars had been unravelled. This proof not only put carbohydrate chemistry on a rational basis but—more importantly for that time—provided unequivocal proof for the validity of the Le Bel–van't Hoff theory of stereoisomerism.[28] It became the basis for the sugar family tree (Fig. 5) as it is—100 years later—in our textbooks today.

The completion of this most remarkable, classic piece of work, accomplished by ingeniously planned organic syntheses and brilliant mathematical reasoning had brought order and clarity to the field. To Fischer it was the incentive for now venturing into topics of much higher complexity, that is into biological phenomena:[29]

> "After the classification of the monosaccharides has essentially been concluded by the establishment of their configurational formulae, it is now obvious to utilize the experiences, which have led to this goal, for the purposes of biological research."

Following the early observations on the fermentability of sugars (Fig. 4), which had more the character of orientative tests than carefully planned experiments, Fischer apparently realized that the ordinary brewer's yeast ("gewöhnliche Brauereihefe") he had been using was not pure, and that therefore the results could be misleading. So he made, together with Hans Thierfelder,[30] a comparative study of natural and synthetic monosaccharides with respect to their behavior towards various families of yeast. This resulted in a landmark paper in the "*Berichte*" of 1894.[31] Fischer, thereby, was in the fortunate position, that his sugar studies had left him with a rich stock of rare sugars—nowhere else in chemistry was such a fine inventory of isomers available—yet some of these were only accessible in small amounts.[31]

> "Since the preparation of the artifical sugars is in part quite laborious and the experiments had to be varied frequently we have used a small fermentation tube of the form shown below to save material" (Fig. 6).

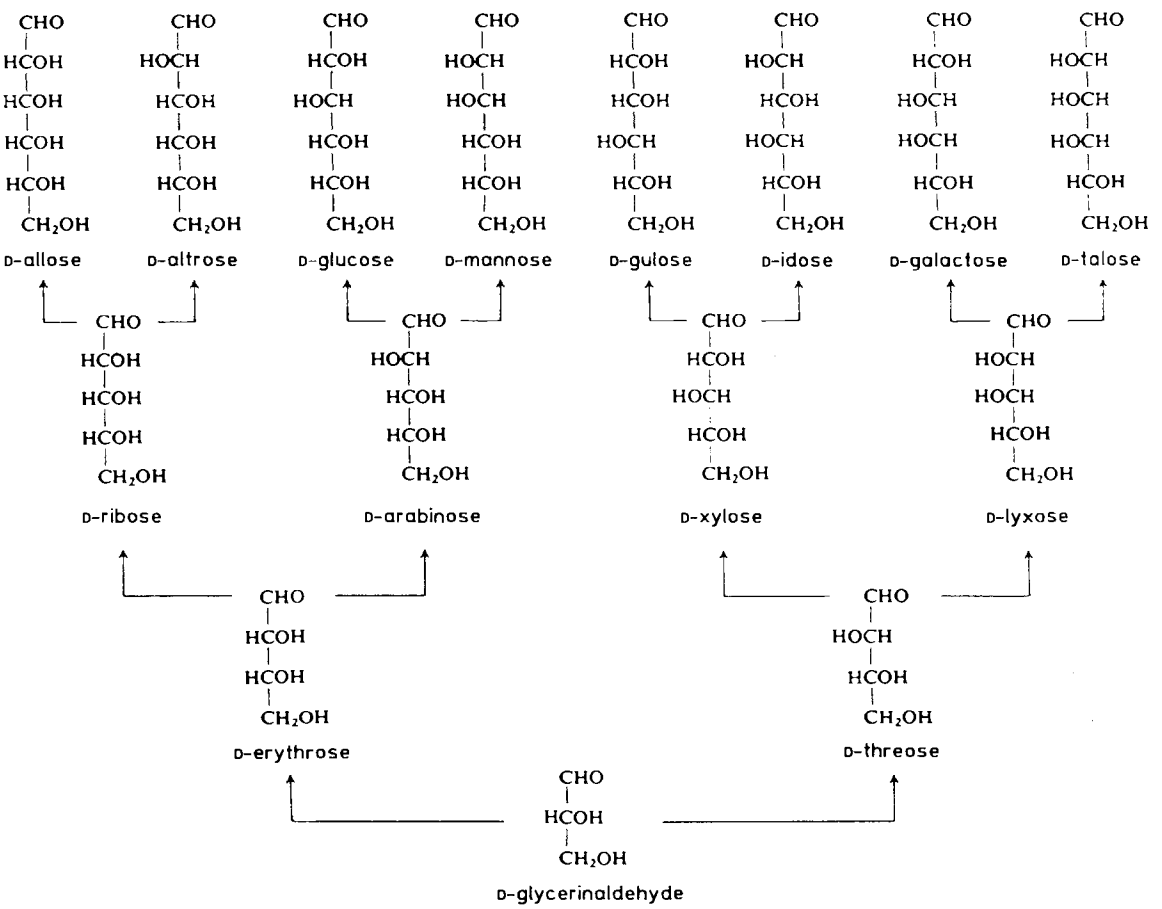


Fig. 5. The sugar family tree of D-aldoses.

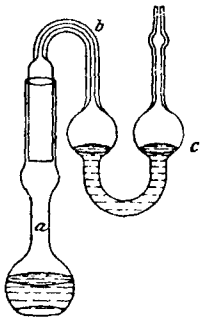


Fig. 6. Semimicro scale assay for the fermentation of sugars by yeasts [31] in original size. a = Fermentation flask, b = S-trap for CO_2 generated, c = aqueous $Ba(OH)_2$. Example: 70 mg sugar in 0.35 mL H_2O, 0.35 mL aqueous yeast abstract; sterilization, addition of 13 mg of a pure yeast species; 3–10 d at 24–28 °C.

This microscale fermentation assay was quite elaborate for the time, allowing one to work with 70 mg of sugar; the bulb holding the sample has a volume of about 1 mL only. It is interesting to perceive today Fischer's keen sense for meticulous observations:[31]

"In all cases, even when the sugar is not fermented, a small amount of carbon dioxide evolves, which covers the surface of the barium hydroxide with a thin layer of carbonate. Since this phenomenon occurs even when no sugar has been added to the solution, it is obviously caused by the small amount of carbohydrate present in the yeast itself or the extract.

The situation is quite different, when the material is readily fermentable: the barium hydroxide is not only becoming strongly turbid, but is neutralized.

Intermediate cases are these, where material has to be brought into a fermentable state first, as with the glucosides; fermentation proceeds slowly ...., yet here too, the amount of carbon dioxide developed is always large enough, that one cannot be in doubt about the real occurrence of fermentation."

Observations of this sort led to the data collected in Scheme 1, a reproduction from the first[31] of four papers to appear on the subject in the second half of 1894:[2, 29, 31, 32] *d*-mannose, *d*-fructose, and, to a lesser extent *d*-galactose resemble *d*-glucose, as does sucrose ("Rohrzucker") and maltose, whilst one of the yeasts ("Milchzuckerhefe") fermented sucrose and lactose ("Milchzucker"), yet left maltose untouched. All of the yeasts were indifferent towards a variety of synthetic sugars.

Fischer seemed to be particularly intrigued by the fact, that *d*-talose, the 2-epimer of galactose, was not fermented (Fig. 7), since he notes:[31]

"*d*-Talose relates configurationally to *d*-galactose as does *d*-mannose to *d*-glucose. As *d*-galactose already ferments less readily than the two others, any further small change in geometry eliminates fermentability altogether."

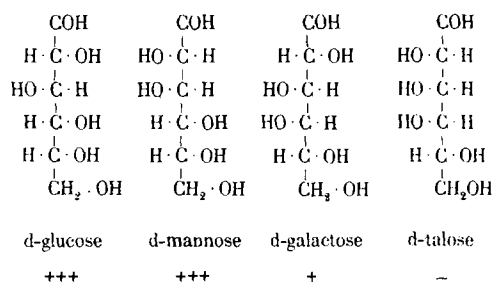


Fig. 7. Fermentability of hexoses by yeast [31].

	d-Mannose	*d*-Fructose	*d*-Galactose	*d*-Talose	*l*-Mannose	*l*-Gulose	Sorbose	*l*-Arabinose	Rhamnose	α-Glucoheptose	α-Glucooctose	Rohrzucker	Maltose	Milchzucker
S. Pastorianus I	†††	†††	†††	–	–	–	–	–	–	–	–	†††	†††	–
S. Pastorianus II	†††	†††	††	–	–		–	–	–	–	–	†††	†††	–
S. Pastorianus III	†††	†††	†††	–	–		–	–	–	–	–	†††	†††	–
S. cerevisiae I	†††	†††	†††	–	–		–	–	–	–	–	†††	†††	–
S. ellipsoideus I	†††	†††	††	–	–		–	–	–	–	–	†††	†††	–
S. ellipsoideus II	†††	†††	†	–	–		–	–	–	–	–	†††	†††	–
S. Marxianus	†††	†††	†††	–	–		–	–	–	–	–	†††	†††	–
S. membranaefaciens	–	–	–	–	–		–	–	–	–	–	–	–	–
Brauereihefe	†††	†††	†††	–	–	–	–	–	–	–	–	†††	†††	–
Brennereihefe	†††	†††	†	–	–	–	–	–	–	–	–	†††	†††	–
S. productivus	†††	†††	–	–	–	–	–	–	–		–	†	†††	–
Milchzuckerhefe	††	†††	†	–	–		–	–	–	–	–	†††	–	†††

††† bedeutet keine Reduktion der Fehlingschen Lösung nach 8 Tagen, also vollständige Vergärung.
†† „ eine ganz schwache Reduktion nach 8 Tagen, also fast vollständige Vergärung.
† „ deutliche Reduktion nach 8 Tagen, aber unzweifelhafte Gärung.
– „ keine Gärung.

Scheme 1. Behavior of sugars towards pure yeasts (from ref. [31]). ††† denotes no reduction of the Fehling's solution after 8 days, thus complete fermentation. †† denotes very weak reduction after 8 days, thus almost complete fermentation. † denotes significant reduction after 8 days, but undoubted fermentation. – denotes no fermentation.

Considerations such as these led to the cautious rationalization, "that the yeast cells with their asymmetrically formed agent are capable of attacking only those sugars of which the geometrical form does not differ too widely from that of *d*-glucose."[31]

On extending this inquiry to natural and artificial glucosides, Fischer found that these materials arrange themselves into distinct groups with respect to their behavior towards air-dried yeast extract and the aqueous extract of bitter almonds ("invertin" and "emulsin", respectively). Although both were later shown to be crude mixtures of enzymes, the former only cleaved α-glucosidic linkages, whereas the other, just as specifically, only hydrolyzed β-glucosides (Table 1).

The second of these four 1894 papers on yeast fermentation carries the unassuming title "influence of the configuration on

Table 1. Fermentability of glycosides [2, 32].

Glycoside	Yeast enzyme (invertin) [a]	Emulsin [b]
methyl-α-D-glucoside	+	–
ethyl-α-D-glucoside	+	–
saccharose	+	–
maltose	+	–
methyl-α-L-glucoside	–	–
methyl-α-D-mannoside	–	–
methyl-α-D-galactoside	–	–
ethyl-α-D-galactoside	–	–
methyl-β-D-glucoside	–	+
phenyl-β-D-glucoside	–	+
methyl-β-D-galactoside	–	+
lactose	–	+

[a] Aqueous extract of air-dried beer yeast (*Saccharomyces cerevisiae*, type Frohberg). [b] Aqueous extract of bitter almonds.

545. Emil Fischer: Einfluss der Configuration auf die Wirkung der Enzyme.

[Aus dem I. Berliner Universitäts-Laboratorium.]
(Vorgetragen in der Sitzung vom Verfasser.)

Das verschiedene Verhalten der stereoisomeren Hexosen gegen Hefe hat Thierfelder und mich zu der Hypothese geführt, dass die activen chemischen Agentien der Hefezelle nur in diejenigen Zucker eingreifen können, mit denen sie eine verwandte Configuration besitzen[1]).

Diese stereochemische Auffassung des Gährprocesses musste an Wahrscheinlichkeit gewinnen, wenn es möglich war, ähnliche Verschiedenheiten auch bei den vom Organismus abtrennbaren Fermenten, den sogenannten Enzymen, festzustellen.

Das ist mir nun in unzweideutiger Weise zunächst für zwei glucosidspaltende Enzyme, das Invertin und Emulsin, gelungen. Das Mittel dazu boten die künstlichen Glucoside, welche nach dem von mir aufgefundenen Verfahren aus den verschiedenen Zuckern und den Alkoholen in grosser Zahl bereitet werden können[1]). Zum Vergleich wurden aber auch mehrere natürliche Producte der aromatischen Reihe und ebenso einige Polysaccharide, welche ich als die Glucoside der Zucker selbst betrachte, in den Kreis der Untersuchung gezogen. Das Ergebniss derselben lässt sich in den Satz zusammenfassen, dass die Wirkung der beiden Enzyme in auffallender Weise von der Configuration des Glucosidmoleküls abhängig ist.

Versuche mit Invertin.

Das Enzym lässt sich bekanntlich aus der Bierhefe mit Wasser auslaugen und soll aus der Lösung durch Alkohol unverändert gefällt werden. Aus den später angeführten Gründen habe ich auf die Isolirung desselben verzichtet. Die nachfolgenden Versuche sind vielmehr direct mit einer klar filtrirten Lösung angestellt, welche durch 15stündige Digestion von 1 Theil lufttrockener Bierhefe (Saccharomyces cerevisiae, Typus Frohberg, Reincultur) mit 15 Theilen Wasser bei 30—35° bereitet war.

[1]) Diese Berichte **27**, 2036.

Fig. 8. Title page of the second [2] of Fischer's four landmark papers in 1894 on the influence of the configuration on the action of enzymes.

the action of enzymes" (Fig. 8), reporting some of these results in a very sober, purely scientific diction.[2] Towards the end—as usually found in the majority of Fischer's publications—he gives clear indications on what he is to do next: incorporation of other enzymes into the study, such as glucase, ptyalin, myrosin, and the ferments of pancreas, and their extension to the rare oligosaccharides, as for example isomaltose, turanose, melibiose and melitriose (Fig. 9). Then, very much towards the end of this paper, in the coda quasi, in musical terms, Fischer tries to sum up and rationalize the observations available. The resulting section contains the crucial metaphor:

> "The restricted action of the enzymes on glucosides may therefore be explained by the assumption that only in the case of similar geometrical structure can the molecules so closely approach each other as to initiate a chemical action. To use a picture I would like to say that enzyme and glucoside have to fit together like lock and key in order to exert a chemical effect on each other. The finding that the activity of enzymes is limited by molecular geometry to so marked a degree, should be of some use in physiological research. Still more important though appears to me the proof, that the previously assumed difference between the chemical activity of a cell and the mode of action of chemical reagents is, factually, non-existent."[2]

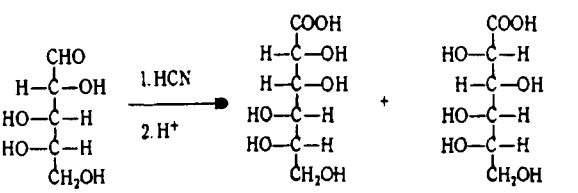
Emil Fischer left many contributions of great brilliance in the annals of science:

- the unravelment of the sugar configurations as the classical piece of exact mathematical reasoning in any experimental science[12]
- the classification of purines[33] and the synthesis of the first nucleosides[34]
- the laying of the chemical and biological foundation of protein chemistry by his extensive work on amino acids, peptides, and proteins,[35]
- the first unifying concept on the structures of the complex natural products depsides and tannins.[36]

But here, an analogy, a metaphor, almost casually thrown in at the end of a paper, develops a life of its own, to become one of the most frequently invoked concepts of the past 100 years. Apparently, the lock-and-key analogy met a conceptual need of the time, for within a very short period it formed an interface between chemistry, biology, and medicine—very much to the surprise of Fischer himself, since he did not expound on it. Particularly, he refrained from going any further—at least in print—although I am sure, in his thoughts, he must have taken this picture to the obvious questions, what turns the key, and what kind of doors are then opened. The only extension to be found in print, in an extensive 43-page review on his investigations on sugars of 1894, is a small refinement:[29]

> "The action of enzymes involves a far-reaching chemical process which takes place readily or not at all. Here, apparently, the geometrical structure exerts such a profound influence on the playing of the chemical affinities, that it appeared legitimate to me to compare the interacting molecules with key and lock.
> If one wants to do justice to the fact, that some yeasts can ferment a larger number of hexoses than others the picture may be completed by the differentiation of main key and special keys."

It was obvious to apply the concept of lock-and-key complementarity to the question of asymmetric synthesis in plants, most notably to the process of assimilation. Along the way of the gradually unfolding interrelationships between the sugars, Fischer, in 1889, had made another key discovery that was to have major bearing on biological questions. He uncovered the phenomenon of asymmetric synthesis:[37] the cyanohydrin extension of natural L-arabinose does not only give L-mannonic acid on hydrolysis, as Kiliani had previously shown,[38] but a second product, the 2-epimeric L-gluconic acid, as evidenced by their distinctly different, well-crystallizing phenylhydrazides:



L-arabinose L-mannonic acid L-gluconic acid

2992

von Leuchtbacterien beweisen will, ist wohl geeignet, ernste Bedenken gegen die Zuverlässigkeit des Resultats zu erwecken. In der That ist denn auch Beyerinck's Ansicht von Schnurmans Stekhoven [1]) sehr bestimmt bestritten worden. Letzterer kommt vielmehr zu dem Schluss, dass das Enzym der Kefirhefe zwar den Rohrzucker und die Raffinose, aber nicht den Milchzucker zerlege. Die Frage, wer hier Recht hat, lässt sich leicht entscheiden, wenn man den Versuch mit reiner Kefirhefe so anstellt, wie er oben für die Kefirkörner beschrieben ist. Ich werde denselben ausführen, so bald mir eine genügende Menge der Hefe zur Verfügung steht.

Ferner beabsichtige ich, noch einige verwandte Enzyme, wie die Glucase, das Ptyalin, Myrosin und die Pancreasfermente zum Vergleiche heranzuziehen und die Versuche auch auf die selteneren Polysaccharide, wie Isomaltose, Turanose, Melibiose, Melitriose, Trehalose, Melezitose, die künstlichen Dextrine etc. zu übertragen. Zweifellos werden sich dann noch mehr solcher Gegensätze zeigen, wie sie zwischen dem Invertin und Emulsin jetzt festgestellt sind.

Aber schon genügen die Beobachtungen, um principiell zu beweisen, dass die Enzyme bezüglich der Configuration ihrer Angriffsobjecte ebenso wählerisch sind, wie die Hefe und andere Mikroorganismen. Die Analogie beider Phänomene erscheint in diesem Punkte so vollkommen, dass man für sie die gleiche Ursache annehmen darf, und damit kehre ich zu der vorher erwähnten Hypothese von Thierfelder und mir zurück. Invertin und Emulsin haben bekanntlich manche Aehnlichkeit mit den Proteïnstoffen und besitzen wie jene unzweifelhaft ein asymmetrisch gebautes Molekül. Ihre beschränkte Wirkung auf die Glucoside liesse sich also auch durch die Annahme erklären, dass nur bei ähnlichem geometrischem Bau diejenige Annäherung der Moleküle stattfinden kann, welche zur Auslösung des chemischen Vorganges erforderlich ist. Um ein Bild zu gebrauchen, will ich sagen, dass Enzym und Glucosid wie Schloss und Schlüssel zu einander passen müssen, um eine chemische Wirkung auf einander ausüben zu können. Diese Vorstellung hat jedenfalls an Wahrscheinlichkeit und an Werth für die stereochemische Forschung gewonnen, nachdem die Erscheinung selbst aus dem biologischen auf das rein chemische Gebiet verlegt ist. Sie bildet eine Erweiterung der Theorie der Asymmetrie, ohne aber eine directe Consequenz derselben zu sein; denn die Ueberzeugung, dass der geometrische Bau des Moleküls selbst bei Spiegelbildformen einen so grossen Einfluss auf das Spiel der chemischen Affinitäten ausübe, konnte meiner Ansicht nach nur durch neue thatsächliche Beobachtungen gewonnen werden. Die bis-

[1]) Koch's Jahresbericht über Gährungsorganismen 1891, 136.

2993

herige Erfahrung, dass die aus zwei asymmetrischen Componenten gebildeten Salze sich durch Löslichkeit und Schmelzpunkt unterscheiden können, genügte dafür sicher nicht. Dass man die zunächst nur für die complicirten Enzyme festgestellte Thatsache bald auch bei einfacheren asymmetrischen Agentien finden wird, bezweifle ich ebensowenig wie die Brauchbarkeit der Enzyme für die Ermittlung der Configuration asymmetrischer Substanzen.

Die Erfahrung, dass die Wirksamkeit der Enzyme in so hohem Grade durch die moleculare Geometrie beschränkt ist, dürfte auch der physiologischen Forschung einigen Nutzen bringen. Noch wichtiger für dieselbe aber scheint mir der Nachweis zu sein, dass der früher vielfach angenommene Unterschied zwischen der chemischen Thätigkeit der lebenden Zelle und der Wirkung der chemischen Agentien in Bezug auf moleculare Asymmetrie thatsächlich nicht besteht. Dadurch wird insbesondere die von Berzelius, Liebig u. A. so häufig betonte Analogie der »lebenden und leblosen Fermente« in einem nicht unwesentlichen Punkte wieder hergestellt. —

Bei der Ausführung obiger Versuche habe ich mich der eifrigen und geschickten Beihülfe des Hrn. Dr. Paul Rehländer erfreut. Ferner bin ich für die Ueberlassung von reingezüchteten Hefen den HH. Dr. H. Thierfelder, Prof. M. Delbrück und Dr. O. Reinke zu grossem Danke verpflichtet.

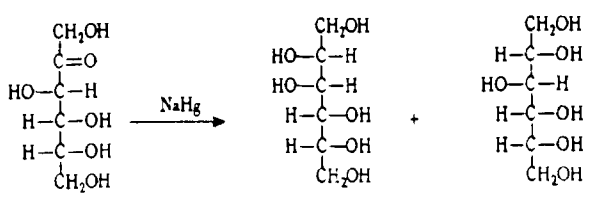
Fig. 9. Final section of Fischer's seminal 1894 paper [2] in which the lock-and-key metaphor was first used.

As it turned out, this is the first example of an asymmetric synthesis recorded in the literature, on which Fischer commented in the following way:[39]

"The simultaneous formation of the two stereoisomeric products on the addition of hydrogen cyanide to aldehydes, which was observed here for the first time, is quite remarkable in theory as well as in practice."

This first example of an asymmetric synthesis was soon to be followed by a second case, since sodium amalgam reduction of D-fructose gave rise to two stereoisomeric products, namely D-mannitol and D-sorbitol.[40] Fischer clearly realized the basic importance of this result:

"The reduction of fructose is the second reaction in the sugar group, which generates two stereoisomeric products due to the formation of an asymmetric carbon atom. The same phenomenon will undoubtedly be observed much more frequently in the future, and most probably will be generally found with all compounds that are asymmetric a priori."



D-fructose D-mannitol D-sorbitol

Four years later, in one of these 1894 papers,[29] the biological significance of these sober chemical findings had been fully realized and applied to assimilation by invoking the lock-and-key concept:

"It seems to me that this concept offers a simple solution for the enigma of natural asymmetric synthesis. According to the plant physiologists, carbohydrate formation takes place in the chlorophyll granule, which itself consists entirely of optically active substances. I can imagine that the formation of carbohydrates is preceeded by the generation of a compound

of carbonic acid or formaldehyde with those substances; and that then, due to the already existing asymmetry of the entire molecule, the condensation to the sugars takes place in an asymmetric fashion too.
Their asymmetry can thus be readily explained by the nature of the material from which they were produced. Of course, they also provide the material for new chlorophyll granules which, in turn, produce active sugar. In this manner, the optical activity propagates from molecule to molecule, as life itself does from cell to cell. Hence, it is not necessary to attribute the formation of optically active substances in the plant to asymmetric forces outside the organism, as Pasteur had supposed. The origin rather lies in the structure of the chlorophyll granule that generates the sugar, and with this conception the difference between natural and artificial synthesis is completely eliminated."

In a lecture of 1894 on "The chemistry of carbohydrates and their importance for physiology" he again advocated this view in more general form:[41]

"Whoever wants to conclusively elucidate the process of assimilation, will have to tackle the more special question, why the plant exclusively generates optically active sugar whilst chemical synthesis leads to the inactive products. This contrast appeared so fundamental to Pasteur, who created the precept of molecular asymmetry, that he considered the generation of active substances to be a privilege of the organism. The progress of science has deprived the highly respected lifeforce of even this last hiding-place; for we are now in a position to artificially prepare such active substances without any assistance from a living organism."

With these words, Fischer had clearly repudiated the accepted view of the time—asserted by Pasteur—that fermentation is inextricably tied to living cells, wherein a "vis vitalis" was supposedly operating. Eduard Buchner is usually credited to have demonstrated in 1897[42] that fermentation can occur outside living cells, thus unequivocally refuting Pasteur's view. The above passage of Fischer in 1894 proves, that he had arrived at this conclusion already three years earlier.

In 1894, when Fischer first used the lock-and-key analogy to illustrate enzyme specifity, he was 42. He lived for another 25 years, during which time he published the imposing number of over 400 further papers.[43] However, he referred to the lock-and-key concept only in another three: in his Nobel lecture in 1902, rather incidentally,[44] in his Faraday lecture at the University of London in 1907,[45] also quite cursorily, and, at the end of an extensive, 28-page review of 1898, with the momentous title "Significance of Stereochemistry for Physiology." Therein,[46] Fischer apparently felt that he had to state the scope of the analogy he had proposed, because others were taking it too far:

"The reasons for these phenomena are in all probability to be found in the asymmetric structure of the enzyme molecule. Although one does not know these substances in a pure state, their similarity with proteins is so close and their generation from these so probable, that they have undoubtedly to be considered as optically active, and, hence, asymmetric molecular forms.
This had led to the hypothesis, that there must be a similarity in the molecular configuration between the enzymes and their object of attack, if reaction is to take place. To make this thought more perspicuous, I have used the picture of lock and key.
I am far from placing this hypothesis side by side to the established theories of our science, and readily admit, that it can only be thoroughly tested, when we are able to isolate the enzymes in a pure state and thus investigate their configuration."[46]

Paul Ehrlich, for example, from 1897 on, introduced the lock-and-key complementarity into the then young discipline of immunology through his so-called "side chain theory of immunity", as illustrated in a publication from 1900[47] (Fig. 10): each cell possesses a number of side chains, which bind toxins in a lock-and-key type manner. The binding of such toxins causes the overproliferation of that particular side chain some of which are set free from the cells as antibodies. In the case of diseases that leave immunity there are so many free "side chains" (antibodies) in the blood that appreciable fixations at the cell cannot occur.

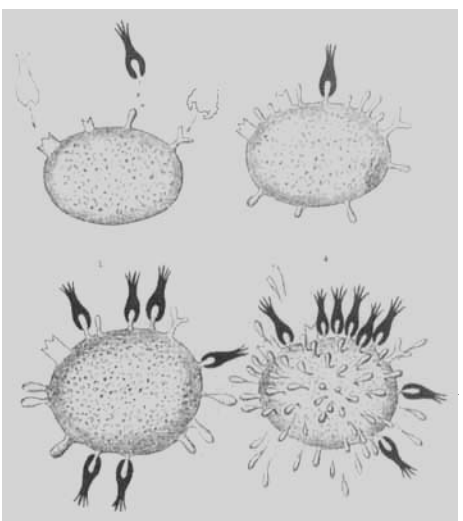


Fig. 10. Ehrlich's side chain theory of immunity as illustrated in 1900 [47].

The lock-and-key complementarity also gained headway in embryology, particularly from 1914 on, when Lillie, at the University of Chicago, invoked it to describe recognition between sperm and cells.[48] He crystallized his ideas on the interaction of the components involved into an explicit lock-and-key diagram (Fig. 11), a dangerously elaborate concept in view of the few secure experimental data available then.

Accordingly, Ehrlich had brought stereocomplementarity from the realm of chemical reactions in solution to reactions on the cell surface, whilst Lillie and others[49] extended it to cell–cell interactions. So, the first two decades following Fischer's use of the lock-and-key analogy saw a rather free, uncontrolled proliferation of the concept from chemistry into medicine and biology—and, along the way, its use became more and more speculative.

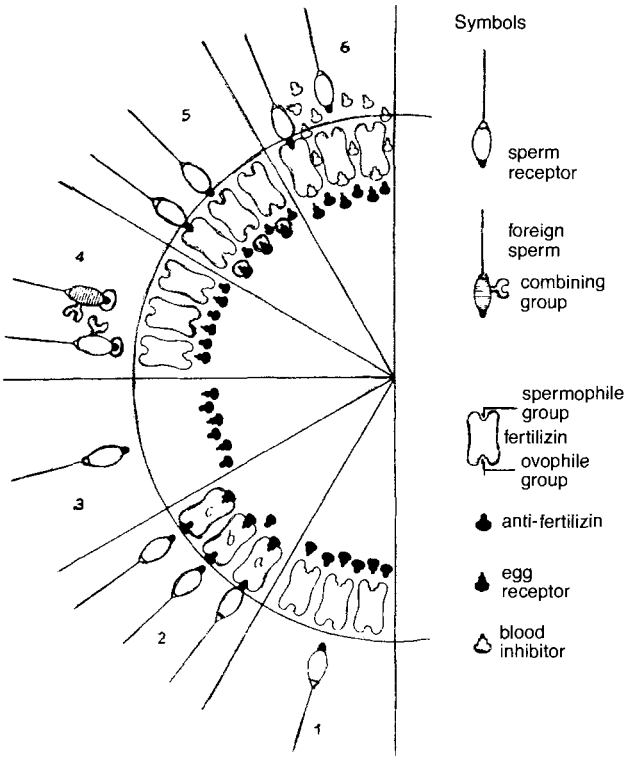


Fig. 11. Lillie's theory of fertilization as diagrammed in 1914 [48]: segment 1 shows the situation before fertilization; in segment 2, the sperm receptor binds to the spermophile group of "fertilizin", activating the ovophile group to bind to the egg receptor. Molecules of antifertilizin combine competitively with this site on other fertilizin molecules to forbid the binding of other sperm. The other segments refer to experiments not relevant to the discussion here.

The passage of time corrects many a distortion of perspective. Both theories survived only insofar as they allowed recognition of the complex relationship in very general terms, and hence, had a favorable influence on the concretization of research activities. Wherever they were used for too detailed analyses, they failed, obviously because the ground of scientifically established facts was left too far behind in the quest to explain phenomena much too complex as to yield to rationalization or comprehension at the time.

Unlike these theories from Ehrlich, Lillie, and others along similar veins,[49] Fischer's lock-and-key analogy still stands in the annals of science—a 100 years later—as a most fertile concept. Maybe, because it was unspecified in its details, thus leaving ample room for the imagination of chemists, biologists, and medical researchers alike.

Fischer had an unfailing intuitive perception for identifying important areas of research in organic chemistry and brought unsurpassed creativity to the conception of experiments and their skilful execution. The most striking feature of Fischer's scientific personality may be found in his pronounced tendency against any sort of theoretical speculation. Two instances may document this attitude further, one concerning the Walden inversion, to which Fischer had contributed[50] and which was controversially discussed around 1912. In a letter to T. W. Richards,[51] Fischer writes:

"I do not derive much pleasure from theoretical things. The occupation with the Walden inversion was rather a digression and recuperation from the extensive work on proteins. Moreover, so many limited heads have now jumped on this question, that the delight thereon is spoiled completely."

The second example refers to the question still open around 1914 on the ring sizes of the fructose and glucose portions of sucrose (formulations see Fig. 12), and how these sugars are

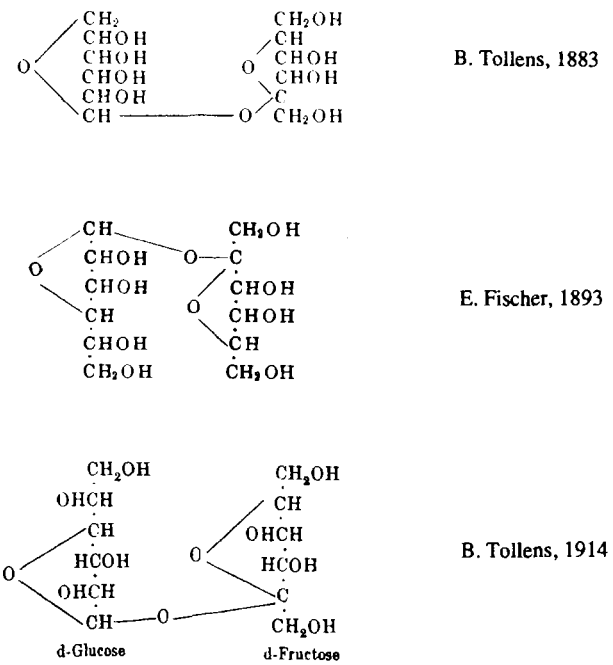


Fig. 12. Structural representations of sucrose by Tollens [53, 55] and Fischer [54].

linked. Fischer clearly states his position,[52] which may rightfully be extended to the lock-and-key picture:

"We know nothing definite on the mode, how the fructose residue is linked in cane sugar, thus leaving huge room for speculation. I, however, gladly renounce to use it."

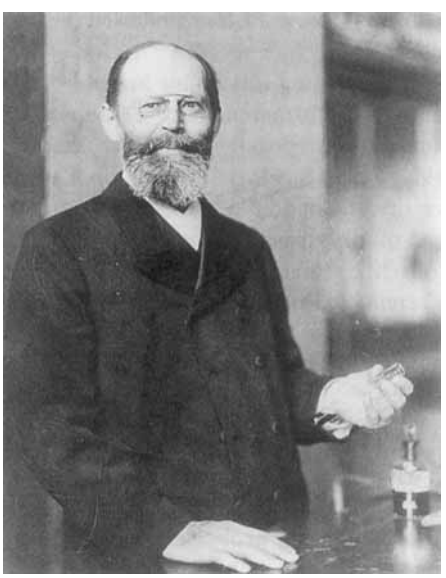


Fig. 13. Emil Fischer around the turn of the century.

In concluding this centennial tribute to one of the really great figures of our science (Figs. 13, 14) and to the lock-and-key concept with which he had a major influence on interrelating chemistry, biology, and medicine, I would like to cite a passage from his 1907 Faraday lecture at the University of London, entitled "Synthetic Chemistry in Relation to Biology", in which he clearly states his conviction to give in one's theoretical reasonings expression only to observed facts:[45]

> "The separation of organic chemistry from biology was necessary during the past century while experimental methods were being elaborated; now, that our science is provided with a powerful armory of analytical and synthetical weapons, chemists can once more renew the alliance both to its own honor and to the advantage of biology. The prospect of obtaining a clearer insight into the wondrous series of processes which constitute animal and vegetable life may well lead organic chemistry and biology to work with definite purpose to a common end.
> In order, as far as possible, to avoid mistakes in this difficult task and to shield ourselves from the disappointment which is the inevitable consequence of exaggerated hopes, we cannot do better than strive to imitate the great example of Faraday, who always, with rare acumen, directed his attention to actual phenomena without allowing himself to be influenced by preconceived opinion, and who in his theoretical conceptions gave expression only to observed facts."

This attitude with respect to the interpretation of experimental results applies to our science today as much as it did a 100 years ago. Especially in the field of molecular recognition which is in a very active phase of its development, we should comply with it most rigorously, as it gives us an unfailing measure of how far we should go with our interpretations today, and what we should leave for the next 100 years.



Fig. 14. Emil Fischer around 1910 in his laboratory at the University of Berlin [6].

Received: August 25, 1994 [A 80 IE]
German version: *Angew. Chem.* **1994**, *106*, 2456

[1] R. Willstätter, *Aus meinem Leben*, Verlag Chemie, Weinheim, 1973, p. 324. "I consider the teaching and study of the historical development of science as essential. Our textbooks fail in this respect."
[2] E. Fischer, *Ber. Dtsch. Chem. Ges.* **1894**, *27*, 2985–2993.
[3] E. Fischer, *Ber. Dtsch. Chem. Ges.* **1875**, *8*, 589–599; G. B. Kauffman, R. P. Ciula, *J. Chem. Educ.* **1977**, *54*, 295.
[4] E. Fischer, *Ber. Dtsch. Chem. Ges.* **1884**, *17*, 579–584.
[5] R. Huisgen, *Angew. Chem.* **1986**, *98*, 297–311; *Angew. Chem. Int. Ed. Engl.* **1986**, *25*, 297–311.
[6] a) The original and numerous other photographs are contained in the Collection of Emil Fischer Papers, housed in the Bancroft Library at the University of California, Berkeley. This scientific bequest consists of 34 boxes of material: lab notes, manuscripts, drafts of his autobiography "Aus meinem Leben", and about 5000 letters, that reached Fischer during his 40-year scientific career; for example, 157 letters during 1889–1915 from his teacher A. von Baeyer, others from F. Beilstein (11), A. Hantsch (56), F. Haber (35), J. H. van't Hoff (31), A. W. Hofmann (5), A. von Kekulé (6), H. Kiliani (16), V. Meyer (46), W. Nernst (67), B. Tollens (20), P. Walden (13), O. Wallach (46), and R. Willstätter (33); Fischer's intense interaction with industry is documented by 181 letters from C. Duisberg (from 1895–1919), from Bayer (271), BASF (54), Boehringer Mannheim (116), Hoechst (50), and Merck (33). The papers eventually reached Berkeley through Fischer's son, Hermann Otto Laurens Fischer [6b] who carried this collection through all the stations of his unusually cosmopolitan career: Privatdozent in Berlin, Professor of Pharmaceutical Chemistry in Basel, Director of the Banting Institute, Toronto, and Professor of Biochemistry at the University of California Berkeley; b) F. W. Lichtenthaler, *Carbohydr. Res.* **1987**, *164*, 1–22.
[7] E. Fischer, *Ber. Dtsch. Chem. Ges.* **1876**, *9*, 880–891; *Justus Liebigs Ann. Chem.* **1878**, *190*, 184–188.
[8] E. Fischer, O. Fischer, *Ber. Dtsch. Chem. Ges.* **1876**, *9*, 891–900; *Justus Liebigs Ann. Chem.* **1878**, *194*, 242–303; *Ber. Dtsch. Chem. Ges.* **1880**, *13*, 2204–2207.
[9] E. Fischer, *Ber. Dtsch. Chem. Ges.* **1881**, *14*, 637–644, 1905–1915; *ibid.* **1882**, *15*, 29–33, 453–456; *Justus Liebigs Ann. Chem.* **1882**, *215*, 253–320.
[10] E. Fischer, F. Jourdan, *Ber. Dtsch. Chem. Ges.* **1883**, *16*, 2241–2245; E. Fischer, O. Hess, *ibid.* **1884**, *17*, 559–568; E. Fischer, *Justus Liebigs Ann. Chem.* **1886**, *236*, 116–126.
[11] P. A. Roussel, *J. Chem. Educ.* **1953**, *30*, 122–125; B. Robinson, *Chem. Rev.* **1963**, *63*, 373–401.
[12] "Emil Fischer's Proof of the Configuration of Sugars: A Centennial Tribute": F. W. Lichtenthaler, *Angew. Chem.* **1992**, *104*, 1577–1593; *Angew. Chem. Int. Ed. Engl.* **1992**, *31*, 1541–1556.
[13] E. Fischer, J. Hirschberger, *Ber. Dtsch. Chem. Ges.* **1888**, *21*, 1805–1809.
[14] E. Fischer, J. Hirschberger, *Ber. Dtsch. Chem. Ges.* **1889**, *22*, 365–376, 1155–1156.
[15] E. Fischer, J. Hirschberger, *Ber. Dtsch. Chem. Ges.* **1889**, *22*, 3218–3224.
[16] R. Gans, W. E. Stone, B. Tollens, *Ber. Dtsch. Chem. Ges.* **1888**, *21*, 2148–2152; R. Gans, B. Tollens, *Justus Liebigs Ann. Chem.* **1888**, *249*, 245–257; R. Reiss, *Ber. Dtsch. Chem. Ges.* **1889**, *22*, 609–613.
[17] E. Fischer, *Aus meinem Leben*, Springer, Berlin, **1987**, pp. 18–20 and 70. (Reprint of the original 1922 version, edited by M. Bergmann, with an English commentary by B. Witkop).
[18] Picture from the congratulatory album of photographs presented to August von Kekulé on the occasion of his 60th birthday (September 6, 1889). The original document is in the collection of Kekulé papers, in the Institut für Organische Chemie, Technische Hochschule Darmstadt.
[19] E. Fischer, J. Tafel, *Ber. Dtsch. Chem. Ges.* **1889**, *22*, 97–101.
[20] E. Fischer, *Ber. Dtsch. Chem. Ges.* **1890**, *23*, 370–394.
[21] E. Fischer, *Ber. Dtsch. Chem. Ges.* **1890**, *23*, 2611–2624.
[22] E. Fischer, J. Hertz, *Ber. Dtsch. Chem. Ges.* **1892**, *25*, 1247–1261.
[23] E. Fischer, R. Stahel, *Ber. Dtsch. Chem. Ges.* **1891**, *24*, 528–539.
[24] E. Fischer, O. Piloty, *Ber. Dtsch. Chem. Ges.* **1891**, *24*, 521–527.
[25] E. Fischer, F. Passmore, *Ber. Dtsch. Chem. Ges.* **1890**, *23*, 2226–2239.

[26] E. Fischer, *Justus Liebigs Ann. Chem.* **1892**, *270*, 64–107.
[27] a) In the Figures 4 and 5 the affiliation of the individual sugars to the D- or L-series has already been made. It should be noted though, that Fischer only introduced the symbols *d* and *l* as late as 1890 [27b] (cf. Scheme 1 and Fig. 7), deriving their meaning from the sign of rotation. Rosanoff in 1906 [27c], and Wohl and Freudenberg in 1923 [27d] brought the use of the *d* and *l* symbols on a logical, genetic basis by selecting the enantiomeric glyceraldehydes as points of reference, such that any sugar belongs to the *d*-series, if it can be derived from *d*-glyceraldehyde by successive Kiliani-Fischer syntheses. The present use of the D- and L-notation [27e] started around 1940; b) E. Fischer, *Ber. Dtsch. Chem. Ges.* **1890**, *23*, 370–394; c) M. A. Rosanoff, *J. Am. Chem. Soc.* **1906**, *28*, 114–121; d) A. Wohl, K. Freudenberg, *Ber. Dtsch. Chem. Ges.* **1923**, *56*, 309–313; e) Rules of Carbohydrate Nomenclature, No. 4 and 5 in *The Carbohydrates, Vol. IIB* (Eds.: W. Pigman, D. Horton), Academic Press, New York, **1970**, p. 809ff.
[28] Aside of ref. [12], there are several pertinent accounts of Fischer's conquest of the sugar configurations, for example C. S. Hudson, "Emil Fischer's Discovery of the Configuration of Glucose", *J. Chem. Educ.* **1941**, *18*, 353–357; "Emil Fischer and His Contribution to Carbohydrate Chemistry". K. Freudenberg, *Adv. Carbohydr. Chem.* **1966**, *21*, 1–38.
[29] E. Fischer, *Ber. Dtsch. Chem. Ges.* **1894**, *27*, 3189–3232; quotation from p. 3228.
[30] Hans Thierfelder (1858–1930) earned his doctorate (Dr. med.) at the University of Rostock (1884), then joined Hoppe-Seyler's group at the University of Strassburg, where he habilitated in 1887 with work on the chemistry and metabolism of glucuronic acid. With Hoppe-Seyler he coedited the 6th edition of the "*Handbuch der physiologisch- und pathologisch-chemischen-Analyse*" (1893). In 1891, he accepted a position at the hygienic institute of the University of Berlin, where he came into contact with Emil Fischer, that eventually led to the joint work on the yeasts [31]. From 1909 on, Thierfelder was professor of physiological chemistry at the University of Tübingen. For a biographical memoir, see: E. Klenk, *Z. Physiol. Chem.* **1931**, *203*, 1–9.
[31] E. Fischer, H. Thierfelder, *Ber. Dtsch. Chem. Ges.* **1894**, *27*, 2031–2037.
[32] E. Fischer, *Ber. Dtsch. Chem. Ges.* **1894**, *27*, 3479–3483.
[33] E. Fischer, *Untersuchungen in der Puringruppe (1882–1906)*, Springer, Berlin, **1907**.
[34] E. Fischer, B. Helferich, *Ber. Dtsch. Chem. Ges.* **1914**, *47*, 210–235.
[35] E. Fischer, *Untersuchungen über Aminosäuren, Polypeptide und Proteine I (1899–1906)*, Springer, Berlin, **1906**; *II (1907–1919)* (Ed.: M. Bergmann), Springer, Berlin, **1923**.
[36] E. Fischer, *Untersuchungen über Depside und Gerbstoffe (1908–1919)*, Springer, Berlin, **1921**, 524 pages.
[37] E. Fischer, F. Passmore, *Ber. Dtsch. Chem. Ges.* **1889**, *22*, 2728–2736; E. Fischer, *ibid.* **1890**, *23*, 2611–2624.
[38] H. Kiliani, *Ber. Dtsch. Chem. Ges.* **1885**, *18*, 3068–3072; **1886**, *19*, 211–227.
[39] E. Fischer, *Ber. Dtsch. Chem. Ges.* **1890**, *23*, 2114–2141; quotation from p. 2134.
[40] E. Fischer, *Ber. Dtsch. Chem. Ges.* **1890**, *23*, 3684–3687.
[41] E. Fischer, Lecture given on August 2, 1894 in Berlin, on the occasion of the foundation day of the School of Military Physicians, A. Hirschwald Verlag, Berlin **1894**, 1–36; quotation from p. 30.
[42] E. Buchner, R. Rapp, *Ber. Dtsch. Chem. Ges.* **1897**, *30*, 2668–2678.
[43] a) Fischer, from about 1896 on, shifted his main research efforts to the systematic exploitation of peptides [35], purines [33], and tannins [36]. Yet he retained a keen interest in sugars [43b] and their action with enzymes; his last two papers [43c], received by the editorial office of *Hoppe-Seyler's Zeitschrift für physiologische Chemie* on July 14, 1919, the day of his death, dealt with sugars, the former being entitled "Einfluss der Struktur der β-Glukoside auf die Wirkung des Emulsins." b) E. Fischer, *Untersuchungen über Kohlenhydrate und Fermente II* (1908–1919), Springer, Berlin, **1922**, 543 pages; c) E. Fischer, *Hoppe-Seyler's Z. Physiol. Chem.* **1919**, *107*, 176–202; *ibid.* **1919**, *108*, 3–8.
[44] *Nobel Lectures Including Presentation Speeches and Laureates Biographies, Chemistry, 1901–1921* (Ed.: Nobel Foundation), Elsevier, Amsterdam, **1966**, pp. 15–39.
[45] E. Fischer, Faraday Lecture on "Synthetical Chemistry in its Relation to Biology", *J. Chem. Soc. (London)* **1907**, *91*, 1747–1765.
[46] "Bedeutung der Stereochemie für die Physiologie": E. Fischer, *Hoppe-Seyler's Z. Physiol. Chem.* **1898**, *26*, 60–87; quotation from p. 82/83.
[47] "On Immunity, with Special Reference to Cell Life": P. Ehrlich, *Proc. R. Soc. London*, **1900**, *66*, 424–448; quotation from p. 433.
[48] "The Mechanism of Fertilization in Arbacia": F. R. Lillie, *J. Exp. Zool.* **1914**, *16*, 523–590.
[49] "Intellectual Traditions in the Life Sciences: Stereocomplementarity": S. F. Gilbert, J. P. Greenberg, *Persp. Biol Med.* **1984**, *28*, 18–34.
[50] E. Fischer, *Justus Liebigs Ann. Chem.* **1911**, *381*, 123–141; *ibid.* **1911**, *386*, 374–386; *ibid.* **1912**, 350–362.
[51] Letter dated November 11, 1912, to Theodore William Richards (1868–1928), professor at Harvard University. Richards did postdoctoral work with W. Ostwald in Leipzig, and in 1907 had an exchange professorship at Fischer's institute at the University of Berlin. In the Emil Fischer papers at the Bancroft Library, Berkeley, CA, there are 39 letters by Richards dated 1905–1915 (originals) and the responses by Fischer (copies).
[52] E. Fischer, *Ber. Dtsch. Chem. Ges.* **1914**, *47*, 1980–1989; quotation from p. 1984.
[53] B. Tollens, *Ber. Dtsch. Chem. Ges.* **1883**, *16*, 921–924; quotation from p. 923.
[54] E. Fischer, *Ber. Dtsch. Chem. Ges.* **1893**, *26*, 2400–2412; quotation from p. 2405.
[55] B. Tollens, *Kurzes Handbuch der Kohlenhydrate*, J. A. Barth Verlag, Leipzig, **1914**, p. 363.

The Key–Lock Theory and the Induced Fit Theory

Daniel E. Koshland, Jr.

It is a great pleasure for me to contribute to this symposium honoring the great scientist Emil Fischer. My graduate thesis required me to synthesize [1-^{14}C]glucose, which introduced me to the famous Fischer–Kiliani synthesis of glucose and mannose from arabinose and HCN.[1] I was also particularly intrigued with his classic key–lock (or template) theory of enzyme specificity,[2, 3] which like all great theories seemed so obvious once one understood it.

This symposium in his honor allows me to pay tribute to Fischer's great contributions to biochemistry varying from natural products chemistry to the key–lock theory, to review some of the history and significance of our induced fit theory, to illustrate the ramifications of those theories in our present era of protein–ligand interactions, and to discuss recent work in our laboratory which is helping to clarify conformational changes and their function. These theories have assumed again a central role in modern health research where the need for drug design requires taking into account the complementarity of fit of Fischer's principle and the flexibility and regulatory implications of the induced fit theory.

The induced fit theory is no more a refutation of Fischer's key–lock principle than the Heisenberg atom was of the Bohr atom or the modern DNA sequences are of the one gene–one enzyme hypothesis. A new theory must explain all the existing facts that pertain to it at the time of its enunciation. Gradually the new theory becomes accepted and then acquires anomalies due to the new facts uncovered after its enunciation. That in turn generates a newer theory which elicits new techniques to test it and its predictions. These new techniques then uncover facts which eventually require further new theories and so on. The new theories are built on components of the old principles. It is said that each scientist stands on the shoulders of the giants who have gone before him. There can be no more honored place than to stand on the shoulders of Emil Fischer.

Limits of the Key–Lock Theory

My first inkling that the Fischer key–lock model needed modification really arose from my consideration of the role of water in biological reactions. I was preparing a lecture for a scientific meeting and decided to consider why some proteins were kinases and others ATPases. The more I thought about the protein, the more astonishing it seemed that water could be prevented from reacting at the active site of a kinase.

In hexokinase, which I took as a typical kinase, the OH group of water was known to be as good a nucleophile as the OH group of a sugar. If glucose is bound very tightly then it could exclude water, and a basic group on the protein would generate a glucosyl oxyanion nucleophile which could attack the ATP. But glucose would not normally saturate the site and could in many physiological circumstances fall to very low levels. Water, at 55 M, would fill up an empty site, and therefore water would be constantly competing with glucose in the nucleophilic attack on ATP. The existence of kinases in the absence of substrate or with only partially filled template type active sites would result in great ATPase activity and an enormous waste of energy.

Once I started thinking along these lines other anomalies came to mind. One example was "noncompetitive inhibition", which was explained by saying that the inhibitor blocked enzyme action but did not affect the binding of the substrate. No key–lock concept was available to explain such a result.

The key–lock (or template principle) could explain why smaller sugars might not react: they would not be attracted to the active site strongly enough to form significant amounts of the ES complex. However, we found that α-methylglucoside was not a substrate but was a tightly bound competitive inhibitor of the enzyme. Thus it was tightly bound, could fit into the site, had the right chemical stereochemistry, but did not react. ("Substrate analog" was used for those chemicals whose chemistry is similar to a substrate but fail to react on the enzyme's surface as in α-methylglucoside, a substrate analog of the enzyme amylomaltase.)

Other reactions raised the same question of smaller chemically logical molecules that nevertheless did not react. And there were also cases in which a bigger substrate analog did not react. As another example, we found that cyclohexaamylose was an inhibitor of β-amylase (an enzyme that cleaved glucosyl bonds in long amylose chains). One could try to explain this on the basis of the key–lock principle by saying that the cyclic amylose was too big and couldn't bind, but we showed it did, in fact, bind (and tightly) but failed to react.[4]

[*] Prof. Dr. D. E. Koshland, Jr.
Department of Molecular and Cell Biology
University of California
229 Stanley Hall 3206, Berkeley, CA 94720 (USA)
Telefax: Int. code + (510) 643-6386

[**] Based on a commemorative lecture at the European Reseah Conference "Supramolecular Chemistry: 100 Years "Lock-and-Key" Principle in Mainz on August 12, 1994.

 © *VCH Verlagsgesellschaft mbH, D-69451 Weinheim, 1994* *0570-0833/94/2323-2375 $ 10.00+.25/0*

Introduction of the Induced Fit Theory

So the induced fit theory[5] was proposed in the following terms "a) the precise orientation of catalytic groups is required for enzyme action, b) the substrate causes an appreciable change in the three-dimensional relationship of the amino acids at the active site, and c) the changes in the protein structure caused by the substrate will bring the catalytic groups into the proper alignment, whereas a nonsubstrate will not."

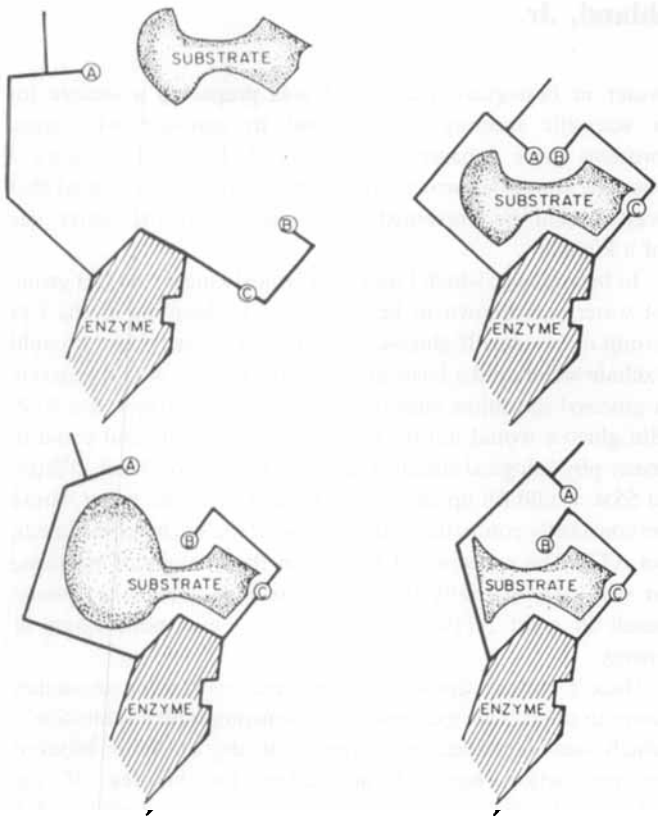


Fig. 1. Schematic model of the induced fit mechanism. Black lines indicate protein chains containing catalytic groups A and B and binding group C. Upper left: substrate and enzyme dissociated. Upper right: substrate with induced change of protein chains to bring A and B into proper alignment for reaction. Lower left: bulky group added to substrate prevents proper alignment of A and B. Lower right: deletion of a group eliminates buttressing action on the chain containing A, so the thermodynamically stable complex has incorrect alignment of A and B.

Pictures to illustrate this concept and how it could explain the previous anomalies are shown in Figure 1 taken from papers published at the time.[6] The theory of Emil Fischer was deep in the hearts of scientists and journal editors, so I had great difficulty getting the original ideas published or convincing skeptics, but we did obtain more evidence from my own laboratory, and soon others joined in. One of the predictions that results from the assumption of a flexible enzyme, namely that a small nonreactive molecule could make up for a structural deficiency in a nonsubstrate (Fig. 2), was established for us by two

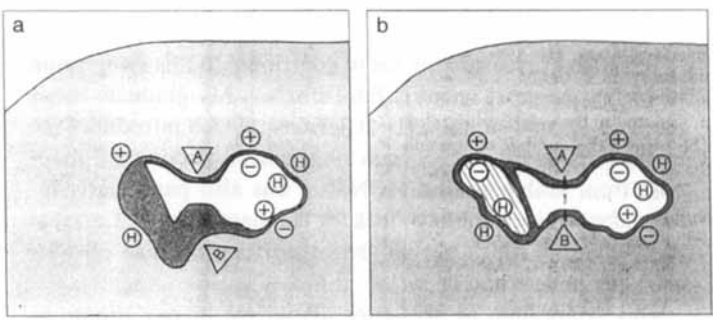
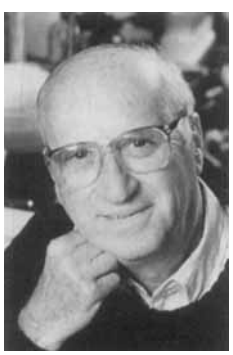


Fig. 2. Activator molecules can, according to the flexible model of enzyme action, help to make a deficient molecule act as a substrate by altering the shape of the enzyme. For example, in the case of a molecule (unshaded) that by itself is too small to induce the proper alignment of catalytic groups, A and B [shown in a)], a second molecule (shaded) can bind immediately adjacent to the deficient molecule [shown in b)] or (not shown here) to a more distant site, thereby inducing a stable shape with the proper alignment of catalytic groups.

laboratories. Sols et al. showed that xylose, a pentose (similar to glucose but lacking the 6-CH_2OH group), made hexokinase a better ATPase,[7a] and Murachi et al.[7b] showed that the nonsubstrate for trypsin, glycine ethyl ester, could react appreciably if ethylamine was added to the incubation mixture. These "regulatory" molecules which did not themselves undergo chemical changes could induce the further conformational changes in an enzyme needed for reaction (as illustrated in Fig. 2).

These indirect chemical assays added to the credibility of the hypothesis, but we needed direct evidence for the predicted induced conformational change in the protein (a proof which was easy later when protein crystallography became available). So Yankeelov and I said we must get a result with protein reactivity



Daniel E. Koshland was born in New York City in 1920. He earned his B. S. degree from the University of California, Berkeley, in 1941, and Ph. D from the University of Chicago in 1949. After two postdoctoral years at Harvard he joined the staff of Brookhaven National Laboratory, and later also of Rockefeller University. In 1965 he joined the faculty of the University of California, Berkeley, where he is currently Professor of Biochemistry and Molecular Biology. He became Editor of Science in 1985. Among his honors are the National Medal of Science, the Edgar Fahs Smith and Pauling Awards of the American Chemical Society, the Rosenstiel Award of Brandeis University, the Waterford Prize, and the Merck Award of the American Society of Biochemistry and Molecular Biology. Included in his fields of interest are the role of conformational changes in enzyme regulation and the elucidation of the catalytic power of enzymes. He demonstrated that bacteria have short-term memory and that purified mammalian cell lines show rudimentary memory. His recent work has emphasized the chemical mechanism of short-term and long-term memory, and the structure–function relationship of receptors.

that tested the key–lock template hypothesis and induced fit. We argued that adding a ligand to a template type enzyme can bury groups but it cannot expose them, whereas an induced fit conformational change could bury some groups and expose others. We picked the enzyme phosphoglucomutase (whose reaction had similarities to hexokinase, and thus we expected it to be an induced fit enzyme)[8] and used the reactivity of its SH group as a test. The experiment illustrated in Figure 3 gave the result we wanted.[8] Ligand binding induced the exposure of an SH group, a result incompatible with the key–lock theory. We likened it to the flexibility of a "hand in glove", which included Fisher's idea of a fit but added the flexibility concept.

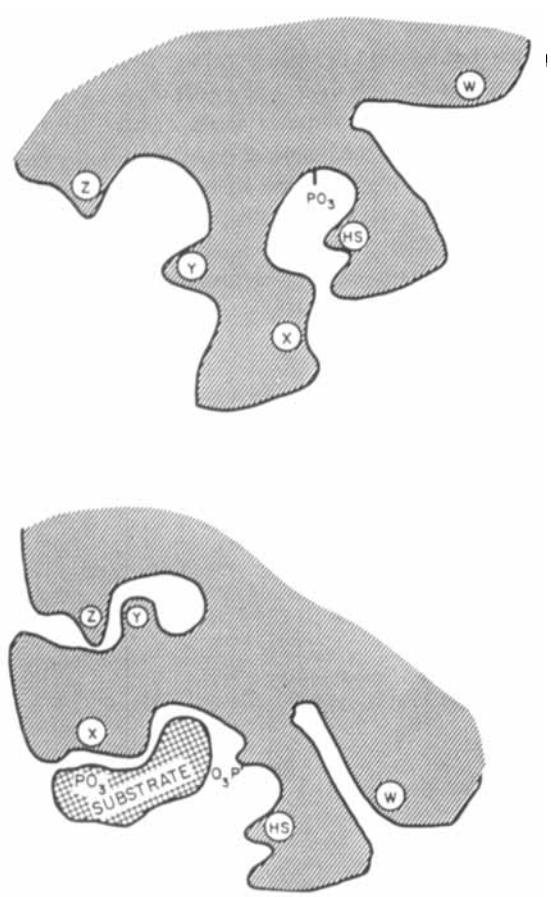


Fig. 3. Schematic illustration of flexibility in the action of phosphoglucomutase. The upper part of the figure represents the enzyme molecule in the absence of substrate. The lower part of the figure represents the change in conformation leading to exposure of –SH and burying of X, Y, Z, and W.

Further support came when the structures of lysozyme[9] and ribonuclease[10] were published because there were definite conformational changes; however, these were small and did not impress many. (Many biologists forgot that C–C and C–O bonds are only 1.5 Å long, so small changes can easily disrupt a catalytic alignment needed to catalyze changes in the bonds.) Then Steitz et al. with carboxypeptidase[11] and Steitz et al. with hexokinase[12] showed conformational changes that were breathtakingly large and highly convincing. Steitz showed that the engulfing of the substrate glucose by hexokinase occurred precisely as the induced fit predicted, thus giving visual proof that ligand-induced conformational changes were real and significant.[12]

Today almost every enzyme has been shown to undergo significant ligand-induced changes. A recent review by Gerstein, Lesk, and Chothia[13] divides these changes into "hinge domain" and "shear" motions and lists 42 enzymes that illustrate major conformational changes. The enzymes that show the least conformational changes are the hydrolases such as the proteases and nucleases—and they are precisely those one might expect to fall in this category, since they do not need to exclude water. The finding of extensive conformational changes in many enzymes is logical, since most enzymes exist in a cytoplasm with many pathways that contain many smaller substrate analogs, for example trioses, which must be prevented from reacting at sites of larger analogous substrates, for example hexoses. If the specificity failed to exclude smaller analogs, poor yields and bad side reactions would occur.

The question then arises as to how big the conformational changes have to be in order to be considered "significant". Some recent evidence indicating some answers to this problem is discussed below.

Isocitrate Dehydrogenase and Small Conformational Changes

We have recently been studying isocitrate dehydrogenase to obtain some clues to the size and significance of conformational changes. We found, for example, that the enzyme was inactivated by phosphorylation,[14] but this phosphorylation, unlike the case of glycogen phosphorylase,[15] involved phosphorylation right at the active site with little resulting change in conformation of the protein.[16–19] We also found very little change in conformation induced by the substrate isocitrate on binding to the protein and were about to conclude that the enzyme was one of those that approximated the Fischer key–lock model. However, we did one more experiment and tested the protein in the presence of the product, α-keto glutarate.[20] In that case the ligand-induced conformational changes were wide spread. Many atoms moved though each movement was rather small. The protein did not fit into the "hinge domain" category of Gerstein, Lesk, and Chothia nor even into the "shear" category, but rather into what might be called a "spider web" category, that is, small interconnected changes occurring over an extensive surface. The changes in each atom were less than an angström but many atoms moved, which suggested that subtleties in alignment were capable of turning an enzyme off or on.

We have also measured the changes in the aspartate receptor of chemotaxis in collaboration with Sung Hou Kim et al.[21] This case fits the shear model more closely, as we postulate that the small changes at the binding site for aspartate can cause a sliding of one helix past another.[22–24] The changes that are generated in the cytoplasmic domain are relatively small – maybe an average change of 0.5 Å—but the conformational change is transmitted from one side of the dimer to the other. In addition we have shown that the receptor shows negative cooperativity[25, 26] in which binding of the first aspartate to a dimer completely blocks aspartate binding to a second aspartate site. The two sites are initially identical, but the ligand-induced changes in the second site reduce the size of the second site so it becomes too small to bind aspartate. The changes are quite

Table 1. Distances between side chains in binding sites in the *Salmonella* aspartate receptor–ligand binding domain.

Amino acids	Separation [Å] in unbound receptor[a]	Separation [Å] in empty site of Asp-bound receptor[a]	Reduction in distance [Å]
Ser-68, Thr-154	8.9	8.1	0.8
Tyr-149, Arg-73	6.9	6.0	0.9
Tyr-149, Arg-64	4.1	3.2	0.9
Phe-150, Arg-73	4.8	3.5	1.3
Ser-68, Arg-69	7.4	6.6	0.8

[a] Distance between closest non-hydrogen atoms.

small in Å (Table 1) but are enough to prevent binding of the aspartate molecule.[26]

Our conclusion is that big movements are important but so are small ones. The important feature from the induced fit theory is that the alignment of catalytic groups and binding groups must be optimized for the transition state, and the attainment of the state is unfavorable energetically unless it is supplied with the energy of the substrate binding. If the protein movements were easy to attain, they would occur spontaneously often enough to have little effect on catalysis. However, a small movement can also be energetically unfavorable, as in the shift of a ferrous atom 0.7 Å into and out of the plane of the heme in hemoglobin.[27] When the small movement needed for catalysis, in the case of an enzyme, is generated by the binding of the substrate, enzyme action occurs.

A second conclusion is that the conformation of the protein is undoubtedly selected during evolution to optimize both the unliganded state and the liganded state. Allosteric sites are often distant from the active site by 20 Å or more, and the conformational changes are far larger than can be explained by a distortion that propagates from one site to another by pure chemical torsions. Those nonbonded forces dampen out too rapidly. Therefore, the conformational change induced by the substrate binding has a long-range effect because it generates and catalyzes the transition from one evolutionarily selected conformation to another.

Summary and Outlook

The basic concept of Emil Fischer's key–lock theory, which explained enzymatic properties of specificity and action for 60 years, required modification to explain discrepancies such as the lack of hydrolytic activity of kinases, noncompetitive inhibition, and other apparent inconsistencies. The new theory, the induced fit theory, incorporated Fisher's concepts of the complementarity of enzyme and substrate but introduced the concept of a flexible enzyme, likened to the fit of a hand in a glove. The flexible enzyme concept not only explained the discrepancies but set the stage for further understanding of *regulation*, *cooperativity*, and *specificity* as described in papers by Pardee,[28] Monod,[29] and our own laboratory, as well as many others. Thus the great work of Emil Fischer lives on in an extension of the theory and application to new problems of chemistry and biochemistry that were impossible to visualize in the 1900s. The new studies focus on the importance of conformational changes, both large and small, and the manner in which they control enzymatic reactions. The findings from modern X-ray crystallography that essentially all enzymes undergo conformational changes induced by substrate binding has made the induced fit theory universally accepted in textbooks and by scientists.

These theories are of increasing importance because of the rise in drug-resistant strains of organisms. Computer-assisted drug design is what we and many others are now developing to prevent the ravages of the new virulent organisms. For that purpose the key–lock theory with a relatively rigid enzyme would be an easier basis for computer designs, but unfortunately the evidence that induced fit theory is closer to reality means that computer programs will have to be a little more sophisticated. However, the modern computer seems clearly up to the challenge, and a rigid enzyme is a good starting point for initial assumption. The flexibility can then be built into subsequent calculations. Moreover, the flexible enzyme allows binding to a "regulatory" or "allosteric" site, which may be a better target for drug therapy in many cases. The finding that very small changes can "turn on" or "turn off" an enzyme is very encouraging in this regard.

This work received financial support from the National Institutes of Health and the National Science Foundation.

[1] F. W. Lichtenthaler, *Angew. Chem.* **1992**, *104*, 1577; *Angew. Chem. Int Ed. Engl.* **1992**, *31*, 1541.
[2] E. Fischer, *Ber. Dtsch. Chem. Ges.* **1890**, *23*, 2611.
[3] E. Fischer, *Ber. Dtsch. Chem. Ges.* **1894**, *27*, 2985.
[4] J. A. Thoma, D. E. Koshland, Jr., *J. Am. Chem. Soc.* **1960**, *82*, 3329.
[5] D. E. Koshland, Jr., *Proc. Natl. Acad. Sci. USA* **1958**, *44*, 98.
[6] a) D. E. Koshland, Jr., *Science* **1963**, *142*, 1533; b) *Cold Spring Harbor Symp. Quant. Biol.* **1963**, *28*, 473.
[7] a) G. Dela Fuente, R. Lagunas, A. Sols, *Eur. J. Biochem.* **1970**, *16*, 226; b) T. Inagami, T. Murachi, *J. Biol. Chem.* **1964**, *229*, 1395.
[8] J. A. Yankeelov, Jr., D. E. Koshland, Jr., *J. Biol. Chem.* **1965**, *240*, 1593.
[9] C. C. F. Blake, D. F. Koenig, G. A. Mair, A. C. J. North, D. C. Phillips, V. R. Sarma, *Nature* **1965**, *206*, 757.
[10] H. W. Wyckoff, K. D. Hardmann, N. M. Allewell, T. Inagami, L. N. Johnson, F. M. Richards, *J. Biol. Chem.* **1967**, *242*, 3984.
[11] T. A. Steitz, M. I. Ludwig, F. A Guiocho, W. N. Lipscomb, *J. Biol. Chem.* **1978**, *242*, 462.
[12] C. M. Anderson, F. H. Zucker, T. A. Steitz, *Science* **1979**, *204*, 375.
[13] M. Gerstein, A. M. Lesk, C. Chothia, *Biochemistry* **1994**, *33*, 6739.
[14] D. C. LaPorte, D. E. Koshland, Jr., *Nature* **1982**, *300*, 458.
[15] L. N. Johnson, D. Barford, *Annual Reviews* **1993**, *22*, 199.
[16] J. H. Hurley, A. M. Dean, J. L. Sohl, D. E. Koshland, Jr., R. M. Stroud, *Science* **1990**, *249*, 1012.
[17] A. M. Dean, D. E. Koshland, Jr., *Science* **1990**, *249*, 1044.
[18] J. H. Hurley, A. M. Dean, D. E. Koshland, Jr., R. M. Stroud, *Biochemistry* **1991**, *30*, 8671.
[19] B. L. Stoddard, A. Dean, D. E. Koshland, Jr., *Biochemistry* **1993**, *32*, 9310.
[20] B. L. Stoddard, D. E. Koshland, Jr., *Biochemistry* **1993**, *32*, 9317.
[21] M. V. Milburn, G. G. Privé, D. L. Milligan, W. G. Scott, J. Yeh, J. Jancarik, D. E. Koshland, Jr., S.-H. Kim, *Science* **1991**, *254*, 1342.
[22] D. L Milligan, D. E. Koshland, Jr., *Science* **1991**, *254*, 1651.
[23] B. A Lynch, D. E. Koshland, Jr., *FEBS Letters* **1992**, *307*, 3.
[24] S. L. Mowbray, D. E. Koshland, Jr., *Cell* **1987**, *50*, 171.
[25] D. L. Milligan, D. E. Koshland, Jr., *J. Biol. Chem.* **1993**, *268*, 19991.
[26] H.-P. Biemann, D. E. Koshland, Jr., *Biochemistry* **1993**, *33*, 629.
[27] M. Perutz, *Proc. Roy. Soc. Lond. Ser. B.* **1990**, *208*, 135.
[28] J. Gerhart, A. Pardee, *J. Biol. Chem.* **1962**, 237, 891.
[29] J. Monod, J. Wyman, J. P. Changeux, *J. Mol. Biol.* **1965**, *12*, 88.

Fine Feathers Make Fine Birds: The Heck Reaction in Modern Garb

Armin de Meijere* and Frank E. Meyer

Dedicated to Professor Wolfgang Lüttke on the occasion of his 75th birthday

The palladium-catalyzed coupling of haloarenes and haloalkenes with alkenes, which was discovered by Richard F. Heck in the late sixties, has been a topic of fluctuating interest; however, in the last six years activity in this area has flourished. Careful choice of substrates and skillful tailoring of reaction conditions lead to impressive sequences consisting of even different reaction types that occur not only in a consecutive mode, but also in a single operation. The well-established Heck reaction, together with other mechanistically related palladium-catalyzed transformations with arene, alkene, and alkyne derivatives, opens the door to a tremendous variety of elegant and highly convergent routes to structurally complex molecules. The reaction is not disturbed by heteroatoms such as oxygen and nitrogen (nor by sulfur and phosphorus with some limitations). The spectrum of recent achievements starts with a range of chemoselective and regioselective monocouplings of highly functionalized substrates with unsymmetrical and multisubstituted reaction partners. Other advances include cascade reactions in which three, four, five, and even eight new C–C bonds are formed to yield oligofunctional and oligocyclic products with impressive molecular complexity. Even the enantioselective construction of complex natural products with quaternary stereocenters has been achieved with Heck reactions in key steps, as exemplified by the synthesis of crinan, picrotoxinin, and morphine. Today, the Heck reaction is indispensible in the arsenal of synthetic methods available to organic chemists. Certainly it is only a matter of time before the Heck reaction is applied in industrial syntheses.

1. Introduction

Like other fields, organic chemistry is subject to fashions. One of the latest fascinating trends is the rapidly developing field of fullerene chemistry.[1] But just as fashions may disappear into the back of the closet after only a short time, relevant discoveries in organic chemistry have often enough slipped into the realm of oblivion or at least have not received the broad attention that their potential would call for.

An example of an important new type of reaction that has been subject to these ups and downs in attention is the palladium-catalyzed arylation or alkenylation of alkenes known as the Heck reaction. Although the reaction was discovered as early as the late sixties by R. F. Heck[2] and initially received much attention as a new method for C–C bond formation, the Heck reaction was not applied and developed in the seventies and eighties to the extent that important synthetic reactions typically are. Only a few research groups continued to explore the scope and limitations of the method.[3]

Since synthetic strategies have become directed increasingly toward both efficiency *and* stereoselectivity, concepts in the past decade have been devised to sequentially form several carbon–carbon bonds in a single synthetic step—if possible, even diastereo- and enantioselectively.[4] Convincing initial success was achieved with radical-initiated cascade cyclizations,[5] but soon metal-mediated and metal-catalyzed reactions were specifically employed.[6] During the mid-eighties many groups recognized that the Heck reaction was underdeveloped and far from being exploited to its full synthetical potential. But this classic reaction experienced a renaissance soon after answers had been found to some important questions regarding the mechanism, the control of substrate selectivity as well as regio- and stereoselectivity, and the increase in efficiency. Now, scarcely a week passes without interesting new publications in this field. In view of this rapid development it would certainly appear reasonable to summarize what the "heck" has been going on recently behind so many laboratory doors.

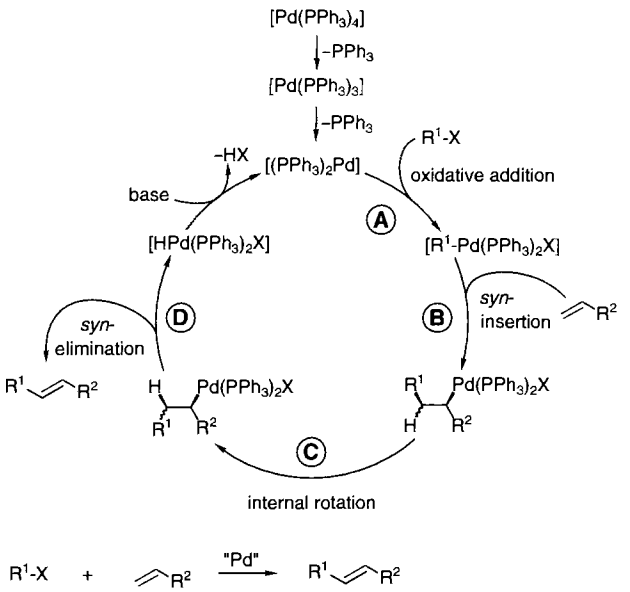
2. A Brief Description: Mechanism, Methods, and New Possibilities

2.1. Mechanism

Even at an early stage in the development of this catalytic reaction into a facile method for the preparation of alkenyl- and aryl-substituted alkenes, reasonable concepts for the mechanism of the Heck reaction emerged, which could serve at least as a working hypothesis (Scheme 1).[3]

[*] Prof. Dr. A. de Meijere, Dr. F. E. Meyer
Institut für Organische Chemie der Universität
Tammannstrasse 2, D-37077 Göttingen (FRG)
Telefax: Int. code +(551) 39 94 75

 © VCH Verlagsgesellschaft mbH, D-69451 Weinheim, 1994 0570-0833/94/2323-2379 $ 10.00+.25/0



Scheme 1. Mechanism of the Heck reaction. R^1 = alkenyl, aryl; R^2 = aryl, alkyl, alkenyl, CO_2R', etc; R' = alkyl; X = I, Br, (Cl), OSO_2CF_3.

Today, a coordinatively unsaturated 14-electron palladium(0) species, usually coordinated with weak donor ligands (tertiary phosphanes), is assumed to be the catalytically active complex. This complex is normally generated in situ. Tetrakis(triphenylphosphane)palladium(0)[7] which occurs as a tris(triphenylphosphane)palladium(0) complex in solution, is frequently employed.[8] After the endergonic loss of a second phosphane ligand[9] the catalytically active species bis(triphenylphosphane)palladium(0) is generated. However, palladium(II) salts such as palladium acetate or bis(triphenylphosphane)palladium dichloride, which are reduced in the reaction medium, are more commonly used.[10] Bis(triphenylphosphane)palladium(0) is a well-characterized compound, accessible by both chemical[11] and electrochemical[12] routes.

In the first step of the catalytic cycle (A in Scheme 1) haloalkenes and haloarenes are commonly assumed to oxidatively add to bis(triphenylphosphane)palladium(0), generating a σ-alkenyl or σ-arylpalladium(II) complex. This reaction should lead to the thermodynamically stable[12, 13] *trans*-σ-alkenyl- or -arylpalladium(II) complex in several steps,[14a, 15, 16] probably via a *cis*-σ-alkenyl- or -arylpalladium(II) intermediate.[15a, c, d]

In the next step an alkene molecule is coordinated, probably after elimination of another phosphane ligand.[17] After both ligands have adopted the *cis* orientation necessary for insertion of the alkene into the σ-alkenyl or σ-aryl C–Pd bond, rotation of the alkene leads to in-plane coordination of the alkene. Finally, the alkene inserts into the σ-alkenyl- or -arylpalladium bond[18] to give a σ-alkylpalladium complex via a four-center transition state (step B).

The rearrangement of complex **1** via σ complex **3** to σ,π complex **5** and the π-allyl complex **6** is an example of a double bond insertion into a σ-aryl C–Pd bond (Scheme 2).[19]

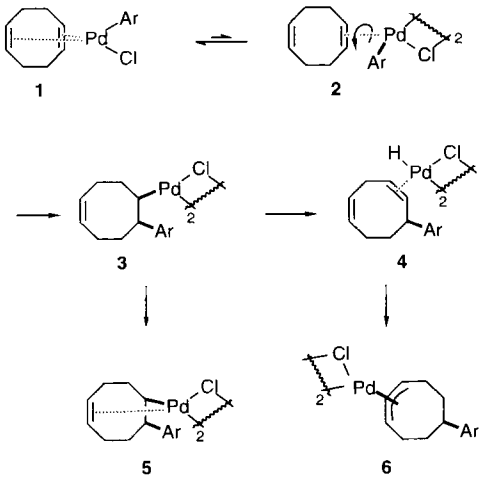
After the *cis*-addition of the alkene, the reaction-terminating β-hydride elimination (step D)[20] can generally occur only after internal rotation (step C) of the generated alkylpalladium species. In this way, the essential *syn* orientation of a β hydrogen is provided for elimination. The catalyst is regenerated after reductive elimination of HX in presence of the base.[21]

2.2. Further Developments

Applications of the Heck reaction in natural product syntheses were until recently[22, 24f] rather limited,[23] despite the potential of this reaction for the arylation and alkenylation of alkenes. This was surely due to the lack of regioselectivity frequently encountered in couplings with unsymmetrical alkenes,



Armin de Meijere, born 1939 in Homberg (Niederrhein), studied chemistry at the Universities of Freiburg and Göttingen and obtained his doctorate at the University of Göttingen with a thesis entitled "The Conformations of the Lower Bicycloalkyls" under the guidance of Prof. Dr. Wolfgang Lüttke. He spent two years as a postdoctoral fellow with Prof. Kenneth B. Wiberg at Yale University in New Haven, CT (USA), and obtained his "Habilitation" in 1971 at the University of Göttingen. He became full professor of organic chemistry at the University of Hamburg in 1977, and returned to the University of Göttingen as a professor of organic chemistry in October 1989. He has served as a member of the Academic Senate at the University of Göttingen, as a dean of the chemistry department in Hamburg, and as the Director of the Institute of Organic Chemistry. Over the years, he has been visiting professor at the University of Wisconsin in Madison, Wisconsin, the IBM Research Laboratory in San José, CA, the Technion in Haifa, Israel, Princeton University in Princeton, NJ, and the University of Aix-Marseille III. He received a fellowship from the Studienstiftung des Deutschen Volkes, obtained the award "Dozentenstipendium" from the Fonds der Chemischen Industrie in 1972, and was elected a member of the Norwegian Academy of Sciences and Letters in 1992. He is editor or member of the editorial board of a number of scientific journals and books. His scientific achievements have been published in over 280 original publications, review articles, and chapters in books. His current research interests include the development of new small-ring building blocks and their application in the synthesis of natural and non-natural compounds; new highly strained polycyclic compounds with interesting properties; application of organometallic complexes and catalysts in organic synthesis; palladium-catalyzed sequential reactions; and carbon compounds and organometallic complexes with unconventional chemical and physical properties.



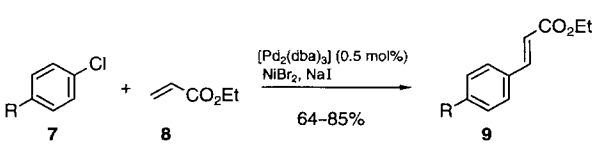
Scheme 2. Ar = C_6F_5.

and the observed isomerizations of the products generated after β-elimination. A further handicap was the restriction of coupling substrates to aryl and alkenyl bromides and iodides. Consequently, there was great interest in the development of coupling substrates that are both more economical and preparatively more easily accessible, and if possible reactive even at lower reaction temperatures.

The nature of the leaving group X also affects the addition rate (ArI > ArBr ≫ ArCl),[24, 25] because the oxidative addition of haloarenes (haloalkenes) to palladium(0) is in many cases the rate-determining step.[12b, 24] Common reaction temperatures lie in the range of 70 to 100 °C, though chloroarenes are practically unreactive under these conditions.[25a, 26]

Meanwhile it has been shown that Heck reactions can be performed at room temperature with aryl diazonium salts,[27] *N*-nitroso-*N*-aryl acetamides,[28] and hypervalent iodo compounds.[29] Interestingly, even haloarenes and haloalkenes react at room temperature when high pressure[30] is applied or phase-transfer catalysts such as tetrabutylammonium chloride[31] are added (conditions according to Jeffery's protocol). Benzyl halides[32] and benzoyl chlorides[33] have also been employed in coupling reactions with alkenes. Further developments are directed towards the use of low-cost chloroarenes that normally do not undergo oxidative addition to palladium(0) under Heck conditions. Some initial successful attempts have been reported on the application of high pressure,[30] the deployment of basic ligands that facilitate oxidative addition,[34] the immediate generation of the catalytically active palladium species,[35] and the nickel dibromide/sodium iodide assisted activation of substituted chloroarenes (Scheme 3).[36]

Alkenyl sulfonates have become important as haloalkene substitutes and are normally easily prepared from the corresponding carbonyl compounds.[37] While the use of alkenyl mesylates and alkenyl tosylates is largely unexplored,[38] many successful reactions with alkenyl trifluoromethanesulfonates



Scheme 3. R = H, COMe, OMe, Me, CN; dba = dibenzylidenacetone.

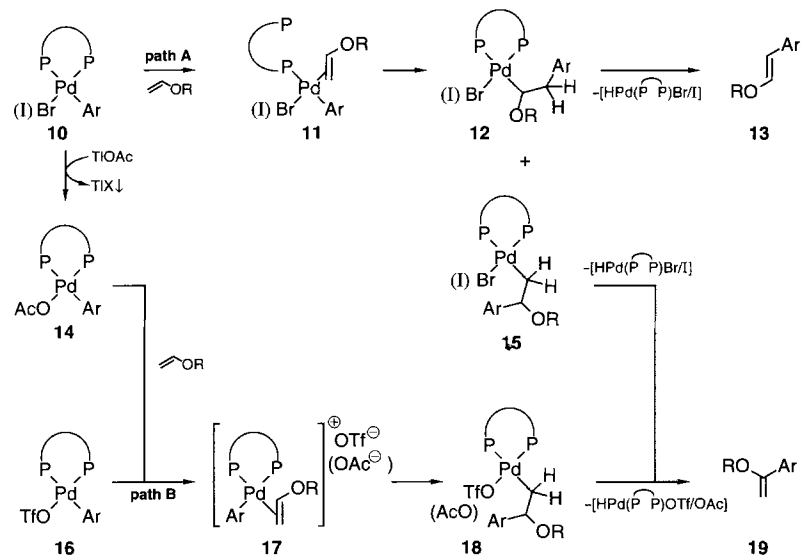
(alkenyl triflates), starting with the early works by Cacchi et al.[39] and Stille et al.,[23m, 40, 41] have demonstrated the advantages of this leaving group. The previously observed inhibition of the reaction following facile oxidative addition of alkenyl triflates to palladium(0) can be prevented by adding lithium chloride to the reaction mixture.[40] Addition of metal halides or tetrabutylammonium halides can also facilitate Heck couplings.[23h, 31, 41a, 42] Detailed studies by Amatore et al.[12a, 43] confirmed the early assumption[40b, c] that halide ions stabilize coordinatively unsaturated and low-valent palladium species. In many cases the Heck reaction is also accelerated by silver(I)[44] and thallium(I) salts.[23a, 45]

Initially, dipolar aprotic solvents such as dimethylformamide (DMF), *N*-methylpyrrolidone (NMP), dimethyl sulfoxide (DMSO), and acetonitrile were common. But ever since the pioneering work by Beletskaya et al.[46] many alkene arylations are also known to proceed superbly in aqueous solution. Thus, excellent results were achieved with water-soluble triarylphosphane ligands in water-containing acetonitrile.[47a] In fact, water accelerates the reaction, especially in the presence of quaternary ammonium salts.[47b]

According to the studies of Hallberg et al.,[48] Teranishi et al.,[49] Choudary et al.,[50] and Zhuangyu et al.[51] the typically homogeneous reaction can also be performed with polymer-bound palladium catalysts. Early investigations concerning intermolecular arylations of unsymmetrically substituted alkenes often revealed only poor regioselectivities,[3a, 52] especially with acyclic enol ethers.[53] In recent years, however, suitable conditions have been developed for the selective α- or β-arylation of enol ethers[54] and enamides.[55] In these arylations the regiochemistry is determined by the decomposition of π complex **11** (Scheme 4, path A)[19] to give either the σ complexes **12** or **15**, or a mixture of both. Although the metal center may be regarded upon insertion as an electron acceptor and the migrating carbon atom as a nucleophile, merely a minor charge separation is actually involved. Therefore, the regioselectivity of insertion is commonly explained by steric considerations.[56, 87b] Nevertheless, electronic effects do indeed play a major role in arylations of acyclic enol ethers.[54b, 57]

Thus, reactions of acceptor-substituted aroyl chlorides provide β-arylalkenyl ethers in good yields.[58a, d] Also, high β-selectivities are achieved in arylations of modified alkenyl ethers, for example 2-(dimethylaminoethyl)-,[58b] 2-(diphenylphosphanoethyl)-, and 2-(diphenylphosphanophenyl)alkenyl ethers.[58c]. On the other hand, the extent of α-alkenylation was improved considerably by using alkenyl triflates.[59] In contrast to previous findings,[60] Cabri et al.[45a, 61] achieved excellent α-regioselectivities with bidentate ligands such as 1,3-bis(diphenylphosphano)propane (DPPP)[45d, 61b, d] and 2,2′-dipyridyls.[61c] Aryl and aroyl halides also give exclusively α regioisomers[61a, d] in presence of thallium(I) acetate.

According to Cabri et al.[61a, d] and Hayashi et al.,[62] the drastic effect that the leaving group on the arene and the addition of silver(I) or thallium(I) salts have on regioselectivity arises from the competition of two different coordination–insertion steps in the Heck reaction. If, after oxidative addition, the counterion in complex **10** is halide, one of the two phosphorus atoms in the bidentate ligand will dissociate from palladium, and an alkene molecule will coordinate instead giving the neutral

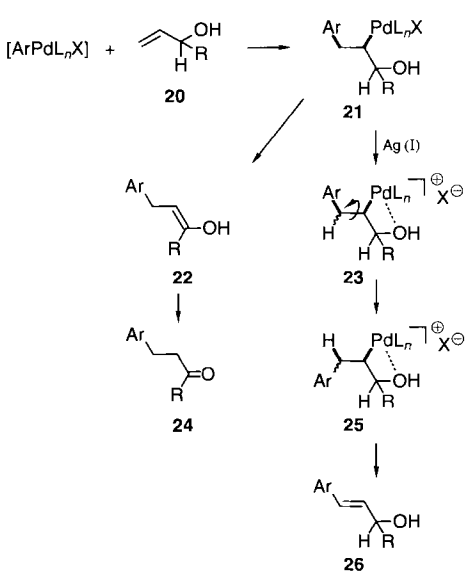


Scheme 4. Ar = aryl; Tf = triflate = CF_3SO_2; P⌒P = diphosphane ligand.

complex **11** (path A in Scheme 4). In **11** the π system of the coordinated enol ether is only slightly polarized, and the electronic effect on the subsequent insertion is subtle, therefore leading to higher preference for β attack. Upon addition of thallium(I) acetate or silver salts to the reaction mixture, the halide ion in complex **10** is presumably replaced by weaker ligands such as acetate to give complex **14**.[63]

In palladium(II) complexes **14** and **16** weak ligands[64] like triflate and acetate readily dissociate giving the cationic complex **17** (path B in Scheme 4). Coordination of the enol ether in these cationic complexes causes a significant polarization of the π system, resulting in a much more directed migration of the aryl residue and an increased proportion of α-substituted product.

The regioselectivity of Heck reactions with unsymmetrical alkenes can therefore be manipulated by specific variation of components in the "catalyst cocktail". But the impact of silver(I) and thallium(I) salts on Pd-catalyzed reactions extends beyond just increasing regioselectivities and enhancing reaction rates.[44a, b, 65] Without these additives, arylations of allyl alcohols **20** afford aldehydes and ketones **24**[66] rather than the β-aryl allylic alcohols **26** (Scheme 5). This may be explained by a faster or more selective β-hydride elimination in intermediate **21**, leading to enol **22**. Similarly, elimination to give allylic alcohol **26** followed by



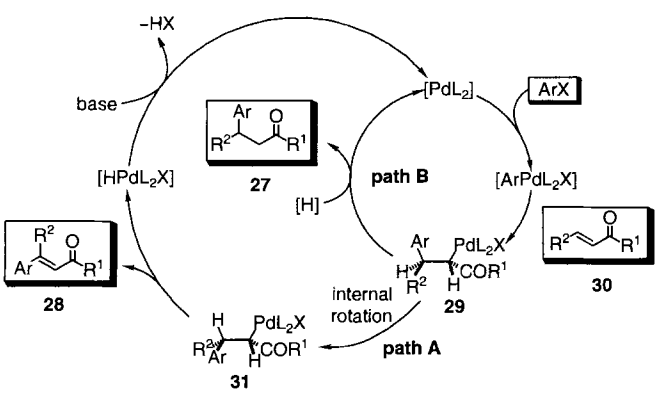
Scheme 5. Ar = aryl; L = ligand; X = halogen; R = alkyl.

readdition of the hydridopalladium species to the double bond[67] and subsequent β-hydride elimination to give the more stable enol **22** also provides a suitable explanation. This type of isomerization consisting of a sequence of β-hydride eliminations, readditions, and renewed elimination is not restricted to allylic alcohols.[68]

These types of Pd-catalyzed isomerizations are suppressed by addition of silver(I) salts.[44] Thus, in the presence of silver carbonate, allylic alcohols can be arylated and alkenylated in palladium-catalyzed reactions.[69] With triflates couplings are achieved without accompanying isomerization, even in the absence of silver salts.[70] The formation of cationic palladium complex **23** is attributed to either silver ion assisted dissociation of **21** or spontaneous dissociation of the triflate leaving group. β-Elimination leading to enol **22** is hindered by the chelating hydroxyl group.[69c, 70] Because of the shortened lifetime of the eliminated hydridopalladium species, its readdition to **26** does not take place.

The complete control of regiochemistry in this example is also impressive. Iodoarenes give, in the presence of phase-transfer catalysts, β regioisomers **22** and **24**.[69] Complementary α-aryl allylic alcohols may be obtained by using aryl triflates and DPPP as a bidentate ligand.[61d] Furthermore, the desilylation reactions in alkenylations with alkenyltrimethylsilanes frequently observed under classical Heck conditions can be avoided by employing alkenyl triflates or iodoalkenes and by adding silver salts.[65, 71]

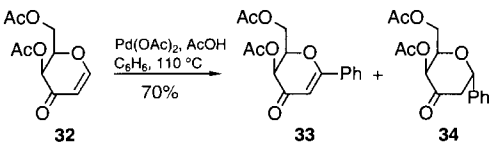
In arylations of β-substituted α,β-unsaturated enones **30** (Scheme 6) varying amounts of different products are frequently



Scheme 6. X = Br, I; R^1 = alkyl, aryl, H; R^2 = alkyl, aryl.

obtained, on account of two competing processes at the stage of alkylpalladium species **29**. On one hand, *syn* β-elimination of $[HPdL_nX]$ (vinylic substitution) may yield the expected Heck reaction product **28** (path A), but the palladium residue in **29** is much more often observed to be protolytically cleaved (path B), giving rise to **27**,[72] the product of 1,4-addition to **30**. In the absence of appropriate reducing agents only low conversions are observed, since palladium leaves the catalytic cycle as Pd^{II}. In contrast to these findings, vinylic substitution is entirely suppressed by 1,4-addition in the presence of trialkylammonium

formate.[73] But β-arylations proceed favorably at least with acyclic α,β-unsaturated enones in the presence of sodium acetate[74] under the conditions developed by Jeffery.[74] However, analogous results cannot be obtained with cyclic α,β-unsaturated enones, as is evident in the arylation of dihydro-γ-pyrone **32** with benzene in the presence of an equimolar amount of palladium acetate.[75] Different reaction conditions lead to varying amounts of both **34**, the product of 1,4-addition, and **33**, that of vinylic substitution (Scheme 7).

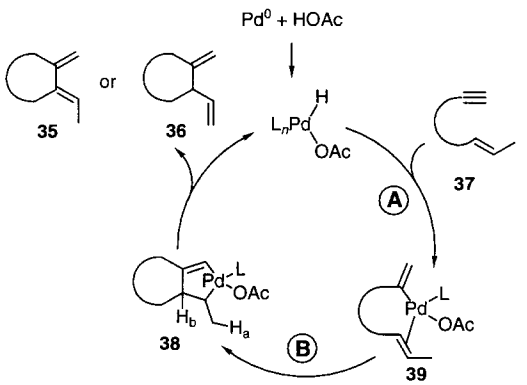


32 **33** **34**

Scheme 7.

Although some of the initial major problems of the Heck reaction (i.e. lack of regioselectivity, product isomerizations, high reaction temperatures, and restriction of substrates to bromides and iodides) have been overcome or almost unraveled, it must be recognized that some of these achievements were literally quite costly. Indeed, the equimolar amounts of silver and thallium salts frequently employed in those first studies are not exactly what one would call inexpensive.

In the mid-eighties Trost et al.[76a] found a both simple and ingenious way out of this dilemma by developing palladium-catalyzed enyne cyclizations[76] (Scheme 8). The atom economy[77]



Scheme 8.

of this reaction equals that of the Diels–Alder reaction.[78] The cycloisomerization of 1,6-enynes **37** to 1,2-dimethylenecycloalkanes **35** or 1-methylene-2-ethenylcycloalkanes **36** is performed with palladium acetate in the presence of acetic acid and phosphane ligands.

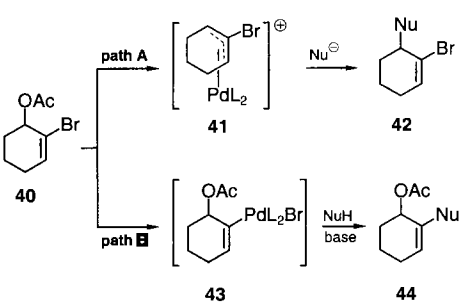
Unlike the Heck reaction, the initial step here is not an insertion of the Pd^0 species into an alkenyl carbon–halogen bond. Instead, acetic acid is oxidatively added to palladium(0), generating a hydridopalladium species.[79] The catalyst then adds to the terminal alkynyl group in enyne **37** with remarkable regio- and chemoselectivity and coordinates the alkenyl group (step A). It is yet unclear how the next intermediate, σ complex **38**, is generated (step B). β-Elimination of H_a or H_b in **38** yields 1,2-dimethylenecycloalkane **35** or the Alder–ene product **36** and regenerates the catalyst [HPdOAc].[80]

Although comparable with the Heck reaction in terms of products and individual mechanistic steps, cycloisomerizations of 1,6-enynes offer an interesting alternative from an economic standpoint. The arduous task of introducing halogen or pseudohalogen substituents to alkenyl groups is not necessary, and difficulties arising from the coordination of halide ions by the catalytically active species can be avoided. Unfortunately, this reaction is still restricted to intramolecular applications, and the initial step of the catalytic cycle, regioselective addition of [HPdOAc] to the terminal alkyne, primarily generates exo-methylenecycloalkanes.

2.3. Variety is the Spice of Life: Ideas and New Concepts

Palladium complexes are of eminant importance in organic synthesis because of the diversity of chemical transformations they catalyze. In addition to Heck reactions and hydrogenations of unsaturated compounds,[81] reactions such as nucleophilic substitutions via π-allylpalladium complexes,[82] the chloroacetoxylation of dienes,[83] couplings with terminal and heteroatom-substituted acetylenes,[84] and stereoselective cross-couplings belong to the modern synthetic chemist's unrelinguishable arsenal of methods.

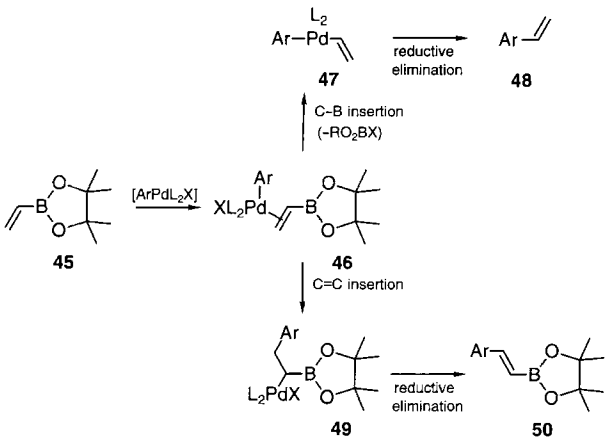
Many parallels in individual mechanistic steps of all these reactions may be perceived and give rise to interesting questions. For example, how do substrates like cyclohexene **40** behave upon reaction with nucleophiles in the presence of a palladium(0) complex (Scheme 9)?[85] The presence of both a vinyl



Scheme 9.

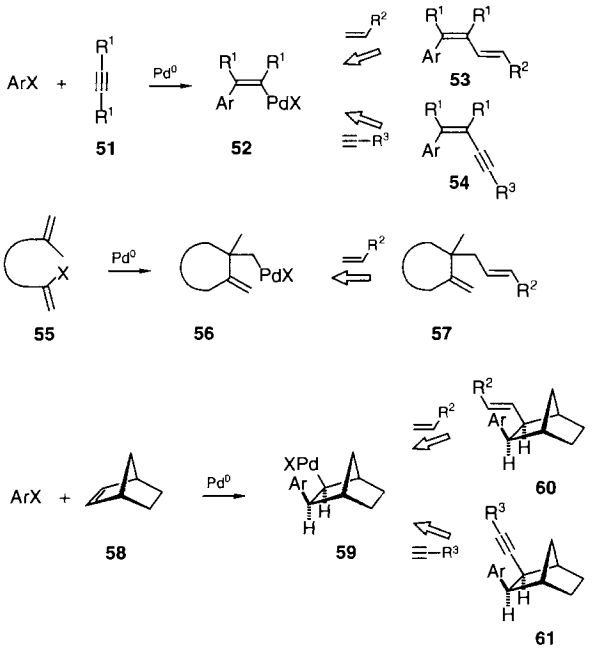
bromide and an allyl acetate group should enable the generation of both a π-allylpalladium complex **41** and σ-alkenylpalladium species **43**, respectively. How do haloarenes react in the presence of Pd^0 complexes with substrates such as ethenyl boronate **45**, which have the potential to react according to a Heck or a Suzuki coupling[22g] (Scheme 10)?[86] Results showed that cyclohexene **40** reacts chemoselectively via cyclohexenylpalladium complex **43** (path B), and ethenyl boronate **45** gives a mixture of styrene **48** and styrylboronate **50**.

Palladium-catalyzed reactions also play an important role in sequential reactions, which are rapidly increasing in popularity. Palladium catalysts initiate reaction cascades in which several carbon–carbon bonds are formed in a single synthetic operation.[4] Heck reactions and mechanistically related transforma-



Scheme 10.

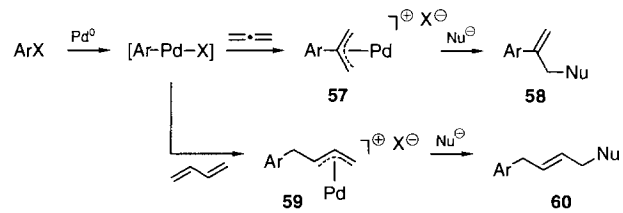
tions with substrates that for steric reasons do not allow termination of the catalytic cycle by the common β-hydride elimination have exceptionally high potential for reaction cascades (Scheme 11).



Scheme 11. Palladium-catalyzed sequential reactions I; R^1 = aryl, $(alkyl)_2COH$, $SiMe_3$; $R^2 \neq$ alkyl; R^3 = alkyl, aryl, CO_2alkyl, $SiMe_3$.

Such a situation arises on addition of a haloarene to disubstituted alkyne **51** in the presence of Pd^0.[87] This addition yields the sufficiently stable and therefore long-lived alkenylpalladium species **52**, which is thus able to undergo further reaction and which also could have been generated by oxidative addition of an appropriate alkenyl halide to palladium(0). β-Hydride elimination is also suppressed in an alkylpalladium halide intermediate of type **56**, which is generated by intramolecular addition of an alkenyl halide to a 1,1-disubstituted double bond as in diene **55**.[32] It can also be advantageous that reductive elimination of [HPdX] typically only occurs if the palladium and hydrogen atoms have a *syn* orientation. Upon addition of arylpalladium halide to the double bond of rigid bicyclic norbornene **58**, alkylpalladium species **59** is generated, which cannot undergo β-hydride elimination. Just like **52** and **56**, intermediate **59** can undergo subsequent intra- and intermolecular reactions with carbon nucleophiles and alkenes.[88] These are only three examples of the formation of two new C–C bonds in a simple two-step sequence.

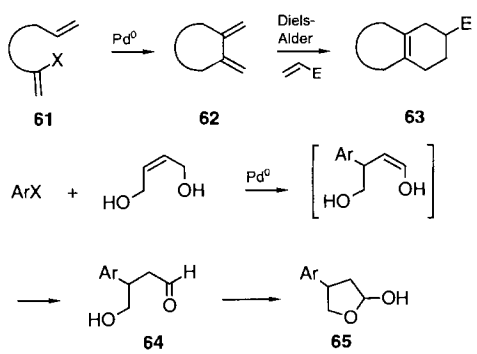
The addition of arylpalladium complexes to polyunsaturated systems such as allenes[89] and 1,3-dienes[90] initiates yet another type of reaction cascade in which two bonds are formed consecutively. The π-allylpalladium complexes **57** and **59** thus generated typically react with various nucleophiles leading to substitution products **58** and **60**, respectively (Scheme 12).



Scheme 12. Palladium-catalyzed sequential reactions II.

In both types of cascades the initial steps are the same as those in the Heck reaction, but in the course of the transformation characteristics of a different reaction type come to fore. The considerable synthetic potential of palladium-catalyzed sequential reactions becomes apparent in these examples. By careful choice of substrate and reaction conditions, several even quite different reaction steps can be performed in a single synthetic operation.

In yet another conceptional approach palladium-catalyzed reactions generate structural elements that can undergo consecutive reactions,[4a] thus allowing additional bond formations.[91] In this context it would appear favorable to assemble 1,3-dienic systems **62** by subjecting bromodienes **61** to a Heck reaction. Subsequently, these 1,3-dienes **62** can serve as reaction partners in Diels–Alder reactions, performed either in the same or in a consecutive synthetic operation (Scheme 13).[92] Haloarenes can be linked to 1,4-butenediol in palladium-catalyzed reactions to yield γ-hydroxyaldehydes **64**, which can react further intramolecularly to provide the corresponding substituted hemiacetals **65**.[93]

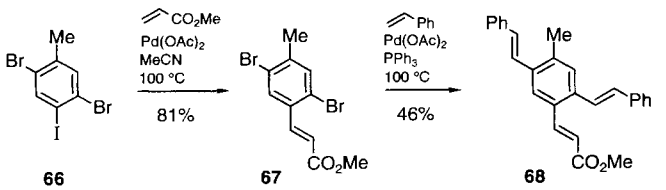


Scheme 13. X = Br, I; E = CO_2alkyl.

During the past six years these astonishingly simple concepts have revealed totally new perspectives for palladium-catalyzed reactions, which have been demonstrated in a whole host of synthetic applications. Thus, in the 25 years following its discovery, the Heck reaction has evolved from a simple alkenylation or arylation of alkenes to an integral part of tunable sequences consisting of various successive transformations in cascade reactions.

3. Heck Couplings with Oligohaloarenes: How Many Are Possible?

Since palladium-catalyzed alkenylations of haloalkenes and haloarenes often proceed in excellent yields, it would appear obvious to also apply this coupling to appropriate oligohalogen derivatives.[94] Heck et al.[95] reported on the twofold coupling of *ortho*- and *para*-diiodobenzene with alkenes at a very early stage. Bromoiodoarenes can also be coupled consecutively to two different alkenes, as was shown in the sequential reaction of 2,5-dibromo-3-iodotoluene (**66**) with methyl acrylate and styrene (Scheme 14).[96] Discrimination is possible with appropriate reaction conditions. When triphenylphosphane is not added, only iodide is replaced by acrylate, whereas upon addition of triphenylphosphane the dibromo derivative **67** reacts with two equivalents of styrene to give **68** (Scheme 14).

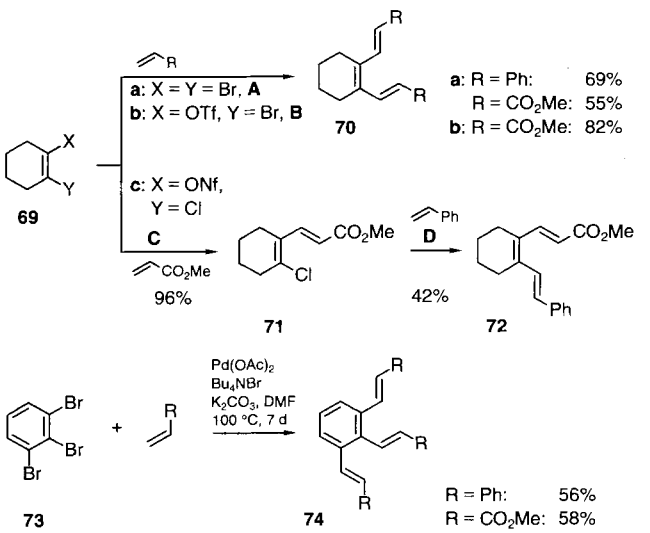


66 **67** **68**

Scheme 14.

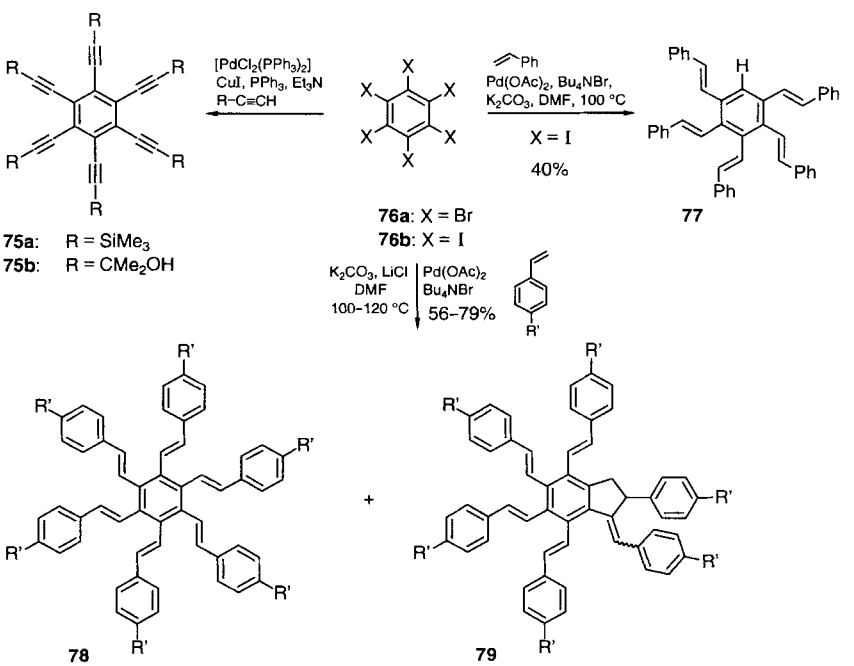
The scope of selectivity control in these multiple couplings can be extended with triflate leaving groups in the multifunctional substrates. The successive coupling of 2-chlorocyclohexenyl nonaflate (**69c**) with methyl acrylate and styrene to yield **72** is a typical example. In contrast, dibromide **69a** and bromotriflate **69b** react with styrene or acrylate under similar conditions to immediately give **70** (Scheme 15).[97]

Although the synthesis of hexaalkynylbenzenes **75** from hexabromobenzene (**76a**) was described some time ago (see Scheme 16),[98] hexaalkenylbenzenes other than hexaethenylbenzene were unknown.[99] Exchange of more than two vicinal halogen substituents on an arene by alkenyl groups failed to take place under Heck's original conditions.[95] However, Jeffery's[31] modified reaction conditions allow the replacement of three, four, five, and even six vicinal halogen substituents by styryl groups.[97, 100] For example, reaction of 1,2,3-tribromobenzene (**73**) with three equivalents of styrene smoothly yields 1,2,3-tristyrylbenzene (**74**) (Scheme 15). Hexaiodobenzene (**76b**) gave pentastyrylbenzene (**77**) in only 40% yield as the major product, apparently because of a side reaction involving protiodepalladation of the (aryl)iodopalladium intermediate.[100] In contrast, hexabromobenzene (**76a**) gave sixfold coupled products **78** with styrene and a whole host of *para*-substituted styrenes in good yields (Scheme 16). However, it proved to be extremely difficult to separate hexastyrylbenzenes **78** from isomers **79**, which were generated in further palladium-catalyzed reactions of *ortho*-dialkenylbenzenes.[101]



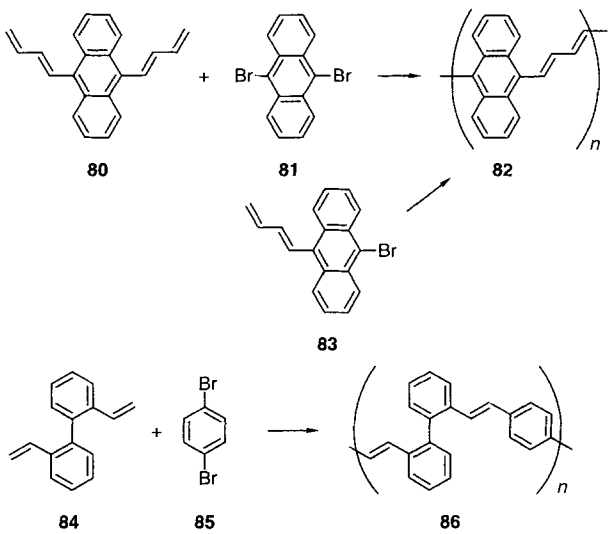
Scheme 15. A: $Pd(OAc)_2$, PPh_3, Et_3N, DMF, 90 °C, 40 h; B: as A but 65 °C, 4 h; C: as A but 60 °C, 24 h; D: $Pd(OAc)_2$, PPh_3, MeCN/THF (3/1), 10 kbar, 60 °C, 3 d. Nf = $C_4F_9SO_2$.

Multiple couplings of *para*-dibromoarenes with dialkenylarenes are also of interest for the synthesis of extended π systems. For example, 9,10-dibromoanthracene (**81**) and 9,10-bis(buta-



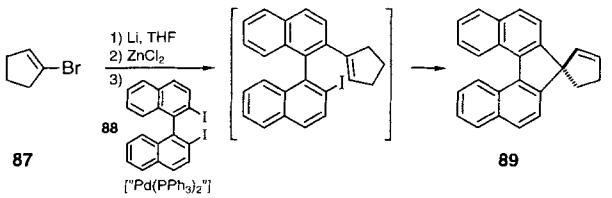
Scheme 16. R' = H, F, CH_3, OCH_3, OC_7H_{15}, $OC_{16}H_{33}$.

dienyl)anthracene (**80**) give oligomers **82** with an average degree of polymerization of 12. These oligomers can also be constructed from the bifunctional monomer **83** (Scheme 17).[102] The analogous coupling of 2,2'-diethenylbiphenyl (**84**) with *para*-dibromobenzene (**85**) led to oligomeric stilbenes **86** with an average degree of polymerization of 15. Compounds **86** are interesting owing to their potential in photochemically induced reactions.



Scheme 17.

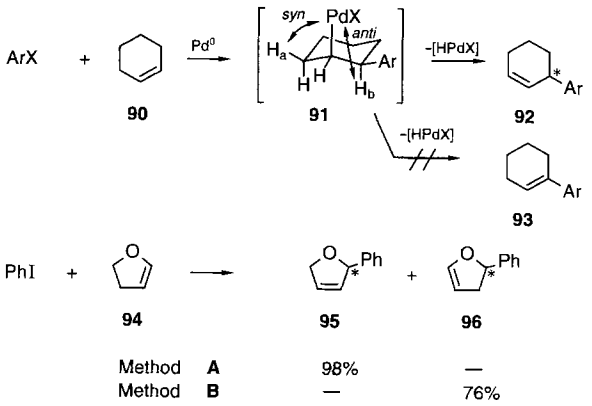
Palladium-catalyzed cross-couplings of dihaloarenes with unsaturated organozinc compounds, followed by an intramolecular Heck reaction offer a yet unexplored area. The interesting spiro compound **89**, for example, is available from 2,2'-diiodo-1,1'-binaphthyl (**88**) and 1-bromocyclopentene (**87**) (Scheme 18).[103]



Scheme 18.

4. Heck Reactions with Cyclic Alkenes: Key to the Construction of Stereogenic Centers

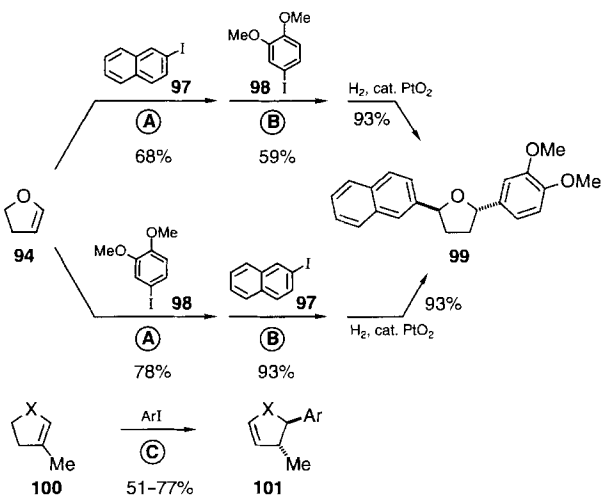
For a long time palladium chemists paid little attention to the intermolecular carbopalladation of cyclic alkenes, because at the high temperatures required, mixtures of double-bond isomers were frequently obtained.[104] But the reaction was never completely ignored, since it offered a possibility of creating new stereogenic centers by linking two sp^2 centers. For example, cis-addition of an arylpalladium species to cyclohexene **90**, followed by syn-elimination of hydrogen atom H_a in intermediate **91** produces 3-arylcyclohexene **92**, but not 1-arylcyclohexene **93**. Elimination of hydrogen atom H_b in the *anti* position does not take place (Scheme 19).



Scheme 19. X = I, Br, OSO_2CF_3. A: 3–4% $Pd(OAc)_2$, 9% PPh_3, 2 equiv Ag_2CO_3, MeCN, 80 °C; B: 2.5% $Pd(OAc)_2$, 1 equiv nBu_4NCl, 3 equiv KOAc, 2.5% PPh_3, DMF.

Thorough studies by Larock et al.[42c–f,l,n,105] led to the development of several experimental procedures with which undesired regioisomer formation can be avoided under very mild conditions.[106] In an impressive example, phenylation of 2,3-dihydrofuran (**94**) in the presence of silver carbonate provides 2-phenyl-2,5-dihydrofuran (**95**).[44,65] In contrast, reaction under Jeffery's[31] conditions affords solely the thermodynamically more stable 2-phenyl-2,3-dihydrofuran (**96**) (Scheme 19).[42n]

When conditions **A** and **B** are applied successively, two different arenes, for example 2-iodonaphthalene (**97**) and 3,4-dimethoxyiodobenzene (**98**), can be introduced to dihydrofuran (**94**) with *trans* stereoselectivity (Scheme 20). Upon catalytic



Scheme 20. X = O, NCO_2Et. A: 3–4% $Pd(OAc)_2$, 9% PPh_3, 2 equiv Ag_2CO_3, MeCN, 80 °C, 24 h; B: 2.5% $Pd(OAc)_2$, 1 equiv nBu_4NCl, 3 equiv KOAc, 2.5% PPh_3, DMF, 80 °C, 24 h; C: 2–6% $Pd(OAc)_2$, 4–12% PPh_3, Et_3N, DMF, 60–80 °C, 3–4 d.

hydrogenation the resulting product gave the *trans*-bisarylte-trahydrofuran **99** in excellent overall yields.[105b] This three-step sequence allows an exceptionally efficient and attractive approach toward potential antagonists of the platelet activating factor.[107] Similar twofold Heck reactions have also been performed with cyclopentene.[108]

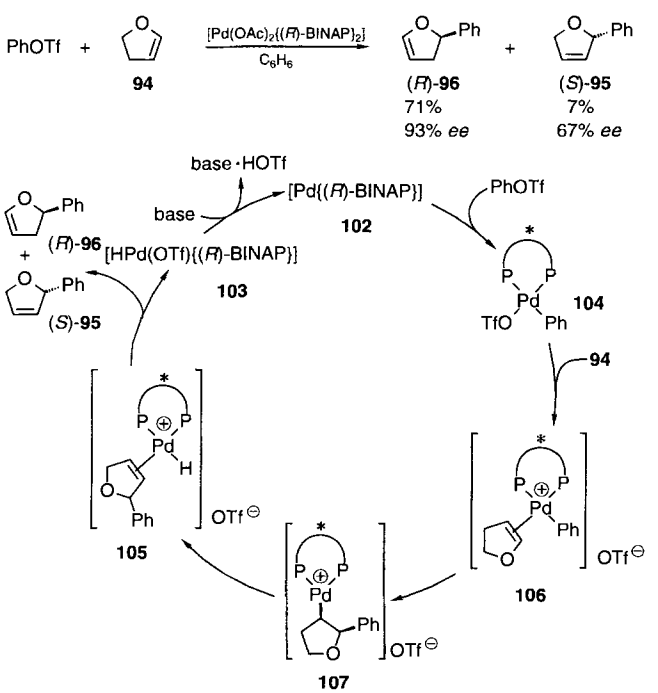
The diastereoselective construction of two stereocenters is also achieved in coupling reactions of 4-substituted 2,3-

dihydrofurans **100** (X = O) and 2,3-dihydropyrroles **100** (X = NCO_2Et). Arylations give exclusively *trans*-configurated products **101** (X = O, NCO_2Et) in good yields.[109]

4.1. The Ultimate Refinement: Heck Reactions with Intermolecular Asymmetric Induction

It is hardly necessary to point out the relevance of asymmetric synthesis in the preparation of chiral compounds. Transition metal induced reactions are increasingly important in the array of methods for the enantioselective construction of new asymmetric centers. Catalytic processes, in which chiral information is transferred from a small portion of the chiral auxiliary in the catalyst to a large portion of the prochiral substrate, are rapidly developing into extremely valuable methods.[110] Among these there are, however, only a few examples of reactions for the catalytic and enantioselective formation of carbon–carbon bonds.[110]

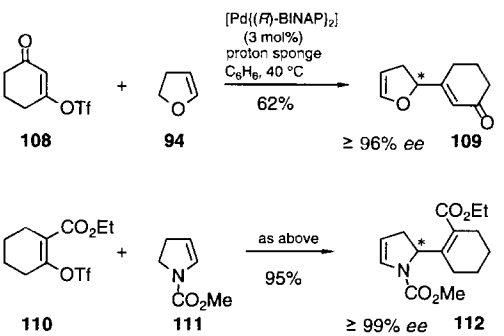
Subsequent to first reports by Overman et al.[111] and Shibasaki et al.[112] on intramolecular asymmetric Heck reactions, Hayashi et al. systematically investigated the ligand-induced asymmetric arylation of dihydrofurans.[10, 113] Whereas coupling with iodoarenes gave only low enantiomeric excesses in the presence of the C_2-symmetrical phosphane ligand (*R*)-1,1′-binaphthalene-2,2′-diylbis(diphenylphosphane) ((*R*)-BINAP), the coupling reaction of 2,3-dihydrofuran (**94**) with phenyl triflate afforded (*R*)-2-phenyl-2,3-dihydrofuran ((*R*)-**96**) with up to 93% enantiomeric excess and up to 71% yield (Scheme 21). In the reaction with iodobenzene, the BINAP ligand apparently dissociates from the intermediate phenylpalladium iodide complex to a certain extent. In contrast, when phenyl triflate is employed in the coupling, the labile triflate ligand dissociates more easily from intermediate **104**, thus generating the cationic complex **106**. Here, the BINAP ligand is much more tightly bound, and asymmetric induction is possible during the addition step leading to **107**.



Scheme 21. BINAP = P⌒P = 1,1′-binaphthalene-2,2′-diylbis(diphenylphosphane).

Quite interestingly, the minor product 2-phenyl-2,5-dihydrofuran (**95**) has the opposite, (*S*), configuration. However, this compound is produced with significantly less enantiomeric excess. It is possible that this is caused by a kinetic resolution effect in the alkene complex **105**; the π-bound palladium hydride in the complex leading to **96** could add again to the double bond (Scheme 21). Base influence is also noteworthy, and the highest enantiomeric excesses were achieved with 1,8-bis(dimethylamino)naphthalene ("proton sponge").[113c]

Regioselectivity and enantioselectivity were even better in reactions of alkenyl triflates with 2,3-dihydrofuran (**94**) and 2,3-dihydropyrroles such as **111**. Under optimized conditions, reactions with **108** and **110** yielded exclusively regioisomers **109** and **112** with enantioselectivities exceeding 96% and 99%, respectively (Scheme 22).

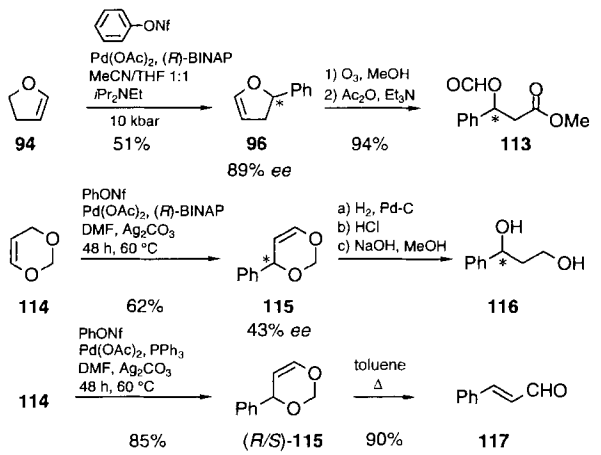


Scheme 22.

Whereas Hayashi et al. obtained good results for intermolecular reactions only with triflates, Shibasaki et al. achieved comparable inductions in intramolecular reactions of iodoalkenes by adding silver salts.[112, 114] These findings support the hypothesis that the generation of a cationic alkenylpalladium complex **106** has a favorable effect on the enantioselectivity (Scheme 21). Nevertheless, Ashimori and Overman[115] obtained good enantioselectivities even with neutral intermediate complexes and halide ligands in the presence of tertiary amines. These and other results[21] suggest a closer investigation of the influence of tertiary amines, which is certainly not just that of a simple base.

4.2. Degradation for Construction—An Interesting Concept

Reiser et al. recently reported[116] on the coupling reactions of aryl nonaflates with 2,3-dihydrofuran (**94**) under high pressure. Enantioselectivities were significantly higher than those obtained in analogous reactions under atmospheric pressure. The enantiopure 2-phenyl-2,3-dihydrofurans (**96**) can be cleaved by ozonolysis, and the resulting aldol derivatives **113** were obtained without loss of chiral information (Scheme 23).[117] A similar reaction sequence[118] is encountered in the enantioselective Heck arylation of 4*H*-1,3-dioxine (**114**), subsequent



Scheme 23. Nf = nonaflate = $C_4F_9SO_2$.

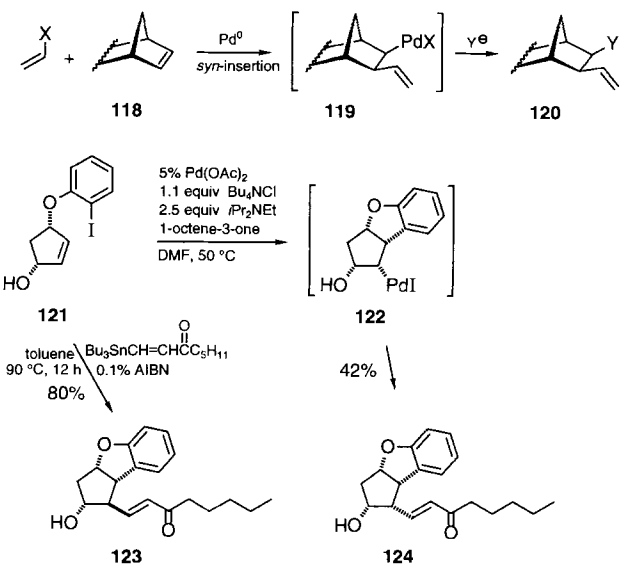
catalytic hydrogenation of phenyldioxine **115**, and acidic cleavage yielding diol **116** (Scheme 23). Although only moderate enantiomeric excess is achieved,[118b] experience shows that a further increase is likely. Another interesting reaction of phenyldioxine **115** is its thermal [4 + 2] cycloreversion to give cinnamic aldehyde **117**. This high-yielding reaction sequence formally corresponds to the β-formyl vinylation of haloarenes, and is thus an alternative to the straightforward arylation of α,β-unsaturated aldehydes under Jeffery's conditions.[31]

4.3. Multiple-Component Reactions: Entropy as the Only Opponent

The concept of stereoselective construction of stereogenic centers by means of Heck reactions becomes even more efficient and elegant when carbopalladations are performed with bridged cycloalkenes such as **118**. In the initially formed halo(β-vinylbicycloalkyl)palladium complex **119** there is no hydrogen atom with a *syn* orientation with respect to the palladium substituent. Therefore, the σ complex has an unusually long lifetime and may undergo intermolecular reaction with a nucleophilic coupling substrate (Scheme 24). In this way two new stereogenic centers can be generated in a single synthetic operation. Three-component couplings like these are suitable for prostaglandin synthesis. The same sequence consisting of carbopalladation and substitution allows the *cis*-selective introduction of two substituents. This differs not only from the previously developed domino reactions (γ-addition of cuprates to cyclopentenones and subsequent alkylation of the resulting enolates[119]), but also from radical domino cyclizations.[120]

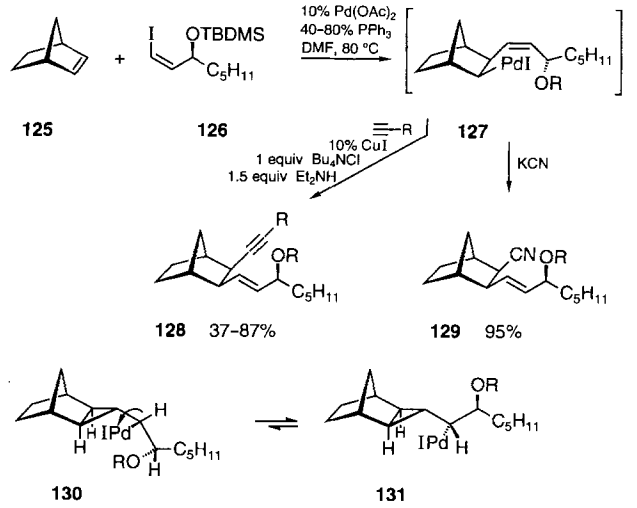
The palladium-induced asymmetric synthesis of the benzoprostacyclin derivative **124** from aryl ether **121** and 1-octen-3-one is an impressing application of this principle. Complementarily, radical-induced cyclization gives the epimeric benzoprostacyclin **123** (Scheme 24).[121]

Torii, Okumoto, et al.[122] have conducted decisive investigations concerning palladium-catalyzed stereoselective intermolecular three-component couplings. In view of the preparation of prostaglandin H (PGH) analogues with 2,3-disubstituted norbornane skeletons, they focused their attention on



Scheme 24. X = I, Br, OSO_2CF_3; Y = nucleophile (e.g. CN); AIBN = 2,2'-azobisisobutyronitrile.

diastereoselective additions to C_s-symmetric norbornene **125** (Scheme 25). Based on early studies by Catellani and Chiusoli[123] as well as by Larock et al. (application of halo-

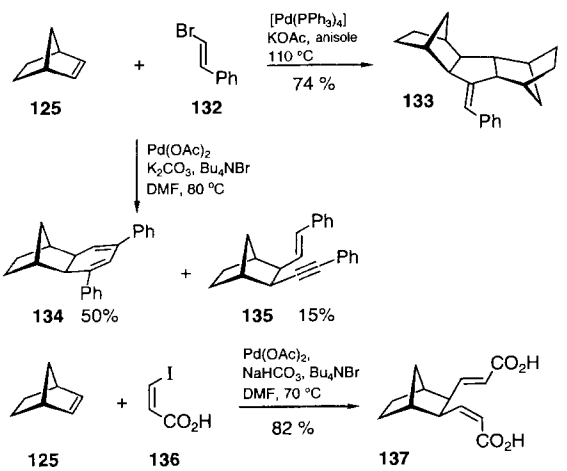


Scheme 25. R = TBDMS = tBuMe$_2$Si.

(alkenyl)mercury compounds as coupling partners[88a, c, 124]), Torii, Okumoto et al. used chiral iodoalkenes **126**. After addition to norbornene (**125**) the alkylpalladium intermediate **127** was captured either with cyanide or terminal alkynes.[122] Not only was *cis*-diastereoselective bis-*exo* coupling observed, but also enantiofacial differentiation of the *meso* substrate norbornene. This asymmetrically induced desymmetrization in the sequential formation of two new carbon–carbon bonds is accompanied by *cis*/*trans* isomerization of the side-chain double bond. A cyclopropylmethylpalladium intermediate **130** is postulated to explain the formation of the more stable *trans* alkene. Rotation about the C–C bond adjacent to Pd leads to the favored conformer **131**, which opens to give the thermodynamically more stable *trans*-alkenyl derivative. Cyclopropane deriva-

tives containing a norbornane skeleton derived from tricyclo[3.2.1.$0^{2,4}$]octane intermediates **130**/**131** have meanwhile been isolated and characterized.[88d, 125]

Halo(norbornyl)palladium intermediates of type **119** (Scheme 24) formed in alkenylations or arylations of norbornene have been identified by reduction with formate,[42b, 125] and also by couplings with organotin compounds[126] and boronates.[127] At least the first step of the domino couplings involving norbornene (**125**) and β-bromostyrene (**132**) proceed analogously and yield **133** and **134**, respectively (Scheme 26). It is not clear why, depending on the selected reaction conditions, two molecules of norbornene react with bromostyrene to give pentacycle **133** with a new five-membered ring,[128] or alternatively only one molecule of norbornene (**125**) reacts with two molecules of **132** to give cyclohexadiene **134**.[129]



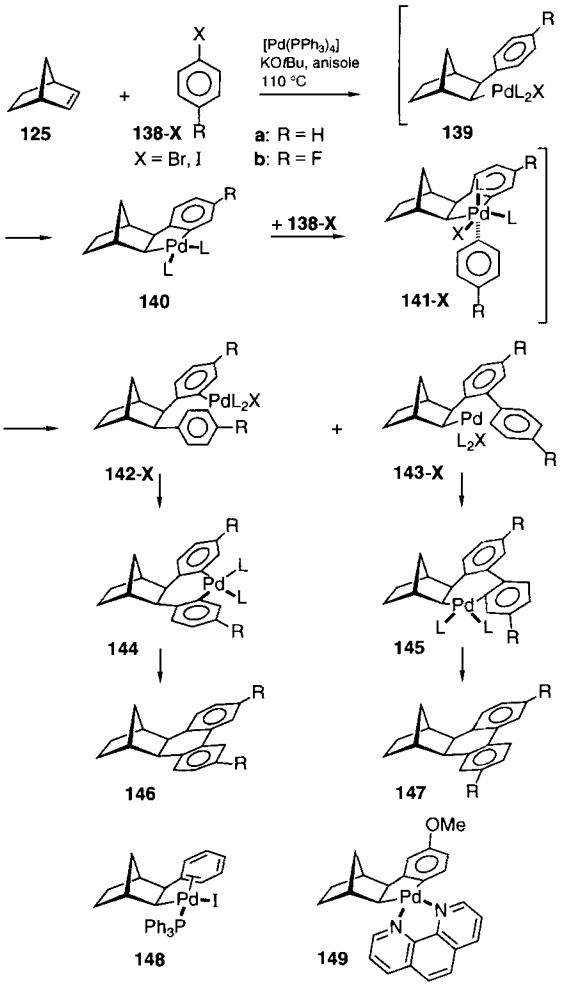
Scheme 26.

Even more puzzling is the finding that *cis*-3-iodoacrylic acid (**136**) reacts under analogous conditions to yield neither the first nor the second kind of product, but the twofold coupled *exo,exo* product **137** with one *cis*- and one *trans*-configurated acrylic acid group.[129] A cyclopropylmethylpalladium intermediate like **131** probably plays a key role in this reaction.

Although the development of palladium-catalyzed multicomponent couplings is still in its infancy, the enormous synthetic potential inherent in this reaction principle is apparent even at this early stage.

4.4. When Heck Reactions Stall: Palladacycles as Intermediates

Some of the above-mentioned palladium-catalyzed sequential couplings with norbornene are not in accord with the common scheme of the Heck reaction. Even haloarenes can react with norbornene to give domino coupling products, provided that other substrates such as alkynes or reducing agents are absent. Thus, upon reaction of iodo- or bromoarenes **138-X** with norbornene (**125**) (in the presence of [Pd(PPh$_3$)$_4$], KO*t*Bu, and anisole at 110 °C), Catellani and Chiusoli obtained the norbornane-annelated 9,10-dihydrophenanthrenes **146** and **147** (Scheme 27).[130] Different reaction conditions (Pd(OAc)$_2$, K_2CO_3, Bu_4NBr, DMF, 80 °C) led to norbornane-annelated

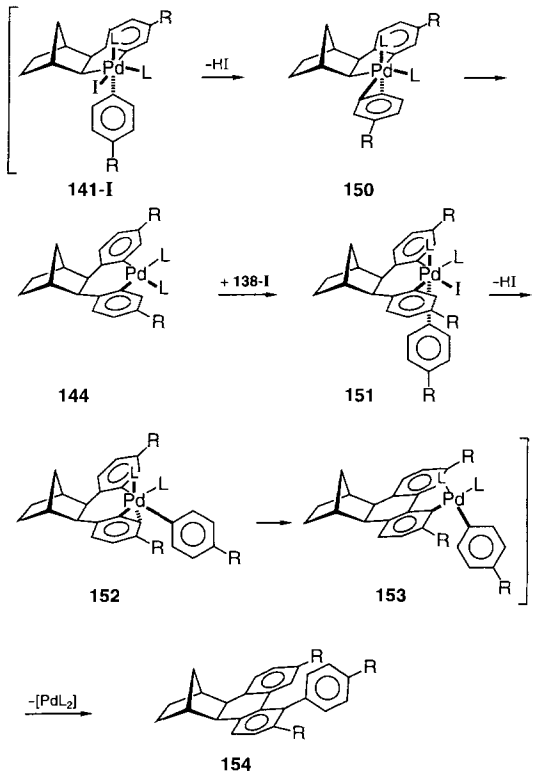


Scheme 27.

4-aryl-9,10-dihydrophenanthrenes **154** exclusively, which apparently were formed from three molecules of **138-X** with one molecule of norbornene (**125**)[131] (see Scheme 28). Both reactions are likely to proceed identically in the first steps. After oxidative addition of the aryl halide to palladium and *exo-syn*-addition of the resulting (aryl)halopalladium complex to **125**, the norbornylpalladium intermediate **139** cyclizes to give palladacycle **140** since it has no coupling partner (Scheme 27). Oxidative addition of another molecule of aryl halide to intermediate **140** gives palladium(IV) complex **141-X**.[132] The structure of intermediate **139** has been corroborated by X-ray structure analysis of complex **148**.[133] The observed η^2-complexation of the phenyl group in **148** provides support for *ortho* activation en route to complex **141-X**. Furthermore, Chiusoli et al.[134] have demonstrated that the well-characterized Pd^{II} complex **149** undergoes facile oxidative additions with a number of reagents.[135]

Reductive elimination in **141-X** can take two directions, leading to Pd^{II} complexes **142-X** and **143-X**, respectively. Repeated *ortho*-CH activation and reductive elimination (via **144**

and **145**) lead to the isomeric products **146** and **147**. Dehydroarene complex **150** can be proposed as an intermediate in the second *ortho*-CH activation (**141-I** → **144**) (Scheme 28). Certain

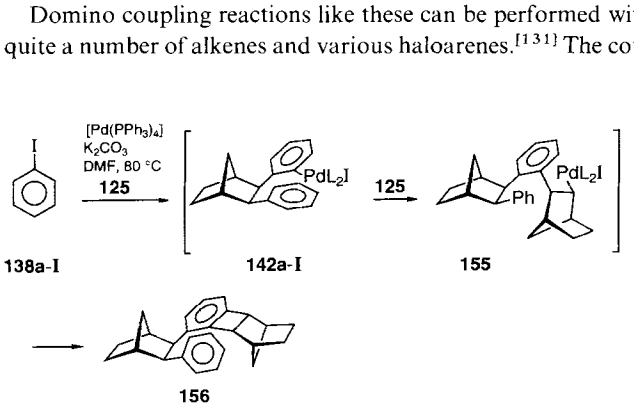


Scheme 28.

conditions lead to a four-component reaction at the stage of the seven-membered palladacycle **144**; oxidative addition of another molecule of iodoarene **138-I** yields the Pd^{IV} complex **151**. Repeated generation of an aryne complex **152**, followed by reductive elimination to give palladium(II) complex **153**, and final reductive elimination regenerates the catalytically active palladium(0) species and provides the 4-aryldihydrophenanthrene derivative **154** (Scheme 28).[131c]

Under yet another set of conditions ($[Pd(PPh_3)_4]$, K_2CO_3, DMF, 80 °C) intermediate **142a-I** reacts with norbornene (**125**) and affords benzocyclobutene **156** apparently via **155** (Scheme 29).[136a]

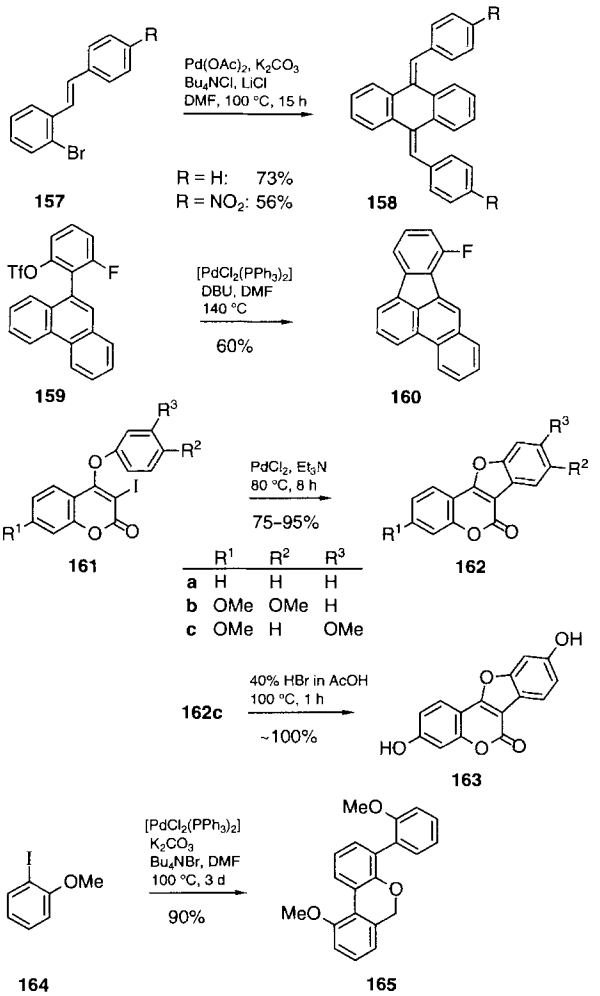
Domino coupling reactions like these can be performed with quite a number of alkenes and various haloarenes.[131] The cou-



Scheme 29.

pling products derived from norbornene and dicyclopentadiene can serve as precursors for diverse polycyclic aromatic compounds.[131c]

By slightly modifying the reaction conditions and the medium the chemistry of palladacycles can be made to proceed selectively, and therefore provides a wealth of interesting perspectives (Scheme 30).[136b] Examples include the dimerization of *ortho*-



Scheme 30. DBU = diazabicycloundecane.

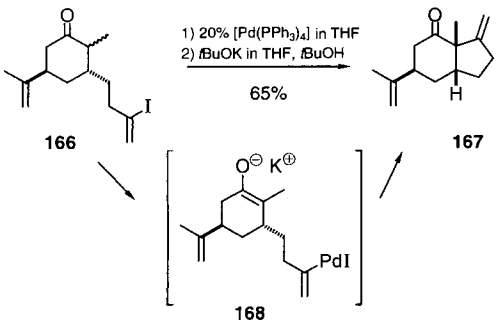
bromostilbenes **157** to give (*Z*)-9,10-dibenzylidenedihydroanthracenes **158**,[100] the synthesis of benzofluoroanthrenes **160** from aryl triflate **159**[137] and of coumestan **162** and coumestrol (**163**) from 4-aryloxy-3-iodo-2*H*-1-benzopyran-2-ones **161**,[138] and the CH activation of *ortho*-methoxy groups as in 2-iodoanisole (**164**) reported by Dyker,[139] leading elegantly to 6*H*-dibenzo[*b*,*d*]pyrans like **165** (Scheme 30).

5. Palladium-Catalyzed Reactions with Nucleophilic Substrates

5.1. Soft Nucleophiles as Reaction Partners

The complexes generated by oxidative addition of haloarenes and haloalkenes to palladium(0) are electrophilic at the substi-

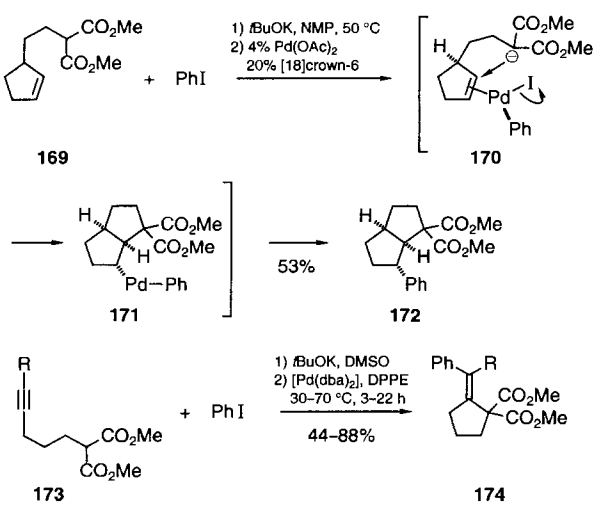
tuted metal center, and can therefore react with carbon nucleophiles other than alkenes, especially with enolate and homoenolate ions, to form new C–C bonds. As Takahashi et al.,[140] Ciufolini et al.,[141] and Piers et al.[142] have shown, palladium-catalyzed intramolecular and intermolecular arylations and alkenylations can be achieved with soft enolate anions. Even quaternary carbon centers may be constructed in this way. The methylenecyclopentane annelation developed by Piers et al. and demonstrated with iodoalkene **166** in Scheme 31 is an interesting alternative to other methods for annelations with five-membered rings.[142] In the mechanism it is assumed that intermediate **168** undergoes an intramolecular nucleophilic substitution, leading to a six-membered palladacycle. Bicycle **167** is subsequently formed by reductive elimination.



Scheme 31.

The formation of substituted cyclopentanes such as **172** and alkylidenecyclopentanes **174** has been investigated fairly thoroughly. These studies focused on intermolecular reactions between iodoarenes and substituted enolates of malonic ester that contain double or triple bonds in the 4'-position (Scheme 32).[143] The results indicate that the electrophilicity of the double or triple bond is enhanced by coordination to the σ-arylpalladium species, and attack of the enolate ion is facilitated (Scheme 32).

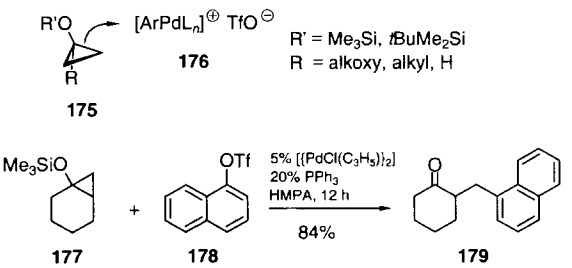
Utimoto, Nozaki, et al.[144] reported at a very early stage on the palladium(II) activation of triple bonds towards nucleophilic



Scheme 32. R = H, CH_3, C_3H_5, CH_2OTHP, $(CH_2)_2OTHP$; NMP = *N*-methylpyrrolidone; DPPE = 1,2-bis(diphenylphosphano)ethane.

attack with carboxylate ions. This method has recently seen a growing number of applications.[145]

Nakamura, Kuwajima et al.[146] have shown that donor-substituted cyclopropane derivatives **175** can be also activated, by cationic arylpalladium complexes **176**, in particular (Scheme 33). The products of a formal arylation of homoenol-

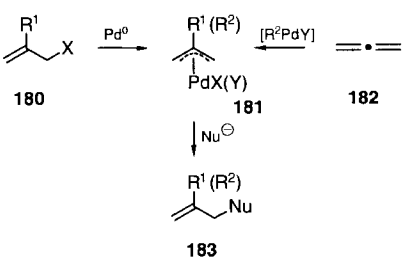


Scheme 33. HMPA = hexamethylphosphoric triamide.

ates are obtained in good yields in the presence of (allyl)chloropalladium, as in the reaction of silyloxycyclopropane **177** with aryl triflate **178**.

5.2. An Unusual Combination: Heck Reactions and π-Allylpalladium Complexes

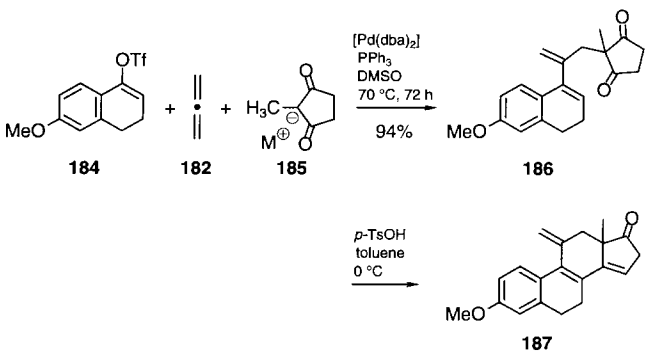
Palladium-catalyzed substitutions of allylic esters **180**, which proceed via π-allylpalladium complexes such as **181**, are well established in the meantime (Scheme 34).[82] In contrast, the



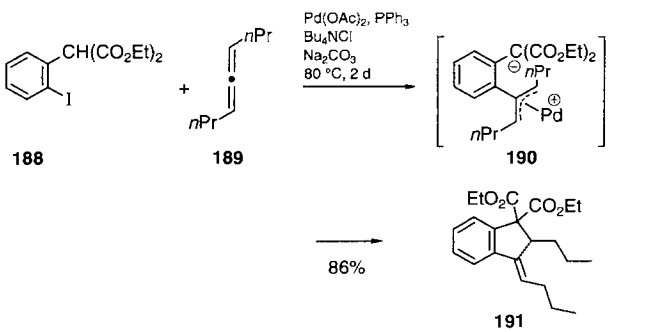
Scheme 34. R^1 = H, alkyl; R^2 = aryl, alkenyl; X = OCOalkyl; Y = I, Br, OSO_2CF_3; Nu = nucleophile.

potential of reactions proceeding through π-allylpalladium intermediates, generated by adding haloarenes, haloalkenes, or the corresponding triflates to allenes **182** and substituted allenes under Pd catalysis, has scarcely been tapped (Scheme 34). π-Allylpalladium intermediates generated in this way have been utilized elegantly by Gore et al.[89, 147] in three-component reactions. For example, allene (**182**), the enol triflate of 6-methoxytetralone (**184**), and the enolate of 2-methylcyclopentane-1,3-dione (**185**) give **186** smoothly and in very good yield (Scheme 35). The steroid skeleton **187** is obtained in just one more step.[148]

In the presence of a palladium catalyst and a base, haloarenes such as **188** containing a CH-acidic group in *ortho* position react regioselectively in inter–intramolecular reactions with allenes such as **189**, giving high yields of annelated arenes like **191** with five-membered rings (Scheme 36).[149] Treatment of 1,3-dienes,[42q, 150] 1,4-dienes,[151] methylenecyclopropanes, and

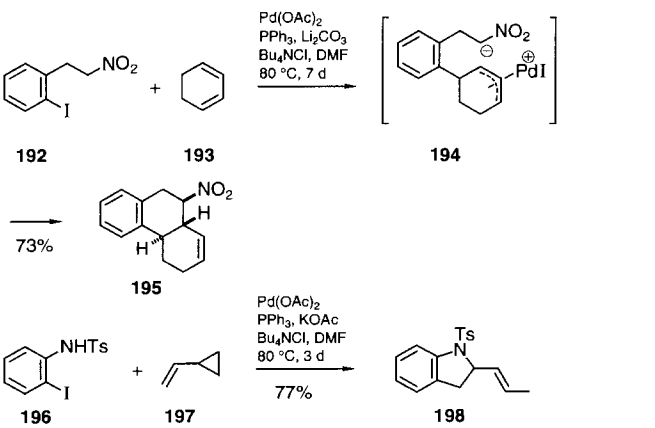


Scheme 35.



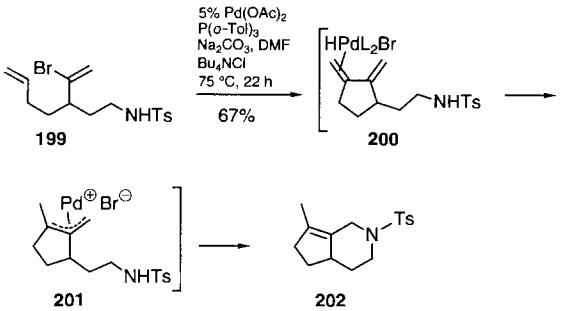
Scheme 36.

ethenylcyclopropanes with arylpalladium intermediates leads to π-allylpalladium complexes, which can be trapped with a variety of nucleophiles. Larock et al. showed that 1,3-cyclohexadiene (**193**)[42q] and *ortho*-(2′-nitroethyl)iodobenzene (**192**) react in the presence of palladium acetate via π-allyl complex **194** to afford the *trans*-configurated tricycle **195** (Scheme 37). Ethenylcyclopropane (**197**) and substituted 2-iodoaniline **196** are transformed analogously into dihydroindole **198**.[152a]



Scheme 37.

Weinreb et al. presented an interesting new approach to nitrogen heterocycles,[153] based on early findings by Heck et al. that coupling reactions of haloalkenes with alkenes in the presence of secondary amines give allylamines.[154] The palladium-catalyzed cyclization of bromo-1,6-diene **199** initially gives 1,3-diene **200**. Readdition of the eliminated halohydridopalladium leads to the π-allylpalladium complex **201**, which then undergoes intramolecular nucleophilic substitution, yielding bicycle **202** (Scheme 38).

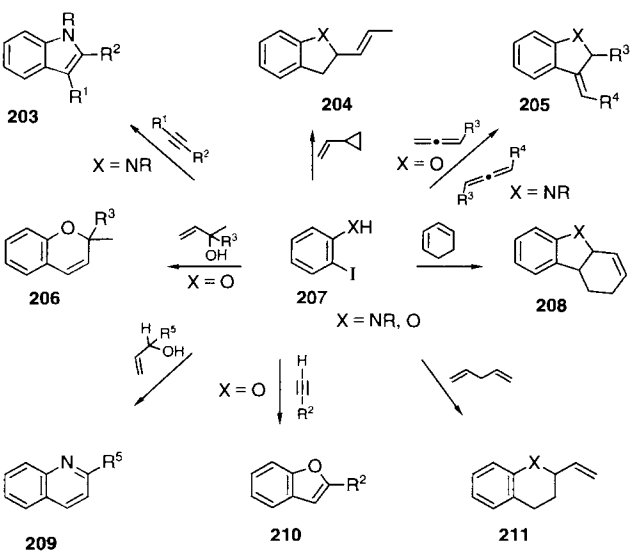


Scheme 38. Tol = tolyl; Ts = tosyl = $CH_3C_6H_4SO_2$.

Interestingly, π-allyl complexes are not generated in palladium-catalyzed arylations of ethenylepoxides, ethenyl oxetanes, or 4-alkenyl-2-azetidinones. Rather, substituted allyl alcohols,[155] homoallyl alcohols,[156] and 5-aryl-3-alkenamides[157] are formed.

5.3. New Routes to Heterocycles: Pd-Catalyzed Heteroannelations

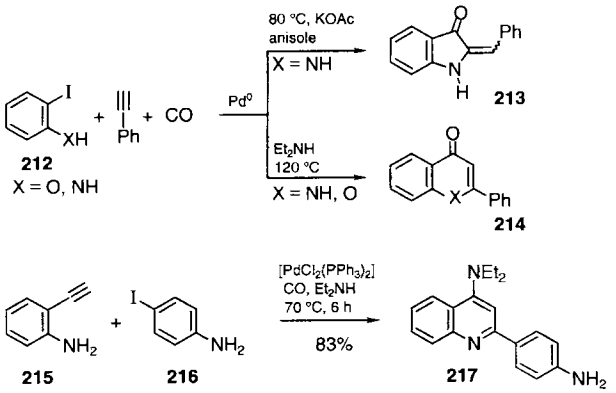
Given the tremendous variety of naturally occurring heterocycles, the development of elegant and efficient synthetic routes to these substances is a desirable goal. Palladium-catalyzed reactions have revealed almost unlimited horizons in this field, which have been documented in a myriad of publications. The array of palladium-catalyzed annelation reactions that *ortho* hetero-substituted iodoarenes **207** can undergo with 1,2-,[149] 1,3-,[42q, 150b] and 1,4-dienes[151] and ethenylcyclopropanes[152] is exemplary (Scheme 39). These reactions, which lead to substi-



Scheme 39. R = H, Me, Ac, Ts; R^1 = alkyl, alkenyl, aryl, CH_2OH; R^2 = alkyl, aryl, CH(OH)aryl, trimethylsilyl, *tert*-butyldimethylsilyl for X = NR; R^3 = alkyl; R^4 = H, alkyl; R^5 = alkyl, aryl.

tuted dihydrobenzofurans and dihydroindoles, also proceed via intermediate π-allylpalladium complexes. Transformations with terminal and internal alkynes afford monosubstituted and disubstituted benzofurans **203**, **210** (X = O)[158] and indoles **203**, **210** (X = N),[159] respectively, in good yields. When allylic alcohols are employed as coupling partners, 2,2-disubstituted chromenes **206**[160] and quinolines **209** are obtained.[161]

New strategies for the annelation of benzene derivatives with five- and six-membered rings rely on the carbonylative coupling of iodo- and bromoarenes with aminophenols[162] and of terminal alkynes with iodophenoles and iodoanilines.[163, 164] In these reactions it is irrelevant whether the heteroatom is at the *ortho* position of the iodoarene **212** or whether it is part of the aryl alkyne as in **215** (Scheme 40).[164] *ortho*-Iodoanilines and *ortho*-iodophenols react with carbon monoxide and phenyl-



Scheme 40.

acetylene in the presence of diethylamine to give 2-substituted 1,4-dihydro-4-oxoquinolines and flavones **214**, respectively. In contrast, *ortho*-iodoaniline yields indoxyl derivatives **213** in anisole, when potassium acetate is used as base.[165] A tremendous number of possible combinations of aryl or alkenyl halides with alkynes or alkenes and alcohols or amines are possible, and their reactions under palladium catalysis lead to a variety of heterocycles.[166]

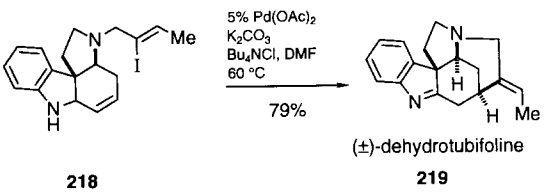
The reaction of 4-iodoaniline (**216**) and (2-aminophenyl)-acetylene (**215**) in diethylamine and exposed to a carbon monoxide atmosphere yields 2-(4′-aminophenyl)-4-diethylaminoquinoline (**217**) in a single synthetic operation.[164]

6. Intramolecular Heck Reactions with Alkenes

6.1. Applied Intramolecular Heck Reactions

For a long time applications of the Heck reaction in the construction of cyclic systems were focused on the preparation of heterocyclic compounds from appropriately substituted haloarenes.[153b, 167] It was not realized until only recently that even complicated ring systems with numerous different functionalities may also be assembled.

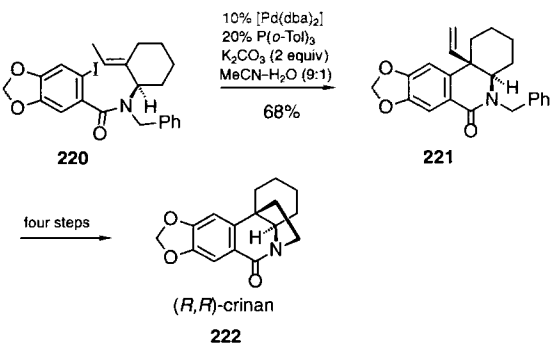
Efforts to develop a generally applicable and stereocontrolled synthesis of *Strychnos* alkaloids led Rawal et al.[168] to the preparation of (±)-dehydrotubifoline (**219**) (Scheme 41). Ring



Scheme 41.

closure of **218** was performed under palladium catalysis in the presence of K_2CO_3 and Bu_4NCl with subsequent enamine–imine tautomerization. The ethylidene group typical for many *Strychnos* alkaloids retains its defined configuration in this transformation.

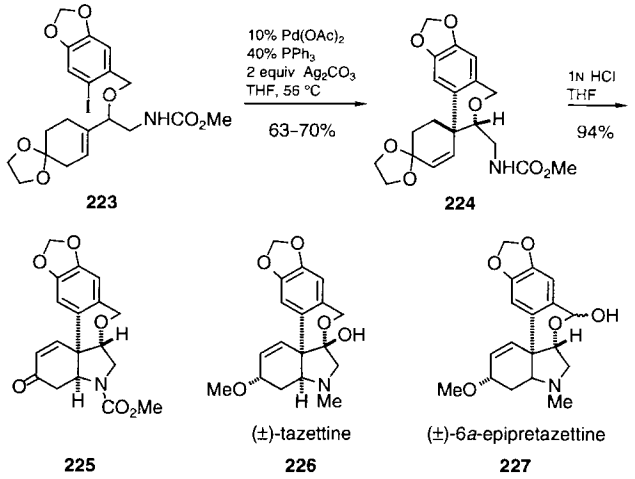
The Heck reaction may even be applied in the construction of tetrasubstituted carbon centers, which are often accessible otherwise only with great difficulty.[42a, p, 44a] Following this strategy, Grigg et al.[42a, p] and in particular Overman et al.[169] have developed new, impressive regioselective and stereoselective routes to a number of complex heterocyclic natural products. (*R,R*)-Crinan (**222**)[23i], an alkaloid from plants in the *Amaryllidaceae* family, has been prepared in a total synthesis in which the key step is the regioselective formation of the central heterocyclic ring (Scheme 42). This was accomplished by an in-



Scheme 42.

tramolecular 6-*exo-trig* reaction of the iodoarene moiety in **220** with the exocyclic double bond on the cyclohexane ring. Interestingly, high yields and high stereoselectivities are possible only when the reaction mixture contains 10% water[47, 170] and when sterically demanding phosphanes are added.[23i]

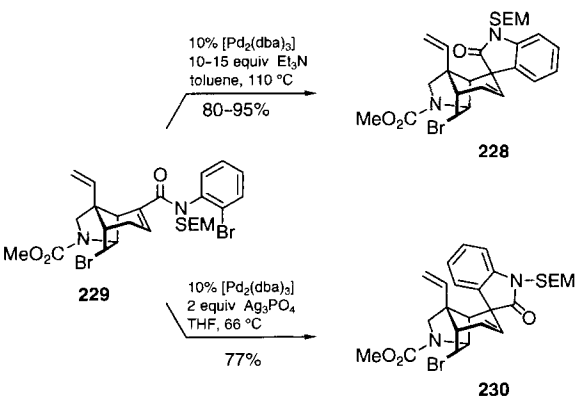
In the syntheses of two other *Amaryllidaceae* alkaloids, tazettine (**226**) and 6*a*-epipretazettine (**227**), the key steps also followed the same principle (Scheme 43).[171] The common precursor is tetracycle **225**. Palladium-catalyzed intramolecular insertion of the iodoarene moiety into the double bond of the appended cyclohexene ring in **223** and subsequent acid-catalyzed rearrangement leads to the 2-benzopyrano[3,4-*c*]hexahydroindole subunit in **225**. Excellent stereoselectivity was observed and the cyclization proceeded as a 6-*exo-trig* ring closure. Compound **225** was thus prepared in 90% yield (63–70% after recrystallization), and provided access to 6*a*-epipretazettine and other related compounds. It should be noted that the intramolecular Heck reaction in **223** required stoichiometric amounts of silver salts. In the formation of tetracycle **225**, which has the relative configuration of the 6*a*-epipretazettines, the



Scheme 43.

Pd–C σ bond and the alkene π bond must be eclipsing in a transition state with a boat conformation.

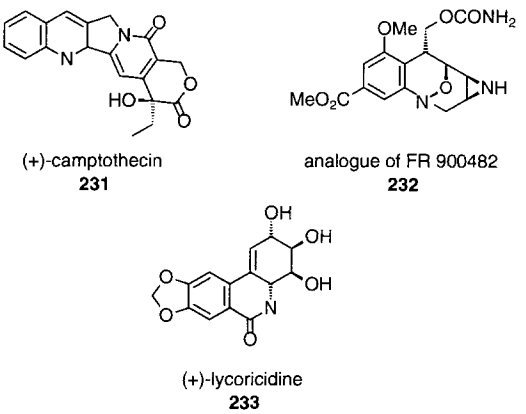
The syntheses of heteropentacycles **228** and **230** by Overman et al.[169, 172] constitute a highlight in the stereoselective construction of compounds containing quaternary carbon centers with sterically demanding substituents (Scheme 44). The dra-



Scheme 44. SEM = $CH_2OCH_2CH_2SiMe_3$.

matic influence of silver salts and various ligands on the stereoselectivity of intramolecular Heck reactions has been impressively demonstrated with the cyclization of tetracyclic acryloyl-2-bromoanilide **229**. In the transition state leading to **228** the 1,3-diaxial interactions between the vinyl group and the oxoindole group make the generation of the pentacyclic oxoindole appear rather unexpected. Additionally, 1,3-diaxial interactions between the ethano bridge and the ligands of the coordinated square-planar alkylpalladium complex (after insertion of the bromoarene moiety) must be allowed for. Formation of pentacycle **228** is greatly favored when the reaction is performed without phosphane ligands. On the other hand, when silver salts are added to the reaction mixture, an almost total reversion of stereoselectivity is observed, thus favoring formation of **230**. The more polar transition state, which is reached via a cationic complex, is favored if the attack occurs from the side of the angular vinyl group. In this way additional coordination of palladium in the complex is facilitated by the vinyl group.

Further examples for natural product syntheses in which intramolecular Heck reactions are important key steps include those of (+)-camptothecin (**231**),[173] the congener **232** of FR 900482,[174] and (+)-lycoricidine (**233**)[23a, 175] (Scheme 45).

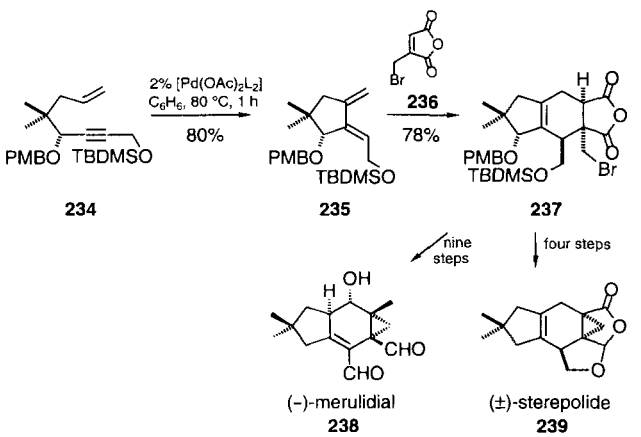


Scheme 45.

Early on, efforts were made to apply palladium-catalyzed alkenylations and especially arylations of double bonds to the synthesis of heterocycles, and these reactions are meanwhile widely applied. However, it took quite a long time before exhaustive and detailed studies were undertaken on the analogous preparations of pure carbocycles. The pioneering work was done by Grigg et al.[42g, 45b, 176a–c] and Negishi et al.[176e–i] in studies of the regioselectivity in cyclizations of acyclic 1- and 2-bromo(or -iodo-)dienes. Although *n-exo-trig* ring closures[177] were found to be generally favored, double bond isomerizations following cyclization often remained a major difficulty. This problem was solved later by adding silver(I) and thallium(I) salts.[44, 45b, 176c]

At the same time Trost et al. developed cycloisomerizations for 1,6-enynes[76] under mild conditions for the construction of carbo- and heterocycles with high regioselectivities and in very good yields. In view of possible synthetic applications, both cycloisomerizations of 1,6(7)-enynes and the selective intramolecular Heck coupling of 2-bromo(or -iodo-)-1,6(7)-dienes to give 1,2-bis(exomethylene)cycloalkanes rapidly gained interest. The latter are suitable substrates for subsequent Diels–Alder reactions.[76a, 92, 176a–c, 178]

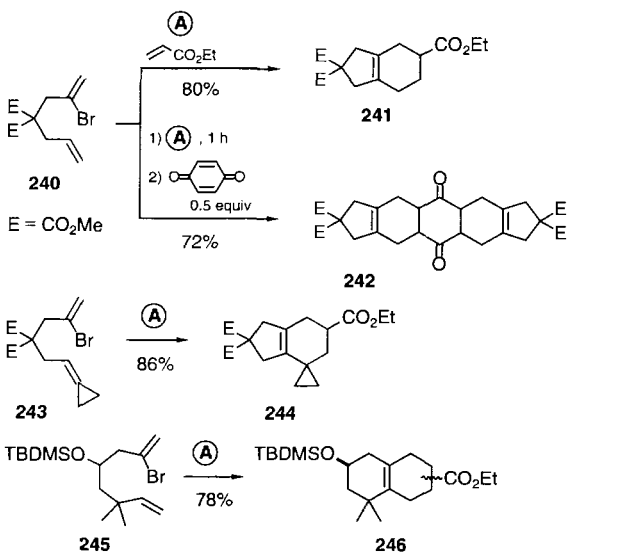
For example, this sequence consisting of a palladium-catalyzed cycloisomerization followed by a Diels–Alder reaction was applied in the syntheses of (±)-sterepolide (**239**)[179] and (−)-merulidial (**238**) (Scheme 46).[180] Both the cycloisomerization of enyne **234** and the Diels–Alder reaction of diene **235** with bromomethyl malonic anhydride (**236**) proceed in good yields. In this synthesis it was essential that formation of the 1,4-diene be suppressed. This was possible with the trialkylsilyloxymethyl group on the alkyne moiety, and the desired 1,3-diene was formed almost exclusively. Analogous Heck reactions performed with corresponding 2-bromo-1,6-dienes having an allylic alcohol function lead preferentially to γ,δ-unsaturated car-



Scheme 46. PMB = *para*-methoxybenzyl; L = P(*o*-Tol)$_3$.

bonyl compounds in the absence of silver(I) or thallium(I) salts.[176d]

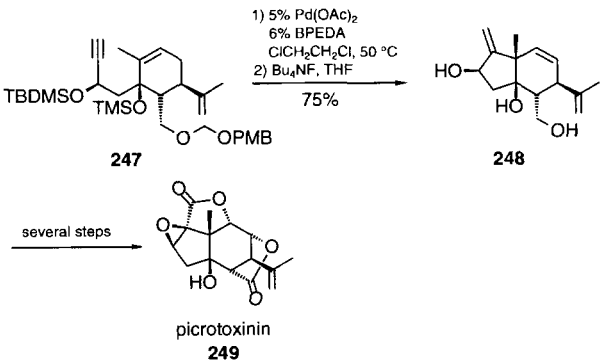
This sequence is normally conducted in two steps, but may also be performed in a one-pot procedure without isolating the intermediate diene, by adding an external dienophile[92] or by making use of a dienophile already present in the intermediate. The intra–intermolecular sequence consisting of Heck and Diels–Alder reactions is feasible only with dienophiles that cannot oxidize the applied catalyst. For example, 2-bromo-1,6-diene **240** reacts smoothly in a one-pot procedure to give bicycle **241** in good yield (Scheme 47). On the other hand, in reactions



Scheme 47. E = CO_2Me; A: 3% $Pd(OAc)_2$, 8% PPh_3, 1.2 equiv Ag_2CO_3, MeCN, 90 °C, 45 min.

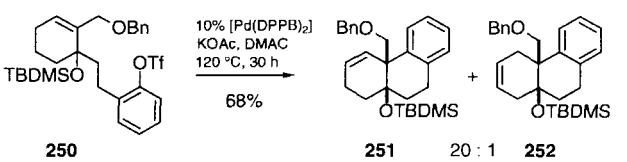
with dienophiles like *para*-benzoquinone, the 1,3-diene must be preformed prior to the addition of the dienophile. Palladium-catalyzed 1,6-enyne cyclizations[76] and subsequent Diels–Alder reactions are also feasible in a one-pot procedure.[92] However, in certain cases bromodienes succeed even when the analogous enyne cycloisomerizations fail. This is demonstrated by bromodiene **243** containing a terminal methylenecyclopropane group, and compound **245**, which both cyclize to form a five- and a six-membered ring, respectively.[181] It is only a matter of time until the combination of metal-catalyzed cyclization and thermal cycloaddition sees its first application in natural product synthesis.

Palladium-catalyzed cycloisomerization is by no means restricted to the preparation of 1,2-bis(exomethylene)cycloalkanes. Other applications include the total syntheses of (−)-dendrobine[182] and picrotoxinin (**249**) (Scheme 48).[76c, 183] The skeleton **248** of **249** was obtained from enyne **247** in very good yield.



Scheme 48. BPEDA = *N*,*N*′-bis(phenylmethylene)-1,2-ethylenediamine; TMS = Me_3Si.

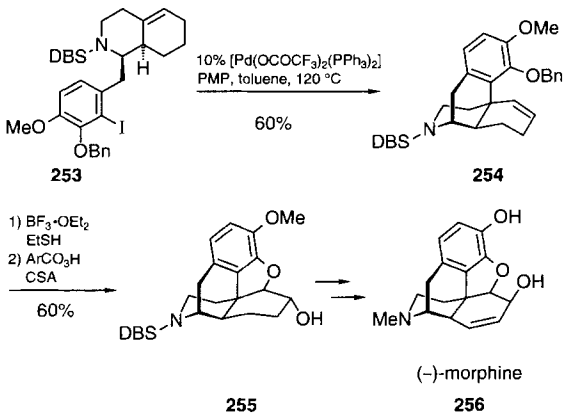
In research directed toward the synthesis of complex cardenolides, Overman et al. examined intramolecular Heck cyclizations with model reactions of triflate **250**, and obtained carbocycles **251** and **252** with the desired *cis* annelation (Scheme 49).[184a]



Scheme 49. DPPB = 1,4-bis(diphenylphosphano)butane. DMAC = *N*,*N*-dimethylacetamide; Bn = benzyl.

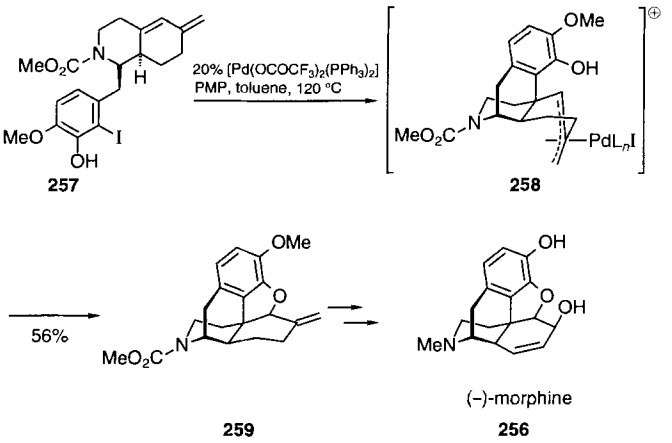
The syntheses of (−)- and (+)-morphine by Overman et al.[184b, 185] constitute further impressive examples, as both enantiomers were prepared for the first time without separation of the diastereomeric intermediates. Again, intramolecular Heck reactions play an important role in Overman's construction of the morphine skeleton. In an initial attempt, an active catalyst obtained from $[Pd(OCOCF_3)_2(PPh_3)_2]$ was used to convert iodoarene **253** into the unsaturated morphinane **254** (Scheme 50). Selective cleavage of the benzyl ether and cyclization of the camphor sulfonate of **254** with 3,5-dinitroperoxybenzoic acid finally yielded pentacycle **255**, which was then transformed via (−)-dihydrocodeinone into (−)-morphine (**256**).[184b]

If, on the other hand, iodoarene **257** is cyclized under palladium catalysis, pentacyclic skeleton **259** is formed directly. In this reaction intramolecular arylation of the 1,3-dienic moiety gives



Scheme 50. DBS = dibenzosuberyl; PMP = 1,2,2,6,6-pentamethylpiperidine; CSA = camphorsulfonic acid; Ar = 3,5-dinitrophenyl.

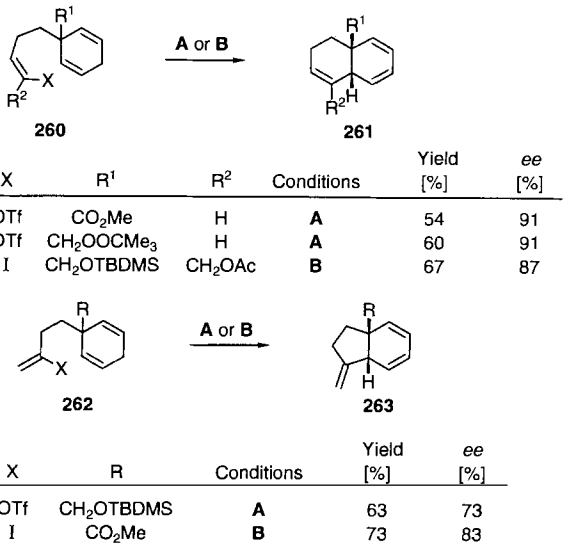
π-allylpalladium complex **258**, the phenolic hydroxy function of which is captured in an intramolecular reaction yielding **259**, a precursor to morphine (Scheme 51).[184c, 185]



Scheme 51.

6.2. Tailored Intramolecular Asymmetric Heck Reactions

The enormous potential of intramolecular Heck reactions has been demonstrated impressively in elegant syntheses of even the most complicated natural product skeletons. Addressing the question of whether these reactions may be performed enantioselectively, Shibasaki et al.[112, 114] and Overman et al.[111, 115] examined the intramolecular Heck reactions of monocyclic iodoalkenes **260** and alkenyl triflates **262** using catalysts that contained chiral ligands (Scheme 52); decalins **261**[114c] and hydroindane derivatives **263**[114d] were obtained with excellent enantioselectivities. Complementary to the asymmetrically induced intermolecular arylations and alkenylations with triflates by Hayashi et al. (see Schemes 21 and 22), reasonable intramolecular inductions were also achieved with iodides upon the addition of silver salts (Scheme 52). With terminal allylsilane groups, these intramolecular reactions regioselectively led to tetrahydroisoquinoline and tetrahydro-1*H*-3-benzazepines with up to 90% enantiomeric excess.[186]

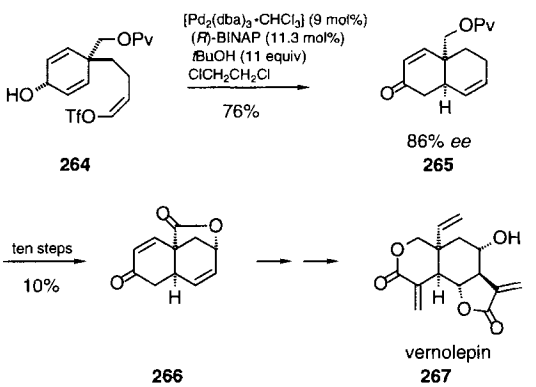


X	R^1	R^2	Conditions	Yield [%]	*ee* [%]
OTf	CO_2Me	H	**A**	54	91
OTf	CH_2OOCMe_3	H	**A**	60	91
I	$CH_2OTBDMS$	CH_2OAc	**B**	67	87

X	R	Conditions	Yield [%]	*ee* [%]
OTf	$CH_2OTBDMS$	**A**	63	73
I	CO_2Me	**B**	73	83

Scheme 52. A: 5% $Pd(OAc)_2$, 10% (*R*)-BINAP, 2 equiv K_2CO_3, benzene or toluene, 60 °C, 49–55 h. B: 10% $[PdCl_2\{(R)\text{-BINAP}\}]$, 2 equiv Ag_3PO_4, 2.2 equiv $CaCO_3$, *N*-methylpyrrolidone, 60 °C, 100 h.

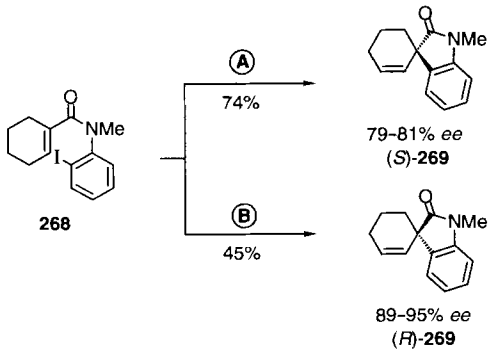
Shibasaki et al. soon applied asymmetric Heck reactions to natural product synthesis.[114g] Cyclization of triflate **264** yielding enone **265** with 86% enantiomeric excess established convenient access to enantiomerically pure **266**, a key intermediate in Danishefsky's synthesis[187] of vernolepin (**267**) (Scheme 53).



Scheme 53. Pv = pivaloyl = $COC(CH_3)_3$.

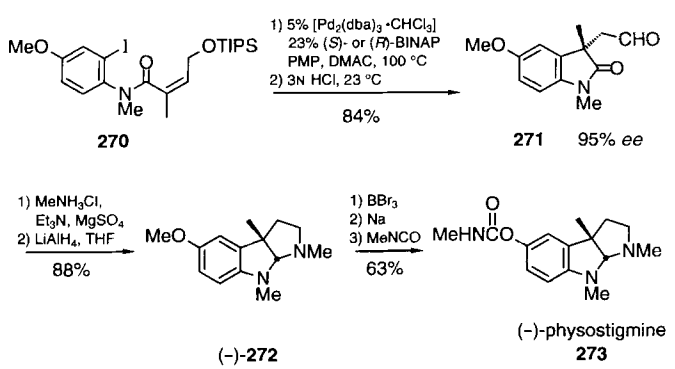
Key intermediates for the synthesis of capnellenols[114b, f] were constructed by asymmetrically induced Heck reaction/anion capture processes,[188] and in the synthesis of (−)-eptazocin a key reaction was the asymmetrically induced generation of a quaternary benzylic carbon center.[114i]

Overman et al.[111, 185] and Grigg et al.[189] first rose to the challenge of the catalytic asymmetric construction of quaternary carbon centers. Amazing results were obtained in the preparation of spirooxoindoles (*S*)-**269** and (*R*)-**269** from **268** (Scheme 54); each product enantiomer was obtained selectively by careful choice of reaction conditions and, remarkably, by applying the exact same enantiomer of the chiral phosphane ligand.[115] It should be noted that despite the absence of silver salts in the latter reaction, very good enantioselectivity was achieved even with an iodoarene.



Scheme 54. A: 5% $[Pd_2(dba)_3]$, 10% (*R*)-BINAP, 2 equiv Ag_2CO_3, $MeCONMe_2$, 60–80 °C. B: 10% $[Pd_2(dba)_3]$, 20% (*R*)-BINAP, 5 equiv 1,2,2,6,6-pentamethylpiperidine, $MeCONMe_2$, 80–100 °C.

These studies culminated in the synthesis of both enantiomers of physostigmine (**273**) (Scheme 55).[190] Palladium-catalyzed cyclizations of iodoarene **270** using (*S*)- and (*R*)-BINAP as

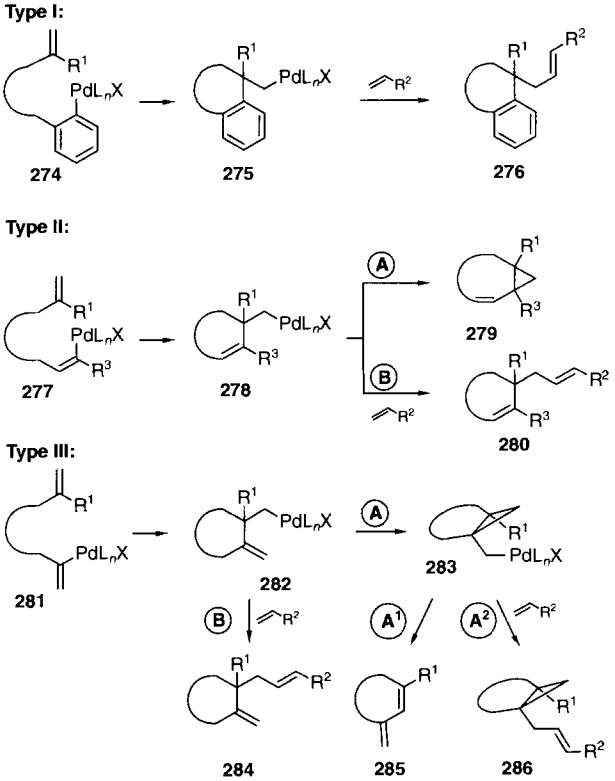


Scheme 55. TIPS = iPr_3Si.

ligands afforded oxoindoles (*S*)-**271** and (*R*)-**271**, respectively, with enantiomeric excesses greater than 95% in each case. After cyclizing condensation of **271** with methylamine, reduction of the products with lithium aluminum hydride furnished (+)- and (−)-esermethole (**272**), respectively. Three further known steps[191] finally completed the syntheses of both (+)- and (−)-physostigmine (**273**) (Scheme 55).

6.3. Obstacles with a Bonus: Neopentylpalladium Intermediates

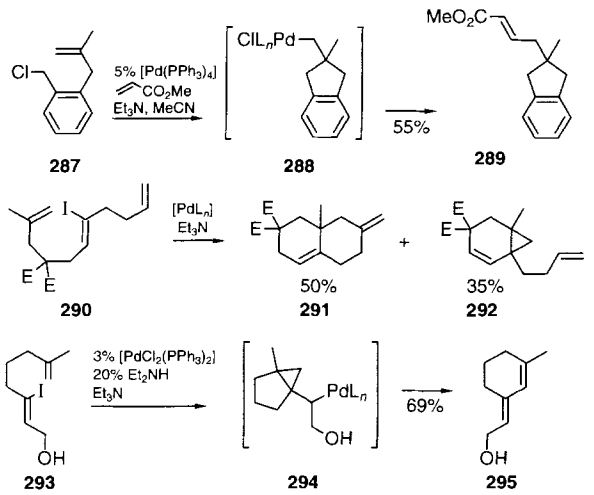
Intramolecular Heck reactions can be extended considerably in scope, when the primary insertion is forced to occur regioselectively at a 2,2-disubstituted double bond, such that β-hydride elimination cannot take place. Three versions of this type of reaction can be distinguished, which depend on the structure of the aryl halide or alkenyl halide initiating the cyclization (Scheme 56). If the initiator is an aryl halide (or benzyl halide) such as the precursor to **274** (type I),[192] then a neopentylpalladium intermediate **275** is generated which reacts intermolecularly with alkene to form an allyl-substituted bicycle **276** in a typical Heck reaction. Intramolecular reaction with the double bond of an alkenyl side chain may also take place, thus forming a further ring.



Scheme 56. R^1 = alkyl; R^2 = aryl, CO_2alkyl, CN, $SiMe_3$; X = I, Br, OSO_2CF_3.

Application of initiating haloalkenes like the precursor to **277** (type II) causes a somewhat more complex reaction course.[193] Even without an additional alkenyl side chain, the generated neopentylpalladium intermediate **278** can react intramolecularly to give alkenylcyclopropane **279** in a 3-*exo-trig* cyclization followed by β-hydride elimination of the (cyclopropylmethyl)palladium intermediate (path A). Alternatively, intermediate **278** may couple intermolecularly with an added alkene to give **280**, or intramolecularly with another alkenyl group in the molecule giving an additional ring (path B). Path A branches further if the double bond of the former haloalkene remains exocyclic after initial cyclization, as in the case of the conversion of **281** to the neopentylpalladium intermediate **282** (type III in Scheme 56). Even after the 3-*exo-trig* ring closure of **282** yielding **283**, the palladium remains in a neopentyl position. Elimination of hydridopalladium halide (or triflate) occurs only with opening of the three-membered ring in a cyclopropylmethyl–homoallyl rearrangement, thus yielding diene **285** (path A^1). On the other hand, allylcyclopropane **286** can be formed by the intermolecular coupling of **283** with an alkene (path A^2). Incidentally, compound **285** is the formal product of a 6-*endo-trig* cyclization of intermediate **281**.

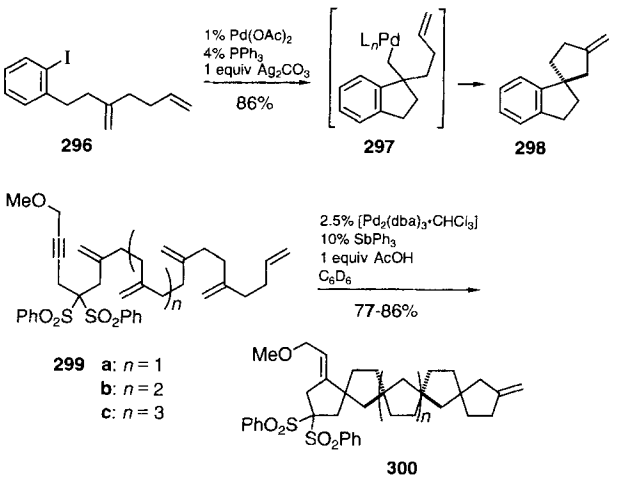
In the long run, kinetics will always determine which path is available for the neopentylpalladium intermediates. The cyclization of benzylic halide **287** in the presence of methyl acrylate gives product **289** according to a type I reaction.[32a] On the other hand, in type II reactions, even the intramolecular capture of the butenyl side chain in iodotriene **290** is only roughly twice as rapid as the 3-*exo-trig* cyclization yielding cyclopropane derivative **292** (Scheme 57).[193] The formation of the formal 6-*endo-trig* product **295** from iododiene **293** is an example of a



Scheme 57. E = CO_2Et.

cyclopropylmethyl–homoallyl rearrangement in a type III reaction.[193]

Little attention has been paid so far to the effect of ligands and halide ions on the course of these reactions.[194] Since Overman et al.[192] succeeded in obtaining spirocycle **298** from iodoarene **296** in good yield (Scheme 58), numerous examples of

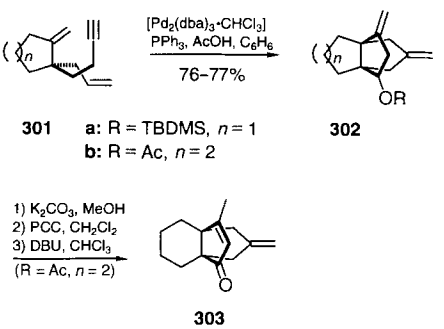


Scheme 58.

neopentylpalladium intermediates used in the formation of complex spirocycles have been published.[45a, 176c, 195] The current record for the maximum number of cyclizations performed in one step is held by the cycloisomerization cascade of heptaenyne **299c**, which finally results in the hexaspiro compound **300c**.[196]

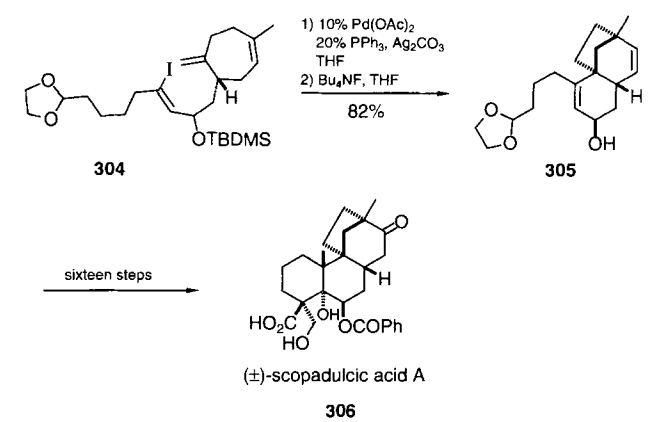
Neopentylpalladium intermediates generated in cycloisomerization reactions from suitable precursors such as **301** can also successfully lead to propellanes **302** (Scheme 59).[198] Hydrolysis, oxidation, and isomerization of the double bond transforms acetoxy derivative **302b** to the enone **303**.

Polyene cyclizations are generally suitable for the synthesis of bridged oligocycles.[193, 195c] The first total synthesis of scopadulcic acid A (**306**), recently reported by Overman et al., is



Scheme 59. PCC = pyridinium chlorochromate.

one of the most convincing demonstrations of the synthetic potential of this method (Scheme 60).[197] The bicyclononane subunit in the tetracyclic skeleton of **306** was constructed in a diastereoselective cyclization of 5-methylenecycloheptene **304**, which led to tricycle **305**.

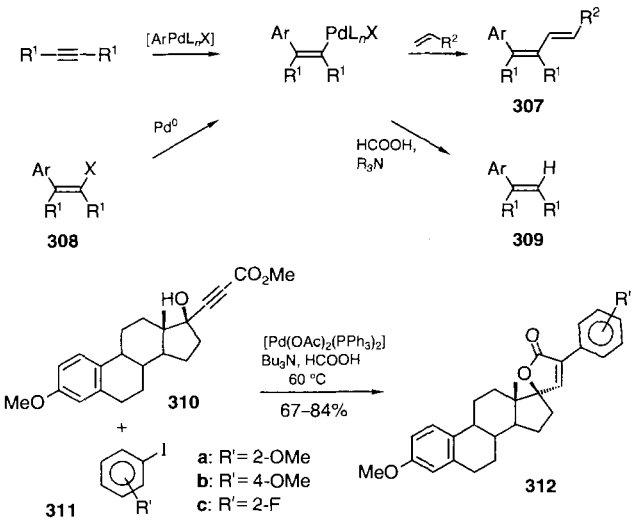


Scheme 60.

7. Chemical Relay Stations: Palladium-Catalyzed Additions to Triple Bonds

7.1. A Domino Sequence Consisting of Intermolecular Addition and Subsequent Intramolecular Reaction

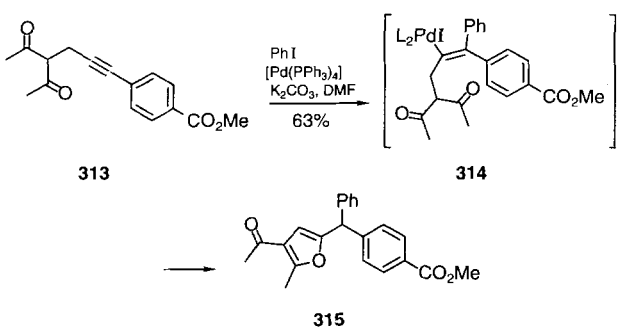
After Cacchi et al. had shown that iodoarenes and α,β-unsaturated carbonyl compounds undergo palladium-catalyzed 1,4-additions in the presence of tertiary amines and formic acid,[73] disubstituted alkynes were allowed to react with iodoarenes under identical conditions (Scheme 61).[87a, b, 198] (Aryl)iodopalladium, generated by oxidative addition of iodoarene to palladium(0), adds to the alkyne, thus creating an intermediate which formally could also have been generated by oxidative addition of the appropriately substituted haloalkene **308** to Pd^0. The intermediate can then react with alkenes to yield dienes **307** or be protiodepalladated, giving rise to **309**. Thus, the alkyne acts as a relay through which the ability of forming carbon–carbon bonds is passed on; in other words, the reactivity of the alkyne to nucleophiles is "switched on" by the addition of the arylpalladium species. Regioselectivity of the addition to



Scheme 61. R^1 = alkyl, aryl, $SiMe_3$; $R^2 \neq$ alkyl.

the alkyne is mainly determined by steric factors. Thus the aryl group is directed preferentially to the sterically less encumbered position.[187b, 198a] This reaction offers interesting possibilities, since arylation of 4-hydroxy-2-alkynoic acid esters such as **310** with iodoarene **311** yields a trisubstituted acrylic ester, which then lactonizes to the substituted butenolide **312** (Scheme 61).

Palladium-catalyzed additions to triple bonds thus afford intermediates capable of forming of further C–C or C–X bonds according to the domino principle. A sequential reaction of this kind is illustrated by the arylation of alkyne **313** with iodobenzene (Scheme 62). The alkenyliodopalladium intermediate **314**

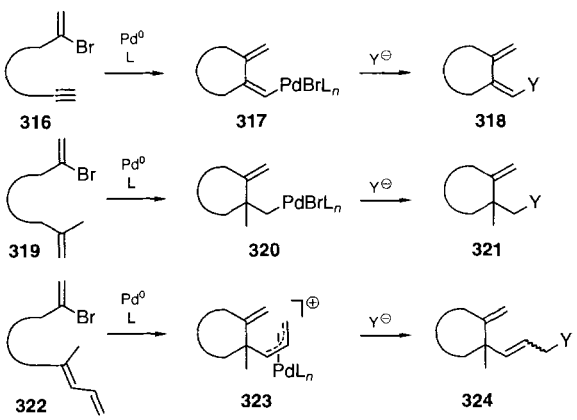


Scheme 62.

is attacked intramolecularly by the enolate ion formed through action of the base. β-Hydride elimination and double bond migration afford trisubstituted furan **315**.[199] Further studies on the preparation of functionalized butenolides,[200a] substituted γ-methylene-γ-butyrolactones,[200b] and substituted 5-alkenyl-2-furanones and 2-alkenyltetrahydrofurans[200c] underline the far-reaching ramifications for synthesis based on this reaction scheme.

7.2. The Sequence Consisting of Cyclization and Anion Capture[201]

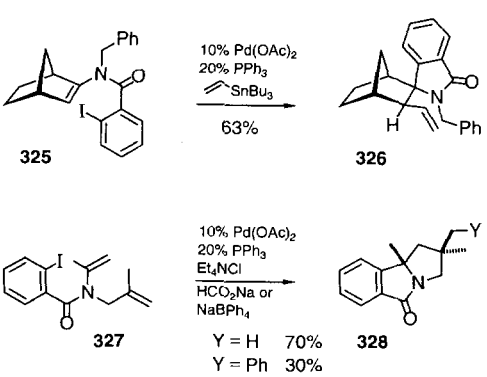
The double bond shifts frequently observed in products of intramolecular Heck reactions can be avoided in intramolecular additions to triple bonds by conducting the reaction under reducing conditions (formic acid/trialkylamine). The scope of this method is, however, by no means restricted to the formation of formal Heck cyclization products by hydride capture.[42i, j] For instance, alkenylpalladium intermediate **317**, generated in the *n-exo-dig* cyclization of bromoenyne **316**, may also be trapped by various "anionic" reagents Y^- (Scheme 63). The pioneering



Scheme 63. Y = H, alkyl, alkenyl, Ph, CN, NR_2, CO_2R; R = alkyl.

work in this field done primarily by Grigg et al. revealed the possibility of a stereospecific group transfer of organotin,[202] -zinc, and -boron compounds,[195a, 203] as well as organoaluminum and -zirconium compounds.[204] Furthermore, intermediates such as **317** may also be captured by oxygen, nitrogen, and carbon nucleophiles.[205] This process is not restricted to just alkenylpalladium species, but can be applied to neopentylpalladium intermediates **320** and π-allylpalladium complexes **323** as well.[42j, 195a, 202, 204]

A frequently encountered problem related to these palladium-catalyzed domino Heck cross-coupling reactions lies in the relative rate of the carbopalladation step in comparison to the rate of group transfer. In reactions involving organozinc compounds the two steps often proceed with comparable rates, thus giving rise to product mixtures. In contrast, coupling reactions with organotin and organozirconium compounds[202, 204] are much more specific, as can be demonstrated by the preparation of spirocycle **326** by reaction of amide **325** with tributylvinylstannane (Scheme 64).[202]

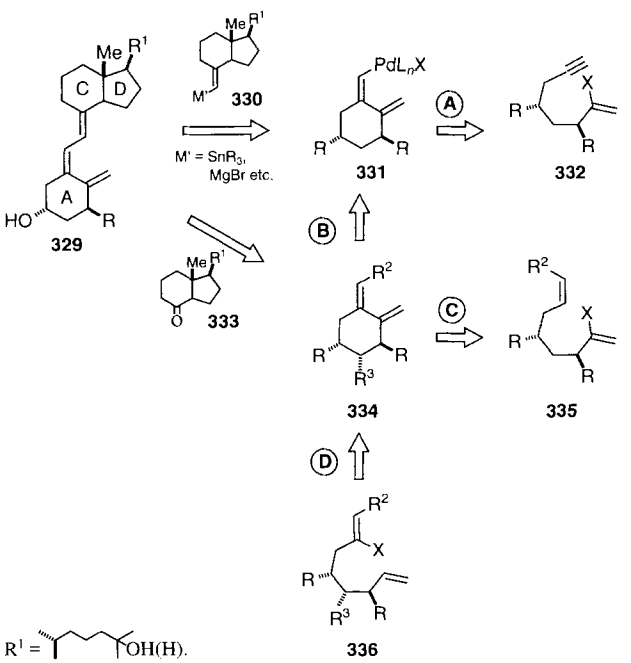


Scheme 64.

Even multiple cyclizations may be performed easily; anion capture with sodium formate or sodium tetraphenylborate occurs only after completion of the cyclization sequence. Grigg et al. performed various transformations in this manner, for example the conversion of iodoarene **327** into tricycle **328** (Scheme 64).[32c, 45a, 195b, e]

7.3. Relay Stations at Work: The Skeleton of Vitamin D and the Enediyne Ring of the Neocarzinostatin Chromophore

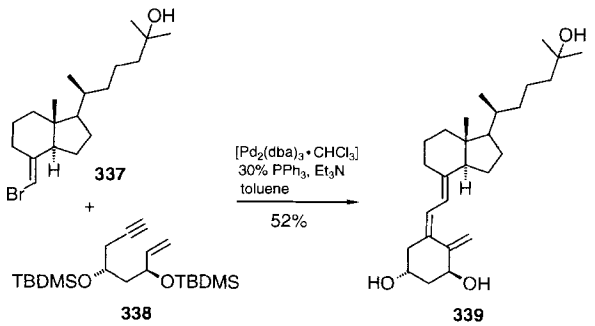
A particular challenge in the synthesis of the hormonally active form of vitamin D_3, 1α,25-dihydroxyvitamin D_3 (**329**; R = OH, $R^1 = CH(CH_3)(CH_2)_3OH$) (Scheme 65), remains the stereoselective preparation of the triene substructure. In the meantime several solutions to this particular problem have been published, each of which has palladium-catalyzed reactions in key steps.



Scheme 65. R = OTBDMS, OCH_2OCH_3, OH, H; $R^2 = CO_2Me$, CH_2OH; X = Br, I.

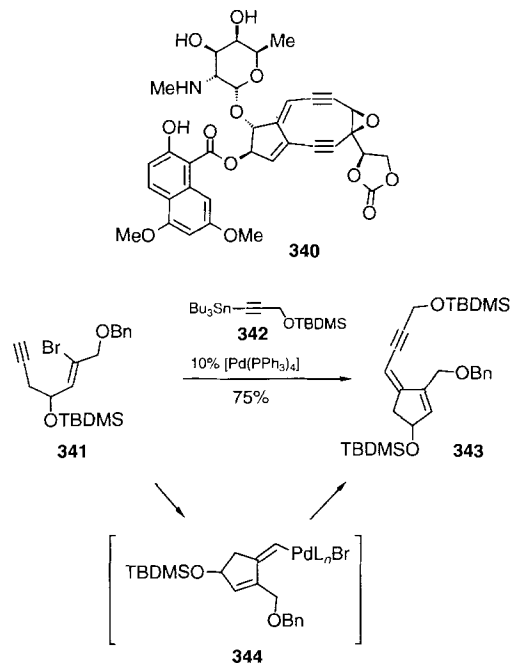
The approaches of Shimizu et al.[206] and Crich et al.[207] (path C), and Mouriño et al.[208] and Takahashi et al.[209] (path D) rely on intramolecular Heck reactions with halodienes **335** and **336**, respectively, for the stereoselective construction of ring A in intermediate **334**. Subsequently, following Kocienski's[210a] protocol, **334** is linked to ketone **333** by a Wittig reaction. The strategy applied by Nuss et al.[211] is even shorter and more elegant. A palladium-catalyzed cyclization–carbonylation sequence is applied to 2-bromo-1,7-enyne **332** in a one-pot procedure to yield cyclic diene **334** via alkenylpalladium species **331** (path A, B) which can then be further transformed according to well-established methods.[210b–c] Intermediate **331** can be trapped directly with metal derivative **330** (alkenylstannane, alkenylmagnesium halide), thus providing the target molecule **329** in a very short sequence indeed (Scheme 65).

Trost et al.[212] demonstrated an elegant and highly convergent reaction cascade in the total synthesis of calcitriol (**339**) (Scheme 66). In this sequence the palladium-catalyzed intermolecular addition of bromoalkene **337** to the terminal alkyne **338** is followed by intramolecular carbopalladation and β-hydride elimination. Desilylation of the cyclized product led directly to calcitriol (**339**) in 52% yield.



Scheme 66.

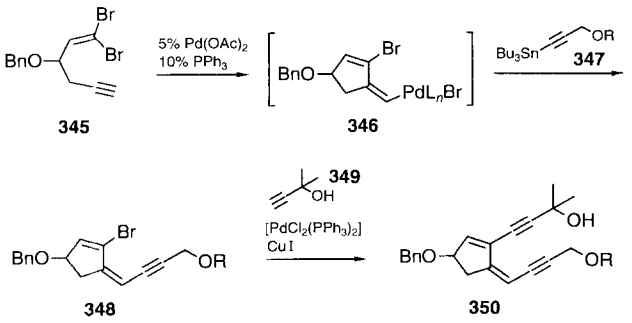
The synthesis of the enediyne ring in the neocarzinostatin chromophore (**340**) is yet another interesting problem that can be tackled successfully with sequential carbometallation/anion capture reactions (Scheme 67). In a first approach Nuss et al.[213a] started with 2-bromo-2,6-enyne **341** which was cyclized to give the alkenylpalladium species **344** and subsequently coupled with stannane **342**, thus yielding dienyne **343**. The second triple bond can be introduced in several subsequent steps.[213b]



Scheme 67.

Sequences published by Torii, Okumoto, et al.[214a] and by Nuss et al.[214b] utilizing 1,1-dibromoalkene **345** as a building

block are even more elegant (Scheme 68). The (*Z*) bromine–vinyl carbon bond reacts preferentially with palladium(0) by oxidative addition, and the resulting intermediate cyclizes to give **346**, which undergoes a selective coupling reaction with

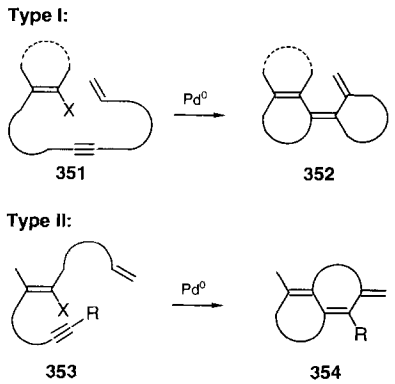


Scheme 68.

stannane **347**. In a second palladium-catalyzed step the bromo substituent, which was originally in the (*E*) position in **345**, is replaced by propargylic alcohol **349**, thus providing the required precursor **350** for the enediyne ring. In spite of uncertainties concerning the mechanism of the cyclization of 1,5-enynes containing a 1,1-dibromovinyl terminus, it may be expected that future efforts in the applications of bifunctional reagents will reveal many new synthetic routes.

7.4. Zip It Up: Carbooligocycles from Cascade Reactions

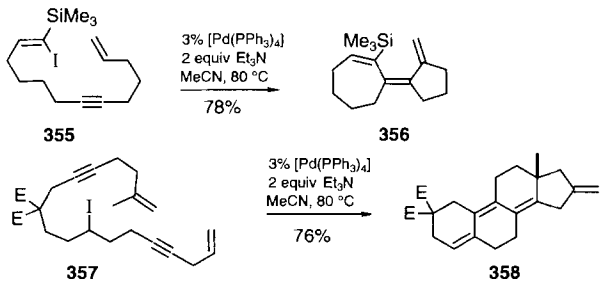
Alkenylpalladium intermediates generated by intramolecular addition of a haloalkene to a triple bond may also be captured by alkenes, either intermolecularly or intramolecularly. Thus, depending on the positions of double and triple bonds in the acyclic precursor, bicycloalkylidenes **352** (type I in Scheme 69)



Scheme 69. R = alkyl, aryl, CO_2alkyl; X = I, Br, OSO_2CF_3.

or annelated ring systems **354** (type II) may be formed. Type I reactions are initiated not only in substrates containing a haloalkenyl unit such as in **351** or **353**, but are also initiated reductively by addition of a hydridopalladium complex (generated in situ) to a terminal triple bond. The latter was demonstrated for the first time by Trost et al. with the reductive cyclization of 1,6-diynes.[215]

An example of a type I reaction is the straightforward cyclization of iododienyne **355** to (methylenecyclopentylidene)-cycloheptane **356** (Scheme 70).[216a] This is not the only demonstration that palladium-catalyzed cyclizations—in contrast to similar radical-initiated reactions—provide easy access to seven-membered rings as well as five- and six-membered rings.



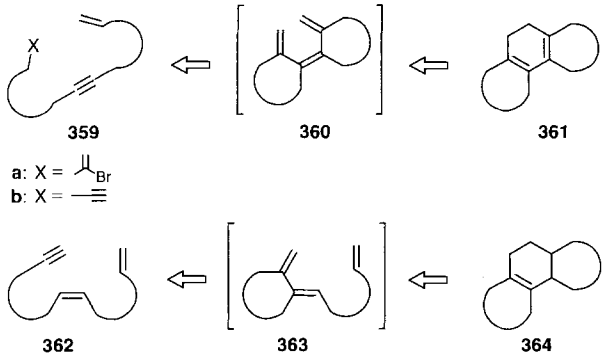
Scheme 70. E = CO_2Et.

Acyclic precursors such as **357** can be subjected to a continuous sequence of more than two carbopalladation steps, thus forming three or more rings. The term "crochet-type reactions" was introduced for carbocation-initiated cyclization cascades[217] because of the analogy with interlinked crochet stitches (see also Scheme 58). In other work Negishi et al. designated their own Pd-catalyzed polycyclizations of acyclic molecules as "zipper" cyclizations, since the two dienoligoyne chains connected by a head piece are multiply linked just like the two sides of a zipper.[216b] The one-step construction of the steroid skeleton **358** through tetracyclization of acyclic precursor **357**[216c] is a good example (Scheme 70). Interestingly, the neopentylpalladium intermediate generated after the third cyclization does not undergo a 3-*exo-trig* cyclization to produce a three-membered ring. Instead, a 5-*exo-trig* ring closure with participation of the terminal double bond predominates (Scheme 70).

7.5. Tactical Combinations: Palladium-Catalyzed Polycyclizations and Intramolecular Reactions

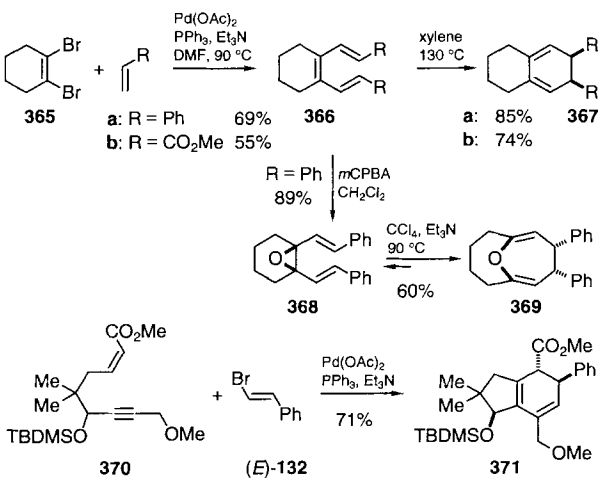
New perspectives for multiple cyclizations may arise when a palladium-catalyzed cyclization sequence leads to a molecule with more than two double bonds in an arrangement that would allow a subsequent thermal intramolecular reaction. Electrocyclic reactions and Diels–Alder reactions are the primary candidates for this second reaction. (*E,Z,E*)-1,3,5-Trienes **360** may be expected from the palladium-catalyzed biscyclizations of 2-bromodienynes **359a** or enediynes **359b**. Subsequent disrotatory electrocyclization of **360** leads to bisannelated cyclohexadienes **361** under comparatively mild conditions (Scheme 71). Alternatively, substituted dienynes **362** are transformed into bis(exoalkylidene)cycloalkanes **363** by palladium-catalyzed cycloisomerization; subsequent intramolecular [4 + 2] cycloaddition then yields bisannelated cyclohexenes **364** (Scheme 71).

The combination of Heck reaction and subsequent electrocyclization was realized for the first time in the preparation of (*E,Z,E*) trienes **366**, in which vicinal dibromides like **365** were



Scheme 71.

coupled with monosubstituted alkenes (Scheme 72).[97, 100, 218] The anticipated electrocyclization did not occur under the applied Heck coupling conditions (90 °C) but at slightly elevated temperature (130 °C) in refluxing xylene.

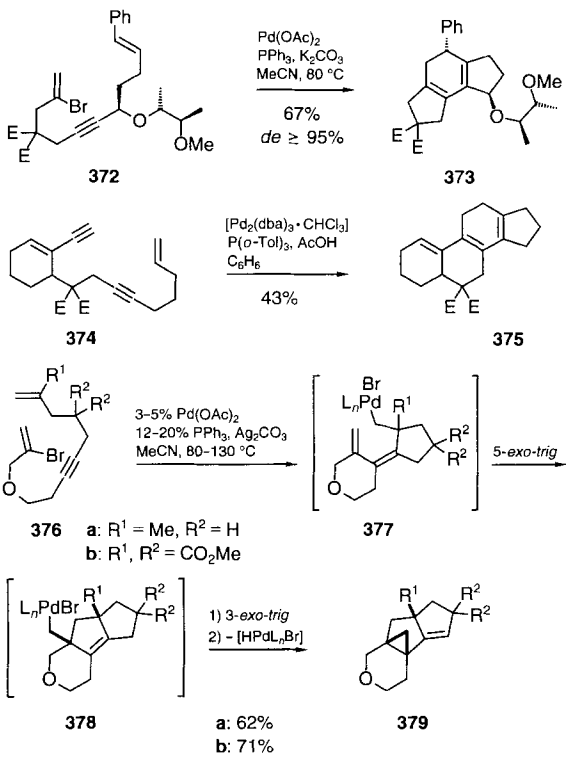


Scheme 72. *m*CPBA = *meta*-chloroperbenzoic acid.

In contrast to these findings, Trost et al.[212b] isolated the bicyclic product **371** from the Heck reaction of enyne **370** with *β*-bromostyrene ((*E*)-**132**) under standard conditions. In this sequence carbopalladation of the triple bond followed by 5-*exo*-*trig* ring closure and subsequent *β*-hydride elimination is assumed; the resulting (*E*,*Z*,*E*) triene is finally transformed into the annelated cyclohexadiene **371** by disrotatory ring closure. The rotaselectivity responsible for the production of only one diastereomer has been explained by interactions between the silyloxy and methoxymethyl substituents (Scheme 72).

Since (*E*,*Z*,*E*) trienes **366** are isolable, they are conducive to diverse applications. Selective epoxidation of the central double bond is feasible, thus yielding dialkenyloxiranes **368**, which can undergo Cope rearrangement at 90 °C.[100] Indeed, the formation of the bridged 1,6-oxacyclodeca-1,5-diene **369** from **366** corresponds to a ring expansion by four carbon atoms (Scheme 72).

In two independent developments[196b, 219, 220] a purely intramolecular reaction cascade was devised, in which two successive Heck reactions yielded a triene, which underwent subsequent 6π electrocyclization. In the first case the sequence is initiated by insertion of palladium into an alkenyl carbon–halogen bond. For unsubstituted dienynes it proved essential to add silver salts to suppress rearrangement products during triene formation.[220a] The disrotatory 6π electrocyclization of terminally substituted 1,3,5-hexatrienes such as that formed from **372** proceeds with remarkable rotaselectivity.[220b, c] Enantiomerically pure 2-bromodienyne **372** thus yielded virtually enantiopure bisannelated cyclohexadiene **373** in good yields (Scheme 73).



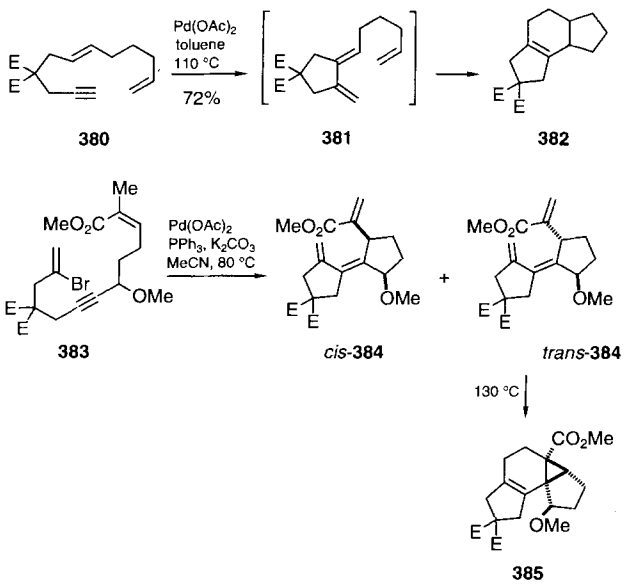
Scheme 73. E = CO_2Et.

The cycloisomerizations of enediynes such as **374** developed by Trost et al. are complementary to these findings, and in part superior. These reactions proceed through an analogous sequence of intermediates, leading to bisannelated cyclohexadienes like **375**.[219] Silver salts may be omitted, as the initial step consists of a chemoselective addition of a hydridopalladium complex (generated in situ) to the terminal triple bond. Moreover, substrates are generally more easily accessible, since haloalkenes are not required. Combined palladium-catalyzed biscyclizations and 6π electrocyclizations have meanwhile matured to such a degree[196b] that it will certainly be only a question of time before this method is applied in natural product synthesis.

An even greater increase of structural complexity in a single synthetic operation may be achieved in palladium-catalyzed transformations of bromodienynes **376**, containing a terminal double bond which is disubstituted at the penultimate carbon atom (Scheme 73). The neopentylpalladium intermediate **377** generated in the second cyclization step undergoes predominantly a 5-*exo*-*trig* cyclization. The resulting intermediate **378** cyclizes once more in a 3-*exo*-*trig* mode before *β*-hydride

elimination yields **379**. Tetracycle **379** is formed with complete diastereocontrol in yields of up to 71%.[220a]

As already mentioned, palladium-catalyzed cycloisomerizations and intramolecular Heck reactions are ideal tools for the construction of bis(exoalkylidene)cycloalkanes,[92] which can continue the reaction cascade in subsequent Diels–Alder reactions, which may even proceed intramolecularly. A nice example of a solely intramolecular sequence is given by the cycloisomerization of dienyne **380**, resulting in the bisannelated cyclohexene **382** (Scheme 74). It should be emphasized that the regiocontrolled formation of conjugated diene **381** is due to the presence of the terminal double bond.[76b,d] Alternatively, the reductive cyclization of 1,6-diynes[215a] may be used to synthesize the 1,3-diene units necessary for intramolecular or intermolecular Diels–Alder reactions. Subsequent to biscyclization of 2-bromodienyne **383** under Heck conditions, an intramolecular Diels–Alder reaction also terminates the reaction sequence leading to the highly strained tetracycle **385** (Scheme 74).[220c]

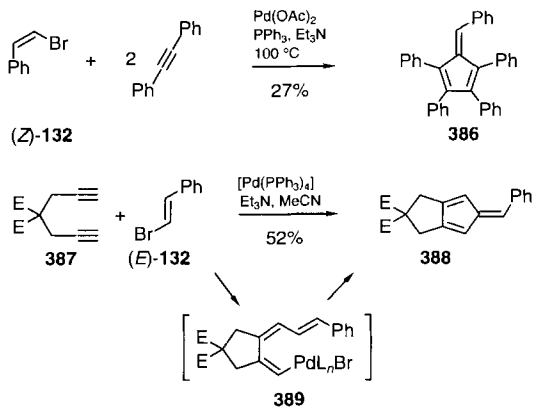


Scheme 74. E = CO_2Et.

7.6. A New Twist on Arene Chemistry: {2+2+2} Assembly of Benzene Derivatives

The efficiency of organometallic reactions manifests itself in numerous transition metal catalyzed and transition metal mediated cyclotrimerizations of alkynes to benzene derivatives.[221] It was merely a question of time before palladium-catalyzed reactions were also applied. However, the first concepts were not amenable to synthetic applications.

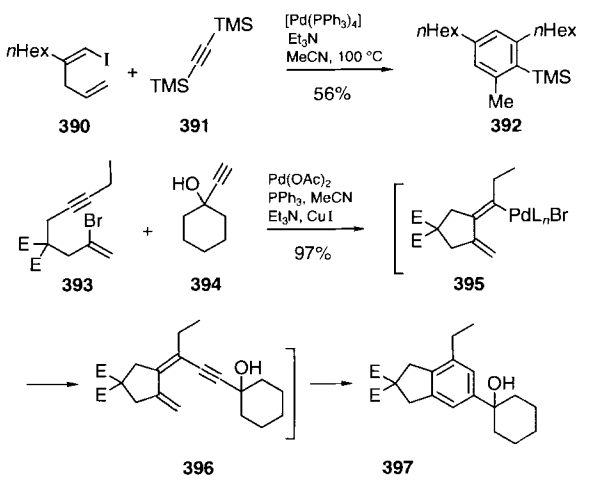
Purely intermolecular {2+2+2} cyclotrimerizations indeed led to benzene derivatives,[222] but the trimerization of unsymmetrically disubstituted alkynes yielded mixtures of at least two regioisomers. Because of this and also the stoichiometric formation of cyclobutadienylpalladium complexes, the synthetic utility of this strategy was extremely limited. Intermolecular Heck reactions were tested with (*Z*)-β-bromostyrene ((*Z*)-**132**) and



Scheme 75. E = CO_2Et.

diphenylacetylene (Scheme 75). The stoichiometry of the reaction no longer created problems, but pentaphenylfulvene (**386**) was obtained in poor yield instead of the anticipated benzene derivative.[223] (*E*)-Bromostyrene ((*E*)-**132**) undergoes a similar transformation upon reaction with diyne **387** under Heck conditions.[224] The 5-*exo-trig* ring closure of the intermediate alkenylpalladium derivative **389** is apparently favored kinetically over a 6-*endo* attack (Scheme 75).

The first promising results were obtained in the palladium-catalyzed reaction of 1-iododiene **390** with alkyne **391** (Scheme 76). Intermolecular addition of the alkenylpalladium intermediate to the triple bond takes place before ring closure occurs, yielding the tetrasubstituted benzene derivative **392**.[216a] Undoubtedly, this approach relies on the tendency of palladium-catalyzed cyclizations to follow Baldwin's rules.[177] Thus, a 4-*exo-trig* ring closure is disfavored kinetically to such an extent that intermolecular addition to the alkyne dominates and is eventually followed by a 6-*exo-trig* ring closure.

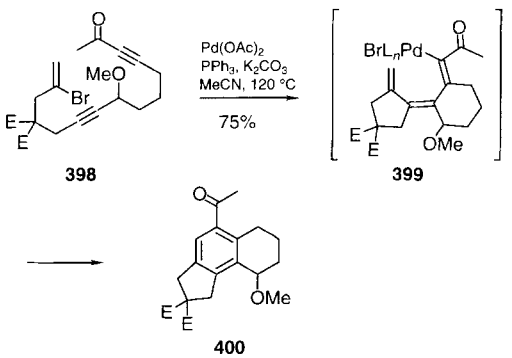


Scheme 76. E = CO_2Et.

Torii, Okumoto et al.[225] have demonstrated the most convincing strategy for the intermolecular trapping of 1,3-dienylpalladium intermediates (generated in situ) with alkynes. Intramolecular cyclization of 2-bromoenyne **393** initially leads to alkenylpalladium species **395**, which is then intermolecularly

coupled with a terminal alkyne **394** to yield dienyne **396**. Spontaneous rearrangement of **396** affords the monoannelated benzene derivative **397** (Scheme 76). Later studies[224, 226] underline the scope of this method and show that diyne cycloisomerizations may also serve as initiators for such sequences.[224a]

The potpourri of palladium-catalyzed preparations of benzene derivatives was completed by a further variant, proceeding entirely intramolecularly (Scheme 77).[227] The acyclic precursor **398** containing a second triple bond leads to the alkenylpalladium species **399** after two successive *n-exo-dig* cyclizations. Yet another ring closure occurs and, after subsequent β-hydride elimination, the angularly bisannelated benzene derivative **400** is formed. It still is unclear whether the last step of this sequence is a direct Heck coupling, or if electrocyclization of **399** first takes place, followed by β-hydride elimination. Needless to say analogous cycloisomerizations of triynes give similar results.[224a]



398 **399** **400**

Scheme 77.

8. Summary and Outlook

Although a reasonable working hypothesis has been established for the mechanism of the palladium-catalyzed arylation and alkenylation of alkenes, the Heck reaction, individual steps are far from being completely understood. Nevertheless, insight into the factors determining these reactions has contributed significantly to the further development and improvement of these methods. Numerous related procedures have emerged from the classic Heck reaction. Chemoselective and regioselective couplings are now possible with the appropriate catalyst cocktail. Indeed, even ligand-controlled enantioselective intermolecular and intramolecular couplings of highly functionalized aryl and alkenyl derivatives with unsymmetrical and oligosubstituted alkenes, cycloalkenes, and unsaturated heterocycles are possible. Oligo couplings and even multiple couplings proceed with astonishing yields, both intermolecularly and intramolecularly.

Reaction cascades have resulted from the skillful combination of the Heck reaction or its initial steps with other palladium-catalyzed procedures such as nucleophilic substitutions (via π-allylpalladium complexes) or thermally controlled transformations like Diels–Alder reactions and 6π electrocyclizations. In these cascades, not just one new C–C bond is formed specifically; two, three, four, and even more new bonds can be formed in a single step. The increase in molecular complexity, accepted nowadays as a measure for the efficiency of a synthetic manipulation, is impressive in these sequential reactions.

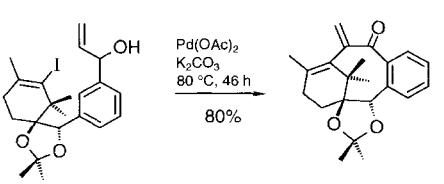
Procedures in which initially formed arylpalladium or alkenylpalladium species are added to a triple or a double bond either (re)generating an alkenyl-, neopentyl-, or even a π-allylpalladium intermediate have proven to be particularly useful for the development of cascade reactions, as these intermediates cannot be removed or at least not so rapidly from the reaction by β-hydride elimination. Instead, they again react with triple bonds and double bonds or with other neutral and anionic nucleophiles. Thus, a triple bond in a molecule behaves like a relay, producing a new reactive intermediate upon the addition of a palladium species.

Up to now, the various possibilities arising from the domino-like combination of several Heck reaction steps with other processes have yet not been exploited to the fullest extent, in spite of numerous successes. In this area chemists' imaginations can run wild. Indeed, the opportunities for the elegant and highly convergent construction of complex natural and non-natural products justify increasing research efforts in this field of palladium-catalyzed bond-forming methods (Heck reactions as well as mechanistically related processes). The anticipation and excitement amongst chemists is a result of a myriad of new discoveries in the recent past. Certainly, the Heck reaction will never again fall into oblivion, since it promises solutions to future preparative challenges. Yet there are still some hurdles to be overcome before a broad application can be realized, especially on an industrial scale. As with almost every new application, selectivity problems will have to be unraveled by carefully matching reaction partners and fine-tuning reaction conditions. Expansion of the spectrum of starting materials, especially to inexpensive chloroarenes and chloroalkenes, remains a desirable goal. In view of a practical industrial application, improvements in catalyst efficiency and catalyst recycling are essential.[35] It remains to be seen whether all these expectations can be met.

Addendum

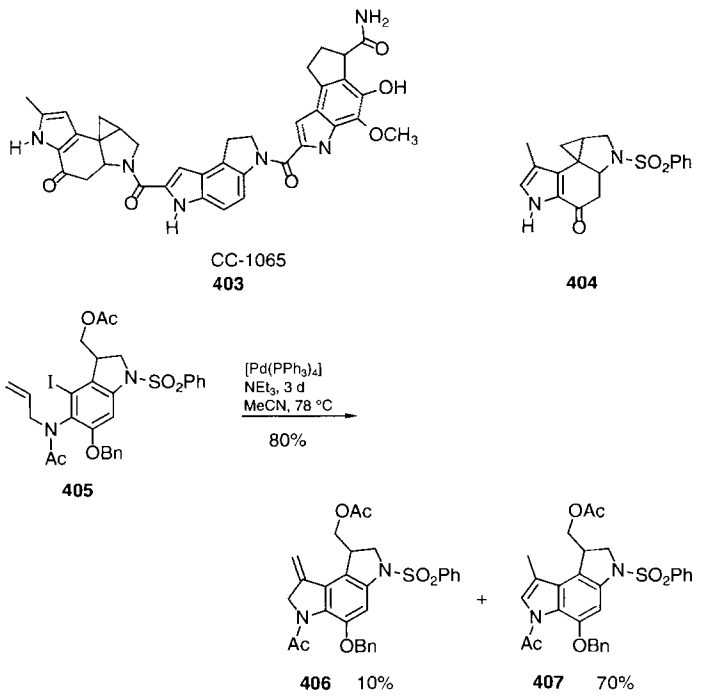
Many new studies have been published since the completion of the final version of this review almost a year ago. These findings have contributed substantially to establishing the Heck reaction in natural product synthesis and have reported progress in catalytically performed asymmetric synthesis.

A short reaction sequence has been demonstrated by Masters et al.,[228] who applied an intramolecular Heck reaction as a key step in the construction of the highly functionalized tricycle **402**, containing the basic tricyclic skeleton of taxol (Scheme 78).



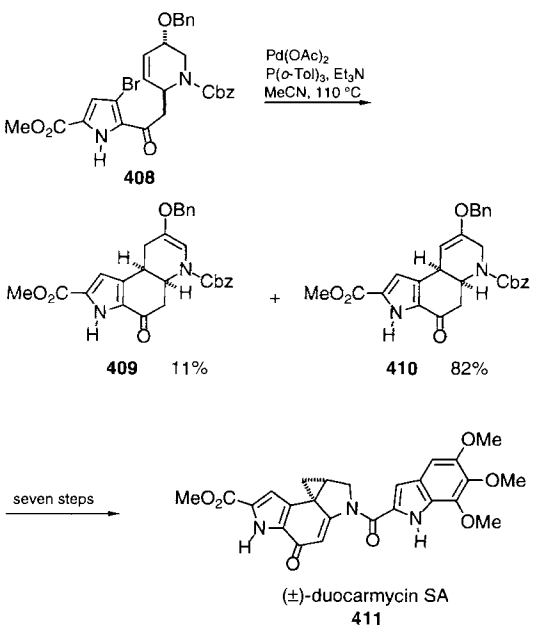
401 **402**

Scheme 78.



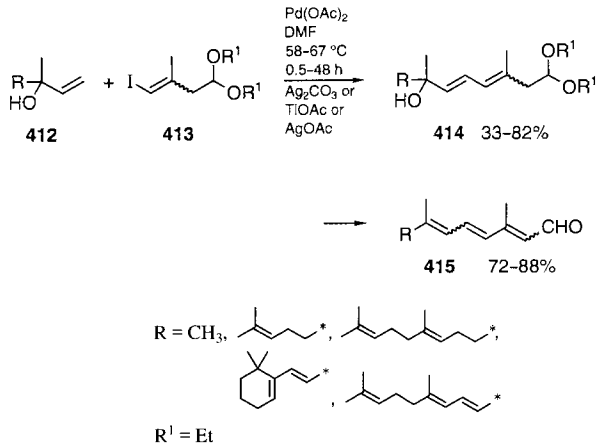
Scheme 79.

Tietze et al.[229] marked progress along a new route to the antitumor antibiotic CC-1065 (**403**) with the successful synthesis of the protected subunit **404** (Scheme 79). One of the two pyrrole rings in the precursor **407** to (±)-N^2-(phenylsulfonyl)-CPI (**404**) may also be obtained by an intramolecular Heck reaction of bicycle **405** (Scheme 79). Natsume et al.[230] applied an intramolecular Heck reaction in a key step of the total synthesis of the antitumor antibiotic (±)-duocarmycin SA (**411**; Scheme 80).



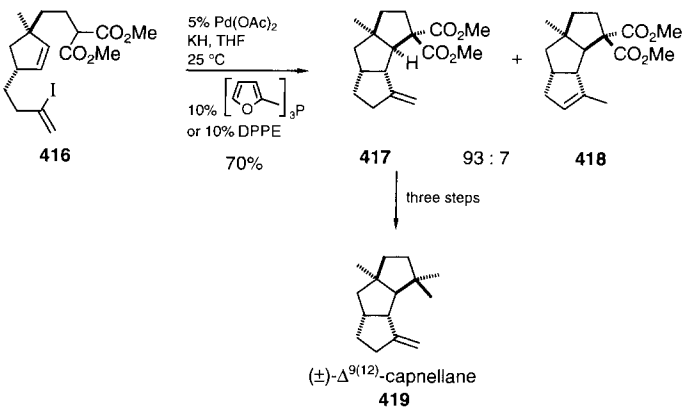
Scheme 80.

An example of a new intermolecular application is the vinylation of tertiary allyl alcohols **412**, giving access to isoprenoid aldehydes **415** (Scheme 81).[231] These results were obtained in the laboratories of Rhône-Poulenc, once again underlining revived interest even in industry in this catalytic transformation.



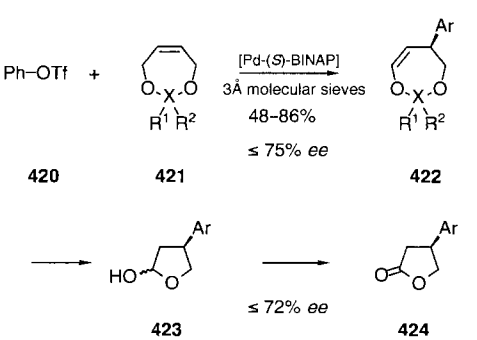
Scheme 81.

Balme et al.[232] reported an interesting new synthesis of the triquinane sesquiterpene (±)-$\Delta^{9(12)}$-capnellane (**419**) (Scheme 82). Biscyclization of the cyclopentene derivative **416** gave tricycle **417** (by-product **418**), which was converted into target molecule **419** in three further steps.



Scheme 82.

The enantioselective arylation of 4,7-dihydro-1,3-dioxepines **421** to yield **422** opens a new chapter in the asymmetric synthesis of γ-butyrolactone derivatives **424** (Scheme 83), which are then accessible in two additional steps via hemiacetal **423**. In this publication Shibasaki et al.[233] also discuss the effect of molecular sieves on reaction rates of asymmetric arylations.



Scheme 83. X = C, Si; R^1,R^2 = CH_3, *t*Bu, H, $(CH_2)_5$.

Studies undertaken by Fuchs et al.[234] Xu et al.,[235] and Pietrusiewicz et al.[236] revealed new substrates for Heck reactions with successful applications of vinylsulfones, phenylvinylphosphinates, and dienylphosphine oxides. Attention should also be drawn to the increasing importance of new ligand classes, especially 1,10-phenanthroline and its derivatives,[237] which have been successfully applied in directing palladium-catalyzed reactions. A myriad of interesting new papers[238–251] have been published in addition to those referred to in this short and somewhat arbitrary selection. And this flood does not promise to end soon.

The authors' own work mentioned in this review was supported financially by the Deutsche Forschungsgemeinschaft, the Volkswagen-Stiftung, the Studienstiftung des Deutschen Volkes, the Alexander-von-Humboldt-Stiftung, the German Academic Exchange Service, and the Fonds der Chemischen Industrie, as well as the companies BASF, Bayer, Degussa, Hoechst, and Hüls AG through generous gifts of chemicals. The authors thank Stefan Beusshausen for preparing the schemes and Dr. Burkhard Knieriem for his careful proofreading of the manuscript in various stages. Our ongoing collaboration with Prof. Dr. Philip J. Parsons, University of Reading, was made possible by a grant within the Academic Research Collaboration (ARC) Programme administered by the German Academic Exchange Service and the British Council.

Received: February 2, 1994 [A 52 IE]
German version: *Angew. Chem.* **1994**, *106*, 2473

[1] a) A. Hirsch, *Angew. Chem.* **1993**, *105*, 1189; *Angew. Chem. Int. Ed. Engl.* **1993**, *32*, 1138; b) *The Chemistry of the Fullerenes*, Thieme, Stuttgart, **1994**, and references therein.

[2] R. F. Heck, *J. Am. Chem. Soc.* **1968**, *90*, 5518.

[3] a) R. F. Heck, *Acc. Chem. Res.* **1979**, *12*, 146; b) *Org. React.* **1982**, *27*, 345; c) in *Fundamental Research in Organometallic Chemistry* (Eds.: M. Tsutsui, Y. Ishii, H. Yaozeng), Van Nostrand Reinhold, New York, **1982**, p. 447; d) *Palladium Reagents in Organic Synthesis*, Academic Press, London, **1985**; e) J. Tsuji, *Organic Synthesis with Palladium Compounds*, Springer, Berlin, **1980**; f) B. M. Trost, T. R. Verhoeven in *Comprehensive Organometallic Chemistry*, *Vol. 8* (Ed.: G. Wilkinson), Pergamon, Oxford, **1982**, p. 799; g) J. Mulzer, H.-J. Altenbach, M. Braun, K. Krohn, H.-U. Reissig, *Organic Synthesis Highlights*, VCH, Weinheim, **1991**, pp. 174ff; h) R. F. Heck in *Comprehensive Organic Synthesis Vol. 4* (Eds.: B. M. Trost, I. Fleming), Pergamon, Oxford, **1991**; i) L. S. Hegedus in *Organometallics in Synthesis* (Ed.: M. Schlosser), Wiley, Chichester, **1994**, pp. 383ff.

[4] Reviews: a) L. F. Tietze, U. Beifuss, *Angew. Chem.* **1993**, *105*, 137; *Angew. Chem. Int. Ed. Engl.* **1993**, *32*, 131; b) T.-L. Ho, *Tandem Organic Reactions*, Wiley, New York, **1992**.

[5] a) B. Giese, *Methoden Org. Chem. (Houben-Weyl) 4th ed. 1952-*, Bd. E 19a, **1989**; b) *Radicals in Organic Synthesis: Formation of Carbon-Carbon Bonds*, Pergamon, Oxford, **1986**; c) D. P. Curran in *Comprehensive Organic Synthesis* (Eds.: B. M. Trost, I. Fleming), Pergamon, Oxford, **1991**.

[6] a) R. L. Hillard, C. A. Parnell, K. P. C. Vollhardt, *Tetrahedron* **1983**, *39*, 905; b) J.-C. Clinet, E. Duñach, K. P. C. Vollhardt, *J. Am. Chem. Soc.* **1983**, *105*, 6710; c) R. L. Funk, K. P. C. Vollhardt, *ibid.* **1977**, *99*, 5483; d) *ibid.* **1979**, *101*, 215; e) *ibid.* **1980**, *102*, 5253; f) K. H. Dötz, *Angew. Chem.* **1975**, *87*, 672; *Angew. Chem. Int. Ed. Engl.* **1975**, *14*, 644; g) *Pure Appl. Chem.* **1983**, *55*, 1689; h) K. H. Dötz, W. Kuhn, *J. Organomet. Chem.* **1983**, *252*, C78; i) U. Schubert, H. Fischer, P. Hofmann, K. Weiss, K. H. Dötz, F. R. Kreissl, *Transition Metal Carbene Complexes*, Verlag Chemie, Weinheim, **1983**; j) K. H. Dötz, *Angew. Chem.* **1984**, *96*, 573; *Angew. Chem. Int. Ed. Engl.* **1984**, *23*, 587; k) A. Llebaria, F. Camps, J. M. Moreto, *Tetrahedron* **1993**, *49*, 1283; l) L. Pages, A. Llebaria, F. Camps, E. Molins, C. Miravitlles, J. M. Moreto, *J. Am. Chem. Soc.* **1992**, *114*, 10449; m) F. Camps, J. Coll, J. M. Moreto, J. Torras, *J. Org. Chem.* **1989**, *54*, 1969; n) *Tetrahedron Lett.* **1987**, *28*, 4745; o) F. Camps, J. M. Moreto, L. Pages, *Tetrahedron* **1992**, *48*, 3147; p) F. Camps, A. Llebaria, J. M. Moreto, L. Pages, *Tetrahedron Lett.* **1992**, *33*, 113; q) *ibid.* **1992**, *33*, 109.

[7] a) F. R. Hartley, *Organomet. Chem. Rev. Sect. A* **1970**, *6*, 119; b) D. T. Rosevear, F. G. A. Stone, *J. Chem. Soc. A* **1968**, 164; c) D. R. Coulson, *Inorg. Synth.* **1972**, *13*, 121.

[8] a) B. E. Mann, A. Musco, *J. Chem. Soc. Dalton Trans.* **1975**, 1673; b) W. Kuran, A. Musco, *Inorg. Chim. Acta* **1975**, *12*, 187.

[9] a) J.-F. Fauvarque, F. Pflüger, M. Troupel, *J. Organomet. Chem.* **1981**, *208*, 419; b) C. Amatore, F. Pflüger, *Organometallics* **1990**, *9*, 2276.

[10] For a discussion on the reducing agent see T. Hayashi, A. Kubo, F. Ozawa, *Pure Appl. Chem.* **1992**, *64*, 421.

[11] a) E.-i. Negishi, T. Takahashi, K. Akiyoshi, *J. Chem. Soc. Chem. Commun.* **1986**, 1338; b) H. Urata, H. Suzuki, Y. Moro-oka, T. Ikawa, *J. Organomet. Chem.* **1989**, *364*, 235; c) F. Camps, E. Chamorro, V. Gasol, A. Guerrero, *Synth. Commun.* **1989**, *19*, 3211.

[12] a) C. Amatore, M. Azzabi, A. Jutand, *J. Organomet. Chem.* **1989**, *363*, C41; b) E.-i. Negishi, *Acc. Chem. Res.* **1982**, *15*, 340.

[13] a) J. P. Collman, L. S. Hegedus, *Principles and Applications of Organotransition Metal Chemistry*, University Science Books, Mill Valley, **1980**; b) J. J. Low, W. A. Goddard III, *J. Am. Chem. Soc.* **1986**, *108*, 6115.

[14] a) J. M. Brown, N. A. Cooley, *Organometallics* **1990**, *9*, 353; b) F. Ozawa, T. Ito, Y. Nakamura, A. Yamamoto, *Bull. Chem. Soc. Jpn.* **1981**, *54*, 1868.

[15] a) P. Fitton, J. E. McKeon, *J. Chem. Soc. Chem. Commun.* **1968**, 4; b) G. K. Anderson, R. J. Cross, *Chem. Soc. Rev.* **1980**, *9*, 185; c) An analogous situation is well documented for platinum complexes: J. Chatt, B. L. Shaw, *J. Chem. Soc.* **1959**, *705*, 4020; J. Rajaram, R. G. Pearson, J. A. Ibers, *J. Am. Chem. Soc.* **1974**, *96*, 2103; d) *cis* Complexes formed by oxidative addition of sterically encumbered aryl halides to palladium(0) have been isolated: H. Urata, M. Tanaka, T. Fuchikami, *Chem. Lett.* **1987**, 751.

[16] J. M. Brown, N. A. Cooley, *J. Chem. Soc. Chem. Commun.* **1988**, 1345.

[17] E. G. Samsel, J. R. Norton, *J. Am. Chem. Soc.* **1984**, *106*, 5505.

[18] a) D. L. Thorn, R. Hoffmann, *J. Am. Chem. Soc.* **1978**, *100*, 2079; b) T. A. Albright, R. Hoffmann, J. C. Thibeault, D. L. Thorn, *ibid.* **1979**, *101*, 3801.

[19] A. C. Albéniz, P. Espinet, Y. Jeannin, M. Philoche-Levisalles, B. E. Mann, *J. Am. Chem. Soc.* **1990**, *112*, 6594.

[20] a) E. H. Brooks, F. Glockling, *J. Chem. Soc. A* **1967**, 1030; b) H. Munakata, M. L. H. Green, *J. Chem. Soc. Chem. Commun.* **1970**, *881*; c) C. Di Bugno, M. Pasquali, P. Leoni, P. Sabatino, D. Braga, *Inorg. Chem.* **1989**, *28*, 1390.

[21] The base has an rate-increasing effect as a ligand: R. Benhaddou, S. Czernecki, G. Ville, *J. Chem. Soc. Chem. Commun.* **1988**, 247.

[22] a) E.-i. Negishi, T. Takahashi, S. Baba, D. E. Van Horn, N. Okukado, *J. Am. Chem. Soc.* **1987**, *109*, 2393; b) E.-i. Negishi, F.-T. Luo, *J. Org. Chem.* **1983**, *48*, 1560; c) C. E. Russell, L. S. Hegedus, *J. Am. Chem. Soc.* **1983**, *105*, 943; d) N. Jabri, A. Alexakis, J. F. Normant, *Tetrahedron Lett.* **1981**, *22*, 959; e) J. K. Stille, B. L. Groh, *J. Am. Chem. Soc.* **1987**, *109*, 813; f) W. J. Scott, J. K. Stille, *ibid.* **1986**, *108*, 3033; g) A. Suzuki, *Pure Appl. Chem.* **1985**, *57*, 1749; h) N. Okukado, D. E. Van Horn, W. L. Klima, E.-i. Negishi, *Tetrahedron Lett.* **1978**, 1027; i) Y. Hatanaka, T. Hiyama, *J. Org. Chem.* **1988**, *53*, 918; j) S. Baba, E.-i. Negishi, *J. Am. Chem. Soc.* **1976**, *98*, 6729; k) H. P. Dang, G. Linstrumelle, *Tetrahedron Lett.* **1978**, *19*, 191; l) T. N. Mitchell, *Synthesis* **1992**, 803.

[23] a) N. Chida, M. Ohtsuka, S. Ogawa, *Tetrahedron Lett.* **1991**, *32*, 4525; b) R. W. Bates, C. J. Gabel, *ibid.* **1993**, *34*, 3547; c) M. Aslam, V. Elango, K. G. Davenport, *Synthesis* **1989**, 869; d) R. J. Alabaster, I. F. Cottrell, D. Hands, G. R. Humphrey, D. J. Kennedy, S. H. B. Wright, *ibid.* **1989**, 598; e) M. Cutolo, V. Fiandanese, F. Naso, O. Sciacovelli, *Tetrahedron Lett.* **1983**, *24*, 4603; f) G. T. Crisp, P. T. Glink, *Tetrahedron* **1992**, *48*, 3541; g) C. A. Busacca, R. E. Johnson, J. Swestock, *J. Org. Chem.* **1993**, *58*, 3299; h) A.-S. Carlström, T. Frejd, *Synthesis* **1989**, 414; i) R. Grigg, V. Santhakumar, V. Sridharan, M. Thornton-Pett, A. W. Bridge, *Tetrahedron* **1993**, *49*, 5177; j) E. C. Taylor, G. S. K. Wong, *J. Org. Chem.* **1989**, *54*, 3618; k) E. C. Taylor, P. S. Ray, *Synth. Commun.* **1987**, *17*, 1865; l) T. Breining, C. Schmidt, K. Polos, *ibid.* **1987**, *17*, 85; m) S. Cacchi, P. G. Ciattini, E. Morera, G. Ortar, *Tetrahedron Lett.* **1988**, *29*, 3117.

[24] a) J. F. Fauvarque, A. Jutand, *Bull. Soc. Chim. Fr.* **1976**, 765; b) *J. Organomet. Chem.* **1977**, *132*, C17; c) *ibid.* **1979**, *177*, 273; d) *ibid.* **1981**, *209*, 109; e) M. Kumada, *Pure Appl. Chem.* **1980**, *52*, 669; f) J. K. Stille, *Angew. Chem.* **1986**, *98*, 504; *Angew. Chem. Int. Ed. Engl.* **1986**, *25*, 508.

[25] a) P. Fitton, E. A. Rick, *J. Organomet. Chem.* **1971**, *28*, 287; b) D. R. Coulson, *J. Chem. Soc. Chem. Commun.* **1968**, 1530.

[26] a) G. W. Parshall, *J. Am. Chem. Soc.* **1974**, *96*, 2360; for exceptions see b) J. B. Davison, N. M. Simon, S. A. Sojka, *J. Mol. Catal.* **1984**, *22*, 349; c) M. Julia, M. Duteil, *Bull. Soc. Chim. Fr.* **1973**, 2790; d) A. Spencer, *J. Organomet. Chem.* **1984**, *270*, 115; e) H. A. Dieck, R. F. Heck, *J. Am. Chem. Soc.* **1974**, *96*, 1133.

[27] a) K. Kikukawa, K. Nagira, K. Wada, T. Matsuda, *Tetrahedron* **1981**, *37*, 31; b) K. Kikukawa, T. Matsuda, *Chem. Lett.* **1977**, 159; c) K. Kikukawa, K. Nagira, N. Terao, F. Wada, T. Matsuda, *Bull. Chem. Soc. Jpn.* **1979**, *52*, 2609; d) W. Yong, P. Yi, Z. Zhuangyu, H. Hongwen, *Synthesis* **1991**, 967.

[28] K. Kikukawa, M. Naritomi, G.-X. He, F. Wada, T. Matsuda, *J. Org. Chem.* **1985**, *50*, 299.

[29] a) R. M. Moriarty, W. R. Epa, A. K. Awasthi, *J. Am. Chem. Soc.* **1991**, *113*, 6315; Pd-catalyzed carbonylations: b) T. Kitamura, I. Mihara, H. Taniguchi, P. J. Stang, *J. Chem. Soc. Chem. Commun.* **1990**, 614; c) M. Ochiai, K. Sumi, Y. Takaoka, M. Kunishima, Y. Nagao, M. Shiro, E. Fujita, *Tetrahedron* **1988**, *44*, 4095.

[30] K. Voigt, U. Schick, F. E. Meyer, A. de Meijere, *Synlett* **1994**, 189.

[31] a) T. Jeffery, *Tetrahedron Lett.* **1985**, *26*, 2667; b) *J. Chem. Soc. Chem. Commun.* **1984**, 1287.

[32] a) G.-z. Wu, F. Lamaty, E.-i. Negishi, *J. Org. Chem.* **1989**, *54*, 2507; b) R. F. Heck, J. P. Nolley, Jr., *ibid.* **1972**, *37*, 2320; c) R. Grigg, S. Sukirthalingam, V. Sridharan, *Tetrahedron Lett.* **1991**, *32*, 2545.

[33] a) C.-M. Andersson, A. Hallberg, *Tetrahedron Lett.* **1987**, *28*, 4215; b) A. Biavati, G. Chiusoli, M. Costa, G. Terenghi, *Transition Met. Chem.* **1979**, *4*, 398; c) K. Hori, M. Ando, N. Takaishi, Y. Inamoto, *Tetrahedron Lett.* **1987**, *28*, 5883; d) G. P. Chiusoli, *Pure Appl. Chem.* **1980**, *52*, 635; e) T.-a. Mitsudo, M. Kadokura, Y. Watanabe, *J. Org. Chem.* **1987**, *52*, 3186.

[34] a) Y. Ben-David, M. Portnoy, D. Milstein, *J. Chem. Soc. Chem. Commun.* **1989**, 1816; b) Y. Ben-David, M. Portnoy, M. Gozin, D. Milstein, *Organometallics* **1992**, *11*, 1995; c) M. Portnoy, Y. Ben-David, D. Milstein, *ibid.* **1993**, *12*, 4734.

[35] a) M. Huser, M.-T. Youinou, J. A. Osborn, *Angew. Chem.* **1989**, *101*, 1427; *Angew. Chem. Int. Ed. Engl.* **1989**, *28*, 1386; b) activation of 1,2-dichloroethene: C. Amatore, M. Azzabi, A. Jutand, *J. Am. Chem. Soc.* **1991**, *113*, 1670; W. A. Herrmann, C. Brossmer, K. Öfele, C.-P. Reisinger, T. Priermeier, M. Beller, H. Fischer, *Angew. Chem.* **1995**, *107*, in press; *Angew. Chem. Int. Ed. Engl.* **1995**, *34*, in press.

[36] J. J. Bozell, C. E. Vogt, *J. Am. Chem. Soc.* **1988**, *110*, 2655.

[37] a) P. J. Stang, W. Treptow, *Synthesis* **1980**, 283; b) J. R. Hassdenteufel, M. Hanack, *Tetrahedron Lett.* **1980**, *21*, 503; c) P. J. Stang, T. E. Fisk, *Synthesis* **1979**, 438.

[38] G. S. Jones, W. J. Scott, *J. Am. Chem. Soc.* **1992**, *114*, 1491.

[39] a) S. Cacchi, E. Morera, G. Ortar, *Tetrahedron Lett.* **1984**, *25*, 2271; b) *ibid.* **1984**, *25*, 4821; c) *Synthesis* **1986**, 320; d) *Tetrahedron Lett.* **1985**, *26*, 1109.

[40] a) W. J. Scott, M. R. Peña, K. Swärd, S. J. Stoessel, J. K. Stille, *J. Org. Chem.* **1985**, *50*, 2302; b) G. T. Crisp, W. J. Scott, J. K. Stille, *J. Am. Chem. Soc.* **1984**, *106*, 7500; c) W. J. Scott, G. T. Crisp, J. K. Stille, *ibid.* **1984**, *106*, 4630.

[41] a) S. Cacchi, P. G. Ciattini, E. Morera, G. Ortar, *Tetrahedron Lett.* **1987**, *28*, 3039; b) R. McCague, *ibid.* **1987**, *28*, 701; c) L. Castedo, A. Mourino, L. A. Sarandeses, *ibid.* **1986**, *27*, 1523; d) S. Cacchi, P. G. Ciattini, E. Morera, G. Ortar, *ibid.* **1986**, *27*, 5541; e) *ibid.* **1986**, *27*, 3931; f) Q.-Y. Chen, Z.-Y. Yang, *ibid.* **1986**, *27*, 1171; g) A. Arcadi, E. Bernocchi, S. Cacchi, L. Caglioti, F. Marinelli, *ibid.* **1990**, *31*, 2463; h) A. Arcadi, S. Cacchi, F. Marinelli, *ibid.* **1989**, *30*, 2581; i) S. Cacchi, A. Lupi, *ibid.* **1992**, *33*, 3939; j) A. Arcadi, E. Bernocchi, S. Cacchi, F. Marinelli, *Tetrahedron* **1991**, *47*, 1525; k) A. Arcadi, S. Cacchi, F. Marinelli, E. Morera, G. Ortar, *ibid.* **1990**, *46*, 7151; l) S. W. Scheuplein, K. Harms, R. Brückner, J. Suffert, *Chem. Ber.* **1992**, *125*, 271.

[42] a) R. Grigg, V. Sridharan, P. Stevenson, T. Worakun, *J. Chem. Soc. Chem. Commun.* **1986**, 1697; b) T. Jeffery, *Synthesis* **1987**, 70; c) R. C. Larock, S. Babu, *Tetrahedron Lett.* **1987**, *28*, 5291; d) R. C. Larock, B. E. Baker, *ibid.* **1988**, *29*, 905; e) R. C. Larock, H. Song, B. E. Baker, W. H. Gong, *ibid.* **1988**, *29*, 2919; f) R. C. Larock, D. E. Stinn, *ibid.* **1988**, *29*, 4687; g) R. Grigg, P. Stevenson, T. Worakun, *Tetrahedron* **1988**, *44*, 2033; h) *ibid.* **1988**, *44*, 2049; i) B. Burns, R. Grigg, V. Sridharan, T. Worakun, *Tetrahedron Lett.* **1988**, *29*, 4325; j) B. Burns, R. Grigg, P. Ratananukul, V. Sridharan, P. Stevenson, T. Worakun, *ibid.* **1988**, *29*, 4329; k) T. Jeffery, *Synth. Commun.* **1988**, *18*, 77; l) R. C. Larock, P. L. Johnson, *J. Chem. Soc. Chem. Commun.* **1989**, 1368; m) H. M. R. Hoffmann, B. Schmidt, S. Wolff, *Tetrahedron* **1989**, *45*, 6113; n) R. C. Larock, W. H. Gong, B. E. Baker, *Tetrahedron Lett.* **1989**, *30*, 2603; o) A. Amorese, A. Arcadi, E. Bernocchi, S. Cacchi, S. Cerrini, W. Fedeli, G. Ortar, *Tetrahedron* **1989**, *45*, 813; p) R. Grigg, V. Sridharan, P. Stevenson, S. Sukirthalingam, *ibid.* **1989**, *45*, 3557; q) R. C. Larock, N. Berrios-Peña, K. Narayanan, *J. Org. Chem.* **1990**, *55*, 3447; r) R. C. Larock, C. A. Fried, *J. Am. Chem. Soc.* **1990**, *112*, 5882; s) C.-M. Andersson, J. Larsson, A. Hallberg, *J. Org. Chem.* **1990**, *55*, 5757; t) C. A. Merlic, M. F. Semmelhack, *J. Organomet. Chem.* **1990**, *391*, C23.

[43] a) C. Amatore, M. Azzabi, A. Jutand, *J. Am. Chem. Soc.* **1991**, *113*, 8375; b) C. Amatore, A. Jutand, A. Suarez, *ibid.* **1993**, *115*, 9531.

[44] a) M. M. Abelman, T. Oh, L. E. Overman, *J. Org. Chem.* **1987**, *52*, 4130; b) M. M. Abelman, L. E. Overman, *J. Am. Chem. Soc.* **1988**, *110*, 2328; c) A. Yamamoto, F. Kawataka, Y. Kayaki, I. Shimizu in ref. [44d]; d) *Seventh IUPAC Symposium on Organo-Metallic Chemistry directed towards Organic Synthesis (OMCOS 7) Abstracts*, Kobe, Japan, September 19–23, 1993, p. 343.

[45] a) R. Grigg, V. Loganathan, S. Sukirthalingam, V. Sridharan, *Tetrahedron Lett.* **1990**, *31*, 6573; b) R. Grigg, V. Loganathan, V. Santhakumar, V. Sridharan, A. Teasdale, *ibid.* **1991**, *32*, 687; c) C. Carfagna, A. Musco, G. Sallese, R. Santi, T. Fiorani, *J. Org. Chem.* **1991**, *56*, 261; d) W. Cabri, I. Candiani, A. Bedeschi, R. Santi, *Tetrahedron Lett.* **1991**, *32*, 1753.

[46] a) N. A. Bumagin, P. G. More, I. P. Beletskaya, *J. Organomet. Chem.* **1989**, *371*, 397; b) N. A. Bumagin, V. V. Bykov, I. P. Beletskaya, *Izv. Akad. Nauk SSSR Ser. Khim.* **1989**, *38*, 2394; English translation: *Bull. Acad. Sci. USSR Div. Chem. Sci. (Engl. Transl.)* **1989**, *38*, 2206; c) *Izv. Akad. Nauk SSSR Ser. Khim.* **1990**, *39*, 2672; English translation: *Bull. Acad. Sci. USSR Div. Chem. Sci. (Engl. Transl.)* **1990**, *39*, 2426; d) I. P. Beletskaya, *Sixth IUPAC Symposium on Organo-Metallic Chemistry directed towards Organic Synthesis (OMCOS 6), Abstracts*, Utrecht, The Netherlands, August 25–29, 1991, p. 67; e) I. P. Beletskaya, in ref. [44d]; f) see also A. L. Casalnuovo, J. C. Calabrese, *J. Am. Chem. Soc.* **1990**, *112*, 4324; g) M. Safi, D. Sinou, *Tetrahedron Lett.* **1991**, *32*, 2025.

[47] a) J. P. Genet, E. Blart, M. Savignac, *Synlett* **1992**, 715; b) T. Jeffery, *Tetrahedron Lett.* **1994**, *35*, 3051.

[48] C.-M. Andersson, K. Karabelas, A. Hallberg, C. Andersson, *J. Org. Chem.* **1985**, *50*, 3891.

[49] a) K. Kaneda, M. Terasawa, T. Imanaka, S. Teranishi, M. Tsutsui, *Fundamental Research in Homogeneous Catalysis, Vol. 3*, Plenum, New York, **1979**, p. 671; b) M. Terasawa, K. Kaneda, T. Imanaka, S. Teranishi, *J. Organomet. Chem.* **1978**, *162*, 403.

[50] a) B. M. Choudary, M. R. Sarma, *Tetrahedron Lett.* **1990**, *31*, 1495; b) B. M. Choudary, M. R. Sarma, K. K. Rao, *ibid.* **1990**, *31*, 5781; c) B. M. Choudary, R. M. Sarma, K. K. Rao, *Tetrahedron* **1992**, *48*, 719.

[51] a) Z. Zhuangyu, P. Yi, H. Honwen, K. Tsi-yu, *Synthesis* **1991**, 539; b) Z. Y. Zhang, H. W. Hu, T. Y. Kao, *React. Polym. Ion Exch. Sorbents* **1988**, *9*, 249; c) *ibid.* **1990**, *12*, 229; d) Z. Zhuangyu, P. Yi, H. Honwen, K. Tsi-yu, *Synth. Commun.* **1990**, *20*, 3563.

[52] For Pd-catalyzed couplings with unsymmetric alkenes see a) N. Okukado, D. E. Van Horn, W. L. Klima, E.-i. Negishi, *Tetrahedron Lett.* **1978**, 1027; b) D. Milstein, J. K. Stille, *J. Am. Chem. Soc.* **1979**, *101*, 4992; c) N. Miyaura, K. Yamada, A. Suzuki, *Tetrahedron Lett.* **1979**, 3437; d) N. Miyaura, A. Suzuki, *J. Chem. Soc. Chem. Commun.* **1979**, 866; e) H. Yoshimoto, H. Itatani, *Bull. Chem. Soc. Jpn.* **1973**, *46*, 2490.

[53] a) I. Arai, G. D. Daves, Jr., *J. Org. Chem.* **1979**, *44*, 21; b) C. B. Ziegler, Jr., R. F. Heck, *ibid.* **1978**, *43*, 2949; c) R. F. Heck, *J. Am. Chem. Soc.* **1968**, *90*, 5535.

[54] a) G. D. Daves, Jr., A. Hallberg, *Chem. Rev.* **1989**, *89*, 1433; b) C.-M. Andersson, A. Hallberg, G. D. Daves, Jr., *J. Org. Chem.* **1987**, *52*, 3529; c) R. N. Farr, R. A. Outten, J. C.-Y. Cheng, G. D. Daves, Jr., *Organometallics* **1990**, *9*, 3151; d) G. D. Daves, Jr., *Acc. Chem. Res.* **1990**, *23*, 201; e) R. A. Outten, G. D. Daves, Jr., *J. Org. Chem.* **1989**, *54*, 29; f) M. A. Tius, X.-q. Gu, J. Gomez-Galeno, *J. Am. Chem. Soc.* **1990**, *112*, 8188; g) M. A. Tius, J. Gomez-Galeno, X.-q. Gu, J. H. Zaidi, *ibid.* **1991**, *113*, 5775; h) D.-I. Kwok, R. N. Farr, G. D. Daves, Jr., *J. Org. Chem.* **1991**, *56*, 3711.

[55] a) K. Nilsson, A. Hallberg, *J. Org. Chem.* **1990**, *55*, 2464; b) H. Iida, Y. Yuasa, C. Kibayashi, *ibid.* **1980**, *45*, 2938.

[56] a) P. G. Ciattini, E. Morera, G. Ortar, *Tetrahedron Lett.* **1991**, *32*, 1579; b) N. M. Doherty, J. E. Bercaw, *J. Am. Chem. Soc.* **1985**, *107*, 2670.

[57] a) T. D. Lee, G. D. Daves, Jr., *J. Org. Chem.* **1983**, *48*, 399; b) A. Hallberg, L. Westfelt, B. Holm, *ibid.* **1981**, *46*, 5414; c) A. Hallberg, L. Westfelt, C.-M. Andersson, *Synth. Commun.* **1985**, *15*, 1131.

[58] a) C.-M. Andersson, A. Hallberg, *J. Org. Chem.* **1988**, *53*, 235; b) C.-M. Andersson, J. Larsson, A. Hallberg, *ibid.* **1990**, *55*, 5757; c) D. Badone, U. Guzzi, *Tetrahedron Lett.* **1993**, *34*, 3603; d) for β-aroylation of enol ethers see ref. [33a] and C.-M. Andersson, A. Hallberg, *J. Org. Chem.* **1988**, *53*, 4257.

[59] C.-M. Andersson, A. Hallberg, *J. Org. Chem.* **1988**, *53*, 2112.

[60] C.-M. Andersson, A. Hallberg, *J. Org. Chem.* **1989**, *54*, 1502.

[61] a) W. Cabri, I. Candiani, A. Bedeschi, S. Penco, R. Santi, *J. Org. Chem.* **1992**, *57*, 1481; b) W. Cabri, I. Candiani, A. Bedeschi, R. Santi, *ibid.* **1990**, *55*, 3654; c) *Synlett* **1992**, 871; d) *J. Org. Chem.* **1992**, *57*, 3558.

[62] F. Ozawa, A. Kubo, T. Hayashi, *J. Am. Chem. Soc.* **1991**, *113*, 1417.

[63] I. Moritani, Y. Fujiwara, S. Danno, *J. Organomet. Chem.* **1971**, *27*, 279.

[64] a) P. J. Stang, M. H. Kowalski, M. D. Schiavelli, D. Longford, *J. Am. Chem. Soc.* **1989**, *111*, 3347; b) P. J. Stang, M. H. Kowalski, *ibid.* **1989**, *111*, 3356; c) R. J. Hinkle, P. J. Stang, M. H. Kowalski, *J. Org. Chem.* **1990**, *55*, 5033.

[65] a) K. Karabelas, A. Hallberg, *Tetrahedron Lett.* **1985**, *26*, 3131; b) K. Karabelas, C. Westerlund, A. Hallberg, *J. Org. Chem.* **1985**, *50*, 3896; c) K. Karabelas, A. Hallberg, *ibid.* **1988**, *53*, 4909; d) *ibid.* **1986**, *51*, 5286.

[66] a) W. Smadja, S. Czernecki, G. Ville, C. Georgoulis, *Organometallics* **1987**, *6*, 166; b) *Tetrahedron Lett.* **1981**, *22*, 2479; c) W. Smadja, G. Ville, G. Cahiez, *ibid.* **1984**, *25*, 1793; d) J. B. Melpolder, R. F. Heck, *J. Org. Chem.* **1976**, *41*, 265; e) A. J. Chalk, S. A. Magennis, *ibid.* **1976**, *41*, 273; f) Y. Tamaru, Y. Yamada, T. Arimoto, Z.-i. Yoshida, *Chem. Lett.* **1978**, 975; g) K. von Werner, *J. Organomet. Chem.* **1977**, *136*, 385; h) Y. Tamaru, Y. Yamada, Z.-i. Yoshida, *J. Org. Chem.* **1978**, *43*, 3396; i) *Tetrahedron Lett.* **1977**, 3365; j) *ibid.* **1978**, 919; k) A. Kasahara, T. Izumi, M. Maemura, *Bull. Chem. Soc. Jpn.* **1977**, *50*, 1021; l) A. J. Chalk, S. A. Magennis in *Catalysis in Organic Synthesis* (Ed.: G. V. Smith), Academic Press, New York, **1977**, p. 139; m) R. F. Heck, *J. Am. Chem. Soc.* **1968**, *90*, 5526.

[67] a) R. C. Larock, D. J. Leuck, L. W. Harrison, *Tetrahedron Lett.* **1988**, *29*, 6399; b) R. C. Larock, K. Takagi, *J. Org. Chem.* **1988**, *53*, 4329; c) R. C. Larock, H. Song, S. Kim, R. A. Jacobson, *J. Chem. Soc. Chem. Commun.* **1987**, 834.

[68] a) R. C. Larock, W.-Y. Leung, S. Stolz-Dunn, *Tetrahedron Lett.* **1989**, *30*, 6629; b) A. P. Wells, W. Kitching, *J. Org. Chem.* **1992**, *57*, 2517.

[69] a) T. Jeffery, *Tetrahedron Lett.* **1991**, *32*, 2121; b) *J. Chem. Soc. Chem. Commun.* **1991**, 324; c) *Tetrahedron Lett.* **1993**, *34*, 1133; d) *ibid.* **1990**, *31*, 6641.

[70] E. Bernocchi, S. Cacchi, P. G. Ciattini, E. Morera, G. Ortar, *Tetrahedron Lett.* **1992**, *33*, 3073.

[71] Desilylation also did not occur in the coupling of alkenyltrimethylsilanes with acetatophenylpalladium generated in situ or with phenylpalladium tetrafluoroborate: a) K. Kikukawa, K. Ikenaga, F. Wada, T. Matsuda, *Tetrahedron Lett.* **1984**, *25*, 5789; b) K. Kikukawa, K. Ikenaga, K. Kono, K. Toritani, F. Wada, T. Matsuda, *J. Organomet. Chem.* **1984**, *270*, 277; c) K. Ikenaga, K. Kikukawa, T. Matsuda, *J. Org. Chem.* **1987**, *52*, 1276.

[72] a) K. S. Chu, G. R. Negrete, J. P. Konopelski, F. J. Lakner, N.-T. Woo, M. M. Olmstead, *J. Am. Chem. Soc.* **1992**, *114*, 1800; b) G. E. Stokker, *Tetrahedron Lett.* **1987**, *28*, 3179.

[73] a) S. Cacchi, F. La Torre, G. Palmieri, *J. Organomet. Chem.* **1984**, *268*, C48; b) S. Cacchi, G. Palmieri, *Synthesis* **1984**, 575; c) S. Cacchi, A. Arcadi, *J. Org. Chem.* **1983**, *48*, 4236; d) A. Arcadi, F. Marinelli, S. Cacchi, *J. Organomet. Chem.* **1986**, *312*, C27; e) A. Arcadi, E. Bernocchi, S. Cacchi, F. Marinelli, *Synlett* **1991**, 27.

[74] A. Amorese, A. Arcadi, E. Bernocchi, S. Cacchi, S. Cerrini, W. Fedeli, G. Ortar, *Tetrahedron* **1989**, *45*, 813.

[75] R. Benhaddou, S. Czernecki, G. Ville, *J. Org. Chem.* **1992**, *57*, 4612.

[76] a) B. M. Trost, M. Lautens, *J. Am. Chem. Soc.* **1985**, *107*, 1781; b) B. M. Trost, *Acc. Chem. Res.* **1990**, *23*, 34; c) *Janssen Chim. Acta* **1991**, *9*, 3; d) B. M. Trost, G. J. Tanoury, M. Lautens, C. Chan, D. T. MacPherson, *J. Am. Chem. Soc.* **1994**, *116*, 4255.

[77] B. M. Trost, *Science* **1991**, *254*, 1471.

[78] a) F. Fringuelli, A. Taticchi, *Dienes in the Diels-Alder Reaction*, Wiley, New York, **1990**; b) W. Carruthers, *Cycloaddition Reactions in Organic Synthesis*, Pergamon, Oxford, **1990**; c) D. Craig, *Chem. Soc. Rev.* **1987**, *16*, 187; d) E. Ciganek, *Org. React.* **1984**, *32*, 1; e) A. G. Fallis, *Can. J. Chem.* **1984**, *62*, 183; f) G. Brieger, J. N. Bennett, *Chem. Rev.* **1980**, *80*, 63; g) D. F. Taber, *Intramolecular Diels-Alder and Alder Ene Reactions*, Springer, Berlin, **1984**.

[79] B. M. Trost, D. C. Lee, F. Rise, *Tetrahedron Lett.* **1989**, *30*, 651.

[80] An alternative reaction mechanism taking into account a palladacyclic intermediate was also discussed, see ref. [76b].

[81] a) P. N. Rylander, *Hydrogenation Methods*, Academic Press, London, **1985**; b) *Catalytic Hydrogenation in Organic Syntheses*, Academic Press, New York, **1979**; c) W. Carruthers, *Some Modern Methods of Organic Synthesis*, 3rd ed., Cambridge, University Press, Cambridge, **1986**, p. 411; d) M. Freifelder, *Catalytic Hydrogenation in Organic Synthesis, Procedures and Commentary*, Wiley-Interscience, New York, **1978**; e) S. Nishimura, U. Takagi, *Catalytic Hydrogenation. Application to Organic Synthesis*, Tokyo Kagaku Dajin, Tokyo, **1987**.

[82] a) B. M. Trost, *Tetrahedron* **1977**, *33*, 2615; b) *Acc. Chem. Res.* **1980**, *13*, 385; c) *Angew. Chem.* **1989**, *101*, 1199; *Angew. Chem. Int. Ed. Engl.* **1989**, *28*, 1173; d) J. Tsuji, I. Shimizu, I. Minami, Y. Ohashi, T. Sugiura, K. Takahashi, *J. Org. Chem.* **1985**, *50*, 1523; e) J. Tsuji, *Acc. Chem. Res.* **1969**, *2*, 144; f) R. Baker, *Chem. Ind. (London)* **1980**, 816; g) J. Tsuji, *Pure Appl. Chem.* **1981**, *53*, 2371; h) B. M. Trost, *ibid.* **1981**, *53*, 2357; i) J. Tsuji, *ibid.* **1982**, *54*, 197; j) *ibid.* **1986**, *58*, 869; k) *Tetrahedron* **1986**, *42*, 4361; l) B. M. Trost, *J. Organomet. Chem.* **1986**, *300*, 263; m) J. Tsuji, *ibid.* **1986**, *300*, 281; n) P. M. Maitlis, P. Espinek, M. J. H. Russel in *Comprehensive Organometallic Chemistry, Vol. 6* (Eds.: G. Wilkinson, F. G. A. Stone, E. W. Abel), Pergamon, Oxford, **1982**, p. 385; o) G. Consiglio, R. M. Waymouth, *Chem. Rev.* **1989**, *89*, 257, and references therein; p) C. G. Frost, J. Howarth, J. M. J. Williams, *Tetrahedron: Asymmetry* **1992**, *3*, 1089.

[83] a) H. Grennberg, S. Faizon, J.-E. Bäckvall, *Angew. Chem.* **1993**, *105*, 269; *Angew. Chem. Int. Ed. Engl.* **1993**, *32*, 263; b) J.-E. Bäckvall, R. B. Hopkins, H. Grennberg, M. M. Mader, A. K. Awasthi, *J. Am. Chem. Soc.* **1990**, *112*, 5160; c) J.-E. Bäckvall, A. K. Awasthi, Z. D. Renko, *ibid.* **1987**, *109*, 4750; d) J.-E. Bäckvall, S. E. Byström, R. E. Nordberg, *J. Org. Chem.* **1984**, *49*, 4619; e) J.-E. Bäckvall, J.-E. Nyström, R. E. Nordberg, *J. Am. Chem. Soc.* **1985**, *107*, 3676; f) J.-E. Bäckvall, R. E. Nordberg, J.-E. Nyström, *J. Org. Chem.* **1981**, *46*, 3479; g) J.-E. Bäckvall, R. E. Nordberg, E. E. Björkman, C. Moberg, *J. Chem. Soc. Chem. Commun.* **1980**, 943; h) J.-E. Bäckvall, A. Gogoll, *Tetrahedron Lett.* **1988**, *29*, 2243; i) J.-E. Bäckvall, R. E. Nordberg, D. Wilhelm, *J. Am. Chem. Soc.* **1985**, *107*, 6892; j) J.-E. Bäckvall, R. E. Nordberg, *ibid.* **1981**, *103*, 4959.

[84] a) K. Sonogashira, Y. Tohda, N. Hagihara, *Tetrahedron Lett.* **1975**, 4467; b) R. Rossi, A. Carpita, M. G. Quirici, M. L. Gaudenzi, *Tetrahedron* **1982**, *38*, 631; c) V. Ratovelomana, G. Linstrumelle, *Synth. Commun.* **1981**, *11*, 917; d) T. F. Tam, R. W. Spencer, E. M. Thomas, L. J. Copp, A. Krantz, *J. Am. Chem. Soc.* **1984**, *106*, 6849; e) E. J. Corey, M. d'Alarcao, *Tetrahedron Lett.* **1986**, *27*, 3589; f) P. Magnus, R. T. Lewis, J. C. Huffman, *J. Am. Chem. Soc.* **1988**, *110*, 6921; g) S. L. Schreiber, L. L. Kiessling, *ibid.* **1988**, *110*, 631; h) A. S. Kende, C. A. Smith, *Tetrahedron Lett.* **1988**, *29*, 4217; i) K. Tomioka, H. Fujita, K. Koga, *ibid.* **1989**, *30*, 851.

[85] G. C. Nwokogu, *Tetrahedron Lett.* **1984**, *25*, 3263.

[86] A. R. Hunt, S. K. Stewart, A. Whiting, *Tetrahedron Lett.* **1993**, *34*, 3599.

[87] a) S. Cacchi, M. Felici, B. Pietroni, *Tetrahedron Lett.* **1984**, *25*, 3137; b) A. Arcadi, S. Cacchi, F. Marinelli, *Tetrahedron* **1985**, *41*, 5121; c) *Tetrahedron Lett.* **1986**, *27*, 6397.

[88] a) R. C. Larock, S. Babu, *Tetrahedron* **1987**, *43*, 2013; b) G. P. Chiusoli, *J. Organomet. Chem.* **1986**, *300*, 57; c) R. C. Larock, S. S. Hershberger, K. Takagi, M. A. Mitchell, *J. Org. Chem.* **1986**, *51*, 2450; d) A. Arcadi, F. Marinelli, E. Bernocchi, S. Cacchi, G. Ortar, *J. Organomet. Chem.* **1989**, *368*, 249.

[89] a) M. Ahmar, B. Cazes, J. Gore, *Tetrahedron Lett.* **1984**, *25*, 4505; b) N. Kopola, B. Friess, B. Cazes, J. Gore, *ibid.* **1989**, *30*, 3963; c) B. Cazes, V. Colovray, J. Gore, *ibid.* **1988**, *29*, 627.

[90] a) T. Jeffery, *Tetrahedron Lett.* **1992**, *33*, 1989; b) M. Uno, T. Takahashi, S. Takahashi, *J. Chem. Soc. Chem. Commun.* **1987**, 785.

[91] R. C. Larock, S. Ding, C. Tu, *Synlett* **1993**, 145, and references therein.

[92] F. E. Meyer, K.-H. Ang, A. G. Steinig, A. de Meijere, *Synlett* **1994**, 191, and references therein.

[93] T. Mandai, S.-i. Hasegawa, T. Fujimoto, M. Kawada, J. Nokami, J. Tsuji, *Synlett* **1990**, 85.

[94] For the synthesis of polyiodobenzenes see D. L. Mattern, *J. Org. Chem.* **1984**, *49*, 3051.

[95] a) J. E. Plevyak, R. F. Heck, *J. Org. Chem.* **1978**, *43*, 2454; b) J. E. Plevyak, J. E. Dickerson, R. F. Heck, *ibid.* **1979**, *44*, 4078.

[96] W. Tao, S. Nesbitt, R. F. Heck, *J. Org. Chem.* **1990**, *55*, 63.

[97] a) A. Lansky, O. Reiser, A. de Meijere, *Synlett* **1990**, *405*; b) K. Voigt, A. Lansky, A. de Meijere, unpublished results.

[98] R. Diercks, J. C. Armstrong, R. Boese, K. P. C. Vollhardt, *Angew. Chem.* **1986**, *98*, 270; *Angew. Chem. Int. Ed. Engl.* **1986**, *25*, 268.

[99] Hexaethenylbenzene was prepared by dehydrobromination of hexakis(1-bromoethyl)benzene: a) J. M. Bollinger, J. J. Burke, E. M. Arnett, *J. Org. Chem.* **1966**, *31*, 1310; b) C. Krüger, M. Yalpani, *Chem. Ber.* **1983**, *116*, 3359.

[100] A. Lansky, A. de Meijere, unpublished results; A. Lansky, Dissertation, Universität Göttingen, **1992**.

[101] G. Rümper, A. de Meijere, unpublished results.

[102] U. Scherf, K. Müllen, *Synthesis* **1992**, 23.

[103] T. J. Katz, A. M. Gilbert, M. E. Huttenloch, G. Min-Min, H. H. Brintzinger, *Tetrahedron Lett.* **1993**, *34*, 3551.

[104] a) N. A. Cortese, C. B. Ziegler, Jr., B. J. Hrnjez, R. F. Heck, *J. Org. Chem.* **1978**, *43*, 2952; b) I. Arai, G. D. Daves, Jr., *ibid.* **1979**, *44*, 21; c) C.-M. Andersson, A. Hallberg, G. D. Daves, Jr., *ibid.* **1987**, *52*, 3529; d) P. J. Harrington, K. A. di Fiore, *Tetrahedron Lett.* **1987**, *28*, 495; e) Y. Tamaru, Y. Yamada, Z.-i. Yoshida, *Tetrahedron* **1979**, *35*, 329; f) I. Arai, G. D. Daves, Jr., *J. Org. Chem.* **1978**, *43*, 4110.

[105] a) R. C. Larock, W. H. Gong, *J. Org. Chem.* **1989**, *54*, 2047; b) *ibid.* **1990**, *55*, 407.

[106] For first intramolecular versions see a) R. Grigg, V. Sridharan, P. Stevenson, T. Worakun, *J. Chem. Soc. Chem. Commun.* **1986**, 1697; b) M. M. Abelman, T. Oh, L. E. Overman, *J. Org. Chem.* **1987**, *52*, 4130.

[107] a) E. J. Corey, C.-P. Chen, M. J. Parry, *Tetrahedron Lett.* **1988**, *29*, 2899; b) S.-B. Hwang, M.-H. Lam, T. Biftu, T. R. Beattie, T.-Y. Shen, *J. Biol. Chem.* **1985**, *260*, 15639.

[108] M. Prashad, J. C. Tomesch, J. R. Wareing, H. C. Smith, S. H. Cheon, *Tetrahedron Lett.* **1989**, *30*, 2877.

[109] a) S. Hillers, O. Reiser, *Synlett* **1995**, in press; b) C. Bubert, O. Reiser, unpublished results.

[110] Recent reviews: a) R. Noyori, H. Takaya, *Acc. Chem. Res.* **1990**, *23*, 345; b) R. Noyori, *Science* **1990**, *248*, 1194; c) I. Ojima, N. Chos, C. Bastos, *Tetrahedron* **1989**, *45*, 6901; d) S. L. Blystone, *Chem. Rev.* **1989**, *89*, 1663; e) H. Brunner in *Topics in Stereochem., Vol. 18* (Eds.: E. L. Eliel, S. H. Wilen), **1989**, p. 129.

[111] N. E. Carpenter, D. J. Kucera, L. E. Overman, *J. Org. Chem.* **1989**, *54*, 5846.

[112] Y. Sato, M. Sodeoka, M. Shibasaki, *J. Org. Chem.* **1989**, *54*, 4738.

[113] a) F. Ozawa, A. Kubo, T. Hayashi, *J. Am. Chem. Soc.* **1991**, *113*, 1417; b) F. Ozawa, T. Hayashi, *J. Organomet. Chem.* **1992**, *428*, 267; c) F. Ozawa, A. Kubo, T. Hayashi, *Tetrahedron Lett.* **1992**, *33*, 1485; d) *Chem. Lett.* **1992**, 2177; e) F. Ozawa, Y. Kobatake, T. Hayashi, *Tetrahedron Lett.* **1993**, *34*, 2505.

[114] a) Y. Sato, M. Sodeoka, M. Shibasaki, *Chem. Lett.* **1990**, 1953; b) K. Kagechika, M. Shibasaki, *J. Org. Chem.* **1991**, *56*, 4093; c) Y. Sato, S. Watanabe, M. Shibasaki, *Tetrahedron Lett.* **1992**, *33*, 2589; d) Y. Sato, T. Honda, M. Shibasaki, *ibid.* **1992**, *33*, 2593; e) M. Shibasaki, Y. Sato, K. Kagechika, *Yuki Gosei Kagaku Kyokaishi* **1992**, *50*, 826; f) K. Kagechika, T. Ohshima, M. Shibasaki *Tetrahedron* **1993**, *49*, 1773; g) K. Kondo, M. Sodeoka, M. Mori, M. Shibasaki, *Tetrahedron Lett.* **1993**, *34*, 4219; h) S. Nukui, M. Sodeoka, M. Shibasaki, *ibid.* **1993**, *34*, 4965; i) T. Takemoto, M. Sodeoka, H. Sasai, M. Shibasaki, *J. Am. Chem. Soc.* **1993**, *115*, 8477.

[115] A. Ashimori, L. E. Overman, *J. Org. Chem.* **1992**, *57*, 4571.

[116] S. Hillers, O. Reiser, *Tetrahedron Lett.* **1993**, *34*, 5265.

[117] S. Hillers, A. Niklaus, O. Reiser, *J. Org. Chem.* **1993**, *58*, 3169.

[118] a) S. Takano, K. Samizu, K. Ogasawara, in ref. [44d]; b) T. Sakamoto, Y. Kondo, H. Yamanaka, *Tetrahedron Lett.* **1992**, *33*, 6845; c) S. Takano, K. Samizu, K. Ogasawara, *Synlett* **1993**, 393.

[119] a) M. Suzuki, T. Kawagishi, R. Noyori, *Tetrahedron Lett.* **1982**, *23*, 5563; b) M. Suzuki, A. Yanagisawa, R. Noyori, *J. Am. Chem. Soc.* **1985**, *107*, 3348; c) C. R. Johnson, T. D. Penning, *ibid.* **1986**, *108*, 5655; d) T. Tanaka, N. Okamura, K. Bannai, A. Hazato, S. Sugiura, K. Tomimori, K. Manabe, S. Kurozumi, *Tetrahedron* **1986**, *42*, 6747; e) J. R. Behling, K. A. Babiak, J. S. Ng, A. L. Campbell, R. Moretti, M. Koerner, B. H. Lipshutz, *J. Am. Chem. Soc.* **1988**,

110, 2641; f) M. Suzuki, A. Yanagisawa, R. Noyori, *ibid.* **1988**, *110*, 4718; g) E. J. Corey, K. Niimura, Y. Konishi, S. Hashimoto, Y. Hamada, *Tetrahedron Lett.* **1986**, *27*, 2199.

[120] D. P. Curran in *Advances in Free Radical Chemistry, Vol. 1* (Ed.: D. D. Tanner), JAI, Greenwich, **1990**, p. 121.

[121] a) R. C. Larock, N. H. Lee, *J. Org. Chem.* **1991**, *56*, 6253; for earlier related work see: b) *J. Am. Chem. Soc.* **1991**, *113*, 7815; c) R. C. Larock, F. Kondo, K. Narayanan, L. K. Sydnes, M.-F. H. Hsu, *Tetrahedron Lett.* **1989**, *30*, 5737; d) R. C. Larock, N. H. Lee, *ibid.* **1991**, *32*, 5911.

[122] a) S. Torii, H. Okumoto, H. Ozaki, S. Nakayasu, T. Tadokoro, T. Kotani, *Tetrahedron Lett.* **1992**, *33*, 3499; b) S. Torii, H. Okumoto, H. Ozaki, S. Nakayasu, T. Kotani, *ibid.* **1990**, *31*, 5319; c) S. Torii, H. Okumoto, T. Kotani, S. Nakayasu, H. Ozaki, *ibid.* **1992**, *33*, 3503.

[123] M. Catellani, G. P. Chiusoli, *Tetrahedron Lett.* **1982**, *23*, 4517.

[124] R. C. Larock, K. Takagi, J. P. Burkhart, S. S. Hershberger, *Tetrahedron* **1986**, *42*, 3759.

[125] M. Catellani, G. P. Chiusoli, W. Giroldini, G. Salermo, *J. Organomet. Chem.* **1980**, *199*, C21.

[126] M. Kosugi, H. Tamura, H. Sano, T. Migita, *Tetrahedron* **1989**, *45*, 961.

[127] M. Catellani, G. P. Chiusoli, S. Concari, *Tetrahedron* **1989**, *45*, 5263.

[128] M. Catellani, G. P. Chiusoli, P. Sgarabotto, *J. Organomet. Chem.* **1982**, *240*, 311.

[129] K. Albrecht, A. de Meijere, *Chem. Ber.* **1994**, *127*, 2539.

[130] a) M. Catellani, G. P. Chiusoli, *J. Organomet. Chem.* **1985**, *286*, C13; b) Review: *Gazz. Chim. Ital.* **1993**, *123*, 1, and references therein.

[131] a) O. Reiser, M. Weber, A. de Meijere, *Angew. Chem.* **1989**, *101*, 1071; *Angew. Chem. Int. Ed. Engl.* **1989**, *28*, 1037; b) K. Albrecht, O. Reiser, M. Weber, A. de Meijere, *Synlett* **1992**, 521; c) K. Albrecht, O. Reiser, M. Weber, B. Knieriem, A. de Meijere, *Tetrahedron* **1994**, *50*, 383.

[132] Palladium(IV) complexes have often been discussed as catalytically active intermediates: a) P. M. Maitlis, F. G. A. Stone, *Chem. Ind. (London)* **1962**, 1865; b) P. M. Maitlis, *The Organic Chemistry of Palladium, Vol. 1*, Academic Press, New York, **1971**, p. 84; c) P. M. Maitlis, P. Espinet, M. J. H. Russel in *Comprehensive Organometallic Chemistry, Vol. 6* (Eds.: G. Wilkinson, F. G. A. Stone, E. W. Abel), Pergamon, Oxford, **1982**, p. 279, and references therein; d) J. F. Stille, K. S. Y. Lau, *J. Am. Chem. Soc.* **1976**, *98*, 5841; e) D. Milstein, J. K. Stille, *ibid.* **1979**, *101*, 4981, 4992; f) S. J. Tremont, H. U. Raman, *ibid.* **1984**, *106*, 5759; g) B. M. Trost, C. Chan, G. Ruhter, *ibid.* **1987**, *109*, 3486; h) H. Azizian, C. Eaborn, A. Pidcock, *J. Organomet. Chem.* **1981**, *215*, 49; i) B. A. Markies, A. J. Canty, M. D. Janssen, A. L. Spek, J. Boersma, G. van Koten, *Recl. Trav. Chim. Pays-Bas* **1991**, *110*, 477; j) Review: A. J. Canty, *Acc. Chem. Res.* **1992**, *25*, 83, and references therein.

[133] a) C.-S. Li, C.-H. Cheng, F.-L. Liao, S.-L. Wang, *J. Chem. Soc. Chem. Commun.* **1991**, 710; b) C.-H. Liu, C.-S. Li, C.-H. Cheng, *Organometallics* **1994**, *13*, 18.

[134] a) M. Catellani, G. P. Chiusoli, *J. Organomet. Chem.* **1988**, *346*, C27; b) M. Catellani, B. E. Mann, *ibid.* **1990**, *390*, 251; c) M. Catellani, G. P. Chiusoli, M. C. Fagnola, *EUCHEM Conference on Nitrogen Ligands in Organometallic Chemistry and Homogenous Catalysis*, Alghero, Italy May 10–15, 1992, OC 18.

[135] For recent papers on oxidative addition to palladium(II) see a) B. A. Markies, A. J. Canty, J. Boersma, G. van Koten, *Organometallics* **1994**, *13*, 2053; C. Dücker-Benfer, R. van Eldik, A. J. Canty, *ibid.* **1994**, *13*, 2412.

[136] a) M. Catellani, G. P. Chiusoli, C. Castagnoli, *J. Organomet. Chem.* **1991**, *407*, C30; b) M. Catellani, G. P. Chiusoli in *Advances in Catalyst Design* (Eds.: M. Graziani, C. N. R. Rao), World Scientific, Singapur, **1991**, p. 243.

[137] a) J. E. Rice, Z.-W. Cai, *Tetrahedron Lett.* **1992**, *33*, 1675; b) *J. Org. Chem.* **1993**, *58*, 1415.

[138] R. Laschober, T. Kappe, *Synthesis* **1990**, 387.

[139] a) G. Dyker, *Angew. Chem.* **1992**, *104*, 1079; *Angew. Chem. Int. Ed. Engl.* **1992**, *31*, 1023; b) *J. Org. Chem.* **1993**, *58*, 234; c) *Tetrahedron Lett.* **1991**, *32*, 7241; d) *Chem. Ber.* **1994**, *127*, 739.

[140] a) M. Uno, K. Seto, S. Takahashi, *J. Chem. Soc. Chem. Commun.* **1984**, 932; b) M. Uno, K. Seto, W. Ueda, M. Masuda, S. Takahashi, *Synthesis* **1985**, 506.

[141] a) M. A. Ciufolini, M. E. Browne, *Tetrahedron Lett.* **1987**, *28*, 171; b) M. A. Ciufolini, H.-B. Qi, M. E. Browne, *J. Org. Chem.* **1988**, *53*, 4149.

[142] E. Piers, P. C. Marais, *J. Org. Chem.* **1990**, *55*, 3454.

[143] a) D. Bouyssi, G. Balme, G. Fournet, N. Monteiro, J. Gore, *Tetrahedron Lett.* **1991**, *32*, 1641; b) G. Balme, D. Bouyssi, R. Faure, J. Gore, B. van Hemelryck, *Tetrahedron* **1992**, *48*, 3891; c) N. Monteiro, J. Gore, G. Balme, *ibid.* **1992**, *48*, 10103; d) G. Fournet, G. Balme, J. Gore, *ibid.* **1991**, *47*, 6293; e) G. Fournet, G. Balme, B. van Hemelryck, J. Gore, *Tetrahedron Lett.* **1990**, *31*, 5147; f) N. Monteiro, G. Balme, J. Gore, *ibid.* **1991**, *32*, 1645; g) G. Fournet, G. Balme, J. Gore, *ibid.* **1989**, *30*, 69.

[144] N. Yanagihara, C. Lambert, K. Iritani, K. Utimoto, H. Nozaki, *J. Am. Chem. Soc.* **1986**, *108*, 2753.

[145] a) A. Arcadi, S. Cacchi, M. Delmastro, F. Marinelli, *Synlett* **1991**, 407; b) D. Bouyssi, J. Gore, G. Balme, *Tetrahedron Lett.* **1992**, *33*, 2811; c) T. Tsuda, Y. Ohashi, N. Nagahama, R. Sumiya, T. Saegusa, *J. Org. Chem.* **1988**, *53*, 2650; d) D. Bouyssi, G. Balme, J. Gore, *Tetrahedron Lett.* **1991**, *32*, 6541.

[146] a) S. Aoki, T. Fujimura, E. Nakamura, I. Kuwajima, *J. Am. Chem. Soc.* **1988**, *110*, 3296; b) T. Fujimura, S. Aoki, E. Nakamura, *J. Org. Chem.* **1991**, *56*, 2809; c) S. Aoki, T. Fujimura, E. Nakamura, I. Kuwajima, *Tetrahedron Lett.* **1989**, *30*, 6541.

[147] a) B. Friess, B. Cazes, J. Gore, *Tetrahedron Lett.* **1988**, *29*, 4089; b) M. Ahmar, B. Cazes, J. Gore, *Tetrahedron* **1987**, *43*, 3453.

[148] V. Gauthier, B. Cazes, J. Gore, *Tetrahedron Lett.* **1991**, *32*, 915.

[149] R. C. Larock, N. G. Berrios-Peña, C. A. Fried, *J. Org. Chem.* **1991**, *56*, 2615.

[150] a) R. C. Larock, C. A. Fried, *J. Am. Chem. Soc.* **1990**, *112*, 5882; b) J. M. O'Connor, B. J. Stallman, W. G. Clark, A. Y. L. Shu, R. E. Spada, T. M. Stevenson, H. A. Dieck, *J. Org. Chem.* **1983**, *48*, 807.

[151] R. C. Larock, N. G. Berrios-Peña, C. A. Fried, E. K. Yum, C. Tu, W. Leong, *J. Org. Chem.* **1993**, *58*, 4509.

[152] a) R. C. Larock, E. K. Yum, *Synlett* **1990**, 529; for examples in which the arylation or vinylation of methylenecyclopropanes does not lead only to formation of alkyl complexes see b) G. Balme, G. Fournet, J. Gore, *Tetrahedron Lett.* **1986**, *27*, 3855; c) G. Fournet, G. Balme, J. Gore, *ibid.* **1987**, *28*, 4533; d) R. Grigg, P. Kennewell, A. Teasdale, V. Sridharan, *ibid.* **1993**, *34*, 153; for further reports on the ring opening of vinylcyclopropanes and cyclobutanes see e) R. C. Larock, S. Varaprath, *J. Org. Chem.* **1984**, *49*, 3432; f) W. Fischetti, R. F. Heck, *J. Organomet. Chem.* **1985**, *293*, 391.

[153] G. D. Harris, Jr., R. J. Herr, S. M. Weinreb, *J. Org. Chem.* **1992**, *57*, 2528.

[154] a) C. K. Narula, K. T. Mak, R. F. Heck, *J. Org. Chem.* **1983**, *48*, 2792; b) L. Shi, C. K. Narula, K. T. Mak, L. Kao, Y. Xu, R. F. Heck, *ibid.* **1983**, *48*, 3894; c) H. A. Dieck, R. F. Heck, *ibid.* **1975**, *40*, 1083; d) B. A. Patel, R. F. Heck, *ibid.* **1978**, *43*, 3898; e) J. I. Kim, B. A. Patel, R. F. Heck, *ibid.* **1981**, *46*, 1067; f) F. G. Stakem, R. F. Heck, *ibid.* **1980**, *45*, 3584.

[155] a) R. C. Larock, S. Ding, *J. Org. Chem.* **1993**, *58*, 804; b) R. C. Larock, S. J. Ilkka, *Tetrahedron Lett.* **1986**, *27*, 2211; c) R. C. Larock, S. K. Stolz-Dunn, *ibid.* **1989**, *30*, 3487.

[156] a) R. C. Larock, S. Ding, C. Tu, *Synlett* **1993**, 145; b) R. C. Larock, S. K. Stolz-Dunn, *ibid.* **1990**, 341; c) *Tetrahedron Lett.* **1988**, *29*, 5069.

[157] R. C. Larock, S. Ding, *J. Org. Chem.* **1993**, *58*, 2081.

[158] a) S. Torii, L. H. Xu, H. Okumoto, *Synlett* **1992**, 515; b) N. G. Kundu, M. Pal, J. S. Mahantny, S. K. Dasgupta, *J. Chem. Soc. Chem. Commun.* **1992**, 41; c) A. Arcadi, F. Marinelli, S. Cacchi, *Synthesis* **1986**, 749; see also d) Y. Kondo, T. Sakamoto, H. Yamanaka, *Heterocycles* **1989**, *29*, 10113.

[159] a) R. C. Larock, E. K. Yum, *J. Am. Chem. Soc.* **1991**, *113*, 6689; b) D. Wensbo, A. Eriksson, T. Jeschke, U. Annby, S. Gronowitz, L. A. Cohen, *Tetrahedron Lett.* **1993**, *34*, 2823.

[160] X. Garcias, P. Ballester, J. M. Saa, *Tetrahedron Lett.* **1991**, *32*, 7739.

[161] R. C. Larock, M.-Y. Kuo, *Tetrahedron Lett.* **1991**, *32*, 569.

[162] R. J. Perry, B. D. Wilson, R. J. Miller, *J. Org. Chem.* **1992**, *57*, 2883.

[163] a) V. N. Kalinin, M. V. Shostakovsky, A. B. Ponomaryov, *Tetrahedron Lett.* **1990**, *31*, 4073; b) S. Torii, H. Okumoto, L. H. Xu, *ibid.* **1991**, *32*, 237; c) V. N. Kalinin, M. V. Shostakovsky, A. B. Ponomaryov, *ibid.* **1992**, *33*, 373.

[164] S. Torii, L. H. Xu, M. Sadakane, H. Okumoto, *Synlett* **1992**, 513.

[165] a) Z.-W. An, M. Catellani, G. P. Chiusoli, *J. Organomet. Chem.* **1990**, *397*, C31; see also b) E. Brocato, C. Castagnoli, M. Catellani, G. P. Chiusoli, *Tetrahedron Lett.* **1992**, *33*, 7433.

[166] Further examples: a) E. Dalcanale, Z.-W. An, L. P. Battaglia, M. Catellani, G. P. Chiusoli, *J. Organomet. Chem.* **1992**, *437*, 375; b) R. C. Larock, C.-L. Liu, H. H. Lau, S. Varaprath, *Tetrahedron Lett.* **1984**, *25*, 4459; c) R. J. Perry, S. R. Turner, *J. Org. Chem.* **1991**, *56*, 6573; palladium(II)-catalyzed cyclizations: d) K. Utimoto, *Pure Appl. Chem.* **1983**, *55*, 1845; e) Y. Fukuda, K. Utimoto, H. Nozaki, *Heterocycles* **1987**, *25*, 297; f) K. Iritani, S. Matsubara, K. Utimoto, *Tetrahedron Lett.* **1988**, *29*, 1799; g) A. Arcadi, S. Cacchi, F. Marinelli, *ibid.* **1989**, *30*, 2581; h) Y. Fukuda, S. Matsubara, K. Utimoto, *J. Org. Chem.* **1991**, *56*, 5812; i) F.-T. Luo, R.-T. Wang, *Tetrahedron Lett.* **1992**, *33*, 6835; j) A. Arcadi, S. Cacchi, F. Marinelli, *ibid.* **1992**, *33*, 3915; k) E.-i. Negishi, T. Nguyen, B. O'Connor, *Heterocycles* **1989**, *28*, 55; formation of indenones: l) R. C. Larock, M. J. Doty, S. Cacchi, *J. Org. Chem.* **1993**, *58*, 4579.

[167] D. S. C. Black, P. A. Keller, N. Kumar, *Tetrahedron* **1992**, *48*, 7601; b) R. Odle, B. Blevins, M. Ratcliff, L. S. Hegedus, *J. Org. Chem.* **1980**, *45*, 2709; c) L. S. Hegedus, T. A. Mulhern, A. Mori, *ibid.* **1985**, *50*, 4282; d) L. S. Hegedus, M. R. Sestrick, E. T. Michaelson, P. J. Harrington, *ibid.* **1989**, *54*, 4141; e) P. J. Harrington, L. S. Hegedus, *ibid.* **1984**, *49*, 2657; f) L. S. Hegedus, *Angew. Chem.* **1988**, *100*, 1147; *Angew. Chem. Int. Ed. Engl.* **1988**, *27*, 1113; g) T. Sakamoto, T. Nagano, Y. Kondo, H. Yamanaka, *Synthesis* **1990**, 215; h) M. Mori, K. Chiba, Y. Ban, *Tetrahedron Lett.* **1977**, 1037; i) P. J. Harrington, L. S. Hegedus, K. F. McDaniels, *J. Am. Chem. Soc.* **1987**, *109*, 4335; j) M. Mori, Y. Ban, *Tetrahedron Lett.* **1979**, 1133; k) M. Mori, I. Oda, Y. Ban, *ibid.* **1982**, *23*, 5315; l) H. Iida, Y. Yuasa, C. Kibayashi, *J. Org. Chem.* **1980**, *45*, 2938; m) J. M. O'Connor, B. J. Stallman, W. G. Clark, A. Y. L. Shu, R. E. Spada, T. M. Stevenson, H. A. Dieck, *ibid.* **1983**, *48*, 807; n) A. Kasahara, T. Izumi, S. Murakami, H. Yanai, M. Takatori, *Bull. Chem. Soc. Jpn.* **1986**, *59*, 927; o) A. P. Kozikowski, D. Ma, *Tetrahedron Lett.* **1991**, *32*, 3317.

[168] a) V. H. Rawal, C. Michoud, *Tetrahedron Lett.* **1991**, *32*, 1695; b) V. H. Rawal, C. Michoud, R. F. Monestel, *J. Am. Chem. Soc.* **1993**, *115*, 3030.

[169] W. G. Earley, T. Oh, L. E. Overman, *Tetrahedron Lett.* **1988**, *29*, 3785.
[170] V. Farina, S. I. Hauck, *Synlett* **1991**, 157.
[171] M. M. Abelman, L. E. Overman, V. D. Tran, *J. Am. Chem. Soc.* **1990**, *112*, 6959.
[172] A. Madin, L. E. Overman, *Tetrahedron Lett.* **1992**, *33*, 4859.
[173] D. L. Comins, M. F. Baevsky, H. Hong, *J. Am. Chem. Soc.* **1992**, *114*, 10971.
[174] K. F. McClure, S. J. Danishefsky, *J. Am. Chem. Soc.* **1993**, *115*, 6094.
[175] T. Hudlicky, H. F. Olivo, *J. Am. Chem. Soc.* **1992**, *114*, 9694.
[176] a) R. Grigg, P. Stevenson, T. Worakun, *J. Chem. Soc. Chem. Commun.* **1984**, 1073; b) *ibid.* **1985**, 971; c) R. Grigg, V. Santhakumar, V. Sridharan, P. Stevenson, A. Teasdale, M. Thornton-Pett, T. Worakun, *Tetrahedron* **1991**, *47*, 9703; d) J.-M. Gaudin, *Tetrahedron Lett.* **1991**, *32*, 6113; e) E.-i. Negishi, J. M. Tour, *ibid.* **1986**, *27*, 4869; f) E.-i. Negishi, Y. Zhang, B. O'Connor, *ibid.* **1988**, *29*, 2915; g) B. O'Connor, Y. Zhang, E.-i. Negishi, *ibid.* **1988**, *29*, 3903; h) Y. Zhang, B. O'Connor, E.-i. Negishi, *J. Org. Chem.* **1988**, *53*, 5588; i) E.-i. Negishi, G. Wu, J. M. Tour, *Tetrahedron Lett.* **1988**, *29*, 6745.
[177] J. E. Baldwin, *J. Chem. Soc. Chem. Commun.* **1976**, 734.
[178] B. M. Trost, D. C. Lee, *J. Org. Chem.* **1989**, *54*, 2271.
[179] B. M. Trost, J. Y. L. Chung, *J. Am. Chem. Soc.* **1985**, *107*, 4586.
[180] a) B. M. Trost, P. A. Hipskind, *Tetrahedron Lett.* **1992**, *33*, 4541; b) B. M. Trost, P. A. Hipskind, J. Y. L. Chung, C. Chan, *Angew. Chem.* **1989**, *101*, 1559; *Angew. Chem. Int. Ed. Engl.* **1989**, *28*, 1502.
[181] K. H. Ang, A. Llebaria, S. Bräse, A. Steinig, F. E. Meyer, A. de Meijere, unpublished results.
[182] B. M. Trost, A. S. Tasker, G. Rüther, A. Brandes, *J. Am. Chem. Soc.* **1991**, *113*, 670.
[183] a) B. M. Trost, D. J. Jebaratnam, *Tetrahedron Lett.* **1987**, *28*, 1611; b) B. M. Trost, lecture at the *EUCHEM-Conference on Palladium in Organic Synthesis*, Sigtuna, Sweden, **1990**.
[184] a) S. Laschat, F. Narjes, L. E. Overman, *Tetrahedron (Symposium in Print "Palladium in Organic Synthesis")* **1994**, *50*, 347; b) C. Y. Hong, N. Kado, L. E. Overman, *J. Am. Chem. Soc.* **1993**, *115*, 11028; c) C. Y. Hong, L. E. Overman, *Tetrahedron Lett.* **1994**, *35*, 3453.
[185] L. E. Overman, *Pure Appl. Chem.* **1994**, *66*, 1423.
[186] L. F. Tietze, R. Schimpf, *Angew. Chem.* **1994**, *106*, 1138; *Angew. Chem. Int. Ed. Engl.* **1994**, *33*, 1089.
[187] S. Danishefsky, P. F. Schuda, T. Kitahara, S. J. Etheredge, *J. Am. Chem. Soc.* **1977**, *99*, 6066.
[188] See also H. Brunner, K. Kramler, *Synthesis* **1991**, 1121.
[189] R. Grigg, M. J. R. Dorrity, J. F. Malone, T. Mongkolaussavaratana, W. D. J. Amilaprasadh Norbert, V. Sridharan, *Tetrahedron Lett.* **1990**, *31*, 3075.
[190] A. Ashimori, T. Matsuura, L. E. Overman, D. J. Poon, *J. Org. Chem.* **1993**, *58*, 6949.
[191] Q.-S. Yu, A. Brossi, *Heterocycles* **1988**, *27*, 745.
[192] a) M. M. Abelman, L. E. Overman, *J. Am. Chem. Soc.* **1988**, *110*, 2328; b) N. E. Carpenter, D. J. Kucera, L. E. Overman, *J. Org. Chem.* **1989**, *54*, 5846.
[193] Z. Owczarczyk, F. Lamaty, E. J. Vawter, E.-i. Negishi, *J. Am. Chem. Soc.* **1992**, *114*, 10091.
[194] B. M. Trost, J. Dumas, *Tetrahedron Lett.* **1993**, *34*, 19.
[195] a) B. Burns, R. Grigg, V. Sridharan, P. Stevenson, S. Sukirthalingam, T. Worakun, *Tetrahedron Lett.* **1989**, *30*, 1135; b) R. Grigg, M. J. Dorrity, J. F. Malone, V. Sridharan, S. Sukirthalingam, *ibid.* **1990**, *31*, 1343; c) R. Grigg, V. Sridharan, S. Sukirthalingam, *ibid.* **1991**, *32*, 3855; d) R. Grigg, A. Teasdale, V. Sridharan, *ibid.* **1991**, *32*, 3859; e) R. Grigg, P. Kennewell, A. J. Teasdale, *ibid.* **1992**, *33*, 7789.
[196] a) B. M. Trost, Y. Shi, *J. Am. Chem. Soc.* **1991**, *113*, 701; b) *ibid.* **1993**, *115*, 9421.
[197] a) D. J. Kucera, S. J. O'Connor, L. E. Overman, *J. Org. Chem.* **1993**, *58*, 5304; see also b) L. E. Overman, D. J. Ricca, V. D. Tran, *J. Am. Chem. Soc.* **1993**, *115*, 2042; c) L. E. Overman, M. M. Abelman, D. J. Kucera, V. D. Tran, D. J. Ricca, *Pure Appl. Chem.* **1992**, *64*, 1813.
[198] a) A. Arcadi, E. Bernocchi, A. Burini, S. Cacchi, F. Marinelli, B. Pietroni, *Tetrahedron* **1988**, *44*, 481; b) *Tetrahedron Lett.* **1989**, *30*, 3465.
[199] A. Arcadi, S. Cacchi, R. C. Larock, F. Marinelli, *Tetrahedron Lett.* **1993**, *34*, 2813.
[200] a) A. Arcadi, S. Cacchi, G. Fabrizi, F. Marinelli, *Synlett* **1993**, 65; b) A. Arcadi, A. Burini, S. Cacchi, M. Delmastro, F. Marinelli, B. R. Pietroni, *J. Org. Chem.* **1992**, *57*, 976; c) R. D. Walkup, L. Guan, M. D. Mosher, S. W. Kim, Y. S. Kim, *Synlett* **1993**, 88.
[201] The term anion trapping was used by Grigg to include transferable groups stemming from anions as well as neutral species and in order to avoid the term cross-coupling.
[202] B. Burns, R. Grigg, P. Ratananukul, V. Sridharan, P. Stevenson, S. Sukirthalingam, T. Worakun, *Tetrahedron Lett.* **1988**, *29*, 5565.
[203] R.-T. Wang, F.-L. Chou, F.-T. Luo, *J. Org. Chem.* **1990**, *55*, 4846.
[204] E.-i. Negishi, Y. Noda, F. Lamaty, E. J. Vawter, *Tetrahedron Lett.* **1990**, *31*, 4393.
[205] a) R. Grigg, V. Sridharan, S. Sukirthalingam, T. Worakun, *Tetrahedron Lett.* **1989**, *30*, 1139; b) N. Chatani, T. Hanafusa, *J. Org. Chem.* **1986**, *51*, 4714.
[206] a) K. Nagasawa, Y. Zako, H. Ishihara, I. Shimizu, *Tetrahedron Lett.* **1991**, *32*, 4937; b) K. Nagasawa, H. Ishihara, Y. Zako, I. Shimizu, *J. Org. Chem.* **1993**, *58*, 2523.
[207] C. Chen, D. Crich, *Tetrahedron Lett.* **1992**, *33*, 1945.
[208] J. L. Mascareñas, A. M. Garcia, L. Castedo, A. Mouriño, *Tetrahedron Lett.* **1992**, *33*, 4365.
[209] T. Takahashi, M. Nakazawa, *Synlett* **1993**, 37.
[210] a) P. J. Kocienski, B. Lythgoe, *J. Chem. Soc. Perkin Trans. 1* **1980**, 1400; b) E. G. Baggiolini, J. A. Iacobelli, B. M. Hennessy, M. R. Uskokovic, *J. Am. Chem. Soc.* **1982**, *104*, 2945; c) E. G. Baggiolini, J. A. Iacobelli, B. M. Hennessy, A. D. Batcho, J. F. Sereno, M. R. Uskokovic, *J. Org. Chem.* **1986**, *51*, 3098; d) M. Kabat, J. Kiegiel, N. Cohen, K. Toth, P. M. Wovkulich, M. R. Uskokovic, *Tetrahedron Lett.* **1991**, *32*, 2343; e) W. H. Okamura, J. M. Aurrecoechea, R. A. Gibbs, A. W. Norman, *J. Org. Chem.* **1989**, *54*, 4072.
[211] J. M. Nuss, M. M. Murphy, R. A. Rennels, M. H. Heravi, B. J. Mohr, *Tetrahedron Lett.* **1993**, *34*, 3079.
[212] a) B. M. Trost, J. Dumas, M. Villa, *J. Am. Chem. Soc.* **1992**, *114*, 9836; b) B. M. Trost, W. Pfrengle, H. Urabe, J. Dumas, *ibid.* **1992**, *114*, 1923.
[213] a) J. M. Nuss, B. H. Levine, R. A. Rennels, M. M. Heravi, *Tetrahedron Lett.* **1991**, *32*, 5243; b) Brückner et al. report on a new approach to a monocyclic dienediyne, which is related to the neocarcinostatin chromophore, by two sequential regioselective Pd-catalyzed couplings in ref. [41 l].
[214] a) S. Torii, H. Okumoto, T. Tadokoro, A. Nishimura, Md. A. Rashid, *Tetrahedron Lett.* **1993**, *34*, 2139; b) J. M. Nuss, R. A. Rennels, B. H. Levine, *J. Am. Chem. Soc.* **1993**, *115*, 6991.
[215] a) B. M. Trost, D. C. Lee, *J. Am. Chem. Soc.* **1988**, *110*, 7255; b) B. M. Trost, R. Braslau, *Tetrahedron Lett.* **1988**, *29*, 1231.
[216] a) Y. Zhang, E.-i. Negishi, *J. Am. Chem. Soc.* **1989**, *111*, 3454; b) E.-i. Negishi, *Pure Appl. Chem.* **1992**, *64*, 323; c) Y. Zhang, G.-z. Wu, G. Agnel, E.-i. Negishi, *J. Am. Chem. Soc.* **1990**, *112*, 8590.
[217] W. S. Johnson, K. Wiedhaup, S. F. Brady, G. L. Olson, *J. Am. Chem. Soc.* **1974**, *96*, 3979, and references therein.
[218] O. Reiser, S. Reichow, A. de Meijere, *Angew. Chem.* **1987**, *99*, 1285; *Angew. Chem. Int. Ed. Engl.* **1987**, *26*, 1277.
[219] B. M. Trost, Y. Shi, *J. Am. Chem. Soc.* **1992**, *114*, 791.
[220] a) F. E. Meyer, P. J. Parsons, A. de Meijere, *J. Org. Chem.* **1991**, *56*, 6487; b) F. E. Meyer, J. Brandenburg, P. J. Parsons, A. de Meijere, *J. Chem. Soc. Chem. Commun.* **1992**, 390; c) F. E. Meyer, H. Henniges, A. de Meijere, *Tetrahedron Lett.* **1992**, *33*, 8039.
[221] Reviews: a) N. E. Schore, *Chem. Rev.* **1988**, *88*, 1081; b) M. J. Winter in *The Chemistry of the Metal-Carbon Bond. Carbon-Carbon Bond Formation Using Organometallic Compounds, Vol. 3* (Eds.: F. R. Hartley, S. Patai), Wiley, New York, **1985**; c) C. W. Bird, *Transition Metal Intermediates in Organic Synthesis, Vol. 1*, Academic Press, New York, **1967**.
[222] a) P. M. Maitlis, *Acc. Chem. Res.* **1976**, *9*, 93; b) G.-z. Wu, S. J. Geib, A. L. Rheingold, R. F. Heck, *J. Org. Chem.* **1988**, *53*, 3238.
[223] L. J. Silverberg, G.-z. Wu, A. L. Rheingold, R. F. Heck, *J. Organomet. Chem.* **1991**, *409*, 411.
[224] a) E.-i. Negishi, L. S. Harring, Z. Owczarczyk, M. M. Mohamud, M. Ay, *Tetrahedron Lett.* **1992**, *33*, 3253; b) E.-i. Negishi, M. Ay, T. Sugihara, *Tetrahedron* **1993**, *49*, 5471.
[225] S. Torii, H. Okumoto, A. Nishimura, *Tetrahedron Lett.* **1991**, *32*, 4167.
[226] F. E. Meyer, Dissertation, Universität Göttingen, **1993**.
[227] F. E. Meyer, A. de Meijere, *Synlett* **1991**, 777.
[228] J. J. Masters, D. K. Jung, W. G. Bornmann, S. J. Danishefsky, *Tetrahedron Lett.* **1993**, *34*, 7253.
[229] L. F. Tietze, T. Grote, *J. Org. Chem.* **1994**, *59*, 192.
[230] H. Muratake, I. Abe, M. Natsume, *Tetrahedron Lett.* **1994**, *35*, 2573.
[231] H. Bienayme, C. Yezeguelian, *Tetrahedron* **1994**, *50*, 3389.
[232] G. Balme, D. Bouyssi, *Tetrahedron* **1994**, *50*, 403.
[233] Y. Koga, M. Sodeoka, M. Shibasaki, *Tetrahedron Lett.* **1994**, *35*, 1227.
[234] a) S. W. Lee, P. L. Fuchs, *Tetrahedron Lett.* **1993**, *34*, 5209; b) Z. Jin, P. L. Fuchs, *ibid.* **1993**, *34*, 5205.
[235] F. Hong, J. Xia, Y. Xu, *J. Chem. Soc. Perkin Trans. 1* **1994**, 1665.
[236] K. M. Pietrusiewicz, M. Kuźnikowski, M. Koprowski, *Tetrahedron: Asymmetry* **1993**, *4*, 2143.
[237] a) W. Cabri, I. Candiani, A. Bedeschi, *J. Org. Chem.* **1993**, *58*, 7421; b) A. Steinig, A. de Meijere, unpublished results; A. Steinig, Diplomarbeit, Universität Göttingen, **1994**.
[238] a) B. M. Trost, C.-J. Li, *Tetrahedron Lett.* **1993**, *34*, 2271; b) B. M. Trost, L. T. Phan, *ibid.* **1993**, *34*, 4735; c) S. Nukui, M. Sodeoka, M. Shibasaki, *ibid.* **1993**, *34*, 4965; d) M. Amat, S. Hadida, J. Bosch, *ibid.* **1993**, *34*, 5005; e) X. Lu, X. Huang, S. Ma, *ibid.* **1993**, *34*, 5963; f) T. Jeschke, D. Wensbo, U. Annby, S. Gronowitz, *ibid.* **1993**, *34*, 6471; g) M. F. Semmelhack, W. R. Epa, *ibid.* **1993**, *34*, 7205; h) R. Grigg, V. Sridharan, *ibid.* **1993**, *34*, 7471; i) S. Torii, H. Okumoto, M. Sadakane, M. V. Shostakovsky, A. B. Ponomaryov, V. N. Kalinin, *Tetrahedron* **1993**, *49*, 6773; j) C. Chen, D. Crich, *ibid.* **1993**, *49*, 7943; k) B. M. Trost, B. A. Czeskis, *Tetrahedron Lett.* **1994**, *35*, 211; l) M. Amat, S. Hadida, J. Bosch, *ibid.* **1994**, *35*, 793; m) D. C. Horwell, P. D. Nichols, E. Roberts, *ibid.* **1994**, *35*, 939; n) Y. Koga, M. Sodeoka, M. Shibasaki, *ibid.* **1994**, *35*, 1227; o) C. S. Cho, K. Tanabe, S. Uemura, *ibid.* **1994**, *35*, 1275; p) Y.

Hatanaka, K.-i. Goda, T. Hiyama, *ibid.* **1994**, *35*, 1279; q) B. M. Trost, L. Zhi, K. Imi, *ibid.* **1994**, *35*, 1361; r) H.-J. Knölker, N. O'Sullivan, *ibid.* **1994**, *35*, 1695; s) C. S. Cho, S.-i. Motofusa, S. Uemura, *ibid.* **1994**, *35*, 1739; t) P. Vittoz, D. Bouyssi, C. Traversa, J. Goré, G. Balme, *ibid.* **1994**, *35*, 1871; u) A. Brown, R. Grigg, T. Ravishankar, M. Thornton-Pett, *ibid.* **1994**, *35*, 2753; v) L. Besson, J. Bazin, J. Goré, B. Cazes, *ibid.* **1994**, *35*, 2881; w) R. Grigg, H. Khalil, P. Levett, J. Virica, V. Sridharan, *ibid.* **1994**, *35*, 3197; x) C. Y. Hong, L. E. Overman, *ibid.* **1994**, *35*, 3453; y) T. Jeffery, J.-C. Galland, *ibid.* **1994**, *35*, 4103; z) K. Ono, K. Fugami, S. Tanaka, Y. Tamaru, *ibid.* **1994**, *35*, 4133.

[239] a) C. S. Nylund, J. M. Klopp, S. M. Weinreb, *Tetrahedron Lett.* **1994**, *35*, 4287; b) R. Grigg, J. Redpath, V. Sridharan, D. Wilson, *ibid.* **1994**, *35*, 4429; c) R. Grigg, P. Fretwell, C. Meerholtz, V. Sridharan, *Tetrahedron* **1994**, *50*, 359; d) Y. Sato, S. Nukui, M. Sodeoka, M. Shibasaki, *ibid.* **1994**, *50*, 371; e) E.-i. Negishi, C. Copéret, T. Sugihara, I. Shimoyama, Y. Zhang, G. Wu, J. M. Tour, *ibid.* **1994**, *50*, 425; f) A. Arcadi, S. Cacchi, V. Carnicelli, F. Marinelli, *ibid.* **1994**, *50*, 437.

[240] a) G. Dyker, J. Körning, P. G. Jones, P. Bubenitschek, *Angew. Chem.* **1993**, *105*, 1805; *Angew. Chem. Int. Ed. Engl.* **1993**, *32*, 1733; b) G. Dyker, *ibid.* **1994**, *106*, 117 and **1994**, *32*, 103; c) L.-F. Tietze, R. Schimpf, *ibid.* **1994**, *106*, 1138 and **1994**, *32*, 1089.

[241] a) G. Dyker, *J. Org. Chem.* **1993**, *115*, 6426; b) T. Hosoya, E. Takashiro, T. Matsumoto, K. Suzuki, *J. Am. Chem. Soc.* **1994**, *116*, 1004; c) B. M. Trost, A. Stephen, K. Hashmi, *ibid.* **1994**, *116*, 2183; d) B. M. Trost, D. L. Romero, F. Rise, *ibid.* **1994**, *116*, 4268; e) B. M. Trost, M. Lautens, G. J. Tanoury, C. Chan, D. T. MacPherson, *ibid.* **1994**, *116*, 4255.

[242] a) R. C. Larock, T. R. Hightower, *J. Org. Chem.* **1993**, *58*, 5298; b) V. H. Rawal, C. Michoud, *ibid.* **1993**, *58*, 5583; c) A. Ashimori, T. Matsuura, L. E. Overman, D. J. Poon, *ibid.* **1993**, *58*, 6949; d) R. J. Perry, B. D. Wilson, *ibid.* **1993**, *58*, 7016; e) J. M. Takacs, S. V. Chandramouli, *ibid.* **1993**, *58*, 7315; f) K. F. McClure, S. J. Danishefsky, G. K. Schulte, *ibid.* **1994**, *59*, 355; g) K. Nozaki, N. Sato, H. Takaya, *ibid.* **1994**, *59*, 2679; h) V. H. Rawal, S. Iwasa, *ibid.* **1994**, *59*, 2685.

[243] a) A. Arcadi, S. Cacchi, G. Fabrizi, F. Marinelli, *Synlett* **1993**, 65; b) I. W. Davies, D. I. C. Scopes, T. Gallagher, *ibid.* **1993**, 85; c) R. D. Walkup, L. Guan, M. D. Mosher, S. W. Kim, Y. S. Kim, *ibid.* **1993**, 88; d) A. Arcadi, S. Cacchi, F. Martinelli, P. Pace, *ibid.* **1993**, 743; e) J. Ji, X. Lu, *ibid.* **1993**, 745; f) M. Terakado, M. Miyazawa, K. Yamamoto, *ibid.* **1994**, 134; g) K. Orito, M. Miyazawa, H. Suginome, *ibid.* **1994**, 245; h) S. Sakuraba, K. Awano, K. Achiwa, *ibid.* **1994**, 291; i) P. Nguyen, S. Todd, D. van den Biggelaar, N. J. Taylor, T. B. Marder, F. Wittmann, R. H. Friend, *ibid.* **1994**, 299.

[244] a) B. M. Trost, V. K. Chang, *Synthesis* **1993**, 824; b) L. F. Tietze, R. Schimpf, *ibid.* **1993**, 876; c) K. Kondo, M. Sodeoka, M. Mori, M. Shibasaki, *ibid.* **1993**, 920; d) M. D. Cliff, S. G. Pyne, *ibid.* **1994**, 681; e) G. McGaffin, A. de Meijere, *ibid.* **1994**, 583.

[245] a) C.-H. Liu, C.-S. Li, C.-H. Cheng, *Organometallics* **1994**, *13*, 18; b) R. A. DeVries, A. Mendoza, *ibid.* **1994**, *13*, 2405.

[246] a) T. Sakamoto, Y. Kondo, H. Yamanaka, *Heterocycles* **1993**, *36*, 2437; b) K. Hirota, H. Kuki, Y. Maki, *ibid.* **1994**, *37*, 563.

[247] a) M. Larhed, C.-M. Andersson, A. Hallberg, *Tetrahedron* **1994**, *50*, 285; b) R. C. Larock, E. K. Yum, H. Yang, *ibid.* **1994**, *50*, 305.

[248] a) T. Sakamoto, Y. Kondo, K. Masumoto, H. Yamanaka, *J. Chem. Soc. Perkin Trans. 1* **1994**, 235; b) Y. Andersson, B. Långström, *ibid.* **1994**, 1395.

[249] a) A. J. Amoroso, J. P. Maher, J. A. McCleverty, M. D. Ward, *J. Chem. Soc. Chem. Commun.* **1994**, 1273; b) F. Ozawa, Y. Kobatake, A. Kubo, T. Hayashi, *ibid.* **1994**, 1323.

[250] G. A. Kraus, H. Kim, *Synth. Commun.* **1993**, *23*, 55.

[251] Y. Fuchita, Y. Takeda, M. Taga, *Inorg. Chim. Acta* **1994**, *216*, 253.

Dendrimers: From Generations and Functional Groups to Functions

Jörg Issberner, Rolf Moors and Fritz Vögtle*

Introduction

When a new idea in science is particularly appealing or "contagious", activity in that area may rapidly reach epidemic proportions.[1] A recent example is the development of dendrimer research in the past few years. A CAS online search shows that the number of publications in this field has increased nearly exponentially over the past decade, and the limit has not yet been reached (Fig. 1).[2-6]

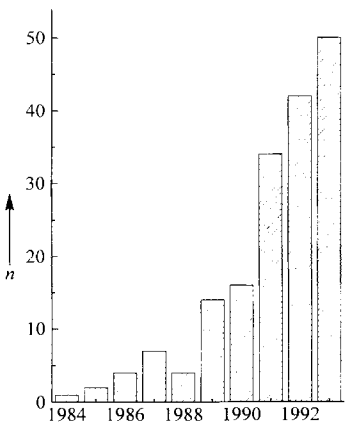


Fig. 1. Number n of publications about dendrimers in the last decade [7].

Up until now the primary goal was the synthesis of dendrimers with high molecular mass and as many generations as possible. Poly(amidoamines) (PAMAM),[6c] polypropylenamines,[8] and silicon dendrimers[9] set "records" for the number of generations, whereas the polyacetylene dendrimer prepared by Moore et al.[10] with the formula $C_{1398}H_{1278}$ and a mass of 18079.53 g mol^{-1} represents the "heavyweight champion" for pure hydrocarbon dendrimers. In the past two years, however, the emphasis has changed, and the synthesis of large, complex molecules has become less important. A first indication of new trends in dendrimer research was, for example, a report in 1991 by Newkome et al.[11] on a chiral dendrimer. In 1992 Shinkai et al. described a "crowned arborol" capable of complexing metal ions with the crown ether units at the periphery of the molecule.[12] We ourselves developed a reversibly photoswitchable dendrimer containing terminal azobenzene units.[13]

These first examples of cascade molecules with functional components point out the new directions in dendrimer research: properties are modified increasingly with functional centers. Not the dendrimer itself but the multiplication of functional components attached to a dendritic skeleton moves into the forefront, and new materials with specific properties (redox, ligand, and liquid crystalline properties, biochemical activity...) are anticipated. Industry has also shown increasing interest in functional cascade molecules for applications in diverse areas such as medical engineering,[14d-j] agrochemistry,[14c] and the development of photocopier toners,[14a,b] as documented by many patents.[14a-c,e,i] Furthermore the potential of dendrimers in pharmaceutical and medical applications,[14f] diagnostic imaging,[14c] and radiation therapy[14g,h] is frequently discussed. Oligoamines[15] were screened for anticancer properties.[16] Recent results and examples for new functional cascade molecules are presented in more detail below.

Dendrimers in Organic and Organometallic Chemistry

The preparation of the first fullerene dendrimer by Fréchet, Wudl, et al. spans two topical areas of supramolecular chemistry.[17] C_{60} and a dendritic benzylic bromide were linked by Williamson ether synthesis. More recently Fréchet et al. obtained the fullerene dendrimer **1** analogously by reaction with a dendritic azide (Scheme 1).[18]

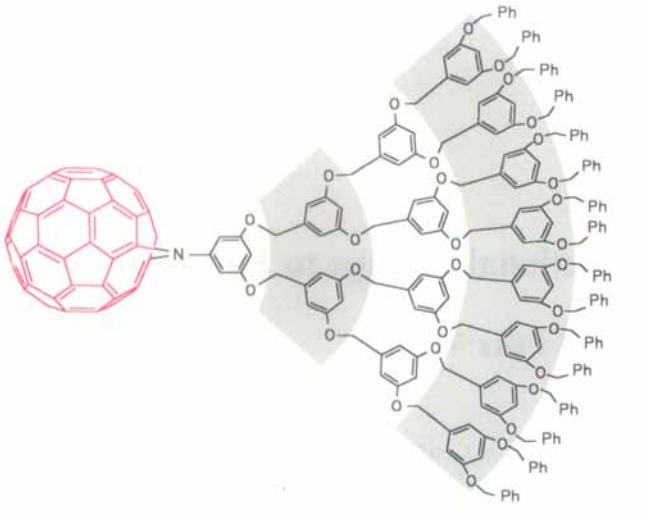
Shinkai et al. reported the synthesis of potentially complexing arborols bearing crown ether units in the core and along the periphery.[12] They provided evidence that these "crowned arborols" **2** not only form complexes with metal ions, but are also able to solubilize myoglobin in organic solvents.

The synthesis of dendrimers **3** with a complexing inner core (hexacyclen = hexaaza[18]crown-6) succeeded in Bonn; hexacyclen was linked with a branching unit which was obtained in a convergent manner.[19] A dendritic imine (multisalen dendrimer) forms the trinuclear complex **4** with cobalt salts.[15]

In most cases the functional units are located on the dendrimer surface, but dendrimers like **3** are now accessible containing a nucleus capable of performing special functions (lu-

[*] Prof. Dr. F. Vögtle, Dipl.-Chem. J. Issberner, Dr. R. Moors
Institut für Organische Chemie und Biochemie der Universität
Gerhardt-Domagk-Strasse 1, D-53121 Bonn (FRG)
Telefax: Int. code + (228)73-5662

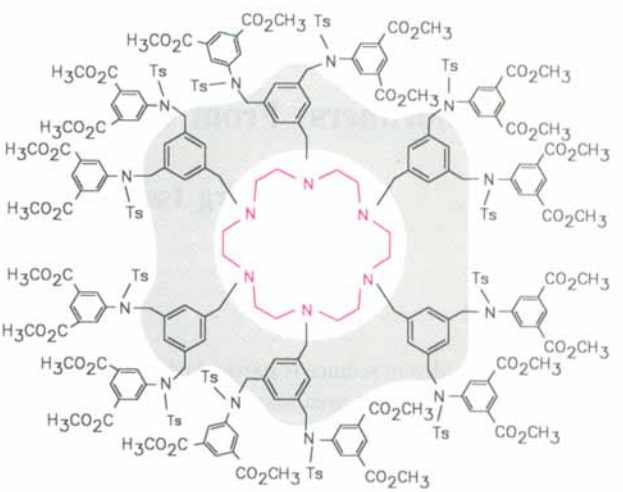
 © VCH Verlagsgesellschaft mbH, D-69451 Weinheim, 1994 0570-0833/94/2323-2413 $ 10.00+.25/0



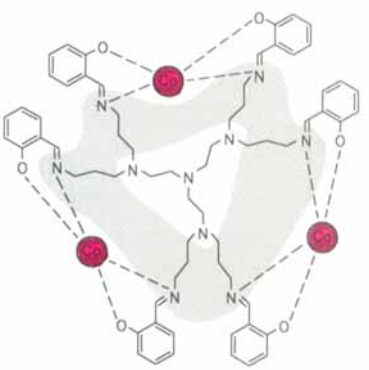
1

Scheme 1. Fullerene-containing dendrimer [18]. Functional units in all formulas are red; every second generation (from the inside to outside, the first, third, fifth etc). is shaded in gray.

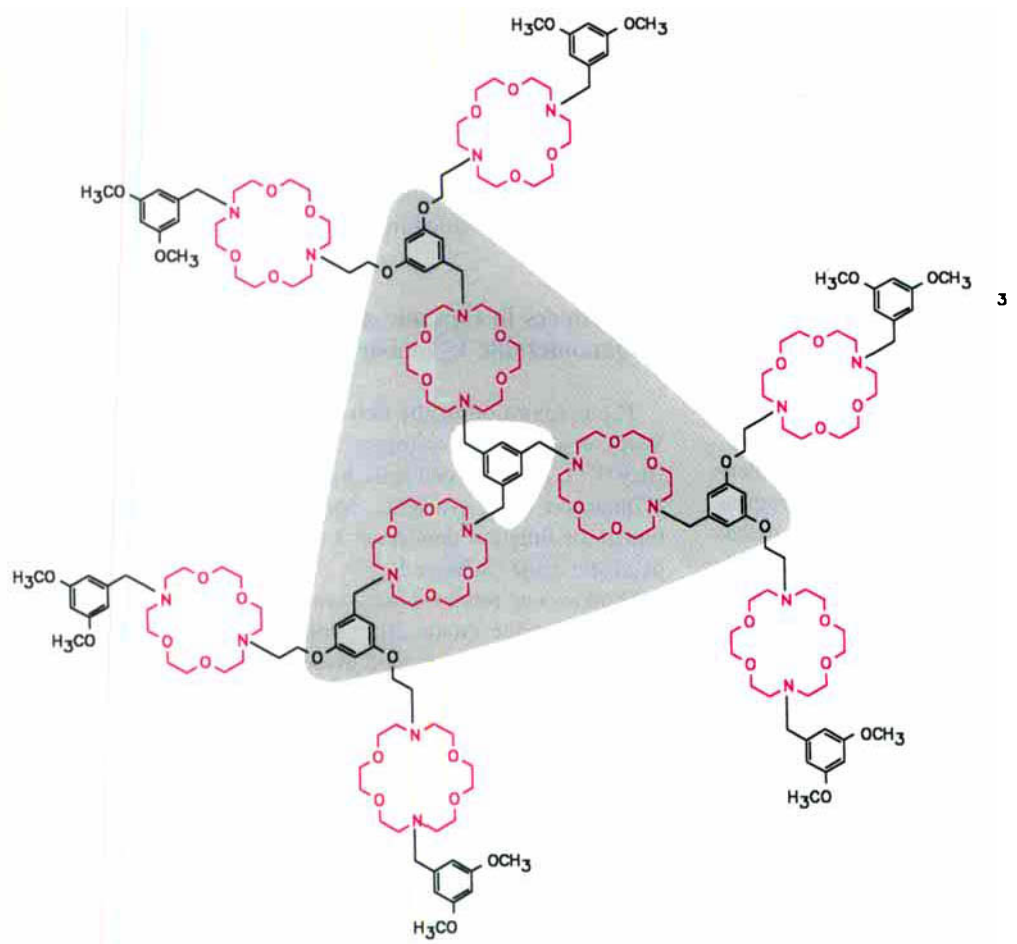
minescence, complexation) which are influenced to some extent (sterically or electronically) by the periphery. Inoue et al. were the first to describe a dendrimer with a metal porphyrin at its center.[20] The convergent synthetic method of Fréchet[17] was used to prepare a dendrimer in which the photoactive metal porphyrin center is sterically shielded. Diederich et al.[21] investigated the influence of the surface groups on the electrochemical behavior of metal porphyrins. Following a divergent synthesis devised by Newkome et al.,[2] they prepared the third-generation porphyrin dendrimer **5**, which has a molecular weight of over 19000. The redox chemistry of **5** strongly contrasts that of non-dendritic zinc porphyrins. The porphyrin nucleus is shielded by a core of electronegative oxygen atoms such that reduction by electrons from the outside is hindered, and conversely oxidation is facilitated. Such structures suggest the development of a "molecular energy collector" with included metal ions for energy absorption. The spontaneous emission of stored energy as light would correspond to an amplification of light intensity (light harvesting effect).



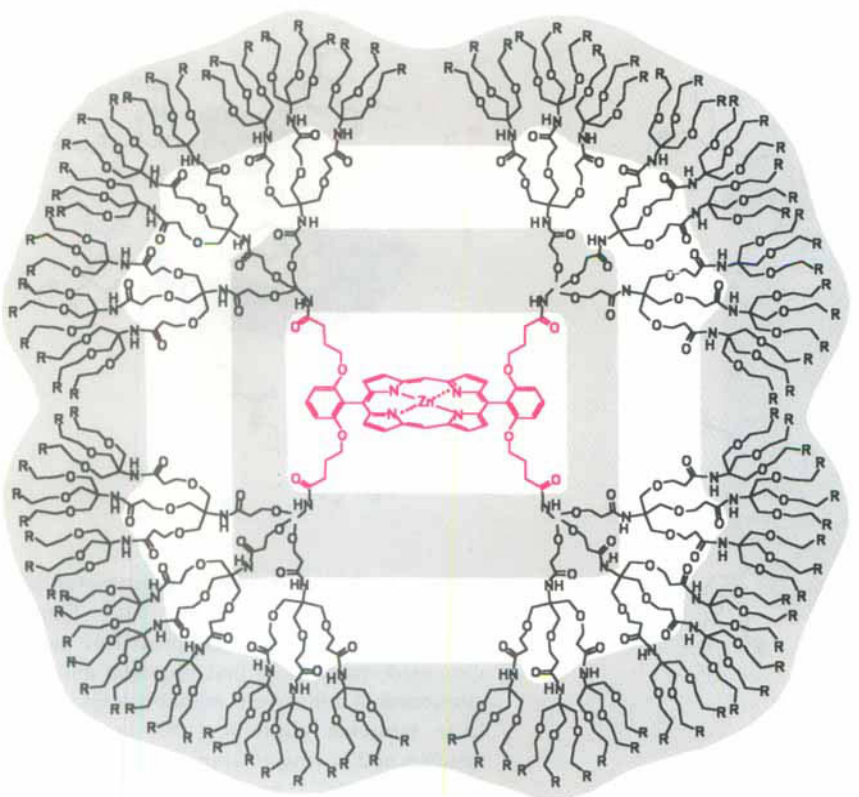
3



4



2



5

The first studies on dendritic metal and nonmetal complexes demonstrate that dendrimers/arborols can be attached to metal centers for the preparation of "supramolecular aggregates".[22–26] The controlled complexation of metal ions at specific binding sites in dendrimer cavities was achieved by Newkome et al., who prepared a dendrimer framework containing triple bonds, which could be complexed by dicobalthexacarbonyl units (**6** in Scheme 2).[27]

A second site-specific reaction within a cascade molecule was reported by Newkome et al. The triple bond containing dendrimer described previously was treated with decaborane $B_{10}H_{14}$. The dendrimer obtained, "boron supercluster" **7**, bears covalently bound borane at defined sites inside the dendrimer.[28, 29] This is not just the complexation of a borane cluster, but an actual reaction with the dendrimer to give a carborane.[29] In this way up to twelve borane clusters can be fixed within a dendrimer. The resulting water-soluble carboranes may find application in catalysis[28, 30] and boron neutron-capture therapy in cancer treatment.[31]

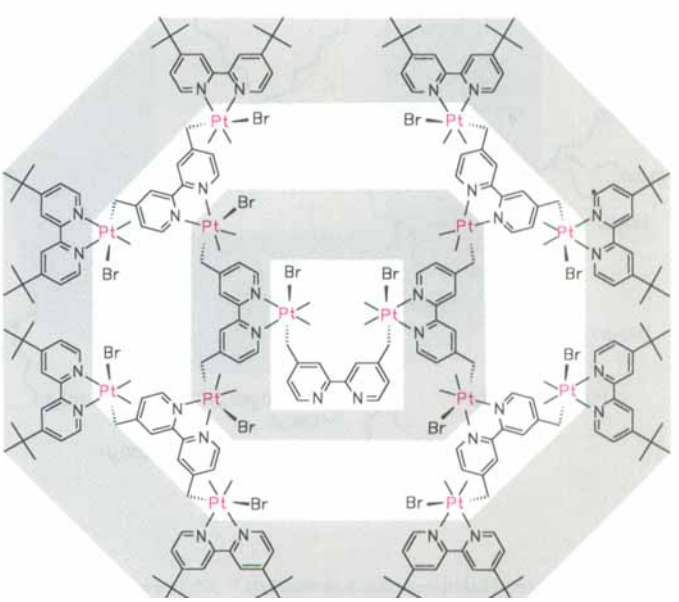
An example of redox-active dendrimers was given by Bryce et al.,[32] who connected benzene tricarboxylic acid trichloride to dendritic tetrathiafulvalene (TTF) as a functional component in **8** (Scheme 2). The cyclic voltammogram of **8** indicates formation of a multiply positively charged species in which the tetrathiafulvalene units do not interact. These new redox-active species may be useful as organic conductors and for the investigation of charge-transfer interactions.

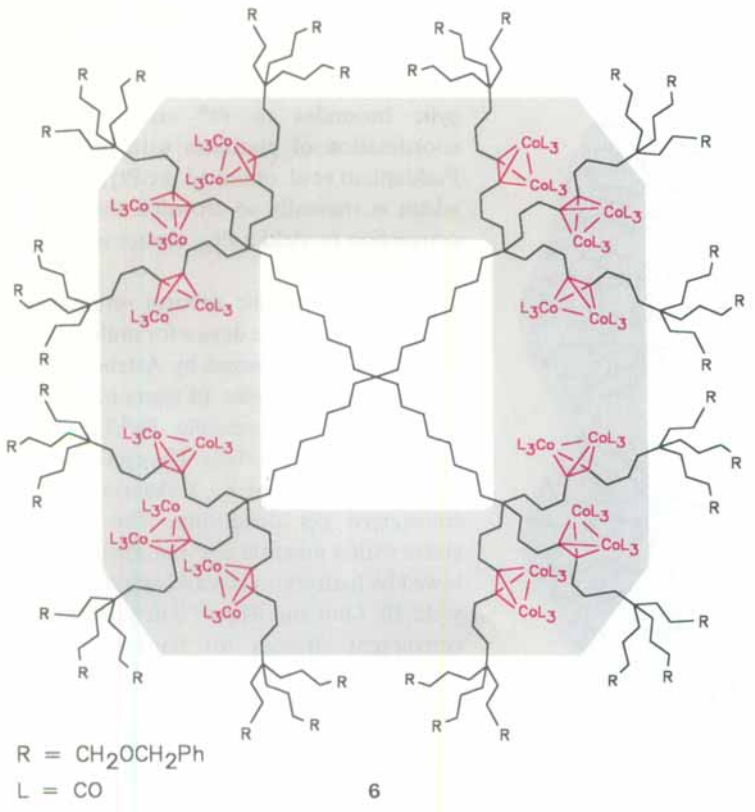
Puddephatt et al.[26] described the synthesis of metal ion containing dendrimers by coordinating bipyridine derivatives to transition metals, which resembles the synthetic strategy developed by Balzani et al.[24] In a convergent synthesis, in other words by repetition of alternating steps (oxidative addition of benzylic bromides to Pt^{II} and subsequent coordination of platinum with bipyridine) Puddephatt et al. obtained the Pt_{14} cluster **9**, which is sterically so crowded that further conversion to yield a Pt_{30} cluster is not possible.[26a]

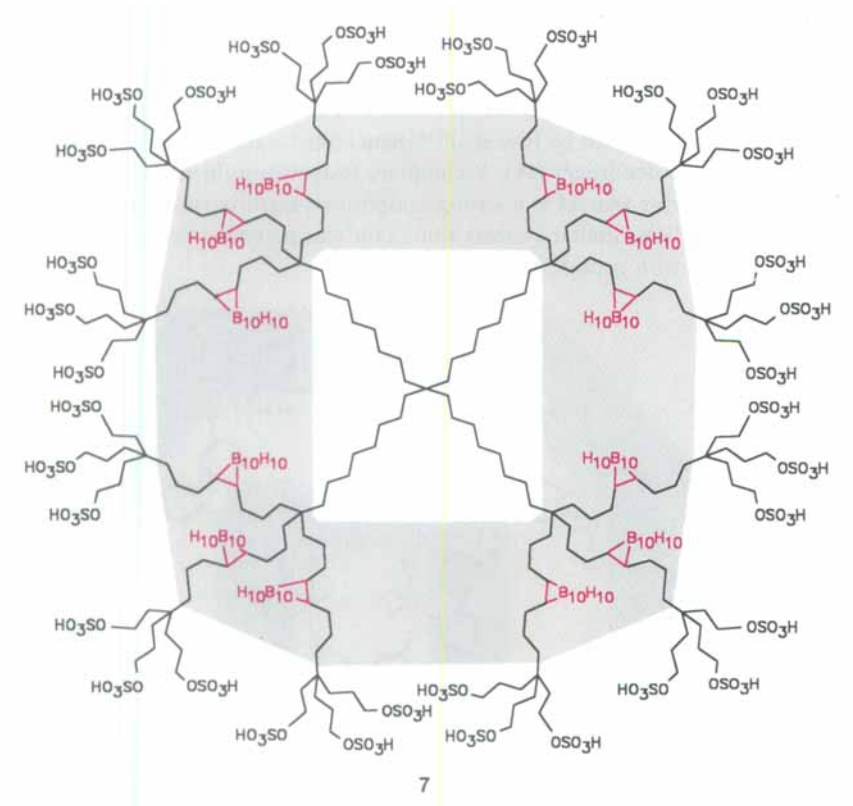
An organometallic arborol serving as a molecular electronic device for multielectron transfer was synthesized by Astruc et al.[23] The nonairon complex **10** bears nine quasi-equivalent and reversible Fe^{II}/Fe^{I} redox equivalents on its surface. The cyclic voltammogram shows that 8 ± 1 electrons can be transferred per dendrimer. The synthesis starts with a ninefold one-pot allylation followed by hydroboration and etherfication to yield **10**. Liao and Moss[33] demonstrated a convergent strategy for hanging organometallic units to the branches of a dendrimer in their synthesis of a molecule with twelve dicarbonylcyclopentadienyl metal complex fragments. Owing to the stability of the metal complexes to oxygen, a convergent strategy was possible.

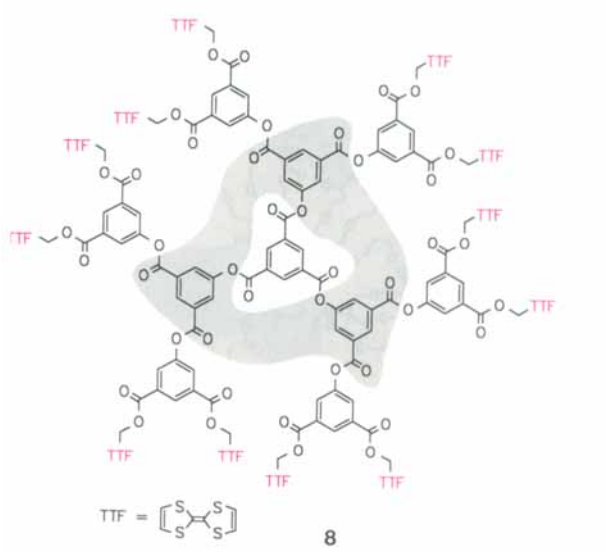
Biochemically Active Dendrimers

The connection of natural products or drugs to a dendritic skeleton is also very promising. The first successful results were published by Roy et al.[34] who linked eight sialinic acid units to a dendrimer (**11**). Preliminary tests with influenza A virus indicate that **11** is a strong inhibitor of erythrocyte hemagglutination. Similar systems among the star polymers were synthesized with peptide residues.[35]









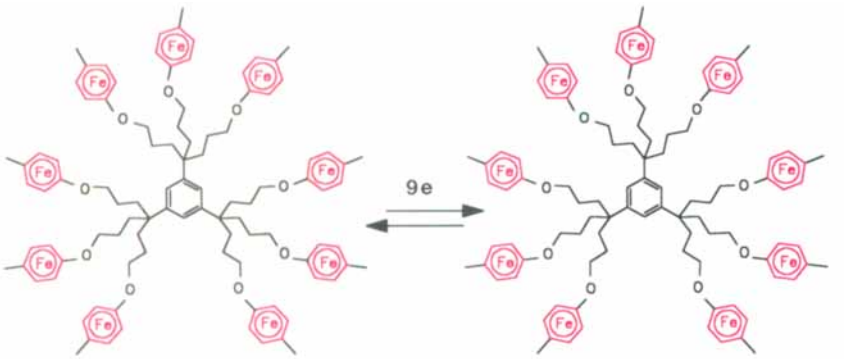
Scheme 2. Examples of functional cascade molecules [27–32]. In **6** and **7** the functional units are located at the inside of the dendrimer; in **8** the functional units (TTF) are along at the periphery of the dendrimer.

Even nucleic acids can be constructed in a dendritic way, as Hudson and Damha showed.[36] In an automated procedure the nucleic acid chains were first prepared and then connected in a divergent manner to give a cascade molecule containing 87 nucleic acid residues and having an approximate molecular weight of 25000. It was necessary to use longer branches for the inner core of the dendrimer than for the periphery. Recently Rao and Tam proved that even peptides can be connected in a dendritic manner.[37] An octameric peptide dendrimer, which could be useful as a synthetic protein, was detected by laser desorption mass spectrometry.

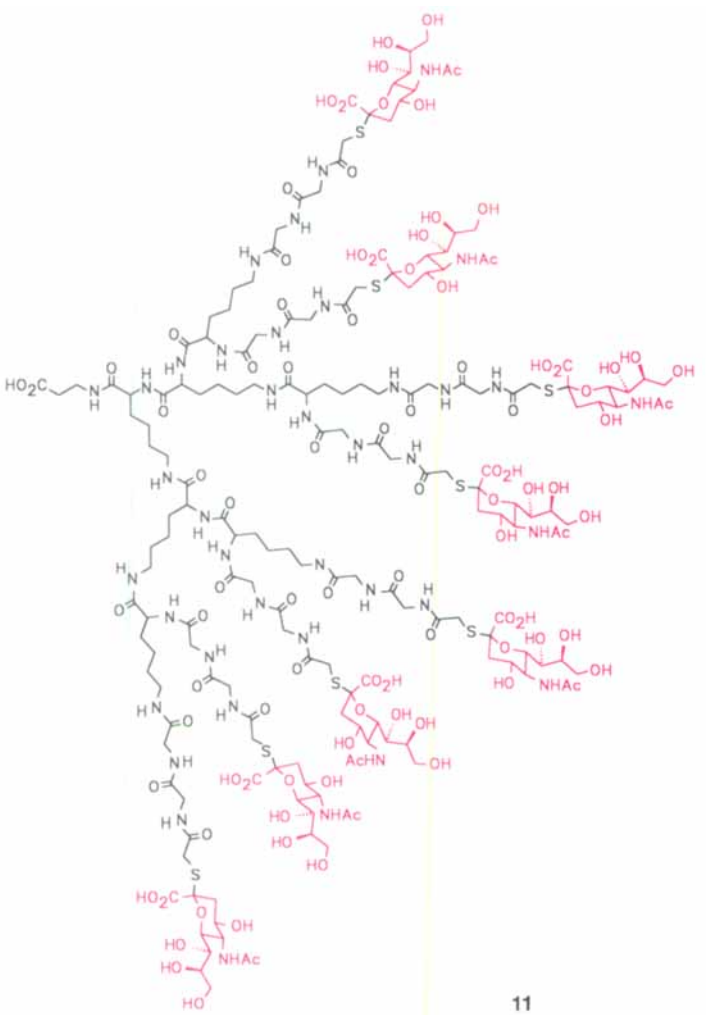
First investigations with cell cultures showed that dendrimers functionalized with amino groups support the transfection of mammalian cells by plasmids.[14d] The controlled synthesis, low toxicity, and pH buffering effect of dendrimers are the main criteria making dendrimers suitable for gene-transfer experiments.

Chiral Dendrimers

Seebach et al.[38] met the challenge of synthesizing chiral dendrimers to investigate the influence of chiral building blocks on the chirality of the whole molecule and to determine whether enantioselective complexation is possible. They achieved dendrimers with a chiral nucleus as well as dendrimers with additional chiral branches. The optical activity of dendrimers with only a chiral nucleus decreases with increasing size of the dendrimer whereas the optical activity of dendrimers that are "fully chiral" correspond to the optical activity of the nucleus. These dendrimers also form quite stable clathrates.



10a $Fe=(CpFe^{II})^+ PF_6^-$ 10b $Fe=CpFe^{I}$



11

A few recent publications have focused on the synthesis of chiral dendrimers by linking chiral units to dendrimer components.[39,40] J. A. Kremers and E. W. Meijer reported on the construction of chiral dendrimers with nonchiral building blocks. They connected four dendrimer branches differing only in the number of generations (generations 0–3) to a pentaerythritol core.[41a] Recent results of Meijer et al. show that dendrimers with chiral terminating units have low or vanishing optical activity with increasing generation number.[41b]

The porous structure of dendrimer with cavities[42] is important for properties like monodispersity and defined surface geometry, in particular for host–guest interactions. The inclusion of small chiral guests within these cavities and subsequent controlled release by chemical processes would be very useful for future medical applications. The examination of the effect of the included guest on the overall chirality may also open new perspectives.

Liquid Crystalline Dendrimers and Dendrimer Layers

The synthesis of liquid crystals is an aspect of dendrimer chemistry with potential industrial applications. Because of the round, flattened shape of many dendrimers, for example, they should be able to form discotic phases.[43] Dendrimers with liquid crystalline properties were reported by different research groups.[44] Kim proposed the synthesis of liquid crystalline polyamides, which he had obtained previously by polymerization, by a more directed, repetitive route. He wanted to optimize the clarification points, which are considerably greater than 100 °C for the polymers.[45]

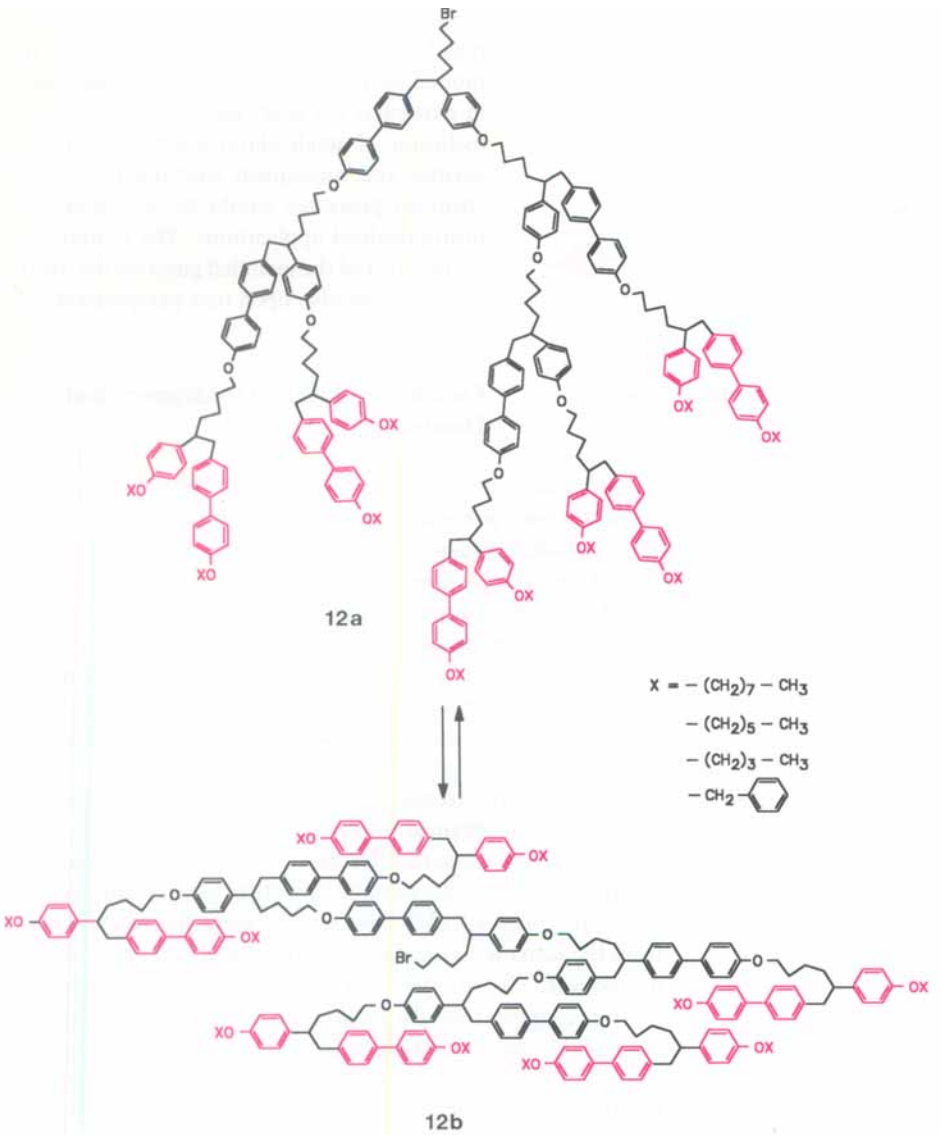
The first thermotropic liquid crystalline dendrimer based on ethers (**12**) was obtained by Percec and Kawasumu.[46,47a] Because of the conformative flexibility of the molecule, **12a** exists in equilibrium with the nematic form **12b**, which exhibits liquid crystalline properties.[45b] The temperature for the transition from the nematic to the isotropic state for X = *n*-octyl, *n*-hexyl lies between 20 and 50 °C. The low transition temperatures for the change from the solid state to the liquid crystalline state make these dendrimers attractive for applications. The control of the transition temperatures seems to be realizable in the future, especially through the stepwise synthesis of dendrimers.

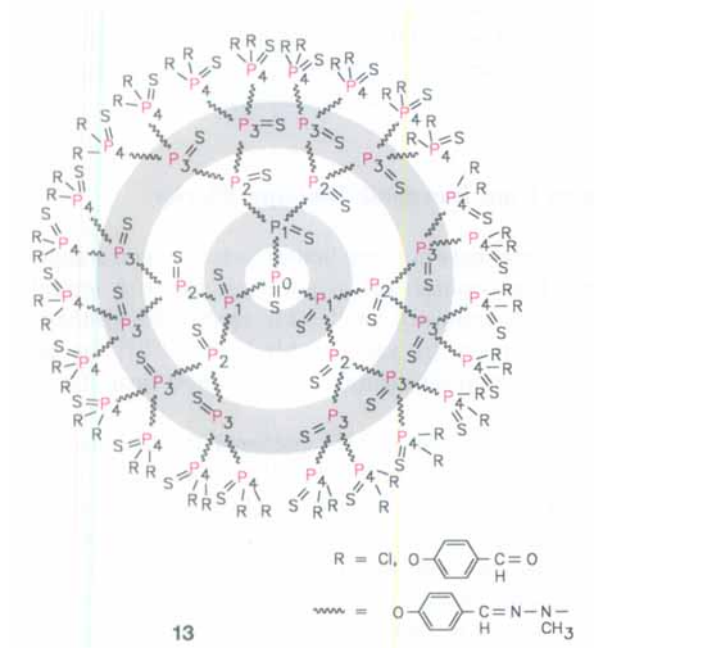
Recently S. Watanabe and S. L. Regen reported the use of dendrimers as building blocks for multilayers.[58] A silicon wafer was coated with $[PtCl_4]^{2-}$ and then treated with the polyamidoamine dendrimer PAMAM (generation 6). Repetition of these coating steps leads to multilayers.

Dendrimers from Inorganic Building Blocks

Recent advances have not been limited to research on organic dendrimers. The synthesis of cascade molecules is a topical area in inorganic chemistry too.[48] The remarkable synthesis of silicon dendrimers by van der Made et al.,[9a,b] for instance, displays impressive simplicity and almost quantitative yield.

Not long ago Majoral et al.[49] prepared the first neutral phosphorus-containing dendrimer **13**.[49] The fourth-generation dendrimer **13** was obtained by reacting $SPCl_3$ and the sodium salt of *para*-hydroxybenzaldehyde and $H_2N-N(Me)P(S)CCl_2$. Analogous reactions with $OPCl_3$ instead of $SPCl_3$ are also possible. The only by-products are NaCl and water, and the dendrimer is formed in almost quantitative yield. Brunner and





Bublak synthesized optically active "inorganic" dendrimers by reaction of optically active metalated pyridamides with 1,2-bis(dichlorophosphino)ethane.[51]

Methods for Analyzing Dendrimers

The analysis of dendrimers has been optimized decisively in the last years. EPR analysis[52] and light scattering experiments[53] have been developed, and new references have emerged for size exclusion chromatography. Until recently common polymers were used as standards for mass detection, but now the dendrimers themselves can serve as standards.[54] Molecules prepared through a repetitive synthesis[55] have well-defined molecular weights which distinguish them from polymers of comparable weight. Another property of many dendrimers is their spherical shape[56] which contrasts that of the more ellipsoidal polymers.

Cavities in Dendrimers

In addition to forming clathrates (see above), dendrimers have been found to encapsulate guest molecules inside their cavities ("dendritic box", "container dendrimers").[57] Suitable methods for inclusion of even large molecules (dyes, spin markers, fluorescence markers) have been developed. After a guest is bound in a defined generation of the dendrimer, the next generation is covalently linked, and the now-closed core binds the guests in the dendrimer cavities either irreversibly or reversibly depending on the size of the guest. Thus dendrimers are clearly supramolecular hosts. If the generation that closes the cavities containing guests is connected to the dendrimer through supramolecular interactions (e.g. hydrogen bonding), this linkage could be broken more easily later. Thus even without guests, dendrimers can be supramolecules. Dendrimers that release guests on changes in pH have been synthesized and hold promise for the targeted application of pharmaceuticals (drug release, drug targeting).

Summary

The variety of the examples listed above documents the status that dendrimer chemistry has attained during the past few years. In this compilation of recent results the trend towards function-

al and application-oriented molecules including biochemically active, photoswitchable, and polymerlike dendrimers is particularly apparent. Dendrimers could have advantages over polymers with regard to viscosity properties and application in high-resolution lithography. Increasing industrial research on dendrimers and the commercial availability of PAMAM[4, 6] and polyamine dendrimers[8] should stimulate further investigations in this field.

German version: *Angew. Chem.* **1994**, *106*, 2507

[1] T. Braun, *Angew. Chem.* **1992**, *104*, 602–603; *Angew. Chem. Int. Ed. Engl.* **1992**, *31*, 588–589.

[2] a) G. R. Newkome, Z. Yao, G. R. Baker, V. K. Gupta, *J. Org. Chem.* **1985**, *50*, 2003–2004; b) G. R. Newkome, A. Nayak, R. K. Behara, C. N. Moorefield, G. R. Baker, *ibid.* **1992**, *57*, 358–362; c) G. R. Newkome, Z. Yao, G. R. Baker, V. K. Gupta, P. S. Russo, M. J. Saunders, *J. Am. Chem. Soc.* **1986**, *108*, 849–850.

[3] a) C. Hawker, J. M. J. Fréchet, *J. Chem. Soc. Chem. Commun.* **1990**, 1010–1013; b) *J. Am. Chem. Soc.* **1990**, *112*, 7638–7647; c) K. L. Wooley, C. Hawker, J. M. J. Fréchet, *ibid.* **1991**, *113*, 4252–4261; d) I. Gitsov, K. L. Wooley, J. M. J. Fréchet, *Angew. Chem.* **1992**, *104*, 1282–1285; *Angew. Chem. Int. Ed. Engl.* **1992**, *31*, 1200–1202; T. M. Miller, E. W. Kwock, T. X. Neehan, *Macromolecules* **1992**, *25*, 3143–3148.

[4] a) D. A. Tomalia, H. Baker, J. R. Dewald, M. Hall, G. Kallos, S. Martin, J. Roeck, J. Ryder, P. Smith, *Polym. J. (Tokyo)* **1985**, *17*, 117–132; b) *Macromolecules* **1986**, *19*, 2466–2468; c) A. B. Padias, H. K. Hall, Jr., D. A. Tomalia, J. R. McConnell, *J. Org. Chem.* **1987**, *52*, 5305–5312; d) D. A. Tomalia, D. M. Hedstrand, M. S. Ferritto, *Macromolecules* **1991**, *24*, 1435.

[5] R. Denkewalter, J. Kole, W. J. Lukasavage (Allied Corp.), US-A 4289872, **1981** [*Chem. Abstr.* **1985**, *102*, 79324q].

[6] Reviews: a) D. A. Tomalia, A. M. Naylor, W. A. Goddard III, *Angew. Chem.* **1990**, *102*, 119–157; *Angew. Chem. Int. Ed. Engl.* **1990**, *29*, 138–175; b) H. B. Mekelburger, W. Jaworek, F. Vögtle, *ibid.* **1992**, *104*, 1609–1614 bzw. **1992**, *31*, 1571–1576; c) D. A. Tomalia, H. D. Durst, *Top. Curr. Chem.* **1993**, *165*, 193–313; d) D. A. Tomalia, *Adv. Mater.* **1994**, *6*, 529–539.

[7] The CAS-online search was performed with the following search terms: dendrimer# or cascade molecule# or cascade polymer# or starhurst dendrimer# or arborol# or dendritic molecule# or repetitive synthes? or pamam (# represents a further character and ? stands for any ending). The number of publications retrieved was nine times higher when only the term dendri? was used.

[8] a) C. Wörner, R. Mülhaupt, *Angew. Chem.* **1993**, *105*, 1367–1370; *Angew. Chem. Int. Ed. Engl.* **1993**, *32*, 1306–1308; b) E. M. M. de Brabander-van den Berg, E. W. Meijer, *ibid.* **1993**, *105*, 1370–1372 and **1993**, *31*, 1308–1311; c) *Chem. Ind. (Düsseldorf)* **1993** (5), 10; d) *Chem. Rund.* **1993**, *15* (4), 3; e) D. Rotman, *Chem. Week* **1993** (4), 32; f) D. A. O'Sullivan, *Chem. Eng. News.* **1993** (8), 20–23.

[9] a) A. W. van der Made, P. W. N. M. van Leeuwen, *J. Chem. Soc. Chem. Commun.* **1992**, 1400–1401; b) A. W. van der Made, P. W. N. M. van Leeuwen, J. C. de Wilde, R. A. C. Brande, *Adv. Mater.* **1993**, *5*, 466–468; c) J. Roovers, P. M. Toporowski, L. L. Zhou, *Polym. Preprints Am. Chem. Soc. Div. Polym. Chem.* **1992**, *33*, 182–183.

[10] a) Z. Xu, J. S. Moore, *Angew. Chem.* **1993**, *105*, 261–263; *Angew. Chem. Int. Ed. Engl.* **1993**, *32*, 246–248; b) *ibid.* **1993**, *105*, 1394–1396 and **1993**, *32*, 1354–1357.

[11] G. R. Newkome, X. Lin, C. D. Weis, *Tetrahedron: Asymmetry* **1991**, *2*, 957.

[12] a) T. Nagasaki, M. Ukon, S. Arimori, S. Shinkai, *J. Chem. Soc. Chem. Commun.* **1992**, 608–610; b) T. Nagasaki, O. Kimura, M. Ukon, S. Arimori, I. Hamachi, S. Shinkai, *J. Chem. Soc. Perkin Trans. 1* **1994**, 75–81.

[13] H. B. Mekelburger, K. Rissanen, F. Vögtle, *Chem. Ber.* **1993**, *126*, 1161–1169.

[14] a) F. M. Winnik, A. R. Davidson, M. P. Breton (Xerox Corp.), US-A 5098475, **1992** [*Chem. Abstr.* **1992**, *117*, 133079p]; b) F. M. Winnik, J. M. Duff, G. G. Sacripante, A. R. Davidson (Xerox Corp.), US-A 5256516 A 931026, **1993** [*Chem. Abstr.* **1993**, *120*, 90707j]; c) D. A. Tomalia, L. R. Wilson (Dow Chemical Co.), CA-A 1316364 A1 930420, **1993** [*Chem. Abstr.* **1993**, *120*, 256197]; d) J. Haenseler, F. Szoka, *Bioconjugate Chem.* **1993**, *4*, 372–379 [*Chem. Abstr.* **1993**, *119*, 174952c]; e) D. Meyer, S. Le Greneur (Guerbet S.A.), FR-A 91/15037, **1991** [*Chem. Abstr.* **1993**, *120*, 72540v]; f) N. A. Peppas, A. B. Argade, *Proc. Int. Symp. Controlled Release Bioact. Mater. 20th 1993* **1993**, 143–144 [*Chem. Abstr.* **1993**, *119*, 233759]; g) R. F. Barth, D. M. Adams, A. H. Soloway, F. Alam, M. V. Darby, *Bioconjugate Chem.* **1994**, *5*, 58–66 [*Chem. Abstr.* **1994**, *120*, 86391j]; h) R. F. Barth, D. M. Adams, A. H. Soloway, F. Alam, *Prog. Neutron Capture Ther. Cancer Proc. Int. Symp. 4th 1990* **1992**, 265–268 [*Chem. Abstr.* **1993**, *118*, 3077w]; i) A. D. Watson (J. R. M. Cockbain; Nycomed Salutar Inc.), US-A 772349, **1993** [*Chem. Abstr.* **1993**, *119*, 220702]; j) J. C. Roberts, Y. E. Adams, D. A. Tomalia, J. A. Mercer-Smith, D. K. Lavallee, *Bioconjugate Chem.* **1990**, *1*, 305–308.

[15] R. Moors, F. Vögtle, *Chem. Ber.* **1993**, *126*, 2133–2135.

[16] Study conducted by the Belgian Departments of Health and Human Services with dendrimer samples provided by the author.

[17] a) K. L. Wooley, C. J. Hawker, J. M. J. Fréchet, F. Wudl, G. Sradnov, S. Shi, C. Li, M. Kao, *J. Am. Chem. Soc.* **1993**, *115*, 9836–9837; b) see also the "Annual Review of Organic Chemistry 1993" ("Jahresrückblick organische Chemie 1993"): *Nachr. Chem. Techn. Lab.* **1994**, *42*, 155–167.

[18] C. J. Hawker, K. L. Wooley, J. M. J. Fréchet, *J. Chem. Soc. Chem. Commun.* **1994**, 925–926.

[19] K. Kadei, R. Moors, F. Vögtle, *Chem. Ber.* **1994**, *127*, 897–903.

[20] R. H. Jin, T. Aida, S. Inoue, *J. Chem. Soc. Chem. Commun.* **1993**, 1260–1262; see also: T. Ema, M. O. Senge, N. Y. Nelson, H. Ogoshi, K. M. Smith, *Angew. Chem.* **1994**, *106*, 1951–1953; *Angew. Chem. Int. Ed. Engl.* **1994**, *33*, 1879–1881.

[21] P. J. Dandliker, F. Diederich, M. Gross, C. B. Knobler, A. Louati, E. M. Sanford, *Angew. Chem.* **1994**, *106*, 1821–1825; *Angew. Chem. Int. Ed. Engl.* **1994**, *33*, 1739–1742.

[22] M. F. Manfrin, L. Setti, L. Moggi, *Inorg. Chem.* **1992**, *31*, 2768–2771.

[23] a) F. Moulines, L. Djakovitch, R. Boese, B. Gloaguen, W. Thiel, J.-L. Fillaut, M.-H. Delville, D. Astruc, *Angew. Chem.* **1993**, *105*, 1132–1133; *Angew. Chem. Int. Ed. Engl.* **1993**, *32*, 1075–1077; b) F. Moulines, B. Gloaguen, D. Astruc, *ibid.* **1992**, *104*, 452–454 and **1992**, *31*, 458–460; c) J.-L. Fillaut, R. Boese, D. Astruc, *Synlett* **1992**, 55–57; d) F. Moulines, L. Djakovitch, J.-L. Fillaut, D. Astruc, *ibid.* **1992**, 57–59.

[24] a) S. Serroni, G. Denti, S. Campagna, A. Juris, M. Ciano, V. Balzani, *Angew. Chem.* **1992**, *104*, 1540–1542; *Angew. Chem. Int. Ed. Engl.* **1992**, *31*, 1493–1495; b) S. Campagna, G. Denti, S. Serroni, M. Ciano, V. Balzani, *Inorg. Chem.* **1991**, *30*, 3728; c) S. Campagna, G. Denti, S. Serroni, M. Ciano, A. Juris, V. Balzani, *ibid.* **1992**, *31*, 2982–2984; d) S. Campagna, G. Denti, S. Sabatino, S. Serroni, M. Ciano, V. Balzani, *J. Chem. Soc. Chem. Commun.* **1989**, 1500; e) G. Denti, S. Campagna, S. Serroni, M. Ciano, V. Balzani, *J. Am. Chem. Soc.* **1992**, *114*, 2944.

[25] E. C. Constable, A. M. W. Cargill Thompson, *J. Chem. Soc. Chem. Commun.* **1992**, 617–619.

[26] a) S. Achar, R. J. Puddephatt, *Angew. Chem.* **1994**, *106*, 895–896; *Angew. Chem. Int. Ed. Engl.* **1994**, *33*, 847–849; b) *J. Chem. Soc. Chem. Commun.* **1994**, 1895–1897.

[27] G. R. Newkome, C. N. Moorefield, *Polym. Preprints Am. Chem. Soc. Div. Polym. Chem.* **1993**, *34*, 75–76.

[28] G. R. Newkome, C. N. Moorefield, J. M. Keith, G. R. Baker, G. H. Escamilla, *Angew. Chem.* **1994**, *106*, 701–703; *Angew. Chem. Int. Ed. Engl.* **1994**, *33*, 666–668.

[29] G. R. Newkome, C. N. Moorefield, *Macromol. Symp.* **1994**, *77*, 1–10.

[30] J. Plesek, *Chem. Rev.* **1992**, *92*, 69.

[31] a) M. F. Hawthorne, *Angew. Chem.* **1993**, *105*, 997–1033; *Angew. Chem. Int. Ed. Engl.* **1993**, *32*, 950–984; b) H. Nemoto, J. G. Wilson, H. Nakamura, Y. Yamamoto, *J. Org. Chem.* **1992**, *57*, 435; c) M. Miuura, D. Gabel, G. Oenbrink, R. G. Fairchild, *Tetrahedron Lett.* **1990**, *31*, 2247; d) H. Ketz, W. Tjarks, D. Gabel, *ibid.* **1990**, *31*, 4003.

[32] M. R. Bryce, W. Devonport, A. J. Moore, *Angew. Chem.* **1994**, *106*, 1862–1864; *Angew. Chem. Int. Ed. Engl.* **1994**, *33*, 1761–1763.

[33] Y.-H. Liao, J. R. Moss, *J. Chem. Soc. Chem. Commun.* **1993**, 1774–1777.

[34] R. Roy, D. Zanini, S. J. Meunier, A. Romanowska, *J. Chem. Soc. Chem. Commun.* **1993**, 1869–1872.

[35] Cf. W. D. Daly, D. Poche, P. S. Russo, I. Negulesco, *Polym. Preprints Am. Chem. Soc. Div. Polym. Chem.* **1992**, *33*, 188–189.

[36] R. H. E. Hudson, M. J. Damha, *J. Am. Chem. Soc.* **1993**, *115*, 2119–2124.

[37] C. Rao, J. P. Tam, *J. Am. Chem. Soc.* **1994**, *116*, 6975–6976.

[38] D. Seebach, J.-M. Lapierre, K. Skobridis, G. Greiveldinger, *Angew. Chem.* **1994**, *106*, 457–458; *Angew. Chem. Int. Ed. Engl.* **1994**, *33*, 440–442.

[39] H.-F. Chow, L. F. Fok, C. C. Mak, *Tetrahedron Lett.* **1994**, *35*, 3547–3550.

[40] a) L. J. Twyman, A. E. Beezer, J. C. Mitchell, *Tetrahedron Lett.* **1994**, *35*, 4423–4424; b) H. Brunner, S. Altmann, *Chem. Ber.* **1994**, *127*, 2285–2296.

[41] a) J. A. Kremers, E. W. Meijer, *J. Org. Chem.* **1994**, *59*, 4262–4266; b) J. F. G. A. Jansen, E. M. M. de Brabander-Van den Berg, E. W. Meijer, *Angew. Chem.*, submitted.

[42] H. Ritter, *GIT Fachz. Lab.* **1994**, *38*, 615–619.

[43] Cf. a) H. R. Christen, F. Vögtle, *Organische Chemie, von den Grundlagen zur Forschung, Vol. II*, Diesterweg Salle + Sauerländer, Frankfurt, **1990**, pp. 490–498; b) F. Vögtle, *Supramolekulare Chemie, eine Einführung*, 2nd ed., Teubner, Stuttgart, **1992**; *Supramolecular Chemistry*, 2nd ed., Wiley, Chichester, **1993**.

[44] Cf. a) V. Percec, J. Heck, *Polym. Preprints Am. Chem. Soc. Div. Polym. Chem.* **1991**, *32*, 263–264; b) V. Percec, C. G. Cho, C. Pugh, D. Tamazos, *ibid.* **1991**, *32*, 257; c) V. Percec, M. Kawasumi, *ibid.* **1993**, *34*, 154–155; d) S. Bauer, H. Fischer, H. Ringsdorf, *Angew. Chem.* **1993**, *105*, 1658–1660; *Angew. Chem. Int. Ed. Engl.* **1993**, *32*, 1589–1592; e) V. Percec, P. Chu, M. Kawasumi, *Macromolecules* **1994**, *27*, 4441–4453

[45] a) Y. H. Kim, *J. Am. Chem. Soc.* **1992**, *114*, 4947–4948; b) *Macromol. Symp.* **1994**, *77*, 21–33.

[46] E. S. Friberg, M. Podzimek, D. A. Tomalia, D. M. Hedstrand, *Mol. Cryst. Liq. Cryst.* **1988**, *164*, 157.

[47] a) V. Percec, M. Kawasumi, *Polym. Preprints Am. Chem. Soc. Div. Polym. Chem.* **1992**, *33*, 221–223; b) *ibid.* **1993**, *34*, 158–160.
[48] For early examples of inorganic dendrimers see: a) K. Rengan, R. Engel, *J. Chem. Soc. Chem. Commun.* **1990**, 1084–1085; b) *ibid.* **1992**, 757–758; c) *J. Chem. Soc. Perkin Trans. 1* **1991**, 987–990; d) H. Uchida, Y. Kabe, K. Yoshino, A. Kawamata, T. Tsumuraya, S. Masamune, *J. Am. Chem. Soc.* **1990**, *112*, 7077–7079; e) E. A. Rebrov, A. M. Muzafarov, V. S. Papkov, A. A. Zhadanov, *Dokl. Akad. Nauk SSSR* **1989**, *309*, 376; f) A. Morikawa, M. Kakimoto, Y. Imai, *Macromolecules* **1991**, *24*, 3469.
[49] a) N. Launay, A.-M. Caminade, R. Lahana, J.-P. Majoral, *Angew. Chem.* **1994**, *106*, 1682–1684; *Angew. Chem. Int. Ed. Engl.* **1994**, *33*, 1589–1592; b) N. Launay, A.-M. Caminade, J.-P. Majoral, *J. Am. Chem. Soc.* **1994**, *114*, in press.
[50] The earlier papers deal exclusively with phosphonium dendrimers.
[51] H. Brunner, P. Bublak, *Synthesis* **1994**, in press.
[52] M. F. Ottavani, S. Bossmann, N. J. Turro, D. A. Tomalia, *J. Am. Chem. Soc.* **1994**, *116*, 661–671.
[53] T.-P. Engelhardt, L. Belkoura, D. Woermann, *Ber. Bunsenges. Phys. Chem.* **1993**, *97*, 33–35.
[54] P. L. Dubin, S. L. Edwards, J. L. Kaplan, M. S. Mehta, D. A. Tomalia, J. Xia, *Anal. Chem.* **1992**, *64*, 2344–2347.
[55] In a repetitive synthetic strategy the size of the molecule increases with each repeated reaction cycle. See R. Moors, F. Vögtle in *Advances in Dendritic Macromolecules Vol. 1*, (Ed.: G. R. Newkome), JAI Greenwich, CT, USA, in press.
[56] M. L. Mansfield, L. I. Klushin, *Macromolecules* **1993**, *26*, 4262–4268.
[57] a) E. W. Meijer, Vortrag COST-Workshop, Stockholm, Mai 1994; b) J. F. G. A. Jansen, E. M. M. de Brabander-van den Berg, E. W. Meijer, *Science* **1994**, *266*, 1226–1229.
[58] S. Watanabe, S. L. Regen, *J. Am. Chem. Soc.* **1994**, *116*, 8855–8856.

Avoid the stampede!



No more elbowing up to the front of the line when the latest copy of **Angewandte Chemie** arrives if you have your own subscription. Fax us.

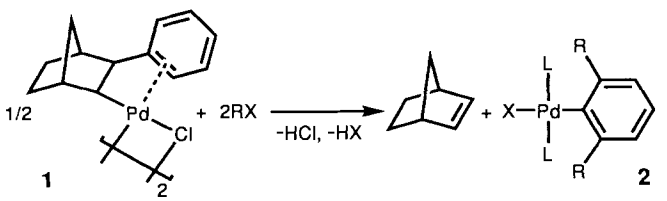
An order form is provided on the last page for your convenience.

VCH

Palladacycles as Intermediates for Selective Dialkylation of Arenes and Subsequent Fragmentation**

Marta Catellani* and Maria Chiara Fagnola

The chemistry of palladium(II) and (IV) metallacycles has attracted much interest in the past years.[1] In particular the metallacycles containing alkyl and arene units recently isolated by us[2] lend themselves to rather complex reactions.[3] We now wish to report an unprecedented reaction sequence of oxidative addition, aromatic substitution, and reductive elimination steps, which ends with spontaneous fragmentation and elimination of the aliphatic part of the metallacycle (Scheme 1).



Scheme 1. X = Br, I; R = alkyl, benzyl; L = DMF, methyl isonicotinate.

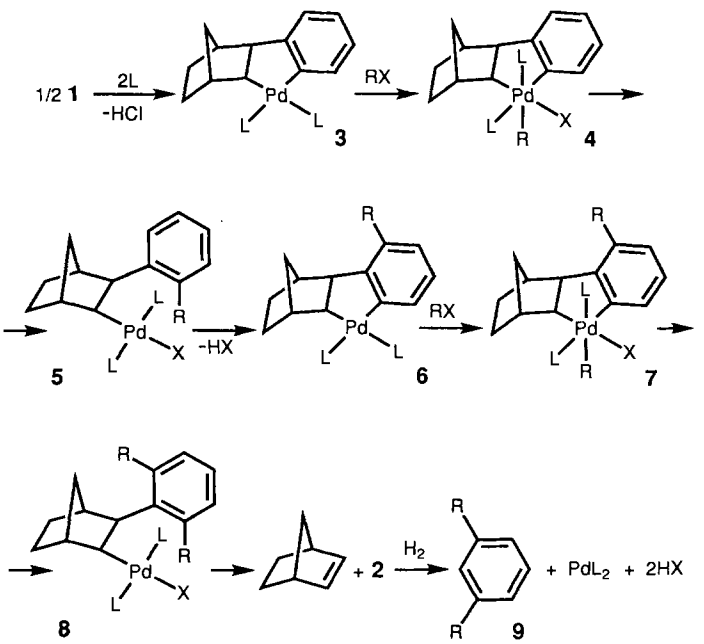
The arylnorbornylhalopalladium complex **1** dissolved in *N*,*N*-dimethylformamide (DMF) reacts with an alkylating agent via metallacycle **3** to form a Pd^{IV} complex (**4**), which spontaneously undergoes reductive elimination to form complex **5**. Complexes of the type **3**–**5** had been previously trapped with phenanthroline as ligand (2L) and fully characterized.[4] Once complex **5** is formed, conditions become favorable for a new ring closure to form complex **6**, which again undergoes oxidative addition to give a Pd^{IV} species (**7**) analogous to **4**, followed by another reductive elimination reaction leading to complex **8**. At this point fragmentation occurs spontaneously by norbornene elimination with formation of the *meta*-dialkylated arylpalladium complex (**2**), which gives arene **9** by treatment with hydrogen or $NaBH_4$.

The position of ligands in the octahedral intermediates **4** and **7** has been inferred from the structure of the complexes containing the bidentate phenanthroline ligands 2L. We cannot exclude, however, a different arrangement still preserving the essential mutually *cis* positions of the R and aryl groups. The four-coordinate square-planar intermediates **5** and **8** are *cis* in the phenanthroline derivative, but in the present case we assume a *trans* arrangement in view of the *trans* structure of the final complex **2**.

[*] Prof. M. Catellani, Dr. M. C. Fagnola
Dipartimento di Chimica Organica e Industriale dell'Università
Via le delle Scienze, 43100 Parma (Italy)
Telefax: Int. code + (521)905472

[**] This work was supported by the Ministero dell'Università e della Ricerca Scientifica e Tecnologica (MURST, Rome) and the Consiglio Nazionale delle Ricerche (CNR, Rome). Mass spectrometric and NMR spectroscopic facilities were provided by Centro Interfacoltà dell'Università di Parma.

In spite of the many steps involved, the reaction occurs simply by treatment of complex **1** (*cis*, *exo*) in DMF with an alkyl or benzyl halide in 1:2 molar ratio under nitrogen at room temperature for 7 h. Beside the *meta*-dialkylated benzene derivative (**9**), small amounts of 2-phenylnorbornanes mono- and dialkylated at the arene ring were obtained by passing hydrogen through the solution. These compounds derive from hydrogenolysis of complexes **5**–**8**, which are present in the final solution after complete conversion of **1**. Although the selectivity of **9** still is high (84–87%), the presence of these species supports the pathway shown in Scheme 2. The formation of nor-



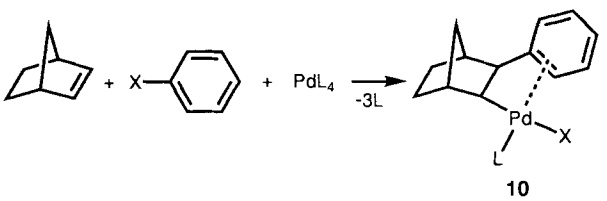
Scheme 2. A possible mechanism for selective dialkylation. X = Br, I; R = alkyl, benzyl; L = DMF, methyl isonicotinate.

bornene was established by mass spectrometry. Similar results were obtained on starting with the palladacycle complex **3** (L = methyl isonicotinate). As further evidence of the proposed mechanism, complex **2** was isolated by addition of the ligand (methyl isonicotinate) at the end of the reaction and removal of the solvent under vacuum and characterized by ^1H NMR spectroscopy.

Fragmentation of **8** to **2** does not occur if the aromatic moiety of phenylnorbornane is not disubstituted; the unexpected cleavage of a C–C bond between aliphatic and aromatic carbon atoms therefore appears to be driven by steric factors. The use of phenanthroline as ligand L does not lead to C–C bond cleavage; instead the reaction proceeds only to the stage of monoalkylation.[4] The fragmentation reported here corresponds to a deinsertion reaction that has been observed in the case of decarbonylation (reversible insertion),[5] but is rather unusual with olefinic compounds. Two related examples deserve

to be mentioned: one by Porri et al., who converted methallylnorbornylnickel acetate into methallylnickel bromide and norbornene by exchange of the acetate with a bromide anion,[6] the other by Maitlis et al., who achieved the elimination of styrene by adding HCl to a 2-pentamethylcyclopentadienyl-2-phenylethylpalladium chloride.[7] In our case, however, elimination is not caused by anion exchange or HCl addition but occurs spontaneously to form an *o,o*-disubstituted aryl group which stabilizes complex **2**[8] with respect to **8**. The elimination of cyclopentadiene from a ruthenacycle containing norbornene[9] is entirely at variance with the behavior reported here, since a retro-Diels–Alder and not a deinsertion reaction is involved in liberation of cyclopentadiene.

Since aryl bromides or iodides are known to react with norbornene in the presence of Pd^0 to give arylnorbornylpalladium complexes of type **10**[10] (Scheme 3), the function of norbornene in the overall process that involves norbornene insertion and deinsertion can be viewed that of a protecting group. It assists in the oxidative addition of alkyl halides and disubstitution of arenes through intermediate palladacycles and is finally expelled.



10

Scheme 3. X = Br, I; L = PPh_3.

Although the reaction is general for alkyl and benzyl halides, *p*-fluorobenzyl bromide proved to be appropriate for our study because it led in good yield to the formation of fluorinated products, which is useful for NMR determinations. Incidentally product **9** (R = *p*-fluorobenzyl) turns out to be an intermediate for the synthesis of polyether–polyketones.[11] Other alkyl halides also react with high yield. It is remarkable that no β-elimination of hydrogen occurs owing to the unfavorable stereochemistry. Thus this general drawback of many metal-catalyzed reactions[12] is absent in the present process.

Experimental Procedure

To complex **1** [10b] (0.100 g, 0.32 mmol) dissolved in anhydrous DMF (8 mL) are added K_2CO_3 (0.090 g, 0.65 mmol) and *p*-fluorobenzyl bromide (0.122 g, 0.64 mmol). The mixture is stirred at room temperature for 7 h under nitrogen. Hydrogen is then bubbled through the solution to precipitate palladium black. After conventional workup and purification by column chromatography with hexane/ethyl acetate as eluent, compound **9** (R = *p*-fluorobenzyl) [13] is obtained in 87% yield together with a small amount of mono- and dialkylated phenylnorbornanes. If instead of passing hydrogen through the reaction mixture, methyl isonicotinate (0.088 g, 0.64 mmol) is added, and DMF is removed under vacuum, complex **2** (L = methyl isonicotinate) [13] is obtained. After filtration through Celite, recrystallization from a mixture of chloroform and hexane gives light orange crystals in 63% yield. Analogously, carrying out the reaction with ethyl iodide as halide (0.100 g, 0.64 mmol) leads to compound **9** (R = ethyl) in 84% yield.

Received: May 3, 1994
Revised version: July 11, 1994 [Z 6896 IE]
German version: *Angew. Chem.* **1994**, *106*, 2559

[1] P. K. Byers, A. J. Canty, B. W. Skelton, A. H. White, *J. Chem. Soc. Chem. Commun.* **1986**, 1722; A. J. Canty, *Acc. Chem. Res.* **1992**, *25*, 83 and references therein; W. de Graaf, J. Boersma, D. Grove, A. L. Spek, G. van Koten, *Recl. Trav. Chim. Pays-Bas* **1988**, *107*, 299; M. Catellani, G. P. Chiusoli, *J. Organomet. Chem.* **1988**, *346*, C27; R. van Asselt, E. Rijnberg, C. J. Elsevier, *Organometallics* **1994**, *13*, 706.

[2] M. Catellani, B. E. Mann, *J. Organomet. Chem.* **1990**, *390*, 251.

[3] M. Catellani, G. P. Chiusoli, *J. Organomet. Chem.* **1985**, *286*, C13; M. Catellani, G. P. Chiusoli, C. Castagnoli, *ibid.* **1991**, *407*, C30; O. Reiser, M. Weber, A. de Meijere, *Angew. Chem.* **1989**, *101*, 1071; *Angew. Chem. Int. Ed. Engl.* **1989**, *28*, 1037; K. Albrecht, O. Reiser, M. Weber, B. Knieriem, A. de Meijere, *Tetrahedron* **1994**, *50*, 383.

[4] G. Bocelli, M. Catellani, S. Ghelli, *J. Organomet. Chem.* **1993**, *458*, C12.

[5] J. Tsuji, K. Ohno, *J. Am. Chem. Soc.* **1968**, *90*, 94; P. I. Graig, M. Green, *J. Chem. Soc. A* **1969**, 157.

[6] M. C. Gallazzi, L. Porri, G. Vitulli, *J. Organomet. Chem.* **1975**, *97*, 131.

[7] T. Hosokawa, P. M. Maitlis, *J. Am. Chem. Soc.* **1972**, *94*, 3238.

[8] J. Chatt, B. L. Shaw, *J. Chem. Soc.* **1959**, 4020.

[9] T. Mitsudo, Y. Watanabe, H. Naruse, T. Kondo, Y. Ozaki, *Angew. Chem.* **1994**, *106*, 595; *Angew. Chem. Int. Ed. Engl.* **1994**, *33*, 580.

[10] a) C.-S. Li, C.-H. Cheng, F.-L Liao, S.-L. Wang, *J. Chem. Soc. Chem. Commun.* **1991**, 710; C.-S. Li, D.-C. Jou, C.-H. Cheng, *Organometallics* **1993**, *12*, 3945; b) H. Horino, M. Arai, N. Inoue, *Tetrahedron Lett.* **1974**, 647.

[11] I. Fuchu, T. Tanabe, S. Fukuoka (Asahi Chemical Industry), JP-A 02160742, **1990** [Chem. Abstr. **1990**, *113*, 190920x]

[12] J. P. Collman, L. S. Hegedus, J. R. Norton, R. G. Finke, *Principles and Applications of Organotransition Metal Chemistry*, University Science Books, Mill Valley, CA, **1987**. To our knowledge only a palladium complex with 2,2'-bipyridyl and fumaronitrile ligands has been shown to prevent β-elimination of hydrogen in a coupling reaction of alkyl halides with Me_4Sn; R. Sustmann, J. Lau, M. Zipp, *Tetrahedron Lett.* **1986**, *27*, 5207.

[13] ^1H NMR data (400 MHz, $CDCl_3$): **9**: $\delta = 7.20$ (t, $J = 7.2$ Hz, 1H, H_5), 7.14–7.08 (4H, AA' part of an AA'BB'X system, protons *meta* to fluorine), 7.02–6.97 (3H, H_4, $H_6 + H_2$ at 6.98), 6.98–6.93 (4H, BB' part of an AA'BB'X system, protons *ortho* to fluorine), 3.90 (4H, CH_2). **2**: ^1H NMR: (400 MHz, $CDCl_3$): $\delta = 8.57$–8.53 (4H, AA' part of an AA'BB' system, protons *ortho* to nitrogen), 7.47–7.42 (4H, BB' part of an AA'BB' system, protons *meta* to nitrogen), 6.98 (t, $J = 7.3$ Hz, 1H, H_4), 6.92–6.84 (4H, AA' part of an AA'BB'X system, protons *meta* to fluorine), 6.79 (d, $J = 7.3$ Hz, 2H, H_3, H_5), 6.75–6.67 (4H, BB' part of an AA'BB'X system, protons *ortho* to fluorine), 4.81 (s, 4H, CH_2), 3.93 (s, 6H, OCH_3).

Diastereomerically Pure Mannich Bases from the Addition of Enamines to Ternary Iminium Salts**

Nikolaus Risch* and Michael Arend

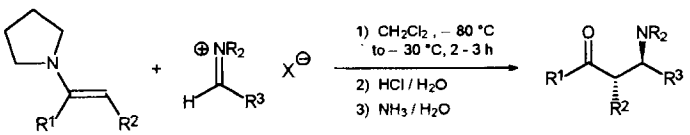
β-Amino carbonyl compounds are an attractive class of substances and are useful polyfunctional synthetic units in a variety of applications, for example, the synthesis of pharmaceutical, plant-protection, and natural products.[2] Efficient access to stereochemically pure Mannich bases, apart from β-amino acids and their derivatives, has hardly been developed until now.[3]

Our method of reacting (*E*)-enamines **1** (derived from aldehydes or ketones) with preformed ternary iminium salts **2** has fundamental advantages over the classic Mannich reaction[2] (Scheme 1). The reaction can be carried out in aprotic solvents, and the high iminium ion concentration guarantees high reaction rates even at low temperatures.

Because of the mild reaction conditions, no unwanted byproducts were formed. Good to excellent yields of almost stereochemically pure β-amino aldehydes or β-amino ketones *anti*-**3** were obtained (Table 1), which were generally crystalline. Ternary iminium salts **2** have long been known and are readily accessible,[4a] but have, surprisingly, in contrast to the methylene iminium salts such as Eschenmoser's salt, hardly

[*] Prof. Dr. N. Risch, Dipl.-Chem. M. Arend
Fachbereich Chemie und Chemietechnik der Universität-Gesamthochschule Warburger Strasse 100, D-33098 Paderborn (FRG)
Telefax: Int. code + (5251) 60-3245

[**] Stereoselective Synthesis of Mannich Bases, Part 2. This work was supported by the Deutsche Forschungsgemeinschaft and the Fonds der Chemischen Industrie. Part 1: [1].



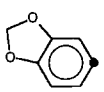
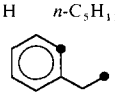
1 2 *anti*-3

Scheme 1. Diastereoselective addition of (*E*)-enamines **1** to ternary iminium salts **2**.

found any applications up until now.[4] Their use allows the scope of the classic Mannich reaction to be extended from amino*methyl*ation to amino*alkyl*ation. In addition, it should be emphasized that our method uses inexpensive, readily available chemicals and can be applied to sensitive substrates (mild reaction conditions).

Surprisingly, our investigations to date have shown (Table 1) that the stereoselectivity of addition is not influenced by the type of (*E*)-enamine or ternary iminium salt used. Variation in R^3, NR_2, and X^- always led to comparable results: with one exception (Table 1, entry 6), the ^1H NMR spectra of the crude products only show the signals for a single diastereoisomer. Similarly, changing the reaction medium from CH_2Cl_2 to the more strongly complexing THF had, at least at low temperatures, no obvious influence on the stereochemistry of the reaction. The fact that the reaction was less stereoselective under reflux in THF than in CH_2Cl_2 is probably explained by the higher temperature (due to the higher boiling point of THF) (Table 1, entry 1c). One product (Table 1, entry 2) was unambiguously assigned the *anti* configuration by comparing its NMR data to those reported in the literature for an authentic sample (X-ray structure analysis available).[3b, c] On the basis of the NMR spectra and considering that the probability of a total reversal of the stereochemical progress of the reaction as a result of the changes made is small, we assume that the other Mannich bases also have the *anti* configuration.

Table 1. Diastereoselective addition of (*E*)-enamines **1** to ternary iminium salts **2**.

Entry	R^1	R^2	R^3	NR_2	X^- [a]	*anti*-**3**: *syn*-**3** [b]	Yield [%]
1a		$(CH_2)_4$	Ph	NMe_2	ClO_4^-	≥99: ≤1	92
1b		$(CH_2)_4$	Ph	NMe_2	Cl^-	≥99: ≤1	94
1c [c]		$(CH_2)_4$	Ph	NMe_2	$AlCl_4^-$	≥99: ≤1	94
2		$(CH_2)_4$	Ph		$AlCl_4^-$	≥99: ≤1	87
3		$(CH_2)_4$	Ph		$AlCl_4^-$	≥99: ≤1	93
4a		$(CH_2)_4$	Ph		$AlCl_4^-$	≥99: ≤1	89
4b		$(CH_2)_4$	Ph		Cl^-	≥99: ≤1	94
5		$(CH_2)_4$			Cl^-	≥96: ≤4	89
6		$(CH_2)_4$	4-NO_2Ph		Cl^-	≥96: ≤4	85
7		$(CH_2)_4$	*i*Pr		Cl^-	≥99: ≤1	76
8	H	*n*-C_5H_{11}	Ph	NMe_2	$AlCl_4^-$	≥99: ≤1	91
9			Ph	NMe_2	$AlCl_4^-$	≥99: ≤1	72
10	Ph	Me	Ph	NMe_2	Cl^-	≥96: ≤4	91

[a] Tetrachloroaluminates are easily accessible (by reaction of the iminium chloride with $AlCl_3$ in CH_2Cl_2 at 0 °C; the tetrachloroaluminates are finally precipitated with Et_2O), only slightly hygroscopic, and therefore especially easy to handle (similar to methylene iminium tetrachloroaluminates) [5]. Because of the formation of an $Al(OH)_3$ precipitate during workup, however, they are less suitable for the preparation of Mannich bases in multigram quantities. Here, better results are obtained by using the freshly prepared iminium chlorides. [b] The diastereoisomeric ratios were always determined for the crude products by means of ^1H or ^{13}C NMR spectroscopy (integration of the signals for CHN protons). [c] Similar results (92%, >99% *ds*) were obtained in THF. Under reflux conditions (10 min), the Mannich base was obtained in 78% yield with 94% *ds* (in THF: 87%, 82% *ds*). Analogous results were obtained with the corresponding chloride and perchlorate. The reaction failed in Et_2O, probably because the iminium salt is practically insoluble in this solvent.

The scope of the method, the consistently high yields, and the excellent *de* values, which are only achieved in exceptional cases—if at all—by other methods, demand that the mechanism of the reaction be examined. The results can basically be explained by a similar model to that described by Seebach et al., namely, a transition state stabilized by electrostatic forces analogous to that formed in the aldol addition.[3e] However, a mechanism of the polar [2s + 2s]-cycloaddition type, such as has already been postulated for numerous reactions between very electron-rich and very electron-poor alkenes,[6] cannot, a priori, be excluded. Evidence in favor of this mechanism includes the fact that the reaction between ynamines and iminium salts is thought to proceed via a four-membered cyclic intermediate.[7]

Elucidation of the mechanism will also give further impetus to the extension of our method to an enantioselective variant,[1] the synthesis of primary and secondary Mannich bases, and the use of (*Z*)-enamines and quaternary iminium salts. It would also be interesting to investigate whether a third stereogenic center can be formed selectively by diastereoselective reactions (e.g., reduction or addition of organometallic compounds) at the prochiral carbonyl group.

Experimental Procedure

anti-3: The reaction was carried out under argon and anhydrous conditions. A solution of the (*E*)-enamine **1** (2.5 mmol) in anhydrous CH_2Cl_2 (2.5 mL) was cooled to −80 °C. The iminium salt **2** (2.5 mmol) was then added in one portion with stirring. The mixture was stirred and the temperature allowed to rise to −30 °C over 2–3 h. In order to ensure a good yield in all cases, it is advantageous to store the reaction mixture at this temperature in a refrigerator for ca. 15 h before workup. Aqueous hydrochloric acid (5 mL, conc. HCl/water 1/1) was then added. The mixture was stirred for ca. 10 min and then extracted several times with Et_2O. Dilute ammonia (25 mL, 25% NH_3/H_2O 1/4) was added with vigorous stirring, and the Mannich base *anti*-**3** was extracted with CH_2Cl_2 or Et_2O (3 × 50 mL, 1 min each time) [8]. The combined organic phases were dried over Na_2SO_4. The solvent was finally removed in a rotary evaporator without heating.

Received: May 28, 1994 [Z6977IE]
German version: *Angew. Chem.* **1994**, *106*, 2531

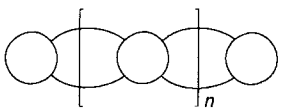
[1] N. Risch, A. Esser, *Liebigs Ann. Chem.* **1992**, 233.
[2] M. Tramontini, L. Angiolini, *Tetrahedron* **1990**, *46*, 1791.
[3] a) J. P. Yardley, H. Fletcher III, P. B. Russel, *Experientia* **1978**, *34*, 1124; b) G. Oszbach, A. Neszmélyi, *Liebigs Ann. Chem.* **1990**, 211; c) A. Neszmélyi, H. Lotter, A. Kiss, I. Pelczer, G. Oszbach, *ibid.* **1991**, 917; d) D. Seebach, C. Betschart, M. Schiess, *Helv. Chim. Acta* **1984**, *67*, 1593; e) D. Seebach, M. Schiess, W. B. Schweizer, *Chimia* **1985**, *39*, 272; f) A. R. Katritzky, P. A. Harris, *Tetrahedron* **1990**, *46*, 987; g) E. G. Nolen, A. Allocco, M. Broody, A. Zuppa, *Tetrahedron Lett.* **1991**, *32*, 73.
[4] a) H. Böhme, M. Haake, *Adv. Org. Chem.* **1976**, *9*, 107; b) E. F. Kleinman in *Comprehensive Organic Synthesis, Vol. 2* (Ed.: B. M. Trost), 1th edition, Pergamon, Oxford, **1991**, p. 893; c) E. Winterfeldt, *J. Prakt. Chem.* **1994**, *336*, 91; d) U. Westerwelle, N. Risch, *Tetrahedron Lett.* **1993**, *34*, 1775; e) U. Westerwelle, A. Esser, N. Risch, *Chem. Ber.* **1991**, *124*, 571.
[5] N. Risch, A. Esser, *Z. Naturforsch. B* **1989**, *44*, 208.
[6] J. E. Baldwin in *Comprehensive Organic Synthesis, Vol. 5* (Ed.: B. M. Trost), 1st ed., Pergamon, Oxford, **1991**, p. 63.
[7] R. Fuks, G. S. King, H. G. Viehe, *Angew. Chem.* **1969**, *81*, 702; *Angew. Chem. Int. Ed. Engl.* **1969**, *8*, 675.
[8] Some Mannich bases of the type *anti*-**3** tend to decompose, to varying extents, in aqueous alkaline solutions. However, this can be almost entirely avoided by rapid workup.

Ladder Polymers with a Heteroacene Skeleton**

Torsten Freund, Ullrich Scherf, and Klaus Müllen*

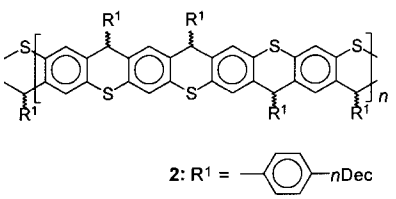
Dedicated to Professor Wolfgang Lüttke on the occasion of his 75th birthday

The synthesis of macromolecular ladder structures of type **1** is a particular challenge for polymer chemistry. With ladder polymers such as these it is possible to compare the form and persistence length of double-stranded polymers with that of their linear analogues.[1] Moreover, in the presence of extended π-conjugation two-dimensional structures have electronic advantages, for example, a lower band gap.[2]

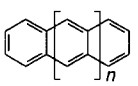


1

Here we describe the synthesis of the high molecular mass heteroacene **2** (*n*Dec = *n*-decyl), which is completely soluble in organic solvents and which, according to spectroscopic investigations, exhibits a defect-free ladder structure. Studies on oligomeric model compounds are particularly important for the investigation into the formation of the polymer and also the subsequent generation of extended π-conjugation in the acene.



2: R^1 = *n*Dec

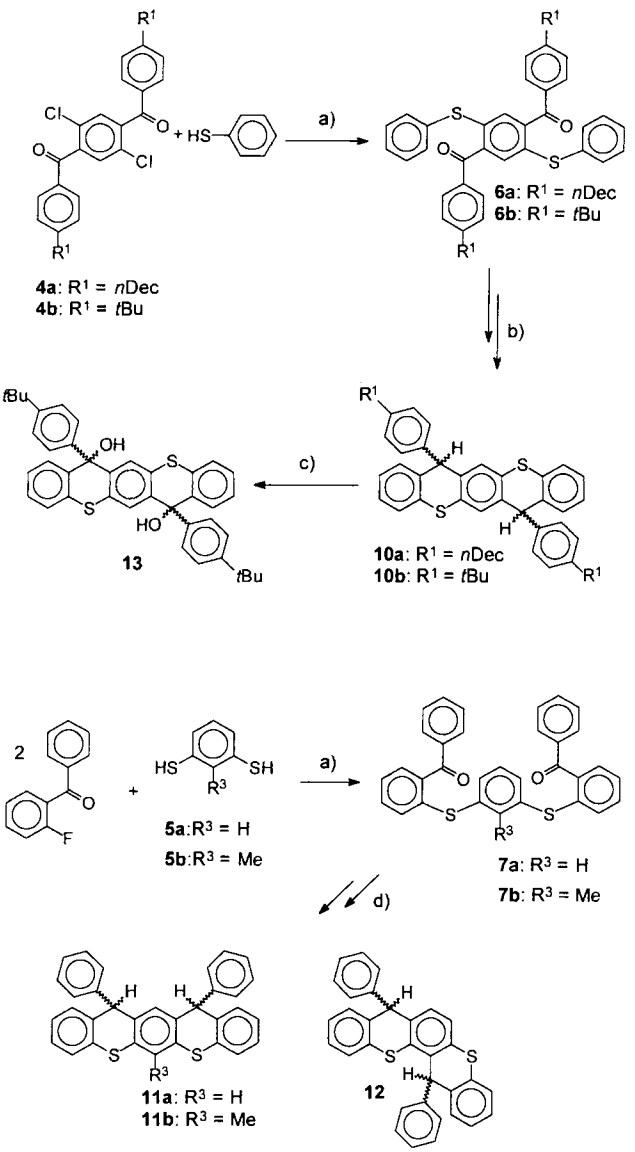


3

In principle, there are two methods available for the synthesis of double-stranded polymers: a "concerted" route with repetitive cycloadditions and a multistep route, in which the linear precursor can undergo polymer-analogous cyclization reactions. In the case of acenes **3** the repetitive Diels–Alder cycloaddition is the preferred method,[3] whereas for the sulfur-containing "polyhydroacene" **2** a multistep synthetic route is required. The starting compound was the terephthalophenone **4a** (see Scheme 2),[4] which can be converted into single-stranded poly(phenylenesulfide)s with benzoyl substituents by nucleophilic aromatic substitution with 1,3-benzenedithiol ("dithioresorcin") (**5a**) or 2-methyl-1,3-benzenedithiol (**5b**). Subsequent cyclization in a sequence of Friedel–Crafts reactions should then yield ladder structures. The phenyl substituents in **4** function as stabilizing substituents on the perimeter of the acene, while the *n*-alkyl groups are essential to achieve sufficient solubility of the rigid polymer backbone.

In model reactions (Scheme 1) **4a** and **4b** can be treated with thiophenolate to give **6a** and **6b** (each in 95% yield), respectively. The diketones **7a** and **7b** are obtained analogously from 2-fluorobenzophenone and the dithioresorcins **5a** and **5b**.[5, 6]

Phenylenesulfide formation of **6**, which proceeds without any detectable side reactions, suggests polycondensation of **4a** with **5a** (Scheme 2). Thus, the dithiolate formed by deprotonation with potassium carbonate in dimethylacetamide replaces both chlorine atoms in **4a** at 120 °C. In this way poly(phenylenesulfide) **8a** is accessible, for example, with molecular weights $M_n = 150000$ and $M_w = 670000$, determined by membrane osmometry and light-scattering, respectively.

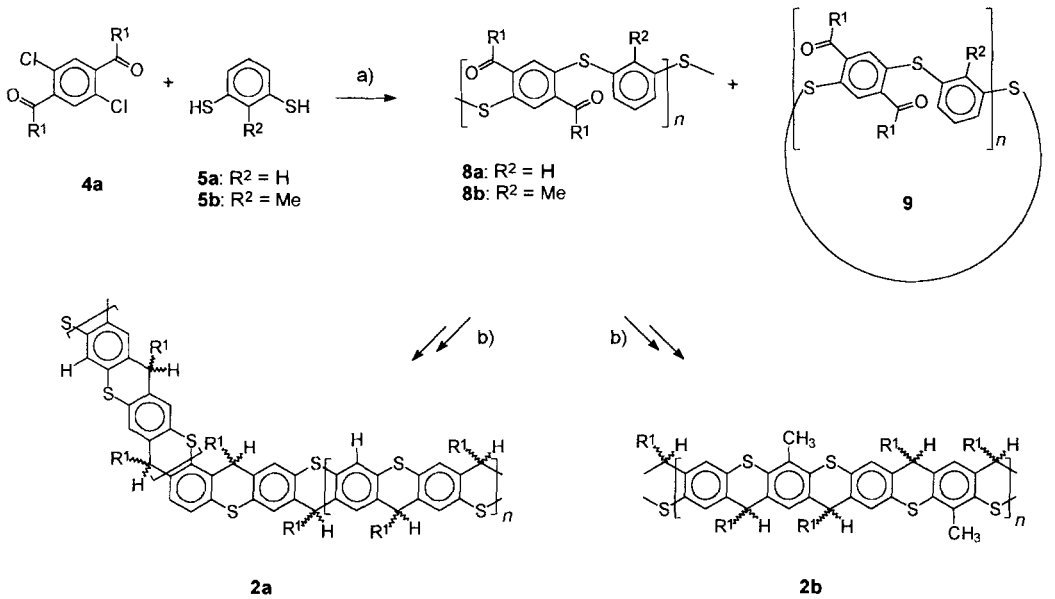


Scheme 1. a) K_2CO_3/dimethylacetamide, 120 °C; b) 1. $LiAlH_4$/THF; 2. $BF_3 \cdot OEt_2/CH_2Cl_2$; c) DDQ/THF 0.5% H_2O; d) **7a**: 1. $LiAlH_4$/THF; 2. $BF_3 \cdot OEt_2/CH_2Cl_2$, **7b**: 1. $LiAlH_4$/THF; 2. $SnCl_4/CH_2Cl_2$.

If polymer **8** is precipitated by pouring the reaction mixture into 10% acetic acid, the gel permeation chromatograms show a bimodal distribution. The maximum in the low molecular mass range is attributed to the formation of cyclic oligomers **9**, which could be shown to contain up to eight repeating units by FD-mass spectrometry. The macrocyclic oligomers **9** can, however, be easily removed from the crude material (dissolved in dichloromethane) by fractional precipitation with acetone. In this way polymer samples of **8a** with narrower molecular mass distribution and number average molecular weights M_n = 50000–110000 are obtained; these samples can be used for investigations into the molecular weight dependence of the subsequent polymer-analogous Friedel–Crafts reactions.

[*] Prof. Dr. K. Müllen, Dipl.-Chem. T. Freund, Dr. U. Scherf
Max-Planck-Institut für Polymerforschung
Ackermannweg 10, D-55128 Mainz (FRG)
Telefax: Int. code + (6131)379-350

[**] T. F. thanks the Verband der Chemischen Industrie for a doctoral stipend.



Scheme 2. a) K_2CO_3/dimethylacetamide, 120 °C; b) 1. $LiAlH_4$/THF; 2. $SnCl_4/CHCl_3$. $R^1 = p\text{-}C_6H_4\text{-}n\text{-}C_{10}H_{21}$.

Dithiol **5b** reacts with diketone **4a** to give the poly(phenylene-sulfide) **8b** (see Scheme 2). In contrast to **8a**, neither a bimodal distribution in the GPC elution profile nor the presence of cyclic oligomers in the FD-mass spectrum could be detected. The isolated material also shows a lower molecular weight and a lower polydispersity ($M_n = 65000$ and $M_w = 140000$) than that of **8a**.

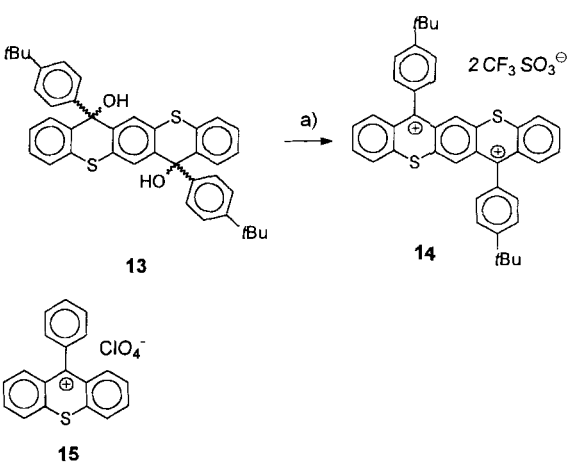
The Friedel–Crafts cyclization route towards ladder structures was initially investigated by using the model compounds **6a**, **6b**, **7a**, and **7b** (see Scheme 1). It was shown that the cyclization of the diketones is significantly inferior to the analogous reaction of the diols. This result confirms observations in the synthesis of ladder-type polyphenylenes.[7] The reaction of the diols obtained from **6a** and **6b** ($LiAlH_4$ in THF) with $BF_3 \cdot OEt_2$ in dichloromethane gave a quantitative yield of **10a** and **10b** as a mixture of the respective diastereomers.

In principle, unlike the cyclization of **6**, regioisomers can be formed by the cyclization of **7**. Although the isomer mixture precipitated after reduction of **7a** and subsequent Friedel–Crafts alkylation with $BF_3 \cdot OEt_2$ in dichloromethane no longer contains any uncyclized diarylmethanol units (^1H and ^{13}C NMR evidence), the bent structures **12** (as a mixture of diastereomers), formed by Friedel–Crafts alkylation in the 2-position of the benzenedithiol group, were detected in addition to the linear annelated systems **11a**. After column chromatography (alumina, CH_2Cl_2/petroleum ether 4:1) and crystallization (CH_2Cl_2/hexane) a pure *cis* isomer of **12** was obtained and its structure determined by crystallography. Thus, it is understandable that 2-methyl-1,3-benzenedithiol (**5b**) is always used as a bifunctional nucleophile, rather than **5a**, to avoid formation of bent substructures during ring closure on route to acenes. Indeed, reaction of the diol obtained from **7b** with $SnCl_4$ in dichloromethane results in a *cis-trans* mixture of diastereomers of the *linear annelated* structure **11b** (see Scheme 1).[8]

The reduction of the polymers **8a** and **8b** to the corresponding polyalcohols with $LiAlH_4$ in THF was quantitative in both cases. Cyclization (see Scheme 2) was also carried out with three equivalents of $SnCl_4$ per reactive group using chloroform as the preferred solvent. This reaction can be conducted in gram-quantities; a polymer concentration of about 4 g polyalcohol per liter of chloroform was chosen, which guarantees that the reaction can take place in an homogeneous medium. Degradation of the polymer does not take place, either during the reduction or during the subsequent ring closure. According to NMR spectroscopic analysis, cyclization products of similar structure are obtained independent of the molecular weight of the sample. The NMR signals of the methine bridges are shown to be of particular diagnostic value, as already seen for the model reactions leading to **10**, **11**, and **12**. No indication of incomplete polymer-analogous cyclization is observed.[9, 10]

The multistep sequences described thus lead to a high molecular weight, completely cyclized, and soluble ladder polymer **2b**. This product should now permit the desired comparison of the form behavior and the persistence length of one- and two-dimensional structures, for example, on the basis of light-scattering and viscosity measurements.[11]

Furthermore, polymer **2b** and model compound **10** are suitable precursors for the preparation of heteropolyacenes with extended conjugated π-electron systems by dehydrogenation or ionization methods. The reaction of **10b** with 2,3-dichloro-5,6-dicyano-*p*-benzoquinone (*DDQ*) in THF in the presence of 0.5 vol.% water led to diol **13** in 96% yield (see Scheme 1). Treatment of **13** with trifluoromethanesulfonic acid in dichlormethane or acetonitrile (Scheme 3) gave a quantitative



Scheme 3. a) Trifluoromethanesulfonic acid/CH_2Cl_2 or CH_3CN.

yield, within seconds, of the stable dication **14**, which was characterized by NMR and electronic absorption spectroscopy (Fig. 1; see also Experimental Procedure). A close relationship of dication **14** with the isoelectronic pentacene could be demonstrated by the electronic absorption spectrum.[11] The longest wavelength absorption of **14** shows, in contrast to that of 9-phenylthioxanthenylium perchlorate (**15**) ($\lambda_{max} = 515$ nm),[12] a

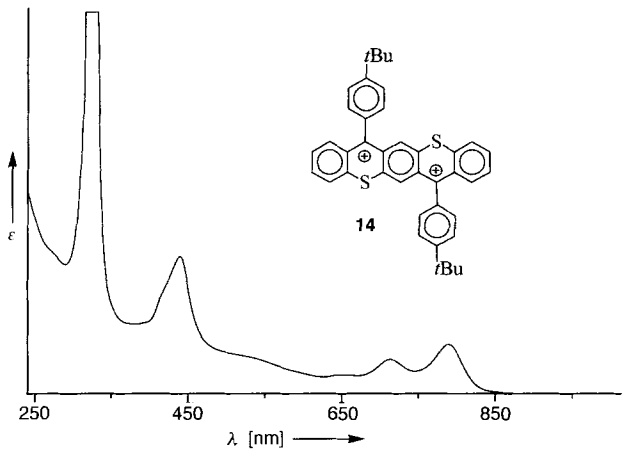
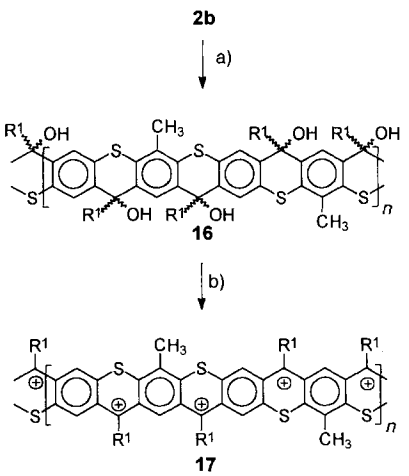


Fig. 1. UV/VIS spectrum of the dication **14**.

marked bathochromic shift, which can be assigned to the smaller band gap of the higher homologue **14**.

Polymer **2b** can be converted, analogous to the formation of **13**, into the polyalcohol **16** by treatment with DDQ in THF/0.5 vol.% H_2O (Scheme 4). The lack of a ^{1}H NMR signal at



Scheme 4. a) DDQ/THF/0.5% H_2O; b) 1. Trifluoromethanesulfonic acid/CH_3CN; 2. Washing with anhydrous CH_3CN. $R^1 = p$-C_6H_4-n-$C_{10}H_{21}$.

$\delta = 5.27$, which stems from the methine bridge in **2b**, substantiates the complete conversion. Characterization of the polycation **17** (analogous to **14**) is prevented by its low solubility (e.g., in dichloromethane, acetonitrile, nitromethane, or trifluoroacetic anhydride). Thus, **16** (in THF) was poured into a thin film from THF solution and this was ionized by using trifluoromethanesulfonic acid in acetonitrile. After washing the product with dry acetonitrile an electronic absorption spectrum was obtained that, based on the longest wavelength absorption at 978 nm, reveals the presence of extended π-conjugated cationic subunits. Examination of the extent of the conversion in the immobilized phase and a more detailed characterization of the ionic polyacene structure **17** will be reported elsewhere.

Experimental Procedure

Dication **14**: 10 mg of a mixture of diastereomers of diol **13** was dissolved in CD_2Cl_2 (1 mL) and treated with one drop of trifluoromethanesulfonic acid. ^{1}H NMR (500 MHz, CD_2Cl_2, 263 K): $\delta = 9.72$ (s, 2H), 8.75 (d, ^3J(H,H) = 8.4 Hz, 2H), 8.75 (m, 4H), 8.57 (m, 4H), 8.18 (t, ^3J(H,H) = 7.8 Hz, 2H), 7.94 (d, ^3J(H,H) = 7.9 Hz, 4H), 7.67 (d, ^3J(H,H) = 7.9 Hz, 4H), 1.54 (s, 18 H); ^{13}C NMR (125 MHz, CD_2Cl_2, 263 K): $\delta = 175.2$, 157.8, 154.1, 142.8, 139.4, 138.8, 137.8, 132.9, 131.7, 131.5, 131.2, 130.6, 128.3, 127.0, 35.6, 30.9. UV/VIS spectrum of **14**: c(**13**) = 2.9×10^{-5} M in 0.05 M trifluoromethanesulfonic acid in acetonitrile: λ_{max} (ε [L mol^{-1} cm^{-1}]) = 323 (64200), 439 (12100), 648 (1280), 706 (2920), 778 (4530).

Received: July 15, 1994 [Z 7121 IE]
German version: *Angew. Chem.* **1994**, *106*, 2547

[1] a) S. A. Jenekhe, P. O. Johnson, *Macromolecules* **1990**, *23*, 4419; b) C. P. Wong, G. C. Berry, *Polymer* **1979**, *20*, 229; c) T. F. Helminiak, G. C. Berry, *J. Polym. Sci. Polym. Symp.* **1978**, *65*, 107; d) C. P. Wong, H. Ohnuma, G. C. Berry, *ibid.* **1978**, *65*, 143; e) U. Scherf, K. Müllen, *Adv. Polym. Sci.*, in press.

[2] a) L. Yu, M. Chen, L. R. Dalton, *Chem. Mater.* **1990**, *2*, 649; b) L. Yu, D. W. Polis, F. Xiao, L. S. Sapochak, M. R. McLean, L. R. Dalton, C. W. Spangler, T. J. Hall, K. O. Havelka, *Polymer* **1992**, *33*, 3239; c) K. Müllen, U. Scherf, *Synthesis* **1992**, *23*; d) H. Naarmann, *Adv. Mater.* **1990**, *2*, 345.

[3] a) A.-D. Schlüter, *Adv. Mater.* **1991**, *3*, 282; b) M. Löffler, A. D. Schlüter, *GIT Fachz. Lab.* **1992**, *1992*, 1101; c) J. P. Mathias, J. F. Stoddart, *Chem. Soc. Rev.* **1992**, *21*, 215; d) S. Wegener, K. Müllen, *Macromolecules* **1993**, *26*, 3037; e) S. Wegener, K. Müllen, *Chem. Ber.* **1991**, *124*, 2101.

[4] Diketones **4a** and **4b** were prepared, according to ref. [7], from 2,5-dichloro-*p*-xylene, which was oxidized with $KMnO_4$ in pyridine to give 2,5-dichloroterephthalic acid (72% yield). The bis-acid chloride obtained with $SOCl_2$ in benzene (85%) then gave **4a** (69% yield) or **4b** (75% yield), respectively, in a Friedel–Crafts acylation with 1-phenyldecane or with *tert*-butylbenzene.

[5] Compound **6b** was synthesized from 2-methylresorcin, according to ref. [6].

[6] H.-J. Kurth, U. Kraatz, F. Korte, *Chem. Ber.* **1973**, *106*, 2419.

[7] U. Scherf, K. Müllen, *Makromol. Chem. Rapid Commun.* **1991**, *12*, 489.

[8] The trityl protons of **11b** show signals at $\delta = 5.55$ and $\delta = 5.50$. The signal for the corresponding carbon atom appears at $\delta = 53.5$ and is not split, in spite of the diastereomer formation observed in the ^{1}H NMR spectrum.

[9] In the ^{1}H NMR spectrum of **2a** the protons of the methine bridges show the signal expected for a triphenylmethane structure at $\delta = 5.25$, as well as an extra signal at $\delta = 5.95$. This result, however, is not attributed to the presence of uncyclized diphenylmethanol groups, since the signals of the alcohol structures at $\delta = 72.8$ in the ^{13}C NMR spectrum have completely disappeared and new signals have appeared at $\delta = 52.0$ and $\delta = 49.0$. Taking into account that the proton of the methine bridge formed by cyclization at the 2-position of the dithioresorcin subunit in the model compound **12** shows a resonance signal at $\delta = 6.0$, it becomes evident that cyclization of the polyalcohol leads to a product **2a**, in which bent substructures also exist. On the other hand, the cyclization of the polyalcohol obtained from **8b** gave, as expected, an exclusively linear annelated product **2b**, the NMR spectrum of which shows only a single signal for the trityl protons at $\delta = 5.27$ and the corresponding ^{13}C NMR signal at $\delta = 52.9$. Even at a signal-to-noise ratio $S/N = 150$ for the ^{1}H NMR signal of the methine bridge, no signals were detected in the range $5.8 > \delta > 6.3$, as would be expected for an incompletely cyclized diphenylmethanol structure. Nevertheless, in the electronic absorption spectrum a band with low intensity was found at $\lambda_{max} = 602$ nm, which can be attributed to partial dehydrogenation during cyclization and thus formation of quinodimethane subunits. This assignment is based on a comparison with the corresponding model compounds and related polymers [10]. The fraction of such structures, which are not detectable in the NMR and IR spectra, is below 1%.

[10] a) U. Scherf, K. Müllen, *Polymer* **1992**, *33*, 2443; b) U. Scherf, *Synth. Met.* **1993**, *55–57*, 767.

[11] *DMS-UV-Atlas Organischer Verbindungen, Vol. 3*, Butterworth, London, and Verlag Chemie, Weinheim, **1966**, spectrum E4/1.

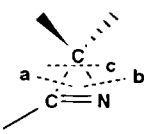
[12] a) C. C. Price, M. Hori, T. Parasaran, M. Polk, *J. Am. Chem. Soc.* **1963**, *85*, 2278; b) O. Convert, J.-P. Le Roux, P.-L. Desbene, A. Defoin, *Bull. Soc. Chim. Fr.* **1975**, 2023.

Thermally Induced Ring Cleavage of a 2*H*-1,2-Azaphosphirene Tungsten Complex**

Rainer Streubel,* Annette Kusenberg, Jörg Jeske, and Peter G. Jones

Dedicated to Professor Reinhard Schmutzler on the occasion of his 60th birthday

Because of their ability to generate 1,3-dipoles as reactive intermediates on ring-opening, unsaturated three-membered heterocycles are of great preparative interest for the generation of five-membered heterocycles.[1] Of three-membered heterocycles possessing the structural element C=N, only the 2*H*-azirenes have been extensively investigated with respect to their ring-opening reactions.[2-4] Thus 2*H*-azirenes with an sp^3-hybridized carbon in the 2-position predominantly display reactions, thermal and photochemical, in which the first step is the breaking of one ring bond (route a and b).[2] In contrast, the 2-methylene-2*H*-azirenes, which have an sp^2-hybridized atom at the 2-position, undergo photochemical reactions that result in ring cleavage (route c)[3] (Scheme 1).



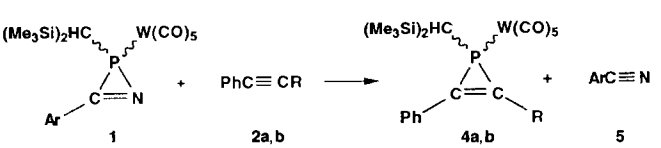
Scheme 1. Schematic representation of the ring-opening reactions of 2*H*-azirenes (the substituents are unspecified; for the 2-methylene-2*H*-azirenes the bonds at the 2-position are formed to the same atom).

We report here the first example of a thermally induced ring cleavage of the 2*H*-1,2-azaphosphirene tungsten complex **1**[5] in the presence of acetylene derivatives and in the presence of benzaldehyde.

The tungsten complex **1** is thermally labile in toluene in the presence of phenylacetylene (**2a**) or diphenylacetylene (**2b**), and the corresponding 1*H*-phosphirene tungsten complexes **4a** and **4b**, respectively, are formed. Since five-membered heterocycles, for example as products of the reaction between **2a,b** and a conceivable 1,3-dipole generated from **1**, were not observed, the assumption of a terminal phosphanediyl tungsten complex **3** as

$[(Me_3Si)_2HCPW(CO)_5]$ **3**

an intermediate seems plausible (cf.[6]). The other product of this reaction, *p*-toluonitrile **5** (Scheme 2), can be identified in the solution by its characteristic C–N valence band in the IR spectrum.[7] The 1*H*-phosphirene tungsten complexes **4a,b** show



Scheme 2. **1, 5:** Ar = *p*-tolyl; und **2a, 4a:** R = H; **2b, 4b:** R = Ph.

NMR spectroscopic data characteristic of this type of compound and this substitution pattern of the ring carbon atoms (Table 1) (cf.[8]). The IR spectroscopic and mass spectrometric data[9] also support the proposed nature of **4a,b**.

Table 1. Selected spectroscopic data of **4a,b** and **7** [a].

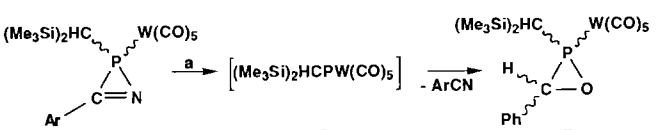
4a: ^{1}H NMR: δ = 0.07 (s, 9 H; $SiMe_3$), 0.25 (s, 9 H; $SiMe_3$), 0.58 (d, ^2J(H,P) = 2.41 Hz, 1 H; PC*H*), 7.48 (m, 3 H; Ph), 7.68 (m, 2 H; Ph), 8.40 (d, ^2J(H,P) = 21.6 Hz; C=C*H*); ^{13}C {^{1}H} NMR: δ = 1.56 (d, ^3J(C,P) = 3.09 Hz; $SiMe_3$), 1.86 (d, ^3J(C,P) = 3.74 Hz; $SiMe_3$), 27.75 (d, ^1J(C,P) = 27.24 Hz; P*C*H($SiMe_3$)$_2$), 124.66 (d, ^1J(C,P) = 6.48 Hz; P*C*H=C), 128.07 (d, ^2J(C,P) = 6.09 Hz; *i*-C), 129.11 (s; *m*-C), 129.24 (d, ^3J(C,P) = 2.64 Hz; *o*-C), 130.82 (s; *p*-C), 145.82 (d, ^1J(C,P) = 17.86 Hz; P*C*=CH), 197.18 (dd, ^2J(C,P) = 8.49 Hz; ^{1}J(C,W) = 108.03 Hz; *cis*-CO), 198.93 (d, ^2J(C,P) = 31.11 Hz; *trans*-CO); ^{31}P {^{1}H} NMR: δ = −136.75 (d, ^1J(P,W) = 272.08 Hz).

4b: ^{1}H NMR: δ = 0.07 (s, 9 H; $SiMe_3$), 0.13 (s, 9 H; $SiMe_3$), 0.27 (d, ^2J(H,P) = 2.98 Hz, 1 H; PC*H*($SiMe_3$)$_2$), 7.33 (m, 6 H; Ph), 7.52 (m, 4 H; Ph); ^{13}C {^{1}H} NMR: δ = 1.06 (d, ^3J(C,P) = 2.87 Hz; $SiMe_3$), 1.74 (d, ^3J(C,P) = 3.18 Hz; $SiMe_3$), 27.89 (d, ^1J(C,P) = 30.28 Hz; P*C*H($SiMe_3$)$_2$), 128.82 (d, ^3J(C,P) = 3.42 Hz; *o*-C), 128.97 (s; *m*-C), 129.18 (d, ^2J(C,P) = 6.22 Hz; *i*-C), 129.99 (s; *p*-C), 136.04 (d, ^1J(C,P) = 12.48 Hz; P(Ph)*C*=), 197.38 (dd, ^2J(C,P) = 8.30 Hz; ^1J(C,W) = 91.78 Hz; *cis*-CO), 198.58 (d, ^2J(C,P) = 30.36 Hz; *trans*-CO); ^{31}P {^{1}H} NMR: δ = −134.60 (d, ^1J(P,W) = 268.64 Hz).

7: ^{1}H NMR: δ = 0.31 (s, 9 H; $SiMe_3$), 0.37 (s, 9 H; $SiMe_3$), 0.88 (d, ^2J(H,P) = 6.16 Hz, 1 H; PC*H*($SiMe_3$)$_2$), 4.34 (d, 1 H, ^2J(H,P) = 2.05 Hz; PhC*H*), 7.47 (m, 3 H; Ph), 8.10 (m, 2 H, Ph); ^{13}C {^{1}H} NMR: δ = 1.66 (d, ^3J(C,P) = 4.26 Hz; $SiMe_3$), 1.97 (d, ^3J(C,P) = 2.29 Hz; $SiMe_3$), 32.49 (d, ^1J(C,P) = 18.96 Hz; P*C*H($SiMe_3$)$_2$), 59.71 (d, ^1J(C,P) = 27.33 Hz; P*C*O), 125.64 (d, ^2J(C,P) = 3.54 Hz; *i*-C), 128.14 (d, ^3J(C,P) = 2.64 Hz; *o*-C), 128.58 (d, ^4J(C,P) = 2.31 Hz; *m*-C), 135.28 (s; *p*-C), 194.85 (dd, ^2J(C,P) = 7.24 Hz; ^1J(C,W) = 125.47 Hz; *cis*-CO), 196.97 (d, ^2J(C,P) = 35.52 Hz, *trans*-CO); ^{31}P {^{1}H} NMR: δ = 40.44 (d, ^1J(P,W) = 308.22 Hz).

[a] All spectra in $CDCl_3$, 25 °C; ^{1}H NMR: 200 MHz, ^{13}C NMR: 50.3 MHz, ^{31}P NMR: 81.0 MHz; the deuterated solvents were used as internal, 85% H_3PO_4 as an external standard.

In order to test further the above interpretation of the reaction of the 2*H*-1,2-azaphosphirene tungsten complex **1** with **2a,b**, the reactivity of **1** with respect to the dipolarophile benzaldehyde **6** was investigated. Complex **1** was treated with a large excess of benzaldehyde (molar ratio 1:20) in toluene at 45 °C. The formation of the corresponding oxaphosphirane tungsten complex **7** again points to the phosphanediyl tungsten complex **3** as the reactive species[10] (Scheme 3). Further confir-



Scheme 3. **1, 7:** Ar = *p*-tolyl. Proposed reaction sequence leading to formation of the oxaphosphirane tungsten complex **7**. a) PhCHO **6**/toluene.

mation of this interpretation is provided by the failure, under these reaction conditions, to observe the formation of [3 + 2] cycloaddition products of a phosphorus analogue to a 1,3-dipolar nitrile ylide with benzaldehyde. It is particularly interesting that the exclusive stereoselective formation of the *RS*/*SR* diastereomer of the oxaphosphirane tungsten complex **7** is observed. This is probably the first example of an effective steric control of a [2 + 1] cycloaddition of a terminal phosphanediyl complex.[11]

The ^{31}P NMR spectroscopic data of **7** (Table 1) show a significant low-field shift for the resonance of the phosphorus atom

[*] Dr. R. Streubel, Dipl.-Chem. A. Kusenberg, Dipl.-Chem. J. Jeske, Prof. Dr. P. G. Jones
Institut für Anorganische und Analytische Chemie der Technischen Universität
Postfach 3329, D-38023 Braunschweig (FRG)
Telefax: Int. code + (531)391-5387

[**] Reactions of 2*H*-1,2-Azaphosphirene Complexes, Part 2. This work was supported by the Fonds der Chemischen Industrie and by BASF AG, Ludwigshafen. Part 1: [5].

at $\delta = 40.44$, compared to the only oxaphosphirane complexes previously known ($\delta = 2.9$ and 3.8).[12] This unusual finding prompted us to investigate the nature of complex **7** more closely by a single-crystal X-ray analysis (Fig. 1).[13]

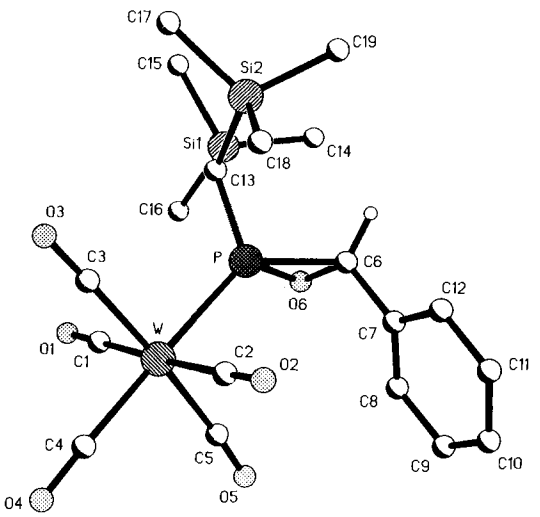


Fig. 1. Structure of compound **7** in the crystal (all H atoms except H6 have been omitted for clarity). Selected bond lengths [pm] and angles [°]: P1-O6 166.8(6), P1-C6 180.2(7), O6-C6 148.0(9), W-P1 246.2(2), P1-C13 179.4(6), C6-C7 149.6(9); O6-P1-C6 50.3(3), O6-C6-P1 60.1(3), O6-P1-C13 107.8(3), C13-P1-C6 108.6(3), C6-O6-P1 69.6(3), O6-C6-C7 116.8(6), C7-C6-P1 122.8(5).

Figure 1 shows for **7** a three-membered P-C-O ring system that is somewhat different from that in the only other known structure of an oxaphosphirane complex;[12] the P1–C6 bond is slightly longer, 180.2(7) vs. 177.8(6) pm,[12] as is the P1–O6 bond, 166.8(6) vs. 165.7(4) pm,[12] whereas the C–O ring bond length remains constant at 148.0(9) pm (cf. C–O 148.0(7) pm[12]). It is notable that the sum of the angles C6-P1-W1, C13-P1-W1, and C13-P1-C6, 357.8°, is close to 360° (cf.[12]). In view of the very similar bond lengths and angles in the phosphanediyl tungsten moieties of **1**[5] and **7**, any structure/reactivity relationships in the ring systems of **1** and **7** remain to be demonstrated.

The cleavage of the 2*H*-1,2-azaphosphirene ring system in **1** and the interesting comparison with the 2-methylene-2*H*-azirenes will form the basis of further investigations.

Experimental Procedure

General preparation of **4a,b**: A solution of **1** (1 mmol) in toluene (3 mL) was treated under nitrogen at room temperature with phenylacetylene **2a** (0.3 g, 2 mmol) or diphenylacetylene **2b** (0.4 g, 2 mmol) and stirred for 2 or 2.5 h, respectively, at 75 °C. The pale brown reaction mixtures were evaporated to dryness under reduced pressure and the products separated by column chromatography on silica (−10 °C, hexane). The eluates were concentrated to about 5 mL under reduced pressure and cooled to −30 °C. The solids thus obtained were washed with a little pentane and freed from residual solvent under high vacuum (10^{-3} mbar). **4a**: Pale yellow powder, yield: 67%, m.p. = 104 °C (decomp.); **4b**: pale yellow powder, yield: 44%, m.p. = 112 °C (decomp.).

7: **1** (0.5 g, 0.75 mmol) in toluene (4 mL) was treated with benzaldehyde (1.5 mL, 15 mmol) and stirred for 9 h at 45 °C. The yellow-brown solution thus obtained was evaporated to dryness under reduced pressure. Subsequent column chromatography on silica (−30 °C, hexane/ether 9:1) afforded **7** as a yellow powder (yield: 56%). Recrystallization from pentane at +6 °C gave pale yellow crystals, yield: 26%, m.p. = 114 °C (decomp.).

Received: August 18, 1994 [Z 7244 IE]
German version: *Angew. Chem.* **1994**, *106*, 2564

[1] R. Huisgen in *1,3-Dipolar Cycloaddition Chemistry* (Ed.: A. Padwa), Wiley, New York, **1984**, pp. 1 ff.
[2] A. Padwa, A. D. Woolhouse in *Comprehensive Heterocyclic Chemistry, Vol. 7* (Eds.: A. R. Katritzky, C. W. Rees), Pergamon Press, Oxford, **1984**, p. 47 and references therein.
[3] a) K. Banert, M. Hagedorn, *Angew. Chem.* **1990**, *102*, 90-92; *Angew. Chem. Int. Ed. Engl.* **1990**, *29*, 103-105; b) K. Banert, M. Hagedorn, E. Knözinger, A. Becker, E.-U. Würthwein, *J. Am. Chem. Soc.* **1994**, *116*, 60-62.
[4] Investigations of ring opening of 1*H*-diazirenes generated as intermediates: a) X. Creary, A. Sky, G. Phillips, D. Alonso, *J. Am. Chem. Soc.* **1993**, *115*, 7584-7592; b) G. Alcaraz, A. Baceiredo, M. Nieger, G. Bertrand, *ibid.* **1994**, *116*, 2159-2160.
[5] R. Streubel, J. Jeske, P. G. Jones, R. Herbst-Irmer, *Angew. Chem.* **1994**, *106*, 115-117; *Angew. Chem. Int. Ed. Engl.* **1994**, *33*, 80-82.
[6] F. Mathey, *Angew. Chem.* **1987**, *99*, 285-296; *Angew. Chem. Int. Ed. Engl.* **1987**, *26*, 275-286.
[7] IR spectrum of the reaction mixture: $\tilde{\nu}_{CN} = 2224\ cm^{-1}$ (C≡N).
[8] F. Mathey, *Chem. Rev.* **1990**, *90*, 997-1025.
[9] Selected IR spectroscopic and mass spectrometric data for **4a,b** and **7**. **4a**: IR (CH_2Cl_2): $\tilde{\nu}$ = 2067 s (C=O), 1977 s (C=O), 1953-1912 vs, b (C=O) cm^{-1}; MS (EI, 70 eV, ^{184}W): *m/z* 616 [M^+]; **4b**: IR (CH_2Cl_2): $\tilde{\nu}$ = 2069 s (C=O), 1979 s (C=O), 1954-1918 vs (C=O) cm^{-1}. MS (EI, 70 eV, ^{184}W): *m/z* = 692 [M^+]. **7**: IR (CH_2Cl_2): $\tilde{\nu}$ = 2073 s (C=O), 1988 s (C=O), 1961–1927 vs, b (C=O) cm^{-1}. MS (CI, pos, NH_3, ^{184}W): m/z 620 [M^+]. Satisfactory C,H elemental analysis for **4a,b** and **7**.
[10] Interestingly, the first synthesis of an oxaphosphirane derivative was by [2 + 1] cycloaddition of hexafluoroacetone with an iminophosphane: G.-V. Röschenthaler, K. Sauerbrey, R. Schmutzler, *Chem. Ber.* **1978**, *111*, 3105-3111.
[11] Cf. sterically controlled [1,4] additions: J. M. Alcaraz, J. Svara, F. Mathey, *Nouv. J. Chim.* **1986**, *10*, 321-326.
[12] S. Bauer, A. Marinetti, L. Ricard, F. Mathey, *Angew. Chem.* **1990**, *102*, 1188-1189; *Angew. Chem. Int. Ed. Engl.* **1990**, *29*, 1166-1167.
[13] Crystal structure analysis of **7**: $C_{19}H_{25}NO_6PSi_2W$, triclinic, space group $P\bar{1}$, $a = 894.3(3)$, $b = 1070.0(3)$, $c = 1400.0(3)$ pm, $\alpha = 87.39(2)$, $\beta = 88.62(2)$, $\gamma = 68.27(2)°$, $U = 1.2431(6)\ nm^3$, $Z = 2$, $\mu = 4.9\ mm^{-1}$, $T = -100$ °C. A colorless tablet 0.8 × 0.32 × 0.1 mm was mounted in inert oil (type RS 3000, Riedel de Haën). A Siemens R3 diffractometer with $Mo_{K\alpha}$ radiation was used to collect 8113 intensities to $2\theta_{max}$ 55°, of which after an absorption correction (Ψ-scans) 5200 independent reflections were used for all calculations (program SHELXL-93: G. M. Sheldrick, University of Göttingen, **1993**). The structure was solved with the heavy atom method and refined anisotropically on F^2. H atoms were included by using a riding model. The final $wR(F^2)$ was 0.115, with a conventional $R(F)$ 0.043 for 262 parameters and 108 restraints. The maximum residual electron density was 2800 e nm^{-3}. Further details of the crystal structure investigation may be obtained from the Fachinformationszentrum Karlsruhe, D-76344 Eggenstein-Leopoldshafen (FRG), on quoting the deposition number CSD-401280.

Porphyrin–Quinone Cyclophanes with Gradually Varied Donor–Acceptor Distances**

Heinz A. Staab,* Achim Feurer, and Ralf Hauck

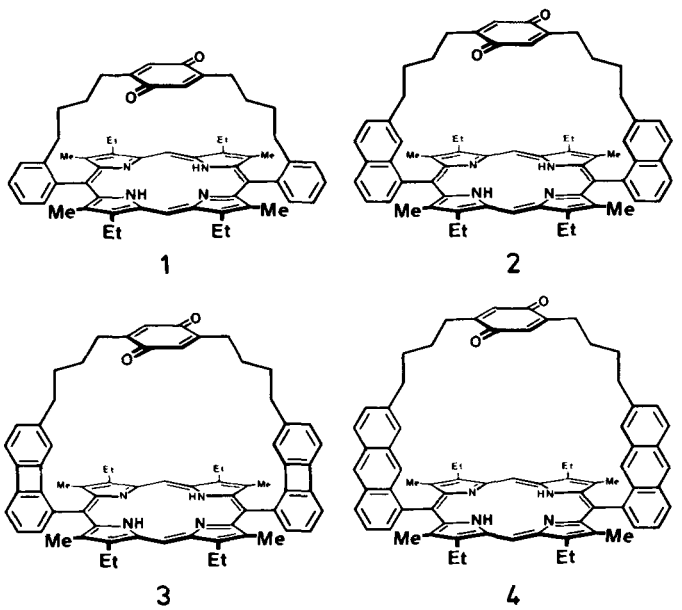
Porphyrin–quinone cyclophanes of type **1** represent especially suitable systems for the investigation of photoinduced electron transfers since the donor and acceptor components are fixed in well-defined spatial orientations. Whereas all other structural parameters remained constant, the electron affinity of the quinone unit and the donor strength of the porphyrin system were varied over a wide range.[1, 2] The cyclophane concept realized in **1** and its doubly bridged analogues[3] was extended to triads of the type porphyrin-quinone(1)-quinone(2) and porphyrin(1)-porphyrin(2)-quinone for the study of multi-

[*] Prof. Dr. H. A. Staab, Dr. A. Feurer, Dr. R. Hauck
Abteilung Organische Chemie
Max-Planck-Institut für medizinische Forschung
Jahnstrasse 29, D-69120 Heidelberg (FRG)
Telefax: Int. code + (6221)486-219

[**] Photoinduced Electron Transfer in Porphyrin–Quinone Cyclophanes, Part 13. Part 12: [4b].

step electron transfer reactions.[4] We now used such porphyrin–quinone cyclophanes for experimental studies of the distance dependence of electron transfer.[5]

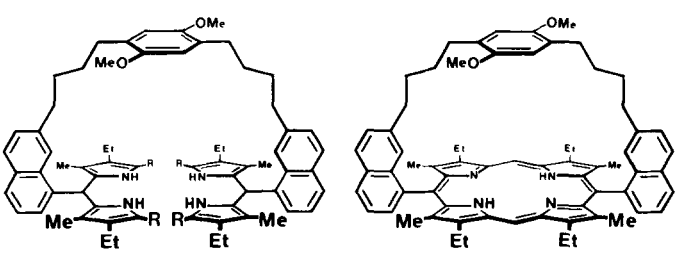
X-ray structure analyses of compounds of type **1** showed[1, 6] that for steric reasons the ring planes of the phenyl substituents in the 5- and 15-positions of the porphyrin units are approximately perpendicular to the plane of the porphyrin system. Thus the linkage of the tetramethylene-quinone-tetramethylene bridge to the *ortho* positions of these phenyl rings has a corresponding spatial orientation. When the phenyl groups of **1** are replaced with 1-naphthyl (**2**), 1-biphenylenyl (**3**), and 1-anthryl groups (**4**), we anticipated that these aryl units would also be positioned

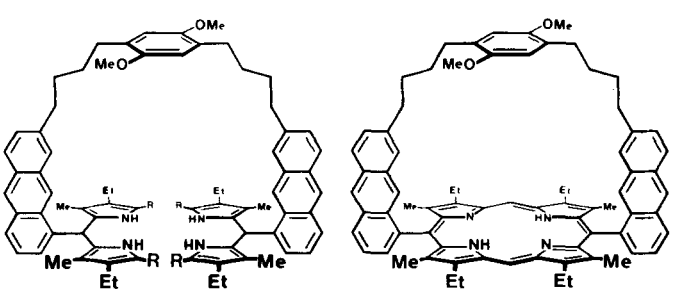


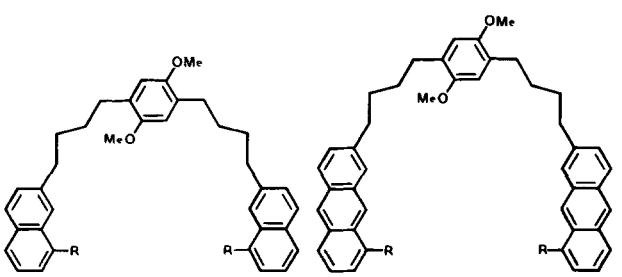
roughly perpendicular to the plane of the porphyrin system, and that the bonds in the 7-positions of these arenes would be oriented parallel to the *ortho* bonds of the phenyl rings of **1**. The same quinone bridge as in **1** attached to the 7-positions of these larger arene spacers would thus be shifted parallel. As a result the porphyrin–quinone distances in the series of compounds **1**–**4** would increase stepwise from about 350 to 900 pm, assuming analogous conformations within the bridges. We report here on the syntheses and properties of **2** and **4** and compare them to those of **1**;[1] the biphenylene system **3** requires a different synthetic route, which so far was used successfully only for cyclophanes having porphyrin units with a different substitution pattern.[7]

The main task in the synthesis of porphyrin–quinone cyclophanes **2** and **4** was the construction of the dialdehydes **7** and **10**, which contain the carbon skeleton of the bridge and the two lateral arene units with substitution patterns suitable for the subsequent porphyrin synthesis. The synthesis of the porphyrin cyclophane system should then be possible in analogy to the preparation of cyclophanes of type **1**.[1]

Reaction of methyl 7-bromomethyl-1-naphthoate[8] with triphenylphosphane provided the corresponding triphenylphosphonium bromide (quantitative yield). Subsequent Wittig reaction with (*E*,*E*)-1,4-bis(2-formyl-1-ethenyl)-2,5-dimethoxybenzene[3] led to 1,4-bis[4-(8-methoxycarbonyl-2-naphthyl)-1,3-butadienyl]-2,5-dimethoxybenzene (mixture of *Z*/*E* isomers, 90–95% yield).[9] Catalytic hydrogenation (Pd/C, methanol/ethyl acetate, 1:1) afforded 1,4-bis[4-(8-methoxycarbonyl-2-naphthyl)butyl]-2,5-dimethoxybenzene (**5**) (90% yield).[9] Compound **5** was reduced with lithium aluminum hydride (THF; 95% yield) to furnish the bis(hydroxymethyl) compound **6**, which was oxidized with pyridinium chlorochromate (celite/magnesium sulfate, dichloromethane; 70–90% yield) to give dialdehyde **7** (m.p. 126–128 °C).[9] The reaction of dialdehyde **7** with 2-benzyloxycarbonyl-3-ethyl-4-methylpyrrole led to the corresponding bis(dipyrrylmethyl) compound **11** (conc HCl, ethanol, 3 h at reflux; 90–95% yield). After hydrogenolysis to **12** (Pd/C, THF, 20 °C; almost quantitative yield), the synthesis was completed by closure of the porphyrin ring in analogy to the synthesis of **1**[1] (triethyl orthoformate, trichloroacetic acid; then dehydrogenation with 2,3-dichloro-5,6-dicyano-1,4-benzoquinone (DDQ)). Purification by chromatography (MPLC, silica gel, hexane/ethyl acetate) and recrystallization from methanol/dichloromethane provided **13** in two crystal modifications with melting points of 289–291 and 325–329° (12% total yield).[9] Subsequent ether cleavage (boron tribromide, dichloromethane) and oxidation with DDQ afforded the corresponding porphyrin–quinone cyclophane **2** (violet crystals; m.p. 314–317 °C, 80% yield).[9]







The porphyrin–quinone cyclophane **4** containing the anthracene spacer was prepared by a reaction sequence resembling that of the synthesis of **2**. Bromination of methyl 7-methylanthracene-1-carboxylate[10] with *N*-bromosuccinimide (NBS) was followed by reaction with triphenylphosphane to give the

 © VCH Verlagsgesellschaft mbH, D-69451 Weinheim, 1994 0570-0833/94/2323-2429 $ 10.00+.25/0

phosphonium salt[9] (61% yield). Subsequent Wittig reaction with 1,4-bis(2-formylethyl)-2,5-dimethoxybenzene[3] afforded the corresponding diene,[9] which was converted to **8**[9] by catalytic hydrogenation (Pd/C, THF, 80% yield). Diester **8** was reduced (lithium aluminum hydride, THF, ca. 95% yield) to furnish the bis(hydroxymethyl) compound **9**,[9] oxidation of which (DMSO, oxalyl dichloride, THF, −75 °C) provided dialdehyde **10** (m.p. 184–186 °C)[9] in almost quantitative yields. Condensation of **10** with 2-benzyloxycarbonyl-3-ethyl-4-methylpyrrole (*p*-toluenesulfonic acid monohydrate, benzene, 48 h, 80 °C, under argon) afforded the corresponding bis(dipyrrylmethyl) compound **14** (53% yield);[9] hydrogenolysis (Pd/C, THF, 24 h, 20 °C) then led to tetracarboxylic acid **15** (72% yield) (in part hydrogenated at the 9,10-positions of the anthracene units). The closure of the porphyrin ring was completed according to the method employed successfully with **1** and **2**[1] (triethyl orthoformate, trichloroacetic acid, dichloromethane; 22 h, 20 °C). Subsequent dehydrogenation with tetrachloro-1,4-benzoquinone and purification by chromatography (MPLC, silica gel, toluene/ethyl acetate, 20:1) provided the porphyrin cyclophane **16** (4.6% yield; recrystallization from methanol/dichloromethane gave violet crystals, m.p. 271–275 °C).[9] The porphyrin–quinone cyclophane **4** was obtained from **16** by ether cleavage (boron tribromide, dichloromethane, 2 h at 20 °C) and then oxidation of the hydroquinone with tetrachloro-1,4-benzoquinone; chromatography (HPLC, silica gel, toluene/ethyl acetate, 30:1) and recrystallization from methanol/dichloromethane provided **4** in the form of a violet microcrystalline powder (m.p. > 350 °C; 19% yield).[11]

In the series of porphyrin–quinone cyclophanes **1**–**4** completely identical conformational relationships in the quinone bridges corresponding to an exactly parallel shift could not be assumed a priori, since with increasing length of the arene spacer the probability of other conformations becomes greater. However, it was evident from the ^{1}H NMR spectra that the quinone–porphyrin distances increased stepwise as desired. The signal of the protons on the quinone ring in **1** is shifted to considerably higher fields ($\delta = 4.15$, s, 2H) as compared to those of simple 2,5-dialkyl-1,4-benzoquinones ($\delta \approx 6.60$) owing to the anisotropy effect of the porphyrin system. The signal arising from the quinone protons in **2**, the cyclophane with naphthalene spacers, is observed at $\delta = 4.92$ (s, 2H), and that of the anthracene analogue **4** at $\delta = 5.96$ (s, 2H; all spectra in CD_2Cl_2, 303 K). This marked reduction in the ring current effect of the porphyrin units provides clear indication of the increasing porphyrin–quinone distance in this series. However, these data correspond to the time average and cannot be assigned to specific conformations which interconvert rapidly on the ^{1}H NMR timescale. Low-temperature ^{1}H NMR spectra[6] of compounds of type **1** demonstrate that the most stable conformations are not the C_2-symmetric structures with parallel and centered quinone and porphyrin rings. Instead, two equivalent mirror-image conformations exist in which the bridges are arranged unsymmetrically; the swinging of the bridges back and forth corresponds to interconversion of the two conformations ("swinging bridge process"). X-ray structure analyses for compounds in this series also displayed these unsymmetrical conformations, in which the quinone rings are tilted toward the average porphyrin plane by roughly 25° and the vertical distances between the center of the quinone ring and the average porphyrin plane are approximately 450 pm.[6]

Similar conformations can be assumed for porphyrin–quinone cyclophane **2** with naphthalene spacers. ^{1}H NMR spectra recorded at low temperatures (down to 145 K) show broadened but unresolved signals for the NH and methine protons of the porphyrin system, as a result of the expected low energy barriers for the swinging bridge process. The X-ray structures of a derivative of **2** with two chloro substituents on the quinone ring and of **13**, the immediate non-quinoid precursor of **2**, are in principle very similar to that of **1**. However, the tilt of the central rings in the bridges is greater (49 and 56°, respectively), and the distances from the center of these rings to the average porphyrin plane increase to 503 and 516 pm, respectively.[12]

The arrangement and distance between the quinone and porphyrin units in the porphyrin–quinone cyclophane **4** with anthracene spacers could not be determined by either low-temperature ^{1}H NMR studies nor by X-ray structure analysis. Calculations of the conformations based on molecular dynamics (MD) simulations, and determination of the geometries of the lowest energy conformations, which in the case of **1** agree quite well with the experimentally determined conformations, indicate that **4** has an extended quinone–porphyrin arrangement with a vertical distance of 952 pm between the quinone center and the porphyrin plane (Fig. 1).[13]

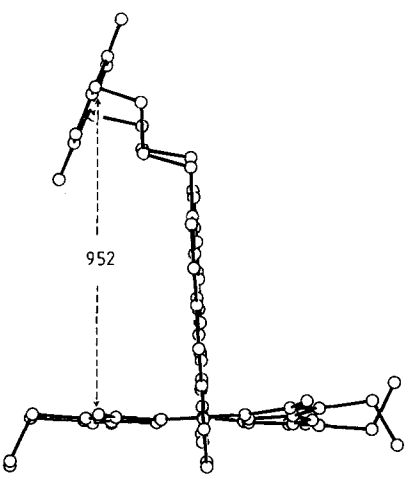


Fig. 1. Lowest energy conformation calculated for **4** (for details on MD simulation see ref. [13]).

UV spectra of porphyrin–quinone cyclophanes **1**, **2**, **4**, and their non-quinoid precursors, as well as the simple 2,8,12,18-tetraethyl-3,7,13,17-tetramethyl-5,15-diphenylporphyrin all show very similar, typical porphyrin absorptions (Soret and Q-bands). The intensities of the emission bands at 630 and 700 nm are, however, dependent on the rate of the photoinduced electron transfer, which leads to radiationless deactivation of the first excited singlet state of the porphyrins competing with fluorescence emission. Comparable values for the emission intensities of the porphyrin–quinone cyclophanes can be obtained from the relative quantum yields φ_{rel} of the fluorescence by comparing the fluorescence intensities of these compounds to those of their immediate non-quinoid precursors. Comparison of the spectra of compounds of type **2** with those of the analogously substituted systems **1**[1] reveals a slight increase of φ_{rel} of fluorescence only marginally outside of the limits of error; in other words, the replacement of the benzene unit by the naphthalene spacer has a rather small effect [$\varphi_{rel} \approx 3 \times 10^{-3}$ (in toluene), 2×10^{-3} (dichloromethane)]. In contrast, for **4** the rate of electron transfer (corresponding to $\varphi_{rel} \approx 0.5$ in toluene) decreases drastically. The magnitude here is in agreement with that found by time-resolved measurements of the fluorescence lifetimes,[14] which appear to correspond to a superposition of

two or three decay times (electron transfer in different conformations?) [**1**: 2 ps (95%); **2**: 3 ps (69%), 25 ps (17%); **4**: 2.4 ns (19%), 5.6 ns (81%); in toluene]. According to these preliminary results the photoinduced electron tranfer becomes slower on going from **2** to **4** by roughly three orders of magnitude. Thus cyclophane **3**, with an intermediate transannular distance, is of particular interest. A systematic investigation of the solvent dependence of the rates of electron tranfer in **1**–**4** seems necessary, since principally different types of solvation cannot be excluded.

Received: August 2, 1994 [Z 7204 IE]
German version: *Angew. Chem.* **1994**, *106*, 2542

[1] H. A. Staab, J. Weiser, M. Futscher, G. Voit, A. Rückemann, C. Anders, *Chem. Ber.* **1992**, *125*, 2285–2301; H. A. Staab, G. Voit, J. Weiser, M. Futscher, *ibid.* **1992**, *125*, 2303–2310; H. A. Staab, C. Krieger, C. Anders, A. Rückemann, *ibid.* **1994**, *127*, 231–236.
[2] H. Heitele, F. Pöllinger, T. Häberle, M. E. Michel-Beyerle, H. A. Staab, *J. Phys. Chem.* **1994**, *98*, 7402–7410; H. Heitele, F. Pöllinger, K. Kremer, M. E. Michel-Beyerle, M. Futscher, G. Voit, J. Weiser, H. A. Staab, *Chem. Phys. Lett.* **1992**, *188*, 270–278.
[3] J. Weiser, H. A. Staab, *Angew. Chem.* **1984**, *96*, 602–603; *Angew. Chem. Int. Ed. Engl.* **1984**, *23*, 623–625; H. A. Staab, J. Weiser, E. Baumann, *Chem. Ber.* **1992**, *125*, 2275–2283.
[4] a) H. A. Staab, M. Tercel, R. Fischer, C. Krieger, *Angew. Chem.* **1994**, *106*, 1531–1534; *Angew. Chem. Int. Ed. Engl.* **1994**, *33*, 1463–1465; b) H. A. Staab, T. Carell, *ibid.* **1994**, *106*, 1534–1536 and **1994**, *33*, 1466–1468; c) F. Pöllinger, H. Heitele, M. E. Michel-Beyerle, M. Tercel, H. A. Staab, *Chem. Phys. Lett.* **1993**, *209*, 251–257.
[5] See M. R. Wasielewski, *Chem. Rev.* **1992**, *92*, 435–461, and references therein; J. W. Evenson, M. Karplus, *Science* **1993**, *262*, 1247–1249.
[6] C. Krieger, M. Dernbach, G. Voit, T. Carell, H. A. Staab, *Chem. Ber.* **1993**, *126*, 811–821.
[7] S. Quazzotti, H. A. Staab, unpublished; B. Kratzer, Diplomarbeit, Universität Heidelberg, **1994**.
[8] Prepared from 7-methyl-1-naphthylamine via 1-bromo-7-methylnaphthalene, methyl 7-methyl-1-naphthoate, and its bromination with bromosuccinimide (A. Feurer, Dissertation, Universität Heidelberg, **1993**).
[9] The elemental analyses, ^{1}H NMR and mass spectra, and other spectroscopic data are in agreement with the assigned structures.
[10] R. Hauck, Diplomarbeit, Universität Heidelberg, **1990**.
[11] The composition of **4** was verified by high-resolution mass spectrometry (LSI-MS positive-ion mode, *m*-nitrobenzyl alcohol/1% trifluoroacetic acid; MH^+ calcd for $C_{74}H_{71}N_4O_2$ 1047.5577, found 1047.5604); the structure was secured by ^{1}H NMR spectroscopy (complete assignment with COSY).
[12] C. Krieger, A. S. Kumar, A. Feurer, H. A. Staab, unpublished.
[13] For detailed information on the conformation calculations see M. Dernbach, Dissertation, Universität Heidelberg, **1993**.
[14] F. Pöllinger-Dammer, H. Heitele, M. E. Michel-Beyerle, unpublished.

Excited-State Carbon Acids: Theoretical Studies of Suberene and Cycloheptatriene

Hans-Martin Steuhl and Martin Klessinger*

Dedicated to Professor Wolfgang Lüttke on the occasion of his 75th birthday

Cyclopentadienyl and cycloheptatrienyl anions in the ground state have a cyclic array of $4N + 2$ and $4N$ π electrons and are expected to be aromatic and antiaromatic, respectively. The hypothesis[1] that in the excited singlet state, ground-state antiaromatic carbanions are stabilized relative to ground-state aromatic carbanions is supported by the recent finding that suberene (**1**) has a much greater propensity to undergo heterolysis of the benzylic C–H bond than fluorene (**2**).[2, 3] Correlation diagrams, as shown in Figure 1 for the deprotonation of the parent hydrocarbons cyclopentadiene (**3**) and cycloheptatriene (**4**), also support this hypothesis.

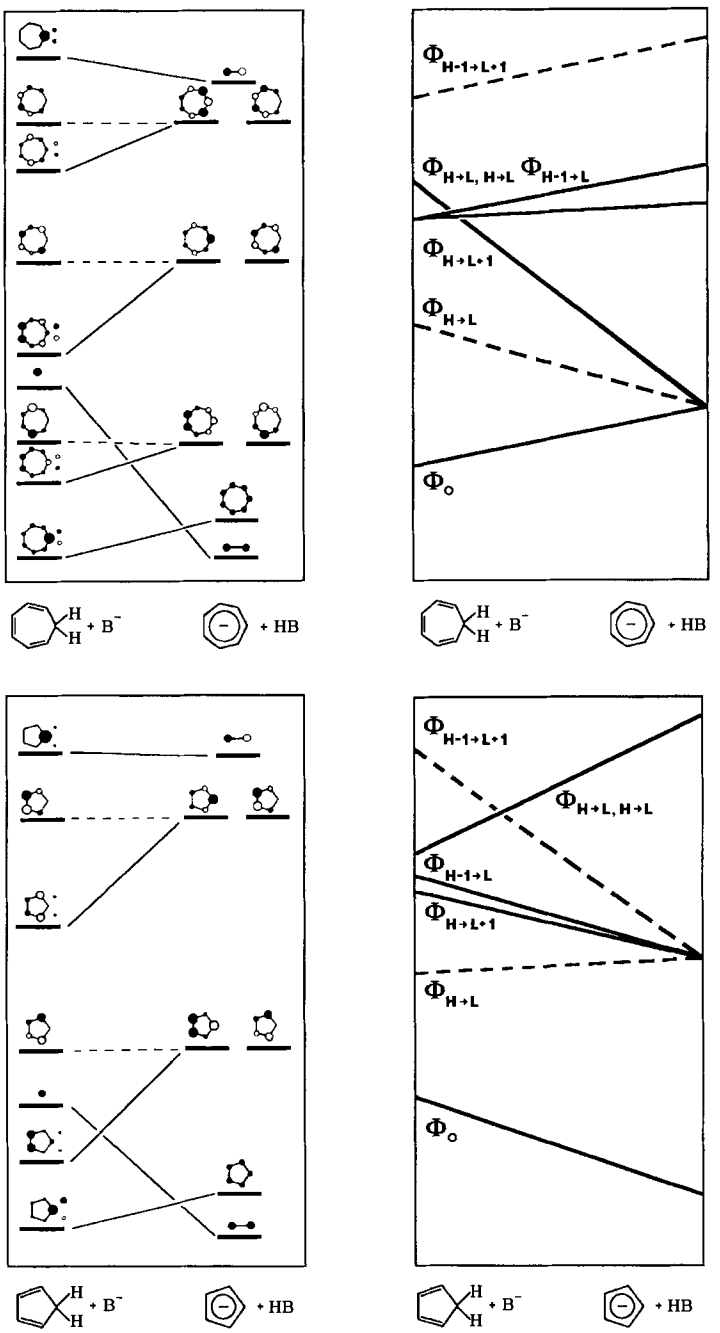
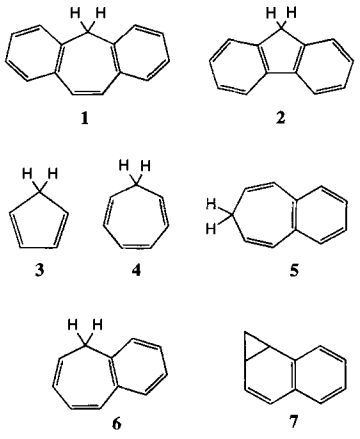


Fig. 1. a) Natural orbital correlation diagrams and b) configuration correlation diagrams for the deprotonation of cycloheptatriene (top) and cyclopentadiene (bottom).

However, while **1** in the excited singlet state is deprotonated by water as base and yields the transient suberenyl anion, on irradiation of **4** a suprafacial [1,7] sigmatropic H-shift[4] and formation of bicyclo[3.2.0]hepta-2,6-diene by intramolecular cyclization[5] occurs. Similarly, the benzo derivatives **5** and **6** showed no evidence for carbon-acidic behavior; instead these compounds reacted exclusively by a very efficient photorear-

[*] Prof. Dr. M. Klessinger, Dipl.-Chem. H.-M. Steuhl
Organisch-chemisches Institut der Universität
Corrensstrasse 40, D-48149 Münster (FRG)
Telefax: Int. code + (251)83-9772

 © VCH Verlagsgesellschaft mbH, D-69451 Weinheim, 1994 0570-0833/94/2323-2431 $ 10.00+.25/0



rangement to give **7** in good yield.[6] The flexibility of **5** and **6** has been mentioned as a possible cause for the difference in photochemical reactivity between these molecules and **1**;[1, 6] the geometric structure or the electronic structure of the excited states could be stated as alternative reasons. To decide between these possibilities and to understand the excited-state carbon-acidic behavior of suberene, we carried out semiempirical MNDOC-CI calculations[7] for the ground and excited states of **1** and **4**, as well as for their anions.

Optimized structures are shown in Figure 2. While **4** is calculated to be planar or nearly planar in the lowest three singlet states S_0, S_1, and S_2,[8] **1** is far from planar in all three states. As a consequence of this nonplanar structure, the two methylene hydrogens of **1** differ considerably with respect to their chemical surroundings as well as to their charge. But the excited state structures of **1** turn out to be rather flexible, the difference in energy between the planar form and the equilibrium conformation being less than 4 kcal mol^{-1} for the S_1 state. A rough estimate of the ground- and excited-state acidity of **1** and **4** from calculation of the ground- and excited-state heats of formation of the corresponding carbanions yields ΔpK_a values of comparable magnitude (ΔpK_a(**1**) = − 52, ΔpK_a(**4**) = − 47). Therefore, the structure and acidity of the excited states cannot explain the different photochemical behavior of **1** and **4**.

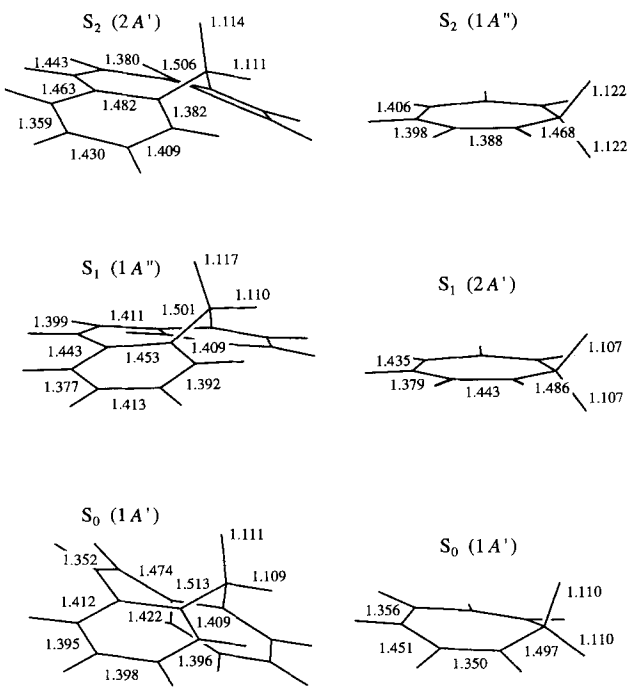


Fig. 2. Optimized structures for the ground and the lowest excited singlet state of suberene (**1**) (left) and cycloheptatriene (**4**) (right). MNDOC-CI results obtained including all single and double excitations with respect to the leading configurations (cf. Table 1) within the active space HOMO−4 to LUMO + 4 for **1** and HOMO−2 to LUMO + 2 for **4**. For the optimization of the excited A' state of **1** the CI had to be further truncated by choosing an excitation index 9/9 [7b]. Vibrational analysis confirmed all stationary points to be true minima.

However, a closer look at the excited-state wave functions in Table 1 reveals that the electronic structure of the lowest excited singlet state of **1** is very different from that of **4**. While for **4** the lowest excited singlet state has the same symmetry as the ground state (A' in C_s), it has a different symmetry (A'') for **1**. The order of vertically excited states, on the other hand, is the same: the A'' state (S_1) lies below the A' state (S_2) for both molecules (Table 1). Therefore, on excited-state relaxation a crossing of states must occur for **4**. This is shown in Figure 3, where the energy of the three lowest singlet states of **1** and **4** is shown as a function of the geometry. Thus, the different photochemical behavior of cycloheptatriene (**4**) and its derivatives on the one hand and of suberene (**1**) on the other is simply due to the fact that excited states of different electronic nature are involved in the photoreactions of these molecules. While in a very short time after vertical excitation into the HOMO → LUMO (H → L) excited A'' state, cycloheptatriene (**4**) will find itself in an excited A' state that may be described by a mixture of the configurations $\Phi_{H\to L,H\to L}$, $\Phi_{H\to L+1}$, and $\Phi_{H-1\to L}$, suberene (**1**) relaxes to the HOMO → LUMO excited A'' state. Only this state is capable of exhibiting excited-state carbon-acidic behavior, as is evident from the correlation diagram shown in Figure 1.

Table 1. Vertical and adiabatic excitation energies [kcal mol^{-1}] of suberene **1** and cycloheptatriene **4** [a].

Excited state[b]	Wave function[c]	**1** ΔE_{vert}	**1** ΔE_{ad}	**4** ΔE_{vert}	**4** ΔE_{ad}
A''	$\Phi_{H\to L}$	98.8	87.5	91.0	84.0
A'	$\Phi_{H\to L,H\to L}$, $\Phi_{H\to L+1}$, $\Phi_{H-1\to L}$	102.1	94.1	91.4	69.2

[a] MNDOC-CI results using the optimized structures and all single and double excitations with respect to all five reference configurations (Φ_0, $\Phi_{H\to L}$, $\Phi_{H\to L,H\to L}$, $\Phi_{H\to L+1}$ and $\Phi_{H-1\to L}$) within the active space specified in the legend of Figure 2 (**1**: 1439 configurations, **4**: 126 configurations). [b] The calculated ground state energies are ΔH_f(**1**) = 138.6 and ΔH_f(**4**) = 65.8 kcal mol^{-1}. [c] Leading contributions to the CI wave function.

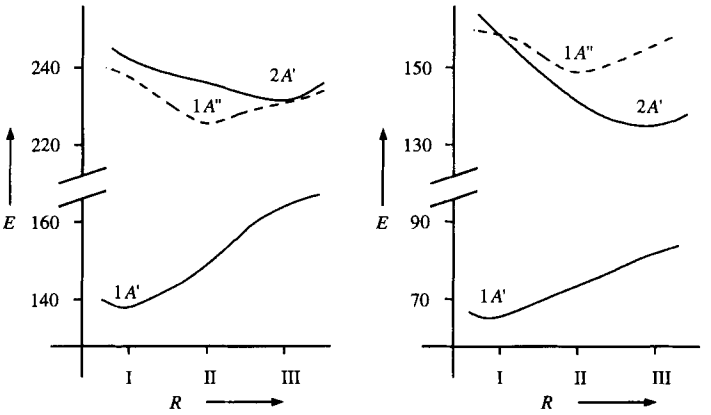


Fig. 3. Energies E [kcal mol^{-1}] of the first three singlet states of suberene (**1**) and cycloheptatriene (**4**) as a function of excited-state relaxation (R). Energies were calculated at the geometries of the $1A'$ ground state (I) and of the $1A''$ (II) and $2A'$ (III) excited states, respectively.

Thus, suberene (**1**) exhibits the expected photochemical reactivity, whereas for cycloheptatriene (**4**) it is not observed, because due to a conical intersection, a fast transition takes place into

the A' state, the characteristic reaction of which is a very efficient [1,7] hydrogen shift. This is in perfect agreement with the observation that though the optically prepared excited state of **4** depopulates within about 25 fs,[11] ground-state **4** is produced only 26 ps after excitation.[12] It also confirms the model proposed to explain this dramatic difference of three orders of magnitude.[12] In addition, this is an indication that in spite of the limitations of semiempirical results as far as absolute accuracy is concerned, the energy difference of merely 0.4 kcal mol^{-1} obtained for the vertical excitation energies of **4** may be significant.

The excited-state acidic behavior observed for **1** might be due to the fact that the photoreactions observed for **4**–**6** are not operative in **1** because they are energetically unfavorable, since the intermediate cannot irreversibly rearomatize to a stable product.[13] This argument, however, is difficult to reconcile with the experimental observation that the [1,7] H shift occurs from a totally symmetric state and the fact that in **1** there is no low-lying state of this symmetry.

Further investigations into the structural and electronic prerequisites for excited-state carbon-acidic behavior are under way.

Received: June 4, 1994 [Z6998IE]
German version: *Angew. Chem.* **1994**, *106*, 2568

[1] P. Wan, D. Shukla, *Chem. Rev.* **1993**, *93*, 571–584.
[2] P. Wan, E. Krogh, B. Chak, *J. Am. Chem. Soc.* **1988**, *110*, 4073–4074.
[3] D. Budac, P. Wan, *J. Org. Chem.* **1992**, *57*, 887–894.
[4] W. R. Roth, *Angew. Chem.* **1963**, *75*, 921–922.
[5] W. G. Dauben, B. Cargill, *Tetrahedron* **1961**, *12*, 186–189.
[6] P. Wan, D. Budac, M. Earle, D. Shukla, *J. Am. Chem. Soc.* **1990**, *112*, 8048–8054.
[7] MNDOC-CI = modified neglect of diatomic overlap correlation, configuration interaction; a) W. Thiel, *J. Am. Chem. Soc.* **1981**, *103*, 1413–1420; A. Schweig, W. Thiel, *ibid.* **1981**, *103*, 1425–1431; b) M. Reinsch, U. Höweler, M. Klessinger, *J. Mol. Struct.* **1988**, *167*, 301–306; c) M. Klessinger, T. Pötter, C. van Wüllen, *Theor. Chim. Acta* **1990**, *80*, 1–17.
[8] Ab initio calculations [9] and electron diffraction studies [10] show that ground state **4** exists in a boat form with a barrier to inversion through the planar form of 5.7 kcal mol^{-1}. These results can be confirmed with the MNDOC-CI method by extending the active space to include non-π orbitals.
[9] S. Saebø, J. E. Boggs, *J. Mol. Struct.* **1982**, *87*, 365–373.
[10] M. Traetteberg, *J. Am. Chem. Soc.* **1964**, *86*, 4265–4270.
[11] P. M. Borell, H. G. Löhmannsröben, K. Luther, *Chem. Phys. Lett.* **1987**, *136*, 371–376.
[12] P. J. Reid, S. D. Wickham, R. A. Mathies, *J. Phys. Chem.* **1992**, *96*, 5720–5724; P. J. Reid, A. P. Shreve, R. A. Mathies, *ibid.* **1993**, *97*, 12691–12699.
[13] We are grateful to one of the referees for pointing out this explanation for the different behavior of **1** and **4**.

"Free" $[Fe(tpp)]^+$ Cation: A New Concept in the Search for the Least Coordinating Anion**

Zuowei Xie, Robert Bau, and Christopher A. Reed*

The search for the least coordinating anion is a major thrust of contemporary chemistry.[1, 2] Coordinatively unsaturated cations such as the silylium ion, R_3Si^+, cannot be isolated in condensed media because of the coordinating nucleophilicity of even the best available counterions.[3] $[Fe(tpp)]^+$, the tetraphenylporphyrinatoiron(III) cation, is another long sought after cation[4] and its geometry has become a yardstick for measuring progress towards the noncoordinating anion ideal. In arene solvents, all anions investigated to date either coordinate to or react with iron to form five-coordinate complexes of the type [Fe(tpp)Y]. We now report that $[Fe(tpp)]^+$ can be isolated from arene solvents with no coordination by the anion. The counterion is a novel complex ion formed from Ag^+ and two equivalents of the least coordinating carborane anion currently known, $Br_6CB_{11}H_6^-$. This introduces a conceptually new strategy for preparing weakly coordinating anions.

Treatment of [Fe(tpp)Br] with one equivalent of $Ag(Br_6CB_{11}H_6)$[5] in dry *p*-xylene at 100 °C, removal of the AgBr precipitate, and vapor diffusion of *n*-hexane gave purple crystals of **1** suitable for X-ray structure determination.[6]

$[Fe(tpp)][Ag(Br_6CB_{11}H_6)_2]\cdot 4(p\text{-xylene})$ **1**

As the stereoscopic view of the packing in the crystal shows (Fig. 1), the crystal structure consists of well-separated, alternating layers of $[Fe(tpp)]^+$ cations and $[Ag(Br_6CB_{11}H_6)_2]^-$ anions. The apparent voids in the structure are filled by several interspersed *p*-xylene solvent molecules (not shown). The complementary sizes of the anion and cation probably contribute to the stabilization of the layered ionic lattice.

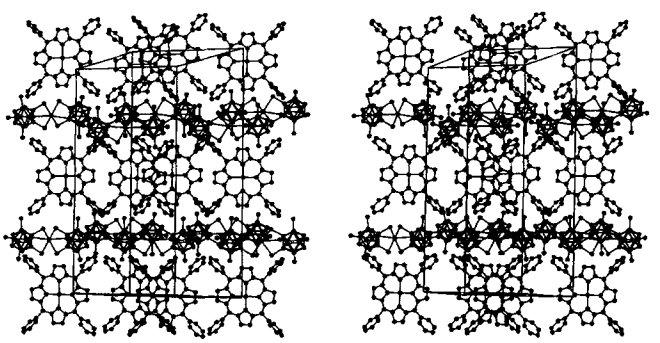


Fig. 1. Stereoscopic view of the packing diagram for **1**. Solvent molecules are omitted for clarity.

The anion (Fig. 2) is a novel variant of the $[AgX_2]^-$ type where X is the icosahedral carborane 7,8,9,10,11,12-hexabromo-*closo*-$CB_{11}H_6^-$. Each carborane is η^3-coordinated to silver through three bromine atoms giving overall octahedral coordination around silver. The generally recognized high affinity of silver(I) for halide ligands may contribute to the stability of this complex ion. Its weak coordinating ability must be related to the

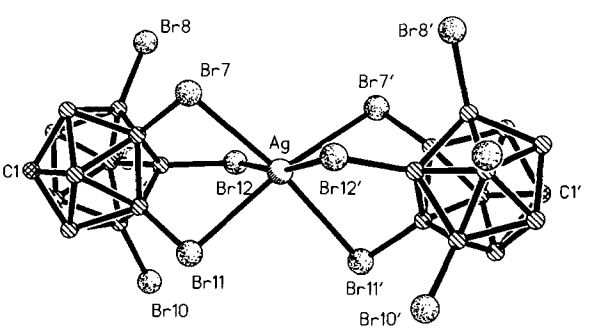


Fig. 2. Perspective view of the anion in **1**: Ag–Br7 = 2.882(3), Ag–Br11 = 2.891(3), Ag–Br12 = 2.865(3) Å.

[*] Prof. C. A. Reed, Dr. Z. Xie, Prof. R. Bau
Department of Chemistry, University of Southern California
Los Angeles, CA 90089-0744 (USA)
Telefax: Int. code + (213)740-0930

[**] This work was supported by the National Institutes of Health (GM 23851), the National Science Foundation (CHE 9407284), and the Research Corporation (R-171).

effective charge reduction brought about by complexation of $Br_6CB_{11}H_6^-$ to Ag^+. By taking the current least coordinating carborane anion,[3, 5] and halving its overall charge, we have lowered its electrostatic attraction to the $[Fe(tpp)]^+$ cation. This is a new concept for lowering the nucleophilicity of an anion and may become an important new general strategy for synthesizing anions that are less coordinating than any presently known.

The $[Fe(tpp)]^+$ cation is shown in Figure 3 along with the two closest approaching solvent molecules. The iron atom lies nearly

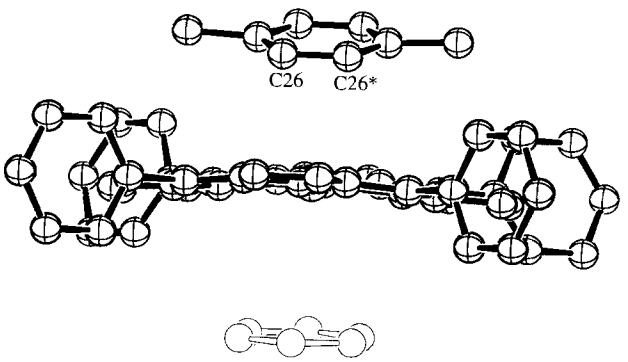


Fig. 3. Perspective view of the $[Fe(tpp)]^+$ cation in **1** with the two closest solvent molecules. The lower *p*-xylene is not well defined crystallographically. Only its arene plane is shown.

in the mean plane of the porphyrin, the Fe–N distances are short (average 1.97(2) Å), and the porphyrin core is slightly ruffled. The porphyrin dimensions are not very different from those of $[Fe(tpp)(FSbF_5)] \cdot C_6H_5F$ (center-to-N distance = 1.974 Å)[7, 8] suggesting that the two closely approaching solvent molecules play a significant role in compensating for the positive charge.

The nature of the solvent interactions can be seen in the side-on view of Figure 3 and the plane projection of Figure 4. The upper *p*-xylene molecule is the more important of the two. It is closer to the porphyrin and is crystallographically well defined by using rigid body refinement procedures. The lower *p*-xylene molecule is about 0.2 Å more distant and, like the other disordered solvent molecules in the lattice, is not well defined crystallographically. Only its arene plane is well defined so we have represented it by an open-bond hexagon. The solvent molecules have many of the general features of π-arene solvates of a number of metalloporphyrins[7, 9, 10] some of which have been shown to have small but demonstrable effects on the coordination geometry.[9] These features include electron-rich carbon atoms relatively close to the metal but not directly over it, a C–C bond approximately straddling a pyrrole N atom, and small dihedral angles between the solvent and porphyrin planes. Some of these features are accentuated in **1**. The dihedral angle of the mean porphyrin plane to the closer, well-defined *p*-xylene plane is 13°, to the other, 5°. The closest approach of a solvent atom to the mean plane of the porphyrin is 2.89 Å to C26. This can be compared to 3.04 Å in [Mn(tpp)]·toluene.[11] The closest Fe–C distance is 2.94 Å to C26, about 0.2 Å shorter than the sum of the covalent radius of Fe^{III} and the van der Waals half-thickness of an arene. The iron atom is drawn 0.07 Å out of the mean plane of the porphyrin core towards the closer, more tilted *p*-xylene.

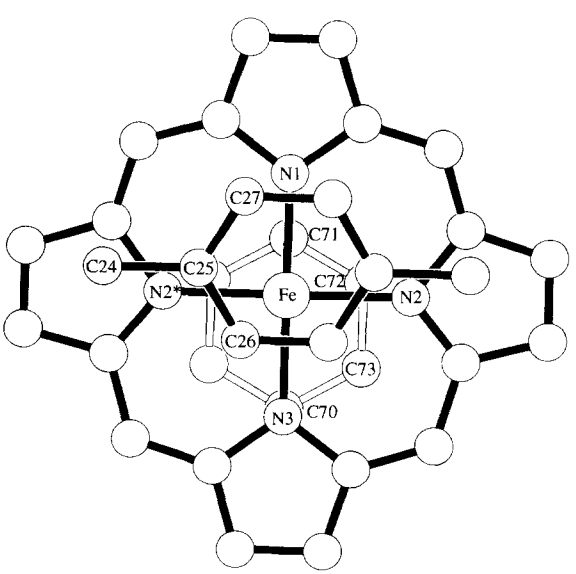


Fig. 4. Projection of the well-defined (front) and less well-defined (hexagon in rear) *p*-xylene molecules onto the mean porphyrin plane.

Thus, the isolation of $[Fe(tpp)]^+$ has been achieved for the first time by providing a) π-donor solvent stabilization of the cation, b) a new least coordinating anion, and c) favorable lattice energetics. The close approach of arene solvent molecules to $[Fe(tpp)]^+$ blurs the distinction between axial ligand and solvate and suggests a continuum between these definitional ideals. Indeed as modern chemistry explores the nature of weak interactions, a vacant coordination site in cationic complexes is becoming increasingly an operational definition rather than a persistent reality.

Received: July 19, 1994 [Z 7143 IE]
German version: *Angew. Chem.* **1994**, *106*, 2566

[1] K. Seppelt, *Angew. Chem. Int. Ed. Engl.* **1993**, *32*, 1025-1027; *Angew. Chem.* **1993**, *105*, 1074-1076; M. Bochmann, *ibid.* **1992**, *31*, 1181-1182 and **1992**, *104*, 1206-1207.
[2] S. H. Strauss, *Chem. Rev.* **1993**, *93*, 927-942.
[3] C. A. Reed, Z. Xie, R. Bau, A. Benesi, *Science* **1993**, *262*, 402-404; G. A. Olah, L. Heiliger, X.-Y. Li, G. K. S. Prakash, *J. Am. Chem. Soc.* **1990**, *112*, 5991-5995; J. B. Lambert, S. Zhang, S. M. Ciro, *Organometallics* **1994**, *13*, 2430-2443.
[4] K. Shelly, C. A. Reed, Y. J. Lee, W. R. Scheidt, *J. Am. Chem. Soc.* **1986**, *108*, 3117-3118.
[5] Z. Xie, T. Jelinek, R. Bau, C. A. Reed, *J. Am. Chem. Soc.* **1994**, *116*, 1907-1913.
[6] Crystal data: purple, $0.2 \times 0.15 \times 0.25$ mm, monoclinic, $C2/m$; $a = 20.984(4)$, $b = 34.980(7)$, $c = 15.994(3)$ Å, $\beta = 129.48(3)°$; $V = 9013(3)$ Å^3, $Z = 4$, $\rho = 1.77$ g cm^{-3}. Data collection: $Cu_{K\alpha}$, 15 kW, 123 K, $2\theta = 3.5-103.5°$, 10554 measured reflections, 4729 independent reflections. Full matrix least squares refinement on $|F|^2$ with 3124 reflections having $F > 4\sigma(F)$, direct methods (SHELXL-93), 436 parameters, calculated H atom positions, Lorentzian polarization, absorption correction, $\mu = 9.547$ mm^{-1}, max 1.00, min 0.365; residual electron density max 0.96, min -0.76 e Å^{-3}, $R = 0.0875$. Further details of the crystal structure investigation are available on request from the Director of the Cambridge Crystallographi Data Centre, 12 Union Road, GB-Cambridge CB2 1EZ (UK), on quoting the full journal citation.
[7] K. Shelly, T. Bartczak, W. R. Scheidt, C. A. Reed, *Inorg. Chem.* **1985**, *24*, 4325-4330.
[8] The center-to-N distance in $[Fe(tpp)(CB_{11}H_{12})]$ is shorter (1.955 Å) but the porphyrin core is significantly more ruffled [4]. Different degrees of ruffling complicate direct comparisons of center-to-N or Fe–N distances amongst related porphyrinatoiron(III) structures.
[9] M. M. Williamson, C. L. Hill, *Inorg. Chem.* **1985**, *24*, 2836-2841.
[10] W. R. Scheidt, Y. J. Lee, *Struct. Bonding (Berlin)* **1987**, *64*, 1-70.
[11] J. F. Kirner, C. A. Reed, Y. J. Lee, W. R. Scheidt, *J. Am. Chem. Soc.* **1977**, *99*, 1093-1101.

$[(Cp^{**}CoH)_2$-μ-$\{\eta^2:\eta^2$-*cis*-μ-$[(C_2H_5)_2Al-CH=CH-Al(C_2H_5)_2]\}]$ and $[\{Cp^*(\eta^2-C_2H_4)CoAl(C_2H_5)\}_2]$: Synthesis and Structure of Unusual Co–Al Cluster Compounds**

Jörg J. Schneider,* Carl Krüger, Matthias Nolte, Ingo Abraham, Teja S. Ertel, and Helmut Bertagnolli

Dedicated to Professor Borislav Bogdanović on the occasion of his 60th birthday

To date, only a few heteronuclear organometallic compounds with transition metal–aluminum bonds are known.[1] In contrast, intermetallic phases such as Co_2Al_5 (Al–Al 2.88, Co–Al 2.43 Å) and Co_2Al_9 (ninefold coordinated Co centers, Al–Al 2.83, Co–Al 2.47 Å) are well characterized.[2] This indicates that compounds with Co–Al bonds are, in principle, stable. The structures of organometallic compounds with this combination of elements could not be determined until now, although the syntheses of $[Co_3(CO)_9Al]$[3] and $[(CO)_3(PMe_3)CoAl\{(NMe_2)(CH_2)_3\}(CH_2tBu)]$[1e] have been reported. Direct Ni–Al interactions have been discussed for the Ni^0-catalyzed alkylaluminum/alkene exchange reaction (nickel effect).[4, 5] Our investigations into the synthesis of homonuclear hydridocobalt cluster compounds show that aluminum bonds directly to alkenyl complex fragments with Group 8 transition metals. In the course of the synthesis, cobalt–aluminum clusters are formed as intermediates. We report here on their structural characterization by means of single-crystal structure analyses and EXAFS spectroscopy. Shortly after our work had been submitted, Schnöckel et al. had success with the first structure determination of a cluster with Ni–Al bonds.[6]

The aluminum hydride **1** reacts slowly with **2** at 60–70 °C to form ethylene and ethane. During the subsequent alcoholysis with methanol or ethanol at −78 °C in pentane, the reaction solution changes color immediately from brown to blackish red. The workup and the fractional crystallization of the reaction mixture leads to the paramagnetic clusters **3** and **4**, as well as the diamagnetic **5**.[7]

$$[Cp^*Co(\eta^2\text{-ethene})_2] + [(C_2H_5)_2AlH] \xrightarrow[-C_2H_5]{70\,^\circ C,\ CH_3C_6H_5} \xrightarrow[C_2H_5OH]{-78\,^\circ C} [(Cp^*Co)_2H_3] + [(Cp^*Co)_3H_4] + [(Cp^*Co)_4H_4]$$

2 **1** **3** **4** **5**

The aprotic workup of the reaction mixture of **1** and **2** in the absence of alcohol (pentane extraction, fractional crystallization of the raw product from ether/pentane) resulted in a 20–30% yield of reddish brown crystals with the analytical composition of **6** as well as unconverted starting material.

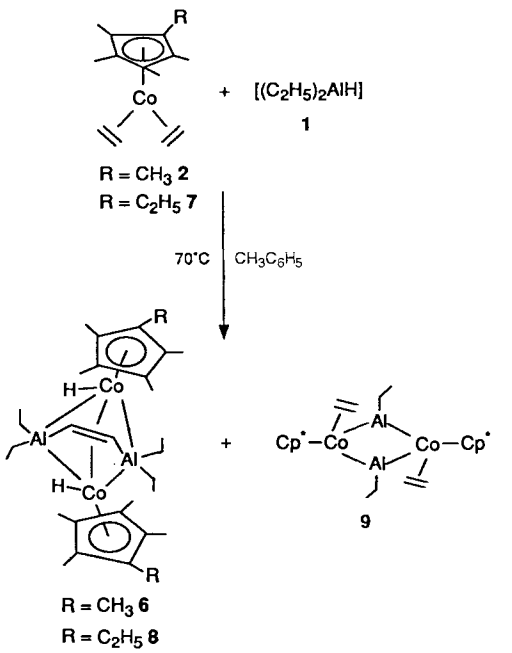
[*] Priv.-Doz. Dr. J. J. Schneider,[+] Prof. Dr. C. Krüger, Dr. M. Nolte
Max-Planck-Institut für Kohlenforschung
Kaiser-Wilhelm-Platz 1, D-45470 Mülheim an der Ruhr (FRG)

[+] New address: Institut für Anorganische Chemie
der Universität–Gesamthochschule
Universitätsstrasse 5–7, D-45117 Essen (FRG)
Telefax: Int. code + (201)183-2402

Dipl.-Phys. I. Abraham, Dr. T. S. Ertel, Prof. Dr. H. Bertagnolli
Institut für Physikalische Chemie der Universität Stuttgart

[**] We thank one of the reviewers for his valuable comments, the Fonds der Chemischen Industrie for financial support, and the Deutsche Forschungsgemeinschaft (Heisenberg Fellowship to J.J.S.). The single-crystal X-ray structure analyses were carried out by C. K. and M. N., the EXAFS analyses by I. A., T. S. E. and H. B. Abbreviations: Cp* = η^5-pentamethylcyclopentadienyl, Cp** = η^5-1,2,3,4-tetramethyl-5-ethylcyclopentadienyl.

A ^{13}C NMR spectrum of **6** with a complete signal set could not be obtained because of the low solubility of the substance. In order to solve the structure of this compound, we attempted to improve the solubility and the crystallization behavior by varying the Cp ligand.



Reaction of the corresponding Cp** starting material **7** with **1** under the same reaction conditions as for the synthesis of **6** led to the analogous compound **8**. The yields of the crystalline product **8** were also between 20–30%. Compounds **6** and **8** gave comparable spectroscopic data. In the mass spectrometer, both decomposed on evaporation in the temperature range 130–150 °C; consequently mainly fragment ions could be observed in the spectra. The most intense signals (100%) in the mass spectra of **6** and **8** are found at *m/z* 527 and 555, respectively. The molecular ions had only low intensity. The sudden formation of ethane could be detected at the beginning of the evaporation of both compounds. The ^1H NMR spectra of **6** and **8** confirm the presence of two hydridic hydrogen atoms; their signals lie in the shift region typical for transition metal hydrides at $\delta = -17.90$ for **6** and $\delta = -18.02$ for **8**. In the IR spectrum of **8** the very broad Co–H stretching vibration lies at 1810 cm^{-1} ($\tilde{\nu}_{1/2}$ = 40 cm^{-1}). A clear designation of the Co–H stretching vibration is not possible for the Cp* derivative **6**. The ^1H NMR signals at $\delta = 1.85$ for **8** and at $\delta = 1.90$ for **6** can be attributed to protons on a C_2 alkene unit. The protons of the various ethyl groups of **8** appear in the ^1H NMR spectrum as three signal groups (each as the expected quartet and triplet).

The molecular structure of the Cp** derivative **8** was solved by means of a crystal structure analysis[8] (Fig. 1). We assume that the Cp* compound **6** has a corresponding structure. In **8**, two 15VE (Cp**CoH) complex fragments, each of which is η^2-bonded to the π-system of the bridging C_2 unit, are connected through a dialuminioethene unit over a twofold axis. One terminal ethyl group of each $[Al(C_2H_5)_2]$ unit is disordered in the crystal. The positions of the hydridic protons on the Co atoms were determined during the resolution of the structure and refined. The nonbonding distance of 3.503 Å between the two Al atoms is very large, even larger than the Co–Co distance

 © VCH Verlagsgesellschaft mbH, D-69451 Weinheim, 1994 0570-0833/94/2323-2435 $ 10.00+.25/0

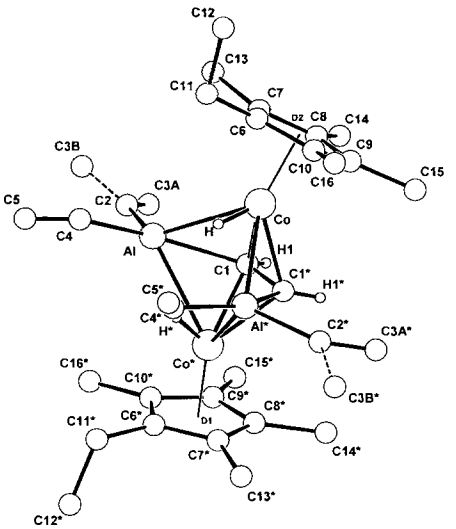


Fig. 1. Molecular structure of **8** in the crystal. Hydrogen atoms on the Cp** rings and on the ethyl groups are not shown. The positions of the carbon atoms C2 and C3 on Al and Al* are disordered (dashed lines). Selected distances [Å] and angles [°]: Co-Al 2.604(1), Co-Al* 2.591(2), Co-C1 1.992(4), Co-Cl* 1.986(4), Al-C1 2.088(4), Co-C6 2.030(4), Co-C7 2.052(4), Co-C8 2.065(5), Co-C9 2.080(5), Co-C10 2.050(4), C1-C1* 1.363(5); C1*-Co-Al 52.1(1), C1*-Co-H 88(2), C1*-Co-Al 81.8(1), Al*-Co-H 47(2), Co-Al-H 57(2), Co*-Al-C1 48.7(1), C1-Al-Co 48.7(1), C1*-C1-Co 70.2(2), Co*-C1-Co 114.2(2), Al-C1-Co 79.3(1).

(Co–Co* 3.338 Å). Because of the absence of an Al–Al bond, the C_2 unit in **8** can be described as a *cis*-dimetalated olefin.[9]

The reaction of **1** with **2** or **7** can be formally considered as the addition of a Lewis acid complex to a coordinatively unsaturated hydrocarbon. This reaction type presents a route to dimetallacycloalkenes.[10] Until now, two structurally characterized examples of this class of compounds existed which contain aluminum.[11] In these, the Al–Al distances of 3.37 Å[11a] and 3.47 Å[11b] are of the same order of magnitude as that in **8**, and are also to be regarded as nonbonding. The length of the olefinic C=C bond in **8** (1.363(5) Å) is comparable with that of other dimetalated olefins[9, 10, 11a] and also only slightly different from that in free ethene (1.34 Å). This would indicate a stronger contribution of the alkene-$\sigma \rightarrow$ donor portion than that of the metal-$\sigma \rightarrow \pi$-acceptor portion to the bond of the Co-dimetallioalkene molecular fragment, which ultimately leads to the short μ-η^2:η^2-coordinated C=C bond in **8**. An almost ideal planar ordering of all four atoms C1, C1*, Al, and Al* was determined for the dialuminioolefin unit in **8** (maximum deviation from the best plane less than $\pm 1.6 \times 10^{-3}$ Å). This indicates that no significant rehybridization of the sp^2 carbon atoms C1 and C1* towards sp^3 hybridization occurs in the formation of the dialuminioethene unit.[12] The Co–Al distances of 2.604(1) Å and 2.598(1) Å in **8** are surprisingly very long in comparison to the Co–Al contacts in **9** (2.336(1), 2.333(1) Å). The atomic distances of both the Co atoms to the C atoms C1 and C1* of the *cis*-dialuminiometalated bridging ethene ligands in **8** are 1.989 Å on average. They are thus clearly shorter than the corresponding Al–C distances to the π bonds of the *cis*-dimetalated olefin units (2.35 Å) in dimeric 1,4-dichloro-2,3,5,6-tetramethyl-1,4-dialumina-2,5-cyclohexadiene.[11a] Structurally characterized complexes of μ-η^2:η^2-bridging alkene ligands, as first observed in **8** for cobalt compounds, were very rare until now (M = Zr,[13] Hf,[14] Sm[15]). An example of a C_2 carbon fragment as a σ-μ-π bridge for four metal atoms is as yet unknown.

When important structural parameters from single-crystal structure analyses are missing, an alternative method for obtaining valuable information on characteristic M–M atomic distances in organometallic complexes is EXAFS spectroscopy. No structural data for **6** is available from single-crystal structure analyses at present. An analysis of the Co-K EXAFS spectra[16] of polycrystalline samples of **6** and **8** show, however, that an analogous structure can be assumed for both. The Fourier transforms of the k^3-weighted $\chi(k)$ functions reveal two coordination shells for the Co atoms in **6** and **8**. The first coordination shell is formed from C atoms at a distance of 2.06(1) Å, the second coordination shell from Al atoms at a distance of 2.56(3) Å (**6**) and 2.59(3) Å (**8**). The Co–Cp_{ring} distances and the Co–Al distances in **6** and **8** determined by the EXAFS method agree very well with those determined in **8** by the single-crystal structure analysis.

The attack of the organoaluminum component on the organocobalt starting materials **2** and **7**, and the π-precoordination of the ethene ligands on the cobalt center are possibly crucial for the formation of the new complex types **6** and **8**. The CH acidity of the protons of the coordinated ethene is greatly increased in this way, and these ligands can thus be eliminated more easily in a consecutive reaction.

A second organometallic component **9** is additionally formed in low yield (< 2%) in the form of red crystals from the product mixture of the reaction of **1** with **2**. In addition to the mass spectroscopic identification, **9** was also characterized by a crystal structure analysis (Fig. 2).[8] We have not yet been able

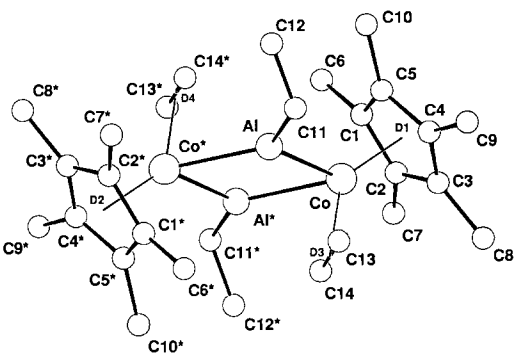


Fig. 2. Molecular structure of **9** in the crystal. Hydrogen atoms not shown. Selected distances [Å] and angles [°]: Al-Al* 2.663(3), Co-Al 2336(1), Co-Al* 2.333(1), Al-C(11) 1.976(3); Co*-Al-Co 110.4(1), Al*-Co-Al 69.6(1), Co-Al-C(11) 123.8(1), Co*-Al-C(11) 125.7(1), C(13)-Co-Al 68.9(1), Al-C(11)-C(12) 119.1(3).

to investigate an analogous product to **9** in the case of the reaction of the Cp** derivative **7**. Formally the two 16VE [Cp*(η^2-ethene)Co] units in **9** are linked by [Al(C_2H_5)] groups. The four-membered ring in **9** is planar, and **9** crystallizes around an inversion center C_i. Due to the space group symmetry, all ligands on the metal atoms are thus arranged as *trans* pairs. No bond exists between the two Co atoms (Co–Co* 3.835(0) Å). The Co–Al distances are 2.336(1) and 2.333(1) Å, and are thus significantly shorter than the distances in **6** and **8**. Comparable data for organometallic compounds do not exist as yet, as **6**, **8**, and **9** are prototypes for such Co–Al clusters. The distance between the two aluminum atoms in **9** of 2.663(3) Å fits reasonably well into the range of Al–Al distances that have already been determined for dimeric alkylaluminum compounds and lies in the region of a bonding Al–Al interaction.[18]

The reaction that leads to the buildup of the heterodinuclear cluster **9**, can be considered as a bimolecular elimination.[23] Al–C bond cleavage occurs at the Co center, resulting elimination of ethane and the formation of Al–Co bonds.

Experimental Procedure

6, **9**: Compound **2** (2.57 g, 10.3 mmol) was dissolved in toluene (100 mL). **1** (1.9 mL, 17 mmol) was added and the mixture stirred at 70 °C for 12 h. The solvent was removed from the resulting reddish brown solution under reduced pressure, and the oily semicrystalline residue extracted first with pentane, then with ether. The greater part of both extracts consisted of red crystals of **6** (pentane, −30 °C); 360 mg (24.2%). MS (EI, 70 eV, evaporation temperature 140 °C), 557(32), 527(100), 471(22), 386(28), 353(28), 264(23), 133(15), 57(26), 28(28), 27(63). – ^{1}H NMR (200 MHz, C_6D_6, 27 °C, TMS): $\delta = -17.9$ (s, 2H), 0.50 (q, 4H), 0.93 (q, 4H), 1.62 (s, 30H), 1.62 (t, 6H, COSY), 1.72 (t, 6H), 1.90 (s, 2H, HC=). – ^{13}C NMR (100 MHz, C_6D_6, 27 °C, TMS): $\delta = 10.1$ (Cp*), 12.47, 12.52, 90.2 (Cp*). – IR (KBr): $\tilde{\nu}$[cm^{-1}] = 525(s), 580(s, br), 620(s), 890(vs), 945(m), 980(m), 1025(s), 1085(s), 1380(vs), 1405(m), 1460(vs, br), 2850, 2910(vs). In addition to this, a few reddish orange crystals of **9** were isolated from the mother liquor. MS (EI, 70 eV, evaporation temperature 160 °C), *m/z* (%): 556(59) [M^+], 528(100), 500(49), 440(41), 377(52), 353(27), 264(32), 27(77). After prolonged cooling at −78 °C, starting material **2** (1.3 g, 5.2 mmol) also crystallized from the pentane extract.

8 was synthesized analogously to **6** by reaction of **7** with **1** (stoichiometry 1:1). Reddish brown crystals of **8** were obtained from the crude oily reaction product by dissolving in diethylether/acetonitrile (3:1) and then cooling slowly, first to 0 °C then to −30 °C. Still more **8** can be obtained, in total up to a yield of approx. 30%, by prolonged cooling of the mother liquor at −30 °C. 555(100), 530(15), 499(45), 278(34), 57(19), 30(12), 28(47). – ^{1}H NMR (200 MHz, C_6D_6, 27 °C, TMS): $\delta = 2.33$ (q, 4H, CH_2 on Cp**), 1.85 (s, 2H, HC=), 1.69 (t, 6H), 1.61 (s, 12H, CH_3 on Cp**), 1.54 (s, 12H, CH_3 on Cp**), 1.54 (t, 6H, COSY-assignment), 0.87 (q, 4H), 0.69 (t, 6H), 0.46 (q, 4H), −18.01 (s). – ^{13}C NMR (100 MHz, C_6D_6, 27 °C, TMS) $\delta = 10.0$, 12.52, 12.56, 14.3, 19.1, 37.7, 89.7, 90.6, 95.5. – IR (KBr): $\tilde{\nu}$ [cm^{-1}] = 2990–2840 (vs), 1820 (m, Co-H), 1480 (m), 1450 (vs), 1405 (s), 1380 (s), 1370 (s), 1305 (m), 1090 (vs), 1050 (s), 1030 (s), 980 (s, br), 950 (s), 910 (s), 895 (vs), 625 (vs), 580 (s), 530 (s), 500 (s). Satisfactory elemental analyses for C, H, Al, and Co were obtained for **6** and **8**.

Received: April 19/ July 27, 1994
Revised version: September 1, 1994 [Z6862/7177IE]
German version: *Angew. Chem.* **1994**, *106*, 2537

[1] a) R. A. Forder, M. L. H. Green, R. E. MacKenzie, J. S. Poland, K. Prout, *J. Chem. Soc. Chem. Comm.* **1973**, 426; b) R. A. Forder, K. Prout, *Acta Crystallogr. Sect. B* **1974**, *30*, 2312; c) S. J. Rettig, A. Storr, B. S. Thomas, J. Trotter, *ibid.* **1974**, *30*, 666; d) J. M. Burlitch, M. E. Leonowicz, R. B. Petersen, R. E. Hughes, *Inorg. Chem.* **1979**, *18*, 1097; e) R. A. Fischer, J. Behm, T. Priermeier, W. Scherer, *Angew. Chem.* **1993**, *105*, 776; *Angew. Chem. Int. Ed. Engl.* **1993**, *32*, 746.

[2] P. J. Black, *Acta Metall.* **1956**, *4*, 172.

[3] K. E. Schwarzhans, H. Steiger, *Angew. Chem.* **1972**, *84*, 587; *Angew. Chem. Int. Ed. Engl.* **1972**, *11*, 535.

[4] a) G. Wilke, *Angew. Chem.* **1988**, *100*, 189; *Angew. Chem. Int. Ed. Engl.* **1988**, *27*, 185; b) *Nova Acta Leopold.* **1991**, *NF65 277*, 105.

[5] K. R. Pörschke, W. Kleimann, Y. H. Tsay, C. Krüger, G. Wilke, *Chem. Ber.* **1990**, *123*, 1267.

[6] C. Dohmeier, H. Krautscheid, H. Schnöckel, *Angew. Chem.* **1994**, *106*, 2570; *Angew. Chem. Int. Ed. Engl.* **1994**, *33*, 2482.

[7] J. J. Schneider, *Z. Naturforsch. B.* **1994**, *49*, 691.

[8] Crystal structure analysis of **8**: $C_{32}H_{60}Al_2Co_2$, $M = 616.7$, crystal size $0.28 \times 0.28 \times 0.46$ mm, monoclinic, space group $C2/c$ (No. 15), $a = 20.230(6)$, $b = 8.723(1)$, $c = 19.922(4)$ Å, $\beta = 106.24(2)°$, $V = 3375.0$ Å^3, $T = 20$ °C, $\rho_{calcd} = 1.21$ g cm^{-3}, $\mu = 10.50$ cm^{-1}, $Z = 4$, Enraf-Nonius CAD4 diffractometer, $\lambda = 0.71069$ Å, measurement method $\omega-2\theta$, 4226 measured reflections [$\pm h, +k, +l$], $[\sin\theta/\lambda]_{max}$ 0.65 Å^{-1}, 3969 independent and 2817 observed reflections [$I > 2\sigma(I)$], 175 refined parameters. The H atomic positions on Co and C1 (Co* and C1*) were found and used in the least-squares refinement, all other H atomic positions were calculated and not used in the least-squares refinement. The positions of the carbon atoms C2 and C3 in the ethyl group are disordered and refined with occupation factors 70:30. $R = 0.053$, $R_w = 0.062$ [$w = 1/\sigma^2(F_0)$], max. residual electron density 0.67 e Å^{-3}. Crystal structure analysis for **9**: $C_{28}H_{48}Al_2Co_2$, $M = 556.6$ g mol^{-1}, crystal size $0.32 \times 0.39 \times 0.46$ mm, monoclinic, space group $P2_1/c$ (No. 14), $a = 8.486(1)$, $b = 17.989(7)$, $c = 9.792(2)$ Å, $\beta = 106.89(1)°$, $V = 1430.3$ Å^3, $\rho_{calcd} = 1.29$ g cm^{-3}, $\mu = 12.32$ cm^{-1}, $F(000) = 592$ e, $Z = 2$, Enraf-Nonius CAD4 diffractometer, $\lambda = 0.71069$ Å, measurement method $\omega-2\theta$, 5412 measured reflections [$\pm h, +k, +l$], $[\sin\theta/\lambda]_{max}$ 0.74 Å^{-1}, 4962 independent and 3808 observed reflections [$I > 2\sigma(I)$], 145 refined parameters, heavy atom method, H atomic positions on the Cp* rings and on the ethyl groups were calculated and not used on least-squares refinement, the H atomic positions on the ethene groups were found and used in the refinement. $R = 0.047$, $R_w = 0.062$ [$w = 1/\sigma^2(F_0)$], max. residual electron density 0.63 e Å^{-3}. Further details of the crystal structure investigation may be obtained from the Fachinformationszentrum Karlsruhe, D-76344 Eggenstein-Leopoldshafen (FRG) on quoting the depository number CSD-58292.

[9] a) D. M. Hoffman, R. Hoffman, *Organometallics* **1982**, *1*, 1299; b) J. T. Mague, *Polyhedron* **1992**, *11*, 677; c) M. Cowie, G. Vasapollo, B. R. Sutherland, J. P. Emett, *Inorg. Chem.* **1986**, *25*, 2648; d) J. T. Mague, *ibid.* **1983**, *22*, 45; e) F. R. Lemke, D. Szalda, R. M. Bullock, *J. Am. Chem. Soc.* **1991**, *113*, 8466; f) W. Kaminski, J. Kopf, G. Thirase, *Liebigs Ann. Chem.* **1974**, 1531.

[10] a) W. Beck, B. Niemer, M. Wieser, *Angew. Chem.* **1993**, *105*, 969; *Angew. Chem. Int. Ed. Engl.* **1993**, *32*, 923; b) D. L. Thorn, R. L. Harlow, *J. Am. Chem. Soc.* **1989**, *111*, 2575.

[11] a) H. Schnöckel, M. Leimkühler, R. Lotz, R. Mattes, *Angew. Chem.* **1986**, *98*, 929; *Angew. Chem. Int. Ed. Engl.* **1986**, *98*, 929; b) H. Hoberg, V. Gotor, A. Milchereit, C. Krüger, J. C. Sekutowski, *ibid.* **1977**, *89*, 563 or **1977**, *16*, 539.

[12] C. Krüger, J. C. Sekutowski, H. Hoberg, R. Krause-Göing, *J. Organomet. Chem.* **1977**, *141*, 141.

[13] F. A. Cotton, P. A. Kibala, *Polyhedron* **1987**, *6*, 645.

[14] a) F. A. Cotton, P. A. Kibala, *Inorg. Chem.* **1990**, *29*, 3192; b) W. Kaminski, J. Hopf, H. Sinn, H. J. Vollmer, *Angew. Chem.* **1976**, *88*, 688; *Angew. Chem. Int. Ed. Engl.* **1976**, *15*, 629.

[15] W. J. Evans, T. A. Ullibarri, J. W. Ziller, *J. Am. Chem. Soc.* **1990**, *112*, 219.

[16] EXAFS measurements on **6** and **8**: Transmission EXAFS measurements were made on polycrystalline samples of **6** and **8** ground with polyethylene at the HASYLAB in Hamburg on the RÖMO II station. Si(311) double crystal monochromator, 30% I_0 reduction with suppression of higher orders by tilting the crystal, N_2 ionization chamber for the I_0 and I_1 measurements, measurement region 7630–8715 eV, measurement points above the absorption edge equidistant in k space, $\Delta k = 0.04$ Å^{-1}, absorption spectra analyzed according to ref. [17]. The positions of the absorption edges in **6** and **8** were determined by folding the region of the spectra near the absorption edge with a group of Gauss functions [17]. The $k^3\chi(k)$ functions for 2 Å$^{-1} \le k \le 12.5$ Å were fitted after Fourier filtering in r space (rectangular window, 1.18 Å $\le r \le$ 2.48 Å for **6**, 1.02 Å $\le r \le$ 2.26 Å for **8**). Scattering amplitude, scattering phases, $S_0^2(k)$ and $\lambda(k)$ according to FEFF V3.1. Fit parameters: R, N, and σ^2 for every coordination shell in **6** and **8**.

[17] T. S. Ertl, H. Bertagnolli, S. Hückmann, U. Kolb, D. Peter, *Appl. Spectrosc.* **1992**, *46*, 690.

[18] D. J. Brauer, C. Krüger, *Z. Naturforsch. B* **1979**, *34*, 1293; ($Al_{van\ der\ Waals}$: 1.531 Å). With reference to $[Al_7Te_{10}]$ (Al–Al 2.660(1) Å) [19], $[\{CH(SiMe_3)_2\}_4Al_2]$ (Al–Al 2.660(1) Å) [20], and $[K_2\{Al(iBu)_{12}\}]$ (Al–Al 2.685 Å) [21], as well as to $[\{\eta^5\text{-Cp*}\}Al]_4$ (Al–Al 2.773(4) Å) [22], the assumption of Al–Al bonds would appear justified. This results in the formulation of **9** as bicyclo[1.1.0]-1,3-dicobalta-2,4-dialuminabutane. Taking the 18 VE rule into consideration, no Al–Al bond can be formulated for **9**, which then results in its formulation as 1,3-dicobalta-2,4-dialuminacyclobutane.

[19] R. Nesper, J. Curda, *Z. Naturforsch. B* **1987**, *42*, 557.

[20] W. Uhl, *Z. Naturforsch. B* **1989**, *43*, 1113.

[21] W. Hiller, K.-W. Klinkhammer, W. Uhl, J. Wagner, *Angew. Chem.* **1991**, *103*, 182; *Angew. Chem. Int. Ed. Engl.* **1991**, *30*, 179.

[22] a) C. Dohmeier, C. Robl, M. Tacke, H. G. Schnöckel, *Angew. Chem.* **1991**, *103*, 594; *Angew. Chem. Int. Ed. Engl.* **1991**, *30*, 564; c) S. Schulz, H. W. Roesky, H. J. Koch, G. M. Sheldrick, D. Stalke, A. Kuhn, *ibid.* **1993**, *105*, 1828 bzw. **1993**, *32*, 1729.

[23] Examples for comparable reactions MR + M′H → M–M′ + RH are known for a series of bimetal combinations M–M′, such as Mo/Al, W/Al, Mo/Ga. See also [10b] and D. G. Tuck in *Comprehensive Organometallic Chemistry, Vol. 1* (Ed.: G. Wilkinson), Pergamon, Oxford, **1982**, p. 954.

Antenna Effect in Multichromophoric Cyclodextrins**

Ludovic Jullien, Josette Canceill, Bernard Valeur,* Elisabeth Bardez, and Jean-Marie Lehn*

By analogy with the antennae pigments of photosynthetic units,[1] a *photochemical antenna* consists of an assembly of chromophores such that 1) the photon-harvesting efficiency is high owing to a large overall cross-section for light absorption and 2) excitation energy is conveyed from the chromophores (directly or after hops from chromophore to chromophore) to an energy acceptor, which converts the absorbed light energy. This acceptor can be a light-emitting species (a lanthanide ion or an organic fluorophore), so that the incident light is converted into light at higher wavelengths; an example is provided by complexes between lanthanide ions and polypyridine ligands,[2] which are promising fluorescent labels for chemical and biological purposes. Other antenna-based photochemical molecular devices can be designed;[3] polynuclear metal complexes have received special attention in this context.[4] The antenna effect has also been studied in light-harvesting polymers having chromophores substituted at intervals along the chains.[5, 6] In the multichromophoric β-cyclodextrins (β-CD) reported to date, the position of the chromophores is much better spatially defined, which is a distinct advantage for the understanding of the energy hopping process.[7, 8] In the course of our work on these systems, we have prepared a new multichromophoric β-CD to mimic the antenna effect occurring in photosynthetic units. We report here on the very efficient energy transfer from seven 6-carboxy-2-naphthyl antenna chromophores to a merocyanine, DCM-OH, included in the cavity (Fig. 1).

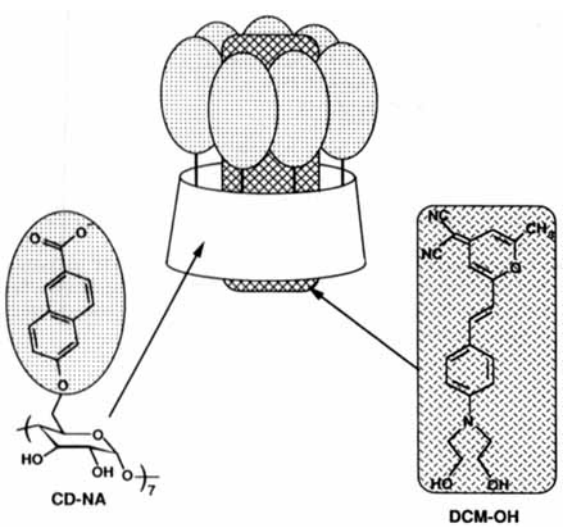


Fig. 1. Schematic representation of the complex between the heptanaphthoate β-cyclodextrin (CD-NA) and the merocyanine DCM-OH.

[*] Prof. Dr. B. Valeur, Dr. E. Bardez
Laboratoire de Chimie Générale (CNRS ER 77)
Conservatoire National des Arts et Métiers
292 rue Saint-Martin, 75003 Paris (France)
Telefax: Int. code + (1)40 27 23 62

Prof. Dr. J.-M. Lehn, Dr. L. Jullien, Dr. J. Canceill
Chimie des Interactions Moléculaires (CNRS UPR 285)
Collège de France
11 Place Marcelin Berthelot, 75005 Paris (France).
Telefax: Int. code + (1)44 27 13 56

[**] This work was supported by the Centre National de la Recherche Scientifique (CNRS). The authors thank Dr. R. Pansu, Ecole Normale Supérieure, Cachan, for his help in the fluorescence decay experiments.

The photosensitive β-CD (CD-NA) was dissolved in a buffer at pH 10, so that the chromophores were in the naphthoate form. The absorption and fluorescence spectra are shown in Figure 2. The fluorescence spectrum consists of two bands. The

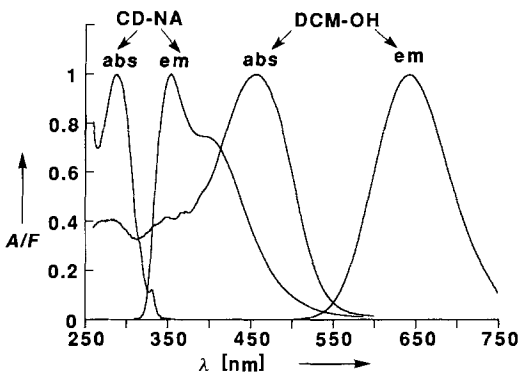


Fig. 2. Absorption and fluorescence spectra of CD-NA and DCM-OH in a buffer at pH 10 containing 5% (v/v) of ethanol; for the sake of clarity, all spectra have been normalized to the same height at the maximum. The molar extinction coefficients at the maximum are 4.35×10^4 and $3.15 \times 10^4\,\text{M}^{-1}\text{cm}^{-1}$ for CD-NA and DCM-OH, respectively; at 300 nm (excitation wavelength), the values are 3.43×10^4 and $1.83 \times 10^4\,\text{M}^{-1}\text{cm}^{-1}$, respectively.

first one with a maximum at 355 nm is similar to the fluorescence spectrum of 2-methoxy-6-naphthoic acid, which at pH 10 is in the naphthoate form. The second band with a maximum at 405 nm is not observed in this model compound under the same conditions; moreover, the excitation spectrum of CD-NA was found to be independent of the observation wavelength (either 355 or 405 nm) and identical to the absorption spectrum. Therefore, the band at 405 nm is assigned to intramolecular excimer formation. Excimers were also identified in β-CD labeled with naphthoyloxy chromophores,[7] but not in those labeled with naphthalene-6-sulfonate residues.[9]

Among dyes that are likely to form an inclusion complex with the cyclodextrin, DCM-OH (4-dicyanomethylene-2-methyl-6-*p*-diethanolaminostyryl-4*H*-pyran),[10] a derivative of the well-known laser dye DCM (4-dicyanomethylene-2-methyl-6-*p*-dimethylaminostyryl-4*H*-pyran), was chosen for the following reasons: 1) good overlap is observed between the absorption spectrum of DCM-OH and the emission spectrum of the naphthoate chromophores (see Fig. 2); 2) its elongated form fits well in the CD-NA interior, and its length is approximately equal to the depth of the cavity plus the length of the linked chromophores; and 3) it is essentially hydrophobic, but partially hydrophilic thanks to the two terminal hydroxyl groups (DCM-OH is fairly soluble in water containing a small amount of ethanol). On the basis of the last two features, efficient complexation of DCM-OH with CD-NA is expected.

Several 2.9 μM solutions of CD-NA in the pH 10 buffer containing 5% (v/v) of ethanol and various amounts of DCM-OH were prepared. The fluorescence of the naphthoate residues (excited at 300 nm) decreases as the concentration of DCM-OH increases. The quenching process can be explained in terms of transfer of excitation energy from the naphthoate residues to DCM-OH; this is confirmed by the concomitant increase in fluorescence intensity of the latter. The contribution of the directly excited DCM-OH molecules (at 300 nm) to this increase was found to be only a small fraction of the overall DCM-OH fluorescence. The evolution of the whole fluorescence spectrum is shown in Figure 3.

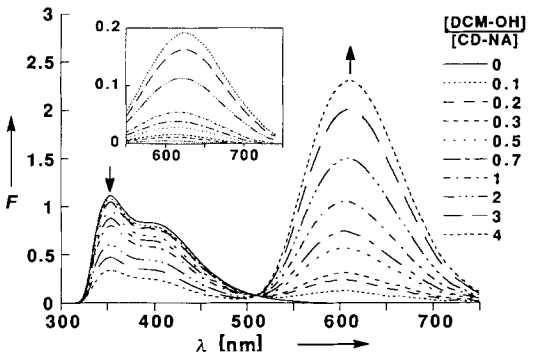


Fig. 3. Evolution of the fluorescence spectrum of a CD-NA solution on addition of DCM-OH in a concentration ratio [DCM-OH]/[CD-NA] = 0 to 4 (solvent: buffer at pH 10 containing 5% (v/v) of ethanol). Excitation wavelength: 300 nm. Insert: contribution from DCM-OH molecules directly excited at 300 nm (this contribution was obtained by measuring the fluorescence spectra upon excitation at 400 nm where CD-NA does not absorb and by multiplication with the ratio of the absorbances at 300 and 400 nm).

The fluorescence decay curves of CD-NA (2.9 μM) upon excitation by a laser pulse at 300 nm were recorded at 355 nm (the time-resolution of the instrument was about 100 ps). In the absence of DCM-OH, the decay is biexponential owing to emission from both monomer and excimer. In the presence of fourfold excess of DCM-OH, the decay was found to be superimposable on the latter (after normalization at the same height at the maximum in order to compensate for the large decrease in fluorescence intensity in the presence of DCM-OH). This means that the efficiency of transfer from the naphthoate chromophores to DCM-OH is very close to 1, and the observed fluorescence at 355 nm is solely due to CD-NA molecules containing no DCM-OH molecule. Considering the very short distances between the naphthoate residues and DCM-OH, both the Förster mechanism (dipole–dipole interaction) and the Dexter mechanism (exchange interaction) are likely to be involved in such a highly efficient energy transfer.

The association of DCM-OH with CD-NA deserves further attention. Information on the complex is provided by fluorescence and circular dichroism spectra. The fluorescence spectrum of DCM-OH is blue-shifted by around 40 nm upon addition of CD-NA, which shows that the averaged microenvironment of DCM-OH is less polar in the complex with CD-NA than in the buffer. More precisely, since the dipole moment of DCM and DCM-OH is much larger in the excited state than in the ground state, a blue shift is due to a reduction of the relaxation of the solvent molecules around the large dipole created upon excitation. Furthermore, the circular dichroism spectrum of DCM-OH in the presence of CD-NA exhibits a positive band in the 380–550 nm range which means[11] that the transition dipole moment of DCM-OH (which is directed along the long axis of the molecule) lies in a cone whose axis is parallel to the symmetry axis of the cyclodextrin.

The stoichiometry of the complex was demonstrated to be 1:1 by means of a Job plot:[12] the variations in fluorescence intensity at 355 nm as a function of the ratio [DCM-OH]/([DCM-OH] + [CD-NA]) at constant [DCM-OH] + [CD-NA] passes through a maximum at 0.5. The most accurate stability constant for the complex was obtained by analysis of the variations in fluorescence intensity at 355 nm as a function of the concentration in DCM-OH. After suitable corrections for inner-filter effects and taking into account the transfer efficiency of 1, a nonlinear least-squares analysis leads to a stability constant of $(1.2 \pm 0.2) \times 10^5$ for the equilibrium (a). Compared to previously

$$\text{CD-NA} + \text{DCM-OH} \rightleftharpoons [\text{DCM-OH} \subset \text{CD-NA}] \quad \text{(a)}$$

reported data on complexes with β-CD molecules,[13] this value is quite high. This can be interpreted in terms of an additional contribution from the naphthoate chromophores: the usual hydrophobic effects operating between the etherlike cyclodextrin walls and lipophilic guests are reinforced by the naphthalene rings of the appended chromophores.

In conclusion, β-cyclodextrins bearing seven naphthoate chromophores form highly stable 1:1 complexes with a merocyanine dye. The antenna effect (i.e., the transfer of excitation energy from the chromophores to the merocyanine) takes place with an efficiency close to 1. It represents a very efficient light conversion process by an absorption–energy-transfer–emission (A–ET–E) sequence in a supramolecular photochemical device.[14] Further studies aimed at the characterization of the excited-state processes are in progress. Other energy acceptors included in the cavity are being considered; special attention is paid to photoreactive acceptors with a view to converting light energy into chemical energy as in natural photosynthetic systems.

Experimental Procedure

CD-NA was prepared from methyl 6-hydroxy-2-naphthoate and heptakis(2,3-di-*O*-acetyl-6-deoxy-6-iodo)cyclomaltoheptanose by nucleophilic substitution [15]. Details of the experimental procedure will be published elsewhere. DCM-OH was synthesized by Dr. J. Bourson according to the general procedure described in ref. [16]. The Britton–Robinson buffer at pH 10 (ionic strength of 0.1 M) was prepared according to ref. [17]. The UV/Vis absorption spectra were obtained with a Kontron Uvikon-940 spectrophotometer. Corrected fluorescence spectra were recorded on a SLM 8000 C spectrofluorometer. All the experiments were performed at 25 °C.

Received: June 27, 1994 [Z 7076 IE]
German version: *Angew. Chem.* **1994**, *106*, 2582

[1] *Antennas and Reaction Centers in Photosynthetic Bacteria* (Ed.: M. E. Michel-Beyerle), Springer, Berlin, **1985**.
[2] B. Alpha, J.-M. Lehn, G. Mathis, *Angew. Chem.* **1987**, *99*, 1310; *Angew. Chem. Int. Ed. Engl.* **1987**, *26*, 266.
[3] V. Balzani, F. Scandola, *Supramolecular Photochemistry*, Ellis Horwood, New York, **1990**.
[4] V. Balzani, in *Photoprocesses in Transition Metal Complexes, Biosystems and Other Molecules. Experiment and Theory* (Ed.: E. Kochanski), Kluwer, Dordrecht, **1992**, p. 233.
[5] J. E. Guillet, *Polymer Photophysics and Photochemistry*, Cambridge University Press, Cambridge, UK, **1985**.
[6] S. E. Webber, *Chem. Rev.* **1990**, *90*, 1469.
[7] M. N. Berberan-Santos, J. Canceill, J. C. Brochon, L. Jullien, J.-M. Lehn, J. Pouget, P. Tauc, B. Valeur, *J. Am. Chem. Soc.* **1992**, *114*, 6427.
[8] M. N. Berberan-Santos, J. Pouget, B. Valeur, J. Canceill, L. Jullien, J.-M. Lehn, *J. Phys. Chem.* **1993**, *97*, 11376.
[9] D. M. Gravett, J. Guillet, *J. Am. Chem. Soc.* **1993**, *115*, 5970.
[10] J. Bourson, D. Doizi, D. Lambert, T. Sacaze, B. Valeur, *Opt. Commun.* **1989**, *72*, 367.
[11] M. Kajtar, C. Horvath-Toro, E. Kuthi, J. Szejtli, *Acta Chim. Acad. Sci. Hung.* **1982**, *110*, 327.
[12] K. A. Connors, *Binding Constants. The Measurement of Complex Stability*, Wiley, Chichester, **1987**.
[13] Y. Inoue, T. Hakushi, Y. Liu, L. H. Tong, B. J. Shen, D. S. Jin, *J. Am. Chem. Soc.* **1993**, *115*, 475.
[14] For A–ET–E conversion in photoactive europium(III) cryptates see ref. [2] and N. Sabbatini, M. Guardigli and J.-M. Lehn, *Coord. Chem. Rev.* **1993**, *123*, 201.
[15] H. H. Baer, A. Vargas Berenguel, Y. Y. Shu, J. Defaye, A. Gadelle, F. Santoyo Gonzalez, *Carbohydr. Res.* **1992**, *228*, 307.
[16] J. Bourson, B. Valeur, *J. Phys. Chem.* **1989**, *93*, 3871.
[17] C. Frugoni, *Gazz. Chim. Ital.* **1957**, *87*, 403.

 © *VCH Verlagsgesellschaft mbH, D-69451 Weinheim, 1994* *0570-0833/94/2323-2439 $ 10.00+.25/0*

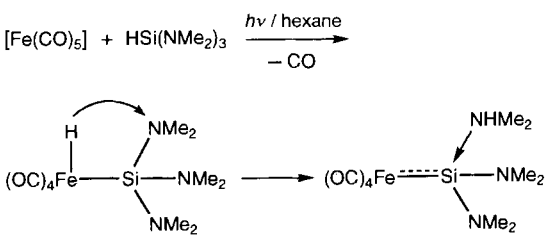
Platinum–Iron Silylene Complexes and Metal-Promoted Substituent Exchange between $Si(NMe_2)_3$ and $P(OEt)_3$ Ligands**

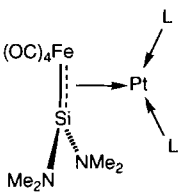
Ulf Bodensieck, Pierre Braunstein,* Werner Deck, Thierry Faure, Michael Knorr, and Christine Stern

The considerable current interest in metal silylene complexes results largely from the need to gain a better understanding of their occurrence, reactivity, and possible role as intermediates in a number of important rearrangements[1] or catalytic reactions, such as the polymerization of silanes or the dehydrogenative coupling of silanes to disilanes.[2]

We reasoned that heterometallic silylenes would represent an important new class of complexes in which the reactivity of the metal–silicon bond could be tuned by varying the nature of the other metal fragment. On the other hand, tris(amino)silyl derivatives of the transition metals should display interesting reactivity patterns, in particular owing to the basicity of the nitrogen atoms. The amino substituents would be expected to have a considerable influence on the properties of the iron–silicon bond. However, the reactivity of tris(amino)silanes towards transition metals has not yet been examined, although tris(amino)silyl complexes have been obtained indirectly.[3] We now attempt to combine these two facets of silicon/transition metal chemistry and report here on the stabilization of a (dimethylamino)silylene complex by an electron-acceptor metal fragment, which leads to formation of heterobimetallic silylene complexes, as well as on an unprecedented iron carbonyl promoted substituent exchange between phosphite and aminosilyl ligands.

In pioneering work, G. Schmid et al. reported the synthesis of the first base-stabilized silylene complex $[Fe(CO)_4\{SiMe_2(NEt_2H)\}]$.[4] We have now synthesized the amine-stabilized bis(dimethylamino)silylene complex **2** by oxidative addition of the Si–H bond of $HSi(NMe_2)_3$ to the photochemically generated $Fe(CO)_4$ species. The hydrido, tris(dimethylamino)silyl complex **1** is the most likely primary product, but is unstable owing to proton migration to the more basic nitrogen atom. However, if tautomer **1** were present in small amounts in the reaction mixture, one could exploit the Fe–H functionality for oxidative addition to a low-valent metal complex with the aim of generating a heterobimetallic complex. This was indeed possible with the isoelectronic system $[HFe\{Si(OMe)_3\}L_4]$ in which the methoxy groups are much less basic than the dimethylamino groups of **1**.[5]





3a L = PPh_3
3b L = $P(p\text{-Tolyl})_3$
3c L_2 = dppe

Reaction of **2** with $[Pt(C_2H_4)(PR_3)_2]$ (R = Ph, *p*-tolyl) resulted in displacement of the dimethylamine ligand from **2** and the Pt-bound ethylene ligand and yielded new complexes, which were assigned the structures **3a,b** on the basis of analytical and spectroscopic data (Table 1). The

Table 1. Selected physical and spectroscopic data for **2**, **3**, **5**, and **6** [a].

2: white powder. FT-IR (KBr): $\tilde{\nu}$(NH) = 3263, (ether): $\tilde{\nu}$(CO) = 1898 (vs), 1910 (vs), 1945 (s), 2024 (s) cm^{-1}; ^1H NMR: δ = 2.21 (s, 18 H; NCH_3); $^{13}C\{^1H\}$ NMR ($CDCl_3$): δ = 39.5 (s, 6C; NCH_3) 216.5 (s, 4C; CO); $^{29}Si\{^1H\}$ NMR: δ = 68.2 (s); MS (FAB^+): *m/z*: 329.0 [M^+].

3a: yellow powder. FT-IR: (toluene): $\tilde{\nu}$(CO) = 1902 (vs, sh), 1938 (m, br), 2009 (vs) cm^{-1}; ^1H NMR (200.1 MHz): δ = 2.52 (s, 12 H; NCH_3); $^{31}P\{^1H\}$ NMR (16 °C): δ = 29.9 (d, ^2J(P,P) = 4, ^1J(P,Pt) = 4884 Hz, 1 P; P *trans* to Fe), 33.3 (d, ^2J(P,P) = 4, ^1J(P,Pt) = 2021 Hz, 1 P; P *trans* to Si); $^{13}C\{^1H\}$ NMR: δ = 39.9 (s, 4C, NMe_2); $^{29}Si\{^1H\}$ NMR (C_6D_6): δ = 113.9 (d, ^2J(Si,P) = 136.4 Hz); MS (FAB^+): *m/z*: 1003.2 [M^+].

3b: yellow powder. FT-IR (toluene): $\tilde{\nu}$(CO) = 1901 (vs sh), 1936 (m br), 2008 (vs) cm^{-1}; ^1H NMR ([D_8]toluene, −15 °C): 2.06 (s, 9 H; CH_3), 2.10 (s, 9 H; CH_3), 2.65 (s, 12 H; NCH_3); $^{31}P\{^1H\}$ NMR ([D_8]toluene, −15 °C): δ = 27.9 (d, ^2J(P,P) = 2.5, ^1J(P,Pt) = 4882 Hz, 1 P; P *trans* to Fe), 32.4 (d, ^2J(P,P) = 2.5, ^1J(P,Pt) = 2053 Hz, 1 P; P *trans* to Si); $^{13}C\{^1H\}$ NMR: δ = 21.0 (s, 3C; CH_3), 21.1 (s, 3C; CH_3), 45.1(s, 4C; NCH_3), 215.4 (s, 4C, CO); $^{195}Pt\{^1H\}$ NMR: δ = −2915 (dd, ^1J(Pt,P^1) = 2041, ^1J(Pt,P^2) = 4876 Hz, 1 Pt; P^1 *trans* to Si, P^2 *trans* to Fe).

3c: yellow powder. FT-IR (toluene): $\tilde{\nu}$(CO) = 1901 (vs sh), 1934 (m br), 2005 (vs) cm^{-1}; ^1H NMR: 1.80 (m, 2 H; CH_2), 2.03 (m, 2 H; CH_2), 2.61 (s, 12 H; NCH_3); $^{13}C\{^1H\}$ NMR: δ = 214.5 (s, 4C, CO); $^{31}P\{^1H\}$ NMR: δ = 52.0 (d, ^2J(P,P) = 18, ^1J(P,Pt) = 4422 Hz, 1 P; P *trans* to Fe), 55.2 (d, ^2J(P,P) = 18, ^1J(P,Pt) = 1840 Hz, 1 P; P *trans* to Si).

5: pale brown crystals. FT-IR (THF): $\tilde{\nu}$(CO) = 1853 (m br), 1940 (vw) cm^{-1}; ^1H NMR: δ = 1.29 (t, ^3J(H,H) = 7.0 Hz, 3 H; $POCH_2CH_3$), 1.33 (t, ^3J(H,H) = 7.0 Hz, 6 H; $SiOCH_2CH_3$), 2.10 (s, 6 H; $SiNCH_3$), 2.80 (d, ^3J(H,P) = 10.2 Hz, 12 H; $PNCH_3$), 4.15 (pseudo-quint., ^3J(H,H) = 7.0, ^3J(H,P) = 8.2 Hz, 2 H; $POCH_2$), 4.28 (m, 4 H; $SiOCH_2$); $^{31}P\{^1H\}$ NMR: δ = 196.8 (s); $^{13}C\{^1H\}$ NMR: δ = 16.5 (d, ^3J(C,P) = 7.8 Hz, 1C; $POCH_2CH_3$), 18.6 (s, 2C; $SiOCH_2CH_3$), 37.5 (s, 2C; $SiNCH_3$), 37.7 (d, ^2J(C,P) = 7.4 Hz, 4C; $PNCH_3$), 59.4 (s, 2C; $SiOCH_2$), 60.3 (s, 1C; $POCH_2$), 215.7 (d, ^2J(C,P) = 28.5 Hz, 3C; CO); $^{29}Si\{^1H\}$ NMR: δ = 57.4 (d, ^2J(Si,P) = 34 Hz); MS (FAB^+): *m/z*: 467.0 [M^+].

6a: white powder. FT-IR (THF): $\tilde{\nu}$(CO) = 1842 (vs), 1869 (s), 1940 (m) cm^{-1}; ^1H NMR: δ = 1.0 (t, ^3J(H,H) = 7.0 Hz, 3 H; $POCH_2CH_3$), 1.31 (t, ^3J(H,H) = 7.0 Hz, 6 H; $SiOCH_2CH_3$), 2.61 (d, ^3J(H,P) = 10.2 Hz, 12 H; $PNCH_3$), 2.97 (s, 6 H; $SiNCH_3$), 3.96 (pseudo-quint., ^3J(H,H) = 7.0 Hz, 2 H; $POCH_2$), 4.24 (m, 4 H; $SiOCH_2$); $^{31}P\{^1H\}$ NMR: δ = 0.8 (s, 1 P; CuP), 190.6 (s, 1 P; FeP); $^{13}C\{^1H\}$ NMR: δ = 16.3 (d, ^3J(C,P) = 8.0 Hz, 1C; $POCH_2CH_3$), 18.7 (s, 2C; $SiOCH_2CH_3$), 37.5 (d, ^2J(C,P) = 7.3 Hz, 4C; $PNCH_3$), 40.1 (s, 2C; $SiNCH_3$), 59.2 (s, 2C; $SiOCH_2$), 60.1 (s, 1C; $POCH_2$), 214.1 (d, ^2J(C,P) = 23.1 Hz, 3C; CO); MS (FAB^+): *m/z*: 791.1 [M^+].

6b: FT-IR (THF): $\tilde{\nu}$(CO) = 1856 (vs), 1880 (s), 1948 (m) cm^{-1}; $^{31}P\{^1H\}$ NMR: δ = 8.0 (s, 1 P; AgP), 193.7 (s, 1 P; FeP).

6c: white powder. FT-IR (THF): $\tilde{\nu}$(CO) = 1879 (vs), 1901 (s), 1964 (m) cm^{-1}; ^1H NMR: δ = 1.07 (t, ^3J(H,H) = 7.0 Hz, 3 H; $POCH_2CH_3$), 1.32 (t, ^3J(H,H) = 7.0 Hz, 6 H; $SiOCH_2CH_3$), 2.59 (d, ^3J(H,P) = 10.3 Hz, 12 H; $PNCH_3$), 3.06 (s, 6 H; $SiNCH_3$), 3.97 (pseudo-quint., ^3J(H,H) = 7.0, ^3J(H,P) = 7.2 Hz, 2 H; $POCH_2$), 4.23 (m, 4 H; $SiOCH_2$); $^{31}P\{^1H\}$ NMR (81.0 MHz, THF/C_6D_6): δ = 42.2 (d, ^3J(P,P) = 12.0 Hz, 1 P; AuP), 188.2 (d, ^3J(P,P) = 12.0 Hz, 1 P; FeP); $^{13}C\{^1H\}$ NMR: δ = 16.4 (d, ^3J(C,P) = 6.4 Hz, 1C; $POCH_2CH_3$), 18.8 (s, 2C; $SiOCH_2CH_3$), 37.0 (d, ^2J(C,P) = 9.1 Hz, 4C; $PNCH_3$), 38.6 (s, 2C; $SiNCH_3$), 58.4 (s, 2C; $SiOCH_2$), 60.0 (s, 1C; $POCH_2$), 216.0 (d, ^2J(C,P) = 19.3 Hz, 3C; CO); MS (FAB^+): *m/z*: 881.0 [$M^+ - NMe_2$].

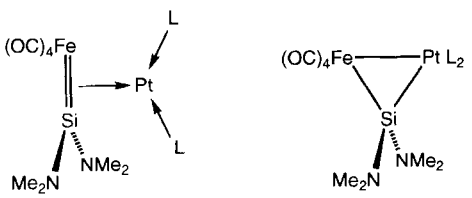
[a] Satisfactory elemental analyses were obtained for the compounds described. ^1H, ^{31}P, ^{13}C, ^{29}Si, and ^{195}Pt chemical shifts are measured relative to external TMS, H_3PO_4, and K_2PtCl_4. Unless otherwise specified, ^1H, ^{31}P, ^{13}C, ^{29}Si, and ^{195}Pt NMR spectra were recorded at 25 °C at 300.1 MHz in C_6D_6, 121.5 MHz in C_6D_6, 75.5 MHz in C_6D_6, 79.5 MHz in $CDCl_3$, and 85.88 MHz in [D_8]toluene, respectively.

[*] Dr. P. Braunstein, Dr. U. Bodensieck, T. Faure, Dr. M. Knorr, C. Stern
Laboratoire de Chimie de Coordination, URA 0416 du CNRS
Université Louis Pasteur
4 rue Blaise Pascal, F-67070 Strasbourg Cedex (France)
Telefax: Int. code + 88 41 60 30.
e-mail: braunst@chimie.u-strasbg.fr
Dr. W. Deck
Albert-Ludwigs-Universität Freiburg
Institut für Anorganische und Analytische Chemie
Albertstrasse 21, D-79104 Freiburg (FRG)

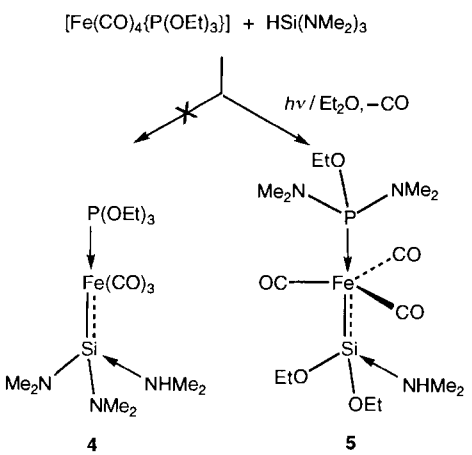
[**] Part of the planned dissertation of C. Stern. We would like to thank Prof. Dr. H. Vahrenkamp for access to the X-ray diffractometer in Freiburg. We are grateful to the Ministère de l'Enseignement Supérieur et de la Recherche (Paris) for a post-doctoral grant to U. B., to the Centre National de la Recherche Scientifique, the Commission of the European Communities (contract CHRX-CT93-0277), and the Alexander von Humboldt-Stiftung (award to P. B.) for financial support, and Johnson Matthey PLC for a generous loan of $PtCl_2$.

$^{31}P\{^1H\}$ NMR spectra of **3a,b** show an AX pattern, which is indicative of two chemically different P nuclei ($^2J(PP) = 4.0$ and 2.5 Hz, respectively; these values are typical for a *cis* arrangement) and is observed for L_2Pt^0 or L_2Pd^0 fragments coordinated to unsymmetrical olefins.[6]

It thus appears that an oxidative addition process does not occur, but rather that the amine ligand in **2** is displaced—more readily than anticipated—to give a silylene complex **3**. The latter is stabilized by an electron-acceptor fragment (i.e. PtL_2) instead of an electron-donor group, as observed so far.[7] It should be noted that base-free silylene complexes have only recently been synthesized and structurally characterized.[8a–e] Bearing in mind the isolobal analogy between $Fe(CO)_4$ and SiR_2, we can relate these molecules to the first platinum η^2-disilene complexes reported recently.[8f] The ^{29}Si NMR chemical shift of **3a** ($\delta = 113.9$) is consistent with a silylene complex, and the $^2J(Si,P_{trans})$ coupling constant of 136.4 Hz indicates that the PtL_2 fragment does not rotate. The Fe–Si–Pt system in **3a** is remarkably stable, since reaction with 1,2-bis(diphenylphosphino)ethane (dppe) led only to displacement of the PPh_3 ligands to give **3c**. In the absence of a crystal structure, we cannot comment on the extent to which the resonance forms **A** and **B** contribute to the actual structure of complexes **3**.



Since electron-donor substituents at Fe should stabilize the Fe–Si double bond, we set out to prepare the phosphite derivative **4**. However, the photochemical reaction of $[Fe(CO)_4\{P(OEt)_3\}]$ with $HSi(NMe_2)_3$ yielded, after workup, a new complex **5** with a singlet in its $^{31}P\{^1H\}$ NMR spectrum at



$\delta = 196.8$. The ^1H NMR spectrum was unexpected: the NCH_3 protons appeared as a singlet and a doublet in a 1:2 ratio, and the CH_2CH_3 protons as two triplets in a 1:2 ratio. An X-ray diffraction study (Fig. 1) allowed full elucidation of the structure of **5** and showed that an unprecedented ligand rearrangement had taken place: two ethoxy groups from the phosphite

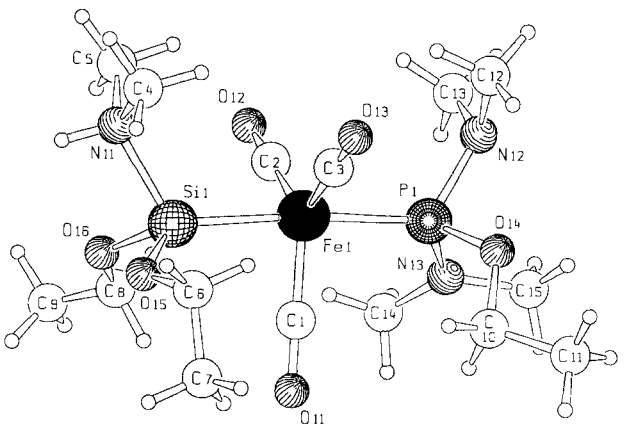


Fig. 1. The crystal structure of one molecule of **5** [13c]. Selected bond lengths [Å] and angles [°]: Fe1–C1 1.747(7), Fe1–C2 1.761(8), Fe1–C3 1.764(7), Fe1–P1 2.186(2), Fe1–Si1 2.218(2), Si1–O15 1.666(5), Si1–O16 1.652(5),Si1–N11 1.916(5), P1–O14 1.618(5), P1–N12 1.695(6), P1–N13 1.661(6); C1-Fe1-C2 120.7(3), C1-Fe1-C3 117.8(3), C2-Fe1-C3 121.2(3), P1-Fe1-Si1 173.4(1), O15-Si1-O16 99.7(2), O15-Si1-N11 95.8(2), O16-Si1-N11 93.9(2), N12-P1-N13 101.8(3), O14-P1-N12 95.2(3), O14-P1-N13 104.1(3).

ligand exchanged with two NMe_2 substituents on the silicon atom; this resulted in the formation of a $HNMe_2$-stabilized (diethoxy)silylene complex.[9] The asymmetric unit of **5** comprises two independent but similar molecules of **5**, which are connected through hydrogen bonds (Fig. 2). The coordination

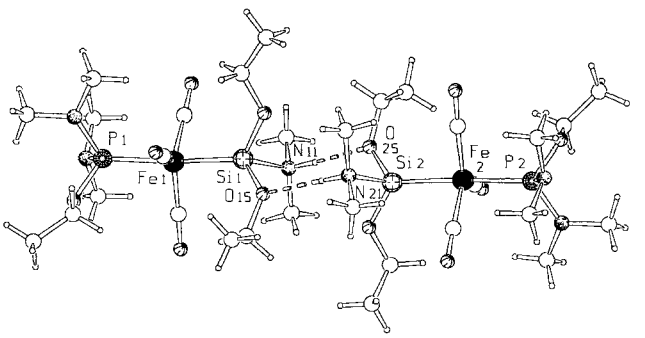


Fig. 2. The pseudo-dimer of **5** resulting from the hydrogen bonds between the molecules [13c].

about the Fe atom is trigonal bipyramidal with a *trans* arrangement of the P-Fe-Si atoms. The metal–Si bond length of 2.218(2) Å [2.216(2) Å in the second molecule] is one of the shortest reported for Fe–silylene complexes.[7] One of the NMe_2 groups attached to P is planar, whereas the other is pyramidal. This is indicative of some π bonding between N and P atoms.[10] In addition, there are mutual hydrogen bonds between two molecules in the solid state, involving the amine H atom of one molecule and the O atom of a SiOEt group of the other molecule. The corresponding distances [N(11)···O(25) = 2.871(7) and N(21)···O(15) = 2.959(7) Å] are consistent with strong interactions;[11] these generate an almost centrosymmetric dimer with a chairlike arrangement of the resulting six-membered ring. The hydrogen bonds contribute significantly to the stabilization of **5** and explain its low solubility in hexane. Accordingly, in donor solvents like THF, the stability of **5** is drastically reduced.

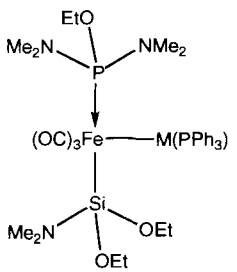
Irradiation or heating of a mixture of $P(OEt)_3$ and $HSi(NMe_2)_3$ did not lead to scrambling of their substituents. The reac-

tion of **2** with $P(OEt)_3$ under similar conditions (*hv*, 4 h, −22 °C) afforded **5** in only 14% yield. These experiments show that the oxophilicity of silicon is sufficient to allow the selective transfer of two OEt substituents from P to Si, but that this reaction requires prior coordination to the metal, preferably of the phosphite ligand. Whether other metals are capable of promoting this reaction, which connects the isosteric pairs M←P/OR and M−Si/NR_2 (or M←P/NR_2 and M−Si/OR) and transforms $P(OEt)_3$ and -$Si(NMe_2)_3$ into $P(OEt)(NMe_2)_2$ and -$Si(OEt)_2(NMe_2)$, is under investigation.

Deprotonation of **5** by KH in THF yielded the metalate complex **7** [$\tilde{\nu}$(CO) (THF) = 1807 (s), 1841 (vs), 1921 (w) cm^{-1};

$K[Fe(CO)_3\{P(OEt)(NMe_2)_2\}\{Si(OEt)_2(NMe_2)\}]$ **7**

$^{31}P\{^1H\}$ NMR(CD_2Cl_2, 25 °C): δ = 207.2], which was reacted with M^I complexes (M = Cu, Ag, Au) to afford the heterobimetallic complexes **6a–c**. The two doublets with $^3J(PP)$ = 12 Hz observed in the $^{31}P\{^1H\}$ NMR spectrum of **6c** confirm the presence of a metal–metal bond. The ^1H NMR data indicate that the substituents of the Fe-bound P and Si ligands have not exchanged further. However, there is a notable shift of the $SiNMe_2$ resonance compared to that of **5**, which is consistent with the change in the nature of the Fe–Si bond in moving from silylene in **5** to silyl in **6**. The IR and $^{31}P\{^1H\}$ NMR data for these complexes are similar to those for complexes such as $[(OC)_3(Ph_3P)\text{-}\{(MeO)_3Si\}Fe\text{-}Au\text{-}(PPh_3)]$.[12] These results indicate that deprotonation of the Si-bound nitrogen atom of **5** restores sufficient basicity to the Fe atom in **7** for the formation of stable (dialkoxy)aminosilyl heterobimetallic complexes.



6a M = Cu
6b M = Ag
6c M = Au

Experimental Procedure

2: A mixture of $[Fe(CO)_5]$ (2.35 g, 12.0×10^{-3} mol) and $HSi(NMe_2)_3$ (3.80 mL, 20.0×10^{-3} mol) in hexane (500 mL) was irradiated with a 150 W lamp for 4 h at −20 °C. A white powder precipitated during irradiation. The solvent was decanted, and the solid collected and dried in vacuo. Yield: 2.77 g (70% based on $[Fe(CO)_5]$.

3a,b: A solution of **2** (1.20×10^{-3} mol) in toluene (20 mL) was added dropwise to a stirred solution of $[Pt(C_2H_4)(PR_3)_2]$ (for **3a**: R = Ph, **3b**: R = *p*-tolyl; 1.20×10^{-3} mol) in toluene (30 mL) at −45 °C. The yellow solution was allowed to warm to room temperature and after completion of the reaction (4 h, monitored by IR) it was evaporated to dryness. Addition of hexane caused precipitation of a yellow product which was filtered off and dried in vacuo. Isolated yield: 1.02 g of **3a** (85%) and 1.02 g of **3b** (78%).

3c: A solution of dppe (0.12 g, 0.30×10^{-3} mol) in toluene (20 mL) was added dropwise to a stirred solution of **3a** (0.30 g, 0.30×10^{-3} mol) in toluene (30 mL) at −45 °C. The orange-yellow solution was slowly evaporated to dryness. Addition of hexane caused precipitation of solid material identified as a mixture of **3c** (80%), $[Pt(dppe)_2]$ (20%), and free PPh_3.

5: A sample of $[Fe(CO)_4\{P(OEt)_3\}]$ (4.0 g, 12.0×10^{-3} mol) and $HSi(NMe_2)_3$ (3.80 mL, 20.0×10^{-3} mol) in diethyl ether (500 mL) was irradiated with a 150 W lamp for 4 h at −20 °C. Concentration and addition of hexane at −20 °C yielded pale brown crystals. Yield: 3.93 g (70% based on $[Fe(CO)_4\{P(OEt)_3\}]$).

6a–c: A solution of **7** in THF (20 mL) was prepared in situ from **5** (0.80×10^{-3} mol) and KH (in excess). This was filtered and added to a stirred suspension of $[MX(PPh_3)]$ (for **6a**: M = Cu, X = Cl; **6b**: M = Ag, X = NO_3; **6c**: M = Au, X = Cl; 0.80×10^{-3} mol) in THF (10 mL) at −45 °C. The mixture was slowly evaporated to dryness. Addition of hexane caused the precipitation of **6a** and **6c**. Complex **6b** was too labile to be isolated in the solid state and was only characterized in solution. Yield: 0.49 g of **6a** (78%) and 0.41 g of **6c** (55%).

Received: June 10, 1994 [Z 7024 IE]
German version: *Angew. Chem.* **1994**, *106*, 2561

[1] a) K. Yamamoto, H. Okinoshima, M. Kumada, *J. Organomet. Chem.* **1971**, *27*, C31; b) H. Okinoshima, K. Yamamoto, M. Kumada, *J. Am. Chem. Soc.* **1972**, *94*, 9263; c) K. H. Pannell, M.-C. Brun, H. Sharma, K. Jones, S. Sharma, *Organometallics* **1994**, *13*, 1075, and references therein.

[2] a) M. Kumada, *J. Organomet. Chem.* **1975**, *100*, 127; b) K. A. Brown-Wensley, *Organometallics* **1987**, *6*, 1590; c) J. Y. Corey, L. S. Chang, E. R. Corey, *ibid.* **1987**, *6*, 1595; d) C. Zybill, D. L. Wilkinson, C. Leis, G. Müller, *Angew. Chem.* **1989**, *101*, 206; *Angew. Chem. Int. Ed. Engl.* **1989**, *28*, 203.

[3] a) G. Thum, W. Malisch, *J. Organomet. Chem.* **1984**, *264*, C5; b) W. Malisch, S. Schmitzer, G. Kaupp, K. Hindahl, H. Käb, U. Wachtler in *Organosilicon Chemistry, from Molecules to Materials* (Eds.: N. Auner, J. Weis), VCH, Weinheim, **1994**, p. 185.

[4] G. Schmid, E. Welz, *Angew. Chem.* **1977**, *89*, 823; *Angew. Chem. Int. Ed. Engl.* **1977**, *16*, 785.

[5] P. Braunstein, M. Knorr, A. Tiripicchio, M. Camellini Tiripicchio, *Angew. Chem.* **1989**, *101*, 1414; *Angew. Chem. Int. Ed. Engl.* **1989**, *28*, 1361.

[6] a) E. R. Hamner, R. D. W. Kemmitt, M. A. R. Smith, *J. Chem. Soc. Chem. Commun.* **1974**, 841; b) J. Andrieu, P. Braunstein, A. D. Burrows, *J. Chem. Res. (S)* **1993**, 380; c) W. A. Herrmann, W. R. Thiel, C. Brossmer, K. Öfele, T. Priermeier, W. Scherer, *J. Organomet. Chem.* **1993**, *461*, 51.

[7] a) C. Zybill, *Top. Curr. Chem.* **1991**, *160*, 1; b) C. Leis, C. Zybill, J. Lachmann, G. Müller, *Polyhedron* **1991**, *10*, 1163; c) R. Corriu, G. Lanneau, C. Priou, *Angew. Chem.* **1991**, *103*, 1153; *Angew. Chem. Int. Ed. Engl.* **1991**, *30*, 1130; d) T. Don Tilley in *The Silicon-Heteroatom Bond* (Eds.: S. Patai, Z. Rappoport), Wiley, New York, **1991**, pp. 245, 309; e) C. Leis, D. L. Wilkinson, H. Handwerker, C. Zybill, *Organometallics* **1992**, *11*, 514; f) H. Handwerker, C. Leis, S. Gamper, C. Zybill, *Inorg. Chim. Acta* **1992**, *198-200*, 763; g) R. J. P. Corriu, G. F. Lanneau, B. P. S. Chauhan, *Organometallics* **1993**, *12*, 2001 and references therein.

[8] a) D. A. Straus, C. Zhang, G. E. Quimbita, S. D. Grumbine, R. H. Heyn, T. Don Tilley, A. L. Rheingold, S. J. Geib, *J. Am. Chem. Soc.* **1990**, *112*, 2673; b) D. A. Straus, S. D. Grumbine, T. Don Tilley, *ibid.* **1990**, *112*, 7801; c) S. D. Grumbine, T. Don Tilley, A. L. Rheingold, *ibid.* **1993**, *115*, 358; d) S. D. Grumbine, T. Don Tilley, F. P. Arnold, A. L. Rheingold, *ibid.* **1993**, *115*, 7884; e) M. Denk, R. K. Hayashi, R. West, *J. Chem. Soc. Chem. Commun.* **1994**, 33; f) E. K. Pham, R. West, *J. Am. Chem. Soc.* **1989**, *111*, 7667.

[9] Crystals of **5**, $C_{15}H_{34}FeN_3O_6PSi$, were grown from a ether/hexane solution of the compound. Data were collected at −90 ± 2 °C. The compound crystallizes in space group $P2_1/a$, a = 15.302(8), b = 17.129(3), c = 18.42(2) Å; β = 109.38(4)°, V = 4556(5) Å^3; Z = 8; μ_{calcd} = 0.818 mm^{-1}; $F(000)$ = 1984. A total of 8180 unique reflections were measured in the range $6.02 \le 2\theta \le 52.58°$, of which 8062 were used for refinement and 5208 with $I > 2\sigma(I)$. The structure was solved by direct methods (hydrogen atoms were introduced in calculated positions) [13a]. Least squares refinement was performed by means of the full matrix on F^2 [13b]. R (obs.) = 0.0743, wR (obs.) = 0.1869. Further details of the crystal structure investigation may be obtained from the Fachinformationszentrum Karlsruhe, D-76344 Eggenstein-Leopoldshafen (FRG), on quoting the depository number CSD-380065.

[10] a) A. H. Cowley, R. E. Davis, K. Remadna, *Inorg. Chem.* **1981**, *20*, 2146; b) D. E. Schiff, J. W. Richardson, Jr., R. A. Jacobson, A. H. Cowley, J. Lasch, J. G. Verkade, *ibid.* **1984**, *23*, 3373.

[11] a) G. A. Jeffrey, W. Saenger, *Hydrogen Bonding in Biological Structures*, Springer, Heidelberg, **1991**; b) G. Boche, C. Boie, F. Bosold, K. Harms, M. Marsch, *Angew. Chem.* **1994**, *106*, 90; *Angew. Chem. Int. Ed. Engl.* **1994**, *33*, 115.

[12] P. Braunstein, M. Knorr, U. Schubert, M. Lanfranchi, A. Tiripicchio, *J. Chem. Soc. Dalton Trans* **1991**, 1507.

[13] a) SHELX-86: G. Sheldrick, *Acta Crystallogr. (Sect. A)* **1990**, *46*, 467; b) SHELX-93 G. Sheldrick, unpublished results; c) E. Keller, *SHAKAL 92, A computer program for the graphic representation of molecular and crystallographic models*, Universität Freiburg **1992**.

The Crystal Structures of Base-Free, Monomeric Arylcopper(I) and Arylsilver(I) Compounds; Two Cases of Mistaken Identity?**

Arne Haaland,* Kristin Rypdal, Hans Peter Verne, Wolfgang Scherer, and Werner Richard Thiel

In 1988 Lingnau and Strähle reported the syntheses of two base-free arylcopper and arylsilver compounds [M(Ar)] (Ar = 2,4,6-$Ph_3C_6H_2$; M = Cu, Ag).[1] X-ray structure analysis showed that both compounds are monomeric in the crystalline phase and yielded the bond lengths Cu–C = 189.0(6) and Ag–C = 190.2(5) pm.[1] These bond lengths remain the only experimentally determined bond lengths between monocoordinate copper or silver centers and carbon, and provide important benchmarks for comparison with Cu–C and Ag–C bond lengths in more complex structures.

Base-free organocopper(I) and organosilver(I) compounds are generally polymeric in the solid phase. Thus CuMes (Mes = 2,4,6-$Me_3C_6H_2$, mesityl) forms a pentamer with a ten-membered ring composed of alternating metal atoms and carbon atoms of the bridging aryl groups, while AgMes forms a cyclic tetramer.[2] 2,4,6-Triisopropylphenylcopper and trimethylsilylmethylcopper both form tetramers in the solid phase.[3, 4]

The close similarity of the Cu–C and Ag–C bond lengths obtained by Lingnau and Strähle is surprising: In the gaseous hydrides MH(g) the Ag–H bond length of 162 pm is 16 pm longer than the Cu–H bond length of 146 pm; in the gaseous monomeric chlorides MCl(g) the Ag–Cl bond length of 228 pm is 23 pm longer than the Cu–Cl bond length of 205 pm.[5] The lengths of the element–carbon bonds in simple methyl derivatives of elements of the fourth period from Zn to Br fall in the relatively narrow range from 193 to 197 pm, while the bond lengths in analogous compounds of elements of the fifth period from Cd to I fall in the range from 211 to 216 pm. The bond between a carbon atom and an element of the fifth period is, on the average, 19 pm longer than that between a carbon atom and an element of the fourth period in the same group.[6] These correlations suggest that if the Cu–C bond length is 189 pm, the Ag–C bond length should be approximately 208 pm.

We have carried out ab initio MO calculations on $CuCH_3$ and $AgCH_3$ to see whether we could reproduce the experimental bond lengths reported by Lingau and Strähle. Structure optimization at the all-electron TZ/MP2 level yielded the bond lengths of 191 pm for Cu–C and 218 pm for Ag–C. Since relativistic effects have been neglected, the value obtained in this manner for the Ag–C bond is expected to be roughly 4 to 8 pm too large.

Before our calculations had been published, they were superseded by more accurate calculations by Bauschlicher et al.[7] Their all-electron calculations on $CuCH_3$ at the TZ + P/MCPF level yielded an optimal Cu–C distance of 193.6 pm; relativistic core potential (RCP) calculations on $AgCH_3$ at the TZ + P/MCPF level yielded an Ag–C distance of 214.6 pm.[7]

[*] Prof. A. Haaland, Dr. K. Rypdal, H. P. Verne
Department of Chemistry, University of Oslo
Box 1033 Blindern, N-0315 Oslo 3 (Norway)
Telefax: Int. code + 22855441

Dipl.-Chem. W. Scherer, Dr. W. R. Thiel
Anorganisch-chemisches Institut der Technische Universität München
Lichtenbergstrasse 4, D-85747 Garching (FRG)
Telefax: Int. code + (89)-32093473

[**] This research was supported by the VISTA program of STATOIL and the Norwegian Academy of Science and Letters. We thank Prof. J. Strähle for helpful correspondence.

We therefore decided to request copies of the X-ray data deposited by Lingnau and Strähle and repeat the structure refinements.[8] Figure 1 top shows the reported structure for [Ag(Ar)]. The calculated thermal displacement parameters of

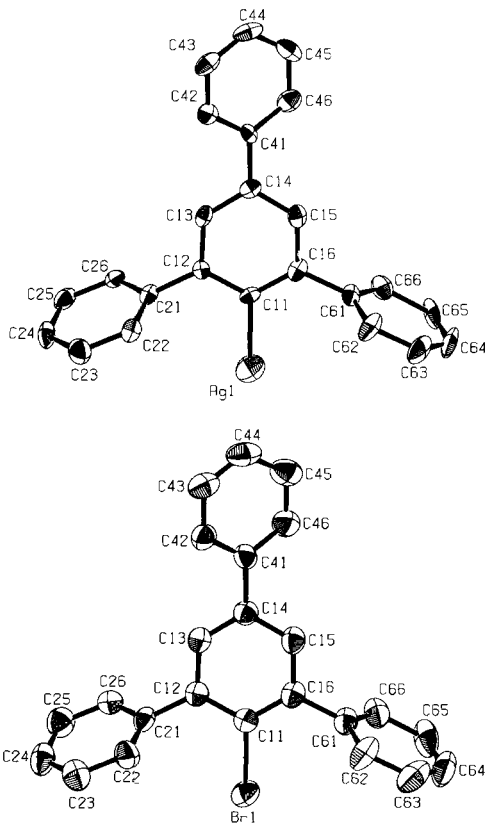


Fig. 1. Top: The published crystal structure of [Ag(Ar)] [1]. The hydrogen atoms are omitted; the thermal ellipsoids correspond to 50% probability. (PLATON drawing, measurement at ambient temperature, extinction correction and empirical absorption (DIFABS) applied. $U_{eq(C)} = 3.2 \times 10^2$ pm^2, $U_{eq(M)} = 5.8 \times 10^2$ pm,^{2}, $R = \Sigma(||F_o| - |F_c||)/\Sigma|F_o| = 0.082$, $R_w = [\sum w(|F_o| - |F_c|)^2/\sum w|F_o|^2]^{1/2} = 0.107$). Bottom: Structure model of BrAr resulting from refinement on the data collected for [Ag(Ar)]. Thermal ellipsoids correspond to 50% probability (no extinction correction applied, weighting scheme ($w = 1/\sigma^2(F_o)$, $U_{eq(C)} = 5.1 \times 10^2$ pm^2, $U_{eq(Br)} = 5.5 \times 10^2$ pm^2, $R = \sum(||F_o| - |F_c||)/\sum|F_o| = 0.041$, $R_w = [\sum w(|F_o| - |F_c|)^2/\sum w|F_o|^2]^{1/2} = 0.030$)).

the carbon atoms, $U_{eq(C)} = 3.2 \times 10^2$ pm^2, are unusually small compared with the corresponding parameter of the metal atom, $U_{eq(M)} = 5.8 \times 10^2$ pm^2. Such a relationship between the thermal parameters indicates that a metal atom was incorrectly identified.[11] Obviously the electron density at the position of the silver atom in the observed Fourier map is much smaller than calculated, and the thermal parameters of the metal and carbon atoms have been adjusted by the least-squares routines to reduce the discrepancy. Lingnau and Strähle also performed an empirical absorption correction (DIFABS) and refined the secondary extinction parameter (as mentioned in the copies of the deposited crystallographic data), which resulted in further reduction of the discrepancy. Refinements of the structure without an extinction correction and using a weighting scheme $w = 1/\sigma^2(F_o)$ result in unreasonable anisotropic thermal displacement parameters, which are also indicative for poor data or an incorrect model.

Refinements based on the "Ag data" and on the assumption that the crystal consisted of pure [Cu(Ar)] (which implies a smaller electron density at the metal atom) proceeded without

 © VCH Verlagsgesellschaft mbH, D-69451 Weinheim, 1994 0570-0833/94/2323-2443 $ 10.00+.25/0

difficulties to yield a significant improvement of the fit (Table 1) and a reasonable ratio of the thermal displacement parameters: $U_{eq(C)}/U_{eq(M)} = 0.88$.[11c] Refinements based on an assumed composition of BrAr (isomorphic replacement of the silver atom by bromine) provide in an even better fit (Table 1 and Fig. 1 bottom). *These results show that the data cannot have been recorded with a crystal of pure [Ag(Ar)].*

Table 1. Unit cell parameters obtained by crystal structure refinements on the data deposited by Lingnau and Strähle [1] (referred to as Ag data and Cu data) and our data for BrAr (Br data) [a].

Data set	Assumed composition	E–C bond length [b] [pm]	R (R_w)	Parameter
Ag data	[Ag(Ar)]	188(1)	0.106 (0.112)	at 18 °C: $P2_1/c$;
	[Cu(Ar)]	188.5(7)	0.051 (0.042)	$a = 1063.6(2)$,
	BrAr	189.5(5)	0.041 (0.030)	$b = 1510.5(4)$,
				$c = 1253.4(4)$ pm;
				$\beta = 113.55(2)°$;
				$V = 1846 \times 10^6$ pm^3
Cu data	[Ag(Ar)]	191(2)	0.118 (0.118)	at 18 °C: $P2_1/c$;
	[Cu(Ar)]	188.4(5)	0.043 (0.036) [c]	$a = 1065.7(4)$,
	BrAr	190.6(5)	0.046 (0.036) [c]	$b = 1508.3(9)$,
				$c = 1252.6(9)$ pm;
				$\beta = 113.61(4)°$;
				$V = 1844 \times 10^6$ pm^3
Br data	[Ag(Ar)]	187(2)	0.107 (0.108)	at 23 ± 1 °C: $P2_1/c$;
	[Cu(Ar)]	187.6(6)	0.042 (0.032) [c]	$a = 1068.0(2)$,
	BrAr	189.2(5)	0.047 (0.034) [c]	$b = 1509.4(1)$,
				$c = 1251.3(2)$ pm;
				$\beta = 113.634(7)°$;
				$V = 1848 \times 10^6$ pm^3

[a] Three structure refinements were carried out with each data set, one under the assumption that the crystal consists of pure [Ag(Ar)], another under the assumption that it consists of pure [Cu(Ar)], and the third under the assumption that it consists of pure BrAr. Refinements based on the composition [Ag(Ar)] were carried out without extinction correction and using a weighting scheme $w = 1/\sigma^2(F_o)$ with isotropic thermal displacement parmeters for carbon atoms; refinements of anisotropic thermal displacement parameters yielded unreasonable results (see text). [b] Ag–C, Cu–C, or Br–C bond. [c] The atom form factors of Cu and Br are apparently too similar to allow distinction of the two elements based on X-ray data [12].

Lingnau and Strähle prepared the two aryl metal complexes from the aryl bromide BrAr, which was treated with magnesium in tetrahydrofuran to give the Grignard compound ArMgBr, which in turn was reacted with solid CuCl or AgCl to yield crystalline, colorless, and air-stable [Cu(Ar)] and [Ag(Ar)] in 65 and 52% yield, respectively. The compounds were characterized by elemental analysis for C and H, but apparently not for the metal or Br.[1]

The ^{1}H and ^{13}C NMR spectra of the two compounds in $CDCl_3$ appear indistinguishable, and identical δ values for all carbons in the two compounds were reported (Table 2).[1b] The ^{1}H spectra contain a number of lines between $\delta = 7.36$ and 7.66; a strong singlet at $\delta = 7.58$ was assigned to H-3 and H-5. The IR spectra are also very similar; both contain a band at 490 cm^{-1} which was assigned to the M–C stretching vibration.[1b] The melting points are given as 121 °C (Cu) and 116 °C (Ag).[1b] The two compounds are isotypic (Table 1).

It would therefore appear possible that Lingnau and Strähle inadvertently exchanged crystals of the arylcopper and arylsilver compounds. Another possibility might be that the Ag data were collected with a crystal containing significant amounts of the starting material BrAr.[13]

Table 2. ^{13}C NMR spectroscopic data of [Cu(Ar)] and [Ag(Ar)] (reported by Lingnau and Strähle [1b]) and of BrAr (our data).

δ ^{13}C{^{1}H} [M(Ar)] [b]	BrAr	Assignment [a]	δ ^{13}C{^{1}H} [M(Ar)] [b]	BrAr	Assignment [a]
144.13	144.11	C-12,16	141.99	141.98	C-21
139.85	139.83	C-14	139.50	139.48	C-41
129.49	129.46	C-22,26	128.87	128.85	C-43,45
128.67	128.64	C-13,15	127.94	127.92	C-23,25
127.76	127.72	C-44	127.58	127.55	C-24
126.98	126.95	C-42,46	122.11	122.08	C-11

[a] From ref. [1b]. [b] M = Cu, Ag.

At this point it may be pertinent to point out that even though organocopper and organosilver compounds generally are very sensitive to oxygen and water, [Cu(Ar)] and [Ag(Ar)] were reported to be air-stable.[1] In addition organosilver compounds are generally light-sensitive, but no such sensitivity is mentioned in ref. [1]. We decided, therefore, to prepare BrAr in order to compare its properties with those reported for the metal analogues.

We found the ^{1}H and ^{13}C NMR spectra of BrAr to be indistinguishable from those reported for [Cu(Ar)] and [Ag(Ar)][1b] (δ(^{13}C) shifts in Table 2). Even the shifts for the *ipso* C atom (C-11) in the three compounds are equal to within $\Delta\delta = 0.03$. The IR spectrum of BrAr is similar to those of [Cu(Ar)] and [Ag(Ar)] reproduced in ref. [1b]. An absorption band is found at 494 cm^{-1} for BrAr, comparable to one at 490 cm^{-1} for [Cu(Ar)] and [Ag(Ar)], which we assign to an out-of-plane skeletal vibration.[14a] The C–Br stretching vibration of aromatic hydrocarbons is usually located in the region from 1075 to 1030 cm^{-1}.[14b] We found an absorption line in the IR spectrum of BrAr at 1073 cm^{-1} which is also present in the IR spectra of [Cu(Ar)] and [Ag(Ar)].[1b] The melting points reported for [Cu(Ar)] and [Ag(Ar)] recrystallized from chloroform/ethanol mixtures fall in the range spanned by the melting points of BrAr recrystallized from different solvents (see Experimental). The crystal structures of the three compounds are isotypic (see Table 1).[15] Refinement of the crystal structure of BrAr yields a C–Br bond length of 189.2(5) pm,[14] which is comparable to that obtained for monobromobenzene by gas electron diffraction (189.8(1) pm).[17]

Finally we have compared the Cu data and the Ag data to the Br data by refining a scaling factor by least squares calculations on the reflections common to the two data sets; this is 621 reflections for Ag and Br data and 646 reflections for Cu and Br data. The Ag data yielded a scaling factor of 30.7(1.6) and an R_w value of 0.050; the Cu data yielded a scaling factor of 22.2(2.2) and an R_w value of 0.052. We feel that the agreement is too close to rule out the possibility that the three data sets were recorded with crystals having the same chemical composition.

Thus we conclude: 1) The crystal used by Lingnau and Strähle[1] to determine the molecular structure of [Ag(Ar)] did not consist of the pure compound. We suggest that the crystal consisted partly or entirely of the starting material. 2) The crystal used by Lingnau and Strähle[1] to determine the structure of [Cu(Ar)] may have consisted partly or entirely of the starting material BrAr. We suggest that the investigation should be repeated before the results of Lingnau and Strähle can be regarded as established.

Experimental Procedure

1-Bromo-2,4,6-triphenylbenzene (BrAr): 1,3,5-Triphenylbenzene (10.0 g, 32.7 mmol) was dissolved in 100 mL of CS_2 in a 250 mL two-necked flask equipped with a reflux condenser and a dropping funnel. After the addition of Fe powder

(0.1 g), bromine (5.49 g, 34.3 mmol) was added dropwise and the mixture stirred for 30 min. The solvent was removed in vacuo, the residue dissolved in diethyl ether, and the solution filtered over Al_2O_3. The crude product was recrystallized from ethanol/diethyl ether. Yield: 10.6 g (84%). The product was pure by gas chromatography (GC/MS). Elemental analysis; calcd (found): C 74.82 (73.99), H 4.45 (4.42). M.p. 128.5 °C from isopropanol (ref. [18]: 129–130 °C); 109 °C from ethanol (ref. [18]: 108 °C). ^{1}H NMR (400 MHz, $CDCl_3$, 25 °C, $CDCl_3$): $\delta = 7.70$ (H-42,46), 7.65 (H-13,15), 7.60 (H-22,26), 7.54 (H-23,25), 7.50 (H-43,45), 7.49 (H-24), 7.43 (H-44). ^{13}C NMR data are listed in Table 2.

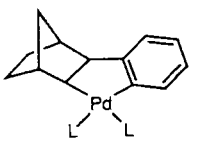
Received: July 11, 1994 [Z 7119 IE]
German version: *Angew. Chem.* **1994**, *106*, 2515

[1] a) R. Lingnau, J. Strähle, *Angew. Chem.* **1988**, *100*, 409; *Angew. Chem. Int. Ed. Engl.* **1988**, *27*, 436; b) R. Lingnau, Dissertation, Universität Tübingen, **1990**.
[2] E. M. Meyer, S. Gambarotta, C. Floriani, A. Chiesi-Villa, C. Guastine, *Organometallics* **1989**, *8*, 1067.
[3] D. Nobel, G. van Koten, A. L. Spek, *Angew. Chem.* **1989**, *101*, 211; *Angew. Chem. Int. Ed. Engl.* **1989**, *28*, 208.
[4] J. A. J. Jarvis, R. Pearce, M. F. Lappert, *J. Chem. Soc. Dalton Trans.* **1977**, 999.
[5] K. P. Huber, G. Herzberg, *Molecular Spectra and Molecular Structure, Vol. IV, Constants of Diatomic Molecules*, Van Nostrand, New York, **1979**.
[6] A. Haaland, *J. Mol. Struct.* **1983**, *97*, 115.
[7] C. W. Bauschlicher, Jr., S. R. Langhoff, H. Partridge, L. A. Barnes, *J. Chem. Phys.* **1989**, *91*, 2399.
[8] The X-ray data for [Ag(Ar)] and [Cu(Ar), referred to in the text as "Ag data" and "Cu data", respectively, had been deposited at the Fachinformationszentrum Karlsruhe [1]. We received 1560 ([Ag(Ar)]) and 1772 ([Cu(Ar)]) independent reflections with $I > 3\sigma(I)$. The numbers of deposited reflections with $I > 3\sigma(I)$ is thus less than those reported by Lingnau and Strähle (1710 and 1946 reflections, respectively). We excluded two reflections of the [Cu(Ar)] data that should be systematically absent. The *R*-factors of the published and deposited data are slightly different in the case of [Ag(Ar)]. An empirical absorption correction (DIFABS) of both data sets had been performed by Lingnau and Strähle. No further corrections were made. All calculations were performed on a DECstation 5000/25 computer with the programs CRYSTALS [9] and PLATON [10].
[9] D. J. Watkin, P. W. Betteridge, J. R. Carruthers, *Crystals User Manual*, Oxford University Computing Laboratory, Oxford, **1986**.
[10] A. L. Spek, *Acta Crystallogr. Sect. A* **1990**, *46*, C34.
[11] a) G. H. Stout, L. H. Jensen, *X-ray Structure Determination*, Wiley-Interscience, New York, **1989**, Chapter 16.4.; b) S. M. Rothstein, M. F. Richardson, W. D. Bell, *Acta Crystallogr. Sect. A* **1978**, *34*, 969; c) J. K. Burdett, *The Importance of Accurate Structure Determination in Inorganic Chemistry* in *Accurate Molecular Structures* (Eds.: A. Domenicano, I. Hargittai), International Union of Crystallography, Oxford University Press, Oxford, **1992**, p. 498.
[12] D. T. Cromer, J. T. Waber, *Int. Tables X-Ray Crystallogr.* **1974**, *IV*, Table 2.2B.
[13] This possibility was first pointed out to us by Prof. J. Strähle.
[14] a) G. Varsanyi, *Assignments for Vibrational Spectra of Seven Hundred Benzene Derivatives*, Académial Kladó, Budapest **1974**; b) M. Hesse, H. Meier, B. Zeeh, *Spektroskopische Methoden der Organischen Chemie*, 4th ed., Thieme, Stuttgart, **1991**.
[15] BrAr crystallizes from a saturated ethanol solution at 23 °C as thin colorless plates (maximum dimensions along direct crystal axes: $0.035 \times 0.45 \times 0.55$ mm). Final cell constants were obtained by least squares refinement of 25 automatically centered high-angle reflections ($30.0° < 2\theta < 36.5°$): $a = 1068.0(2)$, $b = 1509.4(1)$, $c = 1251.3(2)$ pm, $\beta = 113.634(7)°$, $V = 1848 \times 10^6$ pm^3, measurement at 23 ± 1 °C, $\rho_{calcd} = 1.385$ g cm^{-3}, $\mu = 22$ cm^{-3}, $F_{000} = 784$, $Z = 4$, monoclinic crystal system, space group $P2_1/c$ (No. 14), Enraf–Nonius CAD4, $\lambda = 71.073$ pm ($Mo_{K\alpha}$, graphite monochromator), range of measurement $1.0° < \theta < 25°$, ω-scan, scan width $(1.4 + 0.3 \tan\theta)°$ ($\pm 25\%$) before and after each reflection to determine the background, $t_{max} = 60$ s, orientation control reflections were monitored every 200 reflections, and the intensity of three reflections were checked every 3600 s; 6733 measured reflections ($\pm h, +k, \pm l$), 2879 independent reflections of which 1607 had $I > 3\sigma(I)$. A numerical absorption correction based on 7 indexed faces was made. (T_{max}/T_{min} : 51.4/85.8%). 226 least squares parameters; all 25 non-hydrogen atoms with anisotropic thermal parameters; all hydrogen atoms placed in calculated positions and included in the structure factor calculations, but not refined; shift/error < 0.0001. $R = \Sigma(||F_o| - |F_c||)/\Sigma|F_o| = 0.047$, $R_w = [\Sigma w(|F_o| - |F_c|)^2/\Sigma w|F_o|^2]^{1/2} = 0.034$, residual electron density +7.6/ -5.6×10^5 Å e/pm^3. All calculations were performed on a DECstation 5000/25 computer with the programs SDP [16], CRYSTALS [9], and PLATON [10]. Further details of the crystal structure investigation may be obtained from the Fachinformationszentrum Karlsruhe, D-76344 Eggenstein-Leopoldshafen (FRG), on quoting the depository number CSD-58457.
[16] B. A. Frenz, "The Enraf-Nonius CAD4 SDP System", *Computing in Crystallography*, DELFT University Press, Delft, **1978**.
[17] A. Almenningen, J. Brunvoll, M. V. Popik, S. Sokolkov, L. V. Vilkov, S. Samdal, *J. Mol. Struct.* **1985**, *127*, 85.
[18] *Beilsteins Handbuch der Organischen Chemie, E III 5*, Springer, Berlin, **1965**, S. 2564.

Synthesis of Oxa- and Azapalladacycles from Organostannanes**

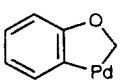
Diego J. Cárdenas, Cristina Mateo, and Antonio M. Echavarren*

Palladium-catalyzed cascade reactions that proceed by means of successive Heck insertions expedite the construction of complex molecules in a single step.[1, 2] A number of more complex sequential reactions proceeding through palladacycles such as **1** show promise in the synthesis of complex targets.[3–5] These cascade reactions are initiated by oxidative addition of aryl halides ArX to a $[Pd^0L_n]$ complex to give $[Pd(Ar)X(L)_2]$.[3, 4] Insertion of norbornene into the Pd–C bond of the arylpalladium complex leads to formation of a labile η^2-aryl complex,[6] which reacts further by intramolecular C–H activation of the aryl ring to form complexes of type **1**.[3, 7, 8] New C–C bonds are formed by reaction of palladacycles such as **1** with alkyl halides to give hexacoordinated Pd^{IV} complexes, followed by reductive elimination.[7, 9–11]

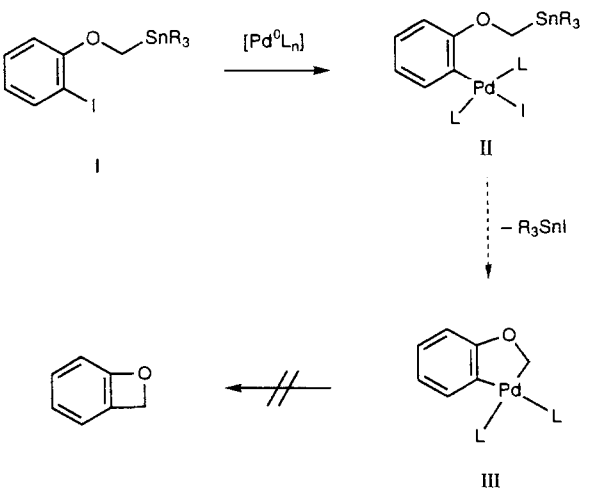


1

Recently, a series of novel palladium-catalyzed cascade reactions leading to the formation of heterocyclic compounds were described by Dyker.[12] In the reaction with *o*-iodoanisole, palladacycle **2** was proposed as an intermediate formed by a new intramolecular C–H activation of the methoxy group.[12, 13] A milder procedure for the synthesis of these intermediate palladacycles could be conceived-based on an intramolecular Stille coupling[14, 15] of an iodoaryl stannane **I** (Scheme 1). Oxidative addition of stannane **I** to a palladium(0) complex would furnish intermediates **II**, which could undergo an intramolecular transmetalation[16] at the OCH_2–Sn bond to give the desired complexes **III**. Endocyclic restriction[17] would disfavor the alternative cleavage of the Sn–R bonds. The reductive elimination of the two



2



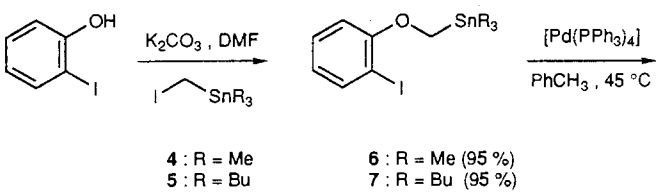
Scheme 1.

[*] Prof. A. M. Echavarren, D. J. Cárdenas, C. Mateo
Departamento de Química Orgánica, Universidad Autónoma de Madrid
Cantoblanco, E-28049 Madrid (Spain)
Telefax: Int. code + (1) 397-3966

[**] This work was supported by the DGICYT (project PB91-0612-C03-02). D. J. C. and C. M. acknowledge the receipt of predoctoral fellowships from the Ministerio de Educación y Ciencia.

mutually *cis* organic ligands is fast in the Stille cross-coupling reaction,[14, 15] even when the elimination leads to the formation of four-membered rings.[18] However, the reductive elimination was expected to be slow in our case, owing to the high energy of the product 2*H*-benzoxete.[19] Herein we report on the successful application of this scheme to the synthesis of oxapalladacycles and an aza derivative related to **2** and the preliminary results on the reactivity of these complexes.

Oxapalladacycle **3** with two triphenylphosphane ligands was synthesized in two steps as shown in Scheme 2. Alkylation of *o*-iodophenol with stannanes **4** or **5**[20] (K_2CO_3, DMF, 70 °C, 15 h) gave **6** and **7**, respectively.[21] Reaction of these stannanes with $[Pd(PPh_3)_4]$ (1 equiv) in toluene at 45 °C for 24 h afforded **3** as an air-stable white powder. The primary oxidative-addition product of the iodoarene to the Pd^0 complex could not be isolated. The structure of **3** was established by ^1H, ^{13}C, and ^{31}P NMR spectroscopy, including heteronuclear correlation experiments (HMQC[22a] and HMBC[22b], Table 1). As expected, **3** did not undergo reductive elimination after prolonged heating in benzene at 80 °C.

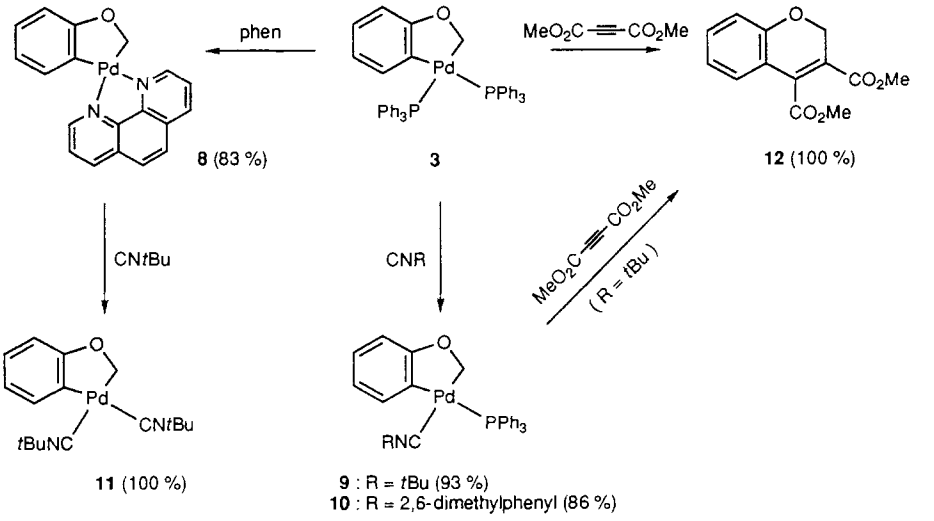


4 : R = Me
5 : R = Bu

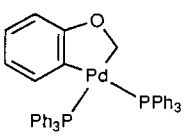
6 : R = Me (95 %)
7 : R = Bu (95 %)

Scheme 2.

Ligand exchange with 9,10-phenanthroline (phen) (10 equiv, CH_2Cl_2, reflux) afforded **8** (Scheme 3). Reaction of **3** with *tert*-butyl- or 2,6-dimethylphenylisocyanide led to complexes **9** and **10**, respectively. The selective substitution of the phosphane *cis* to the aryl ligand reflects the higher *trans* effect of the OCH_2 ligand.[7, 23] Neither substitution of the second phosphane ligand, nor isocyanide insertion reaction[24] were observed under more severe conditions. On the other hand, the metallacycle **11** with two *cis* isocyanide ligands could be prepared from **8** by substitution of the phenanthroline ligand at 23 °C. This organometallic Pd^{II} complex is a rare example of an organopalladium derivative with four Pd–C bonds.[25]



Scheme 3.



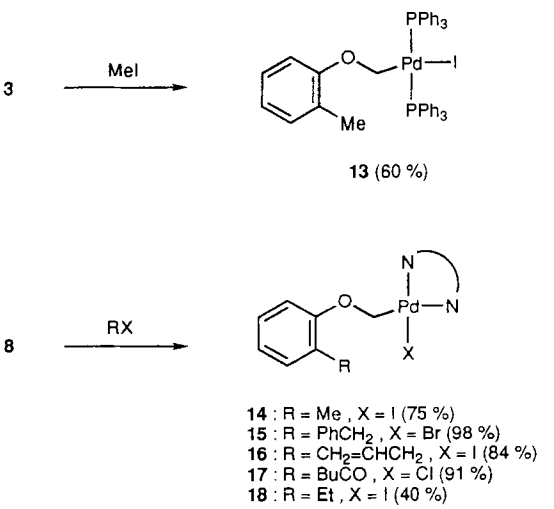
Treatment of **3** with carbon monoxide (3.5 atm, 60 °C, 15 h) failed to give any insertion product. However, dimethyl acetylenedicarboxylate smoothly reacted with **3** ($CHCl_3$, 40 °C, 1 h) by insertion into a C–Pd bond, followed by reductive elimination leading to chromene **12**. The known complex $[Pd(MeO_2CC{\equiv}CCO_2Me)(PPh_3)_2]$ was also isolated in this reaction (91 % yield).[26] Heterocycle **12** could also be obtained in almost quantitative yield by reaction of complex **9** with dimethyl acetylenedicarboxylate (23 °C, 13 h) (Scheme 3).

Oxapalladacycle **3** reacted slowly at 23 °C with methyl iodide in acetone to give **13** after 24 h (Scheme 4). Palladacycle **8** was

Table 1. Selected NMR data ($CDCl_3$) for palladacycles **3** and **24**.

3: ^1H NMR (300 MHz): $\delta = 7.50-7.35$ (m, 12H), 7.32–7.11 (m, 12H), 7.09–7.05 (m, 6H), 6.78 (m, 1H), 6.71 (ddd, $J = 7.9, 2.8, 1.6$ Hz, 1H), 6.61 (tdd, $J = 7.5, 2.5, 1.5$ Hz, 1H), 6.06 (ddt, $J = 7.6, 6.9, 1.6$ Hz, 1H), 5.18 (dd, $J = 5.6, 3.3$ Hz, 2H); $^{13}C\{^1H\}$ NMR (75 MHz; DEPT): $\delta = 174.60$ (dd, $^3J(C,P) = 7.3, 5.5$ Hz; C), 149.27 (dd, $^2J(C,P) = 100.0, 11.7$ Hz; C), 141.71 (dd, $^3J(C,P) = 8.9, 3.0$ Hz; CH), 135.20 (d, $^2J(C,P) = 13.3$ Hz, $CH(PPh_3)$), 134.19 (d, $^2J(C,P) = 13.2$ Hz; $CH(PPh_3)$), 134.03 (dd, $^1J(C,P) = 30.9$ Hz, $^3J(C,P) = 1.9$ Hz; $C(PPh_3)$), 132.10 (dd, $^1J(C,P) = 35.5$ Hz, $^3J(C,P) = 1.8$ Hz; $C(PPh_3)$), 129.84 (d, $^4J(C,P) = 2.0$ Hz; $CH(PPh_3)$), 129.47 (d, $^4J(C,P) = 1.9$ Hz; $CH(PPh_3)$), 127.99 (d, $^3J(C,P) = 9.8$ Hz; $CH(PPh_3)$), 127.76 (d, $^3J(C,P) = 9.3$ Hz; $CH(PPh_3)$), 125.30 (CH), 116.65 (dd, $^4J(C,P) = 7.9, 3.0$ Hz; CH), 107.82 (CH), 93.49 (dd, ^2J (C,P) = 90.8, 6.4 Hz; CH_2); $^{31}P\{^1H\}$ NMR (121.5 MHz): $\delta = 28.39$ (d, $J = 25.6$ Hz, 1P), 25.52 (d, $J = 25.6$ Hz, 1P).

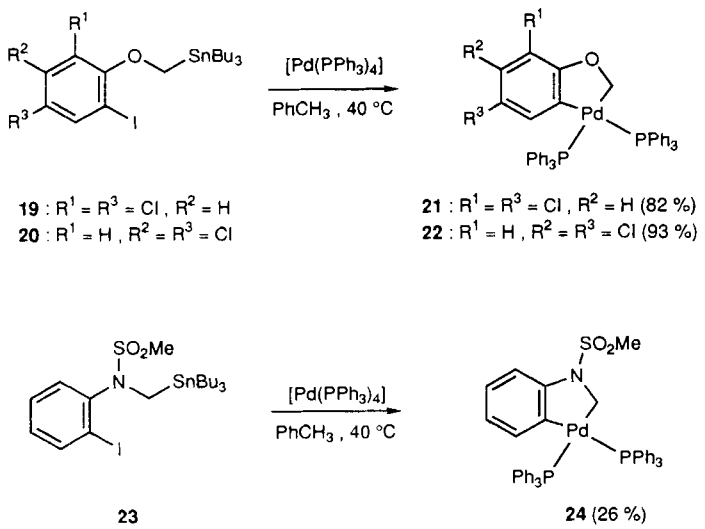
24: ^1H NMR (300 MHz): $\delta = 7.60-7.05$ (m, 31H), 6.82–6.71 (m, 2H), 6.25 (brt, $J = 7.4$ Hz, 1H), 3.98 (dd, $J = 6.6, 4.2$ Hz, 2H), 2.76 (s, 3H); $^{13}C\{^1H\}$ NMR (50 MHz): $\delta = 154.39$ (dd, $^2J(C,P) = 105.3, 8.3$ Hz); 141.66 (brd, $^3J(C,P) = 11.4$ Hz), 135.02 (d, $^2J(C,P) = 13.4$ Hz; PPh_3), 134.03 (d, $^3J(C,P) = 13.8$ Hz; PPh_3), 132.86 (brd, $^1J(C,P) = 44.6$ Hz; PPh_3), 131.83 (brd, $^1J(C,P) = 30.7$ Hz; PPh_3), 129.97 (brs; PPh_3), 129.64 (brs; PPh_3), 128.14 (d, $^3J(C,P) = 8.6$ Hz; PPh_3), 127.81 (d, $^3J(C,P) = 9.2$ Hz; PPh_3), 124.47 (s), 122.54 (brs), 121.66 (brd, $^3J(C,P) = 9.0$ Hz), 115.82 (s), 61.62 (dd, $^2J(C,P) = 88.6, 5.4$ Hz), 33.23 (s); $^{31}P\{^1H\}$ NMR (121.5 MHz): $\delta = 27.45$ (d, $J = 25.8$ Hz, 1P), 25.84 (d, $J = 25.8$ Hz, 1P).



Scheme 4.

more reactive at 23 °C: treatment with methyl iodide, benzyl bromide, allyl iodide,[27] and pentanoyl chloride led to complexes **14**–**17**, respectively, after 1–4 h (Scheme 4). Ethyl iodide reacted more sluggishly with **8** ($CDCl_3$, reflux, 18 h) to give **18**, and starting material was recovered with 2-iodopropane and methyl *p*-toluenesulfonate.[28] The reactions with the alkyl halides probably proceed by oxidative addition to give a Pd^{IV} intermediate, which undergoes aryl–alkyl or aryl–acyl reductive elimination to yield the observed Pd^{II} complexes. The reductive elimination is very selective in these cases, leading to exclusive bond formation with the aryl ligand.[7–11] Surprisingly, reaction of **3** with (*E*)-1-iodo-2-phenylethene in acetone at 23 °C led to (*E*)-triphenylvinylphosphonium iodide and a complex mixture of palladium complexes. The vinyl phosphonium salt could be also prepared by reaction of the vinyl iodide with triphenylphosphane in the presence of catalytic amounts of $[Pd(PPh_3)_4]$.[29] On the other hand, iodobenzene and *o*-iodomethoxybenzene were not reactive with either **3** or **8** even under forcing conditions. The lack of reactivity of the palladacycles with aryl iodides suggests that a more complex reaction pathway not involving Pd^{IV} species may be operating in the formation of aryl–aryl bonds under catalytic conditions.[30]

The synthesis of **3** could be extended to the preparation of substituted oxapalladacycles. Thus, dichloroiodoaryl stannanes **19** and **20** yielded oxapalladacycles **21** and **22**, respectively (Scheme 5). The aminomethyl stannane **23** also reacted with



Scheme 5.

$[Pd(PPh_3)_4]$ to afford the novel azapalladacycle **24** (Table 1) as a white solid that slowly decomposed in $CDCl_3$. The lower yield may be due to decomposition by reductive elimination to give a 1,2-dihydrobenzazete.[31]

The synthesis of oxa- and azapalladacycles described here extends considerably the existing methods for the preparation of metallacycles. These palladacycles are new members of the little studied class of alkyl(aryl)palladium(II) complexes.[3, 8, 11] With the preparation of **3** and related palladacycles, we are now in a position to study their role in the formation of aryl–aryl bonds. In addition, investigations into the catalytic transformations of iodostannanes such as **6**, **7**, and **23** are being pursued.

Received: July 5, 1994 [Z 7099 IE]
German version: *Angew. Chem.* **1994**, *106*, 2529

[1] For leading references, see B. M. Trost, Y. Shi, *J. Am. Chem. Soc.* **1993**, *115*, 9421; Y. Zhang, G. Wu, G. Angel, E. Negishi, *ibid.* **1990**, *112*, 8590; M. M. Abelman, L. E. Overman, *ibid.* **1988**, *110*, 2328; F. E. Meyer, P. J. Parsons, A. de Meijere, *J. Org. Chem.* **1991**, *56*, 6487; B. Burns, R. Grigg, P. Ratananukul, V. Sridharan, P. Stevenson, S. Surkirthalingam, T. Worakun, *Tetrahedron Lett.* **1988**, *29*, 5565.
[2] L. F. Tietze, U. Beifuss, *Angew. Chem.* **1993**, *105*, 137; *Angew. Chem. Int. Ed. Engl.* **1993**, *32*, 131.
[3] M. Catellani, G. P. Chiusoli, C. Castagnoli, *J. Organomet. Chem.* **1991**, *407*, C30; M. Catellani, G. P. Chiusoli, *ibid.* **1992**, *425*, 151; *ibid.* **1992**, *437*, 369, and references therein.
[4] O. Reiser, M. Weber, A. de Meijere, *Angew. Chem.* **1989**, *101*, 1071; *Angew. Chem. Int. Ed. Engl.* **1989**, *28*, 1037; K. Albrecht, O. Reiser, M. Weber, B. Knieriem, A. de Meijere, *Tetrahedron* **1994**, *50*, 383.
[5] For other palladium-catalyzed cascade processes that probably take place through Pd^{IV} metallacycles, see B. M. Trost, A. S. K. Hashmi, *J. Am. Chem. Soc.* **1994**, *116*, 2183; B. M. Trost, G. J. Tanoury, M. Lautens, C. Chan, D. T. MacPherson, *ibid.* **1994**, *116*, 4255, and references therein.
[6] C.-S. Li, C.-H. Cheng, F.-L. Liao, S.-L. Wang, *J. Chem. Soc. Chem. Commun.* **1991**, 710.
[7] C.-H. Liu, C.-S. Li, C.-H. Cheng, *Organometallics* **1994**, *13*, 18.
[8] B. A. Markies, P. Wijkens, H. Kooijman, A. L. Spek, J. Boersma, G. van Koten, *J. Chem. Soc. Chem. Commun.* **1992**, 1420.
[9] M. Catellani, G. P. Chiusoli, *J. Organomet. Chem.* **1988**, *346*, C27; M. Catellani, B. E. Mann, *ibid.* **1990**, *390*, 251; G. Bocelli, M. Catellani, S. Ghelli, *ibid.* **1993**, *458*, C12, and references therein.
[10] A. J. Canty, *Acc. Chem. Res.* **1992**, *25*, 83; C. Dücker-Benfer, R. van Eldik, A. J. Canty, *Organometallics* **1994**, *13*, 2412.
[11] B. A. Markies, A. J. Canty, J. Boersma, G. van Koten, *Organometallics* **1994**, *13*, 2053, and references therein.
[12] a) G. Dyker, *Angew. Chem.* **1992**, *104*, 1079; *Angew. Chem. Int. Ed. Engl.* **1992**, *31*, 1023; b) *J. Org. Chem.* **1993**, *58*, 6426; c) *Chem. Ber.* **1994**, *127*, 739.
[13] For a related process leading to benzocyclobutene derivatives, see G. Dyker, *Angew. Chem.* **1994**, *106*, 117; *Angew. Chem. Int. Ed. Engl.* **1994**, *33*, 103.
[14] J. K. Stille, *Angew. Chem.* **1986**, *98*, 504; *Angew. Chem. Int. Ed. Engl.* **1986**, *25*, 508.
[15] Recent reviews: T. N. Mitchell, *Synthesis* **1992**, 803; K. Ritter, *ibid.* **1993**, 735.
[16] For a synthesis of a different type of palladacycle based on a transmetalation facilitated by chelation, see H. Nishiyama, M. Matsumoto, T. Matsukura, R. Miura, K. Itoh, *Organometallics* **1985**, *4*, 1911.
[17] P. Beak, *Acc. Chem. Res.* **1992**, *25*, 215; M. L. Kurtzweil, D. Loo, P. Beak, *J. Am. Chem. Soc.* **1993**, *115*, 421.
[18] E. Piers, Y.-F. Lu, *J. Org. Chem.* **1988**, *53*, 926; J. C. Bradley, T. Durst, *ibid.* **1991**, *56*, 5459.
[19] W. Adam, L. Hadjiarapoglu, K. Peters, M. Sauter, *J. Am. Chem. Soc.* **1993**, *115*, 8603; W. Adam, M. Sauter, C. Zünkler, *Chem. Ber.* **1994**, *127*, 1115.
[20] D. Seyferth, S. B. Andrews, *J. Organomet. Chem.* **1971**, *30*, 151; D. Seyferth, S. B. Andrews, R. L. Lambert, *ibid.* **1972**, *37*, 69.
[21] J. J. Eisch, J. E. Galle, A. Piotrowski, M.-R. Tsai, *J. Org. Chem.* **1982**, *47*, 5051.
[22] a) A. Bax, S. Subramanian, *J. Magn. Res.* **1986**, *67*, 565; b) A. Bax, M. F. Summers, *J. Am. Chem. Soc.* **1986**, *108*, 2093.
[23] A similar reaction was observed with a nickelacycle related to **3**: J. Cámpora, E. Gutiérrez, A. Monge, P. Palma, M. L. Poveda, C. Ruiz, E. Carmona, *Organometallics* **1994**, *13*, 1728.
[24] Y. Yamamoto, T. Tanase, T. Yanai, T. Asano, K. Kobayashi, *J. Organomet. Chem.* **1993**, *456*, 287, and references therein.
[25] C. H. Davies, C. H. Game, M. Green, F. G. A. Stone, *J. Chem. Soc. Dalton Trans.* **1974**, 357.
[26] H. Urata, H. Suzuki, Y. Moro-oka, T. Ikawa, J. *Organomet. Chem.* **1989**, *364*, 235.
[27] Intermediate Pd^{IV} complexes were observed by ^1H NMR spectroscopy [9,10] in the crude reaction mixtures with benzyl bromide and allyl iodide.
[28] R. G. Pearson, P. E. Figdore, *J. Am. Chem. Soc.* **1980**, *102*, 1541.
[29] For a related synthesis from vinyl triflates, see M. H. Kowalski, R. J. Hinkle, P. J. Stang, *J. Org. Chem.* **1989**, *54*, 2783; R. J. Hinkle, P. J. Stang, M. H. Kowalski, *ibid.* **1990**, *55*, 5033.
[30] A reaction between two aryl–Pd^{II} complexes has been suggested very recently by Dyker for the formation of aryl–aryl bonds [12c].
[31] E. M. Burguess, L. McCullagh, *J. Am. Chem. Soc.* **1966**, *88*, 1580; G. Pfister-Guillouzo, F. Gracian, A. Senio, M. Letulle, J.-L. Ripoll, *Tetrahedron Lett.* **1992**, *33*, 5753; W. Sander, J. Morawietz, *ibid.* **1993**, *34*, 1913, and references therein.

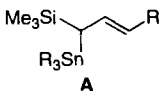
 © VCH Verlagsgesellschaft mbH, D-69451 Weinheim, 1994 0570-0833/94/2323-2447 $ 10.00+.25/0

A Regioselective Palladium-Catalyzed Reduction of 3,3-Heterobimetalated Allylic Acetates—Synthesis and Reactivity of Allylic Bimetallic Compounds**

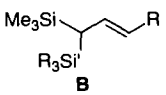
Mark Lautens* and Patrick H. M. Delanghe

Bimetallic reagents have found widespread use in organic synthesis as coupling reagents.[1] These reagents are particularly interesting when a difference in reactivity of the two metals allows selective reaction of one organometallic group.[2]

As part of our continuing interest in the synthesis and reactivity of novel homo- and heterobimetallic reagents containing tin and silicon,[3, 4] we envisioned that stannylsilyl- and disilyl-substituted allylic reagents **A** and **B** would be useful building blocks in organic synthesis.



A

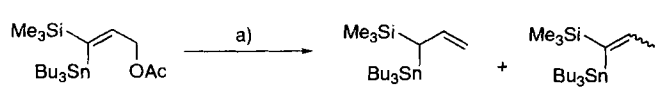


B

Both allylic silanes[5] and allylic stannanes[6] have been shown to be extremely useful reagents for the regio-, diastereo-, and enantioselective construction of C–C bonds. Since allylic stannanes display a higher reactivity towards electrophiles than allylic silanes,[7] selective C–C coupling reactions of the allylic tin moiety of the bimetallic reagent were thought to be feasible. However, there is no general route to these simple bimetallic species.[2c] An appealing and straightforward approach towards **A** via the allyltrimethylsilyl anion yielded predominantly its regioisomer.[8]

The palladium-catalyzed nucleophilic displacement of the acetate unit of allylic acetates by a hydride is ideally suited to achieve this goal. Allylic acetates undergo efficient palladium(0)-catalyzed substitution reactions with a variety of nucleophiles.[9] Control of regiochemistry of the product is determined by the steric hindrance at the termini of the π-allylpalladium intermediate and by the character and size of the incoming nucleophile. Reactions of π-allylpalladium complexes with hydride as a nucleophile are also well known. The regioselectivity observed is highly dependent on the hydride reagent selected: $LiAlH_4$,[10] $Bu_3SnH(D)$,[11] $LiBHEt_3$,[12] and silicon hydrides[13] deliver the hydride at the less substituted terminus of the π-allylic ligand, while hydride generated from formate is delivered selectively to the more substituted position.[14]

When we subjected the allylic acetate **1a** to the reducing conditions of formate in the presence of palladium (2 mol%), **2a** was obtained as the sole product in high yield (Scheme 1).[4] No decomposition of the resulting silylstannyl compound was observed under the reaction conditions. This is quite surprising since allylic stannanes have been used as nucleophiles in the palladium-catalyzed allylation of allylic acetates.[15] Moreover, delivery of the hydride was highly regioselective to the more substituted carbon of the π-allylic ligand.



1a **2a** >99.5:0.5 **3a**

Scheme 1. a) 1 Mol% $[Pd_2(dba)_3]$, 8 mol% PPh_3, 3 equiv HCO_2H, 3 equiv Et_3N, dioxane, 3 h under reflux; 99% yield.

A variety of bimetalated allylic reagents can be prepared in nearly quantitative yield and excellent selectivity (Table 1, entries 1–5). With the alkyl-substituted allylic acetates **1b–d**, only the *E* isomers were obtained. The reaction was generally performed in refluxing dioxane or THF and was complete in 3–24 h. As expected, the allylic chloride **4** reacted even faster (entry 6). Disilyl-substituted allylic groups containing two different silyl moieties can also be obtained. However, while the disilyl-substituted allylic acetate **5a** (tBuMe$_2$Si, Me$_3$Si) reacted almost exclusively at the γ-position (entry 7), the sterically more encumbered substrate **5b** (iPr$_3$Si, Me$_3$Si, entry 8) gave a 2.5:1 mixture of **6b** and **7b**.

Tsuji was the first to show that the ligand plays an important role in the regioselectivity of the hydride delivery.[14c]

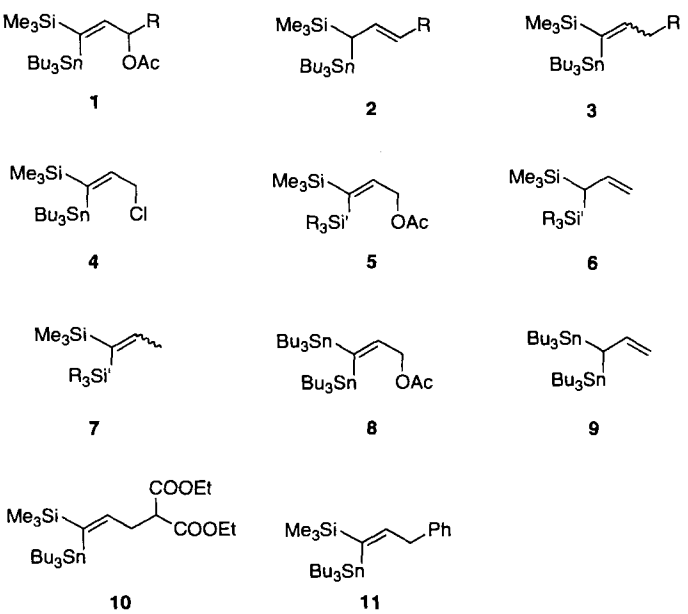


Table 1. Palladium-catalyzed nucleophilic addition to 3,3-bimetallic allylic acetates and chlorides.

No.	Substrate	Method [a]	t [h]	Product(s)	γ: α-Substitution	Yield [%]
1	**1a** (R = H)	A	3	**2a, 3a**	99.6:0.4	99
2	**1a** (R = H)	B	6	**2a, 3a**	99.6:0.4	99
3	**1b** (R = C_2H_5)	A	12	**2b, 3b**	99.6:0.4	99
4	**1c** (R = C_3H_7)	A	12	**2c, 3c**	99.4:0.6	98
5	**1d** (R = c-C_6H_{11})	A	17	**2d, 3d**	99.4:0.6	98
6	**4**	A	1	**2a, 3a**	99.6:0.4	92
7	**5a** (Si' = tBuMe$_2$Si)	A	3	**6a, 7a**	98.9:1.1	85
8	**5b** (Si' = iPr$_3$Si)	A	17	**6b, 7b**	71:29	49
9	**5b** (Si' = iPr$_3$Si)	C	24	**6b, 7b**	88:12	74
10	**8**	B	0.5	**9**	-	-
11	**1a**	D	4	**10**	<1:99	95
12	**1a**	E	4	**11**	-	-

[a] Method A: 3 equiv HCO_2H/Et_3N, 2 mol% $[Pd_2(dba)_3]$, 16 mol% PPh_3, dioxane, 100 °C; method B: 3 equiv HCO_2H/Et_3N, 2 mol% $[Pd_2(dba)_3]$, 16 mol% PPh_3, THF, 65 °C; method C: analogous to method A, except PBu_3 was used instead of PPh_3; method D: $NaCH(COOEt)_2$ was used as the nucleophile; method E: PhZnCl was used as the nucleophile.

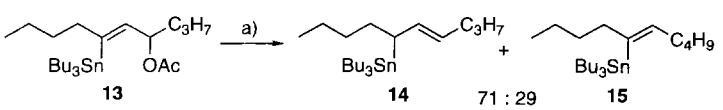
[*] Prof. M. Lautens, P. H. M. Delanghe
Department of Chemistry, University of Toronto
Toronto, Ontario M5S 1A1 (Canada)
Telefax: Int. code + (416)978-6083

[**] This research was supported by the following fellowships: E. W. R. Steacie Fellow, Alfred P. Sloan Foundation Fellow, NSERC (Canada) University Research Fellow, Bio-Mega Young Investigator, Eli Lilly Grantee. P. H. M. D. thanks the Province of Ontario for an Ontario Graduate Scholarship and the University of Toronto for a Simcoe Scholarship.

While typical ratios for hydride attack at the most versus the least substituted position were 95:5 for PPh_3, this ratio improved to 100:0 when PBu_3 was used. With most of the bimetalated allylic acetates (**1a–d** and **5a**) ratios greater than 99:1 were obtained even when PPh_3 was used as the ligand. However, increased selectivity was observed with **5b** when the ligand was changed from Ph_3P to Bu_3P (entry 9). Unfortunately, the distannyl reagent **9** could not be prepared under any of these conditions, presumably due to fast decomposition of the product.

A soft carbon nucleophile such as diethyl sodiomalonate reacted cleanly at the less hindered α-position in 95% yield to give **10** (entry 10). However, the harder phenylzinc choride did not give any of the desired product.

The effect of exchanging silicon for carbon on the regioselectivity of the hydride delivery was also studied. When the alkylstannylated allylic acetate **13** (the Me_3Si group in **1c** is replaced by an *n*-butyl group) was subjected to the same reaction conditions, the selectivity was considerably eroded, and a 71:29 mixture of **14** and **15** was obtained (Scheme 2). To understand this result, the mechanism of hydride transfer must be considered.

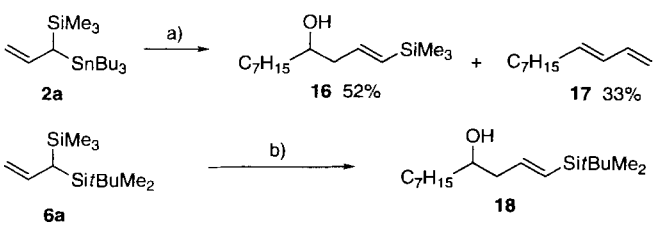


Scheme 2. a) 10 mol% $[Pd_2(dba)_3]$, 80 mol% PPh_3, 3 equiv HCO_2H, 3 equiv Et_3N, dioxane, 17 h at 100 °C; 99% yield.

Tsuji showed that hydride generated from formate is delivered selectively to the more substituted end of the π-allylic ligand in the palladium complex.[14] Recently, a mechanism via an η^1-palladium complex, in which the palladium is coordinated at the least hindered end of the allylic group, was put forward to explain the observed selectivity.[14d] Hydride delivery was proposed to occur intramolecularly at the more hindered terminus of the π-allylic ligand.

Since a butyl group (*A*-value = 1.9)[16] is considerably smaller than a Me_3Si (*A*-value = 2.5),[17] a higher proportion of the η^1-alkyl palladium complex is expected for substrate **1c**. However, this explanation, based exclusively on steric grounds, does not completely explain the results for the extremely hindered substrate **5b**.

We also investigated the reactivity of these bimetallic species with an aldehyde as the electrophile. Treatment of the bimetallic reagent **2a** with octanal in the presence of $BF_3 \cdot OEt_2$ gave the silylated homoallylic alcohol **16** in 52% yield (Scheme 3). No stannyl-substituted homoallylic alcohol was detected. The diene **17** was also isolated in 33% yield. This product presumably arises from a competing, Lewis acid mediated 1,3 shift of the tin substituent in **2a** to give the isomeric bimetallic reagent.[2d] Reaction of this species with the aldehyde, followed by a Peterson elimination of the 1,2-silyl alcohol gives the diene **17**.



Scheme 3. a) 1 equiv $C_7H_{15}CHO$, 1 equiv $BF_3 \cdot Et_2O$, CH_2Cl_2, 10 min at −78 °C. b) 1 equiv $C_7H_{15}CHO$, 1 equiv $BF_3 \cdot Et_2O$, CH_2Cl_2, 2 h at −40 °C; 73% yield.

High selectivity was also observed in the reaction of **6a** with an aldehyde (Scheme 3). Only the Me_3Si group in the disilyl allylic reagent **6a** reacted in the presence of $BF_3 \cdot OEt_2$ to yield the homoallylic alcohol **18** in 73% yield.

In conclusion, the palladium-catalyzed reduction of sensitive bimetallic allylic acetates proceeds with high chemo- and regioselectivity for most cases. The reactivity of these bimetallic reagents towards an electrophile shows that a selective reaction of one of the metals is possible.

Experimental Procedure

2a: To a solution of the allylic acetate **1a** (2.0 g, 4.3 mmol) and PPh_3 (90 mg, 0.34 mmol) in dioxane (15 mL) under nitrogen was added Et_3N (1.8 mL, 13.0 mmol) and HCO_2H (0.49 mL, 13.0 mmol) followed by quick addition of $[Pd_2(dba)_3]$ (39 mg, 0.043 mmol). The mixture was heated at reflux for 3 h. The black solution was diluted with hexanes, washed successively with aqueous $NaHCO_3$ and brine, dried over anhydrous $MgSO_4$, and concentrated in vacuo. The crude oil was filtered through a small plug of silica gel (elution with hexanes) to yield pure **2a** (1.73 g, 99%) as a colorless oil. ^1H NMR (400 MHz, $CDCl_3$): δ = 5.79 (ddd, J(H,H) = 16.5, 12.1, 9.8 Hz, 1H), 4.66 (dd, J(H,H) = 16.5, 2.2 Hz, 1H), 4.62 (dd, J(H,H) = 9.8, 2.2 Hz, 1H), 1.46 (m, 7H), 1.29 (sext, J(H,H) = 7.3 Hz, 6H), 0.88 (t, J(H,H) = 7.3 Hz, 9H), 0.86 (m, 6H), 0.00 (s, 9H); ^{13}C NMR (100 MHz, $CDCl_3$): δ = 139.02 (J(Sn,C) = 42.5 Hz), 109.19 (J(Sn,C) = 46.1 Hz), 29.20 (J(Sn,C) = 19.0 Hz), 27.51 (J(Sn,C) = 59.3 Hz), 22.60 (J(Sn,C) = 183.1, 174.3 Hz), 13.71, 9.99 (J(Sn,C) = 314.2, 301.0 Hz), −0.45 (J(Sn,C) = 10.3 Hz); ^{119}Sn NMR (112 MHz, $CDCl_3$): δ = −16.83; ^{29}Si NMR (80 MHz, $CDCl_3$): δ = 1.18.

18: Octanal (68 mL, 0.44 mmol) was dissolved in 0.5 mL dry CH_2Cl_2, and the flask cooled to −40 °C. $BF_3 \cdot OEt_2$ (0.88 mL, 0.5 M solution in CH_2Cl_2, 0.44 mmol) was added followed by **6a**. The reaction was stirred at −40 °C for 2 h. After aqueous workup, the crude colorless oil was purified by flash chromatography, with pentane to pentane:diethyl ether 10:1 as eluent, to yield 91 mg (73%) of **18**. ^1H NMR (400 MHz, $CDCl_3$): δ = 6.02 (ddd, J(H,H) = 18.6, 7.3, 5.9 Hz, 1H), 5.73 (ddd, J(H,H) = 18.6, 1.5, 1.1 Hz, 1H), 3.64 (m, 1H), 2.37 (dddd, J(H,H) = 13.6, 5.9, 4.4, 1.4 Hz, 1H), 2.19 (dddd, J(H,H) = 13.6, 8.7, 7.3, 1.1 Hz, 1H), 1.54 (d, J(H,H) = 3.7 Hz, 1H), 1.43 (m, 4H), 1.26 (m, 8H), 0.86 (t, J(H,H) = 7.3 Hz, 3H), 0.84 (s, 9H), 0.00 (s, 6H); ^{13}C NMR (100 MHz, $CDCl_3$): δ = 144.09, 131.59, 70.56, 45.20, 36.81, 31.83, 29.64, 29.29, 26.44, 25.65, 22.69, 16.45, 14.13, −6.05, −6.06.

Received: June 6, 1994 [Z 7005 IE]
German version: *Angew. Chem.* **1994**, *106*, 2557

[1] a) Y. Yamamoto, H. Yatagai, K. Maruyama, *J. Am. Chem. Soc.* **1981**, *103*, 3229; b) S. E. Denmark, K. L. Habermas, G. A. Hite, T. K. Jones, *Tetrahedron* **1986**, *42*, 2821; c) O. Desponds, M. Schlosser, *J. Organomet. Chem.* **1991**, *409*, 93; d) K.-T. Kang, J. C. Lee, J. C. U, *Tetrahedron Lett.* **1992**, *33*, 4953; e) Y.-F. Lu, C. W. Harwig, A. G. Fallis, *J. Org. Chem.* **1993**, *58*, 4202.

[2] a) S. Chandrasekhar, S. Latour, J. D. Wuest, B. Zacharie, *J. Org. Chem.* **1983**, *48*, 3810; b) W. S. Johnson, R. Elliott, J. D. Elliott, *J. Am. Chem. Soc.* **1983**, *105*, 2904; c) H. J. Reich, I. L. Reich, K. E. Yelm, J. E. Holladay, D. Gschneidner, *ibid.* **1993**, *115*, 6625; d) G E. Keck, A. Palani, *Tetrahedron Lett.* **1993**, *34*, 3223.

[3] a) M. Lautens, A. H. Huboux, B. Chin, J. Downer, *Tetrahedron Lett.* **1990**, *31*, 5829; b) M. Lautens, P. H. M. Delanghe, *J. Org. Chem.* **1992**, *57*, 798.

[4] All trimethylsilyltributylstannylated allylic alcohols were obtained in good overall yield: a) M. Lautens, A. H. Huboux, *Tetrahedron Lett.* **1990**, *31*, 3105; b) the disilyl-substituted allylic alcohols were prepared by a 1,4-silyl migration reaction: M. Lautens, P. H. M. Delanghe, J. B. Goh, C. H. Zhang, *J. Org. Chem.* **1992**, *57*, 3270; c) acetylation conditions (Ac_2O, pyridine) gave the allylic acetates.

[5] I. Fleming in *Comprehensive Organic Synthesis, Vol.2* (Ed.: B. M. Trost), Pergamon, Oxford, **1991**, p. 563.

[6] M. Pereyre, J.-P. Quintard, A. Rahm, *Tin in Organic Synthesis*, Butterworth, London, **1987**.

[7] a) G. D. Hartman, T. G. Traylor, *Tetrahedron Lett.* **1975**, 939; b) A. Hosomi, T. Imai, M. Endo, H. Sakurai, *J. Organometal. Chem.* **1985**, *285*, 95; c) M. Patz, H. Mayr, *Tetrahedron Lett.* **1993**, *34*, 3393, and references therein.

[8] Deprotonation of allyltrimethylsilane with *s*BuLi in THF/TMEDA, followed by addition of tributyltinchloride, resulted in clean stannylation at the γ-position: a) Y. Yamamoto, Y. Saito, K. Maruyama, *J. Organomet. Chem.* **1985**, *292*, 311; b) G. Fraenkel, A. Chow, W. R. Winchester, *J. Am. Chem. Soc.* **1990**, *112*, 2582; c) G. E. Keck, D. R. Romer, *J. Org. Chem.* **1993**, *58*, 6083.

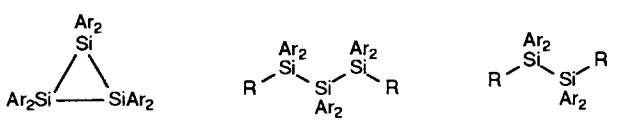
[9] Recent reviews: a) S. A. Godleski in *Comprehensive Organic Synthesis, Vol. 4* (Ed.: B. M. Trost), Pergamon, Oxford, **1991**, p. 585; b) C. G. Frost, J. Howarth, J. M. J. Williams, *Tetrahedron: Asymmetry* **1992**, *3*, 1089.

[10] D. N. Jones, S. D. Knox, *J. Chem. Soc. Chem. Commun.* **1975**, 165.
[11] N. Greenspoon, E. Keinan, *J. Org. Chem.* **1988**, *53*, 3723.
[12] R. O. Hutchins, K. Learn, *J. Org. Chem.* **1982**, *47*, 4380.
[13] E. Keinan, N. Greenspoon, *J. Org. Chem.* **1983**, *48*, 3545.
[14] a) J. Tsuji, T. Yamakawa, *Tetrahedron Lett.* **1979**, 631; b) J. Tsuji, I. Shimizu, I. Minami, *Chem. Lett.* **1984**, 1017; c) J. Tsuji, I. Minami, I. Shimizu, *Synthesis* **1986**, 623; d) D. Mandai, S. Suzuki, T. Murakami, M. Fujita, M. Kawada, J. Tsuji, *Tetrahedron Lett.* **1992**, 33, 2987; e) T. Mandai, T. Matsumoto, J. Tsuji, *Synlett* **1993**, 113; f) T. Hayashi, H Iwamura, Y Uozumi, *Tetrahedron Lett.* **1994**, *35*, 4813.
[15] a) B. M. Trost, E. Keinan, *Tetrahedron Lett.* **1980**, *21*, 2595; b) J. P. Godschalx, J. K. Stille, *ibid.* **1980**, *21*, 2599; c) B. M. Trost, K. M. Pietrusiewicz, *ibid.* **1985**, *26*, 4039; d) A. Gollaszewski, J. Schwartz, *Organometallics* **1985**, *4*, 417.
[16] J. A. Hirsch, *Top. Stereochem.*, **1967**, 199.
[17] W. Kitching, H. A. Olszowy, G. M. Drew, W. Adcock, *J. Org. Chem.* **1982**, *47*, 5153.

Doubly Lithiated Oligosilanes: Synthesis and Structure of the First Vicinal Dilithiodisilane**

Johannes Belzner,* Uwe Dehnert, and Dietmar Stalke*

The cleavage of silicon–silicon σ bonds by alkali metals is a common method for the preparation of metalated silanes. This reaction, however, only proceeds satisfactorily if the silicon centers carry at least one aromatic substituent.[1] The same is true for the reaction of cyclic silanes with alkali metals: while peralkylated cyclosilanes are reduced by alkali metals only to the stage of radical anions,[2] aryl-substituted silacycles undergo bond cleavage to yield synthetically useful difunctional α,ω-dimetallio oligosilanes. The reactions of octaphenyltetrasilane and decaphenylcyclopentasilane with lithium have been studied extensively and have been used for the preparation of numerous organosilicon compounds.[3] To our knowledge, there are no reports about the analogous reactions of cyclotrisilanes with metals. This gap is now filled by the results of the reaction of the cyclotrisilane **1** with lithium metal, which yields, depending on the reaction conditions, either the 1,3-dilithiotrisilane **2a** or the 1,2-dilithiodisilane **3a**.



1 **2** **3**

Ar = 2-(Me_2NCH_2)C_6H_4

2a,3a: R = Li
2b,3b: R = H

The reaction of the cyclotrisilane **1** with two equivalents of lithium in 1,4-dioxane allowed the subsequent isolation of red, extremely air-sensitive crystals of **2a**, which can be smoothly protonated with cyclopentadiene to yield the trisilane **2b**. The ^1H and ^{13}C NMR spectra of **2a** are very concentration- and temperature-dependent, and hence not very useful for structural elucidation, as they primarily contain very broad, strongly overlapping signals. The ^{29}Si NMR spectrum also exhibits two strongly broadened signals at $\delta = -26.5$ and -31.8. Therefore, the identification of the reaction product as the 1,3-dilithiotrisilane **2a** is based primarily on the results of the single-crystal X-ray structure determination.[4]

The crystal structure of **2a** (Fig. 1) indicates that the concept of intramolecular side-chain coordination is, here too, particularly useful—this idea has also been successfully applied to organocopper compounds[8] and compounds containing highly coordinated silicon centers.[9] In **2a** the lithium atoms bound to silicon are coordinated by both amino groups of the neighboring $Me_2NCH_2C_6H_4$ substituents; two chelate rings are thus formed. The average Li–N bond length is 214 pm, significantly longer than that in contact ion pairs of lithium atoms and bases with nitrogen donors.[10] In addition, each lithium atom is coordinated by a single oxygen atom from a dioxane molecule.

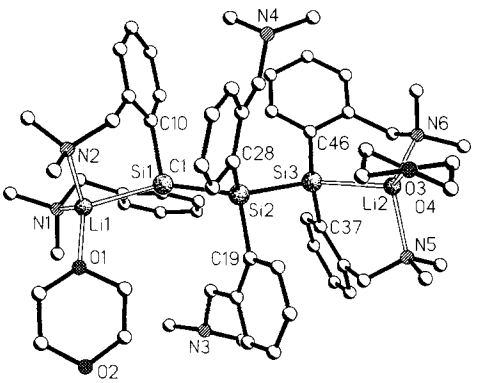


Fig. 1. Crystal structure of **2a**. Three noncoordinated dioxane molecules are omitted for clarity. Selected bond lengths [pm] and angles [°]: Si1–Si2 240.7(3), Si2–Si3 240.1(3), Si1–Li1 255(1), Si3–Li2 254(1), Li1–N1 214(1), Li1–N2 215(1), Li1–O1 197(1), Li2–N5 216(1), Li2–N6 211(1), Li2–O3 199(1); C1-Si1-C10 99.5(3), C19-Si2-C28 101.9(3), C37-Si3-C46 99.8(3), Si1-Si2-Si3 136.9(1), Li1-Si1-Si2 131.6(3), Si2-Si3-Li2 129.7(3).

The average distance between Si and Li is significantly shorter (254.3 pm) than in all other structurally characterized molecular compounds with Si–Li contacts ($[Me_3SiLi]_6$ 265 pm;[11] $[Me_3SiLi(tmeda)_{1.5}]$ 270 pm,[12] tmeda = *N*,*N*,*N*′,*N*′-tetramethylethylenediamine; $[(Me_3Si)_3SiLi(dme)_{1.5}]$ 263 pm,[13] dme = 1,2-dimethoxyethane; $[\{(thf)_3Li\}_2(SiPh_2)_4]$ 271 pm;[14] $[(Me_3Si)_3SiLi(thf)_3]$ 264 and 267 pm;[15] $[Ph_3SiLi(thf)_3]$ 267 pm[16]). The steric demands of the six 2-(Me_2NCH_2)C_6H_4 units cause a distinct stretching of the $LiSi_3Li$ backbone, which assumes an approximately antiperiplanar conformation. The bond angles along the $LiSi_3Li$ chain are significantly larger than ideal tetrahedral angles; the central Si-Si-Si angle is widened to 136.9°.

The reaction of **1** with excess lithium in THF yields a different product: the first 1,2-dilithiodisilane **3a** is obtained in the form of deep red crystals. This compound can also be prepared by treating **2a** with lithium under the same conditions. The single-crystal X-ray structure analysis (Fig. 2) shows that both lithium atoms are coordinated to the silicon centers, as was the case in **2a**.

Compound **3a** crystallizes with two independent molecules per asymmetric unit, which only differ slightly in the orientation of the substituents (the structural parameters of the second mol-

[*] Dr. J. Belzner, Dipl.-Chem. U. Dehnert
Institut für Organische Chemie der Universität
Tammannstrasse 2, D-37077 Göttingen (FRG)
Telefax: Int. code + (551)39-9475
Priv.-Doz. Dr. D. Stalke
Institut für Anorganische Chemie der Universität
Tammannstrasse 4, D-37077 Göttingen (FRG)
Telefax: Int. code + (551)39-2582

[**] This work was supported by the Deutsche Forschungsgemeinschaft and the Fonds der Chemischen Industrie. We thank Prof. M. Rabinovitz for helpful discussions and R. Machinek, Dr. G. Elter, and W. Zolke for assistance with the NMR spectroscopic studies.

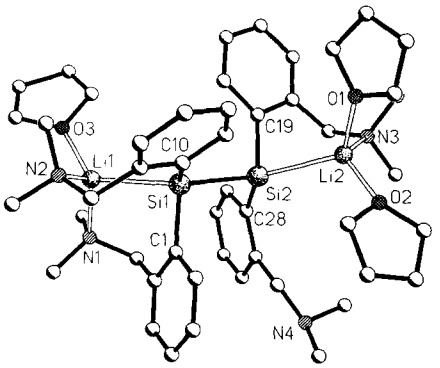


Fig. 2. Crystal structure of **3a**. Selected bond lengths [pm] and angles [°]—the values separated by a slash are those for the chemically equivalent parameter in the second, crystallographically independent molecule: Si1–Si2 238.0(2)/237.7(2), Si1–Li1 254.2(8)/255.0(8), Si2–Li2 258.9(8)/259.0(8), Li1–O3 195(1)/196(1), Li1–N1 217(1)/215(1), Li1–N2 213(1)/215(1), Li2–O1 198(1)/199(1), Li2–O2 196(1)/197(1), Li2–N3 213(1)/214(1); C1-Si1-C10 100.7(2)/99.6(2), C19-Si2-C28 102.0(2)/101.3(2), Li1-Si1-Si2 143.7(2)/143.7(2), Si1-Si2-Li2 134.9(2)/134.7(2).

ecule, not shown in the Figure, are separated from the analogous ones for the first molecule by a slash). The most striking structural feature at first glance is perhaps the different environments of the two lithium atoms: Li1 is coordinated to two Me_2NCH_2 side chains (average Li–N bond length 215.2/215.8 pm) and one thf molecule, while Li2 is surrounded by only one amino group (Li–N 212.8/213.7 pm) and two thf ligands. The two Si–Li bond lengths are not identical (Si1–Li1 254.2/255.0 pm, Si2–Li2 258.9/259.0 pm). Apparently, coordination to two amino side chains brings the Si and Li atoms closer together (cf., 254.3 pm in **2a**). The central Si–Si bond length (238.0/237.7 pm) is typical for a Si–Si single bond and is nearly identical to that in the disilane **3b** (236.4/238.6 pm).[17]

A side-on coordination of the lithium atoms to the central element–element bond,[18] such has been observed for the C–C unit in substituted dilithioethanes, is not found in **3a**. This is presumably a consequence of the intramolecular complexation.

With THF as solvent, the ^{29}Si NMR spectrum of **3a** exhibits a 1:1:1:1 quartet at $\delta = -32.8$.[19] The corresponding $^{29}Si-^{7}Li$ coupling constant (36 Hz) indicates a partially covalent character of the Si–Li bond.[20] However, the fact that the Si–Li bond length is shorter than in other lithiated silicon compounds is not reflected by a larger coupling constant ($[Me_2PhSiLi(thf)_x]$ 51 Hz;[21] $[Ph_3SiLi(thf)_3]$ 45 Hz;[16] $[(Me_3Si)_3SiLi(thf)_3]$ 37.2 Hz;[15] $[\{(thf)_3Li\}_2(SiPh_2)_4]$ 32.8, 40, and 42 Hz[14]).

These results show that the cyclotrisilane **1** is not only a valuable synthetic equivalent to silanediyls $Ar_2Si:$,[22] its reaction with lithium also opens up access to the dilithio compounds **2a** and **3a**, which in turn should be able to function as transfer agents for Si_3 and Si_2 units. Studies to determine the reactivity of these compounds are currently in progress.

Experimental Procedure

All experiments were performed with exclusion of oxygen and moisture. Where possible, the assignments of ^{1}H, ^{13}C, and ^{29}Si NMR signals to atoms of the terminal or central diaryldisilanediyl units in **2a** and **2b** are indicated by the numbers (1,3) or (2), respectively, after the element symbol. The ^{7}Li NMR spectra were calibrated externally with $LiCl/H_2O$.

2a: Lithium shavings (31 mg, 4.47 mmol) were added to a solution of **1** (1.99 g, 2.24 mmol) in dioxane (28 mL). The resulting mixture was stirred for 22 h at 25 °C. The volume of the clear red solution was reduced by about 2/3, and hexane (8 mL) added. Residual lithium was then removed by filtration. Crystallization at 4 °C yielded **2a** as bright red crystals (1.18 g, 49% yield, m.p. 50–60 °C (decomp.)), which still contained 2 equiv of dioxane per molecule of **2a** after solvent removal under high vacuum. ^{1}H NMR (250 MHz, $[D_8]THF$, 25 °C): $\delta = 1.35$ (brs, 12H; NMe_2), 1.93 (s, 24H; NMe_2), 2.3–3.4 (brs, 8H; CH_2), 3.6–4.1 (brs, 4H; CH_2), 6.4–6.9 (brs, 10H), 6.91 (t, $^{3}J = 7.5$ Hz, 4H), 7.18 (d, $^{3}J = 7.2$ Hz, 4H), 7.6–8.1 (brs, 4H; 6-H(1,3)), 8.6–8.9 (brs, 2H; 3-H(2)); ^{7}Li NMR (155.45 MHz, THF/C_6D_6 (5:1), 25 °C): $\delta = 0.90$ (s); ^{29}Si NMR (99.3 MHz, $[D_8]THF$, 25 °C): $\delta = -26.5$ (Si-2), -31.8 (Si-1,3).

2b: A solution of **2a** (1.05 g, 0.93 mmol), which still contained 2.5 equiv of dioxane, in THF (10 mL) was cooled to −78 °C and treated with cyclopentadiene (0.19 mL, 2.33 mmol). The mixture was stirred and allowed to warm to room temperature. The solvent was removed, hexane (15 mL) was added, and undissolved components were removed by filtration. Volume reduction of the filtrate yielded **2b** as hydrolysis-sensitive crystals (0.56 g, 68% yield, m.p. 171–172 °C). ^{1}H NMR (250 MHz, C_6D_6): $\delta = 1.79$ (s, 12H; NMe_2), 2.00 (s, 24H; NMe_2), 3.04 (s, 4H; CH_2), 3.25, 3.27 (AB system, $^{2}J = 14$ Hz, 8H; CH_2), 5.87 (s, $^{1}J(Si,H) = 200.5$ Hz, 2H; SiH), 6.92 (dd, $^{3}J(4,5) = 7.5$ Hz, $^{3}J(5,6) = 7.2$ Hz, 4H; 5-H(1,3)), 7.09 (dd, $^{3}J(3,4) = 7.4$ Hz, $^{3}J(4,5) = 7.5$ Hz, 4H; 4-H(1,3)), 7.22 (dd, $^{3}J(4,5) = 7.5$ Hz, $^{3}J(5,6) = 7.2$ Hz, 2H; 5-H(2)), 7.33 (dd, $^{3}J(3,4) = 7.6$ Hz, $^{3}J(4,5) = 7.5$ Hz, 2H; 4-H(2)), 7.36 (d, $^{3}J(3,4) = 7.4$ Hz, 4H; 3-H(1,3)), 7.71 (d, $^{3}J(5,6) = 7.2$ Hz, 4H; 6-H(1,3)), 7.81 (d, $^{3}J(3,4) = 7.6$ Hz, 2H; 3-H(2)), 8.60 (d, $^{3}J(5,6) = 7.2$ Hz, 2H; 6-H(2)); ^{13}C NMR (62.9 MHz, C_6D_6): $\delta = 45.15$, 45.28 (2 × NMe_2), 63.99, 64.46 (2 × CH_2), 125.98, 128.22, 128.98, 129.05, 129.50, (5 × CH), 135.54, 135.74 (C-1(1,2,3)), 138.43, 138.72 (C-6(1,2,3)), 146.04 (C-2(1,3)), 148.07 (C-2(2)); ^{29}Si NMR (59.6 MHz, C_6D_6): $\delta = -37.5$ (brs), -43.9 (d, $^{1}J(Si,H) = 203$ Hz); MS (70 eV) *m/z* (%): 890 (M^+, <1%), 297 (Ar_2SiH^+, 100).

3a: Lithium shavings (45 mg, 7.38 mmol) were added to a solution of **1** (1.09 g, 1.23 mmol) in THF (18 mL). The resulting mixture was stirred for 3 d at 25 °C. Residual lithium was removed from the clear, deep red solution by filtration, the solution volume was reduced (to ca. 3 mL), and pentane (10 mL) was added. Crystallization at −15 °C yielded **3a** in the form of dark red crystals, which contained 4 equiv of THF per molecule of **3a** (0.87 g, 53% yield, m.p. 45–50 °C (decomp.)). ^{1}H NMR (250 MHz, C_6D_6): $\delta = 1.82$ (brs, 24H; NMe_2), 2.7–3.4 (brs, 8H; CH_2), 6.8–7.1 (m, 4H; 3-H), 7.0–7.3 (m, 8H; 4,5-H), 8.36 (brs, 4H; 6-H); ^{13}C NMR (75.5 MHz, C_6D_6): $\delta = 46.14$ (NMe_2), 67.71 (CH_2), 122.44, 126.08 (C-4,5), 130.23 (C-3), 139.12 (C-6), 142.48 (C-2), 162.20 (C-1); ^{7}Li NMR (155.45 MHz, C_6D_6): $\delta = 1.36$ (s); ^{29}Si NMR (59.6 MHz, THF/C_6D_6 (5:1), 25 °C): $\delta = -32.8$ ($^{1}J(Si,Li) = 36$ Hz).

Received: August 9, 1994 [Z 7224 IE]
German version: *Angew. Chem.* **1994**, *106*, 2580

[1] A. G. Brook, H. Gilman, *J. Am. Chem. Soc.* **1954**, *76*, 278–279; b) H. Gilman, G. D. Lichtenwalter, *ibid.* **1958**, *80*, 608–611.
[2] B. Kirste, R. West, H. Kurreck, *J. Am. Chem. Soc.* **1985**, *107*, 3013–3016.
[3] a) H. Gilman, D. J. Peterson, A. W. Jarvie, H. J. S. Winkler, *J. Am. Chem. Soc.* **1960**, *82*, 2076; b) H. Gilman, G. L. Schwebke, *ibid.* **1963**, *85*, 1016; c) E. Hengge, D. Wolfer, *J. Organomet. Chem.* **1974**, *66*, 413–424.
[4] Crystal structure data for **2a**: $Ar_6Si_3Li_2(dioxane)_2 + 3$dioxane (Ar = 2-$(Me_2NCH_2)C_6H_4$), $M = 1424.05$, triclinic, space group $P\bar{1}$, $a = 1442.6(3)$, $b = 1633.1(3)$, $c = 2025.1(4)$ pm, $\alpha = 66.87(3)$, $\beta = 79.54(3)$, $\gamma = 69.96(3)°$, $V = 4.116(2)$ nm^3, $Z = 2$, $\rho_{calcd} = 1.149$ g cm^{-3}, $F(000) = 1548$, $\lambda = 71.073$ pm, $T = -120$ °C, $\mu(Mo_{K\alpha}) = 0.113$ mm^{-1}, crystal dimensions: 0.6 × 0.4 × 0.4 mm, $8° \le 2\theta \le 45°$; total number of reflections 12625, of which 10698 were independent; all of these were used to refine 952 parameters, with 212 restraints for the 1–2 and 1–3 distances in the coordinated and noncoordinated dioxane molecules; maximum residual electron density: 581 e nm^{-3}, $R1$ ($F > 4\sigma(F)$) = 0.057, $wR2 = 0.161$ (all data) ($R1 = \sum||F_o| - |F_c||/\sum|F_o|$, $wR2 = (\sum w(F_o^2 - F_c^2)^2/\sum w(F_o^2)^2)^{0.5}$. Crystal structure data for **3a**: $Ar_4Si_2Li_2(thf)_3$ (Ar = 2-$(Me_2NCH_2)C_6H_4$), $M = 823.16$, triclinic, space group $P\bar{1}$, $a = 1052.5(2)$, $b = 2155.3(4)$, $c = 2376.2(5)$ pm, $\alpha = 66.26(3)$, $\beta = 89.48(3)$, $\gamma = 88.30(3)°$, $V = 4.932(2)$ nm^3, $Z = 4$, $\rho_{calcd} = 1.109$ g cm^{-3}, $F(000) = 1784$, $\lambda = 71.073$ pm, $T = -120$ °C, $\mu(Mo_{K\alpha}) = 0.113$ mm^{-1}, crystal dimensions: 0.7 × 0.6 × 0.6 mm, $4° \le 2\theta \le 45°$; total number of reflections 12732, of which 12663 were independent; all of these were used to refine 1099 parameters; maximum residual electron density: 470 e nm^{-3}, $R1$ ($F > 4\sigma(F)$) = 0.080, $wR2 = 0.242$ (all data). The data for both structures were collected on a Stoe-AED diffractometer. The intensity measurements were collected, by the $2\theta/\omega$ method, with crystals that were shock-cooled in a drop of oil [5]. The structures were solved by direct methods (SHELXS-90) [6] and refined by the least-squares method vs F^2 [7]. Further details of the crystal structure investigations are available on request from the Cambridge Crystallographic Data Centre, 12 Union Road, GB-Cambridge, CB21EZ, on quoting the full journal citation.
[5] T. Kottke, D. Stalke, *J. Appl. Crystallogr.* **1993**, *26*, 615–619.
[6] G. M. Sheldrick, *Acta Crystallogr. Sect. A* **1990**, *46*, 467–473.
[7] G. M. Sheldrick, SHELXL-93, program for the refinement of crystal structures, Göttingen, **1993**.
[8] a) G. van Koten, J. G. Noltes in *Compehensive Organometallic Chemistry* (Eds.: G. Wilkinson, F. G. A. Stone, E. W. Abel), Pergamon Press, Oxford, **1982**, pp. 709–763; b) G. van Koten, *J. Organomet. Chem.* **1990**, *400*, 283–301.
[9] a) R. J. P. Corriu, C. Guerin, *Adv. Organomet. Chem.* **1982**, *20*, 265–312; b) C. Chuit, R. J. P. Corriu, C. Reye, J. C. Young, *Chem. Rev.* **1993**, *93*, 1371–1448.

[10] a) K. Gregory, P. von R. Schleyer, R. Snaith, *Adv. Inorg. Chem.* **1991**, *37*, 47–142; b) H. Gornitzka, D. Stalke, *Organometallics*, in press; c) U. Olsher, R. M. Izatt, J. S. Bradshaw, N. K. Dalley, *Chem. Rev.* **1991**, *91*, 137–164.
[11] a) T. F. Schaaf, W. Butler, M. D. Glick, J. P. Oliver, *J. Am. Chem. Soc.* **1974**, *96*, 7593–7594; b) W. H. Ilsley, T. F. Schaaf, M. D. Glick, J. P. Oliver, *ibid.* **1980**, *102*, 3769–3774.
[12] B. Teclé, W. H. Ilsley, J. P. Oliver, *Organometallics* **1982**, *1*, 875–877.
[13] G. Becker, H.-M. Hartmann, A. Münch, H. Riffel, *Z. Anorg. Allg. Chem.* **1985**, *530*, 29–42.
[14] G. Becker, H.-M. Hartmann, E. Hengge, F. Schrank, *Z. Anorg. Allg. Chem.* **1989**, *572*, 63–74.
[15] A. Heine, R. Herbst-Irmer, G. M. Sheldrick, D. Stalke, *Inorg. Chem.* **1993**, *32*, 2694–2698.
[16] H. V. R. Dias, M. M. Olmstead, K. Ruhlandt-Senge, P. P. Power, *J. Organomet. Chem.* **1993**, *462*, 1–6.
[17] J. Belzner, N. Detomi, H. Ihmels, M. Noltemeyer, *Angew. Chem.* **1994**, *106*, 1949–1950; *Angew. Chem. Int. Ed. Engl.* **1994**, *33*, 1854–1855.
[18] a) M. Walczak, G. D. Stucky, *J. Organomet. Chem.* **1975**, *97*, 313–323; b) M. Walczak, G. Stucky, *J. Am. Chem. Soc.* **1976**, *98*, 5531–5539; c) A. Sekiguchi, T. Nakanishi, C. Kabuto, H. Sakurai, *ibid.* **1989**, *111*, 3748–3750; d) *Chem. Lett.* **1992**, 867–870.
[19] Experiments to observe the different environments of the Li atoms, which were found in the crystal **3a**, by NMR spectroscopy were not successful, even in such poorly coordinating solvents as [D_8]toluene or C_6H_6.
[20] C. Lambert, P. von R. Schleyer, *Angew. Chem.* **1994**, *106*, 1187–1199; *Angew. Chem. Int. Ed. Engl.* **1994**, *33*, 1129–1140.
[21] U. Edlund, T. Lejon, T. K. Venkatachalam, E. Buncel, *J. Am. Chem. Soc.* **1985**, *107*, 6408–6409.
[22] See, for example, J. Belzner, H. Ihmels, *Tetrahedron Lett.* **1993**, *34*, 6541–6544.

A Chiral Lewis Acid with Two "Metal" Centers: Cooperative Binding of Two Amine Molecules to a Chiral Diboronic Ester**

Kyoko Nozaki, Masanori Yoshida, and Hidemasa Takaya*

Lewis acid/Lewis base interactions are one of the most fundamental types of binding in organic chemistry. Although asymmetric reactions with chiral Lewis acid catalysts are well studied,[1] only a few reports have focused on structural aspects of the interaction of Lewis acids and Lewis bases.[2] Here, we describe the design and synthesis of a chiral Lewis acid having two "metal" centers,[3] *ortho*-bis[(4*R*,5*R*)-4,5-diphenyl-1,3-dioxa-2-borolane-2-yl]benzene (**1a**). This compound contains two dioxaborolane units that can bind two amine molecules cooperatively.[4, 5]

The chiral *ortho*-diboronate **1a** was synthesized along with the *meta* isomer **1b**, *para* isomer **1c**, and analogue **2**, which contains one Lewis-acidic center, and their binding properties with amines were examined. The interaction of *ortho*-diboronate **1a** with benzylamine is unique, as evident in ^{1}H NMR spectra. Thus a mixture of **1a** and benzylamine exhibited the following three notable features: 1) The two originally enantiotopic benzylic protons of the amine appear as a quartet with an AB pattern typical for diastereotopic protons. 2) The signals arising from the NH protons are shifted markedly downfield relative to those of the free benzylamine. 3) The signal due to the methine protons of the dioxaborolane units of **1a** remains a singlet and is only shifted slightly upfield. These results indicate that the amine is complexed with diboronate **1a** and influenced by the chiral surroundings. Since the equilibrium for the formation of the complex at 20 °C is rapid on the NMR timescale, the observed signal of the methine protons in **1a** is a singlet. In sharp contrast to the *ortho*-diboronate **1a**, *meta*- and *para*-diboronates, **1b** and **1c**, and monoboronate **2** show only small changes in their NMR spectra upon mixture with benzylamine under the same conditions, and the benzylic protons of the amine give rise to a singlet.[6] The exceptionally strong binding of **1a** with benzylamine has been demonstrated by titrations of boronates **1a**, **1b**, **1c**, and **2** with the amine (Fig. 1). Titrations of the *ortho*-diboronate **1a** show a characteristic marked saturation effect.

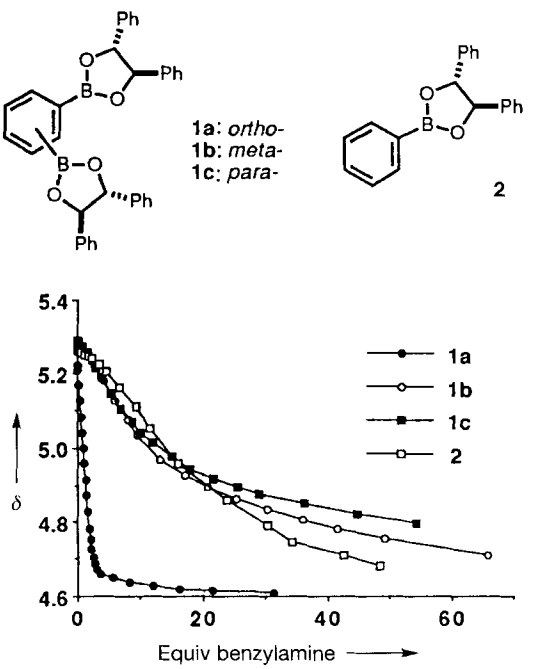


Fig. 1. Titration of boronates **1a–c** and **2** with benzylamine at 20 °C (0.10 M of **1a–c** or **2** in $CDCl_3$). Chemical shifts of the singlets due to the methine protons of the boronates (around $\delta = 5.3$) are plotted against the molar equivalents of added benzylamine.

The complexation ratio of **1a**:benzylamine = 1:2 was determined with a Job plot[7] based on ^{1}H NMR spectroscopic data (conditions: $T = 20$ °C, $[\mathbf{1a}]_{initial} + [amine]_{initial} = 0.05$ M in $CDCl_3$). Maximum complex formation occurred at $[\mathbf{1a}]_{initial}/([\mathbf{1a}]_{initial} + [amine]_{initial}) = 0.33$. Accordingly, the complexation equilibrium of **1a** with benzylamine can be described by Equations (a) and (b). Benesi–Hildebrand analysis[8] indicates that

$$\mathbf{1a} + (amine) \overset{K_1}{\rightleftarrows} \mathbf{1a} \cdot (amine) \quad (a)$$

$$\mathbf{1a} \cdot (amine) + (amine) \overset{K_2}{\rightleftarrows} \mathbf{1a} \cdot (amine)_2 \quad (b)$$

the binding of the second amine molecule to diboronate **1a** is remarkably enhanced compared to that of the first amine molecule ($K_2 \gg K_1$). The plot of $1/[amine]^2_{initial}$ vs $1/\Delta\delta_{observed}$ shows good linearity in the region where $[amine]_{initial} > 10 \times [\mathbf{1a}]_{initial}$ ($[\mathbf{1a}]_{initial} = 0.10$ M). This indicates that the contri-

[*] Prof. Dr. H. Takaya, M. Yoshida, Dr. K. Nozaki
Division of Material Chemistry, Graduate School of Engineering
Kyoto University, Sakyo-ku, Kyoto, 606-01 (Japan)
Telefax: Int. code + (75) 761-8846

[**] This work was supported by a Grant-in-Aid for Developmental Scientific Research (No. 06555272) and by a Grant-in-Aid for Scientific Research (No. 06750885; fellowship for K. N.) both from the Ministry of Education, Science and Culture, Japan. K. N. also thanks The Asahi Glass Foundation for partial financial support.

bution of the 1:1 complex is almost negligible ($K_2 \gg K_1$). Thus the binding constant $K = 18.8\,\mathrm{M}^{-2}$ in Equation (c) can be

$$\mathbf{1a} + 2\,(\text{amine}) \overset{K}{\rightleftarrows} \mathbf{1a}\cdot(\text{amine})_2 \qquad (c)$$

calculated quite simply at 20 °C. The Hill coefficient $n_H = 1.50$ has also been estimated.

^{1}H NMR spectra recorded at −50 °C reveal that only the 1:2 complex consisting of *ortho*-diboronate **1a** and benzylamine is formed regardless of the initial ratios of the two components (Fig. 2). In spectrum C (1:2 initial ratio) complexation is so

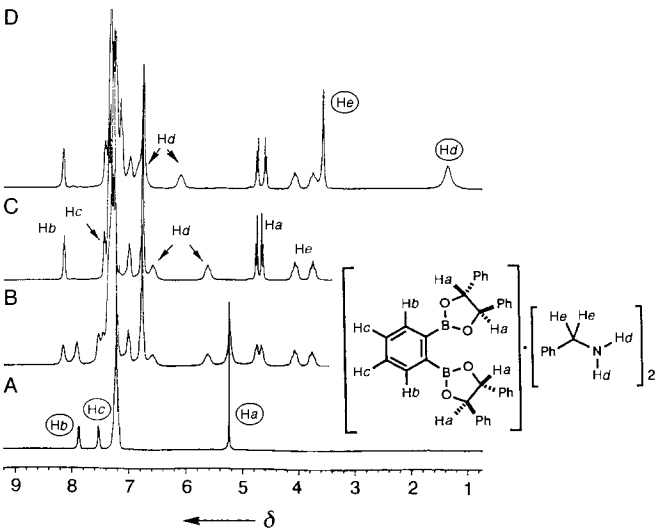
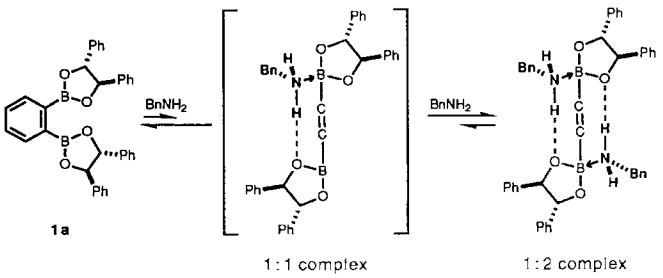


Fig. 2. ^{1}H NMR spectra of a mixture of **1a** (0.10 M) and benzylamine at −50 °C in $CDCl_3$; A: free **1a** without added amine, B: with 1.0 equiv amine (the 1:2 complex and free **1a** are present), C: with 2.0 equiv amine (only the 1:2 complex is present), D: with 4.0 equiv amine (the 1:2 complex and free amine are present). The signals with circled labels are due to free amine.

strong that only the 1:2 complex exists in solution as a single species. Spectra B and D indicate the system to be in the slow-exchange regime, since separated signals are obtained for free and bound **1a** as well as for benzylamine.[9] Thus the absence of any 1:1 complex at −50 °C again strongly suggests the cooperative binding of the two amine molecules to **1a** ($K_2 \gg K_1$).

Two significant structural features in this 1:2 complex can be observed in Figure 2, spectrum C: 1) The methine protons of **1a** (H*a*) give rise to only one AB-type quartet, indicating that the two H*a* protons on each dioxaborolane ring are magnetically nonequivalent, and that the two dioxaborolane groups are equivalent. The C_2-symmetric chiral structure of the 1:2 complex can thus be deduced. 2) A remarkable difference in chemical shift of the two NH protons of benzylamine and a significant downfield shift of one of the two NH protons strongly suggest the presence of a hydrogen bond in addition to the normal Lewis acid/Lewis base complexation.

All these results are clearly accounted for by the structural model shown in Scheme 1. The first amine molecule coordinates with one of the two boron atoms of diboronate **1a**, and at the same time, one NH proton interacts with one of the two oxygen atoms in the other dioxaborolane ring forming a hydrogen bond.[10] As a result, the two dioxaborolane units are conformationally fixed by the two-point binding and provide a suitable binding site for the second amine molecule.[11, 12] This cooperative effect can be realized only with the *ortho*-diboronate **1a**, but



Scheme 1. The central C=C group represents the phenyl unit.

not with the *meta* isomer **1b**, *para* isomer **1c**, or the monoboronate counterpart **2**.

Chiral recognition of the Lewis acid **1a** has also been examined. Titration was carried out at 20 °C for (*R*)- and (*S*)-1-phenylethylamine, and the binding constants for the 1:2 complexes have been estimated to be $K_R = 15.2\,\mathrm{M}^{-2}$ for (*R*)-1-phenylethylamine and $K_S = 18.6\,\mathrm{M}^{-2}$ for the (*S*) isomer at $[\mathbf{1a}]_{initial} = 0.10\,\mathrm{M}$. Thus, chiral recognition at 20 °C is minimal. However, the clear separation of the signals of 1-phenylethylamine suggests the possibility of using **1a** as a chiral NMR shift reagent. For example, spectra of *rac*-1-phenylethylamine (0.40 M in $CDCl_3$) with **1a** (0.10 M) at 20 °C display a pair of doublets ($PhCH(NH_2)CH_3$) and a pair of quartets ($PhCH(NH_2)CH_3$) for the amine.[13] In an analogous experiment with a sample of (*R*)-1-phenylethylamine (60% *ee*) two pairs of doublets and quartets in a ratio of 80:20 are observed.

Thus we have synthesized the chiral Lewis acid **1a** with two "metal" centers and elucidated its unique binding properties to benzylamine. Further studies on the chiral recognition of amines with **1a** and its analogues with other chiral groups on boron atoms are in progress.

Experimental Procedure

1a: (*R,R*)-Diphenyl-1,2-ethanediol (2.87 g, 13.4 mmol) was added to a chloroform solution of a 1:1 mixture of *ortho*-bis(dichloroboryl)benzene and *meta*-bis(dichloroboryl)benzene [14] (6.70 mmol total) at 0 °C. The generated HCl and the solvent were removed at 60 °C under reduced pressure. Recrystallization from CH_3CN afforded **1b** in 35% yield. The mother liquor was concentrated and purified by column chromatography on reversed-phase silica gel (Wakogel LP140C18, CH_3CN, $R_f = 0.75$). Recrystallization from ether–hexane gave **1a** in 33% yield. **1a**: m.p. 85.2–86.0 °C (ether–hexane); $[\alpha]_D^{26.0}$ −15.8 ($c = 0.79$ in $CHCl_3$); ^{1}H NMR (270 MHz, $CDCl_3$, 25 °C, TMS, 0.10 M): $\delta = 5.22$ (s, 4H), 7.12–7.33 (m, 20H), 7.47 (dd, $J = 3.3$, 5.6 Hz, 2H), 7.86 (dd, $J = 3.3$, 5.3 Hz, 2H); ^{13}C NMR (68 MHz, $CDCl_3$ 25 °C, TMS): $\delta = 87.46$, 126.09, 128.25, 128.66, 129.94, 133.84, 139.96 (carbon atoms bound to boron atoms were not observed); ^{11}B NMR (87 MHz, $CDCl_3$, 25 °C, $B(OMe)_3$): $\delta = 20.5$. Anal. Calcd for $C_{34}H_{28}B_2O_4$: C, 78.20; H, 5.40. Found C, 77.94; H, 5.44.

Received: June 23, 1994 [Z 7069 IE]
German version: *Angew. Chem.* **1994**, *106*, 2574

[1] a) Asymmetric boron-catalyzed reactions: L. Deloux, M. Srebnik, *Chem. Rev.* **1993**, *93*, 763. b) A special issue on enantioselective synthesis, *ibid.* **1992**, *92*, 739–1140.

[2] a) A Lewis acid–Lewis base complex in an asymmetric Diels–Alder reaction: J. M. Hawkins, S. Loren, *J. Am. Chem. Soc.* **1991**, *113*, 7794. b) Other recent structural studies, for example: M. T. Reetz, C. M. Niemeyer, M. Harmes, R. Goddard, *Angew. Chem.* **1992**, *104*, 1053; *Angew. Chem. Int. Ed. Engl.* **1992**, *31*, 1017.

[3] Complexation of achiral compounds having two metal centers with Lewis bases: a) M. Simard, J. Vaugeois, J. D. Wuest, *J. Am. Chem. Soc.* **1993**, *115*, 370; b) H. E. Katz in *Inclusion Compounds, Vol. 4* (Eds: J. L. Atwood, J. E. D. Davis, D. D. MacNicol), Oxford University Press, **1991**, p. 391.

[4] A chiral Lewis acid having two "metal" centers has been reported to catalyze asymmetric Diels–Alder reactions in excellent selectivities, but no cooperation between the two metal centers was mentioned: D. Kaufmann, R. Boese, *Angew. Chem.* **1990**, *102*, 568; *Angew. Chem. Int. Ed. Engl.* **1990**, *29*, 545.

[5] General studies on $R_3B{\cdot}NR_3$ complexes: A. Peter, K. Smith, H. C. Brown, *Borane Reagents*; Academic Press: London, **1988**.

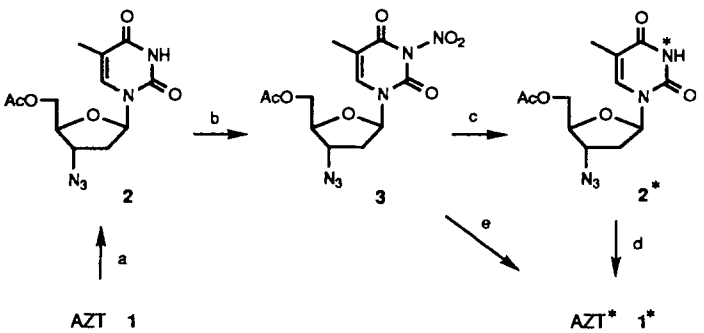
[6] The NMR signals of propylamine (an aliphatic amine) are similar to those of benzylamine in the presence of **1a–c** and **2**.
[7] W. Likussar, D. F. Boltz, *Anal. Chem.* **1971**, *43*, 1265.
[8] A 1:1 complex follows the relationship $1/\Delta\delta_{observed} = 1/\Delta\delta_{complex} + 1/(K \cdot \Delta\delta_{complex} \cdot [amine])$, while a 1:2 complex follows $1/\Delta\delta_{observed} = 1/\Delta\delta_{complex} + 1/(K \cdot \Delta\delta_{complex} \cdot [amine]^2)$. K. A. Connors, *Binding Constants: The Measurement of Molecular Complex Stability*, Wiley, New York, **1987**.
[9] Signals due to the two NH protons of the 1:2 complex moved to even lower field with increasing amounts of amine (Fig. 2, spectrum D). We do not have any proper explanation for this phenomenon at present.
[10] A similar formation of B–N bond coupled with hydrogen bonding has been postulated by Reetz et al; see ref. [2b].
[11] In the 1:2 complex represented in Scheme 1, the two nitrogen atoms are chiral centers. We tentatively draw the structure in which two benzyl groups of the amines occupy the "*exo*" position rather than "*endo*", since space-filling models indicate that this conformation may be sterically less hindered.
[12] Other than the conformational effect in the 1:2 complex, the dipole moment may lead to additional stabilization.
[13] Representative signals in ^{1}H NMR spectrum (270 MHz, $CDCl_3$, 25 °C, TMS): $\delta = 1.22$ (d, $J = 6.6$ Hz, (*S*)-PhCH(CH_3)NH_2), 1.29 (d, $J = 6.6$ Hz, (*R*)-PhCH(CH_3)NH_2), 4.02 (q, $J = 6.6$ Hz, (*R*)-PhC*H*(CH_3)NH_2), 4.12 (q, $J = 6.6$ Hz, (*S*)-PhC*H*(CH_3)NH_2), 4.75 (s, C_6H_4(BOC*H*PhC*H*PhO)$_2$). Assignments of absolute configurations are based on the NMR spectra of **1a** (0.10 M) and (*R*)- or (*S*)-1-phenylethylamine (0.20 M).
[14] D. Kaufmann, *Chem. Ber.* **1987**, *120*, 901.

A Short Route to [3-^{15}N]-3′-Azido-3′-deoxythymidine (N3-Labeled AZT) via 3-Nitro-AZT**

Xavier Ariza, Valentí Bou, Jaume Vilarrasa,* Valya Tereshko, and J. Lourdes Campos

^{15}N-Labeled nucleosides are very useful for gaining insight into nucleic acid structures, drug binding phenomena, and nucleic acid/protein interactions.[1] Once these nucleosides are incorporated into DNA and RNA fragments, the changes that the corresponding ^{15}N–H bonds undergo as a consequence of hydrogen bonding or protonation/deprotonation equilibria can be directly and elegantly monitored by ^{1}H and ^{15}N NMR spectroscopy. In this context, we report here a novel, mild method for the N3-labeling of thymidines and uridines that is illustrated for the case of 3′-azido-3′-deoxythymidine (AZT, **1**), a well-studied nucleoside.[2] The procedure, which may be applied to the final product of any pyrimidine nucleoside synthesis, is based on a selective N-nitration reaction and the substitution of $^{15}NH_3$ for nitramine.[3]

Although it is known that pyrimidine nucleosides may undergo O-nitration on the sugar ring and/or nitration at C5, depending on the substrate and reaction conditions,[4] *N*-nitropyrimidine derivatives have not been reported so far, to the best of our knowledge. To achieve smooth N-nitration and avoid nucleoside hydrolysis and loss of protective groups, we took advantage of our previous experience with amide nitration under mild conditions.[5] Thus, after protecting the hydroxyl group of AZT (**1**),[6] we converted the product **2** into the *N*-nitro compound **3** by treatment with nitric trifluoroacetic anhydride (nitronium trifluoroacetate) generated in situ from appropriate amounts of NH_4NO_3 and $(CF_3CO)_2O$ in CH_2Cl_2 (Scheme 1). This N-nitration reaction gave **3** in 90% yield based on consumed starting material (81% isolated yield).



Scheme 1. a) Ac_2O/Py, 20 °C (96%); b) NO_2OCOCF_3, CH_2Cl_2, 0 °C (90%); c) $^*NH_3$ (i.e. $^{15}NH_3$), CH_3CN/H_2O, 20 °C (67%); d) conc NH_3, MeOH, 20 °C (95%); e) c and d in a one-pot reaction (75%).

5′-*O*-Acetyl-3′-azido-3′-deoxy-3-nitrothymidine (**3**) was identified by the absence of an NH signal in the ^{1}H NMR spectrum and by the large shifts of the signals for C2 and C4 in the ^{13}C NMR spectrum relative to those of **2** ($\Delta\delta = -5$ and -8, respectively). To corroborate its structure we tried to obtain suitable crystals of **3**, but it proved to be an amorphous solid. However, 3′,5′-di-*O*-acetyl-3-nitrothymidine (**4**), prepared similarly in excellent yield from thymidine, afforded good crystals from acetone/hexane. The X-ray structural analysis showed two different conformations of **4** in the asymmetric unit (Fig. 1);[7] the only significant difference between them is the torsion angles involving the 5′ substituent, specifically the O-C5′-C4′-O dihedral angle. The NO_2 group is perpendicular to the plane of the nitrogen ring, as could be expected in view of its close proximity to the two CO groups.

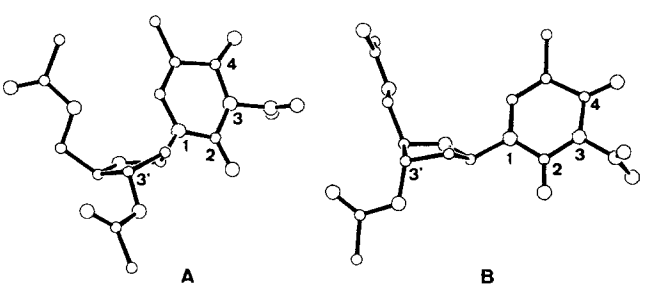


Fig. 1. Molecular structure of 3′,5′-di-*O*-acetyl-3-nitrothymidine (**4**) in the crystal (hydrogen atoms omitted for clarity); the unit cell contains two conformations **A** and **B** of **4** (C2′-*endo*/C3′-*exo*). Selected bond lengths [Å] and angles [°]: **A**: C2–O 1.183(9), C2–N3 1.40(1), N3–NO_2 1.48(1), N3–C4 1.40(1), C4–O 1.20(1); N1-C2-N3 110.5(6), O2-C2-N1 125.8(7), O2-C2-N3 123.6(7), C2-N3-C4 131.3(6), N3-C4-O4 120.6(8), C5-C4-O4 128.3(8), O-N-O 129.9(9); for **B** the values are almost identical.

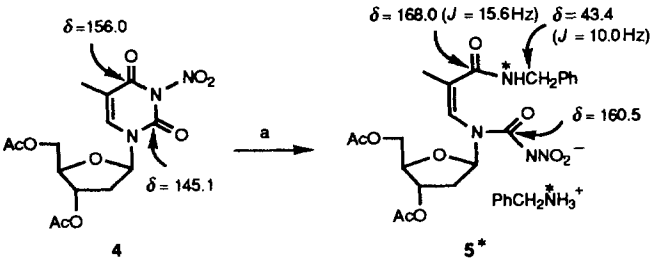
When a solution of **3**, $^{15}NH_4Cl$, and KOH in CH_3CN/H_2O was stirred at room temperature in a closed vial, a smooth reaction gave a much more polar species (according to thin-layer chromatography). After a few days, this reaction intermediate had been converted to a new compound identical to **2**, except

[*] Prof. J. Vilarrasa, X. Ariza, Dr. V. Bou
Departament de Química Orgànica, Universitat de Barcelona
E-08028 Barcelona (Catalonia, Spain)
Telefax: Int. code + (3) 339-7878
Dr. V. Tereshko,[+] Dr. J. L. Campos[+]
Departament d'Enginyeria Química, Universitat Politècnica
E-08028 Barcelona (Catalonia, Spain)
[+] X-ray structure analysis

[**] This research was supported by the Dirección General de Investigación Científica y Técnica (Grants PB86-0137 and PB89-0277 to the Universitat de Barcelona, and Grant PB90-0605 to the Universitat Politècnica) and by the Ministerio de Educatión y Ciencia (fellowships to V. B. and X. A).

for the appearance of some $^1H-^{15}N$ and $^{13}C-^{15}N$ couplings in the NMR spectra. After purification by column chromatography on silica gel a 67% yield of this labeled compound (**2***) was obtained, together with small amounts of the deacetylated product **1***. The proton-coupled ^{15}N NMR spectrum of **2*** showed the expected doublet with $|^1J_{N,H}| = 90.9$ Hz at $\delta = -212.6$, referred to external conc. $H^{15}NO_3$. Deprotection of **2*** under standard conditions, either with a concentrated solution of ammonia in MeOH or with MeOH/HCl, gave almost quantitative yields of [3-^{15}N]-AZT **1*** ($|^1J_{H,N}| = 91.0$ Hz, $|^1J_{C2,N}| = 17.3$ Hz, and $|^1J_{C4,N}| = 9.9$ Hz). Compound **1*** was also obtained in 75% in a one-pot transformation from **3** (see Scheme 1) by adding a 1:1 mixture of aqueous ammonia and MeOH at the end of the labeling reaction.

To gain insight into the mechanism of the reaction of nitro derivatives **3** and **4** with ammonia, which likely involves ring opening and ring closing, we attempted to characterize the polar intermediates by NMR spectroscopy. When benzylamine was used instead of ammonia, these intermediates turned out to be kinetically stable, and their structures could be elucidated. In fact, when **3** or **4** was treated with benzylamine—at least two equivalents were necessary for complete disappearance of starting material—in $CDCl_3$ at 20 °C, we noted in both cases the formation of only one polar compound, which did not cyclize under these conditions. After confirming the assignments of the carbon atoms of **4** and its ring-opened derivative **5** by $^1H-^{13}C$ 2D NMR experiments, we monitored by $^{13}C-\{^1H\}$ NMR spectroscopy the reaction between **4** and ^{15}N-labeled benzylamine leading to the labeled compound **5*** (Scheme 2). The CO group



Scheme 2. a) $PhCH_2{}^*NH_2$, $CDCl_3$, 20 °C.

of **5*** at $\delta = 160.5$, which is related to C2 of the thymidine ring, appeared as a singlet, whereas the CO group of **5*** at $\delta = 168.0$ related to C4 showed a typical $^1J_{C,N}$ splitting. In other words, the attack of benzylamine (and presumably that of ammonia) on 3-nitrothymidines takes place mainly at the C4 position.

Experimental Procedure

3: Trifluoroacetic anhydride (0.560 mL, 4.0 mmol) was added to a suspension of finely powdered NH_4NO_3 (160 mg, 2.0 mmol) in anhydrous CH_2Cl_2 (5 mL) at 0 °C under Ar. The mixture was stirred vigorously at room temperature until the solid dissolved (ca. 1 h) and then cooled again. Compound **2** (309 mg, 1.0 mmol) was introduced, and stirring was maintained at 0 °C for 1 h. After more solvent was added, the reaction mixture was washed with cold phosphate buffer, dried, and concentrated to dryness to give almost pure product (contaminated only with small amounts of starting material). Column chromatography on silica gel (flash chromatography) eluting with CH_2Cl_2/MeOH (98/2) afforded pure **3** (287 mg, 81%); elution with CH_2Cl_2/MeOH (95/5) then provided recovered **2** (32 mg, 10%). Data of **3**: M.p. 81–83 °C (EtOAc/hexane); ^1H NMR (200 MHz, $CDCl_3$): δ = 2.00 (d, J(Me,6) = 1.2 Hz, 3H; Me), 2.14 (s, 3H; MeCO), 2.36–2.62 (m, 2H; H2′, H2″), 4.08–4.44 (m, 4H; H3′, H4′, H5′, H5″), 6.07 (dd, J(1′,2′) = 6.6 Hz, J(1′,2″) = 5.8 Hz, 1H; H1′), 7.33 (q, J(6,Me) = 1.2 Hz, 1H; H6); ^{13}C NMR (50.3 MHz, $CDCl_3$): δ = 12.8 (Me), 20.7 (MeCO), 37.7 (C2′), 60.2 (C3′), 63.0 (C5′), 82.3 (C4′), 86.8 (C1′), 110.7 (C5), 134.9 (C6), 145.0 (C2), 156.1 (C4), 170.1 (*C*OMe).

2*: *N*-Nitro derivative **3** (189 mg, 0.53 mmol) was added to a mixture of $^{15}NH_4Cl$ (145 mg, 2.66 mmol, IC Chemikalien, MSD Isotopes, 99% labeled), powdered KOH (85%, 169 mg, 2.56 mmol), acetonitrile (4 mL), and water (1 mL) in a closed vial, and the solution was stirred at room temperature for a week. Evaporation of the solvent and purification by column chromatography (silica gel, CH_2Cl_2/MeOH 95/5) afforded **2*** (111 mg, 67%) and then **1*** (14 mg, 10%) [8]. Spectral data of **2***: ^1H NMR (200 MHz, $CDCl_3$): δ = 1.94 (d, J(Me,6) = 1.2 Hz, 3H; Me), 2.15 (s, 3H; MeCO), 2.3–2.6 (m, 2H; H2′, H2″), 4.0–4.5 (m, 4H; H3′, H4′, H5′, H5″), 6.13 (t, J(1′,2′) ≈ J(1′,2″) = 6.3 Hz, 1H; H1′), 7.24 (q, J(6,Me) = 1.2 Hz, 1H; H6), 9.66 (d, J(N,H) = 90.9 Hz, 1H; NH); ^{13}C NMR (50.3 MHz, $CDCl_3$): δ = 12.6 (Me), 20.7 (MeCO), 37.5 (C2′), 60.5 (C3′); 63.3 (C5′), 81.6 (C4′), 85.5 (C1′), 111.2 (d, J(C,N) = 6.3 Hz; C5), 135.3 (C6), 150.2 (d, J(C,N) = 18.1 Hz; C2), 163.9 (d, J(C,N) = 10.0 Hz; C4); 170.2 (*C*OMe).

1*: The final mixture from the reaction of **3** (189 mg, 0.53 mmol) with $^{15}NH_4Cl$ and KOH (ca. 5 equiv of each, as above) was treated with an excess of aqueous NH_3 (30%, 15 mL) and MeOH (15 mL) at room temperature for 1 h. Removal of excess reagent and solvents in vacuo, and purification by column chromatography as above gave directly **1*** (107 mg, 75%); ^1H NMR (200 MHz, $CDCl_3$): δ = 1.91 (d, J(Me,6) = 1.2 Hz, 3H; Me), 2.3–2.6 (m, 2H; H2′, H2″), 3.75–4.05 (m, 3H; H4′, H5′, H5″), 4.42 (m, 1H; H3′), 6.08 (t, J(1′,2′) ≈ J(1′,2″) = 6.6 Hz, 1H; H1′), 7.41 (q, J(6,Me) = 1.2 Hz, 1H; H6), 9.64 (d, J(N,H) = 91.0 Hz, 1H; NH); ^{13}C NMR (50.3 MHz, [D$_6$]DMSO): δ = 12.2 (Me), 36.2 (C2′), 60.2 (C3′), 60.8 (C5′), 83.4 (C4′ or C1′), 84.0 (C1′ or C4′), 109.5 (d, J(C,N) = 6.4 Hz; C5), 136.1 (C6), 150.4 (d, J(C,N) = 17.3 Hz, C2), 163.7 (d, J(C,N) = 9.9 Hz; C4).

Received: June 20, 1994 [Z70501E]
German version: *Angew. Chem.* **1994**, *106*, 2535

[1] For some leading references, see: a) B. L. Gaffney, B. Goswami, R. A. Jones, *J. Am. Chem. Soc.* **1993**, *115*, 12607; b) Y. Rhee, C. Wang, B. L. Gaffney, R. A. Jones, *ibid.* **1993**, *115*, 8742, and references therein; c) W. Massefski, A. Redfield, U. D. Sarma, A. Bannerji, S. Roy, *ibid.* **1990**, *112*, 5350; d) D. R. Davis, Z. Yamaizumi, S. Nishimura, C. D. Poulter, *Biochemistry* **1989**, *28*, 4105.

[2] For very recent reviews on anti-HIV nucleosides, see: a) D. M. Huryn, M. Okabe, *Chem. Rev.* **1992**, *92*, 1745; b) C. Périgaud, G. Gosselin, J.-L. Imbach, *Nucleosides Nucleotides* **1992**, *11*, 903.

[3] In an alternative approach based on a stepwise synthesis the label(s) would be incorporated at the very beginning. See: a) J. A. Lawson, J. I. DeGraw in *Nucleic Acid Chemistry, Part 2* (Eds.: L. B. Townsend, R. S. Tipson), Wiley, New York, **1978**, p. 921; b) C. D. Poulter, C. L. Livingston, *Tetrahedron Lett.* **1979**, 755; c) C.-H. Niu, *Anal. Biochem.* **1984**, *139*, 404.

[4] For an excellent review, see: T. Ueda in *Chemistry of Nucleosides and Nucleotides, Vol. 1* (Ed.: L. B. Townsend), Plenum, New York, **1988**, p. 1.

[5] P. Romea, M. Aragonès, J. Garcia, J. Vilarrasa, *J. Org. Chem.* **1991**, *56*, 7038.

[6] Prepared according to the method described by R. P. Glinski, M. S. Khan, R. L. Kalamas, M. B. Sporn, *J. Org. Chem.* **1973**, *38*, 4299.

[7] Enraf-Nonius CAD4 diffractometer with $Cu_{K\alpha}$ radiation and graphite monochromator, crystal dimensions 0.3 × 0.2 × 0.1 mm^3, orthorhombic, space group $P2_12_12_1$, a = 7.832(3), b = 15.695(2), c = 28.076(1) Å, V = 3452(2) Å^3, Z = 8, ρ = 1.43 g cm^{-3}, 5933 collected reflections, 3561 unique reflections, 2220 observed reflections with $F > 2\sigma(F)$, 482 refined parameters, R = 0.067. Further details of the crystal structure investigation are available on request from the Director of the Cambridge Crystallographic Data Centre, 12 Union Road, GB-Cambridge CB2 1EZ (UK), on quoting the full journal citation.

[8] When only 2 equiv of $^{15}NH_4Cl$ and KOH were used and the reaction was carried out at 30 °C the yield of **2*** was 64% (with only 3% of **1***, but 11% of recovered **3**). By using 1.2 equiv of $^{15}NH_4Cl$, 1.0 equiv of KOH, and 1.2 equiv of Et_3N, at 40 °C, the yield was ca. 60% but some label was lost (**2***:**2** = 3:1; i.e., **3** was partially denitrated).

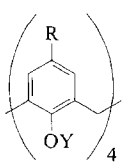
 © VCH Verlagsgesellschaft mbH, D-69451 Weinheim, 1994 0570-0833/94/2323-2455 $ 10.00+.25/0

A Water-Soluble "Bear Trap" Exhibiting Strong Anion Complexation Properties**

Jonathan W. Steed, Ravindra K. Juneja, and Jerry L. Atwood*

Calix[*n*]arenes ($n = 4-8$) have been extensively studied in recent years[1, 2] in connection with a variety of applications in areas such as metal ion extraction,[3, 4] catalysis,[5] and enzyme modeling.[6] The vast majority of this interest has centered around the capacity of calixarenes to form molecular inclusion complexes with a wide varity of guest species,[1, 2, 7, 8] by virtue of hydrophobic cavities formed as a consequence of the conformational properties of the macrocycle.[9] Recently we have embarked upon a program of research designed to modify the electronic properties of calixarene hosts by complexation of the carbocyclic rings of the macrocycle to organotransition metal containing moieties. It is anticipated that the presence of charged metal cations bound directly to the calixarene π network will significantly reduce the electron density within the cavity and allow the incorporation of suitably sized anionic species, especially environmental contaminants such as phosphate and the phosphate residues in biologically important anions such as ATP.[10, 11] Ultimately such complexation may lead to new methods of water purification or inhibition of the conversion of ATP into ADP.

Shinkai and co-workers have already reported some neutral chromium tricarbonyl derivatives of rigidified calix[4]arene tetra-*n*-propyl ethers **1a**.[12, 13] In the present work, however, we have chosen to concentrate upon more robust, air-stable complexes containing the "(arene)Ru^{2+}" moiety which exhibit useful properties such as high positive charge and significant solubility in water.



1a: R = H, Y = *n*Pr
1b: R = Y = H
1c: R = *t*Bu, Y = H

Unsymmetrical bis(arene)ruthenium(II) complexes may be prepared conveniently[14] from the readily available chloro-bridged dimers **2**[15] by treatment with AgX ($X = BF_4$, CF_3SO_3, $\frac{1}{2}SO_4$, etc.) followed by heating in the presence of acid. Accordingly we find that refluxing a trifluoroacetic acid solution of [Ru(*p*-cymene)(acetone)$_3$]X_2 (prepared from **2b**) in the presence of a 0.25 equivalents of calix[4]arene **1b** results in the clean formation of the salt **3**-$(BF_4)_6$ (80% yield), which has a tetrametallic cation arising from the capping of each face of the macrocycle by an (arene)Ru^{2+} fragment and loss of two of the calixarene phenolic protons; the resulting cationic complex has an overall charge of 6 + . Interestingly, direct reaction of excess **2b** with **1b** in refluxing CF_3CO_2H provides the salt **4**-$[H(CF_3CO)_2]_4$ with a bimetallic cation.

$[\{Ru(\eta^6\text{-arene})Cl(\mu\text{-}Cl)\}_2]$

2a: arene = C_6H_6
2b: arene = 4-$MeC_6H_4CHMe_2$
2c: arene = C_6Me_6

$[\{Ru(p\text{-cymene})\}_4(\eta^6{:}\eta^6{:}\eta^6{:}\eta^6\text{-calix[4]arene} - 2H)](BF_4)_6$ **3**-$(BF_4)_6$

$[\{Ru(p\text{-cymene})\}_2(\eta^6{:}\eta^6\text{-calix[4]arene})][H(CF_3CO_2)_2]_4$ **4**-$[H(CF_3CO_2)_2]_4$

Salts **3**-$(BF_4)_6$ and **4**-$[H(CF_3CO)_2]_4$ were characterized by ^1H NMR spectroscopy,[16] which confirmed that the calixarene in **3** is symmetrically substituted. The observation of an AB quartet assigned to the calixarene methylenic bridges suggests that **3** and **4** both assume cone conformations in solution.[9] Both salts are significantly soluble in water and hence may be readily introduced to common water-soluble inorganic anions.

It may seem surprising that **3** should be formed in a doubly deprotonated form even though trifluoroacetic acid is used as the solvent. Previous work upon ruthenium, rhodium, and iridium π complexes with phenol ligands[17-19] has shown, however, that transition metal complexation significantly enhances the acidity of the phenolic protons (because of increased positive charge and the stability of the resulting oxocyclohexadienyl ligand), and hence it seems likely that any more highly charged species formed in the reaction readily release HBF_4 to give the observed hexacationic compounds. We have also noted similar acidity enhancements for related bimetallic pentamethylcyclopentadienyl (Cp*) rhodium and iridium complexes of **1b** and **1c** in which it has proved possible to isolate and characterize salts containing tetra-, tri-, and dicationic complexes $[(MCp^*)_2(\eta^6{:}\eta^6\text{-}p\text{-R-calix[4]arene} - nH)][BF_4]_{4-n}$ (M = Rh, Ir; $n = 0, 1, 2$; R = H, *t*Bu).[20]

The BF_4 salt of complex **3** has also been characterized by X-ray crystallography (Fig. 1).[21] The complex adopts the cone conformation in the solid state with each calixarene ring bound η^6 fashion to a (*p*-cymene)Ru^{2+} fragment (Ru–C = 2.19–2.39 Å). Bonds to the carbon atom attached to the hydroxyl functionality are significantly longer than those to the remaining five atoms of each calixarene ring (Ru–C(1) = 2.367(8) Å

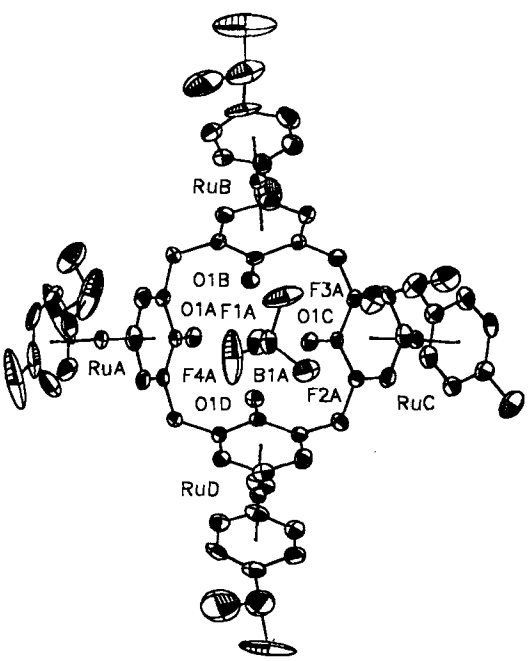


Fig. 1. X-ray crystal structure of **3** and the included tetrafluoroborate ion.

[*] Prof. Dr. J. L. Atwood, Dr. J. W. Steed, Dr. R. K. Juneja
Department of Chemistry, University of Missouri-Columbia
Columbia, MO 65211 (USA)
Telefax: Int. code + (314)882-2754

[**] This work was supported by the U. S. National Science Foundation. We are also grateful to the Science and Engineering Research Council and NATO for a research fellowship (to J. W. S.) and to the University of Alabama for the collection of the X-ray data.

(average), Ru–C(2–6) = 2.22(1) Å (average)), consistent with a partial oxocyclohexadienyl description.[17] In contrast to previous calixarene and calixarene–metal complexes examined in the solid state,[22–25] including the bimetallic iridium(III) species in $[(IrCp^*)_2(\eta^6{:}\eta^6\text{-}p\text{-}tert\text{-butylcalix[4]arene})](BF_4)_3 \cdot Et_2O \cdot NO_2Me$,[20] **3** does not co-crystallize with a molecule of solvent or other guest within the hydrophobic cavity of the calixarene. Instead, withdrawal of electron density from the all four carbocyclic rings by the transition metal centers along with the high charge of the host molecule as a whole results in the incorporation of one of the tetrafluoroborate anions (B1A–F4A) deeply within the cavity. Three of the fluorine atoms are approximately at the level of the upper rim of the calixarene cavity, whilst F1A points directly into the bowl of the molecule. Short contacts of 3.23–3.37 Å are observed between this atom and the calixarene oxygen atoms. Distances from F1A to the centroids of the calixarene rings A and D are 3.10 and 3.15 Å, and to rings B and C 3.41 and 3.46 Å. But the remarkably short F1A···C1A and C1D distances each of 2.85 Å demonstrate the extremely deep penetration of the anion into the cavity. The tight binding of this anionic guest by the metalated host is also highlighted by the relatively small magnitude of the anisotropic thermal parameters for atoms B1A–F4A, which are similar to those of the atoms of the cation. In contrast, thermal parameters for tetrafluoroborate ions in the crystal lattice are commonly large as a result of high thermal motion and/or dynamic disorder.

The deprotonation of two of the calixarene hydroxyl groups is evidenced by the hydrogen bonding network at the base of the calixarene in which the calixarene oxygen atoms are hydrogen bonded in pairs (OA···OB and OC···OD 2.57 Å (average)); the average distance between O atoms not connected by hydrogen bonds (OA–OD and OB–OC) is 2.76 Å. This may be compared with the average distances of 2.40 and 3.14 Å in the lithium salt of the *p-tert*-butylcalix[4]arene dianion.[26]

The remaining five tetrafluoroborate ions, which exhibit larger thermal ellipsoids, occupy positions adjacent to the metal ions within the lattice and form weak hydrogen bonds (ca. 2.9 Å) to a further 1.5 molecules of water located on final difference Fourier syntheses.

Anion metathesis of **3**-$(BF_4)_6$ with $(NBu_4)I$ in nitromethane solution leads to the analogous iodo complex $[\{Ru(p\text{-cymene})\}_4(\eta^6{:}\eta^6{:}\eta^6\text{-calix[4]arene} - 2H)]I_6$ which has also been characterized by X-ray crystallography and demonstrates the inclusion of an iodide anion within the cavity of the macrocycle (I–ring centroid distances 3.60–3.78 Å). Further studies of inclusion reactions with a number of phosphate and polyphosphate anions as well as ATP are currently in progress.

The facile synthesis of **3** and **4**, coupled with our recent reports[29] of trimetallic hosts based upon cyclotriveratrylene and bi- and tetrametallic calixarenes containing rhodium and iridium confirms that bowlic host molecules may be readily modified by direct π complexation to form highly charged, air- and moisture-stable cavity-containing species capable of complexing a wide range of even highly polar guests. It is envisaged that the use of redox-active metal centers such as ruthenium(II/0) bound in close proximity to the cavity in this way will allow the design of redox-active enzyme mimics capable of reducing or oxidizing a bound substrate through electron transfer mediated by the calixarene π network.

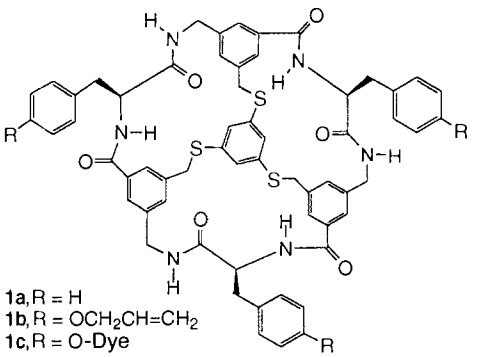
Recieved: June 22, 1994 [Z 7064 IE]
German version: *Angew. Chem.* **1994**, *106*, 2571

[1] C. D. Gutsche, *Calixarenes*, (Ed.: J. F. Stoddart), Royal Society of Chemistry, Cambridge, **1989**
[2] *Calixarenes: A Versatile Class of Macrocyclic Compounds*, (Eds.: J. Vincens, V. Bohmer), Kluwer, Dordrecht, **1991**.
[3] J. L. Atwood in *Cation Binding by Macrocycles*, (Eds.: Y. Inoue, G. W. Gokel), Dekker, New York, **1991**.
[4] T. Nagasaki, S. Shinkai, *Bull. Chem. Soc. Jpn.* **1992**, *65*, 471.
[5] R. Cacciapaglia, L. Mandolini, *Chem. Soc. Rev.* **1993**, *22*, 221.
[6] J. L. Atwood, G. W. Orr, K. D. Robinson, F. Hamada, *Supramol. Chem.* **1993**, *2*, 309.
[7] J. L. Atwood, F. Hamada, K. D. Robinson, G. W. Orr, R. L. Vincent, *Nature (London)* **1991**, *349*, 683.
[8] J. L. Atwood, G. A. Koutsantonis, C. L. Raston, *Nature (London)* **1994**, *368*, 229.
[9] C. D. Gutsche, L. J. Bauer, *J. Am. Chem. Soc.* **1985**, *107*, 6052.
[10] P. D. Beer, Z. Chen, A. J. Goulden, A. Graydon, S. E. Stokes, T. Wear, *J. Chem. Soc. Chem. Commun.* **1993**, 1834.
[11] D. M. Rudkevich, Z. Brzozka, M. Palys, H. C. Visser, W. Verboom, D. N. Reinhoudt, *Angew. Chem.* **1994**, *106*, 480; *Angew. Chem. Int. Ed. Engl.* **1994**, *33*, 467.
[12] H. Iki, T. Kikuchi, S. Shinkai, *J. Chem. Soc. Perkin Trans. 1* **1993**, 205.
[13] T. Kikuchi, H. Iki, H. Tsuzuki, S. Shinkai, *Supramol. Chem.* **1993**, *1*, 103.
[14] M. A. Bennett, T. W. Matheson, *J. Organomet. Chem.* **1979**, *175*, 87.
[15] M. A. Bennett, A. K. Smith, *J. Chem. Soc. Dalton Trans.* **1974**, 233.
[16] **3**-$(BF_4)_6$: ^{1}H NMR ([D$_3$]NO$_2$Me, 200 MHz, 20 °C): $\delta = 6.71$ (s, 16H, *p*-cymene), 6.71 (d, 8H, $J = 5.6$ Hz, calixarene ring), 6.24 (t, 4H, $J = 5.6$ Hz, calixarene ring) 4.35 and 3.49 (AB, 8H, $^2J = 12.3$ Hz, -CH$_2$-), 2.99 (sp, 4H, $J = 6.3$ Hz, C*H*Me$_2$), 2.46 (s, 12H, Me), 1.39 (d, 24H, $J = 6.3$ Hz, CH*Me*$_2$); **4**-$[H(CF_3CO)_2]$: $\delta = 7.09$ (d, 4H, $J = 7.6$ Hz, uncoord. calixarene ring), 6.71 (t, 2H, $J = 7.6$ Hz, uncoord. calixarene ring), 6.6–6.4 (m, 20H, coord. calixarene ring and *p*-cymene), 6.05 (t, 2H, $J = 5.6$ Hz, coord. calixarene ring), 4.40 (d, 4H, $J = 12.8$ Hz, -CH$_2$-), 3.22 (d, 4H, $J = 12.8$ Hz, -CH$_2$-), 2.96 (sp, 4H, $J = 6.9$ Hz, C*H*Me$_2$), 2.44 (s, 12H, Me), 1.32 (d, 24H, $J = 6.9$ Hz, CH*Me*$_2$).
[17] C. White, S. J. Thompson, P. M. Maitlis, *J. Organomet. Chem* **1977**, *127*, 415.
[18] D. J. Cole-Hamilton, R. J. Young, G. Wilkinson, *J. Chem. Soc. Dalton Trans.* **1976**, 1995.
[19] A. Wu, E. R. Biehl, P. C. Reeves, *J. Chem. Soc. Perkin Trans. 2* **1972**, 449.
[20] J. W. Steed, R. K. Juneja, J. L. Atwood, *J. Chem. Soc. Chem. Commun.*, **1994**, 2205.
[21] Crystal data for **3**-$(BF_4)_6$: $C_{68}H_{80}O_4Ru_4 \cdot 6BF_4 \cdot 1.5H_2O$, $M = 1913.50$, dark yellow block, monoclinic, $P2_1/c$, $a = 14.210(3)$, $b = 27.454(5)$, $c = 19.809(3)$ Å, $\beta = 106.85(1)°$, $V = 7396$ Å^3, $Z = 4$, $\rho_{calcd} = 1.72$ g cm^{-3}, $\mu = 8.93$ cm^{-1}. Of 13824 data collected on an Enraf-Nonius CAD4 diffractometer ($Mo_{K\alpha}$, $2\theta = 4–50°$ at 20 °C), 9562 independent reflections were judged observed [$I > 3\sigma(I)$]. Data were corrected for Lorentz, polarization, and absorption effects (ψ-scans). The structure was solved by direct methods (SHELX86 [27]) and refined by alternating least squares and difference Fourier techniques (SHELX76 [28]). The asymmetric unit was found to contain one cation **3**, six tetrafluoroborate ions, and 1.5 molecules of water. The final refinement converged with $R = 0.086$, $R_w = 0.116$. The maximum residual electron density peak was 1.88 e Å^{-3} situated close to one of the ruthenium atoms. Further details of the crystal structure investigation may be obtained from the Director of the Cambridge Crystallographic Centre, 12 Union Road, Cambridge CB2 1EZ (UK), on quoting the full journal citation.
[22] R. Ungaro, A. Pochini, G. D. Andreetti, V. Sangermano, *J. Chem. Soc. Perkin Trans. 2* **1984**, 1979.
[23] G. D. Andreetti, R. Ungaro, A. Pochini, *J. Chem. Soc. Chem. Commun.* **1979**, 1005.
[24] J. L. Atwood, G. W. Orr, F. Hamada, R. L. Vincent, S. G. Bott, K. D. Robinson, *J. Am. Chem. Soc.* **1991**, *113*, 2760.
[25] F. Corazza, C. Floriani, A. Chiesi-Villa, C. Guastini, *J. Chem. Soc. Chem. Commun.* **1990**, 640.
[26] F. Hamada, K. D. Robinson, G. W. Orr, J. L. Atwood, *Supramol. Chem.* **1993**, *2*, 19.
[27] G. M. Sheldrick, *Acta Crystallogr. Sect. A* **1990**, *46*, 467.
[28] G. M. Sheldrick, *SHELX-76*, University of Cambridge, **1976**.
[29] J. W. Steed, P. C. Junk, J. L. Atwood, M. J. Barnes, C. L. Raston, R. S. Burkalter, *J. Am. Chem. Soc.*, **1994**, *116*, 10346.

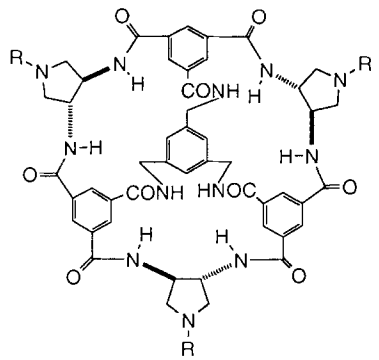
Expeditious Synthesis of a Novel C_3-Symmetric Receptor that Binds Peptides Sequence-Selectively**

Seung Soo Yoon and W. Clark Still*

One of the most exciting recent advances in molecular recognition is the development of synthetic receptors or host molecules that bind biopolymers sequence-selectively.[1] Among the most selective of these is the C_3-symmetric receptor **1**.[2] It binds a variety of biooligomers, including glycosides and both N- and C-protected peptides, with high stereochemical and functional-group selectivity. With simple peptides, for example, **1** binds L peptide residues with enantioselectivities as high as 3 kcal mol^{-1} (>99% *ee*). Though **1** is available by an optimized synthesis,[2b] we sought related receptors that could be prepared by even simpler methods and thus might find practical application to problems of separation. In this regard, **2** and its derivatives are



1a, R = H
1b, R = $OCH_2CH{=}CH_2$
1c, R = O-Dye



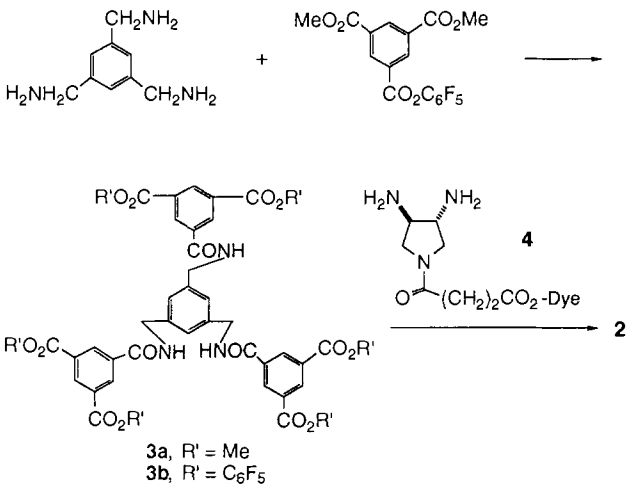
2, R = $CO(CH_2)_2CO_2$-Dye

attractive candidates. Receptors **1** and **2** are closely related in that their cup-shaped binding cavities have both similar dimensions and analogous patterns on their peripheries of unassociated hydrogen-bond donors and acceptors for substrate binding. In this communication, we describe a simple synthesis of **2** and its binding properties as determined by complexation with an encoded combinatorial library[7] of around 50000 acylated tripeptide substrates. As we will show, **2** is a remarkably selective receptor for peptides.

[*] Prof. W. C. Still, S. S. Yoon
Department of Chemistry, Columbia University
New York, NY 10027 (USA)
Telefax: Int. code + (212)932-1289

[**] We acknowledge the support of the National Science Foundation (CHE92 08254).

Our synthesis of **2** (Scheme 1) began with the coupling of three equivalents of pentafluorophenyl dimethyl trimesate to one equivalent of 1,3,5-tri(aminomethyl)benzene to provide **3a** (78% yield). Saponification of all six methyl ester groups and activation as the hexakis(pentafluorophenyl) ester then gave **3b** (30% yield). This material underwent threefold coupling with a (3*R*,4*R*)-3,4-diaminopyrrolidine linked to the dye Disperse Red 1 through a succinyl spacer;[3] three 21-membered rings were formed simultaneously, and the brilliant red receptor **2** was obtained in 26% yield. We should add that a variety of related receptors can be prepared with other 1,2-diamines. For example, reaction of commercially available (1*R*,2*R*)-1,2-diaminocyclohexane with **3b** yielded an analogous receptor (31% yield for the final tricyclization step) in which the pyrrolidine rings are replaced by simple cyclohexanes.



3a, R' = Me
3b, R' = C_6F_5

Scheme 1. Synthesis of receptor **2**.

To establish the binding properties of our new receptor **2**, we treated a dye-labeled receptor with a large collection or library of potential substrates.[2d] The substrate library was synthesized on 50–80 μm Merrifield polystyrene beads in such a way that each bead carried a single library member. The binding experiment simply involved mixing red **2** with the bead-supported library and selecting those beads that turned red. Thus binding of **2** to the entire library (here ca. 50000 acylated tripeptides) could be surveyed in a single experiment.

We used the polymer-supported substrate library[2d] of general structure **5**. We prepared the library using the split

RCO–AA3–AA2–AA1–$NH(CH_2)_5CONHCH_2$–polystyrene **5**

AA*n* (*n* = 1–3) = Gly, D-Ala, L-Ala, O^3-*t*Bu-D-Ser, O^3-*t*Bu-L-Ser, D-Val, L-Val, D-Pro, L-Pro, N^4-trityl-D-Asn, N^4-trityl-L-Asn, N^5-trityl-D-Gln, N^5-trityl-L-Gln, N^6-Boc-D-Lys, N^6-Boc-L-Lys

R = Me, Et, *i*Pr, *t*Bu, *i*Bu, neopentyl (*neo*Pe), trifluoromethyl (TFM), methoxymethyl (MOM), cyclopropyl (*c*Pr), cyclobutyl (*c*Bu), cyclopentyl (*c*Pe), acetoxymethyl (AcOM), Ph, Me_2N, morpholino (Mor)

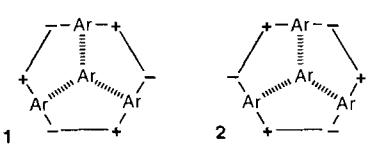
synthesis.[4] Thus, the total possible number of different substrates in the library was 15^4 (50625). To allow for determination of the structure of the substrate on any bead that bound **2**, we employed the binary encoding method that uses electron-capture gas chromatography (ECGC) to analyze tag-encoded structural information.[5]

In the binding assay, a sample of the above peptide library (10 mg, ca. 10^5 beads) was equilibrated with a 50 m > M solution of **2** in $CHCl_3$ (ca. 0.3 mL). After 24 h of agitation, approximately 1% of the beads had developed deep red-orange colorations. These beads carried peptides that bound red **2** most tightly.[6] By measuring the concentration of **2** in solution over the beads at equilibrium, we established that the assay allowed selection of beads having association constants $K_a \geq 3000$. Fifty of these most deeply colored beads were picked under a microscope (4 × magnification), and their tag-encoded structural information was decoded by ECGC. The residue types found in the peptides on these beads are listed in Table 1.

Table 1. Residues R and AA1–AA3 in acylated, protected peptide substrates that are selectively bound by **2** (no. of occurrences from 50 decoded beads in parentheses).

R	AA3	AA2	AA1
MOM (31)	N^5-trityl-D-Gln (31)	Gly (15)	L-Pro (11)
Me_2N (13)	N^4-trityl-D-Asn (7)	N^4-trityl-D-Asn (8)	D-Ala (10)
Et (4)	N^6-Boc-D-Lys (5)	N^5-trityl-D-Gln (5)	D-Pro (9)
Me (2)	N^4-trityl-L-Asn (4)	D-Ala (4)	Gly (7)
	D-Ala (2)	N^5-trityl-L-Gln (3)	N^5-trityl-D-Gln (3)
	Gly (1)	N^6-Boc-D-Lys (3)	N^5-trityl-L-Gln (2)
		L-Val (3)	L-Ala (2)
		N^6-Boc-L-Lys (2)	N^4-trityl-L-Asn (2)
		N^4-trityl-L-Asn (2)	D-Val (2)
		D-Val (2)	O^3-*t*Bu-L-Ser (2)
		L-Ala (1)	
		O^3-*t*Bu-L-Ser (1)	
		O^3-*t*Bu-D-Ser (1)	

In many ways, the binding selectivities of **2** are similar to those recently reported for **1**.[2d] Thus, both receptors show the highest selectivity for residues at the terminus of the peptide chain: they selectively bind certain R groups having three nonhydrogen atoms and AA3 = N^5-trityl-Gln. However, **1** binds AA3 = N^5-trityl-L-Gln, whereas **2** prefers the D isomer. This difference in enantioselection is rationalized by the enantiomeric patterns of hydogen bonding between substrate and groups at the periphery of the binding cavities of **1** and **2** (Scheme 2).



Scheme 2. Schematic representation of receptors **1** and **2**. Ar = aromatic ring; +, − indicate exposed H-bond donors and acceptors, respectively.

According to molecular modeling, these groups surround the opening to the binding cavity and are well positioned to bind substrate through intermolecular hydrogen bonds. Other donors and acceptors of **1** and **2** are unavailable for substrate binding because they project away from the opening to the binding cavity and further are involved in intramolecular hydrogen bonds.

Other selectivity differences between **1** and **2** are found at AA2 (**1** prefers L-Pro, **2** prefers Gly) and AA1 (**1** shows virtually no selectivity, **2** prefers D-Pro, L-Pro or D-Ala) residues. Interestingly, the remarkable preference of **1** for R = cyclopropyl[2d] is absent with **2**. Neither **1** nor **2** bind peptides having R = isopropyl. These and other selectivities were verified by independent binding energy measurements with **2** that showed, inter alia, that changing R = MOM to cyclopropyl or AA3 = N^5-trityl-D-Gln to N^5-trityl-L-Gln diminished binding by 1.3 kcal mol^{-1} relative to the preferred substrate MOMCO–N^5-trityl-D-Gln–Gly–L-Pro ($\Delta G_{binding} = -4.3$ kcal mol^{-1}). These results were obtained by resynthesizing selected substrate sequences and using UV spectrophotometry to quantitate the concentrations of free receptor both before and after treatment with a known quantity of the polymer-supported substrate.

We also carried out an analogous survey of **2** with a substrate library having deprotected peptide side chains (Table 2). Measurement of the concentration of **2** at equilibrium indicated that, in this case, the color assay allowed selection of substrates having $K_a \geq 5000$.

Table 2. Residues R and AA1–AA3 in acylated, deprotected peptide substrates that are selectively bound by **2** (no. of occurrences from 45 decoded beads in parentheses).

R	AA3	AA2	AA1
MOM (12)	D-Gln (23)	L-Gln (18)	L-Pro (23)
Me_2N (10)	D-Val (7)	D-Lys (8)	D-Pro (21)
Ph (6)	D-Lys (4)	L-Lys (3)	D-Gln (1)
Mor (6)	D-Pro (3)	Gly (4)	
Et (4)	D-Ala (2)	D-Gln (3)	
*c*Pr (3)	D-Ser (2)	D-Asn (2)	
Me (1)	D-Asn (2)	D-Ala (2)	
*c*Pen (1)	L-Asn (1)	L-Ala (2)	
*t*Bu (1)	L-Ser (1)	L-Pro (1)	
AcOm (1)		D-Ser (1)	
		L-Ser (1)	

Whereas our previous studies found **1** to have similar selectivities for protected and deprotected peptide substrates, receptor **2** bound a different set of peptides with the deprotected library. It was most discriminating at the internal AA1 site where Pro was strongly preferred. In particular, **2** preferentially bound the sequences with AA3 = D-Gln, AA2 = D amino acid, and AA1 = L-Pro (40% of beads) or with AA2 = L-Gln and AA1 = D-Pro (40% of beads). The relationship between the Pro configuration at the AA1 position and both the configuration and position of the downstream Gln is particularly interesting. This novel Gln–Pro selectivity may reflect the presence of hydrogen bonding between the Gln side chain and amides at the bottom of **2**'s binding cavity—a possibility not available to **1**. The ability of **2** to selectively bind peptide spans with as many as three residues is remarkable for such a small host molecule.

These studies and others soon to be reported suggest that a variety of receptors similar in structure to **1** or **2** have significantly sequence-selective peptide binding properties and that the specific selectivity of such a receptor can be controlled by varying the details of its structure. While the full range of variations that can be tolerated without loss of binding affinity has yet to be established, we have found that the full macrotricyclic framework of **2** is necessary for peptide binding: deletion of the central aromatic linker obliterates tight peptide binding as detected by our solid-phase color assay. Given the simplicity of **2**'s synthesis, its highly selective peptide-binding properties, and the availability of many building blocks for the construction of analogues, it is likely that a variety of C_3-symmetric receptors having a range of peptide sequence selectivies can be prepared along the lines described here.

 © VCH Verlagsgesellschaft mbH, D-69451 Weinheim, 1994 0570-0833/94/2323-2459 $ 10.00+.25/0

Experimental Procedure

3a: To a solution of pentafluorophenyl dimethyl trimesate (0.42 g, 1.04 mmol) and tri(aminomethyl)benzene triHCl salt (86 mg, 0.31 mmol) in 10 mL of dry *N*,*N*-dimethylacetamide (DMA) was added 0.36 mL of iPr_2NEt. After the mixture had been stirred for 8 h, it was concentrated at reduced pressure and purified by flash chromatography (silica gel, 5% MeOH in CH_2Cl_2) to give **3a** as an amorphous white solid (0.20 g, 78%). ^1H NMR ($CDCl_3$) δ = 3.90 (s, 6H), 4.38 (m, 2H), 7.10 (s, 1H), 7.30 (m, 1H), 8.61 (s, 2H), 8.70 (s, 1H); ^{13}C NMR ($CDCl_3$) δ = 165.74, 165.36, 139.11, 134.99, 132.84, 132.18, 130.77, 126.35, 52.44, 43.71; IR (neat) 3324, 2815, 1730, 1674, 1573 cm^{-1}; HR-MS (FAB) for $C_{42}H_{40}N_3O_{15}$: calcd: 827.2537 [$M + H^+$]; found: 827.2539.

2: To **3a** (0.1 g, 0.121 mmol) in THF (5 mL), MeOH (3 mL), and water (1 mL) was added a 1 N NaOH solution (0.85 mL). After stirring for 5 h, the mixture was acidified with 1 N HCl solution and extracted with EtOAc (3 × 50 mL). The extracted hexaacid was dissolved in THF (3 mL) and CH_2Cl_2 (10 mL), and C_6F_5OH (0.15 g, 0.84 mmol) and 1-(3-dimethylaminopropyl)-3-ethylcarbodiimide (EDC) (0.16 g, 0.84 mmol) were added. Stirring for 5 h, concentration, and flash chromatography (silica gel, 20% acetone in CH_2Cl_2) gave **3b** as an amorphous white solid (63 mg, 30%).

A solution of **3b** (44 mg, 0.025 mmol) and **4**·2CF_3CO_2H (63 mg, 0.084 mmol) in DMA (10 mL) was added with stirring to a solution of iPr_2NEt (0.19 mL, 1.09 mmol) in dry THF (200 mL) at room temperature over 20 h by syringe pump. Stirring for an additional 8 h, concentration, and flash chromatography (silica gel, 10% MeOH in CH_2Cl_2) gave **2** as an amorphous red solid (15 mg, 26%). ^1H NMR ($CD_3OD/CDCl_3$ 1/1) δ = 0.70 (t, 3H, J = 7.0Hz), 2.45 (m, 4H), 3.01 (q, 2H, J = 7.0Hz), 3.36 (br.s, 2H), 3.50 (br.s, 2H), 3.74 (m, 1H), 3.92 (m, 1H), 4.12 (m, 4H), 4.58 (m, 1H), 4.68 (m, 1H), 6.64 (d, 2H, J = 9.1Hz), 7.72 (m, 5H), 7.98 (m, 1H), 8.10 (d, 2H, J = 9.0Hz), 8.23 (m, 1H), 8.64 (m, 1H); ^{13}C NMR (1/1 = $CD_3OD/CDCl_3$) δ = 172.82, 170.20, 169.72, 169.61, 167.70, 138.51, 136.06, 133.53, 131.27, 130.54, 130.46, 129.54, 126.72, 125.92, 125.22, 124.37, 124.24, 122.31, 118.85, 112.22, 61.34, 55.74, 50.54, 45.70, 44.42, 38.28, 28.76, 28.27, 27.52, 27.22, 11.94; IR (neat) 3324, 2815, 1720, 1675, 1573 cm^{-1}; MS (FAB) *m*/*z* 2127 [$M + H^+$].

Received: July 25, 1994 [Z 7172 IE]
German version: *Angew. Chem.* **1994**, *106*, 2517

[1] Reviews: H.-J. Schneider, *Angew. Chem.* **1993**, *105*, 890; *Angew. Chem. Int. Ed. Engl.* **1993**, *32*, 848; T. H. Webb, C. S. Wilcox, *Chem. Soc. Rev.* **1993**, 383.

[2] a) J.-I. Hong, S. K. Namgoong, A. Bernardi, W. C. Still, *J. Am. Chem. Soc.* **1991**, *113*, 5111; b) S. D. Erickson, J. A. Simon, W. C. Still, *J. Org. Chem.* **1993**, *58*, 1305; c) R. Liu, W. C. Still, *Tetrahedron Lett.* **1993**, *34*, 2573; d) A. Borchardt, W. C. Still, *J. Am. Chem. Soc.* **1994**, *116*, 373.

[3] (*R*,*R*)-Diaminopyrrolidine preparation: D. R. Reddy, E. R. Thornton, *J. Chem. Soc. Chem. Commun.* **1992**, 172; S. S. Yoon, W. C. Still, *Tetrahedron*, in press.

[4] a) A. Furka, M. Sebestyen, M. Asgedom, G. Dibo, *Abstr. 14th Int. Congr. Biochem.*, Prag, **1988**, *5*, 47; b) *Abstr. 10th Int. Symp. Med. Chem.*, Budapest, **1988**, 288; c) *Int. J. Pept. Protein Res.* **1991**, *37*, 487; d) K. S. Lam, S. E. Salmon, E. M. Hersh, V. J. Hruby, W. M. Kazmierski, R. J. Knapp, *Nature (London)* **1991**, *354*, 82.

[5] M. H. J. Ohlmeyer, R. N. Swanson, L. W. Dillard, J. C. Reader, G. Asouline, R. Kobayashi, M. Wigler, W. C. Still, *Proc. Natl. Acad. Sci. USA* **1993**, *90*, 10922.

[6] Previous studies have shown that the color assay readily distinguishes substrates differing in binding energy by as little as 1.0 kcal mol^{-1}. Control experiments established that bead coloration reflects binding of the peptide and not the dye: neither the dye nor the succinylated dye stained any of the library beads under the assay conditions.

[7] See, for example, P. Eckes, *Angew. Chem.* **1994**, *106*, 1649; *Angew. Chem. Int. Ed. Engl.* **1994**, *33*, 1573.

Single-Step Six-Electron Transfer in a Heptanuclear Complex: Isolation of Both Redox Forms**

Jean-Luc Fillaut, Jorge Linares, and Didier Astruc*

Dedicated to Dr. Jacqueline Zarembovitch

Polymers containing ferrocene units are useful redox catalysts for the modification of electrodes[1] and as biosensors.[2] A new generation of polynuclear compounds intermediate between mononuclear and polymeric complexes has recently appeared—the inorganic[3] and organometallic[4] molecular "trees". These well-defined molecules promise to be useful in the construction of dendrimers,[5] in molecular electronic devices,[6] and in multielectron redox catalysis.[7] $FeCp^+$ can serve as an excellent starting core for molecular trees, since polyalkylation, polyallylation, and polybenzylation of polymethyl arenes leads to various topologies.[7] The reaction of $[FeCp(C_6Me_6)]PF_6$ with excess base and an alkyl halide results in selective hexasubstitution [Eq. (a)].[7]

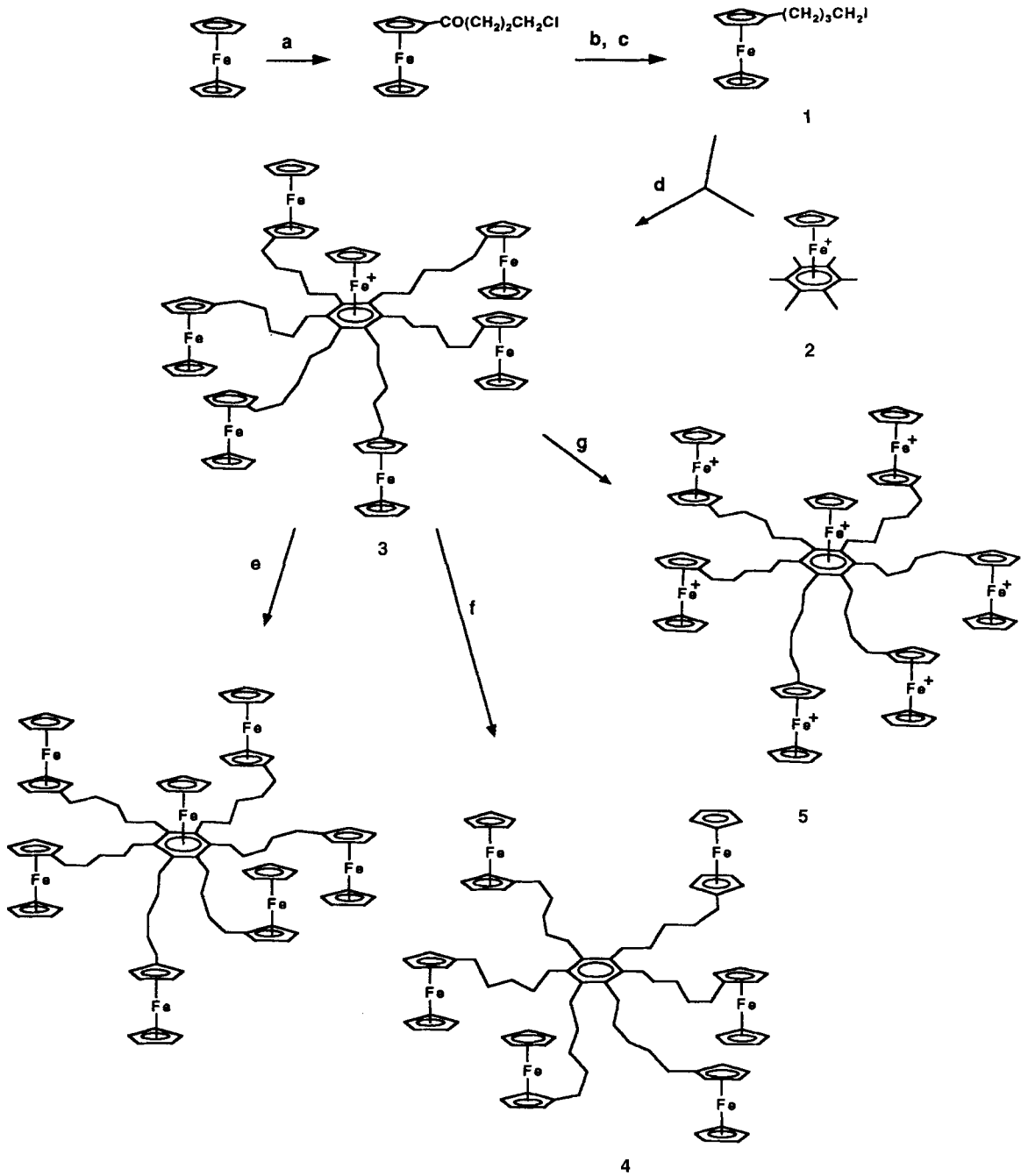
$$[FeCp(C_6Me_6)]PF_6 \xrightarrow[RI\ (R = alkyl)]{KOR'\ (R' = H,\ tBu)} [FeCp\{C_6(CH_2R)_6\}]PF_6 \qquad (a)$$

Since the introduction of organometallic groups on the "branches" is sometimes tedious and requires multistep synthesis,[8a] we have engaged in research aimed at grafting organometallic complexes directly on the branches in the polyalkylation process[8b] and report here our first results. We have isolated and characterized both the reduced and oxidized forms of a heptametallic hexaferrocene system.[9] The central iron units in this complex serve as an internal standard in the determination of the number of ferrocenyl groups on the branches by Mössbauer spectroscopy and cyclic voltammetry.

The 4-ferrocenylbutyl iodide (**1**) was synthesized in the form of orange-red crystals according to Scheme 1. Reaction of a threefold excess of **1** with KOH and $[Fe^{II}Cp(C_6Me_6)]PF_6$ (**2**) gives the PF_6 salt of the heptanuclear Fe^{II} complex cation **3** (orange-red microcrystals) in 65% yield. The Mössbauer spectrum of **3** at 200 K shows a ferrocene doublet with QS = 2.384 mm s^{-1} and IS = 0.487 mm s^{-1} as well as a shoulder for the $[Fe^{II}Cp(arene)]$ doublet at QS = 1.879 mm s^{-1} and IS = 0.487 mm s^{-1}. Photolysis of **3** in CH_3CN in the presence of one equivalent of PPh_3 using visible light gives $[FeCp(PPh_3)(NCMe)_2]PF_6$ and the hexanuclear neutral complex **4** (orange microcrystals) in 96% yield, which results from the selective decomplexation of the central cationic $FeCp^+$ unit. Oxidation of **3** with H_2SO_4 followed by ion exchange with aqueous NH_4PF_6 solution provides the PF_6 salt of the heptanuclear hexaferricinium complex **5** as purple-black microcrystals in 98% yield. The Mössbauer spectrum of **5** at 200 K (as well as at 4 K) shows a Fe^{II} doublet at QS = 1.95 mm s^{-1} and IS = 0.5 mm s^{-1} and a large ferricinium signal at QS = 0.164 mm s^{-1}

[*] Prof. D. Astruc, Dr. J.-L. Fillaut
Laboratoire de Chimie Organique et Organométallique
Université Bordeaux I, URA CNRS N° 35
351, Cours de la Libération, F-33405 Talence Cedex (France)
Telefax: Int. code + 56846646
Dr. J. Linares
Département de Recherches Physiques
Université Pierre et Marie Curie, URA CNRS N° 71
Tour 22, 4, place Jussieu, F-75252 Paris Cedex (France)

[**] This research was supported by the Centre National de la Recherche Scientifique (CNRS), the Universities Bordeaux I and Paris VI, and the Région Aquitaine. We thank Prof. F. Varret and K. Boukheddaden for help with the Mössbauer spectroscopy, S. Treavett for synthetic collaboration, and Dr. F. Moulines for discussions.



Scheme 1: Reagents and conditions: a) $AlCl_3$, $ClCO(CH_2)_2CH_2Cl$ (1.0 equiv), Zn, CH_2Cl_2, 0 °C, 18 h, 72%; b) $LiAlH_4-AlCl_3$ (1.2 equiv.), Et_2O, 0 °C, 16 h, 71%; c) NaI (1.2 equiv), $CH_3COC_2H_5$, 65 °C, 3 h, 95% [10]; d) $[FeCp(C_6Me_6)]PF_6$ (0.05 equiv), KOH (1 equiv), DME, 60 °C, 60 h, 65%; e) +1e (−1.47 V vs SCE); f) *hv*, PPh_3 (1 equiv), CH_3CN, 20 °C, 3 h, 96%; g) 1. H_2SO_4 (40% in H_2O), CH_2Cl_2, 20 °C, 2 min; 2. NH_4PF_6, 98%, or −1e (+0.44 V vs SCE).

and IS = 0.476 mm s^{-1} (Fig. 1). Of particular interest is the fact that the resonance fraction is lower for the outer iron nuclei than for the central one, consistent with a larger thermal motion of the outer Cp_2Fe^+ moieties.

Examination of the electrochemical properties of the hexa- and heptanuclear iron complexes in dimethylformamide (DMF) gave insight into the number and equivalence of the outer ferrocene centers and the influence of the central [FeCp(arene)] group of **3** (Fig. 2). The voltammogram of **3** shows a relative intensity ratio of 6 ± 0.3 between the anodic and cathodic waves, confirming the presence of six ferrocene units. The ΔE_p value of the ferrocene signal, 55 mV at 0.4 Vs^{-1}, indicates that the six ferrocene moieties are electrochemically equivalent. The six ferrocene groups are also oxidized at the same potential in **3** ($E^0 = +0.44$ V vs SCE) as in **4** ($E^0 = +0.45$ V vs SCE) at a scan rate of 400 mVs^{-1}, indicating that the central cationic unit has no influence on the oxidation process. One also notes that all the waves are fully chemically reversible ($I_a/I_c \approx 1$). The formation of Fe^I in the central sandwich group, in particular, is chemically and electrochemically fully reversible on the electrochemical timescale. The diffusion coefficient of **3** is available from the Cotrell equation[1a] by using either the oxidation or the reduction wave ($D_p = 8 \pm 0.5 \times 10^{-6}$ $cm^{-2}s^{-1}$ at 20 °C).

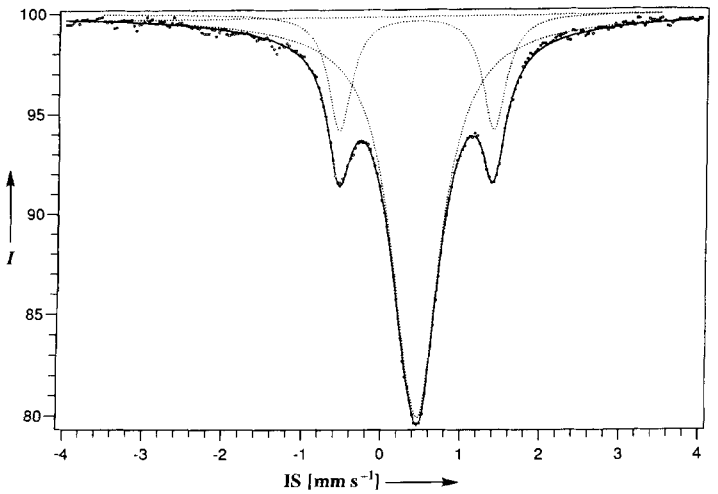


Fig. 1. Mössbauer spectrum of the mixed-valence complex PF_6 salt of **5** at 4.2 K under zero field (standard: iron metal). The shapes and parameters are similar at 78 K and 200 K (see text). The central line is due to the six outer Fe^{III} centers; the external doublet is due to the inner Fe^{II} sandwich.

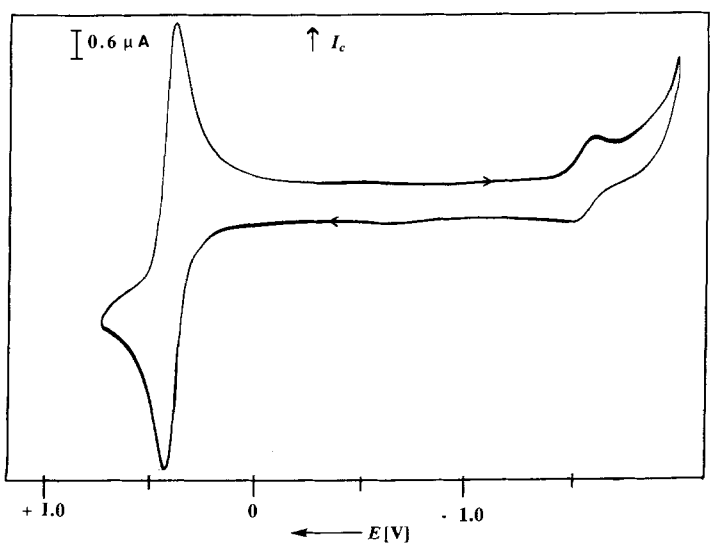


Fig. 2. Cyclic voltammogram of **3** in DMF (concentration ca. 3.4×10^{-3} mol dm^{-3}); supporting electrolyte: 0.1 mol dm^{-3} nBu$_4$BF$_4$. Pt electrode, 20 °C, scan rate 400 mV s^{-1}. Potentials were determined with reference to the SCE.

In conclusion, the $CpFe^+$-induced hexaferrocenylalkylation of C_6Me_6 opens the route to isolable mixed-valence star-shaped molecules with independent redox centers and leads to a fully reversible six-electron redox system which may be useful for multielectron redox catalysis.

Experimental Procedure

Under inert gas, a three-neck round-bottom flask equipped with a condenser was charged with [FeCp(C_6Me_6)]PF_6 (0.36 g, 1 mmol), 4-ferrocenylbutyl iodide (**1**) (6.6 g, 18 mmol), ground KOH (1.12 g, 20 mmol), and 100 mL of dimethoxyethane. The reaction mixture was stirred at 60 °C for 2.5 d under inert gas. Then, the solvent was removed under reduced pressure, and the solid residue was washed with ether (3×30 mL) to remove excess **1**. The cationic organoiron product **3** was extracted as the PF_6 salt, precipitated by addition of pentane, and recrystallized from CH_2Cl_2/ether to give 1.22 g (65 % yield) of orange-red microcrystals of **3**-PF_6, which are soluble in THF, but not in ether.

Received: July 22, 1994 [Z 7159 IE]
German version: *Angew. Chem.* **1994**, *106*, 2540

[1] a) J. B. Flanagan, S. Margel, A. J. Bard, F. C. Anson, *J. Am. Chem. Soc.* **1978**, *100*, 4248; b) F. G. Bordwell, G. D. Cooper, H. Morita, *ibid.* **1957**, *79*, 376; c) T. W. Smith, J. E. Kunder, D. Wychick, *J. Polym. Sci.* **1976**, *14*, 2433.
[2] a) H. A. U. Hill, D. J. Page, N. J. Walton, *J. Electroanal. Chem.* **1987**, *217*, 141; b) Y. Degani, A. Heller, *J. Phys. Chem.* **1987**, *91*, 1285.
[3] a) S. Serroni, G. Denti, S. Campagna, A. Juris, M. Ciano, V. Balzani, *Angew. Chem.* **1992**, *104*, 1540; *Angew. Chem. Int. Ed. Engl.* **1992**, *31*, 1493; b) G. Denti, S. Campagna, S. Serroni, M. Ciano, V. Balzani, *J. Am. Chem. Soc.* **1992**, *114*, 2944.
[4] F. Moulines, L. Djakovitch, R. Boese, B. Gloaguen, W. Thiel, J.-L. Fillaut, M.-H. Delville, D. Astruc, *Angew. Chem.* **1993**, *105*, 1132; *Angew. Chem. Int. Ed. Engl.* **1993**, *32*, 1075.
[5] a) E. Bulheim, W. Wehner, F. Vögtle, *Synthesis* **1978**, 155; b) F. Vögtle, E. Weber, *Angew. Chem.* **1979**, *91*, 813; *Angew. Chem. Int. Ed. Engl.* **1979**, *18*, 753; c) H. B. Mekelburger, W. Jaworek, F. Vögtle, *ibid.* **1992**, *104*, 1609, and **1992**, *31*, 1571; J. Issberner, R. Moors, F. Vögtle, *ibid.* **1994**, *106*, 2507 and **1994**, *33*, 2413; d) D. A. Tomalia, A. M. Taylor, W. A. Goddart III, *ibid.* **1990**, *102*, 119 and **1990**, *29*, 138.
[6] *Molecular Electronics* (Ed.: J.-P. Launay), (*New J. Chem.* **1991**, *15*, 97).
[7] a) D. Astruc in *Mechanisms and Processes in Molecular Chemistry*, (Ed.: D. Astruc), (*New J. Chem.* **1992**, *16*, 305); b) D. Astruc, *Top. Curr. Chem.* **1991**, *160*, 47.
[8] a) J.-L. Fillaut, D. Astruc, *J. Chem. Soc. Chem. Commun.* **1993**, 1320; b) F. Moulines, D. Astruc, *ibid* **1989**, 614.
[9] All new compounds gave satisfactory elemental analysis. NMR spectroscopic data: **1**: ^{1}H NMR ($CDCl_3$): δ = 4.03 (s, 5H, C_5H_5), 4.02, 3.98 (m, 4H, C_5H_4), 3.13 (t, 2H, CH_2), 2.28 (t, 2H, CH_2I), 1.78 (m, 2H, CH_2), 1.57 (m, 2H, CH_2); ^{13}C NMR ($CDCl_3$): δ = 88.59 (*C*-CH_2), 68.56 (C_5H_5), 68.09, 67.23 (C_5H_4), 33.29 (CH_2), 31.92 (CH_2), 28.56 (CH_2), 7.13 (CH_2I). **3**: ^{1}H NMR ($CDCl_3$): δ = 4.38 (s, 5H, $C_5H_5Fe^+$), 4.07 (s, 24H, C_5H_4), 4.03 (s, 30H, C_5H_5), 2.45 (m, 12H, CH_2), 2.35 (m, 12H, CH_2), 1.50 (m, 36H, CH_2); ^{13}C NMR ($CDCl_3$): δ = 103.09 (Ar*C*-C), 89.19 (*C*-CH_2), 77.59 ($C_5H_5Fe^+$), 69.01 (C_5H_5), 68.69, 68.13 (C_5H_4), 32.69 (CH_2), 31.12 (CH_2), 29.56 (CH_2), 29.38 (CH_2), 27.31 (CH_2). **4**: ^{1}H NMR ($CDCl_3$): δ = 4.03 (s, 24H, C_5H_5), 3.98 (s, 30H, C_5H_4), 2.30 (m, 12H, CH_2), 2.27 (m, 12H, CH_2), 1.45 (m, 36H, CH_2); ^{13}C NMR ($CDCl_3$): δ = 115.02 (Ar*C*-C), 89.39 (*C*-CH_2), 68.54 (C_5H_5), 68.16, 67.11 (C_5H_4), 31.20 (CH_2), 31.12 (CH_2), 31.08 (CH_2), 29.78 (CH_2), 29.66 (CH_2).
[10] For useful standard syntheses of closely related ferrocene intermediates, see *Organometallic Compounds of Iron* (Ed.: G. R. Knox), Chapman and Hall, London, 1985.

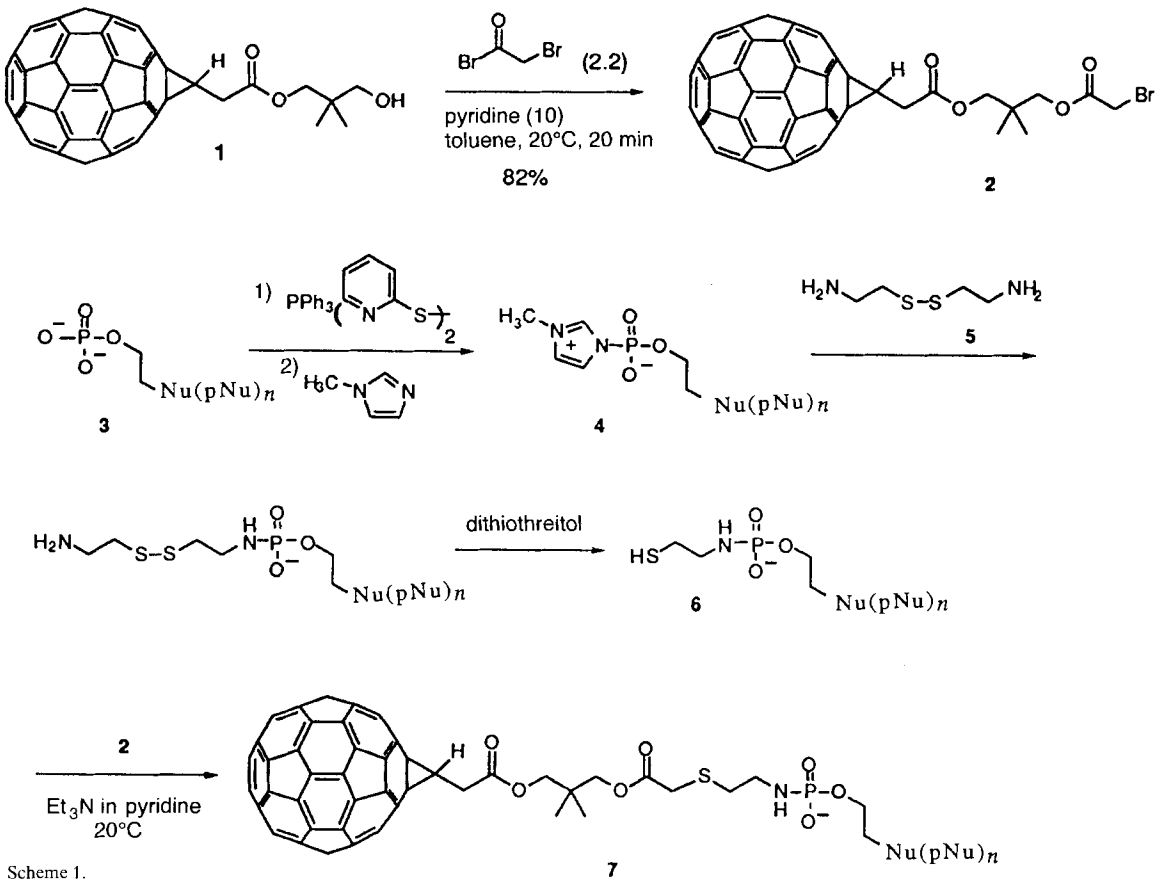
Fullerene–Oligonucleotide Conjugates: Photoinduced Sequence-Specific DNA Cleavage**

Alexandre S. Boutorine, Hidetoshi Tokuyama, Masashi Takasugi, Hiroyuki Isobe, Eiichi Nakamura, and Claude Hélène*

Oligonucleotides can be used to target either single-stranded nucleic acids such as messenger RNA or double-helical DNA.[1, 2] Oligonucleotide binding can block translation of the target mRNA (the *antisense* strategy) or transcription of the targeted gene by triple helix formation (the *antigene* strategy). Attachment of reactive substituents to oligonucleotides can induce irreversible reactions in the target sequence.[2] Hydropho-

[*] Prof. C. Hélène, Dr. A. S. Boutorine, Dr. M. Takasugi
Laboratoire de Biophysique, INSERM U201, CNRS UA 481
Muséum National d'Histoire Naturelle
43 Rue Cuvier, F-75005 Paris (France)
Telefax: Int. code + (1)40793705
Dr. H. Tokuyama, H. Isobe, Prof. E. Nakamura
Department of Chemistry, Tokyo Institute of Technology
O-Okayama, Meguro-Ku, Tokyo 152 (Japan)

[**] E. N. thanks the Japanese Ministry of Education, Science, and Culture for financial support (Grant-in-Aid for Scientific Research on Priority Area no. 06240217). H. T. thanks the Japan Society for the Promotion of Science for a postdoctoral fellowship. The Agence Nationale de Recherche sur le SIDA (ANRS) is acknowledged for a research fellowship to A. B.



Scheme 1.

bic substituents may also be used to improve cell uptake in biological systems.[3, 4] Recent studies on the chemistry of buckminsterfullerenes have revealed a diversity of reactions and provided access to functionalized fullerenes.[5, 6] Reports from three groups[6–8] have demonstrated that suitably modified fullerenes exhibit biological activity towards living cells,[6] enzymes,[6, 7] viruses,[8] and DNA.[6] Irradiation of a mixture of DNA and a detergent-like C_{60} carboxylic acid with low-energy light results in guanine(G)-selective strand cleavage.[6] This base-selective cleavage was ascribed to the action of singlet oxygen generated by photoactivation of the fullerene molecule, and recent experiments demonstrated that the C_{60} carboxylic acid does generate singlet oxygen in water.[9] The G-selective strand cleavage, however, took place randomly, most likely owing to nonselective hydrophobic binding of the C_{60} molecule to DNA. If this assumption is correct, the site selectivity of the G-selective cleavage should dramatically increase once a suitable recognition site is connected to the C_{60} core. Such site-selective photocleavage has been described, for example, for ellipticin and porphyrin derivatives of oligonucleotides.[10, 11] In order to further investigate this possibility, we have synthesized an organofunctional C_{60} bearing a 14-mer oligodeoxynucleotide side chain capable of binding to either a single-stranded target through Watson–Crick hydrogen-bonding interactions, or a double-stranded target by formation of Hoogsteen hydrogen bonds.[12] We report herein that photocleavage reactions do indeed take place at well-defined positions upon irradiation of the oligonucleotide–fullerene conjugate with three different targets, namely, a single-stranded DNA, a duplex DNA, and a duplex DNA with a hairpin structure.

The fullerene–oligonucleotide conjugate **7** was synthesized by alkylation of a deblocked thiol-containing oligonucleotide **6** with bromoacetate **2** (Scheme 1). The moiety **2** was prepared from the methanofullerene derivative **1**.[13] Introduction of a terminal thiol group in the deblocked oligonucleotide **3** was achieved by reaction of the cystamine **5** with the activated phosphate **4**.[14] Treatment with dithiothreitol yielded the thiol **6**, which was alkylated with **2** in pyridine to afford the fullerene–oligonucleotide conjugate **7** with a yield of 30–40%. The conjugate was colored (red-brown), soluble in water, and precipitated in ethanol or $LiClO_4$ in acetone. Purification of **7** by HPLC was not possible because of the irreversible adsorption of the conjugate on modified silica gel supports. On polyacrylamide gels this derivative formed aggregates in the wells. Electrophoresis on 1.0% agarose/0.1% triton X-100 gel revealed one homogeneous colored band migrating more slowly than unmodified oligonucleotide. This technique was used to purify the conjugate from the unreacted oligonucleotide. The sequence of the oligonucleotide is shown in Figure 1.

Three different target oligodeoxynucleotides were used to test the photosensitizing properties of the fullerene–14-mer conjugate: a single-stranded 20-mer, a duplex with 26 base pairs, and a 41-mer hairpin structure with 18 base pairs and a 5 base loop (see sequences in Fig. 1). The complex was irradiated with a 1000 W xenon lamp through a filter absorbing light at wavelengths shorter than 310 nm. The buffer (pH 6.0) contained cacodylate (10 mM), NaCl (50 mM), the target (50–100 nM), and increasing concentrations of the fullerene–14-mer conjugate (1–60 μM). The 20-mer single strand, the 41-mer hairpin, and one of the duplex strands were labeled with ^{32}P at the 5′-end by means of γ-^{32}P-ATP and T4 polynucleotide kinase (Amersham). Analysis by electrophoresis on denaturing 12% polyacrylamide gel was carried out before and after treatment with piperidine (Fig. 2).

 © VCH Verlagsgesellschaft mbH, D-69451 Weinheim, 1994 0570-0833/94/2323-2463 $ 10.00+.25/0

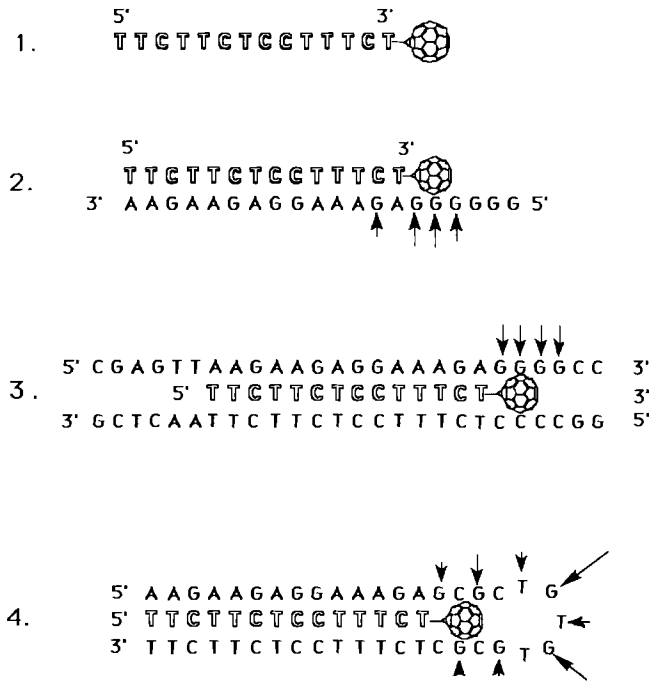


Fig. 1. Structure of oligonucleotide–fullerene conjugate (1) and its complexes with targets: 2. duplex with complementary oligodeoxynucleotide, 3. triple helix, 4. triple helix with hairpin structure. The arrows indicate cleavage sites upon irradiation with light. Lengths of the arrows correspond to intensity of photoinduced cleavage.

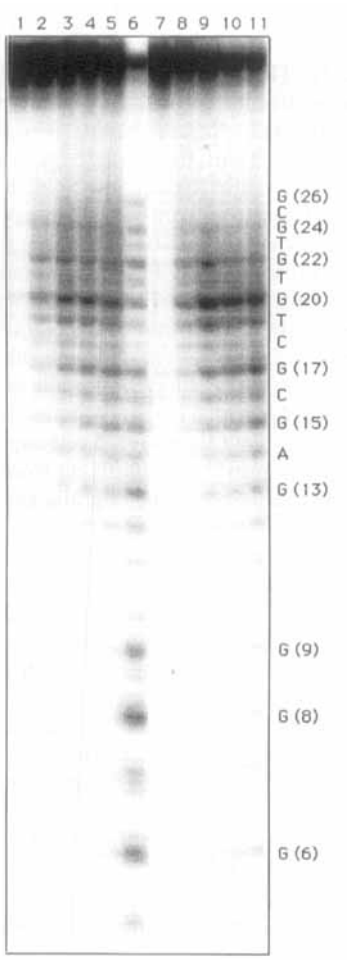


Fig. 2. Gel electrophoresis of the 41-mer hairpin-forming oligonucleotide (100 nM) (see Fig. 1, 4.) after irradiation in the presence of the 14-mer fullerene conjugate (30 μM) in cacodylate (10 mM, pH 6.0) and NaCl (50 mM) at 15 °C. The irradiation times were increased in lanes 1–5 and 7–11, respectively: 0 min (1, 7), 15 min (2, 8), 30 min (3, 9), 45 min (4, 10), and 60 min (5, 11). The two parts of the figure correspond to samples which have not been (1–5) or have been (7–11) treated with piperidine (1 M) at 90 °C for 30 min. The 41-mer was labeled at the 5′-end, and the gels were analyzed with a phosphorimager. Lane 6 indicates the sequence of guanine residues obtained after treatment with dimethyl sulfate and piperidine. The sequence in the region of cleavage and the location of guanine residues are indicated (numbering starts from the 5′-end; see Fig. 1, 4.).

The results of these experiments demonstrate that photocleavage induced by the oligonucleotide–fullerene conjugate occurred at well-defined sites in the duplex, triple helix, and triple helix with hairpin. This is in sharp contrast with the lack of site selectivity in the cleavage by the free C_{60} carboxylic acid.[6] Figure 2 shows the results obtained with the hairpin target. Cleavage was observed at guanines but also at thymine residues (with a lower efficiency). Treatment with piperidine slighthly increased the intensity of the cleavage bands. Comparison with bands generated by piperidine treatment after reaction with dimethyl sulfate (DMS) suggested that fragments obtained by photoinduced cleavage were terminated by a 3′-phosphate. They had the same mobility in the gel as 3′-phosphorylated products of DMS-induced piperidine cleavage. The cleavage sites on the three target sequences are shown in Figure 1. The most reactive guanines were those located in the loop region. With the 26 base pair duplex (devoid of hairpin structure), cleavage occurred at guanines of the purine-containing strand positioned near the 3′-end of the third oligonucleotide strand (Fig. 1). No cleavage was observed on the other strand of the duplex, which did not contain any guanines in the vicinity of the 3′-end of the third strand (the two terminal Gs could not be analyzed owing to their too close proximity to the 5′ label). On the single-stranded target photoinduced cleavage occurred at guanines near the 3′-end of the complementary oligonucleotide–fullerene conjugate (Fig. 1). In all three cases the sites of cleavage were located in the region of the target expected from the known orientation of the oligonucleotide carrying the fullerene derivative: antiparallel orientation with respect to the complementary strand in the duplex and parallel to the oligopurine target sequence in the triplex structures. The enhanced reactivity of guanines in the loop as compared to the stem of the hairpin duplex might be due to a higher accessibility to singlet oxygen in the single-stranded loop, even though the reaction might involve other mechanisms (e.g. electron transfer) resulting from folded structures.

These results indicate that the spherical fullerene terminus on the oligonucleotide chain did not hamper duplex and triplex formation. The cleavage nearly exclusively took place at guanine bases; this is consistent with singlet oxygen mediation. The same profile of site and base selectivity was observed with an oligonucleotide–chlorin conjugate (with the same oligonucleotide sequence), which was shown to generate singlet oxygen upon irradiation and to cleave nucleic acids (results not shown).

In summary, we have shown that fullerene–oligodeoxynucleotide conjugates effectively modify DNA with high site specificity by forming double and triple helices. The present results clearly indicate that fullerene–oligonucleotide conjugates are promising photoprobes for the investigation of gene transcription and mRNA translation. Design of the optimal linker moiety and conditions needed to achieve high efficiency are now under investigation. In addition, the hydrophobicity of the fullerene moiety can be exploited to enhance cell uptake for biological applications.

Received: August 30, 1994 [Z 7279 IE]
German version: *Angew. Chem.* **1994**, *106*, 2526

[1] C. Hélène, J. J. Toulmé, *Biochim. Biophys. Acta* **1990**, *1049*, 99–125.
[2] N. T. Thuong, C. Hélène, *Angew. Chem.* **1993**, *105*, 697–726; *Angew. Chem. Int. Ed. Engl.* **1993**, *32*, 666–690.
[3] A. S. Boutorine, C. Boiziau, T. Le Doan, J. J. Toulmé, C. Hélène, *Biochimie* **1992**, *74*, 485–489.
[4] A. M. Krieg, J. Tonkinson, S. Matson, Q. Zhao, M. Saxon, L. M. Zhang, U. Bhanja, L. Yakubov, C. A. Stein, *Proc. Natl. Acad. Sci. USA* **1993**, *90*, 1048–1052.
[5] F. Diederich, Y. Rubin, *Angew. Chem.* **1992**, *104*, 1123–1146; *Angew. Chem. Int. Ed. Engl.* **1992**, *31*, 1101–1123.

 © VCH Verlagsgesellschaft mbH, D-69451 Weinheim, 1994 0570-0833/94/2323-2464 $ 10.00+.25/0

[6] H. Tokuyama, S. Yamago, E. Nakamura, T. Shiraki, Y. Sugiura, *J. Am. Chem. Soc.* **1993**, *115*, 7918–7919.
[7] S. H. Friedman, D. L. De Camp, R. P. Sijbesma, G. Srdanov, F. Wudl, G. L. Kenyon, *J. Am. Chem. Soc.* **1993**, *115*, 6506–6509.
[8] R. F. Shinazi, R. Sijbesma, G. Srdanov, C. L. Hill, F. Wudl, *Antimicrob. Agents Chemother.* **1993**, *37*, 1707–1710.
[9] H. Tokuyama, E. Nakamura, *J. Org. Chem.* **1994**, *59*, 1135–1138.
[10] L. Perrouault, U. Asseline, C. Rivalle, N. T. Thuong, E. Bisagni, C. Giovannangeli, T. Le Doan, C. Hélène, *Nature* **1990**, *344*, 358–360.
[11] T. Le Doan, D. Praseuth, L. Perrouault, M. Chassignol, N. T. Thuong, C. Hélène, *Bioconjugate Chem.* **1990**, *1*, 108–113.
[12] J. L. Mergny, G. Duval-Valentin, C. H. Nguyen, L. Perrouault, B. Faucon, M. Rougée, T. Montenay-Garestier, E. Bisagni, C. Hélène *Science* **1992**, *256*, 1681–1684.
[13] H. Tokuyama, M. Nakamura, E. Nakamura, *Tetrahedron Lett.* **1993**, *34*, 7429–7432.
[14] A. S. Boutorine, T. Le Doan, J. P. Battioni, D. Mansuy, D. Dupré, C. Hélène, *Bioconjugate Chem.* **1990**, *1*, 350–356.

Bis(pentamethylcyclopentadienyl)(η^3-trimethylenemethane)zirconium: A New Mode of Bonding for the Trimethylenemethane Ligand

Gerhard E. Herberich,* Carsten Kreuder, and Ulli Englert

Trimethylenemethane (tmm) forms a multitude of η^4 complexes with transition metals.[1] For complexes of the early transition metals, only $[Cp^*TaMe_2(tmm)]$[2a] ($Cp^* = \eta^5$-C_5Me_5) and recently $[Cp^*Zr(tmm)(\mu\text{-}Cl)_2Li(tmeda)]$[2b] (tmeda = *N,N,N',N'*-tetramethylethylenediamine) have been described to date.

$[Cp_2^*ZrCl_2]$ reacted with $Li_2[tmm(tmeda)]$[3] to give **1**, which was obtained as deep red crystals in 45% yield. An X-ray structure analysis shows **1** to be a bent metallocene with a side-bound tmm unit (Fig. 1).[4] The angle between the C1,Zr,C2 and C1,C3,C2 planes is only 33.0(9)°; the terminal CH_2 group is bent out of the C1,C3,C2 plane by 7.8(5)°.

$[Cp_2^*Zr(tmm)]$ **1**

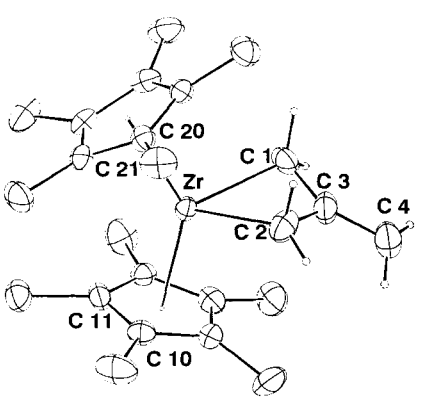
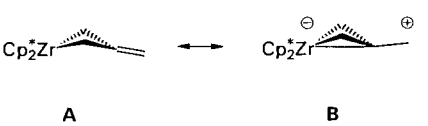


Fig. 1. Crystal structure of **1**. Metallocene angle 136.9(4)°; Zr-C(10 ··· 14) 254.1, Zr-C(20 ··· 24) 256.3 pm (average); Zr-C1 227.7(6), Zr-C2 225.8(7), Zr-C3 263.7(7), C1-C3 149(1), C2-C3 151(1), C3-C4 137.6(9) pm; C1-Zr-C2 66.7(3)°, Zr-C1-C3 86.1(4), Zr-C2-C3 86.4(4), C1-C3-C2 112.2(6), C1-C3-C4 123.4(9), C2-C3-C4 123.7(9).

The binding of the tmm ligand to the Zr atom is unusual. The distances from the metal atom to C1 and C2 (227.7 and 225.8 pm, respectively) are very similar to those in Zr–alkyl complexes ($[Cp_2ZrMe_2]$: 228,[7a] $[Cp_2Zr(CH_2)_2SiMe_2]$: 224 pm[7b]). The distance to the central atom C3 (263.7 pm) is typical for weak interactions (compare, for example, 259.7 pm for C-2/3 in the butadiene complex $[Cp_2Zr(2,3\text{-}Me_2C_4H_4)]$[8] and 263.3–269.2 pm in the η^3-fluorenyl derivative $[CpZr(C_5H_4CMe_2C_{13}H_8)Cl]$[9]); no direct interaction exists between C4 and the Zr center (Zr ··· C4 distance = 388 pm). Thus, η^3 coordination is observed in **1**. Finally, the long C3–C4 bond (137.6(9) pm) shows that the delocalization of the π electrons of the tmm dianion is to a certain extent retained in the complex.

The zirconocene fragment in **1** possesses three valence orbitals with two valence electrons.[10] It is therefore able to form two strong σ bonds with C1 and C2 of the tmm ligand, as in dialkyl derivatives $[Cp_2ZrR_2]$. If the tmm ligand were not bent out of plane, the acceptor orbital of the $[Cp_2^*Zr]$ fragment would be unable to overlap with the π electron pair of the tmm ligand. Only through the observed folding is a σ interaction with C3 possible. This phenomenon has been discussed previously for enedithiolato complexes ($[Cp_2M(S_2C_2R_2)]$ where M = Ti, Mo, W),[10] and is likewise observed for the analogous zircocenes with butadiene[8] and enediolato ligands.[11] The bonding in **1** may be represented according to the valence-bond method by the resonance structures **A** and **B** (Scheme 1).

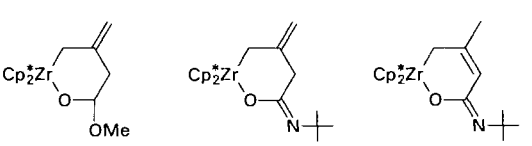


A **B**

Scheme 1.

In the NMR spectrum, the Cp* rings in **1** are equivalent, even at low temperatures (^1H NMR: −90 °C, 500 MHz; ^{13}C NMR: −90 °C, 125.7 MHz). Thus, in solution, the energy barrier for the inversion of the [Zr(tmm)] moiety can only be small ($0 \leq \Delta G^{\neq} <$ ca. 30 kJ mol^{-1}). There is no evidence of high-amplitude motion or disorder of the tmm ligand in the solid state; there are no short distances between the terminal methylene group and neighboring molecules.[12]

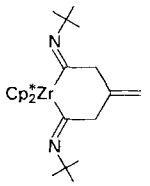
Upon heating, **1** decomposed with cleavage of isobutene. Protonolysis with methanol and phenol generated $[Cp_2^*Zr(OR)_2]$ (R = Me[13] or Ph[14]) and isobutene; no intermediates were detectable by NMR spectroscopy. 2-Butyne and 2,3-dimethylbutadiene did not react with **1**. On the other hand, insertions into polar double bonds were successful. Thus, methyl formate and *tert*-butyl isocyanate react with **1** at 0 °C to form the six-membered ring complexes **2** and **3**, respectively; similar behavior was found with butadiene complexes.[15] On warming, the azaenolato complex **3** with an unconjugated π electron system rearranged quantitatively to give the conjugated isomer **4**.



2 **3** **4**

[*] Prof. Dr. G. E. Herberich, Dr. C. Kreuder, Dr. U. Englert
Institut für Anorganische Chemie der Technischen Hochschule
Professor-Pirlet Strasse, D-52056 Aachen (FRG)
Telefax: Int. code + (241)8888-288

 © VCH Verlagsgesellschaft mbH, D-69451 Weinheim, 1994 0570-0833/94/2323-2465 $ 10.00+.25/0



5

At 0 °C, **1** reacted with *tert*-butyl isonitrile in a double insertion reaction to yield the symmetric diiminoacyl complex **5**. A similar reaction is known for the cyclobutene complex $[Cp_2Zr(PMe_3)(\eta^2\text{-}C_4H_6)]$,[16] whilst the 1-sila-3-zirconacyclobutane $[Cp_2Zr(CH_2)_2SiMe_2]$ undergoes two insertion reactions with C–C coupling of two *t*BuNC molecules.[17]

Experimental Procedure

1: A cooled suspension of $[Cp^*_2ZrCl_2]$ (32.4 g, 0.75 mmol) in THF (0.6 L) and hexane (0.6 L) was treated portionwise at −80 °C with $Li_2[tmm(tmeda)_2]$ (13.8 g, 75 mmol) [3]. The mixture was warmed slowly (18 h) to 20 °C, volatiles were removed in vacuo, and the residue extracted portionwise with hexane (ca. 0.3 L) until the extracts remained colorless. The solution was again evaporated to dryness (finally under high vacuum), and the residue taken up in hexane (0.15 L). The resulting suspension was filtered through sea sand to remove insoluble solid material. Crystallization at −30 °C gave **1** (14.1 g, 45%) as dark red rods [18]; m.p. 105 °C (decomp.); MS: *m/z* (%): 414 (32, M^+), 359 (100, $Cp^*_2Zr - H$); ^1H NMR (C_6D_6): δ = 5.24 (quin, CH_2=), 1.60 (t, $2ZrCH_2$, ^4J = 1.5 Hz), 1.76 (s, 2 Cp*); ^{13}C NMR: δ = 136.9 (s, CC_3), 107.0 (tquin, 154, 6.5 Hz, CH_2=), 56.0 (tm, 133 Hz, $ZrCH_2$), Cp*: 117.5 (s), 10.9 (q, 126 Hz).

2: A solution of **1** (1.27 g) in hexane (50 mL) was treated at 0 °C with HCO_2Me (176 mg). After 2 h, all volatiles were carefully removed in vacuo. Crystallization from hexane at −30 °C gave **2** (1.09 g, 78%) as orange crystals [18]; m.p. 110–120 °C; MS: *m/z* (%): 442 (13, M − MeOH), 287 (100, $Cp^*Zr(OMe)_2^+$); ^1H NMR (C_6D_6): δ = 5.19 (dd, ^3J(5a,6) = 8.6, ^3J(5b,6) = 3.3 Hz, 6-H), 5.04 (t, ^2J(AB) = 2.8 Hz, H_A), 4.66 (dm, ^2J(AB) = 3.2 Hz, H_B) (protons of 4-CH_2= designated as H_A and H_B), 3.27 (s, OMe), 2.55 (ddm, ^2J(5a,5b) = 12.5, ^3J(5b,6) = 3.3 Hz, 5-H_b), 2.26 (ddm, ^2J(5a,5b) = 12.5, ^3J(5a,6) = 8.6 Hz, 5-H_a), 2.18 (dm, ^2J(3a,3b) = 11.0 Hz, 3-H_a), 1.84 and 1.83 (s, Cp*), 1.09 (dm, ^2J(3a,3b) = 11.0 Hz, 3-H_b); ^{13}C NMR: δ = 154.0 (s, C=CH_2), 107.0 (t, 153 Hz, CH_2=), 105.1 (d, 164 Hz, OCH), 54.0 (qd, 140, 4 Hz, OMe), 50.0 and 47.8 (t, 124 Hz, CH_2), Cp*: 119.34 (s), 119.32 (s), 11.52 and 11.47 (q, 126 Hz).

3: A solution of **1** (2.60 g) in hexane (60 mL) was treated at 0 °C with *t*BuNCO (616 mg). After 12 h the precipitated yellow powder was filtered off, and the filtrate concentrated. Further product crystallized at −30 °C as orange platelets (total yield 1.95 g, 61%) [18]; decomp. 160–180 °C; MS: *m/z* (%): 513 (67, M^+), 379 (100, MH − Cp*); ^1H NMR (C_6D_6): δ = 4.99 and 4.70 (dm, ^2J = 3.1 Hz, 4-CH_2=), 3.12 (s, 2 × 5-H), 1.76 (s, 2 Cp*), 1.70 (s, 2 × 3-H), 1.54 (s, *t*Bu); ^{13}C NMR: δ = 158.3 (s, C=CH_2), 151.8 (s, C=N), 107.0 (t, 154 Hz, CH_2=), 53.0 (t, 124 Hz, CH_2), 49.7 (t, 126 Hz, CH_2), *t*Bu: 52.8 (s, CC_3), 32.1 (q, 125 Hz, CMe_3), Cp*: 120.2 (s), 11.3 (q, 125 Hz).

4: Heating of **3** in toluene for 12 h at 60 °C generated **4**. The toluene was replaced with hexane. Further workup as described for **3** afforded **4** as yellow platelets (total yield 60%) [18]; m.p. 67–75 °C; ^1H NMR (C_6D_6): δ = 6.21 (q, ^4J = 1.0 Hz, 5-H), 2.00 (dm, ^4J = 1.0 Hz, 4-Me), 1.75 (s, 2 Cp*), 1.58 (s, *t*Bu), 1.33 (s, 2 × 3-H); ^{13}C NMR: δ = 159.2 (s, CC_3), 148.8 (s, C=N), 129.1 (d, 156 Hz, CH=), 51.5 (t, 123 Hz, CH_2), 32.1 (q, 125 Hz, 4-Me), *t*Bu: 52.7 (s, CC_3), 31.8 (q, 125 Hz, CMe_3), Cp*: 119.7 (s), 11.3 (q, 127 Hz).

5: A solution of **1** (0.51 g) in hexane (30 mL) was treated at 0 °C with *t*BuNC (200 mg). After 2 h the mixture was filtered through sea sand. Concentration of the filtrate to ca. 10 mL gave, after cooling to −30 °C, **5** (240 mg, 35%) as an ochre-colored powder, which decomposed slowly at room temperature; MS: *m/z* (%): 497 (M^+ − *t*BuNC), 360 (100, $Cp^*_2Zr^+$); ^1H NMR (C_6D_6): δ = 4.88 (s, 4-CH_2=), 3.36 (s, 3-/5-CH_2), 1.80 (s, 2 Cp*), 1.48 (s, 2 *t*Bu); $^{13}C\{^1H\}$ NMR: δ = 230.3 (Zr-C=N), 148.3 (CC_3), 109.0 (CH_2=), 58.7 (CH_2), *t*Bu: 47.5, 32.1, Cp*: 115.9, 12.7.

Received: June 9, 1994 [Z 7022 IE]
German version: *Angew. Chem.*, **1994**, *106*, 2589

[1] a) M. D. Jones, R. D. W. Kemmitt, *Adv. Organomet. Chem.* **1987**, *27*, 279–309; b) B. Trost, *Angew. Chem.* **1986**, *98*, 1–22; *Angew. Chem. Int. Ed. Engl.* **1986**, *25*, 1–20; c) G. E. Herberich, T. P. Spaniol, *J. Chem. Soc. Dalton Trans.* **1993**, 2471–2476, and references therein.

[2] a) J. M. Mayer, C. J. Curtis, J. E. Bercaw, *J. Am. Chem. Soc.* **1983**, *105*, 2651–2660; b) G. C. Bazan, G. Rodriguez, B. P. Cleary, *ibid.* **1994**, *116*, 2177–2178.

[3] J. Klein, A. Medlik, *J. Chem. Soc. Chem. Commun.* **1973**, 275–276. The isolated solids have the approximate formula $Li_2[tmm(tmeda)]$.

[4] Crystal structure analysis: ENRAF-Nonius CAD4 diffractometer; $Mo_{K\alpha}$ radiation, graphite monochromator; empirical absorption correction (PSI [5]); intensity data with ω scan collected at 253 K; dark red parallelepiped, 0.3 × 0.3 × 0.2 mm, monoclinic, space group $P2_1/c$ (no. 14); a = 1093.7(8), b = 961.0(4), c = 2060(1) pm, β = 92.4(6)°, V = 2.164(4) nm³, Z = 4, ρ_{calcd} = 1.28 g cm⁻³, $\mu(Mo_{K\alpha})$ = 5.02 cm⁻¹, $F(000)$ = 880; 6879 reflections with $3 < \theta < 24°$ on the half Ewald sphere, 1862 symmetry independent with $I > 3\sigma(I)$ in the structure solution and refinement [6] for 232 parameters; R = 0.041, R_w = 0.047, $w^{-1} = \sigma^2(F_o)$, GOF = 1.19; H atoms in structure factor calculation. Further details of the crystal structure investigation may be obtained from the Fachinformationszentrum Karlsruhe, D-76344 Eggenstein-Leopoldshafen (FRG), upon quoting the depository number CSD-401223.

[5] A. C. T. North, D. C. Phillips, F. S. Mathews, *Acta Crystallogr. Sect. A* **1968**, *24*, 351–359.

[6] B. A. Frenz, *The ENRAF-Nonius CAD4-SDP – a Real-Time System for Concurrent X-Ray Data Collection and Crystal Structure Determination* (*Computing in Crystallography* (Eds.: H. Schenk, R. Olthof-Hazekamp, H. van Koningsveld, G. C. Bassi), Universität Delft, **1978**); SDP-PLUS, version 1.1, **1984**, and VAXSDP, version 2.2, **1985**.

[7] a) W. E. Hunter, D. C. Hrncir, R. V. Bynum, R. A. Pentilla, J. L. Atwood, *Organometallics* **1983**, *2*, 750–755; b) W. R. Tikkanen, J. W. Egan, Jr., J. L. Peterson, *ibid.* **1984**, *3*, 1646–1650.

[8] a) G. Erker, J. Wicher, K. Engel, F. Rosenfeldt, W. Dietrich, C. Krüger, *J. Am. Chem. Soc.* **1980**, *102*, 6344–6346; b) G. Erker, C. Krüger, G. Müller, *Adv. Organomet. Chem.* **1985**, *24*, 1–39; c) H. Yasuda, A. Nakamura, *Angew. Chem.* **1987**, *99*, 745–764; *Angew. Chem. Int. Ed. Engl.* **1987**, *26*, 723–742.

[9] G. M. Diamond, M. L. H. Green, P. Mountford, N. A. Popham, A. N. Chernega, *J. Chem. Soc. Chem. Commun.* **1994**, 103–105.

[10] J. W. Lauher, R. Hoffmann, *J. Am. Chem. Soc.* **1976**, *98*, 1729–1742.

[11] P. Hofmann, M. Frede, P. Stauffert, W. Lasser, U. Thewalt, *Angew. Chem.* **1985**, *97*, 693–694; *Angew. Chem. Int. Ed. Engl.* **1985**, *24*, 712–713.

[12] Shortest contact from the terminal methylene group to its nearest neighbor ca. 270 pm. An inversion is not possible with the given packing of the molecules, since the distance between the terminal methylene group and its nearest neighbor would have to shorten to < 170 pm in order to achieve planarity in the [Zr(tmm)] ring.

[13] J. M. Atkinson, P. B. Brindley, *J. Organomet. Chem.* **1991**, *411*, 131–137.

[14] L. E. Schock, T. J. Marks, *J. Am. Chem. Soc.* **1988**, *110*, 7701–7715.

[15] a) H. Yasuda, T. Okamoto, Y. Matsuoka, A. Nakamura, Y. Kai, N. Kanehisa, N. Kasai, *Organometallics* **1989**, *8*, 1139–1152; b) A. Nakamura, *J. Organomet. Chem.* **1990**, *400*, 35–48, and references therein

[16] R. A. Fisher, S. L. Buchwald, *Organometallics* **1990**, *9*, 871–873.

[17] F. J. Berg, J. L. Peterson, *Organometallics* **1991**, *10*, 1599–1607.

[18] Correct C,H analysis.

Total Synthesis of Soraphen $A_{1\alpha}$

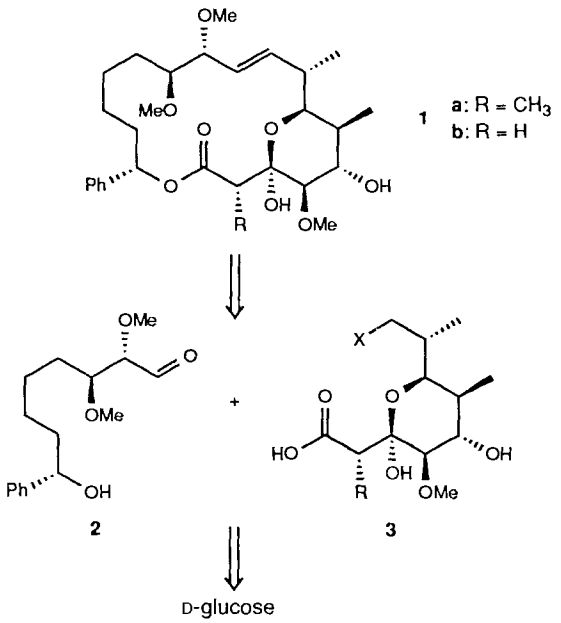
Stephan Abel, Dominik Faber, Ottmar Hüter, and Bernd Giese*

In 1986 a new class of 18-membered macrolides called the soraphens were isolated by H. Reichenbach, G. Höfle et al. as metabolites of the microorganisms *Sorangium cellulosum*.[1] The parent compound, soraphen $A_{1\alpha}$ (**1a**), contains ten stereogenic centers, and the methyl, methoxy, and hydroxy groups of the tetrahydropyran ring occupy axial positions.[2] Due to this chemical structure as well as its antifungal activity, the novel natural product soraphen $A_{1\alpha}$ is an interesting target for synthesis.[3] Herein we report the first total synthesis of soraphen **1a** and 2-norsoraphen **1b**. The retrosynthetic analysis of **1** leads to compounds **2** and **3**, which are both available from D-glucose (Scheme 1). These building blocks were connected by a Julia olefination (**6** + **13** → **14**) as well as a subsequent lactonization (**16** → **1b**). Further key steps of the synthesis involve stereoselective chain elongation (**10** → **11**) and methylation of 2-norsoraphen **1b** resulting in soraphen (**1a**).

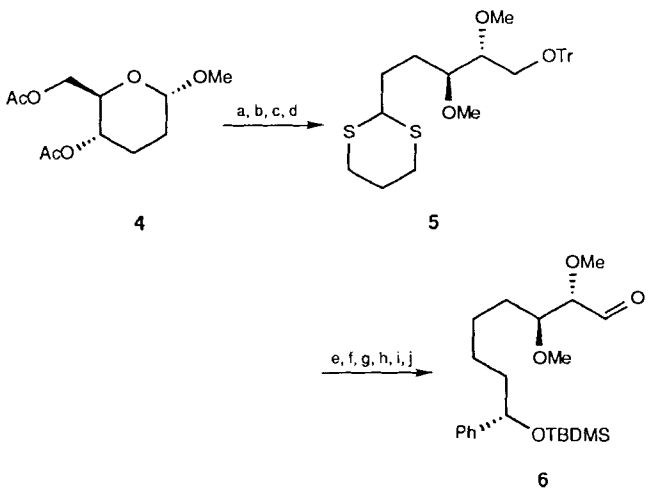
The synthesis of **6**, a silylated derivative of **2**, was accomplished by converting the dideoxysugar **4**[4] into the dithiane **5** and elongating the chain with Corey–Seebach methodology

[*] Prof. Dr. B. Giese, Dr. S. Abel, D. Faber, Dr. O. Hüter
Departement Chemie der Universität
St. Johanns-Ring 19, CH-4056 Basel (Switzerland)
Telefax: Int. code + (61)3226017

[**] This work was supported by Ciba-Geigy. We thank Prof. M. Zehnder and M. Neuburger for performing the crystal structure analysis.



Scheme 1. Retrosynthetic analysis of the soraphens **1**.



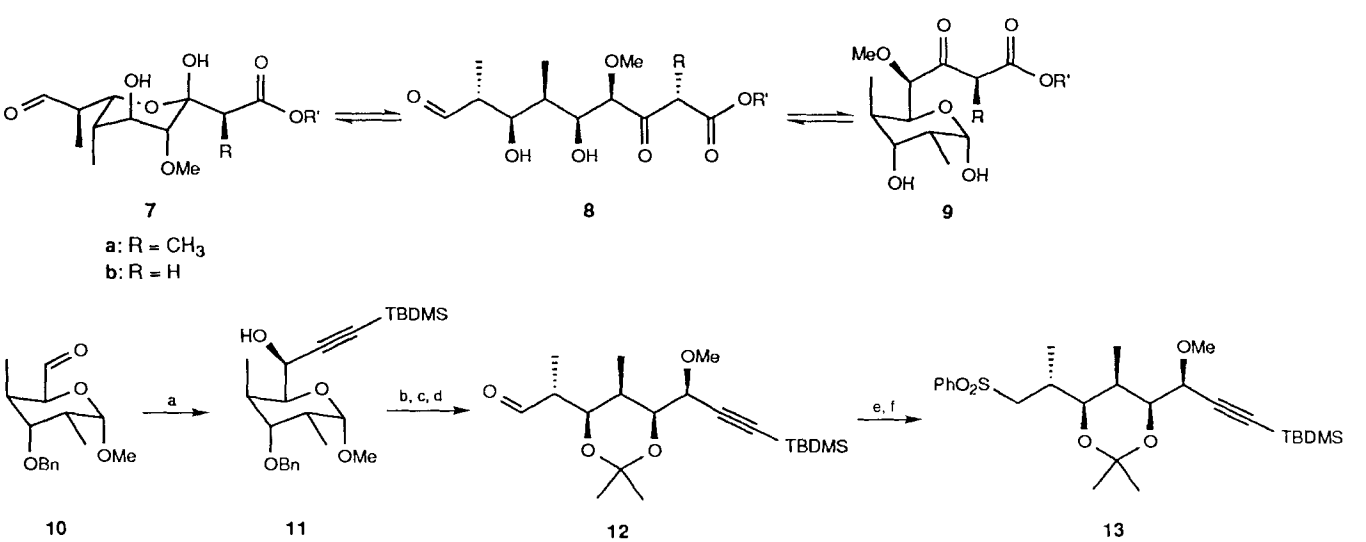
Scheme 2. a) 0.02 M NaOMe, MeOH, 1.5 h, 20 °C, 98%; b) $HS(CH_2)_3SH$, conc HCl, 5 d, 20 °C, 95%; c) triphenylmethylchloride (TrCl), pyridine, 20–60 °C, 36 h, 85%; d) NaH, THF, 1.5 h, 20 °C; Bu_4NI, MeI, 20 h, 0 °C, 71%; e) *n*BuLi, THF, −55 °C, 2 h; (*R*)-phenyloxirane, −35 °C, 5 d, 70%; f) *p*-toluenesulfonic acid, CH_2Cl_2, CH_3OH, 3.5 h, 20 °C, 94%; g) Ni, EtOH, 1 d, 60 °C, 81%; h) *tert*-butyldimethylsilyl chloride (TBDMSCl), imidazole, 4-dimethyl aminopyridine, DMF, 2 h, 0 °C, 95%; i) tetrabutylammonium fluoride (TBAF), THF, 5 h, 0 °C, 86%; j) $(COCl)_2$, DMSO, CH_2Cl_2, 1 h, −78 °C, 90%.

using (*R*)-phenyloxirane (Scheme 2).[5] This reaction sequence allowed the three stereogenic centers of building block **6** to be transferred directly from the starting materials.

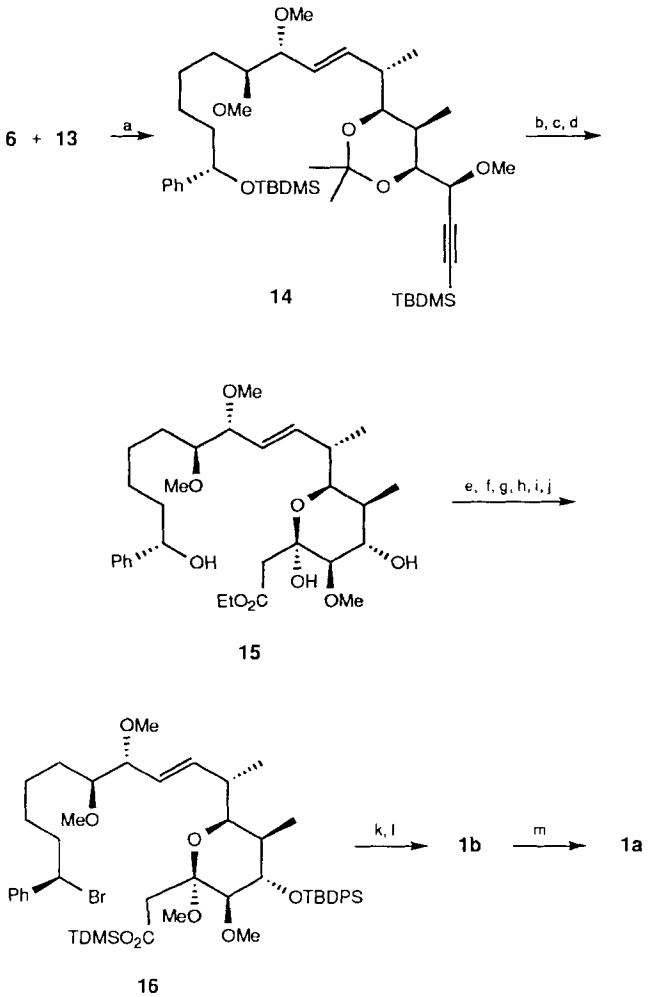
The stereogenic centers of building block **3** were set by conversion of the functional groups of D-glucose. The six-membered ring of **3** has the framework of an L-ketose; its derivative **7**, however, can be transformed into the D-aldose **9** via the acyclic form **8** (Scheme 3). A six-membered ring framework that contains the correct steric arrangement of the functional groups as in **9** is present in aldehyde **10**, which Hanessian et al. obtained from D-glucose.[6]

The chain elongation of the aldehyde in **10** could only be achieved with the desired stereoselectivity and in high yield by using a C_2 unit. Thus the bromomagnesium salt of *tert*-butyldimethylsilylacetylene gave the chelation controlled product (**10** → **11**) stereoselectively in 87% yield.[7] The configuration of **11** was determined by crystal structure analysis.[8] It proved to be advantageous to introduce the missing carboxylic acid group and to hydrolyze the acetylene into the ketone (**14** → **15**) only after connecting the building blocks **6** and **13** by a Julia reaction.[9] To perform the latter, the acetal ring of **11** was opened with propanedithiol and the aldehyde functionality was released with methyl iodide.[10] Subsequent reduction, conversion into the phenyl thioether,[11] and oxidation with *meta*-chloroperbenzoic acid gave rise to sulfone **13**. The Julia reaction produced the (*E*)-isomer **14** selectively as shown by the coupling constant of 14.2 Hz in the ^1H NMR spectrum (Scheme 4).[12] Attempts to carry out the coupling under Wittig reaction conditions remained unsuccessful.

The coupling product **14** still lacks the carboxylic acid function of soraphen, which was introduced with ethyl chlorofor-



Scheme 3. a) H–C≡C–TBDMS, MeLi, $MgBr_2$, 30 min, −30 °C, 87%; b) MeI, Ag_2O, 2 h, 94%, c) $HS(CH_2)_3SH$, $BF_3 \cdot Et_2O$, CH_2Cl_2, 1 h, −20 → 0 °C, 77%; d) $Me_2C(OMe)_2$, 10-camphorsulfonic acid, acetone, 10 h, 20 °C, $CaCO_3$, MeI, CH_3CN, H_2O, 87%; e) $NaBH_4$, EtOH, 45 min, 20 °C; Bu_3P, Ph_2S_2, CH_2Cl_2, 12 h, 20 °C, 81%; f) *m*-chloroperbenzoic acid (MCPBA), $NaHCO_3$, CH_2Cl_2, 45 min, 0–20 °C, 97%.



Scheme 4. a) *t*BuLi, THF, 90 min, −78 °C; BzCl, pyridine, 12 h, 20 °C; 5% Na/Hg, 5 h, −20 °C, 35%; b) Bu_4NF, THF, 1 h, 0 °C, 85%; c) *n*BuLi, $ClCO_2Et$, THF, 1 h, −30 °C, 85%; d) morpholine, THF, 2 h, reflux; 60% CH_3CO_2H, 2 h, 50 °C, 75%; e) TBDPSCl, imidazole, DMF, 7 d, −60 °C, 96%; f) Ac_2O, pyridine, 4-dimethylaminopyridine, 30 min, 0 °C, 98%; g) $HC(OMe)_3$, CH_2Cl_2, MeOH, 4 d, 20 °C, 99%; h) $Ti(OiPr)_4$, 2-(trimethylsilyl)ethanol, 3 d, 100 °C, 90%; i) CsF, DMF, 1 d, 20 °C, 98%; j) thexyldimethylsilyl chloride (TDMSCl), CH_2Cl_2, triethylamine, 20 min, 20 °C; $(CH_3)_2C{=}CBr(NMe_2)$, CH_2Cl_2, triethylamine, 1 h, 20 °C, 91%; k) triethylamine, acetone, H_2O, 15 min, RT; Cs_2CO_3, DMF, 1 d, 20 °C, 50%; l) tetrabutylammonium fluoride, THF, 4 h, 0 °C, 1 M HCl, THF, 1 d, 20 °C, 95%; m) 2 equiv of potassium-2,6-di-*tert*-butylphenoxide, DMF, 1 d, 20 °C; MeI, DMF, molecular sieves (4 Å), 30 min, 0 °C; HCl, THF, 12 h, 20 °C, 70%.

mate after desilylation.[13] Subsequent addition of water across the triple bond via an enamine intermediate followed by cleavage of the protecting groups resulted in the tetrahydropyran ring structure of **15**. Experiments by G. Höfle et al. on the ring-opened soraphen demonstrated that the lactonization is best effected by a substitution reaction of the cesium salt of the carboxylic acid.[14] Therefore, benzyl alcohol **15** and the bromo enamine reported by Ghosez et al.[15] were allowed to react under mild conditions and yielded bromide **16** with complete inversion. The macrocyclization of the cesium carboxylate of **16** (20 °C, 60% yield) produced the soraphen ring structure also with inversion at the benzyl group. Since the methyl group in soraphen $A_{1\alpha}$ (**1a**), that is in α-position to the lactone occupies the thermodynamically favored configuration,[16] it was introduced in the last step of the synthesis. By using two equivalents of potassium 2,6-di*tert*-butylphenoxide, the hemiketal ring of norsoraphen **1b** was opened and deprotonated to give the potassium enolate. To avoid overmethylation, the enolate ion was quenched with an excess of methyl iodide within 30 min at 0 °C. Subsequent cyclization to the hemiketal in acidic medium gave soraphen $A_{1\alpha}$ (**1a**) in 70% yield.

Received: July 20, 1994 [Z 7149]
German version: *Angew. Chem.* **1994**, *106*, 2521

[1] H. Reichenbach, G. Höfle, H. Augustiniak, N. Bedorf, E. Forche, K. Gerth, H. Irschik, R. Jansen, B. Kurze, F. Sasse, H. Steinmetz, W. Trowitzsch-Kienast, EP 282455; [*Chem. Abstr.* **1989**, *111*, 132597].
[2] N. Bedorf, D. Schomburg, K. Gerth, H. Reichenbach, G. Höfle, *Liebigs Ann. Chem.* **1993**, 1017.
[3] J. Rohr, *Nachr. Chem. Tech. Lab.* **1993**, *41*, 889.
[4] M. Böhringer, H.-J. Roth, J. Hunziger, M. Göbel, R. Krishnan, A. Giger, B. Schweizer, J. Schreiber, C. Leumann, A. Eschenmoser, *Helv. Chim. Acta* **1992**, *75*, 1417; R. J. Ferrier, N. Prasad, *J. Chem. Soc. C* **1969**, 570.
[5] E. J. Corey, D. Seebach, *Angew. Chem.* **1965**, *77*, 1134; *Angew. Chem. Int. Ed. Engl.* **1965**, *4*, 1075. The substitution reaction on phenyloxirane resulted in a regioselectivity of 8:1 (−35 °C) in favor of the desired isomer.
[6] S. Hanessian, J.-R. Pougny, I. K. Boessenkool, *Tetrahedron* **1984**, *40*, 1289.
[7] M. T. Reetz, *Angew. Chem.* **1984**, *96*, 542; *Angew. Chem. Int. Ed. Engl.* **1984**, *23*, 556. When using the magnesium salt of acetylene only the desired D-*glycero* isomer **11** was detected. The formation of the L-*glycero* isomer, however, was favored in a ratio of 8:1 when using the triisopropyloxytitanium salt.
[8] Further details of the crystal structure investigation are available on request from the Director of the Cambridge Crystallographic Data Centre, 12 Union Road, GB-Cambridge CB2 1EZ (UK), on quoting the full journal citation.
[9] M. Julia, J.-M. Paris, *Tetrahedron Lett.* **1973**, *14*, 4833.
[10] G. Procter, D. Genin, *Carbohydr. Res.* **1990**, *202*, 81.
[11] I. Nakagawa, T. Hata, *Tetrahedron Lett.* **1975**, *16*, 1409.
[12] For the stereochemistry of the Julia reaction see P. J. Kocienski, B. Lythgoe, S. Ruston, *J. Chem. Soc. Perkin Trans. 1* **1978**, 829.
[13] G. Solladié, C. Hamdouchi, *Synthesis* **1991**, 979.
[14] D. Schummer, B. Böhlendorf, M. Kiffe, G. Höfle in *Antibiotics and Antiviral Compounds* (Eds.: K. Krohn, H. A. Krist, H. Maag), VCH, Weinheim, **1993**, p. 133.
[15] F. Munyemana, A.-M. Frisque-Hesbain, A. Devos, L. Ghosez, *Tetrahedron Lett.* **1989**, *39*, 3077.
[16] Upon treatment of soraphen $A_{1\alpha}$ (**1a**) [2] with base (thermodynamic conditions), no change of configuration occurs at the methylated carbon α to the lactone. The crystal structure of **1a** shows that the methoxy group of the tetrahydropyran ring and the methyl group α to the lactone are in a sterically favorable position relative to each other. In the corresponding *epi* form, however, these methyl and methoxy groups are subject to 1,3-diaxial interactions. This might also be the reason why a possible dimethylation of norsoraphen **1b** can be avoided under appropriate reaction conditions.

Novel Bimetallic Model System for Cytochrome P_{450}: Effect of Membrane Environment on the Catalytic Oxidation**

Albertus P. H. J. Schenning, Dominicus H. W. Hubert, Jan H. van Esch, Martinus C. Feiters, and Roeland J. M. Nolte*

Cytochrome P_{450} catalyzes a variety of oxidation reactions, including the hydroxylation of alkanes and the epoxidation of alkenes.[1] The active site of this membrane-bound enzyme contains a heme function and a thiolate as axial ligand. The catalytic cycle involves the binding of a substrate, reduction of iron(III) to iron(II), and binding and reductive cleavage of molecular oxygen to generate what is formally an oxoiron(V) complex,

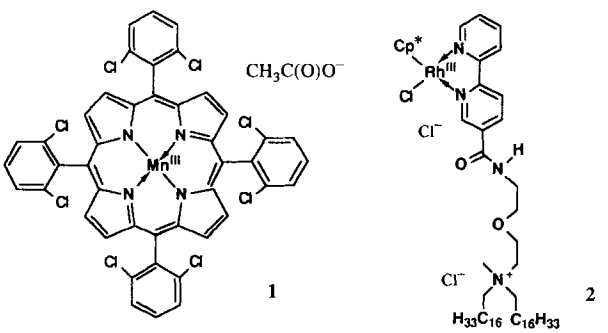
[*] Prof. Dr. R. J. M. Nolte, Dipl.-Chem. A. P. H. J. Schenning, D. H. W. Hubert, Dr. J. H. van Esch, Dr. M. C. Feiters
Department of Organic Chemistry, NSR Center, University of Nijmegen
Toernooiveld, NL-6525 ED Nijmegen (The Netherlands)
Telefax: Int. code + (80)55-34-50

[**] This work was supported by the Netherlands Foundation for Chemical Research (SON) with financial aid from the Netherlands Organization for Scientific Research (NWO).

which transfers its oxygen atom to the bound substrate. The iron center accepts the electrons from NADPH, through mediation of a flavoprotein.

Because of its biological importance—this enzyme plays a crucial role in the metabolism of endogeneous chemicals and xenobiotic compounds—and also because this archetype oxidation catalyst may serve as a model for a new generation of synthetic catalysts, a great deal of research is currently focused on mimicking the action of cytochrome P_{450}.[2] Until now only a few models have been described that incorporate the important features of the natural system, namely molecular oxygen as the oxidant, a metalloporphyrin as catalyst, an electron donor, and a membrane system holding these components.[3] All models have the disadvantage of displaying very low catalytic activity.

During the course of our studies on novel supramolecular catalytic systems, we found that the rhodium complex [$Rh^{III}(\eta^5$-Cp*)(bpy)Cl_2] (Cp* = pentamethylcyclopentadienyl, bpy = 2,2′-bipyridine) is an efficient catalyst for the reduction of manganese(III) porphyrins by sodium formate.[4] We report here on a membrane-bound cytochrome P_{450} mimic that epoxidizes alkenes with good turnover numbers. The system is composed of vesicles containing an α-(aceto)-[5,10,15,20-tetrakis(2,6-dichlorophenyl)-porphyrinato]manganese(III) catalyst ([$Mn^{III}t_{2,6}$-diClPP] **1**),[5] *N*-methylimidazole as axial ligand, and an amphiphilic rhodium(III) complex (**2**)[6] in combination with sodium formate as electron donor. We found that the type of membrane has a dramatic effect on the catalytic activity of the mimic.



1 2

The manganese porphyrin **1** and the rhodium complex **2** were incorporated into positively charged dimethyl-dioctadecylammonium chloride (DODAC)[7] and negatively charged dihexadecylphosphate (DHP)[7] vesicles by the ethanol injection method.[8] Gel permeation chromatography and electron microscopy were used to show that the porphyrin and the rhodium complex were bound to the bilayers of the vesicles and that the vesicle structure was not destroyed by the incorporation procedure. The diameters of the vesicles of both amphiphiles amounted to about 4000 Å. The fluorescence spectra of H_2-$t_{2,6}$-diClPP in both DODAC and DHP vesicles ($T = 70\,^{\circ}C$) showed no effects of self-quenching when the porphyrin to lipid ratio was lower than 0.005. This indicates that below these ratios the porphyrin molecules are not aggregated.[9] The addition of water-soluble quenchers (NaI and $CuSO_4$ in the case of DODAC and DHP vesicles, respectively) to the system did not change the fluorescence spectrum of the vesicle-bound H_2-$t_{2,6}$-diClPP. Most likely the porphyrin is situated in the inner part of the vesicle bilayer. EPR studies, using [$Cu^{II}(t_{2,6}$-diClPP)] instead of **1** revealed that for both vesicle systems the orientation of the porphyrin molecules was parallel to the vesicle surface.[10] The structure of the model system is depicted in Figure 1.

First we investigated the influence of the membrane matrix on the reduction of the manganese(III) porphyrin. To this end the

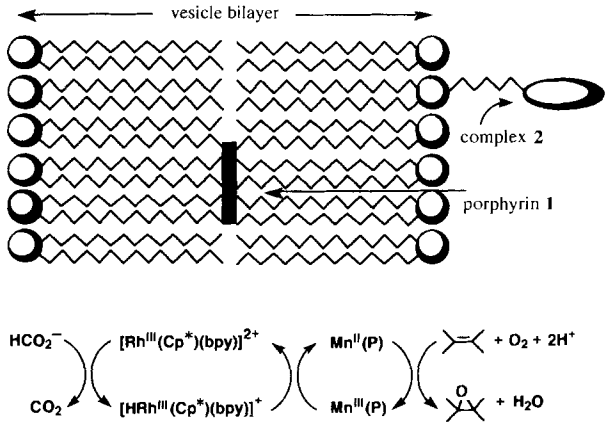


Fig. 1. Schematic representation of the cytochrome P_{450} mimic and the catalyzed reaction.

decrease in the absorption at 660 nm (Mn^{III} porphyrin) and the increase in absorption at 448 nm (Mn^{II} porphyrin) in the UV/VIS spectrum was followed as a function of time, both under an argon atmosphere and in air. The rhodium complex manganoporphyrin ratio was varied from 0.5 to 10. Under argon in DODAC as well as in DHP vesicles, the Mn^{III} porphyrin was reduced at all Rh/Mn ratios tested. The reduction rate was found to increase linearly with the Rh^{III} concentration. At a fixed Rh/Mn ratio the reduction was faster in DODAC vesicles than in DHP vesicles ([Rh]/[Mn] = 1; k_0 (DODAC) > 100 nmol $L^{-1}s^{-1}$, k_0 (DHP) = 20 ± 2 nmol $L^{-1}s^{-1}$). The reduction of Mn^{III} in DODAC vesicles also took place when the reactions were carried out in an air atmosphere. A similar result was obtained for DHP except when the Rh/Mn ratio was equal or less than 1, under which conditions reoxidation of Mn^{II} was observed. In the absence of the Rh^{III} complex or formate no reduction took place. These results indicate that the rhodium-formate system is capable of reducing the membrane-bound Mn^{III} porphyrin and presumably, as observed previously,[4] the rhodium complex acts as a redox-active phase transfer catalyst in this process. The reduction of Mn^{III} is faster in the positively charged vesicles than in the negatively charged ones because the formate concentration is higher at the bilayer/water interface of the former aggregates. The fact that in DODAC vesicles in general and in DHP vesicles with a Rh/Mn ratio higher than 1 no reoxidation of Mn^{II} takes place, indicates that the reduction of manganese is much faster than its reoxidation.

In a second series of experiments we investigated whether our membrane-bound cytochrome P_{450} mimic was able to epoxidize alkenes. The results are listed in Table 1. All substrates tested were epoxidized by the catalytic system based on DHP vesicles. The turnover numbers are higher than those obtained with the two-phase system previously published by us.[4] They are in the same range as those observed for the natural system (1 nmol product per nmol P_{450} per min).[1] Remarkable is the high stability of the catalyst during the reaction, which is in contrast with the two-phase system. The effect of the membrane environment on the catalytic epoxidation became clear when the DHP vesicles were replaced by the DODAC vesicles. In the latter membrane system no epoxidation of alkenes was observed (last two entries of Table 1). Presumably, the concentration of protons is too low to allow the formation of the catalytically active oxomanganese(V)[11] species at the positively charged interface. When the Rh/Mn ratio was increased from 1 to 10 the turnover number of the reaction decreased considerably (Table 1, entry 5). This phenomenon is possibly caused by the fact that more elec-

 © VCH Verlagsgesellschaft mbH, D-69451 Weinheim, 1994 0570-0833/94/2323-2469 $ 10.00+.25/0

Table 1. Epoxidation of alkenes by the membrane-bound cytochrome P_{450} mimic [a].

Entry	Surfactant	Substrate	Product [b]	Turnover number [c]
1	DHP	α-pinene	α-pinene oxide	360
2	DHP	*cis*-stilbene	*cis*-stilbene oxide	45
3	DHP	limonene	limonene oxide	50
4	DHP	styrene	styrene oxide [d]	55
5	DHP [e]	styrene	styrene oxide	5
6	DODAC	styrene	-	0
7	DODAC [e]	styrene	-	0

[a] For reaction conditions see Experimental Procedure. The reaction was followed by GLC for 1 h. No destruction of the catalyst was found after that period. [b] The only product of the reaction was epoxide, which was gradually decomposed into other products. The decomposition processes were independent of the Rh/Mn ratio. No epoxide was formed without vesicles or when any of the components of the catalytic system were omitted. [c] Turnover number [epoxide]/1 per hour, calculated from the initial part of the conversion/time plot. α-Pinene oxide was converted (>90%) into pinocamphone within a period of one hour. Limonene oxide decomposed (±50%) into as yet unidentified products. [d] Styrene oxide and stilbene oxide were stable under the experimental conditions. [e] Rh/Mn molar ratio = 10.

trons become available due to the higher concentration of rhodium centers. As a result a side reaction can take place which produces water (the so-called non-productive pathway[11]).

In summary, we have developed a bimetallic membrane-bound cytochrome P_{450} mimic which catalyzes the epoxidation of alkenes with good turnover numbers. Current work is aimed at developing catalytic systems that display substrate selectivity.

Experimental Procedure

Reduction experiments: The desired amounts of stock solutions of **1**, **2**, *N*-methylimidazole, and DHP or DODAC in chloroform were mixed in a test tube. The solvent was evaporated under a stream of nitrogen to leave a homogeneous film. This film was solubilized in 100 μL ethanol/tetrahydrofuran (1:1, *v*/*v*) and injected in 1.25 mL water at 75 °C. The suspension was purged with argon for 30 min and injected in a cuvette containing 1.25 mL of an ethylmorpholine/sodium formate buffer at 75 °C. Final conditions: 2.4 μM of **1**, 2.4 × *n* μM of **2** (*n* = Rh/Mn molar ratio), 3.95 μM of *N*-methylimidazole, 910 μM DODAC or DHP in ethylmorpholine (50 mM)/sodium formate (250 mM) buffer (pH = 7.0), *T* = 70 °C.

Epoxidation experiments: Final conditions as above, except Rh/Mn molar ratio = 1 and [substrate] = 200 μM. Now the 100 μL solution was directly injected in a 2.5 mL buffered solution at 75 °C. Substrate was added and the reaction mixture was analyzed from time to time by taking a 0.2 mL aliquot to which was added 0.1 mL diethyl ether containing mesitylene as an internal standard. This mixture was shaken vigorously (vortex apparatus) and centrifuged. After phase separation, a 5 μL sample was taken from the diethyl ether layer and analyzed by GLC (column Chrompack, WCOT/CP-SIL5CB, temperature program 70 °C (2 min), 10 K min^{-1} 200 °C (2 min)).

Received: May 2, 1994 [Z 6891 IE]
German version: *Angew. Chem.* **1994**, *106*, 2587

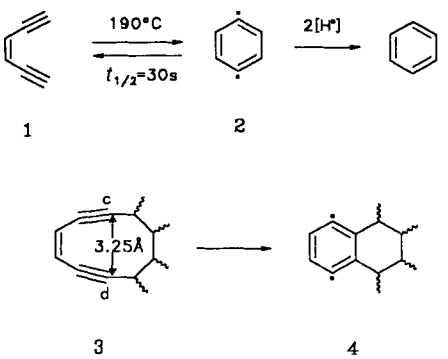
[1] F. P. Guengerich, *J. Biol. Chem.* **1991**, *266*, 10019.
[2] J. P. Collman, X. Zhang, V. J. Lee, E. S. Uffelman, J. I. Brauman, *Science* **1993**, *261*, 1404.
[3] a) J. H. van Esch, M. F. Roks, R. J. M. Nolte, *J. Am. Chem. Soc.* **1986**, *108*, 6093; b) J. T. Groves, R. Neumann, *ibid.* **1989**, *111*, 2900; c) J. T. Groves, S. B. Ungashe, *ibid.* **1990**, *112*, 7796.
[4] P. A. Gosling, J. H. van Esch, M. A. M. Hoffmann, R. J. M. Nolte, *J. Chem. Soc. Chem. Commun.* **1993**, 472.
[5] A. D. Adler, F. L. Longo, F. Kampas, J. Kim, *J. Inorg. Nucl. Chem.* **1970**, *32*, 2443.
[6] a) U. Kölle, M. Grätzel, *Angew. Chem.* **1987**, *99*, 572; *Angew. Chem. Int. Ed. Engl.* **1987**, *26*, 567; b) J. H. van Esch, M. C. Feiters, R. J. M. Nolte, *J. Org. Chem.*, in press.
[7] A. M. Carmona-Ribeiro, *Chem. Soc. Rev.* **1992**, 209.
[8] L. A. M. Rupert, D. Hoekstra, J. B. F. N. Engberts, *J. Am. Chem. Soc.* **1985**, *107*, 2628.
[9] A. P. H. J. Schenning, D. H. W. Hubert, M. C. Feiters, R. J. M. Nolte, unpublished results.
[10] J. H. van Esch, M. C. Feiters, A. M. Peters, R. J. M. Nolte, *J. Phys. Chem.* **1994**, *98*, 5541.
[11] I. Tabushi, M. Kodera, *J. Am. Chem. Soc.* **1986**, *108*, 1101.

1,4-Didehydrobutadiene: The Intermediate in a New Class of Thermally Induced Intramolecular Alkyne Couplings**

Rolf Gleiter* and Joachim Ritter

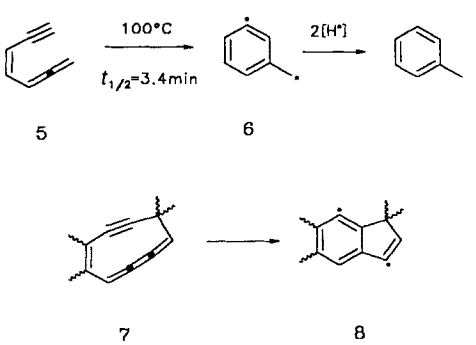
Dedicated to Professor Heinz Dürr on the occasion of his 60th birthday

More than twenty years ago Bergman and co-workers discovered that enediynes such as (*Z*)-hexadiyn-3-ene (**1**) cyclize to give the corresponding 1,4-didehydrobenzenes (**2**) as short-lived intermediates.[1] This reaction occurs at 200 °C with an activation energy of 28 kcal mol^{-1} (Scheme 1).[2a] The recent discovery of the natural antitumor antibiotics calicheamicin, esperamicin, and dynemicin, which contain the cyclic enediyne unit **3**, led to an enormous increase in publications on enediyne chemistry in the last seven years.[3] A common feature in the mechanism of action of these antibiotics is the cycloaromatization of the enediyne unit **3** to give the bicyclic 1,4-didehydrobenzene **4**.



Scheme 1. Cycloaromatization of enediynes.

In the case of neocarzinostatin, the electrocyclization of an initially generated cyclic (*Z*)-cumulene-enyne **7** is proposed as the key step.[4] In related work Myers et al. found that the surprisingly facile cyclization of the open-chain cumulene **5** gives α,3-dehydrotoluene **6** and is an example of a new type of a 1,4-biradical generating reaction (Scheme 2).[5a]



Scheme 2. Cycloaromatization of cumulene-enynes.

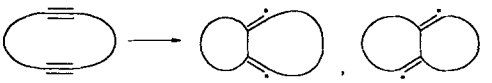
[*] Prof. Dr. R. Gleiter, Dipl.-Chem. J. Ritter
Organisch-chemisches Institut der Universität
Im Neuenheimer Feld 270, D-69120 Heidelberg (FRG)
Telefax: Int. code + (6221)56-4205

[**] This work was supported by the Deutsche Forschungsgemeinschaft, the Fonds der Chemischen Industrie, and the BASF Aktiengesellschaft (Ludwigshafen). J. R. thanks the Studienstiftung des deutschen Volkes for a doctoral fellowship.

The following points concerning the two reactions should be mentioned: 1) The crucial structure parameter influencing the activation energy of the Bergman cyclization is the transannular distance c–d between termini c and d of the triple bonds. Experimental data as well as theoretical investigations reveal that at c–d distances less than about 3.2 Å the enediyne undergoes spontaneous transannular coupling at room temperature.[6] 2) Both the Bergman and the Myers cyclization proceed via a transition state in which the termini of a conjugated 6π electron species are connected.[7] For that reason the antibonding interactions between the in-plane π orbitals are compensated in part by bonding interactions of the out-of-plane π orbitals, and thus the activation energy is less than that of a nonconjugated π system. 3) In terms of thermodynamics the ease of 1,4-diradical generation depends on the energy gap between the alkyne and the diradical. While the Bergman cyclization of **1** is endothermic[2e] with a late transition state, the analogous process for allene-enyne **5** is strongly exothermic and has an early transition state.[2, 5]

One can thus conclude that the formation of a 1,4-diradical from a diyne under moderate conditions requires an electronically activated species (e.g. conjugated enediynes) with a transannular distance between the triple bonds of no more than 3.2 Å. Furthermore the C–C coupling should lead to a diradical with lower σ energy than that of the diyne, and formation of the new π system should lead to at least a partial gain in energy through aromatization or conjugation.

For some time we have been synthesizing a number of strained ten-membered cyclic diynes with c–d distances close to 3 Å.[8] These compounds have strongly split π levels and an enhanced reactivity compared to unstrained alkynes.[8a–g] Thus we wondered whether the reaction of two strongly interacting triple bonds would result in the generation of a corresponding 1,4-didehydrobutadiyne (Scheme 3).



Scheme 3. A possible route to a 1,4-didehydrobuta-1,3-diene.

We report here on our investigations of thermally induced transannular alkyne couplings in 1,6-diazacyclodeca-3,8-diynes.[8e] For instance, heating *N,N'*-diisopropyl-1,6-diazacyclodeca-3,8-diyne **9** (R = *i*Pr) with various organic solvents as trapping agents affords products consistent with a butadiene-1,4-diyl intermediate (Scheme 4). With 1,4-cyclohexadiene as solvent (c(**9**) = 0.04 mol L^{-1}), the overall yield of *trans*-butadienes **10** and **11** is 97%.

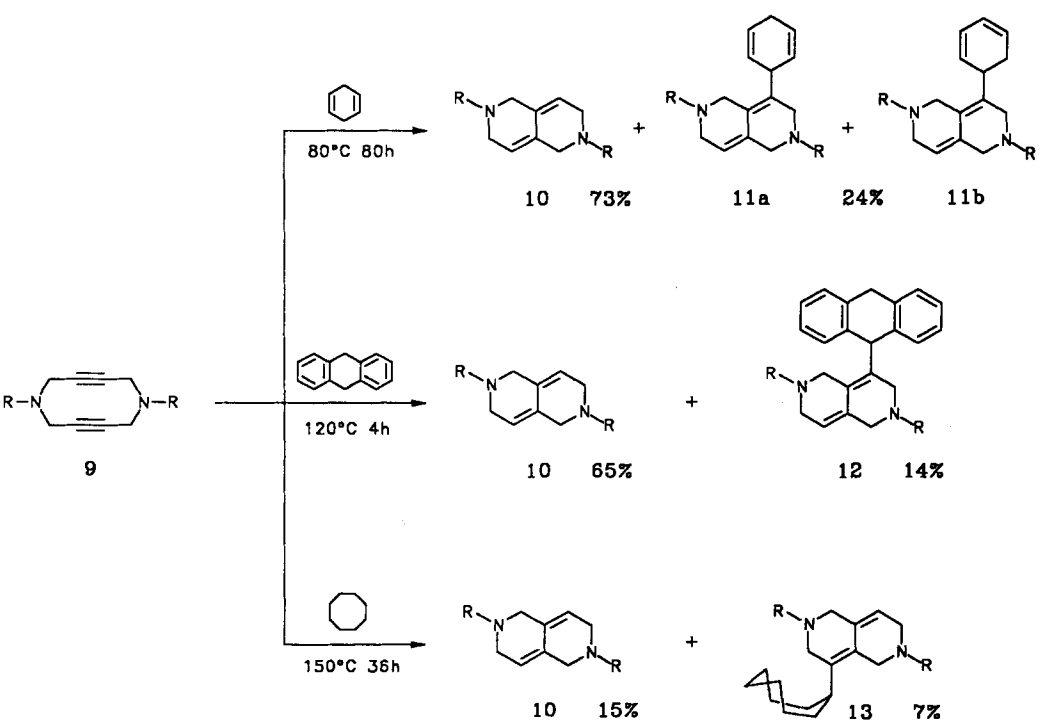
In contrast to the Bergman and Myers cyclization, the reaction rate with respect to the disappearance of the starting material depends on the trapping agent (i.e. solvent). When the reaction is conducted in cyclooctane (c(**9**) = 0.024 mol) at 151 °C nearly quantitative conversion is achieved after 36 h, whereas the reaction time with the more effective hydrogen donor 9,10-dihydroanthracene amounts to only 4 h at 120 °C. The low yield (due to polymerization) for the cyclization/H-abstraction process in solvents that are apparently less effective H donors, such as cyclooctane and *n*-octane, is also consistent with the initial formation of a diradical species.

To account for the results obtained in the thermolysis of **9** we propose the following mechanism (Scheme 5) in which 1,4-didehydrobutadiene **14** occurs as an intermediate. The subsequent hydrogen abstraction from a solvent molecule may lead to a solvent cage radical pair which either results in cage or cage escape reaction products.

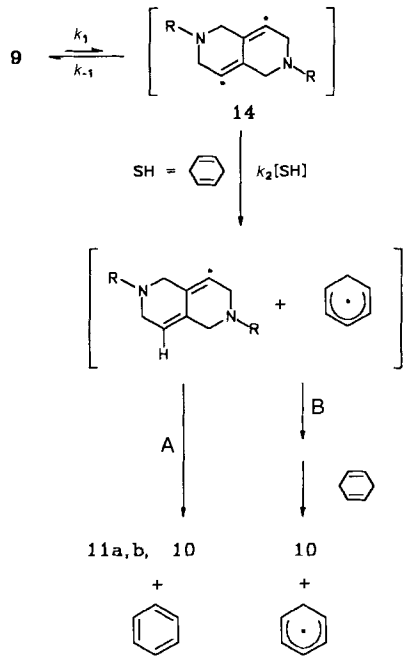
While the radical recombination products with 1,4-cyclohexadiene, 9,10-dihydroanthracene, and *n*-octane are difficult to separate, the only possible low molecular weight cyclooctyl recombination product **13** is obtained as an NMR-pure substance after column chromatography. The NMR data of **10**, **11a/b**, **12**, and **13** are given in Table 1.

It is evident that the reaction rate depends on the dissociation enthalpy of the relevant C–H bond of the solvent. Assuming that the rate constant for the first reaction step k_1 is very small compared to k_{-1} and k_2, we conclude that $k_{-1} \geq k_2$ [SH] should be true, where k_2 is the rate of hydrogen abstraction from a solvent molecule SH. At least in the case of cyclooctane it seems that $E_{a,-1} < E_{a,2}$.

In the course of the first reaction step the alkyne units of **9** have to be distorted in a transoid fashion to diminish the c–d distance and facilitate formation of a bond between C3 and C8. This deformation is well studied for acetylene.[9] We assume that the bending of the alkyne moieties in **9** is supported by a homoconjugative interaction between nitrogen lone pairs and the π and π* orbitals of the triple bonds. This interaction lowers the activation energy for the transannular coupling. Quantum



Scheme 4. Thermolyses of **9** in various solvents; R = isopropyl.



Scheme 5. Proposed mechanism for the thermolyses of **9** in 1,4-cyclohexadiene. A = reaction in solvent cage, B = escape from solvent cage.

Table 1. NMR spectroscopic data of dienes **10**, **11a + b**, **12**, and **13**.

10: ^{1}H NMR (300 MHz, $CDCl_3$): δ = 5.51 (m, 2H; =CH), 3.20 (m, 4H; CH_2N) 3.14 (m, 4H; CH_2N), 2.73 (hept., ^3J = 6.5 Hz, 2H; NCH), 1.06 (d, ^3J = 6.5 Hz, 12H; CH_3); ^{13}C NMR (75.47 MHz, $CDCl_3$): δ = 131.5 (s; =C−), 120.2 (d; =CH), 53.7 (d; NCH), 51.2 (t; CH_2N), 48.3 (t; CH_2N), 18.8 (q; CH_3).

11a + b: ^{1}H NMR (300 MHz, $CDCl_3$): δ = 5.93–5.77 (m, 4H; =CH), 5.58–5.45 (m, 4H; =CH), 3.81 (m, 1H; bisallyl. CH), 3.53–3.42 (m, 1H; allyl. CH), 3.39 (m, 2H; CH_2N), 3.33 (m, 2H; CH_2N), 3.21 (m, 2H; CH_2N), 3.19 (m, 4H; CH_2N), 3.14 (m, 4H; CH_2N), 3.05 (m, 2H; CH_2N), 2.86–2.62 (m, 6H; 4NCH, bisallyl. CH_2), 2.23–2.15 (m, 2H; allyl. CH_2), 1.09–1.05 (m, 24H; CH_3); ^{13}C NMR (75.47 MHz, $CDCl_3$): δ = 133.8, 132.3, 131.4, 131.1 (4 × s; =C−), 128.3, 126.1, 125.9, (3 × d; =CH), 125.6, 125.5 (2 × s, =C−), 125.4, 124.8, 123.6, 119.9, 119.7 (5 × d; =CH), 53.91, 53.90, 53.7, 53.5 (4 × d; NCH), 51.8, 51.7, 50.2, 49.6, 47.6, 47.55, 47.50, 47.1 (8 × t; CH_2N), 37.0, 35.3 (2 × d; CH), 27.1, 25.7 (2 × t; CH_2), 18.83 (q; $2CH_3$), 18.80, 18.69, 18.66, 18.57 (4 × q; CH_3).

12: ^{1}H NMR (300 MHz, $CDCl_3$): δ = 7.21–7.19 (AA'BB', 8H; arom. CH), 5.67, (m, 1H; =CH), 5.16 (m, 1H; CH), 4.18–4.02 (AB, ^2J = 18 Hz, 2H; CH_2), 3.61 (m, 2H; CH_2N), 3.25 (m, 4H; CH_2N), 2.85 (hept., ^3J = 6.5 Hz, 1H; NCH), 2.79 (m, 2H; CH_2N), 2.53 (hept., ^3J = 6.5 Hz, 1H; NCH), 1.10 (d, ^3J = 6.5 Hz, 6H; CH_3), 0.84 (d, ^3J = 6.5 Hz, 12H; CH_3); ^{13}C NMR (75.47 MHz, $CDCl_3$): δ = 136.4, 134.8 (each s; arom. =C−), 133.7, 131.5, 127.7 (3 × s; olef. =C−), 128.3, 127.9, 126.6, 126.5 (4 × d; arom. CH), 120.8 (d; olef. CH), 54.0, 53.1 (2 × d; NCH), 52.7, 48.8, 48.4, 47.9 (4 × t; CH_2N), 44.2 (d; CH), 34.7 (t; CH_2), 18.9, 18.7 (2 × q; CH_3).

13: ^{1}H NMR (300 MHz, $CDCl_3$): δ = 5.43 (m, 1H; =CH), 3.31 (m, 2H; CH_2N), 3.12 (m, 2H; CH_2N), 3.09 (m, 2H; CH_2N), 3.03 (m, 2H; CH_2N), 2.81–2.60 (m, 3H; 2NCH, allyl. CH), 1.08 (d, ^3J = 6.5 Hz, 6H; CH_3), 1.05 (d, ^3J = 6.5 Hz, 6H; CH_3); ^{13}C NMR (75.47 MHz, $CDCl_3$): δ = 138.2, 131.9, 122.9 (3 × s; =C−), 118.6 (d, =CH), 53.9, 53.7 (2 × d; NCH), 52.2, 49.1, 47.7, 47.6 (4 × t; CH_2N), 38.6 (d; CH), 31.6, 26.9, 26.5, 26.4 (4 × t; CH_2), 18.9, 18.8 (2 × q; CH_3).

chemical calculations confirm this hypothesis. Formation of 1,4-didehydrobutadiene **14** leads to a σ framework of lower energy, and the π system has in part lower energy owing to generation of the bicyclic *trans*-butadiene unit with two fused six membered rings. In addition a stabilizing through-bond interaction between the two radical centers occurs. In Table 2 the enthalpy diagrams of the reactions **1** → **2**, **5** → **6**, and **9** → **14** are compared. The values given have been taken from literature[2, 5] or derived from AM1[10a] and MNDO[10b] calculations.[11]

Table 2. Comparison of the reaction enthalpies $\Delta_R H^\circ$ [kcal mol^{-1}] of the reactions **1** → **2**, **5** → **6**, and **9** → **14**; $\Delta_R H^\circ = \Delta_f H^\circ$ (diradical) − $\Delta_f H^\circ$ (alkyne). The $\Delta_f H^\circ$ values used were estimated by triplet singlet AM1/MNDO calculations for the diradicals and alkynes, respectively.

Reaction	$\Delta_R H^\circ$ (AM1)	$\Delta_R H^\circ$ (MNDO)	$\Delta_R H^\circ$ (experiment)
1 → **2**	11	12	13 ± 3 [2e]
5 → **6**	−18	−18	−15 ± 3 [5]
9 → **14**	27	24	

As mentioned previously, the Bergman and Myers cyclizations both include the electrocyclization of a conjugated 6π system to give an arene diradical. The formation of 1,4-didehydrobutadiene **14** is the first example of a related process for nonconjugated diynes in which the activation of the diyne results from homoconjugative interaction with an electron donor. Further experimental and theoretical studies on the scope and limitation of these and related systems are in progress.

Received: July 22, 1994 [Z 7160 IE]
German version: *Angew. Chem.* **1994**, *106*, 2550

[1] R. R. Jones, R. G. Bergman, *J. Am. Chem. Soc.* **1972**, *94*, 660; T. P. Lockhart, P. B. Comita, R. G. Bergman, *ibid.* **1981**, *103*, 4082; T. P. Lockhart, R. G. Bergman, *ibid.* **1981**, *103*, 4091.

[2] a) E. Kraka, D. Cremer, *J. Am. Chem. Soc.* **1994**, *116*, 4929; R. Lindh, J. Persson, *ibid.* **1994**, *116*, 4963; b) P. G. Wenthold, J. A. Paulino, R. R. Squires, *ibid.* **1991**, *113*, 7414; c) S. G. Wierschke, J. J. Nash, R. R. Squires, *ibid.* **1993**, *115*, 11958; d) A. Nicolaides, W. T. Borden, *ibid.* **1993**, *115*, 11951; e) A revised value for $\Delta_R H^\circ$ according to R. R. Squires, Purdue University, West Lafayette, IN, personal communication, cf. refs. [2a, c, d].

[3] For a recent review see K. C. Nicolaou, W.-M. Dai, *Angew. Chem.* **1991**, *103*, 1453; *Angew. Chem. Int. Ed. Engl.* **1991**, *30*, 1387.

[4] A. G. Myers, *Tetrahedron Lett.* **1987**, *28*, 4493; A. G. Myers, P. J. Proteau, T. M. Handel, *J. Am. Chem. Soc.* **1988**, *110*, 7212; A. G. Myers, P. J. Proteau, *ibid.* **1989**, *111*, 1146.

[5] a) A. G. Myers, P. S. Dragovich, E. Y. Kuo, *J. Am. Chem. Soc.* **1992**, *114*, 9369; b) P. G. Wenthold, S. G. Wierschke, J. J. Nash, R. R. Squires, *ibid.* **1993**, *115*, 12611.

[6] See ref. [3] p. 1466 and 1391, respectively, and references therein

[7] Further examples of analogous cyclizations of conjugated $(4n+2)\pi$ systems: a) J. Mayer, F. Sondheimer, *J. Am. Chem. Soc.* **1966**, *88*, 602; b) K. Grohmann, F. Sondheimer, *Tetrahedron Lett.* **1967**, 3121; c) H. A. Staab, A. Nissen, J. Ipaktschi, *Angew. Chem.* **1968**, *80*, 241; *Angew. Chem. Int. Ed. Engl.* **1968**, *7*, 226; d) H. W. Whitlock, Jr., J. K. Reed, *J. Org. Chem.* **1969**, *34*, 874; e) R. H. Mitchell, F. Sondheimer, *Tetrahedron* **1970**, *26*, 2141; f) H. A. Staab, A. Nissen, J. Ipaktschi, *Chem. Ber.* **1971**, *104*, 1182; g) K. N. Bharucha, R. M. Marsh, R. M. Minto, R. G. Bergman, *J. Am. Chem. Soc.* **1992**, *114*, 3120; h) A. G. Myers, N. S. Finney, *ibid.* **1992**, *114*, 10986.

[8] a) R. Gleiter, *Angew. Chem.* **1992**, *104*, 29; *Angew. Chem. Int. Ed. Engl.* **1992**, *31*, 27; b) R. Gleiter, M. Karcher, R. Jahn, H. Irngartinger, *Chem. Ber.* **1988**, *121*, 735; c) R. Gleiter, D. Kratz, V. Schehlmann, *Tetrahedron Lett.* **1988**, *29*, 2813; d) R. Gleiter, J. Ritter, H. Irngartinger, J. Lichtenthäler, *ibid.* **1991**, *32*, 2883; e) *ibid.* **1991**, *32*, 2887; f) R. Gleiter, S. Rittinger, H. Langer, *Chem. Ber.* **1991**, *124*, 357; g) R. Gleiter, R. Merger, B. Nuber, *J. Am. Chem. Soc.* **1992**, *114*, 8921.

[9] C. E. Dykstra, A. J. Arduengo, T. Fukunaga, *J. Am. Chem. Soc.* **1978**, *100*, 6007; O. Eisenstein, G. Proctor, J. D. Dunitz, *Helv. Chim. Acta* **1978**, *61*, 2538; R. W. Strozier, P. Carmella, K. N. Houk, *J. Am. Chem. Soc.* **1979**, *101*, 1340.

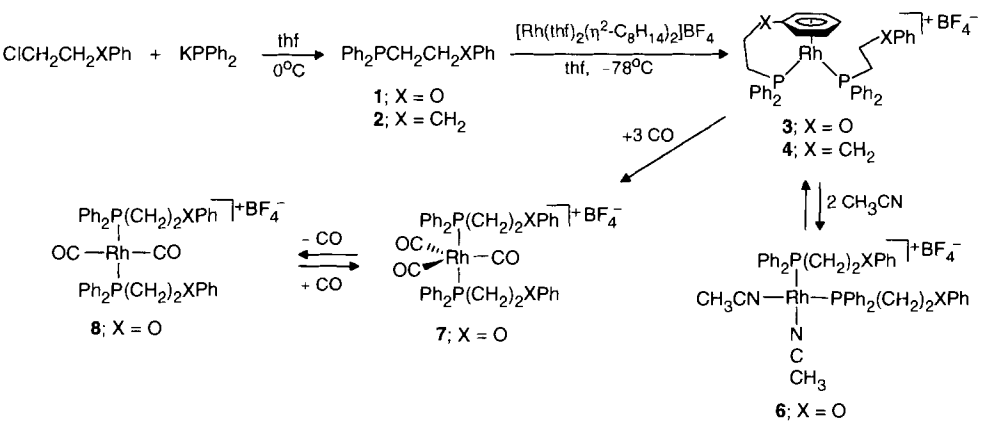
[10] a) M. J. S. Dewar, E. G. Zoebisch, E. F. Healy, J. J. Stewart, *J. Am. Chem. Soc.* **1985**, *107*, 3902; b) M. J. S. Dewar, W. Thiel, *ibid.* **1977**, *99*, 4899.

[11] The $\Delta_R H^\circ$ values for the reaction **1** → **2** based on AM1/MNDO calculations (program MOLEK 9000) are in good agreement with the results of recent ab initio studies: ref. [2c, d].

Novel Rh^I Piano-Stool Complexes with New Hemilabile Ligands Ligating through Phosphane and Arene Groups: Synthesis, Characterization, and Reactivity**

Elizabeth T. Singewald, Chad A. Mirkin,*
Allison D. Levy, and Charlotte L. Stern

Ligands that are hybrids with two types of functional groups, one forming a strong bond with a transition metal and one a weak bond, have been exploited in many areas of homogeneous catalysis including olefin hydrogenation[1] and methanol carbonylation reactions.[2] Such ligands often are referred to as hemilabile ligands because the strongly binding functional groups typically are substitutionally inert and the weakly binding groups are substitutionally labile. For complexes with the late transition metals, the phosphane moiety is often chosen as the substitutionally inert group, and a group ligating through a heteroatom such as O or N is chosen as the substitutionally labile functionality. Herein, we report a new class of hemilabile ligands, **1** and **2**, which are based upon moieties containing phosphane and arene functionalities as ligating groups (Scheme 1). In the design of such ligands we drew upon the observation by others that the arene moiety can be quite labile when bound to a $(PR_3)_2Rh^I$ metal core.[3] We report the synthesis of ligands **1** and **2** and their complexation to Rh^I to form the new η^6-arene-*cis*-phosphane piano-stool complexes **3** and **4**, respectively. In addition to rich arene ligand substitution chemistry, **3** and **4** exhibit two types of novel behavior: 1) the metal-bound η^6-arene ring of the chelated ligand of **3**, but not of **4**, undergoes a fast *intramolecular* exchange with the arene ring of the monocoordinated ligand at moderate temperatures, and 2) both **3** and **4** undergo electrochemically reversible one-electron oxidation reactions to form mononuclear Rh^{II} species.



Scheme 1.

The ligands, $PhXCH_2CH_2PPh_2$ (**1**, X = O; **2**, X = CH_2) were synthesized from the reaction of $PhXCH_2CH_2Cl$ (0.020 mol) with $KPPh_2$ (0.50 M, 40 mL) in THF at 0 °C (Scheme 1). Addition of ligand **1** (1.0 mmol) to a 75 mL solution of $[(\eta^2\text{-}C_8H_{14})_2Rh(thf)_2]BF_4$[4] (0.50 mmol) in THF at −78 °C leads to the formation of **3** in 80% yield. Similarly, compound **4** forms in 75% yield from the addition of ligand **2** (1.0 mmol) to a THF solution of $[(\eta^2\text{-}C_8H_{14})_2Rh(thf)_2]BF_4$ (0.50 mmol) at −78 °C. Recrystallization of **3** and **4** at room temperature from CH_2Cl_2/diethyl ether yielded analytically pure samples of each complex.

Compounds **3** and **4** have been characterized spectroscopically and by single-crystal X-ray diffraction studies. The solid-state structures for **3** and **4** are comparable; therefore in this communication, we will limit our discussion to compound **3** (Fig. 1). The solid-state structure of **3** shows that the complex resembles a piano stool with two legs and the fulcrum at Rh. The C atoms which comprise the η^6-arene ring in **3** are essentially in a plane (mean deviation = 0.02 Å), and the distance from the center of the bound arene to the Rh atom is 1.84 Å. Although there are a few examples of structurally characterized Rh^I complexes with planar η^6-arene ligands, such ligands often adopt boat conformations when bound to Rh^I.[5] The Rh–O1 distance of 3.307(3) Å and the Rh–O2 distance of 4.185(3) Å are well outside of the normal bonding distances for Rh (about 2.2 Å).[1]

Spectroscopic data for **3** and **4** in CD_2Cl_2 at 25 °C are comparable and consistent with the formulated piano-stool structures for these complexes in solution. For example, the ^1H NMR spectrum of **3** in CD_2Cl_2 shows characteristic upfield resonances for the H atoms *ortho* to the O atom in the η^6 coordinated arene at $\delta = 6.75$, at $\delta = 6.88$ for the *meta* H atoms, and at $\delta = 4.63$ for the *para* H atom. These assignments have been confirmed by a 2D COSY experiment and a CH correlation study. The resonance at $\delta = 4.63$ for the *para* H atom of the bound arene is remarkably far upfield for coordinated arene ligands. This phenomenon seems to be common to

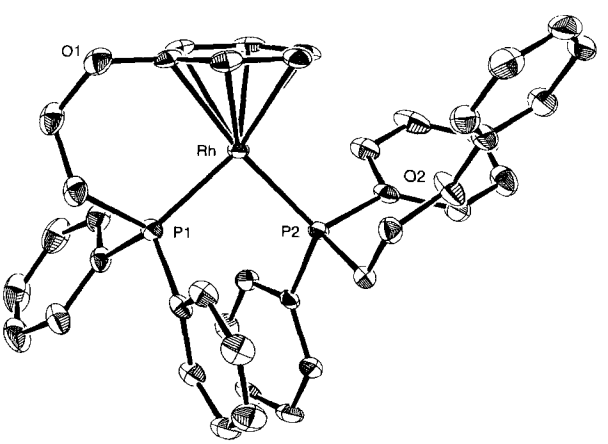


Fig. 1. ORTEP drawing of the cation of **3** in the crystal. Thermal ellipsoids are drawn at 50% probability.

[*] Prof. C. A. Mirkin, E. T. Singewald, A. D. Levy, C. L. Stern
Department of Chemistry, Northwestern University
Evanston, IL 60208 (USA)
Telefax: Int. code + (708)491-7713

[**] This work was supported by the National Science Foundation (NSF, CHE-9121859) and Johnson Matthey (for a loan of $RhCl_3$). C. A. Mirkin acknowledges a Dreyfus Foundation Distinguished New Faculty Award (1991–1996), a Beckman Young Investigator Award (1992–1994), a Naval Young Investigator Award (1994–1997), and a National Science Foundation Young Investigator Award (1993–1998). We are grateful to Prof. Joseph B. Lambert and Dr. Peter N. Nickias for insightful discussions, and Dr. Diana Kushlan for assistance with 2D NMR experiments.

this class of compounds, since **4** also exhibits a resonance in this region ($\delta = 4.68$) for the *para* H atom of its η^6 bound arene ligand.

Compound **3** undergoes an intramolecular exchange reaction between the η^6 bound arene and free arene at moderate temperatures (10–30 °C) in CD_2Cl_2 (Fig. 2). This process, which is

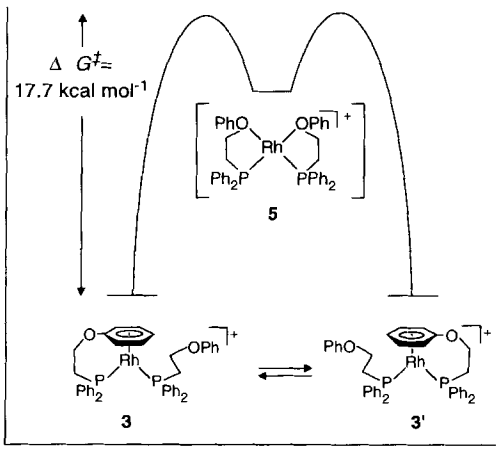


Fig. 2. Energy diagram depicting the exchange reaction between the energetically degenerate compounds **3** and **3'**. Compound **5** is a proposed intermediate; its position within the energy diagram is arbitrarily depicted. The *x* axis represents the reaction coordinate and the *y* axis the energy.

slow even at elevated temperatures (76 °C in [D_8]dioxane) in both the one-dimensional ^1H and ^{31}P NMR experiments, may be detected by a two-dimensional ^1H NMR exchange spectroscopy (EXSY) experiment[6] (Fig. 3). The EXSY experiment confirms that the two ligands undergo dynamic chemical exchange as indicated by the crosspeaks for the *para*-H atoms of the chemically exchanging arene rings, which are at $\delta = 4.63$ and $\delta = 7.00$ for the Rh-bound and unbound forms, respectively. This observation is consistent with a degenerate exchange of the two chemically inequivalent arene ligands in **3**, which is depicted by the interconversion of **3** and **3'** (Fig. 2). The activation parameters $\Delta G^{\neq} = 17.7$ kcal mol^{-1}, $\Delta H^{\neq} = 19.6$ kcal mol^{-1}, and $\Delta S^{\neq} = 6.10$ cal mol^{-1} K^{-1} at 293 K have been determined for this process by performing a variable-temperature (283–303 K) EXSY experiment and modeling the data according to the Eyring equation.[7] Although such reversible ring exchange reactions have never been reported for $Rh^I(PR_3)_2$ fragments, ring exchange reactions have been detected for polyarene complexes of $Cr(CO)_3$, albeit under very forcing conditions (for example, 170 °C, under pressure in C_6D_6).[8] Significantly, under conditions comparable to those used for **3**, compound **4** does not undergo the exchange reaction on a time scale that may be detected by the EXSY experiment.

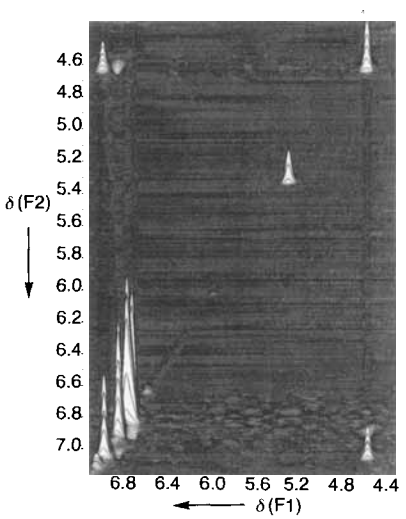


Fig. 3. 2D EXSY spectrum of **3** in CD_2Cl_2 at 30 °C.

Why does **3**, but not **4** undergo fast intramolecular exchange on the EXSY time scale? One explanation is the exchange reaction for **3** is facilitated by its ether groups, which serve as "internal solvent" molecules and allow for the formation of a relatively low energy transition state. Indeed, based on our past work and the work of others, square-planar *cis*-phosphane *cis*-ether complex **5** (Fig. 2) is a reasonable intermediate in the equilibration of **3** and **3'**;[1, 9] thus far, however, it has eluded spectroscopic detection. Since compound **4** does not possess ether moeities, it does not have such a route available to it and would be expected to have a higher energy transition state and a larger energy barrier for arene–arene exchange.

The Rh-bound arene ligand in **3** not only may be displaced intramolecularly, but also intermolecularly with more strongly coordinating ligands such as CO and CH_3CN (Scheme 1). The reaction with CH_3CN demonstrates the extreme lability of the arene–Rh linkage. The addition of four equivalents of CH_3CN to a CD_2Cl_2 solution of compound **3** (32 mg, 0.04 mmol) at −45 °C resulted in clean and quantitative conversion into the *cis*-CH_3CN adduct, **6**. The compound was assigned as the *cis* adduct rather than the *trans* adduct on the basis of the coupling constant ($J_{Rh,P} = 170.5$ Hz).[10] Significantly, the process is reversible, and vacuum evaporation of the solvent from the CD_2Cl_2 solution of **6** leads to quantitative reformation of **3**.

Compound **3** in CH_2Cl_2 also cleanly reacts with CO (1 atm) to form the tricarbonyl complex **7**. However, upon removal of the solvent and CO atmosphere, **7** slowly (4 h at 10^{-5} Torr and 25 °C) loses one CO ligand to form the dicarbonyl complex **8**. Under these conditions, there is no evidence for formation of the *cis* isomer. Addition of CO (1 atm) to a CH_2Cl_2 solution of **8** causes quantitative reformation of the tricarbonyl complex **7**. Interconversions between di- and tricarbonyl complexes containing the $Rh^I(PR_3)_2$ moiety comparable to **7** and **8** have been reported by others.[9]

Another unusual feature of the isoelectronic compounds **3** and **4** is that they each exhibit a reversible electrochemical reaction in CH_2Cl_2/0.1 M nBu$_4$NPF$_6$. The $E_{1/2}$ values for **3** and **4** are 580 mV and 530 mV vs. ferrocene/ferrocenium (Fc/Fc^+), respectively, and show that from an electronic standpoint the two arene ligands **1** and **2** are similar. Furthermore, the steric difference between the O and CH_2 groups in **3** and **4**, respectively, would be expected to be minimal. Therefore, the fluxionality observed in **3**, but not **4**, most likely is due to the ability of **3** to form an intermediate such as **5** that is not chemically possible for **4** (Fig. 2).

Significantly, cyclic voltammetry and rotating disk electrode experiments performed on **3** and **4** (referenced to Fc/Fc^+) show that the observed electrochemical transformations are one-electron oxidations, which suggest that the synthesis of mononuclear Rh^I η^6-arenediphosphane complexes followed by oxidation will provide a reasonable avenue to stable, isolable mononuclear Rh^{II} piano-stool complexes. Although there are many examples of binuclear Rh^{II} complexes and a few examples of mononuclear organometallic Rh^{II} complexes, there are no reported examples of mononuclear Rh^{II} bisphosphane η^6-arene piano-stool complexes.[12]

 © VCH Verlagsgesellschaft mbH, D-69451 Weinheim, 1994 0570-0833/94/2323-2474 $ 10.00+.25/0

Experimental Procedure

All NMR spectra were recorded on a Varian Gemini 300 MHz spectrometer at 20 °C unless otherwise noted. The ^{31}P NMR spectra were referenced to external 85% H_3PO_4. Silica gel (60 Å, 230–400 mesh ASTM) was purchased from Baxter Scientific Products; **1** and **2** were isolated by column chromatography on silica gel with 15% diethyl ether in pentane as the eluent. In each case, the ligand was the only fraction collected. Analytically pure samples were obtained by recrystallization at −20 °C in ethanol (yields: **1**, 70%; **2**, 76%).

1: ^1H NMR (C_6D_6): $\delta = 2.41$ (t, $J(H,H) = 7.7$ Hz, 2H; CH_2P), 3.92 (q, $J(H,H) = J(P,H) = 7.7$ Hz, 2H; CH_2O), 7.40–6.71 (m, 15H; Phs); ^{31}P NMR (C_6D_6): $\delta = -21.8$ (s); MS(EI): (70 eV, 190 °C) *m/z*: 306 [M^+]; anal. calcd. for $C_{20}H_{19}OP$: C 78.42, H 6.25; found: C 78.52, H 6.44.

2: ^1H NMR ($CDCl_3$). $\delta = 1.79$ (m, 2H; $CH_2CH_2CH_2$), 2.09 (dt, $J(H,H) = 7.2$ Hz, $J(P,H) = 4.7$ Hz, 2H; CH_2P), 2.76 (t, $J(H,H) = 7.4$ Hz, 2H; CH_2Ph), 7.43–7.15 (m, 15H; Phs); ^{31}P NMR ($CDCl_3$) $\delta = -15.2$ (s); MS(EI): (70 eV, 190 °C) *m/z*: 304 [M^+]; anal. calcd. for $C_{21}H_{21}P$: C 82.87, H 6.95; found: C 82.62, H 7.07.

3: ^1H NMR (600 MHz, CD_2Cl_2): $\delta = 1.76$ (dt, $J(H,H) = 6.6$, $J(P,H) = 9.6$ Hz, 2H, CH_2P), 2.07 (m, 2H; CH_2P), 4.05 (m, 4H; CH_2O), 4.63 (t, $J(H,H) = 6.1$ Hz, 1H; η^6-*p*-C_6H_5), 6.75 (d, $J(H,H) = 6.2$ Hz, 2H; η^6-*o*-C_6H_5), 6.80 (d, $J(H,H) = 7.8$ Hz, 2H; *o*-C_6H_5O), 6.88 (m, 2H; η^6-*m*-C_6H_5), 7.00 (t, $J(H,H) = 7.4$ Hz, 1H; *p*-C_6H_5O), 7.28–7.47 (m, 22H; Phs); ^{31}P NMR (CD_2Cl_2): $\delta = 32.6$ (dd, $J(Rh,P) = 198.7$ Hz, $J(P,P) = 38.6$ Hz), 34.9 (dd, $J(Rh,P) = 210.4$ Hz, $J(P,P) = 38.6$ Hz); FAB-MS: *m/z*: 715 [M^+]; anal. calcd. for $C_{40}H_{38}O_2P_2RhBF_4$: C 59.88, H 4.77; found: C 59.70, H 4.91.

4: ^1H NMR (400 MHz, CD_2Cl_2): $\delta = 1.44$ (m, 6H; CH_2P, $2\,CH_2CH_2CH_2$), 1.90 (dt, $J(H,H) = 4.8$ Hz, $J(P,H) = 10.4$ Hz, 2H; CH_2P), 2.37 (t, $J(H,H) = 7.2$ Hz, 2H; $CH_2(\eta^6$-Ph)), 2.56 (t, $J(H,H) = 4.8$ Hz, 2H; CH_2Ph), 4.68 (t, $J(H,H) = 6.0$ Hz, 1H; η^6-*p*-C_6H_5), 6.78 (m, 2H; η^6-*m*-C_6H_5), 6.85 (d, $J(H,H) = 7.2$ Hz, 4H; *o*-C_6H_5), 7.44–7.16 (m, 23H; Phs); ^{31}P NMR (CD_2Cl_2): $\delta = 34.6$ (dd, $J(Rh,P) = 203.9$ Hz, $J(P,P) = 40.6$ Hz), 39.8 (dd, $J(Rh,P) = 198.8$ Hz, $J(P,P) = 40.6$ Hz); FAB-MS: *m/z*: 711 [M^+]; anal. calcd. for $C_{42}H_{42}P_2RhBF_4$: C 63.18, H 5.31; found: C 62.63, H 5.50.

6: ^1H NMR (CD_2Cl_2; −45 °C): $\delta = 1.62$ (s, 6H; CH_3CN), 2.11 (m, 4H; CH_2P), 4.46 (m, 4H, CH_2O), 6.79 (d, $J(H,H) = 7.7$ Hz, 4H; *o*-C_6H_5), 6.96 (t, $J(H,H) = 7.3$ Hz, 2H; *p*-C_6H_5), 7.42–7.25 (m, 24H; Phs); ^{31}P NMR (CD_2Cl_2, −45 °C): $\delta = 37.71$ (d, $J(Rh,P) = 170.5$ Hz).

7: ^1H NMR (CD_2Cl_2): $\delta = 3.21$ (m, 4H; CH_2P), 4.32 (m, 4H; CH_2O), 6.58 (d, $J(H,H) = 7.4$ Hz, 4H; (*o*-C_6H_5)O), 6.96 (t, $J(H,H) = 7.4$ Hz, 2H; (*p*-C_6H_5)O), 7.21 (m, 4H; (*m*-C_6H_5)O), 7.64–7.51 (m, 20H; Ph_2P); ^{31}P NMR (for ^{13}CO labeled **7**, CD_2Cl_2, −78 °C): $\delta = 31.5$ (dq, $J(Rh,P) = 71.7$, $J(C,P) = 14.1$ Hz); FAB-MS: *m/z*: 743 [$M^+ - 2CO$].

8: ^1H NMR (CD_2Cl_2): $\delta = 3.20$ (m, 4H; CH_2P), 4.33 (m, 4H; CH_2O), 6.67 (d, $J(H,H) = 8.0$ Hz, 4H; (*o*-C_6H_5)O), 6.98 (t, $J(H,H) = 7.3$ Hz, 2H; (*p*-C_6H_5)O), 7.23 (m, 4H; (*m*-C_6H_5)O), 7.67–7.48 (m, 20H; Ph_2P); ^{31}P NMR (for ^{13}CO labeled **8**, CD_2Cl_2, −78 °C): $\delta = 18.9$ (dt, $J(Rh,P) = 106.8$, $J(C,P) = 15.5$ Hz); IR(CH_2Cl_2): $\nu_{CO} = 1997$ (vs), 1932 (w) cm^{-1}; FAB-MS: *m/z*: 743 [$M^+ - CO$].

Crystal data for **3**: $C_{40}H_{38}O_2P_2RhBF_4$, $0.42 \times 0.26 \times 0.33$ mm, monoclinic, space group = $P2_1/c$, $a = 10.595(3)$, $b = 17.116(5)$, $c = 19.564(5)$ Å, $V = 3545(3)$ Å^3, $\varrho_{calcd} = 1.503$ g cm^{-3}, $2\theta_{max} = 23.9°$, $\mu(Mo_{K\alpha}) = 6.17$ cm^{-1}, $\lambda = 0.71069$ Å, $F(000) = 1640$. Data were collected on an Enraf-Nonius CAD-4 diffractometer at -120 ± 1 °C using the ω-θ scan technique ($2\theta \leq 54.0°$). The data were corrected for Lorentz and polarization effects. In addition, an analytical absorption correction was applied with transmission factors ranging from 0.80–0.86 and a correction for secondary extinction was applied (coefficient = 0.42235×10^{-7}). The structure was solved by Patterson methods (SHELXS-86). Of the 6466 reflections, 5133 with $I > 3.00\,\sigma(I)$ were used in refinement. Refinement of 452 variable parameters (TEXAN 5.0) converged with the residuals of $R = 0.033$ and $R_w = 0.043$ [13].

Received: June 27, 1994 [Z 7077 IE]
German version: *Angew. Chem.* **1994**, *106*, 2524

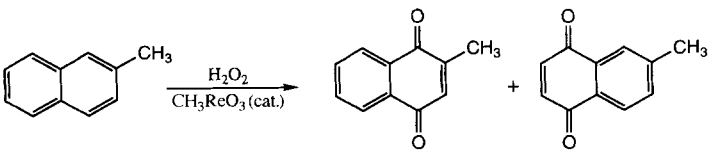
[1] A. M. Allgeier, E. T. Singewald, C. A. Mirkin, C. L. Stern, *Organometallics* **1994**, *13*, 2928.
[2] a) B. D. Vineyard, W. S. Knowles, M. J. Sabacky, G. L. Bachman, D. L. Weinkauff, *J. Am. Chem. Soc.* **1977**, *99*, 5946; b) E. Lindner, B. Andres, *Chem. Ber.* **1988**, *121*, 829.
[3] J. Halpern, D. P. Riley, A. S. C. Chan, J. J. Pluth, *J. Am. Chem. Soc.* **1977**, *99*, 8055.
[4] Postulated as the in situ product of the reaction of 1 equiv of $AgBF_4$ with $[Rh(\eta^2\text{-}C_8H_{14})_2Cl]_x$ in THF; for a synthetic procedure for $[Rh(\eta^2\text{-}C_8H_{14})_2Cl]_x$, see L. Porri, A. Li. Alionetti, G. Allegra, A. Immirzi, *Chem. Commun.* **1965**, 336.
[5] a) J. M. Townsend, J. F. Blount, *Inorg. Chem.* **1981**, *20*, 269, and references therein; b) P. Albano, M. Aresta, M. Manassero, *Inorg. Chem.* **1980**, *19*, 1069; c) J. R. Bleeke, A. J. Donaldson, *Organometallics* **1988**, *7*, 1588.
[6] C. L. Perrin, T. J. Dwyer, *Chem. Rev.* **1990**, *90*, 935.
[7] J. Sandstrom, *Dynamic NMR Spectroscopy*, Academic Press, New York, **1982**.
[8] T. G. Traylor, M. J. Goldberg, *J. Am. Chem. Soc.* **1987**, *109*, 3968.
[9] E. Lindner, Q. Wang, H. A. Mayer, R. Fawzi, M. Steimann, *Organometallics* **1993**, *12*, 1865.
[10] T. G. Appleton, H. C. Clark, L. E. Manzer, *Coord. Chem. Rev.* **1973**, *10*, 333.
[11] F. A. Cotton, R. A. Walton, *Multiple Bonds between Metal Atoms*, Wiley-Interscience, New York, **1982**, p. 311.
[12] K. K. Pandey, *Coord. Chem. Rev.* **1992**, *121*, 1.
[13] Further details of the crystal structure investigation are available on request from the Director of the Cambridge Crystallographic Data Center, 12 Union Road, GB-Cambridge CB21EZ (UK), on quoting the full journal citation.

Homogeneous Catalytic Oxidation of Arenes and a New Synthesis of Vitamin K_3**

Waldemar Adam,* Wolfgang A. Herrmann, Jianhua Lin, Chantu R. Saha-Möller, Richard W. Fischer, and João D. G. Correia

The selective oxidation of arenes is a great challenge for research in catalysis. The oxidants of choice are molecular oxygen and hydrogen peroxide.[1] The preparation of quinones usually requires the direct oxidation of arenes by chromic acid/sulfuric acid.[2] Surprisingly, we have now found that methyltrioxorhenium (MTO) efficiently catalyzes the oxidation of arenes by hydrogen peroxide.[3] This reaction is the key to a much improved synthesis of vitamin K_3, which is of appreciable commercial value as supplement in animal feed.[4]

In acetic acid and in the presence of catalytic amounts of CH_3ReO_3 (2 mol%), 2-methylnaphthalene (**1**) is oxidized by hydrogen peroxide preferentially to the 1,4-quinone **2** (vitamin K_3, "menadione"). At 40 °C and after 4 h the conversion amounts to 81% (quinone yield 67%); in the absence of CH_3ReO_3 under otherwise identical conditions less than 2% conversion takes place. The high regioselectivity is particularly noteworthy: the isomeric 2-methylnaphthoquinones **2** and **3** are



1 **2** **3**

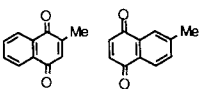
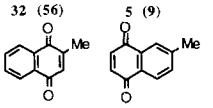
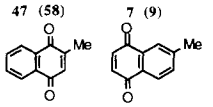
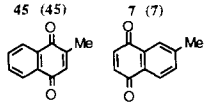
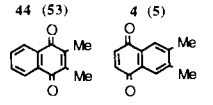
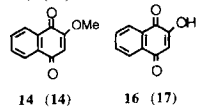
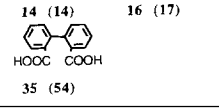
formed in a 7:1 ratio (85% yield of **2**) depending on the reaction conditions and H_2O_2 concentration (10–85% by weight). In the industrial synthesis of vitamin K_3 with chromic acid yields

[*] Prof. Dr. W. Adam, Dr. J. Lin, Dr. C. R. Saha-Möller
Institut für Organische Chemie der Universität
Am Hubland, D-97074 Würzburg (FRG)
Telefax: Int. code + (931)888-4606
Prof. Dr. W. A. Herrmann, Dr. R. W. Fischer,[+] J. D. G. Correia
Institut für Anorganische Chemie der Technischen Universität München
Lichtenbergstrasse 4, D-85747 Garching (FRG)
[+] New address: Hoechst AG, Zentralforschung
D-65926 Frankfurt am Main (FRG)

[**] This work was supported by the Deutsche Forschungsgemeinschaft (Schwerpunktprogramm "Peroxidchemie: Mechanistische und präparative Aspekte des Sauerstofftransfers", and Sonderforschungsbereich 347 "Selektive Reaktionen metallaktivierter Moleküle"), the Bayerische Forschungsstiftung, the Fonds der Chemischen Industrie, the Alexander-von-Humboldt-Stiftung (postdoctoral fellowship for J.L.) and the European Community (postdoctoral fellowship for J.D.G.C.).

of 38–60% are achieved; however, in this stoichiometric oxidation about 18 kg of chromium-containing waste is produced per kg of product.[5a, b] The maximum regioselectivity for the oxidation with H_2O_2 under Pd^{II} catalysis is 66%.[5c] The analogous reaction with 2,3-dimethylnaphthalene provides a 59% yield of 1,4-naphthoquinone and a 1% yield of 5,8-naphthoquinone (conversion 94%, 40 °C, 4 h, 83 wt% H_2O_2 in acetic acid). Phenanthrene is converted under the same conditions into diphenyl-2,2′-dicarboxylic acid in 54% yield (Table 1).

Table 1. Oxidation of arenes with methyltrioxorhenium (MTO) and H_2O_2 [a].

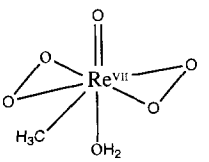
Arene	t [h]	T [°C]	Conversion [%]	M.B. [b] [%]	Products and yields [%] [c]	Selectivity [%]
1	4	20	56	81	 32 (56) 5 (9)	86
1	4	40	81	73	 47 (58) 7 (9)	86
1	4	70	100	52	 45 (45) 7 (7)	86
1	8	40	83 [d]	65	 44 (53) 4 (5)	91
2,3-dimethylnaphthalene	4	40	94 [e]	62	 56 (59) 1 (1)	98
2-methoxynaphthalene	3	20	97	33	 14 (14) 16 (17)	
phenanthrene	5	40	64	71	 35 (54)	

[a] Arene:85% H_2O_2:MTO = 1:7:0.02 (mol ratio) in acetic acid, N_2 atmosphere. [b] M.B. = mass balance of isolated, characterized product and recovered starting material. [c] Yield of isolated product; yields in parenthesis were corrected for conversion of starting material; error ± 4% of stated value. [d] 35% H_2O_2 and acetic anhydride as solvent. [e] Arene:85% H_2O_2:MTO = 1:9:0.02 (mol ratio).

Since water acts as an inhibitor, concentrated H_2O_2 (85%) is preferred. Alternatively, commercially available 35% H_2O_2 in acetic anhydride can be employed; a considerably higher regioselectivity (**2**:**3**) of 10:1 was obtained with this system. The conversions improve for electron-rich arenes. Thus, with 2-methoxynaphthalene at 20 °C and after 3 h up to 97% conversion was achieved. Unfortunately, electron-rich arenes tend to undergo more side reactions, especially overoxidation, and thus the mass balance is quite poor.

Although the binary rhenium oxides ReO_3 and ReO_2 do not catalyze the oxidation of olefins,[6] they can be used instead of CH_3ReO_3 in the oxidation of arenes. These rhenium oxides also activate the oxidant H_2O_2 even at room temperature; with these catalysts the yield of vitamin K_3 amounts to 53% with a regioselectivity of 4:1 (85% H_2O_2 in acetic acid, 4 h, 51% conversion). When the formation of a *para*-quinone is not possible for structural reasons, then hydroxylation occurs instead. Thus, 4-hydroxymesitylene is produced in 73% yield when mesitylene is treated with 85% H_2O_2 in acetic acid in the presence of Re_2O_7 as catalyst (20 °C, 4 h). Without the catalyst, mesitylene does not react under these conditions. These simple rhenium oxides are active in acetic acid and acetic anhydride but not in solvents such as *tert*-butyl alcohol and THF.

Control experiments indicate that this oxidation of arenes proceeds via metal peroxides. The isolated bis(peroxo)rhenium complex **A**[6b, 7] derived from MTO and H_2O_2 reacts with 2-methylnaphthalene *quantitatively* to give 1,4-naphthoquinone **2** in high regioselectivity (>10:1) in acetic acid at 20 °C and 4 h. Analogous to the epoxidation of olefins, the bis(peroxo) complex **A** transfers only *one* of the peroxide oxygen atoms to the arene substrate. When instead of the bis(peroxo) complex **A** the double molar amount of peroxyacetic acid is used, only 29% conversion and an 8% yield of quinone is achieved, even after 4 h at 40 °C. To assure that the consumed peracid is replenished according to Equation (a), the oxidation was conducted with catalytic amounts of the strong acid CF_3CO_2H, since it is known that MTO catalyzes equilibrium (a).[9] MTO serves as a strong Lewis acid.



A

$$CH_3CO_2H + H_2O_2 \rightleftharpoons CH_3CO_3H + H_2O \quad (a)$$

The method described here allows an economic synthesis of vitamin K_3 and related quinone derivatives. The yields and regioselectivities of the oxidation system MTO/H_2O_2/CH_3CO_2H can certainly be optimized, as the stoichiometric control experiment with the bis(peroxo) complex **A** demonstrates. Mechanistic details like those recently reported for the Baeyer–Villiger oxidation should also be clarified.[8] The Re–C bond must not necessarily remain intact in all catalytic oxidations with the methyltrioxorhenium, although the stoichiometric, direct oxidation with **A** speaks for it in the present case. The relatively low amount of H_2O_2 decomposition is an advantage of the MTO/H_2O_2/CH_3CO_2H/arene system. For ReO_3 and Re_2O_7 as much as 20% decomposition may take place when a sevenfold excess of 85% H_2O_2 is employed.

Experimental Procedure

Vitamin K_3: To a solution of 10.0 g (70.3 mmol) of 2-methylnaphthalene (**1**) and 349 mg (1.40 mmol) of MTO [6b] in 150 mL of acetic acid was added dropwise at room temperature 14.3 mL (0.49 mol) of 85% H_2O_2. The reaction mixture was allowed to stir at 40 °C for 4 h under a N_2 atmosphere, before 100 mL of water was added. The mixture was extracted with CH_2Cl_2 (3 × 200 ml). The combined organic phases were washed with 150 mL of water, dried over Na_2SO_4, and concentrated at 20–40 °C/10–20 Torr. The conversion was 81% (GC/MS). The quinone products **2** and **3** were separated from the starting material by column chromatography (silica gel 32–63 μm mesh). Total yield 6.56 g (67% with respect to converted **1**). Recrystallization of the chromatographed product from ethanol afforded the quinone **2** in >98% purity (NMR) and in 58% yield (5.65 g). This method may be applied to other arenes. Depending on the reactivity of the arene, temperatures of 20–70 °C and H_2O_2 concentrations of 10–85% may be employed.

Received May 20, 1994
Revised version: August 4, 1994 [Z 6955 IE]
German version: *Angew. Chem.* **1994**, *106*, 2545

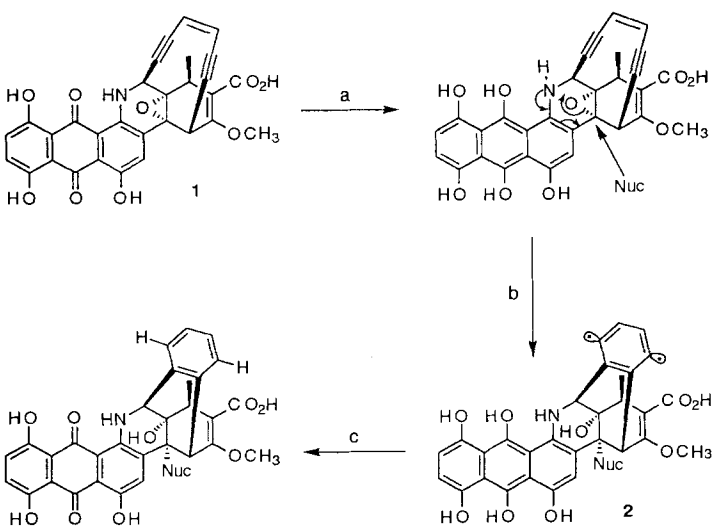
[1] R. A. Sheldon, *Top. Curr. Chem.* **1993**, *164*, 21–43.
[2] Monographs: a) M. Hudlicky, *Oxidations in Organic Chemistry* (*ACS Monogr.* **1990**, *186*); b) R. A. Sheldon, J. K. Kochi, *Metal-Catalyzed Oxidation of Organic Compounds*, Academic Press, New York, **1981**; c) *Organic Syntheses by Oxidation with Metal Compounds* (Eds.: W. J. Mijs, C. R. H. I. de Jonge), Plenum, New York, **1986**; d) *Catalytic Oxidations with Hydrogen Peroxide as Oxidant* (Ed.: G. Strukul), Kluwer Academic Publishers, Dordrecht, **1992**.

[3] W. A. Herrmann, W. Adam, R. W. Fischer, J. Lin, C. R. Saha-Möller, J. D. G. Correia (Hoechst AG), DE-P 4419799.3 **1994**.
[4] Derivatives of vitamin K ("coagulation vitamins") promote the formation of prothrombin and other blood coagulation factors. Vitamin K_3 is mainly used as supplement in animal feed, but has also been employed in the treatment of *Melaena neonatorum* in newly born babies.
[5] a) L. F. Fieser, *J. Biol. Chem.* **1940**, *133*, 391–396; b) R. A. Sheldon, J. Dakka, *Catal. Today* **1994**, *19*, 215–246; c) S. Yamaguchi, M. Inoue, S. Enomoto, *Bull. Chem. Soc. Jpn.* **1986**, *59*, 2881–2884; *Chem. Lett.* **1985**, 827–828.
[6] a) K. A. Jørgensen, *Chem. Rev.* **1989**, *89*, 431–458; b) W. A. Herrmann, R. W. Fischer, M. U. Rauch, W. Scherer, *J. Mol. Catal.* **1994**, *86*, 243–266.
[7] W. A. Herrmann, R. W. Fischer, M. U. Rauch, W. Scherer, *Angew. Chem.* **1993**, *105*, 1209–1212; *Angew. Chem. Int. Ed. Engl.* **1993**, *32*, 1157–1160.
[8] W. A. Herrmann, R. W. Fischer, J. D. G. Correia, *J. Mol. Catal.*, in press.
[9] W. A. Herrmann, F. D. G. Correia, unpublished.

Enediyne Quinone Imines: Truncated, Biologically Active Dynemicin Congeners**

Matthew D. Shair, Taeyoung Yoon, Ting-Chao Chou, and Samuel J. Danishefsky*

The novel enediyne antibiotic dynemicin A (**1**)[1] has stimulated a range of interesting research including DNA cleavage studies,[2] the design of new prodrug constructs,[3a, b, c] and the development of novel methodology directed at total synthesis.[3a, 4] The prevailing assumption[5a, b] concerning the ignition mechanism for the drug to operate as a diyl presupposes reduction of the quinone ring to the hydroquinone. In this way, the lone pair on nitrogen is unleashed to participate in mediating solvent attack on the epoxide (Scheme 1). The opening of this epoxide



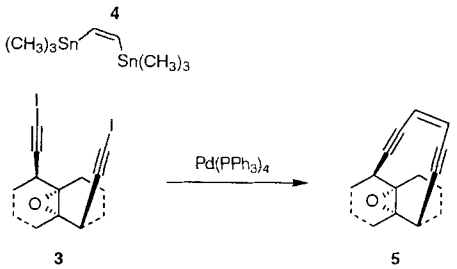
Scheme 1. Mode of action of dynemicin A. a) Reduction, b) Bergman cyclization, c) DNA cleavage through H atom abstraction. Nuc = nucleophile.

[*] Prof. S. J. Danishefsky,[+] M. D. Shair,[+] T. Yoon, T.-C. Chou
Sloan-Kettering Institute for Cancer Research
Laboratory for Bioorganic Chemistry
1275 York Avenue, Box 106, New York, NY 10021 (USA)
Telefax: Int. code + (212)772-8691
[+] Second address: Department of Chemistry, Havemeyer Hall
Columbia University, New York, NY 10027 (USA)

[**] This work was supported by the National Institutes of Health (Grant CA 28824). A predoctoral fellowship from Memorial Sloan-Kettering Cancer Center to M.D.S. is gratefully acknowledged. We thank Professor A. G. Myers for an advanced copy of his manuscript in which related developments are described.

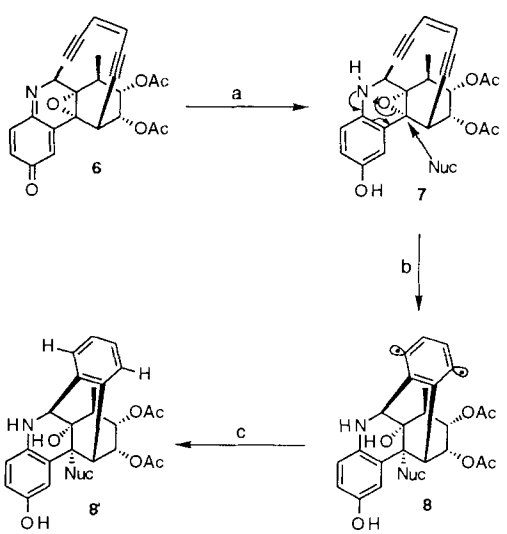
is seen to be a critical prophase in fostering the Bergman (enediyne → 1,4-diyl) transformation.[6] The cytotoxicity of the drug is perceived to arise from the DNA cutting tendency of diyl **2** or its quinone counterpart.[2] The dihydroxynaphthaquinone sector is seen to provide noncovalent contacts for intercalating and directing the drug to its oligonucleotide target.[5b, 7a, b, c]

Recently, we described the synthesis of intermediates generalized as **5** (Scheme 2) by cross coupling of diiodoalkynes of type **3**



Scheme 2. General approach to the palladium-mediated formation of enediynes.

to *cis*-distannylethylenes such as **4** mediated by tetrakis(triphenylphosphane)palladium(0)[8, 9]. Given this capability, we directed our attention to the synthesis of quinone imines such as **6** (Scheme 3). The hope was that such structures might suffer

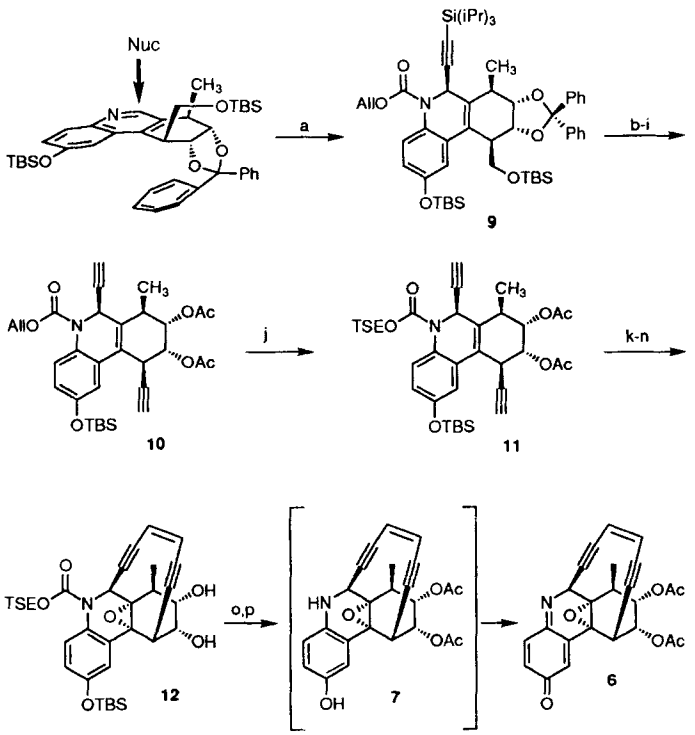


Scheme 3. Proposed mode of action of quinone imine **6**. a) Reduction, b) Bergman cyclization, c) DNA cleavage through H atom abstraction.

reductive activation like dynemicin to set off the cascade **6** → **7** → **8**. It was further perceived that **6** would be accessed by oxidation of a transient hydroisoquinoline precursor such as **7**. Since a system such as **7** is likely to be vulnerable to epoxide opening (and thence to subsequent 1,4-diyl formation), it must be generated under mild conditions from a readily deprotectable carbamate precursor. Given the favorable experiences of our laboratory with unveiling of amines in unstable molecules via (trimethylsilyl)ethoxycarbonyl (TEOC) carbamates,[10a, b] we turned to this protecting group.

We would be unable to carry the TEOC group from the start of the synthesis since it would be necessary to desilylate at several stages along the way while the urethane would remain intact. Accordingly, we prepared the allyl carbamate **9**[8, 11]

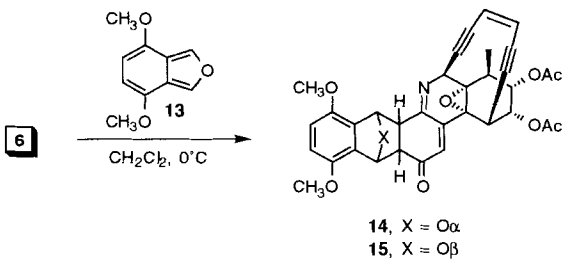
(Scheme 4). Following our recently developed protocol,[8, 9] compound **9** was converted to **10**. Given the eventual need for the palladium-mediated cross coupling reaction, the allyl carbamate was cleaved at the stage of **10** and a TEOC group installed as shown in **11**.[12] Diyne **11** was converted to **12**, and after acylation, the two silyl protecting groups were removed with tetra-*n*-butylammonium fluoride. Rapid oxidation of the resultant fleeting intermediate **7** with $PhI(OAc)_2$ furnished quinone imine **6**. *The conversion of 7 to 6 is to our knowledge, the first example of this type of oxidation of such an epoxy enediyne system, in which the nitrogen is not conjugated to a carbonyl group.*



Scheme 4. Synthesis of 6: a) (TIPS)C≡CMgBr, $ClCO_2All$, THF, −20 °C (75%); b) conc HCl (1 equiv), THF (90%); c) $(COCl)_2$, DMSO, Et_3N, −78 °C (95%); d) Ph_3P, CBr_4, CH_2Cl_2 (90%); e) *n*BuLi, toluene, −78 °C (81%); f) TBAF, THF; g) conc HCl, MeOH; h) NaH, TBSCl; i) Ac_2O, Py, DMAP, CH_2Cl_2 (60% over four steps); j) $Pd(PPh_3)_4$, morpholine, THF, then NaH, TEOCCl (90%); k) NH_2NH_2, THF/MeOH (100%); l) *m*CPBA, CH_2Cl_2 (80%); m) $AgNO_3$, NIS, THF (93%); n) $Pd(PPh_3)_4$, DMF, 70 °C (80%); o) Ac_2O, Py, DMAP, CH_2Cl_2 (96%); p) TBAF, THF, 0 °C, 3 h, then $PhI(OAc)_2$ (60%). TIPS = triisopropylsilyl, All = allyl, DMSO = dimethyl sulfoxide, TBAF = tetra-*n*-butylammonium fluoride, TBS = *tert*-butyldimethylsilyl, DMAP = 4-dimethylaminopyridine, TSE = (trimethylsilyl)ethyl, TEOC = (trimethylsilyl)ethoxycarbonyl, *m*CPBA = *meta*-chloroperbenzoic acid, NIS = *N*-iodosuccinimide, DMF = dimethylformamide.

With a view toward synthesizing dynemicin, or analogues thereof, we have examined the dienophilicity of the quinone imine linkage, in the presence of the bridging enediyne linkage (Scheme 5). The concept was tested with quinone imine **6** and isobenzofuran **13**.[13] In the event, cycloaddition occurred at 0 °C in methylene chloride to furnish an 86% yield of two products formulated as **18** and **19** in a ratio of 2.5:1.[14] Application of cycloadditions to quinone imines to reach dynemicin systems are currently in progress.

While total synthesis remains a major focus in our research directed at these enediyne quinone imines, we have begun to evaluate the biological effects of the transformation **6** → **7** → **8** (Scheme 3). Some promising findings have been obtained.



Scheme 5. Cycloaddition of quinone imine **6** with isobenzofuran **13**.

Compound **6** manifests broad cytotoxicity against a variety of tumor cell lines with an IC_{50} of roughly 5×10^{-4} μM (Table 1). Its potency is considerably greater than that of the widely used drug mitomycin C. For instance, with human promyolytic leukemia cell lines the potency of **6** relative to that of mitomycin C as measured by relative IC_{50} values is approximately 83:1. In acute lymphoblastic T cells (CCRF-CEM), the ratio is about 280:1. In corresponding comparisons with methanesulfonyl-4-(9-acridinylamino)-*m*-anisidide (*m*AMSA)[15] with the same lines, **6** is 70 and 400 times as potent, respectively.

Table 1. Comparison of the cytotoxicity of **6** with that of mitomycin C and *m*AMSA for human promylocytic leukemia cells **A** and human acute lymphoblastic T cells (CCRF-CEM) **B**.

Compound	IC_{50} [μM] for **A**	IC_{50} [μM] for **B**
6	0.00058	0.0005
mitomycin C	0.0484	0.140
*m*AMSA	0.0388	0.199

The properties of compound **6** as a DNA damaging agent have been examined using pBR322 DNA (Fig. 1). Reductive activation with NADPH and dithiothreitol (DTT) were compared, and the former method was found to be more effective. In the nicking assay as well, compound **6** outperformed mitomycin C. Curiously enough, at higher concentrations (500 μM) and under activation by NADPH compound **6** leads to signifi-

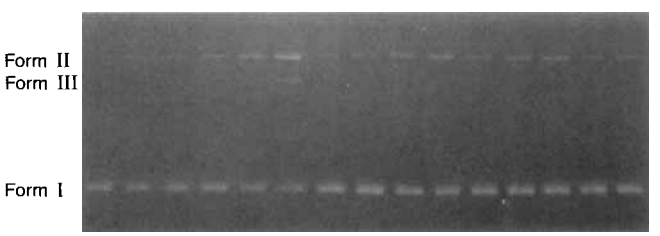


Fig. 1. Cleavage of pBR322 DNa. DNA was incubated in tris(hydroxymethyl)aminomethane (Tris)/HCl buffer (pH 7.5) for 60 min at 37 °C in the presence and absence of NADPH or dithiothreitol (DTT). The reaction mixtures were analyzed by electrophoresis (1% agarose gel, ethidium bromide stain). Track 1: DNA alone; track 2: DNA + NADPH; track 3: DNA + quinone imine **6** (5 μM); track 4: DNA + NADPH + quinone imine **6** (5 μM); track 5: DNA + NADPH + quinone imine **6** (100 μM); track 6: DNA + NADPH + quinone imine **6** (500 μM); track 7: DNA + DTT; track 8: DNA + DTT + quinone imine **6** (5 μM); track 9: DNA + DTT + quinone imine **6** (100 μM); track 10: DNA + DTT + quinone imine **6** (500 μM); track 11: DNA + mitomycin C (5 μM); track 12: DNA + NADPH + mitomycin C (5 μM); track 13: DNA + NADPH + mitomycin C (500 μM); track 14: DNA + DTT + mitomycin C (5 μM); track 15: DNA + DTT + mitomycin C (100 μM).

cant amounts of nonhelical DNA. Given the lack of an apparent intercalating arm, the double-stranded cleavage is noteworthy.

In addition to the in vitro study, a preliminary examination of **6** in various mouse models has been conducted. Compound **6** (0.1–0.5 mg kg^{-1}, i.p. (QD × 5) reduced tumor volume by 42–63% in mice bearing B-16 melanoma or sarcoma 180.[16] In each case where a comparison was drawn, compound **6** outperformed mitomycin C in reduction of tumor mass. That the antitumor properties of **6** arise from diyl intermediate **8** is assumed, but certainly not proven, particularly in the in vivo experiment.

Future studies involving this novel class of enediyne quinone imines will be directed with a view toward their application in the total synthesis of dynemicin A (and congeners thereof) as well as their amenability toward possible development as drugs.

Received: August 19, 1994
Revised version: October 10, 1994 [Z 7252 IE]
German version: *Angew. Chem.* **1994**, *106*, 2578

[1] M. Konishi, H. Ohkuma, K. Matsumoto, T. Tsuno, H. Kamei, T. Miyaki, T. Oki, H. Kawaguchi, G. D. VanDuyne, J. Clardy, *J. Antibiot.* **1989**, *42*, 1449; M. Konishi, H. Ohkuma, T. Tsuno, T. Oki, G. D. VanDuyne, J. Clardy, *J. Am. Chem. Soc.* **1990**, *112*, 3715.

[2] Y. Sugiura, T. Shiraki, M. Konishi, T. Oki, *Proc. Natl. Acad. Sci. USA* **1990**, *87*, 3831.

[3] a) For an excellent review of the chemistry and biology associated with the enediyne antibiotics, see: K. C. Nicolaou, W.-M. Dai, *Angew. Chem.* **1991**, *103*, 1453; *Angew. Chem. Int. Ed. Engl.* **1991**, *30*, 1387; b) K. C. Nicolaou, W.-M. Dai, S.-C. Tsay, V. A. Estevez, W. Wrasildo, *Science* **1992**, *256*, 1387; c) P. A. Wender, C. K. Zercher, S. Beckham, E.-M. Haubold, *J. Org. Chem.* **1993**, *58*, 5867.

[4] J. Taunton, J. L. Wood, S. L. Schreiber, *J. Am. Chem. Soc.* **1993**, *115*, 10378, and references therein.

[5] a) M. F. Semmelhack, J. Gallagher, D. Cohen, *Tetrahedron Lett.* **1990**, *31*, 1521; b) Y. Sugiura, T. Shiraki, M. Konishi, T. Oki, *Proc. Natl. Acad. Sci. USA* **1990**, *87*, 3831.

[6] R. R. Jones, R. G. Bergman, *J. Am. Chem. Soc.* **1972**, *94*, 660; R. G. Bergman, *Acc. Chem. Res.* **1973**, *6*, 25.

[7] For a discussion of the intercalating properties of adriamycin, see: a) F. Arcamone in *Doxorubicin Anticancer Antibiotics*, Academic, New York, **1981**; b) S. Neidle, L. H. Pearl, J. V. Skelly, *Biochem. J.* **1987**, *243*, 1–13; c) A. Wang, G. Ughetto, G. Quigley, A. Rich, *Biochemistry* **1987**, *26*, 1152.

[8] T. Yoon, M. D. Shair, S. J. Danishefsky, G. K. Schulte, *J. Org. Chem.* **1994**, *59*, 3752.

[9] M. D. Shair, T. Yoon, S. J. Danishefsky, *J. Org. Chem.* **1994**, *59*, 3755.

[10] a) S. A. Hitchcock, S. H. Boyer, M. Y. Chu-Moyer, S. H. Olson, S. J. Danishefsky, *Angew. Chem.* **1994**, *106*, 928; *Angew. Chem. Int. Ed. Engl.* **1994**, *33*, 858; b) G. Kim, M. Y. Chu-Moyer, S. J. Danishefsky, *J. Am. Chem. Soc.* **1990**, *112*, 2003.

[11] T. Yoon, Dissertation, Yale University, **1994**.

[12] H. Kunz, C. Unverzagt, *Angew. Chem.* **1984**, *96*, 426; *Angew. Chem. Int. Ed. Engl.* **1984**, *23*, 436.

[13] Isobenzofuran **17** was generated in situ as required: a) R. N. Warrener, *J. Org. Chem.* **1971**, *93*, 2346; G. M. Priestly, R. N. Warrener, *Tetrahedron Lett.* **1972**, 4295.

[14] The 2.5:1 ratio of products obtained in this cycloaddition is believed to arise from *endo*/*exo* selection rather than facial selectivity. While it seems reasonable that cycloaddition occurs on the face opposite to the enediyne, this is unproven.

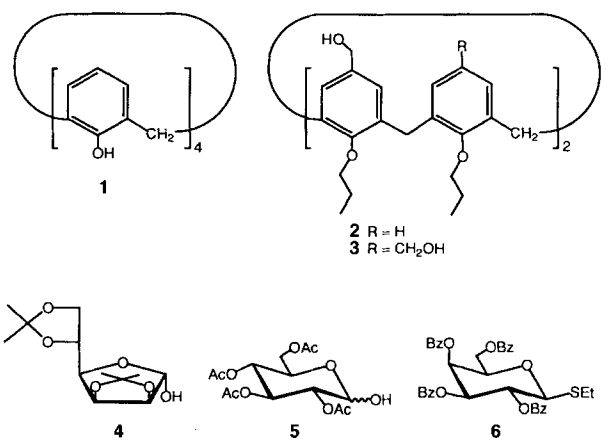
[15] *m*AMSA is a known DNA topoisomerase II inhibitor: N. Osheroff, A. H. Corbett, M. J. Robinson, *Biochemistry* **1993**, *32*, 3638.

[16] The tumor (2×10^6 cells) was innoculated subcutaneously. Treatment began on day 4; three mice were used for the control and for each dose. The tumor size was evaluated seven days after initiation of treatment.

Sugar Calixarenes: Preparation of Calix[4]arenes Substituted at the Lower and Upper Rims with *O*-Glycosyl Groups**

Alberto Marra, Marie-Christine Scherrmann, Alessandro Dondoni,* Alessandro Casnati, Patrizia Minari, and Rocco Ungaro*

Peptide–carbohydrate and carbohydrate–carbohydrate interactions play an important role in biological processes.[1] In order to better understand these interactions and to develop biologically active compounds based on molecular recognition,[2] various synthetic receptors for the specific recognition of peptides[3] and carbohydrates[4, 5, 6] have been synthesized. For example, resorc[4]arenes,[4] cholaphanes,[5] and glycophanes[6] have been used for carbohydrate recognition. Calixarenes[7] represent a class of macrocyclic compounds whose sizes and shapes have been exploited mainly for the recognition of metal ions and apolar organic molecules.[8] Water-soluble nonionic calixarenes[9] are interesting because of their potential use as enzyme mimics and molecular receptors in aqueous solution of highly polar organic molecules, such as amino acids and carbohydrates. In this paper we describe the preparation and complete characterization of well defined sugar calixarenes, which were obtained in good yields by mono- and poly-O-glycosylation of **1** at the phenolic groups (lower rim) and of **2** and **3** at the hydroxymethylene groups (upper rim). Although only the tetrasugar derivative **13** proved to be water-soluble, all these O-glycoside compounds are of interest because they are the first calixarene derivatives bearing chiral polyhydroxylated residues.

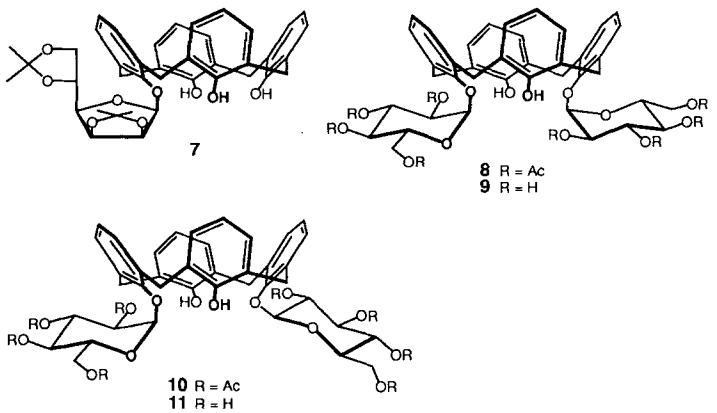


We first addressed the issue of glycosylating the lower rim by Mitsunobu reaction at the phenolic groups.[10, 11] Thus, treatment of calix[4]arene **1** with 1.1 equiv of α-D-mannofuranose diacetonide **4**[12] under standard Mitsunobu conditions (1.5 equiv of diethyl azodicarboxylate (DEAD) and PPh_3,

[*] Prof. A. Dondoni, Dr. A. Marra, Dr. M.-C. Scherrmann
Dipartimento di Chimica, Università di Ferrara
Via L. Borsari 46, I-44100 Ferrara (Italy)
Telefax: Int. code + (532)240709
Prof. R. Ungaro, Dr. A. Casnati, Dr. P. Minari
Dipartimento di Chimica Organica e Industriale, Università di Parma
Viale delle Scienze, I-43100 Parma (Italy)
Telefax: Int. code + (521)905472

[**] We thank Dr. M. Hamdan, Glaxo Research Center, Verona (Italy), for mass spectral determinations.

toluene, 70 °C, 30 min) afforded the monoglycosylated adduct **7** in 71% yield (isolation by flash chromatography on silica gel). The use of 4.4 equiv of **4** and more forcing conditions (refluxing toluene, 3 h) produced a complex mixture of compounds in which mono- and bisglycosides were not present. Indicative of the β-glycosyl linkage[13] in compound **7** was the $J_{1,2}$ value of 3.0 Hz in its ^{1}H NMR spectrum ([D$_6$]DMSO, Table 1). The cone conformation of the macrocycle was assigned on the basis of the chemical shifts and the multiplicity pattern of the proton signals,[7, 14] along with the chemical shifts of the carbon atoms[15] of the methylene bridges. The complete deprotection of the sugar calixarene **7** could not be achieved, since only monodeacetonization (4:1 AcOH:H_2O, room temperature, 6 h; pyridinium *p*-toluenesulfonate (PPTS), MeOH, 90 °C, 1 h) or substantial decomposition (4:1 AcOH:H_2O, 100 °C, 30 min) took place.



The Mitsunobu glycosylation of **1** with 2.2 equiv of tetraacetyl-α,β-D-glucopyranose (**5**)[16] in toluene at room temperature for 1 h afforded, after flash chromatography (4:1 diethyl ether:cyclohexane), an approximately 1:1 mixture of α,α-bisglucoside **8** and α,β-bisglucoside **10** together with several by-products in 50% overall yield.[17] Separation by HPLC (silica gel, 6 μm, 60 Å; 72:28 cyclohexane:ethyl acetate; detection at 280 nm) and crystallization from diethyl ether gave the individual bisadducts in pure form (15% each). The ^{1}H and ^{13}C NMR spectra of these compounds (Table 1) clearly indicated the configuration of the anomeric carbons and the cone conformation[7] of the macrocycle. Moreover, the diametrical 1,3-functionalization in **8** was demonstrated by the presence of only two kinds of diastereotopic carbons for the four ArCH$_2$Ar methylenes in its ^{13}C NMR spectrum.[18] The same assignment of the substitution pattern could not be deduced for **10**, since an

Table 1. Physical data for **2**, **3** and **7**–**13** [a].

2: M.p. 199–200 °C (from hexane); ^{1}H NMR ($CDCl_3$): δ = 6.92 (d, 4H, J = 7.4 Hz; Ar), 6.78 (t, 2H, J = 7.4 Hz; Ar), 6.37 (s, 4H; Ar), 4.45, 3.14 (2 d, 8H, J = 13.2 Hz; 4 ArCH_2Ar), 4.16 (s, 4H; 2 CH_2OH), 3.97, 3.73 (2 t, 8H, J = 7.9 Hz; 4 $CH_3CH_2CH_2$), 2.00–1.86 (m, 8H; 4 $CH_3CH_2CH_2$), 1.05, 0.93 (2 t, 12H, J = 7.4 Hz; 4 $CH_3CH_2CH_2$); CI-MS (CH_4): m/z: 652.6 [M^+]

3: M.p. 271–272 °C (from CH_3OH); ^{1}H NMR ($CDCl_3$): δ = 6.69 (s, 8H; Ar), 4.42, 3.15 (2 d, 8H, J = 13.0 Hz; 4 ArCH_2Ar), 4.34 (s, 8H; 4 CH_2OH), 3.84 (t, 8H, J = 7.5 Hz; 4 $CH_3CH_2CH_2$), 1.94 (ψ-sext, 8H, J = 7.5 Hz; 4 $CH_3CH_2CH_2$), 0.99 (t, 12H, J = 7.5 Hz; 4 $CH_3CH_2CH_2$); CI-MS (CH_4): m/z: 712.6 [M^+]

7: $[\alpha]_D^{20}$ = −43 (c = 1, $CHCl_3$); ^{1}H NMR ($CDCl_3$): δ = 9.91, 9.42, 8.65 (3 s, 3H; 3 OH), 7.20 (dd, 1H, J = 1.6, 7.5 Hz; Ar), 7.08–6.91 (m, 8H; Ar), 6.68, 6.67, 6.61 (3 t, 3H, J = 7.5 Hz; Ar), 5.38–5.33 (m, 2H; H-1, H-2), 4.90–4.85 (m, 1H; H-3), 4.65 (d, 1H, J = 13.8 Hz; H$_{ax}$ of ArCH$_2$Ar), 4.56 (d, 1H, J = 13.0 Hz; H$_{ax}$ of ArCH$_2$Ar), 4.55 (dt, 1H, $J_{4,5}$ = 6.3, $J_{5,6}$ = 5.8 Hz; H-5), 4.34 (d, 1H, J = 13.4 Hz; H$_{ax}$ of ArCH$_2$Ar), 4.23 (d, 1H, J = 13.7 Hz; H$_{ax}$ of ArCH$_2$Ar), 4.14 (d, 2H; 2H-6), 3.68 (dd, 1H, $J_{3,4}$ = 3.8 Hz; H-4), 3.47, 3.46, 3.43, 3.39 (4 d, 4H; H$_{eq}$ of ArCH$_2$Ar), 1.84, 1.57, 1.43, 1.39 (4 s, 12H; 4 CH_3); ^{1}H NMR ([D$_6$]DMSO, selected data): δ = 5.50 (d, 1H, $J_{1,2}$ = 3.0 Hz; H-1), 5.26 (dd, 1H; $J_{2,3}$ = 5.6 Hz; H-2); ^{13}C NMR ($CDCl_3$): δ = 151.1, 150.8, 150.3, 149.4, 134.9, 134.7, 130.0–126.7, 121.5, 121.4, 120.9 (Ar), 113.4, 109.1 (2 O-C-O acetonide), 106.4 (C-1), 79.1 (C-2), 78.5 (C-3), 76.9 (C-4), 73.2 (C-5), 66.4 (C-6), 32.0, 31.8 (2 C), 30.9 (4 ArCH$_2$Ar), 26.7, 25.3 (2 C), 24.2 (4 CH_3); FAB-MS: m/z: 667 [M^+ + H]

8: M.p. 223 °C (from Et_2O); $[\alpha]_D^{20}$ = +95 (c = 0.9, $CHCl_3$); ^{1}H NMR ($CDCl_3$): δ = 7.16–7.09 (m, 4H; Ar), 6.79 (t, 2H, J = 7.5 Hz; Ar), 6.70–6.63 (m, 4H; Ar), 6.59 (t, 2H, J = 7.5 Hz; Ar), 5.85 (dd, 2H, $J_{2,3}$ = 10.3, $J_{3,4}$ = 9.5 Hz; 2H-3), 5.49 (d, 2H, $J_{1,2}$ = 3.7 Hz; 2H-1), 5.40 (s, 2H; 2 OH), 5.26 (dd, 2H, $J_{4,5}$ = 10.4 Hz; 2H-4), 5.20 (dd, 2H; 2H-2), 4.70 (ddd, 2H, $J_{5,6a}$ = 4.8, $J_{5,6b}$ = 2.0 Hz; 2H-5), 4.54 (d, 4H, J = 14.0 Hz, 4H$_{ax}$ of ArCH$_2$Ar), 4.49 (dd, 2H, $J_{6a,6b}$ = 12.4 Hz; 2H-6a), 4.14 (dd, 2H; 2H-6b), 3.40 (d, 4H; H$_{eq}$ of ArCH$_2$Ar), 2.08, 2.04, 2.02, 1.88 (4 s, 24H; 8 CH_3); ^{13}C NMR ($CDCl_3$): δ = 170.9 (2 C), 170.1 (4 C), 169.9 (2 C) (8 CH_3CO), 152.7, 151.9, 131.6–119.7 (Ar), 100.6 (2 C-1), 71.3 (2 C-2), 70.1 (2 C-3), 69.9 (2 C-5), 67.0 (2 C-4), 61.7 (2 C-6), 31.3 (2 ArCH$_2$Ar), 30.8 (2 ArCH$_2$Ar), 20.5–20.2 (8 CH_3CO); FAB-MS: m/z: 1086 [M^+ + H]

9: M.p. 194–197 °C (from MeOH/AcOEt); $[\alpha]_D^{20}$ = +143 (c = 0.8, CH_3OH); ^{1}H NMR (CD_3OD): δ = 7.15–7.09, 7.01–6.96 (2 m, 8H; Ar), 6.76, 6.68 (2 t, 4H, J = 7.5 Hz, Ar), 5.46 (d, 2H, $J_{1,2}$ = 3.9 Hz; 2H-1), 5.05, 3.41 (2 d, 4H, J = 13.5 Hz; 2 ArCH$_2$Ar), 4.72, 3.40 (2 d, 4H, J = 13.0 Hz; 2 ArCH$_2$Ar), 4.53 (ddd, 2H, $J_{4,5}$ = 9.9, $J_{5,6a}$ = $J_{5,6b}$ = 3.3 Hz; 2H-5) 4.29 (dd, 2H, $J_{2,3}$ = 9.9, $J_{3,4}$ = 9.5 Hz; 2H-3), 3.94–3.87 (m, 4H; 4H-6), 3.84 (dd, 2H; 2H-2), 3.62 (dd, 2H; 2H-4)

10: M.p. 242–244 °C (from Et_2O); $[\alpha]_D^{20}$ = +29 (c = 0.9, $CHCl_3$); ^{1}H NMR ($CDCl_3$): δ = 7.17–7.04, 6.82–6.50 (2 m, 12H; Ar), 5.88 (dd, 1H, $J_{2,3}$ = 10.5, $J_{3,4}$ = 9.5 Hz; H-3α), 5.70, 5.28 (2 s, 2H; 2 OH), 5.55 (dd, 1H, $J_{1,2}$ = 8.2, $J_{2,3}$ = 9.4 Hz; H-2β), 5.42 (d, 1H, $J_{1,2}$ = 3.5 Hz; H-1α), 5.34 (dd, 1H, $J_{3,4}$ = 9.5 Hz; H-3β), 5.30 (dd, 1H, $J_{4,5}$ = 10.6 Hz; H-4α), 5.26 (dd, 1H, $J_{4,5}$ = 9.8 Hz; H-4β), 5.14 (dd, 1H; H-2α), 5.07 (ddd, 1H, $J_{5,6a}$ = 3.8, $J_{5,6b}$ = 1.6 Hz; H-5α), 4.87 (d, 1H; H-1β), 4.70–4.61 (m, 3H; H-6aα, 2 H$_{ax}$ of ArCH$_2$Ar), 4.49 (d, 1H, J = 14.5 Hz; H$_{ax}$ of ArCH$_2$Ar), 4.40 (d, 1H, J = 13.2 Hz; H$_{ax}$ of ArCH$_2$Ar), 4.33 (dd, 1H, $J_{6a,6b}$ = 12.6 Hz; H-6bα), 4.25 (dd, 1H, $J_{5,6a}$ = 4.4, $J_{6a,6b}$ = 12.4 Hz; H-6aβ), 4.11 (dd, 1H, $J_{5,6b}$ = 2.5 Hz; H-6bβ), 3.60 (ddd, 1H; H-5β), 3.39–3.28 (m, 4H; 4 H$_{eq}$ of ArCH$_2$Ar), 2.14, 2.04, 1.86 (3 s, 24H; 8 CH_3); ^{13}C NMR ($CDCl_3$): δ = 171.1, 170.7, 170.4, 170.2, 169.8, 169.7, 169.5, 169.3 (8 CH_3CO), 153.0, 152.9, 152.6, 149.1, 134.4–119.2 (Ar), 103.4 (C-1β), 101.0 (C-1α), 72.6 (C-3β), 72.0 (C-5β), 71.9 (C-2α), 70.6 (C-2β), 70.1 (C-3α), 69.4 (C-5α), 68.4 (C-4β), 68.0 (C-4α), 62.0 (C-6α), 61.3 (C-6β), 31.6, 31.3, 31.0, 30.3 (4 ArCH$_2$Ar), 20.6–20.1 (8 CH_3CO); FAB-MS: m/z: 1086 [M^+ + H]

11: M.p. 210–212 °C (from MeOH/AcOEt); $[\alpha]_D^{20}$ = +29 (c = 0.8, CH_3OH); ^{1}H NMR (CD_3OD): δ = 7.18–7.00 (m, 8H; Ar), 6.86, 6.79, 6.69, 6.66 (4 t, 4H, J = 7.5 Hz; Ar), 5.37 (d, 1H, $J_{1,2}$ = 3.8 Hz; H-1α), 5.17 (d, 1H, J = 13.8 Hz; H$_{ax}$ of ArCH$_2$Ar), 4.96 (d, 1H, $J_{1,2}$ = 7.8 Hz; H-1β), 4.74 (d, 2H, J = 13.2 Hz; 2 H$_{ax}$ of ArCH$_2$Ar), 4.66 (d, 1H, J = 13.4 Hz; H$_{ax}$ of ArCH$_2$Ar), 4.64 (ddd, 1H, $J_{4,5}$ = 9.9, $J_{5,6a}$ = $J_{5,6b}$ = 3.2 Hz; H-5α), 4.24 (dd, 1H, $J_{2,3}$ = 10.0, $J_{3,4}$ = 9.2 Hz; H-3α), 3.96 (dd, 1H, $J_{2,3}$ = 9.2 Hz; H-2β), 3.92 (d, 2H; 2H-6α), 3.89 (dd, 1H, $J_{5,6a}$ = 2.3, $J_{6a,6b}$ = 11.9 Hz; H-6aβ), 3.82 (dd, 1H; H-2α), 3.78 (dd, 1H, $J_{5,6b}$ = 5.2 Hz; H-6bβ), 3.67 (dd, 1H; H-4α), 3.66 (dd, 1H, $J_{3,4}$ = 9.0 Hz; H-3β), 3.60 (dd, 1H, $J_{4,5}$ = 9.3 Hz; H-4β), 3.50–3.36 (m, 4H; 4 H$_{eq}$ of ArCH$_2$Ar), 3.33 (ddd, 1H; H-5β)

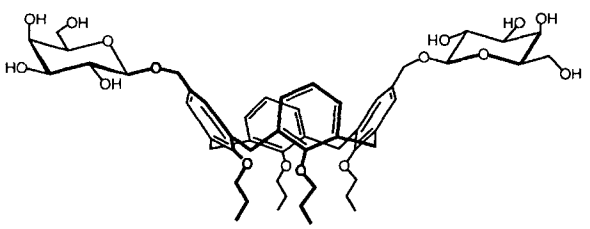
12: M.p. 227–228 °C (from CH_3OH/H_2O); $[\alpha]_D^{20}$ = −25 (c = 0.9, CH_3OH); ^{1}H NMR (CD_3OD): δ = 6.65 (s, 4H; Ar), 6.27–6.16 (m, 6H; Ar), 4.48, 4.20 (2 d, 4H, J = 11.0 Hz; 2 ArCH_2O), 4.24, 2.93 (2 d, 8H, J = 13.3 Hz; 4 ArCH_2Ar), 4.06 (d, 2H, $J_{1,2}$ = 7.7 Hz; 2H-1), 3.71, 3.57 (2 t, 8H, J = 7.5 Hz; 4 $CH_3CH_2CH_2$), 3.62 (dd, 2H, $J_{3,4}$ = 3.3, $J_{4,5}$ = 0.8 Hz; 2H-4), 3.58 (dd, 2H, $J_{5,6a}$ = 4.6, $J_{6a,6b}$ = 11.3 Hz; 2H-6a), 3.53 (dd, 2H, $J_{5,6b}$ = 5.3 Hz; 2H-6b), 3.35 (dd, 2H, $J_{2,3}$ = 9.6 Hz, 2H-2), 3.29 (ddd, 2H; 2H-5), 3.24 (dd, 2H; 2H-3), 1.82–1.66 (m, 8H; 4 $CH_3CH_2CH_2$), 0.85, 0.78 (2 t, 12H, J = 7.4 Hz; 4 $CH_3CH_2CH_2$); ^{13}C NMR (CD_3OD): δ = 158.3, 157.5, 137.0, 136.9, 135.6, 132.2, 130.2, 129.4, 129.3, 123.2 (Ar), 103.7 (2 C-1), 78.0, 77.9 (4 $CH_3CH_2CH_2$), 76.8 (2 C-5), 75.1 (2 C-3), 72.6 (2 C-2), 72.0 (2 ArCH$_2$O), 70.4 (2 C-4), 62.6 (2 C-6), 31.9 (4 ArCH$_2$Ar), 24.5, 24.3 (4 $CH_3CH_2CH_2$), 11.0, 10.6 (4 $CH_3CH_2CH_2$); FAB-MS: m/z: 1000 [M^+ + K]

13: $[\alpha]_D^{20}$ = −33 (c = 0.4, CH_3OH); ^{1}H NMR (CD_3OD): δ = 6.50 (s, 8H; Ar), 4.35, 4.13 (2 d, 8H, J = 11.3 Hz; 4 ArCH_2O), 4.24, 2.94 (2 d, 8H, J = 11.3 Hz; 4 ArCH_2Ar), 4.01 (d, 4H, $J_{1,2}$ = 7.5 Hz; 4H-1), 3.64 (t, 8H, J = 7.4 Hz; 4 $CH_3CH_2CH_2$), 3.61 (dd, 4H, $J_{3,4}$ = 3.3, $J_{4,5}$ = 0.7 Hz; 4H-4), 3.59 (dd, 4H, $J_{5,6a}$ = 7.0, $J_{6a,6b}$ = 11.4 Hz; 4H-6a), 3.52 (dd, 4H, $J_{5,6b}$ = 5.3 Hz; 4H-6b), 3.34 (dd, 4H, $J_{2,3}$ = 9.7 Hz; 4H-2), 3.27 (ddd, 4H; 4H-5), 3.26 (dd, 4H; 4H-3), 1.80–1.68 (m, 8H; 4 $CH_3CH_2CH_2$), 0.82 (t, 12H, J = 7.5 Hz; 4 $CH_3CH_2CH_2$); ^{13}C NMR (CD_3OD): δ = 157.8, 136.2, 132.2, 130.2, 130.1 (Ar), 103.3 (4 C-1), 78.0 (4 $CH_3CH_2CH_2$), 76.8 (4 C-5), 75.0 (4 C-3), 72.5 (4 C-2), 71.7 (4 ArCH$_2$O), 70.4 (4 C-4), 62.6 (4 C-6), 31.9 (4 ArCH$_2$Ar), 24.4 (4 $CH_3CH_2CH_2$), 10.8 (4 $CH_3CH_2CH_2$); FAB-MS: m/z: 1384 [M^+ + K]

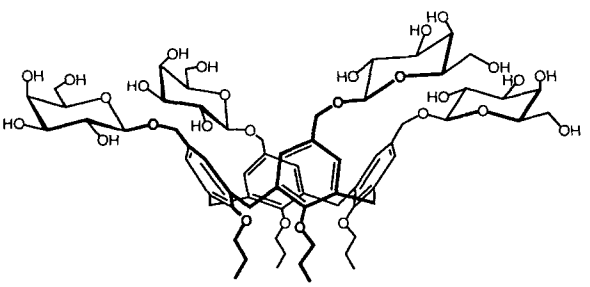
[a] ^{1}H and ^{13}C NMR spectra were recorded at 300 and 75 MHz, respectively.

α,β-bisglycoside should, in any case, show signals due to four different methylene bridges in its NMR spectra. The 1,3-disubstitution pattern of **10** was tentatively assigned by analogy with the isomer **8**.[19] Upon deacetylation with sodium methoxide in methanol, both **8** and **10** provided the corresponding unprotected calix[4]arene glucosides **9** and **11**; however, these compounds proved to be insoluble in water.

For O-glycosylation at the upper rim, we planned to use the symmetrical bishydroxymethylene-substituted calix[4]arene **2**[20] whose cone structure is blocked by four *O*-propyl groups at the lower rim. Moreover, aiming at a totally stereoselective glycosylation,[21] we chose to employ a sugar bearing a participating group at C-2 as glycosyl donor. The stable and readily available ethyl 1-thio-tetrabenzoyl-β-D-galactoside (**6**)[22] (2.4 equiv) was reacted[23] for 30 min at room temperature with the acceptor **2** in the presence of copper(II) triflate (2.4 equiv), acetonitrile, and 4 Å molecular sieves. After quenching with excess Et_3N and evaporation of the solvent, the reaction mixture was filtered through a short column of silica gel (1:1 cyclohexane:ethyl acetate). The solution was concentrated and the residue was treated with sodium methoxide in methanol to afford crude β-linked *O*-galactosyl calixarene **12**. This compound was isolated in pure form (65% yield from **2**) by chromatography on a column of Sephadex LH-20 (1:1 CH_2Cl_2:CH_3OH). In a similar way the calixarene **3**[24] bearing four hydroxymethylene groups, upon treatment with 6 equiv of donor **6**, was transformed into the β-linked derivative **13** in 60% isolated yield. Unlike the bisgalactoside **12**, the tetragalactoside **13** proved to be water-soluble up to 5 mM at room temperature.



12



13

In conclusion, we have described two approaches for the introduction of sugar moieties at either rim of calix[4]arenes. The resultant sugar calixarenes as well as other compounds obtained by these methodologies should provide an entry into molecular recognition of polar chiral substrates, especially carbohydrates, both in water and in organic media.

Received: June 30, 1994 [Z 7087 IE]
German version: *Angew. Chem.* **1994**, *106*, 2533

[1] R. U. Lemieux, *Chem. Soc. Rev.* **1989**, *18*, 347; F. A. Quiocho, *Pure Appl. Chem.* **1989**, *61*, 1293; N. Sharon, H. Lis, *Chem. Br.* **1990**, 679.
[2] *Design and Synthesis of Organic Molecules Based on Molecular Recognition* (Ed.: G. van Bist), Springer, Berlin, **1986**; *Host-Guest Molecular Interactions: from Chemistry to Biology* (*Ciba Found. Symp.* **1991**, *158*).
[3] S. S. Yoon, W. C. Still, *J. Am. Chem. Soc.* **1993**, *115*, 823, and references therein.
[4] Y. Aoyama, Y. Tanaka, S. Sugahara, *J. Am. Chem. Soc.* **1989**, *111*, 5397; F. Diederich in *Cyclophanes, Monographs in Supramolecular Chemistry, Vol. 2* (Ed.: J. F. Stoddart), Royal Society of Chemistry, Cambridge, **1991**.
[5] R.-P. Bonar-Law, A. P. Davis, B. A. Murray, *Angew. Chem.* **1990**, *102*, 1497; *Angew. Chem. Int. Ed. Engl.* **1990**, *29*, 1407.
[6] J. M. Coterón, C. Vicent, C. Bosso, S. Penadés, *J. Am. Chem. Soc.* **1993**, *115*, 10066.
[7] C. D. Gutsche in *Calixarenes, Monograph in Supramolecular Chemistry, Vol. 1* (Ed.: J. F. Stoddart), Royal Society of Chemistry, Cambridge, **1989**; *Calixarenes, a Versatile Class of Macrocyclic Compounds* (Eds.: J. Vicens, V. Böhmer), Kluwer, Dordrecht, **1991**.
[8] S. Shinkai, S. Mori, H. Koreishi, T. Tsubaki, O. Manabe, *J. Am. Chem. Soc.* **1986**, *108*, 2409; P. D. Beer, C. A. P. Dickson, N. Fletcher, A. J. Goulden, A. Grieve, J. Hodacova, T. Wear, *J. Chem. Soc. Chem. Commun.* **1993**, 828; L. Zhang, A. Macias, T. Lu, J. I. Gordon, G. W. Gokel, A. E. Kaifer, *ibid.* **1993**, 1017; R. Ungaro, A. Arduini, A. Casnati, O. Ori, A. Pochini, F. Ugozzoli, *Computational Approaches in Supramolecular Chemistry* (*NATO ASI Ser. Ser. C* **1994**, *371*, 277).
[9] Y. Shi, Z. Zhang, *J. Chem. Soc. Chem. Commun.* **1994**, 375.
[10] O. Mitsunobu, *Synthesis* **1981**, 1.
[11] O-Glycosylations of phenols by the Mitsunobu reaction have been reported: G. Grynkiewicz, *Carbohydr. Res.* **1977**, *53*, c11; A. Lubineau, E. Meyer, P. Place, *ibid.* **1992**, *228*, 191.
[12] O. T. Schmidt, *Methods Carbohydr. Chem.* **1963**, *2*, 318.
[13] This is in agreement with the well known inversion of configuration of secondary alcohols through the Mitsunobu reaction. See ref. [10].
[14] A. Casnati, A. Arduini, E. Ghidini, A. Pochini, R. Ungaro, *Tetrahedron* **1991**, *47*, 2221.
[15] C. Jaime, J. de Mendoza, P. Prados, P. M. Nieto, C. Sanchez, *J. Org. Chem.* **1991**, *56*, 3372.
[16] Compound **5** was prepared according to the method described by T. Itoh, H. Takamura, K. Watanabe, Y. Araki, Y. Ishido, *Carbohydr. Res.* **1986**, *156*, 241.
[17] Reaction with 1.1 equiv of **5** gave a 3:1 mixture of α- and β-monoglucosides (60%) and a mixture of α,α- and α,β-bisglucosides (20%). The separation of α- and β-monoadducts by HPLC was unsuccessful.
[18] The four axial protons of the methylene bridges of **8** are accidentally isochronous, whereas well separated signals were observed for the deacetylated derivative **9**.
[19] Neither **10** nor the deacetylated derivative **11** provided crystals suitable for crystallographic analysis.
[20] Compound **2** was prepared from **1** in 25% yield according to the method described by A. Arduini, A. Casnati, M. Fabbi, P. Minari, A. Pochini, A. R. Sicuri, R. Ungaro, *Supramol. Chem.* **1993**, 235.
[21] For reviews on glycosylation reactions see: H. Paulsen, *Angew. Chem.* **1982**, *94*, 184; *Angew. Chem. Int. Ed. Engl.* **1982**, *21*, 155; K. Toshima, K. Tatsuta, *Chem. Rev.* **1993**, *93*, 1503.
[22] Z. Pakulsky, D. Pierozynski, A. Zamojsky, *Tetrahedron* **1994**, *50*, 2975. We prepared **6** by quantitative perbenzoylation of ethyl 1-thio-β-D-galactopyranoside.
[23] For reviews on thioglycosides see P. Fügedi, P. J. Garegg, H. Löhn, T. Norberg, *Glycoconjugate J.* **1987**, *4*, 97; P. Sinaÿ, *Pure Appl. Chem.* **1991**, *63*, 519.
[24] Compound **3** was prepared from **1** by formylation (T. Komori, S. Shinkai, *Chem. Lett.* **1992**, 901) and subsequent reduction with $NaBH_4$ in EtOH in 90% overall yield.

 © VCH Verlagsgesellschaft mbH, D-69451 Weinheim, 1994 0570-0833/94/2323-2481 $ 10.00+.25/0

$[(CpNi)_2(Cp^*Al)_2]$: Cp*Al as a Bridging Two-Electron Ligand**

Carsten Dohmeier, Harald Krautscheid, and Hansgeorg Schnöckel*

Dedicated to Professor Gerhard Fritz on the occasion of his 75th birthday

Nearly 40 years ago Ziegler and Holzkamp reported the so-called "nickel effect".[1] They discovered that nickel compounds have a remarkable influence on the high pressure polymerization of ethylene in the presence of $[Et_3Al]$. These results initiated intense investigations of the Ziegler–Natta catalysts.

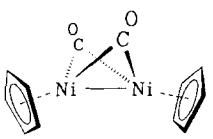
Compounds with direct bonds between the metal atoms of the catalyst components (Al–transition metal) have rarely been described.[2] To our knowledge, no molecular compounds containing the Ni–Al unit have yet been characterized by diffraction methods,[3] even though this type of compound has been discussed in connection with the "nickel effect".[4] Within the scope of our investigations concerning the reactivity of aluminium(I) compounds, we have found a simple route to molecules of this type.

With $[(Cp^*Al)_4]$ as a reducing agent, $[Cp_2Ni]$ can be transformed to the reddish brown complex **1**, which is only slightly

$[(CpNi)_2(Cp^*Al)_2]$ **1**

sensitive towards air and moisture. The diamagnetic nature of **1** is substantiated by sharp ^1H and ^{13}C NMR resonances observed in the range typical for diamagnetic compounds. The unexpectedly high thermal stability of **1** can be deduced from its mass spectrum where the molecular ion is also the base peak.

The spectroscopic results indicate a structure for **1** that can be derived from the well-known carbonyl complex **2**[5] by replacing the CO ligands by Cp*Al units. This proposal is confirmed by the X-ray structure analysis (Fig. 1).[6]



2

The four metal atoms form two three-membered Ni_2Al rings at a dihedral angle of 104.76(9)°. The "substitution" of two Cp*Al units in the tetrahedral compound **3**[7] for two CpNi fragments therefore caused the opening up of one edge of the tetrahedron. This

$[(Cp^*Al)_4]$ **3**

result was expected, since, compared to Cp*Al, every CpNi unit (isolobal with CH) contributes one more electron to the Ni_2Al_2 framework. This interpretation suggests that the Ni and Al atoms are connected by two-center two-electron bonds. Consequently the Al–Al interaction is noticable reduced: compared to that in **3**, the Al···Al distance in **1** (302.4(3) pm) is enlarged by approximately 26 pm, and the planes of the Cp* rings are nearly perpendicular to the Ni_2Al planes; this geometry differs from that of the tetrahedron.

The Ni–Al bonds in **1** (227.4(2)–228.3(2) pm) are about 16 pm shorter than in the intermetallic compound NiAl (CsCl type).[8] Surprisingly, the bond in the diatomic NiAl molecule in the gas phase is also slightly longer than that in **1**.[3] As expected, the Ni···Al distances determined for compounds with the structural unit $Ni(\mu H)Al$ are significantly longer (e.g., 273 pm in ref. [9]). A more detailed discussion of the Ni–Al bonding in **1** is not possible because there are as yet no additional experimental or theoretical data of comparable compounds available.

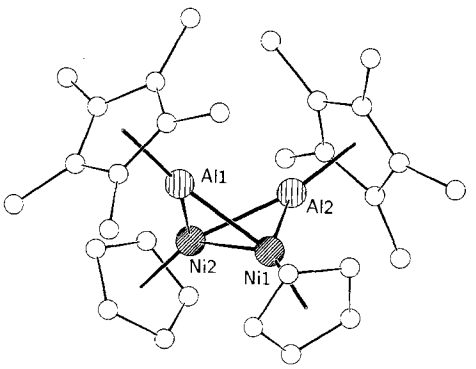


Fig. 1. Molecular structure of **1** (H atoms have been omitted for clarity). Selected bond lengths [pm] (d_{min}, d_{max}, $\bar{d}$) and angles [°]: Ni1–Ni2 248.6(2), Al1···Al2 302.4(3), Al–Ni 227.4(2), 228.3(2), 227.8, Al–C_{Cp} 224.1(7), 226.8(7), 225.3, Ni–C_{Cp} 208.2(8), 218.7(8), 213.1; Ni1–Al1–Ni2 66.04(7), Al2–Ni1–Al1 83.22(8), Al2–Ni2–Ni1 56.91(7), Ni1–Al1–Al2 48.35(7).

The Ni–Ni bond in **1** (248.6(2) pm) is relatively long compared to that in **2** (ca. 236 pm). Similarly, the average Ni–C_{Cp} distance of 213.1 pm is about 4 pm longer than that in **2**.[10] The most probable explanation for these results lies in the different polarities in the butterfly frameworks of **1** and **2**: based on the relative electronegativities, a polarity $Ni^{\delta+}-C^{\delta-}$ is expected for the Ni_2C_2 frame in **2** and $Ni^{\delta-}-Al^{\delta+}$ for Ni_2Al_2 in **1**. This interpretation is consistent with the observation that the average Al–C_{Cp} distances in **1** (225.3 pm) are significantly shorter than in **3** (233.4 pm). Similar short distances between Al and η^5-coordinated Cp* ligands were found for aluminum(III) compounds.[11] The ^{27}Al NMR resonance recorded for **1** ($\delta = +30$) confirms the polarity, since the Al nuclei in **1** are significantly deshielded compared to those in **3** ($\delta = -80$ ppm).

The straightforward synthesis of **1** demonstrates, once more, the high synthetic potential of **3**,[12] which reacts like an electron-rich, selective carbenoid.[13] Compound **1** and its derivatives might be important for the elucidation of the mechanistic details of the "nickel effect" and, furthermore, as single-source precursors for the deposition of bimetallic films by CVD.[14] The properties of **1** as well as the syntheses of other transition metal complexes of Cp*Al are the subject of our current investigations.

Experimental Procedure

1: A solution of 90 mg of $[Cp_2Ni]$ (0.477 mmol) in 3 mL of toluene was slowly added to 46 mg of **3** (0.071 mmol) suspended in 5 mL of toluene at 25 °C. The resulting green solution was heated at 50 °C for 50 h; the color gradually turned to reddish brown. Toluene and the excess of $[Cp_2Ni]$ were removed under vacuum (ca. 10^{-2} mbar) at 50 °C. The residue was suspended in a small amount of *n*-pentane. The resulting reddish brown solution was separated from a colorless compound by filtration [15]. The solution was cooled to 4 °C, and the product **1** was obtained as reddish brown crystals (ca. 40 mg, 72%). The ratio of consumed [Cp*Al] to $[Cp_2Ni]$ was 3:2.

The ESR spectrum of a solution of **1** in benzene exhibits no signal. NMR spectra (300 MHz, C_6D_6, 298 K, Bruker AMX 300): ^1H NMR: $\delta = 5.26$ (10H, Cp), 1.84 (30H, Cp*); ^{13}C NMR: $\delta = 115.3$ (Cp*), 84.4 (Cp), 11.3 (Cp*); ^{27}Al NMR: $\delta = +30$ ($\omega_{1/2} = 1800$ Hz); MS (EI, 70 eV, 155 °C): *m/z* (%): 570 (100) [M^+], 434 (23) [$M^+ - Cp^*H$], and further fragments of lower intensity.

[*] Prof. Dr. H. Schnöckel, Dr. C. Dohmeier, Dr. H. Krautscheid
Institut für Anorganische Chemie der Universität
Engesserstrasse Geb. 30.45, D-76128 Karlsruhe (FRG)
Telefax: Int. code + (721)608-4854

[**] This work was supported by the Deutsche Forschungsgemeinschaft and the Fonds der Chemischen Industrie.

Received: July 8, 1994 [Z 7112 IE]
German version: *Angew. Chem.* **1994**, *106*, 2570

[1] K. Ziegler, *Brennst.-Chem.* **1954**, *35*, 321; K. Ziegler, E. Holzkamp, H. Breil, H. Martin, *Angew. Chem.* **1955**, *67*, 541; K. Fischer, K. Jonas, P. Misbach, R. Stabba, G. Wilke, *ibid.* **1973**, *85*, 1002 and **1973**, *12*, 943.

[2] See, for example, S. K. Boocock, S. G. Shore in *Comprehensive Organometallic Chemistry, Vol. 6* (Eds.: G. Wilkinson, F. G. A. Stone, E. W. Abel), Pergamon, Oxford, **1982**, p. 947; M. J. Taylor, P. J. Brothers in *Chemistry of Aluminium, Gallium, Indium and Thallium* (Ed.: A. J. Downs), Chapman & Hall, London, **1993**, p. 226; R. A. Fischer, J. Behm, T. Priesmeier, W. Scherer, *Angew. Chem.* **1993**, *105*, 776; *Angew. Chem. Int. Ed. Engl.* **1993**, *32*, 746, and references therein.

[3] Recently the diatomic NiAl molecule was characterized by spectroscopic methods ($d = 232.1$ pm): J. M. Behm, C. A. Arrington, M. D. Morse, *J. Chem. Phys.* **1993**, *99*, 6409.

[4] Two main mechanistic models have been discussed: a) species with a multicenter bond Ni(μC)Al have been suggested as important intermediates (G. Wilke, *Angew. Chem.* **1988**, *100*, 189; *Angew. Chem. Int. Ed. Engl.* **1988**, *27*, 185; see also ref. [9]) and b) intermediates with direct Ni–Al bonds were though to be plausible (J. J. Eisch, S. R. Sexsmith, K. C. Fichter, *J. Organomet. Chem.* **1990**, *382*, 273).

[5] E. O. Fischer, C. Palm, *Chem. Ber.* **1958**, *91*, 1725; L. R. Byers, L. F. Dahl, *Inorg. Chem.* **1980**, *19*, 680.

[6] X-ray structure analysis: Stoe Stadi IV diffractometer, $Mo_{K\alpha}$ radiation, unit-cell dimensions (203 K): $a = 948.6(5)$, $b = 976.4(5)$, $c = 1717.3(9)$ pm, $\alpha = 85.22(3)$, $\beta = 76.73(3)$, $\gamma = 70.55(3)^\circ$, $V = 1459.7 \times 10^6$ pm^3, spacegroup $P\bar{1}$ (no. 2), $Z = 2$, $\mu(Mo_{K\alpha}) = 13.66$ cm^{-1}, $2\theta_{max} = 48.3^\circ$, 4657 measured reflections, 4338 symmetry-independent ($R_{int} = 0.032$), 245 parameters (Ni, Al, and C (without disorder) refined anisotropically, disorderd Cp ring at Ni1 and Cp* ring at Al2 refined as riged groups; H atoms were introduced at calculated positions). $R1 = 0.064$ ($I > 2\sigma(I)$), $wR2 = 0.20$ (all data). Further details of the crystal structure investigation may be obtained from the Fachinformationszentrum Karlsruhe, D-76344 Eggenstein-Leopoldshafen (FRG), on quoting the depository number CSD-5843.

[7] C. Dohmeier, C. Robl, M. Tacke, H. Schnöckel, *Angew. Chem.* **1991**, *103*, 594; *Angew. Chem. Int. Ed. Engl.* **1991**, *30*, 564.

[8] K. Becker, F. Ebert, *Z. Phys.* **1923**, *16*, 166; A. J. Bradley, A. Taylor, *Proc. R. Soc. London. Sect. A*, **1937**, *159*, 56.

[9] Compounds of this type can be regarded as model complexes for the mechanism discussed in ref. [4a]. See, for example, K. R. Pörschke, W. Kleinmann, Y.-H. Tsay, C. Krüger, G. Wilke, *Chem. Ber.* **1990**, *123*, 1267.

[10] There are Ni–C_{Cp} distances in the range 208.2(8)–218.7(8) pm; the shortest distances are to the C atoms closest to Al.

[11] See, for exmple, a) C. Dohmeier, H. Schnöckel, C. Robl, U. Schneider, R. Ahlrichs, *Angew. Chem.* **1994**, *106*, 225; *Angew. Chem. Int. Ed. Engl.* **1994**, *33*, 199; b) H.-J. Koch, S. Schulz, H. W. Roesky, M. Noltemeyer, H.-G. Schmidt, A. Heine, R. Herbst-Irmer, D. Stalke, G. M. Sheldrick, *Chem. Ber.* **1992**, *125*, 1107; c) S. Schulz, H. W. Roesky, H. J. Koch, G. M. Sheldrick, D. Stalke, A. Kuhn, *Angew. Chem.* **1993**, *105*, 1828; *Angew. Chem. Int. Ed. Engl.* **1993**, *32*, 1729.

[12] There are two different synthetic routes for the preparation of **3** [7, 11c]. Chemical and physical properties of the two products differ markedly. We will soon report on the reasons for these observations.

[13] For example, cycloadditions (H. Schnöckel, C. Dohmeier, unpublished), insertion into element–element bonds [11a, 11c], and oxidative additions (C. Dohmeier, H. Schnöckel, C. Robl, U. Schneider, R. Ahlrichs, *Angew. Chem.* **1993**, *105*, 1714; *Angew. Chem. Int. Ed. Engl.* **1993**, *32*, 1655).

[14] For CVD (chemical vapor deposition), compare, for example, R. A. Fischer, W. Scherer, M. Kleine, *Angew. Chem.* **1993**, *105*, 778; *Angew. Chem. Int. Ed. Engl.* **1993**, *32*, 748; and references therein; B. Fraser, L. Brandt, W. K. Storall, H. D. Kaez, S. I. Khan, F. Maury, *J. Organomet. Chem.* **1994**, *472*, 317).

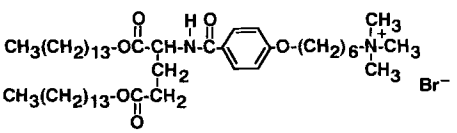
[15] The molar ratio and NMR spectroscopic results of the colorless compound are consistent with the formula [AlCp*Cp_2]. However, this could not be confirmed by mass spectroscopy because of the low volatility of the compound. The yield of **1** is calculated for the reaction 3[Cp*Al] + 2[Cp_2Ni] → **1** + [AlCp*Cp_2].

Mesoscopic Sheets of a Cyano-Bridged Cu–Ni Coordination Complex: Template Synthesis at the Interlayers of Cast Multibilayer Films**

Nobuo Kimizuka, Toyokazu Handa, Izumi Ichinose, and Toyoki Kunitake*

Controlled synthesis and organization of inorganic clusters in diminishing dimensions lie at the heart of mesoscopic science. Conversion of inorganic precursors into desired clusters must be conducted *under mild conditions*, since traditional solid-state synthetic techniques allow little control over such metastable microstructures.[1, 2] Synthetic bilayer membranes display physicochemical characteristics similar to those of biomembranes. Their aqueous dispersions are, in many cases, transformed to self-supporting, multilayered films upon casting on solid substrates. The cast films provide two-dimensional matrices for the preparation of mesoscopic clusters such as quantum-sized CdS particles.[3] Very recently, organization of lead halide aggregates with quantized electronic states was achieved in two-dimensional space through electrostatic interactions with the regularly positioned cationic head groups of the bilayer.[4] These template syntheses have been limited to clusters containing a single type of metal. It is desirable to extend these techniques to the synthesis of heterometallic complexes.[5] We report here on a novel stepwise synthesis of cyano-bridged bimetallic aggregates. These coordination compounds should be of great interest, since their structural characteristics are often associated with novel properties such as molecular magnetism[6] and functional mixed valencies.[6, 7]

Tetracyanonickelate ion $[Ni(CN)_4]^{2-}$ was chosen as a μ-cyano precursor, and copper(II) ion was selected as the second metal component. The stepwise synthesis of the $[Ni(CN)_4]^{2-}$–Cu aggregate at the molecular interlayer was achieved by successively dipping a cast film of **1** first in an aqueous solution of the



1

cyanonickel complex (→**1**-Ni film), and then in an aqueous solution of copper nitrate (→**1**-Ni-Cu film). Incorporation of the cyanonickelate into the film of **1** was confirmed by the appearance of a ν_{CN} band at 2120 cm^{-1} in the IR spectrum. Atomic absorption analysis gave a Ni content corresponding to a **1**:Ni ratio of 2.7:1, which indicates essentially quantitative exchange of bromide ion. Similar stoichiometric exchanges have been reported for lead halide clusters,[4] porphyrins,[8] and myoglobin.[9]

After the second dipping, the resulting **1**-Ni-Cu film showed a group of CN stretching bands at 2195, 2185, and 2175 cm^{-1}, which were shifted to higher wavenumbers from those observed

[*] Prof. Dr. T. Kunitake, N. Kimizuka, T. Handa, I. Ichinose
Department of Chemical Science and Technology
Faculty of Engineering, Kyushu University
Higashi-ku, Fukuoka 812 (Japan)
Telefax: Int. code + (92)632-1842

[**] Contribution No. 996 from the Department of Chemical Science and Technology. We thank Prof. Fumiyuki Nakashio for access to a Seiko SAS 760 instrument for atomic absorption analyses.

for the **1**-Ni film (2120 cm^{-1}). These shifts[10] indicate that the nitrogen atoms of the preorganized cyanonickelate coordinate to the subsequently introduced copper ion, and a cyano-bridged Ni–Cu aggregate forms. The **1**:Ni:Cu ratio estimated from the Ni and Cu contents is 3.4:1.6:1. The presence of an excess of $[Ni(CN)_4]^{2-}$ relative to copper(II) implies that the complex formed is negatively charged. The overall charge of the film appears to be balanced by NO_3^- ions, since a NO stretching band for uncoordinated NO_3^- is observed at 1380 cm^{-1}.

X-ray diffraction patterns of the **1**-Ni-Cu film gave a series of reflections up to 10th order that correspond to a long spacing of 42.8 Å. Therefore, the ordered multibilayer structure remains intact during the stepwise formation of the aggregate. This long spacing is shorter than that of the cast film of **1** alone (d = 66.6 Å). The molecular orientation in the bilayer must have undergone considerable alteration owing to the electrostatic interactions between the cationic bilayer and the anionic Ni–Cu aggregates. A similar change in long spacing was observed for a **1**-$PbBr_4^{2-}$ cast film.[4]

Figure 1 shows ESR spectra of the copper(II) ions in the **1**-Ni-Cu cast film. The cyanonickelate moiety is diamagnetic. In

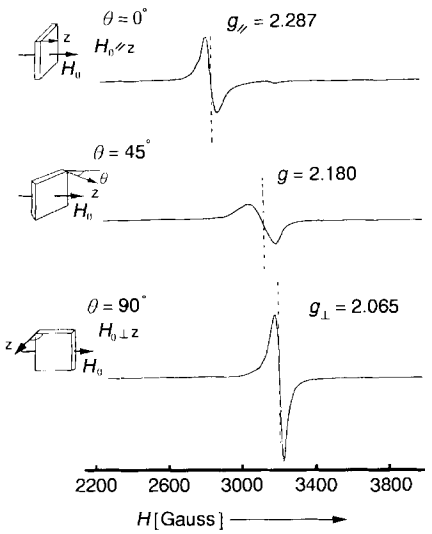


Fig. 1. ESR spectra of a **1**-Ni-Cu film at room temperature; modulation amplitude 12.5 G; microwave frequency 9.208 GHz. θ is the angle between normal of the planes of the film and the applied magnetic field.

recording these spectra the normal of the plane of the film (z axis) was set at angles of 90, 45, and 0° to the applied magnetic field H_0. The hyperfine coupling of the Cu nucleus (I_{Cu} = 3/2) is lost in the aggregate because of spin–spin interactions. A similar observation was reported for the Hofmann-type clathrate $[Cu(NH_3)_2Ni(CN)_4] \cdot 2C_6H_6$.[11] The ESR signals of the **1**-Ni-Cu film at θ = 0° are predominantly of the parallel component ($g_{\parallel}$ = 2.287) and at θ = 90° solely of the perpendicular component ($g_{\perp}$ = 2.065). These g values suggest that the copper ion has square-planar (N coordination) or elongated octahedral coordination (with axial water ligands). The observed angular dependence clearly indicates that the $d_{x^2-y^2}$ orbital of the copper ion is oriented parallel to the bilayer surface. The spectrum observed at θ = 45° has a signal located between these signals (g = 2.180), in contrast to the previous observations of oriented copper chelates[12] and myoglobin.[9] In the latter cases, the $g_{\parallel}$ and $g_{\perp}$ components coexisted in the spectra and showed complementary intensity changes upon variation of the film orientation.

Figure 2 compares the angular dependence of the observed g value with the theoretical angular dependence of the axially symmetric g-factor for a single crystal.[13] The satisfactory agreement clearly indicates that the bimetallic coordination

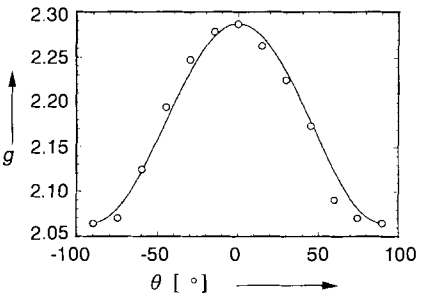


Fig. 2. Values of g (o) as a function of angle θ. The solid line is a theoretical curve obtained by using the following equation [13]: $g^2 = g_{\parallel}^2 \cos^2\theta + g_{\perp}^2 \sin^2\theta$.

compound has a highly oriented two-dimensional structure with long-range order. The copper(II) ions adopt a uniform orientation in the plane without substantial orientational fluctuation[12] in the direction of z axis of the film. When a powdered cast film was used, ESR spectra merely showed the coexistence of the $g_{\parallel}$ and $g_{\perp}$ components without angular dependence.

The stepwise synthesis of the μ-cyano adduct is depicted schematically in Figure 3. It is obvious that the adducts are suffi-

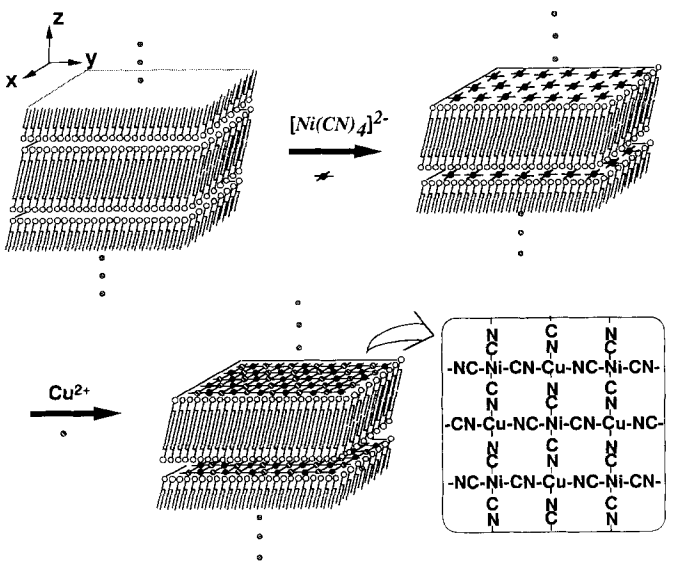


Fig. 3. Idealized representation of the stepwise synthesis of a μ-cyano Ni–Cu aggregate. Top left: cast film of **1**; top right: **1**-Ni film; bottom: **1**-Ni-Cu film and a section of the μ-cyano Ni–Cu aggregate.

ciently large such that orientational fluctuation does not arise in spite of probable undulation of the bilayer surface. The size and shape of the adduct cannot be determined definitely, although the observed Ni:Cu ratio (3:2) is in agreement with an 8 × 8 square-planar lattice.

In conclusion, a highly oriented, bimetallic aggregate was synthesized for the first time by taking advantage of a bilayer template. The repeated dipping process offers a novel approach to the production of bimetallic aggregates with unique electro-optical or quantum-based electronic properties.

Experimental Procedure

Multibilayer cast films were prepared by casting aqueous bilayer dipersions of **1** onto quartz plates or fluoropore membrane filters as described previously [3, 4]. Cast films of **1** were first dipped in an aqueous solution of potassium tetracyanonickel (100 mM) for 5 d at room temperature to effect exchange with bromide ion. The resulting **1**-Ni films were rinsed with deionized water, then dipped in an aqueous solution of copper nitrate (100 mM) for 5 d, and finally dipped in pure water for 10 min to remove unreacted copper ion (**1**-Ni-Cu film). Atomic absorption analysis of Ni and Cu was conducted for the cast films, after they had been dispersed by ultrasonication in aqueous hydrogen chloride (0.1 N) containing 0.25% sodium hypochlorite.

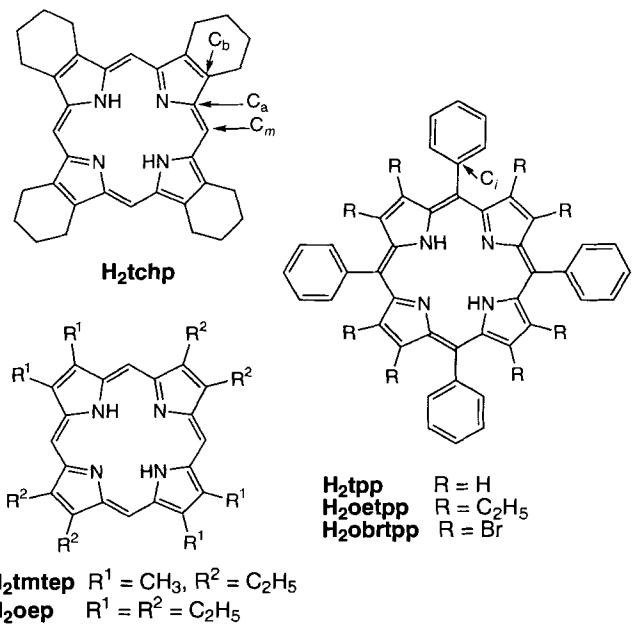
Received: June 21, 1994 [Z 7057 IE]
German version: *Angew. Chem.* **1994**, *106*, 2576

[1] A. Stein, S. W. Keller, T. E. Mallouk, *Science* **1993**, *259*, 1558.
[2] S. Mann, *Nature (London)* **1993**, *365*, 499.
[3] N. Kimizuka, T. Miyoshi, I. Ichinose, T. Kunitake, *Chem. Lett.* **1992**, 2039.
[4] N. Kimizuka, T. Maeda, I. Ichinose, T. Kunitake, *Chem. Lett.* **1993**, 941; *Proc. 3rd IUMRS-Int. Conf. Adv. Mater.* **1993**, in press.
[5] For example H. O. Stumpf, Y. Pei, O. Kahn, J. Sletten, J. P. Renard, *J. Am. Chem. Soc.* **1993**, *115*, 6738.
[6] T. Mallah, S. Thiebaut, M. Verdaguer, P. Veillet, *Science* **1993**, *262*, 1554.
[7] W. M. Laidlaw, R. G. Denning, T. Verbiest, E. Chauchard, A. Parsoons, *Nature (London)* **1993**, *363*, 58.
[8] H. Wakayama, T. Kunitake, unpublished.
[9] I. Hamachi, T. Honda, S. Noda, T. Kunitake, *Chem. Lett.* **1991**, 1121.
[10] K. Nakamoto, *Infrared Spectra of Inorganic and Coordination Compounds*, 2nd ed., Wiley-Interscience, New York, **1970**.
[11] T. Miyoshi, T. Iwamoto, Y. Sasaki, *Inorg. Chim. Acta* **1968**, *2*, 329.
[12] Y. Ishikawa, T. Kunitake, *J. Am. Chem. Soc.* **1991**, *113*, 621.
[13] J. E. Wertz, J. R. Bolton, *Electron Spin Resonance*, McGraw-Hill, New York, **1972**, Chapter 7.

Sterically Strained Porphyrins—Influence of Core Protonation and Peripheral Substitution on the Conformation of Tetra-*meso*-, Octa-β-, and Dodeca-Substituted Porphyrin Dications**

Mathias O. Senge,* Timothy P. Forsyth, Liem T. Nguyen, and Kevin M. Smith

The study of nonplanar porphyrin conformations is currently under active scrutiny with regard to the possible role different macrocycle conformations play in biological processes such as respiration, electron transfer, photosynthesis, and enzyme catalysis.[1a] The synthesis of porphyrins bearing large and sterically interacting substituents at the porphyrin periphery has been used successfully to yield tetrapyrroles with significantly distorted macrocycles.[1, 2] Such compounds were mostly characterized by steric overload of the porphyrin periphery, for example, dodecasubstitution of the *meso*-carbon and β-pyrrole positions. In addition, core substitutions by either protonation of the two hydrogen-free pyrrole nitrogens (porphyrin dications)[3] or preparation of *N*-alkyl or *N*-aryl porphyrins[4] have been shown to lead to significantly distorted macrocycles, owing to steric congestion in the porphyrin core. We were interested in testing how far the macrocycle nonplanarity in dodeca-substituted porphyrins can be increased by a combination of both strategies, namely, core *and* peripheral substitution. Spectroscopic evidence already indicated that compounds such as 22,24-dihydrododecaphenylporphyrin dication are nonplanar in solution, but no detailed structural data were available.[2b] Additionally, only a few crystal structures of tetra-*meso*- or octa-β-substituted porphyrin dications were available for comparison with those of dodecasubstituted porphyrins. These included $[H_4tpp]^{2+}$ (H_2tpp = tetraphenylporphyrin, Scheme 1), which exhibits a nonplanar saddle conformation with pyrrole tilt angles of 33° and β-pyrrole displacements of 0.9–1.16 Å with respect to the mean plane.[3a] In contrast, the porphyrin skeleton in $[H_4oep][RhCl_2(CO)_2]_2$ (H_2oep = octaethylporphyrin) has a planar conformation.[3b]



Scheme 1. Structures of the investigated porphyrins.

The macrocycle of $[H_4tchp][CF_3COO]_2 \cdot 2CF_3COOH \cdot 2H_2O$ (H_2tchp = tetracyclohexa[*b*, *g*, *l*]porphyrin) is, surprisingly, almost planar (Fig. 1).[5, 6a] Two trifluoroacetate (TFA) anions are hydrogen-bonded to the pyrrole hydrogens in a monodentate fashion, with one carboxyl oxygen bonded to two neighboring N–H units on the same face of the porphyrin. In this unique structure, the neighboring pyrrole units are displaced pairwise above and below the mean plane. On the basis

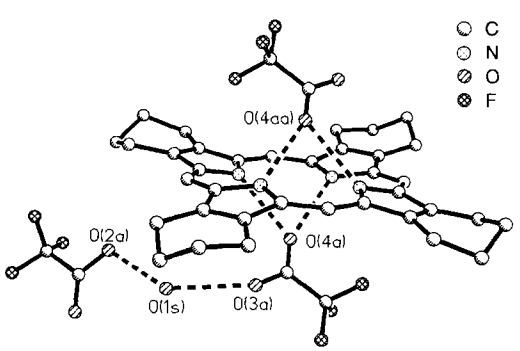


Fig. 1. Crystal structure of $[H_4tchp][CF_3COO]_2 \cdot 2CF_3COOH \cdot 2H_2O$. The associated solvent chain is shown for only one face of the porphyrin. Dashed lines indicate hydrogen bonds. Selected bond lengths [Å]: N(21)–O(4a) 2.727, N(22)–O(4a) 2.760, O(3a)–O(1s) 2.778, O(1s)–O(2a) 2.510.

[*] Dr. M. O. Senge,[+] T. P. Forsyth, L. T. Nguyen, Prof. Dr. K. M. Smith
Department of Chemistry, University of California
Davis CA 95616 (USA)
[+] New address: Institut für Organische Chemie der Freien Universität
Takustrasse 3, D-14195 Berlin (FRG)
Telefax: Int. code + (030) 838-4248

[**] This work was supported by grants from the Deutsche Forschungsgemeinschaft and the National Science Foundation (CHE-93-05577).

of earlier structural data, alternating up-and-down displacement of the N–H units was predicted for all porphyrin dications; this conformation minimizes the steric interaction of the four core hydrogens.[3, 7] The 24 macrocycle atoms show an average deviation from the porphyrin mean plane of 0.129 Å, which is comparable to that found in some sterically unencumbered free-base porphyrins.[8]

In the related compound $[H_4tmtep][ClO_4]_2 \cdot CH_3OH$ (H_2tmtep = tetraethyltetramethylporphyrin), the average deviation from the porphyrin mean plane is 0.173 Å for the macrocycle atoms and 0.37 Å for the C_b atoms; this represents a rather moderate degree of distortion.[6b, 9] In contrast, $[H_4oep][CF_3COO]_2 \cdot 2CF_3COOH$ (Fig. 2)[6c] contains a significantly saddle-distorted macrocycle: the average deviation of the C_b atoms from the mean plane is 0.72 Å (0.333 Å for all 24 macrocycle atoms), which is about 30% smaller than that found in $[H_4tpp]^{2+}$.[3b] On each porphyrin face, a TFA ion acts as a monodentate ligand and binds through a carboxyl oxygen to two opposing N–H protons. The pyrrole rings are twisted with respect to each other by 30.7°; the corresponding value for $[H_4tchp]^{2+}$ is 17°. Thus, octa-β-alkyl-substituted porphyrin dications can have varying degrees of macrocycle distortion, depending on the geometry of the central N–H units. In contrast, all tetra-*meso*-arylporphyrin dications so far studied show similar nonplanar saddle conformations with C_b displacements of about 1–1.2 Å.[10]

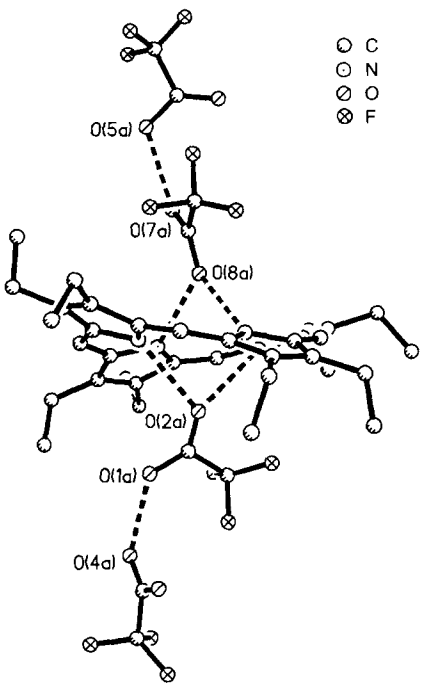


Fig. 2. Crystal structure of $[H_4oep][CF_3COO]_2 \cdot 2CF_3COOH$. Dashed lines indicate hydrogen bonds. Selected bond lengths [Å]: N(21)–O(8a) 2.871, N(23)–O(8a) 2.802, N(22)–O(2a) 2.798, N(24)–O(2a) 2.862, O(1a)–O(4a) 2.501, O(5a)–O(7a) 2.523.

The complex $[H_4oetpp][CH_3COO]_{3/2}[CF_3COO]_{1/2} \cdot 4CH_3COOH \cdot H_2O$ (H_2oetpp = octaethyltetraphenylporphyrin) is an example of a dodeca-substituted porphyrin dication combining both the structural characteristics of oep and tpp with core substitution (Fig. 3).[6d] The dication has a severely distorted macrocycle with C_b atom displacements of 1.357 Å from the porphyrin mean plane (0.612 Å for all macrocycle atoms). The pyrrole rings are tilted by 39.2° with respect to the macrocycle plane and by 53.1° with respect to each other. On each porphyrin face, an acetate ion acts as a bidentate ligand and binds through each carboxyl oxygen atom to an N–H proton. Initial studies on other oetpp dications indicate that the type of anion and the geometry of the hydrogen bonding to the core protons do not exert a major influence on the observed conformation in porphyrin dications.[10]

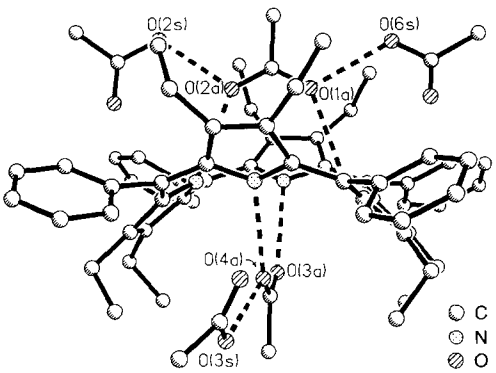


Fig. 3. Crystal structure of $[H_4oetpp][CH_3COO]_{3/2}[CF_3COO]_{1/2} \cdot 2CH_3COOH \cdot H_2O$. The minor TFA component, presumably due to contamination from a prior crystallization, is not shown. Dashed lines indicate hydrogen bonds. Selected bond lengths [Å]: N(21)–O(1a) 2.744, N(23)–O(2a) 2.759, N(22)–O(4a) 2.781, N(24)–O(3a) 2.758, O(4a)–O(3s) 2.596, O(1a)–O(6s) 2.592, O(2a)–O(2s) 2.559. The compound contains an additional acetic acid and water residue (not shown), which are hydrogen-bonded to each other: O(8')–O(9s) 2.288 Å.

The dodeca-substituted free bases and metalloporphyrins have conformations which are about as distorted as or slightly more distorted than the tpp dications. Thus, it might be expected that no further distortion is necessary to accomodate the four pyrrole hydrogens in the corresponding dications. Nevertheless, the $[H_4oetpp]^{2+}$ dication is about 30% more distorted than the corresponding free base, H_2oetpp.[11, 12] It is possible that porphyrins that are already nonplanar due to peripheral steric strain undergo further distortion more easily upon core protonation than do "normal" planar porphyrins. A special feature of *meso*-arylporphyrin dications is the large degree of in-plane rotation of the *meso*-aryl groups (e.g., 21° in $[H_4tpp]^{2+}$).[3a, 10] This feature has been used to account for the increased resonance interaction between the π electron system of the porphyrin macrocycle and the *meso*-aryl groups. This explains the bathochromic shifts of the absorption bands of the tpp dications vs. those of oep dications.[3a, 13] However, inspection of all the structures bearing *meso*-aryl groups[11] yields no evidence for shortening of the C_m–C_i bonds compared to those in the planar H_2tpp.[8c] Thus, the spectroscopic differences between the oep and tpp series reside solely in the electronic effects of the substituents and/or macrocycle conformations. Interestingly, the phenyl tilt angle in $[H_4oetpp]^{2+}$ (39.2°) is actually larger than that observed in $[H_4tpp]^{2+}$, which shows a smaller deviation from planarity. Similarily, compounds like [Cu(oetpp)] show tilt angles of approximately 46°.[2e] Thus, a linear correlation between *meso*-aryl tilt and porphyrin nonplanarity is not possible on the basis of the present data. In general terms, porphyrins that deviate strongly from planarity seem, however, to show a more coplanar arrangement of the aryl rings, which is significantly enhanced by core protonation.

The porphyrin conformation with the largest deviation from planarity observed so far is found in $[H_4obrtpp][CF_3COO]_2 \cdot 0.5CHCl_3$ ($H_2obrtpp$ = octabromotetraphenylporphyrin; Fig. 4).[6e] Overall, the structure is very similar to that of $[H_4oetpp]^{2+}$, with bidentate binding of the TFA carboxyl oxygens to opposing N–H hydrogens. The average deviation of the

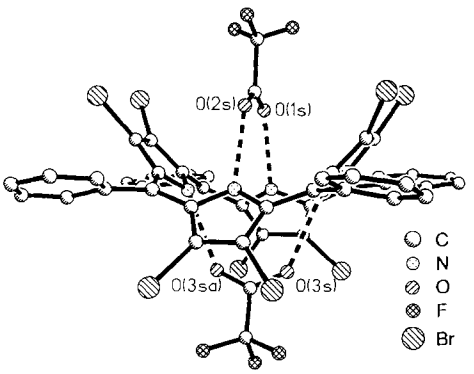


Fig. 4. Crystal structure of $[H_4obrtpp][CF_3COO]_2 \cdot 0.5CHCl_3$. Dashed lines indicate hydrogen bonds. Selected bond lengths [Å]: N(21)–O(2s) 2.744, N(23)–O(1s) 2.648, N(22)–O(3s) 2.685, N(22')–O(3s) 2.658. The compound contains two additional chloroform molecules (not shown) per unit cell.

24 macrocycle atoms from the mean plane is 0.689 Å; the corresponding figure for the C_b atoms is 1.521 Å. The distortion is about 63% greater than in the related octabromotetramesityl free base derivative.[2e] The increase upon protonation of H_2obrtpp is even larger than that observed upon going from H_2oetpp to $[H_4oetpp]^{2+}$. The extreme degree of nonplanarity is also reflected in the angles between the pyrrole rings of 62.1° and those between pyrrole rings and the macrocycle plane of 46.3°. Very surprising is the large in-plane rotation of the phenyl rings with tilt angles as small as 8.8° (average value 10.9°); the aryl rings are almost coplanar with the porphyrin plane. Even at this degree of coplanarity, no evidence for C_m–C_i bond shortening was found. Hence, the phenyl tilt observed in nonplanar porphyrins does not influence the spectroscopic characteristics of the nonplanar porphyrins. Disregarding electronic effects of different substituents or counterions, the bathochromic shifts of the absorption maxima are solely the result of increased macrocycle nonplanarity.

Correlations also exist between increasing macrocycle nonplanarity and selected geometrical characteristics: while most bond lengths and angles remain unaffected by comparison with those of planar porphyrins, increasing nonplanarity leads to a decrease in the N-C_a-C_m and C_a-C_m-C_a angles and an increase in the C_m-C_a-C_b and C_a-C_m-C_i angles. These structural correlations are independent of the way the macrocycle distortion is induced: the same trends are observed in the octa-β-substituted porphyrin dications, whose structure is determined solely by core strain, as in porphyrins with only peripheral steric strain.[2b, d, g–f, 11] These trends are no different in dodeca-substituted porphyrin dications possessing both peripheral and core strain. Since all nonplanar porphyrins described here have the same saddle-shaped distortion, the trends described are the result of the macrocycle distortion alone and not due to local effects of individual substituents, be they core hydrogen atoms or peripheral bulky substituents.

So far no structures of dodeca-substituted porphyrin dications have been found that are not more strongly distorted than the corresponding free base (unlike some oep derivatives). This indicates that sterically strained porphyrins with both β-alkyl and *meso*-aryl substituents behave conformationally like the sterically unencumbered tpp series upon protonation and not like the octaalkyl series. A detailed analysis of the exact geometry of the hydrogens in the core and their influence on the conformation will, especially in the case of the oep series, have to await neutron diffraction studies.

Received: June 16, 1994 [Z 7040 IE]
German version: *Angew. Chem.* **1994**, *106*, 2554

[1] a) K. M. Barkigia, L. Chantranupong, K. M. Smith, J. Fajer, *J. Am. Chem. Soc.* **1988**, *110*, 7566; b) M. O. Senge, *J. Photochem. Photobiol. B* **1992**, *16*, 3.

[2] a) K. M. Barkigia, M. D. Berber, J. Fajer, C. J. Medforth, M. W. Renner, K. M. Smith, *J. Am. Chem. Soc.* **1990**, *112*, 8851; b) C. J. Medforth, M. O. Senge, K. M. Smith, L. D. Sparks, J. A. Shelnutt, *ibid.* **1992**, *114*, 9859; c) D. Mandon, P. Ochsenbein, J. Fischer, R. Weiss, K. Jayarai, R. N. Austin, A. Gold, P. S. White, O. Brigaud, P. Battioni, D. Mansuy, *Inorg. Chem.* **1992**, *31*, 2044; d) M. O. Senge, C. J. Medforth, L. D. Sparks, J. A. Shelnutt, K. M. Smith, *ibid.* **1993**, *32*, 1716; e) L. D. Sparks, C. J. Medforth, M.-S. Park, J. R. Chamberlain, M. R. Ondrias, M. O. Senge, K. M. Smith, J. A. Shelnutt, *J. Am. Chem. Soc.* **1993**, *115*, 581; f) K. M. Barkigia, M. W. Renner, L. R. Furenlid, C. J. Medforth, K. M. Smith, J. Fajer, *ibid.* **1993**, *115*, 3627; g) M. O. Senge, *J. Chem. Soc. Dalton Trans.* **1993**, 3539.

[3] a) A. Stone, E. B. Fleischer, *J. Am. Chem. Soc.* **1968**, *90*, 2735; b) E. Cetinkaya, A. W. Johnson, M. F. Lappert, G. M. McLaughlin, K. W. Muir, *J. Chem. Soc. Dalton Trans.* **1974**, 1236.

[4] D. K. Lavallee, *The Chemistry and Biochemistry of N-Substituted Porphyrins*, VCH. Weinheim, **1987**.

[5] Porphyrin dications are easily prepared by treatment of the respective free base porphyrins [2] with dilute acid in solution. All compounds gave satisfactory analytical data.

[6] Crystal data: a) $[H_4tchp][CF_3COO]_2 \cdot 2CF_3COOH \cdot 2H_2O$: $[C_{36}H_{40}N_4][C_2F_3O_2]_2 \cdot 2CF_3COOH \cdot 2H_2O$, red plate from $CHCl_3/CH_3OH$ + 1% TFA, triclinic, space group $P\bar{1}$, $a = 8.482(2)$, $b = 10.877(2)$, $c = 12.718(2)$ Å, $\alpha = 83.64(2)$, $\beta = 79.61(2)$, $\gamma = 78.43(2)°$, $V = 1127.2(4)$ Å^3, $Z = 2$, 2526 observed reflections with $F > 4.0\sigma(F)$, $\mu = 0.783$ mm^{-1}, $R = 0.059$, $R_w = 0.067$. b) $[H_4tmtep][ClO_4]_2 \cdot CH_3OH$: $[C_{32}H_{44}N_4][ClO_4]_2 \cdot CH_3OH$, red plate from CH_2Cl_2/CH_3OH + 3% $HClO_4$, triclinic, space group $P\bar{1}$, $a = 9.377(4)$, $b = 11.538(4)$, $c = 16.406(7)$ Å, $\alpha = 73.96(3)$, $\beta = 87.56(3)$, $\gamma = 80.97(3)°$, $V = 1684.8(12)$ Å^3, $Z = 2$, 3149 observed reflections with $F > 3.0\sigma(F)$, $\mu = 2.244$ mm^{-1}, $R = 0.093$, $R_w = 0.103$, disorder in one perchlorate anion. c) $[H_4oep][CF_3COO]_2 \cdot 2CF_3COOH$: $[C_{36}H_{40}N_4][C_2F_3O_2]_2 \cdot 2C_2F_3O_2H$, pink block from CH_2Cl_2/CH_3OH + 1% TFA, triclinic, space group $P\bar{1}$, $a = 11.647(4)$, $b = 12.167(5)$, $c = 17.954(7)$ Å, $\alpha = 82.39(3)$, $\beta = 72.61(3)$, $\gamma = 89.27(3)°$, $V = 2405.6(16)$ Å^3, $Z = 2$, 4700 observed reflections with $F > 4.0\sigma(F)$, $\mu = 1.088$ mm^{-1}, $R = 0.114$, $R_w = 0.122$, all TFA units severely disordered. d) $[H_4oetpp][CH_3COO]_{3/2}[CF_3COO]_{1/2} \cdot 4CH_3COOH \cdot H_2O$: $[C_{60}H_{64}N_4][C_2H_3O_2]_{3/2}$ $[C_2F_3O_2]_{1/2} \cdot 4CH_3CO_2H \cdot H_2O$, green block from CH_2Cl_2/CH_3OH + 5% acetic acid, triclinic, space group $P\bar{1}$, $a = 13.219(6)$, $b = 13.667(5)$, $c = 20.144(4)$ Å, $\alpha = 91.29(2)$, $\beta = 98.61(3)$, $\gamma = 108.11(3)°$, $V = 3411(2)$ Å^3, $Z = 2$, 6768 observed reflections with $F > 4.0\sigma(F)$, $\mu = 0.699$ mm^{-1}, $R = 0.081$, $R_w = 0.086$, 1 acetic acid residue disordered. e) $[H_4obrtpp][CF_3COO]_2 \cdot 0.5CHCl_3$: $[C_{44}H_{28}Br_8N_4][C_2F_3O_2]_2 \cdot 0.5CHCl_3$, green hexagon from $CHCl_3/CH_3OH$ + 1% TFA, orthorhombic, space group *Pmma*, $a = 16.358(2)$, $b = 19.437(3)$, $c = 17.629(3)$ Å, $V = 5604(2)$ Å^3, $Z = 4$, 2971 observed reflection with $F > 4.0\sigma(F)$, $\mu = 7.07$ mm^{-1}, $R = 0.063$, $R_w = 0.069$, 1 TFA and the solvent molecule disordered. Instruments used for data collections: a), b), c), and e): Siemens P4 diffractometer with attached rotating anode, 120 K, 2θ-θ-scans, $2\theta_{max} = 112°$, $Cu_{K\alpha}$ radiation (λ = 1.54178 Å); d) Syntex $P2_1$ diffractometer, 130 K, 2θ-θ scans, $2\theta_{max} = 115°$, $Cu_{K\alpha}$ radiation. Programs and refinement strategies used were as described in ref. [2g]. Further details on the crystal structure determinations may be obtained from the Fachinformationszentrum Karlsruhe, D-76344 Eggenstein-Leopoldshafen (FRG) on quoting the depository number CSD-58475.

[7] On the basis of structural data for porphyrin monocations partial sp^3 hybridization of the pyrrole nitrogens has also been suggested as a mechanism for relieving strain in the porphyrin core: N. Hirayama, A. Takenaka, Y. Sasada, E.-I. Watanabe, H. Ogoshi, Z.-I. Yoshida, *Bull. Chem. Soc. Jpn.* **1981**, *54*, 998; C. P. Hrung, M. Tsutsui, D. L. Cullen, E. F. Meyer, Jr., C. N. Morimoto, *J. Am. Chem. Soc.* **1978**, *100*, 6068. We found some evidence for this in the form of residual electron density at 0.8–1 Å from pyrrole nitrogens and outside the pyrrole plane. However, the limited resolution of core protons allows no direct conclusions to this effect.

[8] a) W. R. Scheidt, Y. J. Lee, *Struct. Bonding (Berlin)* **1987**, *64*, 1; b) J. W. Lauher, J. A. Ibers, *J. Am. Chem. Soc.* **1973**, *95*, 5148; c) S. Silvers, A. Tulinsky, *ibid.* **1964**, *86*, 927; M. J. Harmor, T. A. Harmor, J. L. Hoard, *ibid.* **1964**, *86*, 1938.

[9] L. T. Nguyen, M. O. Senge, K. M. Smith, *Tetrahedron Lett.*, in press.

[10] We have obtained a number of other tpp and oetpp dication salts with different counterions, which show similar conformations.

[11] A. Regev, T. Galili, C. J. Medforth, K. M. Smith, K. M. Barkigia, J. Fajer, H. Levanon, *J. Phys. Chem.* **1994**, *98*, 2520.

[12] The related structure of $[H_4oetpp][CH_3COO]_2$ has also been crystallized and shows overall similar characteristics. K. M. Barkigia, M. R. Renner, J. Fajer, K. M. Smith, M. D. Berber, *Acta Crystallogr. C*, in press.

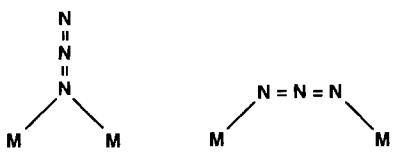
[13] N. Datta-Gupta, T. J. Bardos, *J. Heterocycl. Chem.* **1966**, *3*, 495; E. B. Fleischer, A. L. Stone, *J. Chem. Soc. Chem. Commun.* **1967**, 332.

Alternating Ferro- and Antiferromagnetic Interactions in a Mn^{II} Chain with Alternating End-On and End-to-End Bridging Azido Ligands**

Roberto Cortés, Luis Lezama, J. Luis Pizarro, M. Isabel Arriortua, Xavier Solans, and Teófilo Rojo*

In the last few years we have investigated the role played by pseudohalide ions, in particular the azido ion, in bridging different transition metals with the aim of studying their magnetostructural correlations. As a result, the first dinuclear Ni^{II} compound with bis(μ-end-on-azido) bridges[1] and the first metal compound having bis(μ-end-on-cyanato) bridges[2] were characterized.

Two possible bridging modes: end-to-end (EE) and end-on (EO) (Scheme 1) exist for the azido group. To date, dinuclear[3a, b] and tetranuclear complexes,[3c] and one-dimensional (1D) polymeric systems,[3b] have been synthesized with EO bridges, and dinuclear complexes[4a] and 1D polymeric systems[4b-d] with EE bridges. A complex with an infinite two-dimensional (2D) structure containing both EE and EO forms[5] has also been characterized. The EE bridges give rise to antiferromagnetic[4] and the EO bridges to ferromagnetic[3] interactions between the metal ions even for the Mn^{II} ion with $S = 5/2$.[6] The ferromagnetic behavior in the compounds with the EO bridges has been explained by the spin-polarization concept[7] for angles between 100–105°.



Scheme 1. Possible bridging modes for the azido ligand: Left: EO (ferromagnetic interactions); right: EE (antiferromagnetic interactions).

The different magnetic behavior caused by the two kinds of azido bridges, which is general for different metal ions,[6, 8-10] allows the possibility of obtaining very rare 1D systems with alternating ferro- (through EO bridges) and antiferromagnetic (through EE bridges) exchanges.[11] Such a compound must contain both types of bridging. With this aim in mind we developed a synthesis strategy in which metal and bidentate ligand are used in a 1:1 ratio. This should provide four vacant coordination sites around the metal ion, which should be filled by azide ions. Following this method, we successfully isolated a novel 1D Mn^{II} compound of the empirical formula $[Mn(N_3)_2(bpy)]_\infty$ (bpy = 2,2′-bipyridine) with alternating EO and EE bridges (Fig. 1).

[*] Prof. T. Rojo, Dr. R. Cortés, Dr. L. Lezama
Departamento de Química Inorgánica
Universidad del País Vasco
Aptdo. 644, E-48080 Bilbao (Spain)
Telefax: Int. code + (4)4648500
Prof. M. I. Arriortua, Dr. J. L. Pizarro
Departamento Mineralogía-Petrología, Universidad del País Vasco
Bilbao (Spain)
Prof. X. Solans
Universitat de Barcelona (Spain)

[**] This work has been supported by the Spanish Dirección General de Investigación Científica y Tecnica (DGICYT) (Project PB90-0549) and the University of the Basque Country (UPV 130.310-EB017/92).

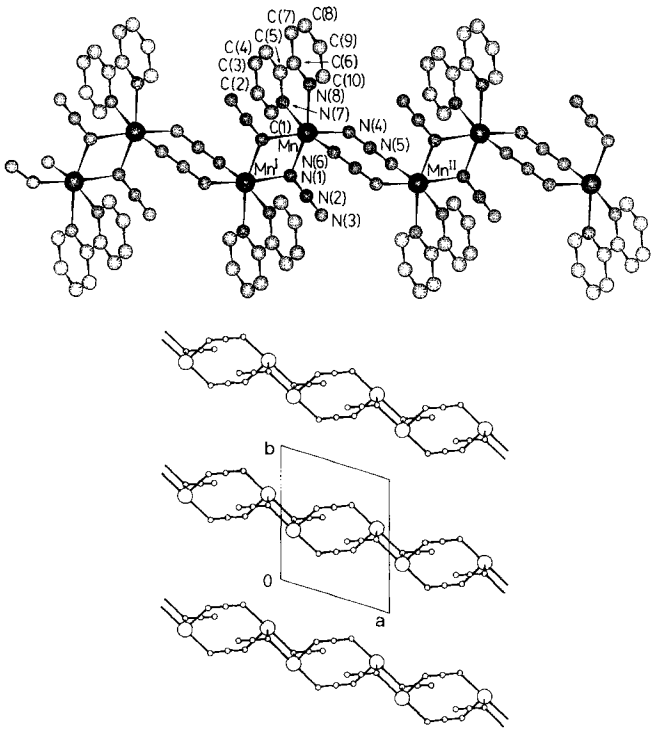


Fig. 1. Crystal structure of $[Mn(N_3)_2(bpy)]_\infty$. Top: View of the chain with alternating end-on and end-to-end coordination of the azido ligand. Bottom: Arrangement of the chains in the *ab* plane (only manganese and nitrogen atoms are shown). Selected distances [Å] and angles [°] (standard deviations in parentheses): Mn-N(1) 2.200(6), Mn-N(4) 2.244(6), Mn-N(6) 2.185(6), Mn-N(7) 2.237(5), Mn-N(8) 2.258(5), Mn-N(1)^{I} 2.276(6); N(1)-Mn-N(4) 92.3(2), N(1)-Mn-N(6) 98.8(2), N(1)-Mn-N(7) 94.3(2), N(1)-Mn-N(8) 162.2(2), N(4)-Mn-N(6) 90.5(2), N(4)-Mn-N(7) 89.5(2), N(4)-Mn-N(8) 98.4(2), N(6)-Mn-N(7) 166.9(2), N(6)-Mn-N(8) 95.3(2), N(7)-Mn-N(8) 71.8(2), Mn-N(1)-Mn^{I} 101.0(2), Mn-N(4)-N(5) 131.1(5), Mn-N(6)-N(5)^{II} 127.3(5); symmetry code: I = $-x, 1-y, 1-z$; II = $1-x, 1-y, 1-z$.

The crystal structure[12] consists of chains in which the Mn^{II} ions are alternatively linked by two EO and two EE azido bridges (Fig. 1). The two nitrogen atoms of the bpy ligand complete a distorted octahedral coordination sphere for each manganese ion. The EO and EE bridges are arranged *cis*, being perpendicular to each other. The Mn-N-Mn angle in the EO mode is 101.0° in good agreement with the results usually obtained for this kind of bridging. For the EE bridges the Mn-N-N angles are 131.1(5)° and 127.3(5)° for a chair conformation of the Mn-$(N_3)_2$-Mn unit and a torsion angle of 41.9°. The intrachain Mn···Mn distances are 3.455(6) Å (EO) and 5.343(5) Å (EE).

ESR measurements show an exchange-narrowed isotropic signal at $g = 2.0$ which is indicative of significant ferromagnetic interactions. A "half-field" signal is also observed. Variable-temperature magnetic susceptibility measurements have been performed on a powdered sample in the range 298 to 2 K with a SQUID SHE magnetometer. A global antiferromagnetic interaction is evident from the magnetic behavior as is shown in Figure 2. The χ_m value increases as the temperature decreases, reaching a rounded maximum at about 55 K and then decreases on cooling down to 2 K. The $\chi_m T$ value at room temperature is 4.0 $cm^3 K mol^{-1}$, smaller than the value expected for an uncoupled Mn^{II} ion. This value decreases with decreasing temperature tending to zero. This compound should exhibit alternating ferromagnetic and antiferromagnetic interactions, since *cis* EO bridges with a bridging angle as observed here are able to mediate a ferromagnetic interaction between the Mn^{II} magnetic cen-

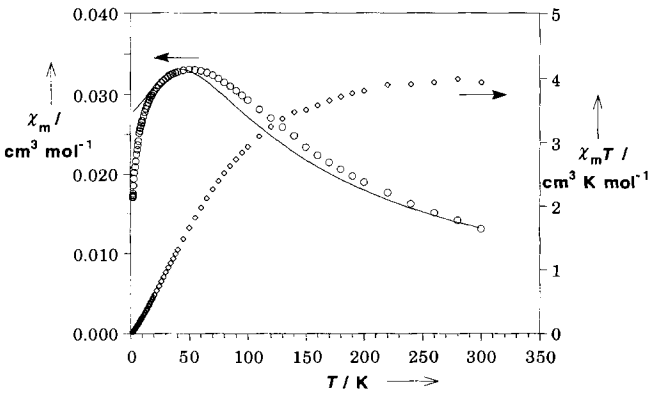


Fig. 2. Plot of $\chi_m T$ (○) and χ_m (○) of $[Mn(N_3)_2(bpy)]_x$ versus T. Solid line: best-fit curve according to Fisher [13a] for a classical or infinite spin linear chain, scaled to a real $S = 5/2$ value.

ters (as has recently been observed in the dinuclear complex $[Mn(N_3)_2(terpy)]_2 \cdot 2H_2O$[6] with an Mn-N-Mn angle of 104.6(2)° and $J/k = +3.5$ K), and the *cis* EE bridges with an M-N-N angle of ≈130° lead to antiferromagnetic coupling.[4a] Consequently, the magnetic behavior of this compound must be explained by assuming a positive J for EO and a negative J' for EE. A tentative fit of the experimental susceptibility to Fisher's equation[13a] for a classical or infinite spin linear chain, scaled to a real spin of 5/2[13b] (Fig. 2), shows a great discrepancy. No formula is available in the literature for an $S = 5/2$ ferro–antiferromagnetic alternating chain and we are now trying to elaborate an adequate model.

Experimental Procedure

A solution of 2,2'-bipyridine (0.15 g, 1 mmol) in methanol (10 mL) was added dropwise to a stirred aqueous solution (20 mL) of $Mn(ClO_4)_2 \cdot 6H_2O$ (0.35 g, 1 mmol). Excess NaN_3 dissolved in water was slowly added. This led to a yellow solution that was filtered and left to stand at room temperature. After several days prismatic, transparent, yellow, X-ray quality single crystals were obtained (yield 0.23 g; 77%).

Received: July 28, 1994 [Z 7185 IE]
German version: *Angew. Chem.* **1994**, *106*, 2520

[1] M. I. Arriortua, R. Cortés, L. Lezama, T. Rojo, X. Solans, M. Font-Bardía, *Inorg. Chim. Acta* **1990**, *174*, 263.
[2] M. I. Arriortua, R. Cortés, J. L. Mesa, L. Lezama, T. Rojo, G. Villeneuve, *Transition Met. Chem.* **1987**, *13*, 371. see also: J. Ribas, M. Monfort, B. K. Ghosh, X. Solans, *Angew. Chem.* **1994**, *106*, 2177–2179; *Angew. Chem. Int. Ed. Engl.* **1994**, *33*, 2087–2089.
[3] a) R. Vicente, A. Escuer, J. Ribas, M. S. El Fallah, X. Solans, M. Font-Bardía, *Inorg. Chem.* **1993**, *32*, 1920; b) J. Ribas, M. Monfort, C. Diaz, C. Bastos, X. Solans, *ibid.* **1994**, *33*, 484; c) J. Ribas, M. Monfort, R. Costa, X. Solans, *ibid.* **1993**, *32*, 695.
[4] a) J. Ribas, M. Monfort, C. Diaz, C. Bastos, X. Solans, *Inorg. Chem.* **1993**, *32*, 3557; b) A. Escuer, R. Vicente, M. S. El Fallah, J. Ribas, X. Solans, M. Font-Bardía, *J. Chem. Soc. Dalton Trans.* **1993**, 2975; c) A. Escuer, R. Vicente, J. Ribas, M. S. El Fallah, X. Solans, M. Font-Bardía, *Inorg. Chem.* **1993**, *32*, 3727; d) R. Cortés, M. K. Urtiaga, L. Lezama, J. L. Pizarro, A. Goñi, M. I. Arriortua, T. Rojo, *ibid.* **1994**, *33*, 4009.
[5] J. Ribas, M. Monfort, X. Solans, M. Drillon, *Inorg. Chem.* **1994**, *33*, 742.
[6] R. Cortés, J. L. Pizarro, L. Lezama, M. I. Arriortua, T. Rojo, *Inorg. Chem.* **1994**, *33*, 2697.
[7] M. F. Charlot, O. Kahn, M. Chaillet, C. Larrieu, *J. Am. Chem. Soc.* **1986**, *108*, 2574.
[8] R. Cortés, M. K. Urtiaga, L. Lezama, J. I. Ruiz de Larramendi, M. I. Arriortua, T. Rojo, *J. Chem. Soc. Dalton Trans.* **1993**, 3685, and references therein.
[9] A. K. Gregson, N. T. Moxon, *Inorg. Chem.* **1982**, *21*, 586.
[10] A. Bencini, C. A. Ghilardi, S. Modollini, A. Orlandini, *Inorg. Chem.* **1989**, *28*, 1958.
[11] a) H. J. M. de Groot, L. J. de Jongh, R. D. Willett, J. Reedijk, *J. Appl. Phys.* **1982**, *53*, 8038; b) C. Benelli, D. Gatteschi, D. W. Carnegie, R. L. Carlin, *J. Am. Chem. Soc.* **1985**, *107*, 2560; c) I. Vasilevesky, N. R. Rose, R. Stenkamp, R. D. Willett, *Inorg. Chem.* **1991**, *30*, 4082; d) G. de Munno, M. Julve, F. Lloret, J. Faus, M. Verdaguer, A. Caneschi, *Angew. Chem.* **1993**, *105*, 1122; *Angew. Chem. Int. Ed. Engl.* **1993**, *32*, 1046.
[12] X-ray structure analysis: Enraf-Nonius CAD4 diffractometer. $Mo_{K\alpha}$, 0.71069 Å, graphite monochromator, 293(2) K. Lorentz-polarization but no absorption corrections. Data collection, solution and refinement: $\omega/2\theta$, standard Patterson methods (SHELSX program) and refined with SHELX93 program. The positions of eight H atoms were located from a difference synthesis. $C_{10}H_8N_8Mn$ ($M_r = 295.18$), triclinic, $P\bar{1}$, $a = 7.547(2)$, $b = 9.137(4)$, $c = 9.960(4)$ Å, $\alpha = 110.76(4)$, $\beta = 104.43(2)$, $\gamma = 100.41(3)°$, $V = 593.9(4)$ Å^3, $Z = 2$, $\rho_{calcd} = 1.651$ g cm^{-3}, $\mu = 11.1$ cm^{-1}, $F(000) = 298$, 2075 unique reflections and 2048 assumed as observed with $I \geq 2\sigma(I)$, 198 parameters, $R(F_o) = 0.055$, $R_w(F_o^2) = 0.125$ and $S = 0.964$. Further details of the crystal structure investigation are available on request from the Director of the Cambridge Crystallographic Data Centre, 12 Union Road, GB-Cambridge CB2 1EZ (UK), on quoting the full journal citation.
[13] a) M. E. Fisher, *Am. J. Phys.* **1964**, *32*, 343; b) R. Dingle, M. E. Lines, S. L. Holt, *Phys. Rev.* **1969**, *187*, 643.

Supramolecular Activation of *para*-Benzoquinone

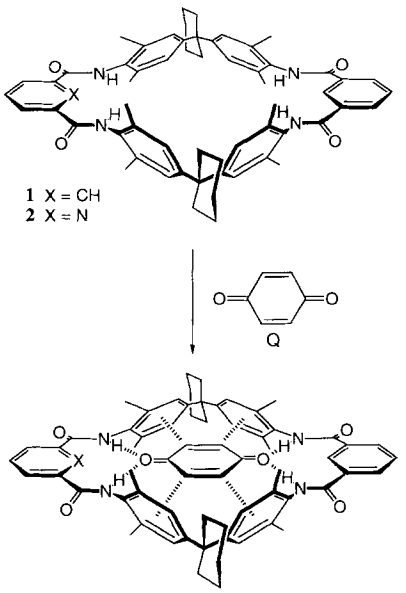
Paula A. Brooksby, Christopher A. Hunter,* A. James McQuillan,* Duncan H. Purvis, Alan E. Rowan, Richard J. Shannon, and Russell Walsh

A key feature of biochemical transformations is chemical activation of a bound substrate by noncovalent interactions with its protein environment. Although great progress has been made in the design of artificial enzymes, few of these systems use a specifically tailored molecular environment to enhance reactivity of the bound substrate,[1] but rather rely on positioning two reactive groups in close proximity.[2] In this paper, we demonstrate how a tailored environment can be used to polarize and activate a noncovalently bound substrate.

Quinones play an important role in photosynthesis. Photosynthetic reaction centers in plants and bacteria contain two closely spaced quinone cofactors, which are the ultimate electron acceptors on the electron transfer pathway and function as a two-electron gate.[3] The properties of the quinones change dramatically on complexation by the protein.[4] In particular, their reduction potentials are between 0.30 and 0.37 V more negative, depending on the particular organism. In an attempt to reproduce these properties, we have developed molecular receptors **1** and **2**, which complex *para*-benzoquinone (Q) through a combination of H-bonds and edge-to-face π–π interactions (Scheme 1).[5, 6] The intermolecular interactions were chosen not only for their molecular recognition properties, but also in the hope that they would cooperatively polarize the guest and modify its chemical properties.

The electrochemical properties of the complexes of Q with **1** and **2** were investigated by cyclic voltammetry. The properties of the two complexes were similar, but due to the low solubility of **1** most of the following discussion will focus on the complex **2** · Q. The experiments were carried out with 10^{-3} M solutions of Q in CH_2Cl_2, a platinum disk electrode, and 0.1 M tetrabutylammonium perchlorate (TBAP) as the supporting electrolyte. The electrolyte may reduce the affinity of Q for the

[*] Dr. A. J. McQuillan, P. A. Brooksby, D. H. Purvis, Dr. A. E. Rowan, Dr. R. Walsh
Department of Chemistry, University of Otago
PO Box 56, Dunedin (New Zealand)
Telefax: Int. code + (34) 797906
Dr. C. A. Hunter, R. J. Shannon
Department of Chemistry, The University
Sheffield S3 7HF (UK)
Telefax: Int. code + (742) 738673



Scheme 1. Two receptors for *para*-benzoquinone.

receptors through competition for the H-bonding sites. However, ^{1}H NMR studies showed that 10^{-2} M concentrations of TBAP had no effect on the binding.

The cyclic voltammogram of Q (Fig. 1a) showed a reversible one-electron reduction with an $E_{1/2}$ of -0.46 V. The reduction peak was at -0.53 V, and the corresponding oxidation peak

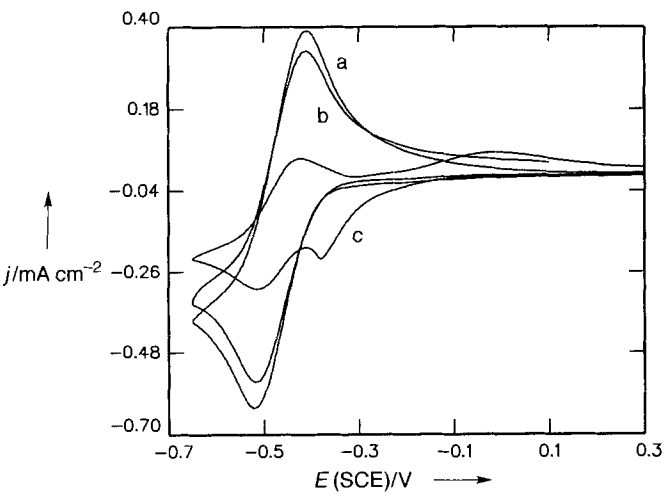


Fig. 1. Cyclic voltammograms of Q in 0.1 M solutions of TBAP in CH_2Cl_2. Platinum disk, 1.6 mm, working electrode. Saturated calomel reference electrode (SCE). Sweep rate 100 mV s^{-1}. a) 1.5×10^{-3} M Q. b) 1.1×10^{-3} M Q and 1.1×10^{-3} M benzanilide. c) 1.0×10^{-3} M Q and 1.0×10^{-3} M **2**.

appeared at -0.39 V. When the experiment was repeated in the presence of **1** or **2** (Fig. 1c), a reduction wave due to free Q was again observed, but a new subsidiary reductive wave appeared at -0.38 V, a shift of 150 mV relative to that of uncomplexed Q. A new oxidative wave also appeared at around 0.00 V, a shift of 390 mV relative to that of uncomplexed Q. The intensity of these new waves increased with increasing receptor concentration. The receptors are not electroactive over the potential range studied; this implies that the new waves are due to the quinone complexes. However, the separation between the reduction and corresponding oxidation peaks of these new waves is too large for the electron transfer to be a simple reversible process. The oxidative wave broadened and moved to higher potentials as the sweep rate was increased. This implies that there is a process which inhibits reoxidation of the quinone radical anion, but we have yet to discover the nature of this process. Protonation of the radical anion by acidic cosolvents leads to similar behavior, but the spectroscopic evidence presented below demonstrates clearly that protonation of the bound radical anion does not occur.

The nature of the species that give rise to the new waves at -0.38 V and 0.00 V was investigated by UV/Vis spectroelectrochemistry. Spectra were recorded as a function of electrode potential from a thin-layer cell.[7] The parent Q absorbs at 244 nm in the UV/Vis region but has no significant absorptions at longer wavelengths, while the semiquinone radical anion ($Q^{\bullet-}$) has very strong absorptions at 326 and 426 nm. This simplifies interpretation of the spectra in Figure 2. The reductive wave at

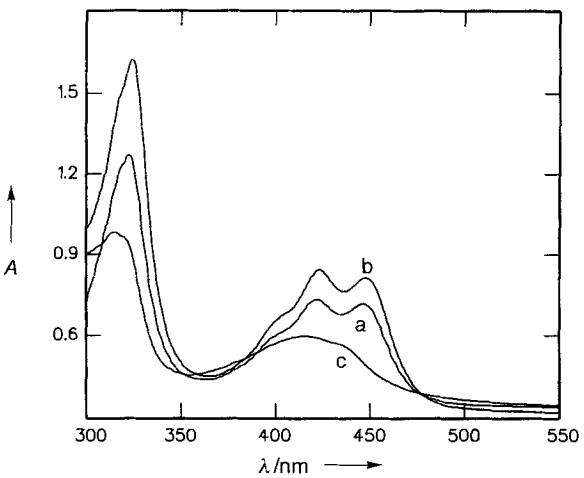


Fig. 2. UV/Vis absorption spectra of partially reduced Q in 0.1 M solutions of TBAP in CH_2Cl_2. The thin-layer electrochemical cell (Pt mesh electrode, 0.35 mm path length) has been described elsewhere [7]. Spectra were recorded at potentials corresponding to comparable stages of reduction. a) 1.5×10^{-3} M Q. b) 1.1×10^{-3} M Q and 1.0×10^{-3} M benzanilide. c) 1.4×10^{-3} M Q and 1.0×10^{-3} M **2**.

-0.38 V correlated with a decrease in the intensity of the Q absorption at 244 nm (not shown) and with the appearance of $Q^{\bullet-}$ absorptions at 324 and 412 nm (Fig. 2c). Similarly, the oxidative wave at $+0.00$ V correlated with the disappearance of the $Q^{\bullet-}$ absorptions. These results demonstrate clearly that the new subsidiary waves in the cyclic voltammogram (Fig. 1c) correspond to the reduction of Q and oxidation of $Q^{\bullet-}$ bound inside the receptor cavity. The spectra of the free and bound $Q^{\bullet-}$ differ significantly (Fig. 2a, c). The 426 nm absorption of $Q^{\bullet-}$ is shifted to shorter wavelength when it is bound inside the receptor, and the vibrational structure is less resolved. This reflects the different molecular environments of the two species.[8]

SNIFTIR experiments were used to probe changes in the hydrogen-bonding interactions that accompany reduction of the quinone complexes.[11] Figure 3 shows the SNIFTIR spectra, which are potential-induced difference spectra. Reduction of free Q is accompanied by a decrease in intensity of the 1669 and 1656 cm^{-1} bands (C=O stretch) and the appearance of $Q^{\bullet-}$ signals at 1505 and 1344 cm^{-1} (Fig. 3a). In the presence of **2**, two additional signals are observed in the difference spectrum (Fig. 3c). These signals are due to changes in the frequencies of the receptor amide stretches on reduction of the bound guest.

 © VCH Verlagsgesellschaft mbH, D-69451 Weinheim, 1994 0570-0833/94/2323-2490 $ 10.00+.25/0

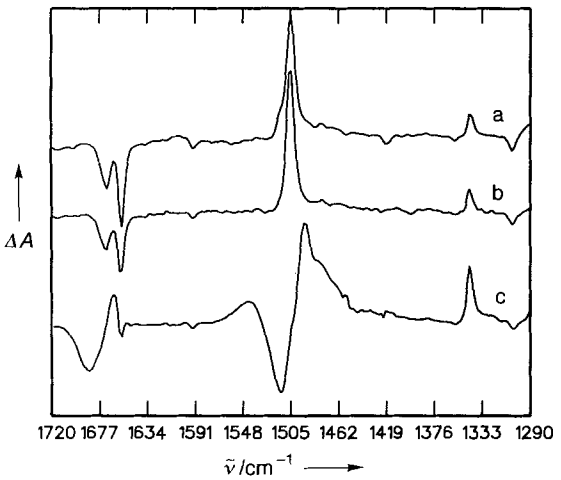


Fig. 3. SNIFTIR spectra of partially reduced Q in 0.1 M solutions of TBAP in CH_2Cl_2. Absorbance differences (ΔA) are due to a potential change from 0.0 to -0.5 V (SCE) in each case. a) 2.0×10^{-3} M Q. b) 1.5×10^{-3} M Q and 1.3×10^{-3} M benzanilide. c) 1.3×10^{-3} M Q and 1.0×10^{-3} M **2**.

The frequency of the amide I stretch shifts from 1686 to 1665 cm^{-1}; this indicates a decrease in the double bond character of the C=O bond. The amide II stretch also shifts from 1515 to 1543 cm^{-1}. It appears that the bound $Q^{\bullet-}$ carbonyl absorption is at 1492 cm^{-1} and that the free $Q^{\bullet-}$ absorption is subsumed in the negative amide II band. These changes imply that reduction of bound Q polarizes the amide bonds in the receptor so that the amide protons become more positive, hydrogen-bond more strongly to the guest, and stabilize the $Q^{\bullet-}$ negative charge.[12] Although such polarization effects are not accounted for by molecular mechanics force fields, calculations with the CHARMm force field also suggest that reduction of the complex is associated with an increase in the strength of the H-bonds, which stabilize the large negative charges on the $Q^{\bullet-}$ oxygen atoms.[9] The calculated H-bond lengths in the **1** · $Q^{\bullet-}$ complex (2.02, 2.04, 2.21, and 2.25 Å) are significantly shorter than in the **1** · Q complex (2.22, 2.31, 2.38, and 2.42 Å).

As a control, we repeated the experiments with benzanilide in place of the receptors. Even at 10^{-2} M concentrations of benzanilide (not shown), no significant changes were observed in the cyclic voltammogram of Q (Fig. 1b). Similarly, the UV/Vis spectroelectrochemical and SNIFTIR experiments gave spectra that were almost indistinguishable from those obtained for Q alone (Fig. 2b and 3b). ^{1}H NMR and FTIR spectra of Q in the presence of 10^{-2} M benzanilide show that there is no intermolecular hydrogen-bonding at these concentrations. Thus the changes in the electrochemical properties of the receptor · Q complexes can be attributed to the formation of a specific 1:1 complex rather than to the presence of amide groups that could interact with the radical anion.

This work demonstrates that if polarizing interactions such as H-bonds perturb the electronic structure of a noncovalently bound substrate in a cooperative manner, then the chemical properties of the substrate can be significantly modified.[10] The interactions that bind the quinone cofactors in photosynthetic reaction centers of purple bacteria involve an H-bond to each of the quinone oxygens, $\pi-\pi$ interactions, and hydrophobic contacts.[3] In addition, the quinones are linked to a non-heme iron(II) ion through a histidine bridge. The role of the iron ion has not been established, but it is thought to stabilize the buildup of negative charge on the semiquinone radical anions.[3] Although these results do not rule out this possibility, they show that H-bonding interactions alone are sufficient to produce a stabilization comparable to that observed in the natural systems. These interactions also appear to slow down reoxidation of the quinone radical anion, which would help prevent charge recombination in the photoinduced electron transfer reactions in the primary events in photosynthesis.

Received: July 9, 1994 [Z 7114 IE]
German version: *Angew. Chem.* **1994**, *106*, 2584

[1] P. Tecilla, S.-K. Chang, A. D. Hamilton, *J. Am. Chem. Soc.* **1990**, *112*, 9586; V. Jubian, R. P. Dixon, A. D. Hamilton, *ibid.* **1992**, *114*, 1120.
[2] H.-D. Lutter, F. Diederich, *Angew. Chem.* **1986**, *98*, 1125; *Angew. Chem. Int. Ed. Engl.* **1986**, *25*, 1125; J. T. Groves, R. Neumann, *J. Am. Chem. Soc.* **1989**, *111*, 2900; T. R. Kelly, C. Zhao, G. J. Bridger, *ibid.* **1989**, *111*, 3744; P. Tecilla, A. D. Hamilton, *J. Chem. Soc. Chem. Commun.* **1990**, 1232; T. Tjivikua, P. Ballester, J. Rebek, Jr., *J. Am. Chem. Soc.* **1990**, *112*, 1249; L. G. Mackay, R. S. Wylie, J. K. M. Sanders, *ibid.* **1994**, *116*, 3141.
[3] a) A. R. Crofts, C. A. Wraight, *Biochim. Biophys. Acta* **1983**, *726*, 149; b) J. Deisenhofer, H. Michel, *Angew. Chem.* **1989**, *101*, 872; *Angew. Chem. Int. Ed. Engl.* **1989**, *28*, 829; c) R. Huber, *ibid.* **1989**, *101*, 849 and **1989**, *28*, 848; d) G. Feher, J. P. Allen, M. Y. Okamura, D. C. Rees, *Nature* **1989**, *339*, 111.
[4] M. R. Gunner, *Curr. Top. Bioenerg.* **1991**, *16*, 319.
[5] C. A. Hunter, *J. Chem. Soc. Chem. Commun.* **1991**, 749.
[6] C. A. Hunter, D. H. Purvis, *Angew. Chem.* **1992**, *104*, 779; *Angew. Chem. Int. Ed. Engl.* **1992**, *31*, 792.
[7] R. S. K. A. Gamage, A. J. McQuillan, B. M. Peake, *J. Chem. Soc. Faraday Trans.* **1991**, *87*, 3653.
[8] A shift to shorter wavelength and loss of vibrational structure due to H-bonding is consistent with an $n-\pi^*$ transition. H. H. Jaffé, M. Orchin, *Theory and Applications of Ultraviolet Spectroscopy*, Wiley, New York, **1962**.
[9] Annealed molecular dynamics simulations were carried out with QUANTA and the CHARMm force field; B. R. Brooks, R. E. Bruccoleri, B. D. Olafson, D. J. States, S. Swaminathan, M. Karplus, *J. Comput. Chem.* **1983**, *4*, 187. Partial atomic charges for Q and $Q^{\bullet-}$ were calculated with MNDO.
[10] The $\pi-\pi$ interactions in this system have a relatively weak electrostatic component, and we assume that they have very little effect on the properties of the substrate. See C. A. Hunter, J. K. M. Sanders, *J. Am. Chem. Soc.* **1990**, *112*, 5525.
[11] Subtractively normalized interfacial Fourier transform infrared spectroscopy (SNIFTIRS) is described by J. K. Foley, *Electroanal. Chem.* **1986**, *14*, 309.
[12] S. Krimm, J. Bandekar, *Adv. Protein Chem.* **1986**, *38*, 181.

$(H_3N(CH_2)_6NH_3)_4[W_{18}P_2O_{62}]\cdot 3H_2O$, a Microporous Solid from Dawson Anions and 1,6-Diaminohexane**

Markus Hölscher, Ulli Englert, Bodo Zibrowius, and Wolfgang F. Hölderich*

The synthesis of solids with defined cavities is the main concern of many current research projects, with a special focus on the preparation of microporous materials containing transition metals. These metal atoms could serve as active sites for oxidation reactions and thus lead to shape-selective reactions due to the defined pore structure of the carrier—a principle that has been well established with zeolites.[1, 2]

[*] Prof. W. F. Hölderich, Dipl.-Chem. M. Hölscher, Dr. B. Zibrowius
Institut für Brennstoffchemie und physikalisch-chemische Verfahrenstechnik der Technischen Hochschule
Worringer Weg 1, 52074 Aachen (FRG)
Telefax: Int. code + (241)873238
Dr. U. Englert
Institut für Anorganische Chemie der Technischen Hochschule Aachen

[**] This work was supported by the state of Nordrhein-Westfalen. We thank F. D. Scherberich and Dr. J. Glinemann (Institut für Kristallographie der Technischen Hochschule Aachen) for powder diffraction measurements and valuable discussions while solving the structure.

 © VCH Verlagsgesellschaft mbH, D-69451 Weinheim, 1994 0570-0833/94/2323-2491 $ 10.00+.25/0

For this reason the isomorphous substitution of silicon in zeolites by other elements has been intensively investigated. Taramasso et al., for instance, could report for the first time on titanium-containing ZSM-5 zeolites in 1983. This material showed catalytic activity in oxidation reactions with H_2O_2.[3] In the case of microporous aluminophosphates, which are closely related to zeolites (alternating AlO_4 and PO_4 tetrahedra form a three-dimensional network), it was shown that phosphorus as well as silicon could be substituted isomorphously by a variety of different metals.[4]

A different kind of approach was made by preparing three-dimensional microporous structures that consisted of the elements phosphorus, oxygen, and transition metal. Rather than using isomorphous substitution, completely new structures and groups of compounds were developed. Haushalter et al. reported on microporous molybdenum phosphates,[5] and Zubieta et al. were successful a short time ago in preparing a vanadium phosphate with elliptical cavities.[6] A microporous cobalt phosphate was prepared by Thomas et al. very recently.[7]

Heteropolyoxometallates of molybdenum and tungsten have been very thoroughly studied and are being used as technical catalysts.[8, 9] For that reason it might be very interesting to prepare these compounds in such a way that they become part of a microporous material. It was our aim to study this new alternative. The Keggin ion $M_{12}XO_{40}^{n-}$ or the Dawson ion $M_{18}X_2O_{62}^{m-}$ (X = P, Si, As, Ge; M = Mo, W; n = 3,4; m = 6) are classic examples. To our knowledge, these heteropolyoxometalates have been crystallized with a large variety of cations, but none of the reported structures showed defined micropores large enough to be useful for shape-selective catalysis.[10] During the course of our investigations to prepare such materials we were able to obtain the first example of that kind. Here we report on the synthesis and characterization of **1**, a reduced Dawson anion that is part of a microporous solid.

$(H_3N(CH_2)_6NH_3)_4[W_{18}P_2O_{62}] \cdot 3H_2O$ **1**

The hydrothermal reaction of tungsten, tungsten oxide, 1,6-diaminohexane, phosphoric acid, and water gave dark blue crystals of **1** in 90% yield.[11] The single-crystal structure analysis showed **1** to consist of discrete Dawson anions surrounded by 1,6-diaminohexane in such a way that the protonated amino groups of one molecule connect two Dawson units. A total of eight alkylammonium groups are in close contact with one anion (Fig. 1). The cavities constructed in this way along the crystallographic c axis have shortest O–O distances of 7.6 × 8.4 Å (internuclei distances). A view of the structure of **1** along the crystallographic b axis shows sheets of anions forming a zigzag chain parallel to the a axis in which every alternate anion lies at the same height (Fig. 2). Between these sheets the 1,6-diaminohexane molecules work as spacers, which likewise form channels. In this projection these openings have shortest O–O distances of 3.6 Å and C–C distances of 9.1 Å. They are too small for organic molecules and contain water molecules, which could be located in the structure analysis. The same is true for the cavities in the a direction, which have dimensions of approximately 3.6 × 8.7 Å.

The Dawson anion is built up from edge- and corner-sharing octahedra encapsulating two phosphorous atoms. In **1** the α-isomer of the anion has crystallized.[17] M–O distances were 1.69–1.71 for terminal oxygens, 1.91–2.08 for μ_2-bridging oxygens, and 2.34–2.38 for μ_3-bridging oxygens. P–O distances varied between 1.54 and 1.59 Å. Our structure determination is in good agreement both with the Dawson[18] and the d'Amour structures of Dawson anions.[19] The anions and the organic dications are connected through hydrogen bonds, and the fact that eight N atoms surround one anion suggests that the Dawson unit is the doubly reduced $[W_{18}P_2O_{62}]^{8-}$. Now we are trying to find evidence for this idea by means of cyclovoltametry. Bond valence calculations do not implicate further protonations.[20] FTIR as well as ^{13}C MAS-NMR and ^{31}P MAS-NMR spectra conformed to expectations.[21, 22, 23] Compound **1** crystallized as a single pure phase, as could be shown by comparing the experimental and the simulated X-ray powder diffraction pattern. Thermoanalyses in air showed that the compound became amorphous at about 200 °C. In the temperature range between 200 and 500 °C the diamine decomposed resulting in a weight loss of 11% (calculated for 1,6-diaminohexane and water of crystallization: 10.7%), and the anion was oxidized, which was observed as a change from dark blue to greenish yellow. To investigate whether the micropore volume is accessible, attempts were made to obtain adsorption isotherms both with

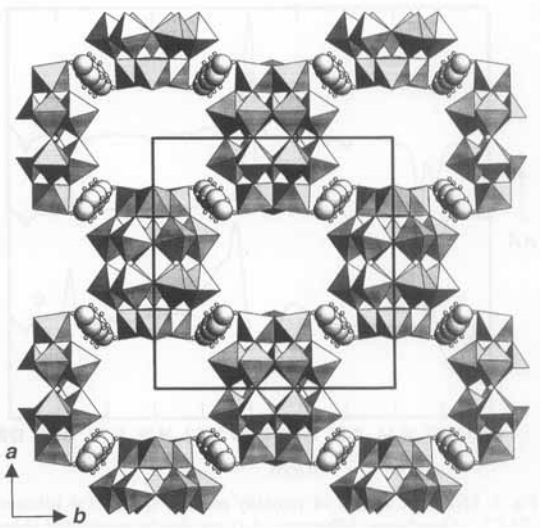


Fig. 1. View of the crystal structure of **1** along the crystallographic c axis. The arrangement of anions (polyhedral representation) and cations (radii arbitrary) forms rectangular openings.

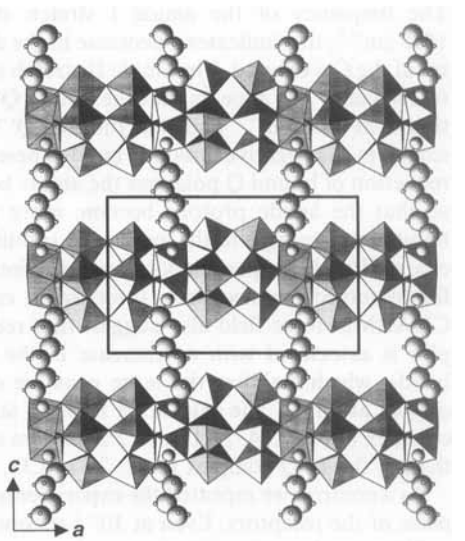


Fig. 2. View of the structure of **1** along the crystallographic b axis. The zigzag chain of polyanions runs parallel to the a axis. The $H_3N(CH_2)_6NH_3$ ions function as spacers in the c direction (carbon: large circles, hydrogen: small circles; nitrogen atoms without hydrogen atoms; radii arbitrary).

nitrogen and water as adsorbate. Finely powdered samples were degassed for 12 hours at temperatures between 100 and 200 °C in a vacuum of 10^{-5} Torr. Under these conditions none of the samples adsorbed nitrogen or water in substantial amounts. We are unable to explain this result at present.

We are also investigating whether the organic spacer influences the formation of the structure as a whole, or whether the choice of the diamine is critical enough to favor the formation of different heteropolyanions. Furthermore, we have started to perform experiments to explore the catalytic potential of **1** in oxidation reactions. We believe that a variety of new interesting compounds should be available, since the preparation of **1** is so surprisingly simple.

Received: July 29, 1994 [Z 7187 IE]
German version: *Angew. Chem.* **1994**, *106*, 2552

[1] W. F. Hölderich, H. van Bekkum in *Introduction to Zeolite Science and Practice* (*Stud. Surf. Sci. Catal.* **1991**, *58*, 631–727).
[2] S. M. Csicsery, *Zeolites* **1984**, *4*, 202–213.
[3] M. Taramasso, G. Perego, B. Notari (Snamprogetti S.p.A., Milan, Italy), US-A 4410501, **1983**.
[4] E. M. Flanigen, B. M. Lok, R. L. Patton, S. T. Wilson in *New Developments in Zeolite Science and Technology*. (*Proc. Int. Conf. Zeolites 7th*. Tokyo **1986**, 103–112).
[5] R. C. Haushalter, L. A. Mundi, *Chem. Mater.* **1992**, *4*, 31–48.
[6] V. Soghomonian, Q. Chen, R. C. Haushalter, J. Zubieta, *Angew. Chem.* **1993**, *105*, 601–603; *Angew. Chem. Int. Ed. Engl.* **1993**, *32*, 610.
[7] J. Chen, R. H. Jones, S. Natarajan, M. B. Hursthouse, J. M. Thomas, *Angew. Chem.* **1994**, *106*, 667–668; *Angew. Chem. Int. Ed. Engl.* **1994**, *33*, 639–640.
[8] M. Misono in *New Frontiers in Catalysis* (*Proc. Int. Congr. Catal. 10th Part A* **1992**, 69).
[9] W. F. Hölderich in *New Frontiers in Catalysis* (*Proc. Int. Congr. Catal. 10th Part A* **1992**, 127).
[10] M. T. Pope in *Compr. Coord. Chem., Vol. 3* (Eds.: G. Wilkinson, R. D. Gillard, J. A. McCleverty), Pergamon, Oxford, **1987**, pp. 1023–1058.
[11] WO_3, W, 1,6-diaminohexane (50% in H_2O), H_3PO_4, and H_2O were mixed in a Teflon beaker of 250 mL volume in molar ratios of 8:1:27:42:4400, inserted into an autoclave, and then kept for 4 d at 200 °C (beaker 45% full). Dark blue crystals of **1** remained after filtration. The crystals were washed with water and air dried. The yield referred to tungsten was 85 to 95%.
[12] a) Crystal structure analysis of **1**: ENRAF-Nonius CAD4; $Ag_{K\alpha}$ radiation (0.5609 Å), graphite monochromator; empirical absorption correction (PSI, [13]); intensity data were collected with ω-2θ scan at 291 K. Dark blue parallelepiped $0.2 \times 0.2 \times 0.2$ mm, orthorhombic space group *Pmmn* (No. 59); $a = 19.839(5)$, $b = 18.682(4)$, $c = 12.605(4)$ Å, $V = 4671(2)$ Å^3, $Z = 2$, $\rho_{calcd} = 3.476$ g cm^{-3}, $\mu(Ag_{K\alpha}) = 121.69$ cm^{-1}, $F(000) = 4320$; 8324 reflexes with $2 < \theta < 24°$, 3652 symmetry independent with $I > 3\sigma(I)$ in structure solution [14] and refinement [15] for 255 parameters; molecular symmetry of the heteropolytungstate *mm*2; except for the oxygen atom of one water molecule which is disorderd, all non-hydrogen atoms were refined anisotropically. Extinction coefficient [16] was refined to 2.6×10^{-7}. $R = 0.057$, $R_w = 0.053$, $w^{-1} = 1/\sigma^2(F_o)$; H atoms unrefined in structure factor calculation; b) Further details on the structure determination of **1** may be obtained from the Fachinformationszentrum Karlsruhe, D-76344 Eggenstein-Leopoldshafen on quoting the depository number CSD-401200.
[13] A. C. T. North, D. C. Phillips, F. S. Mathews, *Acta Crystallogr. Sect. A* **1968**, *24*, 351–359.
[14] G. M. Sheldrick, SHELXS-86, Program for Crystal Structure Solution, Göttingen, **1986**.
[15] B. A. Frenz, The Enraf-Nonius CAD4-SDP – a Real-Time System for Concurrent X-Ray Data Collection and Crystal Structure Determination in *Computing in Crystallography* (Eds.: H. Schenk, R. Olthof-Hazekamp, H. van Koningsveld, G. C. Bassi), University of Delft, SDP-PLUS, Version 1.1 (**1984**) and VAXSDP, Version 2.2 (**1985**).
[16] W. H. Zachariasen, *Acta Crystallogr.* **1963**, *16*, 1139–1144.
[17] R. Contant, R. Thouvenot, *Inorg. Chim. Acta* **1993**, *212*, 41–50.
[18] B. Dawson, *Acta Crystallogr.* **1953**, *6*, 113–126.
[19] H. d'Amour, *Acta Crystallogr. Sect. B* **1976**, *32*, 729–740.
[20] N. E. Breese, M. O'Keeffe, *Acta Crystallogr. Sect. B* **1991**, *47*, 192–197.
[21] IR (KBr disk, characteristic bands): ν[cm^{-1}] = 3449 (m, $\nu(H_2O)$), 3130 (m, $\nu(NH_3^+)$), 2930, 2860 (m, $\nu(CH_2)$), 1080 (m, $\nu(PO_4)$), 943, 912, 819 (vs, ν(W-O)).
[22] The ^{13}C and ^{31}P MAS-NMR spectra were measured on a MSL300 or MSL500 spectrometer using high-power proton decoupling at a resonance frequency of 75.5 MHz and 202.5 MHz, respectively. The contact time for ^{13}C CPNMR spectra was 1 ms. The signals in the ^{13}C NMR spectra at $\delta = 27.8$ and 41.8 (± 0.1 ppm) could be assigned to protonated 1,6-diaminohexane. The ^{31}P NMR spectrum shows three signals at $\delta = -1.2$, -7.2, and -13.0 (± 0.2 ppm) and a shoulder at $\delta = -14.2$. The strongest signal ($\geq 70\%$ of total intensity) at $\delta = -13.0$ can unambiguously be assigned to the phosphorus nuclei in the Dawson anion. The signal at $\delta = -1.2$ is caused by excess phosphoric acid and/or an adduct of phosphoric acid and 1,6-diaminohexane.
[23] R. Massart, R. Contant, J. M. Fruchart, J. P. Ciabrini, M. Fournier, *Inorg. Chem.* **1977**, *16*, 2916–2921.

 © VCH Verlagsgesellschaft mbH, D-69451 Weinheim, 1994 0570-0833/94/2323-2493 $ 10.00+.25/0

New Books

Waste Minimisation: A Chemist's Approach. Edited by **K. Martin, T. W. Bastock.** Royal Society of Chemistry, Cambridge, **1994.** 155 pp., hardcover, £ 39.50.—ISBN 0-85186-585-2

The Laboratory Environment. Edited by **R. Purchase.** Royal Society of Chemistry, Cambridge, **1994.** 258 pp., hardcover, £ 49.50.—ISBN 0-85186-605-0

Organic Reactions Mechanism - 1992. Edited by **A. C. Knipe, W. E. Watts.** Wiley, Chichester, Great Britain, **1994.** 624 pp., hardcover, £ 165.00.—ISBN 0-471-94224-3

Röntgenstrukturanalyse und Rietveldmethode, 5nd Ed. By **H. Krischner, B. Koppelhuber-Bitschnau.** Vieweg, Braunschweig, **1994.** 194 pp., paperback, DM 46.00.—ISBN 3-528-48324-5

Kapillarelektrophorese. Methoden und Möglichkeiten. By **H. Engelhardt, W. Beck, T. Schmitt.** Vieweg, Braunschweig, **1994.** 206 pp., paperback, DM 72.00.—ISBN 3-528-06597-4

Biomedical Polymers. Edited by **S. W. Shalaby.** Carl Hanser, München, **1994.** Hardcover, DM 188.00.—ISBN 3-446-16531-2

Theory of Coronoid Hydrocarbons. (Lecture Notes in Chemistry, Vol. 62). Edited by **S. J. Cyvin, J. Brunvoll, R. Chen et al.** Springer, Heidelberg, **1994.** 297 pp., paperback, DM 90.00.—ISBN 3-540-58138-3

Membrane Processes in Separation and Purification. Edited by **J. G. Crespo.** Kluwer, Dordrecht, **1994.** 520 pp., hardcover, Dfl 385.00.—ISBN 0-7923-2929-5

Synchroton Techniques in Interfacial Electrochemistry. Edited by **C. A. Melendres.** Kluwer, Dordrecht, **1994.** 500 pp., hardcover, Dfl 350.00.—ISBN 0-7923-2844-2

Computational Approaches in Supramolecular Chemistry. Edited by **G. Wipff.** Kluwer, Dordrecht, **1994.** 548 pp., hardcover, Dfl 360.00.—ISBN 0-7923-2767-5

Synthetic Oligosaccharides. Indispensable Probes for the Life Sciences. (ACS Symposium Series No. 560). Edited by **P. Kovác.** American Chemical Society, Washington, **1994.** 304 pp., hardcover, $ 79.95.—ISBN 0-8412-2930-9

Organic-Chemical Drugs and Their Synonyms. By **M. Negwer.** Akademie Verlag, Berlin, **1994.** 3937 pp., hardcover, DM 475.00.—ISBN 3-05-501629-7

Bioregulators for Crop Protection and Pest Control.(ACS Symposium Series No. 557). Edited by **P. A. Hedin.** American Chemical Society, Washington, **1994.** 220 pp., hardcover, $ 59.95.—ISBN 0-8412-2918-X

Lipids in Food Flavors. (ACS Symposium Series No. 558). Edited by **C.-T. Ho.** American Chemical Society, Washington, **1994.** 324 pp., hardcover, $ 89.95.—ISBN 0-8412-2922-8

Sulfur Compounds in Foods. (ACS Symposium Series No. 564). Edited by **C. J. Mussinan, M. E. Keelan.** American Chemical Society, Washington, **1994.** 304 pp., hardcover, $ 79.95.—ISBN 0-8412-2943-0

Interfacial Design and Chemical Sensing. (ACS Symposium Series No. 561). Edited by **T. E. Mallouk, D. J. Harrison.** American Chemical Society, Washington, **1994.** 352 pp., hardcover, $ 94.95.—ISBN 0-8412-2931-7

Biodegradable Plastics and Polymers. Edited by **Y. Doi, K. Fukuda.** Elsevier, Amsterdam, **1994.** 646 pp., hardcover, Dfl 495.00.—ISBN 0-444-81708-5

Atomistic Modeling of Physical Properties of Polymers. (Advances in Polymer Sciene, Vol. 116). Edited by **L. Monnerie, U. W. Suter.** Springer, Heidelberg, **1994.** 388 pp., hardcover, DM 258.00.—ISBN 3-540-57827-7

Probenahme und Aufschluß. Edited by **M. Stoeppler.** Springer, Heidelberg, **1994.** 181 pp., hardcover, DM 98.00.—ISBN 3-540-57491-3

Mathematical Techniques in Crystallography and Materials Science. By **E. Prince.** Springer, Heidelberg, **1994.** 223 pp., hardcover. DM 128.00.—ISBN 3-540-58115-4

Progress in Pacific Polymer Science 3. Edited by **K. P. Ghiggino.** Springer, Heidelberg, **1994.** 437 pp., hardcover, DM 178.00.—ISBN 3-540-57621-5

Porphyric Pesticides. Chemistry, Toxicology, and Pharmaceutical Applications. Edited by **S. O. Duke, C. A. Rebeiz.** American Chemical Society, Washington, **1994.** 312 pp., hardcover, $ 79.95.—ISBN 0-8412-2923-6

New Gmelin Volumes published:

Compounds with Bonds between Tin and Transition Metals of Groups III to VII. Sn. Zinn. Tin (system No. 46). Edited by **U. Krüerke.** Springer, Heidelberg, **1994.** 309 pp., hardcover, DM 1890.00.—ISBN 3-540-93690-4

Compounds with Carbon. Sc, Y, La - Lu. Seltenerdelemente. Rare Earth Elements (system No. 39). Edited by **M Irmler, C. Koeppel, H. Pscheidl et al.** Springer, Heidelberg, **1994.** 362 pp., hardcover, DM 2195.00.—ISBN 3-540-93689-0

Compounds with Se, Te, Po. Mo. Molybdän. Molybdenum (system No. 53). Edited by **H. Katscher, B. Mohsin.** Springer, Heidelberg, **1994.** 165 pp., hardcover, DM 1050.00.—ISBN 3-540-93691-2

Environmental Sampling for Trace Analysis. By **B. Markert.** VCH, Weinheim, **1994.** 282 pp., hardcover, DM 248.00.—ISBN 3-527-30051-1

Enzymkinetik, 2nd Ed. By **S. Bisswanger.** VCH, Weinheim, **1994.** 321 pp., hardcover, DM 118.00.—ISBN 3-527-30032-5

The Chemistry of Metal CVD. Edited by **T. T. Kodas, M. J. Hampden-Smith.** VCH, Weinheim, **1994.** 530 pp., hardcover, DM 228.00/$ 135.00.—ISBN 3-527-29071-0

Deterministisches Chaos. By **H. G. Schuster.** VCH, Weinheim, **1994.** 288 pp., paperback, DM 78.00.—ISBN 3-527-29089-3

Research and Development of Vaccinees and Pharmaceuticals from Biotechnology. By **J.-P. Gregersen.** VCH. Weinheim, **1994.** 173 pp., paperback, DM 98.00/$ 60.00.—ISBN 3-527-30059-7

Biologische Bodensanierung. Edited by **K. Alef.** VCH, Weinheim, **1994.** 269 pp., paperback, DM 78.00.—ISBN 3-527-30058-9

Praktische Qualitätssicherung in der Analytik. By **V. Neitzel, K. Middeke.** VCH, Weinheim, **1994.** 190 pp., paperback, DM 85.00.—ISBN 3-527-28686-1

Umweltchemie. By **C. Bliefert.** VCH, Weinheim, **1994.** 453 pp., paperback, DM 68.00.—ISBN 3-527-28692-6

Molecular Ecology of Rhizosphere Microorganisms. Biotechnology and the Release of GMO's. Edited by **F. O'Gara, D. N. Dowling, B. Boesten.** VCH, Weinheim, **1994.** 177 pp., hardcover, DM 148.00/$ 90.00.—ISBN 3-527-30052-X

Organische Chemie, 2nd Ed. By **A. Streitwieser, C. H. Heathcock, E. M. Kosower.** VCH, Weinheim, **1994.** 1374 pp., hardcover, DM 128.00.—ISBN 3-527-29005-2

Nichtmetallchemie. By **T. M. Klapötke, I. C. Tornieporth-Oetting.** VCH, Weinheim **1994.** 493 pp., hardcover, DM 58.00.—ISBN 3-527-29257-8

Organic Reactions, Vol. 45. Edited by **P. Beak, E. Ciganek, D. Curran et al.** Wiley, Chichester, Great Britain, **1994.** 671 pp., hardcover, £ 79.00.—ISBN 0-471-03161-5

LIMS: Implementation and Management. By **A. S. Nakagawa.** Royal Society of Chemistry, Cambridge, **1994.** 180 pp., hardcover, £ 37.50.—ISBN 0-85186-824-X

Total Quality Management in the Chemical Industry - Strategies for Success. Edited by **G. R. Turner, R. P. Hadfield.** Royal Society of Chemistry, Cambridge, **1994.** 200 pp., hardcover, £ 37.50.—ISBN 0-85186-624-7

Current Topics in the Chemistry of Boron. Edited by **G. W. Kabalka.** Royal Society of Chemistry, Cambridge, **1994.** 406 pp., hardcover, £ 59.50.—ISBN 0-85186-535-6

Chemically Modified Surfaces. Edited by **J. J. Pesek, I. E. Leigh.** Royal Society of Chemistry, Cambridge, **1994.** 223 pp., hardcover, £ 49.50.—ISBN 0-85186-595-X

Chemical Instrumentation. By **R. P. Wayne.** Oxford University Press, Oxford, **1994.** 92 pp., paperback, £ 4.99.—ISBN 0-19-855796-5

Principles and Applications of Electrochemistry 4th Ed. By **D. R. Crow.** Blackie/Chapman & Hall, London, **1994.** 282 pp., paperback, £ 16.99.—ISBN 0-7514-0168-4

Container Molecules and Their Guests. (Monographs in Supramolecular Chemistry). By **D. J. Cram, J. M. Cram.** Royal Society of Chemistry, Cambridge. **1994.** 223 pp., hardcover, £ 49.50.—ISBN 0-85186-972-6

The Role of Oxygen in Improving Chemical Processes. 6th BOC Priestley Conference. Edited by **M. Fetizon, W. J. Thomas.** Royal Society of Chemistry, Cambridge, **1993.** 286 pp., hardcover, £ 57.50.—ISBN 0-85186-725-1

Experimental Toxicology, 2nd Ed. The Basic Issues. Edited by **D. Anderson, D. M. Conning.** Royal Society of Chemistry, Cambridge. **1993.** 566 pp., paperback, £ 25.00.—ISBN 0-85186-461-9

Further Advances in Chemical Information. Edited by **H. Collier.** Royal Society of Chemistry, Cambridge, **1994.** 193 pp., hardcover, £ 45.00.—ISBN 0-85186-545-3

Sugarless - Towards the Year 2000. Edited by **A. J. Rugg-Gunn.** Royal Society of Chemistry, Cambridge, **1994.** 197 pp., hardcover, £ 37.50.—ISBN 0-85186-495-3

The Development of Plastics. Edited by **S. T. I. Mossman, P. J. T. Morris.** Royal Society of Chemistry, Cambridge, **1994.** 120 pp., hardcover, £ 35.00.—ISBN 0-85186-575-5

Electrochemistry and Clean Energy. Edited by **J. A. G. Drake.** Royal Society of Chemistry, Cambridge, **1994.** 104 pp., hardcover, £ 32.50.—ISBN 0-85186-472-4

Biochemistry of Milk Products. Edited by **A. T. Andrews, J. Varley.** Royal Society of Chemistry, **1994.** 182 pp., hardcover, £ 39.50.—ISBN 0-85186-702-2

Waste Incineration and the Environment. Issues in Environmental Science and Technology, Vol. 2. Edited by **R. E. Hester, R. M. Harrison.** Royal Society of Chemistry, Cambridge, **1994.** 158 pp., paperback, £ 15.00.—ISBN 0-85404-205-9

Protecting Groups. By **P. J. Kociénski.** Thieme, Stuttgart, **1994.** 265 pp., paperback, DM 60.00.—ISBN 3-13-135601-4

Food. The Definite Guide. By **T. Coultate, J. Davies.** Royal Society of Chemistry, **1994.** 167 pp, paperback, £ 12.50.—ISBN 0-85186-431-7

Organometallics in Synthesis. A Manual. Edited by **M. Schlosser.** Wiley, Chichester, Great Britain, **1994.** 603 pp., hardcover, £ 60.00.—ISBN 0-471-93637-5

AUTHOR INDEX [*Angew. Chem. Int. Ed. Engl.* **1994**, *33*]

The page numbers in square brackets refer to the German edition [*Angew. Chem.* **1994**, *106*] of *Angewandte Chemie*. Page numbers in round brackets indicate errata.

Abdon, R. L. 2328 [2414]
Abel, S. 2466 [2522]
Abraham, I. 2435 [2537]
Achar, S. 847 [895]
Adam, P. 1166 [1235]
Adam, W. 1107, 1609, 2475 [1159, 1699, 2545]
Adams, R. D. 568 [591]
Adelmann, P. 1651 [1742]
Adolin, G. 1151 [1211]
Aggarwal, V. K. 175 [185]
Ahlrichs, R. 199, 746 [225, 786]
Ahrens, B. 1852 [1966]
Aiyar, J. 855 [925]
Aizenberg, M. 317 [344]
Akazawa, T. 777 [829]
Al-Abed, Y. 1499 [1568]
Alarcón, S. H. 1624 [1708]
Alberti, G. 1594 [1655]
Albrecht, P. 1166 [1235]
Albrecht, S. 1780 [1864]
Aleshkin, A. 91 [106]
Al-Juaid, S. S. 1268 [1336]
Al-Tel, T. H. 1499 [1568]
Altmann, K.-H. 1654 [1735]
Amabilino, D. B. 433, 1286 [450, 1316]
Amin, S. 773 [824]
Anderson, H. L. 429, 655, 1366, 1628 [445, 711, 1427, 1691]
Anderson, P. A. 641 [669]
Ando, W. 659 [723]
Ansari, M. A. 2110 [2200]
Anthamatten, M. 1081 [1150]
Anthony, J. 763 [794]
Antonietti, M. 1869 [1927]
Antonov, D. 91 [106]
Anwander, R. 1285, 1641 [1338, 1725]
Arad, C. 875 [931]
Arce, A. J. 1381, 2193 [1459, 2277]
Arend, M. 2422 [2531]
Argüello, G. A. 1108 [1161]
Ariza, X. 2454 [2535]
Armatage, A. 770, 849 [800, 897]
Armstrong, A. R. 641 [669]
Arnold, J. 95 [119]
Arnold, M. 109 [77]
Arriortua, M. I. 2488 [2520]
Asbrand, M. 749 [791]
Ashton, P. R. 433, 1286, 1503 (1668) [450, 1316, 1563 (1865)]
Assink, R. A. 786 [803]
Astruc, D. 661, 1637, 2460 [715, 1721, 2540]
Atwood, J. L. 2456 [2571]
Auffermann, G. 1112 [1144]
Auf der Heyde, T. 823 [871]
Auner, N. 77 [93]
Austin, D. J. 1797 [1881]
Austin, R. N. 348 [355]
Avent, A. G. 2330 [2406]
Averill, B. A. 2057 [2145]
Ayougou, K. 348 [355]
Azuma, N. 878 [919]

Bacchi, A. 193 [206]
Bach, T. 417 [433]
Back, R. 2332 [2429]
Backhaus, D. 2098 [2167]
Bader, R. F. W. 620 [647]
Badia, A. 2332 [2429]
Baker, G. R. 666 [701]
Baker, R. 2320 [2416]
Bakshi, P. K. 1267 [1332]
Ballschmiter, K. 646 [688]
Bally, T. 1964 [2048]
Balzereit, C. 1487 (1668), 2303, 2306 [1579, 2391, 2394]
Bandel-Schlesselmann, C. 120 [126]
Bao, X. 85 [113]
Baratta, W. 193 [206]
Barbaux, Y. 2100 [2183]
Bardez, E. 2438 [2582]
Bargon, J. 755 [820]
Barluenga, J. 1392 [1451]
Barnes, C. L. 1081 [1150]
Barr, D. 1875 [1960]
Bartik, T. 2199 [2269]
Basché, T. 1723 [1805]
Bashall, A. 429 [445]
Bashir-Hashemi, A. 2059 [2159]
Batail, P. 1379 [1448]
Bats, J. W. 109, 1476 [77, 1559]
Bau, R. 2433 [2566]
Bauch, M. 984 [1041]
Bauer, B. 788 [793]
Baum, G. 1612 [1705]
Baumann, W. 1605, 1850 [1678, 1946]
Baumgarten, M. 1957 [2062]
Baxter, P. N. W. 2284 [2432]
Beale, J. M. 1648 [1733]
Beau, J.-M. 1383 [1457]
Beck, G. 685 [719]
Beck, J. 163 [172]
Beckhaus, H.-D. 996 [1033]
Bedurke, T. 350 [351]
Beer, E. 1087 [1140]
Behar, V. 1468 [1536]
Behrens, U. 987, 1257 [1023, 1364]
Beifuss, U. 1144 [1204]
Beley, M. 1282, 1775 [1359, 1854]
Belgardt, T. 1244, 1351 [1365, 1413]
Belik, P. 559 [601]
Belokon', Y. 91 [106]
Belz, T. 1866 [1919]
Belzner, J. 1854, 2450 [1949, 2580]
Bendix, M. 1955 [2043]
Benedetti, E. 1437 [1502]
Benninghoven, A. 1023 [1075]
Benniston, A. C. 1884 [1956]
Berenguer, J. R. 2083 [2196]
Bergmann, U. 849 [897]
Bergsträsser, U. 1491 [1541]
Berlekamp, M. 1114 [1168]
Berlin, K. 219, 1246 [229, 1356]
Bernabei, I. 2076 [2202]
Bernard, E. 887 [914]
Bernardinelli, G. 1856 [1931]
Berndt, A. 1487 (1668), 2064, 2303, 2306 [1579, 2172, 2391, 2394]
Bertagnolli, H. 45, 2435 [15, 2537]
Bertani, R. 576 [586]
Bertling, U. 1003 [1026]
Bertrand, G. 527, 578 [549, 584]
Beugholt, C. 849 [897]
Bickelhaupt, F. 1611 [1703]
Bierbach, U. 1632 [1701]
Bill, E. 731, 1621 [771, 1697]
Billups, W. E. 313, 1332 [321, 1394]
Binger, P. 197 [213]
Blake, A. J. 195 [208]
Bläser, D. 313 [321]
Bläser, E. 683 [717]
Bloemink, H. I. 1512 [1577]
Blondin, G. 1184 [1223]
Blouet, E. 2100 [2183]
Boche, G. 115, 1161 [90, 1228]
Bochmann, M. 1634 [1715]
Bock, H. 875 [931]
Bockholt, H. 1648 [1733]
Bodenhausen, G. 343 [340]
Bodensieck, U. 2440 [2561]
Boese, R. 201, 313, 661, 869 [211, 321, 715, 934]
Bögge, H. 770, 849 [800, 897]
Böhm, G. 1944 [2024]
Bohme, D. K. 206 [227]
Böhmer, J. 1473 [1556]
Böhmer, V. 214 [230]
Boie, C. 115 [90]
Boldi, A. M. 468 [482]
Bolletta, F. 1501 [1543]
Bolm, C. 1848 [1944]
Bols, M. 1778 [1858]
Bond, M. R. 578, 1253 [584, 1354]
Bonvoisin, J. 2106 [2190]
Bosch, P. 2078 [2157]
Bosold, F. 115, 1161 [90, 1228]
Bossler, H. G. 439 [455]
Bou, V. 2454 [2535]
Boubekeur, K. 1379 [1448]
Boudon, C. 763, 1628 [794, 1691]
Bourdin, B. 1856 [1931]
Bourquard, T. 1601 [1680]
Boutorine, A. S. 2472 [2526]
Boyer, S. H. 858 [928]
Bradley, D. D. C. 655 [711]
Brand, H. 95 [119]
Brandl, H. 1780 [1864]
Bratovanova, E. K. 2302 [2401]
Braum, G. 336 [353]
Braun, J. 2215 [2302]
Braun, P. 336 [353]
Braunschweig, H. 1156 [1243]
Braunstein, P. 2440 [2561]
Brédas, J.-L. 2209 [2281]
Breit, A. 1621 [1697]
Breit, B. 1491 [1541]
Breitmaier, E. 219, 454 (1461), 1246, 1461 [229, 460 (1529), 1356, 1529]
Bremer, M. 1386 [1435]
Bretzke, C. 882 [911]

Breuksch, U. 1960 [2047]
Breunig, H. J. 987 [1023]
Bronger, W. 1112 [1144]
Brooksby, P. A. 2489 [2584]
Brown, D. S. 661 [715]
Brucker, E. A. 2308 [2402]
Brugger, R. 1911 [1987]
Bruna, P. J. 563 [578]
Brunet, L. 742 [812]
Brunner, H. 125, 866, 2214 [130, 941, 2305]
Bryce, M. R. 1761 [1862]
Brzozka, Z. 467 [480]
Bubenitschek, P. 1369 [1444]
Buchholz, D. 1637 [1721]
Buck, J. 1837 (2348) [1954 (2590)]
Budzichowski, T. A. 191 [203]
Buhmann, M. 2337 [2386]
Bunz, U. H. F. 1073 [1127]
Burak, R. 1621 [1697]
Burchard, W. 884 [936]
Burford, N. 1267 [1332]
Burgemeister, T. 1151 [1211]
Bürger, H. M. 442 [459]
Burgess, K. 1182 [1218]
Burgstaller, P. 1084 [1163]
Burlakov, V. V. 1605, 1850 [1678, 1946]
Burrows, R. S. 897 [906]
Bürssner, D. 1772 [1834]
Buschmann, J. 1737 [1813]
Butenschön, H. 636 [664]
Buzek, P. 448 [470]

Cacace, F. 123 [104]
Cahill, P. A. 786 [803]
Calderazzo, F. 193, 1188 [206, 1254]
Caliman, V. 2202 [2284]
Cameron, T. S. 1267 [1332]
Caminade, A.-M. 1589 [1682]
Campos, J. L. 2454 [2535]
Canales, F. 769 [811]
Canceill, J. 2438 [2582]
Capparelli, M. V. 2193 [2277]
Cárdenas, D. J. 2482 [2529]
Carell, T. 1466, 2059, 2061 [1534, 2159, 2162]
Carlier, R. 1379 [1448]
Carrano, C. J. 578, 1253 [584, 1354]
Carré, F. 1097 [1152]
Carrier, S. M. 895 [917]
Carss, S. A. 1624 [1708]
Casnati, A. 1506, 2479 [1551, 2533]
Castagnani, R. 2076 [2202]
Catellani, M. 2421 [2559]
Chai, S. 973 [1050]
Chandrasekhar, J. 1390 [1433]
Chang, H. K. 871 [921]
Chang, Y.-D. 325, 757 [347, 781]
Chapman, W. H., Jr. 73 [110]
Chardon-Noblat, S. 887 [914]
Chauhan, V. S. 970 [1048]
Chen, G. S. 1081 [1150]
Chen, J. 639, 1871 [667, 1922]
Chen, L. 568 [591]
Chen, Q. 757 [781]
Chen, Y. 1607 [1694]
Cheng, T.-Y. 657 [703]
Chiappetta, R. 1184 [1223]
Chicote, M.-T. 1852 [1966]
Chiesi-Villa, A. 2204 [2279]
Chiou, Y.-M. 1886 [1969]
Chisholm, M. H. 191 [203]
Chmielewski, P. J. 779 [805]
Chodorowski-Kimmes, S. 1775 [1854]
Choi, W. 1091 [1148]
Chou, T.-C. 2477 [2578]
Choudhary, V. R. 2104 [2179]
Chrapkowski, A. 863 [903]
Christl, M. 1639 [1719]
Chuit, C. 1097 [1152]
Chu-Moyer, M. Y. 858 [928]
Churchill, M. R. 773 [824]
Clearfield, A. 2324 [2420]
Clegg, W. 451 [463]
Cloke, F. G. N. 2330 [2406]
Colin, J.-C. 1184 [1223]
Collin, J.-P. 1282, 1775 [1359, 1854]
Collins, I. 2320 [2416]
Collman, J. P. 1537 [1620]
Comes, F. J. 1816 [1900]
Conde-Frieboes, K. 753 [822]
Conn, M. M. 1577 [1665]
Connan, J. 1166 [1235]
Conrad, J. 1869 [1927]
Constable, E. C. 2269 [2359]
Cooney, M. J. 869 [934]
Corens, D. 2080 [2154]
Cornils, B. 2144 (2348) [2219]
Coronado, E. 223 [234]
Correia, J. D. G. 2475 [2545]
Corriu, R. J. P. 1097 [1152]
Cortés, R. 2488 [2520]
Couladouros, E. A. 1581 [1669]
Cowley, A. H. 578, 1253, 1370 [584, 1354, 1429]
Crestoni, M. E. 1094 [1157]
Cronje, S. 672 [687]
Crothers, D. M. 855 [925]

Dai, W.-M. 15 [38]
Dandliker, P. J. 1739 [1821]
Danishefsky, S. J. 853, 855, 858, 1468, 1470, 2477 [923, 925, 928, 1536, 1538, 2578]
Daub, J. 1087, 1621 [1140, 1697]
Deck, W. 456, 2440 [467, 2561]
Decken, A. 1370 [1429]
Deeming, A. J. 1381 [1459]
Dehaen, W. 2080 [2154]
Dehnen, S. 746, 2287 [786, 2369]
Dehnert, U. 2450 [2580]
Dehnicke, K. 569, 1726 [599, 1803]
Delanghe, P. H. M. 2448 [2557]
Delhaès, P. 223 [234]
Delville-Desbois, M.-H. 661 [715]
Demiroglou, A. 120 [126]
Deng, J. 1729 [1811]
Denhart, D. 855 [925]
Denker, M. 987 [1023]
Dent, A. J. 1871 [1922]
Derguini, F. 1837 (2348) [1954 (2590)]
Deronzier, A. 887 [914]
Derory, A. 1592 [1660]
Deschamps, E. 1158 [1214]
Desper, J. M. 319 [335]
Dessort, D. 1166 [1235]
Detomi, N. 1854 [1949]
Detzel, M. 1110 [1142]
Devedjiev, I. T. 2302 [2401]
Devonport, W. 1761 [1862]
De Angelis, F. 2076 [2202]
de Bruin, B. 1662 [1741]
De Cian, A. 1592 [1660]
de Gala, S. 853 [923]
de la Maza, A. 2078 [2157]
de Meijere, A. 869, 2379 [934, 2473]
De Mesmaeker, A. 226 [237]
De Munno, G. 1184 [1223]
De Riccardis, F. 2184 [2306]
De Sanctis, Y. 1381, 2193 [1459, 2277]
De Schryver, F. C. 2080 [2154]
De Vos, D. E. 431 [447]
De Witt Scalfaro, P. 2076 [2202]
Dieckmann, T. 277 [284]
Diederich, F. 468, 763, 996, 1366, 1625, 1628, 1739, 2339 [482, 794, 1033, 1427, 1688, 1691, 1821, 2434]
Diedrich, M. K. 1079 [1135]
Dillinger, S. 849 [897]
Diodone, R. 2175 [2267]
Dixon, D. A. 1397 [1454]
Doedens, R. J. 1641 [1725]
Dohmeier, C. 199, 2482 [225, 2570]
Dollé, V. 1176 [1230]
Dondoni, A. 2479 [2533]
Dong, W. 1778 [1858]
Dorn, H. 1352 [1414]
Dougherty, D. A. 1104 [1155]
Doumeix, O. 1383 [1457]
Downing, G. A. 1587 [1653]
Dozol, J.-F. 1506 [1551]
Driess, M. 1484 [1548]
Drillon, M. 1592 [1660]
Dufaud, V. 1285 [1338]
Duffy, N. V. 1497 [1546]
Duschl, C. 1274 [1361]
Dussy, A. 1861 [1941]
Dyker, G. 103 [117]

Eaborn, C. 1268 [1336]
Eaton, P. E. 2220 [2263]
Ebata, K. 1489 [1575]
Ebert, K. H. 987 [1023]
Echavarren, A. M. 2482 [2529]
Eckes, P. 1573 [1649]
Edelmann, F. T. 1618 [1684]
Edwards, A. J. 1093, 1277, 1875 [1166, 1334, 1960]
Edwards, P. P. 641 [669]
Effenberger, F. 1555 [1609]
Eggers, L. 863 [903]
Ehmann, A. 572 [581]
Eichhorn, B. W. 1859 [1973]
Eisenbraun, C. 454 (1461) [460 (1529)]
Eisenmann, B. 749 [791]
Eisenstein, O. 191 [203]
Elie, C. 1861 [1941]
Elling, L. 571 [592]
Ellis, J. E. 1973 [2036]
Ellison, J. J. 1178 [1248]
Ema, T. 1879 [1951]
Enders, D. 1949, 2098 [2033, 2167]
Engels, B. 563 [578]
Englert, U. 201, 991, 1003, 1188, 2465, 2491 [211, 1028, 1026, 1254, 2589, 2552]
Epstein, A. J. 385, 1397 [399, 1454]
Erdmann, P. 1861 [1941]
Erker, G. 197, 1114, 1480, 1955 [213, 1168, 1570, 2043]
Ermer, O. 1755 [1832]
Ernst, L. 1966 [2058]
Ertel, T. S. 45, 2435 [15, 2537]
Ertl, G. 85 [113]
Escamilla, G. H. 666, 1937 [701, 2013]
Eschenmoser, A. 2363 [2455]
Esser, P. 2009 [2093]

Evans, W. J. 1641, 2110 [1725, 2200]
Eversheim, E. 201 [211]

Fabbrizzi, L. 1975 [2051]
Faber, D. 2466 [2522]
Facchin, G. 576 [586]
Fagnola, M. C. 2421 [2559]
Fajer, J. 348 [355]
Famulok, M. 1084, 1827 [1163, 1911]
Fau, S. 2064 [2172]
Faulhammer, D. 1827 [1911]
Faure, T. 2440 [2561]
Faust, R. 1366 [1427]
Faverjon, F. 220 [200]
Fawcett, W. R. 2131 [2239]
Fawzi, R. 321 [363]
Fehlhaber, H.-W. 1844 [1936]
Fehlhammer, W. P. 330 [331]
Fehr, C. 1888 [1967]
Fei, Z. X. 346 [329]
Feiters, M. C. 986, 1662, 2468 [1054, 1741, 2587]
Felicetti, M. 739 [808]
Fenske, D. 746, 1290, 2287 [786, 1311, 2369]
Feringa, B. L. 1458 [1526]
Fernández, E. J. 87 [96]
Fessner, W.-D. 209 [217]
Fettinger, J. C. 1859 [1973]
Feuerer, M. 1087 [1140]
Feurer, A. 2428 [2542]
Field, J. S. 678 [679]
Filla, S. A. 673 [674]
Fillaut, J.-L. 2460 [2540]
Fischer, G. 1415 [1479]
Fischer, J. 348, 1592, 2284 [355, 1660, 2432]
Fischer, M.-R. 217 [220]
Fischer, R. 1463 [1531]
Fischer, R. D. 2165 [2253]
Fischer, R. W. 2475 [2545]
Flórez, J. 1392 [1451]
Floriani, C. 2204 [2279]
Flower, K. R. 2330 [2406]
Fluck, M. 2222 [2265]
Fornarini, S. 1094 [1157]
Forniés, J. 2083 [2196]
Forsyth, T. P. 2485 [2554]
Fox, M. A. 2298 [2384]
Frampton, C. S. 1587 [1653]
Franz, T. 1298 [1308]
Fraser, K. A. 451 [463]
Fréchet, J. M. J. 82, 1644 [123, 1728]
Fredriksen, S. B. 1176 [1230]
Freier, S. M. 226, 1654 [237, 1735]
Frenking, G. 2064 [2172]
Freund, T. 2424 [2547]
Friedrich, S. 676 [705]
Frisch, J. 1609 [1699]
Fritsch, V. 226 [237]
Fröhlich, L. 1971 [2064]
Fröhlich, R. 1480 [1570]
Frost, M. 2111 [2170]
Fuhrhop, J.-H. 350 [351]
Fujii, H. 1660 [1730]
Fujii, N. 652 [693]
Fürstner, A. 751 [779]
Furuchi, I. 1759 [1851]
Furusawa, H. 1750 [1849]
Fusetani, N. 1729 [1811]

Gabbaï, F. P. 578, 1253, 1370 [584, 1354, 1429]
Gade, L. H. 676 [705]
Gadre, S. R. 1390 [1433]
Galindo, J. 1888 [1967]
Gallop, M. A. 339, 1093 [327, 1166]
Gangloff, B. 556 [597]
Gangnus, B. 2296 [2383]
Ganguly, B. 1390 [1433]
Ganis, P. 576 [586]
Gante, J. 1699 [1780]
García-Granda, S. 1392 [1451]
Gardner, D. R. 1859 [1973]
Gasteiger, J. 643, 1189 [671, 1245]
Gates, D. P. 2277 [2367]
Gatzmann, J. 350 [351]
Gauss, J. 448 [470]
Gehrcke, B. 2085 [2175]
Geib, S. J. 446, 1516 [465, 1554]
Geissler, H. 2182 [2296]
Gelerinter, E. 1497 [1546]
Gellman, S. H. 319 [335]
Gennari, C. 2067 [2181]
Gerritz, S. W. 673 [674]
Gersdorff, J. von 2318 [2396]
Gerster, M. 1601 [1680]
Gescheidt, G. 1961 [2056]
Gessler, K. 2209 [2281]
Gestmann, D. 1251 [1326]
Ghosh, B. K. 2087 [2177]
Giannessi, F. 2076 [2202]
Giannini, L. 2204 [2279]
Giannis, A. 178 [188]
Gibson, V. C. 1565 [1640]
Giese, B. 1861, 2466 [1941, 2522]
Giese, S. 461 [473]
Gimenez-Saiz, C. 223 [234]
Gimeno, M. C. 87, 769 [96, 811]
Giolando, D. M. 1981 [2028]
Gisselbrecht, J.-P. 763, 1628 [794, 1691]
Giulieri, F. 1514 [1583]
Gladysz, J. A. 2199 [2269]
Glanz, M. 1733 [1829]
Glaser, M. 1354 [1416]
Glaser, R. 1081 [1150]
Glatthaar, J. 473 [486]
Gleiter, R. 1270, 1272, 1484, 2470 [1340, 1350, 1548, 2550]
Głowiak, T. 779 [805]
Göbel, M. W. 984, 1141 [1041, 1201]
Goddard, R. 197, 879 [213, 908]
Goeldner, M. 1176 [1230]
Gold, A. 348 [355]
Gölitz, P. 1457 [1525]
Gollnick†, K. 2300 [2399]
Gómez-García, C. J. 223 [234]
Gompper, R. 572 [581]
González-Herrero, P. 1852 [1966]
Goodman, M. 1437 [1502]
Goodwin, H. A. 425 [441]
Gopalan, P. 775 [826]
Gorath, G. 788 [793]
Görls, H. 1373 [1421]
Gornitzka, H. 693 [695]
Goto†, T. 978 [1039]
Gould, R. O. 195 [208]
Gözel, G. 749 [791]
Graf, R. 1612 [1705]
Graf von Roedern, E. 687 [684]
Grahn, W. 863, 1966 [903, 2058]
Gramlich, V. 763 [794]
Grand, A. 1397 [1454]
Grandinetti, F. 123 [104]
Grant, C. M. 195 [208]
Greatrex, R. 2298 [2384]
Greaves, G. N. 1871 [1922]
Greenspan, P. D. 2182 [2296]
Greeves, N. 2182 [2296]
Grehl, M. 458, 1480, 1734 [475, 1570, 1815]
Greiveldinger, G. 440 [457]
Grevels, F.-W. 755 [820]
Griesbeck, A. G. 2300 [2399]
Griesinger, C. 332 [338]
Gross, G. 562 [603]
Gross, J. L. 781 [790]
Gross, M. 763, 1628, 1739 [794, 1691, 1821]
Grosshenny, V. 1884 [1956]
Grothe, H. 1482 [1581]
Grove, D. M. 1282 [1359]
Gruber, K. 889 [939]
Grün, F. 1837 (2348) [1954 (2590)]
Grund, S. 350 [351]
Grützmacher, H. 456 [467]
Guardigli, M. 1501 [1543]
Guarini, A. 1188 [1254]
Guarnieri, W. 1734 [1815]
Gudat, D. 982 [1037]
Guénot, P. 2218 [2294]
Guerchais, V. 2218 [2294]
Gügel, A. 559 [601]
Gund, A. 186 [198]
Gut, I. G. 1153 [1240]
Gütlich, P. 425, 2024 [441, 2109]
Guy, R. K. 15, 1581, 1583 [38, 1669, 1672]

Haake, M. 755 [820]
Haaland, A. 2443 [2515]
Habashita, H. 652 [693]
Habermann, N. 884 [936]
Hafkamp, R. J. H. 986 [1054]
Hafner, K. 1479 [1566]
Haggerty, B. S. 1983, 2277 [2053, 2367]
Hahn, A. 350 [351]
Hahn, F. E. 1354, 1356 [1416, 1419]
Hahn, J. 1770 [1824]
Hajra, S. 1169 [1217]
Halbritter, G. 1603 [1676]
Haldimann, R. F. 2339 [2434]
Haley, M. M. 313 [321]
Hallbrucker, A. 691 [677]
Hamada, Y. 1729 [1811]
Hamilton, A. D. 446 [465]
Häming, L. 969 [1052]
Hämmerling, U. 1837 (2348) [1954 (2590)]
Hammerschmidt, F. 341 [334]
Hampel, F. 893, 993, 1952 [901, 1024, 2038]
Hamuro, Y. 446 [465]
Hanack, M. 1646 [1712]
Handa, T. 2483 [2576]
Hänel, R. 1369 [1444]
Hanusa, T. P. 2191 [2300]
Harder, S. 1744 [1830]
Hardt, I. H. 2085 [2175]
Harms, K. 115, 181, 1180 [90, 193, 1238]
Harriman, A. 1884 [1956]
Harris, K. D. M. 649 [698]
Harris, R. K. 1624 [1708]
Hartl, H. 1841 [1929]
Hartmann, H. 572 [581]
Hascall, T. 356, 1000 [350, 1056]
Haselhorst, G. 1473 [1556]

Hasenfratz, C. 2215 [2302]
Hauck, R. 2428 [2542]
Haueisen, R. H. 566 [588]
Hauke, V. 1166 [1235]
Haumann, T. 869 [934]
Hauser, A. 2024 [2109]
Häussermann, U. 2069, 2073 [2147, 2150]
Havlas, Z. 875 [931]
Hawker, C. J. 82 [123]
Heilmann, J. 471 [491]
Hein, M. 1298 [1308]
Heine, A. 113 [121]
Heintz, R. A. 2326 [2389]
Heinz, R. 2080 [2154]
Hélène, C. 2472 [2526]
Helsberg, M. 562 [603]
Hemling, H. 1733 [1829]
Henderson, C. C. 786 [803]
Hendrich, M. P. 1660 [1730]
Hendrickson, D. N. 425 [441]
Henkel, G. 2322 [2422]
Henkel, S. 681 [721]
Henrick, K. 429 [445]
Henschler, D. 1920 [1997]
Herberhold, M. 964 [1016]
Herberich, G. E. 2465 [2589]
Herbst-Irmer, R. 80, 555, 969, 1618, 1621 [115, 577, 1052, 1684, 1697]
Herdtweck, E. 77 [93]
Hergel, A. 1247 [1342]
Herges, R. 255, 993, 1376 [261, 1024, 1441]
Herrmann, G. F. 1241 [1346]
Herrmann, W. A. 105, 1285, 1946, 2144 (2348), 2475 [102, 1338, 2025, 2219, 2545]
Hertwig, R. H. 1192 [1252]
Herzog, A. 967 [1035]
Hesse, M. 327 [360]
Hettrich, R. 203 [215]
Hiatt, A. 183 [195]
Hill, C. 1506 [1551]
Hillhouse, G. L. 657, 1748 [703, 1841]
Hinds, K. 1512 [1577]
Hintzsche, E. 739 [808]
Hirai, K. 873 [944]
Hirsch, A. 437 [453]
Hitchcock, P. B. 463, 1156, 1268, 2202, 2330 [478, 1243, 1336, 2284, 2406]
Hitchcock, S. A. 855, 858 [925, 928]
Hobi, M. 763 [794]
Hochmuth, D. H. 2085 [2175]
Hochstrate, D. 1079 [1135]
Hoffmann, A. 1491 [1541]
Hoffmann, H. M. R. 1280 [1352]
Hoffmann, M. R. 1091 [1148]
Hoffmann, P. 226 [237]
Hoffmann, R. 1462 [1530]
Höfle, G. 1495 [1561]
Hofmann, M. 2202, 2296, 2298, 2303 [2284, 2383, 2384, 2391]
Hofmann, P. 2069 [2147]
Höger, S. 181 [193]
Hölderich, W. F. 2491 [2552]
Hollander, J. 109 [77]
Hollingsworth, M. D. 649 [698]
Holmes, A. B. 2320 [2416]
Hölscher, M. 2491 [2552]
Holstein, W. 1290 [1311]
Holthausen, M. C. 668, 1192 [682, 1252]
Hopf, H. 204, 1099, 1369 [232, 1173, 1444]
Hopkinson, A. C. 206 [227]
Hoppe, D. 1734 [1815]
Hori, K. 878 [919]
Horstmann, S. 785 [818]
Hoshino, M. 777 [829]
Hoss, R. 375 [389]
Hotta, Y. 652 [693]
Houdier, S. 354 [365]
Hrušák, J. 212 [223]
Hsieh, L. C. 339 [327]
Huber, N. W. 105 [102]
Hubert, D. H. W. 2468 [2587]
Huc, I. 1579 [1667]
Huffman, J. C. 191 [203]
Hughbanks, T. 2328 [2414]
Hühnerfuss, H. 882, 2085 [911, 2175]
Hulliger, J. 143 [151]
Hulst, R. 1458 [1526]
Hummel, C. W. 183 [195]
Hunter, C. A. 2313, 2489 [2424, 2584]
Hunter, R. 566 [588]
Hursthouse, M. B. 639 [667]
Hutchison, J. E. 1537 [1620]
Hüter, O. 2466 [2522]

Ibuka, T. 652 [693]
Ichinose, I. 2483 [2576]
Ihmels, H. 1854 [1949]
Ikeda, K. 781 [790]
Ikonnikov, N. 91 [106]
Imhof, W. 1373 [1421]
Ingham, S. L. 1752 [1847]
Inouye, M. 1163 [1226]
Irngartinger, H. 1270 [1340]
Irving, A. 566 [588]
Isaacs, L. 2339 [2434]
Isagawa, K. 1001, 1163 [1021, 1226]
Ishii, A. 777 [829]
Isobe, H. 2472 [2526]
Isobe, K. 1882 [1934]
Isobe, M. 978 [1039]
Isom, H. S. 1253 [1354]
Isozaki, T. 1757 [1856]
Issberner, J. 2413 [2507]
Ito, T. 670 [691]
Ito, Yoshihiko 111 [92]
Ito, Yukishige 1765 [1843]
Iwamoto, T. 1665 [1746]
Izod, K. 1268 [1336]

Jackson, J. E. 775 [826]
Jacobi, D. 685 [719]
Jacobs, P. A. 431 [447]
Jacobs, S. J. 1104 [1155]
Jäger, E.-G. 1363 [1424]
Jäger, V. 1295, 1298 [1305, 1308]
Jähne, G. 562 [603]
Jakubetz, H. 2222 [2265]
James, T. D. 2207 [2287]
Jandeleit, B. 1949 [2033]
Jang, M. 1973 [2036]
Jang, S.-H. 775 [826]
Janiak, C. 1171 [1220]
Janoschek, R. 1484 [1548]
Jansen, M. 563, 683 [578, 717]
Javahery, G. 206 [227]
Jayaraj, K. 348 [355]
Jelínek, T. 1599 [1663]
Jendralla, H. 685 [719]
Jennissen, H. P. 120 [126]
Jepsen, O. 2069 [2147]
Jeske, J. 80, 2427 [115, 2564]
Jespersen, T. M. 1778 [1858]
Jiao, H. 1376 [1441]
Jin, G.-X. 964 [1016]
Jin, Z. 851 [913]
Joachimi, D. 1503 (1668) [1563 (1865)]
Jochem, G. 663 [708]
John, A. 875 [931]
Johnson, B. F. G. 1093 [1166]
Johnson, M. R. 1509 [1572]
Jones, C. 463 [478]
Jones, P. G. 80, 87, 769, 863, 1186, 1369, 1852, 1966, 2427 [115, 96, 811, 903, 1250, 1444, 1966, 2058, 2564]
Jones, R. H. 639 [667]
Journaux, Y. 1184 [1223]
Jülicher, B. 1108 [1161]
Jullien, L. 2438 [2582]
Julve, M. 1184 [1223]
Juneja, R. K. 2456 [2571]
Jung, M. 2222 [2265]

Kabbe, K. 1495 [1561]
Kabe, Y. 659 [723]
Kabuto, C. 1489 [1575]
Kahr, B. 775 [826]
Kallenborn, R. 882 [911]
Kamimura, A. 878 [919]
Kammermeier, B. 685 [719]
Kann, N. 556 [597]
Kappes, M. M. 1651 [1742]
Karam, A. 1381 [1459]
Karfunkel, H. R. 437 [453]
Kastner, F. 1151 [1211]
Kato, T. 1644 [1728]
Kaufmann, D. E. 1832 [1917]
Kaupp, G. 728, 1452, 1459 [768, 1519, 1527]
Kawashima, T. 2094 [2188]
Kawata, S. 1759 [1851]
Kayser, F. 1842 [1962]
Kazmaier, U. 998 [1046]
Keith, J. M. 666 [701]
Keith, T. A. 620 [647]
Kellogg, R. M. 1458 [1526]
Kempe, R. 739, 1605, 1850 [808, 1678, 1946]
Kennedy, J. D. 1599 [1663]
Kent, D. 1437 [1502]
Keppler, B. K. 186 [198]
Kerr, M. A. 781 [790]
Kessler, H. 687 [684]
Keutel, H. 1363 [1424]
Khan, F. A. 1390 [1433]
Khan, M. I. 760 [784]
Khanbabaee, K. 99 [100]
Kharitonov, V. 91 [106]
Kiełkiewicz, J. 214 [230]
Kihara, H. 1644 [1728]
Kikuchi, T. 107 [129]
Kilimann, U. 1618 [1684]
Kim, J. H. 2182 [2296]
Kimizuka, N. 2483 [2576]
Kinkel, J. N. 882 [911]
Kintzel, O. 1354 [1416]
Kira, M. 1489 [1575]
Kirby, A. J. 551 [573]
Kirmse, R. 1497 [1546]
Kirner, S. 352 [346]
Kirschbaum, K. 1981 [2028]
Kirschfeld, A. 2212 [2261]
Kirschning, A. 217 [220]
Kisch, H. 1603 [1676]
Kisters, M. 2308 [2402]
Kitagawa, S. 1759 [1851]

Kitagawa, T. 1882 [1934]
Kiyozumi, Y. 2335 [2427]
Kizilyalli, M. 749 [791]
Klapötke, T. M. 212, 1518, 1575 [223, 1587, 1651]
Klärner, F.-G. 1079 [1135]
Klauck, A. 93 [98]
Kläui, W. 991 [1028]
Klengler, U. 1866 [1919]
Klessinger, M. 2431 [2568]
Klettke, T. 1373 [1421]
Klinkhammer, K. W. 681 [721]
Klüfers, P. 884, 1742, 1863 [936, 1839, 1925]
Klünsch, R. 1770 [1824]
Kniep, R. 749 [791]
Knieriem, B. 863 [903]
Knobler, C. B. 1739 [1821]
Knoch, F. 1603 [1676]
Knölker, H.-J. 1612 [1705]
Knorr, A. 1087 [1140]
Knorr, M. 2440 [2561]
Koch, W. 668, 1192 [682, 1252]
Kochersperger, L. 339 [327]
Kociok-Köhn, G. 1877 [1958]
Köck, M. 332, 753 [338, 822]
Koert, U. 1180, 1873 [1238, 1939]
Köhler, J. U. 1093 [1166]
Köhn, R. D. 1877 [1958]
Kölle, U. 991 [1028]
Kondo, M. 1759 [1851]
Kondo, T. 580, 978 [595, 1039]
König, W. A. 2085 [2175]
Kool, E. T. 1004 [1057]
Köpf, H. 1518 [1587]
Kopf, J. 882 [911]
Koshland, D. E., Jr. 2375 [2468]
Köster, R. 2294 [2380]
Kowalczyk, D. 336 [353]
Kowalski, D. 1114 [1168]
Kozhushkov, S. 869 [934]
Kraatz, H.-B. 2055 [2143]
Krafft, M.-P. 1100, 1514 [1146, 1583]
Kratky, C. 889 [939]
Kratz, T. 1733 [1829]
Kratzer, B. 2177 [2289]
Kraus, A. 559 [601]
Krause, N. 1764 [1845]
Kräutler, B. 889 [939]
Krautscheid, H. 2482 [2570]
Krebs, B. 841, 1363, 1969, 2195 [889, 1424, 2040, 2275]
Kreitmeier, P. 1151 [1211]
Krempner, C. 1615 [1709]
Kretzschmar, G. 2096 [2186]
Kreuder, C. 2465 [2589]
Kreuder, R. 556 [597]
Kreyenschmidt, M. 1957 [2062]
Krickemeyer, E. 770, 849 [800, 897]
Krieger, C. 1463 [1531]
Kroha, H. 562 [603]
Krohn, K. 99 [100]
Krüger, C. 197, 879, 2435 [213, 908, 2537]
Kruizinga, W. H. 1458 [1526]
Kuck, D. 1251 [1326]
Kuhn, A. 555 [577]
Kuhn, N. 1733 [1829]
Kuhnigk, J. 197 [213]
Kula, M.-R. 571 [592]
Kumar, A. 2197 [2272]
Kumar, U. 1644 [1728]
Kündig, E. P. 1856 [1931]
Kunitake, T. 2483 [2576]
Kunz, H. 101, 336, 2096 [87, 353, 2186]
Kunz, R. 330 [331]
Kuribayashi, T. 107 [129]
Kurreck, H. 2318 [2396]
Kusenberg, A. 2427 [2564]
Kuwano, R. 111 [92]
Kybart, C. 1487 (1668) [1579]

Laatsch, H. 422 (1668) [438 (1865)]
Läge, M. 2195 [2275]
Laguna, A. 87, 769 [96, 811]
Laguna, M. 87 [96]
Lahana, R. 1589 [1682]
Lainé, P. 1775 [1854]
Lake, C. H. 773 [824]
Lalinde, E. 2083 [2196]
Lambert, C. 1129 [1187]
Lamparth, I. 437 [453]
Lancaster, S. J. 1634 [1715]
Lang, H. 547 [569]
Langer, H. 1272 [1350]
Lapierre, J.-M. 440 [457]
Lapinte, C. 2218 [2294]
Lappert, M. F. 1156 [1243]
Laschat, S. 458 [475]
Lasic, D. D. 1685 [1765]
Latos-Grażyński, L. 779 [805]
Latour, J.-M. 887 [914]
Laugier, J. 887 [914]
Launay, J.-P. 1775, 2106 [1854, 2190]
Launay, N. 1589 [1682]
Laupp, M. 207 [210]
Lausmann, M. 736 [776]
Lautens, M. 2448 [2557]
La Greca, S. 2184, 2187, 2190 [2306, 2309, 2312]
Lebreton, J. 226 [237]
Legoll, P. 1592 [1660]
Legon, A. C. 1512 [1577]
Lehn, J.-M. 2284, 2438 [2432, 2582]
Lehr, S. 984 [1041]
Leibold, T. 1295 [1305]
Leitner, W. 173 [183]
Lemus, R. H. 781 [790]
Lennox, R. B. 2332 [2429]
Lenoir, C. 1379 [1448]
Lentz, A. 1731 [1827]
Lentz, D. 1315 [1377]
Leonhardt, J. 117 [84]
Leopold, D. 975 [1043]
Leresche, J. E. 2184, 2187, 2190 [2306, 2309, 2312]
Lerner, R. A. 475, 1607 [485, 1694]
Letschert, H.-P. 683 [717]
Levy, A. D. 2473 [2524]
Lewis, J. 1093 [1166]
Lex, J. 731, 736, 2308 [771, 776, 2402]
Ley, S. V. 2290, 2292 [2410, 2412]
Lezama, L. 2488 [2520]
Le Narvor, N. 991 [1028]
Le Paillard, M.-P. 1379 [1448]
Li, T. 183 [195]
Li, W.-S. 676 [705]
Li, X. 643 [671]
Licchelli, M. 1975 [2051]
Lichtenthaler, F. W. 2364 [2456]
Liley, M. 1274 [1361]
Limbach, H.-H. 2215 [2302]
Lin, J. 334, 2475 [357, 2545]
Linares, J. 2460 [2540]
Lind, J. 1259 [1320]
Lindner, E. 321 [363]
Lindner, H. J. 1479 [1566]
Linker, T. 1971 [2064]
Lipka, H. 204 [232]
Lipshutz, B. H. 1842 [1962]
Liskamp, R. M. J. 305, 633 [313, 661]
Liu, F.-Q. 555 [577]
Liu, K. K. C. 855 [925]
Liu, Z.-P. 1842 [1962]
Lloret, F. 1184 [1223]
Lobbia, A. 1737 [1813]
Lobreyer, T. 216 [221]
Lockhart, J. C. 451 [463]
Löffler, M. 2209 [2281]
Lohmüller, M. 1960 [2047]
Lohrenz, J. C. W. 1161 [1228]
Long, N. J. 1752 [1847]
López, L. 1114 [1168]
López-de-Luzuriaga, J. M. 87 [96]
Lorcy, D. 1379 [1448]
Lorenz, V. 1372 [1461]
Lork, E. 1663 [1724]
Louati, A. 1739 [1821]
Lough, A. J. 989 [1019]
Lowe, M. P. 451 [463]
Lueken, H. 736 [776]
Luger, P. 1737 [1813]
Lügger, T. 1354, 1356 [1416, 1419]
Lundt, I. 1778 [1858]
Lüttke, W. 863 [903]
Lutz, M. 2279, 2281 [2372, 2375]
Lynch, V. 1509 [1572]
Lyons, J. E. 1667 [1722]

McCord, D. J. 1332 [1394]
McDaniel, D. H. 897 [906]
McGrath, M. P. 1667 [1722]
MacNicol, D. D. 1587 [1653]
McPartlin, M. 429, 676 [445, 705]
McQuillan, A. J. 2489 [2584]
Maeda, K. 2335 [2427]
Mahdjour-Hassan-Abadi, F. 1841 [1929]
Mahr, N. 97 [82]
Maier, G. 473, 558, 1248 [486, 605, 1347]
Maier, W. F. 471, 1657 [491, 1738]
Majoral, J.-P. 1589 [1682]
Maksić, Z. B. 1192 [1252]
Mal, T. K. 970 [1048]
Mallien, M. 1268 [1336]
Mallinson, P. R. 1587 [1653]
Mandon, D. 348 [355]
Manet, I. 1501 [1543]
Manners, I. 989, 2277 [1019, 2367]
Manzur, J. 2193 [2277]
Marchese, L. 1871 [1922]
Marchetti, F. 193, 1188 [206, 1254]
Marchon, J.-C. 220 [200]
Marian, C. M. 563 [578]
Mark, M. F. 1657 [1738]
Märkl, G. 1151 [1211]
Marmottini, F. 1594 [1655]
Marquard, C. 766 [816]
Marquardt, T. 1459 [1527]
Marra, A. 2479 [2533]
Marsch, M. 115 [90]
Marsmann, H. 1846 [1938]
Martín, A. 2083 [2196]
Martín, E. 1392 [1451]
Martin, S. J. 655 [711]
Maruta, T. 777 [829]
Maruyama, T. 1489 [1575]
Masamune, S. 673 [674]

Maslak, P. 73 [110]
Massa, W. 1487 (1668), 2064, 2303, 2306 [1579, 2172, 2391, 2394]
Mateo, C. 2482 [2529]
Mathey, F. 742, 1158, 1491 [812, 1214, 1541]
Matsubara, Y. 1597 [1658]
Matsumoto, A. 878 [919]
Matsumoto, T. 2316 [2418]
Matsunaga, P. T. 1748 [1841]
Matsunaga, S. 1729 [1811]
Matzinger, S. 1964 [2048]
Maulitz, A. H. 313 [321]
Maury, O. 220 [200]
Mayer, A. 465, 1044 [493, 1097]
Mayer, S. 2222 [2265]
Mayer, T. G. 2177 [2289]
Mayr, H. 788, 938 [793, 990]
Mazéas, D. 1383 [1457]
Mehdi, A. 1097 [1152]
Mehta, G. 1390 [1433]
Meier, H. 465 [493]
Meier, S. 1767 [1818]
Memmler, H. 676 [705]
Ménage, S. 1660 [1730]
Menger, F. M. 346 [329]
Mercier, F. 742 [812]
Merenyi, G. 1259 [1320]
Mertens, R. 1259, 1262 [1320, 1323]
Metz, P. 2195 [2275]
Metzger, J. W. 723 [763]
Metzler, N. 1746 (1988) [1837 (2066)]
Mews, R. 1663 [1724]
Meyer, D. 1592 [1660]
Meyer, F. E. 2379 [2473]
Meyer, H.-J. 1943 [2022]
Michel, R. H. 1651 [1742]
Michel, T. 217 [220]
Miculka, C. 1476 [1559]
Mierke, D. F. 753 [822]
Mihalic, Z. 448 [470]
Miller, C. P. 1516 [1554]
Miller, G. J. 334 [357]
Miller, J. S. 385, 1397 [399, 1454]
Miller, T. A. 962 [1014]
Milne, P. E. Y. 195 [208]
Milstein, D. 317 [344]
Mimura, N. 652 [693]
Minari, P. 2479 [2533]
Mink, C. 1479 [1566]
Minkwitz, R. 1941 [2017]
Mirkin, C. A. 2473 [2524]
Mirlach, A. 1087 [1140]
Misiti, D. 2076 [2202]
Mitsudo, T.-a. 580 [595]
Miwa, Y. 652 [693]
Mizukami, F. 2335 [2427]
Mizuno, K. 2113 [2203]
Möckel, R. 323 [325]
Mocker, M. 862, 1754 [946, 1860]
Mohler, D. L. 313 [321]
Mohn, H. 996 [1033]
Mohr, T. 1110 [1142]
Mokry, L. M. 578 [584]
Möller, E. 1497 [1546]
Möller, K. 882 [911]
Möller, M. H. 2337 [2386]
Moneta, W. 887 [914]
Monflier, E. 2100 [2183]
Monfort, M. 2087 [2177]
Montenbruck, A. 980 [1031]
Montero, M. L. 2103 [2198]
Montserrat, J. M. 1392 [1451]
Moore, A. J. 1761 [1862]
Moorefield, C. N. 666 [701]
Moors, R. 2413 [2507]
Morawietz, M. J. A. 1946 [2025]
Morgan, S. 1964 [2048]
Morin, B. G. 1397 [1454]
Morr, M. 1394 [1439]
Morrow, J. R. 773 [824]
Mortreux, A. 2100 [2183]
Moufid, N. 1601 [1680]
Muck, S. 2076 [2202]
Mühleisen, M. 1186, 1359 [1250, 1431]
Muhler, M. 85 [113]
Mühlhäuser, M. 563 [578]
Müllen, K. 559, 1957, 2424 [601, 2062, 2547]
Müller, Achim 770, 849 [800, 897]
Müller, Armin 562 [603]
Müller, B. 2089 [2164]
Müller, G. 2279, 2281 [2372, 2375]
Müller, R. 1295 [1305]
Müller, T. 277 [284]
Müller, T. J. J. 572 [581]
Müller, W. 996 [1033]
Mullis, K. B. 1209 [1271]
Mulzer, J. 1737 [1813]
Munakata, M. 1759 [1851]
Murcia-Mascarós, S. 1594 [1655]
Müther, M. 1621 [1697]
Muthusamy, S. 2212 [2261]

Nabeshima, T. 1750 [1849]
Nadin, A. 2184, 2187, 2190 [2306, 2309, 2312]
Nagashima, U. 670 [691]
Nakada, M. 183 [195]
Nakai, K. 652, 1001 [693, 1021]
Nakamura, E. 2472 [2526]
Nakanishi, K. 1837 (2348) [1954 (2590)]
Nakatani, Y. 1176 [1230]
Nakayama, J. 777 [829]
Nakazumi, H. 1001 [1021]
Naniwa, Y. 2184 [2306]
Nantermet, P. G. 1581 [1669]
Naruse, H. 580 [595]
Naruta, Y. 1839 [1964]
Narvaez, J. N. 73 [110]
Natarajan, S. 639 [667]
Näther, C. 875 [931]
Natsukawa, K. 1001 [1021]
Naumann, D. 323 [325]
Negura, S. 2222 [2265]
Neiss, T. G. 2326 [2389]
Nelson, J. M. 989 [1019]
Nelson, N. Y. 1879 [1951]
Nesper, R. 843, 2069, 2073 [891, 2147, 2150]
Neuenhofer, S. 1044 [1097]
Neuenschwander, M. 973 [1050]
Neumann, H. 993 [1024]
Neumann, L. 731 [771]
Neumüller, B. 1726 [1803]
Newkome, G. R. 666, 1937 [701, 2013]
Nguyen, L. T. 2485 [2554]
Nickel, T. 879 [908]
Nicolaou, K. C. 15, 183, 781, 1581, 1583, 2184, 2187, 2190 [38, 195, 790, 1669, 1672, 2306, 2309, 2312]
Niecke, E. 353, 982, 1953, 2111 [362, 1037, 2045, 2170]
Nieger, M. 353, 982, 1953, 2111 [362, 1037, 2045, 2170]
Niethammer, D. 2318 [2396]
Nishioka, T. 1882 [1934]
Nishiyama, T. 2113 [2203]
Nixon, J. F. 463, 2202, 2330 [478, 2284, 2406]
Nlate, S. 2218 [2294]
Nobes, R. H. 1667 [1722]
Noda, T. 673 [674]
Noe, C. R. 1476 [1559]
Noguchi, Y. 1163 [1226]
Nolte, M. 2435 [2537]
Nolte, R. J. M. 986, 1662, 2173, 2468 [1054, 1741, 2298, 2587]
Noltemeyer, M. 967, 1351, 1854 [1035, 1413, 1949]
Nöth, H. 663, 1151, 1746 (1988) [708, 1211, 1837 (2066)]
Nozaki, K. 2452 [2574]
Nuber, B. 866, 1272, 1473 [941, 1350, 1556]

Obermeier, H. 2214 [2305]
Ochsenbein, P. 348 [355]
Oehme, G. 2197 [2272]
Oehme, H. 1615 [1709]
Oeschey, R. 866 [941]
Oeser, T. 1270 [1340]
Ogawa, T. 1765 [1843]
Ogoshi, H. 1879 [1951]
Ogura, T. 1882 [1934]
Ohe, K. 781 [790]
Ohff, A. 1605, 1850 [1678, 1946]
Ohgaki, H. 659 [723]
Ohno, F. 2094 [2188]
Ohto, A. 670 [691]
Okada, H. 873 [944]
Okazaki, R. 2094, 2316 [2188, 2418]
Olivier, P. J. 672 [687]
Olivieri, A. C. 1624 [1708]
Olmstead, M. M. 1000 [1056]
Olson, S. H. 858 [928]
Ono, K. 1977 [2030]
Opallo, M. 2131 [2239]
Orlova, S. 91 [106]
Osborn, J. A. 1592 [1660]
Oschkinat, H. 277 [284]
Oshio, H. 670 [691]
Otsuji, Y. 2113 [2203]
Otte, A. R. 1280 [1352]
Otten, A. 1832 [1917]
Ottens-Hildebrandt, S. 1767 [1818]
Ouahab, L. 223 [234]
Ourisson, G. 1176 [1230]
Over, D. E. 220 [200]
Overby, J. S. 2191 [2300]
Ozaki, Y. 580 [595]
Ozawa, Y. 1882 [1934]

Pabel, M. 1835 [1971]
Pacl, H. 1248 [1347]
Padmakumar, R. 2091 [2193]
Padwa, A. 1797 [1881]
Paetzold, P. 201 [211]
Paisdor, B. 1251 [1326]
Pallavicini, P. 1975 [2051]
Palys, M. 467 [480]
Pampaloni, G. 1188 [1254]
Pandey, G. 1169 [1217]
Pandolfo, L. 576 [586]
Pape, A. 2281 [2375]

Parkin, G. 1462 [1530]
Parks, T. M. 1267 [1332]
Parra, J. L. 2078 [2157]
Patz, M. 938 [990]
Pätzel, M. 1295 [1305]
Paver, M. A. 1277, 1875 [1334, 1960]
Pawlik, A. 1966 [2058]
Pearson, D. L. 1360 [1445]
Pebler, J. 569 [599]
Pelizzi, G. 193 [206]
Pelter, A. 851 [913]
Pepi, F. 123 [104]
Perotti, A. 1975 [2051]
Peters, E.-M. 1298, 1639 [1308, 1719]
Peters, K. 1107, 1298, 1639, 1846 [1159, 1308, 1719, 1938]
Peters, K. S. 294 [301]
Peters, T. 88 [79]
Petersen, J. 1663 [1724]
Peterson, B. R. 1625 [1688]
Petkov, D. D. 2302 [2401]
Petrie, S. 206 [227]
Pettinger, B. 85 [113]
Peyerimhoff, S. D. 563 [578]
Pfaffenberger, B. 2085 [2175]
Phan, T. 889 [939]
Pickardt, J. 1731 [1827]
Picken, S. J. 2173 [2298]
Pieles, U. 1654 [1735]
Pierssens, L. J.-M. 1156 [1243]
Pieters, R. J. 1579 [1667]
Pietzsch, H.-J. 1354 [1416]
Pinkos, R. 117 [84]
Pitsinos, E. N. 1583 [1672]
Pizarro, J. L. 2488 [2520]
Plass, W. 849 [897]
Platz, M. S. 1964 [2048]
Plenio, H. 2175 [2267]
Pochini, A. 1506 [1551]
Pohlan, S. 1495 [1561]
Pohlmann, B. 2009 [2093]
Poinsot, J. 1166 [1235]
Polborn, K. 572, 1151, 2300 [581, 1211, 2399]
Ponce, A. 657 [703]
Poojary, D. M. 2324 [2420]
Popelier, P. L. A. 620 [647]
Porsch, M. 1621 [1697]
Pörschke, K.-R. 879 [908]
Porte, A. M. 1182 [1218]
Potenza, D. 2067 [2181]
Power, P. P. 356, 1000, 1178 [350, 1056, 1248]
Prabhakar, B. 2104 [2179]
Praly, J.-P. 751 [779]
Prechtl, F. 1609 [1699]
Priepke, H. W. M. 2290, 2292 [2410, 2412]
Priermeier, T. 105, 1946 [102, 2025]
Prinzbach, H. 117, 2239 [84, 2329]
Pritzkow, H. 203, 216, 456, 1247, 1484 [215, 221, 467, 1342, 1548]
Prosenc, M. H. 1744 [1830]
Proust, A. 849 [897]
Puddephatt, R. J. 847 [895]
Pullen, S. 1875 [1960]
Puls, C. 869 [934]
Purvis, D. H. 2489 [2584]

Que, L., Jr. 1660, 1886 [1730, 1969]

Raabe, G. 1949 [2033]
Rabe, G. W. 2110 [2200]
Rabe, J. P. 2080 [2154]
Rachlewicz, K. 779 [805]
Rack, M. 1646 [1712]
Radom, L. 1667 [1722]
Raithby, P. R. 1093, 1277, 1875 [1166, 1334, 1960]
Rajashankar, K. R. 970 [1048]
Rajca, A. 2091 [2193]
Rajca, S. 2091 [2193]
Rajput, A. M. 2104 [2179]
Ramakumar, S. 970 [1048]
Ramasseul, R. 220 [200]
Ramondenc, Y. 889 [939]
Randolph, J. T. 1470 [1538]
Rasch, M. 2144 (2348) [2219]
Rasmussen, D. R. 1667 [1722]
Ratajczak, H. 770 [800]
Raubenheimer, H. G. 672 [687]
Real, J. A. 1184 [1223]
Rebek, J., Jr. 1577, 1579, 2059, 2061 [1665, 1667, 2159, 2162]
Reber, J.-L. 475 [485]
Rechinger, M. 893 [901]
Reder, A. S. 433, 1286 [450, 1316]
Redlich, H. 1345 [1407]
Reed, C. A. 2433 [2566]
Reed, D. 195 [208]
Reedijk, J. 1632 [1701]
Reetz, M. T. 181 [193]
Reggelin, M. 444, 753 [489, 822]
Regitz, M. 1491 [1541]
Reiffenrath, V. 1386 [1435]
Reijerse, E. J. 1497 [1546]
Reim, J. 1969 [2040]
Rein, T. 556 [597]
Reinhoudt, D. N. 467, 1292, 2345 [480, 1313, 2437]
Reinke, H. 1615 [1709]
Reisenauer, H. P. 1248 [1347]
Reiser, O. 69, 556 [73, 597]
Reisgys, M. 1484 [1548]
Reisner, A. 1966 [2058]
Reller, A. 1352, 1866 [1414, 1919]
Renaud, J. 1581 [1669]
Renaud, P. 1601 [1680]
Rennie, M.-A. 1277, 1875 [1334, 1960]
Renz, M. 1107 [1159]
Ressouche, E. 1397 [1454]
Rétey, J. 1279 [1331]
Reyé, C. 1097 [1152]
Reymond, J.-L. 475, 1607 [485, 1694]
Rheingold, A. L. 657, 1983, 2277 [703, 2053, 2367]
Rhiel, M. 569 [599]
Ribas, J. 2087 [2177]
Ricard, L. 742, 1158, 1491 [812, 1214, 1541]
Riederer, M. 350 [351]
Riess, J. G. 1100, 1514 [1146, 1583]
Rimkus, G. 882, 2085 [911, 2175]
Risch, N. 2422 [2531]
Ritter, J. 2470 [2550]
Rizzoli, C. 2204 [2279]
Robert, A. 1379 [1448]
Roberts, R. J. 1222 [1285]
Röbke, C. 1755 [1832]
Robl, C. 199, 862, 1754 [225, 946, 1860]
Röck, M. 1961 [2056]
Röckel, H. 1270 [1340]
Rodewald, U. 2337 [2386]
Roesky, H. W. 555, 967, 969, 1244, 1351, 1352, 2103 [577, 1035, 1052, 1365, 1413, 1414, 2198]
Rohlfing, C. M. 786 [803]
Röhr, C. 749 [791]
Rohr, J. 1648 [1733]
Rojo, T. 2488 [2520]
Rokicki, G. 214 [230]
Roque, J. P. 2197 [2272]
Rosenthal, U. 1605, 1850 [1678, 1946]
Roth, G. 1651 [1742]
Rothe, M. 1960 [2047]
Röttele, H. 1944 [2024]
Rouquette, H. 1506 [1551]
Rovira, C. 2106 [2190]
Rowan, A. E. 2489 [2584]
Rozenberg, V. 91 [106]
Ruban, A. 2111 [2170]
Rubin, E. 1004 [1057]
Rubin, Y. 1366 [1427]
Rüchardt, C. 996 [1033]
Rudge, A. J. 2320 [2416]
Rudkevich, D. M. 467 [480]
Ruf, M. 2089 [2164]
Ruggiero, C. E. 895 [917]
Ruhlandt-Senge, K. 356, 1178 [350, 1248]
Runge, D. 678, 1255 [679, 1328]
Runsink, J. 2098 [2167]
Russell, C. A. 1277, 1875 [1334, 1960]
Rüther, T. 991 [1028]
Ryabov, A. D. 783 [798]
Rypdal, K. 2443 [2515]

Saalfrank, R. W. 1621 [1697]
Sabbatini, N. 1501 [1543]
Sacchi, D. 1975 [2051]
Sachdev, H. 1746 (1988) [1837 (2066)]
Sadlek, O. 2300 [2399]
Saenger, W. 2209 [2281]
Saha-Möller, C. R. 2475 [2545]
Sakurai, H. 1489 [1575]
Salom, B. 2067 [2181]
Salta, J. 325, 757 [347, 781]
Saluschke, S. 1497 [1546]
Salzer, A. 1003 [1026]
Sandanayake, K. R. A. S. 2207 [2287]
Sander, M. 456 [467]
Sander, W. 766, 1455, 2212 [816, 1522, 2261]
Sanders, J. K. M. 429 [445]
Sandmeyer, F. 197 [213]
Sanford, E. M. 1739 [1821]
Sankar, G. 1871 [1922]
Sano, I. 1757 [1856]
Santarsiero, B. D. 649 [698]
Sarson, L. D. 2313 [2424]
Sasaki, T. 1839 [1964]
Sasayama, M. 1839 [1964]
Sauer, H. 1151 [1211]
Sauvage, J.-P. 1282, 1775 [1359, 1854]
Savin, A. 2069 [2147]
Sawabe, A. 673 [674]
Sawamura, M. 111 [92]
Sawasaki, M. 2113 [2203]
Scafetta, N. 2076 [2202]
Schaeffer, P. 1166 [1235]
Schäfer, Andrea 327 [360]
Schäfer, Annemarie 1846 [1938]
Schäfer, Ansgar 746 [786]
Schäfer, M. 2308 [2402]
Scharf, H.-D. 2009 [2093]
Schauer, C. K. 75 [108]
Schaumann, E. 217 [220]
Scheidt, W. R. 220 [200]
Schenk, W. A. 1609 [1699]

Schenning, A. P. H. J. 1662, 2468 [1741, 2587]
Scherer, O. J. 1110 [1142]
Scherer, W. 1285, 2443 [1338, 2515]
Scherf, U. 2424 [2547]
Scherrmann, M.-C. 2479 [2533]
Schier, A. 327 [360]
Schiessling, H. 125 [130]
Schilbach, W. 982 [1037]
Schimpf, R. 1089 [1138]
Schlaefke, J. 1846 [1938]
Schleyer, P. von R. 216, 448, 1129, 1376, 2202, 2296, 2298, 2303 [221, 470, 1187, 1441, 2284, 2383, 2384, 2391]
Schlingloff, G. 1848 [1944]
Schlögl, R. 85, 311, 1866 [113, 319, 1919]
Schlüter, A.-D. 2209 [2281]
Schmalz, H.-G. 109, 303 [77, 311]
Schmid, U. 1944 [2024]
Schmidpeter, A. 663, 785 [708, 818]
Schmidt, A. 1373 [1421]
Schmidt, H. 188 [240]
Schmidt, R. R. 2177 [2289]
Schmidt, W. 1767 [1818]
Schmidtberg, G. 1960 [2047]
Schmidtchen, F. P. 327 [360]
Schmittel, M. 1961 [2056]
Schmuck, S. 1955 [2043]
Schneider, C. 980 [1031]
Schneider, J. J. 1830, 2435 [1914, 2537]
Schneider, U. 199 [225]
Schnering, H. G. von 1298, 1639, 1846 [1308, 1719, 1938]
Schnick, W. 785 [818]
Schnöckel, H. 199, 862, 1754, 2482 [225, 946, 1860, 2570]
Schoeller, W. W. 2111 [2170]
Scholl, T. 562 [603]
Scholz, A. 1171 [1220]
Scholz, J. 1171, 1372 [1220, 1461]
Schönfels, C. 1780 [1864]
Schreitmüller, J. 646 [688]
Schröder, C. 1499 [1568]
Schröder, D. 212, 1174 [223, 1232]
Schröder, F. 1737 [1813]
Schroth, W. 739 [808]
Schubert, C. 1279 [1331]
Schubert, U. 419 [435]
Schuhmacher, J. 1742, 1863 [1839, 1925]
Schultz, P. G. 339 [327]
Schulz, A. 1844 [1936]
Schulz, S. 969 [1052]
Schulze Tilling, A. 731 [771]
Schumacher, D. 1495 [1561]
Schumann, H. 1171, 1731, 1733 [1220, 1827, 1829]
Schumm, J. S. 1360 [1445]
Schurig, V. 2222 [2265]
Schütz, K. 984 [1041]
Schütz, R. 572 [581]
Schwab, P. 97 [82]
Schwarz, H. 212, 1174 [223, 1232]
Schwarz, W. 681 [721]
Schwarze, M. 2197 [2272]
Schweizer, J. 1397 [1454]
Schwenninger, R. 889 [939]
Schwesinger, R. 2215 [2302]
Schwitter, U. 1861 [1941]
Schwochau, K. 2258 [2349]
Scott, L. T. 869 [934]
Seebach, D. 439, 440, 442 [455, 457, 459]
Seger, B. 884 [936]
Segre, A. 1188 [1254]
Seidel, G. 2294 [2380]
Seidenschwarz, C. 77 [93]
Seiler, P. 763, 1628 [794, 1691]
Selke, R. 2197 [2272]
Senge, M. O. 1879, 2485 [1951, 2554]
Senger, S. 558 [605]
Seppelt, K. 93, 461, 975, 976 [98, 473, 1043, 1044]
Sergeeva, E. 91 [106]
Serrette, A. G. 2342 [2378]
Sessler, J. L. 1348, 1509, 2308 [1410, 1572, 2402]
Seubert, J. 891, 1952 [900, 2038]
Sewald, N. 77 [93]
Shair, M. D. 2477 [2578]
Shannon, R. J. 2489 [2584]
Sharp, P. A. 1229 [1292]
Sheldrick, G. M. 969 [1052]
Shen, G.-J. 1241 [1346]
Shin, J.-H. 1279 [1331]
Shing, T. K. M. 2312 [2408]
Shinkai, S. 2207 [2287]
Shioiri, T. 1729 [1811]
Shiro, M. 777 [829]
Shirsat, R. N. 1390 [1433]
Siebert, W. 203, 1247, 2296 [215, 1342, 2383]
Siegel, J. S. 1721 [1808]
Sieler, J. 739 [808]
Sierks, M. R. 1778 [1858]
Simon, A. 689 [713]
Sinbandhit, S. 2218 [2294]
Sinerius, G. 209 [217]
Singewald, E. T. 2473 [2524]
Skobridis, K. 440 [457]
Skrydstrup, T. 1383, 1778 [1457, 1858]
Smith, J. D. 1268 [1336]
Smith, K. 851 [913]
Smith, K. M. 1879, 2485 [1951, 2554]
Smith, M. 1214 [1277]
Snyder, G. J. 689 [713]
Solans, X. 2087, 2488 [2177, 2520]
Solari, E. 2204 [2279]
Soma, T. 1665 [1746]
Sonntag, C. von 1259, 1262 [1320, 1323]
Sowa, C. E. 1979 [2041]
Spek, A. L. 1282 [1359]
Spencer, N. 433, 1286, 1503 (1668) [450, 1316, 1563 (1865)]
Spickermann, J. 559 [601]
Spiering, H. 2024 [2109]
Spies, H. 1354 [1416]
Spitz, U. P. 2220 [2263]
Spitzner, R. 739 [808]
Sprengard, U. 2096 [2186]
Staab, H. A. 1463, 1466, 2428 [1531, 1534, 2542]
Stabel, A. 2080 [2154]
Stahl, W. 2096 [2186]
Stalke, D. 113, 555, 693, 1244, 1352, 1618, 1621, 2168, 2450 [121, 577, 695, 1365, 1414, 1684, 1697, 2256, 2580]
Stamatis, N. 2303 [2391]
Stec, W. J. 709 [747]
Steed, J. W. 2456 [2571]
Steimann, M. 321 [363]
Stein, M. 1180 [1238]
Steiner, A. 1352 [1414]
Steiner, D. 2064, 2303 [2172, 2391]
Steiner, U. E. 1772 [1834]
Stephan, H.-O. 2322 [2422]
Stephans, J. C. 339 [327]
Stern, C. 2440 [2561]
Stern, C. L. 2473 [2524]
Steuhl, H.-M. 2431 [2568]
Štíbr, B. 1599 [1663]
Still, W. C. 2458 [2517]
Stock, H. 2296 [2383]
Stoddart, J. F. 433, 1286, 1503 (1668) [450, 1316, 1563 (1865)]
Stölting, J. 2195 [2275]
Storre, J. 1244 [1365]
Strähle, J. 207 [210]
Sträter, N. 841 [889]
Streubel, R. 80, 2427 [115, 2564]
Stüer, W. 1981 [2028]
Süling, C. 2080 [2154]
Sun, L. 2318 [2396]
Sundermeyer, J. 678, 1255 [679, 1328]
Sundermeyer, W. 216 [221]
Sunick, D. L. 75 [108]
Süss-Fink, G. 67 [71]
Susuki, S. 878 [919]
Sutter, J.-P. 1282 [1359]
Swager, T. M. 2342 [2378]

Tacke, R. 1186, 1359 [1250, 1431]
Taga, T. 652 [693]
Tai, V. W.-F. 2312 [2408]
Takaoka, Y. 1242 [1343]
Takasugi, M. 2472 [2526]
Takaya, H. 2452 [2574]
Takekuma, H. 1597 [1658]
Takekuma, S. 1597 [1658]
Tallec, A. 1379 [1448]
Tam, E. K. W. 2312 [2408]
Tamai, T. 2113 [2203]
Tamm, M. 1356 [1419]
Tamura, H. 978 [1039]
Tamura, R. 878 [919]
Tanaka, K. 1757 [1856]
Tanaka, S. 1977 [2030]
Tani, K. 2113 [2203]
Tanimoto, N. 673 [674]
Tanner, D. 599 [625]
Temme, B. 1480 [1570]
Tercel, M. 1463 [1531]
Tereshko, V. 2454 [2535]
Termin, A. 1091 [1148]
Terner, J. 348 [355]
ter Meer, H.-U. 996 [1033]
Tesche, B. 1866 [1919]
Theopold, K. H. 2326 [2389]
Theurig, M. 1099 [1173]
Thibault-Starzyk, F. 431 [447]
Thiel, W. R. 2443 [2515]
Thiele, G. 1372 [1461]
Thiele, K.-H. 1372 [1461]
Thiem, J. 1979 [2041]
Thilgen, C. 996 [1033]
Thomann, M. 663 [708]
Thomas, A. 755 [820]
Thomas, J. M. 308, 639, 913, 1871 [316, 667, 963, 1922]
Thorn, J. C. 1512 [1577]
Thornton-Pett, M. 1599 [1663]
Tian, P. 2318 [2396]
Tietze, L. F. 980, 1089 [1031, 1138]
Tillack, A. 1605, 1850 [1678, 1946]
Timmerman, P. 1292, 2345 [1313, 2437]
Tinti, M. O. 2076 [2202]
Toda, F. 878, 1757 [919, 1856]
Toerien, J. G. 672 [687]

Togni, A. 497 [517]
Tokitoh, N. 2316 [2418]
Tokuyama, H. 2472 [2526]
Tolman, W. B. 895 [917]
Tomioka, H. 873 [944]
Tornieporth-Oetting, I. C. 212, 1518 [223, 1587]
Toupet, L. 2218 [2294]
Tour, J. M. 1360 [1445]
Toussaint, J.-M. 2209 [2281]
Traetteberg, M. 204 [232]
Trautwein, A. X. 731, 1621 [771, 1697]
Trendel, J.-M. 1166 [1235]
Trepanier, S. J. 1265 [1357]
Triki, S. 223 [234]
Trofimenko, S. 1983 [2053]
Trommer, M. 766 [816]
Trost, B. M. 2182 [2296]
Truttmann, L. 1964 [2048]
Tschierske, C. 1503 (1668) [1563 (1865)]
Tsuri, T. 2187 [2309]
Tuchagues, J.-P. 887 [914]
Türk, M. 1639 [1719]
Turowska-Tyrk, I. 220 [200]
Tyrra, W. 323 [325]
Tyutyulkov, N. 1957 [2062]
Tzokov, S. B. 2302 [2401]

Ueda, M. 978 [1039]
Ugozzoli, F. 1506 [1551]
Uhlig, G. 1495 [1561]
Ullrich, V. 1911 [1987]
Ungaro, R. 1506, 2479 [1551, 2533]
Unverzagt, C. 1102 [1170]
Uryu, T. 1644 [1728]
Usón, I. 2103 [2198]

Vahrenkamp, H. 2089, 2090 [2164, 2166]
Valeur, B. 2438 [2582]
Valle, G. 576 [586]
Vallombroso, T. M. 73 [110]
Vančik, H. 448 [470]
van Duynhoven, J. P. M. 2345 [2437]
van Eikema Hommes, N. J. R. 216 [221]
van Eldik, R. 783 [798]
van Esch, J. H. 2468 [2587]
van Hoorn, W. P. 1292 [1313]
van Koten, G. 1282 [1359]
van Nostrum, C. F. 2173 [2298]
van Pée, K.-H. 352 [346]
van Rooyen, P. H. 672 [687]
van Schaik, H.-P. 1611 [1703]
van Veggel, F. C. J. M. 1292, 2345 [1313, 2437]
Vázquez de Miguel, A. 1882 [1934]
Veciana, J. 2106 [2190]
Veith, U. 1298 [1308]
Veldman, N. 1282 [1359]
Venanzi, L. M. 497 [517]
Venkatraman, S. 1516 [1554]
Verboom, W. 467, 1292, 2345 [480, 1313, 2437]
Verevkin, S. 996 [1033]
Verne, H. P. 2443 [2515]
Vértesy, L. 1844 [1936]
Veyrat, M. 220 [200]
Vicente, J. 1852 [1966]
Vickers, D. M. 2330 [2406]
Viebrock, H. 1257 [1364]
Vijn, R.-J. 1611 [1703]
Vilarrasa, J. 2454 [2535]
Vincent, S. J. F. 343 [340]
Visser, H. C. 467 [480]
Vivani, R. 1594 [1655]
Voelter, W. 1499 [1568]
Vogel, E. 731, 736, 2308 [771, 776, 2402]
Vogel, H. 1274 [1361]
Vögtle, F. 375, 1767, 2413 [389, 1818, 2507]
Voigt, A. 1352 [1414]
Vollhardt, K. P. C. 313, 661 [321, 715]
von dem Bruch, K. 101 [87]
von der Gönna, V. 982, 2111 [1037, 2170]
Vottéro, P. J. A. 354 [365]

Waezsada, S. D. 1351 [1413]
Wagener, M. 1189 [1245]
Wagenknecht, P. S. 1537 [1620]
Wagner, H. 1873 [1939]
Waldmann, H. 683, 1944 [717, 2024]
Waldmeier, P. 439 [455]
Waldner, A. 226 [237]
Wallenhauer, S. 976 [1044]
Walsh, R. 2489 [2584]
Walther, D. 1373 [1421]
Wang, J. 206 [227]
Wang, P. 1241 [1346]
Wang, S. 1265 [1357]
Wang, Y.-F. 1242 [1343]
Warriner, S. L. 2290 [2410]
Wąsikiewicz, W. 214 [230]
Wassing, W. 321 [363]
Watanabe, T. 670, 873 [691, 944]
Watanabe, Y. 580 [595]
Weber, K. 2239 [2329]
Weber, L. 1077 [1131]
Weghorn, S. J. 1509, 2308 [1572, 2402]
Wegner, G. 2080 [2154]
Wehrung, P. 1166 [1235]
Weickhardt, K. 1848 [1944]
Weidenbruch, M. 1846 [1938]
Weimann, R. 1171, 1731 [1220, 1827]
Weimar, T. 88 [79]
Weinberger, H. 444 [489]
Weiss, E. 1257 [1364]
Weiss, R. 348, 891, 893, 1952 [355, 900, 901, 2038]
Weller, F. 569 [599]
Wenderoth, P. 353, 1953 [362, 2045]
Weng, W. 2199 [2269]
Wengert, S. 2069, 2073 [2147, 2150]
Wentrup, C. 527 [549]
Wenz, G. 803 [851]
Werner, Harald 1866 [1919]
Werner, Helmut 97 [82]
Wesemann, M. 1866 [1919]
Wesendrup, R. 1174 [1232]
Wesolek, M. 1592 [1660]
Wessjohann, L. 959 [1011]
Westerhausen, M. 1493 [1585]
White, A. J. P. 1503 (1668) [1563 (1865)]
White, P. S. 75, 1518 [108, 1587]
Whitesell, C. S. 871 [921]
Whitesell, J. K. 871 [921]
Wieghardt, K. 725, 731, 736, 1473 [765, 771, 776, 1556]
Wiesemann, F. 1363 [1424]
Wilcock, I. 85 [113]
Wild, S. B. 1835 [1971]
Wilde, A. 1280 [1352]
Wilhelm, U. 884 [936]
Wilk, A. 709 [747]
Will, S. 731 [771]
Williams, A. 2067 [2181]
Williams, D. J. 1503 (1668) [1563 (1865)]
Willis, A. C. 1835 [1971]
Willner, H. 1108, 1482 [1161, 1581]
Willner, I. 581 [594]
Winkhofer, N. 1352 [1414]
Winkler, H.-J. 1487 (1668), 2064, 2303, 2306 [1579, 2172, 2391, 2394]
Winkler, I. 562 [603]
Winkler, M. 2279 [2372]
Winkler, T. 1654 [1735]
Winpenny, R. E. P. 195 [208]
Winterfeld, J. 1733 [1829]
Wintner, E. A. 1577, 2059, 2061 [1665, 2159, 2162]
Wipf, P. 1516 [1554]
Wirz, J. 1153 [1240]
Witt, H. 188 [240]
Wočadlo, S. 2064 [2172]
Wolf, J. 97 [82]
Wolf, R. M. 226 [237]
Wolff, G.-J. 454 (1461) [460 (1529)]
Wolff, H.-J. 1772 [1834]
Wollenweber, M. 117 [84]
Wolmershäuser, G. 1110 [1142]
Wolski, A. 1603 [1676]
Womelsdorf, H. 1943 [2022]
Wong, C.-H. 1241, 1242 [1346, 1343]
Wonnemann, R. 1363 [1424]
Wooley, K. L. 82 [123]
Worm, K. 327 [360]
Wrackmeyer, B. 2294 [2380]
Wrasidlo, W. 183, 1581, 1583 [195, 1669, 1672]
Wray, V. 1394 [1439]
Wright, D. S. 1277, 1875 [1334, 1960]
Wright, P. A. 1871 [1922]
Wu, W. 568 [591]
Wulff, G. 188 [240]
Würthwein, E.-U. 2337 [2386]

Xie, Z. 2433 [2566]

Yamamoto, H. 107 [129]
Yamamoto, M. 1176 [1230]
Yamamoto, Y. 652 [693]
Yamashita, Y. 1977 [2030]
Yamazaki, T. 1437 [1502]
Yanagisawa, A. 107 [129]
Yang, Z. 2184, 2187 [2306, 2309]
Yano, Y. 1750 [1849]
Yonkovich, S. 339 [327]
Yoon, S. S. 2458 [2517]
Yoon, T. 853, 2477 [923, 2578]
Yoshida, K. 978 [1039]
Yoshida, M. 2452 [2574]
Yoshida, Z. 1597 [1658]
Youinou, M.-T. 2284 [2432]
Yu, J. 339 [327]
Yue, E. W. 2184, 2187, 2190 [2306, 2309, 2312]
Yuge, H. 1665 [1746]

Zab, K. 1503 (1668) [1563 (1865)]
Zadel, G. 454 (1461) [460 (1529)]
Zahavy, E. 581 [594]
Zak, Z. 967 [1035]
Zamaraev, K. I. 308 [316]
Zeitler, E. 1866 [1919]
Zemlin, F. 1866 [1919]
Zentel, R. 188 [240]
Zervosen, A. 571 [592]
Zhang, B. 2324 [2420]

Zhao, K.-M. 1882 [1934]
Zhao, Y. 1279 [1331]
Zheludev, A. 1397 [1454]
Zhu, N. 2090 [2166]
Zhu, T.-W. 1882 [1934]
Zibrowius, B. 2491 [2552]
Ziche, W. 77 [93]
Ziegler, T. 2272 [2362]
Ziembinski, R. 2277 [2367]
Ziessel, R. 1501, 1884 [1543, 1956]
Ziller, J. W. 1641, 2110 [1725, 2200]
Zimmer, I. 736 [776]
Zimny, B. 1079 [1135]
Zipse, H. 1985 [2019]
Zondervan, C. 1458 [1526]
Zönnchen, P. 1372 [1461]
Zubieta, J. 325, 757, 760 [347, 781, 784]
Zwahlen, C. 343 [340]

INDEX OF AUTHORS AND REVIEWERS OF BOOKS

This index lists separately the names of Authors/Editors and Reviewers, respectively, of books reviewed in *Angew. Chem. Int. Ed. Engl.* **1994**, *33*.

Book Authors

Adloff, J.-P. 1198
Agosta, W. C. 236
Altmann, S. L. 482
Andrews, D. L. 1195
Baer, T. 1669
Baetzold, R. C. 586
Balogh, M. 1892
Barton, D. H. R. 1009
Bein, T. 1009
Bensaude-Vincent, B. 901
Billups, W. E. 2227
Blümich, B. 128
Bochmann, M. 2225
Bonn, G. 1401
Bonnell, D. A. 2226
Brett, A. M. O. 1989
Brett, C. M. A. 1989
Brock, W. H. 901
Bruce, D. W. 585
Brunner, H. 2225
Buerk, D. G. 791
Charsley, E. L. 586
Ciufolini, M. A. 2227
Clark, J. H. 239
Collison, D. 362
Cooper, S. R. 235
Cotton, F. A. 480
Cowan, J. A. 1196
Cox, D. E. 2227
Dehmlow, E. V. 1669
Dehmlow, S. S. 1669
Dvorák, J. 1989
Dwight, K. 1403
Eu, B. C. 481
Fischer, J. E. 2227
FIZ Chemie, 1305
Frank-Kamenetskii, M. D. 1303
Ganellin, C. R. 1783
Gaspar, P. P. 1198
Gasteiger, J. 1671
Georg, G. I. 480
Gileadi, E. 1304
Goldberg, Y. 1669
Golightly, D. W. 231
Göpel, W. 127
Guard, H. E. 1010
Halgas, J. 1012
Hamerloff, S. 2228
Hasegawa, A. 588
Hendra, P. 361
Hennel, J. W. 1670
Hitchman, M. L. 1403
Hoffmann, R. 1303 (1521)
Hoheisel, C. 697
Holtzhauer, M. 234
Homans, S. W. 360
Horváth, O. 483
Hunter, B. K. 1992
Illenberger, E. 479
Imamura, M. 1198
Izumi, Y. 1893
James, L. K. 2118
Jandik, P. 1401
Jensen, K. F. 1403
Jones, C. 361
Kagan, J. 1990
Kaiser, G. 234
Karo, W. 231
Kavan, L. 1989
Kaye, B. 1521
Kemp, T. J. 1785
Keppler, B. K. 1672
Kirst, H. A. 1119
Klinowski, J. 1670
König, W. 1117
Kopecký, J. 483
Koruga, D. 2228
Koryta, J. 1989
Koskinen, A. 1891
Krist, K. 1010
Krohn, K. 1119
Kropf, H. 1891
Kroto, H. W. 2227, 2228
Kuhn, W. 128
Kybett, A. P. 239
Laszlo, P. 1892
Lee, R. E. 1306
Lever, A. B. P. 236
Leznoff, C. C. 236
Lipkowski, J. 2117
Loutfy, R. 2228
Maag, H. 1119
Mabbs, F. E. 362
Macquarrie, D. J. 239
Maddock, A. G. 1198
Marciniec, B. 1893
Mark, H. F. 1117
Mateescu, G. D. 1784
Matsuura, T. 1198
Maurer, H. H. 359
Meinel, C. 232
Merrifield, B. 1990
Mohr, P. 234
Momigny, I. 479
Montaser, A. 231
Moore, E. 587
Moser, W. R. 1671
Müller, U. 479
Ng, C.-Y. 1669
O'Donnell, T. A. 482
Ogura, H. 588
O'Hare, D. 585
Ohashi, Y. 1991
Onaka, M. 1893
Parekh, S. I. 1009
Parker, S. P. 1401
Perlmutter, P. 1197
Petz, W. 1894
Pfleger, K. 359
Platé, N. A. 1013
Powis, I. 1669
Reed, G. 2350
Rehm, H.-J. 2350
Rein, H. 359
Roberts, S. M. 1783
Robinson, G. H. 791
Rocke, A. J. 1195
Ross, P. N. 2117
Rossiter, B. W. 586
Ruckpaul, K. 359
Sanders, J. K. M. 1992
Sandler, S. R. 231
Sano, H. 1198
Schaumann, E. 1891
Schinke, R. 1011
Scholz, H. 232
Sheldon, R. A. 1013
Shimitzky, M. 1783
Silver, J. 1011
Silverman, R. B. 792
Simpkins, N. S. 1404
Slocum, D. W. 1671
Smart, L. 587
Smith, K. 587
Stengers, I. 901
Stevenson, K. L. 483
Stone, F. G. A. 2119
Suami, T. 588
Sullivan, B. P. 1010
Sundareshan, M. 2228
Torrence, V. 1303 (1521)
Traven, V. F. 239
Ulický, L. 1785
Urabe, K. 1893
Valeriu, A. 1784
Walton, D. R. M. 2228
Walton, R. A. 480
Ward, R. S. 2225
Warnes, G. 361
Warrington, S. B. 586
Weber, A. 359
Weinberger, R. 1402
Wenclawiak, B. 1402
Williams, J. M. 1119
Wingender, E. 2349
Winter, M. J. 2225

Withers, J. 2228
Wold, A. 1403
Wolfbeis, O. S. 1673
Yoshihara, K. 1198
Zettlmeier, W. 2225
Zewail, A. 237
Ziegler, C. 127
Zupan, J. 1671

Reviewers

Bahadir, M. 359
Beck, J. 587
Bein, T. 127
Bilitewski, U. 791
Billing, R. 483
Blohm, D. 2350
Broekaert, J. A. C. 231
Bryce, M. R. 1119
Cammenga, H. K. 586
Consiglio, G. 1671
Cook, M. J. 236
Dick, B. 237
Doherty, J. B. 792
Eberhardt, U. 1305
Engelhardt, H. 1401, 1402
Ernsting, N. 1195
Ettre, L. S. 1402
Federsel, H.-J. 1013
Fessner, W.-D. 1012
Fink, M. 1893
Fischer, R. A. 1403
Francke, W. 236
Fuhrhop, J.-H. 1783
Giese, B. 1009
Griesbeck, A. G. 1990
Griesinger, C. 1992
Haeberlen, U. 1670
Harrison, B. 479
Heckl, W. M. 2226
Heinze, J. 1989
Hellwinkel, D. 232
Henrich, E. 1198
Herron, N. 1009
Hirsch, A. 2227, 2228
Hoffmann, S. 1303
Hofmann, U. 234
Holze, R. 361, 2117
Hopf, H. 1303 (1521)
Irion, M. P. 1669
Jaenicke, L. 2118
Jung, G. 1117
Kauffman, G. B. 1117, 1195, 1401, 1990, 2119
Kauffman, L. M. 1117, 1990, 2119
Kaupp, G. 1991
Keeler, J. H. 1784
Kirmse, R. 362
König, B. 2225
Kozikowski, A. P. 588
Krause, N. 1891
Kresse, H. 1013
Kreuzig, R. 359
Krohn, K. 1891
Kühn-Velten, W. N. 359
Laszlo, P. 901
Leitich, J. 483
Leitner, W. 1010
Lippert, B. 1672
Mader, W. 1306
Miethchen, R. 231
Minkwitz, R. 482
Müller-Dethlefs, K. 479
Nieschalk, J. 480
Niessner, R. 1673
Ognyanov, V. I. 588
Pandey, G. 1892, 1893
Pohl, S. 1011
Post, H. 128
Reggelin, M. 360
Reinhoudt, D. N. 235
Reiser, O. 239, 587, 2225
Reuter, H. 585
Rohr, J. 1119
Rösch, N. 482
Roth, G. 1894
Rouvray, D. H. 1785
Schaumann, E. 480
Schinzer, D. 1197
Schmickler, W. 1304
Schmidt, G. 1783
Schmitt, T. 1401, 1402
Schneider, G. 1671
Schnick, W. 1403
Schwalbe, H. 360
Schweizer, M. 2349
Sokolov, I. M. 1521
Sustmann, R. 239
Theil, F. 1669
Tremel, W. 1196
Uhl, W. 791
Wenschuh, E. 1404
Wiesen, P. 1011
Williams, A. F. 480
Winkelmann, J. 697
Woermann, D. 481
Wrede, P. 1671

SUBJECT INDEX [*Angew. Chem. Int. Ed. Engl.* 1994, *33*]

(A second page number to an entry indicates an erratum to the corresponding article.)

(R) = Review Article (H) = Highlight (C) = Short Communication (B) = Book Review (L) = Correspondence

Ab initio calculations
- 1-Alkyl-2,5-(*ortho*-phenylene)-1-carbapentaborane(10) (C) 2296
- A Novel Hexamer of *t*BuC≡P: Synthesis, Structure, and Theoretical Studies (C) 2202
- Are Polar Organometallic Compounds "Carbanions"? The Gegenion Effect on Structure and Energies of Alkali-Metal Compounds (R) 1129
- Excited-State Carbon Acids: Theoretical Studies of Suberene and Cycloheptatriene (C) 2431
- 1(9)-Homocubene and 9-Homocubylidene: Theoretical Investigation of Structures, Energies, and Rearrangement Reactions (C) 668
- *s*-Indacene: A Delocalized, Formally Antiaromatic 12 π Electron System (C) 1192
- Magnetic Properties of Aromatic Transition States: The Diels–Alder Reactions (C) 1376
- New Sulfur- and Selenium-Bridged Copper Clusters; Ab Initio Calculations on $[Cu_{2n}Se_n(PH_3)_m]$ Clusters (C) 746
- Nonclassical 1,2-Diboretanes and 1,2-Diborolanes (C) 2303
- Octaplane: A Saturated Hydrocarbon with a Remarkably Low Ionization Energy Leading to a Cation with a Planar Tetracoordinate Carbon Atom (C) 1667
- Polymorphism and C=N–N=C Conformational Isomers of Azines: X-ray Crystal and Ab Initio Structures of Two Rotational Isomers of Methyl (*para*-Tolyl) Ketone Azine (C) 1081
- The Influence of Charge Distribution on Bond Lengths in the P_4O_6 Framework in Compounds of the Type P_4O_6X (C) 563
- The $S_{RN}2$ Pathway—A Mechanistic Alternative for Radicals in Polar Media? (C) 1985
- The Structures of Alkyl Derivatives of *arachno*-1-$C_3B_4H_{12}$ from Reactions of B_4H_{10} with Alkynes (C) 2298

Acrolein
- Kinetic Resolution of the Acrolein Dimer by Asymmetric Horner–Wadsworth–Emmons Reactions (C) 556

Activation of enzymes
- Activation of Glutathione Reductase by Light: A Novel Approach to Design Redox Photo-Enzymes (C) 581

Adamantylidene
- Matrix Spectroscopy of 2-Adamantylidene, a Dialkylcarbene with Singlet Ground State (C) 1964

Additions
- Conjugate Addition Reactions in Organic Synthesis (B) 1197

Adenosinephosphates
- New Cyclic Derivatives of 3′-Amino-3′-deoxyadenosine-5′-diphosphate, -triphosphate, and -methylenebis(phosphonate) (C) 1394

Agarose
- A Novel Reaction Sequence for the Coupling of Nucleophiles to Agarose with 2,2,2-Trifluoroethanesulfonyl Chloride (C) 120

AIDS
- Conocurvone—Prototype of a New Class of Anti-HIV Active Compounds? (H) 422 (1668)
- Vanadium(II)- and Niobium(III)-Induced, Diastereoselective Pinacol Coupling of Peptide Aldehydes to C_2-Symmetrical HIV-Protease Inhibitors (C) 685

Aldehydes
- On the Nature of Zinc Chloride–Aldehyde Interactions (C) 2089

Aldol reactions
- Catalytic Enantioselective C–C Coupling—Allyl Transfer and Mukaiyama Aldol Reaction (H) 417

Alkali metal compounds
- A New Method for the Synthesis of Heterometallic Complexes: Syntheses and Structures of $[(PhCH_2CH_2NLi)_3Sb(thf)]_2$ and $[Sb_3(cyN)_4(NMe_2)_2]Li$ (C) 1277
- 1,3-Dialkoxycalix[4]arenecrowns-6 in 1,3-Alternate Conformation: Cesium-Selective Ligands that Exploit Cation–Arene Interactions (C) 1506
- Doubly Lithiated Oligosilanes: Synthesis and Structure of the First Vicinal Dilithiodisilane (C) 2450
- Enantioselective Transformations and Racemization Studies of Heteroatom Substituted Organolithium Compounds (H) 175
- Ether-Solvated Sodium Ions in Salts Containing π-Hydrocarbon Anions: Crystallization, Structures, and Semiempirical Solvation Energies (C) 875
- Inversely Coordinating Silanide Ions in an Oligomeric Sodium Alcoholate (C) 216
- [(*N*-Lithio-*N*-mesitylsulfonyloxy-*tert*-butylcarbamate)$_2$ · (thf)$_3$]: Crystal Structure of a Nitrenoid (C) 115
- Metalation of Tris(trimethylsilyl)- and Tris(dimethylphenylsilyl)methane with Methylsodium: The First Dialkylsodate (C) 1268
- Phosphane Coordination to Magnesium: Synthesis and Structure of Bis[*ortho*, *ortho*′-bis{(dimethylphosphino)methyl}phenyl]magnesium (C) 2281
- $Rb_3[Nb_6SBr_{17}]$, the First Compound Containing an Isolated Trigonal-Prismatic Niobium Cluster (C) 1943
- Rearrangement and Selective Transmetalation of Bis(pyridyl)methyllithium (C) 693
- Tetralithiated Dibenzyl(methyl)phosphane (C) 2279
- The Lithocene Anion and "Open" Calcocene—New Impulses in the Chemistry of Alkali and Alkaline Earth Metallocenes (H) 2168
- The Simplest Metallocene Sandwich: the Lithocene Anion (C) 1744
- The Structures of Two Lithium Hydrazides: Is There Electron-Deficient Bonding? (C) 1746 (1988)
- Transannular Addition of Methyllithium to 5,12:6,11-Di[1,2]benzenodibenzo[*a*,*e*]cyclooctene and Its 5,6-Epoxy Derivative (C) 993

Alkaline earth metal compounds
- A Novel Organomagnesium Compound Consisting of Two Triple-Decker Cations $[LMg(\mu\text{-}Me)_3MgL]^+$ and an Octamethyltrimagnesate Anion: $[\{Me_2Mg(\mu\text{-}Me)_2\}_2Mg]^{2-}$ (C) 1257
- $[Be(dad)_2]$: Synthesis and Structure of a Diazabutadieneberyllium Complex (C) 1372
- Phosphane Coordination to Magnesium: Synthesis and Structure of Bis[*ortho*, *ortho*′-bis{(dimethylphosphino)methyl}phenyl]magnesium (C) 2281
- Sensitive and Selective Coloration of Cryptand-Type Crown Spirobenzopyrans for Alkaline-Earth Metal Compounds (C) 1163
- Solvent-Free Volatile Alkoxides of the Alkaline-Earth Elements (C) 105
- Synthesis and Crystal Structure of the "Open" Calcocene $[(tBu_2C_5H_5)Ca\cdot thf]$ (C) 2191
- Synthesis and Molecular Structure of Calcium Bis(trimethylstannanide) · 4 THF (C) 1493
- The Lithocene Anion and "Open" Calcocene—New Impulses in the Chemistry of Alkali and Alkaline Earth Metallocenes (H) 2168

Alkene complexes
- $[(Cp^{**}CoH)_2\text{-}\mu\text{-}\{\eta^2\text{:}\eta^2\text{-}cis\text{-}\mu\text{-}[(C_2H_5)_2Al\text{-}CH=CH\text{-}Al(C_2H_5)_2]\}]$ and $[\{Cp^*(\eta^2\text{-}C_2H_4)CoAl(C_2H_5)\}_2]$: Synthesis and Structure of Unusual Co–Al Cluster Compounds (C) 2435
- Ligands as "Compass Needles": How Orientations of Alkene, Alkyne, and Alkylidene Ligands Reveal π-Bonding Features in Tetrahedral Transition Metal Complexes (R) 1565

Alkenes
- Houben-Weyl. Methoden der Organischen Chemie. Band E15, Teile 1–3. En-X- und In-X-Verbindungen (B) 1891
- Practical and Rapid Vicinal Hydroxylation of Alkenes by Catalytic Ruthenium Tetraoxide (C) 2312

Alkenols
- Intramolecular Photocyclization of ω,ω-Diphenyl-(ω−1)-alken-1-ols by an Exciplex Quenching Mechanism (C) 2113

Alkenyl sulfones
- Iron-Promoted, Regio- and Stereoselective Allylic Substitutions for the Synthesis of Alkenyl Sulfones Substituted at C-3 (C) 1949

Alkoxides
- Solvent-Free Volatile Alkoxides of the Alkaline-Earth Elements (C) 105

Alkylations
- Palladacycles as Intermediates for Selective Dialkylation of Arenes and Subsequent Fragmentation (C) 2421

Alkyne complexes
- $[Cp_2Ti(C\equiv CtBu)_2]$ as an Alkynyl Transfer Reagent: Synthesis and Characterization of the Asymmetrically Bridged Heterodimetallic Complex $[Cp_2Ti(C\equiv CtBu)_2Pt(PPh_3)]\cdot 0.5\,THF$ (C) 2083
- Bis(tetramethylbutynediol)nickel(0), the First Pure Monoalkyne Complex of Nickel and Its Chemistry (C) 1373
- Ligands as "Compass Needles": How Orientations of Alkene, Alkyne, and Alkylidene Ligands Reveal π-Bonding Features in Tetrahedral Transition Metal Complexes (R) 1565

- Towards One-Dimensional Carbon Wires Connecting Single Metal Centers: A Cumulenic C_5 Chain that Mediates Charge Transfer between Rhenium and Manganese Termini (C) 2199

Alkynes
- Complex-Stabilized Alkynyl and Cycloalkenyl Isocyanides (C) 330
- 1,4-Didehydrobutadiene: The Intermediate in a New Class of Thermally Induced Intramolecular Alkyne Couplings (C) 2470
- Electron Delocalization in Ethynyl-Bridged Binuclear Ruthenium(II) Polypyridine Complexes (C) 1884
- Fullerene–Acetylene Hybrids: On the Way to Synthetic Molecular Carbon Allotropes (C) 1366
- Houben-Weyl. Methoden der Organischen Chemie. Band E15, Teile 1–3. En-X- und In-X-Verbindungen (B) 1891
- Triple Bonds in Small Rings: Testing the Limits of Chemical Bonds (H) 1455
- Unexpected Reactions of Acetylenedicarboxylates with Zirconocene Complexes (C) 1850

Allenes
- Nonclassical Stabilization of Planar Allenes: Low Rotational Barriers for Allene Double Bonds (C) 2064

Allylacetates
- A Regioselective Palladium-Catalyzed Reduction of 3,3-Heterobimetalated Allylic Acetates–Synthesis and Reactivity of Allylic Bimetallic Compounds (C) 2448

Allyl cation
- Generation of the Parent Allyl Cation in a Superacid Cryogenic Matrix (C) 448

Allyl halides
- A New Synthesis of 1,3,4-Trideoxy-1,4-iminoglycitols of Varying Chain Length by $(C_3 + C_n)$-Coupling of Allyl Halides with Glyconitrile Oxides (C) 1295

Allylsilanes
- Lewis Acid Promoted [2+2] Cycloaddition of Allylsilanes and Unsaturated Esters: A Novel Method for Cyclobutane Construction (C) 1612
- Liquid Sulfur Dioxide as a Lewis-Acidic Solvent for the Alkylation and Alkoxyalkylation of Allylsilanes (C) 788

Aluminophosphates
- On the Nature of the Active Site in a Co-APO-18 Solid Acid Catalyst (C) 1871

Aluminum compounds
- Coordination Chemistry of Aluminum (B) 791
- $[(Cp^{**}CoH)_2$-μ-$\{\eta^2$:η^2-*cis*-μ-$[(C_2H_5)_2Al$-$CH=CH$-$Al(C_2H_5)_2]\}]$ and $[\{Cp^*(\eta^2$-$C_2H_4)CoAl(C_2H_5)\}_2]$: Synthesis and Structure of Unusual Co–Al Cluster Compounds (C) 2435
- $[(CpNi)_2(Cp^*Al)_2]$: Cp*Al as a Bridging Two-Electron Ligand (C) 2482
- Donor-Stabilized Aluminum(I) Bromide (C) 1754
- Donor-Stabilized Aluminum(II) Bromide (C) 862
- Localization of Electrons in Intermetallic Phases Containing Aluminum (C) 2069
- Oxygen-Induced Structural Transformation of the Polynuclear Organoaluminum Complex $[Al_4(\mu_3$-8-quinolylimide$)_2(CH_3)_8]$ to $[Al_4(\mu_3$-8-quinolylimide$)_2(CH_3)_7(\mu$-$OCH_3)]$ (C) 1265
- $[P_4(Cp^*Al)_6]$: A Compound with an Unusual P_4Al_6 Cage Structure (C) 199
- Reactions of $[(C_5Me_5)ZrF_3]$ with $AlMe_3$—Synthesis and Structure of a Zirconium–Aluminum–Carbon Cluster (C) 967
- Soluble Organic Derivatives of Aluminosilicates with $Al_2Si_2O_4$ and $Al_4Si_2O_6$ Frameworks (C) 2103
- Subvalent Aluminum Halides as Examples of High-Temperature Species in Inorganic Syntheses (H) 1830
- Synthesis and Structure of the First Dimeric Iminoalane Containing an Al_2N_2 Heterocycle (C) 969
- Synthesis of the First Microporous Aluminum Phosphonate with Organic Groups Covalently Bonded to the Skeleton (C) 2335
- The First Carbon–Phosphorus–Aluminum Cage Compounds: Cyclooligomerization of Phosphaalkynes with Trialkylaluminum Compounds (C) 1491
- Unequivocal Partitioning of Crystal Structures, Exemplified by Intermetallic Phases Containing Aluminum (C) 2073

Amide cleavage
- Fast Amide Cleavage under Mild Conditions. An Evolutionary Approach to Bioorganic Catalysis (C) 346

Amidinium ions
- Axially Chiral Amidinium Ions with a Biaryl Skeleton: A New Class of Structure in Host–Guest Chemistry (C) 984

Amino acids
- Synthesis and Structure of the First Titanium(IV) α-Amino Acid Complexes (C) 1518
- Synthesis of a New Unnatural Amino Acid with a Benzodiazepine-Containing Side Chain and Incorporation into a Tripeptide (C) 1737
- Synthesis of Unsaturated Amino Acids by [3,3]-Sigmatropic Rearrangement of Chelate-Bridged Glycine Ester Enolates (C) 998

Amino alcohols
- Simple and Versatile Synthesis of Optically Active 1,2-Amino Alcohols by Grignard Addition to *N,O*-Dibenzylglyceraldimine and -lactaldimine (C) 1298

Aminomalonic acid
- Preparation and C-Alkylation of Peptides with Aminomalonate Building Blocks (C) 439

Aminopolyols
- Regio- and Stereoselective Electrophilic C-Substitution of 2-(*N,N*-Dibenzylamino)-1-,ω-alkanediols by Lithiation of Their Carbamates (C) 1734

Amorphous sulfides
- A Building Principle of Amorphous Chalcogenides of Transition Metals: The "Extrusion" of the Electron Rich Cluster $[Re_4S_2(SO_2)_4(CN)_{10}]^{8-}$ from a-Re_2S_7 (C) 770

Amphiphiles
- Bolaamphiphiles: From Golf Balls to Fibers (H) 1937
- Molecular Golf Balls: Vesicles from Bowl-Shaped Host Molecules (C) 1662
- Stable Flexible Fibers and Rigid Tubules Made from Single-Chain Perfluoroalkylated Amphiphiles (C) 1514

Analysis of proteins
- Ladder Sequencing of Peptides and Proteins—A Combination of Edman Degradation and Mass Spectrometry (H) 723

Analytical methods
- Analysis with Supercritical Fluids: Extraction and Chromatography (B) 1402
- An Anthracene-Based Fluorescent Sensor for Transition Metal Ions (C) 1975
- A Reagent for Determining Optical Purities of Diols by Formation of Diastereomeric Arylboronate Esters (C) 1182
- Chemical Analysis of Inorganic and Organic Surfaces and Thin Films by Static Time-of-Flight Secondary Ion Mass Spectrometry (TOF-SIMS) (R) 1023
- Thermal Analysis—Techniques and Applications (B) 586

Anhydroretinol
- Spectroscopic Studies of Anhydroretinol, an Endogenous Mammalian and Insect *retro*-Retinoid (C) 1837 (2348)

Annulenes
- Tetraaza[14]annulenezirconium(IV) Complexes with Butadiene Ligands and their Relationship with Bis(cyclopentadienyl)-zirconium(IV) Complexes (C) 2204

Anthracenes
- An Anthracene-Based Fluorescent Sensor for Transition Metal Ions (C) 1975

Antibiotics
- Antibiotics and Antiviral Compounds. Chemical Synthesis and Modification (B) 1119
- Biosynthetic Investigations on Pyridazomycin (C) 1648
- Incorporation of L-[Methyl-$^2H_3$]methionine and 2-[Hydroxy-^{18}O]hydroxyethylphosphonic Acid into Fosfomycin in *Streptomyces fradiae*—An Unusual Methyl Transfer (C) 341
- Synthesis of the Anthraquinone Framework of Dynemicin A (C) 781
- The Trehalase Inhibitor Salbostatin, a Novel Metabolite from *Streptomyces albus*, ATCC 21838 (C) 1844

Antibodies
- An Antibody-Catalyzed 1,2-Rearrangement of Carbon–Carbon Bonds (C) 1607
- Enantioselective, Multigram-Scale Synthesis with a Catalytic Antibody (C) 475
- Progress Toward An Antibody Glycosidase (C) 339
- Specific Binding of Antibodies to DNA through Combinatorial Antibody Libraries (H) 1827

Antimony compounds
- $[\{Sb_2(Ncy)_4\}_2Cu_4]$: A Mixed-Metal Antimony(III)/Copper(I) Complex Containing a Cu_4 Square Plane (C) 1875
- A New Method for the Synthesis of Heterometallic Complexes: Syntheses and Structures of $[(PhCH_2CH_2NLi)_3Sb(thf)]_2$ and $[Sb_3(cyN)_4(NMe_2)_2]Li$ (C) 1277
- $[SbN(SbCl)_3(NSbCl_2)(NSiMe_3)_2 \cdot SbCl_3]$, an Unusual Nitridoantimony Complex with a Heterocubane Structure (C) 569
- Trialkylstibanes as Bridging Ligands: Synthesis and Structure of the Dinuclear Complexes $[Rh_2Cl_2(\mu$-Sb*i*Pr$_3)(\mu$-$CR_2)_2]$ (C) 97

Antisense systems
- Amides as a New Type of Backbone Modification in Oligonucleotides (C) 226
- Stereocontrolled Synthesis of Oligo(nucleoside phosphorothioate)s (R) 709
- Synthesis of an Azathymidine and Its Incorporation into Oligonucleotides (C) 1654

Antitumor agents
- A New Application of Modified Peptides and Peptidomimetics: Potential Anticancer Agents (H) 305
- An Unusual Route to Potential Platinum Antitumor Compounds: Synthesis, Reactivity, and Spectroscopic Properties of the Pt^{IV} Complex *fac*-$[PtCl_3(NH_3)_2L]Cl$ (C) 1632
- A Water-Soluble Prodrug of Taxol with Self-Assembling Properties (C) 1583
- Chemistry and Biology of Taxol (R) 15
- Enediyne Quinone Imines: Truncated, Biologically Active Dynemicin Congeners (C) 2477

- Metal Complexes in Cancer Chemotherapy (B) 1672
- Platinum(II) Complexes with Porphyrin Ligands—Additive Cytotoxic and Photodynamic Effect (C) 2214
- Structure of an Antineoplastic Platinum Complex with a Bipyridyl-Crown Ether (C) 186
- Synthesis of C-2 Taxol Analogues (C) 1581
- Synthesis of the Anthraquinone Framework of Dynemicin A (C) 781

Antiviral agents
- Antibiotics and Antiviral Compounds. Chemical Synthesis and Modification (B) 1119
- A Short Route to [3-^{15}N]-3′-Azido-3′-deoxythymidine (N3-Labeled AZT) via 3-Nitro-AZT (C) 2454
- Regioselective Synthesis and Antiviral Activity of Purine Nucleoside Analogues with Acyclic Substituents at N7 (C) 562

Arene complexes
- Cyclotrimerization of Ethyne on the Complex Fragment [(η^1-tBu$_2$PCH$_2$PtBu$_2$)-Ni^0] with Formation of an η^6-Benzene–Nickel(0) Complex (C) 879
- Electron-Reservoir Complexes [Fe^{I}Cp-(arene)] as Selective Initiators for a Novel Electron Transfer Chain Catalyzed Reaction: General Synthesis of Fulvalene-Bridged Homo- and Heterodinuclear Zwitterions (C) 661
- Novel Rh^I Piano-Stool Complexes with New Hemilabile Ligands Ligating through Phosphane and Arene Groups: Synthesis, Characterization, and Reactivity (C) 2473
- [2,6-iPr$_2$C$_6$H$_3$(Me$_3$Si)NTl]$_4$—A Covalent Thallium(I)–Nitrogen Compound with Weak Arene–Thallium Interactions (C) 1351
- Tris(η^4-naphthalene)zirconate(2−) (C) 1973

Arenes
- 2,2′-Bipyrenyl and *para*-Terpyrenyl—A New Type of Electronically Decoupled Oligoarylene (C) 1957
- Homogeneous Catalytic Oxidation of Arenes and a New Synthesis of Vitamin K$_3$ (C) 2475
- Intramolecular [2+2] Cycloadditions of 2,2′-Bis(1-arylvinyl)-Substituted Biphenyls Induced by Photo Electron Transfer (C) 2300
- Ladder Polymers with a Heteroacene Skeleton (C) 2424
- Long-Lived *ipso*-Silylated *p*-Toluenium Ions: Evidence from a Kinetic Isotope Effect (C) 1094
- Palladacycles as Intermediates for Selective Dialkylation of Arenes and Subsequent Fragmentation (C) 2421
- The Crystal Structures of Base-Free, Monomeric Arylcopper(I) and Arylsilver(I) Compounds; Two Cases of Mistaken Identity? (C) 2443
- The Effect of Fusion of Angular-Strained Rings on Benzene: Crystal Structures of 1,2-Dihydrocyclobuta[*a*]cyclopropa[*c*]-, 1,2,3,4-Tetrahydrodicyclobuta[*a,c*]-, 1,2,3,4-Tetrahydrodicyclobuta[*a,c*]-cyclopropa[*e*]-, and 1,2,3,4,5,6-Hexahydrotricyclobuta[*a,c,e*]benzene (C) 313

Aromaticity
- A 1,3-Diboratabenzene (C) 2306
- Benziporphyrin, a Benzene-Containing, Nonaromatic Porphyrin Analogue (C) 1246
- 11,12-Bis(diethylamino)nonatriafulvalene, the First "Aromatic" Nonafulvene (C) 973
- *s*-Indacene: A Delocalized, Formally Antiaromatic 12 π Electron System (C) 1192
- Mills–Nixon Effect: Wherefore Art Thou? (H) 1721
- N-Heteroarene Dianions as Antiaromatic Ligands Bridging two Lanthanocene Moieties (C) 1171
- Synthesis and Structure of the First Hybrid Borazine–Phosphazene Ring (C) 2277

Arsenic compounds
- The First Cycloaddition Reactions of Dimeric Arsenium Cations (C) 1267

Aryl effect
- Cyclopropanes by Nucleophilic Attack of Mono- and Diaryl-Substituted (η^3-Allyl)palladium Complexes: Aryl Effect and Stereochemistry (C) 1280

Asymmetric syntheses
- Absolute Asymmetric Synthesis Solely under the Influence of a Static Homogeneous Magnetic Field? (C) 1459
- A Multiple Five-Membered-Ring-Selective Williamson Reaction as a Key Step in the Stereoselective Construction of 2,5-Linked Oligo(tetrahydrofuran)s (C) 1873
- An Enantioselective Synthesis of Deoxynojirimycin (C) 2320
- A New Synthesis of 1,3,4-Trideoxy-1,4-iminoglycitols of Varying Chain Length by ($C_3 + C_n$)-Coupling of Allyl Halides with Glyconitrile Oxides (C) 1295
- A Novel Approach to the Stereoselective Synthesis of β-Mannosides (C) 1765
- A Novel Route to Diastereomerically Pure (*E*)-Alkene Dipeptide Isosteres from β-Aziridinyl-α,β-enoates by Treatment with Organocopper Reagents (C) 652
- A Short and Highly Stereoselective Synthesis of the 1,10-*seco*-Eudesmanolide Ivangulin (C) 2195
- Asymmetric Diels–Alder Reactions Catalyzed by a Chiral Iron Lewis Acid (C) 1856
- Asymmetric 1,6-Induction in Hetero-Diels–Alder Reactions of Chiral Oxabutadienes for a De Novo Synthesis of Enantiomerically Pure Carbohydrates: Lewis Acid Dependent Reversal of Facial Selectivity (C) 980
- Asymmetric Michael Additions to Chiral α,β-Unsaturated Alkoxycarbene Chromium Complexes (C) 1392
- Asymmetric Synthesis of Biaryls by Intramolecular Oxidative Couplings of Cyanocuprate Intermediates (C) 1842
- Asymmetric Synthesis of Highly Substituted Pyrrolidines by 1,3-Dipolar Cycloadditions of Azomethine Ylides with *N*-Acryloylproline Benzyl Ester (C) 683
- Asymmetric Synthesis of Natural Products (B) 1891
- Attempts to Carry Out Enantioselective Reactions in a Static Magnetic Field (C) 1458
- [2,3] Sigmatropic Wittig Rearrangement of Chiral Allyloxyacetaldehyde Hydrazones in the Diastereo- and Enantioselective Synthesis of Protected, γ,δ-Unsaturated α-Hydroxyaldehydes and Cyanohydrins (C) 2098
- Catalytic Enantioselective C–C Coupling—Allyl Transfer and Mukaiyama Aldol Reaction (H) 417
- Catalytic Enantioselective Protonation of Enolates (C) 1888
- *trans*-Chelating Chiral Diphosphane Ligands Bearing Flexible *P*-Alkyl Substituents (AlkylTRAPs) and their Application to the Rhodium-Catalyzed Asymmetric Hydrosilylation of Simple Ketones (C) 111
- Chiral Aziridines—Their Synthesis and Use in Stereoselective Transformations (R) 599
- Chiroporphyrins: An Approach to Asymmetric Catalysts with Stereocenters Near the Plane of the Porphyrin Ring (C) 220
- Chirotechnology. Industrial Synthesis of Optically Active Compounds (B) 1013
- Cyclopropanes by Nucleophilic Attack of Mono- and Diaryl-Substituted (η^3-Allyl)palladium Complexes: Aryl Effect and Stereochemistry (C) 1280
- Diastereomerically Pure Mannich Bases from the Addition of Enamines to Ternary Iminium Salts (C) 2422
- Diastereoselective Hydroxyalkylation of Enantiomerically Pure 2-Alkenylsulfoximides (C) 444
- Diastereoselective Synthesis of Amino-Substituted Indolizidines and Quinolizidines by the Intramolecular Hetero-Ene Reaction of Prolinal Imine and 2-Piperidine Carbaldimine (C) 458
- Electrostatic vs. Orbital Control of Facial Selectivities in π Systems: Experimental and Theoretical Study of Electrophilic Additions to 7-Isopropylidenenorbornanes (C) 1390
- Enantioselective, Multigram-Scale Synthesis with a Catalytic Antibody (C) 475
- Enantioselective Reactions in a Static Magnetic Field (C) 454 (1461)
- Enantioselective Reactions in a Static Magnetic Field—A False Alarm! (E) 1457
- Enantioselective Transformations and Racemization Studies of Heteroatom Substituted Organolithium Compounds (H) 175
- Handbook of Enantioselective Catalysis with Transition Metal Compounds. Vol. I: Products and Catalysts, Vol. II: Ligands–References (B) 2225
- Increase in the Enantioselectivity of Asymmetric Hydrogenation in Water Influenced by Surfactants or Polymerized Micelles (C) 2197
- Iron-Promoted, Regio- and Stereoselective Allylic Substitutions for the Synthesis of Alkenyl Sulfones Substituted at C-3 (C) 1949
- Nitrogen Donors in Organometallic Chemistry and Homogeneous Catalysis (R) 497
- Optically Active Lactones from a Baeyer–Villiger-Type Metal-Catalyzed Oxidation with Molecular Oxygen (C) 1848
- Oxidation of Metal-Coordinated Thioethers with Dimethyldioxirane—A New Stereoselective Synthesis of Chiral Sulfoxides (C) 1609
- Regio- and Diastereoselective Photooxygenation of Chiral 2,5-Cyclohexadiene-1-carboxylic Acids (C) 1971
- Regio- and Enantioselective Silane-Terminated Intramolecular Heck Reactions (C) 1089
- Regio- and Stereoselective Electrophilic C-Substitution of 2-(*N*,*N*-Dibenzylamino)-1-,ω-alkanediols by Lithiation of Their Carbamates (C) 1734
- Scalemic 2-Formyl-3-hydroxy[2.2]paracyclophane: A New Auxiliary for Asymmetric Synthesis (C) 91
- Simple and Versatile Synthesis of Optically Active 1,2-Amino Alcohols by Grignard Addition to *N*,*O*-Dibenzylglyceraldimine and -lactaldimine (C) 1298
- Stereoselective Reactions of Sulfinylated Benzyl Radicals: Effects of Solvents and Lewis Acids (C) 1601

- Substituent Effects and Complexation Phenomena in the Diastereoselective Protonation of Chiral Enolates (C) 1764
- Synthesis and Reactions of Optically Active Cyanohydrins (R) 1555
- Totally Enantioselective Inversion of Configuration of (*S*)-(+)-Carnitine Derivatives (C) 2076
- Tridentate β-Hydroperoxy Alcohols as Novel Oxygen Donors for the Titanium-Catalyzed Epoxidation of γ,δ-Unsaturated α,β-Diols: A Direct Diastereoselective Synthesis of Epoxy Diols (C) 1107
- Vanadium(II)- and Niobium(III)-Induced, Diastereoselective Pinacol Coupling of Peptide Aldehydes to C_2-Symmetrical HIV-Protease Inhibitors (C) 685

Atomic force microscopy
- Detection and Imaging of Single Molecules by Optical Near-Field Microscopy (H) 1723

Atropisomers
- Asymmetric Synthesis of Biaryls by Intramolecular Oxidative Couplings of Cyanocuprate Intermediates (C) 1842
- Axially Chiral Amidinium Ions with a Biaryl Skeleton: A New Class of Structure in Host–Guest Chemistry (C) 984

Aurophilicity
- Aurophilicity at Sulfur Centers: Synthesis and Structure of the Tetragold(I) Species $[(Ph_3PAu)_4S](CF_3SO_3)_2 \cdot 2CH_2Cl_2$ (C) 769

Autobiographies
- From Small Organic Molecules to Large: A Century of Progress (B) 1117
- Leaving No Stone Unturned: Pathways in Organometallic Chemistry (B) 2119
- Life During a Golden Age of Peptide Chemistry: The Concept and Development of Solid-Phase Peptide Synthesis (B) 1990

Azadiboriridines
- (Iminoboryl)borates $[(tBuN \equiv B)BtBu_2R]^-$ from the Azadiboriridine NB_2tBu_3 (R = Me, Bu) (C) 201

Azaphosphirenes
- Synthesis of the First 2*H*-1-Aza-2-phosphirene Complexes (C) 80
- Thermally Induced Ring Cleavage of a 2*H*-1,2-Azaphosphirene Tungsten Complex (C) 2427

Azasugars
- An Enantioselective Synthesis of Deoxynojirimycin (C) 2320

Azathymidine
- Synthesis of an Azathymidine and Its Incorporation into Oligonucleotides (C) 1654

Azepanediones
- Stereoselective Intramolecular Alkylation of Glycosylimides to Highly Functionalized Bicyclic 2,5-Azepanediones and Heterotricyclic [5.3.1.$0^{2,6}$] Undecanamides (C) 1979

Azines
- Polymorphism and C=N–N=C Conformational Isomers of Azines: X-ray Crystal and Ab Initio Structures of Two Rotational Isomers of Methyl (*para*-Tolyl) Ketone Azine (C) 1081

Aziridines
- Chiral Aziridines—Their Synthesis and Use in Stereoselective Transformations (R) 599

Azo compounds
- Functionalization of Aromatic Azo Compounds by the Cobalt-Catalyzed, Regioselective Double Addition of Tolane: 2,6-Distilbenylazobenzenes and 2,3-Dihydrocinnolines (C) 1603

Benzaldehyde
- Acid-Catalyzed Olefination of Benzaldehyde (C) 1611

Benzene cation
- Molecular Distortion in Reactive Chemical Intermediates (H) 962

Benziporphyrin
- Benziporphyrin, a Benzene-Containing, Nonaromatic Porphyrin Analogue (C) 1246

Benzobisthiete
- 2*H*,5*H*-Benzo[1,2-*b*:4,5-*b*']bisthiete—A Highly Reactive Bisdiene System (C) 465

Benzodiazepines
- Synthesis of a New Unnatural Amino Acid with a Benzodiazepine-Containing Side Chain and Incorporation into a Tripeptide (C) 1737

Benzoquinone
- Supramolecular Activation of *para*-Benzoquinone (C) 2489

Betaines
- Heterodimetal–Betaine Chemistry: Catalytic and Stoichiometric Coupling of Alkynyl Ligands under the Joint Influence of Zirconium and Boron Centers (C) 1480

Biaryls
- Asymmetric Synthesis of Biaryls by Intramolecular Oxidative Couplings of Cyanocuprate Intermediates (C) 1842

Biochemistry
- Binuclear Metal Complexes as Efficient Intermediaries in Biochemically Relevant Hydrolysis Reactions (H) 1141
- Human Oxalate—Really Just an End-Product of Metabolism? (C) 1780
- Inorganic Biochemistry. An Introduction (B) 1196

Biopolymers
- Opportunities for New Chemical Libraries: Unnatural Biopolymers and Diversomers (H) 633

Biosensors
- Biosensors. Theory and Applications (B) 791

Biotechology
- Biotechnology. Vol. 2 Genetic Fundamentals and Genetic Engineering (B) 2349

Bipyridazines
- Self-Assembly and Structure of a 3×3 Inorganic Grid from Nine Silver Ions and Six Ligand Components (C) 2284

Bismuth compounds
- Blue-Violet Pentamethylbismuth (H) 1726
- Methylbismuth(v) Compounds (C) 976

Bis(pyridyl)methyllithium
- Rearrangement and Selective Transmetalation of Bis(pyridyl)methyllithium (C) 693

Blood–brain barrier
- The Absolute Configuration of (+)-α-1,2,3,4,5,6-Hexachlorocyclohexane, and Its Permeation through the Seal Blood–Brain Barrier (C) 882

Bolaamphiphiles
- Assembly Properties of Bolaamphiphiles from Dimeric Acids (C) 2078
- Bolaamphiphiles: From Golf Balls to Fibers (H) 1937

Bond-stretch isomerism
- Bond-Stretch Isomers and Spin-State Isomers: A Comment on the Article "Bond-Stretch Isomers: Fact not Fiction" (C) 1462
- Bond-Stretch Isomers: Fact not Fiction (C) 425

Boron compounds
- A Carbene–Iron Chelate Complex as a Source of a Ferraborane Derivative (C) 2218
- A Chiral Lewis Acid with Two "Metal" Centers: Cooperative Binding of Two Amine Molecules to a Chiral Diboronic Ester (C) 2452
- A 1,3-Diboratabenzene (C) 2306
- A Glucose-Selective Molecular Fluorescence Sensor (C) 2207
- A Highly Distorted and an Undistorted Borirane, C-B-H Hyperconjugation Induced by C-Si-H Hyperconjugation (C) 1487 (1668)
- 1-Alkyl-2,5-(*ortho*-phenylene)-1-carbapentaborane(10) (C) 2296
- A Reagent for Determining Optical Purities of Diols by Formation of Diastereomeric Arylboronate Esters (C) 1182
- A Water-Soluble "Bear Trap" Exhibiting Strong Anion Complexation Properties (C) 2456
- Borophosphates—A Neglected Class of Compounds: Crystal Structures of $Mn^{II}[BPO_5]$ (M^{II} = Ca, Sr) and $Ba_3[BP_3O_{12}]$ (C) 749
- 1-Carba-*arachno*-pentaboranes(10) from Dimethyldi(1-propynyl)silane and Ethyldiboranes(6) (C) 2294
- Chemistry within a Unimolecular Micelle Precursor: Boron Superclusters by Site- and Depth-Specific Transformations of Dendrimers (C) 666
- (Iminoboryl)borates $[(tBuN \equiv B)BtBu_2R]^-$ from the Azadiboriridine NB_2tBu_3 (R = Me, Bu) (C) 201
- Macropolyhedral Boron-Containing Cluster Chemistry: Isolation and Characterization of the First Macropolyhedral Thiaborane, the *arachno*-Type $[9,9'\text{-}S_2B_{17}H_{18}]^-$ Ion (C) 1599
- Macrotricyclic Borane–Amine Adducts: The First Uncharged Synthetic Host Compounds Without Lewis Acid Character, for Anionic Guests (C) 327
- Nonclassical 1,2-Diboretanes and 1,2-Diborolanes (C) 2303
- Nonclassical Stabilization of Planar Allenes: Low Rotational Barriers for Allene Double Bonds (C) 2064
- (η^5-Pentamethylcyclopentadienyl)iron Complexes with η^5-2,3,5-Tricarbahexaboranyl and η^5-2,3-Dihydro-1,3-diborolyl Ligands (C) 203
- Synthesis and Properties of 2,4,6-Trimethylphenylborane (Mesitylborane), a Stable Alternative to Thexylborane (C) 851
- Synthesis and Reactivity of a Naphtho[1,8-*bc*]boret (C) 1247
- Synthesis and Structure of the First Hybrid Borazine–Phosphazene Ring (C) 2277
- The First Structurally Characterized Metal Complex Involving the Free Acid of a New Tris(pyrazolyl)borate as Ligand (C) 1983
- The First Water-Dependent Liquid Clathrate: X-Ray Evidence in the Solid for a C–H···π(Heteroarene)···H–C Interaction (C) 566
- The Structures of Alkyl Derivatives of *arachno*-1-$C_3B_4H_{12}$ from Reactions of B_4H_{10} with Alkynes (C) 2298

Bridgehead functionalization
- Bridgehead Functionalization of Non-Enolizable Ketones: The First Preparatively Useful Methods (C) 2220

Bridging ligands
- A New Oxygen Tripod Ligand and Its First Complexes with p- and d-Block Elements (C) 991
- $[(CpNi)_2(Cp^*Al)_2]$: Cp*Al as a Bridging Two-Electron Ligand (C) 2482

- Cyanide–Isocyanide Isomerism in CN-Bridged Organometallic Complexes (C) 2090
- Mesoscopic Sheets of a Cyano-Bridged Cu–Ni Coordination Complex: Template Synthesis at the Interlayers of Cast Multibilayer Films (C) 2483
- N-Heteroarene Dianions as Antiaromatic Ligands Bridging two Lanthanocene Moieties (C) 1171
- The First Metal Complexes with a Doubly S_3-Bridged Ferrocene Ligand (C) 1752
- Trialkylstibanes as Bridging Ligands: Synthesis and Structure of the Dinuclear Complexes $[Rh_2Cl_2(\mu\text{-Sb}i\text{Pr}_3)(\mu\text{-CR}_2)_2]$ (C) 97

Bromine compounds
- Dibromine Pentoxide Br_2O_5 (C) 975

Butadienes
- 1,1-Di-, 1,2,3-Tri-, and 1,1,4,4-Tetra-*tert*-butyl-1,3-butadiene (C) 1369
- Photoisomerization of Highly Alkylated Butadienes (C) 204

tert-Butylbutadienes
- 1,1-Di-, 1,2,3-Tri-, and 1,1,4,4-Tetra-*tert*-butyl-1,3-butadiene (C) 1369

Cadmium compounds
- Three-Dimensional Interpenetrating Double and Triple Framework Structures in $[Cd(bpy)_2\{Ag(CN)_2\}_2]$ and $[Cd(pyrz)\{Ag_2(CN)_3\}\{Ag(CN)_2\}]$ (C) 1665

Cage compounds
- An Organic Molecule with a Rigid Cavity of Nanosize Dimensions (C) 1292
- From an Insecticide to Plato's Universe—The Pagodane Route to Dodecahedranes: New Pathways and New Perspectives (R) 2239
- Isopagodanes—Precursors of Unusual Cage Ions (C) 117
- Molecular Solids as Ligands in Organometallic Chemistry: $[Cp^*_6Ti_6Na_7F_{19}\cdot 2.5\,thf]$ ($Cp^* = C_5Me_5$) and $[Cp^*_4Ti_4Mg_2F_{12}\cdot 7\,thf]$, Links Between Ionic Solids and Organometallic Compounds (C) 555
- $[P_4(Cp^*Al)_6]$: A Compound with an Unusual P_4Al_6 Cage Structure (C) 199
- Synthesis and Structural Characterization of $[\{(Et_2O)Mg\}_6(NPh)_4Br_4]$: A Magnesium–Imide Cage Species Derived from a Dimagnesylamine Solution (C) 1000
- The First Carbon–Phosphorus–Aluminum Cage Compounds: Cyclooligomerization of Phosphaalkynes with Trialkylaluminum Compounds (C) 1491

Calicheamicins
- A Convergent Total Synthesis of Calicheamicin γ_1^I (C) 858
- Calicheamicin θ_1^I: A Rationally Designed Molecule with Extremely Potent and Selective DNA Cleaving Properties and Apoptosis Inducing Activity (C) 183
- On the DNA Recognition Role of the Carbohydrate Sector in Calicheamicin: A Comparison of DNA Cleaving Capacity of Enantiomeric Calicheamicinones (C) 855

Calixarenes
- An Organic Molecule with a Rigid Cavity of Nanosize Dimensions (C) 1292
- A Novel Type of Stereoisomerism in Calix[4]arene-Based Carceplexes (C) 2345
- A Water-Soluble "Bear Trap" Exhibiting Strong Anion Complexation Properties (C) 2456
- Calixarene-Based Macrocyclic Nonet ($S = 4$) Octaradical and its Acyclic Sextet ($S = 5/2$) Pentaradical Analogue (C) 2091
- 1,3-Dialkoxycalix[4]arenecrowns-6 in 1,3-Alternate Conformation: Cesium-Selective Ligands that Exploit Cation–Arene Interactions (C) 1506
- "Head-to-Tail" Linkage in Double Calix[4]arenes (C) 214
- Sugar Calixarenes: Preparation of Calix[4]arenes Substituted at the Lower and Upper Rims with *O*-Glycosyl Groups (C) 2479

Calorimetry
- Time-Resolved Photoacoustic Calorimetry: From Carbenes to Proteins (R) 294

Calyculin A
- The Synthesis of Naturally Occurring (−)-Calyculin A (C) 673

Capillary electrophoresis
- Capillary Electrophoresis of Small Molecules and Ions (B) 1401
- Practical Capillary Electrophoresis (B) 1402

Carbamates
- $[(N\text{-Lithio-}N\text{-mesitylsulfonyloxy-}tert\text{-butylcarbamate})_2\cdot(thf)_3]$: Crystal Structure of a Nitrenoid (C) 115

Carbanions
- Are Polar Organometallic Compounds "Carbanions"? The Gegenion Effect on Structure and Energies of Alkali-Metal Compounds (R) 1129
- Ether-Solvated Sodium Ions in Salts Containing π-Hydrocarbon Anions: Crystallization, Structures, and Semiempirical Solvation Energies (C) 875
- Phosphane Coordination to Magnesium: Synthesis and Structure of Bis[*ortho*, *ortho*′-bis{(dimethylphosphino)methyl}phenyl]magnesium (C) 2281
- Tetralithiated Dibenzyl(methyl)phosphane (C) 2279

Carbazoles
- Reciprocal Template Effects in a Replication Cycle (C) 1579
- Template Effects in New Self-Replicating Molecules (C) 1577

Carbene complexes
- A Carbene–Iron Chelate Complex as a Source of a Ferraborane Derivative (C) 2218
- A Triosmium Cluster Complex with a Carbene Ligand in an Unusual Coordination Mode (C) 1093
- Chromium Carbene Complexes in Organic Synthesis: Recent Developments and Perspectives (H) 303
- Iron–Carbene Complexes (B) 1894
- New Upswing of Organolanthanoid Research: A Very Promising Revival of Organocerium(IV) Chemistry and the First Stable Lanthanoid(II/III)–Carbene Complexes (H) 2165
- Organolanthanoid–Carbene Adducts (C) 1733
- Reactivity of a Phosphanylcarbene (λ^5-Phosphaacetylene) with Lewis Acids: X-Ray Crystal Structures of the First Carbene–Gallane Complex and *C*-Gallyl-Substituted Phosphorus Ylide (C) 578
- Synthesis and Crystal Structure of a Monocarbene Complex of Copper (C) 672

Carbenes
- An Extremely Long-Lived Triplet Carbene; Reactivity, Optical Absorption, and Kinetics of Highly Congested Diarylcarbenes (C) 873
- Equilibrium between Isocyanide and Carbene Complexes in Coordination Compounds of 2,6-Dihydroxyphenyl Isocyanide (C) 1356
- Matrix Spectroscopy of 2-Adamantylidene, a Dialkylcarbene with Singlet Ground State (C) 1964
- Reactions of an Iminophosphoranylidene Carbenoid (C) 982

Carbocations
- Concerning the Mechanism of α-Elimination: Hypervalent Ion Pairing in an Iodocarbenium Iodide (C) 893
- Generation of the Parent Allyl Cation in a Superacid Cryogenic Matrix (C) 448
- Long-Lived *ipso*-Silylated *p*-Toluenium Ions: Evidence from a Kinetic Isotope Effect (C) 1094
- Molecular Distortion in Reactive Chemical Intermediates (H) 962
- Octaplane: A Saturated Hydrocarbon with a Remarkably Low Ionization Energy Leading to a Cation with a Planar Tetracoordinate Carbon Atom (C) 1667

Carbohydrates
- A Facile One-Pot Synthesis of a Trisaccharide Unit from the Common Polysaccharide Antigen of Group B *Streptococci* Using Cyclohexane-1,2-diacetal (CDA) Protected Rhamnosides (C) 2292
- A Glucose-Selective Molecular Fluorescence Sensor (C) 2207
- A Highly Convergent Synthesis of the Lewis^y Blood Group Determinant in Conjugatable Form (C) 1468
- An Interactive Strategy for the Assembly of Complex, Branched Oligosaccharide Domains on a Solid Support: A Concise Synthesis of the Lewis^b Domain in Bioconjugatable Form (C) 1470
- A Novel Approach to the Stereoselective Synthesis of β-Mannosides (C) 1765
- Asymmetric 1,6-Induction in Hetero-Diels–Alder Reactions of Chiral Oxabutadienes for a De Novo Synthesis of Enantiomerically Pure Carbohydrates: Lewis Acid Dependent Reversal of Facial Selectivity (C) 980
- Biomimetic Phosphonylation and Phosphorylation of Glycoses and Deoxynucleosides (C) 2302
- Carbohydrates—Synthetic Methods and Applications in Medicinal Chemistry (B) 588
- Continuous Enzymatic Synthesis of 2′-Deoxythymidine-5′-(α-D-glucopyranosyl) diphosphate (C) 571
- Conversion of Glycosyl Azides via *N*-Bromoglycosylimines to Aldononitriles (C) 751
- Cyclohexane-1,2-diacetals (CDA): A New Protecting Group for Vicinal Diols in Carbohydrates (C) 2290
- O-Glycoside Syntheses under Neutral Conditions in Concentrated Solutions of $LiClO_4$ in Organic Solvents (C) 1944
- Ring Contractions in Carbohydrates (H) 1345
- Samarium Iodide Induced Intramolecular C-Glycoside Formation: Efficient Radical Formation in the Absence of an Additive (C) 1383
- Stereoselective Intramolecular Alkylation of Glycosylimides to Highly Functionalized Bicyclic 2,5-Azepanediones and Heterotricyclic [5.3.1.$0^{2,6}$] Undecanamides (C) 1979
- Sugar Calixarenes: Preparation of Calix[4]arenes Substituted at the Lower and Upper Rims with *O*-Glycosyl Groups (C) 2479
- Synthesis of a Biantennary Heptasaccharide by Regioselective Glycosylations (C) 1102
- Synthesis of Benzylated Cycloisomaltotri- and -hexaoside (C) 354

- Synthesis of Dihydroxyacetone Phosphate (and Isosteric Analogues) by Enzymatic Oxidation; Sugars from Glycerol (C) 209
- The Selective Blocking of *trans*-Diequatorial, Vicinal Diols; Applications in the Synthesis of Chiral Building Blocks and Complex Sugars (H) 2272

Carbon–carbon coupling
- Catalytic Enantioselective C–C Coupling—Allyl Transfer and Mukaiyama Aldol Reaction (H) 417
- Construction of Carbon Frameworks with the Help of Ruthenium Complexes: 1,5-Cyclooctadiene as a Reagent in Transition Metal Catalyzed Reactions (H) 636
- Copper(II)-Mediated Oxidative Coupling of Bis(dimethylaminomethyl)arylruthenium Complexes to give $[(terpy)Ru^{III}(pincer\text{-}pincer)Ru^{III}(terpy)](CuCl_2)_4$ (C) 1282
- 1,4-Didehydrobutadiene: The Intermediate in a New Class of Thermally Induced Intramolecular Alkyne Couplings (C) 2470
- Fine Feathers Make Fine Birds: The Heck Reaction in Modern Garb (R) 2379
- Iterative Divergent/Convergent Approach to Linear Conjugated Oligomers by Successive Doubling of the Molecular Length: A Rapid Route to a 128 Å-Long Potential Molecular Wire (C) 1360
- Ligand Effects on the Chemoselectivity of Transition Metal Catalyzed Reactions of α-Diazo Carbonyl Compounds (R) 1797
- Reactions at Both Ends of a Dimetalated Olefin: CS_2 Insertion into and Atom Transfer Reactions of $[Re(CO)_4\{trans\text{-}\mu\text{-}HC{=}C(CO_2Me)\}Re(CO)_4(NCMe)]$ (C) 568
- Reactions in Supercritical Carbon Dioxide (H) 1452
- Reactions of C_3O_2 with Stabilized Triphenylphosphoranes $Ph_3P{=}CHX$ (X = CN, COMe, COPh) (C) 576
- Synthesis of Oxa- and Azapalladacycles from Organostannanes (C) 2482
- The First Decaisopropylmetallocene: One-Pot Synthesis of $[Rh(C_5iPr_5)_2]PF_6$ from $[Rh(C_5Me_5)_2]PF_6$ by Formation of 20 Carbon–Carbon Bonds (C) 1637

Carbon compounds
- Novel Carbon Compounds with "Naked" C_n Units (H) 547
- Polyynes—Fascinating Monomers for the Construction of Carbon Networks? (H) 1073

Carbon dioxide
- Active Surface Carbon—A Reactive Intermediate in the Production of Synthesis Gas from Methane and Carbon Dioxide (C) 1657
- Electrochemical and Electrocatalytic Reactions of Carbon Dioxide (B) 1010
- New Ionic, Isoelectronic Analogues of CO_2 and CS_2 (H) 1575
- Reactions in Supercritical Carbon Dioxide (H) 1452
- The Photochemical Activation of Carbon Dioxide Using a Nickel Complex (H) 173

Carbon disulfide
- New Ionic, Isoelectronic Analogues of CO_2 and CS_2 (H) 1575
- Reactions at Both Ends of a Dimetalated Olefin: CS_2 Insertion into and Atom Transfer Reactions of $[Re(CO)_4\{trans\text{-}\mu\text{-}HC{=}C(CO_2Me)\}Re(CO)_4(NCMe)]$ (C) 568

Carbon suboxide
- Reactions of C_3O_2 with Stabilized Triphenylphosphoranes $Ph_3P{=}CHX$ (X = CN, COMe, COPh) (C) 576

Carbonyl complexes
- Homoleptic Noble Metal Carbonyl Cations (H) 1077

Carboranes
- 1-Alkyl-2,5-(*ortho*-phenylene)-1-carbapentaborane(10) (C) 2296
- 1-Carba-*arachno*-pentaboranes(10) from Dimethyldi(1-propynyl)silane and Ethyldiboranes(6) (C) 2294
- Chemistry within a Unimolecular Micelle Precursor: Boron Superclusters by Site- and Depth-Specific Transformations of Dendrimers (C) 666
- "Free" $[Fe(tpp)]^+$ Cation: A New Concept in the Search for the Least Coordinating Anion (C) 2433
- The Structures of Alkyl Derivatives of *arachno*-$1\text{-}C_3B_4H_{12}$ from Reactions of B_4H_{10} with Alkynes (C) 2298

Carnitine
- Totally Enantioselective Inversion of Configuration of (*S*)-(+)-Carnitine Derivatives (C) 2076

Carotenoids
- Spectroscopic Studies of Anhydroretinol, an Endogenous Mammalian and Insect *retro*-Retinoid (C) 1837 (2348)

Cascade reactions
- Fine Feathers Make Fine Birds: The Heck Reaction in Modern Garb (R) 2379
- Syntheses of Cyclopentanols by a Silicon-Induced Cascade Reaction (C) 217

Catalysis
- [2+2] Cycloaddition of Norbornenes with Alkynes Catalyzed by Ruthenium Complexes (C) 580
- Binuclear Metal Complexes as Efficient Intermediaries in Biochemically Relevant Hydrolysis Reactions (H) 1141
- Catalytic Pt^+-Mediated Oxidation of Methane by Molecular Oxygen in the Gas Phase (C) 1174
- Chiroporphyrins: An Approach to Asymmetric Catalysts with Stereocenters Near the Plane of the Porphyrin Ring (C) 220
- Construction of Carbon Frameworks with the Help of Ruthenium Complexes: 1,5-Cyclooctadiene as a Reagent in Transition Metal Catalyzed Reactions (H) 636
- Cooperativity in Rh_2 Complexes: High Catalytic Activity and High Regioselectivity in the Hydroformylation of Olefins (H) 67
- Doubly Bridged *rac*-Metallocenes of Zirconium and Hafnium (C) 1946
- Effects of Metal-Ion Dopants on the Photocatalytic Reactivity of Quantum-Sized TiO_2 Particles (C) 1091
- Enantioselective, Multigram-Scale Synthesis with a Catalytic Antibody (C) 475
- Facile Reduction of a Dialkyl Zirconium(IV) Octaethylporphyrin (OEP) Complex by H_2: Crystal Structure and Spectroscopic Characterization of $[(OEP)Zr\text{-}CH_2SiMe_3]$ (C) 95
- Fast Amide Cleavage under Mild Conditions. An Evolutionary Approach to Bioorganic Catalysis (C) 346
- Handbook of Enantioselective Catalysis with Transition Metal Compounds. Vol. I: Products and Catalysts. Vol. II: Ligands–References (B) 2225
- Homogeneous Catalytic Oxidation of Arenes and a New Synthesis of Vitamin K_3 (C) 2475
- Homogeneous Transition Metal Catalyzed Reactions (B) 1671
- Ligand Effects on the Chemoselectivity of Transition Metal Catalyzed Reactions of α-Diazo Carbonyl Compounds (R) 1797
- Molecular Catalysts for Multielectron Redox Reactions of Small Molecules: The "Cofacial Metallodiporphyrin" Approach (R) 1537
- Molecular Siloxane Complexes of Rare Earth Metals—Model Systems for Silicate-Supported Catalysts? (C) 1285
- Monomer–Dimer Equilibria in Homo- and Heterodinuclear Cationic Alkylzirconium Complexes and Their Role in Polymerization Catalysis (C) 1634
- NiO/CaO-Catalyzed Formation of Syngas by Coupled Exothermic Oxidative Conversion and Endothermic CO_2 and Steam Reforming of Methane (C) 2104
- Nitrogen Donors in Organometallic Chemistry and Homogeneous Catalysis (R) 497
- On the Nature of the Active Site in a Co-APO-18 Solid Acid Catalyst (C) 1871
- Organic Chemistry Using Clays (B) 1892
- Otto Roelen, Pioneer in Industrial Homogeneous Catalysis (R) 2144 (2348)
- Rationally Designed Inorganic Catalysts for Environmentally Compatible Technologies (C) 308
- Reply (C) 311
- Selective Catalysis on Silicon Dioxide with Substrate-Specific Cavities (C) 471
- Solid Supports and Catalysts in Organic Synthesis (B) 587
- Turning Points in Catalysis (R) 913
- Wacker Oxidation of 1-Decene to 2-Decanone in the Presence of a Chemically Modified Cyclodextrin System: A Happy Union of Host–Guest Chemistry and Homogeneous Catalysis (C) 2100
- Zeolite, Clay and Heteropoly Acid in Organic Reactions (B) 1893

Catenanes
- Isomeric Lactam Catenanes and the Mechanism of their Formation (C) 1767
- Olympiadane (C) 1286
- The Two-Step Self-Assembly of [4]- and [5]Catenanes (C) 433

Cations
- Synthesis and Crystal Structure of the First Tetraaminophosphonium Salt $P(NH_2)_4I$ (C) 785

Cavitands
- An Organic Molecule with a Rigid Cavity of Nanosize Dimensions (C) 1292

C_1 building blocks
- Electrochemical and Electrocatalytic Reactions of Carbon Dioxide (B) 1010
- The Photochemical Activation of Carbon Dioxide Using a Nickel Complex (H) 173

Cellulose
- Cellulose in Schweizer's Reagent: A Stable, Polymeric Metal Complex with High Chain Stiffness (C) 884

Cerium compounds
- An Efficient Access to Organocerium(IV) Complexes: Synthesis and Structure of Bis[1,3,6-tris(trimethylsilyl)cyclooctatetraene]cerium(IV) (C) 1618

C-Glycosides
- Samarium Iodide Induced Intramolecular C-Glycoside Formation: Efficient Radical Formation in the Absence of an Additive (C) 1383

C-H acidity
- Excited-State Carbon Acids: Theoretical Studies of Suberene and Cycloheptatriene (C) 2431

C–H activation
- Heterodimetal–Betaine Chemistry: Catalytic and Stoichiometric Coupling of Alkynyl Ligands under the Joint Influence of Zirconium and Boron Centers (C) 1480
- Oxidation of Weakly Activated C–H Bonds (H) 69
- Palladium-Catalyzed C–H Activation of *tert*-Butyl Groups: A Simple Synthesis of 1,2-Dihydroxycyclobutabenzene Derivatives (C) 103

Chalcogen compounds
- Difluoromethyl Compounds of Chalcogens: A NMR Study of the Reactions of $Cd(CF_3)_2 \cdot 2MeCN$ and $ZnBr(CF_3) \cdot 2MeCN$ with Dialkyl Chalcogenides and Boron Trifluoride (C) 323

Chaos theory
- Chaos and Complexity (B) 1521

Charge transfer
- Charge Transfer Photochemistry of Coordination Compounds (B) 483

Charge transfer complexes
- Coexistence of Mobile and Localized Electrons in Bis(ethylene)dithiotetrathiafulvalene (BEDT-TTF) Radical Salts with Paramagnetic Polyoxometalates: Synthesis and Physical Properties of $(BEDT\text{-}TTF)_8[CoW_{12}O_{40}] \cdot 5.5H_2O$ (C) 223

Chelate ligands
- Titanium Complexes with Tripodal Amido Ligands: Building Blocks for Stable Bimetallic Coordination Compounds Containing Highly Polar Metal–Metal Bonds (C) 676

Chemical bonding
- Ligands as "Compass Needles": How Orientations of Alkene, Alkyne, and Alkylidene Ligands Reveal π-Bonding Features in Tetrahedral Transition Metal Complexes (R) 1565
- The Bonding Capability of Imido Complex Fragments of Groups 5–7 with Regard to the Isolobal Relationship (C) 1255
- The Chemical Bond. Structure and Dynamics (B) 237
- The Structures of Two Lithium Hydrazides: Is There Electron-Deficient Bonding? (C) 1746 (1988)

Chemical vapor deposition
- Chemical Vapor Deposition. Principles and Applications (B) 1403

Chemistry imagined
- Chemistry Imagined. Reflections on Science (B) 1303 (1521)

Chemistry of the atmosphere
- Recycling in the Earth's Atmosphere: The OH Radical—Its Importance for the Chemistry of the Atmosphere and the Determination of Its Concentration (R) 1816

Chiral auxiliaries
- Chiral Aziridines—Their Synthesis and Use in Stereoselective Transformations (R) 599
- Scalemic 2-Formyl-3-hydroxy[2.2]paracyclophane: A New Auxiliary for Asymmetric Synthesis (C) 91

Chirality
- A Chiral Lewis Acid with Two "Metal" Centers: Cooperative Binding of Two Amine Molecules to a Chiral Diboronic Ester (C) 2452
- Cooperativity and Transfer of Chirality in Liquid-Crystalline Polymers (C) 188
- The Effect of Chiral Bilayers: Wax Tubes made of (*S*)-Nonacosan-10-ol (C) 350
- The First Zwitterionic, Optically Active Disilicate with Pentacoordinate Silicon (C) 1186

Chlorine compounds
- Effects of $^{35}Cl/^{37}Cl$, ^{13}C Residual Dipolar Coupling on the Variable-Temperature ^{13}C CP/MAS NMR Spectra of Solid, Chlorinated Sodium Acetates (C) 1624
- Optically Active Reference Compounds for Environmental Analysis Obtained by Preparative Enantioselective Gas Chromatography (C) 2085
- The Equilibrium Distribution of Semivolatile Organochloro Compounds between Atmosphere and Surface Water in the Atlantic Ocean (C) 646
- Toxicity of Chlorinated Organic Compounds: Effects of the Introduction of Chlorine in Organic Molecules (R) 1920

Chlorine trioxide
- Chlorine Trioxide: Spectroscopic Properties, Molecular Structure, and Photochemical Behavior (C) 1482

Chlorofluorocarbons
- Ozone Formation through Decomposition of CFCs in the Stratosphere (C) 1108

Cholesterol
- Dissolution of Cholesterol in Water by a Synthetic Receptor (C) 1625
- Increased Selectivity of a Simple Photosensitive Probe in the Presence of Large Proportions of Cholesterol (C) 1176

Chromatography
- Toward Unified Enantioselective Chromatography with a Single Capillary Column Coated with Chirasil-Dex (C) 2222

Chromium compounds
- Asymmetric Michael Additions to Chiral α,β-Unsaturated Alkoxycarbene Chromium Complexes (C) 1392
- Chromium Carbene Complexes in Organic Synthesis: Recent Developments and Perspectives (H) 303
- Cr^{III} and Fe^{III} Complexes with η^3-1,3,5-Triazacyclohexane Ligands (C) 1877
- Unusually Large Isotope Effects on NMR Chemical Shifts of Paramagnetic Organometallic Compounds (C) 2326

Clathrates
- A Clathrate Hydrate of Nitric Oxide (C) 691
- The First Water-Dependent Liquid Clathrate: X-Ray Evidence in the Solid for a $C-H\cdots\pi(Heteroarene)\cdots H-C$ Interaction (C) 566

Clays
- Organic Chemistry Using Clays (B) 1892
- Zeolite, Clay and Heteropoly Acid in Organic Reactions (B) 1893

Clusters
- $[\{Sb_2(Ncy)_4\}_2Cu_4]$: A Mixed-Metal Antimony(III)/Copper(I) Complex Containing a Cu_4 Square Plane (C) 1875
- A Cluster-Bound Triply-Bridging Phosphorus Atom Coordinated to Four $(Ph_3P)Au^+$ Units: $[Fe_3(CO)_9P\{Au(PPh_3)\}_4][BAr_4]$ (C) 75
- A Hexanuclear Gold(I) Complex: $[(Ph_3PAu)_2C(PPh_2AuPPh_2)\}_2](ClO_4)_2$ (C) 87
- A Triosmium Cluster Complex with a Carbene Ligand in an Unusual Coordination Mode (C) 1093
- Cluster Ions (B) 1669
- $[(Cp^{**}CoH)_2\text{-}\mu\text{-}\{\eta^2\text{:}\eta^2\text{-}cis\text{-}\mu\text{-}[(C_2H_5)_2Al\text{-}CH=CH\text{-}Al(C_2H_5)_2]\}]$ and $[\{Cp^*(\eta^2\text{-}C_2H_4)CoAl(C_2H_5)\}_2]$: Synthesis and Structure of Unusual Co–Al Cluster Compounds (C) 2435
- $[Cu_{96}P_{30}\{P(SiMe_3)_2\}_6(PEt_3)_{18}]$, a New Phosphorus-Bridged Copper Cluster (C) 1290
- $[Cu_{44}Se_{22}(PEt_2Ph)_{18}]$ and $[Cu_{44}Se_{22}(PnButBu_2)_{12}]$: Synthesis and Structure of Two Copper Clusters with Isomeric Cu–Se Frameworks (C) 2287
- Desulfurization of Benzo[*b*]thiophene by S/Ru Exchange: Formation and Structure of the Cluster $[Ru_3(CO)_8(C_8H_6)]$ (C) 1381
- Fullercages without Carbon—Fulleranes, Fullerenes, Space-filler-enes? (H) 843
- $[K([18]crown\text{-}6)]^+[Mo_4(\mu_4\text{-}H)(OCH_2tBu)_{12}]^-$, the First Alkoxidohydrido Cluster of Molybdenum. Evidence for a Rare, if not the First, Example of a μ_4-Hydride (C) 191
- Macropolyhedral Boron-Containing Cluster Chemistry: Isolation and Characterization of the First Macropolyhedral Thiaborane, the *arachno*-Type $[9,9'\text{-}S_2B_{17}H_{18}]^-$ Ion (C) 1599
- Metal Complexes of Marine Peptide Metabolites: A Novel Ag_4 Cluster (C) 1516
- $[Mn_4Te_4(SC_3H_7)_4]^{4-}$ and $[Mn_4Te_4(SeC_3H_7)_4]^{4-}$: Novel Heterocubane Clusters of Manganese (C) 2322
- $[Mo_{57}Fe_6(NO)_6O_{174}(OH)_3(H_2O)_{24}]^{15-}$: A Highly Symmetrical Giant Cluster with an Unusual Cavity and the Possibility of Positioning Paramagnetic Centers on Extremely Large Cluster Surfaces (C) 849
- New Sulfur- and Selenium-Bridged Copper Clusters; Ab Initio Calculations on $[Cu_{2n}Se_n(PH_3)_m]$ Clusters (C) 746
- $[(Ph_3PAu)_6(dppeAu_2)(AuCl)_4Pd]$, an Icosahedral Au_{12} Cluster with a Central Pd Atom (C) 207
- $Rb_3[Nb_6SBr_{17}]$, the First Compound Containing an Isolated Trigonal-Prismatic Niobium Cluster (C) 1943
- Reactions of $[(C_5Me_5)ZrF_3]$ with $AlMe_3$—Synthesis and Structure of a Zirconium–Aluminum–Carbon Cluster (C) 967
- Structural and Magnetic Characterization of a Novel Heptanuclear Hydroxo-Bridged Copper(II) Cluster of the Corner-Sharing Dicubane Type (C) 1184

Cobalt compounds
- A Novel Open-Framework Cobalt Phosphate Containing a Tetrahedrally Coordinated Cobalt(II) Center: $CoPO_4 \cdot 0.5\,C_2H_{10}N_2$ (C) 639
- $[(Cp^{**}CoH)_2\text{-}\mu\text{-}\{\eta^2\text{:}\eta^2\text{-}cis\text{-}\mu\text{-}[(C_2H_5)_2Al\text{-}CH=CH\text{-}Al(C_2H_5)_2]\}]$ and $[\{Cp^*(\eta^2\text{-}C_2H_4)CoAl(C_2H_5)\}_2]$: Synthesis and Structure of Unusual Co–Al Cluster Compounds (C) 2435
- Functionalization of Aromatic Azo Compounds by the Cobalt-Catalyzed, Regioselective Double Addition of Tolane: 2,6-Distilbenylazobenzenes and 2,3-Dihydrocinnolines (C) 1603
- On the Nature of the Active Site in a Co-APO-18 Solid Acid Catalyst (C) 1871
- Porphyrins with Biconcave Frameworks (C) 889
- Schiff Base Complexes with Five-Coordinate Cobalt as Dioxygen Activating Sites in Zeolites (C) 431

Cofactors
- Isolation of RNA Aptamers for Biological Cofactors by In Vitro Selection (C) 1084

Complexes with carbon ligands
- A Novel Organomagnesium Compound Consisting of Two Triple-Decker Cations $[LMg(\mu\text{-}Me)_3MgL]^+$ and an Octamethyltrimagnesate Anion: $[\{Me_2Mg(\mu\text{-}Me)_2\}_2Mg]^{2-}$ (C) 1257
- $[Ru_3(CO)_6(\eta^5\text{:}\eta^1\text{-}C_5H_4)_3]$: The First Six-Membered Ru_3C_3 Ring Formed by Insertion of C_5H_4 Units into Metal–Metal Bonds of $[Ru_3(CO)_{12}]$ (C) 2193

- Bifunctional Compounds (B) 2225
- Chemical Bonding (B) 2225
- Equilibrium between Isocyanide and Carbene Complexes in Coordination Compounds of 2,6-Dihydroxyphenyl Isocyanide (C) 1356
- Fluorinated Isocyanides—More than Ligands with Unusual Properties (R) 1315
- Heterodimetal–Betaine Chemistry: Catalytic and Stoichiometric Coupling of Alkynyl Ligands under the Joint Influence of Zirconium and Boron Centers (C) 1480
- Monomer–Dimer Equilibria in Homo- and Heterodinuclear Cationic Alkylzirconium Complexes and Their Role in Polymerization Catalysis (C) 1634
- New Titanium – Boron Complexes with a Planar Tetracoordinate Carbon or a Planar Tricoordinate Phosphorus Center (C) 197
- Organometallics 1. Complexes with Transition Metal–Carbon σ-Bonds (B) 2225
- Organometallics 2. Complexes with Transition Metal–Carbon π-Bonds (B) 2225
- Towards One-Dimensional Carbon Wires Connecting Single Metal Centers: A Cumulenic C_5 Chain that Mediates Charge Transfer between Rhenium and Manganese Termini (C) 2199

Complexes with C_n bridges
- Novel Carbon Compounds with "Naked" C_n Units (H) 547

Complexes with hydrido ligands
- $[(Cp^{**}CoH)_2$-μ-$\{\eta^2:\eta^2$-*cis*-μ-$[(C_2H_5)_2Al$-$CH=CH$-$Al(C_2H_5)_2]\}]$ and $[\{Cp^*(\eta^2$-$C_2H_4)CoAl(C_2H_5)\}_2]$: Synthesis and Structure of Unusual Co–Al Cluster Compounds (C) 2435
- $[K([18]crown\text{-}6)]^+[Mo_4(\mu_4$-$H)(OCH_2tBu)_{12}]^-$, the First Alkoxidohydrido Cluster of Molybdenum, Evidence for a Rare, if not the First, Example of a μ_4-Hydride (C) 191
- Unusually Large Isotope Effects on NMR Chemical Shifts of Paramagnetic Organometallic Compounds (C) 2326

Complexes with nitrogen ligands
- Alternating Ferro- and Antiferromagnetic Interactions in a Mn^{II} Chain with Alternating End-On and End-to-End Bridging Azido Ligands (C) 2488
- A Model for α-Keto Acid Dependent Nonheme Iron Enzymes: Structure and Reactivity of $[Fe^{II}_2(Me_2hdp)_2(bf)](ClO_4)$ (C) 1886
- $[Be(dad)_2]$: Synthesis and Structure of a Diazabutadieneberyllium Complex (C) 1372
- Change of Orientation of Axial Imidazole Ligands in a Cytochrome b Model Complex in Response to a Change in the Oxidation State of the Metal Center (C) 1363
- Copper(II)-Mediated Oxidative Coupling of Bis(dimethylaminomethyl)arylruthenium Complexes to give $[(terpy)Ru^{III}$(pincer-pincer)$Ru^{III}(terpy)](CuCl_2)_4$ (C) 1282
- Cr^{III} and Fe^{III} Complexes with η^3-1,3,5-Triazacyclohexane Ligands (C) 1877
- Electron Delocalization in Ethynyl-Bridged Binuclear Ruthenium(II) Polypyridine Complexes (C) 1884
- Fairly Strong Ferromagnetic Interactions between Imino Nitroxide Ligands through a Diamagnetic Cu^I Ion in $[Cu^I(im\text{-}mepy)_2](PF_6)$ (C) 670
- Hydroxylamine, Hydrazine, and Diazene as Unidentate Ligands in Osmium and Ruthenium Complexes (C) 657
- Lanthanide(III) Tetraamide Macrocyclic Complexes as Synthetic Ribonucleases: Structure and Catalytic Properties of $[La(tcmc)(CF_3SO_3)(EtOH)](CF_3SO_3)_2$ (C) 773
- Luminescent Eu^{3+} and Tb^{3+} Complexes of a Branched Macrocyclic Ligand Incorporating 2,2′-Bipyridine in the Macrocycle and Phosphinate Esters in the Side Arms (C) 1501
- Nitrogen Donors in Organometallic Chemistry and Homogeneous Catalysis (R) 497
- Novel Copper Nitrosyl Complexes: Contributions to the Understanding of Dissimilatory, Copper-Containing Nitrite Reductases (H) 2057
- $[2,6\text{-}i Pr_2C_6H_3(Me_3Si)NTl]_4$—A Covalent Thallium(I)–Nitrogen Compound with Weak Arene–Thallium Interactions (C) 1351
- Pronounced Electronic Coupling in Rigidly Connected N,C,N-Coordinated Diruthenium Complexes over a Distance of Up to 20 Å (C) 1775
- $[SbN(SbCl)_3(NSbCl_2)(NSiMe_3)_2\cdot SbCl_3]$, an Unusual Nitridoantimony Complex with a Heterocubane Structure (C) 569
- Self-Assembly and Structure of a 3×3 Inorganic Grid from Nine Silver Ions and Six Ligand Components (C) 2284
- Structure of an Antineoplastic Platinum Complex with a Bipyridyl-Crown Ether (C) 186
- Synthesis and Structural Characterization of $[\{(Et_2O)Mg\}_6(NPh)_4Br_4]$: A Magnesium–Imide Cage Species Derived from a Dimagnesylamine Solution (C) 1000
- The Bonding Capability of Imido Complex Fragments of Groups 5–7 with Regard to the Isolobal Relationship (C) 1255
- The First Mononuclear Nitrosyl(oxo)-molybdenum Complex: Side-On Bonded and μ_3-Bridging NO Ligands in $[\{MoL(NO)(O)(OH)\}_2]NaPF_6\cdot H_2O$ (C) 1473
- The First Structurally Characterized Metal Complex Involving the Free Acid of a New Tris(pyrazolyl)borate as Ligand (C) 1983
- The Versatility of the Azido Ligand: Linkage of Ni^{II} Centers to Form a Chain with One End-to-End and Three End-On Bridges in Alternation (C) 2087
- Titanium Complexes with Tripodal Amido Ligands: Building Blocks for Stable Bimetallic Coordination Compounds Containing Highly Polar Metal–Metal Bonds (C) 676

Complexes with oxygen ligands
- A New Oxygen Tripod Ligand and Its First Complexes with p- and d-Block Elements (C) 991
- A Thermally Stable Peroxocopper(II) Complex with Unusual μ_4-Coordination of the Peroxo Ligand (C) 1969
- Carboxylatoiron(II) Aggregates: A Novel Fe^{II}_4 Complex with Threefold Symmetry (C) 1660
- Molecular Siloxane Complexes of Rare Earth Metals—Model Systems for Silicate-Supported Catalysts? (C) 1285
- Polar Superstructures Stabilized by Polymeric Oxometal Units: Columnar Liquid Crystals Based on Tapered Dioxomolybdenum Complexes (C) 2342
- Structural and Magnetic Characterization of a Novel Heptanuclear Hydroxo-Bridged Copper(II) Cluster of the Corner-Sharing Dicubane Type (C) 1184
- Synthesis and Structure of the First Organometallic Galloxane Hydroxide $Mes_6Ga_6O_4(OH)_4$ (C) 1244
- Synthesis and Structure of the First Titanium(IV) α-Amino Acid Complexes (C) 1518
- Two-Dimensional Sheets of Tetragonal Copper(II) Lattices: X-Ray Crystal Structure and Magnetic Properties of $[Cu(C_6O_4Cl_2)(C_4H_4N_2)]_n$ (C) 1759
- $[Zr_3Cp_2(O_2CN\text{-}iPr_2)_6(\mu_3\text{-}O)(\mu_2\text{-}CCO)]$, the First Crystallographically Established Ketenylidene Complex; A Model for CO Reductive Cleavage on Metal Surfaces (C) 1188

Complexes with phosphorus ligands
- *trans*-Chelating Chiral Diphosphane Ligands Bearing Flexible *P*-Alkyl Substituents (AlkylTRAPs) and their Application to the Rhodium-Catalyzed Asymmetric Hydrosilylation of Simple Ketones (C) 111
- $[Cp^*Fe(\eta^5\text{-}P_5)]$, a Sandwich Complex with Diverse Ligand Properties (C) 1110
- $[Cu_{96}P_{30}\{P(SiMe_3)_2\}_6(PEt_3)_{18}]$, a New Phosphorus-Bridged Copper Cluster (C) 1290
- $[Cu_{44}Se_{22}(PEt_2Ph)_{18}]$ and $[Cu_{44}Se_{22}$-$(PnButBu_2)_{12}]$: Synthesis and Structure of Two Copper Clusters with Isomeric Cu–Se Frameworks (C) 2287
- New Titanium – Boron Complexes with a Planar Tetracoordinate Carbon or a Planar Tricoordinate Phosphorus Center (C) 197
- Novel Rh^I Piano-Stool Complexes with New Hemilabile Ligands Ligating through Phosphane and Arene Groups: Synthesis, Characterization, and Reactivity (C) 2473
- Platinum-Iron Silylene Complexes and Metal-Promoted Substituent Exchange between $Si(NMe_2)_3$- and $P(OEt)_3$-Ligands (C) 2440
- Propeller Isomerism of the Triphenylphosphane Ligand in Half-Sandwich Ru^{II} Complexes (C) 866
- Thermally Induced Ring Cleavage of a 2*H*-1,2-Azaphosphirene Tungsten Complex (C) 2427

Complexes with silicon ligands
- Platinum-Iron Silylene Complexes and Metal-Promoted Substituent Exchange between $Si(NMe_2)_3$- and $P(OEt)_3$-Ligands (C) 2440

Complexes with sulfur ligands
- $[\{Rh_2Cp^*_2(\mu\text{-}CH_2)_2\}_2(\mu\text{-}S_4)]^{2+}$: A Novel Tetranuclear Cationic Complex with a Rectangular S_4 Unit (C) 1882
- A Postulated Carrier of Gold in Hydrothermal Ore Solutions: Synthesis and Crystal Structure of $[(Ph_3P)_2N]$-$[Au(SH)_2]$, the First Homoleptic Hydrogensulfido Complex (C) 1852
- Homoleptic Thiolato Complexes: Di- and Trinuclear Ti^{IV} Complexes with Unexpected Metal–Sulfur Cores, $[NMe_2H_2]$-$[Ti_2(SMe)_9]$ and $[Ti_3(SMe)_{12}]$ (C) 1981
- Single-Crystal EPR Spectroscopy on $[^{57}Fe(NO)(S_2CNEt_2)_2]$: The "Triplet Signal" in the EPR Spectrum of $[Fe(S_2CNEt_2)_3]$ (C) 1497
- Synthesis and Characterization of Thiolato Complexes with Two-Coordinate Iron(II) (C) 1178
- Synthesis and Structure of $[Ni(SO_2)_6](AsF_6)_2$ and $[Fe(SO_2)_4(FAsF_5)_2]$ (C) 1663
- The First Metal Complexes with a Doubly S_3-Bridged Ferrocene Ligand (C) 1752
- Trigonal-Bipyramidal Technetium and Rhenium Complexes with Tetradentate NS_3 Tripod Ligands (C) 1354

Compound libraries
- A Novel Procedure for the Synthesis of Libraries Containing Small Organic Molecules (C) 2059

- A Solution-Phase Screening Procedure for the Isolation of Active Compounds from a Library of Molecules (C) 2061
- Binary Encoding of Compound libraries (H) 1573
- Expeditious Synthesis of a Novel C_3-Symmetric Receptor that Binds Peptides Sequence-Selectively (C) 2458
- Opportunities for New Chemical Libraries: Unnatural Biopolymers and Diversomers (H) 633
- Specific Binding of Antibodies to DNA through Combinatorial Antibody Libraries (H) 1827

Computer chemistry
- Neural Networks for Chemists. An Introduction (B) 1671
- The Determination of Maximum Common Substructures by a Genetic Algorithm: Application in Synthesis Design and for the Structural Analysis of Biological Activity (C) 1189

Computer simulations
- Theoretical Treatment of Liquids and Liquid Mixtures (B) 697

Conformation
- Conformational Requirements for Sweet-Tasting Peptides and Peptidomimetics (R) 1437
- On the Helicity of Oligomeric Formaldehyde (C) 1476
- Stable Tetrakis(trialkylsilyl)disilenes; Synthesis, X-Ray Structures, and UV/VIS Spectra (C) 1489
- Sterically Strained Porphyrins—Influence of Core Protonation and Peripheral Substitution on the Conformation of Tetra-*meso*-, Octa-β-, and Dodeca-Substituted Porphyrin Dications (C) 2485
- Trigonal Symmetry as a Host Design Element: Novel Conformation of Dodecakis(3,5-dimethylphenylthio)coronene in its 1,4-Dioxane Clathrate (C) 1587

Conjugation
- 2,2′-Bipyrenyl and *para*-Terpyrenyl—A New Type of Electronically Decoupled Oligoarylene (C) 1957
- Iterative Divergent/Convergent Approach to Linear Conjugated Oligomers by Successive Doubling of the Molecular Length: A Rapid Route to a 128Å-Long Potential Molecular Wire (C) 1360
- Nonclassical Stabilization of Planar Allenes: Low Rotational Barriers for Allene Double Bonds (C) 2064
- Stable Soluble Conjugated Carbon Rods with a Persilylethynylated Polytriacetylene Backbone (C) 763

Conocurvone
- Conocurvone—Prototype of a New Class of Anti-HIV Active Compounds? (H) 422 (1668)

Cooperative effects
- A Chiral Lewis Acid with Two "Metal" Centers: Cooperative Binding of Two Amine Molecules to a Chiral Diboronic Ester (C) 2452
- Sixteenfold Deprotonated γ-Cyclodextrin Tori as Anions in a Hexadecanuclear Lead(II) Alkoxide (C) 1863

Coordination
- $[(C_6H_5)_4P]^1_\infty[Cu_3I_4]$—The First Compound with a Helical Chain of Face-Sharing Tetrahedra as a Structural Element (C) 1841
- Alternating Ferro- and Antiferromagnetic Interactions in a Mn^{II} Chain with Alternating End-On and End-to-End Bridging Azido Ligands (C) 2488
- A Thermally Stable Peroxocopper(II) Complex with Unusual μ_4-Coordination of the Peroxo Ligand (C) 1969
- Base-Free Monomeric Organogallium Hydrides (C) 1253
- Bifunctional Compounds (B) 2225
- Bis(pentamethylcyclopentadienyl)(η^3-trimethylenemethane)zirconium: A New Mode of Bonding for the Trimethylenemethane Ligand (C) 2465
- Bis(tetramethylbutynediol)nickel(0), the First Pure Monoalkyne Complex of Nickel and Its Chemistry (C) 1373
- Carboxylatoiron(II) Aggregates: A Novel Fe^{II}_4 Complex with Threefold Symmetry (C) 1660
- Change of Orientation of Axial Imidazole Ligands in a Cytochrome b Model Complex in Response to a Change in the Oxidation State of the Metal Center (C) 1363
- Chemical Bonding (B) 2225
- Equilibrium between Isocyanide and Carbene Complexes in Coordination Compounds of 2,6-Dihydroxyphenyl Isocyanide (C) 1356
- "Free" $[Fe(tpp)]^+$ Cation: A New Concept in the Search for the Least Coordinating Anion (C) 2433
- Hexacoordinate Silicon in a Compound with an F_5SiC Unit (C) 1359
- Hydroxylamine, Hydrazine, and Diazene as Unidentate Ligands in Osmium and Ruthenium Complexes (C) 657
- Inversely Coordinating Silanide Ions in an Oligomeric Sodium Alcoholate (C) 216
- Ligands as "Compass Needles": How Orientations of Alkene, Alkyne, and Alkylidene Ligands Reveal π-Bonding Features in Tetrahedral Transition Metal Complexes (R) 1565
- Linear Coordination Polymers of Copper(II) and Fourfold Deprotonated Sugar Alcohols (C) 1742
- Molecules and Ions with Heptacoordinated Central Atoms (H) 1941
- New Titanium–Boron Complexes with a Planar Tetracoordinate Carbon or a Planar Tricoordinate Phosphorus Center (C) 197
- Novel Rh^I Piano-Stool Complexes with New Hemilabile Ligands Ligating through Phosphane and Arene Groups: Synthesis, Characterization, and Reactivity (C) 2473
- Organometallics 1. Complexes with Transition Metal–Carbon σ-Bonds (B) 2225
- Organometallics 2. Complexes with Transition Metal–Carbon π-Bonds (B) 2225
- Oxygen-Induced Structural Transformation of the Polynuclear Organoaluminum Complex $[Al_4(\mu_3\text{-8-quinolylimide})_2(CH_3)_8]$ to $[Al_4(\mu_3\text{-8-quinolylimide})_2(CH_3)_7(\mu\text{-}OCH_3)]$ (C) 1265
- Sixteenfold Deprotonated γ-Cyclodextrin Tori as Anions in a Hexadecanuclear Lead(II) Alkoxide (C) 1863
- Strategies for Nonmacrocyclic Polythioether Ligands: New Pentacoordinating Architectures (C) 319
- Structural Principles in Seven-Coordinate Subgroup Compounds: The Complex Anions MoF_7^-, WF_7^-, and $ReOF_6^-$ (C) 461
- Structure of a (4 + 4)-Coordinate Silicon Compound, a Precursor of Hypercoordinate Silyl Mono- and Dications (C) 1097
- Synthesis and Structure of $[Ni(SO_2)_6](AsF_6)_2$ and $[Fe(SO_2)_4(FAsF_5)_2]$ (C) 1663
- The First Mononuclear Nitrosyl(oxo)molybdenum Complex: Side-On Bonded and μ_3-Bridging NO Ligands in $[\{MoL(NO)(O)(OH)\}_2]NaPF_6\cdot H_2O$ (C) 1473
- The First Zwitterionic, Optically Active Disilicate with Pentacoordinate Silicon (C) 1186
- The Versatility of the Azido Ligand: Linkage of Ni^{II} Centers to Form a Chain with One End-to-End and Three End-On Bridges in Alternation (C) 2087
- Tris(η^4-naphthalene)zirconate(2−) (C) 1973

Copper compounds
- $[\{Sb_2(Ncy)_4\}_2Cu_4]$: A Mixed-Metal Antimony(III)/Copper(I) Complex Containing a Cu_4 Square Plane (C) 1875
- $[(C_6H_5)_4P]^1_\infty[Cu_3I_4]$—The First Compound with a Helical Chain of Face-Sharing Tetrahedra as a Structural Element (C) 1841
- A Thermally Stable Peroxocopper(II) Complex with Unusual μ_4-Coordination of the Peroxo Ligand (C) 1969
- Cellulose in Schweizer's Reagent: A Stable, Polymeric Metal Complex with High Chain Stiffness (C) 884
- $[Cu_{96}P_{30}\{P(SiMe_3)_2\}_6(PEt_3)_{18}]$, a New Phosphorus-Bridged Copper Cluster (C) 1290
- $[Cu_{44}Se_{22}(PEt_2Ph)_{18}]$ and $[Cu_{44}Se_{22}(PnBurBu_2)_{12}]$: Synthesis and Structure of Two Copper Clusters with Isomeric Cu–Se Frameworks (C) 2287
- Fairly Strong Ferromagnetic Interactions between Imino Nitroxide Ligands through a Diamagnetic Cu^I Ion in $[Cu^I(im\text{-}mepy)_2](PF_6)$ (C) 670
- Linear Coordination Polymers of Copper(II) and Fourfold Deprotonated Sugar Alcohols (C) 1742
- Mesoscopic Sheets of a Cyano-Bridged Cu–Ni Coordination Complex: Template Synthesis at the Interlayers of Cast Multibilayer Films (C) 2483
- New Sulfur- and Selenium-Bridged Copper Clusters; Ab Initio Calculations on $[Cu_{2n}Se_n(PH_3)_m]$ Clusters (C) 746
- Novel Copper Nitrosyl Complexes: Contributions to the Understanding of Dissimilatory, Copper-Containing Nitrite Reductases (H) 2057
- Reductive Disproportionation of NO Mediated by Copper Complexes: Modeling N_2O Generation by Copper Proteins and Heterogeneous Catalysts (C) 895
- Spectroscopic and Reactivity Studies of a Copper-Containing Metallacrown (C) 195
- Structural and Magnetic Characterization of a Novel Heptanuclear Hydroxo-Bridged Copper(II) Cluster of the Corner-Sharing Dicubane Type (C) 1184
- Synthesis and Crystal Structure of a Monocarbene Complex of Copper (C) 672
- The Crystal Structures of Base-Free, Monomeric Arylcopper(I) and Arylsilver(I) Compounds; Two Cases of Mistaken Identity? (C) 2443
- The First Structurally Characterized Metal Complex Involving the Free Acid of a New Tris(pyrazolyl)borate as Ligand (C) 1983
- Two-Dimensional Sheets of Tetragonal Copper(II) Lattices: X-Ray Crystal Structure and Magnetic Properties of $[Cu(C_6O_4Cl_2)(C_4H_4N_2)]_n$ (C) 1759

Coronenes
- Trigonal Symmetry as a Host Design Element: Novel Conformation of Dodecakis(3,5-dimethylphenylthio)coronene in its 1,4-Dioxane Clathrate (C) 1587

Corrigenda 1521, 1668, 1988, 2348
- No Enantioselective Reactions in a Static Magnetic Field (C) 1461

Corroles
- Metallocorroles with Formally Tetravalent Iron (C) 731
Corrphycene
- Corrphycene: A New Porphyrin Isomer (C) 2308
Cross-conjugation
- Expanded Radialenes: A Novel Class of Cross-Conjugated Macrocycles (C) 468
Crown ethers
- A New Class of Novel Macrocyclic Mesogens (C) 1503 (1668)
- Biomimetic Model for a Photosynthetic Reaction Center: A Porphyrin with a Covalently Linked, Redox-Active Crown Ether (C) 2318
- Complexes of Partially Fluorinated Macrocycles with a Metal–Fluorine σ-Donor Bond and Their Suitability as Metal Ion Indicators (C) 2175
- Construction of a Multiwired Molecular Cable of Micrometer Length by a Self-Assembly Process (C) 2173
- Crown Compounds: Toward Future Applications (B) 235
Crystal growth
- Chemistry and Crystal Growth (R) 143
Cubanes
- 1(9)-Homocubene and 9-Homocubylidene: Theoretical Investigation of Structures, Energies, and Rearrangement Reactions (C) 668
Cumulenes
- Synthesis and Structure of the Smallest Cyclic Cumulene; Reaction of 1,3-Diynes with Zirconocene Complexes (C) 1605
Cyanide–isocyanide isomerism
- Cyanide–Isocyanide Isomerism in CN-Bridged Organometallic Complexes (C) 2090
Cyanines
- Phenothiazinyl-Substituted Cyanines: Model Compounds for Molecular Switches (C) 572
Cyanohydrins
- Synthesis and Reactions of Optically Active Cyanohydrins (R) 1555
Cyclizations
- A Novel Photosystem for Harvesting Visible Light to Drive Photoinduced Electron Transfer (PET) Reductions: β-Activation of α,β-Unsaturated Ketones for Radical Cyclizations (C) 1169
- 1,4-Didehydrobutadiene: The Intermediate in a New Class of Thermally Induced Intramolecular Alkyne Couplings (C) 2470
- Intramolecular [2+2] Cycloadditions of 2,2′-Bis(1-arylvinyl)-Substituted Biphenyls Induced by Photo Electron Transfer (C) 2300
- Intramolecular Photocyclization of ω,ω-Diphenyl-(ω−1)-alken-1-ols by an Exciplex Quenching Mechanism (C) 2113
- Novel Optically Active Hydrocarbons in Sediments: Evidence for an Extensive Biological Cyclization of Higher Regular Polyprenols (C) 1166
- Ring Closures on Polymeric Supports—Formation of Extremely Large Macrocycles by Intrapolymeric Cyclooligomerizations (C) 1960
Cycloadditions
- [2+2] Cycloaddition of Norbornenes with Alkynes Catalyzed by Ruthenium Complexes (C) 580
- Asymmetric Synthesis of Highly Substituted Pyrrolidines by 1,3-Dipolar Cycloadditions of Azomethine Ylides with *N*-Acryloylproline Benzyl Ester (C) 683
- Competing Reactions of Silenes: [2+2], [4+2], and [6+2] Cycloadditions with Cycloheptadiene and Cycloheptatriene (C) 77
- Construction of Carbon Frameworks with the Help of Ruthenium Complexes: 1,5-Cyclooctadiene as a Reagent in Transition Metal Catalyzed Reactions (H) 636
- Diastereoselective Reaction of a 1-Phosphaallyl Anion with an Alkyne: Structure of an Isolated Dihydrophospholyl Anion and Stereospecific Protonation to Give 2,3-Dihydrophosphole (C) 1953
- Intramolecular [2+2] Cycloadditions of 2,2′-Bis(1-arylvinyl)-Substituted Biphenyls Induced by Photo Electron Transfer (C) 2300
- Lewis Acid Promoted [2+2] Cycloaddition of Allylsilanes and Unsaturated Esters: A Novel Method for Cyclobutane Construction (C) 1612
- Nitrile Imines: From Matrix Characterization to Stable Compounds (R) 527
- The First Cycloaddition Reactions of Dimeric Arsenium Cations (C) 1267
- The Photochemical Synthesis of Fine Chemicals with Sunlight (R) 2009
Cyclobutaarenes
- A New Synthetic Route to 1,2-Dihydrocyclobutaarenes (C) 1757
Cyclobutabenzenes
- Palladium-Catalyzed C–H Activation of *tert*-Butyl Groups: A Simple Synthesis of 1,2-Dihydroxycyclobutabenzene Derivatives (C) 103
- The Effect of Fusion of Angular-Strained Rings on Benzene: Crystal Structures of 1,2-Dihydrocyclobuta[*a*]cyclopropa[*c*]-, 1,2,3,4-Tetrahydrodicyclobuta[*a,c*]-, 1,2,3,4-Tetrahydrodicyclobuta[*a,c*]-cyclopropa[*e*]-, and 1,2,3,4,5,6-Hexahydrotricyclobuta[*a,c,e*]benzene (C) 313
Cyclobutadienes
- New Types of Metal-Stabilized Cyclobutadiene Superphanes (C) 1272
Cyclobutanes
- Lewis Acid Promoted [2+2] Cycloaddition of Allylsilanes and Unsaturated Esters: A Novel Method for Cyclobutane Construction (C) 1612
Cyclodextrins
- Antenna Effect in Multichromophoric Cyclodextrins (C) 2438
- Cyclodextrins as Building Blocks for Supramolecular Structures and Functional Units (R) 803
- Molecular Recognition of C_{60} with γ-Cyclodextrin (C) 1597
- Sixteenfold Deprotonated γ-Cyclodextrin Tori as Anions in a Hexadecanuclear Lead(II) Alkoxide (C) 1863
- Toward Unified Enantioselective Chromatography with a Single Capillary Column Coated with Chirasil-Dex (C) 2222
- Wacker Oxidation of 1-Decene to 2-Decanone in the Presence of a Chemically Modified Cyclodextrin System: A Happy Union of Host–Guest Chemistry and Homogeneous Catalysis (C) 2100
Cycloheptatrienes
- Excited-State Carbon Acids: Theoretical Studies of Suberene and Cycloheptatriene (C) 2431
Cyclohexanols
- Regio- and Diastereoselective Photooxygenation of Chiral 2,5-Cyclohexadiene-1-carboxylic Acids (C) 1971
Cyclopentanols
- Syntheses of Cyclopentanols by a Silicon-Induced Cascade Reaction (C) 217
Cyclophanes
- 18-, 20-, and 22-Membered Dimetallaortho-, -meta-, and -para[7.7]cyclophanes—The First Typical Metallaphanes (C) 321
- *trans–cis* Isomerization upon One-Electron Oxidation of [12]- and [14]Tetrathiafulvalenophanes (C) 1379
- Porphyrin–Quinone Cyclophanes with Gradually Varied Donor–Acceptor Distances (C) 2428
- Scalemic 2-Formyl-3-hydroxy[2.2]paracyclophane: A New Auxiliary for Asymmetric Synthesis (C) 91
- Supramolecular Activation of *para*-Benzoquinone (C) 2489
- Synthesis and Properties of a Vertically Stacked Porphyrin(1)-Porphyrin(2)-Quinone Cyclophane (C) 1466
- Synthesis and Properties of a Vertically Stacked Porphyrin-Quinone(1)-Quinone(2) Cyclophane (C) 1463
Cyclopropanations
- Cyclopropanation by Methylene Transfer from (η^2-Formaldehyde)zirconocene Complexes (C) 1955
Cyclopropanes
- Cyclopropanes by Nucleophilic Attack of Mono- and Diaryl-Substituted (η^3-Allyl)palladium Complexes: Aryl Effect and Stereochemistry (C) 1280
- Ring Opening of Cyclopropane at 10 K (C) 558
Cyclosporin
- Cyclosporin: A Li- and Ca-Specific Ionophore! (C) 442
Cyclotheonamides
- Synthesis of Cyclotheonamide B and Its Derivatives (C) 1729
Cyclotrimerization
- Cyclotrimerization of Ethyne on the Complex Fragment [(η^1-*t*Bu$_2$PCH$_2$P*t*Bu$_2$)-Ni^0] with Formation of an η^6-Benzene–Nickel(0) Complex (C) 879
Cytochrome P-450
- Relationships between Structure and Function of Cytochrome P-450—Experiments, Calculations, Models (B) 359

Decaphenylferrocene
- Decaphenylferrocene and Decaphenylferrocenium Tetrafluoroborate (C) 1731
Dehydroamino acids
- Synthesis, Crystal and Molecular Structure of Boc-Pro-ΔPhe-Ala-ΔPhe-Ala-OMe; A Pentapeptide with a Novel β-Bend Ribbon Structure (C) 970
- Synthesis of Unsaturated Amino Acids by [3,3]-Sigmatropic Rearrangement of Chelate-Bridged Glycine Ester Enolates (C) 998
Dendrimers
- A "Branched-Monomer Approach" for the Rapid Synthesis of Dendrimers (C) 82
- A General Synthetic Strategy for Neutral Phosphorus-Containing Dendrimers (C) 1589
- Chemistry within a Unimolecular Micelle Precursor: Boron Superclusters by Site- and Depth-Specific Transformations of Dendrimers (C) 666
- Chiral Dendrimers from Tris(hydroxymethyl)methane Derivatives (C) 440
- Dendrimers: From Generations and Functional Groups to Functions (H) 2413
- Dendritic Macromolecules Incorporating Tetrathiafulvalene Units (C) 1761
- Dendritic Porphyrins: Modulating Redox Potentials of Electroactive Chromophores with Pendant Multifunctionality (C) 1739

- Organoplatinum Dendrimers Formed by Oxidative Addition (C) 847
- Single-Step Six-Electron Transfer in a Heptanuclear Complex: Isolation of Both Redox Forms (C) 2460

Denitrification
- Novel Copper Nitrosyl Complexes: Contributions to the Understanding of Dissimilatory, Copper-Containing Nitrite Reductases (H) 2057

Deoxynojirimycin
- An Enantioselective Synthesis of Deoxynojirimycin (C) 2320

Desulfurizations
- Desulfurization of Benzo[*b*]thiophene by S/Ru Exchange: Formation and Structure of the Cluster $[Ru_3(CO)_8(C_8H_6)]$ (C) 1381

Diarylcarbenes
- An Extremely Long-Lived Triplet Carbene; Reactivity, Optical Absorption, and Kinetics of Highly Congested Diarylcarbenes (C) 873

Diazabutadienes
- $[Be(dad)_2]$: Synthesis and Structure of a Diazabutadieneberyllium Complex (C) 1372

Diazaxanthylium salts
- 3,6-Diazaxanthylium Salts: Dyes with a New Chromophore (C) 863

Diazoanthrones
- Photodecomposition of 10-Diazo-2-hexadecylanthrone on Graphite Studied by Scanning Tunneling Microscopy (C) 2080

Diazo carbonyl compounds
- Ligand Effects on the Chemoselectivity of Transition Metal Catalyzed Reactions of α-Diazo Carbonyl Compounds (R) 1797

Diazo compounds
- α-Aryliodonio Diazo Compounds: S_N Reactions at the α-C Atom as a Novel Reaction Type for Diazo Compounds (C) 1952

Dibromine pentoxide
- Dibromine Pentoxide Br_2O_5 (C) 975

Dictionaries
- Comprehensive Dictionary of Physical Chemistry (B) 1785
- Dictionary of Trivial Names/Trivialnamen-Handbuch (B) 1305

Diels–Alder reactions
- A Concise Total Synthesis of (±)-Mamanuthaquinone by Using an *exo*-Diels–Alder Reaction (C) 853
- Asymmetric Diels–Alder Reactions Catalyzed by a Chiral Iron Lewis Acid (C) 1856
- Asymmetric 1,6-Induction in Hetero-Diels–Alder Reactions of Chiral Oxabutadienes for a De Novo Synthesis of Enantiomerically Pure Carbohydrates: Lewis Acid Dependent Reversal of Facial Selectivity (C) 980
- Magnetic Properties of Aromatic Transition States: The Diels–Alder Reactions (C) 1376
- Synthesis of Enediynes through Diels–Alder Addition (C) 1099

Dienone–phenol rearrangement
- An Antibody-Catalyzed 1,2-Rearrangement of Carbon–Carbon Bonds (C) 1607

Dihydroxyacetone phosphate
- Synthesis of Dihydroxyacetone Phosphate (and Isosteric Analogues) by Enzymatic Oxidation: Sugars from Glycerol (C) 209

Dihydroxydehydrocalamenene
- The Total Synthesis of *cis*-7,8-Dihydroxy-11,12-dehydrocalamenene by Regio- and Diastereoselective Alkylation of Chiral η^6-Arenetricarbonylchromium Complexes: An Unexpected Case of Nucleophilic Aromatic *tele*-Substitution with Methoxide as a Leaving Group (C) 109

Dihydroxylations
- Practical and Rapid Vicinal Hydroxylation of Alkenes by Catalytic Ruthenium Tetraoxide (C) 2312

Dimeric acids
- Assembly Properties of Bolaamphiphiles from Dimeric Acids (C) 2078

Diols
- A Reagent for Determining Optical Purities of Diols by Formation of Diastereomeric Arylboronate Esters (C) 1182
- Cyclohexane-1,2-diacetals (CDA): A New Protecting Group for Vicinal Diols in Carbohydrates (C) 2290
- Practical and Rapid Vicinal Hydroxylation of Alkenes by Catalytic Ruthenium Tetraoxide (C) 2312

Dioxiranes
- Dimesityldioxirane—A Dioxirane Stable in the Solid State (C) 2212

Dipeptide isosteres
- A Novel Route to Diastereomerically Pure (*E*)-Alkene Dipeptide Isosteres from β-Aziridinyl-α,β-enoates by Treatment with Organocopper Reagents (C) 652

Disilenes
- Stable Tetrakis(trialkylsilyl)disilenes; Synthesis, X-Ray Structures, and UV/VIS Spectra (C) 1489

Distance geometry calculations
- Determination of the Relative Configuration by Distance Geometry Calculations with Proton–Proton Distances from NOESY Spectra (C) 753

Dithiirane
- The First Isolable Dithiirane by Oxidation of a Dithietane (C) 777

Diversomers
- Opportunities for New Chemical Libraries: Unnatural Biopolymers and Diversomers (H) 633

Diynes
- Synthesis and Structure of the Smallest Cyclic Cumulene; Reaction of 1,3-Diynes with Zirconocene Complexes (C) 1605

DNA
- An Amazing Distortion in DNA Induced by a Methyltransferase (Nobel Lecture) (R) 1222
- Specific Binding of Antibodies to DNA through Combinatorial Antibody Libraries (H) 1827
- Strong, Specific Binding of Six Different DNA Sequences by a Single Conformation–Switching DNA Macrocycle (C) 1004
- Synthetic DNA and Biology (R) 1214
- The Polymerase Chain Reaction (Nobel Lecture) (R) 1209
- Unraveling DNA (B) 1303

DNA cleavage
- Calicheamicin θ_1^1: A Rationally Designed Molecule with Extremely Potent and Selective DNA Cleaving Properties and Apoptosis Inducing Activity (C) 183
- Enediyne Quinone Imines: Truncated, Biologically Active Dynemicin Congeners (C) 2477
- Fullerene–Oligonucleotide Conjugates: Photo-induced Sequence-Specific DNA Cleavage (C) 2472
- On the DNA Recognition Role of the Carbohydrate Sector in Calicheamicin: A Comparison of DNA Cleaving Capacity of Enantiomeric Calicheamicinones (C) 855
- Synthesis and Selective Radical Cleavage of C-4′-Modified Oligonucleotides (C) 1861

Dodecahedranes
- From an Insecticide to Plato's Universe – The Pagodane Route to Dodecahedranes: New Pathways and New Perspectives (R) 2239

Dötz reaction
- Chromium Carbene Complexes in Organic Synthesis: Recent Developments and Perspectives (H) 303

Drugs
- A Short Route to [3-^{15}N]-3′-Azido-3′-deoxythymidine (N3-Labeled AZT) via 3-Nitro-AZT (C) 2454
- Medicinal Chemistry. The Role of Organic Chemistry in Drug Research (B) 1783
- The Organic Chemistry of Drug Design and Drug Action (B) 792

Drug search
- A Novel Procedure for the Synthesis of Libraries Containing Small Organic Molecules (C) 2059
- A Solution-Phase Screening Procedure for the Isolation of Active Compounds from a Library of Molecules (C) 2061

Dyes
- 3,6-Diazaxanthylium Salts: Dyes with a New Chromophore (C) 863
- Synthesis and Structure of New Cationic Squarylium Dyes (C) 1001

Dynamics
- Photodissociation Dynamics (B) 1011

Dynemicins
- Enediyne Quinone Imines: Truncated, Biologically Active Dynemicin Congeners (C) 2477
- Synthesis of the Anthraquinone Framework of Dynemicin A (C) 781

Ecology

- Effects of Metal-Ion Dopants on the Photocatalytic Reactivity of Quantum-Sized TiO_2 Particles (C) 1091
- Mass Spectral and GC Data of Drugs, Poisons, Pesticides, Pollutants and Their Metabolites. Volumes 1–3 (B) 359
- Optically Active Reference Compounds for Environmental Analysis Obtained by Preparative Enantioselective Gas Chromatography (C) 2085
- Ozone Formation through Decomposition of CFCs in the Stratosphere (C) 1108
- Rationally Designed Inorganic Catalysts for Environmentally Compatible Technologies (C) 308
- Recycling in the Earth's Atmosphere: The OH Radical–Its Importance for the Chemistry of the Atmosphere and the Determination of Its Concentration (R) 1816
- The Absolute Configuration of (+)-α-1,2,3,4,5,6-Hexachlorocyclohexane, and Its Permeation through the Seal Blood–Brain Barrier (C) 882
- The Equilibrium Distribution of Semivolatile Organochloro Compounds between Atmosphere and Surface Water in the Atlantic Ocean (C) 646
- Toxicity of Chlorinated Organic Compounds: Effects of the Introduction of Chlorine in Organic Molecules (R) 1920

Electrochemistry
- Electrochemical and Electrocatalytic Reactions of Carbon Dioxide (B) 1010
- Electrochemistry. Principles, Methods, and Applications (B) 1989
- Electrode Kinetics for Chemists, Chemical Engineers, and Material Scientists (B) 1304
- Phase Transitions in Self-Assembled Monolayers Detected by Electrochemistry (C) 2332
- Principles of Electrochemistry (B) 1989
- Structure of Electrified Interfaces (B) 2117

Electronic structure
- $[\{Rh_2Cp^*_2(\mu\text{-}CH_2)_2\}_2(\mu\text{-}S_4)]^{2+}$: A Novel Tetranuclear Cationic Complex with a Rectangular S_4 Unit (C) 1882
- An Extremely Long-Lived Triplet Carbene; Reactivity, Optical Absorption, and Kinetics of Highly Congested Diarylcarbenes (C) 873
- Benzobis(thiadiazole)s Containing Hypervalent Sulfur Atoms: Novel Heterocycles with High Electron Affinity and Short Intermolecular Contacts between Heteroatoms (C) 1977
- 2,2′-Bipyrenyl and *para*-Terpyrenyl—A New Type of Electronically Decoupled Oligoarylene (C) 1957
- Calixarene-Based Macrocyclic Nonet (S = 4) Octaradical and its Acyclic Sextet (S = 5/2) Pentaradical Analogue (C) 2091
- Electron Delocalization in Ethynyl-Bridged Binuclear Ruthenium(II) Polypyridine Complexes (C) 1884
- Localization of Electrons in Intermetallic Phases Containing Aluminum (C) 2069
- Matrix Spectroscopy of 2-Adamantylidene, a Dialkylcarbene with Singlet Ground State (C) 1964
- Thermal and Optical Switching of Iron(II) Complexes (R) 2024
- Unequivocal Partitioning of Crystal Structures, Exemplified by Intermetallic Phases Containing Aluminum (C) 2073

Electron localization
- Localization of Electrons in Intermetallic Phases Containing Aluminum (C) 2069
- Unequivocal Partitioning of Crystal Structures, Exemplified by Intermetallic Phases Containing Aluminum (C) 2073

Electron transfer
- Functionalization of C_{60} Buckminsterfullerene by [8 + 2] Cycloaddition: Spectroscopic and Electron-Transfer Properties of a Tetrahydroazulenofullerene (C) 1087
- Magnetic Spin Effects on Photooxidation Quantum Yields of Ru^{II}-tris(bipyridine) Type Complexes in Magnetic Fields up to 17.5 Tesla (C) 1772
- Porphyrin–Quinone Cyclophanes with Gradually Varied Donor–Acceptor Distances (C) 2428
- Purely Organic Mixed-Valence Molecules with Nanometric Dimensions Showing Long-Range Electron Transfer: Synthesis, and Optical and EPR Studies of a Radical Anion Derived from a Bis(triarylmethyl)Diradical (C) 2106
- Single-Step Six-Electron Transfer in a Heptanuclear Complex: Isolation of Both Redox Forms (C) 2460

Electron-transfer reactions
- A Novel Photosystem for Harvesting Visible Light to Drive Photoinduced Electron Transfer (PET) Reductions: β-Activation of α,β-Unsaturated Ketones for Radical Cyclizations (C) 1169
- Electron-Reservoir Complexes [Fe^{I}Cp(arene)] as Selective Initiators for a Novel Electron Transfer Chain Catalyzed Reaction: General Synthesis of Fulvalene-Bridged Homo- and Heterodinuclear Zwitterions (C) 661
- The Kinetics of Heterogeneous Electron Transfer Reactions in Polar Solvents (R) 2131

Electrophilic additions
- Electrostatic vs. Orbital Control of Facial Selectivities in π Systems: Experimental and Theoretical Study of Electrophilic Additions to 7-Isopropylidenenorbornanes (C) 1390
- Nonreactive Interactions between Ethene and Halogens: Detection of a π-Donor Complex $C_2H_4\cdots BrCl$ by Rotational Spectroscopy (C) 1512

Electrophilicity
- Scales of Nucleophilicity and Electrophilicity: A System for Ordering Polar Organic and Organometallic Reactions (R) 938

Enamines
- A Template Synthesis of Stable Conjugated Primary Enamines from Ketones, Nitriles, and Butadiene (C) 1114

Enantiomeric resolution
- First Resolution of a Free Fluorophosphane Chiral at Phosphorus (C) 1835
- Kinetic Resolution of the Acrolein Dimer by Asymmetric Horner–Wadsworth–Emmons Reactions (C) 556
- Optically Active Reference Compounds for Environmental Analysis Obtained by Preparative Enantioselective Gas Chromatography (C) 2085
- Preparation of Chiral Nitroxide Radicals and Spontaneous Optical Resolution by Recrystallization (C) 878
- Resolution of Racemates by Distillation with Inclusion Compounds (H) 728
- Toward Unified Enantioselective Chromatography with a Single Capillary Column Coated with Chirasil-Dex (C) 2222

Enantioselective protonations
- Enantioselective Protonation of Simple Enolates: Chiral Imide as a Chiral Proton Source (C) 107

Encyclopedias
- McGraw-Hill Encyclopedia of Chemistry (B) 1401

ENDOR spectroscopy
- Biomimetic Model for a Photosynthetic Reaction Center: A Porphyrin with a Covalently Linked, Redox-Active Crown Ether (C) 2318

Enediynes
- A Convergent Total Synthesis of Calicheamicin γ^{I}_{1} (C) 858
- Calicheamicin θ^{I}_{1}: A Rationally Designed Molecule with Extremely Potent and Selective DNA Cleaving Properties and Apoptosis Inducing Activity (C) 183
- 1,4-Didehydrobutadiene: The Intermediate in a New Class of Thermally Induced Intramolecular Alkyne Couplings (C) 2470
- Enediyne Quinone Imines: Truncated, Biologically Active Dynemicin Congeners (C) 2477
- On the DNA Recognition Role of the Carbohydrate Sector in Calicheamicin: A Comparison of DNA Cleaving Capacity of Enantiomeric Calicheamicinones (C) 855
- Synthesis of Enediynes through Diels–Alder Addition (C) 1099
- Synthesis of the Anthraquinone Framework of Dynemicin A (C) 781

Ene reactions
- Diastereoselective Synthesis of Amino-Substituted Indolizidines and Quinolizidines by the Intramolecular Hetero-Ene Reaction of Prolinal Imine and 2-Piperidine Carbaldimine (C) 458

Energy transfer
- Antenna Effect in Multichromophoric Cyclodextrins (C) 2438

Enolates
- Catalytic Enantioselective Protonation of Enolates (C) 1888
- Substituent Effects and Complexation Phenomena in the Diastereoselective Protonation of Chiral Enolates (C) 1764

Enols
- The First Spectroscopic Identification of an Enol Radical Cation in Solution: The Anisyldimesitylethenol Radical Cation (C) 1961

Enol triflate pyranoses
- Enol Triflate Pyranoses, Versatile Reagents for the Formation of Conjugated Systems on Pyranoses (C) 1499

Enzymatic catalysis
- Biocatalysts in Organic Synthesis (B) 1012
- Continuous Enzymatic Synthesis of 2′-Deoxythymidine-5′-(α-D-glucopyranosyl) diphosphate (C) 571
- Enzymatic Grooming of Organic Thin Films (C) 871
- Enzymatic Hydrolysis of Hydrophilic Diethyleneglycol and Polyethyleneglycol Esters of Peptides and Glycopeptides by Lipases (C) 336
- Prostacyclin and Thromboxane Synthase: New Aspects of Hemethiolate Catalysis (R) 1911
- Recombinant Whole Cells as Catalysts for the Enzymatic Synthesis of Oligosaccharides and Glycopeptides (C) 1241
- Synthesis of Dihydroxyacetone Phosphate (and Isosteric Analogues) by Enzymatic Oxidation; Sugars from Glycerol (C) 209
- The Biosynthesis of Nitro Compounds: The Enzymatic Oxidation to Pyrrolnitrin of its Amino-Substituted Precursor (C) 352
- X-Ray Structure Analysis of the Methane Monooxygenase: An Important Step toward Understanding the Oxidation of Methane in Biological Systems (H) 841

Enzyme inhibitors
- Isofagomine, a Potent, New Glycosidase Inhibitor (C) 1778
- On the Mechanism of the Urocanase Reaction: Confirmation of the Structure of the NAD^+-Inhibitor Adduct by Direct ^{13}C-^{13}C Coupling (C) 1279
- Peptidomimetics–Tailored Enzyme Inhibitors (R) 1699
- Remarkable Stereoselectivity in the Inhibition of α-Galactosidase from Coffee Bean by a New Polyhydroxypyrrolidine Inhibitor (C) 1242
- Synthesis of Cyclotheonamide B and Its Derivatives (C) 1729
- Synthesis of Deoxy Sialyl Lewis^x Analogues, Potential Selectin Antagonists (C) 2096
- Synthesis of the First Fully Functionalized Core of the Zaragozic Acids/Squalestatins (C) 2187
- The Synthesis of Naturally Occurring (−)-Calyculin A (C) 673
- The Trehalase Inhibitor Salbostatin, a Novel Metabolite from *Streptomyces albus*, ATCC 21838 (C) 1844
- Total Synthesis of Zaragozic Acid A/Squalestatin S1 (C) 2190
- Zaragozic Acid A/Squalestatin S1: Synthetic and Retrosynthetic Studies (C) 2184

Enzyme mimetics
- Enzyme Mimics (H) 551
- Novel Bimetallic Model System for Cytochrome P_{450}: Effect of Membrane Environment on the Catalytic Oxidation (C) 2468

Enzyme models
- A Mixed-Valent, Unsymmetrical Fe^{II}-Fe^{III} Complex with a Terminal Phenola to Ligand as a Model for the Active Site of Purple Acid Phosphatases (C) 887

- A Model for α-Keto Acid Dependent Nonheme Iron Enzymes: Structure and Reactivity of $[Fe^{II}_2(Me_2hdp)_2(bf)](ClO_4)$ (C) 1886

Enzymes
- Peptidyl-Prolyl *cis/trans* Isomerases and Their Effectors (R) 1415
- Relationships between Structure and Function of Cytochrome P-450—Experiments, Calculations, Models (B) 359

Epoxidations
- Tridentate β-Hydroperoxy Alcohols as Novel Oxygen Donors for the Titanium-Catalyzed Epoxidation of γ,δ-Unsaturated α,β-Diols: A Direct Diastereoselective Synthesis of Epoxy Diols (C) 1107

Epoxy diols
- Tridentate β-Hydroperoxy Alcohols as Novel Oxygen Donors for the Titanium-Catalyzed Epoxidation of γ,δ-Unsaturated α,β-Diols: A Direct Diastereoselective Synthesis of Epoxy Diols (C) 1107

EPR spectroscopy
- Combination of Superexchange and Spin-Polarization Mechanisms Leads to a Novel Hydrocarbon Tetraradical with a High-Spin Ground State (C) 1104
- Electron Paramagnetic Resonance of d Transition Metal Compounds (B) 362
- Ionization and Delocalization in Potassium Zeolite L: A Combined Neutron Diffraction and Electron Spin Resonance Study (C) 641
- Single-Crystal EPR Spectroscopy on $[^{57}Fe(NO)(S_2CNEt_2)_2]$: The "Triplet Signal" in the EPR Spectrum of $[Fe(S_2CNEt_2)_3]$ (C) 1497

Ethylene oxide
- Fullerene Dications as Initiators for Gas-Phase "Ball-and-Chain" Polymerization of Ethylene Oxide; Termination by Cyclization (C) 206

EXAFS spectroscopy
- X-Ray Absorption Spectroscopy of Amorphous Solids, Liquids, and Catalytic and Biochemical Systems—Capabilities and Limitations (R) 45

Fischer, Emil
- 100 Years "Schlüssel-Schloss-Prinzip": What Made Emil Fischer Use this Analogy? (R) 2364

Fluorescence
- Antenna Effect in Multichromophoric Cyclodextrins (C) 2438

Fluorescence spectroscopy
- Fluorescence Spectroscopy. New Methods and Applications (B) 1673

Fluorescent sensors
- An Anthracene-Based Fluorescent Sensor for Transition Metal Ions (C) 1975

Fluorine compounds
- Complexes of Partially Fluorinated Macrocycles with a Metal–Fluorine σ-Donor Bond and Their Suitability as Metal Ion Indicators (C) 2175
- Difluoromethyl Compounds of Chalcogens: A NMR Study of the Reactions of $Cd(CF_3)_2 \cdot 2MeCN$ and $ZnBr(CF_3) \cdot 2MeCN$ with Dialkyl Chalcogenides and Boron Trifluoride (C) 323
- Fluorinated Isocyanides—More than Ligands with Unusual Properties (R) 1315
- Hexacoordinate Silicon in a Compound with an F_5SiC Unit (C) 1359
- Molecular Solids as Ligands in Organometallic Chemistry: $[Cp^*_6Ti_6Na_7F_{19} \cdot 2.5\,thf]$ ($Cp^* = C_5Me_5$) and $[Cp^*_4Ti_4Mg_2F_{12} \cdot 7\,thf]$, Links Between Ionic Solids and Organometallic Compounds (C) 555
- (Pentafluoro-λ^6-sulfanyl)cyclopentadiene and Cyclopentadienylidenetetrafluoro-λ^6-sulfane (C) 93
- Stable Flexible Fibers and Rigid Tubules Made from Single-Chain Perfluoroalkylated Amphiphiles (C) 1514
- Structural Principles in Seven-Coordinate Subgroup Compounds: The Complex Anions MoF_7^-, WF_7^-, and $ReOF_6^-$ (C) 461

Fluorocarbons
- Stable Highly Concentrated Fluorocarbon Gels (C) 1100

Fluorophosphanes
- First Resolution of a Free Fluorophosphane Chiral at Phosphorus (C) 1835

Fluoropyridines
- New Materials for Liquid Crystal Displays: Structure–Property Relationship of 2-Fluoropyridines (C) 1386

Formaldehyde
- On the Helicity of Oligomeric Formaldehyde (C) 1476

Fosfomycin
- Incorporation of L-[Methyl-$^2H_3$]methionine and 2-[Hydroxy-^{18}O]hydroxyethylphosphonic Acid into Fosfomycin in *Streptomyces fradiae*—An Unusual Methyl Transfer (C) 341

Frontier orbitals
- Frontier Orbitals and Properties of Organic Molecules (B) 239

Fullerenes
- 61,61-Bis(trimethylsilylbutadiynyl)-1,2-dihydro-1,2-methanofullerene[60]: Crystal Structure at 100 K and Electrochemical Conversion to a Conducting Polymer (C) 1628
- Buckminsterfullerene Adducts from *Ortho*-Quinodimethanes (C) 559
- Buckminsterfullerenes (B) 2227
- $C_{60}H_4$: Kinetics and Thermodynamics of Multiple Addition to C_{60} (C) 786
- C_{70} Is More Stable than C_{60}: Experimental Determination of the Heat of Formation of C_{70} (C) 996
- Fullercages without Carbon—Fulleranes, Fullerenes, Space-filler-enes? (H) 843
- Fullerene–Acetylene Hybrids: On the Way to Synthetic Molecular Carbon Allotropes (C) 1366
- Fullerene Chemistry in Three Dimensions: Isolation of Seven Regioisomeric Bisadducts and Chiral Trisadducts of C_{60} and Di(ethoxycarbonyl)methylene (C) 437
- Fullerene C_{60}. History, Physics, Nanobiology, Nanotechnology (B) 2228
- Fullerene Dications as Initiators for Gas-Phase "Ball-and-Chain" Polymerization of Ethylene Oxide; Termination by Cyclization (C) 206
- Fullerene–Oligonucleotide Conjugates: Photo-induced Sequence-Specific DNA Cleavage (C) 2472
- Functionalization of C_{60} Buckminsterfullerene by [8 + 2] Cycloaddition: Spectroscopic and Electron-Transfer Properties of a Tetrahydroazulenofullerene (C) 1087
- Molecular Recognition of C_{60} with γ-Cyclodextrin (C) 1597
- On the Mechanism of Fullerene Formation (C) 1866
- Organic Superconductors (Including Fullerenes). Synthesis, Structure, Properties, and Theory (B) 1119
- Preparation and Structure of $C_{76}(S_8)_6$: A First Step in the Crystallographic Investigation of Higher Fullerenes (C) 1651
- Synthesis of a Fully Unsaturated "Molecular Board" (C) 2209
- Taking Fullerenes from Large Molecules to Supramolecules (H) 2269
- Tether-Directed Remote Functionalization of Buckminsterfullerene: Regiospecific Hexaadduct Formation (C) 2339
- The Fullerenes (B) 2227
- The Fullerenes. New Horizons for the Chemistry, Physics and Astrophysics of Carbon (B) 2228

Fulvalenes
- 11,12-Bis(diethylamino)nonatriafulvalene, the First "Aromatic" Nonafulvene (C) 973
- Electron-Reservoir Complexes [Fe^ICp(arene)] as Selective Initiators for a Novel Electron Transfer Chain Catalyzed Reaction: General Synthesis of Fulvalene-Bridged Homo- and Heterodinuclear Zwitterions (C) 661

Furans
- The First Spectroscopic Identification of an Enol Radical Cation in Solution: The Anisyldimesitylethenol Radical Cation (C) 1961

α-Galactosidase
- Remarkable Stereoselectivity in the Inhibition of α-Galactosidase from Coffee Bean by a New Polyhydroxypyrrolidine Inhibitor (C) 1242

Gallium compounds
- Base-Free Monomeric Organogallium Hydrides (C) 1253
- Reactivity of a Phosphanylcarbene (λ^5-Phosphaacetylene) with Lewis Acids: X-Ray Crystal Structures of the First Carbene–Gallane Complex and *C*-Gallyl-Substituted Phosphorus Ylide (C) 578
- Synthesis and Ligative Behavior of a Gallacyclopentadiene (C) 1370
- Synthesis and Structure of the First Organometallic Galloxane Hydroxide $Mes_6Ga_6O_4(OH)_4$ (C) 1244
- The Use of Heterometallic Bridging Moieties To Generate Tractable Lanthanide Complexes of Small Ligands (C) 1641

Gas chromatography
- Optically Active Reference Compounds for Environmental Analysis Obtained by Preparative Enantioselective Gas Chromatography (C) 2085

Gas-phase chemistry
- Gaseous Molecular Ions. An Introduction to Elementary Processes Induced by Ionization (B) 479
- Gas-phase Synthesis of Reactive Molecules Using Adsorbed Reagents (R) 1332

Gels
- Stable Highly Concentrated Fluorocarbon Gels (C) 1100

Genes
- Gene Regulation in Eukaryotes (B) 2349

Genetics
- Biotechnology. Vol. 2 Genetic Fundamentals and Genetic Engineering (B) 2349

Germanium compounds
- Stable Germirane Derivatives (C) 659
- Synthesis and Structure of the Disilagermirane $R_2Ge(SiR_2)_2$ and the Solvent-Separated Ion Pair $[Li([12]crown-4)_2][GeR_3]$; ($R = SiMe_3$) (C) 113
- Synthesis and Structure of the First Stable Germaneselone (C) 2316
- Synthesis, Structures, and Reactions of Two Bis(diaminostannylene)s and a Bis(diaminogermylene) Containing a Central C_6 Ring (C) 1156

Gluconamides
- Tunable Supramolecular Structures from a Gluconamide Containing Imidazole (C) 986
Glutathione reductase
- Activation of Glutathione Reductase by Light: A Novel Approach to Design Redox Photo-Enzymes (C) 581
Glycoconjugates
- A Highly Convergent Synthesis of the Lewis^y Blood Group Determinant in Conjugatable Form (C) 1468
- An Interactive Strategy for the Assembly of Complex, Branched Oligosaccharide Domains on a Solid Support: A Concise Synthesis of the Lewis^b Domain in Bioconjugatable Form (C) 1470
Glycopeptides
- Enzymatic Hydrolysis of Hydrophilic Diethyleneglycol and Polyethyleneglycol Esters of Peptides and Glycopeptides by Lipases (C) 336
- Recombinant Whole Cells as Catalysts for the Enzymatic Synthesis of Oligosaccharides and Glycopeptides (C) 1241
- Synthesis of *N*-Glycopeptide Clusters with Lewis^x Antigen Side Chains and Their Coupling to Carrier Proteins (C) 101
Glycoproteins
- *Aleuria aurantia* Agglutinin Recognizes Multiple Conformations of α-L-Fuc-(1→6)-β-D-GlcNAc-OMe (C) 88
Glycosidases
- Progress Toward An Antibody Glycosidase (C) 339
Glycosylations
- Sugar Calixarenes: Preparation of Calix[4]arenes Substituted at the Lower and Upper Rims with *O*-Glycosyl Groups (C) 2479
- Synthesis of a Biantennary Heptasaccharide by Regioselective Glycosylations (C) 1102
Glycosylimides
- Stereoselective Intramolecular Alkylation of Glycosylimides to Highly Functionalized Bicyclic 2,5-Azepanediones and Heterotricyclic [5.3.1.$0^{2,6}$] Undecanamides (C) 1979
Glycosylimines
- Conversion of Glycosyl Azides via *N*-Bromoglycosylimines to Aldononitriles (C) 751
Gold compounds
- A Cluster-Bound Triply-Bridging Phosphorus Atom Coordinated to Four $(Ph_3P)Au^+$ Units: $[Fe_3(CO)_9P\{Au(PPh_3)\}_4][BAr_4]$ (C) 75
- A Hexanuclear Gold(I) Complex: $[(Ph_3PAu)_2C(PPh_2AuPPh_2)\}_2](ClO_4)_2$ (C) 87
- A Postulated Carrier of Gold in Hydrothermal Ore Solutions: Synthesis and Crystal Structure of $[(Ph_3P)_2N]$-$[Au(SH)_2]$, the First Homoleptic Hydrogensulfido Complex (C) 1852
- Aurophilicity at Sulfur Centers: Synthesis and Structure of the Tetragold(I) Species $[(Ph_3PAu)_4S](CF_3SO_3)_2 \cdot 2CH_2Cl_2$ (C) 769
- Neutral Gold(I) Fluoride Does Indeed Exist (C) 212
- $[(Ph_3PAu)_6(dppeAu_2)(AuCl)_4Pd]$, an Icosahedral Au_{12} Cluster with a Central Pd Atom (C) 207
GPI anchor
- Synthesis of a GPI Anchor of Yeast (*Saccharomyces cerevisiae*) (C) 2177
Grignard reactions
- Enantioselective Reactions in a Static Magnetic Field (C) 454 (1461)
- Simple and Versatile Synthesis of Optically Active 1,2-Amino Alcohols by Grignard Addition to *N*,*O*-Dibenzylglyceraldimine and -lactaldimine (C) 1298
Group theory
- Icons and Symmetries (B) 482

Hafnium compounds
- Hf_3Te_2: A New and Remarkable Layered Compound (C) 2328
Halogen compounds
- Chlorine Trioxide: Spectroscopic Properties, Molecular Structure, and Photochemical Behavior (C) 1482
- Nonreactive Interactions between Ethene and Halogens: Detection of a π-Donor Complex $C_2H_4\cdots BrCl$ by Rotational Spectroscopy (C) 1512
Handbooks
- Comprehensive Handbook on Hydrosilylations (B) 1893
- Peptide and Protein Hormones. Structure, Regulation, Activity. A Reference Manual (B) 1117
Heck reactions
- Fine Feathers Make Fine Birds: The Heck Reaction in Modern Garb (R) 2379
- Regio- and Enantioselective Silane-Terminated Intramolecular Heck Reactions (C) 1089
Helices
- $[(C_6H_5)_4P]^1_\infty[Cu_3I_4]$—The First Compound with a Helical Chain of Face-Sharing Tetrahedra as a Structural Element (C) 1841
- A Convergent Synthesis of 2,5-*trans*-Linked Oligo(tetrahydrofuran)s: Potential Building Blocks for a Polyether Helix with Ion Channel Activity (C) 1180
- Novel Molecular Scaffolds: Formation of Helical Secondary Structure in a Family of Oligoanthranilamides (C) 446
- On the Helicity of Oligomeric Formaldehyde (C) 1476
- 1-Oxa-3,5,7,9-tetraazadecapentaene, a Model Oligonitrile with a Helical Structure in the Crystalline State (C) 2337
Heme proteins
- Change of Orientation of Axial Imidazole Ligands in a Cytochrome b Model Complex in Response to a Change in the Oxidation State of the Metal Center (C) 1363
Hemethiolate enzymes
- Prostacyclin and Thromboxane Synthase: New Aspects of Hemethiolate Catalysis (R) 1911
Heptacoordination
- Molecules and Ions with Heptacoordinated Central Atoms (H) 1941
Heteroarenes
- 3-Phosphonio-1,2-diphosphaindenides and the Electrophilic Substitution of *C*-Phenyl-Substituted Ylides (C) 663
Heterocubanes
- $[Mn_4Te_4(SC_3H_7)_4]^{4-}$ and $[Mn_4Te_4(SeC_3H_7)_4]^{4-}$: Novel Heterocubane Clusters of Manganese (C) 2322
Heterocycles
- $(t\text{BuSi})_2(PC_6H_{11})_3$: A Propellane-Like Cyclosilaphosphane with Remarkable Structure (C) 1484
- Functionalization of Aromatic Azo Compounds by the Cobalt-Catalyzed, Regioselective Double Addition of Tolane: 2,6-Distilbenylazobenzenes and 2,3-Dihydrocinnolines (C) 1603
- 3*H*-Indole (C) 1153
- Phosphindolyl Anions by Elimination from 1-Phosphoallyllithium Complexes – η^5 and η^3 Coordination of a Phospholyl Fragment (C) 353
- Synthesis and Structure of the Disilagermirane $R_2Ge(SiR_2)_2$ and the Solvent-Separated Ion Pair $[Li([12]crown-4)_2][GeR_3]$; $(R = SiMe_3)$ (C) 113
- Synthesis of the First 2*H*-1-Aza-2-phosphirene Complexes (C) 80
- The First Cycloaddition Reactions of Dimeric Arsenium Cations (C) 1267
- Thermally Induced Ring Cleavage of a 2*H*-1,2-Azaphosphirene Tungsten Complex (C) 2427
- Toward Polyphospholes: Synthesis and Structure of an α-Linked Quaterphosphole (C) 1158
Hexachlorocyclohexanes
- The Absolute Configuration of (+)-α-1,2,3,4,5,6-Hexachlorocyclohexane, and Its Permeation through the Seal Blood–Brain Barrier (C) 882
Hexobarbital
- Toward Unified Enantioselective Chromatography with a Single Capillary Column Coated with Chirasil-Dex (C) 2222
High-pressure chemistry
- High-Pressure Synthesis of K_2PtH_6, a Saltlike Hydride with the K_2PtCl_6 Structure (C) 1112
- The Pressure Effect in Pericyclic Rearrangements: the Cope Rearrangement, Electrocyclization, and the Intramolecular Diels–Alder Reaction (C) 1079
History of chemistry
- Die Allianz von Wissenschaft und Industrie. August Wilhelm Hofmann (1818–1892) (B) 232
- Half a Century of Free Radical Chemistry (B) 1009
- Histoire de la chimie (B) 901
- Nobel Laureates in Chemistry, 1901–1992 (B) 2118
- Otto Roelen, Pioneer in Industrial Homogeneous Catalysis (R) 2144 (2348)
- The Fontana History of Chemistry (B) 901
- The Quiet Revolution: Hermann Kolbe and the Science of Organic Chemistry (B) 1195
- Turning Points in Catalysis (R) 913
- 100 Years "Schlüssel-Schloss-Prinzip": What Made Emil Fischer Use this Analogy? (R) 2364
Hofmann, August Wilhelm
- Die Allianz von Wissenschaft und Industrie. August Wilhelm Hofmann (1818–1892) (B) 232
Homocubene
- 1(9)-Homocubene and 9-Homocubylidene: Theoretical Investigation of Structures, Energies, and Rearrangement Reactions (C) 668
Host–guest chemistry
- A Difunctional Receptor for the Simultaneous Complexation of Anions and Cations; Recognition of KH_2PO_4 (C) 467
- A Novel Type of Stereoisomerism in Calix[4]arene-Based Carceplexes (C) 2345
- A Water-Soluble "Bear Trap" Exhibiting Strong Anion Complexation Properties (C) 2456
- Axially Chiral Amidinium Ions with a Biaryl Skeleton: A New Class of Structure in Host–Guest Chemistry (C) 984
- Cyclodextrins as Building Blocks for Supramolecular Structures and Functional Units (R) 803
- Dendrimers: From Generations and Functional Groups to Functions (H) 2413
- 1,3-Dialkoxycalix[4]arenecrowns-6 in 1,3-Alternate Conformation: Cesium-Selective Ligands that Exploit Cation–Arene Interactions (C) 1506

- Dissolution of Cholesterol in Water by a Synthetic Receptor (C) 1625
- Macrotricyclic Borane–Amine Adducts: The First Uncharged Synthetic Host Compounds Without Lewis Acid Character, for Anionic Guests (C) 327
- Mixed-Valence, Tetranuclear Iron Chelate Complexes as Endoreceptors: Charge Compensation Through Inclusion of Cations (C) 1621
- Molecular Golf Balls: Vesicles from Bowl-Shaped Host Molecules (C) 1662
- Redox Control for the Recognition of Ag^+ Ions in a Macrocycle Containing Two SH Groups or an S–S Bridge inside the Cavity (C) 1750
- Resolution of Racemates by Distillation with Inclusion Compounds (H) 728
- Sensitive and Selective Coloration of Cryptand-Type Crown Spirobenzopyrans for Alkaline-Earth Metal Compounds (C) 1163
- Supramolecular Activation of *para*-Benzoquinone (C) 2489
- Taking Fullerenes from Large Molecules to Supramolecules (H) 2269
- Template Syntheses (R) 375
- The Oxovanadium–Organoarsonate System: $[2CH_3OH \subset V_{12}O_{14}(OH)_4(PhAsO_3)_{10}]^{4-}$ and $[2H_2O \subset V_{12}O_{12}(OH)_2(H_2O)_2(PhAsO_3)_{10}(PhAsO_3H)_4]^{2-}$, Clusters with Nanometer Dimensions and Cavities for Neutral Molecules (C) 760
- The Oxovanadium–Organophosphonate System: Complex Cluster Structures $[(VO)_6(tBuPO_3)_8Cl]$, $[(VO)_4\{PhP(O)_2OP(O)_2Ph\}_4Cl]^-$, and $[V_{18}O_{25}(H_2O)_2(PhPO_3)_{20}Cl_4]^{4-}$ with Encapsulated Chloride Anions Prepared from Simple Precursors (C) 757
- The Search for Selective, Neutral Anion Receptors (H) 1832
- Trigonal Symmetry as a Host Design Element: Novel Conformation of Dodecakis(3,5-dimethylphenylthio)coronene in its 1,4-Dioxane Clathrate (C) 1587
- Wacker Oxidation of 1-Decene to 2-Decanone in the Presence of a Chemically Modified Cyclodextrin System: A Happy Union of Host–Guest Chemistry and Homogeneous Catalysis (C) 2100

Hot atom chemistry
- Handbook of Hot Atom Chemistry (B) 1198

Houben-Weyl
- Houben-Weyl. Methoden der Organischen Chemie. Band E15, Teile 1–3. En-X- und In-X-Verbindungen (B) 1891

Hydrazones
- [2,3] Sigmatropic Wittig Rearrangement of Chiral Allyloxyacetaldehyde Hydrazones in the Diastereo- and Enantioselective Synthesis of Protected, γ,δ-Unsaturated α-Hydroxyaldehydes and Cyanohydrins (C) 2098

Hydrides
- Base-Free Monomeric Organogallium Hydrides (C) 1253
- High-Pressure Synthesis of K_2PtH_6, a Saltlike Hydride with the K_2PtCl_6 Structure (C) 1112

Hydroborations
- New Titanium – Boron Complexes with a Planar Tetracoordinate Carbon or a Planar Tricoordinate Phosphorus Center (C) 197

Hydrocarbons
- Novel Optically Active Hydrocarbons in Sediments: Evidence for an Extensive Biological Cyclization of Higher Regular Polyprenols (C) 1166
- Octahydro-1,2,3:4,5,6-dimethenopentalene-2-carbonitrile, the First Derivative of a Yet-Unknown $(CH)_{10}$ Hydrocarbon (C) 1639
- Octaplane: A Saturated Hydrocarbon with a Remarkably Low Ionization Energy Leading to a Cation with a Planar Tetracoordinate Carbon Atom (C) 1667
- Synthesis of Centrohexacyclic Hydrocarbons by the Propellane Route: Centrohexaindan and Tribenzocentrohexaquinane (C) 1251
- Transannular Addition of Methyllithium to 5,12:6,11-Di[1,2]benzenodibenzo[*a,e*]cyclooctene and Its 5,6-Epoxy Derivative (C) 993

Hydroformylations
- Cooperativity in Rh_2 Complexes: High Catalytic Activity and High Regioselectivity in the Hydroformylation of Olefins (H) 67
- Otto Roelen, Pioneer in Industrial Homogeneous Catalysis (R) 2144 (2348)

Hydrogenations
- Increase in the Enantioselectivity of Asymmetric Hydrogenation in Water Influenced by Surfactants or Polymerized Micelles (C) 2197
- In Situ NMR Investigations of Photocatalyzed Hydrogenations with Parahydrogen in the Presence of Metal Carbonyl Compounds of Group 6 (C) 755

Hydrogen bonds
- A Liquid-Crystalline Polymer Network Built by Molecular Self-Assembly through Intermolecular Hydrogen Bonding (C) 1644
- Crystal Structure of 2,5-Di-*tert*-butylhydroquinone: Polar Stacking of Nonpolar Hydrogen-Bonded Sheets with Trigonal Symmetry (C) 1755
- Proton-Transfer-Dependent Reversible Phase Changes in the 4,4'-Bipyridinium Salt of Squaric Acid (C) 181
- The First Water-Dependent Liquid Clathrate: X-Ray Evidence in the Solid for a C–H···π(Heteroarene)···H–C Interaction (C) 566
- Zigzag Channels in the Structure of Sebaconitrile/Urea (C) 649

Hydrolyses
- Binuclear Metal Complexes as Efficient Intermediaries in Biochemically Relevant Hydrolysis Reactions (H) 1141

Hydroperoxides
- The Oxenoid Character of Metalated Hydroperoxides O(M)OR: Oxidation of Organometallic Compounds R'M' to R'OH under Mild Conditions (C) 1161

Hydroquinones
- Crystal Structure of 2,5-Di-*tert*-butylhydroquinone: Polar Stacking of Nonpolar Hydrogen-Bonded Sheets with Trigonal Symmetry (C) 1755

Hydrosilylations
- *trans*-Chelating Chiral Diphosphane Ligands Bearing Flexible *P*-Alkyl Substituents (AlkylTRAPs) and their Application to the Rhodium-Catalyzed Asymmetric Hydrosilylation of Simple Ketones (C) 111
- Comprehensive Handbook on Hydrosilylations (B) 1893

Hydroxyaldehydes
- [2,3] Sigmatropic Wittig Rearrangement of Chiral Allyloxyacetaldehyde Hydrazones in the Diastereo- and Enantioselective Synthesis of Protected, γ,δ-Unsaturated α-Hydroxyaldehydes and Cyanohydrins (C) 2098

Hydroxyalkylations
- Diastereoselective Hydroxyalkylation of Enantiomerically Pure 2-Alkenylsulfoximides (C) 444

Hydroxyl radical
- Recycling in the Earth's Atmosphere: The OH Radical—Its Importance for the Chemistry of the Atmosphere and the Determination of Its Concentration (R) 1816

Hyperconjugation
- A Highly Distorted and an Undistorted Borirane, C-B-H Hyperconjugation Induced by C-Si-H Hyperconjugation (C) 1487 (1668)

Hypervalent compounds
- Concerning the Mechanism of α-Elimination: Hypervalent Ion Pairing in an Iodocarbenium Iodide (C) 893
- Electrostatic Activation of Hypervalent Organo-Iodine Compounds: Bis(onio)-Substituted Aryliodine(III) Salts (C) 891

ICP atomic spectrometry
- Inductively Coupled Plasmas in Analytical Atomic Spectrometry (B) 231

Imides
- Synthesis and Structure of the Magnesium Imide $[(thf)MgNPh]_6$ (C) 356

Imines
- Diastereomerically Pure Mannich Bases from the Addition of Enamines to Ternary Iminium Salts (C) 2422

Iminoalanes
- Synthesis and Structure of the First Dimeric Iminoalane Containing an Al_2N_2 Heterocycle (C) 969

Iminophosphoranes
- Reactions of an Iminophosphoranylidene Carbenoid (C) 982

Immunoassays
- Luminescent Labels—More than Just an Alternative to Radioisotopes? (R) 1044

Immunosorption
- Immunosorption Techniques. Fundamentals and Applications (B) 234

Inclusion compounds
- Zigzag Channels in the Structure of Sebaconitrile/Urea (C) 649

Indacenes
- *s*-Indacene: A Delocalized, Formally Antiaromatic 12 π Electron System (C) 1192

Indigo derivatives
- Concerning the Questionable Existence of Thioxoindigoid Compounds (C) 739

Indoles
- 3*H*-Indole (C) 1153

Indolizidines
- Diastereoselective Synthesis of Amino-Substituted Indolizidines and Quinolizidines by the Intramolecular Hetero-Ene Reaction of Prolinal Imine and 2-Piperidine Carbaldimine (C) 458

Inorganic chemistry
- Inorganic Materials (B) 585

Inositols
- Synthesis of a GPI Anchor of Yeast (*Saccharomyces cerevisiae*) (C) 2177

Interfaces
- Structure of Electrified Interfaces (B) 2117

Intermediates
- Molecular Distortion in Reactive Chemical Intermediates (H) 962

Intermetallic phases
- Localization of Electrons in Intermetallic Phases Containing Aluminum (C) 2069
- Unequivocal Partitioning of Crystal Structures, Exemplified by Intermetallic Phases Containing Aluminum (C) 2073

In vitro selection
- Isolation of RNA Aptamers for Biological Cofactors by In Vitro Selection (C) 1084
Iodine compounds
- $[(C_6H_5)_4P]_\infty^1[Cu_3I_4]$ - The First Compound with a Helical Chain of Face-Sharing Tetrahedra as a Structural Element (C) 1841
- α-Aryliodonio Diazo Compounds: S_N Reactions at the α-C Atom as a Novel Reaction Type for Diazo Compounds (C) 1952
- Concerning the Mechanism of α-Elimination: Hypervalent Ion Pairing in an Iodocarbenium Iodide (C) 893
- Electrostatic Activation of Hypervalent Organo-Iodine Compounds: Bis(onio)-Substituted Aryliodine(III) Salts (C) 891
- Iodine Chains in $(Me_4Sb)_3I_8$ and Discrete Triiodide Ions in Me_4AsI_3 (C) 987
- Small Molecules Stabilized in Inorganic Frameworks: NbI_5 Monomers in the Novel Layered Compound $Nb_7S_2I_{19}$ (C) 334
Ion channels
- A Convergent Synthesis of 2,5-*trans*-Linked Oligo(tetrahydrofuran)s: Potential Building Blocks for a Polyether Helix with Ion Channel Activity (C) 1180
Ionophores
- Cyclosporin: A Li- and Ca-Specific Ionophore! (C) 442
Ions
- Gaseous Molecular Ions. An Introduction to Elementary Processes Induced by Ionization (B) 479
Iron compounds
- A Carbene–Iron Chelate Complex as a Source of a Ferraborane Derivative (C) 2218
- A Mixed-Valent, Unsymmetrical Fe^{II}-Fe^{III} Complex with a Terminal Phenola to Ligand as a Model for the Active Site of Purple Acid Phosphatases (C) 887
- A Model for α-Keto Acid Dependent Nonheme Iron Enzymes: Structure and Reactivity of $[Fe^{II}_2(Me_2hdp)_2(bf)](ClO_4)$ (C) 1886
- Asymmetric Diels–Alder Reactions Catalyzed by a Chiral Iron Lewis Acid (C) 1856
- Bond-Stretch Isomers: Fact not Fiction (C) 425
- Carboxylatoiron(II) Aggregates: A Novel Fe^{II}_4 Complex with Threefold Symmetry (C) 1660
- Change of Orientation of Axial Imidazole Ligands in a Cytochrome b Model Complex in Response to a Change in the Oxidation State of the Metal Center (C) 1363
- Chemistry of Iron (B) 1011
- $[Cp^*Fe(\eta^5\text{-}P_5)]$, a Sandwich Complex with Diverse Ligand Properties (C) 1110
- Cr^{III} and Fe^{III} Complexes with η^3-1,3,5-Triazacyclohexane Ligands (C) 1877
- Decaphenylferrocene and Decaphenylferrocenium Tetrafluoroborate (C) 1731
- "Frec" $[Fe(tpp)]^+$ Cation: A New Concept in the Search for the Least Coordinating Anion (C) 2433
- Iron–Carbene Complexes (B) 1894
- Iron-Promoted, Regio- and Stereoselective Allylic Substitutions for the Synthesis of Alkenyl Sulfones Substituted at C-3 (C) 1949
- Metallocorroles with Formally Tetravalent Iron (C) 731
- Mixed-Valence, Tetranuclear Iron Chelate Complexes as Endoreceptors: Charge Compensation Through Inclusion of Cations (C) 1621
- $[Mo_{57}Fe_6(NO)_6O_{174}(OH)_3(H_2O)_{24}]^{15-}$: A Highly Symmetrical Giant Cluster with an Unusual Cavity and the Possibility of Positioning Paramagnetic Centers on Extremely Large Cluster Surfaces (C) 849
- μ-Oxodiiron(III) Complexes of Porphycenes (C) 736
- (η^5-Pentamethylcyclopentadienyl)iron Complexes with η^5-2,3,5-Tricarbahexaboranyl and η^5-2,3-Dihydro-1,3-diborolyl Ligands (C) 203
- Platinum-Iron Silylene Complexes and Metal-Promoted Substituent Exchange between $Si(NMe_2)_3$- and $P(OEt)_3$-Ligands (C) 2440
- Single-Crystal EPR Spectroscopy on $[^{57}Fe(NO)(S_2CNEt_2)_2]$: The "Triplet Signal" in the EPR Spectrum of $[Fe(S_2CNEt_2)_3]$ (C) 1497
- Single-Step Six-Electron Transfer in a Heptanuclear Complex: Isolation of Both Redox Forms (C) 2460
- Synthesis and Characterization of Thiolato Complexes with Two-Coordinate Iron(II) (C) 1178
- Synthesis and Structure of the First [2$_2$]Metallocenophanes (C) 1479
- The First Metal Complexes with a Doubly S_3-Bridged Ferrocene Ligand (C) 1752
- Thermal and Optical Switching of Iron(II) Complexes (R) 2024
Isocyanides
- Complex-Stabilized Alkynyl and Cycloalkenyl Isocyanides (C) 330
- Equilibrium between Isocyanide and Carbene Complexes in Coordination Compounds of 2,6-Dihydroxyphenyl Isocyanide (C) 1356
- Fluorinated Isocyanides—More than Ligands with Unusual Properties (R) 1315
Isoelectronic analogues
- New Ionic, Isoelectronic Analogues of CO_2 and CS_2 (H) 1575
Isofagomine
- Isofagomine, a Potent, New Glycosidase Inhibitor (C) 1778
Isolobal relationship
- The Bonding Capability of Imido Complex Fragments of Groups 5–7 with Regard to the Isolobal Relationship (C) 1255
Isomerases
- Peptidyl-Prolyl *cis/trans* Isomerases and Their Effectors (R) 1415
Isomerization
- Cyanide–Isocyanide Isomerism in CN-Bridged Organometallic Complexes (C) 2090
- Photoisomerization of Highly Alkylated Butadienes (C) 204
- Propeller Isomerism of the Triphenylphosphane Ligand in Half-Sandwich Ru^{II} Complexes (C) 866
Isotope effects
- Unusually Large Isotope Effects on NMR Chemical Shifts of Paramagnetic Organometallic Compounds (C) 2326
Isotopic labeling
- A Short Route to [3-^{15}N]-3′-Azido-3′-deoxythymidine (N3-Labeled AZT) via 3-Nitro-AZT (C) 2454
Ivangulin
- A Short and Highly Stereoselective Synthesis of the 1,10-*seco*-Eudesmanolide Ivangulin (C) 2195

Keronopsins
- Keronopsins A and B, Chemical Defence Substances of the Marine Ciliate *Pseudokeronopsis rubra* (Protozoa): Identification by Ex Vivo HPLC (C) 1495
Ketenylidene complexes
- $[Zr_3Cp_2(O_2CN\mathit{i}Pr_2)_6(\mu_3\text{-}O)(\mu_2\text{-}CCO)]$, the First Crystallographically Established Ketenylidene Complex; A Model for CO Reductive Cleavage on Metal Surfaces (C) 1188
Ketones
- Bridgehead Functionalization of Non-Enolizable Ketones: The First Preparatively Useful Methods (C) 2220
Kinetics
- Kinetic Theory and Irreversible Thermodynamics (B) 481
- The Kinetics of Heterogeneous Electron Transfer Reactions in Polar Solvents (R) 2131
Kolbe, Hermann
- The Quiet Revolution: Hermann Kolbe and the Science of Organic Chemistry (B) 1195

β-Lactams
- The Organic Chemistry of β-Lactams (B) 480
Lactones
- Optically Active Lactones from a Baeyer–Villiger-Type Metal-Catalyzed Oxidation with Molecular Oxygen (C) 1848
Ladder polymers
- Ladder Polymers and Oligomers Based on Hemiporphyrazine (C) 1646
- Ladder Polymers with a Heteroacene Skeleton (C) 2424
- Synthesis of a Fully Unsaturated "Molecular Board" (C) 2209
Lanthanide compounds
- Lanthanide(III) Tetraamide Macrocyclic Complexes as Synthetic Ribonucleases: Structure and Catalytic Properties of $[La(tcmc)(CF_3SO_3)(EtOH)](CF_3SO_3)_2$ (C) 773
- Luminescent Eu^{3+} and Tb^{3+} Complexes of a Branched Macrocyclic Ligand Incorporating 2,2′-Bipyridine in the Macrocycle and Phosphinate Esters in the Side Arms (C) 1501
- Molecular Siloxane Complexes of Rare Earth Metals—Model Systems for Silicate-Supported Catalysts? (C) 1285
- New Upswing of Organolanthanoid Research: A Very Promising Revival of Organocerium(IV) Chemistry and the First Stable Lanthanoid(II/III)–Carbene Complexes (H) 2165
- N-Heteroarene Dianions as Antiaromatic Ligands Bridging two Lanthanocene Moieties (C) 1171
- Organolanthanoid–Carbene Adducts (C) 1733
- Polynuclear Lanthanide Complexes: Formation of a Selenium-Centered Sm_6 Complex, $[\{(C_5Me_5)Sm\}_6Se_{11}]$, (C) 2110
- The Use of Heterometallic Bridging Moieties To Generate Tractable Lanthanide Complexes of Small Ligands (C) 1641
Laser spectroscopy
- Applied Laser Spectroscopy. Techniques, Instrumentation, and Applications (B) 1195Lead compounds
- Sixteenfold Deprotonated γ-Cyclodextrin Tori as Anions in a Hexadecanuclear Lead(II) Alkoxide (C) 1863
Lewis acids
- Liquid Sulfur Dioxide as a Lewis-Acidic Solvent for the Alkylation and Alkoxyalkylation of Allylsilanes (C) 788

Lewis^b hapten
- An Interactive Strategy for the Assembly of Complex, Branched Oligosaccharide Domains on a Solid Support: A Concise Synthesis of the Lewis^b Domain in Bioconjugatable Form (C) 1470

Lewis^x hapten
- Synthesis of Deoxy Sialyl Lewis^x Analogues, Potential Selectin Antagonists (C) 2096
- Synthesis of *N*-Glycopeptide Clusters with Lewis^x Antigen Side Chains and Their Coupling to Carrier Proteins (C) 101
- The Sialyl Lewis^x Group and its Analogues as Ligands for Selectins: Chemoenzymatic Syntheses and Biological Functions (H) 178

Lewis^y hapten
- A Highly Convergent Synthesis of the Lewis^y Blood Group Determinant in Conjugatable Form (C) 1468

Lipids
- The Effect of Chiral Bilayers: Wax Tubes made of (*S*)-Nonacosan-10-ol (C) 350

Liposomes
- Sterically Stabilized Vesicles (R) 1685

Liquid crystals
- A Liquid-Crystalline Polymer Network Built by Molecular Self-Assembly through Intermolecular Hydrogen Bonding (C) 1644
- A New Class of Novel Macrocyclic Mesogens (C) 1503 (1668)
- Cooperativity and Transfer of Chirality in Liquid-Crystalline Polymers (C) 188
- Dendrimers: From Generations and Functional Groups to Functions (H) 2413
- Liquid Crystal Polymers (B) 1013
- New Materials for Liquid Crystal Displays: Structure–Property Relationship of 2-Fluoropyridines (C) 1386
- Polar Superstructures Stabilized by Polymeric Oxometal Units: Columnar Liquid Crystals Based on Tapered Dioxomolybdenum Complexes (C) 2342
- Synthesis of Very Highly Ordered Liquid Crystalline Phases by Complex Formation of Polyacrylic Acid with Cationic Surfactants (C) 1869

Liquid mixtures
- Theoretical Treatment of Liquids and Liquid Mixtures (B) 697

Lithium perchlorate
- O-Glycoside Syntheses under Neutral Conditions in Concentrated Solutions of $LiClO_4$ in Organic Solvents (C) 1944

Lithocene anion
- The Simplest Metallocene Sandwich: the Lithocene Anion (C) 1744

Lock and key principle
- One Hundred Years Lock-and-Key Principle (R) 2363
- The Key–Lock Theory and the Induced Fit Theory (R) 2375
- 100 Years "Schlüssel-Schloss-Prinzip": What Made Emil Fischer Use this Analogy? (R) 2364

Low-valent compounds
- Donor-Stabilized Aluminum(I) Bromide (C) 1754
- Donor-Stabilized Aluminum(II) Bromide (C) 862
- Subvalent Aluminum Halides as Examples of High-Temperature Species in Inorganic Syntheses (H) 1830
- Tetrakis(hypersilyl)dithallium(*Tl–Tl*): A Divalent Thallium Compound (C) 681

Luminescence
- Luminescent Eu^{3+} and Tb^{3+} Complexes of a Branched Macrocyclic Ligand Incorporating 2,2′-Bipyridine in the Macrocycle and Phosphinate Esters in the Side Arms (C) 1501

Luminescent labels
- Luminescent Labels—More than Just an Alternative to Radioisotopes? (R) 1044

Macrocycles
- A Difunctional Receptor for the Simultaneous Complexation of Anions and Cations; Recognition of KH_2PO_4 (C) 467
- A New Class of Novel Macrocyclic Mesogens (C) 1503 (1668)
- An Organic Molecule with a Rigid Cavity of Nanosize Dimensions (C) 1292
- Complexes of Partially Fluorinated Macrocycles with a Metal–Fluorine σ-Donor Bond and Their Suitability as Metal Ion Indicators (C) 2175
- Crown Compounds: Toward Future Applications (B) 235
- Dialdehyde + Diamine—Polymer or Macrocycle? (C) 125
- Isomeric Lactam Catenanes and the Mechanism of their Formation (C) 1767
- Luminescent Eu^{3+} and Tb^{3+} Complexes of a Branched Macrocyclic Ligand Incorporating 2,2′-Bipyridine in the Macrocycle and Phosphinate Esters in the Side Arms (C) 1501
- New Types of Metal-Stabilized Cyclobutadiene Superphanes (C) 1272
- Redox Control for the Recognition of Ag^+ Ions in a Macrocycle Containing Two SH Groups or an S–S Bridge inside the Cavity (C) 1750
- Ring Closures on Polymeric Supports—Formation of Extremely Large Macrocycles by Intrapolymeric Cyclooligomerizations (C) 1960
- Tether-Directed Remote Functionalization of Buckminsterfullerene: Regiospecific Hexaadduct Formation (C) 2339

Macrolids
- Total Synthesis of Soraphen $A_{1\alpha}$ (C) 2466

Magnesium compounds
- Synthesis and Structural Characterization of $[\{(Et_2O)Mg\}_6(NPh)_4Br_4]$: A Magnesium–Imide Cage Species Derived from a Dimagnesylamine Solution (C) 1000
- Synthesis and Structure of the Magnesium Imide $[(thf)MgNPh]_6$ (C) 356

Magnetic properties
- Alternating Ferro- and Antiferromagnetic Interactions in a Mn^{II} Chain with Alternating End-On and End-to-End Bridging Azido Ligands (C) 2488
- Coexistence of Mobile and Localized Electrons in Bis(ethylene)dithiotetrathiafulvalene (BEDT-TTF) Radical Salts with Paramagnetic Polyoxometalates: Synthesis and Physical Properties of $(BEDT\text{-}TTF)_8[CoW_{12}O_{40}]\cdot 5.5H_2O$ (C) 223
- Combination of Superexchange and Spin-Polarization Mechanisms Leads to a Novel Hydrocarbon Tetraradical with a High-Spin Ground State (C) 1104
- Fairly Strong Ferromagnetic Interactions between Imino Nitroxide Ligands through a Diamagnetic Cu^I Ion in $[Cu^I(im\text{-}mepy)_2](PF_6)$ (C) 670
- Ferromagneto-Structural Correlations in $[Mn(OC_6X_3H_2)_2(bipy)]_2$ Compounds, X = Cl, Br (C) 1592
- Magnetic Properties of Aromatic Transition States: The Diels–Alder Reactions (C) 1376
- $[Mo_{57}Fe_6(NO)_6O_{174}(OH)_3(H_2O)_{24}]^{15-}$: A Highly Symmetrical Giant Cluster with an Unusual Cavity and the Possibility of Positioning Paramagnetic Centers on Extremely Large Cluster Surfaces (C) 849
- Organic and Organometallic Magnetic Materials—Designer Magnets (R) 385
- Pronounced Electronic Coupling in Rigidly Connected N,C,N-Coordinated Diruthenium Complexes over a Distance of Up to 20 Å (C) 1775
- Structural and Magnetic Characterization of a Novel Heptanuclear Hydroxo-Bridged Copper(II) Cluster of the Corner-Sharing Dicubane Type (C) 1184
- Two-Dimensional Sheets of Tetragonal Copper(II) Lattices: X-Ray Crystal Structure and Magnetic Properties of $[Cu(C_6O_4Cl_2)(C_4H_4N_2)]_n$ (C) 1759

Magnetic resonance microscopy
- Magnetic Resonance Microscopy (B) 128

Mamanuthaquinone
- A Concise Total Synthesis of (±)-Mamanuthaquinone by Using an *exo*-Diels–Alder Reaction (C) 853

Manganese compounds
- Alternating Ferro- and Antiferromagnetic Interactions in a Mn^{II} Chain with Alternating End-On and End-to-End Bridging Azido Ligands (C) 2488
- A Structural Model for the Water-Oxidizing Manganese Cluster in Photosystem II (H) 725
- Ferromagneto-Structural Correlations in $[Mn(OC_6X_3H_2)_2(bipy)]_2$ Compounds, X = Cl, Br (C) 1592
- $[Mn_4Te_4(SC_3H_7)_4]^{4-}$ and $[Mn_4Te_4(SeC_3H_7)_4]^{4-}$: Novel Heterocubane Clusters of Manganese (C) 2322
- Novel Bimetallic Model System for Cytochrome P_{450}: Effect of Membrane Environment on the Catalytic Oxidation (C) 2468
- Oxygen Evolution by Oxidation of Water with Manganese Porphyrin Dimers (C) 1839
- The Reactivity of Phosphacymantrenes towards Palladium(II) and Palladium(0) Compounds: Synthesis, Structure, and Chemistry of Pd_2Mn_2 and Pd_3Mn_4 Arrays (C) 742
- Towards One-Dimensional Carbon Wires Connecting Single Metal Centers: A Cumulenic C_5 Chain that Mediates Charge Transfer between Rhenium and Manganese Termini (C) 2199

Mannich bases
- Diastereomerically Pure Mannich Bases from the Addition of Enamines to Ternary Iminium Salts (C) 2422

β-Mannosides
- A Novel Approach to the Stereoselective Synthesis of β-Mannosides (C) 1765

Mark, Herman Francis
- From Small Organic Molecules to Large: A Century of Progress (B) 1117

Mass spectrometry
- An Extraordinarily Violent Molecular Dissociation: The Unprecedented Kinetic Energy Release in the Decomposition of $HONF^+$, a Singly Charged Metastable Ion (C) 123
- Catalytic Pt^+-Mediated Oxidation of Methane by Molecular Oxygen in the Gas Phase (C) 1174
- Chemical Analysis of Inorganic and Organic Surfaces and Thin Films by Static Time-of-Flight Secondary Ion Mass Spectrometry (TOF-SIMS) (R) 1023
- Ladder Sequencing of Peptides and Proteins—A Combination of Edman Degradation and Mass Spectrometry (H) 723

- Mass Spectral and GC Data of Drugs, Poisons, Pesticides, Pollutants and Their Metabolites. Volumes 1–3 (B) 359
- Neutral Gold(I) Fluoride Does Indeed Exist (C) 212

Materials science
- Inorganic Materials (B) 585

Matrix isolation
- C_2H_2Si Isomers: Generation by Pulsed Flash Pyrolysis and Matrix-Spectroscopic Identification (C) 1248
- 1,1-Dimethyl-1*H*-silirene (C) 766
- Gas-phase Synthesis of Reactive Molecules Using Adsorbed Reagents (R) 1332
- Generation of the Parent Allyl Cation in a Superacid Cryogenic Matrix (C) 448
- Matrix Spectroscopy of 2-Adamantylidene, a Dialkylcarbene with Singlet Ground State (C) 1964
- Nitrile Imines: From Matrix Characterization to Stable Compounds (R) 527
- Ring Opening of Cyclopropane at 10 K (C) 558
- Silane Nitrile: Matrix Isolation, Adduct with Hydrogen (C) 473

Medicinal chemistry
- Medicinal Chemistry. The Role of Organic Chemistry in Drug Research (B) 1783

Membrane probes
- Increased Selectivity of a Simple Photosensitive Probe in the Presence of Large Proportions of Cholesterol (C) 1176

Membranes
- Biomembranes. Physical Aspects (B) 1783
- Bolaamphiphiles: From Golf Balls to Fibers (H) 1937
- Novel Bimetallic Model System for Cytochrome P_{450}: Effect of Membrane Environment on the Catalytic Oxidation (C) 2468

Merrifield, Bruce
- Life During a Golden Age of Peptide Chemistry: The Concept and Development of Solid-Phase Peptide Synthesis (B) 1990

Mesolytic bond cleavage
- Free-Energy Relationship for Mesolytic Cleavage of C–C Bonds (C) 73

Metabolites
- Metal Complexes of Marine Peptide Metabolites: A Novel Ag_4 Cluster (C) 1516

Metalations
- Metalation of Tris(trimethylsilyl)- and Tris(dimethylphenylsilyl)methane with Methylsodium: The First Dialkylsodate (C) 1268

Metal halide tellurides
- New Forms and Functions of Tellurium: From Polycations to Metal Halide Tellurides (R) 163

Metallabenzenes
- From Triple-Decker to Metallabenzene: A New Generation of Sandwich Complexes (C) 1003

Metallacrowns
- Spectroscopic and Reactivity Studies of a Copper-Containing Metallacrown (C) 195

Metallacycles
- Desulfurization of Benzo[*b*]thiophene by S/Ru Exchange: Formation and Structure of the Cluster $[Ru_3(CO)_8(C_8H_6)]$ (C) 1381
- Synthesis and Structure of the Smallest Cyclic Cumulene; Reaction of 1,3-Diynes with Zirconocene Complexes (C) 1605
- Thianickelacycles by Ring-Opening Reactions of Cyclic Thioethers and Their Subsequent Carbonylation to Thioesters (C) 1748
- Unexpected Reactions of Acetylenedicarboxylates with Zirconocene Complexes (C) 1850

Metallaphanes
- 18-, 20-, and 22-Membered Dimetallaortho-, -meta-, and -para[7.7]cyclophanes—The First Typical Metallaphanes (C) 321

Metallocenophanes
- Synthesis and Structure of the First [2$_2$]Metallocenophanes (C) 1479

Metalloproteins
- Designer Proteins: On the Art of Synthesizing De Novo Metalloproteins (H) 2055

Metal–metal bonds
- Direct Metal–Metal Bonds Between High and Low Valent Complex Fragments: The Reaction of Metal Bases with the Metal Acids $[Re(NR)_3]^+$ and $[Mo(NR)_2]^{2+}$ (C) 678
- Heterodimetallic Complexes with an Unbridged, Polar Metal–Metal Bond (H) 964
- Titanium Complexes with Tripodal Amido Ligands: Building Blocks for Stable Bimetallic Coordination Compounds Containing Highly Polar Metal–Metal Bonds (C) 676

Metastable ions
- An Extraordinarily Violent Molecular Dissociation: The Unprecedented Kinetic Energy Release in the Decomposition of $HONF^+$, a Singly Charged Metastable Ion (C) 123

Methane
- Catalytic Pt^+-Mediated Oxidation of Methane by Molecular Oxygen in the Gas Phase (C) 1174

Methane monooxygenase
- X-Ray Structure Analysis of the Methane Monooxygenase: An Important Step toward Understanding the Oxidation of Methane in Biological Systems (H) 841

Methyllithium
- Transannular Addition of Methyllithium to 5,12:6,11-Di[1,2]benzenodibenzo[*a*,*e*]cyclooctene and Its 5,6-Epoxy Derivative (C) 993

Methylsodium
- Metalation of Tris(trimethylsilyl)- and Tris(dimethylphenylsilyl)methane with Methylsodium: The First Dialkylsodate (C) 1268

Methyl transfer
- Incorporation of L-[Methyl-$^2H_3$]methionine and 2-[Hydroxy-^{18}O]hydroxyethylphosphonic Acid into Fosfomycin in *Streptomyces fradiae*—An Unusual Methyl Transfer (C) 341

Methyltransferases
- An Amazing Distortion in DNA Induced by a Methyltransferase (Nobel Lecture) (R) 1222

Micelles
- Assembly Properties of Bolaamphiphiles from Dimeric Acids (C) 2078
- Increase in the Enantioselectivity of Asymmetric Hydrogenation in Water Influenced by Surfactants or Polymerized Micelles (C) 2197

Michael additions
- Asymmetric Michael Additions to Chiral α,β-Unsaturated Alkoxycarbene Chromium Complexes (C) 1392

Microporosity
- Preparation and Preliminary Characterization of a Covalently Pillared Zirconium Phosphate–Diphosphonate with Interlayer Microporosity (C) 1594

Mills–Nixon effect
- Mills–Nixon Effect: Wherefore Art Thou? (H) 1721

Mixed-valent compounds
- A Mixed-Valent, Unsymmetrical Fe^{II}-Fe^{III} Complex with a Terminal Phenola to Ligand as a Model for the Active Site of Purple Acid Phosphatases (C) 887
- Mixed-Valence, Tetranuclear Iron Chelate Complexes as Endoreceptors: Charge Compensation Through Inclusion of Cations (C) 1621
- Purely Organic Mixed-Valence Molecules with Nanometric Dimensions Showing Long-Range Electron Transfer: Synthesis, and Optical and EPR Studies of a Radical Anion Derived from a Bis(triarylmethyl)Diradical (C) 2106

Molecular cable
- Construction of a Multiwired Molecular Cable of Micrometer Length by a Self-Assembly Process (C) 2173

Molecular crystals
- Reactivity in Molecular Crystals (B) 1991

Molecular devices
- Sensitive and Selective Coloration of Cryptand-Type Crown Spirobenzopyrans for Alkaline-Earth Metal Compounds (C) 1163

Molecular dynamics
- Porphyrin–Quinone Cyclophanes with Gradually Varied Donor–Acceptor Distances (C) 2428

Molecular recognition
- *Aleuria aurantia* Agglutinin Recognizes Multiple Conformations of α-L-Fuc-(1 → 6)-β-D-GlcNAc-OMe (C) 88
- Conformational Requirements for Sweet-Tasting Peptides and Peptidomimetics (R) 1437
- Expeditious Synthesis of a Novel C_3-Symmetric Receptor that Binds Peptides Sequence-Selectively (C) 2458
- One Hundred Years Lock-and-Key Principle (R) 2363
- Selective Catalysis on Silicon Dioxide with Substrate-Specific Cavities (C) 471
- Self-Assembly of a Dimeric Porphyrin Host (C) 2313
- Strong, Specific Binding of Six Different DNA Sequences by a Single Conformation-Switching DNA Macrocycle (C) 1004
- The Key–Lock Theory and the Induced Fit Theory (R) 2375
- 100 Years "Schlüssel-Schloss-Prinzip": What Made Emil Fischer Use this Analogy? (R) 2364

Molybdenum compounds
- Direct Metal–Metal Bonds Between High and Low Valent Complex Fragments: The Reaction of Metal Bases with the Metal Acids $[Re(NR)_3]^+$ and $[Mo(NR)_2]^{2+}$ (C) 678
- $[K([18]crown-6)]^+[Mo_4(\mu_4\text{-}H)(OCH_2tBu)_{12}]^-$, the First Alkoxidohydrido Cluster of Molybdenum, Evidence for a Rare, if not the First, Example of a μ_4-Hydride (C) 191
- $[Mo_{57}Fe_6(NO)_6O_{174}(OH)_3(H_2O)_{24}]^{15-}$: A Highly Symmetrical Giant Cluster with an Unusual Cavity and the Possibility of Positioning Paramagnetic Centers on Extremely Large Cluster Surfaces (C) 849
- Novel Conjugation of Hetero(macro)cycles and a Pentamolybdodiphosphonate Cage (C) 451
- Polar Superstructures Stabilized by Polymeric Oxometal Units: Columnar Liquid Crystals Based on Tapered Dioxomolybdenum Complexes (C) 2342
- The First Mononuclear Nitrosyl(oxo)molybdenum Complex: Side-On Bonded and μ_3-Bridging NO Ligands in $[\{MoL(NO)(O)(OH)\}_2]NaPF_6 \cdot H_2O$ (C) 1473

Monolayers
- Phase Transitions in Self-Assembled Monolayers Detected by Electrochemistry (C) 2332
Multiple bonds
- A Stannanediyl with a Tin–Carbon Multiple Bond (C) 456
- (Iminoboryl)borates $[(t\mathrm{Bu}N{\equiv}B)B t\mathrm{Bu}_2R]^-$ from the Azadiboriridine $NB_2t\mathrm{Bu}_3$ (R = Me, Bu) (C) 201
- Multiple Bonds Between Metal Atoms (B) 480

Nanostructures
- Nanostructures Based on Molecular Materials (B) 127
Naphtho[1.8-*bc*]boret
- Synthesis and Reactivity of a Naphtho[1,8-*bc*]boret (C) 1247
Natural products
- A Concise Total Synthesis of (±)-Mamanuthaquinone by Using an *exo*-Diels–Alder Reaction (C) 853
- A Convergent Total Synthesis of Calicheamicin γ_1^I (C) 858
- A Facile One-Pot Synthesis of a Trisaccharide Unit from the Common Polysaccharide Antigen of Group B *Streptococci* Using Cyclohexane-1,2-diacetal (CDA) Protected Rhamnosides (C) 2292
- A Short and Highly Stereoselective Synthesis of the 1,10-*seco*-Eudesmanolide Ivangulin (C) 2195
- Asymmetric Synthesis of Natural Products (B) 1891
- A Total Synthesis of (+)-2′*S*,3′*R*-Zoapatanol (C) 2182
- Biosynthetic Investigations on Pyridazomycin (C) 1648
- Chemistry and Biology of Taxol (R) 15
- Composition of Protocyanin, A Self-Assembled Supramolecular Pigment from the Blue Cornflower, *Centaurea cyanus* (C) 978
- First Total Synthesis of (±)-Rabelomycin (C) 99
- Keronopsins A and B, Chemical Defence Substances of the Marine Ciliate *Pseudokeronopsis rubra* (Protozoa): Identification by Ex Vivo HPLC (C) 1495
- New Total Syntheses of Strychnine (H) 1144
- Novel Optically Active Hydrocarbons in Sediments: Evidence for an Extensive Biological Cyclization of Higher Regular Polyprenols (C) 1166
- Spectroscopic Studies of Anhydroretinol, an Endogenous Mammalian and Insect *retro*-Retinoid (C) 1837 (2348)
- Synthesis of a GPI Anchor of Yeast (*Saccharomyces cerevisiae*) (C) 2177
- Synthesis of C-2 Taxol Analogues (C) 1581
- Synthesis of Cyclotheonamide B and Its Derivatives (C) 1729
- Synthesis of *N*-Glycopeptide Clusters with Lewis^x Antigen Side Chains and Their Coupling to Carrier Proteins (C) 101
- Synthesis of the First Fully Functionalized Core of the Zaragozic Acids/Squalestatins (C) 2187
- The First Total Syntheses of Taxol (H) 959
- The Sialyl Lewis^x Group and its Analogues as Ligands for Selectins: Chemoenzymatic Syntheses and Biological Functions (H) 178
- The Synthesis of Naturally Occurring (−)-Calyculin A (C) 673
- The Total Synthesis of *cis*-7,8-Dihydroxy-11,12-dehydrocalamenene by Regio- and Diastereoselective Alkylation of Chiral η^6-Arenetricarbonylchromium Complexes: An Unexpected Case of Nucleophilic Aromatic *tele*-Substitution with Methoxide as a Leaving Group (C) 109
- Total Synthesis of Soraphen $A_{1\alpha}$ (C) 2466
- Total Synthesis of Zaragozic Acid A/Squalestatin S1 (C) 2190
- Zaragozic Acid A/Squalestatin S1: Synthetic and Retrosynthetic Studies (C) 2184
Near-field microscopy
- Detection and Imaging of Single Molecules by Optical Near-Field Microscopy (H) 1723
- Mapping the Electrostatic Potential of Muscarinic and Nicotinic Agonists with Artificial Neural Networks (C) 643
Neural networks
- Neural Networks for Chemists. An Introduction (B) 1671
Neutron diffraction
- The Spin Density Distribution in the Tetracyanoethylene Radical Anion, $[TCNE]^-$, by Single-Crystal Polarized Neutron Diffraction (C) 1397
Nickel compounds
- Bis(tetramethylbutynediol)nickel(0), the First Pure Monoalkyne Complex of Nickel and Its Chemistry (C) 1373
- $[(CpNi)_2(Cp^*Al)_2]$: Cp*Al as a Bridging Two-Electron Ligand (C) 2482
- Cyclotrimerization of Ethyne on the Complex Fragment $[(\eta^1\text{-}t\mathrm{Bu}_2PCH_2Pt\mathrm{Bu}_2)Ni^0]$ with Formation of an η^6-Benzene–Nickel(0) Complex (C) 879
- Mesoscopic Sheets of a Cyano-Bridged Cu–Ni Coordination Complex: Template Synthesis at the Interlayers of Cast Multibilayer Films (C) 2483
- Synthesis and Characterization of the First Compounds Containing a Stable Phosphirenyl Cation: Crystal and Molecular Structure of $[Ni(\eta^3\text{-}PC_2t\mathrm{Bu}_2)(\eta^5\text{-}P_3C_2t\mathrm{Bu}_2)W(CO)_5]$ (C) 2330
- The Photochemical Activation of Carbon Dioxide Using a Nickel Complex (H) 173
- The Versatility of the Azido Ligand: Linkage of Ni^{II} Centers to Form a Chain with One End-to-End and Three End-On Bridges in Alternation (C) 2087
- Thianickelacycles by Ring-Opening Reactions of Cyclic Thioethers and Their Subsequent Carbonylation to Thioesters (C) 1748
Niobium compounds
- $Rb_3[Nb_6SBr_{17}]$, the First Compound Containing an Isolated Trigonal-Prismatic Niobium Cluster (C) 1943
- Small Molecules Stabilized in Inorganic Frameworks: NbI_5 Monomers in the Novel Layered Compound $Nb_7S_2I_{19}$ (C) 334
Nitrenoids
- [(*N*-Lithio-*N*-mesitylsulfonyloxy-*tert*-butylcarbamate)$_2$ · (thf)$_3$]: Crystal Structure of a Nitrenoid (C) 115
Nitric oxide
- A Clathrate Hydrate of Nitric Oxide (C) 691
- Reductive Disproportionation of NO Mediated by Copper Complexes: Modeling N_2O Generation by Copper Proteins and Heterogeneous Catalysts (C) 895
Nitrile imines
- Nitrile Imines: From Matrix Characterization to Stable Compounds (R) 527
Nitriles
- 1-Oxa-3,5,7,9-tetraazadecapentaene, a Model Oligonitrile with a Helical Structure in the Crystalline State (C) 2337
Nitrogen compounds
- Diastereomerically Pure Mannich Bases from the Addition of Enamines to Ternary Iminium Salts (C) 2422
- Monomeric Tris(imino)metaphosphates (C) 2111
- N-Heteroarene Dianions as Antiaromatic Ligands Bridging two Lanthanocene Moieties (C) 1171
- Polymorphism and C=N–N=C Conformational Isomers of Azines: X-ray Crystal and Ab Initio Structures of Two Rotational Isomers of Methyl (*para*-Tolyl) Ketone Azine (C) 1081
- The Biosynthesis of Nitro Compounds: The Enzymatic Oxidation to Pyrrolnitrin of its Amino-Substituted Precursor (C) 352
- The Structures of Two Lithium Hydrazides: Is There Electron-Deficient Bonding? (C) 1746 (1988)
Nitroxide radicals
- Preparation of Chiral Nitroxide Radicals and Spontaneous Optical Resolution by Recrystallization (C) 878
NMR spectroscopy
- A Dictionary of Concepts in NMR (B) 360
- *Aleuria aurantia* Agglutinin Recognizes Multiple Conformations of α-L-Fuc-(1→6)-β-D-GlcNAc-OMe (C) 88
- A Novel Type of Stereoisomerism in Calix[4]arene-Based Carceplexes (C) 2345
- Determination of the Relative Configuration by Distance Geometry Calculations with Proton–Proton Distances from NOESY Spectra (C) 753
- Difluoromethyl Compounds of Chalcogens: A NMR Study of the Reactions of $Cd(CF_3)_2 \cdot 2MeCN$ and $ZnBr(CF_3) \cdot 2MeCN$ with Dialkyl Chalcogenides and Boron Trifluoride (C) 323
- Effects of $^{35}Cl/^{37}Cl$,^{13}C Residual Dipolar Coupling on the Variable-Temperature ^{13}C CP/MAS NMR Spectra of Solid, Chlorinated Sodium Acetates (C) 1624
- FAST NOESY Experiments—An Approach for Fast Structure Determination (C) 332
- Fundamentals of Nuclear Magnetic Resonance (B) 1670
- In Situ NMR Investigations of Photocatalyzed Hydrogenations with Parahydrogen in the Presence of Metal Carbonyl Compounds of Group 6 (C) 755
- Magnetic Resonance Microscopy (B) 128
- Modern NMR Spectroscopy (B) 1992
- On the Mechanism of the Urocanase Reaction: Confirmation of the Structure of the NAD^+-Inhibitor Adduct by Direct ^{13}C-^{13}C Coupling (C) 1279
- Protein Structure Determination with Three- and Four-Dimensional NMR Spectroscopy (R) 277
- Selective Measurement of the Time-Dependence of Transient Overhauser Effects in Magnetic Resonance: Applications to Oligonucleotides (C) 343
- Unusually Large Isotope Effects on NMR Chemical Shifts of Paramagnetic Organometallic Compounds (C) 2326
- 2D NMR. Density Matrix and Product Operator Treatment (B) 1784
Nobel laureates
- Nobel Laureates in Chemistry, 1901–1992 (B) 2118
Nobel lecture
- An Amazing Distortion in DNA Induced by a Methyltransferase (Nobel Lecture) (R) 1222

- Split Genes and RNA Splicing (Nobel Lecture) (R) 1229
- Synthetic DNA and Biology (R) 1214
- The Polymerase Chain Reaction (Nobel Lecture) (R) 1209

Noble metals
- Homoleptic Noble Metal Carbonyl Cations (H) 1077

Nonacosan-10-ol
- The Effect of Chiral Bilayers: Wax Tubes made of (*S*)-Nonacosan-10-ol (C) 350

Nonlinear optics
- Synthesis and Third-Order Nonlinear Optical Properties of a Conjugated Porphyrin Polymer (C) 655

Norbornanes
- Electrostatic vs. Orbital Control of Facial Selectivities in π Systems: Experimental and Theoretical Study of Electrophilic Additions to 7-Isopropylidenenorbornanes (C) 1390

Norbornenes
- [2+2] Cycloaddition of Norbornenes with Alkynes Catalyzed by Ruthenium Complexes (C) 580

Nucleophilic aromatic *tele*-substitution
- The Total Synthesis of *cis*-7,8-Dihydroxy-11,12-dehydrocalamenene by Regio- and Diastereoselective Alkylation of Chiral η^6-Arenetricarbonylchromium Complexes: An Unexpected Case of Nucleophilic Aromatic *tele*-Substitution with Methoxide as a Leaving Group (C) 109

Nucleophilicity
- Scales of Nucleophilicity and Electrophilicity: A System for Ordering Polar Organic and Organometallic Reactions (R) 938

Nucleophilic substitutions
- A Novel Reaction Sequence for the Coupling of Nucleophiles to Agarose with 2,2,2-Trifluoroethanesulfonyl Chloride (C) 120

Nucleoside analogues
- Regioselective Synthesis and Antiviral Activity of Purine Nucleoside Analogues with Acyclic Substituents at N7 (C) 562

Nucleosides
- A Short Route to [3-^{15}N]-3′-Azido-3′-deoxythymidine (N3-Labeled AZT) via 3-Nitro-AZT (C) 2454
- Biomimetic Phosphonylation and Phosphorylation of Glycoses and Deoxynucleosides (C) 2302
- New Cyclic Derivatives of 3′-Amino-3′-deoxyadenosine-5′-diphosphate, -triphosphate, and -methylenebis(phosphonate) (C) 1394

Nucleotides
- Continuous Enzymatic Synthesis of 2′-Deoxythymidine-5′-(α-D-glucopyranosyl) diphosphate (C) 571

Octaplane
- Octaplane: A Saturated Hydrocarbon with a Remarkably Low Ionization Energy Leading to a Cation with a Planar Tetracoordinate Carbon Atom (C) 1667

Olefinations
- Acid-Catalyzed Olefination of Benzaldehyde (C) 1611

Oligoanthranilamides
- Novel Molecular Scaffolds: Formation of Helical Secondary Structure in a Family of Oligoanthranilamides (C) 446

Oligoarylenes
- 2,2′-Bipyrenyl and *para*-Terpyrenyl—A New Type of Electronically Decoupled Oligoarylene (C) 1957

Oligomers
- Iterative Divergent/Convergent Approach to Linear Conjugated Oligomers by Successive Doubling of the Molecular Length: A Rapid Route to a 128Å-Long Potential Molecular Wire (C) 1360

Oligonitriles
- 1-Oxa-3,5,7,9-tetraazadecapentaene, a Model Oligonitrile with a Helical Structure in the Crystalline State (C) 2337

Oligonucleotides
- Amides as a New Type of Backbone Modification in Oligonucleotides (C) 226
- Fullerene–Oligonucleotide Conjugates: Photo-induced Sequence-Specific DNA Cleavage (C) 2472
- Selective Measurement of the Time-Dependence of Transient Overhauser Effects in Magnetic Resonance: Applications to Oligonucleotides (C) 343
- Stereocontrolled Synthesis of Oligo(nucleoside phosphorothioate)s (R) 709
- Synthesis and Selective Radical Cleavage of C-4′-Modified Oligonucleotides (C) 1861
- Synthesis of an Azathymidine and Its Incorporation into Oligonucleotides (C) 1654
- Synthetic DNA and Biology (R) 1214

Oligosaccharides
- Recombinant Whole Cells as Catalysts for the Enzymatic Synthesis of Oligosaccharides and Glycopeptides (C) 1241

Oligosilanes
- Structures of 2-(Me_2NCH_2)C_6H_4-Substituted Oligosilanes (C) 1854

Oligo(tetrahydrofuran)s
- A Convergent Synthesis of 2,5-*trans*-Linked Oligo(tetrahydrofuran)s: Potential Building Blocks for a Polyether Helix with Ion Channel Activity (C) 1180
- A Multiple Five-Membered-Ring-Selective Williamson Reaction as a Key Step in the Stereoselective Construction of 2,5-Linked Oligo(tetrahydrofuran)s (C) 1873

Olympiadane (C) 1286

Organic chemistry
- Sourcebook of Advanced Organic Laboratory Preparations (B) 231

Organic conductors
- 61,61-Bis(trimethylsilylbutadiynyl)-1,2-dihydro-1,2-methanofullerene[60]: Crystal Structure at 100 K and Electrochemical Conversion to a Conducting Polymer (C) 1628

Organic synthesis
- Biocatalysts in Organic Synthesis (B) 1012
- Solid Supports and Catalysts in Organic Synthesis (B) 587

Organometallic compounds
- Are Polar Organometallic Compounds "Carbanions"? The Gegenion Effect on Structure and Energies of Alkali-Metal Compounds (R) 1129

Organometallic magnetic materials
- Organic and Organometallic Magnetic Materials—Designer Magnets (R) 385

Osmium compounds
- A Triosmium Cluster Complex with a Carbene Ligand in an Unusual Coordination Mode (C) 1093
- Hydroxylamine, Hydrazine, and Diazene as Unidentate Ligands in Osmium and Ruthenium Complexes (C) 657

Oxalate
- Human Oxalate—Really Just an End-Product of Metabolism? (C) 1780

Oxathietanes
- Synthesis, Structure, and Thermolysis of a Tetracoordinate 1,2λ^4-Oxathietane (C) 2094

Oxenoids
- The Oxenoid Character of Metalated Hydroperoxides O(M)OR: Oxidation of Organometallic Compounds R′M′ to R′OH under Mild Conditions (C) 1161

Oxidations
- Catalytic Pt^+-Mediated Oxidation of Methane by Molecular Oxygen in the Gas Phase (C) 1174
- Homogeneous Catalytic Oxidation of Arenes and a New Synthesis of Vitamin K_3 (C) 2475
- *trans*–*cis* Isomerization upon One-Electron Oxidation of [12]- and [14]Tetrathiafulvalenophanes (C) 1379
- Novel Bimetallic Model System for Cytochrome P_{450}: Effect of Membrane Environment on the Catalytic Oxidation (C) 2468
- Optically Active Lactones from a Baeyer–Villiger-Type Metal-Catalyzed Oxidation with Molecular Oxygen (C) 1848
- Oxidation of Metal-Coordinated Thioethers with Dimethyldioxirane—A New Stereoselective Synthesis of Chiral Sulfoxides (C) 1609
- Oxidation of Weakly Activated C–H Bonds (H) 69
- Oxygen Evolution by Oxidation of Water with Manganese Porphyrin Dimers (C) 1839
- Oxygen-Induced Structural Transformation of the Polynuclear Organoaluminum Complex [$Al_4(\mu_3$-8-quinolylimide$)_2$ $(CH_3)_8$] to [$Al_4(\mu_3$-8-quinolylimide$)_2$ $(CH_3)_7(\mu$-$OCH_3)$] (C) 1265
- The Oxenoid Character of Metalated Hydroperoxides O(M)OR: Oxidation of Organometallic Compounds R′M′ to R′OH under Mild Conditions (C) 1161
- Wacker Oxidation of 1-Decene to 2-Decanone in the Presence of a Chemically Modified Cyclodextrin System: A Happy Union of Host–Guest Chemistry and Homogeneous Catalysis (C) 2100
- X-Ray Structure Analysis of the Methane Monooxygenase: An Important Step toward Understanding the Oxidation of Methane in Biological Systems (H) 841

Oxygen activation
- Schiff Base Complexes with Five-Coordinate Cobalt as Dioxygen Activating Sites in Zeolites (C) 431

Oxygenations
- Regio- and Diastereoselective Photooxygenation of Chiral 2,5-Cyclohexadiene-1-carboxylic Acids (C) 1971

Ozone
- Ozone Formation through Decomposition of CFCs in the Stratosphere (C) 1108

Pagodanes
- From an Insecticide to Plato's Universe—The Pagodane Route to Dodecahedranes: New Pathways and New Perspectives (R) 2239
- Isopagodanes—Precursors of Unusual Cage Ions (C) 117

Palladium compounds
- Palladacycles as Intermediates for Selective Dialkylation of Arenes and Subsequent Fragmentation (C) 2421
- [$(Ph_3PAu)_6$(dppeAu_2)$(AuCl)_4Pd$], an Icosahedral Au_{12} Cluster with a Central Pd Atom (C) 207
- Synthesis of Oxa- and Azapalladacycles from Organostannanes (C) 2482
- The Reactivity of Phosphacymantrenes towards Palladium(II) and Palladium(0) Compounds: Synthesis, Structure, and Chemistry of Pd_2Mn_2 and Pd_3Mn_4 Arrays (C) 742

Parahydrogen
- In Situ NMR Investigations of Photocatalyzed Hydrogenations with Parahydrogen in the Presence of Metal Carbonyl Compounds of Group 6 (C) 755
Pentalenes
- Octahydro-1,2,3:4,5,6-dimethenopentalene-2-carbonitrile, the First Derivative of a Yet-Unknown $(CH)_{10}$ Hydrocarbon (C) 1639
Pentamethylbismuth
- Blue-Violet Pentamethylbismuth (H) 1726
Peptide hormones
- Peptide and Protein Hormones. Structure, Regulation, Activity. A Reference Manual (B) 1117
Peptide mimetics
- A New Application of Modified Peptides and Peptidomimetics: Potential Anticancer Agents (H) 305
- A Novel Route to Diastereomerically Pure (*E*)-Alkene Dipeptide Isosteres from β-Aziridinyl-α,β-enoates by Treatment with Organocopper Reagents (C) 652
- A Sugar Amino Acid as a Novel Peptidomimetic (C) 687
- Peptidomimetics–Tailored Enzyme Inhibitors (R) 1699
- Preparation and C-Alkylation of Peptides with Aminomalonate Building Blocks (C) 439
- Synthesis of Sulfonamido-Pseudopeptides: New Chiral Unnatural Oligomers (C) 2067
Peptides
- Conformational Requirements for Sweet-Tasting Peptides and Peptidomimetics (R) 1437
- Enzymatic Grooming of Organic Thin Films (C) 871
- Expeditious Synthesis of a Novel C_3-Symmetric Receptor that Binds Peptides Sequence-Selectively (C) 2458
- Life During a Golden Age of Peptide Chemistry: The Concept and Development of Solid-Phase Peptide Synthesis (B) 1990
- Metal Complexes of Marine Peptide Metabolites: A Novel Ag_4 Cluster (C) 1516
- Synthesis, Crystal and Molecular Structure of Boc-Pro-ΔPhe-Ala-ΔPhe-Ala-OMe; A Pentapeptide with a Novel β-Bend Ribbon Structure (C) 970
- Synthesis of a New Unnatural Amino Acid with a Benzodiazepine-Containing Side Chain and Incorporation into a Tripeptide (C) 1737
Pericyclic rearrangements
- The Pressure Effect in Pericyclic Rearrangements: the Cope Rearrangement, Electrocyclization, and the Intramolecular Diels–Alder Reaction (C) 1079
Peroxides
- Jacobson and Heintschel Peroxides (C) 775
Phanes
- New Types of Metal-Stabilized Cyclobutadiene Superphanes (C) 1272
Phase transfer catalysis
- Phase Transfer Catalysis (B) 1669
- Phase Transfer Catalysis. Selected Problems and Applications (B) 1669
Phase transitions
- Phase Transitions in Self-Assembled Monolayers Detected by Electrochemistry (C) 2332
Phenothiazin
- Phenothiazinyl-Substituted Cyanines: Model Compounds for Molecular Switches (C) 572
Phenylalkyne oligomers
- Iterative Divergent/Convergent Approach to Linear Conjugated Oligomers by Successive Doubling of the Molecular Length: A Rapid Route to a 128Å-Long Potential Molecular Wire (C) 1360
Pheromones
- Chemical Communication. The Language of Pheromones (B) 236
Phosgene
- A Kinetic Study of the Hydrolysis of Phosgene in Aqueous Solution by Pulse Radiolysis (C) 1259
Phosphaalkynes
- A Novel Hexamer of tBuC≡P: Synthesis, Structure, and Theoretical Studies (C) 2202
- Novel Trimerization of Phosphaalkynes in the Coordination Sphere of Ruthenium Complexes (C) 463
- Reactivity of a Phosphanylcarbene (λ^5-Phosphaacetylene) with Lewis Acids: X-Ray Crystal Structures of the First Carbene–Gallane Complex and *C*-Gallyl-Substituted Phosphorus Ylide (C) 578
- The First Carbon–Phosphorus–Aluminum Cage Compounds: Cyclooligomerization of Phosphaalkynes with Trialkylaluminum Compounds (C) 1491
Phosphacymantrenes
- The Reactivity of Phosphacymantrenes towards Palladium(II) and Palladium(0) Compounds: Synthesis, Structure, and Chemistry of Pd_2Mn_2 and Pd_3Mn_4 Arrays (C) 742
Phospholes
- Toward Polyphospholes: Synthesis and Structure of an α-Linked Quaterphosphole (C) 1158
Phosphonates
- Preparation and Preliminary Characterization of a Covalently Pillared Zirconium Phosphate–Diphosphonate with Interlayer Microporosity (C) 1594
Phosphorothioates
- Stereocontrolled Synthesis of Oligo(nucleoside phosphorothioate)s (R) 709
Phosphorus compounds
- A Cluster-Bound Triply-Bridging Phosphorus Atom Coordinated to Four $(Ph_3P)Au^+$ Units: $[Fe_3(CO)_9P\{Au(PPh_3)\}_4][BAr_4]$ (C) 75
- A General Synthetic Strategy for Neutral Phosphorus-Containing Dendrimers (C) 1589
- Borophosphates–A Neglected Class of Compounds: Crystal Structures of $Mn^{II}[BPO_5]$ (M^{II} = Ca, Sr) and $Ba_3[BP_3O_{12}]$ (C) 749
- $(t\text{BuSi})_2(PC_6H_{11})_3$: A Propellane-Like Cyclosilaphosphane with Remarkable Structure (C) 1484
- Diastereoselective Reaction of a 1-Phosphaallyl Anion with an Alkyne: Structure of an Isolated Dihydrophospholyl Anion and Stereospecific Protonation to Give 2,3-Dihydrophosphole (C) 1953
- First Resolution of a Free Fluorophosphane Chiral at Phosphorus (C) 1835
- Monomeric Tris(imino)metaphosphates (C) 2111
- Phosphane Coordination to Magnesium: Synthesis and Structure of Bis[*ortho*, *ortho*'-bis{(dimethylphosphino)methyl}phenyl]magnesium (C) 2281
- Phosphindolyl Anions by Elimination from 1-Phosphoallyllithium Complexes—η^5 and η^3 Coordination of a Phospholyl Fragment (C) 353
- Structure of a Mixed Phosphate/Phosphonate Layered Zirconium Compound from Synchrotron X-Ray Powder Diffraction Data (C) 2324
- Synthesis and Characterization of the First Compounds Containing a Stable Phosphirenyl Cation: Crystal and Molecular Structure of $[Ni(\eta^3\text{-}PC_2t\text{Bu}_2)(\eta^5\text{-}P_3C_2t\text{Bu}_2)W(CO)_5]$ (C) 2330
- Synthesis and Crystal Structure of the First Tetraaminophosphonium Salt $P(NH_2)_4I$ (C) 785
- Synthesis and Structure of the First Hybrid Borazine–Phosphazene Ring (C) 2277
- Synthesis of the First Microporous Aluminum Phosphonate with Organic Groups Covalently Bonded to the Skeleton (C) 2335
- Synthesis of the First 2*H*-1-Aza-2-phosphirene Complexes (C) 80
- Tetralithiated Dibenzyl(methyl)phosphane (C) 2279
- The First Carbon–Phosphorus–Aluminum Cage Compounds: Cyclooligomerization of Phosphaalkynes with Trialkylaluminum Compounds (C) 1491
- The Influence of Charge Distribution on Bond Lengths in the P_4O_6 Framework in Compounds of the Type P_4O_6X (C) 563
Phosphorus ylides
- 3-Phosphonio-1,2-diphosphaindenides and the Electrophilic Substitution of *C*-Phenyl-Substituted Ylides (C) 663
- Reactions of an Iminophosphoranylidene Carbenoid (C) 982
- Reactions of C_3O_2 with Stabilized Triphenylphosphoranes $Ph_3P{=}CHX$ (X = CN, COMe, COPh) (C) 576
Phosphorylations
- Biomimetic Phosphonylation and Phosphorylation of Glycoses and Deoxynucleosides (C) 2302
Photoacoustic calorimetry
- Time-Resolved Photoacoustic Calorimetry: From Carbenes to Proteins (R) 294
Photochemistry
- A Novel Photosystem for Harvesting Visible Light to Drive Photoinduced Electron Transfer (PET) Reductions: β-Activation of α,β-Unsaturated Ketones for Radical Cyclizations (C) 1169
- Antenna Effect in Multichromophoric Cyclodextrins (C) 2438
- Charge Transfer Photochemistry of Coordination Compounds (B) 483
- Chlorine Trioxide: Spectroscopic Properties, Molecular Structure, and Photochemical Behavior (C) 1482
- Effects of Metal-Ion Dopants on the Photocatalytic Reactivity of Quantum-Sized TiO_2 Particles (C) 1091
- Increased Selectivity of a Simple Photosensitive Probe in the Presence of Large Proportions of Cholesterol (C) 1176
- Intramolecular [2+2] Cycloadditions of 2,2'-Bis(1-arylvinyl)-Substituted Biphenyls Induced by Photo Electron Transfer (C) 2300
- Intramolecular Photocyclization of ω,ω-Diphenyl-(ω−1)-alken-1-ols by an Exciplex Quenching Mechanism (C) 2113
- Organic Photochemistry: A Visual Approach (B) 483
- Organic Photochemistry. Principles and Applications (B) 1990
- Photodecomposition of 10-Diazo-2-hexadecylanthrone on Graphite Studied by Scanning Tunneling Microscopy (C) 2080
- Photodissociation Dynamics (B) 1011
- Photoisomerization of Highly Alkylated Butadienes (C) 204

- Recycling in the Earth's Atmosphere: The OH Radical—Its Importance for the Chemistry of the Atmosphere and the Determination of Its Concentration (R) 1816
- Regio- and Diastereoselective Photooxygenation of Chiral 2,5-Cyclohexadiene-1-carboxylic Acids (C) 1971
- Stereoselective Intramolecular Alkylation of Glycosylimides to Highly Functionalized Bicyclic 2,5-Azepanediones and Heterotricyclic [5.3.1.$0^{2,6}$] Undecanamides (C) 1979
- The Photochemical Activation of Carbon Dioxide Using a Nickel Complex (H) 173
- The Photochemical Synthesis of Fine Chemicals with Sunlight (R) 2009

Photooxidations
- Magnetic Spin Effects on Photooxidation Quantum Yields of Ru^{II}-tris(bipyridine) Type Complexes in Magnetic Fields up to 17.5 Tesla (C) 1772

Photosynthesis
- A Structural Model for the Water-Oxidizing Manganese Cluster in Photosystem II (H) 725
- Biomimetic Model for a Photosynthetic Reaction Center: A Porphyrin with a Covalently Linked, Redox-Active Crown Ether (C) 2318

Phthalocyanines
- Construction of a Multiwired Molecular Cable of Micrometer Length by a Self-Assembly Process (C) 2173
- Phthalocyanines. Properties and Applications. Vol. 2 (B) 236

Physical chemistry
- Comprehensive Dictionary of Physical Chemistry (B) 1785
- Determination of Thermodynamic Properties (B) 586
- Kinetic Theory and Irreversible Thermodynamics (B) 481

Pinacol coupling
- Vanadium(II)- and Niobium(III)-Induced, Diastereoselective Pinacol Coupling of Peptide Aldehydes to C_2-Symmetrical HIV-Protease Inhibitors (C) 685

Platinum compounds
- $[Cp_2Ti(C\equiv CtBu)_2]$ as an Alkynyl Transfer Reagent: Synthesis and Characterization of the Asymmetrically Bridged Heterodimetallic Complex $[Cp_2Ti(C\equiv CtBu)_2Pt(PPh_3)]\cdot 0.5\,THF$ (C) 2083
- An Easy Route to Homo- and Heteroleptic Biscycloplatinated Complexes without Recourse to Organolithium Compounds (C) 783
- An Unusual Route to Potential Platinum Antitumor Compounds: Synthesis, Reactivity, and Spectroscopic Properties of the Pt^{IV} Complex *fac*-$[PtCl_3(NH_3)_2L]Cl$ (C) 1632
- High-Pressure Synthesis of K_2PtH_6, a Saltlike Hydride with the K_2PtCl_6 Structure (C) 1112
- Organoplatinum Dendrimers Formed by Oxidative Addition (C) 847
- Platinum(II) Complexes with Porphyrin Ligands—Additive Cytotoxic and Photodynamic Effect (C) 2214
- Platinum-Iron Silylene Complexes and Metal-Promoted Substituent Exchange between $Si(NMe_2)_3$- and $P(OEt)_3$-Ligands (C) 2440
- Structure of an Antineoplastic Platinum Complex with a Bipyridyl-Crown Ether (C) 186

Polyacrylic acid
- Synthesis of Very Highly Ordered Liquid Crystalline Phases by Complex Formation of Polyacrylic Acid with Cationic Surfactants (C) 1869

Polycycles
- Octahydro-1,2,3:4,5,6-dimethenopentalene-2-carbonitrile, the First Derivative of a Yet-Unknown $(CH)_{10}$ Hydrocarbon (C) 1639
- Synthesis of Centrohexacyclic Hydrocarbons by the Propellane Route: Centrohexaindan and Tribenzocentrohexaquinane (C) 1251

Polyenes
- 1,1-Di-, 1,2,3-Tri-, and 1,1,4,4-Tetra-*tert*-butyl-1,3-butadiene (C) 1369
- Keronopsins A and B, Chemical Defence Substances of the Marine Ciliate *Pseudokeronopsis rubra* (Protozoa): Identification by Ex Vivo HPLC (C) 1495

Polyethers
- A Convergent Synthesis of 2,5-*trans*-Linked Oligo(tetrahydrofuran)s: Potential Building Blocks for a Polyether Helix with Ion Channel Activity (C) 1180
- A Multiple Five-Membered-Ring-Selective Williamson Reaction as a Key Step in the Stereoselective Construction of 2,5-Linked Oligo(tetrahydrofuran)s (C) 1873

Polymerase chain reaction
- The Polymerase Chain Reaction (Nobel Lecture) (R) 1209

Polymerization
- Monomer–Dimer Equilibria in Homo- and Heterodinuclear Cationic Alkylzirconium Complexes and Their Role in Polymerization Catalysis (C) 1634
- Synthesis and Ring-Opening Polymerization of Highly Strained Ring-Tilted [2]Ruthenocenophanes (C) 989

Polymers
- Ladder Polymers and Oligomers Based on Hemiporphyrazine (C) 1646
- Liquid Crystal Polymers (B) 1013
- Synthesis and Third-Order Nonlinear Optical Properties of a Conjugated Porphyrin Polymer (C) 655
- Synthesis of a Fully Unsaturated "Molecular Board" (C) 2209

Polyoxometalates
- Coexistence of Mobile and Localized Electrons in Bis(ethylene)dithiotetrathiafulvalene (BEDT-TTF) Radical Salts with Paramagnetic Polyoxometalates: Synthesis and Physical Properties of $(BEDT\text{-}TTF)_8[CoW_{12}O_{40}]\cdot 5.5H_2O$ (C) 223
- $(H_3N(CH_2)_6NH_3)_4[W_{18}P_2O_{62}]\cdot 3H_2O$, a Microporous Solid from Dawson Anions and 1,6-Diaminohexane (C) 2491
- $[Mo_{57}Fe_6(NO)_6O_{174}(OH)_3(H_2O)_{24}]^{15-}$: A Highly Symmetrical Giant Cluster with an Unusual Cavity and the Possibility of Positioning Paramagnetic Centers on Extremely Large Cluster Surfaces (C) 849
- Novel Conjugation of Hetero(macro)cycles and a Pentamolybdodiphosphonate Cage (C) 451
- Synthesis and Structure of Oxovanadium(v)-Organophosphonate Cluster Encapsulating a Chloride Ion: $[ClV_7O_{12}(O_3PC_6H_5)_6]^{2-}$ (C) 325
- The Oxovanadium–Organoarsonate System: $[2\,CH_3OH \subset V_{12}O_{14}(OH)_4(PhAsO_3)_{10}]^{4-}$ and $[2\,H_2O \subset V_{12}O_{12}(OH)_2(H_2O)_2(PhAsO_3)_{10}(PhAsO_3H)_4]^{2-}$, Clusters with Nanometer Dimensions and Cavities for Neutral Molecules (C) 760
- The Oxovanadium–Organophosphonate System: Complex Cluster Structures $[(VO)_6(tBuPO_3)_8Cl]$, $[(VO)_4\{PhP(O)_2OP(O)_2Ph\}_4Cl]^-$, and $[V_{18}O_{25}(H_2O)_2(PhPO_3)_{20}Cl_4]^{4-}$ with Encapsulated Chloride Anions Prepared from Simple Precursors (C) 757

Polythioethers
- Strategies for Nonmacrocyclic Polythioether Ligands: New Pentacoordinating Architectures (C) 319

Polyynes
- Hexaspiro[2.4.2.4.2.4.2.4.2.4.2.4]dotetraconta-4,6,11,13,18,20,25,27,32,34,39,41-dodecayne—An Exploding [6]Rotane (C) 869
- Polyynes—Fascinating Monomers for the Construction of Carbon Networks? (H) 1073
- Stable Soluble Conjugated Carbon Rods with a Persilylethynylated Polytriacetylene Backbone (C) 763

Porphycenes
- μ-Oxodiiron(III) Complexes of Porphycenes (C) 736

Porphyrazines
- Ladder Polymers and Oligomers Based on Hemiporphyrazine (C) 1646

Porphyrinoids
- Benziporphyrin, a Benzene-Containing, Nonaromatic Porphyrin Analogue (C) 1246
- Biomimetic Model for a Photosynthetic Reaction Center: A Porphyrin with a Covalently Linked, Redox-Active Crown Ether (C) 2318
- Chiroporphyrins: An Approach to Asymmetric Catalysts with Stereocenters Near the Plane of the Porphyrin Ring (C) 220
- Conformational Effects on the Redox Potentials of Tetraarylporphyrins Halogenated in the β-Pyrrole-Positions (C) 348
- Corrphycene: A New Porphyrin Isomer (C) 2308
- Crystal Structure of a Supramolecular Dimer Formed by π–π Interactions between Two Interlocked Cyclic Zinc Porphyrin Trimers (C) 429
- Dendritic Porphyrins: Modulating Redox Potentials of Electroactive Chromophores with Pendant Multifunctionality (C) 1739
- Enzyme Mimics (H) 551
- Facile Reduction of a Dialkyl Zirconium(IV) Octaethylporphyrin (OEP) Complex by H_2: Crystal Structure and Spectroscopic Characterization of $[(OEP)Zr\text{-}CH_2SiMe_3]$ (C) 95
- Free Acid Porphyrin and Its Conjugated Monoanion (C) 2215
- "Free" $[Fe(tpp)]^+$ Cation: A New Concept in the Search for the Least Coordinating Anion (C) 2433
- Metallocorroles with Formally Tetravalent Iron (C) 731
- Molecular Catalysts for Multielectron Redox Reactions of Small Molecules: The "Cofacial Metallodiporphyrin" Approach (R) 1537
- New Porphyrin Isomers (H) 1348
- New Porphyrinoid Macrocycles Containing Pyridine (C) 219
- μ-Oxodiiron(III) Complexes of Porphycenes (C) 736
- Platinum(II) Complexes with Porphyrin Ligands—Additive Cytotoxic and Photodynamic Effect (C) 2214
- Porphyrin–Quinone Cyclophanes with Gradually Varied Donor–Acceptor Distances (C) 2428
- Porphyrins with Biconcave Frameworks (C) 889
- Self-Assembly of a Dimeric Porphyrin Host (C) 2313

- Sterically Strained Porphyrins—Influence of Core Protonation and Peripheral Substitution on the Conformation of Tetra-*meso*-, Octa-β-, and Dodeca-Substituted Porphyrin Dications (C) 2485
- Synthesis and Properties of a Vertically Stacked Porphyrin(1)-Porphyrin(2)-Quinone Cyclophane (C) 1466
- Synthesis and Properties of a Vertically Stacked Porphyrin-Quinone(1)-Quinone(2) Cyclophane (C) 1463
- Synthesis and Third-Order Nonlinear Optical Properties of a Conjugated Porphyrin Polymer (C) 655
- 5,10,15,20-Tetra-*tert*-butylporphyrin and Its Remarkable Reactivity in the 5- and 15-Positions (C) 1879
- Tetraoxa[22]porphyrin(2.2.2.2) Dication and Tetraoxa[24]porphyrinogens(2.2.2.2) (C) 1151
- Tetra-*p*-tolylporphyrin with an Inverted Pyrrole Ring: A Novel Isomer of Porphyrin (C) 779
- Turcasarin, the Largest Expanded Porphyrin to Date (C) 1509

Propellanes
- Synthesis of Centrohexacyclic Hydrocarbons by the Propellane Route: Centrohexaindan and Tribenzocentrohexaquinane (C) 1251

Prostacyclin
- Prostacyclin and Thromboxane Synthase: New Aspects of Hemethiolate Catalysis (R) 1911

Protecting groups
- A Facile One-Pot Synthesis of a Trisaccharide Unit from the Common Polysaccharide Antigen of Group B *Streptococci* Using Cyclohexane-1,2-diacetal (CDA) Protected Rhamnosides (C) 2292
- Cyclohexane-1,2-diacetals (CDA): A New Protecting Group for Vicinal Diols in Carbohydrates (C) 2290
- The Selective Blocking of *trans*-Diequatorial, Vicinal Diols; Applications in the Synthesis of Chiral Building Blocks and Complex Sugars (H) 2272

Proteins
- Peptidyl-Prolyl *cis/trans* Isomerases and Their Effectors (R) 1415
- Protein Structure Determination with Three- and Four-Dimensional NMR Spectroscopy (R) 277

Protocyanin
- Composition of Protocyanin, A Self-Assembled Supramolecular Pigment from the Blue Cornflower, *Centaurea cyanus* (C) 978

Protonations
- Catalytic Enantioselective Protonation of Enolates (C) 1888
- Diastereoselective Reaction of a 1-Phosphaallyl Anion with an Alkyne: Structure of an Isolated Dihydrophospholyl Anion and Stereospecific Protonation to Give 2,3-Dihydrophosphole (C) 1953
- Enantioselective Protonation of Simple Enolates: Chiral Imide as a Chiral Proton Source (C) 107
- Substituent Effects and Complexation Phenomena in the Diastereoselective Protonation of Chiral Enolates (C) 1764

Proton transfer
- Proton-Transfer-Dependent Reversible Phase Changes in the 4,4'-Bipyridinium Salt of Squaric Acid (C) 181

Purple acid phosphatases
- A Mixed-Valent, Unsymmetrical Fe^{II}-Fe^{III} Complex with a Terminal Phenola to Ligand as a Model for the Active Site of Purple Acid Phosphatases (C) 887

Pyranoses
- Enol Triflate Pyranoses, Versatile Reagents for the Formation of Conjugated Systems on Pyranoses (C) 1499

Pyridazomycin
- Biosynthetic Investigations on Pyridazomycin (C) 1648

Pyrrolidines
- A New Synthesis of 1,3,4-Trideoxy-1,4-iminoglycitols of Varying Chain Length by $(C_3 + C_n)$-Coupling of Allyl Halides with Glyconontrile Oxides (C) 1295
- Asymmetric Synthesis of Highly Substituted Pyrrolidines by 1,3-Dipolar Cycloadditions of Azomethine Ylides with *N*-Acryloylproline Benzyl Ester (C) 683
- Remarkable Stereoselectivity in the Inhibition of α-Galactosidase from Coffee Bean by a New Polyhydroxypyrrolidine Inhibitor (C) 1242

Pyrrolnitrin
- The Biosynthesis of Nitro Compounds: The Enzymatic Oxidation to Pyrrolnitrin of its Amino-Substituted Precursor (C) 352

Quinodimethanes
- Buckminsterfullerene Adducts from *Ortho*-Quinodimethanes (C) 559

Quinones
- Enediyne Quinone Imines: Truncated, Biologically Active Dynemicin Congeners (C) 2477
- Porphyrin–Quinone Cyclophanes with Gradually Varied Donor–Acceptor Distances (C) 2428
- Synthesis and Properties of a Vertically Stacked Porphyrin(1)-Porphyrin(2)-Quinone Cyclophane (C) 1466
- Synthesis and Properties of a Vertically Stacked Porphyrin-Quinone(1)-Quinone(2) Cyclophane (C) 1463

Rabelomycin
- First Total Synthesis of (±)-Rabelomycin (C) 99

Radialenes
- Efficient Synthesis of Heteroradialenes by SN' Reaction (C) 1270
- Expanded Radialenes: A Novel Class of Cross-Conjugated Macrocycles (C) 468

Radical anions
- Purely Organic Mixed-Valence Molecules with Nanometric Dimensions Showing Long-Range Electron Transfer: Synthesis, and Optical and EPR Studies of a Radical Anion Derived from a Bis(triarylmethyl)Diradical (C) 2106
- The Spin Density Distribution in the Tetracyanoethylene Radical Anion, $[TCNE]^{\cdot -}$, by Single-Crystal Polarized Neutron Diffraction (C) 1397

Radical cations
- The First Spectroscopic Identification of an Enol Radical Cation in Solution: The Anisyldimesitylethenol Radical Cation (C) 1961

Radical ions
- Molecular Distortion in Reactive Chemical Intermediates (H) 962

Radicals
- A Kinetic Study of the Hydrolysis of Phosgene in Aqueous Solution by Pulse Radiolysis (C) 1259
- Calixarene-Based Macrocyclic Nonet ($S = 4$) Octaradical and its Acyclic Sextet ($S = 5/2$) Pentaradical Analogue (C) 2091
- Combination of Superexchange and Spin-Polarization Mechanisms Leads to a Novel Hydrocarbon Tetraradical with a High-Spin Ground State (C) 1104
- Determination of the Kinetics of Vinyl Radical Reactions by the Characteristic Visible Absorption Spectra of Vinylperoxyl Radicals (C) 1262
- Half a Century of Free Radical Chemistry (B) 1009
- Preparation of Chiral Nitroxide Radicals and Spontaneous Optical Resolution by Recrystallization (C) 878
- Prostacyclin and Thromboxane Synthase: New Aspects of Hemethiolate Catalysis (R) 1911
- Recycling in the Earth's Atmosphere: The OH Radical—Its Importance for the Chemistry of the Atmosphere and the Determination of Its Concentration (R) 1816
- Samarium Iodide Induced Intramolecular C-Glycoside Formation: Efficient Radical Formation in the Absence of an Additive (C) 1383
- Stereoselective Reactions of Sulfinylated Benzyl Radicals: Effects of Solvents and Lewis Acids (C) 1601
- Synthesis and Selective Radical Cleavage of C-4'-Modified Oligonucleotides (C) 1861
- The $S_{RN}2$ Pathway—A Mechanistic Alternative for Radicals in Polar Media? (C) 1985

Radiochemistry
- Handbook of Hot Atom Chemistry (B) 1198

Radiopharmaceuticals
- Technetium Radiopharmaceuticals—Fundamentals, Synthesis, Structure, and Development (R) 2258

Raman spectroscopy
- Fourier Transform Raman Spectroscopy. Instrumentation and Chemical Applications (B) 361
- Thermal Decomposition of Silver Oxide Monitored by Raman Spectroscopy: From AgO Units to Oxygen Atoms Chemisorbed on the Silver Surface (C) 85

Reaction mechanisms
- A Kinetic Study of the Hydrolysis of Phosgene in Aqueous Solution by Pulse Radiolysis (C) 1259
- An Extraordinarily Violent Molecular Dissociation: The Unprecedented Kinetic Energy Release in the Decomposition of $HONF^+$, a Singly Charged Metastable Ion (C) 123
- α-Aryliodonio Diazo Compounds: S_N Reactions at the α-C Atom as a Novel Reaction Type for Diazo Compounds (C) 1952
- Determination of Reaction Paths for Pentacoordinate Metal Complexes with the Structure Correlation Method (R) 823
- Determination of the Kinetics of Vinyl Radical Reactions by the Characteristic Visible Absorption Spectra of Vinylperoxyl Radicals (C) 1262
- Electrostatic vs. Orbital Control of Facial Selectivities in π Systems: Experimental and Theoretical Study of Electrophilic Additions to 7-Isopropylidenenorbornanes (C) 1390
- Free-Energy Relationship for Mesolytic Cleavage of C–C Bonds (C) 73
- Magnetic Properties of Aromatic Transition States: The Diels–Alder Reactions (C) 1376
- Nonreactive Interactions between Ethene and Halogens: Detection of a π-Donor Complex $C_2H_4 \cdots BrCl$ by Rotational Spectroscopy (C) 1512
- On the Mechanism of the Urocanase Reaction: Confirmation of the Structure of the NAD^+-Inhibitor Adduct by Direct ^{13}C-^{13}C Coupling (C) 1279

- Organizing Principle of Complex Reactions and Theory of Coarctate Transition States (R) 255
- Scales of Nucleophilicity and Electrophilicity: A System for Ordering Polar Organic and Organometallic Reactions (R) 938
- The $S_{RN}2$ Pathway—A Mechanistic Alternative for Radicals in Polar Media? (C) 1985

Reagents
- A Reagent for Determining Optical Purities of Diols by Formation of Diastereomeric Arylboronate Esters (C) 1182
- A Regioselective Palladium-Catalyzed Reduction of 3,3-Heterobimetalated Allylic Acetates–Synthesis and Reactivity of Allylic Bimetallic Compounds (C) 2448
- Enantiosclective Transformations and Racemization Studies of Heteroatom Substituted Organolithium Compounds (H) 175
- Enol Triflate Pyranoses, Versatile Reagents for the Formation of Conjugated Systems on Pyranoses (C) 1499
- O-Glycoside Syntheses under Neutral Conditions in Concentrated Solutions of $LiClO_4$ in Organic Solvents (C) 1944
- On the Nature of Zinc Chloride–Aldehyde Interactions (C) 2089
- Reactions in Supercritical Carbon Dioxide (H) 1452
- Sulphones in Organic Synthesis (B) 1404
- Supported Reagents. Preparation, Analysis and Applications (B) 239
- Synthesis and Properties of 2,4,6-Trimethylphenylborane (Mesitylborane), a Stable Alternative to Thexylborane (C) 851

Rearrangements
- An Antibody-Catalyzed 1,2-Rearrangement of Carbon–Carbon Bonds (C) 1607
- [2,3] Sigmatropic Wittig Rearrangement of Chiral Allyloxyacetaldehyde Hydrazones in the Diastereo- and Enantioselective Synthesis of Protected, γ,δ-Unsaturated α-Hydroxyaldehydes and Cyanohydrins (C) 2098
- Nitrile Imines: From Matrix Characterization to Stable Compounds (R) 527
- Synthesis of Unsaturated Amino Acids by [3,3]-Sigmatropic Rearrangement of Chelate-Bridged Glycine Ester Enolates (C) 998

Receptors
- Expeditious Synthesis of a Novel C_3-Symmetric Receptor that Binds Peptides Sequence-Selectively (C) 2458
- Mapping the Electrostatic Potential of Muscarinic and Nicotinic Agonists with Artificial Neural Networks (C) 643

Redox reactions
- Molecular Catalysts for Multielectron Redox Reactions of Small Molecules: The "Cofacial Metallodiporphyrin" Approach (R) 1537

Redox systems
- Dendritic Porphyrins: Modulating Redox Potentials of Electroactive Chromophores with Pendant Multifunctionality (C) 1739
- Redox Control for the Recognition of Ag^+ Ions in a Macrocycle Containing Two SH Groups or an S–S Bridge inside the Cavity (C) 1750

Reductions
- A Regioselective Palladium-Catalyzed Reduction of 3,3-Heterobimetalated Allylic Acetates–Synthesis and Reactivity of Allylic Bimetallic Compounds (C) 2448
- Enantioselective Reactions in a Static Magnetic Field (C) 454 (1461)
- Facile Reduction of a Dialkyl Zirconium(IV) Octaethylporphyrin (OEP) Complex by H_2: Crystal Structure and Spectroscopic Characterization of [(OEP)Zr-CH_2SiMe_3] (C) 95
- Novel Copper Nitrosyl Complexes: Contributions to the Understanding of Dissimilatory, Copper-Containing Nitrite Reductases (H) 2057
- Reductive Disproportionation of NO Mediated by Copper Complexes: Modeling N_2O Generation by Copper Proteins and Heterogeneous Catalysts (C) 895
- Supramolecular Activation of *para*-Benzoquinone (C) 2489

Rhenium compounds
- A Building Principle of Amorphous Chalcogenides of Transition Metals: The "Extrusion" of the Electron Rich Cluster $[Re_4S_2(SO_2)_4(CN)_{10}]^{8-}$ from a-Re_2S_7 (C) 770
- Direct Metal–Metal Bonds Between High and Low Valent Complex Fragments: The Reaction of Metal Bases with the Metal Acids $[Re(NR)_3]^+$ and $[Mo(NR)_2]^{2+}$ (C) 678
- Reactions at Both Ends of a Dimetalated Olefin: CS_2 Insertion into and Atom Transfer Reactions of $[Re(CO)_4\{trans\text{-}\mu\text{-}HC{=}C(CO_2Me)\}Re(CO)_4(NCMe)]$ (C) 568
- $[Re_2I_2(CO)_6(Se_7)]$, a Coordination Compound of Elemental Selenium with a Transition Metal: a Solution- and Solid-State Study (C) 193
- Towards One-Dimensional Carbon Wires Connecting Single Metal Centers: A Cumulenic C_5 Chain that Mediates Charge Transfer between Rhenium and Manganese Termini (C) 2199
- Trigonal-Bipyramidal Technetium and Rhenium Complexes with Tetradentate NS_3 Tripod Ligands (C) 1354

Rhodium compounds
- $[\{Rh_2Cp^*_2(\mu\text{-}CH_2)_2\}_2(\mu\text{-}S_4)]^{2+}$: A Novel Tetranuclear Cationic Complex with a Rectangular S_4 Unit (C) 1882
- Cooperativity in Rh_2 Complexes: High Catalytic Activity and High Regioselectivity in the Hydroformylation of Olefins (H) 67
- Increase in the Enantioselectivity of Asymmetric Hydrogenation in Water Influenced by Surfactants or Polymerized Micelles (C) 2197
- Ligand Effects on the Chemoselectivity of Transition Metal Catalyzed Reactions of α-Diazo Carbonyl Compounds (R) 1797
- Novel Bimetallic Model System for Cytochrome P_{450}: Effect of Membrane Environment on the Catalytic Oxidation (C) 2468
- Novel Rh^I Piano-Stool Complexes with New Hemilabile Ligands Ligating through Phosphane and Arene Groups: Synthesis, Characterization, and Reactivity (C) 2473
- The First Decaisopropylmetallocene: One-Pot Synthesis of $[Rh(C_5iPr_5)_2]PF_6$ from $[Rh(C_5Me_5)_2]PF_6$ by Formation of 20 Carbon–Carbon Bonds (C) 1637
- Trialkylstibanes as Bridging Ligands: Synthesis and Structure of the Dinuclear Complexes $[Rh_2Cl_2(\mu\text{-}SbiPr_3)(\mu\text{-}CR_2)_2]$ (C) 97

Ring contractions
- Ring Contractions in Carbohydrates (H) 1345

RNA
- Split Genes and RNA Splicing (Nobel Lecture) (R) 1229

RNA aptamers
- Isolation of RNA Aptamers for Biological Cofactors by In Vitro Selection (C) 1084

RNA cleavage
- Lanthanide(III) Tetraamide Macrocyclic Complexes as Synthetic Ribonucleases: Structure and Catalytic Properties of $[La(tcmc)(CF_3SO_3)(EtOH)](CF_3SO_3)_2$ (C) 773

RNA polymerases
- Gene Regulation in Eukaryotes (B) 2349

Roelen, Otto
- Otto Roelen, Pioneer in Industrial Homogeneous Catalysis (R) 2144 (2348)

Rotanes
- Hexaspiro[2.4.2.4.2.4.2.4.2.4.2.4]dotetraconta-4,6,11,13,18,20,25,27,32,34,39,41-dodecayne–An Exploding [6]Rotane (C) 869

Ruthenium compounds
- $[Ru_3(CO)_6(\eta^5{:}\eta^1\text{-}C_5H_4)_3]$: The First Six-Membered Ru_3C_3 Ring Formed by Insertion of C_5H_4 Units into Metal–Metal Bonds of $[Ru_3(CO)_{12}]$ (C) 2193
- A Water-Soluble "Bear Trap" Exhibiting Strong Anion Complexation Properties (C) 2456
- Construction of Carbon Frameworks with the Help of Ruthenium Complexes: 1,5-Cyclooctadiene as a Reagent in Transition Metal Catalyzed Reactions (H) 636
- Copper(II)-Mediated Oxidative Coupling of Bis(dimethylaminomethyl)arylruthenium Complexes to give $[(terpy)Ru^{III}(pincer\text{-}pincer)Ru^{III}(terpy)](CuCl_2)_4$ (C) 1282
- Desulfurization of Benzo[*b*]thiophene by S/Ru Exchange: Formation and Structure of the Cluster $[Ru_3(CO)_8(C_8H_6)]$ (C) 1381
- Electron Delocalization in Ethynyl-Bridged Binuclear Ruthenium(II) Polypyridine Complexes (C) 1884
- From Triple-Decker to Metallabenzene: A New Generation of Sandwich Complexes (C) 1003
- Magnetic Spin Effects on Photooxidation Quantum Yields of Ru^{II}-tris(bipyridine) Type Complexes in Magnetic Fields up to 17.5 Tesla (C) 1772
- Novel Trimerization of Phosphaalkynes in the Coordination Sphere of Ruthenium Complexes (C) 463
- Pronounced Electronic Coupling in Rigidly Connected N,C,N-Coordinated Diruthenium Complexes over a Distance of Up to 20 Å (C) 1775
- Propeller Isomerism of the Triphenylphosphane Ligand in Half-Sandwich Ru^{II} Complexes (C) 866
- Synthesis and Ring-Opening Polymerization of Highly Strained Ring-Tilted [2]Ruthenocenophanes (C) 989

Salbostatin
- The Trehalase Inhibitor Salbostatin, a Novel Metabolite from *Streptomyces albus*, ATCC 21838 (C) 1844

Sandwich complexes
- An Efficient Access to Organocerium(IV) Complexes: Synthesis and Structure of Bis[1,3,6-tris(trimethylsilyl)cyclooctatetraene]cerium(IV) (C) 1618
- A Novel Organomagnesium Compound Consisting of Two Triple-Decker Cations $[LMg(\mu\text{-}Me)_3MgL]^+$ and an Octamethyltrimagnesate Anion: $[\{Me_2Mg(\mu\text{-}Me)_2\}_2Mg]^{2-}$ (C) 1257
- $[Cp^*Fe(\eta^5\text{-}P_5)]$, a Sandwich Complex with Diverse Ligand Properties (C) 1110

- Cyclopropanation by Methylene Transfer from (η^2-Formaldehyde)zirconocene Complexes (C) 1955
- Decaphenylferrocene and Decaphenylferrocenium Tetrafluoroborate (C) 1731
- Doubly Bridged *rac*-Metallocenes of Zirconium and Hafnium (C) 1946
- From Triple-Decker to Metallabenzene: A New Generation of Sandwich Complexes (C) 1003
- New Upswing of Organolanthanoid Research: A Very Promising Revival of Organocerium(IV) Chemistry and the First Stable Lanthanoid(II/III)–Carbene Complexes (H) 2165
- (η^5-Pentamethylcyclopentadienyl)iron Complexes with η^5-2,3,5-Tricarbahexaboranyl and η^5-2,3-Dihydro-1,3-diborolyl Ligands (C) 203
- Single-Step Six-Electron Transfer in a Heptanuclear Complex: Isolation of Both Redox Forms (C) 2460
- Synthesis and Characterization of the First Compounds Containing a Stable Phosphirenyl Cation: Crystal and Molecular Structure of $[Ni(\eta^3\text{-}PC_2tBu_2)(\eta^5\text{-}P_3C_2tBu_2)W(CO)_5]$ (C) 2330
- Synthesis and Crystal Structure of the "Open" Calcocene $[(tBu_2C_5H_5)Ca\cdot thf]$ (C) 2191
- Synthesis and Ligative Behavior of a Gallacyclopentadiene (C) 1370
- Synthesis and Ring-Opening Polymerization of Highly Strained Ring-Tilted [2]Ruthenocenophanes (C) 989
- Synthesis and Structure of the First [2_2]Metallocenophanes (C) 1479
- Synthesis and Structure of the First Titanium(IV) α-Amino Acid Complexes (C) 1518
- Tetraaza[14]annulenezirconium(IV) Complexes with Butadiene Ligands and their Relationship with Bis(cyclopentadienyl)-zirconium(IV) Complexes (C) 2204
- The First Decaisopropylmetallocene: One-Pot Synthesis of $[Rh(C_5iPr_5)_2]PF_6$ from $[Rh(C_5Me_5)_2]PF_6$ by Formation of 20 Carbon–Carbon Bonds (C) 1637
- The First Metal Complexes with a Doubly S_3-Bridged Ferrocene Ligand (C) 1752
- The Lithocene Anion and "Open" Calcocene– New Impulses in the Chemistry of Alkali and Alkaline Earth Metallocenes (H) 2168
- The Simplest Metallocene Sandwich: the Lithocene Anion (C) 1744

Scanning electron microscopy
- Scanning Electron Microscopy and X-Ray Analysis (B) 1306

Scanning tunneling microscopy
- Photodecomposition of 10-Diazo-2-hexadecylanthrone on Graphite Studied by Scanning Tunneling Microscopy (C) 2080
- Scanning Tunneling Microscopy and Spectroscopy. Theory, Techniques, and Applications (B) 2226

Schweizer's reagent
- Cellulose in Schweizer's Reagent: A Stable, Polymeric Metal Complex with High Chain Stiffness (C) 884

Selenium compounds
- $[Cu_{44}Se_{22}(PEt_2Ph)_{18}]$ and $[Cu_{44}Se_{22}(PnButBu_2)_{12}]$: Synthesis and Structure of Two Copper Clusters with Isomeric Cu–Se Frameworks (C) 2287
- New Sulfur- and Selenium-Bridged Copper Clusters; Ab Initio Calculations on $[Cu_{2n}Se_n(PH_3)_m]$ Clusters (C) 746
- Polynuclear Lanthanide Complexes: Formation of a Selenium-Centered Sm_6 Complex, $[\{(C_5Me_5)Sm\}_6Se_{11}]$, (C) 2110
- $[Re_2I_2(CO)_6(Se_7)]$, a Coordination Compound of Elemental Selenium with a Transition Metal: a Solution- and Solid-State Study (C) 193
- Synthesis and Characterization of the First Thiaselanes (C) 1770
- Synthesis and Selective Radical Cleavage of C-4′-Modified Oligonucleotides (C) 1861
- Synthesis and Structure of the First Stable Germaneselone (C) 2316

Self-assembly
- A Liquid-Crystalline Polymer Network Built by Molecular Self-Assembly through Intermolecular Hydrogen Bonding (C) 1644
- Assembly Properties of Bolaamphiphiles from Dimeric Acids (C) 2078
- A Water-Soluble Prodrug of Taxol with Self-Assembling Properties (C) 1583
- Construction of a Multiwired Molecular Cable of Micrometer Length by a Self-Assembly Process (C) 2173
- Designer Proteins: On the Art of Synthesizing De Novo Metalloproteins (H) 2055
- Micrometer-Scale Lateral Structuring of Organic Thiolate Layers through Self-Organization (C) 1274
- Phase Transitions in Self-Assembled Monolayers Detected by Electrochemistry (C) 2332
- Self-Assembly and Structure of a 3 × 3 Inorganic Grid from Nine Silver Ions and Six Ligand Components (C) 2284
- Self-Assembly of a Dimeric Porphyrin Host (C) 2313
- The Two-Step Self-Assembly of [4]- and [5]Catenanes (C) 433
- Tunable Supramolecular Structures from a Gluconamide Containing Imidazole (C) 986

Self-replication
- Reciprocal Template Effects in a Replication Cycle (C) 1579
- Template Effects in New Self-Replicating Molecules (C) 1577

Sensors
- A Glucose-Selective Molecular Fluorescence Sensor (C) 2207
- Complexes of Partially Fluorinated Macrocycles with a Metal–Fluorine σ-Donor Bond and Their Suitability as Metal Ion Indicators (C) 2175

Sesquiterpenes
- A Short and Highly Stereoselective Synthesis of the 1,10-*seco*-Eudesmanolide Ivangulin (C) 2195

Schiff bases
- Dialdehyde + Diamine—Polymer or Macrocycle? (C) 125

Silametallacycles
- Competitive Generation of C–H and C–Si Bonds by Reductive Elimination: Formation of Silametallacycles by Metalation of Silyl Ligands (C) 317

Silicon compounds
- A Regioselective Palladium-Catalyzed Reduction of 3,3-Heterobimetalated Allylic Acetates–Synthesis and Reactivity of Allylic Bimetallic Compounds (C) 2448
- $(tBuSi)_2(PC_6H_{11})_3$: A Propellane-Like Cyclosilaphosphane with Remarkable Structure (C) 1484
- C_2H_2Si Isomers: Generation by Pulsed Flash Pyrolysis and Matrix-Spectroscopic Identification (C) 1248
- Competing Reactions of Silenes: [2+2], [4+2], and [6+2] Cycloadditions with Cycloheptadiene and Cycloheptatriene (C) 77
- 1,1-Dimethyl-1*H*-silirene (C) 766
- Doubly Lithiated Oligosilanes: Synthesis and Structure of the First Vicinal Dilithiodisilane (C) 2450
- Hexacoordinate Silicon in a Compound with an F_5SiC Unit (C) 1359
- Inversely Coordinating Silanide Ions in an Oligomeric Sodium Alcoholate (C) 216
- Long-Lived *ipso*-Silylated *p*-Toluenium Ions: Evidence from a Kinetic Isotope Effect (C) 1094
- Making and Breaking of Si–E (E = C, Si) Bonds by Oxidative Addition and Reductive Elimination Reactions (H) 419
- Metalation of Tris(trimethylsilyl)- and Tris(dimethylphenylsilyl)methane with Methylsodium: The First Dialkylsodate (C) 1268
- Molecular Siloxane Complexes of Rare Earth Metals—Model Systems for Silicate-Supported Catalysts? (C) 1285
- Selective Catalysis on Silicon Dioxide with Substrate-Specific Cavities (C) 471
- Silane Nitrile: Matrix Isolation, Adduct with Hydrogen (C) 473
- Soluble Organic Derivatives of Aluminosilicates with $Al_2Si_2O_4$ and $Al_4Si_2O_6$ Frameworks (C) 2103
- Stable Silanetriols as Building Blocks for the Synthesis of Titanasilasesquioxanes– Model Compounds for Titanium-Doped Zeolites (C) 1352
- Stable Tetrakis(trialkylsilyl)disilenes; Synthesis, X-Ray Structures, and UV/VIS Spectra (C) 1489
- Structure of a (4 + 4)-Coordinate Silicon Compound, a Precursor of Hypercoordinate Silyl Mono- and Dications (C) 1097
- Structures of 2-$(Me_2NCH_2)C_6H_4$-Substituted Oligosilanes (C) 1854
- Synthesis and Structure of the Disilagermirane $R_2Ge(SiR_2)_2$ and the Solvent-Separated Ion Pair $[Li([12]crown\text{-}4)_2][GeR_3]$; (R = $SiMe_3$) (C) 113
- The First Zwitterionic, Optically Active Disilicate with Pentacoordinate Silicon (C) 1186
- The Formation and an Unusual Dimerization of 2-Mesityl-1,1-bis(trimethylsilyl)silene (C) 1615

Silver compounds
- "Free" $[Fe(tpp)]^+$ Cation: A New Concept in the Search for the Least Coordinating Anion (C) 2433
- Metal Complexes of Marine Peptide Metabolites: A Novel Ag_4 Cluster (C) 1516
- Self-Assembly and Structure of a 3 × 3 Inorganic Grid from Nine Silver Ions and Six Ligand Components (C) 2284
- The Crystal Structures of Base-Free, Monomeric Arylcopper(I) and Arylsilver(I) Compounds; Two Cases of Mistaken Identity? (C) 2443
- Thermal Decomposition of Silver Oxide Monitored by Raman Spectroscopy: From AgO Units to Oxygen Atoms Chemisorbed on the Silver Surface (C) 85
- Three-Dimensional Interpenetrating Double and Triple Framework Structures in $[Cd(bpy)_2\{Ag(CN)_2\}_2]$ and $[Cd(pyrz)\{Ag_2(CN)_3\}\{Ag(CN)_2\}]$ (C) 1665

Solar reactors
- The Photochemical Synthesis of Fine Chemicals with Sunlight (R) 2009

Solid-phase synthesis
- Life During a Golden Age of Peptide Chemistry: The Concept and Development of Solid-Phase Peptide Synthesis (B) 1990

- Ring Closures on Polymeric Supports—Formation of Extremely Large Macrocycles by Intrapolymeric Cyclooligomerizations (C) 1960

Solid-state chemistry
- A Novel Open-Framework Cobalt Phosphate Containing a Tetrahedrally Coordinated Cobalt(II) Center: $CoPO_4 \cdot 0.5\ C_2H_{10}N_2$ (C) 639
- Borophosphates—A Neglected Class of Compounds: Crystal Structures of $Mn^{II}[BPO_5]$ (M^{II} = Ca, Sr) and $Ba_3[BP_3O_{12}]$ (C) 749
- Chemistry and Crystal Growth (R) 143
- Evidence of Room-Temperature Superconductivity in the Bi-Sr-Cu-O System (C) 897
- Reactivity in Molecular Crystals (B) 1991
- Solid State Chemistry. An Introduction (B) 587
- Solid State Chemistry. Synthesis, Structure, and Properties of Selected Oxides and Sulfides (B) 1403

Solid-state structures
- Determination of Reaction Paths for Pentacoordinate Metal Complexes with the Structure Correlation Method (R) 823
- Discrete M_6N Octahedra in the Subnitrides $Na_{16}Ba_6N$ and $Ag_{16}Ca_6N$: A Reconsideration of the Ag_8Ca_3 Structure Type (C) 689
- Fullercages without Carbon—Fulleranes, Fullerenes, Space-filler-enes? (H) 843
- Hf_3Te_2: A New and Remarkable Layered Compound (C) 2328
- $(H_3N(CH_2)_6NH_3)_4[W_{18}P_2O_{62}] \cdot 3H_2O$, a Microporous Solid from Dawson Anions and 1,6-Diaminohexane (C) 2491
- Proton-Transfer-Dependent Reversible Phase Changes in the 4,4′-Bipyridinium Salt of Squaric Acid (C) 181
- Structure of a Mixed Phosphate/Phosphonate Layered Zirconium Compound from Synchrotron X-Ray Powder Diffraction Data (C) 2324
- Three-Dimensional Interpenetrating Double and Triple Framework Structures in $[Cd(bpy)_2\{Ag(CN)_2\}_2]$ and $[Cd(pyrz)\{Ag_2(CN)_3\}\{Ag(CN)_2\}]$ (C) 1665
- Two-Dimensional Sheets of Tetragonal Copper(II) Lattices: X-Ray Crystal Structure and Magnetic Properties of $[Cu(C_6O_4Cl_2)(C_4H_4N_2)]_n$ (C) 1759

Solvation energies
- Ether-Solvated Sodium Ions in Salts Containing π-Hydrocarbon Anions: Crystallization, Structures, and Semiempirical Solvation Energies (C) 875

Soraphens
- Total Synthesis of Soraphen $A_{1\alpha}$ (C) 2466

Spin crossover
- Thermal and Optical Switching of Iron(II) Complexes (R) 2024

Spin density distribution
- The Spin Density Distribution in the Tetracyanoethylene Radical Anion, $[TCNE]^{\cdot -}$, by Single-Crystal Polarized Neutron Diffraction (C) 1397

Spin effects
- Magnetic Spin Effects on Photooxidation Quantum Yields of Ru^{II}-tris(bipyridine) Type Complexes in Magnetic Fields up to 17.5 Tesla (C) 1772

Spin-state isomerism
- Bond-Stretch Isomers and Spin-State Isomers: A Comment on the Article "Bond-Stretch Isomers: Fact not Fiction" (C) 1462

Splicing
- Split Genes and RNA Splicing (Nobel Lecture) (R) 1229

Squalestatins
- Synthesis of the First Fully Functionalized Core of the Zaragozic Acids/Squalestatins (C) 2187
- Total Synthesis of Zaragozic Acid A/Squalestatin S1 (C) 2190
- Zaragozic Acid A/Squalestatin S1: Synthetic and Retrosynthetic Studies (C) 2184

Squaric acid
- Proton-Transfer-Dependent Reversible Phase Changes in the 4,4′-Bipyridinium Salt of Squaric Acid (C) 181

Squarylium ions
- Synthesis and Structure of New Cationic Squarylium Dyes (C) 1001

Statistical mechanics
- Theoretical Treatment of Liquids and Liquid Mixtures (B) 697

Stone, F. G. A.
- Leaving No Stone Unturned: Pathways in Organometallic Chemistry (B) 2119

Strained rings
- A New Synthetic Route to 1,2-Dihydrocyclobutaarenes (C) 1757
- 2*H*,5*H*-Benzo[1,2-*b*:4,5-*b*′]bisthiete—A Highly Reactive Bisdiene System (C) 465
- C_2H_2Si Isomers: Generation by Pulsed Flash Pyrolysis and Matrix-Spectroscopic Identification (C) 1248
- Dimesityldioxirane—A Dioxirane Stable in the Solid State (C) 2212
- 1,1-Dimethyl-1*H*-silirene (C) 766
- Gas-phase Synthesis of Reactive Molecules Using Adsorbed Reagents (R) 1332
- Mills–Nixon Effect: Wherefore Art Thou? (H) 1721
- Palladium-Catalyzed C–H Activation of *tert*-Butyl Groups: A Simple Synthesis of 1,2-Dihydroxycyclobutabenzene Derivatives (C) 103
- Stable Germirane Derivatives (C) 659
- Structures of 2-$(Me_2NCH_2)C_6H_4$-Substituted Oligosilanes (C) 1854
- Synthesis and Reactivity of a Naphtho[1,8-*bc*]boret (C) 1247
- The Effect of Fusion of Angular-Strained Rings on Benzene: Crystal Structures of 1,2-Dihydrocyclobuta[*a*]cyclopropa[*c*]-, 1,2,3,4-Tetrahydrodicyclobuta[*a,c*]-, 1,2,3,4-Tetrahydrodicyclobuta[*a,c*]-cyclopropa[*e*]-, and 1,2,3,4,5,6-Hexahydrotricyclobuta[*a,c,e*]benzene (C) 313
- The First Isolable Dithiirane by Oxidation of a Dithietane (C) 777
- Transannular Addition of Methyllithium to 5,12:6,11-Di[1,2]benzenodibenzo[*a,e*]-cyclooctene and Its 5,6-Epoxy Derivative (C) 993
- Triple Bonds in Small Rings: Testing the Limits of Chemical Bonds (H) 1455

Structural chemistry
- Inorganic Structural Chemistry (B) 479

Structure correlation
- Determination of Reaction Paths for Pentacoordinate Metal Complexes with the Structure Correlation Method (R) 823

Structure–activity relationships
- Mapping the Electrostatic Potential of Muscarinic and Nicotinic Agonists with Artificial Neural Networks (C) 643
- Peptide and Protein Hormones. Structure, Regulation, Activity. A Reference Manual (B) 1117

Structure elucidation
- A Novel Type of Stereoisomerism in Calix[4]arene-Based Carceplexes (C) 2345
- Crystal Structure of 2,5-Di-*tert*-butylhydroquinone: Polar Stacking of Nonpolar Hydrogen-Bonded Sheets with Trigonal Symmetry (C) 1755
- Determination of the Relative Configuration by Distance Geometry Calculations with Proton–Proton Distances from NOESY Spectra (C) 753
- Doubly Lithiated Oligosilanes: Synthesis and Structure of the First Vicinal Dilithiodisilane (C) 2450
- FAST NOESY Experiments—An Approach for Fast Structure Determination (C) 332
- Jacobson and Heintschel Peroxides (C) 775
- Nonclassical 1,2-Diboretanes and 1,2-Diborolanes (C) 2303
- Structure of a Mixed Phosphate/Phosphonate Layered Zirconium Compound from Synchrotron X-Ray Powder Diffraction Data (C) 2324
- Synthesis, Crystal and Molecular Structure of Boc-Pro-ΔPhe-Ala-ΔPhe-Ala-OMe; A Pentapeptide with a Novel β-Bend Ribbon Structure (C) 970
- The Crystal Structures of Base-Free, Monomeric Arylcopper(I) and Arylsilver(I) Compounds; Two Cases of Mistaken Identity? (C) 2443

Strychnine
- New Total Syntheses of Strychnine (H) 1144

Subnitrides
- Discrete M_6N Octahedra in the Subnitrides $Na_{16}Ba_6N$ and $Ag_{16}Ca_6N$: A Reconsideration of the Ag_8Ca_3 Structure Type (C) 689

Sugar alcohols
- Linear Coordination Polymers of Copper(II) and Fourfold Deprotonated Sugar Alcohols (C) 1742

Sugar amino acids
- A Sugar Amino Acid as a Novel Peptidomimetic (C) 687

Sulfonamido-pseudopeptides
- Synthesis of Sulfonamido-Pseudopeptides: New Chiral Unnatural Oligomers (C) 2067

Sulfoxides
- Oxidation of Metal-Coordinated Thioethers with Dimethyldioxirane—A New Stereoselective Synthesis of Chiral Sulfoxides (C) 1609

Sulfoximides
- Diastereoselective Hydroxyalkylation of Enantiomerically Pure 2-Alkenylsulfoximides (C) 444

Sulfur compounds
- A Building Principle of Amorphous Chalcogenides of Transition Metals: The "Extrusion" of the Electron Rich Cluster $[Re_4S_2(SO_2)_4(CN)_{10}]^{8-}$ from a-Re_2S_7 (C) 770
- Aurophilicity at Sulfur Centers: Synthesis and Structure of the Tetragold(I) Species $[(Ph_3PAu)_4S](CF_3SO_3)_2 \cdot 2CH_2Cl_2$ (C) 769
- Benzobis(thiadiazole)s Containing Hypervalent Sulfur Atoms: Novel Heterocycles with High Electron Affinity and Short Intermolecular Contacts between Heteroatoms (C) 1977
- 2*H*,5*H*-Benzo[1,2-*b*:4,5-*b*′]bisthiete—A Highly Reactive Bisdiene System (C) 465
- Concerning the Questionable Existence of Thioxoindigoid Compounds (C) 739
- Ladder Polymers with a Heteroacene Skeleton (C) 2424
- (Pentafluoro-λ^6-sulfanyl)cyclopentadiene and Cyclopentadienylidenetetrafluoro-λ^6-sulfane (C) 93
- Preparation and Structure of $C_{76}(S_8)_6$: A First Step in the Crystallographic Investigation of Higher Fullerenes (C) 1651

- Redox Control for the Recognition of Ag^+ Ions in a Macrocycle Containing Two SH Groups or an S–S Bridge inside the Cavity (C) 1750
- Stereoselective Reactions of Sulfinylated Benzyl Radicals: Effects of Solvents and Lewis Acids (C) 1601
- Strategies for Nonmacrocyclic Polythioether Ligands: New Pentacoordinating Architectures (C) 319
- Synthesis and Characterization of the First Thiaselanes (C) 1770
- Synthesis, Structure, and Thermolysis of a Tetracoordinate $1,2\lambda^4$-Oxathietane (C) 2094
- The First Isolable Dithiirane by Oxidation of a Dithietane (C) 777
- Thianickelacycles by Ring-Opening Reactions of Cyclic Thioethers and Their Subsequent Carbonylation to Thioesters (C) 1748

Sulfur dioxide
- Liquid Sulfur Dioxide as a Lewis-Acidic Solvent for the Alkylation and Alkoxyalkylation of Allylsilanes (C) 788

Sulphones
- Sulphones in Organic Synthesis (B) 1404

Super acids
- Super-Acids and Acidic Melts as Inorganic Chemical Reaction Media (B) 482

Superconductors
- Evidence of Room-Temperature Superconductivity in the Bi-Sr-Cu-O System (C) 897
- Organic Superconductors (Including Fullerenes). Synthesis, Structure, Properties, and Theory (B) 1119
- Solvent-Free Volatile Alkoxides of the Alkaline-Earth Elements (C) 105

Supercritical fluids
- Analysis with Supercritical Fluids: Extraction and Chromatography (B) 1402

Supported reagents
- Supported Reagents. Preparation, Analysis and Applications (B) 239

Supramolecular chemistry
- Cyclodextrins as Building Blocks for Supramolecular Structures and Functional Units (R) 803
- Stable Flexible Fibers and Rigid Tubules Made from Single-Chain Perfluoroalkylated Amphiphiles (C) 1514

Surface chemistry
- Active Surface Carbon—A Reactive Intermediate in the Production of Synthesis Gas from Methane and Carbon Dioxide (C) 1657
- Gas-phase Synthesis of Reactive Molecules Using Adsorbed Reagents (R) 1332

Surfaces
- Chemical Analysis of Inorganic and Organic Surfaces and Thin Films by Static Time-of-Flight Secondary Ion Mass Spectrometry (TOF-SIMS) (R) 1023

Surfactants
- Synthesis of Very Highly Ordered Liquid Crystalline Phases by Complex Formation of Polyacrylic Acid with Cationic Surfactants (C) 1869

Sweeteners
- Conformational Requirements for Sweet-Tasting Peptides and Peptidomimetics (R) 1437

Symmetry
- Icons and Symmetries (B) 482

Syngas
- NiO/CaO-Catalyzed Formation of Syngas by Coupled Exothermic Oxidative Conversion and Endothermic CO_2 and Steam Reforming of Methane (C) 2104

Synthesis design
- The Determination of Maximum Common Substructures by a Genetic Algorithm: Application in Synthesis Design and for the Structural Analysis of Biological Activity (C) 1189

Synthesis gas
- Active Surface Carbon—A Reactive Intermediate in the Production of Synthesis Gas from Methane and Carbon Dioxide (C) 1657

Synthetic methods
- Chromium Carbene Complexes in Organic Synthesis: Recent Developments and Perspectives (H) 303
- Conjugate Addition Reactions in Organic Synthesis (B) 1197
- Fine Feathers Make Fine Birds: The Heck Reaction in Modern Garb (R) 2379

Taxol
- A Water-Soluble Prodrug of Taxol with Self-Assembling Properties (C) 1583
- Chemistry and Biology of Taxol (R) 15
- Synthesis of C-2 Taxol Analogues (C) 1581
- The First Total Syntheses of Taxol (H) 959

Technetium compounds
- Technetium Radiopharmaceuticals—Fundamentals, Synthesis, Structure, and Development (R) 2258
- Trigonal-Bipyramidal Technetium and Rhenium Complexes with Tetradentate NS_3 Tripod Ligands (C) 1354

Tellurium compounds
- Hf_3Te_2: A New and Remarkable Layered Compound (C) 2328
- $[Mn_4Te_4(SC_3H_7)_4]^{4-}$ and $[Mn_4Te_4(SeC_3H_7)_4]^{4-}$: Novel Heterocubane Clusters of Manganese (C) 2322
- New Forms and Functions of Tellurium: From Polycations to Metal Halide Tellurides (R) 163
- Synthesis and Structure of $[WOTe_3]^{2-}$ (C) 1859

Template effects
- Reciprocal Template Effects in a Replication Cycle (C) 1579
- Template Effects in New Self-Replicating Molecules (C) 1577

Template syntheses
- A Template Synthesis of Stable Conjugated Primary Enamines from Ketones, Nitriles, and Butadiene (C) 1114
- Mesoscopic Sheets of a Cyano-Bridged Cu–Ni Coordination Complex: Template Synthesis at the Interlayers of Cast Multibilayer Films (C) 2483
- Template Syntheses (R) 375

Tetracyanoethylene
- The Spin Density Distribution in the Tetracyanoethylene Radical Anion, $[TCNE]^{\cdot-}$, by Single-Crystal Polarized Neutron Diffraction (C) 1397

Tetrahydrofurans
- A Convergent Synthesis of 2,5-*trans*-Linked Oligo(tetrahydrofuran)s: Potential Building Blocks for a Polyether Helix with Ion Channel Activity (C) 1180
- A Multiple Five-Membered-Ring-Selective Williamson Reaction as a Key Step in the Stereoselective Construction of 2,5-Linked Oligo(tetrahydrofuran)s (C) 1873

Tetrathiafulvalenes
- Coexistence of Mobile and Localized Electrons in Bis(ethylene)dithiotetrathiafulvalene (BEDT-TTF) Radical Salts with Paramagnetic Polyoxometalates: Synthesis and Physical Properties of $(BEDT\text{-}TTF)_8[CoW_{12}O_{40}]\cdot 5.5H_2O$ (C) 223
- Dendritic Macromolecules Incorporating Tetrathiafulvalene Units (C) 1761
- *trans–cis* Isomerization upon One-Electron Oxidation of [12]- and [14]Tetrathiafulvalenophanes (C) 1379

Textbooks
- Chaos and Complexity (B) 1521
- Electrochemistry. Principles, Methods, and Applications (B) 1989
- Electrode Kinetics for Chemists, Chemical Engineers, and Material Scientists (B) 1304
- Fundamentals of Nuclear Magnetic Resonance (B) 1670
- Inorganic Biochemistry. An Introduction (B) 1196
- Inorganic Structural Chemistry (B) 479
- Organic Photochemistry: A Visual Approach (B) 483
- Principles of Electrochemistry (B) 1989
- Solid State Chemistry. An Introduction (B) 587
- Solid State Chemistry. Synthesis, Structure, and Properties of Selected Oxides and Sulfides (B) 1403
- Sourcebook of Advanced Organic Laboratory Preparations (B) 231

Thallium compounds
- $[2,6\text{-}iPr_2C_6H_3(Me_3Si)NTl]_4$—A Covalent Thallium(I)–Nitrogen Compound with Weak Arene–Thallium Interactions (C) 1351
- Tetrakis(hypersilyl)dithallium(*Tl–Tl*): A Divalent Thallium Compound (C) 681

Theoretical chemistry
- Frontier Orbitals and Properties of Organic Molecules (B) 239
- Theoretical Definition of a Functional Group and the Molecular Orbital Paradigm (R) 620

Thermal analysis
- Thermal Analysis—Techniques and Applications (B) 586

Thermodynamics
- C_{70} Is More Stable than C_{60}: Experimental Determination of the Heat of Formation of C_{70} (C) 996
- Determination of Thermodynamic Properties (B) 586
- Kinetic Theory and Irreversible Thermodynamics (B) 481

Thiaboranes
- Macropolyhedral Boron-Containing Cluster Chemistry: Isolation and Characterization of the First Macropolyhedral Thiaborane, the *arachno*-Type $[9,9'\text{-}S_2B_{17}H_{18}]^-$ Ion (C) 1599

Thiadiazoles
- Benzobis(thiadiazole)s Containing Hypervalent Sulfur Atoms: Novel Heterocycles with High Electron Affinity and Short Intermolecular Contacts between Heteroatoms (C) 1977

Thiaselanes
- Synthesis and Characterization of the First Thiaselanes (C) 1770

Thin films
- Chemical Analysis of Inorganic and Organic Surfaces and Thin Films by Static Time-of-Flight Secondary Ion Mass Spectrometry (TOF-SIMS) (R) 1023
- Enzymatic Grooming of Organic Thin Films (C) 871
- Mesoscopic Sheets of a Cyano-Bridged Cu–Ni Coordination Complex: Template Synthesis at the Interlayers of Cast Multibilayer Films (C) 2483
- Micrometer-Scale Lateral Structuring of Organic Thiolate Layers through Self-Organization (C) 1274
- Supramolecular Architecture. Synthetic Control in Thin Films and Solids (B) 1009

Thioindigo
- 3,3'-Bis(dicyanomethylene)-4,4,4',4'-tetramethyl-2,2'-bithiolanylidene, a Compound Containing the Fundamental Chromophore of Thioindigo: (*E*/*Z*) and Valence Isomers, Thermo- and Photochromism (C) 1966

Thioles
- Micrometer-Scale Lateral Structuring of Organic Thiolate Layers through Self-Organization (C) 1274

Tin compounds
- A Regioselective Palladium-Catalyzed Reduction of 3,3-Heterobimetalated Allylic Acetates–Synthesis and Reactivity of Allylic Bimetallic Compounds (C) 2448
- A Stannanediyl with a Tin–Carbon Multiple Bond (C) 456
- Bis(2,4,6-tri-*tert*-butylphenyl)stannanediyl: A Diarylstannylene without Donor Stabilization (C) 1846
- Synthesis and Molecular Structure of Calcium Bis(trimethylstannanide)·4THF (C) 1493
- Synthesis of Oxa- and Azapalladacycles from Organostannanes (C) 2482
- Synthesis, Structures, and Reactions of Two Bis(diaminostannylene)s and a Bis(diaminogermylene) Containing a Central C_6 Ring (C) 1156

Titanium compounds
- $[Cp_2Ti(C\equiv CtBu)_2]$ as an Alkynyl Transfer Reagent: Synthesis and Characterization of the Asymmetrically Bridged Heterodimetallic Complex $[Cp_2Ti(C\equiv CtBu)_2Pt(PPh_3)]\cdot 0.5\,THF$ (C) 2083
- Effects of Metal-Ion Dopants on the Photocatalytic Reactivity of Quantum-Sized TiO_2 Particles (C) 1091
- Homoleptic Thiolato Complexes: Di- and Trinuclear Ti^{IV} Complexes with Unexpected Metal–Sulfur Cores, $[NMe_2H_2][Ti_2(SMe)_9]$ and $[Ti_3(SMe)_{12}]$ (C) 1981
- Molecular Solids as Ligands in Organometallic Chemistry: $[Cp^*_6Ti_6Na_7F_{19}\cdot 2.5\,thf]$ ($Cp^* = C_5Me_5$) and $[Cp^*_4Ti_4Mg_2F_{12}\cdot 7\,thf]$, Links Between Ionic Solids and Organometallic Compounds (C) 555
- Stable Silanetriols as Building Blocks for the Synthesis of Titanasilasesquioxanes—Model Compounds for Titanium-Doped Zeolites (C) 1352
- Synthesis and Structure of the First Titanium(IV) α-Amino Acid Complexes (C) 1518
- Titanium Complexes with Tripodal Amido Ligands: Building Blocks for Stable Bimetallic Coordination Compounds Containing Highly Polar Metal–Metal Bonds (C) 676

Total syntheses
- A Concise Total Synthesis of (±)-Mamanuthaquinone by Using an *exo*-Diels–Alder Reaction (C) 853
- A Convergent Total Synthesis of Calicheamicin γ_1^I (C) 858
- A Total Synthesis of (+)-2'*S*,3'*R*-Zoapatanol (C) 2182
- First Total Synthesis of (±)-Rabelomycin (C) 99
- New Total Syntheses of Strychnine (H) 1144
- The First Total Syntheses of Taxol (H) 959
- The Total Synthesis of *cis*-7,8-Dihydroxy-11,12-dehydrocalamenene by Regio- and Diastereoselective Alkylation of Chiral η^6-Arenetricarbonylchromium Complexes: An Unexpected Case of Nucleophilic Aromatic *tele*-Substitution with Methoxide as a Leaving Group (C) 109
- Total Synthesis of Soraphen $A_{1\alpha}$ (C) 2466
- Total Synthesis of Zaragozic Acid A/Squalestatin S1 (C) 2190

Toxicology
- Toxicity of Chlorinated Organic Compounds: Effects of the Introduction of Chlorine in Organic Molecules (R) 1920

Trace analysis
- Luminescent Labels—More than Just an Alternative to Radioisotopes? (R) 1044

Transition states
- Organizing Principle of Complex Reactions and Theory of Coarctate Transition States (R) 255

Trifluoroethanesulfonyl chloride
- A Novel Reaction Sequence for the Coupling of Nucleophiles to Agarose with 2,2,2-Trifluoroethanesulfonyl Chloride (C) 120

Trimethylenemethane
- Bis(pentamethylcyclopentadienyl)(η^3-trimethylenemethane)zirconium: A New Mode of Bonding for the Trimethylenemethane Ligand (C) 2465

Trimethylphenylborane
- Synthesis and Properties of 2,4,6-Trimethylphenylborane (Mesitylborane), a Stable Alternative to Thexylborane (C) 851

Triphenylmethyl radical
- Jacobson and Heintschel Peroxides (C) 775

Tris(imino)metaphosphates
- Monomeric Tris(imino)metaphosphates (C) 2111

Trivial names
- Dictionary of Trivial Names/Trivialnamen-Handbuch (B) 1305

Tungsten compounds
- $(H_3N(CH_2)_6NH_3)_4[W_{18}P_2O_{62}]\cdot 3\,H_2O$, a Microporous Solid from Dawson Anions and 1,6-Diaminohexane (C) 2491
- Synthesis and Characterization of the First Compounds Containing a Stable Phosphirenyl Cation: Crystal and Molecular Structure of $[Ni(\eta^3\text{-}PC_2tBu_2)(\eta^5\text{-}P_3C_2tBu_2)W(CO)_5]$ (C) 2330
- Synthesis and Structure of $[WOTe_3]^{2-}$ (C) 1859
- Thermally Induced Ring Cleavage of a 2*H*-1,2-Azaphosphirene Tungsten Complex (C) 2427

Turcasarin
- Turcasarin, the Largest Expanded Porphyrin to Date (C) 1509

Uranium compounds
- A Difunctional Receptor for the Simultaneous Complexation of Anions and Cations; Recognition of KH_2PO_4 (C) 467

Urea
- Zigzag Channels in the Structure of Sebaconitrile/Urea (C) 649

Urocanase
- On the Mechanism of the Urocanase Reaction: Confirmation of the Structure of the NAD^+-Inhibitor Adduct by Direct ^{13}C-^{13}C Coupling (C) 1279

Valence isomerization
- 3,3'-Bis(dicyanomethylene)-4,4,4',4'-tetramethyl-2,2'-bithiolanylidene, a Compound Containing the Fundamental Chromophore of Thioindigo: (*E*/*Z*) and Valence Isomers, Thermo- and Photochromism (C) 1966

Vanadium compounds
- Synthesis and Structure of Oxovanadium(v)-Organophosphonate Cluster Encapsulating a Chloride Ion: $[ClV_7O_{12}(O_3PC_6H_5)_6]^{2-}$ (C) 325
- The Oxovanadium–Organoarsonate System: $[2\,CH_3OH \subset V_{12}O_{14}(OH)_4(PhAsO_3)_{10}]^{4-}$ and $[2\,H_2O \subset V_{12}O_{12}(OH)_2(H_2O)_2(PhAsO_3)_{10}(PhAsO_3H)_4]^{2-}$, Clusters with Nanometer Dimensions and Cavities for Neutral Molecules (C) 760
- The Oxovanadium–Organophosphonate System: Complex Cluster Structures $[(VO)_6(tBuPO_3)_8Cl]$, $[(VO)_4\{PhP(O)_2OP(O)_2Ph\}_4Cl]^-$, and $[V_{18}O_{25}(H_2O)_2(PhPO_3)_{20}Cl_4]^{4-}$ with Encapsulated Chloride Anions Prepared from Simple Precursors (C) 757

Vesicles
- Molecular Golf Balls: Vesicles from Bowl-Shaped Host Molecules (C) 1662
- Sterically Stabilized Vesicles (R) 1685
- Tunable Supramolecular Structures from a Gluconamide Containing Imidazole (C) 986

Vinyl radicals
- Determination of the Kinetics of Vinyl Radical Reactions by the Characteristic Visible Absorption Spectra of Vinylperoxyl Radicals (C) 1262

Vitamins
- Homogeneous Catalytic Oxidation of Arenes and a New Synthesis of Vitamin K_3 (C) 2475

Wacker oxidations
- Wacker Oxidation of 1-Decene to 2-Decanone in the Presence of a Chemically Modified Cyclodextrin System: A Happy Union of Host–Guest Chemistry and Homogeneous Catalysis (C) 2100

Water oxidation
- Oxygen Evolution by Oxidation of Water with Manganese Porphyrin Dimers (C) 1839

X-ray absorption spectroscopy
- X-Ray Absorption Spectroscopy of Amorphous Solids, Liquids, and Catalytic and Biochemical Systems—Capabilities and Limitations (R) 45

Zaragozic acids
- Synthesis of the First Fully Functionalized Core of the Zaragozic Acids/Squalestatins (C) 2187
- Total Synthesis of Zaragozic Acid A/Squalestatin S1 (C) 2190
- Zaragozic Acid A/Squalestatin S1: Synthetic and Retrosynthetic Studies (C) 2184

Zeolites
- A Novel Open-Framework Cobalt Phosphate Containing a Tetrahedrally Coordinated Cobalt(II) Center: $CoPO_4\cdot 0.5\,C_2H_{10}N_2$ (C) 639
- $(H_3N(CH_2)_6NH_3)_4[W_{18}P_2O_{62}]\cdot 3\,H_2O$, a Microporous Solid from Dawson Anions and 1,6-Diaminohexane (C) 2491
- Ionization and Delocalization in Potassium Zeolite L: A Combined Neutron Diffraction and Electron Spin Resonance Study (C) 641
- Schiff Base Complexes with Five-Coordinate Cobalt as Dioxygen Activating Sites in Zeolites (C) 431
- Stable Silanetriols as Building Blocks for the Synthesis of Titanasilasesquioxanes—Model Compounds for Titanium-Doped Zeolites (C) 1352
- Synthesis of the First Microporous Aluminum Phosphonate with Organic Groups Covalently Bonded to the Skeleton (C) 2335

- Zeolite, Clay and Heteropoly Acid in Organic Reactions (B) 1893

Zinc compounds
- Crystal Structure of a Supramolecular Dimer Formed by $\pi-\pi$ Interactions between Two Interlocked Cyclic Zinc Porphyrin Trimers (C) 429
- On the Nature of Zinc Chloride–Aldehyde Interactions (C) 2089

Zirconium compounds
- A Template Synthesis of Stable Conjugated Primary Enamines from Ketones, Nitriles, and Butadiene (C) 1114
- Bis(pentamethylcyclopentadienyl)(η^3-trimethylenemethane)zirconium: A New Mode of Bonding for the Trimethylenemethane Ligand (C) 2465
- Cyclopropanation by Methylene Transfer from (η^2-Formaldehyde)zirconocene Complexes (C) 1955
- Doubly Bridged *rac*-Metallocenes of Zirconium and Hafnium (C) 1946
- Facile Reduction of a Dialkyl Zirconium(IV) Octaethylporphyrin (OEP) Complex by H_2: Crystal Structure and Spectroscopic Characterization of [(OEP)Zr-CH_2SiMe_3] (C) 95
- Monomer–Dimer Equilibria in Homo- and Heterodinuclear Cationic Alkylzirconium Complexes and Their Role in Polymerization Catalysis (C) 1634
- Preparation and Preliminary Characterization of a Covalently Pillared Zirconium Phosphate–Diphosphonate with Interlayer Microporosity (C) 1594
- Reactions of [(C_5Me_5)ZrF_3] with $AlMe_3$—Synthesis and Structure of a Zirconium–Aluminum–Carbon Cluster (C) 967
- Structure of a Mixed Phosphate/Phosphonate Layered Zirconium Compound from Synchrotron X-Ray Powder Diffraction Data (C) 2324
- Synthesis and Structure of the Smallest Cyclic Cumulene; Reaction of 1,3-Diynes with Zirconocene Complexes (C) 1605
- Tetraaza[14]annulenezirconium(IV) Complexes with Butadiene Ligands and their Relationship with Bis(cyclopentadienyl)-zirconium(IV) Complexes (C) 2204
- Tris(η^4-naphthalene)zirconate(2−) (C) 1973
- Unexpected Reactions of Acetylenedicarboxylates with Zirconocene Complexes (C) 1850
- [$Zr_3Cp_2(O_2CNiPr_2)_6(\mu_3\text{-}O)(\mu_2\text{-}CCO)$], the First Crystallographically Established Ketenylidene Complex; A Model for CO Reductive Cleavage on Metal Surfaces (C) 1188

Zoapatanol
- A Total Synthesis of (+)-2′*S*,3′*R*-Zoapatanol (C) 2182